

# Annual Cumulated Index

ACCESSION NOS. A66-10001 to A66-43226

## INTERNATIONAL AEROSPACE ABSTRACTS

PART 1, PERIODICALS SCANNED, SUBJECT INDEX, A - L

1966

VOL. 6

*How To Obtain Publications  
Abstracted--See Page IV*

U. of ILL. LIBRARY

JAN 17 1967

CHICAGO CIRCLE

PUBLISHED BY THE TECHNICAL INFORMATION SERVICE  
AMERICAN INSTITUTE OF AERONAUTICS AND ASTRONAUTICS





Digitized by the Internet Archive  
in 2023



# INTERNATIONAL AEROSPACE ABSTRACTS

Prepared and published by the TECHNICAL INFORMATION SERVICE,  
AMERICAN INSTITUTE OF AERONAUTICS AND ASTRONAUTICS, INC., under  
NATIONAL AERONAUTICS AND SPACE ADMINISTRATION  
Contract No. NSR 33-003-009

TL  
500  
I57  
vol. 6  
pt. 1  
N/C

## ANNUAL CUMULATED INDEX

PART 1  
PERIODICALS SCANNED, SUBJECT INDEX, A - L

VOLUME 6  
JANUARY-DECEMBER  
1966

ACCESSION NUMBERS A66-10001 to A66-43226

**INTERNATIONAL AEROSPACE ABSTRACTS** is published semimonthly by the Technical Information Service, American Institute of Aeronautics and Astronautics, Inc., at Phillipsburg, N. J.  
Editorial and Subscription Offices: 750 Third Avenue, New York, N. Y. 10017  
Telephone 212 TN-7-8300 TWX: 212 867-7265

### SUBSCRIPTION INFORMATION.

Semimonthly issues: United States and Possessions, 1 year, \$25 postpaid; Foreign Countries, 1 year, \$33 postpaid.

Cumulated Index Volumes: United States and Possessions, 1 year, \$25 postpaid; Foreign Countries, 1 year, \$33 postpaid.

Second-class postage paid at Phillipsburg, N. J.

Copyright © 1966 by the American Institute of Aeronautics and Astronautics, Inc.



# CONTENTS

	Pages	
PART 1		
INTRODUCTION .....	iii	
HOW TO OBTAIN PUBLICATIONS ABSTRACTED .....	iv	
CROSS REFERENCES .....	iv	
LIST OF PERIODICALS SCANNED .....	v	— xxiii
SUBJECT INDEX, A - L .....	A1	— A798a
PART 2		
INTRODUCTION .....	iii	
HOW TO OBTAIN PUBLICATIONS ABSTRACTED .....	iv	
CROSS REFERENCES .....	iv	
SUBJECT INDEX, M - Z .....	A799	— A1658
PART 3		
INTRODUCTION .....	iii	
HOW TO OBTAIN PUBLICATIONS ABSTRACTED .....	iv	
PERSONAL AUTHOR INDEX .....	B1	— B738
CONTRACT NUMBER INDEX .....	C1	— C60
MEETING PAPER INDEX .....	D1	— D24
ACCESSION NUMBER INDEX .....	E1	— E148

**STAFF, AIAA Administrator—Technical Information Programs, ROBERT R. DEXTER**  
**STAFF, TECHNICAL INFORMATION SERVICE** Director, JOHN J. GLENNON • Associate Director—  
 Administrative, THOMAS J. MESKEL • Associate Director—Technical, IRENE W. BOGOLUBSKY •  
 Manager—Information Systems, WILLIAM T. MORRIS, JR. • Supervisor—Abstracting Department,  
 DALE D. MCADOO • Chief Librarian, PATRICIA M. MARSHALL

Printed by Sheridan Printing Company, Inc.

Phillipsburg, N. J.



## INTRODUCTION

INTERNATIONAL AEROSPACE ABSTRACTS (IAA) is an abstracting and indexing service covering the world's published literature in the field of aeronautics and space science and technology. IAA is issued semimonthly, on the 1st and 15th of each month.

### Coverage of Published Literature

The following types of publications are covered in IAA:

- Periodicals (including government-sponsored journals) and books.
- Meeting papers and conference proceedings issued by professional societies and academic organizations.
- Translations of journals and journal articles.

### Coverage of Reports ("Unpublished" Literature)

Abstracts and indexes of report literature are issued in SCIENTIFIC AND TECHNICAL AEROSPACE REPORTS (STAR), which is published by the Scientific and Technical Information Division, National Aeronautics and Space Administration.

By special arrangement between NASA and the American Institute of Aeronautics and Astronautics, IAA is issued in coordination with the twice-monthly schedule of STAR, which appears on the 8th and 23rd of each month.

IAA and STAR utilize both identical subject categories and indexes, which are described below.

Thus the two services provide comprehensive access to the national and international unclassified report and published literature of current significance to aerospace science and technology.

### Arrangement of the Semimonthly Issues

IAA is arranged in two major sections:

- (1) Abstracts Section. This section contains complete bibliographic citations with informative abstracts, arranged by appropriate subject categories to facilitate scanning. The subject categories are numbered from 01 to 34, and the scope of each category is outlined in the Table of Contents and again at the beginning of each category in the Abstracts Section. Each abstract is prefixed by the IAA accession number.
- (2) Index Section. Four indexes are contained in this section: Subject, Personal Author, Meeting Paper, and Accession Number. Each index is prefaced by explanatory notes to guide the user to the desired abstract.

### Cumulated Indexes

Cumulated indexes are prepared and issued promptly at the end of each quarter year, with the 4th quarterly being the Annual Index.

Each cumulated index contains the following sections: A—Subject Index, B—Personal Author Index, C—Contract Number Index, D—Meeting Paper Index, and E—Accession Number Index.

### Guide to the Subject Indexes

A GUIDE TO THE SUBJECT INDEXES FOR STAR has been issued by the Scientific and Technical Information Division of NASA. This publication contains an alphabetic listing of the subject headings and cross-references used in both STAR and IAA indexes, which use the same subject terminology.

Subscribers to the IAA Cumulative Indexes may obtain copies of the guide by writing to the AIAA Technical Information Service, 750 Third Avenue, New York, N. Y. 10017.

---

Information regarding SCIENTIFIC AND TECHNICAL AEROSPACE REPORTS and the availability of INTERNATIONAL AEROSPACE ABSTRACTS to organizations having contractual arrangements with NASA may be obtained from the following address:

National Aeronautics and Space Administration  
Scientific and Technical Information Division  
Attention: Code USS-A  
Washington, D. C. 20546



# How to obtain publications abstracted

All publications abstracted are available from the AIAA Technical Information Service.

## LOANS

Individual and Corporate AIAA Members in the United States and Canada, and NASA Centers, may borrow publications without charge. Interlibrary loan privileges are extended to the libraries of government agencies and academic nonprofit institutions in the United States and Canada. The loan period is two weeks, excluding transit time. The borrower pays return postage and insurance.

## PHOTOCOPIES

Documents can be supplied in the form of positive paper copies or negative 35-mm. microfilm.

## MICROFICHE SUBSCRIPTIONS

Documents available on microfiche are identified in INTERNATIONAL AEROSPACE ABSTRACTS by the symbol # following the accession number in the Abstracts Section and in the Report Number and Accession Number Indexes. Microfiche are made in conformity with Federal Microfiche Standards (COSATI) and are 105 x 148.75 mm. (approximately 4 x 6 inches) in size.

Microfiche of documents announced in INTERNATIONAL AEROSPACE ABSTRACTS may be obtained on annual subscription—each subscription covering all IAA-announced documents that are available on microfiche. Approximately 50 per cent of the documents announced each year are available in this manner. Subscriptions are accepted on a current basis, and subscribers will be billed monthly for the actual charges at the rate of \$0.40 per microfiche issued. Individual microfiche continue to be available on a demand basis at \$0.50 each.

## RATES

Positive paper copies	\$0.25 per page
minimum order	\$1.50
Negative 35-mm. microfilm	\$0.20 per frame
minimum order	\$2.50
Microfiche (demand)	\$0.50 per microfiche
Microfiche (subscription)	see above

(Minimum air-mail postage to foreign countries is \$5.00)

*Requests for loans or photocopies may be made by telephone, telegram, TWX, or in person.*

## PLEASE REFER TO THE ACCESSION NUMBER WHEN REQUESTING PUBLICATIONS

NOTE: The AIAA does not sell the publications abstracted, except those issued by the AIAA.

**Address all inquiries and requests to:**

TECHNICAL INFORMATION SERVICE  
AMERICAN INSTITUTE OF AERONAUTICS  
AND ASTRONAUTICS, INC.  
750 Third Avenue, New York, N. Y. 10017

Telephone: 212 TN-7-8300

TWX: 212 867-7265

---

## CROSS REFERENCES

The subject index includes two types of cross references to aid the user of the index in locating the material being sought:

1. "SEE" references (S) direct the user to alternate headings under which material on the subject will be found, for example:

COLUMBIUM  
S NIOBIUM

2. "SEE ALSO" references (SA) refer the user to additional headings in the same subject area, for example:

LUMINESCENCE  
SA ELECTROLUMINESCENCE



The periodicals listed in this section were scanned for material to be announced in *International Aerospace Abstracts* in 1966. The periodicals were received regularly throughout the year in all but a few instances. In the case of titles preceded by an asterisk, only the articles abstracted in *International Aerospace Abstracts* are available. All abstracted articles can be obtained from the AIAA Technical Information Service (see page iv).

BM — Bimonthly

BW — Biweekly

Irreg. — Irregular

M — Monthly

Q — Quarterly

SA — Semiannual

SM — Semimonthly

W — Weekly

## A

*Académie des Sciences (Paris), Comptes Rendus* (see *Académie des Sciences /Paris/, Comptes Rendus, Série A — Sciences Mathématiques, Série B — Sciences Physiques; Académie des Sciences /Paris/, Comptes Rendus, Série C — Sciences Chimiques; and Académie des Sciences /Paris/, Comptes Rendus, Série D — Sciences Naturelles*). Académie des Sciences; Gauthier-Villars & Cie, Paris. W

*Académie des Sciences (Paris), Comptes Rendus, Série A — Sciences Mathématiques, Série B — Sciences Physiques* (formerly *Académie des Sciences /Paris/, Comptes Rendus*). Académie des Sciences; Gauthier-Villars & Cie, Paris. W

*Académie des Sciences (Paris), Comptes Rendus, Série C — Sciences Chimiques* (formerly *Académie des Sciences /Paris/, Comptes Rendus*). Académie des Sciences; Gauthier-Villars & Cie, Paris. W

*Académie des Sciences (Paris), Comptes Rendus, Série D — Sciences Naturelles* (formerly *Académie des Sciences /Paris/, Comptes Rendus*). Académie des Sciences; Gauthier-Villars & Cie, Paris. W

*Académie Polonaise des Sciences, Bulletin, Série des Sciences Mathématiques, Astronomiques et Physiques*. Académie Polonaise des Sciences; Polish Scientific Press, Warsaw. M

*Académie Polonaise des Sciences, Bulletin, Série des Sciences Techniques*. Académie Polonaise des Sciences; Polish Scientific Press, Warsaw. M

*Académie Royale de Belgique, Classe des Sciences, Bulletin*. Académie Royale de Belgique; Office International de Librairie, Brussels. M

*Academy of Sciences, Izvestiya, Atmospheric and Oceanic Physics (Akademiia Nauk SSSR, Izvestiia, Fizika Atmosfery i Okeana)*. American Geophysical Union, Washington, D. C. M

*Academy of Sciences, Izvestiya, Physics of the Solid Earth (Akademiia Nauk SSSR, Izvestiia, Fizika Zemli)*. American Geophysical Union, Washington, D. C. M

*Academy of Sciences, USSR, Bulletin, Physical Series (Akademiia Nauk SSSR, Izvestiia, Serii Fizicheskaiia)*. Columbia Technical Translations, White Plains, N. Y. M

*Accademia Nazionale dei Lincei, Atti, Rendiconti — Classe di Scienze Fisiche, Matematiche e Naturali*. Accademia Nazionale dei Lincei, Rome. M

*ACM, Communications*. Association for Computing Machinery, New York. M

*Acoustical Society of America, Journal*. Acoustical Society of America, New York. M

*Acta Astronomica*. Warsaw. Q

*Acta Astronomica Sinica*. Chinese Astronomical Society, Peking. Q

\**Acta Cardiologica*. Brussels. BM

*Acta Electronica Sinica*. The Chinese Society of Electronics, Peking. Q

*Acta Geophysica Polonica*. Polska Akademia Nauk; Panstwowe Wydawnictwo Naukowe, Warsaw. Q

*Acta Geophysica Sinica*. Chinese Geophysical Society, Peking. Q

*Acta Mechanica*. Springer Verlag, Vienna. Q

*Acta Mechanica Sinica*. Chinese Society of Mechanics, Peking. Q

*Acta Metallurgica*. Pergamon Press, Ltd., Oxford. M

*Acta Meteorologica Sinica*. Chinese Meteorological Society, Peking. Q

\**Acta Oto-Laryngologica*. Stockholm. M

*Acta Physica*. Academiae Scientiarum Hungaricae, Budapest. 8 issues per year

*Acta Physica Polonica*. Polska Akademia Nauk, Instytut Fizyki and Polskie Towarzystwo Fizyczne, Warsaw. M

*Acta Physica Sinica*. Chinese Physical Society, Peking. M

*Acta Polytechnica Scandinavica, Chemistry Including Metallurgy Series*. Scandinavian Council for Applied Research, Stockholm. Irreg.

*Acta Polytechnica Scandinavica, Civil Engineering and Building Construction Series*. Scandinavian Council for Applied Research, Stockholm. Irreg.

*Acta Polytechnica Scandinavica, Electrical Engineering Series*. Scandinavian Council for Applied Research, Stockholm. Irreg.

*Acta Polytechnica Scandinavica, Mathematics and Computing Machinery Series*. Scandinavian Council for Applied Research, Stockholm. Irreg.

*Acta Polytechnica Scandinavica, Mechanical Engineering Series*. Scandinavian Council for Applied Research, Stockholm. Irreg.



# INTERNATIONAL AEROSPACE ABSTRACTS

- Acta Polytechnica Scandinavica, Physics Including Nuclear Series.* Scandinavian Council for Applied Research, Stockholm. Irreg.
- Acta Technica.* Hungarian Academy of Sciences, Budapest. M
- Acta Technica ČSAV.* Československá Akademie Věd, Prague. BM
- Acustica.* S. Hirzel Verlag KG, Stuttgart. BM
- Advanced Energy Conversion.* Pergamon Press, Ltd., Oxford. Q
- Advances in Physics.* Taylor & Francis, Ltd., London. Q
- Aero-Revue.* Aero-Club der Schweiz, Zurich. M
- Aeronautical Quarterly.* Royal Aeronautical Society, London. Q
- Aeronautical Society of India, Journal.* Aeronautical Society of India, New Delhi. Q
- Aeroplane (formerly Aeroplane and Commercial Aviation News).* Temple Press, Ltd., London. W
- Aeroplane and Commercial Aviation News (see Aeroplane).*
- Aerospace Management.* General Electric Co., Missile and Space Division, Valley Forge Space Technology Center, Philadelphia. Q
- Aerospace Medicine.* Aerospace Medical Association, Washington, D. C. M
- L'Aerotecnica.* Associazione Italiana di Aerotecnica, Rome. BM
- AIAA Journal.* American Institute of Aeronautics and Astronautics, Inc., New York. M
- AIAA Student Journal.* American Institute of Aeronautics and Astronautics, Inc., New York. Q
- A.I.Ch.E. Journal.* American Institute of Chemical Engineers, New York. BM
- AIIME, Transactions.* American Institute of Mining, Metallurgical and Petroleum Engineers, New York. BM
- \**Air Engineering.* Aerovox Corporation, Bedford, Mass.; Business News Publishing Co., Detroit. M
- Air et Cosmos.* Air et Cosmos, Paris. W
- Air Line Pilot.* Air Line Pilots Association/International, Chicago. M
- Air Techniques.* Boulogne (Seine), France. BM
- Air University Review.* Aerospace Studies Institute, Maxwell AFB, Ala. BM
- Aircraft Engineering.* Bunhill Publications, Ltd., London. M
- AiRevue.* Brussels. M
- Akademiia Nauk Armianskoi SSR, Doklady.* Akademiia Nauk Armianskoi SSR, Yerevan. 10 issues per year
- Akademiia Nauk Armianskoi SSR, Izvestiia, Fizika.* Akademiia Nauk Armianskoi SSR, Yerevan. BM
- Akademiia Nauk Armianskoi SSR, Izvestiia, Matematika.* Akademiia Nauk Armianskoi SSR, Yerevan. BM
- Akademiia Nauk Armianskoi SSR, Izvestiia, Mekhanika.* Akademiia Nauk Armianskoi SSR, Yerevan. BM
- Akademiia Nauk Armianskoi SSR, Izvestiia, Nauki o Zemle.* Akademiia Nauk Armianskoi SSR, Yerevan. BM
- Akademiia Nauk Armianskoi SSR, Izvestiia, Seriiia Fiziko-Matematicheskikh Nauk.* Akademiia Nauk Armianskoi SSR, Yerevan. 10 issues per year
- Akademiia Nauk Armianskoi SSR, Izvestiia, Seriiia Tekhnicheskikh Nauk.* Akademiia Nauk Armianskoi SSR, Yerevan. 10 issues per year
- Akademiia Nauk Azerbaidzhanskoi SSR, Doklady.* Akademiia Nauk Azerbaidzhanskoi SSR, Baku. M
- Akademiia Nauk Azerbaidzhanskoi SSR, Izvestiia, Seriiia Fiziko-Tekhnicheskikh i Matematicheskikh Nauk.* Akademiia Nauk Azerbaidzhanskoi SSR, Baku. BM
- Akademiia Nauk BSSR, Doklady.* Akademiia Nauk Belorusskoi SSR, Minsk. M
- Akademiia Nauk Estonskoi SSR, Izvestiia, Seriiia Fiziko-Matematicheskikh i Tekhnicheskikh Nauk.* Akademiia Nauk Estonskoi SSR, Tallin. Q
- Akademiia Nauk Gruzinskoi SSR, Soobshcheniia.* Akademiia Nauk Gruzinskoi SSR, Tiflis. M
- Akademiia Nauk Kazakhskoi SSR, Izvestiia, Seriiia Fiziko-Matematicheskikh Nauk.* Akademiia Nauk Kazakhskoi SSR, Alma Ata. M
- Akademiia Nauk Kazakhskoi SSR, Vestnik.* Akademiia Nauk Kazakhskoi SSR, Alma Ata. M
- Akademiia Nauk Latviiskoi SSR, Izvestiia.* Akademiia Nauk Latviiskoi SSR, Riga. M
- Akademiia Nauk Latviiskoi SSR, Izvestiia, Seriiia Fizicheskikh i Tekhnicheskikh Nauk.* Akademiia Nauk Latviiskoi SSR, Riga. BM
- Akademiia Nauk SSSR, Doklady.* Akademiia Nauk SSSR, Moscow. 36 issues per year
- Akademiia Nauk SSSR, Izvestiia, Energetika i Transport.* Akademiia Nauk SSSR, Moscow. BM
- Akademiia Nauk SSSR, Izvestiia, Fizika Atmosfery i Okeana.* Akademiia Nauk SSSR, Moscow. M
- Akademiia Nauk SSSR, Izvestiia, Fizika Zemli.* Akademiia Nauk SSSR, Moscow. M
- Akademiia Nauk SSSR, Izvestiia, Mekhanika (see Akademiia Nauk SSSR, Izvestiia, Mekhanika Zhidkosti i Gaza).*
- Akademiia Nauk SSSR, Izvestiia, Mekhanika Zhidkosti i Gaza (formerly Akademiia Nauk SSSR, Izvestiia, Mekhanika).* Akademiia Nauk SSSR, Moscow. BM
- Akademiia Nauk SSSR, Izvestiia, Metally.* Akademiia Nauk SSSR, Moscow. BM
- Akademiia Nauk SSSR, Izvestiia, Seriiia Biologicheskaiia.* Akademiia Nauk SSSR, Moscow. BM
- Akademiia Nauk SSSR, Izvestiia, Seriiia Fizicheskaiia.* Akademiia Nauk SSSR, Moscow. M
- Akademiia Nauk SSSR, Izvestiia, Seriiia Matematicheskaiia.* Akademiia Nauk SSSR, Moscow. BM
- Akademiia Nauk SSSR, Izvestiia, Tekhnicheskaiia Kibernetika.* Akademiia Nauk SSSR, Moscow. BM
- Akademiia Nauk SSSR, Sibirskoe Otdelenie, Izvestiia, Seriiia Tekhnicheskikh Nauk.* Akademiia Nauk SSSR, Sibirskoe Otdelenie, Novosibirsk. 3 issues per year
- Akademiia Nauk SSSR, Vestnik.* Akademiia Nauk SSSR, Moscow. M
- Akademiia Nauk Turkmeniskoi SSR, Izvestiia, Seriiia Fiziko-Tekhnicheskikh, Khimicheskikh i Geologicheskikh Nauk.* Akademiia Nauk Turkmeniskoi SSR, Ashkhabad. BM
- Akademiia Nauk Uzbekskoi SSR, Izvestiia, Seriiia Fiziko-Matematicheskikh Nauk.* Akademiia Nauk Uzbekskoi SSR, Tashkent. BM



- Akademiia Nauk Uzbekskoi SSR, Izvestiia, Seriiia Tekhnicheskikh Nauk.* Akademiia Nauk Uzbekskoi SSR, Tashkent. BM
- Akademiia Navuk BSSR, Vestsi, Seryia Fizika-Tekhnichnykh Navuk.* Akademiia Navuk Belaruskai SSR, Minsk. Q
- Akusticheskii Zhurnal.* Akademiia Nauk SSSR, Moscow. Q
- Alta Frequenza.* Associazione Elettrotecnica Italiana, Milan. BM
- Aluminium.* Aluminium-Zentrale e.V., Düsseldorf. M
- American Ceramic Society, Bulletin.* American Ceramic Society, Inc., Columbus, Ohio. M
- American Ceramic Society, Journal.* American Ceramic Society, Inc., Columbus, Ohio. M
- American Chemical Society, Journal.* American Chemical Society, Washington, D.C. SM
- American Geophysical Union, Transactions.* American Geophysical Union, Washington, D.C. Q
- American Geriatrics Society, Journal.* Williams and Wilkins Co., Baltimore. M
- American Helicopter Society, Journal.* American Helicopter Society, Inc., New York. Q
- American Industrial Hygiene Association, Journal.* American Industrial Hygiene Association, Cincinnati. BM
- American Journal of Medical Electronics.* United Technical Publications, Garden City, N. Y. Q
- American Journal of Physics.* American Institute of Physics, Inc., New York. M
- American Journal of Physiology.* American Physiological Society, Washington, D.C. M
- American Journal of Psychiatry.* American Psychiatric Association, New York. M
- American Mathematical Society, Bulletin.* American Mathematical Society, Providence. BM
- American Mathematical Society, Proceedings.* American Mathematical Society, Providence. BM
- American Mathematical Society, Transactions.* American Mathematical Society, Providence. M
- American Medical Association, Journal.* American Medical Association, Chicago. W
- American Meteorological Society, Bulletin.* American Meteorological Society, Boston. M
- American Mineralogist.* Mineralogical Society of America c/o U.S. Geological Survey, Washington, D.C. BM
- American Oil Chemists' Society, Journal.* American Oil Chemists' Society, Chicago. M
- American Scientist.* Society of the Sigma XI, Easton, Pa. Q
- American Society of Civil Engineers, Aero-Space Transport Division, Journal.* American Society of Civil Engineers, New York. Q
- American Society of Civil Engineers, Engineering Mechanics Division, Journal.* American Society of Civil Engineers, New York. BM
- American Society of Civil Engineers, Hydraulics Division, Journal.* American Society of Civil Engineers, New York. BM
- American Society of Civil Engineers, Structural Division, Journal.* American Society of Civil Engineers, New York. BM
- American Society of Civil Engineers, Surveying and Mapping Division, Journal.* American Society of Civil Engineers, New York. Q
- \*American Statistical Association, Journal.* American Statistical Association, Washington, D.C. Q
- \*Analytical Biochemistry.* Academic Press, Inc., New York. M
- Analytical Chemistry.* American Chemical Society, Washington, D.C. M
- \*Anatomical Record.* American Association of Anatomists; Wistar Institute of Anatomy and Biology, Philadelphia. M
- Annalen der Physik.* Johann Ambrosius Barth Verlag, Leipzig. Irreg.
- Annales d'Astrophysique.* Centre National de la Recherche Scientifique, Paris. BM
- Annales de Géophysique.* Centre National de la Recherche Scientifique, Paris. Q
- Annales de Physique.* Centre National de la Recherche Scientifique; Bd. Masson & Cie, Paris. BM
- Annales de Radioélectricité.* Groupe de la Compagnie Générale de Télégraphie sans Fil, Paris. Q
- Annales des Télécommunications.* Centre National d'Etudes des Télécommunications, Issy-les-Moulineaux (Seine), France. BM
- Annali di Geofisica.* Istituto Nazionale de Geofisica, Rome. Q
- \*Annals of Mathematical Statistics.* Institute of Mathematical Statistics; Stanford University, Department of Statistics, Stanford. Q
- \*Annals of Otolaryngology and Rhinology.* Annals Publishing Company, St. Louis, Mo. Q
- Annals of Physics.* Academic Press, Inc., New York. M
- APL Technical Digest.* Johns Hopkins University, Silver Spring, Md. BM
- Aplikace Matematiky.* Československá Akademie Věd, Matematický Ústav, Prague. BM
- Applied Materials Research.* Plenum Publishing Corp., New York. Q
- Applied Mechanics Reviews.* American Society of Mechanical Engineers, New York. M
- \*Applied Microbiology.* American Society for Microbiology, Baltimore. BM
- Applied Optics.* Optical Society of America, Inc., Washington, D.C. M
- Applied Physics Letters.* American Institute of Physics, Inc., New York. SM
- Applied Polymer Symposia.* John Wiley & Sons, Inc., New York. Irreg.
- Applied Scientific Research (formerly Applied Scientific Research, Section A).* Martinus Nijhoff, The Hague. Irreg.
- Applied Scientific Research, Section A (see Applied Scientific Research).*
- Applied Solar Energy (Geliotekhnika).* The Faraday Press, Inc., New York. BM
- Applied Spectroscopy.* Society for Applied Spectroscopy, Boston College, Mass.; American Institute of Physics, Inc., New York. BM
- Archiv der elektrischen Übertragung.* S. Hirzel Verlag, K.G., Stuttgart. M
- Archiv für Elektrotechnik.* Springer Verlag, Berlin. Irreg.



- Archiv für Meteorologie, Geophysik und Bioklimatologie, Serie A.* Springer Verlag, Vienna. Irreg.
- Archiv für technisches Messen und industrielle Messtechnik.* Verlag R. Oldenbourg, Munich. M
- Archive for Rational Mechanics and Analysis.* Springer Verlag, Berlin. Irreg.
- \**Archives Internationales de Physiologie et de Biochimie.* Imprimerie Vaillant-Carmanne, S.A., Liège. 5 issues per year
- \**Archives Italiennes de Biologie.* Pisa, Università, Pisa. Q
- \**Archives of Biochemistry and Biophysics.* Academic Press, Inc., New York. M
- Archives of Environmental Health.* American Academy of Occupational Medicine; American Medical Association, Chicago. SA
- \**Archives of Neurology.* American Neurological Association; American Medical Association, Chicago. M
- Archiwum Automatyki i Telemechaniki.* Akademia Nauk, Instytut Automatyki; Państwowe Wydawnictwo Naukowe, Warsaw. Q
- Archiwum Budowy Maszyn.* Polska Akademia Nauk, Komitet Budowy Maszyn, Warsaw. Q
- Archiwum Elektrotechniki.* Wydawnictwo Polskiej Akademii Nauk, Warsaw. Q
- Archiwum Mechaniki Stosowanej.* Académie Polonaise des Sciences, Warsaw. BM
- Arkiv för Astronomi.* Kungliga Svenska Vetenskapsakademien; Almqvist & Wiksells Boktryckeri AB, Stockholm. Irreg.
- Arkiv för Fysik.* Kungliga Svenska Vetenskapsakademien; Almqvist & Wiksells Boktryckeri AB, Stockholm. Irreg.
- Arkiv för Geofysik.* Kungliga Svenska Vetenskapsakademien; Almqvist & Wiksells Boktryckeri AB, Stockholm. Irreg.
- Arkiv för Matematik.* Kungliga Svenska Vetenskapsakademien; Almqvist & Wiksells Boktryckeri AB, Stockholm. Irreg.
- Artificial Satellites* (formerly *Biuletyn Polskich Obserwacji Sztucznych Satelitów*). Polish Academy of Sciences, Warsaw. Q
- ASEA Journal.* ASEA, Västerås, Sweden. M
- ASHRAE Journal.* American Society of Heating, Refrigerating and Air-Conditioning Engineers, Inc., New York. M
- ASLE Transactions.* American Society of Lubrication Engineers; Academic Press, New York. Q
- ASM Transactions Quarterly.* American Society for Metals, Metals Park, Ohio. Q
- ASME Transactions, Series A - Journal of Engineering for Power.* American Society of Mechanical Engineers, New York. Q
- ASME Transactions, Series B - Journal of Engineering for Industry.* American Society of Mechanical Engineers, New York. Q
- ASME Transactions, Series C - Journal of Heat Transfer.* American Society of Mechanical Engineers, New York. Q
- ASME Transactions, Series D - Journal of Basic Engineering.* American Society of Mechanical Engineers, New York. Q
- ASME Transactions, Series E - Journal of Applied Mechanics.* American Society of Mechanical Engineers, New York. Q
- Association for Computing Machinery, Journal.* Association for Computing Machinery, New York. Q
- ASTM Special Technical Publication.* American Society for Testing and Materials, Philadelphia. Irreg.
- Astronautica Acta.* International Academy of Astronautics, International Astronautical Federation; Springer Verlag, Vienna. BM
- Astronautics and Aeronautics.* American Institute of Aeronautics and Astronautics, Inc., New York. M
- Astronautik.* (formerly *Hermann Oberth-Gesellschaft, Mitteilungen*). Hermann Oberth-Gesellschaft, Hannover. BM
- Astronautyka.* Polskie Towarzystwo Astronautyczne, Warsaw. Q
- Astronomical Institutes of Czechoslovakia, Bulletin.* Czechoslovak Academy of Sciences, Prague. BM
- Astronomical Institutes of the Netherlands, Bulletin.* Astronomical Institutes of the Netherlands; North-Holland Publishing Co., Amsterdam. Q
- Astronomical Journal.* American Astronomical Society, Evanston, Ill. M
- Astronomical Society of Japan, Publications.* Astronomical Society of Japan, Tokyo. Q
- Astronomical Society of the Pacific, Leaflet.* Astronomical Society of the Pacific, San Francisco. M
- Astronomical Society of the Pacific, Publications.* Astronomical Society of the Pacific, San Francisco. BM
- Astronomicheskii Zhurnal.* Akademiia Nauk SSSR, Moscow. BM
- L'Astronomie.* Société Astronomique de France, Paris. M
- Astronomie und Raumfahrt.* Deutsche Astronautische Gesellschaft, Berlin. 5 issues per year
- Astronomische Gesellschaft, Mitteilungen.* Astronomische Gesellschaft, Hamburg. Biennial.
- Astronomische Nachrichten.* Akademie Verlag GmbH, Berlin. Irreg.
- Astrophysica Norvegica.* Oslo, University, Institute of Theoretical Astrophysics, Oslo. Irreg.
- Astrophysical Journal.* University of Chicago Press, Chicago. 8 issues per year
- Astrophysical Journal, Supplement Series.* University of Chicago Press, Chicago. 8 issues per year
- Astrophysics (Astrofizika).* The Faraday Press, Inc., New York. Q
- \**Australasian Corrosion Engineering.* Australasian Corrosion Association, North Sydney, Australia. M
- Australian Journal of Physics.* Commonwealth Scientific and Industrial Research Organization, Melbourne. BM
- Australian Journal of Physics, Astrophysical Supplement.* Commonwealth Scientific and Industrial Research Organization, East Melbourne. Irreg.
- Australian Mathematical Society, Journal.* Australian Mathematical Society; P. Noordhoff N. V., Groningen, Netherlands. Q
- Automatica.* Pergamon Press, Ltd., Oxford. Q
- Automation.* Penton Publishing Co., Cleveland. M



*Automation and Remote Control (Avtomatika i Telemekhanika)*. Instrument Society of America, Pittsburgh, Pa. M  
*Automatisme*. Association Française de Régulation et d'Automatisme, Paris. M  
*Aviation Week and Space Technology*. McGraw-Hill, Inc., New York. W  
*Aviatsiia i Kosmonavtika*. Voennoe Izdatel'stvo Ministerstva Oborony SSSR, Moscow. M  
*Aviatsionnaia Tekhnika*. Ministerstvo Vysshego i Srednego Spetsial'nogo Obrazovaniia SSSR; Kazanskii Aviatsionnyi Institut, Kazan. Q  
*Avtomatika*. Akademiia Nauk Ukrainskoi SSR, Kiev. BM  
*Avtomatika i Telemekhanika*. Akademiia Nauk SSSR, Moscow. M

## B

*Babeş-Bolyai, Universitas, Studia, Series Mathematica-Physica*. Babeş-Bolyai, Universitas, Cluj, Rumania. SA  
*Bandung, Institut Teknologi, Madjalah*. Institut Teknologi, Bandung, Indonesia.  
*Battelle Technical Review*. Battelle Memorial Institute, Columbus, Ohio. M  
*Bayerische Akademie der Wissenschaften, mathematisch-naturwissenschaftliche Klasse, Sitzungsberichte*. Bayerische Akademie der Wissenschaften, Munich. Irreg.  
*Beiträge aus der Plasmaphysik*. Deutsche Akademie der Wissenschaften, Berlin. BM  
*Beiträge zur Physik der Atmosphäre*. Akademische Verlagsgesellschaft mbH, Frankfurt/Main. Q  
*Bell Laboratories Record*. Bell Telephone Laboratories, Inc., New York. M  
*Bell System Technical Journal*. American Telephone and Telegraph Co., New York. 10 issues per year  
*Bildmessung und Luftbildwesen*. Herbert Wichmann Verlag, Karlsruhe. Q  
*Biochemical and Biophysical Research Communications*. Academic Press Inc., New York. Irreg.  
*Biochimica et Biophysica Acta*. Elsevier Publishing Co., Amsterdam. W  
*Biophysical Journal*. Biophysical Society, New York. BM  
*BioScience*. American Institute of Biological Sciences, Washington, D. C. M  
*Biuletyn Polskich Obserwacji Sztucznych Satelitów*. (see *Artificial Satellites*).  
*B'lgarska Akademiia na Naukite, Izvestiia na Geofizichniia Institut*. B'lgarska Akademiia na Naukite, Sofia. Irreg.  
*Bolgarskaia Akademiia Nauk, Doklady*. Bolgarskaia Akademiia Nauk, Sofia. M  
*Bollettino di Geofisica Teorica ed Applicata*. Osservatorio Geofisico Sperimentale, Trieste. Q  
*Brennstoff-Chemie*. Verlag W. Girardet, Essen. M  
*Brennstoff-Wärme-Kraft*. VDI-Verlag GmbH, Düsseldorf. M

*Bristol Siddeley Journal*. Bristol Siddeley Engines, Ltd., London. Q  
*British Astronomical Association, Journal*. British Astronomical Association, Hounslow West, Middx., England. 8 issues per year  
*British Electron* (formerly *Electron*). Associated Trade Publications, Ltd., London. Q  
*British Interplanetary Society, Journal*. British Interplanetary Society, London. BM  
*British Journal of Applied Physics*. Institute of Physics and The Physical Society, London. M  
*British Welding Journal*. Institute of Welding and The British Welding Research Association, London. M  
*Brno, Vysoké Učení Technické, Shorník*. Polytechnical Institute, Brno. M  
*Brown Boveri Review*. Brown, Boveri and Co., Ltd., Baden, Switzerland. BM  
*Bucureşti, Institutul Politehnic, Buletinul* (see *Bucureşti, Institutul Politehnic Gheorghe Gheorghiu-Dej, Buletinul*).  
*Bucureşti, Institutul Politehnic Gheorghe Gheorghiu-Dej, Buletinul* (formerly *Bucureşti, Institutul Politehnic, Buletinul*). Bucuresti, Institutul Politehnic Gheorghe Gheorghiu-Dej, Bucharest. BM  
*Bulletin Astronomique*. Centre National de la Recherche Scientifique, Service des Publications; Gauthier-Villars & Cie, Paris. Irreg.  
*Bulletin d'Informations Scientifiques et Techniques*. Dunod Editeur, Paris. M

## C

*Cambridge Philosophical Society, Proceedings*. Cambridge University Press, London. Q  
*Canada, National Research Council, Division of Mechanical Engineering and National Aeronautical Establishment, Quarterly Bulletin*. National Research Council of Canada, Ottawa. Q  
*Canadian Aeronautics and Space Journal*. Canadian Aeronautics and Space Institute, Ottawa. M  
*Canadian Electronics Engineering*. Maclean-Hunter Publishing Co., Ltd., Toronto. M  
*\*Canadian Journal of Microbiology*. National Research Council, Ottawa. BM  
*\*Canadian Journal of Zoology*. National Research Council of Canada, Ottawa. BM  
*Canadian Metallurgical Quarterly*. Canadian Institute of Mining and Metallurgy, Dept. of Mines and Technical Surveys, Ottawa, Canada. Q  
*Canadian Journal of Physics*. National Research Council of Canada, Ottawa. M  
*\*Canadian Journal of Psychology*. Canadian Psychological Association, Toronto. Q  
*Canadian Operational Research Society, Journal*. Canadian Operational Research Society, Ottawa. 3 issues per year  
*Časopis pro Pěstování Matematiky*. Československá Akademie Věd, Matematický Ústav, Prague. Q  
*Československá Akademie Věd, Rozpravy*. Československá Akademie Věd, Prague. Irreg.



*Challenge.* General Electric Co., Missile and Space Division, Philadelphia. Q

*Chalmers Tekniska Högskolas Handlingar.* Chalmers Tekniska Högskola, Göteborg, Sweden. Irreg.

*Chartered Mechanical Engineer.* Institution of Mechanical Engineers, London. M

*Chemia Stosowana, Seria B.* Polish Academy of Sciences, Warsaw. Q

\**Chemical Communications.* Chemical Society, London. SM

*Chemical Engineering Progress.* American Institute of Chemical Engineers, New York. M

*Chemical Engineering Progress, Symposium Series.* American Institute of Chemical Engineers, New York. M

\**Chemical Society of Japan, Bulletin.* Chemical Society of Japan, Tokyo. M

*Chemie-Ingenieur-Technik.* Verlag Chemie GmbH, Weinheim. M

*Chinese Mathematics (Acta Mathematica Sinica).* American Mathematical Society, Providence. Q

*Ciel et Terre.* Société Belge d'Astronomie, de Météorologie et de Physique du Globe, Brussels. BM

*Cobalt.* Centre d'Information du Cobalt, Brussels. Q

*Collins Signal.* Collins Radio Co., Dallas. Q

*Combustion, Explosion, and Shock Waves (Fizika Goreniia i Vzryva).* The Faraday Press, Inc., New York. Q

*Combustion and Flame.* Combustion Institute; Butterworth & Co., Ltd., London. Q

*Communications on Pure and Applied Mathematics.* New York University, Institute of Mathematical Sciences; Interscience Publishers, New York. Q

\**Computer Journal.* British Computer Society, London. Q

*Contamination Control.* American Association for Contamination Control, Los Angeles. M

*Contemporary Physics.* Taylor and Francis, Ltd., London. BM

*Control.* Morgan Brothers (Publishers), Ltd., London. Q

*Control Engineering.* McGraw-Hill Publishing Co., Inc., New York. M

*The Controller.* International Federation of Air Traffic Controllers' Associations, Cologne. Q

*Convair Traveler.* General Dynamics Corporation, Convair Division, San Diego. BM

*Coopération Méditerranéenne pour l'Energie Solaire, Bulletin.* Coopération Méditerranéenne pour l'Energie Solaire /COMPLES/, Madrid.

*COSPAR Information Bulletin.* COSPAR Secretariat, Paris. Irreg.

\**Cryogenic Technology.* Cryogenic Society of America. BM

*Current Science.* Current Science Association, Bangalore, India. SM

*Cybernetics (Kibernetika).* The Faraday Press, New York. BM

*Czechoslovak Journal of Physics, Series B.* Czechoslovak Academy of Sciences, Prague. M

*Czechoslovak Mathematical Journal.* Czechoslovak Academy of Sciences, Prague. Q

## D

*Debrecen Heliophysical Observatory, Publications.* Hungarian Academy of Sciences, Budapest. Irreg.

*Defectoscopy (Defektoskopiia).* Consultants Bureau Enterprises, Inc., New York. BM

*Deutscher Aerokurier.* Deutscher Aero-Club e.V., Frankfurt/Main. M

\**DFL-Mitteilungen.* Deutsche Forschungsanstalt für Luft- und Raumfahrt, Stuttgart. Irreg.

*DGRR, Mitteilungen.* Deutsche Gesellschaft für Raketentechnik und Raumfahrt, Munich. Q

\**Diagnostica.* Göttingen. Q

*Differential Equations (Differentsial'nye Uravneniia).* The Faraday Press, New York. M

*Differentsial'nye Uravneniia.* Izdatel'stvo Nauka i Tekhnika, Minsk. M

*DISA Information.* DISA Elektronik A/S, Herlev, Denmark. Irreg.

*Doc-Air-Espace.* Service de Documentation Scientifique et Technique de l'Armement, Paris. BM

*Dornier-Post.* Dornier-Werke GmbH, Munich. Q

\**Duke Mathematical Journal.* Duke University Press, Durham, N.C. Q

*DVL-Nachrichten.* Deutsche Versuchsanstalt für Luft- und Raumfahrt e.V., Porz-Wahn. Irreg.

## E

*Earth and Planetary Science Letters.* North-Holland Publishing Co., Amsterdam. BM

*L'Echo des Recherches.* Centre National d'Etudes des Télécommunications, Issy-les-Moulineaux (Seine), France. Q

\**Economic Geology.* Economic Geology Publishing Co., Urbana, Ill. 8 issues per year

*EEE — The Magazine of Circuit Design Engineering.* Mactier Publishing Corporation, New York. M

*Eesti NSV Teaduste Akadeemia, Toimetised, Füüsika-Matemaatika- ja Tehnikateaduste Seeria.* Tallinn. Q

\**Ege Universitesi, Fen Fakültesi Ilmi, Raporlar Serisi, Astronomy.* Ege Universitesi, Izmir, Turkey. Irreg.

*Electrical Communication.* International Telephone and Telegraph Corp., New York. Q

*Electrical Engineering in Japan (Denki Gakkai Zasshi).* Institute of Electrical and Electronics Engineers, Inc., New York.

*Electro-Technology.* Conover-Mast Technical Publications Corp., New York. M

\**Electrochemical Society, Journal.* Electrochemical Society, Inc., New York. M

*Electrochimica Acta.* Pergamon Press, Ltd., Oxford. M

\**Electroencephalography and Clinical Neurophysiology.* International Federation of Societies for Electroencephalography and Clinical Neurophysiology; Elsevier Publishing Co., Amsterdam. M

*Electromechanical Design.* Electromechanical Design, Brookline, Mass. M

*Electron* (see *British Electron*).  
*Electronic Age*. Radio Corporation of America, New York. Q  
*Electronic Applications*. N.V. Philips' Gloeilampenfabrieken, Electronic Market Dept., Eindhoven, Netherlands. Q  
*Electronic Capabilities*. U.S. Industrial Publications, Inc., New York. Q  
*Electronic Design*. Hayden Publishing Co., Inc., New York. BW  
*Electronic Engineering*. Morgan Brothers, Ltd., London. M  
*Electronic Industries*. Chilton Co., Philadelphia. M  
*Electronic Packaging and Production*. Milton S. Kiver Publications, Inc., Chicago. M  
*Electronic Progress*. Raytheon Company, Lexington, Mass. BM  
*Electronics*. McGraw-Hill Publishing Co., Inc., New York. BW  
*Electronics and Communications*. Southam Business Publications, Ltd., Ontario. M  
*Electronics and Communications in Japan*. Institute of Electrical and Electronics Engineers, Inc., New York. M  
*Electronics and Power*. Institution of Electrical Engineers, London. M  
*Electronics Letters*. Institution of Electrical Engineers, London. M  
*Electronique*. Editions PEPTA, Paris. M  
*Elektrokhimiia*. Akademiia Nauk SSSR, Moscow. M  
*Elektromekhanika*. Ministerstvo Vysshego i Srednego Spetsial'nogo Obrazovaniia, Novocherkassk, USSR. M  
*Elektronik*. Teknisk Forlag A/S, Copenhagen. M  
*Elektronische Datenverarbeitung*. Friedr. Vieweg & Sohn, Braunschweig. BM  
*Elektronische Rechenanlagen*. Verein deutscher Ingenieure, Nachrichtentechnische Gesellschaft, Munich. BM  
*Elektrosviaz'*. Ministerstvo Sviazi SSSR, Moscow. M  
*Elektrotechnický Obzor*. SNTL - Publishers of Technical Literature, Prague. M  
*Endeavour*. Imperial Chemical Industries, London. Q  
*Endocrinology*. Endocrine Society, Philadelphia. M  
*Energomashinostroenie*. Gosudarstvennyi Komitet Tiazhelogo, Energeticheskogo i Transportnogo Mashinostroeniia pri Gosplane SSSR, Leningrad. M  
*Engelhard Industries Technical Bulletin*. Engelhard Industries, Inc., Newark, N. J. Q  
*The Engineer*. Morgan Brothers (Publishers), Ltd., London. W  
*Engineering*. Engineering, Ltd., London. W  
*Engineering and Science*. California Institute of Technology, Pasadena. M  
*Engineering Bulletin*. Motorola, Inc., Military Electronics Div., Scottsdale, Ariz. Irreg.  
*Engineering Cybernetics (Akademiia Nauk SSSR, Izvestiia, Tekhnicheskaja Kibernetika)*. Institute of Electrical and Electronics Engineers, Inc., New York. BM  
*Engineering Journal*. Engineering Institute of Canada, Montreal. M  
*Engineering Materials and Design*. Heywood and Co., Ltd., London. M

*Entropie*. Editions Barthelemy & Cie, Paris. BM  
*Environmental Engineering*. Society of Environmental Engineers; Kenneth Mason Publications, Ltd., London. BM  
*Environmental Quarterly*. Environmental Publications, Inc., Little Neck, N.Y. Q  
*Ericsson Technics*. Telefonaktiebolaget LM Ericsson, Stockholm. SA  
*Esso Air World*. Esso International, Inc., New York. BM  
*Euratom*. Euratom, Dissemination of Information Directorate, Brussels. Q  
*Eurocontrol*. European Organization for the Safety of Air Navigation, Brussels. SA  
*\*Euronuclear*. Morgan Brothers (Publishers), Ltd., London. M  
*Evaluation Engineering*. A. Verner Nelson Associates, Chicago. BM  
*\*Excerpta Medica International Congress Series*. Excerpta Medica Foundation, Amsterdam. M  
*\*Experimental Brain Research*. Springer Verlag, Berlin. Irreg.  
*Experimental Mechanics*. Society for Experimental Stress Analysis, Westport, Conn. M  
*\*Experimental Neurology*. Academic Press, Inc., New York. BM  
*Explosifs*. Association des Fabricants Belges d'Explosifs et de Recherches Scientifiques, Brussels. Q  
*Explosivstoffe*. Erwin Barth Verlag KG, Mannheim, Germany. M

## F

*\*Faraday Society, Discussions*. Aberdeen University Press, Ltd., Aberdeen. SA  
*Field Service Digest*. Lockheed-California Co., Burbank. Irreg.  
*Fizika*. Ministerstvo Vysshego i Srednego Spetsial'nogo Obrazovaniia SSSR; Tomskii Universitet, Tomsk. BM  
*Fizika Gorenii i Vzryva*. Akademiia Nauk SSSR, Sibirskoe Otdelenie, Novosibirsk. Q  
*Fizika Metallov i Metallovedenie*. Akademiia Nauk SSSR, Sverdlovsk. M  
*Fizika Tverdogo Tela*. Akademiia Nauk SSSR, Moscow. M  
*Flight Comment*. Directorate of Flight Safety, Royal Canadian Air Force, Ottawa. BM  
*Flight International*. Iliffe Transport Publications, Ltd., London. W  
*Flug-Revue*. Vereinigte Motor-Verlage GmbH, Stuttgart. M  
*Flugwelt*. Krausskopf-Flugwelt-Verlag GmbH, Mainz, M  
*Fluid Power International*. Grampian Press, Ltd., London. M  
*Forces Aériennes Françaises*. Comité d'Etudes Aéronautiques Militaires, Paris. M  
*Forschung im Ingenieurwesen*. VDI-Verlag GmbH, Düsseldorf. BM



- France. Ministère de l'Air, Publications Scientifiques et Techniques. Service de Documentation Scientifique et Technique de l'Armement, Paris. Irreg.
- France. Ministère de l'Air, Publications Scientifiques et Techniques, Notes Techniques. Service de Documentation Scientifique et Technique de l'Armement, Paris. Irreg.
- Franklin Institute, Journal. Franklin Institute, Philadelphia. M
- Frequency. Frequency, Inc., Brookline, Mass. BM
- Frequenz. Fachverlag Schiele und Schön, Berlin. M
- Frontier. Illinois Institute of Technology, Research Institute, Chicago. Q
- Fujitsu Scientific and Technical Journal. Fujitsu, Ltd., Kawasaki City, Kanagawa, Japan. SA

## G

- G. E. C. Journal of Science and Technology. General Electric Co., Ltd., London. Q
- Geochimica et Cosmochimica Acta. Pergamon Press, Ltd., Oxford. M
- Geodesy and Aerophotography (Geodeziia i Aerofotos'emka). American Geophysical Union, Washington, D. C. BM
- Geodeziia i Aerofotos'emka. Moskovskii Institut Inzhenerov Geodezii, Aerofotos'emki i Kartografii, Moscow. BM
- Geodeziia i Kartografiia. Gosudarstvennyi Geologicheskii Komitet SSSR, Moscow. M
- Geodezja i Kartografia. Polska Akademia Nauk, Komitet Geodezji, Warsaw. Q
- Geofisica e Meteorologia. Società Italiana di Geofisica e Meteorologia, Genoa. BM
- Geofizicheskii Biulleten'. Akademiia Nauk SSSR, Moscow. Irreg.
- Geofysikální Sborník. Československá Akademie Věd, Geofysikální Ustav, Prague. Annual
- Geofysiske Publikasjoner (Geophysica Norvegica). Norske Videnskaps-Akademi, Oslo. Irreg.
- \*Geological Society of America, Bulletin. Geological Society of America, New York. M
- Geomagnetism and Aeronomy (Geomagnetizm i Aeronomiia). American Geophysical Union, Washington, D. C. BM
- Geomagnetizm i Aeronomiia. Akademiia Nauk SSSR, Moscow. BM
- Geophysical Journal. Royal Astronomical Society, London. M
- Gerlands Beiträge zur Geophysik. Akademische Verlagsgesellschaft Geest & Portig KG, Leipzig. BM
- Glavnaia Geofizicheskaiia Observatoriia imeni A. I. Voeikova, Trudy. Glavnoe Upravlenie Gidrometeorologicheskoi Sluzhby pri Sovete Ministrov SSSR, Leningrad.
- Göttingen, Akademie der Wissenschaften, Nachrichten, Mathematisch-physikalische Klasse. Vandenhoeck & Ruprecht, Göttingen. Irreg.
- Ground Support Equipment. Compass Publications, Inc., Arlington, Va. Q

## H

- \*Harvard Review. Harvard College, Cambridge, Mass. 3 issues per year
- Hawker Siddeley Review. The Hawker Siddeley Group, London. Q
- Helvetica Physica Acta. Schweizerische Physikalische Gesellschaft, Basel. BM
- Hermann Oberth-Gesellschaft, Mitteilungen (see Astronautik).
- High Temperature (Teplofizika Vysokikh Temperatur). American Institute of Physics, Inc., New York. BM
- Hiroshima, University, Journal of Science, Series A - II. Hiroshima, University, Hiroshima. 3 issues per year
- Hochfrequenztechnik und Elektroakustik. Akademische Verlagsgesellschaft Geest & Portig K.G., Leipzig. BM
- La Houille Blanche. Association pour la Diffusion de la Documentation Hydraulique, Grenoble. 8 issues per year
- Hovering Craft and Hydrofoil. Kalerghi-McLeavy Publications, London. M
- Human Factors. Pergamon Press, Ltd., Oxford. BM
- Hydraulics and Pneumatics. Industrial Publishing Corp., Cleveland. M

## I

- Iasi, Institutul Politehnic, Buletinul. Iasi, Institutul Politehnic, Iasi, Rumania.
- IBM Journal of Research and Development. International Business Machines Corp., New York. BM
- Icarus. Academic Press, Inc., New York. BM
- I & EC - Industrial and Engineering Chemistry. American Chemical Society, Washington, D.C. M
- I & EC — Industrial and Engineering Chemistry, Fundamentals. American Chemical Society, Washington, D. C. Q
- I & EC — Industrial and Engineering Chemistry, Process Design and Development. American Chemical Society, Washington, D. C. Q
- I & EC — Industrial and Engineering Chemistry, Product Research and Development. American Chemical Society, Washington, D. C. Q
- IEEE, Proceedings. Institute of Electrical and Electronics Engineers, Inc., New York. M
- IEEE International Convention Record. Institute of Electrical and Electronics Engineers, Inc., New York. Annual
- IEEE Journal of Quantum Electronics. Institute of Electrical and Electronics Engineers, Inc., New York. M
- IEEE Spectrum. Institute of Electrical and Electronics Engineers, Inc., New York. M
- IEEE Transactions on Aerospace and Electronic Systems (formerly IEEE Transactions on Aerospace, IEEE Transactions on Aerospace and Navigational Electronics, IEEE Transactions on Military Electronics, and IEEE Transactions on Space Electronics and Telemetry). Institute of Electrical and Electronics Engineers, Inc., New York. BM



- IEEE Transactions on Antennas and Propagation. Institute of Electrical and Electronics Engineers, Inc. New York. BM
- IEEE Transactions on Audio. Institute of Electrical and Electronics Engineers, Inc., New York. Q
- IEEE Transactions on Automatic Control. Institute of Electrical and Electronics Engineers, Inc., New York. Q
- IEEE Transactions on Bio-Medical Engineering. Institute of Electrical and Electronics Engineers, Inc., New York. Q
- IEEE Transactions on Broadcast and Television Receivers. Institute of Electrical and Electronics Engineers, Inc., New York. 3 issues per year
- IEEE Transactions on Broadcasting. Institute of Electrical and Electronics Engineers, Inc., New York. Irreg.
- IEEE Transactions on Circuit Theory. Institute of Electrical and Electronics Engineers, Inc., New York. Q
- IEEE Transactions on Communication Technology (formerly IEEE Transactions on Communications Systems). Institute of Electrical and Electronics Engineers, Inc., New York. Q
- IEEE Transactions on Education. Institute of Electrical and Electronics Engineers, Inc., New York. Q
- IEEE Transactions on Electromagnetic Compatibility. Institute of Electrical and Electronics Engineers, Inc., New York. Q
- IEEE Transactions on Electron Devices. Institute of Electrical and Electronics Engineers, Inc., New York. M
- IEEE Transactions on Electronic Computers. Institute of Electrical and Electronics Engineers, Inc., New York. BM
- IEEE Transactions on Engineering Management. Institute of Electrical and Electronics Engineers, Inc., New York. Q
- IEEE Transactions on Human Factors in Electronics. Institute of Electrical and Electronics Engineers, Inc., New York. Irreg.
- IEEE Transactions on Industrial Electronics and Control Instrumentation. Institute of Electrical and Electronics Engineers, Inc., New York. Irreg.
- IEEE Transactions on Industry and General Applications (formerly IEEE Transactions on Applications and Industry). Institute of Electrical and Electronics Engineers, Inc., New York. BM
- IEEE Transactions on Information Theory. Institute of Electrical and Electronics Engineers, Inc., New York. Q
- IEEE Transactions on Instrumentation and Measurement. Institute of Electrical and Electronics Engineers, Inc., New York. Q
- IEEE Transactions on Magnetics. Institute of Electrical and Electronics Engineers, Inc., New York. Q
- IEEE Transactions on Microwave Theory and Techniques. Institute of Electrical and Electronics Engineers, Inc., New York. BM
- IEEE Transactions on Nuclear Science. Institute of Electrical and Electronics Engineers, Inc., New York. BM
- IEEE Transactions on Parts, Materials and Packaging (formerly IEEE Transactions on Component Parts and IEEE Transactions on Product Engineering and Production). Institute of Electrical and Electronics Engineers, Inc., New York. Q
- IEEE Transactions on Power Apparatus and Systems. Institute of Electrical and Electronics Engineers, Inc., New York. Irreg.
- IEEE Transactions on Reliability. Institute of Electrical and Electronics Engineers, Inc., New York. Irreg.
- IEEE Transactions on Sonics and Ultrasonics. Institute of Electrical and Electronics Engineers, Inc., New York. Irreg.
- IEEE Transactions on Systems Science and Cybernetics. Institute of Electrical and Electronics Engineers, Inc., New York. Irreg.
- \*Immunochemistry. Pergamon Press, Ltd., Oxford. Q
- Indian Academy of Sciences, Proceedings, Section A. Indian Academy of Sciences, Bangalore. M
- Indian Institute of Science, Journal. Indian Institute of Science, Bangalore. Q
- Indian Journal of Meteorology and Geophysics. India Meteorological Department, Delhi. Q
- Indian Journal of Pure and Applied Physics. Council of Scientific and Industrial Research, New Delhi. M
- Indian Journal of Technology. Council of Scientific and Industrial Research, New Delhi. M
- Industrial Electronics. Iliffe Electrical Publications, Ltd., London. M
- Industrial Laboratory (Zavodskaja Laboratoriia). Instrument Society of America, Pittsburgh. M
- Industrial Quality Control. American Society for Quality Control, Inc., Milwaukee. M
- Industrial Research. Industrial Research, Inc., Beverly Shores, Ind. M
- Information and Control. Academic Press, Inc., New York. BM
- Information Display. Information Display Publications, Inc., Los Angeles. BM
- Infrared Physics. Pergamon Press, Ltd., Oxford. Q
- Ingeniería Aeronáutica y Astronáutica. Asociación de Ingenieros Aeronáuticos, Madrid. BM
- Ingenieur-Archiv. Springer Verlag, Berlin. Irreg.
- \*Inorganic Chemistry. American Chemical Society, Washington, D. C. M
- Institut Fourier, Annales. Grenoble, Université, Grenoble, France.
- Institut Français du Pétrole, Revue. Editions Technip, Paris. M
- Institut Royal Météorologique de Belgique, Publications, Série B. Institut Royal Météorologique de Belgique, Brussels. Irreg.
- Institut Teoreticheskoi Astronomii, Biulleten'. Izdatel'stvo Nauka, Moscow. Irreg.
- Institut Teoreticheskoi Astronomii, Trudy. Akademiia Nauk SSSR, Institut Teoreticheskoi Astronomii; Izdatel'stvo Nauka, Leningrad. Irreg.
- Institute of Mathematics and Its Applications, Journal. Academic Press, Ltd., London. Q
- Institute of Navigation, Journal. Institute of Navigation, London. Q
- Institute of Transport, Journal. Institute of Transport, London. BM
- Institution of Electrical Engineers, Proceedings. Institution of Electrical Engineers, London. M

# INTERNATIONAL AEROSPACE ABSTRACTS

- Institution of Electronic and Radio Engineers, Proceedings.* Institution of Electronic and Radio Engineers, London. BM
- Institution of Engineers (India), Journal, Electronics and Telecommunication Engineering Division.* The Institution of Engineers, Calcutta. 3 issues per year
- Institution of Engineers (India), Journal, Mechanical Engineering Division.* Institution of Engineers, Calcutta. BM
- Institution of Mechanical Engineers, Proceedings.* Institution of Mechanical Engineers, London. BM
- Instituto de Matemática, Astronomía y Física, Boletín.* Cordoba, Universidad Nacional, Cordoba, Argentina. SA
- Instrument Practice.* United Trade Press, Ltd., London. M
- Instrument Review.* Morgan Brothers, Ltd., London. M
- Instruments and Control Systems.* Instruments Publishing Co., Inc., Pittsburgh. M
- Instruments and Experimental Techniques (Pribory i Tekhnika Eksperimenta).* Instrument Society of America, Pittsburgh. BM
- Instytut Lotnictwa, Biuletyn Informacyjny.* Instytut Lotnictwa, Warsaw. BM
- Instytut Lotnictwa, Prace.* Instytut Lotnictwa, Warsaw. Irreg.
- Instytut Maszyn Przepływowych, Prace.* Polska Akademia Nauk, Instytut Maszyn Przepływowych, Gdansk.
- Interavia.* Interavia S. A., Geneva. M
- Inter-Electronique (formerly Revue Générale d'Electronique).* Editions LEPS, Paris. M
- International Chemical Engineering.* American Institute of Chemical Engineers, New York. Q
- International Journal of Control, First Series (formerly Journal of Electronics and Control, 1st Series).* Taylor and Francis, Ltd., London. M
- International Journal of Electronics, First Series (formerly Journal of Electronics and Control, 1st Series).* Taylor and Francis, Ltd., London. M
- International Journal of Engineering Science.* Pergamon Press, Ltd., Oxford. BM
- International Journal of Fracture Mechanics.* P. Noordhoff, Ltd., Groningen, Netherland. Q
- International Journal of Heat and Mass Transfer.* Pergamon Press, Ltd., Oxford. M
- International Journal of Mechanical Sciences.* Pergamon Press, Ltd., Oxford. M
- International Journal of Non-Linear Mechanics.* Pergamon Press, Ltd., Oxford. Q
- International Journal of Powder Metallurgy.* American Powder Metallurgy Institute, New York. Q
- International Journal of Solids and Structures.* Pergamon Press, Ltd., Oxford. Q
- International Science and Technology.* Conover-Mast Publications, Inc., New York. M
- Internationale elektronische Rundschau.* Verlag für Radio-Foto-Kinotechnik GmbH, Berlin. M
- \*Internationale Zeitschrift für angewandte Physiologie einschliesslich Arbeitsphysiologie.* Springer Verlag, Berlin. 3 issues per year
- Inzhenerno-Fizicheskii Zhurnal.* Akademiia Nauk BSSR, Minsk. M
- Inzhenernyi Zhurnal (see Inzhenernyi Zhurnal - Mekhanika Tverdogo Tela).*

- Inzhenernyi Zhurnal - Mekhanika Tverdogo Tela (formerly Inzhenernyi Zhurnal).* Akademiia Nauk SSSR, Moscow. BM
- Iowa State University Bulletin, Iowa Engineering Experiment Station, Engineering Report.* Iowa State University, Ames, Iowa. Irreg.
- \*Irish Astronomical Journal.* Irish Astronomical Society, Armagh, Northern Ireland. M
- ISA Journal.* Instrument Society of America, Pittsburgh. M
- ISA Transactions.* Instrument Society of America, Pittsburgh. Q
- Ishikawajima-Harima Engineering Review.* Ishikawajima-Harima, Tokyo. BM
- Israel Journal of Technology.* Weizmann Science Press of Israel, Jerusalem. Q
- Istanbul Teknik Üniversitesi Bülteni.* Istanbul Teknik Üniversitesi, Istanbul. Annual
- Istanbul Üniversitesi, Fen Fakültesi Mecmuası, Seri C - Astronomi-Fizik-Kimya.* Istanbul Üniversitesi, Istanbul. Q

## J

- \*Japan, Chemical Society, Bulletin.* Japan, Chemical Society, Tokyo. M
- Japan, Defense Academy, Memoirs.* Japan, Defense Academy, Yokosuka, Japan.
- Japan Broadcasting Corporation, Technical Journal.* Nippon Hoso Kyokai, Technical Research Laboratories, Tokyo. BM
- Japan Institute of Metals, Transactions.* Japan Institute of Metals, Sendai. Q
- Japan Society for Aeronautical and Space Sciences, Journal.* Japan Society for Aeronautical and Space Sciences, Tokyo. M
- Japan Society for Aeronautical and Space Sciences, Transactions.* Japan Society for Aeronautical and Space Sciences, Tokyo. M
- \*Japan Society of Mechanical Engineers, Journal.* Japan Society of Mechanical Engineers; Japan Publications Trading Co., Tokyo. M
- Japanese Journal of Aerospace Medicine and Psychology.* Japanese Aerospace Medical and Psychological Society, Tokyo. Irreg.
- Japanese Journal of Applied Physics.* Physical Society of Japan and Japan Society of Applied Physics, Tokyo. M
- Jemná Mechanika a Optika.* Státní Nakladatelství Technické Literatury, Prague. M
- JETP Letters (ZHETF Pis'ma v Redaktsiiu).* American Institute of Physics, Inc., New York. SM
- Journal de Mathématiques Pures et Appliquées.* Gauthier-Villars & Cie, Paris. Q
- Journal de Mécanique.* Gauthier-Villars & Cie, Paris. M
- Journal de Physique (formerly Journal de Physique et le Radium).* Société Française de Physique, Paris. M
- Journal of Air Law and Commerce.* Southern Methodist University, School of Law, Dallas. Q



- Journal of Aircraft.* American Institute of Aeronautics and Astronautics, Inc., New York. BM
- Journal of Algebra.* Academic Press, Inc., New York. Q
- Journal of Applied Mechanics and Technical Physics* (PMTF - Zhurnal Prikladnoi Mekhaniki i Tekhnicheskoi Fiziki). The Faraday Press, Inc., New York. BM
- Journal of Applied Meteorology.* American Meteorological Society, Boston. Q
- Journal of Applied Physics.* American Institute of Physics, Inc., New York. M
- Journal of Applied Physiology.* American Physiological Society, Washington, D. C. BM
- Journal of Applied Polymer Science.* Interscience Publishers, New York. BM
- Journal of Applied Probability.* Michigan State University, Statistics Department, East Lansing. SA
- Journal of Atmospheric and Terrestrial Physics.* Pergamon Press, Ltd., Oxford. M
- Journal of Bacteriology.* American Society for Microbiology, Baltimore. M
- Journal of Biological Chemistry.* American Society of Biological Chemists, Baltimore. M
- Journal of Cell Biology.* Rockefeller Institute Press, New York. M
- Journal of Cellular Physiology.* Wistar Institute of Anatomy and Biology, Philadelphia. BM
- Journal of Chemical and Engineering Data.* American Chemical Society, Washington, D. C. Q
- Journal of Chemical Physics.* American Institute of Physics, Inc., New York. SM
- Journal of Clinical Investigation.* American Society for Clinical Investigation, Inc., Boston. M
- Journal of Comparative and Physiological Psychology.* American Psychological Association, Inc., Washington, D. C. BM
- Journal of Computational Physics.* Academic Press, Inc., New York. Q
- Journal of Differential Equations.* Academic Press, Inc., New York. Q
- Journal of Engineering Physics* (Inzhenerno-Fizicheskii Zhurnal). The Faraday Press, New York. M
- Journal of Engineering Psychology.* Elias Publications, Washington, D. C. Q
- Journal of Environmental Sciences.* Institute of Environmental Sciences, Mt. Prospect, Ill. BM
- Journal of Fluid Mechanics.* Cambridge University Press, London. M
- Journal of Gas Chromatography.* Preston Technical Abstracts Co., Evanston, Ill. M
- Journal of General Psychology.* Virginia, University, Department of Psychology, Charlottesville; The Journal Press, Provincetown, Mass. Q
- Journal of Geomagnetism and Geoelectricity.* Kyoto University, Geophysical Institute, Kyoto, Japan. Q
- Journal of Geophysical Research.* American Geophysical Union, Washington, D. C. SM
- Journal of Heterocyclic Chemistry.* Raymond N. Castle, Albuquerque. BM
- Journal of Immunology.* The Williams & Wilkins Co., Baltimore. M
- Journal of Labelled Compounds.* Brussels. Q
- \*Journal of Lipid Research.* Lipid Research, Inc., New York. Q
- \*Journal of Macromolecular Chemistry.* Marcel Dekker, Inc., New York. Q
- Journal of Materials.* American Society for Testing and Materials, Philadelphia. Q
- Journal of Materials Science.* Chapman & Hall, Ltd., London. Q
- Journal of Mathematical Analysis and Applications.* Academic Press, Inc., New York. BM
- Journal of Mathematical Physics.* American Institute of Physics, Inc., New York. M
- Journal of Mathematics and Mechanics.* Indiana University, Graduate Institute for Mathematics and Mechanics, Bloomington; Technology Press, Cambridge, Mass. BM
- Journal of Mathematics and Physics.* Massachusetts Institute of Technology, Cambridge, Mass. Q
- Journal of Mechanical Engineering Science.* Institution of Mechanical Engineers, London. Q
- Journal of Metals.* American Institute of Mining, Metallurgical and Petroleum Engineers, Inc., New York. M
- \*Journal of Molecular Biology.* Academic Press, Inc., New York. M
- \*Journal of Neurophysiology.* American Physiological Society, Washington, D.C. BM
- Journal of Nuclear Energy, Part C — Plasma Physics, Accelerators, Thermonuclear Research.* Pergamon Press, Ltd., Oxford. BM
- \*Journal of Organic Chemistry.* American Chemical Society, Washington, D.C. M
- \*Journal of Organometallic Chemistry.* Elsevier Publishing Co., Amsterdam. M
- Journal of Photographic Science.* Royal Photographic Society of Great Britain, London. BM
- \*Journal of Phycology.* Phycological Society of America, Baltimore. Q
- Journal of Physical Chemistry.* American Chemical Society, Washington, D. C. M
- \*Journal of Physics and Chemistry of Solids.* Pergamon Press, Ltd., Oxford. M
- \*Journal of Physiology.* Cambridge University Press, London. 3 issues per year
- \*Journal of Polymer Science, Part A.* Interscience Publishers, Inc., New York. M
- \*Journal of Polymer Science, Part B — Polymer Letters.* Interscience Publishers, Inc., New York. M
- \*Journal of Polymer Science, Part C - Polymer Symposia.* Interscience Publishers, Inc., New York. M
- \*Journal of Psychology.* The Journal Press, Provincetown, Mass. BM
- \*Journal of Quantitative Spectroscopy and Radiative Transfer.* Pergamon Press, Ltd., Oxford. Q
- Journal of Research, Section A — Physics and Chemistry.* National Bureau of Standards; Supt. of Documents, Washington, D. C. BM
- Journal of Research, Section B — Mathematics and Mathematical Physics.* National Bureau of Standards; Supt. of Documents, Washington, D. C. Q
- Journal of Research, Section C — Engineering and Instrumentation.* National Bureau of Standards; Supt. of Documents, Washington, D. C. Q



- Journal of Research, Section D — Radio Science* (see *Radio Science*).
- Journal of Scientific and Industrial Research*. Council of Scientific and Industrial Research, New Delhi. M
- Journal of Scientific Instruments*. Institute of Physics and The Physical Society, London. M
- Journal of Sound and Vibration*. Academic Press, Inc., New York. Q
- Journal of Spacecraft and Rockets*. American Institute of Aeronautics and Astronautics, Inc., New York. BM
- Journal of Strain Analysis*. Institution of Mechanical Engineers, London. Q
- Journal of the Astronautical Sciences*. American Astronautical Society, Inc., Baltimore. BM
- Journal of the Atmospheric Sciences*. American Meteorological Society, Boston. BM
- \**Journal of the Experimental Analysis of Behavior*. Society for the Experimental Analysis of Behavior, Inc., Bloomington. Q
- Journal of the Less-Common Metals*. Elsevier Publishing Co., Amsterdam. M
- Journal of the Mechanics and Physics of Solids*. Pergamon Press, Ltd., Oxford. BM
- \**Journal of Theoretical Biology*. Academic Press, Inc., New York. Q
- Journal of Vacuum Science and Technology*. American Institute of Physics, Inc., New York. BM
- \**Journal of Verbal Learning and Verbal Behavior*. Academic Press, Inc., New York. BM
- JSME, Bulletin*. Japan Society of Mechanical Engineers, Tokyo. Q

## K

- Kakioka Magnetic Observatory, Memoirs*. Kakioka Magnetic Observatory, Kakioka, Japan.
- Kerntechnik*. Verlag Karl Thieme KG, Munich. M
- Kexue Tongbao*. Academia Sinica, Peking. SM
- Khimii i Tekhnologiiia Topliv i Masel*. Ministerstvo Neftepererabatyvaiushchei i Neftekhimicheskoi Promyshlennosti SSSR, Akademiia Nauk SSSR, and Nauchno-Tekhnicheskoe Obschestvo Neftianoi i Gazovoi Promyshlennosti, Moscow. M
- Kinetika i Kataliz*. Akademiia Nauk SSSR, Sibirskoe Otdelenie, Novosibirsk. BM
- \**Kongelige Danske Videnskabernes Selskab, Matematisk-Fysiske Skrifter*. Kongelige Danske Videnskabernes Selskab, Copenhagen.
- Koninklijke Nederlandse Akademie van Wetenschappen, Proceedings, Series B*. North-Holland Publishing Co., Amsterdam. 5 issues per year
- \**Konstruktion im Maschinen-, Apparate- und Gerätebau*. Springer Verlag, Berlin. M
- Kosmicheskie Issledovaniia*. Akademiia Nauk SSSR, Moscow. BM
- Kraków, Astronomiczne Obserwatorium, Rocznik, Dodatek Międzynarodowy*. Polska Akademia Nauk, Komitet Astronomii, Krakow. Annual
- Kristallografiia*. Akademiia Nauk SSSR, Moscow. BM

- Kungliga Tekniska Högskolans Handlingar*. Royal Institute of Technology, Stockholm. Irreg.
- \**Kybernetik*. Springer Verlag, Berlin. Annual.
- Kybernetika*. State Technical Library, Prague.
- Kyoto University, Faculty of Engineering, Memoirs*. Kyoto University, Faculty of Engineering, Kyoto, Japan. Q
- Kyoto University, Institute of Astrophysics and Kwasan Observatory, Contributions*. Kyoto, Japan. Irreg.
- Kyushu University, Research Institute for Applied Mechanics, Reports*. Kyushu University, Fukuoka. Irreg.

## L

- Laboratory Practice*. United Trade Press, Ltd., London. M
- Leningradskii Gosudarstvennyi Universitet, Astronomicheskaiia Observatoriia, Trudy*. Leningradskii Gosudarstvennyi Universitet, Leningrad.
- Leningradskii Universitet, Vestnik, Serii Matematiki, Mekhaniki i Astronomii*. Leningradskii Universitet, Leningrad. Q
- \**Life Sciences*. Pergamon Press, Ltd., Oxford. BW
- Light Metals* (Tokyo). Japan Institute of Light Metals, Tokyo. BM
- Lockheed Georgia Quarterly*. Lockheed-Georgia Co., Marietta, Ga. Q
- Lockheed Horizons*. Lockheed-California Co., Burbank, Calif. Q
- Lockheed Orion Service Digest*. Lockheed-California Co., Burbank, Calif. BM
- Lubelskie Towarzystwo Naukowe, Biuletyn, Matematyka-Fizyka*. Lublin University, Lublin, Poland. Irreg.
- Lubrication*. Texaco, Inc., New York. M
- Lubrication Engineering*. American Society of Lubrication Engineers, Park Ridge, Ill. M
- Luftfahrttechnik Raumfahrttechnik*. Verlag Deutscher Ingenieure, Düsseldorf. M

## M

- Machine Design*. Penton Publishing Co., Cleveland. BW
- Machinery*. Machinery Publishing Co., Ltd., Brighton, England. W
- Magnetohydrodynamics (Magnitnaia Gidrodinamika)*. The Faraday Press, Inc., New York. Q
- Magnitnaia Gidrodinamika*. Akademiia Nauk Latvii-skoi SSR, Riga. Q
- Magyar Tudományos Akadémia, Matematikai Kutató Intézet, Közleményei, Series A*. Hungarian Academy of Sciences, Mathematical Institute, Budapest. Q
- Marconi Review*. Marconi Co., Ltd., Chelmsford, Essex. Q



*Maschinenmarkt*. Vogel-Verlag, Würzburg. BW  
*Matematicheskii Institut imeni V. A. Steklova, Trudy*.  
 Akademiia Nauk SSSR, Moscow. Irreg.  
*Matematicheskii Shornik*. Izdatel'stvo Nauka, Moscow.  
 M  
*Matematisko-Fyzikalny Časopis*. Slovenská Akadémia  
 Vied, Bratislava. Q  
*Matematika*. Kazanskii Gosudarstvennyi Universitet,  
 Kazan. BM  
*Materialprüfung*. VDI-Verlag GmbH, Düsseldorf. M  
*Materials Evaluation*. Society for Nondestructive Test-  
 ing, Evanston. M  
*Materials Protection*. National Association of Corrosion  
 Engineers, Inc., Houston. M  
*Materials Research and Standards*. American Society  
 for Testing and Materials, Philadelphia. M  
*Materials Science and Engineering*. Elsevier Publishing  
 Co., Amsterdam. BM  
*Matematica*. Societatea de Științe Matematice și Fizice,  
 Filiala Cluj, Cluj, Rumania. SA  
*Mathematics of Computation*. American Mathematical  
 Society, Providence. Q  
*Mathematika*. University College, Dept. of Mathe-  
 matics, London. SA  
*Mathematische Annalen*. Springer Verlag, Berlin. Q  
*Measurement Techniques (Izmeritel'naia Tekhnika)*. In-  
 strument Society of America, Pittsburgh. M  
*Mechanical Engineering*. American Society of Me-  
 chanical Engineers, New York. M  
*Mechanical Engineering Science, Monograph*. Institu-  
 tion of Mechanical Engineers, London. Irreg.  
*Mechanika*. Politechnika Łódzka, Lodz, Poland. Irreg.  
*Mechanika Teoretyczna i Stosowana*. Polskie Towarzys-  
 two Mechaniki Teoretycznej i Stosowanej, Warsaw.  
 Irreg.  
*Medical Electronics and Biological Engineering*. Inter-  
 national Federation for Medical Electronics, Oxford.  
 Q  
*Medical Opinion and Review*. Medical Opinion and Re-  
 view, New York. M  
*Mekhanika Polimerov*. Akademiia Nauk Latviiskoi  
 SSR, Riga. BM  
*Mérés és Automatika*. Budapest. M  
*Metal Finishing*. Metals and Plastics Publications, Inc.,  
 Westwood, N. J. M  
*Metal Progress*. American Society for Metals, Metals  
 Park, Ohio. M  
*Metal Science and Heat Treatment (Metallovedenie i  
 Termicheskaia Obrabotka Metallov)*. Consultants  
 Bureau Enterprises, Inc., New York. BM  
*Metall*. Metall Verlag GmbH, Berlin. M  
*Metallovedenie i Termicheskaia Obrabotka Metallov*.  
 Ministerstvo Tiazhelogo Mashinostroeniia and Tsen-  
 tral'nyi Nauchno-Issledovatel'skii Institut Tekhnologii  
 i Mashinostroeniia, Moscow.  
*Metallurgia*. Kennedy Press, Ltd., Manchester. M  
*Metalscope*. Brooks and Perkins, Inc., Detroit. Q  
*Metals Engineering Quarterly*. American Society for  
 Metals, Metals Park, Ohio. Q  
*Meteoritics*. Meteoritical Society, New Haven. Irreg.  
*Meteorological Magazine*. Meteorological Office; Her  
 Majesty's Stationery Office, London. M  
*Meteorological Society of Japan, Journal*. Japan Pub-  
 lications Trading Co., Tokyo. BM


*Meteorologische Rundschau*. Springer Verlag, Berlin.  
 BM  
*Métra*. Groupe METRA - Association de Conseillers  
 Scientifiques de Gestion, Paris. Q  
*\*Metrologia*. Springer Verlag, Berlin. Q  
*\*Michigan Mathematical Journal*. University of Michi-  
 gan Press, Ann Arbor. SA  
*Microelectronics and Reliability*. Pergamon Press, Ltd.,  
 Oxford. Q  
*Microwave Journal*. Horizon House, Inc., Dedham,  
 Mass. M  
*Microwaves*. Hayden Microwaves Corp., New York.  
 M  
*Milano, Seminario Matematico e Fisico, Rendiconti*.  
 Seminario Matematico e Fisico, Milan.  
*Military Medicine*. Association of Military Surgeons of  
 the United States, Washington, D. C. M  
*Missili (see Missili e Spazio)*.  
*Missili e Spazio (formerly Missili)*. Associazione Italia-  
 na Razzi, Rome. BM  
*Mitsubishi Denki Laboratory Reports*. Mitsubishi Elec-  
 tric Corp., Central Research Laboratories, Minami  
 Shimizu, Amagasaki, Hyogo Prefecture, Japan. Q  
*\*Molecular Physics*. Taylor & Francis, Ltd., London.  
 Irreg.  
*Monthly Weather Review*. U.S. Weather Bureau, Wash-  
 ington, D. C. M  
*Moskovskii Universitet, Vestnik, Serii I - Matematika,  
 Mekhanika*. Moskovskii Universitet, Moscow. BM  
*Moskovskii Universitet, Vestnik, Serii III - Fizika, As-  
 tronomiia*. Moskovskii Universitet, Moscow. BM  
*Motorola Monitor*. Motorola Semiconductor Products,  
 Inc., Phoenix. BM  
*\*Mutation Research*. Elsevier Publishing Co., Amster-  
 dam. BM

## N

*Nachrichtentechnische Zeitschrift*. Nachrichtentechni-  
 sche Gesellschaft; Friedr. Vieweg & Sohn, Braun-  
 schweig. M  
*Nagoya University, Faculty of Engineering. Memoirs*.  
 Nagoya University, Nagoya, Japan. Irreg.  
*Nagoya University, Research Institute of Atmospherics,  
 Proceedings*. Nagoya University, Nagoya, Japan.  
 Irreg.  
*\*Nantes, Ecole Nationale Supérieure de Mécanique, An-  
 nales*. Ecole Nationale Supérieure de Mécanique,  
 Nantes.  
*\*National Academy of Sciences, Proceedings*. National  
 Academy of Sciences, Washington, D. C. M  
*National Institute of Sciences of India, Proceedings*.  
 National Institute of Sciences of India, New Delhi.  
 BM  
*Nature*. Macmillan & Co., Ltd., London. W  
*\*Naturwissenschaften*. Max Planck-Gesellschaft zur För-  
 derung der Wissenschaften; Springer Verlag, Berlin.  
 SM  
*Naval Research Logistics Quarterly*. U. S. Navy, Office  
 of Naval Research; Supt. of Documents, Washington,  
 D. C. Q



# INTERNATIONAL AEROSPACE ABSTRACTS

- Naval Research Review*. U. S. Navy, Office of Naval Research; Supt. of Documents, Washington, D. C. M
- Navigation*. Institute of Navigation, Washington, D. C. Q
- Navigation* (Paris). Institut Français de Navigation, Paris. Q
- NEC Review*. Nippon Electric Co., Tokyo. Irreg.
- Neue Physik*. Verlag Neue Physik, Vienna. Irreg.
- \**Neues Jahrbuch für Mineralogie, Geologie und Paläontologie, Monatshefte*. E. Schweizerbart'sche Verlagsbuchhandlung, Stuttgart. M
- \**New Scientist*. London. Irreg.
- New York Academy of Sciences, Annals*. New York Academy of Sciences, New York. Irreg.
- Nihon University, Research Institute of Technology, Report*. Nihon University, Tokyo. Irreg.
- Nordrhein-Westfalen, Forschungsberichte*. Westdeutscher Verlag, Cologne. Irreg.
- \**Norelco Reporter*. Philips Electronic Instruments, Mount Vernon, N.Y. Q
- \**Nova Acta Leopoldina*. Deutsche Akademie der Naturforscher Leopoldina, Halle an der Saale. Irreg.
- NTZ-Communications Journal*. Friedr. Vieweg & Sohn, GmbH, Braunschweig. BM
- Nuclear Applications*. American Nuclear Society, Inc., Hinsdale, Ill. BM
- Nuclear Fusion*. International Atomic Energy Agency, Vienna. Q
- \**Nuclear Instruments and Methods*. North-Holland Publishing Co., Amsterdam. M
- \**Nuclear Science and Engineering*. American Nuclear Society, Inc., Hinsdale, Ill. M
- \**Nuclear Structural Engineering*. North-Holland Publishing Co., Amsterdam. BM
- Nucleonics*. McGraw-Hill, Inc., New York. M
- Nukleonika*. Polska Akademia Nauk; Panstwowe Wydawnictwo Naukowe, Warsaw. M
- Nuovo Cimento*. Società Italiana di Fisica, Bologna. SM
- Observatorio de Madrid, Boletín Astronómico*. Observatorio de Madrid, Instituto Geográfico y Catastral, Madrid.
- The Observatory*. Royal Greenwich Observatory, Hailsham, Sussex, England. BM
- 
- \**Ohio Journal of Science*. Ohio State University, Columbus. BM
- \**Oil and Gas Equipment*. Petroleum Publishing Co., Tulsa. M
- \**Oklahoma Academy of Sciences, Proceedings*.  
*L'Onde Electrique*. Société Française des Electroniciens et des Radioélectriciens, Paris. M
- ONERA, TP*. Office National d'Etudes et de Recherches Aérospatiales, Chatillon-sous-Bagneux (Seine), France. Irreg.
- Operations Research*. Operations Research Society of America, Baltimore. BM
- Optica Acta*. Taylor & Francis, Ltd., London. Q

- Optical Society of America, Journal*. Optical Society of America, Inc., Washington, D. C. M
- Optics and Spectroscopy (Optika i Spektroskopiia)*. Optical Society of America, Inc., Washington, D. C. M
- Optika i Spektroskopiia*. Akademiia Nauk SSSR, Leningrad. M
- Ordnance*. American Ordnance Association, Washington, D. C. BM
- Osaka Prefecture, University, Bulletin, Series A - Engineering and Natural Sciences*. Osaka Prefecture, University, Osaka. Irreg.
- Österreichische Akademie der Wissenschaften, Mathematisch-naturwissenschaftliche Klasse, Sitzungsberichte, Abteilung 2*. Österreichische Akademie der Wissenschaften, Vienna. 10 issues per year
- Österreichische Ingenieur Zeitschrift*. Österreichischer Ingenieur- und Architekten-Verein; Springer Verlag, Vienna. M

## P

- Pacific Journal of Mathematics*. Berkeley, Calif. Q
- Papers in Meteorology and Geophysics*. Meteorological Research Institute, Tokyo. SA
- \**Perception and Psychophysics*. Psychonomic Press, Goleta, Calif. M
- \**Perceptual and Motor Skills*. Southern Universities Press, Missoula, Mont. BM
- Periodica Polytechnica, Electrical Engineering Series*. Budapest, Polytechnical University, Budapest. Q
- Periodica Polytechnica, Engineering Series*. Budapest, Polytechnical University, Budapest. Q
- Philips Research Reports*. N. V. Philips' Gloeilampenfabrieken, Eindhoven. BM
- Philips Technical Review*. N. V. Philips' Gloeilampenfabrieken, Research Laboratories, Eindhoven. M
- Philips Telecommunication Review*. N. V. Philips' Telecommunicatie Industrie, Hilversum. Q
- Philosophical Magazine, 8th Series*. Taylor and Francis, Ltd., London. M
- \**Photochemistry and Photobiology*. Pergamon Press, Ltd., Oxford. Q
- Photogrammetric Engineering*. American Society of Photogrammetry, Falls Church, Va. BM
- Photographic Science and Engineering*. Society of Photographic Scientists and Engineers, Washington, D. C. BM
- Physica*. Martinus Nijhoff, The Hague. M
- Physica Status Solidi*. Akademie Verlag GmbH, Berlin. M
- Physical Review, 2nd Series* (formerly *Physical Review, 2nd Series, Section A* and *Physical Review, 2nd Series, Section B*). American Institute of Physics, Inc., New York. SM
- Physical Review, 2nd Series, Section A* (see *Physical Review, 2nd Series*).
- Physical Review, 2nd Series, Section B* (see *Physical Review, 2nd Series*).
- Physical Review Letters*. American Institute of Physics, Inc., New York. SM



*Physical Society, Proceedings.* Institute of Physics and The Physical Society, London. M

*Physical Society of Japan, Journal.* Physical Society of Japan, Tokyo. M

*Physics Letters.* North-Holland Publishing Co., Amsterdam. 4 issues per mo.

*Physics of Fluids.* American Institute of Physics, Inc., New York. M

*Physics of Metals and Metallography (Fizika Metallov i Metallovedenie).* Pergamon Press, Ltd., Oxford. M

*Physics Teacher.* American Institute of Physics, Inc., New York. M

*Physics Today.* American Institute of Physics, Inc., New York. M

*Physikalische Blätter.* Physik Verlag GmbH, Mosbach, Germany. M

*Planetary and Space Science.* Pergamon Press, Ltd., Oxford. M

*Plant and Cell Physiology.* Japanese Society of Plant Physiologists, c/o Institute of Applied Microbiology, University of Tokyo, Tokyo. Q

*Plant Physiology.* American Society of Plant Physiology, Washington, D. C. BM

*Planta.* Springer Verlag, Berlin. SA

*PMM - Journal of Applied Mathematics and Mechanics (Prikladnaia Matematika i Mekhanika).* Pergamon Press, Ltd., Oxford. BM

*PMTF - Zhurnal Prikladnoi Mekhaniki i Tekhnicheskoi Fiziki.* Akademiia Nauk SSSR, Sibirskoe Otdelenie, Novosibirsk. BM

*Point to Point Telecommunications.* Marconi Co., Ltd., Communications Division, Chelmsford, England. 3 issues per year

*Polar Record.* Scott Polar Research Institute, Cambridge. Irreg.

*Polymer Engineering and Science.* Society of Plastics Engineers, Stamford, Conn. Q

*Pomiary, Automatyka, Kontrola.* Naczelna Organizacja Techniczna, Warsaw. M

*Poroshkovaia Metallurgii.* Akademiia Nauk Ukrainskoi SSR, Kiev. BM

*Postepy Astronomii.* Obserwatorium Astronomiczne Politechniki, Warsaw. Q

*Postepy Fizyki.* Polskie Towarzystwo Fizyczne, Warsaw. BM

*Powder Metallurgy.* Powder Metallurgy Joint Group, Iron and Steel Institute and Institute of Metals, London. SA

*Priborostroenie.* Leningradskii Institut Tochnoi Mekhaniki i Optiki, Leningrad. BM

*Pribory i Tekhnika Eksperimenta.* Akademiia Nauk SSSR, Moscow. BM

*Prikladnaia Matematika i Mekhanika.* Akademiia Nauk SSSR, Otdelenie Tekhnicheskikh Nauk, Institut Mekhaniki, Moscow. BM

*Prikladnaia Mekhanika.* Akademiia Nauk Ukrainskoi SSR, Otdelenie Matematiki, Mekhaniki i Kibernetiki, Kiev. M

*Problemy Peredachi Informatsii.* Izdatel'stvo Nauka, Moscow. Q

*Proceedings of Vibration Problems.* Polish Academy of Sciences, Institute of Basic Technical Problems, Warsaw. Q

*Product Engineering.* McGraw-Hill Publishing Co., Inc., New York. BW

*Progress of Theoretical Physics.* Kyoto University, Kyoto, Japan. M

*Protection of Metals (Zashchita Metallov).* Scientific Information Consultants, Ltd., London. BM

*\*Protoplasma.* Springer Verlag, Vienna. Irreg.

*Przegląd Elektroniki.* Polska Akademia Nauk, Komitet Elektroniki i Telekomunikacji and Stowarzyszenie Elektryków Polskich, Sekcja Elektroniki i Telekomunikacji, Warsaw. M

*Przegląd Geodezyjny.* Warsaw. M

*\*Psychonomic Science.* Psychonomic Science, Goleta, Calif. M

## Q

*Quarterly Journal of Mechanics and Applied Mathematics.* Oxford University Press, London. Q

*Quarterly of Applied Mathematics.* Brown University, Providence. Q

## R

*Radio and Electronic Engineer.* British Institute of Radio Engineers, London. M

*\*Radiation Botany.* Pergamon Press, Ltd., Oxford. Q

*Radio Engineering and Electronic Physics (Radiotekhnika i Elektronika).* Institute of Electrical and Electronics Engineers, Inc., New York. M

*Radio Research Laboratories, Journal.* Ministry of Posts and Telecommunications, Radio Research Laboratories, Tokyo. BM

*Radiofizika.* Gor'kovskii Universitet, Gorki. BM

*Radio Science (formerly Journal of Research, Section D - Radio Science).* Environmental Science Services Administration; Supt. of Documents, Washington, D.C. M

*Radiotekhnika.* Nauchno-Tekhnicheskoe Obshchestvo Radiotekhniki i Elektrosvazi, Moscow. BM

*Radiotekhnika (Kiev).* Kievskii Politeknicheskii Institut, Kiev. BM

*Radiotekhnika i Elektronika.* Akademiia Nauk SSSR, Moscow. M

*Raumfahrtforschung.* Deutsche Gesellschaft für Raketentechnik und Raumfahrt, e.V., Stuttgart. Q

*RCA Review.* RCA Laboratories, Princeton, N. J. Q

*La Recherche Aéronautique.* Office National d'Etudes et de Recherches Aéronautiques, Chatillon-sous-Bagneux (Seine), France. BM

*La Recherche Spatiale.* Centre National d'Etudes Spatiales; Dunod Editeur, Paris. M

*Rendezvous.* Bell Aerosystems Co., Buffalo. BM

*Report of Ionosphere and Space Research in Japan.* Science Council of Japan, Ionosphere Research Committee, Tokyo. Q

*Research/Development.* F. D. Thompson Publications, Inc., New York. M



# INTERNATIONAL AEROSPACE ABSTRACTS

- Research Trends.* Cornell Aeronautical Laboratory, Inc., Buffalo. Q
- Review of Scientific Instruments.* American Institute of Physics, Inc., New York. M
- Reviews of Geophysics.* American Geophysical Union, Washington, D. C. Q
- Reviews of Modern Physics.* American Physical Society, New York. Q
- Revista de Aeronáutica y Astronáutica.* Ministerio del Aire, Madrid. M
- Revista Nacional Aeronáutica y Espacial.* Circulo de Aeronáutica, Buenos Aires. M
- Revista Transporturilor.* Asociația Științifică a Inginerilor și Tehnicienilor din Republicii Populare Române, Bucharest. M
- Revue de Physique Appliquée.* Société Française de Physique, Centre National de la Recherche Scientifique, Paris. Q
- Revue Française d'Astronautique.* Société Française d'Astronautique, Paris. BM
- Revue Française de Mécanique.* Société Française des Mécaniciens, Paris. Q
- Revue Générale de l'Air et de l'Espace.* Editions Internationales, Paris. Q
- Revue Générale de l'Electricité.* Comité Electrotechnique Français et de l'Union Technique de l'Electricité, Paris. M
- Revue Générale de Thermique.* Institut Français des Combustibles et de l'Energie and Société Française des Thermiciens, Paris. M
- Revue mble.* Société Anonyme MBLE, Brussels. Q
- Revue Roumaine de Mathématiques Pures et Appliquées.* Académie de la République Populaire Roumaine, Bucharest. 10 issues per year
- Revue Roumaine des Sciences Techniques, Série de Mécanique Appliquée* (formerly *Revue de Mécanique Appliquée*). Académie de la République Populaire Roumaine, Bucharest. BM
- Revue Technique CECLES.* Gauthier-Villars & Cie, Paris. Q
- Ricerca Scientifica* (formerly *Ricerca Scientifica, Parte I: Rivista* and *Ricerca Scientifica, Parte II: Rendiconti, Sezione A*). Consiglio Nazionale delle Ricerche, Rome. M
- Ricerca Scientifica, Parte I: Rivista* (see *Ricerca Scientifica*).
- Ricerca Scientifica, Parte II: Rendiconti, Sezione A* (see *Ricerca Scientifica*).
- Rivista Aeronautica.* Ministero Difesa Aeronautica, Rome. M
- Rivista di Ingegneria.* Milan. M
- Rivista di Medicina Aeronautica e Spaziale.* Rome. Q
- Rivista di Meteorologia Aeronautica.* Servizio Meteorologico d'Aeronautica, Rome. Q
- Roma, Osservatorio Astronomico, Contributi Scientifici.* Osservatorio Astronomico, Rome. Irreg.
- Roma, Università, Scuola d'Ingegneria Aerospaziale, Centro Ricerche Aerospaziali, Atti.* Roma, Università, Rome. Irreg.
- Royal Aeronautical Society, Journal.* Royal Aeronautical Society, London. M
- Royal Astronomical Society, Monthly Notices.* Royal Astronomical Society, London. M
- Royal Astronomical Society, Quarterly Journal.* Royal Astronomical Society, London. Q
- \*Royal Astronomical Society of Canada, Journal.* Royal Astronomical Society of Canada, Toronto. BM
- Royal Meteorological Society, Quarterly Journal.* Royal Meteorological Society, London. Q
- Royal Society (Edinburgh), Proceedings, Section A.* Royal Society of Edinburgh, Edinburgh. Irreg.
- Royal Society (London), Philosophical Transactions, Series A.* Royal Society, London. Irreg.
- Royal Society (London), Proceedings, Series A.* Royal Society, London. Irreg.
- \*Royal Society of New South Wales, Journal and Proceedings.* Royal Society of New South Wales, Sydney. BM
- Rozprawy Inżynierskie.* Polska Akademia Nauk, Instytut Podstawowych Problemów Techniki, Warsaw. Q
- Ruimtevaart.* The Hague. Q
- Russian Chemical Reviews (Uspekhi Khimii).* Chemical Society, London. M
- Russian Journal of Inorganic Chemistry (Zhurnal Neorganicheskoi Khimii).* Chemical Society, London. M
- Russian Journal of Physical Chemistry (Zhurnal Fizicheskoi Khimii).* Chemical Society, London. M
- Russian Mathematical Surveys (Uspekhi Matematicheskikh Nauk).* London Mathematical Society; Macmillan & Co., Ltd., London. BM
- Russian Metallurgy and Mining (Akademiia Nauk SSSR, Izvestiia, Metallurgii i Gornoe Delo).* Scientific Information Consultants, Ltd., London. BM
- Ryan Reporter.* Ryan Aeronautical Co., San Diego. Q

## S

- Science.* American Association for the Advancement of Science, Washington, D. C. W
- Science Journal.* Associated Iliffe Press, Ltd., London. M
- Science Progress.* Science Progress, London. Q
- \*Science Teacher.* National Science Teachers Association, Washington, D.C. 8 issues per year
- Sciences et Industries Spatiales.* SADESI - Société Anonyme d'Editions Scientifiques et Industrielles, Geneva. BM
- Sciences et Techniques.* Société des Ingénieurs Civils de France; Société d'Editions de la rue Blanche, Paris. M
- Scientia.* Milan. M
- Scientia Sinica.* Academia Sinica, Peking. M
- Scientific American.* Scientific American, Inc., New York. M
- Secrétariat Général à l'Aviation Civile, Revue.* Secrétariat Général à l'Aviation Civile, Paris. Irreg.
- Semiconductor Products and Solid State Technology.* Cowan Publishing Corp., New York. M
- Seoul National University, College of Engineering, Science and Engineering Report.* Seoul National University, College of Engineering, Seoul.
- Shell Aviation News.* Shell Oil Co., London. M
- \*Shinkei Kagaku.* Toho University, School of Medicine, Dept. of Physiology, Tokyo. SM

- SIAM Journal on Applied Mathematics* (formerly *Society for Industrial and Applied Mathematics, Journal*). Society for Industrial and Applied Mathematics, Philadelphia. BM
- SIAM Journal on Control* (formerly *Society for Industrial and Applied Mathematics, Journal, Series A — Control*). Society for Industrial and Applied Mathematics, Philadelphia. Q
- SIAM Journal on Numerical Analysis* (formerly *Society for Industrial and Applied Mathematics, Journal, Series B - Numerical Analysis*). Society for Industrial and Applied Mathematics, Philadelphia. Q
- SIAM Review*. Society for Industrial and Applied Mathematics, Philadelphia. Q
- Sibirskii Matematicheskii Zhurnal*. Akademiia Nauk SSSR, Sibirskoe Otdelenie, Novosibirsk. BM
- Siemens Review*. Siemens und Halske AG, Siemens-Schuckertwerke AG, Erlangen. M
- Signal*. Armed Forces Communications and Electronics Association, Washington, D. C. M
- Sky and Telescope*. Harvard College Observatory, Cambridge, Mass. M
- Smithsonian Contributions to Astrophysics*. Smithsonian Institution, Washington, D. C. Q
- SMPTE, Journal*. Society of Motion Picture and Television Engineers, Inc., New York. M
- Società Astronomica Italiana, Memorie*. Gia Società degli Spettroscopisti Italiani, Milan. Q
- Société Royale des Sciences de Liège, Mémoires*. Société Royale des Sciences de Liège, Liege. Annual
- Society for Experimental Biology and Medicine, Proceedings*. Society for Experimental Biology and Medicine, New York. 11 issues per year
- Society for Industrial and Applied Mathematics, Journal* (see *SIAM Journal on Applied Mathematics*).
- Society for Industrial and Applied Mathematics, Journal, Series A — Control* (see *SIAM Journal on Control*).
- Society for Industrial and Applied Mathematics, Journal, Series B — Numerical Analysis* (see *SIAM Journal on Numerical Analysis*).
- Society of Experimental Test Pilots, Technical Review*. Society of Experimental Test Pilots, Lancaster, Calif. Q
- Society of Instrument Technology, Transactions*. Society of Instrument Technology, London. Q
- Society of Licensed Aircraft Engineers and Technologists, Journal* (see *Tech Air*).
- Society of Rheology, Transactions*. American Institute of Physics, Inc., New York. Irreg.
- Solar Energy*. Solar Energy Society, Arizona State University, Tempe. Q
- Solid-State Electronics*. Pergamon Press, Ltd., Oxford. M
- Solid-State Communications*. Pergamon Press, Ltd., Oxford. M
- Soviet Astronomy (Astronomicheskii Zhurnal)*. American Institute of Physics, Inc., New York. BM
- Soviet Electrical Engineering (Elektrotehnika)*. The Faraday Press, Inc., New York. M
- Soviet Electrochemistry (Elektrokhimiia)*. Consultants Bureau Enterprises, Inc., New York. M
- Soviet Engineering Journal (Inzhenernyi Zhurnal)*. The Faraday Press, Inc., New York. BM
- Soviet Materials Science (Fiziko-Khimicheskaiia Mekhanika Materialov)*. The Faraday Press, Inc., New York. BM
- Soviet Mathematics (Akademiia Nauk SSSR, Doklady)*. American Mathematical Society, Providence, R. I. BM
- Soviet Physics — Acoustics (Akusticheskii Zhurnal)*. American Institute of Physics, Inc., New York. Q
- Soviet Physics — Crystallography (Kristallografiia)*. American Institute of Physics, Inc., New York. BM
- Soviet Physics — Doklady (Akademiia Nauk SSSR, Doklady)*. American Institute of Physics, Inc., New York. M
- Soviet Physics — JETP (Zhurnal Eksperimental'noi i Teoreticheskoi Fiziki)*. American Institute of Physics, Inc., New York. M
- Soviet Physics Journal (Fizika)*. The Faraday Press, Inc., New York. BM
- Soviet Physics — Solid State (Fizika Tverdogo Tela)*. American Institute of Physics, Inc., New York. M
- Soviet Physics — Technical Physics (Zhurnal Tekhnicheskoi Fiziki)*. American Institute of Physics, Inc., New York. M
- Soviet Physics — Uspekhi (Uspekhi Fizicheskikh Nauk)*. American Institute of Physics, Inc., New York. BM
- Soviet Powder Metallurgy and Metal Ceramics (Poroshkovaia Metallurgiiia)*. Consultants Bureau Enterprises, Inc., New York. M
- Soviet Radio Engineering (Radiotekhnika /Kiev/)*. The Faraday Press, Inc., New York. BM
- Soviet Radiophysics (Radiofizika)*. The Faraday Press, Inc., New York. BM
- Space*. Cockatrice Press, Ltd., London. M
- Space/Aeronautics*. Conover-Mast Publications, Inc., New York. M
- Space Science Reviews*. D. Reidel Publishing Co., Dordrecht, Netherlands. 9 issues per year
- Spaceflight*. British Interplanetary Society, London. BM
- SPARMO Bulletin*. Solid Particles and Radiation Monitoring Organization, Meudon, France. Q
- SPE Journal*. Society of Plastics Engineers, Inc., Stamford, Conn. M
- Spectra-Physics Technical Memorandum*. Spectra-Physics, Inc., Mountain View, Calif. Irreg.
- Sperry Engineering Review*. Sperry Gyroscope Co., Great Neck, N.Y. Q
- SPIE Journal*. Society of Photo-Optical Instrumentation Engineers, Redondo Beach, Calif. BM
- \*Der Stahlbau*. Wilhelm Ernst & Sohn, Berlin. M
- Sterne und Weltraum*. Verlag Bibliographisches Institut AG, Mannheim. M
- Studia Geophysica et Geodaetica*. Czechoslovak Academy of Sciences; Artia, Prague. Q
- Studii și Cercetări Matematice*. Academia Republicii Populare Romîne, Institutul de Matematica, Bucharest. 10 issues per year
- Sun at Work*. Solar Energy Society, Arizona State University, Tempe, Ariz. Q
- Surface Science*. North-Holland Publishing Co., Amsterdam. Q



## T

- Tech Air* (formerly *Society of Licensed Aircraft Engineers and Technologists, Journal*). Society of Licensed Aircraft Engineers and Technologists, Maidenhead, Berks., England. M
- Tech Engineering News*. Cambridge, Mass. 9 issues per year
- Technika Lotnicza* (see *Technika Lotnicza i Astronautyczna*).
- Technika Lotnicza i Astronautyczna* (formerly *Technika Lotnicza*). Stowarzyszenie Inżynierów i Mechaników Polskich, Warsaw. M
- Technique et Science Aéronautiques et Spatiales*. Association Française des Ingénieurs et Techniciens de l'Aéronautique et de l'Espace, Paris. BM
- La Technique Moderne*. Dunod Editeur, Paris. M
- Technology Week*. American Aviation Publications, Inc., Washington, D.C. W
- \**Technometrics*. American Statistical Association, Washington, D.C. Q
- Tecnica Italiana*. Trieste. M
- Teknisk Tidskrift*. Svenska Teknologföreningen, Stockholm. W
- \**Telecommunication Journal*. Union Internationale des Télécommunications UIT, Geneva. M
- Telecommunications and Radio Engineering. Part I - Telecommunications, Part 2 - Radio Engineering.* (*Elektrosviaz', Radiotekhnika*). Institute of Electrical and Electronics Engineers, Inc., New York. M
- Telefunken-Zeitung*. Telefunken AG, Berlin. Irreg.
- Tellus*. Svenska Geofysiska Föreningen, Stockholm. Q
- \**Tensor*. Tensor Society, Hokkaido University, Faculty of Science, Sapporo. 3 issues per year
- Teoriia Veroiatnostei i ee Primeneniia*. Akademiia Nauk SSSR, Moscow. Q
- Teplofizika Vysokikh Temperatur*. Akademiia Nauk SSSR, Moscow. BM
- \**Tetrahedron Letters*. Pergamon Press, Ltd., Oxford. SM
- \**Texas State Journal of Medicine*. Texas Medical Association, Austin. M
- \**Theoretica Chimica Acta*. Springer Verlag, Berlin. Q
- Theory of Probability and its Applications (Teoriia Veroiatnostei i ee Primeneniia)*. Society for Industrial and Applied Mathematics, Philadelphia. Q
- TNB General Precision Aerospace*. General Precision, Inc., Aerospace Group, Little Falls, N.J. Q
- Tohoku University, Institute of High Speed Mechanics, Reports*. Tohoku University, Sendai. Annual
- Tohoku University, Research Institute for Scientific Measurements, Bulletin*. Tohoku University, Sendai. Irreg.
- Tohoku University, Science Reports, Series 5 - Geophysics*. Tohoku University, Sendai. 3 issues per year
- \**Tokyo, University, Earthquake Research Institute, Bulletin*. Tokyo, University, Tokyo. Q
- Tokyo, University, Institute of Space and Aeronautical Science, Bulletin*. Tokyo, University, Institute of Space and Aeronautical Science, Tokyo. Q

- Tokyo Astronomical Observatory, Tokyo Astronomical Bulletin, Second Series*. Tokyo, University, Tokyo Astronomical Observatory, Tokyo. Irreg.
- Tokyo Institute of Technology, Bulletin*. Tokyo Institute of Technology, Tokyo. Irreg.
- Tokyo, University, Institute of Space and Aeronautical Science, Report*. Tokyo, University, Institute of Space and Aeronautical Science, Tokyo. Q
- Tokyo, University, Tokyo Astronomical Observatory, Annals, Second Series*. Tokyo, University, Tokyo Astronomical Observatory, Tokyo. Q
- Tool and Manufacturing Engineer*. American Society of Tool and Manufacturing Engineers, Milwaukee. M
- Torino, Accademia delle Scienze, Atti*. Torino, Accademia delle Scienze, Turin. Irreg.
- \**Torino, Accademia delle Scienze, Classe di Scienze Fisiche, Matematiche e Naturali, Atti*. Torino, Accademia delle Scienze, Turin. Irreg.
- Toshiba Review*. Tokyo Shibaura Electric Co., Ltd., Tokyo. Q
- Trend in Engineering*. Washington, University, Engineering Experiment Station, Seattle. Q
- TRW Space Log* (formerly *Space Log*). TRW Systems, Redondo Beach, Calif. Q
- \**Tschermaks mineralogische und petrografische Mitteilungen*. Springer Verlag, Vienna. Irreg.
- Tsvetnaia Metallurgii*. Ministerstvo Vysshego i Srednego Spetsial'nogo Obrazovaniia; Severokavkazskii Gornometallurgicheskii Institut, Ordzhonikidze. M

## U

- Ukrains'kii Fizichnii Zhurnal*. Akademiia Nauk Ukrain'skoi RSR, Kiev. M
- Ukrainskii Matematicheskii Zhurnal*. Akademiia Nauk Ukrainskoi SSR, Kiev. BM
- Ultrasonics*. Iliffe Industrial Publications, Ltd., London. Q
- Universidad Industrial de Santander, Revista*. Universidad Industrial de Santander, Bucaramanga, Colombia. Q
- University of Electro-Communications, Reports*. University of Electro-Communications, Tokyo. Annual
- Uspekhi Fizicheskikh Nauk*. Akademiia Nauk SSSR, Moscow. M
- Uspekhi Matematicheskikh Nauk*. Akademiia Nauk SSSR and Moskovskoe Matematicheskoe Obshchestvo, Moscow. BM

## V

- \**VDI-Berichte*. Verein deutscher Ingenieure; VDI-Verlag GmbH, Düsseldorf. Irreg.
- VDI-Forschungsheft*. VDI-Verlag GmbH, Düsseldorf. BM

- VDI Zeitschrift*. VDI-Verlag GmbH, Düsseldorf. 36 issues per year
- Vectors*. Hughes Aircraft Co., Culver City, Calif. Q
- Verti-Flite*. American Helicopter Society, Inc., New York. M
- Vertical World*. Press-Tech, Inc., Evanston, Ill. M
- Le Vide*. Société Française des Ingénieurs et Techniciens du Vide, Nogent-sur-Marne (Seine), France. BM
- \**Virginia, University, Leander McCormick Observatory, Publications*. Charlottesville, Va. Irreg.
- \**Virology*. Academic Press, Inc., New York. M

## W

- Wear*. Elsevier Publishing Co., Amsterdam. BM
- \**Wehrtechnische Monatshefte*. E. J. Mittler & Sohn, Frankfurt/Main. M
- Weight Record*. Society of Aeronautical Weight Engineers, Inc., Fort Worth, Tex. BM
- Welding Journal*. American Welding Society, New York. M
- Weltraumfahrt Raketentechnik*. Umschau-Verlag Frankfurt/Main. BM
- \**Werkstattstechnik*. Springer Verlag, Berlin. M
- Westrex Communicator*. Westrex Communications, New Rochelle, N.Y. BM
- Wireless World*. Iliffe Electrical Publications, Ltd., London. M
- Wissenschaftliche Zeitschrift*. Dresden, Technische Universität, Dresden. BM
- World Aerospace Systems*. Hanover Press, Ltd., London. M

## Z

- Zashchita Metallov*. Akademiia Nauk SSSR, Gosudarstvennyi Komitet Khimicheskoi Promyshlennosti pri Gosplane SSSR, Moscow. BM
- Zeitschrift für angewandte Mathematik und Mechanik*. Akademie-Verlag GmbH, Berlin. M

- Zeitschrift für angewandte Mathematik und Physik*. Birkhäuser Verlag, Basel. BM
- Zeitschrift für angewandte Physik*. Springer Verlag, Berlin. BM
- Zeitschrift für Astrophysik*. Springer Verlag, Berlin. Irreg.
- Zeitschrift für Flugwissenschaften*. Wissenschaftliche Gesellschaft für Luft- und Raumfahrt, e.V., and Deutsche Gesellschaft für Flugwissenschaften, e.V.; Friedr. Vieweg & Sohn, Braunschweig. M
- Zeitschrift für Geophysik*. Deutsche geophysikalische Gesellschaft, Hamburg; Physica-Verlag, Würzburg. BM
- Zeitschrift für Instrumentenkunde*. Wissenschaftliche und technische Geräte und Messwesen; Friedr. Vieweg & Sohn, Braunschweig. M
- Zeitschrift für Metallkunde*. Deutsche Gesellschaft für Metallkunde, e.V.; Riederer-Verlag GmbH, Stuttgart. M
- Zeitschrift für Meteorologie*. Akademie-Verlag GmbH, Berlin. M
- Zeitschrift für Naturforschung, Ausgabe A*. Verlag der Zeitschrift für Naturforschung, Tübingen. M
- Zeitschrift für Naturforschung, Ausgabe B*. Verlag der Zeitschrift für Naturforschung, Tübingen. M
- Zeitschrift für Physik*. Deutsche physikalische Gesellschaft; Springer Verlag, Berlin. Irreg.
- Zentralblatt für Verkehrs-Medizin, Verkehrs-Psychologie, Luft- und Raumfahrt-Medizin*. J. F. Lehmanns Verlag, Munich. Irreg.
- Zeitschrift für Vermessungswesen*. Deutscher Verein für Vermessungswesen; Verlag Konrad Wittwer, Stuttgart. M
- ZHETF Pis'ma v Redaktsiiu*. Akademiia Nauk SSSR, Moscow. SM
- Zhurnal Eksperimental'noi i Teoreticheskoi Fiziki*. Akademiia Nauk SSSR, Moscow. M
- Zhurnal Nauchnoi i Prikladnoi Fotografii i Kinematografii*. Akademiia Nauk SSSR, Moscow. BM
- Zhurnal Tekhnicheskoi Fiziki*. Akademiia Nauk SSSR, Moscow. M
- Zhurnal Vychislitel'noi Matematiki i Matematicheskoi Fiziki*. Akademiia Nauk SSSR, Moscow. BM
- Zprava VZLÚ*. Výzkumný a Zkušební Letecký Ústav, Prague. Irreg.
- Zpravodaj VZLÚ*. Výzkumný a Zkušební Letecký Ústav, Prague. BM





LIST OF SUBJECT HEADINGS OF  
PUBLICATIONS

A Notation of Content, rather than the title of the publication, appears under each subject heading; it is listed under several subject headings which provide multiple access to the subject content of each accession. The IAA accession number is located under and to the right of the Notation of Content. It is preceded by numbers identifying the issue and page of International Aerospace Abstracts where the abstract is located.

To illustrate:

Issue Number	Page Number	Accession Number
03	p0360	A66-12345

## A

## A-4 AIRCRAFT

Overrunning clutches in gas turbines, design, performance characteristics and application to A-4D Skyhawk aircraft, UH-2 helicopter and Curtiss-Wright X-19 VTOL drive systems

[ASME PAPER 66-GT-92] 14 p2300 A66-26996  
Braze hydraulic system design and fabrication for Skyhawk A4B aircraft 17 p2849 A66-33098

## A-6 AIRCRAFT

Inertial platform test station for shipboard maintenance and calibration of platform used in A6A and E2A aircraft, examining accelerometer bias and gyro drift tests 21 p3723 A66-38889

## A-7 AIRCRAFT

Automatic flight control system for A-7A featuring high fixed gain dual channels, series servos and control augmentation in addition to normal attitude and path control functions 01 p0098 A66-10007

Contractor-customer responsibilities for Model A-7 aircraft design in firm fixed price environment

[AIAA PAPER 65-758] 03 p0320 A66-12589  
Automatic flight control system for A-7A featuring high fixed gain dual channels, series servos and control augmentation in addition to normal attitude and path control functions 23 p4088 A66-40983

## A STAR

UV color and flux at 2200 and 2600 angstroms measured for A and B stars, using rocketborne

photometers 10 p1602 A66-21096  
Stellar rotation and position of metallic line stars in color magnitude diagram 20 p3649 A66-37328

## A-11

## S ECHO I SATELLITE

## A-12

## S ECHO II SATELLITE

## ABDOMEN

## S DIGESTIVE SYSTEM

## S INTESTINE

## ABERRATION

Aberration of width of linear image

created by skew rays in composite quadrupole lens 02 p0199 A66-11782

Coarse-wire objective grating method applied to determination of coma-magnitude scale distortion and magnitude errors in long-focus refracting

telescope 05 p0678 A66-15090

Lens primary aberration evaluation using Twyman interferometer, developing exact equations for high-order lens defects 06 p0879 A66-16118

Electro-optical attitude and velocity sensors for interplanetary navigation and stellar aberration and Doppler shift measurements 08 p1252 A66-19502

Concentric circular grid method of testing for aberrations in image-forming optical system and comparison with Ronchi test 09 p1403 A66-20515

Sunspot phenomena and observation as affected by image perturbation caused by atmospheric inhomogeneities 11 p1770 A66-22647

Spatial amplitude of field of ideally parallel laser beam focused by optical systems with spherical aberration 12 p1889 A66-23778

Lens aberration correction using Gabor wavefront reconstruction method to produce hologram of spherically aberrated wavefront emerging from lens 13 p2080 A66-25990

Lateral, radial and rotational shearing interferometry 13 p2080 A66-25993

Wavefront shearing prism interferometer applied to testing of chromatic aberration of simple and compound lenses and waveforms characterizing monochromatic aberrations 14 p2291 A66-27319

Spherical aberration correction by grinding concave mirror to generate aspheric contour 15 p2498 A66-28826

Scherzer theorem on aperture aberration extended to monochromatic nonrelativistic system with electrostatic or magnetic quadrupole fields with common planes of optical symmetry 24 p4239 A66-43215

## ABIOTENESIS

## SA BIOGENESIS

Astrophysical observation and experimental results of organic synthesis bearing on abiogenic formation of biochemical compounds formed from simple precursor in aqueous or aqueous ammonia system 02 p0181 A66-11603

Synthesis by electrical discharge of porphine-like substances imply abiogenic possibility under primitive Earth condition 03 p0331 A66-13261

Nucleic acid molecule reproduction discussing probability of life development under favorable environmental circumstances 06 p0952 A66-15915

Hydrocarbons synthesized abiogenically and those found in terrestrial samples, using gas chromatography and mass spectrometry in connection with terrestrial life 12 p1806 A66-24965

Synthesis of constituents of nucleic acid and protein molecule for artificial production of life 14 p2227 A66-26866

Chemical laboratory experiments on origin, chemical components and structural attributes of life 16 p2638 A66-30357

Book on photochemical origin of life 16 p2641 A66-31745  
Origins of prebiological systems and their molecular matrices - Conference, Wakulla Springs, Florida, October 1963 17 p2849 A66-32083

Molecular reproduction and life origin from meteorite and gaseous condensation on metallic ion and silicate dust 17 p2850 A66-32085

Prebiological organic synthesis stages and mechanisms prior to and during formation

of Earth, noting extraterrestrial organic matter 17 p2850 A66-32087

Solar UV synthesis of nucleoside phosphates from terrestrial atmosphere, discussing irradiation of adenine-ribose-phosphoric acid solution 17 p2851 A66-32090

Nucleic acid constituents synthesis from methane-ammonia-water mixture, hydrogen cyanide and formaldehyde in thermal-radiation environment 17 p2851 A66-32091

Porphine-like substances synthesis from irradiated mixture of pyrrole, benzaldehyde, pyridine and zinc acetate 17 p2851 A66-32092

Biosynthesis evolutionary stages projected from present data, considering bacterial evolution 17 p2852 A66-32093

Thermal polycondensation of free amino acids with polyphosphoric acid 17 p2852 A66-32094

Polymerization of nucleotides from ADP, noting separation of polymer particles from solution as coacervate drops and relation to life origin 17 p2852 A66-32097

Origin of life experiments noting hereditary propagation in macromolecules arising after spontaneous chemical evolution but before self-replicative biological evolution 17 p2853 A66-32100

Molecular biology noting hemoglobin and enzyme cytochrome evolution, amino acid code, ribonucleic acid, etc 17 p2853 A66-32101

Simulation of organismic morphology and behavior by synthetic poly-alpha-amino acids 19 p3284 A66-35573

Origin of constituents of nucleic acid and protein molecules, noting biological molecules synthesis under conditions similar to those prevailing in prebiotic Earth, following Oparin-Haldane hypothesis 20 p3507 A66-38029

## ABLATING MATERIAL

## SA PYROLYTIC MATERIAL

Plasma arc tunnel tests show thermochemical heat of ablation of magnesia strongly dependent on stagnation enthalpy [AIAA PAPER 65-641] 01 p0089 A66-10225

Thermochemical interaction between ablation material and environment during manned reentry, using mainly graphite and composite materials [AIAA PAPER 65-642] 01 p0160 A66-10226

Cermet ablatives for thermal shields in fabrication of nozzles and nose cones [SAE PAPER 650767] 01 p0078 A66-10838

Ablation mechanism for impregnated tungsten materials 02 p0303 A66-11552

Gemini ablative heat shield, noting nonmetallic honeycomb reinforcement of insulative char 02 p0294 A66-11639

Charring ablative materials effectiveness in combined convective and radiative heating as reentry shield 03 p0444 A66-12792

Mutual effects of vaporization, combustion and coking processes during material decomposition in high temperature gas flow 03 p0445 A66-12828

Uncertainties in thermophysical properties of char-forming ablatives in intense convective and radiative heat transfer environments and effect on mathematical and physical models [AIAA PAPER 65-639] 03 p0445 A66-13010

Make wire, light pipe and spring wire ablation sensors development for measuring parameters of heat shield materials for reentry vehicles 03 p0372 A66-13257

Heat transfer through porous ceramics and thermally degraded ablation material, discussing conductivity [ASME PAPER 65-HT-46] 05 p0785 A66-14756

Thermodynamic calculations and experimental measurements to illustrate material properties pertinent to ablation process and to suggest refractory



compounds as ablating materials 05 p0706 A66-15472

Hypersonic wake ionization dependence on ablation products, investigating laminar and turbulent flow regions [AIAA PAPER 65-54] 05 p0793 A66-15778

Insulation materials and processes for aerospace and hydrospace applications - SAMPE Symposium, San Francisco, May 1965 06 p0898 A66-16284

Carbon and graphite textiles use as ablative reinforcements for high temperature phenolic resin systems 06 p0899 A66-16285

Materials and fabrication techniques for ablative hardware composite materials engineering 06 p0899 A66-16286

Performance assurance for phenolic resin refractory fabric materials used for insulation and ablative components in rocket propulsion hardware and reentry heat shields 06 p0899 A66-16287

Continuous bias tape wrapping of ablative components 06 p0885 A66-16288

Fabrication characteristics of ablative plastics prepreg reinforced tape for construction of large rocket nozzles 06 p0885 A66-16289

Optimization of reinforced plastics in ablative rocket nozzle and reentry body application, considering compression molding 06 p0885 A66-16290

Thermal response of ablative materials for nozzles and leading edges in terms of specific thermal and mechanical properties 06 p0899 A66-16291

Low density thermal insulation materials, discussing temperature control, ablation efficiency and processing qualities of materials for missile use 06 p0900 A66-16296

Elastomeric silicone for aerospace electric and thermal insulation, discussing properties, application and new developments 06 p0900 A66-16297

Backside wall temperatures of ablative rocket nozzle exposed to hyperthermal environment treated for backside with heat transfer 07 p1151 A66-17584

Char formation in solid rocket nozzle exit cones made from reinforced plastic predicted from corrosion standpoint 07 p1151 A66-17585

Hypersonic aerodynamic stability and drag of ablating and nonablating models of blunt-faced reentry shape [AIAA PAPER 66-61] 07 p1141 A66-17898

Materials for extreme temperature and g loading during suborbital, manned and superorbital reentry 07 p1051 A66-18303

Visible and near UV radiation intensity profiles for ablating Teflon boundary layer in hot subsonic arc-jet flow at one atmosphere [AIAA PAPER 66-56] 07 p0983 A66-18450

Effectiveness of charring ablators strongly influenced by stream enthalpy level and heating rate 08 p1316 A66-18812

Ablation rates, surface temperature, emittances and reradiated fluxes of heat shield materials heated by irradiation [AIAA PAPER 66-44] 08 p1318 A66-19070

Photographic spectra of ablating plastics in thermodynamic environments related to species and temperatures in boundary layers [AIAA PAPER 66-132] 08 p1318 A66-19071

Low temperature chemical vapor-plating process for obtaining pyrolytic titanium diboride filaments for ablative composites 08 p1244 A66-19140

Microwave scattering system for detection of voids in fiberglass-honeycomb ablative materials causing drop in receiver signal strength 09 p1385 A66-20966

Ablative materials for thermal protection and minimum mass transfer of aircraft flying at hypersonic speeds 10 p1620 A66-21404

Performance and operation of one-inch-square plasma accelerator to simulate reentry velocities [AIAA PAPER 66-180] 10 p1519 A66-21430

Fabrication of ablative liners for solid propellant rocket motor nozzles [AIAA PAPER 65-167] 14 p2375 A66-27872

Transient thermoelastic stresses under thermoelastic and sublimation ablation, noting temperature profile 14 p2402 A66-27970

Ablation materials behavior in high shear environment using Teflon, Pyrex, quartz and phenolic Refrasil as specimens 15 p2616 A66-29280

Momentum deposition in wake of reentry vehicle, discussing behavior of complex materials characterized by heat of ablation 15 p2424 A66-29309

Thermal model for performance of cork insulation on Minuteman missile in launch environment [AIAA PAPER 65-117] 16 p2827 A66-30893

Double wall ablative heat shield panels for manned lifting entry vehicles, noting nylon phenolic and elastomeric silicone ablators [AIAA PAPER 66-506] 16 p2822 A66-31496

Aerothermochemical performance of inorganic fiber-reinforced char forming ablative material [AIAA PAPER 66-435] 17 p3035 A66-32756

Char-layer structural integrity limits application of charring-ablator heat-protection materials to advanced ballistic reentry [AIAA PAPER 66-424] 18 p3239 A66-33642

Elastomeric ablative thermal shield material to meet system requirements for lifting reentry vehicles having lift-drag ratio of 0.5 to 1.5 18 p3240 A66-33801

Streak test excellent acceptance technique for assurance of reproducibility of service life for ablative thrust chamber of Mira 150A variable thrust rocket engine [AIAA PAPER 65-608] 19 p3449 A66-35607

Mutual effects of vaporization, combustion and coking processes during material decomposition in high temperature gas flow 19 p3479 A66-36770

Ogive shape produced by ablation experiments with duralumin spheres in wind tunnel and reentry 20 p3491 A66-37406

Seminfinite flow of axisymmetric flow of viscous thermoelectric gas around blunt body with ablation shield, noting magnetic field effect 20 p3611 A66-38108

Engineering method to determine combined effects of entry and combustion heating on total char regression of ablative nozzle as function of distance from exit plane [ASME PAPER 66-MD-72] 21 p3806 A66-38500

SIC role in ablation chemistry, examining experimental results on char-reinforcement reactions 21 p3834 A66-38710

Calculating specific heat and conductivity of ablating specimens exposed to radiant heat fluxes 22 p3998 A66-40032

Heat transfer equation solution for ablating solid, assuming exponential temperature profile with numerical solution on digital computer by Runge-Kutta method 22 p3998 A66-40035

Plastic laminates use for ablation shields, noting importance of heat flow and comparison of thermal screens 22 p3938 A66-40417

Heat of pyrolysis of resin in silica-phenolic ablator determined from combustion calorimetry measurements of heats of formation 23 p4150 A66-41892

Gemini ablative heat shield, noting nonmetallic honeycomb reinforcement of insulative char 24 p4283 A66-42773

Internal thermal behavior of charring cork with reference to heat shield design 24 p4294 A66-42783

## ABLATING NOSE CONE

Heat transfer and melting ablation about decelerating spherical bodies during planetary atmosphere entry [AIAA PAPER 65-132] 02 p0303 A66-11539

Surface modifications of recovered small-scale plastic models after high speed flight used to estimate extent of laminar and turbulent flow over surface related to ablation studies 02 p0303 A66-11560

Combustion and sublimation in aerothermochemical interaction between dissociated air stream and graphite surface in hypersonic laminar viscous flow [AIAA PAPER 65-42] 03 p0444 A66-12797

Ablation measurement using sensor with radioactive dispersions being carried away with char [AIAA PAPER 65-363] 07 p1034 A66-17812

Laminar and turbulent boundary layer flow

in ablating cones in hypervelocity flight [AIAA PAPER 66-27] 07 p1020 A66-17889

Ablation effects on static and dynamic stability of reentry vehicle [AIAA PAPER 66-51] 07 p1141 A66-17896

Ablation effects on transient thermoelasticity in sem infinite elastic solid 14 p2402 A66-27969

PDE of terminal shape of ablating body as function of time derived, noting mass and energy flow, boundary layer thickness, etc 16 p2628 A66-30219

Axial shear vibrations of long hollow cylinder subjected to time-dependent body forces in axial direction 18 p3257 A66-34581

Laminar and turbulent boundary layer flow in ablating cones in hypervelocity flight [AIAA PAPER 66-27] 21 p3723 A66-38686

Temperature and heat resistant properties of fiberglass-reinforced plastic nose cone in supersonic flight 23 p4132 A66-41421

Ablation effects on static and dynamic stability of reentry vehicle [AIAA PAPER 66-51] 24 p4283 A66-42770

## ABLATION

### SA AERODYNAMIC HEATING

Maximum temperature profile in phenolic resin-siliceous fiber heat shields on ICBM and Mercury spacecraft [AIAA PAPER 65-638] 01 p0162 A66-10596

Solid bodies in plane parallel flow of ideal fluid, discussing one-parameter family of ablation bodies with steady shape 04 p0596 A66-13554

Increased heat of ablation and performance of injection cooling by addition of surface active agent [ASME PAPER 65-WA/HT-49] 05 p0792 A66-15660

Quasi-linearization solution of two-component laminar compressible boundary layer with heat transfer on ablating wall [ASME PAPER 65-WA/HT-41] 05 p0792 A66-15667

Asymmetrical ablation cause of persistent roll resonance in nominally symmetrical reentry vehicles [AIAA PAPER 66-49] 08 p1303 A66-18950

Ablation of blunt metallic body near stagnation point solution using integral equations, noting pressure effect 09 p1472 A66-20833

Approximate solution of ablation of reinforced plastic for heat protection 10 p1621 A66-21500

Mars atmospheric composition and laminar convective heating and ablation studied to predict performance of heat protection systems during entry 13 p2208 A66-25274

Ablation of reentry heat shields, discussing fiberglass reinforced phenolic resin, charring, graphite, radiation, etc 14 p2412 A66-27484

Meteor luminosity/ionization ratio dependence on air density found through analysis of ablation rate of meteor 14 p2387 A66-28172

Ablation effects on transient thermoelastic phenomenon 14 p2416 A66-28343

Meteoroid heating, deformation and fragmentation of melted meteoroids, showing not so loose structure in connection with satellite and rocket encounter 15 p2604 A66-30055

Ribbon ablative thermocouples for 3000 to 5000 degree F range 17 p2924 A66-32038

Ablation and viscoelasticity effects on vibratory response of hollow viscoelastic cylinder 18 p3247 A66-33572

Aerodynamic stability of slender cone under ablation effect including pressure distribution measurement, ablation-flow field interaction, flow analysis during oscillation, etc [AIAA PAPER 66-410] 18 p3045 A66-33635

Ablation analysis in cylindrical coordinates for axisymmetrical configuration of wall materials with temperature-dependent properties and nonlinear heat flux conditions at boundaries [AIAA PAPER 66-542] 20 p3680 A66-38034

Insulation surface regression mechanism in rocket motors, examining ablation corrosion and erosion effects 22 p3970 A66-39872

Simulated meteor ablation tests using artificial meteors of gabbro, basalt and steel in ultrahigh enthalpy plasma jet [ICAS PAPER 66-40] 23 p4147 A66-41009



Time lag effect on dynamic stability determined, using wind tunnel tests with 10 degree cone as test body simulating ablation process by gas injection into boundary layer [AIAA PAPER 66-757] 23 p4008 A66-41330

Ablation velocity, rocket motor working conditions and combustion instabilities for hybrid rockets, using solid fuel and liquid or gaseous oxidizer 24 p4261 A66-42695

**ABORT**

Two Project High Water experiments producing optical, ELF, RF, and radar data on ionospheric abort of large water quantities and expansion process 14 p2289 A66-28417

Aborted Atlas-Centaur launch data of environmental conditions and use in engineering design 14 p2395 A66-28446

**ABORT APPARATUS**

Design requirements for LEM, describing stabilization and control elements of abort system 01 p0140 A66-10046

**ABRASION**

Abrasion of circular self-rotating cutters as function of blade path in material being worked 11 p1710 A66-22860

Abrasion of reverse side of cutter effect on thermal state of cutter during sharpening of steel specimens 11 p1710 A66-22861

**ABRASIVE**

SA DIAMOND

SA QUARTZ

Ultrasonic cutting tools abrasive supply system modification for efficiency increase 01 p0078 A66-10653

Structure of microsurface layer of silicon wafers after polishing with polirrit and crocus and thorium, cerium, chromium, aluminum and titanium oxide 07 p1037 A66-17413

Ultrasonic cutting tools abrasive supply system modification for efficiency increase 12 p1885 A66-24013

**ABSORBER**

SA NEUTRON ABSORBER

SA SHOCK ABSORBER

SA SOLAR ABSORBER

SA VIBRATION ABSORBER

Frequency range of more than 60 gc obtained by introducing microwave absorber into last stage of multistage absorber, improving reflection coefficient 05 p0648 A66-15029

**ABSORPTION**

SA ATMOSPHERIC ABSORPTION

SA AURORAL ABSORPTION

SA ELECTROMAGNETIC ABSORPTION

SA ENERGY ABSORPTION

SA IONOSPHERIC ABSORPTION

SA LIGHT ABSORPTION

SA MAGNETIC ABSORPTION

SA MOLECULAR ABSORPTION

SA OPTICAL ABSORPTION

SA PHOTON ABSORPTION

SA POLAR CAP ABSORPTION

SA RADIATION ABSORPTION

SA THERMAL ABSORPTION

SA X-RAY ABSORPTION

Mass transfer potential in colloidal bodies, discussing relation between water content of dispersed substance and amount of moisture that can be absorbed by it 14 p2416 A66-28329

Absorption of solar neutrinos in deuterium 16 p2792 A66-30144

**ABSORPTION BAND**

SA SCHUMANN-RUNGE BAND SYSTEM

Spectral distribution of UV radiation in ozone band reflected from Earth, assuming Rayleigh scattering 01 p0133 A66-10756

Angular and spectral distribution of outgoing radiation in cloudy atmosphere in spectral range beyond absorption band 01 p0133 A66-10757

Silicon and lead sulfide electron paramagnetic resonance spectra, showing gas action and temperature effect on EPR signal amplitude and absorption lines 01 p0124 A66-10765

Electromagnetic wave absorption and cosmic noise absorption measurements useful in radio communication 01 p0072 A66-11101

Linewidth parameters for self-broadening and foreign gas broadening of water line measured, noting temperature dependent result and Zeeman components 03 p0443 A66-12342

Effect of surface state of cadmium sulfide on fundamental absorption edge and fine structure obtained from gaseous phase in inert atmosphere 03 p0407 A66-12405

Optical absorption spectra of transition elements especially ruby, based on crystal field, ligand field and molecular orbital theories 03 p0408 A66-12500

Light intensity in homogeneous turbid medium for unresolved absorption bands calculated from distribution of photon optical paths in absence of absorption, considering atmospheric scattering 04 p0542 A66-14302

Response of D-region absorption of cosmic noise to passage of totality during eclipse of May 30, 1965 recorded in New Zealand 05 p0668 A66-14798

Growth of absorption bands of natural and synthetic calcium fluoride crystals irradiated with protons from cyclotron at Tomsk Institute 05 p0741 A66-15857

Exponential absorption edge of gallium arsenide 05 p0742 A66-15870

Earth radiation field characteristics from radiation transfer equation for plane model of atmosphere for specific region, considering ozone absorption and molecular scattering 06 p0876 A66-16553

Measurement of exciton absorption of gallium selenide at low temperatures in presence of electric field, noting line broadening and no splitting 06 p0929 A66-16942

Correlation between strength of induced optical absorption G band and strength of features in electron spin resonance spectrum in electron irradiated diamonds 06 p0934 A66-17125

Temperature factors and intensities of absorption bands of molecular vibrational spectrum 07 p1082 A66-17531

Band structure of germanium in vicinity of Brillouin zone center 07 p1097 A66-17533

Displacement of absorption band edge into long wave region by phonon-caused damping 07 p1105 A66-18372

Carbon dioxide absorption bands in Mars atmosphere, transmission, function of carbon dioxide amount and effective surface pressure [AIAA PAPER 66-147] 08 p1290 A66-19072

Silicon and lead sulfide electron paramagnetic resonance spectra, showing gas action and temperature effect on EPR signal amplitude and absorption lines 11 p1748 A66-22276

Short wavelength wing of pure rotation emission spectrum of water vapor measured at various temperatures and nearly constant optical depth, calculating mean spectral absorption coefficient 11 p1739 A66-22952

Image converter tube spectrophotometry of zonal variation of methane absorption bands on Jovian disk in near IR region 12 p1944 A66-23504

Edge absorption of indium-doped cadmium in polarized light, noting exchange interaction between current carriers and Fermi level dependence on carrier concentration 12 p1929 A66-24449

Measurement of shift of cesium absorption lines near series edge, obtaining electron elastic scattering cross section at zero energy by extrapolation of shift 12 p1918 A66-24882

Receiver of hydrogen line interferometer at California Institute of Technology 13 p2182 A66-25551

Organic solvents and water classed according to increase in oscillator strength of absorption bands of praseodymium, samarium, neodymium and erbium ions 13 p2168 A66-25948

Pressure effects of argon on fine structure components of first two members of cesium principal series 13 p2135 A66-26263

Pressure effects of helium on fine structure components of first two members of cesium principal series, noting changes in shift curves 13 p2135 A66-26264

Spectral distribution of UV radiation in ozone band reflected from Earth, assuming Rayleigh scattering 14 p2285 A66-27855

Angular and spectral distribution of outgoing radiation in cloudy atmosphere in spectral range beyond absorption band 14 p2285 A66-27856

Light intensity in homogeneous turbid medium for unresolved absorption bands calculated from distribution of photon optical paths in absence of absorption, considering atmospheric scattering 14 p2327 A66-28216

Earth radiation field characteristics from radiation transfer equation for plane model of atmosphere for specific region, considering ozone absorption and molecular scattering 14 p2289 A66-28225

Absorption bands in thin lead films, vacuum prepared, considering general analysis of elements in group IVA of periodic table 14 p2369 A66-28271

Measurement of single line in P branch of carbon dioxide vibro-rotational absorption band using tuned optical maser spectroscopy, noting presence of shifted frequencies 15 p2512 A66-28691

Optical properties and thermal behavior of new absorption bands in oxygen doped silicon irradiated at low temperatures 15 p2564 A66-28874

Monograph on intensity distribution and polarization of scattered radiation in ozone absorption bands at selected levels of terrestrial Rayleigh atmosphere 16 p2698 A66-31226

Spectral composition of direct solar radiation variation with height of Sun and relation between aerosol absorption band and humidity 17 p2994 A66-32857

Uniaxial stress effect on two-phonon lattice absorption bands of silicon 18 p3154 A66-33920

Isotope shifts for zero-phonon absorption lines associated with radiation induced color centers in lithium fluoride single crystals 18 p3154 A66-33921

Absorption lines and bands in scattering and absorbing medium elucidated by study of distribution of photon optical paths in scattering atmosphere 18 p3230 A66-34148

Resonant enhancement of Raman cross section for phonons in CdS at frequencies near absorption edge 18 p3156 A66-34468

Lowest of UV absorption bands attributed to 4f-5d transition of trivalent rare earth ions in calcium fluoride crystals 19 p3443 A66-36004

Optical absorption edges with nearly parallel bands of aluminum analyzed for all polyvalent metals with simple structures 19 p3401 A66-36391

Image converter tube spectrophotometry of zonal variation of methane absorption bands on Jovian disk in near IR region 20 p3646 A66-37017

Single continuous correlation for total band absorbance of radiating gases 20 p3678 A66-37121

Fermi surface interpretation of band structure, electron energy levels, optical properties and ferromagnetic structure of transition and noble metals 20 p3613 A66-37274

X-ray absorption edge observation by transmittance measurements through thin unbacked metal films in XUV as function of wavelength 20 p3613 A66-37275

Electronic energy band structure and optical properties of heavy rare earth metals 20 p3614 A66-37278

Edge absorption of indium-doped cadmium in polarized light, noting exchange interaction between current carriers and Fermi level dependence on carrier concentration 20 p3619 A66-37681

Random Elsasser band model to compute atmospheric transmission of Earth and Mars for 2-micron carbon dioxide bands 20 p3655 A66-38024

Temperature dependence of absorption bands by localized vibration modes associated with substitutional impurities in phosphorus-doped gallium arsenide 20 p3622 A66-38249

Kjeldaa absorption edge in cryogenic potassium for shear magnetoacoustic wave propagation in spherical metallic Fermi surface with spin density wave ground state 21 p3800 A66-38991

Faraday and Voigt and dispersive magneto-optic effects in semiconductors in crossed field due to energy band transitions 21 p3800 A66-38995

Spontaneous-emission probability and



absolute intensity for IR absorption band of nitrous oxide 22 p3947 A66-39768

IR absorption band growth and decay in spectra of oxygen-doped Si irradiated with fast neutron 22 p3962 A66-40085

New absorption bands in near IR spectrum of Mars found by Fourier spectroscopy via carbon dioxide absorption measurements 22 p3981 A66-40486

Behavior of lambda 6300 angstrom Fraunhofer absorption line in solar spectrum 22 p3984 A66-40850

D-3 helium absorption line on solar disk connected to chromospheric flare origin 22 p3984 A66-40851

Optical depths of titanium I absorption lines in solar spectrum 22 p3984 A66-40853

Measurement of shift of cesium absorption lines near series edge, obtaining electron elastic scattering cross section at zero energy by extrapolation of shift 23 p4097 A66-41089

Absorption lines on Venus spectrograms of rotational fine structure of excited vibrational transition of carbon dioxide 23 p4130 A66-41816

IR active localized vibrational modes absorption in lithium and copper compensated silicon doped gallium arsenide 24 p4251 A66-42298

## ABSORPTION COEFFICIENT

Visibility range of 100-watt lamp and relation to absorption coefficient of tropospheric fog 01 p0096 A66-10223

Extension of study showing that increase in temperature of silicon carbide increases absorption coefficient of defect, for case of heavy particle irradiation 02 p0274 A66-11723

Photoionization and absorption coefficients of carbon oxide measured below 1000 angstroms, using Seya-Namioka scanning vacuum UV monochromator with helium continuum as background 02 p0263 A66-11834

Absorption coefficient for lines with combined Doppler and Lorentz broadening calculated, using Runge-Kutta method, continued fraction expansion and Hermite-Gauss quadrature 03 p0393 A66-13267

Spectroscopic measurements using membrane-type shock tube for: absolute determination of continuous absorption coefficients of negative hydrogen ions 04 p0553 A66-14279

Continuous absorption coefficients for xi-factors of neutral argon, krypton and xenon by spectroscopic measurements using shock tube with membrane 04 p0553 A66-14280

Optical properties of light scattering layer with negative absorption coefficient, discussing layer reflection and transmission 05 p0715 A66-14726

Frequency dependence of resistivity, absorption and emission processes in fully ionized plasma 05 p0726 A66-15245

Source function models and modified mean values of solar photosphere, accounting for limb-darkening and intensity fluctuation data 05 p0763 A66-15283

Carbon dioxide-R-branch lines of 5 mu sub 3 band from integral of absorption coefficient of Martian atmosphere 05 p0763 A66-15288

Optical properties of polycrystalline InSb films noting index of refraction, absorption coefficient and transmission curves 05 p0741 A66-15852

Electric field effect on optical absorption edge, discussing exponential tail influence on magnitude of absorption coefficient 05 p0741 A66-15869

Atmospheric oxygen absorption factor of centimeter and millimeter radio waves 05 p0636 A66-15878

Exciton absorption lines and long wave intrinsic edges of single-crystal CdSe and CdS at low temperatures 06 p0924 A66-16540

Sunspot spectra, determining lithium abundance and ratio of Li 6/Li 7 isotopes 07 p1136 A66-17736

Resonance Raman effect in crystals, discussing spontaneous and simulated scattering efficiency 08 p1259 A66-19233

Radio wave absorption coefficients calculated, using approximations of magnetoionic formulae 09 p1341 A66-19860

Absorption coefficient of water vapor in relative windows of transparency for millimeter and submillimeter radio

waves 09 p1343 A66-20338

Accuracy in determination of light absorption coefficient of semiconductors with reflection coefficients of 0.2 to 0.5 09 p1431 A66-20943

Hopf analytical solution for values of ratio of gray absorption coefficients for insulating and escaping radiation /greenhouse parameter/ assumed constant at all depths, presenting temperature distribution graphs 10 p1605 A66-21204

Radiative heat-flux potential for nongray gas derived, noting origins of vector differential equation for gray gas 12 p1977 A66-23596

Continuous emission and absorption of plasmas by calculating radiation of hydrogen plasma, deriving temperature and pressure conditions under which plasma radiates as black body 12 p1919 A66-23750

Absorption of longitudinal ultrasonic waves in superconductors containing impurity atoms, noting entrainment effect role in energy dissipation of waves 12 p1929 A66-24453

Atmospheric radio wave absorption coefficient and altitude determined and linked to effects of colliding paramagnetic oxygen molecules 13 p2020 A66-25224

Solar limb darkening measured at various wavelengths by Veronique rocket, obtaining data on continuous absorption coefficient 13 p2180 A66-25421

Nonlinear dielectric laser light absorption by neutral gas resulting in avalanche breakdown of gas due to thermal ionization 13 p2090 A66-25425

Nonresonant absorption of radio waves in molecular oxygen 13 p2025 A66-26044

Steady state variation of light intensity with distance for monochromatic light, noting dependence of absorption coefficient on degree of excitation of electronic system 13 p2099 A66-26183

Growth rate of ionization by electron impact in presence of laser beam, elastic and inelastic scattering cross sections, free-free absorption, excitation and ionization coefficients, breakdown times and thresholds 13 p2134 A66-26193

Photometric determination of extinction coefficient for optical scattering in turbid medium 14 p2326 A66-27544

Reflection, transmission and absorption coefficients of circularly polarized electromagnetic wave incident on plasma layer situated in stationary magnetic field 14 p2348 A66-28471

Accuracy in determination of light absorption coefficient of semiconductors with reflection coefficients of 0.2 to 0.5 15 p2557 A66-28531

Radiative energy transfer between concentric spheres separated by absorbing and emitting gas, noting analogy to atmosphere with spherical symmetry 15 p2615 A66-28620

Free carrier absorption on GaAs films which exhibit absorption edge shift to lower energies 15 p2561 A66-28698

High Q Fabry-Perot interferometer for measurement of atmospheric gas losses, particularly water vapor absorption, using coherent light source in 100-300 gc frequency range 15 p2501 A66-29003

Microwave absorption by water vapor and mixtures with other gases between 100 and 300 gc/s, noting increase in absorption attributed to molecular collision-induced polarization 15 p2450 A66-29004

Absorption coefficients for nitrogen and oxygen ion in air at temperatures of 150,000 to 800,000 degrees K 15 p2617 A66-29345

Exciton absorption lines and long wave intrinsic edges of single-crystal CdSe and CdS at low temperatures 15 p2569 A66-29987

Gallium arsenide absorption edge dependence on strong electric fields 16 p2769 A66-30166

Absorption coefficient change due to electric field measured for indirect absorption edges of silicon and germanium, determining energies of phonons taking part in indirect optical absorption 16 p2775 A66-30728

Model potential consisting of Coulomb potential and linear terms in electric field potential, obtaining eigenfunctions of model

and deriving optical absorption coefficient for electric field excitons 16 p2775 A66-30729

Photoelectric yields of alkali halides measured, using rare gas ion chamber to determine flux distribution of helium continuum and obtain absorption coefficients 16 p2754 A66-30855

Linear absorption effect on threshold for self-focusing of laser beam in cadmium sulfide, noting variation of absorption coefficient 16 p2720 A66-31537

Temperature structure of early type stellar atmospheres noting sources of opacity, electron Rayleigh scattering, etc 16 p2806 A66-31703

Visibility range of 100-watt lamp and relation to absorption coefficient of tropospheric fog 17 p2948 A66-31907

Solar corona emission spectrum and narrow passband photography of solar disk, noting measurement of intensity variation and absorption coefficient 17 p2999 A66-32133

Electric field effect for free carrier absorption, determining coefficient for acoustic phonon scattering 17 p2976 A66-32264

Atmospheric ozone absorption coefficients measurement, determining errors in extraterrestrial constant of Dobson spectrophotometer 17 p2923 A66-33359

Absorption coefficient of oxygen gas Schumann-Runge continuum, using microsecond flashing source 18 p3137 A66-33988

Free-free absorption coefficient of electrons in field of neutral carbon atoms calculated per unit electron pressure per carbon atom in static central field exchange approximation 18 p3233 A66-34574

Absorption, radiative recombination and photoconductivity of CdSe 19 p3444 A66-36035

Splitting of ground state of neutral mercury two-hole acceptor in unstressed silicon or germanium evidenced by intensity decrease of photoabsorption peaks 19 p3444 A66-36174

Absorption of polarized electromagnetic waves at zero degrees K in n-type germanium under high uniaxial stress 19 p3446 A66-36396

Weak field effective mass approximation calculations of absorption coefficient in presence of electric field for transitions at normal threshold extended to arbitrary orientation of electric field in solid 19 p3447 A66-36397

Temperature dependence of UV radiation absorption coefficient in quartz undergoing phase transition for several spectral lines 19 p3447 A66-36722

Absorption coefficients for monomers of water vapor and oxygen for various altitudes, noting seasonal variation 20 p3511 A66-37133

Absorption coefficients for nitrogen and oxygen ions in air at temperatures of 150,000 to 800,000 degrees K 20 p3604 A66-37350

Absorption of longitudinal ultrasonic waves in superconductors containing impurity atoms, noting entrainment effect role in energy dissipation of waves 20 p3619 A66-37685

Optical determination of hole concentration dependence in p-type silicon semiconductors by measuring absorption coefficients 21 p3798 A66-38765

Performance of GaAs semiconductor laser with resonator, noting dependence of forbidden zone width and absorption coefficient on free carrier concentration and incident photon energy 21 p3746 A66-38955

Light scattering influence on effective value of extinction coefficient considered as function of optical parameters of medium and of angular characteristics of source and receiver 21 p3760 A66-39361

IR absorption coefficients of water vapor as function of temperature obtained from absorption and emission spectra 22 p3950 A66-40114

Molecular spectroscopy, measuring absorption coefficient at center of carbon dioxide band, determining vibration-rotation transition moment 23 p4076 A66-41179

Kinetic equations in hydrodynamic approximation for weakly reacting and



- excited Bose systems, finding asymptotic expressions for Green function 23 p4055 A66-41412
- Low accuracy of interferometric measurement of coefficient of ultrasound absorption in gas 23 p4068 A66-41414
- Nongray radiation effects on laminar boundary layer of absorbing gas over flat plate, using absorption coefficient with stepwise frequency dependence 23 p4012 A66-41903
- Mass of shaped charge accelerator generated fragments determined via high speed flash X-ray photography of projectiles in flight 24 p4209 A66-42186
- Frequency temperature dependence of longitudinal and transverse hypersonic wave absorption coefficients in quartz and artificial ruby crystal 24 p4255 A66-42514
- ABSORPTION CROSS SECTION**
- Resonance absorption measurements in cesium vapor 02 p0262 A66-11435
- Visible spectrum absorption cross section of trivalent chromium in metastable 2E state of pink ruby 05 p0694 A66-14902
- Solar radiation attenuation in UV region provides data on production of atomic oxygen by photodissociation of oxygen and ion and electron formation by photoionization of nitrogen and oxygen 05 p0748 A66-15022
- Photoabsorption cross section of atomic hydrogen obtained by flowing molecular hydrogen through discharge tube 06 p0913 A66-17042
- Abundance of titanium for solar photosphere model derived from ion lines 07 p1135 A66-17641
- Mie scattering and absorption cross sections for spherical absorbing particles as function of complex refractive index 09 p1405 A66-20512
- Monograph on solar corona physics covering ground based, satellite and sounding rocket observation, spectral emission and absorption lines, ionization mechanism, RF and UV radiation, etc 12 p1949 A66-24069
- Effective capture cross section for holes by singly negatively charged zinc atoms in p-silicon determined by double injection method 14 p2369 A66-28261
- Energy spectrum of primary photoelectron, using data from atmospheric density distribution, fluxes of solar XUV radiations and absorption and ionization cross sections 15 p2574 A66-28906
- Total absorption cross section of carbon monoxide and carbon dioxide in 550-200 angstrom range 15 p2538 A66-28978
- Temperature effect on UV absorption continuum of oxygen, using photoelectric techniques, obtaining absolute absorption cross sections 16 p2695 A66-30711
- Relation between Rydberg series lines observed in absorption spectrum of atomic oxygen and absorption cross sections of Cairns and Samson 17 p2961 A66-32504
- Altitude distribution of atmospheric molecular and atomic hydrogen, showing results of Lyman alpha absorption measurements 17 p2919 A66-32995
- Fluctuation scattering and absorption cross section derived for space and time dispersive plasma 18 p3149 A66-34914
- Absorption cross section of electron systems in bands of diatomic molecules calculated, noting effects of temperature variation 21 p3775 A66-39077
- Photoabsorption cross section of atomic hydrogen by molecular hydrogen flow through discharge tube 23 p4098 A66-41245
- Absorber concentration effect on pulsed laser system noting performance characteristics, threshold energy, pumping dynamics and time parameters 24 p4220 A66-42254
- Nondestructive detection technique of phosphosilicate layer on semiconductor wafers, using IR spectrophotometer 24 p4181 A66-42390
- Absorption cross section, scattering cross section and angular scattering distribution of solid alumina particles emitted in homogeneous solid propellant rocket plume 24 p4294 A66-42778
- ABSORPTION SPECTRUM**
- X-ray L band absorption spectra of rare earth atoms in hexaborides, collecting evidence on valence state 01 p0126 A66-10980
- Elemental abundances in solar atmosphere determined from intensity of absorption lines in solar spectrum 02 p0285 A66-11297
- Forbidden absorption spectrum of ionized iron in solar absorption ascertained with high resolution direct intensity recordings 02 p0286 A66-11353
- Spectral absorption due to parallel bands of nitrous oxide computed for temperatures of 200 and 300 degrees K 02 p0263 A66-12213
- Slant path measurement of atmospheric absorption spectra of 4.3 mu band, using Sun as radiation source 03 p0359 A66-12301
- IR and UV absorption spectra of free radical NCN observed following photolysis of matrix isolated cyanogen nitride 04 p0473 A66-13644
- Absorption contour for fundamental vibration-rotation band of nitrogen oxide compared with pressure broadened spectra 04 p0473 A66-13651
- Interpretation of nuclear magnetic resonance spectra from cobalt alloys containing small amounts of solute atoms 04 p0564 A66-14032
- Absorption spectrum sidebands for quasi-local oscillation in KCl-H crystals 05 p0730 A66-14648
- Transfer equation of solar absorption line developed with split upper level in magnetic field 05 p0759 A66-14870
- Inverse stimulated Raman spectra during Stokes absorption in terms of stimulated emission of optical phonons 05 p0697 A66-15108
- High resolution absorption spectrum of nitrogen in fourth and fifth orders from 1060 to 1520 angstroms 05 p0763 A66-15284
- Potential curves and spectrum absorption of nitrogen, redetermining spectroscopic constants 05 p0763 A66-15285
- Atmospheric thermal radiation calculated from unresolved molecular absorption spectra of atmospheric carbon dioxide and water 05 p0675 A66-15860
- Absorption and emission spectra pertaining to electronic transitions of short-lived molecules C sub 2 and CH present in reaction zone of low-pressure oxyacetylene flames 06 p0969 A66-16126
- Nitrogen and nitrogen-foreign gas mixtures, determining absorption profile shapes, binary and ternary absorption coefficients and molecular quadrupole moment 06 p0908 A66-16281
- Upper atmospheric research using spectroscopic study of absorption bands and night-sky radiation, celestial bodies as UV and X-ray sources and atmospheric light scattering 06 p0876 A66-16310
- Uniaxial and hydrostatic pressure effect on absorption edge spectrum and edge excitation spectrum for visible luminescence diamond 07 p1095 A66-17320
- Emission and absorption lines with anomalous intensity distributions indicate hydroxyl molecule concentrations in Sagittarius A 07 p1133 A66-17462
- Vacuum fusion and IR absorption determination of bulk oxygen content of germanium crystals 07 p1098 A66-17743
- Manganese X-ray emission lines in compound-oxide semiconductor 07 p1105 A66-18369
- Validity of Kirchhoff law for apparent local spectral emittance and absorptance and total flux calculations for spacecraft cavities [AIAA PAPER 65-135] 08 p1316 A66-18793
- Oscillations in impurity photoconductivity and absorption spectra of p-germanium samples 08 p1269 A66-18973
- Fluorescent K-absorption and emission spectra of phosphorus in III-V semiconductor compounds 09 p1426 A66-20192
- Optical double resonance in ruby, discussing absorption transitions from lowest excited state of chromium ion effected by laser pumping 09 p1387 A66-20856
- Raman scattering and IR absorption spectra of gaseous, liquid and crystalline benzoyl benzoic acid and O-and M-toluic acids 09 p1339 A66-20941
- Vertical water vapor distribution to determine absorption function from high altitude measurements of solar IR radiation spectrum 09 p1375 A66-20942
- Temperature and environment effect on absorption spectra of two-level system, using stochastic model and Green function 09 p1348 A66-20959
- Absorption spectra of alkaline, alkaline-earth and rare-gas groups 10 p1557 A66-21095
- IR absorption spectra of oxygen-defect complexes in irradiated silicon 10 p1581 A66-21737
- Vanadium pentoxide-boron oxide-lead oxide system IR absorption spectra and electroconductivity 10 p1582 A66-21917
- Broadening of IR absorption lines by HF local oscillations attributed to either modulation effects or decay processes 10 p1588 A66-22162
- High precision photoelectric scan at 8667-8668 angstrom wavelengths in solar spectrum for identification and abundance of boron 11 p1771 A66-22773
- Absorption spectrum of neutral nitrogen near 500 angstroms, noting vibrational spacings and Rydberg series 11 p1773 A66-22783
- Multifilm absorption spectrum dependence on magnetic interaction, deposition, thickness and quality of ferromagnetic and insulating films 11 p1753 A66-22810
- Spin wave sideband in absorption spectrum at low temperatures for transition of manganese ion in antiferromagnetic manganese fluoride 11 p1740 A66-22970
- He-Ne laser IR radiation emission attenuated by atmospheric methane 11 p1657 A66-23090
- K absorption spectra of germanium and selenium in germanium selenide based on band theory of solids by assuming electrons transfer, using X-ray spectroscopy 11 p1758 A66-23368
- Longitudinal plasma oscillations excited in warm plasma column at microwave frequencies in presence of magnetic field, manifest themselves as absorption peaks near harmonics of electron cyclotron frequency 11 p1748 A66-23395
- Splitting in indirect absorption edge spectrum dependent on direction and magnitude of applied stress and light polarization with respect to stress axis 12 p1927 A66-23721
- Absorption spectrum of germanium at various temperatures and wavelengths and of heavily doped germanium at room temperature, obtaining agreement for both cases with theory of structural absorption of holes 12 p1929 A66-24452
- Coriolis interaction in first and third fundamental frequencies of ozone, noting vibration rotation spectrum and coupling of two states 13 p2016 A66-25373
- UV absorption and excitation spectrum of ruby and sapphire, noting structure and polarization effects, quantum efficiency, etc 13 p2162 A66-25378
- Microwave absorption in compressed carbon dioxide between 150 and 300 gc measured, detecting no losses at 150 gc 13 p2021 A66-25383
- Absorption spectrum sidebands for quasi-local oscillation in KCl-H crystals 13 p2167 A66-25923
- Elliptic cavity design for solid state lasers, discussing multiple reflections, absorption coefficient, refraction losses, etc 13 p2092 A66-25998
- Excited-singlet even parity states of anthracene in near UV, noting role of absorption spectroscopy 13 p2132 A66-26143
- Absorption spectra in optical region when laser radiation and continuous radiation are simultaneously incident on molecular medium 13 p2133 A66-26161
- Far-IR laser molecular spectroscopy including IR laser oscillators, photon noise, detectors and nuclear optics 13 p2100 A66-26195
- Organic gas magnetically tuned laser spectroscopy, discussing resolution, absorption spectra and vibrational deactivation 13 p2100 A66-26197
- Time behavior of 3889 and 5016 angstrom line helium emission during initial transient of RF discharge, noting pressure dependence and signal intensity 13 p2104 A66-26335
- Optical transition of manganese fluoride as function of temperature and magnetic field



in both emission and absorption 14 p2351 A66-26886  
Emission and absorption bands in K spectral region of titanium, using single setup 14 p2314 A66-27371  
Fine-line absorption spectrum anisotropy with respect to crystallographic axis of cadmium sulfide 14 p2308 A66-27646  
Energy level transitions in vacuum UV absorption spectrum of calcium vapor 14 p2337 A66-27704  
Stark broadening effect on solar atmospheric abundance determinations, with results for sodium 14 p2383 A66-27709  
Field-effect-modulated optical absorption spectrum for various values of Ge surface potential 14 p2366 A66-27765  
Absorption lines of quasi-stellar object 3C 191 14 p2387 A66-28131  
Vertical water vapor distribution to determine absorption function from high altitude measurements of solar IR radiation spectrum 15 p2483 A66-28530  
Ruby phosphorescence under intense optical excitation, inferring possible recombination characteristics from initial brightness decay 15 p2558 A66-28607  
Impurity scattering in theory of interband magneto-optical effects, noting inadequacy of first-order perturbation treatment and low and high impurity-atom concentration with weak interaction 15 p2558 A66-28610  
Riometer absorption caused by solar protons and alpha particles in monoenergetic intensities and in spectral distributions 15 p2574 A66-28818  
IR absorption of arsenic monoselenide 15 p2565 A66-29198  
In, Ga and Cu impurity effects on absorption spectrum of zinc telluride 15 p2565 A66-29199  
IR absorption spectrum of neutron bombarded silicon 15 p2565 A66-29202  
Vacuum spectrometer measurement of absorption band of atmospheric water vapor 15 p2542 A66-29346  
Absorption, excitation, and emission spectra of TI-activated NaI single crystals at liquid helium temperatures 15 p2566 A66-29347  
Absorption spectrum of ruby in metastable state 15 p2566 A66-29349  
High energy mountain-altitude nuclear interactions produced by pions and nucleons, pion/proton and neutral/charged interacting particle ratios studied, using multiplate cloud chamber with air Cerenkov counter and absorption spectrometer 15 p2584 A66-29554  
Electron-photon cascades caused by nuclear active component in atmosphere and on gamma rays, atmospheric absorption spectrum of primary nucleons and generation of pions 15 p2584 A66-29556  
Ionized electron centers in irradiated lithium fluoride crystals investigated by observing emission and absorption spectra 15 p2568 A66-29641  
Impurity absorption of LiF crystals in vacuum UV 15 p2568 A66-29729  
Optical properties of complex compounds of divalent platinum, noting absorption spectra, forbidden transitions, etc 15 p2569 A66-29730  
Biological macromolecule detection using thiocarbocyanine dye and observation of absorption spectra changes 15 p2441 A66-29962  
Absorption, photoionization and fluorescence of carbon dioxide measured in regions of strong band and continuous absorption in various spectral ranges 16 p2749 A66-30111  
Auroral excitation rates and molecular vibrational temperatures in nitrogen 2PG from Franck-Condon factors obtained from intensity measurements and high resolution absorption spectral data 16 p2692 A66-30328  
Atomic scattering from perfect crystal, considering effects of absorption potential, surface vibrational modes momentum and energy exchange etc 16 p2752 A66-30389  
Radiative flux divergence for lower few centimeters of atmosphere, accounting for combined effects of water vapor, particle absorption and scattering 16 p2699 A66-31640  
Optical and magnetooptical phenomena in

CdSnAs sub 2, discussing reflection and absorption spectrum, optical activity, double refraction, dielectric constant, etc 16 p2788 A66-31775  
Relation between Rydberg series lines observed in absorption spectrum of atomic oxygen and absorption cross sections of Cairns and Samson 17 p2961 A66-32504  
Continuous source for atomic fluorescence flame spectrometry using 150-watt xenon arc, total consumption atomizer-burner and low resolution monochromator 17 p2870 A66-32551  
Electron scattering interpretation of ionization, emission and absorption line spectra of quasi-stellar object 17 p3004 A66-32928  
IR absorption of arsenic monoselenide 17 p2982 A66-33047  
In, Ga and Cu impurity effects on absorption spectrum of zinc telluride 17 p2982 A66-33048  
IR absorption spectrum of neutron bombarded silicon 17 p2982 A66-33051  
Triatomic carbon spectrum transition bands based on available photographic and densitometric data 17 p3013 A66-33401  
Chemical bonds between rare earth metals and nitrate radicals in lanthanum, gadolinium and yttrium nitrates studied from IR absorption spectra 18 p3063 A66-33842  
Ionization potential, dissociation energy and electron affinity for molecular oxygen 18 p3137 A66-33989  
Solar extinction measurements and interpretation of terrestrial atmosphere microwave absorption spectrum near 1-cm wavelength 18 p3105 A66-34012  
IR and UV absorption spectra of solid HN sub 3 film after photolysis with unfiltered radiation from Hg lamp 18 p3064 A66-34455  
Absorption spectrum of condensed oxygen in 1.26 to 0.3 micron region 18 p3140 A66-34693  
Absorption spectra modification in silica ceramics after gamma irradiation from Co-60 19 p3388 A66-35463  
Broadening of IR absorption lines by HF local oscillations attributed to either modulation effects or decay processes 19 p3441 A66-35776  
Silicon IR absorption spectra at various wavelengths before and after irradiation with neutron fluxes 19 p3442 A66-35821  
Absorption spectra of pure and isotopic impurity crystals of naphthalene in region of first electronic and vibrational/vibron/transition 19 p3402 A66-36067  
Absorption line between 220 and 550 mu in transmission spectra of ruby at liquid nitrogen and helium temperatures 19 p3446 A66-36342  
Ionospheric absorption measurement by A3 method in which field strength of distant CW transmitter is continuously recorded 19 p3351 A66-36359  
Superconductor electromagnetic absorption in energy gap region, examining gap anisotropy, multiple gaps, precursor absorption and magnetic perturbation effect on optical absorption spectrum 20 p3615 A66-37281  
Vacuum spectrometer measurement of absorption band of atmospheric water vapor 20 p3602 A66-37351  
Absorption, excitation, and emission spectra of TI-activated NaI single crystals at liquid helium temperatures 20 p3615 A66-37352  
Absorption spectrum of ruby in metastable state 20 p3615 A66-37354  
Absorption spectra, reflection index and photoelectric emission of tellurium 20 p3618 A66-37566  
Absorption spectrum of germanium at various temperatures and wavelengths and of heavily doped germanium at room temperature, obtaining agreement for both cases with theory of structural absorption of holes 20 p3619 A66-37684  
Receiver with n-type indium antimonide detector for investigating absorption spectra in submillimeter wave range 20 p3561 A66-37999  
Moisture contamination and associated water band absorption spectra recorded by balloon-borne

spectrometer 20 p3554 A66-38206  
Fine structure in direct absorption edge of cleaved type IIA diamond determined from reflectance data obtained from 5.5 to 11.5 ev at room and liquid-nitrogen temperatures 20 p3622 A66-38248  
Absorption spectrum of sulfur hexafluoride in far UV due to electron impact and inelastic scattering and oscillator strengths for three absorption bands 21 p3774 A66-38524  
Spectral characteristics of gases heated by shock waves, noting absorption capacity distribution as function of wavelength 21 p3726 A66-39078  
Emission and absorption capacity of /zero-zero/ band of CN violet system at high temperatures, determining parameters of oscillator system power 21 p3775 A66-39079  
Absorption and dispersion spectrum of laminar gallium selenide crystal 21 p3802 A66-39159  
Stimulated emission, absorption spectra and luminescence of neodymium-activated YAG crystals in pulsed laser 21 p3748 A66-39306  
Experimental excited state band locations and intensities in absorption spectrum of electron transitions in optically pumped ruby laser 21 p3749 A66-39569  
Theoretical excited state absorption spectrum of electron transitions in optically pumped ruby laser 21 p3749 A66-39570  
Indium and thallium first spectra sp2 atom configurations and configuration mixing 22 p3960 A66-39801  
Multiparametric diagnostic technique for optically dense plasma 23 p4102 A66-41451  
Line strengths variation in spectra of HD 124224 and HD 19832 analyzed, establishing anticorrelation of He I variations with variations in temperature 23 p4130 A66-41808  
Evolving synchrotron self-absorption model of extragalactic nonthermal radio sources 23 p4132 A66-42074  
Saturable dyes noting mode selection properties and absorption spectra in bleached state 24 p4220 A66-42253  
Multiple cyclotron resonance absorption lines in degenerate valence bands of Ge semiconductor studied with far IR laser submillimeter spectrometer 24 p4257 A66-42545  
Transmittance of gaseous air components for 1850 angstrom radiation 24 p4234 A66-42818  
Ultrarelativistic muon electromagnetic interaction energy loss due to bremsstrahlung and pair production 24 p4271 A66-42936  
Decay of small temperature perturbations by thermal radiation in atmosphere, noting gray and line absorption, relaxation time constants and numerical computations 24 p4203 A66-42986  
Dipole moment of perchlorofluoride by measuring absolute absorption maximum and linewidth parameters in resonant cavity 24 p4170 A66-43038  
**ABSORPTIVE INDEX**  
Absorptance and emittance of metal surfaces determined via cyclic incident radiation, noting error computation and method accuracy parameters [AIAA PAPER 66-416] 16 p2829 A66-31487  
**AC**  
**S ALTERNATING CURRENT /AC/ ACCELERATION**  
SA ANGULAR ACCELERATION  
SA DECELERATION  
SA IMPACT ACCELERATION  
SA MAGNETOHYDRODYNAMIC ACCELERATION  
SA PARTICLE ACCELERATION  
SA PHYSIOLOGICAL ACCELERATION  
SA PLASMA ACCELERATION  
Condensation in variable acceleration field, especially linear variation occurring in constant cross section rotating thermosyphon [ASME PAPER 64-WA/GTP-2] 02 p0304 A66-11764  
ESG strapdown inertial navigation system based on double integration of acceleration and analysis of electronic gimbal-induced errors 13 p2124 A66-25653  
Acceleration potential method for solving linear problems of wing hydrodynamics



ve interface between fluids differing in  
 asity, for arbitrary Froude  
 13 p2067 A66-26530  
 dynamics of axisymmetric liquid free  
 face following stepwise acceleration  
 ange 16 p2684 A66-30502  
 power spectral density computer program  
 vibration-acceleration  
 17 p2878 A66-33039  
 similarity method for accelerations and  
 ocities 17 p2960 A66-33424  
 linearized three-dimensional potential flow  
 ations for response of liquids in  
 indrical containers to slightly off-axis  
 eleration 17 p2916 A66-33477  
 random acceleration theory using diffusion  
 nsformation of matrix equation into  
 ferential equation 22 p3947 A66-39664  
 overcraft difficulty in accelerating  
 ough hump, noting wave resistance  
 rease for pressure differential between  
 o compartments of cushion with  
 nverse stability skirt 22 p3901 A66-40678  
**ACCELERATION STRESS**  
**G FORCE**  
**PHYSIOLOGICAL ACCELERATION**  
 radiobiological effects caused by ionizing  
 ation in mice pre-exposed to effect of  
 eleration 02 p0182 A66-11664  
 ibration, acceleration and radiation  
 ects on cell division, chromosome  
 avior and mitotic activity of bone  
 marrow and spleen cells in  
 ce 02 p0182 A66-11665  
 space hazards to spacecraft include  
 ume temperatures, micrometeorites, low  
 essures and electromagnetic and  
 puscular radiations 03 p0425 A66-12860  
 prolonged centrifugation effects on growth  
 rgan development of weanling and  
 ure rats 05 p0625 A66-15412  
 ological effects of chronic acceleration  
 died by using birds and animals in  
 etrifuges with specially designed  
 es 06 p0819 A66-16605  
 xperiments with anesthetized dogs  
 ected to g accelerations, observing  
 avior of arterial oxygen saturation and  
 monary ventilation during short  
 ethods 08 p1175 A66-19083  
 human visual acuity as affected by body  
 sition and various g  
 ues 09 p1334 A66-19978  
 ardiac arrhythmias occurring during  
 sitive and negative  
 eleration 09 p1335 A66-20532  
 cetate conversion to lipids and carbon  
 oxide by liver, kidney and inguinal adipose  
 sues of rats under centrifugation  
 ess 09 p1336 A66-20634  
 echanical and physiological factors  
 olved in design, testing and operation of  
 ction seats, examining effects of short  
 ration acceleration 10 p1493 A66-22126  
 EGs of monkeys stimulated cyclically by  
 ole-body vibration, plotting coherence  
 ctions relating brain records to  
 eleration records 12 p1806 A66-24228  
 ardiovascular stress resulting from radial  
 eleration gradient impeding venous  
 urn analyzed by rotation of seated  
 bject about Z axis /Rz/ 12 p1807 A66-25016  
 egetative responses of human organism to  
 gular, linear and Coriolis  
 elerations 13 p2011 A66-26230  
 abrupt angular acceleration effect on man,  
 ling physiological responses such as blood  
 uture, EKG, EEG, cardiovascular,  
 spiratory and nervous reactions,  
 15 p2434 A66-29447  
 entrifugal acceleration effect on sexual  
 aratus, cardiovascular system and  
 spiratory organs of female  
 onkey 15 p2437 A66-29472  
 mall Coriolis accelerations effect on  
 ctional state of human  
 art 15 p2437 A66-29474  
 otations effect on functional state of  
 man cardiovascular and respiratory  
 stems at various angles of inclination of  
 so 15 p2437 A66-29476  
 effect of combined action of accelerations,  
 iration and radiation of nuclei of bone  
 marrow cells in mice 15 p2437 A66-29478  
 lood flow rate in surface veins of brains  
 animals subjected to accelerations, noting  
 ermal transducer 15 p2445 A66-29500  
 igh-explosive driven shock tubes, as

sources of short duration high-pressure  
 supersonic pulses, applied in accelerating  
 large objects 16 p2674 A66-30423  
 Structural mounting of large diameter  
 cylindrical missile section in centrifuge for  
 high acceleration environmental  
 testing 16 p2677 A66-30458  
 Fast rise programmed centrifuge, noting  
 acceleration testing capabilities, power  
 speed control, etc 16 p2679 A66-30473  
 X-ray motion picture recording of change  
 in A-P chest diameter and heart position of  
 five human subjects during transverse  
 centrifuge accelerations of 5G and  
 10G 16 p2639 A66-31119  
 Antidiuretic effect of positive Gz gradient  
 acceleration 17 p2855 A66-32137  
 Correlation between survival time of rats  
 under acceleration stress and cerebral level  
 norepinephrine 17 p2855 A66-32145  
 Pulmonary blood flow distribution under  
 forward accelerations studied by combined  
 use of human centrifuge and radio-isotope  
 scanning 17 p2856 A66-32153  
 Mechanical impedance of human body  
 subjected to vibration combined with  
 various magnitudes of linear  
 acceleration 17 p2863 A66-32154  
 Abstract higher mental functioning of  
 human operator during exposure to  
 transverse acceleration  
 stress 17 p2857 A66-32161  
 Parasympathetic control of heart rate in  
 monkeys under acceleration stress, noting  
 ECG changes and effect of atropine sulfate  
 on change of rate 17 p2857 A66-32176  
 Blood saturation decrease due to regional  
 pulmonary arterial venous shunting during  
 exposure to transverse  
 acceleration 17 p2858 A66-32195  
 Age effect on liver glycogenesis in rats  
 exposed to acceleration  
 stress 17 p2860 A66-32555  
 Physiological reactions of astronauts to  
 acceleration of Voskhod spacecraft  
 characterized by greater emotional stress  
 than during centrifuge  
 simulation 17 p2861 A66-32936  
 Pathomorphological changes in hemopoietic  
 organs of mice under combined effects of  
 proton radiation and vibration and gamma  
 radiation and acceleration 17 p2861 A66-32937  
 Fluctuations in human acoustic sensitivity  
 after 24 hours in room under effect of  
 Coriolis accelerations of various  
 magnitudes 17 p2861 A66-32941  
 Effect of head-to-foot accelerations of up  
 to 10 g on rabbits, noting changes in ECG,  
 EEG, brain histology, etc, leading to  
 ischemic conditions 18 p3060 A66-34408  
 Labyrinthine nystagmus and sensation of  
 turning evoked by impulsive stimuli in yaw,  
 pitch and roll compared for subjects in  
 plane of rotation and in tilted  
 position 24 p4163 A66-42448  
 Cardiopulmonary hemodynamics in dogs  
 under transverse acceleration studied in  
 terms of changes in heart and  
 lungs 24 p4163 A66-42450  
 High acceleration missiles for intercepting  
 enemy ballistic warheads, considering sprint  
 and hibex rockets, noting problems with gap  
 heat, gyro drift, communications,  
 etc 24 p4284 A66-42952  
**ACCELERATION TOLERANCE**

Heat stress and minimal dehydration effect  
 upon human tolerance to positive  
 acceleration 03 p0326 A66-12353  
 Acceleration effect on food reinforced  
 DRL and FR schedules 03 p0325 A66-13175  
 Vibration exposure with varying peak and  
 rms acceleration and frequency in low  
 altitude high-speed flight 03 p0329 A66-13355  
 Breathing mechanics during transverse  
 acceleration, discussing experiments and  
 measurements made on  
 man 04 p0466 A66-14075  
 Electroencephalographic variations in  
 albino rats, discussing transverse  
 acceleration effects before and after  
 splenectomy 06 p0810 A66-15908  
 Neurologic adaptations and audiogenic  
 responses in mice exposed to chronic 2X  
 gravity field, noting development of more  
 efficient circulatory system, growth pattern  
 alterations, etc 07 p0998 A66-17660  
 Short radius onboard centrifugation for  
 simulated gravity during prolonged space

flight, providing zero G at eye level and  
 maximum G at feet 09 p1334 A66-20524  
 Effects of chronic hypohydration on  
 responses to tests of bodily functions,  
 defining set points and mechanisms involved  
 in changes in work  
 performance 09 p1337 A66-20528  
 Positive /headwards/ acceleration effect on  
 vision, cardiovascular system, respiration,  
 kidneys, brain wave patterns and total  
 performance 10 p1490 A66-22123  
 Negative acceleration physiological effect,  
 discussing heart, blood pressure, respiration,  
 vision, etc 10 p1490 A66-22124  
 Transverse acceleration physiological  
 effect, discussing cardiovascular system,  
 respiration, body position,  
 etc 10 p1490 A66-22125  
 Subgravity tower and axis results obtained  
 on man and animals, discussing transition  
 from acceleration to weightlessness and vice  
 versa 11 p1641 A66-22480  
 Physiological reactions of human body to  
 transverse acceleration, examining means of  
 increasing organism resistance to these  
 effects 11 p1643 A66-22575  
 Ejection seat spin rate tests to determine  
 temporary incapacitation  
 possibilities 11 p1647 A66-22576  
 1 g rotating linear acceleration vector  
 producing compensatory nystagmus, noting  
 effects when rotation axis was vertical and  
 horizontal 11 p1643 A66-22579  
 Vestibular reactions of deaf during angular  
 and coriolis accelerations 13 p2010 A66-25892  
 Combined effect of horizontal and vertical  
 accelerations on gravimeter readings  
 mounted on gyroplatform or in Cardan  
 suspension 14 p2297 A66-28111  
 Hypoxemia induced in man by sustained  
 forward acceleration while breathing pure  
 oxygen in five pounds per square inch  
 absolute environment 15 p2430 A66-28659  
 Acceleration stress-induced changes in fat  
 metabolism, level of circulating glucose and  
 corticosterone level in  
 rats 15 p2431 A66-28868  
 Chest-to-back accelerations effect on  
 human electroencephalograms and work  
 capacity 15 p2437 A66-29475  
 Simulation of aircraft crashes to evaluate  
 seating and restraint  
 systems 16 p2680 A66-30480  
 Packaging techniques for telemetry  
 components and systems to withstand gun-  
 launch accelerations up to 250,000  
 g 16 p2651 A66-30561  
 Physical conditioning found to have no  
 effect on human tolerance of positive Gs  
 during gradual or rapid onset centrifuge  
 runs 16 p2640 A66-31123  
 Wind tunnel, simulator and flight test  
 results to evaluate cockpit accelerations,  
 handling qualities and stability and control  
 of jet transports in severe turbulence  
 [AIAA PAPER 65-330] 16 p2634 A66-31317  
 Squirrel monkey physiological response to,  
 and survival under short duration very high  
 acceleration stress 17 p2858 A66-32187  
 Capability of white mice to sustain  
 extreme accelerations after exposure to  
 ionizing radiation 18 p3058 A66-33844  
 Missile and rocket launching with static  
 instability, deriving approximate solution for  
 equations of longitudinal accelerated  
 motion 19 p3470 A66-36083  
 Consequences of heart-to-foot acceleration  
 gradients on tolerance to positive  
 acceleration determined on variable radius  
 centrifuge 19 p3285 A66-36373  
 Human vestibular responses to combined  
 stimulation by angular and linear  
 accelerations tested, noting relation between  
 tolerance and habituation 19 p3287 A66-36647  
 Physiological and mechanical effects of  
 radial accelerations on brain temperature of  
 dog and rabbit 23 p4026 A66-41336  
 Twofold transversely applied 8-g  
 centrifuging effect on functional state of  
 otolithic part of vestibular apparatus of  
 guinea pigs 23 p4026 A66-41337  
 Combined effect of horizontal and vertical  
 accelerations on gravimeter readings  
 mounted on gyroplatform or in Cardan  
 suspension 24 p4212 A66-42699  
 Physiological disturbances caused by action  
 of prolonged accelerations on human  
 organism, examining methods of increasing



maximum g force tolerance  
levels 24 p4166 A66-43136  
Physiological and biomechanical reactions  
of humans exposed to action of g forces,  
examining effects of impact  
acceleration 24 p4166 A66-43137

**ACCELERATOR**  
SA COAXIAL ACCELERATOR  
SA CYCLIC ACCELERATOR  
SA CYCLOTRON  
SA DECELERATOR  
SA ELECTRON ACCELERATOR  
SA HALL ACCELERATOR  
SA HYPERVELOCITY ACCELERATOR  
SA LINEAR ACCELERATOR  
SA PARTICLE ACCELERATOR  
SA PLASMA ACCELERATOR  
SA SYNCHROTRON  
SA VAN DE GRAAFF ACCELERATOR  
Accelerator energies to simulate space  
radiation damage effects in spacecraft  
systems 07 p1018 A66-18145  
Accelerator for jets formed by shaped  
charges, using principles of detonation  
waves 14 p2329 A66-27475

**ACCELEROMETER**  
SA INERTIAL ACCELEROMETER  
SA STRAIN GAUGE ACCELEROMETER  
Test pad stability measurement using two  
accelerometers and recording  
autocolimator 01 p0065 A66-10031  
Accelerometers and gyroscopes tested  
underground, discussing ground motion  
attenuation with depth investigated in Deep-  
Hole program 01 p0051 A66-10038  
Nonorthogonal and redundant  
accelerometer orientations for optimum  
performance 01 p0068 A66-10678  
Preflight checking of aircraft gyroscopes  
and accelerometers noting built-in spin  
detection, torque generator and gimbal  
check 01 p0070 A66-10956  
Angular velocity and linear acceleration  
measurement by three accelerometers  
mounted on three mutually orthogonal  
rotating disks 03 p0369 A66-12667  
Inertial navigation and accelerometers  
deriving law of gyroscopics, noting design of  
gyroscopes like ball and gas bearings, gimbal  
suspension, electrostatic, laser,  
etc 04 p0543 A66-13362  
Various types of acceleration-sensitive  
transducers such as piezoelectric crystal,  
potentiometer, strain gauge, variable  
reluctance and servo force-balance  
accelerometer 04 p0520 A66-13900  
Slide wire accelerometer, considering  
factors responsible for sensitivity loss and  
gain 07 p1031 A66-17410  
Gyroscopes, accelerometers and error  
sources in inertial navigation  
systems 08 p1249 A66-19056  
Vehicle angular velocity determined, using  
configurations with only linear  
accelerometers and no gyroscopes for  
inertial navigation systems 08 p1224 A66-19488  
ONERA laboratory weightlessness  
simulation tests on liquids, accelerometers,  
aerodynamic braking, etc 13 p2058 A66-26371  
ONERA weightlessness simulation  
laboratory investigations of highly sensitive  
accelerometers 13 p2082 A66-26373  
Prediction of flight transient torsional  
acceleration at base of Surveyor spacecraft  
and implementation of pulse qualification  
testing 14 p2392 A66-28001  
Inertial navigation application to  
aeronautics, requiring accelerometers and  
inertial platform with turning motion  
sensors 15 p2536 A66-29893  
Pulse rebalancing of pendulum  
accelerometers for digital output  
requirements 16 p2706 A66-30882  
Angular transducer using Hall effect,  
noting errors due to distortions in magnetic  
circuit and temperature 16 p2709 A66-31577  
Accelerographic and ballistocardiographic  
evidence of increased stroke volume  
secondary to acute high altitude  
hypoxia 17 p2855 A66-32135  
Controlling motion of object directly from  
accelerometer data without need of object  
coordinate determination 17 p3003 A66-32587  
Absolute angular velocity determination  
and distance to center of attraction along  
vertical established by accelerometer

measurements 17 p3003 A66-32588  
Stable equilibrium position of axis of  
rotation of cylinder in rotating chamber  
filled with one or two  
liquids 17 p2928 A66-33498  
Test pad stability measurement using two  
accelerometers and recording  
autocolimator 18 p3110 A66-33815  
Slew plane technique for locating two gyro  
input axes without removing platform from  
test vehicle and with limited optical  
access 18 p3133 A66-34048  
Accelerometer standard designed for  
reciprocity and comparison calibrations of  
vibration transducers 18 p3112 A66-34207  
Inertial sensor performance degradation in  
strapped-down environment, noting gyro  
drift error and accelerometer  
bias 21 p3763 A66-38839  
Gyro and accelerometer errors in ternary  
torqued inertial components mounted on  
surface to surface missile, noting angular  
vibration environment 21 p3764 A66-38848  
Strapdown inertial sensor configuration  
based on time modulated torquing approach  
in gyro and accelerometer  
readout 21 p3764 A66-38849  
Inertial platform test station for shipboard  
maintenance and calibration of platform  
used in A6A and E2A aircraft, examining  
accelerometer bias and gyro drift  
tests 21 p3723 A66-38889

**ACCIDENT INVESTIGATION**  
SA AIRCRAFT ACCIDENT  
INVESTIGATION  
Medical knowledge as aid in preventing  
aircraft accidents and injury through  
investigation of causes and  
results 10 p1495 A66-22142  
Spatial disorientation experiences of Army  
helicopter pilots, noting accident and  
incident statistics, methods of correction,  
etc 11 p1648 A66-22578  
Missile and space system accident potential  
evaluated numerically 20 p3685 A66-37931

**ACCIDENT PREVENTION**  
Plane crash as result of pilots coronary  
disease, discussing prevention and  
rehabilitation 04 p0469 A66-14387  
Supersonic flight control, discussing  
reliability and safety devices, computer  
application and multiplex  
systems 06 p0816 A66-16055  
USAF aircraft accidents involving ten or  
more fatalities 06 p0807 A66-16825  
RAF system of classification of aircraft  
accidents by causes for statistical  
purposes 10 p1494 A66-22139  
Medical knowledge as aid in preventing  
aircraft accidents and injury through  
investigation of causes and  
results 10 p1495 A66-22142  
Contribution of medical science to accident  
prevention, discussing causes, results and  
escape from standpoint of man and  
machine 10 p1495 A66-22143  
Automatic stabilization systems reduce  
accidents due to disorientation, emphasizing  
sensor-servo system for roll axis control  
[SAE PAPER 660201] 13 p1996 A66-26390  
Clinical and medicolegal considerations on  
fatal case of myocardial infarct involving  
military pilot in flight 14 p2229 A66-26813  
EEG experiments on men exposed to  
intermittent photic stimulation under  
simulated IFR conditions produced  
drowsiness as primary  
response 17 p2864 A66-32165  
Closed circuit television applied to data  
transfer in air traffic control, discussing  
accident prevention and information  
provision to aircraft 17 p2874 A66-32356  
Ground testing of large nuclear rockets,  
discussing decontamination requirements to  
maintain safety level with longer running  
times and higher reactor  
levels 19 p3398 A66-36177  
Allotment of probability shares method  
applied to improving safety in design by  
diagnosing failure and probability of  
accident 20 p3494 A66-36999  
Promotion of aviation safety, discussing  
adoption of new accident statistics,  
elimination of catastrophes and STOL  
design extension to medium and long-range  
aircraft 23 p4152 A66-41305

**ACCIDENT PRONENESS**  
Flying skills assessment in relation to

accident liability 20 p3508 A66-36995

**ACCLIMATIZATION**  
SA ADAPTATION  
SA ALTITUDE ACCLIMATIZATION  
SA ENVIRONMENTAL SCIENCE  
SA HEAT ACCLIMATIZATION  
SA HEAT TOLERANCE  
SA HUMAN TOLERANCE  
Heat regulation, acclimatization and human  
tolerance upon exposure to moderate, hot  
and cold temperatures 10 p1489 A66-22119  
Resistance to hypoxia by individuals at  
height of 1650 m trained for high altitude  
climbing, noting  
equipment 15 p2435 A66-29449

**ACCOMMODATION**  
S VISUAL ACCOMMODATION  
**ACCOMMODATION COEFFICIENT**  
SA THERMAL ACCOMMODATION  
COEFFICIENT  
Energy accommodation coefficients  
calculated for gas particles interacting with  
cubic crystal lattice 04 p0548 A66-14142  
Roberts method determining  
accommodation coefficients of gases on bare  
wires leads to erroneous conclusions due to  
thermal inertia of experimental apparatus in  
vicinity of current paths 04 p0545 A66-14170  
Heat transfer during film condensation of  
liquid metal vapor, discussing thermal  
resistance effect of condensation coefficient  
[ASME PAPER 65-HT-29] 05 p0784 A66-14748  
Parametric analogies used to obtain design  
characteristics of thermal and viscosity  
vacuum meters and hot-wire  
anemometers 07 p1031 A66-17412  
Momentum and energy accommodation  
coefficients for moving gas interaction with  
solid surface, with attention to molecular  
mass and velocity flux  
distribution 07 p1083 A66-18135  
Heat transfer during film condensation of  
liquid metal vapor, discussing thermal  
resistance effect of condensation coefficient  
[ASME PAPER 65-HT-29] 11 p1784 A66-22182  
Temperature jump in polyatomic gases,  
discussing nonequilibrium energy  
distribution on boundary  
conditions 11 p1687 A66-22334  
Energy accommodation coefficient variation  
with energy of gas molecules impinging on  
clean surfaces or adsorbed  
monolayers 16 p2645 A66-30391  
Pulsed molecular nitrogen beam-ballistic  
pendulum measurements of normal  
momentum accommodation  
coefficients 16 p2701 A66-30395  
High energy argon atom interactions with  
surfaces and variations in accommodation  
coefficient 16 p2702 A66-30399  
Thermal conductivity and accommodation  
coefficient measurements in gas mixture of  
atomic and molecular  
oxygen 21 p3836 A66-39174  
Revision of Levin average value of  
accommodation coefficient K for iron  
meteoric bodies 22 p3984 A66-40783

**ACCORDION PROJECT**  
Project Accordion data to provide  
information for decisions on horizontal  
separation standards and navigational  
accuracy 07 p1076 A66-17790

**ACCUMULATOR**  
Auxiliary power unit turbine-engine  
starting system analyzed to determine  
sufficiency of selected  
accumulator 16 p2637 A66-31224

**ACETALDEHYDE**  
Radiation-induced solid state explosive  
polymerization of  
acetaldehyde 19 p3295 A66-35333

**ACETATE**  
Nuclear magnetic resonance classification  
of alcohols and hydroxyl groups from FI-19  
spectra of  
trifluoroacetates 15 p2447 A66-29238

**ACETIC ACID**  
Carbon-13 chemical shifts of carboxyl  
carbon atom of acetic, benzoic and mesitoic  
acids in various compositions of sulfuric  
acid 14 p2232 A66-27376  
Conversion of 2-formyl dienone III into  
dienone IV upon irradiation in acetic acid  
followed by base-catalyzed deformation of  
crude photoproduct 15 p2446 A66-28873  
Thermodynamic calculation of explosive  
properties of peracetic acid, using data from  
detonation wave to establish safe limits for



- se of acid 21 p3834 A66-38535
- ETONE
- Stimulated Raman effect in acetone and acetone-carbon disulfide mixtures, noting similarity of Stokes radiation pattern to Raman effect 15 p2513 A66-28881
- ETYLENE
- Mechanical and electro-optical parameters for some acetylene derivatives evaluated from IR spectra 01 p0109 A66-11004
- Behavior of excess radical concentrations, H, OH and O as function of height above reaction zone in premixed acetylene-air flames 03 p0414 A66-12488
- Mechanical and electro-optical parameters for some acetylene derivatives evaluated from IR spectra 09 p1404 A66-19942
- Chemiluminescence in atomic-oxygen-acetylene and atomic-oxygen-carbon monoxide flames attributed to formation of CO in excited and electronic states 22 p3997 A66-39926
- Increase of specific impulse of solid propellants by introducing endothermic groups into binder 23 p4117 A66-41230
- CHONDRITE
- Isotopic composition of xenon extracted from Ca-poor achondrites, noting relation between enstatite achondrites and enstatite chondrites 22 p3983 A66-40558
- Isotopic composition of Xe indicates that two Ca-rich achondrites comprise group of olivine-olivine achondritic meteorites containing fission-produced 24 p4264 A66-42606
- ACID
- ACETIC ACID
- AMINO ACID
- ASPARTIC ACID
- BENZOIC ACID
- CARBOXYLIC ACID
- CYTIDYLIC ACID
- DEOXYRIBONUCLEIC ACID /DNA/
- FATTY ACID
- HYDROCHLORIC ACID
- HYDROFLUORIC ACID
- LACTIC ACID
- NITRIC ACID
- NUCLEIC ACID
- PERCHLORIC ACID
- PHOSPHORIC ACID
- RIBONUCLEIC ACID /RNA/
- SULFURIC ACID
- VALERIC ACID
- Corrosion resistance of titanium and its alloys in solutions of acetic and nitric acids as affected by aluminum additions 06 p0896 A66-16608
- PH FACTOR
- ACOUSTIC ATTENUATION
- Mechanisms of attenuation and amplification of ultrasonic waves in semiconductors 03 p0408 A66-12413
- Use of Brillouin scattering for optical beam modification, spatial distribution of acoustic energy and coherent sound of great intensity 03 p0376 A66-12421
- Ultrasonic attenuation and velocity changes in doped p-type silicon in frequency range from 608 to 960 mc 06 p0851 A66-16460
- Subscale cold-flow rocket motor model used to determine effect of purely geometric variables on acoustic performance leading to axial mode combustion instability [AIAA PAPER 66-110] 06 p0944 A66-17080
- Ultrasonic absorption in superconducting lanthanum explained by two models for loss of energy from low-energy phonon field in London superconductor 09 p1415 A66-20021
- Ultrasonic attenuation in superconductors containing magnetic impurities analyzed, using weak coupling electron gas as model 09 p1416 A66-20022
- Ultrasonic absorption by superconducting indium single crystals, noting nonlinear dependence on sonic field amplitude 09 p1428 A66-20592
- Reflection and transmission of shock waves in porous acoustic absorbers 12 p1913 A66-23822
- Insertion loss of room temperature magnetoelastic waves in yttrium iron garnet from 1.6 to 8.5 gc 16 p2715 A66-30892
- Acoustic wave energy absorption by superconductors in intermediate state 18 p3158 A66-34692
- Acoustic absorption liners for suppressing HF combustion instability in rocket engine combustion chambers [AIAA PAPER 65-585] 19 p3449 A66-35608
- Ultrasonic absorption by superconducting indium single crystals, noting nonlinear dependence on sonic field amplitude 20 p3622 A66-38125
- Longitudinal sound waves attenuation in superconductor with spatially dependent energy gap by Green function method applied to ultrasonic attenuation in type II superconductor 21 p3795 A66-38548
- Ruby laser-induced effect of pulsed pressure on KDP crystal surface and thermal bulk effect on excitation of ultrasonic oscillation in crystal 22 p3932 A66-40318
- Temperature dependence of relaxation-type ultrasound attenuation maxima in plastic deformation of molybdenum and niobium single crystals 22 p3965 A66-40322
- Anisotropic acoustic attenuation measured from surface excitation in novel resonant cavity configuration, discussing validity in quartz and effective viscosity in silicon 22 p3866 A66-40407
- Low accuracy of interferometric measurement of coefficient of ultrasound absorption in gas 23 p4068 A66-41414
- Resonators use for higher sound attenuation in waveguide with sound absorbing cladding 23 p4090 A66-41416
- Ultrasonic wave absorption in GaAs and GaSb compounds at temperatures from 95 to 300 degrees K 23 p4113 A66-41417
- Speech communications effects and temporary threshold shift reduction characteristics of British-made earplugs under quiet and high intensity impulsive noise backgrounds 24 p4168 A66-42857
- ACOUSTIC COMBUSTION
- S COMBUSTION INSTABILITY
- ACOUSTIC DUCT
- Acoustic pressures on vibrating walls for turbulent airflow through rectangular hard-walled duct exposed to traveling sound waves 17 p2905 A66-31944
- ACOUSTIC EXCITATION
- Stress response and fatigue life of acoustically excited brazed steel honeycomb panels for variations in thickness 01 p0147 A66-10133
- Displacement response prediction and fatigue life of honeycomb sandwich panels subjected to acoustic excitation 01 p0149 A66-10141
- Single dispersion relation valid for all collision frequencies for electromagnetic and piezoelectric semiconductor acoustic interactions 01 p0029 A66-10589
- Aeroacoustic excitation of aerospace structures for design purposes, sources being jets of gas turbines and rockets and turbulent boundary layers [SAE PAPER 650823] 01 p0156 A66-10824
- Limited distance of transmission of ultrasonics in air has limited application to remote control systems, proximity indicators, automatic counting and burglar and fire protection 03 p0368 A66-12407
- Frequency response function of lightly damped single-degree of freedom system estimated from truncated measurement of cross-correlation function of white noise excitation and response 05 p0781 A66-15788
- Transducers for exciting and detecting acoustic waves in discharge tube plasmas, discussing requirements, specifications and construction techniques 07 p1032 A66-17496
- Fluid-shell interaction of infinite cylindrical shell submerged in acoustic fluid and subjected to axially propagating step wave 10 p1615 A66-21473
- Elastic constants obtained from longitudinal and transverse acoustic waves propagated in single-crystal indium phosphide 10 p1578 A66-21585
- Cavitation strength of distilled water and distribution of cavitation nuclei, accounting for pressure threshold variance 11 p1688 A66-22607
- Magnetostrictively generated microwave acoustic pulse in thin films of Dy, Ho, Gd and Er 14 p2350 A66-26876
- Acoustically induced cavitation in liquid helium analogous to unfiltered air-saturated water 14 p2334 A66-27663
- Acoustical control of atmospheric boundary layer investigated in wind tunnel for flow velocity range from 5 to 40 m/sec 14 p2277 A66-27862
- Transient acoustoelectric interaction in CdS and ZnS crystals during single transit, measuring electron drift 15 p2563 A66-28758
- Acoustic wave generation and amplification in weakly ionized plasma, explaining sound emission in glow discharge and modulation in plasma afterglow 15 p2556 A66-29808
- Thunderlike acoustic effects associated with extinction of meteors 16 p2796 A66-30272
- Hearing impairment from overexposure to impulsive noise, noting relationship between temporary threshold shift and peak level and duration of impulsive noise 17 p2862 A66-31948
- Forced vibrations of flexible rectangular panel backed by closed rectangular cavity under external acoustic pressure, noting sound transmission into cavity 18 p3250 A66-33674
- Simultaneous existence /triple resonance/ of spin, helical and acoustic waves in ferromagnetic conductor in strong magnetic field 22 p3964 A66-40310
- Unsteady-state solid-propellant combustion subjected to acoustic pressure oscillations, noting effect of combustion parameters 22 p3971 A66-40352
- ACOUSTIC FATIGUE
- Acoustical fatigue in aerospace structures - USAF Conference, Dayton, Ohio, April 1964 01 p0146 A66-10121
- Structural response theory and acoustic fatigue aspects contributing to estimation of fatigue life of aerodynamic structures 01 p0147 A66-10122
- Boundary layer noise and effects of acoustic energy on panel response, panel fatigue and internal sound levels tested with X-15 aircraft 01 p0010 A66-10126
- Fatigue failure in aircraft panels studied by determining spectral densities of response of continuous skin stringer panels under random noise 01 p0147 A66-10130
- Analog computer application to prediction of nonlinear response of panel structure to random forcing function 01 p0148 A66-10134
- Matrix analysis of response of geometrically nonlinear structures to prescribed dynamic loading and effects of thermomechanical midplane preload in prediction of natural frequencies and mode shapes 01 p0148 A66-10135
- Natural frequencies of sheet-stringer panels which do not deflect laterally but rotate when subjected to arbitrary external loads 01 p0148 A66-10137
- Vibration response of steel panels to fluctuating pressures in turbulent boundary layer of wind tunnel compared to random excitation caused by jet noise and siren 01 p0148 A66-10138
- Propagation of fatigue cracks in tensioned plate subjected to acoustic loads 01 p0148 A66-10140
- Dynamic responses of panel shells and complete equipment packages to acoustic inputs to improve fabrication techniques of flight structures 01 p0149 A66-10142
- Acoustic fatigue characteristics of beryllium panels exposed to high intensity random noise 01 p0149 A66-10143
- Increased aluminum panel acoustic resistance due to combination of surface treatment and mylar gasket-universal head mounting technique 01 p0149 A66-10144
- Spectrum shaping of noise generated by broadband siren is possible by introducing air by-pass system and changing rotor shape 01 p0052 A66-10145
- Optimum proportion of surface-damping treatment to surface metal thickness to minimize randomly excited skin surface stresses in stiffened plate structure 01 p0149 A66-10148
- Acoustical fatigue study of propeller duct designed for minimum weight to maintain specified thrust-to-weight ratio 01 p0150 A66-10155
- Acoustic fatigue and acoustically induced



vibration in Titan II and Titan III missiles studied by simulation and wind tunnel scale models 01 p0150 A66-10156

Matrix technique to predict structural fatigue of acoustically loaded structures 01 p0150 A66-10157

Acoustic fatigue testing of 20 fuselage panels of XC-142A VTOL/STOL transport aircraft, using simulated propeller noise 01 p0151 A66-10158

Noise and vibration causing acoustic fatigue leading to deafness of aircrew 06 p0811 A66-18065

Lifting aircraft structures subjected to acoustic pressures, noting estimation of panel joint rms stress 20 p3666 A66-37422

**ACOUSTIC GENERATOR**

Broadband siren spectrum test facility including acoustic chamber, horn network, siren, air supply, instrumentation and controls 01 p0052 A66-10146

Programming method for determining modulation parameters required to change siren sine wave output to random Gaussian noise 01 p0053 A66-10147

Microwave acoustic delay lines made practical by low-loss propagation of microwave phonons at room temperature in single crystals 03 p0331 A66-12412

Mathematical analysis of noise generation mechanism in axial-flow compressor rotors [ASME PAPER 66-GTIN-42] 14 p2372 A66-26987

Longitudinal acoustic wave generation by electrostrictive mixing of two light beams in single crystals of strontium titanate, rutile and z-cut quartz 19 p3400 A66-36073

X-radiation alignment of quartz crystals for generation and detection of reverberating acoustic echoes at liquid-helium temperatures 20 p3624 A66-38409

Oscillator circuit needing no standby power and pulsed on when required, with application to tone generators 21 p3714 A66-39495

**ACOUSTIC IMPEDANCE**

Energy dissipation of acoustic waves propagating in liquid medium and producing cavitation 01 p0106 A66-10417

Acoustic impedance of liquid He 3 under vapor pressure 09 p1391 A66-20012

Acoustic impedance of liquid He 3 under pressure of up to 12.5 atm 09 p1391 A66-20013

150 mc strip-line circulator using Altrron garnet material, noting isolation, insertion loss, input impedance, etc 10 p1514 A66-21910

Energy dissipation of acoustic waves propagating in liquid medium and producing cavitation 11 p1735 A66-22601

Deposition of cadmium selenide films for transducers of electromagnetic energy to acoustic energy at microwave frequencies, noting use of multiple film assemblies 12 p1839 A66-24616

Limitations imposed on upper atmospheric sonic thermometry by lowering of density with increasing altitude 21 p3741 A66-39428

**ACOUSTIC INSTABILITY**

**S COMBUSTION INSTABILITY**

**ACOUSTIC NOZZLE**

Refraction of injected point source of sound by cold nitrogen jet, noting effects of temperature and velocity fields 07 p1080 A66-17500

**ACOUSTIC RADIATION**

Size and position effect, baffle effect and wake and pressure interaction effect of upstream stator on ducted axial flow fan noise 10 p1483 A66-21746

Acoustic power emitted by coaxial subsonic jets in relation to aerodynamic parameter 13 p2063 A66-25432

Unbounded isothermal atmosphere response to time harmonic point disturbances, exact solutions obtained for frequency ranges of acoustic waves, trapped oscillations and gravity 13 p2183 A66-25613

Sound power from nonuniform flow determined by summing surface and volume integral over sound sources 17 p2905 A66-31949

Multipole analysis of acoustic radiation to explore dependence of mass density on functional character of source distribution 17 p2957 A66-31951

Computer-derived contour plots of electric

and magnetic fields for acoustic electromagnetic plane wave pulse incident on wedge 17 p2875 A66-32390

Fluid loading effect on acoustic radiation from point-driven infinite orthotropic plate 18 p3251 A66-33677

Acoustic resonance tube used to change radiation to sound 24 p4213 A66-42854

**ACOUSTIC SCATTERING**

Correlation of large and small scale roughness for plane wave scattering from rough surface 03 p0335 A66-12818

Acoustic-mode scattering theory obtained with tight-binding approximation of band theory and applied to narrow-band semiconduction in organic molecular crystals 04 p0560 A66-13721

One-dimensional self-consistent problems involving interaction between Langmuir and ionic-acoustic plasma oscillations caused by induced combination scattering of former on latter 04 p0556 A66-14418

Acoustic fluctuations from transmission through water whose refractive index varies randomly in space and time related to range from source to receiver, acoustic frequency and scattering medium parameters 05 p0717 A66-15737

Combination scattering of HF electromagnetic and plasma oscillations propagating over longitudinal standing waves of ionic sound 06 p0914 A66-16145

Acoustic detection of micrometeoroids from rockets, discussing experimental setup, calibration methods and analysis of results 09 p1381 A66-20367

Spin-lattice relaxation of conduction electrons in semiconductors of n-InSb type with scattering at acoustical and optical phonons 14 p2358 A66-27083

Combination scattering of HF electromagnetic and plasma oscillations propagating over longitudinal standing waves of ionic sound 15 p2556 A66-29875

Specular returns and diffuse scattering from Moon and ocean bottom 16 p2653 A66-30932

Sonic boom shape distortion due to reflection and scattering by ground surface with finite acoustic impedance 17 p2905 A66-31947

Electric field effect for free carrier absorption, determining coefficient for acoustic phonon scattering 17 p2976 A66-32264

Scattering of ultrasonic waves from turbulence produced by flow through grid in 6 x 6-inch nozzle 18 p3136 A66-35024

Omnidirectional characteristics of scattering of acoustic waves from statistically rough surfaces, measuring scattering cross section as function of incidence and observation angles 21 p3770 A66-38649

Spin-lattice relaxation of conduction electrons in semiconductors of n-InSb type with scattering at acoustical and optical phonons 22 p3967 A66-40839

Brillouin scattering spectra of crystalline quartz, fused quartz and Pyrex glass, noting acoustic modes in crystalline spectrum 23 p4114 A66-41628

Backscatter of electromagnetic waves from rough layer simulated by acoustic backscattering from partially submerged Plexiglas layer 24 p4173 A66-42624

Acousto-optical deflection and modulation devices, considering specific geometries and scattering-efficiency-bandwidth products 24 p4174 A66-42812

**ACOUSTIC SIMULATION**

Response of simple structure to boundary layer noise examined together with response of supported panel to sound field 01 p0055 A66-10132

Model measurement of radar cross section of target with complex outline by use of ultrasonic waves 02 p0189 A66-11366

Simulation of noise transmission through structures under turbulent boundary layer flow shown to be of doubtful value 10 p1520 A66-21744

Elastic wave diffraction on rigid edge analyzed by employing acoustic analogy 13 p1991 A66-25637

Human reaction to noise under various simulated acoustical conditions of space cabin 13 p2015 A66-25890

Stimulus coding in cochlear nucleus, noting different discharge patterns of units in different subdivisions 16 p2641 A66-31187

**ACOUSTIC STABILITY**

Electron heating effect on acoustic instability of weakly ionized plasma in electric field 06 p0914 A66-16143

Sonic instability in piezosemiconductors with negative differential conductivity 10 p1589 A66-22170

Electron heating effect on acoustic instability of weakly ionized plasma in electric field 15 p2556 A66-29873

Influence of relative thickness of elastic case on acoustic stability of radial modes in solid propellant rockets 16 p2791 A66-31474

Combustion instabilities in solid propellant rocket motors, including acoustic and nonacoustic instabilities 18 p3163 A66-34003

Sonic instability in piezosemiconductor with negative differential conductivity 19 p3441 A66-35784

**ACOUSTIC STREAMING**

Thermoacoustic streaming equations, examining effect of sound on free convection from heated cylinder 16 p2828 A66-30992

Acoustic streaming in flow near vibrating membrane and in flow generated by absorption of magnetoacoustic wave 23 p4108 A66-42035

**ACOUSTIC VELOCITY**

Horizontal propagation of sound from jet engine at ground proximity, discussing effects of vector wind, ground absorption and temperature gradient 07 p1080 A66-17730

**ACOUSTIC VIBRATION**

Acoustic, gravitational and gyroscopic oscillation spectra of baroclinic atmosphere over rotating spherical Earth with emphasis on energy composition 01 p0062 A66-10858

Interior and exterior Dirichlet and Neumann problems for LF acoustic oscillations 02 p0261 A66-12153

Unsteady boundary layer flow of multicomponent gas mixtures, investigating combustion instability in liquid and hybrid rocket motors [AIAA PAPER 65-41] 03 p0444 A66-12796

Oscillations in triaxial mirror ellipsoid and quantum conditions, determining natural oscillation frequency and position of acoustic surfaces 03 p0393 A66-13186

Linear vibratory system response to random impulses, describing nonstationary white noise and mean square resonance 07 p1143 A66-17731

Temperature-velocity phase lag of vibrations of air columns excited by heat supply 08 p1320 A66-19555

Turbulence-excited atmospheric velocity, critical frequency of atmosphere, solar atmospheric power spectrum of acoustic field velocity correlation, solar convection zone, etc 11 p1772 A66-22777

Aerodynamic forces on system of N thin slightly twisted profiles in subsonic unsteady flow for small angle of attack, examining acoustic resonance for arbitrary small harmonic oscillations 12 p1798 A66-24436

Test facility for combined sonic and mechanical excitation of flight and surface-vehicle hardware, using electropneumatic transducers 16 p2676 A66-30444

Formula derivation for acoustic conductivity of combustion surface of condensed system 17 p3033 A66-31896

Magnetoacoustic natural oscillations in solid MHD resonators 17 p2971 A66-32787

Dispersion of ion waves in mercury vapor discharges, carrying out spectral analysis of acoustic and plasma oscillations 18 p3146 A66-34234

Sound field parameter dependence of coefficient of heat transfer from horizontal cylinder at near zero Grashof numbers 19 p3478 A66-35751

Acoustic oscillations in solid propellant rocket chambers, discussing cases of small amplitude perturbations and solving wave equations 20 p3628 A66-37387

Rotational axisymmetric mean flow and damping of acoustic waves in solid propellant rocket 21 p3807 A66-38720

Standing ion acoustic waves between cathode and electrically floating auxiliary metal electrode, noting discharges in



mercury vapor between plane oxide-coated cathode and nickel anode 22 p3954 A66-39817  
 Ion-acoustic wave propagation and damping in plasma with negative ions 23 p4104 A66-41505  
 Hamilton variational principle formulation of damped acoustical-structural vibration motion equations, with application to radiation problems 24 p4291 A66-42858  
 High speed photograph analysis of compressed volumes of plasma formed in reaction of colliding supersonic flares of high power pulsed discharge 24 p4244 A66-42875  
 Radiated pressure field due to LF vibration of slender body of revolution expressed as distribution of sources and doublets along body axis 24 p4238 A66-43047  
**COUSTICS**  
**SA NOISE**  
 Acoustic images arising from binaural repetitive wideband acoustic transients, noting tonal harmonic images and two dominant images of impulsive character 05 p0628 A66-15734  
 Design technique for large capacity acoustic instrument 14 p2296 A66-28036  
 Acoustic problems formulated and solved by finite element method of variational calculus, using both force and displacement procedures 17 p2957 A66-31945  
 Acoustics, shock and vibration bibliography of 1959-1965 meetings of Institute of Environmental Sciences 17 p2904 A66-33040  
 Small and low cost voltage-tunable audio filter using field effect transistors as tuning element in place of inductors for space communications 24 p4180 A66-42334  
**ACQUISITION**  
**DATA ACQUISITION**  
**TARGET ACQUISITION**  
**CRYLATE**  
**LUCITE**  
**ACTH**  
**ADRENOCORTICOTROPIN /ACTH/**  
**ACTINIDE**  
 Alpha emitter actinide element application as heat source for isotopic generators, discussing safety precautions required, economy, etc 18 p3134 A66-34056  
 Fluorescence of rare earth, actinide and transition metal ions in insulating crystals as result of optical excitation, discussing spectroscopic properties and operating characteristics 20 p3575 A66-36969  
**ACTINOMETRY**  
 Quantum yield of CO formation from photolysis of carbon dioxide at wavelengths of argon lines 13 p2017 A66-25801  
**ACTIVATION**  
**NEUTRON ACTIVATION**  
**ACTIVATION ENERGY**  
 Neutron flux in atmosphere measured by method of indium 02 p0284 A66-12130  
 Tracer diffusion measurements in beta titanium covering Arrhenius plots, monovacancy and divacancy diffusions and new data for Sc-46, Sn-113 and P-32 03 p0382 A66-12939  
 Compensation dependence of impurity conduction in n-type germanium containing antimony atoms 05 p0743 A66-15876  
 Ripening of defects induced by fast neutrons in germanium in course of low temperature annealing 06 p0937 A66-17143  
 Titanium oxidation characteristics, determining activation energy of scale formation, oxygen absorption of base metal and total oxygen 09 p1389 A66-20613  
 Kinetics and mechanism of enhanced oxidation of platinum in activated oxygen as function of partial pressure of oxygen atoms 09 p1339 A66-20946  
 Numbers theory for lead sulfide photoconducting films, noting balancing of n and p-type impurities, various activation energies, etc 10 p1578 A66-21574  
 Chemical etching revealing dislocations produced by indentation on single crystals of silicon, measuring edge dislocation velocities at various shear stresses and high temperatures, determining activation energy 11 p1750 A66-22492  
 Early interaction stages of metal oxides with carbon, using thermochromatographic method to determine temperature reaction

onset 12 p1892 A66-23518  
 Germanium specimens with various dislocation densities quenched from high temperatures to introduce vacancies, contamination by copper atom diffusion, finding activation energy 12 p1930 A66-24801  
 Annealing of deformed sodium, noting activation energy distribution annealing kinetics, etc 12 p1897 A66-24923  
 Thallium admixture effect on electrical conductivity of crystalline and liquid selenium, noting decrease and increase in conductivity, determining temperature dependency and activation energy 14 p2359 A66-27177  
 Neutron flux in atmosphere measured by method of indium 14 p2377 A66-28087  
 Activation energy and corresponding concentration of unknown donor level in n-type gallium arsenide 16 p2777 A66-31002  
 LF internal friction of beryllium, noting strain amplitude dependency variation with temperature and purity, obtaining activation energies 16 p2724 A66-31265  
 Surface IR photoconductivity spectra of chemically etched p and n silicon, noting energy distribution, activation energies of centers, etc 16 p2788 A66-31774  
 Epitaxial growth of semiconductors in isothermal system approaching thermodynamic equilibrium, noting growth parameters, activation energy, etc 17 p2886 A66-32495  
 Radiotracer investigation of silicon self-diffusion in high purity single crystal material 18 p3153 A66-33609  
 Photoconductivity of thin layers of CdS, noting intrinsic maximum for various dopants, temperature effect, activation energy, etc 18 p3157 A66-34628  
 High temperature rate constants for H-atom transfers involving light atoms evaluated, using hard sphere collision theory 22 p3950 A66-39924  
 Attachment coefficient and temperature dependence of ionic reactions in F layer for various activation energies 22 p3908 A66-39968  
**ACTIVITY**  
**S AURORAL ACTIVITY**  
**S CATALYTIC ACTIVITY**  
**S ENZYME ACTIVITY**  
**S SOLAR ACTIVITY**  
**ACTIVITY /BIOL/**  
**S CATALYTIC ACTIVITY**  
**ACTIVITY CYCLE /BIOL/**  
**S BIOLOGICAL RHYTHM**  
**ACTUATOR**  
**S CARTRIDGE ACTUATED DEVICE**  
**S HYDRAULIC ACTUATOR**  
**S PROPELLANT ACTUATED DEVICE**  
**S SERVOACTUATOR**  
**S SERVOMECHANISM**  
**ADAPTATION**  
**SA ACCLIMATIZATION**  
**SA LIGHT ADAPTATION**  
**SA RETINAL ADAPTATION**  
 Adaptation theory concepts, examining threshold learning process, Markov chain, learning wave, feedback adaptivity, etc 11 p1647 A66-22299  
 Neural, threshold, majority and Boolean logic techniques compared for reliability and efficiency in adaptive machines and data handling systems 11 p1659 A66-22300  
 Adaptation rearrangements in organisms of mice during and after exposure to high concentrations of carbon dioxide 15 p2438 A66-29479  
**ADAPTIVE CONTROL**  
 Empirical Bayes rule obtained from observing unknown signal of stochastic control 02 p0206 A66-11307  
 Computer program and technique for adaptive digital controller that learns switching regions for optimal control of decision-making regulator 04 p0490 A66-13621  
 Adaptive parametric two-input detectors analyzed and compared to nonparametric detector /polarity coincidence correlator/ under assumption of quasi-stationary inputs 06 p0884 A66-16739  
 Active circuit of second order designed with independently variable parameters for use as transfer function model 07 p1003 A66-17819

Algorithm for data transmission system automatic adaptive equalization, employing change of settings during transmission in response to variation in transmission channel characteristics 11 p1656 A66-23088  
 Adaptive analog-to-digital converter using level sensing and current switching 11 p1660 A66-23180  
 Black box analysis from input and output and estimation of subsystem switching by combination of differential approximation, quasi-linearization and dynamic programming technique 11 p1660 A66-23186  
 Automatic control systems, discussing optimal and on-line adaptive control in electricity, nuclear research, steel industry, numerical problems, etc 11 p1679 A66-23272  
 Stability and transient characteristics in single channel sinusoidal perturbation adaptive system 12 p1853 A66-24336  
 Communications satellite system efficiency enhanced by using automatic adaptive voice multiplexer in ground terminal equipment [AIAA PAPER 66-291] 12 p1822 A66-24761  
 Adaptive utilization of communication satellite systems optimizing dynamic traffic handling of combined ground and satellite communications complex, noting network configurations [AIAA PAPER 66-295] 12 p1822 A66-24764  
 Coupling impedance selection for Perceptron-like adaptive pattern recognition system 13 p2045 A66-25338  
 Equalization systems for stochastic processes, discussing automatic adaptive servocontrol, feedback control and vibration simulation equipment 13 p2048 A66-25848  
 Suboptimal control for system with random or deterministic input by frequency domain techniques, differential approximation and quasi-linearization 13 p2055 A66-26096  
 Adaptive on-off communication system for binary data transmission over noisy channel of unknown attenuation 19 p3302 A66-35709  
 On-line and off-line self-organizing control systems for space vehicle application 19 p3333 A66-36661  
 Markov chain hill-climbing scheme for probable fast-time learning absorbing model 19 p3333 A66-36663  
 Estimation method of learning time of time-varying threshold learning processes /TLP/ 19 p3333 A66-36664  
 Algorithm for learning without external supervision and application to learning control systems 19 p3333 A66-36666  
 Rapid parameter identification system for linear time-invariant plant with only input and output measurable 19 p3336 A66-36709  
 Parameter-plane method analysis of nonlinear equations of asymmetric oscillations in adaptive feedback control systems 19 p3338 A66-36740  
 Block diagram of closed loop automatic control system and conditional feedback control system, both with passive adaptation 20 p3536 A66-36883  
 Adaptive control system requirements for launch vehicles includes insensitivity to parameter variations and adjustability as function of measured feedback conditions 20 p3664 A66-38182  
 Mechanical prediction display to improve human behavior in control system 21 p3700 A66-38454  
 Adaptive telemetry applied to data compression, analyzing redundancy reduction, adaptive sampling, data reconstruction, etc 21 p3708 A66-39480  
**ADAPTIVE CONTROL SYSTEM**  
**SA SELF-ADAPTIVE SYSTEM**  
 Adaptive flight control system, using sampled data to identify aircraft parameter, for high performance aircraft 01 p0009 A66-10005  
 Characteristics of linear optimal systems whose performance criterion is defined by minimum of infinite integral of quadratic function of outputs and inputs of system 01 p0049 A66-10016  
 Adaptive coupler providing extended automatic glide slope beam following by compensating for beam convergence 01 p0101 A66-10036  
 Adaption of linear classifier without data repeating and behavior of classifier parameters 04 p0490 A66-13622  
 Redundant data omission for reducing



transmission bandwidth, associated noise vulnerability and optimum  
 prefiltering 04 p0490 A66-13623  
 Changing spectrum of input and output signals related to sensitive element in parametric circuit of adaptive system 04 p0504 A66-13974  
 Adaptive control system with reference model to achieve given performance 05 p0658 A66-15191  
 Optimal adaptive estimation of sampled stochastic process described by initially unknown parameter vector 06 p0865 A66-16740  
 Comparison of adaptive and nonadaptive control systems for lifting entry vehicles [AIAA PAPER 66-48] 06 p0960 A66-17100  
 Model reference adaptive control systems for calculating system variables of sinusoidal or ramp function input signals 08 p1199 A66-18672  
 Dynamic programming approach to nonparametric problem in calculus of variations 09 p1394 A66-20131  
 Automatic parameter tracking model for adaptive control system, using steepest descent procedure for adjusting parameters 09 p1362 A66-20611  
 Synthesis of adaptive control systems by function space methods 09 p1362 A66-20652  
 Property of identification as applied to adaptive control system 13 p2048 A66-25859  
 Components of gradient of performance criterion in adaptive control systems, employing correlation technique by use of time delay 13 p2051 A66-26067  
 Synthesis problem solution for performance criteria defined by time domain sensitivity function, noting controller structure, parametric minimization and operative adjustment of parameters 13 p2051 A66-26071  
 Adaptive servocontrol equalization system using true integrator instead of RC averager in feedback loop and memory circuit 14 p2267 A66-27664  
 Self-oscillations and stability of model reference adaptive systems with constant plant parameters and control response 15 p2476 A66-29991  
 Circuit selection and analysis of model reference nonscanning adaptive system for rapid response controlled plant 15 p2476 A66-29992  
 Energy feedback adaptive control system for elimination of effects of load inertia variations in servomechanisms 16 p2670 A66-30812  
 Model reference adaptive techniques applied to feedback attitude control system to minimize instrumentation 16 p2809 A66-30830  
 Statistical decision theory determination of parameter variations in closed-loop automatic adaptive control system 16 p2670 A66-30880  
 Design of adaptive systems with forced oscillations, using correlation and filter methods 17 p2902 A66-32573  
 Analog computer and logic circuitry combination for variable frequency signal production, noting application to adaptive control systems 18 p3089 A66-33561  
 Sensitivity methods in control theory - International Symposium on Sensitivity Analysis, Dubrovnik, Yugoslavia, August-September 1964 19 p3326 A66-36009  
 Sensitivity analysis and invariant imbedding, discussing application to adaptive control theory and reduction of boundary value problems to initial value problems 19 p3326 A66-36011  
 Doppler tracking loops for antenna array system adaptive to changes in signal and noise levels, maintaining constant SNR in tracking loop 19 p3321 A66-36413  
 Adaptive roll autopilot in air-to-air interceptor missile, noting application of dither principle, simulation results and noise rejection qualities 19 p3398 A66-36691  
 Model reference adaptive control system synthesis based on Liapunov direct method 19 p3335 A66-36698  
 Parameter adjustment model reference adaptive control of nuclear rocket engine, noting design parameters, system performance, propellant savings estimates and dynamic stability 19 p3398 A66-36699

Optimization of time dependent systems in dynamic programming, using forward and backward algorithm 19 p3391 A66-36700  
 Design synthesis of adaptive control system for linear discrete plants with time varying parameters, noisy measurements and statistical and deterministic disturbances 19 p3337 A66-36711  
 Coordinate control theory of self-adapting systems, considering problems of sensitivity, optimization and invariance 20 p3535 A66-36852  
 Experiments and model for adaptation of human controllers to sudden changes in plant dynamics in time-invariant situations 20 p3508 A66-36860  
 Simulation and analysis of adaptive roll autopilot for air to air missile, using limit cycle with small amplitude controlled by gain changing loop 20 p3595 A66-36865  
 Control algorithms synthesis for analytical adaptive control systems with nonlinear plants investigated with hybrid computer 20 p3536 A66-36876  
 General adaptive approach based upon minimizing moments of power density spectrum of system error in feedback control system 20 p3536 A66-36877  
 Parameter adaptation theory of quick-response self-adapting systems subject to parametric disturbance 20 p3536 A66-36884  
 Adaptive decoding technique for analyzing information-carrying signals in order to control signal to noise ratio during transmission time of single compound signal 20 p3522 A66-37384  
 Equations of motion of continuous single loop adaptive control system with scan modulated parameters, noting stability analysis method 24 p4188 A66-42479

## ADAPTIVE FILTER

Filter adapting to spectral density of incoming sampled signal, reconstructing continuous signal from samples 05 p0652 A66-14597  
 Structure of frequency filters in self-adaptive circuit 07 p1005 A66-17404  
 Simulation results of adaptive tracking filter application to stabilization of structural bending modes of SL-B launch vehicle 21 p3821 A66-38877  
 Time varying adaptive filter structure for providing minimum mean square estimate of signal in nonstationary channels for communications satellites 23 p4039 A66-41590  
 Fixed filter structures optimized according to criterion of minimizing average mean square error for nonstationary and statistical description of signals in noise 23 p4039 A66-41591

## ADDITIVE

SA ANTIOXIDANT  
 SA OIL ADDITIVE  
 SA PROPELLANT ADDITIVE  
 Cesium fluoride additive effect on emitter work function and power output of cesium diodes with various emitter materials 05 p0618 A66-15558  
 ADENOSINE MONOPHOSPHATE  
 Occurrence of adenosine monophosphate inhibition of carbon dioxide fixation photosynthetic and chemosynthetic autotrophs 18 p3056 A66-33697  
 ADENOSINE TRIPHOSPHATE /ATP/  
 Ribonucleoside triphosphatase in rabbit reticulocytes, discussing distribution in extracts, behavior in purification of amino acid and properties 17 p2859 A66-32553

## ADHESION

SA BONDING  
 Structural metal adhesion in space environment as affected by time, pressure and temperature 13 p2108 A66-25646  
 Time, pressure and temperature effects on adhesion of structural metals in vacuum and space environment 14 p2316 A66-28005  
 Surface area and condition and effect on adhesion of aluminum plates 14 p2304 A66-28206  
 Nature of forces causing adhesion of coatings produced by plasma jet sputtering techniques 15 p2505 A66-28752  
 Vacuum coating techniques for thin film layers for bonding, examining adhesion, bonding layer reinforcement and surface oxidation 23 p4043 A66-41194  
 Welding and adhesion techniques in aircraft and space vehicle construction -

Conference, Hanover, West Germany, May 1966 23 p4073 A66-41530

Adhesion force of silicates in ultrahigh vacuum as function of load force, temperature, surface roughness and crystal orientation 23 p4131 A66-41848

## ADHESIVE

Strength of adhesive joints showing ratio of normal and shear stress as important parameter, using crack propagation theory 01 p0152 A66-10380  
 Improvement of mechanical properties of structural adhesives and composite materials at cryogenic temperatures 12 p1899 A66-24385  
 Adhesives and sealants in electronics, discussing resin elastomers, epoxies, polyurethanes, polysulfides, outgassing, damping, radiation effects, etc 14 p2318 A66-27103  
 Strength of adhesive-bonded lap joints as affected by changes in temperature and fatigue 14 p2401 A66-27772  
 High temperature insulating adhesives for vacuum applications tested, including outgassing rate, mass spectra of evolved gases, electrical and mechanical properties 17 p2942 A66-31980  
 Rate of setting of adhesive joints in relation to differential thermal contraction of adhesive polymers relative to metal adherend 17 p3019 A66-31986  
 Adhesive bonding of aluminum structures including aircraft and space applications 17 p3023 A66-32266  
 Thermoconductivity, mechanical stress, processing characteristics, etc, of various adhesives used in integrated circuits, noting neoprene cement 18 p3077 A66-34051  
 Nondestructive testing of adhesive bonded structures using ultrasonic-resonant instrument, noting detection of voids and cohesive strength determination 19 p3362 A66-35329  
 Very rapid-curing capsular adhesive developed for use in astronaut-to-space vehicle attachment device 19 p3363 A66-35949  
 Testing of adhesive bonding at high temperatures for use in reentry vehicles, using IR energy on specimen preloaded in shear [ASME PAPER 66-MD-38] 21 p3742 A66-38488  
 Surface treatment of joints for structural adhesive bonding design, material selection and metal surface processing for adhesion [ASME PAPER 66-MD-39] 21 p3742 A66-38489  
 Adhesive performance testing, noting mechanical methods and types of test specimens [ASME PAPER 66-MD-46] 21 p3742 A66-38492  
 Adhesives and joining processes in mechanical quality control 21 p3745 A66-39465  
 Adhesively bonded joints withstand severe thermal shock and have excellent bonding with high strength structural alloys in cryogenic liquids 22 p3937 A66-39778  
 Polybenzimidazole adhesives properties suitable for bonding metals 22 p3926 A66-40275  
 Polybenzimidazole adhesive properties for structural bonding as affected by processing parameters 22 p3937 A66-40276  
 High temperature adhesive properties of epoxy, epoxy-phenolic, polybenzimidazole and polyimide 22 p3937 A66-40278  
 Polyaromatic adhesives for temperature resistant sandwich construction in lap-shear strength and preliminary sandwich evaluations 22 p3926 A66-40279  
 Adhesive strength cured by integrated resistance heaters compared with autoclave and/or press bonding 22 p3926 A66-40280  
 Adhesive and bonding techniques evolution for general and specific use in aircraft and aerospace industry, noting elastomeric and ceramic adhesives 22 p3928 A66-40418  
 Metal adhesives in aircraft and space industry, particularly in construction of laminar and sandwich elements of wings 23 p4073 A66-41532  
 Welding and gluing of third stage of ELDO-A rocket 23 p4073 A66-41533

## ADIABATIC EQUATION

Adiabatic heating and temperature



recovery factor of tubes carrying liquids of high Prandtl number 01 p0165 A66-10905  
 Bogoliubov adiabatic hypothesis in quasi-linear theory of plasma 01 p0115 A66-11088  
 Hydrodynamic equations for one-dimensional, adiabatic, frictionless, ideal-gas flow and general matrix form equations for coupled chemical reaction kinetics of C-H-O/N systems 02 p0303 A66-11533  
 Adiabatic motion determination of charged particle containment in combined mirror-multipole cusp magnetic fields 05 p0718 A66-14712  
 Transient behavior of heated stellar atmosphere, examining unsteady flow caused by sudden application of heat to static adiabatic atmosphere 08 p1286 A66-18541  
 Adiabatic laminar flow in concentric sleeve seal where rotating shaft changes fluid temperature and viscosity  
 ASLE PREPRINT 65AM 4C3]  
 Nonisentropic simple waves in two-dimensional steady flow of ideal gas 08 p1210 A66-19585  
 Scalar formulation of ideal charged adiabatic gas flow in presence of gravitational and electromagnetic fields 10 p1524 A66-21814  
 Positron-helium scattering below positronium threshold, using adiabatic method previously tested in positron hydrogen scattering, presenting phase shifts and momentum transfer cross section computations 13 p2134 A66-26262  
 Violation of second and third adiabatic invariants, examining mirror point change of trapped particles under displacement of guiding centers along force-lines and particle diffusion 13 p2176 A66-26356  
 Adiabatic dispersion into empty space of coaxial gaseous ellipsoid studied by Tsianikov exact solution of equations of gasdynamics 14 p2278 A66-28060  
 Adiabatic compression device for plasmas containing hot ions 14 p2348 A66-28312  
 Characteristic for partially invariant solutions of hydrodynamic equations, specifically adiabatic plane-parallel gas motion 15 p2478 A66-29177  
 Adiabatic invariants and third integrals of motion in periodic potentials in periodically time-dependent Hamiltonian systems of n degrees of freedom 17 p2945 A66-32292  
 Pulsation properties of stellar models representing RR Lyrae stars obtained, using adiabatic and nonadiabatic linearized pulsation equations 20 p3652 A66-37613  
 Adiabatic theory of charged particle motion, considering first-order effects in radius of gyration and Alfvén theory 20 p3603 A66-38303  
 Adiabatic exponents in equations for gas boiling by vaporization 21 p3835 A66-38905  
 Hydraulic analogy methods for simulation of internal gas flows containing combination one 22 p3901 A66-40500  
 Adiabatic motion of auroral particles in model of electric and magnetic fields surrounding Earth, commenting on importance of higher order terms in asymptotic expansion 22 p3914 A66-40561  
 Adiabatic gas flow pattern in plane parallel channel near critical point 22 p3902 A66-40815  
 Adiabatic equation of state for homogeneous compressible anisotropic plasma wave equation invalid for homogeneous case 24 p4243 A66-42639  
 Adiabatic theory and lowest order invariants applied to Van Allen radiation indicate that without collisions particles could remain in geomagnetic field 24 p4240 A66-43110  
 MITTANCE  
 ELECTRIC IMPEDANCE  
 ADRENAL GLAND  
 Electrophysiological study of pituitary-adrenal axis activation during rapid eye movement /REMS/ in human urology patients 17 p2859 A66-32305  
 Correlation of adrenal steroids and alpha frequency in EEG 17 p2860 A66-32556  
 ADRENAL METABOLISM  
 Adaptive responses of adrenal cortex to some environmental stressors, exercise and acceleration 17 p2862 A66-33093

ADRENALINE  
 S EPINEPHRINE  
 ADRENERGICS  
 Performance and physiological effects of adrenalin or insulin in human subjects 06 p0813 A66-16829  
 ADRENOCORTICOTROPIN /ACTH/  
 Adrenocorticotrophin-releasing hormone appears in peripheral blood of rats under physiological stress, noting role of pituitary gland 14 p2228 A66-27811  
 Metabolic correlates of glucocorticoid induction of enzymes in man studied in terms of ACTH induced changes in tryptophan turnover along inducible pathways 24 p4166 A66-43168  
 ADSORPTION  
 Quantum theoretic probability of trapping inert gas atom on solid surface with linear lattice 01 p0108 A66-10634  
 Spectral emissivity calculations for parallel bands of carbon dioxide at 4.3 microns between 150-600 degrees K, comparing experimental measurements with theoretical calculations 03 p0393 A66-13104  
 Gas phase nonideality and mean column pressure effects on sample retention in gas-solid partition chromatographic systems with real carrier gases 04 p0472 A66-13396  
 Adsorption at semiconductor and gel surfaces discussing chemisorption theory, ionizing radiation effect and structural parameters 04 p0563 A66-13768  
 Ultrapurification discussing definition, purification techniques, analytical techniques /e.g. emission and mass spectroscopy/ and role in biochemistry, metals and materials 04 p0474 A66-13867  
 Erected dipole model of adsorbed layer in fluorinated molybdenum filaments exposed to cesium vapor 05 p0737 A66-14986  
 Gas adsorption on molecular sieves, discussing separation caused by electrostatic forces and electric fields 06 p0819 A66-16730  
 Heat capacity of adsorbed He 3 films at temperatures from 0.1 to 4 degrees K, with adsorption surfaces made of monolayers of argon preadsorbed on copper 09 p1392 A66-20020  
 Low-energy electron diffraction studies adsorption of cesium on Si /111/ 10 p1576 A66-21551  
 Germanium dioxide surface adsorption characteristics with respect to water vapor 10 p1583 A66-21983  
 Adsorption of CO radicals on three types of magnesium oxide using EPR techniques, noting spectrum of adsorbed radical, bonding, etc 12 p1916 A66-23619  
 Nitrogen adsorption effect on thermionic emission from polycrystalline tungsten ribbon at high and low applied fields, explaining work function changes 13 p2162 A66-25381  
 Adsorptive phenomena effect on reaction kinetics of electrochemical oxidation involving organic materials on platinum electrode 13 p2017 A66-25676  
 Elutration diagrams in determination of adsorption enthalpies from temperature dependence of retention volume in band maximum 14 p2232 A66-27604  
 Electrostatic theory of physical adsorption applied to gas-solid chromatography, discussing chromatographic inseparability of argon and oxygen at room temperature, prediction of elution order of many gases, etc 16 p2646 A66-30646  
 Thermionic and adsorptive properties of zirconium nitride in cesium vapor, determining current-voltage characteristics and temperature dependence 16 p2755 A66-31732  
 Gas sorption and desorption processes at low pressures, discussing molecular adherence to cold solid surfaces, adsorption mechanism of isotherms, vacuum generation via cryotrapping effect, etc 20 p3605 A66-38088  
 Thermal accommodation coefficients of He on tungsten and hydrogen on hydrogen-covered tungsten at temperatures of 325, 403 and 473 degrees K 23 p4033 A66-42078  
 ADVANCED ORBITING SOLAR OBSERVATORY /AOSO/  
 S AOSO

ADVANCED RANGE INSTRUMENTATION  
 SHIP /ARIS/  
 Calibration of ARIS /Advanced Range Instrumentation Ships/ radars for cross section measurements 04 p0479 A66-13611  
 ADVECTION  
 Short-range forecasting of stratified cloudiness, noting linear dependence between variations in dew point and air temperature near Earth surface for aperiodic processes 16 p2742 A66-30791  
 Wind distribution in atmospheric boundary layer under conditions of advection from pilot balloon observations 20 p3594 A66-38376  
 AE-A  
 S EXPLORER XVII SATELLITE  
 AERIAL PHOTOGRAPHY  
 SA PHOTOGRAMMETRY  
 Structural character of modern black and white aerial photography films and relation to image definition 01 p0068 A66-10694  
 Method for computing base of aerial photograph and maximum altitude for desired resolution 01 p0068 A66-10695  
 Photometric system for measuring linear and angular vibration of aerial photography apparatus 01 p0068 A66-10696  
 Image motion and corresponding loss of resolution from rotational motions of airborne vehicle and camera parameters 02 p0228 A66-11381  
 Multistrip transformation of aerial photographs of mountainous regions to obtain scale maps 02 p0229 A66-11696  
 Multistrip transformation of aerial photographs using rigid special masking frames in accordance with contour line 02 p0231 A66-11971  
 Determination of contrast range of optical images obtained in aerial camera as function of atmospheric and optical factors 03 p0368 A66-12504  
 Operation and uses of triode-based electronic control device for pulse aerial cameras 03 p0368 A66-12505  
 Commercial aerial camera objectives estimated with TsNIIGAIK electron-optical bench 04 p0519 A66-13662  
 Stereometrograph for photographing relief and contours in compilation of topographical charts from vertical aerial photographs 04 p0519 A66-13663  
 Book on French aerial photography, emphasizing methodology rather than reproduction of samples 04 p0523 A66-14380  
 Airborne albedo measurements of ice in Ross Sea, Antarctica, for various solar elevations and altitudes 05 p0669 A66-14937  
 Airborne albedo measurements of various representative underlying surfaces in Antarctica 05 p0669 A66-14938  
 Renovation techniques for topographic maps 06 p0879 A66-16325  
 Color spectrozonal photography used in plotting topographic maps 06 p0881 A66-16752  
 Aerial photography in geology, climatology and urban development 06 p0882 A66-16937  
 Criteria for quality of aerial camera systems including allowances for ground scene properties, photographic grain and human observer, noting role of resolving power and transfer function 07 p1035 A66-18154  
 Combination of geometrical and physical optics with modern system design such as computers, cameras for aerial use, space tracking, etc 09 p1403 A66-20918  
 Large-scale aerial photographs applied to cartography by taking pictures of same area at varying scales 10 p1534 A66-21132  
 Electronic color correction during aerial photograph printing by employing specially programmed computer 10 p1534 A66-21329  
 Hyperaltitude photography, applications and advantages 10 p1535 A66-21523  
 Earth atlas based on high altitude photography, Nimbus and IR imagery and high altitude radar imagery 10 p1532 A66-21527  
 Mutual orientation of oblique aerial photographs at nadir distance greater than 50 degrees for simultaneous rotation of y and z axes of universal autograph 10 p1536 A66-21800  
 Precise airborne geodetic survey system capable of measuring lines up to 900 nautical miles and determining nadir of aerial photographs to 24



ft 10 p1533 A66-22045  
 Mechanical swivel arm that can be used with several types of reflecting stereoscopes for inspecting aerial photographs 11 p1705 A66-22661  
 Flight and navigation procedures and requirements for civil aerial photography 11 p1705 A66-22662  
 Image movement from aircraft velocity for vertical and oblique panoramic cameras 13 p2078 A66-25605  
 Reflector-light source requirements for homogeneous format illumination in night aerial photography 13 p2081 A66-26005  
 Spatial distribution of four cloud fields studied by photometry of aerial photographs, determining statistical parameters 14 p2325 A66-27537  
 Distinct separation of colors on aerial landscape photography 14 p2295 A66-27654  
 Structural character of modern black and white aerial photography films and relation to image definition 15 p2497 A66-28555  
 Method for computing base of aerial photograph and maximum altitude for desired resolution 15 p2497 A66-28556  
 Photometric system for measuring linear and angular vibration of aerial photography apparatus 15 p2497 A66-28557  
 Aerial photograph interpretation of landscape in terms of tone, texture and stereo effect 15 p2500 A66-28967  
 Soviet papers on theory and practice of interpretation of aerial photographs 15 p2503 A66-30004  
 Improvement of negative quality of aerial photographs 15 p2504 A66-30005  
 Spectral brightness of haze and effect on interpretation of aerial photographs 15 p2504 A66-30006  
 Aerial photograph interpretation theory including detection, recognition and interpretation of object on photograph 15 p2504 A66-30007  
 Stereoscopes for aerial photograph interpretation 15 p2504 A66-30009  
 Spectrometric analysis of aerial photograph, using computers 15 p2504 A66-30010  
 Topographic interpretation of aerial photographs 15 p2504 A66-30011  
 Aerial photograph interpretation for sparsely populated regions 15 p2505 A66-30012  
 Landscape interpretation of aerial photographs 15 p2505 A66-30013  
 Soil investigation and geological map preparation from aerial photographs 15 p2505 A66-30014  
 Interpretation of vegetation types from aerial photographs 15 p2505 A66-30015  
 Military aerial mapping program, noting camera lens distortion, shutter, stabilization, films, etc 16 p2703 A66-30511  
 Evaluation of nonstereoscopic pairs of photographs obtained from vertical base by moving camera, determining spatial coordinates of points on photographs 16 p2703 A66-30512  
 Computational photogrammetry, deriving relation between image and object space, using collinearity conditions and orientation matrix 16 p2703 A66-30513  
 Geometrical quality of elements of exterior orientation after double and single point resection in space, noting position determining characteristics of linear and angular parameters 16 p2704 A66-30515  
 Multisensor airborne reconnaissance mission planning and data acquisition 16 p2704 A66-30516  
 Aerial photography of Earth surface, discussing application in Earth and life sciences 17 p2925 A66-32609  
 Integrated elements for aerial surveying and mapping 18 p3109 A66-33739  
 Screening tests to predict potential ability of persons to be trained as aerial photo interpreters 18 p3061 A66-33744  
 Aerial image reproduction on Lith type and extreme resolution emulsions, noting experimental results on sharpness, line width changes and methods of testing with photomicrography 19 p3353 A66-35315  
 Field determination of coordinates of points of mountainous terrain from aerial photographs with known elements of external orientation 19 p3353 A66-35363

Solar altitude relationship to scene luminance for aerial photographs determined by photographic photometry 19 p3358 A66-35816  
 Photogrammetric network for large-area phototriangulation using star-tracking airborne cameras, discussing theoretical and technical aspects 20 p3551 A66-37472  
 Airborne electronic command device for measuring time intervals corresponding to cruising speed/ true flight altitude ratios up to 40 21 p3735 A66-38569  
 Colored spectrozonal aerial photographs in topographic decoding of photographs of wooded regions 21 p3735 A66-38570  
 Distortions in aerial photographs due to errors in cameras, noting determination methods in various countries 22 p3919 A66-40622  
 Spatial distribution of four cloud fields studied by photometry of aerial photographs, determining statistical parameters 24 p4233 A66-42323

## AERIAL RECONNAISSANCE

Analytical aerial triangulation noting accuracy of photographs, stereocomparator, etc 02 p0229 A66-11695  
 Canadian photogrammetry for analytical aerial triangulation, using mathematical model and matrix 04 p0516 A66-13898  
 Aerial observation of sea surface, measuring wind direction, speed, wave direction and period of Gulf Stream along coast 10 p1532 A66-21524  
 Near-real time acquisition of aerial reconnaissance radar imagery from continuously moving and static displays 12 p1808 A66-23921  
 Automatic target recognition, discussing machine analysis problems of aerial reconnaissance data 13 p2124 A66-25657  
 Earth surfaces reflecting and polarizing properties in aerial reconnaissance 17 p2918 A66-32611

## AEROBEE ROCKET

Solar X-ray photographs, describing Aerobee rocket mounted telescope using grazing incidence optics 05 p0763 A66-15289  
 Plasma sheath effects on antenna impedance probe and retarding potential probe installed on two Aerobee 150 rockets 08 p1181 A66-18746  
 Night sky sources for soft X-rays, examining data obtained by Aerobee 4.70 detectors 10 p1598 A66-21102  
 Aerobee rocket measurements of cosmic X-ray sources emanating from Cygnus A, M-87 and galactic supernova remnant Cassiopeia A 13 p2174 A66-25836  
 X-ray emission from Sco X-1 and Crab Nebula sources observed with Aerobee 150 18 p3186 A66-34157  
 Aerobee rocket instrumentation and rocket sounding techniques for investigating far UV auroral emission 20 p3552 A66-37594  
 Particulate contamination control of ultraclean collecting surface for extraterrestrial matter in Aerobee 150 22 p3922 A66-40041  
 Aerobee rocket preliminary tests and FR-1 project 22 p3986 A66-40160  
 FR-1 satellite contact with surrounding plasma ensured by cathode device tested on Aerobee rocket 22 p3876 A66-40163

## AERODYNAMIC CHARACTERISTICS

## SA LATERAL STABILITY AND

## CONTROL

## SA LONGITUDINAL STABILITY AND

## CONTROL

## SA STATIC AERODYNAMIC

## CHARACTERISTICS

Air data equipment trends in subsonic and supersonic control 01 p0033 A66-10680  
 Stopped and slow rotor aircraft configuration for fundamental limitations on forward flight speed of compound helicopters [SAE PAPER 650806] 01 p0012 A66-10847  
 Variable sweepback wing determination of pivot position influence on aerodynamic characteristics while wing is turning, deducing lift and thrust center laws [ONERA TP 272] 02 p0175 A66-11680  
 Aerodynamic characteristics of blower in form of propeller with rim 03 p0314 A66-12536  
 Wind tunnel research of deep stall

aerodynamic characteristics of T tail analyzed as preliminary design guide [AIAA PAPER 65-737] 03 p0317 A66-12547  
 Measured aerodynamic characteristics of cone-cylinder-cone model using magnetic balance system, discussing techniques, errors and data 03 p0315 A66-12773  
 Aerodynamic spacecraft deceleration systems examined by hydraulic analogy, noting Mach number effects on flow disturbances 04 p0507 A66-13533  
 Effect of incompressible fluid flow boundaries on unsteady aerodynamic properties of thin curved profile undergoing small amplitude oscillations 04 p0454 A66-13574  
 Extremal problems in aerodynamics, discussing mathematical and physical models for optimum aerodynamic shape 04 p0455 A66-13995  
 Volterra integral applied to steady supersonic flow past annular wings of various configurations to determine aerodynamic characteristics 04 p0455 A66-14139  
 Aerodynamic characteristics of flat rectangular plate placed normal to flow of highly rarefied gas 04 p0456 A66-14141  
 Aerodynamic characteristics of fixed-geometry double delta wing SST, noting low speed handling improvement due to vortex flow [AIAA PAPER 64-591] 05 p0610 A66-15069  
 Static elastic deformation and associated change of aerodynamic characteristics of flight vehicle subject to aerodynamic and inertia loading 05 p0609 A66-15784  
 Laminar profile characteristics affected by wind tunnel flow turbulence 07 p1018 A66-17857  
 Aerodynamic and heat transfer characteristics of cross-stream wedge in low density aerodynamics, investigating transition from continuum to free molecular flow 07 p0982 A66-18126  
 Numerical computer solutions for several nonlinear gas flow problems in high speed aerodynamics 07 p0983 A66-18143  
 Aerodynamic characteristics of wakes behind hypervelocity bodies [AIAA PAPER 66-53] 08 p1162 A66-18952  
 Peculiarities of aerodynamic characteristics of flow past plate and pointed and blunt slender cones in viscous hypersonic thermodynamically ideal gas 08 p1165 A66-19571  
 Book on thin wing and aerodynamic characteristics in subsonic gas flow 09 p1327 A66-19975  
 Aerodynamic characteristics of arbitrary slender reentry bodies predicted by conformal mapping method 10 p1481 A66-21942  
 Hypersonic wind tunnel measurements to Mach 17 of aerodynamic characteristics of family of hypersonic gliders [ONERA TP 331] 11 p1635 A66-23198  
 Working section size and shape for V/STOL wind tunnels, emphasizing wall effect magnitude limitation, aircraft aerodynamic and propulsion system characteristics 12 p1857 A66-23657  
 Aerodynamic characteristics of shape, constructed by current surfaces of supersonic flows past cones, noting lengthwise variation of cross sections 12 p1798 A66-24431  
 Aerodynamic characteristics of rectangular plates in hypersonic flow of rarefied gas: differing in aspect ratio, thickness and angles of attack, determining maximum lift drag ratio 12 p1798 A66-24444  
 Effect of gap between wing tip and end plates for wing with minimum induced resistance and unrestrained end plates showing aerodynamic characteristics differences between these wings and wing without gaps 13 p1989 A66-25007  
 Three-dimensional plane shock wave intersection in space, noting parameter range for which two solutions exist 13 p1991 A66-2563  
 Double-delta supersonic air transport low speed operational characteristics, noting wind tunnel tests and design parameters 13 p1991 A66-2576  
 ONERA laboratory weightlessness simulation tests on liquids, accelerometers



- aerodynamic braking, etc 13 p2058 A66-26371  
Subsonic business aircraft manufacturing processes and techniques relation to production time and costs [SAE PAPER 660206] 13 p2087 A66-26395  
Aerodynamic characteristics of NAL-16 research rocket of Japan, noting results from transonic and supersonic wind tunnel tests 14 p2220 A66-27670  
Unsteady aerodynamic characteristics of model helicopter rotor operating in vortex ring state, considering thrust and torque fluctuation 16 p2634 A66-31322  
Unsteady aerodynamics of tandem rotor operating in vortex ring 17 p2840 A66-32744  
Vortice effects on aerodynamic characteristics of aircraft and missiles 17 p2841 A66-33081  
Measurement method for aerodynamic damping of helicopter rotors in forward flight 18 p3047 A66-33684  
Aerodynamic pressure on deformable, oscillating and rigid wing surfaces in subsonic flow 18 p3049 A66-34733  
Aerodynamic design criteria for maintaining laminar flow control including instability limit, surface roughness, acoustical environment, etc 18 p3050 A66-34951  
Approximate and characteristic methods to predict effect of gas composition on forces and static stability of planetary entry configurations in air and assumed Martian atmospheres [AIAA PAPER 65-318] 19 p3275 A66-35605  
Wind tunnel research of deep stall aerodynamic characteristics of T tail analyzed as preliminary design guide [AIAA PAPER 65-737] 19 p3280 A66-36491  
Book on aeromechanics of flight vehicles including structure and physical properties of atmosphere, wing characteristics, research methods, aerodynamic characteristics of principal units of aircraft and rockets, etc 21 p3695 A66-39288  
Aerodynamic breakup of liquid drops in flow behind plane shock wave analyzed via high speed photography, noting experimental setup, parameter variation, etc 22 p3899 A66-40198  
Dynamic stability and aerodynamic damping derivative of Apollo launch escape vehicle, using wind tunnel tests [AIAA PAPER 66-770] 22 p3895 A66-40651  
Aerodynamic analysis of complex shapes in hypersonic flow, using digital computer [ICAS PAPER 66-25] 22 p3847 A66-40665  
Supersonic aerodynamic problem of wing-body interaction and solution within lifting-surface theory, using analog method [ICAS PAPER 66-22] 23 p4008 A66-41254  
Annular vortices method applied to determine aerodynamic characteristics of lifting propeller in axial and oblique flows 23 p4010 A66-41785  
**AERODYNAMIC COEFFICIENT**  
**SA LIFT COEFFICIENT**  
Measurements of three coefficients for rectangular, trapezoidal, sweptback, triangular and parabolic wings in subsonic and supersonic flow 07 p0979 A66-17480  
Viscous aerodynamic contributions to forces and moments on front face of blunt lifting reentry vehicle in producing trajectory error [AIAA PAPER 66-464] 16 p2631 A66-31471  
Optimal stochastic control system with control of linear plants approximating characteristics of airframes, allowing plant parameters to vary randomly 19 p3329 A66-36030  
Fluid dynamic fields around slender rotating bodies, discussing simple theories for evaluating aerodynamic coefficients 20 p3492 A66-37431  
Downwash corrections for wings with arbitrary sweepback in open and closed circular wind tunnels with base plate 21 p3694 A66-38936  
Aerodynamic coefficients of large-aspect-ratio fan-in-wing airfoil, noting that velocity field consists of inflow to fan, parallel flow and circulation flow 24 p4158 A66-43050  
**AERODYNAMIC DRAG**  
**AERODYNAMIC FORCE**  
Nonmathematical notes on propeller whirl flutter 02 p0300 A66-11993  
Aerodynamic damping effect on cascading double circular arc blades vibrating in transitory mode 03 p0313 A66-12397  
Pressure distributions on cambered bodies of arbitrary cross section at angle of attack applied to transport fuselage afterbody design [AIAA PAPER 65-718] 03 p0314 A66-12543  
Integration of propulsion systems with airframe, emphasizing aerodynamic lift and drag 05 p0605 A66-14934  
Pressure distribution on oscillating two-dimensional symmetric airfoil in incompressible flow, examining trailing edge angle influence 07 p0982 A66-18133  
Aerodynamic penetration and radius in drag and lift during atmospheric entry process [AIAA PAPER 66-16] 07 p0983 A66-18447  
Cross flow relation to force distribution on circular cylinders curved in plane containing wind vector at subcritical Reynolds number 09 p1328 A66-20746  
Nonstationary supersonic flow in near sonic range, calculating pressure distribution in oscillating profile 09 p1328 A66-20875  
Reentry orbits for manned spacecraft using aerodynamic lift and drag forces for reentry 10 p1606 A66-21264  
Effects on man of direct /escape/ and indirect /aircraft flight/ movement through atmosphere, considering moderate and high-speed aerodynamic forces 10 p1488 A66-22106  
Aerodynamic torque effect on UK-3 satellite precession rate 11 p1777 A66-22966  
Aerodynamics of heavily loaded wing, discussing relation of longitudinal shear before and after deformation of vortex street 11 p1635 A66-23170  
Aerodynamic forces on system of N thin slightly twisted profiles in subsonic unsteady flow for small angle of attack, examining acoustic resonance for arbitrary small harmonic oscillations 12 p1798 A66-24436  
Satellite orbit plane change by external burning aerocruise [AIAA PAPER 65-21] 12 p1954 A66-24695  
Airfoil equilibrium stability under elastic force and uniform wind action 13 p2062 A66-25402  
Mathematical and numerical determinations of aerodynamic forces on harmonically oscillating cylindrical shell under subsonic and supersonic speeds and comparison with slender body theory results 14 p2218 A66-27405  
Aerodynamic forces acting on harmonically oscillating thin profile in stalled plane parallel flow of ideal incompressible fluid 14 p2220 A66-27695  
Potential complex and forces in perfect incompressible fluid at rest at infinity with free vortices determined by pointless profiles excited by arbitrary motion 15 p2479 A66-29637  
Solar environment and aerodynamic drag effect on deflection of structural booms in space [AIAA PAPER 66-502] 16 p2821 A66-31478  
Newtonian formulas for determining pitch and roll and normal force derivatives for various types of conical and spherical bodies 17 p2838 A66-32333  
Aerodynamic forces acting on wings with braking flaps 19 p3275 A66-35365  
Theoretical nonlinear method for calculating aerodynamic forces on low-aspect-ratio wings at high angles of attack and wide range of Mach numbers 20 p3491 A66-36907  
Integration technique for determining unsteady aerodynamic forces at subsonic speeds, noting role of kernel of integral equation 20 p3491 A66-36955  
Book on aerodynamic experiment in machine building, noting self-simulation problems of machines using gas dynamics, analyzing wind tunnels 21 p3694 A66-38743  
Gyrator shape with minimum aerodynamic resistance, discussing cases with constant and varying moment of inertia 21 p3739 A66-39327  
Aerodynamic resistance of cylindrical rotor determined, using method based on formulas for resistance factors of cylindrical surfaces and rotor encasement 21 p3739 A66-39328  
Oblique shock wave formal determination of aerodynamic forces and pressure distribution on delta wings in supersonic or moderately hypersonic flow 21 p3695 A66-39602  
Aerodynamic problem of steady potential flow and added mass in unsteady motion of idealized hemispherical parachute 22 p3845 A66-40591  
Shock tunnel external burning experiments to investigate effects of reactive fuel injection into air stream flowing around body [AIAA PAPER 66-744] 22 p3893 A66-40631  
Free flight model technique in hypervelocity shock tunnel for aerodynamic force and moment measurement by optical instrumentation [AIAA PAPER 66-771] 22 p3847 A66-40652  
Total aerodynamic forces and moments of free flying body in wind tunnel determined from accelerations measured and telemetered by onboard instruments [AIAA PAPER 66-775] 22 p3896 A66-40655  
Side forces and moments on Tomahawk sounding rocket with and without spin at high Reynolds number and Mach 5 [AIAA PAPER 66-754] 23 p4008 A66-41329  
Unsteady supersonic gas flow around lattice of thinly curved plates for calculation of aerodynamic forces and moments acting on oscillating profile 23 p4009 A66-41722  
Displacement detector to provide direct measurement of shear forces in aerodynamics on small surface elements in hotshot wind tunnels 24 p4207 A66-42169  
Piezoelectric balance for aerodynamic force measurements in hypersonic shock tunnel, discussing design, calibration and performance characteristics 24 p4190 A66-42174  
Simultaneous FM telemetry measurement of four aerodynamic forces acting on free flying models in wind tunnel 24 p4209 A66-42190  
**AERODYNAMIC HEAT TRANSFER**  
Equilibrium radiative transport properties of high temperature air coupled with aerodynamic flow field generated by planetary reentry vehicles 01 p0163 A66-10784  
Aerodynamic properties of simple bodies in hypersonic transition regime 08 p1164 A66-19132  
**AERODYNAMIC HEATING**  
**SA AEROTHERMOELASTICITY**  
Theoretical and experimental work in flow field analysis has enhanced ability to predict aerodynamic heating in atmospheric entry 01 p0143 A66-10800  
Preliminary design for optimum combination of insulating and structural materials for hypersonic cruise vehicles 03 p0436 A66-12752  
Glider reentry descent trajectories from near Earth orbit calculated, emphasizing landing accuracy and mechanical and thermal stresses 04 p0584 A66-13525  
Aerodynamic analysis of vapor pressure of tektite glass and bearing on atmosphere entry trajectories of tektites 12 p1952 A66-24895  
Aerodynamic heating of vehicles entering Earth atmosphere at hypersonic speed, noting blunt body concept, radiative and convective heating, heat shield weights, etc 13 p1989 A66-25153  
Aerodynamic heating of ferrous Santa Catharina meteorite 14 p2381 A66-27350  
Thermal model for performance of cork insulation on Minuteman missile in launch environment [AIAA PAPER 65-117] 16 p2827 A66-30893  
Measuring aerodynamic heating of wind-tunnel models by temperature sensitive paint, noting ambient pressure effect 16 p2682 A66-30916  
Stagnation region for body of revolution in analyzing temperature, velocity and atom hypersonic flow with low Reynolds number, concentration under aerodynamic heating 16 p2686 A66-31037  
Gap size effect on pressure and aerodynamic heating over flap of blunt delta wing in hypersonic flow [AIAA PAPER 66-408] 17 p2840 A66-32747  
Australites, external form and structure, describing specific gravity value variation



with size, effect of aerodynamic heating upon atmospheric entry, etc 17 p3007 A66-33288

Prediction characteristics of separated turbulent boundary layers in compression corners used to determine aerodynamic heating distributions and dynamic loading of supersonic vehicles 21 p3724 A66-38730

**AERODYNAMIC LIFT**  
S LIFT

**AERODYNAMIC LOAD**  
SA GUST LOAD

Capability of Cornell Aeronautical Laboratory /CAL/ system for measuring dynamic airloads in wind tunnel [AIAA PAPER 66-15] 06 p0803 A66-17091

Airflow interference theory applied to streamlined wings and bodies undergoing simple harmonic oscillations 07 p0981 A66-18102

Aerodynamic pressure and resistance calculated from gas flow past circular cylinders with piecewise constant diameters 08 p1232 A66-19338

Modified strip analysis method for predicting finite-span, swept or unswept wing flutter at subsonic to hypersonic speeds 09 p1328 A66-20738

Design of control deflections and structural loads of space vehicle for flight stability through atmospheric disturbances [AIAA PAPER 66-350] 12 p1954 A66-24487

Linearized surface pressure distribution on streamlined ducted bodies in axisymmetric flow, considering aerodynamic loading on annular airfoil 13 p1993 A66-26716

Nonstationary aerodynamic load for harmonically oscillating body in fluid flow with constant mean velocity measured, determining errors as functions of system parameters 16 p2630 A66-31302

Aerodynamic and thermal criteria in structural design of aircraft and missiles 20 p3628 A66-37393

Aeroelastic effects due to changes in aerodynamic gain, load factor and structural stresses relative to infinitely stiffened structure in multistage slender missiles 20 p3666 A66-37430

Subsonic aerodynamic loading on harmonically oscillating nonplanar lifting surfaces in kernel-function formulation 21 p3694 A66-38733

Erosion destruction mechanism in polycrystalline graphite, noting effect of gas flow over surfaces, flow pulsation frequency and generated aerodynamic loads 21 p3754 A66-38957

Low speed aerodynamic loading on finite-bladed ducted propeller at zero incidence 22 p3844 A66-40394

Loads on bodies in wakes resulting from crossflow at submerged body or from wake translation over submerged body, noting dynamic instability 22 p3846 A66-40607

Capability of Cornell Aeronautical Laboratory /CAL/ system for measuring dynamic airloads in wind tunnel [AIAA PAPER 66-15] 23 p4051 A66-40977

**AERODYNAMIC NOISE**

Boundary layer noise and effects of acoustic energy on panel response, panel fatigue and internal sound levels tested with X-15 aircraft 01 p0010 A66-10126

Noise problem associated with rocket boosters, possible minimization by radical change of design 02 p0293 A66-11511

Aerodynamically induced vibration in coolers, describing inclined splitter plates for noise and structural vibration elimination 07 p0991 A66-17492

Aerodynamically induced resonance in rectangular cavities resulting from doubly tuned amplification of shear layer unsteadiness by shear layer edge tone and cavity enclosure 18 p3047 A66-33676

**AERODYNAMIC STABILITY**

Operational problems and costs of staged solid-propellant rocket vehicles for atmosphere only, noting aerodynamic stabilization, spin motors, stage separation, jet plume, etc 07 p1140 A66-17612

Hypersonic aerodynamic stability and drag of ablating and nonablating models of blunt-faced reentry shape [AIAA PAPER 66-61] 07 p1141 A66-17898

Free flight dynamic stability measurements indicate that boundary layer transition has

no perceptible effect [AIAA PAPER 64-427] 08 p1161 A66-18810

Stick pushers in new medium range jet transports, noting aerodynamics of aircraft stall 11 p1637 A66-23072

Generalization of Allen-Kelley slender body theory to obtain estimates of two cubic nonlinear aerodynamic damping terms 12 p1795 A66-23593

Static and dynamic stability and drag of blunt-nosed flare-stabilized bodies at velocities up to 8.2 km per second [AIAA PAPER 65-44] 12 p1799 A66-24699

Aerodynamic stability of slender cone under ablation effect including pressure distribution measurement, ablation-flow field interaction, flow analysis during oscillation, etc [AIAA PAPER 66-410] 18 p3045 A66-33635

Flight control system of Saturn V launch vehicle, discussing attitude/altitude rate scheme, gain required and stability achieved 21 p3820 A66-38875

Approximation of aerodynamic stability of coasting vehicle leaving atmosphere at high speeds, assuming linear theory and constant aerodynamic coefficient 22 p3986 A66-40346

Short-periodic motion of tailless glider analyzed to determine degree of overcompensation of flap required for good stability 23 p4016 A66-41784

**AERODYNAMIC VEHICLE**

Magnetic suspension for aerodynamic wind tunnel models in Mach 8 airstream controlled in five degrees of freedom 09 p1364 A66-20664

Book on theory of optimum aerodynamic shapes 11 p1629 A66-22501

Nonequilibrium heat transfer distributions around blunt-nosed aerodynamic bodies, using analytical method, for design analyses of hypervelocity flight vehicles 12 p1799 A66-24715

High performance aerodynamic vehicle design, noting configuration variables, optimum performance parameters, vehicle force characteristics, optimization of hypersonic aircraft performance, etc [AIAA PAPER 66-486] 16 p2635 A66-31476

Dolphin body design for integrating resistance and propulsion mechanisms 19 p3279 A66-36050

**AERODYNAMICS**  
SA FLUID MECHANICS  
SA GAS DYNAMICS  
SA ROTOR AERODYNAMICS

Aerodynamic and heat transfer measurements using interferometer with continuous wave laser as source 01 p0069 A66-10849

Development and stabilization laws of aerodynamic perturbations 01 p0009 A66-11187

Introductory book on hypersonic aerodynamics covering continuum flow of inviscid nonheat-conducting perfect gas and real gas, viscous and low density effects in hypersonic flow 02 p0176 A66-11875

X-15 aircraft and future research noting previous flight data on hypersonic aerodynamics, structural and aerodynamic heating, etc [SAE PAPER 650657] 02 p0179 A66-12238

Text on aerodynamics of wings and bodies, emphasizing matched asymptotic expansion methods for boundary value problems and numerical techniques for loading predictions via computers 03 p0313 A66-12297

Analytic processes for evaluation of supersonic aerodynamics of configuration treating drag, wing design, wrap, interference and sidewash [AIAA PAPER 65-717] 03 p0321 A66-13048

Hydrodynamic systems expressed by kinetic equations, deriving equations of aerodynamics without knowledge of interaction of gas molecules 04 p0510 A66-13879

Solving integral in propeller design and second-order effects in subsonic airfoil theory 05 p0606 A66-15082

X-15 flight problems not encountered during simulation, particularly differences in aerodynamics, control systems, cockpit equipment, etc 07 p1017 A66-17274

Rarified gas dynamics in space flight and hypersonic low density wind tunnel of Goettingen Aerodynamics Research

Facility 07 p1017 A66-17479

Economy of body traveling over given distance at certain velocity and constant air density 07 p0983 A66-18161

Aerodynamics of manometers and mass spectrometers used on rockets and satellites for determination of atmospheric temperature and density 09 p1383 A66-20993

Text on high velocity aerodynamics, including subsonic, supersonic and hypersonic flows, rarefied gases, boundary layer theory and MHD 10 p1479 A66-21057

Variational calculus in one independent variable for optimum aerodynamic shapes and extension to two independent variables 11 p1721 A66-22502

Book on flight dynamics, covering optimum control, multistage rocket trajectory optimization, VTOL aircraft dynamics, autopilot design, etc 11 p1732 A66-23335

General solution for class of initial value problems for systems of aerodynamic equations, constructing reference solution to Cauchy problem involving shock and expansion waves 11 p1694 A66-23363

Development and stabilization laws of aerodynamic perturbations 12 p1797 A66-24005

Aerodynamics of hangar-type engine test facilities, discussing flow stabilization, soundproofing and effect of external winds 12 p1860 A66-24973

Annual report, 1964-65 /Aeronautical Research Laboratories, Australian Defence Scientific Service/ on aerodynamics, guided weapons and systems and flight research 13 p2056 A66-25120

Relativistic aerodynamics, discussing wavefront motion, Thomson and Bernoulli theorems, photon gases, etc, using statistical space-time mechanics 13 p1991 A66-26291

Hydrodynamic systems expressed by kinetic equations, deriving equations of aerodynamics without knowledge of interaction of gas molecules 14 p2275 A66-27569

Hydraulic analogy to compressible gas flow, discussing application to aerodynamic motions, flow visualization, measuring techniques and instrumentation [ASME PAPER 66-FE-16] 17 p2915 A66-33269

Panel flutter at high Mach numbers, using linear plate theory and first-order aerodynamics, noting damping, relation between traveling and standing wave theories, etc 18 p3257 A66-34592

Book on aerodynamics of pure subsonic flow including Earth atmospheric structure, fluid flow laws, boundary layer phenomena, subsonic wind tunnel and Magnus effect 19 p3278 A66-36730

Flight tests on aircraft and analysis by automatic filter, noting structural and aerodynamic problems resulting from use of transient method 21 p3824 A66-38574

Book on aeromechanics of flight vehicles including structure and physical properties of atmosphere, wing characteristics, research methods, aerodynamic characteristics of principal units of aircraft and rockets, etc 21 p3695 A66-39288

Reentry aerodynamics research in Japan including sounding rocket program, optimum reentry trajectory, nonequilibrium flow in nose region of blunt body, wind tunnels, etc [ICAS PAPER 66-36] 22 p3847 A66-40659

Short-duration aerodynamic testing techniques and new usage of hypersonic shock tunnels [AIAA PAPER 66-762] 23 p4052 A66-41331

Integral operator for solving aerodynamic problems for slightly rarefied viscous gas 23 p4054 A66-41356

Propulsion control systems for Concorde aircraft, noting aero-and thermodynamic reasons for power plant variables subject to manipulation 23 p4122 A66-41776

Mass transfer into aerodynamic body flow fields, examining model shear flow in Rayleigh problem for blowing current across gas-solid interface 23 p4058 A66-41900

Aircraft flying up to 6000 miles at Mach numbers up to 8, noting problems in aerodynamics, propulsion, structural weight, cooling, etc 24 p4157 A66-42237

**AEROELASTICITY**  
SA AEROTHERMOELASTICITY  
SA PANEL FLUTTER



# A WING LOADING

Aeroelastic instabilities of simply supported two-dimensional panels in subsonic flow at Mach numbers up to 0.85 [AIAA PAPER 65-772] 03 p0434 A66-12555  
Matrix scheme using two-way spline curves or interpolating low aspect ratio lifting surface mode deflections for use in aeroelastic calculations 05 p0774 A66-15058  
Static elastic deformation and associated change of aerodynamic characteristics of light vehicle subject to aerodynamic and inertia loading 05 p0609 A66-15784  
Free and forced vibrations, static and dynamic stability and aeroelasticity of orthotropic shells and plates in variable temperature field 11 p1781 A66-22614  
Lagrange equation approach to linear aeroelasticity in modern aircraft from structural and aerodynamic data 13 p1997 A66-26696  
Reduction of order of aeroelastic and flutter motion equations while retaining purely elastic contribution of eliminated coordinates, using quasi-static assumption and matrix algebra 14 p2405 A66-27996  
Aeroelastic stability of light aircraft, examining appearance of structural nonlinearities in global vibration test for determining critical flutter speed 17 p3023 A66-32331  
Aeroelastic instability of flat rectangular panels leading, trailing and free lateral edges, noting gap between theoretical and wind tunnel stability test 20 p3491 A66-36952  
Aeroelastic instability of aircraft with automatic pilot, determining domain in which sensor position and other adjustable parameters may vary without risking instability 21 p3695 A66-38580  
Common electronic techniques for studying aeroelasticity in high performance aircraft 21 p3827 A66-38654  
Dynamic aeroelastic motion resulting from inertial and aerodynamic effects, coupled through elastic deformation, applied to jet aircraft, considering flutter, buffet, wakes and turbulence 23 p4015 A66-41035  
Aeroelastic characteristics of Japanese special small rocket, examining body divergence speed and flutter speed of tail fins under flight 23 p4138 A66-41420  
Reverse flow and deformation optimization theories applied to subsonic aeroelasticity of lifting surface in harmonic oscillation, using numerical integration and computer programs 24 p4157 A66-42343

## CROLOGY

Simultaneous lower atmosphere observations with radar and aerological measurements by airborne meteorograph and electrometeorograph 02 p0253 A66-11273  
Aircraft bumpiness conditions in free atmosphere relation to turbulence and other aerological data 18 p3049 A66-34613

## EROMAGNETISM

Comparison of magnetic observations aboard Zaria and aeromagnetic surveying according to magnet plan 08 p1214 A66-19040

## ERONAUTICAL ENGINEERING

Interplay of technology, economics and operation in aircraft design noting VTOL [AIAA PAPER 65-736] 03 p0446 A66-12546  
Text on fundamentals of aircraft gas turbine engine design, including component design and calculation 11 p1762 A66-23310  
Indian National Aeronautics Laboratory annual report 1964-1965 14 p2269 A66-26872  
Bibliographical review of German, French and English texts relative to aeronautical engineering, theoretical and applied 15 p2425 A66-29363  
Progress in aeronautical sciences, noting delta wing vortex sheets, rotating flows, boundary layer flows, etc 17 p2906 A66-32273  
American Helicopter Society, Annual Forum, Washington, D.C., May 1966 17 p2843 A66-32723

## ERONAUTICS

General report of West German Research Institute for Aeronautics and Astronautics for 1964 02 p0216 A66-12073  
Rocket technology and air and space travel research - Annual Meeting, Berlin, West Germany, September 1964 04 p0581 A66-13494  
Aerospace technology including past progress, predictions, minimum and

maximum speeds for safe flight control, economics, propulsion, etc 09 p1472 A66-20164

British influence on world aviation, past, present and future 23 p4151 A66-41258  
Advancement in aeronautics and contribution of Royal Aeronautical Society 23 p4152 A66-42071  
Aeronautical research in U.K. by government establishments, industry and universities 23 p4017 A66-42072

## AERONOMY

Text on atomic and space physics with special emphasis on aeronomy 16 p2804 A66-31316  
Aerospace research programs in India 1965-1966, emphasizing equatorial aeronomy including meteorology up to 170 km 18 p3238 A66-35234  
Soviet book on high latitude research in field of geomagnetism and aeronomy including ionospheric storm, atmospheric absorption, etc 24 p4203 A66-43149

## AEROSOL

### SA ATOMIZATION

Heat and mass transfer in nonuniform gas-suspension flow treated by irreversible thermodynamics 01 p0163 A66-10628  
Influence of absorption of aerosol particles on extinction of solar and sky radiation 02 p0225 A66-12214  
Photographs of passage of Echo II into Earth shadow to determine aerosoles and atmospheric ozone height distribution 03 p0427 A66-12924  
Wooten method for measurement of true light absorption in aerosols, making it unnecessary to make separate light scattering measurement 06 p0906 A66-17032  
Cascade vault sampler for bacterial aerosols 08 p1177 A66-19087  
Critical condition for aerosol deposition from symmetrical flow past solid body, considering case of circular cylinder 08 p1247 A66-19304  
Measurement of radioactivity in air of free atmosphere and interior of cloudy areas and absorption of radioactive aerosols by water droplets 08 p1283 A66-19305

Separation problems of gas and aerosol components in brightness of atmospheric layer for photometric data pertaining to Mars atmosphere 08 p1295 A66-19330  
Difference between values for atmospheric pressure at Martian surface when obtained by photometry or by spectroscopy, due to nonconsideration of light scattering by aerosol particles 08 p1295 A66-19331  
Stable aerosol formation from vapor pressure of hot lava of volcanic eruptions, causing evaporation and condensation from gas phase 10 p1607 A66-21288  
Atmospheric aerosol size distribution from scattered light measurements by rocketborne equipment 11 p1697 A66-22565  
Measurements of decay curves of stored Aitken nuclei with photoelectric nucleus counter show small nonrandom divergences from theoretical curves 11 p1707 A66-23098  
Drift velocity of aerosol particle in field of sound wave distorted by second harmonic 13 p2127 A66-25087

Dispersed material concentration at various cross sections of ascending two-phase gas flow 13 p2065 A66-26484  
Photographs of passage of Echo II into Earth shadow to determine aerosoles and atmospheric ozone height distribution 14 p2380 A66-27273  
Electrical and physical characteristics and distribution density of aerosols in determining microwave scattering and reflection properties in connection with radar angels 14 p2237 A66-27396  
Electrostatic interaction effect on EM wavescattering by atmospheric aerosol particles 14 p2284 A66-27539  
CAT detection from Doppler shift in laser light backscattered from atmospheric aerosol 15 p2500 A66-28930  
Geophysical rocket determination of aerosol scattering coefficient variation from brightness values at 70-450 km heights 15 p2495 A66-30057

Solar radiation absorption by atmospheric water vapor, deriving formulas that include scattering and absorption by aerosol as additional parameter 16 p2691 A66-30228  
Spectral composition of direct solar radiation variation with height of Sun and relation between aerosol absorption band and humidity 17 p2994 A66-32857  
Critical condition for aerosol deposition from symmetrical flow past solid body, considering case of circular cylinder 19 p3393 A66-36041  
Radiation attenuation effect of atmospheric aerosols on all-weather aircraft landing guidance systems using lasers 19 p3397 A66-36051  
Drift velocity of aerosol particle in field of sound wave distorted by second harmonic 21 p3769 A66-38512  
Spectral-transmittance aerosol component for atmospheric haze, taking account of refractive index and polydispersity 21 p3759 A66-38910  
Aerosol component of spectral transmittance of artificial fog, comparing calculated and experimental values for absolute attenuation factor 21 p3759 A66-38916  
Aerosol particle precipitation in surface layer of atmosphere measured by modified method of Alexandrova 21 p3760 A66-39366  
Vertical distribution and transport of radioactive strontium aerosols in rain and air across trade wind inversion at Hawaii 23 p4124 A66-41843  
Electrostatic interaction effect on EM wavescattering by atmospheric aerosol particles 24 p4198 A66-42325  
Laser system for meteorological data using oscilloscope to display return signal, translated as concentrations of matter or aerosols 24 p4226 A66-43044

## AEROSPACE

Russian-English Aerospace Dictionary 05 p0794 A66-15326

## AEROSPACE MEDICINE

### SA BIOASTRONAUTICS

### SA BIOSIMULATION

### SA INJURY

Electrocardiography as related to flying personnel including case histories 01 p0019 A66-10605  
Behavior of right intraventricular conduction in 148 flying cadets under normal sea-level conditions and acute anoxic anoxia 01 p0020 A66-10608  
Medical history of 1056 aviators over 24-year period 01 p0020 A66-10610  
American and Soviet experience considering weightlessness, ionizing radiation, dynamic and biological factors, etc [SAE PAPER 650812] 01 p0021 A66-10819  
Biological problems in extended manned missions caused by low g, artificial atmosphere and absence of terrestrial periodicities 02 p0185 A66-11622  
Effect of delayed feedback in respiratory disease analyzed for behavioral cybernetic theory, using computer-controlled delay 02 p0186 A66-11648  
Forensic medicine in space environment with reference to international responsibility noting risks, medicolegal implications, cybernetics, contamination, pollution, etc 03 p0447 A66-13078  
Space biology and medicine research, stressing flight experiments performed with Russian satellites and spacecraft 04 p0468 A66-14089  
Bibliography of Soviet papers on space medicine and bioastronautics published in 1964 and 1965 06 p0810 A66-15910  
Space medical jurisprudence involved in present and future space technology 06 p0972 A66-16047  
Aerospace medical research of USAF 06 p0815 A66-16049  
Medical wastage of aircrew in Royal Air Force related to age, noting causes 06 p0815 A66-16050  
Postgraduate aviation and space medicine course at University of Rome 06 p0972 A66-16054  
Morphological characteristics and functional data in pilot trainees, noting anthropometric data and vital capacity, oxygen intake, heart rate, etc 08 p1175 A66-19084  
Problems in pilot fitness evaluation, especially physical and emotional capability assessment for flight 09 p1335 A66-20533  
Book on aviation physiology including



atmospheric pressure effect, visual factors in aviation, British Institute of Aviation Medicine, etc 10 p1487 A66-22104

Decompression sickness noting caisson and subatmospheric disease effects, symptoms, causes and prevention 10 p1488 A66-22109

Biological effects of explosive decompression noting parameters such as altitude, pressure differential, compartment volume and rate of pressure loss 10 p1492 A66-22111

Respiration and anoxia, noting anoxic anoxia, reduced oxygen carrying capacity of blood and inadequate flow of oxygenated blood to tissues 10 p1488 A66-22112

Medical knowledge as aid in preventing aircraft accidents and injury through investigation of causes and results 10 p1495 A66-22142

Contribution of medical science to accident prevention, discussing causes, results and escape from standpoint of man and machine 10 p1495 A66-22143

Aviation and space medicine - International Congress, Rome, October 1963 11 p1641 A66-22478

Aeromedical factors of Titan II ICBM support, discussing human factors in missile crew and propellant transfer 11 p1648 A66-22582

Altitude/pressure/vertigo severity and frequency among Swedish RAF pilots 11 p1644 A66-22584

Aerosol deposition in lungs of spacemen under weightless conditions 12 p1806 A66-23920

Acute hemodynamic effects of G-suit inflation, noting elevation of central venous pressure, cardiac output falling due to depressor reflexes and role of ganglionic blockade 12 p1811 A66-25014

Medical evaluation of Martian environment based on Mariner IV photographs and extrapolations from manned flight, noting effects of Martian gravity on astronauts 13 p2014 A66-25293

Preflight medical tests of responses of Soviet cosmonauts Beliaev and Leonov to simulated weightlessness and performance during simulated space walk 13 p2009 A66-25889

Aerospace medical advances in Polish military aviation and pilot testing procedures and equipment, particularly low pressure chamber and centrifuge 14 p2271 A66-28365

Soviet book on physiological methods in astronautics including collection, transmission and procession of medical information from long space flights 15 p2445 A66-29734

Aerospace Medical Association, Scientific Meeting, Las Vegas, April 1966 17 p2853 A66-32134

Particle and droplet contamination of spacecraft cabin atmosphere, examining exogenous and endogenous sources, medical aspects of inhalation and exhalation, effect of weightlessness, etc 17 p2866 A66-32207

R and D clean room complex design for guidance and control systems, noting contamination control, maintenance procedures, cost factors, etc 17 p2903 A66-32209

Contamination control of manned spacecraft, noting problem of biological interactions and methods of monitoring 17 p2866 A66-32211

Accidents involving human error evaluated from medical point of view 18 p3053 A66-34947

Flight activities of Russian cosmonauts in assessment of medical preparedness for orbital flight 19 p3283 A66-35291

Personality development, application of theory to problems of aerospace selection 19 p3294 A66-36378

Flight safety in Soviet civil aviation including takeoff and landing, cruising in airport vicinity, meteorology and medicine 20 p3494 A66-36991

Main stages of development of space biology and medicine in U.S.S.R., discussing biological effects in dogs in suborbital flight vehicles and satellites 24 p4169 A66-43135

Medico-biological methods based on data recording on board rockets and spacecraft and telemetering information to

Earth 24 p4169 A66-43141

**AEROSPACE SYSTEM**

Reliability and maintainability interrelationship in system availability of some aerospace programs 01 p0076 A66-10066

Operational safety analysis techniques according to MIL-S-38130 for aerospace systems 01 p0169 A66-10070

Electronically programmable telemeter using random access multiplexing and stored program control for aerospace missions 01 p0032 A66-11130

Glass properties, formation and application to aerospace systems 07 p1054 A66-18301

Nuclear reactors for space and near-Earth propulsion 07 p1111 A66-18304

Aerospace propulsion systems evaluated and compared from standpoint of cost or effectiveness 08 p1280 A66-18576

Aerospace and electronic systems - IEEE International Convention, New York, March 1966 12 p1818 A66-24600

Aerospace systems - Conference, Seattle, July 1966 20 p3659 A66-37155

Missile and space system accident potential evaluated numerically 20 p3685 A66-37931

**AEROSPACE TECHNOLOGY**

Safety education, management process and aerospace accidents 01 p0169 A66-10073

Safety and management in aerospace industry, noting importance of military specification 01 p0169 A66-10075

Structural system design technique for reliability and weight tradeoffs using designer equations and characteristics of materials, geometry and operational loads 01 p0145 A66-10085

Acoustical fatigue in aerospace structures - USAF Conference, Dayton, Ohio, April 1964 01 p0146 A66-10121

New research techniques from growing space technology for experimental sciences like physics 01 p0134 A66-10209

German participation in aerospace technology noting space transporter design and development 02 p0177 A66-11667

Light alloys for engineering application in armor plates, aerospace and nuclear fields, noting aluminum alloy properties 02 p0244 A66-11745

European Space Technology Center including upper-atmosphere scientific experiments, instrumentation, satellite control, data analysis, etc 03 p0352 A66-12481

Solid state camera system for aerospace application incorporating monolithic phototransistor mosaic sensor, molecular digital readout system, etc 04 p0519 A66-13631

Janes compendium of world aircraft, missiles and rockets 04 p0458 A66-14382

Maintainability guidance as factor in designing for aerospace industry 05 p0646 A66-14634

Roll reduction diffusion bonding for sandwich structures based on solid state diffusion process [SAE PAPER 650778] 05 p0687 A66-15006

French aerospace industry, relationship to French economy, annual expenditures 1958 to 1964 and aircraft exports 05 p0794 A66-15189

Government research and development inventions 06 p0972 A66-16076

Aromatic/heterocyclic polymers from tetraamines reaction with tetraacids at room temperature, developing potential for aerospace application 06 p0901 A66-16299

West Germany and international cooperation in aerospace engine development, noting VTOL aircraft and supersonic and hypersonic spacecraft 06 p0943 A66-16797

Manufacturing methods in space flight technology - German Symposium, Munich, November, 1964 06 p0887 A66-17068

Electron beam welding for in-space welding of spacecraft and space stations noting welding modes, power requirements, environmental influences, etc 06 p0888 A66-17072

Astronautics Year, international astronautical and military space/missile review of 1964 07 p1155 A66-17414

Papers on ceramics emphasizing relationship between microstructure, fabrication techniques and properties, including review of aerospace technological

applications 07 p1050 A66-18293

Civilian and Military Uses of Aerospace-Conference, New York, January 1965 08 p1299 A66-18547

NASA aeronautics and space research including near-Earth, cislunar and interplanetary space, manned flights, meteorology and communications 08 p1321 A66-18549

Factors in shaping policy for aerospace activity, stressing role of scientist 08 p1321 A66-18551

Aerospace industry contribution to science and technology, noting relationship with U.S. Government 08 p1321 A66-18552

Aerospace techniques used for research during International Quiet Sun Years /IQSY/ 08 p1286 A66-18570

Economic aspects of Concorde program, research potential, computational methods and technological progress 08 p1322 A66-19080

IEEE aerospace and navigational electronics conference at Baltimore in October 1965 08 p1250 A66-19487

Effectetics, informetics, control and stability in modern flight vehicle systems [AIAA PAPER 66-131] 08 p1254 A66-19565

Aerospace technology including past progress, predictions, minimum and maximum speeds for safe flight control, economics, propulsion, etc 09 p1472 A66-20164

Book on structure and performance of aerospace industry and governmental relations 09 p1473 A66-20689

European space program of launcher development 11 p1788 A66-22433

Aerospace electronics developments and trends toward more hybrid systems in guidance and control applications 11 p1667 A66-22954

Design-sciences approach for evaluation and selection of materials such as steel, titanium, beryllium, etc, used in idealized structures for aerospace application 11 p1783 A66-23076

U.S. nuclear rocket propulsion program costs, technology and application, noting empirical law of space nuclear program economics 11 p1734 A66-23078

Standardization of machining criteria for aerospace materials, compiling data about tool design, planning, manufacturing, costs, etc, on simple form [ASTME PREPRINT MM66-714] 12 p1887 A66-24418

Scientific and technical program of ESRO including launching of sounding rockets, satellites, space probes, astronomical observatory and scientific interplanetary probe 13 p2211 A66-26293

Machinability data for hard-to-machine materials, noting cost reductions, tool holder test program, cutting fluids, fixtures, producibility, etc [ASTME PAPER MM66-178] 14 p2300 A66-26958

Human factor tests in large-scale operational system testing techniques [ASME PAPER 66-HUF-11] 14 p2229 A66-26967

NASA mission, discussing V/STOL transports, SST and hypersonic cruise vehicles [SAE PAPER 660169] 14 p2416 A66-27282

Defense Materials System control of copper, aluminum and steel and proposed program for readiness and contingency planning of external resources for aerospace industry [SAE PAPER 660286] 14 p2416 A66-27297

Advancement in manufacturing technology in aerospace industry [SAE PAPER 660324] 14 p2301 A66-27301

Aerospace technology, spacecraft and spacecraft systems, launching, control, recovery, etc - Space Congress, Cocoa Beach, Florida, March 1966 14 p2388 A66-28401

European air cargo marketing and air freight industry 15 p2620 A66-29795

Dual-purpose passenger/cargo aircraft noting design, passenger interior system, cargo handling system, compatibility, comparisons, etc 15 p2426 A66-29802

XB-70 technology, developments in materials, equipment and manufacturing



- including steel alloys, welding, etc  
SAE PAPER 660276] 15 p2427 A66-29822
- Manufacture engineer role in producing  
space vehicles, noting S-IC stage of Saturn  
launch vehicle 15 p2511 A66-29834
- Space research programs in Italy since May  
1965 and cooperation with 15 p2602 A66-29940
- JASA 15 p2602 A66-29940
- Aircraft development and goals in  
U.S. 16 p2633 A66-31279
- Aircraft design requirements concerning  
STOL technology emphasizing cost, size  
and propulsion system 16 p2634 A66-31323
- Aerospace life support - Conference,  
American Institute of Chemical Engineers,  
Houston, February 1965 17 p2866 A66-32667
- Effectetics, informatics, control and  
stability in modern flight vehicle systems  
AIAA PAPER 66-131] 18 p3267 A66-33786
- Atlas E/F launch vehicle, discussing  
structure, mission capabilities, launch  
facility, reentry, etc 18 p3245 A66-33890
- SAE PAPER 660444] 18 p3245 A66-33890
- Advanced Atlas launch vehicle technology,  
discussing tank configurations, engine  
ratings, guidance systems, autopilot, thrust  
augmentation, payloads, launch facilities, etc  
SAE PAPER 660445] 18 p3245 A66-33891
- French aerospace industry, production of  
aircraft, engines and missiles, research  
programs, expenditures, etc 18 p3267 A66-33915
- Great Britain, future in space, discussing  
propulsion, nuclear power, satellite orbit,  
guidance, stabilization and attitude  
control 18 p3268 A66-33945
- Aerospace ordnance handbook intended as  
up-to-date reference on design and  
methodology of explosive systems used in  
space technology 18 p3159 A66-34184
- Testing and evaluation of aerospace  
ordnance, considering squibs, detonators,  
fuses and explosive train  
devices 18 p3095 A66-34194
- Quality assurance of aerospace ordnance  
and related devices, discussing factors and  
functions determining performance  
characteristics 18 p3116 A66-34195
- Space technology, Volume 5 - Symposium  
on environmental engineering and society,  
London, April 1966 18 p3230 A66-34208
- USAF Aero Propulsion Laboratory research  
in weapon systems and turbine engines,  
ramjets, etc 18 p3269 A66-34956
- Aerospace electronics - IEEE National  
Conference, Dayton, May 19 p3394 A66-35501
- Life support requirements encountered in  
manned space flights, considering cycle  
involving oxygen, food and water in terms  
of process criteria 19 p3485 A66-36231
- Book on advances in space science and  
technology including solid propellant rocket  
motor cases, solar system exploration  
vehicles, undulation in selenology,  
etc 19 p3464 A66-36311
- Systems analysis for space programs,  
emphasizing systematic quantitative studies  
of reliability and maintainability 20 p3684 A66-37910
- Training problems of reliability engineers  
for aerospace industry 20 p3686 A66-37958
- ASW aircraft performance and technology  
for contact investigation, patrol and convoy  
escort AIAA PAPER 66-727] 20 p3496 A66-38037
- Book on aerospace telemetry covering FM  
data systems, PACM-pulse amplitude-code  
modulation, data compression, etc 21 p3706 A66-39476
- U.S. Government in aerospace research and  
development 22 p4001 A66-40118
- Joining of materials for aerospace systems  
National Symposium, Dayton, November  
1965 22 p3923 A66-40255
- Conventional arc welding processes and  
application to aerospace industry 22 p3925 A66-40267
- Electron beam welding and application to  
aerospace industry, noting basic weld joint  
configurations 22 p3925 A66-40268
- Adhesive and bonding techniques evolution  
for general and specific use in aircraft and  
aerospace industry, noting elastomeric and  
ceramic adhesives 22 p3928 A66-40418
- Advanced spaceborne computer concepts -  
WESCON, Los Angeles, August 1966 22 p3870 A66-40725
- Power and control integrated circuits -  
WESCON, Los Angeles, August 1966 22 p3880 A66-40739
- Welding and adhesion techniques in  
aircraft and space vehicle construction -  
Conference, Hanover, West Germany, May  
1966 23 p4073 A66-41530
- Metal adhesives in aircraft and space  
industry, particularly in construction of  
laminar and sandwich elements of  
wings 23 p4073 A66-41532
- Welding and gluing of third stage of  
ELDO-A rocket 23 p4073 A66-41533
- Hypersonic transport technology,  
considering designs for Mach numbers up to  
14, altitude up to 140,000 ft and 150  
passengers 24 p4159 A66-42238
- Space project planning through detailed  
knowledge and correlation of various  
disciplines, noting role of universities,  
industry and government 24 p4296 A66-42242
- AEROSPACE VEHICLE**
- Aerospace vehicle flight control - SAE and  
NASA Conference, Los Angeles, July  
1965 01 p0102 A66-10661
- Mechanical servoactuator for all-mechanical  
flight control system for aerospace vehicles,  
noting traction transmission effect on  
toroidal actuator, cascading for power  
amplification, etc 01 p0015 A66-10671
- Changes in dynamics of aerospace vehicle,  
flight in low altitude turbulence and  
satellite spin decay 02 p0178 A66-11990
- Optimum structural and thermostructural  
design theory for advanced aerospace  
vehicles 08 p1306 A66-18805
- Meteorological measurement accuracies for  
use in design and operation of aerospace  
vehicles [AIAA PAPER 66-349] 12 p1953 A66-24480
- Aerospacecraft performance optimization  
and design evaluation for airbreathing-rocket  
propulsive systems by variational calculus  
[AIAA PAPER 65-18] 12 p1954 A66-24694
- Determination of number of times per unit  
time that various strength margin levels are  
exceeded under combined random stresses,  
useful to structural design in aerospace  
industry 13 p2195 A66-25592
- Aerospace application of aluminum and its  
alloys 14 p2313 A66-27012
- Hybrid type two-or three-stage aerospace  
vehicle design to place payload in orbit,  
discussing recoverable stages, drives and air  
breathing engines 16 p2635 A66-31682
- Rules for comparing designs of aerospace  
transporters and selecting optimum  
configuration, based on overall cost  
criterion 17 p3040 A66-32375
- First-stage propulsion of aerospace  
transporter, discussing design and  
operational requirements 17 p2990 A66-32377
- Deterministic structural design criteria for  
vehicle systems based on relation between  
management decisions and achieved  
reliability level [AIAA PAPER 66-504] 18 p3250 A66-33659
- High speed hybrid computer simulation of  
aerospace vehicle motion 18 p3094 A66-34068
- Electroexplosive devices in aerospace  
vehicles in two classes, propellants and high  
explosives, noting methods for controlling  
detonation desired effects 20 p3625 A66-37159
- Meteorological measurement systems in  
relation to aerospace problems, using flight  
history of rocket vehicle and root mean  
square accuracy 24 p4214 A66-43043
- AEROTHERMOCHEMISTRY**
- Combustion and sublimation in  
aerothermochemical interaction between  
dissociated air stream and graphite surface  
in hypersonic laminar viscous flow  
[AIAA PAPER 65-42] 03 p0444 A66-12797
- Turbulence in free shear layer in mixing  
region of circular jet, comparing statistical  
characteristics of mathematical and physical  
models [AIAA PAPER 65-805] 03 p0357 A66-13081
- Hypersonic wakes, effects of turbulent  
fluctuations on air ionization reaction rates  
measured by averaging and regrouping  
perturbed source terms of chemical rate  
equations [AIAA PAPER 65-819] 03 p0359 A66-13230
- Aerothermochemical performance of  
inorganic fiber-reinforced char forming  
ablative material [AIAA PAPER 66-435] 17 p3035 A66-32756
- Thermodynamics of combustion and  
concepts of aerothermochemistry using  
Newton-Raphson iteration process, noting  
transfer phenomena of matter, heat and  
momentum 20 p3680 A66-38090
- AEROTHERMODYNAMICS**
- SA AERODYNAMIC HEATING**
- Aerothermodynamic characteristics of  
Apollo command module at hyperbolic Earth  
entry velocities [AIAA PAPER 65-491] 20 p3664 A66-38168
- AEROTHERMOELASTICITY**
- SA AERODYNAMIC HEATING**
- Aerothermoelasticity effect on longitudinal  
stability and control of winged aerospace  
vehicles [AIAA PAPER 64-489] 05 p0775 A66-15075
- AEROZINE**
- Stability of various plastics toward  
hypergolic rocket fuel components aeroxine  
and nitrogen tetroxide 18 p3125 A66-35242
- AFTERBODY**
- S CYLINDRICAL AFTERBODY**
- AFTERBURNER**
- SA GAS TURBINE**
- Correlation study of turbojet afterburner  
combustion efficiency and fuel/air ratio  
setting for maximization of efficiency  
[WSCI 66-1] 18 p3164 A66-34423
- AFTERBURNING**
- Bypass engine development from  
conventional gas turbine to ducted-fan and  
aft-fan engine, noting principle of  
afterburning 14 p2373 A66-27014
- AFTERGLOW**
- SA HELIUM AFTERGLOW**
- SA OXYGEN AFTERGLOW**
- SA PHOSPHORESCENCE**
- Rate coefficients of ion charge exchange  
reaction between atomic oxygen ions and  
oxygen-nitrogen molecules measured at  
thermal energies by afterglow  
method 02 p0263 A66-11505
- Helium-neon gas laser used to determine  
electron density variation, spatial and  
temporal, in afterglow of Z-pinch in H at  
100 mtorr 13 p2104 A66-26239
- Discharge afterglow in low pressure tube  
studied by photomultiplier 13 p2150 A66-26473
- Time resolved electron density  
measurements with microwave  
interferometer used in weak afterglow  
plasma diagnostics 13 p2083 A66-26556
- Helium-neon laser afterglow and  
metastable helium atoms under long pulse  
excitation 14 p2307 A66-27335
- Acoustic wave generation and amplification  
in weakly ionized plasma, explaining sound  
emission in glow discharge and modulation  
in plasma afterglow 15 p2556 A66-29808
- Primary and afterglow emission decay time  
from low temperature gaseous nitrogen  
excited by fast electrons explained by  
possible energy transfer 19 p3404 A66-36799
- Nitrogen ion charge-transfer reaction rates  
with CO and carbon dioxide in pulsed  
flowing afterglow system 21 p3774 A66-38529
- Flow visualization via afterglow produced  
in pure low temperature nitrogen and air by  
electron beam projection 23 p4058 A66-41911
- AFTERIMAGE**
- Characteristics of afterimages produced by  
persisting visual effect after termination of  
illumination 04 p0462 A66-13794
- Decay time of positive afterimage following  
high intensity flashes measured by  
monocular and binocular brightness  
matching 18 p3062 A66-33993
- Psychophysiological fusion linking  
afterimages of separate visual stimuli  
causing artifacts in visual astronomical  
observations 20 p3507 A66-38053
- AGC**
- S AUTOMATIC GAIN CONTROL /AGC/**
- AGE FACTOR**
- Medical wastage of aircrew in Royal Air  
Force related to age, noting  
causes 06 p0815 A66-16050
- Age dependence of resistance of chickens  
to 100 percent oxygen at one atm /OAP/  
noting delayed mortality in adult  
birds 07 p0997 A66-17458
- Age, cardiac output and choice reaction  
time of airline, military and test pilots,  
attempting resolution of data  
discrepancy 12 p1806 A66-24397



Iron and stony meteorite evolution, cosmic radiation ages and space erosion model 14 p2390 A66-28409  
 Age effect on liver glycogenesis in rats exposed to acceleration stress 17 p2860 A66-32555  
 Magnetic spherules in silurian and permian salt samples suggest constant meteoric influx useful in determination of lunar surface age 24 p4198 A66-42435

## AGE HARDENING

## SA PRECIPITATION HARDENING

Aging characteristics of Al-Zn-Mg alloys 03 p0381 A66-12722  
 Cr and Mn effects on aging mechanism and anticorrosion properties of Al-Zn-Mg alloys 03 p0381 A66-12723  
 Martensitic transformation kinetics and maraging mechanism in Fe-Mn-Ni-Ti alloy observed by electron and X-ray diffraction 08 p1236 A66-18762  
 Metastable Ti-Mo-Fe-Al beta-alloy system, discussing metal hardening, heat effects, etc 12 p1893 A66-23761  
 Age hardening response correlated with structural observations of iron-nickel-cobalt alloys 12 p1895 A66-24374  
 Cyclic strain fatigue tests and fatigue failure curve for age-hardened nickel based alloy K-Monel  
 [ASME PAPER 66-MET-9] 14 p2312 A66-26977

Cold work and precipitation hardening effect on tensile and thermal characteristics of gas turbine alloys  
 [ASME PAPER 66-GT-102] 14 p2312 A66-27002

Texture and anisotropic age hardening to improve mechanical properties of AlMgSi alloys 14 p2313 A66-27011  
 Microquenched age-formed titanium alloys and titanium bialloy composites 14 p2313 A66-27093  
 Age hardenable nickel-copper steels with strength achieved by copper phase hardening 16 p2723 A66-30319  
 Microquenched age-formed titanium alloys and titanium Bi-alloy composites, discussing production process using spherical particles produced by rotating electrode  
 [SAE PAPER 660458] 17 p2940 A66-33164  
 Aging behavior and mechanical properties of three wrought high-strength magnesium-yttrium alloys 18 p3122 A66-33751  
 Particle size effects in age hardening of high temperature Ni-based alloys 20 p3586 A66-38094

## AGENA ROCKET

SA ATLAS AGENA LAUNCH VEHICLE  
 Acoustic fatigue characteristics of beryllium panels exposed to high intensity random noise environment 01 p0149 A66-10143  
 Pulse code modulation /PCM/ for telemetry and communication between Gemini spacecraft Agena D satellite and ground stations for data processing and display 01 p0031 A66-10938  
 SNAP 10a/Agena Space System, noting interrelationship of several subsystems and integration with nuclear power unit 12 p1857 A66-23677

## AGING

SA CURING  
 SA STORAGE  
 SA STRAIN AGING  
 Stress-aging, differences from strain-aging and effect on tensile properties of various stainless steels 01 p0085 A66-10409  
 Approximate solution method for unsteady creep of shells within framework of theory of aging 07 p1146 A66-18254  
 Diffuse X-ray scattering in crystal structure of Ni-Be and Cu-Be alloys during first stage of aging due to anisotropic monoclinic lattice distortions 08 p1235 A66-18589  
 Aging of Cu-Ti alloy stimulated by Al additions to 2 percent and retarded by Al additions of 2 to 4 percent 12 p1892 A66-23521  
 Aluminum alloy with various metal additions analyzed for aging, using electron microscope 12 p1898 A66-25022  
 Electrical resistance changes in quaternary alloy during simultaneous occurrence of phase solution coalescence and silicon spheroidization, noting effects of aging and

various metal additions 12 p1898 A66-25023  
 Aging effect on structure of cobalt alloys annealed at 1200 degrees C suggests formation of laminar regions 12 p1898 A66-25030  
 Quenching and slow-cooling effects on ductile-brittle bend-transition temperature of chromium wire 13 p2107 A66-25587  
 Aging behavior of explosively deformed 2219 Al investigated by transmission electron microscopy 13 p2086 A66-25775  
 Aging behavior of rods produced by extrusion of manganese-containing aluminum alloy subjected to solution heat treatment, noting microstructure and mechanical properties 13 p2111 A66-26585  
 Aging of aluminum alloy after quenching and strain hardening, noting Vickers hardness tests, tensile tests, precipitation phases, shearing effect, etc  
 [PST PAPER 423] 14 p2315 A66-27468  
 Effects of heat treatment and aging on phase composition, strength and plasticity of industrial titanium alloys 15 p2522 A66-29178  
 Phase transformations in titanium alloys annealed at high temperatures and subjected to aging processes 15 p2522 A66-29181  
 Structural changes and variations in hardness at high temperatures in titanium alloys, determining aging temperatures producing maximum hardness 15 p2522 A66-29183  
 Kinetics of natural aging process of Al-4 percent Cu alloy, experiments indicate addition of up to 1.0 percent Mg proportionately slows down aging process 16 p2723 A66-30871  
 Silver oxide films by cathodic sputtering, discussing changes in sample preparation and material characteristics due to aging and heat treatment 17 p2976 A66-32262  
 Aging temperature ranges for tensile specimens of equiatomic niobium-zirconium alloys, noting phase diagrams, structural changes, mechanical properties, precipitation hardening, etc 17 p2940 A66-33290  
 Existence and uniqueness of solution in viscoelasticity theory for aging materials, considering four boundary value problems for body subjected to finite deformations 18 p3255 A66-34393  
 Optimum aging temperatures obtained from electric resistance of beryllium alloys containing chromium and zirconium 18 p3124 A66-34406  
 Effects of aging temperature and duration on strength, elongation, yield stress, plasticity and electrical conductivity of Al-Zn-Mg and Al-Zn-Mg-Cu alloys 20 p3585 A66-37698

## AGRICULTURAL AIRCRAFT

Flight tests on various agricultural aircraft noting safety record data 16 p2634 A66-31284

## AILERON

SA SPOILER-SLOT AILERON  
 Aileron traverse effect on amount of coupling from roll to yaw during abrupt aileron roll of conventional aircraft 01 p0011 A66-10175  
 Aileron traverse effect on amount of coupling from roll to yaw during abrupt aileron roll of conventional aircraft 16 p2633 A66-31115  
 Static stability of rolling motion of aircraft for given aileron angle when inertia cross-coupling is present, with numerical solution of nonlinear equations 22 p3848 A66-40493

## AIR

SA ATMOSPHERE  
 SA GAS  
 SA HIGH TEMPERATURE AIR  
 SA UPPER AIR  
 Estimates of collision cross sections for carbon dioxide and air molecules at 200 degrees K with thermal radiation field as error source 01 p0062 A66-10762  
 Whole-body plethysmographic method for determination of total inertia of air breathed by humans, using rectangular coordinates 13 p2011 A66-26323  
 Estimates of collision cross sections for carbon dioxide and air molecules at 200 degrees K with thermal radiation field as error source 14 p2286 A66-27861  
 Reevaluation of data and equations used in calculation of air viscosity coefficient and application to wind tunnel

experiments 16 p2685 A66-30911  
 Laminar boundary layer heat transfer measurements by thick-film calorimeter gauges on flat plate in dissociated and partially ionized air 17 p3039 A66-33483  
 Electrodeless annular discharges in argon and air 18 p3144 A66-34039  
 Air purging of high-performance multilayer insulation system with helium 20 p3675 A66-37064

## AIR BREATHING ENGINE

Jet fuels presently used in military aircraft compared with those for advanced air-breathing weapon systems at high Mach number  
 [SAE PAPER 650804] 01 p0128 A66-10846  
 Performance operation and cost of rockets and airbreathing launch system, noting preliminary designs 02 p0295 A66-11676  
 Effects of improved refractory blade materials and internal cooling on inlet temperatures, design and performance of air breathing engines at supersonic speeds  
 [AIAA PAPER 65-743] 03 p0415 A66-12549  
 Engine thrust and heat mass in air breathing jet engine for space flight 04 p0572 A66-13441  
 High temperature measurement in combustion chambers of air breathing engines discussing optical, pneumatic, acoustic and calorimeter methods 04 p0518 A66-13537  
 Turbo-rocket application to air breathing satellite launcher program describing engine design, performance and weight characteristics 04 p0572 A66-13539  
 High temperature materials for hypersonic air-breathing engines, noting usefulness of coated refractory metals 09 p1435 A66-20670  
 Griffon 02 delta-winged aircraft with composite air breathing turboramjet engine, noting achievements and prospects 11 p1761 A66-23248  
 Thermodynamic process within combustion chamber of propulsive duct, examining potential with reference to feedback and spark discharge 11 p1761 A66-23251  
 Soviet book on automation and control of air breathing gas turbine and ramjet engines 13 p2173 A66-26463  
 Orbital satellite launching systems, problem of increasing percentage orbital payload at minimum cost and advantages of air breathing engines 14 p2391 A66-27010  
 Refractory ceramics for air breathing engine for Mach 7 aircraft, noting zirconia properties 16 p2790 A66-30257  
 Hybrid type two-or three-stage aerospace vehicle design to place payload in orbit, discussing recoverable stages, drives and air breathing engines 16 p2635 A66-31682  
 Air breathing engine designs for winged recoverable boosters 20 p3628 A66-37429  
 Performance, kinetic heating, structural weight and effectiveness of air breathing propulsion for first stage of aerospace transport vehicle  
 [ICAS PAPER 66-28] 22 p3972 A66-40664  
 Bluntness and boundary layer displacement effects on air breathing engine hypersonic inlet flow fields  
 [AIAA PAPER 65-617] 23 p4007 A66-41109  
 Propulsion system development for very high speed winged vehicles application  
 [ICAS PAPER 66-29] 23 p4122 A66-41933  
 Hypersonic cruise vehicles for military and civil requirements, considering air breathing propulsion and structural weight 24 p4296 A66-42241  
 Structural design problems of hypersonic air vehicles with air breathing propulsion, discussing relation to future hypersonic commercial air transport  
 [ICAS PAPER 66-31] 24 p4281 A66-42491

## AIR CARGO HANDLING

Air cargo - International Forum, Chicago, May 1966 15 p2619 A66-29788  
 Air cargo techniques applied to movement of retail merchandise 15 p2620 A66-29792  
 Military air cargo transport technology and logistic systems 15 p2620 A66-29793  
 Air cargo transport development, air freight classification and inventory balancing 15 p2620 A66-29794  
 European air cargo marketing and air freight industry 15 p2620 A66-29795  
 Operational, technical and commercial aspects of air cargo handling and effect on



sales 15 p2620 A66-29798  
 Outlook for air cargo handling indicates  
 reduction of cost and increased efficiency  
 by use of intermodel  
 containers 15 p2620 A66-29799  
 Dual-purpose passenger/cargo aircraft  
 noting design, passenger interior system,  
 cargo handling system, compatibility,  
 comparisons, etc 15 p2426 A66-29802

**IR CONDITIONING**  
**SA COOLING SYSTEM**  
 Air conditioning system of SST Concorde  
 noting reliability 04 p0460 A66-14461  
 Single stage bootstrap air conditioning with  
 two-position turbine nozzle for improved  
 high altitude descent conditions for  
 Concorde SST 09 p1331 A66-20133  
 Personnel comfort and protection from  
 thermal stress, discussing clothing,  
 environmental temperature, metabolic heat  
 production, solar radiation,  
 etc 10 p1492 A66-22120  
 Air conditioning system of SST Concorde  
 noting reliability 11 p1640 A66-22250  
 Vapor-cycle air conditioning for business  
 aircraft, considering weight vs power  
 consumption, compatibility with integrated  
 system and test results  
 [SAE PAPER 660208] 13 p2002 A66-26386  
 Air conditioning development in Beech  
 aircraft  
 [SAE PAPER 660209] 13 p2002 A66-26388  
 Regenerative air conditioning systems of  
 spacecraft cabins for long missions,  
 analyzing principal parameters of gas  
 mixtures for life  
 requirements 24 p4169 A66-43142

**IR COOLING**  
 Air cooled gas turbine rotor and stator  
 airfoils, presenting problem definition,  
 analysis techniques, material application and  
 cascade and engine testing  
 [ASME PAPER 65-WA/GTP-10] 05 p0691 A66-15725  
 Turbine blade and vane cooling in Rolls-  
 Royce nonmilitary aircraft engines, noting  
 side effects on design and development  
 [SAE PAPER 660053] 09 p1433 A66-20151  
 High temperature turbine blade air cooling  
 methods and cyclic and steady state  
 endurance testing  
 [SAE PAPER 660054] 09 p1434 A66-20152  
 Electric machines employing evaporative  
 and universal cooling systems for aircraft  
 use 13 p2041 A66-25902  
 Vaporization cooling of inner wall surface  
 of externally heated cylinder by vortex  
 flow 16 p2829 A66-31162  
 Discharge of cooling air from blades into  
 flow-through part of gas turbine, examining  
 mixing of gas behind blade array with air  
 from blade edges and effect of injected air  
 on turbine efficiency 20 p3627 A66-36913  
 Natural convective heat transfer to gas  
 turbine rotor blade and thermal resistance  
 of cooling system using centrifugal  
 pump 20 p3627 A66-36926  
 Statistical correlation of IR cooling  
 measurements by Tiros II /Channel 2 and  
 Channel 4/ and radiometersonde  
 measurements of radiation divergence within  
 atmospheric layers 22 p3944 A66-40431

**IR CURRENT**  
**SA EKMAN LAYER**  
**SA TURBULENT AIR CURRENT**  
**SA VERTICAL AIR CURRENT**  
 Appleton anomaly of F-2 layer examined,  
 assuming ionization induced horizontal  
 motion of neutral air 08 p1215 A66-19207  
 High precision high-spatial resolution  
 tracer study of low-noise steady air flow in  
 rectangular pipe, emphasizing region within  
 two microns of wall 10 p1524 A66-21804  
 Cylinder rotation in boundary layer of air  
 stream 14 p2273 A66-26785  
 Negative effect of air countercurrents and  
 thermal stresses on performance of cooling  
 systems of gas turbine rotor disks with  
 lateral air flow 15 p2570 A66-28776  
 Pressure distribution, skin friction and  
 heat transfer for sharp- and blunt-nosed  
 slender bodies in hypersonic air  
 flow 17 p2837 A66-32070  
 Air flow luminescence front propagation in  
 electromagnetic shock tube measured, using  
 phase synchronized high-speed  
 photography 21 p3790 A66-39080

**AIR CUSHION VEHICLE**  
**SA GROUND EFFECT MACHINE**  
 Comparison of air cushion vehicles  
 supported by peripheral jets or by air  
 cushion contained in bell-shaped structure,  
 stressing simplicity of  
 latter 12 p1862 A66-23819  
 Air cushion landing gear for aircraft,  
 noting rubber tubing under fuselage forming  
 pneumatic bumper blown up by turbine  
 engine 17 p2848 A66-33082

**AIR DEFENSE SYSTEM**  
 Radar, telecommunication devices, antiraid  
 equipment and computers for air defense  
 system 04 p0494 A66-13693  
 Reliability of missile fire distribution  
 facility, noting transistorization effect on  
 economy 11 p1668 A66-22955  
 Semiautomatic digital data processing  
 system used in ground control of  
 interceptor aircraft, noting track marking on  
 PPI display, control of height radar, radio  
 message transmission, etc 14 p2271 A66-28299  
 U.S. strategic missile and air defense,  
 noting Nike-X system 24 p4297 A66-42950  
 U.S. tactical defense systems noting SAM  
 types, interceptors, technical problems, data  
 handling, radar, etc 24 p4297 A66-42951  
 High acceleration missiles for intercepting  
 enemy ballistic warheads, considering sprint  
 and hibex rockets, noting problems with gap  
 heat, gyro drift, communications,  
 etc 24 p4284 A66-42952

**AIR DUCT**  
 Calibration process for RZ-2 rocket engine,  
 noting changes in orifices, engine  
 performance, influence coefficients,  
 etc 21 p3807 A66-38640

**AIR FREIGHT INDUSTRY**  
 Potential air freight market in next decade  
 forecast as many-fold times present level  
 [SAE PAPER 650782] 01 p0012 A66-10839  
 Air cargo - International Forum, Chicago,  
 May 1966 15 p2619 A66-29788  
 Role of IATA cargo agent in handling air  
 freight shipments 15 p2619 A66-29789  
 Specialized services provided by air freight  
 forwarding industry to shipper and  
 carrier 15 p2619 A66-29790  
 Transportation needs of business in small  
 shipment category, discussing role of air  
 freight 15 p2619 A66-29791  
 Air cargo techniques applied to movement  
 of retail merchandise 15 p2620 A66-29792  
 Air cargo transport development, air  
 freight classification and inventory  
 balancing 15 p2620 A66-29794  
 European air cargo marketing and air  
 freight industry 15 p2620 A66-29795  
 New concepts in railroad management  
 oriented to logistics market and return on  
 investment 15 p2621 A66-29801  
 Civil Aeronautics Board /CAB/ role in air  
 freight industry and in proposed  
 Department of  
 Transportation 15 p2621 A66-29804

**AIR INLET**  
 Air intake with boundary layer trap,  
 examining flow structure under external  
 supersonic pressure and uniformity  
 parameters  
 [ONERA TP 288] 03 p0316 A66-12898  
 ONERA experimental wind tunnel research  
 with jet engine intakes and exits  
 [ONERA TP 292] 05 p0606 A66-15159  
 Air augmented propulsion in liquid  
 hydrogen-LOX rocket booster  
 engines 17 p2990 A66-32376  
 Engine air induction system, engine and  
 integral gear case oil cooling air induction  
 system and nacelle cooling and ventilating  
 air induction systems of XC-142A  
 [AIAA PAPER 66-632] 18 p3048 A66-34435

**AIR JET**  
 Heat transfer coefficient by impingement  
 of two-dimensional air jets  
 [ASME PAPER 65-HT-20] 05 p0605 A66-14742  
 Mean flow pattern of round air jet in  
 ambient airstream parallel to jet  
 axis 06 p0802 A66-16504  
 Heat transfer coefficient by impingement  
 of two-dimensional air jets  
 [ASME PAPER 65-HT-20] 11 p1629 A66-22190  
 Hot wire measurements in radial turbulent  
 incompressible air jet 18 p3045 A66-33593  
 Molecular mixing of cold air jet containing  
 sodium nitrite vapor and slipstream of  
 gasoline-air mixture combustion

products 23 p4149 A66-41793  
 Round turbulent low speed airjet  
 impingement on flat surface and application  
 to theoretical analysis of inviscid rotational  
 flow 23 p4012 A66-42002

**AIR MASS**  
 Total mass of Earth atmosphere computed,  
 using atmospheric pressure and land-height  
 distribution data 09 p1369 A66-19871  
 Investigation of two cold air fronts of  
 polar origin that occurred in Alpine region  
 in April 1962, using data from Tiros  
 IV 11 p1730 A66-23096  
 Turbulence energy balance equation used  
 in air mass transformation  
 problem 20 p3594 A66-38369

**AIR NAVIGATION**  
**SA ALL-WEATHER AIR NAVIGATION**  
**SA TACTICAL AIR NAVIGATION**  
 /TACAN/  
 A-NEW MOD 1 digitally controlled  
 navigation system for antisubmarine warfare  
 aircraft employing Univac CP-754-8 thin film  
 computer 01 p0098 A66-10002  
 Locating low cost aircraft inertial  
 navigation system being designed for  
 compatibility with high performance tactical  
 aircraft 01 p0099 A66-10010  
 SGN-10 Inertial Navigator, pure inertial  
 system with no damping or other external  
 input designed for commercial  
 aircraft 01 p0099 A66-10013  
 Electronic techniques applied to taxiing,  
 takeoff, aerial navigation and  
 landing 02 p0255 A66-11466  
 Doppler radar for aerial navigation noting  
 decoupling of transmitter from receiver,  
 velocity measurement within frequency  
 spectrum, etc 02 p0256 A66-11896  
 Doppler radar performance in air  
 navigation noting calibration error,  
 dispersion, hole-altitude phenomena,  
 etc 02 p0256 A66-11897  
 Aid to air navigation problem discussing  
 reliability and accuracy, hybrid system,  
 redundancy and credibility, display,  
 operational environment and navigation  
 technique 02 p0256 A66-11966  
 Hertzian and IR radiometry applied to  
 temperature determination for use in aerial  
 navigation 02 p0257 A66-12032  
 U.S. papers on air navigation control via  
 artificial satellites, discussing merits and  
 deficiencies 02 p0260 A66-12060  
 Flight control by ground-based radio  
 system discussing aerial navigation safety,  
 operating principles, equipment for VOR  
 and ILS and importance of  
 calibration 03 p0390 A66-13011  
 Helicopter navigation requirements for low  
 altitude sea missions at beyond-horizon  
 distance from supporting ship or shore  
 base 04 p0544 A66-14442  
 Long distance air navigation across North  
 Atlantic 07 p1063 A66-17444  
 International Air Transport Association,  
 Technical Conference, Miami, April 1965,  
 Volume 1 07 p1063 A66-17667  
 SST navigation and air traffic control  
 equipment for NAC-60 aircraft, noting  
 climbout, cruise, position, landing,  
 etc 07 p1067 A66-17687  
 Ferranti navigation display used to monitor  
 and update self-contained navigation system,  
 consisting basically of compass card  
 indicating true or magnetic  
 heading 07 p1067 A66-17688  
 Navigation precision for SST operation  
 having due regard to performance and  
 noise 07 p1069 A66-17709  
 Air traffic control system capacity and  
 navigational requirements for North Atlantic  
 and continental transition areas, discussing  
 relationship to accuracy and flight time  
 economy 07 p1069 A66-17713  
 AN/AVN 1 Astro Navigation Set, remote  
 controlled automatic photoelectric  
 sextant 07 p1073 A66-17766  
 Automatic airborne navigation facilities in  
 civil aircraft 07 p1073 A66-17767  
 Flight tests of navigation systems including  
 hyperbolic system, Doppler system, radio  
 altimeter testing, deviation in gyromagnetic  
 compasses, etc 07 p1073 A66-17770  
 Standardization of air navigation  
 techniques noting equipment  
 standardization, aircraft self-contained  
 capability, lateral standard error, radar



monitoring, etc 07 p1073 A66-17771  
Self-contained and ground-based aids to integrated air navigation system noting costs, crew, display, etc, to be used in SST at VLF 07 p1074 A66-17772  
Receiver for processing lane identification signals for Dectra navigation system and relation to tracking accuracy and probability of error 07 p1074 A66-17773  
Air navigation problems in North Atlantic including separation standards lateral and vertical, SST traffic, collision risk, etc 07 p1074 A66-17774  
Navigation techniques and operational objectives due to computer-generated flight plans of United Air Lines 07 p1074 A66-17777  
Synchronous navigational satellites for ships and planes, noting distance and direction measurement by satellite interferometers 07 p1075 A66-17785  
Project Accordion data to provide information for decisions on horizontal separation standards and navigational accuracy 07 p1076 A66-17790  
Ground based self-phasing and nonrigid airborne arrays for aerial mapping and navigation 08 p1252 A66-19510  
Chart display methods of let-down type, roller type and optical projection for aircraft navigation 10 p1554 A66-21897  
Flight and navigation procedures and requirements for civil aerial photography 11 p1705 A66-22662  
Illumination systems used as visual aids for pilots when approaching airport 12 p1857 A66-24089  
A-NEW MOD 1 digitally controlled navigation system for antisubmarine warfare aircraft employing Univac CP-754-8 thin film computer 13 p2124 A66-25596  
Air navigation problems in North Atlantic including separation standards lateral and vertical, SST traffic, collision risk, etc 13 p2124 A66-25861  
Navigation precision for SST operation having due regard to performance and noise 13 p2125 A66-25868  
Aircraft navigational error parameters combined statistically and used to evaluate wander expected in transport aircraft operating in transoceanic environment 15 p2535 A66-29624  
Inertial navigation application to aeronautics, requiring accelerometers and inertial platform with turning motion sensors 15 p2536 A66-29893  
Inertial navigation for commercial aviation economically justified by fuel economy due to reduced flight time 15 p2536 A66-29894  
Ocean platforms in North Atlantic to house radar and navigational aid for high-density commercial aircraft routes 18 p3131 A66-33559  
Text on theory of automated air navigation, examining methods of flight preparation and precision 22 p3946 A66-40855  
Microwave radiometry feasibility as technique for navigation data-sensing in Army aircraft 23 p4089 A66-41317

**AIR POLLUTION**

Effective planning and operations required for control of air pollution due to increased use of toxic propellants in larger missiles 02 p0183 A66-11491  
Evaluating air pollution hazard to personnel from exhaust gases of Titan II test firings 06 p0819 A66-16493  
Optical radiation absorption and attenuation by atmosphere polluted with carbon dust, including transmission coefficient calculation 09 p1402 A66-20313  
Clean Air Act in relation to toxicology and safety to evaluate atmospheric pollution [AIAA PAPER 66-375] 12 p1907 A66-24501  
Mean droplet size and dispersion of atomized liquids in industrial air determined by microscopic slides and photomicrographs 13 p2066 A66-26489  
Mass spectrometric investigations of interaction of atmospheric ions with molecules of rocket gas release 15 p2495 A66-30061  
Low pollution electric arc air heater of CH9 and CH10 type, using metal electrodes to provide air mass flow rates at 4000 degrees K 20 p3540 A66-36950  
Numerical evaluation of intensity of radiation scattered outward from turbid

atmosphere 20 p3593 A66-38190  
Solargraphic measurements of solar radiation absorption by atmospheric dust and pollutants and effects on solar energy transmission 22 p3912 A66-40244

**AIR PURIFICATION**

Safety measures in working with beryllium, discussing berylliosis prevention, dust reduction, protective suits, etc 05 p0687 A66-14862  
Integrated program approach for contamination control of space cabin atmospheres based on identification, estimation of concentration and system specifications 19 p3293 A66-36238

**AIR SAMPLING**

Cascade vault sampler for bacterial aerosols 08 p1177 A66-19087  
Ice crystallization on solid-insoluble nuclei in high humidity air, noting two measuring methods for nuclei concentration 14 p2327 A66-28134

**AIR SPEED**

Aircraft speed relation to range, endurance and maneuverability capabilities reviewed with regard to military value [SAE PAPER 650797] 05 p0610 A66-15012  
Instrumentation of Polish gliders including altimeters, rate-of-climb, turn and air speed indicators, magnetic compasses, artificial horizon, etc 12 p1882 A66-24386  
Indirectly heated PTC resistor for measurements of low pressures and high air velocities, noting basic circuit and application to heat exchangers 19 p3362 A66-36824

**AIR TO AIR MISSILE**

Air to air missiles describing guidance systems, launching aircraft, maximum range and contractor service 04 p0585 A66-13922  
Tabulation and description of missiles in service or under development 04 p0586 A66-13944  
Adaptive roll autopilot in air-to-air interceptor missile, noting application of dither principle, simulation results and noise rejection qualities 19 p3398 A66-36691  
Simulation and analysis of adaptive roll autopilot for air to air missile, using limit cycle with small amplitude controlled by gain changing loop 20 p3595 A66-36865

**AIR TO AIR REFUELING**

Hypothetical linear programming model for minimizing cost of aerial tanker support of practice bomber mission 06 p0805 A66-16349

**AIR TO SURFACE MISSILE**

Air to ground missiles including dimensions, weight, maximum Mach number, propulsion, status and operational or design problems 04 p0585 A66-13921  
Tabulation and description of missiles in service or under development 04 p0586 A66-13944

**AIR TRAFFIC**

Atmospheric conditions effect on supersonic jet traffic 02 p0178 A66-12030  
Forecasting methods for air passenger traffic between selected city-pairs in U.S. air transport network 02 p0178 A66-12218  
Layout and design of air terminal for Basel, Switzerland, noting passenger accommodation and air traffic problems 05 p0660 A66-15199  
International sanitary regulations and air traffic, noting uniform code for quarantine practices 11 p1647 A66-22479  
Douglas DC-8 super sixty series effect on airport requirements including noise level, runway problems and traffic [SAE PAPER 660281] 15 p2427 A66-29825  
Comparison of air, rail, bus and private car traffic within continental U.S. and within metropolitan France, excluding suburban traffic 20 p3495 A66-37397  
SST in nonoptimum conditions, discussing cost penalties due to navigation error, air traffic conditions, sonic boom restrictions, clear air turbulence and weather 21 p3695 A66-38451

**AIR TRAFFIC CONTROL****SA LANDING AID**

Eurocontrol efforts in optimum safe spacing of aircraft in flight with minimum restrictions by radar observations and pilot reports 01 p0102 A66-10180  
Bretigny experimental control center for studying air traffic control for Eurocontrol 01 p0053 A66-10181

Video maps for air traffic control by associating radar picture with geographic features noting mechanical, optical and electronic components 01 p0022 A66-10486  
Computer flight simulators at Langley discussing Boeing 707 jet, helicopter, air traffic control, orbital rendezvous and docking, lunar navigation and landing 01 p0055 A66-10957  
Electronic techniques applied to taxiing, takeoff, aerial navigation and landing 02 p0255 A66-11466  
Air traffic control methods using radar for long-term planning and solution of West German air traffic control problems 02 p0256 A66-11858  
Satellite functions in air traffic control systems noting position determination, aircraft surveillance, etc 02 p0258 A66-12042  
Telecart C for automatic digital evaluation of data supplied by hyperbolic radio navigation systems 02 p0260 A66-12061  
Self-reported stress-related symptoms among air traffic control specialists /ATCS/ and non-ATCS personnel 03 p0324 A66-12358  
Multiple access satellite-borne reflex repeater for continuous line of sight digital data links and voice transmission for air traffic control 05 p0630 A66-14589  
Milan airport system noting air traffic 05 p0661 A66-15846  
Statistical study of training and job performance measures of Air Traffic Control Specialists representing Enroute, Terminal and Flight Service Station specialties 06 p0973 A66-16821  
Air traffic control simulation system based on digital computer for Eurocontrol 06 p0870 A66-16953  
Long range navigation in jet operations, discussing problems and limitations 07 p1065 A66-17670  
Navigation and air traffic control environment, particularly extent to which lateral and longitudinal separations depend on accuracy of navigation 07 p1065 A66-17676  
Mathematical formulation of lateral and longitudinal separation standards for subsonic and supersonic aircraft operation 07 p1066 A66-17680  
Aircraft separation criteria applied to supersonic transport, describing standards and parameters of air traffic safety 07 p1066 A66-17682  
SST navigation and air traffic control equipment for NAC-60 aircraft, noting climbout, cruise, position, landing, etc 07 p1067 A66-17687  
Location of flight control system for simplifying crew procedure and reducing navigation error in areas of high traffic density 07 p1068 A66-17697  
Air traffic control system capacity and navigational requirements for North Atlantic and continental transition areas, discussing relationship to accuracy and flight time economy 07 p1069 A66-17713  
Simulation of airport with SST aircraft in air traffic control system 07 p1070 A66-17725  
Operational requirements for improved worldwide navigational ability, initially applied in North Atlantic area 07 p1072 A66-17761  
Relation of air traffic control separation to collision risk, applicable to North Atlantic routes 07 p1072 A66-17762  
Model of North Atlantic air space organized as sets of paths at various heights 07 p1072 A66-17763  
Safety and economic factors which determine navigational requirements in long range traffic area 07 p0988 A66-17764  
Air traffic control requirement for navigational capability, taking safety and economy into account 07 p1073 A66-17765  
Air navigation problems in North Atlantic including separation standards lateral and vertical, SST traffic, collision risk, etc 07 p1074 A66-17774  
Combination of moored ocean platforms and transatlantic submarine telephone cables for VHF communication service and other ATC facilities for civil aircraft across North Atlantic 07 p1002 A66-17775  
British Dectra system as long distance navigation aid, detailing increased power and reduction of ambiguities by means of zone and lane



- entification 07 p1075 A66-17789
- Moving map displays for navigation information portrayal, advantages and requirements for subsonic and SST liners 07 p1076 A66-17796
- Air navigation operational requirements for effective air traffic control determined by ICAO Special NAT 07 p1077 A66-17803
- Modern inertial navigation system development, describing accuracy, reliability and operational use of SGN-10 07 p1077 A66-17804
- Air derived separation assurance /ADSA/ systems to avoid in-flight aircraft collisions, detailing range altitude, relative position velocity and projected hazard indicator basic types 07 p1078 A66-18223
- FAA regulation of civilian use of U.S. airspace 08 p1321 A66-18548
- Internal friction and vertical separation effects on airways and traffic control and high altitude deviation in barometric altimeters 08 p1249 A66-18693
- Text on international law of territorial airspace, discussing civil aviation, trespassing and crime aboard aircraft 08 p1322 A66-19237
- Altitude measurement requirements for supersonic transport including flight profile, air traffic control, climb, etc. 09 p1400 A66-20426
- Air collision risk and traffic control in long-range air traffic systems as basis for safe procedural separation 09 p1401 A66-20431
- Standards for air traffic control deviations and relation to size of separation 09 p1401 A66-20432
- Radar detection of sailplanes and other small aircraft aided by aluminum reflecting surfaces 09 p1345 A66-20479
- Air traffic control automation problems 09 p1401 A66-20550
- Clear or secondary radar for air traffic control, noting operating principles, structure, etc. 09 p1346 A66-20555
- International satellite communications, noting application for air traffic, using VHF and 09 p1346 A66-20561
- Vertical separation effect on safety of civil aircraft with type II or III altimeter over North Atlantic 10 p1553 A66-21334
- Operation of VTOL aircraft in vicinity of airport including safety, noise and air traffic control factors 10 p1482 A66-21372
- Air traffic control transponder performance preflight test set, ground-based equipment for fast and positive checkout 11 p1732 A66-22898
- Digital data handling method for air traffic control system employing plan position indicators and video correlator for radar beacon signal analysis 11 p1732 A66-22899
- General purpose computers and cathode ray tube displays used in automation of air traffic control technical 11 p1732 A66-22900
- Role of artificial Earth satellites in air traffic control [AIAA PAPER 66-259] 12 p1910 A66-24734
- Collision prevention in controlled and uncontrolled air space, noting onboard visual surveillance, radar systems, etc. 13 p1213 A66-25233
- Secondary surveillance radar in aiding port traffic through aircraft transponder interrogation 13 p1214 A66-25701
- Air navigation problems in North Atlantic including separation standards lateral and vertical, SST traffic, collision risk, etc. 13 p1214 A66-25861
- Combination of moored ocean platforms and transatlantic submarine telephone cables for VHF communication service and other V/C facilities for civil aircraft across North Atlantic 13 p2058 A66-25862
- Navigation and secondary surveillance radar /SSR/ used in commercial helicopters New York airways [SAE PAPER 660319] 14 p2223 A66-27299
- Legal question in air traffic control concerning recommendation for proof of alt system without limitation on capability 14 p2416 A66-27840
- ST air traffic control and fuel consumption dependence on wind drift and atmospheric temperature 14 p2328 A66-28231
- Proposed one-satellite synchronous satellite system for over-ocean surveillance of aircraft 14 p2329 A66-28364
- Supersonic transport operations, particularly analog computer facility at Langley Research Center and ATC simulator at National Aviation Facilities Experimental Center 15 p2443 A66-28744
- SST air traffic control and arrival and departure simulation 15 p2425 A66-28745
- Air traffic controller performance in detecting possible conflicts among aircraft 15 p2534 A66-29125
- Automatic air traffic control development in France 15 p2534 A66-29126
- Schiphol Airport /Amsterdam/ analog computer installation for air traffic control and flight path calculations, with results displayed on automatic flight progress boards 15 p2534 A66-29311
- Air traffic control in West Germany, considering higher air traffic density and operating speeds 15 p2534 A66-29366
- Separation standards for air traffic control, with analysis of collision risks 15 p2535 A66-29623
- Aircraft navigational error parameters combined statistically and used to evaluate wander expected in transport aircraft operating in transoceanic environment 15 p2535 A66-29624
- Terrain clearance during climb and descent under air traffic control 15 p2535 A66-29627
- Optimum model route structure for North Atlantic subsonic jet traffic 15 p2535 A66-29713
- Possible use of computer as tool for air traffic control 16 p2742 A66-30089
- Navigation satellites as monitoring device by integrating navigational hardware into communications satellite for ATC 16 p2743 A66-30667
- Air traffic control system using primary and secondary radar, radar digitizer and computer complex 16 p2744 A66-31278
- Air traffic control radars, discussing airport surveillance radar /ASR/, precision approach radar /PAR/ and secondary surveillance radar /SSR/ 16 p2666 A66-31444
- Cruising level systems and semicircular rule 17 p2950 A66-32354
- SRT daylight radar display system for air traffic control 17 p2950 A66-32355
- Closed circuit television applied to data transfer in air traffic control, discussing accident prevention and information provision to aircraft 17 p2874 A66-32356
- Flight evaluation using course line computers with pictorial display as navigation aid 17 p2950 A66-32357
- Separation standards and navigation in long-range air traffic control region 17 p2954 A66-33213
- Air traffic control and navigation system for North Atlantic and worldwide all-weather navigation 17 p2956 A66-33224
- Automation in flight safety, noting role of radar, flight control system reliability, data processing system used, etc. 17 p2848 A66-33485
- Separation of aircraft over North Atlantic especially reduced lane width from 120 to 90 n miles 18 p3130 A66-33558
- Role of artificial Earth satellites in air traffic control [AIAA PAPER 66-259] 20 p3659 A66-36931
- Automation of air traffic control, discussing radar, data handling and data communication 20 p3595 A66-37003
- National and international trends in ATC from standpoint of pilot and operator safety 20 p3595 A66-37004
- Quantification of relative contributions of various functions to performance of mission combined with availability and dependability for system effectiveness 20 p3684 A66-37883
- Air traffic control problems posed by advent of supersonic transport may be eased by pictorial navigation display 20 p3598 A66-38185
- Safe separation standards estimation for analyzing long-range air traffic systems, emphasizing flying errors observation in operational conditions 21 p3760 A66-38452
- Costing of parallel route systems for supersonic traffic, examining diurnal traffic patterns, sensitivities to fuel requirements, sonic bang avoidance and layout of track systems 21 p3761 A66-38453
- Air traffic estimation, discussing installation locations and parameters for airport site choice 21 p3838 A66-39433
- Aircraft collision avoidance problems and approaches to solution, discussing air derived separation assurance /ADSA/ 21 p3768 A66-39466
- Narrow band transmitters for response code of secondary radar installations containing identity of aircraft and altitude for air traffic control 21 p3706 A66-39634
- Satellite functions in air traffic control systems noting position determination, aircraft surveillance, etc. 22 p3945 A66-40326
- Japanese air traffic control using real time computer data processing 22 p3945 A66-40617
- Approximation method for maximizing nonlinear separable function with two-sided limitations on unknowns, given common lower boundary for difference modulus of unknowns 23 p4088 A66-41059
- Stability, control, navigation, guidance and air traffic control of hypersonic vehicles noting inertial technology, flight planning and optimal control 24 p4235 A66-42239
- AIR TRANSPORTATION**
- SA CIVIL AVIATION**
- SA SUPERSONIC TRANSPORT**
- Short haul transport systems early and rapid evolution requirements to select first generation vehicles [SAE PAPER 650783] 01 p0012 A66-10840
- Organization of short-distance interurban transportation system based on STOL aircraft of Breguet type 05 p0611 A66-15194
- West German federal air transport authority, scope, organization and objectives 05 p0794 A66-15807
- Short-range aircraft design efficiency and possible reduction in operating cost 06 p0804 A66-15990
- Proposal for control of local service subsidies, noting lack of clearly stated public policy with respect to congressional statements and actions 06 p0973 A66-16401
- Price discrimination and regulation of air transportation, examining history, interplay and evolution 06 p0973 A66-16402
- Air transportation in next fifty years 07 p0985 A66-17226
- Air transport engineering, cost and reliability factors, development possibilities, new design construction phasing, etc. 07 p0987 A66-17488
- Interaction of pilot capabilities and economic factors on future air transport, noting problems with SST, V/STOL, Mach 6 transport craft, etc. 07 p1156 A66-17611
- International Air Transport Association, Technical Conference, Miami, April 1965, Volume 1 07 p1063 A66-17687
- Inertial navigation and guidance systems applied to civil air transport from systems engineering viewpoint 07 p1067 A66-17695
- International Air Transport Association, Technical Conference, Miami, April 1965, Volume 2 07 p1071 A66-17757
- Inertial navigation on north transatlantic route, examining inertial equipment, flight planning and preflight cockpit checks 07 p1076 A66-17798
- Book on political, economic and military analysis of air transport policy and national security 09 p1472 A66-20099
- STOL operations in city center, discussing metropolitan transportation problems 09 p1327 A66-20244
- Terminal facilities, support equipment and operational characteristics of V/STOL aircraft 09 p1330 A66-20696
- Inertial navigation and guidance systems applied to civil air transport from systems engineering viewpoint 13 p2125 A66-25865
- ATA direct operating cost formula for transport aircraft, considering flying operations, maintenance, depreciation and indirect costs [SAE PAPER 660280] 14 p2222 A66-27289
- Costs and operational characteristics of short haul air transportation in mid-1970 and 1980 periods in eastern corridor [SAE PAPER 660332] 14 p2223 A66-27295
- V/STOL aircraft for intercity travel, discussing cost, advantages, technological advances, etc. [SAE PAPER 660318] 14 p2223 A66-27298
- Overcapacity in U.S. international air



transport industry due to transition to jet between 1954 and 1963 14 p2417 A66-27841

Air cargo - International Forum, Chicago, May 1966 15 p2619 A66-29788

Coordinated air-surface transportation microeconomic analysis 15 p2620 A66-29796

Updating of air cargo documentation permitting intranet control and orderly accumulation of statistical information, noting forms and teletype machines 15 p2621 A66-29800

Civil Aeronautics Board /CAB/ role in air freight industry and in proposed Department of Transportation 15 p2621 A66-29804

Helicopter capabilities in solving interurban mass transport problems, particularly cost and time considerations [SAE PAPER 660336] 15 p2427 A66-29835

Helicopter design and application to common carrier transportation, particularly between airport and city [SAE PAPER 660335] 15 p2428 A66-29846

Commercial V/STOL aircraft and systems development, discussing government /FAA/ interest and assistance 16 p2633 A66-31281

Transportation developments for airport planning, emphasizing need to limit carrier transport service to single airport 16 p2682 A66-31283

Short haul air transportation in Europe, noting market development with helicopter techniques and development of more efficient rotor aircraft 23 p4151 A66-41303

Air transportation between 1980 and 2000, noting cost limitation, possible trends, management planning, etc 23 p4152 A66-41304

Passenger and cargo aircraft development 23 p4152 A66-41647

## AIRBORNE EQUIPMENT

Advanced integrated landing system /AILS/ consisting of azimuth and elevation ground station, ground display site and airborne unit, emphasizing scanning-beam technique 01 p0101 A66-10034

Progress in constant speed drive generating systems and control equipment for constant frequency aircraft electric systems [SAE PAPER 650827] 01 p0016 A66-10827

Coordinated program for airborne and ground support equipment testing of Gemini spacecraft and launch vehicle by two different manufacturers 02 p0294 A66-11635

Advisability of West German electronics industry stepping into aviation electronics industry to greater extent 02 p0199 A66-11859

MCS 920M airborne digital computer design, production processes and microelectronic techniques 02 p0193 A66-11931

Worldwide navigation system using existing ground and airborne equipment and limited number of navigation satellites 02 p0259 A66-12054

Airborne equipment modernization through elimination of moving parts and conversion from analog to digital techniques [AIAA PAPER 65-729] 03 p0341 A66-12580

Design and installation of antennae for airborne command and control systems, noting antenna system for SAC Airborne Command Post [AIAA PAPER 65-730] 03 p0334 A66-12581

Implementation of airborne command and control systems, emphasizing communications equipment, data processing facilities, electromagnetic compatibility and aircraft configuration parameters [AIAA PAPER 65-727] 03 p0336 A66-13049

Direct measurements of turbulent thermal flux using airborne pulse type system 04 p0513 A66-13418

Amount of maintenance float determined from relation between maintainability and reliability used to estimate effects of product changes [AIAA PAPER 65-734] 04 p0525 A66-13634

Avionics design using integrated electronics or microelectronics, noting reduction of maintenance requirements 04 p0494 A66-13684

Tests of airborne, gimbal and stabilized mounts of LaCoste-Romberg and Askania-Graf gravity meters conducted in 1962 04 p0524 A66-14452

IR spectral reflectance of terrestrial

atmosphere including ground cover effect, noting data from airborne equipment and instrumented rocket 05 p0669 A66-14947

Airborne laser-radar light detection and ranging /LIDAR/ systems applied to detection of clear air turbulence /CAT/ 05 p0697 A66-15297

Maintenance recordings of aircraft parameters, discussing signal conditioning, economics and application [ISA PREPRINT 1.3-1-65] 05 p0794 A66-15499

Airborne measurement of microwave emission from Earth surface and atmosphere for potential application of radiometry to weather satellite reconnaissance 05 p0675 A66-15765

One-way microelectronic airborne digital data converter intended for use in automatic carrier landings 06 p0824 A66-15969

Preflight and operational status test set /PTS/ using radiating techniques for checking out aircraft electronic equipment without removal from aircraft 06 p0868 A66-15986

Airborne navigation and flight-control equipment for reducing weather minimums to lowest possible level 06 p0907 A66-16427

Cloud raindrop sizes and concentration measurement by airborne flow device 06 p0880 A66-16556

Fault location in modern airborne radar, discussing maintenance reduction techniques and reliability improvement 07 p1006 A66-17495

Aircraft separation criteria applied to supersonic transport, describing standards and parameters of air traffic safety 07 p1066 A66-17682

Airborne computer design free of navigational functions performed by humans, using Doppler equipment 07 p1087 A66-17692

Mechanization of navigational functions for supersonic aircraft within central airborne digital computer, comparing military experience with commercial requirements 07 p1067 A66-17693

DECTRA long range navigational aid, DECTRA airborne receiver and Omnitrac computer 07 p1068 A66-17702

Doppler equipment including planar-array antennas, varactor-multiplier sources, etc, evaluated for third generation Decca series 07 p1068 A66-17703

Flight testing of FAA-Lear Siegler receiver/converter airborne system with Loran-C hyperbolic navigation system 07 p1069 A66-17706

C-band weather radar AVQ-10 incorporating tunnel diode amplifier and p-i-n solid state protector switch 07 p1008 A66-17711

Advanced airborne computer double system applied to fault detection, location, flight management and navigation 07 p1003 A66-17715

Airborne computer-aided navigation system, utilizing letter printer and pictorial display 07 p1070 A66-17718

VOR developments in terms of degree of compatibility with respect to airborne equipment 07 p1075 A66-17787

Reduction of signal power in X-band CW aircraft radar echo 08 p1181 A66-18718

Low cost airborne fixed-point data processor designed to operate with nondestructive readout instructions, constant memory and separate destructive-readout memory 08 p1184 A66-19522

Effect of altitude and camera field-of-view at various degrees on geographic orientation and error in target position, using TV data 08 p1225 A66-19531

Airborne microwave reconnaissance receiver design with almost zero IF 08 p1226 A66-19535

Sky observations with balloon-borne X-ray telescope having sodium iodine scintillator 09 p1442 A66-20466

Airborne camera system used to obtain roll, pitch and heading angles for aircraft during takeoff and landing [AIAA PAPER 65-210] 09 p1330 A66-20744

Aerodynamics of manometers and mass spectrometers used on rockets and satellites for determination of atmospheric temperature and density 09 p1383 A66-20993

Equipment located between Diamant second-stage propulsion unit and jettisonable

rear skirt of third stage including antennas, auxiliary rockets, attitude changing apparatus, control and guidance, etc 10 p1518 A66-21258

X-ray photographs of Sun using Fresnel zone plate camera mounted on Skylark rocket, noting Lyman C-VI emission line in solar spectrum 10 p1607 A66-21291

Onboard equipment designed for transport aircraft landings with visibilities less than 200 ft and runways less than 2600 ft, having all devices duplicated 10 p1554 A66-21368

Ground support equipment /GSE/ concept, onboard checkout system for large space boosters [AIAA PAPER 64-298] 10 p1612 A66-21955

Design of Malfunction Detection System used on board orbiting laboratory type vehicles to monitor and evaluate critical signals 10 p1538 A66-22043

Precise airborne geodetic survey system capable of measuring lines up to 900 nautical miles and determining nadir of aerial photographs to 24 ft 10 p1533 A66-22045

Flight and navigation procedures and requirements for civil aerial photography 11 p1705 A66-22662

Balloon-borne instrument for measuring downward flux of thermal radiation from atmospheric water vapor, using gold doped germanium detector 11 p1706 A66-22888

Computer capability and probable growth in aerospace vehicle applications considered against mission requirement constraints 11 p1659 A66-22959

Spark chamber with vidicon readout for balloon-and satellite-borne high energy gamma ray astronomy analysis, noting Cerenkov counter 12 p1877 A66-23685

Digitized spark chamber for balloon and satellite gamma ray astronomy, noting detector array, high voltage system and data acquisition and handling systems 12 p1877 A66-23687

Automatic handling of information by analog recording on magnetic tape for control, monitoring and maintenance of aircraft 12 p1880 A66-23817

Short term frequency stability affecting resolution and range of Doppler radar noting system and circuit requirements when operating under severe vibration and acoustic environment 12 p1815 A66-24131

Clear air turbulence types at high altitude identified and intensity and wavelength measured by FM instrument, using van der grust probe installed in U-2 aircraft [AIAA PAPER 66-362] 12 p1907 A66-24494

Microwave integrated circuits in radar systems, detailing airborne forward-looking radar, using phased arrays and pulse compression 12 p1840 A66-24621

Simultaneous observations of auroral zone X-ray microbursts, using two balloon-borne radiation detectors separated by 300 km to estimate size of region of electron precipitation 12 p1944 A66-24844

Design of system analyzing operating conditions of jet engine up to overhaul, recording regime of engine revolutions exhaust gas temperatures, accelerations, etc 13 p2076 A66-25077

Airborne checkout system, in-flight maintenance and related signal processing problems 13 p2190 A66-25255

Digital airborne computer for navigation problem solutions including inertial navigation, flight path, time-to-go and arrival time, etc 13 p2124 A66-25883

Electric machines employing evaporative and universal cooling systems for aircraft use 13 p2041 A66-25901

Cross sections of geomagnetic field intensity and ionospheric characteristic obtained by airborne equipment crossings of geomagnetic dip equator 13 p2074 A66-26331

Random error of drift measurements using airborne Doppler radar from observed drift output during short flight over fixed course calculating rms values 13 p2125 A66-26444

Reliability improvement in airborne electronic equipment 13 p2044 A66-26661

Modeling and data reduction techniques for obtaining spectrum signatures of low gal. LF airborne antennas 13 p2044 A66-26774

Ground-based test setup using p-n-p controlled switches, logic circuitry and



- sive relays to analyze telemetered pulse  
 als from four lines of airborne  
 etronic system 14 p2255 A66-27807  
 ound raindrop sizes and concentration  
 asurement by airborne flow  
 ice 14 p2297 A66-28228  
 ratospheric small-ion density  
 asurement from high-altitude jet aircraft,  
 ing dust effect 14 p2297 A66-28334  
 r Force Avionics Laboratory and  
 blem of transition from exploratory  
 elopment to operational  
 dware 15 p2618 A66-28746  
 3 rocket observation of proton and  
 etron fluxes at high altitudes, using solid  
 ce detectors 15 p2574 A66-28910  
 ear air turbulence detection and warning  
 r airborne devices including radar, IR  
 etrum, air temperature probes, ozone  
 ection, etc 15 p2500 A66-28917  
 ear air turbulence detection instrument  
 elopment 15 p2500 A66-28919  
 amera tubes for recording Stratoscope II  
 escope, noting photometric  
 elity 15 p2500 A66-28969  
 FCRL grazing incidence grating  
 nomochromator used with thin window flow  
 ager detector on Aerobee rocket for solar  
 etrum recordings between 30 and 130  
 estroms 15 p2605 A66-30079  
 vionics and  
 nsportation 16 p2830 A66-30087  
 ilitary aerial mapping program, noting  
 mera lens distortion, shutter, stabilization,  
 ms, etc 16 p2703 A66-30511  
 valuation of nonstereoscopic pairs of  
 otographs obtained from vertical base by  
 wing camera, determining spatial  
 rdinates of points on  
 otographs 16 p2703 A66-30512  
 ultisensor airborne reconnaissance  
 sion planning and data  
 uisition 16 p2704 A66-30516  
 yro-stabilized heliostat for airborne  
 ronomy noting design principles, achieved  
 bility, servoloop and mechanical  
 tem 16 p2705 A66-30824  
 yro-stabilized airborne solar eclipse  
 ctrograph, noting wavelength range,  
 rsion accuracy, guidance mechanism,  
 16 p2705 A66-30825  
 ircraft instrumentation for spectroscopic  
 servation of solar middle corona at  
 edium dispersion on May 30,  
 55 16 p2705 A66-30826  
 olarization photography of solar corona,  
 ing apparatus used for separation of K  
 m F component 16 p2705 A66-30827  
 elicopter simulation system for avionic  
 valuation 16 p2682 A66-31248  
 hermostability and control of airborne  
 lectronic equipment in closed-loop forced-  
 cooling systems 16 p2663 A66-31325  
 easibility of monopulse radar used for  
 rborne pictorial radar display as aid to low  
 roach aircraft landing 17 p2950 A66-31964  
 cosmic X-ray sources observed through  
 rket-mounted detectors, noting differences  
 spectra 17 p2994 A66-32970  
 ransfluxor program store for airborne  
 gital computer, noting wiring pattern,  
 onomics, read amplifier,  
 18 p3072 A66-33562  
 Atmospheric density measurements for  
 titudes up to 74 km from X-15 flights  
 ing stagnation pressure method  
 IAA PAPER 66-441] 18 p3104 A66-33646  
 ntegrated elements for aerial surveying  
 d mapping 18 p3109 A66-33739  
 Mark II avionics system used in F-111A  
 ctical fighter for navigation and weapons  
 elivery performance 18 p3076 A66-33958  
 Radiation pattern of ground surveillance  
 dar antenna measured with aid of airborne  
 gal generator 18 p3070 A66-34266  
 ACAN and DME navigation systems,  
 scussing ground stations, airborne  
 quipment and guidance  
 stems 18 p3133 A66-34465  
 nterplanetary magnetic field  
 easurements using flux gate magnetometer  
 nsor mounted on Pioneer VI space probe,  
 ing various graphs 18 p3108 A66-34538  
 Flight data recording and processing  
 stem using magnetic tape for digitally  
 mputing airborne data on flight testing of  
 OL aircraft 18 p3073 A66-34679  
 Primary cosmic radiation modulation study  
 by Ariel I and airborne  
 detector 18 p3180 A66-34770  
 Low-energy protons and electrons of outer  
 radiation belt measured by equipment  
 onboard Cosmos XLI 18 p3196 A66-34872  
 Airborne equipment for study of nucleon  
 interactions at energies in excess of 10  
 trillion ev 18 p3214 A66-35155  
 Built-in tests and periodic testing at field  
 shop level applied to avionic systems  
 operational readiness 19 p3339 A66-35504  
 Microelectronic airborne radar equipment  
 operating in ground mapping, terrain  
 avoidance and air to ground ranging, noting  
 design, packaging, etc 19 p3313 A66-35519  
 Operational environment formulation for  
 airborne navigation radar 19 p3397 A66-35521  
 Microelectronics impact on future airborne  
 radar systems reliability, cost and  
 performance 19 p3314 A66-35522  
 Mission system effectiveness of avionic  
 weapon system predicted by general-purpose  
 computerized technique 19 p3480 A66-35528  
 Airborne UHF telemetry receiver utilizing  
 solid state components and high-density  
 packaging technique 19 p3316 A66-35691  
 Microelectronics in airborne equipment,  
 noting reliability and cost  
 reduction 19 p3360 A66-36261  
 Linear polarization and relative intensity  
 variations of skylight measured with  
 aircraft-mounted telephotopolarimeter  
 during solar eclipse 19 p3349 A66-36346  
 Hydrogen and helium ions formation and  
 destruction, charge transfer, diffusion, role  
 during solar activity, using mass  
 spectrometry, ground radar,  
 etc 19 p3350 A66-36356  
 Airborne data acquisition statistical  
 recorder 19 p3361 A66-36669  
 Real-time data gathering and flight-test  
 technique for aircraft-carried weapons  
 system development  
 testing 20 p3495 A66-37207  
 Automatic built-in test of advanced  
 avionics systems, noting advantages of  
 airborne computer in sequencing, conducting  
 and evaluating in-flight  
 performance 20 p3522 A66-37245  
 Digital testing techniques for analog  
 systems, describing bomb computer set for  
 Phantom F-4D aircraft 20 p3522 A66-37246  
 In-flight stress measurements on coaxial  
 counterrotating helicopter blades, using  
 semiconductor strain gauge with HF  
 telemetric data  
 transmitters 20 p3668 A66-37504  
 Reliability testing programs applied to  
 aircraft electronics equipment and  
 description of development of MIL-STD-  
 781A, exploring relation between reliability  
 prediction and measurement  
 techniques 20 p3570 A66-37936  
 Central Telecommunications Laboratory 882  
 P arithmetical airborne  
 computer 20 p3523 A66-38013  
 Airborne electronic command device for  
 measuring time intervals corresponding to  
 cruising speed/ true flight altitude ratios up  
 to 40 21 p3735 A66-38569  
 Airborne guidance computations using  
 prescribed-h method, representing two-body  
 motion in inertial space, presenting  
 equations for target hitting, circular orbit,  
 etc 21 p3765 A66-38869  
 Airborne photoelectric device for  
 registration of cloud  
 drops 21 p3739 A66-39365  
 Aircraft equipment cooling techniques and  
 systems, particularly natural or free  
 convection 21 p3699 A66-39614  
 Aircraft and spacecraft digital systems  
 including computers for production  
 engineering, ground telemetry and  
 communication with aerospace vehicle and  
 onboard equipment for tracking, guidance  
 and simulation of inflight  
 conditions 21 p3709 A66-39629  
 Clear air turbulence detection and warning  
 by airborne devices including radar, IR  
 spectrum, air temperature probes, ozone  
 detection, etc 22 p3945 A66-40325  
 Turbulent refractivity spectrum and  
 optimization of airborne radar CAT  
 detectors 22 p3944 A66-40429  
 Rotary plate airborne bacteria  
 sampler 22 p3858 A66-40505  
 Ion temperature measurements around 1000  
 km altitude, using ion energy analyzer and  
 mass spectrometer mounted on  
 rocket 22 p3913 A66-40551  
 Number densities and composition of  
 upper atmosphere determined by  
 rocketborne mass spectrometers, estimating  
 temperature variation with  
 altitude 22 p3913 A66-40553  
 Airborne spectrozonal telephotometer used  
 in calculation of photographic brightness  
 coefficient of Earth  
 surface 22 p3919 A66-40621  
 Signal simulator for testing Loran A and  
 Loran C airborne receivers in laboratory,  
 using digital simulator circuits to test  
 dynamic response of tracking  
 circuits 23 p4088 A66-41253  
 Onboard miniaturized telemetry system for  
 stagnation point temperature measurements  
 on free-flight models in ballistic  
 ranges 24 p4209 A66-42189  
 Airborne digital computers role in  
 electronic warfare, navigation and guidance,  
 considering weight, power supply, costs,  
 etc 24 p4177 A66-42245

AIRCRAFT

- SA A-4 AIRCRAFT  
 SA A-6 AIRCRAFT  
 SA A-7 AIRCRAFT  
 SA AGRICULTURAL AIRCRAFT  
 SA ANTISUBMARINE WARFARE  
 AIRCRAFT  
 SA ANTONOV AN-22 AIRCRAFT  
 SA ATTACK AIRCRAFT  
 SA B-58 AIRCRAFT  
 SA BAC 111 AIRCRAFT  
 SA BALLOON  
 SA BEAGLE B-206 AIRCRAFT  
 SA BOEING 707 AIRCRAFT  
 SA BOEING 720 AIRCRAFT  
 SA BOEING 733 AIRCRAFT  
 SA BOEING 737 AIRCRAFT  
 SA BOMBER AIRCRAFT  
 SA BREGUET 941 AIRCRAFT  
 SA BREGUET 942 AIRCRAFT  
 SA BREGUET 1150 AIRCRAFT  
 SA C-5 AIRCRAFT  
 SA C-141 AIRCRAFT  
 SA C-142 AIRCRAFT  
 SA CANADAIR CL-84 AIRCRAFT  
 SA CESSNA 210 AIRCRAFT  
 SA COMMERCIAL AIRCRAFT  
 SA CONCORDE AIRCRAFT  
 SA DASSAULT MIRAGE III AIRCRAFT  
 SA DASSAULT MYSTERE XX  
 AIRCRAFT  
 SA DE HAVILLAND DH-121 AIRCRAFT  
 SA DE HAVILLAND DH-125 AIRCRAFT  
 SA DORNIER DO-31 AIRCRAFT  
 SA DOUGLAS DC-8 AIRCRAFT  
 SA DOUGLAS DC-9 AIRCRAFT  
 SA DRONE  
 SA EXECUTIVE AIRCRAFT  
 SA F-4 AIRCRAFT  
 SA F-5 AIRCRAFT  
 SA F-8 AIRCRAFT  
 SA F-104 AIRCRAFT  
 SA F-111 AIRCRAFT  
 SA FAN-IN-WING AIRCRAFT  
 SA FIAT G-222 AIRCRAFT  
 SA FIGHTER AIRCRAFT  
 SA FIXED-WING AIRCRAFT  
 SA FOKKER F-27 AIRCRAFT  
 SA FOKKER F-28 AIRCRAFT  
 SA GETOL AIRCRAFT  
 SA GLIDER  
 SA GROUND EFFECT MACHINE  
 SA HAMBURGER HFB 320 AIRCRAFT  
 SA HANDLEY PAGE HP-137 AIRCRAFT  
 SA HAWKER P 1127 AIRCRAFT  
 SA HELICOPTER  
 SA HYPERSONIC AIRCRAFT  
 SA ILYUSHIN IL-62 AIRCRAFT  
 SA INTERCEPTOR  
 SA JET AIRCRAFT  
 SA LIGHT AIRCRAFT  
 SA LOCKHEED L-2000 AIRCRAFT  
 SA MANNED AIRCRAFT  
 SA MILITARY AIRCRAFT  
 SA NIHON XS-11 AIRCRAFT  
 SA NORD 600 AIRCRAFT  
 SA NORD 1500 AIRCRAFT  
 SA NUCLEAR AIRCRAFT  
 SA P-3 AIRCRAFT  
 SA PILOTED AIRCRAFT  
 SA PRIVATE AIRCRAFT  
 SA RECONNAISSANCE AIRCRAFT  
 SA ROCKET AIRCRAFT



SA ROTARY WING AIRCRAFT  
 SA SAAB 37 AIRCRAFT  
 SA SAILPLANE  
 SA SEAPLANE  
 SA STOL AIRCRAFT  
 SA SUBSONIC AIRCRAFT  
 SA SUD VJ-101 AIRCRAFT  
 SA SUNRISE S-1600 AIRCRAFT  
 SA SUPERSONIC AIRCRAFT  
 SA T-34 AIRCRAFT  
 SA T-38 AIRCRAFT  
 SA T-39 AIRCRAFT  
 SA TAILLESS AIRCRAFT  
 SA TARGET AIRCRAFT  
 SA TERRAIN FOLLOWING AIRCRAFT  
 SA TILT-WING AIRCRAFT  
 SA TRAINING AIRCRAFT  
 SA TRANSPORT AIRCRAFT  
 SA TURBOPROP AIRCRAFT  
 SA UTILITY AIRCRAFT  
 SA V/STOL AIRCRAFT  
 SA VICKERS VC10 AIRCRAFT  
 SA VTOL AIRCRAFT  
 SA X-15 AIRCRAFT  
 SA X-19 AIRCRAFT  
 SA X-20 AIRCRAFT  
 SA X-21 AIRCRAFT  
 SA X-22 AIRCRAFT  
 SA XB-70 AIRCRAFT  
 SA XC-142 AIRCRAFT  
 SA XV-5 AIRCRAFT  
 Janes compendium of world aircraft, missiles and rockets 04 p0458 A66-14382  
 Aircraft with wings of low aspect ratio 09 p1329 A66-20556  
 Generalized masses of vibrational modes of elastomechanical system determined by three methods 17 p3018 A66-31876

**AIRCRAFT ACCIDENT**  
 Army evaluation and implementation of MIL-S-58077 in system safety engineering of aircraft to eliminate initial high accident rate 01 p0009 A66-10061  
 Aircraft crash loads and motion prediction by set of equations with results correlated by experiments on Lockheed 1649A and Curtiss C-46 01 p0009 A66-10071  
 Naval Aviation Safety Center role in reducing aircraft accidents annually, noting material and man-made accidents 01 p0009 A66-10072  
 Aircraft damage scale constructed from photographs of accident-involved aircraft by method of equal-appearing intervals 02 p0177 A66-11831  
 Historical development of rules governing international cooperation on aircraft accident investigations [AIAA PAPER 65-768] 03 p0446 A66-12591  
 Carrier landing improvements in Fresnel lens optical landing system, emphasizing compensated-meatball stabilization [AIAA PAPER 65-791] 03 p0322 A66-13228  
 USAF aircraft accidents involving ten or more fatalities 06 p0807 A66-16825  
 XB-70A in-flight wing accident, noting damage 07 p0987 A66-17277  
 Marine pilot training to develop visual habit patterns as aid in reducing mid-air collision hazards 07 p0999 A66-17712  
 Air derived separation assurance /ADSA/ systems to avoid in-flight aircraft collisions, detailing range altitude, relative position velocity and projected hazard indicator basic types 07 p1078 A66-18223  
 Passenger injuries due to decompression, impact and explosion from dynamite in rear lavatory of Boeing 707 at high altitude 09 p1336 A66-20522  
 RAF system of classification of aircraft accidents by causes for statistical purposes 10 p1494 A66-22139  
 Human factors in causation of aircraft accidents such as faulty perception, erroneous instrument reading and central nervous system malfunction 10 p1495 A66-22140  
 Results of aircraft accidents in terms of injury and death in-flight, on impact, after impact and during escape 10 p1495 A66-22141  
 Medical knowledge as aid in preventing aircraft accidents and injury through investigation of causes and results 10 p1495 A66-22142  
 Contribution of medical science to accident prevention, discussing causes, results and escape from standpoint of man and machine 10 p1495 A66-22143

Simulation of aircraft crashes to evaluate seating and restraint systems 16 p2680 A66-30480  
 Human factors in B-58 aircraft accidents, considering nose-high landing requirement, pilot fatigue and evaluation of ejection facilities 17 p2864 A66-32166  
 Aircraft accidents resulting from pilot errors of skill and background factors 19 p3294 A66-36439  
 Pilot role in VTOL safety during takeoff and transition phase 19 p3279 A66-36440  
 Medical inquest of Britannia 312 crash near Innsbruck 19 p3294 A66-36441  
 Aircraft accident victim identification techniques 19 p3294 A66-36444  
 Aircraft escape systems design criteria established using military accident statistics, noting drogue parachute and pilot sizes 22 p3850 A66-40610  
 Alcohol induced hypoglycemia as factor in aircraft accidents, noting effect of post mortem changes in blood glucose level 24 p4164 A66-42458

**AIRCRAFT ACCIDENT INVESTIGATION**  
 SR-N5 hovercraft accidents analyzed for prevention of future overturnings or plough-ins 05 p0609 A66-14866  
 Determining whether aircraft was on fire before crash by examination of wreckage fragments 09 p1329 A66-20241  
 French commercial aircraft accident investigation 13 p1994 A66-25232  
 Flight accident casualties, pathological changes in bodies of victims of Comet 4C SA-R7 accident in Italy 14 p2229 A66-26812  
 Hostile long term storage environments, discussing aircraft component condition following extensive exposure 16 p2635 A66-30472  
 Statistical analysis of vertebral fracture in U.S. Navy during 1959-1963 period 16 p2644 A66-31132  
 Accidents involving human error evaluated from medical point of view 18 p3053 A66-34947  
 Civilian aircraft accident investigation in West Germany 19 p3294 A66-36442  
 Air Force pathologist role in accident investigation, noting crash injuries 19 p3294 A66-36443  
 Flying skills assessment in relation to accident liability 20 p3508 A66-36995  
 Swedish aircraft incident /near accident/ documentation and analysis, discussing high rate in air force, prevention and psychophysiological excitation of in-flight tasks 20 p3508 A66-37007

**AIRCRAFT ANTENNA**  
 Linking monopulse radar antennas in aircraft tracking system 04 p0497 A66-13965  
 Correlation between clear air turbulence and aircraft electrical activity, describing corona discharges from DC-8 tail antenna 15 p2426 A66-28922  
 LF electrostatic field characteristics of clear air turbulence, noting theory and application of field sensing antennas, turbulence generated signals, etc 15 p2532 A66-28923  
 VHF aircraft antennas for propagation and communication via synchronous satellite, discussing nose radome yagi and window cavity arrays 20 p3525 A66-37235  
 Antennas for electronic navigation, discussing aircraft and ground based equipment, radiation patterns, restrictions, etc 20 p3597 A66-37719

**AIRCRAFT APPROACH AND LANDING INSTRUMENT**  
 Sectionalized, automatic approach and landing system with monitor channel added developed by Boeing-Bendix for all-weather landing 01 p0101 A66-10033

**AIRCRAFT BRAKE**  
 SA DROGUE PARACHUTE  
 SA WHEEL BRAKE  
 Water, ice and slush effects on traction characteristics of runway pavement, noting aquaplaning and aircraft braking criteria 02 p0216 A66-12223  
 Aircraft braking system, determining energy absorbed during landing or interrupted takeoff 06 p0807 A66-16970  
 Aircraft landing gear design, evaluating undercarriage of research aircraft and weapons systems 07 p0987 A66-17359  
 Hytrol electronic/hydraulic antiskid braking

system for automatic braking pressure modulation in BAC one-eleven 400 series aircraft 07 p0992 A66-18163  
 P-3 tricycle landing gear assembly examining mechanical and hydraulic mechanisms for brakes and steering, using graphic charts 19 p3279 A66-36059

**AIRCRAFT BREATHING APPARATUS**  
 Physiology of breathing at reduced pressure and design of aircraft oxygen system, noting cabin and mask design 10 p1489 A66-22118  
 LOX characteristics for on board breathing equipment including contaminants noxious to people, clogging of equipment, explosiveness and possible use of contaminated LOX 22 p3858 A66-40504

**AIRCRAFT CABIN**  
 SA CABIN ATMOSPHERE  
 SA PRESSURIZED CABIN  
 Approach and landing visibility requirements in terms of information needed by civil pilot 01 p0101 A66-10033  
 Air conditioning system of SST Concordia noting reliability 04 p0460 A66-14464  
 Low humidity and dehydration in jet fuselage, noting water metabolism and effect of various beverages 10 p1491 A66-21333  
 Pressure cabin design and utilization noting relation between air speed and environmental temperature on kinetic heating, contamination of cabin air, pressurization control, sealed cabin advantages, etc 10 p1492 A66-22111  
 Air conditioning system of SST Concordia noting reliability 11 p1640 A66-22255  
 Interior design of BAC 111 short haul jet transport 13 p1994 A66-25566  
 Airliner seat and galley design, investigating loading and safety, comfort convertible seats, upholstery, quick-change seating, etc 21 p3696 A66-39394

**AIRCRAFT CARRIER**  
 Automatic and semiautomatic vectoring and landing capability of U.S. Navy carrier-based aircraft F-4G Phantom II 01 p0099 A66-10000  
 Carrier landing improvements in Fresnel lens optical landing system, emphasizing compensated-meatball stabilization [AIAA PAPER 65-791] 03 p0322 A66-13228  
 One-way microelectronic airborne digital data converter intended for use in automatic carrier landings 06 p0824 A66-15966  
 Versatile avionics shop test /VAST/ system, computerized test system for carrier-based avionics 12 p1838 A66-24666  
 Radiation of prescribed polarization from cross-dipole antenna on aircraft carrier 15 p2447 A66-28555

**AIRCRAFT COMMUNICATION**  
 Frequency diversity can increase degree of compensation for multipath fading and thus improve communication reliability of airborne UHF communications 01 p0031 A66-10877  
 HF antenna coupler noting placement, parts and advantages over long wave antennas 03 p0335 A66-12909  
 Detachable radio relay pods /RRQ-5/ increase range of UHF and VHF communications systems [AIAA PAPER 65-728] 03 p0336 A66-13040  
 VHF aircraft-satellite relay /VASR/ means of improving long-range communications, with flight test results 06 p0825 A66-15966  
 Book on radio wave propagation for aircraft radio communication including frequency ranges, waveguides, ionospheric layer influence, noise, antenna properties, etc 06 p0832 A66-16555  
 International satellite communications: noting application for air traffic, using VHF band 09 p1346 A66-20555  
 Fading and multipath propagation mechanism for communication links involving satellites and aircraft with antenna beams, assuming fading models and estimating margin required for FS teletype transmission [AIAA PAPER 66-294] 12 p1822 A66-24707  
 Transhorizon VHF propagation over ground-air paths and transmission loss 13 p2020 A66-25222  
 Advanced avionics systems for improved surveillance and communications for Army



and-support aircraft 13 p2023 A66-25644  
 satellite communications systems for use  
 pilots passing over empty stretches of  
 or sea 14 p2243 A66-28363  
 eachable radio relay pods /RRQ-5/ to  
 ease range of UHF and VHF  
 munications systems 16 p2654 A66-31326  
 AIAA PAPER 65-728] 16 p2654 A66-31326  
 il aviation communications between  
 and ground controller on over-ocean  
 ts, considering use of VHF and HF and  
 rous satellite to extend 20 p3515 A66-37234  
**RAFT CONFIGURATION**  
 pped and slow rotor aircraft  
 igation for fundamental limitations on  
 ard flight speed of compound  
 eopters [SAE PAPER 650806] 01 p0012 A66-10847  
 plane configuration effect on shape and  
 ntitude of sonic boom pressure signature,  
 ng theoretical and empirical methods  
 AIAA PAPER 65-803] 03 p0320 A66-12599  
 nalytic processes for evaluation of  
 rsonic aerodynamics of configuration  
 ing drag, wing design, wrap,  
 erference and sidewash  
 AIAA PAPER 65-717] 03 p0321 A66-13048  
 mplementation of airborne command and  
 rol systems, emphasizing  
 munications equipment, data processing  
 ities, electromagnetic compatibility and  
 raft configuration parameters  
 AIAA PAPER 65-727] 03 p0336 A66-13049  
 he effect on VTOL aircraft hover and  
 speed handling qualities for helicopter  
 jet VTOL 06 p0806 A66-16813  
 ncorde SST aircraft prototype design  
 evelopment 09 p1329 A66-20132  
 ility of wing mounted pro-rotor pylon  
 ems in fully converted aircraft  
 uration, showing in-plane force  
 erated by blade flapping as destabilizing  
 or 16 p2633 A66-30599  
 an loading on wing of complete aircraft  
 uration determined, using segmented  
 in wind tunnel test technique and  
 t squares method 22 p3895 A66-40649  
 AIAA PAPER 66-768] 22 p3895 A66-40649  
**RAFT CONSTRUCTION**  
**PLASTIC AIRCRAFT**  
**CONSTRUCTION**  
 search, development, test and operation  
 ating devices used in aircraft  
 ruction supply real time data,  
 nsidering human factor, costs,  
 01 p0054 A66-10871  
 OL aircraft construction problems,  
 ularly high performance aircraft  
 oying combination of lift and lift-cruise  
 nes 01 p0012 A66-10923  
 sponsibilities of transport aircraft  
 ructor and subcontractor noting  
 age risk of third party and purchaser,  
 rantees, etc 02 p0306 A66-11748  
 revention of metallic edge corrosion of  
 al aircraft, evaluating surface treatments,  
 ners, epoxy enamels,  
 03 p0380 A66-12318  
 ptimal design for lightweight structures,  
 nsidering material properties, shape and  
 raction forces 06 p0963 A66-16474  
 RT in tool schedule for T-38 trainer and  
 ighter assembly line 10 p1539 A66-21168  
 rplane construction and technology in  
 Force 11 p1636 A66-22846  
 rcraft spinning problems, noting mass  
 istribution and tail design factors for  
 efactory spin recovery  
 aracteristics 11 p1637 A66-23077  
 11 swing-wing /variable-sweep/ aircraft  
 gram 11 p1637 A66-23101  
 et and cold hardening of aluminum-  
 ber-magnesium alloys for application to  
 iles and aircraft skins analyzed, using  
 tron microscope, noting metastable  
 ses 12 p1893 A66-23747  
 bit arc automatic tungsten inert gas  
 on welding and application to joining  
 ular systems in aerospace industry  
**TIME PREPRINT AD66-719]**  
 12 p1886 A66-24410  
 tanium and alloys examined, noting high  
 length-weight ratio, corrosion resistance,  
 trochemical properties, application for  
 rsonic transport, etc 13 p2107 A66-25483  
 ndwich panel composed of plastic  
 ular cells in parts of Hansa

aircraft 13 p1994 A66-25500  
 HS 125 twin-jet 500-mph executive aircraft,  
 construction, pressurization, maintenance,  
 etc 13 p1995 A66-26282  
 Subsonic business aircraft manufacturing  
 processes and techniques relation to  
 production time and costs  
 [SAE PAPER 660206] 13 p2087 A66-26395  
 High by-pass turbofan for business aircraft,  
 comparing jet propulsion system efficiency  
 with fan engines, cost factors and market  
 potentials [SAE PAPER 660221] 13 p2173 A66-26400  
 XB-70 technology, developments in  
 materials, equipment and manufacturing  
 including steel alloys, welding, etc  
 [SAE PAPER 660276] 15 p2427 A66-29822  
 Book on design calculations of elements of  
 aviation construction including elastic  
 parameters for finned fillers, shell torsion,  
 shell stability, etc 16 p2816 A66-31045  
 German HFB tubular aircraft construction  
 techniques and light constructional  
 elements 17 p3023 A66-32301  
 High temperature behavior of organic  
 materials for aircraft, noting elastomers and  
 platomers [ICAS PAPER 66-33] 22 p3938 A66-40660  
 Welding and adhesion techniques in  
 aircraft and space vehicle construction -  
 Conference, Hanover, West Germany, May  
 1966 23 p4073 A66-41530  
 Welding technology in aircraft construction  
 including military aircraft, VTOL, helicopter,  
 TIG method, etc 23 p4073 A66-41531  
 Supersonic transport production problems,  
 discussing Concorde, Lockheed and Boeing  
 projects, machining, shaping and  
 assembling 23 p4073 A66-41649  
 Do 31 system test stand including cockpit  
 with instruments, fuselage frame, wing  
 structure, etc 24 p4192 A66-42488  
**AIRCRAFT CONTROL**  
**SA WING TIP CONTROL**  
 Fail-operative stability augmentation  
 system for C-141 jet transport aircraft yaw  
 control axis, using triple redundant sensors  
 and signaling 01 p0011 A66-10662  
 Aircraft control power requirements  
 provided by lift fan propulsion system for  
 V/STOL flight, noting gas power transfer  
 [SAE PAPER 650831] 01 p0130 A66-10830  
 Prediction display based on computer  
 extrapolated data in aircraft  
 piloting 02 p0187 A66-11985  
 Propulsion-control systems interface for  
 V/STOL hover control in aircraft, using lift  
 plus lift cruise propulsion concept  
 [AIAA PAPER 65-799] 03 p0319 A66-12564  
 Reduced stiffness responses of airplane to  
 longitudinal control, noting elevator flutter  
 and stick-fixed dynamic longitudinal stability  
 [AIAA PAPER 65-784] 03 p0320 A66-12594  
 Experimental fixed and moving-base flight  
 simulator investigation of generalized  
 aircraft longitudinal pilot induced  
 oscillations [AIAA PAPER 65-793] 03 p0352 A66-12596  
 Flying qualities requirements related to  
 control system complexity noting  
 longitudinal, lateral and directional  
 requirements [AIAA PAPER 65-794] 03 p0320 A66-12597  
 Reaction control system for V/STOL  
 aircraft including power source, working  
 fluid, delivery system, thrust producing  
 devices and control point [SAE PAPER 650830] 05 p0610 A66-15014  
 Variable sweep wing effect on supersonic  
 transport stability and control  
 characteristics [AIAA PAPER 64-603] 05 p0610 A66-15068  
 Mixed translation and attitude control  
 system using single cockpit stick for low-  
 speed flight control of VTOL  
 aircraft 05 p0610 A66-15078  
 Accessory power drive, variable sweep  
 wing actuation, hydraulic, electric and  
 environmental control systems of Boeing  
 SST [ASME PAPER 65-AV-13] 05 p0611 A66-15131  
 X-22A variable stability and control VTOL  
 aircraft 06 p0809 A66-16816  
 Control and lift-propulsion systems and  
 model testing of Canadair CL-84 V/STOL  
 tilt-wing aircraft 06 p0804 A66-16818  
 Rolls-Royce RB 108 jet engine, discussing  
 project history, test results and current

application 06 p0943 A66-17021  
 XB-70A, high Mach number handling  
 qualities and suggested improvements  
 through addition of better instrument  
 presentation, automatic flight control,  
 etc 07 p0986 A66-17275  
 Elastic properties of bearing elements of  
 gyrotachometer and effect on frequency of  
 oscillations 07 p1031 A66-17409  
 Utilization of computers to reduce cockpit  
 work load, particularly in SST  
 aircraft 07 p1003 A66-17726  
 Direct lift control as landing approach aid  
 by providing more rapid means of changing  
 and controlling flight path than conventional  
 methods [AIAA PAPER 66-14] 08 p1167 A66-18985  
 Stick pushers in new medium range jet  
 transports, noting aerodynamics of aircraft  
 stall 11 p1637 A66-23072  
 Efficiency factors such as roll scanning  
 methods and pitch control effectiveness in  
 hover control system for VTOL  
 aircraft 11 p1638 A66-23258  
 Control problems in operation of transport  
 aircraft noting degrees of freedom,  
 computer aid, human factor,  
 etc 13 p2047 A66-25497  
 Book on unmanned aircraft and rocket  
 control systems, flight dynamics in  
 conjunction with control processes, design  
 of stabilization and guidance  
 systems 13 p2055 A66-26462  
 Minimum time-of-flight aircraft trajectory  
 between two points with account of Earth  
 sphericity 13 p2125 A66-26481  
 Handling and operation of XB-70 aircraft,  
 noting flight testing, folding wing tips,  
 weight, speed, etc 14 p2222 A66-27284  
 [SAE PAPER 660273] 14 p2222 A66-27284  
 Motion equations for dynamics of aircraft  
 control surface controlled by  
 autopilot 14 p2328 A66-27687  
 Semiautomatic digital data processing  
 system used in ground control of  
 interceptor aircraft, noting track marking on  
 PPI display, control of height radar, radio  
 message transmission, etc 14 p2271 A66-28299  
 Book on automatic control of linear and  
 nonlinear systems, particularly aircraft  
 utilization 16 p2744 A66-31058  
 Discrete control signal effect on crabbing  
 /sideways motion/ of aircraft during floating  
 and after touchdown 17 p2950 A66-32584  
 Flying qualities and aircraft control during  
 tandem rotor helicopter external sling load  
 operations 17 p2846 A66-32742  
 Longitudinal motion of piloted aircraft  
 during rapid dropping of concentrated loads  
 in comparison of numerical solution with  
 flight data 17 p2848 A66-33076  
 Reduced stiffness responses of airplane to  
 longitudinal control, noting elevator flutter  
 and stick-fixed dynamic longitudinal stability  
 [AIAA PAPER 65-784] 19 p3279 A66-36485  
 Multiloop control interaction using  
 linearized technique, noting variable  
 geometry intake loop 20 p3627 A66-36881  
 Experimental maneuver demand aircraft  
 control system, noting design considerations,  
 operation and performance  
 characteristics 20 p3493 A66-36887  
 Transfer response of pilot to steady  
 continuous one-dimensional perturbation of  
 lateral motion of aircraft tested in Boeing  
 707 flight simulator 21 p3701 A66-39832  
 Control laws providing attainment of  
 prescribed attitude and acceleration to  
 prescribed speed in minimum time or fuel  
 consumption for VTOL  
 aircraft 21 p3768 A66-39606  
 Dropping heavy stores from low altitude  
 aircraft, considering stability of store after  
 leaving aircraft and rebound from impact  
 with ground 22 p3850 A66-40616  
 Medical aspects of skill in flying modern  
 aircraft, considering health, personal and  
 environmental factors such as noise levels,  
 placing of controls and barometric pressure  
 [ICAS PAPER 66-19] 22 p3858 A66-40668  
 Pilot dynamic response in bank angle  
 control maneuver simulation of sidewind  
 landing of aircraft [ICAS PAPER 66-14] 22 p3945 A66-40672  
 Optimization of VTOL control concepts  
 with and without stabilization compared  
 with six degree of freedom motion  
 simulator, noting system failure effects and



nonlinear concepts 22 p3851 A66-40675  
 [ICAS PAPER 66-9] 22 p3851 A66-40675  
 Propulsion control systems interface for V/STOL hover control in aircraft, using lift plus lift cruise propulsion concept [AIAA PAPER 65-799] 23 p4015 A66-40985  
 Automatic flight control for VJ 101C VTOL aircraft, noting autopilot function 23 p4016 A66-41931  
 Stability, control, navigation, guidance and air traffic control of hypersonic vehicles noting inertial technology, flight planning and optimal control 24 p4235 A66-42239

## AIRCRAFT DESIGN

## SA HELICOPTER DESIGN

DC-9 maintainability, simplicity and commonality of design with emphasis on reliability 01 p0129 A66-10092  
 F-5/T-38 design philosophy to meet rigorous operational and maintenance requirements 01 p0010 A66-10094  
 Weight and load factor modification of V/STOL aircraft design when aircraft is used as weapon system 01 p0011 A66-10186

Balanced power concept for weight savings in aircraft actuation system consisting of mechanically actuated flight control surface, mechanical servo, flywheel and motor 01 p0015 A66-10670  
 XB-70 vehicle control system sensing, local force application, coupling and adaptability for increasing structural mode damping ratio, thus avoiding disturbing pilot accelerations and structural loads 01 p0103 A66-10672

Statistical analysis of dynamic system response used to design aircraft undercarriage systems [AIAA PAPER 65-710] 01 p0013 A66-10947  
 C-5A aircraft design load criteria for landing gear of large aircraft that must operate from semi-improved airfields [AIAA PAPER 65-711] 01 p0013 A66-10948  
 Airport pavement roughness data and aircraft response data evaluated to determine pavement design and construction criteria [AIAA PAPER 65-712] 01 p0055 A66-10949

Ground and laboratory testing of HFB 320 Hansa considering static, dynamic, wind tunnel and deicing tests 02 p0176 A66-11245  
 Comparative design study of low-disk-loading VTOL concepts including stopped-rotor, tilt-propeller, tilt-wing, transport effectiveness, etc 03 p0318 A66-12551

DC-9 aerodynamic design features and control systems [AIAA PAPER 65-738] 03 p0320 A66-12731  
 Aerodynamic design of Boeing 737 covering data of analytical studies, wind tunnel and flight tests, aerodynamic parameters and drag, flap system size, efficiency, wing geometry and handling qualities [AIAA PAPER 65-739] 03 p0321 A66-13047

Thrust-control system on XC-142A tilt-wing aircraft considered in connection with structural design of aircraft hover, transition and acceleration [AIAA PAPER 65-769] 03 p0321 A66-13063  
 Variable geometry aircraft structural problems including fail-safe criteria, flutter configurations, dynamic loads, etc [AIAA PAPER 65-774] 03 p0438 A66-13064  
 Design and development of U.S. SST program 03 p0322 A66-13105

Hypersonic aircraft and aerodynamic aspects for global transport operation noting shock waves, Mach number and gas dynamics 04 p0453 A66-13504

Aerodynamically conventional low-wing monoplane design for high-performance light aircraft stressed to 8g limit loads, utilizing fiberglass reinforced plastic primary structure 04 p0588 A66-13633  
 Variable-sweep aircraft design, with application to trainer, strike fighter and supersonic transport 04 p0458 A66-13928

Aerodynamics, performance and operational considerations effect on Boeing design of variable sweep supersonic transport aircraft [SAE PAPER 858C] 04 p0458 A66-13929

General Dynamics/Grumman multi-mission variable-sweep fighter for Navy and Air Force 04 p0458 A66-13930

Analytical tool for computer flight testing of VTOL designs, evaluating effects of steady state flight, maneuvers, gust

response and weapon

recoll 04 p0490 A66-14137  
 Effect of canard foreplane on longitudinal long-period perturbed motion of aircraft depends on change in hinge moments with Mach number change 04 p0458 A66-14152  
 Drag decrease in glider aircraft noting wing profile, flow laminarization /boundary layer control/, landing flaps, tail, etc 05 p0607 A66-15200

Future developments in supersonic transport and V/STOL aircraft 05 p0611 A66-15269

Short-range aircraft design efficiency and possible reduction in operating cost 06 p0804 A66-15990

Possible cost reduction with all-wing short-range aircraft, noting ogee design 06 p0804 A66-15993

V/STOL Aircraft Symposium, Wright-Patterson AFB, Ohio, November 1965 06 p0805 A66-16808

Quad tilt propeller, tilt prop/rotor and two direct lift jets for VTOL aircraft compared for design 06 p0806 A66-16811

Control power composition and usage characterized for VTOL aircraft flight control system design 06 p0806 A66-16812

Fokker F-28 Fellowship short-haul passenger aircraft 06 p0807 A66-17166

Optimum operational influence on design of DC-9 cockpit 07 p0988 A66-17704

VC10 C Mk I jet transport for troop transport, freighting, casualty evacuation and refueling 07 p0989 A66-18163

Deep-stall characteristics of T-tailed aircraft configurations and recovery procedures, noting parameters of pitch-up, angle of attack, etc 07 p0989 A66-18446

[AIAA PAPER 66-13] 07 p0989 A66-18446  
 X-20 program for maneuverable hypersonic reentry vehicle, noting boost-glide dynamic soaring 08 p1300 A66-18555

American supersonic commercial air transport design, development and operation 08 p1167 A66-18557

Aircraft design parameter development, discussing supersonic air transport, helicopter and V/STOL design problems, metal fatigue, etc 08 p1167 A66-18707

Military aircraft from design stage through service life, emphasizing flight testing 08 p1322 A66-19017

Thermal management of Lockheed L-2000 supersonic transport heat sources and sinks, considering flight profile, aircraft configuration and heat transfer modes [ASME PAPER 65-AV-40] 09 p1329 A66-20298

Design and propulsion of 2-B version of Lockheed L-2000 SST noting drooping nose, variable geometry inlets, stressed skin construction, etc 09 p1329 A66-20390

XC-142A V/STOL transport aircraft with four-ton payload and 200 nautical mile range radius [AIAA PAPER 64-775] 09 p1330 A66-20735

Reliability factors considered by aircraft designers and manufacturers including bad design, indifferent manufacture, inadequate testing, human error, etc 10 p1538 A66-21134

Aircraft landing gear design and maintenance, noting elimination of sharp corners and radii, weldability criterion, joints, part identification, bushings, etc 10 p1482 A66-21135

Short-haul aircraft design for low direct operating costs, noting various wings 10 p1482 A66-21364

Lift-drag ratio, specific impulse, aspect ratio and weight of payload and power plant considered for STOL aircraft 10 p1483 A66-21398

Aircraft fuselage design in region of center section for case of asymmetric bending 11 p1782 A66-22854

DC-9 Douglas short-and medium-range air transport, discussing takeoff field length, fuel capacity, payload and landing-field length 12 p1800 A66-23754

Boeing 737 twin-jet, discussing wing, fuselage and tail design, aerodynamic wind tunnel tests, stability and control, etc 12 p1801 A66-23785

Optimization criteria for critical parameters for attainment of flight by man powered aircraft 12 p1801 A66-23803

Aircraft electrical system design, power requirements, instrumentation, excess loads,

etc 12 p1803 A66-24387

Basic principles of structural design as applied to aircraft, discussing loads and strengths and effect of accidents and costs 12 p1971 A66-24972

Large transport aircraft design, examining effect of high horizontal stabilizer location on vertical fin [AIAA PAPER 65-331] 13 p1994 A66-25588

Ring wings to develop beneficial aerodynamic interference effects at supersonic speeds 13 p1995 A66-25590

Lockheed supersonic air transport design development 13 p1995 A66-25758

DC-9 maintainability, simplicity and commonality of design with emphasis on reliability 13 p2173 A66-26231

Vapor-cycle air conditioning for business aircraft, considering weight vs power consumption, compatibility with integrated system and test results [SAE PAPER 660208] 13 p2002 A66-26386

Reliability testing of aircraft engine components 13 p2088 A66-26688

Design of V/STOL aircraft including propulsion systems, control and configurations 14 p2222 A66-26924

Aerodynamic concepts and configuration of Mach 3 XB-70A aircraft [SAE PAPER 660274] 14 p2222 A66-27283

Relationship between military and contractors in aircraft development, noting adherence to military specifications, costs, weapons, etc 14 p2416 A66-27812

Aircraft design for gust loads encountered based on power spectral results 14 p2405 A66-27998

Concorde aircraft progress report 14 p2223 A66-28100

Dual-purpose passenger/cargo aircraft noting design, passenger interior system cargo handling system, compatibility, comparisons, etc 15 p2426 A66-29800

Aircraft design for large cargo transport noting aerodynamic efficiency, wing construction, cargo loading, cost estimates, etc 15 p2426 A66-29800

Aircraft mile cost vs seat mile cost, noting payload estimation, profit potential, productivity and other parameters [SAE PAPER 660277] 15 p2427 A66-29822

Design and mission requirements and weight penalties claimed for jet VTOL tactical aircraft 16 p2633 A66-30599

VC 400 VTOL aircraft design, development and performance 16 p2633 A66-30944

Aircraft development and goals U.S. 16 p2633 A66-31277

Aircraft design requirements concerning V/STOL technology emphasizing cost, size and propulsion system 16 p2634 A66-31322

High performance aerodynamic vehicle design, noting configuration variables optimum performance parameters, vehicle force characteristics, optimization of hypersonic aircraft performance, etc [AIAA PAPER 66-486] 16 p2635 A66-31477

Aircraft response data evaluated to determine pavement design and construction criteria [AIAA PAPER 65-712] 16 p2683 A66-31599

Stall prevention device for Beechcraft T-34B aircraft equipped with stall warning wing device 17 p2843 A66-32199

First-stage propulsion of aerospace transporter, discussing design and operational requirements 17 p2990 A66-32377

Transport approach and landing visibility requirements, examining design of forward portion of airplane 17 p2950 A66-32688

Aircraft design to minimize sonic boom pressure field energy 17 p2847 A66-33022

Sonic boom requirements for supersonic transports 17 p2847 A66-33030

Algorithm for cost effectiveness comparison of aircraft tradeoffs of performance vs cost vs time of obtainability 18 p3052 A66-34161

Aerodynamic design criteria for maintaining laminar flow control including instability limit, surface roughness, acoustical environment, etc 18 p3050 A66-34959

Optimum high payload laminar flow control aircraft offer 20 to 25 percent range improvement, indicated by design studies of large logistics aircraft 18 p3053 A66-34959



- VTOL aerodynamics, discussing jet-lift, lift, high-lift boundary layer control, jets, ground simulation and wind-tunnel techniques 19 p3275 A66-35364
- lying characteristics of Falcon fanjet, inch-built aircraft, noting landing, accommodations, soundproofing, 19 p3279 A66-36048
- form and swimming characteristics of phin applied to design of high-speed commercial aircraft and VTOL aircraft 19 p3279 A66-36049
- onic boom reduction by aircraft shape modification 19 p3279 A66-36180
- ost-effectiveness evaluation methodology choosing best aircraft to construct for en purpose 20 p3682 A66-37197
- erodynamic and thermal criteria in ctural design of aircraft and ssiles 20 p3628 A66-37393
- structural design criteria for Concorde craft, including necessity for heat-istant airframe 20 p3666 A66-37400
- terior design techniques in civil aircraft t design and supersonic aircraft eriors 20 p3495 A66-37425
- niform design process AFSCM 375-5 plementation and operating personnel elationships in aircraft 20 p3685 A66-37929
- afety-factor problem in glider design, cussing limiting load concept in form of reme load in exceptional cases of eration 21 p3696 A66-38620
- araging steels for landing gear forgings, ing fabrication, distortion and fatigue ts 21 p3751 A66-39237
- o-31 V/STOL transport aircraft design luding engine, wings, speed, rate of mb, etc 21 p3696 A66-39540
- erodynamic design and development of gle B.206 S aircraft, examining irections for inadequate stability margins aft CG limit 22 p3848 A66-39689
- light testing of Beagle B.206 S aircraft ealed need for forward shift of CG in ries II model due to more powerful gines 22 p3848 A66-39690
- utter of variable geometry aircraft odel as affected by airfoil sweep, pivot d wing-empennage coupling [SAE PAPER 66-12] 22 p3996 A66-40674
- ext on weight reduction techniques for e in monitoring phase of engineering sign, using model 22 p3851 A66-40801
- lications 22 p3851 A66-40801
- erodynamically conventional low wing onoplane design for high performance ht aircraft stressed to 8g limit loads, izing fiberglass reinforced plastic amary structure [AIAA PAPER 65-771] 23 p4015 A66-40980
- ngine thrust requirement comparison for rtical and short takeoff aircraft with same ht mission 23 p4088 A66-41187
- project management of Jaguar Anglo-ench military aircraft in design, test and oduction phases 23 p4151 A66-41217
- etal adhesives in aircraft and space ustry, particularly in construction of minar and sandwich elements of ings 23 p4073 A66-41532
- hort-periodic motion of tailless glider alalyzed to determine degree of ercompensation of flap required for good ability 23 p4016 A66-41784
- ust design procedures based on power etral techniques, considering atmospheric urbulence with aircraft as rigid body with gle degree of freedom [SAE PAPER 66-11] 23 p4017 A66-42073
- ircraft flying up to 6000 miles at Mach mbers up to 8, noting problems in yrodynamics, propulsion, structural weight, oling, etc 24 p4157 A66-42237
- ypersonic transport technology, nsidering designs for Mach numbers up to t, altitude up to 140,000 ft and 150 ssengers 24 p4159 A66-42238
- reguet 1150 high seas reconnaissance craft, noting design features and chnological problems 24 p4159 A66-42489
- V/STOL aircraft design noting very high t generation at very low flight speeds and yload role 24 p4159 A66-42890
- V/STOL aircraft for commercial short-haul nsports, considering turboprops, fan-in wing and propulsion 24 p4159 A66-42891
- Dornier twin engine high wing STOL monoplane design and performance, noting useful space, landing gear, control system, fuselage, cargo, etc 24 p4160 A66-43070
- Design, performance capabilities and operational characteristics of Russian high speed jet aircraft IL-62 with tail-mounted engine 24 p4160 A66-43075
- AIRCRAFT DETECTION**
- In-flight monitoring of advanced aircraft, discussing system requirements and constraints [ISA PREPRINT 1.3-2-65] 05 p0684 A66-15512
- Radar detection of sailplanes and other small aircraft aided by aluminum reflecting surfaces 09 p1345 A66-20479
- Radar separation of closely spaced aircraft by fire-control weapon 10 p1553 A66-21268
- Radar cross sections of full-sized targets in flight measured by dynamic system at L, S and X bands 10 p1499 A66-21605
- Data converter system for conditioning, recovery and display of aircraft position and altitude data permitting real time surveillance by ground observer 16 p2651 A66-30564
- Probability of overlapping intercept by system of random intercepts and application to detection of flying objects in cloudy skies 24 p4231 A66-42472
- AIRCRAFT ENGINE**
- SA GAS TURBINE
- SA JET ENGINE
- McCulloch Model 4318 Drone Target Aircraft Engine for maintainability, reliability, moderate cost and high power-to-weight ratio 01 p0129 A66-10091
- Refractory metals for gas turbine and ramjet aircraft engines, noting niobium and tantalum alloys 02 p0245 A66-11746
- Introduction of programmed milling machines to production of aircraft engines for Czechoslovakian FB series 04 p0525 A66-13763
- Book on matched parameters of gas turbine engines for aircraft including rpm and peripheral speed, calculating parameters for axial-flow compressors, centrifugal compressors, turbojet, turboprop, etc 04 p0573 A66-14004
- Various types of periodically discontinuous combustion, showing improved thermal efficiency applicable to turbine combustion chambers 05 p0787 A66-14962
- Aircraft and propulsion system design matching for long range and endurance aircraft [AIAA PAPER 64-783] 05 p0610 A66-15073
- Pulse jet engine where hot gas discharge rather than developing thrust is used to obtain shaft power [ASME PAPER 65-WA/GTP-6] 05 p0745 A66-15721
- Production and recent developments in gas turbines and propulsive engines in West Germany 06 p0942 A66-16795
- West Germany and international cooperation in aerospace engine development, noting VTOL aircraft and hypersonic and hypersonic spacecraft 06 p0943 A66-16797
- Dual flow engines with high by-pass ratios, considering engine process parameter effects, fuel consumption, efficiency, etc 06 p0944 A66-17025
- XB-70A systems, particularly J-39 engine, including ground aborts, in-flight shutdowns, hydraulic and fuel contamination, nozzle control difficulties, etc 07 p0986 A66-17276
- Engine-overhaul facilities and procedures at BOAC noting use of flow principle, automatic processing and three main sections, engine dismantling, crack detection and static and dynamic balancing 07 p1111 A66-18329
- Isochronous and droop type governors controlling aircraft engines 08 p1282 A66-19765
- Aircraft engine rotating shaft coupling design, noting splined shafts, correct lubrication, flexible members and test results 09 p1383 A66-19863
- SNECMA axial flow transonic compressor development during last ten years 09 p1433 A66-19866
- Dimensional stability and structural integrity of labyrinth seals, considering various mechanical design criteria in application to aircraft gas turbines [SAE PAPER 660048] 09 p1383 A66-20150
- Turbine blade and vane cooling in Rolls-Royce nonmilitary aircraft engines, noting side effects on design and development [SAE PAPER 660053] 09 p1433 A66-20151
- Aircraft turbine lubricant technology for high Mach number engines especially SST, noting stability, autoignition, coking, toxicity, etc [SAE PAPER 660071] 09 p1434 A66-20156
- Aircraft turbine engine oil drain practices, discussing engine design and materials and minimum and maximum drain time [SAE PAPER 660073] 09 p1434 A66-20158
- Means of assessing aviation turbine lubricant quality, considering specification, maintenance, operational factor and equipment strip approach [SAE PAPER 660074] 09 p1434 A66-20159
- Sailplane equipped with auxiliary starting engine, characteristics and application in studying Alpine current 09 p1329 A66-20478
- Engines for supersonic and hypersonic aircraft to be used in next decade, noting suitability for cruise aircraft or boosters 09 p1435 A66-20668
- Propulsion problems for engine of 5000 mph aircraft noting ramjet, cooling, intake, nozzle, etc 09 p1435 A66-20669
- Turbine vanes of aircraft engines and experimental plants, determining structural angle of outlet, maximum thickness and area of profile, setting angle, etc 09 p1328 A66-20761
- Comparison of piston engine with turbojet engine, noting power-weight ratio, specific fuel consumption, performance characteristics, etc 10 p1591 A66-21392
- Supercharging turbojet engine for light aircraft compared to piston and turbojet engines 10 p1591 A66-21393
- Design, operating characteristics, advantages of two-cycle star configuration four-cylinder engine for general-purpose aircraft, noting crankshaft, fuel injection, cooling, etc 10 p1592 A66-21407
- Text on fundamentals of aircraft gas turbine engine design, including component design and calculation 11 p1762 A66-23310
- Shock tube ignition delay study of aircraft engine cooling by hydrocarbon fuels in endothermic heat sinks [AIAA PAPER 65-594] 12 p1934 A66-23588
- Simulation of lubricating oil circulation in aviation turbine engines by constructed model, noting change of viscosity, acid number and electrical conductivity at high temperatures 12 p1803 A66-23751
- Constant oil monitoring system using electric conductivity tester for extending oil life in gas turbine engines [SAE PAPER 650814] 12 p1935 A66-23844
- Book on strength and dynamics of aircraft engines including deformation of shells of revolution, osculation frequencies of various shells, turbine rotor dynamics, etc 12 p1963 A66-24042
- Rarefying of dense frequency spectrum of shell-shaped elements of aircraft engines by corrugating shell surface, determining natural oscillation modes and frequencies 12 p1964 A66-24046
- Combustion deposit fouling and other difficulties in spark plug operation in commercial aircraft [AIAA PAPER 64-779] 13 p2038 A66-25597
- Control of large engine motion from soft mountings during starting and stopping [SAE PAPER 660222] 13 p2088 A66-26399
- U.S. Army program for small gas turbine, noting turbine specific horsepower, component, payload-range curve, etc [ASME PAPER 66-GT-91] 14 p2372 A66-26995
- McCulloch TSIR-5190 highly compounded two-stroke cycle, turbocharged, direct fuel injection, liquid cooled, radial light plane engine [SAE PAPER 660173] 14 p2373 A66-27283
- Commercial air transport in 1972, discussing operating economics, management planning, maintenance costs, etc [SAE PAPER 660321] 14 p2223 A66-27300
- Heat transfer considerations in aircraft-engine design noting fuel, oil and icing



problems 14 p2375 A66-28300  
 Factors affecting useful life of subsonic gas turbine engine components including metallurgical variances, stress-cycle relationships, surface coating, etc [SAE PAPER 660312] 15 p2573 A66-29837  
 Factors extending life of aircraft engine part beyond that available by in-service development of component replacement [SAE PAPER 660313] 15 p2573 A66-29838  
 Turbofan engine fuel consumption, noting high cycle pressure ratio compressor, regenerator, etc 15 p2573 A66-29842  
 Jet engine transient thrust response for V/STOL aircraft 16 p2791 A66-30598  
 Operating stability of turbojet engines improved by use of double-rotor compressor 17 p2992 A66-33487  
 French aerospace industry, production of aircraft, engines and missiles, research programs, expenditures, etc 18 p3267 A66-33915  
 Engine air induction system, engine and integral gear case oil cooling air induction system and nacelle cooling and ventilating air induction systems of XC-142A [AIAA PAPER 66-632] 18 p3048 A66-34435  
 Pneumatic vernier engines in aircraft and spacecraft, discussing weight, gas expansion and gas temperature 20 p3627 A66-36916  
 Aircraft turbine engine oil drain practices, discussing engine design and materials and minimum and maximum drain time [SAE PAPER 660073] 20 p3628 A66-37255  
 Maintainability program for aircraft power plant particularly turbofan engine, noting inspection, failure detection, replacements, etc 20 p3574 A66-37963  
 Irreversible trimmed stalls at high angles of attack for aircraft with aft-mounted engine nacelles and high-or T-tails 20 p3496 A66-38255  
 Aircraft gas turbine starting with automatically controlled electronic unit, noting system design, operation and performance 20 p3540 A66-38299  
 Cyclic characteristics of Joule process applied to processes in jet and propjet engines 21 p3807 A66-38813  
 Beagle B 206 S aircraft power plant, vacuum system, air conditioning system, fire protection, hydraulics, fuel, oxygen, rain protection and deicing equipment 22 p3970 A66-39688  
 Lift fan propulsion system using 62.5-inch lift fans flight tested in XV-5A aircraft from hover to subsonic flight regions [AIAA PAPER 66-739] 22 p3972 A66-40628  
 Dynamic test method for characteristics and interactions of supersonic aircraft propulsion systems, particularly inlet/engine performance and control compatibility aspects [AIAA PAPER 66-741] 22 p3893 A66-40630  
 Aircraft and missile engine development at Saclay Propulsion Test Center /France/ 23 p4053 A66-41648  
 Materials and cooling of aircraft gas turbine engines, noting nickel and tantalum alloys, turbine-inlet temperatures, coatings, etc 23 p4122 A66-41662  
 Power plant development trends and effect on short and vertical takeoff aircraft design, noting improvement in thrust-weight ratio 24 p4262 A66-43051

**AIRCRAFT FUEL**  
 Jet fuels presently used in military aircraft compared with those for advanced air-breathing weapon systems at high Mach number [SAE PAPER 650804] 01 p0128 A66-10846  
 Flammability hazards of aircraft hydrocarbon fuels as function of temperature and pressure based on equilibrium conditions [AIAA PAPER 65-801] 03 p0414 A66-12565  
 Fuels and lubricants with thermally stable molecular structure and antioxidants to meet requirements of supersonic transport 03 p0414 A66-13221  
 SST prospects, history, design and controversy 07 p0985 A66-17203  
 Fuel requirements for high altitude high-Mach number aircraft, noting thermal stability, autooxidation, self-ignition, specific heat, etc 10 p1590 A66-21400  
 1965 supplement to 1958 ASTM manual for

rating aviation fuels by supercharge and aviation methods 14 p2370 A66-27230

**AIRCRAFT FUEL SYSTEM**  
 Microbiological attack in aircraft fuel systems and protective measures 06 p0940 A66-15996  
 Aircraft fuel tank coating corrosion resistance, discussing polyurethane and epoxy material characteristics and application 07 p1053 A66-17491  
 Lucas fuel control system for Spey engine, using rotating metering valves and variable stroke fuel pump [SAE PAPER 660049] 08 p1282 A66-19389  
 Concorde fuel system in cooling application and adjustment of center of gravity through fuel distribution 11 p1637 A66-23168  
 Jet pump development and testing on Lear Jet Model 24 and Model 40, noting fuel pump system performance, requirements and configuration [SAE PAPER 660223] 13 p2002 A66-26398  
 Wear and grease lubrication effects in matched aircraft spline specimens subjected to oscillatory motion 16 p2713 A66-30572  
 USAF CH-3C helicopter V/STOL in flight refueling, discussing requirements, system characteristics and flight tests 17 p2844 A66-32724  
 Concorde supersonic transport aircraft propulsion, fuel supply and storage systems 22 p3848 A66-40415

**AIRCRAFT GUIDANCE**  
 Automatic star trackers for long range aircraft navigation, discussing instrumentation methods and use of pulse code modulation for sensor design 02 p0257 A66-12029  
 Evaluation of minimum-time courses for aircraft and inherent error 02 p0257 A66-12035  
 Decra system with increased power and ambiguity reduction evaluated for long range navigation in North Atlantic 02 p0258 A66-12046  
 Omega hyperbolic radio navigation system for aircraft using eight broadcasting stations 02 p0259 A66-12048  
 USAF Central Inertial Guidance Test Facility for testing aircraft navigation systems 02 p0259 A66-12051  
 Astronomical Guidance System for Air Navigation which detects altitude and azimuth errors resulting from precomputed and preadjusted deviations 02 p0259 A66-12052  
 Future trends in long range aircraft navigation 02 p0260 A66-12058  
 Telecart C for automatic digital evaluation of data supplied by hyperbolic radio navigation systems 02 p0260 A66-12061  
 Radiogeodetic plotting device for piloting aircraft on assigned track 03 p0389 A66-12507  
 Modification of Decra position fixing service in North Atlantic 07 p1063 A66-17446  
 Evaluation of four different types of Doppler radar as long range self-contained navigation aid 07 p1065 A66-17669  
 Long range navigation in jet operations, discussing problems and limitations 07 p1065 A66-17670  
 Air traffic control system capacity and navigational requirements for North Atlantic and continental transition areas, discussing relationship to accuracy and flight time economy 07 p1069 A66-17713  
 Design of Elliott E.5, low cost inertial navigation system for civil aircraft 07 p1071 A66-17727  
 Accuracy of Doppler navigational system obtained from ground information accumulated over 500 North Atlantic crossings 07 p1071 A66-17728  
 Error of airborne Doppler navigation system 07 p1073 A66-17768  
 Self-contained Doppler Navigation System performance over three-year operation 07 p1074 A66-17776  
 Navigation techniques and operational objectives due to computer-generated flight plans of United Air Lines 07 p1074 A66-17777  
 Navigation satellite in aircraft traffic control 07 p1074 A66-17778  
 Long-range navigation system control/display concepts and automation for airline navigation 07 p1074 A66-17779  
 Subsonic and supersonic aircraft navigational systems requirements,

discussing pictorial presentation and effect on command function 07 p1075 A66-17788  
 Navigational inertial system dynamic property analysis at high flight speeds, using hodographic characteristic equation for longitudinal and lateral aircraft motion error determination 09 p1401 A66-20913  
 Navigation satellite in aircraft traffic control 13 p1225 A66-25870  
 Compass system on VC10 provides magnetic heading reference, or alternately, inertial reference for grid navigation 13 p1225 A66-26283  
 Book on unmanned aircraft and rocket control systems, flight dynamics in conjunction with control processes, design of stabilization and guidance systems 13 p2055 A66-26482  
 Prediction and avoidance of atmospheric turbulence affecting large aircraft 17 p2842 A66-31989  
 Switching surface construction using one to one correspondence between points in controllability region and points on surface of n-th order system 17 p2902 A66-32570  
 All-weather operations, head up displays, long-range navigational aids - Conference International Federation of Air Line Pilots Associations, Rotterdam, October 1965 17 p2953 A66-33212  
 Worldwide civilian-aircraft navigation system based on VLF radio using ground stations or satellites 17 p2954 A66-33212  
 Decra long-range navigational system giving area coverage position fixing for multiplicity of North Atlantic transoceanic routes 17 p2954 A66-33212  
 Optimal trajectory problem solution using in-flight guidance computers for control rockets and aircraft under influence of random disturbances 17 p2956 A66-33323  
 Navigation satellite system providing precise position information of aircraft, noting flight tests 19 p3396 A66-35511  
 Radiation attenuation effect of atmospheric aerosols on all-weather aircraft landing guidance systems using lasers 19 p3397 A66-36057

**AIRCRAFT HAZARD**  
 Flammability hazards of aircraft hydrocarbon fuels as function of temperature and pressure based on equilibrium conditions [AIAA PAPER 65-801] 03 p0414 A66-12565  
 Behavioral characteristics of birds that collide with aircraft in flight and methods to reduce such strikes at airport [AIAA PAPER 65-748] 03 p0319 A66-12588  
 Human factors in Concorde SST program 03 p0329 A66-13356  
 Radioactive contaminant detection on surface of high altitude transports, noting passenger protection 04 p0458 A66-14466  
 Spontaneous ignition of inflammable fluid by hot surfaces, particularly high aircraft skin temperatures 15 p2618 A66-29639  
 Siting of static discharger to control nature and occurrence positions of corona to minimize RF noise capable of causing hazard to aircraft navigational aid systems 19 p3282 A66-36675  
 Deformation of solids by impact of liquid and relation to rain damage in aircraft arm missiles, to blade erosion in steam turbine and to cavitation erosion - Meeting, London May 1965 20 p3546 A66-37800

**AIRCRAFT HYDRAULIC SYSTEM**  
 In situ ultrasonic testing of braze hydraulic pipe joints in aircraft, noting superiority over radiography 01 p0079 A66-10977  
 High-performance hydraulic power system for supersonic transport aircraft, using redundancy of three completely separate and functional systems 04 p0459 A66-13788  
 British Lockheed undercarriage and hydraulic system for German HFB 320 Hans aircraft 04 p0458 A66-13939  
 Aircraft landing gear design, evaluation undercarriage of research aircraft arm weapons systems 07 p0987 A66-17735  
 Hydraulic system of De Havilland Buffalo tactical aircraft is self-sufficient 10 p1486 A66-22033  
 Hydraulic system of Cessna 210 aircraft noting component structure, electrical and hydraulic sequencing devices, etc [SAE PAPER 660202] 13 p2002 A66-26398



- multiple quick-disconnect valve used in  
iliary power unit (APU) of aircraft and  
viring several systems at once while  
venting fluid leakage from one system to  
ther 14 p2226 A66-28032
- ized hydraulic system design and  
ication for Skyhawk A4B 17 p2849 A66-33098
- T aircraft fluid power systems and  
ormance, discussing power requirements,  
erials, maintenance, configuration,  
ace temperature distribution, etc  
[AIAA PAPER 66-MD-35] 21 p3697 A66-38487
- ircraft hydraulic system contamination  
ontrol program under clean as you go  
inciple 22 p3851 A66-40043
- riteria for hydraulic fluids for supersonic  
raft noting fluid toxicity, fire hazards,  
compatibility with elastomeric materials,  
24 p4229 A66-42380
- urdon-helix pressure-sensitive switch for  
vehicle hydraulic system of XB-70A  
raft and other instruments operating in  
ere environment 24 p4213 A66-42824
- ## RAFT INDUSTRY
- perational research techniques applied to  
urement and capital investment  
grams of aviation 01 p0170 A66-10341
- nickel-chromium base alloys considering  
raft and industrial gas turbine  
lication 02 p0244 A66-11740
- lanium, beryllium and refractory metals  
roperties and application of their alloys in  
raft industry 02 p0244 A66-11743
- ench aerospace industry, relationship to  
nch economy, annual expenditures 1958  
1964 and aircraft 05 p0794 A66-15189
- ports 05 p0794 A66-15189
- transport engineering, cost and  
ability factors, development possibilities,  
design construction phasing,  
07 p0987 A66-17488
- K aircraft industry mergers, causes,  
ernment policies and  
ory 07 p1156 A66-17490
- erospace industry contribution to science  
echnology, noting relationship with U.S.  
ernment 08 p1321 A66-18552
- ook on structure and performance of  
ospace industry and governmental  
ctions 09 p1473 A66-20689
- ystems effectiveness and F-111, concept,  
applicability, reliability, performance,  
and use during F-111 aircraft  
elopment 11 p1789 A66-23440
- ydrogen embrittlement or fatigue  
length loss avoidance in overhauling and  
pairing of high strength aircraft steel  
onponent 13 p2087 A66-26284
- uality and reliability programs of Cessna  
ircraft Commercial Division covering  
onnel from trainees to scientists  
[AIAA PAPER 66-204] 13 p2087 A66-26384
- ## RAFT INSTRUMENTATION
- ### ALTIMETER
- ### APPROACH AND LANDING INSTRUMENT
- ### FLIGHT INSTRUMENT
- ### FLIGHT LOAD RECORDER
- ### GAUGE
- ### LANDING AID
- ### POSITION INDICATOR
- ### SPEEDOMETER
- ilitary specifications MIL-HDBK-217 and  
R-22256, 22973 and 23094A with respect  
reliability design of aircraft electronic  
ipment 01 p0034 A66-10059
- redicted vs observed avionics reliability  
esign technique, using factual reliability  
of baseline equipment and solid state  
onponent advances 01 p0035 A66-10080
- r data equipment trends in subsonic and  
ersonic control 01 p0033 A66-10680
- omparative merits of visual, audible and  
omposite aircraft warning systems for  
imum human response to causal  
dition 01 p0021 A66-10939
- rediction display based on computer  
rapolated data in aircraft  
iting 02 p0187 A66-11985
- heory of aircraft measurement of gravity  
g gyropatform, ideal gimbal suspension  
three orthogonal string sensors, deriving  
formula for unperturbed gravity value,  
discussing perturbation measurement  
03 p0366 A66-12991
- Automatic in-flight testing capability of  
redundant systems 03 p0353 A66-13051
- [AIAA PAPER 65-732] 03 p0353 A66-13051
- Increased aircraft close-support mission  
effectiveness through optimized selection of  
avionic systems 04 p0458 A66-13685
- Takeoff and overshoot director system for  
jet transport aircraft 05 p0712 A66-14701
- XC-142A Flight Test Program, program  
statistics, aircraft instrumentation and flying  
qualities in hover and transition flight  
regimes 06 p0807 A66-16820
- Stall indicator modification, describing  
design in combination with speed indicator  
LUN-1106 06 p0883 A66-16971
- Magnetic compensation methods which  
eliminate swinging 07 p1032 A66-17684
- Navigation and flight instrument,  
discussing deficiencies of panel-mounted  
navigational command 07 p1033 A66-17685
- Supersonic commercial air transport,  
evaluating communication, navigation and  
identification systems 07 p1066 A66-17686
- Inertial navigation and guidance systems  
applied to civil air transport from systems  
engineering viewpoint 07 p1067 A66-17695
- Feasibility of using perfected gyromagnetic  
compass as heading reference for  
aircraft 07 p1033 A66-17698
- Vertime, navigation system for vertical  
plane control 07 p1069 A66-17716
- Up-dating of self-contained navigational  
aids such as Doppler, inertial and  
Doppler/inertial systems 07 p1070 A66-17717
- Position-attitude-true-heading-steering  
navigation system noting accuracy,  
reliability, maintenance, operational  
requirements and functional  
features 07 p1070 A66-17720
- Compass performance improvement,  
discussing Sperry C-12 compass system  
accuracy, operational features,  
etc 07 p1033 A66-17721
- Controlled direct current applied to flux  
valve to stimulate rotation of aircraft in  
compass swing 07 p1033 A66-17723
- Design criteria and operational  
performance of Doppler-driven map display  
device installed on Trident 07 p1077 A66-17802
- Automatic star trackers for long range  
navigation, discussing associated  
instrumentation methods 07 p1078 A66-17808
- Cockpit flight instrument display in  
integrated navigation system for SST,  
stressing smooth transition in handling from  
enroute navigation to terminal-area and  
approach procedures 07 p1078 A66-17810
- Visual display system providing instrument  
data in one-to-one correspondence with real  
world, using cathode ray tube images of  
horizon and runway projected on aircraft  
windscreen 08 p1034 A66-19764
- Thermal management /heat-sink and  
pressurization and cooling systems/, fuel,  
flying control and hydraulic and electrical  
systems of Lockheed L-2000 SST  
project 09 p1329 A66-20391
- Concorde navigation system noting inertial  
platform, digital computer using integrated  
circuits and  
microminiaturization 09 p1401 A66-20685
- Terrestrial test sites and aircraft flights  
used in preparing for remote sensing from  
Earth orbital spacecraft 10 p1532 A66-21525
- Human factor in design of controls and  
instrumentation in aircraft, discussing man-  
machine dynamics 10 p1494 A66-22135
- Atmospheric parameter determination by  
aircraft measurements, noting applicability  
to supersonic air  
transports 12 p1879 A66-23752
- Instrumentation of Polish gliders including  
altimeters, rate-of-climb, turn and air speed  
indicators, magnetic compasses, artificial  
horizon, etc 12 p1882 A66-24386
- Aircraft electrical system design, power  
requirements, instrumentation, excess loads,  
etc 12 p1803 A66-24387
- Universal turbulence measuring system  
giving quantitative measure of turbulent  
intensity independent of type or speed of  
aircraft, using all-weather sensor  
[AIAA PAPER 66-364] 12 p1906 A66-24476
- Equilibrium temperature gradient  
determined from theoretical calculations and
- balloon and aircraft  
measurements 12 p1875 A66-24872
- Vertime, navigation system for vertical  
plane control 13 p2125 A66-25863
- Inertial navigation and guidance systems  
applied to civil air transport from systems  
engineering viewpoint 13 p2125 A66-25865
- Controlled direct current applied to flux  
valve to stimulate rotation of aircraft in  
compass swing 13 p2079 A66-25866
- Automatic star trackers for long-range  
navigation, discussing associated  
instrumentation methods 13 p2125 A66-25867
- Inertial guidance systems using three-  
gimbal, four-gimbal and ball-type platforms,  
operative control of aircraft, ships and  
ballistic missiles 13 p2125 A66-26140
- Redundant system reliability in aircraft  
design, noting amplifier and filter  
arrangements, diode and quadruplex circuits,  
etc 14 p2247 A66-27015
- Theory of aircraft measurement of gravity  
using gyropatform, ideal gimbal suspension  
and three orthogonal string sensors, deriving  
formula for unperturbed gravity value,  
discussing perturbation measurement  
errors 15 p2483 A66-28666
- Atmospheric temperature changes as factor  
in detection of clear air turbulence,  
especially above 25,000 ft, noting aircraft  
instrumentation used 15 p2532 A66-28918
- Clear air turbulence forecasting for  
aircraft, noting methods employed by  
airlines 15 p2533 A66-28932
- Navigation displays for supersonic  
transports, discussing inductive reasoning,  
system performance verification, initial data  
verification, etc 15 p2535 A66-29625
- Airborne weather radar to detect  
dangerous turbulent condition and other  
phenomena 15 p2452 A66-29626
- Aircraft as platform for solar eclipse  
observation, discussing history, project  
APEQS, navigation problems, aircraft used,  
etc 16 p2705 A66-30822
- Pilot eye movement data by recording eye  
fixations on flight 16 p2644 A66-31273
- Helicopter landing in zero-zero weather,  
describing experiment in England involving  
landing in dense fog 17 p2844 A66-32728
- Automation in flight safety, noting role  
of radar, flight control system reliability, data  
processing system used,  
etc 17 p2848 A66-33485
- Monogram on metrological foundations and  
test methods of aircraft instruments,  
especially navigation  
instruments 18 p3111 A66-34011
- Multisensor display requirements and  
approaches, using as example hypothetical  
two-man advanced tactical  
aircraft 19 p3396 A66-35512
- Solid cryogenics as heat sinks for cooling  
electronic components, particularly IR  
detectors in aircraft and  
spacecraft 20 p3676 A66-37073
- Automatic built-in test of advanced  
avionics systems, noting advantages of  
airborne computer in sequencing, conducting  
and evaluating in-flight  
performance 20 p3522 A66-37245
- Prediction of avionic equipment reliability  
in early design stage, noting equations for  
line replaceable unit (LRU), classification,  
regression techniques,  
etc 20 p3573 A66-37953
- Aircraft instrumentation for oceanographic  
measurement platform including radiation  
thermometer, wave meter and expendable  
bathythermograph  
[AIAA PAPER 66-695] 20 p3496 A66-38036
- Equilibrium temperature gradient  
determined from theoretical calculations and  
balloon and aircraft  
measurements 22 p3912 A66-40333
- Barometric instrument development and  
description of counter-pointer altimeter and  
airspeed indicator 23 p4067 A66-41164
- Head-up aircraft display systems using  
cathode ray tube 23 p4067 A66-41166
- Temperature and humidity variations in  
weak convection over England, noting  
measurement techniques and  
results 24 p4235 A66-43076
- Environmental testing and evaluation of  
useful life of insulation material for aircraft  
electrical equipment operating at 280



degrees C 24 p4229 A66-43083

## AIRCRAFT LANDING

Cause and elimination of vertical oscillations of aircraft landing gear system in motion of aircraft over unpaved airfield 01 p0011 A66-10470

Soft and rough airfield landing gears, discussing ground flotation and shock absorbers for aircraft of several sizes [SAE PAPER 650844] 01 p0011 A66-10834

Analytical landing simulation to analyze dynamic loads and aircraft response, particularly high sink speed landing gear [SAE PAPER 650845] 01 p0011 A66-10835

Carrier landing characteristics of vectored-thrust aircraft obtained in piloted fixed-base flight simulator studies [AIAA PAPER 65-792] 03 p0390 A66-12560

Boeing Lower Minimums Program in terms of certified components and systems for Category II and for Automatic Landing [AIAA PAPER 65-765] 03 p0390 A66-13060

Category II lower weather minimums for aircraft landing of airlines of western world [AIAA PAPER 65-766] 03 p0391 A66-13061

Carrier landing improvements in Fresnel lens optical landing system, emphasizing compensated-meatball stabilization [AIAA PAPER 65-791] 03 p0322 A66-13228

Organization of short-distance interurban transportation system based on STOL aircraft of Breguet type 05 p0611 A66-15194

Design of landing gear for military cargo aircraft and supersonic transports 07 p0985 A66-17255

British and French VTOL landing gear design, describing unique SConc fixed-wing VTOL aircraft 08 p1167 A66-18627

CHSS-2 Haul Down and Handling System for operating large /SH-3A/ helicopter from small ships 10 p1484 A66-21891

Automatic system ensuring landing in absence of visibility and atmospheric turbulence by controlling motion of aircraft leveling out, consisting of time-dependent input signal shaping device and amplifiers 12 p1909 A66-24321

Assisted takeoff and landing for commercial aircraft using short runways [SAE PAPER 660337] 14 p2269 A66-27296

Category II lower weather minimums for aircraft landing of airlines of western world [AIAA PAPER 65-766] 14 p2328 A66-28107

Terrain clearance during climb and descent under air traffic control 15 p2535 A66-29627

Dynamic and steady state flow disturbances encountered by aircraft during carrier landing approach in water tunnel simulation study [AIAA PAPER 65-332] 16 p2634 A66-31319

Landing gears and operation illustrated in modern aircraft 16 p2635 A66-31681

Discrete control signal effect on crabbing /sideways motion/ of aircraft during floating and after touchdown 17 p2950 A66-32584

Air cushion landing gear for aircraft, noting rubber tubing under fuselage forming pneumatic bumper blown up by turbine engine 17 p2848 A66-33082

Landing run and taxiing problems in very low visibility 17 p2952 A66-33206

Technological approaches to use of aircraft on undeveloped or semideveloped field from standpoint of load and terrain roughness 18 p3051 A66-33937

Automatic landing of aircraft in blind flying conditions, Royal Aircraft Establishment equipment accuracy and safety 18 p3133 A66-35243

TALAR, tactical aircraft landing aid-radio uses ground-based Cassegrain antenna, magnetron transmitter and 4-lb receiver in aircraft while providing ILS functions 20 p3596 A66-37232

Discrete control signal effect on lateral motion of aircraft landing in presence of correction, considering slideslip equation 23 p4089 A66-41355

## AIRCRAFT LIGHTING

Aircraft illumination utilizing electroluminescent panels 11 p1640 A66-22666

White light rather than red for illumination of instruments and cockpits 11 p1648 A66-22667

## AIRCRAFT MAINTENANCE

## SA CEMS SYSTEM

Whitney Aircraft system for assurance in gas turbine

engines, discussing management, failure modes, product development and tests 01 p0128 A66-10062

DC-9 maintainability, simplicity and commonality of design with emphasis on reliability 01 p0129 A66-10092

T-53 gas turbine engine used to describe results of maintainability at work 01 p0129 A66-10093

F-5/T-38 design philosophy to meet rigorous operational and maintenance requirements 01 p0010 A66-10094

Aircraft maintenance and maintainability within context of U.S. supersonic transport program 01 p0010 A66-10095

Standard Navy Maintenance and Material Management System /3M System/ detailing aviation portion of maintenance data collection program 01 p0033 A66-10118

RCAF system of aircraft fleet operations management /TC-91/ for unserviceability cost estimate 02 p0178 A66-11992

Corrosion control on aircraft skin, countersinks and fasteners describing tests, sealant coatings, chemical treatments, mechanical barriers, platings on fasteners and organic coatings 03 p0372 A66-12298

Aircraft materials stress corrosion at high temperature discussing test and results on titanium alloys, precipitation hardening steels and superalloys 03 p0380 A66-12299

V/STOL aircraft economic and operational characteristics for commercial service over routes of 150 miles or less [SAE PAPER 650243] 03 p0446 A66-12632

Flight operating techniques influence upon engine maintenance costs and new engine design, specifically Pratt and Whitney JT3C-12 on Boeing 720 aircraft [SAE PAPER 650212] 03 p0322 A66-13220

Training and instruction by means of teaching machines in field of aviation 04 p0469 A66-13508

Maintainability guidance as factor in designing for aerospace industry 05 p0646 A66-14634

Maintenance recordings of aircraft parameters, discussing signal conditioning, economics and application [ISA PREPRINT 1.3-1-65] 05 p0794 A66-15499

Manned aircraft self-contained checkout and fault isolation systems, discussing characteristics and operational concepts [ISA PREPRINT 1.3-3-65] 05 p0684 A66-15513

Safe usage of toxic chemical agents in aircraft maintenance 06 p0816 A66-16056

Radioactive contamination of aircraft and effects on maintenance, discussing washing and monitoring procedures for containment and personnel protection 06 p0816 A66-16059

Leakage detection system for monitoring component test stand hydraulic circuit 06 p0869 A66-16792

XB-70 landing gear inspection, describing hydraulic jack used 06 p0869 A66-16793

Aircraft engine maintenance, discussing line, minor and major services, operating period parameters, overhaul facilities, etc 06 p0943 A66-17024

Fault location in modern airborne radar, discussing maintenance reduction techniques and reliability 07 p1006 A66-17495

Engine-overhaul facilities and procedures at BOAC noting use of flow principle, automatic processing and three main sections, engine dismantling, crack detection and static and dynamic balancing 07 p1111 A66-18329

Aircraft landing gear design and maintenance, noting elimination of sharp corners and radii, weldability criterion, joints, part identification, bushings, etc 10 p1482 A66-21135

Concord SST propulsion system, discussing maintainability, monitoring, closed-loop control systems, nozzle, intake, etc 12 p1935 A66-23707

Maintenance and airworthiness philosophy in aerospace engineering 12 p1801 A66-23858

Airline long-haul maintenance objectives, methods for monitoring maintenance equipment and cost 12 p1801 A66-23859

Cost reduction in aircraft maintenance and servicing 12 p1801 A66-23860

Airline safety maintenance, noting British system of classification of parts into chapter

numbers, ground equipment use testing methods 12 p1857 A66-23861

Airborne checkout system, in maintenance and related signal problems 13 p2190 A66-23862

DC-9 maintainability, simplicity, commonality of design with emphasis on reliability 13 p2173 A66-23863

Digital computer automatic check equipment for maintenance of systems 14 p2269 A66-23864

Aircraft maintenance, ground service and safety precautions for XB-70 [SAE PAPER 660275] 14 p2269 A66-23865

SST flight operations, maintenance servicing compared to subsonic [SAE PAPER 660294] 14 p2222 A66-23866

Automatic preworkshop screening apparatus for determining which components removed from aircraft during maintenance need to be sent to workshop 14 p2224 A66-23867

Douglas DC-8 super sixty series of airport requirements including noise runway problems and traffic [SAE PAPER 660281] 15 p2427 A66-23868

Operation and maintenance of Lockheed 2000 double delta SST aircraft with thrust engine and large delta [SAE PAPER 660295] 15 p2427 A66-23869

Airborne performance analysis multiparameter sampling applied to maintenance and benefits including prediction of impending malfunctions 17 p2842 A66-23870

Nondestructive testing in aircraft maintenance, surveying radiography, ultrasonic testing and eddy current testing 18 p3116 A66-23871

Maintenance and inspection of transport vehicle structures 19 p3278 A66-23872

Contractor components/parts relationship program for Douglas S-IVB space project 20 p3566 A66-23873

Decision table for determining base maintenance policy for aircraft engines 20 p3566 A66-23874

Maintenance Dependency Chart for checking and troubleshooting in missile weapon systems 20 p3566 A66-23875

Microelectronics application to missile maintenance and support of guidance control systems of missile and weapons systems 20 p3567 A66-23876

Lockheed C-5 quantitative maintenance program and application to airworthiness utilization and cost effectiveness 20 p3495 A66-23877

VTOL operational availability comparison simulation model, studying initial tradeoff design, maintenance, logistics manpower and flight operational requirements 20 p3543 A66-23878

Naval weapons A-7A maintenance requirement effect on management design and analysis of early flight data 20 p3496 A66-23879

Maintainability program of F-111 aircraft 20 p3574 A66-23880

Maintainability program for aircraft plant particularly turbofan engine, inspection, failure detection, replacement etc 20 p3574 A66-23881

Molybdenum bisulfide as lubricant for aircraft construction to combat corrosion, facilitate assembly and dismantling of parts and reduce frequency of maintenance 23 p4074 A66-23882

## AIRCRAFT MODEL

Sequence photography of models used study head-on interaction between shock cone in supersonic flight and moving wave [AIAA PAPER 66-57] 08 p1163 A66-23883

Modeling and data reduction technique obtaining spectrum signatures of low LF airborne antennas 13 p2044 A66-23884

Drag force of flexible wire connection between aircraft and ship models and about which they are rotating 21 p3832 A66-23885

## AIRCRAFT NOISE

Sound pressure and acoustic spectrum associated with it calculated for predetermination of ground noise at takeoff period of future aircraft



- ERA TP 250] 02 p0177 A66-11679  
Assessment of aircraft noise and relation  
time duration and discrete tone  
ponents  
[A PAPER 65-802] 03 p0319 A66-12566  
Aircraft noise due to propeller, engine  
transmission, examining reduction  
techniques, comparing with aircraft and  
space transport 04 p0457 A66-13466  
Hearing-intelligibility tests in presence of  
recorded noise from jet and propeller  
aircraft 09 p1338 A66-20957  
Measurement of aircraft noise in vicinity  
airports in connection with land-use  
planning 10 p1483 A66-21745  
Physical and psychological nature of noise  
principles of noise suppression in  
aircraft 10 p1493 A66-22129  
Psychological reactions to jet aircraft  
noise, including behavioral reactions and  
fatigue 12 p1806 A66-24234  
Sequential Noise Output Recording  
Equipment /SNORE/, aircraft engine noise  
facility, for jet noise and compressor  
noise and acoustic absorption materials test  
facility  
[SAE PAPER 66-GT-N-41] 14 p2269 A66-26986  
Field noise-reduction measurements in  
hotel, motel and residential rooms during  
flights of aircraft 17 p2847 A66-33036  
Dynamics of noise and loading actions on  
helicopters, V/STOL aircraft and ground  
test machines 18 p3050 A66-33679  
Noise generation due to mass introduction,  
thrust force and stress in helicopters,  
V/STOL aircraft and ground effect  
engine 18 p3051 A66-33687  
Acoustic isolator-membrane structure for  
soundproofing V/STOL aircraft exposed to  
noise levels with radical saving in  
weight 18 p3051 A66-33688  
Internal noise associated with hovercraft  
propeller 18 p3051 A66-33689  
Noise acceptability as produced by actual  
aircraft flyovers and recorded flyover  
levels judged on relative and absolute  
levels 21 p3721 A66-38647  
Pressure-perturbation produced by  
supersonic aircraft near caustic, deriving  
partial equations 23 p4016 A66-42040  
Interactions among technical, economic and  
social aspects of aircraft noise problem,  
examining relation between thrust and jet  
engine noise  
[SAE PAPER 66-5] 23 p4152 A66-42068  
**AIRCRAFT PART**  
Aircraft landing gear designs in past 12  
years 05 p0611 A66-15134  
Modern landing gear design as function of  
aircraft type and size 13 p1997 A66-25499  
Dynamic Antiresonant Vibration Isolator  
design, operation and capability of  
actively isolating VLF vibrations with high  
static stiffness 17 p2929 A66-32738  
Anti-flap controlled lifting propeller,  
minimizing power and  
inefficiency 21 p3731 A66-39592  
**AIRCRAFT PERFORMANCE**  
Flight program and performance of X-15  
research aircraft noting aerodynamic  
testing, cockpit, controls and handling  
capabilities 01 p0011 A66-10340  
Aircraft speed relation to range, endurance  
maneuverability capabilities reviewed  
in regard to military value  
[SAE PAPER 650797] 05 p0610 A66-15012  
Present and future X-15 aircraft research,  
evaluating flight characteristics, propulsion  
structural materials  
[AA PAPER 64-781] 05 p0610 A66-15072  
Aircraft performance including sink speeds,  
climb speed, absolute thermal strength,  
etc 07 p0989 A66-18057  
Look on aircraft testing techniques for  
aeronautical technical school  
Students 08 p1167 A66-18590  
V/STOL aircraft static and dynamic  
performance measurement technology,  
analyzing application of data processing  
methods 10 p1535 A66-21381  
Being 737 twin-jet, discussing wing,  
tail and tail design, aerodynamic wind  
tunnel tests, stability and control,  
etc 12 p1801 A66-23785  
Factors determining performance  
characteristics of powered aircraft, including  
climb altitude, runway length, air  
temperature, etc 12 p1802 A66-24833  
Flight path optimization methods for given  
aircraft performance  
objectives 13 p1995 A66-25764  
Scramjet aircraft performance capabilities,  
noting operating parameters such as thrust  
coefficient, flight velocity, acceleration, fuel  
consumption, etc 13 p2173 A66-26032  
Effects of nonlinearities in lift and  
pitching moment curves on longitudinal  
motion of aircraft, comparing approximate  
analytical method with computer  
calculations 13 p1995 A66-26285  
Flying qualities of six late-model personal-  
owner aircraft in visual and instrument  
flight  
[SAE PAPER 660219] 13 p1996 A66-26396  
Aircraft utilization and schedule planning,  
optimum use of flight performance, ground  
equipment, facilities and personnel  
[SAE PAPER 660279] 15 p2427 A66-29824  
Data processing techniques for analyzing  
turbulence records and for estimating  
response of aircraft to atmospheric  
turbulence 17 p2843 A66-32329  
Performance spectrum of military aircraft  
noting speed, range, endurance, safety,  
etc 17 p2843 A66-32501  
Flying qualities and aircraft control during  
tandem rotor helicopter external sling load  
operations 17 p2846 A66-32742  
Sonic boom phenomena, noting atmospheric  
dynamic effects, acceleration and lateral  
spread, variations in pressure signatures,  
etc 17 p2847 A66-33026  
Military STOL and conventional civil  
aircraft behavior on rudimentary  
airstrips 18 p3051 A66-33686  
Kestrel /P-1127/ Tripartite V/STOL  
Operational Trials, describing aircraft  
performance, test unit organization, results,  
etc  
[SAE PAPER 660320] 18 p3052 A66-34945  
Laminar flow control /LFC/, aircraft  
performance benefits include increased  
endurance, loiter time and cruise  
altitude 18 p3050 A66-34948  
Flight testing of laminar flow control on  
X-21 aircraft, noting degradation of laminar  
performance in proximity of clouds or  
atmospheric turbulence, feasibility, handling,  
etc 18 p3050 A66-34949  
Optimum high payload laminar flow control  
aircraft offer 20 to 25 percent range  
improvement, indicated by design studies of  
large logistics aircraft 18 p3053 A66-34952  
Liquid methane fueled propulsion system  
for SST application, noting increased  
payload capacity, propellant characteristics  
and design criteria for storage within  
aircraft  
[AIAA PAPER 66-685] 20 p3625 A66-37259  
Common electronic techniques for studying  
aeroelasticity in high performance  
aircraft 21 p3827 A66-38654  
Aircraft in-flight vs ground testing, noting  
better SNR, freedom of jamming and  
decreased parameter requirements for  
vibration and transient  
monitoring 22 p3917 A66-39995  
Fundamental modes of nonervo-assisted  
aircraft control surface 24 p4159 A66-42344  
Optimization of aircraft performance, pilot  
performance and mission completion  
[ICAS PAPER 66-4] 24 p4159 A66-42492  
Dornier twin engine high wing STOL  
monoplane design and performance, noting  
useful space, landing gear, control system,  
fuselage, cargo, etc 24 p4160 A66-43070  
**AIRCRAFT POWER SOURCE**  
Integrated secondary power system to  
provide additional capabilities for supersonic  
aircraft  
[SAE PAPER 650828] 01 p0016 A66-10828  
Engine technology including higher turbine  
operating temperatures, high speed fan and  
nacelle design, increased by-pass ratio and  
improved power plant  
efficiency 06 p0943 A66-16924  
M.A.N. RB 153 jet engine development,  
characteristics and  
capabilities 06 p0943 A66-17019  
Aircraft batteries design, considering  
plastics, separators, alloys and operating  
conditions including thermal stability,  
explosion risks, etc 08 p1173 A66-19658  
Thermal stability of endothermic  
hydrocarbon heat-sink fuels, noting  
application flying in 10 Mach speed  
range 11 p1759 A66-23124  
Small gas turbines, market, technical  
problems, etc  
[ASME PAPER 66-GT-90] 14 p2372 A66-26994  
Incompressible fluid static thrust  
augmentation devices for aircraft propulsion  
for cases of presence and absence of heat  
and work exchange  
[ASME PAPER 66-GT-116] 14 p2373 A66-27008  
Airframe structure and power plant  
configuration effects on transport V/STOL  
performance 17 p2846 A66-32885  
USAF Aero Propulsion Laboratory research  
in weapon systems and turbine engines,  
ramjets, etc 18 p3269 A66-34956  
Nickel-cadmium batteries commercial  
aircraft application and maintenance  
problems 20 p3497 A66-37162  
Sealed nickel-cadmium batteries for  
aircraft-electrical systems, noting T-39B  
aircraft 20 p3497 A66-37163  
Method of weight analysis for constant  
frequency aircraft electrical generating  
system equipment 20 p3498 A66-37171  
Frequency sensing for protection of  
frequency aircraft electric power systems,  
applying storms saturating reactor  
concept 20 p3499 A66-37175  
Function, method of operation, complexity  
and effect on weight and cost for BITE  
/built-in test equipment/ as applied to  
electric power systems for jet  
aircraft 20 p3499 A66-37189  
HF electric power transmission lines in  
aircraft noting effect of frequency, ground  
plane elevation and feeder configuration on  
impedance 20 p3499 A66-37190  
Jet aircraft electric power system  
performance affected by transmission line  
impedances 20 p3499 A66-37191  
Power plant development trends and effect  
on short and vertical takeoff aircraft design,  
noting improvement in thrust-weight  
ratio 24 p4262 A66-43051  
**AIRCRAFT PRODUCTION**  
**SA EQUIPMENT SPECIFICATIONS**  
F-104J production program from Japanese  
standpoint  
[AIAA PAPER 65-804] 03 p0446 A66-12600  
Worldwide F-104 program, discussing  
licensing agreements and weapons system  
management  
[AIAA PAPER 65-776] 03 p0447 A66-13065  
Introduction of programmed milling  
machines to production of aircraft engines  
for Czechoslovakian FB  
series 04 p0525 A66-13763  
Processing techniques in aircraft  
fabrication including explosive,  
electrohydraulic and magnetic  
forming 05 p0688 A66-15195  
Netherlands Nationaal Lucht-en  
Ruimtevaartlaboratorium /NLR/ activities,  
discussing production of Fokker F-27 and F-  
28 aircraft and other  
projects 07 p1017 A66-17204  
Normal startup time for aircraft series  
production run and practical rate  
gradient 09 p1383 A66-19865  
Developments in use of line of balance  
charts in production management  
[ASTME PREPRINT MM66-703] 12 p1886 A66-24414  
Data processing approach for management  
control of aircraft manufacture  
[SAE PAPER 660205] 13 p2211 A66-26391  
V/STOL aircraft for intercity travel,  
discussing cost, advantages, technological  
advances, etc  
[SAE PAPER 660318] 14 p2223 A66-27298  
Maximizing aircraft production and critical  
weapons systems schedule for industrial  
readiness programs  
[SAE PAPER 660287] 15 p2621 A66-29829  
Military aircraft procurement, discussing  
development production cost estimate and  
design 17 p3040 A66-32796  
Military aircraft procurement, discussing  
equipment supply, management control,  
development procedure and value  
engineering 17 p3040 A66-32797  
Production methods for Beagle B.206 S  
aircraft, examining sequence of assembly  
and erection and methods of anticipating  
minimum customer  
requirements 22 p3922 A66-39691



## AIRCRAFT RELIABILITY

### SA AIRWORTHINESS REQUIREMENT SA COMPONENT RELIABILITY SA STRUCTURAL RELIABILITY

Changes to improve reliability of attack aircraft, estimating cost and gains in operational effectiveness 01 p0167 A66-10049

Military specifications MIL-HDBK-217 and MIL-R-22256, 22973 and 23094A with respect to reliability design of aircraft electronic equipment 01 p0034 A66-10059

DC-9 reliability program emphasizing simplicity improved proven components rather than completely new equipment 01 p0010 A66-10088

Triple redundancy with majority logic voting in application for increased safety and reliability of aircraft stability augmentation and/or automatic flight control 01 p0103 A66-10665

Reliability factors in flight controls, particularly automatic landing systems and controls for VTOL aircraft in transitional regime 02 p0231 A66-11863

Verdan digital computer operation in aircraft noting problems of reliability 02 p0194 A66-11965

Aid to air navigation problem discussing reliability and accuracy, hybrid system, redundancy and credibility, display, operational environment and navigation technique 02 p0256 A66-11966

Aircraft Unserviceability Analysis 03 p0322 A66-13107

British short-range aircraft operating cost affected by reliability, design and engines 06 p0804 A66-15991

Reliability factors considered by aircraft designers and manufacturers including bad design, indifferent manufacture, inadequate testing, human error, etc 10 p1538 A66-21134

Dimensionality theory for determining failure rate of aircraft components not in operation 11 p1637 A66-22862

Defining fatigue load environment for business aircraft [SAE PAPER 660215] 13 p2199 A66-26392

British Air Registration Board approach to safety of advanced complex aircraft and assessment of aircraft reliability 13 p2088 A66-26690

Reliability of military aircraft from viewpoint of user 13 p1996 A66-26691

Probability assessment of reliability effect on sortie of patrolling aircraft 13 p1996 A66-26695

Data recording and information transfer for defects in aircraft 16 p2715 A66-31200

Computer program for airborne surveillance system reliability 18 p3052 A66-34212

Optimum number of test aircraft in test program to predetermine endurance and service life of same aircraft in serial production 20 p3493 A66-36921

Predelivery reflight policies role in airplane system reliability, noting failures during various test and retest flights 20 p3495 A66-37178

XB-70A reliability program applied to initial system design stage from inception to present flight test program 20 p3568 A66-37917

UH-1D helicopter reliability determination and maintenance through planned data acquisition, analysis and corrective action program 20 p3572 A66-37946

### AIRCRAFT SAFETY

Safety education, management process and aerospace accidents 01 p0169 A66-10073

Air Force system safety management progress in issuance of new instruction manuals and in revision of system specifications 01 p0169 A66-10074

Safety and management in aerospace industry, noting importance of military specification 01 p0169 A66-10075

Arresting transport type aircraft, preventing overshooting runways, noting field tests 02 p0179 A66-12222

Structural design of transport aircraft to reduce fatalities, analyzing protective shell to withstand ground impact load and fuel containment [AIAA PAPER 65-773] 03 p0434 A66-12592

Computer-directed malfunction checkout of rockets, boosters and modern military aircraft 04 p0526 A66-14020

Supersonic flight control, discussing reliability and safety devices, computer application and multiplex systems 06 p0816 A66-16055

Stall indicator modification, describing design in combination with speed indicator LUN-1106 06 p0893 A66-16971

Mathematical formulation of lateral and longitudinal separation standards for subsonic and supersonic aircraft operation 07 p1066 A66-17680

International Air Transport Association, Technical Conference, Miami, April 1965, Volume 2 07 p1071 A66-17757

Operational requirements for improved worldwide navigational ability, initially applied in North Atlantic area 07 p1072 A66-17761

Optical and atmospheric conditions contributing to visibility loss at high altitude for high-speed aircraft approaching each other with very rapid closing times 10 p1494 A66-22134

Aircraft crew fatigue on long distance jet flights, measuring flight safety parameters such as heartbeat, pulse rate and temperature 12 p1808 A66-23753

North American Sabreliner laminate windshield for bird-proofing pilot compartment [SAE PAPER 660214] 13 p1995 A66-26389

FAA research, development and airworthiness compliance for general aviation aircraft [SAE PAPER 660217] 13 p1996 A66-26394

Rain repellent polymers for aircraft windshields 13 p2116 A66-26544

British Air Registration Board approach to safety of advanced complex aircraft and assessment of aircraft reliability 13 p2088 A66-26690

Aircraft maintenance, ground servicing, and safety precautions for XB-70 aircraft [SAE PAPER 660275] 14 p2269 A66-27286

Airworthiness and operational standards approaches for safety in supersonic transport, noting problems with temperature, altitude, radiation, ozone, etc [SAE PAPER 660293] 14 p2222 A66-27288

Aircraft safety, noting minimization of clear air turbulence, mountain wave and wind shear effects 15 p2533 A66-28933

Clear air turbulence, noting importance of good detection system and history of incidents in six-year period 15 p2426 A66-28934

Flight tests on various agricultural aircraft noting safety record data 16 p2634 A66-31284

Fail-safe concept application to rotorcraft noting fatigue requirements, accident prevention methods, etc 17 p2843 A66-32721

Hughes OH-6A helicopter fail-safe structural composition noting design, fatigue testing, application of redundant design features, etc 17 p2845 A66-32736

Helicopter airframe fatigue testing noting fail-safe design, crack detection, loads applied, test facilities and techniques, etc 17 p3027 A66-32737

Head-up display systems, discussing state of the art and arguments in favor of their use 17 p2952 A66-33202

Separation standards and navigation in long-range air traffic control region 17 p2954 A66-33213

Airworthiness codes for supersonic transports, noting current regulations, codes, etc 18 p3268 A66-34622

FAA safety research on aircraft reliability, discussing power spectral gust design, structural strength, turbine performance and lightning strike effects 20 p3540 A66-36992

Pilot protection from aircraft vibration caused by atmospheric turbulence 20 p3508 A66-36997

Allotment of probability shares method applied to improving safety in design by diagnosing failure and probability of accident 20 p3494 A66-36999

Airline evaluation of aircraft survival equipment, noting Arctic survival exercises and testing 20 p3494 A66-37002

XB-70 aircraft safety program developed during flight tests applied to future SST civil aircraft 20 p3494 A66-37006

Safety-factor problem in glider design, discussing limiting load concept in form of extreme load in exceptional cases of

operation 21 p3696 A66-3861

Promotion of aviation safety, discussing adoption of new accident statistics, elimination of catastrophes and STO design extension to medium and long-range aircraft 23 p4152 A66-4130

### AIRCRAFT SPECIFICATION

AFSC 375 series of systems management manuals with emphasis on specification programs 01 p0168 A66-1000

Reliability problems associated with producing to specification from viewpoint aircraft manufacturer 13 p2088 A66-26690

### AIRCRAFT STABILITY

Aileron traverse effect on amount coupling from roll to yaw during abrupt aileron roll of conventional aircraft 01 p0011 A66-101

Triple redundancy with majority logic voting in application for increased safety and reliability of aircraft stability augmentation and/or automatic flight control 01 p0103 A66-10665

Variable stability system /VSS/ incorporated into X-22A aircraft to obtain flight data on VTOL aircraft [AIAA PAPER 65-706] 01 p0013 A66-109

Preflight checking of aircraft gyroscope and accelerometers noting built-in speed detection, torque generator and gimbal check 01 p0070 A66-109

Free oscillation device for studying dynamic stability of models in hypersonic range of intermittent wind tunnels 02 p0210 A66-112

Changes in dynamics of aerospace vehicle flight in low altitude turbulence at satellite spin decay 02 p0178 A66-119

Vestibulo-ocular disorganization in aerodynamic spin, noting roll plane skull 03 p0325 A66-123

Tail aircraft in deep stall conditions at fixed-base cockpit simulation at large angle of attack [AIAA PAPER 65-781] 03 p0322 A66-130

Wing-fuselage interaction effects on static and dynamic stability at low and moderate hypersonic Mach numbers by small disturbance approximation to shock expansion method [AIAA PAPER 65-719] 04 p0454 A66-135

Pitch, roll and yaw axis stability augmentation system providing automatic failure detection of portions of system at further stability augmentation after a single failure 04 p0544 A66-141

Vibrational analysis of multicomponent systems using Rayleigh-Ritz type approximation, treating cases of fuselage and T tail assembly 04 p0594 A66-143

Aerodynamic coupling between longitudinal and lateral-directional rigid body modes of aircraft trimmed at nonzero sideslip angle and degradation of Dutch roll damping 05 p0606 A66-150

X-22A variable stability and control VTOL aircraft 06 p0809 A66-168

Capability of Cornell Aeronautical Laboratory /CAL/ system for measuring dynamic airloads in wind tunnel [AIAA PAPER 66-15] 06 p0803 A66-170

Aircraft erect and inverted spin characteristics, discussing Hawker-Siddeley Hunter T.Mk. 7 spin properties and application of controls for recovery 07 p0987 A66-174

Deep-stall characteristics of T-tailed aircraft configurations and recovery procedures, noting parameters of pitch-up angle of attack, etc [AIAA PAPER 66-13] 07 p0989 A66-184

Dynamic response of supersonic transport to runway unevenness during takeoff landing 09 p1330 A66-206

Longitudinal stability and controllability characteristics of glider, considering effect of elastic warp of wing 09 p1331 A66-207

Load factor estimation for flights in turbulent conditions by replacing exact transfer function with equivalent statistical model 10 p1482 A66-213

Drone aircraft onboard stabilization circuit design for control signal transmission at transient response irrespective of noise background 11 p1778 A66-233

Aircraft vibration in transonic regime caused by aileron oscillations, eliminated by friction dampers 12 p1801 A66-240



Automatic stabilization of helicopters by using autopilots 12 p1801 A66-24388

Aeronautical stability problems, discussing background, rigid and elastic stability and adaptive control 13 p1994 A66-25582

Lateral stability and control of STOL airplane at low speed 13 p1995 A66-26380

Automatic stabilization systems reduce accidents due to disorientation, emphasizing sensor-servo system for roll axis control [SAE PAPER 660201] 13 p1996 A66-26390

Light aircraft lateral stability augmentation system for wing leveling, noting operation and pilot performance [SAE PAPER 660220] 13 p1996 A66-26397

Text on longitudinal static stability of low-speed aircraft including effect on pilot, flight test, pitch maneuverability, etc 14 p2222 A66-26792

Stabilizing methods for hypersonic aircraft, noting effect of aircraft characteristic parameters on magnitude of balancing coefficients of lifting force 14 p2223 A66-27680

Dynamic programming design of invariant multiloop feedback autostabilizers and matrix-Ricatti equation 14 p2268 A66-28184

Stability of wing mounted pro-rotor pylon systems in fully converted aircraft configuration, showing in-plane force generated by blade flapping as destabilizing factor 16 p2633 A66-30599

Aircraft stabilization for solar eclipse observation, emphasizing use of autopilot for maximum control 16 p2743 A66-30823

Aileron traverse effect on amount of coupling from roll to yaw during abrupt aileron roll of conventional aircraft 16 p2633 A66-31115

Spiral instability in STOL aircraft prevented by larger wing dihedral setting, noting permissible dihedral levels and tests 16 p2634 A66-31395

Wind shear problems in terminal operations, considering effects on aircraft as longitudinal and lateral components 17 p2843 A66-32202

Aeroelastic stability of light aircraft, examining appearance of structural nonlinearities in global vibration test for determining critical flutter speed 17 p3023 A66-32331

Integrated Helicopter Avionics System flight control, noting stability augmentation, long-term motion control, outer and inner loop function separation and fail-safe capability 17 p2951 A66-32730

XV-5A V/STOL aircraft flight testing, noting handling qualities and sequential diversion capability 17 p2844 A66-32731

Lift engine technology, noting effect on operational transport aircraft design, VTOL capabilities, low speed control, etc 17 p2844 A66-32732

Flight control design parameters and performance effects on VTOL aircraft handling qualities, noting manufacture and flight test results 17 p2845 A66-32733

Gust alleviation systems for transport aircraft using linkage, noninteracting and split control 18 p3052 A66-34493

Aircraft bumpiness conditions in free atmosphere relation to turbulence and other aerological data 18 p3049 A66-34613

VTOL aircraft performance characteristics noting flying qualities, hover dynamics, transition flight and variable stability system 18 p3052 A66-34623

Normal modes of vibration in aircraft design, noting mass distribution effect on calculation accuracy 21 p3823 A66-38562

Automatic resonance testing technique for exciting normal modes of vibration of complex aircraft structures 21 p3823 A66-38566

Mechanics of linear vibrations - Symposium, Paris, April 1965 21 p3824 A66-38576

Linearized equilibrium conditions for force densities of aircraft oscillating in flight, determining Rayleigh-Ritz equations, measuring elastomechanical parameters by vibration tests 21 p3825 A66-38579

Aeroelastic instability of aircraft with automatic pilot, determining domain in which sensor position and other adjustable parameters may vary without risking instability 21 p3695 A66-38580

Static stability of rolling motion of aircraft for given aileron angle when inertia cross-coupling is present, with numerical solution of nonlinear equations 22 p3848 A66-40493

Performance of two-dimensional curtain jets of air cushion vehicles based on incompressible flow theory, noting stability criteria 22 p3844 A66-40499

Hovercraft difficulty in accelerating through hump, noting wave resistance increase for pressure differential between two compartments of cushion with transverse stability skirt 22 p3901 A66-40678

Capability of Cornell Aeronautical Laboratory /CAL/ system for measuring dynamic airloads in wind tunnel [AIAA PAPER 66-15] 23 p4051 A66-40977

Stability of vehicle passing from water to air as function of neutral point, maneuver point and center of gravity 23 p4015 A66-40987

Midpath airplane interference to digital transmission in tropospheric radio, considering scattering of radiant energy by atmospheric layers 23 p4040 A66-41594

# AIRCRAFT STRUCTURE

## SA AIRFRAME

Structural response theory and acoustic fatigue aspects contributing to estimation of fatigue life of aerodynamic structures 01 p0147 A66-10122

Computer programming of diagonal tension analysis of flat panels in shear 01 p0152 A66-10345

Engineering exploitation of glass fiber reinforced plastics for aircraft structures [AIAA PAPER 65-762] 03 p0386 A66-12590

Cost barrier breakthrough in air vs surface cargo transportation by structural weight fraction reduction, using new material [AIAA PAPER 65-763] 03 p0382 A66-13058

Aircraft structural design errors due to use of idealized models 04 p0587 A66-13505

Royal Aircraft Establishment facilities in England for aircraft structure testing under supersonic conditions, simulating aircraft takeoff, flight and landing 04 p0508 A66-14021

Supersonic transport design in thermal insulation, structure and air traffic control 06 p0805 A66-16324

Synthetic spherulites in plastic foam and synthetic tube segments in honeycomb form as fillers in sandwich construction 10 p1614 A66-21390

Aircraft structure weight reduction, using redux bending and spot welding instead of bolts and rivets 12 p1963 A66-24036

Basic principles of structural design as applied to aircraft, discussing loads and strengths and effect of accidents and costs 12 p1971 A66-24972

Optimization of minimum weight multirib or multiweb wing box structure subjected to vertical shear and unidirectional bending moment 13 p2195 A66-25593

YS-11 transport aircraft fatigue testing, noting wing fatigue damage and equipment used 13 p2197 A66-26099

Aerospace application of aluminum and its alloys 14 p2313 A66-27012

Forced oscillations of three-layer plate used as vibration dampers for engine components 14 p2400 A66-27696

Starting weight increments in aircraft designs having various structural features and dimensions 14 p2223 A66-27697

Nondestructive metal testing in SST development, noting welded titanium structures 15 p2509 A66-29319

Book on dynamics of elastic structures in free flight 16 p2815 A66-30612

Design, fabrication and test of sandwich construction box beam made of D-43 columbium and Haynes 25 superalloy for use as hot redundant structure for hypersonic vehicles 16 p2816 A66-30894

Aircraft mass and stiffness estimations by displaced frequency method 18 p3254 A66-33949

Maintenance and inspection of air transport vehicle structures 19 p3278 A66-35399

Aircraft structures strength and longevity obtained by applying standards and criteria to design and manufacture including static, fatigue and fail-safe tests 20 p3666 A66-37000

Lifting aircraft structures subjected to

acoustic pressures, noting estimation of panel joint rms stress 20 p3666 A66-37422

Flight tests on aircraft and analysis by automatic filter, noting structural and aerodynamic problems resulting from use of transient method 21 p3824 A66-38574

Response of continuous structure to random forces distributed over surface of structure estimated through normal mode method, exemplifying with aircraft fuselage in vibration 21 p3824 A66-38575

Matrix methods of forces and displacements applied to free oscillations of aircraft structures, proposing procedure yielding coherent mass matrix 21 p3825 A66-38582

Book on manufacturing of welded and soldered structures of aircraft including material selection, plasma and ultrasound techniques, economics, etc 21 p3744 A66-38951

Aircraft materials and structures for extreme ranges of velocity and temperature 22 p3990 A66-40120

Status of aircraft structural design analysis methods, examining structural elastic behavior on basis of stress analysis 23 p4138 A66-41381

# AIRCRAFT TIRE

Landing gear with one to eight wheels, weight, wheel well volume and allowable traffic on heavy airplanes, noting flexible pavement design and tire pressure [SAE PAPER 650799] 01 p0053 A66-10815

Tire traction on wet runways, possible improvement via jets mounted ahead of tires and pavement grooving [AIAA PAPER 65-749] 03 p0319 A66-12585

Aircraft tire performance at high rolling speeds 14 p2223 A66-27711

Static and dynamic forces against pneumatic tire used to predict off-runway takeoff and landing performance [AIAA PAPER 66-328] 16 p2634 A66-31320

Snow runway construction, discussing physical characteristics of snow, mechanical properties related to supporting capacity temperature effect, etc 17 p2904 A66-32933

# AIRCREW

Medical wastage of aircrew in Royal Air Force related to age, noting causes 06 p0815 A66-16050

Noise and vibration causing acoustic fatigue leading to deafness of aircrew 06 p0811 A66-16065

Location of flight control system for simplifying crew procedure and reducing navigation error in areas of high traffic density 07 p1068 A66-17697

Hearing acuity requirements of aircraft personnel, examining discrimination from background noise and acoustic trauma causative factors 10 p1493 A66-22130

German Air Force functional tests for early diagnosis of cardiovascular disease among aircrew, also discussing therapy 16 p2640 A66-31133

Aircrew helmet design for protection against buffeting and against crash impacts 17 p2865 A66-32188

Analogies between nutritional requirements of aircrew and cosmonauts, evaluating physiological factors involved 23 p4029 A66-41204

# AIRFIELD SURFACE MOVEMENT

Soft and rough airfield landing gears, discussing ground flotation and shock absorbers for aircraft of several sizes [SAE PAPER 650844] 01 p0011 A66-10834

Electronic techniques applied to taxiing, takeoff, aerial navigation and landing 02 p0255 A66-11466

Airport operation under low visibility conditions, discussing use of pictorial display to aid in surface movement 17 p2953 A66-33208

# AIRFLOW

Nonequilibrium expansion of air through hypersonic nozzle extended to higher reservoir temperatures and pressures 02 p0303 A66-11565

Two-dimensionality effect on suppression of thermal turbulence in air between two horizontal plates 02 p0218 A66-11954

Air intake with boundary layer trap, examining flow structure under external supersonic pressure and uniformity parameters



[ONERA TP 288] 03 p0316 A66-12898  
Mass transfer by sublimation from surface of stationary or rotating naphthalene cone in axisymmetric airstream 04 p0595 A66-13388  
Hypersonic airflow at alpha angle of attack about flat wing with shock wave on upstream side attached 04 p0454 A66-13572  
Heat transfer and flow in turbulent separated airflow over downward step in plate surface with suction and injection [ASME PAPER 65-WA/HT-2] 05 p0664 A66-15656  
Geometrical approach to investigate airflow toward and within updraft of severe storm cell [AFCLR-SR-32-65] 07 p1061 A66-17368  
Supersonic airflow past blunt body with various dissociation reactions 08 p1165 A66-19192  
Temperature-velocity phase lag of vibrations of air columns excited by heat supply 08 p1320 A66-19555  
Plane nonlinear stationary problem of hill slope winds reduced to set of finite difference equations and solved by simple and matrix factorization combined with iteration by computer 09 p1398 A66-19885  
Nonsteady isentropic compression wave to generate high-velocity air flows with very low ambient dissociation levels 11 p1684 A66-22831  
Flow field near leading edge of heated flat plate in Mach 0.5 airflow 11 p1634 A66-22934  
Severely turbulent airflow at low levels over United Kingdom 11 p1730 A66-23015  
Interferometer apparatus used in combination with Fabry-Perot etalon to study properties of low density air streams 11 p1709 A66-23298  
Heat transfer between longitudinal flow of air and staggered cluster of tubes 11 p1787 A66-23311  
Hydraulic resistance of air flow through porous steel plate 13 p2065 A66-26483  
Mean velocity, rms velocity fluctuations and Reynolds shear stress for air flow at high Reynolds number in rectangular channel partially roughened, measuring turbulence intensity 13 p2070 A66-26703  
Acoustic pressures on vibrating walls for turbulent airflow through rectangular hard-walled duct exposed to traveling sound waves 17 p2905 A66-31944  
Vibrational and rotational nonequilibrium flow effects in hypersonic conical nozzle expansion of nitrogen flows and airflows 17 p2842 A66-33478  
Heat transfer between copper sphere and air flow at normal and reduced pressure for various Reynolds numbers 21 p3835 A66-38904  
Heat transfer between turbulent flow of air and isothermal wall plate and constant thermal flux at surface 21 p3835 A66-38907  
Dissociation of hypersonic airflow past circular cylinder at zero angle of incidence 21 p3695 A66-39230  
Heat transfer and flow in turbulent separated airflow over downward step in plate surface with suction and injection [ASME PAPER 65-WA/HT-2] 22 p3898 A66-40025  
Equation for calculating entrainment ratio of ejectors as function of velocity numbers of two frictionless one-dimensional streams flowing side by side in pressure equilibrium 22 p3899 A66-40371  
Shock tunnel external burning experiments to investigate effects of reactive fuel injection into air stream flowing around body [AIAA PAPER 66-744] 22 p3893 A66-40631  
Balance bridging techniques using air supply lines for powered lift-fan model testing [AIAA PAPER 66-751] 22 p3893 A66-40637  
Surface catalytic and Reynolds number effects on nonequilibrium hypersonic stagnation flow of air or diatomic gas on highly cooled blunt body 22 p3847 A66-40919  
Flows with relaxation involving very rapid flow processes accompanied by reactions without chemical or thermodynamic equilibrium, using characteristics 23 p4014 A66-42048  
Single air flow acceleration and deviation for propulsion and lift of high speed

aircraft, analyzing long-range flight paths [ICAS PAPER 66-41] 23 p4122 A66-42070  
Thermodynamics of real air expansion using state equation applied to large temperature range, including contribution of vibrational energy 24 p4293 A66-42155  
Thermoanemometric and high speed motion-picture photographic experimental analysis of air vortex ring structure 24 p4196 A66-42879  
**AIRFOIL**  
SA HYDROFOIL  
SA LAMINAR FLOW AIRFOIL  
SA SUPERSONIC AIRFOIL  
SA THIN AIRFOIL  
Unsteady airfoil functions evaluated approximately 10 p1479 A66-21345  
Transition region and amplification factor of unstable disturbances in laminar boundary layers with distributed suction 10 p1522 A66-21408  
Prediction of local flow conditions at crest of aerofoil section in sonic stream 13 p1992 A66-26697  
Interference effect for biconvex aerofoil in wind tunnel with slotted liners 13 p1992 A66-26698  
Text on cascade flow through airfoils and application to turbomachine and blade design 14 p2220 A66-27699  
Surface pressure on thin two-dimensional airfoils in transonic flow 15 p2478 A66-29246  
Pressure distribution at low speeds on two-dimensional airfoils with blunt trailing edges at zero incidence, taking into account wake 19 p3278 A66-36751  
**AIRFOIL CHARACTERISTICS**  
Linear cascade of double-circular-arc airfoils in transonic shear flow compared with subsonic flow 03 p0313 A66-12394  
Change rate of pitching moment coefficient upon aerofoil correlated to deflection of flap control for application to wing reversal analysis 06 p0801 A66-16001  
Clearance loss in rectilinear cascade, emphasizing flow separation and vortices shed at blade tips 07 p0980 A66-17483  
Numerical solution of Fredholm integral equation with singularities and application to annular airfoil theory 09 p1396 A66-20626  
Longitudinal stability and controllability characteristics of glider, considering effect of elastic warp of wing 09 p1331 A66-20757  
Unsteady plane motion of pointed airfoil pair, obtaining resultant force and moment of biplane 13 p2062 A66-25400  
Electrical analog method used in determining potential gas flow past airfoil lattice, noting components of solution 13 p2068 A66-26541  
Linearized surface pressure distribution on streamlined ducted bodies in axisymmetric flow, considering aerodynamic loading on annular airfoil 13 p1993 A66-26716  
Helicopter airfoils, discussing design improvement by proper choice of camber and leading edge 17 p2840 A66-32725  
Airfoil pitching motion and flap rotational motion in two-dimensional low supersonic flow in wind tunnels 23 p4053 A66-40975  
Transonic airfoil characteristics correlation for zero incidence in slotted wall wind tunnels 23 p4007 A66-40976  
STOL flying possibilities and limitations, considering aircraft generating high lift by using fixed wing and airfoil features 23 p4016 A66-41774  
First- and second-order theory for uniform shear flow past airfoil, obtaining expressions for pressure, lift and moment coefficients 23 p4011 A66-41879  
Aerodynamic coefficients of large-aspect-ratio fan-in-wing airfoil, noting that velocity field consists of inflow to fan, parallel flow and circulation flow 24 p4158 A66-43050  
**AIRFOIL PROFILE**  
Pressure distribution and skin friction measurements confirming that effects of changing base flow conditions decay with distance upstream along airfoil surface 06 p0801 A66-15999  
Measurements of three coefficients for rectangular, trapezoidal, sweptback, triangular and parabolic wings in subsonic and supersonic flow 07 p0979 A66-17480  
Compressible subsonic flow with symmetric Zhukovskii profile calculated by correspondence principle 07 p1023 A66-18112

Airfoil section testing at transonic speeds aimed at extending NACA low-drag airfoil information 09 p1365 A66-20740  
Slender profile of infinitely thin supersonic wing that provides minimum mean heat-transfer coefficient at given lift-drag ratio 09 p1328 A66-20754  
Book on theory of optimum aerodynamic shapes 11 p1629 A66-22501  
Airfoil cascade oscillation in near-sonic gas flow 12 p1798 A66-24432  
Airfoil equilibrium stability under elastic force and uniform wind action 13 p2062 A66-25402  
Airfoil theory in incompressible flow for boundary layer suction or Helmholtz type wake 16 p2629 A66-31039  
Transonic flow around airfoils and wing profiles in uniform asymptotic transonic stream studied, using hodograph plane and method for smoothing results 16 p2629 A66-31040  
**AIRFOIL SECTION**  
Lift force of airfoil section determined for sudden change in angle of attack, analyzing Prandtl vortex positions 03 p0314 A66-12526  
Rolling moments of five symmetrical, untwisted airfoils of various planform tested in high-speed wind tunnel as functions of angle of attack and angle of yaw 07 p0980 A66-17481  
Airfoil shape construction by conformal mapping and development of analog computer program to plot two-dimensional potential flow about various airfoil sections 16 p2629 A66-31116  
Fluidic system design of single and double airfoil amplifiers based on airfoil surface characteristics 21 p3698 A66-39464  
Lighthill integral transform methods in hodograph transformation theory of plane compressible transonic shock-free potential flows around airfoil sections in solution space of Chaplygin equation [ICAS PAPER 66-26] 23 p4007 A66-41008  
**AIRFOIL THICKNESS**  
Transonic airfoil problem solved via differentiation of airfoil thickness ratio by infinitesimal perturbation method [AIAA PAPER 66-90] 06 p0802 A66-16410  
Jet drag solutions for symmetrical struts of various shapes, thickness ratios and slot widths in quiescent and uniform streaming flow 12 p1800 A66-25005  
Wind tunnel experiments on thin two-dimensional airfoil with sharp leading edge and with jet blowing through mid-chord slot on upper surface in order to control boundary layer and circulation around it 18 p3048 A66-33950  
**AIRFRAME**  
SA FUSELAGE  
SA LANDING GEAR  
Use of monofilament composites of S-glass fibers and epoxy-resin in primary aircraft structure [AIAA PAPER 65-761] 05 p0772 A66-14729  
Structural design of Concorde supersonic airliner, noting airframe strength parameters 10 p1483 A66-21711  
Aircraft structure weight reduction, using redux bending and spot welding instead of bolts and rivets 12 p1963 A66-24036  
Helicopter airfoils, discussing design improvement by proper choice of camber and leading edge 17 p2840 A66-32725  
Hughes OH-6A helicopter fail-safe structural composition noting design, fatigue, testing, application of redundant design features, etc 17 p2845 A66-32736  
Helicopter airframe fatigue testing noting fail-safe design, crack detection, loads applied, test facilities and techniques, etc 17 p3027 A66-32737  
Airframe structure and power plant configuration effects on transport V/STOL performance 17 p2846 A66-32885  
Algorithm used in circuit design, evaluating equivalent strain at critical points of airframe structure, verifying it during fatigue tests 20 p3665 A66-36880  
SH-3A airframe fatigue test facility for automatic simulation of helicopter flight and landing loads 22 p3992 A66-40251  
Use of monofilament composites of S-glass fibers and epoxy-resin in primary aircraft structure [AIAA PAPER 65-761] 23 p4083 A66-40979



# IRFRAME MATERIAL

Fatigue failure in aircraft panels studied by determining spectral densities of response of continuous skin stringer panels under random noise  
excitation 01 p0147 A66-10130

Fatigue crack propagation in airframe materials under axial narrow and broadband random loading 01 p0148 A66-10139

Titanium alloys as basic structural material for supersonic transport noting strength, corrosion resistance, fatigue, etc [SAE PAPER 650789] 01 p0088 A66-10814

Thermal stresses arising at high velocities in aircraft skin consisting of two load-carrying layers separated by filler 09 p1468 A66-20758

Newer titanium alloys compared with present production alloys from closed die forgings in typical airframe and engine configuration 14 p2317 A66-28011

Plastic strain effect on fatigue strength of aircraft skin sheets with hole subjected to constant loading, noting stress concentration at hole 16 p2815 A66-30678

Structural design criteria for Concorde aircraft, including necessity for heat-resistant airframe material 20 p3666 A66-37400

## IRGLOW

### SA ATMOSPHERIC EMISSION

#### SA AURORA

#### SA SKY BRIGHTNESS

#### SA SKY RADIATION

Alternating-light monochromator with Fabry-Perot interferometer for measuring sodium and oxygen lines during twilight and at night 01 p0066 A66-10184

Kinetic temperatures derived from Doppler width of airglow 5577 angstroms /OI/ line measured with Fabry-Perot interferometer 02 p0221 A66-11503

Data concerning planetary scale of intensity variations of 5577 angstrom emission in night airglow 04 p0515 A66-13848

Lunar tidal effect on oxygen green line in night airglow at Honolulu from 1961 to 1963 05 p0668 A66-14801

Zenith intensity of second positive band of molecular nitrogen in dayglow calculated and compared to experimental results 05 p0668 A66-14802

Mid-day dayglow intensities arising from solar ionizing radiation fluorescence 05 p0748 A66-14942

Observation location and instrument vagaries cause discrepancy between photographic and photoelectric interferometric measurements of dayglow at 6300 angstroms 05 p0671 A66-14958

Spectrographic and interferometric techniques used in temperature determinations of auroral and airglow emissions in upper atmosphere 05 p0671 A66-15020

Night airglow intensity measured at Kerguelen Islands in 1963, rejecting observations contaminated by auroral light 05 p0672 A66-15039

Doppler temperatures obtained from 6300 angstrom line of atomic oxygen in airglow 05 p0673 A66-15047

Manned space flight observations include confirmation of normal airglow, Glenn effect and photographs of land and ocean areas that can be compared with lunar and planetary photographs for geologic interpretation 05 p0629 A66-15755

Airglow and auroral radiation and time-space variations 09 p1372 A66-20280

Intensity variation of 6300 angstrom night airglow and rate coefficient of ion-atom interchange reaction 09 p1372 A66-20381

Dayglow at 6300 and 3914 angstroms from rocket soundings and roles of ion recombination and UV dissociation 09 p1374 A66-20887

Night sky luminosity and solar UV reflection from Earth measured by Cosmos XLV 09 p1376 A66-20996

Photographic observations of rocket nightglow 10 p1528 A66-21141

UV night airglow spectrometry 10 p1528 A66-21142

Photometric monitorings of 5577 and 6300 angstrom lines during undisturbed geophysical conditions in South Atlantic 10 p1530 A66-21164

Laboratory duplication of processes exciting airglow, noting green line of oxygen atoms 11 p1699 A66-23116

Brightness of oxygen bands in twilight and day airglow, relating variation to sunspot cycle, ozone dissociation and solar eclipse 11 p1702 A66-23490

Excitation of auroral green line in terrestrial nightglow caused by interaction of three ground state oxygen atoms 11 p1703 A66-23498

Relative intensity measurements of 50 major bands of Lyman-Birge-Hopfield /LBH/ system of nitrogen 12 p1869 A66-23919

Atomic oxygen night sky emission observations with pressure scanning Fabry-Perot interferometer 12 p1873 A66-24837

Wide angle Michelson interferometer for measuring Doppler temperature from width of 5577 angstrom atomic oxygen line in nightglow and aurora 13 p2128 A66-25799

Auroral hydrogen emission in night sky, noting variance with sunspot cycle and magnetic activity 13 p2073 A66-26029

Variations of zodiacal light and airglow, suggesting correlation with solar and lunar cycle 14 p2283 A66-27096

Design and fabrication of automatic all-sky scanning and self-recording photometer for night airglow 14 p2296 A66-27724

Rocketborne photometer data analysis of night sky airglow and spectrum in 6300 angstrom region 15 p2482 A66-28494

Airglow continuum measurement with birefringent filter 15 p2484 A66-28837

Intensity of oxygen red line in night airglow analyzed, obtaining temperature dependence of rate coefficients of ion atom interchange reaction and collisional deactivation, noting red line intensity dependence on solar activity 15 p2484 A66-28905

Excitation temperature of three states of atomic oxygen determined to be 2000 degrees K from intensity ratio of three atomic oxygen 1300 angstrom triplet lines in dayglow 15 p2484 A66-28907

Airglow lines measured through photometers on OGO-II satellite, noting nadir and zenith airglow 15 p2494 A66-30044

Nightglow emission from atomic oxygen caused by dissociative recombination in F region 16 p2694 A66-30707

F-layer nightglow 6300 angstrom emission intensity and electron density data, noting variations in emissions 16 p2694 A66-30708

Spectral lines in atmospheric emission during day and night airglow in review of published works 17 p2917 A66-32026

Height measurement of nightglow by photometric ground triangulation, minimizing previous errors 17 p2917 A66-32524

Mapping 6300 angstrom airglow isophotes from observations of scanning photometer at Haleakala, Hawaii 17 p2918 A66-32534

Upper atmospheric temperature measurement from Doppler line widths of atomic oxygen auroral and nightglow emission, using Michelson interferometer 17 p2919 A66-32993

Variations of 6300 angstrom airglow emission at Sacramento Peak, New Mexico 17 p2919 A66-32994

Monte Carlo calculation of nightglow excitation and maintenance of nighttime ionosphere by low energy protons 18 p3169 A66-34518

Grille spectrometer, noting greater signal to noise ratio than that of scanning Fabry-Perot spectrometer for airglow observations 19 p3353 A66-35378

Lyman alpha airglow observations indicate diurnal variation of atomic hydrogen in thermosphere and exosphere with abundance change with solar activity 19 p3349 A66-36349

Quantitative measurement of free metallic atoms abundance and height distribution from twilight, dayglow and aurora fluorescence 19 p3349 A66-36350

Aerobee rocket measurement of nitric oxide in upper atmosphere, noting fluorescence in airglow layer, emission rate factors and NO densities 19 p3349 A66-36351

Atomic hydrogen and helium emissions in upper atmosphere determined by diffraction spectrophotometer measurement of twilight

airglow and aurora 19 p3350 A66-36352

Diurnal and latitudinal variations in 6300 angstrom nightglow intensity determined along Pacific coast of South America, noting relation between location of antisolar point and equatorial midnight enhancement 19 p3352 A66-36628

Upper atmospheric nitric oxide determined from Aerobee measurement of UV dayglow spectra 20 p3550 A66-37299

Earth albedo estimation, backscattered interplanetary radiation and resonance scattering of dayglow 20 p3553 A66-38194

Intensity measurements on molecular oxygen Herzberg I system emitting in afterglow of microwave discharge, noting dependence of transition moment on internuclear distance 20 p3555 A66-38208

Spatial inhomogeneities in green line of atomic oxygen, using electrophotometry during airglow 22 p3915 A66-40778

Quenching of metastable states by atmospheric particles on basis of rocket measurements of dayglow, noting quenching coefficients of oxygen 22 p3916 A66-40872

Image orthicon slit spectrograph for study of aurora and night glow 22 p3921 A66-40898

Altitude profiles for dayglow emissions excited by molecular ion dissociative recombination, solar radiation fluorescence, oxygen photodissociation, electron collisions and chemical reactions 23 p4064 A66-41680

Molecular nitrogen ions in nocturnal upper atmosphere at middle latitudes, noting space radiation bombardment 23 p4064 A66-41681

Rocket photometric measurements of weak airglow emission at 6300 angstrom oxygen line 24 p4199 A66-42467

Photoelectric photometer using filter that tilts relative to incident light for patrol observation of 5577 angstrom intensity in nightglow 24 p4210 A66-42468

Zodiacal light, airglow and falling atmospheric dust measurements and observations in terms of solar orbiting small diameter particle clouds 24 p4276 A66-42663

## AIRLINE

British short-range aircraft operating cost affected by reliability, design and engines 06 p0804 A66-15991

Lowering total airline operating costs through nonaircraft economizing 06 p0804 A66-15994

Navigation techniques and operational objectives due to computer-generated flight plans of United Air Lines 07 p1074 A66-17777

## AIRPORT

### SA LANDING AID

C-5A aircraft design load criteria for landing gear of large aircraft that must operate from semi-improved airfields [AIAA PAPER 65-711] 01 p0013 A66-10948

Airport pavement roughness data and aircraft response data evaluated to determine pavement design and construction criteria [AIAA PAPER 65-712] 01 p0055 A66-10949

Airport approach standards used to protect approaches to airports 02 p0260 A66-12221

Milan airport system noting air traffic 05 p0661 A66-15846

Lowering total airline operating costs through nonaircraft economizing 06 p0804 A66-15994

Deformation modulus of airfield pavement materials 09 p1365 A66-20697

Airport suitability for delta wing commercial supersonic transport, discussing noise objectives 09 p1365 A66-20698

Operation of VTOL aircraft in vicinity of airport including safety, noise and air traffic control factors 10 p1482 A66-21372

STOL aircraft characteristics compared with VTOL aircraft and helicopter, noting airport layout 10 p1519 A66-21406

Multiple-access worldwide satellite communication system for aircraft terminals with limited antenna gain and transmitter power [AIAA PAPER 66-297] 12 p1823 A66-24765

Douglas DC-8 super sixty series effect on airport requirements including noise level, runway problems and traffic [SAE PAPER 660281] 15 p2427 A66-29825

Airport pavement roughness data and aircraft response data evaluated to determine pavement design and construction criteria



- [AIAA PAPER 65-712] 16 p2683 A66-31590  
Economics of airport facilities and operations, noting safety and regularity problems 20 p3687 A66-38016  
All-weather landing systems in U.K., examining safety and reliability criteria in connection with trident airborne equipment [ICAS PAPER 66-8] 22 p3946 A66-40676  
Dispersal of supercooled fogs over airports by seeding with dry ice [ICAS PAPER 66-7] 23 p4086 A66-41255

## AIRPORT LIGHT

- Airport lighting equipment required to reduce prescribed weather minima, including light for approach, high intensity, runway, flashing, etc 11 p1683 A66-22683  
Airport lighting facilities for aiding aircraft takeoffs and landings in conditions of poor visibility 12 p1859 A66-24832

## AIRPORT PLANNING

- Mathematical model based on control and queueing theory for human controller for turn-round operations on airport apron 03 p0329 A66-12886  
Operational considerations in airport planning [AIAA PAPER 65-746] 03 p0353 A66-13054  
Organization of short-distance interurban transportation system based on STOL aircraft of Breguet type 05 p0611 A66-15194  
Layout and design of air terminal for Basel, Switzerland, noting passenger accommodation and air traffic problems 05 p0660 A66-15199  
FAA regulation of civilian use of U.S. airspace 08 p1321 A66-18548  
Airspace, accessibility and economics studied in quest for airport in New Jersey-New York area 09 p1473 A66-20693  
Methodology for evaluating current and future annual capacity and other operational factors in development of airport systems in metropolitan area 09 p1364 A66-20694  
Airport access, circulation and parking 09 p1365 A66-20695  
Measurement of aircraft noise in vicinity of airports in connection with land-use planning 10 p1483 A66-21745  
Assisted takeoff and landing for commercial aircraft using short runways [SAE PAPER 660337] 14 p2269 A66-27296  
Aircraft utilization and schedule planning, optimum use of flight performance, ground equipment, facilities and personnel [SAE PAPER 660279] 15 p2427 A66-29824  
Super airport planning concepts, satellite and unit terminal, stress decentralization to meet changing demands and increased volume of air traffic [SAE PAPER 660282] 15 p2476 A66-29826  
Airport planning with respect to transportation systems and population centers on Eastern seaboard, noting past experience and future requirements [SAE PAPER 660284] 15 p2477 A66-29828  
Transportation developments for airport planning, emphasizing need to limit carrier transport service to single airport 16 p2682 A66-31283  
Air traffic estimation, discussing installation locations and parameters for airport site choice 21 p3838 A66-39433

## AIRWORTHINESS REQUIREMENT

- Maintenance and airworthiness philosophy in aerospace engineering 12 p1801 A66-23858  
Airworthiness codes for supersonic transports, noting current regulations, codes, etc 18 p3268 A66-34622

## AIRYS STRESS FUNCTION

- SA POISSON RATIO  
Elastic critical load of centrally loaded simply-supported beam which buckles laterally out of plane derived by Airy integral functions 07 p1144 A66-18049  
Airy stress function applied in solving problems for doubly connected regions with contiguous circular boundaries 13 p2204 A66-26432  
Stress intensity factors, strains and rotation in infinite eccentrically cracked strip under uniform tensile stress applied at infinity 24 p4286 A66-42157

## ALANE

- Synthesis of complex lithium aluminum hydride, lithium hexahydroalane, having hydrogen to aluminum ratio greater than four 11 p1649 A66-22400  
Preparation of aluminum difluoramide from

- trimethylamine alane and difluoramine 13 p2018 A66-26501

## ALBEDO

- SA COSMIC RAY ALBEDO  
SA EARTH ALBEDO  
Albedo and planetary radiation simulation to provide field angle and uniformity of intensity for thermal testing 02 p0211 A66-11217  
Approximation of effect of albedo inhomogeneity on flux of short wave radiation leaving Earth 02 p0222 A66-11658  
Airborne albedo measurements of ice in Ross Sea, Antarctica, for various solar elevations and altitudes 05 p0669 A66-14937  
Airborne albedo measurements of various representative underlying surfaces in Antarctica 05 p0669 A66-14938  
Spectral distribution of albedo and luminance at center of disk for diffusing and absorbing planetary atmosphere 07 p1027 A66-17247  
Directional radiative characteristics of conical cavities and relation to reflective characteristics of Moon 07 p1136 A66-17729  
Planetary albedo as affected by solar radiation reflected from surface of red clay soil or white quartz sand 15 p2597 A66-29258  
Geometric albedos and phase integral of planet Mercury compared with Moon 18 p3230 A66-34153  
Iterative solution of equations for diffuse reflection and transmission in finite plane-parallel atmosphere with arbitrary stratification 21 p3734 A66-39220

## ALCOHOL

- SA CHOLESTEROL  
SA ETHYL ALCOHOL  
SA METHYL ALCOHOL  
Critical heat flux under forced motion of underheated alcoholic aqueous solutions 09 p1470 A66-20148  
Paramagnetic resonance spectra of free radicals in hydrogen peroxide and alcohols during intense UV irradiation 11 p1650 A66-23216  
Photoionization of leucocarinols and leucocyanides of malachite green, crystal violet and sunset orange dissolved in straight chain alcohols and chlorinated hydrocarbons 14 p2232 A66-27374  
Nuclear magnetic resonance classification of alcohols and hydroxyl groups from FI-19 spectra of trifluoroacetates 15 p2447 A66-29238  
Alcohol induced hypoglycemia as factor in aircraft accidents, noting effect of post mortem changes in blood glucose level 24 p4164 A66-42458

## ALDEHYDE

- S ACETALDEHYDE  
S FORMALDEHYDE

## ALFVEN WAVE

- SA MAGNETOHYDRODYNAMICS  
Alfven waves and fast magnetosonic waves in nonisothermal plasma with molecular ions traversed by charged particle flux 02 p0268 A66-11771  
Contradictory experiments to determine whether particles responsible for auroral events are solar particles or local particles accelerated by secondary processes 03 p0421 A66-12864  
Nonlinear Alfven waves in Vlasov plasma noting particle trapping 03 p0400 A66-12949  
Velocity and attenuation of Alfven waves in hydrogenous plasma at LF and HF by experiment 03 p0406 A66-13177  
Small amplitude wave propagation in hot ionized gases, noting magnetic field presence 05 p0721 A66-14716  
Hydromagnetic waves in nonisotropic medium in presence of gravitational field 05 p0759 A66-14877  
Plasma velocity in weakly ionized gas with strong magnetic field and neutral component velocity determined independently [AIAA PAPER 66-4] 06 p0916 A66-16255  
Alfven waves in conducting nondissipative fluid permeated by external localized inhomogeneous magnetic field while in equilibrium 07 p1086 A66-17655  
Shock wave propagation in electrically conducting incompressible fluid imbedded in magnetic field 07 p1089 A66-17975  
Helicon and Alfven wave propagation in solid state plasma 07 p1101 A66-18198  
Chronological account of direct observation

- of Alfven waves and helicons in solids, noting propagation through metals and cyclotron absorption 07 p1101 A66-18199  
Polarization and Alfven wave attenuation in Doppler-like change in transverse wave velocity when drift current is passed parallel to magnetic field in solid-bismuth plasma 07 p1102 A66-18209  
Alfven wave propagation in incompressible inviscid infinitely conducting medium by canonical equations of motion 08 p1205 A66-18534  
Alfven wave generation and propagation in low pressure arc discharges of helium, argon, nitrogen and air [AIAA PAPER 66-171] 10 p1560 A66-21425  
Geomagnetic thruster form of Alfven wave propulsion system, using ionospheric plasma contacts [AIAA PAPER 66-257] 10 p1594 A66-21462  
Nonpotential Alfven drift waves and magnetic noise in magnetosonic stationary hydrogen plasma 10 p1569 A66-21964  
Cerenkov electron absorption of Alfven and magnetoacoustic waves in plasma cylinder, obtaining formula for energy absorbed by plasma and damping factor where there is no resonance layer 11 p1743 A66-22443  
Propagation of MHD emissions in Alfven mode along high latitude geomagnetic field lines, auroral zone signal energy penetration and isotropic wave mode transformation 11 p1701 A66-23151  
Propagation modes of small disturbances in homogeneous incompressible magnetoelastic medium at Alfven velocities 12 p1929 A66-24379  
Alfven wave generation in spherical system, determining velocity of MHD waves in longitudinal magnetic field by creating standing wave resonance 12 p1924 A66-24590  
Terminal properties of Alfven waveguides, deriving electrical input impedance of set of coaxial excitor electrodes 13 p2137 A66-25046  
Alfven wave propagation in inhomogeneous magnetic fields satisfying magnetohydrostatic equation and allowing for electric currents solved, using differential equation 13 p2156 A66-26710  
Excitation of Alfven waves in semimetallic plasma at low temperature, noting wave propagation below plasma or cyclotron frequency in magnetic field 14 p2363 A66-27516  
MHD wave generation in sunspots, examining depth of solar magnetic layer that affects magnetic convection 15 p2596 A66-29138  
Induction drag of long cylindrical satellites and Alfven waves emitted from them determining potential and current distribution and effect on energy loss [AIAA PAPER 66-478] 16 p2799 A66-30523  
Wentzel-Kramers-Brillouin method for Alfven wave propagation in medium slowly varying with time 16 p2804 A66-31262  
Conical refraction of magnetosonic waves occurring when Alfven waves propagate at speed of sound in conducting fluid in presence of constant uniform magnetic field 16 p2764 A66-31364  
Alfven waves in bismuth for propagation along magnetic field, noting dielectric constant variation with frequency, effect on real part of refractive index, relaxation time analysis, etc 19 p3443 A66-36006  
Ion cyclotron resonance heating applied to C stellarator plasma formed by ohmic heating, noting Alfven wave generation by Stix coil 19 p3432 A66-36594  
Alfven wave propagation equations used to study electronic properties of semimetals 20 p3615 A66-37282  
Alfven wave propagation in incompressible fluid stratified by inhomogeneous fluid density or magnetic field strength 21 p3791 A66-39170  
Nonpotential Alfven drift waves and magnetic noise in magnetosonic stationary hydrogen plasma 21 p3794 A66-39543  
Field, mass, momentum and energy conservation, entropy and evolution conditions for steady MHD oblique shock discontinuities in perfectly conducting gas flow with Mach and Alfven number parameters 21 p3795 A66-39577  
Alfven shocks for flow of highly



conducting incompressible fluid over blunt body where magnetic and flow vectors are not aligned 22 p3957 A66-40705

**CGAE**

**SA CHLORELLA**

Algatron, device for life support systems in space, providing potable water, oxygen supply, stabilizing human wastes by algal photosynthesis 13 p2015 A66-25702

Extracellular polysaccharides biosynthesis by blue-green alga *Anabaena* 13 p2009 A66-25875

*Clostridium* 13 p2009 A66-25875

Characteristics of sterols naturally occurring in species of *Chlorella* with algae grown heterotrophically on glucose 13 p2009 A66-25876

Inhibition of zoospores of unicellular chlorococcacean alga by soil bacillus through ammonium ion 17 p2860 A66-32833

Two-billion-year-old fossils related to blue-green algae considered in connection with origins of photosynthesis 19 p3285 A66-35794

Algal bioregenerative photosynthetic gas exchange system 19 p3293 A66-36239

**LGEBRA**

**SA BOOLEAN ALGEBRA**

**SA DIFFERENTIAL ALGEBRA**

**SA MATRIX ALGEBRA**

**SA TERNARY ALGEBRA**

Multiplier operators and quotient algebra 05 p0707 A66-15031

Properties of  $n$ -pi operatives and np operatives 06 p0903 A66-16905

Algebraic and graphical methods for evaluating system stability and parameter sensitivity 12 p1854 A66-24382

Derivation of expansion theorem of circuit algebra 16 p2670 A66-31032

Approximate solution of cubic equation with real roots and applications in mechanics 17 p2947 A66-33328

Structure and representations of noncommutative Jordan algebras, using proof of analog of Jacobson coordinatization theorem 18 p3127 A66-34456

Digital computer program for handling algebraic expressions in complex numbers 23 p4042 A66-41739

**LGORITHM**

Approximate solution for differential equations, using algorithm applied to boundary value problem involving linear equation 01 p0091 A66-10164

Nonlinear equations of atmospheric hydrodynamics solved, using numerical algorithm 01 p0096 A66-10751

Algorithm for allocating redundancy among subsystems to achieve maximum system reliability without exceeding multiple constraints on redundancy 02 p0236 A66-11856

Graphs for problems of computing system design automation, specifically finding algorithm for graph scheme construction 02 p0250 A66-12102

Algorithm for determining number of vertices contained in single contact network corresponding to transmission function 03 p0348 A66-12574

Inversion of correlation matrices used to obtain simple numerical algorithms and in construction of self-adjustment algorithms 03 p0338 A66-13036

Algorithms for teaching open-loop optimizing control system correct recognition of situations expressed as regions of complex configuration 04 p0503 A66-13773

Algorithm for designing miniaturized discriminators 04 p0490 A66-13969

Algorithm determining best approximation of bounded function in Chebyshev sense adapted to discrete case 04 p0540 A66-14167

Algorithm determining best approximation in Chebyshev sense of continuous function on segment 04 p0540 A66-14168

Differential correction algorithm in orbit and attitude determination having optimal property in system data error 05 p0635 A66-15800

Extension, modification and analysis of Gorenstein-Zierler decoding algorithm for binary codes of Bose, Ray-Chaudhuri and Hocquenghem /BCH/ correcting erasures and errors 06 p0837 A66-16114

Existence and uniqueness of optimum algorithms proven for application to transformation of potential

fields 06 p0875 A66-16133

Algorithm for optimum control problem based on Pontryagin maximum principle 06 p0902 A66-16424

Algorithm for mathematical expectation and dispersion of two-dimensional random sequences, obtaining linear estimation of norm of meteorological elements minimizing rms error 06 p0905 A66-16550

Algorithm determining end product concentration of mixture for chain isothermal propagation of plane flame 06 p0971 A66-16710

Optimum numerical algorithm for determining elements of inverse of Vandermonde matrix 06 p0866 A66-16751

Algorithm synthesizing sequential circuit from transition matrix, making critical races occurrence impossible during simultaneous relays starting 07 p1013 A66-17384

Algorithm used for synthesis of regular events in asynchronous automatic machines 07 p1014 A66-17437

Statistical problem of control system synthesis, discussing plant algorithm 07 p1014 A66-17438

Algorithm of stochastic search for maximum in determined field 07 p1060 A66-18507

Globally convergent iteration function for solution of polynomial equations according to certain algorithms 09 p1395 A66-20624

Algorithm to automatically ascertain admissible processing sequence for all-digital simulation of analog or analog-hybrid system 10 p1507 A66-21699

Algorithm for optimal parameter choice in reliability control of complex systems, based on dynamic programming 11 p1675 A66-22623

Algorithm for computer eigenfunction solution of boundary value problem involving partial differential equations for stress functions of semimomentless cylindrical shells 11 p1782 A66-22856

Linear cycle set factorization, showing that uniqueness of canonical procedure is incorrect and introducing new cycle division algorithm 11 p1679 A66-23247

Associative parallel processor using word and bit logic and sequential-state-transformation mode, with application to picture processing and pattern recognition 12 p1827 A66-23830

Bernstein form of polynomial with algorithm for determining upper and lower bounds for polynomial in  $x$  in closed interval  $[0, 1]$  14 p2320 A66-27114

Algorithm for perceptron-type recognition systems with input correlator 14 p2264 A66-27203

Algorithm for analyzing transient stress waves generated in cylindrical shell by application of impulsive dynamic loads 14 p2399 A66-27609

Nonlinear equations of atmospheric hydrodynamics solved, using numerical algorithm 14 p2285 A66-27850

Algorithm for mathematical expectation and dispersion of two-dimensional random sequences, obtaining linear estimation of norm of meteorological elements minimizing rms error 14 p2327 A66-28222

Positional coordinates of spacecraft determined by algorithm, using distance from three predetermined points as found by rangefinders 15 p2447 A66-28505

Existence and uniqueness of optimum algorithms proven for application to transformation of potential fields 15 p2483 A66-28667

Algorithm for SHF diagnostics of plane-laminar plasma 15 p2549 A66-28669

Algorithms for numerical determination of asymptotically stable solutions for ordinary differential equations 15 p2526 A66-28734

Optimum algorithm derived for making binary decisions in decision systems of hierarchical structure 15 p2469 A66-29054

Spatial problems in gas dynamics solved by difference methods, discussing supersonic flow 15 p2423 A66-29174

Algorithm from orthogonalization method for obtaining generalized inverse of matrix 15 p2529 A66-29847

Unstable behavior of nonlinear discretization algorithms when perturbation of computation exceeded threshold value 16 p2731 A66-30237

Test system for  $n$ -digit combinative comparison unit realizing special, previously described algorithm 16 p2656 A66-30765

Duality theory of optimal control and resulting duality correspondence between formulation of optimal control and calculus of variations, noting decomposition algorithm 16 p2671 A66-31229

Numerical differentiation by differential quotients, interpolations, Richardson-Romberg algorithm and other methods, including analysis of approximation errors 16 p2658 A66-31347

Inversion of correlation matrices used to obtain simple numerical algorithms and in construction of self-adjustment algorithms 18 p3073 A66-34999

Probe and edge theorems for nonlinear optimization algorithms using stored-program computers 19 p3309 A66-35873

Computer algorithm for geometric programming methods 19 p3309 A66-35874

Gomory all-integer linear programming algorithm based on lexicographical ordering principle and relation to cost function 19 p3309 A66-35876

Algorithm for learning without external supervision and application to learning control systems 19 p3333 A66-36666

Algorithm based on sequential optimization of nonlinear control system 19 p3334 A66-36676

Control algorithms for microminiaturized sampled data digital control systems 19 p3311 A66-36822

Control algorithms synthesis for analytical adaptive control systems with nonlinear plants investigated with hybrid computer 20 p3536 A66-36876

Algorithm used in circuit design, evaluating equivalent strain at critical point of airframe structure, verifying it during fatigue tests 20 p3665 A66-36880

Algorithm for rapid damping of multidimensional system 20 p3670 A66-37675

Dynamic programming for optimal algorithm for external control in presence of noise at system input and output 20 p3538 A66-37746

Computation of adjusted coordinates of artificial Earth satellites on basis of synchronous observations made at two known points on Earth surface 20 p3654 A66-37840

Computer algorithm for recognition and extraction of planar graph from incidence matrix 20 p3523 A66-38279

Algorithms for digital computation of vectors and eigenvalues of matrix 21 p3823 A66-38564

High-speed multiplication for R-11 microminiaturized digital computer, using modified form of Booth algorithm 21 p3707 A66-38676

Symbolic factoring of multivariate polynomial with integer coefficients, noting application of Kronecker method and techniques of implementation 21 p3708 A66-38681

No-gimbal system mechanizations evaluated by flight test and compared for advantages, noting system error 21 p3764 A66-38851

Moments of output coordinates of nonlinear system determined by algorithm based on approximation method, noting application to automatic control system 21 p3758 A66-39283

Iterative algorithms for calculating sum of some series, considering gamma and theta functions 21 p3758 A66-39368

DIVIC /digital variable increment computer/ for solving hyperbolic-navigation problems, examining computational algorithms 22 p3945 A66-40335

Algorithms for numerical determination of asymptotically stable solutions for ordinary differential equations 22 p3939 A66-40442

Algorithm construction for processing of telemetry data in determination of space vehicle trajectories, applying dynamic filtering method 22 p3980 A66-40463

Minimization of logical functions in normal disjunctive form, using Gavrilova method and ALGOL 60 algorithm 22 p3941 A66-40541

Functional analysis applied to optimum control by reduction of variational problem to finite dimensional analysis and calculation of algorithms for use with digital



- computer 24 p4231 A66-42470  
Frequency characteristic and transient  
delta function of plant, using algorithm  
based on correlation  
functions 24 p4188 A66-42483
- ALIGNMENT**  
**SA FIELD-ALIGNED IRREGULARITY**  
/FAI/  
**SA RUNWAY ALIGNMENT**  
Optical metrological and alignment  
methods for fast and accurate rocket thrust  
chamber alignment  
[SAE PAPER 650758] 01 p0078 A66-10836  
Specific initial alignment problems and  
techniques of analytic inertial platform  
systems 04 p0543 A66-13617  
Effect of thermal instability in shop areas,  
static and dynamic loading and floor  
movement on precision fabrication and  
assembly  
[SAE PAPER 650759] 05 p0688 A66-15274  
Three-directional optical square, used with  
alignment telescope, establishes three  
mutually perpendicular lines-of-sight in one  
instrument setting  
[SAE PAPER 650757] 06 p0878 A66-16014  
Alignment of laser mirrors using gas laser  
with highly collimated beam of small  
diameter 13 p2092 A66-25824  
Positioning and aligning operations for  
Titan IIIC solid propellant rocket  
motors 14 p2271 A66-28421  
Slew plane technique for locating two gyro  
input axes without removing platform from  
test vehicle and with limited optical  
access 18 p3133 A66-34048  
Linear filtering technique for estimation of  
azimuth alignment of inertial guidance  
system in presence of disturbances with no  
measurement noise 19 p3398 A66-36689  
Master reference system for reducing sea  
alignment time of aircraft inertial navigation  
systems 21 p3767 A66-38890  
Analytic axes alignment for strapdown  
inertial system, describing computational  
procedures for ground-based and in-flight  
correction of attitude  
parameters 23 p4088 A66-41115  
Resonator misalignment effect on output  
of neon-helium laser with spherical  
mirrors 23 p4079 A66-41830
- ALIPHATIC COMPOUND**  
**S ORGANIC COMPOUND**  
**ALKALI**  
Alkali-ion desorption energies measured on  
polycrystalline refractory metals at low  
surface coverage by electron work  
function 02 p0263 A66-11483  
Alkali and titania analyses of tektites  
before and after G-1 precision  
monitoring 08 p1291 A66-19076  
Nonrandomness in base sequences of  
DNA 21 p3702 A66-38542
- ALKALI HALIDE**  
Dielectric constants of alkali and thallium  
halides determined for various temperatures  
and frequencies, showing results obtained  
on sodium chloride 07 p1108 A66-18417  
Plasma oscillation of valence electrons and  
exciton in alkali halides, measuring  
differential cross section, dispersion relation  
and loss peak in  
spectrum 09 p1430 A66-20844  
Quantitative detection and washing and  
pumping methods for removal of traces of  
water from alkali halides 09 p1339 A66-20874  
Reflection measurements of RbI film in  
UV to observe optical property differences  
between films and single  
crystals 12 p1931 A66-24813  
Strong electron-phonon interaction which  
couples electron to lattice motion in F  
center of alkali halide crystal by measuring  
temperature dependence of F center  
absorption and emission  
bands 15 p2559 A66-28629  
Photoelectric yields of alkali halides  
measured, using rare gas ion chamber to  
determine flux distribution of helium  
continuum and obtain absorption  
coefficients 16 p2754 A66-30855  
Radiation-induced electroconductivity and  
secondary emission in alkali halide single  
crystals under positive ion  
bombardment 17 p2988 A66-33458  
Energy distribution of electrons emitted  
from alkali halide films on Mo substrates  
during positive helium and argon ion

- bombardment 17 p2988 A66-33459  
Magnetic properties of lattice  
imperfections in lithium fluoride, potassium  
chloride and sodium chloride single  
crystals 18 p3157 A66-34499  
Disintegration of alkali halide single  
crystals, polymers and glasses under laser  
radiation, noting parameters of  
disintegration region  
magnitude 18 p3119 A66-34681
- ALKALI METAL**  
**SA CESIUM**  
**SA LITHIUM**  
**SA POTASSIUM**  
**SA RUBIDIUM**  
**SA SODIUM**  
Polarization and exchange effects in slow  
electron scattering from lithium and  
sodium 03 p0393 A66-12325  
Preparation of single crystals of double  
molybdates of Na and La /or other rare  
earth elements/ doped with Nd, Tb or Pr  
for laser application 04 p0529 A66-13478  
Cosmic ray induced lithium and calcium in  
iron meteorites by improved technique of  
potassium isotope  
detection 04 p0580 A66-14487  
Nucleate boiling instability of alkali metals  
noting effects of surface material, chemical  
treatment, heat flux and cavity geometry  
[ASME PAPER 65-HT-22] 05 p0783 A66-14743  
Resonance radiation emitted by alkali  
cloud for ionospheric temperature  
measurement, considering multiple  
scattering and radiative transfer inside  
cloud 05 p0672 A66-15040  
Refractory alloy corrosion, discussing  
columbium and tantalum base tubing alloy  
resistance to refluxing potassium between  
1800 and 2400 degrees F 06 p0894 A66-16071  
Ionization of inert-gas atoms and of  
hydrogen and nitrogen molecules by alkali  
metal ions of energies greater than 1 to 30  
keV 06 p0915 A66-16151  
Densities of binary mixtures of fused alkali  
nitrates with alkaline earth nitrates  
measured by manometric densitometer and  
expressed as linear function of  
temperature 08 p1177 A66-18617  
Cavitation damage in alkali liquid metals  
predicted from properties of water, aviation  
gasoline and sodium-potassium  
eutectic 08 p1211 A66-19721  
Effective excitation cross sections of alkali  
metal atoms during collision with slow  
electrons 09 p1406 A66-20940  
Electron excitation in germanium by alkali  
metal ions, noting effect on electrical  
conductivity 10 p1587 A66-22154  
High activity of alkali metal salts of  
carboxylic acids and substituted phenols as  
synergists for arylamine antioxidants in  
ester-type synthetic lubricating  
oils 11 p1711 A66-23123  
Design and construction of probe  
measuring density of neutral atoms in  
quiescent alkali metal magnetoplasma,  
noting vacuum system, electric circuitry,  
etc 12 p1884 A66-24984  
MHD nuclear electric space power systems  
using noble gases seeded with alkali metal  
vapors as working fluid 13 p1998 A66-25526  
Ionizing collisions between alkali metal  
atoms and gas molecules, with measured  
cross sections applied to physics of atomic  
collisions 13 p2131 A66-25966  
Charge exchange cross section increase  
during single collisions of alkali-metal ions  
with atoms of inert gases and atomic  
hydrogen and nitrogen  
molecules 14 p2336 A66-27155  
Effective excitation cross sections of alkali  
metal atoms during collision with slow  
electrons 15 p2543 A66-28529  
Ionization of inert-gas atoms and of  
hydrogen and nitrogen molecules by alkali  
metal ions of energies greater than 1 to 30  
keV 15 p2548 A66-29881  
Nucleate boiling instability of alkali metals  
noting effects of surface material, chemical  
treatment, heat flux and cavity geometry  
[ASME PAPER 65-HT-22] 16 p2828 A66-30986  
Color centers in alkali metal azides, noting  
change of ion from linear to bent  
configuration 16 p2777 A66-31023  
Dissociation energies of chlorides of  
alkaline-earth metals determined from  
equilibrium reactions of metals with

- chlorine in flames 16 p2830 A66-31617  
Ionization of low temperature supersonic  
plasma jets, noting kinetics of elementary  
processes, gas dynamic parameters and  
effects of combustion and alkali metal  
admixtures 18 p3143 A66-34030  
Electron excitation in germanium by alkali  
metal ions, noting effect on electrical  
conductivity 19 p3440 A66-35760  
Oxygen role in oxidation/reduction  
reaction and polyoxide formation  
mechanisms associated with refractory metal  
corrosion by liquid alkali  
metals 19 p3383 A66-36133  
Welding and annealing procedures for  
fabrication of Nb alloy liquid metal loop and  
operation in boiling alkali  
metals 19 p3370 A66-36130  
Carbon dioxide decomposition and oxygen  
reclamation by chemical reaction with  
electrochemically reduced  
lithium 19 p3292 A66-36230  
Loss rate comparison for alkali plasma  
produced by contact ionization in stellarator  
and toroidal device with minimum mean-  
properties 19 p3428 A66-36588  
Density of lithium, sodium and potassium  
up to 1600 degrees C, using pycnometric  
method, showing dependence of density on  
temperature 20 p3582 A66-36970  
Ultrahigh vacuum optical measurements of  
mirrorlike surfaces of Na, K, Rb and Cs  
prepared in ultrahigh vacuum in wavelength  
region from 3000 to 25,000  
angstroms 20 p3613 A66-37277  
Optical absorption of K, Cs and  
Na 20 p3613 A66-37277  
Charge exchange of protons in alkali metal  
vapors with formation of highly excited  
hydrogen atoms, noting cross section  
reaction mechanism, etc 22 p3953 A66-39760  
Radiation induced chemical decomposition  
in inorganic solids such as alkali metals and  
metallic sulfates 23 p4111 A66-41211  
Optimum seed concentrations of alkali  
metal in rare gas for maximum  
electroconductivity of slightly ionized  
nonequilibrium plasma 23 p4104 A66-41511  
Charge exchange cross section increase  
during single collisions of alkali-metal ions  
with atoms of inert gases and atomic  
hydrogen and nitrogen  
molecules 24 p4239 A66-42970
- ALKALINE EARTH OXIDE**  
**SA BERYLLIUM OXIDE**  
**SA CALCIUM OXIDE**  
**SA MAGNESIUM OXIDE**  
Electrical conductivity of single crystals of  
calcium and strontium  
oxides 10 p1581 A66-21870  
Thermionic emission from barium telluride  
measured by cathodes formed by direct  
reaction of elements and reduction of  
barium tellurate 19 p3436 A66-35420
- ALKALOID**  
**SA STRYCHNINE**  
Mass spectrometry in structural and  
stereochemical problems of 16  
Amaryllidaceae alkaloids 03 p0330 A66-13087  
Constitution of vallesiachotamine isolated  
from Peruvian Apocynaceae Vallesia  
dichotoma Ruiz et Pav 14 p2232 A66-27860
- ALKANE**  
Constants in empirical equation for  
evaluated from viscosities and densities for  
various n-alkanes 03 p0330 A66-12330  
Biologic-type alkanes of indigenous origin  
more than 2.7 billion years old present in  
Precambrian rocks of Sudan  
formation 03 p0325 A66-12360  
Molecular acentricity effect on  
intermolecular pair potential of n-alkane  
homologs and benzene 10 p1495 A66-21800
- ALKYL**  
Thermal degradation of mesoporphyrin  
obtaining various alkylpyrroles and  
hydrocarbons, noting role of controlled  
pyrolysis as adjunct to mass  
spectrometry 15 p2446 A66-28880
- ALKYLATION**  
Friedel-Crafts methylation of decaborane  
determining reactant parameters and  
relationship of decaborane conversion and  
alkylate composition 05 p0629 A66-14540
- ALL-SKY PHOTOGRAPHY**  
All-sky electrophotometer for attachment  
to camera 02 p0227 A66-11350  
Patches and irregular bands and eastward



motions in morning sector of  
 auroras 16 p2693 A66-30336  
 Pulsating auroras observed near  
 equatorward boundary of auroral displays  
 during postbreakup phase with image  
 orthicon TV and  
 photometers 18 p3107 A66-34519  
**ALL-WEATHER AIR NAVIGATION**  
 Sectionalized, automatic approach and  
 landing system with monitor channel added  
 developed by Boeing-Bendix for all-weather  
 landing 01 p0101 A66-10033  
 All-weather landing system for C-141 jet  
 cargo transport using vertical navigation  
 computer for military  
 operations 01 p0101 A66-10035  
 Adaptive coupler providing extended  
 automatic glide slope beam following by  
 compensating for beam  
 convergence 01 p0101 A66-10036  
 Present status of all-weather landing  
 system 02 p0256 A66-11861  
 All-weather landing progress based on  
 improved airborne equipment, pilot  
 qualification, approach lighting and ground  
 environment  
 [AIAA PAPER 65-767] 03 p0391 A66-13062  
 Onboard equipment designed for transport  
 aircraft landings with visibilities less than  
 200 ft and runways less than 2600 ft, having  
 all devices duplicated 10 p1554 A66-21368  
 All-weather landing systems  
 evaluated 11 p1732 A66-23163  
 Fog chamber tests and runway lighting  
 requirements, considering landing, cockpit  
 vision and photometry  
 [AIAA PAPER 65-333] 12 p1857 A66-23801  
 Meteorological environment considerations  
 in terminal flight region relating to all-  
 weather land recovery operations of lifting  
 reentry vehicles  
 [AIAA PAPER 66-360] 12 p1907 A66-24492  
 Instrument low-approach system and low-  
 level precision radio altimeter for all-  
 weather landings 17 p2951 A66-33100  
 All-weather operations, head-up displays,  
 long range navigational aids - Symposium,  
 International Federation of Air Line Pilots  
 Associations, Rotterdam, October  
 1965 17 p2951 A66-33198  
 Head-up display system as aid in bad-  
 weather landing 17 p2951 A66-33199  
 Head-up display systems, discussing state  
 of the art and arguments in favor of their  
 use 17 p2952 A66-33202  
 Blind landing equipment, discussing type  
 191 collimator unit tested on Caravelle  
 aircraft 17 p2952 A66-33203  
 Pilot performance and problems arising  
 during transition from instrument to visual  
 flight in landing approach with low  
 visibility 17 p2952 A66-33204  
 Flight simulator techniques applied to all-  
 weather landing problems 17 p2869 A66-33205  
 Operational all-weather landing system  
 described, examining history and present  
 status of all-weather  
 operations 17 p2953 A66-33211  
 All-weather operations, head up displays,  
 long-range navigational aids - Conference,  
 International Federation of Air Line Pilots  
 Associations, Rotterdam, October  
 1965 17 p2953 A66-33212  
 Pilot acceptance factors in development of  
 all-weather landing and SST navigation  
 systems 17 p2955 A66-33219  
 Air traffic control and navigation system  
 for North Atlantic and worldwide all-  
 weather navigation 17 p2956 A66-33224  
 satellite  
 Radiation attenuation effect of atmospheric  
 aerosols on all-weather aircraft landing  
 guidance systems using  
 lasers 19 p3397 A66-36051  
 Para-Visual Detector, flight director display  
 unit, considered by British European  
 Airways 20 p3595 A66-37005  
 TALAR, tactical aircraft landing aid-radio  
 uses ground-based Cassegrain antenna,  
 magnetron transmitter and 4-lb receiver in  
 aircraft while providing ILS  
 functions 20 p3596 A66-37232  
 V/STOL aircraft human reliability factors  
 and requirements for displays and controls  
 in various operational modes under low  
 altitude, high speed and all-weather  
 conditions 20 p3509 A66-37895  
 Flight electronics equipment and

techniques, discussing communications  
 devices, radio navigation apparatus, all-  
 weather landing and onboard navigation  
 aids 21 p3709 A66-38653  
 Sud-Lear all-weather landing system using  
 automatic guidance 21 p3768 A66-39400  
 All-weather landing systems in U.K.,  
 examining safety and reliability criteria in  
 connection with trident airborne equipment  
 [ICAS PAPER 66-8] 22 p3946 A66-40676  
 Approach and landing system with added  
 monitoring channel for category II weather  
 conditions 23 p4088 A66-41137

## ALLOY

SA ALUMINUM ALLOY  
 SA ANTIMONY ALLOY  
 SA BERYLLIUM ALLOY  
 SA BINARY ALLOY  
 SA BISMUTH ALLOY  
 SA BORON ALLOY  
 SA CADMIUM ALLOY  
 SA CHROMIUM ALLOY  
 SA COBALT ALLOY  
 SA COPPER ALLOY  
 SA ERBIUM ALLOY  
 SA EUTECTIC ALLOY  
 SA GALLIUM ALLOY  
 SA GERMANIUM ALLOY  
 SA GOLD ALLOY  
 SA HAFNIUM ALLOY  
 SA HASTELLOY  
 SA HIGH STRENGTH ALLOY  
 SA HIGH TEMPERATURE ALLOY  
 SA INDIUM ALLOY  
 SA IRON ALLOY  
 SA LANTHANUM ALLOY  
 SA LEAD ALLOY  
 SA LITHIUM ALLOY  
 SA MAGNESIUM ALLOY  
 SA MANGANESE ALLOY  
 SA MERCURY ALLOY  
 SA MOLYBDENUM ALLOY  
 SA NICKEL ALLOY  
 SA NIMONIC ALLOY  
 SA NIOBIUM ALLOY  
 SA PALLADIUM ALLOY  
 SA PERMALLOY  
 SA PLATINUM ALLOY  
 SA RARE EARTH ALLOY  
 SA REFRACTORY ALLOY  
 SA RHENIUM ALLOY  
 SA SILICON ALLOY  
 SA SILVER ALLOY  
 SA TANTALUM ALLOY  
 SA TELLURIUM ALLOY  
 SA TIN ALLOY  
 SA TITANIUM ALLOY  
 SA TUNGSTEN ALLOY  
 SA VANADIUM ALLOY  
 SA WROUGHT ALLOY  
 SA YTTRIUM ALLOY  
 SA ZINC ALLOY  
 SA ZIRCONIUM ALLOY  
 Strength and heat resistance of alloys,  
 particularly low alloy  
 steels 01 p0084 A66-10286  
 Mechanical properties of alloys with aging  
 martensite 05 p0701 A66-14860  
 Alloy steel fracture resistance, describing  
 creep strain effect on gas turbine engine  
 alloys  
 [ASME PAPER 65-WA/MET-13]  
 05 p0703 A66-15685  
 Generation modes of dislocations in  
 ordered alloys from Frank-Read  
 sources 07 p1049 A66-17486  
 Effect of structural transformations /such  
 as aging/ on temperature dependence of  
 stress relaxation criteria of certain  
 alloys 07 p1050 A66-18061  
 Alloy steel fracture resistance, describing  
 creep strain effect on gas turbine engine  
 alloys  
 [ASME PAPER 65-WA/MET-13]  
 12 p1896 A66-24535  
 Aluminum alloy with various metal  
 additions analyzed for aging, using electron  
 microscope 12 p1898 A66-25022  
 Electrical resistance changes in quaternary  
 alloy during simultaneous occurrence of  
 phase solution coalescence and silicon  
 spheroidization, noting effects of aging and  
 various metal additions 12 p1898 A66-25023  
 Refractory metals and metal alloys  
 analyzed regarding electron work function  
 and threshold temperature for surface  
 ionization in all-metal guard ring diode with  
 directly heated wire

[AIAA PAPER 66-223] 13 p2129 A66-25171  
 Effects of notch geometry on mechanical  
 behavior /yield strength, tensile strength,  
 etc/ of duplex annealed quaternary alloy at  
 various temperatures 13 p2109 A66-25856  
 High energy Alnico alloys, discussing  
 crystal growth, anisotropy, recrystallization,  
 etc 14 p2311 A66-26883  
 Cold work and precipitation hardening  
 effect on tensile and thermal characteristics  
 of gas turbine alloys  
 [ASME PAPER 66-GT-102]  
 14 p2312 A66-27002  
 Friction corrosion caused by alternate  
 pivoting of steel ball on plane of light  
 alloy 14 p2302 A66-27934  
 Various factors affecting hardening of  
 KhN35VTiU /EI787/ alloy 15 p2519 A66-28535  
 Kh16N15M2B steel properties and effects  
 of grain size and Nb/C  
 ratio 15 p2519 A66-28536  
 Semiconductor cooler creating hypothermia  
 in small animals, operating on Peltier effect  
 and employing quaternary metal  
 alloy 15 p2444 A66-29497  
 Thermal emf of metallic liquid couples  
 measured as function of thermal difference  
 between junctions and alloys composition,  
 noting correlation between thermodynamic  
 and thermoelectric properties of  
 alloys 16 p2781 A66-31410  
 Amplitude dependence of energy  
 dissipation due to internal friction in metals  
 and alloys of various lattice types under  
 near-resonance loading  
 vibrations 17 p2940 A66-33228  
 Resistance to cavitation flow erosion and  
 cracking in metal alloys studied, using  
 rotating disk in water  
 [ASME PAPER 66-FE-11] 17 p2915 A66-33265  
 Mass spectrometric measurement of  
 distribution of spallation produced  
 chromium nuclides between alloys in iron  
 meteorite 17 p3007 A66-33282  
 Ginzburg-Landau expressions for local  
 tunneling density of states of  
 superconducting alloys and effects of space  
 dependence of order  
 parameter 18 p3159 A66-34709  
 Cryogenic design of aluminum, titanium  
 and steel alloys subjected to uniaxial, 1-to-1  
 biaxial and 2-to-1 biaxial stress  
 states 20 p3583 A66-37094  
 Metal and alloy optical properties and  
 electronic structure - International  
 Colloquium, Paris, September  
 1965 20 p3612 A66-37271  
 Electron energy spectrum for alloyed  
 semiconductors, determining state densities  
 via Thomas-Fermi statistical  
 method 20 p3618 A66-37562  
 Optimum alloying level defined as one  
 beyond which net positive effect is reduced  
 by decline in some product property, noting  
 steels 20 p3585 A66-37697  
 Metallurgical and design characteristics of  
 dispersion strengthened metals as function  
 of temperature  
 [ASME PAPER 66-MD-88]  
 21 p3750 A66-38505  
 Electronic structures of transition metal  
 alloys analyzed, comparing superconducting  
 critical temperatures with H, N and O  
 acting as electron donors 22 p3960 A66-39779  
 Fatigue fracture and crack propagation in  
 ordered alloys due to plastic  
 flow 22 p3989 A66-39891  
 Mechanical properties of VAD23 alloy  
 noting tensile, compression, crushing and  
 shearing strength and notch sensitivity and  
 comparison with D16T  
 alloy 22 p3936 A66-40881  
 X-ray and thermographic methods to study  
 structure and phase composition of alloys  
 belonging to silver indium selenide  
 systems 23 p4112 A66-41279  
 Gas turbine blades fabricated from various  
 alloys tested in stationary turbine burning  
 diesel fuel 23 p4121 A66-41401  
 High cycle fatigue strength of titanium, Cb  
 and Al alloys correlated with constants of  
 logarithmic true stress-true strain  
 curve 24 p4229 A66-43080  
**ALOUETTE I SATELLITE**  
 Whistler in Alouette I satellite VLF  
 recordings, variation of time delay with  
 frequency given by Eckersley law time  
 delay and additive correction



term 05 p0668 A66-14797  
 Delayed cyclotron pulse generation in topside ionosphere deduced from Alouette I data 15 p2452 A66-29678  
 Alouette I topside sounder ionograms of electron cyclotron harmonic resonance and frequency variation 16 p2697 A66-31003  
 Topside ionograms electron density data both at and below orbit of Alouette I satellite 17 p2920 A66-33092  
 Unpredicted period in orbital motion of Alouette I artificial Earth satellite attributed to solar gravitational attraction 19 p3463 A66-35921  
 Alouette I topside ionograms analyzed, discussing mathematical procedures and digital computer programs in use and orbit and electron density profiles 22 p3909 A66-39973  
 Seasonal, diurnal and latitudinal variations of electron density distributions in topside of ionosphere as revealed by Alouette I satellite 22 p3909 A66-39974

**ALOUETTE HELICOPTER**  
**S SUD-AVIATION SA 330 HELICOPTER**  
**ALOUETTE SATELLITE**  
 Effective ion mass in upper ionosphere from electron-density profiles obtained from Alouette satellite, compared with theory 04 p0517 A66-14177  
 Ion distribution and temperature in topside ionosphere from plasma scale height profiles from Alouette electron density data 05 p0667 A66-14788  
 Resonant effects theory observed by sounding equipment on ionospheric satellite Alouette 08 p1212 A66-18620  
 Ringing phenomena in ionospheric magnetoplasma as evidenced by spikes on ionograms from Alouette satellite 14 p2283 A66-27513  
 Ion composition and natural electromagnetic emissions of VLF phenomena observed by Alouette I and II 15 p2496 A66-30074  
 Early results from topside sounder experiments in Alouette II satellite, presenting ionograms, plasma spike, electron number density and scale height 15 p2496 A66-30075  
 Alouette satellite observation of ionospheric cyclotron resonance, obtaining plasma frequency at particular height 17 p2920 A66-33085  
 Correlation of geomagnetic index and plasma scale height in topside ionosphere observed from Alouette topside sounder and planetary geomagnetic data 18 p3169 A66-34517  
 Launch of Alouette II satellite noting experiments on board 20 p3663 A66-37625  
 Occurrence frequency patterns of topside spread-F on Alouette satellite ionograms, discussing radio propagation, magnetic irregularities, electron density-induced refraction, etc 20 p3554 A66-38196  
 Topside ionosphere, emphasizing experiments with incoherent scatter radars and topside sounder satellites 22 p3908 A66-39970  
 Canadian ISIS program for launching of satellites containing enough instrumentation to measure all ionospheric parameters simultaneously 24 p4283 A66-42696

**ALPHA RADIATION**  
**SA LYMAN ALPHA RADIATION**  
 Proton and alpha particle effects on thermal properties of spacecraft and solar concentrator coatings of anodic-coated aluminum, zinc oxide/ potassium silicate, etc [AIAA PAPER 65-649] 01 p0090 A66-10230  
 Recombination radiation in gallium arsenide due to alpha particles 04 p0565 A66-14269  
 Solar cosmic ray generation, discussing proton energy spectrum analysis and wave propagation in interplanetary space 05 p0751 A66-15374  
 Flux of alpha component of primary cosmic radiation determined at top of atmosphere, using nuclear emulsion stack exposed near geomagnetic equator 05 p0756 A66-15529  
 Electron energy diffusion in superconducting thin Sn and In films bombarded by alpha particles observed in terms of IR drop 06 p0927 A66-16755  
 Effectiveness of measurements of X-ray

diffraction intensities as probe of lattice defects introduced in perfect germanium crystals by energetic particle irradiation 06 p0933 A66-17121  
 High speed gross alpha autoradiographic technique to reduce exposure time if silver activated ZnS is used as intensifier 07 p1030 A66-17235  
 Low temperature alpha radiation and subsequent isothermal recovery effects on electron structure of gold, relating resulting failures to Frenkel defects 07 p1048 A66-17303  
 Intensity of cosmic ray alpha particles on July 16, 1959 when counting rates of neutron monitors were near absolute minimum value 07 p1124 A66-17997  
 Measurement of energy required to form one hole-electron pair in gallium phosphide by alpha particles 07 p1107 A66-18407  
 Pulse heights produced when argon, nitrogen and argon-nitrogen mixtures completely stop alpha particles 09 p1405 A66-20680  
 Alpha particle and X-radiation ionizing effects on cerebral astroglial cells and blood vessels of young rats 10 p1487 A66-22020  
 Parameters of dynamic modulation determined from measurements of proton and alpha particle spectra, used in cosmic-ray modulation in interplanetary space 11 p1762 A66-22411  
 Directional intensity and decay time of scintillations from anthracene and p-terphenyl single crystals under alpha particle bombardment 11 p1750 A66-22465  
 Light output of alpha particles in crystalline and vapor anthracene as function of pressure and temperature 14 p2296 A66-27796  
 Riometer absorption caused by solar protons and alpha particles in monoenergetic intensities and in spectral distributions 15 p2574 A66-28818  
 High energy primary cosmic radiation research at Bristol, England, including energy spectra for nuclear interactions, nuclear emulsion stack measurements, alpha production, etc 15 p2583 A66-29550  
 Energy spectra of atmospheric alpha rays at balloon altitude and of alpha rays from graphite nuclear interactions 15 p2583 A66-29551  
 Solar flare analysis by examination of high energy gamma rays, noting solar proton and solar material interaction, energy spectrum, generation of fast protons and alpha particles, etc 15 p2592 A66-30076  
 Alpha emitter actinide element application as heat source for isotopic generators, discussing safety precautions required, economy, etc 18 p3134 A66-34056  
 Angular distributions of elastic and inelastic alpha-particle scattering in even tin isotopes, using 40 mev alpha beam 18 p3138 A66-34166  
 Energy characteristics of 11-year cosmic ray variations, evaluating electromagnetic conditions in interplanetary space for proton, alpha particle and electron variations in energy 18 p3176 A66-34752  
 Electrons, hydrogen and helium nuclei of cosmic radiation as observed in 1964 at average residual pressure of 2.4 mb compared with 1.8 mb obtained in 1963 18 p3187 A66-34819  
 Solar modulation of galactic protons and helium nuclei from 1963 to 1965 18 p3188 A66-34821  
 Balloon-borne Cerenkov scintillation counter for measurements of primary proton and helium spectra and modulations 18 p3188 A66-34822  
 Helium nuclei flux at top of atmosphere shows independence of solar activity 18 p3189 A66-34825  
 Energy spectrum of primary helium nuclei at energies greater than 6 gev 18 p3189 A66-34826  
 Differential rigidity spectrum of alpha particles for R less than 2.5 gv at solar minimum 18 p3189 A66-34827  
 Solar cosmic ray alpha particle relation to PCA and lowest latitude of enhanced ionization 20 p3635 A66-38224  
 Artificial radiation belt sources, noting positrons and alpha particles, nuclear

explosion, etc 20 p3643 A66-38333

**ALTERNATING CURRENT /AC/**  
**SA DIRECT CURRENT /DC/**  
 DC and LF AC characteristics of silicon transistor over collector current range 02 p0200 A66-11877  
 MGD DC crossed field plasma accelerator capable of operating on LF AC current 08 p1262 A66-18822  
 Tunnel junction RF modes driven by AC Josephson current 09 p1417 A66-20033  
 Linear theory of alternating current fluctuations in MHD channel subject to Hall instability of Velikhov 09 p1333 A66-20399  
 Single probe method for measuring semiconductor resistivity, using alternating current, noting tests with germanium and silicon samples 11 p1705 A66-22599  
 Equivalent circuit for cycloconverter valve for AC and DC outputs, noting data on voltage drops 12 p1804 A66-24655  
 Superconductors for mixed AC-DC power transmission and thermal dissipation effect 13 p2030 A66-25217  
 Circuit with single externally driven switch, operated at fundamental frequency gives efficient conversion of DC to AC at that frequency or any specified harmonic circuit 17 p2848 A66-31811  
 Transport of AC disturbance /emission/ noise/ on electron beams magnetically compressed in microwave tubes, deriving power flow invariants 17 p2878 A66-31811  
 Alternating current losses in type I superconductor, showing dependence of magnitude and direction of local magnetic field and transport current 19 p3439 A66-35722  
 Conducting nonmagnetic circular cylinder supported on magnetic field produced by alternating current 19 p3324 A66-35722  
 Measurement of physical quantity converted to form of AC signal, noting ripple-free circuit and several clamping arrangements 21 p3709 A66-38600  
 AC losses and magnetic field aberration associated with use of high-field superconducting wire in adiabatic demagnetization apparatus 21 p3804 A66-39399  
 Electron effective mobility variation in Al for small signals as function of operating frequency of thin film transistors and dielectric diodes 24 p4181 A66-42389

**ALTERNATING CURRENT GENERATOR**  
 Transverse current MHD conduction generators for AC power generation 04 p0459 A66-13466  
 Alternating current thermionic power diode with magnetic regeneration 18 p3163 A66-33811  
 Electrical power control and conditioning subsystem for Manned Orbital Research Laboratory /MORL/, noting Brayton cycle system optimization, alternator and frequency converter selection 20 p3497 A66-37155  
 Cylindrical induction type MHD AC power generator analyzed in terms of cylindrical geometry, neglecting end effects 23 p4017 A66-41588

**ALTIMETER**  
**SA RADAR ALTIMETER**  
**SA RADIO ALTIMETER**  
 Altimetry methods reviewed for altitude in 40,000 to 80,000 ft range, noting calibration and instrument accuracy 02 p0231 A66-11986  
 Accurate and economical determination of static system position errors in pressure altimetry systems by trail cone technique 07 p1034 A66-17776  
 Internal friction and vertical separation effects on airways and traffic control at high altitude deviation in barometric altimeters 08 p1249 A66-18669  
 Pulse-radar altimeter for Saturn launch vehicle incorporating molecular and monolithic integrated circuits 08 p1225 A66-19522  
 Inertial techniques extended to height measurement in supersonic aircraft by simple computing addition to main navigation platform 09 p1400 A66-20422  
 Pressure sensing techniques applied to altimetry in supersonic aircraft 09 p1381 A66-20422  
 Geoscience information acquisition by



- radar return studied by means of terrain target scattering coefficients 14 p2244 A66-28407
- /scatometry/ 14 p2244 A66-28407
- Psychophysiological study of compensatory tracking on digital altimeter display and on combined digital and scale-and-pointer display 17 p2869 A66-33448
- Barometric instrument development and description of counter-pointer altimeter and airspeed indicator 23 p4067 A66-41164
- ALTITUDE**
- SA FLIGHT ALTITUDE**
- SA HIGH ALTITUDE**
- SA LOW ALTITUDE**
- Effect of altitude and camera field-of-view at various degrees on geographic orientation and error in target position, using TV data 08 p1225 A66-19531
- Altitude distribution of combinations of meridional gradients of pressure, temperature and density 19 p3393 A66-35394
- Altitude of lower cloud boundary functional correlation with atmospheric parameters obtained from numerical weather forecast 20 p3593 A66-38366
- ALTITUDE ACCLIMATIZATION**
- Lifetime high altitude environment effect on man, noting Peruvian natives adaptation to constant hypoxia 22 p3854 A66-40112
- ALTITUDE CONTROL**
- Vertice, navigation system for vertical plane control 07 p1069 A66-17716
- Altitude control for VTOL aircraft facilitates control of hovering flight, noting construction, operation principles and performance 10 p1484 A66-21379
- Instrumentation of Polish gliders including altimeters, rate-of-climb, turn and air speed indicators, magnetic compasses, artificial horizon, etc 12 p1882 A66-24386
- Vertice, navigation system for vertical plane control 13 p2125 A66-25863
- Approximate atmospheric entry trajectories on cylindrical planet, noting minor circle turn maneuver and bank angle schedule 21 p3811 A66-38705
- ALTITUDE SIMULATION**
- Design and operation of test stands for ELDO rocket engines under simulated high altitude conditions 10 p1519 A66-21384
- Estimation of starting pressure ratio of axisymmetric ejector-diffuser systems for rocket altitude simulation 10 p1481 A66-21933
- Altitude simulator for adjustment and calibration of high altitude meteorological instruments 14 p2325 A66-27279
- ALTITUDE TEST**
- SA HIGH ALTITUDE TESTING**
- Altitude distribution of atmospheric molecular and atomic hydrogen, showing results of Lyman alpha absorption measurements 17 p2919 A66-32995
- ALTITUDE TOLERANCE**
- Ability of airmen to withstand exposure to supersonic transport 05 p0627 A66-15000
- Altitude effect on metabolic rates of deer mice, noting direct relationship between seasons and metabolic rate at all ambient temperatures 20 p3506 A66-37365
- ALUMINATE**
- Optical absorption spectra of cobalt ion in magnesium aluminate crystal 20 p3621 A66-37822
- ALUMINIZATION**
- Coating of titanium with aluminum and silicon by immersion of titanium samples in molten aluminum or in aluminum/silicon melts 10 p1547 A66-21749
- Plane shock wave compressions of cylindrical and wedge-shaped specimens used to obtain shock Hugoniot of two unreacted, composite and double-base aluminumized propellants 12 p1934 A66-23589
- ALUMINUM**
- SA POWDERED ALUMINUM**
- Aluminum honeycomb sandwich structures under axial compressive loading in reliability safety margin analysis, using derived statistical strength data 01 p0145 A66-10086
- Increased aluminum panel acoustic resistance due to combination of surface treatment and mylar gasket-universal head mounting technique 01 p0149 A66-10144
- Luminous phenomena and electron emission discontinuity in aluminum thin film tunnel diodes 01 p0119 A66-10392
- Aluminum cold cathodes with single mode 6328 angstrom helium-neon gas laser lifetimes exceeding 3000 hours 01 p0043 A66-10855
- Stress criterion for crack growth obtained by testing aluminum sheets with transverse machined cracks 01 p0156 A66-10919
- Radiative recombination in thin film structures observing characteristic of aluminum 01 p0127 A66-11089
- Wide wedge penetration into thick aluminum target, noting adiabatic heating and softening 02 p0300 A66-11854
- Phonon spectra in aluminum single crystals investigated by means of inelastic scattering of slow neutrons 02 p0277 A66-12083
- Thermal resistance across aluminum bolted joints in vacuum environment [ASME PAPER 65-HT-53] 05 p0785 A66-14759
- Techniques of joining aluminum to stainless steel for space vehicle application [SAE PAPER 650754] 05 p0701 A66-15002
- Aluminum diffusion bonding for fabrication of Apollo cold plates, noting alternate bonding techniques 05 p0687 A66-15007
- Fatigue test of 1000 aluminum specimens in order to assess accuracy with which lower tail of probability distribution of failure curve fits experimental results 05 p0774 A66-15056
- Elastic impact and perforation of aluminum plates at minimal velocities by projectiles 05 p0775 A66-15299
- Waves in bars of mechanically unstable materials discussing differential equation of motion, jump conditions, wave velocity and application to annealed aluminum [ASME PAPER 65-WA/APM-22] 05 p0778 A66-15444
- Thin metal diaphragms in shock tubes, discussing bursting characteristics and petalling behavior [ASME PAPER 65-WA/MET-16] 05 p0661 A66-15683
- Metal ignition and combustion of aluminum and beryllium [AIAA PAPER 65-103] 05 p0793 A66-15782
- Neutron activation and cesium-aluminum sputtering in oxygenated gas atmosphere [AIAA PAPER 66-77] 06 p0913 A66-17103
- Microhardness changes in polycrystalline aluminum irradiated by alpha, beta and neutron particles 07 p1092 A66-17305
- Sodium and aluminum content in Pribram meteor measured and compared with other fallen meteorites 07 p1135 A66-17639
- Heat resistance and tensile strength of aluminum filament wire compared to ordinary wire 07 p1049 A66-17869
- Leigh theory concerning effect of electron concentration on elasticity of Al and Al alloys compared with experiment 07 p1053 A66-18520
- Quenched-in vacancy data estimated by analysis of quenched-in resistivity in zone-refined aluminum 08 p1240 A66-19062
- Isothermal annealing effect on internal friction and Young modulus of cold-rolled aluminum with different purities 08 p1240 A66-19088
- Spontaneous ignition of mixtures of aluminum trimethyl and oxygen shows ignition boundary as function of partial pressures of reactants 08 p1321 A66-19801
- Yield stress dependence on strain rates in annealed steel and aluminum subjected to ball-indentation tests 08 p1315 A66-19803
- Influence of crystal-lattice defects on Youngs modulus and damping constant of aluminum 09 p1388 A66-19980
- Magnetic field dependence of microwave surface impedance of superconducting aluminum 09 p1418 A66-20024
- Effect of static magnetic field on millimeter wave absorption in superconducting aluminum at reduced temperature 09 p1416 A66-20025
- Welding characteristics of Ti-7Al-2Cu-1Ta plate including strength, toughness and cracking resistance 11 p1717 A66-22863
- Vacuum effect on fatigue life of aluminum under constant stress cyclic bending deformation 11 p1717 A66-22995
- Magnesium fluoride overcoated aluminum mirrors, discussing thickness monitoring techniques by vacuum UV reflectance measurements 11 p1737 A66-23430
- Surface pit formation in aluminum, discussing effects of vacuum, quenching high temperature and repeated cycling 12 p1897 A66-24921
- Effect of conventional ammunition on aluminum honeycomb paneling, noting reduction of load-bearing and peel-strength properties 13 p2196 A66-25599
- Solar concentrator fabrication for space power conversion systems, emphasizing stretch-formed aluminum method [AIAA PAPER 64-731] 13 p2006 A66-26637
- Crystallization sequences in alkali aluminogermanate glass 14 p2318 A66-26947
- Aerospace application of aluminum and its alloys 14 p2313 A66-27012
- Elastic anisotropic deformation of thin polycrystalline condensed films of Al, Ag and Ni 14 p2359 A66-27184
- High purity aluminum strain rate effects with cold working 14 p2316 A66-27782
- Surface area and condition and effect on adhesion of aluminum plates 14 p2304 A66-28206
- Temperature dependence of Hall emf and electrical resistance of Sendust type Fe-Si-Al alloys 15 p2560 A66-28678
- Heat transfer coefficients between layers of thin film structure on niobium and aluminum substrates at liquid helium temperature 15 p2816 A66-28763
- Spherical substrate converted to parabolic mirror by selective evaporation of aluminum, using silver as nonuniform thickness layer 15 p2499 A66-28841
- Electron-spin paramagnetism effect on critical field of thin aluminum superconductor films 16 p2769 A66-30169
- Laser beam energy profile determined by multiple-layer aluminum foil technique 16 p2719 A66-31217
- Sputtering of aluminum thin films prepared by bell-jar vacuum systems /getter sputtering and standard diode/ for electronic application 16 p2783 A66-31423
- Modes of elastic wave propagation and orientation dependence of dislocation damping in aluminum 16 p2821 A66-31452
- Temperature dependence of magnetization and resistivity in SHF magnesium-aluminum ferrite 16 p2786 A66-31677
- Adhesive bonding of aluminum structures including aircraft and space applications 17 p3023 A66-32266
- Explosive forming process for deep aluminum shells, discussing limits and failure 17 p2930 A66-33091
- Inelastic buckling strength of aluminum columns, plates and beams in compression and in shear 17 p3032 A66-33434
- Waves in bars of mechanically unstable materials, discussing differential equation of motion, jump conditions, wave velocity and application to annealed aluminum [ASME PAPER 65-WA/APM-22] 18 p3247 A66-33571
- Use of balanced filter pairs for nondispersive analysis of aluminum and silicon in aluminum-silicon mixtures 18 p3063 A66-33693
- Metal combustion in porous plug configuration for application to solid propellants, noting aluminum porous plug fabrication [WSCI 66-7] 18 p3161 A66-34420
- Water vapor effects on burning rate of aluminum and magnesium wires at atmospheric pressure [WSCI 66-4] 18 p3264 A66-34421
- Time-resolved spectra of single titanium or aluminum particles burning in laminar gas flow recorded by optically fast slitless spectrograph [WSCI 66-5] 18 p3264 A66-34427
- Singularities of temperature dependence of electric resistivity of aluminum at helium temperatures 19 p3382 A66-36072
- Grain boundary migration in pure aluminum and lead under reversed torsional and bending stresses at elevated temperatures 19 p3386 A66-36365
- High temperature fatigue in pure lead and aluminum observed continuously by microscopic cinecamera combined with fatigue machine 19 p3386 A66-36366
- Optical absorption edges with nearly parallel bands of aluminum analyzed for all polyvalent metals with simple



structures 19 p3401 A66-36391  
Yield strength anisotropy due to preferred orientation estimated by Taylor model, considering cold rolled aluminum 20 p3585 A66-37784  
Shock propagation and attenuation in porous graphite and aluminum foams, noting effects of particle shape and size on materials response to shock loading 20 p3588 A66-38407  
Thin film transmission electron microscopic analysis of stress corrosion of heat-treated aluminum 21 p3749 A66-38471  
Transmission electron microscopy on polycrystalline Al, determining hardening and tensile yield stress variations as function of quenching temperature 21 p3753 A66-39586  
Aluminum foil and plastic film compared for wrapping aerospace hardware for moisture-vapor protection 22 p3922 A66-40038  
Neutron activation investigation of cesium ion sputtering of Al in rarefied oxygen atmosphere 22 p3950 A66-40082  
Deformation of aluminum single crystals during constant load tensile test 22 p3935 A66-40201  
Temperature homogenization effect on structure of industrial aluminum, determining mechanical properties dependency on Fe/Si ratio 23 p4081 A66-41403  
Fatigue behavior of aluminum reinforced with stainless steel wires, considering effects of fiber volume fraction and interfacial bond 23 p4081 A66-41661  
Fatigue testing machine shear strain measurements near cracks on Al flat plate surfaces by observing birefringence 23 p4147 A66-41997  
Effect of chemical attachment in boundary lubrication of aluminum thrust washer using 1-cetene and cetane 24 p4217 A66-42700  
Elastic anisotropic deformation of thin polycrystalline condensed films of Al, Ag and Ni 24 p4257 A66-42732

## ALUMINUM ALLOY

Thermal and microscopic analysis and determination of microhardness, electrical conductivity and emf in titanium-aluminum-oxygen ternary system 01 p0087 A66-10659  
Light alloys for engineering application in armor plates, aerospace and nuclear fields, noting aluminum alloy properties 02 p0244 A66-11745  
Aging characteristics of Al-Zn-Mg alloys 03 p0381 A66-12722  
Zinc effect on mechanical properties and microstructure of Al-Si-Cr-Mg alloy 03 p0382 A66-12724  
Nonconservative motion of jogged screw dislocations in high temperature deformation of Al-Mg alloys 03 p0382 A66-12937  
Effect of aluminum on stability and kinetic decomposition of beta phase in Ti-Mo-Mn alloys 03 p0384 A66-13169  
Effect of varying percentages of constituent elements in alumina dispersion-strengthened copper-nickel alloys, listing creep rupture properties 04 p0534 A66-13378  
Fracture toughness of X7000-series aluminum alloy plate weldments 05 p0686 A66-14695  
Cold deformability of alpha-titanium alloys during strip rolling, showing temperature increase of incipient recrystallization of titanium-aluminum alloys 05 p0699 A66-14699  
Metal inert gas and tungsten inert gas welding of 2014-T6 aluminum noting advantages, structures, weld strengths, etc 05 p0688 A66-15186  
Mean strain cumulative damage and effect in low cycle fatigue of 2024-T351 aluminum alloy, covering strain cycling, fatigue life, residual ductility, etc [ASME PAPER 65-WA/MET-5] 05 p0703 A66-15690  
Plane strain fracture toughness of high strength aluminum alloys measuring techniques and relevant metallurgical factors [ASME PAPER 64-WA/MET-11] 06 p0895 A66-16209  
Selective separation of nickel titanium and nickel aluminum alloys and electrochemical behavior in various electrolytes 06 p0896 A66-16542  
Aluminum alloy surface flaw detection, discussing finishing process methods and

parameters for improving penetrant response 06 p0887 A66-16798  
Aluminum alloy butt fusion welds, discussing ghost lack of fusion phenomenon mechanism, characteristics and causes 06 p0887 A66-16800  
Chemical milling techniques, particularly for aluminum alloys, comprising surface preparation, chemical etching and finishing 06 p0888 A66-17074  
Creep tests to verify validity of coincident axis and constancy of volume postulates of Alcoa 1100-0 aluminum alloy 06 p0968 A66-17178  
Text on die, permanent mold, shell and other processes for casting aluminum and aluminum alloys 07 p1047 A66-17214  
Text on aluminum metal and its alloys, stressing connecting links between classical metallurgy, physics of metals and industrial research 07 p1048 A66-17253  
Torsional fatigue induced slip bands and crack initiation in aluminum-zinc-magnesium alloy at room temperature to 250 degrees C 07 p1048 A66-17485  
Materials for extreme temperature and g loading during suborbital, manned and superorbital reentry 07 p1051 A66-18303  
Transmission electron microscopy structural analysis of dislocations in stress-corrosion cracking of 7075 aluminum alloy 08 p1236 A66-18761  
Aluminum-beryllium base alloys, noting problems of application as construction materials 08 p1239 A66-18904  
Aluminum alloys, tensile properties and testing 08 p1241 A66-19715  
Strain distribution in tensile deformation of aluminum alloy coated with gridded Prussian blue coating 08 p1241 A66-19716  
Elongation and yield strength of wrought aluminum alloys as affected by gauge length and offset in tension and compression tests 08 p1242 A66-19717  
Notch toughness of aluminum alloy sheet and plate with machine-edge and fatigue-cracked notches investigated according to ASTM practice 08 p1242 A66-19718  
Low-temperature mechanical properties and fracture toughness of commercial and extra-low-interstitial grade Ti-6Al-4V-2Sn 08 p1242 A66-19719  
Temperature change effect on cumulative fatigue damage on 24S-T3 aluminum alloy and type 301 stainless steel 08 p1242 A66-19720  
Extensometer system and specimen alignment fixture for cylindrical or flat creep specimens 09 p1465 A66-19949  
Microstructures of rapidly solidified aluminum-chromium-silicon alloys 09 p1389 A66-20804  
Quench aging, heat treatment which rationalizes role of vacancy-solute atom association and effect on precipitation hardening aluminum alloys 10 p1545 A66-21218  
Oxygen and water vapor effects on propagation of fatigue cracks in aluminum alloy sheets 10 p1614 A66-21338  
X-ray determination of elastic constant of pure nickel and alloy with aluminum 10 p1547 A66-21982  
Aging of Cu-Ti alloy stimulated by Al additions to 2 percent and retarded by Al additions of 2 to 4 percent 12 p1892 A66-23521  
Phase determination by electron-probe X-ray microanalysis of nickel aluminide self-bonding coating produced by flame-spraying 12 p1892 A66-23560  
Mechanical properties of butt welded joints in high-strength aluminum alloy sheet, noting tensile strength, welding techniques and test results 12 p1893 A66-23708  
AC resistivity profiles through anodic oxide films on Al and Al alloys 12 p1895 A66-24392  
Aluminum alloy with various metal additions analyzed for aging, using electron microscope 12 p1898 A66-25022  
Kinetics of two-phase decomposition of solid solution of magnesium-aluminum alloy, using X-ray analysis, noting grain orientation and size 12 p1898 A66-25027  
Mechanical property evaluation and reproducibility in six heats of commercial Be-Al alloy 13 p2108 A66-25769

Shot peening for resistance to stress corrosion cracking of high strength steel and aluminum alloys and to improve fatigue life of landing gears, wing spars, jet engine components and other structural parts 13 p2196 A66-25777  
Aging behavior of explosively deformed 2219 Al investigated by transmission electron microscopy 13 p2086 A66-25777  
Fracture characteristics of welds in aluminum alloys evaluated by tear and notch tensile tests 13 p2197 A66-25777  
Metals for liquid propellant rocket system in terms of environments in which performance is required 13 p2109 A66-25777  
Effect of corrosive and surface active media on fatigue strength of aluminum alloys widely used in aircraft construction 13 p2109 A66-25888  
Plastic deformation effects on preage, aluminum-copper alloy structure subjected to 40-75 percent compression 13 p2110 A66-25968  
X-ray method determining diameter of Guinier-Preston I zones and fraction of copper atoms contained in such zones in Al-Cu alloys 13 p2111 A66-26588  
Aging behavior of rods produced by extrusion of manganese-containing aluminum alloy subjected to solution heat treatment, noting microstructure and mechanical properties 13 p2111 A66-26588  
Domain boundaries and superdislocations of structure of Alnico V by thin film electron transmission microscopy 14 p2311 A66-26888  
Section size effect on room-temperature notch strength of H-11 steel, 2014-T6 and 7075-T6 aluminum alloys and Plexiglas [ASME PAPER 66-MET-4] 14 p2312 A66-26977  
Texture and anisotropic age hardening to improve mechanical properties of AlMgSi alloys 14 p2313 A66-27011  
Variation of LN 29546 test for determination of susceptibility of aluminum alloy sheet to coarse grain formation 14 p2313 A66-27011  
Strength of screw-connected aluminum alloys, noting screw grades, coatings, thread inserts required, etc 14 p2301 A66-27255  
Mathematical analysis of relationship between weld strength, maximum temperature and time at temperature of type 2219 aluminum 14 p2302 A66-27344  
Elastoplastic properties of copper, aluminum alloys and brass under explosive load, noting increased temperature effect on elastoplastic wave parameters 14 p2314 A66-27377  
Aging of aluminum alloy after quenching and strain hardening, noting Vicker hardness tests, tensile tests, precipitation phases, shearing effect, etc [PST PAPER 423] 14 p2315 A66-27466  
Creep buckling of column subjected to arbitrary temperature distribution along column, considering aluminum alloy 14 p2403 A66-27997  
Chemical composition effect on fracture properties of Al-Zn-Mg-Cu alloys 14 p2317 A66-28000  
Explosive deformation effect on stress corrosion and mechanical properties of 707 aluminum alloy 14 p2317 A66-28011  
Axially loaded cylindrical structure analyzed for optimum weight construction consistent with cost constraint, emphasizing beryllium-aluminum alloys 14 p2406 A66-28202  
Temperature of container heated during pressing aluminum alloy sections 14 p2304 A66-28202  
Precleaning treatment and coating effect on fatigue strengths of aluminum alloys 15 p2521 A66-29007  
Densities of wrought aluminum alloy computed from rule of mixtures and metallurgical phenomena and compared with observed densities 15 p2522 A66-29007  
Aluminum screw coupling resistance to stresses as affected by profile, thread depth, and composition 15 p2509 A66-29111  
Mechanical properties of Ti-Al-Mo-Zr-Si alloy as affected by varying cooling rate after heat treatment 15 p2523 A66-29191  
Electron microscope investigation of dislocation effect on stress corrosion cracking in aluminum alloy 15 p2523 A66-29411



Hot drape forming of torus and semitoroidal bulkhead segments from aluminum alloys 15 p2511 A66-29831  
 [SAE PAPER 660290] 15 p2511 A66-29831  
 Free energy of aluminum alloy containing two-dimensional Guinier-Preston zones of copper atoms 16 p2722 A66-30307  
 Trace element effect on lifetime of iron-chromium-aluminum heat-resisting alloy 16 p2723 A66-30311  
 Welding of aluminum alloy for S-IC stage of Saturn-Apollo space vehicle 16 p2713 A66-30592  
 Kinetics of natural aging process of Al-4 percent Cu alloy, experiments indicate addition of up to 1.0 percent Mg proportionately slows down aging process 16 p2723 A66-30871  
 Critical stress, stability loss and load carrying capacity of axially compressed thin walled aluminum alloy 16 p2819 A66-31142  
 Estimation of creep in Ti-Al-V alloys by high temperature bending method 16 p2724 A66-31237  
 Alloying elements effect on aluminum corrosion over wide pH range in water, alkali and 0.1N solutions of anions 16 p2725 A66-31392  
 Discoloration in contamination area of aluminum bonds in integrated circuits, noting cause and effect on interconnection bond integrity 16 p2665 A66-31434  
 Vibrational and static plastic deformation effect on structure of 40KhNMA steel and VD 17 aluminum alloy 16 p2728 A66-31800  
 Various heat treat tempers of 2014 Al alloy and corresponding values of eddy current 17 p2940 A66-33099  
 Polycrystalline nickel aluminide lightly deformed at 77, 298 and 900 degrees K exhibit fine slip band structure with mostly screw dislocations 18 p3121 A66-33747  
 Hardness and lattice parameter increase effect on oxidation temperature of internally oxidized Ag-Mg and Ag-Al alloys 18 p3122 A66-33750  
 Characteristic microstresses in plastically deformed iron and aluminum alloy under tensile testing studied by X-ray techniques 19 p3376 A66-35400  
 Specific heat and thermal conductivity of metals at cryogenic temperatures 19 p3381 A66-35849  
 X-ray determination of elastic constant of pure nickel and alloy with aluminum 19 p3381 A66-35864  
 Nickel aluminide structure, examining arrangement of Ti, Cr and W in lattice via X-ray spectroscopy 19 p3381 A66-35928  
 High strength weldable Al alloys with good cryogenic toughness, stress-corrosion cracking resistance and tensile strength 20 p3582 A66-37091  
 Effects of aging temperature and duration on strength, elongation, yield stress, plasticity and electrical conductivity of Al-Zn-Mg and Al-Zn-Mg-Cu alloys 20 p3585 A66-37698  
 Shear mode fatigue fracture in aluminum alloys studied, using fractography, metallography and Laue back reflection technique 20 p3586 A66-37800  
 High strength aluminum alloys, evaluating tensile strength, toughness and stress-corrosion resistance 21 p3751 A66-39234  
 High strength aluminum alloys manufacturing and service experience, fracture characteristics and tables on composition ranges of various alloys 21 p3751 A66-39235  
 Titanium-rich end of Ti-Al solid solution equilibrium diagram 22 p3934 A66-39781  
 Alloys and processes for Titan booster system fabrication, noting mechanical properties and behavior of welded joints 22 p3924 A66-40260  
 Electron beam welding outside of vacuum, discussing performance and tolerance parameters 22 p3924 A66-40261  
 Gas mixtures evaluation for MIG welding aluminum alloy noting nondestructive, mechanical and stress corrosion testing 22 p3925 A66-40266  
 Grain boundary cavity growth in Al-Cu alloy during compressive creep testing 22 p3935 A66-40291  
 Corrosion fatigue strength of duralumin in

presence of stress concentrators, noting parameters of resistance and alloy properties 22 p3935 A66-40679  
 Book on aluminum alloys covering mechanical properties, contact welding, manufacturing, cold deformation, etc 22 p3936 A66-40876  
 Structural, mechanical and corrosion properties of aluminum alloy of various compositions 22 p3936 A66-40877  
 Heat resistance of coarse- and fine-grained D20 aluminum alloy 22 p3936 A66-40878  
 Effect of technological factors on quality of semifinished pressed products of aluminum alloy 22 p3936 A66-40879  
 Spot and seam welding processes effect on behavior of aluminum alloy 22 p3928 A66-40880  
 Mechanical properties of semifinished products, welds and machined sections of high strength V92Ts aluminum alloy 22 p3936 A66-40883  
 Mechanical properties, coefficient of linear expansion and microstructure of aluminum-based sintered-powder alloy containing silicon and nickel 22 p3937 A66-40884  
 Susceptibility to cold deformation of semifinished B95-2 Al-Zn-Mg-Cu alloy products, noting machinability in manufacturing of parts 22 p3928 A66-40885  
 Manufacturing of semifinished pressed products of AD31 Al-Mg-Si alloy, examining coarse-grained structure occurring after hardening and machining 22 p3928 A66-40886  
 Residual stress, crack propagation and fatigue fracture mechanisms in Al alloy sheets with fatigue cracks, for use in wing panels [ICAS PAPER 66-34] 23 p4137 A66-41007  
 Effect of titanium, zirconium, vanadium and cerium additions on properties and macrostructure of aluminum alloy tested in cast and heat treated states 23 p4080 A66-41271  
 Effect of manganese and zirconium additions on recrystallization temperature and grain size of aluminum alloys 23 p4081 A66-41404  
 Nozzle for special small rocket motor, noting weight, construction material and performance 23 p4121 A66-41422  
 Aluminum alloy tube for combustion chamber of Japanese SSR, noting mechanical properties, temperature effects, etc 23 p4081 A66-41424  
 Aluminum and titanium alloys, composite materials and nonmetallic materials for supersonic transports and VTOL aircraft noting intakes, nozzles and variable-geometry wings [ICAS PAPER 66-1] 23 p4016 A66-41932  
 Cold-drawing effect on creep behavior of nickel-aluminum alloy at various temperatures through changes in fracture, precipitates and structure 24 p4227 A66-42309  
 Section size effect on room temperature notch strength of H-11 steel, 2014-T6 and 7075-T6 aluminum alloys and Plexiglas [ASME PAPER 66-MET-4] 24 p4228 A66-42581  
 Vibrational creep of Al alloy at normal temperature, noting plastic deformation magnitudes creep limit equations, etc 24 p4228 A66-42864  
**ALUMINUM ANTIMONIDE**  
 Stoichiometric thin films of AlSb prepared by coevaporation of elements onto glass substrates held at 550 degrees C 02 p0270 A66-11436  
 Weak-field magnetoresistance and impurity activation energy in n-type aluminum antimonide single crystal 08 p1275 A66-19363  
 Thin aluminum antimonide film fabrication for photoelectric cell application 09 p1359 A66-20927  
 Uniaxial compression and hydrostatic pressure effect on piezoresistance and piezo-Hall effects in n-and p-type AlSb 17 p2984 A66-33153  
 Galvanomagnetic effects in p-type aluminum antimonide, discussing field dependence of Hall effect and magnetoresistance 21 p3801 A66-38999  
**ALUMINUM CARBIDE**  
 Aluminum carbide thermodynamic properties over large temperature interval calculated from low-temperature heat capacity and high-temperature relative

enthalpy 04 p0536 A66-13832  
**ALUMINUM COMPOUND**  
 Complex permittivity and permeability of lithium aluminum ferrite in cavity resonator determined, using perturbation theory 01 p0123 A66-10590  
 Aluminum nitrate powder maser doped with ferric ions operation in X-band without external DC magnetic field 02 p0239 A66-11374  
 Thermal diffuse elastic electron scattering in polycrystalline Al foil, using retarding field apparatus 05 p0736 A66-14980  
 Premixed flames of trimethylaluminum vapors and oxygen stabilized at reduced pressure, analyzing stability region, burning velocity and emission spectrum 08 p1318 A66-19199  
 X-ray spectral analysis of chemical bond structure in aluminum semiconductor compounds 08 p1274 A66-19311  
 Plasma oscillation of electrons in aluminum compound eutectoids studied, using energy analysis of electrons passed through thin foil of eutectoid, noting dependency of oscillation energy on component grain size 09 p1429 A66-20843  
 Preparation of aluminum difluoramide from trimethylamine alane and difluoramine 13 p2018 A66-26501  
 Growth of single crystal and polycrystalline thin films of magnesium aluminum oxide and magnesium iron oxide, discussing techniques employed, results, etc 17 p2982 A66-33061  
 Aluminum welding, examining internal defects such as porosity and metallurgical changes in heat effected zone [SAE PAPER 660292] 18 p3117 A66-34944  
 Aluminide-ductile binder composite alloys containing high volume of nickel-aluminum compounds and CoAl prepared by powder blending and hot extrusion 20 p3585 A66-37783  
 Solid state maser oscillator operating in zero field configuration, using ferric ion substituted as impurity in aluminum nitrate host crystal 24 p4221 A66-42551  
**ALUMINUM FLUORIDE**  
 Oxyfluorides relationship to basic aluminic fluorides, discussing difficulties and formation 18 p3064 A66-33928  
**ALUMINUM HYDRIDE**  
**SA LITHIUM ALUMINUM HYDRIDE**  
 Rates and stoichiometry of reaction of aluminum hydride in tetrahydrofuran at zero degrees with selected organic compounds containing representative functional groups 13 p2018 A66-26500  
**ALUMINUM NITRIDE**  
 Aluminum nitride coatings on graphite deposited by introduction of plasma-generating gas into electric arc between tungsten cathode and aluminum filament anode 09 p1392 A66-20149  
 Synthesis conditions for materials of B-Al-N system determined by sintering mixtures of BN plus Al and AlN plus B powder in nitrogen atmosphere 11 p1720 A66-23473  
 Voltage dependence of barrier height in Al-AlN-Mg tunnel junction 13 p2170 A66-26596  
 Aluminum nitride coatings on graphite deposited by introduction of plasma-generating gas into electric arc between tungsten cathode and aluminum filament anode 21 p3754 A66-39419  
**ALUMINUM OXIDE**  
 Deformation resistance and stability dependence of strain-induced distortions in nickel alloys on various aluminum oxide distributions 01 p0087 A66-10749  
 IR-active lattice vibrational spectra of alpha-aluminum oxide and chromium oxide analyzed by reflection and transmission measurements 03 p0380 A66-12341  
 Dielectric relaxation effects, dissipation factor peak and capacitance and conductivity dispersions in pure and doped sapphire single crystals 03 p0409 A66-12638  
 Temperature dependence of Mie scattering, covering absorption and scattering of electromagnetic radiation on spherical aluminum oxide particles 05 p0718 A66-14917  
 Low work function collector with Ba-covered thin aluminum trioxide film electrodes for high efficiency thermionic converters 05 p0621 A66-15575



Manganese oxide effect on kinetics and mechanics of sintering of alumina powder compacts 08 p1243 A66-18774

Model derived describing oxide particle distribution obtained from internal burning cylindrically-perforated aluminized solid propellant grains

[AIAA PAPER 65-10] 08 p1282 A66-19137

X-ray spectral analysis of chemical bond structure in aluminum semiconductor compounds 08 p1274 A66-19311

Tunnel and Schottky in aluminum oxide thin film element 09 p1426 A66-20193

Silicone alumina low temperature low-pressure plastic molding technique for precision forming of ceramic materials for aerospace structural application 10 p1538 A66-21130

Economic process for vapor phase formation of refractory fibers and whiskers using hydrogen, carbon dioxide, carbon monoxide and chlorine source gases [AICE PREPRINT 18A] 10 p1548 A66-21183

Measured thermal conductivities of magnesium oxide, aluminum oxide and zirconium oxide powders 10 p1546 A66-21538

Theoretical expression for thermal conductivities of magnesium oxide, aluminum oxide and zirconium oxide powder 10 p1546 A66-21539

Internal photoemission measurements show potential barrier profile in thin anodically formed aluminum oxide films between metal electrodes 10 p1509 A66-21541

Low temperature chromatographic separation of hydrogen isotopes based on interaction with alumina surface electric fields 11 p1650 A66-23209

Vapor phase process to form aluminum oxide whiskers on nuclei suspended in reacting gas stream 12 p1896 A66-24468

Aluminum oxide inclusions effect on radioactive cobalt 60 autodiffusion observed, noting higher diffusion in samples prepared by powder methods 13 p2110 A66-25964

Voltage dependence of barrier heights in aluminum-aluminum oxide-aluminum tunnel diodes at room and liquid-nitrogen temperatures 13 p2170 A66-26595

Electron energy distribution for emission from aluminum-aluminum oxide-gold thin films 14 p2257 A66-27943

Forging and hot working of SAP samples containing 6-10 percent aluminum oxide 14 p2303 A66-28192

Variations in amount and composition of oxide phase during sintering of compacted aluminum powder, determining aluminum oxide in SAP products 14 p2303 A66-28195

Hardening and softening of nickel-alumina alloys 15 p2519 A66-28533

Photovoltage of aluminum-aluminum oxide-aluminum thin film sandwich with aluminum oxide layer of 60 angstroms measured as function of wavelength and incident light intensity 16 p2778 A66-31076

Hardness and microstructure of sintered alloys of molybdenum with oxides of aluminum and zirconium obtained by powder metallurgy methods 17 p2939 A66-32394

Transmittance of optical materials between 1050 and 3000 angstroms, noting effect of simulated high energy space environment 17 p2979 A66-32615

Dynamic Jahn-Teller effect in excited state vanadium doped aluminum oxide 17 p2981 A66-32717

Combustion behavior of aluminum-ferric oxide thermite with aluminum oxide additions used as combustion model for involatile condensed systems 18 p3259 A66-33718

Deformation resistance and stability dependence of strain-induced distortions in nickel alloys on various aluminum oxide distributions 18 p3124 A66-34983

Alumina high temperature gas discharge tube for investigation of pulsed metal vapor laser oscillations 19 p3374 A66-35810

Factors affecting strength of whisker reinforced metals, noting characteristics [ASME PAPER 66-MD-81] 21 p3750 A66-38504

Thermocompression bonding, discussing aluminum wire connection to substrate material via eyelet bond 23 p4044 A66-41197

Absorption cross section, scattering cross section and angular scattering distribution

of solid alumina particles emitted in homogeneous solid propellant rocket plume 24 p4294 A66-42778

Vacuum furnace for studying high temperature fracture of ceramic materials, noting tests on polycrystalline aluminum oxide 24 p4192 A66-43220

**ALUMINUM 26**

Determination of constancy of cosmic radiation and of terrestrial and cosmic ages of ferrous meteorites by radioactivity of Al 26 and Be 10 20 p3651 A66-37411

**AMBIPOLAR DIFFUSION**

Ambipolar diffusion and electron attachment in photoionized nitric oxide by presence of negative ions, noting electron loss and electron density 03 p0394 A66-12326

Ambipolar diffusion and electron-ion recombination coefficients dependence on electron temperature in afterglow of neon plasmas 04 p0554 A66-14294

Effects of variable ionic mobility on current collection by cylindrical body and of fringing electric field on sheath size, noting role of diffusion 05 p0722 A66-14724

Ambipolar diffusion in magnetic field showing plasma equations of momentum-transfer yield unambiguous steady state solutions 05 p0669 A66-14943

Martian ionospheric observations made by Mariner IV interpreted in terms of model show atmosphere consists mainly of carbon dioxide, low temperature and no thermosphere 06 p0953 A66-16404

Time dependent ambipolar diffusion waves, solving electron density equation 07 p1088 A66-17951

Electron conservation equation and effects of laminar or turbulent flow on breakdown in gases 08 p1206 A66-18933

Ambipolar diffusion parameter calculation by Quinn and Nisbet found erroneous for night F layer 08 p1219 A66-19420

Sounding rocket-released artificial strontium and barium ion cloud motion in upper atmosphere, based on equations of ambipolar diffusion 15 p2491 A66-29950

Ambipolar diffusion of plasma cloud imbedded in ionized gas with homogeneous magnetic field, assuming electric current is not vanishing 15 p2494 A66-30045

Ambipolar potential in magnetoactive cold plasma applied to power generation and effects of electric field on diffusion coefficient 17 p2973 A66-32984

Magnitude of vertical drifts in F-region during high and low sunspot years, considering effect of ambipolar diffusion along geomagnetic lines of force 19 p3347 A66-35923

**AMIDASE**

Dipeptidyl-beta-naphthylamidase activated by chloride in extracts of rat and bovine anterior pituitary glands 13 p2010 A66-25900

**AMIDE**

**SA POLYAMIDE**

Dipeptidyl arylamidase I of bovine pituitary tissue and chloride and sulphydryl activation of seryltyrosyl-beta-naphthylamide hydrolysis 17 p2861 A66-32899

Alpha-chloro alkanoyl valine methyl esters analyzed, finding that diastereoisomeric pairs separation by gas-liquid chromatography can assess steric conditions around amide bond 17 p2871 A66-32932

Cyclomethylenetrinitramine-hexamethylphosphortriamide complex preparation 20 p3627 A66-38416

**AMINE**

**SA AMPHETAMINE**

**SA CATECHOLAMINE**

**SA CYSTEAMINE**

**SA DIFLUORAMINE**

**SA HEXAMETHYLENETETRAMINE**

**SA NITROAMINE**

Crystal and molecular structure of chlorotetraamine /sulfur dioxide/ ruthenium chloride 06 p0820 A66-15939

High sensitivity optical resolution of amine diastereoisomers by gas liquid chromatography 17 p2869 A66-31873

**AMINO ACID**

**SA ASPARTIC ACID**

**SA GLYCINE**

**SA PROTEIN**

**SA TRYPTOPHAN**

Thermal stability to racemization and

resolution of several racemic amino acid diastereomeric derivatives by gas chromatography 01 p0021 A66-1060

Relation of earliest proteins to protocol with tabulated comparison of key properties of acid proteinoids and protein 04 p0461 A66-1336

Total optical resolution of DL-alpha amino acids from supersaturated aqueous solution by seeding with pure crystals of L-or D isomers of amino acid 04 p0473 A66-1345

Amino acid genetic code in which ion sequences in DNA spell out instruction transcribed into RNA and subsequently into proteins 11 p1644 A66-2271

Amino acids dissolved in saline water removed by ligand exchange chromatography 11 p1650 A66-2312

Behavior of synthetic polyribonucleotide in cell-free amino-acid-incorporating system from E coli, noting release of polypeptide chains into supernatant fraction 12 p1805 A66-2353

Crystalline lactic dehydrogenases in reaction with p-hydroxymercuribenzoate 13 p2009 A66-2579

Paleogenetic study of ferredoxin structure reconstructing evolution from amino acid sequence 14 p2228 A66-2781

Structural and functional properties of heart and muscle type subunits of lactate dehydrogenases investigated, using comparative amino acid analysis 15 p2446 A66-2886

Gas chromatography for resolution and separation of racemic amino acids as TFA sec-butanol ester derivatives applied to protein analysis 15 p2446 A66-2886

Pasteur Probe assay of asymmetry of D, amino acids in detection of Martia life 15 p2447 A66-3002

Synthesis of alpha-amino acid l-menthyl esters under mild conditions, using alpha-amino acid N-carboxy anhydride /NCA/ and l-menthol 16 p2646 A66-3118

Resolution method for DL-amino-acids via menthyl ester derivatives and gas-liquid chromatographic analysis of crystalline products 17 p2869 A66-3187

Amino acid content of carbonaceous and noncarbonaceous chondrites and possible origins 17 p2850 A66-3208

Amino acid, peptides and spherule obtained from sparking in closed atmosphere of ammonia, methane, hydrogen and water 17 p2851 A66-3208

Thermal synthesis of amino acids from methane-ammonia-water mixture passing through Earth-crust materials 17 p2851 A66-3208

Thermal polycondensation of free amino acids with polyphosphoric acid 17 p2852 A66-3209

Molecular biology noting hemoglobin an enzyme cytochrome evolution, amino acid code, ribonucleic acid, etc 17 p2853 A66-3210

Ribonucleoside triphosphatase in rabbit reticulocytes, discussing distribution in extracts, behavior in purification of amino acid and properties 17 p2859 A66-3255

Corticosterone injection in rats, assaying amino acid incorporation into liver microsomal and cell-sap protein 17 p2860 A66-3255

Repetitions in polypeptide sequence of cytochromes 18 p3059 A66-3419

Simulation of organismic morphology and behavior by synthetic poly-alpha-amino acids 19 p3284 A66-3557

Amino-acid-sequence determination in peptides using N-fatty acids, mass spectra of peptide derivatives and computer techniques 20 p3510 A66-3705

Gas liquid chromatography resolution of racemic hydroxy and beta-mercapto-amino acids involving suitable derivation of functional group 20 p3510 A66-3760

Optical resolution and absolute configuration of trans-beta-phenylglycidic acid 21 p3702 A66-3844

Stereoselective synthesis of optically active amino acids from menthyl esters and alpha keto acids 23 p4032 A66-4137

**AMMONIA**

**SA LIQUID AMMONIA**

Discrepancy among derived temperatures for cloud tops of Jupiter and Saturn and



expected value for model in simple equilibrium with solar radiation attributed to presence of ammonia 04 p0579 A66-14180

Thermal conductivity of liquid and gaseous ammonia between 20 and 177 degrees C and 1 to 500 atm 05 p0744 A66-15464

Stress-corrosion cracking, rate of weight loss and surface condition of 70-30 copper zinc alloy in concentrated aqueous ammonia 07 p1053 A66-18519

Temperature dependence of crystalline ammonia elastic moduli 10 p1589 A66-22166

Toxic and lethal effect on mice of ammonia in air, noting biological and physiological changes 15 p2439 A66-29494

Tuning of ammonia beam maser resonator based on frequency shift method, noting hysteresis appearance and elimination 16 p2720 A66-31696

UV radiation effect on decomposition of ammonia ejected in upper atmosphere 17 p3013 A66-33402

Temperature dependence of crystalline ammonia elastic moduli 19 p3441 A66-35780

**AMMONIUM COMPOUND**

Crystal structure of ammonium tricyanomethide determined by X-ray diffraction 04 p0474 A66-13833

HF optical modulator using Pockel effect in ammonium and potassium dihydrophosphate single crystals 06 p0889 A66-15899

**AMMONIUM PERCHLORATE**

Steady state composition mechanism of solid /heterogeneous/ propellants noting linear pyrolysis, exothermal oxidizers, fuels, etc [ONERA TP 240] 02 p0278 A66-11681

Ammonium perchlorate spheres combustion in flowing gaseous fuel similar to conditions in solid rocket combustion, noting diffusion flame significance 03 p0414 A66-13225

Temperature at which predecomposition or decomposition of ammonium perchlorate occurs, changed by perchlorate surface treatment and reflected in burning rate of propellant containing perchlorate [CI PAPER WSCI-65-36] 05 p0744 A66-15151

Theoretical detonation characteristics of ammonium perchlorate-polyurethane solid composite propellants 05 p0744 A66-15781

Ignition of ammonium perchlorate composite propellants by convective heating [AIAA PAPER 66-65] 06 p0941 A66-17101

Linear pyrolysis velocity measuring device for ammonium perchlorate in one-dimensional flow 08 p1279 A66-18723

Binder-oxidizer interaction separation in composite solid propellants containing preirradiated ammonium perchlorate 08 p1279 A66-18825

Combustion of ammonium perchlorate propellants in solid propellant rockets 12 p1978 A66-23965

Combustion of composite ammonium perchlorate based propellants near extinction pressure, noting burning rate parameters 13 p2171 A66-25181

Thermal diffusivity of ammonium perchlorate and sodium chloride powders measured as function of porosity and temperature 14 p2370 A66-27414

Ignition mechanisms of solid composite propellants containing ammonium perchlorate as oxidizer 15 p2569 A66-29308

Combustion rate of ammonium perchlorate-polystyrene and ammonium perchlorate-Plexiglas mixtures related to mixture ratio 18 p3260 A66-33720

Burning rate anomalous dependence on particle size for ammonium perchlorate-polystyrene mixture 20 p3679 A66-37703

Ignition of ammonium perchlorate composite propellants by convective heating [ATAA PAPER 66-65] 21 p3806 A66-38689

Ignition of simulated propellants based on ammonium perchlorate, determining empirical relations 22 p3969 A66-40354

Direct-casting polyurethane-ammonium perchlorate-based composite propellant grain manufacture for small rocket motor, noting inspection methods 23 p4119 A66-41432

Erosive burning in rocket engines of radial burning type, using polyurethane/ammonium perchlorate base propellant grains, examining flow channel 23 p4121 A66-41433

Effect of fuel-binders ingredients and

additives on physicomaterial properties of polyurethane-ammonium perchlorate base propellant grains 23 p4119 A66-41434

Halides used as burning rate depressants on combustion stability of polyurethane/ammonium perchlorate base propellants, examining acoustic instability 23 p4119 A66-41435

Effects of isothermal decomposition of gamma ray irradiated orthorhombic crystals of ammonium perchlorate 24 p4170 A66-42421

Chemical interaction among components of CdO, ZnO and PbO admixtures in ammonium perchlorate, noting effect on thermal decomposition 24 p4295 A66-43200

**AMMONIUM PHOSPHATE**

Absolute measurement of optical-rectification coefficient in ammonium dihydrogen phosphate 12 p1912 A66-23715

Continuous wave measurement of optical nonlinearity of ammonium dihydrogen phosphate, using helium-neon laser 12 p1912 A66-23716

**AMMONIUM PICRATE**

Rocket propellant chemistry covering synthesis, properties and capabilities of organic and inorganic rocket fuels 05 p0743 A66-14675

**AMPHETAMINE**

Effect of amphetamine on signal detectability in vigilance task 01 p0020 A66-10616

**AMPHIBIA****S FROG****AMPLIFICATION****S FLUID AMPLIFICATION****S SOUND AMPLIFICATION****AMPLIFICATION FACTOR**

Amplification factor of semiconductors for direct interband transitions and saturation effect 01 p0124 A66-10766

Current amplification factor decrease and input resistance increase with current decrease in transistor circuits in microregime 02 p0207 A66-11414

Linear coefficient of amplification of carbon dioxide subjected to HF excitation field for laser emission 02 p0241 A66-12003

Light flow amplification in inhomogeneous layer taking nonlinearity into account 05 p0692 A66-14725

Amplification factors and optimum matching conditions calculated for complex capacitive diode frequency converters 07 p1005 A66-17347

Maximum gain condition of resonance amplifier for given passband, determining amplification coefficient 07 p1005 A66-17351

Resonant amplifier stage calculations for realizing given passband width and amplification factor 08 p1193 A66-19107

Coherent amplification coefficients of neon lines in helium-neon mixture 08 p1234 A66-19310

Generalization of Manley-Rowe theorem for case in which one or more pumping generators act on nonlinear reactive element 08 p1197 A66-19603

Slow neutron scintillation counter using photomultiplier with nonactivated dynodes, with low amplification factor to measure very low intensity ion beams 09 p1380 A66-20359

Partial amplification factors of multistage cascade amplifier to determine transmission coefficient of follower 09 p1354 A66-20449

Transistor sawtooth-voltage generators with positive feedback and nonlinear distortions correction by amplification factor control 10 p1511 A66-21679

Amplification factor of semiconductors for direct interband transitions and saturation effect 11 p1748 A66-22277

Single pulse operation of lasers, noting energy storage and amplification effect for four-and three-level active medium 12 p1889 A66-23667

Stable self-adjusting system with single adjustable parameter designed, using inverse model of desired transfer function of closed-loop system in feedback control circuit with large amplification factor 12 p1851 A66-24315

Variation of antenna amplification ratio with distance as function of phase error at antenna aperture with exciter off-focus as error source 13 p2030 A66-25225

Weimer triode with contact rectifier for

use as component of microminiature radio circuits, noting effect of contact rectification on current-voltage characteristics and amplifying power of such triodes 13 p2031 A66-25228

Combined automatic control systems with automatic adjustment of amplification coefficient of disturbance controller for error reduction 13 p2045 A66-25300

Silicon UHF power transistor performance, showing parameters of amplifier gain, power output and impedance 13 p2036 A66-25512

Linear power amplification with switching techniques, using pulse width modulation 13 p2036 A66-25522

Nonlinear quantum effect in solid state lasers using paramagnetic crystals, noting Raman effect and gain dependence on pumping power 13 p2098 A66-26172

Current amplification factor of filamentary transistor with intrinsic-conductance semiconductor base 14 p2255 A66-27751

Measuring modulus and phase angle of transistor current gain 15 p2464 A66-29058

Radial amplification dependence over discharge cross section of He-Ne laser 15 p2515 A66-29208

Regenerative helium-neon laser with amplification coefficient of 1000 15 p2516 A66-29352

Charge control analysis of transistor cut-off frequency, noting current amplification factor, transit time of minority carriers, etc 15 p2468 A66-29889

Dependence of amplification factors on emitter current in p-n-p-n silicon rectifiers 15 p2468 A66-29917

Stability analysis of two types of single-stage amplifiers using Dynistor as active element 15 p2468 A66-29920

Double sideband capacitance and resistance modulation of systems and calculation of noise and amplification factors 16 p2666 A66-31561

Radial amplification dependence over discharge cross section of He-Ne laser 17 p2936 A66-33057

Dual control of plant with random amplification factor as Bayesian problem 18 p3089 A66-33738

Fluid amplifier operation characteristics, noting gain, switching circuits, power jet pressure effects, etc 18 p3054 A66-34128

Beam deflection type proportional fluid amplifier, noting pressure and flow gain parameters, transfer characteristics, etc 18 p3054 A66-34129

Generalization of Manley-Rowe theorem for case in which one or more pumping generators act on nonlinear reactive element 18 p3087 A66-34961

Regenerative helium-neon laser with amplification coefficient of 1000 20 p3576 A66-37357

Single pulse operation of lasers, noting energy storage and amplification effect for four-and three-level active medium 22 p3929 A66-39711

Theoretical static I-V characteristics of surface gate dielectric triode and geometric factors influence on amplification factor at cut-off 22 p3872 A66-39746

Criterion for spatial-amplification or nontransmittance using double Laplace transforms in light of complex values of wave vector 22 p3869 A66-40928

Equations of motion of continuous single loop adaptive control system with scan modulated parameters, noting stability analysis method 24 p4188 A66-42479

**AMPLIFIER****SA BEAM-PLASMA AMPLIFIER****SA BISTABLE AMPLIFIER****SA BROADBAND AMPLIFIER****SA CHOPPER****SA CROSSED FIELD AMPLIFIER****SA CURRENT AMPLIFIER****SA DIFFERENTIAL AMPLIFIER****SA ELECTRON MULTIPLIER****SA FEEDBACK AMPLIFIER****SA FLUID AMPLIFIER****SA FREQUENCY AMPLIFIER****SA JET AMPLIFIER****SA KLYSTRON****SA LASER****SA LIGHT AMPLIFIER****SA LIMITER AMPLIFIER****SA MAGNETIC AMPLIFIER**



SA MAGNETOSTATIC AMPLIFIER  
 SA MASER  
 SA OPTICAL AMPLIFIER  
 SA PARAMAGNETIC AMPLIFIER  
 SA PARAMETRIC AMPLIFIER  
 SA PHOTOMULTIPLIER  
 SA PHOTOTUBE  
 SA PREAMPLIFIER  
 SA QUANTUM AMPLIFIER  
 SA SERVOAMPLIFIER  
 SA TRANSFORMER  
 SA TRANSISTOR AMPLIFIER  
 SA TRAVELING WAVE AMPLIFIER  
 SA VOLTAGE AMPLIFIER

Technique for controlling logarithmic amplitude response /LAR/ and regulating logarithmic amplifiers under industrial conditions 01 p0035 A66-10219

Periodic electrostatic focusing scheme for ungridded multicavity klystron amplifier 01 p0044 A66-10932

Price determining factors considered in integrated circuit amplifier for AM receiver 02 p0203 A66-11925

Active RC synthesis using operational amplifier, noting analog computer simulation of transfer function 03 p0339 A66-12434

Equivalent circuits and characteristics of RC amplifier in which source of signal to be amplified, tunnel diode and load are connected in parallel 04 p0497 A66-13918

NEC maser amplifier for radio astronomical observation of Cygnus A, Taurus A and Orion and Omega nebulas 05 p0697 A66-15365

Transfer functions synthesis by passive RC networks with two or three computing amplifiers 06 p0861 A66-16360

Practical stability criterion for tunnel-diode circuit including bias and stabilizing circuits and requiring only plots of modulus of reflection coefficient vs frequency 06 p0858 A66-16986

Noise coefficient of amplifier using microwave modulation-demodulation principle derived by impedance-matrix method 06 p0859 A66-17185

Amplification factors and optimum matching conditions calculated for complex capacitive diode frequency converters 07 p1005 A66-17347

HF pulse rise in high-Q synchronous amplifier with one circuit per stage by approximation method 07 p1009 A66-18069

LF capacitive amplifier taking into account nonlinear-capacitance component which varies with twice heterodyne frequency, proposing equivalent circuits 08 p1193 A66-19108

HF pulse decay in input of slightly detuned multistage synchronous single-circuit amplifier 08 p1198 A66-19737

Harmonic suppression ratios in RF amplifiers calculated, using circuit parameters and applying Fourier transformations 10 p1508 A66-21299

Linear microwave amplification in n-type gallium arsenide bulk semiconductor at room temperature, noting negative conductance and peak gain 10 p1515 A66-22079

Microwave regenerative amplifier using reflex klystron, considering beam current, supply voltages, mismatch, input and output amplitudes, phase lead, etc 11 p1655 A66-22725

Selection of minimum noise temperature for HF amplifiers in SHF receivers 11 p1667 A66-22795

Information recovery from noisy measurements, employing steady quantity measurements, known waveform detection and transfer function evaluation 11 p1656 A66-22825

Circuit design techniques for linear integrated circuits, noting manufacturing methods, achievement of monolithic construction, etc 11 p1670 A66-23243

Noise characteristics, sources and bandwidths of active devices and circuits including transistors, masers, parametric amplifiers, etc, noting causes of noise 12 p1830 A66-23662

Secant correction and dynamic compensation for tracking pedestal servo loop in operational amplifier circuit 12 p1816 A66-24261

Direct-to-home TV broadcasting satellite system for upper UHF, describing

stabilization, thermal control, antenna, power amplifier, etc 12 p1955 A66-24776

[AIAA PAPER 66-309] DC behavior of negative-impedance circuit without internal bias 13 p2045 A66-25201

Noise factor of linear receiving systems in quantum and classical regions, noting role of dual push-pull amplifier and frequency converter 13 p2020 A66-25226

Vibration generator consisting of electrodynamic shake table, control amplifier, drive generator, auxiliary servo equipment and equalization console 13 p2058 A66-25496

Noise and amplification characteristics of millimeter-wave reflex klystron amplifiers 13 p2037 A66-25549

Electron precipitation onto electrodes of quadrupole amplifier and resultant impairment of output current and efficiency 13 p2043 A66-26468

Build-up oscillations in system of two identical parallel-plate capacitors flanking quadrupole capacitor in longitudinal magnetic field 13 p2044 A66-26469

Integrated circuit as exclusive-OR gate or as linear amplifier, using transistor or tunnel diode shunted by resistor 14 p2263 A66-27051

Book on solid state communications and design of equipment using semiconductors 14 p2260 A66-28367

Physical principles in plasma application for amplification and generation of electromagnetic oscillations 16 p2760 A66-30797

Book on nonlinear electron-wave interaction phenomena and application to amplifiers, oscillators and other crossed electric and magnetic field devices 16 p2653 A66-30873

Technique for controlling logarithmic amplitude response /LAR/ and regulating logarithmic amplifiers under industrial conditions 17 p2880 A66-31902

Communication satellite design noting use for educational and commercial purposes, instrumentation applied, etc 17 p2872 A66-31935

Nonlinear operational amplifier with high power switching devices, noting volt-ampere characteristics 18 p3086 A66-34494

Noise coefficient of amplifier using microwave modulation-demodulation principle derived by impedance-matrix method 19 p3314 A66-35543

Microwave power generation and amplification via transistors, noting optimum source and load impedance for microwave transistors under large signal conditions 19 p3319 A66-36166

Single-stage negative resistance reflection amplifier theory based on circuit models for frequency dependent band-limited circulators and broadband negative resistance device 20 p3524 A66-37115

Selection of minimum noise temperature for HF amplifiers in SHF receivers 20 p3525 A66-37132

Time domain characteristics application to pulse amplifier design, noting correlation with results obtained via frequency method 20 p3538 A66-37582

Input admittance, gain and noise performance in dipole antennas with Esaki diodes 20 p3531 A66-37731

Equivalent circuits and characteristics of RC amplifier in which source of signal to be amplified, tunnel diode and load are connected in parallel 20 p3532 A66-37876

Gas laser alignment, obtaining oscillation on three lines of He-Ne laser 22 p3930 A66-39718

Response of automatic gain control amplifier to two narrow-band input signals, examining weak signal suppression and cross-product generation 22 p3875 A66-40059

Slow wave circuit for traveling wave tubes operating in millimeter-wave band, examining attenuator for double-ladder traveling wave amplifier 22 p3877 A66-40187

Microwave regenerative amplifier using reflex klystron, considering beam current, supply voltages, mismatch, input and output amplitudes, phase lead, etc 23 p4045 A66-41463

Low level amplifier for IR receiver for Earth-space IR contrast

study 24 p4180 A66-42341

Multiple large signal theory for TWT amplifiers with restrictive assumptions 24 p4183 A66-42635

### AMPLIFIER DESIGN

Intermodulation effects and rule of thumb for spurious free dynamic range in wideband high sensitivity amplifiers 01 p0044 A66-10929

Parametric amplifier reconstruction by varying capacitance and modulation index while keeping pumping frequency constant 02 p0196 A66-11419

Transistorized LF amplifier design, determining transistor nonlinearity coefficients 02 p0199 A66-11755

Current gain and transconductance of silicon planar transistor for collector currents used in design of DC amplifiers 02 p0200 A66-11886

Thin film integrated wideband amplifier with details on circuit, construction, performance and outline of design process 02 p0202 A66-11916

Long range program on Ubitron TWT amplifier, noting beam synchronism and dispersion characteristics 03 p0338 A66-12433

Harmonic distortion measurements on amplifier stages using vacuum tubes and transistors with antidistortion circuit 03 p0340 A66-12472

Two-stage tuned amplifier design with digital computer 03 p0337 A66-12498

Characteristics of balanced transistor amplifiers with symmetrical directional couplers 03 p0342 A66-12708

Operational amplifier design using normal feedback equations with grounded output voltage for input, discussing frequency response and determination of open-loop gain magnitude 03 p0351 A66-13276

Linear integrated circuits discussing differential and operational amplifiers, development, use, capabilities, new techniques, special designs and reliability 03 p0347 A66-13346

High power wideband RF voltage and power amplifiers covering design, operating characteristics, differences, etc 04 p0494 A66-13683

Fluid state power amplifier discussing design, construction, operation, advantages and limitations 04 p0460 A66-13783

Gain, bandwidth and noise characteristics of UHF parametric amplifier 04 p0498 A66-14042

Automatic gain control circuits, discussing performance and comparing theoretical and experimental results 04 p0501 A66-14408

High performance operational amplifier design, discussing monolithic circuit construction and performance parameters 05 p0642 A66-14563

Microelectronic amplifiers, emphasizing reliability improvement and decreased sensitivity to parameter changes 05 p0643 A66-14564

Octave-broadband tunnel-diode amplifier design with added shunt capacitance and stabilizing circuit 05 p0643 A66-14571

Hyperfrequency parametric amplifier circuit with modulation-demodulation applicable to very rapid pulse transmission 05 p0633 A66-15102

Transistorized common-emitter amplifier design using AC-bypassed emitter resistor to eliminate degeneration effects 06 p0843 A66-16012

HF correction by series induction in transistorized wideband amplifier 06 p0849 A66-16371

Optimal regime for triode amplifier of microwave output 06 p0849 A66-16372

Characteristics of electrochemical cells in which concentration of ionic species in chamber can be varied via applied electrical signal as analog of junction transistor 06 p0852 A66-16632

Paraelectrics as prospective materials for UHF amplifiers with very low noise level 06 p0854 A66-16722

Field effect transistor circuits used to replace bipolar transistors or thermionic devices and action as variable ohmic resistor 06 p0856 A66-16862

Maximum gain condition of resonance amplifier for given passband, determining amplification coefficient 07 p1005 A66-17351



Stability and gain prediction of microwave tunnel diode reflection amplifier, using Smith chart 07 p1007 A66-17508

C-band weather radar AVQ-10 incorporating tunnel diode amplifier and p-i-n solid state protector switch 07 p1008 A66-17711

Proportional axisymmetric fluid-amplifying element, noting operation of three-terminal modulator and application to various amplifiers 07 p0992 A66-18027

Resonant amplifier stage calculations for realizing given passband width and amplification factor 08 p1193 A66-19107

Pulse amplifier with tunnel diode, achieving maximum gain for parallel-connected load and diode 08 p1194 A66-19284

Oscillator design procedure incorporating circuit and equivalent AC model and transfer functions of feedback and amplifier networks 08 p1197 A66-19560

High gain HF transistor amplifier design, considering deviations of device parameters and variations with temperature and bias 08 p1197 A66-19561

Linville technique speeds HF amplifier design, using Smith chart 09 p1351 A66-20165

Papers on fluidics, analyzing digital and fluid amplifier design 09 p1331 A66-20316

Operational pure-fluid amplifier with negative and positive gain designed by electronic principles 09 p1332 A66-20320

Fluid flow and design of fluidic amplifiers, considering flow as two-dimensional and using mathematical solutions 09 p1367 A66-20323

Superregenerative amplifier of backward wave including oscillation spectrum, resonance curve, noise coefficient, etc 09 p1357 A66-20777

One-, two-and three-circuit systems with periodically varying inductance, capacitance and resistance influencing energy transfer, noting application to amplifier design 09 p1363 A66-20782

Superconducting magnet for variable bandwidth traveling wave masers, noting amplifier bandwidth increase via gain reduction 10 p1542 A66-21417

Nonresonant solid state magnetic, semiconductor and dielectric devices, noting operation characteristics, control parameters, etc 10 p1509 A66-21418

Solid state amplifiers using streaming carriers analyzed, noting different role played by collisions when electron stream interacts with TM and TEM waves 10 p1584 A66-22072

Wideband low-level amplifier design and operation 11 p1662 A66-22404

Circuit of two-state pentode resonance amplifier with electronic passband control and slightly varying amplification coefficient 11 p1667 A66-22788

Transistorized power amplifier for CW operation, using switching transistor as key element 12 p1829 A66-23535

Approximate equations for dependence of electron-drift mode over cathode-triode /tetrode/ grid spacing on parameters of UHF triode power amplifier 12 p1830 A66-23733

Klystron and TWT, generating high powers at millimeter wavelengths, combined in single amplifier for radar systems 12 p1839 A66-24614

Monolithic silicon-transistorized integrated amplifier for use as stabilized gain block element in linear circuit 12 p1842 A66-24656

High performance active RC band pass filter design providing for independent adjustment of poles 12 p1843 A66-24675

Matrix methods for design of HF integrated circuit amplifier 12 p1844 A66-24729

Circuit design for high impedance amplifier for control systems, considering input and output impedance and amplifier gain 12 p1844 A66-24731

Integrated circuit selective amplifier for intermediate frequency application, using RC active networks 12 p1846 A66-24915

FET amplifier driving common-emitter bipolar-transistor second stage operated with channel not pinched off 13 p2029 A66-25206

Differential amplifiers using common-collector, isolated and lateral complementary transistor structures, including frequency

response, phase shift, etc 13 p2036 A66-25532

UHF transistor design and performance, noting power gain, stability, low noise figure and correlation between circuit invariants and transistor parameters 13 p2038 A66-25560

High data rate SHF communication receiver for demodulating analog or digital information, noting components 13 p2023 A66-25656

HF correction by series induction in transistorized wideband amplifier 13 p2042 A66-25959

Optimal regime for triode amplifier of microwave output 13 p2042 A66-25961

Band pass characteristics realized by four-layer distributed RC network without series resistance and amplifier scheme used as model for integrated circuits, noting frequency characteristics 13 p2051 A66-26069

Microwave L-band tunnel diode amplifier 14 p2254 A66-27733

Design, power gain and stability of transistorized linear active network HF amplifier 14 p2255 A66-27801

Input and output impedances and gain of hybrid-coil feedback amplifier 14 p2268 A66-28038

HF amplifier design, using two-port theory measurement of Si epitaxial mesa transistor y-parameters, discussing power gain, sensitivity and inherent stability 14 p2261 A66-28372

UHF amplifier design, linear active and coupling networks, loading, admittance-impedance characteristics, etc 14 p2261 A66-28373

Dual transistors for noise and drift reduction in differential direct-coupled amplifier design 14 p2262 A66-28376

Low noise linear amplifier design, noting noise voltage generator-noise current generator and direct noise figure methods 14 p2268 A66-28378

Communications circuit application, examining amplifier, oscillator, mixer converter and transmitter designs 14 p2269 A66-28385

Power conditioning and advanced propulsion system of ionic engine, noting high voltage inverter design and vaporizer heater circuit 14 p2375 A66-28416

Master-graph technique for predicting performance of amplifying and switching systems, using charts which present circuit response to basic step-function inputs 15 p2458 A66-28887

High power sources for millimeter wavelength oscillator and amplifier design 15 p2461 A66-29008

General broadband matching for passive and active 1-port load impedance and application to tunnel diode amplifier 15 p2464 A66-29321

Stability analysis of two types of single-stage amplifiers using Dynistor as active element 15 p2468 A66-29920

Network analysis and amplitude frequency response characteristic of operational amplifier for DC analog computer 16 p2659 A66-30517

Step response of saturating feedback amplifier with single time constant, noting design graph for amplifier gain 16 p2660 A66-30580

Transistorized wideband and pulse type amplifiers for nanosecond frequency range 16 p2664 A66-31357

Fabrication of linear integrated amplifier circuits 16 p2665 A66-31430

Gain-bandwidth product of Hall magnetic amplifier circuits design 16 p2666 A66-31573

X-band strip transmission line tunnel diode amplifier 16 p2667 A66-31648

Microelectronic encoder design problems, considering stability in high gain amplifiers, resistors, capacitors and voltage reference source and low resistance in multiplex switch 17 p2883 A66-32120

Very high input impedance buffer circuit using field effect transistors for voltage sensing in high impedance analog simulator 17 p2886 A66-32381

Solid state transmitter with triggered Si controlled rectifiers /SCRs/ for high power efficiency in LF and ULF bands 17 p2895 A66-33120

Optimum complementary feedback

amplifier design having high input and low output impedances, low noise and stable gain over wide frequency range 18 p3074 A66-33556

Amplifier helping backward diodes as mixers and detectors in microwave systems 18 p3088 A66-35019

Book on analysis and design of transistor circuits including transistor parameters, emitter diode equivalent circuits, FET, amplifiers, noise, etc 18 p3089 A66-35238

Tuning of power amplifiers without standard servoloop and electromechanical variable RF element, for application to transceiver 19 p3324 A66-35515

Gating circuit with MOS transistors for amplifier strobing in low-level signal transmission 19 p3315 A66-35559

Two-stage field effect transistor amplifier with high input resistance and modification of circuit enabling input resistance to be adjusted to infinity 19 p3315 A66-35560

Redundant S band power amplifier achieved through low-loss feedthrough characteristics of QKSL3000 amplitron tube 19 p3316 A66-35682

Parametric amplifier design curves to calculate gain-bandwidth product, noise temperature, pump frequency and idler loading for one-and two-port amplifiers 19 p3319 A66-36031

Black-box approach applied to design of 60-megacycle IF amplifier, considering application of AGC to circuit and design of phase modulator and balanced mixer 19 p3321 A66-36423

Amplifiers using properties of vortex flow confined within flattened cylindrical chamber, considering velocity distribution 19 p3281 A66-36634

Applicability of microelectronic technique to construction of integrated wideband amplifier consisting of symmetrical differential circuit and common-emitter circuit 19 p3323 A66-36818

Circuit of two-state pentode resonance amplifier with electronic passband control and slightly varying amplification coefficient 20 p3525 A66-37128

Quantum paramagnetic traveling wave amplifier using rutile with admixture of chromium and combined with magnet with superconducting coil 20 p3580 A66-37996

Reactance modulation amplifier with semiconductor-diode capacitance analyzed by oscillation theory 21 p3711 A66-38911

Bandpass amplifier design by selecting peak frequencies occurring in active high- and low-pass RC filter sections 21 p3711 A66-39200

Amplifying elements ensuring required dynamic properties of resolving amplifier without calculating entire amplifier circuitry 21 p3712 A66-39252

Superregenerative amplifier of backward wave including oscillation spectrum, resonance curve, noise coefficient, etc 22 p3873 A66-39836

One-, two-and three-circuit systems with periodically varying inductance, capacitance and resistance influencing energy transfer, noting application to amplifier design 22 p3884 A66-39841

Approximate equations for dependence of electron-drift mode over cathode-triode /tetrode/ grid spacing on parameters of UHF triode power amplifier 22 p3875 A66-40076

Scattering parameters for design of HF transistor circuits 22 p3877 A66-40334

HF amplifier design - WESCON, Los Angeles, August 1966 22 p3881 A66-40745

Method of characterization for germanium microwave transistors and circuit design principles for low noise performance 22 p3881 A66-40746

**AMPLITUDE**

**S PULSE AMPLITUDE**

**S SCATTERING AMPLITUDE**

**AMPLITUDE DISTRIBUTION ANALYZER**

Amplitude distribution of pulsed signal envelope at output of narrow band system 02 p0192 A66-12145

Transistorized amplitude discriminator design, operation and test results 05 p0678 A66-15119

Distribution function of zeros in harmonic signals relation to frequency characteristic



of latter undergoing maximum amplitude limitation 07 p1001 A66-17348

Amplitude distributions of radio noise at ELF and VLF related to amplitude distribution of lightning discharges 08 p1184 A66-19403

Amplitude distribution density

measurements of stochastic processes with intensity spectra ranging from 30 cps to 20 kc, using multichannel pulse-height analyzers 12 p1856 A66-24940

Amplitude distribution of pulsed signal envelope at output of narrow band system 14 p2241 A66-28101

Angle of arrival in amplitude-comparison monopulse antenna arrangement including thermal noise as interference and pulsed radar with ideal radar target 23 p4044 A66-41314

**AMPLITUDE MODULATION**

Parametric amplifier reconstruction by varying capacitance and modulation index while keeping pumping frequency constant 02 p0196 A66-11413

Price determining factors considered in integrated circuit amplifier for AM receiver 02 p0203 A66-11925

Psychophysical method measuring effects of several variables on loudness fluctuation of binaural beats when amplitude modulated 05 p0628 A66-15733

Communications and control systems that require faithful transmission of amplitude-modulated signals through linear filters 06 p0823 A66-15964

Yttrium iron garnet filters, noting envelope limiting characteristics for submegacycle range modulating frequencies and response parameters 06 p0845 A66-16089

Helium-neon gas lasers, discussing amplitude variation suppression technique 06 p0892 A66-16670

Shielding effect on modulating microwave ferrite switch in applied magnetic field and relation between inside and outside fields for thin waveguide 06 p0857 A66-16952

Bridge phase modulator with RLC circuit, noting parasitic amplitude modulation elimination 06 p0858 A66-16991

Linear demodulation of AM

electromagnetic wave propagating through dispersive medium 06 p0836 A66-17033

Oscillations in two-circuit parametric oscillator operating on fixed-bias p-n junction 06 p0860 A66-17194

Pulse-amplitude modulator using p-n junction diode for transforming weak input signals by amplifying 07 p1005 A66-17399

Amplitude modulated carrier frequency signal circuit analyzed, showing open loop linear pulse system 07 p1014 A66-17439

Cross modulation in varactor-tuned limiters 08 p1191 A66-18944

AM and FM of transferred electron microwave generators, noting voltage dependence 10 p1515 A66-22094

Semiconductor diode mixer relatively free of modulation distortion and cross modulation 11 p1669 A66-23066

Signal to noise ratio in amplitude-, angle-, and pulse-modulated systems with carrier power exceeding receiver power 12 p1820 A66-24727

Variable premodulation gain to multichannel transmission system for which AM baseband power is proportional to cumulative channel activity, showing improvement of SNR 13 p2020 A66-25151

Optoelectronic amplitude modulator using gallium arsenide diode as carrier source and lead sulfide photoconductor as modulation element 13 p2030 A66-25207

Atmospheric turbulence effects on laser beam propagation, noting beam cross section, phase variation, AM and FM, etc 14 p2235 A66-27035

Models of hybrid AM-PM signal modulated by single sinusoid and having one-sided frequency spectrum described by using MacLaurin series expansions, noting phase relation of sidebands to carrier 14 p2235 A66-27061

Correctors for variations in group propagation time of AM wave transmitted by radio carrier wave, noting circuit analysis for matched and unmatched all-pass IF

filters 14 p2252 A66-27353

Swept frequency antenna gain

measurements, evaluating mismatch losses at feedpoint and obtaining gain-frequency curves 14 p2256 A66-27911

Design and operation of ferrite rectangular waveguide modulator in 5 to 7 gc/s range 14 p2258 A66-27963

Fluorescence lifetime measuring technique employing pulsed or modulated RF discharges applied to emission of second positive and first negative systems of nitrogen 14 p2337 A66-27974

Line width and shifts in molecular spectra of gases, giving general formulas for pressure broadening, phase shift of rotation, amplitude modulation of radiation and rotationally inelastic collisions 16 p2750 A66-30118

Amplitude modulation by transistorized circuits with consideration of sideband slope, signal input resistance and inverse feedback 16 p2654 A66-31029

Energy amplitude detection based on relation between laws describing variation in total energy of oscillation system and variation of modulating function 17 p2888 A66-32706

Resonant frequency change of oscillatory circuit due to nonlinear capacitance of semiconductor diode used as amplitude detector 17 p2898 A66-33523

Simultaneous amplitude-phase modulation of periodic cosmic ray variations, examining properties of satellites produced by these variations for case of true waves 18 p3196 A66-34867

Effect of geomagnetic cavity field on cosmic ray threshold rigidity, using model of cavity field, finding cavity shape produces amplitude in diurnal variation of cosmic ray intensity 18 p3198 A66-34882

Oscillations in two-circuit parametric oscillation operating on fixed-bias p-n junction 19 p3315 A66-35552

Amplitude and phase fluctuations in two-circuit quartz-crystal oscillator with crystal positioned between grid and electron tube cathode 20 p3525 A66-37152

Low-distortion modulation of IR and submillimeter waves, using free-carrier absorption in pair of crossed reverse-biased junction diodes 20 p3528 A66-37452

Semiannual variation in geomagnetic disturbance amplitudes consisting of one-to-one correspondence between average daily amplitude index and solar declination 21 p3732 A66-38635

Amplitude modulation of radiation pulses of two-level paramagnetic maser as affected by inhomogeneous broadening and spinning of resonance line 22 p3929 A66-39652

Light absorption by optically pumped atoms undergoing magnetic resonance, noting modulation amplitudes and modulation frequency limitation for primary interaction 22 p3930 A66-39807

Equations derived for combined single sideband hybrid AM-PM signal 22 p3866 A66-40177

Plasma fluctuation effect on gas laser noise, noting relation between modulation amplitude of light output and frequency noise and oscillation spectrum 23 p4077 A66-41294

AC background in phase of output oscillation of multistage frequency multipliers attributed to presence of HF harmonics in automatic bias circuit 23 p4038 A66-41520

Bridge circuit measurement of phase at UHF and microwave frequencies, examining amplitude modulation and mixer types 24 p4171 A66-42101

AM/PM conversion factor of TWT as function of helix voltage when beam current is varied to keep gain constant 24 p4180 A66-42371

Subsidiary peaks in power spectra of Ci and Kp /magnetic indices/ attributed to amplitude modulation of 27-day components 24 p4201 A66-42607

Edser-Butler band amplitude dependence on modulating effect of interference grating 24 p4212 A66-42819

**AMPLITUDE PROBABILITY ANALYZER**

Amplitude analysis and statistical implications of random data analysis applied

to evaluation of random signals 18 p3135 A66-34498

**AN-22 AIRCRAFT**

**S ANTONOV AN-22 AIRCRAFT**

**ANALOG COMPUTER**

**SA DIGITAL COMPUTER**

**SA HYBRID COMPUTER**

Computer flight simulators at Langley discussing Boeing 707 jet, helicopter, air traffic control, orbital rendezvous and docking, lunar navigation and landing 01 p0055 A66-10957

Harmonic analysis on analog computer by method giving very high Q modeling filters 01 p0034 A66-11024

Simulation method for confirming computations of space vehicle motions continuing after firing around gravity center of vehicle 02 p0215 A66-11673

Parameter variation effect on performance of second order maximum effort /bang-bang/ controller, noting optimum system, stability analysis and analog computer study 02 p0207 A66-11790

Optimization of nonlinear control system with random input using analog computer, automatic optimizer and dimensional analysis 02 p0207 A66-11791

Large signal transient response simulation of p-n junction diode using RC analog network 02 p0200 A66-11882

Analog, digital and hybrid computerized systems for investigating problems in aeronautics and astronautics 02 p0193 A66-11894

Linear circuit for degenerate parametric amplification, using analog computer elements 03 p0332 A66-12425

Active RC synthesis using operational amplifier, noting analog computer simulation of transfer function 03 p0339 A66-12434

Emission factor of radiating inhomogeneous layer determined by Abel integral equation from intensity profile, using analog computer 03 p0398 A66-12524

Plasma diode analog, determining behavior of unsteady state series-parallel systems for thermionic reactor control 05 p0615 A66-15537

Fluid state analog-computation technology, and process control computation systems [ASME PAPER 65-WA/PID-11] 05 p0624 A66-15637

Switching surfaces in three-dimensional phase space obtained by analog computer, for optimizing nonlinear control systems 06 p0862 A66-16361

Navigation equipment for civil use based on miniature inertial platform, analog and digital computers, automatic chart display, etc 07 p1067 A66-17689

Two automatic astronomical navigation and tracking systems compared for accuracy and performance in civil aircraft 07 p1070 A66-17722

HF analog computers for representing algebraic and differential systems and solving problems due to loop instability and drift in DC amplifiers 07 p1003 A66-17818

Torsional vibration analog computer and determination of torsional oscillation frequencies in multimass in-line systems 07 p1144 A66-18164

Analog computers used in modeling of heat conduction and diffusion processes for Fourier differential equation 08 p1319 A66-19427

Gradient systems of differential equations for solution of linear and quadratic programming problems on analog computer 08 p1188 A66-19687

Improvement of transient response of third order servosystems by discrete control of system parameters, noting application of switching circuit 09 p1360 A66-19859

Digital application of fluid amplifiers, examining greater precision, accuracy and reliability of digital systems compared to speed of digital systems 09 p1349 A66-20324

Circuit techniques for performing analog pulse arithmetic, using logarithmic p-n junctions on amplitudes of random nuclear pulses 09 p1356 A66-20604

Analog computer techniques applied to find roots of complex functions, to generate complex functions by Cauchy integral theorem and to scan z plane 10 p1507 A66-21698



- Rail-type plasma gun analysis using analog computer for application to space vehicle propulsion 11 p1743 A66-22405
- Book on analog, digital and hybrid analog-digital computers for random process studies 11 p1659 A66-22864
- Electronic analog computer nonlinear function generation by using silicon carbide varistors 11 p1660 A66-23254
- Nonohmic-resistor analog function generator, using output voltage summation of nonlinear combination channels for input range 11 p1660 A66-23255
- Programming procedures for analog computer solution of problems consisting of more than 250 linear and nonlinear computing elements 11 p1660 A66-23324
- Multipurpose chips for reduction of analog computer integrated circuit cost 12 p1834 A66-24101
- Analog computer, programmed on digital computer, used in examination of lumped and distributed parameter models of cardiovascular system 12 p1809 A66-24230
- Real time system for measuring and analyzing meteorological data for computing launch angles for unguided rocket flights [AIAA PAPER 66-336] 12 p1953 A66-24481
- Analog computer analysis of current readout tunnel diode memory cell 12 p1846 A66-24856
- Parameter variations and stability problem in coarse-fine synchro servos leading to expressions for optimum threshold detector setting 13 p2000 A66-25840
- Synthesis problem solution for time domain sensitivity function, noting controller structure, parametric minimization and operative adjustment of parameters 13 p2051 A66-26071
- Analog computer solution of simplified turbulent viscous layer boundary value problem 13 p2064 A66-26370
- Nonlinear gyroscopic system equations solved by analog computer and verified through method of harmonic linearization 14 p2294 A66-27362
- Motion of material point in central force field, reducing problem to solution of boundary value problem based on Pontryagin maximum principle, using analog computers 14 p2245 A66-28286
- Statistical characteristics of number of pulse periods during unaffected operation of analog computer after malfunction 14 p2246 A66-28354
- Schiphol Airport /Amsterdam/ analog computer installation for air traffic control and flight path calculations, with results displayed on automatic flight progress boards 15 p2534 A66-29311
- L/D ratio for gliding recovery of first stage of launch vehicle, using stage separation conditions as parameters 16 p2807 A66-30348
- Functional time-delay device and integration into analog correlator for analysis of autocorrelation and cross-correlation functions of measured system response signals 16 p2676 A66-30445
- Network analysis and amplitude frequency response characteristic of operational amplifier for DC analog computer 16 p2659 A66-30517
- Discrete transfer functions simulated on analog computer by direct currents 16 p2656 A66-30584
- Simulation of controlled diffusion-type Markov processes applied to two stochastic equations related to problem of misadjustment on analog computer 16 p2656 A66-30763
- Method of approximating functions with aid of orthonormal systems and single channel optimization, using analog computer 16 p2656 A66-30764
- Airfoil shape construction by conformal mapping and development of analog computer program to plot two-dimensional potential flow about various airfoil sections 16 p2629 A66-31116
- Analog computer technique for solving nonlinear ODE system 16 p2658 A66-31263
- X-Y plotter for analog computers, analog to digital converters and digital computers 17 p2925 A66-32313
- Noise rejecting algorithms for ODE solutions with computer, using redundancy, placement of control and feedback techniques 17 p2877 A66-32569
- Analog computer and logic circuitry combination for variable frequency signal production, noting application to adaptive control systems 18 p3089 A66-33561
- Parameter variation effect on self-excited torsional oscillations and sustained frictional vibrations in mechanical systems, comparing results with analog computer predictions 18 p3256 A66-34558
- Gradient systems of differential equations for solution of linear and quadratic programming problems on analog computer 18 p3073 A66-34673
- Analog computer solution of high-order optimal control problem, noting application of Pontryagin maximum principle and extension to two-point boundary value problems 19 p3306 A66-35536
- Analog computer method for reconstruction of data distorted by physical system response noise 20 p3627 A66-36888
- Timing and framing synchronization of PCM communication systems using analog techniques, analyzing transient state and jitter 21 p3705 A66-39226
- Selective amplification of signal voltages in analog computers with integrated circuitry 21 p3716 A66-39623
- True height in-line computation of electron density profile from ionograms, using analog computer in real time 22 p3908 A66-39969
- Laplace transformation simulation by analog computer for real and complex values 22 p3870 A66-39996
- Digital filtering system comprising only few integrated circuits and using addershift register combination, compared with analog devices 23 p4067 A66-41168
- Analog computer analysis of input signals effect on time constant, vibration frequency and overshoot ratio of nonlinear control system 23 p4051 A66-41854
- Resistance network analog method determination of carrier density distribution and charge constant in p-n junction for two-dimensional axisymmetric case 23 p4115 A66-41858
- Versatile electric timer possessing six independent timing channels, useful in analog and hybrid computation 24 p4183 A66-42642
- Electromagnetic analog computer for solving Dirichlet and Neumann equations for half-space and associated geophysical problems 24 p4202 A66-42763
- ANALOG DATA**
- Dynamic data /waveforms/ analysis comparing analog with digital methods for speed, costs, flexibility, reliability, etc [SAE PAPER 650818] 01 p0033 A66-10480
- Limitations of communication system transmitting data from analog source obtained, using theorem in Shannon paper on information theory 06 p0828 A66-16115
- Analog message transmission by optimum angle modulation system and rate distortion function deriving mean square error 09 p1360 A66-19923
- Systematic error in processing series of analog data 11 p1707 A66-23058
- Probability distribution data analysis in real time, using delay-line time-compression storage as information source in analog and digital form 12 p1825 A66-23760
- Analog telemetering system, discussing design, transmitter principle, receiver elements, special features and test results 15 p2451 A66-29361
- Analog form data transmission via FM compared to digital form via phase shift keying, noting accuracy, power and bandwidth required, output signal to noise ratios, etc 18 p3067 A66-33902
- Continuous nonlinear recursive filtering based on Markov processes and state-variable concepts for application to optimum analog demodulation 22 p3868 A66-40717
- ANALOG SIMULATION**
- Analog simulation of operations on stochastic matrices using random transitions in automata aided by relay-contact circuits 03 p0350 A66-13037
- Relationship between three symbolic circuit representations of charge-capacitance effects in 4-terminal field effect transistors 04 p0500 A66-14099
- Analog computer simulation of silicon-controlled rectifier applied to cycloconverter 05 p0612 A66-14639
- Analog computer solution to nonlinear dynamic system model of oscillations associated with cavitating inducers and sequence of trend-and-effect of constituent influences [ASME PAPER 65-FE-14] 06 p0870 A66-16210
- Capacitive biasing transducer is electromechanical analog of parametric system 06 p0860 A66-17199
- Discontinuous system investigated, using oscillating circuit governed by second order differential equation 07 p1015 A66-17830
- Mathematical foundations of analog simulation proceeding from Laplace, diffusion and wave equations 08 p1187 A66-18861
- Potential analog synthesis of linear arrays and radiation pattern representation as function of single complex variable 09 p1356 A66-20605
- Laplace transform and analog computation applied to simulation of heat transfer between wall separated fluids, determining transfer functions and frequency responses 09 p1472 A66-20908
- Two-terminal current-controlled negative resistance devices examined, using equivalent circuit, noting stability criterion, frequency response, etc 10 p1513 A66-21860
- Analog simulation of nonlinearly rigid systems for hard and soft elasticity by electrodynamic analogy methods 11 p1779 A66-22236
- Analog simulation of peak smearing in spectrometers in terms of convolution transforms 13 p2084 A66-26751
- Supersonic transport operations, particularly analog computer facility at Langley Research Center and ATC simulator at National Aviation Facilities Experimental Center 15 p2443 A66-28744
- Analog computer simulation of gas turbine engines for control study, discussing steady state performance and transient response data, surge region, maximum acceleration, etc 15 p2570 A66-28852
- Electronic simulation for evaluation of control concepts and system behavior of regenerative gas turbines 15 p2571 A66-28853
- Gas turbine engine analog simulation for acceleration sensing fuel control studies, comparing results with actual engine performance 15 p2571 A66-28855
- Electronic analog magnetic shield simulator /Magsim/ for producing radiation-protective region around space vehicles 16 p2681 A66-30610
- Analog simulation and performance prediction techniques in reliable circuit design and analysis, emphasizing programming procedures using Monte Carlo and worst-case methods 17 p2877 A66-32302
- Very high input impedance buffer circuit using field effect transistors for voltage sensing in high impedance analog simulator 17 p2886 A66-32381
- Digitally computed tables of Chebyshev approximations of Laplace shift operator transfer function enabling analog simulation of time delay systems 18 p3090 A66-34069
- Analog simulation of operations on stochastic matrices using random transitions in automata aided by relay-contact circuits 18 p3073 A66-35000
- Capacitive biasing transducer is electromechanical analog of parametric system 19 p3356 A66-35557
- Difference analog construction for second-order elliptic differential equation in case of rectangular network 19 p3389 A66-35935
- Hover augmentation system /HAS/ design for analog computer helicopter simulation and flight control 21 p3696 A66-38901
- Analog computation of minimum fuel trajectories with soft landings in uniform gravitational field, using Pontryagin maximum principle to reduce two-point BVP with optimal controllers 23 p4133 A66-41618
- ANALOG-TO-DIGITAL CONVERTER**
- SA DIGITAL-TO-ANALOG CONVERTER**
- Analog-digital transformations in detection of microvariations in geomagnetic field 01 p0061 A66-10691
- Analog-to-digital conversion system for



automatic meteorological data collection and transmitting system 02 p0251 A66-11259  
 Digital IF amplifier for thin film radar receiver 02 p0202 A66-11917  
 Fast analog comparator for hybrid computation using wideband DC amplifier with regenerative feedback circuit providing digital output 03 p0337 A66-12573  
 Nonlinear analog-to-digital converter for more constant accuracy 03 p0338 A66-12988  
 Microminiature Loran-C Receiver/Indicator for analog-to-digital conversion, using integrated circuit 10 p1555 A66-22047  
 SCADS, programming system for simulation of combined analog-digital systems 11 p1659 A66-23109  
 Adaptive analog-to-digital converter using level sensing and current switching 11 p1660 A66-23180  
 Analog-digital transformations in detection of microvariations in geomagnetic field 14 p2286 A66-28035  
 Harmonic analysis of accuracy of reproduction in digital form of operators selecting period of time quantization, duration of analog-to-digital conversion, etc 16 p2669 A66-30758  
 X-Y plotter for analog computers, analog to digital converters and digital computers 17 p2925 A66-32313  
 PCM transmission system based on analog data conversion into binary signals, noting use of Shannon decoder for signal demodulation, circuit design and system properties 19 p3306 A66-36655  
 Digital testing techniques for analog systems, describing bomb computer set for Phantom F-4D aircraft 20 p3522 A66-37246  
 Unit for centralizing AC-carrier measurements onboard VTOL Hawker Siddeley P 1127 aircraft 21 p3741 A66-39475

**ANALYTIC FUNCTION**  
 S CHEMICAL ANALYSIS  
 S CREEP ANALYSIS  
 S CRITICAL PATH ANALYSIS  
 S DATA ANALYSIS  
 S DIFFERENTIAL THERMAL ANALYSIS /DTA/  
 S DIMENSIONAL ANALYSIS  
 S FACTOR ANALYSIS  
 S FLUTTER ANALYSIS  
 S FOURIER ANALYSIS  
 S FREQUENCY ANALYSIS  
 S FUNCTIONAL ANALYSIS  
 S HARMONIC ANALYSIS  
 S MATRIX ANALYSIS  
 S MICROANALYSIS  
 S NEPHANALYSIS  
 S NETWORK ANALYSIS  
 S NUMERICAL ANALYSIS  
 S PREFLIGHT ANALYSIS  
 S QUALITATIVE ANALYSIS  
 S QUANTITATIVE ANALYSIS  
 S REGRESSION ANALYSIS  
 S SEQUENTIAL ANALYSIS  
 S SIGNAL ANALYSIS  
 S SPECTRAL ANALYSIS  
 S STATISTICAL ANALYSIS  
 S STRESS ANALYSIS  
 S SYSTEMS ANALYSIS  
 S TENSOR ANALYSIS  
 S TRAJECTORY ANALYSIS  
 S VECTOR ANALYSIS  
 S WEIGHT ANALYSIS  
 S X-RAY ANALYSIS

**ANALYTIC FUNCTION**  
 SA COMPLEX VARIABLE  
 SA POWER SERIES  
 Representation of arbitrary functions in region of convergence through Dirichlet series expansion 01 p0096 A66-11185  
 Dirichlet series representation of arbitrary analytical functions in convex region of convergence with complex exponent 01 p0096 A66-11186  
 Theory of weight classes for differentiable functions of many variables, with application to boundary value problems for elliptic equations 02 p0250 A66-12099  
 Nonlinear differential-difference equations of form  $Ly$  equals  $f(y)$  solved by using  $f(y)$  as power series in 03 p0387 A66-12614  
 Extremum problem connected with simultaneous approximations of some functions analyzed by polynomials and derivatives 04 p0540 A66-14467

Extremum problems with asymmetrical supplementary conditions in certain classes of analytical functions 04 p0540 A66-14468  
 Resolution of two fundamental problems of elastostatic plane into complex variables under conditions of analytical limits 05 p0775 A66-15096  
 Representation of analytical periodic Fourier transforms of difference operators by sum of squares 05 p0708 A66-15328  
 Boundaries of convexity of star-shaped functions, order alpha, in open circular region  $/0, 1/$  07 p1059 A66-18098  
 Continuation of certain classes of differentiable functions beyond limits of region 07 p1060 A66-18465  
 Boundary value problems of plane theory of ideally plastic bodies, with analytical solutions 08 p1306 A66-18703  
 Three-dimensional problem of isotropic continuous nonaxisymmetrical body of revolution, applying analytic functions of complex variable 08 p1307 A66-18885  
 Position of singularities of analytic continuation of potential /geophysical/ fields 09 p1373 A66-20480  
 Equations for variation of orbital elements in two-body problem with variable mass solved analytically for various laws of mass loss, noting periodic function of eccentric anomaly 10 p1605 A66-21205  
 Analog computer techniques applied to find roots of complex functions, to generate complex functions by Cauchy integral theorem and to scan  $z$  10 p1507 A66-21693  
 Cauchy problem for two-dimensional Laplace equation in infinite strip 11 p1722 A66-22646  
 Cauchy type integral on hypersphere, defining Cauchy principal values, noting role in theory of functions of complex variables 11 p1724 A66-23366  
 Boundary value problem solutions in meteorology 12 p1905 A66-23664  
 Analytical solution for surfaces with longitudinal curvature of larger magnitude than that considered in early forms of boundary layer theory, noting condition for self-similar solutions, main flow, boundary layer equations, etc 12 p1861 A66-23811  
 Representation of arbitrary functions in region of convergence through Dirichlet series expansion 12 p1903 A66-24018  
 Dirichlet series representation of arbitrary analytical functions in convex region of convergence with complex exponent 12 p1903 A66-24019  
 Strong plane shock produced in Al by hypervelocity impact and late stage equivalence examined, using analytical and graphical solution of method of characteristics and realistic state equation 13 p2194 A66-25061  
 Analytic hyperfunction solution of elliptic equation 13 p2117 A66-25473  
 Approximate analytical solutions for distributed parameter networks with parameters as functions of spatial variable, using differential equation that reduces boundary value problem to Sturm-Liouville system 13 p2120 A66-26068  
 Numerical-analytical method of obtaining periodic solutions to  $T$  systems 14 p2321 A66-27160  
 Exact order of best approximations of analytic functions expressible as generalized gap series in Faber polynomials 14 p2321 A66-27338  
 Determination for piecewise analytic  $F(t)$  of what vectors can be represented by bang-bang control having finite number of discontinuities 15 p2469 A66-28514  
 Parametrically analytic solution of infinite differential equation system 15 p2527 A66-29047  
 Classical analytical mechanics applied to mechanics of continua, noting relation between kinetic-stress functions and Ostrogradskii-Hamilton principle and stress tensor and finite deformation 15 p2539 A66-29148  
 Multidimensional hyperbolic equations of any order with discontinuous coefficients, noting conditions for analytic or continuous solution 16 p2734 A66-30782  
 Approximating values of analytic function in form of power series, when region of

interest is outside convergence domain of series, using numerical methods, noting detached shock problem 16 p2735 A66-30944  
 Representation of analytical periodic Fourier transform of difference operators by sum of squares 16 p2735 A66-30966  
 Normality of analytic functions with multiple values, deriving criteria for meromorphic function 16 p2737 A66-31218  
 Polynomials orthogonal with respect to contours, examining analytic function representation via Fourier series expansion of such polynomials 16 p2738 A66-31409  
 Approximate analytical solution for pitching and rolling motion near resonance of sounding rocket, using nonlinear differential equation [AIAA PAPER 66-463] 16 p2811 A66-31470  
 Rational approximation and differential properties at boundary of analytic functions 16 p2739 A66-31796  
 Analytic continuation of power series with aid of lower triangular matrices 16 p2740 A66-31797  
 Continuous functions with given differential properties on perfect measure set and application to Fourier series 16 p2740 A66-31799  
 Maximum error curves for Lanczos selected point method of polynomial solution to ordinary differential equations, using Chebyshev and Legendre functions 17 p2947 A66-32858  
 Analytic solutions for predicting motion of high-thrust rockets applied in guidance and real-time targeting [AIAA PAPER 66-452] 18 p3226 A66-33648  
 Perturbation theories for equations of celestial mechanics, obtaining analytical solutions in terms of Chebyshev polynomial series [AIAA PAPER 66-534] 18 p3226 A66-33664  
 Orthogonal sets of rational functions on unit circle 18 p3128 A66-34700  
 Reduction of plane thermoelastic problem of anisotropic body to determination of three analytical functions of complex variables, solving temperature stress distribution in anisotropic plate 18 p3258 A66-34702  
 Dynamic systems described by nonlinear differential equations containing analytical functions for random initial conditions 18 p3091 A66-34984  
 Position of singularities of analytic continuation of potential /geophysical/ fields 19 p3345 A66-35498  
 Boundary value problem solutions in meteorology 19 p3394 A66-36194  
 Optimal scanning problem variant with simple analytical solution, determining cessation moment 20 p3537 A66-37110  
 Mean value theorem for curves arising in solution of ordinary differential equation by series method 20 p3590 A66-37525  
 Eigenfunction expansion of analytic linear ordinary differential operators of boundary value problem with normalized irregular disintegrating boundary conditions 20 p3592 A66-38432  
 Eigenvalue problem for Laplace operator for two-dimensional region with boundary composed of piecewise-analytical simple closed curves solved by finite difference method 22 p3938 A66-39901  
 Multidimensional hyperbolic equations of any order with discontinuous coefficients, noting conditions for analytic or continuous solution 22 p3939 A66-40444  
 Mixed boundary value problem of the theory of analytic single-value function 23 p4086 A66-41873  
 Analytical method based on Taylor series to substitute linear control system for nonlinear control system 24 p4188 A66-42482

**ANALYTIC GEOMETRY**  
 SA ANNULUS  
 SA CONE  
 SA CYLINDER  
 SA ELLIPSE  
 Passive spaceborne trajectory tracking system design, using tetrahedral tracking geometry 08 p1184 A66-19509

**ANALYTICAL CHEMISTRY**  
 S QUALITATIVE ANALYSIS  
 S QUANTITATIVE ANALYSIS



**ANALYZER**  
**S AMPLITUDE DISTRIBUTION ANALYZER**  
**S AMPLITUDE PROBABILITY ANALYZER**  
**S DIFFERENTIAL ANALYZER**  
**S GAS ANALYZER**  
**S INDICATOR**  
**S SIGNAL ANALYZER**  
**ANATOMY**  
**S BRAIN**  
**S INTESTINE**  
**S LIVER**  
**ANCHORED INTERPLANETARY MONITORING PLATFORM /AIMP/**  
**S EXPLORER XXXIII SATELLITE**  
**ANECHOIC CHAMBER**  
**SA ECHO**  
 Anechoic chamber design for higher measurement accuracies for radar cross section and antenna parameters 10 p1501 A66-21623  
 Anechoic chamber facility for surface field measurement in scattering studies using probes 10 p1520 A66-21638  
 Absorbing materials used in construction of anechoic chambers for electromagnetic waves 20 p3543 A66-37724  
**ANELASTICITY**  
**S INTERNAL FRICTION**  
**ANEMOMETER**  
**SA HOT-WIRE ANEMOMETER**  
**SA SONIC ANEMOMETER**  
 Measurements of pulsation spectra of vertical component of wind velocity, using acoustic anemometer mounted on aircraft 06 p0906 A66-18552  
 Tower and triple theodolite pilot balloon measurements of time and space variability 11 p1730 A66-23380  
 Drag force anemometer utilizing semiconductor strain gauges for measuring horizontal wind speed and direction [AIAA PAPER 66-337] 12 p1882 A66-24482  
 Measurements of pulsation spectra of vertical component of wind velocity, using acoustic anemometer mounted on aircraft 14 p2327 A66-28224  
 Wind tunnel facilities of British Meteorological Office for checking performance and calibration of anemometers 17 p2903 A66-32794  
 Forced convection caused by normal and longitudinal components of flow around hot wire, noting effect of wire length 20 p3544 A66-36928  
 Atmospheric turbulence determined from velocity fluctuations in flight path direction measured by wing-tip mounted hot-wire anemometer 20 p3593 A66-37470  
 Temperature compensated thermoanemometer using bead shaped thermistor, for use in nonisothermal boundary layers 24 p4212 A66-42704  
 Thermoanemometric and high speed motion-picture photographic experimental analysis of air vortex ring structure 24 p4196 A66-42879  
 Low level atmospheric flow structure resolution, noting equipment and results on wind speed variations 24 p4235 A66-43077  
**ANESTHESIOLOGY**  
 Anatomical studies in dog anesthetized with pentobarbital and chlorpromazine and subjected to repeated prolonged positive G 03 p0327 A66-12362  
**ANGLE**  
**S APSIDAL ANGLE**  
**S ELEVATION ANGLE**  
**S PHASE ANGLE**  
**ANGLE OF ATTACK**  
**SA ZERO ANGLE OF ATTACK**  
 Plane transonic gas flow past symmetrical convex profile at zero angle of attack along axis of channel with parallel walls 02 p0176 A66-12171  
 Lift force of airfoil section determined for sudden change in angle of attack, analyzing Prandtl vortex positions 03 p0314 A66-12526  
 Relation between angle of attack envelopes and correlation parameter for spinning bodies entering atmosphere at large inclinations 03 p0432 A66-12811  
 Hypersonic airflow at alpha angle of attack about flat wing with shock wave on upstream side attached 94 p0454 A66-13572  
 Flow properties in turbulent near wake of circular and elliptic cones at zero angle of

attack in Mach 6 flow [AIAA PAPER 66-54] 07 p0980 A66-17897  
 Angle of attack, leading edge sweep and thicknesses effects on hypersonic flow field of slender delta wing 08 p1184 A66-19135  
 Impact tube pressure probe response to free molecular rarefied gas flow for arbitrary angle of attack 11 p1692 A66-22939  
 Numerical solution of problem of supersonic flow at angle of attack past arbitrarily smooth conical bodies 12 p1798 A66-24441  
 Aerodynamic characteristics of rectangular plates in hypersonic flow of rarefied gas differing in aspect ratio, thickness and angles of attack, determining maximum lift-drag ratio 12 p1798 A66-24442  
 Ideal gas flow past infinite circular cone at angle of attack, noting finite-difference method for self-similar solution of Prandtl boundary layer equation 14 p2222 A66-28283  
 Direct numerical method for calculation of supersonic inviscid flow about axisymmetric blunt body at large angle of attack [AIAA PAPER 65-24] 15 p2423 A66-29269  
 Pressure effect on cone caused by spike protruding at angles of attack may provide aerodynamic directional control at supersonic speed 16 p2629 A66-31117  
 Experimental prediction theoretical prediction comparisons of pressure distributions, force and stability coefficients for spherically blunt cone at various angles of attack 17 p2839 A66-32473  
 Navy angle of attack system as aid in transition from propeller airplanes to turbojets, emphasizing application to commercial aircraft 17 p2843 A66-32684  
 Oscillatory motion of angle of attack for space vehicles entering Earth atmosphere at hypersonic speeds from satellite orbits 17 p3016 A66-32893  
 Head wave of frictionless flow of real gas past positioned circular cone for small or zero angles of attack 17 p2842 A66-33169  
 Partial differential equations for three-dimensional inviscid flow solved for flow field over blunt body shapes at various angles of attack, for application to Apollo spacecraft [AIAA PAPER 66-413] 18 p3045 A66-33638  
 Nose bluntness and angle of attack effects on hypersonic flow, noting shock wave deflection decrease of minimum possible shock angle, varying specific heat ratio, convective heating, boundary layer transition, etc [AIAA PAPER 66-414] 18 p3046 A66-33639  
 Tangent cone method extended to determine pressure coefficients of yawed circular cones and ogives at angle of attack 18 p3048 A66-33820  
 Structure of flow past bodies with radial cross section in wind tunnel at various Mach numbers and angles of attack, noting position of shock waves 19 p3276 A66-36473  
 Separation of laminar boundary layer of gas flow from cone as function of angle of attack, Mach number, etc 19 p3277 A66-36478  
 Low speed handling with special reference to super stall, emphasizing rate of change of angle of attack and flight trials of BAC 111 and VC10 aircraft 19 p3280 A66-36748  
 Theoretical nonlinear method for calculating aerodynamic forces on low-aspect-ratio wings at high angles of attack and wide range of Mach numbers 20 p3491 A66-36907  
 Instrument for continuous variation of angle of incidence between ion beam and axis of RF quadrupole mass spectrometer from zero to 90 degrees 20 p3561 A66-38174  
 Irreversible trimmed stalls at high angles of attack for aircraft with aft-mounted engine nacelles and high-or T-tails 20 p3496 A66-38255  
 Mass transfer from cone in supersonic flow in tests performed at zero angle of attack, preserving Mangler transformation which transforms flat plate solution to cone 22 p3843 A66-40036  
 Supersonic flow past pointed bodies of revolution at small angles of attack 24 p4157 A66-42611  
**ANGULAR ACCELERATION**  
 Hypoxic hypoxia and hyperventilation effect on nystagmus induced by angular acceleration 03 p0326 A66-13356

Two-axis pedestal tracking limitations in station vicinity such as angular acceleration, velocity and reacquisition capability [ASME PAPER 65-WA/MD-17] 05 p0635 A66-15522  
 Instantaneous center of vector accelerations of free solid body 11 p1736 A66-22848  
 Cardiovascular stress resulting from radial acceleration gradient impeding venous return analyzed by rotation of seated subject about Z axis /Rz/ 12 p1807 A66-25016  
 Interplanetary trajectory adaptive gyrocompass system, discussing orbital angular velocity, angular acceleration, error sensitivity coefficients, error sources, etc 13 p2124 A66-25256  
 Abrupt angular acceleration effect on man, noting physiological responses such as blood pressure, EKG, EEG, cardiovascular, respiratory and nervous reactions, etc 15 p2434 A66-29447  
 Vestibular neuronal response to rotating linear acceleration vectors, noting generation of compensatory ocular nystagmus 17 p2858 A66-32177  
 Manually imposed angular accelerations during weightlessness period of parabolic flight, obtaining electrooculographic recordings for analyzing nystagmic response 19 p3286 A66-36382  
 Elimination of rate gyro angular acceleration error and scale factor sensitivity to wheel speed by integration of output signal 21 p3767 A66-38895  
**ANGULAR CORRELATION**  
 Optical heterodyne system, discussing angular alignment reduction by signal beam focusing to Airy pattern 05 p0695 A66-14912  
 Angular correlation of photons measured for positrons annihilating in normal and superconducting lead without observing any effect on Fermi surface 07 p1109 A66-18440  
 Positron annihilation of single oriented crystals of vanadium silicide, measuring angular correlation between gamma rays for calculation of Fermi surface 09 p1419 A66-20046  
 Gemini noncoherent pulse radar system using interferometer methods for angle information, noting failures of diode capacitor combination and methods of reliability improvement 13 p2035 A66-25508  
 Bolivian Air Shower Joint Experiment /BASJE/ fast-timing methods compared with arrival directions measured in cloud chamber pictures 18 p3210 A66-35123  
 Subshell photoelectron emission in germanium at angle of 90 degrees to converting X radiation determined for two radiation sources using photographic techniques and track counting method 20 p3621 A66-38096  
**ANGULAR DISTRIBUTION**  
 Extension of measurements in Van Allen belt concerning particle equator crossing at given pitch angle between magnetic mirrors, suggesting repulsing force from equator 01 p0132 A66-10495  
 Angular and spectral distribution of outgoing radiation in cloudy atmosphere in spectral range beyond absorption band 01 p0133 A66-10757  
 Angular distribution of diffusely reflected light flux as function of scattering indicatrix, survival probability of light quantum and conditions of medium illumination 04 p0541 A66-13415  
 Rocket measurements of energetic particles discussing electron fluxes, energy spectra, angular distribution and data 05 p0745 A66-14777  
 Rocket measurement of energetic particles discussing proton flux, energy spectra, pitch angular distribution and data 05 p0746 A66-14778  
 Off-specular peaks in directional distribution of reflected thermal radiation as function of angle of incidence, surface roughness and wavelength [ASME PAPER 65-WA/HT-19] 05 p0790 A66-15845  
 Angular distribution of annihilation gamma quanta in CdS single crystals of high and low resistivity 06 p0928 A66-16921  
 Vertical intensity and angular distributions of penetrating cosmic ray muons measured by scintillators, Geiger counters and neon



flash tubes, underground in India 06 p0877 A66-17039

Angular distribution of secondary particles from interactions in nuclear emulsions, determining energy release ratio in electron photon cascade 07 p1113 A66-17541

Energy spectrum shape and absolute abundance of nuclear active particles at low altitude determined, using ionization calorimeter, plotting angular distribution of particles 07 p1115 A66-17551

Angular moments of lateral-angular distribution functions in electromagnetic cascade theory calculated by method of moments 07 p1116 A66-17561

Cathode sputtering theory, explaining sputtering dependence on ion angle of incidence, with application in electromagnetic isotope separators, etc 08 p1257 A66-18695

Measurement of radiation pattern of ruby laser emission for various resonators and operating regimes, noting laser effect on angular half-width values 10 p1544 A66-22028

Angular distribution of stimulated Raman radiation, discussing axial and off-axial Stokes and surface radiation mechanism 13 p2090 A66-25189

Angular and spectral distribution of outgoing radiation in cloudy atmosphere in spectral range beyond absorption band 14 p2285 A66-27856

Distribution of arrival directions of muon-rich air showers, using equatorial and galactic coordinate systems 15 p2579 A66-29524

Structure of air showers, considering muon components and distribution of arrival directions of muon-rich EAS 15 p2580 A66-29530

Arrival directions of large EAS falling in 10 to 80 degree band of north declination, noting angle, azimuth and sidereal time 15 p2580 A66-29532

Cosmic ray intensities underground and energy spectrum of cosmic ray muons at sea level, tabulating depths, operation time, angular distribution, telescope aperture, etc 15 p2587 A66-29572

Angular distribution and energy loss of fast muons 15 p2547 A66-29594

Measurement of radiation pattern of ruby laser emission for various resonators and operating regimes, noting laser effect on angular half-width values 16 p2718 A66-30847

Off-specular peaks in directional distribution of reflected thermal radiation as function of angle of incidence, surface roughness and wavelength [ASME PAPER 65-WA/HT-19] 16 p2828 A66-30989

Angular discrimination improvement in radar beacon systems using null-type antenna superposed on normal directional beam 17 p2872 A66-31957

Electron angular distribution in copper and gold thin films attributed to individual close interaction scattering phenomena 17 p2987 A66-33314

Angular sizes of sources of Jovian radio bursts measured by using interferometers suggest they are produced by diffraction or focusing process in interplanetary space 18 p3237 A66-35083

Azimuthal angular distributions of secondary particles in cosmic jets, discussing shower particles from fireball model 18 p3215 A66-35163

Angular distribution of high-energy jets analyzed by kinematic approach, assuming constant transverse momentum of secondary pions 18 p3217 A66-35178

Angular distribution of secondary particles in multiple production at high energy, noting multiplicity and inelasticity dependence on primary energy 18 p3218 A66-35181

Data on energy and angular distribution of high energy muons, noting detector and structural bursts 18 p3220 A66-35193

Angular distribution and energy spectrum of cosmic particle showers at large zenith angles analyzed, using ionization calorimeter 18 p3220 A66-35196

Vertical intensity and angular distributions of penetrating cosmic ray muons measured underground by scintillators, Geiger counters, etc 18 p3221 A66-35205

Various light nuclei considered as possible solar neutrino detectors, deriving cross sections and angular distributions of electrons 18 p3223 A66-35216

Effect of binding on distribution in angle of charged particles having suffered scattering with lattice atoms 19 p3403 A66-36172

Orbit determination from only angular data spread over large time 19 p3463 A66-36242

Distorted wave calculation from rotational excitation of molecular hydrogen and molecular deuterium in thermal collisions with atomic hydrogen, presenting angular distributions, cross sections, etc 19 p3403 A66-36329

Secondary ions energy spectra dependent on incidence angle of primary ions for varying escape angles, using molybdenum targets 19 p3403 A66-36454

Book on human spatial orientation and effect on behavior 20 p3508 A66-37011

Mass spectrometer used for analysis of spatial distribution of molecular beams, with data on angular distribution of magnesium atom beam 20 p3559 A66-37522

Radiative heat transfer effect on propagation of plane pressure waves in inviscid nonheat-conducting gas applied in theory of angular intensity distribution of integral radiation 20 p3548 A66-38107

Pitch angle diffusion perturbing relativistic electrons in Van Allen zones and violating adiabatic invariants of electron motion, using Fokker-Planck equation 20 p3641 A66-38328

Omnidirectional characteristics of scattering of acoustic waves from statistically rough surfaces, measuring scattering cross section as function of incidence and observation angles 21 p3770 A66-38649

Charged particle and electromagnetic wave interaction with nonequilibrium plasma, noting conversion of transverse into longitudinal waves and angular distribution of scattered radiation 21 p3781 A66-39011

Langmuir electron oscillation behavior in inhomogeneous plasma in magnetic field when applied at angle to oscillation axis 21 p3781 A66-39012

Angular wind wave spectrum of deep ocean and variations in coastal zone, noting data on energy distribution of spectrum 21 p3760 A66-39362

Pitch-angle dependence of first-order Fermi acceleration of particles trapped between shock front and moving magnetic mirror 21 p3776 A66-39564

Angular distribution of Earth outgoing thermal radiation in IR region measured by geophysical rocket 22 p3913 A66-40470

Angular, spectral and geographical distributions of outgoing fluxes of thermal radiation and Earth albedo measured, using Cosmos satellite 22 p3913 A66-40471

Auroral zone electron source properties deduced from electron fluxes, spectrums and angular distributions measured by rocket flown into breakup phase of IBC I aurora 24 p4199 A66-42584

Auroral zone proton-electron anticorrelations, proton angular distributions and electric fields 24 p4199 A66-42585

Angular distribution of secondaries in elementary multiple high energy production event, evaluating expected frequency of asymmetrical showers 24 p4267 A66-42905

Angular and energy distributions of muons produced by interaction of atmospheric neutrinos with matter underground 24 p4270 A66-42933

**ANGULAR MOMENTUM**

Equations of motion for rigid body with fixed point derived by expression of angular velocity 07 p1080 A66-17845

Dynamic calculation for 2 sigma pi resonant system /meson-baryon/ in P 3/2 state, using Balaz type N/D method 08 p1259 A66-19077

Large-scale aspects of gaseous components of our Galaxy, noting dynamics of gaseous systems with magnetic fields, virial theory, angular momentum, spiral structure of galactic disk, etc 11 p1767 A66-22263

Temporal spectra of atmospheric angular momentum transfer from wind data at

various tropospheric and lower stratospheric levels 11 p1697 A66-22568

High energy cosmic ray jet showers noting energy, angular momentum, collision inelasticity, secondary meson distribution, etc 11 p1763 A66-22705

Solar system origins and planet evolution as subcondensations in differentially rotating medium, discussing orbit and spin angular momentum 12 p1946 A66-23653

Ginzburg-Pitaevskii two-fluid formulation of superfluidity problem describing behavior of helium 2 in rotating annular cylinder, considering constant angular velocity and angular momentum 13 p2128 A66-26272

Energy dependence of elastic resonance scattering of low energy electrons from He, Ne, Ar and nitrogen gases at angles ranging from 8 to 110 degrees 14 p2337 A66-27797

Variation in Earth-Moon distance as result of meteoritic impact 15 p2597 A66-29261

Energy from hydrogen molecule interaction with magnetic field and from hyperfine interaction expressed as products of irreducible spherical tensors 15 p2548 A66-29806

Line width and shifts in molecular spectra of gases, giving general formulas for pressure broadening, phase shift of rotation, amplitude modulation of radiation and rotationally inelastic collisions 16 p2750 A66-30118

Moderately long-range relativistic intermolecular forces, obtaining interaction energies 17 p2960 A66-32401

Relativistic precession measurement using satellite as precise orbiting gyroscope [AIAA PAPER 65-36] 17 p3001 A66-32450

Angular momentum distribution in planetary systems computed, based on mass of star and period of revolution of planet-like companion 18 p3236 A66-34891

Control moment gyroscope for angular momentum transfer with minimum power consumption, noting design and application for free body motion stabilization 19 p3360 A66-35962

Close binary systems involving transfer of angular momentum, considering circulatory patterns of gaseous flow and axial rotation of component stars 21 p3815 A66-39483

Theorem concerning use of instantaneous axis of rotation for simplification of small oscillation equation of angular momentum 22 p3992 A66-40300

Energy, linear and angular momentum conservation principles for elastic body with finite number of defects 23 p4091 A66-41855

**ANGULAR MOTION**

Damping effects on initial angular motion of spinning shell with overturning and yawing moment 09 p1466 A66-20260

Angular velocity effect on radial hydromagnetic oscillations of rotating plasma cylinder 10 p1566 A66-21732

Capacitive torsional vibration transducer for measuring angular displacement of vibrations in engine shaft 12 p1880 A66-23845

Alignment of angular positions of spherical mirror and grating of Fastie-Ebert spectrometer, using bright collimated monochromatic beam of He-Ne laser 13 p2084 A66-26564

Angular transducer using Hall effect, noting errors due to distortions in magnetic circuit and temperature effects 16 p2709 A66-31577

Angular measuring system for radio telescopes, noting application of Raksyn variable capacitor block as nonwearing rotating pinion 18 p3113 A66-34274

Fluid-damped rotary oscillators, discussing angular deflection effect, suspension torsion, electric modulator, mechanical boundary layer forces and static characteristics 19 p3360 A66-36306

Stabilization and control system of Tiros-wheel satellite, using current-carrying coil interaction with geomagnetic field 21 p3821 A66-38878

DME-A satellite attitude control, discussing performance of spin control system 21 p3821 A66-38879

Linear dynamic analysis of angular motion of spinning axisymmetrical rocket or spacecraft, emphasizing rigid body with thrust misalignment and another motion caused by deflection of control surfaces or



jets 22 p3988 A66-40618  
 Angular stabilization of flight vehicle by introduction of cubic terms of variable parameters into control 23 p4088 A66-40968  
 law 23 p4088 A66-40968  
 Angular variation of position of energy loss maxima in indium 23 p4110 A66-41180  
**ANGULAR VELOCITY**  
 Angular velocity and linear acceleration measurement by three accelerometers mounted on three mutually orthogonal rotating disks 03 p0369 A66-12667  
 Plotting Burmeister curves and points from given position, velocity and acceleration of first 3-orders of Ball point for constant angular velocity of mobile plane 03 p0324 A66-13297  
 Equations of motion for rigid body with fixed point derived by expression of angular velocity 07 p1080 A66-17845  
 Unaided visual detection of target satellite for rendezvous purposes, discussing intensity and angular velocity in star field 08 p1176 A66-18815  
 Motion of orthogonal trihedron, determining accurately angular position in translational motion relative to coordinate system 08 p1249 A66-18878  
 Pendulum motion in system of coordinates related to pendulum base, considering damping of absolute and relative angular velocity 08 p1223 A66-18892  
 Vehicle angular velocity determined, using configurations with only linear accelerometers and no gyroscopes for inertial navigation 08 p1224 A66-19488  
 Analogy between eigenvalues for fluid convection and flow stability extended to rotating cylinders with corresponding temperature distribution for given angular velocities 08 p1212 A66-19821  
 Measurement of magnetic field produced by rotating singly and multiply-connected superconductors, formulating macroscopic electrodynamics of rotating body at low angular velocities 09 p1418 A66-20041  
 Solid rotating mercury cylinder, reversibly obeying London equation when cooled through superconducting transition, at given angular velocity 09 p1419 A66-20042  
 Centrifugal-tangential sensor for angular velocity detection, noting dynamics and parameters 09 p1380 A66-20309  
 Perceiving undetectable rotation in semicircular canals by employing self-induced Coriolis stimulation, determining psychophysical functions for direction or rotation discrimination at different yaw velocities 09 p1337 A66-20531  
 Dynamics of pump rotor allowing for hydrodynamic forces arising in seals, determining region of unstable rotor motion and amplitude of oscillations 12 p1964 A66-24049  
 Forced oscillations of coaxial multidisk rotors, allowing for gyroscopic effect and rotating at different angular velocities determined by replacing differential equations with integral equations 12 p1964 A66-24050  
 Vortices disintegration in rotating helium 2 in presence of oscillating disk when container stops rotating, noting role of helium angular velocity 12 p1865 A66-24880  
 Stable resonant spins for planet in eccentric orbit, particularly Mercury rotation, analyzing motion equation for angular position of long axis relative to inertial line fixed in space 12 p1952 A66-24968  
 Stability of commensurate spin angular velocity for Venus, assuming solar tidal torque action and suggesting Venus rotation period is commensurate with synodic period 12 p1953 A66-24969  
 Tachometer measuring angular velocity from time of definite number of rotations, noting diagram of basic circuit 13 p2077 A66-25327  
 Ginzburg-Pitaevskii two-fluid formulation of superfluidity problem describing behavior of helium 2 in rotating annular cylinder, considering constant angular velocity and angular momentum 13 p2128 A66-26272  
 Sensing device of angular velocity vector with respect to inertial system, noting sensitive mass and parasitic terms arising

from nonlinearity 14 p2296 A66-27888  
 Spin angular velocity stability of gyroscope with incompressible fluid-filled cavity as function of three degrees of freedom 14 p2277 A66-28051  
 Stress distribution in thin circular annular disk, rotating with variable angular velocity, having transient shearing stress applied on outer edge 15 p2510 A66-29732  
 Flow in viscous incompressible conducting fluid subjected to magnetic field in concentric cylinders rotating at different angular velocities, assuming planar motion, using differential equations 16 p2757 A66-30214  
 Orbital rendezvous, stressing necessity of measuring absolute angular velocity of line of sight connecting two vehicles, noting details on gyroscopes, coupling, optimization, etc 16 p2743 A66-30314  
 Centrifuge performance, noting angular velocity constancy vibration levels in terms of acceleration, temperature effects, etc 16 p2679 A66-30476  
 Portion of human vestibular system response determined through eyeball counterroll measurement, noting experimental techniques and methods of computing results 16 p2639 A66-30807  
 Angular dependence of spin-lattice relaxation times in ruby evaluated, using second order perturbation wave function and field coupling representation 16 p2781 A66-31220  
 Ancient solar eclipses analyzed, determining secular decrease in angular velocity of Earth by computation based on ephemeris time and astronomical constants 17 p2999 A66-32067  
 Miele solidification principle for uniformly spinning rotor mounted on rigid body applied to case where modulus of angular velocity of rotor is allowed to vary 17 p2909 A66-32478  
 Absolute angular velocity determination and distance to center of attraction along vertical established by accelerometer measurements 17 p3003 A66-32588  
 Longitudinal acceleration and angular velocity of rotation effect on flexural vibration of elongated body of revolution in supersonic flow applied to critical flutter calculation 17 p3027 A66-32603  
 Separated unsteady flow about flat plate rotating impulsively from rest to uniform angular velocity about axis along leading edge, noting torsional oscillations [AIAA PAPER 66-427] 17 p2910 A66-32753  
 Ring laser sensor parameters and characteristics, noting application to measurement of angular rate, mass flow, navigation and guidance 19 p3356 A66-35533  
 Gravity on planets explored by reference system expressing gradient magnitudes, data on equipotential and application to system with continuous rotation in space 19 p3346 A66-35627  
 Ephemeral georotational variations from deviations in quartz oscillator clocks of Paris and Greenwich observatories 19 p3351 A66-36370  
 Motion of arbitrary gyro-stabilizer in central Newtonian force field, applying Liapunov stability conditions for regular precession 19 p3362 A66-36841  
 Semipassive two-gyroscope damper for countering high angular rates of Earth-pointing satellites 20 p3659 A66-36868  
 Velocity and angle dependence of rain erosion for various materials, using rotating arm apparatus with high circumferential speeds 20 p3588 A66-37810  
 Photoelectric photometer used for tracking entry of artificial satellites into shadow of Earth 20 p3518 A66-37839  
 Effect of random fluctuations of voltage and frequency of gyrorotor feed current on change in rotor angular velocity, noting gyro drift 21 p3738 A66-38970  
 Generator of plasma with supercritical rotational velocity in crossed electric and magnetic fields 21 p3789 A66-39063  
 Floating vibratory gyroscope having enhanced sensitivity to angular velocity 21 p3739 A66-39329  
 Human performance analysis based on two criteria, zero and 100 percent legibility of moving targets consisting of black

alphanumeric symbols, finding mean angular velocities 21 p3701 A66-39423  
 Vortices disintegration in rotating helium 2 in presence of oscillating disk when container stops rotating, noting role of helium angular velocity 23 p4053 A66-41087  
 Retrograde rotation of cloud formations of Venus with angular velocity corresponding to one rotation in four days analyzed by high resolution photography 23 p4128 A66-41181  
 Incompressible fluid motion inside cylinder rotating at constant angular velocity with generatrix forming curve 23 p4055 A66-41560  
 Angular velocity of solar corona determined as function of radial distance from Sun including effect of solar wind, magnetic field and viscosity 23 p4130 A66-41811  
**ANHYDRIDE**  
 Synthesis of alpha-amino acid l-menthyl esters under mild conditions, using alpha-amino acid N-carboxy anhydride /NCA/ and l-menthol 16 p2646 A66-31186  
**ANIMAL PERFORMANCE**  
 Cystamine hydrochloride, strychnine nitrate and hexobarbital injections effect on mice subjected to vibration, noting vibration effect on swimming 15 p2431 A66-28740  
 Physiological functioning of monkeys under restricted mobility noting appetite, orientation reflexes, bioelectrical activity of brain, etc 15 p2436 A66-29470  
**ANIMAL STUDY**  
 SA BIRD  
 SA CAT  
 SA CHICKEN  
 SA DOG  
 SA FISH  
 SA MAMMAL  
 SA MONKEY  
 SA MOUSE  
 SA ORGANISM  
 Hypoxia protection on taking of second graft of homologous bone marrow in previously irradiated and grafted mice 01 p0020 A66-10609  
 UV radiation effect on viscosity and optical density of DNA solutions from calf thymus and rat spleen 01 p0018 A66-11193  
 Survival of Earth organisms under environment simulated low pressure, low oxygen, low temperature and low extraterrestrial conditions 02 p0181 A66-11605  
 Alveolar nitrogen concentration and environmental pressure influence upon rate of gas absorption from nonventilated lung in dog 03 p0324 A66-12357  
 Anatomical studies in dog anesthetized with pentobarbital and chlorpromazine and subjected to repeated prolonged positive G 03 p0327 A66-12362  
 Animal temperature sensing for studying effect of prolonged orbital flight on circadian rhythms of pocket mice 03 p0328 A66-12767  
 Heart and breathing rate and electroencephalo-graphic responses of rats during weightlessness 04 p0467 A66-14083  
 Monitoring human performance during manned orbital flight for assessment of central nervous system function, noting animal studies during simulated stresses of space flight 04 p0468 A66-14088  
 Prolonged centrifugation effects on growth and organ development of weanling and mature rats 05 p0625 A66-15412  
 Conduction velocity of single units, verified components of spinocervical tract and over-all conduction velocity determined in dorsal column of cat 06 p0810 A66-15941  
 Animal exposure to low pressure-high oxygen environment noting pressure control, electronic watering device and constant environmental temperature 06 p0815 A66-15942  
 Protective effect of adrenaline, subgaleally injected, on survival time of rats subjected to acute hypoxia 06 p0811 A66-16064  
 Organic superconductor and dielectric IR waveguide, resonator and antenna models of insects sensory hairs, spines and pit pegs 06 p0847 A66-16103  
 Biological effects of chronic acceleration studied by using birds and animals in centrifuges with specially designed cages 06 p0819 A66-16605



Endocrine and metabolic response of restrained dogs to body vibration, nonanesthetized or anesthetized, showing increase in plasma and blood epinephrine 06 p0812 A66-16822

Infantile treadmill experience effect on body weight and resistance to exhaustion in rat 07 p0997 A66-17460

Rats exposed to space cabin atmosphere for two weeks, noting mortality rate, organism functioning, growth rate, etc 07 p0998 A66-17663

Zero-gravity effect on opossum fetus observed by TV system in proposed satellite 08 p1176 A66-18726

Cytoplasmic alterations and fat vacuole formation in pneumocytes of guinea pigs exposed to severe hypoxia in low pressure chamber 08 p1175 A66-18769

Experiments with anesthetized dogs subjected to *g* accelerations, observing behavior of arterial oxygen saturation and pulmonary ventilation during short periods 08 p1175 A66-19083

Experiments with rats under anesthesia subjected to acceleration, noting electroencephalograms 08 p1175 A66-19085

Ionizing radiation effects in mice protected with hypoxia or with chemicals 08 p1175 A66-19086

Acute inhalation toxicity of oxygen difluoride in albino rat 08 p1175 A66-19723

Inhalation toxicity at ambient and reduced pressures in monkeys, dogs and rodents upon exposure to ozone, nitrogen dioxide and carbon tetrachloride 08 p1176 A66-19724

Internal organ injury mechanism of cats subjected to severe vertical sinusoidal vibration and observed by high speed X-ray cinematography 09 p1335 A66-20525

Positive pressure breathing effect on vibration tolerance of mice 09 p1335 A66-20529

Acetate conversion to lipids and carbon dioxide by liver, kidney and inguinal adipose tissues of rats under centrifugation stress 09 p1336 A66-20634

Mice susceptibility to pentobarbital sodium, showing short term fluctuations in toxicity 09 p1338 A66-20964

Mathematical theory relating neuronal geometry to parameters of excitation in unconditioned response of planarians to electric shock 10 p1486 A66-21296

Alpha particle and X-radiation ionizing effects on cerebral astroglial cells and blood vessels of young rats 10 p1487 A66-22020

Subgravity tower and axis results obtained on man and animals, discussing transition from acceleration to weightlessness and vice versa 11 p1641 A66-22480

Vestibular function in conditions of subgravity 11 p1641 A66-22481

Low-gravity vibration stress effects on weight, growth, metabolism, white blood cells and endocrine system of albino Wistar rats 11 p1643 A66-22581

EEG and cortical and subcortical responses analysis of sensory stimulation in restricted dogs and normally reared littermates 11 p1644 A66-22950

Importance of neural site and experimental conditions in determining motivational direction /positive or negative/ produced by electrical stimulation of brain in animals 11 p1644 A66-22976

Miniature long-life telemetry system for implanting in animal to study deep body temperature 11 p1649 A66-23499

EEGs of monkeys stimulated cyclically by whole-body vibration, plotting coherence functions relating brain records to acceleration records 12 p1806 A66-24228

Responses of neuronal elements in visual cortex of unanesthetized cats shown to depend on time interval length 12 p1806 A66-24232

Chromosome injury in mouse bone marrow due to distant ionizing radiation 12 p1806 A66-24396

Continuous exposure of rats to 100 percent oxygen at 450 mm Hg for 64 days shows no physiological effects 12 p1807 A66-25013

Cosmic and UV radiation effects on breakdown of DNA and production of tumors in mice 13 p2008 A66-25642

Holtzman strain experiments on rats, determining if electrical stimulation of

various neural sites produce motivational consequences of appetitive or defensive behavior 13 p2009 A66-25790

Immunochemical studies on interspecies molecular hybrids of hemoglobin 13 p2010 A66-25898

Protein synthesis in liver of adrenalectomized and hypophysectomized rats exposed to centrifugation stress 13 p2010 A66-25899

Spatial interrelations between mitochondrial apparatus of capillary cells and synapses of these cells in utricular receptor of animals at rest and after exposure to accelerations, using electron microscopy 13 p2011 A66-26250

Effect of oxygen deficiency on acoustic organ of cats, determining content of potassium and sodium ions in perilymph, cerebrospinal fluid and blood serum 13 p2011 A66-26251

Changes in shock-evoked response complex /SERC/ recorded from visual cortexes of cats after retinal illumination, noting enhancement of waveform after photic stimulation and role of barbiturate anesthetization 13 p2012 A66-26581

Sodium excretion during extracellular volume expansion and associated changes in renal blood flow and intrarenal blood distribution during natriuresis accompanying saline loading in dogs 13 p2012 A66-26582

Effect of unilateral renal vasodilatation on sodium excretion by infusing acetylcholine into renal artery of dogs 14 p2227 A66-26793

Chronic hypoxia effects on thyroid function of rats, discussing radioiodine trapping and acinar cell length 14 p2227 A66-26811

Adrenocorticotrophin-releasing hormone appears in peripheral blood of rats under physiological stress, noting role of pituitary gland 14 p2228 A66-27811

Effects of alpha glycerophosphate and of palmitoyl-coenzyme A on lipid synthesis in yeast extracts 15 p2429 A66-28616

Ambient pressure effect on tolerance of mice to air blast 15 p2430 A66-28655

High oxygen at reduced pressure effect on metabolism of radioactive acetate in rats 15 p2430 A66-28658

Structural and functional properties of heart and muscle type subunits of lactic dehydrogenases investigated, using comparative amino acid analysis 15 p2446 A66-28864

Long duration flight physiological data on ducks and chickens in closed ecological systems, including oxygen and food requirements and carbon dioxide output 15 p2435 A66-29452

Prolonged optokinetic stimulation effect on rabbits studied by corneoretinal potential changes during eyeball motion 15 p2437 A66-29471

Centrifugal acceleration effect on sexual apparatus, cardiovascular system and respiratory organs of female monkey 15 p2437 A66-29472

Vibration effect on reception of certain organs and tissues of white mice to dye introduced intravenously 15 p2437 A66-29477

Effect of combined action of accelerations, vibration and radiation of nuclei of bone marrow cells in mice 15 p2437 A66-29478

Adaptation rearrangements in organisms of mice during and after exposure to high concentrations of carbon dioxide 15 p2438 A66-29479

Injurious effect of gamma radiation and 660 and 120 mev protons on white mice and protective action of certain pharmacochemics 15 p2438 A66-29480

Effect of shielding individual parts of rats on variations in reaction to radiation during exposure to gamma rays and high energy protons 15 p2438 A66-29481

Pathomorphological changes in hemopoietic organs of mice after irradiation with high energy protons 15 p2438 A66-29482

Preference of mice for oxygen-poor atmosphere after removal from 60 and 90 percent oxygen atmospheres 15 p2439 A66-29489

Increased partial oxygen pressure effect on morphological composition of peripheral blood of rats and mice 15 p2439 A66-29490

Hypoxia in cats and rats due to gradual

and abrupt drops in oxygen content of air 15 p2439 A66-29491

Effects on white mice of exposure to oxygen-enriched air, noting biological and physiological observations 15 p2439 A66-29493

Toxic and lethal effect on mice of ammonia in air, noting biological and physiological changes 15 p2439 A66-29494

Irritability, by injected apomorphine, of emetic center of dogs with functioning and removed labyrinths subjected to various motions 15 p2439 A66-29495

Semiconductor cooler creating hypothermia in small animals, operating on Peltier effect and employing quaternary metal alloy 15 p2444 A66-29497

Electrode implantation in dogs and detection of action currents in vegetative nerves after ten months 15 p2444 A66-29499

Blood flow rate in surface veins of brains of animals subjected to accelerations, noting thermal transducer 15 p2445 A66-29500

Hematocrit index and arterial-blood gas composition in white rats during artificial hypothermia 15 p2440 A66-29511

Simulation of solar flare radiation effects on white mice in spacecraft along circumlunar trajectory 15 p2445 A66-29512

Cardiovascular measurement on anesthetized dogs subjected to vibration, noting recording techniques, instrument sensitivity, etc [AIAA PAPER 66-442] 16 p2642 A66-30622

Low atmospheric pressure and oxygen-rich environment effect on characteristics of uninterrupted long-term exposure to toxic gases of space cabin atmospheres, noting animal testing 16 p2642 A66-30623

Short-term starvation effect on gastric mucosa of weanling vs post-weaned rats 16 p2638 A66-30636

Chronic exposure of rats to gaseous environments of varied composition and pressure, noting exposure capsules, gas flow system, respiratory gas analyzer, etc 16 p2643 A66-30650

Hamsters, mice and rats exposed to elevated oxygen tensions for 60-day periods with nitrogen at high or minimal levels 16 p2640 A66-31125

Blood pressure and heart rate during hypothalamic self-stimulation in dogs, discussing experimental methods and results, physiological response, etc 16 p2640 A66-31154

Receptive field organization of rat retinal ganglion cells, examining maintained impulse activity with stationary spots of light 16 p2640 A66-31184

Stress and dietary influence on direct oxidative pathway of carbohydrate metabolism in jejunal mucosa of rats 16 p2641 A66-31383

Chorioretinal lesion produced by pulsed ruby laser beam and complex changes in retinal excitability in cats 16 p2841 A66-31761

Dendritic arborization of retinal ganglion cells of rat stained in vivo with methylene blue, relating it to receptive field organization of these cells 17 p2849 A66-31995

Immobilization effect on monkeys noting influence on calcium, phosphorus and nitrogen metabolic balance 17 p2855 A66-32140

Nitrogen, phosphorus and calcium determination from perchloric acid digestion, process includes sample collection, preparation, digestion and determination 17 p2870 A66-32143

Correlation between survival time of rats under acceleration stress and cerebral level norepinephrine 17 p2855 A66-32145

Altered physiologic function of dogs produced by exposure to pulsed microwaves including study of combined effect of X-irradiation 17 p2856 A66-32156

Increase of arterial lactate and pyruvate in blood glucose of fasted anesthetized dog after hydrazine injection 17 p2856 A66-32157

Calorimetric study of effects of hydrazine on heat balance, source of metabolic energy and rate of protein catabolism of rats 17 p2856 A66-32158

Toxic effects of hydrazine derivatives tested in dogs, producing methemoglobin and pigmentation in blood 17 p2856 A66-32159



- Effect of 0.6 LD/50 intraperitoneal dose of hydrazine on coagulation mechanism in rats, comparing results with saline injected controls 17 p2857 A66-32167
- Lysosomal enzymes in rats exposed to 100 percent oxygen to determine possibility of accelerated in vivo lipid peroxidation 17 p2857 A66-32169
- Oxygen consumption of rabbits decreases in proportion to inert gas concentration dissolved in tissues 17 p2857 A66-32174
- Parasympathetic control of heart rate in monkeys under acceleration stress, noting ECG changes and effect of atropine sulfate on change of rate 17 p2857 A66-32176
- Vestibular neuronal response to rotating linear acceleration vectors, noting generation of compensatory ocular nystagmus 17 p2858 A66-32177
- Proliferative pulmonary lesions in monkeys under high oxygen concentration for various periods 17 p2858 A66-32181
- Gravitational environment, effect of change on frogs measured using gravitoceptors in vestibular apparatus 17 p2865 A66-32183
- Squirrel monkey physiological response to, and survival under short duration very high acceleration stress 17 p2858 A66-32187
- Hazards of macrofractionated gamma ray irradiation hazards upon Rhesus monkeys 17 p2858 A66-32189
- Myocardiograph study of dogs leading to development of flight-rated vibrophonocardiographic system for monitoring cardiac dynamics in flight environment 17 p2924 A66-32191
- ECG P wave changes due to body tilt in space of rabbits deprived of afferent impulses from pressure-receptive areas 17 p2859 A66-32230
- Medial forebrain bundle, lateral hypothalamic area and reinforcing brain stimulation, discussing self-stimulation 17 p2859 A66-32552
- Ribonucleoside triphosphatase in rabbit reticulocytes, discussing distribution in extracts, behavior in purification of amino acid and properties 17 p2859 A66-32553
- Corticosterone injection in rats, assaying amino acid incorporation into liver microsomal and cell-sap protein 17 p2860 A66-32554
- Age effect on liver glycogenesis in rats exposed to acceleration stress 17 p2860 A66-32555
- Pathomorphological changes in hemopoietic organs of mice under combined effects of proton radiation and vibration and gamma radiation and acceleration 17 p2861 A66-32937
- Vibration exposure of mice 4 and 24 hours prior to irradiation tends to lessen mortality and increase mean longevity 17 p2861 A66-32938
- Radiation-protective agents /anoxia, serotonin, amino thiols/ tend to increase sulfhydryl groups in mice spleen and Ehrlich ascite carcinoma cells 17 p2861 A66-32939
- Space medicine and biology studies of space flight environmental factors based on experiments with animals and manned spacecraft 18 p3056 A66-33699
- Capability of white mice to sustain extreme accelerations after exposure to ionizing radiation 18 p3058 A66-33844
- Neuronal circuitry relations of cat mammillary nuclei derived from neuron population ratio computed from population data 18 p3058 A66-34067
- Effect of head-to-foot accelerations of up to 10 g on rabbits, noting changes in ECG, EEG, brain histology, etc., leading to ischemic conditions 18 p3060 A66-34408
- Ascorbic acid concentration in urine and organs of guinea pigs exposed to high oxygen concentrations 18 p3060 A66-34410
- Effects of radiation protective pharmacological agents /cystamine, serotonin, AET, strychnine, etc/ on animals subjected to centrifugation, for application to astronauts 19 p3283 A66-35292
- Rapid decompression effects on dogs and subhuman primates, studying physical and physiological responses after loss of consciousness and recompression effects 19 p3285 A66-35839
- Effect of sudden intense noise and near vacuum decompression on cardiac rate of anesthetized and unanesthetized dogs 19 p3286 A66-36380
- Residual pathologic changes in central nervous system of dog following rapid decompression to 1 mm Hg 19 p3286 A66-36381
- Response characteristics of lateral geniculate cells of macaque monkey, discussing hue, saturation and brightness encoding in primate color visual system 20 p3504 A66-36946
- Neuronal circuitry and neuron populations of structures in normal animal brains and brains modified by unambiguous lesion arrays 20 p3505 A66-37053
- Myocardial glycogenolysis in rat ventricle and relation to severity of exercise 20 p3505 A66-37058
- Altitude effect on metabolic rates of deer mice, noting direct relationship between seasons and metabolic rate at all ambient temperatures 20 p3506 A66-37365
- Dissociation of rhinencephalic or thalamic self-stimulation and epileptiform activity in rats 20 p3506 A66-37602
- Combination of renal vasodilation and angiotensin infusion effect large changes in renal hemodynamics, excretion and reabsorption of sodium in anesthetized hypopenic dogs 20 p3507 A66-37607
- Partial restraining device for rats in operant conditioning studies 20 p3508 A66-38419
- Liquid breathing effects on dogs in hyperbaric chamber 21 p3699 A66-38447
- Inertial navigation in relation to animal navigation, considering three principal characteristics and biological analogs 21 p3760 A66-38450
- PAH transport mechanism in dogs with hydrazine-depressed para-aminohippurate treated with acetate, 6,8-epidithioacetate and 6,8-epidithioacetamide 22 p3854 A66-39795
- Bioelectric potentials in animals, investigating electrical materials, anatomical sites and means of increasing output and long-term implants 22 p3857 A66-39797
- Sound pressure in external auditory meatus and near center of cat head in absence of animal as function of frequency 22 p3854 A66-40166
- Hypoxia of simulated high altitude exposure prolongs synaptic delay and conduction time in brain system of rats 22 p3855 A66-40403
- Sleep deprivation in rats induced by injections of dextroamphetamine or forced treadmill activity resulted in temporary increase in daily sleep time 22 p3855 A66-40481
- Thromboelastographic investigation of short duration high-intensity chest-to-back impact deceleration in rats 22 p3856 A66-40502
- Respiratory activity and hematological factors of avian blood cells, discussing oxygen consumption, thermal effects, tissue and erythrocyte metabolism 23 p4024 A66-41043
- Physiological and mechanical effects of radial accelerations on brain temperature of dog and rabbit 23 p4026 A66-41336
- Twofold transversely applied 8-g centrifuging effect on functional state of otolithic part of vestibular apparatus of guinea pigs 23 p4026 A66-41337
- Repeated vertical/head-tail vibration effect on functional state of spinal reflex arc of guinea pigs 23 p4026 A66-41338
- Repeated vertical vibration and noise effects on conditioned reflexes of rats 23 p4026 A66-41339
- Vibration effect on bioelectric activity of brain and oxygen consumption, using experimental rats 23 p4027 A66-41340
- Vibration stimulus effect on oxygen metabolism of brain in rats with partial destruction of auditory and vestibular apparatus and in anesthetized control rats 23 p4027 A66-41341
- Vibration effect on conditioned reflexes, oxidation mechanism and electric activity of brain in rats 23 p4027 A66-41342
- Vibration effect on external respiration of rats, noting independence of oxidation metabolism from respiratory changes 23 p4027 A66-41343
- X-ray irradiation effect on venous blood flow in rabbit brain vessels 23 p4027 A66-41344
- Neutron, proton and gamma radiation effect on small animals examined, using conditioned response drinking method 23 p4027 A66-41345
- Gamma and fast neutron radiation effect on nervous activity of mice examined, using conditioned reflex drinking method 23 p4028 A66-41346
- Gamma radiation, fast neutron and proton effect on conditioned and motor responses, nervous activity, excitation and inhibitory processes of white rats 23 p4028 A66-41347
- Effect of total chronic and acute gamma radiation on higher nervous activity of white rats 23 p4028 A66-41348
- Conditioned motor food reflexes of rats exposed to vibration, vibrostand noise and X-ray 23 p4028 A66-41351
- Mortality and histopathology of germ-free rats and mice exposed to pure oxygen, noting effect of chronic respiratory condition 24 p4162 A66-42315
- Cardiopulmonary hemodynamics in dogs under transverse acceleration studied in terms of changes in heart and lungs 24 p4163 A66-42450
- Neuronal spike populations and EEG activity in chronic unrestrained cats, noting multiple unit responses of acceleration/inhibition during behavioral conditioning procedures 24 p4169 A66-43098
- Main stages of development of space biology and medicine in U.S.S.R., discussing biological effects in dogs in suborbital flight vehicles and satellites 24 p4169 A66-43135
- Electromagnetic and corpuscular radiation hazards to astronauts deduced from data on dogs 24 p4166 A66-43140
- Electric impedance measurements in hippocampus, amygdala and midbrain reticular formation during altering, orienting and discriminative responses in cat 24 p4166 A66-43167
- ANION**
- SA ANODE
- SA CATION
- Spectroscopic measurements using membrane-type shock tube for absolute determination of continuous absorption coefficients of negative hydrogen ions 04 p0553 A66-14279
- ANISOTROPIC FLUID**
- Hydromagnetic stability of interface formed by two superposed columns of dilute plasmas with anisotropic pressure 01 p0116 A66-11198
- Definition, equations, static and dynamic problems and normal and shear stress functions of subfluids 03 p0354 A66-12531
- Current distribution for cylindrical dipole of infinite length immersed in homogeneous lossless magnetotonic anisotropic ionosphere 06 p0827 A66-16033
- Stationary flow of viscous incompressible anisotropically conducting fluid in coaxial channel 11 p1743 A66-22235
- Current distribution and input impedance of infinite cylindrical antenna in anisotropic plasma, treating it as boundary value problem 11 p1661 A66-22396
- Steady flow of anisotropic conducting medium in half-space under influence of magnetic field 13 p2142 A66-25632
- Instability of unbounded anisotropic plasma containing beam 13 p2149 A66-26039
- Surface electron density in magnetoplasmas and microwave reflection from anisotropic plasma surface 13 p2149 A66-26241
- Compressivity tensors as parameters to characterize two-fluid compressible plasma in external magnetic field 13 p2149 A66-26273
- Input impedance of small loop of uniform electric current immersed in anisotropic cold magnetoplasma calculated by induced emf method 15 p2548 A66-28593
- H-plane bifurcation of parallel plate waveguide filled with anisotropic plasma 15 p2457 A66-28597
- Generalized model of ideal compressible anisotropic fluid, determining dependence of free energy on density gradient 16 p2689 A66-31517
- Optimum MHD generators using anisotropic plasma, discussing conducting-gas MHD flow, Hall effect, ion slip effect,



etc 18 p3152 A66-35075  
 Turnstile multiple-probe microwave  
 polarimeter for anisotropic plasma  
 diagnostics 20 p3609 A66-37630  
 Potentials for cylindrical warm plasmas,  
 noting anisotropic effects caused by  
 external magnetic field 20 p3611 A66-38362  
 Periodic flows of orientable anisotropic  
 fluids tending to be unoriented at rest  
 considered through linear equations which  
 predict resonance  
 phenomenon 21 p3727 A66-39173  
 Homogeneous rotating low density plasma  
 permeated by magnetic field with  
 anisotropic velocity distribution may exhibit  
 hose instability as well as gravitational  
 instability 21 p3794 A66-39562  
 Radiation in relativistically moving  
 anisotropic plasma medium, noting Lorentz  
 type transformation of plasma electron  
 volume density 23 p4105 A66-41638

**ANISOTROPIC MATERIAL**  
 Electromagnetic wave propagation through  
 multilayer isotropic and anisotropic  
 structure 01 p0025 A66-10525  
 Anisotropy of ytterbium iron garnet and  
 ytterbium-doped yttrium iron garnet crystals  
 measured by torque method in applied  
 magnetic fields 04 p0563 A66-13812  
 Anomalous behavior of radiation resistance  
 of antennas in anisotropic  
 media 04 p0500 A66-14101  
 Photocapacitative effect for determining  
 degree of anisotropy of zinc sulfide with  
 stacking faults 04 p0571 A66-14498  
 Theoretical anisotropic energy gap of  
 superconducting lead when photon density  
 of states is principal source of gap  
 anisotropy 05 p0741 A66-15866  
 Dyadic Green function for anisotropic and  
 compressible media based on reformulation  
 of governing equations for electromagnetic  
 phenomena in compressible anisotropic  
 plasma 06 p0832 A66-16455  
 Two-fluid anisotropic warm plasma,  
 characterizing macroscopic electromagnetic  
 properties via compressivity and  
 permittivity tensor and  
 permeability 06 p0920 A66-16975  
 Model of elastoplastic body undergoing  
 strain hardening, examining microstresses  
 via internal viscosity 07 p1143 A66-17629  
 Anisotropic transverse magnetoplasma  
 effects in cubic semiconductors, examining  
 reflectance and elliptic  
 polarization 07 p1102 A66-18204  
 Approximate method for examining stress-  
 strain state of anisotropic body with  
 elliptical holes via reduction to infinite  
 algebraic system 08 p1304 A66-18591  
 Generalized strength criterion for  
 anisotropic materials with different tensile,  
 compression and shear  
 strengths 08 p1307 A66-18881  
 Balanced anisotropic photoelectromagnetic  
 effect in germanium 09 p1413 A66-20003  
 Collective energy losses by plasmas in  
 crystals caused by excitation of volume or  
 surface plasmons 09 p1427 A66-20350  
 Radiation resistance of linear current strip  
 of finite width immersed in uniaxially  
 anisotropic plasma 09 p1408 A66-20370  
 Structural anisotropy coefficients of  
 crystallization in carbon-graphite materials  
 from X-ray and linear expansion  
 data 10 p1548 A66-21240  
 UHF ferrites as magnetically anisotropic  
 media in which electromagnetic wave  
 propagation rate assumes two values and  
 magnetic permeability is of tensor  
 nature 11 p1658 A66-23233  
 Torsional stress distributed on ends and  
 lateral face of anisotropic rod with variable  
 elastic moduli 12 p1969 A66-24353  
 Equation relating sound velocity in  
 polymer sample with angle between axes of  
 molecules and fibers of  
 sample 13 p2113 A66-25910  
 Cross section for inelastic scattering of  
 electromagnetic radiation by electron  
 density fluctuations in anisotropic solids,  
 using laser sources, investigating Landau  
 and collision damping of  
 plasmons 13 p2132 A66-26153  
 Compression of anisotropic fiber  
 monofilaments extended to measurements of  
 expansion of horizontal diametral plane and

contact widths for polyethylene  
 terephthalate and nylon, as function of  
 load 13 p2115 A66-26306  
 Stress-strain relations for laminar  
 anisotropic medium from known mechanical  
 properties of layers for application to fiber-  
 reinforced plastics 13 p2205 A66-26451  
 Ghost modes in open microwave resonator  
 waveguides containing dielectric slabs of  
 rectangular geometry with anisotropic  
 dielectric constant 14 p2246 A66-26796  
 Radiation due to time-harmonic source and  
 field solution of electric dipole in moving  
 uniaxial anisotropic medium by Minkowski  
 theory 14 p2234 A66-26861  
 Magnetoionic couplings and electromagnetic  
 wave propagation in horizontally stratified  
 layer of gyrotropic  
 medium 14 p2283 A66-27125  
 Cross correlation of satellite signals  
 through slab containing small anisotropic  
 irregularities 14 p2237 A66-27398  
 Theoretical and experimental investigations  
 of electromagnetic scattering by conducting  
 cylinder coated with anisotropic ferrite  
 sheath magnetized along  
 axis 15 p2449 A66-28594  
 Bending center of prismatic anisotropic rod  
 of arbitrarily asymmetrical cross  
 section 15 p2608 A66-28774  
 Steady state creep equations derived for  
 anisotropic material under multiaxial stress  
 states, based on perfect plasticity  
 analogies 16 p2820 A66-31275  
 Hot electrons in anisotropic semiconductor,  
 considering case of scattering by acoustic  
 phonons within one energy valley with  
 nondegenerate bottom 17 p2977 A66-32318  
 Specimen anisotropy during tensile  
 elongation to rupture of composite solid  
 propellants, based on analysis of dilatational  
 behavior 17 p2989 A66-32451  
 Hertzian contact of anisotropic bodies,  
 reducing problem to one of evaluating  
 contour integrals by Fourier transform  
 method 17 p3029 A66-32792  
 Admittance problem of cylindrical antenna  
 in homogeneous anisotropic medium  
 formulated and analyzed, using Fourier  
 transforms and Wiener-Hopf  
 technique 17 p2897 A66-33428  
 Structural anisotropy coefficients of  
 crystallization in carbon-graphite materials  
 from X-ray and linear expansion  
 data 19 p3388 A66-35863  
 Diffraction of electromagnetic plane by  
 half-plane in uniaxially anisotropic medium  
 solved in terms of Sommerfeld  
 approximation 19 p3304 A66-36284  
 Photoelastic Wertheim law in general  
 tensor coordinate system derived for  
 linearly anisotropic or isotropic  
 homogeneous matter 19 p3474 A66-36320  
 Properties of anisotropic continuous media  
 with energy and stresses depending on  
 deformation-tensor gradients and other  
 tensor magnitudes 19 p3476 A66-36833  
 Linear elastostatic BVPs for  
 inhomogeneous anisotropic elastic body  
 including existence-uniqueness theorem,  
 based on Korn inequality 21 p3755 A66-38463  
 Generalized reciprocity theorem for  
 antenna systems containing anisotropic  
 media and antenna systems radiating  
 directly through arbitrary  
 apertures 21 p3711 A66-38835  
 Three-dimensional linear-anisotropic  
 elasticity with inertia effects analyzed in  
 isotropic and anisotropic Cosserat continua,  
 deriving static and kinematic  
 components 23 p4141 A66-41945  
 Displacement matrix analysis of three-  
 dimensional anisotropic and inhomogeneous  
 elastically deformable bodies represented as  
 tetrahedral assemblies 23 p4146 A66-41989  
 Design synthesis relationship derived for  
 primary structural weight of membrane type  
 pressure vessels of anisotropic  
 materials 24 p4286 A66-42151  
 Anisotropy in mechanical properties of  
 lamellar solids due to abrasiveness,  
 examining wear and surface damage  
 produced by laminar solid on metal during  
 slipping and hardness 24 p4229 A66-42701  
 Electromagnetic wave transmission through  
 and reflection from homogeneous nonlinear  
 anisotropic slab between two linear isotropic  
 media 24 p4173 A66-42706

Electromagnetic propagation in slowly  
 rotating anisotropic dielectric single band  
 waveguide modulator 24 p4175 A66-42967

**ANISOTROPIC PLATE**  
 Critical loads for anisotropic plates on  
 various configurations and boundary  
 conditions, detailing stability of rectangular  
 plate and orientation of  
 axes 01 p0154 A66-10477  
 Large amplitude oscillation of anisotropic  
 triangular plates 04 p0591 A66-14202  
 Classical theory of bending of anisotropic  
 plates, using asymptotic integration method  
 and expressing stressed state as sum of  
 three stressed states 07 p1145 A66-18255  
 Stress-strain state of infinite plate with  
 two holes of different diameter solved  
 using integral equation derived for two-  
 dimensional problem in elasticity theory for  
 anisotropic medium 08 p1314 A66-19577  
 Elastoplastic behavior of anisotropic plate,  
 elastically uniform in depth, using  
 asymptotic integration for bending  
 problem 12 p1966 A66-24057  
 Elastic bending of anisotropic plates with  
 stresses represented by Legendre  
 polynomial series 12 p1968 A66-24344  
 Stability of rectangular transversely  
 isotropic plate hinged at three sides under  
 uniform pressure applied to two opposite  
 hinged sides 13 p2205 A66-26451  
 Stress distribution in anisotropic plate with  
 form of infinite wedge loaded at vertex by  
 concentrated force 17 p3018 A66-31833  
 Bending problem of anisotropic plate  
 solved by method of small  
 parameter 17 p3030 A66-32811  
 Reduction of plane thermoelastic problem  
 of anisotropic body to determination of  
 three analytical functions of complex  
 variables, solving temperature stress  
 distribution in anisotropic  
 plate 18 p3258 A66-34702  
 Stress and strain fields caused by straight  
 line dislocation located in anisotropic elastic  
 plate 20 p3671 A66-38111  
 Bending of nonorthotropic clamped plates  
 solved, using small parameter  
 method 21 p3826 A66-38611  
 Stability of circular transversely isotropic  
 plates under various attachment conditions  
 along contour based on Ambartsumian plate  
 theory 21 p3826 A66-38611  
 Bending problems of transversely isotropic  
 circular plates based on Ambartsumian  
 theory of anisotropic  
 plates 21 p3830 A66-38982  
 Stress distribution in elastically  
 nonhomogeneous rotating thin circular disk  
 of varying thickness of anisotropic  
 material 21 p3745 A66-39595  
 Nonlinear differential equations for  
 cylindrically anisotropic plates, noting error  
 of Wolmir method 22 p3988 A66-39651  
 Bending of anisotropic elliptical plate  
 weakened by elliptical hole solved by  
 infinite system of linear algebraic  
 equations 23 p4138 A66-41444  
 Vibrations of transversal-isotropic circular  
 plates solved, using refined theory  
 anisotropic plates 23 p4138 A66-41444  
 Linear viscoelastic bending analysis of  
 anisotropic plates 23 p4145 A66-41977

**ANISOTROPIC SHELL**  
 Uniqueness of mixed problem of  
 anisotropic body dynamic thermoelasticity  
 when radiative heat transfer is absent, using  
 thermodynamics and Onsager  
 relations 02 p0300 A66-12007  
 Matrix displacement analysis of anisotropic  
 shells, determining bending and membranal  
 stiffnesses of triangular element and effects  
 of initial strains 06 p0961 A66-16007  
 Asymptotic integration of elasticity theory  
 equations and analysis of stressed state of  
 anisotropic shell 15 p2609 A66-28997  
 Hooke law analysis of dynamic stability of  
 closed circular cylindrical anisotropic shell  
 compressed by longitudinal  
 force 15 p2609 A66-29147  
 Thermal stresses in anisotropic hollow  
 cylinder by arbitrary radial temperature  
 distribution 17 p3020 A66-31919  
 Stability of structurally anisotropic circular  
 cylindrical shell under nonuniform  
 compression 21 p3829 A66-38977

**ANISOTROPY**  
 SA CRYSTAL STRUCTURE



Anisotropy of scattering in tellurium, correlating cyclotron frequency data and alvanomagnetic measurements 05 p0738 A66-15353

Diffuse X-ray scattering in crystal structure of Ni-Be and Cu-Be alloys during first stage of aging due to anisotropic monoclinic lattice distortions 08 p1235 A66-18589

Perturbation solutions of stress and deformation problems for homogeneous anisotropic shells constructed from orthotropic material 08 p1309 A66-19004

Perpendicular anisotropy of Ni and Fe films and saturation magnetization under various pressures 08 p1270 A66-19011

Electron microscopic estimation of perpendicular anisotropy of magnetic thin film originating from nonmagnetic grain boundaries 08 p1270 A66-19012

Magnetocrystal anisotropy of hexagonal ferromagnetic substances in neighborhood of Curie point 08 p1273 A66-19249

Magnetic measurements and exchange interactions in thin anisotropic ferromagnetic films 09 p1410 A66-19905

Cosmic ray distribution intensity over celestial sphere determined, detecting anisotropy against background of isotropic variations, using spherical analysis 09 p1439 A66-20220

Electromagnetic-wave radiation peculiarities in homogeneous anisotropic dispersive magnetic plasma 09 p1343 A66-20342

Strain anisotropy matrix analysis 09 p1466 A66-20462

Anisotropy of scattering in tellurium, correlating cyclotron frequency data and alvanomagnetic measurements 09 p1431 A66-20894

Singlet and triplet pairs coexistence in anisotropic superconductor 10 p1583 A66-21971

Reverse magnetization and energy of anisotropy of single crystal ferromagnetic films 11 p1754 A66-22815

Coercive force of single crystal iron films with two-axial magnetic anisotropy 11 p1754 A66-22817

Induced anisotropy of ferromagnetic atom pairs and magnetostriction stresses in Fe-Ni thin films subject to annealing 11 p1755 A66-22818

Turbulent channel flow, discussing friction law anisotropy and homogeneity, vortex flow, channel viscosity, etc 12 p1860 A66-23532

Anisotropy of weak cosmic ray bursts studied by examining diurnal variations for rays with increased solar flare activity 12 p1942 A66-24178

Microwave Faraday effect in n-type germanium, discussing Faraday rotation, ellipticity, magnetoabsorption, complex conductivity tensor elements and measurement of microwave polarization anisotropy 14 p2349 A66-26826

High energy Alnico alloys, discussing crystal growth, anisotropy, recrystallization, etc 14 p2311 A66-26883

Uniaxial permalloy film anisotropy at cryogenic temperatures and magnetization characteristics 14 p2355 A66-26914

Fine-line absorption spectrum anisotropy with respect to crystallographic axis of cadmium sulfide 14 p2308 A66-27646

Anisotropy and annealing behavior in extrinsic single-crystal tellurium studied by measuring electric resistivity and Hall coefficient 15 p2562 A66-28725

Anisotropic vector functions of vector argument connected with crystal symmetry 15 p2526 A66-28951

Temperature dependence of line width and anisotropy field in Mn substituted MnO 15 p2565 A66-29028

Structure of air showers, considering muon components and distribution of arrival directions of muon-rich AS 15 p2580 A66-29530

Anisotropy of arrival directions of extensive air showers /EAS/ with one or more high energy nuclear active particles 15 p2580 A66-29531

Magnetic anisotropy of vacuum deposited permalloy films under applied magnetic field

and obliquely incident molecular beam 16 p2773 A66-30686

Anisotropy of electrical resistance of indium in magnetic field shown to be nearly absent, confirming absence of open Fermi surface 17 p2977 A66-32315

Apparent HF stability of highly anisotropic plasma, noting charge exchange and trapped proton energy spectrum 18 p3142 A66-33671

Anisotropy of secondary electron emission in ion bombarded Si single crystals, using electron microscope 19 p3445 A66-36340

Effects of nonmagnetic impurities upon anisotropy of superconducting energy gap 21 p3797 A66-38559

Singlet and triplet pairs coexistence in anisotropic superconductor 21 p3805 A66-39550

Induced uniaxial anisotropy energy of manganese-bearing ferrites, noting effect of metal additives 24 p4253 A66-42360

Anisotropy of cosmic rays in N-S direction determined by comparison of intensity variations observed in Arctic and Antarctic regions 24 p4263 A66-42464

## ANNEALING

Superconducting transition temperatures measured for various tin-gallium compositions in quenched and annealed states 02 p0271 A66-11482

Dependence of magnetic moment and thermal coefficient of permanent magnets on annealing temperature and length/diameter ratio 02 p0232 A66-12147

Molybdenum machine parts produced by plasma powdering process, noting improvement due to annealing 04 p0525 A66-13434

Audiofrequency hysteresis loops and initial permeabilities of single-crystal yttrium iron garnet cores with annealing and silicon substitution 04 p0562 A66-13750

Isochronal annealing from 80 to 360 degrees K of defects induced by 45-mev electrons in floating zone and pulled n-type silicon 05 p0742 A66-15873

Thorium dioxide strengthened nickel and nickel molybdenum alloys, discussing production via selective reduction, strength, creep rupture, stability and ductility characteristics 06 p0893 A66-15943

Radiation damage resistance and characteristics of aluminum- and boron-doped silicon solar cells, noting annealing 06 p0809 A66-16567

Gamma irradiated germanium at zero degrees C, studying annealing of recombination center, obtaining life times from transient decay of photoconductivity 06 p0934 A66-17126

Ripening of defects induced by fast neutrons in germanium in course of low temperature annealing 06 p0937 A66-17143

Ion damage and successive annealing of germanium observed by electron microscope 07 p1097 A66-17528

Zone melting effect on mechanical properties of niobium on isochronal annealing after cold swaging 07 p1052 A66-18351

Diffraction contrast analysis, using transmission electron microscope, of two-dimensional defects present in mechanically damaged silicon after annealing 07 p1109 A66-18516

Isothermal annealing effect on internal friction and Young modulus of cold-rolled aluminum with different purities 08 p1240 A66-19088

Annealing and diffusion processes effect on lifetime of minority carriers in p-silicon used in production of rectifiers 08 p1272 A66-19245

Molybdenum single crystal dislocation redistribution and subgrain boundaries formation during annealing at high temperatures 09 p1391 A66-20873

Tensile, static notch, stress rupture, creep and salt stress corrosion tests at appropriate temperatures, evaluating effect of solution annealing temperatures of Ti-8Al-1Mo-1V 12 p1892 A66-23625

Carbide formation from beta-titanium and graphite 12 p1895 A66-24377

Annealing of deformed sodium, noting activation energy distribution annealing kinetics, etc 12 p1897 A66-24923

Cosmic annealing of Chesterville meteorite 14 p2330 A66-27349

Anisotropy and annealing behavior in extrinsic single-crystal tellurium studied by measuring electric resistivity and Hall coefficient 15 p2562 A66-28725

Phase transformations in titanium alloys annealed at high temperatures and subjected to aging processes 15 p2522 A66-29181

Hardenability /ratio between phase transformation and cooling rates at given point of sample cross section/ in several titanium alloys after annealing 15 p2522 A66-29190

Effect of annealing and aging on structure, hardness, strength and plasticity of VT15 alloy welds 15 p2523 A66-29192

Effect of annealing in magnetic field on structural and magnetic properties of thin films prepared from nickel alloy 16 p2774 A66-30695

Effect of annealing on thin gold films sandwiched between two evaporated layers of zinc sulfide, presenting resistance curves 16 p2779 A66-31083

Arsenic overpressure, obtained by including metallic arsenic along with gallium arsenide, depresses defect concentration identifying primary defect species as arsenic monovacancies 16 p2779 A66-31086

Annealing of lightly deformed columbium single crystals with parallel twins or parallel and intersecting twins 16 p2726 A66-31461

Fluorescence bands produced by electron bombardment of ZnSe show threshold of annealing stages of radiation damage 17 p2985 A66-33154

Recrystallization of Ge and Si thin films and structural changes due to electron bombardment and thermal annealing 17 p2988 A66-33456

Temperature dependence of sputtering yields of germanium under low energy ion bombardment, observing atom ejection patterns above annealing temperatures 19 p3436 A66-35422

Welding and annealing procedures for fabrication of Nb alloy liquid metal loop and operation in boiling alkali metals 19 p3370 A66-36139

Chemical vapor deposited thermoprotective coatings for tungsten- and molybdenum-based refractory alloys, discussing diffusion barrier selection, interfacial microhardness, high temperature diffusion-annealing tests, etc 19 p3383 A66-36142

Molybdenum machine parts produced by plasma powdering process, noting improvement due to annealing 20 p3575 A66-38136

Radiative recombination in annealed electron irradiated zinc doped gallium arsenide 24 p4250 A66-42229

Superconductivity degradation in betungsten structure compounds, niobium selenide and niobium aluminide, noting tin loss and transition temperature for high temperature annealing 24 p4257 A66-42614

Birefringence recording device for measurements within very short wavelengths, describing photoelastic applications for identifying degrees of annealing and homogeneity of glass 24 p4292 A66-42965

## ANNUAL VARIATION

Atmospheric ozone variations, distributions, continents and planetary circulation according to IGY data 05 p0674 A66-15222

Annual variations of ionospheric absorption at medium and long wavelengths measured by A3 method at midlatitudes 08 p1220 A66-19779

Annual variation of auroral absorption attributed to frictional interaction between streaming plasma and geomagnetic field 10 p1530 A66-21161

Correlation between amplitudes and phase angles of first two harmonics of monthly mean Sq and solar activity for period 1905-1960 14 p2376 A66-27395

Speculative mean monthly Arctic stratospheric temperatures estimated from radiosonde and meteorological rocket wind and temperature data 16 p2696 A66-30928

Low and medium frequency absorption measurements at steep ionospheric incidence for demonstrating diurnal, annual and sunspot cycle changes in lower



ionosphere 19 p3351 A66-36360  
 Iterative method for extracting annular and Chandlerian terms of variation of Earth rotation from experimental data of universal time 20 p3550 A66-37410  
 Magnetosphere tail, annular magnetospheric configurative variation and seasonal variation in polar cap magnetic intensity 20 p3657 A66-38229  
 Annual variations of ionospheric absorption at medium and long wavelengths measured by A3 method at midlatitudes 21 p3732 A66-38775

**ANNULAR FLOW**  
 Behavior of unassisted annular cowed compressor intakes under cross-flow conditions [AIAA PAPER 65-707] 01 p0130 A66-10945  
 Heat transfer and shear between coaxial cylinders of different temperatures for large Knudsen numbers 03 p0445 A66-12959  
 Conductive heat transfer through gases contained between two concentric cylinders, comparing results with different methods [ASME PAPER 65-HT-4] 04 p0595 A66-13390  
 Laminar flow of viscous electrically conducting fluid through annular channel in presence of transverse magnetic field 04 p0551 A66-13824  
 Laminar and turbulent flow in eccentric annular ducts compared 04 p0511 A66-13938  
 Heat transfer by laminar forced convection for dissipative fluid in annulus calculated, using complex variable method 04 p0598 A66-14211  
 Film boiling of saturated nitrogen flowing upward in vertical heated tube, noting annular-flow regime change to vapor matrix [ASME PAPER 65-WA/HT-26] 05 p0793 A66-15677  
 Radial variation of circumferential-average flow properties inside turbomachine blade row [ASME PAPER 65-WA/GTP-1] 05 p0608 A66-15717  
 Slip and compressibility effect on velocity and pressure drop characteristics of rarefied gas flows in rectangular and annular ducts [ASME PAPER 65-FE-20] 06 p0871 A66-16218  
 Temperature distribution in homogeneous eccentric annular layer with constant internal heat generation 06 p0971 A66-16471  
 Vortex flow of incompressible viscous fluid bounded by two parallel finite flat plates [AIAA PAPER 66-88] 07 p1026 A66-18454  
 Annular flow and two-dimensional forced convective boiling heat transfer to hydrogen in nucleate and film boiling regimes 08 p1316 A66-18832  
 Similarity hypothesis applied to turbulent flow in annulus 09 p1366 A66-20177  
 Heat convection in vertical annular tube filled with mechanically incompressible viscous liquid 09 p1471 A66-20823  
 Unsteady motion of viscous incompressible liquid flow between two concentric cylinders 09 p1368 A66-20828  
 Radial variation of circumferential-average flow properties inside turbomachine blade row [ASME PAPER 65-WA/GTP-1] 10 p1480 A66-21501  
 Behavior of unassisted annular cowed compressor intakes under cross-flow conditions [AIAA PAPER 65-707] 10 p1594 A66-21890  
 Heat-transfer coefficient for annular dispersed flows in absence of vaporization, explaining high values obtained by flux profile effect 12 p1973 A66-23523  
 Elastico-viscosity, cross-viscosity and suction variation effects on rheological behavior of fluid moving steadily past porous circular cylinder and between two coaxial right circular cylinders 12 p1865 A66-24808  
 Temperature effect on motion stability of fluid between rotating cylinders 14 p2415 A66-28323  
 Vortex tube with double row nozzle, discussing energy separation efficiency, velocity profile, temperature characteristics, etc 16 p2685 A66-30801  
 Incompressible viscous conducting flow between two concentric cylinders in radial magnetic field 16 p2765 A66-31376  
 Flow field, pressure drop and friction factor characteristics of turbulent flow in

eccentric annular ducts 16 p2690 A66-31656  
 Resistance coefficient calculation procedure for turbulent flow in circular pipes extended to case of annular conduits 17 p2906 A66-32034  
 Viscous incompressible fluid motion between two parallel planes and between two co-axial circular cylinders with one boundary moved by impulse 17 p2916 A66-33418  
 High performance annular Hall-current accelerator using radial magnetic field and axial electric field with cesium as propellant [AIAA PAPER 65-300] 19 p3450 A66-35614  
 Pulsating laminar flow of viscous incompressible conducting fluid in annular channel between circular cylinders under radial magnetic field, solving MHD equations 19 p3432 A66-36643  
 Annular vortices method applied to determine aerodynamic characteristics of lifting propeller in axial and oblique flows 23 p4010 A66-41785  
 Sliding magnetic field effect on electric current in conducting annular channel flow, noting energy-transfer efficiency and acoustic resonance 23 p4107 A66-42030  
 Slow steady viscous flow through annulus between porous circular cylinders with uniform arbitrary injection and suction velocities, calculating wall porosity effect on velocity and pressure distributions 24 p4193 A66-42156

**ANNULAR JET**  
 Fluid digital amplifiers of axisymmetric focused jet design, based on focused-jet stalling effect known in ground effect vehicle aerodynamics 09 p1332 A66-20322  
 Ground effect takeoff and landing /GETOL/ aircraft, noting problems in controlling it and configurations of annular jet 16 p2635 A66-31396

**ANNULAR NOZZLE**  
 Unsteady laminar forced and free convection in coaxial sector tubes in presence of constant axial temperature gradient, accounting for oscillation and resonance 13 p2210 A66-26719  
 Feasibility of rocket motor using detonation wave rotating in annular combustion chamber wherein propellant is injected continuously and expelled through annular nozzle 18 p3162 A66-33807  
 Annular nozzle shapes established via method of straight line characteristics, noting flow patterns at various regions 23 p4009 A66-41731

**ANNULAR PLATE**  
 Approximate yield conditions for perfectly plastic annular plate under combined tension and bending, noting shallow shell problem 03 p0437 A66-12932  
 Classical theory of flexural motions of elastic plates used to determine natural frequencies of uniform annular plates for nine combinations of boundary conditions 10 p1616 A66-21490  
 Membrane creep and plastic deformation of annular flat plate bounded by concentric circles and subjected to evenly distributed pressure 12 p1958 A66-23710  
 Plate loaded over ring-shaped zone, determining bending moment, torque and shearing force 12 p1967 A66-24111  
 Linearized surface pressure distribution on streamlined ducted bodies in axisymmetric flow, considering aerodynamic loading on annular airfoil 13 p1993 A66-26716  
 Stress distribution in thin circular annular disk, rotating with variable angular velocity, having transient shearing stress applied on outer edge 15 p2510 A66-29732  
 Elastic large-deflections of annular membrane treated by modified Föppl-von Karman equation 17 p3024 A66-32359  
 Stress-strain state of annular plate made of incompressible nonlinear elastic material, noting power function describing relation between maximum tangential stress and displacement 17 p3026 A66-32596  
 Stability of annular plate with nonuniform stress field and nodal diameters arising with stability loss, obtaining solution for radial force intensity ratio 17 p3026 A66-32597  
 Elastoplastic bending of thin annular plates with free inner edge, based on Mises yield condition and Hencky stress-strain relation 20 p3671 A66-38102

Lateral buckling of annular plate compressed radially at inner or outer edge 20 p3674 A66-38229  
 Time-dependent stress distribution annular hereditary-elastic cylindrically anisotropic plate 22 p3989 A66-3989

**ANNULUS**  
 Elastic strip and elastic annulus differential-difference equations, using Fourier transforms and analytic continuation 11 p1780 A66-2247  
 Series in function of complex variable applied to mixed problem of equilibrium of annulus 15 p2607 A66-286  
 Plane contact problem for circular ring a elastic or absolutely rigid disk, using method of successive approximations 18 p3252 A66-337

**ANODE**  
 SA ANION  
 SA CATHODE  
 Progressive modification of anode surface of negative point-to-plane system used in corona discharge with microcrystals becoming seat of luminous phenomena 03 p0395 A66-129  
 Anode current in cut-off smooth-beam magnetron 14 p2248 A66-270  
 Additional measurements from electrostatic magnetic field interactions and power limitations in coaxial filament and anode geometry in electron bombardment heater thruster 17 p2990 A66-3247  
 Hydrogen ions detected near anode of glow discharge at various pressures, using mass spectrometer 19 p3410 A66-3647  
 Transient charge and discharge currents in tantalum oxide with anodic electrolyte at tantalum oxide with anodic metal 19 p3448 A66-367  
 Anodic oxidation process for sliced examining current flow in strong electric field as function of time, Curie-Schweidler law and Tafel law 19 p3448 A66-367  
 Electrolysis of wet hydrogen fluoride noting analysis of anode products by gas chromatography and water content measurement by IR spectroscopy 23 p4118 A66-412

**ANOMALY**  
 SA GEOMAGNETIC ANOMALY  
 SA MAGNETIC ANOMALY  
 Bjerrhammar gravimetric boundary value problem with gravity reduction defined integral equation 19 p3345 A66-353  
 Anomalous photocurrent generation transistors, noting carrier generation a transport processes 20 p3526 A66-373  
 Anomalous photovoltaic effect in semiconductor Ge, Si, CdTe and GaAs thin films due to photodiffusion and microtransitions 20 p3620 A66-377

**ANOXIA**  
 Effects of cold and abnormal atmosphere discussing tolerance limits to hypercapnia anoxia induced hypothermia and hypoxia 04 p0464 A66-140  
 Respiration and anoxia, noting anoxia, reduced oxygen carrying capacity blood and inadequate flow of oxygenated blood to tissues 10 p1488 A66-221  
 Increased blood circulation for compensating anoxia by changes in cardiac output, blood distribution and red blood cell volume 10 p1489 A66-221  
 Anoxia effect on central nervous system forms of personality, vision and consciousness impairment 10 p1489 A66-221  
 Anoxia induced changes in normal cellular metabolism as evidenced by oxidative reduction system, lactic acid and glucose content and nerve conduction 10 p1489 A66-221  
 Radiation-protective agents /anoxia, serotonin, amino thiols/ tend to increase sulfhydryl groups in mice spleen a Ehrlich ascites carcinoma cells 17 p2861 A66-328  
 Prolonged exposures to acute anoxia cause reductions in viability of hydrated r seeds, findings suggest helium may harmful as atmospheric component manned space capsules 22 p3855 A66-404

**ANTARCTICA**  
 Radiation measurements made at Antarctic station at Mirny including solar radiative total radiation and short and long wave



- reflection and radiation  
 alance 02 p0220 A66-11260  
 Comparison of diurnal variations of  
 onization level in F region at geographically  
 and geomagnetically conjugate stations in  
 Arctic and Antarctic 04 p0516 A66-13851  
 Airborne albedo measurements of ice in  
 loss Sea, Antarctica, for various solar  
 elevations and altitudes 05 p0669 A66-14937  
 Airborne albedo measurements of various  
 representative underlying surfaces in  
 Antarctica 05 p0669 A66-14938  
 Cosmic radiation measured by neutron  
 monitor in Antarctic during enhanced solar  
 activity in September 1963, determining  
 ares connected with particles producing  
 orbrush effects 07 p1118 A66-17642  
 Effects of AZA and PCA on radio wave  
 ropagation in Antarctic, noting reliability  
 nd radiation power  
 equirements 12 p1817 A66-24275  
 Rocket observation of atmospheric density  
 t high latitudes in Arctic and Antarctic  
 ocations  
 AIAA PAPER 66-345] 12 p1872 A66-24485  
 Flows and fractures as types of  
 eformation occurring on Earth under huge  
 ads of ice suggested by isostatic  
 ompensation of Antarctica, Arctic basin and  
 aciated region in North  
 merica 12 p1875 A66-24894  
 Satellite signals wave polarization by  
 onosphere above  
 Antarctic 18 p3106 A66-34366  
 Glassy spherules found in precipitate of  
 melted ice in Antarctica may be cosmic dust  
 articles /microtektites/ 19 p3465 A66-36389  
 Antarctic pack ice boundaries established  
 rom TV and IR pictures taken by Nimbus I  
 eteorological satellite 21 p3735 A66-39491  
 Double cloud vortex near Antarctica  
 etected by Nimbus I high resolution  
 R 22 p3942 A66-40053
- ANTENNA  
 A AIRCRAFT ANTENNA  
 A CASSEGRAIN ANTENNA  
 A DIPOLE ANTENNA  
 A DIRECTIONAL ANTENNA  
 A HELICAL ANTENNA  
 A HORN ANTENNA  
 A LENS ANTENNA  
 A LOG PERIODIC ANTENNA  
 A LOG SPIRAL ANTENNA  
 A LOOP ANTENNA  
 A MICROWAVE ANTENNA  
 A MONOPULSE ANTENNA  
 A MULTIPLE BEAM INTERVAL  
 A SCANNER /MUBIS/  
 A OMNIDIRECTIONAL ANTENNA  
 A RADAR ANTENNA  
 A RADIO ANTENNA  
 A SHUNT  
 A SLOT ANTENNA  
 A SPIRAL ANTENNA  
 A STEERABLE ANTENNA  
 A TRACKING ANTENNA  
 A TURNSTILE ANTENNA  
 A TWO-REFLECTOR ANTENNA  
 A WAVEGUIDE ANTENNA  
 A YAGI ANTENNA  
 Advanced satellite antennas and their  
 physico-electrical  
 characteristics 01 p0046 A66-11128  
 Multiple antenna based on corner reflector  
 sed in absorption measurements in  
 agnetically conjugate  
 egions 03 p0334 A66-12661  
 Circular waveguides for antenna lead-ins  
 nd suitability as line sections and  
 omponents of communication  
 ystems 03 p0345 A66-13237  
 Radiation resistance of antennas in  
 yroelectric media 04 p0492 A66-13424  
 Multipurpose feed system for 60-ft  
 araboloid antennas 04 p0493 A66-13616  
 Wind forces and moments on parabolic  
 ntennas supported above  
 round 04 p0495 A66-13803  
 Factors in evaluating antenna  
 esign 04 p0500 A66-14121  
 Coma-corrected, mono-and multifrequency  
 iffraction reflector antennas, examining  
 eed system, electronic scanner and  
 ibrations 05 p0648 A66-14911  
 Admittance of thin long linear antenna  
 mbedded in uniaxial medium and inclined  
 t angle theta to axis of  
 medium 06 p0848 A66-16279
- Electrically small antennas that distribute  
 tuning and matching components over entire  
 antenna volume to achieve lowest coupling  
 loss 06 p0850 A66-16428  
 Resonant endfire antennas formed by open  
 cavity with radiating elements coupled to  
 cavity field 06 p0853 A66-16657  
 Plasma sheath effects on antenna  
 impedance probe and retarding potential  
 probe installed on two Aerobee 150  
 rockets 08 p1181 A66-18746  
 Parabolic antenna design for millimeter  
 wavelength radio telescope  
 [AIAA PAPER 64-423] 08 p1202 A66-18814  
 Method of induced emf and integral  
 antenna equation 08 p1197 A66-19605  
 Kliatskin objections and improvements  
 concerning integral equation describing  
 current distribution in rectilinear  
 antenna 08 p1197 A66-19607  
 Antennas in ionized medium - Colloquium,  
 Paris, June 1965 09 p1339 A66-19841  
 Evaluation and comparison of methods of  
 calculating antenna impedance in ionized  
 medium 09 p1349 A66-19844  
 Radiative and capacitive terms of  
 impedance of finite cylindrical antenna  
 calculated in magnetoplasma with losses by  
 using Kogelnik theory 09 p1349 A66-19845  
 Antenna impedance behavior in plasma  
 related to radio astronomy, emphasizing  
 electrically small antennas used in space  
 vehicles 10 p1507 A66-21118  
 Diurnal changes in total ionospheric  
 electron content measured, using Randle  
 Cliff antenna 10 p1530 A66-21162  
 Millimeter wavelength brightness  
 temperatures of Mars, Jupiter and Saturn  
 calculated from antenna  
 temperatures 11 p1769 A66-22532  
 Phase variation dependence at receiver  
 output on polarization of wave incident on  
 antenna of phase measuring  
 system 12 p1817 A66-24277  
 Alteration of antenna spatial frequency  
 response due to time constant of radiometer  
 and scan velocity 12 p1837 A66-24311  
 Spacecraft communication link antenna  
 design, noting Earth coverage from  
 synchronous orbit, attitude stability, beam  
 width limits, construction, etc  
 [AIAA PAPER 66-306] 12 p1823 A66-24773  
 Implementation of electronically despun  
 satellite antenna system considering limits  
 of impracticability because of excessive  
 weight, control power, etc  
 [AIAA PAPER 66-325] 12 p1844 A66-24795  
 Antenna requirements for satellite  
 communications system ground stations,  
 discussing antenna and mount  
 designs 13 p2038 A66-25575  
 Radiation due to axially oriented electric  
 dipole situated on axis of infinite cylindrical  
 column of insulating free space surrounded  
 by uniaxially anisotropic  
 plasma 13 p2026 A66-26103  
 Prolate spheroidal antennas, discussing  
 spheroidal wave functions, confocal plasma  
 sheath effects and influence of DC magnetic  
 field 14 p2249 A66-27129  
 Analysis of antenna parameters for  
 determining equivalent radius of noncircular  
 antennas 14 p2253 A66-27531  
 Calibration of communication satellite  
 Earth station antenna system, using radio  
 stars 14 p2238 A66-27532  
 Fixed and mobile versions of antenna  
 portion of Iris telemetry and remote control  
 systems 14 p2253 A66-27547  
 Radiation efficiency of short whip antenna  
 with loading coil cooled to 77 degrees K and  
 4.2 degrees K at approximately 20 mc  
 frequency 14 p2257 A66-27925  
 Antenna cost, efficiency, noise, minimum  
 detectable signal and signal temperature  
 relationships 14 p2257 A66-27928  
 Permanent magnetized ferrite antenna  
 waveguide windows for improving EM wave  
 transmission through plasma and reducing  
 transmission losses during  
 reentry 14 p2241 A66-27930  
 Antenna and propagation - IEEE  
 International Symposium, Washington, D.C.,  
 August 1965 15 p2454 A66-28566  
 Beam scan at millimeter wavelengths  
 obtained from ferrite antenna  
 aperture 15 p2455 A66-28574  
 Antenna synthesis of prescribed
- configuration requiring minimum  
 current 16 p2666 A66-31555  
 Admittance problem of cylindrical antenna  
 in homogeneous anisotropic medium  
 formulated and analyzed, using Fourier  
 transforms and Wiener-Hopf  
 technique 17 p2897 A66-33428  
 Maximum and minimum power absorbed by  
 antenna connected through coaxial  
 transmission line to transmitter under  
 unmatched conditions 18 p3078 A66-34168  
 Design and construction of large steerable  
 antennas - IEE Conference, London, June  
 1966 18 p3079 A66-34262  
 Losses due to uniform rainwater layers on  
 antenna 18 p3095 A66-34290  
 Wind effects on antenna structures studied  
 to determine feasibility of operation without  
 radome in various weather  
 conditions 18 p3083 A66-34291  
 Bowl-distortion and dynamic measurements  
 of reflector profile of modified Goonhilly  
 no. 1 antenna 18 p3085 A66-34313  
 Reflector construction for radar and  
 communications antennas, discussing  
 materials, surface configuration and relative  
 costs 18 p3096 A66-34326  
 Kliatskin objections and improvements  
 concerning integral equation describing  
 current distribution in rectilinear  
 antenna 18 p3087 A66-34963  
 Book on principles of antenna design,  
 discussing fundamental laws of  
 electromagnetism, Maxwell equations and  
 practical forms 19 p3312 A66-35311  
 Book on antenna analysis and antenna  
 types 20 p3524 A66-37008  
 Japanese ground antennas for use with  
 communications satellites Teistar, Relay and  
 Syncom 20 p3530 A66-37718  
 Antenna types and designs for aircraft,  
 cars and trains 20 p3530 A66-37720  
 Boundary value problem of wave equation  
 with application to antenna theory of  
 singular integral  
 equations 20 p3531 A66-37730  
 Input resistance of short filamental  
 antenna in warm isotropic plasma from  
 kinetic /Vlasov equation/ rather than  
 hydrodynamic approach 22 p3874 A66-39939  
 FR-1 satellite components and antennas for  
 VLF signals 22 p3986 A66-40158  
 FR-1 satellite receiving antennas and  
 adaptation for measuring  
 circuits 22 p3876 A66-40161  
 Electron collection from VLF receiving  
 antennas and plasma-density probe on board  
 FR-1 satellite, using cathode-grid  
 device 22 p3876 A66-40162  
 Antenna in interplanetary plasma, noting  
 fluctuation noise in exosphere and radiation  
 impedance when exposed to solar  
 wind 22 p3877 A66-40466  
 Surface contour and structural  
 requirements of reflecting panels of  
 multiplate antenna, examining  
 manufacturing, installation and cost  
 advantages 23 p4138 A66-41259  
 Signal excitation in negatively charged  
 antenna rod in effect of unfocused laser  
 beam 24 p4224 A66-42753
- ANTENNA ARRAY  
 SA LINEAR ARRAY  
 Radiation from dielectric coated cylindrical  
 core loop antenna surrounded by lossy  
 plasma sheath 01 p0040 A66-10552  
 Reggia-Spencer phase shift for X-band  
 scanning antenna 01 p0042 A66-10581  
 Cross-polarized radiation beams of  
 rectangular waveguide antennas with slot  
 arrays, determining radiation pattern for  
 center-fed case 02 p0198 A66-11523  
 Eagle arrays obtained by substituting for  
 continuous or discrete phase inverters  
 simpler controlled and more stable ones,  
 noting radiation patterns 02 p0198 A66-11753  
 Approximation of band-limited function by  
 sum of cosines arising in design of phased  
 array antennas 03 p0342 A66-12709  
 Transformation technique enables any  
 aperture distribution of circular array to be  
 electronically rotated by phasing techniques  
 for linear array 03 p0344 A66-13018  
 Aperture antenna subdivided into reflector,  
 horn, lenses, surface and leaky wave  
 antennas 04 p0491 A66-13403  
 Minimal number of controlled elements for  
 antenna array of point transmitters with



electrical scanning distributed uniformly along straight line 04 p0483 A66-14049

Circular array phased to produce main beam in one direction by feeding elements from set of series-connected phase shifts 04 p0500 A66-14105

Energy calculation as time function required to switch toroidal ferrimagnetic core from one remanent state to another, considering core type used in antenna phased arrays 05 p0642 A66-14564

Current and directive gain for maximum directivity of orthogonal antenna array with individual elements possessing directivity 05 p0651 A66-15879

Relationship between two-and three-channel monopulse systems, with some logical extensions to various symmetrical configurations 06 p0824 A66-15981

Concentric ring antenna arrays with low sidelobes, estimating currents from Fourier-Bessel series 06 p0825 A66-16017

Antenna array excitation for maximum power gain in terms of network parameters defined at input terminals 06 p0843 A66-16022

Minimization of grating lobes in slotted waveguides as array elements by using linearly nonuniform array with equal power division between elements 06 p0827 A66-16034

Integration of Poynting vector over real and imaginary space to determine input admittance of one slot in infinite planar array as function of beam pointing direction 06 p0827 A66-16041

Impedance variation in scanning arrays approximated without beam forming and steering system 06 p0850 A66-16398

Equation determining maximum spacing between adjacent array elements in scanned antenna, considering sidelobe level 06 p0851 A66-16456

Angular-frequency sensitivity of antenna arrays and relation to feeder waveguide 06 p0859 A66-17183

Optimum geometry of nonuniformly spaced antenna arrays improves relation between beamwidth and sidelobe levels 08 p1192 A66-19098

Compact multielement antenna with omnidirectional radiation pattern in horizontal plane and compressed in vertical plane 08 p1193 A66-19106

Comparison of detection and resolution performance of multiplicative and additive aerial array in presence of noise 08 p1193 A66-19119

High-directional spherical antenna array, determining shape of radiation pattern as function of orientation of individual antennas and amplitude distribution of excitation currents 08 p1197 A66-19608

Book on antenna systems of non-Soviet communication links via satellites 09 p1342 A66-19974

Ground antenna for satellite tracking and orbit calculation 09 p1355 A66-20587

Diffraction of plane electromagnetic wave at planar array consisting of thin rectangular plates 09 p1347 A66-20787

Antenna array and radiometer selection for orbiting LF radio astronomical observatory 10 p1507 A66-21122

Shortest short-backfire antenna with two plane reflectors spaced about half-wavelength apart 10 p1510 A66-21648

Celestially referenced electronic space tracking system for augmenting accuracy of existing antenna 10 p1505 A66-21895

Ground diffraction pattern caused by radio wave reflection from F region, using array of three aerials 11 p1651 A66-22374

Space-tapered array analysis, noting that very few yield reasonably low sidelobe level and none are optimum 11 p1662 A66-22542

Wide-angle impedance matching /WAIM/ method reducing variation of reflection coefficient with scan angle and polarization by dielectric sheet located in front of array antenna face 11 p1663 A66-22547

Moderately superdirective antenna with directivity slightly greater than uniform-current distribution of same size 11 p1664 A66-22560

Unequally spaced array antennas, noting broadband characteristics, high resolution, radiation patterns, etc 11 p1664 A66-22637

Cross correlation radar system for mapping of target distribution 12 p1813 A66-23789

Asymmetric nonuniformly spaced antenna array design by orthogonal function expansion of radiation pattern, using Schmidt orthogonal method 12 p1836 A66-24301

Phase shifters for signals arriving from North-South arm elements of Northern Cross radio telescope reflector antenna array 12 p1836 A66-24304

Antennas, microwaves, electron devices - IEEE International Convention, New York, March 1966 12 p1838 A66-24613

Superdirective array of normal mode helical dipoles 12 p1840 A66-24625

Explicit relation between mutual coupling and radiation pattern of array antenna evaluated via scattering formalism, based on spherical modes 12 p1841 A66-24627

Nonuniformly spaced antenna array synthesis using lambda function via Chebyshev-Gauss quadrature and Hankel transform 12 p1841 A66-24629

Fresnel zone beam scanning antenna array, considering patterns, maximum scan ability and effect of interelement spacing 12 p1841 A66-24633

Electronically despun switched antenna using variable phase shifters to control phase of incident power to circular array of elements [AIAA PAPER 66-302] 12 p1844 A66-24769

Electronic self-steering techniques applied to satellite communications systems with high gain antennas, noting transdirective array and self-phasing array [AIAA PAPER 66-326] 12 p1824 A66-24796

Vertical incidence fading amplitude experiment using array of receiving antennas, obtaining data on ground diffraction pattern of reflected radio waves, noting correlation function shapes 12 p1824 A66-24840

Bilinear transformation reduces linear uniformly spaced array to examination of rational fraction on imaginary axis of complex plane 13 p2029 A66-25202

High resolution East-West antenna array for solar studies designed to operate at 408 mc 13 p2180 A66-25428

Radar observation of Sun, noting continuous wave transmitter, antenna, etc 13 p2022 A66-25537

Aperture synthesis technique for increasing information rate to radio astronomy array by rejecting restriction of fractional bandwidths 13 p2037 A66-25553

Antenna drive with feedback control system for radio telescope, noting design, construction and operation 13 p2038 A66-25640

Antenna array response to pulse compression signals, showing dependence of array response on compressed pulse shape 13 p2023 A66-25665

Noise suppression, signal reception, and polarization measurement in cross correlated antennas as function of dipoles imbedded in random field, surrounding noise field and coherency matrix of cross correlation function 13 p2044 A66-26746

Yagi-Uda antenna array discussing wave theory of semiinfinite and finite arrays, excitation by reflected wave proportional to incident wave and King-Sandler theory 14 p2255 A66-27907

Swept frequency antenna gain measurements, evaluating mismatch losses at feedpoint and obtaining gain-frequency curves 14 p2256 A66-27911

Log periodic Yagi-Uda dipole antenna array and extension of frequency bandwidth 14 p2256 A66-27920

Theoretical gains and current distribution in supergain endfire antenna arrays 14 p2256 A66-27922

Distant-field antenna model of current sheet array used to approximate ultimate decay of mutual coupling in planar array antenna 14 p2257 A66-27926

Asymptotic behavior of coupling coefficients of infinite array of thin walled rectangular waveguide 14 p2257 A66-27927

Gain optimization problem for antenna arrays responding to quasi-monochromatic periodic signal 14 p2240 A66-27929

Antenna array output SNR and directive

gain indices optimization 15 p2455 A66-2855

Passive series fed generation of multiple radar beam from single aperture 15 p2455 A66-2855

Multibeam hexagonal triangular-grip planar arrays 15 p2455 A66-2855

Phase array antenna system based on 4 element subarray 15 p2455 A66-2855

Internally and externally observable mutual coupling effects and seriousness in closely spaced arrays used for electronic scanning application 15 p2456 A66-2855

Cumulative coupling and impedance mismatch and radiation pattern problems in large uniformly spaced flat phase array 15 p2456 A66-2855

Wide angle impedance matching /WAIM/ of planar array antenna by dielectric sheet for reduction of reflection coefficient variation with scan angle and polarization 15 p2456 A66-2855

Dichroic Cassegrain subreflector utilized array of nonresonant elements 15 p2457 A66-2855

Antenna array receiving line-of-sight ground-to-ground transmissions over 28-km path, measuring amplitude and relative phase of arriving wave, noting perturbations in amplitude 15 p2461 A66-2855

Eigenvalues design method for nonuniformly spaced arrays that will approximate any required radiation pattern 15 p2463 A66-2904

Large aperture antenna arrays analyzed as means of increasing space communication capability 17 p2872 A66-3195

Angular discrimination improvement in radar beacon systems using null-type antenna superposed on normal directional beam 17 p2872 A66-3195

Height finding technique using phase-space principle for radar system with single antenna and feed structure 17 p2872 A66-3195

Minimal number of controlled elements in antenna array of point transmitters with electrical scanning distributed uniformly along straight line 17 p2884 A66-3225

Probability distribution of phase difference between two spaced antennas excited by random fan of rays plus specular component 17 p2874 A66-3235

Haar theorem for synthesis of nonuniformly spaced linear discrete antenna arrays 17 p2886 A66-3235

Beam position selection and antenna location connection to receiver processing channels in multiple-beam receiver system 18 p3074 A66-3325

Beamwidth and operating regions for patterns for space tapered arrays 18 p3074 A66-3325

Calibration of spherical reflector at Arecibo Ionospheric Observatory antennas using analytical photogrammetric methods 18 p3075 A66-3374

Coherent optical system for simplifying signal processing from antenna arrays in simultaneous beam forming and correlation 18 p3069 A66-3425

High scanning frequency for transmitting radar information to vehicles with beams arranged to form coded pulse signal 18 p3070 A66-3425

Vertically-fed steerable parabolic reflector system for communications satellite Earth station 18 p3081 A66-3425

Antenna design techniques, describing methods of improvement in resolution and sensitivity of radio telescopes 18 p3081 A66-3425

Accuracy limitations in control of construction of large steerable parabolic antennas 18 p3081 A66-3425

Electronic compensation for phase errors in surface profile of reflecting antennas 18 p3081 A66-3425

Optimum number of arrays for hemispherical coverage in electronically steerable antenna 18 p3084 A66-3435

Antenna structure analysis by finite element method and energy method considering Cassegrain antenna 18 p3255 A66-3435

High-gain surface wave antenna arrays for satellite communication, comparing volumetric array and parabolic dish antenna 18 p3085 A66-3435



High-directional spherical antenna array, determining shape of radiation pattern as function of orientation of individual antennas and amplitude distribution of excitation currents 18 p3088 A66-34964

Statistical characteristics of radiation pattern of antenna array with randomly positioned radiators determined from density distribution of radiators 19 p3311 A66-35306

Angular-frequency sensitivity of antenna arrays and relation to feeder waveguide 19 p3314 A66-35541

Information theory criterion applied to nonlinear processing antenna systems yielding optimum system, considering SNR 19 p3318 A66-35885

Current magnitude and phase associated with individual elements of slot Yagi-type antenna array on planar and curved surfaces 19 p3321 A66-36406

Doppler tracking loops for antenna array system adaptive to changes in signal and noise levels, maintaining constant SNR in tracking loop 19 p3321 A66-36413

Space factor of linear array with isotropic sources determined, using illumination function and convolution theorem 19 p3321 A66-36414

Directive gain characteristics of nonuniformly spaced arrays, plotting values representing gain of space tapered arrays as function of elements, optimized gain vs number of elements, etc 19 p3321 A66-36415

VHF aircraft antennas for propagation and communication via synchronous satellite, discussing nose radome yagi and window cavity arrays 20 p3525 A66-37235

Japanese antenna engineering, discussing linear, microwave, slot and plate antennas, arrangement, radiation and temperature characteristics, etc 20 p3529 A66-37704

Antenna radiation pattern synthesis for various array distributions, noting methods applied 20 p3529 A66-37706

Slot antenna research, discussing arrays and polarization characteristics 20 p3530 A66-37710

Folded antennas, discussing Franklin array and current distribution via equivalent circuit analysis and application for TV transmission and reception 20 p3530 A66-37712

Scanning antenna operating principles, noting adjustment of directivity to receive radio waves from long distance 20 p3530 A66-37713

Medium frequency, FM, VHF and UHF TV broadcasting and receiving antennas 20 p3530 A66-37717

Formula derivation for directivity of short endfire antenna array, obtaining current amplitude and phases for maximum gain 20 p3531 A66-37725

Multielement antenna scanning grid-phasing method having random function distribution at aperture 20 p3533 A66-37994

Transhorizon microwave propagation measurements using rapidly scanning phased-array antenna 20 p3520 A66-38356

Iterated theoretical admittance of cylindrical antenna, determining effective length and approximating ideal independent susceptance 20 p3534 A66-38365

Point detector array design for optimal detection of known spatially invariant signal fields corrupted by additive, zero-mean, covariance-separable and spatially isotropic noise field 21 p3711 A66-39136

Short distance receiving radiation field pattern of phase-biased array of two isotropic point antennas 21 p3713 A66-39373

Erectable antenna for S-band communication between LEM and Earth 21 p3714 A66-39522

Diffraction of plane electromagnetic wave at planar array consisting of thin rectangular plates 22 p3862 A66-39846

Rake system equipment for tropospheric scatter, noting delay-resolution capabilities and circuit stability 22 p3865 A66-40067

Space antenna arrays - WESCON, Los Angeles, August 1966 22 p3881 A66-40747

Adaptive antenna system circuitry for maximum signal to noise ratio of signals reaching ground station from deep space probe 22 p3881 A66-40750

Antenna patterns for spacecraft antenna

array with aperiodic arrangement of large elements provide high aperture efficiency 22 p3882 A66-40751

Electronically despun antenna and electronically controlled phase shifters to increase transmitter output power for spin-stabilized communication satellites 23 p4036 A66-41142

Auroral disturbances resulting in multipath distortion in propagation by ionospheric reflection and description of chirp ionosonde and antenna systems 23 p4036 A66-41143

Angle of arrival in amplitude-comparison monopulse antenna arrangement including thermal noise as interference and pulsed radar with ideal radar target 23 p4044 A66-41314

Spaced antenna reception by quadratic addition of signals providing efficient operation at various statistical characteristics of radio channel 23 p4038 A66-41518

Complexity and reliability of telemechanics systems and distribution law of number of interrogations for telemechanics systems with dispersed objects 23 p4038 A66-41570

Impedance of flat strip antenna embedded in planar dielectric slab surrounded by layers of compressible isotropic electron plasma 23 p4047 A66-41639

Jupiter radiation recorded almost every night with antenna arrays shows emission dependency on Jupiter longitude and Io position 23 p4131 A66-41817

Antenna systems for deep space communication emphasizing ground station, balancing of ground antenna aperture with spacecraft performance, arrays, etc 24 p4171 A66-42244

Wide frequency bandwidth properties of arrays of shunt slots in ridged waveguide 24 p4187 A66-43194

**ANTENNA COUPLER**

SA ELECTROMAGNETISM

SA ENERGY TRANSFER

SA IMPEDANCE MATCHING

SA TRANSMISSION LINE

Noise performance of antennafier and advantage when added to receiver system 03 p0339 A66-12448

HF antenna coupler noting placement of parts and advantages over long wire antennas 03 p0335 A66-12999

Symmetrical transverse electromagnetic-mode directional couplers, deriving formulas for functional parameters and insertion-loss function 06 p0844 A66-16083

TEM-mode coupled-transmission-line directional couplers, determining equal-ripple polynomials and tabulating parameters 06 p0844 A66-16084

Internally and externally observable mutual coupling effects and seriousness in closely spaced arrays used for electronic scanning application 15 p2456 A66-28583

Errors in Gemini rendezvous radar interferometer due to antenna ellipticity and coupling of adjacent antennas 17 p2876 A66-33437

Coupling situations involving two flush-mounted antennas such as those used in space vehicles, noting interference problems and use of nomographs 19 p3313 A66-35514

Generalized method of calculating multielement antenna and feeder system 21 p3712 A66-39250

Waveguide directional couplers using inclined slots, considering broad-to-narrow cross and broadwall parallel guide configuration 22 p3878 A66-40546

Large, small and infinite phased array antennas and coupling effects 22 p3881 A66-40749

HF transmitter multicoupler for connecting several transmitters to single antenna 23 p4046 A66-41548

**ANTENNA FIELD**

Directional properties of surface antennas with linear, squared and cubic phase distortions for symmetrical and asymmetrical amplitude distribution laws 01 p0035 A66-10220

Impedance behavior and frequency dependence of radiation pattern of wideband sheet antenna 01 p0036 A66-10366

Slotted-sphere antenna immersed in compressible plasma 01 p0037 A66-10513

Three parameter antenna pattern synthesis using nonlinear computer programming technique derived from method of steepest descent 01 p0044 A66-10934

Radiation patterns of transversely polarized corner reflector antenna, using image method 01 p0044 A66-10937

Electromagnetic field and radiation pattern of Hertzian electric dipole antenna in conical sheath 02 p0191 A66-11803

Tuning of lens and mirror antennas with circularly polarized radiation patterns 02 p0192 A66-11848

Beam width of two antenna systems measured and compared for accuracy in determining plasma density 02 p0269 A66-11969

Electromagnetic excitation of spherical radially laminar medium with interfaces solved rigorously by derived algorithm 03 p0331 A66-12286

Reciprocity of radiation patterns of receiving and transmitting antennas in assessing performance 03 p0341 A66-12523

Design and installation of antennae for airborne command and control systems, noting antenna system for SAC Airborne Command Post [AIAA PAPER 65-730] 03 p0334 A66-12581

Linear superdirectional antennas discussing directional properties and formulas for optimal directive gain stability 03 p0337 A66-13315

Antenna characteristics, design and selection noting use in broadcasting, radio navigation, etc 04 p0491 A66-13401

Plasma sheaths on radiation patterns of antennas on hypersonic vehicles, noting permittivity and transmission loss 04 p0474 A66-13426

Sampling of independent orthogonally polarized antenna output to increase signal levels at least 10 decibels over one-antenna systems 04 p0481 A66-13729

Algorithm derived for processing packet of binary-quantized signals according to maximum likelihood for various types of target fluctuations 04 p0482 A66-13919

Anomalous behavior of radiation resistance of antennas in anisotropic media 04 p0500 A66-14101

Basic radar equation, giving geometrical relationship between radar antenna and target based on antenna gain, aperture and target cross section 04 p0484 A66-14107

Radiation field of single-filament logarithmic-elliptical helical antenna, assuming traveling wave along helix 04 p0501 A66-14408

Fresnel gain of aperture antenna, developing rigorous analytical formula for circular aperture antennas with parabolic tapered illumination 05 p0651 A66-15837

Field of linear array consisting of coaxial spherical antennas, each representing pair of hemispheres separated by narrow clearance with applied voltage 05 p0651 A66-15880

Field amplitude and phase measurements close to number of driven periodic arrays of monopoles used to determine frequency dependence of propagation constant 06 p0825 A66-16016

Cylindrical receiving and scattering antennas, determining current from admittance, charge distribution and near field for incident plane wave 06 p0827 A66-16036

Radiation pattern of slotted-cylinder antenna in presence of inhomogeneous lossy plasma 06 p0827 A66-16045

Current distribution on L-band loop antenna composed of four quarter-circular sections 06 p0850 A66-16446

Blake procedure effectiveness and applicability in computing beam loss of radars, extrapolating for rapid-scan systems 06 p0832 A66-16452

Field-strength measurements at 11 gc over 35 km near-optical path for receiving antenna of variable height in shadow of two knife edges 06 p0836 A66-16982

Aerial radiation patterns, discussing determination through near field pattern processing 06 p0858 A66-16994

Tuning antennas of radio telescopes with flat reflectors by in-phase addition of reflected fields 06 p0859 A66-17193

Circuitry of system for simultaneously



obtaining several independent radiation patterns from one ultra-short-wave receiving antenna 07 p1005 A66-17344

Effect of various geometries on performance and characteristics of helical antennas, considering input impedance and radiation pattern 07 p1006 A66-17474

Electromagnetic field near highly conducting cylindrical antenna of finite length excited by plane electromagnetic wave 08 p1189 A66-18668

Wideband annular-zone directional antenna, with individual radiators arranged in log-periodic concentrated groups on ring fed by conical line 08 p1190 A66-18682

Polarization pattern dependence on phase-amplitude distribution of field at microwave antenna aperture 08 p1190 A66-18912

Spatial radiation patterns of curved high-directivity antenna array as function of amplitude distribution and directivity 08 p1191 A66-18913

Multimode antennas, discussing mode and mode generation, radiation sum and difference pattern control, discontinuity reflections, monopulse antennas, etc 08 p1191 A66-18945

Compact multielement antenna with omnidirectional radiation pattern in horizontal plane and compressed in vertical plane 08 p1193 A66-19106

Radiation pattern of two annular slot-coupled antennas mounted on elongated spheroid 08 p1193 A66-19187

Power flux distribution of symmetrical wave outside and inside antenna septum with anisotropic medium 08 p1193 A66-19189

High-gain narrow-pulse radar antenna with rectangular beam shape in vertical plane, noting design requirements and experimental results 08 p1196 A66-19511

Antenna radiation shows relationship to tangential component of electric field intensity along antenna 08 p1197 A66-19606

High-directional spherical antenna array, determining shape of radiation pattern as function of orientation of individual antennas and amplitude distribution of excitation currents 08 p1197 A66-19608

Transient processes in thin open-loop and closed-loop antennas studied by method that takes transmission line processes into account 08 p1199 A66-19759

Antenna radiation pattern in anisotropic medium such as ionosphere in presence of Earth magnetic field 09 p1340 A66-19842

Admittance measurements for antenna in ionosphere, effect of local magnetic field variations, plasma frequency and gyrofrequency 09 p1341 A66-19854

Transient condition effects on radiation resistance and expansion in linear antennas 09 p1352 A66-20348

Radiation resistance of linear current strip of finite width immersed in uniaxially anisotropic plasma medium 09 p1408 A66-20370

Cross-polarization radiation of axisymmetric mirror antennas 09 p1353 A66-20448

Potential analog synthesis of linear arrays and radiation pattern representation as function of single complex variable 09 p1356 A66-20605

Polarization patterns of microwave antennas with sine-phase /complex/ apertures of rectangular, circular, annular or rhombic form 09 p1356 A66-20771

Antenna field calculations in Fresnel and induction regions 09 p1356 A66-20772

Error assessment in antenna radiation patterns at small distances by means of collimator which shapes plane wave region 09 p1358 A66-20807

Anechoic chamber design for higher measurement accuracies for radar cross section and antenna parameters 10 p1501 A66-21623

Radar range with discretely located passive reflectors for obtaining full scale bistatic radar cross section measurement 10 p1501 A66-21625

Sand table simulation of full-scale ground-plane range 10 p1502 A66-21631

Microwave transmission tests in pure air plasma using hypersonic shock tunnel, obtaining electron density and collision frequency profiles, predicting propagation path signal loss and antenna radiation

pattern distortion [AIAA PAPER 66-173] 11 p1742 A66-22211

Aperture field of leaky-wave antenna of finite length 11 p1661 A66-22394

Angular autocorrelation function of circular-aerial radiation 11 p1662 A66-22397

Correlation method measuring far-field patterns of large-aperture antennas, using radio star sources and auxiliary antenna for providing reference signal for cross correlation with test antenna signal 11 p1662 A66-22540

Tube shaped and solid cylinder antennas compared, calculating surface current distribution and radiation patterns 11 p1662 A66-22543

Feed polarization incident upon conic reflector in antenna system specified in terms of crossed electric and magnetic dipoles 11 p1663 A66-22544

Geometrical theory of diffraction applied to calculation of radiation pattern and impedance of monopole antenna 11 p1663 A66-22545

Electrical and mechanical features of millimeter-wave antenna facility, including measurement of lunar surface during eclipse of December 1963 11 p1770 A66-22551

Radiation characteristics of dielectric coated half-wave resonant slot antenna, examining effects of improper dielectric scaling 11 p1663 A66-22553

Minor lobe suppression in rectangular horn antenna through utilization of high impedance choke flange 11 p1663 A66-22556

Exact expressions for antenna-tracking parameters when transmitter-receiver scattering angle is constant 11 p1653 A66-22557

Quasi-optical design of lens-fed millimeter-wavelength antenna combination whose radiation is of azimuthally symmetric split-beam type 11 p1663 A66-22559

Angular sectors of transparency of scanning antennas with periodic waveguide 11 p1666 A66-22718

Antenna theory, analyzing radio astronomical methods such as antenna axis, radiation pattern, gain, efficiency, etc 11 p1658 A66-23219

Nonsteady radiation field of antenna systems for arbitrary signals via Huygen-Kirchhoff principle 11 p1670 A66-23225

Radiating mechanisms in reflector antenna system including aperture radiation, direct feed radiation and diffracted radiation 11 p1673 A66-23481

Antenna orientation effect on polarization components of radio waves reflected from ionosphere, noting occurrence and properties of magnetoionic component of polarization 12 p1869 A66-24273

Asymmetric nonuniformly spaced antenna array design by orthogonal function expansion of radiation pattern, using Schmidt orthogonal method 12 p1836 A66-24301

Field intensity and polarization characteristics of turnstile antenna with arbitrary phase and amplitude relationship between two exciting elements 12 p1838 A66-24610

Far field simulation of antennas with complex aperture distribution functions 12 p1840 A66-24624

Explicit relation between mutual coupling and radiation pattern of array antenna evaluated via scattering formalism, based on spherical modes 12 p1841 A66-24627

Pattern synthesis method for linear array using integral mean of Fourier approximation 12 p1841 A66-24628

Approximate theory for lumped impedance loaded traveling wave linear antenna, considering possibility of nondissipative loading 12 p1841 A66-24631

Fresnel and Fraunhofer patterns of overmoded feeds and reflector antennas 12 p1841 A66-24632

Fading and multipath propagation mechanism for communication links involving satellites and aircraft with antenna beams, assuming fading models and estimating margin required for FSK teletype transmission [AIAA PAPER 66-294] 12 p1822 A66-24763

Variation of antenna amplification ratio

with distance as function of phase error at antenna aperture with exciter off-focus and error source 13 p2030 A66-25222

Radiation pattern excitation of elongated impedance spheroid by annular slot with uniform field distribution 13 p2042 A66-26044

Modeling and data reduction techniques for obtaining spectrum signatures of low gain LF airborne antennas 13 p2044 A66-26744

Optimum antenna placement within metallic enclosure 13 p2044 A66-26744

First-order formula for component of electric field very near surface and parallel to axis of perfectly conducting center-driven cylindrical antenna 14 p2247 A66-26866

Radiation pattern of dielectric antenna using integral equations, noting differences between real antenna and idealized linear traveling wave antenna 14 p2250 A66-27144

Random error effect on directional gain of sectional parabolic antenna with automatic phasing, setting sections effectively by three control points method 14 p2250 A66-27144

Emission of axisymmetric parabolic antenna with antiphase field distribution at aperture, calculating radiation pattern of principal and cross polarization components of field 14 p2250 A66-27144

High directional antenna with variable aperture and signal processing after frequency conversion 14 p2251 A66-27232

Radiation characteristics of horn antenna analyzed, using edge diffraction theory, noting intensity at backlobe and far sidelobe 14 p2255 A66-27902

Broadband slotted cone antenna exhibiting multioctave bandwidth properties in UHF/VHF range 14 p2256 A66-27911

Mutual and self-impedance of linear antennas in interface between dielectric layers computed, noting cases of symmetric and antisymmetric excitations 14 p2256 A66-27911

Endfire effect in dielectric foam rods and mode control by varying dielectric constant of rod 14 p2256 A66-27922

Stationary phase technique synthesis of continuous linear antenna and integral equation for determining radiation pattern 14 p2259 A66-28151

Vector potential representation of planar logarithmic spiral antenna field 14 p2259 A66-28151

Linear superdirectional antennas, discussing directional properties and formulas for optimal directive gain, stability 14 p2242 A66-28282

Electromagnetic and acoustic wave coupling in homogeneous compressible isotropic plasma and diffraction by half plane due to sharp structural discontinuities in antenna configurations 15 p2448 A66-28558

Antenna tolerance theory, presenting axial loss of gain and pattern degradation as function of reflector surface rms error 15 p2462 A66-29022

Eigenvalues design method for nonuniformly spaced arrays that will approximate any required radiation pattern 15 p2463 A66-29022

Radiation pattern of dielectric coated cylindrical core loop antenna in lossy plasma sheath 15 p2452 A66-29711

Ionospheric sounding using random diffusion of electromagnetic wave by ionospheric plasma with continuous wave through two separate antennas 16 p2653 A66-30955

Transmitting antenna of Cassegrain type, noting conical horn, primary and secondary mirror, etc 16 p2661 A66-30955

Geometrical characteristics of framework and reflecting surface of ionospheric diffusion probe antenna, noting specifications on design, manufacture, erection, alignment and adjustment 16 p2662 A66-30955

Coherent optical systems in signal processing techniques, information theory and antenna pattern simulation 16 p2657 A66-31224

Design and testing of cross polarized feed for 10 ft diameter parabolic dish, noting coincidence of focal and aperture plane 16 p2666 A66-31566

Boresight shift in phase sensing monopulse antennas due to reflected signal 16 p2667 A66-31644



Equivalent linear antenna substitution for antenna with plane aperture in statistical analysis of antennas 17 p2879 A66-31861

Directional properties of surface antennas with linear, squared and cubic phase distortions for symmetrical and asymmetrical amplitude distribution laws 17 p2880 A66-31903

Determination of radio brightness distribution across sky dependent upon conditions of radio telescope operation 17 p2999 A66-32236

Characteristics of lunar radio emission considered, taking into account averaging effect of antenna radiation pattern 17 p2999 A66-32237

Optimization of radiation characteristics of satellite mounted antennas 17 p2894 A66-32990

Radiation characteristics of circular aperture and linear antenna with partially coherent illumination 18 p3074 A66-33536

Radiation fields of center-fed cylindrical antenna surrounded by plasma sheath, graphically presenting far-field patterns and surface wave fields 18 p3141 A66-33538

Radiation from spherical aperture antenna immersed in compressible plasma 18 p3066 A66-33541

Beamwidth and operating regions of patterns for space tapered arrays 18 p3074 A66-33543

Array of circumferential slots on large cylinder as omnidirectional antenna 18 p3074 A66-33544

Source distribution determination from radiation pattern and field amplitudes expressed as Fourier transform pair 18 p3066 A66-33545

Near field phase and amplitude measurements of small radiating structures, using standard microwave equipment 18 p3075 A66-33619

Instant antenna patterns for estimating far field characteristics, noting location of peaks and zeros of radiation patterns, voltage ratios, etc 18 p3077 A66-34063

Radiation pattern of ground surveillance radar antenna measured with aid of airborne signal generator 18 p3070 A66-34266

Tolerance theory for parabolic reflector antenna, noting gain and radiation-pattern distortion 18 p3082 A66-34285

Diffraction pattern analysis of fields generated by hoghorn-fed Cassegrain antenna operating in Fresnel zone 18 p3083 A66-34289

Optimum shape of feed patterns for paraboloidal antennas 18 p3083 A66-34293

Improved feed synthesis using multimodes for large circular paraboloids at Parkes 18 p3084 A66-34310

Amplitude-comparison tracking antenna utilizing parabolic reflector, determining parameters from radiation patterns 18 p3086 A66-34396

High-directional spherical antenna array, determining shape of radiation pattern as function of orientation of individual antennas and amplitude distribution of excitation currents 18 p3088 A66-34964

Radiation pattern of linear nonequidistant antenna array 19 p3311 A66-35307

Tuning antennas of radio telescopes with flat reflectors by in-phase addition of reflected fields 19 p3314 A66-35551

Coupled waveguides structure proposed as leaky-wave antenna, extending previous coupled-mode theory 19 p3320 A66-36401

Broadband signals effect on far-zone field of linear arrays studied in terms of energy radiation pattern 19 p3320 A66-36402

Electric dipole radiation through finite conical plasma sheath about reentry vehicle, calculating radiation pattern 19 p3304 A66-36403

Radiation pattern synthesis for circular aperture horn antennas, assuming aperture distribution consisting of fields of cylindrical waveguide modes and by linear combination of radiation pattern functions 19 p3320 A66-36404

Scale model of submerged VLF antenna using lossy ceramic powder to model ice and snow for submarine communication, geophysics, etc 19 p3321 A66-36416

Radiated fields for plasma external to dielectric coating surrounding biconical

antenna, equivalent circuit developed for terminating impedance 19 p3305 A66-36422

Radio astronomy instrumentation, describing antenna parameters, design characteristics, instrumentation needs, etc 20 p3524 A66-36962

Gain loss ratio between one antenna and two antennas used to analyze antenna gain loss for long-range tropospheric propagation of ultrashort waves 20 p3525 A66-37124

Dual beam technique and antenna used to observe variations in flux of radiosource 3C 273 20 p3650 A66-37344

Axially oriented point source current and filament with triangular current distribution in magnetoionic medium, examining ion sheath effect on radiation characteristics 20 p3516 A66-37624

Near electric field of antenna in magnetoactive plasma, noting frequency effect 20 p3529 A66-37637

Antennas with leaky wave characteristics, noting similarities and differences with wave diffraction 20 p3529 A66-37707

Power transmission, gain, directivity pattern and reception between large aperture antennas in near-field region 20 p3529 A66-37709

Antenna measurement for input impedance, gain and directivity characteristics 20 p3531 A66-37722

Algorithm derived for processing packet of binary-quantized signals according to maximum likelihood for various types of target fluctuations 20 p3518 A66-37877

Vehicle structures combining as antenna functions, using spaces between bolts of flange joints as slot antennas 20 p3533 A66-38260

Two-dimensional reflector with large angular field theoretically and experimentally studied, using geometrical optics 21 p3710 A66-38745

Generalized reciprocity theorem for antenna systems containing anisotropic media and antenna systems radiating directly through arbitrary apertures 21 p3711 A66-38835

Radio astronomy satellite with extendible antennas achieves gravity gradient stabilization while receiving electromagnetic radiation, analyzing dynamic behavior and effect of passive damper 21 p3820 A66-38863

Parabolic reflector design modified to reduce temperature noise level by increasing diameter and extending cylindrical mantle around antenna rim 21 p3714 A66-39513

Radio source flux density relation to antenna temperature studied, using antenna integral and convolute integral 22 p3862 A66-39814

Polarization patterns of microwave antennas with sine-phase /complex/ apertures of rectangular, circular, annular or rhombic form 22 p3873 A66-39830

Antenna field calculations in Fresnel and induction regions 22 p3873 A66-39831

Bornis U function applied to design of electron tube having drift space between collector and grid controlling current 22 p3876 A66-40173

Angular sectors of transparency of scanning antennas with periodic waveguide 23 p4045 A66-41456

Antenna radiation theory, noting reiteration of incorrectness of infinity catastrophe theory and application to oscillating dipole in uniaxial medium 23 p4047 A66-41633

Radiation resistance of antennas in magnetoplasma, considering inapplicability of reversible power concept to steady state mode 23 p4047 A66-41634

Propagation and radiation of radio waves from dielectric coated prolate spheroidal core loop antenna surrounded by plasma sheath 24 p4184 A66-42745

# ANTHEUS AIRCRAFT

S ANTONOV AN-22 AIRCRAFT

# ANTHRACENE

Directional intensity and decay time of scintillations from anthracene and p-terphenyl single crystals under alpha particle bombardment 11 p1750 A66-22465

Excited-singlet even parity states of anthracene in near UV, noting role of absorption spectroscopy 13 p2132 A66-26143

Light output of alpha particles in crystalline and vapor anthracene as function of pressure and temperature 14 p2296 A66-27796

Recombination rate of electron-hole pairs in anthracene determined and compared with theoretical value based on hypothesis of Coulomb capture in dielectric 14 p2369 A66-28272

Transitions and excited states in anthracene, using two-photon spectroscopy 16 p2717 A66-30203

Current decay in anthracene irradiated by gamma ray 18 p3157 A66-34476

# ANTHROPOMETRY

SA BODY MEASUREMENT /BIOL/

SA HUMAN ENGINEERING

Morphological characteristics and functional data in pilot trainees, noting anthropometric data and vital capacity, oxygen intake, heart rate, etc 08 p1175 A66-19084

Mass measurement of man in zero gravity environment, discussing laboratory device using linear harmonic motion 17 p2924 A66-32171

Text evaluating application of human body size and mechanical capabilities to equipment design for man-machine integration 23 p4030 A66-41619

# ANTIBIOTICS

Physiologically active compounds and cultured antibiotic fluids used to eliminate effects of ionizing beta radiation on plant seeds 15 p2438 A66-29487

# ANTIBODY

SA ANTIGEN

SA GAMMA GLOBULIN

Virus purification methods including density gradient centrifugation, liquid-phase partition, etc, evoke high antibody levels 09 p1333 A66-19899

Antibody globulin coupled to diazotized aminoaryl derivative of carboxymethyl-cellulose to form immunoadsorbent for extracting antigens 12 p1805 A66-23568

# ANTICYCLONE

SA CYCLONE

Lower atmospheric diurnal variations in air temperature, directional wind velocity and gradients, during clear anticyclonic weather 16 p2742 A66-30774

# ANTIFERROELECTRICITY

Temperature dependence of dielectric properties of antiferroelectrics of perovskite structure in SHF range 10 p1589 A66-22168

Temperature dependence of dielectric properties of antiferroelectrics of perovskite structure in SHF range 19 p3441 A66-35782

# ANTIFERROMAGNETISM

SA FERROMAGNETISM

SA HYSTERESIS

Gyrotropic properties in simple and canted two-sublattice antiferromagnetics in small static magnetic field 01 p0122 A66-10569

Low temperature excitation spectrum for ferro- and antiferromagnets with large crystalline field splittings 05 p0741 A66-15867

Phase transitions theory analyzed by simple self-consistent equations including ferromagnetism, antiferromagnetism, liquid-gas condensations and melting and freezing 09 p1424 A66-20076

Low temperature measurement of magnetic susceptibility of CdS single crystals with manganese impurity, considering effects of antiferromagnetic exchange 09 p1424 A66-20078

Spin wave sideband in absorption spectrum at low temperatures for transition of manganese ion in antiferromagnetic manganese fluoride 11 p1740 A66-22970

Minimum electric resistivity of chromium in antiferromagnetic state shows no disappearance in longitudinal magnetic field 19 p3444 A66-36071

Physics of ferro- and antiferromagnetism - All-Union Conference, Sverdlovsk, U.S.S.R., July 1965 20 p3616 A66-37475

Spectral analysis of interacting electromagnetic, plasma and spin waves in antiferromagnetic semiconductors and metals with easy-axis and plane type anisotropy 21 p3804 A66-39311

# ANTIGEN

SA ANTIBODY

SA GAMMA GLOBULIN

Virus purification methods including density gradient centrifugation, liquid-phase



partition, etc, evoke high antibody levels 09 p1333 A66-19899  
C and D antigens of coxsackievirus, centrifugation separation and similarity to poliomyelitis 09 p1335 A66-20633  
Antibody globulin coupled to diazotized aminoaryl derivative of carboxymethyl-cellulose to form immunoadsorbent for extracting antigens 12 p1805 A66-23568

ANTIGRAVITY

S GRAVITY

ANTIMATTER

Theory of antimatter applied to cosmology and development of metagalactic system, discussing ambiplasma 04 p0578 A66-14009  
Comets hypothesized to consist of antimatter, originating from parts of galaxy consisting entirely of antimatter 11 p1774 A66-23039

Carbon 14 content in growth rings of tree 60 km from epicenter of 1908 explosion of Tungus meteorite, considering antimatter as possible explosion cause 18 p3233 A66-34553

Ambiplasma sources of positronium, protonium and muonium radiation, theorizing that quasars may be ambiplasmas containing admixtures of matter and antimatter 24 p4280 A66-43027

ANTIMISSILE MISSILE

Intercepting moving completed powered-flight of ICBM missile 04 p0581 A66-13458  
Ballistic missile defense and national security, discussing defense system requirements, strategy types, etc 08 p1322 A66-18560

Digital simulation of guidance and control of exoatmospheric interceptor missiles for study of parameter variations effect on overall mission effectiveness 20 p3596 A66-37230

ANTIMONIDE

S ALUMINUM ANTIMONIDE

S CADMIUM ANTIMONIDE

S CESIUM ANTIMONIDE

S GALLIUM ANTIMONIDE

S INDIUM ANTIMONIDE

S ZINC ANTIMONIDE

ANTIMONY

Antimony ionization in p-germanium single crystals, based on diffusion of Sb into Ge 12 p1930 A66-24460

Energy levels and interband oscillator strengths of antimony calculated in Brillouin zone by pseudopotential method, predicting polarization effects and spin-orbit splittings 19 p3446 A66-36392

Alfven wave propagation equations used to study electronic properties of semimetals 20 p3615 A66-37282

Antimony ionization in p-germanium single crystals, based on diffusion of Sb into Ge 20 p3620 A66-37692

Cs-Sb film thickness measurement method in various compositions and relation between thickness and composition 24 p4251 A66-42301

Antimony abundance in meteorites determined by neutron activation analysis 24 p4274 A66-42432

ANTIMONY ALLOY

Thermal and electrical properties of copper antimony telluride/tin telluride system as function of composition 01 p0116 A66-10190

Electronic band structure of BiSb alloy tunnel junction for various Sb concentrations 16 p2770 A66-30178

ANTIMONY COMPOUND

Electron spin resonance of radical cations produced by oxidation of aromatic hydrocarbons with antimony pentachloride 03 p0330 A66-12336

Thermoelectric properties of solid solution of germanium telluride in copper antimony telluride 23 p4114 A66-41572

Magnesium antimonide and magnesium bismuthide as materials for power generating thermocouples 24 p4227 A66-42111

ANTIOXIDANT

Fuels and lubricants with thermally stable molecular structure and antioxidants to meet requirements of supersonic transport 03 p0414 A66-13221

ANTIPARTICLE

Microscopic model of symmetry between particle and antiparticle populations in expanding universe 23 p4131 A66-42065

ANTISUBMARINE WARFARE AIRCRAFT

A-NEW MOD 1 digitally controlled navigation system for antisubmarine warfare aircraft employing Univac CP-754-8 thin film computer 01 p0098 A63-10002

CHSS-2 Haul Down and Handling System for operating large /SH-3A/ helicopter from small ships 10 p1484 A66-21891

New antisub aircraft operating from ships and land bases 11 p1637 A66-23161

A-NEW MOD 1 digitally controlled navigation system for antisubmarine warfare aircraft employing Univac CP-754-8 thin film computer 13 p2124 A66-25596

ASW aircraft performance and technology for contact investigation, patrol and convoy escort [AIAA PAPER 66-727] 20 p3496 A66-38037

ANTONOV AN-22 AIRCRAFT

Principal civil aircraft at 26th Aeronautical and Space Exhibition, detailing AN 22 Antaeus cargo aircraft 07 p0989 A66-17820

ANVIL

Robustness, axial alignment and low friction through limited angular excursion of pivot, noting lapping fixture and anvil assembly 24 p4218 A66-43222

AOSO

Stabilization, communication, data handling and power subsystem requirements for AOSO [AIAA PAPER 64-333] 08 p1303 A66-18817

AOSO stabilization and control system for solar experiments, noting closed loop stability and gain stability 21 p3819 A66-38854

APERIODIC FUNCTION

Optimal control and trajectory optimization in aperiodic discrete time functional systems 11 p1681 A66-23422

Volterra series analysis of aperiodic solutions to certain second order integrodifferential equations with nonlinear damping and nonlinear restoring force 16 p2737 A66-31334

APERTURE

Fresnel gain of aperture antenna, developing rigorous analytical formula for circular aperture antennas with parabolic tapered illumination 05 p0651 A66-15837

Polarization patterns of microwave antennas with sine-phase /complex/ apertures of rectangular, circular, annular or rhombic form 09 p1356 A66-20771

Aperture field of leaky-wave antenna of finite length 11 p1661 A66-22394

Radiation pattern from circular aperture with symmetrical inphase illumination described by Neumann series, noting sidelobe level 11 p1652 A66-22398

Far field simulation of antennas with complex aperture distribution functions 12 p1840 A66-24624

Equivalent linear antenna substitution for antenna with plane aperture in statistical analysis of antennas 17 p2879 A66-31861

Radiation pattern synthesis for circular aperture horn antennas, assuming aperture distribution consisting of fields of cylindrical waveguide modes and by linear combination of radiation pattern functions 19 p3320 A66-36404

Polarization patterns of microwave antennas with sine-phase /complex/ apertures of rectangular, circular, annular or rhombic form 22 p3873 A66-39830

Antenna patterns for spacecraft antenna array with aperiodic arrangement of large elements provide high aperture efficiency 22 p3882 A66-40751

Scherzer theorem on aperture aberration extended to monochromatic nonrelativistic system with electrostatic or magnetic quadrupole fields with common planes of optical symmetry 24 p4239 A66-43215

APOGEE

Results of approximate computation of rocket apogee from data on flight duration between different trajectory points 14 p2383 A66-27815

APOLLO PROJECT

SA LUNAR EXPLORATION SYSTEM

FOR APOLLO /LESA/

SA LUNAR LAUNCH

SA LUNAR MOBILE LABORATORY

/MOLAB/  
Apollo manned space flight program including mission profile, spacecraft and

constituent systems 01 p0143 A66-10799

Basic navigation concepts and techniques used by MIT Instrumentation Laboratory to design Apollo guidance and navigation system 02 p0254 A66-11313

Evolution of navigation systems in Mercury and Apollo manned space vehicles and role of astronaut plays in design of system 02 p0293 A66-11373

Apollo hardware and technology for future manned space exploration, noting MORV spacecraft use 02 p0288 A66-11503

Apollo extension systems, developing technology for long-term manned space mission 02 p0293 A66-11503

Ground support equipment and launch installations for Apollo launch operation and testing 02 p0215 A66-11633

Gemini and Apollo Earth-orbital programs 02 p0185 A66-11633

Apollo Extension Systems program for exploiting capabilities in Saturn/Apollo space vehicle system 02 p0293 A66-11633

Structural, propulsion, guidance and flight control systems of Saturn IB and V Apollo launch vehicles 02 p0294 A66-11633

Navigation concepts and techniques for Apollo manned lunar landing mission 02 p0260 A66-12053

Apollo space suit design discussing construction, purpose and operating conditions of liquid-cooled life support system 03 p0328 A66-12673

Integrated operating mode of Apollo mission simulator with mission control center for combined training of Apollo flight and ground crews [AIAA PAPER 65-266] 03 p0353 A66-12773

Voice communication in space discussing Gemini subsystem, Apollo Command Module system and laser communication techniques 04 p0477 A66-13553

Apollo unified S-band system covering station locations, uplink and downlink spectrums, spacecraft gross parameters, theory of operation, etc 04 p0478 A66-13553

Practice techniques for maintaining astronaut psychomotor skills during extended missions, with star sighting and flight control test results 05 p0626 A66-14633

Conditioning and isolation of Apollo stabilization and control system signals using field effect transistors 05 p0646 A66-14633

Aluminum diffusion bonding for fabrication of Apollo cold plates, noting alternate bonding techniques [SAE PAPER 650779] 05 p0687 A66-15063

Space flight posture of U.S. at completion of AES program and alternate approaches for further lunar exploration and exploitation [SAE PAPER 650833] 05 p0760 A66-15033

Apollo spacecrew training from simulation and actual past space flights [ASME PAPER 65-WA/HUP-17] 05 p0628 A66-15613

Man in Project Apollo including module and module docking, lunar landing, maneuvering, reentry, etc 07 p1140 A66-17213

Apollo and LEM mission simulators, noting computer complex providing real time simulation, mathematical models, telemetry display equipment, aural effects, etc 07 p1018 A66-18333

S-band tracking and communication systems to connect 15 ground stations with large parabolic antennas and Apollo command module and lunar excursion module 07 p1018 A66-18333

Apollo lunar landing spacecraft design, noting command, service, lunar excursion module, etc 08 p1300 A66-18553

Design and program for Apollo Lunar Excursion Module, noting propulsion, guidance, control, ground support, etc 08 p1300 A66-18553

Astronaut selection and crew preparation procedures for Gemini and Apollo programs 08 p1176 A66-18553

Television camera system circuit design, mission requirements and optical response for Apollo mission to Moon 08 p1222 A66-18773

Apollo extension system /AES/ for lunar surface exploration [SAE PAPER 660145] 08 p1296 A66-19333

Gemini and Apollo space programs, present



status, future plans and development trends 09 p1453 A66-20168  
 Gemini and Apollo Earth Orbital flights as precursors to Apollo extension and ORL Earth Orbital missions 10 p1611 A66-21528  
 Astronomical research possibilities, using manned Earth orbital spacecraft 10 p1608 A66-21531  
 Post-Apollo experiments for space 11 p1775 A66-23075  
 Manned space flight program management noting system efficiency, cost factors, reliability and performance reports based on Apollo project 11 p1789 A66-23437  
 Weather support problems in Gemini and Apollo programs [AIAA PAPER 66-334] 12 p1953 A66-24475  
 Evolutionary manned interplanetary exploration program with modular elements used for flyby, orbital capture and Mars landing, noting influence of Apollo program 13 p2179 A66-25241  
 Servo tester with automatic data acquisition and reduction /STADAR/, discussing design and operational capability in Apollo program 13 p2027 A66-25661  
 Audio signal processing techniques in future space exploration, discussing channel capacity, speech processing, bandwidth narrowing, etc 13 p2025 A66-26024  
 Fuel cell power plant for Apollo command and service module from engineering viewpoint [AIAA PAPER 64-748] 13 p2007 A66-26649  
 Structural dynamics/manned space flight relation, discussing man-machine dynamics, Apollo command module LF studies, pilot control of spacecraft and launch vehicle, etc 14 p2230 A66-28017  
 Apollo Manned Space Flight Network /MSFN/ tracking and communications systems for tracking lunar spacecraft 15 p2450 A66-28748  
 High reliability digital test command system for use as part of prelaunch acceptance checkout equipment for Apollo program 15 p2460 A66-28989  
 Apollo/Saturn S-II telemetry data processing systems 16 p2652 A66-30567  
 Lunar charting for project 16 p2743 A66-30669  
 Digital guidance and control computer used in Apollo Guidance and Navigation System 18 p3073 A66-33874  
 Design of Apollo project lunar-based telemetry system for transmitting experiment data to Earth for one year 19 p3300 A66-35671  
 Mobility aids for wheeled surface vehicles and flyers for Apollo lunar surface exploration 19 p3340 A66-35963  
 Apollo Spacecraft Test Data Evaluation System, noting functions, operation and performance 20 p3662 A66-37247  
 Acceptance checkout system for checkout assistance to Apollo CSM and LEM facilities during countdown, discussing system configuration variability, composition and operation 20 p3543 A66-37579  
 Apollo command service module /CSM/ parts management 20 p3684 A66-37882  
 Training seminar for reliability surveyors organized by NASA, particularly for Apollo program, noting content, participation, methodology, etc 20 p3686 A66-37957  
 Trajectories for manned lunar landing, discussing various mission alternatives in planning and realized stages and Apollo project characteristics 20 p3656 A66-38032  
 LEM program history and management in RCA, discussing Apollo mission studies and initial assignments 21 p3822 A66-39516  
 Apollo mission evolution, with particular reference to lunar descent, landing, takeoff and rendezvous performed by LEM 21 p3822 A66-39517  
 Cassegrain monopulse tracking antenna for LEM and Command Module rendezvous guidance 21 p3714 A66-39524  
 Apollo environmental control system simulation chamber for suit and manned system evaluation and operational verification 22 p3892 A66-40241  
 Dynamic stability and aerodynamic damping derivative of Apollo launch escape vehicle, using wind tunnel tests [AIAA PAPER 66-770] 22 p3895 A66-40651

Navigation, guidance and control system instrumentation for Apollo manned lunar landing mission [AGARDOGRAPH 105] 24 p4236 A66-43124  
**APOLLO SPACECRAFT**  
**SA COMMAND MODULE**  
**SA LUNAR EXCURSION MODULE**  
**/LEM/**  
**SA SERVICE MODULE**  
 Communication system for 1969 Apollo spacecraft 01 p0037 A66-10502  
 Apollo spacecraft for manned near-Earth orbital mission, noting Apollo command and service modules and Lunar Excursion Module 02 p0288 A66-11508  
 Automatic control in space reviewing tracking techniques, IR horizon sensors, Apollo spacecraft guidance computer and control systems and terminal guidance system of Surveyor spacecraft 03 p0351 A66-13258  
 Complex and hand-held instrumental devices for celestial navigation, noting Apollo scanner and sextant assembly 04 p0521 A66-14024  
 Data processing procedures of Apollo onboard navigation system for determination of position and velocity 05 p0712 A66-14640  
 Man, system and vehicle simulation program for landing and docking phases of Apollo lunar landing mission 08 p1202 A66-18577  
 Construction and design of Apollo spacecraft, examining high temperature aluminum and titanium alloys and fabricating methods 10 p1545 A66-21217  
 Design and fabrication of computer subsystems for Apollo guidance and navigation systems 13 p2027 A66-25781  
 Thermal protection system for Apollo command module 14 p2393 A66-28004  
 Model tests for determination of structural response of Apollo command module to water impact 14 p2393 A66-28020  
 Integrated checkout of Apollo payloads, command module, lunar excursion module and service module 14 p2271 A66-28423  
 Human response to predicted Apollo landing impacts in selected body orientations 15 p2430 A66-28663  
 Simulated lunar landing maneuver of Apollo spacecraft, determining pilot control problems and handling qualities 16 p2743 A66-30886  
 Manned spaceflight analytical instrumentation uses design tradeoff of reduction in size with loss of versatility 17 p2867 A66-32677  
 Partial differential equations for three-dimensional inviscid flow solved for flow field over blunt body shapes at various angles of attack, for application to Apollo spacecraft [AIAA PAPER 66-413] 18 p3045 A66-33638  
 Checkout criteria and requirements for manned spacecraft, specifically Apollo [AIAA PAPER 65-284] 18 p3093 A66-33791  
 Automatic control systems for attitude control of Apollo spacecraft 18 p3244 A66-33876  
 Guidance and navigational system hardware for Apollo Command Module and LEM 18 p3132 A66-33877  
 Apollo LEM ECS and main subsystems design emphasizing maintenance of pressure, temperature, relative humidity and oxygen at safe levels 18 p3062 A66-33956  
 Microelectronics pulse code modulation /PCM/. multiplexer-encoder for Apollo spacecraft, emphasizing packaging techniques, discussing advance circuit design techniques 19 p3317 A66-35707  
 Implementation and individual units design for DATA-CORE telemetry processing system utilized in data acquisition and processing from Saturn/Apollo 19 p3307 A66-35708  
 Central static inverter used to establish 1250-v, 115/200-v, three-phase 400-cps AC power distribution for Apollo Spacecraft Command and Service Module 20 p3498 A66-37170  
 Entry Monitor System /EMS/ for maneuverable spacecraft, interpreting display relationship to entry trajectory control [AIAA PAPER 65-495] 20 p3592 A66-38160  
 Aerothermodynamic characteristics of

Apollo command module at hyperbolic Earth entry velocities [AIAA PAPER 65-491] 20 p3664 A66-38168  
 Theoretical and experimental data on Apollo command module during water impact 20 p3684 A66-38169  
 Sequential and concurrent chemical engineering operations in solid-propellant Apollo launch motor manufacturing 22 p3968 A66-39867  
 Detached shock wave determination for calculation of shock layer or wake, discussing theories of conic and explosive wave methods for application to Apollo space capsule 22 p3900 A66-40416  
 Base-mounted landing rocket system for Apollo-type vehicle evaluated for heat-shield water pressure, ground effect, vehicle dynamics, etc 22 p3987 A66-40612  
 Land landing system for Apollo spacecraft with roll control, steerable parachutes and landing rocket 22 p3987 A66-40613  
 Premature pressure vessel failure prevention in Apollo spacecraft 23 p4072 A66-41124  
 Apollo launch escape tower electroexplosive bolts produced heat transfer to surrounding structural members, obtaining sound intensity maps 23 p4119 A66-41310  
 Apollo spacecraft parts screening program, showing dependence on reliability for mission success 24 p4216 A66-42090  
 Onboard calculation for navigation and guidance of Apollo mission vehicle [AGARDOGRAPH 105] 24 p4236 A66-43125  
 Inertial measurement unit and pulse torquing of Apollo spacecraft, noting components and operation [AGARDOGRAPH 105] 24 p4215 A66-43126  
 Apollo guidance computer, discussing memory storage, central processing unit and sequence generator [AGARDOGRAPH 105] 24 p4236 A66-43128  
 Apollo spacecraft attitude control, noting phases of application [AGARDOGRAPH 105] 24 p4284 A66-43129  
**APPARATUS**  
**S ABORT APPARATUS**  
**S AIRCRAFT BREATHING APPARATUS**  
**S HYPERSONIC TEST APPARATUS**  
**S INSTRUMENT**  
**S LABORATORY APPARATUS**  
**S LOADING APPARATUS**  
**S MEASURING APPARATUS**  
**S MICROWAVE APPARATUS**  
**S NONELECTRONIC APPARATUS**  
**S OXYGEN APPARATUS**  
**S PENDULUM APPARATUS**  
**S PHOTOELECTRIC APPARATUS**  
**S PHOTOGRAPHIC APPARATUS**  
**S SPRAYING APPARATUS**  
**S TIMING APPARATUS**  
**S VAPOR PRESSURE APPARATUS**  
**S VESTIBULAR APPARATUS**  
**S WIND TUNNEL APPARATUS**  
**APPLICATIONS TECHNOLOGY SATELLITE /ATS/**  
 Gravity gradient stabilization system and sensor subsystem for attitude determination and flight test data on gravity gradient components of applications technology satellite /ATS/ 21 p3820 A66-38859  
**APPROACH AND LANDING**  
 Approach and landing visibility requirements in terms of information needed by civil pilot 01 p0101 A66-10032  
 Lateral-directional handling qualities of large transport, examining factors involved in pilot maneuvers 01 p0101 A66-10037  
 Propeller control at low airspeed on turboprop engines in any fixed-wing aircraft, with special reference to thrust or drag in approach and landing [AIAA PAPER 65-709] 01 p0013 A66-10946  
 Airport approach standards used to protect approaches to airports 02 p0260 A66-12221  
 Propeller control at low airspeed on turboprop engines in any fixed-wing aircraft, with special reference to thrust or drag in approach and landing [AIAA PAPER 65-709] 09 p1329 A66-20242  
 Fog chamber tests and runway lighting requirements, considering landing, cockpit vision and photometry [AIAA PAPER 65-333] 12 p1857 A66-23801  
 Illumination systems used as visual aids for pilots when approaching



airport 12 p1857 A66-24089  
 Lateral-directional handling qualities of large transport, examining factors involved in pilot maneuvers 16 p2634 A66-31318  
 Transport approach and landing visibility requirements, examining design of forward portion of airplane 17 p2950 A66-32683  
 Manual steering, hybrid guidance system, in-flight computations and trajectory for automatic descent and landing system for LEM 21 p3768 A66-38899  
 Approach and landing system with added monitoring channel for category II weather conditions 23 p4088 A66-41137

**APPROACH AND LANDING INSTRUMENT SA AIRCRAFT APPROACH AND LANDING INSTRUMENT**  
 Adaptive coupler providing extended automatic glide slope beam following by compensating for beam convergence 01 p0101 A66-10036  
 Feasibility of monopulse radar used for airborne pictorial radar display as aid to low approach aircraft landing 17 p2950 A66-31964  
 Instrument low-approach system and low-level precision radio altimeter for all-weather landings 17 p2951 A66-33100  
 Head-up display used during transition from instrument to visual contact in Category II operations based on pilot sensitivity to movement and peripheral vision 17 p2953 A66-33210

**APPROACH CONTROL**  
 Spacecraft guidance during distant approach stage of rendezvous with orbital station and information on rotation of sighting line 18 p3245 A66-33885

**APPROXIMATION**  
 S BORN APPROXIMATION  
 S BOUSSINESQ APPROXIMATION  
 S OSEEN APPROXIMATION  
 S PADE APPROXIMATION  
 S POHLHAUSEN SOLUTION  
 S QUADRATURE APPROXIMATION  
 S SOMMERFELD APPROXIMATION

**APPROXIMATION METHOD**  
 Approximate solution for differential equations, using algorithm applied to boundary value problem involving linear equation 01 p0091 A66-10164  
 Velocity distribution in turbine stage with compressible medium for repeating axial velocity profile derived, employing approximation method 01 p0130 A66-10211  
 Approximate calculation of Wiener integration 01 p0092 A66-10317  
 Charge trapped in electron or ion beams at pressures below breakdown determined from general integro-differential equation, using approximation method 01 p0111 A66-10375  
 Attached coordinate system for approximate solution of compression waves emitted by expanding sphere at constant rate in ideal medium 01 p0057 A66-10420  
 Approximate determination of flow characteristics around multistage nonstationary blade configuration, using singularity method 01 p0006 A66-10442  
 Intermediate stages of wave-type bending process in elastic plate investigated by system of approximate methods 01 p0157 A66-10983  
 Covariance matrix approximation and conservative error volume estimate 02 p0249 A66-11568  
 Approximation method reproducing assigned time functions by using exponential polynomials in synthesis problems of electrical circuits 02 p0207 A66-11752  
 Approximate solution of principal boundary value problem of electrostatics 02 p0262 A66-12246  
 Approximation method for momentary peak shaft loads, computing starting and stalling torques of power transmission system 02 p0238 A66-12266  
 Successive approximations for variational problems in control theory including pulse amplitude and pulse width modulation, using quasi-linearization techniques 03 p0349 A66-12685  
 Approximation of band-limited function by sum of cosines arising in design of phased array antennas 03 p0342 A66-12709  
 Continuous periodic functions approximation by Fejer and arithmetic means 03 p0388 A66-12712

Class of periodic functions for which given method of summation gives trigonometric approximation of optimal order 03 p0388 A66-12713  
 Scalar quantity spectrum in statistically stationary turbulent velocity field, using closure approximations to provide unified comparison, noting eddy diffusivity, transfer function, etc [AIAA PAPER 65-814] 03 p0357 A66-13082  
 Method which for given relation yields high order approximation for any type of transistor 03 p0345 A66-13239  
 Uniqueness of optimum approximation sums of single variable functions for multivariable functions in Lebesgue space 04 p0538 A66-13485  
 Approximation of spherical functions by analogs of Fejer and Vallee-Poussin sums 04 p0539 A66-13486  
 Number theoretic method to approximate solution of linear integral equations 04 p0539 A66-13488  
 Reduction of Rabotnov approximate equation describing steady creep in circular cylindrical shells, under axisymmetric loading, to system of integral equations 04 p0588 A66-13567  
 Successive linearization for variational problems of flight mechanics 04 p0458 A66-13698  
 Approximate determination of correct detection probability in optimum signal reception of unknown phase 04 p0482 A66-13913  
 Local gravity anomalies for circular cylinder with vertical axis, discussing solution to direct and inverse problems of quantitative interpretation of fields 04 p0516 A66-13960  
 Rotating polytrope structure analyzed, using approximation technique of integrating outwards from center and inward from surface 04 p0578 A66-14018  
 Bergeron and first approximation method for solving problems of unsteady fluid flow in pipeline 04 p0511 A66-14157  
 Extremum problem connected with simultaneous approximations of some functions analyzed by polynomials and derivatives 04 p0540 A66-14467  
 Approximation formulas for minimum and maximum roots of nth order polynomials 05 p0707 A66-14624  
 Approximate solution of first biharmonic problem for spatial simply-connected finite region 06 p0902 A66-16231  
 Linear dynamical systems with weak coupling solved approximately, noting examples and definition 06 p0862 A66-16362  
 Maximum accuracies of parameter estimates for complex signals reflected from several points 06 p0837 A66-17191  
 Approximate methods for plotting logarithmic frequency responses of discrete systems with and without time lag, noting PAM systems 07 p1012 A66-17382  
 Approximate method determining nonstationary thermal fields in solid bodies with thermal capacity and thermoconductivity coefficient depending linearly on temperature 07 p1148 A66-17392  
 Point-matching method, approximate technique for wave equations of uniform waveguides with very general cross sections 07 p1007 A66-17510  
 Radiant transport with isotropic scattering, evaluating approximate solutions for reflection and transmission of parallel plane radiation 07 p1152 A66-17589  
 Approximation theorem and uniqueness theorem for abstract equations with almost periodic coefficients 07 p1056 A66-17603  
 Networks method applied to approximate solution of heat conduction equation for spatial boundary conditions with aid of theory of hypermatrices 07 p1153 A66-17863  
 Optimum control calculated by iteration method 07 p1016 A66-17910  
 Approximate solution of magnetospheric free boundary for steady state interaction between field-free streaming plasma and magnetic dipole 07 p1088 A66-17952  
 Second approximation of compressible subsonic flow over given wing profile reduced to regular Dirichlet problem 07 p0981 A66-18110  
 Hypersonic gas flow past axisymmetric

slender blunt body by Chernyi approximate method 07 p0983 A66-1814  
 Nonsimilar solution of incompressible boundary layer over flat plate in presence of shear flow, using approximate method 08 p1204 A66-1852  
 Approximate method for examining stress-strain state of anisotropic body with elliptical holes via reduction to infinite algebraic system 08 p1304 A66-1855  
 General relation between third-order approximation stress function and complete displacement function in problem of finite plane deformations of incompressible materials 08 p1304 A66-1855  
 Stress concentration study using third-order approximation operators for tangential stress components of cylindrical shell with elliptical, triangular and square holes 08 p1305 A66-1855  
 Scattering by small discontinuities in single or multimode waveguides by lowest order approximation 08 p1189 A66-1860  
 Reentry guidance by threshold network, storage of precomputed optimum command, using analogy of surface approximation problem in N plus one-dimensional space [AIAA PAPER 66-52] 08 p1249 A66-1899  
 Lunar crater distribution measurements from Ranger VII photographic data analysis deriving approximate expression for secondary distribution 08 p1297 A66-1941  
 Approximation method solution for elastoplastic distribution of stresses infinite plane with square hole for case compressive force plane deformation 08 p1313 A66-1941  
 Digital simulation of magnetic hysteresis using analytic approximation of magnetic curves by seventh degree polynomials 08 p1187 A66-1951  
 Approximate method for solving inverse scattering of radio waves from conducting bodies of complex shape 08 p1185 A66-1961  
 Uniform approximation by polynomial solutions for differential equation 08 p1245 A66-1961  
 Phased oscillator stability solved, using hydrodynamic approximation 08 p1266 A66-1961  
 Schuessler-elliptic low pass filters, discussing solution of approximation problem for low pass filters with good transient response 08 p1198 A66-1974  
 Radio wave absorption coefficients, calculated, using approximations of magnetoionic formulae 09 p1341 A66-1986  
 Intrinsic noise effect on synchronization of self-excited oscillators, determining phase diffusion coefficient, frequency fluctuation spectra and spectral line length 09 p1344 A66-2034  
 Approximate analysis of spacecraft trajectories in circular extra-atmospheric, anaorbital flight 09 p1457 A66-2051  
 Runge-Kutta fourth order formula used to obtain approximate solution to differential equations 09 p1395 A66-2063  
 Numerical integration of coupled first order ODE of greatly differing time constant 09 p1395 A66-2063  
 Power series drawbacks as tool for numerical solution of differential equations 09 p1395 A66-2063  
 Deriving interpolatory type quadrature formula by inverting linear systems of differentiation formulas 09 p1395 A66-2063  
 Tensor product analysis of alternative direction implicit iteration techniques for approximate solution of elliptic partial differential equations 09 p1396 A66-2063  
 Approximate solution for elasticity problems, noting mathematical determination of stress distribution in any homogeneous isotropic body 09 p1468 A66-2066  
 Characteristic TWT equation solved for large space-charge parameter 09 p1357 A66-2071  
 Transistorized LR oscillator design using piecewise linear approximation in oscillation theory 09 p1357 A66-2071  
 Floquet form of solution to system of linear differential equations with periodic parameters 09 p1363 A66-2071  
 Upper atmosphere temperature and pressure measured with manometers mounted on rockets, using method of



successive approximations 09 p1375 A66-20988  
 Monte Carlo linear extrapolation of  
 multivariable functions, introducing  
 truncation procedure which saves on  
 machine time and serves for variance  
 reduction 10 p1549 A66-21215  
 Comparing modified method of averaging  
 and two-variable expansion procedure in  
 nonlinear oscillations of autonomous  
 system 10 p1555 A66-21344  
 Unsteady airfoil functions evaluated  
 approximately 10 p1479 A66-21345  
 Aerodynamic forces of oscillating lifting  
 surfaces of large aspect ratio in subsonic  
 range investigated by approximation  
 method 10 p1479 A66-21378  
 Bimodal formulation applied to chemical  
 reactions in turbulent wake flow behind  
 hypersonic spheres, using quasi-one-  
 dimensional model 10 p1480 A66-21771  
 Multidimensional radiation transport  
 equations for nonscattering quasi-  
 equilibrium gray gas obtained by spherical  
 harmonic approximation  
 [ATAA PAPER 65-81] 10 p1621 A66-21774  
 Phased oscillator stability solved, using  
 hydrodynamic  
 approximation 10 p1568 A66-21835  
 Computational solution of functional  
 differential equations, using successive  
 approximations 10 p1551 A66-21922  
 Approximation of continuous and  
 differentiable functions by algebraic  
 polynomials on closed  
 interval 10 p1551 A66-21976  
 Theorems for uniform approximations by  
 algebraic and trigonometric rational  
 functions, noting application in determining  
 functional properties 10 p1552 A66-21984  
 Model approximation method for induced  
 elastic and thermal characteristics of  
 materials reinforced by circular cylindrical  
 fibers 11 p1720 A66-22231  
 Successive approximations method for  
 calculating optimum regimes of some  
 systems with distributed parameters, using  
 gradient procedure 11 p1674 A66-22357  
 Diffraction by conducting cylinder solved  
 by approximation method, using expanded  
 series of diffraction field of cylinder with  
 polygonal section 11 p1662 A66-22464  
 Hartree-Fock approximation method for  
 calculating efficiencies of multiple-photon  
 processes 11 p1737 A66-22495  
 Successive approximation method for  
 elastic-plastic plane stress-strain  
 analysis 11 p1781 A66-22690  
 Shock structure calculations from kinetic  
 theory, using ellipsoidal distribution  
 function 11 p1690 A66-22912  
 Theoretical and machine aspects of  
 ignoring singularity in approximate  
 integration, relating uncertain cases to  
 diophantine  
 approximation 11 p1722 A66-22981  
 Computational aspects of uniform  
 polynomial approximation to function and  
 derivative 11 p1722 A66-22983  
 Error bounds in best approximation of  
 given function in Banach space constrained  
 by inequality  
 relationships 11 p1722 A66-22984  
 Numerical analysis of thin cylindrical shell  
 under action of external forces for small  
 deformations, using first-order  
 theory 11 p1783 A66-23016  
 Multidimensional spline theory generalized  
 from one-dimensional spline theory and  
 preserving minimum curvature, best  
 approximation and convergence  
 properties 11 p1723 A66-23182  
 Mathematical approximation for alpha of  
 drift transistors derived in terms of  
 equivalent dominant pole and excess  
 phase 11 p1671 A66-23245  
 Successive approximation methods of  
 solving optimal control problems, based on  
 variational calculus and Euler-Lagrange  
 equation 11 p1679 A66-23273  
 Parameter estimation utilizing state vector  
 model, regression methods, asymptotic  
 methods, etc 11 p1680 A66-23278  
 Approximation of function of many  
 variables by linear  
 methods 11 p1723 A66-23313  
 Takeoff dynamics of VTOL aircraft, noting  
 thrust-weight ratio, wing load, initial thrust  
 angle, engine tilt, etc 11 p1733 A66-23339

Graphical-analytical method using  
 successive approximations determines  
 guided missile trajectory 11 p1734 A66-23344  
 Approximation methods for matrix  
 computation, considering characteristic  
 roots 11 p1723 A66-23361  
 Linear approximation method for  
 continuous periodic functions based on  
 theorems concerning relation between  
 triangular matrix and continuity modulus of  
 subset of functions 11 p1724 A66-23365  
 Schauder-type solution estimates to first  
 boundary value problem for parabolic  
 equations of order 2p 12 p1901 A66-23663  
 Construction of rational second order  
 kernels with aid of rational functions of  
 order n, applying result to theory of  
 approximation of  
 functions 12 p1902 A66-23765  
 Space and time dependent randomly  
 distributed stress and temperature fields in  
 cylinder with deformable surface calculated,  
 using approximation  
 method 12 p1959 A66-23864  
 Transformation relation for prestress  
 tensor in problem of indifferent equilibrium  
 of elastic bodies derived, using  
 approximation method 12 p1959 A66-23865  
 Approximate solution of equation with  
 normally distributed  
 operators 12 p1902 A66-23899  
 Approximation of expectation values for  
 nonequilibrium properties via perturbation  
 theory, obtaining values for molecular  
 polarizability 12 p1917 A66-23935  
 Quantitative information regarding validity  
 of certain approximations applicable to  
 sandwich plate analysis 12 p1960 A66-23972  
 Approximate determination of flexural  
 vibrations of shells of revolution with  
 vibrations involving appearance of nodal  
 lines along generatrix and meridional  
 directions 12 p1964 A66-24047  
 Supersonic flow around blunt body  
 calculated via integral relations, using  
 simultaneous approximation function in two  
 directions 12 p1797 A66-24208  
 Solution of Kepler equation by stepwise  
 approximation, discussing elliptical orbit,  
 parabolic ellipse and hyperbolic  
 orbit 12 p1950 A66-24398  
 Hypersonic flow of inviscid gas past cone,  
 obtaining solution for entire flow including  
 turbulent boundary layer and velocity field,  
 using zero approximation  
 method 12 p1798 A66-24440  
 High performance active RC band pass  
 filter design providing for independent  
 adjustment of poles 12 p1843 A66-24675  
 Strong plane shock produced in Al by  
 hypervelocity impact and late stage  
 equivalence examined, using analytical and  
 graphical solution of method of  
 characteristics and realistic state  
 equation 13 p2194 A66-25061  
 Statistical distribution of first occurrence  
 and recurrence of crossing of given level in  
 continuous random process determined,  
 using approximate forms and exponential  
 distribution 13 p2116 A66-25141  
 Successive approximations to determine  
 vector in theory of optimal  
 control 13 p2045 A66-25294  
 Monte Carlo calculations of cross section  
 magnitude of electron-positive-molecular-ion  
 dissociative  
 recombination 13 p2130 A66-25375  
 Numerical values describing molecular  
 rainbow scattering in Airy approximation for  
 12-6 potential 13 p2130 A66-25379  
 Plane electromagnetic wave diffraction by  
 narrow strip-grating, obtaining reflection  
 coefficient via optical approximation  
 method 13 p2021 A66-25395  
 Approximate solution of Navier-Stokes  
 equations applicable to viscous and  
 incompressible fluids 13 p2062 A66-25429  
 Explicit approximate solution for  
 distribution of constraints along wall of  
 revolution assuming limiting equilibrium and  
 for case of system with discontinuity  
 line 13 p2195 A66-25443  
 Second order approximation and  
 perturbation theory applied to determine  
 effect of instantaneous pulse on oscillation  
 amplitude 13 p2127 A66-25451  
 Quasi-linear approximation method and  
 Poisson equation used in determining static

fields and electron redistribution in plasma  
 waveguides 13 p2039 A66-25678  
 Integral relations method to reduce by  
 approximation PDEs to ODEs or to algebraic  
 or transcendental  
 equations 13 p2119 A66-25854  
 Method for automatically adjusting  
 networks for best approximation to desired  
 responses, using iterative gradient  
 techniques, constraint equations and Carroll  
 programming technique 13 p2051 A66-26070  
 Iterative approximation of rational transfer  
 function in Laplace transform variable s,  
 optimal with respect to given input and  
 output time functions, and deviation from  
 desired output-input-time functional  
 relation 13 p2054 A66-26087  
 Ionization cross section for rare gases and  
 hydrogen atoms calculated from  
 perturbation theory, noting ruby laser  
 photon absorption 13 p2133 A66-26188  
 Stressed state of isotropic elastic medium  
 with two circular holes solved, using  
 approximation method for concentrated  
 loads 13 p2202 A66-26417  
 Approximation method for determining  
 limit and breaking load for infinite brittle  
 body weakened by plane crack, noting crack  
 propagation 13 p2203 A66-26423  
 Stress-strain state of plate with circular  
 hole, noting stress concentration, material  
 creep properties and solution by successive  
 approximation 13 p2204 A66-26436  
 Nonlinear ordinary differential equations  
 applicable to damped oscillatory circuits  
 with exploding wires, obtaining conservation  
 law and approximate solutions by Picard  
 method 13 p2129 A66-26667  
 Approximation method for evaluating body  
 flexibility effects on slender aircraft static  
 stability, noting application to sounding  
 rocket 13 p1994 A66-26734  
 Justification for multiple isothermal layer  
 approximation to real atmospheric acoustic-  
 gravity wave propagation 14 p2234 A66-26857  
 Equations from hydrodynamic equations,  
 determining steady state fields and currents  
 in plasma caused by microwave field, using  
 quasi-linear  
 approximation 14 p2341 A66-27153  
 Approximation of variable time delays and  
 design of constant and variable delay  
 circuits, noting simulation of delays in  
 automatic control systems by  
 computers 14 p2266 A66-27528  
 V-I characteristics of tunnel diode by  
 approximation method of polynomials of  
 degree no higher than  
 sixth 14 p2254 A66-27739  
 Results of approximate computation of  
 rocket apogee from data on flight duration  
 between different trajectory  
 points 14 p2383 A66-27815  
 Molodenskii first approximation equations  
 used in determination of characteristics of  
 terrestrial gravitational field, noting  
 techniques to average  
 corrections 14 p2288 A66-28213  
 Laminar fluid flow in channel generated by  
 arbitrary generatrix, allowing for interaction  
 between boundary layer and flow core,  
 calculating boundary  
 layer 14 p2278 A66-28316  
 Approximate synthesis of second-order  
 optimum system with controlled  
 coefficients 14 p2269 A66-28479  
 Polynomial approximation method for  
 determining satellite orbits from large-time-  
 interval trajectory  
 measurements 15 p2592 A66-28488  
 Successive linearization for variational  
 problems of flight  
 mechanics 15 p2425 A66-28539  
 Input and output coupling constants of  
 spin-2 mesons with two pseudo-scalar  
 mesons obtained by producing resonances at  
 experimentally observed  
 positions 15 p2544 A66-28947  
 Minimax problem for pursuit problem of  
 two linearly controlled objects describable  
 by identical differential  
 equations 15 p2526 A66-28948  
 Boundary between applicability ranges of  
 network and steepest descent methods in  
 equation integration of Timoshenko theory  
 in analysis of plate  
 deformation 15 p2608 A66-28962  
 Iterative derivation of approximation of



real function by exponential series 15 p2527 A66-29056

Kosmodamianskii approximate method for solution of tension problem of isotropic plate with two similar circular holes reinforced by rigid rings 15 p2613 A66-29431

Approximation method for solution of bending problem of isotropic plate resting on rigid columns to cover case of anisotropic plate with reinforced elliptic hole 15 p2613 A66-29434

Approximate solution of free axisymmetric oscillations of circular structurally orthotropic plate of specific laws of variable thickness 15 p2613 A66-29436

Uniqueness, existence and stability of solutions to polyvibrant systems with delayed remainder and arguments 15 p2528 A66-29652

Approximate method, using power polynomials, for calculating distance between detached shock wave and profile 15 p2425 A66-29721

Multicategory pattern recognition, noting mathematical treatment, dimensional and correlational effects, etc 15 p2453 A66-29774

Approximation method for thermal diffusion factor of almost Lorentzian gas mixture with better convergence properties than Chapman-Enskog approximation 16 p2824 A66-30119

Planar subsonic flow around circular cylinder using Kisseleff approximation method for compressible fluid 16 p2627 A66-30210

Hermite interpolation combined with Ritz method for numerical approximation of solution of two-point boundary value problems 16 p2732 A66-30243

Differential approximation linearization technique compared with Galerkin method 16 p2732 A66-30265

Approximation method for limit Nusselt number for channels of nonuniform geometrical configuration and linearly variable wall temperature 16 p2684 A66-30677

Unperturbed motion for follow-up systems in critical case of double zero root, noting stability and correspondence of root to solution of first approximation equation 16 p2733 A66-30738

Closed-loop automatic control system with univalued substantially nonlinear element, using approximation of characteristics by Fourier series 16 p2669 A66-30754

Approximation method determining follow-up failure conditions for nonlinear automatic systems in presence of control and noise signals 16 p2669 A66-30755

Function approximation from finite number of arbitrary points, using iteration methods 16 p2734 A66-30760

Reliability of finite automata determined from analysis of elements capable of misalignment, input errors and structural design 16 p2669 A66-30761

Method of approximating functions with aid of orthonormal systems and single channel optimization, using analog computer 16 p2656 A66-30764

Approximate analysis of nonlinear systems similar to harmonic oscillators, using Chaplygin theory of differential inequalities 16 p2705 A66-30781

Uniform approximation by polynomial solutions for differential equation 16 p2736 A66-30982

Error estimates for approximation formulas for Bessel functions and Hankel functions obtained, using Luke trapezoidal rule 16 p2736 A66-31021

Harmonic approximation of infinite crystal dynamics problem, noting collisional case and action of external force on atoms 16 p2820 A66-31169

Segmental differential approximation in system identification with data available 16 p2656 A66-31227

Generalization of Barbier-Eddington approximation, for inversion of darkening law 16 p2803 A66-31258

Collision cross sections of ions in isoelectronic sequence of lithium, noting dipolar transitions of type  $2s$  to  $np$  16 p2754 A66-31261

Numerical differentiation by differential quotients, interpolations, Richardson-Romberg algorithm and other methods,

including analysis of approximation errors 16 p2858 A66-31347

Approximate substitution of ordinary dynamical systems for systems with retardation by increasing order of ordinary differential equations 16 p2748 A66-31505

Improved Donnell equations for concentrated load of circular cylindrical shell 16 p2823 A66-31717

Flowgraph techniques for closed systems, discussing properties, approximation method, topology equation, frequency response, constraints, oscillatory and stochastic processes, etc 17 p2898 A66-31954

Steady state circuit analysis of basic linear parametric amplifier using successive approximation 17 p2880 A66-32058

Approximate calculation of free convective heat transfer in rectangular region 17 p3034 A66-32562

Necessary condition for optimal control in nonlinear automatic control system determined, using method of successive approximations 17 p2902 A66-32574

Successive approximation solution to integral kinetic equation and corrections to moments of distribution function for viscous and rarefied gases 17 p2909 A66-32585

Assessment of error of method of successive approximations in determination of circular plate deflections 17 p3026 A66-32598

Computer solution using Bubnov-Galerkin method to determine concentrated force effect on shallow spherical dome 17 p3026 A66-32601

Electron capture detector parameters in pulse sampling mode analyzed, noting kinetic processes, temperature effect, etc 17 p2961 A66-32660

Approximation theory by generalized rational functions 17 p2947 A66-32843

Section moments of inertia by approximation method 17 p3030 A66-32967

Iteration scheme based on Newton approximation method applied to two-dimensional and rotationally symmetric flows past obstacles 17 p2913 A66-33066

Radar return from perfectly reflecting target in presence of second medium, obtaining first approximation for return and accounting for multiple reflections and dispersion 17 p2876 A66-33104

Point matching method calculation of cut-off frequencies and field configurations of waveguides with general cross section 17 p2896 A66-33278

Textbook on numerical solution of initial value problems and approximate numerical integration 17 p2948 A66-33436

Approximate solution of boundary layer problems by variational techniques, using multiparameter approach 18 p3096 A66-33594

Rational approximations for lower natural frequencies of uniform beam with concentrated mass or rotary inertia obtained by expanding eigenvalue equation into power series 18 p3249 A66-33599

Solution method for use when linear combinations of given approximate solutions are used for representing exact solution of general ordinary linear homogeneous differential equation 18 p3125 A66-33627

Plane contact problem for circular ring and elastic or absolutely rigid disk, using method of successive approximations 18 p3252 A66-33710

Approximation method for compressible laminar heat transfer to blunt axisymmetric bodies in high speed flow 18 p3048 A66-33824

Approximation techniques for determination of optimum uniform or nonuniform quantizer 18 p3068 A66-33904

Approximation solution to plane bend problem in thin rod of variable rigidity 18 p3254 A66-33933

Diffraction of linearly polarized electromagnetic wave by coaxial cylinders, deriving approximate solution for wavelengths smaller than distance between cylinder centers 18 p3068 A66-33977

Correction of magnetic measurements made by Mariner II, noting use of second-order approximation for interplanetary magnetic field 18 p3106 A66-34333

N/D and determinantal methods of partial wave dispersion relations applied to Yukawa potential scattering 18 p3138 A66-34453

Transport properties of ionized monatomic gases, using Chapman-Enskog-Burnett approximation method for determination of thermal conductivity, diffusion coefficient and viscosity 18 p3149 A66-34927

Approximate method for solving inverse scattering of radio waves from convex conducting bodies of complex shape 18 p3072 A66-34967

Asymptotic expression for difference between continuous periodic function and typical mean of Fourier series 18 p3128 A66-35011

Approximation technique for flow graph that eliminates nonessential equivalent circuit elements, providing for derivation of most concise model with preassigned accuracy 18 p3092 A66-35044

Radiation transport in spectral lines and consecutive photon absorptions and emissions, discussing contemporary theories, approximation methods and applications 18 p3120 A66-35073

Dispersion degree of coherent scattering regions, microdeformation and packing defects probability in fcc metals determined, using approximation method 19 p3438 A66-35498

Maximum accuracies of parameter estimates for complex signals reflected from several points 19 p3297 A66-35544

Stratification with bottom heating analysis, using approximate integral approach 19 p3477 A66-35631

Error in plane-layer approximation of boundary layer emission associated with gray gas flow past plane plate 19 p3341 A66-35758

Reduction of variance by least squares polynomial approximations, noting exact functional dependence of variance on degree of polynomial 19 p3388 A66-35833

Two-dimensional problems in which heat flow is predominantly in one direction solved by approximate methods, noting constant profile of temperature role 19 p3478 A66-35852

Missile and rocket launching with static instability, deriving approximate solution for equations of longitudinal accelerated motion 19 p3470 A66-36068

Approximation of continuous and differentiable functions by algebraic polynomials on closed interval 19 p3390 A66-36182

Theorems for uniform approximations by algebraic and trigonometric rational functions, noting application in determining functional properties 19 p3390 A66-36188

Schauder-type solution estimates to first boundary value problem for parabolic equations of order  $2p$  19 p3390 A66-36188

Approximation technique for analysis of two-dimensional boundary layer flows with arbitrary external velocity distribution 19 p3341 A66-36322

Approximation method for transitive section calculation of turbulent jet obtaining velocity profiles for initial arbitrary sections 19 p3276 A66-36446

Numerical approximation of Riemann integration for plane gas flow at supersonic speeds 19 p3276 A66-36478

Approximation method for checking stability of compression members in rigid joint space truss or stability against out-of-plane buckling of compression members in rigid-joint plane truss 19 p3475 A66-36488

Propagation of spherically symmetric cylindrically symmetric and plane waves examined via analytic perturbation method in solving gas dynamics equation for nonstationary compressible flow 19 p3343 A66-36667

Approximation theory for calculating linearized subsonic and supersonic flow over pulsating bodies with low aspect ratio noting structure of flow field 19 p3277 A66-36667

Iterative approximation method for solution of proper elements/eigenvalue/Sturm-Liouville equation 19 p3392 A66-36747

Fourth-order multipoint iterative method for solving equations which cost or function and two derivative evaluations per iteration, for use in root finding 19 p3392 A66-36747

Transfer process effect on stability



- plane flame front, deriving revised  
approximate solution for large finite  
keynolds numbers 19 p3479 A66-36829
- Synthesis parametry of ensemble-averaged  
second-order polynomial approximation to  
performance index of optimal guidance  
linear feedback control system 20 p3589 A66-36858
- Unimodal function minimum located by  
successive approximations to interval of  
uncertainty 20 p3589 A66-36903
- Approximate solution for dipole radiator  
field in space containing two conducting  
ong cylinders with parallel  
axes 20 p3512 A66-37146
- Maximum sample excursions of Kiefer-  
Wolfowitz stochastic approximation  
processes 20 p3590 A66-37364
- Self-focusing and self-trapping of intense  
light beams in nonlinear medium examined,  
using approximations of geometrical optics  
and accounting for diffraction  
effects 20 p3602 A66-37372
- Monotony principle for linear  
approximations to determine upper and  
lower bounds of minimum deviation in  
approximating functions of real variable by  
generalized polynomials 20 p3590 A66-37529
- Monograph on approximate analysis of  
randomly excited nonlinear controls,  
discussing feedback system performance,  
functional and quasi-functional  
representation, zero mean systems,  
etc 20 p3538 A66-37577
- Open and closed-loop network synthesis  
using transient-response  
approximation 20 p3538 A66-37581
- Approximate method of integrating  
linearized equation for laminar boundary  
layer to establish relations of velocity  
distribution with friction  
stress 20 p3546 A66-37679
- Approximate determination of correct  
detection probability in optimum signal  
reception of unknown  
phase 20 p3518 A66-37871
- Bounds on reliability, life distributions and  
open problems for  
structures 20 p3574 A66-37964
- Monograph on solving shell stability  
dynamic problems by geometric  
approximation 20 p3671 A66-37983
- Second approximation of transonic theory  
as laws for thin bodies 20 p3493 A66-37988
- Successive approximation method for  
solving fundamental equations of nonlinear  
flexural vibration for rectangular elastic  
plate, noting effect of temperature and  
large amplitude 20 p3672 A66-38236
- Atmospheric turbulence coefficient  
determination from flow fluctuations,  
measuring error as function of observation  
duration 20 p3594 A66-38379
- Sudden approximation applied to rotational  
transition probabilities and inelastic total  
cross sections for scattering of homonuclear  
atomic molecules by  
atoms 21 p3774 A66-38526
- Extension of pairing theory of  
superconductivity to electron-phonon  
coupling, applying Landau quasi-particle  
approximation 21 p3796 A66-38552
- Krylov-Bogoliubov method applied to linear  
differential equations, noting transcendental  
functions and error  
analysis 21 p3755 A66-38596
- Approximate method for solution of  
dynamic stability problem of shafts  
subjected to pulsating moment and constant  
axial force 21 p3743 A66-38621
- Metric vector space with one-dimensional  
linear subspace not  
approximating 21 p3756 A66-38809
- Energy transport by electromagnetic  
waves, using successive  
approximations 21 p3770 A66-38946
- Approximate method for determining  
damping factors of mechanical oscillatory  
systems with many degrees of freedom  
described by linear differential equations of  
-th order with constant  
coefficients 21 p3770 A66-38971
- Generalized Rolle and Bernstein theorems  
applied to polynomial approximation of  
ordinary differential equations over compact  
linear space 21 p3758 A66-39259
- Moments of output coordinates of  
nonlinear system determined by algorithm  
based on approximation method, noting  
application to automatic control  
system 21 p3758 A66-39283
- Nonlinear automatic system with logical  
device analyzed in presence of external  
action, obtaining harmonic linearization  
coefficients 21 p3719 A66-39284
- Difference approximations to PDEs of fluid  
dynamics used to determine necessary  
condition for stability, examining advective,  
diffusive and inertial  
terms 21 p3730 A66-39471
- Approximation of nonlinear characteristics  
of conservative vibrations by two polygon  
characteristics chosen so that mechanical  
energy of system remains  
same 21 p3833 A66-39599
- Amplitude friction effect in single degree  
of freedom vibrating system by developing  
amplitude into approximate trigonometric  
series 22 p3917 A66-39669
- Characteristic TWT equation solved for  
large space-charge  
parameter 22 p3874 A66-39838
- Transistorized LR oscillator design using  
piecewise linear approximation in oscillation  
theory 22 p3874 A66-39843
- Time dependent Ising-model description of  
binary liquid mixture near critical  
temperature 22 p3947 A66-39922
- Conditions under which optimal wave  
functions satisfy various time-dependent  
Hellmann-Feynman  
theorems 22 p3947 A66-39923
- Asymptotic formulas for approximate  
solutions of Cauchy problem by difference  
techniques, considering error of tabulated  
elements 22 p3939 A66-40154
- Addition of uniform and Gaussian  
distributions, exact and approximate  
solutions 22 p3939 A66-40171
- Statistical properties of dynamic response  
of structure to random load field, examining  
simple deterministic  
loadings 22 p3993 A66-40359
- Euler-Lambert equation for orbital transfer  
in Newtonian field solved by approximate  
method 22 p3981 A66-40475
- Nonlinear boundary value problem for  
temperature distribution in convex solid  
with radiation boundary  
condition 22 p3999 A66-40565
- Supersonic flow around blunt body  
calculated via integral relations, using  
simultaneous approximation function in two  
directions 22 p3844 A66-40572
- Approximate solution of PDE for heat  
transfer in uniform-property universal  
turbulent boundary layer 22 p4001 A66-40923
- Reduction of PDE system of heat transfer,  
using Hermitian approximating polynomials  
to obtain solution to initial  
system 23 p4041 A66-40971
- Approximate solution of boundary value  
problems in elasticity theory as applied to  
thin plate theory, using homogeneous  
equations 23 p4136 A66-41000
- Analytical approximate solution of motion  
equations for ballistic vehicles during  
atmospheric entry, examining velocity and  
inclination angle error dependence on height  
eccentricity and apogee radius  
[ICAS PAPER 66-38] 23 p4007 A66-41010
- Approximation method for maximizing  
nonlinear separable function with two-sided  
limitations on unknowns, given common  
lower boundary for difference modulus of  
unknowns 23 p4088 A66-41059
- Particle-in-cell /PIC/ method for  
approximate solution of propagation and  
reflection of plane shock waves in dusty  
gases 23 p4054 A66-41158
- Disperse material heating by simultaneous  
radiative and convective energy with  
temperatures expressed as integral  
equations 23 p4148 A66-41270
- Successive approximation method for  
optimization of nonlinear systems of  
ordinary differential equations with  
limitations on phase  
coordinates 23 p4084 A66-41352
- Reciprocal theorems of best  
approximations of complex variable,  
considering domain restricted by finite  
number of smooth curves forming nonzero  
angles at junction points 23 p4084 A66-41353
- Supersonic gas flow problems around  
lattice of conical blades solved in any  
approximation of perturbation  
theory 23 p4008 A66-41358
- Electric microfields in plasma taken as  
system of charged particles moving in  
uniform neutralizing background, using  
approximations and Monte Carlo  
study 23 p4101 A66-41363
- Kinetic equations in hydrodynamic  
approximation for weakly reacting and  
excited Bose systems, finding asymptotic  
expressions for Green  
function 23 p4055 A66-41412
- Stochastic form of decaying isothermal  
second-order reactions, comparing exact  
solution with various closure  
approximations 23 p4055 A66-41498
- Quasi-linear approximation for turbulent  
plasma obtained via Wiener-Hermite  
functional expansion for electric field and  
distribution function 23 p4104 A66-41504
- Phase plane method in study of transfer  
functions of higher order relay  
servosystems 23 p4050 A66-41613
- Approximate solution to digital sequential  
least squares estimation of eigenstates of  
nonlinear processes 23 p4050 A66-41614
- Approximate solution of certain mixed  
plane boundary value problems involving  
isotropic elastic body 23 p4140 A66-41836
- One-dimensional approximation analysis of  
excess carrier density distribution in  
illuminated semiconductor and radiative  
recombination effects 23 p4115 A66-41857
- Approximate second-order supersonic delta  
wing theory taking into account second-  
order differential equation via approximate  
particular integral 23 p4011 A66-41897
- Approximate integral method for  
determining thermal boundary layer and  
heat transfer on flat plate with insulated  
surface 23 p4150 A66-41920
- Perturbation approximations of order  
greater than unity used to study behavior of  
oscillator 23 p4096 A66-41946
- Inviscid hypersonic flow past flat wings at  
large angle of attack analyzed, using  
homogeneous layer concept of shock layer  
theory 23 p4013 A66-42014
- Rational one-dimensional theory of wave  
propagation and vibrations in elastic bars  
with rectangular cross  
section 24 p4284 A66-42137
- Dumbbell librations of satellites in elliptic  
orbits of small eccentricity determined via  
WKBJ approximation 24 p4272 A66-42158
- Stability of solution obtained in first  
approximation, introducing concept of  
quantity gamma for n-dimensional  
systems 24 p4230 A66-42216
- Thermodynamics and approximation theory  
of viscoelastic materials, developing  
Coleman-Noll theory, thermodynamic theory  
for fluids, etc 24 p4288 A66-42278
- Drift approximation of motion equations  
for relativistic charged particle in  
electromagnetic field, adiabatic trap, HF  
magnetic field, etc 24 p4241 A66-42332
- Local approximation of continuous periodic  
function by Fourier  
series 24 p4231 A66-42513
- Analytical method for studying pattern of  
flow from nozzle into vacuum used to  
calculate plume shape for rocket exhausting  
into hypersonic stream 24 p4158 A66-42790
- Reentry heat flux condition transformation  
into specified convective coefficients and  
temperatures, accounting for variation of  
flux with wall  
temperature 24 p4261 A66-42795
- Method of weighted residuals /MWR/,  
Galerkin method and variational method  
compared for approximate solution of  
differential equations 24 p4232 A66-42836
- Approximate solution of variation problems  
in heat explosion theory, noting difficulty  
resulting from heat libration dependence on  
temperature 24 p4295 A66-42884
- Equations from hydrodynamic equations,  
determining steady state fields and currents  
in plasma caused by microwave field, using  
quasi-linear  
approximation 24 p4244 A66-42973
- Approximation method for calculating  
transient temperature field in solid for case  
where heat-transfer coefficient  
varies 24 p4296 A66-43224

APSIDAL ANGLE

Optimum impulsive transfer between



elliptic and noncoplanar circular orbits, noting paths with up to three apsidal impulses 09 p1459 A66-20884

**APTITUDE**

**SA PERSONNEL SELECTION**  
Criteria for aircrew selection, describing aptitude and performance tests used by RAF 10 p1494 A66-22137

**ARC**

**S AURORAL ARC**  
**S CARBON ARC**  
**S ELECTRIC ARC**  
**S MAGNETIC ANNULAR ARC**  
**S MERCURY ARC**  
**S PLASMA ARC**

**ARC CHAMBER**  
Variable-volume arc chamber in Ling-Temco-Vought hypervelocity wind tunnel, examining design, performance and calibration technique 11 p1686 A66-22843  
Cylindrically symmetric plasma column produced by wall-stabilized arc constrained to operate within transparent tube 13 p2148 A66-25822  
Stagnation-point heat-transfer measurements in partially dissociated supersonic air arc tunnel 17 p3040 A66-33484  
Hypersonic plasma generator for reentry vehicles with arc tunnel experimental data and analysis of nonequilibrium chemical reaction between cesium atoms and ionized air species 20 p3497 A66-37158  
Lanthanum germanide synthesis using arc furnace, noting chemical properties 20 p3584 A66-37416  
High temperature high density carbon plasma production in arc chamber of shock tube 22 p3955 A66-40092

**ARC DISCHARGE**  
Equilibria and stability of confined arc column noting electron temperature, temperature gradients and radiative transport [AIAA PAPER 65-541] 01 p0109 A66-10182  
Nonlinear effect of modulation by propagating wave in arc discharge 01 p0110 A66-10349  
Book on UV radiation covering arcs, incandescent radiation sources, solar radiation, transmission, reflection, detectors and application 01 p0107 A66-10979  
High pressure argon arc with intense continuum as possible source in UV radiometry 02 p0212 A66-11225  
Fluid-transpiration plasma source and liquid-cooled mechanically sealed short arc source for solar simulation 02 p0213 A66-11229  
Compact arc lamps, arcs in enclosed quartz glass filled with gas or vapor, most powerful and concentrated sources of UV, near IR and visible radiation 02 p0213 A66-11231  
Spectral radiance measurements for vortex stabilized arcs in argon, oxygen, air and nitrogen 02 p0263 A66-11232  
Dispersion relation of density waves in low pressure arc discharges 02 p0269 A66-11953  
Performance of vortex-stabilized arc radiation source in which arc current, gas pressure, gas flow rate and nozzle diameter are prime variables 02 p0270 A66-12209  
Arc column parameters calculated for argon atmosphere, obtaining curves of thermal-electrical conductivity vs temperature and conductivity zone vs temperature 03 p0398 A66-12511  
Plasma density enhancement in arc discharge by applying converging magnetic field 04 p0551 A66-13742  
Inhomogeneous plasma from hot-cathode arc discharge at various pressures using various gases, recording oscillations from plasma instability with Langmuir probes 04 p0552 A66-13868  
Inhomogeneous plasma from hot-cathode arc discharge at various pressures using various gases, recording oscillations from plasma instability with Langmuir probes 05 p0727 A66-15459  
Current-voltage characteristics of low-voltage arc in cesium vapor, noting ionization process 06 p0915 A66-16150  
Electron concentration and temperature distribution in argon DC arc measured with hot wire probe 06 p0918 A66-16834  
Transition probabilities and line-shape parameters for three argon lines in wall-stabilized Ar arc containing trace of

H 08 p1261 A66-18766  
Demountable high-power xenon arc lamp with replaceable silica discharge tube 08 p1168 A66-19296  
Radial inhomogeneity, temperature dependence and ion and atom concentration of growing luminous cloud from arc discharge 08 p1266 A66-19771  
Vapor jet pressure and velocity in heavy-current arc between two graphite electrodes, comparing results from universal 09 p1368 A66-20826  
Alfven wave generation and propagation in low pressure arc discharges of helium, argon, nitrogen and air [AIAA PAPER 66-171] 10 p1560 A66-21425  
High density plasma with high optical emissions produced by wall stabilized pulsed arc discharge in xenon, noting absorptivity and electric conductivity [AIAA PAPER 66-184] 10 p1561 A66-21433  
Auxiliary arc heating hollow cylindrical cathode and preionization of interelectrode space, obtaining thermionic emission [AIAA PAPER 66-191] 10 p1562 A66-21437  
Vacuum arc thruster experiments in development of electric propulsion system for spacecraft [AIAA PAPER 66-202] 10 p1592 A66-21444  
Ion engine arcing frequency from micrometeoroid impact [AIAA PAPER 66-205] 10 p1592 A66-21446  
Discharge and exhaust beam of small low-power DC magnetic expansion thruster [AIAA PAPER 66-195] 11 p1743 A66-22216  
Arc discharge in cesium vapor within diode, noting plasma parameter distribution in electrode spacing during low, luminous and arc discharge phases 13 p2142 A66-25681  
Operation and performance characteristics of shock tube using arc discharge heating of driver gas, noting results on radiative emission from aerodynamic plasmas 13 p2059 A66-26711  
Arc discharges in supersonic flows, discussing problem of obtaining stable transverse electric arc in supersonic plasma jet 14 p2375 A66-28177  
Arc cathodes as heat sources in low pressure gas flows, noting loss of material and other effects 14 p2346 A66-28178  
Large annular steady state stable hot-electron plasma blanket formed by magnetically trapping electrons originating in intense arc gas 14 p2347 A66-28304  
Quasi-steady-state operation of arc thruster obtained with pulse time of few hundred microseconds, producing continuous plasma stream [AIAA PAPER 65-338] 15 p2572 A66-29276  
Current-voltage characteristics of low-voltage arc in cesium vapor, noting ionization process 15 p2429 A66-29880  
Magnetic properties of thin Permalloy films prepared in glow and arc discharge in inert gas 16 p2774 A66-30692  
Axially flowing gas through arc discharge, examining effect on I-V characteristic and radial temperature distribution in arc column 16 p2762 A66-31159  
Pressure rise in inner region of hydrogen arc discharge in axial magnetic field 16 p2764 A66-31352  
Electric conductivity parameters for plasma gap formed by discharge in argon and potassium mixture in electric-arc heater 16 p2766 A66-31601  
Plasma plate and cylinder oscillation compatibility with radiation from positive argon column at four discrete frequency bands and low pressure 17 p2962 A66-31815  
Velocity of arc wind measured for various magnetic fields and distances above arc path, using temperature probe and dragmeter 17 p2969 A66-32639  
Symptomatic behavior and anode regimes of arc for electric arc with superimposed subsonic flow of argon [AIAA PAPER 66-479] 17 p2970 A66-32768  
Dissociation rate of undiluted carbon monoxide behind strong shock waves produced in arc discharge shock tube [AIAA PAPER 66-518] 18 p3063 A66-33660

**ARC GENERATOR**  
Origin of arc in hollow anode of argon high pressure arc plasma generator shown to be not static 02 p0264 A66-11241

**ARC HEATING**  
Large solar simulator using interreflector to collect energy from high pressure arc 02 p0214 A66-11231  
Arc temperature field with transpiration, cooled anode in argon atmosphere measured by spectroscopy, noting semiluminous region [AIAA PAPER 65-94] 02 p0303 A66-11531  
Spectroscopic analysis of helium plasma heated by reflected shock in T-tube discussing luminous front and preceding shock 09 p1409 A66-20851  
Arc plasma generator for anode research noting design operation techniques and results [AIAA PAPER 66-162] 10 p1485 A66-21681  
Arc heating, self-magnetic acceleration and supersonic flow in plasma thruster [AIAA PAPER 66-237] 11 p1760 A66-22221  
Arc-driven vortex type heater-accelerator for possible use in reentry flight simulation 11 p1684 A66-22833  
Excitation temperature measurement of arc-heated argon plasma jet by spectroscopic method at supersonic nozzle outlet 12 p1920 A66-23851  
Enthalpy of gas stream, calorimeter surface treatment and heat transfer measurement errors in arc-heated tests 14 p2411 A66-27421  
Electrical discharge probe for transient density measurements in rarefied gas flow noting density range, flow velocity, etc 16 p2701 A66-30316  
High intensity fast molecular beams obtained by skimming and collimating core of supersonic plasma jet from arc-heated source 16 p2760 A66-30416  
Argon arc torch as compact heat source for thermophysical studies 17 p2928 A66-33501  
Arc burning mechanism of vortex-stabilized plasmatrons, noting effect of arc shunting on volt-ampere characteristics 18 p3143 A66-34011  
Error analysis of absorbed energy flux density and ignition exposure time data accuracy, precision and confidence limit estimates for arc image furnace ignition experiments [AIAA PAPER 66-669] 18 p3261 A66-34221  
Arc heated impulse wind tunnel facilities including Mach 16 contoured nozzle [AIAA PAPER 66-759] 22 p3894 A66-40611  
Gas heating in wall stabilized electric arc with axial flow applied to nitrogen arc obtaining highest enthalpy flux and efficiency 24 p4295 A66-43011

**ARC JET**  
Optical processes effect on integral wall plasma radiation to determine atmospheric pressure and temperature 03 p0399 A66-12811  
Visible and near UV radiation intensity profiles for ablating Teflon boundary layer in hot subsonic arc-jet flow at or near atmosphere [AIAA PAPER 66-56] 07 p0983 A66-18411  
Large vacuum facility tests of MPD arc thruster [AIAA PAPER 66-117] 08 p1282 A66-19011  
Current density distribution in MPD arc jet exhaust measured, using Hall effect sensors [AIAA PAPER 66-116] 09 p1433 A66-20011  
Varying instability frequency in simulated arc jet-Hall accelerator [AIAA PAPER 66-156] 10 p1559 A66-21411  
Friction factors and mean electric conductivity for argon arc plasma flow examining laminar-turbulent flow modes [AIAA PAPER 66-189] 10 p1561 A66-21411  
Criterion of electron-heavy particle thermal nonequilibrium encountered in subsonic arc jet plasma at pressure of 1 atm [AIAA PAPER 66-192] 10 p1562 A66-21411  
Lithium, ammonia and hydrogen-fueled MPD arc jets [AIAA PAPER 66-239] 12 p1936 A66-24511  
Experiments with arc jet characterized by composite electromagnetic and vortex stabilization and propelled by hydrogen, nitrogen, noting heat loss through electrodes 14 p2373 A66-27011  
Lithium-hydrogen bipropellant arc jet 14 p2374 A66-27411  
Transpiration cooling of hemispherical models in arc jet wind tunnel to obtain mass injection effects into boundary layer of aerodynamic



- configuration 14 p2412 A66-27446  
Liquid cooled high specific impulse arc jet engine has measured engine thrust not completely aerodynamic in nature  
[AIAA PAPER 64-669] 14 p2374 A66-27470  
Laminar argon arcjet mixing with coaxial flow of cool helium, considering turbulent characteristics and heat transfer  
[AIAA PAPER 65-587] 17 p3033 A66-32442  
Profile of ionized calcium resonance lines radiated from arc plasma jet observed by Fabry-Perot etalon 17 p2970 A66-32714  
Large vacuum facility tests of MPD arc thruster  
[AIAA PAPER 66-117] 21 p3777 A66-38716  
Langmuir type probe in argon arc jet, discussing surface contamination problems, causes of high electron temperature and development of automatic cleaning technique 22 p3899 A66-40368  
Photometric device for measuring propagation velocity of light fluctuations in arc-heated plasma jet 24 p4212 A66-42776  
Energy storage film capacitors for pulsed plasma thrusters developed for coaxial plasma gun and pulsed arc gun  
[AIAA PAPER 65-337] 24 p4261 A66-42780  
**ARC LAMP**  
Optical conversion efficiencies computed from spectral distribution measurements of pulsed and continuous xenon arc discharges 08 p1259 A66-19703  
Model L/C water-cooled DC power supply for short arc lamps, noting SCR selection 16 p2635 A66-30495  
Maximum efficiency contour /MEC/ source collector designed for compact arc sources used in solar simulators 16 p2681 A66-30508  
Four-foot diameter solar radiation simulator system using single xenon arc source and closed-loop heat exchange system for electrode cooling 22 p3887 A66-40206  
**ARC MELTING**  
Solid solution and carbide strengthened arc melted alloys of hafnium with tungsten and ternary alloys of tantalum, columbium, rhenium and carbon 06 p0894 A66-16078  
Grain size effects on tensile and creep properties of arc-melted and electron-beam-melted tungsten 07 p1048 A66-17475  
**ARC WELDING**  
**SA PLASMA ARC WELDING**  
**SA SPOT WELDING**  
Out-of-position gas metal-arc and gas tungsten-arc welding of fuel and LOX tanks of S-1C Booster for Saturn V 02 p0235 A66-11467  
Arc welding of two stainless maraging steels 02 p0235 A66-11468  
Inherent self-control of arc made possible by elimination of drift in current source output and electrode feed rate 02 p0236 A66-12226  
Notch-tough high-strength butt welds in alloy titanium plate with gas metal-arc welding, using spray type or short circuiting metal transfer 02 p0236 A66-12228  
HF multiple-seam arc welding unit that produces six welds simultaneously 03 p0374 A66-13118  
Alternating current rectified by tungsten electrodes of argon shield welding unit and DC component generated affects arc welding performance 03 p0375 A66-13121  
Effects of drop formation on rate, duration and size of welding and quality of welds in submerged-arc welding 03 p0375 A66-13123  
Submerged arc welding of 18 percent maraging steel 05 p0685 A66-14516  
Short-circuiting gas metal-arc welding of high nickel alloys for manufacture of liquid rocket engine components with aerospace quality 05 p0686 A66-14691  
Electrode tip geometry effect on characteristics of gas tungsten arc welding operating in cathode spot mode 05 p0686 A66-14693  
Theoretical and experimental evaluation of arc-image welding technique using solar energy as high temperature source 05 p0686 A66-14694  
Argon-arc welding of 3-mm high-strength steel sheet and molten slag arcless electric welding of 100-mm high-strength steel plate 08 p1231 A66-19168  
Fusion welding processes dependent upon electric heat source 09 p1384 A66-20610  
Submerged arc welding of Ti-Ni-Co-Mo maraging steel 10 p1539 A66-21169  
Fabrication of 260-inch diameter rocket cases by automatic gas tungsten arc welding techniques, using 18 percent nickel maraging steel 10 p1540 A66-21767  
Spray transfer gas metal-arc welding of titanium plate, using flux backing technique 13 p2087 A66-26016  
Porosity at weld fusion zone-base material interface in gas tungsten-arc and electron beam welds of tantalum 13 p2110 A66-26018  
Argon arc and resistance diffusion /vacuum/ welding of Ti and Ti alloys and protective metallic coating deposition on welded parts 13 p2110 A66-26027  
Gas shielded metal arc welding, discussing power sources, wire feed mechanism, torch and carbon dioxide cylinders 13 p2088 A66-26764  
Pulsed spray arc welding compared with continuous spray processes 14 p2301 A66-27342  
Porosity in titanium arc welds, noting sources of gas evolution and probable causative gases, particularly molecular hydrogen and oxygen 14 p2302 A66-27346  
Gas tungsten arc welding process automation based on feedback control concept 16 p2715 A66-31435  
Welding characteristics of four advanced commercial columbium base alloys using gas tungsten arc and electron beam processes 16 p2725 A66-31437  
Electron beam welding suitable for joining tungsten sheet for fabrication of solid rocket nozzles and nozzle accessories 19 p3369 A66-36128  
Quantitative analysis of drops of material transferred during arc welding 21 p3743 A66-38938  
Vacuum pressure effect on separation distance for arcing of DC current between spacecraft material 21 p3771 A66-39214  
Conventional arc welding processes and application to aerospace industry 22 p3925 A66-40267  
Plasma arc welding of aerospace materials, comparison with TIG method, penetration of thick sections, tests, etc 22 p3926 A66-40272  
**ARCTIC**  
Comparison of diurnal variations of ionization level in F region at geographically and geomagnetically conjugate stations in Arctic and Antarctic 04 p0516 A66-13851  
Arctic short-wave atmospheric radiation absorption, long-wave radiation loss, and tropospheric radiation balance 12 p1949 A66-24203  
Rocket observation of atmospheric density at high latitudes in Arctic and Antarctic locations  
[AIAA PAPER 66-345] 12 p1872 A66-24485  
Flows and fractures as types of deformation occurring on Earth under huge loads of ice suggested by isostatic compensation of Antarctica, Arctic basin and glaciated region in North America 12 p1875 A66-24894  
Speculative mean monthly Arctic stratospheric temperatures estimated from radiosonde and meteorological rocket wind and temperature data 16 p2696 A66-30928  
**ARGENTINA**  
Aerospace studies in Argentina during 1964 using rockets and balloons and including winds, E layer, satellite tracking, etc 09 p1458 A66-20706  
Space research in Argentina in 1965 15 p2602 A66-29942  
**ARGON**  
High pressure argon arc with intense continuum as possible source in UV radiometry 02 p0212 A66-11225  
MHD experiments with high enthalpy flow of argon 03 p0445 A66-13214  
Potassium content and K-A ages of 18 amphoteric chondrites determined from isotope dilution 04 p0580 A66-14486  
Heat transfer from Ar and Xe to end wall of shock tube measured, using thin film gauge monitored by IR photocell 05 p0782 A66-14705  
Speed of sound in ionized argon, noting electronic excitation influence 05 p0723 A66-15167  
High-pressure pulse arc created by discharging capacitor bank through steadily burning argon arc 06 p0919 A66-16874  
Atmospheric argon effect on hypersonic stagnation point convective heat transfer, using arc-heated shock tube simulating flight velocities up to 34,000 fps  
[AIAA PAPER 66-29] 07 p1153 A66-17891  
Ionization rate behind shock waves in argon, allowing for excitation and ionization by atom-atom collisions 07 p1020 A66-17938  
Neutral atomic beam used to measure total ionization cross section of argon atoms incident on low density argon gas 07 p1083 A66-18421  
Extraterrestrial dust as atmospheric argon source and influx of black spherules 08 p1287 A66-18770  
Thermodynamic parameters of carbon dioxide and argon mixture behind straight shock wavefront 09 p1470 A66-20146  
Pulse heights produced when argon, nitrogen and argon-nitrogen mixtures completely stop alpha particles 09 p1405 A66-20680  
Free piston argon shock tunnel using helium as driver gas, considering interface shock, pressure and stagnation point heat transfer  
[AIAA PAPER 66-169] 10 p1519 A66-21419  
Heat transfer measurement to side wall of shock tube behind incident shock wave in argon and xenon  
[AIAA PAPER 66-160] 10 p1560 A66-21428  
Ionization phenomena in argon due to laser radiation by measuring electron density and energy as time function after laser pulse initiation at different gas pressures and preionized conditions  
[AIAA PAPER 66-176] 10 p1565 A66-21690  
Argon-oxygen phase diagram determined by X-ray diffraction 11 p1650 A66-23208  
Shock compression of liquid argon at very high pressures and temperatures by reflecting shock wave from tungsten wall for testing interatomic potential 11 p1694 A66-23210  
Thermal decomposition of difluorocarbene radical diluted in argon analyzed behind incident shock waves at high temperatures 12 p1811 A66-23623  
Electrical precursors in immediate vicinity of ionizing shock waves in argon analyzed, using model describing electron diffusion through shock 12 p1923 A66-24579  
Metal wall ionized argon lasers, discussing use of water-cooled quartz discharge channels, CW lasers, development of satisfactory metal, etc 13 p2091 A66-25555  
Electron impact excitation mechanism of argon-ion continuous and long pulse lasers 13 p2102 A66-26206  
Transition probabilities and lifetimes in ionized argon gas lasers 13 p2102 A66-26207  
Pressure effects of argon on fine structure components of first two members of cesium principal series 13 p2135 A66-26263  
Differential scattering of ionized helium on neon and argon and ionized argon on argon measured at various relative energies and scattering angles 13 p2135 A66-26269  
Static pressure distributions in supersonic nozzle flows of dissociated hydrogen plus argon 14 p2219 A66-27442  
Argon flow through long tube compared with Weber theoretical model, applying classical continuum equations 14 p2274 A66-27444  
Argon diffusion from biotite of mica schist due to intrusion of dyke analyzed on basis of thermal metamorphism and isotope migration 14 p2364 A66-27848  
Ionization cross sections for low energy collisions of neutral nitrogen molecules or neutral argon atoms, using asymmetric charge transfer 14 p2337 A66-27980  
Motion of potassium ions in argon, using apparatus for simultaneous measurement of mobility and diffusion coefficients 14 p2345 A66-28140  
Intensity growth and decay in Ar and Hg lines after switching on mercury vapor discharge lamps filled with Ar 15 p2542 A66-29716  
Fundamental vibration spectrum of HD in liquid argon, noting rotation-translation coupling, quantized translational energy levels and perturbation treatment of interaction 16 p2645 A66-30120



Spatial distribution of high energy Ar atoms scattered by various surfaces 16 p2753 A66-30398  
High energy argon atom interactions with surfaces and variations in accommodation coefficient 16 p2702 A66-30399  
Thin film heat transfer gauges to measure axial extent of curved shock fronts in argon 17 p2908 A66-32416  
Measurable range of ionizational relaxation behind shock front in argon extended to equilibrium region by mm-wave technique 17 p2912 A66-32982  
Argon arc torch as compact heat source for thermophysical studies 17 p2928 A66-33500  
Electrodeless annular discharges in argon and air 18 p3144 A66-34039  
Radiation spectra of plasma jets from IR to UV, determining electron density and argon excitation temperature, noting bremsstrahlung 18 p3144 A66-34103  
Polarization difference in elastic scattering of proton from Ar 40 and Ca 40 due to spin-orbit force difference 18 p3140 A66-35037  
Light energy measurements made with argon bomb used as chemically powered laser pump 19 p3373 A66-35388  
Sputtering yields of various semiconducting single crystals under argon ion bombardment 19 p3436 A66-35420  
Temperature dependence of dissociative recombination coefficients in argon according to hypotheses of Bates and Palgarno 19 p3404 A66-36758  
Numerical calculations of parameters of steady state HF high pressure vortical discharge of argon in air 20 p3607 A66-36975  
P-V-T behavior of argon, nitrogen and argon-nitrogen gas 20 p3677 A66-37089  
Thermodynamic parameters of carbon dioxide and argon mixture behind straight shock wavefront 21 p3836 A66-39417  
Intracavity interferometer laser measurements of power gain and output in single-frequency Ar laser and 6328-angstrom Ne isotope shift 22 p3932 A66-40110  
Temperature measurement in shock tubes and transition probabilities of argon spectrum lines from emission intensities 22 p3956 A66-40406  
Methane/deuterium exchange reaction rate measured in shock tube, using vibrational excitation mechanism to explain data 22 p3860 A66-40903  
Charge exchange cross sections for argon ions incident on hydrogen and deuterium measured over energy range of 30 to 1000 ev, taking into account ion-molecule reactions 23 p4098 A66-41267  
Shock tube monitoring of electron-generation rate in argon-xenon ionization cross section implies that atom-atom processes in noble gases ionization cross section is independent of electronic structure 23 p4099 A66-42080  
Time resolved emission measurements for Cr-Ar mixtures in three spectral regions and ionization occurrence in excited state inelastic collisions 23 p4033 A66-42083  
Argon entropy diagram calculation from sound velocity data and P-V-T relation 24 p4238 A66-42887

ARGON PLASMA

Acceleration and dynamics of argon plasma in inductive hydrodynamic shock tube 01 p0113 A66-10638  
Origin of arc in hollow anode of argon high pressure arc plasma generator shown to be not static 02 p0264 A66-11241  
Argon arc stabilized by cooled walls, considering radiation calculated with aid of dependences describing transport properties of argon plasma 02 p0265 A66-11390  
Arc column parameters calculated for argon atmosphere, obtaining curves of thermal-electrical conductivity vs temperature and conductivity zone vs temperature 03 p0398 A66-12511  
Spectral line energy emitted by homogeneous argon plasma 03 p0399 A66-12715  
Current, potential electron and atom temperature distributions between anode and cathode in low pressure crossed-field plasma accelerator 03 p0416 A66-12784  
Thermal conductivity measurements of

argon plasma produced by stabilized electrical arc 03 p0399 A66-12825  
Electrical conductivity of argon plasma 03 p0400 A66-12834  
Electrical characteristics of plasma torch types with plasma jets used in buildup welding 03 p0374 A66-13120  
Probes in atmospheric pressure argon plasma where ion diffusion is function of temperature 03 p0406 A66-13280  
Spatial distribution and temporal decay of electron and atom concentrations in pulsed /argon afterglow/ plasma measured with laser interferometer 04 p0551 A66-13741  
High pressure high current argon discharge, calculating statistical variations of photon radiation, electron and ion densities 05 p0720 A66-14504  
Reflected shock waves in helium and argon plasmas noting electron density, Saha equations and Newtonian technique 05 p0720 A66-14505  
Isentropic expansion of argon plasma in Laval nozzle, discussing parallel flow parameters, frozen flow, thermodynamic equilibrium, energy balance, etc 05 p0720 A66-14509  
Output spectra of argon ion laser in ring resonator and two mirror resonators 05 p0694 A66-14904  
Electric arc interaction with argon flow analyzed in crossed convective and magnetic fields [ASME PAPER 65-WA/ENER-1] 05 p0728 A66-15626

Nonequilibrium ionization of K-seeded or Na-seeded argon for MHD generators, noting current density-electric field characteristics 05 p0625 A66-15811  
Boundary layer between argon plasma and solid wall at atmospheric pressure 05 p0728 A66-15815  
Electron temperature spectroscopy for atmospheric argon plasmas, sodium vapor seeded at high temperatures, noting relationship with current density 06 p0915 A66-16178  
Electron concentration and temperature distribution in argon DC arc measured with hot wire probe 06 p0918 A66-16834  
Argon plasma temperatures measured by spectral method in internal and external arc plasmatrons, using copper impurity line 06 p0918 A66-16837  
Sorption of low energy argon ions by titanium films as function of ion energy, density of ion beam and method of preparation of film 06 p0928 A66-16886  
Behavior of small cylindrical Langmuir probe in steady low density flow of argon plasma

[AIAA PAPER 66-5] 07 p1034 A66-17880  
Electrical characteristics of supersonic MHD generator with arc heated argon plasma, noting discharge modes 07 p0993 A66-18311  
Transition probabilities and line-shape parameters for three argon lines in wall-stabilized Ar arc containing trace of H 08 p1261 A66-18766  
Variation of electron temperature and number density, ion current density and plasma potential through low density Hall current ion accelerator as function of magnetic field strength [AIAA PAPER 66-76] 08 p1262 A66-18994  
Electron temperature variation in argon MGD channel in crossed magnetic and electrical fields 08 p1263 A66-19174  
Magnetic field effect on electron temperature, number of ionization events and potential gradient in argon and neon HF discharge 08 p1264 A66-19186  
Spectral line energy emitted by homogeneous argon plasma 09 p1406 A66-19946

High voltage vortex arc radiation source for producing reliable quantifiable plasmas, noting argon spectral distribution [AIAA PAPER 66-186] 10 p1561 A66-21434  
Friction factors and mean electrical conductivity for argon arc plasma flow, examining laminar-turbulent flow modes [AIAA PAPER 66-189] 10 p1561 A66-21436  
Criterion of electron-heavy particle thermal nonequilibrium encountered in subsonic arc jet plasma at pressure of 1 atm [AIAA PAPER 66-192] 10 p1562 A66-21438

Electric arc interaction with argon flow analyzed in crossed convective and magnetic fields [ASME PAPER 65-WA/ENER-1] 10 p1563 A66-21501

Laser induced gas breakdown at high pressures, noting effect of plasma density on index of refraction via optical frequency resonance measurement 10 p1542 A66-2156  
Anomalous diffusion and instabilities of argon plasma in strong magnetic field 10 p1564 A66-21561

Arc plasma generator for anode research noting design operation techniques and results

[AIAA PAPER 66-162] 10 p1485 A66-21681  
Variation of thermal radiation emitted with mass flow rate of argon plasma torch 10 p1621 A66-21798

Electron temperatures in hot argon potassium discharges determined, using ratio of electron energy slopes from floating double-probe curve 10 p1568 A66-21801

Spectral line shift in low-power spark discharge argon plasma, noting line broadening and incomplete ionization 10 p1572 A66-22028

RF electromagnetic fields to control state of flowing thermal plasma

[AIAA PAPER 66-166] 11 p1742 A66-22213

Temperature and electron concentration in HF induction discharge argon plasma investigated by optical method 11 p1745 A66-22581

Spectroscopic investigation of argon jet temperature at outlet of plasmatron nozzle, measuring temperature of plasma jet 11 p1745 A66-22581

Feasibility of using Langmuir probe for measuring statistical properties of unsteady or turbulent electron-rich plasmas [AIAA PAPER 65-544] 12 p1919 A66-23581

Excitation temperature measurement of arc-heated argon plasma jet by spectroscopic method at supersonic nozzle outlet 12 p1920 A66-23881

Harmonic generation in short magnetized plasma column from helical oscillation near critical magnetic field for helical instability 12 p1925 A66-24828

Free jet of arc heated low-density supersonic argon plasma examined, measuring radiative mechanisms, electron temperatures, thrust, jet structure, etc [AIAA PAPER 66-163] 13 p2138 A66-25161

Conductivity of ionized gas in DC discharge in argon for various magnetic field intensities 13 p2139 A66-25468

HF and LF alternating electric field effect on weakly ionized argon, temperature modulation and production of harmonics 13 p2141 A66-25448

Cylindrically symmetric plasma column produced by wall-stabilized arc constrained to operate within transparent tube 13 p2148 A66-25828

Resonance peaks due to electromagnetic scattering by argon plasma jet observed during change in electron concentration, noting dependence of scattering on argon flow rate and electric power of arc 14 p2341 A66-27113

Thermal radiation from argon plasma arc of wall-stabilized type with Poiseuille flow, comparing experimental measurements with theoretical reentry predictions [AIAA PAPER 65-546] 15 p2551 A66-29221

Electron temperature correlation with excitation in temperature in argon plasma established, using spectral analysis and Langmuir probe 15 p2555 A66-29768

Spectral line shift in low-power spark discharge argon plasma, noting line broadening and incomplete ionization 16 p2760 A66-30801

Spectroscopic data from argon arc nitrogen supersonic plasma jets, noting line width, intensity, temperature, etc 16 p2763 A66-31111

Electronic relaxation of shock-heated nonequilibrium argon plasma flow by microscopic-macroscopic treatment [AIAA PAPER 66-476] 16 p2765 A66-31421

Conductivity and electron-ion recombination coefficient in argon determined from collision cross sections of electrons with neutral particles 16 p2755 A66-31511



- Electric conductivity parameters for plasma  
p formed by discharge in argon and  
tassium mixture in electric-arc  
ater 16 p2766 A66-31601  
Continuous-emission coefficient of argon  
asma in 2500 to 7500 angstrom range at  
emperatures from 11,500 to 12,500 degrees  
16 p2766 A66-31602  
Plasma plate and cylinder oscillation  
mpatibility with radiation from positive  
gon column at four discrete frequency  
nds and low pressure 17 p2962 A66-31815  
radial temperature distribution within  
gon plasma column determined  
ectroscopically at various arc currents,  
ting argon  
ermoconductivity 17 p2966 A66-32427  
Electron temperature determination in  
gon plasma as function of distance  
asured to axis of inductive  
ndings 17 p2974 A66-33255  
ypersonic argon beam flow past  
indrical thermal nozzle 17 p2974 A66-33287  
Composition, heat conduction and radiative  
ergy transfer characteristics of hydrogen  
d argon plasmas produced by arc in  
indrical channel with cooled  
alls 18 p3142 A66-34023  
Thermal conductivity coefficient  
perimentally determined for argon plasma  
atmospheric pressure and temperatures  
om 10,000 to 13,000 degrees  
18 p3144 A66-34038  
onization outside equilibrium and  
axation of ionization in cesium seeded  
gon 18 p3144 A66-34102  
Atmospheric argon Poiseuille plasma arc  
stability in axial magnetic field examined,  
ting frequency and shapes of stability  
rves 18 p3149 A66-34916  
Particle concentration and luminescence  
ensity correlation with electron cyclotron  
requency in stationary SHF argon discharge  
magnetic field 18 p3152 A66-35080  
Population temperatures within argon-  
icium plasma generated by reflected  
rodynamic shock determined by spectral  
e-reversal method 19 p3409 A66-36332  
Open air welding of titanium, noting nozzle  
esign for optimum shielding, argon gas  
ow rate and magnitude of electrode  
tension 19 p3371 A66-36633  
Thermal conductivity measurements of  
gon plasma produced by stabilized  
ectrical arc 19 p3433 A66-36767  
Electric conductivity of argon  
asma 19 p3433 A66-36776  
Heat-flux density transmitted by relatively  
oad low-velocity argon plasma jet to  
ritical cold plate 20 p3608 A66-37461  
Simplified model of relation between  
ectron concentration and ionization rate in  
eady-state inert gas discharge column  
adding to contraction of  
lumn 20 p3608 A66-37464  
nstrument for continuous variation of  
ngle of incidence between ion beam and  
ls of RF quadrupole mass spectrometer  
om zero to 90 degrees 20 p3561 A66-38174  
Electric conductivity of magnetically  
lanced arc in transverse argon flow at  
atmospheric pressure 21 p3777 A66-38718  
Electric field intensity of helium and argon  
c column as affected by pressure and  
urrent intensity 21 p3783 A66-39021  
Stabilization of long high-pressure argon  
c achieved by rotation of gas for radiation  
asurement 21 p3783 A66-39022  
onization and secondary effects during  
flection of shock waves in  
gon 21 p3726 A66-39086  
Behavior of small cylindrical Langmuir  
obe in steady low density flow of argon  
asma  
[IAA PAPER 66-5] 22 p3918 A66-40350  
Conductivity of potassium-seeded argon  
asma, assuming variable collision cross  
ctions and Maxwellian distribution for  
ectrons 22 p3951 A66-40363  
Langmuir type probe in argon arc jet,  
cussing surface contamination problems,  
uses of high electron temperature and  
velopment of automatic cleaning  
chnique 22 p3899 A66-40368  
onization relaxation in impure shock-  
ated argon studied by magnetic mass  
ectrometer 22 p3899 A66-40380  
F induced gas plasma at 250-300  
kc/s 22 p3956 A66-40401  
Spectroscopic measurements of electron  
densities and temperatures in argon-  
hydrogen plasma jet 23 p4068 A66-41290  
Electron and neutral atom densities in  
helium and argon afterglow plasma obtained  
by two helium-neon laser interferometers,  
noting temporal dependence of electron  
decay 23 p4101 A66-41364  
Temperature profiles across argon plasma  
arc calculated from measured radiation  
intensities at arc currents from 1 to 400  
amp 23 p4104 A66-41495  
Resonance peaks due to electromagnetic  
scattering by argon plasma jet observed  
during change in electron concentration,  
noting dependence of scattering on argon  
flow rate and electric power of  
arc 24 p4244 A66-42971  
**ARGON 40**  
Thermal history of Bruderheim meteorite  
showing loss of 90 percent radiogenic argon  
40 20 p3651 A66-37591  
**ARIEL I SATELLITE**  
Data from ion energy spectrometer  
mounted on Ariel I satellite indicating  
increased concentration of oxygen ions  
during afternoon at high  
altitudes 01 p0061 A66-10498  
Ariel I measurement of ionospheric  
electron density, temperature and ion  
composition 03 p0366 A66-12877  
**ARIEL II SATELLITE**  
Sunlight attenuation reaching Ariel II  
satellite after passing through Earth  
atmosphere along almost horizontal  
path 05 p0672 A66-15023  
Satellite Ariel II receiver for measuring  
cosmic radio noise, using dipole  
antenna 05 p0769 A66-15841  
Sky brightness and cosmic radio emission  
in satellite Ariel II 05 p0769 A66-15842  
**ARIEL SATELLITE**  
Ariel II /UK-2/ international satellite  
environmental test  
program 14 p2394 A66-28426  
**ARIS**  
S ADVANCED RANGE  
INSTRUMENTATION SHIP /ARIS/  
**ARITHMETIC**  
High-speed multiplication for R-11  
microminaturized digital computer, using  
modified form of Booth  
Algorithm 21 p3707 A66-38676  
Automatic detection and correction of  
errors in digital computers by using residue  
arithmetic, whether caused by arithmetic  
operations or data transmission  
operations 23 p4042 A66-41602  
Theoretical methods for reliable machine  
design, comparing redundant residue  
number system code with linear codes and  
majority voting  
techniques 23 p4042 A66-41603  
**AROMATIC COMPOUND**  
**SA BENZENE**  
Aromatic hydrocarbons in carbonaceous  
chondrites investigated by time-of-flight  
mass spectrometry and hypothesized as  
formed in solar nebula under  
thermodynamic  
equilibrium 01 p0136 A66-10436  
Carbonaceous chondrite in stony  
meteorites, noting presence of organized  
elements and microfossils 02 p0289 A66-11604  
Properties of polyaromatic C-ethers for use  
as high temperature lubricants with  
outstanding gear load-carrying capability  
[ASLE PREPRINT 65-LC-2] 02 p0238 A66-12260  
Electron spin resonance of radical cations  
produced by oxidation of aromatic  
hydrocarbons with antimony  
pentachloride 03 p0330 A66-12336  
Aromatic/heterocyclic polymers from  
tetraamines reaction with tetraacids at room  
temperature, developing potential for  
aerospace application 06 p0901 A66-16299  
Raman scattering and IR absorption  
spectra of gaseous, liquid and crystalline  
benzoyl benzoic acid and O-and M-toluic  
acids 09 p1339 A66-20941  
Directional intensity and decay time of  
scintillations from anthracene and p-  
terphenyl single crystals under alpha  
particle bombardment 11 p1750 A66-22465  
Properties of polyaromatic C-ethers for use  
as high temperature lubricants with  
outstanding gear load-carrying capability  
[ASLE PREPRINT 65-LC-2] 12 p1889 A66-24987  
Synthesis of polyimidazopyrrolones, using  
previous macromolecular synthesis of ladder  
segments of aromatic-heterocyclic  
polymers 13 p2017 A66-26290  
Electron transfer from alkali metals to  
aromatic hydrocarbons, examining rate of  
chain scission in case of poly(4-vinyl  
biphenyl/ and poly(alpha/ vinyl  
naphthalene/ 17 p2870 A66-32300  
Polyaromatic adhesives for temperature  
resistant sandwich construction in lap-shear  
strength and preliminary sandwich  
evaluations 22 p3926 A66-40279  
Formation of organic compounds under  
conditions of thermal equilibrium, noting  
aromatic compounds in solar nebula and  
gases activated to plasma  
state 22 p3860 A66-40483  
Aromatic hydrocarbon synthesis by passing  
methane through silica gel at high  
temperature 23 p4032 A66-41306  
**ARRAY**  
S ANTENNA ARRAY  
S LINEAR ARRAY  
S PHASED ARRAY  
**ARSENIC**  
Thermoconductivity of germanium alloyed  
with arsenic and gallium depends on  
impurity type starting from certain impurity  
concentration 14 p2359 A66-27178  
IR absorption of arsenic  
monoselenide 15 p2565 A66-29198  
Arsenic overpressure, obtained by  
including metallic arsenic along with gallium  
arsenide, depresses defect concentration  
identifying primary defect species as arsenic  
monovacancies 16 p2779 A66-31086  
IR absorption of arsenic  
monoselenide 17 p2982 A66-33047  
**ARSENIC COMPOUND**  
Propagation of LF helicon waves in  
strongly doped cadmium arsenide and  
indium antimonide 03 p0410 A66-12944  
Dielectric losses and permittivity of  
vitreous semiconductor arsenic trisulfide  
with silver impurity 06 p0929 A66-16922  
Donor impurity effect on direct-indirect  
transition in gallium arsenic phosphide,  
particularly at low  
temperature 13 p2170 A66-26590  
Indium arsenic antimonide single crystals  
in p-n junction laser 16 p2721 A66-31767  
Electrical and physicochemical properties  
of silver doped arsenic  
sulfide 17 p2981 A66-32876  
Epitaxial growth of bulk quality GaAs on  
GaAs and Ge substrates, using hydrogen  
stream saturated at room temperature with  
arsenic chloride 24 p4251 A66-42307  
**ARSENIDE**  
S GALLIUM ARSENIDE  
S INDIUM ARSENIDE  
**ARTIFICIAL CLOUD**  
Rain effect on visibility through windshield  
tested in large wind tunnel including  
construction, calibration and removal  
devices 02 p0176 A66-11204  
Time variation in radiance of contaminant  
glow clouds released in upper atmosphere,  
noting solar radiation  
scattering 02 p0221 A66-11474  
Solar wind study by observing effect on  
artificially produced clouds of barium and  
strontium compounds 07 p1029 A66-17833  
Atmospheric motions from sodium cloud  
firings in 80 to 200 km height region, noting  
internal gravity waves, atmospheric tides  
and drift 15 p2489 A66-29661  
Sounding rocket-released artificial  
strontium and barium ion cloud motion in  
upper atmosphere, based on equations of  
ambipolar diffusion 15 p2491 A66-29950  
Atmospheric decay of rocket-released Li  
due to diffusion, wind and chemical  
reaction 16 p2697 A66-31008  
Shock wave and glow cloud of nitrogen  
dioxide released at 110 km  
altitude 19 p3345 A66-35492  
Aerosol component of spectral  
transmittance of artificial fog, comparing  
calculated and experimental values for  
absolute attenuation 21 p3759 A66-38916  
Rocket observation of upper atmospheric  
wind around ionospheric E layer by sodium



release method, noting cloud drift 24 p4199 A66-42466

**ARTIFICIAL GRAVITY**

Interior design problems in artificial g spacecraft simulator 02 p0185 A66-11624  
Rotating artificial gravity system for manned orbital vehicles and stations requiring no expenditure of propulsive mass to attain full vehicle rotation 02 p0294 A66-11632  
Planar motion examined for space station having cable-connected manned compartment and counterweight configuration [AIAA PAPER 64-493] 03 p0431 A66-12742  
Physiological and psychomotor test performed in revolving space station simulator for design criteria for spacecraft with artificial gravity 06 p0815 A66-16051  
Artificial gravity through slow rotation to solve weightlessness problem in long manned space flights, considering cardiovascular deconditioning and biological problems of rotating environments 06 p0817 A66-16237  
Short radius onboard centrifugation for simulated gravity during prolonged space flight, providing zero G at eye level and maximum G at feet 09 p1334 A66-20524  
Psychological and physiological reaction to Coriolis effect under artificial gravitational field simulated in rotating space station 15 p2443 A66-28682

**ARTIFICIAL INTELLIGENCE**

SA BIOSIMULATION  
SA GAME THEORY  
On-line and off-line self-organizing control systems for space vehicle application 19 p3333 A66-36661  
Frog retina layered model, stereoscopic system and decision/control system in connection with robot data reduction in Voyager missions 24 p4168 A66-43081

**ARTIFICIAL RADIATION BELT**

Brazilian magnetic anomaly as observed by Sputnik V and VI and five satellites of Cosmos series 09 p1446 A66-21036  
Star Fish radiation belt discrepancy between theoretical and experimental values may be due to explosion in belt of naturally trapped protons 18 p3170 A66-34530  
Artificial radiation belt sources, noting positrons and alpha particles, nuclear explosion, etc 20 p3643 A66-38338  
Spatial distribution and time decay of intensities of geomagnetically trapped electrons from high altitude nuclear burst 20 p3643 A66-38339  
Transient behavior of energetic electrons in artificial radiation belts analyzed via satellite observations 20 p3643 A66-38341  
Electron spectra made with five-channel magnetic electron spectrometer from Star Fish explosion and from outer radiation belt 20 p3643 A66-38343  
High altitude nuclear detonations, discussing data on trapped radiation, values of empirical and theoretical spectra and artificial radiation belts 20 p3643 A66-38344  
Energetic electrons from shock heating of exosphere, discussing formation of artificial radiation belt via MHD shock wave heated and density gradient accelerated electrons 20 p3644 A66-38346

**ARTIFICIAL RESPIRATION**

Resuscitative device combining nonbreathing valve and squeeze bag, noting advantages 17 p2864 A66-32173

**ARTIFICIAL SATELLITE****S SATELLITE****ARYL**

High resolution ESR spectra of acyclic semidione radical anions and single aryl substituent cations 15 p2447 A66-29817

**ASCENT TRAJECTORY**

Plane trajectory with multistage rocket in minimum climb-time 02 p0296 A66-11703  
Two-dimensional ascending trajectories used to determine performance and structural parameters of reusable high altitude research rocket 04 p0584 A66-13524  
Electrochemical and chemiluminescent ozone sensor performance, using analysis of comparative ascents 04 p0517 A66-14451  
Climb profiles by SST pilot evaluated by simulator study using instrument, Mach altitude display and flight director 07 p0988 A66-17783  
Conically spiraling ascent or descent

trajectory of spacecraft in application of jet lift, noting characteristic mission parameters 09 p1457 A66-20557  
Flight trajectory analysis of body in vertical ascent from planet under constant thrust, by numerical integration of motion equations 13 p2188 A66-26292  
Effect of air mixture application on optimum ascent trajectories and ratio of payload to takeoff weight of carrier rocket configurations 16 p2790 A66-30345  
Booster rocket ascent trajectory optimization, using steepest ascent method [AIAA PAPER 64-663] 16 p2801 A66-30883  
Analytic solution in terms of modified Bessel functions of synergetic turn in exponential atmosphere, using spacecraft engines only for drag cancellation and orbit trimming [AIAA PAPER 66-487] 16 p2811 A66-31493  
Guidance scheme for control of multistage rocket vehicle through ascent phase of complex space mission [AIAA PAPER 64-640] 20 p3597 A66-38156

**ASCORBIC ACID METABOLISM**

Ascorbic acid concentration in urine and organs of guinea pigs exposed to high oxygen concentrations 18 p3060 A66-34410

**ASIA**

S CHINA  
S INDIA  
S JAPAN  
S U.S.S.R.

**ASPARTIC ACID**

Flight fatigue treatment by acetyl-aspartic acid and citrulline, noting improved reaction to acoustic and visual stimuli 17 p2859 A66-32232

**ASPECT RATIO**

Prandtl lifting line classical theory of high aspect ratio wings as singular perturbation problem yields asymptotic expansions of Navier-Stokes solution 07 p0982 A66-18124  
Rotational derivative coefficients of angular wing of arbitrary aspect ratio situated in ideal incompressible media 08 p1162 A66-18875  
Inviscid hypersonic flow over compression side of delta wing of moderate aspect ratio 12 p1796 A66-23605  
Electrical analogy for wing in unsteady supersonic flow, determining distribution of lifting power for various aspect ratios 13 p1990 A66-25405  
Circulation distribution over rectangular wings, based on Chushkin algorithm and lifting surface equation calculated by digital computer 13 p2068 A66-26540  
Cut-off wavelength of transverse electrostatic wave mode in ridged rectangular waveguide of arbitrary aspect ratio 14 p2257 A66-27951  
Flow analysis of swept back blades in water tunnel, noting flow patterns, surface pressure distribution, lift-drag ratio, etc 18 p3049 A66-34649  
Low speed three-stage axial flow compressor tests at aspect ratios of one, two and four [AIAA PAPER 66-613] 19 p3275 A66-35359  
Approximation theory for calculating linearized subsonic and supersonic flow over pulsating bodies with low aspect ratio, noting structure of flow field 19 p3277 A66-36641  
Lateral fluid jet visualization for spanwise launching on wing model with low aspect ratio in subsonic flow 21 p3731 A66-39593  
Polar auroral radar system using ionospheric propagation effects for aspect sensitive backscatter 22 p3916 A66-40811

**ASTEROID****SA METEOR**

Age of Martian craters investigated, based on asteroid collision and certain spatial distribution 01 p0136 A66-10439  
Minor planets and ephemeris calculations with bibliography 02 p0292 A66-12262  
Improved orbital data for 36 minor planets 02 p0292 A66-12263  
Moon, Martian satellites and minor planetoids for possible use in refueling space ships by generating propellants from natural chemical planetary resources 04 p0577 A66-13577  
Spatial distribution and motion of known asteroids analyzed in order to avoid or maximize encounters in planning space

**flight**

[AIAA PAPER 66-149] 06 p0957 A66-1710  
Retrograde rotation of Venus established by radar observations is attributed to collision with 200-km diam asteroid 09 p1452 A66-2012  
Various hypotheses concerning meteorite origin, noting relation with asteroids, fireball origin, chondrules, etc 09 p1460 A66-2092  
Orbital elements of 13 asteroids, using digital computer and taking Jupiter and Saturn perturbations into account 10 p1606 A66-2126  
Bronzite and hypersthene chondrites evaluating lunar or asteroidal origin 12 p1948 A66-2390  
Positions of asteroids 1221 /Amor/ and 1948 OA /Object Wirtanen/ from photographs taken at Tautenburg, East Germany 12 p1950 A66-2439  
Lunar and asteroidal meteorites 14 p2382 A66-2760  
Tables of improved orbital data for 15 minor planets prepared by use of BESM electronic computer 17 p2995 A66-3184  
Declinations of minor planets Vesta and Pallas according to observations on vertical circle at Goloseevo in 1954-1962 17 p2995 A66-3184  
Minor planets, comets and satellite motions and positions in outline of present research 17 p2998 A66-3202  
Photographic observations of minor planet at Sydney during 1964 17 p3003 A66-3282  
Possible adaptation of asteroids to support human life for indefinite periods of time 19 p3285 A66-3624  
Meteorites from asteroids in hypothesis based on chemical composition, structure and gas absorption age 20 p3647 A66-3704  
Bias free statistics of orbital elements of asteroids 20 p3656 A66-3802  
Martian surface markings, brightness along optical equator, crater erosion, asteroid collision and yellow dust clouds 22 p3981 A66-4052  
Spatial distribution and motion of known asteroids analyzed in order to avoid or maximize encounters in planning space flight [AIAA PAPER 66-149] 23 p4127 A66-4111  
Tables of observational statistics of comets, minor planets and natural satellites 24 p4273 A66-4220  
Origin, population, orbital characteristics, surface structure and chemical composition of asteroids /meteorite type/ in solar system 24 p4276 A66-4266  
Asteroid belt flyby spacecraft concept based on Atlas family with potential growth for Jupiter flyby 24 p4278 A66-4269

**ASTRONOMICS****S ASTRONAUTICS****ASTROBIOLOGY****S BIOASTRONAUTICS****S EXTRATERRESTRIAL LIFE****ASTRODYNAMICS**

Book on methods in astrodynamics and celestial mechanics including libration points, satellite motion, orbit determination, optimization, optimal control, etc 19 p3460 A66-3588

**ASTROMETRY**

Astrometry current status, examining establishment of coordinate system and determination of astronomical constants 03 p0427 A66-1292  
System of astronomical constants adopted in 1965 by International Astronomical Union for introduction in 1968, discussing difficulties in consistency, compatibility and durability 03 p0429 A66-1319  
Astronomical constants system approved by International Astronomical Union at Hamburg in August 1964 05 p0759 A66-1488  
New techniques in astronomy - Conference Kazan, U.S.S.R., May 1964 05 p0679 A66-1520  
Prime-focus field of Maksutov telescope system on Mount Kanobil, U.S.S.R. noting objective, mirror and tests for distortion and accuracy in astrometry 05 p0680 A66-1520  
Solar flare photographic observation presenting development of flare and associated prominences on limb 07 p1118 A66-1762  
Reduction of diffracted light for



astrometry near Sun 07 p1035 A66-18036  
 Determining coordinates of astrogeodetic grid points by Molodenskii integral formulas and accuracy estimation by astrogravimetric interpolation of 08 p1217 A66-19345  
 Planetary nebulas noting observational problems, parallax, proper motion, distance, etc 11 p1787 A66-22260  
 Interferometric determination of radio source positions and use of Royal Radar Establishment 11 p1657 A66-23191  
 Nutation constant for absolutely solid Earth from recent astronomical unit and lunar mass measurements 12 p1867 A66-23513  
 Astrometry current status, examining establishment of coordinate system and determination of astronomical constants 14 p2380 A66-27271  
 Classical theory of tidal oscillations of plumb line acting under solar and lunar tidal forces 15 p2596 A66-29142  
 Measurement of distance to Moon by optical radar, discussing ruby laser/photomultiplier apparatus and procedure 16 p2647 A66-30291  
 Determining coordinates of astrogeodetic grid points by Molodenskii integral formulas and accuracy estimation by astrogravimetric interpolation of 19 p3348 A66-36053  
 Nutation constant for absolutely solid Earth from recent astronomical unit and lunar mass measurements 20 p3549 A66-37027  
 Astronomical techniques on occurrence and nature of planets outside solar system 20 p3656 A66-38027  
**STRON THERMONUCLEAR REACTOR**  
 Astron facility experiments on injection of very intense pulses of relativistic electrons into cylindrical azimuthally symmetric magnetic trap 19 p3423 A66-36551  
 Electron injection and E-layer buildup in Astron device theoretically studied by one-dimensional model, using Green functions for self-electric and self-magnetic fields 19 p3423 A66-36552  
**STRONAUT**  
**SA PILOT**  
 Crew survival goals in system design for manned space mission derived from comparative examination of mortality rates of overall society [ASME PAPER 65-WA/HUF-18] 05 p0627 A66-15694  
 Astronauts with thin shielding in radiation exposure from heavy nuclei in solar particle beams 09 p1336 A66-20521  
 Effects of radiation protective pharmacological agents /cystamine, pherotonin, AET, strychnine, etc/ on animals subjected to centrifugation, for application to astronauts 19 p3283 A66-35292  
 Effect of man walking inside or outside of satellite on attitude 21 p3818 A66-38843  
 Analogies between nutritional requirements of aircrew and cosmonauts, evaluating physiological factors involved 23 p4029 A66-41204  
**STRONAUT LOCOMOTION**  
 Mathematical model study of three-mass retrieval technique using anchor mass in space for future Gemini extravehicular operation 16 p2812 A66-31538  
 Space cabin simulator to test premise that in-flight physical exercise can be used for early detection of deteriorative trends for mission preservation 17 p2924 A66-32172  
 Extravehicular astronaut maneuvering and retrieval using thrusting devices and tether lines 19 p3290 A66-35956  
 Low-thrust jet fitted shoe for zero-gravity movement 19 p3290 A66-35957  
 Astronaut maneuvering unit, discussing experiments, performance requirements, design concepts, system tradeoffs, packaging and configuration 19 p3290 A66-35958  
 Extravehicular maneuvering techniques research, discussing manual locomotion methods, powered units, computer simulation, zero-g flight and space tests 19 p3291 A66-35960  
 Modular maneuvering unit for crew members providing independent propulsion, life support, power supply and communication capability 19 p3450 A66-35961  
 Computer simulation and performance

prediction of MMU astronaut maneuvering system, discussing acceleration, velocity, displacement, fuel consumption, propulsion efficiency 19 p3291 A66-35964  
 Extravehicular environment and mobility constraints affecting design of anthropomorphic space suit for working astronaut 19 p3291 A66-35972  
 Cleaning techniques for zip gun or hand-held maneuvering unit and environmental life support system or ventilation control module used for astronaut White walk in space 22 p3886 A66-40039  
**ASTRONAUT PERFORMANCE**  
**SA PILOT PERFORMANCE**  
 Measurement schedules effect on work load of astronaut performing navigation function, stressing tradeoff between number of measurements and accuracy level 01 p0102 A66-10044  
 Physiological test results on cosmonauts during Voskhod I and II flights including electrocardiograms, electroencephalograms, pneumograms, blood tests, spacesuit parameters, etc 01 p0017 A66-10416  
 Ionizing radiation dosimetry for space pilots on short-and long-term space flights 01 p0021 A66-10803  
 Problem areas in long duration manned space flight noting vehicle maintenance, extravehicular activities, visual skill performance, spacecraft control, etc [SAE PAPER 650809] 01 p0021 A66-10818  
 American and Soviet experience considering weightlessness, ionizing radiation, dynamic and biological factors, etc [SAE PAPER 650812] 01 p0021 A66-10819  
 Radiation hazard for cosmonaut inside or outside space from Earth radiation belt, considering electron radiative effect, tissue sensitivity, etc 02 p0182 A66-11663  
 Astronaut selection including dynamic testing, discussing examination methods, biological parameters, laboratory and radiological procedures, blood chemistry techniques, etc 04 p0469 A66-14064  
 Biological hazards of radiation exposure of man in space discussing recovery, delayed effect, injury treatment and dose 04 p0467 A66-14078  
 Vestibular sickness susceptibility under conditions of weightlessness 04 p0467 A66-14082  
 Spatial orientation disturbances and vegetative disorders occurring in cosmonauts during space flight due to disturbances in physiological interplay of sensing mechanisms governing space perception 04 p0468 A66-14084  
 Man-machine relationship during space flight 04 p0471 A66-14085  
 Perception of apparent vertical without visual cues depending on longitudinal axes of body and head to direction of resultant acceleration above 1 g 04 p0468 A66-14086  
 Space biology and medicine research, stressing flight experiments performed with Russian satellites and spacecraft 04 p0468 A66-14089  
 Astronaut physiological responses to space flight conditions measured for clinical or experimental purposes 04 p0471 A66-14091  
 Comparison of manned and unmanned spacecraft 04 p0472 A66-14092  
 Practice techniques for maintaining astronaut psychomotor skills during extended missions, with star sighting and flight control test results 05 p0626 A66-14635  
 LEM mission and pilot role in spacecraft control including guidance and control systems, retromaneuvering, landing-site inspection, etc 05 p0713 A66-15166  
 Physiological and psychomotor test performed in revolving space station simulator for design criteria for spacecraft with artificial gravity 06 p0815 A66-16051  
 Clinical aspects of interplanetary flights noting models of future cosmic diseases, automation of diagnostics, medical aid aboard spacecraft, etc 06 p0815 A66-16052  
 Simulation and environment effect on astronaut performance in space to understand work-task effort 06 p0817 A66-16239  
 Two-man space station simulator for 15-day integrated test program, primarily to study maintenance of operational mission element 06 p0868 A66-16242

Flight crew capability determined for Manned Orbital Research Laboratory /MORL/ 06 p0818 A66-16243  
 Human performance measurement capability and limitations for defining mans role in future space missions 06 p0818 A66-16244  
 Book on physiological and medical observations on cosmonauts Bykovskii and Tereshkova during simultaneous flights in Vostok V and VI 06 p0820 A66-16917  
 Correlation analysis to study reactions of human cardiovascular system during space flight of Voskhod 06 p0814 A66-17175  
 Water balance test for investigation of kidney functions of astronauts of Voskhod I spacecraft 06 p0814 A66-17176  
 Man in Project Apollo including module to module docking, lunar landing, maneuvering, reentry, etc 07 p1140 A66-17279  
 Human performance capabilities in space based on laboratory and spaceflight research 08 p1176 A66-18581  
 Human adjustment to shift in day-night cycle and effect of space flight on sleep and activity cycles of astronauts 08 p1174 A66-18582  
 Upper atmosphere and outer space research carried out by U.S.S.R. in 1964, including cosmonaut responses and launching tables 09 p1458 A66-20691  
 Layman book on lunar exploration including topographical data, lunar water, food, shelter and travel, space suits, working conditions, etc 10 p1609 A66-21900  
 Measurement schedules effect on work load of astronaut performing navigation function, stressing tradeoff between number of measurements and accuracy level 10 p1554 A66-21953  
 Emotional problems of astronauts during space flight 11 p1642 A66-22488  
 Extraterrestrial environment and calculation of realistic metabolic requirements for astronauts 11 p1648 A66-23003  
 Pre-and postflight medical examinations of Voskhod I cosmonauts 11 p1645 A66-23049  
 Mars exploration by astronauts, considering Mariner IV observations, noting low pressure and temperature, existence of frozen hydrosphere, etc 12 p1952 A66-24723  
 Model for social system for extended-duration spaceflight crews subject to isolation, confinement and/or stress 13 p2013 A66-25279  
 Medical evaluation of Martian environment based on Mariner IV photographs and extrapolations from manned flight, noting effects of Martian gravity on astronauts 13 p2014 A66-25293  
 Preflight medical tests of responses of Soviet cosmonauts Beliaev and Leonov to simulated weightlessness and performance during simulated space walk 13 p2009 A66-25889  
 Vestibular reactions of deaf during angular and coriolis accelerations 13 p2010 A66-25892  
 Physiological responses of astronauts Komarov, Feoktistov and Egorov during 24-hour orbital flight 13 p2011 A66-26229  
 Electrocardiogram P wave changes relation to body position changes in space 14 p2227 A66-26810  
 Role of man in space exploration, noting astronauts personal reports, scientific ability, superiority over instruments, etc 14 p2229 A66-26919  
 Structural dynamics/manned space flight relation, discussing man-machine dynamics, Apollo command module LF studies, pilot control of spacecraft and launch vehicle, etc 14 p2230 A66-28017  
 Experimental psychological testing and role in choice and training of cosmonauts 15 p2434 A66-29442  
 Entropy concept of information theory applied to space flight physiological data analysis 15 p2444 A66-29461  
 Electroencephalograms, cutaneous galvanic reactions and electrooculograms of Nikolaev, Popovich, Bykovskii and Tereshkova as recorded during space flight 15 p2436 A66-29463  
 Biological and medical tests during training and flight of Russian



astronauts 15 p2436 A66-29464  
Physiological reactions of Russian astronauts under prolonged weightlessness, noting motor activity, heart and pulse beat, breathing rates, arterial pressure, etc 15 p2436 A66-29467  
Soviet book on physiological methods in astronautics including collection, transmission and procession of medical information from long space flights 15 p2445 A66-29734  
Lowering of psychic tone, absentmindedness and vigilance decline during astronaut weightlessness on long space flights 15 p2442 A66-30003  
Simulated lunar landing maneuver of Apollo spacecraft, determining pilot control problems and handling 16 p2743 A66-30886  
Simulation testing pilot performance in orbiting Gemini spacecraft based on tracking rate errors and fuel consumption 17 p2872 A66-31963  
Psychiatric evaluation of candidates for space mission, developing rank order of candidates and stressing empathic approach of psychiatrist 17 p2862 A66-31982  
Visual requirements of space missions, discussing navigation, rendezvous and docking, lunar landing and lunar exploration 17 p2862 A66-32136  
Simulated orbital flights with extravehicular activities, determining incidence and severity of flyers bends due to decompression and exercise 17 p2856 A66-32148  
Factors affecting determination of selenographic latitude and longitude by astronaut landed on Moon, defining selenocentric system and lunar prime meridian 17 p3001 A66-32344  
Physiological reactions of astronauts to acceleration of Voskhod spacecraft characterized by greater emotional stress than during centrifuge simulation 17 p2861 A66-32936  
Flight activities of Russian cosmonauts in assessment of medical preparedness for orbital flight 19 p3283 A66-35291  
Weightlessness effects on man with data from Voskhod flights 19 p3284 A66-35568  
Human performance in space simulation chambers and physiological limitations 19 p3288 A66-35838  
Space tool kit development and evaluation program, examining design requirements for in-orbit and lunar surface repair and assembly tasks 19 p3363 A66-35948  
Controller, employing voice recognition principle, for attitude control system of astronaut maneuvering unit in various space tasks 19 p3291 A66-35973  
Man/machine problems in performance of space maintenance, noting conditions for shirtsleeve and pressurized suit, glove-tool interface, etc 19 p3292 A66-35974  
Heart rate response to Valsalva maneuver performed regularly during space flight suggests application to development of astronaut orthostatic intolerance 19 p3286 A66-36376  
Vestibular tolerance differences among members of crew of Voskhod to 24-hour stay in zero-weight environment 19 p3286 A66-36377  
Physical and psychological aspects of man in space, examining oxygen supply, temperature extremes, meteorites, radiation and effects of confinement, isolation and sensory impoverishment 19 p3287 A66-36645  
Extravehicular activity during Voskhod II flight, discussing motion and orientation of Soviet cosmonaut in space 21 p3701 A66-39337  
Mars exploration by astronauts, considering Mariner IV observations, noting low pressure and temperature, existence of frozen hydrosphere, etc 22 p3976 A66-39775  
Storage, dumping and regeneration techniques in air, water and food needed to keep astronauts alive 22 p3857 A66-40022  
Life support systems for crew comfort and safety, considering thermal and radiation environmental control, carbon dioxide removal, cryogenic gas storage, etc 22 p3857 A66-40129  
Astronaut observation in Gemini and Mercury space flights that stars cannot be

seen in daytime, noting first-magnitude stars and background illumination 22 p3982 A66-40523  
Preflight consideration of astronaut performance testing program for Gemini XI flight, noting manual operations and devices used 24 p4168 A66-42742  
Psychological effects of velocity and hermetic compartments on astronaut performance 24 p4166 A66-43146  
**ASTRONAUT TRAINING**  
**SA PILOT TRAINING**  
Program for engineering development of integrated spacecraft environmental control and life support systems and solution of man-machine integration problems [SAE PAPER 650813] 01 p0021 A66-10820  
Integrated operating mode of Apollo mission simulator with mission control center for combined training of Apollo flight and ground crews [AIAA PAPER 65-266] 03 p0353 A66-12777  
Apollo spacecrew training from simulation and actual past space flights [ASME PAPER 65-WA/HUF-17] 05 p0628 A66-15695  
Two-man space station simulator for 15-day integrated test program, primarily to study maintenance of operational mission element 06 p0868 A66-16242  
Psychophysical orientation mechanisms of man under weightlessness simulation, gravity conditions encountered on Earth, in orbital flight and during free floating in space 06 p0814 A66-17177  
System costs and pharmacological techniques as function of exercise program designed to maintain space crew physical fitness 07 p0999 A66-17658  
Astronaut selection and crew preparation procedures for Gemini and Apollo programs 08 p1176 A66-18578  
Training and selection procedures used at USAF Aerospace Research Pilot School 08 p1176 A66-18579  
Medical tests of spacemen Beliaev and Lenov during training and orbital flight 15 p2442 A66-28502  
Spacecraft crew training, noting universal multipurpose, complex and specialized functional training 15 p2443 A66-29440  
Astronaut training based on environmental factors, rated efficiency and physical and mental condition 15 p2443 A66-29441  
Immunological reactions of Russian spacemen before and after space flight 15 p2436 A66-29468  
Visual simulation device for aircraft pilot and astronaut 16 p2643 A66-30952  
Integrated mission simulation technique tests pilot reliability for seven-day manned lunar mission [AIAA PAPER 65-275] 18 p3061 A66-33792  
T-27 Space Flight Simulator, for extravehicular activity training, utilizing closed-circuit TV system 19 p3291 A66-35966  
First half of Gemini program noting design, prelaunch operations, astronaut training, EVA, etc 19 p3469 A66-35977  
Rescue teams for manned testing in environmental chamber for Gemini spacecraft noting personnel, chamber and personal equipment, test operations and rescue function and drill 22 p3857 A66-40240  
Engineering psychology of man-machine interface and relation to spacecraft piloting and systems control 24 p4169 A66-43147  
Professional training of Soviet astronauts, instilling high resistance to weightlessness, isolation, radiation, acceleration and other space flight stimuli 24 p4169 A66-43148  
**ASTRONAUTICS**  
**SA BIOASTRONAUTICS**  
**SA SPACE NAVIGATION**  
Rocket technology and air and space travel research - Annual Meeting, Berlin, West Germany, September 1964 04 p0581 A66-13494  
Astronautics education for RAF and USAF officers 06 p0972 A66-15920  
Astronautics Year, International astronomical and military space/missile review of 1964 07 p1155 A66-17414  
Scientific experiments for manned orbital flight - Goddard Memorial Symposium, Washington, D.C., March 1965 10 p1607 A66-21517  
Space travel and

exploration 12 p1946 A66-23672  
Monograph on manned space flight discussing environment, crew, spacecraft navigation, guidance, control, communications, etc 16 p2809 A66-30872  
Aviation and astronautics - Conference, Tel Aviv and Haifa, February 1966 17 p2912 A66-33062  
Legal aspects of spacecraft, space station and space navigation 19 p3483 A66-36272  
Handbook on theory of space flight and navigation of spaceships in interplanetary space, emphasizing characteristics of space trajectories, rocket engines and space vehicles 21 p3812 A66-38944  
**ASTRONAVIGATION**  
**S CELESTIAL NAVIGATION**  
**ASTRONOMICAL COORDINATE**  
**SA PLANETARY LONGITUDE**  
**SA SOLAR LONGITUDE**  
**SA SOLAR POSITION**  
Meridian astronomy methods including determination of instrumental errors, derivation of systems of right ascension and declinations and determining systematic errors 05 p0761 A66-15084  
Six faint radio sources identified with quasi-stellar objects, radio positions agreed with optical positions 05 p0764 A66-15242  
Data compilation on 21 new quasi-stellar radio sources including optical positions 05 p0764 A66-15242  
Orbital, geocentric, heliocentric and heliographic positions of cometary nuclei and tails in ecliptic or parabolic orbit 08 p1292 A66-19112  
Determining coordinates of astrogodetic grid points by Molodenskii integral formula and accuracy estimation by astrogravimetric interpolation of deviations 08 p1217 A66-19341  
Trajectory analysis and Birkhoff rings in restricted three-body problem in three-dimensional coordinate system 09 p1453 A66-20232  
Computer calculation of apparent positions of stars and Sun by reduction of mean stellar coordinates 10 p1604 A66-21122  
Matrix techniques for finding geomagnetic field strength in solar ecliptic coordinate system 11 p1699 A66-23022  
Directional accuracy of chords and angles in geocentric equatorial coordinate system in stellar triangulation 12 p1867 A66-23572  
Synoptic chart of chromosphere and sunspots, discussing coordinate systems, faculae, solar filaments, etc 12 p1948 A66-23972  
Positions of asteroids 1221 /Amor/ and 1948 OA /Object Wirtanen/ from photographs taken at Tautenburg, East Germany 12 p1950 A66-24352  
Absolute direction in space and control of stellar triangulation equations 12 p1875 A66-24872  
Compensated coordinates of artificial Earth satellites from synchronous observations at two given points on Earth surface 12 p1824 A66-24872  
Electronic trispheration, three-dimensional analog of triangulation, for long distance geodetic surveys 12 p1875 A66-24932  
Nomogram construction for transformation of astronomical object position from one spherical coordinate system to another using trigonometric functions 16 p2737 A66-31332  
Jupiter Red Spot coordinate measurements from recent plates 17 p3006 A66-33012  
Stars and galaxies in field of 18 southern radio sources observed in Australia 18 p3237 A66-35082  
Radio source identification between declinations -20 and -30 degrees 18 p3238 A66-35082  
564 radio sources between declinations and 20 degrees from Parkes catalogue 18 p3238 A66-35232  
Determining coordinates of astrogodetic grid points by Molodenskii integral formula and accuracy estimation by astrogravimetric interpolation of deviations 19 p3348 A66-36052  
IAU system of geocentric astronomical constants for ellipsoid Earth 20 p3653 A66-37762  
Zenith attraction value determined by simplified Bauschinger method, considering



- meteor position 20 p3653 A66-37795  
 Solar longitude according to Verrier and Newcomb 20 p3653 A66-37796  
 Directional accuracy of chords and angles in geocentric equatorial coordinate system 21 p3732 A66-38659
- ## ASTRONOMICAL MAP
- Graphical device for transformation between horizon system of coordinates and equatorial system, noting construction techniques, operation and application 09 p1381 A66-20395  
 Astronomical satellite application to sky mapping, stellar photometry, interstellar grains and gas study and statistical stellar sampling 15 p2594 A66-28987
- ## ASTRONOMICAL MODEL
- Magnetohydrostatic models of long-duration sunspot of depth 1000 km 06 p0954 A66-16466  
 Observed line spectra of nine quasi-stellar radio sources representation for single temperature, electron density and ionization level 09 p1456 A66-20416  
 Evolution of 9 solar masses stellar model of population I initial composition from main sequence through core helium burning 11 p1773 A66-22781  
 Model of oscillating cosmos which rejuvenates during contraction 14 p2378 A66-27021  
 Cosmological models for studying infinite universe 14 p2379 A66-27225  
 Principle of matter inexhaustibility applied to construction of finite and infinite cosmological models 14 p2379 A66-27227  
 Soft X-ray spectrum of Sun analyzed, using isothermal model of quiet corona providing representation of line intensities of C and Mg ions 17 p2994 A66-32657  
 Physicochemical quantitative analysis of cometary nucleus-coma buildup relationship, discussing gas liberation, entropy and enthalpy variation, change of state and gross energy balance 17 p3010 A66-33374  
 Grid computations of model atmospheres for A-type stars, considering effects of Balmer-line blanketing 18 p3227 A66-33762  
 Solar wind models analyzed, taking into account solar ejected high-velocity gas jets and southward component of interplanetary magnetic field 18 p3167 A66-34339  
 Galactic model for studying hydromagnetic stability of spiral arm in which field lines are helices around axis 18 p3237 A66-35043  
 Astronomical model for diffusion of galactic cosmic rays in solar system, based on zonal character of solar activity 20 p3630 A66-37329  
 Meteorite size prior to entering atmosphere, noting radius and use of isotope activity 21 p3812 A66-38953  
 General relativity theory, examining Schwarzschild surface which allows matter and light to pass through in one direction only 21 p3774 A66-39532  
 Solar rotation rate determined from longitudinal motion of sunspots, noting parameters of observation 21 p3816 A66-39555  
 Simulator for star motion in proximity of Sun consisting of sphere upon whose surface stars are uniformly distributed 22 p3977 A66-40001  
 Electromagnetic field of concentric rotating mass shells, noting Machian effects on cosmological models with near-Schwarzschild radius 22 p3948 A66-40525  
 Theoretical model for high energy phase of solar flares including radio bursts, proton acceleration and plasma cloud ejection 22 p3973 A66-40535  
 Theoretical model for quasars characterizes them as galactic flares, based on study of high energy phenomena associated with solar flares 22 p3982 A66-40536  
 Result of testing cosmological models with red shift magnitude observations of cluster galaxies and quasi-stellar radio sources 23 p4125 A66-41066
- ## ASTRONOMICAL OBSERVATORY
- ### SA CELESTIAL OBSERVATION
- ### SA OAO
- ### SA SOLAR OBSERVATORY
- Equal altitude method for calculating deviations of vertical, geographical coordinates and time correction for radio time signal from astronomical measurements 01 p0063 A66-11099  
 Steerable radio telescopes noting Mark I radio telescope at Jodrell Bank, England 01 p0139 A66-11156  
 Photographic, photometric and polarimetric observation of Mars from 1954 to 1958 at Pic du Midi noting seasonal variation of surface markings, clouds, diameter, etc 02 p0286 A66-11355  
 Catalog of radio telescope sky survey covering declination range between plus 40 and plus 44 degrees 05 p0759 A66-14806  
 Night airglow intensity measured at Kerguelen Islands in 1963, rejecting observations contaminated by auroral light 05 p0672 A66-15039  
 Experimental astronomical dome of glass-fiber-reinforced plastic distinguished by lightness, stability, smooth and silent operation and ease of assembly 05 p0660 A66-15219  
 Effect of lateral refraction and thermal conditions near Pavlov passage instrument on azimuthal position values and time measurement results 05 p0766 A66-15424  
 Radio astronomy observatory at Nancay, reviewing principles of electromagnetic radiation in Hertzian range 06 p0869 A66-16936  
 Antenna array and radiometer selection for orbiting LF radio astronomical observatory 10 p1507 A66-21122  
 Astronomical research possibilities, using manned Earth orbital spacecraft 10 p1608 A66-21531  
 Solar chromosphere observations in 1960-1963 by Istanbul University, noting flares, filaments, observation duration, etc 10 p1609 A66-21833  
 Astronomical yearbook of Cracow Observatory covering ephemerides of 787 eclipsing binaries, Lagrangian points, precession coefficients, etc 11 p1768 A66-22333  
 Annual astronomical almanac compiled by Madrid Observatory 11 p1770 A66-22638  
 Astronomical instruments and observation procedures for soft X-rays and extreme UV radiation 12 p1880 A66-23944  
 Manned orbiting astronomical observatories would enable astronomer astronauts to erect large sensors in space and avoid atmospheric effects 13 p2192 A66-25689  
 German and Austrian astronomical observatories reports on personnel, equipment, projects and publications 13 p2189 A66-26736  
 Lunar astronomical research, establishment of lunar observatory and mathematical model for analysis of logistics implications 14 p2390 A66-28410  
 Swiss space research program, apparatus and experiments 15 p2600 A66-29904  
 National report on space research in Sweden 15 p2601 A66-29933  
 Tabular data on magnetic storms and on geomagnetic and solar data furnished by Swiss Federal Observatory 16 p2801 A66-30726  
 Collected reports on new development of telescopic, photometric, spectrometric, meteorological, interferometric and detection equipment at various solar and stellar observatories 17 p2923 A66-32020  
 Lunar photography with 74-inch reflector of Helwan Observatory, detailing original negatives 17 p3006 A66-33018  
 Meteorological observations of Earth from lunar surface 19 p3455 A66-35286  
 Space systems for astronomical observations including OAO, rocket and balloon programs and manned space observatories 19 p3466 A66-36648  
 Solar physics, Communications of Shemakha Astrophysical Observatory 22 p3984 A66-40849
- ## ASTRONOMICAL PHOTOGRAPHY
- ### SA ELECTRONIC PHOTOGRAPHY
- ### SA HELIOGRAPHY
- ### SA LUNAR PHOTOGRAPHY
- ### SA SATELLITE PHOTOGRAPHY
- ### SA SPACE PHOTOGRAPHY
- Image translation from plate into coordinate system on another plate using homographic coordinates of object applied to astrometry 01 p0135 A66-10276  
 Reduction of photographic positions for arbitrary optical center 03 p0370 A66-12923
- Time-referencing of moment of photographing to determine satellite coordinates with aid of reference stars 04 p0524 A66-14394  
 Meteor photography by instantaneous exposure technique, effective tool for studying shape, dimensions and brightness distribution 05 p0759 A66-14884  
 Optical systems with improved aperture ratios, noting concentric optical system with corrected chromatic aberrations for photographing meteors, satellites, auroras, etc 05 p0679 A66-15203  
 Improved photographic images of meteors, using method of instantaneous exposure 05 p0681 A66-15218  
 Jupiter in 1964/65 photographic observation 11 p1771 A66-22648  
 Hybrid narrow band filter compared with Lyot filter, noting long-term instability and need for temperature control 11 p1706 A66-22892  
 Error analysis for statescope or radar altimeter phototriangulation readings and radio geodetic coordinate photography phototriangulation 12 p1867 A66-23517  
 Positions of asteroids 1221 /Amor/ and 1948 OA /Object Wirtanen/ from photographs taken at Tautenburg, East Germany 12 p1950 A66-24399  
 Comet Tomita-Gerber-Honda, noting direct photored photograph, spectrum of head and spectrum of tail 13 p2182 A66-25577  
 Reduction of photographic positions for arbitrary optical center 14 p2291 A66-27272  
 Flare initiated filament oscillations, noting photographic measurement of oscillation frequencies 15 p2573 A66-28646  
 Photographs from observatories of comet Ikeya-Seki discovered in constellation Hydra 16 p2804 A66-31309  
 Photographic atlas of Moon, particularly Ranger VII transmissions and Pic-du-Midi ground observation, with discussion of lunar physical and dynamic properties 16 p2807 A66-31747  
 Solar magnetic field measurements noting magnetic flux, development of bipolar magnetic region, etc 17 p2996 A66-31918  
 Solar corona emission spectrum and narrow passband photography of solar disk, noting measurement of intensity variation and absorption coefficient 17 p2999 A66-32133  
 Geocentric velocity of Leonids measured via meteor radar equipment 17 p3000 A66-32339  
 Earth shadow enlargement during lunar eclipse, noting contacts of lunar formations with shadow 17 p3000 A66-32341  
 Photographic observations of minor planets at Sydney during 1964 17 p3003 A66-32822  
 Data from ground photography of Mars covering portions of Mariner IV path, noting position of oases and canals 17 p3005 A66-33008  
 Rapid drift in longitude of small dark spot on south edge of Jupiter North Temperate Belt, noting sinusoidal displacement characteristics and measurement with blue and UV photography 17 p3005 A66-33009  
 Telescopic and photographic observation of cometary structure, particularly coma region 17 p3010 A66-33377  
 Comet Moorhouse III photographic analysis, noting tail motion, composition, angular motion of rays, etc 17 p3012 A66-33395  
 Astronomical photography of solar disk, revealing facula at 2190 angstroms and producing limb darkening curves 18 p3236 A66-34899  
 Thermal history, chemical composition and interior of Moon evaluated from Ranger VII, VIII and IX and terrestrial photographs 19 p3456 A66-35438  
 Lunar and Planetary Laboratory of University of Arizona, summarizing conclusions concerning lunar surface 19 p3457 A66-35440  
 Brightness of white corona in vicinity of solar prominences determined by trichromatic selection from color pictures of Sun during eclipse 19 p3454 A66-36610  
 Lunar profiles determined from photographs of annular solar eclipses of 1962 and 1963 20 p3655 A66-38021  
 Error analysis for statescope or radar altimeter phototriangulation readings and radio geodetic coordinate photography



phototriangulation 21 p3732 A66-38661  
Photographic data on iron meteor 36221  
noting trajectory, velocity, light curve, orbit  
and spectral emission 22 p3977 A66-39860  
intensities  
Retrograde rotation of cloud formations of  
Venus with angular velocity corresponding  
to one rotation in four days analyzed by  
high resolution 23 p4128 A66-41181  
photography

# ASTRONOMICAL PHOTOMETRY

Optical thickness, phase variation and  
albedo of rings A and B of  
Saturn 05 p0758 A66-14804  
Coarse-wire objective grating method  
applied to determination of coma-magnitude  
scale distortion and magnitude errors in  
long-focus refracting  
telescope 05 p0678 A66-15090  
Iris microphotometer on MF-2  
base 05 p0681 A66-15215  
20-inch mirror telescope with photoelectric  
astrophotometer for photometric,  
colorimetric and polarimetric  
measurements 05 p0683 A66-15419  
Photocathode scanned storage tube for  
detection of faint optical  
images 06 p0883 A66-17016  
Secular variations in absolute brightness of  
periodic comets attributed to instrumental  
and geometrical effects 07 p1133 A66-17519  
Isophotometric representation of solar  
corona, using photographs of equal  
density 07 p1136 A66-17735  
Separation problems of gas and aerosol  
components in brightness of atmospheric  
layer for photometric data pertaining to  
Mars atmosphere 08 p1295 A66-19330  
Difference between values for atmospheric  
pressure at Martian surface when obtained  
by photometry or by spectroscopy, due to  
nonconsideration of light scattering by  
aerosol particles 08 p1295 A66-19331  
Photometric examination of brightness  
distribution along disk of  
Mars 08 p1295 A66-19332  
Spectral reflecting power curve for  
Martian disk center compared with  
terrestrial equivalent 08 p1295 A66-19333  
MF-4 microphotometer modifications  
eliminating dependence of readings on  
brightness fluctuations of illuminating lamp  
and permitting negative processing in terms  
of intensity 08 p1224 A66-19336  
Optical parameters of Mars atmosphere and  
surface from photometric data for spherical  
and elongated scattering  
indicatrices 08 p1295 A66-19337  
Absolute calibration of Arizona  
Photometry 09 p1402 A66-20293  
UV color and flux at 2200 and 2600  
angstroms measured for A and B stars,  
using rocketborne  
photometers 10 p1602 A66-21096  
Zodiacal light and atmospheric continuum  
examined via new photoelectric 30-cm  
telescope 10 p1526 A66-21125  
Millimeter wavelength brightness  
temperatures of Mars, Jupiter and Saturn  
calculated from antenna  
temperatures 11 p1769 A66-22532  
Photoelectric observations and orbital  
solutions of BV 267, obtaining new light  
elements, system light change and orbital  
solutions 11 p1769 A66-22533  
Koval method for correcting distortions in  
photometric cross sections for Martian disk  
brightness distribution 12 p1944 A66-23502  
Image converter tube spectrophotometry of  
zonal variation of methane absorption bands  
on Jovian disk in near IR  
region 12 p1944 A66-23504  
Design parameters of astronomical camera  
for lunar charting 12 p1876 A66-23644  
Evidence that Martian maria corresponds  
to elevated land areas, citing radiometric  
measurement results 13 p2189 A66-26601  
Spectrophotometric measurements of ring  
nebula NGC 7662 in  
Andromeda 14 p2386 A66-28121  
Temperature and radii of nova  
photospheres 16 p2800 A66-30640  
Photometric measurements of solar flares  
and prominences for central intensities in  
hydrogen alpha 16 p2804 A66-31397  
Lunar topography and cartography, noting  
application to lunar atlas preparation,  
absence of magnetic field,

etc 17 p2999 A66-32132  
Photoelectric photometry of comet  
Everhart 1964 h, noting density of carbon  
radicals and CN 17 p3000 A66-32338  
molecules  
Photometry of nuclear condensation used  
to determine dimensions of cometary  
nuclei 17 p3009 A66-33369  
Resolution spectra and photometric  
profiles of comet heads in monochromatic  
light and physical state and chemical  
composition of comets 17 p3011 A66-33383  
Equidensitometric photographic  
isophotometry of comets and other luminous  
objects 17 p3011 A66-33385  
Integrated brightness observations of  
comets, using Baker-Nunn satellite tracking  
camera 17 p3011 A66-33386  
Cometary trail classification using  
Bredikhin method, noting  
spectrophotometric data on meteoritic  
microstructure 17 p3012 A66-33393  
Comet Humason photographic analysis  
noting tail movement, curvature and  
emanation of lateral jets 17 p3012 A66-33398  
Polarization and visible and IR reflectivity  
studies of Mars indicate that hematite is  
stable form on Martian  
surface 18 p3228 A66-34016  
Geometric albedos and phase integral of  
planet Mercury compared with  
Moon 18 p3230 A66-34153  
Thermal contrast of satellite eclipse  
shadows and band structure during 1965  
apparition of Jupiter 18 p3230 A66-34156  
Photoelectron counter stellar photometer  
noting design, applicability of secondary  
electron multipliers, etc 18 p3113 A66-34617  
Lunar photometric brightness variational  
function based on JPL study of Moon  
topology 18 p3235 A66-34656  
Optical photometric properties of lunar  
surface, discussing brightness effects, solar  
wind, albedo, reflectivity, backscatter,  
chemical composition, ion bombardment  
effects, etc 19 p3457 A66-35444  
Mass and diameter of planet Pluto  
determined by gravitational effects on orbits  
of Neptune and Uranus and photometric  
detection of occultations 19 p3463 A66-35945  
Koval method for correcting distortions in  
photometric cross sections for Martian disk  
brightness distribution 20 p3646 A66-37015  
Image converter tube spectrophotometry of  
zonal variation of methane absorption bands  
on Jovian disk in near IR  
region 20 p3646 A66-37017  
Digital video system for measuring  
broadband spectral intensity of stars and  
coordinates onboard OAO 20 p3557 A66-37202  
Pinhole photometric observation of umbra  
intensity profiles of large  
sunspot 21 p3808 A66-38469  
Multicolor photometric work on bright  
stars by Lunar and Planetary  
Laboratory 21 p3811 A66-38523  
IR astronomical measurements for  
computation of bolometric corrections and  
effective temperatures of stars of various  
spectral types 21 p3815 A66-39486  
IR photometric measurement of Comet  
1965f, noting absolute intensity dependence  
on distance from Sun, tail intensities and  
nature of particle  
emissions 21 p3816 A66-39557  
Primary nucleus splitting in comet Ikeya-  
Seki, noting mechanics and velocity of  
splitting process 22 p3977 A66-39861  
Photographic photometry of comet Ikeya-  
Seki using telescope in red region of  
spectrum, obtaining stellar  
magnitude 22 p3977 A66-39862  
Martian surface markings, brightness along  
optical equator, crater erosion, asteroid  
collision and yellow dust  
clouds 22 p3981 A66-40520  
Comparison of faint and bright solar  
prominences, analyzing hydrogen and  
metallic spectra of three bright and four  
faint prominences 23 p4126 A66-41074  
Liquid filter cell for telescopes, using half-  
saturated solution of cupric sulfate to block  
red leak of UG filter  
glass 23 p4071 A66-41927

# ASTRONOMICAL SPECTRUM

Spectral data of Galilean satellites of  
Jupiter 03 p0427 A66-12919  
Enhanced intensity of forbidden lines of

neutral oxygen in 28 planetary nebulae  
spectra linked to lower ionization  
levels 05 p0759 A66-14877  
Fabry-Perot fine etalon in astronomical us,  
such as H-alpha emission line profile  
measurement 05 p0681 A66-1521  
Detection of 3.1 micron mu cephei  
absorption band due to interstellar ic  
particles 05 p0768 A66-15777  
Comet spectrum analysis and variation  
with distance of comet from  
Sun 06 p0952 A66-15944  
Three Sun-mass star evolution from main  
sequence to helium exhaustion in core  
noting chronology of  
process 08 p1288 A66-18777  
Spectrographic analysis of Ikeya-Seki  
comet 08 p1289 A66-18799  
Indicatometric measurement of Martia  
surface composition, noting loamy an  
dustlike limonites, terra rossa and  
ferruginized soils 08 p1295 A66-19333  
Spectra of lunar occultations of emissio  
source 3C 273 08 p1297 A66-19444  
Variations in optical spectrum of quasi  
stellar radio source 3C  
345 09 p1456 A66-20414  
Earth, balloon and satellite spectroscopy  
observations of Mars to determine  
atmospheric composition and pressure a  
surface level 10 p1602 A66-21066  
Rocket and satellite observations of L  
radio waves from extragalactic  
sources 10 p1603 A66-21111  
Photoelectric observations and orbital  
solutions of BV 342, obtaining light elemen  
and light curve data 11 p1769 A66-22533  
Lunar spectral reflectivity distributio  
determined by comparison of lunar spectra  
with solar spectrum and spectra of earl  
star classes 12 p1945 A66-23504  
Hydrogen and helium spectra of gaseous  
nebulae in theory and  
observation 13 p2183 A66-25611  
IR reflection spectrum of Jupiter from  
second flight of Stratoscope II, discussin  
deep absorption features 13 p2184 A66-25611  
Empirical curve of growth on S/I line o  
1-0 hydrogen quadrupole band obtained  
laboratory and planetary hydrogen  
quadrupole spectra corrected for  
saturation 13 p2184 A66-25624  
Spectral data of Galilean satellites o  
Jupiter 14 p2380 A66-27266  
Absorption lines of quasi-stellar object 3C  
191 14 p2387 A66-28132  
Daylight observations of 1965 f comet,  
noting influence on solar corona, spectra a  
various wavelengths, polarization data an  
results of photoelectric  
scans 15 p2592 A66-28644  
Solar eclipse coronal isotopes, noting  
spectrum in region of maximum visual  
sensitivity, eulipticity figures, Luderndorff  
coefficient, luminosity gradients,  
etc 15 p2593 A66-28867  
High resolution power spectrum o  
international magnetic character, showing  
two subsidiary peaks on both sides of 27-day  
period 16 p2695 A66-30711  
Aircraft instrumentation for spectroscopic  
observation of solar middle corona a  
medium dispersion on May 30,  
1965 16 p2705 A66-30826  
Solar class 2 flares, noting activity on  
September 16, 1963, associated ionospheric  
disturbances, etc 16 p2795 A66-31149  
Quasi-stellar object origin noting spectrum,  
intensity distance, etc 17 p2995 A66-31910  
Spatial cross-correlation analyses between  
radial velocity and continuum brightness  
fluctuations of solar disk center  
spectrograms 17 p2996 A66-31919  
Mars disk intensity, noting  
spectrophotometric measurements in search  
for limonite near IR spectral  
features 17 p2997 A66-31922  
Cosmic radio source strength, explaining  
spectral output from substructures o  
3C-273 17 p3007 A66-33084  
Rotational line intensities of lambda 4300  
band of CH in spectrum of comet  
Ikeya 17 p3010 A66-33379  
Continuous spectrum of comet Alcock  
/1963 b/ observed with quartz spectrograph  
at Haute-Provence observatory in  
France 17 p3011 A66-33386  
Cometary trail classification using



- Bredikhin method, noting  
spectrophotometric data on meteoritic  
microstructure 17 p3012 A66-33393
- Laboratory work on comets, discussing  
spectroscopic data, incompleteness of  
knowledge of dissociation energies and  
ionization potentials, etc 17 p3012 A66-33400
- Cometary and hydrocarbon flame spectra  
compared, discussing Swan, HCO and other  
band systems 17 p3013 A66-33404
- Physical characteristics of ten periodic  
comets compared, considering continuum,  
triatomic carbon radical and other emissions  
intensity tail and photometric  
parameters 17 p3014 A66-33412
- Nonsolar absorption lines in spectra of  
inner three Galilean satellites of  
Jupiter 18 p3230 A66-34155
- Spectra of lunar occultations of emission  
source 3C 273 18 p3232 A66-34478
- Quasi-stellar radio source characteristics,  
noting methods of identification, emission of  
high energy particle flux,  
etc 18 p3176 A66-34751
- Catalog of neutral H-line profiles at 21 cm  
wavelength noting intensity, radial velocity,  
line widths, etc 19 p3460 A66-35792
- Stellar evolution of stars between 1 and 3  
solar masses, noting nuclear reactions and  
chemical composition 19 p3467 A66-36792
- Lunar spectral reflectivity distribution  
determined by comparison of lunar spectra  
with solar spectrum and spectra of early  
star classes 20 p3646 A66-37019
- Spectral study of Jupiter, Saturn and rings  
of Saturn, determining methane  
concentration in cloud  
layers 20 p3647 A66-37035
- Interferometric observation of cosmic  
emission at OH frequency, noting emission  
source dimensions 21 p3814 A66-39268
- High resolution spectroscopic study of  
comets, examining mechanism involved in  
excitation of cometary  
spectra 21 p3816 A66-39533
- Abundance and temperature of carbon  
dioxide in Martian atmosphere, noting  
implications, observation methods and  
results 21 p3816 A66-39558
- New absorption bands in near IR spectrum  
of Mars found by Fourier spectroscopy via  
carbon dioxide absorption  
measurements 22 p3981 A66-40486
- Forms of red shift magnitude relation for  
Friedmann type relativistic model  
universes 23 p4125 A66-41046
- Absorption lines on Venus spectrograms of  
rotational fine structure of excited  
vibrational transition of carbon  
dioxide 23 p4130 A66-41816
- 3 cm hydrogen line from solar flares,  
estimating line-to-continuum ratio during  
flare 23 p4124 A66-41928
- Planetary atmosphere resolution spectrum  
noting carbon dioxide lines, radiation  
transfer, composition, temperatures,  
pressures, etc 24 p4277 A66-42667
- Venus atmosphere noting pressure induced  
absorption in carbon dioxide-nitrogen  
atmosphere as indicated in decline of  
microwave brightness  
temperature 24 p4277 A66-42668
- Maser amplifier based on UV continuum  
pumping from nearby stars, explaining 18-cm  
OH emission from anomalous H-2  
regions 24 p4280 A66-43042
- ASTRONOMICAL TELESCOPE**  
**SA RADIO TELESCOPE**  
Multiple passband monochromatic filter  
used in telescopes for spectrophotometry of  
red shifts of distant  
galaxies 02 p0227 A66-11352
- Designing space telescopes to perform  
astronomical observations from Earth orbit  
and integration into manned  
spacecraft 02 p0229 A66-11627
- Slit spectrograph theory of Bowen for use  
with medium size astronomical  
telescopes 02 p0229 A66-11701
- High-speed aplanatic catadioptric telescope  
system with all optical elements having  
spherical surfaces only, noting refracting  
and reflecting telescopes 05 p0679 A66-15204
- Prime-focus field of Maksutov telescope  
system on Mount Kanobil, U.S.S.R. noting  
objective, mirror and tests for distortion  
and accuracy in  
astrometry 05 p0680 A66-15205
- Optical system of RM-700 astronomical  
telescope, analyzing prime focus and  
Cassegrain focus 05 p0680 A66-15206
- Deformation calculation of RM-700  
telescope mounting 05 p0680 A66-15207
- Telescope components and subassemblies,  
covering structural element analysis  
techniques on experimental  
basis 05 p0680 A66-15208
- Astronomical telescope, discussing support  
mechanism design for constant mirror  
shape 05 p0680 A66-15209
- Long-focus horizontal telescope with  
coelostat for photographing position of  
Moon 05 p0681 A66-15217
- Stellar diurnal variation determined during  
reduced solar activity from crossed-  
telescope and neutron monitor  
data 05 p0754 A66-15396
- 20-inch mirror telescope with photoelectric  
astrophotometer for photometric,  
colorimetric and polarimetric  
measurements 05 p0683 A66-15419
- Minimum field of view required for rapid  
accurate navigation star identification-  
acquisition established between 25 and 30  
degrees 06 p0906 A66-16247
- New solar telescope and spectrograph  
installed at Kwasan Observatory, Kyoto,  
Japan 06 p0879 A66-16331
- Instrumental effects distorting data of  
telescopically observed meteors analyzed by  
simultaneous observation with various  
binocular telescopes and naked  
eye 07 p1135 A66-17635
- Reflection spectrum of clouds in Venus  
atmosphere measured, using telescope  
mounted on helium balloon, noting details of  
instrument 07 p1137 A66-18055
- Signal-generating astronomical sensors,  
describing Stratoscope II balloon-borne  
telescope 08 p1222 A66-18732
- Light polarization of twilight and daytime  
sky at various wavelengths, using telescope-  
polarimeter system with various color  
filters 08 p1217 A66-19335
- Feedback method for reducing errors of  
counter telescopes due to missed counts and  
accidental coincidences 09 p1379 A66-20235
- Zodiacal light and atmospheric continuum  
examined via new photoelectric 30-cm  
telescope 10 p1526 A66-21125
- Orbiting eye /space telescope/ construction  
featuring membrane optics with smooth and  
symmetric surfaces, inflatable body and  
laser transceiver 12 p1876 A66-23646
- Short period variations in cosmic ray  
intensity, using neutron monitors, cubic  
telescopes, etc, analyzed with superhigh  
statistical precision 12 p1943 A66-24186
- Image dissector for lunar observation in  
conjunction with Earth-based telescope,  
noting efficiency of resolution contrast  
sensitivity 12 p1883 A66-24678
- Radiotelescope of 40-sec-of-arc resolving  
power, composed of compound  
interferometers with small  
antennas 13 p2058 A66-25569
- Plane grating monochromator illuminated  
by convergent light for scanning  
spectrometers on astronomical  
telescopes 13 p2080 A66-25988
- Design and construction of 106-cm  
Cassegrain-type reflector telescope at Pic du  
Midi observatory 13 p2081 A66-26233
- Accuracy of radio astronomy measurements  
of wavelength, frequency, position,  
brightness distribution and flux density  
compared with optical  
measurements 15 p2594 A66-28982
- Balloon-carried automatic telescope-  
spectrometer observation of Venus upper  
atmosphere and determination of water  
vapor content 16 p2797 A66-30352
- Gyro-stabilized heliostat for airborne  
astronomy noting design principles, achieved  
stability, servoloop and mechanical  
system 16 p2705 A66-30824
- Gyro-stabilized airborne solar eclipse  
spectrograph, noting wavelength range,  
dispersion accuracy, guidance mechanism,  
etc 16 p2705 A66-30825
- Collected reports on new development of  
telescopic, photometric, spectrometric,  
meteorological, interferometric and  
detection equipment at various solar and  
stellar observatories 17 p2923 A66-32020
- Orbiting of manned astronomical  
telescopes, noting advantages over  
instruments hampered by Earth  
atmosphere 19 p3468 A66-35795
- Spectral receiver of Nancy radiotelescope  
of correlation type, for extragalactic  
observations on 21-cm neutral hydrogen  
band 19 p3319 A66-36259
- Systems design analysis of lunar survey  
viewfinder /LSV/ consisting of pointing and  
tracking telescope for high-resolution lunar  
surface survey 20 p3558 A66-37225
- Sidereal anisotropy indicated for charged  
galactic cosmic radiation obtained by  
celestial scanning, using narrow angle muon  
telescope 21 p3808 A66-38466
- Reduced-scale models for predicting image  
degradation due to nonuniform temperatures  
and resulting deformations of structural and  
optical elements in large spaceborne  
telescopes 22 p3889 A66-40215
- Telescope field of view requirements for  
human recognition of navigation  
stars 22 p3946 A66-40860
- Liquid filter cell for telescopes, using half-  
saturated solution of cupric sulfate to block  
red leak of UG filter  
glass 23 p4071 A66-41927
- Diagrams of computers calculating parallax  
angle of azimuthally mounted astronomical  
telescopes 24 p4211 A66-42484
- Radar astronomy methods permit  
determination of range from echo delay,  
rotation rate from dispersion of echo and  
surface dielectric constant from reflectivity  
measurements 24 p4280 A66-43198
- ASTRONOMICAL UNIT**  
Improved determination of astronomical  
unit as result of radar measurements of  
Venus 03 p0429 A66-13114
- System of astronomical constants adopted  
in 1965 by International Astronomical Union  
for introduction in 1968, discussing  
difficulties in consistency, compatibility and  
durability 03 p0429 A66-13195
- Radar astronomy investigations of Venus,  
Mars, Jupiter, Mercury and Moon, discussing  
surface and rotational characteristics to  
establish astronomical  
unit 04 p0578 A66-13963
- ASTRONOMY**  
**SA INFRARED ASTRONOMY**  
**SA RADAR ASTRONOMY**  
**SA RADIO ASTRONOMY**  
**SA SELENOLOGY**  
Catalog of observations on auroral  
phenomena in Western Europe below  
geomagnetic latitude of 55 degrees for years  
1601 to 1700 01 p0139 A66-11104
- Theoretical and experimental studies in  
astronomy and astrophysics, relating them to  
physical and mathematical  
sciences 02 p0285 A66-11296
- Communications of Lunar and Planetary  
Laboratory 02 p0287 A66-11493
- Cosmic triangulation systems assessing  
polar method for determining geodetic  
satellite coordinates and inherent error  
estimation and correction 03 p0361 A66-12502
- Electron-optical converters in  
astronomy 05 p0681 A66-15212
- Astronomical Society Conference, Eisenach,  
Thuringia, East Germany, September  
1965 07 p1134 A66-17630
- Astronomical observations from space  
vehicles - International Astronomical Union  
Symposium, Liege, Belgium, August  
1964 10 p1596 A66-21078
- Chinese-English/English-Chinese  
astronomical and astrophysical  
dictionary 12 p1949 A66-24200
- New astronomical techniques for  
observations outside Earth atmosphere,  
noting X-ray sources and neutron  
stars 14 p2378 A66-26915
- Arguments pro and con on Milankovitch  
astronomical theory of climatic  
changes 15 p2489 A66-29266
- Monographs from Lunar and Planetary  
Laboratory of University of Arizona,  
1965 15 p2603 A66-29968
- Interstellar medium survey including cloud  
structure and velocity field of interstellar  
gas, galactic magnetic field,  
etc 16 p2799 A66-30575
- Total eclipse of Sun, November 12, 1966,  
classical theory of solar eclipses and  
procedure for automatic computation,  
including charts and tables with



- results 16 p2801 A66-30821  
 Book on spherical astronomy including celestial coordinate systems, parallax, diurnal motion, precession and nutation, time measurement, etc 16 p2806 A66-31738  
 Transactions of International Astronomical Union, Volume 12A, Reports on astronomy 17 p2997 A66-32018  
 Book of astronomical literature published in 1964 17 p3000 A66-32326  
 Space astronomy discussing history, solar XUV, galactic UV, galactic X-rays and gamma rays, visible and IR observations, laboratory astrophysics, etc 17 p3002 A66-32549  
 Papers on astronomy and astrophysics including objective prisms, lunar gravity, relativistic degenerate gas, solar system, etc 21 p3812 A66-38820  
 Annual review of astronomy and astrophysics, Volume 4, covering measurements in IR, polarization of cosmic radio waves, pulsation theory, etc 21 p3815 A66-39482

## ASTROPHYSICS

- Collected works of K. E. Tsiolkovskii on astronomy, natural science and technology 01 p0135 A66-10295  
 Dimensions, form and structure of entire known universe, examining discontinuous emission of energy from stars as they cool 01 p0135 A66-10299  
 Theoretical and experimental studies in astronomy and astrophysics, relating them to physical and mathematical sciences 02 p0285 A66-11296  
 Space physics - Proceedings of Summer School, Alpbach, Austria, July-August 1963 03 p0419 A66-12839  
 Textbook on celestial mechanics, meridian astronomy, instrumentation, solar research and astrophysics 05 p0760 A66-15087  
 Fundamental problems in cosmic radiation astrophysics 05 p0752 A66-15379  
 Cosmic rays and problems in space physics - Conference, Yakutsk, U.S.S.R., August 1962 06 p0945 A66-16568  
 Stellar neutrino emission mechanism and neutrino-electron scattering 06 p0946 A66-16570  
 Interferometric techniques in visual and radio regions for astrophysics 07 p1035 A66-18151  
 Text on sources of stellar energy, internal structure of stars and evolution of stars 09 p1447 A66-20090  
 Milky Way composition and light radiation characteristics, outlining definitions, basic relations, star categories, color diagrams, etc 09 p1454 A66-20288  
 Data on stars having space velocity greater than 65 km/sec 11 p1767 A66-22261  
 Stellar dynamics of Galactic system, discussing relations between density and velocity distributions of stars 11 p1767 A66-22262  
 Chinese-English/English-Chinese astronomical and astrophysical dictionary 12 p1949 A66-24200  
 Relativistic astrophysics covering evolution of moderate to supermassive stars, radiation and gravitational field and stellar collapse 14 p2385 A66-27948  
 Dynamic stability of supermassive stars with nuclear-energy generation, noting rotation and limiting mass for hydrogen burning 14 p2385 A66-28117  
 Temperature and radii of nova photospheres 16 p2800 A66-30640  
 Review of literature on planets, natural satellites, Moon and origin of solar system 17 p2998 A66-32023  
 Space astronomy discussing history, solar XUV, galactic UV, galactic X-rays and gamma rays, visible and IR observations, laboratory astrophysics, etc 17 p3002 A66-32549  
 Nature and origin of comets - International Colloquium on Astrophysics, Liege, Belgium, July 1965 17 p3008 A66-33367  
 Cometary origin through survey of literature for last 13 years 17 p3013 A66-33405  
 Upper limit on fractional binding energy of nonrotating magnetoturbulent supermassive star and for mass which can reach radiative equilibrium 18 p3229 A66-34141  
 Semiconvective zone in very massive stars

- during hydrogen burning, noting factors leading to instability 18 p3229 A66-34142  
 Stellar formation rate in young clusters according to simultaneous formation hypothesis and continuous formation hypothesis 18 p3229 A66-34143  
 Stellar evolution - International Conference, Goddard Institute for Space Studies, New York, November 1963 19 p3466 A66-36788  
 Interferometric techniques in visual and radio regions for astrophysics 21 p3735 A66-38508  
 Papers on astronomy and astrophysics including objective prisms, lunar gravity, relativistic degenerate gas, solar system, etc 21 p3812 A66-38820  
 Annual review of astronomy and astrophysics, Volume 4, covering measurements in IR, polarization of cosmic radio waves, pulsation theory, etc 21 p3815 A66-39482  
 Soviet papers on problems of astrophysics 23 p4125 A66-41072

## ASYMPTOTIC FUNCTION

- Matched asymptotic expansion to derive dynamical displacements of infinite elastic space embedded with light rigid axisymmetric body 02 p0299 A66-11806  
 Laplace transform technique to develop asymptotic solutions to integral equations describing influence of scattering law on radiation damage displacement cascade 02 p0245 A66-11946  
 Asymptotic solution of some nonstationary boundary value problems of cylindrical surface 02 p0250 A66-12098  
 Global asymptotic stability problem for complex high order system solved by transformation into interconnected set of lower subsystems 05 p0654 A66-14608  
 Asymptotic theory of photoionization chamber noting charged particle densities, sheath equations and quasi-neutral plasma 05 p0721 A66-14717  
 Asymptotic behavior of solutions of boundary value problem for second-order elliptic equations 07 p1056 A66-17602  
 Richardson critical number and asymptotic equation applied to stably stratified ground atmospheric layer 07 p1062 A66-17924  
 Prandtl lifting line classical theory of high aspect ratio wings as singular perturbation problem yields asymptotic expansions of Navier-Stokes solution 07 p0982 A66-18124  
 Conservation laws involving mass, momentum and energy applied to asymptotic properties of hypersonic flow 09 p1327 A66-20266  
 Construction method for asymptotic series of given class of functions and application to diffraction theory 09 p1394 A66-20459  
 Asymptotic behavior of probability distributions and density functions of processes with independent increments 09 p1397 A66-20645  
 Asymptotic representation of maximum of normal stationary process over large time interval 09 p1397 A66-20647  
 Asymptotic behavior, at plus infinity, of first order linear differential-difference-delay equation solutions, discussing asymptotic oscillatory number 10 p1549 A66-21224  
 Unilateral estimates under conditions of asymptotic stability of solutions to differential equations with unbounded operators 10 p1552 A66-21985  
 Approximate solutions of second order differential equations for nonlinear electronic circuits with strong disturbance 11 p1676 A66-22735  
 Asymptotic expansions to heat-transfer rate for laminar boundary layer flow at small or large Prandtl number 11 p1786 A66-23012  
 Approximate oscillatory solution of second order linear equations, with application to Bessel equation 11 p1724 A66-23425  
 Blast wave theory with and without entropy layer effect, determining asymptotic flow, far downstream of blunted nose, past given body 12 p1861 A66-23808  
 Richardson critical number and asymptotic equation applied to stably stratified ground atmospheric layer 12 p1905 A66-23885  
 Sufficient conditions for boundedness of

- solutions of nonlinear differential equations and oscillatory and asymptotically stable solutions 12 p1904 A66-24193  
 Asymptotic behavior of two-dimensional inviscid flow at infinite Mach number past power-law body, considering flow over flat plate and blunt body followed by cylindrical afterbody 13 p2060 A66-25156  
 Species diffusion in frozen hypersonic boundary layer with Falkner-Skan velocity profiles, where surface is linear, given as Meili transform, constructing series and asymptotic expansion of surface concentration 13 p2060 A66-25156  
 Existence and stability of periodic motions in dynamic systems applied to analysis of uniformly asymptotically stable solutions of differential equations 15 p2525 A66-28508  
 Stability analysis of symmetrically loaded thin walled spherical shell, noting construction of asymptotic expansion, error estimation and application of elasticity theory 15 p2608 A66-28952  
 Asymptotic behavior of solution to ordinary differential equation, noting transformation to nearly diagonal system of first order 16 p2733 A66-30741  
 Asymptotic behavior of nonlinear integral equations with certain conditions on kernels and nonlinearities 16 p2738 A66-31703  
 Asymptotic efficiency for maximum likelihood estimator 17 p2946 A66-32298  
 Discreteness conditions for spectrum of one-term differential operator, considering asymptotic distribution of eigenvalues 18 p3126 A66-33933  
 Asymptotic behavior of transition probability matrices, analyzing limit theorems involving capacities in Markov chains 19 p3389 A66-35984  
 Unilateral estimates under conditions of asymptotic stability of solutions to differential equations with unbounded operators 19 p3390 A66-36190  
 Interpretation of results obtained by Liapunov method, using parallelepiped imbedded in region of asymptotic stability 19 p3337 A66-36712  
 Flight stability, discussing quasi-critical case in neighborhood of asymptotic stability boundary of autonomous systems and that of variable system parameters 21 p3696 A66-39594  
 Energy spectral density of ideal sonic boom pressure signatures and equations for HF and LF asymptotic spectral behavior 22 p3848 A66-40307  
 Approximate solutions of second-order differential equations for nonlinear electronic circuits with strong disturbance 23 p4049 A66-41477  
 Transcendental case of dynamical asymptotic stability of motion of autonomous system with one zero 23 p4090 A66-41551
- ASYMPTOTIC METHOD**  
 Asymptotic behavior of solution to system of differential equations with random limited coefficients 01 p0095 A66-10733  
 Cauchy problem for linearized Boltzmann equation in kinetic theory of gases 01 p0107 A66-11017  
 Spectral matrix of fourth-order differential operator on half-axis 02 p0250 A66-12107  
 Text on aerodynamics of wings and bodies emphasizing matched asymptotic expansion methods for boundary value problems and numerical techniques for loading predictions via computers 03 p0313 A66-12297  
 Existence of stable periodic solution of Liénard equation, using asymptotic methods 03 p0392 A66-12615  
 Asymptotic solution of Dirichlet problem for diffusion processes and small parameters in elliptic equations with discontinuous coefficients 03 p0388 A66-12923  
 Derivation of asymptotic form of Green's function, using hydrodynamic approximation method 04 p0510 A66-13871  
 Asymptotic methods for hydrodynamic stability of slightly nonuniform plasma 05 p0727 A66-15262  
 Book on asymptotic expansions in powers of small parameter applied to nonsteady oscillations in nonlinear systems with one or more degrees of freedom 05 p0776 A66-15322  
 Effective transformation and asymptotic behavior of class of nonlinear differential



- equations 05 p0709 A66-15343
- Asymptotic solutions of second-order ordinary differential equations in region containing irregular singularity of rank one, with application to Whittaker functions 05 p0710 A66-15475
- Asymptotic solutions of second-order differential equations having irregular singularity of arbitrary rank 05 p0710 A66-15476
- Asymptotic error estimates in solving elliptic equations of fourth order by method of finite differences 05 p0710 A66-15477
- Asymptotic solutions for viscous flow of transparent radiating gas in stagnation region, using method of matched inner and outer expansions [AIAA PAPER 66-105] 06 p0871 A66-16254
- Shell linear theory, discussing classical elasticity theory, bending equations, edge effect and asymptotic theory 06 p0962 A66-16350
- Asymptotic solutions of problems in wave propagation, examining electromagnetic field equations, hyperbolic equations, radiation from sources, etc 06 p0835 A66-16900
- Gas flow dissipation in transonic plane-symmetric nozzle, obtaining asymptotic solutions for flow parameter 07 p0979 A66-17264
- Asymptotic behavior of solutions of ordinary linear differential equations involving continuous complex valued functions 07 p1058 A66-17913
- Circulation distribution for swept-back wing of finite span and large aspect ratio in subsonic flow by asymptotic method 07 p0981 A66-18033
- Statistical approach to derivation of quadrature formulas 07 p1061 A66-18510
- Asymptotic formulas derived, describing stress-strain state of circular cylindrical shell subject to concentrated heating 08 p1305 A66-18602
- Asymptotic solution of problem of thin spherical shell free vibration for axisymmetric and general cases 08 p1308 A66-18888
- Dynamics of two-channel automatic control systems taking into account nonlinear interaction between channels 08 p1201 A66-19676
- Saddle point, Watson transformation and residue series in survey of asymptotic methods for HF scattering 10 p1498 A66-21596
- Asymptotic expansions of double and multiple integrals occurring in diffraction theory, using stationary phase method 10 p1550 A66-21850
- Chaplygin asymptotic series solution method for differential equation systems 10 p1551 A66-21915
- Asymptotic method of integral estimation of space-time broadband random vibrations boundary value problem for elastic systems 11 p1781 A66-22616
- Liapunov first method and applicability to asymptotic stability of stationary points of nonlinear differential systems 11 p1721 A66-22641
- Asymptotic solution of rarefied gas flow, using free molecular approximations 11 p1692 A66-22919
- Asymptotic approximations in hydrodynamic stability problems including Couette, spiral and parallel shear flows 12 p1860 A66-23548
- Asymptotic theory where limit  $R$  / Rayleigh number/ approaches infinity 12 p1976 A66-23550
- Stability of two-dimensional parallel flows, using Orr-Sommerfeld equation and adjoint equation with asymptotic solution 12 p1861 A66-23809
- Asymptotic series solution to problem of laminar film condensation on nonisothermal vertical plate, considering inertia and convection effects 12 p1978 A66-23996
- Extended Dirichlet problem for cross section of cylindrical shell, showing asymptotic solution is valid, approximation to Dirichlet integral applied to electrostatic problem of condenser and closed tubes torsion 12 p1968 A66-24196
- Asymptotic solution to motion of solid containing cylindrical or spherical cavities filled with viscous liquid 12 p1863 A66-24356
- Asymptotic solution, valid in physical space, obtained for kinetic layers in slip flow of linearized Couette problem 12 p1865 A66-24589
- Aerodynamic resistance of transonic wing profile analyzed, using asymptotic flow at long distance downstream of shocks 13 p1990 A66-25456
- Free oscillation of thin elastic shell, using asymptotic method for integrating dynamic equations in classical linear theory 13 p2196 A66-25630
- Motion equation for rotation of Mercury solved by asymptotic expansion 13 p2187 A66-26287
- Derivation of asymptotic form of Green function, using hydrodynamic approximation method 14 p2275 A66-27578
- Orthotropic-elasticity solutions applied to wave propagation in infinite cylindrical shell, obtaining asymptotic solutions for HF range 14 p2400 A66-27662
- Asymptotic stability of equilibrium states of nonholonomic systems 14 p2336 A66-28052
- Exact solutions for unsteady two-dimensional gas dynamics equations for self-similar flow behind shocks and expansion waves 14 p2278 A66-28143
- Nonhomogeneous solid sphere radiative cooling asymptotic representation based on heat conduction theory by Laplace transforms 14 p2414 A66-28144
- Statistical thermodynamics analysis of interaction limit problem for real system 14 p2414 A66-28277
- Asymptotic estimates of characteristic values of differential equation with periodic coefficients 15 p2524 A66-28507
- Asymptotic integration of elasticity theory equations and analysis of stressed state of anisotropic shell 15 p2609 A66-28963
- Asymptotic methods of nonlinear mechanics, involving averaging for differential equations, applied to motion equations of satellites and resonance in electric circuits 15 p2541 A66-29162
- Asymptotic solutions of boundary value problems for elastic semiinfinite circular cylindrical shells by removing restriction of slow circumferential variation 15 p2609 A66-29239
- Rational approximation of transcendental functions for cylindrical cavity subject to internal pressure 15 p2528 A66-29254
- Effective transformation and asymptotic behavior of class of nonlinear differential equations 15 p2530 A66-29979
- Asymptotic behavior of solutions to equations for laminar boundary layer far from wall 16 p2684 A66-30582
- Asymptotic behavior of solutions of ordinary linear differential equations involving continuous complex valued functions 16 p2736 A66-30976
- Robbins-Monro stochastic approximation method extended and results applied to least squares method 17 p2946 A66-32296
- Large deflections of symmetrically loaded shallow membrane shells of revolution, considering existence of boundary layer near edges and using asymptotic analysis 17 p3025 A66-32480
- Random delay effect on excitation of vibrations in nonlinear systems, using Krylov-Bogoliubov method 17 p2958 A66-32710
- Asymptotic methods of nonlinear mechanics applicable to nonlinear differential equations with random arguments 17 p2958 A66-32711
- Asymptotic theory of spherical electrostatic probe in collision-dominated partially ionized gas by quasi-linearization 18 p3146 A66-34583
- Asymptotic expression for difference between continuous periodic function and typical mean of Fourier series 18 p3128 A66-35013
- Generalized method of averaging and von Zeipel method as applied to perturbed Hamiltonian system of appropriate form [AIAA PAPER 65-687] 19 p3462 A66-35893
- Derivative-expansion method of first-order asymptotic expansion of takeoff of satellite from circular orbit by small thrust inclined at finite angle to radius vector [AIAA PAPER 65-688] 19 p3462 A66-35894
- Matched asymptotic expansions and patched conics used to simplify flyby interplanetary trajectories [AIAA PAPER 65-689] 19 p3462 A66-35895
- Asymptotic representations of perturbation methods used to solve differential equations of satellite orbit mechanics 19 p3462 A66-35897
- Asymptotic solution of nonlinear hyperbolic equation in gas dynamics, with applications in explosion theory, astrophysics, etc 19 p3390 A66-36200
- Asymptotic property derived for particular solutions of Hamilton-Jacobi equation of conservative systems with two degrees of freedom 19 p3401 A66-36252
- Asymptotic calculation of effect of small tangential thrust on satellite motion, problem solved for satellite orbit in first and second approximation 19 p3472 A66-36842
- Dynamics of two-channel automatic control systems taking into account nonlinear interaction between channels 20 p3538 A66-37268
- Asymptotic representation of systems of nonlinear differential equations, setting up lemmas and theorems 20 p3590 A66-37484
- Asymptotic solutions of differential equations of mass transfer with chemical reaction without assumptions concerning kinematics, showing existence of five regimes 20 p3679 A66-37789
- Block diagonalization theorem for linear ordinary differential equation systems and applications 21 p3755 A66-38597
- Asymptotic forms exhibited by powers of nonnegative matrix, discussing index of convergence and associated values 21 p3755 A66-38602
- Decomposition of system of linear differential equations, using asymptotic techniques of Krylov and Bogoliubov 22 p3940 A66-40459
- Adiabatic motion of auroral particles in model of electric and magnetic fields surrounding Earth, commenting on importance of higher order terms in asymptotic expansion 22 p3914 A66-40561
- Asymptotic method for solving equations of theory of elasticity and mathematical physics 22 p3996 A66-40687
- Correct conductance and susceptance of infinite cylindrical antenna determined via asymptotic evaluation of parametric integrals 23 p4047 A66-41636
- Viscous supersonic flow near wall with large local curvature, using asymptotic solutions to Navier-Stokes equations 23 p4056 A66-41721
- Asymptotic solutions for viscous flow of transparent radiating gas in stagnation region, using method of matched inner and outer expansions [AIAA PAPER 66-105] 23 p4057 A66-41881
- Asymptotic solution of broadband random vibration BVP for elastic systems, based on excitation spectral width and natural frequency density 23 p4142 A66-41953
- Incompressible viscous flow around right angle corner, noting effect of geometry on boundary layer and cross flow 24 p4194 A66-42410
- Book on asymptotic methods of integrating linear differential equations with varying coefficients, emphasizing equations for oscillatory processes 24 p4231 A66-42613
- Asymptotic behavior of solution to system of differential equations with random limited coefficients 24 p4232 A66-42749
- Linear second-order partial differential equations of elliptic type analyzed, using maximum principle and barrier functions 24 p4233 A66-43065
- ATHENA ROCKET**
- Real time ground computer for Athena system and input/output data requirements in multiprocessing jobs 12 p1827 A66-23836
- Motion equations, attitude and ignition time of third and fourth stage of USAF Athena, noting solution derivation using Taylor series constraints, accuracy, etc 16 p2743 A66-30908
- ATLANTIC AIRCRAFT**
- S BREGUET 1150 AIRCRAFT**
- ATLANTIC OCEAN**
- Spherules from Atlantic Ocean sediments studied by electron microprobe, noting terrestrial alteration and contamination of surfaces 16 p2803 A66-31222



## ATLAS AGENA LAUNCH VEHICLE

Comet mission study using space probes boosted by Atlas Agena and Atlas Centaur launch vehicles for interception from 1967 to 1975 04 p0577 A66-13579

Comet missions, discussing spacecraft exploration criteria for short period and long period first-aparition comets 06 p0952 A66-15923

Communication satellite design noting use for educational and commercial purposes, instrumentation applied, etc 17 p2872 A66-31935

Selection of elliptic orbit for solar probe craft without undue perihelion growth [AIAA PAPER 64-646] 19 p3459 A66-35601

## ATLAS CENTAUR LAUNCH VEHICLE

Comet mission study using space probes boosted by Atlas Agena and Atlas Centaur launch vehicles for interception from 1967 to 1975 04 p0577 A66-13579

Atlas-Agena and Atlas-Centaur launch vehicles to investigate comets 06 p0951 A66-15903

Aborted Atlas-Centaur launch data of environmental conditions and use in engineering design 14 p2395 A66-28446

Suitability of Saturn IB/Centaur and Atlas/Centaur launched solar-electric propulsion vehicles for performing 0.1-AU solar probe mission [AIAA PAPER 66-496] 17 p2991 A66-32773

## ATLAS LAUNCH VEHICLE

Physical and biological blast effects from explosive fragmentation of gaseous nitrogen flight pressurized Atlas missile without propellants [AIAA PAPER 65-195] 16 p2810 A66-30897

Atlas E/F launch vehicle, discussing structure, mission capabilities, launch facility, reentry, etc [SAE PAPER 660444] 18 p3245 A66-33890

Advanced Atlas launch vehicle technology, discussing tank configurations, engine ratings, guidance systems, autopilot, thrust augmentation, payloads, launch facilities, etc [SAE PAPER 660445] 18 p3245 A66-33891

## ATMOSPHERE

SA AIR  
SA CABIN ATMOSPHERE  
SA EARTH ATMOSPHERE  
SA EXOSPHERE  
SA FREE ATMOSPHERE  
SA GAS  
SA IONOSPHERE  
SA LOWER ATMOSPHERE  
SA LUNAR ATMOSPHERE  
SA MID-LATITUDE ATMOSPHERE  
SA NONGRAY ATMOSPHERE  
SA OZONOSPHERE  
SA PLANETARY ATMOSPHERE  
SA SOLAR ATMOSPHERE  
SA SPACE CABIN ATMOSPHERE  
SA STANDARD ATMOSPHERE  
SA STELLAR ATMOSPHERE  
SA STRATOSPHERE  
SA TROPOPAUSE  
SA TROPOSPHERE  
SA UPPER ATMOSPHERE

Cosmic space physics - All-Union Conference, Moscow, June 1965 09 p1460 A66-20986

Soviet papers on atmospheric boundary layer, wind profiles, meteorological effects, etc 16 p2741 A66-30769

Propagation modes of infrasonic waves in isothermal atmosphere with constant horizontal winds and under effect of gravity 17 p2959 A66-33032

Graphite and C-H-O gas phase equilibrium at high temperatures and pressures in implication of Earth ocean and atmosphere development 17 p3015 A66-33432

Solution method for nuclear cascade equation representing process of propagation of pions through atmosphere 24 p4270 A66-42925

## ATMOSPHERE EXPLORER

S EXPLORER XVII SATELLITE

ATMOSPHERE EXPLORER-A

S EXPLORER XVII SATELLITE

## ATMOSPHERE MODEL

Equations of quasi-stationary mean flow of momentum and heat on spherical Earth averaged over long period and over latitude circle 02 p0221 A66-11574

Average atmosphere encountered by geomagnetically trapped

protons 03 p0364 A66-12676

Cyclogenesis prediction by two-level primitive equation model with constant static stability for two cases characterized by typical baroclinic development 05 p0711 A66-14936

Earth atmosphere, discussing properties of high altitude neutral atmosphere combined with measurement of solar output variations 05 p0675 A66-15743

Emission and absorption of radiant energy in model Martian atmosphere composed of 15 percent carbon dioxide and 85 percent nitrogen by volume 05 p0768 A66-15777

Martian ionospheric observations made by Mariner IV interpreted in terms of model show atmosphere consists mainly of carbon dioxide, low temperature and no thermosphere 06 p0953 A66-16404

Homogeneous isotropic turbulence in atmosphere model showing accretion qualities for small droplets during diffusion dissociation 08 p1212 A66-18673

Abundance of molecules, ions and atoms in late-type dwarf, giant and supergiant atmospheres 08 p1288 A66-18781

Nine-level general circulation model of atmosphere for resolving surface boundary layer fluxes as well as radiative transfer by ozone, carbon dioxide and water vapor 08 p1213 A66-18924

Numerical experiment with general circulation model with simple hydrologic cycle 08 p1247 A66-18925

Cumulus cloud simulation by dropping solid piece of carbon dioxide into hot water 08 p1248 A66-19388

Static diffusion models of upper atmosphere with density and composition determined for wide exospheric temperature ranges 09 p1370 A66-19901

Planetary environments in various models 09 p1454 A66-20287

Neutron star atmosphere models for determining, surface temperature, cooling time and X-ray emission 10 p1599 A66-21103

Harris and Priester model used to compute amplitude of diurnally varying component of horizontal pressure acceleration, showing increase with altitude 10 p1529 A66-21150

Numerical experiments with large-scale seasonal forcing, treating six different heating fields in general circulation model for periods of five and 100 years 10 p1530 A66-21273

Upper atmosphere model for calculating neutral properties from 100 to 10,000 km as function of local time and solar activity 10 p1531 A66-21280

Nickel abundance in solar spectrum determined, based on atmospheric model 11 p1772 A66-22774

Blanketing and convection effect on theoretical models of solar photosphere 11 p1772 A66-22775

Modified Eliassen finite difference grid solution of primitive hydrostatic equations system for barotropic and baroclinic model of atmosphere 11 p1730 A66-22946

Atmospheric density models for solar radiation cycle variation in upper atmosphere [AIAA PAPER 66-355] 12 p1951 A66-24490

Computer program for predicting satellite long-term orbit decay and digital simulation of atmosphere and reentry conditions [AIAA PAPER 66-357] 12 p1951 A66-24491

Mars atmosphere definition important in advanced landing vehicle design with increased payload capability and reduced complexity [AIAA PAPER 65-22] 12 p1952 A66-24697

Goldberg method for determining Doppler widths in calculations of depth dependence of solar turbulence 13 p2183 A66-25615

Upper atmospheric model of variations for solar minimum conditions based on satellite drag and rocket sounding 13 p2073 A66-26130

Justification for multiple isothermal layer approximation to real atmospheric acoustic-gravity wave propagation 14 p2234 A66-26857

Response of atmosphere to impulsive point disturbances 14 p2386 A66-28123

Atmospheric model describing generation of clear air turbulence /CAT/, noting horizontal shear effect 15 p2532 A66-28915

Atmosphere models for seasonal and latitudinal variation in thermosphere as

function of solar flux and geomagnetic index 15 p2492 A66-3003

Numerical model of Earth atmosphere used to compute hydro-and thermodynamic evolution of global moist atmosphere, considering solar heating, evaporation, etc 16 p2697 A66-3094

Stability of baroclinic axially symmetric vortex on F plane to axially symmetric disturbances 16 p2700 A66-3164

Ten micron stellar flux measurements of 42 stars with 200 inch Hale telescope and predictions of model atmospheres and line blanketing theory 17 p3000 A66-3226

Grid computations of model atmospheres for A-type stars, considering effects of Balmer-line blanketing 18 p3227 A66-3376

Three-dimensional polarizations of high latitude micropulsations derived for conjugate point observatories from hydromagnetic wave-ionospheric current model 18 p3107 A66-3452

Equatorial electrojet model construction to fit direct measurements 19 p3348 A66-3592

Physical structure of upper atmosphere given by pressure and density scale height and mean molecular mass due to diffusion 19 p3349 A66-3634

Negative ion density and composition in lower ionosphere 19 p3350 A66-3635

Atmospheric models, comparing Chamberlain evaporative and solar breeze models, Opik and Singer evaporative model and Parker solar wind model 19 p3465 A66-3660

Photospheric structure and temperature distributions, determined from center limb variations of central intensities in neutral titanium lines, used in connection with model atmosphere 19 p3465 A66-3660

CIRA 1965, COSPAR International Reference Atmosphere covering mean atmospheric structure variations from 30 to 100 km and from 120 to 800 km 19 p3352 A66-3679

Thermal escape of neutral hydrogen and distribution in Earth thermosphere, noting collision in transition regions 20 p3549 A66-3729

Baroclinic instability of quasi-geostrophic perturbation to zonal wind in two-layer inviscid model, examining short wavelength cut-off in terms of potential vorticity 20 p3550 A66-3746

Least squares iterative procedure for resolving individual particle distributions comprising model atmosphere density profile above 110 km 20 p3551 A66-3751

Equations describing motion of satellite in Paetzold-Zschoerner model of Earth atmosphere 20 p3654 A66-3784

Modified Eliassen finite difference grid solution of primitive hydrostatic equations system for barotropic and baroclinic model of atmosphere 20 p3593 A66-3785

Transmission and coupling resonance of hydromagnetic disturbances in nonuniform model magnetosphere calculated by approximate dipole coordinates valid near equatorial plane 21 p3734 A66-3921

British stratospheric and mesospheric temperature measurements compared with values from available atmospheric models 22 p3913 A66-4051

Statistical properties of phase and amplitude fluctuations during total reflection of waves from ionospheric layer 22 p3869 A66-4076

Mariner IV models of three Mars atmospheric layers analogous to terrestrial E, F-1 and F-2 layers, considering relative mass densities, temperatures, carbon dioxide photodissociation and ionization profile 23 p4129 A66-4177

## ATMOSPHERIC ABSORPTION

Visibility range of 100-watt lamp and relation to absorption coefficient of tropospheric fog 01 p0096 A66-1022

Aurora position and brightness determination by S-180 camera as affected by such factors as distortion and vignetting 02 p0226 A66-1134

Graphical method to determine detection range for narrow IR windows in dependence of atmospheric absorption and emission 02 p0223 A66-12064

Influence of absorption of aerosol particles on extinction of solar and sky



radiation 02 p0225 A66-12214  
 Slant path measurement of atmospheric  
 absorption spectra of 43 mu band, using  
 Sun as radiation source 03 p0359 A66-12301  
 Relationship between phase-structure  
 function and statistics governing geometric  
 shape of randomly distorted wave  
 front 03 p0391 A66-12302  
 Energy flux of electron beam absorbed by  
 atmosphere derived from resulting intensity  
 of first negative system of molecular  
 nitrogen 05 p0670 A66-14948  
 Atmospheric oxygen absorption factor of  
 centimeter and millimeter radio  
 waves 05 p0636 A66-15878  
 Absorption effect on Rayleigh atmosphere,  
 calculating reflected and transmitted  
 intensities and polarizations for C  
 wavelength pair used for Umkehr  
 measurements 07 p1028 A66-17364  
 Characteristics of solar radio bursts in  
 microwave region and measurements of  
 atmospheric absorption and solar flux at 17  
 gc/s 07 p1028 A66-17419  
 Theoretical model of isolated Lorentz line  
 of IR absorption by gases applied to  
 atmospheric optics and spectroscopy  
 problems 08 p1248 A66-19307  
 Estimation of ozone concentration at  
 altitudes of 44 to 102 km from nighttime  
 geophysical rocket measurements of  
 atmospheric brightness 08 p1221 A66-19796  
 Vertical temperature and humidity  
 distributions of atmosphere determined  
 from satellite measurements of carbon  
 dioxide and water-vapor absorption  
 bands 09 p1376 A66-20999  
 Solar X-ray and UV radiation  
 measurements by monitoring satellite,  
 including instrumentation 10 p1598 A66-21085  
 Atmospheric radio wave absorption  
 coefficient and altitude determined and  
 linked to effects of colliding paramagnetic  
 oxygen molecules 13 p2020 A66-25224  
 Atmospheric absorption in IR region,  
 noting effects of water vapor, ozone, carbon  
 dioxide and collision-induced dipole  
 moments 13 p2075 A66-26603  
 Mass calculation for absorbing gases such  
 as water vapor, carbon dioxide and ozone  
 along oblique paths between two arbitrary  
 points in atmosphere, considering vertical  
 distribution, refraction and Earth  
 curvature 14 p2284 A66-27541  
 Diurnal variation of average energy  
 spectrum of auroral X-rays observed from  
 balloon flights, assessing effect of  
 atmospheric absorption 14 p2376 A66-27614  
 Effect of radiative sound absorption in  
 atmosphere, calculating absorption due to  
 radiation by water vapor in far-IR rotation  
 spectrum 14 p2334 A66-27659  
 Atmospheric propagation of radio waves at  
 wavelength of 33 mm 14 p2240 A66-27919  
 Contaminating effect of water vapor in  
 optical path of spectrometer on  
 measurements of stratospheric water vapor  
 absorption 15 p2530 A66-28601  
 Radiometric measurements of atmospheric  
 absorption at 600 gc/s by DICKE type  
 superheterodyne receiver, using harmonic  
 mixing 15 p2450 A66-28999  
 Vacuum spectrometer measurement of  
 absorption band of atmospheric water  
 vapor 15 p2542 A66-29346  
 UV solar radiation absorption in upper  
 atmosphere determined from measurement  
 of photoelectron currents emitted by planar  
 metallic orthogonal photocathodes onboard  
 Cosmos II satellite 15 p2592 A66-30051  
 Solar radiation absorption by atmospheric  
 water vapor, deriving formulas that include  
 scattering and absorption by aerosol as  
 additional parameter 16 p2691 A66-30228  
 Visibility range of 100-watt lamp and  
 relation to absorption coefficient of  
 tropospheric fog 17 p2948 A66-31907  
 Atmospheric ozone absorption coefficients  
 measurement, determining errors in  
 extraterrestrial constant of Dobson  
 spectrophotometer 17 p2923 A66-33359  
 Solar extinction measurements and  
 interpretation of terrestrial atmosphere  
 microwave absorption spectrum near 1-cm  
 wavelength 18 p3105 A66-34012  
 Theoretical model of isolated Lorentz line  
 of IR absorption by gases applied to  
 atmospheric optics and spectroscopy

problems 19 p3400 A66-36043  
 Radio wave absorption factors in  
 atmospheric water vapor and oxygen,  
 deriving expressions for effective length,  
 mean temperature and total vertical  
 absorption 20 p3512 A66-37134  
 Vacuum spectrometer measurement of  
 absorption band of atmospheric water  
 vapor 20 p3602 A66-37351  
 Microwave antenna design elements, feed  
 equipment and performance  
 characteristics 20 p3530 A66-37716  
 Sound absorption in air at 1/3-octave  
 frequency intervals as function of humidity  
 and temperature at normal atmospheric  
 pressure for studies in room  
 acoustics 21 p3769 A66-38648  
 Estimation of ozone concentration at  
 altitudes of 44 to 102 km from nighttime  
 geophysical rocket measurements of  
 atmospheric brightness 21 p3733 A66-38792  
 Direct solar radiation predetermination and  
 extinction coefficient 22 p3912 A66-40243  
 Solargraphic measurements of solar  
 radiation absorption by atmospheric dust  
 and pollutants and effects on solar energy  
 transmission 22 p3912 A66-40244  
 Nocturnal high altitude ozone distribution  
 determined, using small geophysical  
 sounding rockets with Moon as light source  
 to measure atmospheric absorption of UV  
 radiation 22 p3914 A66-40559  
 Absorption and brightness temperature  
 variations of atmosphere on basis of  
 statistical characteristics of vertical  
 temperature and humidity  
 structures 23 p4087 A66-41802  
 Mass calculation for absorbing gases such  
 as water vapor, carbon dioxide and ozone  
 along oblique paths between two arbitrary  
 points in atmosphere, considering vertical  
 distribution, refraction and Earth  
 curvature 24 p4198 A66-42326  
 Venus atmosphere noting pressure induced  
 absorption in carbon dioxide-nitrogen  
 atmosphere as indicated in decline of  
 microwave brightness  
 temperature 24 p4277 A66-42668  
 Stellar extinction measurements made in  
 Gemini IX flight, determining existence and  
 location of Link layer from airglow  
 study 24 p4280 A66-43026

## ATMOSPHERIC ATTENUATION

Aerosol component of transparency  
 attenuation coefficient relation to humidity  
 characteristics of individual atmospheric  
 layers 04 p0513 A66-13417  
 Ultrashort wave attenuation and damping  
 on long open tracks, discussing wave  
 scattering and reflection in inhomogeneous  
 atmosphere 04 p0482 A66-14006  
 Atmospheric spatial inhomogeneities  
 degradation in radar signal-target  
 information 04 p0486 A66-14120  
 Sunlight attenuation reaching Aries II  
 satellite after passing through Earth  
 atmosphere along almost horizontal  
 path 05 p0672 A66-15023  
 Atmospheric attenuation of light with  
 average turbulence 08 p1248 A66-19319  
 Atmospheric optics noting attenuation,  
 reflectance, flux and optical  
 radiation 09 p1398 A66-20274  
 Electromagnetic wave propagation in  
 meteorology and geophysics, noting  
 expression for refractive modulus in  
 troposphere, considering attenuation and  
 backscattering 09 p1343 A66-20276  
 Beer and square root law compared in  
 relation to use for atmospheric extinction  
 correction in IR  
 spectrum 09 p1372 A66-20292  
 Optical radiation absorption and  
 attenuation by atmosphere polluted with  
 carbon dust, including transmission  
 coefficient calculation 09 p1402 A66-20313  
 Illuminance of Earth shadow at three  
 wavelengths by numerical integration,  
 accounting for light attenuation, ozone  
 absorption and extinction, Rayleigh  
 scattering and refractive beam  
 divergence 11 p1770 A66-22570  
 He-Ne laser IR radiation emission  
 attenuated by atmospheric  
 methane 11 p1657 A66-23090  
 Ultrashort wave attenuation and damping

on long open tracks, discussing wave  
 scattering and reflection in inhomogeneous  
 atmosphere 12 p1813 A66-23868  
 High-resolution interference spectrometer  
 to observe water vapor absorption in 500 to  
 1500 gc region 13 p2020 A66-25203  
 Q band propagation test carried out over  
 12-km path, comparing rainfall attenuation  
 with rainfall rate over path, noting scatter  
 of measured values 13 p2023 A66-25567  
 Attenuation of coherent optical waves  
 propagating in troposphere, noting molecular  
 scattering, bending of refractive index  
 homogeneities due to temperature gradients  
 in air, etc 15 p2448 A66-28578  
 Atmospheric optical properties and  
 directional reflectances of ocean water and  
 other surfaces, for unobscured low  
 Sun 15 p2531 A66-28832  
 Humidity attenuation in 8 to 13 micron IR  
 window used in radiance measurement from  
 orbiting satellite 15 p2531 A66-28848  
 Millimeter wave transmission and reception  
 of television signals, examining picture  
 quality and tropospheric scintillation and  
 attenuation relative to  
 weather 15 p2450 A66-28997  
 Atmospheric turbidity measurements over  
 India, using daily direct solar radiation  
 measurements for selected spectral regions  
 and entire spectrum 15 p2485 A66-29065  
 Possible use of IR radiation to improve  
 visibility through fog, including atmospheric  
 attenuation effects and radiant energy  
 source 16 p2740 A66-30088  
 Flux density of nonthermal radio sources  
 at 8000 mc noting measurement correction,  
 correlation between curvature index spectral  
 index and component  
 separation 17 p2995 A66-31911  
 Direct measurement of attenuation length  
 of extensive air showers through  
 water 18 p3212 A66-35136  
 Radiation attenuation effect of atmospheric  
 aerosols on air-weather aircraft landing  
 guidance systems using  
 lasers 19 p3397 A66-36051  
 Detectability of coronal IR lines due to  
 Mg, Al and Si ions with practicable IR  
 spectrometers and photoconductive  
 detectors, considering atmospheric  
 attenuation 20 p3649 A66-37333  
 Aerosol component of spectral  
 transmittance of artificial fog, comparing  
 calculated and experimental values for  
 absolute attenuation  
 factor 21 p3759 A66-38916  
 Fog transmittance attenuation factor,  
 comparing photometric values and values  
 calculated from microstructural observations,  
 using flow trap 21 p3759 A66-38917

## ATMOSPHERIC CHEMISTRY

Electrochemical and chemiluminescent  
 ozonesonde performance, using analysis of  
 comparative ascents 04 p0517 A66-14451  
 Physics of lower thermosphere studied by  
 using conditions applying to oxygen  
 atmosphere and oxygen-nitrogen  
 atmosphere 05 p0671 A66-15018  
 Upper atmospheric helium ion chemical  
 loss process, distribution of nitrogen ion and  
 rate coefficient of helium ion-molecular  
 nitrogen reaction 11 p1701 A66-23153  
 Oxygen photochemical equilibrium above  
 150 km, assuming dominant role of radiative  
 recombination above 120  
 km 15 p2486 A66-29089  
 Chemical release at high altitudes in order  
 to obtain information about atmosphere by  
 ground observation 16 p2697 A66-31012  
 Aerosol particle precipitation in surface  
 layer of atmosphere measured by modified  
 method of Alexandrova 21 p3760 A66-39366

## ATMOSPHERIC CIRCULATION

### SA WIND CIRCULATION

Nonlinear equations of atmospheric  
 hydrodynamics solved, using numerical  
 algorithm 01 p0096 A66-10751  
 Stationary distribution of ozone density  
 with height in presence of long waves in  
 atmosphere, solving continuity equation for  
 ozone and considering photochemical  
 processes 01 p0062 A66-10752  
 Planetary wave analysis using zonal  
 harmonics in connection with atmospheric  
 circulation and weather  
 forecasting 01 p0064 A66-11106  
 Phases of lower stratospheric circulation



and temperature variation 02 p0221 A66-11571

Stratospheric dynamics north of 40 degrees N with reference to kinetic energy variation, wave disturbances and shallow layer 02 p0253 A66-11572

Equations of quasi-stationary mean flow of momentum and heat on spherical Earth averaged over long period and over latitude circle 02 p0221 A66-11574

Dynamic equations in quasi-static and quasi-solenoidal approximations to describe synoptic meteorologic processes in spherical coordinate system 04 p0540 A66-13412

Air currents and temperature distribution in stratosphere and mesosphere in Northern Hemisphere from rocket observation 04 p0513 A66-13438

Vorticity equation describing properties of large-scale atmospheric motions 04 p0542 A66-14304

Cumuli above sea in spite of stable layer between sea surface and cloud boundary, noting condensation around salt particles penetrating ascending thermals 04 p0542 A66-14306

Cellular convection in conditionally unstable atmosphere, determining preferred areas of ascending and descending regions and current distribution 05 p0666 A66-14542

Positions of monthly mean troughs and ridges in Northern Hemisphere from 1949 to 1963 05 p0711 A66-14939

Correction to paper on rocket studies of sporadic-E ionization and ionospheric winds 05 p0671 A66-14957

Air motions and physical factors affecting general circulation in mesosphere and lower thermosphere 05 p0711 A66-15027

Climatic conditions at Earth surface, relation to long-term planetary trends in atmospheric circulation 05 p0712 A66-15221

Atmospheric ozone variations, distributions, continents and planetary circulation according to IGY data 05 p0674 A66-15222

Numerical experiment where conditionally unstable environment was present for study of cumulus-like circulations developed from initial state 06 p0905 A66-16267

Cumulus modification experiment using station network, radiosonde and pilot balloon stations, cameras, radar data, etc 06 p0905 A66-16268

Reflection and ducting of atmospheric acoustic-gravity waves whose temperature and horizontal wind velocity vary arbitrarily with height 06 p0876 A66-16278

Nonlinear stability of zonal flows in two-dimensional quasi-solenoidal model when absolute eddy is monotonic function of width 06 p0905 A66-16549

Skua Meteorological Rocket program including analysis of stratospheric winter circulation and spring reversal and temperature soundings on Outer Hebrides 07 p1063 A66-18336

Closed vertical and horizontal air circulation effect on steady state distribution of ozone in Earth atmosphere 08 p1213 A66-19031

Ionospheric drift in F region compared with overall circulation in troposphere and stratosphere 08 p1214 A66-19048

Time-space spectral analysis of meteorological fields based on time-dependent spectra of wind velocity, temperature, pressure and turbulent pulse and heat fluxes 09 p1397 A66-19883

Macro-turbulent transfer and meridional circulation in northward drift of atmospheric ozone 09 p1370 A66-19891

Empirical wind structure models, considering mean wind as height function, wind shear, tropospheric wind profiles for vehicle design, etc 09 p1398 A66-20271

Model atmosphere structural parameters and improvement proposals for 1964 COSPAR International Reference Atmosphere 09 p1375 A66-20989

Numerical experiments with large-scale seasonal forcing, treating six different heating fields in general circulation model for periods of five and 100 years 10 p1530 A66-21273

System of equations derived for dynamics of convective atmospheric vortices for model with unstable stratification and basic vorticity 10 p1530 A66-21274

Inaccuracy in rocketsonde data on HF of midwinter easterlies in stratosphere over Cape Kennedy 10 p1531 A66-21281

Temporal spectra of atmospheric angular momentum transfer from wind data at various tropospheric and lower stratospheric levels 11 p1697 A66-22566

Sudden increase in radioactive fallout traced to stratospheric origin due to debris age exceeding assumed mean tropospheric residence time of one month 11 p1699 A66-23095

Investigation of two cold air fronts of polar origin that occurred in Alpine region in April 1962, using data from Tiros IV 11 p1730 A66-23096

Mean wind vector shear and shear interval and standard deviation, examining correlation 11 p1730 A66-23097

Winds in upper atmosphere as revealed by sodium vapor trails explained on basis of prevailing and tidal components critically analyzed 11 p1701 A66-23147

Kinetic energy generation and dissipation in large-scale atmospheric circulation, using six months aerological data from North American network 11 p1731 A66-23487

Changes in current kinetic theory of NO-O reaction, based on observation of release of nitric oxide in E region 11 p1703 A66-23494

Terrestrial atmosphere circulation and circulation of solar photophere 14 p2282 A66-26928

Synoptics of stratosphere and stratospheric warming of winter of 1963 14 p2283 A66-27095

Entrainment problem, convective clouds and atmospheric thermal convection 14 p2325 A66-27280

Nonlinear equations of atmospheric hydrodynamics solved, using numerical algorithm 14 p2285 A66-27850

Stationary distribution of ozone density with height in presence of long waves in atmosphere, solving continuity equation for ozone and considering photochemical processes 14 p2285 A66-27851

Cumuli above sea in spite of stable layer between sea surface and cloud boundary, noting condensation around salt particles penetrating ascending thermals 14 p2327 A66-28219

Nonlinear stability of zonal flows in two-dimensional quasi-solenoidal model when absolute eddy is monotonic function of width 14 p2327 A66-28221

Behavior of superpressure balloons in vertical air currents, noting various combinations of wind speed and wave amplitude 15 p2426 A66-28941

Atmospheric motions from sodium cloud firings in 80 to 200 km height region, noting internal gravity waves, atmospheric tides and drift 15 p2489 A66-29661

Wind shear theory of formation of temperate zone blanketing sporadic E layers, noting motion equation for ions in ionospheric E region 15 p2490 A66-29948

Meteorological Rocket Network observations of complex circulation system in middle and upper atmosphere 15 p2491 A66-29953

Diurnal and semidiurnal oscillations in atmospheric density, temperature, pressure and wind in subtropical Southern Hemisphere 15 p2491 A66-29964

Meteorological rocket measurement of wind patterns noting velocities, turbulences, stratospheric diffusion coefficients, etc 15 p2492 A66-30028

Average rotational speed of upper atmosphere above 200 km evaluated from changes in orbital inclinations of 13 satellites 15 p2496 A66-30082

Mars atmospheric circulation, diurnal heating, thermal tides and effects on Earth atmosphere 16 p2797 A66-30353

Atmospheric wind measurement technique utilizing acoustic noise of rocket exhaust [AIAA PAPER 66-440] 16 p2741 A66-30601

Dynamic influence of orography on atmospheric motion examined, using fluid mechanics analogy with periodicity as boundary condition 16 p2699 A66-31637

Initial value problem for small amplitude wave perturbations solved on zonal atmospheric flow with constant vertical shear and vanishing temperature lapse

rate 16 p2699 A66-31637

Organized convection as photographed by Gemini astronauts 18 p3129 A66-3421

Atmospheric circulation - International Space Science Symposium, Argentina, Mar 1965 19 p3346 A66-3563

EOLE system consisting of balloons and satellite, interrogation for synoptic data on atmospheric circulation over Southern Hemisphere 19 p3346 A66-3563

Balloon sounding of Southern Hemisphere by global horizontal sounding technique /GHOST/, providing data on atmospheric circulation 19 p3279 A66-3563

Hydrodynamic and thermodynamic equations for biennial variations of zonal atmospheric circulation in equatorial area 19 p3346 A66-3564

Meteorological rocket network observation of gross global circulation patterns in stratosphere and mesosphere for analysis of vertical structure and synoptic processes 19 p3347 A66-3564

Atmospheric circulation and eddy diffusion based on thermal structure, oxygen transport continuity and sodium trail spreading in thermosphere 19 p3347 A66-3564

Quasi-geostrophic wave motions of inertial gravity wave type and Rossby wave type in equatorial area 19 p3348 A66-3605

Latitudinal effect on behavior of ionospheric absorption determined by absorption measurements at four stations 19 p3350 A66-3636

Pressure gradients in F region from model atmosphere, estimating from motion equations variation of magnitude and direction of wind with local time, season and epoch of solar cycle 19 p3352 A66-3662

Quasi-geostrophic instability of disturbance of small amplitude in baroclinic zonal flow, caused by barotropic, baroclinic or critical layer instabilities 20 p3550 A66-3746

Vertical velocities in atmospheric motions, noting pressure and temperature field distributions and application of computer to solve obtained equations 20 p3593 A66-3775

Internal atmospheric gravity waves in isothermal medium, solving hydrodynamic equations, determining wave propagation in realistic atmosphere for range of wave parameters, wind amplitude, reflected energy, etc 20 p3554 A66-3820

Horizontal temperature gradient produced by water body effect on distribution of wind velocity and direction in atmospheric boundary layer 20 p3594 A66-3837

Wind distribution in atmospheric boundary layer under conditions of advection from pilot balloon observations 20 p3594 A66-3837

Polar vortex breakdown and explosive warming in upper stratosphere in numerical tests based on observed height pattern noting kinetic energy 21 p3759 A66-3920

Ionization irregularities in bottomside an topside ionosphere, noting circulation effect 22 p3911 A66-3998

Planetary scale atmospheric circulations of Jupiter and Saturn using fluid dynamics, noting rotation effects 23 p4129 A66-4167

Atmospheric ozone data on basis of meteorological observations and synoptic maps on ship in Atlantic 23 p4065 A66-4180

Rocket observation of upper atmospheric wind around ionospheric E layer by sodium release method, noting cloud drift 24 p4199 A66-4246

Stress, eddy viscosity and viscous dissipation estimations in jet stream obtained during Project TOPCAT in Australia, using aircraft soundings 24 p4234 A66-4298

**ATMOSPHERIC COMPOSITION**

Stable elementary particle detection of mass greater than that of proton in hydrogen, deuterium and atmospheric air sample, using mass spectrometer 01 p0060 A66-1025

Atomic hydrogen reaction with HO-2 as a source of hydrogen molecules in lower thermosphere 02 p0221 A66-1150

Further evidence of correlation of atmospheric ozone and relative sunspot number 02 p0222 A66-1182

Aerospace Breathing Chart used in analytical evaluation of breathable atmospheres and emergency oxygen system



[AIAA PAPER 65-723] 03 p0328 A66-12544  
 Redetermination of isotopic composition of  
 atmospheric neon resulting from  
 measurements of neon in  
 meteorites 04 p0517 A66-14323  
 Atmospheric ozone concentration variation  
 during total eclipse of sun affected by limb  
 darkening and solar radiation  
 intensity 05 p0666 A66-14545  
 Mass spectrometer application to  
 measurement of chemical and ionic  
 composition of upper  
 atmosphere 05 p0676 A66-14683  
 Terrestrial helium loss by speculated  
 reaction between helium metastables and  
 oxygen atoms 05 p0669 A66-14940  
 Solar radiation attenuation in UV region  
 provides data on production of atomic  
 oxygen by photodissociation of oxygen and  
 ion and electron formation by  
 photoionization of nitrogen and  
 oxygen 05 p0748 A66-15022  
 Human thermal comfort prediction in  
 oxygen-nitrogen  
 atmospheres 06 p0817 A66-16235  
 Nature and momentum spectra of nuclear  
 active particle flux at low altitudes,  
 determining root mean square  
 error 07 p1115 A66-17552  
 Nucleon passage through atmosphere and  
 meson production data including nuclear  
 cascade intensity, gamma ray production,  
 etc, and mean free path values for nucleon  
 interaction 07 p1115 A66-17553  
 Atmospheric argon effect on hypersonic  
 stagnation point convective heat transfer,  
 using arc-heated shock tube simulating  
 flight velocities up to 34,000 fps  
 [AIAA PAPER 66-29] 07 p1153 A66-17891  
 Extraterrestrial dust as atmospheric argon  
 source and influx of black  
 spherules 08 p1287 A66-18770  
 Measurement of radioactivity in air of free  
 atmosphere and interior of cloudy areas and  
 absorption of radioactive aerosols by water  
 droplets 08 p1283 A66-19305  
 Probability of presence of nitrogen, oxygen  
 and water in atmosphere of Venus, based on  
 spectroscopic studies 08 p1294 A66-19323  
 Separation problems of gas and aerosol  
 components in brightness of atmospheric  
 layer for photometric data pertaining to  
 Mars atmosphere 08 p1295 A66-19330  
 Total mass of Earth atmosphere computed,  
 using atmospheric pressure and land-height  
 distribution data 09 p1369 A66-19871  
 Liquid and particulate content of  
 atmosphere noting surface rates of rainfall,  
 particle size distribution, cloud data,  
 aerosols, etc 09 p1398 A66-20272  
 Earth atmosphere composition noting  
 extent and effects of ozone, absorption,  
 ionization, electron attachment and  
 detachment, etc 09 p1371 A66-20273  
 Spectral distribution of direct sunlight at  
 Earth surface at sea level, as function of air  
 mass and concentration of aerosol, ozone  
 and water vapor 09 p1375 A66-20962  
 Data compendium on neutral composition  
 of atmosphere at altitudes from 100 to 200  
 km, noting nitrogen and oxygen  
 concentration values from optical and mass  
 spectroscopic studies 09 p1376 A66-20991  
 Earth, balloon and satellite spectroscopic  
 observations of Mars to determine  
 atmospheric composition and pressure at  
 surface level 10 p1602 A66-21065  
 Seasonal variation of atmospheric ozone,  
 determining via IR method total amount and  
 vertical distribution 10 p1526 A66-21124  
 Reconciling observed ozone distribution in  
 atmosphere with that of photochemical  
 theory, using accepted rate  
 constants 10 p1531 A66-21278  
 Atmospheric properties important to  
 aviation and aerospace medicine including  
 composition, weather conditions, radiation,  
 temperature effect at various heights,  
 etc 10 p1553 A66-22105  
 Atmospheric aerosol size distribution from  
 scattered light measurements by  
 rocketborne equipment 11 p1697 A66-22565  
 Carbon 14 content of dendrochronologically  
 dated tree rings used to determine  
 atmospheric C-14 variation over past six  
 millennia 11 p1697 A66-22568  
 Secular variation of atmospheric  
 radiocarbon concentration, noting

dependence on geomagnetic field  
 strength 11 p1698 A66-22569  
 Vertical distribution of neutral composition  
 of atmosphere between 100 and 200 km,  
 comparing mass spectrometer with optical  
 measurement 11 p1698 A66-23038  
 Height dependence of albedo in Earth  
 upper atmosphere, calculating total quantity  
 of neutral hydrogen in  
 ionosphere 11 p1699 A66-23044  
 Ozone photochemistry in atmosphere  
 containing hydrogen, calculating equilibrium  
 vertical distribution, rate of formation of  
 hydroxyl, diurnal variation,  
 etc 11 p1700 A66-23138  
 Influence coefficients for computation of  
 atmospheric components of reentry vehicle  
 circular error probable /CEP/, using Bliss  
 adjoint method, noting effects of certain  
 inadequacies on system performance  
 [AIAA PAPER 66-358] 12 p1908 A66-24517  
 Finite-difference scheme for short-term  
 operational weather forecasts from two-level  
 model atmosphere 12 p1909 A66-24870  
 equations 12 p1909 A66-24870  
 Three-color photometric study of  
 atmospheric extinction by dust particles  
 from lunar eclipse photoelectric  
 measurements of Mare Crisium  
 region 13 p2185 A66-25810  
 Stable elementary particle detection of  
 mass greater than that of proton in  
 hydrogen, deuterium and atmospheric air  
 samples, using mass  
 spectrometer 13 p2131 A66-25968  
 Radio astronomy studies of Venus and  
 Mars noting surface properties, atmospheric  
 structure, etc 13 p2186 A66-26031  
 Limitation on oxygen concentration in  
 possible primitive atmospheres examined via  
 physical and photochemical  
 factors 13 p2186 A66-26122  
 Atmospheric observation with advanced  
 light radar, noting equipment characteristics,  
 molecular scattering mechanism,  
 etc 13 p2122 A66-26133  
 Atmospheric distribution profiles of ozone  
 noting formation, elimination, effect on  
 terrestrial heat losses, UV absorption,  
 etc 13 p2073 A66-26318  
 Soviet monograph on atmospheric  
 exploration using rockets and satellites,  
 covering meteorological and geophysical  
 instrumentation, measurement parameters,  
 etc 13 p2083 A66-26502  
 Altitude simulator for adjustment and  
 calibration of high altitude meteorological  
 instruments 14 p2325 A66-27279  
 Drag coefficient of spherical satellites at  
 various heights, based on gas-surface  
 interactions and atmospheric  
 composition 14 p2382 A66-27617  
 Mass spectrometry of composition and  
 density of neutral atmosphere, noting  
 diffuse separation of  
 gases 14 p2285 A66-27621  
 Composition and temperature variation of  
 thermosphere, using mass spectrometry and  
 optical methods 14 p2285 A66-27622  
 Atmospheric exploration with lidar, noting  
 high resolution and  
 sensitivity 15 p2530 A66-28600  
 Atmospheric mixing time and lifetime of  
 atomic and molecular oxygen at high  
 altitude, noting agreement with barometric  
 distribution law, concentration pattern,  
 etc 15 p2486 A66-29088  
 Estimation of ion formation rate at various  
 altitudes in ionosphere and zenith angles  
 during low and high solar activity  
 periods 15 p2487 A66-29105  
 Mars upper atmosphere and single-layer  
 ionosphere UV photoionization, temperature  
 profile and chemical  
 composition 15 p2598 A66-29417  
 Seasonal-latitude variations in lower  
 thermospheric density, temperature and  
 composition 15 p2490 A66-29820  
 Rocket measurement of diurnal variation  
 of ozone profiles above maximum  
 concentration level 15 p2495 A66-30058  
 Atmospheric neutral and ion composition  
 and ionization radiation rates from rocket  
 data compared with electron densities  
 around 200 km 15 p2496 A66-30081  
 Neutral particle densities of nitrogen,  
 molecular and atomic oxygen and argon in  
 upper atmosphere, noting density profile

irregularities, diffusive separation altitude,  
 etc 15 p2497 A66-30086  
 Chronic exposure of rats to gaseous  
 environments of varied composition and  
 pressure, noting exposure capsules, gas flow  
 system, respiratory gas analyzer,  
 etc 16 p2643 A66-30650  
 Atomic-to-molecular oxygen concentrations  
 ratio values in upper atmosphere used to  
 determine strength of turbulent mixing in  
 atmosphere, noting definition of turbopause  
 height 16 p2694 A66-30704  
 Mars atmosphere models based on Mariner  
 IV occultation deriving electron number  
 density, temperature, pressure, mass  
 density, etc, noting carbon dioxide  
 presence 16 p2800 A66-30713  
 Dust flux in upper atmosphere and on  
 polar ice sheets 16 p2696 A66-30931  
 Electromagnetic spectrum of upper  
 atmosphere examined, using microwave  
 techniques, noting molecular rotation of  
 gases with permanent electric or magnetic  
 dipole moments 16 p2698 A66-31044  
 Atmospheric ozone and effect on  
 geophysics, noting concentration at ground  
 level, distribution, temperature, origin,  
 etc 16 p2700 A66-31744  
 Methane content of upper atmosphere  
 determined by Fabry-Perot interferometer  
 measurement of radiation transmission in  
 methane absorption band 17 p2926 A66-32948  
 Variations in atmospheric radio carbon  
 activity related to secular variations in  
 carbon-14 production rate, carbon residence  
 times and carbon reservoir  
 times 18 p3104 A66-33552  
 Variation in radiocarbon content in  
 atmosphere studied from measurement of  
 concentration in wood sample nearly 2000  
 years old 18 p3199 A66-34889  
 Venus atmosphere, surface temperature  
 and radiation  
 characteristics 19 p3460 A66-35799  
 Nitrogen temperature and density in  
 thermosphere region from thermosphere  
 probe data, examining inconsistency with  
 satellite drag estimates 19 p3349 A66-36347  
 Aerobee rocket measurement of nitric  
 oxide in upper atmosphere, noting  
 fluorescence in airglow layer, emission rate  
 factors and NO densities 19 p3349 A66-36351  
 Atomic hydrogen and helium emissions in  
 upper atmosphere determined by diffraction  
 spectrophotometer measurement of twilight  
 airglow and aurora 19 p3350 A66-36352  
 Auroral spectrum emission intensity in  
 upper atmosphere used to determine  
 densities of metastable atoms and molecules  
 and rates of dissociation and  
 ionization 19 p3350 A66-36353  
 Upper atmospheric nitric oxide determined  
 from Aerobee measurement of UV dayglow  
 spectra 20 p3550 A66-37299  
 Small-scale fluctuations in vertical  
 distribution of atmospheric ozone analyzed,  
 examining possible transport mechanisms in  
 Southern Hemisphere 20 p3551 A66-37469  
 Possible enhancement to low-energy  
 atmospheric proton flux induced by passage  
 of Ikeya-Seki comet examined, using  
 balloon-borne scintillation counter and pulse  
 height analysis  
 techniques 20 p3631 A66-37617  
 Statistical characteristics of atmospheric  
 ozone distribution, determining  
 autocorrelation and cross correlation  
 functions, concentration and temperature  
 profiles 20 p3552 A66-37751  
 Ionization and constitution of neutral  
 atmosphere, including solar EUV, X-ray and  
 corpuscular sources 22 p3905 A66-39944  
 Finite-difference scheme for short-term  
 operational weather forecasts from two-level  
 model atmosphere  
 equations 22 p3943 A66-40331  
 Prolonged exposures to acute anoxia cause  
 reductions in viability of hydrated rye  
 seeds, findings suggest helium may be  
 harmful as atmospheric component in  
 manned space capsules 22 p3855 A66-40480  
 Cylindrical functions for calculating free  
 oscillations of Saturn rings and estimation  
 of upper limit to mass of ring if motion is  
 stable against axisymmetric  
 perturbations 23 p4125 A66-41063  
 Muon production in atmosphere and energy



- dependence of positive excess 24 p4271 A66-42938  
 Detecting concentration of nitric oxide in metastable state in upper atmosphere, using giant-pulse Raman laser sources 24 p4203 A66-43022  
 Low level atmospheric flow structure resolution, noting equipment and results on wind speed variations 24 p4235 A66-43077
- ATMOSPHERIC CONDITION EFFECT**  
**SA WEATHER FORECASTING**  
 Atmospheric conditions effect on supersonic jet traffic 02 p0178 A66-12030  
 Determination of contrast range of optical images obtained in aerial camera as function of atmospheric and optical factors 03 p0368 A66-12504  
 Atmospheric model applied to fogs forming in valley bottoms and data acquisition in connection with this phenomenon 03 p0389 A66-12705  
 Changes in apparent radio path length of ground-to-ground microwave links caused by atmospheric changes 04 p0481 A66-13730  
 Propagation of optical waves through atmosphere, considering attenuation of optical waves and noise generation 04 p0545 A66-13756  
 Automatic atmospheric measuring system at Marshall Space Flight Center 05 p0661 A66-15485  
 Extensive air showers and intensity of cosmic rays of moderate energy 06 p0949 A66-16586  
 Solar absorptance and thermal emittance of vacuum-deposited aluminum, zinc oxide-potassium silicate white paint and high emissivity black paint after exposure to salt atmosphere [AIAA PAPER 66-41] 07 p1053 A66-17892  
 Effect of space environment on ceramic materials, considering atmosphere /including vacuum/, thermal, radiation and meteoroid environments 07 p1147 A66-18307  
 Two-year study of solar seeing conditions with recording monitor near Sydney, Australia indicates average of 23 sec per hour of observation 11 p1768 A66-22365  
 Meteorological effects on atmospheric concentrations of radon beta activity in ground proximity, noting effects of wind, temperature, radioactive precipitation and atmospheric scavenging 11 p1731 A66-23489  
 Magnetospheric and upper atmospheric meteorological effects on cosmic ray intensity variation and solar corpuscular streams 12 p1940 A66-24163  
 Factors connected with atmospheric dynamic processes, applying hydrodynamic equations to wind field and pressure field variations 12 p1909 A66-24786  
 SST flight performance as affected by wind, temperature and radiation 14 p2224 A66-28233  
 Preference of mice for oxygen-poor atmosphere after removal from 60 and 90 percent oxygen atmospheres 15 p2439 A66-29489  
 Thunderlike acoustic effects associated with extinction of meteors 16 p2796 A66-30272  
 Barotropic atmospheric model for forecasting in tropics, discussing wind analysis area covered, accuracy, etc 17 p2948 A66-31943  
 Effect of stratified atmospheric models on sonic boom generated by aircraft in steady level flight, using propagation of weak shock waves theory as base for analysis 17 p2847 A66-33024  
 Sonic boom phenomena, noting atmospheric dynamic effects, acceleration and lateral spread, variations in pressure signatures, etc 17 p2847 A66-33026  
 Regression calculations correlating daily average meson intensity with barometric pressure, atmospheric temperature and neutron monitor intensity 18 p3195 A66-34862  
 Daily correction of meson diurnal variation for ground-level air temperature and barometric pressure effects 18 p3195 A66-34863  
 Energy spectrum of cosmic ray diurnal variation determined from IGY neutron monitor data by introducing upper energy cut-off parameter 18 p3195 A66-34864  
 Altitude distribution of combinations of meridional gradients of pressure, temperature and density 19 p3393 A66-35394  
 Morning humidity variation relation to dew content and visibility of atmosphere, noting role of water vapor 19 p3393 A66-35395  
 Coherent laser light use in atmospheric communications system, discussing effect of atmospheric turbulence and small vibrations on coherent detection efficiency and SNR 20 p3511 A66-36930  
 Polar cap absorption and upper atmosphere solar-terrestrial disturbances due to solar flare and type IV outburst 20 p3636 A66-38227  
 Biological effect of atmospheric conditions and physical and psychological factors on living organisms 24 p4165 A66-43134
- ATMOSPHERIC CONDUCTIVITY**  
 LF anisotropic electric conductivity in upper atmosphere, noting Hall current 08 p1214 A66-19050  
 Weather forecasting from atmospheric electric conductivity measurements, noting polarization by neutrinos 11 p1729 A66-22865  
 Radiative energy transfer between concentric spheres separated by absorbing and emitting gas, noting analogy to atmosphere with spherical symmetry 15 p2615 A66-28620  
 Laser communications system design, describing range equation, modulation and detection techniques, atmospheric effects, etc 20 p3515 A66-37257  
 Optical communication systems, discussing available equipment, transmission characteristic, lack of long distance operation reliability, etc 24 p4174 A66-42805
- ATMOSPHERIC DENSITY**  
**SA SPACE DENSITY**  
 Atmospheric density and heating as function of altitude determined from satellite drag measurements [AIAA PAPER 65-507] 01 p0134 A66-10192  
 Formula for average rate of atmospheric particle fallout in terms of height-averaged values of density and viscosity of atmosphere 01 p0097 A66-10760  
 San Marco project, joint effort of NASA and Italian Space Commission to launch satellite for atmospheric and ionospheric measurements 01 p0143 A66-10809  
 Atmospheric density calculations from observing Sputnik III satellite, examining solar activity effect 03 p0361 A66-12624  
 Increased diurnal amplitude in density of thermosphere between 200 and 300 km for decreasing solar activity 05 p0671 A66-15019  
 Seasonal variation in short-wave signal absorption at different latitudes reflected in seasonal variation of gas density and ionospheric absorption at D region and lower E region 05 p0672 A66-15025  
 Atmospheric density effects on frequency of extensive air showers 06 p0948 A66-16578  
 First-order perigee to perigee changes in nonequatorial orbital elements due to spherical, rotational, exponential, time-invariant atmospheric drag 06 p0955 A66-16909  
 Contraction of satellite orbits due to atmospheric drag, extending theory to atmosphere with day-to-night sinusoidal variation with air density 07 p1132 A66-17256  
 Effect of Earth oblateness on lifetime of satellite in time-varying atmospheric density [AIAA PAPER 66-63] 07 p1139 A66-18451  
 Static diffusion models of upper atmosphere with density and composition determined for wide exospheric temperature ranges 09 p1370 A66-19901  
 Earth atmosphere physical properties including temperature, density, pressure and water vapor 09 p1398 A66-20270  
 Lower atmospheric density measurements through light scattering from Q-spoiled ruby laser beam, using optical radar detector 09 p1373 A66-20398  
 Shock wave propagation in atmosphere whose density is exponentially decreasing 09 p1367 A66-20405  
 Atmospheric structure in lower thermosphere, examining grenade clouds to determine density 09 p1375 A66-20892  
 Atmospheric density distribution at altitude from 200 to 300 km, based on Soviet satellite observations during minimum solar activity 09 p1375 A66-20990  
 Wave reflection in density-inhomogeneous atmosphere from plane solid obstacle larger than wavelength 11 p1735 A66-22601  
 Existence of significant latitudinal variation in density from 200 to 800 km 12 p1868 A66-23554  
 Data on satellite orbits used for Earth figure, upper atmosphere density, solar radiation, etc, 12 p1868 A66-23637  
 Upper atmosphere temperature, pressure and density determined by photographic observations of meteors, based on calculating height of homogeneous atmosphere 12 p1870 A66-24299  
 Atmospheric environment effects on Saturn IB launch vehicle design, showing density profiles for various altitudes and listing extremes of thermodynamic variables at specific altitudes [AIAA PAPER 66-347] 12 p1906 A66-24477  
 U.S. Standard Atmosphere supplements 1966 [AIAA PAPER 66-342] 12 p1906 A66-24488  
 Rocket observation of atmospheric density at high latitudes in Arctic and Antarctic locations [AIAA PAPER 66-345] 12 p1872 A66-24488  
 Atmospheric density models for solar radiation cycle variation in upper atmosphere [AIAA PAPER 66-355] 12 p1951 A66-24499  
 Mars atmosphere and ionosphere analyzed by measuring effect on radio occultation of planet, determining shape, atmospheric density profile, diurnal variations, etc 13 p2178 A66-25230  
 Falling sphere, solar XUV radiation absorption and pressure gauge mass spectrometry for density measurements of thermosphere, comparing results and noting discrepancies 14 p2284 A66-27611  
 Air density at heights near satellite perigee by analyzing changes in satellite orbit 14 p2382 A66-27616  
 Distribution and variation of atmospheric density over thermosphere, including auroral region, noting wind motion and high altitude circulation 14 p2382 A66-27616  
 Density variation observed from satellites in upper atmosphere 14 p2284 A66-27611  
 Density distribution in exosphere, particularly Maxwellian velocity distribution disturbed by light particle escape 14 p2284 A66-27620  
 Mass spectrometry of composition and density of neutral atmosphere, noting diffuse separation of gases 14 p2285 A66-27622  
 Formula for average rate of atmospheric particle fallout in terms of height-averaged values of density and viscosity of atmosphere 14 p2327 A66-27859  
 Atmospheric drag effect on satellite trajectories in eccentric orbits, assuming spherical atmosphere with exponentially distributed density 14 p2384 A66-27882  
 Meteor luminosity/ionization ratio dependence on air density found through analysis of ablation rate of meteor 14 p2387 A66-28177  
 Energy spectrum of primary photoelectron using data from atmospheric density distribution, fluxes of solar XUV radiations and absorption and ionization cross sections 15 p2574 A66-28906  
 Density, temperature and wind data of strato- and mesosphere, together with water vapor measurements in central tropical Pacific, using rocket and balloon soundings 15 p2485 A66-28937  
 Rejection of Jones ionospheric mode where Venus microwave emission is attributed to free-free electron emission analyzing formation of dense Cytherean ionosphere 15 p2597 A66-29258  
 Extensive air showers at various atmospheric depths analyzed, using hodoscope counters and ionization chambers, noting differential spectra of densities 15 p2580 A66-29526  
 Drag coefficients and absolute atmospheric densities at high altitudes calculated, using spin and orbital decays of Explorer VI satellite conjugated with models of surface particle interaction 15 p2489 A66-29818  
 Latitudinal and seasonal variations in atmospheric densities during low solar activity obtained by inflatable air density satellites 15 p2490 A66-29819  
 Seasonal-latitudinal variations in lower



- thermospheric density, temperature and composition 15 p2490 A66-29820
- Shape and location of diurnal bulge in upper atmosphere, analyzing density and temperature distribution at high latitude from satellite drag data 15 p2490 A66-29821
- Falling sphere measurements of atmospheric density, noting temperature and density profiles, pressure distribution, etc 15 p2494 A66-30041
- Mars atmospheric density determined from photoelectric measurements of eclipses of Phobos 15 p2604 A66-30049
- Cosmos satellite observational values of atmospheric density during low solar activity 15 p2496 A66-30083
- Day-to-night and semiannual variations in exospheric density during low solar activity from observations of Echo II orbital period changes 15 p2497 A66-30084
- Atmospheric density statistics from cumulative frequencies for seasons as function of altitude for design of booster vehicles 16 p2741 A66-30602
- Anderson hypothesis on semiannual variation in upper atmosphere density and relation to geomagnetic latitude effects, analyzing Samos II motion 17 p2920 A66-33087
- Atmospheric density measurements for altitudes up to 74 km from X-15 flights using stagnation pressure method [AIAA PAPER 66-441] 18 p3104 A66-33646
- Upper atmospheric density determination from data of satellite orbit evolution, noting effect of solar activity 19 p3343 A66-35253
- Falling sphere experiment instrumentation for aerospace density determination including sensor, transit-time accelerometer and telemetry system 19 p3356 A66-35672
- Atmospheric density and scale height from satellite 1964-30A decay 19 p3463 A66-35922
- Meteorological rocket measurements of diurnal oscillations of pressure and density in upper stratosphere and lower mesosphere 20 p3551 A66-37515
- Least squares iterative procedure for resolving individual particle distributions comprising model atmosphere density profile above 110 km 20 p3551 A66-37516
- Processing of satellite observations obtained within INTEROBS program dealing with atmospheric density determination and calculation of satellite orbital elements 20 p3518 A66-37847
- Upper atmospheric density determination on basis of changes in orbital elements of artificial Earth satellites 20 p3553 A66-37850
- Satellite orbit determination and air density and scale height analysis, using visual observation 23 p4128 A66-41359
- Time dependent behavior of temperature and density in monoconstituent atmosphere under diurnal photoheating and cooling by conduction, analyzing effect of atmosphere rotation eastward 23 p4064 A66-41678
- ATMOSPHERIC DIFFUSION**
- Diffusion from elevated point source into turbulent atmosphere flow over horizontal ground 01 p0061 A66-10483
- Diffusion of heavy contaminant in turbulent atmosphere, approximating vertical wind profile and turbulent diffusion coefficient by power functions of height 01 p0096 A66-10754
- Vertical and horizontal turbulent diffusion in lower atmospheric layer as two-layer problem 04 p0513 A66-13442
- Observed and predicted standard deviations compared for cross-wind deposits 04 p0541 A66-13670
- Diffusion of toxic fumes driven by winds of variable velocity from given site over irregular terrain 10 p1553 A66-21580
- Model of high energy collision processes, based on terms of four-momentum transfer and spectra variation, used for calculation of atmospheric diffusion of heavy triplets produced by primary cosmic radiation 11 p1741 A66-23190
- Atmospheric diffusion study to determine toxic hazard exclusion distances for rocket launching personnel under operating conditions [AIAA PAPER 66-376] 12 p1907 A66-24502
- Ablation particulate dispersion in atmosphere estimation by calculating particle deposit concentration at Earth surface [AIAA PAPER 66-379] 12 p1951 A66-24504
- Light diffusion of Martian atmosphere measured by spectroscopic evaluation of polarization variation from disk center to edge 13 p2181 A66-25461
- Concentration distribution at Earth surface associated with precipitation of cloud of interacting particles forming dust source, due to turbulent scattering in time and space 13 p2122 A66-26248
- Diffusion of heavy contaminant in turbulent atmosphere, approximating vertical wind profile and turbulent diffusion coefficient by power functions of height 14 p2326 A66-27853
- Average rate of eddy mixing obtained from some eddy transport problems in thermosphere, noting molecular diffusion 15 p2490 A66-29945
- Atmospheric diffusion coefficients by measuring radial growth of chemiluminous trails deposited in upper atmosphere 16 p2695 A66-30712
- Atmospheric decay of rocket-released Li due to diffusion, wind and chemical reaction 16 p2697 A66-31008
- Vertical atmospheric distribution of Rn, Tn and short-lived decay products under stationary conditions 16 p2698 A66-31345
- Terrestrial aureole structure in daylight, twilight and night and explanation for luminous particles observed in wake of Voskhod spacecraft 19 p3347 A66-35646
- Altitude of lower cloud boundary functional correlation with atmospheric parameters obtained from numerical weather forecast 20 p3593 A66-38366
- Meteorological characteristics for atmospheric boundary layer under stationary conditions, considering thermal stability and turbulent energy 20 p3593 A66-38367
- Molecular diffusion coefficient calculated in 130-200 km region from time variation of radiance distribution from glow clouds produced by grenade detonation 21 p3734 A66-39339
- Concentration distribution at Earth surface associated with precipitation of cloud of interacting particles forming dust source, due to turbulent scattering in time and space 22 p3942 A66-39710
- Effective diffusion cross section for meteor atoms in atmosphere, using Thomas-Fermi-Dirac and dumbbell molecule models 22 p3983 A66-40764
- Upward heat flux with vanishing counter potential temperature gradient in lower atmosphere and in laboratory experiments 24 p4202 A66-42983
- ATMOSPHERIC ELECTRIC FIELD**
- Lightning discharges investigated by oscillographic method in field laboratory at Pirkuli in 1963 01 p0096 A66-10191
- Particle-field interaction in magnetosphere discussing categories, properties, scale model experiments, etc 03 p0363 A66-12646
- Electrical effect of large meteorite moving in lower atmosphere 04 p0577 A66-13846
- Electrostatic fluxmeter measuring electrostatic field in atmosphere 04 p0523 A66-14307
- Precipitation formation considering collision efficiency of different-size droplets, noting influence of gravitational and electric fields, space charge, atmospheric turbulence, etc 06 p0905 A66-16269
- Electrical structure of thunderstorms, particularly weak portion of squall line thunderstorm complex, using aircraft photography, radar data, etc 06 p0905 A66-16270
- Ionospheric plasma diffusion, noting electric field effect in derived equation of continuity for F region 08 p1215 A66-19206
- True height variations of F-2 layer for bay disturbances of geomagnetic field obtained from ionograms, assuming they are caused by horizontal electric field 08 p1216 A66-19213
- Design feasibility of dipole antenna for measuring electric fields at VLF from satellite moving through ionosphere 09 p1340 A66-19848
- Magnetospheric electric fields, noting implications of magnetic storm theories 10 p1528 A66-21149
- Strong electric-field radiosonde for thunderclouds, noting sounding results 11 p1725 A66-22198
- Doppler frequency changes in vertically incident and reflecting sounding wave associated with geomagnetic disturbances yields information on ionospheric electric field 14 p2234 A66-26856
- Meteor stream effect on atmospheric electric field variation 14 p2284 A66-27543
- Electrostatic fluxmeter measuring electrostatic field in atmosphere 14 p2297 A66-28220
- Correlation between clear air turbulence and aircraft electrical activity, describing corona discharges from DC-8 tail antenna 15 p2426 A66-28922
- LF electrostatic field characteristics of clear air turbulence, noting theory and application of field sensing antennas, turbulence generated signals, etc 15 p2532 A66-28923
- Critical electric field for charged droplets atomizing, noting spark discharge and ion concentration in clouds 16 p2742 A66-31109
- Lightning flash mechanisms and electric field strengths in clouds 21 p3759 A66-38533
- Atmospheric electric field change compensation during measuring air-Earth ionic conduction and electron precipitation current densities 22 p3920 A66-40804
- Meteor stream effect on atmospheric electric field variation 24 p4198 A66-42327
- ATMOSPHERIC ELECTRICITY**
- SA LIGHTNING**
- Electric conductivity, electric field and space charge of atmosphere under fair weather or thunderstorms 09 p1371 A66-20275
- Tornado dehydration and burning effects in terms of conventional hot wind mechanism, corona discharge mechanism and new ring-current mechanism 13 p2122 A66-26126
- Giant-pulse laser-induced atmospheric electric breakdown causing optical frequency discharge 13 p2134 A66-26194
- Atmospheric electrode effect equations solved for case with no nuclei and convection and constant ionization 17 p2922 A66-33350
- Atmospheric electrode effect where condensation nuclei are present 17 p2922 A66-33351
- Autocorrelation statistical method applied to atmospheric electricity 17 p2923 A66-33363
- Photometric studies of lightning with correlated photographs of discharge channels to determine photoelectric pulse profile characteristics 18 p3129 A66-34018
- Sferics from lightning from warm cloud, noting microsecond pulse-train format and temporal duration 22 p3942 A66-39678
- Visibility and small ion density correlated by comparing light scattering with ion attachment processes on airborne scatters 23 p4065 A66-41842
- ATMOSPHERIC EMISSION**
- SA AIRGLOW**
- Terrestrial albedo of 40 to 190 kev X-rays measured, using directional detectors at balloon altitude 03 p0419 A66-12683
- Spectral emissivity calculations for parallel bands of carbon dioxide at 4.3 microns between 150-600 degrees K, comparing experimental measurements with theoretical calculations 03 p0393 A66-13104
- IR emission observation used to deduce composition, temperature and energy budget of stratosphere and mesosphere 05 p0672 A66-15024
- Airborne measurement of microwave emission from Earth surface and atmosphere for potential application of radiometry to weather satellite reconnaissance 05 p0675 A66-15765
- Statistical radio emission characteristics of cloudy atmosphere 06 p0837 A66-17181
- Space correlation of main emission lines for night sky emission spectra and altitude distribution of sodium luminescence 15 p2495 A66-30060
- Naturally occurring electromagnetic radiation in audiofrequency range studied at Kiruna Geophysical Observatory 16 p2691 A66-30232
- Spectral lines in atmospheric emission during day and night airglow in review of



published works 17 p2917 A66-32026  
 Atmospheric radio noise variations at LF  
 noting daytime increases, distribution of  
 mean source localizations, solar activity  
 effect, etc 18 p3104 A66-33960  
 Statistical radio emission characteristic of  
 cloudy atmosphere 19 p3297 A66-35539  
 ULF radio emission of upper atmosphere  
 and other related geophysical phenomena,  
 analyzing hisses, choruses and contribution  
 to Earth radiation belt 20 p3551 A66-37487  
 Search for 22.235 gc/s emission line from  
 stratospheric water vapor, noting absence of  
 noise temperature enhancement 22 p3916 A66-40810  
 Temperature profiles across argon plasma  
 arc calculated from measured radiation  
 intensities at arc currents from 1 to 400  
 amp 23 p4104 A66-41495  
 Altitude profiles for dayglow emissions  
 excited by molecular ion dissociative  
 recombination, solar radiation fluorescence,  
 oxygen photodissociation, electron collisions  
 and chemical reactions 23 p4064 A66-41680

**ATMOSPHERIC ENERGETICS**  
 Acoustic, gravitational and gyroscopic  
 oscillation spectra of baroclinic atmosphere  
 over rotating spherical Earth with emphasis  
 on energy composition 01 p0062 A66-10858  
 Coupling coefficients in high energy region  
 of Earth atmosphere, considering  
 interactions between primary nucleons and  
 nuclei of air atoms 06 p0950 A66-16594  
 Atmospheric energetics during January-  
 February 1963 stratospheric warming  
 investigated, using spectral energy equations  
 for zonal and eddy kinetic and potential  
 energies 07 p1027 A66-17360  
 Heat transfer and mass flux expressions  
 for recombination interactions at solid-gas  
 interface due to transport of atomic and  
 ionized particles to spacecraft in  
 ionosphere 08 p1161 A66-18747  
 Kinetic energy variations in different parts  
 of baric centers during atmospheric  
 motion 08 p1217 A66-19301  
 Charge transfer and charge rearrangement  
 in atmospheric ion-neutral particle  
 collisions 10 p1557 A66-21143  
 Differential equations describing air  
 movement, heat exchange and exchange of  
 moisture 11 p1730 A66-22942  
 Energy conversion between four different  
 forms of kinetic energy in  
 atmosphere 15 p2489 A66-29662  
 Generalized vertical coordinate system for  
 application in atmospheric  
 dynamics 18 p3129 A66-33965  
 Kinetic energy variations in different parts  
 of baric centers during atmospheric  
 motion 19 p3348 A66-36038  
 Differential equations describing air  
 movement, heat exchange and exchange of  
 moisture 20 p3593 A66-37855  
 Frontogenetic potentialities of wind  
 deformation fields determined, using  
 mathematical model of  
 atmosphere 24 p4234 A66-42979

**ATMOSPHERIC ENTRY**  
 Theoretical and experimental work in flow  
 field analysis has enhanced ability to predict  
 aerodynamic heating in atmospheric  
 entry 01 p0143 A66-10800  
 Planetary entry trajectory control of  
 manned vehicles for Earth and Mars  
 atmospheres 03 p0431 A66-12741  
 Orbiter injected sterilized ballistic skipout  
 capsule for in-flight Martian stratosphere  
 measurements, using nonablative heat shield  
 and outside atmospheric propulsion  
 maneuvers [AIAA PAPER 65-23] 03 p0431 A66-12764  
 Glider reentry descent trajectories from  
 near Earth orbit calculated, emphasizing  
 landing accuracy and mechanical and  
 thermal stresses 04 p0584 A66-13525  
 Calculating meteor braking from  
 theoretical and observational data, showing  
 braking dependence on zenith  
 distance 04 p0577 A66-13844  
 Meteor radiation curves showing that  
 integral radiation calculated for  
 nondisintegrating meteoric body is greater  
 than observed radiation 04 p0577 A66-13845  
 Convective and radiative heat transfer  
 during atmospheric reentry examined, using  
 double-diaphragm shock tube operated in  
 expansion tube mode 11 p1684 A66-22828

Aerodynamic analysis of vapor pressure of  
 tektite glass and bearing on atmosphere  
 entry trajectories of 12 p1952 A66-24895  
 Aerodynamic heating of vehicles entering  
 Earth atmosphere at hypersonic speed,  
 noting blunt body concept, radiative and  
 convective heating, heat shield weights,  
 etc 13 p1989 A66-25153  
 High-temperature gas radiance in simulated  
 planetary atmosphere at various entry  
 velocities 13 p1990 A66-25169  
 [AIAA PAPER 66-183] Manned Mars entry and landing, discussing  
 aerobraking as feasible entry 13 p1991 A66-25272  
 mode Problem of operational flexibility in Mars  
 landing mission, discussing use of lifting  
 vehicles 13 p1991 A66-25273  
 Mars atmospheric composition and laminar  
 convective heating and ablation studied to  
 predict performance of heat protection  
 systems during entry 13 p2208 A66-25274  
 Inviscid equilibrium gas stability  
 characteristics for pointed and spherically  
 blunt bodies in unsteady supersonic flight in  
 Mars atmosphere 13 p1991 A66-25275  
 Monograph on atmospheric reentry,  
 discussing reentry trajectories, atmospheric  
 kinematics, reentry flow fields,  
 etc 13 p1993 A66-26466  
 Hypersonic wake studies in ballistic missile  
 research program, discussing reentry of  
 hypervelocity vehicles, laminar flow,  
 atmospheric turbulence, 14 p2218 A66-27402  
 Recovery of interplanetary vehicles by low  
 thrust braking outside 14 p2391 A66-27472  
 atmosphere Global coverage by banked aeroglide  
 atmospheric entry from spherical Earth  
 analysis of bank-speed schedule and  
 necessary L/D 14 p2395 A66-28453  
 Reentry scattering due to equilibrium  
 incidence without using Allen  
 hypothesis 16 p2796 A66-30315  
 Material properties and thermal inputs on  
 heat shields for Mars entry, noting  
 importance of insulation vs ablation due to  
 uncertainties in radiant heating  
 inputs 16 p2809 A66-30895  
 Terrestrial origin of tektites, noting  
 possible connection with cometary collision  
 and evidence of lunar origin for  
 some 16 p2802 A66-30926  
 Wind tunnel test of dynamic stability  
 characteristics of spherically blunted 10  
 degree cones [AIAA PAPER 66-465] 17 p2841 A66-32764  
 Second-order theory used to provide nearly  
 exact solution for entry mechanics including  
 solution of nonoscillating and oscillating  
 trajectories [AIAA PAPER 66-488] 17 p3016 A66-32771  
 Oscillatory motion of angle of attack for  
 space vehicles entering Earth atmosphere at  
 hypersonic speeds from satellite 17 p3016 A66-32893  
 Oscillatory trajectories in atmospheric  
 entry of lifting vehicles at subcircular  
 speeds and constant angles of attack with  
 initial conditions deviating from equilibrium  
 glide 17 p3016 A66-33065  
 Basic shock layer radiation data obtained  
 in shock tube and free-flight ballistic range  
 facilities, applicable to Venus or Mars  
 atmosphere entry [AIAA PAPER 66-421] 18 p3046 A66-33641  
 Optimum entry vehicle design using  
 aerobraking for manned Earth entry at  
 hyperbolic speeds, examining blunted conic,  
 biconic and tetrahedral configurations  
 [AIAA PAPER 66-489] 18 p3239 A66-33657  
 Friable structure of meteorites, examining  
 disintegration under aerodynamic pressure  
 in atmosphere 18 p3227 A66-33838  
 Simulator results on guidance and control  
 during supercircular atmospheric entry  
 maneuvers 18 p3244 A66-33878  
 Atmospheric reentry trajectory of space  
 vehicle at orbital velocities and constant  
 lift-drag ratio 18 p3244 A66-33879  
 Disintegration of meteoric bodies in  
 terrestrial atmosphere, disputing conclusion  
 of Kramer 19 p3455 A66-35271  
 Figure that results from disintegration of  
 package of plates during fall through  
 atmosphere, deriving equations for

rotational motion of 20 p3493 A66-38118  
 plates Approximate atmospheric stability of  
 aerodynamic entry trajectories  
 on cylindrical planet, noting minor circle  
 turn maneuver and bank angle  
 schedule 21 p3811 A66-38705  
 Meteorite size prior to entering  
 atmosphere, noting radius and use of  
 isotope activity 21 p3812 A66-38953  
 nomogram Approximation of aerodynamic stability of  
 coasting vehicle leaving atmosphere at high  
 speeds, assuming linear theory and constant  
 aerodynamic coefficient 22 p3986 A66-40346  
 Reentry simulation systems using MHD  
 accelerators, technical difficulties,  
 performance and efficiency  
 [ICAS PAPER 66-39] 22 p3996 A66-40661

**ATMOSPHERIC HEAT BUDGET**  
 Thermal balance of Earth in light of IGY  
 data 05 p0674 A66-15223  
 Mesosphere of integral terrestrial  
 thermal radiation field determined from  
 outgoing radiation, cloudiness and satellite  
 data 07 p1029 A66-17922  
 Mesosphere of integral terrestrial  
 thermal radiation field determined from  
 outgoing radiation, cloudiness and satellite  
 data 12 p1869 A66-23883  
 Upper atmosphere radiative and heat flux,  
 balance and dynamics from balloon-borne  
 measurements 19 p3347 A66-35641  
 Monthly variations in Southern Hemisphere  
 heat budget calculated from Tiros satellite  
 radiation measurements 19 p3347 A66-35642  
 Energy and momentum budget of  
 atmosphere above tropopause determined by  
 computing momentum and heat transports  
 from wind and temperature observations up  
 to 30 km 19 p3347 A66-35643  
 Turbulence energy balance equation used  
 in air mass transformation 20 p3594 A66-38369  
 problem Solar radiation control for changing  
 meteorological conditions in lower  
 atmospheric layer 20 p3594 A66-38373  
 Angular distribution of Earth outgoing  
 thermal radiation in IR region measured by  
 geophysical rocket 22 p3913 A66-40470

**ATMOSPHERIC HEATING**  
 Atmospheric density and heating as  
 function of altitude determined from  
 satellite drag measurements  
 [AIAA PAPER 65-507] 01 p0134 A66-10192  
 Stationary heat sources effect on  
 convective fluxes in unstable  
 atmosphere 04 p0513 A66-13413  
 Cellular convection in horizontal layers  
 heated from below, noting effect of critical  
 Rayleigh number and width-height ratio of  
 cells 05 p0666 A66-14543  
 Transient behavior of heated stellar  
 atmosphere, examining unsteady flow caused  
 by sudden application of heat to static  
 adiabatic atmosphere 08 p1286 A66-18541  
 Thermospheric heating effect on F-region  
 ionization and electron density in daily basis  
 study 08 p1218 A66-19404  
 Phase difference between atmospheric  
 large-scale disturbances and heating due to  
 sea-surface evaporation and turbulent  
 exchange 11 p1694 A66-22199  
 Radiant heat flux in spectral region from 4  
 to 40 microns at various atmospheric  
 levels 11 p1698 A66-22945  
 Radiation effect on hydrodynamic shock  
 wave parameter distribution for bodies  
 entering dense atmospheric layers at  
 supersonic velocities 11 p1635 A66-23051  
 Radiant heat flux in spectral region from 4  
 to 40 microns at various atmospheric  
 levels 20 p3553 A66-37858  
 Dynamic stability of waves in stratosphere,  
 examining vertical transfer of energy from  
 troposphere to stratosphere weakened at  
 tropopause 21 p3734 A66-39219

**ATMOSPHERIC IMPURITY**  
 Gaseous impurity distribution /oxygen/  
 between scale and diffusion layer after heat  
 treatment of various titanium  
 alloys 05 p0699 A66-14700  
 Deposition of black magnetic spherules  
 from atmosphere at two stations in New  
 Mexico believed to be of extraterrestrial  
 origin 09 p1370 A66-19879  
 Kinetics of oxidation of various  
 atmospheric contaminants over several  
 catalysts tested in catalytic reactor



[AICE PREPRINT 26C] 10 p1491 A66-21190  
Kinetics of oxidation of various  
atmospheric contaminants over several  
catalysts tested in catalytic reactor  
[AICE PREPRINT 26C] 17 p2888 A66-32680  
Impurities effect on electrical conductivity  
of air between 1000 and 10,000 degrees  
K 19 p3406 A66-35743  
Bomb debris motion following Star Fish  
test, noting formation of MHD shock wave,  
production of stationary plasma through X-  
ray ionization and collision in neutral  
air 20 p3644 A66-38345  
Gerdien-condenser rocketborne probe used  
to measure ion densities in D region of  
atmosphere 22 p3905 A66-39947  
**ATMOSPHERIC IONIZATION**  
Tropospheric ion mobility distribution,  
conductivity and densities above exchange  
layer 02 p0222 A66-11824  
D-region atmospheric processes such as  
electron attachment, photo and other  
detachment processes, recombination and  
neutralization as studied in  
laboratory 03 p0362 A66-12640  
Particle bombardment produces ionized  
layers in high latitude ionosphere similar to  
sporadic E layers of lower  
latitudes 03 p0363 A66-12657  
Ionic reactions and photoionization  
processes in D, E and F regions of  
ionosphere 03 p0365 A66-12874  
Ionizing radiation as potential lightning  
hazard, noting lightning protection device  
for medical and industrial  
buildings 03 p0423 A66-13266  
Correlation dependence of F-2 layer on  
solar wave energy entering Earth  
atmosphere 04 p0515 A66-13850  
French FR-1 satellite for observation of  
ionized layers of atmosphere by propagation  
of VLF waves in  
ionosphere 04 p0586 A66-14385  
Atmospheric ionization, discussing  
formation of different ionospheric  
regions 05 p0675 A66-15744  
Hypersonic wake ionization dependence on  
ablation products, investigating laminar and  
turbulent flow regions  
[AIAA PAPER 65-54] 05 p0793 A66-15778  
Ultrahigh-energy primary cosmic ray  
particle interactions cause electron photon  
cascades and muon  
emission 07 p1117 A66-17570  
Extensive air shower high energy gamma  
rays in upper third  
of  
atmosphere 07 p1118 A66-17575  
Mean free path for nucleon-light atom  
interaction changed from 75 to 90 g/sq cm  
affecting air shower  
characteristics 07 p1118 A66-17575  
Papers on interactions of space vehicles  
with ionized atmosphere 08 p1302 A66-18742  
Shock wave induced thermal ionospheric  
ionization from Tungusk explosion of 1908,  
with recalculation of shock  
magnitude 08 p1290 A66-19053  
Position determination of equatorial  
boundary of abnormally high nocturnal  
atmospheric ionization for various levels of  
planetary magnetic  
activity 08 p1221 A66-19793  
Ionospheric ionization  
physics 09 p1371 A66-20279  
Upper atmospheric parameters that control  
daytime electron density distributions in F-1  
region determined with use of N/h/  
profiles 09 p1372 A66-20369  
Dayglow at 6300 and 3914 angstroms from  
rocket soundings and roles of ion  
recombination and UV  
dissociation 09 p1374 A66-20887  
Bremsstrahlung produced during stoppage  
of electrons generated by thunderstorms can  
create ionized columns extending to  
ionospheric heights 10 p1529 A66-21158  
Equilibrium theory of ionization transport  
in ionosphere predicts tendency for thin  
layers of overdense ionization to form in E  
region 10 p1531 A66-21279  
Surface boundary layer charge of  
isothermal atmosphere of fully ionized  
equilibrium plasma in gravitational  
field 10 p1609 A66-21813  
Anomalous ionization of lower ionosphere  
at medium latitudes during worldwide  
geomagnetic storm result in increased radio  
wave absorption in

ionosphere 11 p1696 A66-22416  
Lower ionosphere ionization for quiet and  
disturbed Sun calculated for comparison of  
experimental and theoretical values for  
electron concentration and effective  
recombination 11 p1696 A66-22417  
Outer radiation belt particle penetration  
into stratosphere, accounting for increased  
total ionizing radiation recorded at  
Murmansk 11 p1762 A66-22426  
Critique of local ionospheric electron  
concentration determined by dispersion  
method with aid of satellite and new  
ionization maximum 11 p1697 A66-22428  
Substantiating possibility of determining  
local electron concentration by dispersion  
method with aid of satellites and new  
ionization maximum 11 p1697 A66-22429  
Chemical and photochemical reactions  
controlling ion composition of atmosphere  
between 150 and 300 km 11 p1699 A66-23041  
Meteor trail formation by ionization,  
examining HF radio wave reflection in  
communications field 12 p1947 A66-23795  
Wind velocity measurement using radar  
detection of artificially ionized air column  
by radioactive source 12 p1908 A66-24516  
[AIAA PAPER 66-404] 12 p1908 A66-24516  
Threshold data for ruby and neodymium  
laser pulse-induced breakdown in Xe, Ar,  
Kr, Ne, He, oxygen, nitrogen, air and carbon  
dioxide 13 p2100 A66-26191  
Sporadic E ionization, considering sheets  
and winds 14 p2282 A66-26854  
Extraterrestrial dust as possible cause of  
background ionization and stratification in  
sporadic E layer 14 p2282 A66-26855  
Plasma due to high-altitude nuclear  
explosion and effect on radar  
propagation 14 p2237 A66-27510  
Stratospheric small-ion density  
measurement from high-altitude jet aircraft,  
noting dust effect 14 p2297 A66-28334  
E layer ionization and characteristic  
number as affected by solar X radiation in  
44-60 angstrom range 15 p2487 A66-29097  
Frequency correlation of ionospheric radio  
waves in inhomogeneous thin layer medium  
and effect of irregular horizontal ionization  
gradients 15 p2451 A66-29111  
Ion composition and effective  
recombination coefficient variation of  
ionosphere in study of X and UV radiation  
ionization of E layer 15 p2495 A66-30059  
Mass spectrometric investigations of  
interaction of atmospheric ions with  
molecules of rocket gas  
release 15 p2495 A66-30061  
Maximum ionization in ionospheric F  
region around geomagnetic equator, noting  
instruments and observed  
variations 16 p2697 A66-30995  
E-2 layer of atmosphere, discussing  
maxima, minima, variations and shielding  
effect of E-layer 17 p2918 A66-32877  
Cosmic radio wave absorption dependence  
on frequency and number of electron-ion  
collisions during atmospheric magnetic  
storms 19 p3344 A66-35267  
Rocket probe measurements indicate  
existence of maximum ion concentration in  
stratosphere and lower ion concentration at  
equator than at  
midlatitudes 19 p3345 A66-35288  
RF mass spectrometer with small  
dimensions and power requirements and  
high sensitivity designed for analysis of  
upper atmosphere ion and neutral  
composition 19 p3353 A66-35289  
Aerobee rocket measurement of nitric  
oxide in upper atmosphere, noting  
fluorescence in airglow layer, emission rate  
factors and NO densities 19 p3349 A66-36351  
Siting of static discharger to control  
nature and occurrence positions of coronas  
to minimize RF noise capable of causing  
hazard to aircraft navigational aid  
systems 19 p3282 A66-36752  
Air ionization effect on vigilance task  
performance, noting smaller decrement for  
environment containing negative  
ions 20 p3504 A66-36933  
Anomalous enhancement of F-2 ionization  
in high latitude around geomagnetic noon  
due to formation of irregularity or new  
layer around locality 20 p3658 A66-38234  
Upper atmospheric parameters that control  
daytime electron density distributions in F-1

region determined with use of N/h/  
profiles 20 p3636 A66-38235  
Position determination of equatorial  
boundary of abnormally high nocturnal  
atmospheric ionization for various levels of  
planetary magnetic  
activity 21 p3733 A66-38789  
Height distributions for atmospheric  
ionization rate and Balmer radiation  
resulting from precipitation of auroral  
protons 21 p3734 A66-39338  
Ionization and constitution of neutral  
atmosphere, including solar EUV, X-ray and  
corpuscular sources 22 p3905 A66-39944  
Riometric data on ionospheric absorption  
applied to determination of dissociative  
recombination coefficient, noting  
atmospheric ionization by fragment gamma-  
radiation 22 p3973 A66-40468  
Ionic reaction in nitrogen-oxygen system,  
discussing reactions of He and N  
ions 23 p4063 A66-41039  
Variation in energy of energetic electron  
precipitating into atmosphere as function of  
initial energy, pitch, angle and altitude,  
neglecting scattering  
effect 24 p4262 A66-42463  
Pressurized Ar-filled ionization chamber  
response to charged particles in cosmic  
radiation determined as function of  
atmospheric depth 24 p4264 A66-42604  
High energy particle interactions initiate  
large ionization bursts, noting pion  
production 24 p4267 A66-42907  
Extent of maximum in altitude dependence  
curve for extensive air showers, noting  
energy dissipation among secondary  
particles 24 p4270 A66-42927  
**ATMOSPHERIC MOISTURE**  
**S HUMIDITY**  
**ATMOSPHERIC NEUTRON FLUX**  
Neutron flux in atmosphere measured by  
method of indium  
activation 02 p0284 A66-12130  
Detection of slow neutrons escaping from  
atmosphere by counters filled with boron  
fluoride onboard high altitude  
balloons 05 p0754 A66-15401  
Neutron albedo flux at 45 degree  
geomagnetic latitude 07 p1121 A66-17982  
Neutron intensity increase observed by  
boron fluoride proportional counter at high  
altitude associated with auroral zone X-ray  
event 07 p1121 A66-17983  
Intensity of cosmic ray alpha particles on  
July 16, 1959 when counting rates of  
neutron monitors were near absolute  
minimum value 07 p1124 A66-17997  
High-energy neutron emission from Sun  
studied by balloon-borne nuclear emulsion  
recording of proton track colliding with  
neutron 13 p2175 A66-26349  
Neutron flux in atmosphere measured by  
method of indium  
activation 14 p2377 A66-28087  
Barometric air pressure correction anomaly  
for nucleonic component monitors, noting  
time variation in attenuation  
coefficients 18 p3194 A66-34856  
Attenuation and multiplicity effect used as  
indexes of properties of radiation recorded  
by IGY neutron monitors in lower  
atmosphere 18 p3194 A66-34859  
Modulation data for primary cosmic ray  
spectrum at low rigidities determined from  
daily latitude curves of cosmic ray nucleonic  
component obtained from IGY neutron  
monitors 18 p3194 A66-34860  
Counting rate of high latitude NM-64  
neutron monitors, examining dependence on  
atmospheric temperature and water vapor  
content 18 p3195 A66-34861  
Smooth curves of cosmic ray neutron  
component intensity variations compared  
with H component of geomagnetic field  
during IGY and IGC 18 p3196 A66-34868  
Atmospheric neutron flux measured by  
balloons, using polyethylene-moderated  
boron fluoride counter 18 p3197 A66-34875  
Low energy fast cosmic ray neutrons,  
measurements of energy spectrum and  
primary intensity variations, using organic  
scintillator in field of photomultiplier  
tube 18 p3199 A66-34885  
Solar minimum measurements of fast  
neutrons at high altitude using balloons and  
rockets carrying anthracene-plastic  
phoswich 24 p4262 A66-42293



ATMOSPHERIC NOISE  
 S ATMOSPHERICS  
 ATMOSPHERIC PRESSURE  
 SA BAROMETER  
 SA ISOBAR  
 Soviet, Swedish and Norwegian data on solar activity and barometric pressure, showing corpuscular flux effect on barometric pressure even at Earth surface 01 p0060 A66-10272  
 Survival of Earth organisms under environment simulated low pressure, low oxygen, low temperature and low extraterrestrial conditions 02 p0181 A66-11605  
 Numerical objective analysis for stratospheric constant pressure data at various levels 02 p0254 A66-11983  
 High precision digital atmospheric-pressure recorder that does not require mercury barometer readings for barogram processing 02 p0232 A66-12148  
 Temperature of hydrogen plasma jet at atmospheric pressure by measuring electric field on profile of Stark broadened line 03 p0403 A66-12973  
 Probes in atmospheric pressure argon plasma where ion diffusion is function of temperature 03 p0406 A66-13280  
 Geomagnetic relationship of daily variation of cosmic ray neutron intensity corrected for barometric pressure variation at various ground stations 03 p0423 A66-13360  
 Optimization of fin geometry to maximize free-convection heat transfer in air at atmospheric pressure [ASME PAPER 65-HT-12] 05 p0783 A66-14738  
 Atmospheric pressure variation at troposphere, relation to solar activity 05 p0759 A66-14882  
 Simulated flights evaluating verbal communication intelligibility in oxygen breathing mixtures at low atmospheric pressures compared with results obtained in room air at ground level 06 p0813 A66-16827  
 Difference between values for atmospheric pressure at Martian surface when obtained by photometry or by spectroscopy, due to nonconsideration of light scattering by aerosol particles 08 p1295 A66-19331  
 Earth atmosphere physical properties including temperature, density, pressure and water vapor 09 p1398 A66-20270  
 Earth, balloon and satellite spectroscopic observations of Mars to determine atmospheric composition and pressure at surface level 10 p1602 A66-21065  
 Book on aviation physiology including atmospheric pressure effect, visual factors in aviation, British Institute of Aviation Medicine, etc 10 p1487 A66-22104  
 Pressure cabin design and utilization, noting relation between air speed and environmental temperature on kinetic heating, contamination of cabin air, pressurization control, sealed cabin advantages, etc 10 p1492 A66-22110  
 High precision digital atmospheric-pressure recorder that does not require mercury barometer readings nor barogram processing 14 p2297 A66-28103  
 Quasi-stationary solar corpuscular fluxes, examining effect on atmospheric pressure in Earth polar cap regions 15 p2576 A66-29134  
 Distribution of solar-tropospheric disturbances over Earth surface, based on simultaneous observations of 103 U.S.S.R. stations 15 p2533 A66-29135  
 Spherical semipassive probe for density/altitude and pressure/altitude profile of planetary atmospheres, notably Mars and Venus 16 p2801 A66-30889  
 Slide-wire microbarometer with pressure changes transformed into frequency changes of output signal designed for operation on moving objects 16 p2709 A66-31795  
 Electric conductivity in low voltage atmospheric pressure gas discharge, noting Maxwellian electron density distribution 17 p2968 A66-32484  
 Hot flame gases ionization by electron reactions at atmospheric pressure 18 p3137 A66-34116  
 Barometric coefficients of Leeds IGY and NM-64 neutron monitors, noting variation from solar minimum to maximum 18 p3194 A66-34857  
 Latitude and altitude survey in North

America made by road transport carrying neutron monitor, meson telescope, mercury barometer, etc 18 p3198 A66-34879  
 Barometric effect and density spectrum of photon-initiated EAS 18 p3208 A66-35115  
 muons  
 Empirical formula for calculating surface wind conditions from barometric field 19 p3394 A66-36453  
 Comparison of magnitude of collision frequency of electrons in D and E regions obtained by satellites, rockets, etc, with cross sections measured in laboratory 19 p3352 A66-36627  
 Book on physiological responses of healthy mammals to natural changes or extremes of physical environment, considering heat, cold, light, atmospheric pressure and water 20 p3505 A66-37253  
 Meteorological rocket measurements of diurnal oscillations of pressure and density in upper stratosphere and lower mesosphere 20 p3551 A66-37515  
 Phase relationships of normal stress perturbations in cylindrical combustor operating near atmospheric pressure with premixed air and natural gas 20 p3680 A66-38038  
 Sound absorption in air at 1/3-octave frequency intervals as function of humidity and temperature at normal atmospheric pressure for studies in room acoustics 21 p3769 A66-38648  
 Increased ambient pressure effect on hearing function in divers 22 p3853 A66-39787  
 E layer properties noting role of pressure, temperature, composition and recombination coefficient when varying with height and time 22 p3907 A66-39960  
 Graphical determination of atmospheric pressure from rocketsonde temperature measurements 22 p3943 A66-40056  
 Two-layer model of pressure jump produced by mountains 22 p3944 A66-40966

## ATMOSPHERIC RADIATION

## SA SKY RADIATION

## SA STRATOSPHERE RADIATION

Angular and spectral distribution of outgoing radiation in cloudy atmosphere in spectral range beyond absorption band 01 p0133 A66-10757  
 Equations for reflecting effect of underlying surfaces on long wave radiation fluxes in free atmosphere 01 p0062 A66-10761  
 Five-year measurements of circumglobal radiation and of short wave radiation from lateral half-spaces 02 p0220 A66-11258  
 Radiation measurements made at Antarctic station at Mirny including solar radiation, total radiation and short and long wave reflection and radiation balance 02 p0220 A66-11260  
 Interpretation of inverse relationship between long-lasting radioactivity and relative humidity in near-ground layer of atmosphere 02 p0279 A66-11261  
 Atmospheric source of diurnal variation of cosmic radiation whose properties undergo substantial variation 02 p0281 A66-11337  
 Solar UV radiation measurements in stratosphere for calculating ozone production 02 p0283 A66-11573  
 Approximation of effect of albedo inhomogeneity on flux of short wave radiation leaving Earth 02 p0222 A66-11658  
 Solar radiation measurements made in four stations from 1957 to 1963 show dependence of atmospheric long-wave radiation on water-vapor pressure and cloudiness 04 p0542 A66-13818  
 Isotropic scattering of radiation from point source in finite atmosphere bounded by totally absorbing spherical shell, deriving iterative series solution 04 p0548 A66-13828  
 Dependence of vertical structure parameters of atmospheric temperature and humidity fields on atmospheric long-wave radiation field, noting transport equation 04 p0542 A66-14303  
 Time and altitude dependence of 55-mev trapped protons in South Atlantic region detected by nuclear emulsions onboard satellites 05 p0747 A66-14784  
 Atmospheric radiation calculations emphasizing carbon dioxide and nitrous oxide absorption spectrum, spectral energy distribution, quasi-statistical band model,

etc 05 p0748 A66-14918  
 Atmospheric showers and high energy nuclear-active particles 05 p0756 A66-15410  
 Atmospheric thermal radiation calculated from unresolved molecular absorption spectra of atmospheric carbon dioxide and water 05 p0675 A66-15860  
 Nuclear interaction at high energies, discussing active component structure ionization calorimeter application, energy spectrum of particles, etc 07 p1113 A66-17536  
 Ascending and descending fluxes of long wave radiation in free winter atmosphere as affected by temperature stratification, water-vapor distribution and clouds 07 p1029 A66-17923  
 Intensity variation of nucleonic component of atmospheric cosmic radiation, geomagnetic threshold rigidity and calculation of cosmic ray equator 08 p1284 A66-19398  
 Neutrino detecting equipment located in South African mine, discussing theory of neutrino production 08 p1285 A66-19600  
 Radiometersonde observations of atmospheric IR irradiance, noting measurement results with improved equipment 09 p1369 A66-19869  
 Equilibrium air total radiation mechanism, vacuum UV radiation and relation to hypervelocity entry studied, using shock tube blunt model test flow [AIAA PAPER 66-103] 09 p1469 A66-20087  
 Primary ultrahigh energy cosmic radiation composition analyzed, using Cerenkov flash 09 p1437 A66-22050  
 IR radiation source, characteristics, transmission and detection, noting atmospheric absorption and emission, IR celestial backgrounds, etc 09 p1371 A66-20277  
 Reflectivity of atmospheric shock front determined, using laser range finder and wide-bandwidth dual-beam oscilloscope 09 p1367 A66-20396  
 Angular distribution of IR radiation of Earth and atmosphere from rocket and balloon sounding 09 p1376 A66-20997  
 IR radiation in upper atm layers investigated by rocket and balloon, noting solar radiation effect 09 p1377 A66-21006  
 Interpretation of outgoing IR radiation data from meteorological satellites, including cloud cover identification and Earth surface temperature 10 p1525 A66-21046  
 Diurnal properties of horizontal geomagnetic micropulsation field in New Zealand, noting variation of period, field rotation and direction of oscillating vector 10 p1529 A66-21152  
 Meteorological satellite terrestrial UV radiation and cloud formation photographic data interpretation 11 p1728 A66-22317  
 Atmospheric high resolution transmission in carbon dioxide bands between 12 and 18 microns evaluated, using mixed Doppler-Lorentz broadening and new method for slant-path calculations 11 p1736 A66-22881  
 Radioactivity of Cosmos III satellite after U.S. thermonuclear explosion over Johnston Island 11 p1764 A66-23053  
 Ascending and descending fluxes of long wave radiation in free winter atmosphere as affected by temperature stratification, water-vapor distribution and clouds 12 p1869 A66-23884  
 Arctic short-wave atmospheric radiation absorption, long-wave radiation loss, and tropospheric radiation balance 12 p1949 A66-24203  
 Spectral and vertical distribution of atmospheric IR radiation flux divergence for five model atmospheres, noting dependence on sighting angle 12 p1874 A66-24868  
 IR radiation measurement from Earth-space transition region /project TACITE/ 13 p2192 A66-25498  
 Intensity and polarization of radiation diffusely transmitted and reflected by Rayleigh atmosphere for optical thickness from 1.0 to 10.0 13 p2072 A66-25806  
 Effect of aperture and atmospheric turbidity on readings of pyrheliometers considered, based on measurements concerning radiation intensity within solar aureole 14 p2282 A66-26930  
 IGY and IGC data on atmospheric washout of radioactive fission products by precipitation 14 p2376 A66-27540



Angular and spectral distribution of outgoing radiation in cloudy atmosphere in spectral range beyond absorption band 14 p2285 A66-27856

Equations for reflecting effect of underlying surfaces on long wave radiation fluxes in free atmosphere 14 p2285 A66-27860

Dependence of vertical structure parameters of atmospheric temperature and humidity fields on atmospheric long-wave radiation field, noting transport equation 14 p2327 A66-28217

Outgoing Earth and atmospheric radiation observed in IR spectrum at various altitudes by geophysical balloons and rockets 15 p2483 A66-28739

Cosmos-65 spectrophotometric measurements of atmosphere-reflected UV radiation spectra 15 p2485 A66-29076

Air showers size, lateral distribution and arrival direction at 5,200 m altitude 15 p2578 A66-29521

Energy spectra of atmospheric alpha rays at balloon altitude and of alpha rays from graphite nuclear interactions 15 p2583 A66-29551

Cosmic ray showers, discussing high energy interactions of nuclear active particles, intensity and energy spectra of gamma rays and muons, young air showers, ionization bursts, etc 15 p2584 A66-29555

Atmospheric high-energy cosmic ray cascade, using fire ball and gev-range nucleon isobars in model 15 p2586 A66-29565

Radiation data measured by Tiros IV satellite for determination of global distribution of atmospheric water vapor 15 p2533 A66-30029

Vertical profile of atmospheric radiative balance from balloon-borne actinometry at 25 to 32 km 16 p2698 A66-31344

Radiant equilibrium temperature of opaque absorbing body relation to radiative temperature variations of air 18 p3265 A66-34611

Energy spectra of muon, electron and N components of extensive air showers /EAS/ 18 p3210 A66-35129

Airborne scintillation counter-spark chamber observations of particle energy flow and incident zenith angle distribution of air showers 18 p3211 A66-35131

Extensive air showers /EAS/, discussing lateral distribution function variation with atmospheric density, primary energy dissipation, shower front radius of curvature, etc 18 p3211 A66-35133

Design and test flying of transistorized sonde used with Suomi-Kuhn radiometer for measurement of heat loss by long wave radiation from atmosphere 19 p3353 A66-35316

Galactic and atmospheric X-ray characteristics determined by two scintillation counters borne on sounding rocket booster 19 p3452 A66-35354

Tiros IV atmospheric IR radiation measurements and application to weather analysis, using quasi-global synoptic maps of troposphere relative humidity 19 p3393 A66-35637

Ionosphere as anisotropic dissipative medium where charged particles random thermal motion acts as thermal radiation source, noting relation between driven AC conduction current density and applied AC electric field intensity 19 p3352 A66-36630

Random Elsasser band model to compute atmospheric transmission of Earth and Mars for 2-micron carbon dioxide bands 20 p3655 A66-38024

Atmospheric thermal radiation in clouds and rainfall causing antenna radio noise, considering long waves due to heterodyning of molecular radiations 20 p3520 A66-38143

Numerical evaluation of intensity of radiation scattered outward from turbid atmosphere 20 p3593 A66-38190

Solar terrestrial physics - Symposium, Japan, December 1965 20 p3634 A66-38211

Transfer equation for radiation escape from semiinfinite atmosphere with nonconservative scattering 21 p3808 A66-38639

Vacuum UV radiation in equilibrium air measured by photoelectric gauge 21 p3835 A66-38732

Total solar radiation intensity

measurements by pyranometric and heliographic methods, noting relation to sunshine duration 21 p3733 A66-39101

Spectral and vertical distribution of atmospheric IR radiation flux divergence for five model atmospheres, noting dependence on sighting angle 22 p3912 A66-40329

Statistical correlation of IR cooling measurements by Tiros II /Channel 2 and Channel 4/ and radiometersonde 22 p3944 A66-40431

Low level amplifier for IR receiver for Earth-space IR contrast study 24 p4180 A66-42341

Vertical profile of atmospheric radiative balance from balloon-borne actinometry at 25 to 32 km 24 p4201 A66-42652

Energy spectra of muonic and electronic neutrinos in atmosphere 24 p4270 A66-42930

Decay of small temperature perturbations by thermal radiation in atmosphere, noting gray and line absorption, relaxation time constants and numerical computations 24 p4203 A66-42986

## ATMOSPHERIC REFRACTION

### SA LIGHT TRANSMISSION

Aerial observation of rare halo formation consisting of small ring, large ring, secondary sun of small ring, horizontal ring and extraordinary secondary sun 02 p0220 A66-11263

Simultaneous lower atmosphere observations with radar and aerological measurements by airborne meteorograph and electrometeorograph 02 p0253 A66-11273

Vertical profile of refractive index in lower atmospheric layer measured by modified A-22-IV radio probe on captive balloon 02 p0253 A66-11274

Diurnal and seasonal variations in refractive index of atmosphere near Earth surface based on meteorological station data in Transbaikalian region 02 p0253 A66-11275

Polar interferometric method for measuring north-south component of ultrashort wave refraction in ionosphere and optical thickness gradient 02 p0190 A66-11415

Astronomical and parallax refraction determined for satellites, elevated targets and meteors inside and outside atmosphere 03 p0429 A66-13199

Manned space flight observations include confirmation of normal airglow, Glenn effect and photographs of land and ocean areas that can be compared with lunar and planetary photographs for geologic interpretation 05 p0629 A66-15755

Orientation of satellite-borne dipole emitter and influence on ground-based recording of Faraday effect 07 p1028 A66-17455

Frequency-dependent ionospheric refraction effects on Doppler shift of satellite signals 08 p1181 A66-18714

Brightness calculation of aureole visible in daytime at Earth edge from spacecraft 08 p1217 A66-19302

Optical turbulence simulation with small transparent solid bodies immersed in index-matching liquids 08 p1186 A66-19702

Photoelectric focus and seeing monitor for solar telescopes, noting atmospheric blurring 09 p1382 A66-20513

Sunspot phenomena and observation as affected by image perturbation caused by atmospheric inhomogeneities 11 p1770 A66-22647

Refraction angle of radio waves in troposphere and stratosphere, using refractive index of air 11 p1658 A66-23220

Electronic trispheration, three-dimensional analog of triangulation, for long distance geodetic surveys 12 p1875 A66-24936

Mass calculation for absorbing gases such as water vapor, carbon dioxide and ozone along oblique paths between two arbitrary points in atmosphere, considering vertical distribution, refraction and Earth curvature 14 p2284 A66-27541

Atmospheric refraction data acquisition using radiating source, receiver/transmitter and receiver/recorder 14 p2285 A66-27842

Atmospheric refraction dependence on wavelength solved numerically 15 p2483 A66-28644

Atmospheric refractive index variation

measured by microwave refractometer 16 p2693 A66-30337

Height distributions of atmospheric refractive index variations over Japan 16 p2653 A66-30798

Conical refraction of magnetosonic waves occurring when Alfvén waves propagate at speed of sound in conducting fluid in presence of constant uniform magnetic field 16 p2764 A66-31364

Variational method calculation of refraction angle in inhomogeneous laminar medium, using approximate integration of series of exponential functional of electron concentration 17 p2873 A66-32241

Brightness calculation of aureole visible in daytime at Earth edge from spacecraft 19 p3348 A66-36039

Tropospheric and ionospheric refraction, aspect sensitivity and height of radio aurora, backscatter radar aurora observation and geomagnetic field anomalies 20 p3520 A66-38199

Spectral-transmittance aerosol component for atmospheric haze, taking account of refractive index and polydispersity 21 p3759 A66-38910

Tropospheric duct propagation above sea in experiment and mode theory of Booker and Walkinshaw 22 p3863 A66-39934

Turbulent refractivity spectrum and optimization of airborne radar CAT detectors 22 p3944 A66-40429

Mass calculation for absorbing gases such as water vapor, carbon dioxide and ozone along oblique paths between two arbitrary points in atmosphere, considering vertical distribution, refraction and Earth curvature 24 p4198 A66-42326

Refraction due to acoustic focusing of sound waves in lower troposphere, noting effect of wind profile 24 p4203 A66-43108

## ATMOSPHERIC SCATTERING

### SA LIGHT SCATTERING

### SA WAVE SCATTERING

Time variation in radiance of contaminant glow clouds released in upper atmosphere, noting solar radiation scattering 02 p0221 A66-11474

Radiation transport in optically thick medium where natural wings of lines are important and 1304 OI triplet in upper atmosphere 02 p0282 A66-11501

Angular volume-scattering functions measured as function of scattering angle for natural fogs in atmosphere, using coherent and incoherent radiation 02 p0262 A66-12211

Ground-based absolute measurements of energy in solar spectrum using relative aureole criterion of atmospheric scattering 03 p0422 A66-12912

Upper atmospheric observation using normal-pulse ruby laser techniques, presenting height distribution curves of scattered light 04 p0528 A66-13376

Isotropic scattering of radiation from point source in finite atmosphere bounded by totally absorbing spherical shell, deriving iterative series solution 04 p0548 A66-13828

Light intensity in homogeneous turbid medium for unresolved absorption bands calculated from distribution of photon optical paths in absence of absorption, considering atmospheric scattering 04 p0542 A66-14302

Upper atmospheric research using spectroscopic study of absorption bands and night-sky radiation, celestial bodies as UV and X-ray sources and atmospheric light scattering 06 p0876 A66-16310

Diffusive reflection of light from and passage through optically thick atmosphere with nonspherical indicatrix 07 p1080 A66-17921

Measurement of light scattering matrix in lower atmosphere, discussing apparatus and results 08 p1247 A66-19303

Model of Mars atmosphere and surface close to terrestrial conditions, with scattering atmospheric spectrum and surface covered with limonitic dust 08 p1295 A66-19329

Optical parameters of Mars atmosphere and surface from photometric data for spherical and elongated scattering indicatrices 08 p1295 A66-19337

Power loss of optical-heterodyne system with angle tracking in signal propagation



through turbulent medium 08 p1185 A66-19701

Average transfer function from statistics of wave-front distortions in light propagating through atmosphere 08 p1256 A66-19705

Visible and IR radiation observations made above atmosphere 10 p1603 A66-21107

Radiative transfer and imperfect scattering in planetary atmospheres from Chapman approach 11 p1776 A66-23414

Diffusive reflection of light from and passage through optically thick atmosphere with nonspherical indicatrix 12 p1913 A66-23882

Ruby laser optical radar detection of upper atmospheric backscattering 12 p1818 A66-24395

Wavelength dependence of angel echoes, using radar backscatter from clear atmosphere 12 p1825 A66-24890

Nonuniqueness of solutions of nonlinear integral equation for Chandrasekhar S-function for homogeneous semiinfinite atmosphere 13 p2127 A66-25612

Solar near-IR scattering by sunlit terrestrial clouds as affected by cloud type, altitude and scattering angle 13 p2073 A66-25989

Laser radiation coherence property deterioration and molecular scattering during propagation through turbulent atmosphere 14 p2236 A66-27131

Ground-based absolute measurements of energy in solar spectrum using relative aureole criterion of atmospheric scattering 14 p2376 A66-27261

Measurement apparatus and procedure for aureole scattering function in lowest layer of atmosphere 14 p2325 A66-27536

Electrostatic interaction effect on EM wave scattering by atmospheric aerosol particles 14 p2284 A66-27539

Angular divergence effect of light beam on illuminance of turbid scattering medium 14 p2326 A66-27542

Concepts, symbols, units and nomenclature for transmission of radiant flux through Earth /variable density/ atmosphere 14 p2335 A66-27776

Light intensity in homogeneous turbid medium for unresolved absorption bands calculated from distribution of photon optical paths in absence of absorption, considering atmospheric scattering 14 p2327 A66-28216

Solar UV reflection and scattering from Earth atmosphere, use in determining total concentration and vertical distribution of ozone 15 p2486 A66-29090

Kaon decay contribution to sea level muon flux at large zenith angles, using Ashton and Wolfendale procedure 15 p2588 A66-29579

Rocketborne spectrograph measurement of UV reflectivity of Venus and Jupiter, noting atmospheric Rayleigh scattering effects 15 p2603 A66-29963

Atmospheric refractive index variation measured by microwave refractometer 16 p2693 A66-30337

Monograph on intensity distribution and polarization of scattered radiation in ozone absorption bands at selected levels of terrestrial Rayleigh atmosphere 16 p2698 A66-31226

Ground reflection effect on polarization of radiation scattered from top of Rayleigh atmosphere, using Fresnel and Lambert models [AIAA PAPER 66-514] 16 p2699 A66-31498

Lidar detection of backscatter from upper atmosphere 17 p2875 A66-32929

Upper atmospheric light scattering of vertically fired ruby-laser pulse 17 p2922 A66-33348

Absorption lines and bands in scattering and absorbing medium elucidated by study of distribution of photon optical paths in scattering atmosphere 18 p3230 A66-34148

Diffuse reflection by planetary inhomogeneous atmosphere with albedo for single scattering decreases exponentially with optical depth 18 p3230 A66-34149

High resolution spectrophotometric system for measuring atmospheric transmittance spectra 18 p3130 A66-34610

Measurement of light scattering matrix in

lower atmosphere, discussing apparatus and results 19 p3393 A66-36040

Book on atmospheric optics of twilight phenomena 19 p3394 A66-36732

Numerical evaluation of intensity of radiation scattered outward from turbid atmosphere 20 p3593 A66-38190

Loss rates of trapped electrons by atmospheric collisions 20 p3640 A66-38321

Transfer equation for radiation escape from semiinfinite atmosphere with nonconservative scattering 21 p3808 A66-38639

Iterative solution of equations for diffuse reflection and transmission in finite plane-parallel atmosphere with arbitrary stratification 21 p3734 A66-39220

Solar radiation passage through Earth atmosphere in triplet lines O I, considering molecular hydrogen absorption and brightness distribution of radiation 22 p3973 A66-40472

Daytime sky brightness relationship to atmospheric anisotropic light scattering 22 p3917 A66-40960

Monograph on absorption, scattering and attenuation of light and IR radiation in atmosphere 23 p4087 A66-41272

Multiple air scattering in mesosphere as function of zenith distance of Sun and brightness of twilight sky 23 p4087 A66-41803

Complete Rayleigh scattered field within homogeneous plane parallel atmosphere, noting scalar transfer equation extension 23 p4065 A66-41813

Measurement apparatus and procedure for aureole scattering function in lowest layer of atmosphere 24 p4233 A66-42322

Electrostatic interaction effect on EM wave scattering by atmospheric aerosol particles 24 p4198 A66-42325

Velocity characteristics of clear-air dot angel echoes determined via Doppler radar measurements 24 p4234 A66-42990

**ATMOSPHERIC STRATIFICATION**

Geostrophic coefficient of friction dependence on stratification from wind profile measurements at lower atmospheric layer 06 p0906 A66-16555

Richardson critical number and asymptotic equation applied to stably stratified ground atmospheric layer 07 p1062 A66-17924

Earth atmosphere layers described according to thermal structure 09 p1371 A66-20269

Internal gravity wave propagation in thermally stratified atmosphere 11 p1697 A66-22567

Richardson critical number and asymptotic equation applied to stably stratified ground atmospheric layer 12 p1905 A66-23885

Extraterrestrial dust as possible cause of background ionization and stratification in sporadic E layer 14 p2282 A66-26855

Geostrophic coefficient of friction dependence on stratification from wind profile measurements at lower atmospheric layer 14 p2328 A66-28227

Thermal stratification and thermostability effects on turbulent diffusion approximated by Swinbank exponential wind profile 15 p2530 A66-28603

Numerical analysis of wind velocity profile measurements and theoretical calculation of profile by numerical methods, based on geostrophic friction coefficient 16 p2741 A66-30771

Vertical wind shear effect on development and structure of convection, noting perturbation growth rate and unstable stratification 16 p2742 A66-31110

Nonstationary models of cumuli and thermals in stratified atmosphere 18 p3130 A66-34606

Annual frequency of noctilucent clouds linked to low temperatures in mesopause region 19 p3345 A66-35396

Physical structure of upper atmosphere given by pressure and density scale heights and mean molecular mass due to diffusion 19 p3349 A66-36348

Atmospheric stratification effect on radiative thermal flux, including diagrams for flux estimate from temperature gradient 20 p3594 A66-38372

Stepped structure of sunrise fall observed at various frequency bands of atmospheric activity suggest it is due to wave

propagation between Earth and E and D layers 21 p3706 A66-39374

Radio wave diffraction in stratified troposphere solved for case of exponential refractivity profile 22 p3863 A66-39935

Relation between diurnal, seasonal and cyclic variations of stratifications in E layer and fine structure of sporadic E layer and E-2 layer 22 p3914 A66-40761

Wind and temperature profiles for constant flux atmospheric boundary layer in lapse stratification implying relation between eddy transfer coefficient ratio and stability parameter 24 p4202 A66-42982

**ATMOSPHERIC TEMPERATURE**

**SA IONOSPHERIC TEMPERATURE**

**SA ISOTHERM**

Planetary temperature including oceans and atmosphere related to types of organic life, gravity, specific heat and thickness of atmosphere 01 p0136 A66-10301

Temperature and wind velocity fields of stationary atmospheric boundary layer derived from semiempirical turbulence theory 01 p0062 A66-10859

Magnetic storm accompanied by Forbush decreases taking into account atmospheric temperature, noting cyclonic storm origin 02 p0282 A66-11388

Kinetic temperatures derived from Doppler width of airglow 5577 angstroms /OI/ line measured with Fabry-Perot interferometer 02 p0221 A66-11503

Phases of lower stratospheric circulation and temperature variation 02 p0221 A66-11571

Stratospheric monthly temperature variation at latitude 15 degrees N between 25 to 55 km in phase angles and amplitude 02 p0223 A66-11959

Air currents and temperature distribution in stratosphere and mesosphere in Northern Hemisphere from rocket observation 04 p0513 A66-13438

Harmonic analysis of solar diurnal and semidiurnal variations of wind, pressure and temperature in stratosphere, comparing observed and wind-derived heights and temperature 04 p0515 A66-13672

Dependence of vertical structure parameters of atmospheric temperature and humidity fields on atmospheric long-wave radiation field, noting transport equation 04 p0542 A66-14303

Ionospheric F region electron density and electron and ion temperatures measured by ground-based radar backscatter 05 p0670 A66-14950

Photometric measurements of twilight brightness for upper atmospheric temperature determination 05 p0674 A66-15528

Atmospheric temperature of route of SST and influence on navigation, fuel management and operating economics 07 p0988 A66-17694

Atmospheric diurnal variation investigated, using temperature controlled high-counting neutron and meson monitors 07 p1126 A66-18008

Correction of cosmic ray meson intensity monitor counting rates for atmospheric temperature variation 07 p1127 A66-18012

Temperature changes in entire atmosphere and effect on diurnal variation of meson component of cosmic rays 07 p1129 A66-18025

Dynamical properties of solar wind and solar corona atmosphere with extended temperature bound strongly by gravity 07 p1132 A66-18263

Variations in vertical temperature and humidity profiles used to determine underlying terrestrial surface temperature from outgoing radiation 09 p1398 A66-19888

Relation between ascending fluxes of Earth and troposphere long-wave IR radiation and temperature of mean energy level 09 p1398 A66-19889

Effect of atmospheric temperature changes on diurnal variation of meson component, using temperature coefficient and crossed telescopes methods 09 p1439 A66-20219

Earth atmosphere physical properties including temperature, density, pressure and water vapor 09 p1398 A66-20270

Upper atmosphere temperature and pressure measured with manometers mounted on rockets, using method of



successive approximations 09 p1375 A66-20988  
 Aerodynamics of manometers and mass spectrometers used on rockets and satellites for determination of atmospheric temperature and density 09 p1383 A66-20993  
 Fields of outgoing radiation in 8-12 micron region, calculating surface temperature and effective water vapor content 11 p1698 A66-22943  
 Atmospheric conditions during total eclipse of February 15, 1961 in France, particularly temperature curves 12 p1868 A66-23533  
 Mars upper atmosphere thermal structure from spectroscopic measurements and Mariner IV occultation experiment 12 p1947 A66-23660  
 High temperature anomaly in stratosphere over Australia during 1963-64 12 p1871 A66-24464  
 Monthly temperature variations in tropical stratosphere and mesosphere between 25 and 80 km [AIAA PAPER 66-344] 12 p1872 A66-24474  
 Flight data used to determine relationship between atmospheric temperature changes and clear air turbulence occurrence at jet altitudes [AIAA PAPER 66-365] 12 p1906 A66-24477  
 Two-channel satellite-borne radiometric system to furnish temperature information for SST flight planning, discussing conceptual design, operating mode and data handling procedures [AIAA PAPER 66-372] 12 p1872 A66-24500  
 Heat transfer equations for rocketborne stratospheric temperature sensor in form of spherical bead thermistor and experimental analysis of physical, thermodynamic and electrical characteristics of rocketsonde [AIAA PAPER 66-385] 12 p1882 A66-24508  
 Laboratory studies of heat balance in rocketsonde thermistors for measurement of upper air temperature, noting dissipation constant and solar radiation effect [AIAA PAPER 66-386] 12 p1883 A66-24509  
 High altitude mesospheric temperature measurements, discussing air-to-sensor heat transfer mechanism, bead thermistor and descent rate [AIAA PAPER 66-388] 12 p1908 A66-24510  
 Atmospheric vertical temperature profile determined from outgoing radiation spectrum, evaluating error probability and accuracy 12 p1874 A66-24869  
 Structural constant of temperature fluctuations in atmosphere determined by methods involving turbulent energy dissipation velocity and velocity distribution probability 12 p1875 A66-24871  
 Atmospheric noise temperature spectra observed from satellite at wavelength near rotational lines of water vapor molecule 13 p2075 A66-26742  
 Breakdown of biennial oscillation of ozone and of lower stratospheric temperature of Southern Hemisphere and relation to sunspot cycle observations 14 p2286 A66-27904  
 Dependence of vertical structure parameters of atmospheric temperature and humidity fields on atmospheric long-wave radiation field, noting transport equation 14 p2327 A66-28217  
 Nonoptimum flight conditions effects on SST fuel performance, noting sonic boom and atmospheric temperature variations 14 p2224 A66-28230  
 SST air traffic control and fuel consumption dependence on wind drift and atmospheric temperature 14 p2328 A66-28231  
 Low atmospheric temperature and humidity changes beneath subsidence inversion above Southern England 15 p2530 A66-28599  
 Exospheric temperature, scale heights and mean molecular weight up to 3500 km derived from satellite accelerations in 1964 15 p2484 A66-28819  
 Clear air turbulence detection and warning by airborne devices including radar, IR spectrum, air temperature probes, ozone detection, etc 15 p2500 A66-28917  
 Atmospheric temperature changes as factor in detection of clear air turbulence, especially above 25,000 ft, noting aircraft instrumentation used 15 p2532 A66-28918  
 Clear air turbulence detection by measuring associated air temperature

gradient by airborne IR radiometer 15 p2500 A66-28927  
 Vertical atmospheric temperature and wind distribution in optimal parametric representations 15 p2489 A66-29775  
 Seasonal-latitude variations in lower thermospheric density, temperature and composition 15 p2490 A66-29820  
 Diurnal and semidiurnal oscillations in atmospheric density, temperature, pressure and wind in subtropical Southern Hemisphere 15 p2491 A66-29964  
 Mass spectrometric measurements of upper atmosphere temperature 15 p2495 A66-30062  
 Air-temperature and wind profiles in atmospheric boundary layer and dependence upon stability criteria of ground layer 16 p2741 A66-30772  
 Speculative mean monthly Arctic stratospheric temperatures estimated from radiosonde and meteorological rocket wind and temperature data 16 p2696 A66-30928  
 Atmospheric heat and moisture transfer during developing cloud conditions 16 p2742 A66-31342  
 Upper atmospheric temperature measurement from Doppler line widths of atomic oxygen auroral and nightglow emission, using Michelson interferometer 17 p2919 A66-32993  
 Objective analysis of wind and temperature distribution in vertical cross section through atmosphere derived from radiosonde and rawinsonde data 17 p2949 A66-33336  
 Upper air sounding analysis using electronic computer 17 p2921 A66-33340  
 Ambient temperature measurements from radiosondes flown on constant-level balloons 17 p2949 A66-33342  
 Atmospheric contribution to diurnal variation of cosmic ray meson intensity at Deep River, Canada 17 p2994 A66-33429  
 Temporal variations in temperature and drift velocity in ionosphere determined from nighttime variations of F-region electron density profiles at Puerto Rico 18 p3107 A66-34522  
 Numerical solution of integral form of radiative transfer equation from measurements in finite set of spectral intervals for deducing atmospheric temperature profiles, using satellites 18 p3129 A66-34554  
 Difficulties and instabilities accompanying inversion of radiance data to infer temperature structure related to interdependence existing among nominally independent measurements 18 p3130 A66-34555  
 Atmospheric temperature profile determination by satellite-borne IR spectrometer, noting instrument design 18 p3113 A66-34556  
 Optimum averaging periods in measurements of wind velocity profile, temperature gradient, vertical thermal turbulent flow and atmospheric drag 18 p3130 A66-34609  
 Radiant equilibrium temperature of opaque absorbing body relation to radiative temperature variations of air 18 p3265 A66-34611  
 Cosmic ray intensities in stratosphere over Antarctica and Murmansk, noting differences not due to low energy primary particles or temperature 18 p3196 A66-34869  
 Fields of outgoing radiation in 8-12 micron region, calculating surface temperature and effective water vapor content 20 p3553 A66-37856  
 Substantial pulse type stratospheric temperature fluctuations over Armenia based on diurnal observations 21 p3734 A66-39293  
 Limitations imposed on upper atmospheric sonic thermometry by lowering of density with increasing altitude 21 p3741 A66-39428  
 Clear air turbulence detection and warning by airborne devices including radar, IR spectrum, air temperature probes, ozone detection, etc 22 p3945 A66-40325  
 Atmospheric vertical temperature profile determined from outgoing radiation spectrum, evaluating error probability and accuracy 22 p3912 A66-40330  
 Structural constant of temperature fluctuations in atmosphere determined by methods involving turbulent energy

dissipation velocity and velocity distribution probability 22 p3912 A66-40332  
 British stratospheric and mesospheric temperature measurements compared with valves from available atmospheric models 22 p3913 A66-40519  
 Time dependent behavior of temperature and density in monoconstituent atmosphere under diurnal photoheating and cooling by conduction, analyzing effect of atmosphere rotation eastward 23 p4064 A66-41678  
 Absorption and brightness temperature variations of atmosphere on basis of statistical characteristics of vertical temperature and humidity structures 23 p4087 A66-41802  
 Atmospheric heat and moisture transfer during developing cloud conditions 24 p4234 A66-42650  
 Temperature and humidity variations in weak convection over England, noting measurement techniques and results 24 p4235 A66-43076

## ATMOSPHERIC TIDE

Atmospheric tidal oscillations, Coriolis forces dominate diurnal tide causing small scale depth 05 p0672 A66-15026  
 Spherical harmonic analysis of diurnal surface pressure oscillation indicates that it can be represented by wave traveling westward with Sun 07 p1027 A66-17224  
 Possible effects of oceans on atmospheric lunar tide 07 p1061 A66-17363  
 Vertical distribution of heights of lower boundary of polar auroras, examining dependence on intensity and lunar hour angle 08 p1220 A66-19782  
 Upper atmospheric diurnal tide determined via sodium vapor trail measurements 11 p1701 A66-23146  
 Prevailing and tidal wind shears in sporadic E region determined from 29 sodium vapor trails 14 p2280 A66-26840  
 Annual variations in atmospheric lunar tides attributed primarily to vertical shear of zonal wind systems 16 p2698 A66-31112  
 Vertical and horizontal structure of negative eigenvalue modes of diurnal atmospheric oscillation 18 p3107 A66-34524  
 Tidal dissipation function in solar system, examining cases having appreciable evolution since origin of planets and satellites 20 p3655 A66-38023  
 Dynamical effects of liquid nucleus of Earth in diurnal terrestrial tides 20 p3553 A66-38068  
 Vertical distribution of heights of lower boundary of polar auroras, examining dependence on intensity and lunar hour angle 21 p3732 A66-38778  
 Diurnal heating of ozonosphere near stratopause level results in diurnal temperature variation of 15 degrees C and development of tidal circulation in stratospheric wind field 22 p3916 A66-40874  
 Tidal circulation system induced by stratospheric wind field perturbations via diurnal ozonospheric heating 24 p4203 A66-42985

## ATMOSPHERIC TURBULENCE

### SA CLEAR AIR TURBULENCE

Diffusion from elevated point source into turbulent atmosphere flow over horizontal ground 01 p0061 A66-10483  
 Air data equipment trends in subsonic and supersonic control 01 p0033 A66-10680  
 Atmospheric density variations due to turbulence incorporated in analysis of nonsymmetrical tensor of turbulent momentum transfer 02 p0220 A66-11257  
 Karman vortex street pattern of mesoscale eddies in wake of islands [AIAA PAPER 65-16] 02 p0221 A66-11548  
 Parametric fluctuations of spatially restricted light beam in turbulent atmosphere 02 p0191 A66-11838  
 Evaporation as molecular diffusion from large rough surface into random-lived internal scale turbulent eddies 02 p0223 A66-11960  
 Changes in dynamics of aerospace vehicle, flight in low altitude turbulence and satellite spin decay 02 p0178 A66-11990  
 Optical scintillation frequency noting propagation of electromagnetic and acoustic waves in turbulent atmosphere 02 p0262 A66-12207  
 Soviet monograph on continuous



measurement of cosmic ray mu component, covering experimental apparatus, data analysis, atmospheric dynamics, etc 03 p0423 A66-13287

Vibration exposure with varying peak and rms acceleration and frequency in low altitude high-speed flight 03 p0329 A66-13355

Statistical characteristics of fluctuations in radio emission of atmosphere producing turbulent pulsations and displacements of hydrometeorological formations in scan field of radiotelescope, noting distribution function 04 p0517 A66-14046

Wind velocity, vertical wind profile and temperature fluctuations in near-water air layer measured, noting differences from pulsation measurements 04 p0542 A66-14300

Vertical distribution of turbulence and wind velocity characteristics in atmospheric boundary layer, considering temperature stratification in boundary layer 04 p0542 A66-14301

Two-point correlation function expressed in terms of structural function of velocity field 04 p0542 A66-14305

Atmospheric whistler activity, discussing anomaly of low geographic latitude detection and various propagation modes at Rabat, Morocco from 1956 to 1958 05 p0673 A66-15048

Airborne laser-radar light detection and ranging /LIDAR/ systems applied to detection of clear air turbulence /CAT/ 05 p0697 A66-15297

Phase perturbation of optical beams due to atmospheric turbulence, using modulated interferometer to produce Doppler beats between two coherent beams 06 p0909 A66-16434

Measurements of pulsation spectra of vertical component of wind velocity, using acoustic anemometer mounted on aircraft 06 p0906 A66-16552

Atmospheric turbulence, power fluctuation and radar detection in laser systems design 07 p1041 A66-17294

Mesoscale eddies in wake of islands describing properties, characteristic parameters via Karman vortex street pattern, drag theory and empirical observation 07 p1061 A66-17365

Separable nongeostrophic baroclinic stability problem of Eady 07 p1062 A66-17373

Random process theory analysis of equipment performance for measuring time spectra of turbulent fluctuations in lower atmosphere 09 p1398 A66-19886

Spectra of vertical turbulent thermal fluxes and momenta in lower atmospheric layer, including review of relevant literature sources 09 p1398 A66-19893

Accurate calibration of Doppler winds for use in computation of mesoscale wind fields 09 p1399 A66-20728

Tiros IV satellite photographs of various storms, relating equivalent black body temperatures shown on IR analysis to cloud height 09 p1399 A66-20731

Low altitude turbulence model for aircraft gust load estimation related to meteorological parameters, terrain conditions and height [AIAA PAPER 65-14] 09 p1400 A66-20741

System of equations derived for dynamics of convective atmospheric vortices for model with unstable stratification and basic vorticity 10 p1530 A66-21274

Stability of baroclinic circular vortex in incompressible inviscid fluid for axially symmetric disturbances 10 p1530 A66-21275

Winter jet stream structure and turbulence over Australia 10 p1552 A66-21317

Load factor estimation for flights in turbulent conditions by replacing exact transfer function with equivalent statistical model 10 p1482 A66-21385

Phase difference between atmospheric large-scale disturbances and heating due to sea-surface evaporation and turbulent exchange 11 p1694 A66-22199

Monin-Obukhov similarity theory for turbulent structure of thermally stratified surface layer of atmosphere 11 p1725 A66-22266

Four wind profiles analyzed for vertical scale structure and wind shear in mesosphere due to falling sphere 11 p1729 A66-22564

Turbulence-excited atmospheric velocity, critical frequency of atmosphere, solar atmospheric power spectrum of acoustic field velocity correlation, solar convection zone, etc 11 p1772 A66-22777

Severely turbulent airflow at low levels over United Kingdom 11 p1730 A66-23015

Time and height variations of temperature, wind speed and moisture content during dissipation of low level jet on May 14, 1962 before sunrise near Dallas 11 p1730 A66-23379

Directional fluctuations in light waves propagating from edge of solar disk caused by atmospheric turbulence 12 p1913 A66-23775

Light intensity fluctuations along inclined inhomogeneous path with variable turbulence characteristics in lower atmospheric layer 12 p1913 A66-23776

Statistical research on g-loadings and atmospheric turbulence in field of structural strength limits for sporting gliders 12 p1801 A66-23855

Automatic system ensuring landing in absence of visibility and atmospheric turbulence by controlling motion of aircraft leveling out, consisting of time-dependent input signal shaping device and amplifiers 12 p1909 A66-24321

Universal turbulence measuring system giving quantitative measure of turbulent intensity independent of type or speed of aircraft, using all-weather sensor [AIAA PAPER 66-364] 12 p1906 A66-24476

Ballistic wind and density predictions, measuring wind and D-value at 500 mb, calculating missile response to atmospheric effects [AIAA PAPER 66-359] 12 p1906 A66-24478

Wind and turbulence distribution caused by barriers and complex surfaces adjacent to missile launching sites [AIAA PAPER 66-335] 12 p1906 A66-24483

Design of control deflections and structural loads of space vehicle for flight stability through atmospheric disturbances [AIAA PAPER 66-350] 12 p1954 A66-24487

Relationship between atmospheric gust criteria and performance of supersonic inlet and propulsion [AIAA PAPER 66-367] 12 p1801 A66-24495

Unbounded isothermal atmosphere response to time harmonic point disturbances, exact solutions obtained for frequency ranges of acoustic waves, trapped oscillations and gravity 13 p2183 A66-25613

Northward momentum transfer across asymmetric jet in three-dimensional atmosphere analyzed, using initial value problem, noting energy transfer and transformation 13 p2064 A66-26128

Atmospheric radio noise in tropics, noting structural characteristics such as amplitude probability, pulse rate distribution of noise envelope, effects of thunderstorms, etc 14 p2234 A66-27034

Atmospheric turbulence effects on laser beam propagation, noting beam cross section, phase variation, AM and FM, etc 14 p2235 A66-27035

Laser radiation coherence property deterioration and molecular scattering during propagation through turbulent atmosphere 14 p2236 A66-27131

Hypersonic wake studies in ballistic missile research program, discussing reentry of hypervelocity vehicles, laminar flow, atmospheric turbulence, etc 14 p2218 A66-27402

Disturbance propagation in baroclinic atmosphere in presence of radiation and turbulent heat conduction 14 p2325 A66-27535

Effective early warning system to enable pilot to cope with clear air turbulence /CAT/ 14 p2326 A66-27819

Vertical distribution of turbulence and wind velocity characteristics in atmospheric boundary layer, considering temperature stratification in boundary layer 14 p2327 A66-28215

Two-point correlation function expressed in terms of structural function of velocity field 14 p2327 A66-28218

Measurements of pulsation spectra of vertical component of wind velocity, using acoustic anemometer mounted on aircraft 14 p2327 A66-28224

Head-on collision between two pressure jumps in two-layer atmospheric 14 p2289 A66-28335

Quantitative assessment of deterioration that light beam undergoes on passing through turbulent atmosphere 15 p2448 A66-28579

Plane wave propagation statistics in turbulent atmosphere 15 p2448 A66-28582

Economic effects of turbulence on airline operations, considering costs on temporary grounding for repairs, passenger injuries, information dissemination on turbulence, etc 15 p2618 A66-28916

Errors in wind speed measurements under conditions of turbulence, noting quantitative aspects of lateral, vertical and data processing errors 15 p2533 A66-28940

Lower thermospheric turbulence investigated for scale size, turbulent velocity spectra and energy dissipation rate 15 p2491 A66-29954

Rocket observation of upper atmospheric winds, noting wind shear, velocity, pressure, wind vector rotation, etc 15 p2492 A66-30027

Experimental data analysis of turbulence of atmospheric boundary layer 16 p2696 A66-30770

Large and small-scale atmospheric eddy velocities and scale lengths estimated, noting eddy Reynolds number ascertained from dispersion of chemical contaminants 16 p2696 A66-30927

Wing penetration into zone of sharply localized gust, deriving equations for forces and moments acting on wing 16 p2630 A66-31292

Wind tunnel, simulator and flight test results to evaluate cockpit accelerations, handling qualities and stability and control of jet transports in severe turbulence [AIAA PAPER 65-330] 16 p2634 A66-31317

Pulsation spectrum of vertical wind-velocity component at 70 m 16 p2742 A66-31343

Prediction and avoidance of atmospheric turbulence affecting large aircraft 17 p2842 A66-31989

Statistical characteristics of fluctuations in radio emission of atmosphere producing turbulent pulsations and displacements of hydrometeorological formations in scan field of radiotelescope, noting distribution function 17 p2917 A66-32212

Data processing techniques for analyzing turbulence records and for estimating response of aircraft to atmospheric turbulence 17 p2843 A66-32329

Fluctuations in mean refractive index over long path through turbulent atmosphere examined, using Michelson interferometer with He-Ne laser source 17 p2948 A66-32618

Optimal gain settings for atmospheric turbulence in 407 Jimsphere wind profiles [AIAA PAPER 66-484] 17 p2902 A66-32770

Aircraft bumpiness conditions in free atmosphere relation to turbulence and other aerological data 18 p3049 A66-34613

Nature of middle-latitude ionospheric perturbations 19 p3344 A66-35262

Semiempirical law for spectrum of wind velocity fluctuations and energy in lower layer of atmosphere 19 p3393 A66-35332

Turbulence coefficient and mean altitude of atmospheric boundary layer determined from diurnal temperature variations and wind profile 19 p3348 A66-35939

Coherent laser light use in atmospheric communications system, discussing effect of atmospheric turbulence and small vibrations on coherent detection efficiency and SNR 20 p3511 A66-36930

Pilot protection from aircraft vibration caused by atmospheric turbulence 20 p3508 A66-36997

Atmospheric turbulence determined from velocity fluctuations in flight path direction measured by wing-tip mounted hot-wire anemometer 20 p5593 A66-37470

Energy balance equation obtained from turbulent winds from chemical release studies and turbulent diffusion analysis of globe expansion 20 p3554 A66-38205

Wind velocity profile for nonstationary atmospheric boundary layer, noting effect of time-dependent variations on turbulence and pressure gradient coefficient 20 p3594 A66-38368



- Atmospheric turbulence coefficient  
determination from flow fluctuations,  
measuring error as function of observation  
uration 20 p3594 A66-38379
- Jet flow turbulence characteristics,  
calculating vertical wind velocity pulsation  
component, determining thermodynamic  
characteristics of 20 p3595 A66-38381
- Internal turbulence scale for convection  
ets determined, using measurements of  
ight intensity 21 p3760 A66-39357
- uctuations 21 p3760 A66-39357
- Doppler radar measurements of wind  
elocity horizontal components variation in  
ain and snow, calculating time correlation  
nd structural functions for neutral and  
nstable stratifications 21 p3760 A66-39358
- Clear air turbulence near jet stream,  
discussing velocity profiles and various  
eteorological parameters 22 p3902 A66-39677
- High altitude turbulence in presence of  
trong jet stream or under influence of  
rographic systems 22 p3942 A66-39730
- Multichannel computer controlled Mobile  
Micrometeorological Observation System,  
automatic data acquisition, processing and  
ecording system for observational analyses  
of turbulence of atmospheric boundary  
ayer 22 p3943 A66-40427
- Dependence of complex optical transfer  
unction of image forming system on  
horizontal range through turbulent  
tmosphere 22 p3949 A66-40890
- Atmospheric turbulence effect on laser  
eam intensity 23 p4035 A66-41030
- istribution 23 p4035 A66-41030
- Atmospheric turbulence effect on  
requency spectra of light intensity  
uctuations examined, using He-Ne  
aser 23 p4035 A66-41031
- Atmospheric turbulence statistical  
characteristics dependence on stratification  
nd elevation from heat flux and wind  
riction stress 23 p4087 A66-41800
- Characteristics 23 p4087 A66-41800
- Spectral characteristics of turbulence in  
presence of mean velocity and temperature  
adients 23 p4087 A66-41801
- Vertical wind gradient variation and energy  
variation at height ranging from 80 to 140  
m and relation to gravity waves and upper  
tmosphere turbulence 23 p4066 A66-41849
- ust design procedures based on power  
pectral techniques, considering atmospheric  
urbulence with aircraft as rigid body with  
ngle degree of freedom 23 p4017 A66-42367
- ICAS PAPER 66-11] 23 p4017 A66-42073
- Disturbance propagation in baroclinic  
tmosphere in presence of radiation and  
urbulent heat conduction 24 p4233 A66-42321
- Tropospheric propagation using laser as  
ransmitter, analyzing effects of Benard  
ells, turbulence, wind shear,  
etc 24 p4171 A66-42367
- Pulsation spectrum of vertical wind-  
elocity component at 70 24 p4234 A66-42651
- n 24 p4234 A66-42651
- Spectral density measurement for  
atmospheric turbulence by method based on  
nversion of Rice 24 p4195 A66-42855
- Formulas 24 p4195 A66-42855
- Stability of two-dimensional boundary layer  
low in rotating tank with small inflow  
analyzed, using perturbation 24 p4197 A66-42981
- heory 24 p4197 A66-42981
- Air motion probe via Doppler radar, noting  
alculation of speed, direction and  
pplication to wind variance 24 p4234 A66-42989
- analysis 24 p4234 A66-42989
- ATMOSPHERICS
- SA STATIC ELECTRICITY
- SA SUDDEN ENHANCEMENT OF  
ATMOSPHERICS /SEA/
- SA WHISTLER
- Thermal noise radiation in microwave  
egion from lower 04 p0474 A66-13379
- tmosphere 04 p0474 A66-13379
- Atmospheric radio noise bursts arising  
rom radiation fields of electrical discharge  
n LF band at Bangalore, 04 p0475 A66-13428
- ndia 04 p0475 A66-13428
- Prediction curves showing expected  
median and upper and lower decile levels of  
tmospheric radio noise power in tropics for  
requencies from 10 kc to 30 04 p0488 A66-14376
- nc 04 p0488 A66-14376
- Confirmation of systematic and random  
variations of noise parameters in tropics by  
4-year period of measurement of  
atmospheric radio noise 04 p0488 A66-14377
- Noise from terrestrial lightning discharges  
as source of interference to satellite radio  
reception 05 p0633 A66-14955
- Aerospace studies in Argentina during 1964  
using rockets and balloons and including  
winds, E layer, satellite tracking,  
etc 09 p1458 A66-20706
- Detection range of 500-kc/sec sferics  
determined by examination of data taken  
during severe weather events and during  
zero background 09 p1399 A66-20729
- condition 09 p1399 A66-20729
- Integrated field intensity of atmospherics  
analysis compared to continuous wave  
method for data acquisition for radio  
systems design 10 p1496 A66-21073
- Spaceborne observations of radio noise  
from 0.7 to 7.0 mhz and dependence on  
terrestrial environment 10 p1603 A66-21115
- SEA effect at VLF 11 p1651 A66-22373
- Frequency spectra of atmospherics and  
atmospheric radio noise at frequencies of 1  
to 100 kc from day and night observations  
in Pacific Ocean 11 p1652 A66-22418
- Polarization of atmospheric pulses due to  
successive reflections at ionosphere in echo  
type atmospherics 12 p1873 A66-24839
- Amplitude probability distribution of  
atmospheric noise, noting effect of  
bandwidth change 13 p2026 A66-26567
- Flux density, polarization characteristics  
and position measurements for type IV  
bursts in meter and microwave  
range 14 p2378 A66-26933
- Atmospheric noise FSK error probabilities  
for envelope detection 14 p2243 A66-28352
- receiver 14 p2243 A66-28352
- Crossing rate distribution of atmospheric  
noise at various frequencies in LF and MF  
bands, examining relation to amplitude  
probability distributions 16 p2652 A66-30613
- Ionospheric effects over Delhi of Russian  
high altitude nuclear explosions in Central  
Asia and of U.S.A. explosions at Johnston  
Island, autumn 1962 17 p2918 A66-32695
- Lightning discharge radiating sferics near  
Gulf of Mexico and west coast of  
U.S. 17 p2923 A66-33358
- Frequency distribution of atmospherics  
emitted by multiple lightning  
discharges 20 p3553 A66-38075
- Stepped structure of sunrise fall observed  
at various frequency bands of atmospherics  
activity suggest it is due to wave  
propagation between Earth and E and D  
layers 21 p3706 A66-39374
- Diurnal cyclic intensity variations of  
atmospheric radio noise at stations widely  
spaced over globe 22 p3915 A66-40782
- Automatic radio atmospherics recorder for  
simultaneous observation of waveform and  
energy spectrum 23 p4069 A66-41663
- ATOM
- S HELIUM ATOM
- S HYDROGEN ATOM
- S INTERSTITIAL ATOM
- S METASTABLE ATOM
- S NITROGEN ATOM
- S OXYGEN ATOM
- S RECOIL ATOM
- ATOM CONCENTRATION
- Spatial distribution and temporal decay of  
electron and atom concentrations in pulsed  
/argon afterglow/ plasma measured with  
laser interferometer 04 p0551 A66-13741
- Normal atom concentration in cesium and  
mercury vapors during pulse  
discharge 15 p2545 A66-29343
- Free sodium atom distribution in upper  
atmosphere related to diurnal and nocturnal  
variation 15 p2491 A66-30018
- Diurnal variation of hydrogen atom  
concentration at base of exosphere,  
including effects of lateral flow of gas  
around Earth 17 p2919 A66-32996
- Atomic concentration measurement in  
discharged nitrogen, oxygen and  
hydrogen 18 p3139 A66-34507
- Equilibrium deviation occurring in plasma  
with variable kinetic temperature due to  
radiation transport within plasma volume  
and outflow beyond limits of  
volume 20 p3606 A66-36973
- Normal atom concentration in cesium and
- mercury vapors during pulse  
discharge 20 p3604 A66-37348
- Electron and neutral atom densities in  
helium and argon afterglow plasma obtained  
by two helium-neon laser interferometers,  
noting temporal dependence of electron  
decay 23 p4101 A66-41364
- ATOMIC BATTERY
- Out-of-pile thermionic power system using  
inert gas for heat transfer from reactor to  
converter, noting creep-rupture problem of  
materials 23 p4023 A66-41767
- ATOMIC BEAM
- Atomic beam lasers, particularly for  
population inversion in levels of optical  
transition 01 p0082 A66-10448
- Atomic beam lasers, particularly for  
population inversion in levels of optical  
transition 03 p0380 A66-13311
- Neutral atomic beam used to measure total  
ionization cross section of argon atoms  
incident on low density argon  
gas 07 p1083 A66-18421
- Beam source producing atomic and  
molecular hydrogen by molecular  
dissociation at high  
temperatures 07 p1084 A66-18492
- Hot plasma probed with atomic beam in  
presence of intense self-radiation flux and  
magnetic field impulse  
scattering 10 p1571 A66-22011
- History and development of atomic  
frequency standard, discussing newest  
atomic oscillators 12 p1880 A66-24122
- Atomic frequency standard fluctuation,  
instability due to noise and atomic beam  
frequency stability 12 p1881 A66-24125
- Atomic-beam technique for studying Stark  
effect in optical D-line transition in cesium  
and rubidium 19 p3402 A66-35993
- Hot plasma probed with atomic beam in  
presence of intense self-radiation flux and  
magnetic field impulse  
scattering 19 p3407 A66-36095
- High frequency-stability EM wave source,  
applying thermal excitation methods to  
pencil quantum generator in IR  
region 21 p3749 A66-39336
- High frequency-stability EM wave source,  
applying thermal excitation methods to  
pencil quantum generator in IR  
region 22 p3929 A66-39706
- ATOMIC CLOCK
- Time measurement as applied to aerial  
navigation noting atomic clocks, time  
transmission by ionospheric propagation of  
electromagnetic radiation,  
etc 02 p0257 A66-12031
- Fluctuations since 1956 in period of Earth  
rotation obtained in universal atomic time  
with photographic zenith tube at Neuchatel  
Observatory 07 p1135 A66-17633
- Flying clock experiment with traveling  
cesium beam clocks 11 p1703 A66-22251
- High stability clocks for trajectory  
measurement with oscillator, using atomic or  
molecular transitions 11 p1708 A66-23198
- [ONERA TP 311] 11 p1708 A66-23198
- Frequency fluctuations in frequency  
standards, analyzing noise and finite  
observation time effects and atomic  
standard characteristics, using  
servocontrolled oscillator 12 p1881 A66-24123
- Quartz crystal oscillators and effect on  
precise time measurements by atomic  
clocks 12 p1881 A66-24129
- Statistical analysis of noise quality of  
atomic frequency standards including  
masers 12 p1881 A66-24130
- Joint experiment of U.S. Naval Observatory  
and Japan Radio Research Laboratories for  
synchronizing standard time pulses, using  
Relay II satellite 12 p1818 A66-24473
- Cesium beam atomic time and frequency  
standards 13 p2079 A66-25874
- Atomic maser clocks rotation with Earth,  
deriving formula for relative drift at widely  
separated localities arising from local  
gravitational potentials 16 p2745 A66-30187
- Atomic and molecular frequency standards,  
considering use of cesium 17 p2927 A66-33244
- Atomic clocks, frequency standards of  
atomic beam resonators, masers and gas  
cells and application to space  
research 18 p3110 A66-33982
- Atomic time standards, describing cesium  
beam standard, ammonia maser and gas-cell  
type clocks 19 p3354 A66-35468



Ephemeral georotational variations from deviations in quartz oscillator clocks of Paris and Greenwich 19 p3351 A66-36370  
 Iterative method for extracting annual and Chandlerian terms of variation of Earth rotation from experimental data of universal time 20 p3550 A66-37410  
 Relativistic effect of atomic clocks, noting error and magnitude increase with experiment duration 22 p3948 A66-40476  
 Atomic clocks and synchronization for space research 22 p3920 A66-40794

# ATOMIC COLLISION

## SA MOLECULAR COLLISION

Helium afterglow discussing stability of collisional-radiative recombination of ions with electrons and neutral particles 04 p0547 A66-13652  
 Ionization rate behind shock waves in argon, allowing for excitation and ionization by atom-atom collisions 07 p1020 A66-17938  
 Effective excitation cross sections of alkali metal atoms during collision with slow electrons 09 p1406 A66-20940  
 Molecular oxygen dissociation resulting from collisions with neon and argon metastable atoms in auroral afterglow 11 p1696 A66-22419  
 Structure of conducting and insulating liquids as affected by interatomic forces 11 p1693 A66-22979  
 Numerical values describing molecular rainbow scattering in Airy approximation for 12-6 potential 13 p2130 A66-25379  
 Low energy atomic collisions, considering Schrodinger equation for proton interchange 13 p2130 A66-25380  
 Ionizing collisions between alkali metal atoms and gas molecules, with measured cross sections applied to physics of atomic collisions 13 p2131 A66-25966  
 Amplification of interaction of atoms and of pulsed or periodic cooling of transparent media produced by laser beam, noting changes in kinetic energy of atoms 13 p2093 A66-26021  
 Effective excitation cross sections of alkali metal atoms during collision with slow electrons 15 p2543 A66-28529  
 Average diffusion cross section for elastic collisions of electrons with heavy particles, comparing calculated and measured values 15 p2551 A66-29225  
 Interaction of nuclear active particles with atomic nuclei, using ionization chamber at 3260 m above sea level 15 p2584 A66-29558  
 Output power frequency response of single mode helium neon laser, determining effects of atomic collisions on frequency response of individual atoms 15 p2518 A66-29812  
 Cesium ionization cross section measurement from threshold to 50 ev, noting apparatus used and results obtained 15 p2548 A66-29814  
 Atomic scattering from perfect crystal, considering effects of absorption potential, surface vibrational modes momentum and energy exchange etc 16 p2752 A66-30389  
 Interactions occurring when beam of thermal atoms strikes surface 16 p2753 A66-30396  
 Spatial distribution of high energy Ar atoms scattered by various surfaces 16 p2753 A66-30398  
 Interaction between atoms of solid surface and gas phase, obtaining closed-form solution of motion equations 16 p2753 A66-30786  
 Electronic relaxation of shock-heated nonequilibrium argon plasma flow in microscopic-macroscopic treatment [AIAA PAPER 66-476] 16 p2765 A66-31475  
 Collision cross sections and energy scattering of atoms with slow electrons 18 p3137 A66-34024  
 Born cross sections for double-transition collisions of hydrogen atoms 18 p3138 A66-34150  
 Energy transfer in low velocity inelastic atomic collisions 19 p3401 A66-35464  
 Transitions induced by electron impact between all ground-state terms of atomic systems with computed cross sections satisfying unitarity 19 p3463 A66-35990  
 Relaxation of optically pumped Rb atoms on paraffin-coated walls, using Franzen

sequence, analyzing physical meaning of optical signal 19 p3374 A66-35992  
 Distorted wave calculation from rotational excitation of molecular hydrogen and molecular deuterium in thermal collisions with atomic hydrogen, presenting angular distributions, cross sections, etc 19 p3403 A66-36329  
 Neutral-impurity scattering and scaled electron-hydrogen-atom collision problem for hydrogenic-type impurities in semiconductor studied by method using highly spin-polarized carriers 19 p3448 A66-36763  
 Recharge cross section in collisions of slow atoms or ions involving interparticle transfer of one electron 20 p3604 A66-36987  
 Bomb debris motion following Star Fish test, noting formation of MHD shock wave, production of stationary plasma through X-ray ionization and collision in neutral air 20 p3644 A66-38345  
 Classical cross section for producing specified energy transfer in collision of two particles in laboratory system applied to atomic collision cross sections 21 p3774 A66-38544  
 Collision integrals, effective cross sections and deflection angles for Morse potential calculated, using dimensionless relative kinetic energy of pair of atoms 21 p3775 A66-39073  
 Atomic collisions, excitation, transfer processes and energy level transition probabilities in plasma of gas lasers 21 p3748 A66-39305  
 Coupled equations for open-channel components of wave function derived in total-angular-momentum representation in Feshbach approach to scattering theory for rigid rotator and atom 22 p3950 A66-39914  
 Initial phase of shock produced ionization in argon, krypton and xenon to elucidate atom-atom ionization reaction to determine cross section 23 p4098 A66-42079

## ATOMIC ENERGY

### S NUCLEAR ENERGY

## ATOMIC EXCITATION

Modifications of impulse approximation allowing for motion of bound electrons, providing simple analytic expressions for atomic ionization and detachment cross sections 03 p0394 A66-12328  
 FM laser oscillation theory discussing effect of arbitrary atomic line shape, saturation, mode pulling, power output, sideband amplitude, distortion, etc 04 p0530 A66-13954  
 Structural changes in radiation field following quantum reemission after photoexcitation of atom when true absorption is low 05 p0765 A66-15416  
 Solid state laser system, describing quantum mechanical treatment of self-sustained oscillation for one mode 07 p1044 A66-17817  
 Excitation cross sections of helium lines in electron/atom collisions 07 p1044 A66-17874  
 Frequency stabilization of gas lasers, using atomic resonance and interferometers 07 p1045 A66-18357  
 Coherent excitation of mercury resonance state by irradiation with light modulated at Larmor frequency 08 p1233 A66-19089  
 Gas laser emission solution by determining emission field density dependence on resonator parameters, relaxation characteristics and atom excitation in gas discharge plasma 08 p1234 A66-19271  
 Regularities in solid substance vaporization from probe surface in plasma arc allowing quantitative control without change in atomic excitation characteristics 08 p1266 A66-19770  
 Galactic center dynamics revealed by hydroxyl radicals present in interstellar medium, noting detection of radio emissions caused by star-excited atoms and molecules 09 p1453 A66-20239  
 Effective excitation cross sections of alkali metal atoms during collision with slow electrons 09 p1406 A66-20940  
 Effective excitation cross sections for resonance doublets of cesium and rubidium, using slow electrons 10 p1544 A66-21981  
 Degree of excitation of metastable state determined, using luminescence saturation phenomenon, calculating population of working level of laser

substance 10 p1544 A66-22020  
 Quantum mechanical nonlinear theory of intensity and phase fluctuations of homogeneously broadened laser noise 11 p1711 A66-22460  
 Lifetimes of orientation and alignment of excited atomic states examined in level crossing and optical double resonance experiments employing polarized light 11 p1740 A66-22960  
 First order wave function of helium due to one- and two-electron excitation determined by solving differential equations, noting contribution to second order energy 11 p1741 A66-23400  
 Pulse excitation of volume of gas to coherently radiating state applied to beam maser spectrometer 12 p1879 A66-23730  
 Thermionic energy converter energy loss through resonance emission and excited atom diffusion, accounting for de-excitation at electrodes 12 p1922 A66-24210  
 Differences between thermodynamic equilibrium of hydrogen plasma, accounting for increased atomic energy levels 13 p2141 A66-25430  
 Consistency of Gunn effect with excitations of conduction band electrons from high mobility minimum to low mobility valleys 13 p2164 A66-25510  
 Electron impact excitation mechanism of argon-ion continuous and long pulsed lasers 13 p2102 A66-26200  
 Measurement of total cross section for excitation of metastable atoms of helium by electron bombardment 13 p2135 A66-26260  
 7P terms of excited chromium configurations examined, using level crossing and double resonance spectroscopy, noting core polarization 13 p2135 A66-26260  
 Values for contribution of core polarization to hyperfine structure of excited states of chromium compared theoretically and experimentally, extracting core contribution to magnetic field 13 p2135 A66-26260  
 Rotational excitation of oxygen by slow electrons, calculating electron energies quadrupole moments and energy loss rates 13 p2135 A66-26270  
 Semiconductor GaAs quantum generator with two-photon absorption of neodymium laser emission 14 p2307 A66-27150  
 Effective excitation cross sections of alkali metal atoms during collision with slow electrons 15 p2543 A66-28529  
 Ruby phosphorescence under intense optical excitation, inferring possible recombination characteristics from initial brightness decay 15 p2558 A66-28860  
 Excitation temperature of three states of atomic oxygen determined to be 200 degrees K from intensity ratio of three atomic oxygen 1300 angstrom triplet lines by dayglow 15 p2484 A66-28900  
 Calculation of effective excitation cross sections of hydrogen atoms for collision with nitrogen molecules and hydrogen atoms 15 p2545 A66-29210  
 Transverse and axial magnetic field effects on gas lasers, deriving expression for atomic and macroscopic polarization, determining oscillation mode characteristics, frequency responses, etc 15 p2518 A66-29810  
 Pressure dependent energy loss process determined in atomic light analysis of helium positive column, noting molecular-ion concentration relation to 3 D superpopulation 16 p2750 A66-30110  
 Collective oscillations of atoms in Hartree-Fock approximation 16 p2751 A66-30150  
 Degree of excitation of metastable state determined, using luminescence saturation phenomenon, calculating population of working level of laser substance 16 p2718 A66-30840  
 Electron vibration spectra of light absorption in molecular crystals, taking oscillation frequency changes as principle mechanism of exciton-phonon interaction 16 p2780 A66-31170  
 Collision cross sections of ions in isoelectronic sequence of lithium, noting dipolar transitions of type 2s to np 16 p2754 A66-31260  
 Semiconductor lasers with high power efficiency obtained via electron beam excitation on crystals of mixed cadmium sulfide-selenide alloy 16 p2720 A66-31530



Probability of atomic excitation by electron bombardment 18 p3143 A66-34033  
 Individual efficiency curves for excitation of two metastable electron energy states of helium by electron impact 18 p3139 A66-34504  
 Optical pumping of rubidium atoms, describing design and operation of equipment, concepts of resonance, atomic orientation, nuclear magnetic moments, etc 18 p3120 A66-35028  
 Optical pumping of rubidium atoms, treating oriented atoms as magnetized macroscopic gyroscope 18 p3120 A66-35029  
 Effective excitation cross sections for resonance doublets of cesium and rubidium, using slow electrons 19 p3402 A66-35860  
 Approximation method using sum rules for energy shift in atomic system due to interaction of electrons with vacuum electromagnetic field applied to hydrogen, helium and lithium atom ground states and hydrogen molecule 19 p3402 A66-35995  
 High energy cross sections for electron excitations of excited hydrogen atoms in which principal quantum number is changed by 2 19 p3409 A66-36327  
 Excitation of ground state hydrogen atoms by fast protons, evaluating total Born cross section in limit of infinitely massive protons 19 p3403 A66-36333  
 Atomic energy levels in plasma, considering energy spectrum of hydrogen-like atom in plasma, based on cut-off Coulomb potential model 20 p3607 A66-37373  
 FORTRAN program for calculation of approximate total half-intensity line widths of several spectral lines for atoms in common analytical flames 20 p3605 A66-37758  
 Electron excitation of high eigenstates of hydrogen atom and convergence of total wave function expansion 21 p3774 A66-38532  
 Beam foil excitation technique application in measuring mean lives of 2p and 3p levels of hydrogen 21 p3774 A66-38543  
 Gas laser frequency and emitted power dependence on resonator tuning 21 p3748 A66-39308  
 Collisional excitation in Van de Graaff accelerator of beams of light elements producing light emission in 2700-6600 angstrom range 21 p3776 A66-39396  
 Ground state resonance, noting absence of Doppler broadening of signals in forward scattered light 22 p3931 A66-39810  
 Thermionic energy converter energy loss through resonance emission and excited atom diffusion, accounting for de-excitation at electrodes 22 p3957 A66-40583  
 Collective oscillations of electron shells of atom, discussing energy, excitation and damping 22 p3959 A66-40940  
 Spectrophotometry of four bright prominences with respect to kinetic temperature, Doppler half-widths and population levels 23 p4126 A66-41075  
 Semiconductor GaAs quantum generator with two-photon absorption of neodymium laser emission 24 p4226 A66-43085  
**ATOMIC EXPLOSION**  
**S NUCLEAR EXPLOSION**  
**ATOMIC GAS**  
**SA DIATOMIC GAS**  
**SA MONATOMIC GAS**  
 Bethe approximation of ionization cross sections of excited states of atomic hydrogen by high energy electrons 06 p0912 A66-17037  
 Interaction mechanism between internal gravity waves and radiative photochemical processes, noting solar radiation absorption, heat of atomic oxygen recombination, etc 13 p2073 A66-26129  
 Atmospheric mixing time and lifetime of atomic and molecular oxygen at high altitude, noting agreement with barometric distribution law, concentration pattern, etc 15 p2486 A66-29088  
 Spatial distribution of high energy Ar atoms scattered by various surfaces 16 p2753 A66-30398  
 Breakdown by neodymium glass laser radiation in atomic and molecular gases, determining power densities, noting relation of pressure to breakdown power 16 p2718 A66-30938  
 Altitude distribution of atmospheric molecular and atomic hydrogen, showing

results of Lyman alpha absorption measurements 17 p2919 A66-32995  
 Lyman alpha airglow observations indicate diurnal variation of atomic hydrogen in thermosphere and exosphere with abundance change with solar activity 19 p3349 A66-36349  
 Thermal conductivity and accommodation coefficient measurements in gas mixture of atomic and molecular oxygen 21 p3836 A66-39174  
**ATOMIC PHYSICS**  
**S NUCLEAR PHYSICS**  
**ATOMIC RECOMBINATION**  
 Inviscid supersonic nozzle flow of ideal dissociating gas, sudden freezing, equilibrium-recombination mechanism and velocity distribution [AIAA PAPER 66-1] 08 p1163 A66-18983  
 Dissociated laminar boundary layer with heterogeneous recombination 10 p1524 A66-21805  
 Nonequilibrium effects in recombination dissociation kinetics, using iterative perturbation procedure 11 p1738 A66-22884  
 Excitation of auroral green line in terrestrial nightglow caused by interaction of three ground state oxygen atoms 11 p1703 A66-23498  
 High resistivity silicon single crystals, discussing carrier lifetime, photoconductivity and recombination levels 17 p2987 A66-33312  
 Measurement apparatus for studying kinetics of catalytic recombination of gas atoms at solid surfaces of refractory metals, semiconductors and dielectrics 21 p3735 A66-38522  
 Recombination of carbon monoxide and atomic oxygen in expansion wave at high temperature in single pulse shock tube 22 p3860 A66-40527  
 Plasmoid-like RF helium plasma, noting molecular ion formation and destruction leading to evaluation of lower limit for molecular collisional-radiative recombination coefficient 22 p3957 A66-40908  
**ATOMIC STRUCTURE**  
 Long-range interatomic forces from thermal energy spectra, elastic scattering cross sections for atomic beams and limiting curve of dissociation 16 p2751 A66-30161  
 Theoretical band structure, Fermi surface, electronic structure, magnetic and optical properties of rare earth metals 20 p3614 A66-37277  
 Electronic energy band structure and optical properties of heavy rare earth metals 20 p3614 A66-37278  
 Free-atomic pseudopotentials, sizes, s-p splittings and pseudowave functions 22 p3951 A66-40910  
 Cross section for lambda, kappa and sigma particle production in cosmic ray interaction with C, Cu and Pb nuclei dependent on atomic weight of target material 24 p4268 A66-42911  
**ATOMIZATION**  
**SA AEROSOL**  
**SA LIQUID ATOMIZATION**  
 Average heat of atomization in correlating physical properties of vitreous semiconductor 08 p1268 A66-18655  
 Plasma atomization of molybdenum, discussing variable process parameter effects on size grading of spherical powdered molybdenum 08 p1238 A66-18895  
 Atomization of fluids by using nozzles and rotating disks, comparative analysis between these methods and applications 13 p2059 A66-25076  
 Three-dimensional Hueckel molecular orbital calculations performed on series of molecules made from atoms of H, C, N, O, F and Cl 23 p4031 A66-41223  
 Atomization of water drops by high speed airstreams, noting dependency on time 23 p4016 A66-42053  
**ATP**  
**S ADENOSINE TRIPHOSPHATE /ATP/**  
**ATS**  
**S APPLICATIONS TECHNOLOGY**  
**SATELLITE /ATS/**  
**ATTACK AIRCRAFT**  
 Changes to improve reliability of attack aircraft, estimating cost and gains in operational effectiveness 01 p0187 A66-10049  
 Boundary layer control for improvement of lift at lower angles of attack by carrier-

based supersonic aircraft [AIAA PAPER 65-751] 03 p0321 A66-13055  
 Assault helicopter cost and system effectiveness in mission of delivering cargo from carrier to landing zone, evaluating avionics system [AIAA PAPER 64-785] 05 p0610 A66-15079  
 Attack aircraft optimized for attack and strike 07 p0987 A66-17283  
**ATTENUATION**  
**S ABSORPTION**  
**S ACOUSTIC ATTENUATION**  
**S ATMOSPHERIC ATTENUATION**  
**S FADING**  
**S MICROWAVE ATTENUATION**  
**S NOISE ATTENUATION**  
**S RADAR ATTENUATION**  
**S RADIO ATTENUATION**  
**S SHOCK WAVE ATTENUATION**  
**S WAVE ATTENUATION**  
**ATTENUATION COEFFICIENT**  
 Visible and IR radiation attenuation by artificial fogs found to depend on droplet size and distribution 01 p0097 A66-10860  
 Aerosol component of transparency attenuation coefficient relation to humidity characteristics of individual atmospheric layers 04 p0513 A66-13417  
 Attenuation coefficients deduced in lower atmosphere near Rome, using IGY cosmic ray neutron monitor 07 p1032 A66-17465  
 Q band propagation test carried out over 12-km path, comparing rainfall attenuation with rainfall rate over path, noting scatter of measured values 13 p2023 A66-25567  
 Surface wave propagation along plasma column noting discharge tube properties, density distribution variation with magnetic field, attenuation due to collisional losses, etc 17 p2970 A66-32651  
 Horn radiators with high attenuation capabilities, noting design features, application to parabolic antennas, etc 17 p2894 A66-32989  
 Ultrasonic attenuation in lithium fluoride from liquid helium to room temperature, finding anharmonic attenuation of slow transverse mode to vary with frequency 19 p3447 A66-36398  
 Short distance expansion method used to calculate ground radio wave propagation over mixed path on spherical Earth 19 p3305 A66-36421  
 Uppsala IGY-neutron monitor multiplicity measurements indicate increase of attenuation coefficient with increasing multiplicity 20 p3632 A66-38079  
 Ultrasonic attenuation coefficient of transverse wave in gapless superconductor, noting effect on critical field and parameter amplitude 21 p3797 A66-38558  
 Amplifying elements ensuring required dynamic properties of resolving amplifier without calculating entire amplifier circuitry 21 p3712 A66-39252  
 Horowitz minimum sensitivity decomposition does not lead to optimally sensitive networks for selected class of RC networks 24 p4181 A66-42372  
**ATTENUATOR**  
 Wideband UHF-power regulator design, based on use of electrically controllable semiconductor attenuator 09 p1358 A66-20795  
 Electron density in gas-discharge attenuator with hollow cathode 09 p1358 A66-20811  
 Field effect transistor application to linear amplifier and attenuator circuits 11 p1673 A66-23470  
 P-i-n diode coaxial attenuators and levers noting design, performance parameters and application 12 p1831 A66-23812  
 Computer program with data compilation, using equivalent circuit for p-i-n diode, employed in design of coaxial wideband variable attenuator 14 p2246 A66-26833  
 Formula derived for estimating reflection coefficient of cylindrical resistive-film attenuator for traveling wave tube 16 p2660 A66-30617  
 Wideband UHF-power regulator design, based on use of electrically controllable semiconductor attenuator 22 p3874 A66-39854  
 Slow wave circuit for traveling wave tubes operating in millimeter-wave band, examining attenuator for double-ladder traveling wave amplifier 22 p3877 A66-40187



## ATTITUDE

SA HORIZONTAL ATTITUDE

SA PITCH ATTITUDE

SA SATELLITE ATTITUDE

DISTURBANCE

SA YAW ATTITUDE

Staff flight test design velocity comparison technique for estimating in-flight inertial platform attitude 18 p3132 A66-34044

## ATTITUDE CONTROL

SA FLIGHT CONTROL

SA HORIZON SENSING

SA ROLL CONTROL

SA SATELLITE ATTITUDE CONTROL

Automatic flight control system for A-7A featuring high fixed gain dual channels, series servos and control augmentation in addition to normal attitude and path control functions 01 p0098 A66-10007

Self-organizing adaptive systems for spacecraft attitude control in which reward-punishment reinforcement process is used to obtain on-line synthesis of plant actuation signals 01 p0140 A66-10019

Reentry guidance for manned Mars mission return considering capture and acceleration control, skip range and terminal range controls 01 p0101 A66-10041

Design requirements for LEM, describing stabilization and control elements of abort system 01 p0140 A66-10046

Availability concept in attitude control system for manned Mars expedition 01 p0018 A66-10084

Pulse operated bipropellant control valve design for attitude control systems of space vehicles 01 p0015 A66-10668

Spacecraft attitude control system selection constraints and tradeoffs of components 01 p0142 A66-10681

Attitude control by means of reaction wheel driven by photoelectronically commutated DC torquer 02 p0179 A66-11278

Brushless DC reaction wheel operation, examining use of current limiting to achieve constant torque 02 p0179 A66-11279

Three-axis control system of Mariner IV for midcourse maneuver, communication, scientific instruments orientation, etc 03 p0430 A66-12480

Star pattern recognition system for spacecraft attitude control [AIAA PAPER 64-652] 03 p0390 A66-12755

Solar sail attitude stabilizer integration with thermionic power generation to obtain weight, simplicity and reliability advantages 03 p0431 A66-12762

Thrust modulation with minimum limit cycle in bang-bang system, reducing fuel consumption for spacecraft attitude control system 03 p0432 A66-13206

Low thrust cold gas reaction jet system for small spacecraft with nitrogen, ammonia, Freon-12 and Freon-14, analyzing thrust chamber pressure history [ASME PAPER 65-WA/AUT-11] 05 p0624 A66-15608

V/STOL Aircraft Symposium, Wright-Patterson AFB, Ohio, November 1965 06 p0805 A66-16808

Reference-point results applied to variations in laminar heat transfer to total vehicle over range of vehicle attitudes and associated trajectories [AIAA PAPER 66-28] 07 p0980 A66-17890

Navigation, guidance and control of spacecraft in interplanetary space, considering free-fall flight and thrust-vector stabilization during accelerated flight 08 p1248 A66-18586

Spinning rocket attitude measured from geomagnetic field and solar cell data, using digital computer technique, noting instrumentation 08 p1225 A66-19492

Three-axis limit cycle operation of reaction jet attitude stabilization system 08 p1304 A66-19515

Equipment located between Diamant second-stage propulsion unit and jettisonable rear skirt of third stage including antennas, auxiliary rockets, attitude changing apparatus, control and guidance, etc 10 p1518 A66-21258

Influence on stability of masses which are in relative motion with respect to projectile determined, noting engine thrust effect on attitude control system performance 10 p1611 A66-21386

Ion thruster, including mercury feed system and shielded neutralizer, designed and tested for spacecraft station keeping and attitude control

[AIAA PAPER 66-247] 10 p1593 A66-21456  
Telemetry and data processing systems and sensor equipment of Mariner IV including TV camera, magnetometer, ion chamber, plasma probe, etc 11 p1778 A66-23115

Impulse bit-size, gas consumption and specific impulse of cold-gas attitude control reaction jet system 12 p1954 A66-24710

Stabilite system, three-axis attitude control system utilizing single reaction wheel [AIAA PAPER 66-307] 12 p1955 A66-24774

Spacecraft attitude perturbation due to meteoroid impacts, anisotropy of incident flux and possibility of steady state disturbance torque 14 p2392 A66-27878

Boresighted scanning star tracker for precise attitude sensing and control of sounding rocket 14 p2329 A66-28452

Versatile air-bearing table with three-axis attitude control system for variety of nonspinning zero-g space stations 15 p2534 A66-29362

High precision attitude control system using pulse width modulation evaluated by hardware fabrication and digital computer simulation 15 p2606 A66-29651

Test program for Gemini Attitude Control and Maneuver Electronics /ACME/ system, establishment and execution 16 p2676 A66-30438

Model reference adaptive techniques applied to feedback attitude control system to minimize instrumentation 16 p2809 A66-30830

Two-dimensional dynamic analysis of probe and drogue docking concept noting design, operation and performance 16 p2809 A66-30896

Torque-free precession of spin stabilized spacecraft, showing thrust misalignment as cause for final burnout impulse 16 p2810 A66-30903

Motion equations, attitude and ignition time of third and fourth stage of USAF Athena, noting solution derivation using Taylor series constraints, accuracy, etc 16 p2743 A66-30908

Rocket attitude determined by simultaneous measurement of geomagnetic field and electromagnetic field generated by radio wave transmitted by rocket-mounted dipole 16 p2810 A66-30958

Pilot performance evaluation method based on analysis of control of aircraft attitude in fixed wing aircraft 17 p2864 A66-32162

Dynamical attitude equations for rotational motion of set of  $n$  rigid bodies interconnected by dissipative elastic joints and subjected to arbitrary forces and torques 17 p3001 A66-32345

Systems and operation of quantized data attitude control system for spacecraft [AIAA PAPER 64-660] 18 p3240 A66-33787

Solar alignment system for Skylark rocket attitude control, describing system composition, operation and results 18 p3243 A66-33856

Optimum three-dimensional attitude control of spacecraft with two pairs of reaction jets 18 p3244 A66-33863

Automatic control systems for attitude control of Apollo spacecraft 18 p3244 A66-33876

Ion engine satellite control system noting design and laboratory tests [AIAA PAPER 65-417] 19 p3450 A66-35616

Control moment gyroscope for angular momentum transfer with minimum power consumption, noting design and application for free body motion stabilization 19 p3360 A66-35962

Controller, employing voice recognition principle, for attitude control system of astronaut maneuvering unit in various space tasks 19 p3291 A66-35973

Linear filtering technique for estimation of azimuth alignment of inertial guidance system in presence of disturbances with no measurement noise 19 p3398 A66-36689

Rigid body rotational attitude control in three dimensions with linear transformation as output variable, noting advantages, applications and results 19 p3471 A66-36693

Liapunov method synthesis of time variable nonlinear multivariable systems deriving simplified control law for tracking of linear noninteracting model 19 p3335 A66-36699

Acquisition phase of attitude control function of space vehicle, using noisy measurements on one state 20 p3658 A66-36861

Automatic self-monitor techniques for attitude and heading reference systems 20 p3596 A66-37184

Combined computer and physical simulation of manual tracking system for coupled-camera photography of one space vehicle from another when viewfinder is used 20 p3597 A66-37234

Nitrogen powered hydraulic attitude control system of Little Joe II solid propellant launch vehicle for flight testing escape mechanism used on Apollo 20 p3499 A66-37314

Adaptive control system requirements for launch vehicles includes insensitivity to parameter variations and adjustability as function of measured flight conditions 20 p3664 A66-38182

Low-thrust rockets for spacecraft attitude control, noting subliming solid rockets 21 p3807 A66-38806

Second-order solution for strapped-down attitude computation compared with first order solution 21 p3763 A66-38842

Rotating spacecraft attitude changes due to energy dissipation from angular deformation treated by modal method 21 p3819 A66-38844

Spacecraft attitude reference system using passive temperature control device and four gyros in skewed position 21 p3764 A66-38853

Flight control system of Saturn V launch vehicle, discussing attitude/attitude rate scheme, gain required and stability achieved 21 p3820 A66-38875

Simulation results of adaptive tracking filter application to stabilization of structural bending modes of SI-B launch vehicle 21 p3821 A66-38877

Attitude control system/engine control system for hover control of VTOL aircraft 21 p3697 A66-38902

Attitude, translation and descent engine control for attitude and position control of LEM 21 p3808 A66-39518

Mechanical and thermal requirements of attitude, translation and descent engine controls of Lunar Excursion Module /LEM/ 21 p3808 A66-39519

Automatic flight control system for A-7A featuring high fixed gain dual channels, series servos and control augmentation in addition to normal attitude and path control functions 23 p4088 A66-40983

Control moment gyros with reaction control jet torque sources for attitude control of spinning and nonspinning space stations [AIAA PAPER 65-405] 23 p4132 A66-41097

Apollo spacecraft attitude control, noting phases of application [AGARDOGRAPH 105] 24 p4284 A66-43129

## ATTITUDE GYRO

Error sources in strapdown inertial attitude reference system consisting of three pulse torqued gyros and digital differential analyzer 21 p3763 A66-38840

Strapdown attitude reference system with two rotor gyros using gas bearing in space vehicle 21 p3763 A66-38847

Control moment gyros with reaction control jet torque sources for attitude control of spinning and nonspinning space stations [AIAA PAPER 65-405] 23 p4132 A66-41097

Error sources in strapdown inertial attitude reference system consisting of three pulse torqued gyros and digital differential analyzer 23 p4088 A66-41101

IMU /inertial measurement unit/ gyrocompass as attitude reference in space 24 p4214 A66-42955

Space vehicle guidance and navigation, noting instrument techniques, gyroscopic units for reference coordinate realization, inertial navigation systems, etc [AGARDOGRAPH 105] 24 p4235 A66-43123

## ATTITUDE INDICATOR

Unconventional attitude sensors required to make strapped-down gimballess inertial



guidance system practical 01 p0139 A66-10004  
Bubble level for sensing local vertical of attitude stabilized 08 p1223 A66-18816  
satellite  
Electro-optical attitude and velocity sensors for interplanetary navigation and stellar aberration and Doppler shift measurements 08 p1252 A66-19502  
High reliability system for sensing excessive and potentially dangerous turning rates of Gemini launch vehicle 08 p1225 A66-19525  
Spatial disorientation experiences of Army helicopter pilots, noting accident and incident statistics, methods of correction, etc 11 p1648 A66-22578  
Attitude detectors, characteristics and performance 12 p1879 A66-23745  
Tiro IX satellite design and performance, noting wheel configuration, TV camera, control systems, etc 15 p2606 A66-28968  
**AUDIO EQUIPMENT**  
Distortion measurement by total harmonic distortion analysis and intermodulation distortion analysis 01 p0037 A66-10499  
In-flight entertainment system discussing video, audio and motion picture systems 02 p0231 A66-12015  
Auditory threshold location and uncertainty as function of tone parameters and fatigue examined for pulsed and continuous tones, using Bekesy audiometer 09 p1337 A66-20954  
**AUDIOFREQUENCY**  
**SA SOUND WAVE**  
Design and performance of two multirange current transformers for audio frequencies operating 400 hz to 10 khz with minimum error 07 p1004 A66-17215  
Stability of vertical water jet examined by imposing audiofrequency disturbances 13 p2060 A66-25133  
**AUDIOLOGY**  
**SA DEAFNESS**  
**SA HEARING**  
Difference between earphone /MAP/ and sound field /MAF/ threshold sound pressure levels /SPL/ for spondee 09 p1338 A66-20955  
**AUDITORY FATIGUE**  
Auditory threshold location and uncertainty as function of tone parameters and fatigue examined for pulsed and continuous tones, using Bekesy audiometer 09 p1337 A66-20954  
Psychological reactions to jet aircraft noise, including behavioral reactions and auditory fatigue 12 p1806 A66-24234  
Human auditory response under conditions of intermittent long-term action of medium intensity sound 15 p2435 A66-29451  
Noise effect on human performance 20 p3504 A66-36932  
Human engineering of acoustic fatigue for optimum data processing performance [ASME PAPER 66-MD-25] 21 p3700 A66-38481  
**AUDITORY PERCEPTION**  
**SA HEARING**  
Information processing in auditory neural mechanism, examining synthesis operation of cortex neurons and function of centrifugal nerve paths 02 p0180 A66-11365  
Auditory threshold location and uncertainty as function of tone parameters and fatigue examined for pulsed and continuous tones, using Bekesy audiometer 09 p1337 A66-20954  
Hearing acuity requirements of aircraft personnel, examining discrimination from background noise and acoustic trauma causative factors 10 p1493 A66-22130  
Inter- and intramodal comparisons of light and tone durations in two-alternative forced-choice situation, noting possible judgment errors 13 p2015 A66-25789  
Human subjects making comparisons of duration of two tones in forced choice situation for signal with same or different intensities 14 p2229 A66-27309  
Fluctuations in human acoustic sensitivity after 24 hours in room under effect of Coriolis accelerations of various magnitudes 17 p2861 A66-32941  
Binaural unmasking of tones masked by broadband Gaussian noise including theoretical work on equalization and cancellation model 21 p3702 A66-38646

Vibration stimulus effect on oxygen metabolism of brain in rats with partial destruction of auditory and vestibular apparatus and in anesthetized control rats 23 p4027 A66-41341  
**AUDITORY SENSATION AREA**  
Stochastic behavior of primary auditory neurons illustrated by functional model subjected to steady HF sinusoidal tone bursts 01 p0019 A66-10400  
Stimulus coding in cochlear nucleus, noting different discharge patterns of units in different subdivisions 16 p2641 A66-31187  
**AUDITORY SIGNAL**  
Audio signal processing techniques in future space exploration, discussing channel capacity, speech processing, bandwidth narrowing, etc 13 p2025 A66-26024  
**AUDITORY STIMULUS**  
**SA NOISE**  
Behavior and physiological correlates of human response time to high intensity auditory stimuli 02 p0187 A66-11832  
Temperature effect on amplitude of cochlear microphonic and on latency action potential of auditory nerve 06 p0812 A66-16405  
Sound pressure in external auditory meatus and near center of cat head in absence of animal as function of frequency 22 p3854 A66-40166  
Response patterns to tone-burst stimulation of cochlear nucleus and dependency on stimulus parameters 22 p3855 A66-40375  
**AUDITORY TASK**  
Performance sharing when two audio visual vigilance tasks are performed concurrently 11 p1646 A66-23374  
Information feedback and psychophysical variables in two-alternative temporal forced-choice auditory-signal-detection task 18 p3063 A66-35023  
**AUREOLE**  
Fast photoionization aureole detection and cloud of concentrated long-lived ionization from spark shock wave in laser beam 01 p0080 A66-10263  
Fast photoionization aureole detection and cloud of concentrated long-lived ionization from spark shock wave in laser beam 03 p0379 A66-13308  
Brightness calculation of aureole visible in daytime at Earth edge from spacecraft 08 p1217 A66-19302  
Measurement apparatus and procedure for aureole scattering function in lowest layer of atmosphere 14 p2325 A66-27536  
Brightness calculation of aureole visible in daytime at Earth edge from spacecraft 19 p3348 A66-36039  
Fast overlap of microwave radiation by ionization aureole of spark in laser beam 19 p3376 A66-36719  
Measurement apparatus and procedure for aureole scattering function in lowest layer of atmosphere 24 p4233 A66-42322  
**AURORA**  
**SA AIRGLOW**  
**SA POLAR AURORA**  
**SA RADIO AURORA**  
Monographs on auroras, geomagnetic disturbances and ionosphere at high latitudes 01 p0064 A66-11160  
Micropulsations of Earth magnetic field and relation to various types of auroras 04 p0515 A66-13849  
Visible and invisible aurora discussing morphology, occurrence, magnetic activity, absorption, geophysical and energy particle 05 p0675 A66-15746  
Rocket and satellite data contribution to new physical description of aurora in which Earth magnetosphere acts like gigantic cathode ray tube 06 p0875 A66-16015  
Relative intensity measurements of 50 major bands of Lyman-Birge-Hopfield /LBH/ system of nitrogen 12 p1869 A66-23919  
Auroras, frequency, geographical distribution, types, evolutionary processes and auroral phenomena 15 p2482 A66-28517  
Auroral occurrence rate at zenith as function of latitude for magnetically quiet and magnetically disturbed periods 15 p2486 A66-29092  
Patches and irregular bands and eastward motions in morning sector of auroras 16 p2693 A66-30336

Equatorward motions of auroras 17 p2923 A66-33356  
**AUROLAL ABSORPTION**  
Shift of anomalous absorption region from riometric observation 02 p0225 A66-12138  
Electron density and collision frequency observation during auroral absorption event, discussing rocket experiment techniques and results of analysis 03 p0363 A66-12645  
Auroral type of riometer absorption and magnetic disturbances for stations situated at different longitudes in auroral zone 03 p0364 A66-12660  
Untamated solar cosmic ray data obtained when polar cap absorption events removed toward magnetic poles from auroral zones 03 p0418 A66-12662  
Auroral absorption height obtained from statistical satellite data on average precipitation rate of electrons in auroral zone as function of energy 03 p0364 A66-12663  
Electron energy spectrum during auroral absorption measured by Nike-Cajun analyzer 03 p0366 A66-12880  
Energy flux of electron beam absorbed by atmosphere derived from resulting intensity of first negative system of molecular nitrogen 05 p0670 A66-14948  
Auroral phenomena in integral-invariant coordinate system, discussing pole-centered circular nature of isochasms in geomagnetic dipole coordinates 06 p0876 A66-16280  
Auroral absorption measured, using riometers compared with energetic particle fluxes simultaneously detected by passing satellite, showing absorption and particle flux correlation 09 p1374 A66-20881  
Annual variation of auroral absorption attributed to frictional interaction between streaming plasma and geomagnetic field 10 p1530 A66-21161  
Effects of AZA and PCA on radio wave propagation in Antarctic, noting reliability and radiation power requirements 12 p1817 A66-24275  
Radio wave absorption at high latitudes dependent on frequency, noting AZA and PCA are inversely proportional to powers of frequency 12 p1817 A66-24276  
Auroral absorption at 18-mc/s in middle latitudes, noting daily and seasonal variation 13 p2074 A66-26361  
Auroral absorption of cosmic radio noise which is not identical at magnetic conjugate point 13 p2076 A66-26743  
Shift of anomalous absorption region from riometric observation 14 p2287 A66-28094  
Auroral absorption of cosmic radio radiation recorded by shipboard station drifting in North Geographic Pole region in winter 1963-64 15 p2487 A66-29099  
Auroral absorption of cosmic radio noise 18 p3238 A66-35086  
Auroral absorption analysis during geomagnetic storm, noting satellite measurement of energetic particles 20 p3642 A66-38335  
Sudden cosmic radio noise absorption, polar cap absorption and auroral absorption 24 p4202 A66-42832  
**AUROLAL ACTIVITY**  
Nocturnal auroral drift in meridional direction 01 p0064 A66-11163  
Ionospheric, auroral and geomagnetic observation at Syowa Base, Antarctic 02 p0222 A66-11684  
Current theories for auroral excitation, general excitation and ionization by fast particles in air and relation between luminosity and ionization in aurora 03 p0418 A66-12656  
Effects connected with auroras and magnetic storms in lower ionosphere considering radio wave attenuation, cosmic ray absorption, etc 03 p0365 A66-12854  
E-layer disturbances caused by particles impinging upon atmosphere during auroras noting ionization, X-rays and electrical conductivities 03 p0365 A66-12858  
Contradictory experiments to determine whether particles responsible for auroral events are solar particles or local particles accelerated by secondary processes 03 p0421 A66-12864  
Auroral zone X-ray bursts and polar magnetic substorms 03 p0422 A66-12873  
Ionospheric disturbances traveling at



subauroral latitudes compared at different altitudes 04 p0514 A66-13481

Dipole latitude of auroral activity during periods of zero and very weak magnetic disturbance 04 p0517 A66-14375

Neutron intensity increase observed by boron fluoride proportional counter at high altitude associated with auroral zone X-ray event 07 p1121 A66-17983

Penetration of interplanetary plasma into magnetosphere, connected to aurorae and magnetic storms, noting that plasma need not behave like magnetofluid 07 p1138 A66-18081

Aurora production via magnetic field induction during geomagnetic storms by ring current growth in Van Allen belt region 07 p1029 A66-18088

Polar electrojet causing magnetic substorms in high latitudes flows westward along closed oval curve and is connected with auroral activity and outer radiation belt 08 p1216 A66-19216

Airglow and auroral radiation and time-space variations 09 p1372 A66-20280

Comparison between auroral effects and experimentally observed electron leakage from magnetic mirror with electron acceleration 09 p1373 A66-20471

HF noise signals and association with auroral disturbances analyzed, using data from IGY network of backscatter sounders 11 p1701 A66-23154

Diurnal variation of average energy spectrum of auroral X-rays observed from balloon flights, assessing effect of atmospheric absorption 14 p2376 A66-27614

Short-lived oscillation in light emitted in active aurora 14 p2286 A66-27985

Canadian space program including nonmilitary activities, upper atmosphere research, rocket sounding, aurora studies, satellite use, etc 15 p2601 A66-29937

Polar magnetic substorms associated with westward traveling surge 16 p2693 A66-30334

Poleward motion of auroral bands in midnight sector during early phase of auroral substorm and cause of planetary scale auroral displays 16 p2693 A66-30335

Proton data from rocket flight into breakup phase of IBC-I aurora, noting proton movement in atmosphere 16 p2794 A66-30701

VLF emission associated with flickering aurora 16 p2696 A66-30721

ESRO-I satellite design and auroral activity study 16 p2810 A66-31000

Dynamics of geomagnetic tail, noting transformation of magnetic energy into kinetic energy due to pinch instability and auroral activity phenomena 18 p3106 A66-34162

Pulsating auroras observed near equatorward boundary of auroral displays during postbreakup phase with image orthicon TV and photometers 18 p3107 A66-34519

Riometer recordings at high geomagnetic latitude of intense and sporadic absorption events correlated with occurrence of auroral and geomagnetic disturbances 18 p3108 A66-34531

Ascent and descent in 80-year cycles of solar activity based on Schöve decadal numbers of auroral frequency 18 p3239 A66-35246

Auroral oval, auroral substorm and relations with internal magnetospheric structure during growth and decay of ring current and neutral sheet 20 p3549 A66-37296

Electron precipitation in auroral zones caused by magnetospheric instability 20 p3609 A66-37820

Magnetospheric tail instabilities, auroral electron acceleration and deformation due to dipole magnetic field acceleration of plasma particles 20 p3635 A66-38222

Nonadiabatic and adiabatic acceleration and diffusion of particles trapped in Earth magnetic field, examining particle drift, trapping boundary, auroral substorms and bounce resonances 20 p3658 A66-38326

Upper atmospheric phenomena and particle precipitations noting ionization cross section, energy and spatial distribution and auroral activities 20 p3642 A66-38334

Enhanced activity in ionospheric E region at Cape Hallett and Campbell Island for

information on diurnal variation and sunspot cycle changes of overhead and auroral activity 22 p3916 A66-40809

Image orthicon slit spectrograph for study of aurora and night glow 22 p3921 A66-40898

Auroral zone electron source properties deduced from electron fluxes, spectrums and angular distributions measured by rocket flown into breakup phase of IBC I aurora 24 p4199 A66-42584

Auroral zone proton-electron anticorrelations, proton angular distributions and electric fields 24 p4199 A66-42585

Auroral zone microbursts associated with geomagnetic storms, negative magnetic bays and electron precipitation observed by balloon and rocket 24 p4201 A66-42600

**AURORAL ARC**

Homogeneous auroral arcs orientation and relation to magnetic disturbance currents 01 p0064 A66-11164

Aurora heights determined from wide-angle photographs at Tiksi Bay in 1964 support existence of coastal effect 02 p0224 A66-12121

Visibility conditions for fibrous structure of auroral arcs and bands 04 p0516 A66-13863

Aurora heights determination from wide format photographs, presenting data concerning upper and lower edges and vertical length of homogeneous arcs 08 p1213 A66-19029

Aurora relations with ionospheric currents responsible for magnetic disturbance, noting sign of bay 08 p1215 A66-19054

Aurora heights determined from wide-angle photographs at Tiksi Bay in 1964 support existence of coastal effect 14 p2287 A66-28080

**AURORAL BOMBARDMENT**

Behavior patterns exhibited by polar ionospheric phenomena indicated by statistical analysis of IGY data 03 p0364 A66-12664

Lunar X-ray detectability, noting generation by solar wind electron bombardment and flux intensity 09 p1459 A66-20885

**AURORAL ECHO**

Particle bombardment produces ionized layers in high latitude ionosphere similar to sporadic E layers of lower latitudes 03 p0363 A66-12657

Connection between occurrence of auroral green line of atomic oxygen and head echo by meteors suggests common mechanism for both phenomena 07 p1135 A66-17636

Radio auroral echoes and correlation to geomagnetic disturbance 08 p1215 A66-19205

Data on Northern Hemisphere radio aurora obtained on radar located in England, showing delay in onset of auroral echoes following sudden commencement, depending on local time of SC occurrence 11 p1695 A66-22375

Theoretical calculation of propagation path geometry of VHF aurora backscatter communications compared with experimental observations 19 p3306 A66-36653

Auroral radar echo wavelength dependence determined by two-frequency radar at Homer, Alaska 24 p4172 A66-42593

Auroral radio reflections in analysis of polar current eddy structure, noting effect of geomagnetic and solar activity 24 p4205 A66-43157

**AURORAL ELECTROJET**

Location of latitude over which aurora current passes as function of geomagnetic storm intensity 02 p0225 A66-12139

Ring current growth tendency prior to sudden magnetospheric compression 08 p1219 A66-19406

Auroral electrojet index and universal time variations, discussing polar disturbance statistics 10 p1528 A66-21144

Localization and motion of energetic electron precipitation regions during negative magnetic bays, noting similarity of motion to that of auroral electrojets 10 p1599 A66-21147

Magnetospheric electric fields, noting implications of magnetic storm theories 10 p1528 A66-21149

Location of latitude over which aurora current passes as function of geomagnetic storm intensity 14 p2287 A66-28095

Growth and decay of ring current and

polar electrojet, using magnetic storm examples 22 p3974 A66-40562

**AURORAL EMISSION**

Catalog of observations on auroral phenomena in Western Europe below geomagnetic latitude of 55 degrees for years 1601 to 1700 01 p0139 A66-11104

Correlation of hydrogen emission and oxygen line in diffusive auroras and sporadic E layer 01 p0064 A66-11162

Short period fluctuations in intensity of auroral luminescence and relation to geomagnetic fluctuations 01 p0065 A66-11161

Book on geo-and heliophysical effects in cosmic rays and auroras 02 p0280 A66-11329

Pulsations of aurora luminescence and irregular quasi-periodic oscillations of geomagnetic field 02 p0224 A66-12120

Rocket-mounted spectrometer with solid state detectors for measuring interaural energy spectra of auroral electrons and protons in 40-104 keV range 03 p0369 A66-12650

Balloon measurements of solar protons and auroral X-rays discussing radiation detector flight techniques, instrumentation and results 03 p0417 A66-12654

Auroras and magnetic storm models including those of Chapman and Ferraro, Alfven, and Axford and Hines, noting magnetization of solar plasma 03 p0365 A66-12856

Geomagnetic disturbances and related visual auroras noting pulsations, excitation processes, etc 03 p0365 A66-12857

Visual aurora morphology and dynamics, luminosity curves, angular and energy distributions of auroral electrons, etc 03 p0365 A66-12858

Cometary emissions and excitation processes and prediction of major atomic and molecular emissions of UV spectrum of aurora 03 p0425 A66-12869

Rocket launching through aurora of high luminosity spectrograph and liquid ammoniated to study behavior under solar radiation 03 p0426 A66-12870

Appearance frequency and brightness distribution of band and other auroral forms 04 p0516 A66-13864

Pearl micropulsations in auroral zone at Flin Flon, Manitoba 05 p0667 A66-14790

Night airglow intensity measured at Kerguelen Islands in 1963, rejecting observations contaminated by auroral light 05 p0672 A66-15039

ULF radiation of polar lights, detailing apparatus for receiving and recording signals 06 p0876 A66-16592

Molecular oxygen dissociation resulting from collisions with neon and argon metastable atoms in auroral afterglow 11 p1696 A66-22419

Rocketborne measurements of electron precipitation and relative brightness of ionized molecular nitrogen ion and atomic oxygen auroral emissions 11 p1764 A66-23139

Excitation of auroral green line in terrestrial nightglow caused by interaction of three ground state oxygen atoms 11 p1703 A66-23498

Pitch-angle distribution and differential energy spectrum of polar aurora protons penetrating Earth atmosphere 12 p1870 A66-24283

Auroral hydrogen emission in night sky, noting variance with sunspot cycle and magnetic activity 13 p2073 A66-26029

Simultaneous IR emission and auroral X-ray observations from high altitude balloon flights 14 p2376 A66-27399

Pulsations of aurora luminescence and irregular quasi-periodic oscillations of geomagnetic field 14 p2287 A66-28079

Fast auroral waves differ from flaming aurora in which waves of luminosity appear to converge toward magnetic zenith 15 p2484 A66-28820

Dependence of frequency distribution of auroral displays in zenith on latitude and local time in magnetically quiet and disturbed periods analyzed by all-sky camera network in Northern Hemisphere 15 p2488 A66-29227

Relation between frequency spectrum of pulsations in auroral luminosity and energy spectrum of auroral electrons, using photometer 15 p2489 A66-29235



- Proton bombardment for generation of polar glow aurora 16 p2693 A66-30338
- UV emissions in 1000-1350 angstrom range measured from rocket launched into aurora from Fort Churchill 17 p2917 A66-32523
- Upper atmospheric temperature measurement from Doppler line widths of atomic oxygen auroral and nightglow emission, using Michelson interferometer 17 p2919 A66-32993
- Tilting interference filter photometer to investigate morphology of hydrogen emission and relation to visible aurora 18 p3109 A66-35087
- Time structure of auroral X-rays at Swedish and Finnish locations, using simultaneous balloon flights 19 p3452 A66-35562
- Energy spectrum of auroral X-rays in range from 20 to 150 kev according to balloon measurements show remarkable diurnal variation 19 p3452 A66-35563
- Quantitative measurement of free metallic atoms abundance and height distribution from twilight, dayglow and aurora fluorescence 19 p3349 A66-36350
- Atomic hydrogen and helium emissions in upper atmosphere determined by diffraction spectrophotometer measurement of twilight airglow and aurora 19 p3350 A66-36352
- Auroral spectrum emission intensity in upper atmosphere used to determine densities of metastable atoms and molecules and rates of dissociation and ionization 19 p3350 A66-36353
- Energy spectrum of primary auroral electrons determined from vertical luminosity profiles of 16 auroral arcs 20 p3550 A66-37297
- Aerobee rocket instrumentation and rocket sounding techniques for investigating far UV auroral emission 20 p3552 A66-37594
- Height distributions for atmospheric ionization rate and Balmer radiation resulting from precipitation of auroral protons 21 p3734 A66-39338
- Upper and lower limits to expected alpha and beta hydrogen and helium line emissions due to protons and alpha particles penetrating auroral atmosphere 22 p3913 A66-40554
- Initial energy spectrum and flux of low energy protons responsible for luminescence of hydrogen in auroras 22 p3974 A66-40753
- Spatial distribution of auroral radio signal reflection centers based on radar observations 22 p3915 A66-40777
- Height-luminosity distribution of auroral hydrogen beta emission measured with rocket mounted photometer 23 p4065 A66-41690
- AURORAL IONIZATION**
- Discrepancies in data concerning aurora type sporadic ionization in E region obtained by various high latitude stations 02 p0225 A66-12136
- Visible and invisible aurora discussing morphology, occurrence, magnetic activity, absorption, geophysical and energy particle 05 p0675 A66-15746
- Ionization structure of polar auroras from spatial distribution of radar-reflecting zones, taking into account magnetic field variations 12 p1871 A66-24293
- Discrepancies in data concerning aurora type sporadic ionization in E region obtained by various high latitude stations 14 p2287 A66-28092
- Elementary geomagnetic polar disturbances, lip-shaped auroral ionization patterns and existence of energetic electrons on night side of magnetosphere 15 p2485 A66-28909
- AURORAL SPECTROSCOPY**
- Double-focusing miniaturized beta-spectrometer for measuring low energy electrons within small band spread associated with auroral phenomena 03 p0369 A66-12651
- Artificial aurora, describing time delays between intensity variations of high altitude nuclear explosion generated spectral lines 05 p0667 A66-14789
- Spectrographic and interferometric techniques used in temperature determinations of auroral and airglow emissions in upper atmosphere 05 p0671 A66-15020
- Wide angle Michelson interferometer for measuring Doppler temperature from width of 5577 angstrom atomic oxygen line in nightglow and aurora 13 p2128 A66-25799
- Brightness fluctuations in quiet-form auroras, noting peaks and anisotropy of spectrum 14 p2286 A66-27983
- Power spectrum analysis of intensity variation of pulsating aurora from Tromso during winter 1964/65 15 p2488 A66-29234
- Upper and lower limits to expected alpha and beta hydrogen and helium line emissions due to protons and alpha particles penetrating auroral atmosphere 22 p3913 A66-40554
- AURORAL TEMPERATURE**
- Rotational temperatures derived from molecular nitrogen ion in aurora along with simultaneous height measurements 02 p0223 A66-11833
- Auroral excitation rates and molecular vibrational temperatures in nitrogen 2PG from Franck-Condon factors obtained from intensity measurements and high resolution absorption spectral data 16 p2692 A66-30328
- AURORAL ZONE**
- Auroral zone absorption, reporting periodic variation of sporadic E layer in Antarctica, considering magnetospheric time-of-flight spectrometer effect 01 p0061 A66-10497
- Geomagnetic pulsation pc-5 in and near auroral zones based on data collected during IGY period, noting local time dependence 01 p0062 A66-10889
- Progressive change in worldwide current systems and auroral zone electrojets of geomagnetic bays examined with magnetic data during IGY 01 p0063 A66-10890
- Broadband VLF emissions observed to determine whether whistler mode signals appearing below ionosphere travel toward polar regions and at low latitude from auroral zone 01 p0012 A66-10893
- Diurnal velocity variations of ionospheric wind in auroral zones and disturbance daily solar variation 01 p0064 A66-11161
- Corpuscular flux entry zone and spiral time distribution of disturbance maxima 01 p0133 A66-11165
- Relative position of solar disturbance daily variations mean flux system compared with auroral region of same period 01 p0065 A66-11169
- Ionosphere electron content near auroral zone obtained from differential Faraday observations of multifrequency beacon satellite Explorer XXII, noting corpuscular radiation role 02 p0223 A66-12017
- Charged particles in auroral zone, measuring energy and pitch angle distribution of electrons and protons with rocket mounted solid state detectors 03 p0417 A66-12653
- Enhanced audiofrequency electromagnetic radiation between 500 and 1000 cps recorded in auroral zone by swept-frequency analyzer 03 p0418 A66-12659
- Electric current system arising from sudden enhancement of ionospheric conductivity in auroral zone 04 p0516 A66-13853
- Structure of Arctic auroral zone in period of minimum solar activity 05 p0673 A66-15050
- Time-agreement of sudden commencements indicated by geomagnetic micropulsation results from Byrd Station and Great Whale river 06 p0875 A66-16271
- Occurrence frequency of midlatitude geomagnetic transition bays and relation to spatial movement of overhead electrojet current systems 08 p1218 A66-19395
- Spatial and temporal character of fast variations in auroral zone X-rays, describing balloon experiment and results 08 p1284 A66-19397
- Diurnal variation of aurora zone geophysical disturbances, examining VLF phenomena including noise, aurora and ionospheric absorption 09 p1372 A66-20375
- Latitudinal dependence of geomagnetic disturbance magnitude along noon and midnight meridians for different seasons, noting effect on auroral zone 09 p1373 A66-20386
- Morphological analysis of daily variability of geomagnetic field regular daily changes, noting current systems in polar and nonpolar regions 10 p1526 A66-21126
- Energy spectrum of auroral zone X-rays, noting electron precipitation and diurnal pattern for occurrence of bremsstrahlung 10 p1599 A66-21145
- Energy spectrum for auroral zone X-rays, measuring simultaneously bremsstrahlung X-rays and ionospheric absorption 10 p1599 A66-21146
- VHF hiss zone morphology and correlation with particle precipitation events, from Alouette I satellite observations 11 p1700 A66-23136
- Auroral zone, ionospheric scattering and nongreat-circle HF propagation statistically analyzed 11 p1700 A66-23141
- Propagation of MHD emissions in Alfvén mode along high latitude geomagnetic field lines, auroral zone signal energy penetration and isotropic wave mode transformation 11 p1701 A66-23151
- X-ray produced auroral light emission in air and excitation of second positive and first negative bands in nitrogen 11 p1765 A66-23152
- Auroral zone electron flux and relation to broadbeam radiowave absorption 11 p1703 A66-23495
- Corpuscular intrusions into Earth magnetosphere involving entire auroral zone and occurring only on night side 12 p1871 A66-24296
- Enhanced ionization along midnight auroral zone during elementary geomagnetic disturbances 12 p1872 A66-24472
- Simultaneous observations of auroral zone X-ray microbursts, using two balloon-borne radiation detectors separated by 300 km to estimate size of region of electron precipitation 12 p1944 A66-24841
- Radioactive debris over Fairbanks, Alaska, on February 18, 1965, investigating bremsstrahlung X-rays in auroral zone 12 p1875 A66-24896
- Distribution and variation of atmospheric density over thermosphere, including auroral region, noting wind motion and high altitude circulation 14 p2382 A66-27618
- Auroral zone position changes as function of magnetic activity and time of day 15 p2486 A66-29091
- Diurnal and seasonal variations of sporadic layer in auroral zone 15 p2487 A66-29098
- Temporal variation in scintillation rate spectrum of satellite signals analyzed in auroral zone 16 p2691 A66-30231
- Correlation of simultaneous optical and radio auroral data showing that radio wave scattering belt includes visual auroral belt 16 p2692 A66-30329
- Electron precipitation in auroral zone, using observations from riometer, balloon, rocket and satellite experiments 17 p2917 A66-32363
- Data on geophysical phenomena at magnetically conjugate points on Earth including cosmic noise absorption, conjugacy of visual auroras, magnetic variations, VLF phenomena, etc 19 p3453 A66-35981
- Statistical analysis of diurnal variation in southern boundary of aurora, HF backscatter records and geomagnetic latitude of dayside aurora 20 p3553 A66-38193
- Precipitation of electrons and protons into atmosphere from inside magnetosphere, within auroral zone and at polar caps 20 p3640 A66-38320
- Electron density profile measurements in auroral zone D layer during quiet ionospheric conditions, using partial reflection method 22 p3906 A66-39951
- Latitudinal and diurnal variations of ionospheric electron content near auroral zone in winter from Faraday rotation data 22 p3911 A66-39985
- Auroral disturbances resulting in multipath distortion in propagation by ionospheric reflection and description of chirp ionosonde and antenna systems 23 p4036 A66-41143
- AUSFORMING**
- Ausforming effect on rolling contact fatigue life of M-50 bearing steel [ASME PAPER 65-LUB-9] 04 p0536 A66-14243
- Ausforming, process of plastically deforming austenitic steel at high temperatures, without recrystallization and prior to transformation 13 p2107 A66-25639



## AUSTENITIC STEEL

## SA MARTENSITIC STEEL

Heat resistance in air of four industrial austenitic-ferrite steels with low nickel content at 750-1050 degrees C, noting oxide scale formation 01 p0088 A66-10988

Heat treatment cycle effect on mechanical properties of corrosion resistant precipitation hardened steel AM 355 in terms of metallographic structure 02 p0242 A66-11304

Interface discontinuities from improper heat balance and effects on fatigue life of spot welded joint in austenitic stainless steel 02 p0235 A66-11469

Tensile testing study of hardening mechanisms when niobium carbide precipitation occurs during deformation of 18Cr/12Ni/Nb austenitic stainless steel at 650 degrees C 02 p0246 A66-12195

Mechanical characteristics of columbium steels and synthetic iron-carbon-niobium alloys as function of temperature at which they are converted to austenite 03 p0381 A66-12540

Temperature effect of plastic deformation on aging kinetics of heat resistant austenitic steels 03 p0385 A66-13171

Stress effect on negative creep in chromium-nickel-titanium steels, noting temperature effect and specific volume change 05 p0699 A66-14684

Effect of gamma phase aging and phase cold hardening on austenitic strength of Fe-Ni-Ti steels, noting martensitic point and segregation 05 p0699 A66-14689

Impact strength of austenitic stainless steel welds discussing effects of heat treatment, carbon and ferrite content [ASME PAPER 65-WA/MET-1] 05 p0704 A66-15692

Austenitic chromium-nickel-manganese steel, describing temperature effects on crystal structure and experimental techniques 05 p0704 A66-15819

Maraging steel response to heat treatment including formability, machinability, stress-corrosion resistance and cold-working behavior of austenitic and martensitic phases 08 p1239 A66-18959

Feasibility, reliability and applicability of maraging steels 08 p1240 A66-18960

Aus-bay quenching, heat treatment process which minimizes distortion and increases tensile strength 10 p1545 A66-21219

Effect of molybdenum, niobium and tungsten on structure and properties of nitrogen containing austenitic chromium-manganese steels 12 p1893 A66-23726

High temperature plastic deformation and hardening effects on brittleness, strength and viscosity of austenitic steel and alloys 13 p2106 A66-25328

Ausforging, process of plastically deforming austenitic steel at high temperatures, without recrystallization and prior to transformation 13 p2107 A66-25639

Elastic and plastic deformation of polycrystalline metals exposed to ultrasonic load and high temperatures 15 p2523 A66-29601

Surface finishing effect on stress corrosion resistance of austenitic stainless steels 17 p2942 A66-33445

Austenite-martensite interface dislocations in stainless steel shown as probable pinned Shockley partials 18 p3123 A66-33927

Optimum alloying level defined as one beyond which net positive effect is reduced by decline in some product property, noting steels 20 p3585 A66-37697

Electron microprobe for studying thermoelectric materials and heat-resistant steel for gas-turbine blading 24 p4211 A66-42507

## AUSTRALIA

Upper atmosphere sounding rocket program in increased space research activities in Australia 09 p1458 A66-20707

Winter jet stream structure and turbulence over Australia 10 p1552 A66-21317

Meteorological interpretation of Tiros satellite photographs of Australian area 11 p1728 A66-22319

Annual report, 1964-65 /Aeronautical Research Laboratories, Australian Defence Scientific Service/ on aerodynamics, guided weapons and systems and flight

research 13 p2056 A66-25120  
Australian space program noting rocket soundings, Beacon satellites, station development, etc 15 p2600 A66-29909

## AUSTRIA

German and Austrian astronomical observatories reports on personnel, equipment, projects and publications 13 p2189 A66-26736

Space research activities in Austria 15 p2601 A66-29934

## AUTOCORRELATION

Autocorrelation and spectral density of energy of stationary electromagnetic wave expressed as function of same parameters of its component trains of waves 01 p0106 A66-10645

Itinerant oscillator model of liquids covering classical velocity autocorrelation function of atom and neutron scattering experiments 04 p0547 A66-13809

Numerical characteristics of signal-noise mixture at output of autocorrelation device for sinusoidal signal and Gaussian noise 04 p0501 A66-14407

Single-sideband optical correlator using ultrasonic transducer for variable reference function 06 p0881 A66-16641

Relationship between geometric optic and autocorrelation approach to lunar and planetary radar echoes for Gaussian autocorrelation function 09 p1341 A66-19870

Statistics of product of Gaussian noise process and pseudorandom binary code 09 p1342 A66-19919

Cross correlation and autocorrelation functions of nonstationary signals based on optimal approximation of ensemble correlation function for one pair of signals 10 p1517 A66-21694

Vibrational analysis, discussing spectrum analyzers, correlation and autocorrelation analysis and hybrid and digital computer applications 12 p1970 A66-24722

Electron irregularity size and motion in interplanetary medium determined from radio source scintillation phenomena 13 p2182 A66-25571

Two-time probability distribution function, autocorrelation function, Liouville equation and fluctuation theory of plasma kinetics 13 p2156 A66-26685

Autocorrelation and hypergeometric function applied in evaluating response of nonlinearities to Gaussian noise 14 p2287 A66-27726

High resolution power spectrum of international magnetic character, showing two subsidiary peaks on both sides of 27-day period 16 p2695 A66-30719

Autocorrelation functions and spectra for mechanical systems subjected to random vibrations 16 p2823 A66-31687

[ONERA TP-340] Oscillatory component in solar granulation continuum brightness fluctuations, secondary maxima in temporal autocorrelation functions and power spectra 17 p2996 A66-31920

Autocorrelation statistical method applied to atmospheric electricity 17 p2923 A66-33363

Frequency measurement using autocorrelator as frequency discriminator, noting technique and high-noise sensitivity 19 p3306 A66-36657

Improper random process where impulse occurrence times constitutes stationary point process, noting autocorrelation function and spectral density 22 p3885 A66-40870

Autocorrelation as pulse compression system, giving effective time resolution as inverse of correlation bandwidth and compression ratio of time resolution to signal duration 23 p4034 A66-41022

Stochastic process explaining statistical properties of radar echo patterns 24 p4175 A66-42987

## AUTOIONIZATION

## S SELF-IONIZATION

## AUTOMATIC CONTROL

## SA CYBERNETICS

## SA SERVOCONTROL

Automatic flight control system for A-7A featuring high fixed gain dual channels, series servos and control augmentation in addition to normal attitude and path control functions 01 p0098 A66-10007

Sectionalized, automatic approach and landing system with monitor channel added developed by Boeing-Bendix for all-weather landing 01 p0101 A66-1003

Automated techniques for providing reliability assurance in launch operations of Saturn IB space vehicle 01 p0052 A66-1011

Optimum prognosis for random processes by applying asymptotically optimal succession of automatic systems 01 p0050 A66-1065

Difficulties in control system synthesis for launch vehicles exhibiting severe mode interaction 01 p0104 A66-1067

Realizable transfer function of closed-loop automatic control system calculated with aid of minimum mean square error criterion 01 p0051 A66-1070

Probability of averting failure in system containing automatic safety devices 01 p0043 A66-1070

Statistical characteristics of angular drift velocity of gyrostabilizer employing floating gyroscopes 01 p0068 A66-1071

Propeller control at low airspeed of turboprop engines in any fixed-wing aircraft with special reference to thrust or drag approach and landing 01 p0013 A66-1094

[AIAA PAPER 65-709] Gradient method of solving terminal control problems in linear automatic control system 01 p0051 A66-1101

Transient process of nonlinear automatic system calculated by numerical digital computer method based on convolution integral 01 p0045 A66-1102

Optimal transfer function of linear automatic system determined from criterion of minimum mean square error 02 p0206 A66-1131

Disturbance signals used to synthesize optimal structure of rapid action automatic systems 02 p0206 A66-1131

Stability of automatic control system with variable structure studied for application to stabilization of linear objects whose parameters vary quite rapidly within wide limits 02 p0207 A66-1131

Comparison of differentiating and integrating correction circuits for stability of forced gyrostabilizers for high value of amplification coefficient 02 p0226 A66-1131

Hot wire Wheatstone bridge used in automatic control and method to obtain linear response in large speed fields 02 p0229 A66-1176

Human pilot behavior compared with automatic pilots in terms of adaptability response time and reliability 02 p0187 A66-1186

Control problems associated with stable platforms using single-axis integrating gyroscopes including axes design, drift due to vibration and compensation 03 p0390 A66-1253

Stability of automatic control system with nonlinear elements, obtaining quadratic equations by using Liapunov method 03 p0349 A66-1270

Optimal control approach and uncertainty to feedback control problems 03 p0349 A66-1299

Time lapse in variable-structure automatic control systems 03 p0350 A66-1304

Cybernetics role in space flight including control circuits for guidance and electronic equipment automation and development 04 p0469 A66-1349

Automatic command control system using phonetic voice pattern recognition 04 p0469 A66-1349

Automatic control in captive testing of large space-vehicle propulsion systems and components 04 p0507 A66-1361

Control system 465L used by Strategic Air Command noting automated functions, data processing, integration of human and electronic elements, etc 04 p0507 A66-1368

Frequency characteristics of pulse automatic control systems determined by auxiliary pulse system 04 p0502 A66-1370

Automatic control of flow rate and pressure in mixing process involving several components 04 p0504 A66-1377

Sampled-data control systems analyzed by signal flow graphs 04 p0504 A66-1377

Noise rejection improvement of class of



automatic control systems by means of nonlinear control laws 04 p0504 A66-13976  
Pitch, roll and yaw axis stability augmentation system providing automatic failure detection of portions of system and further stability augmentation after any single failure 04 p0544 A66-14136  
Centralized vibration control of vibration testing noting details of automatic equalizers, switching panel, data reduction, etc 04 p0508 A66-14446  
Limited transients for certain single-loop systems containing nonlinear amplifier and linear system 05 p0656 A66-14727  
Man-powerplant reliability interface, emphasizing manned vs automatic sensing and control 05 p0627 A66-15013  
[SAE PAPER 650810] 05 p0627 A66-15013  
Book on theory of random functions in probability methods for automatic control systems 05 p0657 A66-15066  
Book on structural synthesis of high-accuracy automatic control systems with large stable amplification 05 p0657 A66-15086  
Digital electrometric device with automatic discrete compensation 05 p0680 A66-15211  
Book on asymptotic expansions in powers of small parameter applied to nonsteady oscillations in nonlinear systems with one or more degrees of freedom 05 p0776 A66-15327  
Invariance provided for in nonlinear control systems by reducing problem to construction of inverse operator 05 p0709 A66-15342  
Automation of equalizer consisting of delay line with adjustable taps 06 p0831 A66-16343  
Determination of automatic control in automatically controlled plants 06 p0862 A66-16419  
Nonlinear automatic control system, discussing optimum tuning via parametric stability region 06 p0863 A66-16528  
Automatic relay systems, describing self-oscillation induced parameter variation 06 p0863 A66-16530  
Graphic-analytical method for calculating optimum adjustment of disturbance-compensating system incorporating dynamic elements 06 p0863 A66-16532  
Frequency domain stability criteria, discussing generation and validity of stability criteria 06 p0864 A66-16736  
Upper bound on dynamic/transient and steady state/quantization error in digital control systems, using direct method of Liapunov 06 p0865 A66-16741  
Optimum numerical algorithm for determining elements of inverse of Vandermonde matrix 06 p0866 A66-16751  
Synthesis of automation elements and finite automata in graphical form 07 p1012 A66-17383  
Mean time of failureless operation of duplicated devices with automatic control and switching 07 p1013 A66-17388  
Technique for evaluating accuracy of nonlinear automatic system using structural diagrams 07 p1013 A66-17430  
Nonlinear optimal filtration problem solved, using quasi-orthogonal representations of random functions 07 p1014 A66-17432  
Fault location in modern airborne radar, discussing maintenance reduction techniques and reliability improvement 07 p1006 A66-17495  
Slope quantized binary pulse code modulation by coding signal slopes with unidigit 1/0 pulses, using special feedback circuit and threshold in coder comparator 07 p1002 A66-18248  
Constant time loci in phase-plane and isoclines for nonlinear and piecewise linear systems 07 p1016 A66-18345  
Practical determination of stability region of equilibrium point of second-order nonlinear recurrence with real variables 08 p1255 A66-18639  
Semiconductor diodes and transistors applied to temperature measurement and control, examining automation application 08 p1221 A66-18697  
Thyatron temperature regulator, operation and application 08 p1223 A66-18799  
Mathematical foundations of analog simulation proceeding from Laplace, diffusion and wave

equations 08 p1187 A66-18861  
Microminiaturization in control equipment and computers 08 p1194 A66-19300  
Intermediate text on dynamic analysis and automatic control 08 p1200 A66-19464  
Dynamics of two-channel automatic control systems taking into account nonlinear interaction between channels 08 p1201 A66-19676  
Attenuation factor and degree of stability of automatic control systems determined by Mikhailov criterion and Chebyshev polynomials 08 p1201 A66-19684  
Wiener problem applied to synthesis of automatic control system incorporating minimum phase, nonminimum phase or unstable element 08 p1201 A66-19686  
Reliability of automatic control systems, considering properties of controlled plant, taking error probability in control as criterion 08 p1201 A66-19691  
Propeller control at low airspeed on turboprop engines in any fixed-wing aircraft, with special reference to thrust or drag in approach and landing 09 p1329 A66-20242  
[AIAA PAPER 65-709] 09 p1329 A66-20242  
Pure-fluid amplifier in automatic control 09 p1331 A66-20299  
Automatic system dynamics analysis, considering variations of random parameters, determining reliability of representative servosystems 09 p1361 A66-20302  
Predicting change in state of automatic control system, using correlation analysis 09 p1361 A66-20304  
Sensitivity of transistor multiple loop feedback amplifier to parameter variations evaluated via replacement with equivalent circuit systems 09 p1355 A66-20603  
Generation of Liapunov functions for second method solution of stability problems in automatic control 09 p1362 A66-20650  
Automatic control systems commutable rigid feedback to create astaticism in variable structured systems 09 p1364 A66-20912  
Automatic time-domain equalizer consisting of delay line with adjustable taps 10 p1503 A66-21649  
Pneumatic fluid elements used in automatic control systems, noting viscous fluid properties and application to turbine rpm control 10 p1486 A66-21753  
Equations of linear automatic control systems decomposed 10 p1518 A66-21979  
Sufficient conditions of optimality having control region dependent on phase coordinates 10 p1518 A66-21980  
Theoretical and engineering aspects of applying predicting systems to automatic guidance and control 11 p1673 A66-22201  
Lowering order of transfer function of automatic control system based on use of generalized integral quadratic estimates of transient processes of system 11 p1673 A66-22203  
Optimization of terminal state of controlled system when equations of motion contain derivatives of control parameters 11 p1674 A66-22350  
Optimum control in nonlinear automatic control systems and linear systems with distributed parameters 11 p1674 A66-22352  
Absolute stability of automatic control system with allowances for external load of hydraulic servomotor 11 p1674 A66-22358  
Generalized statistical linearization method for multivariable systems and arbitrary periodic and random signal effect on nonlinear automatic system 11 p1674 A66-22359  
Rms approximation theory applied to linear self-adaptive models 11 p1674 A66-22360  
Realizable transfer function of closed-loop automatic control system calculated with aid of minimum mean square error criterion 11 p1675 A66-22618  
Probability of averting failure in system containing automatic safety devices 11 p1664 A66-22620  
Statistical characteristics of angular drift velocity of gyrostabilizer employing floating gyroscopes 11 p1705 A66-22625  
Forced sliding regimes in automatic control systems 11 p1675 A66-22640  
Spontaneous switching from closed to open state observed in four-layer silicon diodes

serving as keying elements in automatic systems 11 p1667 A66-22743  
Variable-structure system dynamics in sliding regime investigated, using structural analysis methods of infinite gain and relay systems 11 p1676 A66-22755  
Design of variable structure automatic control system frequency characteristics, using harmonic linearization 11 p1677 A66-22763  
Automatic control theory application to null-balance processing of spectral data generated by vidicon television camera 11 p1706 A66-22890  
Automatic control - Conference, Rensselaer Polytechnic Institute, Troy, New York, June 1965 11 p1659 A66-23108  
Nonlinear servomechanism analyzed, using Fokker-Planck equation, discussing tracking failure 11 p1670 A66-23224  
Automatic control systems, discussing optimal and on-line adaptive control in electricity, nuclear research, steel industry, numerical problems, etc 11 p1679 A66-23272  
Relations between coefficients of characteristic equation of automatic systems and parameters of root loci with hyperbolic branches 11 p1680 A66-23325  
Adaptation, learning and self-learning in automatic systems, discussing stochastic approximation, pattern recognition, adaptive filters, etc 11 p1680 A66-23332  
Existence of Liapunov functions for problem of Lure with removal of complete controllability and observability 11 p1681 A66-23451  
Self-diagnosable DX-1 computer design to achieve maximum operational availability 12 p1828 A66-23843  
Optimum prognosis for random processes by applying asymptotically optimal succession of automatic systems 12 p1848 A66-24006  
Automatic control system relay represented by means of limit toward which continuous function tends when chosen parameter increases indefinitely 12 p1848 A66-24029  
Overall stability of equilibrium position in critical Liapunov case, using extension of Malkin method 12 p1848 A66-24030  
Systems design of automatic dynamic control for piloted aircraft, discussing stability, accuracy, response and behavior to external perturbations 12 p1803 A66-24090  
Bang-bang damping rate on system components with time delay and lag 12 p1850 A66-24263  
Two theorems on Liapunov second method, discussing related automatic control system techniques and asymptotic system stability 12 p1850 A66-24264  
Automation of control processes - International Federation on Automatic Control Congress, Basel, Switzerland, August-September 1963 12 p1850 A66-24314  
Control of radio telescope, noting servosystem ability to keep tracking position errors and wind-caused error within certain limits 12 p1851 A66-24319  
Control system of microwave antenna positioning used in communication satellite tracking, noting servosystems, converter, Leonard drive, control panel, etc 12 p1817 A66-24320  
Pressure regulation in equalization chamber of model blowdown wing tunnel used at various Mach numbers, calculating compressed-air flow through control valve and characteristics of transfer function 12 p1857 A66-24322  
Discrete and self-adaptive systems - International Federation on Automatic Control Congress, Basel, Switzerland, August-September 1963 12 p1851 A66-24323  
Stability and quality evaluation of nonlinear sampled data control systems using Popov criteria for continuous nonlinear systems 12 p1852 A66-24325  
Applicability and limitations of analytical methods in study of nonlinear sampled data automatic control systems 12 p1852 A66-24326  
Automatic system optimization techniques using independent random trial signals, relying on correlation functions 12 p1853 A66-24332  
Dominant operator method to determine characteristic of self-adaptive automatic



control system 12 p1853 A66-24335  
 Space structure welding-automation system consisting of Sciaky-welding system, automation control and seam-tracking system [ASTME PREPRINT MS66-708] 12 p1886 A66-24409  
 System approach and requirements of particular switching system of Automated Patching System /Aps/ for use on Atlantic Missile Range /AMR/ 12 p1818 A66-24596  
 Automatic control, systems science, cybernetics, biomedical engineering, human factors - IEEE International Convention, New York, March 1966 12 p1854 A66-24634  
 Control problems regarding space developments, considering automation, reliability, computer role, human operator, etc 13 p2056 A66-25231  
 Combined automatic control systems with automatic adjustment of amplification coefficient of disturbance controller for error reduction 13 p2045 A66-25300  
 Phase stability of system of particles in cyclic accelerator with automatic frequency correction of accelerating field, noting kinetic equation method 13 p2147 A66-25748  
 Equalization systems for stochastic processes, discussing automatic adaptive servocontrol, feedback control and vibration simulation equipment 13 p2048 A66-25848  
 Automatic control system stability reserve using amplitude phase criteria with respect to modulus and phase 13 p2049 A66-26055  
 Method for automatically adjusting networks for best approximation to desired responses, using iterative gradient techniques, constraint equations and Carroll programming technique 13 p2051 A66-26070  
 Synthesis problem solution for performance criteria defined by time domain sensitivity function, noting controller structure, parametric minimization and operative adjustment of parameters 13 p2051 A66-26071  
 Nonlinear signal comparators in feedback structures used for input-output invariance of single piecewise constant parameter 13 p2054 A66-26090  
 Sensitivity comparison of closed-loop and open-loop systems 13 p2054 A66-26092  
 Automatic stabilization systems reduce accidents due to disorientation, emphasizing sensor-servo system for roll axis control [SAE PAPER 660201] 13 p1996 A66-26390  
 Soviet book on automation and control of air breathing gas turbine and ramjet engines 13 p2173 A66-26463  
 Synthesis of automatic control system for tracking random moving coordinate solved by dynamic programming methods 13 p2055 A66-26467  
 Meteorological data from weather satellites equipped with TV and IR sensors, noting Automatic Picture Taking /APT/ recorder 14 p2289 A66-26806  
 Random error effect on directional gain of sectional parabolic antenna with automatic phasing, setting sections effectively by three control points method 14 p2250 A66-27141  
 Effect of relay response time on dynamic properties of automatic system incorporating linear group and relay element with pure delay 14 p2264 A66-27358  
 Synthesis of linear automatic control system with constant parameters for integral Q-factor, noting effect of small parameters on properties of optimum system 14 p2265 A66-27521  
 Solution of optimum filtering problems when input signals of automatic control system are described by different differential equations at successive time intervals 14 p2265 A66-27523  
 Approximation of variable time delays and design of constant and variable delay circuits, noting simulation of delays in automatic control systems by computers 14 p2266 A66-27528  
 Minimum effort control problem in rotund reflexive Banach space and extension to Hilbert space under bounded linear transformation 14 p2266 A66-27631  
 Automatic control of wideband vibration testing of nonrigid structure with wide range of acceleration levels requiring computation of feedback signal 14 p2267 A66-27665  
 Motion control for nonlinear system with

small initial perturbation 14 p2267 A66-27673  
 Autocorrelation and hypergeometric function applied in evaluating response of nonlinearities to Gaussian noise 14 p2267 A66-27726  
 Automatic preworkshop screening test apparatus for determining which components removed from aircraft during ground maintenance need to be sent to workshop 14 p2224 A66-28298  
 Frequency characteristics of pulse automatic control systems determined by auxiliary pulse system 15 p2469 A66-28544  
 Automatic device for reversible hypothermia in living organism, considering parameters of physiological functions, included in logic circuits 15 p2444 A66-29498  
 Plant physiological process measuring devices for automatic growth control in closed system 15 p2445 A66-29506  
 Dynamic characteristics of automatic control plants determined, using term-by-term integration of differential equations 15 p2475 A66-29768  
 Invariance provided for in nonlinear control systems by reducing problem to construction of inverse operator 15 p2530 A66-29977  
 Graphic analysis of behavior of stepwise extremal control system adapted to process showing inertia after static characteristic 16 p2668 A66-30585  
 Closed-loop automatic control system with unvalued substantially nonlinear element, using approximation of characteristics by Fourier series 16 p2669 A66-30754  
 Approximation method determining follow-up failure conditions for nonlinear automatic systems in presence of control and noise signals 16 p2669 A66-30755  
 Nonlinear automatic control system, discussing optimum tuning via parametric stability region construction 16 p2670 A66-30838  
 Graphic-analytical method for calculating optimum adjustment of disturbance-compensating system incorporating dynamic elements 16 p2670 A66-30839  
 Instruments and measurements, automatic control - International Conference, Stockholm, September 1964 16 p2706 A66-30879  
 Statistical decision theory determination of parameter variations in closed-loop automatic adaptive control system 16 p2670 A66-30880  
 Automatic level-control systems requirements for powerline carrier engineering 16 p2654 A66-31028  
 Book on automatic control of linear and nonlinear systems, particularly aircraft utilization 16 p2744 A66-31058  
 Automatic control systems with carrier frequency information transmission channel, deriving transfer functions 16 p2672 A66-31552  
 Stability of pulse-type automatic system described by matrix algebra 16 p2673 A66-31793  
 Reliability of back-up system with consideration of failures in switches and automatic control systems 17 p2880 A66-31904  
 Nonlinear automatic systems analyzed by reduction to first and second order systems by linear nonsingular transformation of variables 17 p2901 A66-32250  
 Synthesis method for automatic control systems, examining controller design for turbo-prop engine 17 p2901 A66-32311  
 Necessary condition for optimal control in nonlinear automatic control system determined, using method of successive approximations 17 p2902 A66-32574  
 Stability of automatic systems for tracking point targets, noting nonlinear dependence of signals on channel mismatch and its limiting values 17 p2902 A66-32579  
 Nonstationary automatic control systems design by reaction quenching method 17 p2902 A66-32580  
 Reliability of stand-by system with automatic reserve cut-in, considering probability method 17 p2888 A66-32709  
 Level quantization effect in statistical analysis of closed-loop digital automation systems 18 p3089 A66-33736  
 Peaceful uses of automation in outer space - Symposium, International Federation of

Automatic Control, Stavanger, Norway, June 1965 18 p3240 A66-33844  
 Automatic starter for nuclear reactor rocket engine with automatic power control system 18 p3133 A66-33874  
 Automatic control systems for attitude control of Apollo spacecraft 18 p3244 A66-33870  
 Nonlinear control laws for takeoff and landing of circular-orbit winged glide space vehicle 18 p3132 A66-33880  
 Operational circuits found in measuring devices and in regulation or control systems for low power signal transformation for space application 18 p3076 A66-33888  
 Spacecraft trajectories prediction under discrete control 18 p3228 A66-33886  
 Automatic control equipment for FR-1 and D-1 satellites 18 p3246 A66-33981  
 Attenuation factor and degree of stability of automatic control systems determined by Mikhailov criterion and Chebyshev polynomials 18 p3091 A66-34677  
 Wiener problem applied to synthesis of automatic control system incorporating minimum phase, nonminimum phase or unstable element 18 p3091 A66-34677  
 Reliability of automatic control systems considering properties of controlled plants taking error probability in control as criterion 18 p3091 A66-34677  
 Optimal set of parameters for radioelectronic equipment automatic control using nonlinear programming 18 p3091 A66-34981  
 Dynamics of nonlinear control systems by constructing cross sections of parameter space 18 p3091 A66-34981  
 Variable-structure automatic control system with switchable phase-shifting filters for linear plants, converting error signal to control switching device 18 p3092 A66-34999  
 Stability analysis of automatic control systems with random parameters, applying Mikhailov criterion 18 p3092 A66-34999  
 Time lapse in variable-structure automatic control systems 18 p3092 A66-35004  
 Graphical analysis of extremal control system stepwise adapted to process with extremal characteristic located between two first-order linear operators 19 p3324 A66-35581  
 Mikhailov criterion for exponential polynomials, determining existence of zeros in right half-plane 19 p3388 A66-35824  
 Equations of linear automatic control systems decomposed asymptotically 19 p3324 A66-35851  
 Sufficient conditions of optimality having control region dependent on phase coordinates 19 p3325 A66-35851  
 Automatic system with stored experience, examining probability density of useful signal 19 p3325 A66-35947  
 Self-oscillations of pulse type extremum system with plant having extremal characteristics shaped by multiplication of two coordinates 19 p3325 A66-35981  
 Invariance effect for finite number of coordinates in infinite dimensional automatic control system 19 p3325 A66-35981  
 Synthesis of automatic control systems for linear plants with variable parameters satisfying specified performance criteria 19 p3328 A66-36024  
 Stability, reproducibility and sensitivity of combined systems of automatic control with variable structure determined by presence of sliding mode region 19 p3329 A66-36021  
 Automatic control - Conference, University of Washington, Seattle, August 1966 19 p3330 A66-36660  
 Algorithm based on sequential optimization of nonlinear control system 19 p3334 A66-36676  
 Optimum discrete information system and relations between measurement quality decisions and system performance 19 p3310 A66-36681  
 Distributed parameter systems in discrete time models compared with response obtained by approximating transcendental transfer function with root factor and other approximations 19 p3282 A66-36683  
 Sequential estimation on states of linear systems disturbed by white noise, determining relations between covariance matrices 19 p3338 A66-36736



Microminiaturization in automatic control equipment and digital computers - Symposium, International Federation of Automatic Control and International Federation for Information Processing, Munich, October 1965 19 p3322 A66-36806

Automatic tracking radar control via nonstationary filter, noting design principle and operation 20 p3536 A66-36866

Control algorithms synthesis for analytical adaptive control systems with nonlinear plants investigated with hybrid computer 20 p3536 A66-36876

Forced modes of automatic continuous system with linear controlled plant with variable dynamic properties and learning model self-adjusted by search modulation 20 p3536 A66-36878

Equivalent transfer function of linear two-channel system of automatic control, discussing system stability dependence on cross links 20 p3537 A66-36891

Transient processes in linear automatic control systems dependent on parameters which appear when differential equations of analyzing system are transformed by Laplace-Karson method 20 p3537 A66-36892

Stability and quality of automatic control of plant with pure time delay, using regulator with constant and switching parameters 20 p3537 A66-36894

Automation of air traffic control, discussing radar, data handling and data communication 20 p3595 A66-37003

Space packaged automatic checkout system for aerospace vehicles including test equipment, control, measurement capability and computer program 20 p3542 A66-37244

Dynamics of two-channel automatic control systems taking into account nonlinear interaction between channels 20 p3538 A66-37268

Automatic control of spacing of Fabry-Perot interferometers to transmit at given wavelength 20 p3558 A66-37286

Operational reliability of finite automatic systems in terms of entropy in individual components 20 p3538 A66-37486

Effectiveness of shock-absorber parameters of instrument with weakly damped sensitive elements 20 p3560 A66-37677

Temperature automatic control system in photographic laboratory compensating for humidity changes by using semiwet bulb controller 20 p3561 A66-38049

Semiautomatic mechanical system for evaluation of rocket booster test stand oscillograms 20 p3561 A66-38065

Aircraft gas turbine starting with automatically controlled electronic unit, noting system design, operation and performance 20 p3540 A66-38299

Photoelectric solar power plant for water pumps in grazing areas noting design, construction and automatic control system testing 20 p3503 A66-38438

Automatic feedback table leveling system, noting tilt to simulate aerodynamic drag 21 p3722 A66-38887

Damping by hemispheric torquing to actively control spin axis in rotor while remaining unchanged with respect to case fixed reference 21 p3737 A66-38896

Autonomy in multiply connected variable structure automatic control systems 21 p3719 A66-39247

Moments of output coordinates of nonlinear system determined by algorithm based on approximation method, noting application to automatic control system 21 p3758 A66-39283

Nonlinear automatic system with logical device analyzed in presence of external action, obtaining harmonic linearization coefficients 21 p3719 A66-39284

Synthesis of control device for class of nonlinear sampled data system, obtaining processes with minimum control time 21 p3719 A66-39286

Time domain analysis and synthesis of time-varying linear sampled data automatic control system with separable impulsive responses 21 p3719 A66-39429

Effect of signal frequency maladjustment and automatic phase control circuit parameters on amplitude and phase shift of reflex amplifier, analyzing filtering properties 22 p3875 A66-40071

Adaptation, learning and self-learning in automatic systems, discussing stochastic approximation, pattern recognition, adaptive filters, etc 22 p3884 A66-40412

Book on synthesis of multiloop control systems for application to automatic control and computer circuit construction 22 p3885 A66-40854

Text on theory of automated air navigation, examining methods of flight preparation and precision 22 p3946 A66-40855

Stability of automatic control systems with nonlinearity and nonunique equilibrium state 23 p4048 A66-40967

Analytical design of controllers for linear autonomous systems of arbitrary order 23 p4048 A66-40969

Automatic flight control system for A-7A featuring high fixed gain dual channels, series servos and control augmentation in addition to normal attitude and path control functions 23 p4088 A66-40983

Stable transmission of given transient response in closed loop nonlinear servosystem under fixed initial condition and in presence of possible disturbances 23 p4048 A66-41393

Recognition and prediction systems, developing criteria for resolvable arguments 23 p4041 A66-41395

Automatic control system analysis via space-state method, using n first-order differential equation 23 p4049 A66-41399

Spontaneous switching from closed to open state observed in four-layer silicon diodes serving as keying elements in automatic systems 23 p4046 A66-41481

Automatic tracking from video signals, discussing characteristics of single and multiple gate trackers and measured performance 23 p4089 A66-41672

Motion stability conditions of plant equipped with automatic control device in certain critical cases 24 p4236 A66-42213

Chemical and electrical energies in manufacturing noting role of numerical control, hydrostatic processes, forming, electrochemical machining, etc 24 p4217 A66-42336

Analog and digital controls used in electron beam welding and metal working machinery including electron beam milling machine 24 p4217 A66-42345

Input signal level for stability loss or self-oscillations in automatic control system, using analysis for nonlinear systems with forced vibrations 24 p4188 A66-42476

Diagrams of computers calculating parallax angle of azimuthally mounted astronomical telescopes 24 p4211 A66-42484

Absolute stability of specific class of nonlinear pulsed automatic systems, noting error signal and amplitude modulation 24 p4189 A66-42948

**AUTOMATIC DATA PROCESSING SYSTEM**

Mass spectrometric electron impact ionization potentials rapidly obtained by electronic control and automatic data processing systems 07 p1091 A66-18489

Satellite Telemetry Automatic Reduction System /STARS/ capable of processing data at capacity of 200 million data points per day [ISA PAPER 7.2-2-65] 10 p1507 A66-21904

Automatic recording, printing and punching of meteorological data from signals measured by automatic bridges and potentiometers on high tower of Institute of Applied Geophysics 16 p2704 A66-30776

RT Data Automation System automatically controls and synchronizes data-gathering sequence of cruise instruments of Mariner IV spacecraft 19 p3307 A66-35668

Automatic telemetry checkout station for Saturn V systems using real time signal digitizer and general purpose computer 19 p3339 A66-35677

Automatic, multichannel system for data recording and processing obtained in studies of ionospheric structural inhomogeneities, containing magnetic-tape memory and device for digital tape memory and device for digital computer input 22 p3920 A66-40772

Steady and dynamic loads on tandem rotor, controls and airframe flight tested with Army helicopter, using automatic data processing [AIAA PAPER 66-735] 23 p4008 A66-41324

## AUTOMATIC FREQUENCY CONTROL

Automatic frequency control of laser local oscillator for heterodyne detection of laser signal and use of 2.5 gc frequency offset to permit retrieval of microwave data 05 p0633 A66-14908

Mean square phase fluctuations at phase detector input of automatic frequency control system with proportional integrating filter 06 p0859 A66-17192

Nonlinear forced oscillations in phase automatic frequency control system, accounting for nonlinearity of system 07 p1001 A66-17353

Filtering properties of frequency-stability transport circuits of molecular beam generator, noting design considerations for high efficiency 09 p1353 A66-20442

Residual difference between oscillator frequencies used to investigate noise immunity of phase automatic frequency control 14 p2236 A66-27245

Mean square phase fluctuations at phase detector input of automatic frequency control system with proportional integrating filter 19 p3324 A66-35550

## AUTOMATIC GAIN CONTROL /AGC/

Automatic gain control of emitter current to increase dynamic range and calculate amplitude characteristics of transistorized resonance amplifier 04 p0496 A66-13914

Automatic gain control circuits, discussing performance and comparing theoretical and experimental results 04 p0501 A66-14409

Single-pulse detection probability data for system with instantaneous automatic gain control and 5/1 bandwidth ratio obtained by Monte Carlo simulation 06 p0841 A66-15957

Amplitude and phase direction-finding characteristics of monopulse automatic tracking system operating on sum-difference principle 08 p1190 A66-18911

Automatic gain control for reducing dynamic range of signals at output of phase radio range finder, noting effect of parasitic phase shifts 14 p2236 A66-27356

Diode bridge variable attenuator used to overcome error signals and harmonic distortion in wide range AGC 14 p2267 A66-27805

Black-box approach applied to design of 60-megacycle IF amplifier, considering application of AGC to circuit and design of phase modulator and balanced mixer 19 p3321 A66-36423

Automatic gain control of emitter current to increase dynamic range and calculate amplitude characteristics of transistorized resonance amplifier 20 p3532 A66-37872

Response of automatic gain control amplifier to two narrow-band input signals, examining weak signal suppression and cross-product generation 22 p3875 A66-40059

## AUTOMATIC LANDING SYSTEM

Automatic and semiautomatic vectoring and landing capability of U.S. Navy carrier-based aircraft F-4G Phantom II 01 p0099 A66-10009

All-weather landing system for C-141 jet cargo transport using vertical navigation computer for military operations 01 p0101 A66-10035

Automatic landing equipment for 707/720 airplanes used under low visibility conditions noting autopilot, auto-throttle, yaw damper, etc 01 p0103 A66-10663

Outer loop control mechanization for automatic landing systems associated with flight control, noting series servo concept as compared to parallel servo mechanization 01 p0014 A66-10664

Electronic techniques applied to taxiing, takeoff, aerial navigation and landing 02 p0255 A66-11466

Present status of all-weather landing system 02 p0256 A66-11861

Reliability factors in flight controls, particularly automatic landing systems and controls for VTOL aircraft in transitional regime 02 p0231 A66-11863

Autoland, stalling and jet V/STOL systems for flight testing of aircraft [AIAA PAPER 65-783] 03 p0318 A66-12557

Head-up display /HUD/ developed for automatic landing in civil aircraft 03 p0329 A66-12884

Boeing Lower Minimums Program in terms of certified components and systems for Category II and for Automatic Landing



- [AIAA PAPER 65-765] 03 p0390 A66-13060  
All-weather landing progress based on improved airborne equipment, pilot qualification, approach lighting and ground environment
- [AIAA PAPER 65-767] 03 p0391 A66-13062  
One-way microelectronic airborne digital data converter intended for use in automatic carrier
- landings 06 p0824 A66-15969  
Inertial navigation systems for automatic landing, using category I instrument landing system 07 p1069 A66-17714  
Schuler tuned inertial system as flight sensor and control of VTOL aircraft translational velocity during hover phase and landing 07 p1070 A66-17724  
Feasibility of using Elliott Automatic Landing System, developed for medium-haul aircraft, on short-haul aircraft 10 p1553 A66-21361  
Automatic landing development in autopilot and autoflares for Trident aircraft 10 p1553 A66-21362  
All-weather landing systems evaluated 11 p1732 A66-23163  
Automatic system ensuring landing in absence of visibility and atmospheric turbulence by controlling motion of aircraft leveling out, consisting of time-dependent input signal shaping device and amplifiers 12 p1909 A66-24321  
Flight control systems, automatic landing devices and inertial navigation with gyros 15 p2534 A66-29365  
Guidance control technique for soft automatic lunar landing 16 p2743 A66-30887  
Operational all-weather landing system described, examining history and present status of all-weather operations 17 p2953 A66-33211  
Automatic landing system on trident aircraft 18 p3131 A66-33560  
Automatic landing of aircraft in blind flying conditions, Royal Aircraft Establishment equipment accuracy and safety 18 p3133 A66-35243  
Para-Visual Detector, flight director display unit, considered by British European Airways 20 p3595 A66-37005  
Manual steering, hybrid guidance system, in-flight computations and trajectory for automatic descent and landing system for LEM 21 p3768 A66-38899  
Sud-Lear all-weather landing system using automatic guidance 21 p3768 A66-39400  
Information and failure warnings monitoring by flight crew during autopilot operation, particularly during very low visibility landing
- [ICAS PAPER 66-17] 22 p3945 A66-40671  
All-weather landing systems in U.K., examining safety and reliability criteria in connection with trident airborne equipment
- [ICAS PAPER 66-8] 22 p3946 A66-40676  
Duplicate monitored system for automatic landing control of VC10 and Concorde 23 p4088 A66-41163  
VC10 test flight of autoflare and automatic landing instrumentation 23 p4015 A66-41165
- ### AUTOMATIC PATTERN RECOGNITION
- Automatic pattern recognition and application to space navigation 04 p0543 A66-13511  
Automatic vortex recognition system for Tiros satellite photograph analysis, noting phases of development and results obtained 16 p2658 A66-31251  
Images of automatic recognition system for two-dimensional patterns move in rapid nonstop manner across stationary scanning unit composed of bank of photodiodes 21 p3705 A66-39145  
Pattern recognition computer operating under automatic control and stored program control for data transfers, system operation, man-machine interface and display operations 23 p4041 A66-41056
- ### AUTOMATIC PICTURE TRANSMISSION
- /APT/  
Automatic picture transmission of Nimbus I meteorological satellite, considering frequency choice, vehicle position, antenna, image reception, etc 08 p1180 A66-18612  
Incorrect input-induced errors in meteorological satellite photogrids 11 p1704 A66-22318  
Device for automatically feeding experimental curve coordinates in large quantities into digital computer for high noise level photographic image 11 p1659 A66-22432  
Graphical method by which small local users of meteorological satellite pictures can identify geographical position of features in image
- [AIAA PAPER 66-439] 16 p2708 A66-31467  
APT signal reception from Nimbus and Tiros satellites, describing APT equipment and signal conversion 20 p3518 A66-37849  
High resolution IR scanning system and vidicon automatic picture transmission of Nimbus II and ground station printout instrumentation 21 p3821 A66-39497
- ### AUTOMATION
- Gas tungsten arc welding process automation based on feedback control concept 16 p2715 A66-31435  
Legal problems in space law, noting automation and new space public domain 19 p3484 A66-36220  
Behavioral analysis of stochastic automata in random media, discussing automata design with quasi-linear behavior and expedient behavior 20 p3537 A66-36895
- ### AUTOMATON
- SA FINITE-STATE MACHINE  
Analog simulation of operations on stochastic matrices using random transitions in automata aided by relay-contact circuits 03 p0350 A66-13037  
Probability analysis of finite automata with unreliable binary elements and regular structural design 03 p0350 A66-13038  
Coding states of partial automaton where memory-element transition functions depend on minimum possible number of variables 03 p0338 A66-13041  
Comparison of manned and unmanned spacecraft 04 p0472 A66-14092  
Global search of performance surface to find parameters optimizing performance of learning control system, using variable structure stochastic automaton 05 p0653 A66-14598  
Common framework for automata theory and control theory 06 p0863 A66-16619  
Algorithm used for synthesis of regular events in asynchronous automatic machines 07 p1014 A66-17437  
Infinite automata theory and structural logical design of digital machines 11 p1659 A66-22707  
Minimizing number of states of automaton with consideration of transition 11 p1676 A66-22708  
Abstract automata analysis based on solution of system of equations in algebra of events 11 p1676 A66-22709  
Limit behavior of closed system of automata with random input 11 p1676 A66-22710  
Automata theory and control theory analytically compared for general and linear systems and tolerance 11 p1680 A66-23275  
Probabilistic automata as generalization of deterministic and nondeterministic finite model, theorems and concept of definiteness 12 p1853 A66-24338  
Random distribution function of nonfailure operation time, taking into account exponential time distribution law of fault occurrence 16 p2672 A66-31407  
Probabilistic logical analysis of neurons and neurophysiological functional organization of core of reticular formation 18 p3056 A66-33761  
Analog simulation of operations on stochastic matrices using random transitions in automata aided by relay-contact circuits 18 p3073 A66-35000  
Probability analysis of finite automata with unreliable binary elements and regular structural design 18 p3092 A66-35001  
Coding states of partial automaton where memory-element transition functions depend on minimum possible number of variables 18 p3074 A66-35004  
Self-reproducing array with simple programming using finite automaton as basic unit 19 p3306 A66-35335  
Learning control system design, discussing hill-climbing and pattern recognition schemes in framework of statistical decision,
- automata and information theory 19 p3333 A66-36662  
Asymptotically optimal stochastic automata in random medium, discussing penalization 23 p4051 A66-41840
- ### AUTOMOBILE
- SAE handbook, 1966, supplies definitions testing methods, measurement methods and data for engineering materials, machine elements and vehicle components 10 p1540 A66-21700
- ### AUTONOMIC NERVOUS SYSTEM
- SA CENTRAL NERVOUS SYSTEM  
Interaction between optokinetic and vestibulo-ocular responses during head rotation in various planes 11 p1643 A66-22587  
Blood pressure and heart rate during hypothalamic self-simulation in dogs, discussing experimental methods and results, physiological response, etc 16 p2640 A66-31154
- ### AUTOPILOT
- Evolution of Honeywell first generation adaptive autopilot inner loop and application to F-94, F-101, X-15 and X-20 vehicles 01 p0099 A66-10000  
Category II lower weather minimums for aircraft landing of airlines of western world [AIAA PAPER 65-766] 03 p0391 A66-13062  
Flight evaluation of long range inertial navigation and steering in autopilot and manual operation 07 p1076 A66-17792  
Optimum autopilot design for maneuverable lifting bodies 11 p1733 A66-23342  
Drone aircraft onboard stabilization circuit design for control signal transmission and transient response irrespective of noise background 11 p1778 A66-23348  
Automatic pilot consisting of guidance system for flight trajectory control and stabilization system for angular acceleration control 12 p1909 A66-23815  
Automatic stabilization of helicopters by using autopilots 12 p1801 A66-24388  
Motion equations for dynamics of aircraft control surface controlled by autopilot 14 p2328 A66-27687  
Category II lower weather minimums for aircraft landing of airlines of western world [AIAA PAPER 65-766] 14 p2328 A66-28107  
Duplex pitch channel in Hawker Siddeley Trident autopilot for glide path extension and flareout control 14 p2328 A66-28229  
Aircraft stabilization for solar eclipse observation, emphasizing use of autopilot for maximum control 16 p2743 A66-30823  
Textbook on automatic guidance of missiles and space vehicles 17 p2951 A66-33151  
Simulator results on guidance and control during supercircular atmospheric entry maneuvers 18 p3244 A66-33879  
Evolution of Honeywell first generations adaptive autopilot inner loop and application to F-94, F-101, X-15 and X-20 vehicles 19 p3397 A66-36483  
Adaptive roll autopilot in air-to-air interceptor missile, noting application of dither principle, simulation results and noise rejection qualities 19 p3398 A66-36691  
Simulation and analysis of adaptive roll autopilot for air to air missile, using limit cycle with small amplitude controlled by gain changing loop 20 p3595 A66-36865  
Aeroelastic instability of aircraft with automatic pilot, determining domain in which sensor position and other adjustable parameters may vary without risking instability 21 p3695 A66-38580  
Information and failure warnings monitoring by flight crew during autopilot operation, particularly during very low visibility landing
- [ICAS PAPER 66-17] 22 p3945 A66-40671
- ### AUTORADIOGRAPHY
- Autoradiography of components of a disassembled nuclear reactor as final phase in evaluating performance of experimental Kiwi rocket engine 06 p0907 A66-16430  
High speed gross alpha autoradiographic technique to reduce exposure time if silver activated ZnS is used as intensifier 07 p1030 A66-17235  
Autoradiography used to determine dislocation density in germanium, silicon and copper single crystals, with aid of tagged atoms 24 p4257 A66-42535



# AUXILIARY POWER SOURCE

## SA CHEMICAL AUXILIARY POWER SOURCE

Rechargeable chemical batteries using nickel-cadmium and silver-cadmium electrodes and chemical reaction 01 p0014 A66-10365  
Integrated secondary power system to provide additional capabilities for supersonic aircraft  
[SAE PAPER 650828] 01 p0016 A66-10828  
X-15 research vehicle auxiliary power system discussing operation, hardware and major components 01 p0016 A66-10829  
New cathode and electrolyte materials for high energy electrochemical batteries 05 p0612 A66-15307  
Noble gas-filled thermionic converter characteristics, performance and application 05 p0617 A66-15555  
Cesium diode with cylindrical molybdenum emitter and niobium collector fueled with uranium dioxide in out pile test 05 p0618 A66-15557  
Current and power gain of noble gas filled converter as affected by auxiliary emitter position to electrode and geometry 05 p0618 A66-15560  
Negative resistance of dynatron type and oscillations in reverse current range of cesium thermionic energy converter 05 p0620 A66-15572  
Solar-heated thermionic generator design and fabrication evaluation, considering mirror configurations 05 p0623 A66-15598  
Cavitation damage in high-temperature liquid metal pumps for Rankine cycle space power plants studied in water model 07 p1038 A66-18175  
Mercury lubricated hybrid bearings for lubrication requirements of mercury Rankine Silent Compact Auxiliary Power (SCAP) system  
[ASLE PREPRINT 65AM 3A3] 07 p1039 A66-18288  
Auxiliary power devices using solar, chemical and nuclear sources 07 p0992 A66-18305  
Automatic battery formation system for silver-cadmium electrochemical cells 08 p1169 A66-19505  
Charge current control circuit for nickel-cadmium cells with control electrodes 08 p1169 A66-19506  
Silicon photovoltaic cells in economic solar energy conversion on Earth 08 p1174 A66-19665  
Auxiliary turbine power generator using gas from solid propellant 09 p1333 A66-20331  
Fuel cell development in U.S., Europe and Great Britain, noting design, performance and problems 11 p1639 A66-22247  
Auxiliary power generating systems for 24-man space laboratory, evaluating power requirements, cost, weight and deployed area  
[AIAA PAPER 64-719] 13 p2004 A66-26614  
Shaft-power turbine design, including rotor vibration problems, computer high speed testing, application as auxiliary power supply in turbojets, etc  
[ASME PAPER 66-GT-87] 14 p2225 A66-26992  
Small gas turbines, market, technical problems, etc  
[ASME PAPER 66-GT-90] 14 p2372 A66-26994  
Multiple quick-disconnect valve used in auxiliary power unit (APU) of aircraft and serving several systems at once while preventing fluid leakage from one system to another 14 p2226 A66-28032  
Auxiliary power unit turbine-engine starting system analyzed to determine sufficiency of selected accumulator 16 p2637 A66-31224  
Auxiliary propulsion for satellite attitude control 17 p2990 A66-32374  
Bismuth telluride alloy solar thermoelectric flat plate generators applied to auxiliary power systems for exploratory missions toward Sun 20 p3497 A66-37166  
Dynamic power generating systems using Rankine and Brayton cycles for space application 20 p3598 A66-37256  
Electrochemical power generator using silver cathode and zinc anode 21 p3698 A66-39474  
Nuclear power systems using radioisotope

and reactor power sources 22 p3946 A66-40127  
Nuclear reactor as power source in remote location 23 p4089 A66-41608  
Reciprocating engine for space power, noting power capacity as function of piston displacement 23 p4022 A66-41762  
Spacecraft turboelectric generation system using superconducting field as stator and rotor as armature to deliver 5000 vdc 23 p4023 A66-41764  
Potassium Rankine-cycle space power plant design for four turbine inlet temperature levels, noting construction materials 23 p4023 A66-41765

## AVALANCHE

### SA ELECTRON AVALANCHE

Punch-through avalanche phenomena, describing fast rise pulse production in junction transistors of variable base width 05 p0651 A66-15840  
Avalanche multiplication factors other than impact ionization leading to breakdown in p-n junctions 06 p0850 A66-16445  
Microwave power generation from avalanching diffused and epitaxial silicon and gallium arsenide varactor diodes 06 p0851 A66-16462  
Gas breakdown by laser can be accounted for by both microwave breakdown theory and inverse bremsstrahlung 06 p0893 A66-17040  
Silicon diode microwave oscillators and amplifiers, noting application of avalanche transit time for increased efficiency of p-n junctions 10 p1515 A66-22090  
Microwave generation with conventional transistors in avalanche mode, describing circuit, mounting construction and avalanche oscillator frequency 12 p1830 A66-23757  
Threshold energy for avalanche multiplication in semiconductors obtained from energy band structure and crystal momentum conservation in ionization process 13 p2157 A66-25035  
Nonlinear dielectric laser light absorption by neutral gas resulting in avalanche breakdown of gas due to thermal ionization 13 p2090 A66-25425  
Sensitivity and operation of IR detector using avalanche multiplication in microplasmas in silicon junctions, noting SNR at room temperature 13 p2164 A66-25490  
Circuit of step voltage generator using two transistors operating in avalanche breakdown regime 16 p2664 A66-31358

## AVALANCHE RECTIFIER

One-sided avalanche injection in n-p-p diodes as cause of negative resistance for carrier concentrations smaller than impurity concentration 10 p1515 A66-22085  
Noise current spectrum of Read type avalanche diode with ideal uniform avalanche behavior in thin zone 10 p1515 A66-22086  
Spectral density of white noise generated in uniformly multiplying p-n junction calculated for any distribution of injected carriers 10 p1515 A66-22087  
Electronic tuning effects through DC avalanche current variation in negative-resistance diode 10 p1515 A66-22088  
Time dependence of multiplication and refinement in silicon technology needed to establish uniform multiplication for Read diode prototype 10 p1515 A66-22089  
Avalanche breakdown voltages of abrupt and linearly graded p-n junction in Ge, Si, GaAs and GaP 14 p2356 A66-27027  
Microplasma breakdown in high voltage avalanche rectifiers, considering leakage current and junction impurity dislocation migration 14 p2363 A66-27583  
Controlled noise generation at high pulse rate with avalanche diodes, noting spectral voltage density and temperature coefficient 15 p2458 A66-28894  
Phase locking range of avalanche diode CW oscillator to external microwave signal by direct injection 15 p2463 A66-29042  
Low noise photodiodes with avalanche multiplication for high sensitivity, noting capability for low intensity wideband signal detection, performance in IR region, etc 17 p2880 A66-31934  
Solid state high speed pulse generators

utilizing avalanche transistor 17 p2893 A66-32927  
Avalanche transistor generation of jitter-free nanosecond current pulses for driving GaAs laser diodes at low temperatures 20 p3528 A66-37453  
Differential minority carrier storage circuit with avalanche pulse energization and fast rise/fall adjustable length pulse output 22 p3872 A66-39717  
Coupling of two avalanche diode oscillators to obtain increased continuous wave microwave power output 22 p3877 A66-40180  
Voltage control by means of Zener diode, transistor and variable-gain amplifier circuit 23 p4044 A66-41214  
Avalanche radiation from bulk of long thin forward-biased p-n-p silicon diodes 24 p4180 A66-42258  
Curves computed for avalanche multiplication and Zener tunneling for gallium arsenide specimens of various thicknesses 24 p4258 A66-42958

## AVIATION

### S AERONAUTICS

### S CIVIL AVIATION

### S MILITARY AVIATION

## AXIAL COMPRESSION

Electrical resistivity and Hall coefficient of undoped n-type gallium arsenide with carrier concentrations measured at various temperatures as function of uniaxial compression and hydrostatic pressure 03 p0412 A66-13149  
Statistical study of linear buckling of circular cylindrical shells under axial compression, showing preferred mode shape [ASME PAPER 65-APMW-23] 04 p0592 A66-14224  
Strain dependence of impurity conductivity measured in compensated p-type germanium, using uniaxial compression 06 p0922 A66-16171  
Deleterious effect of heterogeneity on stability of composite cylindrical shells under axial compression 06 p0968 A66-17083  
Strain energy method used to examine stability and supercritical strains of rib-reinforced cylindrical shells under axial compression 08 p1305 A66-18595  
Stress-strain state of elastic space, examining circular crack for axial tensile load effects 08 p1305 A66-18597  
Axisymmetric creep in cylindrical shells, noting creep buckling collapse after high temperature compression loading [AIAA PAPER 66-123] 08 p1308 A66-19002  
Elastic general instability of orthotropically stiffened cylinders under axial compression [AIAA PAPER 66-139] 08 p1308 A66-19003  
Edge conditions effect on elastic stability of cylindrical shells extended to additional combinations of boundary conditions, considering cylinders under axial compression 08 p1310 A66-19144  
Idealized cylindrical shell buckling under axial compression derived from generalized integral expression 08 p1310 A66-19166  
Microwave reflection measurements for precursor in electromagnetically driven shock tube, discussing axial distribution and electron density 09 p1409 A66-20855  
Statistical study of linear buckling of circular cylindrical shells under axial compression, showing preferred mode shape [ASME PAPER 65-APMW-23] 10 p1615 A66-21474  
Structural efficiency of orthotropic materials for cylindrical shells under axial load, including examination of fibrous composites characteristics [AIAA PAPER 65-73] 12 p1956 A66-23583  
Dynamic buckling of imperfection sensitive models, specifically cylindrical shells under axial compression 12 p1957 A66-23590  
Stability and buckling of core-filled axially compressed circular cylinder 12 p1957 A66-23603  
Initial deflection effect on stability of rib-reinforced cylindrical shells under axial compression 12 p1967 A66-24109  
Stability analysis of shells of revolution with curvilinear generatrices under axial compression, using strain energy technique 12 p1967 A66-24110  
Imperfections and edge restraint effect on buckling of axially compressed



- cylinders 14 p2404 A66-27988  
 Longitudinal stiffeners eccentricity /one-sidedness/ effect on buckling strength of axially compressed cylinders 14 p2404 A66-27989  
 Supersonic flutter of circular cylindrical shells subjected to internal pressure and axial compression [AIAA PAPER 65-407] 15 p2610 A66-29281  
 Stiffener eccentricity and end moment effect on stability of cylindrical panel in axial compression 15 p2610 A66-29283  
 Stability analysis of elastic axially compressed orthotropic glass-fiber-reinforced-plastic cylindrical shell with linear heredity properties 15 p2611 A66-29341  
 Metal hardening by explosive loading under near triaxial compression determined by charged power and independent of plastic deformation magnitude 15 p2523 A66-29599  
 Cylindrical thin shells with axial stringers under axial compression 15 p2614 A66-29636  
 Bending stresses in cylindrical shell with rigid circular inclusion examined under axial tension and internal pressure [AIAA PAPER 66-525] 16 p2813 A66-30526  
 Critical stress, stability loss and load carrying capacity of axially compressed thin walled aluminum alloy rods 16 p2819 A66-31142  
 Weight savings derived from use of contrasting ring, stringer and wall materials in J-stiffened axially compressed cylinders [AIAA PAPER 66-508] 16 p2821 A66-31480  
 Heterogeneity effect on multilayer composite cylindrical shell stability under axial compression 17 p3025 A66-32454  
 Thin circular cylindrical shell behavior in axial compression, noting buckling under stress, boundary condition detail effects, etc 17 p3031 A66-33064  
 Propellant composition influence on finite-amplitude axial wave mode instability in solid propellant rockets [AIAA PAPER 66-600] 18 p3161 A66-34431  
 Ring stringer eccentricity effects on structural optimization of stiffened axially compressed cylinders 20 p3672 A66-38166  
 Shell stability in Euler formulation, taking into account actual redistribution of stresses that results from initial deflection and creep, noting buckling of closed cylindrical shell under axial compression 21 p3829 A66-38978  
 Postbuckled equilibrium configurations of axially compressed circular cylindrical shell determined from large deflection theory and principle of stationary potential energy 22 p3993 A66-40340  
 Structural efficiency of orthotropic materials for cylindrical shells under axial load, including examination of fibrous composites characteristics [AIAA PAPER 65-73] 23 p4138 A66-41107  
 Energy method application to buckling of axially compressed cylindrical shells with ring-stiffened edges, noting upper and lower bounds and critical rigidity ratio 23 p4140 A66-41912  
 Stress distribution and displacements in neighborhood of circular hole in cylindrical shell subjected to load such as torsion or axial compression 23 p4142 A66-41959  
 Large deflection postbuckling analysis of thin walled oval cylinders under axial compression 23 p4143 A66-41961  
 Approximate finite deflection analysis of buckling of long slightly curved panels in axial compression 23 p4143 A66-41963  
 Postbuckling behavior of circular cylindrical shell locally buckled under axial compression 23 p4143 A66-41964  
 Classical critical stress values for buckling of thin walled circular cylindrical shells in axial compression as function of edge conditions 23 p4143 A66-41965
- AXIAL FLOW**  
 Torsional oscillations of plane with large suction effect on magnitude of induced axial steady inflow toward surface of disk 01 p0057 A66-10429  
 Incompressible laminar axisymmetric near wake behind very slender cylinder in axial flow 02 p0175 A66-11527  
 Couette flow, unpressurized axial flow in annular gap between two cylinders and flow between two rotating cylinders, taking into account energy dissipation and dependence of viscosity on temperature 04 p0512 A66-14423  
 Corrugation growth on infinitely conducting fluid sheets, discussing acceleration induced by constant axial and linearly increasing currents 06 p0871 A66-16276  
 Doppler broadened Cv spectral line from theta pinch and microscopic plasma velocities by reducing axial motion effect 07 p1086 A66-17654  
 Arc plasma generator for anode research, noting design operation techniques and results [AIAA PAPER 66-162] 10 p1485 A66-21687  
 Hypersonic rarefied gas flow in short ducts, measuring wall static pressure and stream total pressure distributions 11 p1634 A66-22932  
 Free-molecule flow through conical tubes noting mass transport, axial momentum, energy, flow distribution and speed ratio 11 p1635 A66-22938  
 Noise measurement in axial flow fans for military vehicle cooling installations 14 p2220 A66-27567  
 Annular vortices method applied to determine aerodynamic characteristics of lifting propeller in axial and oblique flows 23 p4010 A66-41785
- AXIAL FLOW COMPRESSOR**  
**SA CENTRIFUGAL COMPRESSOR**  
 Acoustical fatigue study of propeller duct designed for minimum weight to maintain specified thrust-to-weight ratio 01 p0150 A66-10155  
 Axial compressors with nonuniform inlet flow, investigating size of gap between blade rows and rotating stall 01 p0008 A66-10953  
 Correction factors derived for avoiding formation of stagnation cores near hub of axial compressors 01 p0008 A66-11094  
 Performance of blade rows in transonic axial-flow compressor for V/STOL aircraft 03 p0313 A66-12393  
 Rotating stall and blade row interference in axial compressor 03 p0313 A66-12395  
 Visualizing rotating stall in axial compressor simulated by rotary-cascade machine using water 03 p0313 A66-12396  
 Book on matched parameters of gas turbine engines for aircraft including rpm and peripheral speed, calculating parameters for axial-flow compressors, centrifugal compressors, turbojet, turboprop, etc 04 p0573 A66-14004  
 Outlet angle in axial compressor cascades, accounting for effect of shear flows, Bernoulli surface rotation and flow separation [ASME PAPER 65-WA/FE-2] 05 p0608 A66-15714  
 Multiple stage axial flow compressor with blades staggered differently at different stages 06 p0801 A66-16000  
 Theory of highly rarefied cascade flow and proposal for new axial flow molecular pump in free molecule range 06 p0803 A66-16945  
 Flow through straight slot cascade, investigating application to axial compressors for optimum slot parameters 06 p0803 A66-16968  
 SNECMA axial flow transonic compressor development during last ten years 09 p1433 A66-19866  
 Number of working blades effect on magnitude of total work coefficient and other characteristics of axial radial compressor 09 p1435 A66-20763  
 Vibration suppression in axial flow compressors, discussing blade root damping and pin hole stress 09 p1469 A66-20968  
 Versatile facility applicable as high-speed annular cascade wind tunnel or as transonic axial flow test compressor 12 p1859 A66-24928  
 Stress analysis of rim-straddling fastenings for axial compressor and turbine blades 13 p2171 A66-25081  
 Mathematical analysis of noise generation mechanism in axial-flow compressor rotors [ASME PAPER 66-GTIN-42] 14 p2372 A66-26987  
 Recent progress in aerodynamic design of axial flow compressors and components in U.S. [ASME PAPER 66-GT-95] 14 p2217 A66-26998
- Adjustable stator blades in axial compressors, noting advantages of system for constant-speed electric or variable-speed turbine drives 14 p2373 A66-27017  
 Vibration suppression in axial flow compressors, discussing blade root damping and pin hole stress 15 p2468 A66-29926  
 Two-stage radial-flow turbomolecular vacuum pump noting design, measured and predicted performance, application, etc 16 p2710 A66-30382  
 New type of vacuum pump is multistage axial compressor known as /turbomolecular/ pump 16 p2715 A66-31308  
 Noise sources in axial flow fans, including broad frequency band lift fluctuations, turbulent wakes, velocity fluctuations, etc 17 p2989 A66-31946  
 Transonic stage design in axial compressor 17 p2838 A66-32310  
 Low speed three-stage axial flow compressor tests at aspect ratios of one, two and four [AIAA PAPER 66-613] 19 p3275 A66-35359  
 Recent progress in aerodynamic design of axial flow compressors and components in U.S. [ASME PAPER 66-GT-95] 19 p3278 A66-36756  
 Inhomogeneity of axial velocity component in or near blades forming impeller intake of radial compressor attributed to flow deflection 24 p4158 A66-43067
- AXIAL FLOW TURBINE**  
 Velocity distribution in turbine stage with compressible medium for repeating axial velocity profile derived, employing approximation method 01 p0130 A66-10211  
 Three-dimensional incompressible viscous flow calculated for axial-flow turbine stage of given blade profile, verified by computer method developed from cascade theory 05 p0605 A66-14961  
 M.A.N. RB 153 jet engine development, characteristics and capabilities 06 p0943 A66-17019  
 Ducted axial flow fan noise generation and noise spectrum 10 p1483 A66-21743  
 Size and position effect, baffle effect and wake and pressure interaction effect of upstream stator on ducted axial flow fan noise 10 p1483 A66-21746  
 Computer programs for efficiency predictions of axial flow turbines, using Ainley-Mathieson and Soderberg methods of loss correlation 13 p1991 A66-26224  
 CERCOR glass-ceramic axial flow rotary regenerator as inexpensive component for gas turbine regeneration [ASME PAPER 66-GT/107] 14 p2301 A66-27004  
 Graduate level textbook on axial flow turbine design, examining useful thermodynamic/fluid mechanic concepts, cascade potential flow, turbine efficiency, etc 17 p2991 A66-32991  
 Flow transition from propeller in free stream to axial pump in cylindrical shroud for impeller clearance between zero and infinity 21 p3695 A66-39499
- AXIAL LOAD**  
 Prebuckling deformation and stress-strain distributions in clamped thin cylindrical shell subjected to axial load, determining effect of boundary supports 02 p0297 A66-11557  
 Fracture strength of two rocket-nozzle-grade graphites under ten biaxial stress states at room temperature 03 p0435 A66-12637  
 Creep buckling, examining two-hinged H-section long column under distributed axial load and effect on buckling time, column deflection and numerical results of example 03 p0436 A66-12720  
 Reduction of Rabotnov approximate equation describing steady creep in circular cylindrical shells, under axisymmetric loading, to system of integral equations 04 p0588 A66-13567  
 Linear small deflection theory and statistical analysis in dynamic buckling of thin cylindrical shell under axial impact [ASME PAPER 65-APMW-17] 04 p0592 A66-14218  
 Reynolds equation for compressible and incompressible lubrication for load coefficients and attitude angles of axial



- groove cylindrical bearings  
[ASME PAPER 65-LUB-16] 04 p0528 A66-14248
- Parametric response of elastic columns  
discussing longitudinal inertia effects,  
analytic stability criteria and results  
[ASME PAPER 65-WA/APM-13] 05 p0777 A66-15435
- Collapse under end load of pressurized  
axially stiffened thin  
cylinders 07 p1147 A66-18282
- Self-oscillating hydraulic vibration  
apparatus capable of generating high cyclic  
actuating power for testing  
purposes 07 p1147 A66-18389
- Stresses and elongation of U-shaped  
bellows subjected to axial load solved by  
elastic theories of plates and  
shells 08 p1314 A66-19549
- Postbuckling behavior of metal plate strip  
subjected to opposing axial loads, using  
nonlinear bending theory  
[ASME PAPER 65-AV-3] 11 p1780 A66-22470
- Critical impact load under which  
axisymmetric deformation of perfect elastic  
isotropic cylindrical shell becomes unstable  
determined, using deflection  
theory 12 p1959 A66-23746
- Linear small deflection theory and  
statistical analysis in dynamic buckling of  
thin cylindrical shell under axial impact  
[ASME PAPER 65-APMW-17] 12 p1961 A66-23980
- Parametric response of elastic columns,  
discussing longitudinal inertia effects,  
analytic stability criteria and results  
[ASME PAPER 65-WA/APM-13] 12 p1961 A66-23985
- Photoelastic solution of distribution of  
stresses around centrally located elliptical  
hole in plate of finite width subjected to  
uniform axial loading 12 p1962 A66-23991
- Extensive creep deformation of thin zero-  
moment shell of revolution under action of  
internal and axial load 12 p1966 A66-24059
- Time to viscous failure of tubes subjected  
to internal pressure and axial  
load 12 p1967 A66-24066
- Stability of cylindrical nonlinearly elastic  
shell under axial loads applied to shell  
ends 15 p2607 A66-28766
- Deformation of finned conical shell under  
axial load 15 p2608 A66-28781
- Stiffness, carry-over factor and fixed-end  
moment of axially loaded nonuniform  
members under tension or  
compression 17 p3024 A66-32397
- Creep behavior of selected polypropylene  
monofilament under axial  
loading 17 p3029 A66-32789
- Boundary value problems in secondary  
creep of circular thin shells under  
axisymmetric loading, giving solutions for  
deformation rates and stress  
resultants 17 p3030 A66-32891
- Bending behavior of spherical shells  
through second-order differential equation  
with complex coefficients, noting effect of  
load 18 p3253 A66-33765
- Crack propagation, damage and fatigue  
fracture in plane rods with transverse cut  
under single step and multistep axial  
load 20 p3666 A66-37307
- Impact of elastic conical shell of revolution  
moving with constant axial velocity toward  
rigid obstacle 21 p3827 A66-38692
- Comparison between theoretical and  
experimental measurements of rotation  
caused by axial load on highly twisted bars  
following stress relieving 23 p4138 A66-41380
- AXIAL PUMP**
- Working process of axial-inflow  
turbomolecular pump for ultrahigh vacuum,  
noting pressures reached during  
tests 19 p3371 A66-36617
- AXIAL STRESS**
- Cylinders subjected to internal and  
external pressure and axial stress with  
equations for radial and tangential  
direction 02 p0299 A66-11706
- Equations of plastic interaction curves for  
cross section of beam subject to uniaxial  
stress and under simultaneous bending  
moment and normal force, using power  
series 03 p0442 A66-13306
- Biaxial uniform stressed state of physically  
nonlinear plate with circular  
hole 04 p0589 A66-14145
- Free steady state jet subject to axial  
tension applied to Newtonian liquids, noting  
effect of flow variables on dimensionless  
criterion 04 p0512 A66-14209
- Asymptotic expressions for axial stress in  
thin viscoelastic shells due to longitudinal  
impact obtained, using Laplace transform,  
determining viscosity effect on propagating  
wave shape  
[ASME PAPER 65-WA/APM-10] 05 p0776 A66-15432
- Plastic deformation effect on strain energy  
release rate, examining axial rigidity of  
plate with central propagating crack under  
uniaxial tension  
[ASME PAPER 65-WA/MET-9] 05 p0780 A66-15687
- Asymptotic expressions for axial stress in  
thin viscoelastic shells due to longitudinal  
impact obtained, using Laplace transform,  
determining viscosity effect on propagating  
wave shape  
[ASME PAPER 65-WA/APM-10] 10 p1615 A66-21476
- Transport properties of III-V and II-VI  
semiconducting compounds with zincblende  
structure under uniaxial stress, calculating  
galvanomagnetic coefficients, Faraday effect,  
plasma frequency, etc 10 p1578 A66-21665
- Evaluations for multiaxial-stress properties  
of ceramic materials including elastic and  
plastic strength, stiffness, ductility,  
resilience, etc 12 p1958 A66-23631
- Hydrodynamics of free steady state jet  
subject to axial tension, numerical  
computation of perturbation corrections for  
Newtonian jets 12 p1797 A66-24031
- Plastic deformation effect on strain energy  
release rate, examining axial rigidity of  
plate with central propagating crack under  
uniaxial tension  
[ASME PAPER 65-WA/MET-9] 12 p1970 A66-24539
- Biaxial behavior of titanium sheet,  
obtaining stress states, yield strength, burst  
strength, etc  
[ASME PAPER 66-MET-6] 14 p2312 A66-26974
- Steady state creep equations derived for  
anisotropic material under multiaxial stress  
states, based on perfect plasticity  
analogies 16 p2820 A66-31275
- Model-forming process in which plane flat  
sheet is stretched by pair of loads  
producing biaxial principal stresses,  
examining stress ratios, loads and plastic  
strains 18 p3247 A66-33573
- Comparison of characteristic roots arising  
from Fluegge and Donnell theories, when  
certain amount of axial prestress is imposed  
on circular cylinder 19 p3474 A66-36345
- Absorption of polarized electromagnetic  
waves at zero degrees K in n-type  
germanium under high uniaxial  
stress 19 p3446 A66-36396
- In-plane stiffness matrices for composite  
cylinders of filament winding determined by  
internal pressure, axial tension and torsion  
tests 20 p3666 A66-37440
- Optimal control of elastic flight vehicles,  
describing axis oscillations by equations of  
beam with variable cross  
section 21 p3768 A66-39279
- AXIAL pressure asymmetry produced by  
Hall effect in linear pinch  
discharge 23 p4104 A66-41512
- AXIS**
- S ROTOR AXIS**
- AXISYMMETRIC BODY**
- Matched asymptotic expansion to derive  
dynamical displacements of infinite elastic  
space embedded with light rigid  
axisymmetric body 02 p0299 A66-11806
- Supersonic and hypersonic flow fields  
around plane and axisymmetric bodies and  
inlets obtained by nonlinear characteristics  
method 04 p0454 A66-13519
- Computer analysis of axisymmetric free  
vibrations of orthotropic shells of revolution  
and elastic rings  
[AIAA PAPER 65-109] 05 p0781 A66-15790
- Hypersonic gas flow past axisymmetric  
slender blunt body by Chernyi approximate  
method 07 p0983 A66-18142
- Asymptotic solution of problem of thin  
spherical shell free vibration for  
axisymmetric and general  
cases 08 p1308 A66-18888
- Extended physical optics methods for  
calculating nose-on echo area of  
axisymmetric thin bodies having sharp  
apices 10 p1500 A66-21617
- Newtonian flow model minimization of  
pressure drag of slender axisymmetric two-  
dimensional body subjected to isoperimetric  
constraints 11 p1631 A66-22511
- Optimum minimal-drag shape of slender  
axisymmetric body in free molecular  
flow 11 p1632 A66-22526
- Optimum nose form determination for  
minimum drag in free-molecule flow of  
asymmetric body 11 p1635 A66-22937
- Uniqueness theorem of axisymmetric  
exterior traction boundary value problem in  
linear elastostatics theory 12 p1971 A66-24818
- Laminar separated hypersonic flow over  
spiked bodies in gun tunnel for analyzing  
parameters influencing heat transfer rates  
in reattachment region 14 p2218 A66-27403
- Axisymmetric solid motion about fixed  
point under constant momentum, using  
chain fractions and Lagrange  
method 14 p2336 A66-28063
- Similarity law for longitudinal contours of  
optimum bodies minimizing drag in  
hypersonic and low subsonic free molecular  
flows constrained on length, base width,  
wetted area, etc 14 p2221 A66-28183
- Direct numerical method for calculation of  
supersonic inviscid flow about axisymmetric  
blunt body at large angle of attack  
[AIAA PAPER 65-24] 15 p2423 A66-29269
- Contact process of linearly viscoelastic  
axisymmetric die, for case of  
noncommutative operators 15 p2611 A66-29342
- Supersonic flow over downstream-facing  
step on circumference of ducted  
axisymmetric body used in flow  
reattachment, measuring surface pressure  
distributions 17 p2839 A66-32440
- Periodic solutions of axisymmetric shell  
theory equations for displacement of shells  
of revolution and bending of thin walled  
rods 17 p3026 A66-32593
- Supersonic wind tunnel measurements in  
turbulent wake of axisymmetric slender  
body [AIAA PAPER 66-453] 18 p3046 A66-33649
- Laminar, transitional and turbulent  
boundary layer flows with adverse pressure  
gradient on axisymmetric blunted conical  
flared body at Mach 10 10
- [AIAA PAPER 66-493] 18 p3047 A66-33658
- Approximation method for compressible  
laminar heat transfer to blunt axisymmetric  
bodies in high speed flow 18 p3048 A66-33824
- Optimum stabilization problem for  
axisymmetric satellite, considering fuel  
consumption 19 p3467 A66-35277
- Optimum stabilization of axisymmetric  
satellite by system of n reactive  
jets 22 p3986 A66-40464
- Linear dynamic analysis of angular motion  
of spinning axisymmetrical rocket or  
spacecraft, emphasizing rigid body with  
thrust misalignment and another motion  
caused by deflection of control surfaces or  
jets 22 p3988 A66-40618
- Body shapes providing minimum wave  
resistance to supersonic flow of perfect gas,  
considering bodies around which flow causes  
bound shock waves 23 p4009 A66-41717
- AXISYMMETRIC DEFORMATION**
- Plastic analysis of conical shells of  
revolution under axisymmetric loads based  
on approximate parabolic hypercylindrical  
yield 01 p0153 A66-10445
- Critical load of ellipsoidal end faces of  
cylindrical reservoir assuming deformation  
beyond critical load is  
axisymmetric 01 p0155 A66-10657
- Four types of axisymmetric distribution of  
stresses and displacements in infinitely long  
rod of circular cross section with  
discontinuous boundary  
conditions 01 p0155 A66-10713
- Axisymmetrical stressed state of three-  
dimensional models exposed to transmitted  
light determined from photoelasticity by  
polarized method 01 p0158 A66-10986
- Plate theory for case of thin elastic  
deformable circular plate under rotationally  
symmetrical stress 02 p0296 A66-11243
- Large axisymmetric nonlinear elastic or  
plastic deformations of zero-moment circular



conical shells 04 p0590 A66-14160  
 Donnell-type nonlinear theory for  
 instability of cylindrical shell subjected to  
 axisymmetric moving loads with constant  
 velocity [ASME PAPER 65-APMW-35] 04 p0594 A66-14235  
 Finite element structural analysis of  
 stresses and displacements in axisymmetric  
 solids of arbitrary geometry [AIAA PAPER 65-143] 05 p0781 A66-15786  
 Nonlinear axisymmetric deformation of  
 shallow spherical shells subjected to  
 dynamic loads 05 p0781 A66-15791  
 Asymptotic solution to elasticity theory  
 problem for hollow isotropic cylinder of  
 finite dimensions and small thickness under  
 axisymmetric load distributed over entire  
 surface 07 p1144 A66-18183  
 Simplified calculation of axisymmetric  
 bending of annular three-layer plates with  
 lightweight filler by use of initial parameter  
 method 08 p1313 A66-19437  
 Stress-strain calculations for thin walled  
 axisymmetric shells with arbitrarily shaped  
 midplane based on second-order  
 theory 10 p1614 A66-21383  
 Large deflections of spherical shells under  
 concentrated loads, obtaining curves for  
 axisymmetric deformations 10 p1616 A66-21493  
 Axisymmetric imperfections effect on  
 elastic buckling of spherical caps under  
 uniform pressure 10 p1617 A66-21785  
 Edge effect in case of finite pipe under  
 arbitrary axisymmetrical load, determining  
 radial displacement 11 p1782 A66-22851  
 Aircraft fuselage design in region of  
 center section for case of asymmetric  
 bending 11 p1782 A66-22854  
 Critical impact load under which  
 axisymmetric deformation of perfect elastic  
 isotropic cylindrical shell becomes unstable  
 determined, using deflection  
 theory 12 p1959 A66-23746  
 Critical load of ellipsoidal end faces of  
 cylindrical reservoir, assuming deformation  
 beyond critical load is  
 axisymmetric 12 p1963 A66-24015  
 Inverse problem of stressed state of elastic  
 plate reinforced by members of known  
 rigidity under axisymmetric  
 load 12 p1967 A66-24107  
 Axisymmetric creep of circular cylindrical  
 shells taking into account axial  
 forces 12 p1968 A66-24347  
 First boundary value problem for general  
 case of axisymmetric stressed state of body  
 of revolution, using biharmonic solution of  
 Love and Grodskii 13 p2196 A66-25636  
 Axisymmetric deformation of cylindrical  
 shell consisting of many layers of glass  
 fabric connected by polymer  
 mass 16 p2823 A66-31626  
 Hollow metallic O rings used for sealing as  
 thin shells under axisymmetric  
 loading 17 p3020 A66-32002  
 Transient wave processes of deformation in  
 spherical shell under load abruptly applied  
 to geometrical pole 17 p3029 A66-32805  
 Donnell-type nonlinear theory for  
 instability of cylindrical shell subjected to  
 axisymmetric moving loads with constant  
 velocity [ASME PAPER 65-APMW-35] 18 p3248 A66-33574  
 Stress analysis of junction of thin elastic  
 shells of revolution, considering  
 axisymmetric wind and sinusoidal load  
 distributions 18 p3253 A66-33804  
 Moment theory for thin spherical elastic  
 shells under axisymmetric loading, noting  
 role of Poisson ratio 19 p3474 A66-35851  
 Stiffness method for analysis of elastic-  
 plastic shells of revolution with  
 axisymmetric loading implemented by step-  
 by-step method of integration in computer  
 program 20 p3667 A66-37482  
 Three-dimensional and axisymmetric  
 problem in elasticity theory with particular  
 reference to  
 photoelasticity 23 p4135 A66-40989  
 Structural dynamics of axisymmetric  
 deformation of semiinfinite plastic  
 cylindrical shell under concentrated ring  
 impact 23 p4147 A66-41999  
 Axisymmetric bending problem of idealized  
 elastic rigidly-plastic two-layer circular

plates, deriving exact mathematically strict  
 solutions and uniqueness  
 conditions 24 p4290 A66-42443  
 Numerical integration of equations of Love  
 first approximation for thin isotropic shells,  
 presenting results for torus and flask having  
 variable wall thickness 24 p4292 A66-42964  
**AXISYMMETRIC FLOW**  
 Axially symmetric potentials represented  
 as mean values in integral operators given  
 for Stokes-Beltrami  
 equations 01 p0058 A66-10505  
 Transonic flow in throat of plane  
 axisymmetric nozzle determined by taking  
 velocity potential in form of power series  
 and determining coefficients of series from  
 set of recurrence  
 equations 01 p0007 A66-10714  
 Boundary layer on spherically blunted  
 cones in supersonic air flow at given wall  
 temperature and thermally insulated wall,  
 graphing calculation 01 p0008 A66-11016  
 Inlet region of laminar meridional flow in  
 arbitrarily shaped narrow gap between two  
 axisymmetrically formed  
 walls 02 p0217 A66-11585  
 Viscosity effect on transition between  
 axisymmetric and nonaxisymmetric flow  
 regimes of vertical rotating annulus of  
 liquid 02 p0223 A66-11826  
 Nonisothermal wall problem for vertical  
 right circular cone in laminar free  
 convection for fluids with low Prandtl  
 numbers 02 p0305 A66-12200  
 Similar flows about axisymmetric bodies  
 rotating in fluid at rest 03 p0354 A66-12351  
 Axisymmetric modes and frequency  
 vibration of thin conical shells subjected to  
 rapid surface heating [AIAA PAPER 65-788] 03 p0434 A66-12558  
 Geometric shape of axisymmetric shock  
 waves from point source explosion in  
 nonhomogeneous medium 03 p0355 A66-12621  
 Turbulent mixing of axisymmetric jet of  
 partially dissociated nitrogen with ambient  
 air, establishing mixing and decay  
 characteristics 03 p0359 A66-13231  
 Thermal energy transfer in base portion of  
 stagnant region obtained from plane and  
 axisymmetric flow  
 equations 04 p0454 A66-13570  
 Closed form solution of axisymmetric  
 transonic flow about  
 obstacle 05 p0665 A66-15796  
 Propagation of shock wave of gas flow  
 from axisymmetric nozzle 06 p0802 A66-16422  
 Axisymmetric MHD flows classified by  
 configuration of electromagnetic  
 field 07 p1090 A66-18123  
 Power characteristics of linear  
 axisymmetric flow of ideal incompressible  
 conducting gas with Hall effect in two-  
 component magnetic field 08 p1168 A66-18863  
 Thermal stresses due to axisymmetric heat  
 flow past spherical cavity inside long  
 circular cylinder solved by stress functions  
 and thermoelastic displacement  
 potentials 08 p1313 A66-19547  
 Numerical method for calculating flow,  
 including gas reactions and nonequilibrium,  
 behind given axisymmetric detached shock  
 wave 10 p1481 A66-21892  
 Hydrodynamic problem of nonviscous liquid  
 flow past two spheres solved, using new  
 method of solution 10 p1525 A66-21919  
 Unsteady two-dimensional axisymmetric  
 plasma flows, classifying isentropic or  
 incompressible flows according to magnetic  
 field configurations 11 p1746 A66-23234  
 Inviscid flow of compressible conducting  
 gas with aligned magnetic field through  
 axially symmetric Laval nozzle in various  
 transition regions 11 p1636 A66-23256  
 Shock layer approximation used in inverse  
 hypersonic blunt body  
 problem 12 p1795 A66-23574  
 Axisymmetric liquid nitrogen turbulent jet  
 propagating under supercritical pressure in  
 gaseous nitrogen medium 12 p1864 A66-24446  
 Axisymmetric shock wave formation at  
 nozzle exit when jet pressure is less than  
 ambient pressure 12 p1799 A66-24447  
 Wake dimensions growth and turbulent  
 energy decay in incompressible  
 axisymmetric wakes surveyed, using hot-  
 wire anemometer in low speed wind tunnel

[ASME PAPER 65-FE-8] 12 p1799 A66-24556  
 Axisymmetric convection between two  
 rotating disks, noting secondary flow and  
 viscous effects of Ekman  
 layers 12 p1980 A66-24941  
 Anisotropic grid-generated turbulence  
 passed through axisymmetric nozzle of small  
 contraction ratio followed by straight  
 section 12 p1866 A66-24947  
 Heat exchange between axisymmetric jet  
 flow and plate situated normal to  
 flow 13 p2208 A66-25311  
 Linearized surface pressure distribution on  
 streamlined ducted bodies in axisymmetric  
 flow, considering aerodynamic loading or  
 annular airfoil 13 p1993 A66-26716  
 Axisymmetric supersonic flow involving  
 shock waves applied to flow near vertex  
 region of pointed bodies of revolution with  
 arbitrary geometry 14 p2218 A66-27354  
 Nonequilibrium inviscid flow about  
 arbitrarily shaped body with detached shock  
 waves, using method with time derivative  
 and bypassing boundary conditions  
 [AIAA PAPER 65-24] 14 p2218 A66-27404  
 Plane or axisymmetric hypersonic ideal gas  
 flow in divergent nozzle with parabolic wall  
 shape 14 p2221 A66-28056  
 Structure of axisymmetric core of spiraling  
 fluid with high vorticity 17 p2907 A66-32277  
 Current-carrying incompressible fluid  
 confined between two axisymmetrically  
 deformed nonconducting coaxial  
 tubes 17 p2966 A66-32420  
 Mangler rectilinearization of axisymmetric  
 laminar boundary layer flows and Prandtl  
 boundary layer hypotheses, applicability to  
 non-Newtonian fluids 17 p2912 A66-33041  
 Flow field of highly underexpanded  
 axisymmetric jet impinging on flat convex  
 or concave surface calculated by modified  
 inverse method 18 p3100 A66-34606  
 Transonic flow in axisymmetric nozzles  
 with nearly sharp wall curvatures, extending  
 Friedrich equations 21 p3693 A66-38681  
 Rotational axisymmetric mean flow and  
 damping of acoustic waves in solid  
 propellant rocket 21 p3807 A66-38720  
 Conicoidal MHD shock wave in  
 axisymmetric hypersonic viscous-layer  
 flow 21 p3727 A66-39188  
 Velocity distribution of fluctuating  
 axisymmetric flow of incompressible second  
 order fluid near stagnation  
 point 21 p3728 A66-39346  
 Von Karman integral concept for  
 incompressible laminar boundary layers  
 extended to second-order for two-  
 dimensional or axisymmetric flow by  
 generalizing definition of displacement and  
 momentum thickness 22 p3898 A66-40137  
 Weakly perturbed supersonic flows in  
 presence of arbitrary number of  
 nonequilibrium physicochemical  
 processes 22 p3901 A66-40684  
**AXISYMMETRY**  
 Growth of symmetrical plane cracks in  
 axial symmetry and plain  
 strain 17 p3018 A66-31927  
**AZIDE**  
 IR and UV absorption spectra of free  
 radical NCN observed following photolysis  
 of matrix isolated cyanogen  
 nitride 04 p0473 A66-13644  
**AZIMUTH**  
 SA SOLAR AZIMUTH  
 Accurate and permanent data obtained for  
 true-north referencing, using  
 photography 01 p0065 A66-10030  
 Azimuth and latitude determination  
 without time recording based on observation  
 of stars at same horizontal  
 elevation 02 p0255 A66-11694  
 Azimuth and latitude determination  
 without time recording based on observation  
 of stars at same horizontal  
 elevation 02 p0255 A66-11702  
 Spatial properties of rapid geomagnetic  
 fluctuations, noting correlation and epoch  
 differences between distant stations azimuth  
 distributions and Parkinson plane  
 effects 08 p1219 A66-19416  
 Breadboard microwave pointing device with  
 attached RF source comprising azimuth  
 angle measuring system, with application in  
 geodesy, tropospheric propagation,  
 etc 10 p1538 A66-22048  
 Photographic determination of azimuth



orientation with respect to north celestial pole 19 p3358 A66-35827  
Azimuth reference system design and stability, noting flight simulator installation 21 p3723 A66-38888  
Azimuthal mismatch of two Cardan suspensions when used to determine azimuth of distant object in relation to moving object 21 p3770 A66-38968  
Azimuth of line between Potsdam and Ucharest from Echo I satellite photographs 22 p3903 A66-39694  
Inertial navigation for civil airline operations, noting azimuth alignment made by automatic gyrocompassing [CAS PAPER 66-6] 22 p3946 A66-40677

## METHYLENE BLUE

## O COMPOUND

Synthesis of polyimidazopyrrolones, using previous macromolecular synthesis of ladder segments of aromatic-heterocyclic polymers 13 p2017 A66-26290

## POLYBENZIMIDAZOLE

## PHOTOBACTER

Ribonuclease effect on polymerase activity in *Azotobacter vinelandii* used to verify theory that RNA polymerase is inhibited by RNA produced in reaction 20 p3510 A66-37790

## P-1 AIRCRAFT

## P-6 AIRCRAFT

## P-3 AIRCRAFT

## P-4 AIRCRAFT

## B

## B-58 AIRCRAFT

Human factors in B-58 aircraft accidents, considering nose-high landing requirement, pilot fatigue and evaluation of ejection facilities 17 p2864 A66-32166

## B-6 AIRCRAFT

## B-72 AIRCRAFT

## B-70 AIRCRAFT

## B-70 AIRCRAFT

## B-70 AIRCRAFT

## B-70 AIRCRAFT

UV color and flux at 2200 and 2600 angstroms measured for A and B stars, using rocketborne photometers 10 p1602 A66-21096

Absolute magnitude of magnetic star HR 732 11 p1776 A66-23429

Intrinsic rotation of Orion B stars with weak He lines, discussing color-magnitude diagram 23 p4130 A66-41815

## B-6 AIRCRAFT

## B-206 AIRCRAFT

## B-111 AIRCRAFT

Hydrol electronic/hydraulic antiskid braking system for automatic braking pressure modulation in BAC one-eleven 400 series aircraft 07 p0992 A66-18165

Interior design of BAC 111 short haul jet transport 13 p1994 A66-25565

Low speed handling with special reference to super stall, emphasizing rate of change of angle of attack and flight trials of BAC 111 and VC10 aircraft 19 p3280 A66-36748

Detail parts production out of Flomat, structural material composed of polyester resin and woven glass reinforcement for AC 111 20 p3562 A66-37424

## BACK INJURY

Statistical analysis of vertebral fracture in U.S. Navy during 1959-1963 period 16 p2644 A66-31132

## BACKGROUND EFFECT

USAF whole body gamma spectrometry in support of Air Force aerospace mission 07 p0999 A66-17664

Standard system for radar cross section error determination, noting calibration techniques, background level reduction methods, etc 10 p1504 A66-21660

Background gamma and electron fluxes reduction in charged-particle spectroscopy with fast-gated electronics 19 p3359 A66-35918

## BACKGROUND NOISE

Random-phase pulsed signal detection by contrast reception techniques against background of normal correlated noise 02 p0191 A66-11757  
Sampling techniques for extraction of periodic signals from background of random

noise 03 p0333 A66-12470

Statistical decision theory, applying Neyman-Pearson test, used to detect and discriminate signal 04 p0485 A66-14113

Probability density and distribution functions associated with noise and signal plus noise in radar IF, after linear and square law detector, and after these detectors with subsequent video integration 04 p0485 A66-14115

Formal variance of measurement error in frequency and phase of harmonic signal in narrow-band noise 08 p1201 A66-19688

Hearing acuity requirements of aircraft personnel, examining discrimination from background noise and acoustic trauma causative factors 10 p1493 A66-22130

Detection of fluctuating signal packets from noise background with unknown parameters 11 p1658 A66-23223

Detectability criterion for signal received against random noise 14 p2242 A66-28151

Statistical theory for optimum direction-finding system for space-time signal processing against wide-band fluctuation noise background 17 p2872 A66-31851

Formal variance of measurement error in frequency and phase of harmonic signal in narrow-band noise 18 p3091 A66-34674

Two-step procedure for high energy signal detection against noise background, based on statistical probability 19 p3296 A66-35296

Optimal detection of signals by spatially distributed receiving system against random noise background, using space-time signal selection method 20 p3517 A66-37744

Simultaneous estimate of delay time and drift of carrier frequency during nonoptimum reception against correlated noise background 20 p3519 A66-38002

Approximately minimax detection of vector signal on Gaussian background 22 p3939 A66-40188

Random dispersive wave intensity detection and measurement in presence of noise 23 p4037 A66-41499

Optimum detection of Markov signals against noise background in case of discrete time 24 p4188 A66-42474

Noise limitations in obtaining three-dimensional images by holographic techniques, considering graininess of photographic emulsion 24 p4212 A66-42752

## BACKGROUND RADIATION

Ionospheric effect on spectrum of general background galactic radio emission below 10 mc/s 02 p0284 A66-12192

Cosmic ray contribution to background of NaI scintillation spectrometers noting counting rate, surrounding material and atomic number 05 p0678 A66-14967

Optimum signal to noise ratio photon detector and relation to high background radiation 10 p1505 A66-21842

Miniature proportional counters with low background level for determining ultrasmall quantities of Ar 37 and H 3 10 p1610 A66-22017

Continuous radio emission in our Galaxy, discussing radio stars, background features, corona, emission mechanisms, etc 11 p1787 A66-22259

Type IV radio event of February 1965, noting four bursts preceded by decreases in background radiation intensity interpreted as absorption of type IV 12 p1952 A66-24966

Solar noise in optical communications, background radiation dependence on detector aperture, noise power and application to GaAs diodes and gas lasers 13 p2024 A66-25833

Night sky darkness explained as limitation of background radiation by various factors in static, steady state and evolving universes 13 p2075 A66-26602

HF brightness intensity of cosmic background radiation at 20.7 cm wavelength may be primordial fireball residue of big-bang cosmology 18 p3171 A66-34717

Miniature proportional counters with low background level for determining ultrasmall quantities of Ar 37 and H 3 19 p3453 A66-36103

Electron densities, magnetic field strength and energetic particle fluxes in

magnetosphere determined, using VLF background radiation 22 p3911 A66-39990

Microwave background radiation field accounted for by integrated effect of population of radio sources if CN excitation is collisional in origin 22 p3978 A66-40004

Kaufman assumption regarding universe expansion considered untenable because it requires intergalactic hydrogen temperature to remain constant while hydrogen has expanded in volume 22 p3978 A66-40008

Cosmic microwave background radiation, considering statistically homogeneous and isotropic but nonuniform distribution of matter 22 p3978 A66-40009

Potential sensitivity of energy radiation detectors, examining measurement error causes for radiation power of natural and artificial sources 24 p4172 A66-42523

## BACKSCATTER

Directional reflective coating consisting of cylindrical dielectric fibers oriented perpendicular to absorbing substrate [AIAA PAPER 65-671] 01 p0160 A66-10232

Relative backscatter coefficients for 16-mc backscatter from land and sea 02 p0190 A66-11472

Minimization of radar cross section of thin cylinder by central loading, calculating backscatter field 05 p0632 A66-14842

Plane electromagnetic wave scattering at rectangular conducting strips, examining front end backscattering and current distribution measurements 05 p0649 A66-15121

Radar backscatter cross section from turbulent wakes 05 p0635 A66-15797

New aspect function applied to radar signal return from ground approximates measured data more accurately than any other aspect function 06 p0826 A66-16031

Cross section measurement for electromagnetic backscattering of laser beams from rough aluminum and magnesium oxide surfaces 08 p1182 A66-18930

Multifrequency radar as remote sensor for exploration of Earth and Moon surfaces, examining variation of backscattering with change in wavelength 09 p1341 A66-19868

Angular dependence of mean power backscattered from Moon and Venus indicates greater smoothness of Venus surface 09 p1452 A66-20127

Current distribution along circular loop antenna, obtaining backscattering patterns as function of rotation angle 10 p1510 A66-21592

Short-pulse scattering by simple geometric shapes useful for heuristic models of electromagnetic scattering, illustrating creeping-wave return 10 p1500 A66-21618

Short pulse radar return of cone-sphere measured to determine contribution of individual scattering elements to total scattered field, noting creeping wave contribution 10 p1502 A66-21636

Auroral zone, ionospheric scattering and nongreat-circle HF propagation statistically analyzed 11 p1700 A66-23141

HF noise signals and association with auroral disturbances analyzed, using data from IGY network of backscatter sounders 11 p1701 A66-23154

Surface roughness and tolerances in model scattering experiments, noting shape perturbation consequences, frequency characteristics wave behavior, etc 11 p1658 A66-23406

Backscattered and surface fields for acoustically hard and soft prolate spheroids at end-on incidence computed, using tabulation of spheroidal functions 12 p1815 A66-24119

Ruby laser optical radar detection of upper atmospheric backscattering 12 p1818 A66-24395

Wavelength dependence of angel echoes, using radar backscatter from clear atmosphere 12 p1825 A66-24890

Clear air turbulence detection with optical radar, using spectral analysis of backscattered Doppler-shifted light particle formation mapping via correlates of rough flying conditions 15 p2450 A66-28920

CAT detection by radar backscatter measurement of radio refractive index eddies 15 p2532 A66-28925

CAT detection from Doppler shift in laser



light backscattered from atmospheric aerosol 15 p2500 A66-28930  
 HF backscattering by plane electromagnetic wave incident on concentric conducting sphere covered with concentric layers of different materials, noting refractive index value 16 p2647 A66-30224  
 Correlation of simultaneous optical and radio auroral data showing that radio wave scattering belt includes visual auroral belt 16 p2692 A66-30329  
 Stimulated Brillouin scattering from nitrogen and methane using giant pulse laser, noting convergence angle of backscattered beam sound, velocity measurement, etc 17 p2961 A66-32627  
 Lidar detection of backscatter from upper atmosphere 17 p2875 A66-32929  
 Backscatter returns from ionospheric sporadic E on sea and land 17 p2923 A66-33357  
 End-fire radar echo of long thin body minimized by impedance loading technique 18 p3065 A66-33535  
 Phase fluctuations of ground-backscattered signals recorded, noting phase stability of sporadic E-layer-supported and F-2-layer-supported ground backscatter 18 p3071 A66-34534  
 Theoretical calculation of propagation path geometry of VHF aurora backscatter communications compared with experimental observations 19 p3306 A66-36653  
 Depolarization of electromagnetic waves backscattered from rough surface boundary 20 p3515 A66-37293  
 Statistical analysis of diurnal variation in southern boundary of aurora, HF backscatter records and geomagnetic latitude of dayside aurora 20 p3553 A66-38193  
 Earth albedo estimation, backscattered interplanetary radiation and resonance scattering of dayglow 20 p3553 A66-38194  
 Physical-optics solution for backscattering from concave ring singularity 20 p3521 A66-38364  
 Backscattering characteristics of overdense essentially collisionless spherical plasma explained by surface wave interference 22 p3955 A66-40108  
 Vector scatter theory for backscatter of circularly polarized waves from Moon and Venus 22 p3866 A66-40174  
 Modified Fock function for current distribution in penumbra and shadow region of plane electromagnetic wave incident upon convex cylinder, with application to backscattering 23 p4040 A66-41637  
 16-megacycle backscatter echoes from sporadic E region recorded near Brisbane, Australia, examining dimensions of horizontally moving irregularities 23 p4064 A66-41685  
 Coherent CW superheterodyne radar system for studying backscattering from hypersonic velocity projectile wakes 24 p4191 A66-42196  
 Daily and seasonal variation of long distance propagation related to horizontal ionospheric gradients, particularly height of layer on wave path 24 p4174 A66-42739

**BACKWARD WAVE**  
 Uniform ferrite slow wave structure analysis of parameters, discussing three applications 01 p0040 A66-10554  
 Formed point contact gallium arsenide backward diodes compared with conventional millimeter-wave diodes show advantage as low level baseband current detectors 08 p1189 A66-18658  
 Superregenerative amplifier of backward wave including oscillation spectrum, resonance curve, noise coefficient, etc 09 p1357 A66-20777  
 Time-and space-resolved measurements on self-excited moving striations and on low pressure glow discharge to externally excited pulses 10 p1564 A66-21565  
 Surface and interface waves in plasma gaps, discussing backward wave 10 p1564 A66-21584  
 Backward diode application to microwave circuit design, discussing characteristics of stripline mount with probe detector 15 p2457 A66-28886  
 Frequency converters using traveling wave and backward wave tubes, noting current-

wave amplitude distribution, velocity and voltage 16 p2666 A66-31550  
 Flow structure and heat transfer for rearward facing step in supersonic flow, discussing critical Reynolds number, flow through lip shock, etc 17 p2913 A66-33068  
 Birefringence of certain crystals sufficiently large to allow collinear backward wave interaction of three electromagnetic waves with signal frequency tunable over large portion of IR spectrum 21 p3771 A66-39113  
 Superregenerative amplifier of backward wave including oscillation spectrum, resonance curve, noise coefficient, etc 22 p3873 A66-39836

**BACKWARD WAVE OSCILLATOR**  
 Coupled monotron analysis of band-edge oscillations in high power traveling wave tubes, discussing electron beam interaction with coupled-cavity structure 06 p0855 A66-16768  
 Gain-bandwidth product determined for traveling wave quantum amplifiers with regeneration by partially reflecting mirrors 11 p1711 A66-22727  
 Mode separation in bifilar-helix backward-wave oscillator 21 p3712 A66-39228  
 Backward wave oscillator /BWO/ design parameters and components 22 p3880 A66-40736  
 Gain-bandwidth product determined for traveling wave quantum amplifiers with regeneration by partially reflecting mirrors 23 p4078 A66-41465

**BACTERIA**  
 SA AZOTOBACTER  
 SA HYDROGENOMONAS  
 SA SPORE  
 SA VIRUS  
 Contamination of carbonaceous chondrites by ordinary viable microorganisms, isolating three types of bacteria on various meteorites 03 p0325 A66-13339  
 Cascade vault sampler for bacterial aerosols 08 p1177 A66-19087  
 Resistance transfer factor episome analyzed by measuring inactivation by cobalt gamma radiation, phosphorus and tritium, suggesting existence of DNA 14 p2228 A66-27308  
 Biological procession of human secretions and water regeneration by Chlorella in bacterial colony 15 p2440 A66-29501  
 Enteric microbial flora changes in man exposed 56 days to oxygen-helium atmosphere 18 p3058 A66-33777  
 Cosmic radiation and space flight effects on lysogenic bacteria and human cells in culture 21 p3700 A66-39315  
 Space diet effect on aerobic and anaerobic microflora of human feces 22 p3854 A66-39796  
 Bacteria survival and mutation in radiation environment on Voskhod I and II 22 p3855 A66-40474

**BACTERIOLOGY**  
 Characteristics, fine structure and mode of functioning of bacterial cell and artificial synthesis possibility 11 p1644 A66-22713  
 Number of viable aerobes and anaerobes accumulating on stainless steel surface in clean room during one year under various conditions, for spacecraft sterilization purposes 13 p2015 A66-25797  
 Inhibition of zoospores of unicellular chlorococcacean alga by soil bacillus through ammonium ion 17 p2860 A66-32833  
 Oral, cutaneous and aerosol bacteriological evaluation of astronaut exposed to oxygen-helium atmosphere at low pressure 18 p3058 A66-33778  
 Survival and growth of Bacillus cereus and B. subtilis in simulated Martian environment of diurnal temperature cycling and low moisture and oxygen 19 p3284 A66-35576  
 Rotary plate airborne bacteria sampler 22 p3858 A66-40505

**BACTERIOPHAGE**  
 Proton tunneling and mutation rate of Escherichia coli B To T1 and T2 phage resistance in water 13 p2008 A66-25788

**BAFFLE**  
 Damping of liquid oscillations in cylindrical tanks, determining rigid and flexible baffle loss coefficients, baffle efficiency and maximum bending stress

[AIAA PAPER 66-97] 08 p1207 A66-1900

**BALLOUT**  
 S EJECTION  
 S PARACHUTING

**BAKER-NUNN CAMERA**  
 Tesseral harmonics of coordinates using Baker-Nunn data and geopotential and dynamical procedures, noting iterative cycle for correction determination 15 p2491 A66-2999  
 Integrated brightness observations of comets, using Baker-Nunn satellite tracking camera 17 p3011 A66-3338

**BALANCE**  
 SA COMPENSATOR  
 SA HEAT BALANCE  
 SA MASS BALANCE  
 SA MICROBALANCE  
 SA STRAIN GAUGE BALANCE  
 SA WATER BALANCE  
 SA WIND TUNNEL BALANCE  
 Book on dynamic and static balancing of rotating machine parts and devices, particularly gyroscopes, noting effect of bearings, vibration causes, etc 09 p1383 A66-2093

**BALANCE EQUATION**  
 SA MOTION EQUATION  
 SA PRESSURE FIELD  
 SA VORTICITY EQUATION  
 Stabilizing methods for hypersonic aircraft noting effect of aircraft characteristics, parameters on magnitude of balancing coefficients of lifting force 14 p2223 A66-2766  
 Balance equations derived from kinetic equations for nonequilibrium plasmas considering radiative processes and inelastic collisions between electrons and atoms 16 p2766 A66-3160  
 Friction and imbalance moments relative to gimbal axes and effects on gyroverlock motion under starting conditions 21 p3739 A66-3933  
 Balance equations for heterogeneous continua - substances consisting of materials distinct, possibly interacting constituents derived from classical continuum physics viewpoint 21 p3772 A66-3934  
 Ion energy balance equation for ionosphere including effects of O, He, and H ions thermoconductivity and cooling by atomic hydrogen and helium 24 p4198 A66-4243

**BALL BEARING**  
 Model analysis of radial oscillations of shaft with pounding of ball bearings 02 p0299 A66-1186  
 Ball bearing lubrication with vapor from volatile organic compounds for wide temperature range and long term operation [ASLE PREPRINT 65-LC-24] 02 p0237 A66-1224  
 Operating performance of deep groove ball bearing used for gas turbine at high duty values 03 p0372 A66-1246  
 Microslip between ball and track in ball thrust bearings with ball subjected to forced and spin moment 04 p0527 A66-1423  
 Compressive residual stress effects of surface layers of through-hardened bearing steels produced by prenitriding before hardening [ASME PAPER 65-WA-CF-7] 05 p0690 A66-1562  
 Properties of helical delay line used to feed frequency scanned X-band array, noting role of ball bearing inserted in helix 06 p0854 A66-1668  
 Lift in spherical ball bearings with a lubrication calculated, taking into account inertial term in general equations of aerodynamics, gap variability and compressibility 08 p1232 A66-1969  
 Lubricants for space environment, noting experiences with satellites and application to ball bearings and electrical contacts 13 p2086 A66-2573  
 Book on design and utilization of antifriction bearings 13 p2087 A66-2625  
 Motion equations for radial oscillation of shaft with ball bearing chatter 14 p2305 A66-2847  
 Jet oil lubrication and scavenging technique for 20 mm high speed ball bearing [ASLE PAPER 66AM 1B4] 16 p2710 A66-3040  
 Ball bearing life operating in vacuum with



molybdenum disulfide and oils as lubricant  
ASLE PAPER 66AM 7A3]

Split-inner-race ball bearings design for  
use as thrust bearings on aircraft gas  
urbines  
ASME PAPER 66-LUBS-10]

Jet oil lubrication and scavenging  
technique for 20 mm high speed ball  
bearing  
ASLE PAPER 66AM 1B4]

16 p2712 A66-30416

17 p2931 A66-33183

22 p3928 A66-40657

ALLISTIC CAMERA

Calibration procedures and statistical  
analysis for error reduction in ballistic  
camera lead-screw type  
comparator 02 p0228 A66-11380

BRL ballistic camera system noting optical  
and mechanical characteristics, measurement  
and computer synchronization

methods 10 p1537 A66-21872

Spectral ballistic camera instrument  
providing relative intensity data and  
scintillation information on missiles and  
emissive body

jectories 21 p3735 A66-38607

ALLISTIC MISSILE

SA INTERCONTINENTAL BALLISTIC

MISSILE /ICBM/

Low cost inertial guidance system

commands missile attitude so that modified  
ballistic trajectory is followed along direct  
line of sight to target 01 p0098 A66-10003

Reliability and maintainability concepts  
applied to solid propellant subsystems of  
mobile ballistic missiles 01 p0129 A66-10108

Relative advantages of ballistic missiles  
and orbital ferries for placing payloads in  
orbit 02 p0306 A66-11862

Rarefied hypersonic flow at high Mach  
numbers and stagnation temperatures  
encountered by ballistic missiles and  
satellites, noting air plasma with magnetic  
field

AIAA PAPER 65-754] 03 p0354 A66-12588

Evaluation of methods for estimating  
circular error probable /CEP/ or system  
accuracy of ballistic missiles employing  
inertial navigation

systems 04 p0544 A66-14444

Maximum range of ballistic missile with  
given burnout speed and altitude, optimum  
angle obtained by geometrical  
means 05 p0760 A66-14891

Optimization of multistage ballistic missile  
system operating in drag environment by  
solution of physical discontinuity problems  
[AIAA PAPER 66-91] 06 p0959 A66-16406

Military aspects of U.S. space program,  
reviewing work from ballistic missile to  
Manned Orbiting

laboratory 08 p1321 A66-18550

Ballistic wind and density predictions,  
measuring wind and D-value at 500 mb,  
calculating missile response to atmospheric  
effects

AIAA PAPER 66-359] 12 p1906 A66-24478

Real time system for measuring and  
analyzing meteorological data for computing  
launch angles for unguided rocket flights  
[AIAA PAPER 66-336] 12 p1953 A66-24481

Inertial guidance systems using three-  
gimbal, four-gimbal and ball-type platforms,  
operative control of aircraft, ships and  
ballistic missiles 13 p2125 A66-26140

Hypersonic wake studies in ballistic missile  
research program, discussing reentry of  
hypervelocity vehicles, laminar flow,  
atmospheric turbulence,

te 14 p2218 A66-27402

Recovery locations and techniques for  
atmospheric reentry vehicles in normal  
flight and impact 14 p2395 A66-28454

Reentry scattering due to equilibrium  
incidence without using Allen

hypothesis 16 p2796 A66-30315

Optimum flight of axially propelled  
nonlifting vehicles through resisting medium  
calculated by calculus of variations  
[AIAA PAPER 66-485] 16 p2799 A66-30524

High speed computer technique for  
simulating test design parameters for  
evaluation of ballistic-weapon system  
accuracy

AIAA PAPER 65-222] 16 p2809 A66-30888

Downrange radar and optical data  
reduction used for evaluation of ejection

velocities of ballistic missile penetration

aids at deployment

[AIAA PAPER 66-405] 16 p2804 A66-31464

Stellar inertial guidance system composed  
of integral inertial platform-stellar sensor  
combination, airborne digital computer and  
power supply for Polaris

missile 18 p3132 A66-34042

Preflight and in-flight testing of stellar  
sensor subsystem for guidance of ballistic  
missiles 18 p3111 A66-34046

Approximation of aerodynamic stability of  
coasting vehicle leaving atmosphere at high  
speeds, assuming linear theory and constant  
aerodynamic coefficient 22 p3986 A66-40346

Optimization multistage ballistic missile  
system operating drag environment by  
solution of physical discontinuity problems  
[AIAA PAPER 66-91] 22 p3986 A66-40362

Problems arising in production and  
implementation of ballistic missiles and  
spacecraft programs 23 p4074 A66-41652

SYSTEM /BMEWS/ P

Ballistic missile defense and national  
security, discussing defense system  
requirements, strategy types,

etc 08 p1322 A66-18560

BALLISTIC RANGE

UV radiation from shock-heated nitrogen  
measured by ballistic flight through  
nitrogen-neon mixture

[AIAA PAPER 66-422] 17 p3035 A66-32751

Ballistic range blast-traversal testing  
technique using scale models containing fast  
response FM telemetry system modulated by  
capacitance type pressure transducer  
[AIAA PAPER 66-777] 23 p4053 A66-41333

Moving source scanning spectrometer for  
ballistic range radiometry noting spectral  
resolution, operation and performance  
characteristics 24 p4208 A66-42180

High velocity impact range diagnostic  
instrumentation including timing and  
triggering devices, laser and spark  
photography, radiation monitors, ballistic  
pendulum, etc 24 p4191 A66-42187

Onboard miniaturized telemetry system for  
stagnation point temperature measurements  
on free-flight models in ballistic  
ranges 24 p4209 A66-42189

BALLISTIC TRAJECTORY

Maximum ballistic rocket trajectory range  
in view of Earth rotational and curvature  
effects 11 p1734 A66-23346

Computer program for predicting satellite  
long-term orbit decay and digital simulation  
of atmosphere and reentry conditions  
[AIAA PAPER 66-357] 12 p1951 A66-24491

Restoration of trajectory without known  
initial point, considering ballistic missile  
trajectory 24 p4171 A66-42340

BALLISTIC VEHICLE

Orbiter injected sterilized ballistic skipout  
capsule for in-flight Martian stratosphere  
measurements, using nonablative heat shield  
and outside atmospheric propulsion  
maneuvers

[AIAA PAPER 65-23] 03 p0431 A66-12764

Booster rocket survey of U.S. and Western  
Europe 10 p1612 A66-21958

Externally caused radio frequency  
interference /RFI/ in electronic subsystems  
of ballistic vehicles at orbital  
altitudes 13 p2027 A66-26744

Internal ballistic considerations in hybrid  
rocket design, noting throttling and regimes  
of operation involving effects of surface-or  
gas-phase reaction kinetics

[AIAA PAPER 66-628] 20 p3663 A66-38035

Ballistic reentry vehicle recovery via low  
speed water impact or air snatch after  
vehicle has flown unperturbed trajectory  
down to altitude of maximum dynamic  
pressure 22 p3986 A66-40597

Airdrop, delivery of personnel, supplies  
and equipment from aircraft in flight,  
increased effectiveness through new family  
of low-cost cargo parachutes, ballistically  
deployed reserve parachute and extraction-  
force transfer coupling 22 p3850 A66-40614

Analytical approximate solution of motion  
equations for ballistic vehicles during  
atmospheric entry, examining velocity and  
inclination angle error dependence on height  
eccentricity and apogee radius

[ICAS PAPER 66-38] 23 p4007 A66-41010

Chemical effects on RF attenuation during

reentry for blunt-nosed lifting vehicles and  
sphere-cone ballistic

vehicles 24 p4158 A66-42782

BALLISTICS

SA INTERIOR BALLISTICS

SA PENETRATION BALLISTICS

Burning rate equation and constant volume  
burning of solid propellant to determine  
ballistic properties 15 p2617 A66-29606

Dispersionless ballistics patterns of  
weapons analyzed as check on reported  
computer program 16 p2831 A66-31147

BALLISTOCARDIOGRAM

Triaxial ballistocardiogram in weightless  
environment 18 p3056 A66-33715

BALLISTOCARDIOGRAPHY

Accelerographic and ballistocardiographic  
evidence of increased stroke volume  
secondary to acute high altitude  
hypoxia 17 p2855 A66-32135

BALLOON

SA HIGH ALTITUDE BALLOON

PROGRAM

SA METEOROLOGICAL BALLOON

SA ROBIN BALLOON

High altitude balloons for scientific  
research noting zero-pressure  
balloon 05 p0611 A66-15271

Venus probe design of expandable balloon-  
type instrument package capable of entry  
into and of static equilibrium within Kaplan  
atmosphere 14 p2392 A66-27887

Saturn booster recovery by means of drag  
balloon which converts to hot air balloon for  
final recovery 22 p3987 A66-40608

BALLOON FLIGHT

Cosmic ray intensity measured during  
geomagnetically quiet and active days from  
1959 to 1963 by using balloon flights, noting  
role of ionization, Forbush effect,  
etc 07 p1124 A66-18000

IR spectroscopic observations with balloon-  
borne telescope, Stratoscope

II 10 p1603 A66-21108

Radioactive debris over Fairbanks, Alaska,  
on February 18, 1965, investigating  
bremsstrahlung X-rays in auroral  
zone 12 p1875 A66-24896

High altitude balloons used to carry  
scientific instruments 14 p2222 A66-26926

Balloon flight near peak of solar cycle in  
search for solar and cosmic gamma  
rays 18 p3169 A66-34515

Time structure of auroral X-rays at  
Swedish and Finnish locations, using  
simultaneous balloon

flights 19 p3452 A66-35562

Upper limits resulting from search for  
solar photons in 100-kev to 2-mev range  
from balloon observations 22 p3973 A66-40549

Spark chamber system designed to detect  
gamma rays in cosmic radiation on high  
altitude balloon flights 24 p4215 A66-43212

BALLOON SOUNDING

Polyethylene balloons for atmospheric  
research in France 01 p0011 A66-10361

Vertical distribution of atmospheric ozone  
measured by balloon-borne Sun-seeking  
guidance system and light-scattering gypsum  
screen 01 p0071 A66-11044

Vertical profile of refractive index in  
lower atmospheric layer measured by  
modified A-22-IV radio probe on captive  
balloon 02 p0253 A66-11274

Mountain lee waves at White Sands Missile  
Range investigated by balloon

soundings 02 p0253 A66-11970

Balloon measurements of solar protons and  
auroral X-rays discussing radiation detectors,  
flight techniques, instrumentation and  
results 03 p0417 A66-12654

Height, wind speed and direction errors  
arising from radar tracking with level  
balloons 04 p0541 A66-13667

Electrons, hydrogen nuclei and helium  
nuclei observed in primary cosmic radiation  
by balloon in 1963, discussing integral  
intensity and differential energy  
spectrums 05 p0746 A66-14780

Detection of slow neutrons escaping from  
atmosphere by counters filled with boron  
fluoride onboard high altitude  
balloons 05 p0754 A66-15401

Flux and energy spectrum of primary  
electron component measured by balloon at  
period near solar activity

minimum 06 p0944 A66-16075

Cumulus modification experiment using



station network, radiosonde and pilot balloon stations, cameras, radar data, etc 06 p0905 A66-16268

Balloon-borne scintillation counters combined with Cerenkov counter for measuring primary cosmic ray charge and energy spectra during 07 p1123 A66-17994

1963 Spectral variation of low energy galactic cosmic ray protons and helium nuclei measured by balloon flights 07 p1123 A66-17995

Reflection spectrum of clouds in Venus atmosphere measured, using telescope mounted on helium balloon, noting details of instrument 07 p1137 A66-18055

Spatial and temporal character of fast variations in auroral zone X-rays, describing balloon experiment and results 08 p1284 A66-19397

Sky observations with balloon-borne X-ray telescope having sodium iodine scintillator 09 p1442 A66-20466

Aerospace studies in Argentina during 1964 using rockets and balloons and including winds, E layer, satellite tracking, etc 09 p1458 A66-20706

Localization and motion of energetic electron precipitation regions during negative magnetic bays, noting similarity of motion to that of auroral electrojets 10 p1599 A66-21147

Balloon-borne instrument for measuring downward flux of thermal radiation from atmospheric water vapor, using gold doped germanium detector 11 p1706 A66-22888

Vertical distribution of atmospheric ozone measured by balloon-borne Sun-seeking guidance system and light-scattering gypsum screen 11 p1709 A66-23291

Mesoscale perturbations in vertical wind velocity profiles obtained from superpressure balloons tracked by FPS-16 radars 11 p1731 A66-23381

Motion equations for stable rising balloon systems which consider effects of apparent mass and wind accelerations, using radar tracking [AIAA PAPER 66-398] 12 p1802 A66-24513

Simultaneous observations of auroral zone X-ray microbursts, using two balloon-borne radiation detectors separated by 300 km to estimate size of region of electron precipitation 12 p1944 A66-24841

Equilibrium temperature gradient determined from theoretical calculations and balloon and aircraft measurements 12 p1875 A66-24872

French EOLE experiment for measuring tropospheric parameters, describing balloon transponder, balloon and spacecraft electronic packages, telemetry, etc 12 p1956 A66-24934

Degree of clustering expected from 500-mb horizontal sounding system, using stream functions and velocity potentials derived from historical tapes of National Meteorological Center 13 p2121 A66-25815

Diurnal variation of average energy spectrum of auroral X-rays observed from balloon flights, assessing effect of atmospheric absorption 14 p2376 A66-27614

Outgoing Earth and atmospheric radiation observed in IR spectrum at various altitudes by geophysical balloons and rockets 15 p2483 A66-28739

Behavior of superpressure balloons in vertical air currents, noting various combinations of wind speed and wave amplitude 15 p2426 A66-28941

Camera tubes for recording Stratoscope II telescope, noting photometric fidelity 15 p2500 A66-28969

Crab Nebula X-ray spectrum from 16-120 kev by balloon 16 p2792 A66-30143

Balloon-carried automatic telescope-spectrometer observation of Venus upper atmosphere and determination of water vapor content 16 p2797 A66-30352

Small-scale wind variations in stratosphere and mesosphere studied by high resolution Robin falling-sphere soundings 16 p2740 A66-30510

Vertical profile of atmospheric radiative balance from balloon-borne actinometry at 25 to 32 km 16 p2698 A66-31344

Automatic reduction of recorded flight data from balloons equipped with radiation

detectors and SPARMO

telemetry 17 p2926 A66-33148

Launching balloon measurements of cosmic ray intensity as function of atmospheric depth at cosmic equator 17 p2994 A66-33150

Ambient temperature measurements from radiosondes flown on constant-level balloons 17 p2949 A66-33342

Flux and energy spectrum of primary electron component measured by balloon at period near solar activity minimum 18 p3187 A66-34814

Balloon observation of high energy primary electrons with counter system 18 p3187 A66-34816

Low energy galactic cosmic radiation studies by high altitude balloon flights carrying nuclear emulsions, including solar activity, energy and intensity spectra, etc 18 p3189 A66-34829

Balloon flight data obtained at 50 and 65 degrees N geomagnetic latitude on spectra of primary cosmic ray hydrogen and helium nuclei, using Cerenkov scintillator technique 18 p3190 A66-34831

Balloon-borne nuclear emulsion detection of solar cosmic ray heavy nuclei during solar burst 18 p3190 A66-34836

Balloon-borne nuclear emulsion detection of finite fluxes of low energy cosmic ray heavy nuclei and interstellar cosmic radiation propagation 18 p3191 A66-34838

Balloon-borne Cerenkov scintillation counter measurements of energy spectra of primary cosmic radiation heavy nuclei at various geomagnetic latitudes 18 p3191 A66-34840

Skyhook balloon flight Geiger counter cosmic ray monitor measurements of energy and charge spectra of galactic rays at solar minimum 18 p3192 A66-34847

Balloon-borne scintillation counter measurements of isotopic composition, energy/nucleon and rigidity spectra of primary cosmic helium nuclei 18 p3193 A66-34848

Spark chamber experimental investigation of flux of high energy gamma rays at high altitudes near magnetic equator 18 p3193 A66-34849

Balloon flight experiment to search for celestial sources of X-rays in energy range 20 to 58 kev 18 p3193 A66-34852

Atmospheric neutron flux measured by balloons, using polyethylene-moderated boron fluoride counter 18 p3197 A66-34875

Energy spectrum of auroral X-rays in range from 20 to 150 kev according to balloon measurements show remarkable diurnal variation 19 p3452 A66-35563

EOLE system consisting of balloons and satellite, interrogation for synoptic data on atmospheric circulation over Southern Hemisphere 19 p3346 A66-35638

Balloon sounding of Southern Hemisphere by global horizontal sounding technique /GHOST/, providing data on atmosphere circulation 19 p3279 A66-35639

Balloon measurements of cosmic ray hydrogen and helium nuclei at locations with nominal geomagnetic threshold rigidities 19 p3452 A66-35926

Possible enhancement to low-energy atmospheric proton flux induced by passage of Ikeya-Seki comet examined, using balloon-borne scintillation counter and pulse height analysis techniques 20 p3631 A66-37617

Moisture contamination and associated water band absorption spectra recorded by balloon-borne spectrometer 20 p3554 A66-38206

Wind distribution in atmospheric boundary layer under conditions of advection from pilot balloon observations 20 p3594 A66-38376

Cosmic X-ray source near direction of north galactic pole, noting empirical results from balloon observations 21 p3810 A66-39267

Equilibrium temperature gradient determined from theoretical calculations and balloon and aircraft measurements 22 p3912 A66-40333

Upper wind evaluation by pilot and radiosonde balloon radar tracking for flat Earth and effects of Earth curvature 22 p3943 A66-40428

Balloon-borne spark chamber observations of cosmic gamma rays from 30 to 500

mev 23 p4124 A66-4206

Radiosonde for high altitude balloon soundings using large polyethylene balloon to carry payloads of electronics, cosmic ray and nuclei counters 23 p4087 A66-4208

Flux and energy spectrum of low energy heavy nuclei of primary cosmic radiation measured by balloon-mounted nuclear emulsion stacks 24 p4284 A66-4260

Vertical profile of atmospheric radiative balance from balloon-borne actinometry at 25 to 32 km 24 p4201 A66-4265

Cosmic ray electron sign ratio and absolute flux measured by balloon-borne equipment 24 p4272 A66-4304

### BALLUTE

#### SA PARACHUTE

First-stage decelerator and stabilization balloon system for payload recovery for Mach 4 and 10 flight 04 p0585 A66-1353

Parachutes and other devices for slow body falling through air including Rogall wing, ballute, ribbon parachute and vortex ring parachute 24 p4160 A66-4319

#### BALMER SERIES

Stark broadening of Balmer lines in hydrogen plasma produced by alternating axial magnetic field induced by coil surrounding discharge tube 03 p0400 A66-1293

Absolute magnitude of magnetic star HD 1732 11 p1776 A66-2342

Grid computations of model atmosphere for A-type stars, considering effects of Balmer-line blanketing 18 p3227 A66-3376

Height distributions for atmospheric ionization rate and Balmer radiation resulting from precipitation of auroral protons 21 p3734 A66-3933

#### BANACH SPACE

Stability theorems concerning unconditionality of bases, considering Riesz theorem and Banach and Gilbert spaces 01 p0093 A66-1040

Optimal control problems in Banach spaces; discussing extension to infinite dimension, and application to distributed parameter systems 04 p0506 A66-1399

Stability of solutions of Cauchy problem for linear hyperbolic differential equations 07 p1056 A66-1760

Existence and convergence theorems for minimizing sequences for extremum problems in presence of constraints 10 p1551 A66-2197

Unilateral estimates under conditions of asymptotic stability of solutions to differential equations with unbounded operators 10 p1552 A66-2198

Error bounds in best approximation of given function in Banach space constrained by inequality relationships 11 p1722 A66-2298

Stability and boundedness for solutions of class of complex differential systems obtained in terms of Liapunov-like functions 11 p1725 A66-2342

Estimates of solutions to second order differential equations generalized to include inequalities with Schwarz derivative numbers 12 p1902 A66-2376

Minimum effort control problem in reflexive Banach space and extension to Hilbert space under bounded linear transformation 14 p2266 A66-2763

Variational problem in Banach space including optimal control problems, deriving conditions for extremality and Pontryagin maximum principle 15 p2473 A66-2937

Existence theorem of recurrent solution to differential equations defined in Banach space for dynamic and nondynamic systems 16 p2735 A66-3078

Nonlinear parabolic equations, considering existence, uniqueness theorems, abstract Cauchy problem, etc 17 p2946 A66-3230

Existence and convergence theorems for minimizing sequences for extremum problems in presence of constraints 19 p3390 A66-3618

Unilateral estimates under conditions of asymptotic stability of solutions to differential equations with unbounded operators 19 p3390 A66-3619

Well-posed BVP for linear partial differential system and relation of weak solution with two Banach spaces 21 p3754 A66-3845



Existence theorem of recurrent solutions  
of differential equations defined in Banach  
space for dynamic and nondynamic  
systems 22 p3940 A66-40447  
Error free recovery of signals from  
regularly spaced samples in terms of  
completeness of sets of nonharmonic  
exponentials 24 p4189 A66-43202  
**BAND**  
ABSORPTION BAND  
BLOCH BAND  
CONDUCTION BAND  
E-BAND  
ENERGY BAND  
ERROR BAND  
FORBIDDEN BAND  
FREQUENCY BAND  
K-BAND  
L-BAND  
PHOTOLUMINESCENT BAND  
POSITIVE BAND  
SCHUMANN-RUNGE BAND SYSTEM  
SLIP BAND  
SPECTRAL BAND  
SWAN BAND  
**BAND PASS FILTER**  
Open periodic structures applied as high  
power limited passband loss filter in  
microwave radar and communications  
transmitters 01 p0044 A66-10935  
Multiple passband monochromatic filter  
used in telescopes for spectrophotometry of  
red shifts of distant  
galaxies 02 p0227 A66-11352  
Figure of merit and methods of finding  
optimal filters for pulse-forming networks,  
taking into account frequency response as  
well as time response 02 p0208 A66-11910  
Working characteristics of transmission  
channel, calculating relationships between  
probability characteristics and output signal  
to noise ratio, considering band  
filter 04 p0496 A66-13903  
Coaxial helical resonator for VHF filters  
with sharp selectivity 05 p0644 A66-14578  
Hyperfrequency parametric amplifier  
circuit with modulation-demodulation  
applicable to very rapid pulse  
transmission 05 p0633 A66-15102  
Microwave filters, discussing cascaded lines  
of cavities, band pass and band stop filters,  
group delay, dissipation loss,  
etc 06 p0844 A66-16080  
Interdigital band pass filters and related  
coupled structures, deriving exact  
equivalent circuits from impedance  
matrices 06 p0845 A66-16085  
Circular TE sub 011 mode, trapped mode  
band pass filters, discussing energy radiation  
mechanism, design, operation and test  
results 06 p0845 A66-16087  
Frequency and resonance characteristics of  
two- and three-circuit band filters used in  
parallel spectral analysis 06 p0848 A66-16135  
Design and construction procedures for  
band-passed matched filter with 200 mc  
center frequency 06 p0853 A66-16658  
Filter used as input/output network in  
resonant transfer system, noting steady  
state passband and transient  
response 06 p0853 A66-16668  
Four formulas for Kuroda identities for  
band pass and band stop transmission line  
filters, noting role of transient  
response 06 p0854 A66-16685  
Suppression of FM in parallel signal  
channels, using Mix-On-Self /MOS/  
loop 06 p0834 A66-16858  
Maximum gain condition of resonance  
amplifier for given passband, determining  
impedance coefficient 07 p1005 A66-17351  
Quadrature modulation single-sideband  
circuit as frequency translating two-port,  
comparing performance with conventional  
modulator-with-SSB filter  
circuit 07 p1015 A66-17746  
Two-frequency volume resonator with  
independent tuning within wide frequency  
band 08 p1191 A66-18918  
Possible amplitude-frequency and phase-  
frequency characteristics of selective  
systems with smooth passband control and  
nonminimal phase 09 p1352 A66-20294  
Phase frequency characteristics of two- and  
three-circuit band pass filters used in radio  
receiving devices 09 p1354 A66-20450  
Band pass filter network with constant  
input resistance over entire frequency

range 10 p1517 A66-21655  
Exponential resonators in filters and  
matching networks, determining reactance  
or susceptance frequency behavior by  
plotting curves with analog  
computer 11 p1661 A66-22382  
Coaxial helical resonator for VHF filters  
with sharp selectivity 11 p1666 A66-22688  
Hybrid narrow band filter compared with  
Lytot filter, noting long-term instability and  
need for temperature  
control 11 p1706 A66-22892  
Ten-element band pass filter section and  
derivatives with classification of image-  
impedance functions 11 p1669 A66-23113  
Jacobi elliptic functions for designing low-  
pass filters whose attenuation is represented  
by universal normalized  
curve 12 p1829 A66-23661  
High performance active RC band pass  
filter design providing for independent  
adjustment of poles 12 p1843 A66-24675  
Calculation of loss in interdigital and  
combine filters due to finite conductivity of  
materials 13 p2029 A66-25204  
Band pass characteristics realized by four-  
layer distributed RC network without series  
resistance and amplifier scheme used as  
model for integrated circuits, noting  
frequency characteristics  
variation 13 p2051 A66-26069  
Passband filters with three coupled  
circuits, determining circuit characteristics  
by method based on use of right angle  
triangles 13 p2043 A66-26315  
Passband filters with three coupled  
circuits 14 p2246 A66-26802  
Junction filters for eight channels in SHF  
range with provision for 1800 paths, noting  
bandpass width signal mixing for antenna  
feed, attenuation, capability,  
etc 14 p2252 A66-27351  
Correctors for variations in group  
propagation time of AM wave transmitted  
by radio carrier wave, noting circuit analysis  
for matched and unmatched all-pass IF  
filters 14 p2252 A66-27353  
Transfer function for quadrature  
modulation single band signal generating all-  
pass filter, using differential operational  
amplifier 14 p2253 A66-27586  
Octave band all-pass filter with  
electronically tunable  
limiter 15 p2463 A66-29037  
Pole-sharing method for reducing number  
of poles required for synthesis of bank of  
contiguous bandpass  
filters 15 p2463 A66-29038  
Lumped-constant filters whose bandpass  
depends only on one parameter of  
transmission coefficient, having lower  
bandpass for given transient process delay  
time 15 p2464 A66-29120  
Formula involving two impedances leads to  
equations for positive real functions, for  
application to power gain of symmetric and  
antisymmetric filters 15 p2464 A66-29322  
Pulse generator network synthesis and low-  
pass/ bandpass  
conversion 17 p2900 A66-32198  
Asymmetrical property of binary  
pseudorandom noise generators, noting  
Gaussian probability density function in  
output of low pass filter 17 p2894 A66-33110  
Bandpass filter design with three coupled  
circuit and determination of amplitude  
curve and circuit  
constants 17 p2895 A66-33243  
Half-wavelength resonators as capacitive-  
gap strip-line bandpass-type microwave  
filters, discussing parameter derivation for  
equivalent circuit and Cohn synthesis  
method 18 p3087 A66-34621  
Possible amplitude-frequency and phase-  
frequency characteristics of selective  
systems with smooth passband control and  
nonminimal phase 18 p3087 A66-34958  
Synthesis of HF multicircuit band filters  
with indirect couplings 19 p3312 A66-35324  
Working characteristics of transmission  
channel, calculating relationships between  
probability characteristics and output signal  
to noise ratio, considering band  
filter 20 p3531 A66-37861  
Bandpass amplifier design by selecting  
peak frequencies occurring in active high-  
and low-pass RC filter  
sections 21 p3711 A66-39200

Multiple access to ideal bandpass limiter  
channel in pseudonoise system  
analysis 23 p4040 A66-41593  
Small and low cost voltage-tunable audio  
filter using field effect transistors as tuning  
element in place of inductors for space  
communications 24 p4180 A66-42334  
**BANDWIDTH**  
Synchronous tuning of microwave filters  
involving small changes in rejection  
bandwidth and being consistent with  
Chebyshev response 01 p0044 A66-10936  
Helix traveling wave tube using beryllium  
oxide ceramic as supporting medium for  
wide band slow-wave  
structures 02 p0200 A66-11879  
Gain-bandwidth limitations for physically  
realizable systems obtained in integral form  
by employing generalized representation  
theorem for bounded-real  
functions 02 p0208 A66-11904  
Gain and bandwidth narrowing in  
regenerative helium-xenon laser  
amplifier 03 p0376 A66-12308  
Data control constant-bandwidth frequency  
system and tricom system discussed as  
examples of better methods of taking  
advantage of communication frequency  
spectrum 04 p0480 A66-13727  
Digital computer research program for  
reducing bandwidth schemes and quality for  
picture transmission 05 p0676 A66-14820  
Optical ultrasonic delay lines as correlators  
and variable code matched filters to achieve  
large time-bandwidth products and high data  
rates 05 p0631 A66-14821  
Fabry-Perot interferometer using wire  
grids instead of glass plates, covering  
operation, advantages and bandwidth  
characteristics 05 p0682 A66-15355  
Traffic aspects of communications systems  
involving single wideband facilities carrying  
simultaneously traffic of various bandwidths  
and group switching to meet individual  
traffic requests 06 p0830 A66-16334  
Gain-bandwidth limitations and optimum  
design of noninverting frequency converters  
comprised of parametric conductance in  
parallel with parametric capacitance pumped  
in time-quadrature 07 p1017 A66-18348  
Noise spectrum and noise factor of  
semiconductor switching elements, including  
transistors and electron tubes, as function  
of bandwidth 13 p2041 A66-25897  
Impedance transforming compensated  
balance to unbalanced line transformer  
/balun/, discussing  
bandwidths 14 p2258 A66-27959  
PCM picture transmission, pseudorandom  
scanning, noise, bandwidth compression and  
digital simulation 15 p2450 A66-28785  
Bandwidth of nonoverdriven abrupt-  
junction varactor-frequency doubler,  
deriving upper bounds for minimum  
constant T for lossless  
case 15 p2465 A66-29323  
Pump modulation factor of various GaAs  
and Si varactor diodes under operating  
conditions, noting experimental bandwidth  
gain via increased shot  
noise 16 p2663 A66-31017  
Three-cavity extended-interaction klystron  
with cavities consisting of resonated  
sections of bar structure tested in pulsed  
operation, noting relation between cavity  
length and efficiency 16 p2663 A66-31020  
Simple diode parametric amplifier,  
discussing bandwidth and noise  
measurements, compensating circuits for  
gain-frequency response  
improvement 17 p2892 A66-32917  
Sampling techniques for conversion of  
broadband signal into multiple narrow  
bandwidth and reconversion back to original  
signal 19 p3302 A66-35705  
PCM bandwidth halving and twin working  
method of superimposing two PCM channels  
in frequency band occupied by one PCM  
channel 19 p3305 A66-36625  
Ground-state spin memory in excited state  
of ruby under broadband optical pumping,  
observing change in relative populations of  
Zeeman components 20 p3578 A66-37596  
Broadening frequency bandwidth of full-  
wave directive loop antennas employing  
reflectors and directors 20 p3531 A66-37727  
Equivalent width of waveguides by  
considering wave propagation in direction



perpendicular to waveguide axis 21 p3712 A66-39225

Contrawound helical antenna with independent control of polarization bandwidth and gain used for receiving or low-power transmitting 21 p3714 A66-39496

Wide stop bandwidths from quasi-optical filters formed from iterations of dielectric slabs demonstrated at millimeter wavelengths 22 p3877 A66-40181

Inverse transfer function of pulse-forming network for binary code transmission with small intersymbol interference in time domain and narrow bandwidth in frequency domain 22 p3866 A66-40182

Autocorrelation as pulse compression system, giving effective time resolution as inverse of correlation bandwidth and compression ratio of time resolution to signal duration 23 p4034 A66-41022

VHF power modulator devised to give broadband output signals within frequency range of 66 to 184 megacycles at 2.5 mw and 50 ohms impedance 24 p4184 A66-42644

**BANG-BANG CONTROL**

Parameter variation effect on performance of second order maximum effort /bang-bang/ controller, noting optimum system, stability analysis and analog computer study 02 p0207 A66-11790

Thrust modulation with minimum limit cycle in bang-bang system, reducing fuel consumption for spacecraft attitude control system 03 p0432 A66-13206

Nonlinear servomechanisms using bang-bang control mode 07 p1016 A66-17850

Extension of optimal guidance method of Kelley and Breakwell to systems containing bang-bang control component, consisting of rescaling of time variable 08 p1250 A66-19145

Lapunov second method applied to stability of general second order bang-bang control systems 12 p1850 A66-24259

Bang-bang damping rate on system components with time delay and lag 12 p1850 A66-24263

Determination for piecewise analytic F/t/ of what vectors can be represented by bang-bang control having finite number of discontinuities 15 p2469 A66-28514

Iterative gradient method application to trajectory optimization problems, noting feasibility to systems with continuous bang-bang controls 17 p2903 A66-33254

Optimum control laws for bilinear system, using distributed parameter model with optimizing procedures including bang-bang control and optimum feedback control 20 p3598 A66-36856

Bang-bang principle in problem of epsilon-stabilization of linear control systems extended to systems of arbitrary dimension 23 p4051 A66-41874

**BAR**

**SA ELASTIC BAR**

**SA PRISMATIC BAR**

Longitudinal oscillations of Voigt body bar whose characteristics vary with time and are bounded 06 p0964 A66-16475

Limit load of flat notched bars subject to tension, discussing rupture force magnitude, plastic strain occurrence, rupture stress and yield limit curves, etc 14 p2398 A66-27394

Coupled-modal equations for arbitrary vibratory system, with example for longitudinal vibrations of bar 22 p3992 A66-40298

Elastic-plastic and stress shock wave propagation in finite-length bar with monotone decreasing cross-sectional area 22 p3995 A66-40509

**BARANY CHAIR**

Barany hypothesis tested to clarify mechanism of caloric nystagmus by use of zero gravity environment 17 p2857 A66-32168

**BARBITURATE**

**S PENTOBARBITAL SODIUM**

**BARIUM**

Polarization effects in magnetic and nonmagnetic barium plus bismuth oxide and magnesium-zinc ferrites when subjected to DC low-voltage electric fields 03 p0409 A66-12690

Fuel cells using metallic barium as fuel electrode and oxygen or chlorine as cathode, noting net energy densities 08 p1172 A66-19656

Sounding rocket-released artificial

strontium and barium ion cloud motion in upper atmosphere, based on equations of ambipolar diffusion 15 p2491 A66-29950

Low pressure combination of barium and cesium vapors for reduction of transport-affected losses in thermionic energy converters, noting work function and V-I characteristics 18 p3055 A66-34584

Barium ion concentration computed from Ba II 4554 angstrom line and Lyman alpha radiation intensity in lower chromosphere 20 p3646 A66-37013

**BARIUM COMPOUND**

Conditions for formation of barium and gold compound for semiconductor 04 p0570 A66-14365

Conditions for formation of barium and gold compound for semiconductor 14 p2369 A66-28264

Thermionic emission from barium telluride measured by cathodes formed by direct reaction of elements and reduction of barium tellurate 19 p3436 A66-35426

Electrical properties of barium plumbate noting conductivity, Hall field, thermoelectromotive force, magnetization, etc 24 p4253 A66-42382

**BARIUM FERRITE**

Cation distribution in barium hexaferrites 10 p1589 A66-22169

Cation distribution in barium hexaferrites 19 p3441 A66-35783

**BARIUM FLUORIDE**

Frequency and temperature effects on dielectric properties of calcium, strontium and barium fluorides 10 p1577 A66-21561

Self-lubricating properties of composites of porous nickel and nickel-chromium alloy impregnated with barium fluoride-calcium fluoride eutectic [ASLE PAPER 66AM 1C2] 16 p2710 A66-30404

UV transmittance of LiF and BaF under various storage conditions 18 p3134 A66-34001

**BARIUM TITANATE**

Optical phase modulator using ferroelectric barium titanate crystal plate 01 p0117 A66-10240

Strain-free electro-optic effect in single crystal barium titanate as function of temperature between 10 and 120 degrees C 01 p0126 A66-10969

Semiconductor characteristics of barium titanate with n-type conductivity produced after heat treatment with hydrogen and doping with lanthanum 02 p0273 A66-11716

Curie temperature, static dielectric constant and electro-optic coefficient of large single crystals of barium titanate 03 p0411 A66-13007

Amplitude distribution of ultrasonic vibrations of excited disk of barium titanate ceramic polarized perpendicularly to faces 04 p0559 A66-13471

Boundary layer thickness responsible for anomalous lattice distortions of colloidal barium titanate 04 p0571 A66-14492

Structure, electrical properties and paramagnetic resonance absorption of barium titanate with admixtures of oxides of triple valent element 05 p0730 A66-14651

Barium titanate single crystals at infralow frequencies investigated for polarization, effective permittivity and coercive field 06 p0928 A66-16713

Reversing permittivity of barium titanate single crystals measured, using lithium chloride solution for electrodes 06 p0926 A66-16714

Permittivity of barium titanate single crystals with laminar domain structure 06 p0926 A66-16715

Polarization and domain structure of barium titanate single crystals with double hysteresis loop 06 p0926 A66-16716

UHF dispersion in barium titanate ferroelectric crystals explained as microwave scattering 06 p0926 A66-16717

Slow polarization processes of barium titanate in weak field 06 p0927 A66-16718

Classification of ions capable of replacing Ti in barium titanate 06 p0927 A66-16719

Permittivity of barium titanate ferroceramic materials determined by various methods 06 p0927 A66-16721

Electromechanical hysteresis and relaxation effects in piezoelectric ceramics 06 p0927 A66-16722

Temperature autostabilization in barium and strontium titanate solid solutions during dielectric heating 06 p0927 A66-16722

Electric properties of thin ferroelectric films of barium titanate compound 06 p0927 A66-16722

Pyroelectrical effect in barium titanate ceramics used for weak thermal radiation recording 06 p0881 A66-16722

Polycrystalline barium titanate ceramic with nonlinear resistance-temperature characteristic that rises steeply at ferroelectric Curie point 07 p1100 A66-18152

Surface layers on ferroelectric barium titanate crystals, noting parameters of R induced electroluminescence 07 p1107 A66-18402

Interferometric measurement of large indices of refraction, noting applicability and accuracy 09 p1403 A66-20510

Barium titanate transition front structure noting similarity to ferroelectric and nonferroelectric crystal structure 10 p1582 A66-21882

Quadratic electro-optical effect in paraelectric phase of barium titanate single crystals as affected by temperature 10 p1587 A66-22155

Polar vapor effects on dielectric properties of barium titanate single crystals with metal admixtures 11 p1749 A66-22293

Ultrasonic piezoelectric investigation of asymmetric polarizability of barium titanate crystal 11 p1757 A66-23250

Minimum internal energy calculation of anisotropic oxygen polarizability and Lorentz correction in barium titanate crystal 11 p1758 A66-23402

Piezoelectric constants of polycrystalline ferroelectrics of barium titanate type, noting dependence on ceramic sintering temperature and applied constant voltage 13 p2160 A66-25099

Current limitation by space charge in polycrystalline barium titanate, noting voltage-ampere characteristics and hysteresis effects 13 p2164 A66-25478

Structure, electrical properties and paramagnetic resonance absorption of barium titanate with admixtures of oxides of triple valent element 13 p2167 A66-25920

Semiconductor properties of reduced barium titanate analyzed by electron spin resonance measurements at various temperatures 14 p2359 A66-27132

Flame spraying method for conversion of pure barium titanate into glass, noting dielectric Curie temperature 15 p2524 A66-29681

Doping and firing atmosphere effects on electric resistivity of polycrystalline barium titanate, noting oxidation of small grain and positive temperature coefficient effect on large grain 17 p2978 A66-32404

Piezoelectric voltage of barium titanate with stabilized domains 18 p3153 A66-33631

Quadratic electro-optical effect in paraelectric phase of barium titanate single crystals as affected by temperature 19 p3440 A66-35767

Work function of semiconducting barium titanate as function of temperature for testing Heywang theory of polycrystalline material anomalous resistance behavior 20 p3616 A66-37404

Humidity effect on ferroelectric properties of barium titanate with tantalum oxide admixture, noting growth of dielectric constant and crystal polarization 20 p3617 A66-37553

X-band spectrometric observation of ESR of trivalent gadolinium in reduced barium titanate 21 p3797 A66-38756

Mushroom-shaped barium titanate sensor for shock tube pressure recording, noting high acoustic insulation, mechanical strength and vacuum tightness 21 p3738 A66-39099

Ferroelectric transducers, discussing feasibility of using ceramic transducers as pulsed power supplies 21 p3741 A66-39504

Existence of twins in single crystalline films of barium titanate, obtaining electron diffraction patterns 21 p3805 A66-39581

Reflectance measurement of barium titanate single crystal as function of temperature 21 p3805 A66-39583

Barium titanate rods as nonlinear element of S-band resonant cavity microwave



parametric amplifier, noting variation of  
 ermittivity of rods with percentage of  
 arium titanate 22 p3872 A66-39736  
 Sputtering, slurry and doctor-blade  
 echniques for depositing thin thermistor  
 films of lanthanum-doped barium-strontium-  
 titanate for bolometer  
 application 23 p4109 A66-41127  
 Barium titanate semiconductors containing  
 controlled amounts of neodymium prepared,  
 showing dependence of electrical properties  
 on preparative conditions and amount of  
 rare earth 23 p4109 A66-41128  
**BARCKHAUSEN EFFECT**  
**ANOMALOUS FERROMAGNETISM**  
 Anomalous Barkhausen effect in  
 ferromagnetic alloys 01 p0117 A66-10239  
 Magnetic interaction between layers of  
 two-layer ferromagnetic film, discussing  
 inhomogeneity effects, Barkhausen jumps,  
 reverse magnetization nuclei,  
 etc 16 p2774 A66-30689  
**BAROCLINIC WAVE**  
 Acoustic, gravitational and gyroscopic  
 oscillation spectra of baroclinic atmosphere  
 over rotating spherical Earth with emphasis  
 on energy composition 01 p0062 A66-10858  
 Index of clear air turbulence in sloping  
 baroclinic layer 02 p0253 A66-11575  
 Dynamic equations in quasi-static and  
 quasi-solenoidal approximations to describe  
 synoptic meteorologic processes in spherical  
 coordinate system 04 p0540 A66-13412  
 Separable nongeostrophic baroclinic  
 stability problem of Eady 07 p1062 A66-17373  
 Origin of stellar magnetic fields, examining  
 surface distortions on star due to magnetic  
 field 09 p1448 A66-20095  
 Disturbance propagation in baroclinic  
 atmosphere in presence of radiation and  
 turbulent heat conduction 14 p2325 A66-27535  
 Effect of radiative and photochemical  
 processes on stability of two level baroclinic  
 flow, noting low and high shear instability,  
 wavelength, phase speed,  
 etc 16 p2700 A66-31644  
 Quasi-geostrophic instability of disturbance  
 of small amplitude in baroclinic zonal flows  
 caused by barotropic, baroclinic or critical  
 layer instabilities 20 p3550 A66-37467  
 Baroclinic instability of quasi-geostrophic  
 perturbation to zonal wind in two-layer  
 inviscid model, examining short wavelength  
 cutoff in terms of potential  
 vorticity 20 p3550 A66-37468  
 Finite amplitude disturbances in baroclinic  
 atmosphere, considering interaction with  
 zonal current and effect of upward eddy  
 transport upon time change of mean static  
 stability 21 p3759 A66-39205  
 Disturbance propagation in baroclinic  
 atmosphere in presence of radiation and  
 turbulent heat conduction 24 p4233 A66-42321  
**BAROMETRIC**  
 Slide-wire microbarometer with pressure  
 changes transformed into frequency changes  
 of output signal designed for operation on  
 moving objects 16 p2709 A66-31795  
 Freiberg radiosonde aneroid capsule design  
 modification, using U-shaped axle which is  
 synchronized with capsule  
 reflections 18 p3110 A66-33964  
 Barometric instrument development and  
 description of counter-pointer altimeter and  
 pressure indicator 23 p4067 A66-41164  
**BAROMETRIC PRESSURE**  
**ATMOSPHERIC PRESSURE**  
**BAROTRAUMA**  
 Otic barotrauma caused by difference  
 between atmospheric pressure and middle  
 ear cavity pressure arising during flight,  
 compression chamber tests, etc, and leading  
 to deafness 10 p1488 A66-22107  
 Effects and causes of sinus barotrauma  
 pressure differential between sinuses and  
 outside atmosphere/ noting prevention,  
 treatment and  
 side effects 10 p1488 A66-22108  
**BAROTROPIC FLOW**  
**BAROCLINIC WAVE**  
 Quasi-Lagrangian study of inviscid  
 barotropic fluid for analysis of certain  
 geostrophic jet flows 02 p0222 A66-11825  
 Contribution of divergent wind components  
 to energy exchange between baroclinic and  
 barotropic components 09 p1399 A66-20726  
 Equations describing motion of barotropic  
 fluid with free surface solved, using finite

difference methods based on two-step Lax-  
 Wendroff scheme 13 p2121 A66-25814  
 Difference system and boundary conditions  
 for primitive-equation barotropic  
 forecast 17 p2948 A66-31942  
 Barotropic atmospheric model for  
 forecasting in tropics, discussing wind  
 analysis area covered, accuracy,  
 etc 17 p2948 A66-31943  
 Quasi-geostrophic instability of disturbance  
 of small amplitude in baroclinic zonal flows  
 caused by barotropic, baroclinic or critical  
 layer instabilities 20 p3550 A66-37467  
**BARREL**  
**S LAUNCHING DEVICE**  
**BARRIER LAYER**  
**SA JUNCTION**  
 Dependence of barrier height of metal-  
 semiconductor systems on metal work  
 function, surface states and thickness of  
 interfacial layer 02 p0271 A66-11438  
 Nonlinear properties of complete tunnel  
 diode equivalent circuit emphasizing  
 conductance, susceptance and oscillatory  
 characteristics of barrier  
 layer 03 p0346 A66-13317  
 Photoconduction model for illuminated lead  
 sulfide films with shunt path increase  
 during barrier modulation 10 p1578 A66-21575  
 Superconducting systems partitioned by  
 thin barriers allow supercurrents to pass  
 through, noting magnetic field penetration  
 into barrier, AC supercurrents, structure in  
 DC, current-voltage characteristics of  
 barrier, etc 11 p1756 A66-22978  
 Ultrasonic generation and amplification in  
 CdS crystals with barrier layer under  
 constant drift field 13 p2159 A66-25085  
 Abrupt p-n junction irregularities in  
 barrier layer where Poisson equation is  
 reducible to quadrature 14 p2348 A66-26798  
 Properties of hydrothermally grown  
 single crystals of tetragonal lead monoxide,  
 with contacts applied by metal  
 evaporation 14 p2359 A66-27099  
 Nonlinear properties of complete tunnel  
 diode equivalent circuit emphasizing  
 conductance, susceptance and oscillatory  
 characteristics of barrier  
 layer 14 p2260 A66-28290  
 Double barrier transmission resonance in  
 metal thin film triode 15 p2563 A66-28731  
 Wave diffraction in rectangular waveguides  
 passing through double ribbon  
 barriers 19 p3311 A66-35299  
 Chemical vapor deposited thermoprotective  
 coatings for tungsten and molybdenum-based  
 refractory alloys, discussing diffusion barrier  
 selection, interfacial microhardness, high  
 temperature diffusion-annealing tests,  
 etc 19 p3383 A66-36142  
 Ultrasonic generation and amplification in  
 CdS crystals with barrier layer under  
 constant drift field 21 p3795 A66-38510  
 Barrier height determination in thin film  
 sandwich tunnel diodes, using value of  
 internal electric field and electric tunnel  
 method 22 p3959 A66-39720  
 Deep centers in conducting n-type GaAs  
 and production of Schottky  
 layer 22 p3963 A66-40088  
 I-V characteristics of junction diode with  
 antibarrier layer and oxide film pressed on  
 rear contact 23 p4045 A66-41445  
**BARYON**  
**SA MESON-BARYON RESONANCE**  
 Kinematics of collapse and discussion of  
 observable properties of baryons and  
 collapsing stars 05 p0757 A66-14524  
 High energy nuclear interaction and  
 particle structures covering meson, baryon,  
 composition and dimensional  
 analysis 05 p0749 A66-15351  
 Nonconservation of baryon and  
 cosmological theory, discussing creation of  
 matter in discrete manner around isolated  
 pockets with strong gravitational  
 fields 11 p1774 A66-23067  
**BASE**  
**S ALKALI**  
**S LUNAR BASE**  
**BASE FLOW**  
 Base bleeding effect on near-wake  
 structure for very low Reynolds  
 number 03 p0355 A66-12805  
 Base flow and near wake problem at very  
 low Reynolds numbers, using general  
 solution of Stokes equation of motion for

two-dimensional and axisymmetric  
 flows 04 p0456 A66-14469  
 Base flow and near wake problem at very  
 low Reynolds numbers, discussing influence  
 of inertia terms by using Oseen  
 approximation 04 p0456 A66-14470  
 Effect of interaction of dissipating and  
 isentropic currents on flow at base region  
 of bodies moving with hypersonic  
 velocity 05 p0607 A66-15314  
 Punch-through avalanche phenomena,  
 describing fast rise pulse production in  
 junction transistors of variable base  
 width 05 p0651 A66-15840  
 Pressure distribution and skin friction  
 measurements confirming that effects of  
 changing base flow conditions decay with  
 distance upstream along airfoil  
 surface 06 p0801 A66-15999  
 Hypersonic boundary layer separation and  
 expansion at shoulder of blunt based  
 body 21 p3693 A66-38683  
 Model of laminar hypersonic base flow  
 region of slender bodies, introducing base  
 height and Reynolds number variation of  
 base pressure ratio 22 p3843 A66-40345  
**BASE HEATING**  
 Base heating of launch vehicles examined  
 by studying heat transfer processes in two-  
 dimensional recirculation zone behind blunt  
 trailing edge in Mach 3 wind tunnel  
 [AIAA PAPER 65-825] 04 p0454 A66-13690  
 Base heating in Saturn S-IV stage from  
 exhaust reversal, comparing flight and scale  
 model data  
 [AIAA PAPER 66-45] 05 p0770 A66-15037  
 Base heating scaling criteria for four-  
 engine rocket cluster operating at high  
 altitude  
 [AIAA PAPER 65-826] 05 p0771 A66-15851  
 Heat transfer in base flow region,  
 determining parameter of correlation for  
 hydrogen injection and combustion, adiabatic  
 flame temperature, heating rates and  
 recovery temperature  
 [AIAA PAPER 66-108] 06 p0970 A66-16408  
 Base thermal environment measured on  
 flight tests of eight-engine LOX/RP-1  
 propelled Saturn I booster  
 [AIAA PAPER 65-212] 14 p3391 A66-27873  
 Short duration technique providing  
 simulation of thermodynamic properties and  
 composition of exhaust products of liquid  
 and solid propellant rocket engines  
 [AIAA PAPER 66-760] 22 p3894 A66-40643  
 Density and temperature measurement in  
 base region flow field of clustered rocket  
 model, using electron beam  
 technique 24 p4210 A66-42200  
**BASE PRESSURE**  
 Ratio base pressure of spherical cone in  
 turbulent flow at zero angle of  
 attack 05 p0609 A66-15804  
 Mach number, Reynolds number and  
 boundary layer trip devices effect on base  
 pressure 14 p2219 A66-27443  
 Variation problem solution in hypersonic  
 gas dynamics, noting intake portion  
 construction for body with minimum  
 resistance for limited length and flat  
 end 15 p2477 A66-28956  
 ONERA research on use of magnetic  
 suspension systems in hypersonic wind  
 tunnels and measurement of base pressure  
 and heat transfer rates 16 p2683 A66-31699  
 Turbulent supersonic base pressure for  
 Chapman-Korst flow model of separated  
 flows 17 p2906 A66-32077  
 Base, recompression and laminar near wake  
 regions of cones in hypersonic  
 flow 17 p2838 A66-32438  
 Nozzle precombustion chamber base  
 pressure for sudden pulsating sonic flow  
 propagation 17 p2909 A66-32582  
 Base pressure behind ridge in separated  
 supersonic flow of compressible gas  
 determined for case of turbulent  
 mixing 18 p3103 A66-35053  
 Base pressure approximation for two-  
 dimensional isentropic supersonic flow and  
 separation supersonic  
 flow 19 p3277 A66-36476  
 Base pressure and flow parameters near  
 trailing edges of axisymmetric blunt bodies  
 in supersonic flow 20 p3492 A66-37678  
 Model of laminar hypersonic base flow  
 region of slender bodies, introducing base  
 height and Reynolds number variation of



base pressure ratio 22 p3843 A66-40345  
Supersonic and hypersonic wake flow dependence on near wake pressure, using momentum integral method 24 p4158 A66-42775

**BATHYTHERMOGRAPH**

Aircraft instrumentation for oceanographic measurement platform including radiation thermometer, wave meter and expendable bathythermograph [AIAA PAPER 66-695] 20 p3496 A66-38036

**BATTERY**

SA ATOMIC BATTERY  
SA DRY CELL BATTERY  
SA ELECTRIC CELL  
SA ELECTRODE  
SA ELECTROLYTE  
SA NICKEL-CADMIUM BATTERY  
SA SILVER-CADMIUM BATTERY  
SA SILVER-ZINC BATTERY  
SA STORAGE BATTERY  
SA THERMAL BATTERY  
SA ZINC-SILVER OXIDE BATTERY

Heat dissipation values for spacecraft silver oxide-zinc primary and nickel oxide-cadmium secondary batteries determined with calorimeter 03 p0323 A66-12772

Load-voltage battery charger power-optimizing regulator for maintaining continuous maximum power loading on solar cells under various environments 08 p1169 A66-19495

Batteries - International Symposium at Brighton, England in September 1964 08 p1169 A66-19641

Design and operation of radioisotope-powered battery using direct beta-particle collection to negatively charge electrode, noting choice of isotope, dielectric, collector, etc 08 p1172 A66-19657

Aircraft batteries design, considering plastics, separators, alloys and operating conditions including thermal stability, explosion risks, etc 08 p1173 A66-19658

Three-day battery capable of operation at temperature of 425 degrees C for use on lunar and planetary probes 13 p1999 A66-25691

Organic and liquid ammonia electrolyte systems in combination with active anode materials to achieve high energy output battery system [AIAA PAPER 64-750] 13 p2007 A66-26651

Improved operating characteristics of solid-electrolyte cell at room temperature by using silver sulfur iodide 18 p3055 A66-34901

Open circuit half-cell potentials of calcium in thiocyanate-liquid ammonia solutions 18 p3055 A66-34902

Nonaqueous lithium-nickel halide batteries capabilities and limitations, explaining methods of selection and evaluation of solvent, solutes and combinations for electrolytes 23 p4021 A66-41752

**BAYESIAN STATISTICS**

Bayesian statistics in combining analytically derived design reliability data with available test data for reliability estimates 01 p0169 A66-10078

Empirical Bayes rule obtained from observing unknown signal of stochastic control 02 p0206 A66-11307

Bayesian approach in reliability evaluation, noting point estimation and confidence interval 03 p0335 A66-12902

Filtering techniques for estimating nonlinear discrete-time processes, including Bayesian estimation and weighted least squares approach 05 p0656 A66-14631

Bayes risk function of sequential games, discussing recurrence formula, decision rule and approximate computational method in pattern recognition problems 05 p0639 A66-15838

Construction of Bayes estimator, using prior estimates of random parameter, with mean square error less than that of maximum-likelihood estimator when a prior distribution of parameter is unknown 12 p1816 A66-24195

System with unknown failure-rate parameter undergoing reliability test of accept-reject variety, based on Bayesian context 12 p1888 A66-24670

Dynamic programming recursive estimation of modal trajectory for nonlinear non-Gaussian noise and comparison with Bayesian estimation and case of Gaussian

white noise 13 p2053 A66-26086

Predicting structural reliability by recent developments in statistics, reliability, cost effectiveness analysis and decision theory [AIAA PAPER 66-503] 16 p2714 A66-30607

Dual control of plant with random amplification factor as Bayesian problem 18 p3089 A66-33738

Abundance of individual effects /pt, bp, bps/ of geomagnetic pulsations and variations at Goettingen and Fuerstenfeldbruck stations 18 p3105 A66-34096

Performance criterion for adaptive pattern classification system, noting approximation to optimum Bayes discriminant function 19 p3333 A66-36665

Adaptive pattern classification system, based on typical patterns or training samples used by system to determine decision procedure that does not require a priori knowledge of probability density of class pattern vectors 20 p3522 A66-37666

Bayesian methods applied to structural design selection with known reliability without confidence coefficient 20 p3572 A66-37944

Bayesian statistics applied to reliability and maintainability transactions 20 p3574 A66-37967

Canonical theory approximation of optimum or Bayes detection procedures in critical limiting threshold mode of operation 21 p3705 A66-39146

**BCC**

S BODY CENTERED CUBIC /BCC/ CRYSTAL

**BE-A**

Total electron content from S-66 satellite received at nine stations, using differential Faraday technique 15 p2491 A66-30017

**BE-B**

S EXPLORER XXII SATELLITE

**BEACON**

S RADAR BEACON

S RADIO BEACON

BEACON EXPLORER-A

S BE-A

BEACON EXPLORER-B

S EXPLORER XXII SATELLITE

BEACON SATELLITE

Accurate tracking of Beacon-Explorer orbiting optical reflectors, using pulsed ruby laser beams 09 p1341 A66-19902

Beacon observations of differential Doppler and Faraday effects from analysis of signals emitted by Explorer XXII satellite 15 p2453 A66-30069

Ionospheric electron content over Ahmedabad and Bombay from differential Faraday rotations of plane polarized radio waves from Beacon satellite 21 p3734 A66-39229

Diurnal variation of ionospheric irregularities, using differential Doppler method for analysis of data transmitted by Beacon satellite 24 p4200 A66-42596

**BEAGLE B-206 AIRCRAFT**

British Executive and General Aviation /BEAGLE/ and development of Beagle B.206 S twin-engine executive aircraft 22 p3847 A66-39686

Airframe and landing gear of Beagle B.206 S series II low-wing monoplane of all-metal stressed skin construction 22 p3848 A66-39687

Beagle B.206 S aircraft power plant, vacuum system, air conditioning system, fire protection, hydraulics, fuel, oxygen, rain protection and deicing equipment 22 p3970 A66-39688

Aerodynamic design and development of Beagle B.206 S aircraft, examining corrections for inadequate stability margins at aft CG limit 22 p3848 A66-39689

Flight testing of Beagle B.206 S aircraft revealed need for forward shift of CG in series II model due to more powerful engines 22 p3848 A66-39690

Production methods for Beagle B.206 S aircraft, examining sequence of assembly and erection and methods of anticipating minimum customer requirements 22 p3922 A66-39691

**BEAM**

S ATOMIC BEAM

S BOX BEAM

S CANTILEVER BEAM

S CURVED BEAM

S ELECTRON BEAM

S GAMMA RAY BEAM

S I-BEAM

S ION BEAM

S MOLECULAR BEAM

S NEUTRAL BEAM

S OPTICAL BEAM SCANNING

S PARTICLE BEAM

S PHOTON BEAM

S PROTON BEAM

S RADAR BEAM

S RECTANGULAR BEAM

**BEAM COLUMN**

Beam forced vibration with harmonically time-variant motion produced by uniform distributed load, assuming one boundary condition is nonlinear 01 p0157 A66-1092

Boundary value problem of elastic/viscoplastic beams solved, using iteration method, noting wave propagation and effect of shear and inertia of axial motion of beam in motion equation 14 p2397 A66-2738

Operational calculus in determining strength and deflection of material [PST PAPER NT-147] 14 p2401 A66-2775

Pure bending of beams with hole 15 p2612 A66-2942

Dynamic hinge concept for determining fundamental frequency of beam vibration in terms of equivalent system 15 p2614 A66-2961

Stresses and deflections of biaxially loaded columns calculated from exact solution of biaxial bending equation 17 p3024 A66-3239

Elastic stresses around holes in webs of simply-supported wide-flange beams under uniform load 17 p3024 A66-3239

Shear coefficient in Timoshenko beam theory 18 p3248 A66-3358

Thin walled box beams under nonuniform torsion treated by energy method 19 p3472 A66-3531

Beam column supported by linear rotational and extensional springs representing elasticity of test rig, used in analog study of thermal buckling behavior of thin cylindrical shells 21 p3828 A66-3870

**BEAM CURRENT**

AM/PM conversion factor of TWT as a function of helix voltage when beam current is varied to keep gain constant 24 p4180 A66-4237

**BEAM-PLASMA AMPLIFIER**

Dynamic behavior of beam-plasma amplifier 01 p0038 A66-1051

Effect of nonzero plasma electron temperature considered in electron beam-plasma interaction wave growth computation 01 p0112 A66-1053

Electric wave growth and amplification in electron beam interaction with plasma in microwave amplifier, noting longitudinal inhomogeneity 01 p0112 A66-1053

Electron beam-plasma interactions used to predict occurrence of amplifying wave having growth rates maximizing near to electron plasma frequency 04 p0552 A66-1403

Beam plasma amplifier operation noting interaction region, millimeter wave operation, technological problems, etc 12 p1839 A66-2461

Ion cyclotron instabilities in bounded cold beam-plasma system, noting growth rate parameters, instability conditions, etc 13 p2138 A66-2519

Excited electron plasma nonlinear oscillations, beam-plasma interaction, Langmuir probe measurement of frequency and density, amplification of superimposed RF electric field, etc 15 p2552 A66-2940

Instability of three-component plasma system studied to analyze beam-plasma interaction, noting restraining effect of electrons on instability of beam-ion coupling 21 p3792 A66-3918

Monochromatic longitudinal wave amplification by charged particle beam in nonlinear plasma, noting amplitude dependence on coordinate 24 p4243 A66-4252

Parametric amplification in beam-plasma system and generation of stationary waves 24 p4258 A66-4300

**BEAM SWITCHING**

Photographic film used for quantitative



- measurements of intensity distribution in Q-switched laser beam 05 p0695 A66-14920
- Atmospheric turbulence effects on laser beam propagation, noting beam cross section, phase variation, AM and FM, etc 14 p2235 A66-27035
- Phased array antenna system for multidirectional transmission and reception of focused beams with high gain 17 p2872 A66-31936
- Beam position selection and antenna lead connection to receiver processing channels in multiple-beam receiver system 18 p3074 A66-33527
- Probability of recurrent event defined over state r-th-order Markov chain, specifically probability of events in Bernoulli sequence 21 p3757 A66-39103
- Laser beam deflection and scanning techniques 24 p4175 A66-42817
- BEAM WAVEGUIDE**
- Statistics of beam waveguide light-ray propagation extended to include correlations between displacements of different lenses 05 p0634 A66-15179
- Design of intentional bends of beam waveguide, giving relations between waveguide parameters and radius of curvature of guide axis 06 p0846 A66-16093
- Mode losses of single iteration in confocal beam waveguide resonator and transmission systems with circular lenses separated by twice focal length 06 p0848 A66-16107
- Random irregularities caused by mechanical distortion in lenses, reflectors or diaphragms of optical beam waveguides and increases in diffraction attenuation 09 p1345 A66-20491
- Irregularities of iris type beam waveguide, noting transmission loss during principal lightwave propagation 11 p1712 A66-22736
- Beam waveguides for long distance electromagnetic wave transmission at optical wavelengths described by theory of focusing antennas 11 p1656 A66-22737
- Equation governing properties encountered in Gaussian beam propagation represented graphically on impedance chart, showing relation between Gaussian mode and geometrical optics 11 p1656 A66-23089
- Optical guides stressing lens type beam waveguide 13 p2022 A66-25538
- Transverse beam width and phase constant of nonsquare law media for light propagation in imperfect lenslike media requiring repeater techniques 13 p2127 A66-25539
- Random variations in beam waveguide components and effects on light propagation 13 p2024 A66-25939
- Dual mode frequency discriminator for microwave source frequency stability, discussing application of beam waveguide resonator 17 p2895 A66-33274
- Irregularities of iris type beam waveguide, noting transmission loss during principal lightwave propagation 23 p4078 A66-41474
- Beam waveguides for long distance electromagnetic wave transmission at optical wavelengths described by theory of focusing antennas 23 p4037 A66-41475
- BEARING**
- SA BALL BEARING
- SA FOIL BEARING
- SA GAS BEARING
- SA JOURNAL BEARING
- SA ROLLER BEARING
- SA THRUST BEARING
- Bistable vibration of rotors in bearing clearance [ASME PAPER 65-WA/MD-1] 05 p0689 A66-15520
- Partial porous metal bearings performance during steady state operation with full film of lubricant, determining pressure distribution [ASME PAPER 65-WA/LUB-3] 05 p0689 A66-15526
- Correlation equation estimating pitting fatigue life of bearings from minimal rolling contact rig data [ASME PAPER 65-WA/CF-5] 05 p0690 A66-15624
- Service life of antifriction bearings represented by Weibull distribution law, with computer method for parameters and density function 06 p0886 A66-16486
- Flexible unbalanced rotating shaft, discussing vibration of system with axial symmetry in asymmetric bearings 07 p1037 A66-17733
- Thin section bearings used to solve spatial needs and temperature problems of high altitude flying 08 p1229 A66-18827
- High temperature bearing lubricant requirements for jet engine lubrication systems [SAE PAPER 660072] 09 p1383 A66-20157
- Operation, maintenance and installation of friction and nonfriction bearings, noting characteristics, problems, etc 11 p1711 A66-22951
- Powder metal bearings manufacture noting shapes, sizes, tolerances, materials, design, installation, etc 12 p1885 A66-24100
- Pressure distribution of viscous electrically conducting fluid in lubricating layer of cylindrical bearing 12 p1887 A66-24425
- Oil cushion resilience in hydrodynamic bearings, examining effect on dynamic behavior of unsymmetrical shaft with one disk 12 p1889 A66-24999
- Book on design and utilization of antifriction bearings 13 p2087 A66-26281
- MHD inclined slider bearing with azimuthal magnetic field, noting load capacity 15 p2509 A66-29407
- Liquid solid film lubrication of hydrodynamic bearings, including effects of solid particles in liquid base lubricant [ASLE PAPER 66AM 5DE] 16 p2711 A66-30412
- Rolling friction studies of intermetallic and zirconium oxide for control surface bearings for space reentry vehicle [ASLE PAPER 66AM 5D4] 16 p2712 A66-30413
- SNAP-8 reactor oscillating bearings to provide low friction self-lubrication at 1150 degrees F 16 p2712 A66-30414
- Bearing capacity of shallow spherical shell freely supported along contour and subjected to action of uniformly distributed normal pressure 16 p2823 A66-31632
- Starting friction and kinetic friction of PTFE fabric-lined spherical bearings and deflection and permanent set under static loading 17 p2929 A66-31932
- Shaft-rotor system with bearing configuration such that load-deflection relation at rotor is nonlinear and radially symmetric, noting harmonic whirl and free undamped vibrations 17 p2930 A66-32892
- Operating lifetime of porous bearings, discussing dependence on quality of impregnating lubricant 17 p2930 A66-33143
- Steady-state and dynamic characteristics of full circular bearing and centrally loaded arc bearing presented in design charts for turbulent lubrication analysis [ASME PAPER 66-LUBS-4] 17 p2931 A66-33178
- Superconducting bearing operating on conservation of fluxoid in closed loop of superconductor 18 p3116 A66-34243
- Load-supporting capacity of vertical plasma cylinder contained by axial pinch effect analyzed for applications to bearings with electrically conducting lubricants 23 p4101 A66-41293
- Laser beam effect on hydrodynamic bearings, discussing microcracks and critical energy, explaining breakdowns 23 p4078 A66-41409
- BED REST**
- Exercise tolerance, plasma volume, red cell mass, total blood volume and orthostatic tolerance during four weeks of bed rest 03 p0326 A66-13354
- Long-term lower body negative pressure in supine position effect on deterioration in cardiovascular function of man during prolonged bed rest 15 p2430 A66-28657
- Bed rest and water immersion effects on plasma volume and catecholamine response to tilting, noting urinary excretion of norepinephrine and epinephrine 15 p2430 A66-28661
- Prolonged hypokinesia effect on human resistance to transverse g-forces, detailing respiratory and circulatory systems, motor response and visual acuity 15 p2437 A66-29473
- Hypoxia and lower body negative pressure effects on blood volume, and orthostatic and physical tolerance after four weeks of hypoxic bed rest 16 p2640 A66-31124
- Lower body negative pressure effect on blood volume and orthostatic tolerance during prolonged bed rest 17 p2858 A66-32178
- Medical problems of weightlessness 18 p3059 A66-34365
- Tilt table response and blood volume changes associated with 30 days of bed rest, evaluating time required to recover from cardiovascular deconditioning 22 p3853 A66-39785
- BEECH MILITARY AIRCRAFT**
- S T-34 AIRCRAFT
- BEEHIVE PROJECT**
- S PROPELLANT
- BEHAVIOR**
- S CONDITIONED RESPONSE
- S GROUP BEHAVIOR
- S HUMAN BEHAVIOR
- S LEARNING
- S TRAINING
- BEHRENS-FISHER PROBLEM**
- Optimum similar solutions of Behrens-Fisher problem 07 p1060 A66-18506
- BELL MILITARY AIRCRAFT**
- S X-22 AIRCRAFT
- BELLOWS**
- Stresses and elongation of U-shaped bellows subjected to axial load solved by elastic theories of plates and shells 08 p3134 A66-19549
- Dynamic instability in undamped bellows face seals operating in cryogenic environment with torsional oscillation and diametrical rocking as primary motion [ASLE PAPER 66AM 2CE] 16 p2711 A66-30408
- Numerical analysis of stress-strain rate of sylphon bellows, using differential equations 16 p2820 A66-31145
- BELTRAMI FLOW**
- Stress function and displacement vector for linear, homogeneous, isotropic and elastic material body occupying bounded simply connected region of space 21 p3772 A66-39354
- Vector equations of steady incompressible viscous flow in absence of extraneous forces, discussing Beltrami flow, doubly laminar flow and plane flow 21 p3728 A66-39435
- Continuum mechanical Cartesian tensor analysis theorem on completeness of Beltrami stress function 23 p4139 A66-41544
- BENDING**
- SA ELASTIC BENDING
- Circle and sphere theorems for biharmonic equation and application to displacement field of stressed plate under pure bending, noting singularities 01 p0093 A66-10427
- Error estimates in application of linear plate theory to deflection and stress determination as function of boundary conditions, correlation between geometric plate parameters and load distribution 08 p1305 A66-18599
- Quenching and slow-cooling effects on ductile-brittle bend-transition temperature of chromium wire 13 p2107 A66-25587
- Heat resistance, bending and tensile creep of multicomponent Ti alloys 15 p2519 A66-28534
- Bending center of prismatic anisotropic rod of arbitrarily asymmetrical cross section 15 p2608 A66-28774
- Equivalent mass matrix for rectangular plate elements in bending, noting coordinate system 15 p2610 A66-29306
- Bending problem of three-layer plates with fillers 16 p2817 A66-31050
- Arbitrary bending of hinged thin plate reinforced with circular ring 16 p2819 A66-31141
- Periodic solutions of axisymmetric shell theory equations for displacement of shells of revolution and bending of thin walled rods 17 p3026 A66-32593
- Bending problem of anisotropic plates solved by method of small parameter 17 p3030 A66-32811
- Bending behavior of spherical shells through second-order differential equation with complex coefficients, noting effect of load 18 p3253 A66-33765
- Die friction effects on plane stress and plane strain in plastic bending of steel and titanium alloy beams 21 p3745 A66-39528



Membrane force in axisymmetric elastoplastic bending of clamped thin circular plate 23 p4142 A66-41951  
 Successive approximation analysis of large deflections of elastoplastic shell under bending deformation and load carrying capacity 24 p4290 A66-42440

## BENDING DIAGRAM

Four-point loading bend test on specimen of full plate thickness with sharp notch to 20 percent depth, with ductility criterion as fully plastic angle of bend before fracture 08 p0965 A66-16492

## BENDING FATIGUE

Constrained stress-strain test of Ni-Cr-Mo steel carried out on plane bending plastic fatigue testing machine 02 p0243 A66-11580  
 Slow-bend impact testing of embrittlement of zirconium by hydrogen 06 p0895 A66-16356  
 Fatigue damage of metals under mean stress investigated by X-ray diffraction 08 p1314 A66-19551  
 Stress concentrations in fatigue bending of perforated rectangular and tapered plates studied by photoelastic means 08 p1315 A66-19802  
 Aircraft fuselage design in region of center section for case of asymmetric bending 11 p1782 A66-22854  
 Sintered aluminum powder endurance under bending stresses and cladding effect on fatigue resistance 14 p2318 A66-28198  
 Notched and unnotched bending fatigue strength of machined work hardened AISI type 305 stainless steel affected by cold worked surface layer with high compressive residual stresses 15 p2521 A66-29073  
 Bending stresses in cylindrical shell with rigid circular inclusion examined under axial tension and internal pressure [AIAA PAPER 66-525] 16 p2813 A66-30526  
 Grain boundary migration in pure aluminum and lead under reversed torsional and bending stresses at elevated temperatures 19 p3388 A66-36365  
 Infinitely small bending deformations of convex surfaces with boundary condition of generalized slip, formulating boundary value problem for bending of surface 22 p3995 A66-40450  
 Structural integrity studies of gravitational and inertial loading effects on British solid propellant grains 23 p4115 A66-41112  
 Strength test results on special small rocket covering bending, stiffness and internal pressure strength of various components 23 p4133 A66-41423

## BENDING MOMENT

Size effect of bending and twisting fatigue strength by calculating probability of flaws on surface 02 p0243 A66-11581  
 Shells and tubes subjected to internal and external pressures including analysis of transition theory for sheet-bending, considering creep rupture and relaxation 03 p0438 A66-12696  
 Equations of plastic interaction curves for cross section of beam subject to uniaxial stress and under simultaneous bending moment and normal force, using power series 03 p0442 A66-13306  
 Tangential force and bending moment effect on behavior of internal stresses and moments near application point in spherical shell analysis 04 p0588 A66-13585  
 Semizero-moment shell with one edge braced by elastic support with small rigidity for deformation out of plane, noting magnitude of critical stress 04 p0588 A66-13586  
 Brazier effect and overlap effect in bending of slit thin walled circular tubes [ASME PAPER 65-APMW-20] 04 p0592 A66-14221  
 Contact of two axisymmetric plates, showing ability of Reissner theory to overcome classical theory problems [ASME PAPER 65-APMW-28] 04 p0593 A66-14226  
 Component balancing alone can provide better balanced high-speed rotor than common practice of balancing complete assembly of balanced components 06 p0888 A66-16433  
 Full plastic moments in struts, analyzing problem of member subjected to combined axial stress and unequal major-axis bending moments at ends 07 p1142 A66-17257

Series solution for deflection of rectangular plate subjected to concentrated load at arbitrary location, using Green function 08 p1310 A66-19161  
 Stress-strain state of shell having one end clamped and other under concentrated bending moments and concentrated force acting along generatrix solved by integral equation 08 p1314 A66-19579  
 Brazier effect and overlap effect in bending of slit thin walled circular tubes [ASME PAPER 65-APMW-20] 12 p1961 A66-23976

Variational method for determining frequencies and modes of oscillation of pinned variable incidence blade 12 p1965 A66-24052  
 Two-dimensional problems in moment theory of elasticity for multiply coupled regions weakened by finite number of arbitrarily distributed circular holes 12 p1987 A66-24106  
 Plate loaded over ring-shaped zone, determining bending moment, torque and shearing force 12 p1987 A66-24111  
 Concentrated forces and bending moments effect on shallow cylindrical shell 12 p1987 A66-24113  
 Strain gauge load measuring transducer operating in bending mode and based on elastic properties of epoxide glass fabric laminate 12 p1884 A66-24985  
 Book on stress-strain analysis including photoelastic investigations of bending impact on cantilever beam 13 p2198 A66-26298  
 Bending moment of thin nonlinearly elastic plates, noting dependence of coefficient of moment concentration on external load and material properties 13 p2203 A66-26429  
 Three-dimensional statically indeterminate frame with rigid nodes, noting effect of bending moments for shifting forces 13 p2207 A66-26498  
 Design of composite structures of minimum weight, using flat-bottomed cylindrical tank, noting continuity condition of radial bending moment of plate and shell 14 p2395 A66-27174  
 Pure bending of orthotropic plate with curvilinear hole reinforced by rigid ring 15 p2812 A66-29425  
 Approximation method for solution of bending problem of isotropic plate resting on rigid columns to cover case of anisotropic plate with reinforced elliptic hole 15 p2813 A66-29434  
 Transverse cut-out effect on fatigue strength of rotating shaft under constant bending load, noting fatigue stress concentration factor 16 p2815 A66-30679  
 Dynamic plastic bending of cantilever and variation in strength of mild steel with strain rate, considering shear force at hinge 16 p2815 A66-30808  
 Fatigue tests at high stress levels under rotating bending of carbon steel and roll material, analyzing stress-strain behavior in plastic fatigue process 16 p2815 A66-30809  
 Bending moment, longitudinal force, radial displacement and transverse deflection of circular plate undergoing elastoplastic bending accompanied by radial tension 16 p2822 A66-31622  
 Contact of two axisymmetric plates, showing ability of Reissner theory to overcome classical theory problems [ASME PAPER 65-APMW-28] 18 p3248 A66-33581  
 Multiply connected orthotropic plate of variable thickness, discussing bending stresses, load distribution, temperature distribution and boundary load 18 p3256 A66-34492  
 Finite creep equations derived for circular sandwich plate under lateral pressure, considering bending moments and tensile forces 19 p3472 A66-35392  
 Instrumentation of bending moments on large space boosters, discussing ground wind restrictions, telemetry system used, data transmission link, etc 19 p3356 A66-35678  
 Differential equations for deformations of nonuniform flat plates bent into cones 19 p3473 A66-35850  
 Bending of elliptical anisotropic plate with two elliptic holes 20 p3669 A66-37668  
 Elastic-plastic axisymmetric bending of circular cylindrical shell with constant and

variable thickness 20 p3670 A66-37677  
 Response data for uniform beam supports, on nonlinear springs and subjected to shock demonstrating usefulness of shock spectra in design situations 20 p3671 A66-37977  
 Elastoplastic bending of thin annular plate with free inner edge, based on Mises yield condition and Hencky stress-strain relation 20 p3671 A66-38101  
 Nonstationary forces and bending and torsional moments along wing computed using punch card system 20 p3674 A66-38441  
 Bending of isotropic thin plate in moment theory of elasticity, noting Kirchhoff-Lov hypothesis from which relations for bending moment torque and shear force are obtained 22 p3991 A66-40151  
 Plate and rod systems to test abrupt intensive heating effects, discussing dynamic stresses and bending moments via approximate equations 23 p4137 A66-41001  
 Critical bending angles of rollers used in shaping profiled rings and casings with titanium alloy flanges 23 p4075 A66-41761  
 Membrane theory of convex shells and approaches to construction of general moment theory of elastic shells 23 p4141 A66-41933

## BENDING THEORY

Strains and internal force in bending of two coupled orthotropic plate strips of different rigidity under effect of uniformly distributed loads 01 p0152 A66-10401  
 Flexural waves propagating over plate with thin obstacles exerting both head-on and moment impedance 01 p0152 A66-10411  
 Bending problem of circular orthotropic plate on elastic base under axisymmetric load 01 p0153 A66-10461  
 Bending of elastic rectangular plate uniformly transverse loaded along axes of symmetry 01 p0154 A66-10461  
 Bearing reactions and stresses of bridge analyzed by calculating bending of rectangular plate with two supported and two free parallel sides 01 p0155 A66-10711  
 Dynamic stability of elastic and rigid rod under longitudinal impact 03 p0441 A66-13291  
 Bending of rigidly fastened square plate with deflections 03 p0442 A66-13301  
 Maximum stress on flat plate stress corrosion strip with ends rotated 90 degrees, using nonlinear bending theory [ASME PAPER 64-WA-AV-3] 04 p0589 A66-14021  
 Bending of plate of arbitrary trapezoidal planform for various support conditions and combinations thereof 04 p0589 A66-14141  
 Shaft deflection at any point determined by geometric method for shaft diameter selection 05 p0687 A66-14991  
 Finite-difference equations derived and applied at or near flexural discontinuities in plates subjected to bending 05 p0774 A66-15061  
 Linear elastic theory of thin shells considering membrane and bending theories of open and closed cylindrical shell 05 p0775 A66-15081  
 Buckling of cantilever cylindrical shell with transverse end load inducing shear stresses and bending stresses in middle surfaces 05 p0781 A66-15801  
 Book on stress analysis and elastic body vibration covering stress and strain, bending moment, shearing forces, mechanical vibration, torsion, columns, oscillation, etc 07 p1142 A66-17236  
 Higher order approximations derived for bending equations of isotropic homogeneous thermoelastic plates 07 p1142 A66-17286  
 Classical theory of bending of anisotropic plates, using asymptotic integration method and expressing stressed state as sum of three stressed states 07 p1145 A66-18252  
 Errors in approximation equations for dynamic bending of cylindrical rod 08 p1308 A66-18889  
 Small parameter method determination of pure bending and torsion of thin plate with circular hole, where material of plate obeys nonlinear elasticity law 08 p1312 A66-19435  
 Transition process whereby plate approaches limiting load state under effect of transverse load that creates torques and bending moments in plate cross sections 08 p1312 A66-19436  
 Simplified calculation of axisymmetric



- bending of annular three-layer plates with lightweight filler by use of initial parameter method 08 p1313 A66-19437
- Large displacement bending of rods for constant deformation cross section, negligible shearing forces and exponential stress-strain relation 08 p1314 A66-19580
- Spherical shell bending examined, using quasi-linear stress-strain relationship 09 p1465 A66-19857
- Finite bending of cylindrical plates, evaluating numerical values of stress distribution in baryte sheet 09 p1465 A66-19861
- Deflection of thin circular plate under eccentric loading using complex variables, obtaining expressions in series form 09 p1467 A66-20581
- Bending of orthotropic plates and beams supported by elastic layer under uniform transverse load, noting effect of length-width ratio change 10 p1615 A66-21410
- Iterative procedure to obtain numerical solutions of von Karman equations for rectangular plates with finite deflections 10 p1615 A66-21477
- Optimum study of anticlastic deformations of elastic strips with tapered edges, using Newton-Raphson iteration method 11 p1780 A66-22328
- Postbuckling behavior of metal plate strip subjected to opposing axial loads, using nonlinear bending theory [ASME PAPER 65-AV-3] 11 p1780 A66-22470
- Flexural waves propagating over plate with thin obstacles exerting both head-on and moment impedance 11 p1780 A66-22802
- Permanent deformations in circular plates subjected to uniformly distributed impulses compared with predictions of bending theory of rigid-plastic plates 11 p1781 A66-22612
- Cylindrical bending theory for rectangular three-layer sandwich plate supported at opposite ends under variable load 11 p1783 A66-23019
- Self-equilibrating bending of complete circular cylindrical shells described by first harmonic terms of Fourier series for displacement components 12 p1962 A66-24004
- Optimum depth, minimum area design charts for laterally supported structural beams in pure bending, discussing weight parameters, elastic buckling, material characteristics, etc 12 p1968 A66-24201
- Deflections, moments and shears of circular ring plate under transverse load, comparing classical and improved theory of deformation 13 p2195 A66-25180
- Stress concentration for cylindrical bending of plates with holes, deriving equations and evaluating errors in classical theory 13 p2203 A66-26424
- Boundary conditions in bending theory of reinforced shells, noting decreased stress concentration obtained by reinforcement ring 13 p2204 A66-26431
- Nonlinear bending theory of three-layered simply supported plates 14 p2396 A66-27379
- Pure bending of beams with hole 15 p2612 A66-29424
- Symmetric bending of circular orthotropic plate of systematically variable thickness for different types of loading 15 p2613 A66-29435
- Sandwich panel bending under thermal and mechanical loads; solving differential equations for temperature distribution, transverse load and uniform edge compression with boundary conditions 16 p2812 A66-30218
- Bending equations of orthotropic three-layer plates with rigid filler 16 p2818 A66-31055
- Book on bending theories of sandwich plates including use of Fourier series, stress-strain state, trigonometry, deflection theory, etc 16 p2818 A66-31100
- Monograph on nonlinear bending theory of three layer plates, covering mathematical theory of elasticity stress-strain diagrams, Galerkin method, maximum deflection criteria, etc 16 p2819 A66-31136
- Longitudinal bending of elastic truncated conical shell subjected to edge loads 17 p3020 A66-32001
- Stresses and deflections of biaxially loaded columns calculated from exact solution of biaxial bending equation 17 p3024 A66-32395
- Bending behavior under lateral loads and stretching effects due to in-plane forces described by two uncoupled differential equations governing circular plates 18 p3253 A66-33803
- Bending characteristics of tapered cylindrical shells, discussing edge and internal influence 18 p3253 A66-33806
- Approximation solution to plane bend problem in thin rod of variable rigidity 18 p3254 A66-33933
- Monograph on thin walled rods under bending and torsion, discussing calculations in lightweight structure design 18 p3254 A66-33966
- Nearly inextensional deformations of cylindrical shells, noting bending theory 18 p3256 A66-34489
- Extension of Vlasov bending theory for thin shells to include shells with undamped solutions, obtaining partial differential equations for normal deflection and stress function 19 p3472 A66-35466
- Bending of plane electromagnetic waves around elliptically ideally conducting cylinder of infinite length and around parallel circular dielectric cylinder, with solution as Mathieu-type series 19 p3303 A66-36064
- Book on strength, stiffness and stability of sandwich structural elements for structural designer, emphasizing practical applicability 20 p3666 A66-37010
- Rigorous solutions for loadings applied at apex of spherical shell, noting cases of concentrated radial and tangential force, concentrated moment about polar and planar axis, etc 20 p3670 A66-37761
- Bending of thin rectangular sandwich plate of three layers with small flexure 21 p3829 A66-38812
- Hydraulic support system for free-flight simulation with Saturn V-Apollo vehicle, discussing stability requirements, upper bounds of system design, conversion from nonlinear to linear model, etc 21 p3722 A66-38876
- Simulation results of adaptive tracking filter application to stabilization of structural bending modes of SI-B launch vehicle 21 p3821 A66-38877
- Bending problems of transversely isotropic circular plates based on Ambartsumian theory of anisotropic plates 21 p3830 A66-38980
- Mixed bending problem of eccentric ring solved by coordinate system with origin at center of outer boundary of cut 21 p3831 A66-39290
- Bending of anisotropic cylindrical bodies with curved axis under transverse force 21 p3833 A66-39595
- Nonlinear differential equations for cylindrically anisotropic plates, noting errors of Wolmir method 22 p3988 A66-39698
- Two-dimensional elastic equilibrium problems in reinforced plates with holes and bending theory problems in reinforced thin plates 23 p4137 A66-41003
- Bending of anisotropic elliptical plate weakened by elliptical hole solved by infinite system of linear algebraic equations 23 p4138 A66-41447
- Linear viscoelastic bending analysis of anisotropic plates 23 p4145 A66-41975
- BENDING VIBRATION**
- Calculation method for natural bending pulsations of continuous medium extended to case of torsion 01 p0154 A66-10843
- Intermediate stages of wave-type bending process in elastic plate investigated by system of approximate methods 01 p0157 A66-10983
- Equations for rotational motion of satellite and rods with end loads as stabilizer, considering rods elastic deformation caused by load bending 02 p0295 A66-11651
- Resonant frequency of circular cylindrical shells under initial stress 02 p0301 A66-12165
- Behavior of centrally compressed rod beyond proportionality limit, noting system stability 04 p0590 A66-14162
- Asymptotic analysis for equations of axisymmetric vibrations of thin shells [ASME PAPER 65-WA/APM-15]
- Numerical technique to determine vibration characteristics of disk-like structures in turbine engine [ASME PAPER 65-WA/GTP-8] 05 p0777 A66-15437
- Shaft deflections in turbopumps from cavitation-induced unbalanced hydrodynamic forces in inducer 05 p0639 A66-15723
- Fatigue stress analysis, using graphical technique for complex problem of bending and torsional out-of-phase variable frequency vibrations 07 p1038 A66-18174
- Harmful oscillation elimination from high rpm gyroscopic centrifuge by introducing one elastic bearing into dynamic system 07 p1147 A66-18342
- Exact solution of wave field of point vibrator operator on free plate in form of elastic strip, comparing theory and measurement 08 p1307 A66-18877
- Formula for numerical values of propagation rates of flexural harmonic waves of various lengths 11 p1780 A66-22605
- Frequency characteristics of bending vibrations of bounded rods with electromechanical feedback, possibility of artificially attenuating resonance vibrations and conditions for self-excitation 11 p1780 A66-22605
- Parallelogrammic elements in solution of deflection and natural frequency of rhombic cantilever plate 13 p2194 A66-25088
- Calculation of natural twisting and bending vibrations of beam whose characteristics vary along length 13 p2198 A66-26237
- Dilatational wave resonance scattering of waterborne sound waves on hollow cylinder excited to oscillation by incident sound 14 p2401 A66-27983
- Flexural vibration of uniform shafts treated by impedance techniques and traveling-wave concepts 14 p2400 A66-27683
- Bending-torsional flutter of uniform swept wing with velocity component aerodynamic-strip theory 17 p3022 A66-32015
- [AIAA PAPER 66-475] 17 p3028 A66-32767
- Bending oscillations of semiminfinite beam with moving end 17 p3030 A66-32815
- Free flexural vibration of cylindrical shells stiffened by equidistant ring frames treated by finite difference calculus 17 p3030 A66-32815
- Subharmonic vibrations during resonant testing of thin walled beams for coupled torsional and bending vibrations 18 p3250 A66-33673
- Frequency characteristics of bending vibrations of bounded rods with electromechanical feedback, possibility of artificially attenuating resonance vibrations and conditions for self-excitation 18 p3256 A66-34559
- Reissner-Uflyand-Mindlin PDEs for circular ring flexural vibrations under transverse shear and rotary inertia 21 p3822 A66-38513
- Longitudinal, torsional and flexural free vibration of elastic slender bar of variable cross section with nonhomogeneous properties 22 p3992 A66-40297
- Mass point transfer matrix for coupled bending-torsion of swept wing and tail surfaces 22 p3992 A66-40299
- Orthogonality condition for eigenvalue problem of out-of-plane twist-bending vibrations of elastic ring for various sets of boundary conditions 23 p4134 A66-40986
- Nonlinear flexural vibrations of thin circular rings analyzed, using Galerkin procedure on motion equations 23 p4139 A66-41693
- BENZENE**
- Self-consistent field calculations of benzene molecule using Gaussian expansion functions, considering 42 electrons and finding interspersions of sigma and pi levels 24 p4285 A66-42142
- Crystallization kinetics of tri-alpha-naphthyl benzene in large temperature range, noting transition in morphology, crystal growth rate and viscosity 04 p0473 A66-13648
- Molecular acentricity effect on intermolecular pair potential of n-alkane homologs and benzene 08 p1179 A66-19595
- Coupling of adjacent axial modes in external Raman resonator observed as first Stokes frequency with benzene as Raman medium and Q-switched ruby laser as pump 10 p1495 A66-21803



source 21 p3747 A66-39109  
Triplet states of liquid benzene and  
toluene studied, using biacetyl  
phosphorescence  
sensitization 23 p4032 A66-42077

**BENZOIC ACID**  
Raman scattering and IR absorption  
spectra of gaseous, liquid and crystalline  
benzoyl benzoic acid and O-and M-toluic  
acids 09 p1339 A66-20941

**BERGMAN OPERATOR**  
Bergman integral operator to generate  
families of transonic flow patterns which  
yield Ringleb pattern as special  
case 17 p2909 A66-32498

**BERNOULLI EQUATION**  
Change of variables for generalization of  
Konyukov second-order nonlinear  
differential equation, using Bernoulli and  
Riccati equations 09 p1393 A66-19917  
Pitot tube technique for measuring  
velocity profiles, using Bernoulli equation in  
stress measurement in laminar viscoelastic  
flow 22 p3898 A66-40010  
Fluidmagnetic buoyancy effects in  
ferrohydrodynamic /FHD/ flows and  
implications of Ernschaw levitation  
theorem 23 p4057 A66-41885

**BERNOULLI THEOREM**  
Proof of irreducibility of Bernoulli  
polynomial, using Norlund  
notation 01 p0093 A66-10386  
Bernoulli theorem development and  
extension 17 p2911 A66-32819  
Probability of recurrent event defined over  
t-state r-th-order Markov chain, specifically  
probability of events in Bernoulli  
sequence 21 p3757 A66-39103

**BERYLLIUM**  
Acoustic fatigue characteristics of  
beryllium panels exposed to high intensity  
random noise 01 p0149 A66-10143  
Beryllium properties and fabrication  
process in space 01 p0085 A66-10364  
Beryllium technology noting fabrication  
methods, physical and mechanical properties,  
toxicity, low transverse ductility,  
application, etc 02 p0244 A66-11739  
Titanium, beryllium and refractory metals  
properties and application of their alloys in  
aircraft industry 02 p0244 A66-11743  
Metal ignition and combustion of aluminum  
and beryllium  
[AIAA PAPER 65-103] 05 p0793 A66-15782  
Radiative recombination in p-n junctions  
produced by diffusion of beryllium into  
GaAs with very high electron  
concentration 07 p1096 A66-17325  
Stacking faults and Burger vector  
dislocations in twin crystals of beryllium  
observed by electron  
microscopy 08 p1235 A66-18651  
Papers on beryllium properties and  
metallurgy, emphasizing application as  
construction material, ductility improvement  
and processing 08 p1237 A66-18839  
Powder metallurgy of beryllium, discussing  
manufacturing, compacting and  
sintering 08 p1237 A66-18840  
Melting and casting techniques in  
purification and production of beryllium,  
discussing vacuum induction and  
ingots 08 p1230 A66-18841  
Beryllium rolling and sheet metal  
fabrication, discussing billeting and  
temperature conditions in foil  
manufacture 08 p1230 A66-18842  
Extrusion process for complex beryllium  
structures, noting die-wear  
problem 08 p1230 A66-18843  
Beryllium powder forging, working  
temperatures and use of steel  
cans 08 p1230 A66-18844  
Forging techniques for vacuum hot-pressed  
unclad beryllium metal billets, noting  
temperature effect 08 p1230 A66-18845  
Metal-metal joining techniques for  
beryllium 08 p1230 A66-18846  
Surface treatment and coating for  
beryllium corrosion and surface  
damage 08 p1230 A66-18847  
Physical, thermal, electrical and optical  
properties of beryllium 08 p1238 A66-18849  
Mechanical properties of beryllium S-200  
and I-400 QMV hot-pressed block, S-200  
cross-rolled sheet and I-400 in extruded and

forged condition 08 p1238 A66-18850  
Beryllium ductility in fabrication as  
affected by single crystal slip and fracture  
and improvement by grain  
control 08 p1238 A66-18851  
Research trends of commercial beryllium  
as affected by physical and alloy  
properties 08 p1238 A66-18853  
Health hazards in handling and processing  
beryllium and its compounds, noting effect  
on lungs and reviewing AEC  
recommendations 08 p1177 A66-18854  
Suitability of beryllium reinforced plastics  
and various light metals for application in  
manned space stations 10 p1545 A66-21216  
High temperature equilibria among vapor  
species produced by fluorination of  
beryllium in Knudsen effusion cell, using  
mass spectrometer, deriving dissociation  
energy 12 p1811 A66-23621  
Oxidation of hot pressed and extruded  
beryllium during heating in air at various  
temperatures and for various heating  
times 12 p1897 A66-24902  
Rational compression curves and plastic  
deformation mechanism of cast and drawn  
polycrystalline beryllium 13 p2106 A66-25356  
Energy spectra of ions emitted by  
beryllium, carbon and molybdenum heated  
by laser 13 p2131 A66-25479  
Beryllium diffusion into gallium arsenide in  
/111/ plane with various electron  
concentrations through vacuum  
deposition 14 p2358 A66-27087  
Ductility and production techniques of  
cross rolled beryllium sheet  
[SAE PAPER 660291] 14 p2313 A66-27287  
Diffusion saturation of industrial iron,  
molybdenum, Kh18N9T steel and ZhS6-K  
alloy with powdered beryllium  
mixture 15 p2520 A66-28538  
Heat capacity of high purity beryllium  
measured at temperatures below 30 degrees  
K 16 p2775 A66-30727  
LF internal friction of beryllium, noting  
strain amplitude dependency variation with  
temperature and purity, obtaining activation  
energies 16 p2724 A66-31265  
Ti-Be system phase diagram, noting  
solubility and formation of eutectoid and  
eutectic 18 p3121 A66-33725  
Beryllium single crystal plasticity increased  
due to preprogrammed  
load 18 p3124 A66-34404  
Negative temperature coefficient of  
electrical resistance, anomalous Hall  
constant and magnetoresistance constant for  
thin films of Be and Pb 18 p3157 A66-34627  
Effect of chemical chromate film on high  
temperature oxidation behavior of  
beryllium 19 p3386 A66-36437  
Beryllium properties and application in  
aerospace noting alloy sheet fabrication,  
temperature effect, toxicity, impact tests,  
etc 21 p3752 A66-39239  
Joining processes effect on mechanical  
properties and metallurgical structure of  
beryllium 22 p3925 A66-40264  
Adhesively joined beryllium structures for  
extreme temperature application, noting  
properties in various  
conditions 22 p3926 A66-40277  
Temperature measurements of laser sparks  
from relative intensity of X-ray flux  
transmitted through beryllium foils of  
different thickness 22 p3933 A66-40421  
Beryllium diffusion into gallium arsenide in  
/111/ plane with various electron  
concentrations through vacuum  
deposition 22 p3967 A66-40843

**BERYLLIUM ALLOY**  
Diffuse X-ray scattering in crystal  
structure of Ni-Be and Cu-Be alloys during  
first stage of aging due to anisotropic  
monoclinic lattice  
distortions 08 p1235 A66-18589  
Solid solubility of Be in W and properties  
of tungsten-richest  
beryllide 08 p1235 A66-18623  
Beryllium-containing alloys, properties and  
effect of beryllium  
addition 08 p1237 A66-18848  
Powder metallurgy development of  
sintered alloys of magnesium with MgO and  
magnesium-beryllium alloys with high  
oxidation resistance 10 p1544 A66-21200  
Mechanical property evaluation and  
reproducibility in six heats of commercial

Be-Al alloy 13 p2108 A66-25769  
Welded beryllium-copper structures,  
techniques and properties 13 p2086 A66-26015  
Axially loaded cylindrical structures  
analyzed for optimum weight construction  
consistent with cost constraint, emphasizing  
beryllium-aluminum alloys 14 p2406 A66-28023  
Abnormal X-ray interference pattern  
change during aging of nickel-beryllium  
alloys 18 p3124 A66-34405  
Optimum aging temperatures obtained  
from electric resistance of beryllium alloys,  
containing chromium and  
zirconium 18 p3124 A66-34406

**BERYLLIUM COMPOUND**  
Beryllium and beryllium compounds are  
components of most efficient chemical fuels,  
theoretically known but extremely  
toxic 03 p0414 A66-12907  
Aluminum-beryllium base alloys, noting  
problems of application as construction  
materials 08 p1239 A66-18904  
Hot wire-drawn beryllium recrystallization  
analyzed by hardness measurement and  
micrography, noting dependence on initial  
deformation 13 p2107 A66-25358  
Production process for gun-drilling of holes  
in beryllium, noting filtration techniques,  
and clamping fixture  
[ASTME PAPER MR66-185] 14 p2300 A66-26959  
Thermodynamic and physical properties of  
beryllium hydroxide at four temperatures in  
1567-1808 degrees K range, with computation  
of free energy of  
formation 14 p2370 A66-27372

**BERYLLIUM OXIDE**  
Brittle and plastic behavior of hot-pressed  
polycrystalline BeO noting stress corrosion,  
fractography and X-ray rocking  
curves 05 p0701 A66-14933  
Anisotropic broadening of X-ray diffraction  
lines and increase in lattice perimeter  
resulting from neutron irradiation of  
beryllium oxide powder 06 p0896 A66-16539  
BeO properties and relationship to  
microstructure and fabrication  
variable 07 p1051 A66-18297  
Beryllium oxide properties, fabrication and  
application 08 p1243 A66-18852  
AMRA high speed tensile tester analysis of  
dynamic stress-strain behavior in beryllium  
oxide in flexure and in  
compression 13 p2115 A66-26114  
Anisotropic broadening of X-ray diffraction  
lines and increase in lattice perimeter  
resulting from neutron irradiation of  
beryllium oxide powder 15 p2524 A66-29986  
X-ray diffraction analysis of single crystal  
silicon film grown on several natural faces  
of BeO by thermal decomposition of silane  
and hydrogen reduction of silicon  
tetrachloride 16 p2782 A66-31420  
Interstitial dislocation loops in beryllium  
oxide irradiated at high  
temperatures 19 p3398 A66-35495

**BERYLLIUM POISONING**  
Safety measures in working with beryllium,  
discussing berylliosis prevention, dust  
reduction, protective  
suits, etc 05 p0687 A66-14862

**BERYLLIUM 10**  
Determination of constancy of cosmic  
radiation and of terrestrial and cosmic ages  
of ferrous meteorites by radioactivity of Al  
26 and Be 10 20 p3651 A66-37411

**BESSEL FUNCTION**  
SA LÖMMEL FUNCTION  
Solving integrals with Bessel functions as  
integrand 01 p0095 A66-11001  
Ellipsoidal wave equation /differential  
equation with ellipsoidal coordinates/  
solution expressed as Neumann  
series 02 p0249 A66-11579  
Oscillating coaxial cylinder viscometer to  
determine rheological properties of  
viscoelastic materials, using Bessel function  
approximations 05 p0678 A66-14969  
Rate of decrease of coefficients in  
expansion of potential of body of revolution  
into series of spherical  
functions 06 p0909 A66-16425  
Transversely isotropic cylindrical shell  
vibrations solved via Bessel function for  
flexural, axisymmetric and torsional  
modes 07 p1143 A66-17499  
Helium-neon gas discharge intensification  
for 6328A laser wavelength, discussing



measurement techniques, gain parameters and results 08 p1232 A66-18632  
 Rectilinear and smooth multiwave transition 08 p1191 A66-18922  
 Computation and measurement of Hall potentials and flow field perturbations in MGD flow of axisymmetric free jet 08 p1266 A66-19815  
 Sturm-Liouville series expansion of Bessel functions and Bessel differential equation eigenvalue function 09 p1394 A66-20578  
 Approximate oscillatory solution of second order linear equations, with application to Bessel equation 11 p1724 A66-23425  
 Nonuniformly spaced antenna array synthesis using lambda function via Chebyshev-Gauss quadrature and Hankel transform 12 p1841 A66-24629  
 Bessel type lambda function for describing properties of dipoles 12 p1841 A66-24630  
 Statistical theory of electronic energies, calculating binding energy at theoretical equilibrium separation of molecular hydrogen ion 13 p2130 A66-25370  
 Force-free paramagnetic model and force-free Bessel function model of stability of feeble pinch, presenting numerical calculations using Newcomb criterion 13 p2144 A66-25720  
 Solution of quasi-static problem in thermoelasticity for cylinder with time dependent boundary conditions obtained as series of Bessel functions and error functions 14 p2397 A66-27385  
 Imaginary eigenvalue existence and zeros of modified Bessel function 15 p2528 A66-29243  
 Effect of harmonic distortion on Bessel-zero technique for FM deviation measurement used in calibration of carrier deviation and FM signal generator instruments 15 p2467 A66-29857  
 FM error calculation via comparison of demodulated output with input 16 p2649 A66-30544  
 Frequency spectrum of FM signal for carrier modulation by any number of subcarriers 16 p2649 A66-30547  
 Interaction between atoms of solid surface and gas phase, obtaining closed-form solution of motion 16 p2753 A66-30786  
 Error estimates for approximation formulas for Bessel functions and Hankel functions obtained, using Luke trapezoidal rule 16 p2736 A66-31021  
 Analytic solution in terms of modified Bessel functions of synergetic turn in exponential atmosphere, using spacecraft engines only for drag cancellation and orbit trimming 16 p2811 A66-31493  
 Krylov-Bogolubov method applied to linear differential equations, noting transcendental functions and error analysis 21 p3755 A66-38596  
 Transient resonant response of inhomogeneously broadened nuclear spin system to pulsed electromagnetic field represented as series of Bessel functions modulated by time-varying coefficients 22 p3950 A66-40093  
 Uniqueness theorem for particular inverse problem of plane wave perpendicularly incident on long cylinder of complex refractive index 22 p3866 A66-40455  
 Nonaxisymmetric temperature fields for orthotropic hollow cylinder and sphere solved using Bessel functions, noting heat transfer between external and internal surfaces 22 p4000 A66-40693  
**ETA RADIATION**  
**SA LYMAN BETA RADIATION**  
 Minimization of radiation absorption in order to measure soft beta radiations in solids, liquids and gases 01 p0070 A66-10874  
 Metallic corrosion measurement by radiation backscattering and radiation induced X-rays 04 p0536 A66-13933  
 Film thickness measurements on printed circuit-board material plated with gold over copper, using X-ray emission and absorption and beta ray backscatter test methods 06 p0886 A66-16429  
 Beta-electron in nuclear photoemulsion study of primary cosmic ray properties 06 p0880 A66-16600  
 Design and operation of radioisotope-

powered battery using direct beta-particle collection to negatively charge electrode, noting choice of isotope, dielectric, collector, etc 08 p1172 A66-19657  
 Physical pattern of high altitude fission cloud and motion of gamma and beta fission fragments captured by geomagnetic field and observed by Cosmos satellite 11 p1764 A66-23043  
 Physiologically active compounds and cultured antibiotic fluids used to eliminate effects of ionizing beta radiation on plant seeds 15 p2438 A66-29487  
 Direction of collapsing star determined by detecting generated neutrino front by time delay method 18 p3223 A66-35217  
 Solar neutrino detection via -neutrino-chlorine reaction, discussing energy level positions and probabilities of beta transition 18 p3223 A66-35219  
**BETHE-HEITLER FORMULA**  
 Approximate differential operator replacing integral operator, taking ionization losses into account in electromagnetic cascade theory 24 p4269 A66-42923  
**BETHE-SALPETER EQUATION**  
**SA WAVE FUNCTION**  
 Lamb shift in lithium isotope measured by determining lifetime from photon emission and employing analog formula of Bethe and Salpeter 11 p1739 A66-22948  
**BIACETYL**  
 Sensitized and unsensitized phosphorescence and energy transfer properties of series of aliphatic alpha diketones in fluid solution 12 p1916 A66-23620  
**BIBLIOGRAPHY**  
 Survey of literature on thermodynamics from bibliographies in journals on heat and mass transfer and ASME symposia 01 p0160 A66-10178  
 Laser bibliography covering devices and related systems for period January-June 1965 02 p0239 A66-11372  
 Bibliography of current aspects of exobiology dealing with solar system, life detection system, origin of life and life in universe 02 p0182 A66-11612  
 International Satellite Bibliography including orbital theory, lunar-satellite motion, artificial asteroids, geomagnetic field, geodesy, navigation, etc 03 p0424 A66-12457  
 Bibliography of Soviet papers on space medicine and bioastronautics published in 1964 and 1965 06 p0810 A66-15910  
 Bibliography on semiconductor reliability classified under applications /computers, radio, spacecraft, etc/, costs, devices, environments, networks, production, etc 06 p0848 A66-16308  
 Soviet and foreign papers on physics of boiling including heat transfer, heat release, bubbling processes, kinetics and sonic aspects of boiling and bibliography 09 p1469 A66-20100  
 Heat Transfer Bibliography 09 p1470 A66-20180  
 Bibliography of articles on radar reflectivity and related subjects, 1957-1964 10 p1500 A66-21614  
 Bibliography of open literature on lasers, Part V 11 p1712 A66-22876  
 Review of published papers on stress-strain of perforated shells, including bibliography 13 p2201 A66-26402  
 Heat transfer bibliography of 32 Japanese works including heat transfer application, phase change, separated flow, radiation, transpiration and mass transfer 14 p2410 A66-26937  
 Heat transfer bibliography of Russian works including conductive, convective and radiant heat transfer, phase and chemical conversions, mass transfer, etc 14 p2410 A66-26938  
 Bibliographical review of German, French and English texts relative to aeronautical engineering, theoretical and applied 15 p2425 A66-29363  
 Dual-flow and single-flow jet engines 15 p2572 A66-29364  
 Flight control systems, automatic landing devices and inertial navigation with gyros 15 p2534 A66-29365  
 Bibliography of holograms 16 p2702 A66-30433

Radiation and structure of solar atmosphere, bibliographic review discussing solar spectrum, photosphere, chromosphere, corona, eclipses of 1962 and 1963, etc 17 p2997 A66-32022  
 Lunar motion and shape, reviewing observational and theoretical work of various observatories and laboratories 17 p2998 A66-32024  
 Book of astronomical literature published in 1964 17 p3000 A66-32326  
 Bibliography of programmed low-thrust trajectories and optimal low-thrust trajectories 17 p3001 A66-32350  
 Acoustics, shock and vibration bibliography of 1959-1965 meetings of Institute of Environmental Sciences 17 p2904 A66-33040  
 Heat transfer bibliography including listing of works on boundary layer flow, phase change, channel flow, MHD conduction, etc 17 p3037 A66-33043  
 Heat transfer bibliography of Russian works, including listing of works on thermodynamics, heat conduction, radiant and convective heat transfer processes, phase change, mass transfer, drying processes, etc 17 p3037 A66-33044  
 Soviet bibliography on heat and mass transfer 18 p3267 A66-35062  
 Bibliography on metal fatigue in aircraft structures, 1955-1959 19 p3473 A66-35800  
 Classified bibliography on optimization consisting of techniques, stochastic optimization and problem formulation 19 p3309 A66-35886  
 Heat transfer literature published in 1965 on conduction, channel flow, boundary layer flow, separated flow, transfer mechanism, etc 20 p3678 A66-37117  
 Annotated bibliography on R and D management with book abstracts 20 p3683 A66-37732  
 Soviet and foreign papers on physics of boiling covering heat transfer, heat release, bubbling processes, kinetics and sonic aspects of boiling, including bibliography 21 p3834 A66-38509  
 Laser bibliography July-December 1965, including references to holograms 21 p3749 A66-39541  
**BIHARMONIC EQUATION**  
**SA ELASTICITY**  
 Circle and sphere theorems for biharmonic equation and application to displacement field of stressed plate under pure bending, noting singularities 01 p0093 A66-10427  
 Approximate solution of first biharmonic problem for spatial simply-connected finite region 06 p0902 A66-16231  
 Basic biharmonic problem for any singly or doubly connected region with piecewise-smooth boundary solved by method of summary representations 11 p1778 A66-22225  
 Stress state of weakly curved cylindrical shell analyzed, finding biharmonic function from given boundary value of partial derivatives 13 p2197 A66-25853  
**BILLET**  
 Microwave attenuation method of measuring parameters of motion of billet during sheet stamping 11 p1710 A66-22859  
**BINARY ALLOY**  
 Joining and metal deposition portion of time-temperature effects on gold-aluminum thermocompression bonds 01 p0049 A66-11154  
 Binary systems of niobium pentoxides with various oxides for improvement of oxidation behavior of niobium alloys 03 p0386 A66-13210  
 Individual and combined effects of tungsten, molybdenum and zirconium additions on hardness of recrystallized niobium at various temperatures 05 p0699 A66-14698  
 Regularities in hardness variations in niobium binary alloy 05 p0704 A66-15821  
 Cobalt-vanadium-boron system, discussing phases with boron coordination number 8 07 p1047 A66-17225  
 Binary boron-metal systems, except B-Cu, show large miscibility gaps in liquid state 07 p1052 A66-18353  
 Conditions of preparation and properties of pseudobinary boron carbide-boron silicide hard alloys 08 p1239 A66-18899  
 Electrochemical and corrosion behavior of Al-based Fe, Ni, Ti, Cu and Sb alloys and intermetallic compounds 09 p1390 A66-20840



Temperature dependence of electrical resistivities of dilute binary alloys, using phenomenological approach of Krishnan and Bhatia 11 p1718 A66-23387

Book on niobium alloys including binary and ternary alloys, physical, chemical and mechanical properties, electron structure, heat treatment, resistance, etc 12 p1893 A66-23654

Electronic structure and Seebeck coefficient for chromium-iron alloys from 125 to 625 degrees K, emphasizing phonon drag and electron diffusion effects 14 p2310 A66-26879

Depressing effect of hafnium and zirconium on work function of tungsten, tantalum, niobium and rhenium 14 p2314 A66-27369

Hardening and softening of nickel-alumina alloys 15 p2519 A66-28533

Sigma-type phase occurrence in austenitic superalloys, discussing electron/atom density, residual matrix composition, etc 16 p2725 A66-31456

Chemical activities of cadmium and magnesium in binary Mg-Cd alloys based on vapor pressure measurement by Knudsen effusion method 18 p3121 A66-33729

Aging behavior and mechanical properties of three wrought high-strength magnesium-yttrium alloys 18 p3122 A66-33751

Plessite composition and texture, discussing possible origin in terms of meteorite thermal history 19 p3480 A66-35732

Order-to-disorder structural transition in binary alloys studied by method based on spectral parameters of probability distribution of various atomic configurations 19 p3402 A66-35938

Critical temperatures of binary alloy films in which major constituent is superconducting amorphous bismuth 19 p3444 A66-36007

X-ray analysis of crystal structure relationships among transition elements in binary and ternary aluminide alloys 20 p3586 A66-38092

Equilibrium diagram and existence corroboration of Ti-Rh alloy 20 p3586 A66-38093

Regularities in hardness variations in niobium binary alloy 23 p4081 A66-41386

**BINARY CODE**

Pseudorandom binary coded waveforms as modulating functions for radar signals, noting autocorrelation function 04 p0486 A66-14119

Optical ultrasonic delay lines as correlators and variable code matched filters to achieve large time-bandwidth products and high data rates 05 p0831 A66-14821

Transformations with correlation function unaltered, changing generalized Barker sequences 06 p0880 A66-18113

Extension, modification and analysis of Gorenstein-Zierler decoding algorithm for binary codes of Bose, Ray-Chaudhuri and Hocquenghem /BCH/ correcting erasures and errors 06 p0837 A66-18114

Statistics of product of Gaussian noise process and pseudorandom binary code 09 p1342 A66-19919

Simultaneous error correction and burst error detection, using binary linear cyclic codes 09 p1347 A66-20643

Telemetric technique based on data modulation and coding for satellite data transfer, stressing noise suppression, operation flexibility, error correction, etc 11 p1651 A66-22386

Residual error probability for cyclic binary code data transmission on symmetrically random noise channels 14 p2245 A66-26795

Electrohydraulic digital actuator design and conversion of discrete electric input signal in binary code to linear motion 14 p2227 A66-28366

Binary block codes simultaneously correcting additive and synchronization errors in data transmission systems 15 p2452 A66-29680

Transistor-tunnel diode RC emitter circuit for binary numeration 17 p2888 A66-32841

Asymmetrical property of binary pseudorandom noise generators, noting Gaussian probability density function in output of low pass filter 17 p2894 A66-33110

Cyclic product codes operating in variable redundancy modes used in communications systems, noting protection against errors 19 p3296 A66-35336

Existence of q-ary uniform convolutional codes where q is any prime-power, noting error-correcting ability comparable to familiar maximal-length block codes 21 p3704 A66-39138

Self-synchronizing codes derived from binary cyclic codes 21 p3720 A66-39635

Photographic data recorder noting simultaneous event and data recording capability 22 p3917 A66-39994

Inverse transfer function of pulse-forming network for binary code transmission with small intersymbol interference in time domain and narrow bandwidth in frequency domain 22 p3866 A66-40182

**BINARY DATA**

Algorithm derived for processing packet of binary-quantized signals according to maximum likelihood for various types of target fluctuations 04 p0482 A66-13919

Optimum threshold and associated error probability for detecting binary optical signals 06 p0833 A66-16683

Binary FM signal originating from single frequency source 06 p0835 A66-16861

Component characteristic determining conversion probability of input signal to output signal allowing for random dispersion of transmission characteristics of individual components 07 p1013 A66-17385

Static and dynamic characteristics of four-layer semiconductor switches as components of binary storage circuits 09 p1356 A66-20627

Pseudorandom binary sequential digital simulation of feedback control systems subjected to random input signals 13 p2030 A66-25211

Phase coherent digital M-ary transmission with binary waves through Gaussian channel 13 p2022 A66-25554

Frequency domain design of time-limited binary signals imbedded in colored Gaussian noise 13 p2052 A66-26078

Statistical properties of input signals and effect on structure of optimal binary system of signal reception 14 p2236 A66-27173

Optimum algorithm derived for making binary decisions in decision systems of hierarchic structure 15 p2469 A66-29054

Quadratic integral equation solution for bandlimited signal design for binary communication, using memoryless correlation detection 19 p3296 A66-35339

Adaptive on-off communication system for binary data transmission over noisy channel of unknown attenuation 19 p3302 A66-35709

Low error probabilities in binary communication systems estimated by statistics of bivariate extreme-value theory 20 p3514 A66-37211

Algorithm derived for processing packet of binary-quantized signals according to maximum likelihood for various types of target fluctuations 20 p3518 A66-37877

Matter exchange, period change and orbital element variation in close binary system 21 p3812 A66-38824

Optimum recognition of binary signals passed through channels with random parameters, examining case where variances are equal and case of exact estimation of parameters 21 p3705 A66-39147

Design formulae and comparative tables of three n-input universal logic circuits 22 p3883 A66-39727

Plurality-count diversity combiner for fading M-ary transmission, noting nonbinary alphabets with plurality count combining for transmission of binary data 22 p3865 A66-40069

**BINARY FLUID**

Chapman-Enskog kinetic gas theory calculation of diffusion coefficient of binary gas mixture 17 p3035 A66-32694

Rotating Couette flow of miscible binary liquid mixture between two coaxial cylinders 18 p3102 A66-34924

Concentration profile of heavy species for binary fluid mixture under body force from uniformly mixed upstream condition, considering inviscid hydrodynamical model 18 p3103 A66-34925

**BINARY INTEGRATION**

Optimum number of phase-quantization

steps in phase-shift keying communications system for maximum data transmission rate, using binary integration method 08 p1183 A66-19097

Binary communications integral equations in complex variable functions and application of Fourier transform for bandlimited signals 23 p4085 A66-41537

**BINARY MIXTURE**

Reflectance and emittance properties of binary coatings in sintered or compacted powder form in terms of properties of pure components [AIAA PAPER 65-670] 01 p0090 A66-10231

Interaction virial coefficient of binary gas mixtures by Guggenheim-McGlashan method 05 p0718 A66-15527

Stagnation point heat transfer for binary air diffusion model including dissociation and ionization 05 p0665 A66-15775

Heat conductivity of binary gas mixtures compared with theoretical and experimental results 07 p1155 A66-18159

Densities of binary mixtures of fused alkali nitrates with alkaline earth nitrates measured by manometric densitometer and expressed as linear function of temperature 08 p1177 A66-18617

Two-phase flow of evaporating cryogen in condensing binary mixture related to Gibbs potentials [AIAA PAPER 65-7] 08 p1318 A66-19153

Theoretical formulae for thermal diffusion of binary gas mixtures 08 p1320 A66-19569

Asymptotic steady state solution to problem of thermal separation of components across shear layer between cold jet mixture and hot ambient gas 09 p1470 A66-20178

Neutral disparate mass mixtures, replacing Boltzmann collision integrals by relaxation-type kinetic models with model equation terms ordered according to mass ratio, deriving two-fluid transport equations 10 p1523 A66-21802

Prediction of thermal conductivity of binary mixture of solids, particularly solid propellants utilizing metallic filaments 10 p1590 A66-21957

Shock wave structure in binary gas mixtures that are monatomic and chemically inert, using Mott-Smith method 11 p1691 A66-22914

Accuracy and applicability of approximate formulas describing heat conductivity of binary gas mixture 11 p1787 A66-23318

Detonation limits for binary mixtures of tetramethylsilane with oxygen, analyzing factors controlling transition from detonation to deflagration, noting condensation effects 13 p2209 A66-26303

Nonequilibrium laminar boundary layer of binary dissociating gas determined by solving nonlinear partial differential equations governing system [AIAA PAPER 65-129] 14 p2274 A66-27406

Hypothesis that system sodium fluoride-yttrium trifluoride serves as model for each of binary systems of rare earth trifluorides SmF<sub>3</sub> to LuF<sub>3</sub> with sodium fluoride 14 p2315 A66-27466

Thermodynamic characteristics of two volumes of binary gas mixture connected through capillary tube 14 p2415 A66-28324

Thermal diffusion factor of binary gas mixtures, discussing some relatively unknown characteristics 17 p3033 A66-32041

Liquid-vapor phase equilibria of neon-normal hydrogen system 20 p3676 A66-37087

Low temperature liquid-vapor equilibrium in neon-oxygen system at pressures up to 5000 psi from 63 to 152 degrees K 20 p3601 A66-37088

Time dependent Ising-model description of binary liquid mixture near critical temperature 22 p3947 A66-39922

Orientation relaxation in symmetrical-top gases and binary gas mixtures, noting prediction of cross sections from kinetic theory data for molecules 22 p3860 A66-40901

**BINARY STAR**

**SA ECLIPSING BINARY STAR**

Elements of eclipsing binary spherical stars determined from Fourier transforms of their light curves by defining characteristic functions of system 02 p0285 A66-11298

Gravitational emission from double star systems 06 p0955 A66-16779



- Classical spectroscopic binary star orbit determination techniques to provide orbital elements for lunar satellite tracked by Earth-based Doppler radar [AIAA PAPER 86-40] 08 p1298 A66-19727
- Origin of binary system by splitting of single star into two components due to rotational instability during contraction of star 09 p1455 A66-20407
- Angular momenta associated with orbital motion of close binaries is not due to localization of galactic rotation of prestellar media 09 p1456 A66-20408
- Superconducting behavior of various close packed low symmetry intermediate phases in various binary systems, noting relation between transition temperature and composition 12 p1928 A66-23939
- Electron scattering responsible for variable polarization in V444 13 p2184 A66-25624
- Cygni 13 p2184 A66-25624
- Classical spectroscopic binary star orbit determination techniques to provide orbital elements for lunar satellite tracked by Earth-based Doppler radar 18 p3234 A66-34596
- Angular momentum distribution in planetary systems computed, based on mass of star and period of revolution of planet-like companion 18 p3236 A66-34891
- Gravitational emission from double star systems 19 p3456 A66-35376
- Close binary systems involving transfer of angular momentum, considering circulatory patterns of gaseous flow and axial rotation of component stars 21 p3815 A66-39483
- Pulsation in cepheid instability strip in H-R diagram, giving equations for spherically symmetric motion 21 p3816 A66-39489
- BINARY SUMMATOR**
- Binary counter circuit, discussing relevance to solid state design, performance and operation 06 p0857 A66-16973
- Digital counter synthesis for fixed base and periodic sequence-variable base counters with various feedback loops 09 p1361 A66-20606
- Scope display width expansion via simple switching circuit with binary counter and several resistors 10 p1508 A66-21300
- Integrated circuit binary counters using majority logic current mode gate element 14 p2255 A66-27803
- Binary adder and other pneumatic logic elements producing any two-valued function of three two-valued input parameter by proper arrangement of input jet nozzles 20 p3496 A66-36862
- BINARY-TO-DECIMAL CONVERSION**
- Active two-input pure fluid OR-NOR gate fabrication by logic binary-to-decimal converter [ASME PAPER 85-WA/AUT-13] 05 p0624 A66-15606
- BINAURAL HEARING**
- Voice communication channels expansion, using mans binaural listening capability 02 p0187 A66-11828
- Psychophysical method measuring effects of several variables on loudness fluctuation of binaural beats when amplitude modulated 05 p0628 A66-15733
- Acoustic images arising from binaural repetitive wideband acoustic transients, noting tonal harmonic images and two dominant images of impulsive character 05 p0628 A66-15734
- Binaural interaction phenomena, examining end point of lateralization for dichotic clicks 09 p1337 A66-20952
- Masking-level differences/MLD/ for 600-cps low-pass transient noise explored as function of interaural time difference, interaural intensity difference and combinations of both 09 p1338 A66-20956
- Binaural unmasking of tones masked by broadband Gaussian noise including theoretical work on equalization and cancellation model 21 p3702 A66-38646
- BINDER**
- S ADHESIVE**
- S PROPELLANT BINDER**
- BINDING ENERGY**
- Strain field calculation from linearized elasticity theory for vacancies and dislocations in diamond structure valence crystals 06 p0938 A66-17147
- Correlation energy effect on dissociation and binding energies of diatomic and polyatomic molecules 07 p1000 A66-18343
- Binding energy between oxygen atom and dislocation in tantalum by measuring critical temperature at which discontinuous yield disappears on heating 07 p1052 A66-18514
- Structure of conducting and insulating liquids as affected by interatomic forces 11 p1693 A66-22979
- Statistical theory of electronic energies, calculating binding energy at theoretical equilibrium separation of molecular hydrogen ion 13 p2130 A66-25370
- Simplified method of evaluating thermal and ionizing energies from fission of uranium atoms 16 p2744 A66-30436
- O-O and O-N clusters in niobium detected via internal friction and elastic aftereffect measurements, noting equilibrium, kinetic properties, binding enthalpy, etc 18 p3121 A66-33728
- Upper limit on fractional binding energy of nonrotating magnetoturbulent supermassive star and for mass which can reach radiative equilibrium 18 p3229 A66-34141
- Effect of binding on distribution in angle of charged particles having suffered scattering with lattice atoms 19 p3403 A66-36172
- BINOMIAL COEFFICIENT**
- Betti numbers shown to be equal to binomial coefficients of torus, determining minimal set of van Hove critical points 15 p2559 A66-28624
- BINOMIAL THEOREM**
- Variables/attributes/error/propagation /VAEP/ method of system estimation from performance parameters, using binomial analysis 20 p3568 A66-37919
- BIOASTRONAUTICS**
- SA AEROSPACE MEDICINE**
- Cybernetics methods suited to complex systems associated with bioastronautics 01 p0021 A66-10807
- Basic environmental problems of man in space - International Symposium, Paris, October 1962 04 p0463 A66-14063
- Biological characteristics and physical conditions of space flights, such as low pressure, ionizing radiation, noise, acceleration, weightlessness, artificial atmosphere, feeding problems, etc 04 p0464 A66-14066
- Soviet biological and physiological investigations in rockets and satellites, particularly nonpathological character of physiological reactions to stress factors 04 p0466 A66-14076
- Space biology and medicine research, stressing flight experiments performed with Russian satellites and spacecraft 04 p0468 A66-14089
- Bibliography of Soviet papers on space medicine and bioastronautics published in 1964 and 1965 08 p0810 A66-15910
- Spacecraft crew monitoring system for evaluating performance capabilities and physiological state 08 p0818 A66-16241
- Neurologic adaptations and audiogenic responses in mice exposed to chronic 2X gravity field, noting development of more efficient circulatory system, growth pattern alterations, etc 07 p0998 A66-17660
- Basic physical/biological phenomena studied under zero-g conditions in Earth orbital spacecraft 10 p1491 A66-21529
- Pre- and postflight medical examinations of Voskhod I cosmonauts 11 p1845 A66-23049
- Environmental parameters affecting spacecrew comfort during weightlessness and optimization of comfort 14 p2231 A66-28412
- Soviet monographs on problems of space biology 15 p2431 A66-29439
- Human reaction to simulated landing impact overload, including analysis of EKG, kinetocardiogram, blood pressure and respiration data 15 p2443 A66-29445
- Space flight problems in maintaining personal hygiene 15 p2435 A66-29456
- Human physiological and hygienic problems when confined in closed system of circulating biological substances 15 p2443 A66-29457
- Sport-type knit suit indicated as most suitable astronaut clothing in small-volume cabin during comfortable microclimatic conditions 15 p2443 A66-29458
- Spacecraft-cabin microatmosphere composition, theoretically analyzing applicability of helium-oxygen mixtures 15 p2444 A66-29459
- Biological cybernetics applied to physiological studies during space flight, examining mathematical modelling, biological control and statistical dynamics techniques 15 p2444 A66-29460
- Immunological reactions of Russian spacemen before and after space flight 15 p2436 A66-29468
- Periodometer automatic analysis of periodic diurnal variations in EEG observations of six healthy men 15 p2440 A66-29503
- Maximum photosynthetic capacity for Chlorella determined experimentally from cell reproduction rates 15 p2440 A66-29505
- Book on extraterrestrial biology covering origin processes of life, planets, life detection, etc 16 p2639 A66-30874
- Oral, cutaneous and aerosol bacteriological evaluation of astronaut exposed to oxygen-hellum atmosphere at low pressure 18 p3058 A66-33778
- Life support requirements encountered in manned space flights, considering cycle involving oxygen, food and water in terms of process criteria 19 p3485 A66-36231
- Water-circulation-cooled space suit, discussing heat dissipation mechanism, body temperature maintenance, metabolic rates, astronaut comfort, etc 20 p3509 A66-38164
- Experimental biology in space, discussing goals, contributions and future potentials 24 p4164 A66-42670
- Book on space biology and medicine covering interplanetary trajectories, biological effects of prolonged and impact accelerations, weightlessness and cosmic radiation 24 p4165 A66-43130
- Main stages of development of space biology and medicine in U.S.S.R., discussing biological effects in dogs in suborbital flight vehicles and satellites 24 p4169 A66-43135
- Electromagnetic and corpuscular radiation hazards to astronauts deduced from data on dogs 24 p4166 A66-43140
- Professional training of Soviet astronauts, instilling high resistance to weightlessness, isolation, radiation, acceleration and other space flight stimuli 24 p4169 A66-43143
- BIOCHEMICAL FUEL CELL**
- Biochemical processes used to produce fuels for fuel-cell batteries, including fermentation processes involving microorganisms acting on carbohydrates 05 p0612 A66-15306
- Commercial fuel cells, noting biochemical, regenerative and low temperature carbon monoxide fuel cell 07 p0996 A66-18476
- BIOCHEMISTRY**
- SA PHYSIOCHEMISTRY**
- Astrophysical observation and experimental results of organic synthesis bearing on abiogenic formation of biochemical compounds formed from simple precursor in aqueous or aqueous ammonia system 02 p0181 A66-11603
- Martian life possibilities discussing its atmosphere, clouds, violet layer, temperature and biological interpretation of dark areas 02 p0181 A66-11607
- Electron micrographs from fraction I protein of Chinese cabbage leaves, noting substructure in individual particle 06 p0811 A66-16119
- Origination of organic matter and distribution of invisible bodies capable of supporting life 06 p0811 A66-16322
- Endocrine and metabolic response of restrained dogs to body vibration, nonanesthetized or anesthetized, showing increase in plasma and blood epinephrine 06 p0812 A66-16822
- Substrate specificity of proteolytic enzyme thermolysin /Thermolase/ isolated from bacterial cultures 09 p1338 A66-20582
- Characteristics, fine structure and mode of functioning of bacterial cell and artificial synthesis possibility 11 p1844 A66-22713
- Forms of water in biologic systems - Conference, New York, October 1964 11 p1844 A66-22987
- Structured water forms in biological systems, relationship to macromolecular system, detection and evaluating electron



- microscopy 11 p1645 A66-22992
- Crystalline lactic dehydrogenases in reaction with p-hydroxymercuribenzoate in urea 13 p2009 A66-25796
- Biochemical mutation, DNA, RNA and microorganisms infecting wing tanks of jet aircraft 13 p2011 A66-26546
- Synthesis of constituents of nucleic acid and protein molecule for artificial production of life 14 p2227 A66-26866
- Paleogenetic study of ferredoxin structure, reconstructing evolution from amino acid sequence 14 p2228 A66-27810
- Automatic chemical processing systems for extraterrestrial biochemical investigations 14 p2233 A66-28414
- Effects of alpha glycerophosphate and of palmitoyl-coenzyme A on lipid synthesis in yeast extracts 15 p2429 A66-28616
- Physicochemical processes in memory, learning, consciousness and other mental processes in man 15 p2431 A66-28671
- Chromatography on carboxymethyl cellulose to obtain fractions containing predominantly single bands of malate dehydrogenases 15 p2446 A66-28871
- Biological macromolecule detection using thiacarbocyanine dye and observation of absorption spectra changes 15 p2441 A66-29962
- Chemical laboratory experiments on origin, chemical components and structural attributes of life 16 p2638 A66-30357
- Cellulose and derivatives and coupling with biochemical substances 16 p2646 A66-31155
- Biochemical experiments aimed at explaining rapid eye movement sleep /REMS/ 16 p2641 A66-31399
- Book on photochemical origin of life 16 p2641 A66-31745
- Stereospecific hydrolytic action of acylase studied by gas-liquid chromatography 17 p2869 A66-31871
- Origins of prebiological systems and their molecular matrices - Conference, Wakulla Springs, Florida, October 1963 17 p2849 A66-32083
- Role of light in chemical and biochemical evolution noting photosynthetic reactions depending on chlorophylls, pigment system, etc 17 p2853 A66-32102
- GLC-mass spectrometric stereoisomer discrimination as means of detecting biological processes 18 p3059 A66-34372
- Space diet effect on aerobic and anaerobic microflora of human feces 22 p3854 A66-39796
- Chloride requirement for cathepsin C 24 p4165 A66-43099
- Molecular and ultrastructural correlates of function in neuron, neuronal nets and brain studied, using genetic and immunological concepts 24 p4165 A66-43102
- BIOCONTROL SYSTEM**
- SA MUSCULAR SYSTEM**
- SA RESPIRATORY SYSTEM**
- Probability state variable device /neurotron/, operation, functions and application 06 p0819 A66-16807
- Human accommodative system, investigating absence of odd-error signal mechanism under restricted monocular viewing conditions 06 p0819 A66-16850
- Electromagnetic energy transport between coils or coils external to human body and coil implanted inside body is increased by using suitable ferrite core for receiving coil 06 p0820 A66-16852
- Computational analysis employing digital computers to evaluate hypoxic stress reactions in man 07 p0998 A66-17659
- Eye control in relation to visual process, showing derivation of position information from pointing of eyeball 12 p1807 A66-23645
- BIOCOURIER PROJECT**
- S LIFE SCIENCE**
- BIODYNAMICS**
- Relative specific energy capabilities of fish and birds and body structure relative to environment 01 p0017 A66-10200
- Effect of varying strain rate on physical properties of bone and muscle tissue, measuring load and time displacement with constant-velocity compression test machine [ASME PAPER 65-WA/HUF-9] 05 p0626 A66-15699
- BIOELECTRIC POTENTIAL**
- Microcircuit internal medical sensors with

- high electronic gain and lower sensitivity transducers 11 p1647 A66-22298
- Electrophysiological study of responses of central nervous system on action of some factors of space flight 11 p1642 A66-22489
- Bioelectric potentials in animals, investigating electrical materials, anatomical sites and means of increasing output and long-term implants 22 p3857 A66-39797
- BIOELECTRICITY**
- Utilization of microorganisms to generate electrical energy 05 p0627 A66-15478
- Physiological functioning of monkeys under restricted mobility noting appetite, orientation reflexes, bioelectrical activity of brain, etc 15 p2436 A66-29470
- Vibration effect on bioelectric activity of brain and oxygen consumption, using experimental rats 23 p4027 A66-41340
- BIOENGINEERING**
- SA HUMAN ENGINEERING**
- Automatic control, systems science, cybernetics, biomedical engineering, human factors - IEEE International Convention, New York, March 1966 12 p1854 A66-24634
- BIOGENESIS**
- SA ABIOTENESIS**
- Constitution of vallesiachotamine isolated from Peruvian Apocynaceae Vallesia dichotoma Ruiz et Pav 14 p2232 A66-27865
- Biogenesis, chemical evolution, detection of extraterrestrial life and future automated biological laboratory to explore Mars 16 p2798 A66-30361
- BIOGENY**
- Isolation and identification of biogenic steranes and pentacyclic triterpanes in Eocene shale 12 p1805 A66-23539
- BIOINSTRUMENTATION**
- Biochemical monitoring systems for spacecraft operation, considering parotid secretion and diagnostic and calibration stability [ISA PREPRINT 1.2-3-65] 05 p0627 A66-15503
- Telemetric Universal Sensor /TELUS/ describing measurement, processing and control of biological data from terrestrial and aerospace sources [ISA PREPRINT 1.2-2-65] 05 p0683 A66-15506
- In-flight measurement, describing human pulse wave velocity detection system principles, design and application [ISA PREPRINT 1.2-4-65] 05 p0638 A66-15509
- Bioinstrumentation and monitoring device which relates complex environmental variables to development of psychophysiological stress evaluation for controlling environment of space capsules 06 p0878 A66-15963
- Recording sampling system for measuring energy incident on biological system exposed to laser beam 07 p1030 A66-17293
- Advances in biomedical computer applications - Conference, N.Y. Academy of Sciences, June 1965 12 p1809 A66-24227
- Physiological study and instrumentation of pigtail Macaque under extended exposure to near-zero gravity environment 13 p2014 A66-25514
- Subminiature high-performance biopotential telemetry system with inexpensive components and simple construction 13 p2015 A66-25795
- Automatic systems for diagnostic medical tests onboard spacecraft, using algorithms given in matrix form 15 p2444 A66-29462
- Biological and medical tests during training and flight of Russian astronauts 15 p2436 A66-29464
- System measuring various respiratory parameters using hybrid computer for monitoring and instrumentation 16 p2643 A66-31125
- Biomedical equipment for manned space flight, noting characteristic requirements, specifications and design 17 p2862 A66-32139
- Instrumentation for biophysical data acquisition for pressure-suited test subjects in space environment simulation testing 19 p3289 A66-35840
- Biological telecommunication, discussing application of microtelemeters for measurement of physiological processes and responses in animal and human subjects [ASME PAPER 66-MD-27] 21 p3700 A66-38483
- BIOKINETIC THEORY**
- Performance and physiological effects of

- adrenalin or insulin in human subjects 06 p0813 A66-16822
- Computational analysis employing digital computers to evaluate hypoxic stress reactions in man 07 p0998 A66-17659
- Eye control in relation to visual process, showing derivation of position information from pointing of eyeball 12 p1807 A66-23645
- Life support system in spacecraft cabin circulation of biological substances 24 p4166 A66-43140
- BIOLOGICAL CELL**
- SA CHROMOSOME**
- SA CYTOLOGY**
- SA ERYTHROCYTE**
- SA NUCLEUS**
- Physical state of water in living cell and model systems such as collagen and wool 11 p1645 A66-22992
- Microbiological and cytological experiments in Vostok spacecraft, noting behavior of lysogenic E coli K-12 culture and normal and cancerous human cells 15 p2436 A66-29466
- Dendritic arborization of retinal ganglion cells of rat stained in vivo with methylene blue, relating it to receptive field organization of these cells 17 p2849 A66-31990
- Microsphere used as cell model, when produced by solution and condensation of proteinoid, for understanding of cellular life origin 17 p2852 A66-32098
- Buffering capacity of substances liberated by Chlorella expressed in terms of van Slyke buffer index, noting changes in pH 17 p2860 A66-32833
- DNA synthesis in cultured mammalian cells stimulated by UV light, using radioautography and density gradient centrifugation 19 p3287 A66-36438
- BIOLOGICAL EFFECT**
- SA PATHOLOGICAL EFFECT**
- SA PHYSIOLOGICAL RESPONSE**
- Biological problems in extended manned missions caused by low g, artificial atmosphere and absence of terrestrial periodicities 02 p0185 A66-11622
- Vibration, acceleration and radiation effects on cell division, chromosome behavior and mitotic activity of bone marrow and spleen cells in mice 02 p0182 A66-11666
- Biological effects of laser radiation with reference to intact animals, primate eyes and skin and malignant tumors of animals and human origin 03 p0325 A66-12998
- Space radiation of solar and cosmic origin and biological effects, examining DNA structure and radiation induced changes 04 p0463 A66-13899
- Biological effects of cosmic radiation under laboratory and flight conditions on various craft to study measures for pharmacological and biological protection 04 p0466 A66-14077
- Biological hazards of radiation exposure of man in space discussing recovery, delayed effect, injury treatment and dose 04 p0467 A66-14078
- Laser beam use in biology and medicine noting interaction of electromagnetic radiation with biological systems, hazards diagnostics, therapeutics, etc 04 p0534 A66-14453
- Detonation and decompression research comparing biological effects of explosive decompression and detonation 06 p0811 A66-16087
- Biological effects of chronic acceleration studied by using birds and animals in centrifuges with specially designed cages 06 p0819 A66-16800
- Rats exposed to space cabin atmosphere for two weeks, noting mortality rates, organism functioning, growth rate, etc 07 p0998 A66-17663
- Correlation between solar corona and Wolf number, examining intensity variation effect on chemical and biological tests 07 p1136 A66-17846
- Biosatellite for TV monitoring of development of opossum embryonic fetus in space environment 08 p1174 A66-18581
- Acute inhalation toxicity of oxygen difluoride in albino rat 08 p1175 A66-19723
- Inhalation toxicity at ambient and reduced pressures in monkeys, dogs and rodents upon exposure to ozone, nitrogen dioxide



and carbon tetrachloride 08 p1176 A66-19724  
Text on life into space covering space biology, extraterrestrial environment, temperature, pressure, acceleration, radiation effects, etc 10 p1492 A66-22062  
Physiological effects of pressure breathing and aveolar oxygen tension at high altitude 10 p1489 A66-22117  
Personnel comfort and protection from thermal stress, discussing clothing, environmental temperature, metabolic heat production, solar radiation, etc 10 p1492 A66-22120  
Cathodic depolarization theory of bacterial corrosion, using Desulfovibrio desulfuricans with benzyl viologen as electron acceptor 11 p1647 A66-22303  
Psychological and medical aspects of human confinement, isolation and sensory deprivation 11 p1642 A66-22485  
Vasovagal syncope induced by application of negative pressure to lower half of human body, noting effect on lung CO diffusing capacity 11 p1643 A66-22580  
Low-gravity vibration stress- effects on weight, growth, metabolism, white blood cells and endocrine system of albino Wistar rats 11 p1643 A66-22581  
Biological effect on mice of bombardment by protons of 120 mev 11 p1645 A66-23055  
Response of tissue culture cells to low magnetic fields, noting no quantitative growth differences 12 p1807 A66-25015  
Optical ray tracing to predict focusing characteristics of laser light in refractive targets, calculating heating effects in target, noting target geometry, refractive index, thickness of skin layers, etc 13 p2090 A66-25531  
Laser safety standards, discussing nature of photobiological mechanisms responsible for tissue damage upon exposure to laser radiation 14 p2309 A66-27775  
Ambient pressure effect on tolerance of mice to air blast 15 p2430 A66-28655  
Long duration flight physiological data on ducks and chickens in closed ecological systems, including oxygen and food requirements and carbon dioxide output 15 p2435 A66-29452  
Antiradiation protection and relative biological effectiveness of seldom-ionizing radiation 15 p2435 A66-29455  
Biological experiments under flight conditions in Vostok spacecraft, noting reproduction of Drosophila melanogaster and effect of weightlessness and cosmic radiation on hereditary structures 15 p2436 A66-29465  
Space flight effect on living cells examined by using higher plants as biological dosimeters 15 p2436 A66-29469  
Vibration effect on reception of certain organs and tissues of white mice to dye introduced intravenously 15 p2437 A66-29477  
Effects on white mice of exposure to oxygen-enriched air, noting biological and physiological observations 15 p2439 A66-29493  
Toxic and lethal effect on mice of ammonia in air, noting biological and physiological changes 15 p2439 A66-29494  
Biological effects of confining fish in sealed aquarium with and without Chlorella 15 p2440 A66-29504  
Planetary quarantine constraints, noting prevention of Martian atmosphere contamination 15 p2441 A66-29966  
Pulmonary blood flow distribution under forward accelerations studied by combined use of human centrifuge and radio-isotope scanning 17 p2856 A66-32153  
Altered physiologic function of dogs produced by exposure to pulsed microwaves including study of combined effect of X-irradiation 17 p2856 A66-32156  
Increase of arterial lactate and pyruvate in blood glucose of fasted anesthetized dog after hydrazine injection 17 p2856 A66-32157  
Calorimetric study of effects of hydrazine on heat balance, source of metabolic energy and rate of protein catabolism of rats 17 p2856 A66-32158  
Toxic effects of hydrazine derivatives tested in dogs, producing methemoglobin and pigmentation in blood 17 p2856 A66-32159  
Microbial profiles of 20 men under simulated space conditions indicates that

certain men can go unwashed six weeks 17 p2856 A66-32160  
Magnetic effects on reproduction and metabolism of normal and diseased mammalian cells in vivo and in vitro 17 p2859 A66-32229  
Theoretical molecular mechanism of chemical radio-protection based on stabilization of defects of damaged biological structures by molecular adsorption 17 p2861 A66-32940  
Seed water content influence on oxygen effect as detected in gamma irradiated barley seeds and prolonged post-storage period in terms of biological effect and paramagnetic resonance 22 p3855 A66-40378  
Biological effect of atmospheric conditions and physical and psychological factors on living organisms 24 p4165 A66-43134  
Main stages of development of space biology and medicine in U.S.S.R., discussing biological effects in dogs in suborbital flight vehicles and satellites 24 p4169 A66-43135  
**BIOLOGICAL MODEL**  
Organic superconductor and dielectric IR waveguide, resonator and antenna models of insects sensory hairs, spines and pit pegs 06 p0847 A66-16103  
**BIOLOGICAL RHYTHM**  
Animal temperature sensing for studying effect of prolonged orbital flight on circadian rhythms of pocket mice 03 p0328 A66-12767  
Flight fatigue studies, discussing parametric evaluation of crew performance on overseas flights 06 p0816 A66-16057  
Human adjustment to shift in day-night cycle and effect of space flight on sleep and activity cycles of astronauts 08 p1174 A66-18582  
Light effect on rhythmic excretion of water and electrolytes in humans 09 p1335 A66-20534  
Random lighting exposure effects in rats and changes caused in adrenal cortical function, circadian rhythm, endocrine system, group running activity, etc 15 p2429 A66-28487  
Daily physiological rhythm changes associated with light intensity and color, noting body temperature oscillations vs light intensity, heart rate changes, etc 15 p2441 A66-29959  
Book on physiological responses of healthy mammals to natural changes or extremes of physical environment, considering heat, cold, light, atmospheric pressure and water 20 p3505 A66-37253  
Miniaturized implantable biotelemetry transducer for study of metabolic rhythms in extraterrestrial life 24 p4167 A66-42674  
NASA Biosatellite Program exploring dynamic space flight effects on terrestrial organisms and Earth diurnal rotation effect on biological rhythm 24 p4168 A66-42675  
**BIOLOGY**  
SA BACTERIOLOGY  
SA ECOLOGY  
SA GENETICS  
SA MICROBIOLOGY  
SA MORPHOLOGY  
SA PHYSIOLOGY  
SA PROTOBIOLOGY  
SA RADIOBIOLOGY  
Biological and engineering problems in spacecraft sterilization, noting heat treatment 15 p2445 A66-29996  
Radiation detectors in radiobiology, photobiology and nuclear medicine 19 p3289 A66-35907  
Chemico-physical and biological fluctuation and causality dependence on space phenomena 21 p3811 A66-38630  
**BIOMAGNETICS**  
Effect of extremes in magnetic environment on physiological behavior 08 p1174 A66-18585  
**BIOMECHANICS**  
Similarity concept applied to study of work done by living creatures in various situations 01 p0017 A66-10302  
Total simulation system mass effect on certain human force outputs in tractionless environments 19 p3293 A66-36243  
Text evaluating application of human body size and mechanical capabilities to equipment design for man-machine

integration 23 p4030 A66-41619  
Physiological and biomechanical reactions of humans exposed to action of g forces, examining effects of impact acceleration 24 p4166 A66-43137  
**BIOMETRICS**  
SA REGRESSION ANALYSIS  
Plant physiological process measuring devices for automatic growth control in closed system 15 p2445 A66-29506  
**BIONICS**  
S CYBERNETICS  
**BIOPHYSICS**  
SA RADIOBIOLOGY  
Collected works of K. E. Tsiolkovskii on astronomy, natural science and technology 01 p0135 A66-10295  
Exobiology concepts suggest that apparent inherent limitations on temperature, pressure or chemical environment for living matter are geocentric 02 p0181 A66-11602  
Gate control system role in pain mechanism, noting specificity and pattern theories 03 p0325 A66-13337  
Relative contribution of stapedial reflex to remote and contralateral remote masking 09 p1337 A66-20953  
Response of tissue culture cells to low magnetic fields, noting no quantitative growth differences 12 p1807 A66-25015  
Proton tunneling and mutation rate of Escherichia coli B To T1 and T2 phage resistance in water 13 p2008 A66-25788  
General cosmological problem /GCP/ based on unified field theory involving cosmological expansion, oscillation and organic evolution, discussing quadrant mechanics, entropy, ether, minimum time problem, etc 14 p2389 A66-28408  
Relationship between biology and physics 18 p3060 A66-34454  
**BIOREGENERATION**  
Electrolysis-Hydrogenomonas bacterial bioregenerative life support system for manned space flight of long duration 06 p0815 A66-15929  
Biological procession of human secretions and water regeneration by Chlorella in bacterial colony 15 p2440 A66-29501  
Chemical methods for carbon dioxide conversion for oxygen recovery, including relationship to biological processes 19 p3293 A66-36235  
Algal bioregenerative photosynthetic gas exchange system 19 p3293 A66-36239  
**BIOSATELLITE**  
NASA biosatellite study of organism in space environment, with emphasis on weightlessness and radiation effect 07 p0999 A66-17615  
Design of recoverable biosatellite spacecraft for studying effects of space environment on living organisms 08 p1301 A66-18580  
Biosatellite for TV monitoring of development of opossum embryonic fetus in space environment 08 p1174 A66-18583  
Self-contained environmental control system for biosatellite study of prolonged effects of weightlessness and radiation [AICE PREPRINT 19D] 10 p1491 A66-21186  
NASA Biosatellite Program exploring dynamic space flight effects on terrestrial organisms and Earth diurnal rotation effect on biological rhythm 24 p4168 A66-42675  
**BIOSENSOR**  
S BIOINSTRUMENTATION  
**BIOSIMULATION**  
SA ARTIFICIAL INTELLIGENCE  
Analog method for simulating visual receptor network as model for inhibitory interaction in retina 06 p0819 A66-16849  
Analog computer, programmed on digital computer, used in examination of lumped and distributed parameter models of cardiovascular system 12 p1809 A66-24230  
**BIOT METHOD**  
Biot variational method applied to transient heating of porous half-space from which gas escapes [AIAA PAPER 65-118] 03 p0444 A66-12766  
Approximation method for calculating transient temperature field in solid for case where heat-transfer coefficient varies 24 p4296 A66-43224  
**BIOTECHNOLOGY**  
Medical knowledge as aid in preventing



aircraft accidents and injury through investigation of causes and results 10 p1495 A66-22142

**BIPROPELLANT**

Pulse operated bipropellant control valve design for attitude control systems of space vehicles 01 p0015 A66-10668  
Flow rate distribution and mixing ratio of two impinging jets in simulation of bipropellant liquid rocket system, using hypergolic propellants 02 p0278 A66-11590  
Lithium-hydrogen bipropellant arc jet 14 p2374 A66-27426

**BIRD**

SA CHICKEN  
SA PIGEON

Relative specific energy capabilities of fish and birds and body structure relative to environment 01 p0017 A66-10200  
Behavioral characteristics of birds that collide with aircraft in flight and methods to reduce such strikes at airports [AIAA PAPER 65-748] 03 p0319 A66-12584  
Radar cross sections of ducks and chickens at vertical polarization and 400 mc 10 p1503 A66-21647  
North American Sabreliner laminate windshield for bird-proofing pilot compartment [SAE PAPER 660214] 13 p1995 A66-26389  
Long duration flight physiological data on ducks and chickens in closed ecological systems, including oxygen and food requirements and carbon dioxide output 15 p2435 A66-29452  
Respiratory activity and hematological factors of avian blood cells, discussing oxygen consumption, thermal effects, tissue and erythrocyte metabolism 23 p4024 A66-41043

**BIREFRINGENCE**

Mechanical double refraction of unsaturated copolymer polyesters of styrene subjected at different temperatures to constant tensile stress [ONERA TP 276] 04 p0538 A66-14242  
Temperature dependence of optical birefringence on single crystals of lead zirconate-titanate solid solution measured, noting they are optically negative 08 p1269 A66-19006  
Polarization and birefringence of photoelastoplastic medium 11 p1781 A66-22613  
Mechanical and optical measurements on plasticized polyvinyl chloride, photoviscoelastic stress analysis and wave propagation effects 14 p2318 A66-27767  
Fundamental equations for birefringence of isotropic elastic solids and isotropic viscous fluid derived from Toupin theory of photoelasticity and stress optics 14 p2408 A66-28388  
Calibration of birefringent filter photometer 15 p2499 A66-28845  
Stress in viscoelastic polystyrene in Aroclor flowing in straight, converging and diverging channels 16 p2686 A66-31043  
Resonant birefringence in potassium vapor under influence of electric field of ruby laser emission 19 p3375 A66-36066  
Laser light modulation by Pockels or Kerr effect for application to telecommunications system, examining electrical birefringence modulation 19 p3304 A66-36262  
Uniqueness theorems concerning lossless birefringent networks and effects on transmittance of changing sign of crystal angles and output 20 p3599 A66-36943  
Maxwell-Lorentz field equations for Couette flow birefringence of Rivlin-Ericksen viscoelastic fluid and Noll simple fluid 21 p3724 A66-38761  
Birefringence of certain crystals sufficiently large to allow collinear backward wave interaction of three electromagnetic waves with signal frequency tunable over large portion of IR spectrum 21 p3771 A66-39113  
Optical dispersion and dispersion of birefringence, noting photoelastic methods and stress-strain optical coefficients 22 p3994 A66-40437  
Fatigue testing machine shear strain measurements near cracks on Al flat plate surfaces by observing birefringence 23 p4147 A66-41997

Adhesive backed birefringent tape for separation of thin film and printed circuit master drawings with near perfect registration for microelectronic production masking purposes 24 p4180 A66-42312  
Photoelectric photometer using filter that tilts relative to incident light for patrol observation of 5577 angstrom intensity in nightglow 24 p4210 A66-42468  
Self-trapping of laser beam due to diffraction from dielectric waveguide arising from permittivity increase of birefringent beam 24 p4222 A66-42554  
Birefringence recording device for measurements within very short wavelengths, describing photoelastic applications for identifying degrees of annealing and homogeneity of glass 24 p4292 A66-42965

**BIREFRINGENT COATING**

Photoelastic experiment by birefringent coating method to determine stress analysis applicable for any elastic body 02 p0298 A66-11583  
Dynamic strains and transient deformations on opaque body surfaces measured, using bonded birefringent strip 12 p1961 A66-23988  
Minimization technique for light scatter due to diffuse mirrored birefringent coatings used in performing photoelastic studies by fringe multiplication 18 p3257 A66-34563  
Stress-strain determination in elastoplastic problems with aid of photoelastic epoxy resin coating 23 p4135 A66-40990  
Direct determination of oblique incidence coefficients in birefringent coatings and models, eliminating error sources 24 p4292 A66-42863

**BISMUTH**

Recrystallization of bismuth films by controlled melting and resolidification 05 p0732 A66-14668  
Transport theory based on relaxation time applied to bismuth, deriving analytic expressions for electric resistance, thermoconductivity and Hall, Seebeck and Nernst coefficients 07 p0990 A66-17237  
Polarization and Alfvén wave attenuation in Doppler-like change in transverse wave velocity when drift current is passed parallel to magnetic field in solid-bismuth plasma 07 p1102 A66-18209  
Pronounced quantum effects of solid-bismuth plasma properties at quantum limit and low temperature 07 p1082 A66-18212  
Quantum size effects in thin bismuth film and specific resistance, Hall effect and reluctivity 13 p2160 A66-25107  
Magnetic hysteresis and switching property of manganese-bismuth thin magnetic films epitaxially grown by vapor deposition technique 14 p2355 A66-26913  
Excitation of Alfvén waves in semimetal plasma at low temperature, noting wave propagation below plasma or cyclotron frequency in magnetic field 14 p2363 A66-27516  
Temperature dependence of Hall effect and conductivity of lead telluride single crystals containing bismuth 14 p2364 A66-27645  
Quantum size effects in thin bismuth film and specific resistance, Hall effect and reluctivity 16 p2771 A66-30286  
Alfvén wave propagation equations used to study electronic properties of semimetals 20 p3615 A66-37282  
Elastoresistance effects in evaporated bismuth films, deposited on glass and epoxy resin substrates, used as strain gauges and transducers 22 p3962 A66-40046  
Criticism of identification of bismuth lines with lines of solar spectrum based on analysis of new tracings of solar spectrum by Kachalov 24 p4278 A66-42709  
Thermoelectric power measurement method for thin bismuth lamella, obtaining Peltier and Thomson coefficients 24 p4258 A66-43010

**BISMUTH ALLOY**

Electrical resistivity, Hall effect and magnetoresistance of bismuth antimony single crystal solid solutions 02 p0272 A66-11712  
Electronic band structure of BiSb alloy tunnel junction for various Sb concentrations 16 p2770 A66-30178

Critical temperatures of binary alloy films in which major constituent is superconducting amorphous bismuth 19 p3444 A66-36007

**BISMUTH COMPOUND**

Temperature dependence of dielectric permittivity and relative expansion of bismuth ferrite in large temperature intervals, detecting phase transitions 14 p2357 A66-27078  
Fermi surface of metals and semimetals and quantum oscillations in ultrasonic attenuation and magnetic susceptibility of InBi 14 p2366 A66-27763  
Temperature dependence of dielectric permittivity and relative expansion of bismuth ferrite in large temperature intervals, detecting phase transition 22 p3967 A66-40834  
Magnesium antimonide and magnesium bismuthide as materials for power generating thermocouples 24 p4227 A66-42111

**BISMUTH OXIDE**

Polarization effects in magnetic and nonmagnetic barium plus bismuth oxide and magnesium-zinc ferrites when subjected to DC low-voltage electric fields 03 p0409 A66-12690

**BISMUTH TELLURIDE**

Thermoconductivity decrease of bismuth-telluride based solid solutions due to forbidden bandwidth and majority and minority carrier mobility 01 p0127 A66-11029  
Assembly for determining thermal conductivity coefficients of liquid bismuth selenide-bismuth telluride semiconductor at 970 to 1280 degrees C 06 p0882 A66-16839  
Transverse reluctance of bismuth telluride in pulsed magnetic fields revealing fine structure of Shubnikov-De Haas oscillations, interpreted as spin-splitting of Landau levels 16 p2786 A66-31695  
Bismuth telluride alloy solar thermoelectric flat plate generators applied to auxiliary power systems for exploratory missions toward Sun 20 p3497 A66-37166

**BISTABLE AMPLIFIER**

Electronic relays with bistable elements based on nonlinear circuits with p-n junction capacitance 15 p2468 A66-29923

**BISTABLE CIRCUIT**

Transient processes in nonlinear trigger circuit with capacitive p-n junction used in bistable trigger systems 11 p1670 A66-23226  
Monostable and bistable counting circuits: synthesis and analysis of volt-ampere characteristics 11 p1678 A66-23238  
Bistable fluid elements without moving parts for switching fluid currents showing stability against load and supply pressure fluctuation 19 p3283 A66-36810  
Operating characteristics of pneumatic bistable element using Coanda effect, examining correlation between outlet flow and pressure and feed pressure 21 p3697 A66-38802

**BIT SYNCHRONIZATION**

Bit synchronization of coded messages transmitted by telemetering 03 p0333 A66-12474  
Operational test instrument for PCM bit synchronizers/signal conditioners, discussing importance of bit decision errors 16 p2659 A66-30541

**BLACK ARROW LAUNCH VEHICLE**

Rocket engines for Black Arrow satellite launcher, noting solid propellant motor in third stage, payload mass ratio, etc 16 p2791 A66-30349

**BLACK BODY RADIATION**

Thermal radiation absorption by droplet or spray during ignition and combustion of atomized liquid fuels 01 p0164 A66-10899  
Photographic pyrometer using variable-density filter noting temperature master curve, attenuation, calibration and error sources 02 p0229 A66-11518  
Surface cooling effect on accuracy of black body coefficient determination for highly heated materials 03 p0444 A66-12518  
IR radiation of refractory solids with radiation properties of flame-sprayed ceramic coatings, determining normal spectral emittance, integrated normal total emittance and IR intensity curves at 1300 K 03 p0386 A66-13100  
Doppler effect discussing relativistic form, transmission in dispersive media, broadening



of spectral lines, black body radiation, rocket and satellite tracking, navigation and application 04 p0546 A66-14383  
High temperature air-carbon plasma noting black body radiation, atomic constants and thermodynamic equilibrium 04 p0599 A66-14460  
Solar thermonuclear process, radiation phenomena, structural measurements, observations and properties 05 p0767 A66-15757  
Planckian black body approximation used to simulate and assign star magnitudes for nonhuman photodetector, considering relationship between star brightness and stellar spectra 07 p1003 A66-18332  
Thermal radiation into space of limited areas of inner walls of space radiators determined, assuming cylinder and cone are isothermal black body radiators 08 p1317 A66-18835  
IR fluctuations radiated by fluid mechanical turbulence of hot shear layers analyzed, assuming gas mixture is black body [AIAA PAPER 66-107] 08 p1206 A66-18955  
Radiometers observations of atmospheric IR irradiance, noting measurement results with improved equipment 09 p1369 A66-19869  
Radio observation of Mercury, Venus, Mars, Saturn and Uranus and black body temperatures of planets 09 p1450 A66-20110  
High temperature black body as spectral radiance standard for high intensity arc 09 p1471 A66-20504  
Cylindrical black body furnace with graphite resistance built in France, attaining 1600 degrees C, for calibration of radiation pyrometers 09 p1383 A66-20909  
Effects of long-wave radiation exchange near Earth surface, extrapolating air temperature measurements to ground to estimate surface temperature, obtaining equivalent black body temperature of ground 11 p1702 A66-23155  
Continuous emission and absorption of plasmas by calculating radiation of hydrogen plasma, deriving temperature and pressure conditions under which plasma radiates as black body 12 p1919 A66-23750  
Black body radiation law deduced from astochastic electrodynamics 14 p2414 A66-28173  
Equilibrium binary correlations in classical relativistic homogeneous electron gas 14 p2336 A66-28275  
Thermal conductivity coefficient and integral hemispherical degree of blackness of niobium at temperatures above 1000 degrees C 15 p2523 A66-29217  
Cosmic black body radiation at 2.6 mm wavelength from 2.7 to 3.4 degrees K, noting CN molecules 16 p2793 A66-30199  
Pyrheliometers, noting performance, application, environmental effects and calibration based on black body radiation 16 p2703 A66-30509  
Inverse Compton X-ray and gamma ray flux due to high energy electron interaction with cosmic blackbody radiation at 3.5 degrees K 17 p2992 A66-31914  
Black body radiation, pressure and temperature dependences of equilibrium composition, enthalpy, specific heat and electron density of air-carbon plasmas 18 p3144 A66-34040  
IR emitting flares, examining major parameters governing methods of analysis and performance 18 p3135 A66-34192  
High temperature light source with substantially continuous spectral emission for UV absorption spectroscopy approximating black body in visible and near UV region 19 p3353 A66-35314  
Reduced blackness coefficients measured for coaxial system of tungsten-molybdenum surfaces by calorimetric method 20 p3674 A66-36984  
IR fluctuations radiated by fluid mechanical turbulence of hot shear layers analyzed, assuming gas mixture is black body [AIAA PAPER 66-107] 22 p3899 A66-40351  
**BLACK BRANT II MISSILE**  
Development of 23KS20000 motor for Black Brant IIB vehicle with emphasis on internal ballistics 06 p0942 A66-16702

**BLACK BRANT MISSILE**  
Canadian Black Brant research rocket program for upper atmospheric sounding 13 p2184 A66-25700  
**BLACK KNIGHT ROCKET**  
Environment influence on design and development of Black Knight rocket engine 18 p3163 A66-34211  
Environment influence on design and development of Black Knight rocket engine 24 p4261 A66-42573  
**BLACKOUT**  
**S SYNCOPE**  
**BLADE**  
SA COMPRESSOR BLADE  
SA IMPELLER BLADE  
SA PROPELLER BLADE  
SA ROTOR BLADE  
SA STATOR BLADE  
SA TURBINE BLADE  
SA VANE  
Abrasion of circular self-rotating cutters as function of blade path in material being worked 11 p1710 A66-22860  
Calculation method for vibrations of twisted pinned blades under combined bending and torsion 12 p1965 A66-24053  
Nonrectilinear blade rows with zero thickness when produced by conformal transform 20 p3491 A66-36986  
Rapid opening mechanical gate valve consisting of blade assembly, blade catcher and primer holder used in conjunction with hypervelocity free flight range experiments 24 p4162 A66-43219  
**BLASIUS FLOW**  
Eigenvalues and norms arising in flow description represented by perturbations of Blasius solution 03 p0356 A66-12810  
Finite-difference method for computing transient velocity profiles in laminar boundary layer around two-dimensional cylinder, noting Blasius flow oscillations 14 p2274 A66-27434  
Effect of unsteady longitudinal vortices on Blasius profile in traditional boundary layer of flat plate 14 p2279 A66-28461  
Blasius series for heat and mass transfer in two-dimensional boundary layers, discussing velocity and concentration profiles 20 p3678 A66-37122  
**BLAST**  
**SA JET BLAST EFFECT**  
Similar solutions of partial differential flow equations for cylindrical blast uniform flow shock wave and determination of blast wave velocity 14 p2344 A66-27633  
Ambient pressure effect on tolerance of mice to air blast 15 p2430 A66-28655  
Blast environment simulation developing high pressures of relatively long duration, noting helical winding of cord explosive 16 p2681 A66-30501  
Interaction of first and second shocks of blast-bow wave in double-driver shock tube, examining stagnation point pressure prediction methods [AIAA PAPER 66-409] 17 p2840 A66-32748  
Blast waves in inviscid gaseous medium devoid of heat conduction and viscosity but with finite conductivity 20 p3609 A66-37536  
Weak oblique blast impingement on slender hypersonic wedge 21 p3724 A66-38726  
**BLAST LOADING**  
Fracture time for thin spherical shells subjected to internal blast loading 04 p0586 A66-13411  
Clamped circular rigid-plastic plates under blast loading distributed over surface [ASME PAPER 65-APMW-34] 04 p0593 A66-14234  
Drucker stability hypothesis indicates strain rate as dominant fracture criteria for thin spherical shell under blast loading 07 p1141 A66-17211  
Dynamic buckling of circular cylindrical aluminum shells subjected to axial blast loads [AIAA PAPER 66-82] 08 p1308 A66-18996  
Dynamic transient response of cylindrical shell to internal pressure pulse generated by blast wave 12 p1959 A66-23799  
Stress wave propagation in inhomogeneous rod applied to measurement of dynamic overpressure on moving vehicle subjected to sudden intense blast loading 14 p2409 A66-28398  
Energy method for analysis of lowest mode

symmetrical buckling of thin shell shallow spherical caps and cylindrical arches under blast loading 15 p2610 A66-29291  
Clamped circular rigid-plastic plates under blast loading distributed over surface [ASME PAPER 65-APMW-34] 18 p3247 A66-33569  
Equations of motion for inelastic large deformations of circular membranes subjected to blast loading, useful in metal forming 18 p3252 A66-33763  
Clamped circular plates of rigid plastic material under uniformly distributed blast loading, noting parameters of permanent central deflection 20 p3673 A66-38277  
Dynamic buckling of circular cylindrical aluminum shells subjected to axial blast loads [AIAA PAPER 66-82] 21 p3828 A66-38728  
**BLEED-OFF**  
Effect of bleeding air behind compressor for VTOL stabilization on dynamic behavior of jet engine 10 p1591 A66-21405  
**BLIND LANDING**  
**S INSTRUMENT LANDING SYSTEM**  
**BLINDNESS**  
**S FLASH BLINDNESS**  
**S VISION**  
**BLOCH BAND**  
Pseudopotential method for determining temperature-dependent electric resistance of lithium, neglecting free electron approximation and examining electron-phonon interaction 04 p0566 A66-14316  
Optical pumping on He 4 atom in metastable level, examining modulation of light in absorption in longitudinal and transverse beams and obtaining magnetic resonance curves 22 p3930 A66-39808  
**BLOCH WALL**  
**SA FERROMAGNETISM**  
**SA MAGNETIC DOMAIN**  
Anomalous Barkhausen effect in ferromagnetic alloys 01 p0117 A66-10239  
Coercive force for Bloch wall displacement of thin magnetic films coupled with stripe domain neon-iron films 11 p1758 A66-23359  
Minimum internal energy and magnetization distribution for two parallel Bloch walls in thin films 14 p2353 A66-26899  
Magnetic relaxation and high temperature effect of Bloch wall stabilization in ferrite Mn-Fe 15 p2565 A66-29052  
**BLOCK DIAGRAM COMPILER /BLODIB/**  
Digital computer simulation of sampled data communication system using Block Diagram Compiler, B [BLODIB/] 13 p2028 A66-25937  
**BLOOD**  
Erythropoieting properties and polyglobulia-inducing techniques 14 p2227 A66-26814  
Increased partial oxygen pressure effect on morphological composition of peripheral blood of rats and mice 15 p2439 A66-29490  
Hematocrit index and arterial-blood gas composition in white rats during artificial hypothermia 15 p2440 A66-29511  
Human blood enzyme response to 56-day exposure to oxygen-helium atmosphere at 258 mm Hg total pressure 18 p3057 A66-33771  
Dissociation and reassociation reactions of hemocyanin mixtures analyzed by electron microscopy, noting original molecular structures 18 p3060 A66-34459  
Macromolecular organization of hemocyanins and apohemocyanins as revealed by electron microscopy 18 p3060 A66-34460  
Continuous in vivo recording of partial pressure of arterial carbon dioxide and oxygen by mass spectrography 21 p3701 A66-39494  
**BLOOD CIRCULATION**  
**SA BRAIN CIRCULATION**  
**SA CAPILLARY CIRCULATION**  
**SA CARDIORESPIRATORY SYSTEM**  
**SA CARDIOVASCULAR SYSTEM**  
**SA CIRCULATORY SYSTEM**  
**SA CORONARY CIRCULATION**  
**SA OCULAR CIRCULATION**  
**SA PERIPHERAL CIRCULATION**  
Increased blood circulation for compensating anoxia by changes in cardiac output, blood distribution and red blood cell volume 10 p1489 A66-22113  
Cardiovascular stress resulting from radial acceleration gradient impeding venous



return analyzed by rotation of seated subject about Z axis /Rz/ 12 p1807 A66-25016  
Pulmonary blood flow distribution under forward accelerations studied by combined use of human centrifuge and radio-isotope scanning 17 p2856 A66-32153

**BLOOD COAGULATION**

Effect of 0.6 LD/50 intraperitoneal dose of hydrazine on coagulation mechanism in rats, comparing results with saline injected controls 17 p2857 A66-32167

**BLOOD FLOW**

Respiration and anoxia, noting anoxic anoxia, reduced oxygen carrying capacity of blood and inadequate flow of oxygenated blood to tissues 10 p1488 A66-22112

Sodium excretion during extracellular volume expansion and associated changes in renal blood flow and intrarenal blood distribution during natriuresis accompanying saline loading in dogs 13 p2012 A66-26582

Blood flow measurement by indicators by taking samples in situ-dyes, thermolulution, krypton 85 14 p2230 A66-27552

Electromagnetic and ultrasonic flow measurement of blood flow rate for cardiocirculatory physiology, discussing future application of nuclear resonance and laser 14 p2230 A66-27553

Blood flow rate in surface veins of brains of animals subjected to accelerations, noting thermal transducer 15 p2445 A66-29500

Lower body negative pressure effect on blood volume and orthostatic tolerance during prolonged bed rest 17 p2858 A66-32178

Change pattern in human cerebral blood flow during time immediately following initiation of carbon dioxide inhalation 18 p3056 A66-33691

X-ray irradiation effect on venous blood flow in rabbit brain vessels 23 p4027 A66-41344

Oscillating two-phase flow through rigid circular pipe investigated to understand blood cells effects on changes in shape of pressure pulse wave 23 p4058 A66-41916

Wave propagation, dispersion and energy transfer in arterial blood flow considered as fluid dynamics, noting finite amplitude effects in circulatory system and flow control mechanism 23 p4062 A66-42058

**BLOOD GROUP**

S ERYTHROCYTE  
S HEMATOPOIETIC SYSTEM  
S THROMBIN

**BLOOD PLASMA**

Exercise tolerance, plasma volume, red cell mass, total blood volume and orthostatic tolerance during four weeks of bed rest 03 p0326 A66-13354

Toxicological effect of hydrazine and monomethylhydrazine in blood serum of rats 05 p0626 A66-14642

Free and esterified cholesterol in plasma extracts determined by fluorometric means 13 p2017 A66-25871

Bed rest and water immersion effects on plasma volume and catecholamine response to tilting, noting urinary excretion of norepinephrine and epinephrine 15 p2430 A66-28661

Acceleration stress-induced changes in fat metabolism, level of circulating glucose and corticosterone level in rats 15 p2431 A66-28868

Physiological factors in decompression sickness, noting recompression, plasma replacement, etc 16 p2638 A66-30624

Toxic effects of hydrazine derivatives tested in dogs, producing methemoglobin and pigmentation in blood 17 p2856 A66-32159

**BLOOD PRESSURE**

SA MANOMETER  
SA TONOMETER

Effects of water immersion, recumbency and activity without negative breathing pressures, measuring heart rate and blood pressure with and without tilting 11 p1642 A66-22573

Systolic and diastolic blood pressures continuously measured without direct arterial puncture effected, using digital pressure cuff on one arm and brachial cuff on other 12 p1810 A66-25010

Cardiovascular measurement on anesthetized dogs subjected to vibration, noting recording techniques, instrument sensitivity, etc 16 p2642 A66-30622

[AIAA PAPER 66-442] 16 p2642 A66-30622  
Sympathetic nervous system integrity following water immersion evaluated by measuring plasma-free fatty acid responses to passive tilting 16 p2639 A66-30649  
Blood pressure and heart rate during hypothalamic self-simulation in dogs, discussing experimental methods and results, physiological response, etc 16 p2640 A66-31154

Arterial blood pressure, visual accommodation power, vital capacity and body weight of pilots and tower controllers 18 p3059 A66-34407

Theoretical and experimental analysis of Korotkoff sounds at diastole which are interpreted as dynamic instability induced by application of pressure cuff 19 p3286 A66-36431

Tilt table response and blood volume changes associated with 30 days of bed rest, evaluating time required to recover from cardiovascular deconditioning 22 p3853 A66-39785

**BLOWDOWN WIND TUNNEL**

Pressure and temperature distribution measurements in test chamber of hypersonic blow-down wind tunnel located at University of Tokyo 01 p0053 A66-10632

Pressure regulation in equalization chamber of model blowdown wing tunnel used at various Mach numbers, calculating compressed-air flow through control valve and characteristics of transfer function 12 p1857 A66-24322

Blowdown-type high-speed linear cascade wind tunnel with variable exit pressure, Mach and Reynolds numbers permit boundary layer control 12 p1859 A66-24927

Shock-on-shock test facility converted from combustion driver shock tunnel, noting model surface transient pressure results [AIAA PAPER 66-764] 24 p4192 A66-42571

**BLOWER****SA BELLOWS****SA FAN**

Reduction gears, mechanical systems and automation of modern propellers, rotors and blowers 01 p0014 A66-11061

Aerodynamic characteristics of blower in form of propeller with rim 03 p0314 A66-12536

**BLOWING****SA INJECTION**

Parameter predicting transition from low to medium blowing rate in arc with transpiration cooled anode 08 p1168 A66-19156

Monograph on clearance losses between rotating blade of propeller and annular duct, determining reduction by blade blowing 09 p1327 A66-20454

Blowing system effect on fog dispersion over limited area 20 p3595 A66-38380

Mass transfer into aerodynamic body flow fields, examining model shear flow in Rayleigh problem for blowing current across gas-solid interface 23 p4058 A66-41900

Similarity solutions of boundary layer equations for blowing through porous surface, obtaining skin friction 24 p4194 A66-42541

**BLUE STREAK MISSILE**

Design and manufacture of Blue Streak satellite launcher structure, noting propellant tank 06 p0888 A66-17070

Blue streak structural problems, noting loading from ground handling to flight and strength in relation to upper stages 21 p3818 A66-38641

**BLUFF BODY**

Wake from bluff bodies interaction with initially laminar boundary layer [AIAA PAPER 66-126] 06 p0875 A66-17096

Cavitation effects on periodic wakes behind symmetric wedges, noting Strouhal number variation [ASME PAPER 65-FE-15] 12 p1864 A66-24549

Turbulent jet theory, thermal ignition theory and flameout characteristics of bluff body flame stabilizers 14 p2413 A66-27694

**BLUNT BODY**

Wake pressure of blunt body moving at supersonic speed calculated by analysis of curved half-jet mixing 01 p0007 A66-10630

Vorticity distribution in wake of circular cylinder oscillating in unperturbed flow, using Burger linearization of Navier-Stokes equations 01 p0007 A66-10715

Boundary layer on spherically blunted cones in supersonic air flow at given wall temperature and thermally insulated wall, graphing calculation results 01 p0008 A66-11016

Hypersonic laminar near wake of blunt bodies considered in terms of dual region model [AIAA PAPER 65-52] 03 p0315 A66-12789

Numerical solutions for inviscid nitrogen gas flows over circular cylinder where nonequilibrium prevails through nose region 03 p0317 A66-13211

Drag of body of revolution with blunt base substantially reduced by mounting disk behind body with smaller diameter than body 05 p0606 A66-15059

Heat transfer to blunt bodies with catalytic and noncatalytic surfaces in nonequilibrium dissociated hypersonic flow [AIAA PAPER 66-3] 05 p0609 A66-15850

Hypersonic aerodynamic stability and drag of ablating and nonablating models of blunt-faced reentry shape [AIAA PAPER 66-61] 07 p1141 A66-17898

Oscillating pressure effect on shock wave detachment and shape at blunt body surface 07 p1023 A66-18108

Hypersonic perfect gas flow around slightly blunted plate, discussing analogy between asymptotic shock behavior and explosion theory 07 p0981 A66-18109

Steady flow interactions of supersonic airstream and jet blown from hemispherical and flat body noses 07 p0982 A66-18137

Hypersonic gas flow near blunt body, examining entropy effects 07 p0983 A66-18140

Hypersonic gas flow past axisymmetric slender blunt body by Chernyi approximate method 07 p0983 A66-18142

High resolution equilibrium radiation spectra for shock layer of blunt bodies at reentry velocities and radiative recombination of N and O ions [AIAA PAPER 66-104] 07 p0984 A66-18458

Supersonic airflow past blunt body with various dissociation reactions 08 p1165 A66-19192

Nonequilibrium inviscid flow behind blunt body shock wave analysis, using series truncation and reducing truncation error 08 p1166 A66-19816

Nucleate boiling heat transfer considered as heat transfer into liquid near front of flow past blunt nosed body 09 p1471 A66-20824

Ablation of blunt metallic body near stagnation point solution using integral equations, noting pressure effect 09 p1472 A66-20833

Instability of hypersonic shock layer flow over blunt bodies with surface cavities coupled to dynamic stability of body 10 p1619 A66-21156

Thermal insulation of hypersonic blunt body by central coolant injection formation of insulating layer between body and high temperature freestream 10 p1481 A66-21797

Minimum pressure drag for nonslender hypersonic body calculated, using normalized coordinates 11 p1631 A66-22515

Shape of nonslender body of revolution for minimum total drag in viscous hypersonic flow at Newtonian pressure distribution and constant friction 11 p1631 A66-22516

Transversal contour of minimum pressure drag for body with noncircular cross section 11 p1631 A66-22517

Minimal-drag shape of nonslender body of revolution in diffuse free molecular flow 11 p1632 A66-22527

Shock layer approximation used in inverse hypersonic blunt body problem 12 p1795 A66-23574

Transient loading of rectangular and right circular cylinders by shock waves in air numerically determined by time dependent Eulerian method [AIAA PAPER 65-4] 12 p1860 A66-23581

Modified Newtonian-Prandtl Meyer approximation technique to determine pressure distribution over blunt body 12 p1796 A66-23600



Blast wave theory with and without entropy layer effect, determining asymptotic flow, far downstream of blunted nose, past given body 12 p1861 A66-23808

Supersonic viscous gas flow near blunt body numerically determined by equations similar to Navier-Stokes equations 12 p1796 A66-23900

Supersonic flow around blunt body calculated via integral relations, using simultaneous approximation function in two directions 12 p1797 A66-24208

Radiative heat transfer near stagnation point of blunt body in hypersonic flow, noting effect on convective heat transfer 12 p1978 A66-24241

Boundary value problems in plane and axisymmetric hypersonic flow of viscous ideal gas past blunt body 12 p1797 A66-24343

Supersonic air flow past blunt bodies and equilibrium physicochemical conversion effects 12 p1797 A66-24426

Heat transfer and mass transfer near stagnation point during injection and suction of various gases through blunt body surface 12 p1979 A66-24427

Static and dynamic stability and drag of blunt-nosed flare-stabilized bodies at velocities up to 8.2 km per second [AIAA PAPER 65-44] 12 p1799 A66-24699

Nonequilibrium heat transfer distributions around blunt-nosed aerodynamic bodies, using analytical method, for design analyses of hypervelocity flight vehicles 12 p1799 A66-24715

Aerodynamic heating of vehicles entering Earth atmosphere at hypersonic speed, noting blunt body concept, radiative and convective heating, heat shield weights, etc 13 p1989 A66-25153

Estimates of expected relative magnitudes of convective and radiative heat transfer at stagnation point of blunt body for superorbital speeds and altitudes with continuum flow 13 p1989 A66-25154

Supersonic flow past blunt body by Taylor series expansion from shock wave, Newton-Busemann expansion, truncated series expansion from axis, etc, and comparison with numerical solutions 13 p1989 A66-25155

Asymptotic behavior of two-dimensional inviscid flow at infinite Mach number past power-law body, considering flow over flat plate and blunt body followed by cylindrical afterbody 13 p2060 A66-25156

Viscous hypersonic blunt body problem examined, using Newtonian thin-shock-layer theory, slip effect, Navier-Stokes shock structure, etc 13 p1990 A66-25157

Approximate shape of detached shock wave calculated and results compared with empirical findings obtained by supersonic wind tunnel experiments 13 p1990 A66-25452

Rotational flow properties in ideal inviscid shear layer about arbitrarily shaped blunt-nosed body in hypersonic flow 13 p1993 A66-26727

Pressure distribution and shock standoff distance on spherically blunt cones in supersonic wind tunnel 14 p2220 A66-27968

Blockage corrections for streamline blunt-based bodies of revolution in closed wind tunnel 14 p2271 A66-28186

Approximate iterative calculation of non-Newtonian supersonic gas flow past highly blunt bodies 15 p2423 A66-28959

Conditions at head shock wave in viscous hypersonic flow past blunt body for study of boundary layer separation 15 p2423 A66-28960

Direct numerical method for calculation of supersonic inviscid flow about axisymmetric blunt body at large angle of attack [AIAA PAPER 65-24] 15 p2423 A66-29269

Integral relations method for flow field calculations of blunt body entries for determining convective heat flux to reentry body 15 p2424 A66-29305

Extension to MHD hypersonic stagnation flow theory of Bush, including viscous term and solving boundary value problem from both ends at once 15 p2424 A66-29307

Diatomic gas flow past blunt bodies, noting effect of oscillation and dissociation relaxation on mean 16 p2627 A66-30100

Unsteady interaction between blunt bodies and shock wave, comparing reflected shock

wave velocity decrease for plane spherically blunted cylinders 16 p2685 A66-30788

Hypersonic flow past blunt body near stagnation point examined, noting surface layer, characterized by increased density and decreased entropy of gas 16 p2630 A66-31305

Diffusion flame for stagnation mixing layer created by jet fuel injected into oxidant stream at stagnation region of blunt body 17 p3033 A66-32447

Experimental prediction theoretical prediction comparisons of pressure distributions, force and stability coefficients for spherically blunt cone at various angles of attack 17 p2839 A66-32473

Gap size effect on pressure and aerodynamic heating over flap of blunt delta wing in hypersonic flow [AIAA PAPER 66-408] 17 p2840 A66-32747

Wind tunnel test of dynamic stability characteristics of spherically blunted 10 degree cones [AIAA PAPER 66-465] 17 p2841 A66-32764

Implicit finite difference method applied to plane hypersonic flow over blunt circular cylinder 17 p2842 A66-33170

Integral relations method formulation of inverse blunt body problem and corresponding shock wave under supersonic flow of perfect gas 17 p2842 A66-33333

Inviscid hypersonic flow of perfect gas past symmetric two-dimensional and axisymmetric blunt bodies at angle of attack [AIAA PAPER 66-411] 18 p3045 A66-33636

Nose bluntness and angle of attack effects on hypersonic flow, noting shock wave deflection decrease of minimum possible shock angle, varying specific heat ratio, convective heating, boundary layer transition, etc [AIAA PAPER 66-414] 18 p3046 A66-33639

Optimum entry vehicle design using aerobreaking for manned Earth entry at hyperbolic speeds, examining blunted conic, biconic and tetrahedral configurations [AIAA PAPER 66-489] 18 p3239 A66-33657

Approximation method for compressible laminar heat transfer to blunt axisymmetric bodies in high speed flow 18 p3048 A66-33824

Free shear layer diffusion and vortex formation region behind bluff bodies 18 p3049 A66-34669

Separated shock wave distance from free flying blunt body influence by real gas oscillation excitation 19 p3341 A66-35746

Nonstationary flow past various bodies in wake of plane shock wave, noting cylinders 19 p3276 A66-36461

Newtonian variational problem for pressure on surface of nonshallow body moving at hypersonic velocity 19 p3276 A66-36472

Pressure distribution at low speeds on two-dimensional airfoils with blunt trailing edges at zero incidence, taking into account wake 19 p3278 A66-36751

Base pressure and flow parameters near trailing edges of axisymmetric blunt bodies in supersonic flow 20 p3492 A66-37678

Semiinfinite flow of axisymmetric flow of viscous thermoelectric gas around blunt body with ablation shield, noting magnetic field effect 20 p3611 A66-38108

Hypersonic boundary layer separation and expansion at shoulder of blunt based body 21 p3693 A66-38683

Nose-region flow of blunt body moving in supersonic or hypersonic speeds solved by variety of numerical methods 21 p3693 A66-38700

Applicability of inverse blunt-body computer program /Norair/ to supersonic and transonic flow problems 21 p3694 A66-38731

Density distribution and shock wave profile of rarefied gas slip flows past blunt bodies determined, using multibeam interferometer 21 p3724 A66-38903

Eulerian finite difference method for solving time-dependent equations of motion for compressible fluid flow, noting shock wave diffraction, supersonic blunt body interaction with shock wave, etc 21 p3730 A66-39472

Hypersonic gas flow past blunt body problem solved by integral correlation method, taking into account radiation effects and gas dynamic parameter

distribution in shock wave layer 22 p3897 A66-39902

Detached shock wave determination for calculation of shock layer or wake, discussing theories of conic and explosive wave methods for application to Apollo space capsule 22 p3900 A66-40416

Supersonic flow around blunt body calculated via integral relations, using simultaneous approximation function in two directions 22 p3844 A66-40572

Shock impingement on blunt body in hypersonic flow, noting alteration of flow and local heat transfer rate near impingement point [AIAA PAPER 66-756] 22 p3846 A66-40641

Alfven shocks for flow of highly conducting incompressible fluid over blunt body where magnetic and flow vectors are not aligned 22 p3957 A66-40705

Surface catalyticity and Reynolds number effects on nonequilibrium hypersonic stagnation flow of air or diatomic gas on highly cooled blunt body 22 p3847 A66-40919

Bluntness and boundary layer displacement effects on air breathing engine hypersonic inlet flow fields [AIAA PAPER 65-617] 23 p4007 A66-41109

Supersonic unsteady state three-dimensional flow around blunted bodies with detached shock wave 23 p4009 A66-41718

Similarity laws in hypersonic flow of real gas around thin blunted bodies, particularly bodies with rough lateral surface 23 p4009 A66-41720

Heat transfer to blunt bodies with catalytic and noncatalytic surfaces in nonequilibrium dissociated hypersonic flow [AIAA PAPER 66-3] 23 p4150 A66-41878

Distance of transition to turbulence of wake measured behind spherical and blunted-cone models at hypersonic speeds in ballistic range 23 p4011 A66-41883

Secondary injection induced shock shape and vertex location solved by equivalent blunt body in supersonic flow 23 p4058 A66-41899

Diameter and location of wake neck and trailing wake shock for pointed and blunt slender hypersonic cones 23 p4012 A66-41919

Inviscid flow near stagnation point of blunt body in hypersonic stream, using thin shock layer theory with very small density ratio 23 p4013 A66-42013

Three-dimensional supersonic gas flow past smooth blunt bodies, considering gas dynamic equations for mixed and purely supersonic regions 23 p4013 A66-42016

Radiometer system with photomultiplier tube for measuring absolute radiation from hypervelocity projectile flow fields 24 p4208 A66-42181

Chemical effects on RF attenuation during reentry for blunt-nosed lifting vehicles and sphere-cone ballistic vehicles 24 p4158 A66-42782

Velocity gradient on blunt axisymmetric bodies in stagnation region if pressure distribution is known, using isentropic flow equations 24 p4158 A66-42798

# BMEWS

S BALLISTIC MISSILE EARLY WARNING SYSTEM /BMEWS/

# BOATTAIL

Drag of body of revolution with blunt base substantially reduced by mounting disk behind body with smaller diameter than body 05 p0606 A66-15059

# BODY

S AXISYMMETRIC BODY  
S BLUFF BODY  
S BLUNT BODY  
S CELESTIAL BODY  
S DUCTED BODY  
S ELASTIC BODY  
S FINNED BODY  
S FLARED BODY  
S FLEXIBLE BODY  
S HUMAN BODY  
S INELASTIC BODY  
S LENTICULAR BODY  
S LIFTING BODY  
S MISSILE BODY  
S REENTRY BODY  
S RIGID BODY  
S ROTATING BODY  
S SLENDER BODY  
S STREAMLINE BODY



- S SUBMERGED BODY  
 S SYMMETRICAL BODY  
 S THIN BODY  
 S TWO-DIMENSIONAL BODY  
 S WING BODY
- BODY CENTERED CUBIC /BCC/ CRYSTAL**  
 Slip-induced fracture of polycrystalline Cr, Mo and W and bcc transition metals V, Fe, Nb and Ta 01 p0085 A66-10376  
 Crystalline structure on fatigue noting changes of body-centred metals and face-centred and hexagonal metals 02 p0245 A66-11948  
 Three-stage hardening in tantalum single crystals deformed in tension over limited range of orientations, temperatures and strain rates 02 p0246 A66-12194  
 Properties of chromium particles obtained by vaporization of metal in argon at low pressure, noting cubic shape, electron diffraction pattern, etc 06 p0894 A66-16185  
 Transmission electron microscopy observation of microhardness of shock-hardened iron and bcc iron-based alloy structures 08 p1236 A66-18758  
 Martensitic transformation of Ni-Fe alloy from fcc to bcc lattice, noting stress produced by chemical free energy difference between austenite and martensite structure 15 p2520 A66-28649  
 AMO method applied to bcc crystal of hydrogen atoms, taking into account all many-center integrals 15 p2543 A66-28784  
 Two oxycarbide phases in zirconium-carbon-oxygen compositions found in zirconia-carbon mixtures at high temperatures, giving X-ray diffraction patterns indexed as fcc at various lattice parameters 16 p2729 A66-30246
- BODY FLUID**  
**SA WATER**  
 Nuclear fast red technique of calcium in serum, parotid fluid and urine in weightless state 03 p0329 A66-13347  
 Biochemical monitoring systems for spacecraft operation, considering parotid secretion and diagnostic and calibration stability [ISA PREPRINT 1.2-3-65] 05 p0627 A66-15503  
 Lower body negative pressure used to restore hydration after recumbency diuresis following bed rest 06 p0813 A66-16823  
 Effects of 9-alpha-fluorohydrocortisone on metabolic changes occurring during six days of bed rest, including water and sodium retention, hematocrit decrease, plasma increase, etc 06 p0813 A66-16824  
 Low power radio transmitters implanted to telemeter physiological information, discussing drift caused by body fluid permeability 06 p0820 A66-16854  
 Mathematical model, using computer, to determine fluid and electrolyte distribution in principal body compartments of young 70-kg human male 12 p1809 A66-24229  
 Parotid fluid collection technic for determining in-flight biochemical responses for 17-OHCS levels 22 p3854 A66-39791
- BODY KINEMATICS**  
 Electromagnetic energy transport between coils or coils external to human body and coil implanted inside body is increased by using suitable ferrite core for receiving coil 06 p0820 A66-16852  
 Approximation method for evaluating body flexibility effects on slender aircraft static stability, noting application to sounding rocket 13 p1994 A66-26734  
 Stress wave propagation in inhomogeneous rod applied to measurement of dynamic overpressure on moving vehicle subjected to sudden intense blast loading 14 p2409 A66-28398  
 Plasma flows past bodies in magnetic field, using plasma gun, analyzing downstream wake of ordinary hydrodynamic shock wave 15 p2553 A66-29743  
 Disturbances about solid body in flowing low density plasma applied to satellite-ionosphere interactions and Langmuir probe data analysis 16 p2759 A66-30373  
 Flat rigid body motion with respect to coincident fixed plane with point on body constrained to move on fixed line in plane 17 p2932 A66-33419  
 Braking of bodies moving in rarefied plasma 19 p3275 A66-35256  
 Structure of flow past bodies with radial cross section in wind tunnel at various Mach numbers and angles of attack, noting position of shock waves 19 p3276 A66-36473
- BODY MEASUREMENT**  
**SA ANTHROPOMETRY**  
 USAF whole body gamma spectrometry in support of Air Force aerospace mission 07 p0999 A66-17664
- BODY MEASUREMENT /BIOL/**  
**SA ANTHROPOMETRY**  
**SA ELECTROCARDIOGRAPHY**  
 Mass measurement of man in zero gravity environment, discussing laboratory device using linear harmonic motion 17 p2924 A66-32171
- BODY OF REVOLUTION**  
**SA DISK**  
**SA ELLIPSOID**  
**SA OGIVE**  
 Three-dimensional laminar boundary layer on body of revolution at small incidence at its stability 01 p0055 A66-10203  
 Masses attached to body of revolution estimated by Vandrey method of calculating disturbed velocity potential of flow of ideal fluid 01 p0058 A66-10462  
 Supersonic flow past pointed bodies of revolution in calculation of initial ratio of shock to body curvature and initial surface pressure gradient 01 p0007 A66-10631  
 Smoothing of intersection of surfaces of revolution with quadrics of revolution 02 p0297 A66-11244  
 Similar flows about axisymmetric bodies rotating in fluid at rest 03 p0354 A66-12351  
 Forced convective heat transfer from isothermal and nonisothermal uniformly spinning bodies of revolution obtained by similar flow analysis [ASME PAPER 64-WA/HT-15] 04 p0595 A66-13387  
 Method for steady state heat conduction of bodies of revolution 04 p0596 A66-13439  
 Electromagnetic wave diffraction by moving bodies of revolution subjected to pulsed radiation when spatial dimension of impulse may be less than linear dimension of body 04 p0483 A66-14050  
 Drag of body of revolution with blunt base substantially reduced by mounting disk behind body with smaller diameter than body 05 p0606 A66-15059  
 Longitudinal motion effect on lateral vibrations of prolate body of revolution in ideal fluid 05 p0775 A66-15315  
 Real flow and interference effects of body of revolution and stabilizing surfaces when at small angle of attack [ASME PAPER 65-FE-5] 06 p0801 A66-16212  
 Rate of decrease of coefficients in expansion of potential of body of revolution into series of spherical functions 06 p0909 A66-16425  
 Ellipsoid of revolution of large aspect ratio with axis of revolution perpendicular to uniform flow at infinity analyzed for small Reynolds number 06 p0873 A66-16995  
 Incompressible laminar boundary layer equations for flow due to jet against body of revolution extending to infinity in absence of pressure gradient but with axially symmetrical swirl 07 p0981 A66-18045  
 Three-dimensional problem of isotropic continuous nonaxisymmetrical body of revolution, applying analytic functions of complex variable 08 p1307 A66-18885  
 Unperturbed highly supersonic flow past thin profiles and bodies of revolution with generatrix equations, using law of plane cross sections for solution 09 p1328 A66-20765  
 Turbulent boundary layer in subsonic or supersonic flow past pinched-waist bodies of revolution at various Mach numbers and pressure gradients 10 p1480 A66-21387  
 Book on theory of optimum aerodynamic shapes 11 p1629 A66-22501  
 Variational calculus in one independent variable for optimum aerodynamic shapes and extension to two independent variables 11 p1721 A66-22502  
 Shape determination of bodies of revolution minimizing pressure drag in linearized supersonic flow 11 p1630 A66-22505  
 Nonslender bodies of revolution with minimum pressure drag, noting derivation of minimizing curves for Newtonian flow 11 p1631 A66-22514
- Minimum pressure drag for nonslender hypersonic body calculated, using normalized coordinates 11 p1631 A66-22515  
 Shape of nonslender body of revolution for minimum total drag in viscous hypersonic flow at Newtonian pressure distribution and constant friction coefficient 11 p1631 A66-22516  
 Minimal-drag shape of nonslender body of revolution in diffuse free molecular flow 11 p1632 A66-22527  
 Stress-strain state of shells of revolution of variable thickness and elastic parameters under effect of external loads and secondary strains obtaining strain, equilibrium and elasticity equations 12 p1963 A66-24043  
 Approximate determination of flexural vibrations of shells of revolution with vibrations involving appearance of nodal lines along generatrix and meridional directions 12 p1964 A66-24047  
 First boundary value problem for general case of axisymmetric stressed state of body of revolution, using biharmonic solution of Love and Grodskii 13 p2196 A66-25636  
 Shells produced by rotation of second-order curves about axis of symmetry evaluated for symmetric and antisymmetric loads 13 p2202 A66-26418  
 Stability loss of shells of revolution under effect of axial compression and radial pressure with no restrictions on generatrix curvature, using strain energy method 13 p2206 A66-26454  
 Velocity pattern in turbulent wake behind symmetric body and conservation of temperature and enthalpy in wake in cylindrical polar coordinates when incoming flow is nonuniform 13 p1992 A66-26704  
 Axisymmetric supersonic flow involving shock waves applied to flow near vertex region of pointed bodies of revolution with arbitrary geometry 14 p2218 A66-27354  
 Eigenvalues of truncated cones of revolution with degenerate poles and various rigidities and geometries 14 p2400 A66-27686  
 Blockage corrections for streamline blunt-based bodies of revolution in closed wind tunnel 14 p2271 A66-28186  
 Differential equations describing elastic shells of revolution under physical nonlinearities, noting positive stresses in buckling zone 15 p2611 A66-29422  
 Forced torsional vibrations of pointed bodies of revolution 15 p2510 A66-29437  
 Computer program for axisymmetric nonlinear behavior of stiffened elastic shells of revolution with variable thickness, calculating collapse pressures [AIAA PAPER 66-529] 16 p2814 A66-30527  
 Laminar boundary layer separation in supersonic flow on body with symmetry of revolution 16 p2629 A66-30583  
 Reissner variational formulation of temperature distribution boundary value problem of axisymmetric thermal stresses in isotropic sandwich shells of revolution [AIAA PAPER 66-528] 16 p2814 A66-30611  
 Stagnation region of solid body of revolution in low density hypersonic flow with low Reynolds number 16 p2629 A66-31033  
 Thin body of revolution with annular shield with zero wave resistance in supersonic axial linearized flow 16 p2629 A66-31036  
 Stagnation region for body of revolution in analyzing temperature, velocity and atom hypersonic flow with low Reynolds number, concentration under aerodynamic heating 16 p2686 A66-31037  
 Electromagnetic wave diffraction by moving bodies of revolution subjected to pulsed radiation when spatial dimension of impulse may be less than linear dimension of body 17 p2873 A66-32216  
 Large deflections of symmetrically loaded shallow membrane shells of revolution, considering existence of boundary layer near edges and using asymptotic analysis 17 p3025 A66-32480  
 Periodic solutions of axisymmetric shell theory equations for displacement of shells of revolution and bending of thin walled rods 17 p3026 A66-32593  
 Longitudinal acceleration and angular



velocity of rotation effect on flexural vibration of elongated body of revolution in supersonic flow applied to critical flutter calculation 17 p3027 A66-32603

Stress analysis of junction of thin elastic shells of revolution, considering axisymmetric wind and sinusoidal load distributions 18 p3253 A66-33804

Quantitative examination of Saint Venant principle in context of elastostatic boundary problems, i.e., axisymmetric pure torsion of bodies of revolution 19 p3473 A66-35485

Three-dimensional heat conduction of body of revolution of arbitrary shape for exponential temperature-time relationship 20 p3678 A66-37112

Nonsteady state zero-moment creep in shells of revolution with clamped edges under internal pressure, finding change range in stresses in time 21 p3826 A66-38612

Limiting equilibrium of compression-and tension-bent shallow shell of revolution 22 p3991 A66-40149

Doubly curved axisymmetric shell construction for structural analysis of shells of revolution, using direct stiffness method 22 p3993 A66-40339

Cylindrical shell analysis for short segments of shells of revolution with axisymmetric edge-loading and variable wall thickness, using matrix method 22 p3994 A66-40369

Mach number and body geometry effects on stability characteristics of oscillation in supersonic regime of bodies of revolution 22 p3844 A66-40373

Three-dimensional and axisymmetric problem in elasticity theory with particular reference to photoelasticity 23 p4135 A66-40989

Supersonic flow past pointed bodies of revolution at small angles of attack 24 p4157 A66-42611

Radiated pressure field due to LF vibration of slender body of revolution expressed as distribution of sources and doublets along body axis 24 p4238 A66-43047

**BODY SWAY TEST**

Bed rest and water immersion effects on plasma volume and catecholamine response to tilting, noting urinary excretion of norepinephrine and epinephrine 15 p2430 A66-28661

ECG P wave changes due to body tilt in space of rabbits deprived of afferent impulses from pressure-receptive areas 17 p2859 A66-32230

**BODY TEMPERATURE**

Surface temperature of solid bodies measured by crayons, thermography, hardness, etc, particularly heat transfer tubes, current-carrying bodies, etc 12 p1882 A66-24408

Potential on hot body in plasma as function of surface temperature and plasma characteristics, considering case where photoemission is present 15 p2595 A66-29087

Parabolic equations describing periodic oscillatory processes that occur in certain electrolytic systems, oil gushers and relay regulation of body temperature 24 p4230 A66-42218

**BODY TEMPERATURE /BIOL/**

**SA HYPOTHERMIA**

**SA SKIN TEMPERATURE /BIOL/**

Animal temperature sensing for studying effect of prolonged orbital flight on circadian rhythms of pocket mice 03 p0328 A66-12767

Body heat storage experiments conducted to physiological limit in pressurized suits 06 p0817 A66-16238

Daily physiological rhythm changes associated with light intensity and color, noting body temperature oscillations vs light intensity, heart rate changes, etc 15 p2441 A66-29959

Harness-mounted temperature sensor for prolonged monitoring of human skin temperature 16 p2643 A66-31128

Radio telemetry for acquisition of Circadian rhythm data on ambulatory animal, including deep body temperature, heart rate, locomotor activity and oviposition 22 p3856 A66-39792

Physiological and mechanical effects of radial accelerations on brain temperature of dog and rabbit 23 p4026 A66-41336

**BODY TEMPERATURE REGULATION**

Aircrew body heat loss from cold water immersion and developments in heating systems and insulative clothing 15 p2442 A66-28656

**BODY WEIGHT**

Prolonged centrifugation effects on growth and organ development of weanling and mature rats 05 p0625 A66-15412

Infantile treadmill experience effect on body weight and resistance to exhaustion in rat 07 p0997 A66-17460

**BODY-WING COMBINATION**

Pressure distribution along wing and body of wing-body combination 14 p2221 A66-28185

**BOEING 707 AIRCRAFT**

Automatic landing equipment for 707/720 airplanes used under low visibility conditions noting autopilot, auto-throttle, yaw damper, etc 01 p0103 A66-10663

Boundary layer control high lift system for high speed aircraft, using ejector for momentum augmentation and air bleed from propulsion system 05 p0610 A66-15070

[AIAA PAPER 64-589] Serviceability and accuracy of Sperry C-12 compass system on Boeing 707-320C aircraft from June to October 07 p1065 A66-17673

Serviceability and accuracy of dual Doppler installation on Boeing 707-320C aircraft 07 p1065 A66-17674

AD560 Doppler Radar sensor and computer in Boeing 707-138 aircraft 07 p1076 A66-17794

**BOEING 720 AIRCRAFT**

Flight operating techniques influence upon engine maintenance costs and new engine design, specifically Pratt and Whitney JT3C-12 on Boeing 720 aircraft 03 p0322 A66-13220

[SAE PAPER 650212] Pressurization effect on fuselage drag of Boeing 720 jetliner based on boundary layer measurement 05 p0606 A66-15077

**BOEING 733 AIRCRAFT**

SST flight operations, maintenance and servicing compared to subsonic aircraft [SAE PAPER 660294] 14 p2222 A66-27290

**BOEING 737 AIRCRAFT**

Aerodynamic design of Boeing 737 covering data of analytical studies, wind tunnel and flight tests, aerodynamic parameters and drag, flap system size, efficiency, wing geometry and handling qualities [AIAA PAPER 65-739] 03 p0321 A66-13047

Boeing 737 twin-jet short haul airliner, featuring wing-mounted engines and advanced technology 10 p1481 A66-21074

Boeing 737 twin-jet, discussing wing, fuselage and tail design, aerodynamic wind tunnel tests, stability and control, etc 12 p1801 A66-23785

Boeing 737 short-haul jet transport aircraft design problems, including engine placement, wing design, lift system, body shape, performance, economics, etc 15 p2426 A66-29735

**BOGOLIUBOV THEORY**

First approximations of kinetic theory for homogeneous and unstable plasma obtained from generalized Bogoliubov method 01 p0111 A66-10389

Bogoliubov adiabatic hypothesis in quasi-linear theory of plasma 01 p0115 A66-11088

Low temperature excitation spectrum for ferro- and antiferromagnets with large crystalline field splittings 05 p0741 A66-15867

Spectrum and eigenstates of Bardeen-Cooper-Schrieffer /BCS/ reduced Hamiltonian in theory of superconductivity 08 p1276 A66-19446

Chapman-Enskog method applied to equations obtained when Bogoliubov functional assumption is introduced into BBGKY hierarchy, determining transport coefficients 14 p2276 A66-27640

Prekinetic equations for multicomponent plasma, generalizing Bogoliubov theory 18 p3148 A66-34906

Potential of average force experienced by charge in plasma calculated from Bogoliubov-Born-Green-Kirkwood-Yvon equations of classical statistical mechanics without linearization 19 p3406 A66-35996

Quantum theory of laser model, deriving kinetic equations for radiation and single-particle density matrices, using Bogoliubov expansion procedure 19 p3374 A66-36008

**BOHR THEORY**

Theorem on quotients of complex-valued almost periodic functions of one real variable containing Bohr theorem 06 p0904 A66-17043

**BOILING**

**SA EVAPORATION**

**SA FILM BOILING**

**SA NUCLEATE BOILING**

**SA VAPORIZATION**

Book on boiling heat transfer and two-phase flow 06 p0971 A66-16610

Minimum heat transfer levels and vapor formation in boiling liquid metals 06 p0972 A66-16843

Pool boiling potassium, discussing heat flux behavior, experimental setup and results for burnout heat flux 07 p1152 A66-17593

Nucleation and boiling liquids phenomena, using Clapeyron equation in expressing saturation curve 07 p1154 A66-18029

Boiling heat transfer in liquid metals including boiling instability, superheats, two-phase flow, forced convection, heat flux, etc 08 p1316 A66-18684

Contact area of boiling bubbles observed through electroconductive glass/heating surface/ into tank 08 p1320 A66-19556

Time variation in boiling heat transfer caused by bubble generation 08 p1320 A66-19557

Soviet and foreign papers on physics of boiling including heat transfer, heat release, bubbling processes, kinetics and sonic aspects of boiling and bibliography 09 p1469 A66-20100

Critical heat flux under forced motion of underheated alcoholic aqueous solutions 09 p1470 A66-20148

Reversible thermodynamics laws applied to boiling, assuming uniform temperature and pressure for vapor and liquid phases 12 p1974 A66-23531

Critical heat flow for propagated heat exchange crises during boiling of liquid 14 p2410 A66-26787

Correlations between Lennard-Jones potential parameters and critical and boiling point constants of 28 nonpolar and 17 polar gases 15 p2618 A66-29718

Thermodynamic analysis of Hg-Cd and Hg-Bi alloys, noting enthalpies and entropies of mixing, boiling point and phase diagrams, vapor pressure measurements, etc 17 p3037 A66-33289

Vapor-fin heat rejection system employing boiling-condensing cycle, noting performance characteristics 18 p3055 A66-34381

Soviet and foreign papers on physics of boiling covering heat transfer, heat release, bubbling processes, kinetics and sonic aspects of boiling, including bibliography 21 p3834 A66-38509

**BOILING WATER REACTOR**

Thermal conditions in boiling liquids including container wall damage-flux density relationship, stable and unstable boiling in bubble evaporation region and film vaporization 07 p1154 A66-18066

Delay time for bubble formation associated with heating surface thermal layer formation in water moderated reactors 17 p2956 A66-32271

**BOLOMETER**

Electric resistivity of carbon resistor material determined as temperature function, calculating static response characteristics of carbon bolometer 02 p0228 A66-11445

Thermoelectric cooling of IR detectors, examining thermistor bolometers and photoconductive detectors 08 p1221 A66-18683

Output power of CW laser measured by wire bolometer in form of plane single-layer spiral as sensitive element 09 p1381 A66-20364

Output power of CW laser measured by wire bolometer in form of plane single-layer spiral as sensitive element 19 p3353 A66-35321

Sputtering, slurry and doctor-blade techniques for depositing thin thermistor films of lanthanum-doped barium-strontium-titanate for bolometer application 23 p4109 A66-41127

Bolometer mount efficiency measurement technique by impedance



method 24 p4205 A66-42104  
 Precision microwave power measurement  
 methods noting calorimetry, bolometry and  
 thin film 24 p4184 A66-42649

**BOLT**  
 High strength structural bolts under static  
 loadings of tension and 02 p0301 A66-12241  
 shear  
 Load partition in double-lap butt joints for  
 bearing type connections including  
 expressions for stress-strain relationship and  
 bolt shear deformation 02 p0302 A66-12242  
 Stress distribution in bolted fastenings  
 noting effects of internal and external  
 forces on deformation, energy and screw  
 mechanism and methods of  
 calculation 06 p0964 A66-16480  
 Aluminum screw coupling resistance to  
 stresses as affected by profile, thread depth  
 and composition 15 p2509 A66-29118  
 Stress level for crack initiation and  
 propagation and delayed failures in stainless  
 steel used for bolts 17 p2941 A66-33442

**BOLTZMANN DISTRIBUTION**  
 Axial variation of plasma column density in  
 nonuniform axial magnetic field determined  
 by theory for ambipolar diffusion and  
 Boltzmann transport 06 p0917 A66-16649  
 Self-consistent equilibrium configuration of  
 s-component plasma representing infinitely  
 extended plane layer consisting of periodic  
 sequence of current  
 quasi-filaments 07 p1085 A66-17646  
 Temperature and environment effect on  
 absorption spectra of two-level system,  
 using stochastic model and Green  
 function 09 p1348 A66-20959  
 Boltzmann modulus used to predict stress-  
 strain design parameters of viscoelastic  
 materials, including time as  
 variable 11 p1783 A66-23172  
 Small two-dimensional oscillations in XY  
 plane for isothermal magnetosphere in  
 uniform gravitational field, postulating  
 Boltzmann equilibrium density  
 distribution 12 p1943 A66-24282  
 Existence of dense and dilute distinct  
 phases in one-dimensional classical fluids  
 consisting of finite particles obeying  
 Boltzmann statistics and potential wells of  
 finite range 18 p3099 A66-34203  
 Wall term in Boltzmann H relationship  
 leads to increase in entropy for solutions to  
 Boltzmann equations 19 p3401 A66-35584

**BOLTZMANN EQUATION**  
**SA CHAPMAN-ENSKOG METHOD**  
 Equilibrium thermodynamics from  
 transport theory including interaction  
 studied up to second virial coefficient,  
 determining velocity of first sound and zero  
 sound 01 p0161 A66-10327  
 Kinetic theory of Lorentz plasma in  
 rotating magnetic fields and electromagnetic  
 fields based on Boltzmann  
 equation 01 p0113 A66-10640  
 Cauchy problem for linearized Boltzmann  
 equation in kinetic theory of  
 gases 01 p0107 A66-11011  
 Existence and uniqueness of Cauchy  
 problem for Boltzmann equation describing  
 flow past convex body of rarefied gas of  
 structureless particles 02 p0261 A66-12022  
 Locally Maxwellian solution of Boltzmann  
 kinetic equation 02 p0251 A66-12182  
 Equation for singlet distribution function  
 as quantum-mechanical analog of Boltzmann  
 equation 03 p0391 A66-12340  
 Cylindrical plasma rotational velocity  
 formulas derived by calculating Boltzmann  
 collision integral in stationary momentum  
 equation 04 p0556 A66-14339  
 Boltzmann-Landau equation to calculate  
 transport coefficients of moderately dense  
 quantum gases 04 p0549 A66-14478  
 Adherence of gas to wall, investigating  
 Boltzmann equations for perfect fluid,  
 Prandtl-type flow and state of rest  
 fluid 05 p0661 A66-14535  
 Microinstabilities in collisionless plasma  
 due to Boltzmann  
 equation 05 p0726 A66-15253  
 Structure of solutions of chain of  
 equations for deriving Boltzmann kinetic  
 equation of gases 05 p0663 A66-15344  
 Solution to Liouville equation, obtaining  
 expression for singlet distribution function  
 for system under arbitrary perturbation

from equilibrium, leading to solution of  
 linear Boltzmann  
 equation 06 p0912 A66-16633  
 Hot electron transfer from light mass  
 central valley to surrounding heavy-mass  
 satellite valleys in n-type gallium arsenide,  
 indium phosphide and cadmium telluride  
 analysis based on Boltzmann  
 equation 06 p0929 A66-17035  
 Convergence of Chapman-Enskog expansion  
 for linearized Boltzmann equation, using  
 perturbation theory 07 p1081 A66-17935  
 methods  
 Two-fluid shock wave model involving  
 Boltzmann equation and inelastic collision  
 theory for rarefied gas 08 p1204 A66-18524  
 Anomalies in low temperature properties  
 of noble metal alloys such as thermoelectric  
 power and nonmonotonic behavior of  
 resistivity with  
 temperature 08 p1274 A66-19362  
 Width of strong shock wave front and  
 transition layers estimated, using Boltzmann  
 kinetic equation and  
 H-theorem 08 p1209 A66-19478  
 Kinetic model construction of maximum  
 number of Boltzmann collision integral  
 properties 08 p1259 A66-19577  
 Collisional transition between lower  
 atmosphere and collisionless exosphere  
 analyzed, using integral formulation of  
 Boltzmann equation and collision  
 models 09 p1459 A66-20882  
 Exact solutions of Boltzmann equation with  
 Maxwellian distribution  
 law 10 p1557 A66-21316  
 Neutral disparate mass mixtures, replacing  
 Boltzmann collision integrals by relaxation-  
 type kinetic models with model equation  
 terms ordered according to mass ratio,  
 deriving two-fluid transport  
 equations 10 p1523 A66-21802  
 Perpendicular shock wave structure in  
 plasma, using Boltzmann ionized gas  
 equations 10 p1566 A66-21812  
 Boltzmann equation for Gunn effect in  
 GaAs, discussing scattering processes,  
 unjustifiability of use of drifted Maxwell  
 distribution, etc 10 p1583 A66-22067  
 Cauchy problem for linearized Boltzmann  
 equation, deriving high accuracy equations  
 of motion of rarefied  
 gases 11 p1735 A66-22338  
 Numerical calculations of axially symmetric  
 two-dimensional steady expansions of  
 monatomic gas, using approximate  
 Boltzmann equation with Krook collision  
 term 11 p1690 A66-22908  
 Iterative solution to shock wave structure  
 in highly rarefied flows through kinetic  
 theory and full Boltzmann  
 equation 11 p1690 A66-22910  
 Boltzmann equation behavior, at large  
 Knudsen numbers, for free molecular  
 interactions with infinite collision cross  
 section 11 p1691 A66-22918  
 Discrete ordinate technique for solution of  
 distribution function of linearized Boltzmann  
 equation, with application to Couette  
 flow 11 p1692 A66-22923  
 Internal flow problems in free, nearly free  
 molecular regimes and higher transition  
 flows, using Boltzmann equation and series  
 expansion to solve integral equation for  
 surface collision density 11 p1693 A66-22940  
 Breakdown regime of diffusion-controlled  
 HF resonance gas discharge analyzed  
 kinetically, solving Boltzmann equation for  
 electron distribution  
 function 11 p1740 A66-23081  
 Relaxation of isotropic distribution of test  
 particles in homogeneous background gas,  
 including nonzero temperature  
 effects 11 p1741 A66-23390  
 Boltzmann transport equation solution for  
 electrons in ionized gas with nonuniform  
 electron concentration 12 p1916 A66-23728  
 Gradient  
 Fourier transform of time-dependent  
 density-density correlation function  
 calculated from linearized Boltzmann  
 equation for Maxwell  
 molecules 12 p1917 A66-24584  
 Brillouin scattering by gases as  
 experimental test of kinetic theory away  
 from hydrodynamic  
 regime 12 p1917 A66-24585  
 Transport coefficients of moderately dense

gas calculated by three methods based on  
 correlation function or generalized  
 Boltzmann equation 12 p1979 A66-24586  
 Boltzmann transfer equation for electrons  
 and generation of nonlinear second harmonic  
 of current density in inhomogeneous  
 plasma 12 p1924 A66-24806  
 Milne-Eddington model in heat and mass  
 transfer, showing analogy between radiation  
 and particle transfer and correspondence to  
 simplified Boltzmann  
 equation 13 p2208 A66-25162  
 Landau damping of transverse oscillations  
 in collisionless plasma at ion cyclotron  
 resonance and collisional damping in zero-  
 temperature plasma 13 p2142 A66-25706  
 Binary-collision expansion for viscosity of  
 two-dimensional gas of hard disks, showing  
 dynamical origin of divergence appearing in  
 first correction of Boltzmann  
 equation 13 p2136 A66-26276  
 Rarefied gas mechanics based on  
 Boltzmann equation with prescribed  
 boundary conditions 13 p2071 A66-26726  
 Space and time dependence of particle  
 density and current in semiconductor  
 material 14 p2356 A66-27045  
 Existence and uniqueness of Cauchy  
 problem for Boltzmann equation describing  
 flow past convex body of rarefied gas of  
 structureless particles 14 p2334 A66-27573  
 Finite difference solution of nonlinear  
 boundary value problem of Landau-Vlasov  
 equation for charged particle for Maxwellian  
 distribution function 14 p2344 A66-27625  
 First order in density corrections to  
 transport coefficients of moderately dense  
 gas /viscosity and thermoconductivity/,  
 using Boltzmann equation 14 p2276 A66-27636  
 Integral equations defining transport  
 coefficients of moderately dense gas  
 obtained from Boltzmann equation shown to  
 be identical to first order in density, with  
 results obtained by autocorrelation function  
 method 14 p2276 A66-27639  
 Chapman-Enskog method applied to  
 equations obtained when Bogoliubov  
 functional assumption is introduced into  
 BBGKY hierarchy, determining transport  
 coefficients 14 p2276 A66-27640  
 Boltzmann equation for gas acted upon by  
 relativistic forces in fibered state  
 space 14 p2335 A66-27938  
 Quasi-linear perturbation theory of  
 transverse electromagnetic waves from  
 instabilities in nonthermal magnetoactive  
 plasma, using Boltzmann equation, applied to  
 magnetospheric MHD  
 emissions 14 p2286 A66-27982  
 Solution to dispersion equation of  
 linearized Boltzmann equation in kinetic  
 theory of rarefied gases, noting root  
 behavior and distribution function  
 structure 14 p2278 A66-28285  
 Second law of thermodynamics, discussing  
 Clausius and Boltzmann mathematical  
 expressions of entropy, role of  
 irreversibility and relationship between  
 increase of entropy and increase of  
 disorder 15 p2616 A66-29062  
 Rarefied gas flow described by Boltzmann  
 equation 15 p2477 A66-29175  
 Electromagnetic propagation in weakly  
 ionized plasma, deriving electronic  
 distribution function and dielectric  
 permittivity tensor 15 p2552 A66-29331  
 Boltzmann equation for Pitot tube  
 problem, using distribution function,  
 deriving equations for rarefied gas flow in  
 impact tube under hypersonic and adiabatic  
 conditions 15 p2481 A66-29739  
 Small-signal energy conservation theorem  
 for one-dimensional multiveLOCITY electron  
 beam according to Boltzmann and  
 multistream descriptions 15 p2467 A66-29755  
 Moment equations from collisionless  
 Boltzmann equation solved by  
 transformation into polarized  
 coordinates 15 p2555 A66-29784  
 Structure of solutions of chain of  
 equations for deriving Boltzmann kinetic  
 equation of gases 15 p2482 A66-29972  
 Collisionless Boltzmann and Maxwell  
 equations for plasma instability of plasma  
 without external magnetic field for  
 transverse oscillation propagating  
 perpendicular to streams 16 p2760 A66-30817  
 Iterative solution to Krook-Boltzmann



- kinetic equation noting Navier-Stokes numerical solution, computation and analysis of distribution function within shock wave 16 p2685 A66-30945
- Monte Carlo solutions to two molecular flow problems, heat transfer between parallel walls and shock wave profile-computer programmed in Boltzmann equation analysis 16 p2686 A66-30946
- Mathematical model for analysis of wave propagation in linearized vertically nonuniform partially ionized gas, proceeding from Maxwell and Boltzmann equations 16 p2761 A66-31005
- Trapped electron effect and stationary longitudinal wave propagation in Maxwellian hot plasma based on exact solution of nonlinear collisionless Boltzmann equation compatible with equilibrium electron distribution 16 p2761 A66-31009
- Secondary electron interaction with solid state plasma, noting energy distribution, Boltzmann equation solution, etc 16 p2789 A66-31783
- Nonlinear theoretical derivation of creep equations for three-dimensional processes in polymers, based on Boltzmann-Volterra creep heredity concept using stress-strain summation 17 p2943 A66-32807
- Linearized model of Boltzmann equation to examine problems of kinetic theory of nonuniform gases 17 p2911 A66-32961
- Boltzmann equation, interpreted in terms of certain correlation functions known as product densities, applied to fluctuation theorem and gases and liquids not in equilibrium 18 p3136 A66-34706
- High magnetic field limit of shock wave in steady state model plasma moving along x axis studied transverse to magnetic field 18 p3148 A66-34905
- Potential of average force experienced by charge in plasma calculated from Bogoliubov-Born-Green-Kirkwood-Yvon equations of classical statistical mechanics without linearization 19 p3406 A66-35996
- Microwave transmission through turbulent plasma of Zeta machine, examining transport theory by use of Boltzmann equation 19 p3429 A66-36584
- Nonrelativistic equations of bulk motion of relativistic /cosmic ray/ gas derived by taking moments of collisionless Boltzmann equation 20 p3649 A66-37327
- Electron energy distribution function obtained by Druyvesteyn analysis in low-current positive column neon discharge compared with theoretical distribution function 20 p3608 A66-37463
- Critical parameters in Poisson-Boltzmann equation of steady state thermal explosion theory, noting temperature gradient 20 p3680 A66-38047
- Density of steady state gas flow expanding from viscous to molecular flow regime approximately calculated 21 p3723 A66-38507
- Asymptotic time behavior of longitudinal waves in one-dimensional plasma of relativistic electrons and stationary ions studied, using collisionless Boltzmann equation 21 p3775 A66-39189
- Electron-collision-induced magnetoplasma instability, using Boltzmann equation for wave dispersion 21 p3794 A66-39571
- Boltzmann-Krook equation in Knudsen layers for Rayleigh shear flow and related flow of rarefied gas 21 p3731 A66-39578
- Boltzmann equation for dilute monatomic gases, discussing asymptotic interpretation of Hilbert and Chapman-Enskog theories 23 p4097 A66-42011
- Numerical solution of Boltzmann kinetic equation for weakly ionized plasma in thermoelectronic converter 24 p4239 A66-42871
- Convective processes in magnetoactive plasma flows transverse to homogeneous magnetic fields, based on multifluid equations derived from Boltzmann equation for ionization and recombination reaction 24 p4245 A66-43069
- BOLTZMANN-VLASOV EQUATION**
- Initial value problem for Boltzmann-Vlasov and Poisson equation for one-dimensional plasmas 06 p0915 A66-16161
- Response of spherical plasma probe to alternating potentials determined by Boltzmann-Vlasov equation together with Maxwell equations 11 p1746 A66-23070
- Transverse magnetic field effect on drifting hot plasma resonance peaks, noting oscillation mechanism and application of successive moments of Boltzmann equation 13 p2144 A66-25725
- Instability of three-or four-component beam plasma for various coupling waves, graphically analyzing dispersion equation derived from Boltzmann-Vlasov equations 18 p3146 A66-34472
- Third moment equation derived from Boltzmann-Vlasov equation for wave propagation in plasmas with very strong magnetic field used instead of state equation 20 p3521 A66-38363
- BOLZA PROBLEM**
- Variational and optimal control theory discussing extension of McShane and Pontryagin methods to general problem of Bolza 04 p0505 A66-13988
- Lagrange and Mayer problems of optimal control of cost 11 p1680 A66-23277
- Necessary conditions of calculus of variations applicable to optimization of control processes dependent on discontinuity point time and location 16 p2672 A66-31520
- Deduction procedure for generalized Clebsch necessary condition for singular extremals for which final form of accessory minimum problem is nonsingular Bolza problem 22 p3940 A66-40530
- BOMBARDMENT**
- S AURORAL BOMBARDMENT
- S ELECTRON BOMBARDMENT
- S ION BOMBARDMENT
- S NEUTRON BOMBARDMENT
- BOMBER AIRCRAFT**
- Hypothetical linear programming model for minimizing cost of aerial tanker support of practice bomber mission 06 p0805 A66-16349
- Flexibility in strategic retaliatory weapons offered by bombers and missiles, discussing defense capability offered by SAC 08 p1322 A66-18558
- Weight empty estimation methods evaluated for transports and bombers ranging in weight from 78 to 488 klb 11 p1783 A66-23002
- BONDING**
- SA ADHESION
- SA CERAMIC BONDING
- SA CHEMICAL BOND
- SA DIFFUSION BONDING
- SA JOINT
- SA METAL BONDING
- SA METAL-METAL BONDING
- SA MOLECULAR BONDING
- SA RESIN BONDING
- SA SOLDERING
- SA WELDING
- Photoelastic investigation of stresses in cemented joints, particularly scarf and butt bonding 02 p0298 A66-11582
- Thermocompression bonding applied to integrated circuits of semiconductor and thin film type, noting resistance, ultrasonic and electron beam welding 12 p1846 A66-24916
- Thermoconductivity, mechanical stress, processing characteristics, etc, of various adhesives used in integrated circuits, noting neoprene cement 18 p3077 A66-34051
- Nondestructive testing of adhesive bonded structures using ultrasonic-resonant instrument, noting detection of voids and cohesive strength determination 19 p3362 A66-35329
- Tungsten and tungsten composite fabrication by gas-pressure-bonding process 19 p3368 A66-36123
- Testing of adhesive bonding at high temperatures for use in reentry vehicles, using IR energy on specimen preloaded in shear [ASME PAPER 66-MD-38] 21 p3742 A66-38488
- Adhesives and joining processes in mechanical quality control 21 p3745 A66-39465
- Adhesively bonded joints withstand severe thermal shock and have excellent bonding with high strength structural alloys in cryogenic liquids 22 p3937 A66-39778
- Microbonding difficulties in joining flat pack circuits to printed circuit boards, examining parallel gap welding connections
- with board material and use of dissimilar metals 23 p4043 A66-41189
- Face-bonding technique for attaching semiconductor chips to thin film or similar circuits 23 p4043 A66-41193
- Vacuum coating techniques for thin film layers for bonding, examining adhesion, bonding layer reinforcement and surface oxidation 23 p4043 A66-41194
- BONE**
- SA RIB
- Stress-strain relationships for tension, compression and shear of femoral bone loaded longitudinally and transversely [ASME PAPER 65-WA/HUF-7] 05 p0626 A66-15698
- Effect of varying strain rate on physical properties of bone and muscle tissue, measuring load and time displacement with constant-velocity compression test machine [ASME PAPER 65-WA/HUF-9] 05 p0626 A66-15699
- Bone calcium loss during two weeks of simulated weightlessness, using X-ray wedge technique 11 p1643 A66-22577
- BONE MARROW**
- Hypoxia protection on taking of second graft of homologous bone marrow in previously irradiated and grafted mice 01 p0020 A66-10609
- Chromosome injury in mouse bone marrow due to distant ionizing radiation 12 p1806 A66-24396
- Effect of combined action of accelerations, vibration and radiation of nuclei of bone marrow cells in mice 15 p2437 A66-29478
- BOOLEAN ALGEBRA**
- Necessary conditions for realization of Boolean threshold function by means of real threshold elements 04 p0504 A66-13968
- Book on switching theory covering circuit synthesis and analysis, Boolean algebra, functional theory, relay type network, etc 06 p0861 A66-16197
- Ternary-pentary majority algebra, Boolean-to-majority function conversion, and derivative identities 08 p1188 A66-19672
- Neural, threshold, majority and Boolean logic techniques compared for reliability and efficiency in adaptive machines and data handling systems 11 p1659 A66-22300
- Multithreshold threshold element design, discussing realization based on Boolean functions, network synthesis employing transformation technique and logical design application 13 p2039 A66-25803
- Integrated circuit binary counters using majority logic current mode gate element 14 p2255 A66-27803
- Ternary-pentary majority algebra, Boolean-to-majority function conversion and derivative identities 20 p3522 A66-37264
- Parallel evaluation of Boolean function in search memory via multiwrite 20 p3523 A66-38017
- Boolean algebraic analysis of AND, OR, NAND and NOR functions in electronic integrated circuits 21 p3720 A66-39625
- BOOM**
- SA SONIC BOOM
- Solar environment and aerodynamic drag effect on deflection of structural booms in space [AIAA PAPER 66-502] 16 p2821 A66-31478
- BOOSTER**
- Engine thrust and heat mass in air breathing jet engine for space flight 04 p0572 A66-13441
- Design and comparison of apogee impulse systems developed for booster rocket thrust augmentation 04 p0573 A66-13541
- Engines for supersonic and hypersonic aircraft to be used in next decade, noting suitability for cruise aircraft or boosters 09 p1435 A66-20668
- Instrumentation of bending moments on large space boosters, discussing ground wind restrictions, telemetry system used, data transmission link, etc 19 p3356 A66-35678
- Turbine engines and ramjet for SST and space boosters 22 p3971 A66-40123
- Economics of various orbital boosters from completely expendable to completely recoverable vehicles, noting concept of cost-optimum vehicle 23 p4133 A66-41775
- BOOSTER RECOVERY**
- Saturn S-IVB stage adaptation for complete stage recovery by incorporating modification



kit including all recovery system elements 17 p3016 A66-32372  
 Recoverable space boosters, discussing technological and economic aspects of reuse 19 p3469 A66-36082  
 Rescuing men and equipment in space by manned rescue craft, unmanned craft, personal ejection capsules, etc 20 p3665 A66-38254  
 Saturn S-IVB stage adaptation for complete stage recovery by incorporating modification kit including all recovery system elements 22 p3986 A66-39776  
 Saturn booster recovery by means of drag balloon which converts to hot air balloon for final recovery 22 p3987 A66-40608

# BOOSTER ROCKET

## S ROCKET BOOSTER

## BOOTSTRAP EQUATION

Liquid hydrogen flow system performance during startup transient of nuclear rocket measured in full-scale simulated engine system, approximating in-flight exhaust conditions 12 p1911 A66-23699  
 Elementary particle theory, interactions at accelerator energies, bootstrap mechanism for generating bound states and resonances and Regge pole concept applied to high energy scattering 15 p2545 A66-29548

## BORANE

### SA DECBORANE

### SA DIBORANE

### SA PENTABORANE

Molecular configuration of bis /ortho-dodecacarborane/ determined by three-dimensional X-ray crystallography 06 p0822 A66-16631  
 Fine structure of vibrational-rotational spectrum of difluoroborane and difluoroborane-d 08 p1178 A66-18935  
 Pyrolysis of boranes using mass spectrometer at increasing temperatures, observing tetraborane, diborane, pentaboranes, etc 12 p1812 A66-23632  
 Spectroscopic analysis of isotope shift between tetraborane /10/ and pentaborane /11/ 15 p2446 A66-29236  
 Chemical kinetics of borane and diborane compounds, decomposition rates and molecular dissociation energy 15 p2447 A66-29237

## BORATE

Mass spectra of isotopically labeled tetraboranes obtained under zero ion source contact conditions, observing parent peak and metastable transition 16 p2647 A66-31379

## BORIDE

### SA DIBORIDE

### SA HEXABORIDE

### SA TITANIUM BORIDE

Metallographic identification of borides in Udimet 700 08 p1237 A66-18765  
 Saturation conditions and alloying elements effect on depth, phase composition and properties of borided layer 14 p2316 A66-27831

## BORN APPROXIMATION

Ionization cross section of ground state helium cation by electron impact in Born exchange approximation 04 p0549 A66-14312  
 Radiation unit of length, calculating path-length for passage of high-energy electrons and photons through matter 06 p0912 A66-16575  
 Vibrational excitation cross sections of diatomic molecules calculated, using Born approximation by including polarization interaction between incident electron and molecule 06 p0912 A66-16630  
 Quantitative comparison of systematic approaches to generation of inelastic impact cross section with aid of simple universal excitation cross section function [AIAA PAPER 66-150] 06 p0913 A66-17097  
 Born approximation applied to electromagnetic scattering from finite cone to determine radar cross section 10 p1500 A66-21616  
 Born approximation of cross sections for electron and proton impact ionization of Na and Mg 11 p1737 A66-22496  
 Born-exchange and Ochkur approximations used to calculate electron impact ionization cross sections for He, Li, Be, Na and Mg atoms in ground states 11 p1737 A66-22497  
 Electron impact ionization cross section of H/2s/ and H/2p/ in Born A, Born B, Born-Ochkur and classical

approximations 11 p1738 A66-22498  
 Bethe-Born approximation and partial ionization cross sections of singly and doubly charged helium and neon ions 14 p2336 A66-26830  
 Bethe-Born approximation and partial ionization cross sections of argon, krypton and xenon ions 14 p2336 A66-26831  
 Quantitative comparison of systematic approaches to generation of inelastic impact cross section with aid of simple universal excitation cross section function [AIAA PAPER 65-150] 15 p2545 A66-29268  
 Slow electron excitation cross section for polar molecule rotational and vibrational transitions based on Born approximation and point-dipole interaction 15 p2545 A66-29395  
 Augmented Born approximation based on variational principles applied to electromagnetic scattering from inhomogeneous dielectric spheres of finite extent 18 p3071 A66-34452  
 Second Born and Born-exchange approximations used in calculation of ionization cross sections for Fe XV and Fe XVI 19 p3403 A66-36325  
 Excitation of ground state hydrogen atoms by fast protons, evaluating total Born cross section in limit of infinitely massive protons 19 p3403 A66-36333  
 Born approximation for phase shift of microwaves scattered from underdense cylindrical plasma used to determine plasma electron density 21 p3794 A66-39572  
 Excitation of hydrogen molecule from ground state to B and C electronic states by electron impact, using one-center wave functions of Huzinaga together with Born approximation 23 p4098 A66-41360

## BORN-INFELD THEORY

Relativistic electrodynamics of moving medium, discussing Maxwell-Minkowski equations, Born equations, field vector transformations, etc 12 p1915 A66-24650

## BORON

Boron addition induced nickel heat resistance measured by internal friction as function of elastic oscillations 05 p0699 A66-14690  
 Radiative lifetimes of strongest vacuum UV multiplets of B I, B II, C I, C II, N I and N II measured by phase shift method 07 p1083 A66-18423  
 Anomalous diffusion of boron parallel and perpendicular to dislocation arrays in grain boundary contained in silicon 10 p1574 A66-21356  
 Boron, Volume 2, Preparation, properties and application 10 p1579 A66-21718  
 Semiconductor properties including conductivity, resistivity, band gap, optical absorption, etc, analyzed on very pure and doped beta-rhombohedral boron 10 p1579 A66-21719  
 Electrical and optical experiments performed on single crystals of beta-rhombohedral boron, noting resistivity decrease and differences between thermal and optical band gap 10 p1579 A66-21720  
 Optical and electrical constants of beta-rhombohedral boron 10 p1579 A66-21721  
 Electric and photoconductivity of vacuum sintered and zone refined semiconductor boron 10 p1579 A66-21722  
 Trap dominated conductivity changes and optical absorption phenomena in near IR in crystalline beta-rhombohedral boron 10 p1580 A66-21723  
 Electron paramagnetic resonance, electrical conductivity and impurity diffusion in doped boron 10 p1580 A66-21724  
 Magnetoresistance of crystalline beta-rhombohedral boron and amorphous boron film as function of magnetic field, temperature, specimen purity and crystal orientation 10 p1580 A66-21725  
 Vacuum deposited amorphous boron films, presenting structure, optical measurements and electrical properties 10 p1580 A66-21726  
 Boron filament tensile and flexural strength affected by surface and internal flaws with chemical polishing 10 p1548 A66-21728  
 Boron semiconductor devices acting as contactless switches, based on current vs voltage characteristics of boron 10 p1511 A66-21729  
 High precision photoelectric scan at 8667-

8668 angstrom wavelengths in solar spectrum for identification and abundance of boron 11 p1771 A66-22777  
 Dispersion hardening of titanium carbide by boron doping from critical resolved shear stress measurements 11 p1719 A66-2339  
 Role of discontinuous fibers /whiskers/ in forming composites and how reinforcing parameters and processing vary from those used in continuous fibers systems, noting differences between boron and fiberglass whisker characteristics 13 p2113 A66-2531  
 Single-configuration open-shell calculation for ground state of boron isoelectronic sequence, using doublet-spin-state wave function 16 p2750 A66-3012  
 Boron film characteristics and preparation by direct resistance heating of elements boron filaments 16 p2778 A66-3107  
 Changes in massive amorphous boron filaments by heat treatments under reduced pressures and in presence of inert gases 17 p2943 A66-3285  
 Structural chemistry of boron compounds analyzed by X-rays, examining effects of increasing boron-to-metal ratio of boron-containing crystal structure 18 p3064 A66-3438  
 Boron abundance in Sun from B I line and solar spectra 19 p3458 A66-3549

## BORON ALLOY

Vacuum thermal etching of nickel and etc figure development by boron addition 03 p0383 A66-1312

## BORON CARBIDE

Conditions of preparation and properties of pseudobinary boron carbide-boron silicide hard alloys 08 p1239 A66-1889  
 Apparatus for melting boron carbide inductively on water-cooled hearth, noting application to other refractory materials 13 p2088 A66-2656  
 Hydrocarbon fuel cell anodes containing boron carbide as support for platinum electrocatalyst 14 p2226 A66-2790  
 Boron carbide as potential substitute for platinum as catalyst for fuel cell cathodes 14 p2227 A66-2817

## BORON CHLORIDE

Dichloroborane synthesized in quantitative yields by thermal hydrogenation of boron trichloride 05 p0629 A66-1458

## BORON COMPOUND

Surface ionization of Cs atoms on lanthanum hexaboride cathode with intrinsic thermionic emission of cathode observed from mass-spectrometric measurement of ion current 06 p0912 A66-1688  
 Rotating bomb calorimetric technique determining accurate values of enthalpy of combustion of boron and boron compounds 08 p1178 A66-1906  
 Compressive strength and instability failure mechanism in uniaxial boron fiber metal matrix composite material 08 p1240 A66-1911  
 High temperature, electrically insulating refractory tubes of boron carbonitride for protection of metal thermocouples 17 p2944 A66-331  
 Inorganic thin film surface finish for boron filaments, noting improved adhesion organic resins and high temperature oxidation resistance 23 p4082 A66-4187

## BORON FLUORIDE

Detection of slow neutrons escaping from atmosphere by counters filled with boron fluoride onboard high altitude balloons 05 p0754 A66-1541  
 Neutron intensity increase observed from boron fluoride proportional counter at high altitude associated with auroral zone X-ray event 07 p1121 A66-1791  
 Atmospheric fast cosmic ray neutron flux measurements, using boron fluoride recording neutron counter 15 p2584 A66-2958  
 Atmospheric neutron flux measured by balloons, using polyethylene-moderated boron fluoride counter 18 p3197 A66-3481  
 Electrical conductivities of boron trifluoride in chlorine and bromine trifluorides studied as function of temperature and concentration 19 p3295 A66-3633

## BORON HYDRIDE

Chemistry of decaborane and structure and reactivity of stable derivatives 11 p1649 A66-2291



- Molecular orbital method for boron hydrides from self-consistent field, analyzing dipole moments, ionization potentials, molecular charge distributions, wave functions, etc 17 p2870 A66-32851  
Methylene blue action in reversing decabore-mediated norepinephrine depletion 22 p3853 A66-39788
- BORON NITRIDE**  
Interaction energies of Ne, Ar, Kr, Xe N-2 and CH-4 near semiinfinite hexagonal boron nitride lattice at potential minimum 08 p1178 A66-18936  
Synthesis conditions for materials of B-Al-N system determined by sintering mixtures of BN plus Al and AlN plus B powder in nitrogen atmosphere 11 p1720 A66-23473  
Chemical stability of silver graphite, molybdenum disulfide, zinc oxide, boron nitride, muscovite and phlogopite mica solid lubricants 16 p2715 A66-31675
- BORON OXIDE**  
Vanadium pentoxide-boron oxide-lead oxide system IR absorption spectra and electroconductivity 10 p1582 A66-21917  
Composition and combustion products of boron at 300 to 3200 degrees K and heat of formation of boron oxide 16 p2830 A66-31604
- BOSE-EINSTEIN STATISTICS**  
High pressure high current argon discharge covering statistical variations of nonblack body, photon and IR radiation and measurement with InSb photodiode 05 p0720 A66-14507  
Flux quantization, Josephson tunneling and persistent currents in superconductor studied by model of charged Bose gas at zero K 09 p1417 A66-20034  
Ground state energy of charged Bose gas obtained from pair Hamiltonian and Green functions 11 p1741 A66-23392  
Bose-Einstein distribution function for quantum photons from amplified spontaneous emission 14 p2307 A66-27195  
Near-Bose-Einstein probability distribution of photoelectron counts produced by He-Ne gas laser narrow band Gaussian light source operating slightly below oscillation threshold 16 p2717 A66-30645  
Kinetic equations in hydrodynamic approximation for weakly reacting and excited Bose systems, finding asymptotic expressions for Green function 23 p4055 A66-41412  
Bose-Einstein distribution function for quantum photons from amplified spontaneous emission 24 p4226 A66-43093
- BOSON**  
Magnetic properties of ideal gas of charged bosons and fermions as affected by dimensionality n of containing space 03 p0409 A66-12630  
Hypothesis of two intermediate bosons to explain K-2 meson anomalous decay, exploring relation to gravitational and cosmological theories 05 p0718 A66-15348  
Magnetization using Hartree-Fock approximation in terms of boson distribution for uniformly interacting spins system 07 p1084 A66-18441  
Normal ordering method of solving boson equations leading to closed solutions of Schroedinger and density operator equations in certain cases only 17 p2945 A66-32293  
Charged Bose gas, discussing ground-state energy, excitation spectra and plasmon-particle interactions, using Bohm-Pines and Bogoliubov approximations 18 p3140 A66-34729
- BOSON FIELD**  
Superfluid hydrodynamics and kinetic theory of superfluids, noting relation of macroscopic concepts of Bardeen-Cooper-Schrieffer theory to microscopic characteristics 09 p1415 A66-20006  
One-boson Lee model of solvable field theory with nontrivial charge and mass renormalization as example of Lehmann-Symanzik-Zimmermann formalism 12 p1917 A66-24098
- BOUNDARY**  
**S FLUID BOUNDARY**  
**S FREE BOUNDARY**  
**S GRAIN BOUNDARY**  
**S INTERFACE**  
**S JET BOUNDARY**  
**BOUNDARY LAYER**  
**SA COMPRESSIBLE BOUNDARY LAYER**
- SA DRAG**  
**SA HYPERSONIC BOUNDARY LAYER**  
**SA LAMINAR BOUNDARY LAYER**  
**SA THERMAL BOUNDARY LAYER**  
**SA THREE-DIMENSIONAL BOUNDARY LAYER**  
**SA TURBULENT BOUNDARY LAYER**  
Free convection boundary layers on horizontal flat plate 01 p0161 A66-10434  
Vorticity distribution in wake of circular cylinder oscillating in unperturbed flow, using Burger linearization of Navier-Stokes equations 01 p0007 A66-10715  
Boundary layer effect on thrust of small rocket engines with high expansion ratio nozzles 01 p0130 A66-10791  
Temperature and wind velocity fields of stationary atmospheric boundary layer derived from semiempirical turbulence theory 01 p0062 A66-10859  
Graduate-level text on engineering MHD establishing bridge with plasma physics, using particle /microscopic/ and continuum approaches 01 p0114 A66-10978  
MHD boundary layer development on body set in motion by jerking movement where rate of formation of flow around body is greater than boundary layer 02 p0264 A66-11386  
Similarity of two-dimensional and axisymmetric boundary-layer flows for purely viscous non-Newtonian fluids 02 p0218 A66-11951  
Generalized dimensional analysis applied to wind distribution in planetary boundary layer, using motion 02 p0223 A66-11981  
Asymptotic representation of solutions for boundary layers near weak shock waves in conical flows 02 p0176 A66-12181  
Hydrodynamic flow against rotating disk noting magnetic field effect on torque, boundary layer thickness and velocity profile, applying motion equation 03 p0399 A66-12689  
Mathematical model for predicting heat transfer in vicinity of protuberances 03 p0444 A66-12763  
Falkner-Skan similar solutions for effects of longitudinal surface curvature on incompressible laminar boundary layer flows 03 p0355 A66-12786  
Unsteady boundary layer flow of multicomponent gas mixtures, investigating combustion instability in liquid and hybrid rocket motors [AIAA PAPER 65-41] 03 p0444 A66-12796  
Electrostatic probe performance interpreted by taking into account MGD boundary layer 03 p0399 A66-12800  
Pressure field of supersonic flow around hemi-axisymmetric body resting on flat plate 03 p0316 A66-12804  
Pohlhausen method application to stagnation point flow, noting failure for case of stretch wall caused by exclusion of MHD boundary layer compatibility condition 03 p0356 A66-12807  
Air intake with boundary layer trap, examining flow structure under external supersonic pressure and uniformity parameters [ONERA TP 288] 03 p0316 A66-12898  
Inner-outer expansion technique applied to MGD Rayleigh problem with infinite conductivity 04 p0549 A66-13368  
Effect of incompressible fluid flow boundaries on unsteady aerodynamic properties of thin curved profile undergoing small amplitude oscillations 04 p0454 A66-13574  
Thin ferromagnetic Fe-Ni films, discussing elastic tensile stresses on structure of interdomain boundaries and distribution of magnetization vectors 04 p0563 A66-13876  
Numerical solution of two-dimensional Navier-Stokes equations for confined wake formed by merging of two-plane Poiseuille flow streams 04 p0511 A66-13936  
Laminar flow development of incompressible - Newtonian fluid in hydrodynamic entrance region of flat duct 04 p0511 A66-13939  
Boundary layer relation between viscosity laws of perfect gas and equilibrium dissociating air 04 p0456 A66-14158  
Qualitative and quantitative solution of linearized approximations to boundary layer equations, noting free jet and wall-slot injection into moving stream [ASME PAPER 65-APMW-6] 04 p0512 A66-14212  
Vertical distribution of turbulence and wind velocity characteristics in atmospheric boundary layer, considering temperature stratification in boundary layer 04 p0542 A66-14301  
Diffusion in supersonic duct flow composed of boundary layers, with application to hypersonic inlet with internal compression [AIAA PAPER 64-245] 05 p0606 A66-15071  
Pressurization effect on fuselage drag of Boeing 720 jetliner based on boundary layer measurement 05 p0606 A66-15077  
Shielding of surface from parallel thermal radiation beams by distributed injection of fluid containing absorbing particles into boundary layer flow over surface near stagnation point [ASME PAPER 65-WA/HT-21] 05 p0789 A66-15643  
Temperature dependent thermal conductivity, considering one-dimensional plate problem with linearly varying heat conduction and constant-volumetric specific heat [ASME PAPER 65-WA/HT-29] 05 p0793 A66-15675  
Stagnation point heat transfer for binary air diffusion model including dissociation and ionization 05 p0665 A66-15775  
Dorodnitsyn approximate solution method applied to Crocco forms of first and second order incompressible two-dimensional boundary layer equations 05 p0685 A66-15776  
Boundary layer solutions for Rayleigh problem in MGD with Hall effect, using Karman-Pohlhausen technique 05 p0728 A66-15779  
Streamline curvature effect on mixing within boundary layer, deriving magnitude of concentration and pressure 05 p0665 A66-15798  
Boundary layer between argon plasma and solid wall at atmospheric pressure 05 p0728 A66-15815  
Influence of suction or injection in boundary layer flow past vertical flat porous plate in presence of uniform magnetic field 06 p0969 A66-16181  
Real flow and interference effects of body of revolution and stabilizing surfaces when at small angle of attack [ASME PAPER 65-FE-5] 06 p0801 A66-16212  
Experimental method to produce fully developed flow in relatively short channel length 06 p0871 A66-16221  
Shell linear theory, discussing classical elasticity theory, bending equations, edge effect and asymptotic theory 06 p0962 A66-16350  
MHD stagnation-point flow, discussing incompressible viscous conducting fluid boundary layer behavior 06 p0916 A66-16355  
Flow through straight slot cascade, investigating application to axial compressors for optimum slot parameters 06 p0803 A66-16968  
Similarity solutions of boundary layer equations with algebraic decay for viscous incompressible fluid inside infinite circular cone 06 p0873 A66-16996  
MHD boundary layer equations with explicit solutions for longitudinal field in plane stationary incompressible laminar flow 06 p0920 A66-17007  
Flow field study of shock wave and boundary layer development at leading edge of sharp flat plate in rarefied hypersonic flow [AIAA PAPER 66-31] 06 p0803 A66-17082  
MHD traveling wave converter, determining frictional fluid losses due to boundary flow and calculating performance 07 p0990 A66-17240  
Rotationally symmetric flow of non-Newtonian fluid in presence of infinite rotating disk, solving Navier-stokes equation and determining velocity profiles 07 p1019 A66-17258  
Modified Karman-Pohlhausen pulse integral equation for calculating boundary layers is more accurate when seeking flow separation point 07 p1019 A66-17391  
Pressure gradient influence on velocity profile in boundary layer of plate with



semicircular transverse ribs 07 p0979 A66-17449  
 Pressure dependency in oxidation of platinum above 800 degrees C explained by boundary layer diffusion mechanism 07 p1000 A66-17476  
 Boundary layer flow of rotating sphere by series expansion from pole, discussing eruption at equator 07 p1021 A66-18046  
 Fluid dynamics - Symposium, Zakopane, Poland, September 1963 07 p1021 A66-18101  
 Lagrangian similarity hypothesis to determine structure of turbulence that arises during fluid flow over rough rigid wall 07 p1022 A66-18103  
 Effectiveness of stagnant layer of radiating gas in shielding surface from radiation flux formulated as integral equation, with heat transfer results presented graphically 07 p1155 A66-18346  
 Visible and near UV radiation intensity profiles for ablating Teflon boundary layer in hot subsonic arc-jet flow at one atmosphere [AIAA PAPER 66-56] 07 p0983 A66-18450  
 Surface pressure, heat transfer coefficient, wave structure and shock disturbances of inviscid supersonic flow field along corner of intersecting wedges [AIAA PAPER 66-128] 07 p0984 A66-18462  
 Nonsimilar solution of incompressible boundary layer over flat plate in presence of shear flow, using approximate method 08 p1204 A66-18529  
 Stagnation point velocity and pressure distribution over heat-sink shielded reentry vehicle to test boundary layer heat transfer theories 08 p1161 A66-18811  
 Boundary layer equation transformation, using special curvilinear coordinates 08 p1206 A66-18872  
 Velocity profile of main section of axisymmetric turbulent jet of incompressible fluid flowing into homogeneous companion flow of same fluid 08 p1206 A66-18876  
 Nine-level general circulation model of atmosphere for resolving surface boundary layer fluxes as well as radiative transfer by ozone, carbon dioxide and water vapor 08 p1213 A66-18924  
 Mass transfer and first order boundary layer effects on sharp cone drag [AIAA PAPER 66-33] 08 p1163 A66-18954  
 Photographic spectra of ablating plastics in thermodynamic environments related to species and temperatures in boundary layers [AIAA PAPER 66-132] 08 p1318 A66-19071  
 Schlichting two-dimensional unsteady boundary layer problem results extended to three-dimensional periodic boundary layers 08 p1208 A66-19341  
 Book on two-dimensional laminar boundary layers with and without suction noting velocity profile role, wind tunnel models, transition measurements, etc 08 p1208 A66-19355  
 Unsteady flow of second order fluid near stagnation point on harmonically oscillating flat plate 08 p1212 A66-19814  
 Approximate solutions with error estimate for stationary boundary layer with desired distribution of pressure and mass transfer along wall 08 p1166 A66-19828  
 Stationary nonviscous plane flow of conducting plasma in narrow channel subject to transverse magnetic field and Hall effect, using sectionized electrodes, noting boundary layer near anode 09 p1407 A66-20135  
 Resistance due to viscous shear on circular cylinder in oscillating stream calculated by boundary layer equations formulated in polar coordinates 09 p1367 A66-20262  
 Deformation from stress in thin walled pressure vessels determined by differential equation from boundary layer problem 09 p1467 A66-20488  
 Boundary layer theory applied to solution of problems of combined heat and mass transfer, using approximate single-parameter integral method 09 p1367 A66-20703  
 Nucleate boiling heat transfer considered as heat transfer into liquid near front of flow past blunt nosed body 09 p1471 A66-20824  
 Nonequilibrium transport properties and electron relaxation at cooled surface of

partially ionized argon 10 p1559 A66-21270  
 Local boundary layer approximations of first order for steady laminar convection flow produced by nonuniform axisymmetric heating or cooling of infinite horizontal surface 10 p1620 A66-21276  
 Initial velocity and density conditions for three-dimensional boundary layer equations, noting wakes and jets 10 p1522 A66-21303  
 Boundary layer effect on lift and drag characteristics of hypersonic lifting bodies 10 p1480 A66-21409  
 Qualitative and quantitative solution of linearized approximations to boundary layer equations, noting free jet and wall-slot injection into moving stream [ASME PAPER 65-APMW-6] 10 p1523 A66-21470  
 Ion density profiles in boundary layers associated with supersonic flow of shock heated air over flat plate measured by cylindrical and flush-mounted electrostatic probes [AIAA PAPER 66-159] 10 p1565 A66-21686  
 Rapid expansion of supersonic boundary layer and application to vortical flow of near wake 10 p1480 A66-21772  
 Velocity overshoot within boundary layer in alternating laminar air flow near mouth of square channel 10 p1524 A66-21827  
 Compressibility effect on flow in MHD boundary layer of semiminfinite thermally insulated flat plate 10 p1525 A66-21847  
 Relative effect of restrictive orifices, venturis or nozzles on measurement accuracy of fluid flow rates in pipes 11 p1703 A66-22207  
 Heat transfer and pressure data extended from classical thin boundary layer regime to near-free-molecule flow in study of low density effects in hypersonic wedge flows 11 p1633 A66-22928  
 Flow over sharp and blunt flat plates at zero angle of attack in hypersonic shock tunnel, measuring surface skin friction, heat transfer, static pressure and shock layer pitot pressure 11 p1633 A66-22929  
 First-order boundary proximity effect on Stokes resistance of body, using integral equation approach 11 p1693 A66-23008  
 Kinetic energy generation and dissipation in large-scale atmospheric circulation, using six months aerological data from North American network 11 p1731 A66-23487  
 Variational extremal principles for continuum systems, analyzing various approaches to boundary layer flow 12 p1975 A66-23544  
 Asymptotic theory where limit  $R/\text{Rayleigh number}$  approaches infinity 12 p1976 A66-23550  
 Polynomials used to solve theoretical cascade problems exemplified by two-dimensional incompressible flow through nonstreamlined blades 12 p1796 A66-23786  
 Surface pressure fluctuations produced by boundary layer turbulence developed above rigid plane surface 12 p1862 A66-23820  
 Two-dimensional stagnation point flow of elastic-viscous liquid 12 p1862 A66-23956  
 Liquid film flow stability, considering two-dimensional perturbations, hydrodynamic friction with allowance for finite curvature radius of bounding surface 12 p1864 A66-24435  
 Compressor cascade flow with blades of different thickness ratio for variable Mach and Reynolds numbers, measuring turbulence level influence on loss coefficients, secondary flow parameters, etc 12 p1799 A66-24553  
 Elastico-viscosity, cross-viscosity and suction variation effects on rheological behavior of fluid moving steadily past porous circular cylinder and between two coaxial right circular cylinders 12 p1865 A66-24808  
 Free convection film boiling heat transfer from isothermal vertical plate to subcooled stagnant liquid, using two-phase boundary layer theory 12 p1980 A66-24907  
 Saturated and surface film boiling from horizontal isothermal plate in longitudinal flow field analysis, based on two-phase boundary layer theory, correlating heat transfer and skin friction characteristics 12 p1980 A66-24908  
 Laminar hypersonic flow past sphere based

on constant-density approximation, solving Navier-Stokes equations and comparing with values of shock Reynolds number 12 p1800 A66-24943  
 Viscous hypersonic blunt body problem examined, using Newtonian thin-shock-layer theory, slip effect, Navier-Stokes shock structure, etc 13 p1990 A66-25157  
 Heat exchange between axisymmetric jet flow and plate situated normal to flow 13 p2208 A66-25313  
 Engineering method for calculating distribution of convective heat transfer for continuous boundary layer gas flow past body 13 p2208 A66-25316  
 Quasi-linear approximation method and Poisson equation used in determining static fields and electron redistribution in plasma waveguides 13 p2039 A66-25678  
 Metal-ceramic boundary structures and reactions, considering metal-oxide and metal-glass interfaces, ionic and covalent bonds, oxidation, reduction, solution and precipitation 13 p2108 A66-25767  
 Hot-wire analysis of permanent sound fields during varied flow velocity around flat plate boundary layer, noting resonance effect of sound amplitude 13 p2063 A66-25901  
 Velocity profile within boundary layer region for flow of second-order fluid past symmetrical cylinder determined for nondimensional parameter formed by velocity and material constants 13 p2068 A66-26666  
 Interaction of boundary layer produced by vortex flow of viscous electrically conducting fluid over disk with axial magnetic field and relation to MHD generator and hydromagnetic capacitor 13 p2156 A66-26707  
 Solutions of nonstationary equations of plane laminar MHD boundary layer, using transformation to specialized form of curvilinear coordinates 14 p2338 A66-26773  
 Cylinder rotation in boundary layer of air stream 14 p2273 A66-26785  
 Boundary layer generation for viscous incompressible fluid flow past rigid wall or obstacle to which fluid adheres 14 p2274 A66-26940  
 Heat transfer equation to find temperature distribution in two-dimensional and circular jets 14 p2274 A66-27378  
 Mach number, Reynolds number and boundary layer trip devices effect on base pressure 14 p2219 A66-27443  
 Periodically excited boundary layer disturbances above flat plate in water flow scanned by hot-wire anemometer under various conditions 14 p2275 A66-27477  
 Thin ferromagnetic Fe-Ni films, discussing elastic tensile stresses on structure of interdomain boundaries and distribution of magnetization vectors 14 p2363 A66-27581  
 Vertical distribution of turbulence and wind velocity characteristics in atmospheric boundary layer, considering temperature stratification in boundary layer 14 p2327 A66-28215  
 Ideal gas flow past infinite circular cone at angle of attack, noting finite-differences method for self-similar solution of Prandtl boundary layer equation 14 p2222 A66-28283  
 Laminar fluid flow in channel generated by arbitrary generatrix, allowing for interaction between boundary layer and flow core, calculating boundary layer 14 p2278 A66-28316  
 Heat and mass transfer process in reacting boundary layer of compressible gas in laminar flow along semiinfinite porous plate 14 p2416 A66-28484  
 Oscillatory pressures in idealized annular boundary layer apply to panel flutter of circular cylindrical shell in supersonic flow 15 p2610 A66-29282  
 Quasi-linearization applied in boundary layer calculations, noting simple flow over solid surface 15 p2479 A66-29299  
 PDE of terminal shape of ablating body as function of time derived, noting mass and energy flow, boundary layer thickness, etc 16 p2628 A66-30219  
 Free stream turbulence effects on heat transfer rates evaluated by boundary layer approximation 16 p2824 A66-30302  
 Reduction of thick boundary layers in low density wind tunnel by applying suction to



nozzle, using high-speed  
cryopump 16 p2673 A66-30381

Soviet papers on atmospheric boundary layer, wind profiles, meteorological effects, etc 16 p2741 A66-30769

Numerical analysis of wind velocity profile measurements and theoretical calculation of profile by numerical methods, based on geostrophic friction 16 p2741 A66-30771

Air-temperature and wind profiles in atmospheric boundary layer and dependence upon stability criteria of ground layer 16 p2741 A66-30772

Short-range forecasting of stratified cloudiness, noting linear dependence between variations in dew point and air temperature near Earth surface for aperiodic processes 16 p2742 A66-30791

Airfoil theory in incompressible flow for boundary layer suction or Helmholtz type wake 16 p2629 A66-31039

Flow of turbulent incompressible fluid downstream from step-shaped wall, determining velocity fields in isobaric region, considering existence of boundary layer thickness at separation point 16 p2687 A66-31205

Energy relationships for efficiency of propulsors which induct boundary layer flow on submerged body of revolution [AIAA PAPER 65-234] 16 p2688 A66-31330

Numerical solution of MHD equations for boundary layer conducting gas flow near flat plate when velocity distribution of external flow obeys power law 16 p2764 A66-31366

Two-dimensional MHD jet flow of conducting fluid in coplanar magnetic field and nonstationary flow past body with magnetic field perpendicular to surface 16 p2765 A66-31402

MHD boundary layer flow of incompressible conducting rotational fluids over infinite dielectric disk 16 p2765 A66-31403

Three-dimensional flow separation of plane boundary layer caused by half delta wing on flat plate using Cooke small cross-flow method and Maskell separation criterion [AIAA PAPER 66-428] 16 p2631 A66-31465

Effect of oscillatory relaxation of air boundary layer on flow characteristics around wedge 16 p2632 A66-31629

Boundary layer development at free surface formed from uniform shear flow 16 p2691 A66-31657

Asymptotic behavior of horn-shaped vortex sheet in neighborhood of x-axis 17 p2905 A66-31840

Jet flow effect on electrical discharge in conducting viscous fluid based on magnetic boundary layer theory 17 p2964 A66-31895

Strip film schlieren interferometry to investigate interaction of reflected shock with incident shock boundary layer 17 p2908 A66-32415

Large deflections of symmetrically loaded shallow membrane shells of revolution, considering existence of boundary layer near edges and using asymptotic analysis 17 p3025 A66-32480

Secondary flow for supersonic boundary layers with or without swept edges, noting effect of compressibility and heat transfer on reverse flow 17 p2840 A66-32485

Modified Pohlhausen method applied to velocity profile for MHD boundary layer problems 17 p2968 A66-32490

Displacement thickness for boundary layers with surface mass transfer 17 p2909 A66-32491

Boundary conditions in viscous interaction theory, noting boundary layer growth effect on outer inviscid flow 17 p2909 A66-32492

Temperature and pressure distribution for fluid flow through porous matrix, noting chemical reaction, heat transfer, boundary layer flow, etc [AIAA PAPER 66-423] 17 p2910 A66-32752

Elasticoviscosity and cross viscosity of second-order fluid effects on advancement over infinite flat plate 17 p2912 A66-32981

Turbulent flow near boundary and equations for mass- or heat-transfer coefficient in terms of turbulent diffusion coefficient and thermal diffusivity 17 p3037 A66-33042

Approximate solution of boundary layer

problems by variational techniques, using multiparameter approach 18 p3096 A66-33594

Terminal shock-boundary layer interaction on slender cone-cylinder payloads at supersonic speeds and resulting flow separation [AIAA PAPER 66-471] 18 p3250 A66-33653

Wind tunnel experiments on thin two-dimensional airfoil with sharp leading edge and with jet blowing through mid-chord slot on upper surface in order to control boundary layer and circulation around it 18 p3048 A66-33950

Three-dimensional flow separation about immersed surfaces 18 p3098 A66-34019

Shock wave boundary layer interactions and shear flow regimes in hypersonic inlet flows [AIAA PAPER 66-606] 18 p3049 A66-34447

Boundary layer equations for nonstationary plane flow of viscous incompressible fluid 18 p3100 A66-34545

Boundary layer of steady incompressible plane crossed fields MHD flow at large Reynolds number 18 p3147 A66-34663

Critical parameters and flow characteristics of swept wings with full-chord laminar flow, noting boundary layer disturbance effects 18 p3050 A66-34950

Aerodynamic design criteria for maintaining laminar flow control including instability limit, surface roughness, acoustical environment, etc 18 p3050 A66-34951

Plasma half-space impedance for diffusive electron reflection from plasma vacuum boundary, noting damping decrement of surface electromagnetic wave, electric field Fourier components and absorption capacity 18 p3151 A66-35065

Numerical integration of boundary layer equations for dissociating gas flows, determining heat flow near stagnation point 19 p3341 A66-35739

Error in plane-layer approximation of boundary layer emission associated with gray gas flow past plane 19 p3341 A66-35752

Navier-Stokes equations solutions for incompressible fluid representing boundary layer flows with suction along corners or cylindrical bodies 19 p3341 A66-35855

Stress field on epitaxial dislocation line in weakly alloyed titanium, calculating energy of phase boundary and contribution of latter to plastic deformation 19 p3381 A66-35929

Turbulence coefficient and mean altitude of atmospheric boundary layer determined from diurnal temperature variations and wind profile 19 p3348 A66-35939

Approximation technique for analysis of two-dimensional boundary layer flows with arbitrary external velocity distribution 19 p3341 A66-36321

MHD boundary layer at conducting wall of plane channel treated by numerical method 19 p3410 A66-36459

Self-simulating solutions of nonstationary turbulent mixing in some aerodynamic problems, considering shock interaction with boundary layer 19 p3276 A66-36462

Navier-Stokes equations for plane interface with stagnation point formed by expelling different gas from leading edge of airfoil opposite to main flow 19 p3277 A66-36635

Book on aerodynamics of pure subsonic flow including Earth atmospheric structure, fluid flow laws, boundary layer phenomena, subsonic wind tunnel and Magnus effect 19 p3278 A66-36730

Boundary layer behavior in fully ionized two-temperature plasma 19 p3433 A66-36827

Plane viscous problem of gas motion through weak straight line discontinuity of acceleration, noting formation of boundary layer 19 p3278 A66-36845

Blasius series for heat and mass transfer in two-dimensional boundary layers, discussing velocity and concentration profiles 20 p3678 A66-37122

Electrical control of boundary layer flip-flop fluidistor by disruptive discharges between electrodes producing pneumatic pressure shocks that switch output flow 20 p3501 A66-37648

Horizontal temperature gradient produced by water body effect on distribution of wind velocity and direction in atmospheric

boundary layer 20 p3594 A66-38375

Wind distribution in atmospheric boundary layer under conditions of advection from pilot balloon observations 20 p3594 A66-38376

Elliptic boundary problem with small parameter, constructing boundary layer function 21 p3755 A66-38541

Boundary layers with coupled heat and mass transfer for large enthalpy per unit mass of injected material, based on linearity of perturbation equations 21 p3834 A66-38704

Boundary layer equations of MHD free convection from heated horizontal plate in vertical uniform magnetic field 21 p3776 A66-38707

Boundary layer growth effect on tailored interface operation of shock tunnel 21 p3721 A66-38719

Short-circuit effects by metal walls and influence on plasma boundary stability 21 p3791 A66-39177

Approximate solution of two-dimensional boundary layer problem using Rayleigh-Ritz method, coordinate functions and interpolation 21 p3831 A66-39351

Wind profiles obtained from meteorological tower plotting wind velocity, normalized by value of friction velocity, as function of measurement heights 21 p3759 A66-39356

Stationary nonviscous plane flow of conducting plasma in narrow channel subject to transverse magnetic field and Hall effect, using sectionized electrodes, noting boundary layer near anode 21 p3793 A66-39407

Boundary layer equation solution along vertical hot plate for constant plate temperature, noting use of Blasius technique 21 p3837 A66-39590

Velocity distribution for inlet flow in finite radial diffuser 21 p3731 A66-39591

Book on flow and thermal boundary layers including laminar and turbulent flow velocity profiles, Prandtl equation, heat transfer problems, etc 22 p3897 A66-39702

Viscous drag on flat plate in supersonic flow injected with gas in boundary layer, examining exit cone of rocket nozzle 22 p3970 A66-39875

Shielding of surface from parallel thermal radiation beams by distributed injection of fluid containing absorbing particles into boundary layer flow over surface near stagnation point [ASME PAPER 65-WA/HT-21] 22 p3997 A66-40026

Experimental boundary layer study on hovering rotors using evaporative chemical films, pressure probes and hot wire anemometers 22 p3843 A66-40249

Flow field study of shock wave and boundary layer development at leading edge of sharp flat plate in rarefied hypersonic flow [AIAA PAPER 66-31] 22 p3844 A66-40349

Total boundary layer mass flow with mass transfer at wall 22 p3899 A66-40370

Flow pattern of three-dimensional interaction of oblique shock with boundary layer obtained when shock generated by wedge spanning supersonic wind tunnel interacts with side wall 22 p3901 A66-40491

Book on MHD covering fundamental equations, boundary conditions, incompressible flow, steady flow MHD simple and shock waves, etc 22 p3957 A66-40619

Wind tunnel tests of sonic boom phenomena, noting weak pressure field measurement, construction of extremely small models, boundary layer effects, etc [AIAA PAPER 66-765] 22 p3894 A66-40646

Panel flutter analysis via forced vibration technique noting frequency coalescence, flutter boundary and experimental technique [AIAA PAPER 66-769] 22 p3895 A66-40650

Solution of motion and energy equations in boundary layer of main portion of vortex jet 22 p3902 A66-40817

Two-dimensional problem for layer with mixed boundary conditions, obtaining solutions for Fredholm integral equations and relations for temperature distribution 22 p4001 A66-40930

Time lag effect on dynamic stability determined, using wind tunnel tests with 10 degree cone as test body simulating ablation process by gas injection into boundary layer



- [AIAA PAPER 66-757] 23 p4008 A66-41330  
Monograph on kinetic theory of plasmas, deriving state equation, Maxwell equation for plasma-magnetic field interaction and boundary layer heat transfer expressions 23 p4102 A66-41400  
Initial air-side boundary layer effect on ignition of slot injected gaseous hydrogen by hot supersonic air stream [AIAA PAPER 66-644] 23 p4149 A66-41513  
Asymptotic expansion of electromagnetic field scattered from convex cylinder near grazing incidence, using boundary layer theory 23 p4038 A66-41546  
Liquid drop flow in twisted fan-shaped nonisothermal jet allowing change in viscosity coefficient in flow field, using boundary layer equations 23 p4055 A66-41567  
Time of establishment of steady state mixing in plane and axially symmetrical jets determined, using self-similar motions in unsteady state boundary layer and free turbulence 23 p4010 A66-41734  
Mass transfer and first-order boundary layer effects on sharp cone drag [AIAA PAPER 66-33] 23 p4011 A66-41877  
Turbulent viscous-interaction parameter in connection with boundary layer growth in presence of mass transfer, examining comparison of effects of strong and weak interactions 23 p4058 A66-41902  
Similar solution of laminar mixing of curved half-jet and curvature effect of boundary layer flow along curved surface 23 p4059 A66-42003  
Short-range weather forecasting based on principles of fluid dynamics 23 p4087 A66-42017  
Boundary layer problems in rotating flows, noting similarity solutions and including general momentum-integral solution 23 p4061 A66-42044  
Unification of various small-epsilon theories of real gas flows based on assumption of specific-heat ratio near unity 23 p4151 A66-42050  
Friction and turbulent heat transfer as function of Reynolds number applied to missile rounded-off forebody, delta wings, etc, using boundary layer equations 23 p4151 A66-42056  
Power conversion enhancement of acoustic-electromagnetic wave coupling across plasma-air boundary by suitable thickness and charged particle density 24 p4241 A66-42304  
Incompressible viscous flow around right angle corner, noting effect of geometry on boundary layer and cross flow 24 p4194 A66-42410  
Similarity solutions of boundary layer equations for blowing through porous surface, obtaining skin friction 24 p4194 A66-42541  
Wind and temperature profiles for constant flux atmospheric boundary layer in lapse stratification implying relation between eddy transfer coefficient ratio and stability parameter 24 p4202 A66-42982
- BOUNDARY LAYER COMBUSTION**  
Laminar diffusion flame occurring in mixing zone between undiluted fuel and undiluted oxidizer by process of molecular diffusion 03 p0443 A66-12489  
Combustion and sublimation in aerothermochemical interaction between dissociated air stream and graphite surface in hypersonic laminar viscous flow [AIAA PAPER 65-42] 03 p0444 A66-12797  
Turbulent velocity fluctuation field in isothermal boundary layer with homogeneous injection and combustion [AIAA PAPER 65-820] 04 p0510 A66-13689  
Thermal oxidation kinetics of silicon, describing diffusion process, oxide layer boundary reactions and space charge effects on initial phase 07 p1106 A66-18401  
Flame properties as function of flame gases 14 p2414 A66-28142  
Diffusion combustion in laminar boundary layer between two plane-parallel co-current streams 14 p2416 A66-28485  
Diffusion combustion in turbulent compressible gas flow 17 p3036 A66-32827  
Feasibility of rocket motor using detonation wave rotating in annular combustion chamber wherein propellant is injected continuously and expelled through annular nozzle 18 p3162 A66-33807  
Hydrogen combustion in air above solid noncatalytic wall heated to 800 degrees C, examining diffusion equation for slow combustion and laminar boundary layer flow over noncatalytic wall 19 p3479 A66-36249
- BOUNDARY LAYER CONTROL**  
SA FLUTTER  
SA POROUS BOUNDARY LAYER CONTROL  
Boundary layer control /BLC/ high lift system used as integral part in design of F-4 Mach 2 plus Navy interceptor [AIAA PAPER 65-714] 01 p0013 A66-10951  
Drag reduction measurements on porous cylindrical bodies with blunt nose and tail sections, using area suction [AIAA PAPER 65-561] 02 p0175 A66-11564  
Flight experiments to assess stalling behavior and handling problems arising in design, maintenance and operation of suction wing for high lift [AIAA PAPER 65-750] 03 p0319 A66-12586  
Boundary layer control for improvement of lift at lower angles of attack by carrier-based supersonic aircraft [AIAA PAPER 65-751] 03 p0321 A66-13055  
Laminar boundary layer control wind tunnel results, using perforated plastic reinforced by glass fiber 04 p0453 A66-13513  
Boundary layer control by blowing, analyzing turbulent boundary layer for flow about flat plate of incompressible fluid with intense cross flows 04 p0509 A66-13573  
Incompressible laminar boundary layer for plate with slot suction at high Reynolds number 04 p0509 A66-13654  
Boundary layer control high lift system for high speed aircraft, using ejector for momentum augmentation and air bleed from propulsion system 05 p0610 A66-15070  
[AIAA PAPER 64-589] 05 p0610 A66-15070  
Drag decrease in glider aircraft noting wing profile, flow laminarization /boundary layer control/, landing flaps, tail, etc 05 p0607 A66-15200  
Fluoric control devices physical mechanisms, including jet-on-jet and turbulence amplifiers, vortex and boundary layer control devices [ASME PAPER 65-WA/AUT-21] 05 p0624 A66-15615  
Direct lift control as landing approach aid by providing more rapid means of changing and controlling flight path than conventional methods [AIAA PAPER 66-14] 08 p1167 A66-18985  
Boundary layer control /BLC/ high lift system used as integral part in design of F-4 Mach 2 plus Navy interceptor [AIAA PAPER 65-714] 12 p1801 A66-24095  
Blowdown-type high-speed linear cascade wind tunnel with variable exit pressure, Mach and Reynolds numbers permit boundary layer control 12 p1859 A66-24927  
Decreasing secondary flows in spatial boundary layer on porous plate by boundary layer control /BLC/ through suction or blowing, using Prandtl partial differential equations 13 p2065 A66-26460  
Acoustical control of atmospheric boundary layer investigated in wind tunnel for flow velocity range from 5 to 40 m/sec 14 p2277 A66-27862  
Flow loss in conical diffusers with boundary layer suction through single slit 16 p2629 A66-30813  
High-lift jet-pump boundary layer control system for STOL short haul S-1600 transport 16 p2633 A66-31282  
Boundary layer control on walls by means of longitudinal vortices created by row of wings in shape of swallow tail 17 p2907 A66-32328  
Boundary layer control using smoke tunnel, discussing sources and scale of tunnel turbulence 17 p2912 A66-32965  
Laminar flow control /LFC/, aircraft performance benefits include increased endurance, loiter time and cruise altitude 18 p3050 A66-34948  
Self-preserving flow in outer part of two-dimensional curved turbulent wall jet for constant ratio of jet thickness to wall radius of curvature 22 p3844 A66-40489  
Boundary layer suction in two-component fluid flow around plate solved by method of partial averaging 23 p4056 A66-41568
- Comparison of lifting characteristics of profile with air ejection onto slotted and unslotted flaps, examining dependence on jet impulse coefficient 23 p4010 A66-41795  
Boundary layer control of conducting fluid by transverse magnetic field and spanwise electric field 23 p4107 A66-41904  
Approximate solution of second-order incompressible boundary layer equations, using mathematical model reformulated for application in vicinity of separation point 23 p4058 A66-41924  
Pliant coatings applied to streamlined bodies to reduce hydrodynamic drag by stabilizing laminar boundary layer against transition to turbulence 23 p4059 A66-41943
- BOUNDARY LAYER NOISE**  
Boundary layer noise and effects of acoustic energy on panel response, panel fatigue and internal sound levels tested with X-15 aircraft 01 p0010 A66-10126  
Spectral energy distribution modified by finite Mach number effects and structural response to boundary layer turbulence and susceptibility to changes in mean flow Mach number 01 p0005 A66-10129  
Response of simple structure to boundary layer noise examined together with response of supported panel to sound field 01 p0055 A66-10132  
Vibration response of steel panels to fluctuating pressures in turbulent boundary layer of wind tunnel compared to random excitation caused by jet noise and siren 01 p0148 A66-10138  
Aeroacoustic excitation of aerospace structures for design purposes, sources being jets of gas turbines and rockets and turbulent boundary layers [SAE PAPER 650823] 01 p0156 A66-10824  
Noise problem associated with rocket boosters, possible minimization by radical change of design 02 p0293 A66-11511  
Magnetoacoustic wave in rarefied plasma, examining nonstationarity of motion, wave front behavior, wave energy absorption and magnetic field profile 06 p0921 A66-17056
- BOUNDARY LAYER SEPARATION**  
SA LAMINAR BOUNDARY LAYER SEPARATION  
Separating force determined for boundary layer of nonsedimentating suspension of various configurations 01 p0060 A66-11092  
Upstream length of turbulent boundary layer separation ahead of compression corner or flare 05 p0666 A66-15801  
Displacement thickness of boundary layer with blowing for arbitrary shaped bodies, noting stagnation flow 05 p0666 A66-15802  
Compressor blade cascade in flow with boundary layer separation, calculating velocity distribution and blade angle 06 p0803 A66-16967  
Asymptotic steady state solution to problem of thermal separation of components across shear layer between cold jet mixture and hot ambient gas 09 p1470 A66-20178  
Theoretical determination of buffeting limits of wings, using boundary layer theory, obtaining Reynolds number effect on location of buffeting limits 10 p1479 A66-21377  
Turbulent boundary layer separation in supersonic flow 12 p1797 A66-24112  
Turbulence and separation in boundary layer and relation to wing design 14 p2217 A66-26925  
Conditions at head shock wave in viscous hypersonic flow past blunt body for study of boundary layer separation 15 p2423 A66-28960  
Laminar boundary layer separation in supersonic flow on body with symmetry of revolution 16 p2629 A66-30583  
Three-dimensional boundary layer separation, assuming zero friction 16 p2630 A66-31286  
Drag on cylinders of various height mounted on flat plate, noting dependence of compression region length on cylinder diameter during analysis of boundary layer separation phenomena 17 p2909 A66-32493  
Laminar separation in supersonic and hypersonic flow analyzed in gun tunnel, noting concept of incipient separation and free interaction principle [AIAA PAPER 66-455] 17 p2910 A66-32761



Shock-induced boundary layer separation on supersonic intake, using hodograph technique for flow structure analysis 17 p2841 A66-32896

Laminar, transitional and turbulent boundary layer flows with adverse pressure gradient on axisymmetric blunted conical flared body at Mach 10 10

[AIAA PAPER 66-493] 18 p3047 A66-33658

Laminar film condensation of vapor flow along flat plate and cylindrical surface 18 p3261 A66-34362

Supersonic diffuser for eliminating separation of boundary layer in isentropic compression 19 p3276 A66-36084

Separation of laminar boundary layer of gas flow from cone as function of angle of attack, Mach number, etc 19 p3277 A66-36478

Localized convection coefficient for hypersonic separation line along delta wing leading edge calculated, using Mangler and Stewartson transformation 20 p3492 A66-37818

Hypersonic boundary layer separation and expansion at shoulder of blunt based body 21 p3693 A66-38683

Prediction characteristics of separated turbulent boundary layers in compression corners used to determine aerodynamic heating distributions and dynamic loading of supersonic vehicles 21 p3724 A66-38730

Boundary layer solutions to two-dimensional stationary viscous incompressible flow past finite object under vanishing skin friction 23 p4060 A66-42009

Separation point of laminar boundary layer before dihedral, determining conservation of momentum and mass 23 p4013 A66-42010

Velocity profile in isobaric zone downstream from step-shaped wall in case of incompressible fluid 24 p4197 A66-43002

**BOUNDARY LAYER STABILITY**

Three-dimensional laminar boundary layer on body of revolution at small incidence at its stability 01 p0055 A66-10203

Nonlinear buckling of rectangular plates emphasizing calculations of thrust magnitude for boundary value problem, Von Karman equations, etc 03 p0435 A66-12612

Electrodynamic jump conditions and momentum-energy laws at arbitrary moving boundary derived three-dimensionally 06 p0917 A66-16435

Linear stability of laminar boundary layers for asymptotic suction profile, obtaining solution of inviscid equation in terms of hypergeometric function 06 p0874 A66-16998

Self-preserving development in turbulent boundary layer in strong adverse pressure gradient described by two-layer model 06 p0874 A66-17001

Ablation effects on static and dynamic stability of reentry vehicle [AIAA PAPER 66-51] 07 p1141 A66-17896

Unsteady oscillations of boundary layer interaction with shock waves in lower transonic region 07 p1022 A66-18106

Russian monograph on MHD of liquid metals, discussing application for transport and technological treatment of metals, molten salts and slags 08 p1266 A66-19566

Increased mass transfer from flat plate caused by wake from cylinders located near boundary layer edge 08 p1211 A66-19682

Small transverse flow effect on spanwise perturbation of two-dimensional boundary layer of flat plate 08 p1166 A66-19820

Stability of laminar boundary layers and wakes at hypersonic speeds, noting existence conditions for subsonic disturbances and effect of hot wake core 13 p2061 A66-25165

Turbulent flow intensity measured in turbulent wake of small fence along flat plate covered with flabby skin, for analysis of drag reduction in aerodynamics 13 p2063 A66-25598

Simultaneous diffusion of momentum and energy in turbulent mixing, noting static and stagnation properties, density and temperature variations, flow pattern, etc 13 p2070 A66-26721

Finite-difference method for computing transient velocity profiles in laminar boundary layer around two-dimensional cylinder, noting Blasius flow oscillations 14 p2274 A66-27434

Effect of unsteady longitudinal vortices on

Blasius profile in traditional boundary layer of flat plate 14 p2279 A66-28461

Stability of idealized laminar boundary flow, determining phase velocity, amplification rate and wave number of all disturbances 16 p2686 A66-30948

Response of two-dimensional laminar boundary layer to fluctuating free stream or surface oscillation 17 p2908 A66-32443

Laminar boundary layer stability of incompressible fluid at elastic surface 19 p3342 A66-36463

Behavior of solution of system of equations for unsteady boundary layer of two-dimensional liquid as time approaches infinity 19 p3343 A66-36826

Flight testing of laminar flow control on full-scale swept wings, examining total pressure probes, wing wake drag and boundary layer stability utilizing pressure transducer [AIAA PAPER 66-734] 22 p3846 A66-40625

Laminar boundary layer in incompressible liquid, noting effect of variation of kinematic viscosity and density on stability 23 p4056 A66-41725

Stability of laminar boundary layers at concave wall with vortex type disturbance introduced by interference baffles 23 p4060 A66-42022

Ablation effects on static and dynamic stability of reentry vehicle [AIAA PAPER 66-51] 24 p4283 A66-42770

Instability of laminar Ekman boundary layer, obtaining critical values of Reynolds numbers, perturbation growth rates and equilibrium finite amplitude solutions 24 p4197 A66-42980

Stability of two-dimensional boundary layer flow in rotating tank with small inflow analyzed, using perturbation theory 24 p4197 A66-42981

**BOUNDARY LAYER TRANSITION**

**SA TURBULENCE**

Surface modifications of recovered small-scale plastic models after high speed flight used to estimate extent of laminar and turbulent flow over surface related to ablation studies 02 p3033 A66-11560

Laminar boundary layer transition on highly cooled 10 degree cone in hypersonic flow, using heat gauges to study turbulent burst propagation 03 p0315 A66-12788

Laminar to turbulent transition along aluminum plate in free convection measured, using hot-wire probes 04 p0596 A66-13515

Intermittency profiles of turbulent boundary layers for various pressure gradients to determine relationship between descriptive quantities and form factor of velocity profile 04 p0508 A66-13516

Helium II film free-convection heat transfer, discussing mathematical analysis for vertical flat plate and horizontal circular cylinder [ASME PAPER 65-WA/HT-10] 05 p0791 A66-15652

Effect of initial flow turbulence on optimum suction of fluid from boundary layer of porous plate 06 p0872 A66-16468

Controlled three-dimensional roughness effect on hypersonic laminar boundary layer transition [AIAA PAPER 66-26] 06 p0804 A66-17092

Wake from bluff bodies interaction with initially laminar boundary layer [AIAA PAPER 66-126] 06 p0875 A66-17096

Laminar and turbulent boundary layer flow in ablating cones in hypervelocity flight [AIAA PAPER 66-27] 07 p1020 A66-17889

Velocity profiles of transitional viscous boundary layer for plane Poiseuille flow 07 p1023 A66-18120

Free flight dynamic stability measurements indicate that boundary layer transition has no perceptible effect [AIAA PAPER 64-427] 08 p1161 A66-18810

Surface oscillations in bounded cold plasma with charged particle fluxes along stationary magnetic field 08 p1262 A66-18982

Hypersonic shock tunnel study, examining effects of roughness, bluntness and angle of attack on boundary layer transition 08 p1166 A66-19813

Transition region and amplification factor of unstable disturbances in laminar boundary layers with distributed

suction 10 p1522 A66-21408

Transition from near free molecular flow at leading edge of flat plate in rarefied hypersonic flow to continuum boundary layer flow downstream 11 p1633 A66-22925

Correlation for boundary layer transition on sharp slender cones with heat transfer, using wind tunnel and free flight data 12 p1799 A66-24708

Convective heat transfer to flat plate and at stagnation point in partially ionized equilibrium air boundary layer, noting heating rates 13 p2210 A66-26720

Simulated fish propulsion analysis of boundary layer transition and vortex chain shedding 13 p2071 A66-26725

Boundary layer transition measurements on swept wings with supersonic leading edges 14 p2219 A66-27439

Longitudinal pressure gradient effect on evolution of finite three-dimensional perturbation in transition boundary layer of upper surface of wing section near critical Reynolds number 15 p2423 A66-28521

Transition delay and skin friction drag reduction by considering boundary layer flow over flexible aerodynamic surface [AIAA PAPER 66-430] 16 p2688 A66-31466

Laminar boundary layer transition in hypersonic shock tunnel of cone, noting effect of high Mach numbers and tip surface roughness, using surface heat transfer gauges [AIAA PAPER 66-494] 17 p2841 A66-32772

Nose bluntness and angle of attack effects on hypersonic flow, noting shock wave deflection decrease of minimum possible shock angle, varying specific heat ratio, convective heating, boundary layer transition, etc [AIAA PAPER 66-414] 18 p3046 A66-33639

Laminar and turbulent boundary layer flow in ablating cones in hypervelocity flight [AIAA PAPER 66-27] 21 p3723 A66-38686

Effect of mass injection into cavity on hypersonic boundary layer transition and on heating downstream 21 p3835 A66-38734

Boundary layer transition on downstream surface of sharply pointed cones when angle of incidence is slight and boundary layer is attached throughout 23 p4007 A66-41172

Two-dimensional roughness element effect on boundary layer transition, noting free stream turbulence level influence on amplification rate of disturbance 23 p4060 A66-42020

Laminar turbulent transition in freestream boundary layer behind axisymmetric and plane nozzle 23 p4061 A66-42036

Transitions between phases and states of crystallographic order in films, noting conditions for preferential nucleation and analogies between two- and three-dimensional phase diagrams 24 p4251 A66-42305

Pressure effects of flexible walls on boundary layer transition in turbulent pipe inlet flow 24 p4195 A66-42859

**BOUNDARY LUBRICATION**

Silicone copolymers lubricants containing both trifluoropropyl and haloophenyl substitution to cover wide temperature range [ASLE PREPRINT 65-LC-5] 02 p0237 A66-12233

Self-excited torsional vibrations of power transmission drives under boundary lubrication, developing rotating shaft/bearing relations 05 p0772 A66-14643

Hydromagnetically squeezed films between two conducting surfaces used as lubricator, discussing load capacity, pressure and time of approach [ASME PAPER 65-LUBS-6] 06 p0884 A66-16202

Silicone copolymer lubricants containing both trifluoropropyl and haloophenyl substitution to cover wide temperature range [ASLE PREPRINT 65-LC-5] 12 p1889 A66-24990

Surface roughness effect on boundary friction for various loads, speeds and lubricants [ASLE PREPRINT 65 AM 6AZ] 13 p2085 A66-25367

Lubrication characteristics of dry unbonded and bonded molybdenum sulfide films for varying speed, load, humidity and



metal substrate  
[ASLE PREPRINT 65AM 5C1] 14 p2302 A66-27773

Idle time effect on static friction studied under boundary lubrication conditions, using compression tester and press-fit test specimens  
[ASLE PAPER 66AM 1C1] 16 p2710 A66-30403

Effect of chemical attachment in boundary lubrication of aluminum thrust washer using 1-cetene and cetane 24 p4217 A66-42700

### BOUNDARY VALUE

Asymptotically accurate estimates of Bubnov-Galerkin method error in eigenvalue problem as applied to boundary value problem 01 p0091 A66-10162

Approximate solution for differential equations, using algorithm applied to boundary value problem involving linear equation 01 p0091 A66-10164

Heat potential theories applied to boundary value problem for heat conduction equation 01 p0160 A66-10167

Mixed boundary value problem for second order hyperbolic equation with discontinuous coefficients having time derivatives 01 p0092 A66-10187

Eigenfunction expansions of convenient fourth order equation constructed examining convergence, method for summing various associated series and solution of boundary value plate problems 01 p0154 A66-10484

Generalization of Wiener-Hopf integral equation in class of mixed boundary value problems 01 p0094 A66-10506

Thermodynamic paradox consisting of boundary value problem with mathematical inconsistency observed in rectangular waveguides loaded with magnetized ferrite 01 p0121 A66-10540

Solution of ferrite boundary value problem in rectangular waveguide and resolution of Lewin paradox 01 p0028 A66-10560

Simplified leading-edge flow boundary value problem of Bhatnager-Gross-Krook equation solved by finite difference method 01 p0058 A66-10633

Four types of axisymmetric distribution of stresses and displacements in infinitely long rod of circular cross section with discontinuous boundary conditions 01 p0155 A66-10713

Perturbation of boundary value problem for second order hyperbolic equation 01 p0095 A66-10927

Straight lines method applied to Dirichlet and Neumann boundary value problem for certain nonself-adjoint two-dimensional second order elliptic equations 01 p0095 A66-11014

Coupling method for determining natural oscillations of ideal incompressible liquid in vessel consisting of two regions 01 p0059 A66-11017

Stress function for linear viscoelastic problems where body shape, boundary condition type or both vary with time 02 p0298 A66-11576

Asymptotic solution of some nonstationary boundary value problems of cylindrical surface 02 p0250 A66-12098

Theory of weight classes for differentiable functions of many variables, with application to boundary value problems for elliptic equations 02 p0250 A66-12099

Mixed boundary value problem in bounded region for Navier-Stokes equations and discontinuity equation 02 p0219 A66-12101

Nonlinear boundary value problem solution as applied to effect of uniformly distributed pressure and concentrated load on spherical dome 02 p0301 A66-12174

Spectral theory applied to elliptical boundary value problem with eigenvalue parameters 02 p0251 A66-12229

Proof of boundary regularity connected with inhomogeneous systems of partial differential equations leading to elliptic boundary value problems 02 p0251 A66-12231

Approximate solution of principal boundary value problem of electrodynamic 02 p0262 A66-12246

Text on aerodynamics of wings and bodies, emphasizing matched asymptotic expansion methods for boundary value problems and numerical techniques for loading predictions via computers 03 p0313 A66-12297

Monograph on boundary problems for linear parabolic systems with complex coefficients 03 p0386 A66-12456

Elastic equilibrium of rectangular prism with given stress-vector components at lateral surfaces and displacements at faces 03 p0435 A66-12635

Finite plane stretching of neo-Hookean strip bonded at ends treated by principle of stationary potential 03 p0435 A66-12669

Time optimization problem involving dynamic programming, boundary value problem, differential equations and optimal control 03 p0349 A66-12687

Spectral functions of generalized second-order differential equations with boundary conditions at singular end 03 p0388 A66-13115

Optimum motion in central force field, discussing orbital transfer for circular orbits when energy source is controllable 04 p0576 A66-13560

Electrohydrostatic boundary equations solving two-and three-dimensional axisymmetric situation and sessile drop problem 04 p0545 A66-13808

Reflection coefficients of plane wave field in grid-earth system, using averaged boundary conditions 04 p0482 A66-13907

Nonlinear eigenvalue problem for equilibrium state of rotating rod solved by perturbation procedures and Leray-Schauder degree theory 04 p0589 A66-13948

Bounds for Dirichlet energy integral in terms of arbitrary vector 04 p0539 A66-13949

Geometrical aspects of optimal processes, discussing existence of limiting surfaces in cost augmented state space, state equations, maximum principle and functional equations for optimal trajectories 04 p0505 A66-13990

Theory of differential equations discussing extremal problems for generalization of optimal control problem 04 p0505 A66-13994

Book on MHD including kinematic aspect, magnetic force effects, boundary conditions, MGD, etc 04 p0556 A66-14384

Solution to boundary value problems associated with artificial satellite, lunar impact trajectory and interplanetary trajectory 04 p0579 A66-14445

Boundaries of stability sector of nonlinear controlled systems with delay, deriving criterion for designing maximum boundaries 05 p0657 A66-15114

Expansion in eigenfunctions of not self-conjugate boundary value problem for differential equation with singularity at zero 05 p0709 A66-15339

Exact solution for Green function of open spherical shell subjected to harmonically oscillating concentrated load and any consistent boundary conditions  
[ASME PAPER 65-WA/APM-24] 05 p0778 A66-15446

Electron temperature distribution in plasma diode, discussing electron transport properties and current-voltage characteristics 05 p0615 A66-15535

Cavitation bubble collapse in venturi, discussing flow characteristics under large pressure gradient  
[ASME PAPER 65-WA/FE-20] 05 p0663 A66-15610

Heat transfer and velocity characteristics of thermal and hydrodynamic laminar flow in ducts of arbitrary cross section, considering boundary conditions at wall  
[ASME PAPER 65-WA/HT-13] 05 p0790 A66-15650

Boundary value problem solution for composite media applied to cooling of composite cylinder by convection at outer surface  
[ASME PAPER 65-WA/HT-52] 05 p0792 A66-15664

Axial thermal gradient stresses in finite length thin cylinders, evaluating distinct boundary conditions  
[ASME PAPER 65-WA/MET-17] 05 p0780 A66-15682

Superimposed vibrations, corresponding to different propagation constants for same frequency parameter, satisfy boundary conditions at flat surfaces of cylinder 05 p0781 A66-15739

Complex variable functions, discussing boundary properties for holomorphic

continuous unit disk with constant absolute value on boundary 06 p0901 A66-16007

Numerical solution to Laplace equation in two dimensions, subject to boundary conditions imposed by conducting surfaces and dielectrics, applied to transmission line problems 06 p0846 A66-16097

Oblique incidence on plane boundary between two general gyrotropic plasma media, evaluating reflection and transmission coefficients 06 p0913 A66-16137

Book on point matching technique for solving boundary value problems of elasticity theory for multiply connected regions 06 p0962 A66-16245

Traveling magnetic wave plasma accelerator, discussing representative MHD equations, force and output power parameters and energy relations  
[AIAA PAPER 66-72] 06 p0942 A66-16257

Axisymmetric dynamic response of ring supported cylinder to time dependent loads discussing boundary conditions and differential equations of motions  
[AIAA PAPER 66-83] 06 p0962 A66-16261

Oscillating disk induced flow, discussing mathematical formulation of flow field produced by finite-amplitude rotational oscillations 06 p0872 A66-16357

Conversion of gravity reduction problem into internal boundary value problem which is solved by finite difference methods 06 p0876 A66-16416

Stress and strain analysis of sandwich plates, formulating and solving problem of bending for transversally isotropic layers and light core 06 p0964 A66-16477

Optical absorption of metal films in region of transformation to dielectric, discussing valence and conduction band separation mechanism 06 p0924 A66-16518

Pseudo-convex functions, discussing existence criteria, properties and application 06 p0864 A66-16623

Motion of solid body with cavity filled with viscous incompressible fluid at small Reynolds number, reducing hydrodynamic problem to solution of stationary linear boundary value problems 06 p0873 A66-16707

One-dimensional unsteady motions of heat conducting gas in which heat conduction has significant role, formulating boundary value problems with self-similar solutions 06 p0917 A66-16709

Heat conductivity problems for two-and three-layer systems solved by splitting boundary conditions and dividing system into single layers 06 p0972 A66-16842

Solution of boundary value problems for partial differential equations 06 p0903 A66-16903

Exact measurement of local temperature determining grain boundary temperature gradient, describing probe 06 p0882 A66-16938

Complete resolution of concentrated loads of limiting contour, determining spectrum of functional linear operator attached to interior region 06 p0967 A66-17061

Cylindrical beam plasma system immersed in finite longitudinal magnetic field deriving dispersion equation for approximate boundary conditions 06 p0921 A66-17161

Traveling wave MHD converter basic equations, accounting for magnetic potential difference in iron via generalized boundary conditions 07 p0991 A66-17242

Rotating non-Newtonian fluid, discussing stabilizing and destabilizing effect of circular magnetic field for cross-viscous parameter variation 07 p1019 A66-17259

Beam on elastic supports, determining fundamental frequency of free oscillation for one weak nonlinear boundary condition 07 p1142 A66-17260

Elastically nonhomogeneous sphere under uniform pressure, determining parameters of plastic deformation 07 p1142 A66-17262

Optimal control for systems whose behavior is described by ordinary and differential equations set with initial and boundary conditions 07 p1013 A66-17426

Transversely isotropic cylindrical shell vibrations solved via Bessel function for flexural, axisymmetric and torsional modes 07 p1143 A66-17499

Unsteady heat conduction in finite homogeneous region of arbitrary geometry



- and initial conditions with inhomogeneous boundary conditions 07 p1150 A66-17578
- Boundary value problem for parabolic equation in closed region 07 p1056 A66-17599
- Asymptotic behavior of solutions of boundary value problem for second-order elliptic equations 07 p1056 A66-17602
- Second order degenerate elliptic and parabolic equations, giving smoothness theorems of solutions 07 p1056 A66-17604
- Cauchy and boundary value problem for second-order nonlinear ordinary differential equations 07 p1056 A66-17607
- Solvability of general mixed boundary value problems for multidimensional hyperbolic integro-differential equation of arbitrary order with analytic coefficients 07 p1056 A66-17608
- Stability of solutions of Cauchy problem for linear hyperbolic differential equations 07 p1056 A66-17609
- Popov-related stability results for feedback systems proved via bounded solutions for functional equations 07 p1015 A66-17756
- Boundary problems concerning linear integro-differential equations with caloric operator and delayed arguments 07 p1057 A66-17842
- Regularization of ordinary differential operator trace in region of regular boundary conditions 07 p1057 A66-17855
- Slow decay of solution of initial boundary value problem for wave equation in unbounded region 07 p1059 A66-17970
- Existence and uniqueness theorems for invariant-imbedding nonlinear ODE systems for absorption loss rate satisfying Lipschitz condition 07 p1059 A66-17972
- Existence of subsonic jets issuing from curved symmetric channels in plane 07 p0981 A66-18030
- Data analysis from Explorer XIV satellite, noting magnetic field measurements in tail of geomagnetic cavity 07 p1029 A66-18086
- Plasma and magnetic field data from Explorer X, emphasizing correlation with multiple crossings of geomagnetic cavity boundary on dark hemisphere of Earth 07 p1029 A66-18087
- Elastic equilibrium of rectangular parallelepiped when boundary conditions on surface are given in terms of displacements 07 p1146 A66-18253
- Steady state radiative transport through homogeneous spherical medium, applying invariance principles of Ambartsumian and Chandrasekhar 07 p1155 A66-18339
- Certain inequalities for solutions of elliptic equations and derivatives near metric region 07 p1060 A66-18466
- One-dimensional heat flow to cool wall, discussing effects of compressibility and variable thermal conductivity 08 p1205 A66-18540
- Equivalence of oscillating electric field on plasma boundary, with specularly reflecting bounding wall, to unbounded plasma with planar oscillating grid at wall position 08 p1261 A66-18546
- Mixed boundary value problem for velocity potential of unsteady perturbation flow past oscillating thin profile in inviscid compressible gas at subsonic speeds 08 p1205 A66-18674
- Boundary value problems of plane theory of ideally plastic bodies, with analytical solutions 08 p1306 A66-18703
- Reflection of radio waves incident on boundary surfaces, noting application to Kraus effect theory 08 p1182 A66-18753
- Temperature fluctuations of elastic isotropic cylinder, obtaining temperature equilibrium equations and reducing three-dimensional problems of thermoconductivity and thermoelasticity to boundary value problems 08 p1307 A66-18886
- Errors in approximation equations for dynamic bending of cylindrical rod 08 p1308 A66-18889
- Small perturbations of parabolic boundary value problem 08 p1245 A66-19114
- Edge conditions effect on elastic stability of cylindrical shells extended to additional combinations of boundary conditions, considering cylinders under axial compression 08 p1310 A66-19144
- Scintillation observations of satellite signals noting latitude, diurnal, seasonal and sunspot cycle variations 08 p1183 A66-19208
- Optimal feedback control and bounding hypersurface of allowable perturbations in linear plant regulator, noting multiplier equation 08 p1200 A66-19543
- Approximate methods for integration of equations of plane isentropic motion of gas at supersonic velocities 08 p1165 A66-19572
- Boundary problems for differential and integro-differential equations 08 p1245 A66-19631
- Diffusion controlled mechanism for operation of nickel hydroxide electrode, analyzing corresponding boundary value problem and predicting electrochemical behavior 08 p1171 A66-19647
- Dynamic problems of transversely isotropic half-space and elastic layer, solving contact and boundary value problems 08 p1315 A66-19708
- Optimum processes in systems with distributed parameters described by partial differential equations 08 p1202 A66-19710
- Wave propagation equations in inhomogeneous warm plasma, emphasizing separation into quasi-electromagnetic and dynamic components 08 p1266 A66-19736
- Spherical shell bending examined, using quasi-linear stress-strain relationship 09 p1465 A66-19857
- Modified Cochran method giving valid expansions for singular perturbation problems in heat transfer 09 p1469 A66-20084
- Free boundary problem for heat equation with heat input at melting interface 09 p1470 A66-20264
- Green function-eigenvalue relationship on closed smooth boundary of open dimensional region 09 p1394 A66-20265
- Monograph on potential methods in theory of elasticity, basing boundary value solution on theory of singular integral equations 09 p1466 A66-20332
- Fredholm integral equation system for magnetic currents induced on wedge under impedance boundary condition 09 p1344 A66-20441
- Computer program for numerical solution of uniform hollow waveguides with boundaries of arbitrary shape 09 p1346 A66-20607
- Bounds for two-dimensional discrete harmonic Green function used in boundary problems 09 p1395 A66-20621
- Tensor product analysis of alternating direction implicit iteration techniques for approximate solution of elliptic partial differential equations 09 p1396 A66-20637
- Approximate solution for elasticity problems, noting mathematical determination of stress distribution in any homogeneous isotropic body 09 p1468 A66-20642
- Second-order linear equations with nonnegative characteristic form in analysis of first boundary value problem 09 p1397 A66-20734
- Approximate solution of nonlinear heat conduction problems for boundary conditions of first and third kind, using Leibenson integral relations 09 p1471 A66-20750
- Boundary condition constraint method for generalizing R-matrix theory, permitting use of shell model as basis for nuclear-reaction calculations 09 p1405 A66-20822
- Differential equations describing boundary conditions at front of change of aggregation state, computing temperature field 09 p1471 A66-20825
- Optical absorption of metal films in region of transformation to dielectric, discussing valence and conduction band separation mechanism 09 p1431 A66-20899
- Numerical solution of laminar boundary layer momentum, energy and diffusion differential equations for heat and mass transfer on moving continuous flat surface with injection or suction 10 p1619 A66-21053
- Stability and dissipation in second and third-order fluid approximations of boundary value problems for unsteady simple shear flow [AICE PREPRINT 21F] 10 p1521 A66-21188
- Integration of Laplace transformed elastokinetic equations, examining stress function, displacement vector field and boundary and initial value problems 10 p1555 A66-21226
- Boundary value problem for wave propagation on cylindrical anisotropic dielectric rod solved for hybrid modes 10 p1496 A66-21307
- Perturbation technique solution for MHD flow in closed regions with symmetric flow properties and axial boundary conditions 10 p1563 A66-21543
- Impurity atom diffusion through narrow diffusion mask opening determined by relaxation method 10 p1512 A66-21762
- Book on problems of mathematical physics noting integral transforms, curvilinear coordinates, integral equations and other solution techniques 10 p1556 A66-21766
- Solar plasma flow around geomagnetic cavity studied by numerical blunt body analog, proposing MGD boundary pressure as condition for self-consistent solution [AIAA PAPER 65-121] 10 p1533 A66-21775
- Boundary condition effects in magnetic mirror compression experiment, noting dependence of transition from unstable to quasi-stable plasma containment on density and lifetime 10 p1568 A66-21824
- Boundary value solutions applied to class of rotating disk flows, including examining convergence of successive approximation scheme 10 p1525 A66-21849
- Theorems and corollaries describing bounds for quadratic Liapunov functions 10 p1551 A66-21918
- Boundedness and uniform boundedness of nonhomogeneous systems, obtaining necessary and sufficient conditions for existence of solutions 10 p1551 A66-21920
- Electromagnetic wave diffraction around finite perfectly conducting cone 10 p1506 A66-21924
- Time reversal heat conduction problems in thermodynamical system with known boundary conditions solved for various structures 10 p1623 A66-22060
- Stressed state in medium length cylindrical shell with arbitrary closed transverse contour and method of solving it 10 p1618 A66-22178
- Numerical solution of heat conduction and gas dynamics equations by sifting over separate regions 11 p1785 A66-22339
- Current distribution and input impedance of infinite cylindrical antenna in anisotropic plasma, treating it as boundary value problem 11 p1661 A66-22396
- Elastic strip and elastic annulus differential-difference equations, using Fourier transforms and analytic continuation 11 p1780 A66-22439
- Boundary value problem for stress concentration at spherical cavity in field of isotropic tension for deformable microstructure 11 p1781 A66-22615
- Nonlinear circuit theory, discussing invariant imbedding, dynamic programming and quasi-linearization 11 p1675 A66-22629
- Algorithm for computer eigenfunction solution of boundary value problem involving partial differential equations for stress functions of semimomentless cylindrical shells 11 p1782 A66-22856
- Alternating direction schemes for heat equation in general cross sections with M space dimensions and nonlinear equations 11 p1722 A66-22982
- Torsional oscillations of fluid sphere with rigid boundary in uniform magnetic field 11 p1745 A66-23007
- Numerical analysis of thin cylindrical shell under action of external forces for small deformations, using first-order theory 11 p1783 A66-23016
- Nonlinear boundary value problem for elliptic PDE continuous over composite region 11 p1723 A66-23030
- Optimal control program satisfying all boundary conditions, noting application to thrust vector control 11 p1733 A66-23336
- Dynamic programming method for approximate solution of gliding flight and minimum time to climb problems in boundary value theory 11 p1778 A66-23349
- Uniqueness theorems for second-order linear elliptic and parabolic equations with discontinuous boundary values 11 p1724 A66-23362
- Mechanical flow processes and variational methods based on fluctuation theory, noting relations on minimum entropy production,



two-dimensional laminar flow of incompressible fluid, etc 12 p1975 A66-23543  
Eigenfunction expansions and scattering theory for free-space wave equation in exterior region 12 p1912 A66-23563  
Schauder-type solution estimates to first boundary value problem for parabolic equations of order 2p 12 p1901 A66-23663  
Boundary value problem solutions in meteorology 12 p1905 A66-23664  
Estimates of solutions to second order differential equations generalized to include inequalities with Schwarz derivative numbers 12 p1902 A66-23768  
Subinterval optimization technique for final value control system with magnitude constraint on control variable 12 p1848 A66-23852  
Quasi-linear boundary value problems solved with Galerkin convergence method 12 p1902 A66-23863  
Eigenfunctions for laminar flow in porous two-dimensional channel subject to certain boundary conditions 12 p1862 A66-23994  
Boundary value problem of acoustic point source antenna within compressible plasma region with assumed rigid boundary, noting acoustic power conversion into electromagnetic waves 12 p1920 A66-24116  
Axisymmetric problems of heat conductivity theory for layer with one constant boundary and one circular boundary solved by paired integral equations method 12 p1978 A66-24207  
Majorants of solutions of first boundary problem for second order linear elliptic equations 12 p1904 A66-24238  
Boundary value problem solution constructed as expansion of particular solutions of Chaplygin equation in region bounded by parabolic line and two characteristics 12 p1904 A66-24240  
Boundary value problems in plane and axisymmetric hypersonic flow of viscous ideal gas past blunt body 12 p1797 A66-24343  
Heat conduction problem simulation, using moving interfaces, solving Stefan and Verigin problems 12 p1978 A66-24371  
Plane stationary problem of heat conduction for mixed boundary conditions solved, using Fredholm integral equation with symmetrical kernel 12 p1979 A66-24372  
Maximized elliptic equations, Dirichlet problem, distance function solution, maximum principle, removable singularity, etc 12 p1905 A66-24401  
Charge sheath role at discharge wall in determining boundary conditions for LF wave in low pressure discharge, using hydrodynamical model 12 p1923 A66-24571  
Ion acoustic waves propagating along cylindrical plasma column analyzed, deriving boundary condition at plasma surface 12 p1923 A66-24572  
Uniqueness theorem of axisymmetric exterior traction boundary value problem in linear elastostatics theory 12 p1971 A66-24818  
Orr-Sommerfeld equation regarding stability of parallel flows solved for large Reynolds number, using inner and outer expansion theory 12 p1866 A66-24944  
Two-dimensional Stokes flows for functions time-periodic with common frequency, noting analogy to oscillations of long cylinder in viscous fluid 12 p1867 A66-24963  
Theorems associated with surface parabolic potentials 13 p2116 A66-25334  
Mathematical programming methods for solving nonlinear state-constrained discrete optimal control problems 13 p2047 A66-25352  
Reducing optimal control variational problems to limit problem associated with Hamilton-Jacobi equation 13 p2047 A66-25423  
Cold forming of metals, noting thin tube flow boundary variation with permanent deformation due to torsion and tension 13 p2195 A66-25455  
Maximum friction along jet path in mixing zone at constant pressure applied in finding irrotational wall velocity 13 p2063 A66-25468  
First boundary value problem for general case of axisymmetric stressed state of body of revolution, using biharmonic solution of Love and Grodskii 13 p2196 A66-25636  
Plasma stability with plane boundary, noting effect of perturbed electric field, particle trajectory and equilibrium distribution 13 p2144 A66-25726

Weak, strict and strict-weak Levi conditions defined in complex variables, noting conditions for holomorphy and coincidence of functions 13 p2118 A66-25787  
Stress state of weakly curved cylindrical shell analyzed, finding biharmonic function from given boundary value of partial derivatives 13 p2197 A66-25853  
Equation for elliptical system in plane singly connected region, satisfying specified boundary condition 13 p2119 A66-25903  
Boundary value problem for quasi-linear elliptic equations degenerating parabolically on boundary of region D lying in upper half-plane 13 p2119 A66-25904  
Existence and uniqueness of solution for first boundary value problem of system of specified mixed-type differential equations 13 p2119 A66-25905  
Deriving nearly periodic solutions for Sobolev equation with near periods dependent on spatial variables, constructing solutions for boundary value problem of Hopf equations 13 p2119 A66-25906  
Schauder-type boundary estimates for solution of directional-derivative problem of parabolic equation in noncylindrical region 13 p2120 A66-25909  
Dirichlet problem for elliptical system, showing solvability of inhomogeneous system with uniform boundary values for half-plane and circle cases 13 p2120 A66-26008  
Second-order elliptical operator for m-dimensional Euclidean space with open region bounded by closed surface 13 p2120 A66-26010  
Approximate analytical solutions for distributed parameter networks with parameters as functions of spatial variable, using differential equation that reduces boundary value problem to Sturm-Liouville system 13 p2120 A66-26068  
Analog computer solution of simplified turbulent viscous layer boundary value problem 13 p2064 A66-26370  
Stressed state of spherical shallow shells determined by satisfying boundary conditions and using infinite sets of algebraic equations 13 p2202 A66-26412  
Static boundary value problem for shallow shells with multiply connected sections 13 p2202 A66-26414  
Boundary conditions in bending theory of reinforced shells, noting decreased stress concentration obtained by reinforcement ring 13 p2204 A66-26431  
Airy stress function applied in solving problems for doubly connected regions with contiguous circular boundaries 13 p2204 A66-26432  
Conformal mapping of unit circle onto given, singly connected or multiply connected region bounded by simple closed contour 13 p2204 A66-26433  
Self-similar solutions for Mises equation of boundary value problem in incompressible gas flow 13 p2065 A66-26486  
Net-point method determination of two finite-difference systems for systems of Navier-Stokes equations 13 p2066 A66-26504  
Nonsteady motion of slender body near interface between fluids of different densities 13 p2067 A66-26536  
Inviscid hypersonic flow of nonuniform incident stream over wedge, noting vorticity effects, perturbation equations and boundary conditions 13 p1992 A66-26665  
Electrical analogy for turbulent liquid metal heat transfer in noncircular duct entrance region, solving Fourier equation, determining fluid boundary conditions, temperature distribution, etc 13 p2210 A66-26717  
Optimal control problems described by classical boundary problems for equations of parabolic and hyperbolic type 14 p2263 A66-26768  
Boundary problem describing plane jet steady state flow of ideal incompressible fluid, reducing solution to nonlinear integro-differential equations 14 p2272 A66-26775  
First boundary value problem for nonlinear second order differential equations 14 p2320 A66-26942  
Boundary value problems for minimal surface equation 14 p2320 A66-26943  
Electrodynamic boundary conditions at moving boundary, determining fields in

interior of semiinfinite fixed channel 14 p2235 A66-2704  
Uniqueness of operator spectral function of self-adjoint boundary value problem involving second-order differential equation with operator coefficients 14 p2320 A66-2715  
Green function of high degree of self adjoint expansion of elliptic operator generated by differential expression in smooth inside domain and on smooth part of boundary 14 p2321 A66-2716  
Regularity properties of functions from domains of definition of minimum and maximum operators for general elliptic problem with inhomogeneous boundary conditions 14 p2321 A66-2716  
Solution of quasi-static problem in thermoelasticity for cylinder with time dependent boundary conditions obtained as series of Bessel functions and error functions 14 p2397 A66-2738  
Boundary value problem of elastic/viscoplastic beams solved, using iteration method, noting wave propagation, and effect of shear and inertia of axial motion of beam in motion equation 14 p2397 A66-2738  
Solution of boundary value problem for three-dimensional wave equation applied to supersonic gas flow past wing in presence of shock wave, obtaining velocity potential 14 p2218 A66-2738  
Stresses and displacements in circular cylinder of transversely isotropic material for mixed boundary conditions, obtaining solution by using partial differential equation 14 p2397 A66-2738  
Finite difference solution of nonlinear boundary value problem of Landau-Vlasov equation for charged particle for Maxwellian distribution function 14 p2344 A66-2762  
Decay of solutions of initial boundary value problem for hyperbolic equations in unbounded regions 14 p2322 A66-2762  
Green matrix of periodic boundary value problem for system of linear differential equations 14 p2322 A66-2767  
Thermal stresses in finite cylinder with prescribed temperature distribution on curved lateral surface and with ends in contact with smooth insulating plates 14 p2400 A66-2772  
Variational problem of designing maximum draft nozzle supersonic section for three dimensional supersonic flow 14 p2221 A66-2805  
Finite difference method solution of parabolic and hyperbolic partial differential equations in one space variable 14 p2324 A66-2814  
Nonlinear and constrained variational problems in search theory and boundary value problem construction by maximum principle 14 p2324 A66-2819  
Motion of material point in central force field, reducing problem to solution of boundary value problem based on Pontryagin maximum principle, using analog computers 14 p2245 A66-2828  
Basic equations and methods for transverse MHD flow analysis when Hall currents are not suppressed, noting set of suitable simplifications, restrictive conditions and boundary value considerations 14 p2346 A66-2830  
Thermoelasticity equations describing harmonic vibrations of medium solved via singular integral equation 14 p2408 A66-2839  
Stresses and coupled-stresses generated by dislocation in isotropic media treated in terms of boundary value problem for Cosserat medium 14 p2409 A66-2846  
Dual integral equation and dual series analysis and application to mixed boundary value problems in elasticity, hydrodynamic, and electrostatics 15 p2526 A66-2895  
Dual integral equations in elasticity theory noting Mehler-Fok transformation of spherical functions, Fredholm equation and application to mixed boundary value problems 15 p2526 A66-2895  
Asymptotic solutions of boundary value problems for elastic semiinfinite circular cylindrical shells by removing restriction on slow circumferential variation 15 p2609 A66-2923  
Stabilization of unstable two-point boundary value problems, noting field



- method for avoiding computer storage problems during integration of related differential equations 15 p2528 A66-29292
- Extension to MHD hypersonic stagnation flow theory of Bush, including viscous term and solving boundary value problem from both ends at once 15 p2424 A66-29307
- Singular integral equations for thermoelasticity equations describing harmonic oscillations of medium, applied in boundary value problems 15 p2611 A66-29419
- Instability of nonlinearly viscoelastic column under finite compression, noting boundary conditions, application to buckling problem, types of stability loss, etc 15 p2615 A66-29720
- Lagrangian multiplier method applied to mixed boundary value problems such as stresses due to temperature changes in semiinfinite slab 15 p2615 A66-29733
- Linear initial value problems involving first order differential equations transformed into higher order systems and treated as boundary value problems, using numerical techniques 15 p2529 A66-29773
- Sandwich panel bending under thermal and mechanical loads, solving differential equations for temperature distribution, transverse load and uniform edge compression with boundary conditions 16 p2812 A66-30218
- Error bounds based on a priori inequalities for solutions of boundary value problems for linear elliptic partial differential equations 16 p2731 A66-30236
- Linear integral operators applied to singular differential equations and to computations of compressible fluid flows 16 p2683 A66-30241
- Hermite interpolation combined with Ritz method for numerical approximation of solution of two-point boundary value problems 16 p2732 A66-30243
- Linearized unsteady supersonic potential flow theory formulation of boundary value problem of aerodynamic forces on oscillating cylinder and comparison with two-dimensional quasi-steady and slender body approximations 16 p2628 A66-30259
- Nonlinear deformation theory of plasticity for plane strain which approximates isotropic hardening of von Mises loading surface by isotropic hardening piecewise linear loading surface 16 p2812 A66-30260
- General boundary conditions for second-order ordinary differential operators 16 p2733 A66-30630
- Riemann-Hilbert boundary value problem for elliptic systems of linear partial differential equations of first order 16 p2733 A66-30651
- Uniqueness and solution estimates to boundary value problems, noting solvability correlation with existence of Green function 16 p2733 A66-30739
- Solution of heat-conduction equation over functional spaces possessing fractional derivatives with respect to time, applied as solution to first boundary value problem 16 p2827 A66-30779
- Uniqueness of solution to second and third boundary value problems for second-order elliptic equation in presence of boundary singular points 16 p2734 A66-30783
- Normal solvability of Dirichlet problem for Bitsadze elliptic system, noting conditions under which homogeneous problem has nonzero regular solutions 16 p2734 A66-30784
- Solution of boundary value problems describing two-dimensional flow in plastic regions 16 p2815 A66-30789
- Intrinsic electric field of rarefied ion-electron plasma in external magnetic field and plasma stability, noting use of Galerkin method to determine plasma layer slippage 16 p2760 A66-30790
- General boundary value problems for general elliptic systems with discontinuous coefficients 16 p2735 A66-30965
- Expansion in eigenfunctions of not self-conjugate boundary value problem for differential equation with singularity at zero 16 p2735 A66-30969
- Boundary problems for differential and integro-differential equations 16 p2736 A66-30980
- Boundary value problem of temperature stresses of rectangular orthotropic plates solved, using separation of variables method 16 p2818 A66-31067
- Thermoelastic problem for plate with prismatic inclusion of rectangular cross section discussing stress, elastic deformation, displacement potential, etc 16 p2818 A66-31108
- Variational solution of simultaneous stability equations boundary value problem for transverse displacements and stress state 16 p2819 A66-31137
- Steady motion of viscous incompressible fluid between concentric spheres, injecting and ejecting fluid through inlet and outlet holes, describing boundary conditions by series expansion 16 p2687 A66-31294
- Shape and stability of liquid-gas interface in annular tank in force field determined by numerical integration of boundary value problem and eigenvalue [AIAA PAPER 66-425] 16 p2689 A66-31488
- Rigid revolution paraboloid pressure on plates and membranes with contour consisting of straight line segments 16 p2822 A66-31509
- Boundary conditions for existence of damped solutions to plane problem in elasticity theory for half-strip with stress-free longitudinal edges 16 p2822 A66-31525
- Dynamic influence of orography on atmospheric motion examined, using fluid mechanics analogy with periodicity as boundary condition 16 p2699 A66-31637
- Axiomatic theory of Dirichlet problem applicable to nonlinear PDEs and to systems of PDEs 16 p2738 A66-31704
- Solution of particular elementary boundary value problem using new set of orthogonal functions 16 p2739 A66-31726
- Book on similarity theory and physical interpretation, examining boundary value problems, dimensional analysis, etc 16 p2739 A66-31751
- Rational approximation and differential properties at boundary of analytic functions 16 p2739 A66-31796
- Mixed boundary value problem for parabolic hypoelliptic equation with two independent variables treated by modified potential method 16 p2740 A66-31798
- Finite difference estimation of boundary value problem errors 17 p2945 A66-31878
- Difference system and boundary conditions for primitive-equation barotropic forecast 17 p2948 A66-31942
- Symmetrical stress wave propagation in thin plate with small, circular hole at center, noting boundary conditions and solutions via Laplace transforms and by method of characteristics 17 p3022 A66-32012
- Kohn-Kato bounds for natural frequencies of axial shear vibrations for solid circular bar, extending calculations through conformal transformations for bar with many-lobed plane curved boundary 17 p3022 A66-32014
- Stress concentration factor for infinite plate in tension containing doubly symmetrical hole with three intersecting circles forming boundary 17 p3023 A66-32081
- Stochastic equation applied to investigating second boundary value problem for parabolic differential equations with small parameters 17 p2946 A66-32297
- Nonlinear parabolic equations, considering existence, uniqueness theorems, abstract Cauchy problem, etc 17 p2946 A66-32307
- Heat transfer problems solved, using Pohlhausen solution for phase-space trajectory, noting effect of boundary conditions and application of analog computer 17 p3034 A66-32497
- Arc operation under nonsteady electrical inputs, noting initial conditions, energy equation solution, temperature profiles, application of Green function for moving boundary problem, etc [AIAA PAPER 66-480] 17 p2970 A66-32769
- Stationary boundary value problem of Navier-Stokes equation for incompressible viscous fluids 17 p2911 A66-32817
- Evolution of two different homogeneous media separated by straight wall with arbitrary transmission and reflection properties, noting heat flow, vibration, diffusion coupled vibration, etc 17 p3036 A66-32842
- Boundary value problems in secondary creep of circular thin shells under axisymmetric loading, giving solutions for deformation rates and stress resultants 17 p3030 A66-32891
- Intensity of emergent radiation in finite homogeneous slab absorbing and scattering it isotropically, viewed as boundary value problem determined by imbedding techniques 17 p3037 A66-33012
- Thin circular cylindrical shell behavior in axial compression, noting buckling under stress, boundary condition detail effects, etc 17 p3031 A66-33064
- Textbook on differential equations with deviating arguments, covering existence theorems, linear equations, stability theory, boundary value problems, etc 17 p2947 A66-33188
- External gravity field and geodetic boundary value problem 17 p2921 A66-33195
- Loading of thin ring airfoil in unbounded spherical source flow field, calculating vortex distribution, strength, etc [ASME PAPER 66-FE-3] 17 p2914 A66-33259
- Direct method in calculus of variations for boundary value problem of Mangoron type 17 p2948 A66-33416
- Initial boundary value problems involving Maxwell equations in isotropic media solved numerically 18 p3065 A66-33533
- Equivalence between scalar three-dimensional diffraction problems in homogeneous medium and two-dimensional diffraction problems in inhomogeneous medium with inverse square permittivity profile 18 p3065 A66-33534
- Exact solution for Green function of open spherical shell subjected to harmonically oscillating concentrated load and any consistent boundary conditions [ASME PAPER 65-WA/APM-24/] 18 p3248 A66-33576
- Thrust programming in central gravitational field, discussing reduction of Mayer-Bolza variational problem to boundary value problem for system of nonlinear differential equations 18 p3241 A66-33846
- Sufficient conditions for boundedness of solutions of linear system of differential equations with variable coefficients 18 p3126 A66-33929
- Discreteness conditions for spectrum of one-term differential operator, considering asymptotic distribution of eigenvalues 18 p3126 A66-33931
- Infinite boundary value problem solution for third-order differential equations obtained in convergent series form 18 p3126 A66-33974
- Differential inequality theorem for boundary value problem involving second-order differential equation 18 p3126 A66-33975
- Existence, uniqueness and periodicity of solutions to boundary value problems for quasi-linear ODEs on topological space of continuous mappings 18 p3127 A66-34138
- Partial differential equation describing transient conduction in multidimensional inhomogeneous media solved by method based on use of known boundary conditions 18 p3262 A66-34380
- Existence and uniqueness of solution in viscoelasticity theory for aging materials, considering four boundary value problems for body subjected to finite deformations 18 p3255 A66-34393
- Additional conditions for boundary value problem with directional derivative in heat conduction 18 p3127 A66-34544
- Transverse propagation of waveguide modes in conducting cylindrically stratified magnetoplasma analogous to VLF radio waves propagating in Earth-ionosphere 18 p3071 A66-34565
- Asymptotic theory of spherical electrostatic probe in collision-dominated partially ionized gas by quasi-linearization 18 p3146 A66-34583
- Boundary value problem of Stokes equations proving branching for flow between two rotating concentric cylinders and nonexistence of singular flow 18 p3101 A66-34659
- Flow of incompressible viscous fluid subject to conditions governed by Navier-Stokes equation, examining fluid velocity as time tends to infinity 18 p3101 A66-34660



Mixed initial boundary value problem for wave equation in three space dimensions, proving existence of generalized solution 18 p3128 A66-34662

Variational principle applied to boundary value problems in kinetic theory, specifically examining Kramer problem, plane Couette flow and plane Poiseuille flow 18 p3102 A66-34919

Transverse boundary effects on ionic-acoustic wave propagation in magnetoplasma 18 p3150 A66-34938

Plane steady state problem solved in thermoconductivity theory in case of boundary conditions of third kind for regions of special shape 18 p3267 A66-35055

Bjerhammar gravimetric boundary value problem with gravity reduction defined by integral equation 19 p3345 A66-35393

Quantitative examination of Saint Venant principle in context of elastostatic boundary problems, i.e., axisymmetric pure torsion of bodies of revolution 19 p3473 A66-35485

Analog computer solution of high-order optimal control problem, noting application of Pontryagin maximum principle and extension to two-point boundary value problems 19 p3306 A66-35536

Perturbation method solution of rectangular waveguide boundary value problem filled with transversely magnetized semiconductor or plasma 19 p3317 A66-35716

Displacement boundary value problem in classical linear elastostatics, deriving ellipticity condition for uniqueness theorem 19 p3474 A66-35852

Asymptotic solutions for large time obtained for predominantly mechanical mode of one-dimensional solution of coupled thermoelastic equations 19 p3400 A66-35853

Vector formulation of boundary value optimization problems 19 p3388 A66-35871

Comparison of parameter hunting procedures and implementation techniques for solving higher order boundary value problems with rapid convergence [AIAA PAPER 65-693] 19 p3462 A66-35900

Low thrust trajectory optimization, using Newton-Raphson method to solve nonlinear two-point boundary value problem [AIAA PAPER 65-698] 19 p3462 A66-35904

Solution of mixed boundary and Cauchy problem for system of PDE 19 p3389 A66-35933

Third boundary problem solution for two-dimensional equation of thermal conductivity in arbitrary region by locally one-dimensional method 19 p3478 A66-35934

Difference analog construction for second-order elliptic differential equation in case of rectangular network 19 p3389 A66-35935

Sensitivity analysis and invariant imbedding, discussing application to adaptive control theory and reduction of boundary value problems to initial value problems 19 p3326 A66-36011

Solution of two-point boundary problems in optimal control syntheses in which sensitivity coefficients for differential equations satisfy jump conditions at discontinuity point 19 p3327 A66-36017

Eigenvalue problems for systems of ordinary differential equations resolved computationally by use of quasi-linearization technique 19 p3310 A66-36046

Schauder-type solution estimates to first boundary value problem for parabolic equations of order 2p 19 p3390 A66-36193

Boundary value problem solutions in meteorology 19 p3394 A66-36194

Theorems associated with surface parabolic potentials 19 p3390 A66-36195

Diffraction of electromagnetic plane by half-plane in uniaxially anisotropic medium solved in terms of Sommerfeld approximation 19 p3304 A66-36284

Min-H Strategy in deriving two iterative methods for rapid convergence to optimum solutions for nonlinear variational two-point boundary value problems 19 p3466 A66-36677

Nonlinear and nonstationary finite differential system identification by quasi-linearization and differential approximation 19 p3335 A66-36701

Iterative approximation method for solution of proper elements /eigenvalue/ of Sturm-Liouville equation 19 p3392 A66-36783

Elastic deformation of unbounded

transversely isotropic body with internal plane-circular slot under slot surface load 19 p3476 A66-36839

Iterative solution of time optimal control boundary value problem resulting from application of Pontryagin maximum principle 20 p3535 A66-36850

Weierstrass necessary condition and basic equations for optimal control of initial or boundary states of continuum mechanical MHD and hypersonic partial differential systems 20 p3535 A66-36853

Asymptotic behavior of solutions to boundary value and initial problems for ODE with small parameter, using functions of power law boundary layer 20 p3590 A66-37109

Continuous plane with circular inclusion with different elastic properties, giving solution in form of boundary equation in random variable 20 p3668 A66-37530

Application of Rayleigh principle to obtain sharp upper bounds for increase of first eigenvalue of membrane submitted to parallel and equidistant rectilinear constraints 20 p3669 A66-37544

Electric analogs construction for stability and oscillation of elastic system 20 p3670 A66-37674

Boundary value problem of wave equation with application to antenna theory of singular integral equations 20 p3531 A66-37730

Plane linearly polarized electromagnetic wave diffraction on several spheres forming linear system, showing solution of boundary value problems 20 p3603 A66-37754

Solvability and methods of solution of boundary value problems noting uniqueness, potential theory application in solving polyharmonic equations and second-order equation 20 p3591 A66-37757

Reflection coefficients of plane wave field in grid-Earth system, using averaged boundary conditions 20 p3518 A66-37865

Ablation analysis in cylindrical coordinates for axisymmetrical configuration of wall materials with temperature-dependent properties and nonlinear heat flux conditions at boundaries [AIAA PAPER 66-542] 20 p3680 A66-38034

Boundary conditions of downstream singularity in nonadiabatic flames 20 p3680 A66-38048

Magnetospheric boundary phenomena, noting dependence of charged particle observations on character of associated magnetic fields 20 p3641 A66-38329

Boundary value problems for Sturm-Liouville-type equation with asymptotic formula derived for eigenfunctions 20 p3592 A66-38420

Boundary value problems with natural boundary conditions solved by representing desired solution by finite sum 20 p3592 A66-38423

Eigenfunction expansion of analytic linear ordinary differential operators of boundary value problem with normalized irregular discontinuous boundary conditions 20 p3592 A66-38432

Linear elliptic partial differential systems, eigenvalue and boundary value problems - Johns Hopkins University, Lectures, March-May 1965 21 p3754 A66-38457

Well-posed BVP for linear partial differential system and relation of weak solution with two Banach spaces 21 p3754 A66-38458

Semiweak solutions of elliptic BVP, particularly generalized Dirichlet problem 21 p3754 A66-38461

Existence and uniqueness theorems for Dirichlet problem of second-order linear elliptic equation, Neumann BVP, mixed BVP and oblique derivative problem 21 p3754 A66-38462

Linear elastostatic BVPs for inhomogeneous anisotropic elastic body including existence-uniqueness theorem, based on Korn inequality 21 p3755 A66-38463

Elliptic BVP in equilibrium theory of thin plates employing iterated Laplace operator 21 p3822 A66-38464

Elliptic singular integro-differential operators on smooth compact manifold without and with boundary 21 p3756 A66-38626

Closed loop optimization of fixed

configuration systems termed specific optimal control solved by applying Pontryagin maximum principle to reduce problem to two-point boundary value problem 21 p3718 A66-38662

Mathematical model of linear guidance law to dynamical system, noting reduction of two-point boundary value class error 21 p3765 A66-38870

Existence of angular boundary values of harmonic function in sphere 21 p3757 A66-38902

Computer analysis of cylindrical shell stability under uniform external pressure and critical pressure determination for various boundary conditions 21 p3829 A66-38970

Energy transport mechanism in magnetosphere analyzed by study of character of three-dimensional hydromagnetic waves in uniform cold plasma 21 p3734 A66-39218

Existence conditions of solution to two-point boundary value problem for ordinary nonlinear any order differential equation 21 p3757 A66-39248

Necessary and sufficient conditions for matrix satisfying discrete maximum principle and difference methods for numerically solving second-order elliptic boundary value problem 21 p3757 A66-39258

Dynamic behavior of soap film stretched between two coaxial rings, assuming potential energy of this surface to be proportional to surface area 21 p3772 A66-39352

Stress function and displacement vector for linear, homogeneous, isotropic and elastic material body occupying bounded simply connected region of space 21 p3772 A66-39352

Extension of extremum principles concerned with velocity fields for boundary value problems of incompressible rigid viscoplastic /Bingham/ solid 21 p3832 A66-39440

Flight stability, discussing quasi-critical case in neighborhood of asymptotic stability boundary of autonomous systems and that of variable system parameters 21 p3696 A66-39594

Bending of anisotropic cylindrical bodies with curved axis under transverse force 21 p3833 A66-39595

Haag general synchronization theory for oscillating systems with one degree of freedom applied to boundary value problems for multivibrating systems 21 p3774 A66-39607

Boundary value problem for equation of mixed type with two intersecting parabolic lines of degeneration, reducing it to integral equation with solution in half-plane 21 p3758 A66-39613

Boundary value problem for isothermal unidirectional deformation of hyperelastic material applied to inflation of thick walled sphere 22 p3988 A66-39673

Book on boundary value problems and partial differential equations for electric circuits and other engineering problems 22 p3938 A66-39703

Heat equation solution by use of Crandall optimum finite difference method with boundary discontinuity 22 p3997 A66-40029

Hamilton principle, motion equations, natural boundary conditions and constitutive relations for finite deformation of one-dimensional curved elastica and radial motion and stability of circular ring 22 p3990 A66-40138

Wiener-Hopf and series solutions to BVP of indentation stresses and displacements in infinite hollow elastic cylinder for axisymmetric punch of finite length and arbitrary profile 22 p3990 A66-40139

Stressed state near round opening in orthotropic cylindrical shell solved for various loading and boundary conditions by Bubnov-Galerkin variational method 22 p3990 A66-40145

Effect of stiffening ribs on stressed-strained state of shallow symmetrically loaded conical shells, noting reduction of boundary value problem to integration of differential equations 22 p3991 A66-40150

Mixed boundary value problem in elasticity of circular and quarter-plane



segments 22 p3991 A66-40153  
 Conformal mapping technique applied to boundary value problem of plane wave diffraction by perfectly conducting elliptic cylinder, noting integral 22 p3866 A66-40185  
 Cauchy and boundary value problems for second-order hyperbolic equations 22 p3939 A66-40189  
 Uniqueness of solution to second and third boundary value problems for second-order elliptic equation in presence of boundary singular points 22 p3940 A66-40445  
 Normal solvability of Dirichlet problem for Bitsadze elliptic system, noting conditions under which homogeneous problem has nonzero regular solutions 22 p3940 A66-40446  
 Infinitely small bending deformations of convex surfaces with boundary condition of generalized slip, formulating boundary value problem for bending of surface 22 p3995 A66-40450  
 Nonlinear boundary value problem for temperature distribution in convex solid with radiation boundary condition 22 p3999 A66-40565  
 Axisymmetric problems of heat conductivity theory for layer with one constant boundary and one circular boundary solved by paired integral equations method 22 p4000 A66-40571  
 Book on numerical processes in differential equations including initial value and boundary value problems 22 p3941 A66-40620  
 Small parameter method to study steady state flow of viscous incompressible fluid in journal bearing 22 p3928 A66-40688  
 Matrix functions and use in problems of heat and mass transfer 22 p4000 A66-40820  
 Projection method for obtaining upper and lower bound estimates of solutions to elliptic equations 22 p3942 A66-40914  
 Variational techniques in solving BVPs for nonlinear plastic, elastoplastic and viscous media and in predicting existence, uniqueness and equilibrium conditions 23 p4136 A66-40996  
 Shell dynamical integral and integro-differential BVPs for linear deformable shells, examining reciprocity theorem and Kirchhoff-Lowe hypothesis 23 p4136 A66-40997  
 Soviet literature survey of exact and approximate solution of two- and three-dimensional mixed boundary value problems in theory of elasticity 23 p4136 A66-40999  
 Approximate solution of boundary value problems in elasticity theory as applied to thin plate theory, using homogeneous equations 23 p4136 A66-41000  
 Axisymmetric dynamic response of ring supported cylinder to time dependent loads, discussing boundary conditions and differential equations of motions [AIAA PAPER 66-83] 23 p4138 A66-41106  
 Parameters of dynamic systems described by PDEs determined by replacing PDE with integral equation and eliminating via recursion process terms resulting from initial and boundary conditions 23 p4084 A66-41396  
 Initial broadening of diffusion flame sheet caused by nonvanishing equilibrium constant determined, using method of inner and outer expansions 23 p4148 A66-41500  
 Rall theorem on variational principle for linear elastodynamic BVPs on Hilbert space 23 p4138 A66-41538  
 Existence and uniqueness theorems in Poincare-Liapunov theory for multipoint control boundary value problems 23 p4085 A66-41539  
 Invariant imbedding and scattering of light in one-dimensional medium with moving boundary, noting relaxation of photon emission and Doppler frequency shift 23 p4087 A66-41540  
 Wiener-Hopf solution of thermoconductivity boundary value problems 23 p4149 A66-41558  
 Proof of existence of boundary value solutions for various mixed component equations by reduction to singular integral equation 23 p4085 A66-41562  
 Analog of Galerkin method for solving boundary value problems and quasi-linear operator equations 23 p4086 A66-41569

Pontryagin maximum principle applied to solution of optimal control problems by hybrid computer, using digital parameter optimizer to solve two-point boundary value problem 23 p4042 A66-41601  
 Numerical solution of BVP for optimal control parameters in trajectory analysis 23 p4051 A66-41617  
 Boundary conditions for unique solution to linearized warm plasma equations 23 p4105 A66-41640  
 Fredholm integral equations obtained in study of boundary value problem occurring in thin shallow shell theory 23 p4140 A66-41835  
 Approximate solution of certain mixed plane boundary value problems involving isotropic elastic body 23 p4140 A66-41836  
 Thermal transport in channel-gas flow, discussing integral equation and power series solution 23 p4150 A66-41869  
 Mixed boundary value problem of theory of analytic single-value function 23 p4086 A66-41873  
 Boundary value problem of steady two-dimensional MHD flow of viscous incompressible fluid past rigid plate 23 p4106 A66-41875  
 Trefftz method applied to derivation of integral for general boundary value problem in classical theory of elasticity 23 p4144 A66-41968  
 Inviscid hypersonic flow past flat wings at large angle of attack analyzed, using homogeneous layer concept of shock layer theory 23 p4013 A66-42014  
 Generalized solution to linear second-order parabolic equation showing that first boundary value problem has unique solution, obtaining estimates of Holder norms of solutions 24 p4231 A66-42233  
 Classical character of generalized solution of boundary value problem for general nonlinear Navier-Stokes equations 24 p4231 A66-42235  
 Benard convection between free bounding surfaces for ranges of Rayleigh and Prandtl numbers achieving steady state with motion of single large cell, evaluating eigenfunction amplitudes 24 p4293 A66-42409  
 Graphical construction and geometrical interpretation of particular analytical solution for determining ionic orbits subject to certain boundary conditions 24 p4277 A66-42685  
 Bifurcated parallel plate waveguide solution extended to solution of open ended parallel plate waveguide radiating into space 24 p4184 A66-42703  
 Isentropic two-dimensional nonstationary flow of polytropic gas adjoining region with quiescent gas, constructing approximate picture of motion near arbitrary discontinuities 24 p4195 A66-42723  
 Net point method determination of two finite difference systems for systems of Navier-Stokes equations 24 p4195 A66-42724  
 Hilbert parametrix method of solving linear BVPs for second-order elliptic PDEs, using Green functions 24 p4232 A66-42740  
 Weak and strict solution existence theorem for initial-boundary value problem for nonlinear hyperbolic equation in relativistic quantum mechanics 24 p4237 A66-42829  
 Single second-order oblique derivative problem with elliptic operator 24 p4232 A66-42830  
 Two mixed boundary value problems of infinite elastic cylinder under torsion solved by dual integral equation with differentiation of boundary conditions 24 p4291 A66-42843  
 Numerical solution of linear boundary value problems 24 p4233 A66-43201

# **BOUNDARY VALUE PROBLEM**

Torsion of elastic rectangular bar with similarly distributed external tangential loads applied at both ends 24 p4289 A66-42436

# **BOUSSINESQ APPROXIMATION**

Temperature distribution in flow past sphere, discussing time dependent form of Boussinesq transformation [ASME PAPER 65-HT-38] 05 p0784 A66-14752  
 Boussinesq approximation for hydrodynamic stability of natural thermal convection of fluid between two parallel vertical planes and calculation of critical

Reynolds number 15 p2617 A66-29399  
 Energy method applied to stability of flows governed by nonlinear Boussinesq equations, establishing universal stability region in Reynolds-Rayleigh number plane 19 p3478 A66-36199  
 Thermal convection in horizontally infinite layer of fluid confined between rigid heat conducting plates driven by temperature difference 23 p4151 A66-42055

# **BOW SHOCK**

Model of Fermi acceleration at shock front developed and applied to Earth bow shock 13 p2184 A66-25620  
 Electron acceleration near Earth bow shock measured, using Explorer XVIII satellite, noting solar wind effect, energy spectrum in radiation belt and magnetospheric boundary, etc 13 p2175 A66-26355  
 Time required for detached bow shock to reach equilibrium 17 p2840 A66-32483  
 Interaction of first and second shocks of blast-bow wave in double-driver shock tube, examining stagnation point pressure prediction methods [AIAA PAPER 66-409] 17 p2840 A66-32748  
 Energy spectrum change of group of electrons being convected downwind in magnetosheath and behind Earth bow shock 18 p3170 A66-34521  
 Shock wave instability and mass flow accommodation for ribbon-type parachutes, noting canopy porosity and free stream Mach number 22 p3845 A66-40594

# **BOWEN HYPOTHESIS**

Slit spectrograph theory of Bowen for use with medium size astronomical telescopes 02 p0229 A66-11701

# **BOX BEAM**

Deformation of cantilever parallelogram box beam 12 p1969 A66-24365  
 Design, fabrication and test of sandwich construction box beam made of D-43 columbium and Haynes 25 superalloy for use as hot redundant structure for hypersonic vehicles 16 p2816 A66-30894

# **BRAGG EQUATION**

Temperature effect on diffraction curve profile for Bragg case using triple crystal spectrometer, observing intrinsic temperature effect due to thermal motion 06 p0923 A66-16186  
 Existence of vortex lines in superconducting niobium in mixed state demonstrated via neutron diffraction 09 p1420 A66-20050  
 Integral equations describing multiple neutron Bragg reflections in mosaic crystal 11 p1742 A66-23409  
 Horizontal deflection in TV display produced by Bragg reflection of laser light by ultrasonic waves in water 24 p4212 A66-42816

# **BRAIN**

SA CEREBRAL CORTEX  
 SA ELECTROENCEPHALOGRAPHY  
 SA HYPOTHALAMUS

Alpha particle and X-radiation ionizing effects on cerebral astroglial cells and blood vessels of young rats 10 p1487 A66-22020  
 Importance of neural site and experimental conditions in determining motivational direction /positive or negative/ produced by electrical stimulation of brain in animals 11 p1644 A66-22976  
 Holtzman strain experiments on rats, determining if electrical stimulation of various neural sites produce motivational consequences of appetitive or defensive behavior 13 p2009 A66-25790  
 Correlation between survival time of rats under acceleration stress and cerebral level norepinephrine 17 p2855 A66-32145  
 Neuronal circuitry relations of cat mammillary nuclei derived from neuron population ratio computed from population data 18 p3058 A66-34067  
 Neuronal circuitry and neuron populations of structures in normal animal brains and brains modified by unambiguous lesion arrays 20 p3505 A66-37053  
 Operant conditioning of single unit responses, considering hippocampus and midbrain tegmentum 20 p3506 A66-37601  
 Spectral analysis of human EEG generators in posterior cerebral regions 20 p3506 A66-37604  
 Hypoxia of simulated high altitude



- exposure prolongs synaptic delay and conduction time in brain system of rats 22 p3855 A66-40403
- Physiological and mechanical effects of radial accelerations on brain temperature of dog and rabbit 23 p4026 A66-41336
- Vibration effect on bioelectric activity of brain and oxygen consumption, using experimental rats 23 p4027 A66-41340
- Molecular and ultrastructural correlates of function in neuron, neuronal nets and brain studied, using genetic and immunological concepts 24 p4165 A66-43102

**BRAIN CIRCULATION**

- Rheographic regional method for evaluation of cerebral and ocular circulation in cardiac and cerebrovascular disease 04 p0463 A66-14002
- Blood flow rate in surface veins of brains of animals subjected to accelerations, noting thermal transducer 15 p2445 A66-29500
- Change pattern in human cerebral blood flow during time immediately following initiation of carbon dioxide inhalation 18 p3056 A66-33691
- X-ray irradiation effect on venous blood flow in rabbit brain vessels 23 p4027 A66-41344

**BRAKE**

- SA AIRCRAFT BRAKE
- SA WHEEL BRAKE
- Aerodynamic forces acting on wings with braking flaps 19 p3275 A66-35365
- Minimum of maximum overload in braking of vehicle in atmosphere, examining aerodynamic lift on basis of Pontryagin maximum principle 22 p3986 A66-40465

**BRASS**

- Stress-corrosion cracking, rate of weight loss and surface condition of 70-30 copper zinc alloy in concentrated aqueous ammonia 07 p1053 A66-18519
- Diffusivity, elastic modulus and stacking fault energy effect on high temperature creep behavior of alpha brasses 11 p1717 A66-22996
- X-ray study of 16 monolith and powdered brass samples with 30.07 to 40.1 percent copper, indicating two phase fields for gamma region of Cu-Zn system 12 p1896 A66-24866

**BRAYTON CYCLE**

- Brayton cycle nuclear space power systems and heat transfer components 01 p0016 A66-10913
- Recuperative Brayton cycle for nuclear-electric spacecraft power supplies [AIAA PAPER 64-757] 13 p2005 A66-26620
- Brayton-cycle space power system, describing solar collector, heat receiver/storage unit, recuperator, radiator and gas bearings [AIAA PAPER 64-726] 13 p2006 A66-26635
- Thermal energy storage using solar Brayton cycle cavity receiver with lithium fluoride heat storage [AIAA PAPER 64-727] 13 p2006 A66-26636
- Gas lubricated bearings used in Brayton cycle closed-loop system turbomachinery in design of two-shaft power plant [ASME PAPER 66-GT/CLC-9] 14 p2300 A66-26982
- Closed Brayton cycle for onboard generation of space vehicle electric power from solar, isotope and nuclear reactor energy source [ASME PAPER 66-GT/CLC-10] 14 p2224 A66-26983
- Design of 500-kwe closed Brayton cycle power conversion system, analyzing various turbomachinery configurations hermetically sealed and operating on gas bearings [ASME PAPER 66-GT/CLC-15] 14 p2225 A66-26985
- Brayton cycle, Rankine cycle and thermoelectric systems considered as radioisotope secondary power systems for MOL [ASME PAPER 65-AV-18] 16 p2636 A66-30856
- Electrical power control and conditioning subsystem for Manned Orbital Research Laboratory /MORL/, noting Brayton cycle, system optimization, alternator and frequency converter selection 20 p3497 A66-37157
- Dynamic power generating systems using Rankine and Brayton cycles for space application 20 p3598 A66-37256

- Closed Brayton cycle power system for space vehicles, discussing closed loop and major components 23 p4020 A66-41750
- Plutonium-238 radioisotope Brayton cycle power system design and vehicle integration 23 p4021 A66-41754
- High temperature testing and evaluation of graphite helical-screw expanders and compressors for use with inert gas Brayton cycle 23 p4075 A66-41755

**BRAZIL**

- Space research activities in Brazil 15 p2601 A66-29935

**BRAZING**

- SA SOLDERING
- SA WELDING
- In situ ultrasonic testing of brazed hydraulic pipe joints in aircraft, noting superiority over radiography 01 p0079 A66-10973
- Brazing and diffusion bonding of titanium alloys to similar and dissimilar materials in high vacuum or inert gas [SAE PAPER 650752] 05 p0687 A66-15001
- Techniques of joining aluminum to stainless steel for space vehicle application [SAE PAPER 650754] 05 p0701 A66-15002
- High remelt temperature brazing of Ta-10W honeycomb structures by brazing with pure titanium, using diffusion sink concept 13 p2109 A66-25774
- Chromium-vanadium alloys for brazing tungsten to molybdenum in engine application 13 p2087 A66-26020
- Brazed hydraulic system design and fabrication for Skyhawk A4B aircraft 17 p2849 A66-33098
- Brazed lap joints between stainless steel and tantalum or Ta-10W alloy obtained with pure copper or silver-copper-base brazing alloys 19 p3367 A66-36112
- Refractory metal brazing alloys developed for producing brazed refractory metal sandwich panels 19 p3367 A66-36113
- High-temperature brazing materials for niobium and tungsten with tensile-shear strengths in excess of 7000 psi at 2500 degrees F 19 p3367 A66-36114
- Reactive brazing alloys evaluated for columbium alloy foil brazing in order to avoid erosion and embrittlement of conventional brazing alloys 19 p3367 A66-36115
- Exothermic brazing of refractory metals, tabulating braze filler metals that formed acceptable joints with molybdenum, tungsten and TZM alloy 19 p3367 A66-36117
- Brazing and cladding research on refractory metals offers dependability and continuity of protective layers and abrasion resistance in extreme environments 19 p3368 A66-36119
- Protective coatings for titanium and tantalum refractory alloy brazing envelopes, offering ephemeral protection from oxidation at ultrahigh temperatures 19 p3384 A66-36143
- Solid state welding and brazing for surface layer bonding 22 p3925 A66-40269

**BREAKDOWN**

- S ELECTRIC BREAKDOWN
- S VOLTAGE BREAKDOWN
- S VORTEX BREAKDOWN

**BREATHING**

- S AIRCRAFT BREATHING APPARATUS
- S HIGH ALTITUDE BREATHING
- S LIQUID BREATHING
- S OXYGEN BREATHING
- S PRESSURE BREATHING
- S RESPIRATION
- BREATHING MODE
- Dynamic behavior of aircrew breathing equipment considering cyclic flow response tests, stability problems, measurement techniques and human respiratory impedance 03 p0329 A66-13350

**BREATHING VIBRATION**

- Thermal events in diurnal breathing cycle and vapor loss reduction in volatile liquid storage [AICE PREPRINT 11C] 10 p1521 A66-21181
- Liquid instability of vibrating partially filled elastic tank, emphasizing resonant breathing mode and frequency response 20 p3672 A66-38153

**BREGUET 941 AIRCRAFT**

- Breguet 941 STOL aircraft advantages over conventional commercial jet aircraft to solve

- requirements imposed on airport facilities 02 p0177 A66-1174
- Breguet 941 STOL aircraft design and performance, noting maximum lift coefficient and single-shaft power plant 10 p1483 A66-2171
- Breguet 941 STOL aircraft, considering possibilities as television relay platform with Citroen ID 19 station wagon 14 p2238 A66-2767
- BREGUET 942 AIRCRAFT**
- Organization of short-distance interurban transportation system based on STO aircraft of Breguet type 05 p0611 A66-1519
- BREGUET 1150 AIRCRAFT**
- Breguet 1150 high seas reconnaissance aircraft, noting design features and technological problems 24 p4159 A66-4248
- BREMSTRABLUNG**
- SA X-RAY
- Transition and bremsstrahlung spectrum from measurement of energy dependence of visible and UV radiation emitted from electron bombarded Ag targets 01 p0108 A66-1019
- Radiation hazard for cosmonaut inside outside spaceship from Earth radiation belt, considering electron radiative effect, tissue sensitivity, etc 02 p0182 A66-1166
- Galactic X-ray astronomy discussing neutron stars, thermal bremsstrahlung and synchrotron radiation 02 p0290 A66-1186
- Cut-off of ruby laser emission by pulse electron and bremsstrahlung radiation, using adiabatic temperature 03 p0377 A66-1244
- Enhanced bremsstrahlung from thermal plasmas containing nonthermal electrons 03 p0401 A66-1295
- Solar flares, discussing continuous electromagnetic radiation, hard X-ray radiation and microwave radio bursts 05 p0752 A66-1537
- Gas breakdown by laser can be accounted for by both microwave breakdown theory and inverse bremsstrahlung 06 p0893 A66-1704
- Accuracy of calculation of energy losses by fast muons, considering cases of bremsstrahlung, direct pair production and nuclear cascades 07 p1117 A66-1756
- Periodic variations in luminosity of quasars, stellar radio sources related to fluctuations of main parameters of magnetic bremsstrahlung mechanism 07 p1134 A66-17620
- Anomalous bremsstrahlung and anomalous cyclotron radio emission from partially ionized gases in 20 to 1000 m range 08 p1263 A66-1901
- Bremsstrahlung produced during stoppage of electrons generated by thunderstorms can create ionized columns extending to ionospheric heights 10 p1529 A66-2115
- Bremsstrahlung, recombination radiation and electromagnetic emission from high temperature high density plasmas 10 p1566 A66-2170
- Radioactive debris over Fairbanks, Alaska, on February 18, 1965, investigating bremsstrahlung X-rays in auroral zone 12 p1875 A66-2489
- Bremsstrahlung of nonrelativistic plasmas: treating nondegenerate electron component of plasma simultaneously with degenerate component by applying Fermi-Dirac distribution 12 p1925 A66-2499
- Nonlinear dielectric laser light absorption by neutral gas resulting in avalanche breakdown of gas due to thermal ionization 13 p2090 A66-2542
- Charge particle acceleration through electron absorption of bremsstrahlung photons 14 p2375 A66-2725
- Emission from hot low-density plasma due to bremsstrahlung, radiative recombination and electron collision-induced line emission 14 p2345 A66-2812
- Experimental evidence of inverse bremsstrahlung and electron-impact ionization in low pressure argon ionized by giant pulse laser 15 p2544 A66-2911
- Plasma electron temperature measure from soft X-ray bremsstrahlung absorption by beryllium foil 16 p2756 A66-3009
- Plasma bremsstrahlung power derived from relativistic, nonrelativistic and electron beams 17 p2965 A66-3225
- X-ray spectrum produced by thermal



bremsstrahlung of gas, taking Gaunt factor into account 18 p3200 A66-35049  
 EAS RF emission detection, discussing enhanced Cerenkov radiation, mutual coherence effects, diffraction, Fresnel zones, Coulomb-field bremsstrahlung, etc 18 p3208 A66-35117  
 One-dimensional cascade theory of photon-electron showers for light and heavy substances, taking into account polarization of medium upon cross section for electron bremsstrahlung 18 p3213 A66-35145  
 Bremsstrahlung and pair production processes as regarded in cascade theory of showers 18 p3213 A66-35146  
 Bremsstrahlung of electron impinging on fixed center of force and subsequent anomalous interaction, noting similar effect in strong interactions 18 p3218 A66-35183  
 Delta electrons formed in interstellar hydrogen-galactic ray collision 19 p3452 A66-35283  
 Visible and UV transition radiation, bremsstrahlung and plasma due to electron bombardment of metal surfaces 20 p3604 A66-37280  
 Ultrarelativistic muon electromagnetic interaction energy loss due to bremsstrahlung and pair production 24 p4271 A66-42936

**BRIDGE**  
 SA WHEATSTONE BRIDGE  
 SA WIRE BRIDGE CIRCUIT  
 Bearing reactions and stresses of bridge analyzed by calculating bending of rectangular plate with two supported and two free parallel sides 01 p0155 A66-10711  
 Diode gate design, using bridge circuit to eliminate spurious gating signals 14 p2267 A66-27802  
 Diode bridge variable attenuator used to overcome error signals and harmonic distortion in wide range 14 p2267 A66-27805  
 AGC 14 p2267 A66-27805  
 Bridge circuit measurement of phase at UHF and microwave frequencies, examining amplitude modulation and mixer types 24 p4171 A66-42101  
 Thermistor temperature sensing bridge for temperature control of liquid volume 24 p4214 A66-43033

**BRIGHTNESS**  
 SA LUMINESCENCE  
 SA LUMINOSITY  
 SA SKY BRIGHTNESS  
 X-ray photograph confirmation in 1964 of solar brightness distribution derived from ionospheric observations during solar minimum in 1954 04 p0579 A66-14179  
 Brightness dependence of pulse arc on power per unit length of arc, estimating charged particle density and plasma temperature 06 p0919 A66-16875  
 Secular variations in absolute brightness of periodic comets attributed to instrumental and geometrical effects 07 p1133 A66-17519  
 Apparent magnitude of periodic comet Oterma calculated from relation between absolute brightness and computed ephemerides 07 p1134 A66-17521  
 Brightness calculation of aureole visible in daytime at Earth edge from spacecraft 08 p1217 A66-19302  
 Brightness temperature measurements on illuminated side of Venus at 10.6 cm challenges Troitski theory of planetary radiation emission 08 p1297 A66-19457  
 Millimeter wavelength brightness temperatures of Mars, Jupiter and Saturn calculated from antenna temperatures 11 p1769 A66-22532  
 Brightness of oxygen bands in twilight and day airglow, relating variation to sunspot cycle, ozone dissociation and solar eclipse 11 p1702 A66-23490  
 Koval method for correcting distortions in photometric cross sections for Martian disk brightness distribution 12 p1944 A66-23502  
 Supercooled water droplets hypothesized in Venus cloud layer, based on radiometric observation in SHF range 12 p1944 A66-23503  
 Brightness fluctuations in quiet-form auroras, noting peaks and anisotropy of spectrum 14 p2286 A66-27983  
 Millimeter wavelength solar radiation consisting of thermal, slowly varying active and burst components and eclipse measurements of brightness

distribution 15 p2594 A66-29001  
 Brightness distribution in corona during solar eclipse of May 30, 1965 16 p2796 A66-30279  
 Initial pulse in luminous emission of discharge laser, using photomultiplier preceded by mobile iris, determining geometrical distribution of discharge brightness 16 p2719 A66-31209  
 Brightness temperature measurements on illuminated side of Venus at 10.6 cm challenges Troitski theory of planetary radiation emission 18 p3232 A66-34486  
 Lunar photometric brightness variational function based on JPL study of Moon topology 18 p3235 A66-34656  
 Profiles of isophotes and relative intensities for Aristarchus region of Moon taken during total eclipse on December 19, 1964 18 p3237 A66-35048  
 Optical photometric properties of lunar surface, discussing brightness effects, solar wind, albedo, reflectivity, backscatter, chemical composition, ion bombardment effects, etc 19 p3457 A66-35444  
 Brightness calculation of aureole visible in daytime at Earth edge from spacecraft 19 p3348 A66-36039  
 Koval method for correcting distortions in photometric cross sections for Martian disk brightness distribution 20 p3646 A66-37015  
 Supercooled water droplets hypothesized in Venus cloud layer, based on radiometric observation in SHF range 20 p3646 A66-37016  
 Brightness curves used to determine geometrical and physical parameters of eclipsing binary systems containing component with extended spherical atmosphere 20 p3647 A66-37031  
 Venus brightness temperature and polarization of integral radio emission at 3.75 cm wavelength 20 p3648 A66-37044  
 Photoelectric photometer used for tracking entry of artificial satellites into shadow of Earth 20 p3518 A66-37839  
 Water vapor mass below upper limit of Earth cloud cover estimated through Earth brightness measurements 21 p3735 A66-39360  
 Airborne spectrozonal telephotometer used in calculation of photographic brightness coefficient of Earth surface 22 p3919 A66-40621  
 Brightness variation from center to limb for Sun in submillimeter and IR range calculated from some available models of solar atmosphere 24 p4278 A66-42708

**BRIGHTNESS DISCRIMINATION**  
 Brightness discrimination and brightness contrast of human and animal eyes in suprathreshold luminance difference 04 p0461 A66-13791  
 Interpretation of some particular features in brightness distribution of twilight sky 06 p0876 A66-16554  
 Interpretation of some particular features in brightness distribution of twilight sky 14 p2289 A66-28226  
 Ruby phosphorescence under intense optical excitation, inferring possible recombination characteristics from initial brightness decay 15 p2558 A66-28607  
 Luminescence in December 1964 lunar eclipse, noting brightness measurement results in Mare Nubium region 16 p2800 A66-30644  
 Oscillatory component in solar granulation continuum brightness fluctuations, secondary maxima in temporal autocorrelation functions and power spectra 17 p2996 A66-31920  
 Solar active region analysis at radio frequencies, using fan or pencil beam scanning and superposition of wide beam transit curves 17 p3007 A66-33083  
 Lunar occultation and identification of MSH 19-27 radio source, noting computer analysis of brightness distribution 18 p3225 A66-33549  
 Increment threshold of vision cannot be used as reliable index of visual brightness due to variable and complex relation 20 p3504 A66-36947  
 Effect of color and brightness contrast, direction of contrast and contrast values on legibility of circular dial 21 p3701 A66-39420

**BRILLOUIN EFFECT**  
 Use of Brillouin scattering for optical beam modification, spatial distribution of

acoustic energy and coherent sound of great intensity 03 p0376 A66-12421  
 Brillouin scattering in liquids examining velocity, frequency and lifetime of thermally excited hypersonic sound waves, using laser light sources 03 p0376 A66-12422  
 Stimulated Brillouin and Raman scattering in gases, discussing sound velocity calculation from frequency shift and argon, hydrogen and nitrogen 04 p0531 A66-13981  
 Molecular anisotropy of propagation of intense light beam, noting Raman and Brillouin effects 05 p0696 A66-15106  
 Brillouin scattering of light by phonons and phonon maser in derivation of conservation theorems from basic equations 07 p1045 A66-18397  
 Forced Mandelstam-Brillouin scattering in gases, determining hypersonic velocity for three gases 09 p1408 A66-20770  
 Gas spectroscopy of laser-induced stimulated Brillouin effect in high pressure oxygen 11 p1715 A66-23432  
 Brillouin scattering by gases as experimental test of kinetic theory away from hydrodynamic regime 12 p1917 A66-24585  
 Coupled wave formalism, giving unified description of parametric down conversion of light, stimulated Brillouin and Raman effects, etc, stressing exponential character of gain 13 p2132 A66-26156  
 Discrepancy between calculated and experimental values for Raman gain in pulsed laser suggests higher energy distribution due to light trapping or Brillouin scattering 13 p2096 A66-26157  
 Interaction between stimulated Brillouin and Raman scattering in carbon sulfide, using optical resonator and laser beam 13 p2097 A66-26162  
 Stimulated Brillouin scattering in anisotropic media, showing excitation and propagation of stimulated phonons at radio frequencies 13 p2097 A66-26163  
 Multiple stimulated Brillouin emission exhibited by liquids exposed to pulsed ruby laser, noting scattering events, Stokes orders identification and iteration mechanism 13 p2097 A66-26164  
 Stimulated Brillouin scattering in quartz analyzed, noting amplification, Stokes wave generation and ruby gain 13 p2097 A66-26165  
 Dispersion and absorption of hypersonic waves analyzed by examining Brillouin scattering as function of scattering angle 13 p2133 A66-26167  
 Forced Mandelstam-Brillouin scattering in gases, determining hypersonic velocity for three gases 14 p2341 A66-27305  
 Dispersion relations for waves propagating along warm homogeneous isotropic plasma columns immersed in dielectric medium 15 p2549 A66-28713  
 Scattered light spectrum of thermal sound waves used to provide velocity and absorption data about hypersonic waves in several liquids 16 p2745 A66-30300  
 Stimulated Brillouin scattering from nitrogen and methane using giant pulse laser, noting convergence angle of backscattered beam sound, velocity measurement, etc 17 p2961 A66-32627  
 Stimulated Brillouin scattering in ferroelectric triglycine sulphate crystals and Rochelle salt exhibiting second-order phase transition, measuring scattering threshold as temperature function 20 p3620 A66-37770  
 Brillouin scattering spectra of crystalline quartz, fused quartz and Pyrex glass, noting acoustic modes in crystalline spectrum 23 p4114 A66-41628

**BRILLOUIN FLOW**  
 SA ELECTRON BEAM  
 Power flow of cyclotron modes propagating in waveguide filled with cold collisionless axially magnetized plasma studied by Brillouin diagram 20 p3612 A66-38398

**BRILLOUIN ZONE**  
 Fermi surface shape and size determination and thermoconductivity and conduction electron properties in metals 18 p3155 A66-34135  
 Optical absorption edges with nearly parallel bands of aluminum analyzed for all polyvalent metals with simple structures 19 p3401 A66-36391  
 Energy levels and interband oscillator



strengths of antimony calculated in Brillouin zone by pseudopotential method, predicting polarization effects and spin-orbit splittings 19 p3446 A66-36392

#### BRISTOL-SIDDELEY BS-53 TURBOFAN ENGINE

Recent developments in vectored-thrust Pegasus turbofan engine used in V/STOL subsonic strike fighters 04 p0573 A66-13931

#### BRISTOL-SIDDELEY OLYMPUS 593

##### TURBOJET ENGINE

Concord SST propulsion system, discussing thrust, flight requirements, medium compression ratio straight jet engine, intake, exhaust, etc 12 p1935 A66-23706

Olympus 593 B engine design and characteristics for Concorde application 13 p2172 A66-25564

Concorde supersonic transport aircraft propulsion, fuel supply and storage systems 22 p3848 A66-40415

#### BRITTLENESS

##### SA EMBRITTLEMENT

##### SA HARDNESS

Brittle fracture paths completely predictable and those predictable after initial random propagation 01 p0152 A66-10378

Irreversible tempering brittleness of spring steel with Mn, Cr, Si and C 01 p0086 A66-10452

Mechanical proof test used to reduce variability and screen out weaker elements of brittle materials with widely scattered strength values 03 p0436 A66-12754

Fracture of brittle bodies with cracks subjected to tension and compression 03 p0441 A66-13291

Critical loads causing brittle-rupture equilibrium cracks that develop near elliptical holes in bodies that remain elastic up to fracture 03 p0441 A66-13298

Synthesis and fabrication methods for intermetallic carbides, borides, beryllides, nitrides and silicides, decreasing susceptibility to brittle fracture 07 p1051 A66-18298

Brittle fracture in ceramic materials, noting Griffith theory on crack propagation, plastic deformation occurrence, stress distribution effect, etc 07 p1054 A66-18499

Plastic properties of brittle materials analyzed by hydrostatic pressure, using double ring, calculating radial pressure on sample, between rings, etc 08 p1305 A66-18600

Deformation of double ring used in compression tests to study stress-strain state of brittle and ceramic materials 08 p1313 A66-19438

Front and zone of fractures originating in brittle elastic body under influence of high pressure arising on wall of cavity within body 08 p1313 A66-19475

Gas-bearing facilities for determining axial stress-strain and lateral strain of brittle materials to high temperature 08 p1242 A66-19722

High-chromium ferrite steel Kh25T brittleness at 475 degrees C investigated, using neutron structural analysis 09 p1391 A66-20872

Hydrogen effect on strength, plasticity and brittleness of metals with fcc lattice at various temperatures and hydrogen concentrations 12 p1894 A66-23763

Niobium addition effect on mechanical properties of steel, noting improvement of tensile strength and cold brittleness threshold decrease 12 p1897 A66-24899

Quenching and slow-cooling effects on ductile-brittle bend-transition temperature of chromium wire 13 p2107 A66-25587

Propagation of brittle cracks in body under compression, discussing theory of resistance of brittle bodies to compression 13 p2196 A66-25629

Approximation method for determining limit and breaking load for infinite brittle body weakened by plane crack, noting crack propagation 13 p2203 A66-26423

Effect of stress concentrations on load carrying capacity of brittle materials of nonuniform microstructure, considering iron plates with holes 13 p2205 A66-26441

Self-sustained fracture of stressed brittle body with assessment of fragment mean dimension 14 p2399 A66-27594

Brittle materials failure theory for cases where presence of plane deformation or plane stressed state is assumed, using Griffith theory 16 p2822 A66-31510

Ceramic structural design, discussing laboratory specimen design, brittle material strength, boundary conditions, statistical parameters, etc 18 p3125 A66-33733

Joint strength analysis for brittle materials 22 p3927 A66-40283

Self-sustained fracture of stressed brittle body with assessment of fragment mean dimension 24 p4291 A66-42734

#### BROADBAND AMPLIFIER

Disk and parasitic resonance of broadband and small circulators for UHF and VHF 01 p0040 A66-10551

Standard amplifier building blocks used in systems design, stressing manufacture by silicon integrated circuit processes 02 p0203 A66-11924

Broadband tunable tunnel diode oscillator in waveguide mounting, noting role of variable capacitor 03 p0339 A66-12450

Octave-broadband tunnel-diode amplifier design with added shunt capacitance and stabilizing circuit 05 p0643 A66-14573

Traveling wave transistor for HF medium-power application, device is also broadband amplifier whose circuit uses distributed elements 06 p0853 A66-16645

Tunnel diode series inductance and stray capacitance effect on gain and bandwidth of broadband reflection type amplifiers 07 p1007 A66-17509

Wideband DC amplifier operating with double full-wave signal transformation 11 p1664 A66-22621

Broadband X to K band varactor frequency doubler, noting efficiency increase by replacing variable resistance element with varactor 12 p1832 A66-23908

Tunnel diode amplifier for broadband radio communication using integrated circuits, noting noise figure, stability and saturation effect 12 p1840 A66-24623

Solid state tuned RF radiometric receiver using low-noise broadband tunnel diode amplifier 14 p2290 A66-27063

Broadband slotted cone antenna exhibiting multioctave bandwidth properties in UHF-VHF range 14 p2256 A66-27912

Relation between transistors and distortion in line amplifiers used for repeaters or multicouplers, noting generation of harmonics and intermodulation products, distortion sources in transistors, etc 14 p2262 A66-28381

General broadband matching for passive and active 1-port load impedance and application to tunnel diode amplifier 15 p2464 A66-29321

Broadband semiconductor diode frequency multipliers, examining performance, noise theory, realization and frequency multiplication mechanism 17 p2890 A66-32904

Broadband semiconductor diode frequency multipliers, examining performance, noise theory, realization and frequency multiplication mechanism 18 p3075 A66-33564

Solid state millimeter wave receivers for space vehicle environments, discussing integral mixer IF amplifiers, oscillators and varactor multipliers 22 p3879 A66-40733

VHF power modulator devised to give broadband output signals within frequency range of 66 to 184 megacycles at 2.5 mw and 50 ohms impedance 24 p4184 A66-42644

SA POTASSIUM BROMIDE

SA SILVER BROMIDE

Concave-convex growth spirals due to screw dislocation in nickel bromide 15 p2563 A66-28730

BROMINE

Photochemical studies of oxygen-ozone and carbon dioxide equilibria with bromine UV lamp 04 p0473 A66-13397

BROMINE COMPOUND

Cis-and trans-beta-bromostyrene reaction with lithium diphenylphosphide in tetrahydrofuran producing cis-and trans-beta-styryldiphenylphosphine, discussing proton magnetic resonance and configuration retention 14 p2232 A66-27498

Electrical conductivity variation with temperature of chlorine and bromine trifluoride, noting maximum conductivity

below freezing point of chlorine trifluoride 23 p4118 A66-41241

#### BROWNIAN MOTION

Self-field electron kinetic reaction to electromagnetic propagation in three-fluid Brownian plasma 01 p0110 A66-10330

Dirichlet problem solved by probability density for Brownian particle, using Fredholm integral equation 01 p0094 A66-10730

Book on kinetic theory of simple liquids including equilibrium properties, time-dependent system, Markov processes, Brownian motion, transport coefficients, etc 08 p1209 A66-19461

Optimization of five second and third-order systems with saturating and relay controllers and with random Brownian Motion input 11 p1674 A66-22222

Dirichlet problem solved by probability density for Brownian particle, using Fredholm integral equation 24 p4232 A66-42740

BRUDERHEIM METEORITE

Xenon, radiogenic Xe 129R and krypton contents and xenon and krypton isotopic composition of Bruderheim meteorite 08 p1297 A66-19401

Thermal history of Bruderheim meteorite showing lost of 90 percent radiogenic argon 40 20 p3651 A66-37591

BUBBLE

Size distribution law for dimensions of gas bubbles formed during cavitation in turbulent flow of liquid 06 p0870 A66-16191

Numerical analysis of collapse of spherical bubble in compressible fluid including surface tension, viscosity and adiabatic compression of gas within bubble [ASME PAPER 65-FE-16] 06 p0870 A66-16211

Terminal rise velocity of small distorted gas bubbles in liquid of small viscosity 06 p0874 A66-17001

Violent bubble behavior in liquids contained in vertically vibrated tanks caused by water hammer type of resonance [AIAA PAPER 66-86] 06 p0875 A66-17091

Bubble coalescence in longitudinally vibrated liquid column 07 p1025 A66-18171

Behavior of individual cavitation bubbles in cavitating flows of water and liquid Mercury, using two-dimensional Plexiglas venturi 07 p1025 A66-18171

Contact area of boiling bubbles observed through electroconductive glass/heating surface/into tank 08 p1320 A66-19550

Time variation in boiling heat transfer caused by bubble generation 08 p1320 A66-19550

Saturated vapor spherical bubble collapse in uniformly subcooled liquids 08 p1320 A66-19550

Cavitation strength of distilled water and distribution of cavitation nuclei, accounting for pressure threshold variance 11 p1688 A66-22601

Devitrification of glass around collapsed bubbles in tektites, noting formation mechanism 11 p1773 A66-22961

Relationship between shock wave phenomena during collapse of cavitation bubbles in water and temperature and gas content of water 13 p2060 A66-25091

Size distribution law for dimensions of gas bubbles formed during cavitation in turbulent flow of liquid 13 p2064 A66-25911

Conditions under which gas bubbles arise in organs and physiological fluids of living organism during pressure drop 13 p2011 A66-26571

Motion of gas bubble in weightless viscous fluid with temperature gradient 14 p2273 A66-26786

Bubble boiling model of nucleation and growth of bubble on heating surface 14 p2411 A66-27138

Violent bubble behavior in liquids contained in vertically vibrated tanks caused by water hammer type of resonance [AIAA PAPER 66-86] 16 p2685 A66-30911

Delay time for bubble formation associated with heating surface thermal layer formation in water moderated reactors 17 p2956 A66-32271

Mass transfer in gas-liquid dispersions noting effect of flow rate, bubble size etc 18 p3266 A66-34736

Dimensional and experimental analyses of



helium bubble motion in liquid  
 nitrogen 20 p3545 A66-37104  
 Munroe jet formation when small cavity or bubble in liquid is subjected to impact or shock 20 p3546 A66-37804  
 Relationship between shock wave phenomena during collapse of cavitation bubbles in water and temperature and gas content of water 21 p3723 A66-38516  
 Linear flow equation motion of fluid with suspended impurities, noting that under certain assumptions velocity fields can be described by family of potential functions 21 p3729 A66-39448  
 Marangoni flow, motion of liquid surfaces under influence of surface tension gradients, explaining high fluxes obtained in boiling heat transfer 22 p3999 A66-40303  
 Viscosity, surface tension and inclination angle effect on motion of long bubbles in closed tubes 22 p3900 A66-40388  
 Two-dimensional bubble contours in steady state turbulence-free flow of ideal incompressible fluid, obtaining solution for all internal pressures 24 p4232 A66-43064  
**BUBBLE CHAMBER**  
 Ruby laser with concentric resonator as illumination source of bubble chamber 01 p0084 A66-11189  
 Laser simulated nucleation in bubble chamber, comparing sensitivity with radioactively stimulated nucleation 10 p1557 A66-21583  
 Nucleate saturated pool boiling over horizontal plate, noting bubble development relation to boiling through heat exchange 12 p1973 A66-23528  
 Ruby laser with concentric resonator as illumination source of bubble chamber 12 p1890 A66-24010  
**BUCKLING**  
 SA COMPRESSION BUCKLING  
 SA CREEP BUCKLING  
 SA ELASTIC BUCKLING  
 SA EULER BUCKLING  
 SA SHELL STABILITY  
 SA STRAIN  
 SA STRESS  
 SA THERMAL BUCKLING  
 Small amplitude vibrations of rectangular panel relative to static buckled configuration 02 p0301 A66-12164  
 Linear small deflection theory and statistical analysis in dynamic buckling of thin cylindrical shell under axial impact [ASME PAPER 65-APMW-17] 04 p0592 A66-14218  
 Nonconservative loading on linear two-degree of freedom elastic system, discussing damping effects on equilibrium stability [ASME PAPER 65-WA/APM-17] 05 p0777 A66-15439  
 Torsional instability of cantilevered bars, describing effects of distributed nonconservative compressive load at free end [ASME PAPER 65-WA/APM-19] 05 p0777 A66-15441  
 Collapse of pressurized axially stiffened thin cylinder 06 p0967 A66-16933  
 Inextensional buckling of thin conical shell under axial compression [AIAA PAPER 66-125] 07 p1148 A66-18461  
 Buckling loads of reinforced cylindrical shells, discussing size and placement of stiffening members 10 p1614 A66-21391  
 Torsional instability of cantilevered bars, describing effects of distributed nonconservative compressive load at free end [ASME PAPER 65-WA/APM-19] 12 p1961 A66-23979  
 Linear small deflection theory and statistical analysis in dynamic buckling of thin cylindrical shell under axial impact [ASME PAPER 65-APMW-17] 12 p1961 A66-23980  
 Nonconservative loading on linear two-degree of freedom elastic system, discussing damping effects on equilibrium stability [ASME PAPER 65-WA/APM-17] 12 p1961 A66-23983  
 Buckling, postbuckling and imperfection sensitivity of cylinders and shells 14 p2404 A66-27987  
 Buckling characteristics of eccentrically stiffened cylindrical shells under hydrostatic pressure loading and vibration, buckling and

flutter characteristics of stiffened flat plates [AIAA PAPER 65-370] 15 p2610 A66-29285  
 Energy method for analysis of lowest mode symmetrical buckling of thin shell shallow spherical caps and cylindrical arches under blast loading 15 p2610 A66-29291  
 Mechanical strength of plastic buckling of sheet metals under lateral hydraulic loads 15 p2510 A66-29778  
 Local buckling in curved two-dimensional manifolds, detailing experimental exposition of phenomenon in stability and deformation of shallow spherical shell 17 p3021 A66-32005  
 Torsion of slit overlapped thin walled tubes, noting change in slope at point of first instability in torque-twist relationship 18 p3253 A66-33802  
 Space-frame radome design and buckling analysis for wind and deadweight static load using digital computers 18 p3095 A66-34299  
 Buckling, postbuckling and imperfection sensitivity of cylinders and shells 22 p3992 A66-40337  
 Postbuckled equilibrium configurations of axially compressed circular cylindrical shell determined from large deflection theory and principle of stationary potential energy 22 p3993 A66-40340  
 Initial buckling under shear stress of long clamped plate with parallel edges reinforced by stiffener mesh, noting flexural and torsional rigidity of stiffeners 22 p3995 A66-40495  
**BUDGET**  
 S ENERGY BUDGET  
**BUFFALO AIRCRAFT**  
 S DE HAVILLAND DHC-5 AIRCRAFT  
**BUFFER**  
 Very high input impedance buffer circuit using field effect transistors for voltage sensing in high impedance analog simulator 17 p2886 A66-32381  
 Buffering capacity of substances liberated by Chlorella expressed in terms of van Slyke buffer index, noting changes in pH 17 p2880 A66-32831  
**BUFFER STORAGE**  
 Buffer storage in digital radar smoothing irregular output data flow, noting decreasing bandwidth requirements 11 p1654 A66-22656  
**BUFFETING**  
 HF response of shell-type structures to buffeting aerodynamic environment [AIAA PAPER 66-81] 06 p0968 A66-17086  
 Theoretical determination of buffeting limits of wings, using boundary layer theory, obtaining Reynolds number effect on location of buffeting limits 10 p1479 A66-21377  
 Transonic buffeting effects on hammerhead shaped payloads analyzed, using power spectral techniques and wind tunnel tests 20 p3672 A66-38170  
**BULK MODULUS**  
 Plastic deformation in body under uniform pressure, establishing necessary condition for existence of uniform stressed state in inhomogeneous body 07 p1142 A66-17261  
 Continuous fluid film self-acting cylindrical journal bearing theory and design data, introducing isothermal bulk modulus into lubrication equations [ASLE PREPRINT 65AM 3A2] 07 p1039 A66-18285  
 Spherically divergent stress pulses in linear viscoelastic solids, measuring change in shape of polyethylene polymethyl methacrylate and polystyrene blocks 09 p1393 A66-20662  
 Overall elastic moduli of inhomogeneous system composed of various solid phases firmly bonded together at arbitrary concentration 17 p3029 A66-32791  
**BULKHEAD**  
 Hot drape forming of torus and semitoroidal bulkhead segments from aluminum alloys [SAE PAPER 660290] 15 p2511 A66-29831  
**BULLPUP MISSILE**  
 Value analysis as cost reduction factor, using production of Bullpup A and B missiles as example 11 p1711 A66-23060  
**BUOY**  
 S FLOTATION SYSTEM  
**BUOYANCY**  
 SA RAYLEIGH NUMBER  
 Axial temperature variation in turbulent buoyancy-controlled diffusion

flame 08 p1319 A66-19202  
 Turbulent heat transfer effect on gas stratification in field of Archimedes forces 12 p1979 A66-24429  
 Streamlines in Benard convection cells induced by surface tension and buoyancy 15 p2478 A66-29247  
 Buoyancy and magnetohydrostatic stability of magnetic body immersed in magnetizable fluid 16 p2749 A66-31757  
 Buoyancy in convecting ideal dissociating gas analyzed, obtaining solution for one-dimensional unsteady free mixing 18 p3103 A66-34931  
 Fluidmagnetic buoyancy effects in ferrohydrodynamic /FHD/ flows and implications of Ernschaw levitation theorem 23 p4057 A66-41885  
**BURGER EQUATION**  
 Two physical-space and two spectral solutions of Burger equation which are exact, viscous and nonsteady 18 p3103 A66-34930  
**BURNER**  
 SA AFTERBURNER  
 Hydrogen/oxygen and hydrogen/air flame temperature experiments on porous fuel flame burner 20 p3680 A66-38042  
**BURNING PROCESS**  
 S COMBUSTION  
**BURNING RATE**  
 SA FLAME PROPAGATION  
 Nonuniqueness of stationary solutions to system of equations in burning theory with piecewise invariable reaction rate and thermoconductivity and diffusion coefficients 06 p0970 A66-16345  
 Electronic timer for rocket, controlling duration of burning time 08 p1188 A66-18616  
 Premixed flames of trimethylaluminum vapors and oxygen stabilized at reduced pressure, analyzing stability region, burning velocity and emission spectrum 08 p1318 A66-19199  
 Combustion of solid rocket propellants, using potassium nitrate as oxidizer and phenol formaldehyde as fuel 08 p1319 A66-19201  
 Servomechanism measurement of solid propellant burning rate 08 p1227 A66-19697  
 Book on quasi-stationary conditions in open systems with short reaction times in solid propellant rocket engines 09 p1432 A66-20487  
 Hybrid rocket engine performance noting stable fuel burning, burning rate, thrust modulation, ignition delay and use of tricomponent fuels 10 p1594 A66-21715  
 Ballistic performance change in spinning rocket motors attributed to internal gas dynamics and combustion effects, noting grain geometry influence 10 p1590 A66-21945  
 Nonuniqueness of stationary solutions to system of equations in burning theory with piecewise invariable reaction rate and thermoconductivity and diffusion coefficients 11 p1785 A66-22340  
 Combustion of composite ammonium perchlorate based propellants near extinction pressure, noting burning rate parameters 13 p2171 A66-25181  
 Combustion of hydrazine droplets burning in hydrazine vapor investigated via suspended droplet technique [AIAA PAPER 65-355] 14 p2370 A66-27413  
 Quasi-steady spherically symmetric burning of monopropellant liquid droplet in stagnant atmosphere 14 p2412 A66-27560  
 Organic flame temperatures and burning velocities at various fuel-air ratios measured, noting band intensity, effect of diluents, etc 14 p2413 A66-27723  
 Schlieren photographs of spark ignition in turbulent gas mixture flows and analysis of ignition delay and burning velocity 15 p2616 A66-29069  
 Burning rate equation and constant volume burning of solid propellant to determine ballistic properties 15 p2617 A66-29606  
 Stabilization of lifted diffusion flame in turbulent methane jet flow field and measurements of gas flow velocity, turbulence and gas composition 15 p2479 A66-29608  
 Liquid hydrazine decomposition process to determine what chemical or physical changes may be occurring that cause breaks in burning rate/ pressure curves, measuring flame temperature and light



emission 15 p2570 A66-29610  
Weightlessness effect on flame ignition, burning rate, self-extinguishment, etc 16 p2825 A66-30487  
Effect of spin on internal ballistics of solid propellant motor  
[AIAA PAPER 66-523] 16 p2791 A66-31485  
Five halogenated hydrocarbons and effect on flame speed of  
methane 17 p3032 A66-31881  
Formula derivation for acoustic conductivity of combustion surface of condensed system 17 p3033 A66-31896  
Burning properties of oxygen-nitrogen and oxygen helium spacecraft atmospheres determined for increasing safety of crew members in case of emergency 17 p3033 A66-32147  
Pressure dependence of burning rate of stoichiometric fuel-oxidizer mixtures 17 p3036 A66-32825  
Burning velocity in turbulent stream of homogeneous mixture 17 p3036 A66-32826  
Combustion rate of ammonium perchlorate-polystyrene and ammonium perchlorate-Plexiglas mixtures related to mixture ratio 18 p3260 A66-33720  
Computer programs for combustion rates of hydrogen-air mixture 18 p3063 A66-33830  
Saturn IVB vehicle constraints noting burning time, associated design problems, performance requirements, propellant management, etc  
[SAE PAPER 660441] 18 p3245 A66-33889  
Water vapor effects on burning rate of aluminum and magnesium wires at atmospheric pressure  
[WSCI 66-4] 18 p3264 A66-34421  
Propellant composition influence on finite-amplitude axial wave mode instability in solid propellant rockets  
[AIAA PAPER 66-600] 18 p3161 A66-34431  
Cinephotomicrographic studies of metallized fuel-rich propellants with high aluminum powder content, discussing composition, burning rates, etc  
[AIAA PAPER 66-616] 18 p3162 A66-34433  
Ignition pressure transient of rocket motor, discussing initial ignition event, flame spreading and final chamber filling, convective heating effect on burning rate, etc  
[AIAA PAPER 66-666] 18 p3165 A66-34449  
Combustion rate in simultaneous heterogeneous-homogeneous reactions on particle surfaces of catalytic agents added 18 p3265 A66-34550  
Mathematical model of combustion instability in solid propellant rocket engines, noting system dynamic behavior, appearance of limit cycle and effect of large amplitude oscillations on burning rate 20 p3627 A66-36889  
Digital computer analysis of kinetic equations for CO burning in presence of hydrogen 20 p3679 A66-37702  
Burning rate anomalous dependence on particle size for ammonium perchlorate-polystyrene mixture 20 p3679 A66-37703  
Reaction rates of decomposition burning of small spheres of liquid hydrazine 20 p3626 A66-38043  
Distance/time records, drag coefficients and Reynolds numbers of single freely-falling drops of pentane, heptane and benzene burning in cold atmosphere 20 p3626 A66-38044  
Equilibrium control and burning rate control of solid propellant in heat exchanger 20 p3629 A66-38155  
Hybrid rocket combustion mechanism, burning rate, mass transfer coefficient, throttling effects and grain design  
[AICE PREPRINT 34C] 22 p3970 A66-39877  
Ignition and controlled burning of liquid oxygen-liquid methane mixture, evaluating use as rocket monopropellants  
[AICE PREPRINT 28E] 22 p3969 A66-39880  
Japanese Aeronautical Research Institute Solid Rocket and Special Small Rocket projects, examining propellant design for performance requirements 23 p4132 A66-41418  
Erosive burning in rocket engines of radial burning type, using polyurethane/ammonium perchlorate base propellant grains, examining flow channel constriction 23 p4121 A66-41433

Halides used as burning rate depressants on combustion stability of polyurethane/ammonium perchlorate base propellants, examining acoustic instability 23 p4119 A66-41435  
Analog computation of minimum fuel trajectories with soft landings in uniform gravitational field, using Pontryagin maximum principle to reduce two-point BVP with optimal controllers 23 p4133 A66-41618

## BURNOUT

Torque-free precession of spin stabilized spacecraft, showing thrust misalignment as cause for final burnout impulse 16 p2810 A66-30903

## BURST

## SA METEOR BURST

## SA RADIO BURST

Thin metal diaphragms in shock tubes, discussing bursting characteristics and petalling behavior  
[ASME PAPER 65-WA/MET-16] 05 p0661 A66-15683

Simultaneous error correction and burst error detection, using binary linear cyclic codes 09 p1347 A66-20643

## BUTADIENE

Statistical variability of ultimate properties for eight samples of SBR-sulfur gum vulcanizates 05 p0706 A66-15460

## BUTYLENE

## S ISOBUTYLENE

## S POLYISOBUTYLENE

## BY-PASS ENGINE

High bypass high-pressure ratio cycles in turbofans for increased subsonic transport range  
[AIAA PAPER 65-795] 03 p0415 A66-12561

Optimum design of by-pass engine with exhaust and by-pass flow mixing, noting thrust and efficiency 04 p0572 A66-13536

Engine technology including higher turbine operating temperatures, high speed fan and nacelle design, increased by-pass ratio and improved power plant efficiency 06 p0943 A66-16924

Dual flow engines with high by-pass ratios, considering engine process parameter effects, fuel consumption, efficiency, etc 06 p0944 A66-17025

Intake requirements and cold efflux of high-bypass turbofan engines can be turned to advantage by integrated installation arrangements which reduce long-haul operating costs 09 p1434 A66-20392

High by-pass turbofan for business aircraft, comparing jet propulsion system efficiency with fan engines, cost factors and market potentials  
[SAE PAPER 660221] 13 p2173 A66-26400

Bypass engine development from conventional gas turbine to ducted-fan and aft-fan engine, noting principle of afterburning 14 p2373 A66-27014

Exhaust mixing process in Rolls-Royce bypass jet engines, noting stream mixing in common duct with corrugated metal interface on inlet side 17 p2990 A66-32079

High bypass high-pressure ratio cycles in turbofans for increased subsonic transport range  
[AIAA PAPER 65-795] 19 p3279 A66-36490

## C-5 AIRCRAFT

C-5A aircraft design load criteria for landing gear of large aircraft that must operate from semi-improved airfields  
[AIAA PAPER 65-711] 01 p0013 A66-10948

Handling qualities research for C-5A, noting inconsistencies in magnitudes of parameters and parameters to be specified  
[AIAA PAPER 65-740] 03 p0317 A66-12548

Lockheed C-5A military jet transport design 11 p1636 A66-22332

New high by-pass ratio turbofan engine for C-5A subsonic transport aircraft  
[SAE PAPER 660323] 15 p2428 A66-29843

Lockheed C-5 quantitative maintainability program and application to air-vehicle utilization and cost 20 p3495 A66-37891

Uniform design process AFSCM 375-5 implementation and operating personnel interrelationships in aircraft

industry 20 p3685 A66-3792

## C-BAND

C-band weather radar AVQ-10 incorporating tunnel diode amplifier and p-i-n solid state protector switch 07 p1008 A66-1772

TWT delivering CW power in L, S, C and X-band designed for space environment considering size, weight, voltage, etc, and comparing klystrons, amplifiers, circuit design, etc  
[AIAA PAPER 66-308] 12 p1844 A66-2472

Temperature stable high power C band digital many-phased-array-radar phase shifter 13 p2035 A66-2552

## C-141 AIRCRAFT

Fail-operative stability augmentation system for C-141 jet transport aircraft yaw control axis, using triple redundant sensor and signaling 01 p0011 A66-1062

C-141 aircraft automatic navigation system, self-contained and with redundant modes of operation, ensures all-weather mission reliability 07 p1078 A66-1782

## C-142 AIRCRAFT

Acoustic fatigue testing of 20 fuselage panels of XC-142A VTOL/STOL transport aircraft, using simulated propeller noise 01 p0151 A66-1012

Landing gear design challenges for V/STOL service XC-142A and relative success/failure  
[SAE PAPER 650843] 01 p0012 A66-1082

Structural dynamics of XC-142A tilt-wing VTOL aircraft including flutter, vibration, environmental acoustics, etc  
[AIAA PAPER 65-790] 03 p0318 A66-1252

XC-142A tri-service V/STOL aircraft specifications, considering control and transmission systems and flight test results 03 p0321 A66-1282

Thrust-control system on XC-142A tilt-wing aircraft considered in connection with structural design of aircraft hover, transition and acceleration  
[AIAA PAPER 65-769] 03 p0321 A66-1302

Flight controls of tilt wing XC-142A aircraft, noting mechanization and operation of wing and flap control system 06 p0809 A66-1682

## CABIN ATMOSPHERE

## SA PRESSURIZED CABIN

## SA SPACE CABIN ATMOSPHERE

Spacecraft cabin atmosphere, comparison of pure oxygen with two-gas atmosphere 06 p0814 A66-1592

Supersonic aircraft artificial atmosphere, discussing linear relationship between imperceptible perspiration and ambient water vapor pressure 06 p0815 A66-1602

Low humidity and dehydration in jet fuselage, noting water metabolism and effect of various beverages 10 p1491 A66-2132

Pressure cabin design and utilization, noting relation between air speed and environmental temperature on kinetic heating, contamination of cabin atmosphere, pressurization control, sealed cabin advantages, etc 10 p1492 A66-2212

## CABLE

## S COAXIAL CABLE

## S TRANSMISSION LINE

## CABLE FORCE RECORDER

Rotating orbiting cables, determining lateral vibration in orbital plane via mathematical model analysis  
[AIAA PAPER 66-98] 06 p0962 A66-1622

## CADMIUM

## SA NICKEL-CADMIUM BATTERY

Photovoltaic effect in thin ternary semiconductor of Cd-Te-Hg 07 p1092 A66-1722

Identification of mass series and mass values in Fermi surface of cadmium cyclotron resonance compared with results for zinc 10 p1581 A66-2172

## CADMIUM ALLOY

Superconducting transition temperatures of Cd-Hg alloys covering complete composition range, considering effect of ordering 07 p1109 A66-1842

Electric Ag-CdO contacts obtained by internal high temperature oxidation method 08 p1239 A66-1892

Indium-cadmium alloy superconducting transition temperatures for varying compositions, noting electronic structure 13 p2169 A66-2822



Semiconductor lasers with high power efficiency obtained via electron beam excitation on crystals of mixed cadmium-sulfide-selenide alloy 16 p2720 A66-31533

Chemical activities of cadmium and magnesium in binary Mg-Cd alloys based on vapor pressure measurement by Knudsen effusion method 18 p3121 A66-33729

**CADMIUM ANTIMONIDE**

Optical constants of CdSb determined for photon energies up to 2 eV from reflectivity measurements and Kramers-Kronig dispersion relation 02 p0275 A66-11967

Electrical conductivity, Hall effect and thermoelectric power as function of temperature in CdSb single crystals strongly doped with silver 02 p0275 A66-11968

Magnetoresistance effect on p- and n-type cadmium antimonide single crystals for various arrangements of electric and magnetic fields 11 p1756 A66-23017

Gold and silver doping effect on Hall effect, electroconductivity thermal emf and conductivity of CdSb 17 p2984 A66-33145

**CADMIUM COMPOUND**

Temperature dependence of electric conductivity and Hall effect of single crystal cadmium tin arsenide 01 p0126 A66-11026

Stationary and kinetic methods determining parameters of sensitizing recombination r-center in high resistivity monopolar photoconductors 02 p0273 A66-11718

Propagation of LF helicon waves in strongly doped cadmium arsenide and indium antimonide 03 p0410 A66-12944

Liquids used in manometers for pressure and pressure difference measurement in rarefied gases, considering cadmium boron tungstate, polymethylsiloxanes, etc, noting lack of toxicity, low viscosity, etc 03 p0371 A66-13204

Diamond-like semiconductors in glassy state, investigating structure and characteristics of cadmium-germanium-arsenide 07 p1106 A66-18383

P-type cadmium tin arsenide crystals, plotting temperature dependences of specific electroconductivity, Hall coefficient and thermal electromotive force 08 p1277 A66-19622

Electrical capacity of galvanic cell and crystal habit and surface property effects on porous cadmium hydroxide electrode electrochemical properties 08 p1171 A66-19644

Cadmium and indium thiogermanates, properties and synthesis 14 p2361 A66-27339

Conduction band in cadmium arsenide semiconductor, measuring transport phenomena 15 p2560 A66-28635

Physical properties of thin films of CdS and CdSe formed by vacuum deposition analyzed as function of deposition and processing conditions 16 p2782 A66-31422

Optical and magnetooptical phenomena in CdSnAs sub 2, discussing reflection and absorption spectrum, optical activity, double refraction, dielectric constant, etc 16 p2788 A66-31775

P-type cadmium tin arsenide crystals, plotting temperature dependences of specific electroconductivity, Hall coefficient and thermal electromotive force 17 p2984 A66-33136

Sensitivity of cadmium sulfate-based photovoltaic cells in short wave region 21 p3798 A66-38915

Semiconducting properties of cadmium tetraphosphide 24 p4253 A66-42361

**CADMIUM FLUORIDE**

Laser regime with giant pulses generated in dysprosium doped cadmium fluoride under continuous pumping by xenon lamps, obtaining Q factor modulation by rotating prism 08 p1234 A66-19376

Optical absorption and reflectivity of single crystals of strontium fluoride and cadmium fluoride in far UV 17 p2974 A66-31844

Effect of anomalous dispersion on stimulated emission spectrum of doped cadmium fluoride crystals 17 p2977 A66-32317

Laser regime with giant pulses generated in dysprosium doped cadmium fluoride under continuous pumping by xenon lamps, obtaining Q factor modulation by rotating prism 18 p3119 A66-34178

**CADMIUM SELENIDE**

N-type conductive cadmium selenide single crystals investigated for heat treatment and Hall effects in selenium vapor 01 p0127 A66-11194

Interband Faraday rotation at liquid-nitrogen temperature in CdS-CdSe mixed crystals 02 p0274 A66-11722

Cadmium selenide thin film transistors /TFT/ where electron mobility values exceed bulk single crystal values 02 p0276 A66-11979

Electrical properties of cadmium selenide evaporated films prepared on substrates at various substrate temperatures 03 p0409 A66-12725

Cadmium sulfide and cadmium selenide, discussing optical absorption, energy band structure, effective band-masses and composition changes of crystals in polarized light 05 p0731 A66-14656

Cadmium sulfide and cadmium selenide recombination centers, discussing temperature dependence of electron capture cross sections 05 p0731 A66-14661

Exciton absorption lines and long wave intrinsic edges of single-crystal CdSe and CdS at low temperatures 06 p0924 A66-16540

Forced emission from electron-excited cadmium selenide 10 p1544 A66-22174

Potential distribution in p-type selenium layer adjacent to n-type cadmium selenide in cut-off direction 11 p1757 A66-23231

Edge absorption of indium-doped cadmium in polarized light, noting exchange interaction between current carriers and Fermi level dependence on carrier concentration 12 p1929 A66-24449

Deposition of cadmium selenide films for transducers of electromagnetic energy to acoustic energy at microwave frequencies, noting use of multiple film assemblies 12 p1839 A66-24616

Cadmium sulfide and cadmium selenide, discussing optical absorption, energy band structure, effective band-masses and composition changes of crystals in polarized light 13 p2167 A66-25931

Cadmium sulfide and cadmium selenide recombination centers, discussing temperature dependence of electron capture cross sections 13 p2168 A66-25936

Laser oscillations in CdSe and CdS bombarded by fast electron beam 14 p2306 A66-27031

Laser-generation-type luminescence CdS-CdSe crystals exposed to double photon excitation from ruby laser 14 p2308 A66-27647

Exciton absorption lines and long wave intrinsic edges of single-crystal CdSe and CdS at low temperatures 15 p2569 A66-29987

CdSe-Au-Ge metal base transistor fabricated, based on fact that Ge-Au junction barrier is low and CdSe-Au junction is Schottky 16 p2660 A66-30615

Lattice vibrational properties of hexagonal CdSe 16 p2778 A66-31075

Expanded single crystal hetero-transitions in CdS-CdSe system 16 p2787 A66-31734

Distribution of recombination centers over energy levels of CdS-CdSe solid solutions 16 p2787 A66-31737

Forced emission from electron-excited cadmium selenide 19 p3441 A66-35788

Absorption, radiative recombination and photoconductivity of CdSe 19 p3444 A66-36035

Time-dependent response of polycrystalline cadmium selenide thin film transistor to transient high energy radiation 20 p3525 A66-37316

Spectral characteristics of two-photon optical excitation and light emission from CdSe semiconductor laser with modulated Q-factor 20 p3578 A66-37565

Edge absorption of indium-doped cadmium in polarized light, noting exchange interaction between current carriers and Fermi level dependence on carrier concentration 20 p3619 A66-37681

Light emission from semiconducting cadmium selenide crystals when not excited with photons, electron beam or tunneling, noting association with acoustoelectric field domain 20 p3620 A66-37767

Direct measurement of dispersion

properties of cadmium sulfide and CdS-CdSe crystals, using Obreimov-Fresnel diffraction method, growing crystals by synthesis 21 p3799 A66-38926

Spatial distributions of carrier concentration and internal field in cadmium selenide for various voltages, measuring conductivity and Hall coefficient 23 p4112 A66-41292

Failure mechanisms of CdS and CdSe thin film FETs noting volt-ampere characteristics, temperature, electrical stress and humidity effects 24 p4181 A66-42381

**CADMIUM-SILVER BATTERY**

**S SILVER-CADMIUM BATTERY**

**CADMIUM SULFIDE**

Space and time dependence of increased phonon population /amplitude of lattice vibration/ in amplifying cadmium sulfide crystal 01 p0122 A66-10575

Isothermal cross section of phase diagram of Zn-Cd-S and sulfide films 01 p0125 A66-10781

Moire patterns of two superposed cadmium sulfide crystals observed by Lang method of X-ray observation 01 p0126 A66-10968

Range formula calculation of neodymium ion concentration in two samples of CdS crystals after bombardment at 200 keV Nd ion energies 01 p0126 A66-10970

Indirect transition and temperature dependence of absorption limit in single crystal cadmium sulfide 01 p0126 A66-11006

Interband Faraday rotation at liquid-nitrogen temperature in CdS-CdSe mixed crystals 02 p0274 A66-11722

Capture and recombination levels in CdS single crystals examined from photoconductivity analysis 02 p0277 A66-12087

Effect of surface state of cadmium sulfide on fundamental absorption edge and fine structure obtained from gaseous phase in inert atmosphere 03 p0407 A66-12405

Vacuum deposition of cadmium sulphide ultrasonic transducers for generating longitudinal or linearly polarized shear waves 03 p0368 A66-12410

Beating effect of current oscillations in cadmium sulfide due to nonuniform illumination and indicating sinusoidal oscillations of different frequencies and comparable amplitude 03 p0408 A66-12453

Cuprous oxide-cadmium sulfide junction photocells enhanced in photosensitivity and rectifying properties by exposure to periods of light and darkness 03 p0413 A66-13190

CdS single crystal optical generator during excitation by ruby laser, discussing two-photon absorption coefficient at 300 degrees K for radiation flux densities 04 p0529 A66-13874

Recombination parameters in CdS determined from kinetics and IR quenching of photocurrent relative to available illumination 04 p0584 A66-14257

Two ohmic electrodes or one ohmic and one barrier electrode for current-voltage stable-negative characteristic of cadmium sulfide, noting IR radiation effects 04 p0568 A66-14351

Electron collision-ionization avalanches in cadmium sulfide crystal due to electric field intensities 04 p0570 A66-14489

Conductivity dependence of acoustoelectric effect in cadmium sulfide samples 05 p0731 A66-14653

Cadmium sulfide and cadmium selenide, discussing optical absorption, energy band structure, effective band-masses and composition changes of crystals in polarized light 05 p0731 A66-14656

Cadmium sulfide and cadmium selenide recombination centers, discussing temperature dependence of electron capture cross sections 05 p0731 A66-14661

Quenching and enhancement of dark conductivity in high resistivity photosensitive single crystals of cadmium sulfide 05 p0732 A66-14663

Crystalites of CdS in obliquely evaporated film on relative intensity of X-ray diffraction peaks 05 p0736 A66-14975

High strain sensitivity in CdS evaporated films, noting effects of tension and/or compression on film resistance 05 p0736 A66-14977

Luminescence decay of electron bombarded



CdS, measuring time constants 05 p0737 A66-15173  
 Fine structure exhibited by near IR absorption and emission spectra of copper ions in ZnS and CdS crystals recorded at low temperatures 05 p0742 A66-15874  
 Storage stability, moisture degradation and thermal cycling durability of cadmium sulfide-copper sulfide thin film solar cells 06 p0808 A66-16012  
 Current voltage characteristics of cadmium sulfide semiconductors showing departures from Ohm law associated with ultrasonic amplification, crystal length and increasing conductivity 06 p0923 A66-16183  
 Low temperature copper diffusion limits frequency range of cadmium sulfide shear mode diffusion layer transducer 06 p0851 A66-16461  
 Exciton absorption lines and long wave intrinsic edges of single-crystal CdSe and CdS at low temperatures 06 p0924 A66-16540  
 Coherent current oscillations observed in dark conductive In-doped CdS at 77 and 300 degrees K 06 p0925 A66-16659  
 Current oscillations in nonuniformly illuminated cadmium sulfide, examining effects of variation in parameters 06 p0925 A66-16664  
 Angular distribution of annihilation gamma quanta in CdS single crystals of high and low resistivity 06 p0928 A66-16921  
 Second sound in semiconductors, interpreting signal following amplification in CdS crystal as diffraction caused by anisotropy of amplification coefficient 06 p0930 A66-17055  
 Lattice vacancies and interstitials in II-VI compounds of cadmium sulfide and zinc selenide caused by electron bombardment often determine advantages or limits of material 06 p0935 A66-17130  
 Space-charge-limited currents and electron traps in CdS crystals thermally stimulated after electron injection 07 p1097 A66-17738  
 Electron energy levels in CdS single crystals from Hall effect, conductivity and space-charge-limited current measurements 07 p1098 A66-17739  
 Depletion layer 1000 mc transducers for producing or detecting hypersonic waves in solids, using CaS or GaAs for high acoustoelectrical conversion efficiency 07 p1009 A66-17827  
 Laser emission in pure cadmium sulfide crystals bombarded by electron beams 08 p1233 A66-18650  
 Group II-VI semiconductors, examining theory of bound exciton complexes, lattice vibrations, phonon-assisted edge emission and higher energy bands 08 p1271 A66-19239  
 Contact-making process in cadmium sulfide crystals, examining influence on plasma electron efficiency in glow discharge effect 08 p1272 A66-19243  
 Secondary illumination effect on intrinsic photovoltage and photocurrent excited in certain spectral region in cadmium sulfide crystals with gold and indium contact 08 p1272 A66-19244  
 Rise and decay of photoconductivity of cadmium sulfide single crystals with superlinear photocurrent illumination characteristics 08 p1272 A66-19248  
 Postdeposition vacuum heat treatments of cadmium sulfide films, examining effect on photocurrent and photocurrent to dark current ratio 08 p1273 A66-19258  
 Time resolved photoluminescence spectra of two green broad emission bands in CdS as function of temperature, attributing new structure to transverse optical phonons 08 p1276 A66-19368  
 Generation in cadmium sulfide during two-photon optical excitation by ruby laser with modulated Q-factor 08 p1277 A66-19620  
 Metallography of cadmium crystals with copper impurities obtained by sublimation from copper powder, noting that copper solubility is limited 08 p1277 A66-19623  
 Indirect transition and temperature dependence of absorption limit in single crystal cadmium sulfide 09 p1411 A66-19944  
 Effect of electric field and crystalline dimensions on position of optical absorption edge in cadmium sulfide thin films obtained by vacuum deposition 09 p1412 A66-19995  
 Low temperature measurement of magnetic

susceptibility of CdS single crystals with manganese impurity, considering effects of antiferromagnetic exchange 09 p1424 A66-20078  
 Photoimpedance measurement as function of AC field of CdS crystals coated with SiO films or situated between polystyrene foils 09 p1425 A66-20189  
 CdS-type superlinear photoconductivity due to excitation from localized levels 09 p1426 A66-20195  
 Extrinsic and intrinsic surface states and photoelectronic properties of insulating CdS crystals 09 p1427 A66-20256  
 Spectral dependence of photovoltaic effect CdS-CdSe heterojunction 09 p1427 A66-20482  
 Stationary IR quenching of photocurrent in CdS, discussing recombination channels 09 p1428 A66-20538  
 Characteristics of cadmium sulfide photocells and p-n junction photocells, using germanium or silicon 09 p1355 A66-20573  
 Cadmium sulfide based film photoresistors insensitive to moisture and long exposure to air 09 p1429 A66-20820  
 Film-type photocell consisting of p-n heterojunction between copper oxide and cadmium sulfide with secondary maximum in sensitivity 09 p1429 A66-20821  
 Metal oxide semiconductor /MOS/ transistors constructed on single crystal cadmium sulfide, noting transconductance, gate source, gate drain capacitance, etc 09 p1360 A66-20980  
 Direct piezoelectric coupling to surface elastic waves by spatially periodic electrode, noting measurements in quartz plate and CdS film 10 p1533 A66-21068  
 Contact barriers on insulating semiconductor cadmium sulfide measurements, based on pulsed light and bridge 10 p1573 A66-21245  
 Phonon series in cadmium sulfide single crystal emissions at low temperature range 10 p1583 A66-22025  
 LF photocurrent noise intensity, spectrum and photoresponse in CdS single crystals 10 p1588 A66-22157  
 Isothermal cross section of phase diagram of Zn-Cd-S and sulfide films 11 p1749 A66-22294  
 Cadmium sulfide space charge limited diodes, noting current voltage characteristics and field and electron density distributions 11 p1668 A66-23026  
 Spatial variation of electric field in amplifying CdS measured, using electro-optic effect to study acoustic flux from thermal noise 11 p1758 A66-23356  
 Coupling of ordinary and extraordinary electromagnetic waves in CdS induced by external magnetic field or stress 12 p1926 A66-23719  
 CdO films as transparent ohmic contacts with CdS /single crystal and film type/ photoconductor 12 p1927 A66-23771  
 IR radiation effect on photovoltaic effect in cadmium sulfide excited by visible light 12 p1927 A66-23772  
 Capacitive probe measurements of potential fluctuation in current-oscillating CdS crystals under ultrasonic amplification conditions at room temperature 12 p1931 A66-24812  
 Current saturation in CdS crystals 12 p1931 A66-24814  
 Ultrasonic generation and amplification in CdS crystals with barrier layer under constant drift field 13 p2159 A66-25085  
 Photoelectric properties and relaxation time of polycrystalline layers of cadmium sulfide are highly dependent on substrate temperature 13 p2160 A66-25097  
 Crystallites in evaporated film of CdS on Au and Al films studied by X-ray diffraction 13 p2161 A66-25196  
 Negative resistance in cadmium sulfide single crystal 13 p2162 A66-25198  
 Microwave emission from crystal of n-type CdS illuminated by mercury lamp or laser in strong electric field 13 p2162 A66-25199  
 Surface photovoltage measured in vapor-deposited cadmium sulfide using metal-insulator-semiconductor-structures, noting surface potential analysis as applied to thin film field effect 13 p2164 A66-25487  
 Cadmium sulfide single crystal preparation

by zone sublimation method, analyzing structure via X-ray diffraction and obtaining photosensitivity curves 13 p2165 A66-25687  
 Stationary and kinetic determination parameters of capturing recombinative centers in CdS single crystal 13 p2166 A66-25687  
 Effects of recoil in semiconductor with thermal-neutron-absorption cross section measuring changes in luminescence and conductive properties of CdS 13 p2166 A66-25700  
 Conductivity dependence of acoustoelectric effect in cadmium sulfide samples 13 p2167 A66-25900  
 Cadmium sulfide and cadmium selenide discussing optical absorption, energy band structure, effective band-masses and composition changes of crystals in polarized light 13 p2167 A66-25900  
 Cadmium sulfide and cadmium selenide recombination centers, discussing temperature dependence of electron capture cross sections 13 p2168 A66-25900  
 Laser oscillations in CdSe and CdS bombarded by fast electron beam 14 p2306 A66-27000  
 UV absorption and dispersion of cadmium sulfide crystals and energy band structure 14 p2356 A66-27000  
 Influence of trapping on acousto-electric effect in piezoelectric semiconductor noting ultrasound absorption and experimental results in cadmium sulfide 14 p2359 A66-27100  
 CdS single crystal optical generator during excitation by ruby laser, discussing two photon absorption coefficient at 300 degrees K for radiation flux densities 14 p2308 A66-27500  
 Fine-line absorption spectrum anisotropy with respect to crystallographic axis in cadmium sulfide 14 p2308 A66-27600  
 Laser-generation-type luminescence CdS-CdSe crystals exposed to double photon excitation from ruby laser 14 p2308 A66-27600  
 Two ohmic electrodes or one ohmic and one barrier electrode for current-voltage stable-negative characteristic of cadmium sulfide, noting IR radiation effects 14 p2368 A66-28200  
 Structural defects arising during growth and heat treatment of CdS single crystals studied, using anomalous transmission of X rays 15 p2557 A66-28500  
 High amplitude LF current and optical transmission oscillations in CdS single crystals under high electric field and monochromatic illumination near fundamental absorption edge 15 p2558 A66-28600  
 Impurity photovoltaic effect in cadmium sulfide, noting radiative enhancement of spectral response upon illumination with green light 15 p2561 A66-28700  
 Two parallel carrier capture mechanisms in single recombination center in cadmium sulfide 15 p2563 A66-28700  
 Transient acoustoelectric interaction in CdS and ZnS crystals during single transition measuring electron drift 15 p2563 A66-28700  
 Exciton absorption lines and long wave intrinsic edges of single-crystal CdSe and CdS at low temperatures 15 p2569 A66-29900  
 Beam trapping in cadmium sulfide noting threshold, trapping length, refractive index change and Stokes radiation 16 p2716 A66-30100  
 Phonon series in cadmium sulfide single crystal emissions at low temperature range 16 p2776 A66-30800  
 Linear absorption effect on threshold for self-focusing of laser beam in cadmium sulfide, noting variation of absorption coefficient 16 p2720 A66-31500  
 Electric conductivity of CdS single crystals in atmosphere, dry air, oxygen, water vapor, carbon dioxide and in transverse electric field 16 p2786 A66-31700  
 Dark conductivity of cadmium sulfide single crystals as affected by contact voltage and transverse electric field 16 p2786 A66-31700  
 Expanded single crystal hetero-transition in CdS-CdSe system 16 p2787 A66-31700  
 Distribution of recombination centers over energy levels of CdS-CdSe solid



- solutions 16 p2787 A66-31737  
Gamma radiation and fast neutron effects on dark resistance, photoconductivity, majority carrier mobility, recombination kinetics, etc. in CdS single crystal 16 p2787 A66-31765  
Spatial periodic modulation of high field domain in cadmium sulfide 17 p2974 A66-31813  
Magnitude of DC conductivity change in CdS by microwave phonons at liquid helium temperature explained with piezoelectric polaron effect 17 p2975 A66-31886  
Current oscillations, negative resistance and high field domain transition in dark conductive cadmium sulfide crystals 17 p2975 A66-31940  
Generation in cadmium sulfide during two-photon optical excitation by ruby laser with modulated Q-factor 17 p2936 A66-33134  
Metallography of cadmium crystals with copper impurities obtained by sublimation from copper powder, noting that copper solubility is limited 17 p2984 A66-33137  
Spectra and intensity vs excitation level and spatial distribution vs current density determined for optical radiation by electron excited cadmium sulfide 17 p2937 A66-33308  
Current-voltage characteristics peculiarities of fine cadmium sulfide single crystals with nonohmic contacts 17 p2986 A66-33311  
Current oscillation observations in photoconductive cadmium sulfide crystal 17 p2987 A66-33317  
Changes in piezoelectric constants of cadmium sulfide crystal caused by illumination and on mechanical vibration caused by fluctuation of carrier injection from electrodes 18 p3153 A66-33613  
Cadmium sulfide thin films as ultrasonic transducers, obtaining mixed or pure vibration modes via crystalline axis orientation 18 p3111 A66-34085  
Resonant enhancement of Raman cross section for phonons in CdS at frequencies near absorption edge 18 p3156 A66-34468  
Photoconductivity of thin layers of CdS, noting intrinsic maximum for various dopants, temperature effect, activation energy, etc 18 p3157 A66-34628  
Spectral distribution of relative quantum yield of photoluminescence in polycrystalline cadmium sulfide films 18 p3158 A66-34694  
Evaporated and recrystallized CdS layers, discussing electron mobility, level distribution, capture cross section and techniques of measurement 19 p3435 A66-35408  
Spatial distribution of acoustoelectric field in photoconductive CdS measurement under conditions of current saturation, determining carrier drift mobility 19 p3435 A66-35415  
Steady state open-circuit photovoltage in some monocrystalline CdS samples found to be due to generation of free minority carriers 19 p3437 A66-35476  
Concentration and lifetime of minority carriers in cadmium sulfide determined by method based on optically induced changes in concentration 19 p3437 A66-35477  
Layer of CdS crystals photoconduction measurements suggesting change in space charge under illumination due to increase of free electron concentration in volume 19 p3438 A66-35478  
LF photocurrent noise intensity, spectrum and photoresponse in CdS single crystals 19 p3440 A66-35771  
Texture and electric conductivity of cadmium sulfide thin films 19 p3442 A66-35865  
Electron-phonon interaction phenomena observed in GaAs and CdS, examining current saturation, ultrasonic emission by charge carriers and acoustic amplification 19 p3445 A66-36256  
Lampert double injection theory for CdS diodes with negative resistance I-V characteristic curve 20 p3535 A66-38435  
Ultrasonic generation and amplification in CdS crystals with barrier layer under constant drift field 21 p3795 A66-38510  
Direct measurement of dispersion properties of cadmium sulfide and CdS-CdSe crystals, using Obreimov-Fresnel diffraction method, growing crystals by synthesis 21 p3799 A66-38926  
Modulation by ultrasonic diffraction of 10.6 micron laser radiation in photoelastic CdS, GaAs and Si crystals 21 p3747 A66-39112  
Photoconductive and luminescent behavior of undoped cadmium sulfide single crystals at room temperature under laser excitation 21 p3748 A66-39165  
Varying excitation intensity effects on edge emissions from pure and doped CdS powder samples, noting electron-hole recombination mechanisms 21 p3802 A66-39202  
Applications for ferroelectric cold conductors and GaAs light-sensitive diodes, examining supersonic amplification in CdS 21 p3716 A66-39620  
UV absorption and dispersion of cadmium sulfide crystals and energy band structure 22 p3966 A66-40823  
Optical thickness measurement of nonabsorbing dielectric film when it is inconvenient to apply overlay film to measure thickness by Fizeau fringe shift 22 p3968 A66-40889  
Precision polishing technique for optical and microwave acoustical surfaces with overall flatness of one-eighth wavelength of light and parallel to 6 inches 23 p4067 A66-41248  
Structural defects arising during growth and heat treatment of CdS single crystals studied, using anomalous transmission of X-rays 23 p4112 A66-41284  
P-type conductivity and stored electron charge densities in high resistivity cadmium sulfide crystals 23 p4114 A66-41625  
Single crystal wurtzite CdS luminescence as function of exciting intensity, noting shift of overlapping band structure of green-edge emission indicative of electron-hole recombination 24 p4219 A66-42250  
Recrystallization of evaporated CdS layers in environment containing various elements, obtaining oxygen enhanced crystal growth 24 p4253 A66-42356  
Optical properties and energy structure parameters calculation for CdS-CdTe crystals 24 p4253 A66-42362  
Failure mechanisms of CdS and CdSe thin film FETs noting volt-ampere characteristics, temperature, electrical stress and humidity effects 24 p4181 A66-42381  
Surface pinned layer-like field inhomogeneities in cadmium sulfide, investigating visibility of field layer by corresponding shift of absorption edge, using Franz-Keldysh effect 24 p4254 A66-42427  
**CADMIUM TELLURIDE**  
Recombination radiation of p-n junctions in CdTe-ZnTe system crystals for various current densities and molecular compositions 01 p0125 A66-10780  
Cadmium telluride laser with electron excitation 01 p0084 A66-11188  
Impurities effect on electrification of cadmium telluride dust, specifically n and p types, with electrification increasing with impurity concentration 06 p0928 A66-16891  
Specific conductivity, Hall, Nernst-Ettingshausen and thermoelectric transfer effects in InAs-CdTe and InAs-ZnTe alloys 09 p1428 A66-20539  
Photovoltaic cells based on p-n junctions of ternary Cd-Te-Hg films, noting fabricating methods for n-or p-types 09 p1431 A66-20926  
Distribution coefficient and electrical behavior of indium in cadmium telluride crystals, using In 114 /half-life 49 days/ as tracer 10 p1574 A66-21352  
Diffusion of selenium in cadmium telluride, using radioactive Se as tracer 10 p1574 A66-21353  
Recombination radiation of p-n junctions in CdTe-ZnTe system crystals for various current densities and molecular compositions 11 p1749 A66-22293  
Elastoresistance coefficients for n-type cadmium telluride determined at 300 and 195 degrees K 12 p1926 A66-23713  
Cadmium telluride laser with electron excitation 12 p1890 A66-24009  
Photoconductivity and optical transmission of cadmium-indium-telluride, noting temperature dependence 13 p2165 A66-25685  
Field effect measurements in n-and p-type CdTe at room temperature and pressure 15 p2558 A66-28612  
Spontaneous and coherent photoluminescence in cadmium mercury telluride crystals excited optically by GaAs diode laser. 15 p2517 A66-29390  
Resistivity increase in Cadmium Telluride, attributed to conduction band separation due to deionization into impurity levels 16 p2768 A66-30131  
Hexagonal crystal structure growth of CdTe thin film 19 p3438 A66-35480  
Injection luminescence in forward-biased CdTe p-n junction diode 23 p4112 A66-41298  
Optical properties and energy structure parameters calculation for CdS-CdTe crystals 24 p4253 A66-42362  
Pressure deformation of band structure of HgTe-CdTe alloys determined from measurements of Hall effect and resistivity 24 p4258 A66-43009  
**CAJUN ROCKET**  
**S NIKE-CAJUN ROCKET**  
**CALCITE**  
Compressional wave velocity in limestones, marbles and single crystal of calcite under hydrostatic pressure to 20 kbar 19 p3351 A66-36337  
**CALCIUM**  
H-line of calcium ion analyzed from spectrograms of chromospheric spicules 01 p0131 A66-10277  
Green corona before birth and after death of calcium pike in intensity plot vs heliographic latitude 09 p1455 A66-20379  
Bone calcium loss during two weeks of simulated weightlessness, using X-ray wedge technique 11 p1643 A66-22577  
Energy level transitions in vacuum UV absorption spectrum of calcium vapor 14 p2337 A66-27704  
Profile of ionized calcium resonance lines radiated from arc plasma jet observed by Fabry-Perot etalon 17 p2970 A66-32714  
Final character figures of calcium bright foci for IGY 18 p3235 A66-34735  
Cosmic ray produced lithium and calcium in iron meteorites 18 p3236 A66-34890  
Open circuit half-cell potentials of calcium in thiocyanate-liquid ammonia solutions 18 p3055 A66-34902  
Polarization difference in elastic scattering of proton from Ar 40 and Ca 40 due to spin-orbit force difference 18 p3140 A66-35037  
Ionized calcium luminescence in large chromospheric flare, noting K line broadening due to nonthermal turbulent motions 23 p4126 A66-41078  
**CALCIUM FLUORIDE**  
Ruby laser radiation effect on fluorescence and laser action in dysprosium doped calcium fluoride crystals 01 p0082 A66-10718  
Plastic deformation spitting and evolution of spectral lines and excited level structure of europium ion in alkaline-earth fluoride crystals 03 p0409 A66-12717  
Germanium films deposited on heated crystal calcium fluoride substrates in vacuum system 05 p0732 A66-14667  
Growth of absorption bands of natural and synthetic calcium fluoride crystals irradiated with protons from cyclotron at Tomsk Institute 05 p0741 A66-15857  
Chemical and thermal stability of fluoride solid lubricants measured and tested for aerospace environment [ASLE PREPRINT 65AM 5C5] 07 p1039 A66-18284  
Frequency and temperature effects on dielectric properties of calcium, strontium and barium fluorides 10 p1577 A66-21561  
Microstructure of epitaxial germanium films deposited on calcium fluoride substrates, noting parameters of deposition 13 p2158 A66-25063  
Magnetization induced by circularly polarized laser light incident on nonabsorbing material, in absence of external magnetic field, in doped calcium fluoride proportional to light intensity and Verdet constant 13 p2131 A66-26142  
Pulsed nuclear resonance experiment on neodymium doped calcium fluoride, determining relaxation time 14 p2336 A66-27638  
Stimulated emission from samarium-doped calcium fluoride crystal excited by ruby laser 15 p2516 A66-29358  
Laser lines due to energy transfer from color centers to erbium ions in calcium fluoride crystals irradiated by gamma



ray 16 p2717 A66-30278  
Self-lubricating properties of composites of porous nickel and nickel-chromium alloy impregnated with barium fluoride-calcium fluoride eutectic  
[ASLE PAPER 66AM 1C2] 16 p2710 A66-30404  
Solid state CW optically pumped microwave maser, using divalent thulium doped calcium fluoride 18 p3117 A66-33614  
Lowest of UV absorption bands attributed to 4f-5d transition of trivalent rare earth ions in calcium fluoride 19 p3443 A66-36004  
Stimulated emission from samarium-doped calcium fluoride crystal excited by ruby laser 20 p3577 A66-37362  
Ruby laser radiation effect on fluorescence and laser action in dysprosium doped calcium fluoride crystals 20 p3579 A66-37656  
Electron paramagnetic resonance and optical spectra of trivalent erbium in type II crystals of calcium fluoride disclose existence of cubic, tetragonal and trigonal sites 22 p3961 A66-39916

**CALCIUM METABOLISM**  
Nuclear fast red technique of calcium in serum, parotid fluid and urine in weightless state 03 p0329 A66-13347

**CALCIUM OXIDE**  
Electrical conductivity of single crystals of calcium and strontium oxides 10 p1581 A66-21878

**CALCIUM TUNGSTATE**  
Addition of molybdenum to neodymium doped calcium tungstate laser material increases susceptibility to photolytic coloring and changes vacuum reduction coloring spectra 04 p0561 A66-13732  
Laser oscillation in calcium tungstate crystals activated with trivalent praseodymium 05 p0694 A66-14898  
Continuous optical quantum generator operating at room temperature on calcium tungstate doped with neodymium ions 09 p1386 A66-19956

**CALCULUS**  
SA DIFFERENTIAL EQUATION  
SA INTEGRAL EQUATION  
SA OPERATIONAL CALCULUS  
SA VARIATIONAL CALCULUS  
SA VECTOR CALCULUS  
Numerical calculus and physical calculus - Colloquium, Henri Poincare Institute, Paris, May 1963  
[PST PAPER NT-147] 14 p2323 A66-27790  
Mean value theorem for curves arising in solution of ordinary differential equation by series method 20 p3590 A66-37525

**CALIBRATION**  
SA STANDARDIZATION  
SA WIND TUNNEL CALIBRATION  
Intercalibration of cosmic ray neutron monitors at nine European sea level stations and deduction of daily latitude effect in 1963 01 p0132 A66-10321  
Vacuum gauge calibration at lower pressures necessitates transfer to secondary standard and extrapolation of this calibration to range of interest 01 p0067 A66-10491  
Calibration of spectral apparatus for visible region of spectrum with measurements of spectral fluxes of total and scattered radiation, atmospheric spectral transparency, etc 01 p0133 A66-10755  
Evaluation and calibration of missile and space tracking systems including test-by-test analysis, lofted rockets, self-calibrating systems, etc 01 p0053 A66-10805  
Shock and vibration measurement system with error correcting techniques including dynamic calibration data, noise detection, etc  
[SAE PAPER 650820] 01 p0069 A66-10822  
Thermal shock and wrinkled diaphragms effect on calibration of pressure transducers 01 p0070 A66-10887  
Laboratory vibratory stand for calibrating sensors of oscillatory motion 01 p0070 A66-11020  
Calibration procedures and statistical analysis for error reduction in ballistic camera lead-screw type comparator 02 p0228 A66-11380  
Lincoln sphere for radar calibration, noting measurements before and after launching 03 p0430 A66-12449

Tunable calibrated impedance for measurement of unknown terminations in millimeter range and based on reflection coefficient adjustments 03 p0371 A66-13242  
Calibration of ARIS /Advanced Range Instrumentation Ships/ radars for cross section measurements 04 p0479 A66-13611  
Assured performance calibration discussing statistical quality control, instrument variability, vacuum tube and digital voltmeter histories, calibration costs, etc 04 p0520 A66-13941  
Shipboard inertial navigation system recalibration, using periodic position information from communications satellite 05 p0712 A66-14604  
High altitude aircraft for calibration of solar cells and extrapolation of data to obtain outer space short circuit current 06 p0808 A66-16013  
Checking and calibration of aircraft compasses, discussing compass base at Dublin Airport and effect of lightning strikes 07 p1032 A66-17675  
Accurate and economical determination of static system position errors in pressure altimeter systems by trail cone technique 07 p1034 A66-17792  
HF magnetic probes for measurement of transient magnetic fields in linear pitch devices and Helmholtz coil calibration 07 p1037 A66-18491  
Light source having absolute spectral energy distribution for standardizing star tracker calibration 08 p1252 A66-19501  
Indicator design for semiconductor strain gauges, discussing basic circuitry, calibration and stability 08 p1226 A66-19599  
Solar cell orbital performance measurement, discussing apparatus, V-I characteristics, spectral response and calibration 08 p1174 A66-19664  
Power of solar cell array in space predicted from comparative measurements in earth sunlight of given solar panel and monitor with known output in space 09 p1331 A66-20171  
Absolute calibration of Arizona Photometry 09 p1402 A66-20293  
Accurate calibration of Doppler winds for use in computation of mesoscale wind fields 09 p1399 A66-20728  
Cylindrical black body furnace with graphite resistance built in France, attaining 1600 degrees C, for calibration of radiation pyrometers 09 p1383 A66-20909  
First order error analysis, radar antenna calibration technique and polarization scattering matrix 10 p1501 A66-21627  
Photometric standards which are references for measurement of sources of energy in visual and near visual portion of electromagnetic spectrum 11 p1736 A66-22671  
Lincoln radar calibration sphere ejected from Titan III-A transtage to calibrate all but large-scale radar installations 11 p1777 A66-22875  
Calibration problem of load-measuring instruments solved, using automatic digital voltmeter  
[ASTME PREPRINT IQ66-705] 12 p1882 A66-24412  
Sensor calibrations using NBS standard of spectral irradiance, as used for Mariner IV Canopus sensor 13 p2080 A66-25986  
Self-calibration and automatic correction for wavelength response of monochromator-filter-detector system 14 p2292 A66-27323  
Calibration curve for Preston tubes in supersonic flow obtained by reference-temperature method 14 p2294 A66-27452  
Calibration of communication satellite Earth station antenna system, using radio stars 14 p2238 A66-27532  
Maintaining of flow similarity in calibration of nozzle type water meters for study of working processes of pumps 14 p2225 A66-27698  
Utilization of confidence interval concept for instrument calibration 14 p2296 A66-27818  
Calibration of spectral apparatus for visible region of spectrum with measurements of spectral fluxes of total and scattered radiation, atmospheric spectral transparency, etc 14 p2285 A66-27854  
Gravimeter error in recording of Earth tides, examining leveling and calibration problems 14 p2298 A66-28400

Range instrumentation systems calibrating and evaluation at Air Force Eastern Test Range 14 p2272 A66-28444  
Calibrating geodetic and geophysical errors effect on Minuteman trajectory, noting instrument errors 14 p2390 A66-28444  
Carbon dioxide to calibrate instruments for carbon determination in metals 15 p2445 A66-28612  
Calibration ensuring optimal instrument performance, using statistical quality control, noting background of Assurance Performance Calibration program 15 p2508 A66-28812  
Calibration of birefringent filter photometer 15 p2499 A66-28844  
Radiation measurement error using Eppley radiation sensors in Antarctic 15 p2503 A66-29664  
Voltage output characteristics of axial gradient heat flux transducers employing thermoelectric temperature difference sensing 16 p2702 A66-30422  
Pyrheliometers, noting performance, application, environmental effects and calibration based on black body radiation 16 p2703 A66-30562  
Lens decentering distortion using thin prism and Conrady models, noting application of precise calibration technique analytical photogrammetry 16 p2746 A66-30512  
Calibration and testing of temperature measuring devices in -200 to 3000 degrees C 16 p2704 A66-30632  
High accuracy variable area meteorological calibrations with multiple gases 16 p2704 A66-30672  
Calibration of spherical reflector at Arecibo Ionospheric Observatory antennas using analytical photogrammetric methods 18 p3075 A66-33742  
Accelerometer standard designed for reciprocity and comparison calibrations of vibration transducers 18 p3112 A66-34202  
Frequency standard system using quartz servo-oscillators for design and testing of high-stability frequency sources 18 p3087 A66-34702  
Constant current sources consisting of sealed ionization chambers for calibrating electrometers 19 p3357 A66-35802  
Strain gauge strip chart error determination, elimination and effects on accuracy of electric calibration 19 p3360 A66-36302  
Calibration of turbine flow meter on air against pitot tube traverse, considering random scatter 19 p3362 A66-36752  
Digital computers used in error calculation in calibration curves of turboengines and other pneumatic devices 20 p3555 A66-36922  
Calibration device for flow and volume meters for liquid rocket engine propellant 20 p3561 A66-38062  
Calibration test for photorheological method of stress analysis in plastically flowing body under plastic work or creep deformation 20 p3671 A66-38102  
Calibration process for RZ-2 rocket engine noting changes in orifices, engine performance, influence coefficients, etc 21 p3807 A66-38642  
Inertial platform test station for shipboard maintenance and calibration of platform used in A6A and E2A aircraft, examining accelerometer bias and gyro drift tests 21 p3723 A66-38882  
Radio astronomy measurements requiring absolute intensity calibrations, noting flux densities and measurements of very dark areas of sky 21 p3815 A66-39482  
Quantitative photographic determinations of laser beam power density distributions and Q-switched ruby oscillator-amplifier system divergence characteristics 23 p4075 A66-41032  
Error of measurement of mean square value of fluctuation signals due to voltmeter calibration 23 p4038 A66-41523  
Shutters, lenses, vidicons, data rates and calibration techniques for TV cameras of Rangers VI, VII, VIII and IX 23 p4070 A66-41671  
Piston manometer calibration for precision pressure measurement 24 p4213 A66-42822

**CALIBRATOR**  
Valve arrangement for calibrating



- piezoelectric shock tunnel transducers used in pressure measurements 24 p4213 A66-42823
- CALORIC REQUIREMENT**  
**S NUTRITIONAL REQUIREMENT**  
**CALORIC STIMULUS**  
 Barany hypothesis tested to clarify mechanism of caloric nystagmus by use of zero gravity environment 17 p2857 A66-32168
- CALORIMETER**  
 Pulse energy and power of lasers under continuous operating conditions measured, using calorimeters, photoelectric effect of radiation, etc 03 p0379 A66-13205  
 Heat conduction in thermocouples with lateral heat leakages applied to calibration of microcalorimeters of Calvet type 05 p0679 A66-15174  
 Energy spectrum shape and absolute abundance of nuclear active particles at low altitude determined, using ionization calorimeter, plotting angular distribution of particles 07 p1115 A66-17551  
 Specific heat of liquids with constant volume determined, using, pycnometer cell, obtaining formula for specific heat in terms of measurable thermal parameters 13 p2077 A66-25354  
 Ionization calorimeter for measuring primary cosmic ray components, discussing nuclear interactions, energy spectra, EM cascades, etc 13 p2175 A66-26011  
 Enthalpy of gas stream, calorimeter surface treatment and heat transfer measurement errors in arc-heated tests 14 p2411 A66-27425  
 Calorimeter bomb combustion of hydrocarbons and fluoro-substituted hydrocarbons with nitrogen trifluoride and nitrogen trifluoride-oxygen mixtures and mass spectrometric analysis 15 p2570 A66-29609  
 Transfer efficiency of theta pinch in converting capacitively stored electrical energy to plasma energy measured, using calorimeter technique 16 p2761 A66-31090  
 Bench-top calorimeter for determining radiation and convection in small-scale combustion of fuel [WSCI 66-14] 18 p3113 A66-34425  
 Energy and power of Q-switched neodymium glass laser measured, using calorimetric devices, vacuum photodiodes, etc 18 p3120 A66-34904  
 Electron-photon and nuclear active components energy of young air showers measured by ionization calorimeter, determining inelasticity coefficient 18 p3206 A66-35100  
 Ionization calorimetry of energy spectrum of leading particles in cores of EAS compared with data from model 18 p3206 A66-35101  
 Spectrum of nuclear active component of cosmic rays determined by nuclear calorimeter 18 p3217 A66-35171  
 Meson properties analyzed underground by spark calorimeter operated by telescope of Geiger counters 18 p3220 A66-35194  
 Angular distribution and energy spectrum of cosmic particle showers at large zenith angles analyzed, using ionization calorimeter 18 p3220 A66-35196  
 Electron-photon cascade showers recorded with ionization calorimeter, determining influence of value of radiation length on form of mean cascade curve 18 p3221 A66-35198  
 Interaction of 1000 bev particles by ionization calorimeter technique suggests free path of nuclear active particles in atmosphere decreases as particle energy increases 24 p4267 A66-42908  
 Ionization calorimeter measurement of number of particles in electron photon cascade with energy transferred from ionization calorimeter 24 p4269 A66-42924
- CALORIMETRY**  
**SA THERMOMETRY**  
 Specific heat of gadolinium near Curie point, discussing measuring procedure and line drawing of calorimetric setup 01 p0118 A66-10252  
 Atomic heat of titanium, vanadium and chromium in high temperature range, discussing parameters and experimental techniques 05 p0698 A66-14511  
 Diluted nickel alloys, describing calorimetric determination of specific heat at low temperatures 06 p0897 A66-16939  
 Rotating bomb calorimetric technique, determining accurate values of enthalpy of combustion of boron and boron compounds 08 p1178 A66-19068  
 Specific heat of iron, cobalt and nickel in high temperature range measured, using quasi-adiabatic operating calorimeter 08 p1240 A66-19255  
 Calorimetric and magnetic measurements of dilute titanium alloys with other transition elements, distinguishing between homogeneous and nonhomogeneous transitions 09 p1419 A66-20045  
 Magnetocaloric effects in high-field superconductor, noting magnetic field-induced temperature variation effects on thermally isolated superconducting alloy specimen 09 p1420 A66-20051  
 Superheating of linear high polymer polyethylene crystals, evaluating time dependence of melting, differential thermal analysis and calorimeter techniques 12 p1899 A66-23937  
 Calorimetric measurement of local temperatures in nitrogen plasma jet at atmospheric and subatmospheric pressures [DGR PAPER 66-002] 13 p2082 A66-26493  
 Calorimetric measurement of local temperatures and velocities in weakly ionized nitrogen plasma at subsonic velocity and thermodynamic equilibrium 14 p2294 A66-27487  
 Direct measuring radiation calorimeter developed for determining radiant heat flux of solid propellant gas flame in rocket combustion chambers [AIAA PAPER 65-358] 18 p3159 A66-33814  
 Heat transfer in wake of reflected shock wave in reacting gases, using calorimetry and shock tube technique 21 p3727 A66-39095  
 Precision microwave power measurement methods noting calorimetry, bolometry and thin film 24 p4184 A66-42649
- CAMBERED WING**  
 Pressure distributions on cambered bodies of arbitrary cross section at angle of attack applied to transport fuselage afterbody design [AIAA PAPER 65-718] 03 p0314 A66-12543  
 Lift coefficient in two-dimensional smoke wind tunnel noting symmetrical, cambered and leading double-edge slot wing section 03 p0317 A66-13216
- CAMERA**  
 SA BAKER-NUNN CAMERA  
 SA BALLISTIC CAMERA  
 SA FRAMING CAMERA  
 SA HIGH SPEED CAMERA  
 SA LALLEMAND CAMERA  
 SA TELEVISION CAMERA  
 Aurora position and brightness determination by S-180 camera as affected by such factors as distortion and vignetting 02 p0226 A66-11345  
 S-180-S spectral camera characteristics of spectral sensitivity, distortion and slit width effect 02 p0226 A66-11346  
 High speed streak camera using electronic control circuits, light amplifier and time calibrator 02 p0230 A66-11816  
 Stereocamera for determining spatial orientation of cosmic particle tracks in large diffusion chamber 03 p0368 A66-12503  
 Camera for precision satellite observations accurate to one inch in determining position and to less than 0.002 seconds in determining moment of measurement 03 p0370 A66-13200  
 Commercial aerial camera objectives estimated with TsNIIGAIK electron-optical bench 04 p0519 A66-13662  
 Simple rotating drum streak camera covering principle, design, construction and application 04 p0520 A66-13940  
 Sinusoidal rocking-motion camera, advantages in satellite tracking such as light grasp gain, speed error insensitivity, clock switch operation, etc 05 p0682 A66-15370  
 Stereoscopic camera system design for use on lunar orbiting vehicle including illumination, lunar albedo, resolution and signal to noise ratio 08 p1222 A66-18734  
 Metric photography techniques utilizing stroboscopic light in highlight camera and rotating disk camera 10 p1534 A66-21229  
 Space photography, camera-film systems and TV/videotape systems for space environments 11 p1707 A66-23162  
 Design parameters of astronomical camera for lunar charting 12 p1876 A66-23644  
 Panoramic facsimile camera providing IR and visible spectrum imagery designed for unmanned space operation, noting construction, weight, etc 13 p2077 A66-25236  
 Military aerial mapping program, noting camera lens distortion, shutter, stabilization, films, etc 16 p2703 A66-30511  
 Polarization photography of solar corona, noting apparatus used for separation of K from F component 16 p2705 A66-30827  
 Smear resolution losses in ground target photographs for maneuverable target-tracking reconnaissance cameras, noting MOL simulation 17 p2925 A66-32351  
 Aerial mapping camera for photogrammetric research, examining three systems of correcting for film distortion 18 p3110 A66-33740  
 Rotating prism design for continuous image compensation cameras, application to UV and IR regions of spectrum 19 p3354 A66-35384  
 Pinhole array camera for multiple image production for integrated circuits 19 p3354 A66-35385  
 Dielectric-tape camera borne by meteorological satellite to provide high-quality photographs of Earth cloud cover 20 p3557 A66-37204  
 Cameras for recording data related to orbit of Earth satellites, noting technique in which tracks on photograph are chopped into discrete segments of length related to satellite velocity 20 p3560 A66-37841  
 Photographic radar system employing Q-switched ruby laser, Mullard type 6929 image tube and conventional camera 21 p3736 A66-38796  
 Photography of small freely moving particles undergoing heat and mass transfer, using beam splitter to align two cameras on drop 22 p3917 A66-39675  
 Distortions in aerial photographs due to errors in cameras, noting determination methods in various countries 22 p3919 A66-40622  
 Advanced imaging techniques for Metro camera for space applications 23 p4070 A66-41670
- CAMERA SHUTTER**  
 Photographic equipment using image converter tube as electronic shutter with exposure times from 0.5 to 5000 microseconds 23 p4070 A66-41674
- CAMOUFLAGE**  
**S RADAR ABSORBING MATERIAL**  
 /RAM/
- CANADA**  
 Canadian aerospace research including study of high latitude atmospheric phenomena by universities and government 09 p1458 A66-20710  
 Canadian space program including nonmilitary activities, upper atmosphere research, rocket sounding, aurora studies, satellite use, etc 15 p2601 A66-29937  
 Trends in short-haul transportation in Canada 24 p4296 A66-42261
- CANADAIR CL-84 AIRCRAFT**  
 V/STOL Canadair CL-84, evaluating control and lift propulsion system 05 p0609 A66-14767  
 Control and lift-propulsion systems and model testing of Canadair CL-84 V/STOL tilt-wing aircraft 06 p0806 A66-16818  
 Flight characteristics and test program of CL-84 light tilt-wing V/STOL Army support vehicle 07 p0986 A66-17271  
 Stability and control test program for Canadair CL-84 tilt-wing V/STOL aircraft prototype [SAE PAPER 660315] 15 p2427 A66-29839  
 CL-84 V/STOL flight simulation at Canadair through design, development and flight testing of flapped tilt-wing prototype [ICAS PAPER 66-18] 24 p4159 A66-42493
- CANADIAN SATELLITE**  
**S ALOUETTE I SATELLITE**  
**S ISIS SATELLITE**
- CANARD**  
 Effect of canard foreplane on longitudinal long-period perturbed motion of aircraft depends on change in hinge moments with Mach number change 04 p0458 A66-14152



## CANONICAL PROBLEM

- Transformation of error ellipsoid in motion of material point, with selection of invariant parameters 06 p0954 A66-16423
- Isoperimetric problems of controlled systems of continuous functions solved, using Lure canonical transformations 07 p1012 A66-17376
- Relativistic perturbed oscillator, solving problem via canonical transformation 07 p1080 A66-17498
- Perturbed motion stability in critical cases, examining canonical systems 07 p1082 A66-18184
- Alfven wave propagation in incompressible inviscid infinitely conducting medium by canonical equations of motion 08 p1205 A66-18534
- Linear cycle set factorization, showing that uniqueness of canonical procedure is incorrect and introducing new cycle division algorithm 11 p1679 A66-23247
- Transformation of canonical system of differential equations with rapidly varying periodic coefficients into canonical system with constant coefficients 12 p1902 A66-23764
- Extension of dynamics to arbitrary systems of differential equations, proposing universal canonical structure generalizing Hamiltonian structure 15 p2539 A66-29145
- Canonical form for two-terminal nonlinear RLC network first-order ordinary differential equations 15 p2472 A66-29371
- Invariant imbedding as basis for integration theory for canonical equations of motion with parallels to Jacobi theory 17 p2947 A66-32500
- Generalized Lur coordinates used in canonical forms for controllable systems, with applications to optimal nonlinear feedback 20 p3535 A66-36848
- Canonical theory approximation of optimum or Bayes detection procedures in critical limiting threshold mode of operation 21 p3705 A66-39146
- Direct solution method for canonical equations resulting from elimination of terms of first-order general planetary theory 23 p4127 A66-41174
- CANOPY**
- Filling process of solid cloth parachute canopies of flat circular and 10 percent extended skirt types operating under finite mass conditions 22 p3845 A66-40592
- CANTILEVER BEAM**
- Transfer functions of cantilever beam and clamped-edge square plate determined by cross-correlation methods 01 p0148 A66-10136
- Optimal surface damping in two-layered cantilever for random periodic loading decreasing in symmetrical cycle 01 p0160 A66-11180
- Residual stress in epitaxial silicon film on sapphire measured by cantilever beam technique 05 p0733 A66-14673
- Torsional instability of cantilevered bars, describing effects of distributed nonconservative compressive load at free end [ASME PAPER 65-WA/APM-19] 05 p0777 A66-15441
- Effect of initial strains on flange reinforced cantilever beam, using triangular elements with linearly varying strains 06 p0961 A66-16004
- Beam deflection in creep bending for statically determinate and indeterminate cases [ASME PAPER 64-WA/MET-9] 06 p0961 A66-16208
- Self-oscillating hydraulic vibration apparatus capable of generating high cyclic actuating power for testing purposes 07 p1147 A66-18389
- Longitudinal and lateral natural frequencies of cantilever bars with concentrated end masses for axial and transverse excitation 09 p1468 A66-20936
- Stress corrosion cracking test employing precracked bar stressed in bending, noting apparatus and results on martensitic steel and titanium alloy 12 p1958 A66-23647
- Torsional instability of cantilevered bars, describing effects of distributed nonconservative compressive load at free end [ASME PAPER 65-WA/APM-19] 12 p1961 A66-23979

- Deformation of cantilever parallelogram box beam 12 p1969 A66-24365
- Photoelastic intensity variations in glass beam following impact of steel ball, registering values 13 p2198 A66-26300
- Pointwise 13 p2198 A66-26300
- Ballistic pendulum technique to measure permanent plastic deformation of shallow circular arches subject to explosive impulse loading 15 p2610 A66-29294
- [AIAA PAPER 65-408] 15 p2610 A66-29294
- Approximate formulas for upper and lower values of natural frequencies for transverse vibrations of cantilever bars of variable cross section 16 p2813 A66-30299
- Dynamic plastic bending of cantilever and variation in strength of mild steel with strain rate, considering shear force at hinge 16 p2815 A66-30808
- Frequency equation for free vibration of uniform cantilever beam carrying concentrated mass and moment of inertia at tip 17 p3030 A66-32966
- Dynamic absorber tuning and damping of resonance of cantilever beams excited by sinusoidally varying force 17 p3030 A66-33034
- Stability of bending-torsional equilibrium of cantilevered bar subjected at end to follower force, as in case of wing under jet, determining critical thrust 19 p3475 A66-36432
- Static and dynamic stability loss of nonconservative mechanical systems describing buckling of clamped-free rod and stability loss of cantilever beam subjected to bending 20 p3672 A66-38267
- Support flexibility effect on natural frequency free vibrations of uniform cantilever carried by mass supported on string 21 p3833 A66-39608
- Oscillation of tubular cantilevers conveying fluid, discussing theoretical conditions of stability 22 p3994 A66-40408
- Oscillation of tubular cantilevers conveying fluid, checking stability aspects of theory and accounting for internal and viscous damping 22 p3994 A66-40409
- CANTILEVER PLATE**
- Parallelogrammic elements in solution of deflection and natural frequency of rhombic cantilever plate 13 p2198 A66-26237
- Free vibration of trapezoidal cantilever plates with swept-back leading edge 16 p2823 A66-31666
- Ritz method for solving elastic stability of rectangular cantilever plate in flows moving in direction perpendicular and parallel to clamped edge of plate 23 p4139 A66-41787
- CANTILEVER WING**
- Taper ratio effects on transonic flutter characteristics of series of thin cantilever wings with 45 degree sweptback and aspect ratio 4 13 p2199 A66-26381
- CAPACITANCE**
- SA RLC CIRCUIT**
- Synchronization of reflex klystron loaded with resonator with nonlinear capacitance from p-n junction of semiconductor diode at third harmonic of external signal 03 p0342 A66-12626
- Photocapacitive effect for determining degree of anisotropy of zinc sulfide with stacking faults 04 p0571 A66-14498
- Regenerative heat exchangers, covering heat transfer and pressure loss characteristics of glass ceramic matrix materials [ASME PAPER 65-HT-35] 05 p0784 A66-14750
- Capacitance-voltage curves in MOS devices indicating difference in relaxation time of surface states 06 p0940 A66-17163
- MOS capacitance measurements, utilizing graphical relations between silicon surface parameters 06 p0940 A66-17165
- Capacitive biasing transducer is electromechanical analog of parametric system 06 p0860 A66-17199
- Effect of fast states with discrete energy levels and quasi-continuous spectrum on capacitance of silicon dielectric film-metal structure 08 p1274 A66-19308
- Electrical capacity of galvanic cell and crystal habit and surface property effects on porous cadmium hydroxide electrode electrochemical properties 08 p1171 A66-19644
- Room temperature capacitance voltage characteristics and built-in diffusion voltages

- in n Ge-n Si double saturation heterojunction 09 p1411 A66-199
- Parametric mixing action resulting from pumping emitter capacitance in transistors 09 p1355 A66-206
- Capacitance of alloyed p-n junctions in type InSb is inversely proportional square root of bias voltage 09 p1429 A66-208
- Field effect transistor input capacitance in pinch-off region derived by using two parallel coupled condensers as equivalent 10 p1510 A66-216
- Reactance of gallium arsenide buffer oscillator in oscillating state, plotting value together with capacitance 12 p1835 A66-241
- Load capacitance method for measurement of quartz crystal parameters 12 p1845 A66-248
- Double-layer capacitance of solid silver bromide determined against platinum and gold electrodes, using electrochemical cell 12 p1933 A66-250
- Capacitance transducer characteristics at applications as fuel gauge, level detector, interface detector, pressure and proximity sensors, etc 13 p2078 A66-253
- Carrier concentration and minority carrier lifetime measurement in MOS epitaxial layers by capacitance method 13 p2164 A66-254
- Capacitance type ferrite transducer consisting of polycrystalline yttrium garnet of high resistivity 14 p2252 A66-272
- Silicon film MOS transistors with extremely low capacitance produced by diffusion of source and drain regions entirely through film 15 p2459 A66-288
- Capacitance variation of gold n-type gallium arsenide surface barrier diode when illuminated, applied to light detector frequency modulation, etc 15 p2463 A66-290
- Density and location of surface states at silicon-silicon dioxide interface determined by analyzing capacitance-voltage characteristics of MOS diode 15 p2567 A66-294
- Results derived from dissipative four-terminal networks applied to varactor converter, leading to capacitance variation determination as function of polarizing potential 16 p2662 A66-309
- Behavior of incremental and fundamental capacitances appearing in varactor analyzed as function of voltage 16 p2662 A66-309
- Space charge density in p-n junction found to be unrelated to charge density assumed in Schottky theory 17 p2979 A66-326
- Low temperature silicon variable capacitance diodes for use in low noise band parametric amplifier 17 p2890 A66-329
- Photoeffect on barrier capacitance of p-n junction 17 p2988 A66-333
- Resonant frequency change of oscillator circuit due to nonlinear capacitance of semiconductor diode used as amplitude detector 17 p2898 A66-335
- Half-wavelength resonators as capacitive gap strip-line bandpass-type microwave filters, discussing parameter derivation for equivalent circuit and Cohn synthesis method 18 p3087 A66-346
- Capacitance transducer for measuring capacitance ratios with minimum environmental problems, noting wide application range 19 p3355 A66-354
- Capacitive transducer principle, describing basic circuit, performance characteristics and sensitivity factors 19 p3355 A66-354
- Capacitive biasing transducer is electromechanical analog of parametric system 19 p3356 A66-355
- Silicon variable capacitance diodes with high-voltage sensitivity produced by low temperature epitaxial growth technique 20 p3528 A66-374
- Frequency multiplication using diffusion capacitance with derivation of efficiency expression 20 p3519 A66-380
- Bias voltage dependence of capacitance in n-type silicon p-n junctions with voltage breakdown 20 p3621 A66-380
- Photoreponse measurements of depletion capacitance and diffusion potential of Gallium Schottky-Barrier diodes 20 p3534 A66-383
- Reactance modulation amplifier with semiconductor-diode capacitance analyzed by



oscillation theory 21 p3711 A66-38911  
 Distribution of capacitive photo-emf over surface of semiconductor determined by measuring value created by scanning surface of sample with narrow modulated-light beam 22 p3965 A66-40316  
 Conductance and capacitance of metal-insulator-semiconductor diodes or any two-terminal complex admittance plotted automatically as function of applied bias 22 p3882 A66-40897  
 Amplification processes in parametrically regenerated circuit with simultaneous complex variation of capacitance and attenuation 23 p4038 A66-41517  
 Three-circuit system with circuits connected by nonlinear capacitance applied to frequency converters, amplifiers, etc 23 p4049 A66-41565  
 Nonuniform thickness of dielectric films effect on capacitance and tunnel currents of elements with metal-insulator-metal structure 24 p4254 A66-42387  
 MOS transistor structures with enhancement mode of operation, discussing fabrication processes via V-C characteristics, temperature effects on performance, etc 24 p4181 A66-42389  
 Thyristor circuit, basis for capacitive switching circuits, expressing switching capacitance by DC source 24 p4181 A66-42485  
**CAPACITIVE FUEL GAUGE**  
 Fluid content measurement in storage tanks under zero-g conditions discussing gas law system, trace material, capacitive panel and RF methods [AIAA PAPER 65-365] 19 p3340 A66-35611  
 Fuel and propellant gauging, using method of capacitance change induced by liquid dielectrics 20 p3664 A66-38251  
**CAPACITOR**  
 Charged Styropor ball motions in free float between plates of perforated capacitor with alternating electric field 01 p0119 A66-10374  
 Comparison of inflector unmatched with line with matched one using additional capacitors, showing both devices have identical electric and time characteristics 01 p0046 A66-11057  
 Embedment stress effects on electrical characteristics of encapsulated components, presenting capacitor test results 02 p0247 A66-11287  
 Microelectronics and results achieved in relays, switches, variable capacitors and potentiometers 02 p0205 A66-11943  
 Developments in capacitor design particularly electrolytic, ceramic and mica types 03 p0347 A66-13331  
 Metal oxide semiconductor structures in integrated circuits as high and low resistances, inverters and AC amplifiers 05 p0643 A66-14569  
 Capacitor reliability as function of voltage and temperature of dielectric and environmental conditions 06 p0839 A66-15951  
 Book on theoretical and engineering problems arising in capacitor discharge technique of pulse generation 06 p0878 A66-16046  
 Surface state density variations on metal oxide semiconductor capacitors due to gamma radiation 06 p0925 A66-16646  
 High-pressure pulse arc created by discharging capacitor bank through steadily burning argon arc 06 p0919 A66-16874  
 Measuring temperature coefficient and drift for small capacitors, noting design and environmental control 09 p1359 A66-20921  
 High voltage capacitor discharge from Marx circuit, using stepup transformer 10 p1486 A66-21862  
 Text on high speed optical pulse technology, lasers and measuring techniques, emphasizing capacitor discharge application 10 p1538 A66-22063  
 Coaxial capacitor for measuring density of fluids in both liquid and gaseous phase over wide range of temperatures and pressures 11 p1707 A66-22961  
 Transient processes resulting from instantaneous application of constant potential difference to plasma capacitor plates 12 p1922 A66-24216  
 Interaction of boundary layer produced by vortex flow of viscous electrically conducting fluid over disk with axial magnetic field and relation to MHD generator and hydromagnetic capacitor 13 p2156 A66-26707  
 Harmonic linearization technique to examine characteristics of oscillatory circuits with nonlinear capacitors 14 p2250 A66-27167  
 Capacitors for monolithic integrated circuits 14 p2252 A66-27306  
 Surface charge sign effect on capacitor photoelectromotive force in semiconductors and photoinduced contact potential change 15 p2559 A66-28628  
 Space charge polarization in glass films, discussing parameters of shift of capacitance-voltage characteristics, diffusion coefficient in metal-glass-silicon dioxide-silicon double-layer capacitor 16 p2779 A66-31089  
 Compatible thin film resistor-capacitor process using nichrome and alumina-silica glass for silicon integrated circuits 16 p2667 A66-31595  
 Deuterium plasma containment and stability in theta pinch configuration using megajoule capacitor banks, studying density, temperature and radial distribution 19 p3413 A66-36505  
 MOS capacitance of p-type silicon in inversion layer and ion drift in fringing field 22 p3872 A66-39744  
 Transient processes resulting from instantaneous application of constant potential difference to plasma capacitor plates 22 p3878 A66-40580  
 Optimal lumped constant dispersive network design with inductors and capacitors functioning independently 23 p4034 A66-41015  
 Electrical properties and fabrication of zinc oxide-bismuth oxide low Q capacitor with high apparent dielectric constant over wide frequency range 24 p4180 A66-42311  
 Energy storage film capacitors for pulsed plasma thrusters developed for coaxial plasma gun and pulsed arc gun [AIAA PAPER 65-337] 24 p4261 A66-42780  
**CAPE KENNEDY**  
 Objectives, effectiveness and results of reliability program at Kennedy Space Center /KSC/ referring to Saturn launches 01 p0141 A66-10106  
 Effective planning and operations required for control of air pollution due to increased use of toxic propellants in larger missiles 02 p0183 A66-11491  
 Inaccuracy in rocketsonde data on HF of midwinter easterlies in stratosphere over Cape Kennedy 10 p1531 A66-21281  
 Programmable patching system at Cape Kennedy for communications network composed of two individual switching subsystems, using solid state devices and glass-reed relays 14 p2233 A66-26805  
**CAPILLARY**  
 Optimum ionizer structure, examining cesium transport through tungsten capillaries [AIAA PAPER 66-207] 12 p1922 A66-24529  
 Modified Poiseuille equation for gas flow through capillaries, applicable to flow regimes extending from molecular to viscous flow 21 p3725 A66-38943  
**CAPILLARY CIRCULATION**  
 Localization caused by capillary effects in gas-liquid interface such as epidermis and wicks depends upon gas phase unsaturated with liquid vapor 03 p0355 A66-12779  
 Heat pipes as heat removal systems in space thermionic power supplies, discussing laminar, turbulent flow and heat transfer efficiency 05 p0789 A66-15542  
 Thermal diffusion coefficient and composition of gas mixtures by measuring gas flow rate in capillary tube as function of viscosity 07 p1148 A66-17394  
 Approximate theory for electrokinetic phenomena in capillary flows, determining interaction between mechanical and electrical energy 08 p1174 A66-19829  
 Distribution of permeable solute during Poiseuille flow in capillary tubes, deriving equations, noting flow dependence on permeability but not on diffusion constant 19 p3285 A66-35711  
 Leak specifications for gas-filled electronic enclosures, discussing molecular, slow viscous, capillary and ordinary leak patterns 24 p4182 A66-42574

**CAPILLARY WAVE**

Growth and excitation of surface waves on capillary liquid jet stressed by electric field 07 p1087 A66-17946  
 Gas flow and self-diffusion in capillaries 17 p2909 A66-32652  
 Capillary gas flow and self-diffusion as affected by pressure ranging from free molecule to continuum regimes 17 p2910 A66-32653  
 Geometric dimensional, plasma temperature and pressure effects on capillary discharge with evaporating wall /CDEW/ 18 p3143 A66-34028

**CAPSULE**

S ESCAPE CAPSULE  
 S MERCURY CAPSULE  
 S SPACE CAPSULE

**CAPTURE**

S ELECTRON CAPTURE

**CAPTURE EFFECT**

Field effect theory in semiconductors with capture centers, noting basic equation, quadrature expressions, etc 11 p1751 A66-22732  
 Traveling wave beats created by ring laser on rotating platform, noting frequency division rotating rate and capture band parameters 13 p2089 A66-25102  
 Stationary and kinetic determination of parameters of capturing recombination centers in CdS single crystal 13 p2166 A66-25686  
 Plastic deformation effect on carrier capture in silicon 14 p2358 A66-27090  
 Two parallel carrier capture mechanisms at single recombination center in cadmium sulfide 15 p2563 A66-28738  
 Formation mechanism of ionospheric narrow sporadic E layers by high energy electron fluxes captured by geomagnetic field 15 p2488 A66-29110  
 Traveling wave beats created by ring laser on rotating platform, noting frequency division rotating rate and capture band parameters 16 p2717 A66-30281  
 Rarefied supersonic flow condensation on cold flat plate, noting capture coefficients, shock wave behavior, etc 16 p2825 A66-30383  
 Temperature dependence of lifetime of electrons and holes in GaAs, noting trapping effect of recombination centers and capture levels 16 p2787 A66-31771  
 Integrated flux distributions in neutron capture in stars 17 p2997 A66-31924  
 Evaporated and recrystallized CdS layers, discussing electron mobility, level distribution, capture cross section and techniques of measurement 19 p3435 A66-35408  
 Plastic deformation effect on carrier capture in silicon 22 p3967 A66-40846  
 Capture effect on I-V characteristics of junction diodes and injection coefficients in forbidden transition zone 23 p4045 A66-41444  
 Field effect theory in semiconductors with capture centers, noting basic equation, quadrature expressions, etc 23 p4113 A66-41470  
 Optical heterodyne receiver antenna properties, noting effective aperture of capture cross section vs directional tolerance and detection of doppler shifts in liquid scattered coherent light 24 p4174 A66-42809  
**CARAVELLE AIRCRAFT**  
 S SUD-AVIATION SE-210 AIRCRAFT  
**CARBIDE**  
 SA ALUMINUM CARBIDE  
 SA BORON CARBIDE  
 SA CHROMIUM CARBIDE  
 SA HAFNIUM CARBIDE  
 SA NIOBIUM CARBIDE  
 SA SILICON CARBIDE  
 SA STEEL  
 SA TANTALUM CARBIDE  
 SA TITANIUM CARBIDE  
 SA TUNGSTEN CARBIDE  
 SA URANIUM CARBIDE  
 SA VANADIUM CARBIDE  
 SA ZIRCONIUM CARBIDE  
 Refractory metal carbide solubility in cobalt dependent on carbon content, crystal structure and metal-carbon bonds 01 p0085 A66-10287  
 Solid solution and carbide strengthened arc melted alloys of hafnium with tungsten and ternary alloys of tantalum, columbium,



- rhenium and carbon 06 p0894 A66-16078  
 Vacuum diffusion welding of zirconium, niobium and tantalum carbides to high-melting niobium, tantalum, molybdenum and tungsten 06 p0887 A66-16696  
 Optimum conditions for preparation of complex carbide alloys containing scandium carbide 07 p1049 A66-17903  
 Thermal shock resistant carbides, using arc-casting techniques, noting microstructure, phase diagram, mechanical properties, etc 07 p1055 A66-18504  
 Book on refractory metals and cemented carbides /hard metals/, discussing pressing and sintering techniques, testing methods, properties under stress, etc 12 p1893 A66-23739  
 Effect of preparation conditions on formation of carbide phases in iron-carbon thin films, using vacuum condensation 12 p1933 A66-25025  
 Extremely high thermal shock resistance in group IVA carbides of carbide-graphite composites fabricated, using vacuum arc melting and casting techniques 15 p2524 A66-29287  
 Large quantities of high-purity carbides and carbide solid solutions produced by auxiliary metal bath in carbon tube furnace 16 p2723 A66-30638  
 Powder metallurgy methods for obtaining products of complex form from sintered carbides 16 p2715 A66-31679  
 Chemical bonds in carbides and nitrides of transition metals, obtaining atomization heat of compound and effective charges of transition atomic nuclei 19 p3386 A66-36425  
 Niobium dissolution kinetics in iron carbide 19 p3386 A66-36447  
 Compressive tests on WC-Co cemented alloys including preparation of sample, equipment, behavior and failure mode [ASME PAPER 66-MD-80] 21 p3750 A66-38503  
 Optimum conditions for preparation of complex carbide alloys containing scandium carbide 21 p3752 A66-39403  
 Solid solutions of titanium, tungsten, chromium prepared by carbidization of mixtures in hydrogen medium and obtained as fine-grained carbide powders 22 p3934 A66-39865
- CARBOHYDRATE**  
 SA CELLULOSE  
 SA GLUCOSE  
 SA GLYCOGEN  
 SA NUCLEOSIDE  
 Stratigraphic distribution of carbohydrate residues in middle Devonian Onondaga beds of Pennsylvania and western New York and application to paleontology and paleoecology 22 p3912 A66-40133
- CARBOHYDRATE METABOLISM**  
 Stress and dietary influence on direct oxidative pathway of carbohydrate metabolism in jejunal mucosa of rats 16 p2841 A66-31383  
 Increase of arterial lactate and pyruvate in blood glucose of fasted anesthetized dog after hydrazine injection 17 p2856 A66-32157
- CARBON**  
 SA DIAMOND  
 SA FERRITE  
 SA GRAPHITE  
 Electric resistivity of carbon resistor material determined as temperature function, calculating static response characteristics of carbon bolometer 02 p0228 A66-11445  
 Graphite and carbon steel case hardening by chromium 05 p0702 A66-15111  
 Effects of nitrogen and carbon on low temperature embrittlement of vanadium, noting transition temperature increases 05 p0702 A66-15488  
 Carbon diffusion into titanium and zirconium nitrides, noting carbide layer parabolic growth rate and experimental techniques 05 p0704 A66-15817  
 Radiation from carbon particle clouds produced by research rocket motors [ATAA PAPER 66-133] 06 p0970 A66-16413  
 Measurement of equilibrium fractions of helium ions present in helium beams scattered at zero degrees through carbon foils 06 p0912 A66-17038  
 Interaction mean free path of nuclear-active particles in iron determined by measuring number of interactions in each iron layer in ionization calorimeter 07 p1115 A66-17550  
 Interaction of vanadium, niobium and tantalum diborides with carbon 07 p1049 A66-17904  
 Data on combustion of pyrolyzing solids as applicable to combustion chambers of hybrid propulsion devices, placing emphasis on coal 07 p1154 A66-18028  
 Radiative lifetimes of strongest vacuum UV multiplets of B I, B II, C I, C II, N I and N II measured by phase shift method 07 p1083 A66-18423  
 Carbon and tungsten effects compared on tensile flow stress recovery of molybdenum 08 p1237 A66-18764  
 Carbon seals for gas turbine evaluated in statistically designed test method 08 p1232 A66-19381  
 Thermal dissociation in interactions of carbon with carbon dioxide and oxygen 08 p1320 A66-19639  
 Carbon deposition boundaries and other constant parameter curves in triangular representation of C-H-O equilibria, with application to fuel cells 11 p1639 A66-22243  
 Energy spectra of ions emitted by beryllium, carbon and molybdenum heated by laser 13 p2131 A66-25479  
 Photochemical decomposition of carbon suboxide and spectroscopic observation of carbon atom reactions with nitrogen, hydrogen and deuterium at 4.2 degrees K 14 p2233 A66-27975  
 Kh16N15M2B steel properties and effects of grain size and Nb/C ratio 15 p2519 A66-28536  
 Kinetics of highly endothermic carbon-silica reaction for silica-reinforced resin systems 17 p2943 A66-32453  
 Rotational and vibrational temperature of diatomic C in comets derived from high resolution spectra, considering transition probabilities in R and P branches 17 p3010 A66-33380  
 Total number of cyanide molecules and diatomic carbon free radicals and density distribution in head of Arend-Roland 1957 III comet 17 p3010 A66-33381  
 Triatomic carbon spectrum transition bands based on available photographic and densitometric data 17 p3013 A66-33401  
 Deformation characteristics of 0.90 percent carbon steel wire studied for structures and strengthening mechanisms 18 p3122 A66-33754  
 Free-free absorption coefficient of electrons in field of neutral carbon atoms calculated per unit electron pressure per carbon atom in static central field exchange approximation 18 p3233 A66-34574  
 Carbon/graphite material /carbiterx/, physical, thermal, mechanical and chemical properties 18 p3125 A66-34618  
 Values of Morse potential for interaction of atoms in diatomic molecules carbon, CO and CN 21 p3775 A66-39072  
 100-200 ksi yield-strength notched steels for high-toughness weldments, discussing quenched and tempered steels, maraging steels, heat treatment effects, etc 21 p3751 A66-39193  
 Interaction of vanadium, niobium and tantalum diborides with carbon 21 p3752 A66-39404  
 Melting point and microhardness of carbon-saturated TiC-VC solid solutions, noting temperature of eutectic of TiC-VC with graphite 22 p3934 A66-39866  
 Rate constants for atomic and molecular hydrogen ion transfer from tri- and tetra-atomic carbon paraffins to propylene and cyclopropane molecular ions 22 p3861 A66-40905  
 Correlation between chemi-ionization in flames containing organic fuels and heat of oxidation of carbon in fuel molecule 23 p4147 A66-41154  
 Ceylon and artificial graphite behavior under very high pressure, examining problem of metallic phase of carbon 24 p4229 A66-42751  
 Inelasticity in carbon particle nuclei interactions evaluated by variation with depth of energy of electron photon shower in thick absorber 24 p4268 A66-42910  
 Carbon solubility in Ta, Nb and V at temperatures from 1500 degrees C to eutectic temperatures 24 p4228 A66-43068
- CARBON ARC**  
 Carbon arc solar simulator with nonconsumable tungsten rod negative electrode operating continuously over 10 hours 02 p0213 A66-11231  
 Carbon joint and nonconsumable negative electrode design for carbon arc solar simulator 10 p1521 A66-21931  
 Electron concentration in AC carbon arc determined from H-beta linewidth 11 p1748 A66-23410  
 Maecker-Boldt cascade arc in argon a radiance standard, noting superiority over carbon arc, especially in UV 16 p2767 A66-31699
- CARBON COMPOUND**  
 SA FLUOROCARBON  
 SA HYDROCARBON  
 Early interaction stages of metal oxides with carbon, using thermochromatographic method to determine temperature reaction onset 12 p1892 A66-23512  
 Syntheses of three macromolecular chlorocarbons, studying structure and configuration, noting high thermal stability and chemical inertness 12 p1812 A66-23633  
 K emission band of graphite examined using grazing incidence spectrometer and Gaussian window function 12 p1931 A66-24808  
 Photoelectric photometry of comet Everhart 1964 h, noting density of carbon radicals and CN molecules 17 p3000 A66-32334
- CARBON DIOXIDE**  
 Estimates of collision cross sections for carbon dioxide and air molecules at 20 degrees K with thermal radiation field at error source 01 p0062 A66-10761  
 Carbon dioxide reduction systems using chemical, electrochemical and thermoelectric energy 02 p0185 A66-11641  
 Linear coefficient of amplification of carbon dioxide subjected to HF excitation field for laser emission 02 p0241 A66-12001  
 Shock tube measurements of carbon dioxide dissociation in argon mixtures at 6000 to 11,000 degrees K 03 p0443 A66-12331  
 Spectral emissivity calculations for parallel bands of carbon dioxide at 4.3 microns between 150-600 degrees K, comparing experimental measurements with theoretical calculations 03 p0393 A66-13101  
 State equation for carbon dioxide describing gaseous and liquid phases and left and right boundary curves at temperatures and pressures 04 p0572 A66-13668  
 Molecular collision cross sections discussing vibrational excitation of carbon dioxide by collision with molecular hydrogen 04 p0548 A66-13811  
 Cluster ion formation by electric retarding field, measuring spectrum and size distribution in condensed supersonic molecular beams of carbon dioxide 05 p0718 A66-14501  
 Atmospheric radiation calculations emphasizing carbon dioxide and nitrous oxide absorption spectrum, spectral energy distribution, quasi-statistical band models, etc 05 p0748 A66-14911  
 Carbon dioxide-R-branch lines of 5 mu sun 3 band from integral of absorption coefficient of Martian atmosphere 05 p0763 A66-15281  
 Electron paramagnetic resonance spectrum of carbon dioxide when absorbed on UV irradiated magnesium oxide 05 p0630 A66-15766  
 Atmospheric thermal radiation calculations from unresolved molecular absorption spectra of atmospheric carbon dioxide and water 05 p0875 A66-15866  
 Internal and vibrational partition functions of carbon dioxide and rotational line intensities arising from transitions from ground and first excited states 06 p0907 A66-15948  
 Carbon dioxide frost as thermal insulation for hypersonic spacecraft, noting conductivity 06 p0989 A66-16301  
 CW laser action in carbon dioxide-helium mixtures 06 p0890 A66-16388  
 Carbon dioxide absorption bands in Mars atmosphere, transmission, function of carbon dioxide amount and effective surface



- pressure  
[AIAA PAPER 66-147] 08 p1290 A66-19072  
Cumulus cloud simulation by dropping  
solid piece of carbon dioxide into hot  
water 08 p1248 A66-19388  
Thermal dissociation in interactions of  
carbon with carbon dioxide and  
oxygen 08 p1320 A66-19639  
Thermodynamic parameters of carbon  
dioxide and argon mixture behind straight  
shock wavefront 09 p1470 A66-20146  
Transmission of IR radiation from flames  
through various carbon dioxide  
pathlengths 09 p1471 A66-20509  
Regenerative separation and recovery of  
carbon dioxide from manned atmospheres,  
using metallic oxides  
[AICE PREPRINT 26D] 10 p1491 A66-21191  
Free convection heat transfer to carbon  
dioxide near critical point, noting free,  
turbulent and oscillating  
flow 10 p1619 A66-21271  
Carbon dioxide effect on shattering of  
freezing water drops, using methanol-cooled  
chamber with variable temperature  
control 10 p552 A66-21290  
Oxidation of artificial graphitic carbon 14  
oxidized to carbon 14 dioxide in presence of  
nonsterile soils, noting inhibition of  
biological activity by electron beam  
irradiation 11 p1649 A66-22304  
Spectral emissivity measurements of  
carbon dioxide at high  
temperatures 11 p1738 A66-22870  
Atmospheric high resolution transmission  
in carbon dioxide bands between 12 and 18  
microns evaluated, using mixed Doppler-  
Lorentz broadening and new method for  
slant-path calculations 11 p1738 A66-22889  
Free energy of pure fluids as function of  
thermodynamic temperature determined  
from measurements of internal energy,  
noting case of carbon  
dioxide 12 p1981 A66-24997  
Carbon dioxide relaxation processes in  
shock waves, measuring density variation,  
vibrational energy, relaxation time, shock  
density profile, etc 13 p2061 A66-25161  
Chemical system and reaction rates behind  
strong shock waves in mixtures of carbon  
dioxide and nitrogen used to study entry  
conditions into Mars 13 p2062 A66-25276  
Interferogram interpretation to determine  
carbon dioxide concentration in air  
mixture 13 p2208 A66-25315  
Microwave absorption in compressed  
carbon dioxide between 150 and 300 gc  
measured, detecting no losses at 150  
gc 13 p2021 A66-25383  
IR laser radiation with power of 5.7 watts  
in vicinity of 10.69  $\mu$ m in sealed tube  
containing pure carbon dioxide excited by  
AC or DC current 13 p2131 A66-25410  
Quantum yield of CO formation from  
photolysis of carbon dioxide at wavelengths  
of argon lines 13 p2017 A66-25801  
Vertical temperature distribution in  
Martian atmosphere, noting insensitivity to  
surface pressure and carbon dioxide  
variations 13 p2186 A66-26132  
He-Ne laser homodyne spectrometer  
observation of broadening of spectral profile  
of light scattered from carbon dioxide near  
critical temperature and density due to  
density fluctuations 13 p2133 A66-26168  
Atmospheric absorption in IR region,  
noting effects of water vapor, ozone, carbon  
dioxide and collision-induced dipole  
moments 13 p2075 A66-26603  
Gas shielded metal arc welding, discussing  
power sources, wire feed mechanism, torch  
and carbon dioxide  
cylinders 13 p2088 A66-26764  
Vibrational-rotational line strengths and  
widths in carbon dioxide, using carbon  
dioxide-neon laser 14 p2306 A66-27030  
Jet boundary determination of  
underexpanded two-phase carbon dioxide  
supersonic nozzle flow 14 p2219 A66-27445  
Estimates of collision cross sections for  
carbon dioxide and air molecules at 200  
degrees K with thermal radiation field as  
error source 14 p2286 A66-27861  
Carbon dioxide to calibrate instruments for  
carbon determination in  
metals 15 p2445 A66-28617  
Measurement of single line in P branch of  
carbon dioxide vibro-rotational absorption  
band using tuned optical maser  
spectroscopy, noting presence of shifted  
frequencies 15 p2512 A66-28691  
IR spectral reflectance of water frost and  
solid carbon dioxide 15 p2501 A66-28977  
Total absorption cross section of carbon  
monoxide and carbon dioxide in 550-200  
angstrom range 15 p2538 A66-28978  
Adaptation rearrangements in organisms of  
mice during and after exposure to high  
concentrations of carbon  
dioxide 15 p2438 A66-29479  
Intensive Chlorella culture need of carbon  
dioxide concentration in closed and  
controlled air-carbon dioxide  
system 15 p2440 A66-29508  
Absorption, photolysis and  
fluorescence of carbon dioxide measured in  
regions of strong band and continuous  
absorption in various spectral  
ranges 16 p2749 A66-30111  
Rate constant for atomic oxygen ion  
destruction by carbon dioxide measured in  
pulsed flowing afterglow  
system 16 p2645 A66-30115  
Fast ion molecule reaction in carbon  
dioxide analyzed, using mass  
spectrometer 16 p2645 A66-30116  
Photolysis of carbon dioxide and molecular  
oxygen, using 1470 angstrom radiation to  
produce atomic oxygen 16 p2645 A66-30117  
Hypoxic hypoxia attenuation mechanism by  
carbon dioxide enrichment of air  
intake 16 p2638 A66-30273  
Mars atmosphere models based on Mariner  
IV occultation deriving electron number  
density, temperature, pressure, mass  
density, etc, noting carbon dioxide  
presence 16 p2800 A66-30713  
Photolysis of carbon dioxide, using 1633  
angstrom line of bromine  
lamp 16 p2646 A66-30862  
Optical transition probability and  
broadening cross section obtained from  
absorption measurements in carbon dioxide  
and mixtures with other  
gases 17 p2933 A66-31938  
Carbon dioxide control for manned  
spacecraft, discussing regenerative methods  
for eliminating system weight dependence  
on mission duration 17 p2863 A66-32141  
Regenerative sorbents for removal of  
carbon dioxide with minimal drying of  
process air stream 17 p2865 A66-32186  
Continuous flow, solid state  
electrochemical device for simultaneous  
carbon dioxide removal and oxygen  
generation 17 p2867 A66-32675  
[AICE PREPRINT 47E] 17 p2867 A66-32675  
Regenerative separation and recovery of  
carbon dioxide from manned atmospheres,  
using metallic oxides  
[AICE PREPRINT 26D] 17 p2868 A66-32681  
Carbon dioxide laser principle and  
performance 17 p2936 A66-33247  
High-power molecular laser based on  
vibrational-rotational energy level, noting  
carbon dioxide-neon-helium laser  
design 17 p2936 A66-33248  
Spectrographic investigation of  
luminescence of carbon monoxide and  
dioxide excited by collisions with  
accelerated ions 17 p2961 A66-33403  
Carbon dioxide supersaturation and  
condensation in supersonic nozzles in terms  
of stagnation pressures, temperatures, and  
expansion rates 17 p3039 A66-33476  
Change pattern in human cerebral blood  
flow during time immediately following  
initiation of carbon dioxide  
inhalation 18 p3058 A66-33691  
Occurrence of adenosine monophosphate  
inhibition of carbon dioxide fixation  
photosynthetic and chemosynthetic  
autotrophs 18 p3056 A66-33697  
Laser action in closed molecular system  
with mixture of carbon dioxide, nitrogen  
and water vapor, noting coupling-out plate  
reflectivity and population  
inversion 19 p3373 A66-35433  
Vibrational relaxation of carbon dioxide in  
mixtures with noble  
gases 19 p3295 A66-35494  
Carbon dioxide decomposition and oxygen  
reclamation by chemical reaction with  
electrochemically reduced  
lithium 19 p3292 A66-36234  
Chemical methods for carbon dioxide  
conversion for oxygen recovery, including  
relationship to biological  
processes 19 p3293 A66-36235  
Carbon dioxide control by enzymatic  
reaction in spacecraft atmosphere by hydro-  
lyase and multienzyme  
system 19 p3293 A66-36240  
Heat transfer in turbulent carbon dioxide  
pipeflow at supercritical  
region 20 p3674 A66-36983  
Vibrational relaxation measurements in  
carbon dioxide, using induced-fluorescence  
technique 20 p3578 A66-37595  
Identification of number of lines at 11  
microns emitted from pulsed carbon dioxide  
laser as P branch of carbon dioxide  
vibrational transition 20 p3579 A66-37629  
Random Elsasser band model to compute  
atmospheric transmission of Earth and Mars  
for 2-micron carbon dioxide  
bands 20 p3655 A66-38024  
Nitrogen ion charge-transfer reaction rates  
with CO and carbon dioxide in pulsed  
flowing afterglow system 21 p3774 A66-38529  
Supersonic nozzle flow of dissociated  
oxygen, nitrogen and carbon  
dioxide 21 p3694 A66-39089  
Carbon dioxide flow density in wake of  
shock wave front 21 p3726 A66-39091  
Peculiarities in Mach reflection of shock  
waves traveling in carbon dioxide gas and  
nitrogen at velocities of order of 2000  
m/sec 21 p3728 A66-39094  
Thermodynamic parameters of carbon  
dioxide and argon mixture behind straight  
shock wavefront 21 p3836 A66-39417  
Thermal conductivity of carbon dioxide in  
critical region interpreted, considering gas  
as mixture of clusters and heat transfer due  
to formation and breaking of  
clusters 21 p3837 A66-39454  
Abundance and temperature of carbon  
dioxide in Martian atmosphere, noting  
implications, observation methods and  
results 21 p3816 A66-39558  
Carbon dioxide dissociation rate measured  
from 3000 to 5000 degrees K, considering  
decrease in temperature and increase in  
density caused by endothermic  
dissociation 22 p3859 A66-39915  
Thermal model of Martian surface suggests  
solid carbon dioxide composition of polar  
caps, studying diurnal and annual  
temperature variations at various  
latitudes 22 p3981 A66-40482  
Induced microwave absorption in carbon  
dioxide studied at frequency of 9260 mc/sec  
over temperature range from 270 to 500  
degrees K and pressures as high as 95  
atm 22 p3985 A66-40909  
Molecular spectroscopy, measuring  
absorption coefficient at center of carbon  
dioxide band, determining vibration-rotation  
transition moment 23 p4076 A66-41179  
Competition, hysteresis and reactive Q-  
switching in carbon dioxide lasers at 10.6  
microns, using moving mirror  
technique 23 p4079 A66-41831  
Absorption lines on Venus spectrograms of  
rotational fine structure of excited  
vibrational transition of carbon  
dioxide 23 p4130 A66-41816  
Conductivity modulation by heavy-to-light  
hole transitions in p-type germanium noting  
carrier lifetime and ringing of laser  
pulse 24 p4219 A66-42249  
Planetary atmosphere resolution spectrum  
noting carbon dioxide lines, radiation  
transfer, composition, temperatures,  
pressures, etc 24 p4277 A66-42687  
Venus atmosphere noting pressure induced  
absorption in carbon dioxide-nitrogen  
atmosphere as indicated in decline of  
microwave brightness 24 p4277 A66-42688  
Kinetics of dissociation of carbon dioxide  
gas molecules behind shock wave  
front 24 p4196 A66-42882  
**CARBON DIOXIDE CONCENTRATION**  
Carbon dioxide induced mild hypoxia,  
correction of alterations on performance of  
psychologic and psychomotor  
systems 07 p0998 A66-17661  
Secular variation of atmospheric  
radiocarbon concentration, noting  
dependence on geomagnetic field  
strength 11 p1698 A66-22569



Conditioned reflex role in information of subthreshold stimuli of respiratory system in dogs subjected to electric shock and carbon dioxide increase 14 p2228 A66-27185

Variations in atmospheric radio carbon activity related to secular variations in carbon-14 production rate, carbon residence times and carbon reservoir times 18 p3104 A66-33552

**CARBON DIOXIDE REMOVAL**

**S AIR PURIFICATION**

**CARBON DISULFIDE**

CW laser oscillation between 11.48 and 11.55 microns from nitrogen-carbon disulfide system 06 p0890 A66-16384

Interaction between stimulated Brillouin and Raman scattering in carbon disulfide, using optical resonator and laser beam 13 p2097 A66-26162

Laser oscillation in flash photolysis of carbon disulfide and oxygen to form CO 17 p2933 A66-31941

Carbon disulfide traveling wave Kerr cells with identical microwave and dielectric constants, noting light modulator construction at microwave frequencies 24 p4185 A66-42814

**CARBON MONOXIDE**

Variations of equivalent line widths of first overtone of carbon monoxide band at transition from photosphere to facula, estimating temperature difference 01 p0131 A66-10278

Manufacture of propellants by aerogel carbothermal process involving reduction of silicates with methane and/or carbon [SAE PAPER 650835] 01 p0053 A66-10831

Photoionization and absorption coefficients of carbon oxide measured below 1000 angstroms, using Seya-Namioka scanning vacuum UV monochromator with helium continuum as background 02 p0263 A66-11834

Integrated intensity measurements on fundamental and first overtone band systems of carbon monoxide between 2500 and 5000 degrees K 04 p0596 A66-13647

CW gas laser, measuring vibrational rotational translation frequencies of carbon monoxide 04 p0531 A66-13984

Laser action on rotational transitions of 10-9, 9-8, 8-7, 7-6 and 6-5 vibrational bands of ground electronic state CO 07 p1046 A66-18424

Commercial fuel cells, noting biochemical, regenerative and low temperature carbon monoxide fuel cell 07 p0996 A66-18476

Saturation problem for middle sections of CO solar spectral lines, using thin layer absorption concept 08 p1297 A66-19453

Vasovagal syncope induced by application of negative pressure to lower half of human body, noting effect on lung CO diffusing capacity 11 p1643 A66-22580

Closed ecological systems and endogenous formation of CO in plant and animal tissues 11 p1648 A66-23048

Adsorption of CO radicals on three types of magnesium oxide using EPR techniques, noting spectrum of adsorbed radical, bonding, etc 12 p1916 A66-23619

Quantum yield of CO formation from photolysis of carbon dioxide at wavelengths of argon lines 13 p2017 A66-25801

Total absorption cross section of carbon monoxide and carbon dioxide in 550-200 angstrom range 15 p2538 A66-28978

Diffusion and dissociation of CO molecules in solar atmosphere 15 p2596 A66-29139

Physiological, psychological and biochemical effects on humans after 8-hr inhalation of low carbon monoxide concentration 15 p2435 A66-29448

Dissociation layer heights on Venus, Mars and Jupiter, noting CO flame airglow intensities 15 p2604 A66-30050

Carbon monoxide adsorption on tungsten surface as affected by temperature, noting sticking probability of molecules striking clean or covered surfaces 16 p2721 A66-30108

Laser oscillation in flash photolysis of carbon disulfide and oxygen to form CO 17 p2933 A66-31941

Spectrographic investigation of luminescence of carbon monoxide and dioxide excited by collisions with accelerated ions 17 p2961 A66-33403

Dissociation rate of undiluted carbon monoxide behind strong shock waves

produced in arc discharge shock tube [AIAA PAPER 66-518] 18 p3063 A66-33660

Saturation problem for middle sections of CO solar spectral lines, using thin layer absorption concept 18 p3232 A66-34482

Hydroxyl radical concentration in rarefied CO flame by EPR method 18 p3265 A66-34551

Electric quadrupole transition in fourth positive system of CO observed in bands of electric dipole allowed transition 19 p3404 A66-36800

Digital computer analysis of kinetic equations for CO burning in presence of hydrogen 20 p3679 A66-37702

Nitrogen ion charge-transfer reaction rates with CO and carbon dioxide in pulsed flowing afterglow system 21 p3774 A66-38529

Values of Morse potential for interaction of atoms in diatomic molecules carbon, CO and CN 21 p3775 A66-39072

Chemical reactor on-site manufacture of propellant oxygen from metallic silicates found on Moon 22 p3977 A66-39895

[AICE PREPRINT 46C]

Chemiluminescence in atomic-oxygen-acetylene and atomic-oxygen-carbon suboxide flames attributed to formation of CO in excited and electronic states 22 p3997 A66-39926

Analytic solution for ignition kinetics of dry carbon monoxide-oxygen reaction obtained, assuming initiation reaction followed by chain-branching steps 22 p3998 A66-40115

Recombination of carbon monoxide and atomic oxygen in expansion wave at high temperature in single pulse shock tube 22 p3860 A66-40527

**CARBON STEEL**

**S STEEL**

**CARBON TETRACHLORIDE**

Carbon and ethylene tetrachloride ultrasonic modulators applied to IR laser heterodyne experiments on InAs photodiode 11 p1714 A66-23353

**CARBON 13**

Carbon-13 chemical shifts of carboxyl carbon atom of acetic, benzoic and mesitoic acids in various compositions of sulfuric acid 14 p2232 A66-27376

**CARBON 14**

Secular variations of cosmic ray produced carbon 14 in 150 wood samples up to 2000 years old 05 p0747 A66-14795

C 14 content in tree rings, Tungusk meteor and supernova explosions 05 p0765 A66-15334

Oxidation of artificial graphitic carbon 14 oxidized to carbon 14 dioxide in presence of nonsterile soils, noting inhibition of biological activity by electron beam irradiation 11 p1649 A66-22304

Carbon 14 content of dendrochronologically dated tree rings used to determine atmospheric C-14 variation over past six millennia 11 p1697 A66-22568

Phosgenation procedure for synthesis of carbon-14 labeled isocyanates, noting isotope distribution in compounds 14 p2231 A66-26871

C 14 content in tree rings, Tungusk meteor and supernova explosions 15 p2603 A66-29981

Variations in atmospheric radio carbon activity related to secular variations in carbon-14 production rate, carbon residence times and carbon reservoir times 18 p3104 A66-33552

Carbon 14 content in growth rings of tree 60 km from epicenter of 1908 explosion of Tungus meteorite, considering antimatter as possible explosion cause 18 p3233 A66-34553

Variation in radiocarbon content in atmosphere studied from measurement of concentration in wood sample nearly 2000 years old 18 p3199 A66-34889

Solar activity variations, C 14 production by cosmic rays and reevaluation of C 14 dating 24 p4265 A66-42738

**CARBONACEOUS METEORITE**

Aromatic hydrocarbons in carbonaceous chondrites investigated by time-of-flight mass spectrometry and hypothesized as formed in solar nebula under thermodynamic equilibrium 01 p0136 A66-10436

Carbonaceous chondrite in stony meteorites, noting presence of organized elements and microfossils 02 p0289 A66-11604

Rubidium-strontium ages of chondrules and

carbonaceous chondrites 02 p0290 A66-11604

Chemical composition of meteorites a micropaleontological evidence of existing meteoric biological carbonaceous chondrites 08 p1287 A66-18476

Origin of diamonds in Canyon Diablo a Novo Urei meteorites 09 p1447 A66-19600

Mineralogical, chemical and microscopic analyses of carbonaceous chondrites reveal presence of substances usually synthesized by living cells on Earth 11 p1771 A66-22700

Organic matter in Orgueil meteorite a chemical equilibrium in solar nebula 13 p2185 A66-25801

Organic matter in carbonaceous chondrites as forming from chemical equilibrium in solar nebula 13 p2185 A66-25801

Inhomogeneities, inclusions and interbrecciation in meteoritic material including carbon-rich samples 14 p2384 A66-27800

Carbonaceous meteorite analysis, indicating possible biological substances 18 p3232 A66-34482

Chemical composition of meteorites a micropaleontological evidence of existing meteoric biological carbonaceous chondrites 19 p3459 A66-35500

Sulfur compounds analysis in lipid extracts from Orgueil meteorite support concept of low temperature environment on parent body and differ from petroleum 20 p3648 A66-37702

Cl, Br and I contents in carbonaceous chondrites measured by activation analysis 21 p3814 A66-39200

Statistical petrographic analysis of meteorite and carbonaceous chondrite evolution on Moon and Mars from rock photographs 23 p4132 A66-42814

**CARBONATE**

Molten carbonate fuel cell system performance evaluated from engineering and economic aspects [AIAA PAPER 64-747] 13 p2007 A66-26600

**CARBONIC ANHYDRASE**

Carbon dioxide control by enzymatic reaction in spacecraft atmosphere by hydrolase and multienzyme system 19 p3293 A66-36200

**CARBOXYL GROUP**

Carbon-13 chemical shifts of carboxyl carbon atom of acetic, benzoic and mesitoic acids in various compositions of sulfuric acid 14 p2232 A66-27376

Conversion of 2-carboxy-3-keto-9-methoxy-10-unsaturated hexahydronaphthalene into 5,6-fused products on irradiation in aqueous alkaline media, observing photochemical rearrangements 24 p4170 A66-42300

**CARBOXYLIC ACID**

High activity of alkali metal salts of carboxylic acids and substituted phenols synergists for arylamine antioxidants ester-type synthetic lubricating oils 11 p1711 A66-23100

**CARCINOTRON**

Submillimeter wave mixing of output of carcinotron and output of klystron crossed-waveguide harmonic generator 15 p2463 A66-29000

**CARDIOGRAM**

**S BALLISTOCARDIOGRAM**

**S ELECTROCARDIOGRAM**

**S PHONOCARDIOGRAM**

**S VIBROCARDIOGRAM**

**CARDIOGRAPHY**

**SA BALLISTOCARDIOGRAPHY**

**SA ELECTROCARDIOGRAPHY**

Impedance plethysmographic system for monitoring right ventricular output obtain cardiac output 17 p2924 A66-32100

**CARDIORESPIRATORY SYSTEM**

**SA BLOOD CIRCULATION**

Cardiac and respiratory changes in spacemen under light physical strain during Voskhod I orbital flight 13 p2010 A66-25801

Real time cardiorespiratory rate monitoring for data converter on Gemini space program 19 p3288 A66-35700

Liquid breathing effects on dogs hyperbaric chamber 21 p3699 A66-38400

Maximum exercise tolerance in healthy aircrew members limited by cardiac output 24 p4163 A66-42400

Flack Test for cardiorespiratory integrity noting heart rate response 24 p4164 A66-42400



**CARDIOVASCULAR SYSTEM**  
**SA BLOOD CIRCULATION**  
**SA CAPILLARY**

Behavior of right intraventricular conduction in 148 flying cadets under normal sea-level conditions and acute anoxic anoxia 01 p0020 A66-10608

Observations on heart rates and cardiodynamics during prolonged weightlessness, discussing immersion experiment on animals 04 p0465 A66-14073

Effect of weightlessness on cardiovascular, neuromuscular and autonomic nervous systems 06 p0810 A66-15904

Correlation analysis to study reactions of human cardiovascular system during space flight of Voskhod 06 p0814 A66-17175

Positive /headwards/ acceleration effect on vision, cardiovascular system, respiration, kidneys, brain wave patterns and total performance 10 p1490 A66-22123

Analog computer, programmed on digital computer, used in examination of lumped and distributed parameter models of cardiovascular system 12 p1809 A66-24230

Age, cardiac output and choice reaction time of airline, military and test pilots, attempting resolution of data discrepancy 12 p1806 A66-24397

Cardiovascular stress resulting from radial acceleration gradient impeding venous return analyzed by rotation of seated subject about Z axis /Rz/ 12 p1807 A66-25016

Long-term lower body negative pressure in supine position effect on deterioration in cardiovascular function of man during prolonged bed rest 15 p2430 A66-28657

Rotations effect on functional state of human cardiovascular and respiratory systems at various angles of inclination of torso 15 p2437 A66-29476

Cardiovascular measurement on anesthetized dogs subjected to vibration, noting recording techniques, instrument sensitivity, etc [AIAA PAPER 66-442] 16 p2642 A66-30622

Hypoxia and lower body negative pressure effects on blood volume, and orthostatic and physical tolerance after four weeks of hypoxic bed rest 16 p2640 A66-31124

German Air Force functional tests for early diagnosis of cardiovascular disease among aircrew, also discussing therapy 16 p2640 A66-31133

Cardiovascular deconditioning from weightlessness treated by 9-alpha-fluorohydrocortisone 17 p2858 A66-32180

Exercise performance and cardiovascular response of man exposed for 56 days to oxygen-helium atmosphere 18 p3057 A66-33772

Space cardiology, discussing methods of biological telemetry such as ECG, seismocardiography, kinetocardiograph, arterial oscillography, etc 18 p3059 A66-34364

Consequences of heart-to-foot acceleration gradients on tolerance to positive acceleration determined on variable radius centrifuge 19 p3285 A66-36373

Heart rate response to Valsalva maneuver performed regularly during space flight suggests application to development of astronaut orthostatic intolerance 19 p3286 A66-36376

Tilt table response and blood volume changes associated with 30 days of bed rest, evaluating time required to recover from cardiovascular deconditioning 22 p3853 A66-39785

**CARET WING**

Wind tunnel testing of delta-like lifting bodies at low, supersonic and hypersonic speeds, noting lift to drag ratios and off-design performance of caret wave-rider wings [ICAS PAPER 66-24] 23 p4007 A66-41011

**CARGO**

Role of IATA cargo agent in handling air freight shipments 15 p2619 A66-29789

Future improvements in economic and service performance of cargo carriers in surface modes of transportation 15 p2620 A66-29797

**CARGO AIRCRAFT**  
**S TRANSPORT AIRCRAFT**  
**ARNOT ENGINE**

Practical Phillips cycle for low temperature

refrigeration, noting equal coefficient of performance to that of ideal Carnot cycle under isothermal conditions 09 p1472 A66-20879

Carnot function and relationship to second law of thermodynamics 13 p2209 A66-25860

**CAROTID SINUS REFLEX**

Internal carotid artery insufficiency in neuro-ophthalmic and aeromedical implications, noting ophthalmodynametry in flight qualification 24 p4164 A66-42457

**CARRIER**

SA AIRCRAFT CARRIER

SA MAJORITY CARRIER

SA MINORITY CARRIER

Anisotropic absorption of electromagnetic waves by hot carriers in germanium 02 p0277 A66-12082

Recombination of nonequilibrium charge carriers in p-type indium antimonide, using steady state photomagnetolectric effect 08 p1272 A66-19246

Magnetic field effect on energy distribution and slowing-down times of nonequilibrium carriers in semiconductors when excitation source creates electron-hole pairs 12 p1929 A66-24451

Electric conductivity and thermal emf of solid solutions of silicon-germanium with near silicon composition and various current-carrier concentrations and test temperatures 12 p1929 A66-24454

Excitation of axial oscillation modes in semiconductor lasers analyzed, based on rate equations for chemical potentials of carriers and number of photons 12 p1890 A66-24455

Amplitude probability density of random stationary signal potential and variation of free carriers in germanium semiconductor at near-ambient temperature 13 p2170 A66-26758

Temperature variation and carrier concentration effects on density-of-states effective mass, polar and dipolar thermoconductivity, electron and phonon scattering and electron-phonon interaction in doped Si-Ge alloys 14 p2365 A66-27759

Slow wave interaction with drifting stream of carriers, including collision and diffusion effects, noting TWT and acoustic semiconductor amplifier cases 17 p2878 A66-31820

Carrier travel time in transistor region where changeover from neutral region to depletion layer takes place 18 p3076 A66-33936

Acousto-thermal effect in semiconductors in which carriers are characterized by isotropic effective mass and relaxation time, both dependent on energy 18 p3154 A66-33944

Effect of reduction of breakdown voltage by external illumination of oxide protected planar diode or by nonequilibrium carriers drifting in surface channel 20 p3528 A66-37493

Reflectivity of heavily doped samples of p-type gallium arsenide of known carrier concentration and determination of dependence of effective mass upon carrier concentration 20 p3619 A66-37631

Magnetic field effect on energy distribution and slowing-down times of nonequilibrium carriers in semiconductors when excitation source creates electron-hole pairs 20 p3619 A66-37683

Electric conductivity and thermal emf of solid solutions of silicon-germanium with near silicon composition and various current-carrier concentrations and test temperatures 20 p3619 A66-37686

Excitation of axial oscillation modes in semiconductor lasers analyzed, based on rate equations for chemical potentials of carriers and number of photons 20 p3579 A66-37687

Carrier motion equation in Gunn diode in terms of average drift velocity and diffusion coefficient 20 p3534 A66-38402

Isochronal and isothermal stage II recovery in high energy electron irradiated n-type InSb semiconductor, based on Hall coefficient and electroconductivity 21 p3800 A66-38994

N-type Ge hot carrier Hall mobility, magnetoresistance, Maxwellian energy distribution, electron-electron and intervalley electron-phonon collisions 21 p3801 A66-38997

IR absorption, reflectivity and transmission

in n-type gallium arsenide single crystals at room temperature due to impurities and high carrier concentration 21 p3805 A66-39580

Carrier density, mobility and space-charge-limited current in p-type silicon 22 p3962 A66-40049

Spatial distributions of carrier concentration and internal field in cadmium selenide for various voltages, measuring conductivity and Hall coefficient 23 p4112 A66-41292

Multiple access to ideal bandpass limiter channel in pseudonoise system analysis 23 p4040 A66-41593

Scattering mechanism in space charge region as possible explanation of temperature fluctuations of carrier mobility in n-and p-type indium arsenide 23 p4115 A66-41829

One-dimensional approximation analysis of excess carrier density distribution in illuminated semiconductor and radiative recombination effects 23 p4115 A66-41857

Resistance network analog method determination of carrier density distribution and charge constant in p-n junction for two-dimensional axisymmetric case 23 p4115 A66-41858

Anisotropic thermoelectric power in semiconductors as result of combined phonon and impurity scattering or in presence of carrier with anisotropic effective mass 24 p4252 A66-42352

Decaying free carrier concentration increase in GaAs when subjected to increased level of drive during first cycle 24 p4253 A66-42370

**CARRIER FREQUENCY**  
**SA RADIO FREQUENCY**

Carrier frequency stabilization of FM laser with respect to center of atomic gain profile, using small distortion present in laser oscillation 01 p0083 A66-10966

Rate of intercarrier energy exchange in semiconductor by intraband collisions within Maxwellian distribution of carriers 04 p0566 A66-14314

Degradation of correspondence between reference and modulated carriers by arbitrary offset in time-frequency space in random channel 06 p0831 A66-16342

Received field strength dependence on maximum and minimum usable carrier frequency range for ionospheric scattering 06 p0836 A66-17034

Amplitude modulated carrier frequency signal circuit analyzed, showing open loop linear pulse system 07 p1014 A66-17439

Volt-ampere and current carrier mobility characteristics of semiconductors with electron-phonon bonds proportional to applied field 10 p1582 A66-21968

Amplification of electromagnetic waves in solid state plasma in presence of carrier drift in external electric and magnetic fields 10 p1586 A66-22147

Secondary emission effect on LF noises near carrier frequency of continuously operating high power TWT output signal 11 p1655 A66-22724

Extremely rapid propagation deformations in phase envelope of rectangular-type carrier pulse with extended spectrum 13 p2031 A66-25424

Active transistor modulators for carrier frequency engineering, noting noise reduction, lower power requirements and modulation-filter matching 13 p2032 A66-25485

Gating circuit concept, using carrier frequency approach, applied to inverter, converter and cycloconverter circuits 13 p2043 A66-26296

T-type carrier-frequency RC correcting circuits calculated by equivalent transfer function 14 p2264 A66-27205

Frequency deviations in carrier frequencies of ionospherically propagated HF radio waves produced by fluctuations in solar ionizing radiation 14 p2286 A66-27903

Optical and electrical characteristics of n-type indium oxide films prepared by spraying, noting relation between carrier mobility and particular impurity used 15 p2559 A66-28623

Automatic control systems with carrier frequency information transmission channel,



deriving transfer functions 16 p2872 A66-31552

Amplification of electromagnetic waves in solid state plasma in presence of carrier drift in external electric and magnetic fields 19 p3440 A66-35761

Simultaneous estimate of delay time and drift of carrier frequency during nonoptimum reception against correlated noise background 20 p3519 A66-38002

Rheoelectric integrator simulation method for charge carrier lifetime determination in transistor 21 p3713 A66-39320

Volt-ampere and current carrier mobility characteristics of semiconductors with electron-phonon bonds proportional to applied field 21 p3805 A66-39547

Peak power of pulse modulated RF carrier measured by sequential comparison with reference carrier 22 p3872 A66-39728

Secondary emission effect on LF noises near carrier frequency of continuously operating high power TWT output signal 23 p4037 A66-41462

**CARRIER INJECTION**

Properties of long forward-biased diodes operating in double-injection regime 03 p0346 A66-13318

Long-wave recombination radiation of germanium associated with optical transitions involving photon emission and current carrier heating 04 p0568 A66-14348

Distribution of high plasma density along semiconductor rod, noting surface recombination rate and assuming existence of high level injection at one end of rod 06 p0923 A66-16176

Dependence of lifetime on injected level in high-energy electron-irradiated silicon with production of total displacements per primary recoil event 06 p0939 A66-17156

Carrier temperature injected into InSb effect on shape of direct intrinsic line 07 p1095 A66-17317

Effect of injection of charge carriers on recombination lifetime in GaAs diode laser 07 p1042 A66-17331

Efficiency of DC electroluminescence produced when minority carriers are injected into n-type ZnSe crystals depends on injection efficiency at contacts 07 p1097 A66-17342

Nonisothermal gaseous transport of hot injected plasma in semiconductor 07 p1103 A66-18213

Lifetime degradation rate due to cobalt gamma irradiation reduced in p-silicon due to electron injection at low temperature 07 p1106 A66-18400

Single injection measurements in n-type silicon at liquid-helium temperatures under transient conditions, using pulse measurements 07 p1107 A66-18414

Doppler effects of injected carriers of semiconductor detected in microwave fields, used to measure semiconductor plasma drift velocity 08 p1270 A66-19060

Fluctuation of electric field distributions within germanium sample when one contact of sample is used to inject holes 09 p1412 A66-19994

AC current measurement to determine contribution in semiconductors, which appears as displacement current, from space charge caused by injected and alternatively modulated carriers 09 p1432 A66-20970

One-sided avalanche injection in n-p-p diodes as cause of negative resistance for carrier concentrations smaller than impurity concentration 10 p1515 A66-22085

Spectral density of white noise generated in uniformly multiplying p-n junction calculated for any distribution of injected carriers 10 p1515 A66-22087

Dependence of recombination-generation current and injection coefficient of p-n junction on forward bias voltage 11 p1666 A66-22730

Indium antimonide diodes of various base thickness for high injection levels, results in graphical form applied to magnetic diode production 11 p1666 A66-22740

High injection theories of transport in p-n junctions and transistors in charge neutrality approximation 11 p1756 A66-23020

Double injection in long p-p-n diffused silicon junctions subjected to heat treatment, noting donor density energy level

and electrical properties 11 p1756 A66-23027

VHF power modulation receivers using germanium injection modulators produce no additional noise at frequencies around 25 cps 11 p1670 A66-23228

Injection and extraction of hot electrons in n-n heterojunctions with rapid Maxwellization of electron gas, negative resistance and semiconductor characteristics 13 p2186 A66-25920

Injection-current dependence of intensity of recombination radiation of separate bands in gallium arsenide 14 p2249 A66-27084

Long diode theory not limited by conditions of quasi-neutrality, noting V-I characteristics 14 p2254 A66-27744

Long-wave recombination radiation of germanium associated with optical transitions involving photon emission and current carrier heating 14 p2368 A66-28245

Properties of long forward-biased diodes operating in double-injection regime 14 p2280 A66-28292

Injection of minority carriers at field-induced junction near silicon-silicon dioxide interface 15 p2459 A66-28897

Capacitive current injected by collector effect on internal reaction of plane transistor 16 p2660 A66-30587

Relation between time of voltage buildup and length of diode base in p-n junction at high injection levels 16 p2776 A66-30866

Phase shift lifetime of excess carriers in semiconductors under sinusoidal injection, showing decrease as injection frequency increases 16 p2784 A66-31451

Electroluminescence of silicon carbide diodes 16 p2668 A66-31781

Instability of Sb and Au-doped n-type germanium during carrier injection, examining current-voltage and frequency characteristics and illumination 17 p2974 A66-31858

Strong injection in nondegenerated p-n junction producing electron-hole plasma in n region near junction 17 p2986 A66-33307

Changes in piezoelectric constants of cadmium sulfide crystal caused by illumination and on mechanical vibration caused by fluctuation of carrier injection from electrodes 18 p3153 A66-33613

Transient behavior of current to applied voltage step for semiconductor structure with double injection behavior in initial and final states 19 p3435 A66-35406

Efficiency limitation factors in radiative recombination in electroluminescent GaAs diodes, examining contribution of majority and minority carriers injected into P region 19 p3319 A66-36284

Plasma confinement experiments with electron injection parallel to cusped magnetic field axis in nonadiabatic regime 19 p3422 A66-36549

Astron facility experiments on injection of very intense pulses of relativistic electrons into cylindrical azimuthally symmetric magnetic trap 19 p3423 A66-36551

Electron injection and E-layer buildup in Astron device theoretically studied by one-dimensional model, using Green functions for self-electric and self-magnetic fields 19 p3423 A66-36552

Steady state donor-acceptor recombination rate and effects on diode current and injection electroluminescence, using Shockley-Read-Hall semiconductor phenomenological model 21 p3800 A66-38993

Injection-current dependence of intensity of recombination radiation of separate bands in gallium arsenide 22 p3882 A66-40840

Dependence of recombination-generation current and injection coefficient of p-n junction on forward bias voltage 23 p4045 A66-41468

Indium antimonide diodes of various base thickness for high injection levels results in graphical form applied to magnetic diode production 23 p4045 A66-41478

Space-charge-limited current dependence on time in semiconductor taking trapping into account 24 p4252 A66-42350

Time dependence of space-charge limited current in Fe-doped p-silicon used for determining capture probability, noting retrapping significance 24 p4252 A66-42351

Charge transport through hemispherical metal contacts on semiconductors,

calculating V-I characteristics and injection ratios 24 p4254 A66-42351

**CARRIER MODULATION**

**SA PULSE MODULATION**

Qualitative interpretation of negative resistance by impact ionization of deep level impurities noting temperature, impurity concentration and energy level 05 p0735 A66-14618

Spectral density of FM baseband wave when it is quantized random facsimile signal 05 p0634 A66-15111

Helicons in n-type silicon and germanium calculating collective modes of electrons external magnetic field from frequency and wavelength-dependent conductivity tensor 06 p0923 A66-16176

Power spectrum of random phase modulated carrier, assuming rectangular spectrum for modulating signal 06 p0853 A66-18666

Behavior of carrier mobility in semiconductors with layered structure, with carriers acting as mobile particles in state of independent layers 06 p0929 A66-16180

AC current measurement to determine contribution in semiconductors, which appears as displacement current, from space charge caused by injected and alternatively modulated carriers 09 p1432 A66-20970

Microwave circuit design using transmission line, noting single-sideband suppressed carrier modulator, tunnel diode in low-noise amplifiers, etc 10 p1512 A66-21712

Nomograph for FM/FM telemetry system design 12 p1815 A66-24111

Diode quad modulator suppresses carrier 65 db in high capacity communication system 14 p2247 A66-28866

Coherent transmission of optical radiation from laser source and use of RF subcarrier placed on optical beams for wideband communications purposes 14 p2244 A66-28400

Propagation velocity and attenuation variation effect in coaxial cables frequency modulated carrier evaluated using IBM 1620 computer 16 p2649 A66-30611

Response of phase-locked loop near threshold to input consisting of modulated carrier and white Gaussian noise, noting ratio of SNR 18 p3070 A66-34280

Computer optimization of baseband design of angle-modulated unified carrier space ground communication link 19 p3299 A66-35611

Conductivity modulation by heavy-to-light hole transitions in p-type germanium noting carrier lifetime and ringing of laser pulse 24 p4219 A66-42211

**CARRIER ROCKET**

**S LAUNCH VEHICLE**

**CARRIER SYSTEM**

Indirect optical transitions in semiconductors due to photons and impurities, noting absorption and emission of photons, avalanche and long wavelength radiation 02 p0273 A66-11740

Carrier circuit techniques applied to fluorescence amplifier control systems 09 p1332 A66-20311

Edge absorption of indium-doped cadmium in polarized light, noting exchange interaction between current carriers and Fermi level dependence on carrier concentration 12 p1829 A66-24411

Carrier concentration and minority carrier lifetime measurement in MOS epitaxial layers by capacitance method 13 p2164 A66-25411

Edge absorption of indium-doped cadmium in polarized light, noting exchange interaction between current carriers and Fermi level dependence on carrier concentration 20 p3619 A66-37611

**CARTAN SPACE**

Dirac equation for spin-half particles curved space-time formulated by using Cartan calculus, applied to treatment neutrinos in homogeneous nonisotropic universes and plane wave geometries 12 p1905 A66-24511

**CARTESIAN COORDINATE**

Stereographic mapping of plane Cartesian coordinate grid onto sphere for position navigation use 09 p1401 A66-20911

Relations among vibrational frequencies isotopically substituted molecules when on one Cartesian coordinate of any atom



- involved in motion, obtaining general valence-force-constant matrix 14 p2336 A66-27373
- Best straight line calculated by least squares method 16 p2736 A66-31007
- MHD wave equation for compressible infinitely conducting fluid formulated in Cartesian tensor form 18 p3103 A66-34935
- Flat elliptical crack in infinite elastic medium under shear stress at infinity 22 p3995 A66-40457
- Continuum mechanical Cartesian tensor analysis theorem on completeness of Beltrami stress function 23 p4139 A66-41544
- CARTOGRAPHY**
- SA MAPPING**
- Tables and maps of geomagnetic coordinates corrected by higher order spherical harmonic terms 01 p0082 A66-10888
- Reseau techniques application to cartographic photography to improve analytical procedures, reduce mensuration errors and aid in automating systematic corrections 02 p0228 A66-11382
- Multistrip transformation, of aerial photographs of mountainous regions to obtain scale maps 02 p0229 A66-11896
- Renovation techniques for topographic maps 06 p0879 A66-16325
- Nearly ideal cartographic projections of variable type and reduction of certain functional to minimum 08 p1217 A66-19346
- Graphical device for transformation between horizon system of coordinates and equatorial system, noting construction techniques, operation and application 09 p1381 A66-20395
- Large-scale aerial photographs applied to cartography by taking pictures of same area at varying scales 10 p1534 A66-21132
- Twelve monthly world maps of daily means of total solar radiation incident on horizontal surface 11 p1702 A66-23156
- Cylindrical coordinate system describing geomagnetic field analyzed, noting consequences in magnetic cartography when going from field to time gradients 12 p1875 A66-24970
- Statistical comparison of lunar maps of U.S. Army with Baldwin maps, determining true precision of individual values on both maps 13 p2177 A66-25119
- Soil investigation and geological map preparation from aerial photographs 15 p2505 A66-30014
- Lunar charting for project Apollo 16 p2743 A66-30669
- Graphical method by which small local users of meteorological satellite pictures can identify geographical position of features in image [AIAA PAPER 66-439] 16 p2708 A66-31467
- Lunar topography and cartography, noting application to lunar atlas preparation, absence of magnetic field, etc 17 p2999 A66-32132
- Nearly ideal cartographic projections of variable type and reduction of certain functional to minimum 19 p3348 A66-36054
- CARTRIDGE**
- Neutron radiographic techniques to solve nondestructive testing problem of pyrotechnic cartridge inspection 21 p3806 A66-39153
- CARTRIDGE ACTUATED DEVICE**
- SA THRUSTOR**
- Propellant actuated device /PAD/ functions by using cartridge type energy source wherein chemical reaction is controlled without sonic orifice 18 p3160 A66-34188
- CASCADE**
- SA ELECTRON PHOTON CASCADE**
- Comparing VHF cascade circuits with double diffusion silicon planar transistors and metal oxide field effect planar transistors 04 p0501 A66-14133
- Upper laser states deriving population through cascade transitions from higher layer states of argon ion noting consistency of laser output current dependence with current dependence of cascade rate 20 p3579 A66-37774
- Possibility of realization of multicascade tunnel diode frequency doublers without intercascade amplification 20 p3533 A66-38009
- Stability of solutions to inverse problems in cascade theory, analyzing case when equilibrium spectrum of particles is specified 24 p4269 A66-42922
- CASCADE FLOW**
- Conformal mapping to calculate exit flow velocity of compressible frictionless subsonic flow through plane blade cascade 01 p0005 A66-10212
- Velocity changes and concomitant losses in rotating transonic blade cascade 01 p0005 A66-10213
- Mach number effect on secondary losses of straight turbine-blade configuration at high subsonic velocities 01 p0007 A66-10924
- Axial compressors with nonuniform inlet flow, investigating size of gap between blade rows and rotating stall 01 p0008 A66-10953
- High subsonic flow passing choked flat plate cascade with comparatively small pitch chord ratio 02 p0175 A66-11305
- Three-dimensional theory of incompressible and inviscid flow through mixed flow turbomachines [ASME PAPER 64-WA/GTP-1] 02 p0176 A66-11765
- Laplace transform technique to develop asymptotic solutions to integral equations describing influence of scattering law on radiation damage displacement cascade 02 p0245 A66-11946
- Linear cascade of double-circular-arc airfoils in transonic shear flow compared with subsonic flow 03 p0313 A66-12394
- Aerodynamic damping effect on cascading double circular arc blades vibrating in translatory mode 03 p0313 A66-12397
- Outlet angle in axial compressor cascades, accounting for effect of shear flows, Bernoulli surface rotation and flow separation [ASME PAPER 65-WA/FE-2] 05 p0608 A66-15714
- Supersonic cascade tunnel to evaluate compressor blade performance [ASME PAPER 65-WA/GTP-4] 05 p0661 A66-15719
- Theory of highly rarefied cascade flow and proposal for new axial flow molecular pump in free molecule range 06 p0803 A66-16945
- Flow through straight slot cascade, investigating application to axial compressors for optimum slot parameters 06 p0803 A66-16968
- Clearance loss in rectilinear cascade, emphasizing flow separation and vortices shed at blade tips 07 p0980 A66-17483
- Supercavitating flow past straight cascade of arbitrary hydrofoils 07 p1024 A66-18169
- Assessment of current methods of calculating flows through cascade turbines 08 p1162 A66-18862
- Pseudoshocks in pipe flow in supersonic compressors represented as diffusion process, noting application in cascade and rotor configuration 10 p1479 A66-21363
- Supersonic retardation cascades for lossless reduction of supersonic flow to subsonic in turbines and compressors 10 p1591 A66-21380
- Secondary flows in turbine cascades, obtaining correlations between velocity distributions and circulations along span by expanding Fourier series 11 p1632 A66-22664
- Polynomials used to solve theoretical cascade problems exemplified by two-dimensional incompressible flow through nonstreamlined blades 12 p1796 A66-23786
- Analytic design of turbine blades based on inviscid isentropic supersonic vortex flow theory and performance in cascades 12 p1796 A66-23800
- Airfoil cascade oscillation in near-sonic gas flow 12 p1798 A66-24432
- Compressor cascade flow with blades of different thickness ratio for variable Mach and Reynolds numbers, measuring turbulence level influence on loss coefficients, secondary flow parameters, etc 12 p1799 A66-24553
- Text on cascade flow through airfoils and application to turbomachine and blade design 14 p2220 A66-27699
- Supersonic cascade tunnel used to evaluate compressor blade performance [ASME PAPER 65-WA/GTP-4] 16 p2673 A66-30340
- Turbine blades suitable for supersonic relative inlet velocities and performance in cascade 17 p2841 A66-32889
- Graduate level textbook on axial flow turbine design, examining useful thermodynamic/fluid mechanic concepts, cascade potential flow, turbine efficiency, etc 17 p2991 A66-32991
- Aerodynamics of propulsion plants, discussing cascade flow parameters, sub and supersonic flows, rocket gas cooling, acceleration of electrically conducting gases, etc 19 p3343 A66-36749
- Pressure distribution of steady flow through cascade of closely spaced circular cylinders 23 p4010 A66-41778
- CASCADE WIND TUNNEL**
- Blowdown-type high-speed linear cascade wind tunnel with variable exit pressure, Mach and Reynolds numbers permit boundary layer control 12 p1859 A66-24927
- Versatile facility applicable as high-speed annular cascade wind tunnel or as transonic axial flow test compressor 12 p1859 A66-24928
- CASE**
- S MISSILE CASE**
- S MOTOR CASE**
- CASE BONDED PROPELLANT**
- Ultrasonic testing of solid propellant rocket motors, describing technique for separation of propellant from steel combustion chamber 09 p1385 A66-20965
- Forced vibration function for stresses and displacements in viscoelastic thick-walled cylinder case-bonded to thin shell, noting pressure and strain effect [AIAA PAPER 65-173] 10 p1817 A66-21784
- Cast-double-base propellant mechanical behavior and failure during slow cooling and rapid pressurization of case-bonded rocket motors [AIAA PAPER 65-161] 12 p1934 A66-24704
- Photoelastic analysis of stress and strain distributions of case-bonded propellant grains, calculating internal pressure and dependence on mechanical properties of grain material 23 p4120 A66-41440
- CASSEGRAIN ANTENNA**
- 85-ft paraboloid antenna with new type of Cassegrainian feed system for satellite communication ground station at Nova Scotia 02 p0189 A66-11362
- Design and electrical properties of 25-meter Cassegrainian antenna installed at Raisting ground station for radio communications via satellites 08 p1190 A66-18681
- USN contributions to space communications, noting Syncom program, communications by Moon relay, design of antenna aboard Kingsport vessel, etc [AIAA PAPER 66-270] 12 p1820 A66-24743
- Dichroic Cassegrain subreflector utilizing array of nonresonant elements 15 p2457 A66-28590
- Ground clutter shields for L-band radar using 60-ft parabolic reflector with Cassegrain geometry 15 p2457 A66-28596
- Transmitting antenna of Cassegrain type, noting conical horn, primary and secondary mirror, etc 16 p2681 A66-30955
- Phase error and associated cross-polarization effects in Cassegrain-fed microwave antenna 18 p3074 A66-33528
- Low-cost ground station design for satellite communications, with emphasis on Cassegrain reflector antenna and drive system 18 p3093 A66-33868
- Conical beam scanning by nutating subreflector in Cassegrain antenna system, showing most favorable motion pattern from point of view of electrical performance 18 p3082 A66-34282
- Shadow and diffraction effect of spars on Cassegrain antenna system gain performance 18 p3082 A66-34283
- Diffraction pattern analysis of fields generated by hoghorn-fed Cassegrain antenna operating in Fresnel zone 18 p3083 A66-34289
- Antenna structure analysis by finite-element method and energy method, considering Cassegrain antenna 18 p3255 A66-34312
- Cassegrain satellite tracking antenna with 40-ft diameter, considering reflector geometry and feed design 18 p3085 A66-34319
- R.R.E. North Site Cassegrain aerial system for monopulse tracker radar 18 p3086 A66-34322
- Millimeter wavelength parabolic reflector



- with Cassegrain feed system 18 p3095 A66-34325
- Cassegrain monopulse tracking antenna for LEM and Command Module rendezvous guidance 21 p3714 A66-39524
- CASSEGRAIN OPTICS**
- Optical system of RM-700 astronomical telescope, analyzing prime focus and Cassegrain focus 05 p0680 A66-15206
- Design and construction of 106-cm Cassegrain-type reflector telescope at Pic du Midi observatory 13 p2081 A66-26233
- Sun pumped continuous wave one-watt YAG crystal laser, noting equipment setup and output duration 17 p2934 A66-32620
- CASSIOPEIA A**
- Flux density of Cas A measured, using horn-reflector antenna, response compared with output of reference-noise source 05 p0762 A66-15278
- Aerobee rocket measurements of cosmic X-ray sources emanating from Cygnus A, M-87 and galactic supernova remnant Cassiopeia A 13 p2174 A66-25836
- CASTIGLIANO VARIATIONAL THEOREM**
- Compatibility conditions derived from Castigliano principle by three-dimensional stress function 02 p0299 A66-11804
- CASTING**
- SA INVESTMENT CASTING**
- SA PROPELLANT CASTING**
- Lightweight steel and superalloy casting design, describing avoidance of shrinking, ceramic-shell molds, X-ray standards and weld repair [ASME PAPER 65-MD-3] 05 p0688 A66-15132
- Text on die, permanent mold, shell and other processes for casting aluminum and aluminum alloys 07 p1047 A66-17214
- Thermal shock resistant carbides, using arc-casting techniques, noting microstructure, phase diagram, mechanical properties, etc 07 p1055 A66-18504
- Precision casting based on directional solidification resulting in longitudinal columnar grains with preferred orientation, eliminating transverse grain boundaries in gas turbine elements 09 p1388 A66-20153
- [SAE PAPER 660055] 09 p1388 A66-20153
- Composite casting as metallurgical bonding technique, noting application to weight reduction and increase of corrosion resistance 13 p2086 A66-25779
- Extremely high thermal shock resistance in group IVA carbides of carbide-graphite composites fabricated, using vacuum arc melting and casting techniques 15 p2524 A66-29287
- Casting technique based on directional solidification for nickel and cobalt alloys used in gas turbine blades [AIAA PAPER 65-742] 23 p4079 A66-40973
- CAT**
- Hypoxia in cats and rats due to gradual and abrupt drops in oxygen content of air 15 p2439 A66-29491
- Superacute hypoxia in cats exposed to pure nitrogen followed by artificial respiration 15 p2439 A66-29492
- Chorioretinal lesion produced by pulsed ruby laser beam and complex changes in retinal excitability in cats 16 p2641 A66-31761
- CATALYST**
- SA ELECTROCATALYST**
- SA ENZYME**
- Boron carbide as potential substitute for platinum as catalyst for fuel cell cathodes 14 p2227 A66-28174
- Performance analysis of carbon-supported platinum-ruthenium alloy catalysts with respect to anodic oxidation of methanol in acid electrolyte 17 p2870 A66-31898
- Criteria for selection of mixed metal oxides that can be used as catalysts in oxygen-hydrogen batteries 17 p2871 A66-32949
- CATALYTIC ACTIVITY**
- Macrokinetics of homogeneous-heterogeneous processes in moving media and estimates of initial material concentration in core and boundary layer regions of reaction vessel flow 06 p0971 A66-16543
- Heat transfer rate to stagnation point of catalytic surface placed in slow flow of dissociated oxygen from glow discharge tube and atom-molecule diffusion coefficient 06 p0822 A66-16632

- Concentration profile in laminar boundary layer frozen to wall by catalytic chemical reaction 07 p1019 A66-17245
- Water vapor influence on latitudinal and seasonal distribution of stratospheric ozone concentration explained via Hampson chemical mechanism 08 p1216 A66-19209
- Kinetics of oxidation of various atmospheric contaminants over several catalysts tested in catalytic reactor [AICE PREPRINT 26C] 10 p1491 A66-21190
- Catalytic dehydrogenation of hydrocarbons over chromia-alumina catalyst in absence of added hydrogen to determine heat sink capability 11 p1650 A66-23119
- Methylcyclohexane dehydrogenation over platinum-alumina in absence of excess hydrogen, yielding toluene and hydrogen 11 p1650 A66-23122
- JP-5 fuel-air mixture ignition by platinum catalytic igniters, using ramjet engine baffle combustors 13 p2171 A66-25594
- Properties of laminar boundary layer undergoing surface catalysis with two reactants and two products obeying Langmuir-Hinshelwood mechanism, solving concentration field by integral equation 13 p2019 A66-26663
- Catalytic efficiency of noncatalysts interferes with accuracy of measurement, noting necessity of oxygen treatment of noncatalytic surfaces 15 p2502 A66-29310
- Extraterrestrial life detection based on catalysis of oxygen exchange between labeled oxyanions and water, noting equipment 15 p2441 A66-29961
- Kinetics of oxidation of various atmospheric contaminants over several catalysts tested in catalytic reactor [AICE PREPRINT 26C] 17 p2868 A66-32680
- Dipeptidyl arylamidase I of bovine pituitary tissue and chloride and sulphydryl activation of seryltyrosyl-beta-naphthylamide hydrolysis 17 p2861 A66-32899
- Combustion rate in simultaneous heterogeneous-homogeneous reactions on particle surfaces of catalytic agents added 18 p3265 A66-34550
- Boundary conditions and rate equations in surface-catalyzed reactions 18 p3064 A66-34598
- Diffusion of chemically frozen partially dissociated gas over surfaces with discontinuous catalytic 18 p3266 A66-34928
- Catalytic combustion of cyclohexane, cyclohexene and benzene, determining significance of combustion via computer program 18 p3266 A66-35022
- Periodic volt-ampere curves of anode oxidation mechanism of hydrocarbons, alcohols, ketones, aldehydes and carboxylic acid to carbon dioxide, using Raney platinum catalyst 19 p3295 A66-36291
- Purification of turbine oil by hydrogenation, using Al-Co-Mo catalyst 20 p3575 A66-38382
- Measurement apparatus for studying kinetics of catalytic recombination of gas atoms at solid surfaces of refractory metals, semiconductors and dielectrics 21 p3735 A66-38522
- Surface catalytic and Reynolds number effects on nonequilibrium hypersonic stagnation flow of air or diatomic gas on highly cooled blunt body 22 p3847 A66-40919
- CATAPULT**
- S LAUNCHING**
- S TAKEOFF SYSTEM**
- CATECHOLAMINE**
- Bed rest and water immersion effects on plasma volume and catecholamine response to tilting, noting urinary excretion of norepinephrine and epinephrine 15 p2430 A66-28661
- Urinary excretion of 3-methoxy-4-hydroxymandelic acid during dreaming sleep in man 16 p2638 A66-30635
- CATENARY CURTAIN**
- Mechanics of catenaries for structures and machines in space, noting equations for behavior [AIAA PAPER 66-99] 07 p1037 A66-17899
- CATHODE**
- SA ANODE**
- SA CATHION**
- SA COLD CATHODE**
- SA HOT CATHODE**
- SA PHOTOCATHODE**

- SA THERMIONIC CATHODE**
- Cathode sputtering theory, explaining sputtering dependence on ion angle of incidence, with application in electromagnetic isotope separators, etc 08 p1257 A66-1869
- Potential striae determined in hollow cathode plasma 08 p1264 A66-1918
- Mass and energy transfer characteristics of cathode attachment zone in high intensity arcs [AIAA PAPER 66-187] 11 p1742 A66-22215
- Design of gravity-independent force-free liquid-metal cathode providing unlimited cathode life in gas discharge devices and mercury electron-bombardment thrusters [AIAA PAPER 66-245] 13 p2106 A66-2517
- Enhanced photoelectron emission between 200 and 1300 angstroms, using polygonal cathode to absorb incident radiation 13 p2131 A66-25828
- Boron carbide as potential substitute for platinum as catalyst for fuel cell cathodes 14 p2227 A66-28174
- Arc cathodes as heat sources in low pressure gas flows, noting loss of material and other effects 14 p2346 A66-28178
- Inverse brush cathode design that functions like brush cathode in producing negative glow plasma 15 p2550 A66-28728
- Relation between laser parameters and cathode diameter in excitation of He-N mixture by discharge of hollow cylinder 15 p2516 A66-29358
- Model of discharge in electron bombardment thrusters noting mechanism and interplay between discharge plasma and cathode [AIAA PAPER 66-244] 16 p2791 A66-31152
- Surface microstructure of cathode oxide coatings using carbon replicas 16 p2789 A66-31808
- Physical principles of cathode electronics All-Union Conference, Leningrad, October 1965 17 p2988 A66-33458
- Current source for vacuum tube circuits delivering constant and fairly large current from cathode of pentode 18 p3079 A66-34248
- Zr-coated tungsten cathode in reducing divergence of electron beam emission 18 p3088 A66-35078
- Relation between laser parameters and cathode diameter in excitation of He-N mixture by discharge of hollow cylinder 20 p3576 A66-37368
- Cathode current density distribution, bearing minimum radius and location and electrode current interception, using computer techniques on electron guns 20 p3528 A66-37498
- Thermoconductive energy transfer from cathode of low pressure gas discharge 20 p3679 A66-38018
- Cesium-plasma diode effect dependence of material output of cathode in vacuum plotting short circuit current vs vapor pressure, voltage distribution, etc 22 p3952 A66-39758
- Field intensities and electron distribution functions in hollow cathode, graphs show potential distribution along cathode axis 22 p3953 A66-39758
- Standing ion acoustic waves between cathode and electrically floating auxiliary metal electrode, noting discharges of mercury vapor between plane oxide-coated cathode and nickel anode 22 p3954 A66-39818
- Uniform-current-density thermionic and secondary electron emission from dense plasma interaction with negatively biased solid surface at high temperature under high current arc cathode simulated conditions 23 p4107 A66-41908
- CATHODE RAY TUBE**
- SA ELECTRON GUN**
- Electron image of CRT cathode formed directly on view screen, eliminating emission patchiness from oxide coated tubes 01 p0036 A66-10398
- Cathode ray curve tracer for differentiated current-voltage characteristics of tunnel diode 01 p0046 A66-11048
- Cathode ray tube measurements indicate that noise in cathodoluminescence is mainly caused by shot noise of primary beam 02 p0206 A66-12168
- Continuous moving-scene display system for output of airborne mapping sensors such



as radars, microwave radiometers and IR scanners 06 p0878 A66-15966  
 Cathode development noting increased lifetime, high emission capability and application 06 p0855 A66-16806  
 CRT control display console models, console selection pointers, computer programming requirements, etc 07 p1003 A66-17879  
 Image, display and storage tube for scan conversion, digital storage and signal processing 07 p1036 A66-18270  
 Visual display system providing instrument data in one-to-one correspondence with real world, using cathode ray tube images of horizon and runway projected on aircraft windscreens 08 p1203 A66-19764  
 Text on electron optics covering principles and application, electron lenses, cathode ray tubes, mass and beta ray spectrographs, quadrupole systems, image converters, etc 09 p1402 A66-20333  
 Electrical damage to cathode ray tube safety glass attributed to current passing through cathode ray tube face and safety glass as result of ionic conduction 10 p1504 A66-21659  
 General purpose computers and cathode ray tube displays used in automation of air traffic control technical aids 11 p1732 A66-22900  
 Cathode ray curve tracer for differentiated current-voltage characteristics of tunnel diode 11 p1671 A66-23290  
 Electron-beam-controlled CRT scanlaser 13 p2091 A66-25557  
 Apparatus for teaching and research in electron physics including emitters, cathode ray tubes, electron multipliers and mass spectrometer 18 p3088 A66-35033  
 Luminescent surfaces and structures for information display, discussing cathode ray tube, image intensifier for night vision, spectral emission, etc 19 p3312 A66-35338  
 CRT oscilloscope tracer device for relay units and relay parameter influence on operational characteristics 19 p3358 A66-35835  
 Gas pressure effect on excitation of 4.38-ev level in Pb during hollow cathode discharge in magnetic field 20 p3579 A66-37780  
 Retinal analogs of three-dimensional forms produced on CRT for three-dimensional oscillographic display system 23 p4047 A66-41596  
 Cathode ray tube device for digital video processing of Ranger pictures 23 p4071 A66-41677  
**CATION**  
 SA ANION  
 SA CATHODE  
 Electron spin resonance of radical cations produced by oxidation of aromatic hydrocarbons with antimony pentachloride 03 p0330 A66-12336  
 Ionization cross section of ground state helium cation by electron impact in Born exchange approximation 04 p0549 A66-14312  
 Organic cations effect on laser threshold of solutions of tetrakis form of europium benzoyltrifluoroacetate 07 p1046 A66-18418  
 Cation distribution in barium hexaferrites 10 p1589 A66-22169  
 Cation distribution in barium hexaferrites 19 p3441 A66-35783  
 Heat of formation of perfluoroammonium ion estimated from thermochemical correlations and compared with estimates by means of Kapustinskii approximation for lattice energies 23 p4031 A66-41222  
**CAUCHY INTEGRAL**  
 Boundary properties of Cauchy integrals and harmonically conjugate functions in regions having rectifiable boundary 07 p1059 A66-18097  
 Analog computer techniques applied to find roots of complex functions, to generate complex functions by Cauchy integral theorem and to scan z plane 10 p1507 A66-21693  
**CAUCHY LAW**  
 Existence and formal uniqueness theorem of partial linear differential equations with Cauchy conditions on characteristic multiple hyperplane 01 p0095 A66-11075  
 Boundary conditions producing simple waves in Green-elastic and Cauchy-elastic materials that generate three-dimensional

unsteady deformations 06 p0874 A66-17010  
 Attenuation factor and degree of stability of automatic control systems determined by Mikhailov criterion and Chebyshev polynomials 08 p1201 A66-19684  
 Cauchy type integral on hypersphere, defining Cauchy principal values, noting role in theory of functions of complex variables 11 p1724 A66-23366  
 Attenuation factor and degree of stability of automatic control systems determined by Mikhailov criterion and Chebyshev polynomials 18 p3091 A66-34670  
**CAUCHY PROBLEM**  
 Liubich generalization of Laplace transform as related to Cauchy problem 01 p0094 A66-10651  
 Existence of explicit stable difference scheme in correct Cauchy problem for linear systems of partial differential equations with constant coefficients 01 p0094 A66-10654  
 Cauchy problem for linearized Boltzmann equation in kinetic theory of gases 01 p0107 A66-11011  
 Cauchy problem for infinite order linear differential equation 02 p0250 A66-12019  
 Existence and uniqueness of Cauchy problem for Boltzmann equation describing flow past convex body of rarefied gas of structureless particles 02 p0261 A66-12022  
 Comparison lemma for determining uniqueness of solution to Cauchy problem for ordinary differential equations 02 p0251 A66-12243  
 Cauchy problem of heat conduction equation and inversion of Weierstrass transform on certain symmetrical Riemann spaces 03 p0444 A66-12714  
 Singular perturbation for mixed Cauchy problem relative to equation with second-order partial linear hyperbolic derivatives 05 p0708 A66-15094  
 Charged fluid in presence of electromagnetic induction and thermal exchange, noting Cauchy problem, thermodynamic and heat equations 05 p0787 A66-15101  
 Cauchy problem for hyperbolic singular convolution-type integral equation 05 p0708 A66-15320  
 Cauchy problem for first-order nonlinear equation 05 p0709 A66-15360  
 Correct solvability of Cauchy problem for parabolic systems with coefficients satisfying Dini condition 06 p0902 A66-16534  
 Cauchy problem at infinity for certain nonlinear systems of ordinary differential equations 06 p0903 A66-16704  
 Width of influence zone for heat conduction equation in Cauchy problem 06 p0971 A66-16711  
 Classes of uniqueness for solutions of Cauchy problem and representation of positively defined kernels 07 p1056 A66-17598  
 Second order degenerate elliptic and parabolic equations, giving smoothness theorems of solutions 07 p1056 A66-17604  
 Cauchy and boundary value problem for second-order nonlinear ordinary differential equations 07 p1056 A66-17607  
 Stability of solutions of Cauchy problem for linear hyperbolic differential equations 07 p1056 A66-17609  
 Uniqueness theorem for Cauchy problem for heat equation, using Poisson representation 07 p1153 A66-17839  
 Poisson representation and Cauchy problem for heat equation, with improved results over previous paper 07 p1153 A66-17843  
 Two-tangents method for numerical solution of Cauchy problem for system of ordinary differential equations 07 p1058 A66-17911  
 Three-dimensional Cauchy-Poisson problem for waves in viscous fluid 07 p1026 A66-18196  
 Approximate methods for integration of equations of plane isentropic motion of gas at supersonic velocities 08 p1165 A66-19572  
 Cauchy problem for elliptic system 09 p1396 A66-20632  
 Cauchy problem for linearized Boltzmann equation, deriving high accuracy equations of motion of rarefied gases 11 p1735 A66-22338  
 Cauchy problem for two-dimensional Laplace equation in infinite strip 11 p1722 A66-22646  
 Global solutions of Cauchy problem for

quasi-linear first-order differential equations in several space variables 11 p1722 A66-22895  
 General solution for class of initial value problems for systems of aerodynamic equations, constructing reference solution to Cauchy problem involving shock and expansion waves 11 p1694 A66-23363  
 Liubich generalization of Laplace transform as related to Cauchy problem 12 p1903 A66-24022  
 Existence of explicit stable difference scheme in correct Cauchy problem for linear systems of partial differential equations with constant coefficients 12 p1903 A66-24023  
 Cauchy problem for infinite order linear differential equation 12 p1903 A66-24024  
 Necessary and insufficient conditions for well-posed Cauchy problems verified by Fourier analysis 13 p2118 A66-25828  
 Modified Cauchy problem in Bitsadze representation with smoothness conditions imposed on initial conditions and on coefficients of pertinent parabolic equation 13 p2119 A66-25907  
 Asymptotic solution of Cauchy problem for integro-differential equation with small parameter associated with derivative 13 p2119 A66-25908  
 Protter criterion for correctness of Cauchy problem for second-order degenerate hyperbolic equation 13 p2120 A66-26246  
 Cauchy problem of first-order nonlinear partial differential equations 13 p2121 A66-26503  
 Maximum property of Cauchy problem for wave operator 14 p2320 A66-28941  
 Existence and uniqueness of Cauchy problem for Boltzmann equation describing flow past convex body of rarefied gas of structureless particles 14 p2334 A66-27573  
 Uniqueness theorems of Cauchy problem for parabolic equations of heat conduction 14 p2322 A66-27630  
 Estimation of proximity of solution for Cauchy problem of nonlinear differential equations, formulating six theorems 14 p2325 A66-28279  
 Emersion and impulse ring waves, examining rigorous solution of classic Cauchy-Poisson problem with finite energy 15 p2480 A66-29647  
 Generalized Cauchy representations and resonance phenomena 16 p2747 A66-30637  
 Certain incorrect Dirichlet and Cauchy problems of potential theory for elliptic and parabolic equations 16 p2733 A66-30744  
 Correct solvability of Cauchy problem for parabolic systems with coefficients satisfying Dini condition 16 p2735 A66-30972  
 Nonlinear parabolic equations, considering existence, uniqueness theorems, abstract Cauchy problem, etc 17 p2946 A66-32307  
 Pointwise bounds for solutions to Cauchy problem for elliptic systems of partial differential equations, using extension of Payne and Trytten results 19 p3388 A66-35487  
 Solution of mixed boundary and Cauchy problem for system of PDE 19 p3389 A66-35933  
 Protter criterion for correctness of Cauchy problem for second-order degenerate hyperbolic equation 19 p3390 A66-36196  
 Incorrect problems of mathematical physics examined and illustrated by classical Cauchy problem for Laplace equation 20 p3591 A66-37756  
 Powers of integral operator generated by Cauchy problem for second-order hyperbolic equation solved by Riesz method of analytical continuation 21 p3756 A66-38739  
 Differential inequality theorems applied to hyperbolic differential equation, discussing Riemann functions and sufficient conditions for characteristic and Cauchy problems for quasi-linear Bianchi equation 21 p3757 A66-39232  
 Stress function and displacement vector for linear, homogeneous, isotropic and elastic material body occupying bounded simply connected region of space 21 p3772 A66-39354  
 Poisson representation of solutions to Cauchy problem for heat equation, showing applicability of Nicolescu method of imaginary reflection 21 p3837 A66-39612  
 Asymptotic formulas for approximate solutions of Cauchy problem by difference



techniques, considering error of tabulated elements 22 p3939 A66-40154

Cauchy and boundary value problems for second-order hyperbolic equations degenerating within and on boundary of region 22 p3939 A66-40189

Cauchy problem of first-order nonlinear partial differential equations 22 p3939 A66-40439

Stability of trivial solution to system of linear differential equation with distributed delay, determining majorant of solutions to Cauchy problems 22 p3941 A66-40797

Navier-Stokes equations solutions for coefficient of viscosity tending to zero become solution to Euler equations in Cauchy problem for equations of hydromechanics 24 p4193 A66-42232

**CAVITATION**

**SA WAKE**

Energy dissipation of acoustic waves propagating in liquid medium and producing cavitation 01 p0106 A66-10417

Numerical analysis of collapse of spherical bubble in compressible fluid including surface tension, viscosity and adiabatic compression of gas within bubble [ASME PAPER 65-FE-16] 06 p0870 A66-16215

Two-dimensional cavity flow of ideal fluid with small unsteady disturbances in gravity free field 06 p0870 A66-16216

[ASME PAPER 65-FE-18] 06 p0870 A66-16216

Cavitation in fluid machinery - ASME Symposium, Chicago, November 1965 07 p1024 A66-18166

Energy dissipation of acoustic waves propagating in liquid medium and producing cavitation 11 p1735 A66-22601

Cavitation effects on periodic wakes behind symmetric wedges, noting Strouhal number variation 12 p1864 A66-24549

[ASME PAPER 65-FE-15] 12 p1864 A66-24549

Relationship between shock wave phenomena during collapse of cavitation bubbles in water and temperature and gas content of water 13 p2060 A66-25091

Acoustically induced cavitation in liquid helium analogous to unfiltered air-saturated water 14 p2334 A66-27663

Quadrant edge orifice meter performance under cavitating conditions, noting discharge coefficient curves 17 p2915 A66-33263

[ASME PAPER 66-FE-9] 17 p2915 A66-33263

Cavitation effect on discharge coefficient of standard flow nozzles 17 p2915 A66-33266

[ASME PAPER 66-FE-12] 17 p2915 A66-33266

Spectral study of ultrasonic shock waves emitted by cavitation on square-section bends, applications include erosion fatigue problem and cavitation detection 18 p3101 A66-34644

Cavitation phenomena induced by ultrasonic waves experimentally studied, using ultrasonic erosion tests and high speed photography 18 p3101 A66-34645

Accelerated cavitation damage in liquid sodium and mercury of stainless steels and superalloys under consideration for use in liquid metal power conversion systems 19 p3380 A66-35804

Water and mercury cavitation damage on solids in cavitating venturi tunnels consisting of single event symmetrical craters and irregular fatigue-type failures 20 p3586 A66-37813

Cavitation erosion research, examining correlation between drop impact erosion and constricted tube and vibratory cavitation erosion tests 20 p3588 A66-37814

Relationship between shock wave phenomena during collapse of cavitation bubbles in water and temperature and gas content of water 21 p3723 A66-38516

Grain boundary self-diffusion coefficient variation with applied stress and production of lattice vacancies applied to cavity growth in high temperature fatigue of Mg 23 p4081 A66-41714

**CAVITATION FLOW**

Tandem interference effects of supercavitating struts within framework of two-dimensional inviscid irrotational and linearized hydrodynamic theory 01 p0057 A66-10443

Solid surface interaction of atoms and molecules of wedge cavity in rarefied free molecular gas stream 04 p0456 A66-14143

Cavitation bubble collapse in venturi,

discussing flow characteristics under large pressure gradient [ASME PAPER 65-WA/FE-20] 05 p0663 A66-15610

Laminar heat transfer and pressure distribution in open cavity supersonic flow, noting heat-transfer coefficient [ASME PAPER 65-WA/HT-37] 05 p0608 A66-15670

Size distribution law for dimensions of gas bubbles formed during cavitation in turbulent flow of liquid 06 p0870 A66-16199

Energy distribution in cavitation bubble collapsing at interface between liquid and solid approximated by localized explosion in ideal gas 06 p0870 A66-16200

Analog computer solution to nonlinear dynamic system model of oscillations associated with cavitating inducers and sequence of trend-and-effect of constituent influences [ASME PAPER 65-FE-14] 06 p0870 A66-16210

Pressure peaks in hydraulic actuator inertia load aggravated in presence of valve overlap, noting cavitation damage [ASME PAPER 65-FE-4] 06 p0808 A66-16213

Flow field in rectangular cavities at low Reynolds number 07 p1020 A66-17941

Predicting onset of cavitation for surface irregularity on parent body 07 p1024 A66-18167

Hydrofoil profile and surface roughness effect on cavitation performance 07 p1024 A66-18168

Jet inducer with multiple nozzles calibrated in liquid mercury and water to minimize feed pump performance degradation due to off-design operation and cavitation 07 p1025 A66-18170

Jet pump cavitation correlation by similarity parameter 07 p1025 A66-18171

Cavitation testing of high efficiency shear force pump and pump rotor, considering air content and cavitation parameters 07 p1038 A66-18172

Bubble coalescence in longitudinally vibrated liquid column 07 p1025 A66-18173

Shaft deflections in turbopumps from cavitation-induced unbalanced hydrodynamic forces in inducer 07 p1038 A66-18174

Cavitation damage in high-temperature liquid metal pumps for Rankine cycle space power plants studied in water model 07 p1038 A66-18175

Cavitation induced between rotating and stationary cylinder in vaporizing liquid within gap of simulated electric motor configuration 07 p1039 A66-18176

Behavior of individual cavitation bubbles in cavitating flows of water and liquid Mercury, using two-dimensional Plexiglas venturi 07 p1025 A66-18177

Motion picture on cavitation hysteresis, details on test apparatus, noting cavitation delay time 07 p1025 A66-18178

Cavitation performance testing in water of mixed flow pump 07 p1039 A66-18179

Impeller 07 p1039 A66-18179

Cavitation damage in alkali liquid metals predicted from properties of water, aviation gasoline and sodium-potassium eutectic 08 p1211 A66-19721

Pressure coefficient criterion for transition between two- and three-dimensional turbulent cavity flow 10 p1523 A66-21791

Cavitation strength of distilled water and distribution of cavitation nuclei, accounting for pressure threshold variance 11 p1688 A66-22607

Nonlinear two-dimensional cavity theory for choked unsymmetric flow over flat plate at arbitrary attack angle, noting variation of lift and drag coefficients [ASME PAPER 65-FE-13] 12 p1864 A66-24544

Cavitation delay time variation with velocity, size, dissolved air content, liquid tension, flow history and surface characteristics [ASME PAPER 65-FE-9] 12 p1864 A66-24552

Cavitating and noncavitating flows past plano-convex hydrofoil, noting oscillation frequency dependence on attack angle, tunnel velocity and cavitation number [ASME PAPER 65-FE-3] 12 p1865 A66-24557

Size distribution law for dimensions of gas bubbles formed during cavitation in turbulent flow of liquid 13 p2064 A66-25915

Energy distribution in cavitation bubble

collapsing at interface between liquid and solid approximated by localized explosion in ideal gas 13 p2064 A66-25915

Water entry cavity for missiles, noting parameters, cavity development and collapse, etc 13 p2071 A66-2677

Shock waves from empty cavity collapsing with spherical symmetry on small solid sphere 13 p2071 A66-2677

Strouhal number relation to cavitation erosion effect of circular cylinder model placed in closed circuit channel, in critical and supercritical Reynolds number range 14 p2275 A66-2766

Cavity depth for waterdrop impacts against water, discussing apparatus, equation for cavity depth, effect of gravitation potential energy, liquid surface behavior etc 15 p2477 A66-2877

Flutter conditions for finite-span hydrofoil under partial cavitation or supercavitation 16 p2688 A66-3133

Hubless inducer with shroud eliminating vane clearance cavitation, noting test data, suction speed, interrelation of boundary layer transition and cavitation, etc [ASME PAPER 66-FE-8] 17 p2932 A66-3326

Resistance to cavitation flow erosion and cracking in metal alloys studied, using rotating disk in water [ASME PAPER 66-FE-11] 17 p2915 A66-3326

Fluid dynamic characteristics of propeller pumps in presence of oscillatory cavitation, noting performance of J-2 rocket engine system [AIAA PAPER 66-559] 18 p3246 A66-3446

Cavitation behavior of Herschel-type venturi tube, noting constant flow for varying venturi profile 18 p3114 A66-3464

Optimum fully cavitating hydrofoils having analytic profiles at zero cavitation number investigated by Levi-Civita method 19 p3342 A66-3642

Cavitation flow of water and ethyl alcohol in venturi tube, noting effect of varying vapor concentration and thermodynamic properties 20 p3544 A66-3692

Munroe jet formation when small cavity of bubble in liquid is subjected to impact of shock 20 p3546 A66-3780

Hydrodynamic implosion mechanism and impact of liquid jets formed by collapsing cavitation bubbles, examining damage to solid boundaries 20 p3547 A66-3783

Frequency of wake shedding from circular cylinder in water flow with values above critical Reynolds number, noting eddy generation and drag coefficient dependence on cavitation number 20 p3548 A66-3803

Cavitational flow past curvilinear airfoil constructed according to Ryabushinski scheme 20 p3548 A66-3817

Approximation method for wall effect in cavitation flow around bodies in water tunnel, examining effect of solid boundary on resistance factor 23 p4056 A66-4172

Intensity and scale effect of cavitation damage investigated by closed circuit hydrodynamic test devices 23 p4057 A66-4188

**CAVITY**

**SA CHAPMAN-FERRARO CAVITY**

Torsion problem of nonhomogeneous infinite circular cylinder with symmetrical located spherical cavity 03 p0442 A66-1330

Cyclotron radius, magnetospheric boundary and Debye length scaling parameters for magnetospheric cavity arising from solid wind-induced geomagnetic storm and visibility of quasi-Van Allen belts 14 p2269 A66-2712

Bistable flow in hemispherical cavity induced by external stream, noting skew position 14 p2274 A66-2743

Convective heat transfer in centrifugal force field of cavity between two rotating disks in turbulent gas flow 14 p2375 A66-2769

Three-dimensional photoelasticity calculation of stresses in spheres with concentric spherical cavities under diametral compression 14 p2401 A66-2776

Stress concentration near circular cavity in nonlinearly deformable material 15 p2608 A66-2878

Local emissivity of vertex point of diffusional or V-groove cavity, noting dependence on wall material, angle factor



and agreement with theoretical solution 17 p3035 A66-32613

Elastic stress field due to spherical inclusion or cavity in infinite exterior region, deriving potential energy dependent on strains, noting skin effects and stress concentration factor 19 p3474 A66-36427

Numerical extrapolation solution of kernel-characterized integral equations for apparent emissivity of conical and cylindrical cavities 20 p3681 A66-38298

Griffith type crack propagation due to localized thermal stress at holes, cavities, penny-shaped cracks and inclusions disturbing uniform heat flow 23 p4146 A66-41993

Shape and motion of cavities in steady planar supercavitating flows, noting transverse gravity field effect on Helmholtz flow past forebody experiencing drag alone 23 p4062 A66-42059

Dual transverse electric mode cavity preselector loaded with large nonferrous metallic perturbation plug 24 p4179 A66-42102

**CAVITY RESONANCE**

**SA RESONANT CAVITY**

Beat frequencies and coherence properties in circularly polarized atomic transitions of gaseous lasers with axial magnetic fields 07 p1046 A66-18429

Beat frequency and rotation of polarization plane in He-Ne laser with axial magnetic field 07 p1046 A66-18430

Thin conducting susceptances in circular TE-11 and TM-01 waveguides measured by cavity-resonance method 08 p1198 A66-19750

Simplified measurement of Q of microwave transmission cavities 12 p1816 A66-24148

Asymptotic solution to motion of solid containing cylindrical or spherical cavities filled with viscous liquid 12 p1863 A66-24356

Small oscillations of pendulum with spherical cavity filled with viscous incompressible liquid 12 p1882 A66-24357

Frequency sweep method of measuring relaxation times and determining Q value in high Q superconducting cavities 14 p2258 A66-27955

Aerodynamically induced resonance in rectangular cavities resulting from doubly tuned amplification of shear layer unsteadiness by shear layer edge tone and cavity enclosure 18 p3047 A66-33676

Electromagnetic cavity resonances in rotating systems investigated through covariant space-time formulation of classical electromagnetic field theory 18 p3119 A66-34451

Laser mirror transducer decoupling from mechanical resonances of laser cavity 19 p3374 A66-35813

Microwave cavity resonant frequency sampler for direct oscilloscope-photographic recording of electron density, recombination and diffusion time in decaying plasma 21 p3740 A66-39389

**CAVITY RESONATOR**

General mode structure and eigenvalues of cavities containing ferrite magnetized in axial direction 01 p0027 A66-10547

Fabry-Perot resonators compared with cavity resonators and microwave interferometers for plasma diagnostics, noting electron density application 03 p0398 A66-12525

Intensity distribution in Fabry-Perot interferometer producing resonant waves for large Fresnel number applied in model for filament-form laser mechanism 03 p0379 A66-13097

High power microwave filters discussing dominant mode and harmonic filters, design, parameters, application and limitation 04 p0493 A66-13677

Mode selective characteristics of plane-parallel dielectric plate as reflector for ruby laser resonator 04 p0533 A66-14330

Rectangular waveguide filter with trapped mode resonators, describing operation, energy handling characteristics and application 06 p0845 A66-16086

Resonant endfire antennas formed by open cavity with radiating elements coupled to cavity field 06 p0853 A66-16657

Electromagnetic propagation in rotating systems, classic analysis of mode-splitting phenomena caused by rotation of cavity

resonator 11 p1658 A66-23266

Instrumentation for measurement of short-term frequency stability of microwave sources 12 p1816 A66-24134

Stripline cavity resonator for low microwave frequency measurements of magnetic and dielectric properties of ferrites 12 p1881 A66-24156

Resonator cavity measurement of microwave Faraday effect in low resistivity semiconductors 14 p2349 A66-26799

Spurious X-band output signals observed during interaction of dual reflex klystron cavities and klystron beams 14 p2258 A66-27956

Stability conditions of two-photon processes, analyzing combination and double radiation by matter placed in resonator cavity 17 p2874 A66-32242

Cavity natural resonant frequencies in cylindrically stratified magnetoplasma examined by exact harmonic series solution 18 p3072 A66-34566

Faraday rotation obtained with pulsed high-field magnets for controlling laser cavities 19 p3372 A66-35380

Theory of steady multimode oscillation of solid state laser extended to cavities with inefficient end mirrors or losses dependent on frequency 23 p4077 A66-41274

Transient ionization levels of hypersonic velocity projectile wakes measured by open microwave resonators phase shift observation 24 p4209 A66-42194

Transmission resonant cavity measurements of electron line densities and collision frequencies in ionized wakes of hypervelocity projectiles 24 p4191 A66-42195

Electron number densities measured behind shock wave in pressure driven shock tube by microwave resonant cavity technique and by electrostatic quasi-Langmuir probe 24 p4191 A66-42197

**CELESCOPE PROJECT**

Tradeoff for high reliability program, discussing development of satellite equipment for Celestscope project 15 p2507 A66-28796

**CELESTIAL BODY**

Sovereignty with respect to outer space especially celestial bodies and space stations, noting international law for free exploration, navigation, etc 03 p0447 A66-13075

Codification to determine international law of celestial bodies resulted in formulation of general principles 03 p0448 A66-13079

Iterative determination of space flight trajectory and velocity represented as sum of Kepler motions about celestial bodies 18 p3234 A66-34635

Space law in planetary explorations 19 p3482 A66-36211

Legal status of Moon and celestial bodies 19 p3483 A66-36213

Celestial bodies nature and structure effect on space flights, detailing interplanetary space properties and orbital motion 24 p4280 A66-43131

**CELESTIAL GEODESY**

Cosmic triangulation systems assessing polar method for determining geodetic satellite coordinates and inherent error estimation and correction 03 p0361 A66-12502

Effect of Moon phase and celestial latitude on lunar modulation of geomagnetic activity 10 p1529 A66-21157

Directional accuracy of chords and angles in geocentric equatorial coordinate system in stellar triangulation 12 p1867 A66-23515

Error analysis for statorscope or radar altimeter phototriangulation readings and radio geodetic coordinate photography phototriangulation 12 p1867 A66-23517

Absolute direction in space and control of stellar triangulation equations 12 p1875 A66-24874

Electronic trispheration, three-dimensional analog of triangulation, for long distance geodetic surveys 12 p1875 A66-24936

Directional accuracy of chords and angles in geocentric equatorial coordinate system in stellar triangulation 21 p3732 A66-38659

Error analysis for statorscope or radar altimeter phototriangulation readings and radio geodetic coordinate photography phototriangulation 21 p3732 A66-38661

Glossary of gravimetric and celestial

geodesy 23 p4063 A66-41525

**CELESTIAL MECHANICS**

**SA ASTRODYNAMICS**

**SA PERTURBATION THEORY**

Finite collision time for artificial celestial body moving under influence of Newtonian force from attractive center 01 p0137 A66-10794

Classification of all nonplanar motions in problem of two fixed gravitation centers of arbitrary masses corresponding to real potential 02 p0292 A66-12234

Terrestrial gravitational potential determined by observation of satellite motion, assuming trajectory is determined solely by force field 03 p0428 A66-13027

Textbook on celestial mechanics, meridian astronomy, instrumentation, solar research and astrophysics 05 p0760 A66-15087

Solution of extremal problems of celestial mechanics 05 p0764 A66-15318

Equilibrium shape of Moon, assuming homogeneity computing mean rotation configuration and pertinent single parameter equilibrium shapes 07 p1133 A66-17304

Resonance cases and small divisors in third integral of motion used to calculate galactic orbits on plane of symmetry of nonaxisymmetric galaxy 08 p1296 A66-19353

Trajectory analysis and Birkhoff rings in restricted three-body problem in three-dimensional coordinate system 09 p1453 A66-20251

Book on celestial mechanics considering Laplace-Newcombe method, Hill planet and lunar methods, periodic orbits methods, etc, using differential equations 09 p1459 A66-20916

Book on mathematics underlying celestial mechanics, including central force problem, n-body problem, Hamilton-Jacobi and perturbation theories 11 p1776 A66-23202

Hamiltonian mechanics applied to planetary and artificial satellite motion problems 12 p1950 A66-24402

Numerical methods of celestial mechanics and Airy method computation of trigonometric series with numerical coefficients 12 p1950 A66-24403

Inclined periodic solutions of restricted three-body problem in form of orbit parameters 13 p2185 A66-25809

Soviet monograph on celestial mechanics of satellites and space probes covering trajectory problems, two-and three-body systems, space flight duration between two points, etc 13 p2188 A66-26465

Book on satellite orbital flight trajectory theory and celestial mechanics 15 p2595 A66-29128

Analytical mechanics, motion stability, celestial ballistics - All-Union Conference, Moscow, January-February 1964 15 p2538 A66-29144

Poincare-von Ziepel procedure in celestial mechanics applied to satellite motion about oblate Earth 16 p2796 A66-30263

Lagrange theorem extended for solution of three-body problem to regular configurations of more than three particles 16 p2804 A66-31393

Mars spacecraft guidance and navigation requirements, noting entry trajectory, possible guidance errors and gravitational constant uncertainty [AIAA PAPER 66-532] 16 p2744 A66-31501

Celestial mechanics covering two-body problem, planetary and asteroid theory, interplanetary trajectories, lunar probe, spherical harmonics, etc 17 p2997 A66-32019

Satellite orbit stability discussing proof of Haseltine formal stability theorem, doubly periodic expansions, satellite motion around oblate curve, etc 17 p2999 A66-32065

K-orthogonality for inversion of state transition matrices 17 p2946 A66-32482

Perturbation theories for equations of celestial mechanics, obtaining analytical solutions in terms of Chebyshev polynomial series [AIAA PAPER 66-534] 18 p3226 A66-33664

Dynamical system of two degrees of freedom, with application to restricted problem and lunar theory 18 p3234 A66-34654

Book on methods in astrodynamics and celestial mechanics including libration points, satellite motion, orbit determination, optimization, optimal control,



- etc 19 p3460 A66-35887  
Theory and application of motion associated with equilibrium configurations of dynamical systems applied to astronomy and space dynamics 19 p3461 A66-35888  
Effect of Sun perturbations on motion near Earth-Moon equilateral libration points [AIAA PAPER 65-683] 19 p3461 A66-35890  
Libration point motion in restricted four-body problem and stable trajectory determination for Earth-Moon-Sun system, noting effect of initial configurations of system [AIAA PAPER 65-684] 19 p3461 A66-35891  
Restricted three-body problem in plane, with two equal masses and nonperiodic orbits 20 p3653 A66-37798  
Critical values of satellite orbit inclinations accounting for effects of first-order perturbations and mean anomaly 20 p3654 A66-37853  
Coplanar orbit transfers by tangential impulses at apse point in graphical presentation of solutions 20 p3657 A66-38176  
Difference assessment between secular and long period perturbations generated by similar initial conditions for celestial mechanics problems 22 p3985 A66-40959  
Spin-orbit coupling in solar system, examining resonant spin rates for one-and two-body planet/ satellite systems with eccentric orbits 24 p4272 A66-42203
- CELESTIAL NAVIGATION**  
Recognition procedure identifying given star constellation despite erroneous scanning, for application in celestial navigation 01 p0102 A66-10619  
Star pattern recognition system for spacecraft attitude control [AIAA PAPER 64-652] 03 p0390 A66-12755  
Remote extraterrestrial surface navigation, discussing image-tube based stellar field acquisition system 04 p0543 A66-13590  
Complex and hand-held instrumental devices for celestial navigation, noting Apollo scanner and sextant assembly 04 p0521 A66-14024  
Minimum field of view required for rapid accurate navigation star identification-acquisition established between 25 and 30 degrees 06 p0906 A66-16247  
Two automatic astronomical navigation and tracking systems compared for accuracy and performance in civil aircraft 07 p1070 A66-17722  
Astronavigation applied to piston aircraft and supersonic jets, advantages and shortcomings 07 p1076 A66-17797  
Manual control sextant sighting performance for space navigation, using simulated and real celestial targets 10 p1554 A66-21894  
Electro-optical celestial guidance system with miniaturized computer and scanning sensor 12 p1909 A66-24104  
Recognition procedure identifying given star constellation despite erroneous scanning, for application in celestial navigation 13 p2123 A66-25179  
Electro-optical automatic celestial guidance system for spacecraft and satellites 13 p2124 A66-25643  
Automatic instrumentation for celestial sightline tracking of spacecraft 18 p3132 A66-33871  
Autonomous celestial and selenocentric spacecraft navigation and orbit prediction without using ground tracking stations 20 p3598 A66-38253
- CELESTIAL OBSERVATION**  
Modulation type radiometer with input parametric converter used for observation of weak radiation from Moon, Jupiter and other celestial sources 04 p0520 A66-13883  
Comet Ikeya-Seki /1965f/ discussing visual, telescopic and spectral observation 04 p0578 A66-14022  
Meridian astronomy methods including determination of instrumental errors, derivation of systems of right ascensions and declinations and determining systematic errors 05 p0761 A66-15089  
Spectroscopic observations of Sun-grazing Ikeya-Seki Comet /1965f/ at minimum possible heliocentric distance 05 p0761 A66-15100  
Disappearance of Saturn rings every 15 years due to profile view, thinness and lack of self-luminosity 07 p1136 A66-17813  
Sky observations with balloon-borne X-ray telescope having sodium iodine scintillator 09 p1442 A66-20466  
Astronomical observations from space vehicles - International Astronomical Union Symposium, Liege, Belgium, August 1964 10 p1596 A66-21078  
Possible atmosphere detection on J-II and J-III satellites revealed by excess brightness on eclipse reappearance 10 p1604 A66-21202  
Planetary nebulas noting observational problems, parallax, proper motion, distance, etc 11 p1767 A66-22260  
Two-year study of solar seeing conditions with recording monitor near Sydney, Australia indicates average of 23 sec per hour of observation 11 p1768 A66-22365  
Halley comet motion during return of 1910, obtaining orbits via differential correction procedures, including perturbation by all planets but Pluto 11 p1769 A66-22531  
Annual astronomical almanac compiled by Madrid Observatory 11 p1770 A66-22638  
Comet observations in IQSY 11 p1771 A66-22768  
Astronomical and orbital data of comet Ikeya-Seki noting elements for parabolic orbit, elliptical orbit, etc 13 p2188 A66-26319  
Daylight observations of 1965 f comet, noting influence on solar corona, spectra at various wavelengths, polarization data and results of photoelectric scans 15 p2592 A66-28645  
Modulation type radiometer with input parametric converter used for observation of weak radiation from Moon, Jupiter and other celestial sources 15 p2503 A66-29695  
Streaking fireball of January 14, 1965, analyzing position, motion and brightness 15 p2601 A66-29939  
Comet Ikeya-Seki near perihelion passage 16 p2694 A66-30657  
Aircraft as platform for solar eclipse observation, discussing history, project APEQS, navigation problems, aircraft used, etc 16 p2705 A66-30822  
Aircraft stabilization for solar eclipse observation, emphasizing use of autopilot for maximum control 16 p2743 A66-30823  
Photographs from observatories of comet Ikeya-Seki discovered in constellation Hydra 16 p2804 A66-31309  
Sunspot cycles from 1954 to 1964, considering difference in activity observed in Northern and Southern Hemispheres 16 p2804 A66-31311  
Photographic observations of minor planets at Sydney during 1964 17 p3003 A66-32822  
Telescopic and photographic observation of cometary structure, particularly coma region 17 p3010 A66-33377  
Weak comets in vicinity of Sun during solar eclipse 17 p3010 A66-33382  
Empirical decision-making techniques, determining nature of quasi-stellar source or galaxy 18 p3234 A66-34616  
Sidereal anisotropy indicated for charged galactic cosmic radiation obtained by celestial scanning, using narrow angle muon telescope 21 p3808 A66-38466  
Evidence for natural ephemeral Earth satellite including latitude and longitude, date, time, azimuth and elevation of observations 22 p3978 A66-40005  
Bottom-moored sonar beacons surveyed in absolute position coordinates, noting transmitter-receiver and celestially augmented inertial navigator and error minimization techniques 22 p3945 A66-40323  
Astronaut observation in Gemini and Mercury space flights that stars cannot be seen in daytime, noting first-magnitude stars and background illumination 22 p3982 A66-40523  
Venus phase simulator experiment indicating anomaly due to observer 23 p4128 A66-41208  
Orbit determination for comet 1965 F Seki-Ikeya, projecting collision with Sun at perihelion 23 p4129 A66-41573  
Tables of observational statistics on comets, minor planets and natural satellites 24 p4273 A66-42205  
Zodiacal light, airglow and falling atmospheric dust measurements and observations in terms of solar orbiting small diameter particle clouds 24 p4276 A66-42666  
Stellar extinction measurements made in Gemini IX flight, determining existence and location of Link layer from airglow study 24 p4280 A66-43026  
Interplanetary space and celestial observations from ground stations, satellite and space rockets 24 p4280 A66-43131
- CELESTIAL SPHERE**  
Cosmic ray distribution intensity over celestial sphere determined, detecting anisotropy against background of isotropic variations, using spherical analysis 09 p1439 A66-20222  
Night sky and zodiacal light polarization near 5000 angstroms over celestial sphere noting dependence of zodiacal light distribution on angular distance from sun 16 p2698 A66-31252  
Book on spherical astronomy including celestial coordinate systems, parallax, diurnal motion, precession and nutation, time measurement, etc 16 p2806 A66-31732
- CELL**  
S BIOLOGICAL CELL  
S ELECTRIC CELL  
S ELECTROCHEMICAL CELL  
S FUEL CELL  
S GALVANIC CELL  
S GAS CELL  
S HEXAGONAL CELL  
S KERR CELL  
S KNUDSEN CELL  
S PARTICLE IN CELL TECHNIQUE  
S PHOTOCONDUCTIVE CELL  
S PHOTOELECTRIC CELL  
S PHOTOVOLTAIC CELL  
S SOLAR CELL
- CELL DIVISION**  
SA MITOSIS  
Mitotic phases of Tradescantia paludosa microspores as affected by spaceflight factors of Voskhod I 10 p1486 A66-21981  
Text on evolution, interpreting function of body organs in terms of chemical processes and tracing development of complex organic molecules 10 p1487 A66-22066  
Response of tissue culture cells to low magnetic fields, noting no quantitative growth differences 12 p1807 A66-25013  
Maximum photosynthetic capacity for Chlorella determined experimentally from cell reproduction rates 15 p2440 A66-29502  
Magnetic effects on reproduction and metabolism of normal and diseased mammalian cells in vivo and in vitro 17 p2859 A66-32222
- CELLULOSE**  
SA NITROCELLULOSE  
SA WOOD  
Antibody globulin coupled to diazotized aminoaryl derivative of carboxymethyl cellulose to form immunoadsorbent for extracting antigens 12 p1805 A66-23566  
Cellulose and derivatives and coupling with biochemical substances 16 p2646 A66-31151
- CEMS SYSTEM**  
SA AIRCRAFT MAINTENANCE  
Manned aircraft self-contained checkout and fault isolation systems, discussing characteristics and operational concept [ISA PREPRINT 1.3-3-65] 05 p0684 A66-15511
- CENTAUR LAUNCH VEHICLE**  
SA ATLAS CENTAUR LAUNCH VEHICLE  
Test program for thermal-vacuum testing of Centaur vehicle components 16 p2808 A66-30481
- CENTAUR PROJECT**  
Centaur project with assessment of reliability of explosive one-shot devices 14 p2394 A66-28444
- CENTRAL ELECTRONIC MANAGEMENT SYSTEM /CEMS/**  
S CEMS SYSTEM
- CENTRAL NERVOUS SYSTEM**  
SA AUTONOMIC NERVOUS SYSTEM  
Human stress reactions to three-day march, sleep deprivation, food and oxygen starvation, noting changes in central nervous system functions 04 p0467 A66-14086  
Anoxia effect on central nervous system in forms of personality, vision and consciousness impairment 10 p1489 A66-22114  
Electrophysiological study of responses of central nervous system on action of some factors of space flight 11 p1642 A66-22487



Physiological study and instrumentation of pigtail Macaque under extended exposure to near-zero gravity environment 13 p2014 A66-25514

Residual pathologic changes in central nervous system of dog following rapid decompression to 1 mm Hg 19 p3286 A66-36381

Soviet papers on effect of space flight factors on functions of central nervous system 23 p4025 A66-41334

Peculiarities in effects of ionizing radiation on space vehicle crew and on functioning of central nervous system 23 p4026 A66-41335

Vibration stimulus effect on oxygen metabolism of brain in rats with partial destruction of auditory and vestibular apparatus and in anesthetized control rats 23 p4027 A66-41341

Vibration effect on conditioned reflexes, oxidation mechanism and electric activity of brain in rats 23 p4027 A66-41342

**CENTRAL NERVOUS SYSTEM DEPRESSANT**

S MEPROBAMATE

S PENTOBARBITAL SODIUM

**CENTRAL NERVOUS SYSTEM STIMULANT**

S EPINEPHRINE

S NOREPINEPHRINE

S STRYCHNINE

**CENTRIFUGAL COMPRESSOR**

Flow field in centrifugal compressor impeller [ASME PAPER 65-WA/GTP-7] 05 p0608 A66-15722

Boundary layer influence on performance of centrifugal-compressor impellers, measuring discharge velocity profile [ASME PAPER 65-WA/FE-7] 05 p0609 A66-15728

Boundary layer influence on performance of centrifugal-compressor impellers, measuring discharge velocity profile [ASME PAPER 65-WA/FE-7] 12 p1799 A66-24538

Shaft sealing systems on centrifugal compressors, noting labyrinth, restrictive ring shaft, liquid film and mechanical and special seals [ASME PAPER 66-MD-42] 21 p3742 A66-38490

**CENTRIFUGAL FORCE**

Stresses calculated in centrifugal impeller with cover disk by two-dimensional stress analysis and digital computer program [ASME PAPER 65-WA/FE-17] 05 p0780 A66-15701

Fatigue testing of structure, using machines producing loads by centrifugal forces 06 p0965 A66-16488

MHD plasma accelerator with circular autostable path where centrifugal force is balanced by spontaneous centripetal MHD force 09 p1410 A66-20985

Equations for translatory motion of lifting body moving at hypersonic speed, considering Earth sphericity, noting effect of centrifugal forces 13 p2193 A66-26448

Rotary deployment and stabilization mechanisms for solar collectors [AIAA PAPER 64-732] 13 p2005 A66-26631

Concentration profile of heavy species for binary fluid mixture under body force from uniformly mixed upstream condition, considering inviscid hydrodynamical model 18 p3103 A66-34925

**CENTRIFUGAL PUMP**

Liquid-metal heat transport fluid circulation, discussing molten lithium pump development and testing for high performance mobile nuclear plants [ASME PAPER 65-WA/FE-18] 05 p0689 A66-15611

Canned motor pump for nitrogen tetroxide or hazardous liquids, noting ball bearings, chemical materials, balancing drum and helium leak tested motor parts [ASME PAPER 65-WA/FE-3] 05 p0691 A66-15715

Hydraulic performance and sensitivity of various configurations of centrifugal pumps to tip clearance effects [ASME PAPER 64-WA/FE-17] 06 p0884 A66-16211

Jet pump cavitation correlation by similarity parameter 07 p1025 A66-18171

Liquid-metal heat transport fluid circulation, discussing molten lithium pump

development and testing for high performance mobile nuclear plants [ASME PAPER 65-WA/FE-18] 10 p1539 A66-21502

Cermet face seals for inert gas environment sealing shaft of liquid-metal pumps employing conventional lubrication system [ASLE PREPRINT 65AM 4C4] 10 p1540 A66-22039

Three-dimensional flow visualization approach to complex flow characteristics in centrifugal impeller [ASME PAPER 66-GT-83] 14 p2274 A66-26989

Geometrically different volutes effect on impeller of centrifugal pump performance, discussing radial thrust, head and runout capacity [ASME PAPER 66-FE-14] 17 p2932 A66-33268

Centrifugal pump for liquid metal power-transmission in flight control systems [ASME PAPER 66-FE-20] 17 p2932 A66-33273

Natural convective heat transfer to gas turbine rotor blade and thermal resistance of cooling system using centrifugal pump 20 p3627 A66-36926

**CENTRIFUGAL STRAIN**

Anatomical studies in dog anesthetized with pentobarbital and chlorpromazine and subjected to repeated prolonged positive G 03 p0327 A66-12362

Protein synthesis in liver of adrenalectomized and hypophysectomized rats exposed to centrifugation stress 13 p2010 A66-25899

**CENTRIFUGE**

**SA HUMAN CENTRIFUGE**

Acceleration effect on food reinforced DRL and FR schedules 03 p0325 A66-13175

Harmful oscillation elimination from high rpm gyroscopic centrifuge by introducing one elastic bearing into dynamic system 08 p1307 A66-18877

Biophysical property similarities of several human enteroviruses as shown by density gradient ultracentrifugation of virus mixtures 13 p2009 A66-25872

Tables for evaluation of Faxen approximation to solution of Lamm equation 14 p2320 A66-27115

Aerospace medical advances in Polish military aviation and pilot testing procedures and equipment, particularly low pressure chamber and centrifuge 14 p2271 A66-28365

Structural mounting of large diameter cylindrical missile section in centrifuge for high acceleration environmental testing 16 p2677 A66-30458

Fast rise programmed centrifuge, noting acceleration testing capabilities, power speed control, etc 16 p2679 A66-30473

Centrifuge performance, noting angular velocity constancy vibration levels in terms of acceleration, temperature effects, etc 16 p2679 A66-30476

Consequences of heart-to-foot acceleration gradients on tolerance to positive acceleration determined on variable radius centrifuge 19 p3285 A66-36373

Twofold transversely applied 8-g centrifuging effect on functional state of otolithic part of vestibular apparatus of guinea pigs 23 p4026 A66-41337

**CENTRIPETAL FORCE**

MHD plasma accelerator with circular autostable path where centrifugal force is balanced by spontaneous centripetal MHD force 09 p1410 A66-20985

Degree of partiality effect on centripetal turbine operation 23 p4122 A66-41799

**CENTURION AIRCRAFT**

S CESSNA 210 AIRCRAFT

**CEPHEID**

Second postulate of special theory of relativity proved by existence of short period Cepheids 05 p0759 A66-14888

Computation method used in pulsation of Lyrae models extended to models of Cepheid variables, noting instability of appropriate period, mass size, luminosity and velocity curves 20 p3650 A66-37339

Pulsation in cepheid instability strip in H-R diagram, giving equations for spherically symmetric motion 21 p3816 A66-39489

**CERAMIC BONDING**

Insulating materials, discussing impregnated refractory ceramic foams for

high energy hybrid motors 06 p0899 A66-16293

Hybrid circuit rejects avoided by using ceramic channels and ultrasonic bonders during assembly of active semiconductor devices and integrated circuits to thin film network 10 p1512 A66-21759

Metal-ceramic boundary structures and reactions, considering metal-oxide and metal-glass interfaces, ionic and covalent bonds, oxidation, reduction, solution and precipitation 13 p2108 A66-25767

Ceramic structural design, discussing laboratory specimen design, brittle material strength, boundary conditions, statistical parameters, etc 18 p3125 A66-33733

Strength of ceramic specimens with parallel cylindrical holes, noting strength/weight characteristics during compression loading 21 p3753 A66-38677

Adhesive and bonding techniques evolution for general and specific use in aircraft and aerospace industry, noting elastomeric and ceramic adhesives 22 p3928 A66-40418

Thermocompression bonding, discussing aluminum wire connection to substrate material via eyelet bond 23 p4044 A66-41197

**CERAMIC COATING**

Heat resistant ceramic coating on steel produced by gas-flame spraying of refractory oxides investigated for effective heat conductivity and integral radiative capacity 03 p0443 A66-12514

IR radiation of refractory solids with radiation properties of flame-sprayed ceramic coatings, determining normal spectral emittance, integrated normal total emittance and IR intensity curves at 1300 K 03 p0386 A66-13100

Oxidation-resistant ceramic coatings for tungsten, tantalum, molybdenum and niobium 07 p1051 A66-18300

Continuous hot pressing apparatus design, operation, production economy and results with oxidic materials and metals 16 p2709 A66-30255

**CERAMICS**

**SA CERMET**

Design and fabrication techniques for high voltage impulse generation by conversion of mechanical to electrical energy, using piezoelectric ceramics 01 p0016 A66-10916

Powdered or densified nonconductive ceramic materials analyzed by spark source mass spectrography based on use of conducting probe 02 p0188 A66-11294

Ceramics technology noting properties, high temperature and corrosion resistance, brittleness, comparison with metals, etc 02 p0248 A66-11741

Nucerite, ceramic-metal composite with high mechanical strength and abrasion resistance noting crystal structure, application, properties, etc 02 p0244 A66-11742

Piezoelectric crystals and ceramics properties that affect application in electroacoustic transducers 03 p0408 A66-12408

Heat transfer through porous ceramics and thermally degraded ablation material, discussing conductivity [ASME PAPER 65-HT-46] 05 p0785 A66-14756

Metal fiber reinforced ceramics 05 p0705 A66-14817

Radiation damage to crystalline lattices by energetic particles, discussing consequences on physical behavior of solids, particularly ceramics 05 p0738 A66-15471

Thermodynamic calculations and experimental measurements to illustrate material properties pertinent to ablation process and to suggest refractory compounds as ablating materials 05 p0706 A66-15472

Electromechanical hysteresis and relaxation effects in piezoelectric ceramics 06 p0927 A66-16722

Polarization and volt-ampere characteristics of ferroelectrics simultaneously under static and alternating fields 06 p0854 A66-16726

Papers on ceramics emphasizing relationship between microstructure, fabrication techniques and properties, including review of aerospace technological applications 07 p1050 A66-18293

Relation between fabrication, microstructure and properties of solid



ceramics 07 p1051 A66-18294  
Oxide ceramics fabrication, with particular attention to microstructure 07 p1053 A66-18296  
Composite ceramic systems consisting of metallic or organic phase and ceramic phases, microstructure, mechanical strength and thermal expansion 07 p1051 A66-18299  
Refractory materials properties used in nuclear fuel element 07 p1079 A66-18302  
Effect of space environment on ceramic materials, considering atmosphere (including vacuum/), thermal, radiation and meteoroid environments 07 p1147 A66-18307  
Text on modern ceramics, principles and concepts 07 p1054 A66-18495  
Ductility in polycrystalline single phase ceramics, noting behavior at room and high temperature of single crystal structure, dislocation, etc 07 p1054 A66-18498  
Brittle fracture in ceramic materials, noting Griffith theory on crack propagation, plastic deformation occurrence, stress distribution effect, etc 07 p1054 A66-18499  
Interrelationship among fabrication procedures, microstructure and properties of ceramic materials, noting dependencies on porosity, grain size, temperature, pressure, etc 07 p1054 A66-18500  
Structural design with ceramic materials, using prestraining and prestressing for improved tensile and impact strength and stiffness 07 p1054 A66-18501  
Casting of plastic-ceramic dies 08 p1229 A66-18687  
Construction of hot forming tool made of fused silica ceramic 08 p1229 A66-18691  
Liquid titanium reaction with nonmetallic refractory ceramics, Ti melting behavior and electron-probe microstructural analysis 08 p1236 A66-18759  
Temperature and bias characteristics of ceramics of Pb/Zr-Ti-O-3 and its families, using schematic model on reorientations of 180 and 90 degree domains 08 p1243 A66-19061  
Ceramic and graphite fibers and whiskers, Air Force sponsored monograph 09 p1392 A66-20475  
Silicone alumina low temperature low-pressure plastic molding technique for precision forming of ceramic materials for aerospace structural application 10 p1538 A66-21130  
Evaluations for multiaxial-stress properties of ceramic materials including elastic and plastic strength, stiffness, ductility, resilience, etc 12 p1958 A66-23631  
Explosive compaction of ceramic materials 12 p1900 A66-24720  
CERCOR glass-ceramic axial flow rotary regenerator as inexpensive component for gas turbine regeneration [ASME PAPER 66-GT/107] 14 p2301 A66-27004  
Stannic oxide ceramic formation and dielectric constant and resistivity measurements and evaluations 14 p2362 A66-27499  
Superconductivity in ceramic mixed titanates 16 p2770 A66-30180  
Special ceramics - Symposium, British Ceramic Research Association, Stoke-on-Trent, U.K., July 1964 16 p2728 A66-30244  
Preparation and mechanical properties of spinel, discussing microstructure, transverse and compressive strength and Young's modulus 16 p2730 A66-30251  
Ceramic materials selection for principal high temperature components of gas turbines 16 p2790 A66-30256  
Rupture strength increase in tungsten and molybdenum chopped wires silicide coated by pack diffusion and incorporated in mullite matrix by vacuum hot pressing [ACS PAPER 7-C-65F] 16 p2723 A66-30949  
High temperature compressive deformation equipment for ceramic materials noting loading, alignment and stress-strain measurement 16 p2682 A66-30950  
Behavior of ceramic insulating materials under nonisothermal conditions at high temperatures 16 p2731 A66-31605  
Absorption spectra modification in silica ceramics after gamma irradiation from Co-60 19 p3388 A66-35463  
Scale model of submerged VLF antenna using lossy ceramic powder to model ice

and snow for submarine communication, geophysics, etc 19 p3321 A66-36416  
Optimum fabrication of microelectronic devices by interconnection of integrated circuits on ceramic substrates 19 p3323 A66-36820  
Honeycomb structure, examining assembly, skin delamination at spars or terminal fitting, glasscloth radome and inspection techniques 20 p3671 A66-37827  
Mechanical properties of metallic and ceramic fibers in metallic matrices and refractory fibers in ceramic matrices 21 p3751 A66-39231  
Ceramic fiber reinforcement of steel, aluminum, nickel and titanium alloys 21 p3752 A66-39242  
Mechanical-type filters used in electronic circuits including quartz filters, piezoelectric materials, metallic resonators, ceramic converters, torsion resonators and miniaturized filters 21 p3717 A66-39628  
Velocity of sound vibration in partially plated piezoelectric ceramics differs in plated region and unplated region due to piezoelectric effect 22 p3877 A66-40186  
Fired circuitry application to ceramic substrates by thick film process and use of thin films on ceramic and glass substrates by vapor deposition 23 p4043 A66-41126  
Fuel cells with ceramic electrolyte operating at high temperatures, calculating voltage and efficiency 24 p4161 A66-42503  
**CEREBRAL CORTEX**  
Responses of neuronal elements in visual cortex of unanesthetized cats shown to depend on time interval length 12 p1806 A66-24232  
Perceptual masking and enhancements of two flashes in evoked cortical potentials recorded by electroencephalography 23 p4029 A66-41549  
Internal carotid artery insufficiency in neuro-ophthalmic and aeromedical implications, noting ophthalmodynamometry in flight qualification 24 p4164 A66-42457  
Neuronal spike populations and EEG activity in chronic unrestrained cats, noting multiple unit responses of acceleration/inhibition during behavioral conditioning procedures 24 p4169 A66-43098  
**CEREBRUM**  
Electric impedance measurements in hippocampus, amygdala and midbrain reticular formation during altering, orienting and discriminative responses in cat 24 p4166 A66-43167  
**CERENKOV COUNTER**  
Balloon-borne scintillation counters combined with Cerenkov counter for measuring primary cosmic ray charge and energy spectra during 1963 07 p1123 A66-17994  
Cerenkov counter measurement of nuclear component of cosmic rays onboard Elektron II satellite as function of solar activity during IQSY 10 p1595 A66-21043  
Spark chamber with vidicon readout for balloon-and satellite-borne high energy gamma ray astronomy analysis, noting Cerenkov counter 12 p1877 A66-23685  
Operation of scintillation and Cerenkov counters used for recording cosmic radiation, noting design, amplitude properties, collection of scintillating light from phosphor, etc 12 p1882 A66-24185  
Cosmic ray anisotropy and gamma rays in Orion analyzed, using Geiger counter and Cerenkov telescope 15 p2579 A66-29525  
High energy mountain-altitude nuclear interactions produced by pions and nucleons, pion/proton and neutral/charged interacting particle ratios studied, using multiplate cloud chamber with air Cerenkov counter and absorption spectrometer 15 p2584 A66-29554  
High altitude cosmic ray measurements by Cerenkov scintillator counter system near solar minimum 17 p2994 A66-33147  
Balloon-borne Cerenkov scintillation counter for measurements of primary proton and helium spectra and modulations 18 p3188 A66-34822  
Balloon flight data obtained at 50 and 65 degrees N geomagnetic latitude on spectra of primary cosmic ray hydrogen and helium nuclei, using Cerenkov scintillator technique 18 p3190 A66-34831

Balloon-borne Cerenkov scintillation counter measurements of energy spectra of primary cosmic radiation heavy nuclei at various geomagnetic latitudes 18 p3191 A66-34840  
Cerenkov counter using sulfur hexafluoride gas as radiator developed for study of isotopic composition of helium nuclei in primary cosmic radiation 18 p3193 A66-34853  
Cerenkov counter measurements of primary cosmic ray heavy nuclei made by Elektron II satellite 18 p3199 A66-34886  
Anisotropy of muon-rich extensive air showers examined by observation, using large area air Cerenkov detector at 60 degrees zenith angle 18 p3205 A66-35095  
Transition region of pulse spectrum from EAS particle density recordings by Cerenkov and scintillation detectors 18 p3207 A66-35110  
Cerenkov and scintillation counters responses to electron-photon EAS 18 p3208 A66-35113  
Air shower detection with radio receiving system, broadband band helical antenna and Cerenkov particle detector 18 p3115 A66-35119  
EAS front structure and normal energy transfer determined from pulse forms recorded by Cerenkov detectors 18 p3210 A66-35126  
Airborne equipment for study of nucleon interactions at energies in excess of 10 trillion ev 18 p3214 A66-35155  
Two detector elements developed for 2000-ton neutrino detector, noting cylindrical spark counter and Cerenkov counter 18 p3096 A66-35224  
Balloon measurements of cosmic ray hydrogen and helium nuclei at locations with nominal geomagnetic threshold rigidities 19 p3452 A66-35926  
Large air Cerenkov counter construction and performance characteristics for use in distinguishing protons and pions in cosmic radiation in 10-45 gev energy region 23 p4072 A66-42086

**CERENKOV RADIATION****SA COSMIC RADIATION****SA GAMMA RADIATION**

Radiation characteristics of point charge moving along direction of external magnetostatic field in warm anisotropic plasma 01 p0111 A66-10509  
Propagation, interaction and scattering of electromagnetic waves on diffusing inhomogeneous cylindrical plasma beam 01 p0027 A66-10550  
Possibility of determining electron concentration and magnetic field of plasma by measuring drift wave frequencies 02 p0291 A66-12114  
Cerenkov radiation by charge moving lengthwise in magnetic field of cold plasma, determining radiation spectrum range and total radiation energy 03 p0397 A66-12389  
Ultrasonic waves and electrons in piezoelectric semiconductors, noting role of acoustoelectric fields and propagating collective sound waves 03 p0408 A66-12414  
High energy proton from local radio sources, using telescopic system for Cerenkov effect detection of broad atmospheric showers 05 p0753 A66-15389  
Traveling wave characteristics of Cerenkov interaction studied by circular waveguide with electron beam flow 06 p0850 A66-16441  
High energy photons from discrete sources of cosmic radiation, verifying radio source electron production through proton-nucleon-matter interaction 06 p0947 A66-16572  
Spectral distributions for current and field fluctuations in nonequilibrium plasma located in external magnetic field 06 p0918 A66-16868  
Primary ultrahigh energy cosmic radiation composition analyzed, using Cerenkov flash 09 p1437 A66-20205  
Ultrahigh energy primary cosmic ray energy spectrum calculated from EAS particle-number spectrum 09 p1437 A66-20206  
Cerenkov radiation in circularly symmetrical waveguide filled with uniform dielectric in presence of flowing modulated electron stream 09 p1351 A66-20258  
Spatial scattering of associated electromagnetic waves arising during passage of fast charged particles through



semiconductors, noting role of Cerenkov radiation 09 p1428 A66-20596  
 Transition radiation relative to dispersion of dielectric permittivity for charged particle passing through boundary between two media 09 p1410 A66-20930  
 Cerenkov measurements of high energy gamma ray flux from quasi-stellar radio sources in mountains near Dublin 10 p1599 A66-21105  
 Cerenkov electron absorption of Alfvén and magnetoacoustic waves in plasma cylinder, obtaining formula for energy absorbed by plasma and damping factor where there is no resonance layer 11 p1743 A66-22443  
 Cerenkov radiation from charge spiralling in warm plasma under action of infinite magnetostatic field 11 p1745 A66-22494  
 Cerenkov radiation by charge moving lengthwise in magnetic field of cold plasma, determining radiation spectrum range and total radiation energy 13 p2139 A66-25394  
 Separation of radio emission of extensive air showers /EAS/ polarized in East-West direction from usual Cerenkov radiation 13 p2175 A66-26023  
 Possibility of determining electron concentration and magnetic field of plasma by measuring drift wave frequencies 14 p2385 A66-28073  
 High Q open resonator using two-conical optics and capable of traveling wave resonances at millimeter and submillimeter wavelengths 15 p2461 A66-29011  
 Ion motion effect on spectral region and energy density of Cerenkov excitation produced by charge moving in cold magnetoactive plasma 16 p2755 A66-30091  
 Quasi-linear approximation of Cerenkov and cyclotron damping of electromagnetic waves in magnetoactive plasma, considering collisions of wave-absorbing resonance particles with plasma 16 p2762 A66-31173  
 Increase of mean photon energies by mechanism related to Cerenkov plasmon-induced acceleration of charged particles 17 p2965 A66-32254  
 Frequency range in which Vavilov-Cerenkov surface wave exists in plasma-vacuum boundary 17 p2968 A66-32540  
 Radio noise bursts from Jupiter at decimeter wavelengths noting Cerenkov emission, Doppler-shifter cyclotron emission and escaped-whistler models 18 p3225 A66-33550  
 EAS RF emission detection, discussing enhanced Cerenkov radiation, mutual coherence effects, diffraction, Fresnel zones, Coulomb-field bremsstrahlung, etc 18 p3208 A66-35117  
 Jodrell Bank experiment testing Askarian hypothesis on radio pulses coincident with EAS under mutual coherence effects and checking coherent condition, internal reflection, shower energy, threshold and polarization 18 p3209 A66-35118  
 Solar and sidereal time variations of small air showers measured by array of water Cerenkov detectors 18 p3213 A66-35143  
 Primary intensity and primary spectrum at energies of trillion ev determined from atmospheric Cerenkov light 18 p3217 A66-35173  
 Spatial scattering of associated electromagnetic waves arising during passage of fast charged particles through semiconductors, noting role of Cerenkov radiation 20 p3622 A66-38130  
 Resonance excitation and Cerenkov damping of HF plasma oscillations 21 p3780 A66-39004  
 Cerenkov absorption of whistlers in nonhomogeneous plasma cylinder, noting electron heating 21 p3780 A66-39005  
**ERIUM**  
 Direct, Orbach and Raman paramagnetic relaxation measurements for trivalent cerium ion present as dilute impurity in lanthanum magnesium hydrate 19 p3443 A66-36001  
**ERIUM COMPOUND**  
 X-ray diffraction from cerium deformed at room temperature to form extrinsic stacking fault 02 p0272 A66-11710  
 Emission of Auer-Welsbach mixture in flames 16 p2827 A66-30852

**CERMET**

Cermet ablatives for thermal shields in fabrication of nozzles and nose cones [SAE PAPER 650767] 01 p0078 A66-10838  
 Refractory material cermet fabrication, discussing techniques of preparation, fuel-metal compatibility and fuel canning 05 p0713 A66-15585  
 Porous cermets of iron, bronze and stainless steel efficiently arrest flame of burning gas mixtures 06 p0897 A66-16694  
 Similarity theory applied to thermal shock resistance of brittle cermets 06 p0897 A66-16699  
 Deformation of double ring used in compression tests to study stress-strain state of brittle and cermet materials 08 p1313 A66-19438  
 Cermet face seals for inert gas environment sealing shaft of liquid-metal pumps employing conventional lubrication system [ASLE PREPRINT 65AM 4C4] 10 p1540 A66-22039  
 Cermet film microcircuit characteristics and design 13 p2029 A66-25126  
 Oxide-base cermets prepared by infiltration with silver and silver alloys, noting dispersion strengthening, bend creep, impact loading, etc, for gas-turbine application 16 p2730 A66-30250  
 Structure and electrical resistance as function of temperature for Nichrome-silicon monoxide cermet films on single crystal Si substrates 16 p2783 A66-31425  
 Pressing of two-component sintered materials 16 p2728 A66-31676  
 Thick film techniques, discussing applications, limitations, passive elements and design characteristics of cermet element 17 p2882 A66-32107  
 TiN-Mo cermet production by hot pressing and microstructure and phase composition, noting Ti-N production method 17 p2939 A66-32392  
 Hardness and microstructure of sintered alloys of molybdenum with oxides of aluminum and zirconium obtained by powder metallurgy methods 17 p2939 A66-32394  
 Element distribution in cermet alloys of W-Ni-Fe system determined by X-ray spectral analysis 17 p2940 A66-32848  
 Durability of cutting tool alloys for producing porous cermet ball bearings, noting effect of pearlite in cermets 17 p2930 A66-32850  
 Physical and mechanical properties of cermets obtained by sintering powdered iron at high temperatures under dynamic impact compression 20 p3583 A66-37413  
 Heat resistance of refractory alloys containing nickel, cobalt, tungsten, niobium, etc, and cermets, noting application in rocket engines 24 p4228 A66-43049  
**CESIUM**  
 Photon radiation effect on ionization of cesium vapor 05 p0615 A66-15533  
 Cesium thermionic converter with tungsten cathode and nickel anode improved operation by increasing cesium pressure 05 p0617 A66-15551  
 Constants A and B of cesium superfine structure calculated from magnetic sublevel intersections 05 p0741 A66-15859  
 Excited state of cesium lifetime determined from double magnetic resonance experiments 09 p1406 A66-20944  
 Low-energy electron diffraction studies adsorption of cesium on Si /111/ 10 p1576 A66-21551  
 Effective excitation cross sections for resonance doublets of cesium and rubidium, using slow electrons 10 p1544 A66-21981  
 Flying clock experiment with traveling cesium beam clocks 11 p1703 A66-22251  
 Optimum ionizer structure, examining cesium transport through tungsten capillaries [AIAA PAPER 66-207] 12 p1922 A66-24529  
 Measurement of cross section for excitation of cesium atom by electron impact in prethreshold energy region, using electron trap method 12 p1925 A66-24878  
 Measurement of shift of cesium absorption lines near series edge, obtaining electron elastic scattering cross section at zero energy by extrapolation of shift 12 p1918 A66-24882

Cesium beam atomic time and frequency standards 13 p2079 A66-25874  
 Pressure effects of argon on fine structure components of first two members of cesium principal series 13 p2135 A66-26263  
 Pressure effects of helium on fine structure components of first two members of cesium principal series, noting changes in shift curves 13 p2135 A66-26264  
 Photoelectric yield and energy distribution for clean-cleaved cesium-covered /111/ surfaces of silicon and germanium 14 p2365 A66-27755  
 Atomic standards of frequency and second of ephemeris time, discussing frequency of Cs 133 transition at zero field 14 p2296 A66-27899  
 Excited state of cesium lifetime determined from double magnetic resonance experiments 15 p2543 A66-28532  
 Electron spin resonance in rubidium and cesium observed, using selective transmission technique 16 p2750 A66-30145  
 Conduction electron spin resonance in rubidium and cesium observed, using reflection technique 16 p2750 A66-30146  
 Excitation cross sections of cesium in collisions with slow electrons 17 p2989 A66-33507  
 Effective excitation cross sections for resonance doublets of cesium and rubidium, using slow electrons 19 p3402 A66-35860  
 Atomic-beam technique for studying Stark effect in optical D-line transition in cesium and rubidium 19 p3402 A66-35993  
 Output characteristics of cesium thermionic converter as function of size of electrode gap, using device with movable air-cooled stainless steel anode 22 p3853 A66-40943  
 Measurement of cross section for excitation of cesium atom by electron impact in prethreshold energy region, using electron trap method 23 p4099 A66-41085  
 Measurement of shift of cesium absorption lines near series edge, obtaining electron elastic scattering cross section at zero energy by extrapolation of shift 23 p4097 A66-41089  
 Excitation cross sections of cesium in collisions with slow electrons 24 p4249 A66-42122  
**CESIUM ANTIMONIDE**  
 Fast-acting nonselective light emission receiver for wavelengths from 250 to 800 millimicrons 08 p1223 A66-19286  
**CESIUM COMPOUND**  
 Electron work function analysis using cesium compounds vapor combinations in thermionic energy converter, noting role of vapor pressure 05 p0619 A66-15562  
**CESIUM DIODE**  
 Cesium diode parameters and operating characteristics in arc mode not requiring specific ion generating mechanism for interpretation 05 p0615 A66-15538  
 Cesium filled diodes measured at various cathode temperatures, noting effect of ions generated in interelectrode space on current 05 p0728 A66-15549  
 Ignited mode of current voltage characteristics of thermionic diodes 05 p0617 A66-15550  
 Phenomenology of ignited cesium diode discharge noting saturation mode, obstructed mode and ball of fire 05 p0728 A66-15552  
 Thermionic converters with two alkalines using graphite insertion composites for imparting supplementary degree of freedom to cesium plasma diode 05 p0617 A66-15554  
 Cesium diode with cylindrical molybdenum emitter and niobium collector fueled with uranium dioxide in out pile test 05 p0618 A66-15557  
 Cesium fluoride additive effect on emitter work function and power output of cesium diodes with various emitter materials 05 p0618 A66-15558  
 Maximum obtainable efficiencies of cesium diodes with cesium fluoride additive from experimental U-I curves 05 p0618 A66-15559  
 Cesium diode thermionic converter, noting design, operation, application 10 p1485 A66-21515  
 Time resolution of laser-induced electron emission from cesium diode at high laser power 16 p2719 A66-31135



Large amplitude oscillations with frequencies corresponding to ion transit times in thermal cesium plasma diodes with parallel plane construction 19 p3313 A66-35425

Inert gas effect on performance characteristics of cesium thermionic converter, noting saturation current increase 22 p3853 A66-40944

Thermionic energy conversion phenomena and advances, detailing Cs diode and optimum ideal performance 23 p4021 A66-41756

## CESIUM ENGINE

Discrepancy between observed ion production rate in cesium thermionic converter and Saha-Langmuir equation prediction suggests locality of ion formation 05 p0612 A66-14984

Electric rocket propulsion system requirements for space propulsion, comparing capabilities with chemical and electrical rockets 08 p1280 A66-18575

Electron-ion emitting characteristics of various electrode materials with cesiated surfaces for cesium contact ion thrusters [AIAA PAPER 66-208] 10 p1592 A66-21447

Plasma measurements in cesium electron bombardment ion engine indicate that reversed cathode-anode configuration improves radial ion distribution [AIAA PAPER 66-246] 10 p1593 A66-21455

Life testing of electron-bombardment cesium ion engine designed for power-to-thrust ratio of 160 kw/lb [AIAA PAPER 66-233] 10 p1594 A66-21701

Surface ionization engine development, considering life testing of sastrugi thrusters [AIAA PAPER 66-236] 11 p1760 A66-22219

Development and performance of cesium ion engines for satellite control, noting lifetime, fuel consumption reliability, thrust vector control, etc [AIAA PAPER 66-234] 13 p2172 A66-25173

Multistrip cesium contact thrusters, integral focus life test engine and various integral focus ionizers [AIAA PAPER 66-235] 13 p2172 A66-25174

Cesium contact ion engine construction and performance and engine neutralizer [AIAA PAPER 65-375] 16 p2791 A66-30906

Computer program for current profile and trajectory analysis for cesium contact thruster leading to integral focus configuration of multistrip contact engines for long space missions [AIAA PAPER 66-206] 16 p2792 A66-31690

High performance annular Hall-current accelerator using radial magnetic field and axial electric field with cesium as propellant [AIAA PAPER 65-300] 19 p3450 A66-35614

Comparison of electromagnet and permanent magnet versions of electron bombardment cesium ion engine [AIAA PAPER 65-373] 19 p3450 A66-35617

## CESIUM FLUORIDE

Cesium fluoride additive effect on emitter work function and power output of cesium diodes with various emitter materials 05 p0618 A66-15558

Maximum obtainable efficiencies of cesium diodes with cesium fluoride additive from experimental U-I curves 05 p0618 A66-15559

## CESIUM ION

Focusing and accelerating electrode materials for cesium contact ion engines, noting advantages of copper, beryllium and molybdenum [AIAA PAPER 64-684] 02 p0278 A66-11537

Fission heated generator using cesium ion space charge neutralization for operation in pile 05 p0620 A66-15568

Neutron activation and cesium-aluminum sputtering in oxygenated gas atmosphere [AIAA PAPER 66-77] 06 p0913 A66-17103

Theory and operation of cesium thermionic converter 07 p0995 A66-18322

Sputtering yields of aluminum, copper and titanium measured as function of cesium ion energies for use as electrodes on cesium ion engines [AIAA PAPER 66-203] 10 p1575 A66-21445

Ion propulsion by electrostatic acceleration of cesium ions subjected to transverse magnetic field, using negative space charge sheath [AIAA PAPER 66-256] 10 p1563 A66-21461

Residual gas effect on work function vs

critical temperature for surface ionization of cesium on porous tungsten 10 p1594 A66-21778

Cesium ion emission patterns obtained from rear-fed porous refractory metals, using thermal emission microscope [AIAA PAPER 66-220] 11 p1746 A66-23086

Ionization characteristics of various porous metal ionizers and suitability for use in cesium contact thrusters [AIAA PAPER 66-218] 11 p1756 A66-23094

Cesium-vapor ion electrostatic drives for long-term space flight 11 p1761 A66-23129

Secondary emission of excited cesium atoms during bombardment of molybdenum and tantalum by fast cesium ions 14 p2338 A66-28248

Radioactive tracer technique to measure yield and angular distribution of copper sputtered from monocrystalline target subject to cesium ion bombardment [AIAA PAPER 65-379] 15 p2566 A66-29290

Cesium ionization cross section measurement from threshold to 50 ev, noting apparatus used and results obtained 15 p2548 A66-29814

Cesium ion tubes advantages over conventional tubes including ability to study electron-inertia effects 17 p2888 A66-32823

Cesium ion source evolved from surface ionization on porous refractory metal ionizers 18 p3138 A66-34240

Low thrust divergent flow cesium-on-tungsten contact ionization electrostatic thruster for satellite attitude control and stationkeeping missions [AIAA PAPER 66-569] 20 p3628 A66-37051

Hypersonic plasma generator for reentry vehicles with arc tunnel experimental data and analysis of nonequilibrium chemical reaction between cesium atoms and ionized air species 20 p3497 A66-37158

Neutron activation investigation of cesium ion sputtering of Al in rarefied oxygen atmosphere 22 p3950 A66-40082

## CESIUM PLASMA

Ionic waves amplified by collective behavior in alkali plasma obtained by contact ionization of cesium or potassium vapors on surface of two coaxial tantalum cylinders 01 p0110 A66-10331

Oscillation frequency and amplitude variation with parameters of contact-ionization cesium plasma device 01 p0111 A66-10391

Electron-ion recombination rate and effective ionization calculated for cesium plasma by Bates method 03 p0398 A66-12510

Oscillation and Maxwellian distribution of electrons in cesium 03 p0403 A66-12968

Electrostatic ionic instability of cesium Q type machines for hot plasma-beam interactions in VLF range in sheath and plasma 03 p0404 A66-12984

Comparing data of two Langmuir probes placed in cesium plasma generator 04 p0550 A66-13476

Cesium plasma thermionic converter, calculating voltage drop in emitter, collector and plasma 05 p0615 A66-15536

Heat transfer measured at different conditions of diode operation, obtaining data on plasma properties and electrode sheaths 05 p0616 A66-15546

Prototype of cesium plasma converter implementing heavy-duty electric power generator with nuclear reactor as primary energy source 05 p0617 A66-15547

Arc mode thermionic converter output characteristics relationship to neutralization plasma properties 05 p0620 A66-15570

Cesium plasma created in thermionic converter investigated by Langmuir probe to determine potential, gain, velocity and oscillations 05 p0620 A66-15571

Emitter of thermionic converter with cesium plasma heated by solar energy, determining electric power values 05 p0623 A66-15595

Current-voltage characteristics of low-voltage arc in cesium vapor, noting ionization process 06 p0915 A66-16150

Conductivity and transfer coefficients calculated from electron scattering in cesium plasma 06 p0918 A66-16836

Solar energy powered cesium-plasma thermionic converter, noting development,

output and application 09 p1333 A66-20924

Weak collisions effect on ion waves instability in cesium plasma solved via linearized Fokker-Planck equation 10 p1568 A66-21823

Relative drift between ions in adjacent layers exciting Kelvin-Helmholtz instability analyzed in thermally ionized cesium plasma, noting range of frequency oscillations 12 p1923 A66-24577

Design and construction of probe measuring density of neutral atoms in quiescent alkali metal magnetoplasma, noting vacuum system, electric circuitry, etc 12 p1884 A66-24984

Disturbance of thermal equilibrium of weakly ionized cesium contact plasma due to wall losses measured by Langmuir probe 13 p2137 A66-25117

Arc discharge in cesium vapor within diode, noting plasma parameter distribution in electrode spacing during low, luminous, and arc discharge phases 13 p2142 A66-25681

Drift instabilities in thermionic plasmas, noting excitation of LF oscillations with finite perturbation amplitude around cathode ion sheath 13 p2145 A66-25729

Multicomponent transport theory to compute cesium plasma transport properties over range of conditions wherein it changes from pure single component gas to mixture and then to completely charged particles gas 13 p2147 A66-25751

Diffusion coefficient measurement in fully ionized cesium plasma, using potassium plasma pulse launching techniques 13 p2155 A66-26680

Excitation of ion-acoustic waves in potassium-cesium plasma when passing current through it, finding natural frequencies of system when plasma is drifting along axis 15 p2550 A66-29214

Microwave scattering from large amplitude oscillations in cesium plasma, noting cross-section magnitude and nonlinear effects 15 p2556 A66-29810

Current-voltage characteristics of low-voltage arc in cesium vapor, noting ionization process 15 p2429 A66-29880

Plasma probe for dense isothermal cesium plasma, noting electron concentration and temperatures, potential distribution, etc 16 p2756 A66-30102

Gravitational instability of magnetoplasma in radial electric field, noting resistive drift modes, stabilization criterion effect of Coriolis force, Landau damping, etc 17 p2966 A66-32425

Ionization outside equilibrium and relaxation of ionization in cesium seeded argon 18 p3144 A66-34102

Two-stream instability for longitudinal waves in plasma traversed by ion beam 18 p3148 A66-34909

Plasma model representing phenomena occurring in cesium thermionic converters operating in collisional ignited mode 19 p3406 A66-35429

Atomic time standards, describing cesium beam standard, ammonia maser and gas-cell type clocks 19 p3354 A66-35468

Temperature and pressure of cesium plasma in wake of incident and reflected shock wave 21 p3790 A66-39075

Cesium plasma of Q device used in study of stability of plasma devices with slanted, nonconducting end plates 21 p3792 A66-39187

Cesium-plasma diode effect dependence on material output of cathode in vacuum, plotting short circuit current vs vapor pressure, voltage distribution, etc 22 p3952 A66-39752

LF drift waves observed in thermally ionized cesium plasma in magnetic field, with variable curvature 23 p4106 A66-41710

LF oscillation modes in TOPSY thermally generated cesium plasma devices investigated as function of plasma parameters 24 p4240 A66-42299

## CESIUM VAPOR

Low voltage arc in cesium vapor for case in which free-path length of particles is small compared to electrode spacing 01 p0016 A66-10702

Resonance absorption measurements in cesium vapor 02 p0262 A66-11435

Nonisothermal pulse discharge column in argon-cesium and helium-cesium systems



with produced plasma studied for nonisothermic conductivity 03 p0398 A66-12508

Shifts in output frequency of cesium vapor magnetometer due to temperature, light intensity and orientation, noting Zeeman component and geomagnetic field 05 p0678 A66-14968

Negative resistance of dynatron type and oscillations in reverse current range of cesium thermionic energy converter 05 p0620 A66-15572

Electron and ion emission of material in presence of cesium vapor, noting use as emitters 05 p0622 A66-15579

Thermodynamic validity of two cesium adsorption theories analyzed from semiclassical approach and electronegativity approach 05 p0622 A66-15581

Contact potential difference measurements for adsorption of cesium on polycrystalline tungsten surfaces in cesium vapor 05 p0622 A66-15582

Electron mobility in potassium and cesium DC glow discharges at low electron temperature 05 p0728 A66-15809

Solar radiation effect on Langmuir frequency, noting ionization of cesium vapor at low potential differences 09 p1409 A66-20925

Low voltage arc in cesium vapor for case in which free-path length of particles is small compared to electrode spacing 11 p1640 A66-23307

Atomic frequency standard fluctuation, instability due to noise and atomic beam frequency stability 12 p1881 A66-24125

Normal atom concentration in cesium and mercury vapors during pulse discharge 15 p2545 A66-29343

Increasing sturdiness of glass-to-metal seals in cesium vapors 15 p2429 A66-29707

Plasma probe in thermal emission converter with high cesium vapor, noting parameters of diffusion, electron concentration, etc 16 p2756 A66-30103

Electron temperature measurements in low voltage arc in saturated cesium vapor 16 p2756 A66-30105

Heat conductivity coefficient of cesium vapor at temperatures from 1000 to 1600 degrees K and 1 to 5 torr measured by hot tungsten filament method 18 p3142 A66-34022

Plasma Separator Thrustor, advanced ion thruster design based on independent operation and optimization of plasma source and plasma extraction system [AIAA PAPER 66-598] 18 p3163 A66-34217

Low pressure combination of barium and cesium vapors for reduction of transport-affected losses in thermionic energy converters, noting work function and V-I characteristics 18 p3055 A66-34584

Corrosion tests on eight refractory metals and alloys in liquid lithium and cesium vapors 19 p3383 A66-36136

Normal atom concentration in cesium and mercury vapors during pulse discharge 20 p3604 A66-37348

Electron and ion emission from polycrystalline surface of Be, Ti, Cr, Ni, Cu, Pt and type-304 stainless steel in cesium vapor 20 p3623 A66-38400

**CESSNA 210 AIRCRAFT**

Hydraulic system of Cessna 210 aircraft, noting component structure, electrical and hydraulic sequencing devices, etc [SAE PAPER 660202] 13 p2002 A66-26385

**CF-104 AIRCRAFT**

S F-104 AIRCRAFT

**CH-3 HELICOPTER**

SA SIKORSKY S-61 HELICOPTER

USAF CH-3C helicopter V/STOL in flight refueling, discussing requirements, system characteristics and flight tests 17 p2844 A66-32724

**CH-53 HELICOPTER**

CH-53A helicopter design, testing, reliability and flight characteristics 07 p0988 A66-17494

**CHAMBER**

S ANECHOIC CHAMBER

S ARC CHAMBER

S BUBBLE CHAMBER

S CLOUD CHAMBER

S COMBUSTION CHAMBER

S ENVIRONMENTAL CHAMBER

S FLOW CHAMBER

S ION CHAMBER

S IONIZATION CHAMBER

S LOW PRESSURE CHAMBER

S PLENUM CHAMBER

S PRESSURE CHAMBER

S ROCKET CHAMBER

S SPARK CHAMBER

S TEST CHAMBER

S VACUUM CHAMBER

**CHAMBER PRESSURE**

Low thrust cold gas reaction jet system for small spacecraft with nitrogen, ammonia, Freon-12 and Freon-14, analyzing thrust chamber pressure history [ASME PAPER 65-WA/AUT-11] 05 p0624 A66-15608

Response of Langmuir probes in rocket exhaust jets, noting sensitivity to chamber temperature and pressure and alkali metal concentration 14 p2294 A66-27421

Cryopumping, titanium-sublimation and ion-pumping mechanisms studied for exhausting vacuum chambers to simulate outer space 16 p2677 A66-30456

Solid propellant ignition and ignition propagation for rocket exhaust and hypergolic-type igniters 18 p3161 A66-34225

Igniter performance in solid propellant rocket motors, examining mass discharge rate effect on chamber pressure transients [AIAA PAPER 66-680] 18 p3161 A66-34227

**CHANCE-VOUGHT MILITARY AIRCRAFT**

S A-7 AIRCRAFT

S C-142 AIRCRAFT

S F-8 AIRCRAFT

S XC-142 AIRCRAFT

**CHANDRASEKHAR EQUATION**

Transfer equation of solar absorption line developed with split upper level in magnetic field 05 p0759 A66-14870

Internal diffuse radiation field computed in finite homogeneous isotropically scattering slab illuminated by parallel rays of radiation 10 p1556 A66-21923

Nonuniqueness of solutions of nonlinear integral equation for Chandrasekhar S-function for homogeneous semiinfinite atmosphere 13 p2127 A66-25612

**CHANNEL**

Channel shape effect on current-voltage characteristics in channel transistors 04 p0496 A66-13906

Electrical and gas dynamical parameters effect on length of linear constant Mach number MHD duct, assuming gas is ionized by neutron irradiation in expansion nozzle preceding duct and electron recombination takes place in duct 13 p2000 A66-25739

Stability of automatic systems for tracking point targets, noting nonlinear dependence of signals on channel mismatch and its limiting values 17 p2902 A66-32579

Channel shape effect on current-voltage characteristics in channel transistors 20 p3532 A66-37864

Error probabilities in binary transmission of signals over selectively fading diversity channels containing specular and scatter type components 22 p3864 A66-40058

Distortion of FM signals after being processed through time-invariant channels with nonlinear phase characteristic and fluctuating amplitude 22 p3864 A66-40061

**CHANNEL CAPACITY**

Parallel decoding for discrete channel with statistically independent noise 02 p0189 A66-11404

Mathematical structure and characteristics of codes used in transmission over nonsymmetric channels 02 p0209 A66-12020

Channel capacity of communications satellite repeater, deriving link capacities of radio teletype and voice channels 04 p0478 A66-13597

Relationship between distribution entropy and variation in distribution of almost-periodic channels 05 p0638 A66-15361

Coding theorems for almost-periodic channels 05 p0638 A66-15362

Monitoring of discrete state discrete transition Markov source whose states are input letters to memoryless discrete noisy channel 06 p0860 A66-16189

Signal optimization for digital communication system over channel characterized by rational transfer function and Gaussian noise having

memory 06 p0829 A66-16192

Degenerate parametric amplifier receiving two oppositely modulated input waves, improving noise figure 07 p1010 A66-18152

Tunnel diode voltage-controlled oscillator to expand FM system channel capacity 07 p1010 A66-18246

Synchronism between transmitting and receiving terminal of transmission systems, particularly single channel systems, using code pulse modulation 09 p1346 A66-20546

Ultimate performance of m-ary transmissions, showing signal filtering by use of energy measurement 10 p1505 A66-21837

Random and burst channel error affects output signal-to-noise ratio of delta modulation system 13 p2019 A66-25145

Variable premodulation gain to multichannel transmission system for which AM baseband power is proportional to cumulative channel activity, showing improvement of SNR 13 p2020 A66-25151

Shannon model for capacity of time-continuous and time-discrete Gaussian channel with inputs perturbed by independent noise random variable 13 p2024 A66-25938

Audio signal processing techniques in future space exploration, discussing channel capacity, speech processing, bandwidth narrowing, etc 13 p2025 A66-26024

Quantum information generalizes classical Shannon concept 13 p2025 A66-26045

Quantum communication channel entropy and information analysis using noncommutative output and input variables, including waveguide carrying capacity thermal noise calculations 13 p2025 A66-26046

Mathematical structure and characteristics of codes used in transmission over nonsymmetric channels 14 p2266 A66-27571

Error detection techniques for maximizing average rate of information transmitted through burst error channel 14 p2243 A66-28346

Maximum channel capacity of tandem link multichannel troposcatter systems for specified noise level 14 p2243 A66-28347

Four-and five-horn tracking feeds for large antennas, emphasizing sum channel gain in five-horn feed 18 p3083 A66-34292

PCM bandwidth halving and twin working method of superimposing two PCM channels in frequency band occupied by one PCM channel 19 p3305 A66-36625

Cathode ray oscillograph-directional antenna recordings of electromagnetic pulses from lightning discharges 20 p3553 A66-38081

Laboratory environment simulation of multipath propagation interference effects on low channel capacity FM systems 22 p3865 A66-40066

**CHANNEL FLOW**

**SA ANNULAR FLOW**

Laminar flow through parallel and uniformly porous walls of different permeability 01 p0057 A66-10425

Simple wave interaction in polytropic rarefied gases flowing from parallel wall channel 01 p0006 A66-10473

Flow stability theorem for viscous homogeneous and incompressible fluid through infinitely long cylindrical pipe of arbitrary cross section 01 p0058 A66-10504

Flow structure in initial length of MHD channel of square cross section taking longitudinal magnetic field nonuniformities into account 01 p0113 A66-10699

Eddy conductivity, eddy viscosity and dimensionless ratio of diffusivity for mercury flowing in tube 01 p0164 A66-10904

Adiabatic heating and temperature recovery factor of tubes carrying liquids of high Prandtl number 01 p0165 A66-10905

Two-phase flow and heat transfer for boiling liquid nitrogen in horizontal tubes 01 p0165 A66-10909

Graduate-level text on engineering MHD establishing bridge with plasma physics, using particle /microscopic/ and continuum approaches 01 p0114 A66-10978

Axisymmetric steady flow of incompressible viscous fluid in circular tube of constant porosity treated by small parameter method 01 p0059 A66-11003

Electrically conducting two-dimensional



compressible flow in traveling wave plasma accelerator, noting effect of nonuniform magnetic field 01 p0115 A66-11085

Transfer of heat or nonstationary mass in circular cylindrical laminar flow tube 01 p0166 A66-11086

Hall currents effect during acceleration of plasma intrinsic magnetic field 02 p0264 A66-11384

MHD flow analyzed in entrance region of parallel-plate channel 02 p0267 A66-11531

Collisionless mass flow of ionized gas through channel with imposed magnetic field [AIAA PAPER 65-124] 02 p0267 A66-11535

Equation of velocity distribution of fluid in duct, evaluating effect of eddy activity on second derivative 02 p0218 A66-11759

Plasma velocity field determined from glow discharge in crossed fields propagating along rectangular channel, two walls being dielectrics and other two electrodes 02 p0268 A66-11786

Plane transonic gas flow past symmetrical convex profile at zero angle of attack along axis of channel with parallel walls 02 p0176 A66-12171

Motion of medium of variable electric conductivity in rectangular channel situated in magnetic field 02 p0270 A66-12172

Heat transfer and friction for laminar flow of gas in circular tube at high heating rate, using finite difference method 02 p0304 A66-12198

Quasi-one-dimensional ionized gas motion through channels of arbitrary cross section in crossed electrical and magnetic field 03 p0398 A66-12516

Local heat transfer during turbulent gas flow in pipe for large temperature differences, describing test apparatus and results 03 p0443 A66-12517

Shear flow influence on sound attenuation in lined duct, considering upstream and downstream propagation 03 p0356 A66-12822

Free convection heat transfer in partially enclosed channel flow, noting effect of vertical fin geometry and temperature [ASME PAPER 64-WA/HT-33] 04 p0595 A66-13386

Transient heat transfer between thin circular tube and incompressible fluid, considering radial conduction and heat loss [ASME PAPER 65-HT-2] 04 p0595 A66-13393

Plasma flow discussing flow mode stabilization in channel formed by two electrodes, flow parameters and plasma conductivity 04 p0529 A66-13553

Electrokinetic transducers to measure potential fluctuations of turbulent flow of tap water in open channel 04 p0509 A66-13664

Laminar flow development of incompressible Newtonian fluid in hydrodynamic entrance region of flat duct 04 p0511 A66-13939

Bergerson and first approximation method for solving problems of unsteady fluid flow in pipeline 04 p0511 A66-14157

Hydrodynamic behavior of mercury in laminar and turbulent flow in tube, discussing effect of vacuum and protective gas 04 p0511 A66-14185

Effect of heat removal through MHD channel walls on stability of temperature distribution during electrical discharge in gas between two planes 04 p0557 A66-14421

Two-dimensional flow of inviscid nonheat-conducting gas with variable conductivity in crossed constant electric and arbitrary magnetic fields 04 p0557 A66-14422

Motion, temperature distribution, concentration and change in electric conductivity of ionized gas in initial section of plane channel 04 p0557 A66-14432

MHD flow in rectangular ducts, discussing laminar motion of conducting liquid under uniform transverse magnetic field 04 p0558 A66-14475

Slow viscous shear flow past plate midway between two walls studied analytically, using Stokes approximation 05 p0605 A66-14702

Transition flow of nitrogen through short circular tubes with length-to-diameter ratios from 0.005 to 1 and pressure ratios from 1 to 20 05 p0605 A66-14704

Stability diagrams for MGD channel flow of conducting fluid for different coplanar

magnetic field intensities 05 p0721 A66-14710

Effect of asymmetrical heating on turbulent heat transfer in rectangular duct [ASME PAPER 65-HT-11] 05 p0782 A66-14735

Integral approximations for skin friction and heat transfer in MHD channel flow [ASME PAPER 65-HT-15] 05 p0783 A66-14739

Thermal flow meter incorporating effect of axial conduction [ASME PAPER 65-HT-19] 05 p0676 A66-14741

Optimum electrode arrangement in MHD channel, taking into account Hall effect 05 p0722 A66-14996

Laminar flow in two-dimensional channel with uniformly porous walls through which fluid is uniformly injected 05 p0662 A66-15057

Heat losses from turbulent gas flowing through poorly insulated pipe where heat lost from outer surface is by free convection and radiation, solving heat equation [ASME PAPER 65-WA/HT-16] 05 p0790 A66-15648

Film boiling of saturated nitrogen flowing upward in vertical heated tube, noting annular-flow regime change to vapor matrix [ASME PAPER 65-WA/HT-26] 05 p0793 A66-15677

Generalized equation of choking for two or more unmixed streams flowing in same channel, noting relevance to ejector principle 05 p0665 A66-15773

Experimental method to produce fully developed flow in relatively short channel length 06 p0871 A66-16221

Stabilized flow of two-phase incompressible viscous media in cylindrical tube 06 p0871 A66-16312

Quasi-steady flow relations to study wave action in duct with gauze 06 p0873 A66-16932

Secondary flow in fully-developed turbulent flow in straight channels, noting Reynolds number effect, directional characteristics of local wall shear stress, etc 06 p0873 A66-16997

Interaction or coupling of radiation with conduction and convection mechanisms in nonisothermal nongray gas flowing in entrance region of tube with isothermal black walls [AIAA PAPER 66-136] 06 p0875 A66-17090

Convective heat transfer in thin rectangular channels commonly found in nuclear reactor fuel assemblies 07 p1148 A66-17299

Stability criterion for flow in interspace between two parallel arbitrarily curved walls 07 p0980 A66-17482

Unsteady, combined free and forced convective MHD channel flow of conducting fluid through transverse magnetic field 07 p1085 A66-17580

Quasi-one-dimensional unsteady hydromagnetic wave flow of ideal inviscid compressible conducting fluid in nonuniform ducts 07 p1089 A66-17962

Existence of subsonic jets issuing from curved symmetric channels in plane 07 p0981 A66-18030

Tube gas flow theory applicable to laminar flow, slip flow, transition region of flow and free molecular flow 07 p1023 A66-18131

Rotation vector increase derived for secondary incompressible fluid flow in curved channels 07 p1023 A66-18134

Wave action in duct with gauze calculated, using steady flow relations including pressure loss coefficients 07 p1026 A66-18281

Nonsteady flow through square-edged orifice in pipe 07 p1026 A66-18283

EGD power generation including functioning, coupling, broad and narrow channels, expanding momentum channel, efficiency, etc 07 p0993 A66-18313

Electric power generation using monopolar charged particles in fluid flow 07 p0994 A66-18315

Analogy between gas flow through convergent/divergent nozzles and open side-contracted channel 08 p1205 A66-18628

Two-dimensional steady MGD flow of ideal thermally nonconducting fluid with infinite conductivity, when magnetic intensity and velocity are orthogonal 08 p1261 A66-18675

Convective heat transfer and artificially turbulent flow through roughened corrugated channels 08 p1317 A66-18864

Transition regime mass flow rate and longitudinal pressure distribution along short tube with bellmouth entry 08 p1207 A66-19131

Charge density distribution, electric field strength and flow rate of turbulent flow of incompressible fluid in flat nonconducting channel 08 p1263 A66-19172

Electron temperature variation in argon MGD channel in crossed magnetic and electrical fields 08 p1263 A66-19174

End effects on viscoelastic polymer flow through capillary tube 08 p1209 A66-19552

Stability of set of Jeffery-Hamel profiles, approximating profiles in two-dimensional divergent channels, investigated by numerical solution of Orr-Sommerfeld problem 08 p1212 A66-19823

Approximate theory for electrokinetic phenomena in capillary flows, determining interaction between mechanical and electrical energy 08 p1174 A66-19829

Vorticity growth when steady heat current is applied to liquid He 2 in narrow tube 09 p1366 A66-20017

Superfluid critical velocity in He 2 isothermal gravitational flow in narrow channels 09 p1366 A66-20018

Critical velocities and supercritical velocity dissipation effects in isothermal flow of liquid He 2 in narrow channels 09 p1366 A66-20019

Modified Cochran method giving valid expansions for singular perturbation problems in heat transfer 09 p1469 A66-20084

Heat transfer in laminar flow between parallel porous walls with discontinuous change in wall temperature 09 p1470 A66-20176

Laminar fully-developed flow of water between parallel flat plates examined, using motion equation with experimental values for viscosity, conductivity, specific heat and density 09 p1470 A66-20179

Visualization of flow in transverse plane across main stream past cylinder 09 p1364 A66-20600

Turbulent heat transport coefficient of various fluids in pipes measured, obtaining formula from experimental data 09 p1367 A66-20702

Free convection thermal transfer in narrow horizontal channels and infinitely wide channels 09 p1471 A66-20704

One-dimensional adiabatic compressible gas flow in cylindrical tube taking into account Reynolds number variations along tube and compressibility effect on friction factor 09 p1368 A66-20827

Two-dimensional steady potential subsonic flow of compressible fluid past circular cylinder between two parallel walls 10 p1522 A66-21323

Pseudoshocks in pipe flow in supersonic compressors represented as diffusion process, noting application in cascade and rotor configuration 10 p1479 A66-21363

Condensing characteristics of mercury vapor flowing in horizontal single tubes examined in crossflow-nitrogen-cooled and NaK-cooled condensers 10 p1621 A66-21463

High precision high-spatial resolution tracer study of low-noise steady air flow in rectangular pipe, emphasizing region within two microns of wall 10 p1524 A66-21804

Cylindrical Poiseuille flow of rarefied gas for inverse Knudsen number from zero to 10 10 p1524 A66-21806

Velocity overshoot within boundary layer in alternating laminar air flow near mouth of square channel 10 p1524 A66-21827

Hydromagnetic stability of current-carrying fluid between two coaxial cylinders with radii ratio 0.05 to 0.9 10 p1568 A66-21829

Thermal flow meter incorporating effect of axial conduction [ASME PAPER 65-HT-19] 11 p1703 A66-22187

Combined free and forced laminar convection heat transfer inside inclined circular tubes of varying position [ASME PAPER 65-WA/HT-3] 11 p1785 A66-22191

Relative effect of restrictive orifices, venturis or nozzles on measurement accuracy of fluid flow rates in pipes 11 p1703 A66-22207

Stationary flow of viscous incompressible anisotropically conducting fluid in coaxial



- channel 11 p1743 A66-22235
- Hydraulic resistance coefficient 11 p1688 A66-22592
- dependence on Reynolds and Hartmann numbers in turbulent flow of conducting fluid through tube in magnetic field 11 p1743 A66-22337
- Turbulent heat transport coefficient of various fluids in pipes measured, obtaining formula from experimental data 11 p1688 A66-22592
- Clamping conditions effect on critical flow rate of fluid moving through pipe, taking into account direction and friction forces on stability 11 p1782 A66-22853
- Rate of effusion for gas flow through orifice and application to fluorine gas dissociation energy 11 p1688 A66-22880
- Hypersonic rarefied gas flow in short ducts, measuring wall static pressure and stream total pressure distributions 11 p1634 A66-22932
- Flow structure in initial length of MHD channel of square cross section, taking longitudinal magnetic field nonuniformities into account 11 p1747 A66-23301
- Heat transfer in turbulent flow of incompressible fluid in plane curved channel 11 p1694 A66-23317
- Turbulent channel flow, discussing friction flow anisotropy and homogeneity, vortex flow, channel viscosity, etc 12 p1860 A66-23532
- MHD duct flow under circular and radial magnetic field 12 p1920 A66-23954
- Eigenfunctions for laminar flow in porous two-dimensional channel subject to certain boundary conditions 12 p1862 A66-23994
- Flow parameters of incompressible ideal fluid in axisymmetric curvilinear channel, obtaining and solving nonlinear differential equation 12 p1863 A66-24243
- Larmor precession of charged particles effect on nonstationary temperature field in plane channel 12 p1922 A66-24361
- Critical Reynolds numbers for oscillating fluid in tube in region of laminar-turbulent transition 12 p1864 A66-24448
- Turbulent radial channel flow without swirl between parallel disks having both supersonic and subsonic regions, determining pressure distribution and normal shock [ASME PAPER 65-FE-11] 12 p1799 A66-24547
- Radial diffuser using swirl-free incompressible flow between narrowly spaced disks of radial channel and supply-pipe outlet [ASME PAPER 65-FE-12] 12 p1864 A66-24548
- Initial flow in entrance of straight circular pipe computed as refinement of Atkinson and Goldstein solution 12 p1867 A66-24980
- Pipeflow simulation by triggered monostable multivibrator driving chopper as logarithmic function generator 13 p2027 A66-25220
- Nonstationary two-dimensional channel flow of compressible electrically conducting fluid subject to traveling magnetic field 13 p2140 A66-25422
- Excess velocity profiles in confined jets in presence of uniform transverse magnetic field, confirming affinity hypothesis 13 p2140 A66-25433
- MHD channel flow as affected by extremities 13 p2141 A66-25474
- Two-dimensional analysis of flow in electrofluid dynamic generator showing effect of radial fields and viscous forces on performance, stressing effect on electrical breakdown of gas, noting basic equations 13 p2001 A66-26257
- MHD channel flow as affected by nonuniform and anisotropic electric conductivity and boundary effects 13 p2150 A66-26339
- Drag coefficient of gas flow in circular tube at transonic velocity 13 p2065 A66-26485
- One-dimensional gas flow in tube with heat transfer 13 p2066 A66-26488
- Transition from laminar to turbulent flow, establishing critical Reynolds number of 2223 for steady pipeflow 13 p2069 A66-26702
- Mean velocity, rms velocity fluctuations and Reynolds shear stress for air flow at high Reynolds number in rectangular channel partially roughened, measuring turbulence intensity 13 p2070 A66-26703
- Pipe flow turbulent temperature fluctuation measurements in mercury and ethylene glycol with fast response thermocouple 14 p2410 A66-26936
- End effects in steady state MHD J x B accelerator, noting voltage and current distribution and eddy-current geometry 14 p2342 A66-27430
- Solution of boundary layer equation for two-dimensional laminar steady motion of viscous incompressible fluid in convergent channel with suction at wall 14 p2276 A66-27728
- Effect of instantaneous change in viscosity on laminar vortex of flow through suddenly widening pipe 14 p2277 A66-27933
- Channel flow of inviscid fluid with tensor conductivity considered when flow leaves transverse magnetic field, noting spatial distribution and ohmic power loss for application in MHD generators 14 p2346 A66-28302
- Laminar adiabatic gas flow in parallel plane channel taking place up to 3/4 of critical velocity 14 p2278 A66-28315
- Laminar fluid flow in channel generated by arbitrary generatrix, allowing for interaction between boundary layer and flow core, calculating boundary layer 14 p2278 A66-28316
- Laminar flow of incompressible fluid in rectangular channel, determining temperature distribution over channel cross section and thermal flux through wall for case of energy dissipation 14 p2415 A66-28317
- Unsteady flow of viscous liquid through tube of rectangular cross section under nonuniform pressure gradient assumed to be linear function of time 14 p2279 A66-28462
- Pressure drop for non-Newtonian flow in inlet length of straight channel 14 p2279 A66-28464
- Two-dimensional laminar MHD flow in convergence channel with uniform input, finding effect of flow convergence on boundary development for arbitrary magnetic field induction 15 p2549 A66-28638
- One-dimensional flow through nozzle and stability of weakly ionized plasma with induced Hall current 15 p2550 A66-28958
- Hysteresis effects in one-dimensional conducting gas flow through rectangular MHD converter channel with constant magnetic gap and variable electron spacing 15 p2428 A66-29219
- Two-dimensional isothermal liquid flow electrically conducting in channel under electromagnetic fields, finding self-modeling solutions, using Jacobi functions 15 p2551 A66-29221
- Motion of non-Newtonian liquid through two coaxial curved pipes, noting relation between pressure gradient and outflow rate, curvature effect and secondary flow 15 p2479 A66-29397
- Forced convection heat transfer in symmetrical ducts when fluid is liquid metal, examining new prediction methods for engineering analysis and design 16 p2824 A66-30304
- Steady flow of highly rarefied ionized gas through channel with magnetic field solved by Monte Carlo method obtaining density, energies, wall shear stress, etc 16 p2759 A66-30371
- Approximation method for limit Nusselt number for channels of nonuniform geometrical configuration and linearly variable wall temperature 16 p2684 A66-30677
- Linearized supersonic flows in quasi-cylindrical tubes and wall form determination from given pressure distribution 16 p2629 A66-31038
- Stress in viscoelastic polystyrene in Aroclor flowing in straight, converging and diverging channels 16 p2686 A66-31043
- Annular diaphragms to produce turbulent flow in tubes 16 p2828 A66-31065
- Heat transfer between turbulent supersonic air stream and circular water-cooled tube at Mach 1 to 4, using two-dimensional flow model 16 p2829 A66-31161
- Steady flow of conducting dissociating gas in channel of constant cross section in presence of magnetic field 16 p2687 A66-31165
- Velocity profile of incompressible and electrically conducting flow in entrance region of constant area MHD channel 16 p2763 A66-31255
- Natural frequency of fluid oscillations in complex pipelines 16 p2687 A66-31296
- Numerical analysis of stabilization of one-component conducting plasma in two-dimensional coaxial duct 16 p2763 A66-31307
- Optimum operation modes of MHD converter 16 p2637 A66-31368
- Laminar-turbulent transition conditions in MHD channel flow 16 p2764 A66-31370
- MHD fluid flow in rectangular channels with allowance for finite wall conductivity 16 p2764 A66-31371
- Effect of single or periodic disturbances on intermittency in pipe flow at various Reynolds numbers, noting relation of disturbance input frequency to output frequency of turbulent slugs 16 p2688 A66-31394
- Diffusive corrosion processes caused in circular tubes by reactive fluid simulated by rotating disk electrodes 16 p2728 A66-31597
- Constant flow velocity and constant Mach number flow problems in MHD generator of minimal length for given temperature drop at output and internal efficiency 16 p2638 A66-31611
- Critical flow rate, critical pressure ratio and critical mass flow of dissipative adiabatic nozzle and pipeflow of ideal gas 16 p2690 A66-31635
- Malkus theory in weakly-conducting turbulent liquid flow between parallel plates in transverse magnetic field, noting velocity profile and transition region 16 p2766 A66-31652
- Heat transfer of forced laminar convection in multiply connected regions 16 p2830 A66-31708
- Resistance coefficient calculation procedure for turbulent flow in circular pipes extended to case of annular conduits 17 p2906 A66-32034
- Convective heat transfer during subsonic and supersonic gas flow in inlet section of cylindrical tube 17 p3034 A66-32561
- Velocity and temperature profiles, hydrodynamic elements, heat transfer and friction coefficients of turbulent incompressible flow through circular and flat tube 17 p2909 A66-32583
- MHD approximation of laminar duct and channel flow of electroconductive viscous Newtonian fluid 17 p2971 A66-32861
- Self-similar solutions of two-dimensional laminar flow of incompressible electroconductive fluid in channel in crossed electric and magnetic fields, using Jacobi elliptic integrals 17 p2971 A66-32866
- Steady-state axially-symmetric channel flow of ionized gas in external electromagnetic field in one-dimensional approximation 17 p2971 A66-32867
- Longitudinal Faraday emf, thermoelectric and Hall effects on channel flow of ionized gas 17 p2972 A66-32868
- Geometric, gasdynamic and electromagnetic parameters of one-dimensional flow of conducting gas with Hall effect for maximum power tapping from channel electrodes 17 p2972 A66-32869
- Effect of sudden enlargements and contractions in flow area on single pressure waves in gases in pipes, covering incident waves of various pressure amplitudes 17 p2841 A66-32890
- Laminar flow velocity field and pressure distribution in inlet region of rectangular ducts [ASME PAPER 66-FE-7] 17 p2914 A66-33261
- Photocurrent and leakage current in zinc diffused GaAs junction diodes in terms of channel effect 17 p2987 A66-33319
- Viscous incompressible fluid motion between two parallel planes and between two co-axial circular cylinders with one boundary moved by impulse 17 p2916 A66-33418
- Forced convection heat transfer for liquid metal flow in rectangular channels with prescribed wall heat fluxes and heat sources in fluid stream 17 p3038 A66-33468
- Gas-phase heat-transfer augmentation by steady and alternating electric field in pipeflow 17 p3039 A66-33473
- Fully developed laminar incompressible flow in stepped rectangular channel, with velocity profiles obtained by variational



method 18 p3097 A66-33596  
 Transverse magnetic field effects on heat transfer in turbulent flow of mercury in circular iron tube 18 p3145 A66-34109  
 Channel flow general equations including nonviscous uniform flow, steady flow, stagnation state and speed of sound in ideal gas 18 p3098 A66-34121  
 Laminar steady incompressible nonuniform flow in rectangular duct, stream tube and pipe 18 p3099 A66-34124  
 Hartree solution of MHD laminar boundary layer incompressible conducting fluids, specifically considering flow at inlet to semiinfinite flat channel 18 p3147 A66-34636  
 MHD flow with parabolic velocity at entrance region of flat channel 18 p3149 A66-34915  
 Drag coefficient of turbulent flow of electrically conducting liquid metal in MHD channels of round cross section 19 p3407 A66-36098  
 Optimization of MHD generating duct by varying cross-sectional area and electrical loading 19 p3281 A66-36372  
 Hydraulic-approximation equations in calculating MHD channel flows 19 p3410 A66-36458  
 MHD boundary layer at conducting wall of plane channel treated by numerical method 19 p3410 A66-36459  
 Free-molecular flow of rarefied gas in plane channels or through cells of heat conducting grid whose cells are smaller than mean free path of gas 19 p3277 A66-36480  
 Pulsating laminar flow of viscous incompressible conducting fluid in annular channel between circular cylinders under radial magnetic field, solving MHD equations 19 p3432 A66-36643  
 Electromagnetic field effect on heat transfer during laminar flow of electrically conducting incompressible fluid in flat channel 20 p3607 A66-36980  
 Spatial correlation coefficients and transverse temperature perturbation scales during turbulent nonisothermal flow of mercury in circular pipe 20 p3607 A66-36982  
 Heat transfer in turbulent carbon dioxide pipeflow at supercritical region 20 p3674 A66-36983  
 Electric field in MHD generator channel under mixed boundary conditions solved by Wiener-Hopf technique, evaluating ohmic losses 20 p3500 A66-37491  
 Differential equations for quasi-homogeneous MHD flow of electrically conducting medium at low magnetic Reynolds numbers 20 p3611 A66-38109  
 Calculation of heat transfer in laminar flows of structurally viscous fluids in tubes with constant thermoconductivity, heat capacity and density 20 p3681 A66-38122  
 Fading multipath channel behavior simulator for communication system performance study 20 p3534 A66-38359  
 Supersonic turbulent flow in low temperature plasma accelerator with rapid boundary layer growth 21 p3693 A66-38684  
 Wall conductance effect on stability of Hartmann flow in curved channel, solving eigenvalue problem via Galerkin method 21 p3777 A66-38762  
 Quantities and relations for describing two-phase flows, kinematics and kinetics of both phases of laminar pipeflow 21 p3724 A66-38933  
 Unsteady convective heat transfer of incompressible fluid between two solid channel walls 21 p3728 A66-39340  
 Heat transfer in laminar flow of Bingham material through circular pipe, taking into account dissipation effect 21 p3836 A66-39441  
 Dissipation of sheet of heated air in turbulent air flow in pipe 21 p3836 A66-39445  
 Slip flow in hydrodynamic entrance region of tube and parallel plate channel determined by solving linearized momentum equation 21 p3730 A66-39459  
 Steady laminar flow of viscous incompressible fluid through two-dimensional channel with fluid sucked or injected with different velocities through uniformly porous parallel walls 21 p3730 A66-39461  
 Laminar forced-convective heat transfer for dissipative fluid in tube bounded by

concentric circles 21 p3837 A66-39610  
 Steady state equations for one-dimensional flow of conducting medium through channel of MHD generator in homogeneous magnetic field 22 p3952 A66-39692  
 MOS capacitance of p-type silicon in inversion layer and ion drift in fringing field 22 p3872 A66-39744  
 Active component of voltage behavior in channel of helium pulse discharge measured, obtaining time dependence of channel resistance, input velocity and energy magnitude 22 p3953 A66-39755  
 Heat losses from turbulent gas flowing through poorly insulated pipe where heat lost from outer surface is by free convection and radiation, solving heat equation [ASME PAPER 65-WA/HT-16] 22 p3997 A66-40027  
 Mean viscous dissipation and bulk temperature variation in incompressible fully developed duct heat transfer, using Green theorem 22 p3998 A66-40033  
 Viscosity, surface tension and inclination angle effect on motion of long bubbles in closed tubes 22 p3900 A66-40388  
 MHD flow in rectangular channel due to periodic pressure gradient at high Hartmann number 22 p3957 A66-40704  
 Laminar heat transfer in plane channel with nonuniform temperature field at inlet 22 p4000 A66-40812  
 Adiabatic gas flow pattern in plane parallel channel near critical point 22 p3902 A66-40815  
 Erosive burning in rocket engines of radial burning type, using polyurethane/ammonium perchlorate base propellant grains, examining flow channel constriction 23 p4121 A66-41433  
 Unsteady air flow discharge coefficients compared for sharp-edged orifices with steady flow values 23 p4009 A66-41700  
 Approximation method for wall effect in cavitation flow around bodies in water tunnel, examining effect of solid boundary on resistance factor 23 p4056 A66-41727  
 Steady state flow of liquid metal in MGD channel of rectangular section, noting magnetic field effect on resistance factor 23 p4106 A66-41729  
 Hydraulic loss decrease in complex pipeline owing to wire grating 23 p4024 A66-41798  
 Thermal transport in channel-gas flow, discussing integral equation and power series solution 23 p4150 A66-41869  
 Steady fully developed MHD channel flow of viscous electrically conducting fluid studied by Galerkin method under applied magnetic and electric fields 23 p4107 A66-41886  
 Oscillating two-phase flow through rigid circular pipe investigated to understand blood cells effects on changes in shape of pressure pulse wave 23 p4058 A66-41916  
 Plasma flow processes in slip type traveling wave accelerator investigated to determine degree to which one-dimensional channel flow is used in design and scaling laws 23 p4053 A66-41917  
 Pressure fluctuations under turbulent boundary layer or in pipe flow, noting surface deflection effect and pressure representation 23 p4061 A66-42027  
 Heat transfer in incompressible viscous fluid between two nearly parallel walls with harmonically varying distance, determining velocity field and temperature distribution 23 p4150 A66-42029  
 Turbulent heat transfer coefficient in smooth pipes at high Prandtl numbers has higher value than when turbulence is not assumed 23 p4151 A66-42054  
 Flow coefficient of elliptical cylindrical pipe, analyzing boundary layer at exit for various Reynolds numbers, noting velocity profile 23 p4014 A66-42057  
 Finite difference method solution of Navier-Stokes equations and applicability to cylindrical-channel viscous flow at small Reynolds numbers 23 p4062 A66-42061  
 Motion equations, shear stress and skin friction for three-dimensional flow in conical pipes 23 p4014 A66-42062  
 Turbulent momentum transfer mechanism in separated flow region of rectangular

cavity facing oncoming turbulent boundary layer 24 p4193 A66-42154  
 Temperature distribution of laminar channel flow with tangential stress and wall temperature 24 p4294 A66-42720  
 Micropolar fluid theory with derivation of motion equation, constitutive equations and boundary conditions, noting channel flow 24 p4195 A66-42828  
 Pressure effects of flexible walls on boundary layer transition in turbulent pipe inlet flow 24 p4195 A66-42859  
 Stroboscopic instantaneous velocity measurements near wall in turbulent flow of water in channel and analysis of viscous layer turbulent pulsations 24 p4196 A66-42880  
 Laminar flow of fluid with varying viscosity in tube with walls at constant temperature, analyzing equations of motion and equations for conservation of energy 24 p4197 A66-42991  
 Flow behind shock wave in long tube analyzed by time effect and integrating equations, using Galerkin method 24 p4197 A66-42997  
 Channel flow deriving equation for proper turbulence spectrum and expression for spectrum of dynamic and turbulent quantities 24 p4197 A66-43061  
 MHD flow, examining effects of finite electric conductivity on basic flows due to compression and shear 24 p4246 A66-43115  
 Generalization of experimental data on hydraulic resistance in tubes with ribbon turbulizers for laminar flow with macrovortices and turbulent flow 24 p4198 A66-43223

## CHAPLYGIN EQUATION

Approximate methods for integration of equations of plane isentropic motion of gas at supersonic velocities 08 p1165 A66-19572  
 Boundary value problem solution constructed as expansion of particular solutions of Chaplygin equation in region bounded by parabolic line and two characteristics 12 p1904 A66-24240  
 Exact solution derived for gas jet flow with three characteristic high subsonic velocities, using Falkovich extension of Chaplygin hodographic method 15 p2425 A66-29850  
 Problems of various subsonic gas jets of finite width around dihedral obstacle solved with Chaplygin hodographic method 16 p2627 A66-30207  
 Subsonic flow around circular cylinders using three alternate hodographic approximations to Chaplygin law 16 p2627 A66-30208  
 Approximation of Chaplygin plane motion equations of gas flow at high supersonic velocities 16 p2688 A66-31304  
 Improved Chaplygin solutions to ordinary differential equations 18 p3126 A66-33955  
 Chaplygin equation solution translating current function and velocity potential from physical into hodograph plane 19 p3342 A66-36474  
 Existence of solution for equilibrium problem of circular symmetrically loaded membrane with stress-free contour proven by Chaplygin method 19 p3476 A66-36838  
 Lighthill integral transform methods in hodograph transformation theory of plane compressible transonic shock-free potential flows around airfoil sections in solution space of Chaplygin equation [ICAS PAPER 66-26] 23 p4007 A66-41008  
 Singular solutions for Chaplygin equations using generalized wave functions, noting iteration method for finding wave equation corresponding to first terms of expansion series 23 p4085 A66-41561

## CHAPMAN-ENSKOG METHOD

## SA BOLTZMANN EQUATION

Convergence of Chapman-Enskog expansion for linearized Boltzmann equation, using perturbation theory 07 p1081 A66-17935  
 Chapman-Enskog method applied to equations obtained when Bogoliubov functional assumption is introduced into BBGKY hierarchy, determining transport coefficients 14 p2276 A66-27640  
 Approximation method for thermal diffusion factor of almost Lorentzian gas mixture with better convergence properties than Chapman-Enskog



approximation 16 p2824 A66-30119  
 Measuring and calculating methods for dilute gas transport properties independent of fluid dynamic environment in which they operate 16 p2825 A66-30306  
 Boltzmann equation for dilute monatomic gas, discussing asymptotic interpretation of Hilbert and Chapman-Enskog theories 23 p4097 A66-42011  
 Dissipative mechanism in cylindrical plasma confined by axial magnetic field noting coefficients, linear transport relations, equations of change, Chapman-Enskog expansion and anomalous effects 24 p4246 A66-43112  
**CHAPMAN-FERRARO CAVITY**  
 Chapman-Ferraro hollows for system of parallel line currents enveloped by stratified corpuscular flux 22 p3975 A66-40806  
**CHAPMAN-JOUGET FLAME**  
 Heterogeneous detonations, discussing polydisperse and monodisperse spray detonations and liquid fuel film shock-induced combustion [AIAA PAPER 66-109] 06 p0969 A66-16256  
 Propagation of combustion-wave, consisting of flame front and shock wave passing down tube closed at one end, in presence of magnetic field in undisturbed gas at rest 06 p0874 A66-17002  
 Detonation in gaseous mixtures and in condensed phase, reviewing aerodynamic theory 15 p2617 A66-29315  
 Ionized gas flow rate behind detonation wave used with Chapman-Jouguet condition to determine speed of sound in reaction products 16 p2687 A66-31160  
 Heterogeneous detonations, discussing polydisperse and monodisperse spray detonations and liquid fuel film shock-induced combustion [AIAA PAPER 66-109] 17 p3037 A66-33237  
 Ideal detonation wave and Chapman-Jouguet condition, considering plane permanent and shock waves 18 p3266 A66-34721  
**CHAPMAN-JOUGET THEORY**  
 Imploding cylindrical shock wave production through imploding detonation waves in oxygen-acetylene mixtures, using Chapman-Jouguet theory 08 p1204 A66-18523  
 One-dimensional CJ detonation existence as self-sustaining phenomenon 08 p1208 A66-19203  
**CHAPMAN SHEAR LAYER**  
 Improved HF prediction using ray tracing techniques to determine F-2 layer scale heights and scale height h for alpha-Chapman electron density distribution 08 p1217 A66-19218  
**CHAR**  
 Char generation and determination of thermal conductivity function under simulated entry heating conditions [AIAA PAPER 65-640] 01 p0162 A66-10597  
 Char formation in solid rocket nozzle exit cones made from reinforced plastic predicted from corrosion standpoint 07 p1151 A66-17585  
 Metallographic technique for encapsulating char layers of plastics tested under reentry conditions to preserve them for microscopic examination 10 p1545 A66-21223  
 Char-layer structural integrity limits application of charring-ablator heat-protection materials to advanced ballistic reentry [AIAA PAPER 66-424] 18 p3239 A66-33642  
 Engineering method to determine combined effects of entry and combustion heating on total char regression of ablative nozzle as function of distance from exit plane [ASME PAPER 66-MD-72] 21 p3806 A66-38500  
**CHARACTER RECOGNITION**  
 Standardization of characters for optical character recognition, class B, using merit curve technique 02 p0193 A66-11598  
 Line structured pattern by vidicon tube and beam control logic 03 p0337 A66-12438  
**CHARACTERISTIC EQUATION**  
 Simple semigroup treatment of problems involving powers of nonnegative matrices 02 p0249 A66-11255  
 Stability limit on forward gain in control systems with small time delay by approximating exponential in characteristic

equation 02 p0207 A66-11877  
 Model consisting of closed rectangular box with one vibrating panel, comparing results of one-term approximation with orthogonal-mode solution 03 p0437 A66-12809  
 Book on motion stability using Liapunov method noting motion equations, perturbing forces effect on equilibrium, instability, Lagrange theorem, etc 03 p0393 A66-13286  
 Perturbed-motion damping for characteristic equation with null root or two imaginary roots 05 p0717 A66-15313  
 Integral curves of particular ordinary differential equation containing singularity 11 p1721 A66-22642  
 Relations between coefficients of characteristic equation of automatic systems and parameters of root loci with hyperbolic branches 11 p1680 A66-23325  
 Root locus methods applied to synthesis of linear multivariable control systems for noninteraction 12 p1855 A66-24644  
 Orr-Sommerfeld equation regarding stability of parallel flows solved for large Reynolds number, using inner and outer expansion theory 12 p1866 A66-24944  
 Stability and sensitivity requirements considered simultaneously in control system design, minimizing time domain sensitivity index and incorporating transient response characteristics 13 p2052 A66-26073  
 Stability of control systems with distributed parameters and hysteresis-curve-type nonlinearity for various critical cases of system characteristic equation 16 p2668 A66-30750  
 Operating characteristics equations of energy converters constructed of anisotropic materials and subjected to physically meaningful constraints 19 p3281 A66-36292  
 Characteristic equation for linear flutter problem of elastic cylindrical shell immersed in gas flow, discussing energy radiation, traveling wave propagation and discontinuity problem 22 p3995 A66-40510  
 Motion stability conditions of plant equipped with automatic control device in certain critical cases 24 p4236 A66-42213  
**CHARACTERISTIC FUNCTION**  
 Elements of eclipsing binary spherical stars determined from Fourier transforms of their light curves by defining characteristic functions of system 02 p0285 A66-11298  
 Characteristic functions of rectifier contact multipoles extended to multipoles containing closing contacts of internal and external relays 05 p0658 A66-15330  
 Decomposition of probability laws that possess specific type of characteristic function 07 p1061 A66-18511  
 Boundary value problem solution constructed as expansion of particular solutions of Chaplygin equation in region bounded by parabolic line and two characteristics 12 p1904 A66-24240  
 Generalized quadratic detection system with n entries, evaluating probability law of output function by derivation of cumulants from second characteristic function 13 p2027 A66-25450  
 Graph analysis by connectivity considerations, based on generating and characteristic functions, noting application to sampled data systems, discrete Markov processes, computer programs, etc 15 p2453 A66-29771  
 Characteristic functions of rectifier contact multipoles extended to multipoles containing closing contacts of internal and external relays 15 p2475 A66-29975  
 Elliptic restricted problem of three bodies, discussing analytical determination of characteristic exponent to equilibrium solutions [AIAA PAPER 65-685] 19 p3461 A66-35892  
 Analyzer of characteristic function of random phase of quasi-harmonic signal using statistics 20 p3529 A66-37520  
 Numerical differentiation formulas for coefficients of given characteristic function, using tabulated Stirling numbers 22 p3938 A66-39904  
 Characteristic operator of Markov process on smooth manifold 24 p4230 A66-42210  
**CHARACTERISTIC METHOD**  
 Method of characteristics applied to three-dimensional supersonic flow equations for compressible inviscid gas 07 p0982 A66-18130

Inviscid supersonic flow fields of reacting gas mixture around pointed bodies calculated, using characteristics method 08 p1164 A66-19128  
 Three-dimensional supersonic gas flow past truncated cone with shock separation calculated by method of characteristics 11 p1629 A66-22336  
 Liapunov first method and applicability to asymptotic stability of stationary points of nonlinear differential systems 11 p1721 A66-22641  
 Strong plane shock produced in Al by hypervelocity impact and late stage equivalence examined, using analytical and graphical solution of method of characteristics and realistic state equation 13 p2194 A66-25061  
 Legendre transformation and characteristics of MGD potential equation 13 p2142 A66-25708  
 Direct numerical solution by method of characteristics for hyperbolic partial differential equation of Timoshenko beam under moving force 14 p2398 A66-27423  
 Difference equations arising when one-velocity kinetic equation is solved by characteristics method, estimating error 14 p2338 A66-28280  
 Points in interior and boundary of three-dimensional supersonic gas flow determined, using characteristic method, deriving difference equations 14 p2278 A66-28284  
 Unified treatment of nonlinear partial differential equations, considering solution technique in engineering application 16 p2739 A66-31740  
 Symmetrical stress wave propagation in thin plate with small, circular hole at center, noting boundary conditions and solutions via Laplace transforms and by method of characteristics 17 p3022 A66-32012  
 Propagation along rays or bicharacteristics for two equations with partial linear derivatives having two unknowns and coefficients which are indefinitely differentiable 17 p2945 A66-32280  
 Propagation of cylindrical shear waves in nonhomogeneous elastic bodies treated by method of characteristics [AIAA PAPER 66-444] 17 p3027 A66-32757  
 Method of characteristics computer code applied to partial differential equations of inviscid fluid, calculating flow fields [AIAA PAPER 66-412] 18 p3097 A66-33637  
 Load characteristics and characteristic curves for proportional and bistable fluid amplifier noting output, input and dynamic effects 18 p3054 A66-34133  
 Multiple rocket engine exhaust plumes calculated by method of characteristics and finite difference and compared with schlieren data [AIAA PAPER 66-651] 18 p3264 A66-34448  
 Gas flow formation ahead of flame front in circular and rectangular shock tubes analyzed, based on high speed photographs and method of characteristics 21 p3836 A66-39097  
 Annular nozzle shapes established via method of straight line characteristics, noting flow patterns at various regions 23 p4009 A66-41731  
 Flows with relaxation involving very rapid flow processes accompanied by reactions without chemical or thermodynamic equilibrium, using characteristics method 23 p4014 A66-42048  
 General theory of mixed problems for two-dimensional hyperbolic system of any order with continuous and discontinuous coefficients 24 p4230 A66-42220  
**CHARACTERISTICS**  
 S AERODYNAMIC CHARACTERISTICS  
 S AIRFOIL CHARACTERISTICS  
 S FLIGHT CHARACTERISTICS  
 S FLOW CHARACTERISTICS  
 S PERFORMANCE CHARACTERISTICS  
 S POLARIZATION CHARACTERISTICS  
 S VOLT-AMPERE CHARACTERISTICS  
**CHARGE**  
 SA ELECTROSTATIC CHARGING  
 SA EXPLOSIVE  
 SA ION CHARGE  
 SA SHAPED CHARGE  
 SA SPACE CHARGE  
 Built-in surface charge on thermally oxidized silicon as function of exposed



crystal face orientation 09 p1411 A66-19929  
 Charge-controlled /p-n-p/ transistors, discussing three-dimensional asymmetric model, dynamic characteristics and switching time calculation 09 p1355 A66-20569  
 Charge motion in Hf accelerator described by nonadiabatic approximation in magnetic field under action of polarized wave 15 p2553 A66-29639  
 Power dissipation in input and output matching networks of varactor doubler for calculating true input and output powers from semiconductor bulk material, noting charge storage occurrence 15 p2466 A66-29674  
 Schrodinger equation in semiconductor with N atoms containing dislocation, vacancy or other defect, noting phase shift and local charge neutrality 16 p2775 A66-30730  
 MOS transistor characteristics based on model in which bulk charge due to ionized impurity in semiconductor and difference between electrostatic potential and voltage drop in channel are included 16 p2662 A66-31015  
 Thermal noise theory extended for insulated gate /MOS/ FET with gate voltage induced channel structure by including bulk charge from ionized impurities in semiconductor substrate 16 p2663 A66-31016

**CHARGE DISTRIBUTION**  
 Charge distribution in ion beams after passage through nitrogen and inert gases 02 p0267 A66-11724  
 Cerenkov radiation by charge moving lengthwise in magnetic field of cold plasma, determining radiation spectrum range and total radiation energy 03 p0397 A66-12389  
 Relationship between field singularities of electrostatic theory and equations for fixed charge and dipole models, including geometrical distributions 03 p0391 A66-12404  
 Cylindrical receiving and scattering antennas, determining current from admittance, charge distribution and near field for incident plane wave 06 p0827 A66-16036  
 Photoelectric storage tube capable of long term integration of faint optical images, employing as storage target low density layer of KCl for increased charge multiplication 06 p0883 A66-17017  
 Potential and forces acting on charged body in rarefied plasma flow 07 p1090 A66-18141  
 Carrier number fluctuation in semiconductor conduction band due to generation and recombination of charge carriers 07 p1105 A66-18371  
 Diffusion technique preparation of GaP p-n junctions and relation of p-i-n junction electric field calculation to Baraff carrier ionization rate theory 07 p1108 A66-18415  
 Potential and charge density distributions derived for stationary charged sphere and charged body moving through plasma 08 p1261 A66-18744  
 Charge density distribution, electric field strength and flow rate of turbulent flow of incompressible fluid in flat nonconducting channel 08 p1263 A66-19172  
 Effect of surface charging on superconducting transition temperature, locating negative charges at oxide-oxygen interface in experiments with thallium films 09 p1419 A66-20043  
 Effect of orientation of silicon substrate on surface charge density and properties of silicon-silicon dioxide interface 10 p1573 A66-21346  
 Space charge theory of one-dimensional, monoenergetic, unipolar and bipolar currents traversing on otherwise evacuated space between infinite plane parallel electrodes 10 p1557 A66-21572  
 Unified theory of cold plasma nonlinear oscillations /Dolph/ fails to apply to traveling wave solutions 10 p1569 A66-21921  
 Density of free carriers in semiconductor conduction band varying with electric field, noting growth and phase velocity of RF wave of small amplitude 10 p1584 A66-22070  
 Heat treatment and ionizing irradiations effect on charge distribution and number of surface states in silicon-silicon dioxide system 12 p1932 A66-24824  
 Cerenkov radiation by charge moving lengthwise in magnetic field of cold plasma,

determining radiation spectrum range and total radiation energy 13 p2139 A66-25394  
 Motion equation of viscous oil flow under action of electric forces caused by surface charge 13 p2070 A66-26709  
 Influence of p and n doping on electrification of dust of Ge monocrystals grown from zone-melted material 14 p2364 A66-27717  
 Formula derivation for dynistor delay time and switching-on time on basis of system of charge equations 14 p2254 A66-27741  
 Charging effect of Ag-Au alloys and other properties determined by perturbation theory 14 p2365 A66-27754  
 Durham horizontal spectrograph measurements of charge ratio of cosmic ray muons at sea level 15 p2588 A66-29574  
 Muon charge ratio derived from inelastic collision model of pion production, considering just average multiplicities 15 p2588 A66-29575  
 Effect of electrical charge on surface of glass substrate on nucleation density and initial growth structure of thin films of gold prepared by evaporation under ultrahigh vacuum 15 p2466 A66-29683  
 Fragmentation probabilities, charge spectrum and interaction mean free paths of relativistic heavy nuclei in primary cosmic radiation investigated in stack of nuclear emulsions 16 p2795 A66-31010  
 Limits to charge groups classified according to structure and geometry into linear dipole-type concentrated moments analyzed, using generalized functions 16 p2823 A66-31713  
 FET structures with linearly graded junctions noting maximum gain configuration, transconductance expression, etc 17 p2895 A66-33116  
 X-ray irradiated MOS structure behavior, noting ionic charge motion in oxidized silicon that depends on electric field 18 p3155 A66-34083  
 Charge distributions in systems of nucleons and pions with given total isotopic spin and charge 18 p3219 A66-35191  
 Theoretical distribution of charges and potential in vicinity of metal-dielectric barrier in absence and presence of applied field 19 p3448 A66-36753  
 Field and charge density distributions in semiconductor with hot electrons, showing domain movement type oscillations due to stationary wave propagation 20 p3617 A66-37555  
 Quasi-oscillations of cold sharply bounded plasmas, noting surface charge role in scattering and AC probe resonances 20 p3611 A66-38361  
 Nonlinear theory of parametric excitation applied to modulated wide beams of uniform cross section, analyzing propagation in such beams of charge density oscillations 21 p3781 A66-39013  
 Unified method for evaluation of electron-repulsion integrals for Slater-type orbitals 22 p3949 A66-39912  
 Carrier density, mobility and space-charge-limited current in p-type silicon 22 p3962 A66-40049  
 MOS work function difference effect on surface charge density and orientation calculations for Si-silicon dioxide interfaces 22 p3962 A66-40050  
 Charge distribution in thermally grown silicon dioxide and silicon n-type inversion layer 22 p3962 A66-40087  
 Taxonomy of electric charges in Si-silicon dioxide metal insulator semiconductor /MIS/ systems under presence or absence of bias 22 p3877 A66-40178  
 Resistance network analog method determination of carrier density distribution and charge constant in p-n junction for two-dimensional axisymmetric case 23 p4115 A66-41858  
 Small charge asymmetry and entropy of hot universe, finding rational solution for almost-charge symmetrical case 24 p4280 A66-43057

**CHARGE EXCHANGE**  
**SA RESONANCE CHARGE EXCHANGE**  
 Charge exchange and ionization cross sections for hydrogen ions passing through ordinary and heavy hydrogen 01 p0107 A66-10194

Secondary emission ratio and multiplication constant of electron-ion oscillatory discharge 06 p0919 A66-16872  
 Measurement of effective cross sections of double charge of hydrogen, lithium, sodium and potassium ions in gases, considering error due to unequal scattering of primary and secondary particles 12 p1918 A66-24876  
 Charge exchange cross section increase during single collisions of alkali-metal ions with atoms of inert gases and atomic hydrogen and nitrogen 14 p2336 A66-27155  
 Effective ionization and charge exchange areas of certain gases undergoing collisional ionization by accelerated ions 17 p2961 A66-32954  
 Charge exchange loss of confined thermal plasma in mirror magnetic field 17 p2972 A66-32975  
 Apparent HF stability of highly anisotropic plasma, noting charge exchange and trapped proton energy spectrum 18 p3142 A66-33671  
 Exchange pairs spectrum analysis based on observation of nonlinear splitting of EPR signals of pairs of exchange-coupled chromium ions in corundum 18 p3154 A66-33943  
 Instability effect in n-channel silicon MOS transistors bombarded with ionizing radiation 20 p3528 A66-37317  
 Ionization of oxygen examined, using charge exchange in double mass spectrometer, noting break in electron impact ionization efficiency curve and constructing breakdown graph 20 p3605 A66-38097  
 Charge exchange of protons in alkali metal vapors with formation of highly excited hydrogen atoms, noting cross section, reaction mechanism, etc 22 p3953 A66-39762  
 Optical charge exchange in silicon carbide analyzed, using electron paramagnetic resonance 22 p3964 A66-40311  
 Measurement of effective cross sections of double charge of hydrogen, lithium, sodium and potassium ions in gases, considering error due to unequal scattering of primary and secondary particles 23 p4097 A66-41083  
 Charge exchange cross sections for argon ions incident on hydrogen and deuterium measured over energy range of 30 to 1000 ev, taking into account ion-molecule reactions 23 p4098 A66-41267  
 Charge exchange cross section increase during single collisions of alkali-metal ions with atoms of inert gases and atomic hydrogen and nitrogen 24 p4239 A66-42975

**CHARGE SEPARATION**  
 Charge separation into film about symmetrically gravitating body at high temperatures and small Debye radius 03 p0396 A66-12290  
 Wave propagation along magnetic field in collisionless plasma taking charge separation effect into account 13 p2148 A66-26036

**CHARGE TRANSFER**  
 Grid dispersion mobility dependence on temperature in p-type Ge, noting discrepancy of theoretical and experimental results 08 p1273 A66-19257  
 Photomicrographic analysis of reactions during charging and discharging of nickel-cadmium alkaline cells 08 p1170 A66-19643  
 Size-effect problem affecting charge transport coefficients in thin films 09 p1428 A66-20577  
 Charge transfer between nitrogen ions and oxygen atoms, calculating cross sections 09 p1405 A66-20681  
 Charge transfer and charge rearrangement in atmospheric ion-neutral particle collisions 10 p1557 A66-21143  
 Charge-carrier concentration and mobility in thin silicon specimens 10 p1589 A66-22172  
 Potential sweep method for organic and adsorption analyses, showing relation between galvanostatic and fast potential sweep transients, noting mathematical analysis of current-potential transients 12 p1812 A66-25000  
 Space and time dependence of particle density and current in semiconductor material 14 p2356 A66-27045  
 Ionization cross sections for low energy collisions of neutral nitrogen molecules or neutral argon atoms, using asymmetric



charge transfer 14 p2337 A66-27980  
 Charge-carrier concentration and mobility in thin silicon specimens 19 p3441 A66-35786  
 Chemical kinetics of electron plasma reactions, discussing energy states, ion-molecule reactions, charge transfer, transport properties, phase interactions, etc 21 p3702 A66-38448  
 Nitrogen ion charge-transfer reaction rates with CO and carbon dioxide in pulsed flowing afterglow system 21 p3774 A66-38529  
 Charge transfer between water drops relevance to radiation problem and efficiency of conversion of electrostatic to electromagnetic energy 22 p3942 A66-39679  
 Reaction rates for charge transfer reactions of carbon monoxide with oxygen and carbon dioxide measured at 300 degrees K in pulse-discharge flowing afterglow system 22 p3859 A66-39907  
 Thermal energy Ar charge transfer reactions measured in pulsed-discharge flowing-afterglow system with mass spectrometer detection 22 p3860 A66-39927  
 Hall effect in poly-n-vinylcarbazole-iodine charge-transfer complex, noting sign discrepancy of majority carrier 22 p3963 A66-40109  
 Surface charge mobility measurement method applied to Si and Ge and time variation of surface conductivity 23 p4110 A66-41183  
 Charge transport through hemispherical metal contacts on semiconductors, calculating V-I characteristics and injection ratios 24 p4254 A66-42388  
 Cross sections for charge transfer reactions of nitric oxide with atomic and molecular ions of oxygen and nitrogen 24 p4200 A66-42590

**CHARGED PARTICLE**  
 SA ALPHA RADIATION  
 SA BETA RADIATION  
 SA COULOMB POTENTIAL  
 SA CYCLOTRON RESONANCE  
 SA DEUTERON  
 SA ELECTRON  
 SA MESON  
 SA NUCLEAR PARTICLE  
 SA PARTICLE CHARGING  
 SA PARTICLE TRAJECTORY  
 SA POSITRON  
 SA PROTON  
 SA QUARK

Focused laser as accelerating cavity for cyclic particle accelerator 01 p0080 A66-10328  
 Charged Styropor ball motions in free float between plates of perforated capacitor with alternating electric field 01 p0119 A66-10374  
 Ionization chamber for measuring interplanetary space radiation, using Geiger-Mueller counter as secondary detector 01 p0073 A66-11115  
 Magnetic moment of charged particle as function of initial particle motion, particle distance from axis of field and asymptotic behavior of field 02 p0268 A66-11775  
 Charged particle interaction with magnetic field of toroidal solenoid, taking into account self-consistent polarization fields and short-circuit currents 02 p0268 A66-11777  
 Series of self-quenched Geiger counters for visual detection in cosmic rays of unstable charged particles decaying within millisecond 03 p0417 A66-12281  
 Structure of disturbed plasma in thermodynamic equilibrium situated near charged solid surface ideally reflecting incident particles 03 p0397 A66-12381  
 Nonlinear oscillations of plasma behind formation front of charged particles 03 p0397 A66-12383  
 Charged particle motion in field of plane traveling wave and acceleration by transverse wave 03 p0397 A66-12387  
 Relationship between laws of electron temperature and charged particle concentration fall-off in helium plasma diffusion flow 03 p0398 A66-12520  
 Reflection and transmission of charged particles incident on plane moving plasma shock with small thickness compared to Larmor radius of particles 04 p0552 A66-14019  
 Recombination of nonequilibrium charge carriers in indium arsenide, noting radiative and impact recombination 04 p0569 A66-14357  
 Solution for group properties of equations

for monoenergetic charged-particle beam extended to beam in presence of stationary background and multivelocity and multicomponent beams 04 p0556 A66-14417  
 Adiabatic motion determination of charged particle containment in combined mirror-multipole cusp magnetic fields 05 p0718 A66-14712  
 Asymptotic theory of photolizationization chamber noting charged particle densities, sheath equations and quasi-neutral plasma 05 p0721 A66-14717  
 Interaction between charged particle beams and plasma in linear stage and saturation stage, using spectroscopic method 05 p0722 A66-14896  
 Physics of cosmic rays - All-Union Conference, Apatity, U.S.S.R., August 1964 05 p0749 A66-15372  
 Low energy charged particle measurements, describing satellite mounted spherical electrostatic analyzer 05 p0751 A66-15373  
 Series of self-quenched Geiger counters for visual detection in cosmic rays of unstable charged particles decaying within millisecond 05 p0756 A66-15453  
 Particles in radiation belt of Earth, considering motion in dipole field, sources, loss processes, etc 05 p0756 A66-15745  
 Instability of plasma supported under gravity by magnetic field, considering collisions between charged and neutral particles dominate over charged particle interaction 06 p0915 A66-16180  
 Survey in satellite era of energetic particle radiations, plasmas and magnetic fields in space, including solar wind, solar cosmic rays, etc 06 p0951 A66-16612  
 Brightness dependence of pulse arc on power per unit length of arc, estimating charged particle density and plasma temperature 06 p0919 A66-16875  
 Angular distribution of secondary particles from interactions in nuclear emulsions, determining energy release ratio in electron photon cascade 07 p1113 A66-17541  
 Identification of charged fast particles in nuclear emulsions, measuring multiple scattering of protons and mesons along track with various kinetic energies 07 p1114 A66-17543  
 Ratio of energy of electron-photon component and energy of charged mesons in interaction between nucleons and iron nuclei 07 p1114 A66-17548  
 Radiation by ultrahigh energy muons in lamellar medium, noting frequency 07 p1117 A66-17566  
 Stochastic acceleration of charged particles in randomly time-varying electromagnetic fields 07 p1084 A66-18426  
 Particle distribution in neighborhood of charged sphere in weakly ionized rarefied plasma 08 p1263 A66-19022  
 Formula for energy deposition from charged particle beams used in techniques for shielding nuclear particles from space 08 p1259 A66-19124  
 Kinetic equations, considering free and bound charges in weakly ionized hydrogen plasma, noting self-consistent approximation for second distribution function 08 p1265 A66-19375  
 Fermi acceleration of charged particles in shock transition region beyond magnetosphere 08 p1219 A66-19407  
 South latitude cosmic-ray plateau determined by measuring cosmic radiation-caused charged particle and neutron fluxes 08 p1284 A66-19415  
 Simplification of equations for two-temperature plasma composed of electrons, singly charged ions and neutral atoms, noting effect of viscosity and thermal force 08 p1265 A66-19468  
 Plasma diagnostics by spectroscopic techniques, measuring polarity dependences of temperature and charged particle concentration for flows with shock wave and periodic structure 08 p1265 A66-19470  
 Superconducting persistent magnets, cryogenic pumping and other low temperature techniques for measuring gravitational forces on charged particles 09 p1379 A66-20083  
 Spatial scattering of associated electromagnetic waves arising during

passage of fast charged particles thorough semiconductors, noting role of Cerenkov radiation 09 p1428 A66-20596  
 Transition radiation relative to dispersion of dielectric permittivity for charged particle passing through boundary between two media 09 p1410 A66-20930  
 Earth radiation belts, summarizing present knowledge and noting as-yet-unknown particle acceleration mechanism 09 p1444 A66-21021  
 Spherical electrostatic analyzers on Cosmos XII, Cosmos XV and Elektron II satellites 09 p1445 A66-21029  
 Outer radiation belt with energies between 100 ev and 10 to 40 keV 09 p1446 A66-21039  
 Cosmic rays during flights of Sputniks and Cosmos satellites investigated by analysis of charged particle fluxes obtained by gas discharge counter 10 p1595 A66-21042  
 Colloidal thruster with hot cathode charged colloidal particle source [AIAA PAPER 66-255] 10 p1593 A66-21460  
 Loss rates of charged particles from ohmically-heated discharges in C-Stellarator, showing confinement time parameters 10 p1568 A66-21825  
 Intensities and ratios of intensities of Be, B and S nuclei determined near geomagnetic equator in India, using nuclear emulsion stack 10 p1600 A66-21844  
 Charged particle radial distribution determination as function of amplitude of HF magnetic field, using diffusion in discharge induced by HF traveling H-wave 10 p1570 A66-21998  
 Large transverse velocity components imparted to charged particles by passing particles through magnetic field prior to injection into trap 10 p1570 A66-22000  
 Linear theory of resonance excitation of oscillations in plasma by fast-charged particle beam 10 p1571 A66-22015  
 Charged particle motion determined by gravitational-electromagnetic field properties with motion equations following from integrability condition of field equations 11 p1735 A66-22343  
 Charged particle fluxes of 1 kev energy measured by spherical electrostatic analyzer aboard Cosmos XV 11 p1762 A66-22423  
 Cerenkov radiation from charge spiralling in warm plasma under action of infinite magnetostatic field 11 p1745 A66-22494  
 Model of high energy collision processes, based on terms of four-momentum transfer and spectra variation, used for calculation of atmospheric diffusion of heavy triplets produced by primary cosmic radiation 11 p1741 A66-23190  
 Sources and effects of electrical charge accumulation and dissipation on spacecraft 11 p1778 A66-23485  
 Cosmic dust particles of interplanetary space hypothesized to carry electrical charges, based on irregularities in zodiacal light, night airglow and noctilucent clouds 12 p1945 A66-23510  
 Measurement of differential energy spectra of protons, helium nuclei and heavy nuclei by cosmic radiation telescopes mounted on POGO and Pioneer satellites 12 p1877 A66-23684  
 Threadlike equatorial current ring and effect on geomagnetic cut-off rigidity of directed cosmic radiation 12 p1941 A66-24172  
 Spectrum, energy and radiation field of charge moving above anisotropically conducting surface 12 p1921 A66-24206  
 Motion of charged particles in rotating and fixed magnetic fields, using drift approximation equations to determine field parameters 12 p1921 A66-24209  
 Hot-wire anemometer determination of electron and ion temperature, neutral particle temperature, concentration and velocity and potential of partially ionized helium plasma 12 p1882 A66-24223  
 Larmor precession of charged particles effect on nonstationary temperature field in plane channel 12 p1922 A66-24361  
 Charged particle motion in time dependent axially symmetric magnetic field, using drift theory of plasma radial compression 12 p1922 A66-24462  
 Measurement of effective cross sections of double charge of hydrogen, lithium, sodium and potassium ions in gases, considering



error due to unequal scattering of primary and secondary particles 12 p1918 A66-24876

Charged particle excitation of weakly damped MHD waves in metal placed in magnetic field 12 p1825 A66-25021

Structure of disturbed plasma in thermodynamic equilibrium situated near charged solid surface ideally reflecting incident particles 13 p2139 A66-25386

Nonlinear oscillations of plasma behind formation front of charged particles 13 p2139 A66-25388

Charged particle motion in field of plane traveling wave and acceleration by transverse wave 13 p2139 A66-25392

Wave propagation during gyroresonance interaction, noting nonlongitudinal characteristics of waves generated in magnetosphere between beams of charged particles 13 p2072 A66-25462

Charged particles in nonadiabatic magnetic traps, noting behavior in mirror machine with spatially modulated central field, using model with square wave modulation 13 p2145 A66-25727

Triple correlative function solution for plasma system of charged particles and collision integral for pair correlative function 13 p2148 A66-25941

Amplification and attenuation of plasma wave by quasi-neutral charged particle flux on boundary between two plasmas 13 p2148 A66-26035

Electrohydrodynamic phenomena associated with motion of charged particle in plasma, showing that disturbance produced depends on particle speed 13 p2154 A66-26669

Meteor ablation, analyzing size and velocity distributions of meteor showers, noting how hydration in secondary particles promotes formation of charged particles which contribute to noctilucent cloud formation 14 p2378 A66-27094

Energy loss of fast-charge particle passing through weakly turbulent magnetoactive plasma 14 p2340 A66-27136

HF potential for motion of charged particle in combined quasi-static magnetic and HF electromagnetic field 14 p2341 A66-27198

Finite difference solution of nonlinear boundary value problem of Landau-Vlasov equation for charged particle for Maxwellian distribution function 14 p2344 A66-27625

Recombination of nonequilibrium charge carriers in indium arsenide, noting radiative and impact recombination 14 p2368 A66-28255

Charged particle acceleration by coherent radiation 14 p2348 A66-28313

Stoermer method solution of charged particle motion in field of magnetic dipole situated in external uniform magnetic field antiparallel to dipole magnetic moment vector 15 p2482 A66-28491

Charge particle flux in Earth radiation belt as observed by Cosmos 15 p2573 A66-28496

XVII

Adiabatic motion of charged particles in space- and time-variant magnetic field studied, using guiding-center approximation 15 p2574 A66-28902

Concentration waves excited by internal modulation of charged particle concentrations in cross section of plasma flow analyzed for various velocities of flow 15 p2550 A66-29212

Charged particle motion in Van Allen belts, examining effect of nondipole terms on mirror point distributions 15 p2489 A66-29314

Core structure and properties of extensive air showers, stressing lateral density structure of charged particles and energy of nuclear active component 15 p2579 A66-29527

Extremely collimated nuclear interactions in carbon induced by collisions of charged cosmic ray particles in energy region 20-100 gev 15 p2585 A66-29559

Vertical drift of charged particles effect on electron density profile as cause of seasonal variations in ionospheric absorption 15 p2490 A66-29944

Role of corpuscular radiation in lower ionosphere formation, noting charged particle flux, energy spectra, etc 15 p2591 A66-30024

Subsonic parachute-borne blunt probes for charged particle measurement in

ionosphere 15 p2493 A66-30039

Distribution of charged particles of different energies escaping from magnetic trap in which spiral moving electron fluxes are created 16 p2755 A66-30094

Temporary capture of charged particles in static magnetic bottle, based on resonant perturbations and Stoermer neck 16 p2760 A66-30588

Critical electric field for charged droplets atomizing, noting spark discharge and ion concentration in clouds 16 p2742 A66-31109

Cross sections for sticking electrons to spherical charged particles, considering Debye screening distance of Coulomb force field 16 p2754 A66-31158

Perturbation of electron density at large distances from body at high velocity in collisionless plasma under steady external magnetic field 16 p2762 A66-31181

Thick lithium drifted semiconductor silicon detectors for investigation of fluctuations of energy loss by high and intermediate energy particles 16 p2755 A66-31389

Solar radiation protection based on charged particle motion through magnetic field of solenoid 16 p2811 A66-31481

[AIAA PAPER 66-512]

Explosive driven magnetic generator applied to investigate electric, optical and elastic properties of various substances, plasma physics and charged particle accelerator 16 p2637 A66-31585

Emission spectrum of copper atom used to measure temperature and concentration of charged particles in DC-arc plasma burning under water 16 p2766 A66-31600

Plasma injected into magnetic trap with aid of conical theta pinch investigated to determine ion and electron energy, lifetime and charged particle concentration variation 17 p2969 A66-32546

Charged particle distribution in hollow cylinder shaped positive plasma column during diffusion and helical instability in longitudinal magnetic field 17 p2969 A66-32548

Strong axial magnetic field effect on constant current discharge in continuous-duty ion laser, noting plasma diffusion, charged particle density and laser output decrease 17 p2936 A66-33117

Electron-ion emission pattern distribution obtained by pulsed laser focusing on solid target 17 p2937 A66-33256

Force action on charged spherical dust particles in cometary atmospheres, noting interaction with ions 17 p3012 A66-33399

Charged particle effect in Van Allen zone on short circuit currents of photovoltaic cells on D-1A satellite 18 p3053 A66-33980

Spectroscopic measurements of cold plasma charged particle concentrations, specifically spectral broadening due to Stark effect, forbidden-line intensities affected by internal electric fields and autoionization line intensities 18 p3143 A66-34032

Kinetic equations, considering free and bound charges in weakly ionized hydrogen plasma, noting self-consistent approximation for second distribution function 18 p3146 A66-34177

Distribution of charged particles in plasma column situated in interspace between two coaxial cylinders 18 p3147 A66-34698

Differential spectra of charge components of primary cosmic ray heavy nuclei at different solar modulation levels and effects of interstellar propagation 18 p3191 A66-34839

Skyhook balloon flight Geiger counter cosmic ray monitor measurements of energy and charge spectra of galactic rays at solar minimum 18 p3192 A66-34847

Hypothetical mechanism of earthward radial drift of charged particles, noting albedo neutron decay, proton belt, etc 18 p3197 A66-34876

Cerenkov counter measurements of primary cosmic ray heavy nuclei made by Elektron II satellite 18 p3199 A66-34886

Unifield field theory equation for energy loss rate of charged particle moving in plasma, considering screened Coulomb potential and dielectric permeability 18 p3150 A66-34937

Charged particle radial distribution determination as function of amplitude of

HF magnetic field, using diffusion in discharge induced by HF traveling H-wave 18 p3151 A66-34975

Large transverse velocity components imparted to charged particles by passing particles through magnetic field prior to injection into trap 18 p3151 A66-34977

Linear nonrelativistic motion of charged particle in field of traveling electromagnetic wave 18 p3092 A66-35073

Charged particle beam interaction with plasma, determining electron-ion temperatures and HF field 18 p3152 A66-35074

Calculations of energy loss of relativistic charged particles in dielectric media compared with mass operator and perturbation theory calculations and with oxygen experiment 18 p3221 A66-35201

Muons and neutrinos from energetic celestial objects, discussing charge ratio, rate and equipment used 18 p3224 A66-35226

High resolution magnetic hodoscope performance for charged particle analysis, measuring momentum response spectrum and experimental error due to instrumental effects 18 p3115 A66-35228

Transfer coefficients of charged particles trapped in magnetic field of Earth studied, examining concept of sudden pulses as basic mechanism 19 p3451 A66-35260

Charged particle motion and penetration of magnetosphere in proximity of neutral point as result of solar wind-geomagnetic field interaction 19 p3405 A66-35281

Charged particle motion in field of magnetic dipole situated in external magnetic field /magnetospheric G region/, using Stoermer method 19 p3451 A66-35282

Role of particle channeling in affecting results from crystal-line detectors used for charged particle and nuclear scattering 19 p3359 A66-35912

Background gamma and electron fluxes reduction in charged-particle spectroscopy with fast-gated electronics 19 p3359 A66-35918

Motion of isolated energetic charged particle in simple force-free magnetic field with rectilinear lines of force 19 p3400 A66-35925

Linear theory of resonance excitation of oscillations in plasma by fast-charged particle beam 19 p3407 A66-36101

Effect of binding on distribution in angle of charged particles having suffered scattering with lattice atoms 19 p3403 A66-36172

Dielectric function for homogeneous plasma calculated, using fluctuation dissipation theorem 19 p3409 A66-36289

Collective interactions of charged particle beams with plasma produced by electron beam, noting power loss of electron beam coincides with power of HF oscillations caused by interaction 19 p3416 A66-36524

Cosmic dust particles of interplanetary space hypothesized to carry electrical charges, based on irregularities in zodiacal light, night airglow and noctilucent clouds 20 p3646 A66-37023

Electron temperatures and concentrations of charged particles behind strong shock wave in air measured, noting techniques, maximal values and accuracy 20 p3545 A66-37369

Spatial scattering of associated electromagnetic waves arising during passage of fast charged particles through semiconductors, noting role of Cerenkov radiation 20 p3622 A66-38130

Correlation of magnetic fields and energetic electrons on IMP I satellite, noting depression in geomagnetic tail region, electron fluxes and diamagnetic effect 20 p3633 A66-38201

Adiabatic theory of charged particle motion, considering first-order effects in radius of gyration and Alfvén theory 20 p3603 A66-38303

Charged particles and plasma in geomagnetic field, noting diffusion of trapped particles and acceleration by Fermi mechanism and wave acceleration 20 p3640 A66-38319

Magnetospheric boundary phenomena, noting dependence of charged particle observations on character of associated



magnetic fields 20 p3641 A66-38329  
 Magnetospheric models, discussing role of fast magnetospheric merging in connection with charged particle acceleration and magnetospheric configuration 20 p3641 A66-38330  
 Adiabatic theory of distorted motion of charged particles in geomagnetic field, showing dependence on equatorial pitch angle 20 p3642 A66-38332  
 Magnetospheric plasma instabilities, discussing resistive, flute type, whistler and HF two-energy component electrostatic loss-cone instability 20 p3642 A66-38333  
 Sideral anisotropy indicated for charged galactic cosmic radiation obtained by celestial scanning, using narrow angle muon telescope 21 p3808 A66-38466  
 Quantum statistical approach to interaction of electromagnetic waves with hot plasma, noting renormalization of Coulomb interaction between charged particles 21 p3776 A66-38545  
 Plasma injection from coaxial plasma gun into magnetic trap with opposite fields 21 p3788 A66-39055  
 Charged particle motion in magnetic traps of acute geometry, examining particle trajectories by numerical integration 21 p3788 A66-39056  
 Rarefied plasma in magnetic trap with oppositely moving magnetic fields, examining charged particle motion 21 p3788 A66-39057  
 Nonadiabatic magnetic trap energy redistribution during charged particle motion in spatially periodic magnetic field 21 p3788 A66-39058  
 Closed magnetic trap for transverse-to-longitudinal conversion of energy of particles moving in spatially periodic magnetic field 21 p3788 A66-39059  
 Electron, charged particle density spectrum and temperature measurements in arc jet of partially ionized argon 21 p3790 A66-39082  
 Fast charged particle and electromagnetic field fluctuations interaction with nonequilibrium plasma 21 p3791 A66-39155  
 Nonlinear theory of fast-particle motion in helical toroidal magnetic fields, using averaging techniques to obtain adiabatic invariants describing nonlinear oscillatory motions 21 p3792 A66-39295  
 Wave theory calculation of moments of velocity change of charged particle in magnetoplasma 21 p3794 A66-39573  
 Energy loss of charged particles during passage through weakly turbulent plasma in magnetic field with HF oscillations 22 p3952 A66-39751  
 Plasma spectrography in shock tube, determining charged particle concentration 22 p3953 A66-39760  
 Charged particle collisions effect on drift instability of low pressure plasma studies, using Landau collision integral as model collision integral 22 p3956 A66-40192  
 Charged particle radiation shielding in space of solar cell panels by use of concentrator geometry 22 p3852 A66-40512  
 Spectrum, energy and radiation field of charge moving above anisotropically conducting surface 22 p3956 A66-40570  
 Motion of charged particles in rotating and fixed magnetic fields, using drift approximation equations to determine field parameters 22 p3956 A66-40573  
 Hot-wire anemometer determination of electron and ion temperature, neutral particle temperature, concentration and velocity and potential of partially ionized helium plasma 22 p3919 A66-40585  
 Behavior of wave function for system of charged particles near coalescence of any two of them, noting electron-nucleus cusp conditions for diatomic molecules 22 p3861 A66-40904  
 Measurement of effective cross sections of double charge of hydrogen, lithium, sodium and potassium ions in gases, considering error due to unequal scattering of primary and secondary particles 23 p4097 A66-41083  
 Magnetic pumping heating rate for plasma, using conversion of organized energy into random energy by charged particle collisions 23 p4100 A66-41250  
 Electric microfields in plasma taken as system of charged particles moving in

uniform neutralizing background, using approximations and Monte Carlo study 23 p4101 A66-41363  
 Second term obtained in asymptotic series for second adiabatic invariant of charged particle motion in static magnetic field and found to vanish at mirror points 23 p4103 A66-41491  
 Potential oscillations in neutral completely ionized plasma-neutral charged-particle beam system in HF electric field and growth rate of plasma instability 23 p4106 A66-41707  
 Electric field effects on collision efficiency of charged cloud droplets 23 p4065 A66-41846  
 Power conversion enhancement of acoustic-electromagnetic wave coupling across plasma-air boundary by suitable thickness and charged particle density 24 p4241 A66-42304  
 Motion of single charged particle inside plasma accelerator with static electric and magnetic fields, showing periodicity of radial motion with time 24 p4241 A66-42397  
 Monochromatic longitudinal wave amplification by charged particle beam in nonlinear plasma, noting amplitude dependence on coordinate 24 p4243 A66-42520  
 Pressurized Ar-filled ionization chamber response to charged particles in cosmic radiation determined as function of atmospheric depth 24 p4264 A66-42604  
 Interplanetary exploration space mission objectives, discussing magnetic fields, energetic particles, cosmic radiation, etc 24 p4264 A66-42660  
 Distributions of extensive air showers with either fixed number of charged particles or muons, using Geiger counter and scintillation counter 24 p4268 A66-42914  
 Ratio of energy flux in nuclear active component to energy flux in electron photon component in extensive air showers with given numbers of particles 24 p4269 A66-42918  
 High energy muon flux in interference radiation incident to fast charged particle constant-speed trajectories through periodic laminar medium 24 p4271 A66-42939  
 RK-1-F radiosonde for stratosphere measurements of X-ray photon energy spectrum, charged particle density and X-ray photon density 24 p4213 A66-42941  
 Three-dimensional voltage traps for charged particles, using equilibrium equations with or without thermal agitation 24 p4245 A66-42996  
 Dispersion equation for cyclotron electromagnetic waves for magnetoactive plasma injected with charged particles 24 p4245 A66-43016  
 HF potential for motion of charged particle in combined quasi-static magnetic and HF electromagnet field 24 p4246 A66-43096  
 Book on theory and application of plasma physics including adiabatic charged particle motion, MHD characteristics, shock waves and hydromagnetic flow 24 p4246 A66-43109  
 Statistical mechanics methods applied to plasma, deducing kinetic equation 24 p4246 A66-43111  
**CHART**  
 SA GRAPH  
 SA MAP  
 SA POLARIZATION CHART  
 Compressibility charts for nonpolar and slightly polar substances in gaseous and liquid states and in two-phase region, using four independent parameters [ASME PAPER 65-WA/PID-1]  
 05 p0793 A66-15680  
 Stability and gain prediction of microwave tunnel diode reflection amplifier, using Smith chart 07 p1007 A66-17508  
 Automatic dynamic chart display, integrating navigation system as well as situation display and link with computer, for monitoring and updating self-contained system 07 p1067 A66-17690  
 Chart display methods of let-down type, roller type and optical projection for aircraft navigation 10 p1554 A66-21897  
 Mixer cross products of mixer frequency charts to determine spurious responses with respect to desired output 13 p2040 A66-25825

Sputnik III data application to plotting of total magnetic field intensity chart above U.S.S.R., using spherical harmonic analysis 19 p3345 A66-35290  
**CHASSIS**  
 Dynamic logic chassis analyzer /DLCA/, diagnostic tool for isolating faults to circuit card or component level in programmer test station /PTS/ and component test station /CTS/ ground support equipment 14 p2260 A66-28266  
 Forced-cooled electronic chassis development history 20 p3527 A66-37347  
**CHEBYSHEV APPROXIMATION**  
 Synchronous tuning of microwave filters involving small changes in rejection bandwidth and being consistent with Chebyshev response 01 p0044 A66-10936  
 Resonant frequency equation for line segment with reactive loads at both ends, using Chebyshev principle 02 p0199 A66-11754  
 Algorithm determining best approximation of bounded function in Chebyshev sense adapted to discrete case 04 p0540 A66-14167  
 Algorithm determining best approximation in Chebyshev sense of continuous function on segment 04 p0540 A66-14168  
 Frequency analysis of wideband RL and RLC phase shifters, using Chebyshev polynomials 04 p0501 A66-14406  
 Distributed stepped impedance low-pass prototype filter, giving impedance values for filters with Chebyshev equal-ripple characteristics 06 p0844 A66-16082  
 Symmetrical transverse electromagnetic-mode directional couplers, deriving formulas for functional parameters and insertion-loss function 06 p0844 A66-16083  
 Chebyshev approximation for function in equation of thermogravimetric data plot 07 p1149 A66-17470  
 Tensor product analysis of alternating direction implicit iteration techniques for approximate solution of elliptic partial differential equations 09 p1396 A66-20637  
 Computational aspects of uniform polynomial approximation to function and derivative 11 p1722 A66-22983  
 Discrete-sample curve fitting using Chebyshev polynomials and approximate determination of optimal trajectories via dynamic programming 12 p1850 A66-24257  
 Computation method of damped resonance frequencies for system of equal masses, spring constants and viscous damping coefficients 13 p2194 A66-25140  
 Minimax polynomial approximation of degree n to continuous function 14 p2323 A66-27779  
 Filter design minimizing maximum value of estimation error over all admissible signal waveforms 15 p2474 A66-29380  
 Approximation theory by generalized rational functions 17 p2947 A66-32843  
 Maximum error curves for Lanczos selected point method of polynomial solution to ordinary differential equations, using Chebyshev and Legendre functions 17 p2947 A66-32858  
 Perturbation theories for equations of celestial mechanics, obtaining analytical solutions in terms of Chebyshev polynomial series  
 [AIAA PAPER 66-534] 18 p3226 A66-33664  
 Discrete time signal estimation, noting minimum mean square error, minimax estimation, etc 18 p3068 A66-33905  
 Digitally computed tables of Chebyshev approximations of Laplace shift operator transfer function enabling analog simulation of time delay systems 18 p3090 A66-34069  
 Attenuation factor and degree of stability of automatic control systems determined by Mikhailov criterion and Chebyshev polynomials 18 p3091 A66-34670  
 Auxiliary polynomials for direct determination of Chebyshev interpolation polynomial 19 p3389 A66-35936  
 Optimal control of dynamic systems with minimax type performance index, discussing application of proposed method of solution 19 p3334 A66-36686  
 Gain specification of linear controller for large launch booster, using new application of linear control theory 19 p3471 A66-36687  
 Monotony principle for linear approximations to determine upper and



lower bounds of minimum deviation in approximating functions of real variable by generalized polynomials 20 p3590 A66-37529

Generalized Rolle and Bernstein theorems applied to polynomial approximation of ordinary differential equations over compact linear space 21 p3758 A66-39259

Approximately minmax detection of vector signal on Gaussian background 22 p3939 A66-40188

Optimum microwave filters with even number of sections, using first-order Chebyshev polynomial to obtain equivalent circuit 23 p4037 A66-41515

**CHECKOUT EQUIPMENT**

**SA CEMS SYSTEM**

**SA SPACE VEHICLE CHECKOUT PROGRAM**

Preflight checking of aircraft gyroscopes and accelerometers noting built-in spin detection, torque generator and gimbal check 01 p0070 A66-10956

Functional system integration as means of displaying complex electrical and electronic systems to minimize initial design, equipment checkout and trouble shooting problems 02 p0306 A66-11637

Automatic in-flight testing capability of redundant systems [ATAA PAPER 65-732] 03 p0353 A66-13051

Probable reliability of measurement accuracies and decision limits for system checkout 03 p0347 A66-13336

Subsystem checkout in operation termed on-line checkout, noting use of digital computer with random noise signals and role of correlation and transfer functions 04 p0493 A66-13608

Mathematical model that takes into account factors involved in detecting faults as well as MTBF and MTTR for prediction of equipment availability 04 p0494 A66-13682

Error in checkout systems for space or weapon systems 08 p1223 A66-18740

Digital computers to control automatic test equipment 08 p1187 A66-18741

Automated ground station, with computer controlled telemetry system, for Saturn launch vehicle checkout 09 p1347 A66-20675

Ground support equipment /GSE/ concept, onboard checkout system for large space boosters [ATAA PAPER 64-298] 10 p1612 A66-21935

Design of Malfunction Detection System used on board orbiting laboratory type vehicles to monitor and evaluate critical signals 10 p1538 A66-22043

Air traffic control transponder performance preflight test set, ground-based equipment for fast and positive checkout 11 p1732 A66-22898

SNAP-10A instrumentation and control subsystems and ground test program 12 p1911 A66-23676

Self-diagnosable DX-1 computer design to achieve maximum operational availability 12 p1828 A66-23843

Versatile avionics shop test /VAST/ system, computerized test system for carrier-based avionics 12 p1838 A66-24606

Design requirements for checkout equipment to support advanced carrier-based airborne early warning /AEW/ aircraft 12 p1858 A66-24607

Parameters for selection of miniaturized integrated circuit computer for onboard checkout systems 12 p1829 A66-24612

Airborne checkout system, in-flight maintenance and related signal processing problems 13 p2190 A66-25259

Digital computer automatic checkout equipment for Saturn spacecraft 13 p2057 A66-25260

Digital computer automatic checkout equipment for maintenance of avionic systems 14 p2269 A66-27157

Automatic preworkshop screening test apparatus for determining which components removed from aircraft during ground maintenance need to be sent to workshop 14 p2224 A66-28298

Onboard testing and checkout of manned space vehicles 14 p2272 A66-28424

Checkout procedure for automatic test systems, checkout error probability and relation to tolerance limits 17 p2888 A66-32777

Onboard checkout requirements and

application for advanced space missions [SAE PAPER 660461] 17 p2904 A66-33166

Maintenance on long-duration manned space flight facilitated by maintenance job aid information stored in high density retrieval and display system 19 p3309 A66-35950

Space packaged automatic checkout system for aerospace vehicles including test equipment, control, measurement capability and computer program 20 p3542 A66-37244

Acceptance checkout system for checkout assistance to Apollo CSM and LEM facilities during countdown, discussing system configuration variability, composition and operation 20 p3543 A66-37579

Deterministic and quasi-deterministic class of electronic failure predictions as prevention strategy for use in aerospace system test or checkout program 20 p3566 A66-37887

Maintenance Dependency Chart for design checking and troubleshooting in missile and weapon systems 20 p3566 A66-37889

Atoll computer programming language for spacecraft checkout systems and automatic support operations in Saturn launch vehicle 20 p3544 A66-38257

**CHELATE COMPOUND**

**SA CHEMICAL LASER**

Rare earth chelates preparation, luminescence behavior and laser action 05 p0741 A66-15833

Organic cations effect on laser threshold of solutions of tetrakis form of europium benzoyltrifluoroacetate 07 p1046 A66-18418

Preparation and physical properties of polytricyanoethylene /TCNE/ copper chelate film, noting electric conductivity and heat treatment effect 10 p1574 A66-21348

Deuterium isotope effect on thresholds of europium chelate lasers, noting solvent thermal effects 13 p2105 A66-26598

Ionic fluorescence of europium chelates, suitability as laser materials, noting energy transfer role in population inversion 14 p2315 A66-27463

Organic laser systems including luminescence for achieving laser action, fluorescent and phosphorescent systems and chemistry and spectroscopic properties of rare earth chelates 20 p3576 A66-36970

Fluorescence quantum efficiencies of octa-coordinated europium homogeneous and mixed chelates in organic solvents, noting effect of oxygen removal 23 p4030 A66-41153

Spectroscopic, chemical and laser properties of piperidinium salt of europium tetrakis 24 p4226 A66-43034

**CHEMICAL ANALYSIS**

Ultrapurification discussing definition, purification techniques, analytical techniques /e.g. emission and mass spectroscopy/ and role in biochemistry, metals and materials 04 p0474 A66-13867

Rare gas content of stony meteorites measured by dissolving diverse mineral fractions in solvents on step-by-step basis 04 p0580 A66-14497

Grinding technique for accurate and proportional subdivision of chondritic meteoritic specimen and separation of metallic and silicate components for chemical analysis 08 p1179 A66-19095

Coordination of substituted pyridine N-oxides with oxovanadium /IV/ cations, noting stoichiometric variations with changes 09 p1339 A66-20878

Hot-pressed high-purity polycrystalline MgO 12 p1900 A66-24721

Chemical analysis of permanent and trace organic gases in 30-day manned experiment, using gas chromatography 12 p1811 A66-25011

Interferogram interpretation to determine carbon dioxide concentration in air mixture 13 p2208 A66-25315

Neutron analysis techniques for determining hydrogen presence on lunar or planetary surfaces, based on measurement of gamma radiation 14 p2233 A66-28105

Automatic chemical processing systems for extraterrestrial biochemical investigations 14 p2233 A66-28414

Nitrogen, phosphorus and calcium determination from perchloric acid digestion, process includes sample collection, preparation, digestion and determination 17 p2870 A66-32143

Chemical analysis of stony meteorites with

sharp boundaries between light and dark structure, noting differences found in achondrites and chondrites 17 p3007 A66-33281

Use of balanced filter pairs for nondispersive analysis of aluminum and silicon in aluminum-silicon mixtures 18 p3063 A66-33693

Phase anomaly detected by chemical test D during decreasing phase of last solar cycle 21 p3732 A66-38629

Isotopic composition of lithium in chondrules from Bruderheim and Bjurboie meteorites 22 p3975 A66-39681

Rare gas isotope composition of Estherville mesosiderite and Haralaya, Juvinas, Shergotty and Stannern achondrites 22 p3975 A66-39682

Diffuramine chemistry for understanding nature of N-F and N-X bonds, electron distributions and existence and stabilities of N-F radicals and ions 23 p4031 A66-41233

Oxalate determination in two methods based on photochemical decomposition of ferric oxalate complexes in aqueous acidic solution 24 p4171 A66-43166

**CHEMICAL AUXILIARY POWER SOURCE**

Organic and liquid ammonia electrolyte systems in combination with active anode materials to achieve high energy output battery system [ATAA PAPER 64-750] 13 p2007 A66-26651

**CHEMICAL BOND**

**SA COVALENT BOND**

**SA HYDROGEN BOND**

Conformal sets of aromatic and other conjugated compounds, noting that sum of combustion heat of compounds in one set equals sum of compounds in other set 03 p0442 A66-12333

Approximate natural orbitals for four electron wavefunctions for Be and LiH obtained by diagonalization of appropriate first order reduced density matrices 06 p0910 A66-16165

Affinity and stoichiometry of binding of 1-anilino-8-naphthalene sulfonate /ANS/ to apomyoglobin and apohemoglobin 08 p1177 A66-18701

X-ray spectral analysis of chemical bond structure in aluminum semiconductor compounds 08 p1274 A66-19311

Nonpolar solutes on structure of water and hydrophobic bond in protein stability in aqueous solutions 11 p1649 A66-22988

Classification of titanium alloying elements by effect on strength of chemical bonds in process of formation of alpha-solid solutions 12 p1892 A66-23519

Chemical behavior of metallic elements predicted by periodic table, noting formation of liquid and solid metallic solutions, binary and complex metallides and nature of chemical bond 12 p1896 A66-24897

Spin-free derivation of Pauling rules for evaluating matrix elements for spin-free Hamiltonian over anti-symmetric Slater bond functions 16 p2754 A66-30860

Alpha-chloro alkanoyl valine methyl esters analyzed, finding that diastereoisomeric pairs separation by gas-liquid chromatography can assess steric conditions around amide bond 17 p2871 A66-32932

Chemical bonds between rare earth metals and nitrate radicals in lanthanum, gadolinium and yttrium nitrates studied from IR absorption spectra 18 p3063 A66-33842

German papers on metal physics, chemical bonds in crystals and ferromagnetism 19 p3439 A66-35712

Quantum theoretical ferromagnetic behavior of chemical bonds in transition metals and Hartree-Fock calculation of atomic orbitals 19 p3439 A66-35713

EPR detection of dangling bonds at surface of silica and quartz, noting inhomogeneous expansion 19 p3445 A66-36341

Chemical bonds in carbides and nitrides of transition metals, obtaining atomization heat of compound and effective charges of transition atomic nuclei 19 p3386 A66-36425

Extended Hueckel method calculations of bonding in N, F oxidizers 23 p4030 A66-41220

Diffuramine chemistry for understanding nature of N-F and N-X bonds, electron distributions and existence and stabilities of N-F radicals and ions 23 p4031 A66-41233



**CHEMICAL COMPOSITION**

Electrolytic isolation and precise composition of intermetallic phase of titanium silicide formed in alloys of system Ti-Al-Fe-Si-B-Cr 02 p0245 A66-11994

Organized elements of Orgueil meteorite by quantitative fluorescence microscopy, correlating morphology with chemical composition 03 p0429 A66-13353

Fe and Mn variation in tektites, significance in identification of parent material 04 p0575 A66-13454

Partition functions in equilibrium chemical composition and thermodynamic properties of nitrogen and oxygen plasmas 07 p1087 A66-17936

Diffusion and regular model of motion of cosmic rays, noting dependence of applicability to cosmic ray fluxes on chemical composition 09 p1443 A66-20598

Solar chemical composition by analysis of UV resonance lines 10 p1602 A66-21090

Schlesinger reaction and chemical composition of mixed hydride reagents 11 p1649 A66-22399

Superconducting behavior of various close packed low symmetry intermediate phases in various binary systems, noting relation between transition temperature and composition 12 p1928 A66-23939

Chemical composition and origin of moldavites, noting densities, refractive indices, oxide content, rubidium-strontium ratio, etc 13 p2187 A66-26234

Phosgenation procedure for synthesis of carbon-14 labeled isocyanates, noting isotope distribution in compounds 14 p2231 A66-26871

Chemical composition of meteorites and classification into siderites, siderolites and aerolites, noting method for determining age and origin 14 p2383 A66-27651

Irtrans 1 to 5 chemical composition and far IR transmittance measured by vacuum grating spectrometer 15 p2524 A66-28847

Fe-Ni-P system and structure of iron meteorites 15 p2603 A66-29967

Major element analysis of chemical composition of Georgia tektite 17 p3004 A66-32931

OH production by sublimation and gas hydrate occurrence in cometary nuclei 17 p3009 A66-33373

Energy spectrum, possible chemical composition and anisotropy of ultrahigh energy primary cosmic radiation 18 p3213 A66-35147

Stellar evolution of stars between 1 and 3 solar masses, noting nuclear reactions and chemical composition 19 p3467 A66-36792

Diffusion and regular model of motion of cosmic rays, noting dependence of applicability to cosmic ray fluxes on chemical composition 20 p3633 A66-38132

Origin and chemical composition of cohenite in meteorites and temperature dependence of weight-percentage content 22 p3981 A66-40479

Phase and chemical compositions of structural components forming in iron-nickel-chromium alloys with aluminum and titanium content 22 p3936 A66-40787

**CHEMICAL COMPOUND**

**SA INORGANIC COMPOUND**

**SA ORGANIC COMPOUND**

**SA POTTING COMPOUND**

Synthesis of complex lithium aluminum hydride, lithium hexahydroaluminum, having hydrogen to aluminum ratio greater than four 11 p1649 A66-22400

Sliding contact wear under very dry high altitude or space conditions due to lack of contact film prevented by using chemical compounds like graphite or lithium carbonate 12 p1888 A66-24664

Hypothesis that system sodium fluoride-yttrium trifluoride serves as model for each of binary systems of rare earth trifluorides SmF<sub>3</sub> to LuF<sub>3</sub> with sodium fluoride 14 p2315 A66-27466

Chemical protection from radiation exposure-induced genetic changes 15 p2438 A66-29484

Physiologically active compounds and cultured antibiotic fluids used to eliminate effects of ionizing beta radiation on plant seeds 15 p2438 A66-29487

Thermoconductivity and electrical

resistivity measurements with derived Lorentz functions for various compounds, using longitudinal heat flow 16 p2771 A66-30252

**CHEMICAL EFFECT**

Intensity of solar corona, Wolf number and biological and chemical tests conducted in Italy 04 p0577 A66-13817

Chemical durability of lithium silicate glass as result of crystallization 12 p1901 A66-24864

Injurious effect of gamma radiation and 660 and 120 mev protons on white mice and protective action of certain pharmacochemics 15 p2438 A66-29480

Effect of chemical attachment in boundary lubrication of aluminum thrust washer using 1-cetene and cetane 24 p217 A66-42700

Chemical effects on RF attenuation during reentry for blunt-nosed lifting vehicles and sphere-cone ballistic vehicles 24 p4158 A66-42782

**CHEMICAL ENERGY**

Carbon dioxide reduction systems using chemical, electrochemical and thermal energy 02 p0185 A66-11641

Discrepancy between measured value of N-H bond dissociation energy in hydrazine and value suggested by other chemical evidence 07 p1000 A66-17463

Chemical potential and integral equation for correlation functions of classical fluids, using Percus method when functions exhibit cluster properties 14 p2276 A66-27637

Martensitic transformation of Ni-Fe alloy from fcc to bcc lattice, noting stress produced by chemical free energy difference between austenite and martensite structure 15 p2520 A66-28649

Liquid junction cell design, noting equation integration for ideal diffusion potential and salt effects potential for heteroionic junctions of uniform ionic strength and cation concentration 20 p3502 A66-38188

Chemical energy conversion to electromagnetic energy by flux compression, discussing process and obtained efficiency 21 p3698 A66-39502

Dynamic conversion of solar and chemical energy, discussing power conditioning, Brayton-cycle system with inert gas and spacecraft batteries 22 p3851 A66-40128

**CHEMICAL ENGINEERING**

Heat transfer - AICE and ASME Conference, Cleveland, August 1964 07 p1149 A66-17576

Industrial technology and cost estimate of chemical machining metal removal process [ASTME PAPER MR66-155] 14 p2299 A66-26953

Heat transfer - AICE and ASME Conference, Los Angeles, August 1965 18 p3261 A66-34375

Sequential and concurrent chemical engineering operations in solid-propellant Apollo launch motor manufacturing 22 p3968 A66-39867

Lunar environmental effects and logistics problems in industrial chemical processing of lunar resources [AICE PREPRINT 46A] 22 p3977 A66-39894

Equipment design and weight estimates for lunar production of oxygen and water 22 p3977 A66-39896

**CHEMICAL EQUILIBRIUM**

**SA MOLECULAR DISSOCIATION**

Stagnation point viscous shock layer equations for three-component gas model in chemical nonequilibrium and binary gas model in vibrational and chemical nonequilibrium, noting heat transfer rates 08 p1164 A66-19125

Nonequilibrium internal distributions effect on rates of chemical gas-phase exchange reactions 11 p1650 A66-23212

Phase equilibrium diagram of Ti-Co-Al system at 800 degree C, based on X-ray and Microstructural analyses 12 p1893 A66-23762

Phase behavior in helium-xenon system exhibiting gas-gas equilibria 13 p2018 A66-26444

Numerical solution of steady state jump equations for normal ionizing shock waves in hydrogen, assuming upstream and downstream states at chemical equilibrium 13 p2154 A66-26661

Law of mass action derivation of chemical equilibrium ionization of multitemperature

system when electron and heavy particle temperature differ 15 p2551 A66-29218

Photolysis of carbon dioxide, using 1633 angstrom line of bromine lamp 16 p2646 A66-30862

Inequalities of chemical thermodynamics with partial equilibrium 21 p3836 A66-39087

Formation of organic compounds under conditions of thermal equilibrium, noting aromatic compounds in solar nebula and gases activated to plasma state 22 p3860 A66-40483

**CHEMICAL EXPLOSION**

Safety requirements for handling and testing unstable materials, particularly hydrazinium diperchlorate /HP sub 2/ solid propellant oxidizer 12 p1812 A66-24469

**CHEMICAL FUEL**

Beryllium and beryllium compounds are components of most efficient chemical fuels theoretically known but extremely toxic 03 p0414 A66-12907

**CHEMICAL KINETICS**

Rarefied hydrogen flame interaction between hydrogen atoms and molecules of certain organic, aliphatic and cyclic compounds 01 p0161 A66-10414

Hydrodynamic equations for one-dimensional, adiabatic, frictionless, ideal-gas flow and general matrix form equations for coupled chemical reaction kinetics of C-H-O /N/ systems 02 p0303 A66-11533

Radiolysis of pure liquid nitrogen tetroxide, detailing product formation kinetics and effects of added oxygen and nitric oxide 02 p0188 A66-11593

High temperature kinetics of difluoroamino radical decomposition in excess argon studied behind incident shock waves 03 p0413 A66-12337

Reaction kinetics of tetrafluorohydrazine with fluorine to yield nitrogen trifluoride measured by colorimetric technique 04 p0472 A66-13395

Kinetic studies of hydroxyl radicals in shock waves, considering recombination via particular reaction in lean hydrogen-oxygen mixtures 04 p0596 A66-13646

Extremal concentrations in laminar flow of incompressible viscous liquid along tube of constant cross section, noting recombination reactions 04 p0597 A66-13695

Thermistor for measuring rate of liquid-phase exothermal and endothermal reactions in terms of heat loss, considering condensation polymerization of terephthalyl chloride with ethylene glycol in dioxane solution 05 p0787 A66-14959

Chemical kinetics of nonequilibrium combustion of propane-air and ethane-air mixtures in one-dimensional flow, including ignition delay and reaction time [CI PAPER WSCI-65-19] 05 p0788 A66-15143

Computed high temperature rate constants for hydrogen atom transfers involving light elements, noting activation energies for exothermic reactions [CI PAPER WSCI-65-24] 05 p0629 A66-15148

Kinetic studies of high temperature carbon-silica reactions in charred silica-reinforced phenolic resins [CI PAPER WSCI-65-25] 05 p0788 A66-15149

Rates and activation parameters determined from nuclear magnetic resonance spectra for degenerate isomerizations of disubstituted benzofurazan oxides 05 p0629 A66-15155

Vibrational excitation effect in hydrogen-deuterium exchange 05 p0718 A66-15156

Burning modes in initially unmixed reactants, describing stagnation region formation by interaction of opposed flows of fuel and oxidant [AIAA PAPER 66-71] 06 p0969 A66-16258

Fuel drop ignition, discussing parametric extension of quasi-flame surface theory to higher reaction orders and arbitrary stoichiometric ratios [AIAA PAPER 66-70] 06 p0970 A66-16415

Macrokinetics of homogeneous-heterogeneous processes in moving media and estimates of initial material concentration in core and boundary layer regions of reaction vessel flow 06 p0971 A66-16543

Kinetic equations of complex reactions derived, using conical graphs, reducing reversible reaction problems to problems of



Irreversible kinetics 06 p0822 A66-16544  
 Oxidation kinetics of pure tungsten and tungsten alloys with various niobium content at high test temperatures 07 p1050 A66-18065  
 Thermal oxidation kinetics of silicon, describing diffusion process, oxide layer boundary reactions and space charge effects on initial phase 07 p1106 A66-18401  
 Kinetics of reactions in iodide method of growing epitaxial germanium layers 08 p1268 A66-18797  
 Relativistic hydrodynamics of relaxation, discussing limiting cases depending on chemical reaction and annihilation rates and pair growth 08 p1206 A66-18974  
 Kinetics of hydroxyl radical in aqueous solution, examining electron spin resonance spectrum as function of flow rate, temperature and mixture composition 08 p1178 A66-19066  
 Water vapor influence on latitudinal and seasonal distribution of stratospheric ozone concentration explained via Hampson chemical mechanism 08 p1216 A66-19209  
 Diffusion controlled mechanism for operation of nickel hydroxide electrode, analyzing corresponding boundary value problem and predicting electrochemical behavior 08 p1171 A66-19647  
 Deposition kinetics of solid phases on electrodes of second kind, noting conditions affecting crystal growth and lattice formation 08 p1171 A66-19648  
 Chemical reaction kinetics and gas dynamics combined to analyze processes occurring in combustion chambers and nozzles of jet and rocket engines 10 p1620 A66-21367  
 Hypersonic flow of air past circular cylinder with nonequilibrium oxygen dissociation, including dissociation of free stream 10 p1479 A66-21375  
 Reaction rate of atomic oxygen with nitrous oxide in shock tube at high temperatures 11 p1649 A66-22881  
 Nonequilibrium effects in recombination dissociation kinetics, using iterative perturbation procedure 11 p1738 A66-22884  
 Upper atmospheric helium ion chemical loss process, distribution of nitrogen ion and rate coefficient of helium ion-molecular nitrogen reaction 11 p1701 A66-23153  
 Nonequilibrium internal distributions effect on rates of chemical gas-phase exchange reactions 11 p1650 A66-23212  
 Kinematic computer calculations of energy distribution among products of repulsive, mixed and attractive energy release exothermic reactions 11 p1787 A66-23213  
 Ion-molecule reaction rates and recombination coefficients from mass spectrometric ionospheric data 11 p1702 A66-23492  
 Kinetics of two-phase decomposition of solid solution of magnesium-aluminum alloy, using X-ray analysis, noting grain orientation and size 12 p1898 A66-25027  
 Chemical reactions in gas flows including relation between dissociation and recombination kinetics, thermal decomposition of hydrazine, kinetics of high temperature air, etc, analyzed, using shock tube 13 p2016 A66-25160  
 Chemical system and reaction rates behind strong shock waves in mixtures of carbon dioxide and nitrogen used to study entry conditions into Mars atmosphere 13 p2062 A66-25276  
 Nitrogen adsorption effect on thermionic emission from polycrystalline tungsten ribbon at high and low applied fields, explaining work function changes 13 p2162 A66-25381  
 Experimental analysis of regression rates in hybrid rocket engines for both chemical kinetics and gas dynamics domains 13 p2173 A66-26369  
 Carbon-13 chemical shifts of carboxyl carbon atom of acetic, benzoic and mesitoic acids in various compositions of sulfuric acid 14 p2232 A66-27376  
 Nitrogen tetroxide dissociation equations 14 p2371 A66-27829  
 General cosmological problem /GCP/ based on unified field theory involving cosmological expansion, oscillation and organic evolution, discussing quadrant mechanics, entropy, ether, minimum time

problem, etc 14 p2389 A66-28408  
 Chemical kinetics of borane and diborane compounds, decomposition rates and molecular dissociation energy 15 p2447 A66-29237  
 Rate constant of ion molecular processes in ionosphere, tabulating results of laboratory analyses 15 p2495 A66-30054  
 Rate constant for atomic oxygen ion destruction by carbon dioxide measured in pulsed flowing afterglow system 16 p2645 A66-30115  
 Dissociation rate of diatomic molecular fluorine 16 p2646 A66-30863  
 Temperature and structure effect on hydride precipitation kinetics in titanium, using resistometric technique, noting nucleation problem 16 p2724 A66-31266  
 Numerical computation of quasi-equilibrium nozzle flows with finite rate chemical kinetics [AIAA PAPER 66-636] 18 p3048 A66-34220  
 Kinetic factors in diffusion flames, noting fuel/ oxidizer ratios, equilibrium in terms of flame geometry, burning of metallic elements, etc [WSCI 66-10] 18 p3263 A66-34419  
 Measurement of hydrogen-fluorine kinetics at high temperatures [AIAA PAPER 66-637] 18 p3064 A66-34437  
 Mathematical analysis of thermal wave technique for linear kinetics from viewpoint of solid-liquid interface motion 18 p3265 A66-34508  
 Internal ballistic considerations in hybrid rocket design, noting throttling and regimes of operation involving effects of surface-or gas-phase reaction kinetics [AIAA PAPER 66-628] 20 p3663 A66-38035  
 Chemi-ionization in reaction zones of hydrocarbon-oxygen or hydrocarbon air flames, noting association with abnormal excitation of hydroxyl radical 20 p3626 A66-38046  
 Space chamber molecular kinetics, noting importance of molecular flux upon simulation fidelity and effect of various gases and chamber geometry on flux profile 20 p3544 A66-38161  
 Chemical kinetics of electron plasma reactions, discussing energy states, ion-molecule reactions, charge transfer, transport properties, phase interactions, etc 21 p3702 A66-38448  
 Elementary gas phase reactions involving atoms and radicals by mass spectroscopic and diffusion cloud methods 21 p3702 A66-38472  
 Hydrogen bonding kinetics in free radical liquid-phase reactions 21 p3702 A66-38520  
 Nitrogen ion charge-transfer reaction rates with CO and carbon dioxide in pulsed flowing afterglow system 21 p3774 A66-38529  
 Numerical data for common solid state reaction equations which are functions of alpha, fraction of material reacted in time, t 21 p3797 A66-38594  
 SiC role in ablation chemistry, examining experimental results on char-reinforcement reactions 21 p3834 A66-38710  
 Inviscid hypersonic nonequilibrium flow of three-component gas past circular cone, using exact reaction-rate equations to correct solution first obtained from approximate equations 21 p3693 A66-38711  
 Thermodynamic and reaction kinetic parameters in solid rocket motor efficiency, examining Le Chatelier effect of environmental pressure, influence of propellant temperature and system thermal losses 22 p3970 A66-39873  
 Reaction rates for charge transfer reactions of carbon monoxide with oxygen and carbon dioxide measured at 300 degrees K in pulse-discharge flowing afterglow system 22 p3859 A66-39907  
 Kinetics of monosilane pyrolysis, detailing gaseous and solid product formation, surface effects and experiments with added gases 22 p3999 A66-40410  
 Methane/deuterium exchange reaction rate measured in shock tube, using vibrational excitation mechanism to explain data 22 p3860 A66-40903  
 Kinetics of dissociation of carbon dioxide gas molecules behind shock wave front 24 p4196 A66-42882

## CHEMICAL LASER

Self-pumping chemical laser theory and operation, noting chemical pumping 13 p2104 A66-26382  
 Deuterium isotope effect on thresholds of europium chelate lasers, noting solvent thermal effects 13 p2105 A66-26598  
 Chemical pumped UV laser action through thermal decomposition of dimethyl peroxide 15 p2513 A66-28836  
 Laser oscillation in flash photolysis of carbon disulphide and oxygen to form CO 17 p2933 A66-31941  
 Light energy measurements made with argon bomb used as chemically powered laser pump 19 p3373 A66-35388  
 Fluorescence quantum efficiencies of octa-coordinated europium homogeneous and mixed chelates in organic solvents, noting effect of oxygen removal 23 p4030 A66-41153  
 CW laser action in holmium-doped erbium trioxide with dominant pumping by energy transfer between ions 24 p4222 A66-42555

## CHEMICAL MILLING

Chemical milling techniques, particularly for aluminum alloys, comprising surface preparation, chemical etching and finishing 06 p0888 A66-17074  
 Chemical milling of columbium reentry vehicle skin panels using powdered metallurgy, vacuum processing, refractory alloy sheet rolling and electron beam welding [ASTME PREPRINT MR66-712] 12 p1886 A66-24417  
 Tooling and manufacturing technique and requirements for controlled removal of metal by chemical and electrochemical processes [ASTME PAPER MR66-165] 14 p2300 A66-26957

## CHEMICAL PROPERTY

Effect of tantalum carbide additions on mechanical, thermal and chemical properties of WC-TiC-Co alloys 08 p1239 A66-18902  
 Resin compacts prepared by high temperature compression of hardened resins mixed with unhardened resins, noting strength, thermal behavior and physicochemical properties 13 p2113 A66-25911  
 Comparative calculation used in computation of physicochemical properties of hydrides, including densities of beryllium hydride, entropy of cesium hydride, crystal lattice energy of rubidium deuteride, etc 13 p2018 A66-26327  
 Rare earth research - Conference, Phoenix, April 1964 14 p2361 A66-27460  
 Chemical and physical properties of samarium dicarbide, prepared by heating samarium sesquioxide with graphite, using X-ray analysis, hydrolytic studies, etc, noting structure 14 p2362 A66-27465  
 Suboxides of tantalum, examining formation, stability, structure and properties 16 p2722 A66-30221  
 Chemical stability of silver graphite, molybdenum disulfide, zinc oxide, boron nitride, muscovite and phlogopite mica solid lubricants 16 p2715 A66-31675  
 Lanthanum germanide synthesis using arc furnace, noting chemical properties 20 p3584 A66-37416  
 Spectroscopic, chemical and laser properties of piperidinium salt of europium tetrakis 24 p4226 A66-43034

## CHEMICAL PROPULSION

Requirements and performance expectations of chemical and nuclear propulsion systems for manned Mars and Venus missions 06 p0942 A66-16499  
 Hypergolic ignition and restart in Plexiglas window hybrid rocket motor, including oxidizer flow transient, flame propagation, chamber pressurization rates, etc [AIAA PAPER 66-69] 07 p1111 A66-18452  
 Liquid chemical propulsion rocket engines development problems, specifically propulsion system for Titan rocket 08 p1280 A66-18572

## CHEMICAL REACTION

SA ALKYLATION  
 SA DECOMPOSITION  
 SA DEHYDRATION  
 SA DEHYDROGENATION  
 SA DISSOCIATION  
 SA ELECTROLYSIS



SA EXOTHERMIC REACTION  
SA FRIEDEL-CRAFT REACTION  
SA HILL REACTION  
SA HYDROGENATION  
SA HYDROLYSIS  
SA ION EXCHANGE  
SA IONIC REACTION  
SA NITRATION  
SA OXIDATION  
SA PHOTOCHEMICAL REACTION  
SA POLYMERIZATION  
SA SYNTHESIS

Chemical reaction occurring between low temperature plasma jet and nearly inviscid fluid /water/ 02 p0264 A66-11388

Equation solution for flame propagatin in gas mixture with first-order exothermic chemical reaction 02 p0302 A66-11392

Atomic hydrogen reaction with HO-2 as source of hydrogen molecules in lower thermosphere 02 p0221 A66-11504

Chemical reaction between iron and extreme pressure agents like chlorine and sulfur for corrosion mechanism analysis [ASLE PREPRINT 65-LC-11] 02 p0237 A66-12254

Chemical inhibition of pentaborane-oxygen reaction in development of improved fire protection systems 03 p0413 A66-12487

Reaction of molecular hydrogen with oxygen in absence of molecular oxygen at various temperatures, using stirred reactor with mass spectrometer 04 p0473 A66-13649

High temperature analysis of mechanism and kinetics of tetrafluoroethylene decomposition and oxidation in excess argon behind shock waves, using UV absorption and mass spectrometry 04 p0571 A66-13650

Rapid irreversible second-order chemical reactions in turbulent wake of cylinder 04 p0455 A66-13937

Convective mass exchange in heterogeneous chemical reactions in laminar flow along wall 04 p0597 A66-14186

Dichloroborane synthesized in quantitative yields by thermal hydrogenation of boron trichloride 05 p0629 A66-14540

Chemical evolution studied by finding and reconstructing chemical reactions that might have occurred among primeval molecules on surface of Earth 05 p0629 A66-15017

Immiscibility and rapid interface reaction rate as cause of disruption in nitrogen tetroxide-hydrazine impinging jets [CI PAPER WSCI-65-20] 05 p0743 A66-15145

Nucleosynthesis in stars including light element reactions, helium and carbon burning, neutrino processes, etc 05 p0719 A66-15764

Kinetics of HF decomposition in HF mixtures behind incident shock waves over various temperature ranges, using IR emission 06 p0941 A66-16127

Aromatic/heterocyclic polymers from tetraamines reaction with tetraacids at room temperature, developing potential for aerospace application 06 p0901 A66-16299

Ignition of hydrogen-oxygen-argon mixtures containing small amounts of hydrocarbons and bromine substituted hydrocarbons in shock tubes 06 p0822 A66-16634

Interaction of thionyl chloride with chlorides of aluminum, titanium silicon, niobium, tantalum and oxychlorides of phosphor and vanadium 07 p1050 A66-18059

Thermodynamic stability and reaction kinetics of solids at high temperature 07 p1054 A66-18496

Inviscid supersonic flow fields of reacting gas mixture around pointed bodies calculated, using characteristics method 08 p1164 A66-19128

Heat capacity expression due to chemical reaction, relating composition variations and binary diffusion coefficient with Lewis number, presenting integral equation for system enthalpy 08 p1318 A66-19164

Oxygen reduction in sealed nickel-cadmium cells 08 p1171 A66-19646

Particle formation involving homogeneous condensation by mixing reaction technique for eventual development of colloid thruster [AIAA PAPER 66-254] 10 p1593 A66-21459

Approximate method for analyzing chemically reacting turbulent flow fields having initial homogeneities [AIAA PAPER 65-37] 10 p1523 A66-21770

Bimodal formulation applied to chemical reactions in turbulent wake flow behind hypersonic spheres, using quasi-one-dimensional model 10 p1480 A66-21771

Schlesinger reaction and chemical composition of mixed hydride reagents 11 p1649 A66-22399

Oxygen interacting with zinc oxide and UV-irradiated magnesium oxide studied, using electron paramagnetic resonance techniques 12 p1916 A66-23618

Syntheses of three macromolecular chlorocarbons, studying structure and configuration, noting high thermal stability and chemical inertness 12 p1812 A66-23633

Chemical reaction between iron and extreme pressure agents like chlorine and sulfur for corrosion mechanism analysis [ASLE PREPRINT 65-LC-11] 12 p1889 A66-24993

Reactivity of titanium alloy oxidizer tank with nitrogen tetroxide oxidizer under vibration analyzed for LEM when subjected to impact 13 p2111 A66-26222

Analytical solution to rate equations for branching chain reactions of hydrogen-oxygen reaction under shock tube conditions, for application to ignition problems 13 p2018 A66-26442

Rates and stoichiometry of reaction of aluminum hydride in tetrahydrofuran at zero degrees with selected organic compounds containing representative functional groups 13 p2018 A66-26500

Properties of laminar boundary layer undergoing surface catalysis with two reactants and two products obeying Langmuir-Hinshelwood mechanism, solving concentration field by integral equation 13 p2019 A66-26663

Hydrazine hydrate interaction with halogenides of tetravalent germanium in aqueous organic solvents 14 p2231 A66-27137

Cis- and trans-beta-bromostyrene reaction with lithium diphenylphosphide in tetrahydrofuran producing cis- and trans-beta-styryldiphenylphosphine, discussing proton magnetic resonance and configuration retention 14 p2232 A66-27498

Critical injection parameter on porous plate with turbulent boundary layer, noting conditions of neutralization reaction 16 p2684 A66-30324

New synthesis of o-nigrophenylacetaldehyde 16 p2646 A66-30621

Cobalt doping effect on magnetic properties of nickel thin films prepared by chemical precipitation 16 p2774 A66-30694

Atmospheric decay of rocket-released Li due to diffusion, wind and chemical reaction 16 p2697 A66-31008

Chemical release at high altitudes in order to obtain information about atmosphere by ground observation 16 p2697 A66-31012

Kinetics of highly endothermic carbon-silica reaction for silica-reinforced resin systems 17 p2943 A66-32453

Ignition and combustion mechanism of liquid propellant consisting of aliphatic alcohols and mixed acid, using calcium and potassium permanganates as catalysts 17 p2989 A66-32458

Temperature and pressure distribution for fluid flow through porous matrix, noting chemical reaction, heat transfer, boundary layer flow, etc [AIAA PAPER 66-423] 17 p2910 A66-32752

Diamant French satellite launching examining combustion stability during ignition, vibrations, chemical reactions between oxidizer and pressure feed system, etc 17 p3017 A66-33236

Ion-molecular reactions of hydrogen with inert gases caused by low energy electrons in low temperature plasmas, considering energy level populations, reaction cross sections, etc 18 p3064 A66-34026

H, C, N, O, Cl, Ca and Al negative ion formation in plasma, noting role of continuous radiation, formation temperature and metastable and stable states 18 p3144 A66-34041

Dissociation and reassociation reactions of hemocyanin mixtures analyzed by electron microscopy, noting original molecular structures 18 p3060 A66-34459

Chemical vapor deposition technique for materials for electron devices including preferred orientation, high purity material, special layer structures, etc 18 p3125 A66-34619

Catalytic combustion of cyclohexane, cyclohexene and benzene, determining significance of combustion via computer program 18 p3266 A66-35022

Chemical methods for carbon dioxide conversion for oxygen recovery, including relationship to biological processes 19 p3293 A66-36235

Chemical processes in low temperature plasma, noting high energy densities, enthalpies, etc 20 p3606 A66-36900

General theorems for dissociated and chemically reacting compressible laminar unsteady two-component boundary layers derived, based on Nirenberg maximum principle 20 p3510 A66-37524

Fatiguing at room temperature resulting in observable diffusion of silver into copper, using precipitation reaction to analyze influence of large number of vacancies 20 p3584 A66-37618

Asymptotic solutions of differential equations of mass transfer with chemical reaction without assumptions concerning kinematics, showing existence of five regimes 20 p3679 A66-37789

Reactions between silica and graphite studied in vacuum from 1445 to 1765 degrees C by continuously measuring amount of carbon monoxide formed 21 p3753 A66-38593

Solid solutions of titanium, tungsten, chromium prepared by carbidization of mixtures in hydrogen medium and obtained as fine-grained carbide powders 22 p3934 A66-39865

Analytic solution for ignition kinetics of dry carbon monoxide-oxygen reaction obtained, assuming initiation reaction followed by chain-branching steps 22 p3998 A66-40115

Homogeneous isotopic exchange reaction between hydrogen and deuterium in single-pulse shock tube with excess argon 22 p3860 A66-40902

Large-signal AC field effect experiments with A and B real surfaces of indium antimonide exposed to various chemical reactions and high electric field described by tunnel equation 23 p4111 A66-41185

Hydrolytic reactions of nitrogen fluorides, noting inertness of nitrogen trifluoride to pure water and reaction with aqueous base to give nitrite and fluoride 23 p4118 A66-41242

Q-switch pulsed ruby laser irradiation-induced chemical dissociation and ionization in residual gases 23 p4079 A66-42076

Homogeneous gas phase and surface reactions based on mass transfer mechanism during quenching of oxygen-nitrogen mixtures from high temperatures 24 p4170 A66-42134

Chemical interaction among components of CdO, ZnO and PbO admixtures in ammonium perchlorate, noting effect on thermal decomposition 24 p4295 A66-43200

CHEMICAL REACTOR

Theory of homogeneous-heterogeneous radical reactions in turbulent flow in one-dimensional elongated reactor with high Peclet number 08 p1179 A66-19379

Newton-Raphson method iterative solution of two-point boundary value problem and application to trajectory optimization and tubular reactor design 11 p1680 A66-23276

Refrigerated mass spectrometer inlet serving also as low temperature reactor and rough separative device for compounds stable only at very low temperatures 16 p2645 A66-30420

Mass spectrometric analysis of contents of flow reactor in which diborane at low pressure was pyrolyzed, varying temperature, flow time, surfaces, etc 17 p2871 A66-32853

Chemical reactor on-site manufacture of propellant oxygen from metallic silicates found on Moon [AICE PREPRINT 46C] 22 p3977 A66-39895

Arc image stagnation-flow reactor for measuring gas-solid reaction rates between 2000 and 3000 degrees K 24 p4216 A66-43214

CHEMICAL RELAXATION

SA GAS FLOW



## SA SHOCK WAVE

Linearized wave equation of supersonic flow with single relaxation process, using model gas mixture 06 p0874 A66-17003

Simple waves in one-dimensional nonsteady nonmagnetic relaxation hydrodynamic flows of chemically reacting compressible gases 07 p1020 A66-17965

Chemical relaxation effects in nozzle flow by measuring high temperatures created by detonation waves in shock tube, using hydrocarbon mixtures 12 p1977 A66-23748

Equation for laminar boundary layer on flat plate in viscous compressible gas flow under chemical relaxation, solved by approximate method in series form 12 p1863 A66-24244

Book on shock wave relaxation processes, discussing laws governing statistical equilibrium, thermal dislocation and ionization, nonequilibrium zones behind shock wavefront, plasma shock propagation, etc 14 p2277 A66-27788

Relaxation processes behind shock wave in free stream partially dissociated and vibrationally excited by monitoring time history of radiative emission in shock tube [AIAA PAPER 66-519] 17 p2911 A66-32775

## CHEMICAL STERILIZATION

Accidental biological contamination of planets during space exploration, noting different physical and chemical sterilization methods 02 p0184 A66-11609

## CHEMILUMINESCENCE

## SA AIRGLOW

Time variation in radiance of contaminant glow clouds released in upper atmosphere, noting solar radiation scattering 02 p0221 A66-11474

Electrochemical and chemiluminescent ozone-sensor performance, using analysis of comparative ascents 04 p0517 A66-14451

Flame as source of emission of visible UV and IR radiation and ionization source for certain combinations of fuels and oxidants 08 p1317 A66-18856

Changes in current kinetic theory of NO-O reaction, based on observation of release of nitric oxide in E region 11 p1703 A66-23494

Glow-discharge shock tube examination of chemiluminescent, surface-catalytic and gas-phase reaction rates, noting temperature dependence of NO-O and CO-O chemiluminescent reactions 13 p2016 A66-25368

Catalytic efficiency of noncatalysts interferes with accuracy of measurement, noting necessity of oxygen treatment of noncatalytic surfaces 15 p2502 A66-29310

Chemiluminescent technique for flow visualization using electrochemical system and water tunnel 15 p2476 A66-29688

Atmospheric diffusion coefficients by measuring radial growth of chemiluminous trails deposited in upper atmosphere 16 p2695 A66-30712

Simulation of upper atmosphere NO release in low density wind tunnel indicating light output of NO-O chemiluminescent reaction depends on O concentration 19 p3405 A66-36804

Chemiluminescent NO-O-atom reaction, determining effect of change of emission intensities and third 20 p3604 A66-37309

Unfocused ruby laser radiation field-biphenyl compound interaction, resulting luminescence and apparent multiphoton absorption 21 p3745 A66-38528

Chemiluminescence in atomic-oxygen-acetylene and atomic-oxygen-carbon suboxide flames attributed to formation of CO in excited and electronic states 22 p3997 A66-39926

## CHEMISORPTION

Sticking coefficients for interaction of molecular oxygen with clean semiconductor surfaces assuming immobile adsorption process 03 p0408 A66-12406

Adsorption at semiconductor and gel surfaces discussing chemisorption theory, ionizing radiation effect and structural parameters 04 p0563 A66-13768

Interaction between hydrogen and various titanium alloys, noting correlation between sorption capacity of alloys and type of phase diagram 07 p1050 A66-18064

Photoadsorption effect on semiconductor

surfaces determined as function of various parameters, noting role of external electric field 08 p1276 A66-19378

Extrinsic and intrinsic surface states and photoelectronic properties of insulating CdS crystals 09 p1427 A66-20256

Correlation and prediction of adsorption levels of gaseous contaminants for removal from space cabin atmospheres

[AICE PREPRINT 26B] 10 p1491 A66-21189

Antibody globulin coupled to diazotized aminoaryl derivative of carboxymethyl-cellulose to form immunoadsorbent for extracting antigens 12 p1805 A66-23568

Potential sweep method for organic and adsorption analyses, showing relation between galvanostatic and fast potential sweep transients, noting mathematical analysis of current-potential transients 12 p1812 A66-25000

Nitrogen adsorption effect on thermionic emission from polycrystalline tungsten ribbon at high and low applied fields, explaining work function changes 13 p2162 A66-25381

Irreversible form of chemisorption by semiconductor as affected by volume impurity and reaction with chemisorbate 13 p2017 A66-25696

Correlation and prediction of adsorption levels of gaseous contaminants for removal from space cabin atmospheres

[AICE PREPRINT 26B] 17 p2868 A66-32679

GaAs field emission cathode microscopy patterns prepared by chemical etching and low temperature field

desorption 20 p3623 A66-38393

Change in thermionic emission current of palladium wire at 1000 degrees C due to exposure to molecular and atomic-hydrogen beams 22 p3859 A66-39913

## CHEMISTRY

## S AEROTHERMOCHEMISTRY

## S ATMOSPHERIC CHEMISTRY

## S BIOCHEMISTRY

## S ELECTROCHEMISTRY

## S GEOCHEMISTRY

## S NUCLEAR CHEMISTRY

## S ORGANIC CHEMISTRY

## S PHOTOCHEMISTRY

## S PHYSICAL CHEMISTRY

## S PHYSIOCHEMISTRY

## S PLASMA CHEMISTRY

## S POLYMER CHEMISTRY

## S PROPELLANT CHEMISTRY

## S RADIOCHEMISTRY

## S STEREOCHEMISTRY

## S SURFACE CHEMISTRY

## S THERMOCHEMISTRY

## CHICKEN

Age dependence of resistance of chickens to 100 percent oxygen at one atm /OAP/, noting delayed mortality in adult birds 07 p0997 A66-17458

## CHILD LAW

Space charge theory of one-dimensional, monoenergetic, unipolar and bipolar currents traversing on otherwise evacuated space between infinite plane parallel electrodes 10 p1557 A66-21572

## CHINA

Chinese-English/English-Chinese astronomical and astrophysical dictionary 12 p1949 A66-24200

## CHIRP SIGNAL

Oblique ionospheric sounding at medium-sweep frequencies, noting performance of chirp techniques 14 p2233 A66-26771

Computer programming of pulse compression by active and passive generation, noting differences between sidelobe structures of generation 22 p3883 A66-39714

## CHLORELLA

Physiological-ecological investigations of Chlorella cultures as link in closed ecological system 01 p0018 A66-10981

Characteristics of sterols naturally occurring in species of Chlorella with algae grown heterotrophically on glucose 13 p2009 A66-25876

Biological procession of human secretions and water regeneration by Chlorella in bacterial colony 15 p2440 A66-29501

Biological effects of confining fish in sealed aquarium with and without Chlorella 15 p2440 A66-29504

Maximum photosynthetic capacity for

Chlorella determined experimentally from cell reproduction rates 15 p2440 A66-29505

Intensive Chlorella culture need of carbon dioxide concentration in closed and controlled air-carbon dioxide system 15 p2440 A66-29508

Dense continuous Chlorella culture growth at various illumination levels 15 p2440 A66-29509

Intensive Chlorella culture consumption of mineral-nutrition elements 15 p2440 A66-29510

Optimum temperature conditions for cultivating thermophilic strains of Chlorella under varying radiant flux intensities 16 p2644 A66-31589

Buffering capacity of substances liberated by Chlorella expressed in terms of van Slyke buffer index, noting changes in pH 17 p2860 A66-32831

High respiration rate of Chlorella maintained by blue-green light 19 p3287 A66-36435

Difference spectra of glucose cultures of Chlorella vulgaris beyernick indicate increased pigmentation in white light and monochromatic light over dark controls 20 p3507 A66-37791

Photillumination effect on growth rate of Chlorella vulgaris, discussing action spectrum and mechanism of light requirement for heterotrophic growth 20 p3507 A66-37792

## CHLORIDE

## SA BORON CHLORIDE

## SA CARBON TETRACHLORIDE

## SA LANTHANUM CHLORIDE

## SA LITHIUM CHLORIDE

## SA NITROSYL CHLORIDE

## SA POLYVINYL CHLORIDE

## SA POTASSIUM CHLORIDE

## SA SILICON TETRACHLORIDE

## SA SILVER CHLORIDE

## SA SODIUM CHLORIDE

## SA TITANIUM CHLORIDE

## SA TUNGSTEN CHLORIDE

Interaction of thionyl chloride with chlorides of aluminum, titanium silicon, niobium, tantalum and oxchlorides of phosphor and vanadium 07 p1050 A66-18059

Chloride requirement for cathepsin C 24 p4165 A66-43099

## CHLORINE

Cl 36 in stony meteorites produced by spallation reactions and neutron capture 04 p0579 A66-14318

Microwave discharge-fast flow to investigate interaction between molybdenum surface and chlorine 06 p0821 A66-16155

Production rates of Cl 36 and Ar 39 in metallic and stone phases of Leedey chondrite 12 p1948 A66-23904

New inner-shell resonance lines in highly ionized sulfur and chlorine from high-energy theta-pinch plasma light source 14 p2338 A66-28130

Chlorine-fluorine mixture combustion, examining flame speeds, temperatures and burned gas composition [WSCI 66-31] 18 p3263 A66-34415

Predicted capture rate in chlorine experimentator detecting solar neutrinos, using set of nuclear parameters, showing CNO cycle and proton-proton chain contribution to solar energy generation 21 p3809 A66-38657

Fluorine, chlorine and other trace elements determined through differentiated tephritic dolerite sill from Tasmania using statistical techniques, showing hydroxyl lattice sites by chlorine and fluorine 24 p4198 A66-42364

## CHLORINE COMPOUND

## SA PERCHLORIC ACID

Syntheses of three macromolecular chlorocarbons, studying structure and configuration, noting high thermal stability and chemical inertness 12 p1812 A66-23633

Chloride alkoxide of pentavalent tungsten, obtaining UV, IR, NMR and EPR spectra, molecular weight, etc 16 p2646 A66-30620

## CHLORINE FLUORIDE

## S PERCHLORYL FLUORIDE

## CHLORINE TRIFLUORIDE

Chlorine trifluoride analysis using combination of gas chromatography and IR spectrophotometry, noting column containing trichloroethylene 23 p4032 A66-41239

Electrical conductivity variation with



temperature of chlorine and bromine trifluoride, noting maximum conductivity below freezing point of chlorine trifluoride 23 p4118 A66-41241

**CHLOROETHYLENE**  
S TRICHLOROETHYLENE  
**CHLOROPHYLL**  
Hydroquinone and oxygen effects on photovoltaic characteristics of optically excited chlorophyll 06 p0812 A66-16357  
Chlorophyll distribution in mechanically fragmented spinach 11 p1645 A66-23195  
Role of light in chemical and biochemical evolution noting photosynthetic reactions depending on chlorophylls, pigment system, etc 17 p2853 A66-32102  
Complete fractionation of bacteriochlorophyll and degradation products by two rapid methods, using small amount of Rhodospirillum rubrum 17 p2859 A66-32308

**CHLOROPLAST**  
Chlorophyll distribution in mechanically fragmented spinach 11 p1645 A66-23195  
Photoreduction of viologen dyes analyzed with chloroplasts, noting oxygen evolution and photophosphorylation efficiency, reduction potentials, etc 16 p2638 A66-30647  
Isolation of morphologically intact and photochemically functional chloroplasts from marine chrysomonad Hymenomonas sp 16 p2638 A66-30648  
Kinetics and spectral characteristics of photoinhibition of spinach chloroplast reactions 24 p4163 A66-42316

**CHOKER**  
Generalized equation of choking for two or more unmixed streams flowing in same channel, noting relevance to ejector principle 05 p0665 A66-15773

**CHOLESTEROL**  
Free and esterified cholesterol in plasma extracts determined by fluorometric means 13 p2017 A66-25871

**CHONDRITE**  
SA ACHONDRITE  
SA CARBONACEOUS METEORITE  
Aromatic hydrocarbons in carbonaceous chondrites investigated by time-of-flight mass spectrometry and hypothesized as formed in solar nebula under thermodynamic equilibrium 01 p0136 A66-10436  
Rubidium-strontium ages of chondrules and carbonaceous chondrites 02 p0290 A66-11961  
Gallium concentrations in iron phases of several chondritic meteorites 02 p0290 A66-11962  
Contamination of carbonaceous chondrites by ordinary viable microorganisms, isolating three types of bacteria on various meteorites 03 p0325 A66-13339  
Potassium content and K-A ages of 18 amphoterite chondrites determined from isotope dilution technique 04 p0580 A66-14486  
Metal grains in 34 chondritic meteorites examined by electron microprobe 07 p1133 A66-17459  
Mineralogy and chemistry of Farmington hypersthene chondrite, examining microtexture aspects such as metal globules, grain shapes and troilite orientation 08 p1290 A66-19073  
Enstatite chondrites comprise well-defined group of meteorites distinct from other chondrite groups in chemical and mineralogical composition 08 p1291 A66-19074  
Chondritic meteorites shed light on role of oxidation-reduction equilibria in formation of terrestrial planets 08 p1291 A66-19075  
Grinding technique for accurate and proportional subdivision of chondritic meteoritic specimen and separation of metallic and silicate components for chemical analysis 08 p1179 A66-19095  
Bronzite and hypersthene chondrites, evaluating lunar or asteroidal origin 12 p1948 A66-23903  
Production rates of Cl 36 and Ar 39 in metallic and stone phases of Leedey chondrite 12 p1948 A66-23904  
Bjurböle chondrite and several separated phases, analyzed for rubidium-strontium age 14 p2388 A66-28338  
Iron and stony meteorite evolution, cosmic

radiation ages and space erosion model 14 p2390 A66-28409  
Neutron activation analysis of K-Ar age for Barwell, England olivine-hypersthene chondrite of December, 1965 16 p2807 A66-31760  
Amino acid content of carbonaceous and noncarbonaceous chondrites and possible origins 17 p2850 A66-32086  
Chemical analysis of stony meteorites with sharp boundaries between light and dark structure, noting differences found in achondrites and chondrites 17 p3007 A66-33281  
Chondritic meteorite chemical composition and fractional mechanisms in study of chondrite origin 17 p3015 A66-33430  
Melting of solid bodies in chondrule size, discussing accumulation mechanisms involving electrostatic acceleration and gas motions 18 p3225 A66-33622  
Chondrite meteorite that fell in Barwell, England, December 24, 1965, may have weighed 200 pounds before fragmentation, breakup occurred at extremely low altitude 18 p3228 A66-34053  
Cosmic radiation age spectrum of chondrites by calculation based on interplanetary erosion rate, discussing asteroidal origin for meteorites 18 p3232 A66-34528  
Rare gas mass spectrometric analysis of He, Ne and Ar in Bursa and Canakkale chondrites 20 p3651 A66-37578  
Cl, Br and I contents in carbonaceous chondrites measured by activation analysis 21 p3814 A66-39260  
Chondrules origin, discussing possible production by lightning in primitive Laplace type nebula 22 p3981 A66-40477  
Chainpur and similar, apparently primitive, chondritic meteorites may be precursors of ordinary chondrites 22 p3981 A66-40485  
Isotopic composition of xenon extracted from Ca-poor achondrites, noting relation between enstatite achondrites and enstatite chondrites 22 p3983 A66-40558  
Statistical petrographic analysis of meteorite and carbonaceous chondrite evolution on Moon and Mars from rocket photographs 23 p4132 A66-42075  
Amphoterite chondrite, St. Mesmin, noting primordial rare gases associated with dark portions 24 p4274 A66-42610  
Load pressures realized in early history of chondrites indicate parent body of lunar or half-lunar dimensions and formation from jadeditic pyroxene 24 p4279 A66-43023

**CHOPPER**  
Static drift in epitaxial planar silicon transistor choppers 01 p0035 A66-10208  
Chopper using complimentary transistors for converting DC voltage into square wave pulses 14 p2246 A66-26801  
Very low DC voltage measurement using chopper principle, based on resistance effect and employing magnetically controlled resistances 16 p2701 A66-30274  
Transformerless chopper built with integrated circuits, noting low power consumption, offset voltages and HF operation 16 p2661 A66-30660  
Current distribution and input resistance of T type, corner and bent tape vibrators powered by lumped electromotive force, using method of integro-differential equations 23 p4045 A66-41457  
FET characteristics in chopping and analog switching applications 24 p4182 A66-42500

**CHORUS PHENOMENON**  
SA WHISTLER  
ULF radio emission of upper atmosphere and other related geophysical phenomena, analyzing hisses, choruses and contribution to Earth radiation belt 20 p3551 A66-37487

**CHROMATE**  
SA POTASSIUM CHROMATE  
Chromate waste treatment methods, noting hexavalent chromium reduction method and ion-exchange method 21 p3743 A66-38769

**CHROMATOGRAPHY**  
SA GAS CHROMATOGRAPHY  
SA THIN LAYER CHROMATOGRAPHY  
Split-stream chromatographic injection parameters including optimum component velocity, column flow, mixing tube cross section, etc 10 p1534 A66-21294  
Amino acids dissolved in saline waters

removed by ligand exchange chromatography 11 p1650 A66-23128  
Low temperature chromatographic separation of hydrogen isotopes based on interaction with alumina surface electric fields 11 p1650 A66-23209  
Wavefront shearing prism interferometer applied to testing of chromatic aberration of simple and compound lenses and waveforms characterizing monochromatic aberrations 14 p2291 A66-27319  
Chromatography on carboxymethyl cellulose to obtain fractions containing predominantly single bands of malate dehydrogenases 15 p2446 A66-28871  
Electrostatic theory of physical adsorption applied to gas-solid chromatography, discussing chromatographic inseparability of argon and oxygen at room temperature, prediction of elution order of many gases, etc 16 p2646 A66-30646  
Pressure gradient elution technique for rapid and quantitative chromatographic separation of purine and pyrimidine bases 22 p3860 A66-40402  
Achromatization of holograms using two-lens configuration 24 p4211 A66-42626  
Column chromatography used to determine hydrocarbons present in Moonie crude oil from Queensland, Australia, that is two hundred million years old 24 p4170 A66-43024

**CHROMIUM**  
Nickel-chromium base alloys considering aircraft and industrial gas turbine application 02 p0244 A66-11740  
Cr and Mn effects on aging mechanism and anticorrosion properties of Al-Zn-Mg alloys 03 p0381 A66-12723  
Visible spectrum absorption cross section of trivalent chromium in metastable 2E state of pink ruby 05 p0694 A66-14902  
Graphite and carbon steel case hardening by chromium 05 p0702 A66-15111  
Sintering and electroforming of complex shapes of pure chromium from hexavalent chromium bath with fluoride ions as catalyst 05 p0702 A66-15135  
Properties of chromium particles obtained by vaporization of metal in argon at low pressure, noting cubic shape, electron diffraction pattern, etc 06 p0894 A66-16185  
L-band traveling-wave maser for radio astronomy research at 21 cm uses chromium-doped rutile 06 p0891 A66-16640  
Resistive properties of vacuum-deposited chromium films determined by grain size and impurity content 07 p1098 A66-17741  
Highly porous chromium materials prepared by sintering of powdered compacts in hydrogen atmosphere 07 p1049 A66-17901  
Electronic structure of refractory compounds based on X-ray study of chromium spectra 09 p1391 A66-20871  
Quenching and slow-cooling effects on ductile-brittle bend-transition temperature of chromium wire 13 p2107 A66-25587  
Values for contribution of core polarization to hyperfine structure of excited states of chromium compared theoretically and experimentally, extracting core contributions to magnetic field 13 p2135 A66-26268  
Layered film of Cr and NiFe exhibit biased hysteresis loop in easy axis direction and asymmetric hysteresis loops in hard axis direction 14 p2353 A66-26901  
Chromium doped ruby whiskers grown by vapor phase reaction, determining chromium concentrations, noting whisker growth morphologies 15 p2561 A66-28706  
Self-lubricating properties of composites of porous nickel and nickel-chromium alloy impregnated with barium fluoride-calcium fluoride eutectic [ASLE PAPER 66AM 1C2] 16 p2710 A66-30404  
Paramagnetic iron and chromium ion impurities effect on absorption spectrum and microhardness of rutile single crystals 16 p2786 A66-31733  
Hamiltonian describing EPR spectrum of trivalent chromium ion in ordered lithium-aluminum spinel and rhombic distortion causing deviation of axes in octahedron electric field 16 p2787 A66-31763  
Mass spectrometric measurement of distribution of spallation produced chromium nuclides between alloys in iron meteorite 17 p3007 A66-33282



Exchange pairs spectrum analysis based on observation of nonlinear splitting of EPR signals of pairs of exchange-coupled chromium ions in corundum 18 p3154 A66-33943

Minimum electric resistivity of chromium in antiferromagnetic state shows no disappearance in longitudinal magnetic field 19 p3444 A66-36071

Splitting of EPR lines of trivalent Cr ion in zinc tungstate by external electric field, noting angular dependence and corresponding spin Hamiltonians 20 p3615 A66-37370

L-band traveling wave maser using chromium doped rutile, discussing inverted susceptibility as figure of merit 20 p3580 A66-38239

Highly porous chromium materials prepared by sintering of powdered compacts in hydrogen atmosphere 21 p3752 A66-39401

Fractional metastable-state population measurements of Cr ions in ruby crystal under Q-switching operation 23 p4077 A66-41288

Time resolved emission measurements for Cr-Ar mixtures in three spectral regions and ionization occurrence in excited state inelastic collisions 23 p4033 A66-42083

**CHROMIUM ALLOY**

Polythermal and isothermal cross sections of phase diagram of titanium-niobium-chromium system at high temperatures 01 p0086 A66-10453

Polycrystalline niobium elastic properties and effects of alloying with chromium and iron 03 p0383 A66-13128

Molybdenum effect on properties of chromium-nickel alloy, noting hardness and strength 11 p1716 A66-22748

Nickel-chromium alloys with niobium in study of precipitation hardening and hardness 11 p1716 A66-22749

Structure and wear resistance of chromium-molybdenum deposits, noting parameters of electrolytic deposition, Amsler machine tests, etc [ONERA TP 319] 12 p1894 A66-24366

Chromium-vanadium alloys for brazing tungsten to molybdenum in engine application 13 p2087 A66-26020

High temperature oxidation of two ductile Cr-Ru alloys with composition near bcc alpha-phase solubility limit analyzed by four different techniques 16 p2721 A66-30220

Transformation process effect on superconducting behavior of titanium-chromium alloy 16 p2722 A66-30308

Precipitation behavior of nickel-molybdenum and nickel-molybdenum-chromium alloys 16 p2722 A66-30310

Trace element effect on lifetime of iron-chromium-aluminum heat-resisting alloy 16 p2723 A66-30311

Metastable phase composition diagram for alloys of titanium-chromium system 16 p2727 A66-31567

Electric resistance and thermal expansion of Ti-Nb-Cr alloys, noting phase composition 19 p3387 A66-36450

Nitrogen addition effect on heat resistance of chromium-manganese-austenitic alloys 20 p3584 A66-37695

Long-time relaxation persistence in heat resistant nickel-chromium alloy 20 p3584 A66-37696

Metallography, roentgenography and differential thermal analysis of composition temperature ranges of chromium-germanium phases 23 p4082 A66-41825

Magnetic transformation and effect of plastic strain on shear modulus of Fe-Cr-Ni alloys 24 p4227 A66-42310

**CHROMIUM CARBIDE**

Heat resistant chromium carbide coating with silicate binder applied to steel 06 p0896 A66-16609

Vapor composition, evaporation rate and vapor pressure above chromium carbides determined by effusion method combined with mass spectrometry 14 p2310 A66-26791

Solid solutions of titanium, tungsten, chromium prepared by carbidization of mixtures in hydrogen medium and obtained as fine-grained carbide powders 22 p3934 A66-39865

**CHROMIUM COMPOUND**

IR-active lattice vibrational spectra of

alpha-aluminum oxide and chromium oxide analyzed by reflection and transmission measurements 03 p0380 A66-12341

Isostructural and jadeite mineral called ureyite found as rare emerald-green grains in iron meteorites Coahuila, Toluca and Hex River Mountains 05 p0674 A66-15197

7P terms of excited chromium configurations examined, using level crossing and double resonance spectroscopy, noting core polarization 13 p2135 A66-26267

Inverted susceptibility, inversion ratio, line widths and spin-lattice relaxation times for maser operation point in chromium-doped cobalt potassium cyanate 18 p2718 A66-30934

**CHROMIUM STEEL**

Corrosion resistance and anodic behavior of Kh18N9 steels with various nickel-manganese-carbon-titanium contents 01 p0088 A66-10987

Brittle creep susceptibility of heat resistant chromium steels reduced by proper thermal treatment 03 p0384 A66-13162

Design properties, application and fabricability of super 12-Cr steels 04 p0535 A66-13638

Chromium nickel steel hardening as result of martensitic transformation and aging 05 p0701 A66-14861

Super chromium steel survey, including applications in gas turbines and aerospace industries, physical and mechanical properties, thermal stability, corrosion resistance, etc 09 p1387 A66-19953

Alloying elements effect on anodic corrosion and passivation of stainless steels 09 p1390 A66-20837

Endurance and creep of chromium steels with extended thermal treatment 11 p1716 A66-22746

Chromium steel strength and corrosion resistance improvement by molybdenum and tungsten addition 11 p1716 A66-22747

Phase composition effect on relaxation stability of chromium steel used for helical spring 11 p1716 A66-22750

Effect of molybdenum, niobium and tungsten on structure and properties of nitrogen containing austenitic chromium-manganese steels 12 p1893 A66-23726

**CHROMOSOME**

**SA BIOLOGICAL CELL**

**SA GENETICS**

Chromosome configuration and mitosis impairment in micropores Tradescantia paludosa due to space flight effects of Voskhod I 11 p1645 A66-23050

Chromosome injury in mouse bone marrow due to distant ionizing radiation 12 p1806 A66-24396

Radiosensitivity differences in yeast cells in terms of differences in chromosome-replication and genetic-structure-restitution intensities 15 p2438 A66-29486

Vibration effects on chromosomes of Tradescantia paludosa and other micropores subjected to Vostok satellite conditions 18 p3058 A66-33781

**CHROMOSPHERE**

Chromospheric emission lines of magnesium iodine analyzed, calculating hydrogen concentration and ionization degree at 1000 km 01 p0134 A66-10269

Electron concentration, length and temperature of limb chromospheric flare, using steady state equation of hydrogen atom 01 p0131 A66-10270

H-line of calcium ion analyzed from spectrograms of chromospheric spicules 01 p0131 A66-10277

Chromospheric and coronal propagation of disturbing agents generating changes in intensity of solar radio emission 02 p0287 A66-11489

Spicules of solar chromospheric disk identified in H-alpha line 02 p0292 A66-12190

Quiet chromosphere and corona noting line intensity and coronal electron and kinetic temperature 03 p0420 A66-12841

Cooling of lower chromosphere contributed to radiation in individual spectral lines 03 p0427 A66-12915

Spectroscopic observation of chromospheric limb structure 03 p0428 A66-13112

Appearance of active regions of Sun associated with 10 to 20 percent increase in convection velocity 05 p0761 A66-15091

Relation between Forbush decreases and

chromospheric flares, obtaining longitudinal distributions before and after onset, using statistics 05 p0753 A66-15394

Motion of material in solar atmosphere, analyzing horizontal inhomogeneities necessary in understanding energy transfer from granulation layer into chromosphere 07 p1138 A66-18076

Sunspot activity in quiet part of Sun between spot areas related to solar chromosphere structure 10 p1604 A66-21133

Solar chromosphere observations in 1960-1963 by Istanbul University, noting flares, filaments, observation duration, etc 10 p1609 A66-21833

Synoptic chart of chromosphere and sunspots, discussing coordinate systems, faculae, solar filaments, etc 12 p1948 A66-23910

Small two-dimensional oscillations in XY plane for isothermal magnetosphere in uniform gravitational field, postulating Boltzmann equilibrium density distribution 12 p1943 A66-24282

Properties of stellar chromospheres 13 p2177 A66-25134

Macroscopic inhomogeneities in solar atmosphere, noting vertical velocity fluctuations in chromosphere, oscillation spectrum, etc 13 p2183 A66-25616

Gamma photon flux from solar Na 22 disintegration emitted by Sun after chromospheric eruption 13 p2176 A66-26760

Cooling of lower chromosphere contributed to radiation in individual spectral lines 14 p2380 A66-27264

Solar prominences, proton flares and chromospheric flares in intensity of corona and solar radio emission and sunspots, noting maxima during eleven-year solar activity cycle 15 p2576 A66-29136

Chromospheric eruption distribution in time 18 p3228 A66-33912

Statistical correlation between decameter type III and type III/V solar radio bursts and microwave bursts and chromospheric flares 18 p3234 A66-34615

Magnesium 3 line profiles observed on solar disk and chromosphere used in determining empirical source function variations and chromospheric profiles 19 p3465 A66-36611

Barium ion concentration computed from Ba II 4554 angstrom line and Lyman alpha radiation intensity in lower chromosphere 20 p3646 A66-37013

Intensity and center-to-limb variation of continuous solar spectrum for several models of chromosphere 20 p3650 A66-37340

Thermal instability of small amplitude disturbances in solar chromosphere, showing linear wave amplification 20 p3654 A66-38019

Solar chromosphere observations, noting distribution of spicules and role in coronal heating 20 p3656 A66-38051

Emission rim formation at filaments caused by chromospheric excitation by radiation reflected from filament 23 p4126 A66-41077

Excitation of H-alpha lines in solar chromosphere from internal and external sources, noting theoretical and empiric results 23 p4127 A66-41080

**CHRONOTRON**

**SA PULSE RATE**

**SA TIME DELAY**

Feedback to quadrupole that incorporates device for converting voltage into time parameter of periodic sequence of pulses and vice versa 11 p1671 A66-23334

Feedback to quadrupole that incorporates device for converting voltage into time parameter of periodic sequence of pulses and vice versa 22 p3877 A66-40414

**CINEFLUOROGRAPHY**

X-ray image intensifier in conjunction with motion picture film sequencing of thrust chamber image during hot firing to obtain failure analysis data 13 p2079 A66-25819

**CINEMATOGRAPHY**

**SA LUNAR CINEMATOGRAPHY**

Cinematographic system in which capacitor-discharge pulses are substitutes for high speed shutter 03 p0368 A66-12465

Microscope modification for time-lapse cinematography noting holding camera stand, deflecting light mirror, culture chamber,



etc. 05 p0677 A66-14865  
 High velocity motions in solar flares, using high time-resolution monochromatic cinematography 07 p1130 A66-18074  
 Low speed flow visualization technique using light-pulse illuminated plastic particles suspended in revolving bowl of brine 09 p1364 A66-20399  
 Cinephotomicrographic studies of metallized fuel-rich propellants with high aluminum powder content, discussing composition, burning rates, etc [AIAA PAPER 66-616] 18 p3162 A66-34433

**CIRCADIAN RHYTHM**  
 Geomagnetic micropulsations, noting diurnal patterns of phase difference, propagation medium dispersive characteristics, signal velocities, etc 10 p1529 A66-21151  
 Thermal events in diurnal breathing cycle and vapor loss reduction in volatile liquid storage [AICE PREPRINT 11C] 10 p1521 A66-21181  
 Primary shift of phase of circadian periodicity effected by time displacement for physiological functions 19 p3285 A66-36374  
 Radio telemetry for acquisition of Circadian rhythm data on ambulatory animal, including deep body temperature, heart rate, locomotor activity and oviposition 22 p3856 A66-39792

**CIRCLE**  
 SA MOHR CIRCLE  
 SA RING  
 Circle and sphere theorems for biharmonic equation and application to displacement field of stressed plate under pure bending, noting singularities 01 p0093 A66-10427

**CIRCUIT**  
 SA BISTABLE CIRCUIT  
 SA EXPLODING CONDUCTOR CIRCUIT  
 SA FLIP-FLOP  
 SA INDUCTOR  
 SA INTEGRATED CIRCUIT  
 SA LC CIRCUIT  
 SA LINEAR CIRCUIT  
 SA LOGIC CIRCUIT  
 SA LOOP  
 SA MAGNETIC CIRCUIT  
 SA MICROCIRCUIT  
 SA MICROWAVE CIRCUIT  
 SA PHASE DETECTOR  
 SA PNEUMATIC CIRCUIT  
 SA PRINTED CIRCUIT  
 SA RLC CIRCUIT  
 SA SHORT CIRCUIT  
 SA SWITCHING CIRCUIT  
 SA TRANSISTOR CIRCUIT  
 SA VARACTOR DIODE CIRCUIT  
 SA WIRE BRIDGE CIRCUIT  
 Plotting and analysis of oriented graphs of electrical circuits of any complexity by considering them as N poles 01 p0050 A66-10218  
 Determination of output voltage of square law device ascertained from input voltage 01 p0050 A66-10221  
 Two-parabola type multiplying circuit constructed on principle of z plane consisting of linear superposition of at least two substitute planes 01 p0043 A66-10879  
 Circuit application of diode matrix memory for permanent information storage in computers 01 p0049 A66-11150  
 Gain-bandwidth limitations for physically realizable systems obtained in integral form by employing generalized representation theorem for bounded-real functions 02 p0208 A66-11904  
 Bandwidth expansion of crystal filters by spacing frequency response characteristics in relay circuit at suitable distances from each other 03 p0342 A66-12895  
 High stability control circuit operating tuning fork in constant amplitude self-excitation circuit, using mechanical oscillator excited by fundamental wave of amplified feedback voltage 03 p0371 A66-13243  
 Theory of poles and zeros applied to nonlinear networks, discussing shift 04 p0502 A66-13383  
 Linear system using differential circuits for indirect measurement of perturbations 04 p0503 A66-13771  
 Automatic pulse shaper circuits at pulse length independent of input signal amplitude 04 p0495 A66-13886

Zero conversion loss obtained for certain frequency change using second-order ideal ring modulator with reactive idler circuit at normal output terminals 04 p0500 A66-14094  
 Photovoltaic effect and principles upon which operation of photodiodes are based, including analysis of photovoltaic circuits to determine operating parameters 04 p0524 A66-14456  
 Circuit response to HF circuits for transistorized amplifiers determined, using polar diagram, noting feedback effect and vectorial analysis 05 p0647 A66-14681  
 Hyperfrequency parametric amplifier circuit with modulation-demodulation applicable to very rapid pulse transmission 05 p0633 A66-15102  
 Operating principles of pulse and frequency modulation, using step-recovery diodes as circuit elements 05 p0651 A66-15835  
 Discrete simulation technique using electrical circuit for finite-difference approximation of initial differential equations, noting functional potentiometers 07 p1055 A66-17201  
 Amplitude modulated carrier frequency signal circuit analyzed, showing open loop linear pulse system 07 p1014 A66-17439  
 Discontinuous system investigated, using oscillating circuit governed by second order differential equation 07 p1015 A66-17830  
 Waveguide resonators equivalent to series circuit, obtaining expressions for various parameters 08 p1192 A66-19105  
 One-, two- and three-circuit systems with periodically varying inductance, capacitance and resistance influencing energy transfer, noting application to amplifier design 09 p1363 A66-20782  
 Filter with two tuned circuits and distributed coupling based on equations for complex values of tuned circuit currents, noting formulas for mutual impedance 10 p1510 A66-21673  
 Comparing basic parameters of common high power pulse-transformer circuits, considering parasitic time constants and winding impedance 10 p1511 A66-21680  
 Radio waves and circuits - URSI Conference, Tokyo, September 1963 11 p1653 A66-22626  
 Nonlinear systems including oscillators, frequency multipliers, limiters, etc, driven by periodic carrier, deriving circuit theory for small perturbations propagated throughout system 12 p1848 A66-24136  
 Three-phase half-wave inverter circuit consisting of ring of three SCRs and converting DC into AC power supplied into zigzag motor load 12 p1804 A66-24662  
 Vacuum-evaporation method of fabricating thin film circuits, using resistance-heating process or electron beam gun 12 p1847 A66-24954  
 Low energy independent-discharge three-element sputtering system and use in thin film fabrication 12 p1847 A66-24955  
 Tachometer measuring angular velocity from time of definite number of rotations, noting diagram of basic circuit 13 p2077 A66-25327  
 Parameter indeterminacy in system identification for mathematical model with adjustable parameters matched to system output by feedback 13 p2054 A66-26091  
 Magnetic amplifier telemetry encoder circuit, using silicon controlled rectifiers /SCR/, for application in satellites and rockets 14 p2263 A66-27062  
 Behavior of resonator quantum devices, using oscillating circuit with quasi-linear negative conductance 14 p2260 A66-28167  
 Auto-oscillations in relay systems, discussing parameters, stability region boundaries and clearance effect 15 p2469 A66-28550  
 Asymptotic methods of nonlinear mechanics, involving averaging for differential equations, applied to motion equations of satellites and resonance in electric circuits 15 p2541 A66-29162  
 Automatic pulse shaper circuits at pulse length independent of input signal amplitude 15 p2466 A66-29698  
 Evolution and present status of electronic circuit components including manufacturing and component

applications 15 p2468 A66-29890  
 Plotting and analysis of oriented graphs of electrical circuits of any complexity by considering them as N poles 17 p2898 A66-31901  
 Determination of output voltage of square law device ascertained from input voltage 17 p2898 A66-31905  
 Bandpass filter design with three coupled circuit and determination of amplitude curve and circuit 17 p2895 A66-33243  
 constants 17 p2895 A66-33243  
 Parametric amplifier based on two-port circuit, employing idler frequency equal to difference between pump and signal frequency, noting negative resistance 18 p3086 A66-34391  
 Noise characteristics at integrator input in nonstationary regime 19 p3311 A66-35297  
 Circuitry of automatic surface tension measurement device 20 p3559 A66-37502  
 Fluid circuit theory, discussing transmission lines, matching, pulse forming and definitions of current and voltage analogies 20 p3500 A66-37643  
 Electric analog approximation of static and dynamic performance of Kearfott ball valve switching device, discussing application to complex circuit design 20 p3501 A66-37650  
 Measurement of physical quantity converted to form of AC signal, noting ripple-free circuit and several clamping arrangements 21 p3709 A66-38606  
 One-, two- and three-circuit systems with periodically varying inductance, capacitance and resistance influencing energy transfer, noting application to amplifier design 22 p3884 A66-39841  
 Man-machine merger in computer aided design of circuits, examining changes in circuit parameters caused by component tolerances, simulation of component failure, feasibility and circuit optimization 23 p4072 A66-41252  
 Three-circuit system with circuits connected by nonlinear capacitance applied to frequency converters, amplifiers, etc 23 p4049 A66-41565  
 MOS equivalent circuit for small signal HF operation of insulated gate field effect transistor in pinch-off mode, using differential equation 24 p4183 A66-42638

**CIRCUIT BOARD**  
 Thermal compression bond failures in internal electric interconnects on circuit boards of advanced Minuteman guidance system 01 p0049 A66-11152  
 Carrier-mother board rack approach to microcircuit interconnection and packaging 02 p0195 A66-11322  
 Automated flat pack welding design, discussing operational functions and major components 02 p0234 A66-11323  
 Multilayer printed wiring for reliable Pershing module program 02 p0197 A66-11461  
 Integrated logic circuit design through breadboard, model assembly, system development, final layout, construction and testing 02 p0204 A66-11939  
 Thin copper clad laminates and problems arising in application to multilayer printed circuit boards 03 p0347 A66-13330  
 Multilayer circuit boards for interconnecting integrated circuits in computer and other large systems 04 p0498 A66-14015  
 Multilayer circuit board defect detection and repairing using computer-controlled IR radiometer 04 p0498 A66-14016  
 Digital systems research model design containing logic gates in integrated circuit packages 09 p1356 A66-20676  
 Breadboard microwave pointing device with attached RF source comprising azimuth angle measuring system, with application in geodesy, tropospheric propagation, etc 10 p1538 A66-22048  
 Protective coating of printed circuit assemblies against humidity, salt spray and other adverse environmental factors 11 p1665 A66-22679  
 Table of interconnecting device for use with printed circuit board 13 p2043 A66-26309  
 Ministick packaging system for integrated circuits 14 p2249 A66-27109  
 Multilayer printed circuits and interconnection methods 15 p2465 A66-29668



Integrated circuit connecting and packing, discussing cost flexibility and performance characteristics 18 p3086 A66-34399

**CIRCUIT PROTECTION**

Fuel cell reliability maximized and weight minimized for space mission power requirement [AIAA PAPER 64-746] 13 p2007 A66-26647

Circuit overloading protection using automatic reset, breakers and fuses 14 p2249 A66-27120

Thermal analysis of ceramic-based hybrid microcircuits, using lumped-constant electrical analog 16 p2667 A66-31594

**CIRCUIT RELIABILITY**

System reliability prediction limited when it does not take into account out-of-tolerance operation due to component variation with environmental changes, electric stresses and aging 01 p0167 A66-10055

Stress survival matrix test in evaluating reliability of monolithic silicon integrated circuit, measuring safety margin and performance parameter drift 01 p0035 A66-10082

Reliability and design factors for space power conditioning equipment examining peak power, component part specifications, integrated circuits and failure analysis 02 p0180 A66-11283

High-reliability microwave printed circuits using copper-clad polyethylene dielectric materials 02 p0195 A66-11288

Miniaturization in improving weapon system component availability, transportability and reliability 02 p0198 A66-11464

Packaging techniques interrelated with design specification and manufacturing capabilities noting integrated circuit system, circuit reliability and thermal resistance 02 p0200 A66-11891

Microminiaturization, three-dimensional stacking, ceramic printed, thin film, hybrid and integrated circuits, discussing reduction in system size, weight and primary power requirement and improved reliability 03 p0343 A66-13001

Linear integrated circuits discussing differential and operational amplifiers, development, use, capabilities, new techniques, special designs and reliability 03 p0347 A66-13340

Avionics design using integrated electronics or microelectronics, noting reduction of maintenance requirements 04 p0494 A66-13684

High performance operational amplifier design, discussing monolithic circuit construction and performance parameters 05 p0642 A66-14567

Reliability of integrated circuits noting stress test schedules, failure rates and sources 05 p0650 A66-15369

Radiation test data on solid state equipment of tracking and command system in SNAP-10A environment 05 p0740 A66-15495

Yields, costs and reliability of monolithic integrated circuits 05 p0650 A66-15496

Thermionic reactor network reliability as function matrix network and converter reliability 05 p0623 A66-15596

Reliability, life and relevance of circuit design in electromechanical switching devices 06 p0839 A66-15946

Predictions of future trends of reliability engineering, with particular reference to impact of microelectronics 06 p0839 A66-15952

Reliability of integrated circuits 06 p0856 A66-16925

Algorithm synthesizing sequential circuit from transition matrix, making critical races occurrence impossible during simultaneous relays starting 07 p1013 A66-17384

Reliability of logical elements and systems with given probabilities of individual elements 07 p1013 A66-17387

Determination of length of deductive circuits of recycling memories and oscillators 09 p1352 A66-20357

Integrated circuit reliability control and determination 09 p1354 A66-20565

Convergence, oscillation, functional stability and reliability of m-by-1 homogeneous polyfunctional nets under

iteration 10 p1517 A66-21691

Redundant microelectronic system and reliability 11 p1661 A66-22272

Time to failure and mean recovery time calculated for system with recoverable elements 11 p1667 A66-22787

Reliability and failure mechanisms of integrated circuits 11 p1669 A66-23158

Current mode technique for worst-case design analysis of electronic networks 11 p1678 A66-23179

Reliability, life and relevance of circuit design in electromechanical switching devices 12 p1831 A66-23791

Reliability technique viewed as broad discipline encompassing entire field of traditional design, production and maintenance 12 p1832 A66-24071

Redundancy method based on circuit failure asymmetries for reliability improvement in digital circuits 12 p1842 A66-24668

Reliability improvement through redundancy at various system levels in analog systems 12 p1844 A66-24733

Metal oxide silicon integrated circuits subsystem size, weight, power and cost compared with double diffused counterpart 12 p1845 A66-24848

Properly controlled high-stress life testing used to evaluate failure rate of high reliability solid state components of integrated circuits 12 p1846 A66-24913

Yield and reliability of integrated electronic devices and electronic digital systems, using redundant components by triplicating voting 12 p1846 A66-24914

Optimum tests for check of working order of system with minimal material losses of safe or fault system functioning 13 p2045 A66-25298

Near minimal set of tests detecting all single faults in combinational logic net, using shortcut methods 13 p2040 A66-25804

Book on measurement of specific electronic parameters in circuit design 13 p2042 A66-26121

Reliability assessment techniques for microelectronics, considering integrated circuits, testing procedures, etc 13 p2043 A66-26226

Reliability improvement in airborne electronic equipment 13 p2044 A66-26692

Tolerance range of multicomponent circuit calculated from tolerance limit of individual component 15 p2474 A66-29766

Tolerance limits for structural components in power-filter circuit design, calculating fluctuations of damping property and phase fluctuations in multiply divided circuits 16 p2663 A66-31031

Discoloration in contamination area of aluminum bonds in integrated circuits, noting cause and effect on interconnection bond integrity 16 p2665 A66-31434

Nomograms published in Electronic Design from 1963 to 1966 covering prototype, testing, costs, selection and avoidance of pitfalls 17 p2881 A66-32103

Step-stress technique to induce failures in integrated circuits to pinpoint source of reliability problems 17 p2882 A66-32114

Approximation technique for flow graph that eliminates nonessential equivalent circuit elements, providing for derivation of most concise model with preassigned accuracy 18 p3092 A66-35040

Book on feedback circuit analysis covering circuit stability, closed loop transient response, frequency response, compensating networks, etc 20 p3537 A66-37047

Time to failure and mean recovery time calculated for system with recoverable elements 20 p3525 A66-37127

Silicon nitride as possible replacement for silicon dioxide in highly stable and reliable semiconductor devices, especially insulated-gate field effect transistor circuits 21 p3710 A66-38827

Rake system equipment for tropospheric scatter, noting delay-resolution capabilities and circuit stability 22 p3865 A66-40067

Specification and assessment of electronic equipment reliability, emphasizing statistical aspects of optimal cost/reliability estimation 22 p3883 A66-40961

Microcircuit joints evaluated, using

metallurgical process 23 p4072 A66-41192

Face-bonding technique for attaching semiconductor chips to thin film or similar circuits 23 p4043 A66-41193

Miniature welding of joints, discussing wire-to-wire welding and advantages over soldered connections in light of environmental parameters 23 p4043 A66-41195

Weld quality control in cross wire welding of assemblies in circuit small quantity manufacture 23 p4044 A66-41196

Optimum use of microelectronic reliability data in system development, discussing relation to sources 24 p4179 A66-42099

**CIRCULAR CONE**

Collisionless plasma flow over cone when flow velocity is greater than ion wave speed [AIAA PAPER 65-125] 02 p0267 A66-11534

Dissociation or ionization effects of air on inviscid hypersonic flow past circular cone with attached shock wave 03 p0316 A66-12928

Tropospheric scatter common volume, describing derivation for two intersecting circular cones 06 p0833 A66-16682

Directional radiative characteristics of conical cavities and relation to reflective characteristics of Moon 07 p1136 A66-17729

Flow properties in turbulent near wake of circular and elliptic cones at zero angle of attack in Mach 6 flow [AIAA PAPER 66-54] 07 p0980 A66-17897

Ideal gas flow past infinite circular cone at angle of attack, noting finite-difference method for self-similar solution of Prandtl boundary layer equation 14 p2222 A66-28283

Natural frequencies of torsional vibrations of circular cone possessing cylindrical anisotropy 16 p2823 A66-31633

Inviscid hypersonic flow past circular cone at finite angle of attack with attached shock wave in presence of dissociation air behind shock wave 17 p2837 A66-32033

Static pitching moment coefficient determination from location of center of pressure in right circular cone, using Newtonian impact mechanics 17 p2840 A66-32494

Head wave of frictionless flow of real gas past positioned circular cone for small or zero angles of attack 17 p2842 A66-33169

Tangent cone method extended to determine pressure coefficients of yawed circular cones and ogives at angle of attack 18 p3048 A66-33820

Inviscid hypersonic nonequilibrium flow of three-component gas past circular cone, using exact reaction-rate equations to correct solution first obtained from approximate equations 21 p3693 A66-38711

Perturbation analysis of radiative cooling in shock layers and radiative heat transfer effects on hypersonic flow over wedge and circular cone 23 p4011 A66-41882

**CIRCULAR CYLINDER**

Stress distribution in symmetrically loaded circular cylinders obtained by solving directly equilibrium and compatibility equations 01 p0151 A66-10202

Vorticity distribution in wake of circular cylinder oscillating in unperturbed flow, using Burger linearization of Navier-Stokes equations 01 p0007 A66-10715

Vortex streets behind circular cylinders and flat plates analyzed, using photography and hot wire techniques, noting role of walls and wakes 03 p0354 A66-12321

Torsion problem of nonhomogeneous infinite circular cylinder with symmetrically located spherical cavity 03 p0442 A66-13302

Turbulence wake suppression in Karman vortex street of circular cylinders by controlling transverse oscillations of vortex generating cylinder in transition range 04 p0453 A66-13514

Cyclic edge loading effect on circular reinforced cylindrical shells 04 p0589 A66-14147

Three-dimensional linear elasticity problems in homogeneous transversely isotropic elastic materials like infinite circular cylinder, using potential function method [ASME PAPER 65-WA/APM-26] 05 p0778 A66-15447

Propagation in rectangular and circular cylindrical waveguide containing inhomogeneous dielectric varying linearly and quadratically 06 p0848 A66-16108



Heat conduction for solid circular cylinder with nonuniform boundary conditions 06 p0970 A66-16327

Rotating non-Newtonian fluid, discussing stabilizing and destabilizing effect of circular magnetic field for cross-viscous parameter variation 07 p1019 A66-17259

Flow of compressible fluid about circular cylinder at Mach number less than unity solved, using small parameter method 08 p1161 A66-18608

Perturbation solutions of stress and deformation problems for homogeneous anisotropic shells constructed from orthotropic material [AIAA PAPER 66-141] 08 p1309 A66-19004

Critical condition for aerosol deposition from symmetrical flow past solid body, considering case of circular cylinder 08 p1247 A66-19304

Thermal stresses due to axisymmetric heat flow past spherical cavity inside long circular cylinder solved by stress functions and thermoelastic displacement potentials 08 p1313 A66-19547

Resistance due to viscous shear on circular cylinder in oscillating stream calculated by boundary layer equations formulated in polar coordinates 09 p1367 A66-20262

Cross flow relation to force distribution on circular cylinders curved in plane containing wind vector at subcritical Reynolds number 09 p1328 A66-20746

Elastic general instability collapse pressure of ring-reinforced circular cylindrical shell subjected to uniform external pressure 10 p1613 A66-21318

Electromagnetic scattering by cylinder with inhomogeneous sheath 11 p1652 A66-22392

Leading edge pressure distributions measured on circular cylinders in normal cross flow, obtaining data from tests in arc-heated perfect gas and variable atmosphere wind tunnels 11 p1686 A66-22845

Transport properties, thermoconductivity, molecular collision and viscosity of polyatomic gas of circular cylindrical molecules with hemispherical caps 11 p1741 A66-23215

Stability and buckling of core-filled axially compressed circular cylinder 12 p1957 A66-23603

Elastico-viscosity, cross-viscosity and suction variation effects on rheological behavior of fluid moving steadily past porous circular cylinder and between two coaxial right circular cylinders 12 p1865 A66-24808

Lift, drag and inertial forces due to uniform unsteady flow with constant acceleration past fixed circular cylinder, determining vorticity flux 13 p1993 A66-26705

Shock tube study of high temperature gas flow around circular cylinders caused by electrical discharge 14 p2218 A66-27348

Stresses and displacements in circular cylinder of transversely isotropic material for mixed boundary conditions, obtaining solution by using partial differential equation 14 p2397 A66-27388

Yaw effect on vortex shedding from circular cylinder at low Reynolds number 14 p2219 A66-27440

Normally incident plane electromagnetic wave scattering by circular cylinder coated with radially stratified sheath 14 p2238 A66-27587

Strouhal number relation to cavitation erosion effect of circular cylinder models placed in closed circuit channel, in critical and supercritical Reynolds number range 14 p2275 A66-27634

Scattering of plane electromagnetic wave at infinite circular cylinder with spatially varying dielectric constant 14 p2242 A66-28155

Hooke law analysis of dynamic stability of closed circular cylindrical anisotropic shell compressed by longitudinal force 15 p2609 A66-29196

Torsion of hollow circular cylinder, consisting of arbitrary number of cylindrically orthotropic layers, by stress exerted on cylindrical boundary 15 p2613 A66-29432

Plane rotational motion of incompressible fluids in presence of homogeneous porous circular cylinder 15 p2481 A66-29856

Subsonic flow around circular cylinders using three alternate hodographic approximations to Chaplygin law 16 p2627 A66-30208

Planar subsonic flow around circular cylinder using Kisseleff approximation method for compressible fluid 16 p2627 A66-30210

Natural oscillations of three-layer circular cylindrical shells with freely supported and clamped edges 16 p2818 A66-31056

Variational solution of simultaneous stability equations boundary value problem for transverse displacements and stress state 16 p2819 A66-31137

Local heat transfer rates and pressure distributions over windward half of yawed circular cylinder at Mach 8 16 p2630 A66-31254

Strouhal and Reynolds numbers relation from data on vortex streets of circular cylinder in two-dimensional flow 16 p2688 A66-31299

Velocity spikes in near-wake of circular cylinders held transversely to air stream 16 p2690 A66-31654

Three dimensional character of wake of circular cylinder at three Reynolds numbers utilizing hot wire anemometers 16 p2632 A66-31659

Plane electromagnetic wave diffraction at two parallel circular cylinders for TM and TE polarization 17 p2879 A66-31862

Thermal stresses in anisotropic hollow cylinder by arbitrary radial temperature distribution 17 p3020 A66-31997

Two-dimensional excitation problem of circular cylinder with surface impedance varying over cylinder circumference 17 p2874 A66-32247

Stress-strain law and finite torsion of homogeneous circular cylinder, noting deformation and force needed to keep final state of body in equilibrium 17 p3025 A66-32499

Laminar boundary layer on cylinder with symmetric cross section bounded by two equal circular arcs 17 p2911 A66-32837

Finite-difference calculation of MHD flow of conducting fluid past circular cylinder in transverse magnetic field based on Navier-Stokes equation 17 p2971 A66-32862

Implicit finite difference method applied to plane hypersonic flow over blunt circular cylinder 17 p2842 A66-33170

Torsion of nonlinear viscoelastic circular cylinder in terms of stress tensors prescribed by time-functionals of finite strains 17 p3032 A66-33332

Three-dimensional linear elasticity problems in homogeneous transversely isotropic elastic materials like infinite circular cylinder, using potential function method [ASME PAPER 65-WA/APM-26] 18 p3248 A66-33582

Variational formulation of equilibrium stability of nonlinear elastic circular cylindrical panel under radial stress 18 p3251 A66-33704

Forced convection heat transfer coefficient of single pin fixed on plate, deriving expression for case corresponding to infinite circular cylinder 18 p3266 A66-34647

Conducting nonmagnetic circular cylinder supported on magnetic field produced by alternating current 19 p3324 A66-35729

Navier-Stokes equations solutions for incompressible fluid representing boundary layer flows with suction along corners of cylindrical bodies 19 p3341 A66-35855

Critical condition for aerosol deposition from symmetrical flow past solid body, considering case of circular cylinder 19 p3393 A66-36041

Bending of plane electromagnetic waves around elliptically ideally conducting cylinder of infinite length and around parallel circular dielectric cylinder, with solution as Mathieu-type series 19 p3303 A66-36064

Comparison of characteristic roots arising from Fluegge and Donnell theories, when certain amount of axial prestress is imposed on circular cylinder 19 p3474 A66-36345

Arbitrary motion of circular cylinder in ideal fluid near wall, using Fourier series 19 p3342 A66-36468

Pulsating laminar flow of viscous incompressible conducting fluid in annular channel between circular cylinders under radial magnetic field, solving MHD equations 19 p3432 A66-36643

Approximate solution for dipole radiator field in space containing two conducting long cylinders with parallel axes 20 p3512 A66-37146

Total cross sections for arbitrarily oriented dielectric circular cylinders used in obtaining extinction and polarization by realistically oriented interstellar particles, noting refractive index 20 p3649 A66-37325

Frequency of wake shedding from circular cylinder in water flow with values above critical Reynolds number, noting eddy generation and drag coefficient dependence on cavitation number 20 p3548 A66-38012

Thermoelastic stresses in elastic strips and cylinders, computing numerical value along axes and centers of elements 21 p3826 A66-38590

Velocity field and suction effects on viscoelastic flow past porous circular cylinder 21 p3724 A66-38709

Axisymmetric temperature field determination in cylindrical bodies 21 p3835 A66-38908

Dissociation of hypersonic airflow past circular cylinder at zero angle of incidence 21 p3695 A66-39230

Influence coefficients for semiinfinite and infinite circular cylindrical elastic shell subject to self-equilibrating edge loads 22 p3995 A66-40451

Instability of long thin circular cylinders under axial compression, bending, torsion, shear and external pressure [ICAS PAPER 66-32] 22 p3996 A66-40663

Slow steady flow of viscous incompressible fluid between two coaxial circular cylinders with axial roughness 23 p4054 A66-41122

Scattering of plane elastic compressional pulse by circular cylindrical cavity in infinite homogeneous isotropic linear elastic solid 23 p4145 A66-41984

Slow steady viscous flow through annulus between porous circular cylinders with uniform arbitrary injection and suction velocities, calculating wall porosity effect on velocity and pressure distributions 24 p4193 A66-42156

Plane stationary elastic wave diffraction by stress-free circular cylinder, noting cylindrical cavity case 24 p4175 A66-42841

**CIRCULAR ORBIT**

Optimal rotation of plane of circular orbit by transverse thrust force, deriving differential equations for rotational maneuver 02 p0289 A66-11653

Circular orbit effect on asymptotically stable stationary rotations of axisymmetrical satellite 03 p0430 A66-12485

First-order perigee to perigee changes in nonequatorial orbital elements due to spherical, rotational, exponential, time-invariant atmospheric drag 06 p0955 A66-16909

First-order perturbation solution to problem of minimum-fuel orbit transfer in form of equal slope guidance constraint [AIAA PAPER 66-11] 07 p1137 A66-17883

Trajectory analysis and Birkhoff rings in restricted three-body problem in three-dimensional coordinate system 09 p1453 A66-20251

Approximative analysis of spacecraft trajectories in circular extra-atmospheric anaorbital flight 09 p1457 A66-20574

Optimum impulsive transfer between elliptic and noncoplanar circular orbits, noting paths with up to three apsidal impulses 09 p1459 A66-20884

Gravitational perturbations of circular satellite orbit [AIAA PAPER 65-550] 14 p2381 A66-27418

Plane change split techniques for circularly orbiting satellite by aerodynamic propulsive and impulsive maneuvers 14 p2384 A66-27894

Perturbation of near circular orbits by Earth gravitational potential 17 p3005 A66-32997

Nonlinear control laws for takeoff and landing of circular-orbit winged glide space vehicle 18 p3132 A66-33880

Torque on rigid body in circular orbit in gravitational central field derived, using



body-centered coordinate system aligned with gravity gradient  
vector 18 p3237 A66-35030  
Infinitesimal economic pulse transfers between quasi-circular noncoplanar orbits 19 p3459 A66-35583  
Derivative-expansion method of first-order asymptotic expansion of takeoff of satellite from circular orbit by small thrust inclined at finite angle to radius vector [AIAA PAPER 65-688] 19 p3462 A66-35894  
Time of rendezvous of two satellites, one on circular and one on elliptical orbit 19 p3470 A66-36247  
Rendezvous maneuver with effect of velocity changes on orbital transfer of near-Earth satellite 20 p3663 A66-37532  
Optimum trajectories between material points moving along same orbit in gravitational field of spherically symmetric central body, obtaining numerical solutions for circular initial orbit 22 p3980 A66-40462

**CIRCULAR PLATE**  
Bending problem of circular orthotropic plate on elastic base under axisymmetric load 01 p0153 A66-10467  
Flexible satellite attitude control, analyzing satellite as thin circular plate with application to radio telescopes, noting vibration modes and nonlinear gyroscopic coupling terms 01 p0142 A66-10674  
Characteristics of flexible circular plate, considering stress and strain in friction zone at clamped section 01 p0160 A66-11181  
Plate theory for case of thin elastic deformable circular plate under rotationally symmetrical stress 02 p0296 A66-11243  
Large deflection analysis of circular ring plates under uniform transverse force along inner edge 02 p0298 A66-11584  
Circular and annular plates calculated by method of networks using polar coordinates 03 p0439 A66-13125  
Large deflection analysis of elliptical plate of lenticular section subjected to uniform temperature gradient through thickness 03 p0440 A66-13271  
Minimum weight circular plate under two independent systems of loading, noting Tresca yield condition 04 p0587 A66-13487  
Poisson-Kirchhoff plate theory for axisymmetric motions of circular elastic plates [ASME PAPER 65-APMW-7] 04 p0591 A66-14213  
Clamped circular rigid-plastic plates under blast loading distributed over surface [ASME PAPER 65-APMW-34] 04 p0593 A66-14234  
Plane disk design calculations for uniform strength under asymmetric and axisymmetric load 07 p1038 A66-18096  
Poisson-Kirchhoff plate theory for axisymmetric motions of circular elastic plates [ASME PAPER 65-APMW-7] 10 p1616 A66-21485  
Permanent deformations in circular plates subjected to uniformly distributed impulses, compared with predictions of bending theory of rigid-plastic plates 11 p1781 A66-22612  
Creep laws in terms of generalized stress-strain rates formulated, noting secondary deformation, Tresca criterion and associated flow rule 12 p1963 A66-24037  
Inverse problem of stressed state of elastic plate reinforced by members of known rigidity under axisymmetric load 12 p1967 A66-24107  
Inner boundary layer existence in circular plate under symmetric tensile stress obtained by asymptotic method 12 p1968 A66-24345  
Von Karman equations for axisymmetric nonlinear bending circular plates 12 p1969 A66-24363  
Deflections, moments and shears of circular ring plate under transverse load, comparing classical and improved theory of deformation 13 p2195 A66-25180  
Airy stress function applied in solving problems for doubly connected regions with contiguous circular boundaries 13 p2204 A66-26432  
Symmetric bending of circular orthotropic plate of systematically variable thickness for

different types of loading 15 p2613 A66-29435  
Approximate solution of free axisymmetric oscillations of circular structurally orthotropic plate of specific laws of variable thickness 15 p2613 A66-29436  
Creep bending of circular plate with temperature gradients, using iterative technique 16 p2813 A66-30269  
Deflection of uniformly loaded circular plate supported at discrete points equally spaced along circumference of concentric circle 16 p2820 A66-31274  
Bending moment, longitudinal force, radial displacement and transverse deflection of circular plate undergoing elastoplastic bending accompanied by radial tension 16 p2822 A66-31622  
Von Karman plate equations specialized to describe large symmetric deflections of circular membranes 17 p3020 A66-31999  
Complex variable method to solve problem of circular elastic plate elastically restrained at edge and subjected to arbitrary concentrated force 17 p3020 A66-32000  
Assessment of error of method of successive approximations in determination of circular plate deflections 17 p3026 A66-32598  
Load carrying capacity of circular plates under antisymmetric load 17 p3029 A66-32806  
Clamped circular rigid-plastic plates under blast loading distributed over surface [ASME PAPER 65-APMW-34] 18 p3247 A66-33569  
Transverse displacement of circular plate containing radial crack examined, using small deflection theory 18 p3249 A66-33597  
Bending behavior under lateral loads and stretching effects due to in-plane forces described by two uncoupled differential equations governing circular plates 18 p3253 A66-33803  
Strain-energy exposition of creep deflection theory and Ritz-Rayleigh method prediction of creep deformations of laterally loaded circular plates 18 p3256 A66-34561  
Clamped circular plates of rigid plastic material under uniformly distributed blast loading, noting parameters of permanent central deflection 20 p3673 A66-38277  
Bending problems of transversely isotropic circular plates based on Ambartsumian theory of anisotropic plates 21 p3830 A66-38980  
Load carrying capacities of rotationally symmetric plates and shells for limited anisotropic behavior and different yield stresses in tension and compression 21 p3831 A66-39375  
Stress distribution in elastically nonhomogeneous rotating thin circular disk of varying thickness of anisotropic material 21 p3745 A66-39597  
Vibrations of transversal-isotropic circular plates solved, using refined theory of anisotropic plates 23 p4138 A66-41448  
Membrane force in axisymmetric elastoplastic bending of clamped thin circular plate 23 p4142 A66-41951  
Plastic theory of structures for collapse under highly localized loading 24 p4286 A66-42152  
Axisymmetric bending problem of idealized elastic rigidly-plastic two-layer circular plates, deriving exact mathematically strict solutions and uniqueness conditions 24 p4290 A66-42443

**CIRCULAR POLARIZATION**  
Tuning of lens and mirror antennas with circularly polarized radiation patterns 02 p0192 A66-11848  
Circularly polarized monopulse feed system for use with parabolic reflectors generates response independent of return-signal polarization 06 p0851 A66-16448  
Beat frequencies and coherence properties in circularly polarized atomic transitions of gaseous lasers with axial magnetic fields 07 p1046 A66-18429  
Two-element interferometer to investigate Jupiter decimeter circularly polarized radiation 08 p1288 A66-18789  
Lifetimes of orientation and alignment of excited atomic states examined in level crossing and optical double resonance experiments employing polarized light 11 p1740 A66-22969  
Near-isotropic circularly polarized

antenna 13 p2035 A66-25503  
Circularly polarized tracking feed in Haystack antenna 13 p2035 A66-25504  
Propagation of circularly polarized electromagnetic waves in circular semiconductor cylinder surrounded by metal tube and immersed in DC magnetic field 13 p2169 A66-26238  
Propagation of circularly polarized plane electromagnetic waves through helium plasma along direction of static magnetic field, determining electron density 13 p2154 A66-26672  
Hooke law extension to include term expressing dependence of stress on spatial variation of strain, noting rotation of polarization plane in sound wave propagation in isotropic medium 14 p2334 A66-27478  
Direction, frequency and polarization of radio emission from galactic OH determined by hypothesis of stimulated emission 21 p3814 A66-39213  
Linearly and circularly polarized fields in laser amplifier interaction with axial magnetic field, emphasizing combination tone production 23 p4079 A66-41624  
Radar scattering equations for transmitting and receiving circularly polarized waves in terms of characteristics for linear polarization 24 p4171 A66-42374  
Anomalous circular polarization of hydroxyl radical 18-cm radiation from cosmic sources 24 p4272 A66-43188

**CIRCULAR SHELL**  
Deformation of circular membrane containing central rigid disk under axisymmetrically distributed load 04 p0590 A66-14150  
Thin circular cylindrical shell behavior in axial compression, noting buckling under stress, boundary condition detail effects, etc 17 p3031 A66-33064  
Stability of structurally anisotropic circular cylindrical shell under nonuniform compression 21 p3829 A66-38976  
Longitudinal and tangential local and strip loads effect on magnitude of forces, moments and displacements in circular cylindrical shell 23 p4139 A66-41788  
Nonlinear flexural vibrations of thin circular rings analyzed, using Galerkin procedure on motion equations 24 p4285 A66-42142  
Prestressed circular membrane shell subjected to uniform radial line load, determining stresses and displacements from material properties, internal pressure and original size 24 p4288 A66-42272

**CIRCULAR TUBE**  
Transient heat transfer between thin circular tube and incompressible fluid, considering radial conduction and heat loss [ASME PAPER 65-HT-2] 04 p0595 A66-13393  
Entrance region Newtonian flow analysis in tube of circular cross section for possible use in viscometry and flow stability studies [AICE PREPRINT 19D] 04 p0511 A66-13935  
Free convection on laminar forced flow heat transfer in horizontal circular tube [ASME PAPER 65-HT-23] 05 p0783 A66-14744  
Pressure drop in entrance region of abrupt inlet circular tube for continuum laminar flow conditions [ASME PAPER 65-WA/APM-5] 05 p0663 A66-15428  
Dynamic stability of circular elastic rods, noting iteration method analysis of nonlinear coupling effect between axial force and curvature in forced in-plane vibrations 09 p1467 A66-20638  
Pressure drop in entrance region of abrupt inlet circular tube for continuum laminar flow conditions [ASME PAPER 65-WA/APM-5] 10 p1523 A66-21471  
Rarefied gas flow in hydrodynamic entrance region of circular tube, noting variation with density level, velocity profile and pressure drop for developing flow 13 p2070 A66-26713  
Heat transfer rate in thermal inlet of circular tube, describing experimental apparatus and observational results 14 p2411 A66-27313  
Free convection on laminar forced flow heat transfer in horizontal circular tube [ASME PAPER 65-HT-23] 16 p2828 A66-30983  
Kohn-Kato bounds for natural frequencies



of axial shear vibrations for solid circular bar, extending calculations through conformal transformations for bar with many-lobed plane curved boundary 17 p3022 A66-32014

Vaporization of liquid fuel injected in heated horizontal circular pipe for straight and swirl air flow, noting increased rate of vaporization in swirl airflow for increased heat supply 18 p3265 A66-34490

Heat transfer in laminar flow of Bingham material through circular pipe, taking into account dissipation effect 21 p3836 A66-39441

Screening of sound in infinite tube with circular cross section and finite wall thickness placed in compressible fluid 21 p3729 A66-39444

Gaseous dispersion in laminar flow through circular tube with mass transfer to retentive layer 22 p3900 A66-40411

Oscillating two-phase flow through rigid circular pipe investigated to understand blood cells effects on changes in shape of pressure pulse wave 23 p4058 A66-41916

**CIRCULATION**

S ATMOSPHERIC CIRCULATION

S BLOOD CIRCULATION

S PERIPHERAL CIRCULATION

S WIND CIRCULATION

**CIRCULATOR**

Three-port waveguide circulator design analyzed with X-band, using manganese ferrite 01 p0038 A66-10524

4-port E-plane cross junction ferrite circulator analyzed in X-band 01 p0039 A66-10532

Wideband junction circulator design with maximum product of isolation and frequency bandwidth but maintaining minimum temperature and DC magnetic field variation 01 p0040 A66-10548

Disk and parasitic resonance of broadband and small circulators for UHF and VHF 01 p0040 A66-10551

Lumped parameter circulators for 80-400 mc/s range 01 p0041 A66-10566

Configuration of broadband waveguide Y circulator 01 p0041 A66-10578

150 mc strip-line circulator using Altron garnet material, noting isolation, insertion loss, input impedance, etc 10 p1514 A66-21910

Ferrites for resonance-directional insulators and circulators, noting properties at microwave frequencies and applicability 11 p1664 A66-22659

Circulators from lumped circuit elements examined, calculating coil properties and analyzing construction 11 p1664 A66-22660

Flow graph analysis of lossless nonideal 3- and 4-port junction circulators for visualizing scattering matrices and calculating coefficients of combined networks 17 p2896 A66-33277

Coupled waveguide circulator in which secondary waveguide is loaded with distributed nonreciprocal attenuation along coupling length 18 p3075 A66-33566

**CIRCULATORY SYSTEM**

SA BLOOD CIRCULATION

SA CAPILLARY

Exercise tolerance, plasma volume, red cell mass, total blood volume and orthostatic tolerance during four weeks of bed rest 03 p0326 A66-13354

Physiological problems of weightlessness discussing motion sickness, fluid volume control and chronic effects on circulatory system 04 p0465 A66-14071

Prolonged hypokinesia effect on human resistance to transverse g-forces, detailing respiratory and circulatory systems, motor response and visual acuity 15 p2437 A66-29473

Wave propagation, dispersion and energy transfer in arterial blood flow considered as fluid dynamics, noting finite amplitude effects in circulatory system and flow control mechanism 23 p4062 A66-42058

**CIRCUMPOLAR VORTEX WIND**

Stability of expanded circumpolar vortex, using available record of 700-mb subtropical westerly index values for five-day means from 1943 through 1965 07 p1062 A66-17372

**CISLUNAR SPACE**

Velocities of dust particles in cislunar space 05 p0762 A66-15266

Density fluctuation effect on radar

determination of total electron content in terms of recent cislunar density measurement 17 p2917 A66-32520

Electric propulsion for transfer mission between parking orbits in cislunar space under optimum payload 17 p2992 A66-33238

**CIVIL AVIATION**

SA AIR TRANSPORTATION

SA BOEING 733 AIRCRAFT

Approach and landing visibility requirements in terms of information needed by civil pilot 01 p0101 A66-10032

Steady growth of commercial aviation over next years will be limited by economics, not technology 02 p0178 A66-12070

Head-up display /HUD/ developed for automatic landing in civil aircraft 03 p0329 A66-12884

West German federal air transport authority, scope, organization and objectives 05 p0794 A66-15807

Proposal for control of local service subsidies, noting lack of clearly stated public policy with respect to congressional statements and actions 06 p0973 A66-16401

Navigation equipment for civil use based on miniature inertial platform, analog and digital computers, automatic chart display, etc 07 p1067 A66-17689

Mechanization of navigational functions for supersonic aircraft within central airborne digital computer, comparing military experience with commercial requirements 07 p1067 A66-17693

Inertial navigation and guidance systems applied to civil air transport from systems engineering viewpoint 07 p1067 A66-17695

Two automatic astronomical navigation and tracking systems compared for accuracy and performance in civil aircraft 07 p1070 A66-17722

Frequency pattern for transmission from ground stations providing worldwide unambiguous navigation aid for civil aircraft, noting airborne equipment 07 p1073 A66-17769

Air navigation problems in North Atlantic including separation standards lateral and vertical, SST traffic, collision risk, etc 07 p1074 A66-17774

Combination of moored ocean platforms and transatlantic submarine telephone cables for VHF communication service and other ATC facilities for civil aircraft across North Atlantic 07 p1002 A66-17775

Military inertial navigation equipment applied to civil aircraft, evaluating accuracy, reliability and cost 07 p1077 A66-17799

Principal civil aircraft at 26th Aeronautical and Space Exhibition, detailing AN 22 Antaeus cargo aircraft 07 p0989 A66-17820

French Air Regulation 2054 applicable to sailplanes, considering effect on design speed and gust loads 07 p0989 A66-17822

Civilian and Military Uses of Aerospace-Conference, New York, January 1965 08 p1299 A66-18547

FAA regulation of civilian use of U.S. airspace 08 p1321 A66-18548

Book on political, economic and military analysis of air transport policy and national security 09 p1472 A66-20099

STOL operations in city center, discussing metropolitan transportation problems 09 p1327 A66-20244

Airport suitability for delta wing commercial supersonic transport, discussing noise objectives 09 p1365 A66-20698

Supersonic business aircraft design problems related to payload and range 12 p1800 A66-23643

Air navigation problems in North Atlantic including separation standards lateral and vertical, SST traffic, collision risk, etc 13 p2124 A66-25861

Combination of moored ocean platforms and transatlantic submarine telephone cables for VHF communication service and other ATC facilities for civil aircraft across North Atlantic 13 p2058 A66-25862

Inertial navigation and guidance systems applied to civil air transport from systems engineering viewpoint 13 p2125 A66-25865

Engine reliability data for four Rolls-Royce civil aircraft engines 13 p2174 A66-26694

Assisted takeoff and landing for commercial aircraft using short runways

[SAE PAPER 660337] 14 p2269 A66-27296

Commercial air transport in 1972, discussing operating economics, management planning, maintenance costs, etc [SAE PAPER 660321] 14 p2223 A66-27300

Medical aspects of commercial jet pilot fatigue, examining effects of socio-economic and off-duty activities 15 p2442 A66-28665

Specialized services provided by air freight forwarding industry to shipper and carrier 15 p2619 A66-29790

Civil Aeronautics Board /CAB/ role in air freight industry and in proposed Department of Transportation 15 p2621 A66-29804

Aircraft utilization and schedule planning, optimum use of flight performance, ground equipment, facilities and personnel [SAE PAPER 660279] 15 p2427 A66-29824

Super airport planning concepts, satellite and unit terminal, stress decentralization to meet changing demands and increased volume of air traffic [SAE PAPER 660282] 15 p2476 A66-29826

Operation and maintenance of Lockheed L-2000 double delta SST aircraft with high thrust engine and large delta wings, designed to meet civil aviation requirements [SAE PAPER 660295] 15 p2427 A66-29832

Helicopter design and application to common carrier transportation, particularly between airport and city [SAE PAPER 660335] 15 p2428 A66-29846

Inertial navigation for commercial aviation economically justified by fuel economy due to reduced flight time 15 p2536 A66-29894

Commercial V/STOL aircraft and systems development, discussing government /FAA/ interest and assistance 16 p2633 A66-31281

Future civil VTOL aircraft potentialities and limitations 17 p2846 A66-32886

Aviation and astronautics - Conference, Tel Aviv and Haifa, February 1966 17 p2912 A66-33063

Navigational display types and requirements for civil aircraft 17 p2956 A66-33223

Canadian labor market for commercial helicopter pilots 18 p3268 A66-34624

Civil aviation safety - International Symposium, Stockholm, April 1966 20 p3493 A66-36990

Flight safety in Soviet civil aviation including takeoff and landing, cruising in airport vicinity, meteorology and medicine 20 p3494 A66-36991

Civil aviation communications between pilot and ground controller on over-ocean flights, considering use of VHF and HF and synchronous satellite to extend VHF 20 p3515 A66-37234

Interior design techniques in civil aircraft seat design and supersonic aircraft interiors 20 p3495 A66-37425

Flight recorder utilization in British civilian jet and turboprop aircraft 21 p3696 A66-38603

Intermediate visual acuity testing of senior airline pilots, including separate testing of each eye with trifocal chart and artificial accommodation measurement 22 p3857 A66-39799

Inertial navigation for civil airline operations, noting azimuth alignment made by automatic gyrocompassing [ICAS PAPER 66-6] 22 p3946 A66-40677

Hypersonic cruise vehicles for military and civil requirements, considering air breathing propulsion and structural weight 24 p4296 A66-42241

**CL-84 AIRCRAFT**

S CANADAIR CL-84 AIRCRAFT

**CLADDING**

Explosion cladding for bonding similar and dissimilar metals without intermediate metal or externally applied heat 03 p0380 A66-12317

Nuclear fuel-cladding diffusion and interactions in uranium-tungsten and uranium-molybdenum systems, covering compatibility, transport rate, thermal cycling effects and cladding surface contamination 05 p0714 A66-15588

Clad metals concept applied to low energy contact using materials system, analyzing material, mechanical and electrical properties of thin precious metal inlays 12 p1930 A66-24666



- Explosive cladding for strong metal-metal bonds  
[ASTME PAPER AD66-112] 14 p2299 A66-26951
- Heat treatment of titanium alloy sheets clad with industrial trial-grade titanium for preventing surface oxidation and hydrogen absorption 15 p2522 A66-29191
- Brazing and cladding research on refractory metals offers dependability and continuity of protective layers and abrasion resistance in extreme environments 19 p3368 A66-36119
- CLAMP**
- Ty-Block injection-molded nylon cable-anchoring device with adjustable nylon strap for clamping cables 11 p1709 A66-22674
- CLASSIC AIRCRAFT**
- S ILYUSHIN IL-62 AIRCRAFT
- CLASSICAL MECHANICS**
- Discrete plasma model describing particle behavior by classical mechanics equations, used for interaction between fast moving bodies and rarefied plasma 09 p1378 A66-21020
- Turbulent vortices in quantum and classical fluid and time dependent meniscus depth of water, He I and He II 10 p1525 A66-21965
- Asymptotic stability of equilibrium states of nonholonomic systems 14 p2336 A66-28052
- Routh theorem describing motion stability of holonomic systems applied to nonholonomic systems, specifically Bobylov spherical gyroscope 14 p2297 A66-28062
- Classical analytical mechanics applied to mechanics of continua, noting relation between kinetic-stress functions and Ostrogradskii-Hamilton principle and stress tensor and finite deformation 15 p2539 A66-29148
- Investigation methods for multidimensional dynamic systems, including parametric dependence, bifurcation theory and phase-propagation separation structure 15 p2541 A66-29165
- Revision of fundamental laws of Newtonian mechanics, noting condition when relativity principle is not obeyed 16 p2748 A66-31400
- Turbulent vortices in quantum and classical fluid and time dependent meniscus depth of water, He I and He II 21 p3731 A66-39544
- CLAVACIN**
- IR spectrum of clavacin structure 05 p0629 A66-15107
- CLAY**
- S SOIL
- CLEAN ROOM**
- SA ENVIRONMENTAL CONTROL
- Number of viable aerobes and anaerobes accumulating on stainless steel surface in clean room during one year under various conditions, for spacecraft sterilization purposes 13 p2015 A66-25797
- Environmental control manufacture discussing cleaning, design and maintenance problems, historical background, etc 17 p2903 A66-32208
- R and D clean room complex design for guidance and control systems, noting contamination control, maintenance procedures, cost factors, etc 17 p2903 A66-32209
- Contamination problems in space program, discussing clean room equipment, maintenance, cleaning problems, etc 17 p2866 A66-32210
- Contamination control of manned spacecraft, noting problem of biological interactions and methods of monitoring 17 p2866 A66-32211
- Contamination control and space program, objectives, achievements, NASA courses, etc 17 p2868 A66-32894
- CLEANING**
- SA PURIFICATION
- Field cleaning of corrosion resistant steel tubing for LOX and pneumatic service 22 p3922 A66-40040
- CLEAR AIR TURBULENCE**
- Index of clear air turbulence in sloping baroclinic layer 02 p0253 A66-11575
- Clear air turbulence detection and prediction by laser, radiometer, radar and other devices  
[AIAA PAPER 65-800] 03 p0370 A66-13072
- Airborne laser-radar light detection and ranging /LIDAR/ systems applied to detection of clear air turbulence /CAT/ 05 p0697 A66-15297
- Occurrence frequency and intensity of clear air turbulence as function of altitude between 20,000 and 75,000 ft  
[AIAA PAPER 65-13] 09 p1400 A66-20742
- Clear air turbulence, considering energy source by transfer from large to small flow in gravity wave spectra, noting shear role and motion equations 10 p1552 A66-21289
- Flight data used to determine relationship between atmospheric temperature changes and clear air turbulence occurrence at jet altitudes  
[AIAA PAPER 66-365] 12 p1906 A66-24477
- Clear air turbulence types at high altitude identified and intensity and wavelength measured by FM instrument, using vane gust probe installed in U-2 aircraft  
[AIAA PAPER 66-362] 12 p1907 A66-24494
- Clear air turbulence detection with laser Doppler optical radar  
[AIAA PAPER 66-374] 12 p1818 A66-24498
- Clear air turbulence structure, noting measurement results obtained by Canberra aircraft and TOPCAT project, energy yield of gravitational shearing waves, etc 13 p2122 A66-26127
- Effective early warning system to enable pilot to cope with clear air turbulence /CAT/ 14 p2326 A66-27819
- Light detection and ranging /LIDAR/ technique use in atmospheric research, particularly meteorological factors important to aviation and rocket operations  
[AIAA PAPER 65-464] 14 p2309 A66-27892
- Measurements of maser beam propagated through atmosphere, emphasizing beam broadening and signal fluctuation due to clear air turbulence 15 p2448 A66-28581
- National Air Meeting on Clear Air Turbulence, Washington, D.C., February 1966 15 p2531 A66-28911
- Wind shear, gravity waves and Richardson number in relation to clear air turbulence /CAT/ 15 p2425 A66-28912
- Present state of knowledge on physical causes of clear air turbulence /CAT/ 15 p2426 A66-28913
- Synoptic analysis of nature and cause of clear air turbulence 15 p2531 A66-28914
- Atmospheric model describing generation of clear air turbulence /CAT/, noting horizontal shear effect 15 p2532 A66-28915
- Clear air turbulence detection and warning by airborne devices including radar, IR spectrum, air temperature probes, ozone detection, etc 15 p2500 A66-28917
- Atmospheric temperature changes as factor in detection of clear air turbulence, especially above 25,000 ft, noting aircraft instrumentation used 15 p2532 A66-28918
- Clear air turbulence detection instrument development 15 p2500 A66-28919
- Clear air turbulence detection with optical radar, using spectral analysis of backscattered Doppler-shifted light particle formation mapping via correlates of rough flying conditions 15 p2450 A66-28920
- Clear air turbulence research methods, noting structural analysis, computer application, satellite photography, etc 15 p2532 A66-28921
- Correlation between clear air turbulence and aircraft electrical activity, describing corona discharges from DC-8 tail antenna 15 p2426 A66-28922
- LF electrostatic field characteristics of clear air turbulence, noting theory and application of field sensing antennas, turbulence generated signals, etc 15 p2532 A66-28923
- Radar refractivity fluctuations and wavelength dependence of reflectivity in clear air turbulence regions 15 p2532 A66-28924
- CAT detection by radar backscatter measurement of radio refractive index 15 p2532 A66-28925
- CAT detection by radiometric measurement of mm wave emission from oxygen molecules and measurement of ambient air temperature and temperature gradient 15 p2532 A66-28926
- Clear air turbulence detection by measuring associated air temperature gradient by airborne IR radiometer 15 p2500 A66-28927
- Airborne laser radar investigation of clear air turbulence 15 p2533 A66-28928
- CAT detection from Doppler shift in laser light backscattered from atmospheric aerosol 15 p2500 A66-28930
- CAT detection by photometric star tracking system from moving aircraft 15 p2500 A66-28931
- Clear air turbulence forecasting for aircraft, noting methods employed by airlines 15 p2533 A66-28932
- Aircraft safety, noting minimization of clear air turbulence, mountain wave and wind shear effects 15 p2533 A66-28933
- Clear air turbulence, noting importance of good detection system and history of incidents in six-year period 15 p2426 A66-28934
- Pilot techniques for control of passenger transport aircraft during CAT or thunderstorm 15 p2426 A66-28935
- Clear air turbulence, examining detection, forecasting and piloting techniques when passing through CAT 17 p2948 A66-32201
- Airborne IR system to detect temperature discontinuities characterizes some forms of clear air turbulence /CAT/  
[AIAA PAPER 65-459] 19 p3360 A66-36482
- Worldwide long-range navigation satellite /Navsat/, noting use with inexpensive black box, clear-air turbulence mapping and position definition in relation to high ground 20 p3598 A66-38259
- SST in nonoptimum conditions, discussing cost penalties due to navigation error, air traffic conditions, sonic boom restrictions, clear air turbulence and weather 21 p3695 A66-38451
- Clear air turbulence near jet stream, discussing velocity profiles and various meteorological parameters 22 p3902 A66-39677
- Tropopause detection by radar, examining detection of high altitude clear-air turbulence by radar and forward-scatter techniques 22 p3912 A66-40304
- Clear air turbulence detection and warning by airborne devices including radar, IR spectrum, air temperature probes, ozone detection, etc 22 p3945 A66-40325
- Turbulent refractivity spectrum and optimization of airborne radar CAT detectors 22 p3944 A66-40429
- Clear air turbulence detection and prediction by laser, radiometer, radar and other devices  
[AIAA PAPER 65-800] 23 p4066 A66-40981
- Stress, eddy viscosity and viscous dissipation estimations in jet stream obtained during Project TOPCAT in Australia, using aircraft soundings 24 p4234 A66-42984
- Velocity characteristics of clear-air dot angle echoes determined via Doppler radar measurements 24 p4234 A66-42990
- CLEAVAGE**
- Cleavage characteristics of copper plate under explosive load determined and interpreted, taking finite failure time into account 10 p1613 A66-21238
- Cleavage characteristics of copper plate under explosive load determined and interpreted, taking finite failure time into account 19 p3474 A66-35861
- Lithium cleavage of unsaturated vicinal di-tert-phosphines producing lithium diphenylphosphide 24 p4170 A66-42889
- CLIMATOLOGY**
- Climatic conditions at Earth surface, relation to long-term planetary trends in atmospheric circulation 05 p0712 A66-15221
- Numerical experiment with general circulation model with simple hydrologic cycle 08 p1247 A66-18925
- Twelve monthly world maps of daily means of total solar radiation incident on horizontal surface 11 p1702 A66-23156
- Model simulation study of economic value of improved methods of translating weather information into operational terms 11 p1731 A66-23488
- Long wave radiation and total radiation balance at Earth surface in Arctic region, based on Stefan-Boltzmann formula 12 p1869 A66-24202
- Arctic short-wave atmospheric radiation absorption, long-wave radiation loss, and



tropospheric radiation  
balance 12 p1949 A66-24203  
Arguments pro and con on Milankovitch astronomical theory of climatic changes 15 p2489 A66-29266  
High latitude density regime in upper stratosphere inferred from Arctic and Antarctic observations 17 p2922 A66-33343  
Climatology of surface temperature which meets most engineering design requirements 20 p3593 A66-38180  
WSR radar four-year climatology of thunderstorm penetrations of tropopause at ten locations in U.S. 22 p3944 A66-40430

**CLINICAL MEDICINE**  
Clinical aspects of interplanetary flights noting models of future cosmic diseases, automation of diagnostics, medical aid aboard spacecraft, etc 06 p0815 A66-16052  
Clinical observations and tests of solitary confinement on neurotic pilots 11 p1642 A66-22486  
Alternobaric /pressure/ vertigo severity and frequency among Swedish RAF pilots 11 p1644 A66-22584  
Clinical and medicolegal considerations on fatal case of myocardial infarct involving military pilot in flight 14 p2229 A66-26813

**CLOCK**  
SA ATOMIC CLOCK  
BTC-2 master clock provides basic information and reference signals for operation of various units of satellite tracking and telemetry 14 p2295 A66-27550  
Receiver design and results of dual VLF transmissions for obtaining timing information 19 p3357 A66-35693  
Experimental meteor burst system for microsecond synchronization of isolated clocks 20 p3515 A66-37227

**CLOCK PARADOX**  
Conditions satisfied by transformation equations connecting inertial and relativistic accelerated systems are deduced for rectilinear motion 03 p0392 A66-12609  
Time contraction physically explained for objects moving with velocities significant with respect to velocity of light 21 p3817 A66-39600

**CLOSE PACKED STRUCTURE**  
Superconducting behavior of various close packed low symmetry intermediate phases in various binary systems, noting relation between transition temperature and composition 12 p1928 A66-23939

**CLOSED CIRCUIT TELEVISION**  
Operational space flight simulator using closed-circuit TV with pinhole optics 10 p1518 A66-21231  
Closed circuit television applied to data transfer in air traffic control, discussing accident prevention and information provision to aircraft 17 p2874 A66-32356  
T-27 Space Flight Simulator, for extravehicular activity training, utilizing closed-circuit TV system 19 p3291 A66-35966

**CLOSED CYCLE**  
Compact Ackeret-Keller closed cycle thermodynamic nuclear turbine power plant [ASME PAPER 66-GT/CLC-6] 14 p2329 A66-26980  
Nonconventional application of electric power-generating closed-cycle gas turbines [ASME PAPER 66-GT/CLC-8] 14 p2224 A66-26981  
Graphical matching solution for gas turbine power plant closed cycle systems [ASME PAPER 66-GT/CLC-14] 14 p2224 A66-26984  
Liquid phase compression in closed cycle gas turbine by using particular working fluids for application to nuclear power stations [ASME PAPER 66-GT-111] 14 p2411 A66-27005  
Jet compression requirements for circulating working medium in closed cycle magnetoplasmadynamics /MPD/ electrical power generator [AIAA PAPER 65-466] 19 p3280 A66-35621  
High speed stable system through combination of hunting-type control system without closed cycles designed for plant optimization, with recycling type controller 22 p3883 A66-39661  
Closed Brayton cycle power system for space vehicles, discussing closed loop and

major components 23 p4020 A66-41750

**CLOSED ECOLOGICAL SYSTEM**  
SA LIFE SUPPORT SYSTEM  
SA OXYGEN PRODUCTION  
SA SPACE CABIN ATMOSPHERE  
SA SPACECRAFT ENVIRONMENT  
Physiological-ecological investigations of Chlorella cultures as link in closed ecological system 01 p0018 A66-10981  
Life support closed cycles for missions to outer space lasting 12 months or longer, considering recovery and replenishing of water, food and oxygen from wastes 07 p0998 A66-17229  
Closed ecological systems and endogenous formation of CO in plant and animal tissues 11 p1648 A66-23048  
Soviet monographs on problems of space biology 15 p2431 A66-29439  
Long duration flight physiological data on ducks and chickens in closed ecological systems, including oxygen and food requirements and carbon dioxide output 15 p2435 A66-29452  
Human physiological and hygienic problems when confined in closed system of circulating biological substances 15 p2443 A66-29457  
Human waste nutrient assimilation by Chinese cabbage plants grown in air-moisture medium in closed system 15 p2440 A66-29507  
Intensive Chlorella culture need of carbon dioxide concentration in closed and controlled air-carbon dioxide system 15 p2440 A66-29508  
Intensive Chlorella culture consumption of mineral-nutrition elements 15 p2440 A66-29510  
Trace contaminant control in closed environments as requirement for safe air in habitable areas of manned spacecraft [AICE PREPRINT 26A] 17 p2867 A66-32676  
Carbon dioxide decomposition and oxygen reclamation by chemical reaction with electrochemically reduced lithium 19 p3292 A66-36234  
Chemical methods for carbon dioxide conversion for oxygen recovery, including relationship to biological processes 19 p3293 A66-36235  
Integrated program approach for contamination control of space cabin atmospheres based on identification, estimation of concentration and system specifications 19 p3293 A66-36238  
Closed universe models with two values of Hubble expansion 21 p3817 A66-39560  
Physicochemical methods of creating life support systems in spacecraft cabins 24 p4169 A66-43143  
Life support system in spacecraft cabins based on biological circulation of substances 24 p4166 A66-43144

**CLOSED LOOP SYSTEM**  
Realizable transfer function of closed-loop automatic control system calculated with aid of minimum mean square error criterion 01 p0051 A66-10706  
Discontinuities occurring in closed loop optimal control problems when using maximum principle 02 p0207 A66-11899  
Graphical method for determining closed-loop frequency response of nonlinear feedback control systems 03 p0349 A66-13021  
Optimum stabilization of tumbling satellite, using Hamilton-Jacobi method 04 p0585 A66-13676  
Frequency domain stability criteria, discussing generation and validity of stability criteria 06 p0864 A66-16736  
Optimal control system terminal condition sensitivity, examining parameter variation effects on open loop, feedback and optimal open loop adjacent to closed loop control 06 p0864 A66-16738  
Series analysis of closed-loop system containing loaded hydraulic valve, with equations of motion and response of system to ramp input and Coulomb load 06 p0810 A66-16915  
Closed loop gain of multiple feedback circuit determined, using return-difference matrix analysis 07 p1015 A66-17754  
Fluidic closed-loop digital position-speed servocontrol system without moving parts, using pulsed air 07 p0991 A66-17878

Transient processes in thin open-loop and closed-loop antennas studied by method that takes transmission line processes into account 08 p1199 A66-19759  
Sensitivity of transistor multiple loop feedback amplifier to parameter variations evaluated via replacement with equivalent circuit systems 09 p1355 A66-20603  
Recovery of reusable products of human excretory wastes in closed-loop life support systems for long-duration manned spaceflight [AICE PREPRINT 19B] 10 p1491 A66-21185  
Closed loop MPD power generation at low temperatures and analysis of nonequilibrium processes in magnetoactive flow [AIAA PAPER 66-168] 10 p1486 A66-21689  
Electric output and gas conductivity of cesium-seeded helium closed-loop MPD generator with auxiliary ionization 11 p1639 A66-22246  
Realizable transfer function of closed-loop automatic control system calculated with aid of minimum mean square error criterion 11 p1675 A66-22618  
Free oscillation stability of closed-loop self-adjusting system with several parameters, noting two methods of measuring relative damping 11 p1677 A66-22760  
Stable self-adjusting system with single adjustable parameter designed, using inverse model of desired transfer function of closed-loop system in feedback control circuit with large amplification factor 12 p1851 A66-24315  
Stability of pulse frequency modulated closed-loop control systems determined, using state variables which define system output and error 12 p1855 A66-24640  
Manual closed-loop control systems analysis, discussing operator dynamics for permanent procedural variables 12 p1855 A66-24641  
Root locus methods applied to synthesis of linear multivariable control systems for noninteraction 12 p1855 A66-24644  
Synthesis of closed loop optimal system with nonlinearity and integral criterion 13 p2047 A66-25475  
Component failure examples of Gemini rendezvous radar, emphasizing need for closed loop reliability program 13 p2039 A66-25786  
Algorithm for optimal controller design with closed loop characteristics 13 p2053 A66-26081  
Sensitivity comparison of closed-loop and open-loop systems 13 p2054 A66-26092  
Closed loop hydraulic high-speed universal testing machine and simulation of high strain rate conditions 13 p2197 A66-26108  
Gas lubricated bearings used in Brayton cycle closed-loop system turbomachinery in design of two-shaft power plant [ASME PAPER 66-GT/CLC-9] 14 p2300 A66-26982  
Optimum controller design for systems with unlimited delay 14 p2264 A66-27340  
Restrictions placed on transfer function of linear system with input and output coordinates in presence of given plant in control loop 14 p2265 A66-27522  
Motion equations and simulation of spin-stabilized interplanetary spacecraft closed-loop pitch control system, using low-thrust gas jet torquers with rate gyro sensors 14 p2392 A66-27881  
Tunable precision frequency source using phase locked variable frequency oscillator for mobile radio sets 15 p2451 A66-29313  
Closed loop active networks with distributed RC elements, noting circuit composition, parameters and application 15 p2471 A66-29327  
Closed-loop automatic control system with unvalued substantially nonlinear element, using approximation of characteristics by Fourier series 16 p2669 A66-30754  
Statistical decision theory determination of parameter variations in closed-loop automatic adaptive control system 16 p2670 A66-30880  
Thermostability and control of airborne electronic equipment in closed-loop forced-air cooling systems 16 p2663 A66-31325  
Liquid filled electrostatic generation, noting charge transporting and insulating



function of liquid helium 17 p2848 A66-31814  
 Maximum increase in system error due to computer round-off errors for closed loop linear sampled data 17 p2900 A66-32075  
 Trial and error method for constructing closed loop harmonic response locus of control system with one nonlinear element 18 p3089 A66-34010  
 Superconducting bearing operating on conservation of fluxoid in closed loop of superconductor 18 p3116 A66-34243  
 Experimental antenna with closed loop profile control, noting light sensor application and fast response characteristics 18 p3081 A66-34278  
 Phase characteristics and amplitude of correcting device ensuring closed loop mechanical system stability at critical frequency 18 p3092 A66-34995  
 Sensitivity of closed loop optimal control system to parameter variations and external perturbations 19 p3324 A66-35581  
 Optimization of control loop type for minimum threshold which is function of modulation index, obtaining results using sine wave modulation 19 p3301 A66-35695  
 Near-threshold behavior of phase-locked devices, noting phase error processes 19 p3301 A66-35697  
 Block sensitivity coefficient analysis in application of method of transformed circuits to closed-loop control systems, noting dynamic accuracy problem 19 p3327 A66-36014  
 Distributed parameter systems in discrete-time models compared with response obtained by approximating transcendental transfer function with root factor and other approximations 19 p3282 A66-36683  
 Closed loop control system for space vehicle guidance, formulating efficient steering algorithm 19 p3471 A66-36685  
 Linear optimal control techniques for design of control system for short-range stationkeeping of large assault helicopter 19 p3280 A66-36688  
 Multiloop flight control system root sensitivity to open loop parameter variation, describing method of 19 p3335 A66-36690  
 Criterion for optimum design of quantizer imbedded in closed loop dynamic system is optimization of overall system performance expressed by variational criterion 19 p3336 A66-36707  
 Explicit method for calculating closed-loop gains defining stability boundary and subsequent phase margin boundaries of two-loop linear feedback system 19 p3337 A66-36716  
 Sequential estimation on states of linear systems disturbed by white noise, determining relations between covariance matrices 19 p3338 A66-36736  
 Simulation and analysis of adaptive roll autopilot for air to air missile, using limit cycle with small amplitude controlled by gain changing loop 20 p3595 A66-36865  
 Closed loop control system combined with air beating technology for measurement of multicomponent microforces 20 p3555 A66-36870  
 Multiloop control interaction using linearized technique, noting variable geometry intake loop 20 p3627 A66-36881  
 Block diagram of closed loop automatic control system and conditional feedback control system, both with passive adaptation 20 p3536 A66-36883  
 Computer model analysis of functional relationships of human operator information handling and control in closed loop tracking situation 20 p3509 A66-37236  
 Open and closed-loop network synthesis using transient-response approximation 20 p3538 A66-37581  
 LF combustion oscillation analyzed by theory of dynamical stability of closed feedback loop 20 p3681 A66-38103  
 Closed loop optimization of fixed configuration systems termed specific optimal control solved by applying Pontryagin maximum principle to reduce problem to two-point boundary value problem 21 p3718 A66-38668  
 Pneumatic servomotor synthesis by root loci technique providing direct insight into

effects of parameter changes on system response 21 p3697 A66-39216  
 Four-foot diameter solar radiation simulator system using single xenon arc source and closed-loop heat exchange system for electrode cooling 22 p3887 A66-40206  
 Multiloop flight control system root sensitivity to open-loop parameter variation, describing method of 22 p3884 A66-40360  
 Selection of size of hydraulic servomotor with rotary hydraulic motor controlled by electrohydraulic spool valve to reduce open-loop gain for given closed-loop stiffness 22 p3852 A66-40515  
 Pontryagin maximum principle minimization of time frequency transition in white noise driven phase-locked loop 23 p4048 A66-41316  
 Stable transmission of given transient response in closed loop nonlinear servosystem under fixed initial condition and in presence of possible disturbances 23 p4048 A66-41393  
 Digital simulation study of acquisition capabilities of phase-locked loop in presence of noise 23 p4050 A66-41616  
 Closed Brayton cycle power system for space vehicles, discussing closed loop and major components 23 p4020 A66-41750  
 Nonlinear behavior of second-order phase locked loop in presence of noise, discussing probability distribution of phase error, statistical properties of loop behavior, etc 24 p4172 A66-42618  
 Differential absorption and Faraday rotation in D region, using closed loop feedback system and two signals of different frequencies 24 p4205 A66-43218  
**CLOSURE LAW**  
 Scalar quantity spectrum in statistically stationary turbulent velocity field, using closure approximations to provide unified comparison, noting eddy diffusivity, transfer function, etc [AIAA PAPER 65-814] 03 p0357 A66-13082  
 Evolution of scalar quantity spectrum in statistically stationary isotropic turbulent velocity field determined by closure approximation theory 12 p1865 A66-24583  
 Singularities in closed universes, discussing closed solutions to Einstein equations and inevitability of singularity, based on Hawking theorem 21 p3771 A66-39266  
**CLOTHING**  
 S FLIGHT CLOTHING  
 S HELMET  
 S PROTECTIVE CLOTHING  
 S SHOE  
**CLOUD**  
 SA ARTIFICIAL CLOUD  
 SA CUMULUS CLOUD  
 SA ELECTRON CLOUD  
 SA NOCTILUCENT CLOUD  
 SA PARTICLE CLOUD  
 SA ZODIACAL DUST CLOUD  
 Aerial observation of rare halo formation consisting of small ring, large ring, secondary sun of small ring, horizontal ring and extraordinary secondary sun 02 p0220 A66-11263  
 Effectiveness and reliability of radar observation of clouds in absence of precipitation 02 p0252 A66-11264  
 Comparison of simultaneous radar and aircraft observation of upper boundary of clouds 02 p0252 A66-11265  
 Variation of radio echo in different types of clouds allows identification from vertical variations in radar reflectivity 02 p0252 A66-11267  
 Statistical relations between weather conditions and geometry of radio echoes produced by cloud and precipitation fields 02 p0252 A66-11268  
 Determination of cloud-top altitude by GT-5 manned space flight mission 05 p0712 A66-15482  
 Cloud raindrop sizes and concentration measurement by airborne flow device 06 p0880 A66-16556  
 Initiation of precipitation in vigorous convective clouds traced to cluster of three shower cells which produce radar echo close to -30 C level [AFCL-SR-32-65] 07 p1062 A66-17369  
 Observations of vertical motion and

particle size of growing thunderstorm moving overhead, using pulsed Doppler radar 10 p1552 A66-21277  
 Observational study of cloud forms in vicinity of jet streams as viewed from ground and Tiros meteorological satellite 11 p1727 A66-22316  
 Synoptic interpretation of tropical land convection over Philippines 11 p1728 A66-22322  
 Low cloud characteristics over Sea of Japan during winter 11 p1729 A66-22324  
 Origin of cloud streaks extending over Pacific Ocean near Japan during winter monsoon 11 p1729 A66-22325  
 Effect of supersonic aircraft on cirrus formation and climate, noting influence of combustion products on stratosphere [AIAA PAPER 66-369] 12 p1907 A66-24497  
 Cloud raindrop sizes and concentration measurement by airborne flow device 14 p2297 A66-28228  
 Radar resolution capability for cloud detection 16 p2740 A66-30225  
 Radar observation of cloud with sharply defined base and slow descent 16 p2740 A66-30226  
 Atmospheric heat and moisture transfer during developing cloud conditions 16 p2742 A66-31342  
 Cloud height measurement by optical radar systems 17 p2949 A66-32884  
 Water-vapor mixing ratios near cloudtops of Venus decreases with altitude at rates comparable to Earth 20 p3655 A66-38020  
 Altitude of lower cloud boundary functional correlation with atmospheric parameters obtained from numerical weather forecast 20 p3593 A66-38366  
 Radiation effect on position of lower cloud boundary 20 p3594 A66-38370  
 Long-wave radiative heat transfer between clouds and free atmosphere as basic factor in weather forecasting 20 p3594 A66-38371  
 Cloud and fog droplet spectra rearrangement due to external conditions calculated from distribution function of water content 20 p3594 A66-38374  
 Double cloud vortex near Antarctica detected by Nimbus I high resolution IR 22 p3942 A66-40053  
 Atmospheric heat and moisture transfer during developing cloud conditions 24 p4234 A66-42650  
**CLOUD CHAMBER**  
 Particle localization in spark chamber and ion drift in Wilson cloud chamber, noting experimental result of simultaneous observation of identical particles 09 p1379 A66-20233  
 Density spectrum of extensive air showers at very large densities from cloud chamber study 15 p2580 A66-29534  
 High energy mountain-altitude nuclear interactions produced by pions and nucleons, pion/proton and neutral/charged interacting particle ratios studied, using multiplate cloud chamber with air Cerenkov counter and absorption spectrometer 15 p2584 A66-29554  
 Nuclear interaction characteristics in brass and carbon, noting production by neutral and charged cosmic ray particles, observation methods, energy spectrum, etc 15 p2585 A66-29560  
 Electron-muon similarities and multiple pion production by high energy muons, using accelerators and cloud chamber 15 p2546 A66-29576  
 Electron pair production by high energy muons, noting application of Monte Carlo method for appearance of low energy with high energy partner below target plate 15 p2546 A66-29583  
 Multiple penetrating particles underground, noting interaction of muons with matter at 148 meters water equivalent 15 p2546 A66-29584  
 Electromagnetic interactions and collisions of particles in cores of EAS studied, using GM counters, plastic scintillators and Wilson cloud chambers 18 p3207 A66-35107  
 Response to EAS electron-photon cascade of plastic scintillator, cloud chamber and Geiger counter tray compared 18 p3208 A66-35112



Bolivian Air Shower Joint Experiment /BASJE/ fast-timing methods compared with arrival directions measured in cloud chamber pictures 18 p3210 A66-35123  
Cloud chamber EAS density spectrum measurements at 2285 m 18 p3210 A66-35124  
Tskhra-Tskaro installation for study of high-energy cosmic particle interaction with matter 18 p3218 A66-35182

## CLOUD COVER

Probability of clear lines-of-sight estimated from sunshine and cloud cover observation 08 p1248 A66-19386  
Long-wave radiation flux in optically dense horizontally-stratified layer of clouds as it ascends from lower into upper troposphere with given temperature and humidity 09 p1398 A66-19894  
Venus cloud layer and brightness temperature from radiometric microwave observations from nocturnal side of planet 09 p1451 A66-20112  
Interpretation of outgoing IR radiation data from meteorological satellites, including cloud cover identification and Earth surface temperature 10 p1525 A66-21046  
Synoptic scale storm development stages traced by Tiros satellite photography of associated cloud vortex patterns 11 p1727 A66-22314  
Orographic precipitation areas on windward side of mountains in outer region of typhoon and convective clouds along warm front accompanied by storm 11 p1728 A66-22320  
Simultaneous occurrence and statistical distribution of clouds over separated cities in U.S. 12 p1907 A66-24493  
[AIAA PAPER 66-361] 12 p1907 A66-24493  
Conventional rawin, pibal and surface wind data compared with photoreconnaissance data, showing cumulus population and patterns over Florida 14 p2325 A66-26927  
Automatic cloud cover picture interpretation 18 p3128 A66-33741  
Radiant energy transfer below cloud cover in Venus atmosphere, noting greenhouse effect caused by atmosphere containing components capable of IR absorption 22 p3980 A66-40469  
Probability of overlapping intercept by system of random intercepts and application to detection of flying objects in cloudy skies 24 p4231 A66-42472

## CLOUD GLACIATION

Sferics from lightning from warm cloud, noting microsecond pulse-train format and temporal duration 22 p3942 A66-39678

## CLOUD PHOTOGRAPH

Gridding error in graphical rectification of satellite photographs eliminated by adopting coupled rotation of principal lines 06 p0882 A66-16782  
Satellite picture interpretation of cloud patterns, emphasizing scale identification and dependence on other meteorological parameters 11 p1726 A66-22308  
Cloud identification from Tiros satellite photographs, noting element identification of order of 1 km 11 p1726 A66-22309  
Tiros photographs of tropical cumulus and cirrus clouds along vertical wind shear vector 11 p1726 A66-22310  
Maximum wind velocity in tropical storms and hurricanes estimated from cloud patterns in satellite pictures 11 p1727 A66-22313  
Tiros satellite photograph study of cloud structure related to two major classes of frontal bands 11 p1727 A66-22315  
Incorrect input-induced errors in meteorological satellite photogrids 11 p1704 A66-22318  
Fog and low stratus clouds studied, using Tiros VII photographs of North Pacific fog 11 p1728 A66-22323  
Photomosaic of cloud system distribution made from Tiros IX photographs 14 p2325 A66-27281  
Spatial distribution of four cloud fields studied by photometry of aerial photographs, determining statistical parameters 14 p2325 A66-27537  
Organization and size of cloud systems in relation to maximum wind speed, using Tiros satellite pictures 15 p2533 A66-29663  
Automatic cloud cover picture interpretation 18 p3128 A66-33741

Vertical motion of moisture fields and saturation deficit determination from nephanalysis of Tiros cloud photographs for operational quantitative precipitation forecasting /QPF/ 22 p3943 A66-40054  
Digital computer processing of Tiros, Nimbus and Essa vidicon cloud pictures for machine nephanalyses, discussing rectification orbital mosaics and calibration effects for future Essa flights 22 p3943 A66-40055  
Spatial distribution of four cloud fields studied by photometry of aerial photographs, determining statistical parameters 24 p4233 A66-42323

## CLOUD PHOTOGRAPHY

Stereo pairs taken at one-and two-minute intervals in photogrammetry of initiation of cumulus clouds over mountainous terrain 07 p1062 A66-17371  
Cloud altitude determination from single satellite photograph, using Sun altitude 07 p1063 A66-18481  
Thermal and wind structures related to major cloud bands of Tiros-photographed extratropical vortices 08 p1248 A66-19384  
ITC on satellite photographs and use of photographs of cirrus for high level analysis 11 p1727 A66-22311  
Meteorological satellite terrestrial UV radiation and cloud formation photographic data interpretation 11 p1728 A66-22317  
Cumulus to cumulonimbus convection over mountains and dissipation of stratus and sea fog when moving inland, using Tiros photographs 11 p1728 A66-22321  
Diagnostic-cycle routine, collection of computer-programmed techniques for interpretation of meteorological satellite videograph observations 11 p1731 A66-23486  
Reliability of locating jet streams by means of cloud patterns in Tiros pictures, determining most definitive characteristics of those patterns 13 p2121 A66-25813  
High resolution IR radiometer on Nimbus I satellite for providing detailed night cold information 17 p2927 A66-33344  
Triangulation technique for correlating trail points on films of chemical cloud releases in space from two different sites to determine winds and wind shear 18 p3110 A66-33743  
Organized convection as photographed by Gemini astronauts 18 p3129 A66-34214  
Dielectric-tape camera borne by meteorological satellite to provide high-quality photographs of Earth cloud cover 20 p3557 A66-37204  
Martian atmosphere and crust analyzed, based on Mariner IV cloud photographs 20 p3655 A66-38022  
Meteorological studies from manned spacecraft discussing interpretation of cloud pictures and optical inhomogeneity of tropo- and stratosphere 21 p3760 A66-39363  
High resolution IR scanning system and vidicon automatic picture transmission of Nimbus II and ground station printout instrumentation 21 p3821 A66-39497

## CLOUD PHYSICS

Combined effect of turbulent gravitational and electrostatic coagulation on growth rate of cloud droplets estimated by two-layer model of process 01 p0096 A66-10658  
Growth of ice crystals freely falling in atmosphere and form when produced by cloud element coagulation analyzed, using low pressure chamber 01 p0097 A66-11105  
Radar reflectivity of developing convective clouds statistically related to state of turbulence and thunderstorm hazard 02 p0252 A66-11270  
Equations describing crystallization process in low level clouds as function of ice crystal penetration from upper clouds or from artificial seeding 02 p0254 A66-12023  
Angular volume-scattering functions measured as function of scattering angle for natural fogs in atmosphere, using coherent and incoherent radiation 02 p0262 A66-12211  
Cumuli above sea in spite of stable layer between sea surface and cloud boundary, noting condensation around salt particles penetrating ascending thermals 04 p0542 A66-14306  
Microstructural fluctuation in low clouds, investigating cloud droplet spectra and fluctuation of absolute total

concentration 05 p0712 A66-15115  
Cloud physics - International Conference, Tokyo and Sapporo, Japan, May 1965 06 p0904 A66-16266  
Numerical study of initiation of cumulus clouds over mountainous terrain 07 p1062 A66-17370  
Spectral density of vertical wind gusts in clouds calculated, including turbulent energy dissipation rates in cloud strata 09 p1398 A66-19884  
Statistical theory of inert particle fluctuations applied to fine structure of clouds and formation of cloud-particle spectrum 09 p1398 A66-19890  
Liquid and particulate content of atmosphere noting surface rates of rainfall, particle size distribution, cloud data, aerosols, etc 09 p1398 A66-20272  
Tiros IV satellite photographs of various storms, relating equivalent black body temperatures shown on IR analysis to cloud height 09 p1399 A66-20731  
Crystallization kinetics in supercooled cloud under natural conditions 11 p1725 A66-22196  
Precipitation distribution in frontal clouds measured from aircraft 11 p1725 A66-22265  
Heat and humidity transfer effects and turbulent exchange influence on cloud formation 11 p1730 A66-22941  
Differential equations describing air movement, heat exchange and exchange of moisture 11 p1730 A66-22942  
Observation of noctilucent and nacreous clouds from satellites 11 p1730 A66-22944  
Internal wave ripples from fluid impacts on base of stably stratified fluid region, calculating particular case of single ripple in viscous fluid 11 p1693 A66-23009  
Preferred thunderstorm development near surface boundary between maritime tropical air masses and dry air masses, defining radar echo areas 11 p1731 A66-23382  
Solar near-IR scattering by sunlit terrestrial clouds as affected by cloud type, altitude and scattering angle 13 p2073 A66-25989  
Electrostatic interaction effect on EM waves scattering by atmospheric aerosol particles 14 p2284 A66-27539  
Cumuli above sea in spite of stable layer between sea surface and cloud boundary, noting condensation around salt particles penetrating ascending thermals 14 p2327 A66-28219  
Two Project High Water experiments producing optical, ELF, RF, and radar data on ionospheric abort of large water quantities and expansion process 14 p2289 A66-28417  
Cloud top heights and areal coverage obtained from satellite IR measurements, noting error estimation and effect of cloud size on accuracy 15 p2485 A66-28938  
Sounding rocket-released artificial strontium and barium ion cloud motion in upper atmosphere, based on equations of ambipolar diffusion 15 p2491 A66-29950  
Martian clouds analysis and topographical relationships, discussing white and yellow classification and frequency of occurrences 15 p2602 A66-29951  
Homogeneous nucleation of water vapor determined by laser beam scattering from cloud 16 p2716 A66-30121  
Critical electric field for charged droplets atomizing, noting spark discharge and ion concentration in clouds 16 p2742 A66-31109  
Precipitation model explaining formation of rain drops from clouds less than several kilometers thick, assuming Gaussian frequency distribution of vertical currents 18 p3130 A66-35015  
Precipitation occurrence in fluctuating updraft 18 p3130 A66-35018  
Heat and humidity transfer effects and turbulent exchange influence on cloud formation 20 p3593 A66-37854  
Differential equations describing air movement, heat exchange and exchange of moisture 20 p3593 A66-37855  
Observation of noctilucent and nacreous clouds from satellites 20 p3593 A66-37857  
Lightning flash mechanisms and electric field strengths in clouds 21 p3759 A66-38533  
Airborne photoelectric device for registration of cloud



drops 21 p3739 A66-39365  
Turbulent refractivity spectrum and optimization of airborne radar CAT detectors 22 p3944 A66-40429  
Electric field effects on collision efficiency of charged cloud droplets 23 p4065 A66-41846  
Electrostatic interaction effect on EM waves scattering by atmospheric aerosol particles 24 p4198 A66-42325  
Heterogeneous formation of seed crystals on wettable and nonwettable condensation nucleus in supercooled water droplets 24 p4234 A66-42756

## CLOUD SEEDING

Nucleation of ice formation in supercooled clouds as result of lightning-initiated sound waves 04 p0542 A66-13674  
Resonance radiation emitted by alkali cloud for ionospheric temperature measurement, considering multiple scattering and radiative transfer inside cloud 05 p0672 A66-15040  
Urea effective ice nucleant in supercooled clouds due to endothermic heat of solution and high solubility 13 p2122 A66-26125

## CLUSTER

## SA STAR CLUSTER

Degree of clustering expected from 500-mb horizontal sounding system, using stream functions and velocity potentials derived from historical tapes of National Meteorological Center 13 p2121 A66-25815  
Thermal conductivity of carbon dioxide in critical region interpreted, considering gas as mixture of clusters and heat transfer due to formation and breaking of clusters 21 p3837 A66-39454

## CLUTCH

Overrunning clutches in gas turbines, design, performance characteristics and application to A-4D Skyhawk aircraft, UH-2 helicopter and Curtiss-Wright X-19 VTOL drive systems [AIAA PAPER 66-GT-92] 14 p2300 A66-26996

## COALESCENCE

Condensed phase particle growth in rocket nozzle by particle collision and coalescence [AIAA PAPER 66-639] 18 p3164 A66-34438  
Behavior of wave function for system of charged particles near coalescence of any two of them, noting electron-nucleus cusp conditions for diatomic molecules 22 p3861 A66-40904

## COANDA EFFECT

Attraction switching through use of parallel secondary injection in Coanda-effect nozzle 03 p0355 A66-12775  
Flow of thin jets in vicinity of solid walls with diverging profiles 07 p1026 A66-18230  
Fluid devices as affected by delay for signal transmission in lines, jet behavior and Coanda effect 13 p2062 A66-25366  
Stream-interaction amplifiers and uses in fluidic circuits, discussing momentum exchange, pressure differential and Coanda effect 18 p3053 A66-33898  
Operating characteristics of pneumatic bistable element using Coanda effect, examining correlation between outlet flow and pressure and feed pressure 21 p3697 A66-38802

## COATING

## SA BIREFRINGENT COATING

## SA CERAMIC COATING

## SA CLADDING

## SA DOPING

## SA ELECTROPLATING

## SA FILM

## SA FINISH

## SA FLAME SPRAYING

## SA GLASS COATING

## SA PLASTIC COATING

## SA PLATING

## SA PROTECTIVE COATING

Electrolytic titanium coating properties, covering porosity coating elimination by repeated electrolysis 04 p0536 A66-14005  
Deformation components of photoelastic coatings of shells affected by errors due to rotation of direction of principal deformations 08 p1307 A66-18883  
Refractory oxides from alkoxides for group IVB transition and rare-earth metals applied to powders and coating of zirconia materials by thermal decomposition 16 p2730 A66-30249  
Test chamber to simulate vacuum and heat sink characteristics of space, measuring optical constants of

coatings 16 p2680 A66-30491  
Space environment degradation of thermal control coatings tested by experimental packages on Pegasus I, II and III [AIAA PAPER 66-419] 18 p3239 A66-33640  
Condensation tests in smooth and porous coated tubes in multi-g centrifugal acceleration fields for increasing heat transfer coefficient of condensing nitrogen 18 p3262 A66-34379  
Electrolytic titanium coating properties, covering porosity coating elimination by repeated electrolysis 22 p3935 A66-40547

## COAXIAL ACCELERATOR

## SA PLASMA ACCELERATOR

Exhaust of pinched plasma from axial orifice involves electromagnetic current profile diffraction and thermal expansion of gas column [AIAA PAPER 65-92] 02 p0267 A66-11536  
Velocity and momentum of high current steady state coaxial plasma noting mass flow, exhaust velocity, thrust, arc voltage and power 02 p0267 A66-11559  
Electrode erosion impurities effect on performance of coaxial plasma source in fast particle generation mode 02 p0268 A66-11778  
Langmuir probe velocity and acceleration measurements for coaxial Hall accelerators [AIAA PAPER 66-196] 10 p1562 A66-21441  
Radio locator for position of plasmoids from coaxial injector 10 p1570 A66-22007  
Plasmoid acceleration by coaxial accelerator 10 p1571 A66-22009  
Sufficiently pure plasmoids obtained, using coaxial plasma gun operating in waiting regime 10 p1571 A66-22010  
Energy distribution of hydrogen plasma from coaxial gun 10 p1571 A66-22013  
Energy efficiency trends in two-stage repetitively pulsed coaxial plasma accelerator 12 p1935 A66-23578  
Performance characteristics of two-stage pulsed coaxial plasma engine [AIAA PAPER 66-240] 12 p1935 A66-24518  
Particle collection and emission spectra observation in repetitively pulsed coaxial plasma accelerator [AIAA PAPER 66-197] 12 p1936 A66-24521  
Delays effect on performance of coaxial plasma guns with about 20 kv applied, shown to produce fast burst of clean plasma containing pure hydrogen ion 13 p2000 A66-25750  
Distribution of current and associated field in coaxial plasma gun, noting plasmoid formation from drift 13 p2153 A66-26521  
High energy particle generation in coaxial plasma gun studied by discharge-current curve 13 p2153 A66-26522  
Plasma contamination by electrode material in coaxial accelerator reduced by longitudinal magnetic field 13 p2153 A66-26523  
Predicted and observed calorimetric exhaust efficiencies of capacitor powered coaxial plasma guns [AIAA PAPER 65-340] 15 p2551 A66-29275  
Coaxial plasma accelerator experiments, determining relation with plasma front velocity, density profile and temperature 17 p2972 A66-32871  
Coaxial plasma gun performance in longitudinal magnetic field, noting conditions of generation of single plasmoid 18 p3151 A66-35070  
Plasmoid structure produced by coaxial plasma gun with interchangeable polarity electrodes, noting experimental setup, particle velocity, density, energy, etc 18 p3151 A66-35071  
Hydrogen density in coaxial plasma injector prior to application of high voltage to electrodes, noting experimental setup and results 18 p3151 A66-35072  
Radio locator for position of plasmoids from coaxial injector 19 p3407 A66-36091  
Plasmoid acceleration by coaxial accelerator 19 p3407 A66-36093  
Sufficiently pure plasmoids obtained, using coaxial plasma gun operating in waiting regime 19 p3407 A66-36094  
Energy distribution of hydrogen plasma from coaxial gun 19 p3407 A66-36097  
Current jet and plasma produced by coaxial plasma gun which is source of abundant slow deuterium plasma and fast plasma, examining acceleration

mechanism 19 p3425 A66-36565  
Plasma generating gun using coaxial electrodes, gas injection and preionization device for regulation with plasma purification by injection into magnetic field with double curvature 19 p3427 A66-36572  
Neutral mass density measurements in repetitively pulsed coaxial plasma accelerator 21 p3776 A66-38690  
Fast plasmoid produced by coaxial plasma accelerator, examining mass and energy spectra of plasma ion component 21 p3785 A66-39035  
Energy-and mass-spectrum measurements of ions from plasmoids from coaxial plasma source, examining plasma acceleration mechanism inside source 21 p3785 A66-39036  
Plasmoid composition effect on electrode geometry in coaxial plasma gun, decreasing impurity concentration by gun design and electrode material choice 21 p3785 A66-39037  
Plasma jet motion from coaxial plasma gun through magnetic field of quadrupole lens, examining interaction of plasma with magnetic field 21 p3788 A66-39054  
Pinch phenomena and current distribution in coaxial plasma gun 23 p4101 A66-41295  
Energy storage film capacitors for pulsed plasma thrusters developed for coaxial plasma gun and pulsed arc gun [AIAA PAPER 65-337] 24 p4261 A66-42780

## COAXIAL CABLE

Coupling between coaxial line and plasma waveguide for three configurations, step, abrupt and tapered transitions 01 p0038 A66-10521  
Complex susceptibility measured, using voltage induced in loop around ferromagnetic core situated at short-circuit end of coaxial line 05 p0716 A66-15028  
Varactor evaluation using series resonance and determination of impedance locus of coaxially mounted varactors 07 p1008 A66-17513  
Dielectric loaded waveguides, defining surface, transverse and longitudinal impedances in analogy with circuit theory definition 08 p1200 A66-19121  
Generator for high-voltage pulses with pulses shaped by two-section length of line with transformation by pulse transformer employing coaxial cable windings 08 p1194 A66-19282  
Microwave frequency feedthrough for vacuum systems suitable for use up to X-band, using Teflon-filled rigid type coaxial line 08 p1197 A66-19700  
Self-compensation of phase angle of Diane station coaxial cable of discontinuous disk structure throughout wide temperature range 10 p1511 A66-21709  
Propagation of quasi-TEM mode in ferrite-filled coaxial line 10 p1506 A66-21913  
Propagation velocity and attenuation variation effect in coaxial cables on frequency modulated carrier evaluated, using IBM 1620 computer 16 p2649 A66-30542  
Diffraction of linearly polarized electromagnetic wave by coaxial cylinders, deriving approximate solution for wavelengths smaller than distance between cylinder centers 18 p3068 A66-33977  
Microwave coaxial termination as low temperature noise-reference source, noting variation of VSWR with voltage and frequency 18 p3077 A66-34078  
Thermal conductivity measurements for hydrogen via coaxial cylindrical cell noting temperature, pressure effects, residual and conductivity values 19 p3479 A66-36290  
Electromagnetic interference shielding for conductors that excludes interference energy caused by both magnetic and electric fields over broad frequency range 20 p3499 A66-37195  
Diffusion controlled breakdown theory applied to compute breakdown potential of helium in coaxial geometry by solving continuity equation 23 p4105 A66-41584  
Design and performance analysis of HF analog and digital circuit, using double-transistor in which signal is fed to transistor stage via coaxial cable 24 p4184 A66-42646

## COAXIAL FLOW

Mean flow pattern of round air jet in ambient airstream parallel to jet axis 06 p0802 A66-16504



Propagation of microwaves through circular cylindrical metallic guide filled with two different dielectrics 06 p0857 A66-16951

Stationary flow of viscous incompressible anisotropically conducting fluid in coaxial channel 11 p1743 A66-22235

Oscillation of viscoelastic liquid between stationary outer coaxial cylinder and vibrating inner coaxial cylinder 11 p1688 A66-22440

Mixed flow of two gases through coaxial cylindrical tubes separated by perforated plate 14 p2273 A66-26782

Electric and magnetic-field parameters measured during discharge half-cycle in coaxial plasma source 21 p3785 A66-39038

Second-order fluid flow over finite rotating disk enclosed within coaxial cylindrical casing 21 p3729 A66-39452

Steady liquid flow between rotating coaxial cylinders with arbitrary dependence of viscosity on temperature 22 p3902 A66-40814

**COAXIAL TRANSMISSION**

Reflection and transmission coefficients of magnetically biased YIG ferrimagnetic resonator loaded in aperture of iris in coaxial transmission line 05 p0641 A66-14555

Fundamental electromagnetic wave propagation in coaxial line filled with inhomogeneous dielectric 06 p0823 A66-15886

Nanosecond electromagnetic pulse dispersion in longitudinally magnetized plasma confined in coaxial transmission line 06 p0826 A66-16026

Coaxial transmission line with adjustable harmonic phase delay equalizer network 06 p0848 A66-16105

Precision coaxial standard and component designs based on constant impedance, coplanar compensation and mechanical tolerance sensitivity 10 p1514 A66-21907

P-i-n diode coaxial attenuators and levers noting design, performance parameters and application 12 p1831 A66-23812

Mode selective coaxial directional couplers for measurement of unwanted harmonics effect 13 p2044 A66-26745

Maximum and minimum power absorbed by antenna connected through coaxial transmission line to transmitter under unmatched conditions 18 p3078 A66-34168

**COBALT**

Cobalt electrode performance in high temperature fuel cells, presenting V-I characteristics 01 p0014 A66-10358

Oxidation kinetics of tantalum-iron and tantalum-cobalt alloys and iron and cobalt at 500-900 degrees C 04 p0535 A66-13696

Martensitic transformation in alloys with aging martensite, discussing effects on molybdenum, Fe-Ni alloy, cobalt and titanium 05 p0700 A66-14859

Effect of tantalum carbide additions on mechanical, thermal and chemical properties of WC-TiC-Co alloys 08 p1239 A66-18902

Crystal structure and allotropic transformation of cobalt and thermal, thermodynamic, electrical and magnetic properties 08 p1240 A66-18961

Specific heat of iron, cobalt and nickel in high temperature range measured, using quasi-adiabatic operating calorimeter 08 p1240 A66-19255

Fe, Ni and Co in gallium arsenide determined by tunnel spectroscopy 08 p1278 A66-19624

Changes in domain structure of cobalt films as function of substrate temperature during sputtering and transformation from poly- to single-crystal structure 11 p1753 A66-22803

Magnetic and semiconducting properties of solid solutions of LaMnO sub 3 and LaCoO sub 3 14 p2353 A66-26900

Fe, Ni and Co in gallium arsenide determined by tunnel spectroscopy 17 p2984 A66-33138

Optical absorption spectra of cobalt ion in magnesium aluminate crystal 20 p3621 A66-37822

Butler iron meteorite composition, noting unusually high cobalt and germanium content and low cooling rate 22 p3978 A66-40013

**COBALT ALLOY**

Refractory metal carbide solubility in

cobalt dependent on carbon content, crystal structure and metal-carbon bonds 01 p0085 A66-10287

Silicon and iron effects on embrittlement of cobalt-base alloy 01 p0085 A66-10357

Thermodynamic properties of cobalt-molybdenum alloys determined by emf method measured between 1170 and 1470 degrees K 01 p0088 A66-10940

Thermodynamic properties of cobalt-niobium alloys determined by emf method measured between 1275 and 1425 degrees K 01 p0088 A66-10941

Creep and fracture of series of nickel-cobalt alloys due to variation in stacking fault energy, noting incidence of annealing twins 02 p0245 A66-11947

High temperature nickel and cobalt superalloys for turbojet engines [AIAA PAPER 65-741] 03 p0382 A66-13052

Casting technique based on directional solidification for nickel and cobalt alloys used in gas turbine blades [AIAA PAPER 65-742] 03 p0382 A66-13053

Interpretation of nuclear magnetic resonance spectra from cobalt alloys containing small amounts of solute atoms 04 p0564 A66-14032

Plastic deformation effect on physical and mechanical properties of hard cylindrical samples of tungsten-cobalt alloy 07 p1049 A66-17905

MAR-M 509, new cast cobalt-base superalloy for high temperature service, noting creep strength, aging, microstructure, oxidation resistance, etc 08 p1239 A66-18958

Effect of thermal and thermomagnetic treatment of nickel-cobalt ferrite single crystal on rotational magnetic hysteresis losses 09 p1412 A66-19883

Residual stress-strain state of WC-Co alloys by changing sample size during process 09 p1389 A66-20806

Plastic deformation preceding fracture in tungsten carbide-cobalt alloys 11 p1717 A66-22994

Hardness, coercive force, saturation induction and electric conductivity during precipitation hardening of two Co-Ni alloys with Ti and Al admixtures 12 p1894 A66-23967

Age hardening response correlated with structural observations of iron-nickel-cobalt alloys 12 p1895 A66-24374

Aging effect on structure of cobalt alloys annealed at 1200 degrees C suggests formation of laminar regions 12 p1898 A66-25030

Structural, physical and mechanical properties of hard alloys formed by sintering powdered VK 15 tungsten cobalt alloy with nonuniformly distributed carbide phase 15 p2520 A66-28753

X-ray investigation of niobium-cobalt system 16 p2725 A66-31457

Cobalt and nickel eutectic alloys modification with selected elements for high temperature application, noting microstructure and tensile behavior 16 p2726 A66-31460

Structural and physical properties of WC-TaC-Co and WC-NbC-Co alloys studied by metallographic, electrochemical and X-ray methods 17 p2939 A66-31970

Structural transformations in alnico alloy with titanium studied by X-ray 18 p3123 A66-34401

Plastic deformation effect on physical and mechanical properties of hard cylindrical samples of tungsten-cobalt alloy 21 p3752 A66-39405

Casting technique based on directional solidification for nickel and cobalt alloys used in gas turbine blades [AIAA PAPER 65-742] 23 p4079 A66-40973

Notch and heat treatment effect on compressive buckling of WC/Co alloys 24 p4228 A66-43063

**COBALT COMPOUND**

Electrical and magnetic properties of cobalt telluride /gamma phase/ to verify semiconductive character 04 p0559 A66-13479

Cobalt-vanadium-boron system, discussing phases with boron coordination number 8 07 p1047 A66-17225

Optical absorption, energy level structure and exchange interactions of cobalt and

sodium cobalt fluoride ions 14 p2357 A66-27075

Inverted susceptibility, inversion ratio, line widths and spin-lattice relaxation times for maser operation point in chromium-doped cobalt potassium cyanate 16 p2718 A66-30934

Phase relations in cobalt niobate-cobalt tantalate system noting structural characteristics, solubility, phase transitions, etc 17 p2940 A66-33062

**COBALT OXIDE**

Short-time high temperature oxidation of cobaltous oxide 16 p2646 A66-30671

**COBALT 60**

Recombination process of electron-hole pairs in germanium irradiated with cobalt 60 gamma rays, using photovoltaic effect in p-n junctions 06 p0938 A66-17146

Aluminum oxide inclusions effect on radioactive cobalt 60 autodiffusion observed, noting higher diffusion in samples prepared by powder methods 13 p2110 A66-25964

Gamma irradiation from Co 60 effect on indium antimonide, determining defect formation on dose and limiting position of Fermi level for n-and p-type material 20 p3617 A66-37552

**COCHLEAR**

Temperature effect on amplitude of cochlear microphonic and on latency action potential of auditory nerve 06 p0812 A66-16405

Effect of oxygen deficiency on acoustic organ of cats, determining content of potassium and sodium ions in perilymph, cerebrospinal fluid and blood serum 13 p2011 A66-26251

Response patterns to tone-burst stimulation of cochlear nucleus and dependency on stimulus parameters 22 p3855 A66-40375

**COCK AIRCRAFT**

S ANTONOV AN-22 AIRCRAFT

**COCKPIT**

SA AIRCRAFT CABIN

Cockpit display correction methods used in design of Trident aircraft 03 p0328 A66-12882

Human perceptual mechanism defined by psychological research and applied to aircraft cockpit display design 03 p0329 A66-12883

Optimum operational influence on design of DC-9 cockpit 07 p0988 A66-17704

White light rather than red for illumination of instruments and cockpits 11 p1648 A66-22667

Flight deck display for future aircraft projects, emphasizing vertical scale director instruments for cockpit display 11 p1649 A66-23250

**COCKPIT SIMULATOR**

Mixed translation and attitude control system using single cockpit stick for low-speed flight control of VTOL aircraft 05 p0610 A66-15078

Wind tunnel, simulator and flight test results to evaluate cockpit accelerations, handling qualities and stability and control of jet transports in severe turbulence [AIAA PAPER 65-330] 16 p2634 A66-31317

British fixed-base aircraft cockpit simulator experiments, testing pilot performance when relying on windshield display as primary information source 17 p2865 A66-32182

Cockpit displays associated with low altitude high-speed flight, emphasizing shift toward designing around man 19 p3287 A66-35508

Extravehicular activity /EVA/ mission simulation, discussing design parameters effect on operating characteristics 19 p3469 A66-35969

**CODE**

S BINARY CODE

S ERROR DETECTING CODE

S GENETIC CODE

S PULSE CODE MODULATION /PCM/

S SYNCHRONIZATION CODE

**CODING**

SA DECODING

SA ENCODING

SA PROGRAMMING

SA PULSE COMPRESSION

Point-to-point contouring systems noting procedures, codes and cost savings [ASTME PREPRINT MS66-725] 12 p1887 A66-24423



## CODING SYSTEM

SA DECODER  
SA ENCODER

Cluster finding technique for determining and coding subclasses in pattern recognition problems 01 p0034 A66-10894

Textbook on communication engineering emphasizing random processes, information and detection theory, statistical communication theory, applications, etc 03 p0335 A66-12992

Value of information concept relating Shannon information theory to theory of optimal solutions 03 p0336 A66-13034

Coding states of partial automaton where memory-element transition functions depend on minimum possible number of variables 03 p0338 A66-13041

Binary pulse sequence conversion to pseudoternary codes for data transmission 04 p0474 A66-13423

False-signal probability in telemetry signals using group distribution and group variable-performance codes 04 p0504 A66-13776

Coding theorems for almost-periodic channels 05 p0638 A66-15362

Nonorthogonal coding in communicating through dispersive or multipath fading channels for increased data rate without increased bandwidth 06 p0835 A66-16866

Properties, symmetries, code matrices and Euler paths for linear graphs used as models for physical systems, considering planar triply connected graphs 07 p1057 A66-17747

Slope quantized binary pulse code modulation by coding signal slopes with unidigit 1/0 pulses, using special feedback circuit and threshold in coder comparator 07 p1002 A66-18248

Optimized hybrid unidigit pulse code modulation system, noting use of secondary feedback loop and equalization of gain/frequency characteristic of coder 08 p1186 A66-19740

Pulse code modulation coder, using delay line as coding network 08 p1186 A66-19744

Generation, selection and implementation of burst-error-detecting and -correcting Fire code, using computed

tables 10 p1496 A66-21513

Linearly separable codes for adaptive threshold networks for pattern recognition 10 p1507 A66-21696

Information assimilation from conspicuity coding of updated alphanumeric information, comparing relative effects of individual and group displays 12 p1809 A66-23927

Lincoln Experimental Terminal /LET/ signal processing system, design, operation and application 13 p2022 A66-25516

Abridged Hamming and Fire code efficiency with respect to randomly distributed disturbances 14 p2245 A66-26794

Information theory, role in communication systems, detailing coding systems 14 p2239 A66-27808

Polyphase coding modulation system with additive white Gaussian noise, finding channel capacity bounds on maximum rate and error exponent 15 p2452 A66-29659

Improvements to be realized through use of single channel black coded communication system 17 p2873 A66-31967

High scanning frequency for transmitting radar information to vehicles with beam arranged to form coded pulse signal 18 p3070 A66-34257

Value of information concept relating Shannon information theory to theory of optimal solutions 18 p3072 A66-34997

Coding states of partial automaton where memory-element transition functions depend on minimum possible number of variables 18 p3074 A66-35004

Space telecommunications techniques, examining reduction of all transmissions to digital type, using current theoretical coding methods and recurrent codes and block codes for error detection 20 p3516 A66-37432

Coding scheme using noiseless feedback link to improve communication over noisy forward link, assuming no bandwidth constraint 21 p3704 A66-39142

Coding scheme using noiseless feedback link to improve communication over noisy forward link, assuming band-limited signals 21 p3704 A66-39143

Communication design techniques for coding set of discrete memoryless channels where transmitter and receiver have no knowledge of channels

selected 21 p3705 A66-39144

Computer code packages for radiation shielding calculations 21 p3769 A66-39392

Modulation and demodulation for probabilistic coding, noting error chances and interrelations affecting performance of communications system 21 p3707 A66-39636

N-orthogonal phase-modulated codes generalized from first-order Reed-Muller codes and biorthogonal

signals 21 p3721 A66-39641

Matrix interpretive codes including SELMA, FORTRAN and

ALGOL 23 p4042 A66-41740

## COEFFICIENT

S ABSORPTION COEFFICIENT

S ACCOMMODATION COEFFICIENT

S AERODYNAMIC COEFFICIENT

S ATTENUATION COEFFICIENT

S BINOMIAL COEFFICIENT

S COHERENCE COEFFICIENT

S CORRELATION COEFFICIENT

S DIFFUSION COEFFICIENT

S DISCHARGE COEFFICIENT

S DRAG COEFFICIENT

S FLOW COEFFICIENT

S FRICTION COEFFICIENT

S FRICTION-LOSS COEFFICIENT

S HEAT-TRANSFER COEFFICIENT

S INFLUENCE COEFFICIENT

S IONIZATION COEFFICIENT

S LIFT COEFFICIENT

S NOZZLE THRUST COEFFICIENT

S ONSAGER PHENOMENOLOGICAL

COEFFICIENT

S PRESSURE COEFFICIENT

S RECOMBINATION COEFFICIENT

S REFLECTION COEFFICIENT

S REGRESSION COEFFICIENT

S RESISTANCE COEFFICIENT

S SCATTERING COEFFICIENT

S SEEBECK COEFFICIENT

S SORET COEFFICIENT

S THERMAL ACCOMMODATION

COEFFICIENT

S THERMAL EXPANSION COEFFICIENT

S TRANSPORT COEFFICIENT

## COHENITE

Origin and chemical composition of cohenite in meteorites and temperature dependence of weight-percentage content 22 p3981 A66-40479

## COHERENCE COEFFICIENT

EEGs of monkeys stimulated cyclically by whole-body vibration, plotting coherence functions relating brain records to acceleration records 12 p1806 A66-24228

Doppler shift and high velocity mirror translation effects on mutual optical coherence function of gas laser Michelson interferometers 19 p3354 A66-35387

## COHERENT LIGHT

Interference effects at thin transparent cylindrical glass fibers exposed to coherent light from He-Ne laser 01 p0081 A66-10368

Switching with optical signals classifying polycrystalline noncoherent and coherent types of optoelectronic devices 02 p0200 A66-11890

Coherence theory for collimation and focusing of time-averaged intensity of pulsed multimode laser radiation 02 p0242 A66-12205

Ultimate sensitivity limit and photoelectron statistics for photomultiplier lit by coherent and noncoherent light 03 p0377 A66-12473

Book on modern optics including laser and coherent light, geometrical optics, lens systems, instruments, etc 03 p0392 A66-12623

Semiconductor application to coherent optical transducers and spatial filters 05 p0647 A66-14822

Pulsed IR laser simulating radiation-induced transient ionizations in semiconductor devices and circuits 05 p0693 A66-14853

Mixed integration techniques used for signal detection having coherence time less than duration when propagating through time-varying medium 06 p0828 A66-16112

Phase perturbation of optical beams due to atmospheric turbulence, using modulated interferometer to produce Doppler beats between two coherent

beams 06 p0909 A66-16434

Triangular resonator for coherent light sources, considering natural oscillations and energy withdrawal 06 p0893 A66-16883

Spontaneous emission noise effects on coherence properties of laser 10 p1542 A66-21550

Coherent light recording and reproduction system 11 p1711 A66-22270

Equations obtained from Hamiltonian for coupling, first Stokes line, first anti-Stokes line and coherent field for Raman laser 11 p1711 A66-22490

Coherent laser light for conventional and unconventional photographic situations 11 p1705 A66-22670

Absolute wavelength stability of helium neon laser measured by direct interferometric comparison with Hg 198 standard lamp 11 p1712 A66-22868

Weakly focusing transparent media properties and guided transmission of coherent light beams with relatively small loss 11 p1657 A66-23091

Two-beam interferometry by wavefront reconstruction from hologram recorded with coherent background successively interfered in same latent image 11 p1708 A66-23204

Holograms and wavefront reconstruction techniques involving prismatic refraction of monochromatic and coherent laser light causing interference pattern on photographic emulsion 13 p2076 A66-25144

Coherent light recording/reproducing techniques based on Debye theory of coherent light source focusing 13 p2091 A66-25541

Magnitude and phase of complex spatial coherence of He-Ne laser beam 13 p2104 A66-26334

Reconstitution in space of curve recorded photographically by displacement of luminous point illuminated by coherent light 13 p2082 A66-26343

Two-beam interferometry in coherence theory 14 p2330 A66-26965

Bose-Einstein distribution function for quantum photons from amplified spontaneous emission 14 p2307 A66-27195

Laser detection of coherent light and superheterodyne and nonlinear parametric studies in optical spectrum 14 p2309 A66-27821

Attenuation of coherent optical waves propagating in troposphere, noting molecular scattering, bending of refractive index homogeneities due to temperature gradients in air, etc 15 p2448 A66-28578

Coherent emission from trivalent holmium ions in rare earth substituted yttrium aluminum garnet, noting three energy transfer combinations in YAG 15 p2512 A66-28690

Kinetic theory of two-photon absorption from single mode of radiation field, noting dependence on coherence properties of field 15 p2544 A66-28943

Influence of object contrast upon partially coherent image formation 15 p2501 A66-28979

Thermal effects in various media due to laser beam 15 p2515 A66-29209

Giant coherent light pulse generation by Q-factor-modulated laser 16 p2719 A66-31183

Partial coherence theory, discussing mutual coherence function, coherent fields, imaging theory, etc 16 p2748 A66-31241

Coherent optical systems in signal processing techniques, information theory and antenna pattern simulation 16 p2657 A66-31242

Coherence properties of optical fields, examining interference effects, intensity fluctuations, photoelectric effects and pulsations 16 p2749 A66-31584

Coherence conditions effects on electromagnetic field density operators and photon density distribution in single excited mode 17 p2957 A66-31975

Optical coherence functions and properties from statistical viewpoint for application to spectroscopy and stellar interferometry 17 p2957 A66-31987

Thermal effects in various media due to laser beam 17 p2936 A66-33058

Measuring amplification of coherent optical radiation in neon-helium filled tube 17 p2938 A66-33512

Parrent theorem in coherence theory



proved, using Fourier-Stieltjes integrals 18 p3118 A66-33987

Coherent laser-type light generators with capability of adjusting frequency over visible spectrum 19 p3375 A66-36265

Holography principles, discussing basic equation, Fourier transform holograms and hologram interferometry 20 p3556 A66-36929

Coherent laser light use in atmospheric communications system, discussing effect of atmospheric turbulence and small vibrations on coherent detection efficiency and SNR 20 p3511 A66-36930

Partially coherent light, noting distinction between narrow-band coherent and incoherent sources 20 p3575 A66-36935

Transformation coefficient and secondary radiation pattern when doubling frequency of focused coherent light beam in approximation of given primary-beam field 20 p3576 A66-37145

Spectrum of spatial frequencies of object analyzed through Michelson method 21 p3738 A66-39130

Holography, discussing potential uses, frozen wave fields, holograms at X-ray wavelength and stress 21 p3739 A66-39199

Signal processing by coherent and incoherent light systems for application in seismology, radar, speech recognition, etc 22 p3862 A66-39734

Magnetic resonance in He 3 ground states examined through interaction with metastable atoms in gas discharge, observing transfer of transverse magnetization by collision 22 p3931 A66-39809

Traveling-wave phase modulation of coherent light propagating in anisotropic medium 22 p3933 A66-40867

Photon time-of-arrival distribution measured in highly monochromatic and spatially coherent light beam from low pressure Hg discharge 23 p4076 A66-41265

Frequency tuning of coherent emission over vibronic continuum of phonon-terminated optical masers by thermal tuning and wavelength-selective feedback 23 p4077 A66-41369

Measuring amplification of coherent optical radiation in neon-helium filled tube 24 p4219 A66-42125

Pulsed laser holograph and problem of overcoming limited coherence 24 p4211 A66-42560

Gas-discharge CW lasers, particularly He-Ne, carbon dioxide, argon-ion and pulsed self-terminating lasers, discussing classification, power output and gain, Doppler width, coherence and noise 24 p4224 A66-42801

Horizontal deflection in TV display produced by Bragg reflection of laser light by ultrasonic waves in water 24 p4212 A66-42816

Bose-Einstein distribution function for quantum photons from amplified spontaneous emission 24 p4226 A66-43093

**COHERENT RADAR**

Distance-and velocity-measurement errors in coherent-pulse systems with periodic modulation law 06 p0837 A66-17180

Master oscillator stability requirements for coherent radar systems 12 p1835 A66-24132

Distance-and velocity-measurement errors in coherent-pulse systems with periodic modulation law 19 p3297 A66-35538

Radar partial coherence theory for clutter construction relationship to radar cross section, waveform coding, output signal, mutual coherence function and random noise 23 p4037 A66-41312

Coherent CW superheterodyne radar system for studying backscattering from hypersonic velocity projectile wakes 24 p4191 A66-42196

**COHERENT RADIATION**

Coherence properties of helium-neon laser with superimposed modes examined by interference pattern 01 p0081 A66-10337

Sharply directional coherent radiation generation by synchronized lasers or multimirrored resonator of single laser 01 p0083 A66-11007

Scattering of radio waves by oscillating reradiators randomly arranged on planar absorbing discontinuity 02 p0190 A66-11409

Semiconductor and dielectrics for generation of coherent short-wave radiation, using electron beam for excitation 04 p0568 A66-14346

Optically connected laser constructed on gallium arsenide p-n junction, noting coherent radiation 04 p0533 A66-14363

History and development of molecular amplification by stimulated emission of radiation, noting various laser types 05 p0696 A66-15034

Rare earth chelates preparation, luminescence behavior and laser action 05 p0741 A66-15833

Spontaneous radiation and nonresonant losses as dominant effects in conversion of incoherent light into coherent induced radiation 06 p0889 A66-15891

Coherent radiation from gallium arsenide p-n junction formed by beryllium diffusion, noting radiative recombination with zinc 07 p1105 A66-18378

Beat frequencies and coherence properties in circularly polarized atomic transitions of gaseous lasers with axial magnetic fields 07 p1046 A66-18429

Laser emission in pure cadmium sulfide crystals bombarded by electron beams 08 p1233 A66-18650

Coherent excitation of mercury resonance state by irradiation with light modulated at Larmor frequency 08 p1233 A66-19089

Gallium arsenide luminescent diodes with triangular resonator producing coherent emission at high density 08 p1193 A66-19195

Coherent amplification coefficients of neon lines in helium-neon mixture 08 p1234 A66-19310

Sharply directional coherent radiation generation by synchronized lasers or multimirrored resonator of single laser 09 p1386 A66-19945

Coherent radiation effect on stability of crossed field electron beam, noting raising of potential of space vehicle 10 p1564 A66-21544

Coherent behavior of light-quantum field in quantum electrodynamics, noting explicit terms of correlation and characteristic field conditions for nth order coherence 12 p1913 A66-23727

Pulse excitation of volume of gas to coherently radiating state applied to beam maser spectrometer 12 p1879 A66-23731

Coherence properties of quantized electromagnetic field and hierarchy of correlation functions for complex field operators 13 p2128 A66-26218

Unitarity conditions for photon echo detectors of coherent radiation 13 p2128 A66-26219

Spatial selective fading as random process, discussing spatial coherence, wave number dispersion profile, time delay profile, etc, in ionospheric propagation 14 p2234 A66-26859

Laser radiation coherence property deterioration and molecular scattering during propagation through turbulent atmosphere 14 p2236 A66-27131

Semiconductor and dielectrics for generation of coherent short-wave radiation, using electron beam for excitation 14 p2368 A66-28242

Optically connected laser constructed on gallium arsenide p-n junction, noting coherent radiation 14 p2310 A66-28262

Charged particle acceleration by coherent radiation 14 p2348 A66-28313

Laser lines due to energy transfer from color centers to erbium ions in calcium fluoride crystals irradiated by gamma ray 16 p2717 A66-30278

Truncated equations describing coherent radiation of excited chromium ions in ruby situated in traveling wave resonator 16 p2720 A66-31547

Minimum spectral line width, threshold current density, radiation-peak displacement and possible recombination mechanism for GaSb laser diode p-n junctions in coherent radiation 16 p2721 A66-31764

Spontaneous and induced coherent radiation from indium antimonide electron-hole plasma 16 p2721 A66-31768

Coherent emission of indium arsenide phosphide p-n junction 16 p2721 A66-31788

Focused laser coherent radiation-induced

degradation of solid methylene and gas chromatographic analysis of reaction products 17 p2933 A66-31870

Coherent plasma radio wave emission ineffective for quasar, Crab Nebula and supernovae remnants 17 p2996 A66-31913

Laser oscillation in flash photolysis of carbon disulphide and oxygen to form CO 17 p2933 A66-31941

Oscillation conditions for feedback lasers, superradiant directionally coherent emission lasers and coherence brightened emission lasers 17 p2934 A66-32628

Laser based on excitation of gallium phosphorus arsenide solid solution by beam of fast electrons 17 p2937 A66-33304

Coherence in radiation peaks of ruby laser studied through interference field 17 p2938 A66-33510

Radiation characteristics of circular aperture and linear antenna with partially coherent illumination 18 p3074 A66-33536

Laser action on several hyperfine transitions in Mn I 18 p3118 A66-34000

EAS RF emission detection, discussing enhanced Cerenkov radiation, mutual coherence effects, diffraction, Fresnel zones, Coulomb-field bremsstrahlung, etc 18 p3208 A66-35117

Jodrell Bank experiment testing Askarian hypothesis on radio pulses coincident with EAS under mutual coherence effects and checking coherent condition, internal reflection, shower energy, threshold and polarization 18 p3209 A66-35118

Spatial coherence measurement of He-Ne laser output 19 p3373 A66-35592

Selective feedback and saturation mechanisms of Raman lasers using secondary Raman lines, emphasizing cyclohexane 20 p3579 A66-37777

Coherent radiation generation in IR region by nonlinear optics 20 p3582 A66-38429

Coherent radiation generation in IR region by nonlinear optics 21 p3746 A66-38962

Born approximation for phase shift of microwaves scattered from underdense cylindrical plasma used to determine plasma electron density 21 p3794 A66-39572

Coherent radiation generation in electron-hole indium antimonide plasma, discussing emission spectrum 22 p3965 A66-40319

Doppler frequency shift for radio waves radiating coherently from satellite in ionosphere, considering electron concentration and angles of refraction 22 p3869 A66-40779

Coherence in radiation peaks of ruby laser studied through interference field 24 p4218 A66-42124

Coherent amplification of RF radiation in cosmic space 24 p4265 A66-42754

Quenching of stimulated Raman scattering of coherent radiation by two-photon absorption in organic liquids 24 p4226 A66-43039

**COHERENT SCATTERING**

Angular volume-scattering functions measured as function of scattering angle for natural fogs in atmosphere, using coherent and incoherent radiation 02 p0262 A66-12211

Barrat theory of multiple scattering of magnetic resonance radiation, accounting for vapor dispersion and photon propagation time 05 p0697 A66-15172

Spatial structure for second harmonic generated in anisotropic medium by finite-aperture light beam 08 p1233 A66-18969

Multiple scattering effects on propagation of coherent optical signals studied for laser communications 15 p2448 A66-28580

Dispersion degree of coherent scattering regions, microdeformation and packing defects probability in fcc metals determined, using approximation method 19 p3438 A66-35496

Optical superheterodyne reception of coherent signals scattered by diffuse surface 20 p3516 A66-37456

Spatial distribution of hot electrons coherently scattering in thin Au film 23 p4115 A66-42063

**COHERENT SOURCE**

Plasma electron concentration measured by Fabry-Perot interferometer partially filled



with gas-discharge plasma and incorporating ruby laser 03 p0375 A66-12294

Intensity distribution in Fraunhofer diffraction patterns of slit and apertures illuminated by partially coherent light 18 p3118 A66-33986

**COHERENT TRANSMISSION**

Coherent nonlinear interaction of two electromagnetic waves in plasma, noting F layer radio communication 01 p0029 A66-10594

Phase coherent and nonphase coherent coded communications systems, discussing theoretical word error probability vs signal to noise ratio 04 p0478 A66-13593

Thermal phase noise and VCO effects at ground receiver output of coherent two-way Doppler communication system 08 p1304 A66-19133

Coherent transmission of optical radar from laser source and use of RF subcarriers placed on optical beams for wideband communications purposes 14 p2244 A66-28404

Linear instability of laser propagation in fluid with coupling between light and medium 18 p3120 A66-35034

Statistical communication theory, examining problem of selecting set of M equipowered finite duration waveforms to minimize error rate for coherent channel perturbed by white Gaussian noise 21 p3704 A66-39140

**COHESION**

**SA ADHESION**

Relation of compressibility with cohesive energy and molecular volume for dielectric solids, noting confirmation of relation for 45 crystalline compounds 08 p1244 A66-19254

**COHOMOLOGY**

**S FUNCTION SPACE**

**COIL**

**SA ELECTROMAGNET**

**SA INDUCTOR**

**SA MAGNETIC COIL**

**SA MAGNETIC FIELD COIL**

**SA SOLENOID**

Circuitors from lumped circuit elements examined, calculating coil properties and analyzing construction 11 p1664 A66-22660

Plasma stream conductivity and velocity measurement, using systems of primary coil and several secondary coils 22 p3921 A66-40899

**COLD CATHODE**

Cold cathode gas discharge controlled by magnetic field in design of plasma switch 01 p0042 A66-10582

Aluminum cold cathodes with single mode 6328 angstrom helium-neon gas laser lifetimes exceeding 3000 hours 01 p0043 A66-10855

Brush cathode used in abnormal glow region, determining features of produced plasma 02 p0196 A66-11429

Present state of cold cathode development 03 p0345 A66-13235

HF noise from electron avalanches and relation to mechanism of cold cathode arc 04 p0502 A66-14480

Voltage stabilization using cold cathode trigger tubes 05 p0647 A66-14769

Cold cathode magnetron gauge characteristics and striking characteristics of gaseous discharge 13 p2078 A66-25647

**COLD FLOW TEST**

Subscale cold-flow rocket motor model used to determine effect of purely geometric variables on acoustic performance leading to axial mode combustion instability [AIAA PAPER 66-110] 06 p0944 A66-17080

Two-phase cold-flow modeling analysis for rocket nozzle, noting deviations from one-dimensional flow for static pressures on nozzle shape [AICE PREPRINT 44F] 22 p3971 A66-39881

**COLD FORMING**

Cold forming of metals, noting thin tube flow boundary variation with permanent deformation due to torsion and tension 13 p2195 A66-25455

**COLD HARDENING**

Effect of gamma phase aging and phase cold hardening on austenitic strength of Fe-Ni-Ti steels, noting martensitic point and segregation 05 p0699 A66-14689

Microquenched age-formed titanium alloys and titanium bialloy composites 14 p2313 A66-27093

**COLD NEUTRON**

Radiographic examination through steel using cold neutrons produced by placing polycrystalline beryllium neutron filter and single crystal bismuth gamma-ray filter in beam tube 06 p0884 A66-17030

**COLD PLASMA**

**S COLLISIONLESS PLASMA**

**S RAREFIED PLASMA**

**COLD PRESSING**

Atomic site changes in cold pressure welding of metal 16 p2710 A66-30309

**COLD TOLERANCE /BIOL/**

Effects of cold and abnormal atmosphere discussing tolerance limits to hypercapnia, anoxia induced hypothermia and hypoxia 04 p0464 A66-14067

Flying personnel protection, discussing human organism tolerance to sudden immersion in cold water and protective stratospheric suits 06 p0816 A66-18062

**COLD TRAP**

Spectral analyses of residual gases using mass spectrometer, noting vacuum equipment and effects of backing and cold-trapping 19 p3361 A66-36615

**COLD WEATHER**

Investigation of two cold air fronts of polar origin that occurred in Alpine region in April 1962, using data from Tirois IV 11 p1730 A66-23096

**COLD WEATHER TESTING**

Airline evaluation of aircraft survival equipment, noting Arctic survival exercises and testing 20 p3494 A66-37002

**COLD WORKING****SA STRETCH FORMING**

Norton-Hoff creep parameters by cold working tests and relaxation tests 05 p0771 A66-14534

Effect of structure and volume cold-working related to structural factors on notched samples of steels subjected to cyclic stresses 07 p1048 A66-17441

Oxygen content effect on recovery of cold worked tantalum investigated by measuring Snoek damping, electric resistivity and dynamic E modulus 11 p1717 A66-22997

Cold work and precipitation hardening effect on tensile and thermal characteristics of gas turbine alloys [ASME PAPER 66-GT-102] 14 p2312 A66-27002

High purity aluminum strain rate effects with cold working 14 p2316 A66-27782

Heat treatment effect on superconducting properties of cold-worked niobium, noting results of magnetization, critical current and resistivity measurements 15 p2564 A66-28760

Notched and unnotched bending fatigue strength of machined work hardened AISI type 305 stainless steel affected by cold worked surface layer with high compressive residual stresses 15 p2521 A66-29073

VT14-16 titanium alloys strength and plasticity with cold working and heat treatment 15 p2522 A66-29188

Cold working effect on room temperature tensile properties of TiNi intermetallic compound 18 p3123 A66-33756

High temperature properties and recrystallization of heat-resistant alloy A-286 experimentally studied, noting faster occurrence of overaging with increased cold working 19 p3376 A66-35357

Internal friction as function of temperature in cold worked tantalum and niobium containing oxygen and nitrogen 19 p3387 A66-36729

Susceptibility to cold deformation of semifinished B95-2 Al-Zn-Mg-Cu alloy products, noting machinability in manufacturing of parts 22 p3928 A66-40885

Structural steel design specifications, discussing anisotropy, stress-strain in tension and compression, cold working effects, etc 24 p4289 A66-42285

Cold-drawing effect on creep behavior of nickel-aluminum alloy at various temperatures through changes in fracture, precipitates and structure 24 p4227 A66-42309

**COLLAPSE**

**SA GRAVITATIONAL COLLAPSE**

Collapse loading of rotationally symmetric cylindrical shell 15 p2609 A66-29253

Computer program for axisymmetric nonlinear behavior of stiffened elastic shells of revolution with variable thickness,

calculating collapse pressures [AIAA PAPER 66-529] 16 p2814 A66-30527

**COLLECTOR**

**SA CONCENTRATOR**

**SA DUST COLLECTOR**

**SA SOLAR COLLECTOR**

**SA VENUS FLY TRAP ROCKET**

Dependence in transistorized multistage amplifiers of Q on resistances in collector loops 02 p0206 A66-12270

Dependence in transistorized multistage amplifiers of Q on resistances in collector loops 12 p1831 A66-23874

Reverse current across collector-base junction in transistor 12 p1844 A66-24822

Collector target complex eliminating target life time and test equipment contamination by sputtered target material, applied in testing of electrical propulsion systems [AIAA PAPER 66-500] 17 p2991 A66-32774

Secondary breakdown in transistors, noting effect of irregularities in collector base junction and tunneling sites 17 p2894 A66-33108

**COLLISION**

**SA ATOMIC COLLISION**

**SA COULOMB COLLISION**

**SA ELASTIC COLLISION**

**SA ELECTRON COLLISION**

**SA INELASTIC COLLISION**

**SA IONIC COLLISION**

**SA METEORITE COLLISION**

**SA MOLECULAR COLLISION**

**SA PARTICLE COLLISION**

Collision effects on full-wave and ray-optics virtual height computations for LF radio waves reflected from stratified ionosphere 20 p3521 A66-33360

**COLLISION AVOIDANCE NAVIGATION**

Air traffic control requirement for navigational capability, taking safety and economy into account 07 p1073 A66-17765

Air derived separation assurance /ADSA/ systems to avoid in-flight aircraft collisions, detailing range altitude, relative position velocity and projected hazard indicator basic types 07 p1078 A66-18223

Air collision risk and traffic control in long-range air traffic systems as basis for safe procedural separation standards 09 p1401 A66-20431

Collision prevention in controlled and uncontrolled air space, noting onboard visual surveillance, radar systems, etc 13 p2123 A66-25233

Separation standards for air traffic control, with analysis of collision risks 15 p2535 A66-29623

Nuclear radiation anticollision instrumentation for guidance systems of helicopters and other vehicles, both air and surface 17 p2926 A66-33097

Separation of aircraft over North Atlantic especially reduced lane width from 120 to 90 n miles 18 p3130 A66-33558

Safe separation standards estimation for analyzing long-range air traffic systems, emphasizing flying errors observation in operational conditions 21 p3760 A66-38452

Radar displays of true and relative motion to ensure collision avoidance by ships in restricted visibility 21 p3761 A66-38455

Aircraft collision avoidance problems and approaches to solution, discussing air derived separation assurance /ADSA/ 21 p3768 A66-39466

**COLLISION PARAMETER**

Langevin equation used to study interaction between radio wave and plasma, taking into account collisions between electrons and heavy ions and electric field caused by group displacement 01 p0022 A66-10322

Impact process beyond limits of Hertz theory 01 p0154 A66-10478

Single dispersion relation valid for all collision frequencies for electromagnetic and piezoelectric semiconductor acoustic interactions 01 p0029 A66-10589

Finite collision time for artificial celestial body moving under influence of Newtonian force from attractive center 01 p0137 A66-10794

Electron collision cross sections of atoms and molecules of argon, helium, nitrogen and dissociation products of carbon dioxide by dual beam radiolysis methods to study low temperature plasma behind shock



- front 02 p0268 A66-11780
- Approximation formulas for certain collision integrals of gas transport 03 p0395 A66-12836
- Current convection modification in low pressure plasma in magnetic field when collision frequency is less than all other characteristic frequencies 06 p0917 A66-16627
- Atmospheric absorption in IR region, noting effects of water vapor, ozone, carbon dioxide and collision-induced dipole moments 13 p2075 A66-26603
- Molecular inelastic collision cross sections from radiometer force curve 15 p2543 A66-28782
- Knudsen gauge designed by university sophomores, measuring molecular collision cross sections 15 p2498 A66-28787
- Collision cross sections of ions in isoelectronic sequence of lithium, noting dipolar transitions of type 2s to np 16 p2754 A66-31261
- Approximation formulas for certain collision integrals of gas transport 19 p3404 A66-36778
- Classical cross section for producing specified energy transfer in collision of two particles in laboratory system applied to atomic collision cross sections 21 p3774 A66-38544
- Conductivity of potassium-seeded argon plasma, assuming variable collision cross sections and Maxwellian distribution for electrons 22 p3951 A66-40363
- COLLISION RATE**
- Electron density, collision frequency and electron drift velocity obtained from plasma column interaction with electromagnetic wave on physically separated helix 01 p0025 A66-10537
- Electron density and collision frequency in lower D region measured by rocket sounding 03 p0366 A66-12879
- Plasma-electromagnetic interaction control by seeding with charged particles to obtain large collision frequency 04 p0480 A66-13626
- Collision effect on coupling of ion-acoustic waves to neutral acoustic waves at diffuse boundary consisting of partially ionized gas 07 p1088 A66-17955
- Class of exact solutions for one-dimensional single-relaxation equation with arbitrary collision frequency 08 p1316 A66-18532
- Effective electron collision frequency from electron temperature profile for ionospheric heating in F region 11 p1697 A66-22499
- Initial one-dimensional density discontinuity propagation in terms of mean free time between collisions 11 p1689 A66-22905
- D-region electron distribution, collision frequency and amplitudes of partially reflected waves 13 p2075 A66-26739
- Dislocation rate magnitudes and relative collision frequencies influencing relaxation profiles in diatomic gases 14 p2274 A66-27447
- Noncollisional damping effects limiting amplitude of resonance peaks experimentally verified, using mercury plasma discharges 14 p2346 A66-28270
- Hall effect in collision dominated gaseous plasma immersed in uniform magnetic field 17 p2969 A66-32629
- Collision frequency control application to control plasma-electromagnetic interaction [IEEE PAPER CP-65-444] 18 p3068 A66-33907
- Comparison of magnitude of collision frequency of electrons in D and E regions obtained by satellites, rockets, etc, with cross sections measured in laboratory 19 p3352 A66-36627
- Plasma density and collision frequency diagnostics using extraordinary transverse wave 21 p3790 A66-39067
- Microwave plasma diagnostics using longitudinal radio wave propagation 21 p3790 A66-39068
- Velocity dependent collision frequency effect on harmonic generation in ionized gas through which electromagnetic wave passes 21 p3792 A66-39180
- LF incompressible waves and gradient instabilities in ionosphere 21 p3733 A66-39183
- Microwave cavity resonant frequency sampler for direct oscilloscope-photographic recording of electron density, recombination and diffusion time in decaying plasma 21 p3740 A66-39389
- Exact solution for transverse electromagnetic wave in plasma with diffuse boundary, noting reflection and transmission coefficients 22 p3952 A66-39719
- Faraday rotation experiment for determination of electron density and collision frequency observations in arctic D region 22 p3905 A66-39946
- Collision frequency in E and D regions of ionosphere for electrons and neutral molecules 22 p3906 A66-39948
- Partial reflections utilizing different amplitudes of ordinary and extraordinary backscattered waves for electron number densities and collision frequency measurement in lowest ionosphere 22 p3906 A66-39949
- Winter variability of electron number density and collision frequency in lower ionosphere measured, using partial reflection method 22 p3906 A66-39950
- Collision frequency gradient effect on weak partial reflections from ionosphere 22 p3906 A66-39952
- Electron density and collision frequency profiles for D region obtained through simultaneous measurement of radio wave phase and amplitude interaction 22 p3906 A66-39953
- Generalized full wave theory equations derived for EM plane wave propagation through magnetoionic medium for electron collision frequencies proportional to electron energy 22 p3869 A66-40805
- Ionospheric cross modulation analysis by computer-oriented simulation process, noting D region electron density and collision frequency profiles 23 p4041 A66-41641
- Transmission resonant cavity measurements of electron line densities and collision frequencies in ionized wakes of hypervelocity projectiles 24 p4191 A66-42195
- COLLISION WARNING DEVICE**
- EEG experiments on men exposed to intermittent photic stimulation under simulated IFR conditions produced drowsiness as primary response 17 p2864 A66-32165
- COLLISIONLESS PLASMA**
- Perturbation theory of nonlinear oscillations in collisionless plasma 01 p0109 A66-10256
- Nonlinear kinetic equation of self-similar motion of rarefied collisionless electron-ion plasma 01 p0109 A66-10260
- Linear oscillations in relativistic Maxwellian plasma, detailing dispersion relations in collisionless cold electron-beam system 01 p0110 A66-10326
- Ionic waves amplified by collective behavior in alkali plasma obtained by contact ionization of cesium or potassium vapors on surface of two coaxial tantalum cylinders 01 p0110 A66-10331
- Saturation and short-time behavior of unstable ion waves in collisionless alkali plasmas in thermal equilibrium 01 p0110 A66-10339
- One-dimensional collisionless plasma in computer simulation with randomized electrons compared with static theory for equivalent diode 01 p0112 A66-10591
- Weak turbulence in media with decay spectrum, analyzing second component of collision term with isotropic model 02 p0264 A66-11385
- Collisionless plasma flow over cone when flow velocity is greater than ion wave speed [AIAA PAPER 65-125] 02 p0267 A66-11534
- Collisionless mass flow of ionized gas through channel with imposed magnetic field [AIAA PAPER 65-124] 02 p0267 A66-11535
- Equilibrium configuration of plasma confined by magnetic field on kinetic equations of particle drift without considering collisions 02 p0268 A66-11781
- Excitation of collisionless shock waves in rarefied plasma, examining neutron radiation and charged particle flux at chamber walls and magnetic field structure in plasma volume 04 p0557 A66-14431
- Space and time dependence of decaying resonant oscillations excited in collisionless plasma by infinitesimally small pulsed dipole 05 p0721 A66-14714
- Shock wave formation in collisionless plasma investigating magnetic compression pulse, electron density and radial magnetic field profile 05 p0722 A66-14720
- Dispersion equation for LF electronic oscillations in electron beam Maxwell collision-free plasma 05 p0722 A66-14722
- Oscillation frequency of plasma and corresponding collision frequency calculated, using Vlasov equation 05 p0725 A66-15242
- Collisionless plasma theory, discussing characteristics and mechanisms of magnetosphere 05 p0674 A66-15250
- Microinstabilities in collisionless plasma due to Boitzmann equation 05 p0726 A66-15253
- Laminar Landau collisionless damping of finite amplitude disturbances in collision-free plasmas 05 p0727 A66-15257
- Dissipative mechanisms in laminar shocks in collisionless plasmas, using analogy between shocks and hydraulic jumps in water 05 p0727 A66-15258
- Separation constants for finite gyromagnetic plasmas, discussing ion motion effects 06 p0826 A66-16024
- Two models /for collisional heating and collisionless transit-time heating/ of cylindrical plasma heated by oscillating magnetic field 07 p1086 A66-17652
- Behavior of small cylindrical Langmuir probe in steady low density flow of argon plasma [AIAA PAPER 66-5] 07 p1034 A66-17880
- Nonlinear interaction between ordinary and extraordinary wave modes for collisionless cold magnetoplasma 07 p1090 A66-18203
- Collisionless damping of nonlinear plasma oscillations, with exact solution of Vlasov equation for resonant electrons 08 p1260 A66-18537
- Computer simulation of randomization of electrons in collisionless plasma 08 p1260 A66-18538
- Noncollisional damping modifies HF plasma resonance 08 p1261 A66-18644
- Transformation of longitudinal waves into transverse waves in weakly turbulent plasma 08 p1262 A66-18979
- Strong collisionless shock wave excitation in deuterium plasma 08 p1266 A66-19479
- Hydrodynamic equations describing strongly rarefied collisionless plasma 10 p1572 A66-22035
- Harmonic wave generation by EM plane wave normally incident on collisionless plasma with linear density profile 11 p1652 A66-22548
- Plasma edge phenomena in unified Langmuir treatment for probe in collisionless plasma 12 p1925 A66-24816
- Potential profile around negatively biased spherical and cylindrical ion probes in collisionless plasma computed numerically 13 p2142 A66-25707
- LF flute instability of collisionless plasma in curved mirror-type magnetic field 13 p2143 A66-25718
- Ray-optic theory to determine microwave transmission through collisionless turbulent plasma in Fraunhofer and Fresnel regions 13 p2147 A66-25753
- Perturbation theory of nonlinear oscillations in collisionless plasma 13 p2148 A66-25973
- Nonlinear kinetic equation of self-similar motion of rarefied collisionless electron-ion plasma 13 p2148 A66-25977
- Necessary conditions for stability of collisionless guiding center plasma, sufficient for stability of equilibrium configurations whose distribution functions are bell shaped 13 p2154 A66-26671
- MHD wave propagation along uniform magnetic field in cold plasma solved in terms of Jacobean elliptic functions 14 p2340 A66-27134
- Particle distribution in low density collisionless plasma in vicinity of moving charged body smaller than Debye radius 14 p2284 A66-27556
- Information theory for describing electric and magnetic fields of one-dimensional collisionless plasma 14 p2346 A66-28274
- Electromagnetic and plasma wave propagation in inhomogeneous compressible isotropic collisionless electron plasma bounded by closed surface in free



space 15 p2449 A66-28592

Bounds on density fluctuations and electrostatic oscillation spectrum for homogeneous collisionless plasma according to Maxwell-Vlasov equation 15 p2554 A66-29749

Moment equations from collisionless Boltzmann equation solved by transformation into polarized coordinates 15 p2555 A66-29784

Collisionless Boltzmann and Maxwell equations for plasma instability of plasma without external magnetic field for transverse oscillation propagating perpendicular to streams 16 p2760 A66-30817

Trapped electron effect and stationary longitudinal wave propagation in Maxwellian hot plasma based on exact solution of nonlinear collisionless Boltzmann equation compatible with equilibrium electron distribution 16 p2761 A66-31009

Perturbation of electron density at large distances from body at high velocity in collisionless plasma under steady external magnetic field 16 p2762 A66-31181

Plasma wave quasi-linear theory, noting nonlinear effect treatment via distribution function, electric field, Fourier component decay, etc 17 p2966 A66-32422

Nonlinear ionic-acoustic wave propagation in collisionless hot electron plasma with at least one cold ion stream 17 p2973 A66-32976

Dispersion and modes of MHD wave propagation in collisionless plasma 17 p2973 A66-32977

Incapability of looping trajectories existing in finite amplitude hydromagnetic waves propagating across magnetic field in quasi-neutral cold collision-free plasma 18 p3148 A66-34908

Reflection and loss of particles in collisionless plasma in one-dimensional magnetic mirror field in presence of parallel electric field 18 p3148 A66-34910

Density field calculation for collisionless expansion of moving cylindrical gas cloud, with Maxwellian random velocity distribution superimposed on uniform initial velocity 18 p3103 A66-34933

Set of fluid equations in finite Larmor radius obtained by systematic asymptotic expansion, using gyration period and radius as small space and time parameters 18 p3150 A66-34965

Growth of unstable collisionless plasma waves to turbulent state, decay of turbulent state and concomitant anomalous diffusion 19 p3415 A66-36519

Stability of low pressure confined plasma taking into account effect of particle collisions, analyzing equilibrium configuration stability 19 p3417 A66-36529

Electromagnetic instabilities in collisionless plasma obtained, using Liapunov function 19 p3423 A66-36554

Plasma convergence, structure and heating by collisionless cylindrical shock waves, discussing wave front 19 p3424 A66-36560

Nonrelativistic equations of bulk motion of relativistic /cosmic ray/ gas derived by taking moments of collisionless Boltzmann equation 20 p3649 A66-37327

Macroscopic hydromagnetic equations with magnetic viscosity for collisionless plasma, determining Larmor radius ratio to characteristic length, using Vlasov equation in drift frame 20 p3610 A66-38054

Shock waves in rarefied magnetoplasma and collisionless shock waves ahead of geomagnetic cavity in solar wind 20 p3611 A66-38221

Power flow of cyclotron modes propagating in waveguide filled with cold collisionless axially magnetized plasma studied by Brillouin diagram 20 p3612 A66-38398

Excitation of collective motions in collisionless plasma in magnetic field for case of large temperature anisotropy 21 p3783 A66-39024

Noncollision ergodic shock wave propagating in plasma situated in magnetic field and thermal oscillation effect on thermonuclear kinetics 21 p3787 A66-39052

Asymptotic time behavior of longitudinal waves in one-dimensional plasma of relativistic electrons and stationary ions studied, using collisionless Boltzmann equation 21 p3775 A66-39189

Transmission and coupling resonance of hydromagnetic disturbances in nonuniform model magnetosphere calculated by approximate dipole coordinates valid near equatorial plane 21 p3734 A66-39217

Behavior of small cylindrical Langmuir probe in steady low density flow of argon plasma [AIAA PAPER 66-5] 22 p3918 A66-40350

Dispersion relation for hydromagnetic waves in infinite collisionless plasma in static magnetic field, using numerical solutions 23 p4103 A66-41488

Electrostatic probe in collisionless plasma wherein sheath joins region of ambipolar diffusion 23 p4104 A66-41494

**COLLOID**

SA ELECTROPHORESIS

SA SOLID SUSPENSION

Stability and surface tension of colloidal graphite dispersions in absence and presence of nonelectrolytes 21 p3754 A66-39150

Particle spectrum determination by inversion of scattering data for high concentrations of sol 21 p3760 A66-39364

**COLLOIDAL GENERATOR**

Particle formation involving homogeneous condensation by mixing reaction technique for eventual development of colloid thruster [AIAA PAPER 66-254] 10 p1593 A66-21459

Negatively charged colloid generation by electrostatic spraying, with capillaries arrayed alternately positive and negative [AIAA PAPER 66-251] 10 p1594 A66-21702

**COLLOIDAL PROPELLANT**

Comparison of various electrostatic thrusters and proposed low pressure colloidal power converter for high payload lunar and planetary missions [AIAA PAPER 66-211] 10 p1592 A66-21448

Colloidal thruster with hot cathode charged colloidal particle source [AIAA PAPER 66-255] 10 p1593 A66-21460

Propellant properties and particle formation efficiency determined for homogeneous condensation-type colloid thruster [AIAA PAPER 66-253] 11 p1760 A66-22221

Colloid particle electrostatic thrusters for lunar ferry missions in specific impulse range 1000-3000 sec 12 p1937 A66-24903

**COLOR PERCEPTION**

Two photocells with positive and negative photoconductivity used in model simulating human color vision and anomalies 18 p3061 A66-33843

Vector transformation properties of tristimulus color-coordinates used to characterize human visual sensation 18 p3111 A66-33992

Adaptive color shifts due to chromatic adaptation interpreted as linear mappings 20 p3504 A66-36942

Response characteristics of lateral geniculate cells of macaque monkey, discussing hue, saturation and brightness encoding in primate color visual system 20 p3504 A66-36946

Sensitivity to color differences as function of step size 20 p3505 A66-36948

Iterative transformation of chromaticity coordinates of Munsell samples into another coordinate system with transformed value spacing in accordance with perceptual color spacing 21 p3773 A66-39397

Effect of color and brightness contrast, direction of contrast and contrast values on legibility of circular dial 21 p3701 A66-39420

**COLOR PHOTOGRAPHY**

Standing wave read-only memory based on Lippmann color photography for information storage 05 p0636 A66-14819

Color spectrozonal photography used in plotting topographic maps 06 p0881 A66-16752

Electronic color correction during aerial photograph printing by employing specially programmed computer 10 p1534 A66-21329

Color hologram for white light reconstruction constructed from three-dimensional diffusely reflecting objects 18 p3109 A66-33611

Solar prominence in color photography, using filtering system for H and D lines 20 p3648 A66-37284

Colored spectrozonal aerial photographs in topographic decoding of photographs of wooded regions 21 p3735 A66-38570

White light reflection holography extended to recording of volume holograms in emulsions on sheet film 24 p4220 A66-42260

**COLOR TELEVISION**

Color TV for exploration of space environment, noting techniques for signal transmission via satellites 08 p1180 A66-18611

**COLORIMETRY**

Nuclear fast red technique of calcium in serum, parotid fluid and urine in weightless state 03 p0329 A66-13347

Toxicological effect of hydrazine and monomethylhydrazine in blood serum of rats 05 p0626 A66-14664

20-inch mirror telescope with photoelectric astrophotometer for photometric, colorimetric and polarimetric measurements 05 p0683 A66-15419

Vector transformation properties of tristimulus color-coordinates used to characterize human visual sensation 18 p3111 A66-33992

**COLUMBIUM**

**S NIOBIUM**

**COLUMN**

SA BEAM COLUMN

SA TAPERED COLUMN

SA VERTEBRAL COLUMN

Parametric response of elastic clamped-free column, noting agreement between theory and experiments for first three spatial and first four temporal modes 04 p0594 A66-14391

Creep buckling of columns under axially nonuniform temperature distribution 12 p1969 A66-24364

Creep buckling of column with nonuniform vertical temperature distribution 14 p2408 A66-28344

Flexure of thin elastic plate clamped to rigid columns, determining functions of complex variable 15 p2613 A66-29433

Approximation method for solution of bending problem of isotropic plate resting on rigid columns to cover case of anisotropic plate with reinforced elliptic hole 15 p2613 A66-29434

Elastic deformation of biaxially loaded columns of thin-wall open cross section with initial imperfections 17 p3032 A66-33435

**COMBUSTIBLE FLOW**

Structure and function of wind tunnel used in supersonic combustion processes 04 p0572 A66-13538

Local heat transfer to immersed cylinder in transonic cross flow for gaseous stream 07 p1150 A66-17581

Flow field of two-dimensional Bunsen flame according to source sheet approximation 07 p1154 A66-17940

Imploding cylindrical shock wave production through imploding detonation waves in oxygen-acetylene mixtures, using Chapman-Jouguet theory 08 p1204 A66-18523

Nonequilibrium chemical reaction effect on decay in spontaneous explosion for reactive expelled gas and inert expelling gas 08 p1179 A66-19482

Approximate method for analyzing chemically reacting turbulent flow fields having initial homogeneities [AIAA PAPER 65-37] 10 p1523 A66-21770

Hybrid rocket combustion regression rate and turbulent boundary layer mass transfer 14 p2412 A66-27449

Unsteady flow field, combustion processes and interaction regions during shock propagation in solid-propellant rocket combustors 17 p2991 A66-32486

**COMBUSTION**

SA AFTERBURNING

SA BOUNDARY LAYER COMBUSTION

SA DEFLAGRATION

SA FLAME

SA FUEL COMBUSTION

SA HYBRID COMBUSTION

SA HYDROCARBON COMBUSTION

SA HYPERSONIC COMBUSTION

SA INTERNAL COMBUSTION ENGINE

SA METAL COMBUSTION

SA PROPELLANT COMBUSTION

SA SUPERSONIC COMBUSTION

Nonlinear system of partial differential equations describing one-dimensional combustion process of gas mixture 15 p2616 A66-28961

Laminar and turbulent diffusion flame combustion mechanisms, stabilization, flame



ionization, Bunsen burner, fuel gas jet eddy diffusion, etc 15 p2616 A66-29068

Flame propagation theory using one-dimensional model and radial temperature variation to obtain dependence of propagation velocity on thermal-diffusivity coefficient 16 p2830 A66-31515

Thermoplastic surface response to intense surface heating exposure, examining linear pyrolysis of polymethyl methacrylate [WSCJ 66-24] 18 p3263 A66-34418

Polymer flammability measured in terms of minimum oxygen content needed for burning, noting effect of various agents for reducing flammability 20 p3680 A66-38040

**COMBUSTION CHAMBER**

**SA ROCKET CHAMBER**

Developing combustion chamber for MHD generator experimentation 01 p0130 A66-10216

Three kerosene-HTP propellant rocket engines for satellite launching, noting combustion chambers 02 p0279 A66-11675

Parameter relationship governing construction of models for combustion of liquid fuels in rocket engines 02 p0279 A66-11707

Combustion phenomena in model combustion chamber of lift jet engine in terms of efficiency, pressure loss and extinction limit 03 p0443 A66-12400

Energy balances for combustion chambers of gas turbines by electronic computer 03 p0416 A66-13202

High temperature measurement in combustion chambers of air breathing engines discussing optical, pneumatic, acoustic and calorimeter methods 04 p0518 A66-13537

Calculation of mean temperature of mixture burning in flame tube of annular combustion chamber 04 p0597 A66-13760

Various types of periodically discontinuous combustion, showing improved thermal efficiency applicable to turbine combustion chambers 05 p0787 A66-14962

Propulsive duct combustion chamber with application of feedback and spark discharge for VTOL and aircraft propulsion 05 p0744 A66-14997

Heat-and fatigue-resistant metal alloys for construction of jet aircraft combustion chambers, including 18 NiCoMo alloy suitable for temperatures up to 650 degrees C 05 p0704 A66-15806

Data on combustion of pyrolyzing solids as applicable to combustion chambers of hybrid propulsion devices, placing emphasis on coal 07 p1154 A66-18028

Combustion chamber of propulsive duct including duct potential, feedback, reed-type valve, aerodynamic valve, Venturi design, fuel control, etc 07 p1110 A66-18162

Nondestructive test method using fluorescent penetrant techniques for detecting intergranular surface attack on Inconel-X thrust chamber 07 p1040 A66-18392

Chamber pressure balanced piston nozzle for fast depressurization to bring about combustion quenching 08 p1281 A66-18833

Chemical reaction kinetics and gas dynamics combined to analyze processes occurring in combustion chambers and nozzles of jet and rocket engines 10 p1620 A66-21367

Control system of supersonic combustion, using spectral intensity ratio, monitoring combustion chamber in two wavelength regions 10 p1622 A66-21948

Three kerosene-HTP propellant rocket engines for satellite launching, noting combustion chambers 11 p1760 A66-22435

Thermodynamic process within combustion chamber of propulsive duct, examining potential with reference to feedback and spark discharge 11 p1761 A66-23251

Mixing processes for isothermal and nonisothermal simulation of flows in combustion chambers 13 p2210 A66-26490

Shock wave/flame front interaction in cylindrical chamber 14 p2412 A66-27438

Hydrodynamic processes in combustion chamber and production of two-phase combustion mixture 14 p2276 A66-27713

Nozzle precombustion chamber base pressure for sudden pulsating sonic flow propagation 17 p2909 A66-32582

Radiant heat transfer from hot solid combustion products to combustion chamber walls [AIAA PAPER 65-559] 18 p3260 A66-33811

Axial pressure gradient change with geometry in combustion chambers formed by cylindrical and conical sections, using rocket motors burning LOX and JP-5A 19 p3450 A66-35624

Model study of aerodynamic oscillations in ramjet diffuser and combustion chamber prior to booster separation in ramjet missile indicates that venting may solve problem 19 p3468 A66-35630

Plasma velocity measurements in and outside plasmatron nozzle and free stream from combustion chamber as function of flow rate of stabilizing gas and combustion chamber 20 p3609 A66-37567

Ablation analysis in cylindrical coordinates for axisymmetrical configuration of wall materials with temperature-dependent properties and nonlinear heat flux conditions at boundaries [AIAA PAPER 66-542] 20 p3680 A66-38034

Hypergolic liquid propellant combinations, noting effect of feed pressure, injection tube diameter and fluid free path on ignition process in combustion chamber 20 p3626 A66-38140

Project Scorpio USAF Cellular Combustion Chamber Program for cost reduction and injection pattern simplification in liquid propellant rocket engines 20 p3629 A66-38256

Simulation of rocket engine starting transients via shock tube combustion drivers, discussing diaphragm rupture effect on combustion, acceleration and burst pressure [AIAA PAPER 66-761] 22 p3972 A66-40644

Pressure variation induced by ignition of air-hydrocarbon mixtures studied by strioscopic cinematography and simultaneous pressure measurement 23 p4148 A66-41176

Aluminum alloy tube for combustion chamber of Japanese SSR, noting mechanical properties, temperature effects, etc 23 p4081 A66-41424

Compressible fuel mixture deflagration perturbation stability in induction regime characteristic of heat-stressed combustion chambers of rocket engines 23 p4122 A66-41790

Pressure, temperature, gas velocity, thrust and specific impulse of rocket combustion chambers determined, using differential equation and Runge-Kutta method 24 p4261 A66-42743

**COMBUSTION EFFICIENCY**

Burning modes in initially unmixed reactants, describing stagnation region formation by interaction of opposed flows of fuel and oxidant [AIAA PAPER 66-71] 06 p0969 A66-16258

Rotating bomb calorimetric technique, determining accurate values of enthalpy of combustion of boron and boron compounds 08 p1178 A66-19068

Limiting conditions of temperature, gas flow rate and heat removal for combustion of methane in atomic oxygen, calculating heat balance of process 16 p2827 A66-30792

Burning properties of oxygen-nitrogen and oxygen helium spacecraft atmospheres determined for increasing safety of crew members in case of emergency 17 p3033 A66-32147

Ignition and combustion mechanism of liquid propellant consisting of aliphatic alcohols and mixed acid, using calcium and potassium permanganates as catalysts 17 p2989 A66-32458

Kinetic factors in diffusion flames, noting fuel/oxidizer ratios, equilibrium in terms of flame geometry, burning of metallic elements, etc 18 p3263 A66-34419

Correlation study of turbojet afterburner combustion efficiency and fuel/air ratio setting for maximization of efficiency [WSCJ 66-1] 18 p3164 A66-34423

Aluminum particle combustion noting changes from preignition to burnout, flame structure, particle geometry, etc 18 p3266 A66-35021

Catalytic combustion of cyclohexane, cyclohexene and benzene, determining significance of combustion via computer

program 18 p3266 A66-35022

Combustion efficiency measurement of jet-engine systems, noting role of static pressure in outflow nozzle 20 p3681 A66-38443

Hydraulic analogy methods for simulation of internal gas flows containing combination zone 22 p3901 A66-40500

Combustion of atomized liquid fuels, noting optimum value of atomization fineness affecting completeness of combustion 24 p4293 A66-42208

**COMBUSTION HEAT**

Conformal sets of aromatic and other conjugated compounds, noting that sum of combustion heat of compounds in one set equals sum of compounds in other set 03 p0442 A66-12333

Opposed jet diffusion flames subjected to electrostatic fields, estimating volumetric heat release rate and mass flow behavior [ASME PAPER 65-WA/ENER-3] 05 p0789 A66-15628

Convective heat transfer measurements for partially dissociated carbon monoxide and hydrogen with high Lewis number [ASME PAPER 65-WA/HT-27] 05 p0793 A66-15676

Heat of combustion of tricarbonyl-cyclopentadienylmanganese 08 p1279 A66-18798

Pressure and temperature distribution in flow of combustion products in presence of transverse magnetic field 11 p1786 A66-22596

Opposed jet diffusion flames subjected to electrostatic fields, estimating volumetric heat release rate and mass flow behavior [ASME PAPER 65-WA/ENER-3] 16 p2825 A66-30341

Direct measuring radiation calorimeter developed for determining radiant heat flux of solid propellant gas flame in rocket combustion chambers [AIAA PAPER 65-358] 18 p3159 A66-33814

Liquid methane as fuel for SST propulsion in terms of cost, combustion heat and cooling capacity 24 p4261 A66-42240

**COMBUSTION INSTABILITY**

Pulse technique employing gunpowder charges to evaluate combustion instability in solid propellant rocket motors 03 p0416 A66-13106

Gas combustion and detonation instability 04 p0597 A66-13901

Acoustic combustion instability of solid fuel rocket dependence on response of burning propellant surface to sound field 05 p0744 A66-15783

Heterogeneous detonations, discussing polydisperse and monodisperse spray detonations and liquid fuel film shock-induced combustion [AIAA PAPER 66-109] 06 p0969 A66-16256

Subscale cold-flow rocket motor model used to determine effect of purely geometric variables on acoustic performance leading to axial mode combustion instability [AIAA PAPER 66-110] 06 p0944 A66-17080

Nonacoustic combustion instability of aluminized composite propellant [AIAA PAPER 66-111] 06 p0941 A66-17105

Coupling of conversion process and internal field related to effect of injector design on unstable burning of liquid propellant rocket motors 08 p1282 A66-19136

Flame wavelength during vibrational combustion of gas mixtures in tubes 14 p2415 A66-28327

Gas combustion and detonation instability 17 p3033 A66-32064

Heterogeneous detonations, discussing polydisperse and monodisperse spray detonations and liquid fuel film shock-induced combustion [AIAA PAPER 66-109] 17 p3037 A66-33237

Combustion instabilities in solid propellant rocket motors, including acoustic and nonacoustic instabilities 18 p3163 A66-34003

Propellant composition influence on finite-amplitude axial wave mode instability in solid propellant rockets [AIAA PAPER 66-600] 18 p3161 A66-34431

Combustion instability in MMH-NTO liquid rocket engine as affected by propellant mixture ratio, injection velocity, droplet size and distribution and chamber pressure [AIAA PAPER 66-603] 18 p3164 A66-34432

Phase relationships of normal stress



perturbations in cylindrical combustor operating near atmospheric pressure with premixed air and natural gas 20 p3680 A66-38038

Unstable combustion products of glow discharge, discussing effect of propagation rate of hydrogen-oxygen flame 21 p3834 A66-38473

Propellant deflagration control for interaction between fluid dynamic disturbance and propellant combustion reaction 22 p3969 A66-39874

Unsteady-state solid-propellant combustion subjected to acoustic pressure oscillations, noting effect of combustion parameters 22 p3971 A66-40352

Nonacoustic combustion instability of aluminumized composite propellant [AIAA PAPER 66-111] 22 p3970 A66-40355

Static firing tests of HT-110 engines with high slenderness ratio using slow burning polyurethane propellant 23 p4121 A66-41428

Measurement and analysis of oscillatory combustion during static firing tests of HT-110 engines by means of pressure indicators and recorded signal playback system 23 p4121 A66-41429

Static firing tests on special small rockets /SSR/ with different igniter cases and combustion instabilities 23 p4119 A66-41436

**COMBUSTION PHYSICS**

Oxygen and combustion, examining mechanisms of flame combustion and study of heat transmission 01 p0166 A66-11091

Pulsating combustion compared with steady combustion as means of increasing energy conversion 01 p0166 A66-11093

Physical and mathematical models in combustion theory of Zeldovich, Frank and Kamenetski 03 p0444 A66-12702

Ammonium perchlorate spheres combustion in flowing gaseous fuel similar to conditions in solid rocket combustion, noting diffusion flame significance 03 p0414 A66-13225

Temperature inhomogeneities in flame jet in condensed system as affected by flow agitation, carbon particles and metal particles 04 p0597 A66-13697

Physics of spark discharges igniting gaseous mixtures, noting increase in thermal power of discharge by gas preionization resulting from energy redistribution 06 p0919 A66-16877

Detonations in gaseous mixtures and in condensed phase, examining effects of pressure, temperature and confinement on normal detonation 12 p1980 A66-24932

Two-phase self-ignition of isooctane-air mixture, considering preignition phase and temperature zones 13 p2209 A66-25695

Laminar air flow past porous plate through which fuel and oxidizer mixture is injected, deriving diffusion combustion processes that develop in laminar boundary layer 14 p2371 A66-28318

Thermal ignition of flowing gas mixtures at nonreactive noncatalytic hot surfaces 16 p2830 A66-31634

Accelerating particulate flow studied, using blowdown system for component velocities and friction 17 p2916 A66-33471

Solid propellant characteristics for application to supersonic combustion, tabulating combustion properties of selected fuels and solid propellants [WSCI 66-32] 18 p3161 A66-34416

Increasing mass flow through gas turbine without additional work from compressor and consequently increasing thermal efficiency, noting combustion problem [WSCI 66-17] 18 p3164 A66-34424

Overall structure of combustion process in jet flow of hydrocarbon-air mixtures stressing conditions for ramjet engines, noting flame propagation angles, flow computation, etc [AIAA PAPER 66-573] 18 p3264 A66-34444

Combustion of solid or hybrid propellants with one or more solid phases, noting properties, erosive and hybrid combustion, etc 18 p3165 A66-35240

Hydrogen combustion in air above solid noncatalytic wall heated to 800 degrees C, examining diffusion equation for slow combustion and laminar boundary layer flow over noncatalytic wall 19 p3479 A66-36249

Compressed-gas dispersion effect on gas turbine engine operation, deriving spraying

law, jet stream, penetration depth, etc 21 p3808 A66-38934

Hybrid rocket combustion mechanism, burning rate, mass transfer coefficient, throttling effects and grain design [AICE PREPRINT 34C] 22 p3970 A66-39877

Measurement and analysis of oscillatory combustion during static firing tests of HT-110 engines by means of pressure indicators and recorded signal playback system 23 p4121 A66-41429

Combustion mechanism of composite propellants including solid propellant combustion rate measurements, flames spectrography, temperature at propellant surface, etc 23 p4122 A66-41660

Flame of homogeneous gas mixture in terms of similarity criteria applied to combustion process analysis 24 p4295 A66-42883

Approximate solution of variation problems in heat explosion theory, noting difficulty resulting from heat liberation dependence on temperature 24 p4295 A66-42884

**COMBUSTION PRODUCT**

Steady state composition mechanism of solid /heterogeneous/ propellants noting linear pyrolysis, exothermal oxidizers, fuels, etc [ONERA TP 240] 02 p0278 A66-11681

Equilibrium combustion products of generalized hydrocarbons with oxygenated air, with charts on enthalpy, entropy, molecular weight, specific heat ratio, etc [ASME PAPER 65-WA/ENER-2] 05 p0789 A66-15627

Combustion process of isothermal quasi-stationary porous particle for Stokes streamline regime 08 p1321 A66-19773

Line-of-sight IR spectral temperature profile measurements in inhomogeneous hot gas 09 p1382 A66-20505

Book on thermodynamic properties of combustion gases 12 p1978 A66-24192

Trails arising in wake of fan-type jets in transverse gas flow during uniform fuel-air mixture combustion 14 p2413 A66-27693

Electroconductivity of combustion products of propane-air mixture determined by double Langmuir probes 15 p2617 A66-29312

Composition and combustion products of boron at 300 to 3200 degrees K and heat of formation of boron oxide 16 p2830 A66-31604

Ionization processes in hot products of combustion processes /flame gases/ as weak plasma media, noting flame properties, mass spectroscopy, electron concentration, etc 18 p3260 A66-34106

Low temperature plasma conductivity of combustion products, particularly of exhaust gases in duct of MHD oscillator 18 p3145 A66-34107

Performance calculations for propellants in terms of composition and enthalpy and principles of rocket engines 19 p3449 A66-36287

Thermodynamics of combustion and concepts of aerothermochemistry using Newton-Raphson iteration process, noting transfer phenomena of matter, heat and momentum 20 p3680 A66-38090

Heat of formation of oxygen difluoride for reaction with hydrogen, using Parr fluorine combustion bomb containing metal ampoule employing burst diaphragm 23 p4118 A66-41238

Molecular mixing of cold air jet containing sodium nitrite vapor and slipstream of gasoline-air mixture combustion products 23 p4149 A66-41793

**COMBUSTION STABILITY**

Stability criterion for steady state combustion of powder with variable surface temperature under constant pressure 02 p0302 A66-11400

Unsteady boundary layer flow of multicomponent gas mixtures, investigating combustion instability in liquid and hybrid rocket motors [AIAA PAPER 65-41] 03 p0444 A66-12796

Oscillations in liquid fuel rocket combustion chambers covering LF and HF theory, stability requirements and optimal performance criteria 04 p0594 A66-14463

Combustion instability in liquid propellant rocket motors causing pressure fluctuations [CI PAPER WSCI-65-22] 05 p0788 A66-15144

Heat transfer in base flow region,

determining parameter of correlation for hydrogen injection and combustion, adiabatic flame temperature, heating rates and recovery temperature [AIAA PAPER 66-108] 06 p0970 A66-16408

Development of 23KS20000 motor for Black Brant IIB vehicle with emphasis on internal ballistics 06 p0942 A66-16702

Impact-induced combustion in hypersonic ramjet engines, determining hypersonic fuel-air mixing from hydrogen concentration at Laval nozzle outlet 10 p1591 A66-21359

Propellant injection distribution effect on transverse modes of liquid rocket engine instability [AIAA PAPER 65-613] 12 p1977 A66-23581

Small disturbances and effect on processes of fast combustion of inflammable /compressible mixture 14 p2374 A66-27690

Laminar and turbulent diffusion flames combustion mechanisms, stabilization, flame ionization, Bunsen burner, fuel gas jet eddy diffusion, etc 15 p2616 A66-29068

Influence of relative thickness of elastic case on acoustic stability of radial modes in solid propellant rockets 16 p2791 A66-31474

Linear stability boundary for acoustic modes in cylindrical solid-propellant rocket 17 p2990 A66-32479

Diamant French satellite launching /examining combustion stability during ignition, vibrations, chemical reactions/ between oxidizer and pressure feed system, etc 17 p3017 A66-33236

Combustion behavior of aluminum-ferroc oxide thermite with aluminum oxides additions used as combustion model for involatile condensed systems 18 p3259 A66-33718

Combustion rate of ammonium perchlorate-polystyrene and ammonium perchlorate-Plexiglas mixtures related to mixture ratio 18 p3260 A66-33720

Pressure deflagration limit of high energy solid propellants increased to superatmospheric pressures by composition changes [AIAA PAPER 66-679] 18 p3163 A66-34226

T-burner tests for combustion stability evaluation of hydrazine diperchlorate [AIAA PAPER 66-599] 18 p3264 A66-34430

Acoustic absorption liners for suppressing HF combustion instability in rocket engine combustion chambers [AIAA PAPER 65-585] 19 p3449 A66-35608

Combustion stability development with storable propellants for liquid rocket engines, showing coupling between technology and engine system [AIAA PAPER 65-614] 19 p3448 A66-35609

Small perturbation method applied to combustion stability of high explosives taking into account heat release in K phase 19 p3477 A66-35740

Discontinuity characteristics of trough-shaped flame stabilizers for combustion in wake of poorly streamlined body during period of ignition arrest 20 p3674 A66-36915

Stability analysis of one-dimensional steady laminar flame propagation with conductive heat loss 20 p3680 A66-38045

LF combustion oscillation analyzed by theory of dynamical stability of closed feedback loop 20 p3681 A66-38103

Laplace transform applied to small pressure variations effect on gunpowder burning stability 20 p3681 A66-38121

Vaporization and atomization theoretically calculated to be controlling parts of combustion process in determining rocket combustion instability [AICE PREPRINT 28D] 22 p3971 A66-39879

Pressure record of HF combustion oscillations observed in solid propellant rocket motor developed under special small rocket /SSR/ program 23 p4121 A66-41430

Halides used as burning rate depressants on combustion stability of polyurethane/ammonium perchlorate base propellants, examining acoustic instability 23 p4119 A66-41435

Solid propellant combustion stability and physicomachanical properties evaluated by measuring and calculation procedure 23 p4120 A66-41437

**COMBUSTION TEMPERATURE**

Calculation of mean temperature of mixture burning in flame tube of annular



combustion chamber 04 p0597 A66-13760  
 Combustion temperatures of explosives  
 PETN, hexogyn and tetryl in constant  
 pressure bomb in nitrogen  
 atmosphere 08 p1316 A66-18795  
 Ignition temperatures of powdered metals  
 in simulated atmospheres of Venus and Mars  
 suggest potential chemical energy  
 sources 11 p1786 A66-22458  
 Flame expansion rate in turbulent flow of  
 homogeneous inflammable mixture at  
 ignition temperatures from 423 to 823  
 degrees K 14 p2374 A66-27691  
 Chlorine-fluorine mixture combustion,  
 examining flame speeds, temperatures and  
 burned gas composition  
 [WSCI 66-31] 18 p3263 A66-34415  
 Thermal self-ignition theory employing  
 general functions of temperature  
 characterizing reaction rate of  
 explosive 19 p3477 A66-35741  
**COMBUSTION VIBRATION**  
**S INSTABILITY**  
**COMBUSTION WAVE**  
 Simple rotating drum, streak camera  
 covering principle, design, construction and  
 application 04 p0520 A66-13940  
 Propagation of combustion wave, consisting  
 of flame front and shock wave passing down  
 tube closed at one end, in presence of  
 magnetic field in undisturbed gas at  
 rest 06 p0874 A66-17002  
 Flame generation of pressure waves and  
 wave-combustion front interactions in  
 detonation processes treated by nonsteady  
 gas dynamics 07 p1155 A66-18118  
 Onset of retonation, laser technology and  
 high repetition-high resolution schlieren  
 stroboscopic wave phenomena  
 records 08 p1318 A66-19200  
 One-dimensional CJ detonation existence as  
 self-sustaining  
 phenomenon 08 p1208 A66-19203  
 Heat conduction equation for convective  
 flow applied to gunpowder combustion  
 under harmonic pressure  
 variation 08 p1280 A66-19486  
 Finite strength spherical shock wave  
 propagation due to explosion into  
 inhomogeneous nongravitating and self-  
 gravitating systems 08 p1211 A66-19810  
 Exothermal discontinuities propagation in  
 conducting media without restricting  
 magnetic field orientation, noting velocity  
 and energy released, showing that existence  
 of propagation velocities leads to two  
 detonation modes 13 p2149 A66-26260  
 Formula derivation for acoustic  
 conductivity of combustion surface of  
 condensed system 17 p3033 A66-31896  
 Solid propellant ignition, discussing  
 deflagration wave propagation along gas-  
 solid grain surface, flux equilibrium  
 equation, etc  
 [AIAA PAPER 66-668] 18 p3165 A66-34441  
 Combustion front pressure rise associated  
 with burning of condensed systems with  
 surface pressure greater than ambient  
 pressure 19 p3478 A66-35748  
 Generation of pressure wave by explosion  
 of condensed phase fuel particles dispersed  
 in gaseous oxidizer  
 [AIAA PAPER 65-357] 22 p3999 A66-40357  
**OMBUSTOR**  
**SA ROCKET COMBUSTOR**  
 JP-5 fuel-air mixture ignition by platinum  
 catalytic igniters, using ramjet engine baffle  
 combustors 13 p2171 A66-25594  
**OMET**  
 Motions in tail of comet Humason from  
 photographs taken at different  
 intervals 02 p0287 A66-11487  
 Three additional members of  
 transplutonian comet family, listing  
 approximate orbital  
 elements 02 p0287 A66-11488  
 Orbit of comet 1947 VI in least-squares  
 adjustment with respect to planetary  
 perturbations 02 p0287 A66-11495  
 Final orbit of Johnson  
 comet 02 p0293 A66-12264  
 Spacecraft-comet rendezvous trajectory  
 analyzed in terms of comet properties and  
 spacecraft capabilities to determine  
 feasibility of interception mission  
 [AIAA PAPER 63-413] 03 p0424 A66-12739  
 Cometary emissions and excitation  
 processes and prediction of major atomic

and molecular emissions of UV spectrum of  
 aurora 03 p0425 A66-12869  
 Rocket launching through aurora of high  
 luminosity spectrograph and liquid ammonia  
 to study behavior under solar  
 radiation 03 p0426 A66-12870  
 Comet mission study using space probes  
 boosted by Atlas Agena and Atlas Centaur  
 launch vehicles for interception from 1967  
 to 1975 04 p0577 A66-13579  
 Comet Ikeya-Seki /1965f/ discussing visual,  
 telescopic and spectral  
 observation 04 p0578 A66-14022  
 Spectroscopic observations of Sun-grazing  
 Ikeya-Seki Comet /1965f/ at minimum  
 possible heliocentric  
 distance 05 p0761 A66-15100  
 Finding coordinates of solar apex from  
 distribution of cometary perihelia and  
 cometary statistics 05 p0761 A66-15129  
 Mass accretion and variation in shape and  
 dimensions of comet  
 orbits 05 p0761 A66-15130  
 Photoelectric measurements of C sub 2, C  
 sub 3, CH and CN band strengths in near  
 nuclear region of Comet Ikeya  
 1964f 05 p0762 A66-15282  
 Atlas-Agena and Atlas-Centaur launch  
 vehicles to investigate  
 comets 06 p0951 A66-15903  
 Comet missions, discussing spacecraft  
 exploration criteria for short period and  
 long period first-apparition  
 comets 06 p0952 A66-15923  
 Comet spectrum analysis and variations  
 with distance of comet from  
 Sun 06 p0952 A66-15944  
 Comet gas production rate calculated from  
 whiplike icy-conglomerate model, considering  
 energy balance between solar radiation and  
 reradiation plus evaporation by  
 comet 06 p0956 A66-17011  
 Secular variations in absolute brightness of  
 periodic comets attributed to instrumental  
 and geometrical effects 07 p1133 A66-17519  
 Sudden decrease in brightness of Encke  
 comet in 1964 07 p1134 A66-17520  
 Apparent magnitude of periodic comet  
 Oterma calculated from relation between  
 absolute brightness and computed  
 ephemerides 07 p1134 A66-17521  
 Orbit determination of Everhart  
 comet 07 p1134 A66-17522  
 Effects of commensurability with mean  
 motion of Jupiter upon distribution of mean  
 motions of short-periodic  
 comets 07 p1135 A66-17640  
 Spectrographic analysis of Ikeya-Seki  
 comet 08 p1289 A66-18791  
 Hypersonic collisionless source flow  
 analysis of comet dust tail model, assuming  
 composition consists of small dust particles  
 acted upon by solar radiation pressure  
 [AIAA PAPER 66-32] 08 p1289 A66-18948  
 Orbital, geocentric, heliocentric and  
 heliographic positions of cometary nuclei  
 and tails in ecliptic or parabolic  
 orbit 08 p1292 A66-19198  
 Comet atmosphere analyzed for neutral  
 particle distribution, acceleration and  
 velocity variations relative to Sun,  
 brightness, etc 10 p1605 A66-21207  
 Orbits of Tsuchinshan 1 /1965b/ and  
 Tsuchinshan 2 /1965c/ 10 p1606 A66-21266  
 Halley comet motion during return of 1910,  
 obtaining orbits via differential correction  
 procedures, including perturbation by all  
 planets but Pluto 11 p1769 A66-22531  
 Comet observations in  
 IQSY 11 p1771 A66-22768  
 Comets hypothesized to consist of  
 antimatter, originating from parts of galaxy  
 consisting entirely of  
 antimatter 11 p1774 A66-23039  
 Comet nucleus as source situated in  
 stationary supersonic solar plasma flux  
 subject to laws of  
 hydrodynamics 12 p1945 A66-23508  
 Distribution of atoms and molecules in  
 comet head, assuming particles may be  
 created and annihilated during dissociation  
 and ionization 12 p1945 A66-23509  
 Launching of artificial comets into orbit to  
 evaluate theories of cometary  
 structure 12 p1945 A66-23569  
 Comet Tomita-Gerber-Honda, noting direct  
 photoreduced photograph, spectrum of head and

spectrum of tail 13 p2182 A66-25577  
 Astronomical and orbital data of comet  
 Ikeya-Seki noting elements for parabolic  
 orbit, elliptical orbit, etc 13 p2188 A66-26319  
 Daylight observations of 1965 f comet,  
 noting influence on solar corona, spectra at  
 various wavelengths, polarization data and  
 results of photoelectric  
 scans 15 p2592 A66-28645  
 Orbit of Comet 1959 IX  
 /Mrkos/ 15 p2593 A66-28647  
 Cometary origin of Tungusk meteorite of  
 1908 supported by analysis of space  
 trajectory and observed nightglow at time  
 of fall 15 p2595 A66-29129  
 Cometary motion in outer solar system  
 region, taking galactic nucleus as perturbing  
 body 15 p2596 A66-29141  
 Ionization process in comets does not  
 depend on solar electromagnetic or  
 corpuscular radiation, considering it as  
 intrinsic property of cometary  
 atmospheres 15 p2598 A66-29267  
 Radio observations of comet Ikeya-Seki at  
 frequencies above 160 mc 16 p2694 A66-30656  
 Comet Ikeya-Seki near perihelion  
 passage 16 p2694 A66-30657  
 Type I comet tail origin due to energetic  
 electrons in shock structure, noting inertial  
 slowing down of interplanetary field lines  
 trapped in solar wind 16 p2801 A66-30919  
 Terrestrial origin of tektites, noting  
 possible connection with cometary collision  
 and evidence of lunar origin for  
 some 16 p2802 A66-30926  
 Photographs from observatories of comet  
 Ikeya-Seki discovered in constellation  
 Hydra 16 p2804 A66-31309  
 BESM-2 computer program for calculating  
 parabolic comet orbit from three  
 observations 17 p2877 A66-31808  
 Minor planets, comets and satellites  
 motions and positions in outline of present  
 research 17 p2998 A66-32025  
 Past and future comet orbits, examining  
 value of auxiliary anomaly in Makover  
 method as function of heliocentric distance  
 of perihelion 17 p3000 A66-32337  
 Photoelectric photometry of comet  
 Everhart 1964 h, noting density of carbon  
 radicals and CN  
 molecules 17 p3000 A66-32338  
 Nature and origin of comets - International  
 Colloquium on Astrophysics, Liege, Belgium,  
 July 1965 17 p3008 A66-33367  
 Cometary nuclei discussing brightness,  
 models, evidence from photometry,  
 spectrography, dynamic properties of nuclei,  
 and meteors 17 p3009 A66-33368  
 Photometry of nuclear condensation used  
 to determine dimensions of cometary  
 nuclei 17 p3009 A66-33369  
 Radioactive heating effect on icy  
 conglomerate cometary nucleus and splitting  
 from solar heat shock 17 p3009 A66-33370  
 Comet flares and cometary nuclear  
 structure, specifically considering  
 Schwassman-Wachmann I 17 p3009 A66-33371  
 Evolution of gases from cometary nuclei by  
 sublimation or desorption 17 p3009 A66-33372  
 OH production by sublimation and gas  
 hydrate occurrence in cometary  
 nuclei 17 p3009 A66-33373  
 Physicochemical quantitative analysis of  
 cometary nucleus-coma buildup relationship,  
 discussing gas liberation, entropy and  
 enthalpy variation, change of state and gross  
 energy balance 17 p3010 A66-33374  
 Dimensions, shape spectra and models of  
 head of comet with atmosphere having dust  
 part much less important than gas  
 part 17 p3010 A66-33375  
 Collisions in inner region of cometary  
 head, structure of emission bands and  
 formation of free radicals 17 p3010 A66-33376  
 Telescopic and photographic observation of  
 cometary structure, particularly coma  
 region 17 p3010 A66-33377  
 Cometary diameter variation determined  
 with heliocentric distance for eight comets,  
 noting solar wind effect 17 p3010 A66-33378  
 Rotational line intensities of lambda 4300  
 band of CH in spectrum of comet  
 Ikeya 17 p3010 A66-33379  
 Rotational and vibrational temperature of  
 diatomic C in comets derived from high  
 resolution spectra, considering transition  
 probabilities in R and P



branches 17 p3010 A66-33380  
 Total number of cyanide molecules and diatomic carbon free radicals and density distribution in head of Arend-Roland 1957 III comet 17 p3010 A66-33381  
 Weak comets in vicinity of Sun during solar eclipse 17 p3010 A66-33382  
 Resolution spectra and photometric profiles of comet heads in monochromatic light and physical state and chemical composition of comets 17 p3011 A66-33383  
 Numerical calculation of relative intensity distribution of solid particles in cometary head, neglecting interparticle collisions 17 p3011 A66-33384  
 Integrated brightness observations of comets, using Baker-Nunn satellite tracking camera 17 p3011 A66-33386  
 Mie theory estimation of mass of dust component of cometary atmospheres observed from 1954 to 1964 17 p3011 A66-33387  
 Selection of comet intercept missions based on predictability of future returns, obtainability of spectroscopic data from Earth during intercept and launch energy limitations 17 p3011 A66-33388  
 Continuous spectrum of comet Alcock /1963 b/ observed with quartz spectrograph at Haute-Provence observatory in France 17 p3011 A66-33389  
 Solar wind and type I comet tails, noting solar wind and plasma velocities as compared with Mariner II measurements 17 p3012 A66-33391  
 Cometary and hydrocarbon flame spectra compared, discussing Swan, HCO and other band systems 17 p3013 A66-33404  
 Cometary origin through survey of literature for last 13 years 17 p3013 A66-33405  
 Hyperbolic comets and Oort hypothesis of cometary cloud, discussing probability distribution and existence of interstellar source 17 p3013 A66-33406  
 Rapid secular decrease in absolute brightness and commensurability effects with mean motion of Jupiter studied in evolution of short periodic comets 17 p3013 A66-33407  
 Secular brightness changes in periodic comets and relation to solar activity 17 p3013 A66-33408  
 Solar wind proton, solar flare proton and galactic ray effect on interstellar solids /comet/ 17 p3013 A66-33409  
 Orbital inclinations relation to comets direction of approach, noting transition between long and short period comets 17 p3014 A66-33410  
 Comet cosmogony of Lagrange and problems of solar system, including volcanic processes in planetary bodies, geophysical and geological arguments, etc 17 p3014 A66-33411  
 Physical characteristics of ten periodic comets compared, considering continuum, triatomic carbon radical and other emissions intensity tail and photometric parameters 17 p3014 A66-33412  
 Dynamical aspects of Oort hypothesis on cometary origin 17 p3014 A66-33413  
 Comet nuclei as principal source of meteorites, discussing dynamical arguments, orbital characteristics and exposure age 17 p3014 A66-33414  
 Interstellar molecules relation to corresponding cometary phenomena 17 p3014 A66-33415  
 Solar wind interactions with natural and artificial comets, discussing charge, momentum and energy transfer, Coulomb collision, plasma instabilities, ion clouds, etc 18 p3169 A66-34354  
 MHD and fluid dynamics interpretation of solar wind-comet interaction 18 p3169 A66-34355  
 Solar wind interaction with type I comet tails in interplanetary magnetic field 18 p3231 A66-34356  
 Solar wind particle density dependence on heliographic latitude due to solar magnetic field channeling 18 p3237 A66-35047  
 Photographic interpretation of shape of tail of comet Ikeya-Seki /1965 f/ and computation of velocity of particles in solar wind 19 p3459 A66-35588  
 Gas tails of brighter comets that may

reach 150,000,000 km in length reveal direction and velocity of solar wind 19 p3452 A66-35797  
 Comet nucleus as source situated in stationary supersonic solar plasma flux subject to laws of hydrodynamics 20 p3646 A66-37021  
 Distribution of atoms and molecules in comet head, assuming particles may be created and annihilated during dissociation and ionization 20 p3646 A66-37022  
 Comet disintegration as basic source of interplanetary dust based on zodiacal isophots 20 p3549 A66-37037  
 Solar wind flow past comet, obtaining minimum radius of comet 20 p3647 A66-37041  
 Possible enhancement to low-energy atmospheric proton flux induced by passage of Ikeya-Seki comet examined, using balloon-borne scintillation counter and pulse height analysis 20 p3631 A66-37617  
 Divergence of gas and dust tails of comets calculated, using moving coordinate with origin at comet head 20 p3653 A66-37797  
 Monte Carlo experiments on cometary origin of meteorites and asteroids in solar system and random orbits of stray bodies 21 p3812 A66-38825  
 Solar corpuscular radiation, discussing schemes of molecular transformations in comets for propene, water, acetylene, carbon dioxide and ammonia 21 p3809 A66-39125  
 MHD analysis of luminescence and widening of tail of Finsler 1937 V Comet passing through solar corpuscular stream containing frozen-in magnetic field 21 p3814 A66-39277  
 High resolution spectroscopic study of comets, examining mechanism involved in excitation of cometary spectra 21 p3816 A66-39533  
 Optimum launch and transfer conditions for two concentrations of orbits within meteor stream associated with Kreutz group of sun-grazing comets in space mission 22 p3976 A66-39859  
 Primary nucleus splitting in comet Ikeya-Seki, noting mechanics and velocity of splitting process 22 p3977 A66-39861  
 Photographic photometry of comet Ikeya-Seki using telescope in red region of spectrum, obtaining stellar magnitude 22 p3977 A66-39862  
 IR I and visual V magnitudes of comet Ikeya-Seki determined, using photoelectric measurements 22 p3977 A66-39863  
 Orbit determination for comet 1965 F Seki-Ikeya, projecting collision with Sun at perihelion 23 p4129 A66-41573  
 Tables of observational statistics on comets, minor planets and natural satellites 24 p4273 A66-42205  
 Cometary nature and phenomena, emphasizing uncertainty of composition of icy snowbank, physical interaction of gases and dust with solar wind and solar radiation 24 p4276 A66-42662

## COMMAND CONTROL

Automatic command control system using phonetic voice pattern 04 p0469 A66-13496  
 Subsonic and supersonic aircraft navigational systems requirements, discussing pictorial presentation and effect on command function 07 p1075 A66-17788  
 NASA Space Tracking and Data-Acquisition Network, describing command telemetry, tracking handling and recording system operations 08 p1180 A66-18587  
 Real-time command and control of Gemini and other entry vehicles by variational techniques 08 p1254 A66-19544  
 Mission-dependent Deep Space Instrumentation Facility equipment designed in support of Pioneer spacecraft program including command encoder, computer buffer and demodulator synchronizer 19 p3315 A66-35670  
 Control laws providing attainment of prescribed attitude and acceleration to prescribed speed in minimum time or fuel consumption for VTOL aircraft 21 p3768 A66-39606

## COMMAND MODULE

SA SERVICE MODULE

Hybrid computer simulation of lunar excursion module and maneuvers with orbiting command service module 12 p1828 A66-2383  
 Fuel cell power plant for Apollo command and service module from engineering viewpoint [AIAA PAPER 64-748] 13 p2007 A66-2664  
 Structural dynamics/manned space flight relation, discussing man-machine dynamics Apollo command module LF studies, pilot control of spacecraft and launch vehicle etc 14 p2230 A66-2801  
 Model tests for determination of structural response of Apollo command module water impact 14 p2393 A66-2802  
 Integrated checkout of Apollo payloads command module, lunar excursion module and service module 14 p2271 A66-2842  
 Guidance and navigational system hardware for Apollo Command Module and LEM 18 p3132 A66-3387  
 Central static inverter used to establish 1250-v, 115/200-v, three-phase 400-cps AC power distribution for Apollo Spacecraft Command and Service Module 20 p3498 A66-3717  
 Apollo command service module /CSM/ parts management 20 p3684 A66-3788  
 Theoretical and experimental data on Apollo command module during water impact 20 p3664 A66-3816

## COMMAND SYSTEM

SA DIGITAL COMMAND SYSTEM  
 Optimization of terrain following performance for supersonic fighter aircraft developing usable command signal 01 p0102 A66-1004  
 Spurious commands and error probability in project RELAY command systems, describing spacecraft equipment 03 p0333 A66-1256  
 Design and installation of antennae for airborne command and control systems, noting antenna system for SAC Airborne Command Post [AIAA PAPER 65-730] 03 p0334 A66-1258  
 Information assimilation from conspicuity coding of updated alphanumeric information, comparing relative effects of individual and group displays 12 p1809 A66-2392  
 Optimization of terrain following performance for supersonic fighter aircraft, developing usable command signal 19 p3397 A66-3648

## COMMERCIAL AIRCRAFT

SA SUPERSONIC COMMERCIAL AIRCRAFT  
 TRANSPORT /SCAT/  
 SA TRANSPORT AIRCRAFT  
 Breguet 941 STOL aircraft advantages over conventional commercial jet aircraft to solve requirements imposed on airport facilities 02 p0177 A66-11744  
 V/STOL aircraft economic and operational characteristics for commercial service over routes of 150 miles or less [SAE PAPER 650243] 03 p0446 A66-12632  
 CH-53A helicopter design, testing, reliability and flight characteristics 07 p0988 A66-17494  
 Design of Elliott E.5, low cost inertia navigation system for civil aircraft 07 p1071 A66-17727  
 Takeoff load distribution predetermination for commercial transport craft based on appropriate weight ratios 12 p1800 A66-23784  
 French commercial aircraft accident investigation 13 p1994 A66-25232  
 Fixed shaft turboprop flight control system for business and utility aircraft [SAE PAPER 660218] 14 p2225 A66-27119  
 Costs and operational characteristics of short haul air transportation in mid-1970 and 1980 periods in eastern corridor [SAE PAPER 660332] 14 p2223 A66-27295  
 Three types of cosmic ray measurement on commercial aircraft, using single Geiger Muller counter 15 p2591 A66-29675  
 Navy angle of attack system as aid in transition from propeller airplanes to turbojets, emphasizing application to commercial aircraft 17 p2843 A66-32684  
 Head-up display system design for civil aircraft including SST and current subsonic jets 17 p2952 A66-33200  
 V/STOL aircraft for commercial short-haul transports, considering turboprops, fan-in



- wing and propulsion 24 p4159 A66-42891
- COMMITTEE ON SPACE RESEARCH
- S COSPAR
- COMMUNICATION
- S AIRCRAFT COMMUNICATION
- S ELECTROSTATIC COMMUNICATION
- S GROUND-AIR-GROUND COMMUNICATION
- S INTERPLANETARY COMMUNICATION
- S INTERSTELLAR COMMUNICATION
- S LASER COMMUNICATION
- S LUNAR COMMUNICATION
- S RADIO COMMUNICATION
- S REENTRY COMMUNICATION
- S SATELLITE COMMUNICATION
- S SPACE COMMUNICATION
- S SPACECRAFT COMMUNICATION
- S TELECOMMUNICATION
- S TELEGRAPHY
- S TELEMETRY
- S TELEVISION
- S TRANSOCEANIC COMMUNICATION
- S VOICE COMMUNICATION
- S WIDEBAND COMMUNICATION
- COMMUNICATION SYSTEM
- SA DEFENSE COMMUNICATIONS SYSTEM /DCS/
- SA DIGITAL COMMUNICATIONS SYSTEM
- SA SPACECRAFT COMMUNICATIONS SYSTEM
- Communication system for 1969 Apollo spacecraft 01 p0037 A66-10502
- Satellite communication, noting satellite and ground terminal design performance criteria 01 p0030 A66-10804
- Long-distance free space microwave circuits noting repeater stations on satellites, satellite orbit, type of traffic handled, equipment, ground stations, etc 01 p0030 A66-10861
- Pulse code modulation /PCM/ for telemetry and communication between Gemini spacecraft Agena D satellite and ground stations for data processing and display 01 p0031 A66-10938
- Development, organization and legal bases of satellite communication system developed by U.S., noting details on COMSAT 02 p0306 A66-11888
- Maximizing flow from source to sink in lossy communication net in which flow through edge is attenuated 02 p0208 A66-11905
- Elliott MCS 920 computer controlled trunk exchange for military area communication network 02 p0194 A66-11932
- Electronic systems in marine, air and space transportation noting radar, ultrasonic devices, computer techniques, etc 02 p0206 A66-12033
- Satellite navigation systems for marine and aircraft industry global, all-weather position determination and communications noting range measurement, range rate, NASA techniques, etc 02 p0260 A66-12237
- FM by mechanical tuning of cavity setting in gallium arsenide crystals for application to communication system 03 p0332 A66-12428
- White noise loading of multichannel communication systems 03 p0333 A66-12492
- Implementation of airborne command and control systems, emphasizing communications equipment, data processing facilities, electromagnetic compatibility and aircraft configuration parameters [AIAA PAPER 65-727] 03 p0336 A66-13049
- Detachable radio relay pods /RRQ-5/ to increase range of UHF and VHF communications systems [AIAA PAPER 65-728] 03 p0336 A66-13050
- Circular waveguides for antenna lead-ins and suitability as line sections and components of communication systems 03 p0345 A66-13237
- Book on channel construction for data transmission using phase-shift keying, considering relative phase telegraphy and noting subassemblies, noise effect, etc 03 p0336 A66-13285
- Scientific research using instruments in space vehicles, noting direct observations of Moon, Venus, Mars, global communications, meteorology, geodetic and navigation satellites, etc 04 p0575 A66-13361
- Phase coherent and nonphase coherent coded communications systems, discussing theoretical word error probability vs signal to noise ratio 04 p0478 A66-13593
- Nonlinear time-variant phase-lock loop differential equation for arbitrary loop voltage-controlled oscillator sweep voltages used in aerospace tracking and communication systems 04 p0502 A66-13605
- Earth-to-space communications using millimeter-wave region of spectrum, noting atmospheric attenuation, propagation losses, etc 04 p0479 A66-13607
- Book on electronic systems constituting space communications systems, noting orbital motions, space environment, noise, propagation, satellites, etc 04 p0481 A66-13816
- UHF voice communications system for 412L Air Weapons Control System discussing transmitter, receiver and compliance testing 04 p0497 A66-13964
- Optimum message decoding in communication systems with pulse code modulation, using minimum square-error criterion 04 p0489 A66-14415
- Communication system using pulse code modulation with polarized light, deriving bit error probability 05 p0631 A66-14594
- Transient response of narrow-band networks to narrow-band signals, using Laplace transforms with positive frequencies 05 p0652 A66-14595
- Communications and control systems that require faithful transmission of amplitude-modulated signals through linear filters 06 p0823 A66-15964
- Error probability computation for incoherent diversity reception in multichannel communications 06 p0828 A66-16111
- Limitations of communication system transmitting data from analog source obtained, using theorem in Shannon paper on information theory 06 p0828 A66-16115
- Maximum likelihood detection of band limited binary signals perturbed by Gaussian noise and intersymbol interference 06 p0829 A66-16193
- Traffic aspects of communications systems involving single wideband facilities carrying simultaneously traffic of various bandwidths and group switching to meet individual traffic requests 06 p0830 A66-16334
- Communication through unknown or random channel, using part of transmission energy to identify channel parameters by receiver 06 p0830 A66-16337
- Reliability of probabilistic communication network 06 p0830 A66-16338
- Supersonic commercial air transport, evaluating communication, navigation and identification systems 07 p1066 A66-17686
- Doppler frequency shift and effect on single-sideband HF communication systems for supersonic transport 07 p1001 A66-17699
- Combination of moored ocean platforms and transatlantic submarine telephone cables for VHF communication service and other ATC facilities for civil aircraft across North Atlantic 07 p1002 A66-17775
- Degenerate parametric amplifier receiving two oppositely modulated input waves, improving noise figure 07 p1010 A66-18152
- Polaris nuclear powered submarine defense capability, noting mobility advantages and command communications system 08 p1322 A66-18559
- Arc-sine modulation method of overcoming amplitude nonlinearities in transmission systems 08 p1186 A66-19741
- Data pulsed transmission over electron-injection laser communication system, using continuous waves 09 p1385 A66-19934
- Linear system induced amplitude-frequency and phase-frequency distortions 09 p1361 A66-20296
- Navigation and communication systems using satellites and ground stations economically, by digital techniques 09 p1400 A66-20425
- Orbiting telecommunications satellite network, noting application and necessary launch vehicles 09 p1464 A66-20562
- Output signal and noise components determination from difference-frequency amplifier of two-channel receiver 10 p1504 A66-21671
- Comparison of sequential and nonsequential detection systems with uncertainty feedback, showing performance as function of peak-to-average power ratio 10 p1518 A66-21838
- Scientific research using instruments in space vehicles, noting direct observations of Moon, Venus, Mars, global communications, meteorology, geodetic and navigation satellites, etc 12 p1946 A66-23639
- Digital computer simulation of stochastic multibeam communications channel with long-distance tropospheric propagation of ultrashort waves 12 p1812 A66-23732
- Macroscopic factors affecting performance of microwave communication systems in plasma channels including absorption, refraction, dispersion, depolarization, nonlinear and random effects 12 p1813 A66-23793
- Improvement on Montgomery prediction of error probability in intermittent system operating during short intervals when SNR is above certain threshold level 12 p1816 A66-24138
- Operation results of Mariner and Pioneer telecommunication systems, including system design and future capabilities 12 p1819 A66-24609
- Future pattern of communications satellite systems, reviewing world requirements for telephony, telex, TV and radio [AIAA PAPER 66-319] 12 p1824 A66-24790
- Data processing centers integration through ground and satellite telecommunications networks for global information network [AIAA PAPER 66-331] 12 p1824 A66-24798
- Computational aids /charts and nomographs/ applicable to gross design of satellite communication systems 13 p2020 A66-25150
- Hybrid PCM-FM communication system, noting quantization error and threshold characteristics 13 p2020 A66-25218
- Deep space network /DSN/ for navigational and communications support to NASA lunar and planetary space programs 13 p2021 A66-25248
- Link design and transmission rates for entry and surface measurements during space exploration to Mars 13 p2021 A66-25249
- Direct and relay link communication from Martian surface station 13 p2021 A66-25250
- Combination of moored ocean platforms and transatlantic submarine telephone cables for VHF communication service and other ATC facilities for civil aircraft across North Atlantic 13 p2058 A66-25862
- Programmable patching system at Cape Kennedy for communications network composed of two individual switching subsystems, using solid state devices and glass-reed relays 14 p2233 A66-26805
- Diode quad modulator suppresses carrier 65 db in high capacity communication system 14 p2247 A66-26869
- Information theory, role in communication systems, detailing coding systems 14 p2239 A66-27808
- Book on solid state communications and design of equipment using semiconductors 14 p2260 A66-28367
- Passive satellite communications system for conventional and specialized networks, discussing new materials and satellite configurations 14 p2244 A66-28402
- Book on automatic communication switching systems, logic, logical switching components, storage elements, relay centers, etc 15 p2465 A66-29644
- Polyphase coding modulation system with additive white Gaussian noise, finding channel capacity bounds on maximum rate and error exponent 15 p2452 A66-29659
- Noise performance of X-band microwave sources, using transistorized crystal oscillators and amplifiers and varactor frequency multipliers for application to communication systems 15 p2465 A66-29672
- Dual polarized high-power synthetic conical scan tracking system at various frequency ranges for parabolic reflector used in communication link 16 p2650 A66-30552
- Communication effectiveness over VLF paths impaired by variability of VLF field strength due to modal interference effects 16 p2653 A66-30723
- Symmetry measurements in



communications device and systems, noting error 16 p2707 A66-31030

Detachable radio relay pods /RRQ-5/ to increase range of UHF and VHF communications systems [AIAA PAPER 65-728] 16 p2654 A66-31326

Analog communication over randomly time varying channels 16 p2654 A66-31331

Improvements to be realized through use of single channel black coded communication system 17 p2873 A66-31967

Increased transmission capability of radio communications link by applying multifrequency manipulation and multipositional amplitude manipulation 17 p2875 A66-32702

Modulators with constant input resistance applied to FDM communications systems for simplification or elimination of filters 18 p3066 A66-33565

Communication systems at microwave and optical frequencies for future Mars missions 18 p3067 A66-33793

Multilevel narrow-band digital FM modem noting design principles, signal to noise ratio vs error rates, etc 18 p3067 A66-33900

Binary synchronous communication in additive non-Gaussian noise, discussing optimal nonlinear detector for digital data transmission through non-Gaussian channels 18 p3067 A66-33901

Communications system design consisting of sequential encoder-decoder in conjunction with modulation detection system 18 p3067 A66-33903

Mathematical representation of latitude-longitude point pairs for intersection of figure of Earth and plane defined by central ray of signal scattered between communications sites 18 p3068 A66-33908

Computer model study of diversity augmented vehicular radio relay communication system in man-made noise environment 18 p3069 A66-34167

Linear system induced amplitude-frequency distortions 18 p3091 A66-34959

Cyclic product codes operating in variable redundancy modes used in communications systems, noting protection against errors 19 p3296 A66-35336

Optimal design of one-way and two-way coherent communication links for space communication 19 p3300 A66-35667

Extreme value statistics estimation of low error probabilities in binary communication systems 19 p3301 A66-35688

Personal telemetry system design and operation 19 p3301 A66-35689

Transceiver subsystem of two-way voice communication system consisting of ear device and master station 19 p3288 A66-35694

Adaptive on-off communication system for binary data transmission over noisy channel of unknown attenuation 19 p3302 A66-35709

System consisting of communications satellites distributed in nonsynchronous orbits and set of ground stations, formulating link scheduling problem as optimum control 19 p3303 A66-35884

Legal problems involved in space communications systems and organizations, assessing rule of ITU in outer space technology 19 p3483 A66-36219

Scale model of submerged VLF antenna using lossy ceramic powder to model ice and snow for submarine communication, geophysics, etc 19 p3321 A66-36416

Book on antenna analysis and antenna types 20 p3524 A66-37008

Recognition of fading signals transmitted by channels with unknown parameters, considering optimum reception technique based on arbitrary law 20 p3515 A66-37382

Antenna types and designs for aircraft, cars and trains 20 p3530 A66-37720

U.S. Lunar Orbiter program 20 p3663 A66-38063

Integral criterion based on absolute value of error, integral-square-ideal error, used as measure of distortion of communication system 20 p3539 A66-38285

Fading multipath channel behavior simulator for communication system performance study 20 p3534 A66-38359

Communication possibility over memoryless channel with computational iterative decoding scheme that is asymptotically

complex 21 p3704 A66-39141

Communication design techniques for coding set of discrete memoryless channels where transmitter and receiver have no knowledge of channels selected 21 p3705 A66-39144

Timing and framing synchronization of PCM communication systems using analog techniques, analyzing transient state and jitter 21 p3705 A66-39226

Communication network response to arbitrary transients calculated by digital computer, permitting replacement of analytic-function wave forms by lists of equal-interval sample values 22 p3883 A66-39724

Optimal design of one-way and two-way coherent communication links for space communication 22 p3864 A66-40060

Transient response of narrow band networks to narrow band signals, using Laplace transforms with positive frequencies 22 p3864 A66-40063

Digital computer simulation of stochastic multibeam communications channel with long-distance tropospheric propagation of ultrashort waves 22 p3865 A66-40075

Satellite communications - WESCON, Los Angeles, August 1966 22 p3867 A66-40709

Manual scheduling technique for allocating military satellite and ground resources to comply with input communications requirements and resources capabilities 22 p3868 A66-40711

Signal and receiver-parameter optimization for additive noise channels with feedback link 22 p3868 A66-40719

Signal systems design approach to problems of communication and radar systems, discussing channel and constraint modeling, data processor performance and signal optimization 22 p3868 A66-40720

Solid microminiature semiconducting materials and devices for microwave communications noting germanium and silicon role, microcircuits, plasma effects, floating zone techniques, etc 24 p4186 A66-43078

## COMMUNICATION THEORY

SA INFORMATION THEORY  
SA STATISTICAL COMMUNICATION THEORY

Textbook on communication engineering emphasizing random processes, information and detection theory, statistical communication theory, applications, etc 03 p0335 A66-12992

Textbook employing signal analysis theory in treating linear systems and communication theory including Fourier series, Fourier and Laplace transforms, convolution integral, etc 03 p0336 A66-13073

Slope quantized binary pulse code modulation by coding signal slopes with undigit 1/0 pulses, using special feedback circuit and threshold in coder comparator 07 p1002 A66-18248

Deriving Erlang lost-signal formula for congestion problem 08 p1184 A66-19236

Signal to noise ratios of AM, FM and PM systems applied to FM-FM receiver 08 p1185 A66-19563

Separation of harmonic components of function E/t/ by double differentiation with subsequent integration 08 p1185 A66-19602

Series solution for average wave field in medium with random inhomogeneities by using Green function for wave equation 09 p1343 A66-20335

Geometrical approximation of amplitude and surface-curvature parameters of wavefront reflected or refracted from curvilinear boundary interface 09 p1343 A66-20336

Morphological method of analysis for space communications, suitable for problems with independent unknowns 09 p1345 A66-20542

Modulation theory, discussing phase-envelope relation for band limited wave in terms of Fourier series 14 p2234 A66-27032

Method of coherent addition of signals to calculate noise resistance of diversity reception 14 p2236 A66-27170

Optimal communication system selection methods 18 p3069 A66-34254

Separation of harmonic components of function E/t/ by double differentiation with subsequent integration 18 p3128 A66-34960

PCM transmission system based on analog data conversion into binary signals, noting use of Shannon decoder for signal demodulation, circuit design and system properties 19 p3306 A66-36653

Antenna radiation pattern synthesis for various array distributions, noting methods applied 20 p3529 A66-37707

Antennas with leaky wave characteristics noting similarities and differences with wave diffraction 20 p3529 A66-37707

Slot antenna research, discussing array and polarization characteristics 20 p3530 A66-37713

Folded antennas, discussing Franklin array and current distribution via equivalent circuit analysis and application for TV transmission and reception 20 p3530 A66-37713

Short wave transmission station conduction, noting shielding to prevent interference from TV transmission 20 p3543 A66-37722

Varactor frequency multipliers, discussing application in low-power ultra-short-wave devices in moving objects for communication purposes 21 p3709 A66-38623

Interchannel generation transfer and multichannel generation in laser with four unsplit levels, noting radiation density, temperature effect and variations in coefficients of losses 21 p3746 A66-38958

Modulation and demodulation for probabilistic coding, noting error chances and interrelations affecting performance of communications system 21 p3707 A66-38633

Radar detection probability in presence of unknown parameters, covering pulse-to-pulse, partial and fully coherent cases 21 p3707 A66-38633

Run-length encodings, determining explicit form of Huffman coding when applied to geometric distribution 21 p3758 A66-39648

State-variable techniques application to communication and radar problems WESCON, Los Angeles, August 1966 22 p3868 A66-40711

Optimum realizable linear filter role in some communication problems, considering detection and continuous estimation 22 p3879 A66-40710

Autocorrelation function and energy spectrum of radiotelegraph signal, noting channel parameter dependency on transmission speed 23 p4036 A66-41050

IEEE Region Six Conference, Tucson, April 1966, Volume 1 23 p4039 A66-41580

## COMMUNICATIONS DEVICE

## SA LIGHT COMMUNICATION DEVICE

Tabulated reliability data on communications systems components for possible application to other fields 12 p1833 A66-24081

Solid state communications devices, discussing HF small signal amplifiers transistor circuits, varactor diodes for frequency multiplier chains, etc 14 p2261 A66-28368

Reflector construction for radar and communications antennas, discussing materials, surface configuration and relative costs 18 p3096 A66-34326

## COMMUNICATIONS SATELLITE

## SA EARLY BIRD SATELLITE

## SA ECHO SATELLITE

## SA INTELSAT SATELLITE

## SA RELAY SATELLITE

## SA SYNCHRONOUS COMMUNICATIONS

## /SYNCOM/ SATELLITE

## SA TELSTAR SATELLITE

Echo II program to launch passive communications satellite that will maintain spherical shape and surface smoothness after loss of inflatable pressure 01 p0145 A66-11122

International TV communications using satellite relaying systems noting Telstar, Relay and Syncom satellites and frequency sharing, video bandwidth, etc 02 p0190 A66-11519

Satellite systems and ground site networks for global surveillance communication nets and synthesis 04 p0475 A66-13460

Communications satellite technology problems discussing synchronization of orbit, attitude stabilization, lifetime and power supply 04 p0475 A66-13499

Communications satellite transponder



discussing system requirements for RF conversion and 04 p0492 A66-13595  
Multiple-access communications satellite discussing modulation and reception techniques for small stations 04 p0478 A66-13596  
Channel capacity of communications satellite repeater, deriving link capacities of radio teletype and voice channels 04 p0478 A66-13597  
Feasibility study indicates that cap-type microwave reflectors can be used as communication satellites 04 p0586 A66-13927  
Shipboard inertial navigation system recalibration, using periodic position information from communications satellite 05 p0712 A66-14604  
Military communications satellite system noting radio frequency, TWT amplifier, synchronous altitude, etc [AIAA PAPER 65-323] 05 p0633 A66-15170  
Moiniva type communication satellite, discussing optimum orbital requirements for maximum coverage, phasing, etc 06 p0952 A66-15907  
Early Bird satellite technology including design parameters, structure, power supply, control system and test program 06 p0958 A66-15921  
Digital range measurement used in design of instantaneous communications handover system for medium altitude multisatellite system 06 p0831 A66-16340  
Solid state output devices in communication satellites 06 p0850 A66-16399  
Traffic needs of communications satellites including random-passing, station-keeping/phased-passing/ and geostationary satellites 06 p0959 A66-16495  
Telecommunications satellite developments and prospects, discussing salient characteristics and traffic requirements 06 p0960 A66-16954  
Possible infringement liability regarding unlicensed transmission of copyrighted works via communications satellites 07 p1155 A66-17227  
Worldwide civilian communications satellite system concept, discussing agreements between U.S. and foreign governments on corporation establishment 08 p1179 A66-18568  
Defense Communication Satellite Program for reliable worldwide military communications 08 p1179 A66-18569  
Design and electrical properties of 25-meter Cassegrainian antenna installed at Raisting ground station for radio communications via satellites 08 p1190 A66-18681  
Time division method of multiple access to military communications satellite by several ground stations 08 p1180 A66-18713  
Medium-capacity satellite receiving system for multiplex FM telephony transmission 08 p1183 A66-18947  
Omega location and satellite reporting for worldwide observation and navigation systems 08 p1252 A66-19508  
Book on antenna systems of non-Soviet communication links via satellites 09 p1342 A66-19974  
Utilitarian space applications, discussing communications, weather, geodetic and navigation satellites and high speed aircraft 09 p1453 A66-20169  
Worldwide satellite communications systems dependence on solution of political, sociological, economic and legal problems 09 p1342 A66-20250  
Transmitters for satellite communications 09 p1345 A66-20545  
Italian participation in COMSAT 09 p1473 A66-20548  
International satellite communications, noting application for air traffic, using VHF band 09 p1346 A66-20561  
Orbiting telecommunications satellite network, noting application and necessary launch vehicles 09 p1464 A66-20562  
Unmanned and manned satellites for communication and terrestrial navigation, noting future plans of NASA 10 p1496 A66-21534  
Gc/s nitrogen-cooled nondegenerate parametric amplifier, noting design, application and operation 10 p1513 A66-21857

Commercial communications satellite for random, phased and synchronous medium altitude, noting design, specifications and operation 11 p1777 A66-22454  
Exact equations derived which can provide all permissible satellite-link assignments for communication satellite scheduling program 12 p1816 A66-24150  
Control system of microwave antenna positioning used in communication satellite tracking, noting servosystems, converter, Leonard drive, control panel, etc 12 p1817 A66-24320  
Future impact of communications satellites on society [AIAA PAPER 66-260] 12 p1981 A66-24735  
Global Commercial Communication Satellite using cylindrical spin stabilized satellite [AIAA PAPER 66-266] 12 p1954 A66-24739  
Satellite providing optimum communications to military users, noting gyroscopic stabilization of antennas, major characteristics, etc [AIAA PAPER 66-267] 12 p1955 A66-24740  
Characteristics and performance of synchronous satellite military communication system [AIAA PAPER 66-268] 12 p1859 A66-24741  
Initial Defense Communications Satellite Project /IDCSP/, current status, objectives and subsystems [AIAA PAPER 66-269] 12 p1820 A66-24742  
Lincoln Experimental Terminal /LET/ system, ground antenna, RF and signal processing equipment for communications via several satellites [AIAA PAPER 66-272] 12 p1821 A66-24745  
Commercial communications satellite system, impact and problems [AIAA PAPER 66-273] 12 p1981 A66-24746  
Manpower projections and problems for communications satellites, discussing requirements for research, development, production and operation [AIAA PAPER 66-275] 12 p1982 A66-24748  
Communications satellites, legal analysis and prognosis [AIAA PAPER 66-277] 12 p1982 A66-24749  
Multiple access modulation techniques /frequency-division, time-division, spread-spectrum and pulse-address/ for use in communications satellites [AIAA PAPER 66-278] 12 p1821 A66-24750  
Time division multiple access /TDMA/ modulation technique for satisfying anticipated demand by many small users for communication satellite facilities [AIAA PAPER 66-279] 12 p1821 A66-24751  
Communications satellites for small nations, describing requirements of worldwide multiple access system [AIAA PAPER 66-281] 12 p1821 A66-24753  
Interference ratios in space telecasting, considering methods of control for cochannel broadcasting [AIAA PAPER 66-283] 12 p1821 A66-24754  
Synchronous stationary satellite system for networking television and radio material to broadcast stations, noting frequency requirements and constraints [AIAA PAPER 66-284] 12 p1821 A66-24755  
Launch vehicle parameter design for optimal support of communications satellites [AIAA PAPER 66-285] 12 p1955 A66-24756  
Effects of varying orbital parameters, including number of satellites, orbit altitude, positioning, tracking accuracy, cost effectiveness, etc, on establishment and maintenance of communications satellite system [AIAA PAPER 66-286] 12 p1955 A66-24757  
Parameters of satellite communication system control and scheduling function, emphasising distinction between scheduling model and scheduling algorithm [AIAA PAPER 66-288] 12 p1822 A66-24759  
Communications satellite system efficiency enhanced by using automatic adaptive voice multiplexer in ground terminal equipment [AIAA PAPER 66-291] 12 p1822 A66-24761  
Adaptive utilization of communication satellite systems optimizing dynamic traffic handling of combined ground and satellite communications complex, noting network configurations [AIAA PAPER 66-295] 12 p1822 A66-24764  
Multiple-access worldwide satellite communication system for aircraft terminals

with limited antenna gain and transmitter power [AIAA PAPER 66-297] 12 p1823 A66-24765  
Design, efficiency and reliability of electric power system related to mission and orbit of communications satellites [AIAA PAPER 66-299] 12 p1804 A66-24766  
Wideband solid state intermediate frequency repeater for communications satellites, using waveguide-cavity diode down converter transistor amplifier and varactor up converter [AIAA PAPER 66-300] 12 p1823 A66-24767  
Increased oscillation stability and efficiency of traveling wave tubes for global satellite communications systems [AIAA PAPER 66-301] 12 p1844 A66-24768  
Requirements for gravity gradient stabilization of medium and synchronous altitude communication satellite systems using zero gain antennas, noting stabilization accuracy, stationkeeping effects, etc [AIAA PAPER 66-303] 12 p1955 A66-24770  
Nuclear power systems for future communications satellites, noting reactor, radioisotope, power system and thermoelectric power conversion equipment [AIAA PAPER 66-305] 12 p1804 A66-24772  
Spacecraft communication link antenna design, noting Earth coverage from synchronous orbit, attitude stability, beam width limits, construction, etc [AIAA PAPER 66-306] 12 p1823 A66-24773  
Direct-to-home TV broadcasting satellite system for upper UHF, describing stabilization, thermal control, antenna, power amplifier, etc [AIAA PAPER 66-309] 12 p1955 A66-24776  
Items affecting information transmitted from payload landed on remote planet to Earth via communications satellite including orbit, transmission policy and orbit injection error effect on communication capability [AIAA PAPER 66-314] 12 p1823 A66-24780  
Lunar communication satellites, discussing satellite relay, librational, random, and synchronous satellite design, lunar orbits, etc [AIAA PAPER 66-315] 12 p1823 A66-24781  
Communications requirements for manned deep space missions, using optical links, with PPM, PCM/PL and coherent reception for each link [AIAA PAPER 66-317] 12 p1823 A66-24782  
Social and legal questions posed by development of large-scale information grids [AIAA PAPER 66-318] 12 p1982 A66-24789  
Long-range projections of demand for intercontinental communication satellite systems and use as basis for business decisions [AIAA PAPER 66-322] 12 p1982 A66-24792  
Implementation of electronically despun satellite antenna system considering limits of impracticability because of excessive weight, control power, etc [AIAA PAPER 66-325] 12 p1844 A66-24795  
Electronic self-steering techniques applied to satellite communications systems with high gain antennas, noting transdirective array and self-phasing array [AIAA PAPER 66-326] 12 p1824 A66-24796  
Parametric analysis, penalty-effectiveness tradeoff and system selection for communications satellites, using block digital computer synthesis with subroutines for operational requirements [AIAA PAPER 66-330] 12 p1824 A66-24797  
International Telecommunications Satellite /INTELSAT/ Consortium and COMSAT participation in program [AIAA PAPER 66-332] 12 p1982 A66-24799  
Antenna drive with feedback control system for radio telescope, noting design, construction and operation 13 p2038 A66-25640  
Lower ionosphere guidance of HF and VHF waves for global communications, outlining computer simulation of phenomenon of whispering galleries 13 p2023 A66-25780  
Design and principles of operation of Relay, Teistar, Syncom, Early Bird and project ATC communications satellites 13 p2193 A66-25858  
Development of satellite communication systems, discussing tentative launching schedule through 1969 14 p2243 A66-28361  
Military communications satellite



developments, describing worldwide network of ground stations and 15 to 22 satellites in near-synchronous equatorial orbit 14 p2243 A66-28362

Synchronous orbit tracking and communication satellite using electronically steered antenna, tracking interferometers and low-powered solid state transmitter-receiver components 14 p2244 A66-28405

Navigation satellites as monitoring device by integrating navigational hardware into communications satellite for 16 p2743 A66-30667

ATC 16 p2743 A66-30667

Book on communications satellites design, testing, operation and power systems for Echo, Telstar, Relay, Syncom, ground stations, etc 16 p2809 A66-30877

Unclassified information concerning military communication satellite system 16 p2655 A66-31650

Graphical method extended to problems of interference between terrestrial line-of-sight radio relay systems and communication satellite systems 17 p2871 A66-31816

Communication satellite design noting use for educational and commercial purposes, instrumentation applied, etc 17 p2872 A66-31935

Phased array antenna system for multidirectional transmission and reception of focused beams with high gain 17 p2872 A66-31936

Time-dependent coverage area design parameter for Comsat systems in elliptical orbits, assuming spherical Earth and Keplerian orbits 17 p3002 A66-32472

U.S. progress in space applications program including communications, geodesy, meteorology and navigation 17 p3040 A66-32692

Optimization of radiation characteristics of satellite mounted antennas 17 p2894 A66-32990

Satellite broadcasting system for TV, international shortwave and high fidelity FM communication 18 p3066 A66-33783

Satellite orbiting via radio command guidance, discussing results with communications and weather satellites, guidance system used, control methods, etc 18 p3131 A66-33848

Mounting problem for land-borne and ship-borne antennas for tracking synchronous, subsynchronous and other communications satellites 18 p3070 A66-34263

Multiple-element steerable Earth-station antenna for communicating with communications satellite 18 p3080 A66-34264

Vertically-fed steerable parabolic reflector system for communications satellite Earth station 18 p3081 A66-34271

System consisting of communications satellites distributed in nonsynchronous orbits and set of ground stations, formulating link scheduling problem as optimum control 19 p3303 A66-35884

French booster projects for orbiting stationary communication satellites, noting SEREB/solid propellant/ and LRBA/liquid propellant/ 19 p3469 A66-36047

Commercial space communication and growth of regional-national organizations 19 p3481 A66-36205

COMSAT and commercial era in space 19 p3482 A66-36210

Objections of Soviet bloc to COMSATCO 19 p3485 A66-36229

Determination method for acquisition time, azimuth of satellite and duration of contact between tracking stations and satellites in general elliptic orbits 19 p3305 A66-36619

Multiple-access systems and characteristics in communications satellite applications, specifically frequency-division multiplex and spread-spectrum modes 20 p3511 A66-36897

Japanese ground antennas for use with communications satellites Telstar, Relay and Syncom 20 p3530 A66-37718

Guidance equations for positioning spin stabilized communications satellite in circular orbit, noting velocity adjustments, using Monte Carlo simulation 21 p3764 A66-38864

Electronic navigation system for marine applications, using communications satellite as data relay link 22 p3945 A66-40324

Long distance communications satellite, considering effect on traditional methods

and organization of global communication system 22 p3867 A66-40699

Comsat Operations Center for support of International Telecommunications Satellites 22 p3867 A66-40710

Coverage and overlap of communications satellites in circular equatorial orbits for multiple-access intercommunication 22 p3870 A66-40964

Electronically despun antenna and electronically controlled phase shifters to increase transmitter output power for spin-stabilized communication satellites 23 p4036 A66-41142

Time varying adaptive filter structure for providing minimum mean square estimate of signal in nonstationary channels for communications satellites 23 p4039 A66-41590

Electromagnetic compatibility of communications satellites, tropospheric scatter and line-of-sight microwave systems operating in same frequency band 23 p4040 A66-41597

Multiple large signal theory for TWT amplifiers with restrictive assumptions 24 p4183 A66-42635

**COMMUTATION**

Commutation relations obtained from commutation operator applied to potential and field intensity 21 p3732 A66-38662

**COMMUTATOR**

SA DECOMMUTATOR

Electronically switched DC motor commutated by light beam directed onto photodiodes 11 p1640 A66-23167

Thyristors for forced-commutated static converter, noting turn-on and turn-off behavior 13 p2029 A66-25115

Configuration-space photon number operators in quantum optics, discussing photoelectric measurements of field, photon localization in space-time regions, commutator formalisms, etc 15 p2543 A66-28942

Flexible commutation system for routing numerous signal-carrying leads to centrally located multiplexer for Saturn 16 p2649 A66-30540

Differential low level junction field effect transistor commutators performance and characteristics for design considerations 19 p3317 A66-35702

High-power nanosecond commutator for control of spark chambers, laser shutters, etc 22 p3933 A66-40945

**COMPARATOR**

Calibration procedures and statistical analysis for error reduction in ballistic camera lead-screw type comparator 02 p0228 A66-11380

Fast analog comparator for hybrid computation using wideband DC amplifier with regenerative feedback circuit providing digital output 03 p0337 A66-12573

Design and performance of two multirange current transformers for audio frequencies operating 400 hz to 10 khz with minimum error 07 p1004 A66-17215

Nonlinear signal comparators in feedback structures used for input-output invariance of single piecewise constant parameter 13 p2054 A66-26090

Basic circuit, sensitivity and mode of operation of balanced magnetic core comparator 24 p4187 A66-43179

**COMPASS**

SA GYROCOMPASS

SA MAGNETIC COMPASS

SA SOLAR COMPASS

Checking and calibration of aircraft compasses, discussing compass base at Dublin Airport and effect of lightning strikes 07 p1032 A66-17675

Controlled direct current applied to flux valve to stimulate rotation of aircraft in compass swing 07 p1033 A66-17723

Controlled direct current applied to flux valve to stimulate rotation of aircraft in compass swing 13 p2079 A66-25866

Compass system on VC10 provides magnetic heading reference, or alternately, inertial reference for grid navigation 13 p2125 A66-26283

**COMPENSATION**

SA TEMPERATURE COMPENSATION

Digital electrometric device with automatic discrete compensation 05 p0680 A66-15211

Compensation and decompensation in

ferromagnetic alloys viewed as electrical interaction of spins 12 p1930 A66-2468

**COMPENSATOR**

Three quarter-wave compensating method for measuring phase difference in visual spectral region 01 p0066 A66-10219

**COMPENSATORY TRACKING**

Manual closed-loop control systems analysis, discussing operator dynamics for permanent procedural variables 12 p1855 A66-2464

Visual and tactile display for compensator tracking, noting conditions for minimum error, mean square error, etc 16 p2644 A66-3127

Psychophysiological study of compensator tracking on digital altimeter display and of combined digital and scale-and-pointer display 17 p2869 A66-3344

**COMPILER PROGRAM**

SA BLOCK DIAGRAM COMPILER /BLODIB/

Universal programming languages and processors, survey and new concepts 12 p1826 A66-2382

New block diagram compiler for sampled data system simulation 12 p1826 A66-2382

Digital computer simulation of sampled data communication system using Block Diagram Compiler, B 13 p2028 A66-2593

Human factor aspects of digital computer programming for simulator control, discussing application and operation 17 p2869 A66-3344

**COMPLEX**

S LAUNCH COMPLEX

**COMPLEX VARIABLE**

SA ANALYTIC FUNCTION

SA MAXIMUM PRINCIPLE

SA RIEMANN SURFACE

Inverse problem of Khavinson and Khavinson approximated for complex plane sets 02 p0250 A66-1209

Heat transfer by laminar forced convection for dissipative fluid in annulus calculated using complex variable method 04 p0598 A66-1421

Resolution of two fundamental problems of elastostatic plane into complex variable under conditions of analytical limits 05 p0775 A66-1509

Complex variable functions, discussing boundary properties for holomorphic continuous unit disk with constant absolute value on boundary 06 p0901 A66-1600

Theorem on quotients of complex-valued almost periodic functions of one real variable containing Bohr theorem 06 p0904 A66-1704

Complete solution of problem of branching of solution of nonlinear equation in multidimensional case 07 p1056 A66-1760

Estimates of Taylor coefficients in theory of regular function of several complex variables 07 p1056 A66-1760

Perturbation method in theory of dynamic stability of systems with distributed parameters, discussing linear Hamiltonian equation in separable Hilbert space 07 p1056 A66-1760

Resolving matrix of normal system of ordinary linear differential equations in complex independent variable for multiply connected fields 07 p1057 A66-1783

Boundaries of convexity of star-shaped functions, order alpha, in open circular region /0, 1/ 07 p1059 A66-1809

Three-dimensional problem of isotropic continuous nonaxisymmetrical body of revolution, applying analytic functions of complex variable 08 p1307 A66-1888

Position of singularities of analytic continuation of potential /geophysical/ fields 09 p1373 A66-20480

Deflection of thin circular plate under eccentric loading using complex variables, obtaining expressions in series form 09 p1467 A66-20581

Potential analog synthesis of linear arrays and radiation pattern representation as function of single complex variable 09 p1356 A66-20605

Heuristical method solving zeros of complex function, transcendental or algebraic, of complex variable, applicable to computation of eigenvalues of general matrix 10 p1548 A66-21214



- Markov direct and inverse problems involving complex value functions on bicomact Hausdorff space and polynomials, with coefficients satisfying linearly independent constraints 10 p1549 A66-21235
- Stress concentration at semicircular notch in semiinfinite plate calculated by Savin complex-variable method 10 p1616 A66-21494
- Cauchy type integral on hypersphere, defining Cauchy principal values, noting role in theory of functions of complex variables 11 p1724 A66-23366
- Mathematical analysis of analogies between theory of heat conduction and theory of functions of complex variable 12 p1977 A66-23562
- Weak, strict and strict-weak Levi conditions defined in complex variables, noting conditions for holomorphy and coincidence of functions 13 p2118 A66-25787
- Dirichlet problem deviation from Bitsadze system with Noetherian properties, giving Hausdorff normal solvability conditions for inhomogeneous problem 13 p2120 A66-26009
- Distribution of complex eigenvalues of three-dimensional Schroedinger equation, showing location of poles of scattering matrix and role of wave function 13 p2026 A66-26249
- Locating zeros of complex functions by computing topological index 13 p2121 A66-26326
- Series in function of complex variable applied to mixed problem of elastic equilibrium of annulus 15 p2607 A66-28697
- Flexure of thin elastic plate clamped to rigid columns, determining functions of complex variable 15 p2613 A66-29433
- Complex variable theory of flame surface interaction and flow field of two-dimensional V-shaped flame simulated by source and sink sheets 15 p2617 A66-29605
- First-order linear elliptic system with areolar derivatives involving  $n$  unknown complex functions 16 p2738 A66-31706
- Book on jet theory in ideal fluids, covering compressible flow, steady jet flow, infinite flow past polygonal obstacle, unsteady flow, etc 16 p2632 A66-31746
- Complex variable method to solve problem of circular elastic plate elastically restrained at edge and subjected to arbitrary concentrated force 17 p3020 A66-32000
- Complex analysis of equilibrium equations in two-dimensional theory of elasticity 17 p3025 A66-32592
- Integral representation providing one-to-one correspondence between functions of  $n$  complex variables and complex-valued harmonic functions of  $n$  plus 1 real variables 18 p3126 A66-33837
- Reduction of plane thermoelastic problem of anisotropic body to determination of three analytical functions of complex variables, solving temperature stress distribution in anisotropic plate 18 p3258 A66-34702
- Position of singularities of analytic continuation of potential /geophysical/ fields 19 p3345 A66-35498
- Markov direct and inverse problems involving complex value functions on bicomact Hausdorff space and polynomials, with coefficients satisfying linearly independent constraints 19 p3389 A66-36182
- Feedback control system behavior, examining influence of values of structural parameters and variations in domain of complex variable 21 p3718 A66-38806
- Distribution of complex eigenvalues of three-dimensional Schroedinger equation, showing location of poles of scattering matrix and role of wave function 22 p3947 A66-39708
- Construction of Cayley-Dickson type and involution type bimodules for composition algebras 22 p3939 A66-40002
- Reciprocal theorems of best approximations of complex variable, considering domain restricted by finite number of smooth curves forming nonzero angles at junction points 23 p4084 A66-41353
- Binary communications integral equations in complex variable functions and application of Fourier transform for bandlimited signals 23 p4085 A66-41537
- Digital computer program for handling algebraic expressions in complex numbers 23 p4042 A66-41739
- Reinforced semiinfinite under concentrated loads, noting flange stress magnitude and distribution 24 p4285 A66-42144
- ### COMPONENT
- #### S SPACECRAFT COMPONENT
- #### COMPONENT RELIABILITY
- System reliability prediction limited when it does not take into account out-of-tolerance operation due to component variation with environmental changes, electric stresses and aging 01 p0167 A66-10055
- Predicted vs observed avionics reliability in design technique, using factual reliability data of baseline equipment and solid state component advances 01 p0035 A66-10080
- DC-9 reliability program emphasizing simplicity improved proven components rather than completely new equipment 01 p0010 A66-10088
- Reliability and reproducibility of SIL-TEMP 84 fabric used as reinforced filler in ablative components and high temperature insulating material in rockets and missiles 01 p0089 A66-10089
- Machining processes effect on reliability of engine components and methods for detecting failure and failure susceptibility 01 p0077 A66-10104
- Reliability and design factors for space power conditioning equipment examining peak power, component part specifications, integrated circuits and failure analysis 02 p0180 A66-11283
- Worst case design for high reliability welded electrical connections, emphasizing encapsulation stresses and quantitative parameter 02 p0234 A66-11325
- Miniaturization in improving weapon system component availability, transportability and reliability 02 p0198 A66-11464
- Avionic equipment reliability improvement through highly reliable components, noting Minuteman 03 p0343 A66-12903
- Noise characteristics of semiconductor devices turned to advantage by using noise measurements for reliability analysis, noting noise types and transistor irregularities effect on noise 03 p0345 A66-13217
- Statistical base for intuitive reliance on validity of conventional component qualification testing 04 p0528 A66-14447
- Reliability of complicated systems based on rarity of component failures 05 p0688 A66-15367
- Nonhazardous and nondestructive method for testing pressure regulating valves, using simulated gas flow and pressure [ASME PAPER 65-WA/AUT-7] 05 p0661 A66-15707
- Degradation analysis for selection of components for space application 05 p0650 A66-15824
- Parts reliability in USAF and Department of Defense specifications 05 p0691 A66-15829
- Spacecraft microelectronic device failure modes and mechanisms 05 p0650 A66-15830
- NASA procurement technique including incentive contracting, improved performance, timely delivery and reduced cost 05 p0795 A66-15831
- Reliability, life and relevance of circuit design in electromechanical switching devices 06 p0839 A66-15946
- Environmental conditions and circuit design effect on various types of resistors, examining quality of manufacture and economics of reliability 06 p0839 A66-15947
- Prediction and engineering assessment in early design, particularly mean time between failures of electronic equipment 06 p0839 A66-15948
- Reliability of electronic systems, discussing redundant systems, series and parallel grouping and exponential survival law 06 p0839 A66-15950
- Capacitor reliability as function of voltage and temperature of dielectric and environmental conditions 06 p0839 A66-15951
- Reliability of electronic equipment needed to increase availability and reduce maintenance cost 06 p0840 A66-15953
- Bibliography on semiconductor reliability classified under applications /computers, radio, spacecraft, etc/, costs, devices, environments, networks, production, etc 06 p0848 A66-16308
- Principles and statistics behind life-test plans of MIL-STD-690 Life Test Sampling Procedures for Established Levels of Reliability and Confidence in Electronic Parts Specifications 06 p0886 A66-16332
- Lifetime of semiconductor devices determined from noise levels 06 p0860 A66-17195
- Beach and ratchet marks plus component geometry information and stresses to pinpoint fatigue failure in service 08 p1306 A66-18634
- Space radiation environment and guidelines for designing satellite electronic equipment for reliable operation in space 08 p1301 A66-18731
- System reliability by analyzing reliability of components in connection with operation of logic structures 08 p1187 A66-19447
- Radiation effects on electronic components noting sensitivity to gamma, fast neutron and electron radiation 09 p1359 A66-20969
- Component tolerance and measuring error effects on noise measurements 11 p1652 A66-22384
- Dimensionality theory for determining failure rate of aircraft components not in operation 11 p1637 A66-22862
- Trigger functioning, failure due to grid voltage and transistor parameter changes, and reliability parameters of computer and control elements 11 p1677 A66-23032
- Engineering problems in SNAP reactor component irradiation program, including material compatibility, vacuum equipment selection and operation and contaminants within chamber 12 p1857 A66-23674
- SNAP-10A instrumentation and control subsystems and ground test program 12 p1911 A66-23676
- Long-term storage effects on reliability of electronic equipment, covering testing results and available data on failure rates 12 p1830 A66-23755
- Reliability, life and relevance of circuit design in electromechanical switching devices 12 p1831 A66-23791
- Reliability of electronic systems, discussing redundant systems, series and parallel grouping and exponential survival law 12 p1831 A66-23792
- Electronic equipment failures, which show characteristic dependence on time, divided into initial, chance and wear-out failures 12 p1832 A66-24074
- Inherent reliability of equipment estimated during design stage, using component failure data 12 p1833 A66-24075
- Truncation method for determining life characteristics of electronic components such as transistors and vacuum tubes before testing to destruction 12 p1833 A66-24078
- Tabulated reliability data on communications systems components for possible application to other fields 12 p1833 A66-24080
- Component failure-rate testing by inspection or sampling, noting recommendations of advisory groups 12 p1833 A66-24081
- Component reliability, especially in transistors, noting techniques, design, tests and mounting as monolithic circuits 12 p1833 A66-24082
- Defense equipment reliability noting specifications, field data collection, control plan, etc 12 p1833 A66-24083
- Queuing model digital simulation techniques used to determine reliability of stand-by system with maintenance station 12 p1834 A66-24085
- Accelerated life tests of germanium transistors, with failure percentage plotted against time 12 p1834 A66-24086
- Microwave component testing accuracy and analysis of error sources 12 p1833 A66-24725
- Accelerated testing of transistors, resistors and capacitors to determine reason for certain types of component failure 12 p1844 A66-24728
- Design, efficiency and reliability of electric power system related to mission and orbit of communications satellites [AIAA PAPER 66-299] 12 p1804 A66-24766
- Standard redundancy techniques for determining reliability of series elements



and interchangeable stand-by components in digital circuits 12 p1888 A66-24821

Defect analysis by device sectioning, noting techniques, application in crystallography, electronics, etc 12 p1845 A66-24849

Reliability testing of electronic components at low stress levels, showing higher failure rates and different failure distributions than at maximum ratings 12 p1846 A66-24911

Properly controlled high-stress life testing used to evaluate failure rate of high reliability solid state components of integrated circuits 12 p1846 A66-24913

Sterilization requirements of spacecraft electronic systems and relation to equipment reliability 13 p2013 A66-25269

Reliability, durability and reduction of failure probability in radioisotope energy source design 13 p2085 A66-25285

Optimum nonlinear inertialess conversion of signals from several devices, taking into account unreliability in operation 13 p2045 A66-25296

Reliability of nonelectronic components in electronic system, noting failure modes, rates, mechanism, etc 13 p2085 A66-25655

Test system design, discussing operative systems and equipment for Sea Vixen radar and Seaslug Mark I missile 13 p2058 A66-25698

Component failure examples of Gemini rendezvous radar, emphasizing need for closed loop reliability program 13 p2039 A66-25786

Military and spacecraft electronic component testing, specifications and reliability programs 13 p2086 A66-25846

Extrapolating reliability ratings of electronic components and materials tested at high stress to low stress performance 13 p2043 A66-26220

Reliability testing of aircraft engine components 13 p2088 A66-26689

Reliability problems associated with producing to specification from viewpoint of aircraft manufacturer 13 p2088 A66-26693

Causes of failure and guidelines for design of solid state lasers 14 p2309 A66-27669

Component testing and system reliability at various confidence limits for serially connected systems 14 p2305 A66-28428

Structural component reliability analysis for rocket engine propellant tanks, noting variance testing of hemisphere strength for statistical tolerance limits 15 p2507 A66-28795

Component and pyrotechnic production sampling applied to reentry vehicle program, noting technique for selecting size, frequency and quantity of components for testing 15 p2507 A66-28798

Effect of limited quantity and short delivery requirement orders for electronic components in reliability and quality control 15 p2508 A66-28803

Military relay reliability, design factors, manufacturing control, etc 15 p2460 A66-28990

Electronic component reliability and control program 15 p2465 A66-29667

Silicon planar transistor design noting accelerated life test, failure data, etc 15 p2466 A66-29675

Tolerance range of multicomponent circuit calculated from tolerance limit of individual component 15 p2474 A66-29766

Creep fatigue, thermal cycling, vibration control, transient thermal response control, structural loads and hot part reliability relating to long-life jet engine failure [SAE PAPER 660311] 15 p2572 A66-29836

Instability of current distribution related to problem of reliability in transistor electronics 15 p2468 A66-29915

Hostile long term storage environments, discussing aircraft component condition following extensive exposure 16 p2635 A66-30472

Reliability of finite automata determined from analysis of elements capable of misalignment, input errors and structural design 16 p2669 A66-30761

Tolerance limits for structural components in power-filter circuit design, calculating fluctuations of damping property and phase fluctuations in multiply divided circuits 16 p2663 A66-31031

Airborne performance analysis by multiparameter sampling applied to aircraft

maintenance and benefits including prediction of impending malfunctions 17 p2842 A66-31959

Peak power stresses in semiconductor device testing for space power equipment, using photo methods 17 p2880 A66-31984

Step-stress technique to induce failures in integrated circuits to pinpoint source of reliability problems 17 p2882 A66-32114

Accuracy analysis method for radioelectronic circuits, noting statistical-test method 17 p2897 A66-33517

Reliability of complex electronic device incorporating great number of components 18 p3087 A66-34957

Lifetime of semiconductor devices determined from noise levels 19 p3315 A66-35553

Ion engine satellite control system noting design and laboratory tests [AIAA PAPER 65-417] 19 p3450 A66-35616

Component reliability and failure rates in aerospace electric power systems with relays 20 p3525 A66-37180

System effectiveness, Volume 5 - Reliability and Maintainability Conference, New York, July 1966 20 p3563 A66-37879

Contractor components/parts reliability program for Douglas S-IVB stage project 20 p3566 A66-37880

Deterministic and quasi-deterministic class of electronic failure predictions as prevention strategy for use in aerospace system test or checkout program 20 p3566 A66-37887

Materials problems affecting system effectiveness, reliability and maintainability in aerospace industry 20 p3567 A66-37896

Performance degradation and system failures in metal-metal, metal-oxide and metal-semiconductor systems 20 p3532 A66-37900

Economics of Ownership structure and cost effectiveness in microelectronic systems 20 p3684 A66-37904

Ultrahigh reliability medium-power lightweight TWT design 20 p3532 A66-37906

Identifying critical elements /parts and components/ as criteria for system design tradeoff at system and circuit levels 20 p3568 A66-37916

Reliability program, determining assurance and stabilization trend by analysis of lots applied to testing high reliability parts for Saturn V inertial guidance system 20 p3570 A66-37934

Electronic data processing used to analyze AFM 66-1 maintenance data on USAF T-38 supersonic jet trainer for reliability monitoring 20 p3572 A66-37945

Information center concept for accurate acquisition and processing of parts, materials and components reliability and maintainability information for task performance 20 p3572 A66-37947

Solderability test procedure for predicting solder joint reliability 20 p3572 A66-37948

Systems tests coverage for data processing system 20 p3523 A66-37950

Saturn S-II stage project uses ground testing of flight vehicle to achieve high statistical confidence in high reliability 20 p3572 A66-37951

Bounds on reliability, life distributions and open problems for structures 20 p3574 A66-37964

Lunar Excursion Module /LEM/ reliability program, discussing engineering, manufacturing and techniques of design and qualification testing of electronic components 21 p3714 A66-39520

Component characteristics in integrated circuits 21 p3716 A66-39621

FR-1 satellite component reliability program 22 p3876 A66-40159

Man-machine merger in computer aided design of circuits, examining changes in circuit parameters caused by component tolerances, simulation of component failure, feasibility and circuit optimization 23 p4072 A66-41252

Electronic component reliability test program review including test planning, objectives and relation of types of review to projects 23 p4152 A66-41605

Mariner 1964 parts screening program including philosophy, program implementation, screening results and

conclusions 24 p4178 A66-42081

Apollo spacecraft parts screening program showing dependence on reliability for mission success 24 p4216 A66-42099

Reliability prediction, failure rates, failure safe design and packaging of integrated circuit and MOS-FET microminiaturized electronic equipment 24 p4179 A66-42099

Parts sterilization at Jet Propulsion Laboratory 24 p4180 A66-42299

### COMPOSITE FUNCTION

Composite state vector method for linear time-varying system 05 p0655 A66-14611

Monograph on continuous maximum principle covering design and control of industrial and process engineering systems: dynamic programming, process optimization, etc 12 p1901 A66-23533

Construction of Cayley-Dickson type an involution type bimodules for composition algebras 22 p3939 A66-40001

### COMPOSITE MATERIAL

#### SA CERMET

Thermochemical interaction between ablation material and environment during manned reentry, using mainly graphite and composite materials [AIAA PAPER 65-642] 01 p0160 A66-10222

Structural composite materials component development program emphasizing design and fabrication [AIAA PAPER 65-760] 03 p0386 A66-13053

Use of monofilament composites of S-glass fibers and epoxy-resin in primary aircraft structure [AIAA PAPER 65-761] 05 p0772 A66-14722

#### Fiber composite materials - ASM Seminar

Metals Park, Ohio, October 1964 05 p0700 A66-14801

Origin and properties of fiber composite materials 05 p0705 A66-14801

Strength of whiskers in fiber composite materials 05 p0705 A66-14801

Influence of fiber and matrix characteristics on mechanics of deformation and fracture of fibrous composite 05 p0773 A66-14811

Unidirectional solidified eutectic alloys as reinforced composites 05 p0700 A66-14811

Macromechanics of stress state at interface of composite material 05 p0700 A66-14811

Strength of fiber reinforced metals: examining fracture mode 05 p0700 A66-14811

Elastic modulus and ultimate tensile strength of fibers and fiber composites 05 p0705 A66-14811

Destructive and nondestructive testing of fiber composite materials 05 p0773 A66-14811

Strengthening metals by using oxide fibers as reinforcements 05 p0700 A66-14811

Metal fiber reinforced ceramics 05 p0705 A66-14811

Structural mechanics and critical conditions of fiber composite materials 05 p0773 A66-14901

High energy protons in synchrocyclotron testing of polyethylene, aluminum, lead and titanium hydride 05 p0627 A66-15111

Stress-strain behavior of tungsten fiber reinforced copper composites, discussing room-temperature tensile and dynamic modulus tests 05 p0702 A66-15321

Electron and ion emission of material in presence of cesium vapor, noting use as emitters 05 p0622 A66-15571

Fracturing model of surface-hardened materials with triaxial stress at subsurface interface from loading [ASME PAPER 65-MET-2] 06 p0961 A66-16204

Materials and fabrication techniques for ablative hardware composite materials engineering 06 p0899 A66-16286

Optimum reinforced composite strength of glass-reinforced plastics depends on filament geometry factors such as filament content, orientation and dimensions [AIAA PAPER 66-142] 06 p0901 A66-17081

Composite materials manufacture and application to high temperatures, with evaluation of various binders and filaments 06 p0898 A66-17110

Survey of composite materials and structures 07 p1053 A66-17846

Composite ceramic systems consisting of metallic or organic phase and ceramic phases, microstructure, mechanical strength



and thermal expansion 07 p1051 A66-18299  
 Validity of three-dimensional photoelastic analysis of composite models of dissimilar materials in nonhomogeneous elastic field problems 08 p1310 A66-19225  
 Tensile properties of composites of tungsten or molybdenum wire uniaxially aligned in copper matrix 09 p1393 A66-20661  
 Strength of structural composites of orthotropic materials with arbitrary thickness and orientation including lamination and anisotropy effects [AIAA PAPER 65-75] 10 p1617 A66-21781  
 Model approximation method for induced elastic and thermal characteristics of materials reinforced by circular cylindrical fibers 11 p1720 A66-22231  
 Sintered W and W plus additive billets used to test feasibility of producing fiber-bearing composites by elongation during extrusion 11 p1715 A66-22537  
 Glass-resin interaction of filament-wound composites, determining material properties and application to high performance pressure vessels 11 p1783 A66-23121  
 Improvement of mechanical properties of structural adhesives and composite materials at cryogenic temperatures 12 p1899 A66-24385  
 Surface area, complexes and water effect on properties of carbon fiber resin composites 13 p2111 A66-25166  
 Naval Ordnance Laboratory /NOL/ multiaxial fatigue test for failure mechanisms in fiber-reinforced composite materials involving cyclic stress under controlled environmental conditions 13 p2113 A66-25312  
 Composite casting as metallurgical bonding technique, noting application to weight reduction and increase of corrosion resistance 13 p2086 A66-25779  
 Composite materials, noting fibrous composites using whiskers, fabrication including spray-up, filament winding, etc, mechanical properties, application for rocket nozzles, heat shields, etc 14 p2318 A66-27228  
 Spacecraft metal-metal composites consisting of continuous filaments in metal matrix 14 p2317 A66-28013  
 Graphite composites suitability for use on hypersonic entry vehicle components 14 p2319 A66-28014  
 Lightweight packageable structurable materials capable of expansion, erection and rigidization in space 14 p2317 A66-28016  
 Microquenched age-formed titanium alloys and titanium Bi-alloy composites, discussing production process using spherical particles produced by rotating electrode [SAE PAPER 660458] 17 p2940 A66-33164  
 Elastic and plastic properties of fiber-reinforced and continuous skeleton tungsten-copper composite materials 17 p2941 A66-33425  
 Nozzle cooling and infiltrant loss from infiltrated refractory metal composites at high gas propellant temperature 19 p3385 A66-36157  
 Aluminum-ductile binder composite alloys containing high volume of nickel-aluminum compounds and CoAl prepared by powder blending and hot extrusion 20 p3585 A66-37783  
 Whisker composite materials, discussing potential of whiskers, utilization of whisker strength, whisker growth, handling whiskers and composite properties 20 p3588 A66-38183  
 Factors affecting strength of whisker reinforced metals, noting characteristics [ASME PAPER 66-MD-81] 21 p3750 A66-38504  
 Mechanical properties of metallic and ceramic fibers in metallic matrices and refractory fibers in ceramic matrices 21 p3751 A66-39231  
 Bonding of similar and dissimilar alloys by composite casting for aerospace use 22 p3926 A66-40273  
 Approximation of elastic constants of unidirectional fiber reinforced composite material from constituent material properties, including longitudinal modulus, transverse modulus and Poisson ratio 22 p3993 A66-40342  
 Composite thermal coating consisting of refractory facing and slightly heat-conducting decomposing

lining 22 p4000 A66-40818  
 Structural composite materials component development program emphasizing design and fabrication [AIAA PAPER 65-760] 23 p4083 A66-40978  
 Use of monofilament composites of S-glass fibers and epoxy-resin in primary aircraft structure [AIAA PAPER 65-761] 23 p4083 A66-40979  
 Fatigue behavior of aluminum reinforced with stainless steel wires, considering effects of fiber volume fraction and interfacial bond 23 p4081 A66-41661  
 Aluminum and titanium alloys, composite materials and nonmetallic materials for supersonic transports and VTOL aircraft noting intakes, nozzles and variable-geometry wings [ICAS PAPER 66-1] 23 p4016 A66-41932  
 Fiber geometry effect on shear stress distribution in composite materials 24 p4292 A66-42861  
**COMPOSITE PROPELLANT**  
**SA BI-PROPELLANT**  
 Manufacturing large production quantities of precise solid propellant mixtures to meet space booster propulsion system [SAE PAPER 650766] 05 p0743 A66-15005  
 Temperature at which predecomposition or decomposition of ammonium perchlorate occurs, changed by perchlorate surface treatment and reflected in burning rate of propellant containing perchlorate [CI PAPER WSCI-65-36] 05 p0744 A66-15151  
 Theoretical detonation characteristics of ammonium perchlorate-polyurethane solid composite propellants 05 p0744 A66-15781  
 Physical model of composite solid propellant combustion which includes oxidizer particle size and surface heat generation [AIAA PAPER 66-112] 06 p0941 A66-17098  
 Ignition of ammonium perchlorate composite propellants by convective heating [AIAA PAPER 66-65] 06 p0941 A66-17101  
 Nonacoustic combustion instability of aluminized composite propellant [AIAA PAPER 66-111] 06 p0941 A66-17105  
 Solid, heterogeneous and gas phase ignition theories of solid propellants [AIAA PAPER 66-64] 08 p1280 A66-19728  
 Prediction of thermal conductivity of binary mixture of solids, particularly solid propellants utilizing metallic filaments 10 p1590 A66-21957  
 Plane shock wave compressions of cylindrical and wedge-shaped specimens used to obtain shock Hugoniot of two unreacted, composite and double-base aluminized propellants 12 p1934 A66-23589  
 Combustion of ammonium perchlorate propellants in solid propellant rockets 12 p1978 A66-23965  
 Bonding strength of polyurethane and polybutadiene composite propellants in cast-in-case rocket motors depends on propellant cohesive strength 12 p1934 A66-24706  
 Combustion of composite ammonium perchlorate based propellants near extinction pressure, noting burning rate parameters 13 p2171 A66-25181  
 Strain rate and pressure effects on tensile behavior of viscoelastic composite solid propellant 13 p2171 A66-26116  
 High speed testing to determine viscoelastic properties of composite propellant polymers, for use in solid propellant rockets 13 p2115 A66-26119  
 Periodic processes in combustion mechanism of composite propellants 14 p2412 A66-27489  
 Laboratory burners used as experimental analogs of actual propellant deflagration process, examining dependence of composite solid propellant deflagration on mixture ratio [WSCI 66-25] 18 p3161 A66-34417  
 Solid, heterogeneous and gas phase ignition theories of solid propellants [AIAA PAPER 66-64] 18 p3162 A66-34580  
 Microwave attenuation magnitude associated with exhaust plasma of nonaluminized and aluminized composite propellant 21 p3807 A66-38687  
 Ignition of ammonium perchlorate composite propellants by convective heating [AIAA PAPER 66-65] 21 p3806 A66-38689  
 Continuous pneumatic mixing of liquid and

solid propellant ingredients into composite type propellant 22 p3968 A66-39669  
 Castable composite high energy propellants manufacturing techniques, discussing economy based on batch mixing and continuous processing 22 p3969 A66-39870  
 Nonacoustic combustion instability of aluminized composite propellant [AIAA PAPER 66-111] 22 p3970 A66-40355  
 Physical model of composite solid propellant combustion which includes oxidizer particle size and surface heat generation [AIAA PAPER 66-112] 22 p3970 A66-40356  
 Direct-casting polyurethane-ammonium perchlorate-based composite propellant grain manufacture for small rocket motor, noting inspection methods 23 p4119 A66-41432  
 Erosive burning in rocket engines of radial burning type, using polyurethane/ammonium perchlorate base propellant / grains, examining flow channel constriction 23 p4121 A66-41433  
 Combustion mechanism of composite propellants including solid propellant combustion rate measurements, flames spectrography, temperature at propellant surface, etc 23 p4122 A66-41660  
**COMPOSITE STRUCTURE**  
 Optimization of viscoelastic damping materials for use in specific composite systems of metal skins and damping viscoelastic layers 01 p0150 A66-10151  
 Macromechanisms of composite structure damping, using viscoelastic materials as in extensional and shear deformation 05 p0772 A66-14552  
 Deleterious effect of heterogeneity on stability of composite cylindrical shells under axial compression [AIAA PAPER 66-140] 06 p0968 A66-17083  
 Compression instability of unidirectional composites consisting of regularly spaced arrays of axially loaded columns supported by elastic filler [AIAA PAPER 66-143] 08 p1309 A66-19005  
 Griffon 02 delta-winged aircraft with composite air breathing turbofanjet engine, noting achievements and prospects 11 p1761 A66-23248  
 Design of composite structures of minimum weight, using flat-bottomed cylindrical tank, noting continuity condition of radial bending moment of plate and shell 14 p2395 A66-27174  
 Stresses in composite spheroids of two different isotropic elastic materials under compressive forces acting along common axis of revolution 14 p2397 A66-27391  
 Stresses and strains in anisotropic multilayered thick walled circular cylinder subjected to radial pressure [AIAA PAPER 65-174] 14 p2402 A66-27869  
 Modes and frequencies of transverse vibrations of composite beams 15 p2610 A66-29339  
 Heterogeneity effect on multilayer composite cylindrical shell stability under axial compression 17 p3025 A66-32454  
 Tungsten and tungsten composite fabrication by gas-pressure-bonding process 19 p3368 A66-36123  
 Composite structures of glass-fiber reinforced resin and other materials for launch shell structures [AIAA PAPER 65-286] 20 p3672 A66-38165  
 Adhesively joined beryllium structures for extreme temperature application, noting properties in various conditions 22 p3926 A66-40277  
 Fiber composites construction from infiltrated powder compacts 23 p4080 A66-41068  
**COMPOSITION**  
**S ATMOSPHERIC COMPOSITION**  
**S CHEMICAL COMPOSITION**  
**S GAS COMPOSITION**  
**S IONOSPHERIC COMPOSITION**  
**S LUNAR COMPOSITION**  
**S METEORITIC COMPOSITION**  
**S PLASMA COMPOSITION**  
**S WATER CONTENT**  
**COMPOUND**  
**S CHEMICAL COMPOUND**  
**S INORGANIC COMPOUND**  
**S PLATINUM COMPOUND**  
**S RUBIDIUM COMPOUND**



## COMPRESSIBILITY

Compressibility charts for nonpolar and slightly polar substances in gaseous and liquid states and in two-phase region, using four independent parameters  
[ASME PAPER 65-WA/PID-1]

Two-fluid anisotropic warm plasma, characterizing macroscopic electromagnetic properties via compressivity and permittivity tensor and permeability

Governing equations for electromagnetic phenomena in lossy magnetoionic media in terms of compressivity tensor, deriving wave equations which are decoupled, giving resulting uncoupled differential equations

Compressibility law corresponding to Tomotika and Tamada generalized approximation for transonic flow, noting Tomotika and Tamada gas

Compressibility factor chart for hydrocarbon-hydrogen and nitrogen-hydrogen gas mixtures, correlating pressure and temperature, using state equation

Energy equation of boundary layer in heat-insulating part of flat wall used to derive equations for gas heat shield efficiency, demonstrating effect of nonisothermicity and compressibility

## COMPRESSIBILITY EFFECT

Velocity distribution in turbine stage with compressible medium for repeating axial velocity profile derived, employing approximation method

Compressibility effect on velocity distribution and gradient at stagnation point in plane subsonic jet incident at arbitrary angle on infinite plate

Electromagnetic problems in anisotropic and compressible plasma solved by characterizing compressibility as compressivity tensor

Externally pressurized foil gas bearings, employing successive approximations method to solve Reynolds equation for fluid and equilibrium equation for foil

Slip and compressibility effect on velocity and pressure drop characteristics of rarefied gas flows in rectangular and annular ducts

One-dimensional heat flow to cool wall, discussing effects of compressibility and variable thermal conductivity

Relation of compressibility with cohesive energy and molecular volume for dielectric solids, noting confirmation of relation for 45 crystalline compounds

Pressure dependent critical temperature and magnetic field of superconducting transitions in metals

One-dimensional adiabatic compressible gas flow in cylindrical tube taking into account Reynolds number variations along tube and compressibility effect on friction factor

Compressibility effect on flow in MHD boundary layer of semilinear thermally insulated flat plate

Effect of incompressibility of substance on gravitational instability, deriving dispersion equation and comparing results with problem of incompressible fluids

Transient response of value-controlled actuator with inertial loading to step input excitation, considering fluid compressibility

Linearization of Rayleigh problem for viscous compressible conducting fluid, considering compressibility effects by evaluating solution of pressure equation

Instability due to coupling between compressibility and resistivity in cylindrical plasma with surface currents, noting growth rate near acoustic velocity phase

Apparatus for determining dynamic compressibility, creep behavior and viscoelastic properties of polymers

Stability loss of shells of revolution under effect of axial compression and radial pressure with no restrictions on generatrix curvature, using strain energy method

Velocity distribution of subsonic flow around von Mises profile, noting compressibility corrections

Secondary flow for supersonic boundary layers with or without swept edges, noting effect of compressibility and heat transfer on reverse flow

Compressibility of material in stability problems of elastoplastic plates and shells

Pressure dependent critical temperature and magnetic field of superconducting transitions in metals

Free convection boundary layer along isothermal plate, using equation of laminar compressible flow and heat transfer, noting profile dependency upon wall coordinate

Boundary layer on spherically blunted cones in supersonic air flow at given wall temperature and thermally insulated wall, graphing calculation

Integral method based on method of moments to investigate compressible laminar boundary layers

Quasi-linearization solution of two-component laminar compressible boundary layer with heat transfer on ablating wall

Separation of gas mixture in curved supersonic flow, noting parameters of concentration gradient profile variation

Corresponding compressible and incompressible jets and wakes in boundary layer equations of turbulent and laminar cases

Hydrodynamic theory relating velocity decrement and curvature of gaseous detonation to conditions at explosive inert interface

Similar solution of differential equations for compressible laminar boundary layers in case of insulated walls

Properties of compressible boundary layers with heat transfer and arbitrary pressure gradients calculated, using integral equation and correlation concept for application in hypersonic flows

Analytical methods for studying turbulent boundary layers at high Mach numbers, comparing theory and experiments for flat plate flow, predicting boundary layer properties around hypersonic configurations

Skin friction methods compared for problem of turbulent compressible boundary layer on flat plate at hypersonic Mach numbers

Turbulent boundary layers in compressible and incompressible flow, examining pressure gradients, temperature distribution and heat transfer effects

General theorems for dissociated and chemically reacting compressible laminar unsteady two-component boundary layers derived, based on Nirenberg maximum principle

Similar solutions for compressible boundary layers with heat transfer and blowing or suction

Compressible turbulent boundary layer on flat plate, noting correspondence between compressible and incompressible flow, numerical results on skin friction and heat transfer, etc

Flow of unsteady compressible boundary layer over semilinear flat plate whose temperature exceeds free stream temperature

Unsteady compressible boundary layer equations solved when wall temperature is perturbing about zero and steady mean

Throttle devices to control compressible gas flow, using gas dynamics laws

Configuration synthesis and optimal utilization of supersonic favorable interference to obtain high lift-drag ratios

Particle in cell method for calculation of supersonic wake flow, noting transient effects for flow initiated by shock diffraction

Losses when compressible and constant density fluids flow across abrupt enlargements and contractions

Axisymmetric integral nozzle design with subsonic /contraction/ and supersonic /effuser/ parts for compressible flow

Fluid dynamics - Symposium, Zakopane, Poland, September 1963

Second approximation of compressible subsonic flow over given wing profile reduced to regular Dirichlet problem

Compressible subsonic flow with symmetric Zhukovskii profile calculated by correspondence principle

Laminar boundary layer problems for compressible and incompressible fluids

Velocity profiles in point-to-point mapping of compressible turbulent boundary layers into constant density flows

Quasi-steady compressible fluid flow and thrust analysis in accelerating nozzles and channels subject to constant axial acceleration or gravitation

Friction resistance of compressible turbulent gas flow through initial section of cooled pipe with large gas-wall temperature gradients

Rarefied compressible gas flow analysis by study of collisions between molecules, molecule-surface collisions and distance molecules travel between collisions

Two-dimensional isoenergetic compressible mixing of jet with fluid at rest for laminar and turbulent mixing

Viscosity and thermoconductivity effects on asymptotic sonic flow structure near profiles and bodies of revolution

Compressible laminar boundary layer equations solved, noting wall flow and suction problem

Handbook of generalized gas dynamics including one-dimensional gas dynamics, compressible flow tables, gamma function, isentropic flow, etc

Low Reynolds number flow past sphere for cases involving density and temperature variations, noting compressibility, transport properties and viscous dissipation

Successive approximation method for compressibility in subsonic flow around elliptical cylinder

Mass transfer, friction and heat transfer analyzed and calculated for turbulent boundary layers in compressible flow

Flow of compressible conducting gas around symmetrical wing in longitudinal magnetic field

Book on jet theory in ideal fluids, covering compressible flow, steady jet flow, infinite flow past polygonal obstacle, unsteady flow, etc

Diffusion combustion in turbulent compressible gas flow

Hydraulic analogy to compressible gas flow, discussing application to aerodynamic motions, flow visualization, measuring techniques and instrumentation

Theoretical and physical limitations restricting hydraulic analogy to compressible gas flow

Approximation method for compressible laminar heat transfer to blunt axisymmetric bodies in high speed flow

One-dimensional theory of compound-compressible nozzle flow

[ASME PAPER 65-WA/PTC-1]

[ASME PAPER 65-AV-44]

[ASME PAPER 65-WA/HT-41]

[ASME PAPER 65-WA/PTC-1]

[ASME PAPER 65-WA/PTC-1]

[ASME PAPER 65-WA/PTC-1]

[ASME PAPER 65-WA/PTC-1]

[ASME PAPER 65-WA/PTC-1]

[ASME PAPER 65-WA/PTC-1]

[ASME PAPER 65-WA/PTC-1]

[ASME PAPER 65-WA/PTC-1]

[ASME PAPER 65-WA/PTC-1]

[ASME PAPER 65-WA/PTC-1]

[ASME PAPER 65-WA/PTC-1]

[ASME PAPER 65-WA/PTC-1]

[ASME PAPER 65-WA/PTC-1]

[ASME PAPER 65-WA/PTC-1]

[ASME PAPER 65-WA/PTC-1]

[ASME PAPER 65-WA/PTC-1]

[ASME PAPER 65-WA/PTC-1]

[ASME PAPER 65-WA/PTC-1]

[ASME PAPER 65-WA/PTC-1]

[ASME PAPER 65-WA/PTC-1]

[ASME PAPER 65-WA/PTC-1]

[ASME PAPER 65-WA/PTC-1]

[ASME PAPER 65-WA/PTC-1]

[ASME PAPER 65-WA/PTC-1]



Skin friction coefficient predictions in turbulent compressible flow, using design nomograph based on Spalding-Chi method 18 p3100 A66-34603

Inertia and pressure effects on energy potential of homogeneous and isotropic turbulence in weakly compressible medium 18 p3100 A66-34608

Propagation of spherically symmetric, cylindrically symmetric and plane waves examined via analytic perturbation method in solving gas dynamics equation for nonstationary compressible flow 19 p3343 A66-36638

Multistep axisymmetrical supersonic exit cones optimum geometry design diagram based on external oblique and normal compression shock 20 p3628 A66-36927

Nozzle-like exact solutions for subsonic and supersonic compressible axisymmetric flow 21 p3723 A66-38701

Oblique detonation impacts in pentolite on iron treated by methods of plane steady compressible flow, discussing regular and shock Mach reflection and expansion 21 p3727 A66-39172

Yield criterion and stress-strain increment relations dependent on isotropic pressure for nonhardening elastic-plastic compressible material 21 p3832 A66-39442

Eulerian finite difference method for solving time-dependent equations of motion for compressible fluid flow, noting shock wave diffraction, supersonic blunt body interaction with shock wave, etc 21 p3730 A66-39472

Laminar mixing of two parallel streams of compressible fluid stability with respect to supersonic disturbances 22 p3900 A66-40385

Numerical solution of continuity equation for transient compressible flow in closed vessel 24 p4193 A66-42135

**COMPRESSIBLE FLUID**

Equations for one-dimensional flow of ideal compressible polytropic fluid obtained by transforming dynamical equation for longitudinal vibrations of nonlinear model string 02 p0219 A66-12160

Impact of rigid or flexible body on surface of compressible fluid, noting impact of rigid wedge and linear supersonic airfoil theory [ASME PAPER 65-WA/UNT-3] 05 p0663 A66-15600

Reciprocity relations in compressible plasma and application to antennas 06 p0827 A66-16040

Numerical analysis of collapse of spherical bubble in compressible fluid including surface tension, viscosity and adiabatic compression of gas within bubble [ASME PAPER 65-FE-16] 06 p0870 A66-16215

Compressible fluid flow, discussing simple wave supersonic flow mechanism for bodies with developable surfaces 06 p0802 A66-16352

Simple waves in one-dimensional nonsteady nonmagnetic relaxation hydrodynamic flows of chemically reacting compressible gases 07 p1020 A66-17965

Existence of subsonic jets issuing from curved symmetric channels in plane 07 p0981 A66-18030

Air disturbances due to small transverse vibrations of finite span thin wing with variable velocity 07 p0981 A66-18111

Shock wave propagation in lower half-space filled with compressible fluid 07 p1026 A66-18256

Flow of compressible fluid about circular cylinder at Mach number less than unity solved, using small parameter method 08 p1161 A66-18608

MHD model of cyclone, considering motion of type of rotating ideal compressible conducting fluid 08 p1213 A66-19023

Stability of motion of spherically symmetric mass of compressible gas with constant space density in absence of gravitational field 08 p1298 A66-19483

Two-dimensional steady potential subsonic flow of compressible fluid past circular cylinder between two parallel walls 10 p1522 A66-21323

Influence of boundaries on wave propagation in compressible warm plasma 10 p1566 A66-21730

Separation of electromagnetic and plasma modes in two-fluid lossy compressible plasma, deriving field quantities from two

Helmholtz equations 11 p1653 A66-22561

Inviscid flow of compressible conducting gas with aligned magnetic field through axially symmetric Laval nozzle in various transition regions 11 p1636 A66-23256

Transition solution of physical state across plane nonrelativistic MHD shock of finite strength in compressible dissipationless perfect gas in uniform magnetic field 12 p1923 A66-24578

Hydrodynamic equation for ideal compressible fluid in case of steady three-dimensional vortex motion solved via two second order PDEs 12 p1865 A66-24867

Nonstationary two-dimensional channel flow of compressible electrically conducting fluid subject to traveling magnetic field 13 p2140 A66-25422

Compressivity tensors as parameters to characterize two-fluid compressible plasma in external magnetic field 13 p2149 A66-26273

Electrical analog method used in determining potential gas flow past airfoil lattice, noting components of solution 13 p2068 A66-26541

Slot admittance for two-layer compressible plasma sheath-ion sheath in plasma half-space 14 p2235 A66-27128

Heat and mass transfer process in reacting boundary layer of compressible gas in laminar flow along semiinfinite porous plate 14 p2416 A66-28484

Electromagnetic and plasma wave propagation in inhomogeneous compressible isotropic collisionless electron plasma bounded by closed surface in free space 15 p2449 A66-28592

Planar subsonic flow around circular cylinder using Kisseleff approximation method for compressible fluid 16 p2627 A66-30210

Linear integral operators applied to singular differential equations and to computations of compressible fluid flows 16 p2683 A66-30241

Energy dissipation due to deformation of magnetic field in compressible conducting medium near zero field 16 p2762 A66-31182

Dynamic law for pressure variation in throttle chamber of hydraulic control booster, taking into account fluid compressibility and change in discharge coefficient 16 p2637 A66-31219

Generalized model of ideal compressible anisotropic fluid, determining dependence of free energy on density 16 p2689 A66-31517

Flow visualization in compressible fluids, examining optical techniques and Toepler schlieren system 18 p3094 A66-34134

Numerical solution for complete Navier-Stokes equations for one-dimensional time-dependent propagation of compressible viscous thermally conducting diatomic gas, including presence of traveling shock wave 18 p3102 A66-34918

MHD wave equation for compressible infinitely conducting fluid formulated in Cartesian tensor form 18 p3103 A66-34935

Helical flows of viscous compressible fluids for homogeneous and inhomogeneous flows 18 p3103 A66-34942

Base pressure behind ridge in separated supersonic flow of compressible gas determined for case of turbulent mixing 18 p3103 A66-35053

General relativistic field equations of compressible fluid sphere with variable polytropic index 20 p3545 A66-37465

Entry problem of thin symmetric wedge impinging normally on free surface of compressible inviscid liquid, neglecting gravitational effects 20 p3547 A66-37981

Hamilton principle extended to compressible MHD flow of perfect conducting fluid 20 p3610 A66-37987

Screening of sound in infinite tube with circular cross section and finite wall thickness placed in compressible fluid 21 p3729 A66-39444

Impact of rigid or flexible body on surface of compressible fluid, noting impact of rigid wedge and linear supersonic airfoil theory [ASME PAPER 65-WA-UNT-3] 21 p3731 A66-39531

Hydrodynamic equation for ideal

compressible fluid in case of steady three-dimensional vortex motion solved via two second order PDEs 22 p3899 A66-40328

Lighthill integral transform methods in hodograph transformation theory of plane compressible transonic shock-free potential flows around airfoil sections in solution space of Chaplygin equation [ICAS PAPER 66-26] 23 p4007 A66-41008

Impedance of flat strip antenna embedded in planar dielectric slab surrounded by layers of compressible isotropic electron plasma 23 p4047 A66-41639

Velocity discontinuity surface instability and fluid compressibility effect on stationary flows 23 p4059 A66-42006

**COMPRESSION**

SA AXIAL COMPRESSION

SA DECOMPRESSION

SA METEORITIC COMPRESSION

SA PULSE COMPRESSION

Test apparatus for continuous measurement of stress relaxation in metals which are plastically prestrained in compression 09 p1466 A66-19950

Shock compression of liquid argon at very high pressures and temperatures by reflecting shock wave from tungsten wall for testing interatomic potential 11 p1694 A66-23210

Liquid phase compression in closed cycle gas turbine by using particular working fluids for application to nuclear power stations [ASME PAPER 66-GT-111] 14 p2411 A66-27005

Elasticity equations for materials with different resistance to tension and compression 17 p3025 A66-32590

Compression per stack layer varying as power of layer thickness when multilayer structures are compressed under loads of up to 5 x 10 super 3 lbf 20 p3667 A66-37480

Megaton and decamegaton dynamic pressure production by blast-type compression of thick walled pipe with core subjected to internal implosion, giving theoretical foundations /Part I/ 23 p4091 A66-41859

Megaton and decamegaton dynamic pressure production by blast-type compression of thick walled pipe with core subjected to internal implosion, for case of graphite core /Part II/ 23 p4091 A66-41860

**COMPRESSION BUCKLING**

Buckling of imperfect cylindrical shells under axial compression and external pressure 02 p0298 A66-11563

Shear instability type accompanying shear deformation of structures and normal to compressive load direction [AIAA PAPER 65-770] 03 p0434 A66-12554

Initial deformation effect on upper critical load of spherical shell under uniform distributed external pressure 04 p0590 A66-14148

Behavior of centrally compressed rod beyond proportionality limit, noting system stability 04 p0590 A66-14162

Stiffened cylinder buckling behavior under compressive load, noting analysis methods [AIAA PAPER 65-79] 05 p0781 A66-15787

Dynamic buckling of circular cylindrical aluminum shells subjected to axial blast loads [AIAA PAPER 66-82] 08 p1308 A66-18996

Compression instability of unidirectional composites consisting of regularly spaced arrays of axially loaded columns supported by elastic filler [AIAA PAPER 66-143] 08 p1309 A66-19005

Compressive strength and instability failure mechanism in uniaxial boron fiber-metal matrix composite material 08 p1240 A66-19139

Von Karman-Donnell large-displacement equations for thin circular cylindrical shells extended by considering larger term numbers in Fourier series representing radial displacements after buckling 08 p1309 A66-19143

Idealized cylindrical shell buckling under axial compression derived from generalized integral expression 08 p1310 A66-19166

New parameter, dimensionless fraction of particle volume irreversibly dislocated by plastic deformation during compression, permits calculation of powder compression



process and constants 10 p1540 A66-21507

Structural efficiency of orthotropic materials for cylindrical shells under axial load, including examination of fibrous composites characteristics [AIAA PAPER 65-73] 12 p1956 A66-23583

Dynamic buckling of imperfection sensitive models, specifically cylindrical shells under axial compression 12 p1957 A66-23590

Stability analysis of shells of revolution with curvilinear generatrices under axial compression, using strain energy technique 12 p1967 A66-24110

Longitudinal stiffeners eccentricity /one-sidedness/ effect on buckling strength of axially compressed cylinders 14 p2404 A66-27989

Filament overwrapped metallic cylindrical pressure vessels show greater efficiency ratio and buckling strength 14 p2405 A66-27992

Stability of three-layer cylindrical shells under compression, load and combined action 16 p2817 A66-31053

Thin circular cylindrical shell behavior in axial compression, noting buckling under stress, boundary condition detail effects, etc 17 p3031 A66-33064

Inelastic buckling strength of aluminum columns, plates and beams in compression and in shear 17 p3032 A66-33434

Exact analytic solution, in confluent hypergeometric functions, to problem of stability of conical shell under uniformly distributed longitudinal compressive forces 18 p3252 A66-33709

Approximation method for checking stability of compression members in rigid-joint space truss or stability against out-of-plane buckling of compression members in rigid-joint plane truss 19 p3475 A66-36489

Finite deflection and stability equations for circular cylindrical shells stiffened in longitudinal and circumferential direction 19 p3475 A66-36636

Postbuckling behavior of clamped infinite flat strip under action of shearing forces analyzed based on von Karman equations 20 p3669 A66-37531

Static and dynamic stability loss of nonconservative mechanical systems describing buckling of clamped-free rod and stability loss of cantilever beam subjected to bending 20 p3672 A66-38267

Inelastic buckling of rod with initial slight sinusoidal deflection subjected to short-term longitudinal compressive dynamic load 20 p3672 A66-38268

Lateral buckling of annular plate compressed radially at inner or outer edge 20 p3674 A66-38294

Dynamic buckling of circular cylindrical aluminum shells subjected to axial blast loads [AIAA PAPER 66-82] 21 p3828 A66-38728

Stability of structurally anisotropic circular cylindrical shell under nonuniform compression 21 p3829 A66-38976

Variational theorems for creep of shallow cylindrical shells, noting buckling and snap-through of square cylindrical panel compressed along generatrix 21 p3829 A66-38977

Critical buckling load at middle plane of variable-rigidity plate 21 p3832 A66-39376

Instability of long thin circular cylinders under axial compression, bending, torsion, shear and external pressure [ICAS PAPER 66-32] 22 p3996 A66-40663

Structural efficiency of orthotropic materials for cylindrical shells under axial load, including examination of fibrous composites characteristics [AIAA PAPER 65-73] 23 p4138 A66-41107

Approximate finite deflection analysis of buckling of long slightly curved panels in axial compression 23 p4143 A66-41963

Slenderness ratio and compressive buckling stress in plates with stiffeners oriented parallel to direction of applied loads 24 p4289 A66-42286

Notch and heat treatment effect on compressive buckling of WC/Co alloys 24 p4228 A66-43063

## COMPRESSION. LOADING

Uniform compression effect on Curie temperature of ferromagnetic compound EuO 01 p0118 A66-10254

Stability of thin walled cylindrical dural shells under creep during compression and bending 02 p0297 A66-11396

New materials in compression packings and O rings such as fibers, metals, plastics and homogeneous materials 04 p0525 A66-13782

Stress-volume results between 20 and 140 kbar for germanium shock loaded in one-dimensional strain 07 p1108 A66-18419

Strain energy method used to examine stability and supercritical strains of rib-reinforced cylindrical shells under axial compression 08 p1305 A66-18595

Plastic deformation effect on critical temperature and magnetic field of superconducting junctions in titanium under uniform high compression loads 09 p1428 A66-20591

Flexure of semiinfinite nonsymmetric three-layer plate under steady transverse compression, using state equation to determine load values impairing equilibrium of plate 09 p1468 A66-20760

Zeta phase in tantalum-carbon system, noting diffusionless transformation of carbon-deficient lattice under compressive stress 12 p1892 A66-23566

Load capacity of condensing vapor-lubricated long self-acting journal bearing, examining two-phase and single-phase regions [ASME PAPER 65-LUBS-5] 12 p1888 A66-24554

Propagation of brittle cracks in body under compression, discussing theory of resistance of brittle bodies to compression 13 p2196 A66-25629

Plastic deformation effects on preaged aluminum-copper alloy structure subjected to 40-75 percent compression 13 p2110 A66-25965

Uniform compression effect on Curie temperature of ferromagnetic compound EuO 13 p2168 A66-25971

Compression of anisotropic fiber monofilaments extended to measurements of expansion of horizontal diametral plane and contact widths for polyethylene terephthalate and nylon, as function of load 13 p2115 A66-26306

Stresses in composite spheroids of two different isotropic elastic materials under compressive forces acting along common axis of revolution 14 p2397 A66-27391

Heated cylindrical shell with braces subjected to given compression and internal pressure, having elastic beams along edges, analyzing local deformations effect on shell strength and stability 14 p2400 A66-27684

Permanent compressive deformation of pyrolytic graphite rapidly heated to very high temperatures and loaded in C direction 14 p2318 A66-27877

Conductivity of compressed powdered refractory compounds found to be exponential function of ratio between material/compact densities 15 p2520 A66-28749

Hooke law analysis of dynamic stability of closed circular cylindrical anisotropic shell compressed by longitudinal force 15 p2609 A66-29196

High temperature compressive deformation equipment for ceramic materials noting loading, alignment and stress-strain measurement 16 p2682 A66-30950

Stress-strain state of plane containing crack in nonuniform field of compression stresses, deriving pressure at contact surface 18 p3252 A66-33714

Temperature, time and loading conditions for adhesion or cohesion of structural metals in vacuum 18 p3117 A66-34651

Compressive load effects on heat flux through multilayer insulation 20 p3675 A66-37062

Plastic deformation effect on critical temperature and magnetic field of superconducting junctions in titanium under uniform high compression loads 20 p3622 A66-38124

Strength of ceramic specimens with parallel cylindrical holes, noting strength/weight characteristics during compression loading 21 p3753 A66-38677

Reinforced cylindrical shell stability under axial compressive force, using linear and quasi-linear formulation 22 p3990 A66-40146

Limiting equilibrium of compression-and-tension-bent shallow shell of revolution 22 p3991 A66-40149

Progressive plastic buckling of cylindrical shells under axial compressive load, noting nonsymmetric patterns 22 p3994 A66-40432

Stability of ideal plate under compression loading beyond elastic limit 24 p4290 A66-42437

## COMPRESSION. TESTING

High speed compression of viscoplastic thin disk between smooth dies considering inertia effects 02 p0299 A66-11690

Structural analysis and experimental verification of sandwich panels with thin plastic-film facings and foam-plastic cores under compression and bending loads 03 p0437 A66-12769

Piezomagneto-resistance on compressive stress for antimony-alloyed germanium, observing magnetic field induction 04 p0569 A66-14358

Mechanical testing methods, discussing quasi-static and fatigue fracture due to tensile compressive load and cyclic deformation characteristics of materials 04 p0537 A66-14399

Compressive residual stress effects on surface layers of through-hardened bearing steels produced by prenitriding before hardening [ASME PAPER 65-WA/CF-7] 05 p0690 A66-15625

Poisson ratio for viscoelastic materials undergoing large strains measured, using compression test [ASME PAPER 65-WA/RP-8] 05 p0706 A66-15629

Deformation of double ring used in compression tests to study stress-strain state of brittle and cermet materials 08 p1313 A66-19438

Changes in fine structure of powdered copper during compression, determining dislocation density and disorientation angles, noting plastic deformation cause as packing defect occurrence 10 p1546 A66-21505

Boundary condition effects in magnetic mirror compression experiment, noting dependence of transition from unstable to quasi-stable plasma containment on density and lifetime 10 p1568 A66-21824

Sliding friction and compression testing of rigid polyurethane foams 13 p2112 A66-25303

Rational compression curves and plastic deformation mechanism of cast and drawn polycrystalline beryllium 13 p2106 A66-25356

Resin-impregnated material response to compression testing at intermediate strain rates 13 p2114 A66-26112

AMRA high speed tensile tester analysis of dynamic stress-strain behavior in beryllium oxide in flexure and in compression 13 p2115 A66-26114

State equation analysis from tensile or compression test data and influence of strain, strain rate and temperature on strain-hardening curve for metals such as Al, Cu, Pb, etc 14 p2397 A66-27393

Piezomagneto-resistance on compressive stress for antimony-alloyed germanium, observing magnetic field induction 14 p2368 A66-28256

Compressive creep in thermoplastic materials measured, using simple test cell apparatus 14 p2319 A66-28483

Idle time effect on static friction studied under boundary lubrication conditions, using compression tester and press-fit test specimens [ASLE PAPER 66AM 1C1] 16 p2710 A66-30403

Drag on cylinders of various height mounted on flat plate, noting dependence of compression region length on cylinder diameter during analysis of boundary layer separation phenomena 17 p2909 A66-32493

Compressive tests on WC-Co cemented alloys including preparation of sample, equipment, behavior and failure mode [ASME PAPER 66-MD-80] 21 p3750 A66-38503

Load carrying capacities of rotationally symmetric plates and shells for limited anisotropic behavior and different yield stresses in tension and compression 21 p3831 A66-39375

Megagauss magnetic field generation by



- explosives and related experiments - Conference, Frascati, Italy, September 1965 21 p3773 A66-39501
- Grain boundary cavity growth in Al-Cu alloy during compressive creep testing 22 p3935 A66-40291
- Mechanical properties of VAD23 alloy noting tensile, compression, crushing and shearing strength and notch sensitivity and comparison with D16T alloy 22 p3936 A66-40881
- Changes in fine structure of powdered copper during compression, determining dislocation density and disorientation angles, noting plastic deformation cause as packing defect occurrence 23 p4081 A66-41526
- COMPRESSION TESTING MACHINE**  
Simple auxiliary torsion testing device for use with universal tension-compression testing machines 01 p0151 A66-10201
- Apparatus for determining dynamic compressibility, creep behavior and viscoelastic properties of polymers 13 p2115 A66-26115
- COMPRESSION TUBE**  
Homogeneous dissociation kinetics of gas examined by means of adiabatic compression apparatus attached to mass spectrometer 13 p2079 A66-25821
- COMPRESSION WAVE**  
Attached coordinate system for approximate solution of compression waves emitted by expanding sphere at constant rate in ideal medium 01 p0057 A66-10420
- Shock wave structure for gas with discrete velocity distribution, examining compression and reflection from plane surface, Broadwell model and increase in specific mass 03 p0354 A66-12538
- Dynamic flexural buckling of rods within axial plastic compression wave, noting strain-hardening law [ASME PAPER 65-APMW-32]
- 04 p0593 A66-14232
- Separation of gases from isotopes in compression shock produced in expanding gas flow past obstruction, dependent on gas density and hydrokinetic properties of components 06 p0875 A66-17052
- Stability of expanding corona against radial compressional waves 09 p1455 A66-20403
- Nonsteady isentropic compression wave to generate high-velocity air flows with very low ambient dissociation levels 11 p1684 A66-22831
- Time-dependent variation of cross sectional area used to generalize classical theory of elastic-plastic loading waves in thin rods 12 p1960 A66-23949
- Ultrasonic observation of magnetization and flux jumping in superconducting niobium-zirconium alloy, analyzing field penetration effect on temperature dependent compressional wave absorption structure 13 p2159 A66-25071
- Acoustic waves and convection effect on asymmetries of weak to medium-strong solar lines 13 p2183 A66-25614
- Circumventing turbine inlet temperature limitation of gas turbines by direct fluid-to-fluid energy exchanger, using isentropic compression waves to avoid shock losses [ASME PAPER 66-GT-117]
- 14 p2373 A66-27009
- Exact solutions for unsteady two-dimensional gas dynamics equations for self-similar flow behind shocks and expansion waves 14 p2278 A66-28143
- Dynamic flexural buckling of rods within axial plastic compression wave, noting strain-hardening law [ASME PAPER 65-APMW-32]
- 18 p3247 A66-33567
- Compressional wave velocity in limestones, marbles and single crystal of calcite under hydrostatic pressure to 20 kbar 19 p3351 A66-36387
- Gas flow formation ahead of flame front in circular and rectangular shock tubes analyzed, based on high speed photographs and method of characteristics 21 p3836 A66-39097
- Screening of sound in infinite tube with circular cross section and finite wall thickness placed in compressible fluid 21 p3729 A66-39444
- COMPRESSOR**  
**SA AXIAL FLOW COMPRESSOR**
- SA CENTRIFUGAL COMPRESSOR
- SA DATA COMPRESSOR
- SA FAN
- SA MULTISTAGE COMPRESSOR
- SA SUPERSONIC COMPRESSOR
- SA TRANSONIC COMPRESSOR
- First phase of thermodynamic development of compressor for 490 hp turboprop engine, test procedures and data evaluation 13 p2171 A66-25077
- Flow diagram for dimensioning of jet compressors to plot irreversible mixing, noting shape of mixing channel, design guidelines, etc 16 p2632 A66-31645
- Pressure distribution of gas-lubricated spiral-groove thrust bearing or compressor [ASME PAPER 66-LUBS-1]
- 17 p2931 A66-33176
- COMPRESSOR BLADE**  
Axial compressors with nonuniform inlet flow, investigating size of gap between blade rows and rotating stall 01 p0008 A66-10953
- Measurement instrumentation of compressor blade vibrations of Rolls-Royce lifting turbojets during testing 02 p0226 A66-11203
- Root rigidity and damping capacity of vibrating turbine and compressor blade mountings 03 p0372 A66-12398
- Internal friction and elastic modulus of compressor and turbine blade materials 03 p0372 A66-12399
- Photoelastic analysis and theoretical considerations to minimize stress concentration of blade joints of compressor and turbine of jet engine 03 p0373 A66-12402
- Supersonic cascade tunnel to evaluate compressor blade performance [ASME PAPER 65-WA/GTP-4]
- 05 p0661 A66-15719
- Helicopter rotor blade and engine erosion by sand and seawater 06 p0804 A66-15997
- Multiple stage axial flow compressor with blades staggered differently at different stages 06 p0801 A66-16000
- Microscopic fatigue crack production in compressor blades, describing methods and application to ultrasonic nondestructive testing 06 p0966 A66-16799
- Compressor blade cascade in flow with boundary layer separation, calculating velocity distribution and blade angle 06 p0803 A66-16967
- Clearance loss in rectilinear cascade, emphasizing flow separation and vortices shed at blade tips 07 p0980 A66-17483
- Number of working blades effect on magnitude of total work coefficient and other characteristics of axialradial compressor 09 p1435 A66-20763
- Vibration suppression in axial flow compressors, discussing blade root damping and pin hole stress 09 p1469 A66-20988
- Compressor cascade flow with blades of different thickness ratio for variable Mach and Reynolds numbers, measuring turbulence level influence on loss coefficients, secondary flow parameters, etc 12 p1799 A66-24553
- Recent progress in aerodynamic design of axial flow compressors and components in U.S. [ASME PAPER 66-GT-95]
- 14 p2217 A66-26998
- Vibration suppression in axial flow compressors, discussing blade root damping and pin hole stress 15 p2468 A66-29926
- Supersonic cascade tunnel used to evaluate compressor blade performance [ASME PAPER 65-WA/GTP-4]
- 16 p2673 A66-30340
- Intake flow maldistribution excitation of rotor blade vibration in V-STOL predicted by blade velocity triangles method 18 p3050 A66-33680
- Low speed three-stage axial flow compressor tests at aspect ratios of one, two and four [AIAA PAPER 66-613]
- 19 p3275 A66-35359
- Recent progress in aerodynamic design of axial flow compressors and components in U.S. [ASME PAPER 66-GT-95]
- 19 p3278 A66-36756
- Early detection of impending failure in aircraft turbines 20 p3629 A66-37828
- Wake motion through moving blade row, demonstrating chopping phenomenon via hot-wire anemometer traces taken downstream of rotor 24 p4157 A66-42583
- COMPRESSOR EFFICIENCY**  
Behavior of unassisted annular cowed compressor intakes under cross-flow conditions [AIAA PAPER 65-707]
- 01 p0130 A66-10945
- Performance of blade rows in transonic axial-flow compressor for V-STOL aircraft 03 p0313 A66-12393
- Rotating stall and blade row interference in axial compressor 03 p0313 A66-12395
- Wall curvature effect on performance of high pressure ratio single-stage compressor [ASME PAPER 65-WA/GTP-12]
- 05 p0745 A66-15727
- Number of working blades effect on magnitude of total work coefficient and other characteristics of axialradial compressor 09 p1435 A66-20763
- Parametric analysis of supersonic compressors, determining relative efficiencies of various leading and trailing guide vane configurations 10 p1479 A66-21365
- Behavior of unassisted annular cowed compressor intakes under cross-flow conditions [AIAA PAPER 65-707]
- 10 p1594 A66-21890
- Aerodynamic characteristics of compressor entry ducts under natural and simulated conditions 13 p1992 A66-26491
- Graphical matching solution for gas turbine power plant closed cycle systems [ASME PAPER 66-GT/CLC-14]
- 14 p2224 A66-26984
- Graduate level textbook on axial flow turbine design, examining useful thermodynamic/fluid mechanic concepts, cascade potential flow, turbine efficiency, etc 17 p2991 A66-32991
- Busemann inlet flow field calculation for hypersonic speeds, considering internal-compression inlet geometry and performance 20 p3493 A66-38178
- COMPRESSOR ROTOR**  
**SA TURBINE WHEEL**  
Fatigue life of aircraft gas turbine compressor disks subjected to cyclic loading 11 p1710 A66-22691
- Mathematical analysis of noise generation mechanism in axial-flow compressor rotors [ASME PAPER 66-GTIN-42]
- 14 p2372 A66-26987
- Gas turbine compressor rotor and power shaft fabrication using electron beam welding 22 p3924 A66-40258
- High temperature testing and evaluation of graphite helical-screw expanders and compressors for use with inert gas Brayton cycle 23 p4075 A66-41755
- COMPTON EFFECT**  
Isotropic photon gas interacting with electron plasma with Maxwellian distribution via Compton effect 05 p0722 A66-14721
- Compton scattering of laser photons, noting transformation into gamma radiation photons upon collision with high energy electrons 07 p1044 A66-17816
- Opacity due to Compton scattering at relativistic temperatures in semidegenerate electron gas 08 p1258 A66-18779
- Magnitude of Compton effect of nuclear reactor operation in space 08 p1254 A66-19593
- Monte Carlo method analysis of electron photon cascade 09 p1436 A66-20134
- Compton process argument for quasar relative nearness to our Galaxy and contrast between Compton and synchrotron radiation scattering effects 12 p1950 A66-24389
- Scattering of electron beam by standing waves of photons inside laser cavity corresponds to stimulated Compton effect 13 p2096 A66-26155
- Annealing effects of gamma ray irradiation on MOS FET increase donor surface state density 15 p2567 A66-29413
- Inverse Compton X-ray and gamma ray flux due to high energy electron interaction with cosmic blackbody radiation at 3.5 degrees K 17 p2992 A66-31914
- Compton-effect produced by thermal photons on relativistic electrons in solar atmosphere 19 p3454 A66-35247
- Space nuclear reactor induction of positive potential and remedy by ambient plasma or positive-ion source 19 p3398 A66-35493
- Inverse Compton scattering effect in quasars, examining assumption that they are



at cosmological distances 22 p3980 A66-40399

**COMPUTATION**

**SA INTERPOLATION**

Survey of IR measurement techniques and computational methods in radiant heat transfer [AIAA PAPER 65-657] 01 p0162 A66-10598

Economical difference scheme of continuous computation for numerical solution to Stefan problem having multiple spatial dimensional variables and phases 01 p0166 A66-11009

Matrix inversion by rank annihilation, discussing memory storage requirements, overlapping input time with computing time, number of computations, etc 09 p1395 A66-20625

Iterative method for computing optimum values of parameters for best agreement in least squares sense between given values and corresponding calculated values 10 p1507 A66-21213

Heuristical method solving zeros of complex function, transcendental or algebraic, of complex variable, applicable to computation of eigenvalues of general matrix 10 p1548 A66-21214

Kinematic computer calculations of energy distribution among products of repulsive, mixed and attractive energy release exothermic reactions 11 p1787 A66-23213

Approximation methods for matrix computation, considering characteristic roots 11 p1723 A66-23361

Computational aids /charts and nomographs/ applicable to gross design of satellite communication systems 13 p2020 A66-25150

Lower bounds on computation times of certain input-output transformations and tradeoff relation between computation time and dimensionality of Turing machine tapes 13 p2027 A66-25802

Computational photogrammetry, deriving relation between image and object space, using collinearity conditions and orientation matrix 16 p2703 A66-30513

Book on methods in computational physics including numerical simulation of Earth atmosphere, computation of propeller design and stellar evolution, etc 16 p2735 A66-30942

Numerical problems in application of Urabe results in considering periodic nonlinear differential systems, obtaining Galerkin approximations 16 p2737 A66-31231

Survey of IR measurement techniques and computational methods in radiant heat transfer [AIAA PAPER 65-657] 19 p3477 A66-35595

**COMPUTER**

**SA ANALOG COMPUTER**

**SA CONTROL SIMULATOR**

**SA COUNTING RATE COMPUTER**

**SA DATA PROCESSING**

**SA DATA TRANSMISSION**

**SA DIGITAL COMPUTER**

**SA FINITE-STATE MACHINE**

**SA HYBRID COMPUTER**

**SA IBM 709 COMPUTER**

**SA IBM 7090 COMPUTER**

**SA INFORMATION RETRIEVAL**

**SA PARAMETRON**

**SA VOCODER**

Standardization of characters for optical character recognition, class B, using merit curve technique 02 p0193 A66-11598

Multiplex measuring device and choice of analog or digital computers in electronic measurement 02 p0230 A66-11792

Elliott MCS 920 computer controlled trunk exchange for military area communication network 02 p0194 A66-11932

Microminiaturized LCT 822 P computer for general aerospace navigation 02 p0257 A66-12034

Book on systems engineering problems and tools for solution noting energy, materials, modeling, simulation, computers, control, statistics, signals, etc 02 p0307 A66-12280

Moore and Mealy diagrams in analysis and synthesis of finite automations 03 p0337 A66-12376

Noncontact elements of transfluxor-based alpha detecting system 04 p0490 A66-13777

Utilization of computers to reduce cockpit work load, particularly in SST aircraft 07 p1003 A66-17726

Man-machine systems involved in on-line

man/ computer interaction, manned space systems, satellite communication and display systems 14 p2230 A66-27820

Dynamic logic chassis analyzer /DLCA/, diagnostic tool for isolating faults to circuit card or component level in programmer test station /PTS/ and component test station /CTS/ ground support 14 p2260 A66-28266

Possible use of computer as tool for air traffic control 16 p2742 A66-30089

Navigational information conversion from digital readout to pictorial display 16 p2743 A66-30670

AFIPS Joint Computer Conference, Boston, April 1966 16 p2656 A66-31239

On-line computers in steerable aerial control system for satellite tracking 18 p3073 A66-34314

Central Telecommunications Laboratory 882 P arithmetical airborne computer 20 p3523 A66-38013

High availability computer systems - WESCON, Los Angeles, August 22 p3871 A66-40743

Pattern recognition computer operating under automatic control and stored program control for data transfers, system operation, man-machine interface and display operations 23 p4041 A66-41056

Literature survey of content-addressable and associative memory systems, noting hardware, logical operations, speed, cost, etc 24 p4177 A66-43184

**COMPUTER DESIGN**

Circuit with tunnel-diode-based active element for dynamic memory used to store regenerated information 01 p0046 A66-11048

Power dissipation as sum of quiescent power and transient power dissipation, considering n-channel metal-oxide-semiconductor and MOS complementary logic circuits 01 p0047 A66-11138

Basic emitter coupled logic gate provides fastest nonsaturating gate for high speed computer 01 p0048 A66-11142

Packaging method for integrated circuits based on flow soldering components through printed wiring boards to be used in digital computer design 02 p0204 A66-11940

Graphs for problems of computing system design automation, specifically finding algorithm for graph scheme construction 02 p0250 A66-12102

Content addressable memory systems promise increased computational capability for Army data processing 04 p0490 A66-13686

Logical and computing devices, discussing construction of homogeneous functional structure using integral circuits 04 p0494 A66-13704

Modular synthesis of sequential machines, discussing external variable dependent single memory element devices 05 p0637 A66-14927

Reliability and fault-masking in n-variable two-input and multiple input NOR trees discussing system, function and signal-state reliability measures 05 p0648 A66-14928

One-tape off-line Turing machines covering crossing sequences, recognition problems and computation times 05 p0637 A66-14929

Self-repairing digital computer, discussing switching mechanism activated diagnostic procedure and failed circuitry replacement 05 p0637 A66-14930

Book on switching theory covering circuit synthesis and analysis, Boolean algebra, functional theory, relay type network, etc 06 p0861 A66-16197

Fluidic devices, discussing design, equivalence to logic circuits, fluid amplifier application to build flip-flops, etc 06 p0809 A66-16794

Binary counter circuit, discussing relevance to solid state design, performance and operation 06 p0857 A66-16973

Functional requirements for computer navigational system for Concorde aircraft 07 p1065 A66-17672

DECTRA long range navigational aid, DECTRA airborne receiver and Omnitrac computer 07 p1068 A66-17702

CRT control display console models, console selection pointers, computer programming requirements, etc 07 p1003 A66-17879

Combination of geometrical and physical

optics with modern system design such as computers, cameras for aerial use, space tracking, etc 09 p1403 A66-20918

Parallelism incorporated in large computers for increasing computational power, including internally overlapped and uniform and multiple instruction 10 p1506 A66-21212

DC-9 flight simulator using monolithic-integrated-circuit GP-4 11 p1683 A66-22687

Computer 11 p1683 A66-22687

Circuit with tunnel-diode-based active element for dynamic memory used to store regenerated information 11 p1671 A66-23295

American Federation of Information Processing Societies, Joint Computer Conference, Las Vegas, November 1965 12 p1825 A66-23824

Lockheed multiprocessor simulation system /LOMUSS I/, data processing system for computer design and analysis 12 p1827 A66-23832

Salient hardware, software, and operational features of machine for automatic graphics interface to computer /MAGIC/ operating display system 12 p1827 A66-23835

Digital differential analyzer /DDA/ design for high speed solution of differential equations common in aerospace problems 12 p1828 A66-23841

Self-diagnosable DX-1 computer design to achieve maximum operational availability 12 p1828 A66-23843

Specialized procedures for constructing diversified types of optimum control systems for discrete dynamic processes 12 p1852 A66-24327

Parameters for selection of miniaturized integrated circuit computer for onboard checkout systems 12 p1829 A66-24612

Triple modular redundancy /TMR/ computer organization used in digital computer design for Apollo Command Module 13 p2027 A66-25258

Design and fabrication of computer subsystems for Apollo guidance and navigation systems 13 p2027 A66-25781

Multithreshold threshold element design, discussing realization based on Boolean functions, network synthesis employing transformation technique and logical design application 13 p2039 A66-25803

Thin film hybrid packaging method for series of computer logic circuits designed to operate at 100-mc clock rate 14 p2260 A66-28267

Logical and computing devices, discussing construction of homogeneous functional structures using integral circuits 15 p2454 A66-28545

Low-cost computer design using electro-optics for information processing 16 p2657 A66-31240

Papers on RCA computer progress 17 p2877 A66-32510

Monolithic silicon integrated circuit application in design of two third-generation computers 17 p2877 A66-32511

Monolithic silicon integrated circuit used for current-mode logic of RCA Spectra 70/45 and 70/55 computers 17 p2886 A66-32512

Batch fabrication of large-capacity memory stacks, using integration of monolithic-ferrite stack with integrated MOS circuitry 17 p2886 A66-32515

Developmental memory using monolithic-ferrite integrated arrays of magnetic storage elements provides cost and power savings 17 p2886 A66-32516

Quality of digital smoothing filters with finite transient time improved by rational choice of delay 17 p2878 A66-33491

Logic and operation principle of model of recording device for high speed readout of digital and alphabetic information from digital computer 17 p2928 A66-33494

TRW Systems MARCO 4418, small high-speed lightweight reliable digital computer, for use in manned space missions 19 p3306 A66-35503

Miniaturization of logic components for modular and monolithic integrated circuits in computer design 21 p3708 A66-39624

Advanced spaceborne computer concepts - WESCON, Los Angeles, August 1966 22 p3870 A66-40725

On board computer simultaneously processing spaceborne data including life support, energy management, human



performance control, etc 22 p3871 A66-40726  
 Book on synthesis of multiloop control systems for application to automatic control and computer circuit construction 22 p3885 A66-40854  
 Man-machine merger in computer aided design of circuits, examining changes in circuit parameters caused by component tolerances, simulation of component failure, feasibility and circuit optimization 23 p4072 A66-41252  
 Computer operational center for orbiting space laboratory that will navigate, arrange experiments and devise work schedules 24 p4177 A66-42335  
 Diagrams of computers calculating parallax angle of azimuthally mounted astronomical telescopes 24 p4211 A66-42484  
 Lasers applied to logic, memory, input-output and data transmission-linkages parts of computers 24 p4225 A66-42804  
 Apollo guidance computer, discussing memory storage, central processing unit and sequence generator [AGARDOGRAPH 105] 24 p4236 A66-43128  
**COMPUTER METHOD**  
 General purpose computers for solution of problems in creative design 01 p0033 A66-10863  
 Transient process of nonlinear automatic system calculated by numerical digital computer method based on convolution integral 01 p0045 A66-11021  
 Analog, digital and hybrid computerized systems for investigating problems in aeronautics and astronautics 02 p0193 A66-11894  
 Computer logical gates for characteristics of large systems as local guidance control and regulation systems of plants 03 p0348 A66-12603  
 Zero-crossing data and decision-making procedures used by computer in recognition of vowels 03 p0338 A66-13020  
 Computer algorithm determination of nonlinear system dynamics, using least squares method 05 p0636 A66-14605  
 All-optical computer techniques, noting semiconductor laser digital devices for near future 05 p0637 A66-14824  
 Computer calculation of relative populations of atomic energy levels not in thermodynamic equilibrium 05 p0718 A66-14871  
 Fifth-order Runge-Kutta formulas including extensions of Radau, Lobatto, Newton-Cotes and Legendre-Gauss quadratures 05 p0707 A66-14892  
 Three-dimensional incompressible viscous flow calculated for axial-flow turbine stage of given blade profile, verified by computer method developed from cascade theory 05 p0605 A66-14961  
 In-flight monitoring of advanced aircraft, discussing system requirements and constraints [ISA PREPRINT 1.3-2-65] 05 p0684 A66-15512  
 Manned aircraft self-contained checkout and fault isolation systems, discussing characteristics and operational concepts [ISA PREPRINT 1.3-3-65] 05 p0684 A66-15513  
 Matrix methods in dimensional analysis discussing algebraic, matrix and shortcut methods [ASME PAPER 65-WA/MD-20] 05 p0710 A66-15523  
 Supersonic flight control, discussing reliability and safety devices, computer application and multiplex systems 06 p0816 A66-16055  
 Extension, modification and analysis of Gorenstein-Zierler decoding algorithm for binary codes of Bose, Ray-Chaudhuri and Hocquenghem /BCH/ correcting erasures and errors 06 p0837 A66-16114  
 Sounding rocket instability, covering exact and approximate solution and Magnus moment coefficient for hypersonic rolling vehicle /Sandia Nitehawk rocket system/ [AIAA PAPER 66-62] 06 p0958 A66-16252  
 Synthesis of planetary screw-cam mechanism of optimum efficiency, using digital computer 06 p0886 A66-16313  
 Blake procedure effectiveness and applicability in computing beam loss of radars, extrapolating for rapid-scan systems 06 p0832 A66-16452  
 Service life of antifriction bearings

represented by Weibull distribution law, with computer method for parameters and density function 06 p0886 A66-16486  
 Convex programming problems, developing parametric gradient method for approximate solution 06 p0838 A66-16526  
 Decomposition of mixed-set distributions into normal distributions using graphing and analog computer methods 07 p1003 A66-17381  
 Ozone decomposition effect upon heat transfer determined, using differential energy and material balance equations 07 p1152 A66-17595  
 Computational analysis employing digital computers to evaluate hypoxic stress reactions in man 07 p0998 A66-17659  
 Computer method calculation of minimum time track, using quasi-optical law of refraction 07 p1066 A66-17681  
 Advanced airborne computer double system applied to fault detection, location, flight management and navigation 07 p1003 A66-17715  
 Airborne computer-aided navigation system, utilizing letter printer and pictorial display 07 p1070 A66-17718  
 Numerical computer solutions for several nonlinear gas flow problems in high speed aerodynamics 07 p0983 A66-18143  
 Digital computer determination of coefficients of transfer function from impulse response in time domain 07 p1060 A66-18334  
 Numerical control using computer-aided design /CAD/ equipment 08 p1228 A66-18686  
 Digital computers to control automatic test equipment 08 p1187 A66-18741  
 Trajectory possibilities for Venus swingby mission and role in manned exploration of Mars [AIAA PAPER 66-37] 08 p1290 A66-18988  
 Microminiaturization in control equipment and computers 08 p1194 A66-19300  
 Contractor performance on cost type contracts evaluated by comparing actual and allocated costs, using NASA PERT facilities 08 p1322 A66-19460  
 Spinning rocket attitude measured from geomagnetic field and solar cell data, using digital computer technique, noting instrumentation 08 p1225 A66-19492  
 Processing signal information from digital rate gyros and accelerometers in analytic, gimballless inertial platform 08 p1253 A66-19530  
 Computer calculation of transistor amplifier performance from measured y-parameters 09 p1349 A66-19898  
 Stellar evolution and evolutionary sequences, use of high speed computer methods and application to age determination of stars 09 p1448 A66-20098  
 Digital computer recomputation of stability transition curves in Hill-Meissner equation 09 p1395 A66-20623  
 ESRO/ELDO Space Documentation Service, describing system characteristics, NASA agreement, indexing and search strategy 09 p1473 A66-20658  
 Automated ground station, with computer controlled telemetry system, for Saturn launch vehicle checkout 09 p1347 A66-20675  
 Computer calculation of apparent positions of stars and Sun by reduction of mean stellar coordinates 10 p1604 A66-21131  
 Monte Carlo linear extrapolation of multivariable functions, introducing truncation procedure which saves on machine time and serves for variance reduction 10 p1549 A66-21215  
 Hamel and Cypkin methods, used to determine free oscillation of plus-or-minus servomechanism, applied to transfer function of certain type 10 p1517 A66-21283  
 Electronic color correction during aerial photograph printing by employing specially programmed computer 10 p1534 A66-21329  
 Radar cross section of metal bodies covered by thin plasma calculated, using computer technique, noting modification of TE and TM mode reflection coefficients 10 p1503 A66-21645  
 BRL ballistic camera system noting optical and mechanical characteristics, measurement and computer synchronization methods 10 p1537 A66-21872  
 Computer controlled visual display 11 p1680 A66-22269

Numerical solution of heat conduction and gas dynamics equations by sifting over separate regions 11 p1785 A66-22339  
 Validity of two approximations for removing corners and slope discontinuities from cylindrical metallic bodies in digital approach to Maxwell equations 11 p1653 A66-22563  
 Microdensitometer for evaluating photographically recorded images for direct use as computer input 11 p1705 A66-22672  
 Numerical solution to first geodetic problem of ellipsoid of rotation, using iterative application of Runge-Kutta method to differential equations of geodetic line 11 p1698 A66-22767  
 Algorithm for computer eigenfunction solution of boundary value problem involving partial differential equations for stress functions of semimomentless cylindrical shells 11 p1782 A66-22856  
 General purpose computers and cathode ray tube displays used in automation of air traffic control technical aids 11 p1732 A66-22900  
 Computer capability and probable growth in aerospace vehicle applications considered against mission requirement constraints 11 p1659 A66-22959  
 Real time on-line man-computer graphics system that may obviate need for special-purpose, complex and cumbersome computations 11 p1660 A66-23176  
 Diagnostic-cycle routine, collection of computer-programmed techniques for interpretation of meteorological satellite videograph observations 11 p1731 A66-23486  
 Numerical solutions of problems in gas dynamics in U.S.S.R., using computers stressing methods for solving systems of nonlinear partial differential equations 12 p1861 A66-23807  
 Hybrid computer methodology and electronic data processing applied to quality evaluation of test operations 12 p1828 A66-23837  
 Schumann-ELF natural background samples recorded in three components at separated points resolved by analog and digital methods into constituent modes for comparison 12 p1815 A66-24115  
 Advances in biomedical computer applications - Conference, N.Y. Academy of Sciences, June 1965 12 p1809 A66-24227  
 Mathematical model, using computer, to determine fluid and electrolyte distribution in principal body compartments of young 70-kg human male 12 p1809 A66-24229  
 Responses of neuronal elements in visual cortex of unanesthetized cats shown to depend on time interval length 12 p1806 A66-24232  
 Terminal reentry and dynamics evaluation computer program for small particles, using point-mass calculation during initial phase and determining drag coefficient [AIAA PAPER 66-380] 12 p1951 A66-24505  
 Influence coefficients for computation of atmospheric components of reentry vehicle circular error probable /CEP/, using Bliss adjoint method, noting effects of certain inadequacies on system performance [AIAA PAPER 66-358] 12 p1908 A66-24517  
 Comparison of frequency shift keyed and phase shift keyed pulse compression systems via digital computer simulation 12 p1819 A66-24602  
 Versatile avionics shop test /VAST/ system, computerized test system for carrier-based avionics 12 p1838 A66-24606  
 Digital computer analytical method for simulation of worst shock conditions for subassembly shock testing 12 p1829 A66-24726  
 Parametric analysis, penalty-effectiveness tradeoff and system selection for communications satellites, using block digital computer synthesis with subroutines for operational requirements [AIAA PAPER 66-330] 12 p1824 A66-24797  
 Computer method for determination of distribution of low lying ionization, using ordinary and extraordinary wave traces in ionograms 12 p1873 A66-24838  
 General theory of optimal processes, discussing general version of maximum principle 13 p2116 A66-25342  
 Consistency of Gunn effect with excitation



of conduction band electrons from high mobility minimum to low mobility valleys 13 p2164 A66-25517

Research development effectiveness evaluation, with computer determining resource allocation 13 p2058 A66-26033

Control system design, analyzing sensitivity of system performance to parameter variations by obtaining time domain measure of sensitivity 13 p2050 A66-26062

Numerical integration methods requiring least computation time for truncation error when applied to ordinary differential equations, comparing Butcher with Runge-Kutta, Adams, etc 13 p2121 A66-26324

DATAN, curve fitting process to approximate data and elimination of problems for programming engineer by data analysis 13 p2028 A66-26325

Locating zeros of complex functions by computing topological index 13 p2121 A66-26326

Comparative calculation used in computation of physicochemical properties of hydrides, including densities of beryllium hydride, entropy of cesium hydride, crystal lattice energy of rubidium deuteride, etc 13 p2018 A66-26327

Computational method for cylinders under external pressure, switching from testing in plastic field to elastic field without gaps 13 p2199 A66-26328

Clear air turbulence research methods, noting structural analysis, computer application, satellite photography, etc 15 p2532 A66-28921

Stabilization of unstable two-point boundary value problems, noting field method for avoiding computer storage problems during integration of related differential equations 15 p2528 A66-29292

Spectrometric analysis of aerial photograph, using computers 15 p2504 A66-30010

Momentum and energy accommodation for hypervelocity gas particles on crystal surface, using Lennard Jones potential and approximating lattice by system of independent forced harmonic oscillators 16 p2752 A66-30388

Selection, flow and transference of technology in large electronics aerospace firm, noting methodology, planning, market area selection, etc 16 p2830 A66-30400

Computer system for control of deceleration of electrodynamic shaker during vibration test 16 p2678 A66-30465

Propagation velocity and attenuation variation effect in coaxial cables on frequency modulated carrier evaluated, using IBM 1620 computer 16 p2649 A66-30542

Apollo/Saturn S-II telemetry data processing systems 16 p2652 A66-30567

Simulation of controlled diffusion-type Markov processes applied to two stochastic equations related to problem of misadjustment on analog computer 16 p2656 A66-30763

Improved Monte Carlo method for calculating steady state monatomic rarefied-gas flows, using computer for calculating possibility of collision in given geometrical cell 16 p2753 A66-30787

Convex programming problems, developing parametric gradient method for approximate solution 16 p2656 A66-30836

Two-dimensional dynamic analysis of probe and drogue docking concept noting design, operation and performance 16 p2809 A66-30896

Hybrid analog/digital techniques for signal processing, noting performance advantages at relatively low cost and applications to linear transformation, function generation, correlation functions, etc 16 p2658 A66-31250

Automatic vortex recognition system for Tiros satellite photograph analysis, noting phases of development and results obtained 16 p2658 A66-31251

Air traffic control system using primary and secondary radar, radar digitizer and computer complex 16 p2744 A66-31278

Planetary motion representation using trigonometric series and computer evaluation techniques 17 p2998 A66-32043

Digital computer method for formulating state space equations for active RLC networks 17 p2900 A66-32055

Electronic computer technique for dividing phase space of transistorized circuit into linearity regions 17 p2885 A66-32253

Heat transfer problems solved, using Pohlhausen solution for phase-space trajectory, noting effect of boundary conditions and application of analog computer 17 p3034 A66-32497

Digital computer to decode digitized or sampled PCM waveform 17 p2875 A66-32502

Digital computer analysis of mission parameters governing spacecraft thermal behavior 17 p3034 A66-32513

Noise rejecting algorithms for ODE solutions with computer, using redundancy, placement of control and feedback techniques 17 p2877 A66-32569

Axially symmetric or two-dimensional electrode system with emitting surface, discussing convergence and accuracy criteria of iteration methods 17 p2887 A66-32700

Integrated Helicopter Avionics System flight control, noting stability augmentation, long-term motion control, outer and inner loop function separation and fail-safe capability 17 p2951 A66-32730

Propellant tanking computer system for monitoring and controlling Saturn IB and Saturn V vehicles [SAE PAPER 660454] 17 p2904 A66-33162

Onboard checkout requirements and application for advanced space missions [SAE PAPER 660461] 17 p2904 A66-33166

Radiation control of ruby laser by diffraction modulator with traveling ultrasonic wave, noting computer solution of kinetic equations of population balance, radiation density, characteristic damping, etc 17 p2938 A66-33515

Lunar occultation and identification of MSH 19-27 radio source, noting computer analysis of brightness distribution 18 p3225 A66-33549

Computational method for determination corridors of launch vehicle trajectory and impact dispersions [AIAA PAPER 66-483] 18 p3226 A66-33656

Complex component design using man-computer system with graphic input/output devices, discussing application for digital computer circuit card design [SAE PAPER 660459] 18 p3116 A66-33897

Computer model study of diversity augmented vehicular radio relay communication system in man-made noise environment 18 p3069 A66-34167

Stress and deflection determination in trusses with pin or rigid joints, using digital computer 18 p3255 A66-34275

Stresses and deflections in inhomogeneous sandwich shells calculated via computer programs 18 p3255 A66-34286

Computer code study of magnetospheric trapped-particle drift under influence of magnetic field gradient, magnetic line curvature, electric rotational field and electric field across tail of magnetosphere 18 p3168 A66-34350

Catalytic combustion of cyclohexane, cyclohexene and benzene, determining significance of combustion via computer program 18 p3266 A66-35022

New solution method for nuclear cascade equation for nucleons and charged pions 18 p3206 A66-35105

Computer iteration scheme for calculating arbitrary hyperbolic transfer orbit in field of attracting center, based on Gauss equations 19 p3455 A66-35278

Analog computer solution of high-order optimal control problem, noting application of Pontryagin maximum principle and extension to two-point boundary value problems 19 p3306 A66-35536

LEM Data Reduction System that performs concurrent data processing and telemetry conversion on computer time-shared arrangement 19 p3299 A66-35662

Automatic telemetry checkout station for Saturn V systems using real time signal digitizer and general purpose computer 19 p3339 A66-35677

Lens design by computer methods known as Flair and Triplet 19 p3399 A66-35824

Adaptive subfield method for solution of variational problems by dynamic programming, applicable to pinpoint problem 19 p3310 A66-36651

Amino-acid-sequence determination in peptides using N-fatty acids, mass spectra of peptide derivatives and computer techniques 20 p3510 A66-37057

Computer analysis of interference in complex network resulting from common impedance coupling of signals 20 p3538 A66-37196

IBM 7094 programmed in FORTRAN IV used to determine sidebands in FM with complex periodic modulation functions 20 p3522 A66-37212

Automatic built-in test of advanced avionics systems, noting advantages of airborne computer in sequencing, conducting and evaluating in-flight performance 20 p3522 A66-37245

Digital testing techniques for analog systems, describing bomb computer set for Phantom F-4D aircraft 20 p3522 A66-37246

Computation method used in pulsation of Lyrae models extended to models of Cepheid variables, noting instability of appropriate period, mass size, luminosity and velocity curves 20 p3650 A66-37339

Cathode current density distribution, beam minimum radius and location and electrode current interception, using computer techniques on electron guns 20 p3528 A66-37490

Acceptance checkout system for checkout assistance to Apollo CSM and LEM facilities during countdown, discussing system configuration variability, composition and operation 20 p3543 A66-37579

Vertical velocities in atmospheric front motions, noting pressure and temperature field distributions and application of computer to solve obtained equations 20 p3593 A66-37750

FORTRAN program for calculation of approximate total half-intensity line widths of several spectral lines for atoms in common analytical flames 20 p3605 A66-37758

Computerized cost-effectiveness model for large payload test vehicle system of 50-150 launch program 20 p3684 A66-37901

Parallel evaluation of Boolean function in search memory via multiwrite 20 p3523 A66-38017

Internal ballistic considerations in hybrid rocket design, noting throttling and regimes of operation involving effects of surface-or gas-phase reaction kinetics [AIAA PAPER 66-628] 20 p3663 A66-38035

Computer algorithm for recognition and extraction of planar graph from incidence matrix 20 p3523 A66-38279

Bomb debris motion following Star Fish test, noting formation of MHD shock wave, production of stationary plasma through X-ray ionization and collision in neutral air 20 p3644 A66-38345

Nonstationary forces and bending and torsional moments along wing computed, using punch card system 20 p3674 A66-38442

Free vibration analysis techniques for computers and derivation from past methods 21 p3823 A66-38561

Computer program for numerical solution of ODE systems, noting generation of symbolic solutions via Taylor series expansion 21 p3707 A66-38679

Solution of systems of polynomial equations by elimination procedure, using coding in LISP and FORMAC 21 p3707 A66-38680

Symbolic factoring of multivariate polynomial with integer coefficients, noting application of Kronecker method and techniques of implementation 21 p3708 A66-38681

Optimization of efficiency of gas turbine cycles with heat recovery by finite difference method using digital computer 21 p3807 A66-38805

Computational limitations of onboard orbiting computers such as fixed point arithmetic, limited word length and solution techniques 21 p3766 A66-38884

Computer analysis of cylindrical shell stability under uniform external pressure and critical pressure determination for various boundary conditions 21 p3829 A66-38979

Eulerian finite difference method for solving time-dependent equations of motion for compressible fluid flow, noting shock



- p wave diffraction, supersonic blunt body interaction with shock wave, etc 21 p3730 A66-39472
- 
- Electronic computer for topological and geometrical considerations in space structures analysis 21 p3708 A66-39534
- 
- Computer and model analysis as design tools in structural engineering 21 p3708 A66-39535
- 
- Communication network response to arbitrary transients calculated by digital computer, permitting replacement of analytic-function wave forms by lists of equal-interval sample values 22 p3883 A66-39724
- 
- Computation of impulsive and short-term perturbing forces effect on body in elliptical orbit, using Tschauner-Hempel equations 22 p3979 A66-40327
- 
- Transient heat conduction problems solved by high capacity computers 22 p3999 A66-40379
- 
- Automated minimum weight structural design for various load conditions, integrating matrix displacement analysis and operations research 22 p3995 A66-40490
- 
- Minimization of logical functions in normal disjunctive form, using Gavriloova method and ALGOL 60 algorithm 22 p3941 A66-40541
- 
- Automatic testing equipment, examining role of computer in reliability, quality of testing and time and cost savings 22 p3892 A66-40543
- 
- Associative memory organizational approaches for onboard data processing of spacecraft 22 p3871 A66-40727
- 
- Computer ray tracing study of image-forming in eyes as affected by pupil size, refractive indices and curvatures of cornea and lens 23 p4025 A66-41149
- 
- Supersonic aerodynamic problem of wing-body interaction and solution within lifting-surface theory, using analog method [ICAS PAPER 66-22] 23 p4008 A66-41254
- 
- LF pulse propagation, describing measurement technique and Fourier transform of signal 23 p4039 A66-41588
- 
- General method for determining real solutions of set of nonlinear simultaneous equations, using digital computer 23 p4086 A66-41923
- 
- Radiation control of ruby laser by diffraction modulator with traveling ultrasonic wave, noting computer solution of kinetic equations of population balance, radiation density, characteristic damping, etc 24 p4219 A66-42128
- 
- Rivet attached stringer effect on stress concentration in thin elastic sheet with crack solved, using computer calculations 24 p4285 A66-42143
- 
- Pressure, temperature, gas velocity, thrust and specific impulse of rocket combustion chambers determined, using differential equation and Runge-Kutta method 24 p4261 A66-42743
- 
- Monte Carlo analysis of plasma of heavy ions, obtaining thermodynamic properties, potential energy and pair distribution 24 p4245 A66-43036
- 
- Book on space navigation guidance and control covering manned lunar landing guidance, pulse torquing and inertial measurement units, computer utilization, control systems, etc [AGARDOGRAPH 105] 24 p4235 A66-43122
- 
- COMPUTER PROGRAM**
- 
- SA DATA PROCESSING
- 
- SA FORTRAN
- 
- SA MINIMUM VARIANCE ORBIT DETERMINATION /MINIVAR/
- 
- SA ROCKET COMPUTER PROGRAM
- 
- SA STRESS COMPUTER PROGRAM
- 
- Computerized tools and constant analysis for real time experiment flight management planning system 02 p0306 A66-11638
- 
- Computer processing of data obtained from panoramic vertical sounding of ionosphere to separate reliable portions of height-frequency characteristic from total 02 p0224 A66-12122
- 
- Computer program for average values of critical frequency of F-2 layer and deviation 02 p0224 A66-12125
- 
- Computer program and technique for adaptive digital controller that learns switching regions for optimal control of decision-making regulator system 04 p0490 A66-13621
- 
- Control system 465L used by Strategic Air Command noting automated functions, data processing, integration of human and electronic elements, etc 04 p0507 A66-13687
- 
- Computer-directed malfunction checkout of rockets, boosters and modern military aircraft 04 p0526 A66-14020
- 
- Digital computer calculation of linear transistor amplifier performance from two-port y-parameter measurements 05 p0645 A66-14587
- 
- Digital computer simulation for phase-locked loops used as narrow-band tracking filters in space communications and radar systems 05 p0652 A66-14590
- 
- Iterative procedure for analyzing linear electrical networks by digital computer 05 p0638 A66-15127
- 
- Monte Carlo computer program for simulation of thermal radiation among opaque surfaces in vacuum [ASME PAPER 65-WA/HT-40] 05 p0792 A66-15668
- 
- Stresses calculated in centrifugal impeller with cover disk by two-dimensional stress analysis and digital computer program [ASME PAPER 65-WA/FE-17] 05 p0780 A66-15701
- 
- Automatic recognition of spoken digit programs, using low bandwidth measures related to articulatory rather than to acoustic properties of speech 05 p0629 A66-15735
- 
- Automatic program conversion system for operations with radioactive materials 06 p0838 A66-16604
- 
- Best-fit sphere approximation to general aspheric lens surface, discussing computer program 09 p1402 A66-20514
- 
- Computer program for numerical solution of uniform hollow waveguides with boundaries of arbitrary shape 09 p1346 A66-20607
- 
- Algorithm to automatically ascertain admissible processing sequence for all-digital simulation of analog or analog-hybrid system 10 p1507 A66-21699
- 
- Digital simulation languages, discussing history, input format, effectiveness, programming error diagnostics, etc 12 p1826 A66-23826
- 
- Computer program for teaching senior graduate engineering course in application of matrices 12 p1828 A66-23842
- 
- Computer program for predicting satellite long-term orbit decay and digital simulation of atmosphere and reentry conditions [AIAA PAPER 66-357] 12 p1951 A66-24491
- 
- Computer oriented manned orbiting laboratory with reduced crew duties, noting computer role in navigation problems, repairs, continuous ion thrust, etc 13 p2190 A66-25245
- 
- Computer graphics in communication 13 p2085 A66-25364
- 
- Computer programs for efficiency predictions of axial flow turbines, using Ainley-Mathieson and Soderberg methods of loss correlation 13 p1991 A66-26224
- 
- Electromagnetic wave propagation near missiles during hypersonic atmospheric reentry and computer program for determination of dissociated and ionized particle density in nonequilibrium nitrogen-plasma flow 13 p2150 A66-26374
- 
- Computer program with data compilation, using equivalent circuit for p-n diode, employed in design of coaxial wideband variable attenuator 14 p2246 A66-26833
- 
- Dynamic unified structural analysis method in computer program, calculating stiffness matrix to obtain natural frequencies and mode shapes 14 p2405 A66-27997
- 
- Computer processing of data obtained from panoramic vertical sounding of ionosphere to separate reliable portions of height-frequency characteristic from total 14 p2287 A66-28081
- 
- Computer program for average values of critical frequency of F-2 layer and deviation 14 p2287 A66-28083
- 
- Structural analysis by network theory, matrix formulation and computer programs 15 p2614 A66-29613
- 
- Subroutines and functions of BE VISION, package of FORTRAN programs for drawing orthographic views of combinations of plane and quadric surfaces 15 p2510 A66-29770
- 
- Graph analysis by connectivity considerations, based on generating and characteristic functions, noting application to sampled data systems, discrete Markov processes, computer programs, etc 15 p2453 A66-29771
- 
- PROP computer program written in FORTRAN for ATLAS computer for refinement of satellite orbital parameters 15 p2603 A66-30000
- 
- Computer program for axisymmetric nonlinear behavior of stiffened elastic shells of revolution with variable thickness, calculating collapse pressures [AIAA PAPER 66-529] 16 p2814 A66-30527
- 
- Dispersionless ballistics patterns of weapons analyzed as check on reported computer program 16 p2831 A66-31147
- 
- Computer program for current profile and trajectory analysis for cesium contact thruster leading to integral focus configuration of multistrip contact engines for long space missions [AIAA PAPER 66-206] 16 p2792 A66-31690
- 
- BESM-2 computer program for calculating parabolic comet orbit from three observations 17 p2877 A66-31808
- 
- Analog simulation and performance prediction techniques in reliable circuit design and analysis, emphasizing programming procedures using Monte Carlo and worst-case methods 17 p2877 A66-32302
- 
- Power spectral density computer program for vibration-acceleration calculation 17 p2878 A66-33039
- 
- General processor and postprocessor elements of numerical control computer system 17 p2930 A66-33090
- 
- Transfluxor program store for airborne digital computer, noting wiring pattern, economics, read amplifier, etc 18 p3072 A66-33562
- 
- Method of characteristics computer code applied to partial differential equations of inviscid fluid, calculating flow fields [AIAA PAPER 66-412] 18 p3097 A66-33637
- 
- Computer programs for combustion rates of hydrogen-air mixture 18 p3063 A66-33830
- 
- Digital simulator program /MIMIC/, discussing operation, application to parallel systems and advantages over MIDAS system 19 p3306 A66-35535
- 
- Flexible lens design program system for determining optimum solution to set of requirements 19 p3399 A66-35825
- 
- Computer programs for generalized orthonormal optimization problems and variations such as multilayer optical filter design 19 p3308 A66-35869
- 
- Probe and edge theorems for nonlinear optimization algorithms using stored-program computers 19 p3309 A66-35873
- 
- Optimal computer search and application to engineering design 19 p3309 A66-35875
- 
- Maintenance problems in long space missions by simulation type computer program 19 p3469 A66-35976
- 
- Design of digital computer program of Monte Carlo variety for analyses of self-contained orbital navigation systems for satellites, including error source categories 20 p3595 A66-36871
- 
- Digital computers used in error calculation in calibration curves of turboengines and other pneumatic devices 20 p3555 A66-36923
- 
- Digital computer optimization program, determining minimum weight fuel cell primary power system for MOLAB 20 p3496 A66-37156
- 
- Payload integration in space experimentation, discussing commonality, flight and load matrices, experiment-spacecraft-ground system interfaces, computer methods, etc 20 p3662 A66-37186
- 
- Space packaged automatic checkout system for aerospace vehicles including test equipment, control, measurement capability and computer program 20 p3542 A66-37244
- 
- Intensity and center-to-limb variation of continuous solar spectrum for several models of chromosphere 20 p3650 A66-37340
- 
- Stiffness method for analysis of elastic-plastic shells of revolution with axisymmetric loading implemented by step-by-step method of integration in computer program 20 p3667 A66-37482
- 
- Critical Human Performance and



- Evaluation /CHPAE/ Program 20 p3509 A66-37893
- Digital computer program for solution of space-charge-flow problem applied to design of thrusters with variable thrust vector, analyzing two ion-thruster configurations with aid of computer 20 p3629 A66-38179
- Applicability of inverse blunt-body computer program /Norair/ to supersonic and transonic flow problems 21 p3694 A66-38731
- Computer code packages for radiation shielding calculations 21 p3769 A66-39392
- Digital computer program for static worst case design of diode transistor logic 22 p3870 A66-40396
- Logical processing units and interconnection networks design noting reliability, fault diagnosis, computer coordination of data and control processes, etc 22 p3871 A66-40728
- Digital computer program for analysis and weight optimization of thermoelectric generators for space applications 24 p4161 A66-42119
- Computer technique for constitutive equations of viscoelastic modulus, using Laplace transform and Volterra integral equation, applied to data on solid propellants 24 p4289 A66-42279
- Computer program for parametric analysis and trajectory simulation for axisymmetric planetary entry vehicles 24 p4283 A66-42792
- Computer program for calculating average lengths of weather radar echoes and pattern bandedness from exponential function approximations to pattern autocorrelation coefficients 24 p4234 A66-42988
- Onboard calculation for navigation and guidance of Apollo mission vehicle [AGARDOGRAPH 105] 24 p4236 A66-43125
- ### COMPUTER PROGRAMMING
- #### SA LINEAR PROGRAMMING
- #### SA REDUNDANCY ENCODING
- Power series expansions as solutions to differential equations, using electronic computers 01 p0091 A66-10163
- Solution to linear programming problems, using iterative method 01 p0050 A66-10170
- Computer programming of diagonal tension analysis of flat panels in shear 01 p0152 A66-10345
- Three parameter antenna pattern synthesis using nonlinear computer programming technique derived from method of steepest descent 01 p0044 A66-10934
- Computation of values for resistances shunting sections of tapped potentiometers from data using two alternative digital computer programs 02 p0200 A66-11884
- Mechanization of synchronous sequential machines with minimal shift registers, using algorithm 03 p0337 A66-12572
- Machine dependence of degree-of-difficulty relation for recursive functions, considering Turing machine as programmed computer 04 p0489 A66-13366
- Programming techniques for optimizing computer use especially in space tracking network 04 p0489 A66-13609
- Arbitrary quasi-orthogonals for calculating flow distribution in turbomachine, noting digital computer calculations 05 p0662 A66-14989
- Data collection system with small on-line computer that monitors stress, temperature, pressure and other physical parameters of environmental laboratory vacuum and temperature chambers [ISA PREPRINT 1.12-1-65] 05 p0638 A66-15502
- Digital computer programming for design of cylindrical vessels 08 p1306 A66-18604
- Power supply system of OAO consisting of solar cells, energy storage device, power controller, etc, and simulation program via digital computer 08 p1168 A66-19493
- Gradient systems of differential equations for solution of linear and quadratic programming problems on analog computer 08 p1188 A66-19687
- Computer code for stress and displacement of shells of revolution under axisymmetric loading 09 p1469 A66-20967
- Generation, selection and implementation of burst-error-detecting and -correcting Fire code, using computed tables 10 p1496 A66-21513
- Analog computer techniques applied to find roots of complex functions, to generate complex functions by Cauchy integral theorem and to scan  $z$  plane 10 p1507 A66-21693
- Advanced Data Management computer programming to provide generalized routines for functions common to large class of command and management problems 10 p1623 A66-22050
- Device for automatically feeding experimental curve coordinates in large quantities into digital computer for high noise level photographic image 11 p1659 A66-22432
- Computer input language for minor engineering calculation 11 p1659 A66-22712
- SCADS, programming system for simulation of combined analog-digital systems 11 p1659 A66-23109
- Programming procedures for analog computer solution of problems consisting of more than 250 linear and nonlinear computing elements 11 p1660 A66-23224
- Guidance by parabolic extrapolation of short-range missile toward pre-established target controlling it aerodynamically, noting finder, computer and navigational errors 11 p1734 A66-23500
- American Federation of Information Processing Societies, Joint Computer Conference, Las Vegas, November 1965 12 p1825 A66-23824
- User-oriented computer programming system using Flexowriter modified to construct new two-dimensional programming language 12 p1826 A66-23828
- Flow of data and control information from apparatus to computer and use of microprogrammed controller 12 p1827 A66-23829
- Management problems of large aerospace computer installation, considering actual costs of change and aspects of turn-around problem 12 p1827 A66-23831
- Management of large physical systems, detailing characteristics of mission planning for Mars exploration including process optimization, computer programming, systems engineering, etc 13 p2179 A66-25238
- Decomposition technique by which convex control programming problem, having coupled subsystem constraints, can be decomposed into smaller subproblems 13 p2117 A66-25349
- Programming under uncertainty and stochastic optimal control for two-stage system treated by derivation of equivalent convex program 13 p2047 A66-25351
- COBLOC programming system for all-digital simulation of operation of large mode-controlled hybrid computers, noting inclusion of patchable logic simulation 13 p2028 A66-25805
- Method for automatically adjusting networks for best approximation to desired responses, using iterative gradient techniques, constraint equations and Carroll programming technique 13 p2051 A66-26070
- Computer programming method for analysis of complex systems 13 p2028 A66-26474
- Programmable patching system at Cape Kennedy for communications network composed of two individual switching subsystems, using solid state devices and glass-reed relays 14 p2233 A66-26805
- Computer design of programmable demultiplexer for multiformat PCM telemetry data 14 p2246 A66-28432
- Arbitrary quasi-orthogonals for calculating flow distribution in turbomachine, noting digital computer calculations [ASME PAPER 65-WA/GTP-2] 16 p2684 A66-30344
- Iterative solution to Krook-Boltzmann kinetic equation noting Navier-Stokes numerical solution, computation and analysis of distribution function within shock wave 16 p2685 A66-30945
- Monte Carlo solutions to two molecular flow problems, heat transfer between parallel walls and shock wave profile-computer programmed in Boltzmann equation analysis 16 p2686 A66-30946
- Molecular-kinetics experiments /trajectory calculation of particle interaction/ using digital computer iterative method for theoretical comparison 16 p2656 A66-30947
- Stability of idealized laminar boundary flow, determining phase velocity, amplification rate and wave number of all disturbances 16 p2686 A66-30948
- AFIPS Joint Computer Conference, Boston, April 1966 16 p2656 A66-31239
- Upper air sounding analysis using electronic computer 17 p2921 A66-33340
- Gradient systems of differential equations for solution of linear and quadratic programming problems on analog computer 18 p3073 A66-34673
- Optimization techniques - Symposium, Carnegie Institute of Technology, Pittsburgh, April 1965 19 p3307 A66-35867
- Optimizing procedures using Fortran II FAP programming on IBM 709/7090 computers, comparing eight known techniques 19 p3308 A66-35868
- Computer algorithm for geometric programming methods 19 p3309 A66-35874
- Iterative approximation method for solution of proper elements /eigenvalue/ of Sturm-Liouville equation 19 p3392 A66-36783
- Parallel evaluation of Boolean function in search memory via multiwrite 20 p3523 A66-38017
- Digital programming and topological optimal filter design incorporating nonideal lossy elements 20 p3533 A66-38281
- Program controlled device for applying tensile force and torque to thin walled tubular specimen during analysis of creep under stress 21 p3827 A66-38618
- Computer programming of pulse compression by active and passive generation, noting differences between sidelobe structures of generation 22 p3883 A66-39714
- Programmed oscillators to control Doppler tracking radar systems for space communications and radar astronomy 22 p3862 A66-39731
- Integration of near equilibrium flows in propulsive nozzles, estimating length of transition region from equilibrium condition to kinetic solution [AICE PREPRINT 28C] 22 p3971 A66-39884
- Digital computer programming to evaluate designs until optimality is found in aerospace structures 22 p3922 A66-40023
- Programming tasks optimization through infinite iteration procedure 22 p3941 A66-40542
- Rational and optimal programming of electronic computers, noting application to structural mechanical problems 23 p4137 A66-41005
- Convex programming procedure yielding algorithm for tuning out system from possible resonance zone 23 p4090 A66-41408
- Digital computer program for handling algebraic expressions in complex numbers 23 p4042 A66-41739
- Matrix interpretive codes including SELMA, FORTRAN and ALGOL 23 p4042 A66-41740
- Digital computer techniques for computation of lunar disturbing function 24 p4273 A66-42204
- ### COMPUTER SIMULATION
- #### SA ANALOG SIMULATION
- #### SA DIGITAL SIMULATION
- One-dimensional collisionless plasma in computer simulation with randomized electrons compared with static theory for equivalent diode 01 p0112 A66-10591
- Analytical landing simulation to analyze dynamic loads and aircraft response, particularly high sink speed landing gear [SAE PAPER 650845] 01 p0011 A66-10835
- Computer flight simulators at Langley discussing Boeing 707 jet, helicopter, air traffic control, orbital rendezvous and docking, lunar navigation and landing 01 p0055 A66-10957
- Computer simulation of pattern recognition system employing same variables as human visual system and using cell assemblies and contour projection 01 p0034 A66-10963
- Task loading effect on pilot performance in computer simulated low altitude high speed flight 02 p0187 A66-11829
- Hybrid computer simulation system for aeronautical and astronautical test work 02 p0215 A66-11893
- Automatic pattern recognition and



application to space navigation 04 p0543 A66-13511

Neutralizer configurations, immersed and withdrawn filaments, for given ion gun based on two-dimensional computer simulation of ion-beam neutralization [AIAA PAPER 65-380] 05 p0723 A66-15168

Jet engine models applicable to analog and Dynasor simulation for transient performance analysis [ASME PAPER 65-WA/MD-16] 05 p0745 A66-15521

Total tactical radar system, describing integrated system, operational functions and computer simulation 06 p0823 A66-15955

Saturn V diphasic data modem, describing computer system for prelaunch checkout 06 p0868 A66-15989

Heuristic approach to reinforcement learning control systems, describing operation and simulation on IBM 1710-GEDA hybrid computer 06 p0864 A66-16734

Simulation of airport with SST aircraft in air traffic control system 07 p1070 A66-17725

Model of North Atlantic air space organized as sets of paths at various heights 07 p1072 A66-17763

Computer simulation of randomization of electrons in collisionless plasma 08 p1260 A66-18538

Onboard lunar orbital navigation system simulation, using minimum variance estimation 08 p1249 A66-18818

Support Evaluation Technique for computer simulation, evaluation and control of complex logistic problems 08 p1203 A66-19527

One-tape off-line Turing machine, analyzing characteristics and computation time minimization 10 p1506 A66-21075

Electro-optic system superiority over radio and inertial techniques for space navigation determined by simulation 10 p1554 A66-21893

Book on analog, digital and hybrid analog-digital computers for random process studies 11 p1659 A66-22864

Digital computer simulation of stochastic multibeam communications channel with long-distance tropospheric propagation of ultrashort waves 12 p1812 A66-23732

New block diagram compiler for sampled data system simulation 12 p1826 A66-23827

Hybrid computer simulation of lunar excursion module and maneuvers with orbiting command service 12 p1828 A66-23839

Analog computer, programmed on digital computer, used in examination of lumped and distributed parameter models of cardiovascular system 12 p1809 A66-24230

Lower ionosphere guidance of HF and VHF waves for global communications, outlining computer simulation of phenomenon of whispering galleries 13 p2023 A66-25780

Flight simulation of SST transport using hybrid computer 13 p2028 A66-26330

Circulation distribution over rectangular wings, based on Chushkin algorithm and lifting surface equation calculated by digital computer 13 p2068 A66-26540

Mathematical models for logistics planning providing complete analysis of requirements through computer simulation 14 p2245 A66-27122

Nonlinear gyroscopic system equations solved by analog computer and verified through method of harmonic linearization 14 p2294 A66-27362

Neutralizer configurations, immersed and withdrawn filaments, for given ion gun based on two-dimensional computer simulation of ion-beam neutralization [AIAA PAPER 65-380] 14 p2342 A66-27411

Tracking interruption probability in second order astatic system, obtaining solution from Fokker-Planck equation and computer simulation 14 p2265 A66-27524

Approximation of variable time delays and design of constant and variable delay circuits, noting simulation of delays in automatic control systems by computers 14 p2266 A66-27528

Missile propellant explosion simulation by digital computer with estimate of physical parameters 14 p2395 A66-28445

L/D ratio for gliding recovery of first

stage of launch vehicle, using stage separation conditions as parameters 16 p2807 A66-30348

Discrete transfer functions simulated on analog computer by direct currents 16 p2656 A66-30584

Quasi-redundant system reliability, solving differential equations for repair environment via computer 16 p2714 A66-30665

Nonstationary problem of linear filtering in presence of additive noise solved by computer simulation 16 p2669 A66-30762

High speed computer technique for simulating test design parameters for evaluation of ballistic-weapon system accuracy [AIAA PAPER 65-222] 16 p2809 A66-30888

Large launch vehicle cryogenic propellant logistics including storage and production capacity optimization, cost and heat loss analyses by computer simulation [AIAA PAPER 65-259] 16 p2789 A66-30900

Numerical model of Earth atmosphere used to compute hydro-and thermodynamic evolution of global moist atmosphere, considering solar heating, evaporation, etc 16 p2697 A66-30943

Helicopter simulation system for avionic evaluation 16 p2682 A66-31248

Simulation of fourth order type I linear system, using one-operational amplifier and two-terminal network consisting of four resistors and four capacitors 16 p2672 A66-31385

Three-stage time division switching network with pulse shifting and direct junctors using computer simulation for blocking probability estimation 17 p2878 A66-31812

Computer solution using Bubnov-Galerkin method to determine concentrated force effect on shallow spherical dome 17 p3026 A66-32601

Loss of power effects on helicopter at high speeds, noting combination of blade analysis with motion equations, application of computer simulation, etc 17 p2845 A66-32735

Propellant tanking computer system for monitoring and controlling Saturn IB and Saturn V vehicles [SAE PAPER 66-0454] 17 p2904 A66-33162

Human factor aspects of digital computer programming for simulator control, discussing application and operation 17 p2869 A66-33449

T-27 space flight simulator design, system performance and use for training and research at USAF Aerospace Research Pilot School [AIAA PAPER 65-265] 18 p3093 A66-33789

Sensitivity of linear and nonlinear systems to parameter variations studied by analog computer simulation 18 p3089 A66-33910

High speed hybrid computer simulation of aerospace vehicle motion 18 p3094 A66-34068

Computer-simulated mathematical model of thermal environmental effects on expulsion system design parameters for liquid-propellant gas-generator rocket engine [AIAA PAPER 66-686] 18 p3183 A66-34228

Three-fluid hydromagnetic computer code for studying dynamic phase of small theta-pinch, noting effects of impurity ionization and radiation losses 18 p3148 A66-34911

Computer simulation and performance prediction of MMU astronaut maneuvering system, discussing acceleration, velocity, displacement, fuel consumption, propulsion efficiency 19 p3291 A66-35964

Maintenance problems in long space missions by simulation type computer program 19 p3469 A66-35976

Parameter evaluation of delta modulation encoding techniques for image communication applications by computer simulation 20 p3513 A66-37201

VTOL operational availability computer simulation model, studying initial and tradeoff design, maintenance, logistics, manpower and flight operational requirements 20 p3543 A66-37909

Monte Carlo technique of importance sampling applied to estimating probability of occurrence of rare event in complex system by fault tree simulation 20 p3543 A66-37912

High-speed rotor operation in bearing clearances, discussing induction of nonlinear

vibration, harmonic generation and computer simulation results [ASME PAPER 66-MD-1] 21 p3741 A66-38474

Gravity gradient satellite stabilization and performance analyzed, using computer simulation of motion equations, including eddy current dampers, solar effect, orbital eccentricity, etc 21 p3819 A66-38857

Computer simulation techniques, including stochastic phenomena and computer-computer applications performance evaluation 21 p3708 A66-39432

Laplace transformation simulation by analog computer for real and complex values 22 p3870 A66-39996

Digital computer simulation of stochastic multibeam communications channel with long-distance tropospheric propagation of ultrashort waves 22 p3865 A66-40075

Computer simulation experiments design for industrial systems, considering variance techniques, multiple ranking procedures, sequential sampling and spectral analysis 22 p3870 A66-40132

Conceptual analytical method for simulating lunar surface environment, using computer program for parametric curves 22 p3888 A66-40210

Saturn computer design and fault simulation on IBM 7090 22 p3871 A66-40744

**CONCENTRATION**

S ATOM CONCENTRATION

S CARBON DIOXIDE CONCENTRATION

S STRESS CONCENTRATION

**CONCENTRATOR**

SA COLLECTOR

Determination of refractive index of polyethylene terephthalate film necessary in calculations of surface shape of film concentrators 20 p3603 A66-37738

Charged particle radiation shielding in space of solar cell panels by use of concentrator geometry 22 p3852 A66-40512

**CONCENTRIC CYLINDER**

Cavitation induced between rotating and stationary cylinder in vaporizing liquid within gap of simulated electric motor configuration 07 p1039 A66-18176

Electromagnetic scattering from infinite cylinder at oblique orientation 15 p2537 A66-28976

Heat transfer in liquids situated in gap between coaxial cylinders in presence of natural convection, determining effective thermal conductivity coefficient for water and ethanol 16 p2825 A66-30325

Hydrodynamical modification of Heller treatment of mixing and unmixing of viscous fluid between two rotating cylinders 16 p2685 A66-30940

Incompressible viscous conducting flow between two concentric cylinders in radial magnetic field 16 p2765 A66-31376

Viscous incompressible fluid motion between two parallel planes and between two co-axial circular cylinders with one boundary moved by impulse 17 p2916 A66-33418

Thermoconductivity through rarefied gases at rest contained between concentric cylinders, varying pressure 19 p3478 A66-36061

Radiant heat transfer between concentric cylinders determined by extending validity of Rosseland diffusion approximation by introducing temperature jump boundary condition at gas solid surface 21 p3837 A66-39462

**CONCORDE AIRCRAFT**

PERT programming applied to design and manufacture of joint Anglo-French Concorde aircraft 02 p0305 A66-11599

Human factors in Concorde SST program 03 p0329 A66-13357

Air conditioning system of SST Concorde noting reliability 04 p0460 A66-14461

Olympus 593 jet engine for Concorde SST, development, performance and reliability 05 p0744 A66-14768

Functional requirements for computer navigational system for Concorde aircraft 07 p1065 A66-17672

Design status of Concorde navigation system, discussing basic system, interconnection with autopilot and flight director system and optional equipment 07 p1078 A66-17805



Economic aspects of Concorde program, research potential, computational methods and technological progress 08 p1322 A66-19080

Concorde SST aircraft prototype design and development 09 p1329 A66-20132

Single stage bootstrap air conditioning with two-position turbine nozzle for improved high altitude descent conditions for Concorde SST 09 p1331 A66-20133

Concorde navigation system noting inertial platform, digital computer using integrated circuits and microminiaturization 09 p1401 A66-20685

Structural design of Concorde supersonic airframe, noting airframe strength parameters 10 p1483 A66-21717

Air conditioning system of SST Concorde noting reliability 11 p1640 A66-22250

Concorde fuel system in cooling application and adjustment of center of gravity through fuel distribution 11 p1637 A66-23168

Olympus 593 B engine design and characteristics for Concorde application 13 p2172 A66-25564

Concorde aircraft progress report 14 p2223 A66-28106

Concorde aircraft front and rear auxiliary landing gear noting geometry, steering and anti-shimmy control, etc 16 p2633 A66-30317

Main landing gear design for Concorde SST 17 p2846 A66-32950

Biological hazard of radiation doses to which passengers of high-flying Concorde aircraft may be subjected, considering use of in-flight warning meter 19 p3452 A66-35796

Structural design criteria for Concorde aircraft, including necessity for heat-resistant airframe material 20 p3666 A66-37400

Concorde supersonic transport aircraft propulsion, fuel supply and storage systems 22 p3848 A66-40415

Duplicate monitored system for automatic landing control of VC10 and Concorde 23 p4088 A66-41163

Design characteristics and marketing prospects of Concorde SST 23 p4015 A66-41301

Supersonic transport production problems, discussing Concorde, Lockheed and Boeing projects, machining, shaping and assembling 23 p4073 A66-41649

Propulsion control systems for Concorde aircraft, noting aero-and thermodynamic reasons for power plant variables subject to manipulation 23 p4122 A66-41776

British-French cooperation in aeronautics, discussing Concorde SST, variable geometry aircraft, Olympus 593 turbojet, etc 23 p4016 A66-42069

**CONDENSATION**

**SA CORONAL CONDENSATION**

**SA FILM CONDENSATION**

**SA NUCLEATION**

Condensation in underexpanded jet issuing from sonic orifice into quiescent atmosphere 01 p0007 A66-10617

Air condensation in hypersonic wind tunnel strongly related to flow expansion rate 01 p0059 A66-10808

Sticking coefficients for interaction of molecular oxygen with clean semiconductor surfaces assuming immobile adsorption process 03 p0408 A66-12406

Cumuli above sea in spite of stable layer between sea surface and cloud boundary, noting condensation around salt particles penetrating ascending thermals 04 p0542 A66-14306

Potassium condensing tests of horizontal multitube convective and radiative condensers operating at vapor temperatures from 1250 to 1500 degrees F 05 p0786 A66-14932

Liquid metal condensation, noting two-phase turbulent condensation mechanism and determining heat transfer coefficients 07 p1152 A66-17592

Propellant properties and particle formation efficiency determined for homogeneous condensation-type colloid thruster [AIAA PAPER 66-253] 11 p1760 A66-22221

Measurements of decay curves of stored Aitken nuclei with photoelectric nucleus counter show small nonrandom divergencies

from theoretical curves 11 p1707 A66-23098

Load capacity of condensing vapor-lubricated long self-acting journal bearing, examining two-phase and single-phase regions [ASME PAPER 65-LUBS-5] 12 p1888 A66-24554

Condensation in underexpanded jet issuing from sonic orifice into quiescent atmosphere 13 p1990 A66-25178

Detonation limits for binary mixtures of tetramethylsilane with oxygen, analyzing factors controlling transition from detonation to deflagration, noting condensation effects 13 p2209 A66-26303

Cumuli above sea in spite of stable layer between sea surface and cloud boundary, noting condensation around salt particles penetrating ascending thermals 14 p2327 A66-28219

Oblique condensation discontinuities calculated during flow of supercooled water vapor in supersonic jets 16 p2690 A66-31608

Preparation temperature and condensation rate effect on current carrier mobility in lead selenide and telluride films 16 p2787 A66-31769

Detonations in explosive gaseous mixtures and detonations in condensed phase, discussing three-dimensional vibratory phenomena, wall effects and transition between deflagration and detonation 17 p3036 A66-32846

Carbon dioxide supersaturation and condensation in supersonic nozzles in terms of stagnation pressures, temperatures, and expansion rates 17 p3039 A66-33476

Condensation tests in smooth and porous coated tubes in multi-g centripetal acceleration fields for increasing heat transfer coefficient of condensing nitrogen 18 p3262 A66-34379

Molecular-kinetic resistance effect on heat exchange in Nusselt-type vapor condensation on vertical plate and in vapor-bubble growth in superheated liquid 19 p3479 A66-36310

Vapor condensation effects on wind tunnel measurements, noting relation between air-moisture and flow field, shock wave intensity increase and density measurements on circular airfoils 22 p3843 A66-39697

**CONDENSATION PUMP**

**SA VACUUM PUMP**

Hydrogen ion intrusion into stainless steel surface measured with apparatus in which hydrogen and helium condensation pumps provide ultrahigh vacuum 13 p2108 A66-25754

Rarefied supersonic flow condensation on cold flat plate, noting capture coefficients, shock wave behavior, etc 16 p2825 A66-30383

Hydrogen pumping by means of phenomenon of hydrogen absorption by solid layer of carbon dioxide condensed at temperature of 20.4-14 degrees K 19 p3400 A66-36099

**CONDENSER**

**S CAPACITOR**

**S GERDIEN CONDENSER**

**CONDITIONED RESPONSE**

**SA LEARNING**

**SA REFLEX**

Food reinforcement of pigeons, comparing two types of extinction following fixed ratio training, noting response rate variation 09 p1336 A66-20876

Conditioned reflex role in information of subthreshold stimuli of respiratory system in dogs subjected to electric shock and carbon dioxide increase 14 p2228 A66-27185

Repeated vertical vibration and noise effects on conditioned reflexes of rats 23 p4026 A66-41339

Vibration effect on conditioned reflexes, oxidation mechanism and electric activity of brain in rats 23 p4027 A66-41342

Neutron, proton and gamma radiation effect on small animals examined, using conditioned response drinking method 23 p4027 A66-41345

Gamma and fast neutron radiation effect on nervous activity of mice examined, using conditioned reflex drinking method 23 p4028 A66-41346

Gamma radiation, fast neutron and proton effect on conditioned and motor responses, nervous activity, excitation and inhibitory processes of white rats 23 p4028 A66-41347

Effect of total chronic and acute gamma

radiation on higher nervous activity of white rats 23 p4028 A66-41348

Conditioned motor food reflexes of rats exposed to vibration, vibrostand noise and X-ray 23 p4028 A66-41351

Possible sustention of observing behavior in pigeons by stimuli of chain schedule or by stimuli correlated with passage of time in interval schedules 24 p4167 A66-42366

Neuronal spike populations and EEG activity in chronic unrestrained cats, noting multiple unit responses of acceleration/inhibition during behavioral conditioning procedures 24 p4169 A66-43098

**CONDUCTING MEDIUM**

Electrohydrostatic boundary equations solving two- and three-dimensional axisymmetric situation and sessile drop problem 04 p0545 A66-13808

One-dimensional unsteady flow of ideal compressible finite conductivity medium in presence of mass forces and plane magnetic field 04 p0516 A66-13856

Radiation from vertical magnetic dipole in inhomogeneous stratified media above horizontal conducting plane, noting Hertz potential as contour integral 04 p0483 A66-14041

Non-one-dimensional solutions of MHD equations for axisymmetric motion of electrically conducting gas in magnetic field 04 p0552 A66-14153

Two-dimensional flow of inviscid nonheat-conducting gas with variable conductivity in crossed constant electric and arbitrary magnetic fields 04 p0557 A66-14422

MHD flow in rectangular ducts, discussing laminar motion of conducting liquid under uniform transverse magnetic field 04 p0558 A66-14475

Electrophoretic motion of dielectric particle determined from flow rate of liquid metals and semiconductors near infinite plane 05 p0733 A66-14688

Formalism for determining linearized hydromagnetic wave phenomena in perfectly conducting plasma permeated by static magnetic multipole field 05 p0720 A66-14709

Corrugation growth on infinitely conducting fluid sheets, discussing acceleration induced by constant axial and linearly increasing currents 06 p0871 A66-16276

Shock wave propagation in electrically conducting incompressible fluid imbedded in magnetic field 07 p1089 A66-17975

Electromagnetic interaction between moving conducting ring and magnetic field inducing voltage in search coil 07 p1091 A66-18416

Explosive wave propagation during cylindrical and plane explosions in ideal electrically conducting gas, taking account of counterpressure and magnetic field 08 p1208 A66-19372

Steady state exothermal hydromagnetic discontinuity in perfectly conducting gas for arbitrarily oriented magnetic field 08 p1267 A66-19822

True heat capacity of solid heat-resistant dielectric or conducting materials at high temperatures 09 p1470 A66-20141

Induction synchronous MGD generator fed with jet of varying-conductivity working medium 10 p1484 A66-21313

Electromagnetic wave diffraction around finite perfectly conducting cone 10 p1506 A66-21924

Stationary flow of viscous incompressible anisotropically conducting fluid in coaxial channel 11 p1743 A66-22235

Hydraulic resistance coefficient dependence on Reynolds and Hartmann numbers in turbulent flow of conducting fluid through tube in magnetic field 11 p1743 A66-22337

Stability of forward and rearward slug flows due to motion of body through perfectly conducting liquid with embedded magnetic field 11 p1746 A66-23011

Input impedance of spherical emitter in infinite homogeneous isotropic conducting medium 11 p1656 A66-23031

Plane electromagnetic wave scattering by conducting cylinder surrounded by hot magnetoplasma sheath 11 p1657 A66-23112

Magnetic forces effect on laminar wall jet of electrically conducting incompressible



fluid of constant properties 12 p1796 A66-23594  
 Electromagnetic properties of gases interacting with magnetic fields whose conductivity increases with temperature 12 p1919 A66-23642  
 Hot-wire anemometer applications to turbulence measurements in conducting liquids and vacuum deposition of quartz film on coated hot-film probe 12 p1880 A66-23848  
 High speed photography determination of current cut-off and recurrent breakdowns during electrical discharges in water 12 p1922 A66-24221  
 Pressure distribution of viscous electrically conducting fluid in lubricating layer of cylindrical bearing 12 p1887 A66-24425  
 X-ray radiation effect on electrical conductivity of liquid organic semiconductors obtained on diethyl ether base with halogen derivatives of benzene, methane, etc 13 p2160 A66-25096  
 Plane wave diffraction by infinitely conducting network representing diffracted electric field by Rayleigh expansion 13 p2021 A66-25457  
 Electric field force dragging of fine jets from surface of conducting fluid in form of cylinder and hemispheroid on earthed plate 13 p2129 A66-26301  
 Laminar ducted flow of viscous electrically conducting fluid under uniform arbitrarily oriented magnetic field for rectangular duct with nonconducting walls 14 p2342 A66-27407  
 Impedance integral evaluation for antenna loop immersed in conducting medium 14 p2256 A66-27923  
 Theoretical and experimental investigations of electromagnetic scattering by conducting cylinder coated with anisotropic ferrite sheath magnetized along axis 15 p2449 A66-28594  
 Ferrite-air interface in waveguide with conducting thin film coated core solved by use of boundary condition or impedance condition 15 p2565 A66-29053  
 Approximation of electrical conductivity change in ideally conducting gas in turbulent MGD flow 15 p2551 A66-29220  
 Flow in viscous incompressible conducting fluid subjected to magnetic field in concentric cylinders rotating at different angular velocities, assuming planar motion, using differential equations 16 p2757 A66-30214  
 HF backscattering by plane electromagnetic wave incident on imperfectly conducting sphere covered with concentric layers of different materials, noting refractive index value 16 p2647 A66-30224  
 Steady flow of conducting dissociating gas in channel of constant cross section in presence of magnetic field 16 p2687 A66-31165  
 Energy dissipation due to deformation of magnetic field in compressible conducting medium near zero field 16 p2762 A66-31182  
 Conical refraction of magnetosonic waves occurring when Alfvén waves propagate at speed of sound in conducting fluid in presence of constant uniform magnetic field 16 p2764 A66-31364  
 Numerical solution of MHD equations for boundary layer conducting gas flow near flat plate when velocity distribution of external flow obeys power law 16 p2764 A66-31366  
 Busbar effect on interaction between conducting fluid flow and traveling wave magnetic field created by long line with concentrated inductance and capacitance, deriving line gain 16 p2765 A66-31374  
 Incompressible viscous conducting flow between two concentric cylinders in radial magnetic field 16 p2765 A66-31376  
 Reynolds analogy computation of heat transfer coefficient of turbulent electroconducting liquids in transverse magnetic field 16 p2765 A66-31401  
 Two-dimensional MHD jet flow of conducting fluid in coplanar magnetic field and nonstationary flow past body with magnetic field perpendicular to surface 16 p2765 A66-31402  
 Excitation of electroacoustic lateral waves in compressible plasma in contact with conducting boundaries 17 p2962 A66-31817

Viscous forces influence on instability of liquid conductor model of hard-core pinch 17 p2964 A66-32032  
 Hall current effect on capillary instability of finitely conducting liquid jet carrying axial volume current 17 p2908 A66-32432  
 MHD approximation of laminar duct and channel flow of electroconductive viscous Newtonian fluid 17 p2971 A66-32861  
 Finite-difference calculation of MHD flow of conducting fluid past circular cylinder in transverse magnetic field based on Navier-Stokes equation 17 p2971 A66-32862  
 MHD flow of electroconductive fluid in transverse magnetic field 17 p2971 A66-32863  
 Electric and magnetic fields effect on three-dimensional laminar boundary layer of conducting fluid near line of intersection of two surfaces 17 p2971 A66-32865  
 Self-similar solutions of two-dimensional laminar flow of incompressible electroconductive fluid in channel in crossed electric and magnetic fields, using Jacobi elliptic integrals 17 p2971 A66-32866  
 Steady-state axially-symmetric channel flow of ionized gas in external electromagnetic field in one-dimensional approximation 17 p2971 A66-32867  
 Geometric, gasdynamic and electromagnetic parameters of one-dimensional flow of conducting gas with Hall effect for maximum power tapping from channel electrodes 17 p2972 A66-32869  
 Conducting fluid flow velocity measuring technique using properties of pulsed electromagnetic field 17 p2926 A66-32873  
 Unsteady slip flow of electrically conducting viscous fluid over porous flat plate under transverse magnetic field 17 p2973 A66-32980  
 Explosive wave propagation during cylindrical and plane explosions in ideal electrically conducting gas, taking account of counterpressure and magnetic field 18 p3099 A66-34171  
 Conductive sheet analogy applied to steady heat conduction problem, noting evaluation without use of potentiometers 18 p3265 A66-34491  
 Transverse propagation of waveguide modes in conducting cylindrically stratified magnetoplasma analogous to VLF radio waves propagating in Earth-ionosphere 18 p3071 A66-34565  
 Hartree solution of MHD laminar boundary layer incompressible conducting fluids, specifically considering flow at inlet to semiminfinite flat channel 18 p3147 A66-34636  
 Transitions of steady flows of conducting gases through two successive oblique MHD shock waves 18 p3147 A66-34726  
 Lagrange equation for symmetric, nonhomotropic, spherical, cylindrical and one-dimensional unsteady flow of perfectly conducting gas behind normal shock wave of variable strength 18 p3102 A66-34728  
 Force-free magnetic fields generated by orthogonal current systems in unbounded conducting fluid 18 p3151 A66-35032  
 Optimum MHD generators using anisotropic plasma, discussing conducting-gas MHD flow, Hall effect, ion slip effect, etc 18 p3152 A66-35075  
 Conducting nonmagnetic circular cylinder supported on magnetic field produced by alternating current 19 p3324 A66-35729  
 Bending of plane electromagnetic waves around elliptically ideally conducting cylinder of infinite length and around parallel circular dielectric cylinder, with solution as Mathieu-type series 19 p3303 A66-36064  
 Self-similar motions in variable conducting fluid in strong magnetic field 20 p3607 A66-36988  
 Method for calculating distribution of electric potential above conducting media with parallel interfaces for general case of  $n$  layers and arbitrary resistivities of base 20 p3551 A66-37512  
 Resistance and heat transfer coefficient relation theoretically determined for flow of electrically conducting liquid in magnetic field 20 p3679 A66-37614  
 Hamilton principle extended to compressible MHD flow of perfect conducting fluid 20 p3610 A66-37987  
 Differential equations for quasi-

homogeneous MHD flow of electrically conducting medium at low magnetic Reynolds numbers 20 p3611 A66-38109  
 Two-dimensional problem of current distribution on surface of permeable electrodes adjacent to flow of conducting medium under Hall effect 20 p3611 A66-38110  
 Field, mass, momentum and energy conservation, entropy and evolution conditions for steady MHD oblique shock discontinuities in perfectly conducting gas flow with Mach and Alfvén number parameters 21 p3795 A66-39577  
 Steady state equations for one-dimensional flow of conducting medium through channel of MHD generator in homogeneous magnetic field 22 p3952 A66-39692  
 Uniform magnetic field effect on plane acceleration wave propagation and growth in homogeneously deformed perfectly electroconductive elastic material 22 p3955 A66-40135  
 Four-point probe technique to measure conductivity of epitaxial layers on conducting substrates 23 p4110 A66-41157  
 EHD traveling potential wave interaction inducing electroconvection in slightly conducting current without electrical contact with flow 23 p4104 A66-41496  
 Boundary layer control of conducting fluid by transverse magnetic field and spanwise electric field 23 p4107 A66-41904  
 Velocity field of conducting fluid interaction with electromagnetic fields, noting applications to electric propulsion, MGD power generation and reentry 24 p4240 A66-42281  
 Plane laminar jet of incompressible conducting fluid propagating homogeneous magnetic field at magnetic Reynolds number 24 p4196 A66-42872  
 Propagation of weak shock wave in heterogeneous conducting medium in presence of magnetic field 24 p4238 A66-42874  
**CONDUCTION**  
**S IONIC CONDUCTION**  
**CONDUCTION BAND**  
 Thermoelectric emf related to entropy in quantizing magnetic field in semiconductor with polyellipsoidal conduction band 04 p0564 A66-14252  
 Hall effect and resistivity measurements on high resistance  $n$ -silicon related to formation conditions at low temperature of level placed at 160 meV from conduction band 06 p0935 A66-17128  
 Pronounced quantum effects of solid-bismuth plasma properties at quantum limit and low temperature 07 p1082 A66-18212  
 Carrier number fluctuation in semiconductor conduction band due to generation and recombination of charge carriers 07 p1105 A66-18371  
 CdS-type superlinear photoconductivity due to excitation from localized levels 09 p1426 A66-20195  
 Electron tunneling in semiconductors with degenerate band structure 10 p1581 A66-21739  
 Negative-conductance amplification and Gunn effect oscillations in two-valley semiconductors 10 p1583 A66-22066  
 Density of free carriers in semiconductor conduction band varying with electric field, noting growth and phase velocity of RF wave of small amplitude 10 p1584 A66-22070  
 Dependence of threshold field for Gunn oscillations on energy minima separation, noting decrease under uniaxial stress 10 p1584 A66-22073  
 Spin resonance of donor electron in Ge and anisotropic line width in relation to dislocation stress 11 p1750 A66-22463  
 Magnetoresistance of reduced and doped strontium titanate to investigate band structure 12 p1927 A66-23722  
 Negative conductivity, induced by nonequilibrium state in semiconductors, due to short electron lifetime in conduction band 13 p2160 A66-25101  
 Consistency of Gunn effect with excitation of conduction band electrons from high mobility minimum to low mobility valleys 13 p2164 A66-25517  
 Gunn effect in gallium arsenide, noting negative differential electron mobility at high electric fields in conduction



- band 13 p2165 A66-25546  
Hall coefficient increase with temperature and electron transition to second conduction band in InSb 15 p2558 A66-28614  
Conduction band in cadmium arsenide semiconductor, measuring transport phenomena 15 p2560 A66-28635  
Resistivity increase in Cadmium Telluride, attributed to conduction band separation due to deionization into impurity levels 16 p2768 A66-30131  
Negative conductivity, induced by nonequilibrium state in semiconductors, due to short electron lifetime in conduction band 16 p2771 A66-30280  
Effect of thermal population of /000/ and /100/ conduction bands on elastic constants of heavily doped n-type germanium 16 p2778 A66-31070  
Optical reflection, transparency and Faraday effect for indium antimonide, calculating effective electron mass, relation between energy and wave number, etc 16 p2788 A66-31777  
State density for highly doped semiconductor in magnetic field, obtaining results at near Fermi level energies and at bottom of conduction band 16 p2788 A66-31779  
Magnitude of DC conductivity change in CdS by microwave phonons at liquid helium temperature explained with piezoelectric polaron effect 17 p2975 A66-31886  
Quantum theory of electric conductivity of semiconductors with nonstandard band, discussing influence of spin splitting of Landau levels on oscillations of transverse magnetoresistance in n-InSb 17 p2978 A66-32508  
Dangling bonds and dislocations in semiconductors, noting existence of core charge dependent localized state in gap caused by local decrease in atom density 17 p2985 A66-33155  
Steady state distribution functions for photoexcited carriers in semiconductors bands determined by competition between intraband intercarrier collisions and recombination processes 18 p3154 A66-33919  
Conduction band structure of KCl calculated by overlapping-plane-wave method 18 p3156 A66-34470  
Sb concentration and ESR linewidth of Sb donors in compensated and uncompensated n-silicon 18 p3156 A66-34475  
Suggested origin of low energy tails in radiative recombination spectra due to degenerate conduction band 19 p3437 A66-35475  
Dipole scattering of electrons in germanium and silicon whose conduction-band structure is described by many-valley model, using distribution function and computing relaxation-time ratio 19 p3446 A66-36393  
Quasi-localized states associated with high-energy conduction-band minima in semiconductors, particularly Se-doped GaSb, plotting pressure-dependence of photoluminescence 20 p3618 A66-37598  
Electron tunneling from metal to doped indium antimonide through oxide layer measured, obtaining characteristics of conductance vs applied voltage for n-and p-type crystals 20 p3620 A66-37769  
Magneto-optical phenomena studied by extension of wavelength range of electroreflectance measurements in solids using electrolyte into near IR 23 p4111 A66-41263  
Charge carrier mobility by combining conductance with thermogravimetric measurements 24 p4250 A66-42295
- CONDUCTION ELECTRON**  
Interaction of conduction electrons with lattice vibrations in semiconductor produces additional transmission bands or disappearance of resonance absorption region 04 p0564 A66-14251  
Rise and decay of photoconductivity of cadmium sulfide single crystals with superlinear photocurrent illumination characteristics 08 p1272 A66-19248  
Anisotropic effect of interelectronic scattering on semiconductor conductivity of ellipsoidal isoenergetic surface 09 p1411 A66-19981  
Conduction electron interaction with spin wave in ferromagnetic superconductor, noting decay and damping 09 p1430 A66-20867  
Coexistence of superconductivity and ferromagnetism in alloy containing paramagnetic impurities explained by spin-orbit interaction of conduction electrons 13 p2169 A66-26566  
Spin-lattice relaxation of conduction electrons in semiconductors of n-InSb type with scattering at acoustical and optical phonons 14 p2358 A66-27083  
Effective-mass approximation of conduction electron scattering in very thin films 14 p2360 A66-27192  
Conduction electron spin resonance in rubidium and cesium observed, using reflection technique 16 p2750 A66-30146  
Electronic density of states of superconducting ferromagnetic alloys determined by static electron-impurity exchange interaction 16 p2768 A66-30148  
Ferromagnetic semiconductors with exchange interaction due to conduction electrons 17 p2986 A66-33306  
Thermal emf of semiconductors in strong magnetic field, examining formation of spherically symmetric zone subject to arbitrary conduction-electron energy dispersion law 22 p3960 A66-39824  
Cross section of slow neutron scattering in superconductors and polarization of scattered electrons 22 p3964 A66-40308  
Spin-lattice relaxation of conduction electrons in semiconductors of n-InSb type with scattering at acoustical and optical phonons 22 p3967 A66-40839  
Effective-mass approximation of conduction electron scattering in very thin films 24 p4259 A66-43090
- CONDUCTIVE HEAT TRANSFER**  
**S THERMOCONDUCTIVITY**  
**CONDUCTIVITY**  
SA ATMOSPHERIC CONDUCTIVITY  
SA ELECTRIC CONDUCTIVITY  
SA IONOSPHERIC CONDUCTIVITY  
SA PHOTOCONDUCTIVITY  
SA PLASMA CONDUCTIVITY  
SA SUPERCONDUCTIVITY  
SA THERMOCONDUCTIVITY  
Complex longitudinal microwave magnetoconductivity and permittivity of n-type silicon at 77 degrees K, noting influence of DC magnetic field 13 p2159 A66-25066
- CONDUCTIVITY METER**  
Heat conductivity measurement of solids at 200 to 1000 degrees C from radial thermal flux, specifically Armco iron and stainless steel 03 p0443 A66-12513  
Heat conductivity measurement of solids to determine exact values of experimental error 04 p0521 A66-14187  
Electric conductivity of plasma measured by miniature immersed coil with RF magnetic field 10 p1561 A66-21431  
[AIAA PAPER 66-181] Plasma jet electrical conductivity, using inductances with different diameters as measurement device 18 p3144 A66-34101  
Electrodeless probe, consisting of single-layer coil enclosed in insulating tube, for plasma conductivity measurements 18 p3112 A66-34110  
Plasma stream conductivity and velocity measurement, using systems of primary coil and several secondary coils 22 p3921 A66-40899  
Thermoconductivity of small thermoelectric samples measured, using disk-shaped resistance heater 24 p4248 A66-42110
- CONDUCTOR**  
SA ELECTRIC CONDUCTOR  
SA EXPLODING CONDUCTOR  
SA PHOTOCONDUCTOR  
SA SEMICONDUCTOR  
SA SUPERCONDUCTOR  
SA THERMAL CONDUCTOR  
SA TRANSMITTER  
Effective resistivity of metal-plate conductor with single ellipsoidal Fermi surface and specularly reflecting boundaries is independent of thickness 14 p2364 A66-27706  
Electromagnetic interference shielding for conductors that excludes interference energy caused by both magnetic and electric fields over broad frequency range 20 p3499 A66-37195
- CONE**  
SA CIRCULAR CONE  
SA NOSE CONE  
SA ROTATING CONE  
SA SLENDER CONE  
Relationship of laminar wake width to wake transition distance for cones 02 p0175 A66-11561  
Tabulated values of ratio of cone surface pressure-pressure at shock 02 p0175 A66-11570  
Frequencies of free lateral resonant vibration of conical beams and truncated wedges for all combinations of simply supported, clamped and free end conditions 10 p1616 A66-21491  
Born approximation applied to electromagnetic scattering from finite cone to determine radar cross section 10 p1500 A66-21616  
Extended physical optics methods for calculating nose-on echo area of axisymmetric thin bodies having sharp apices 10 p1500 A66-21617  
Radar cross section of flat base dielectric cones, noting parameters such as cone angle, size, wavelength, etc 10 p1503 A66-21646  
Hypersonic flow of inviscid gas past cone, obtaining solution for entire flow including turbulent boundary layer and velocity field, using zero approximation method 12 p1798 A66-24440  
Minimum-weight analysis of hydrostatically compressed ring-stiffened cone, showing that previous data derived for cylinders in same condition might be useful 12 p1970 A66-24702  
Experimental prediction theoretical prediction comparisons of pressure distributions, force and stability coefficients for spherically blunt cone at various angles of attack 17 p2839 A66-32473  
Laminar boundary layer transition in hypersonic shock tunnel of cone, noting effect of high Mach numbers and tip surface roughness, using surface heat transfer gauges 17 p2841 A66-32772  
[AIAA PAPER 66-494] Pressure and temperature profiles in turbulent wake behind cone at Mach 5 17 p2842 A66-33472  
Estimation of shock induced pressure rise on wedge or conical body for various Mach numbers, noting variation of blast-induced pressure ratio with incidence angle 19 p3275 A66-35634  
Differential equations for deformations of nonuniform flat plates bent into cones 19 p3473 A66-35850  
Mass transfer from cone in supersonic flow in tests performed at zero angle of attack, preserving Mangler transformation which transforms flat plate solution to cone 22 p3843 A66-40036  
Time lag effect on dynamic stability determined, using wind tunnel tests with 10 degree cone as test body simulating ablation process by gas injection into boundary layer [AIAA PAPER 66-757] 23 p4008 A66-41330
- CONFERENCE**  
Ion guidance and control - AIAA Conference, Minneapolis, August 1965 01 p0097 A66-10001  
Reliability and maintainability - Annual Conference, Los Angeles, July 1965, Volume 4, Practical techniques and application 01 p0074 A66-10048  
Acoustical fatigue in aerospace structures - USAF Conference, Dayton, Ohio, April 1964 01 p0146 A66-10121  
Materials - ASTM International Conference, Philadelphia, February 1964 01 p0085 A66-10291  
Microwave behavior of ferrimagnetics and plasmas - IEE Conference, London, September 1965 01 p0022 A66-10507  
Aerospace vehicle flight control - SAE and NASA Conference, Los Angeles, July 1965 01 p0102 A66-10661  
Heat transfer - National Conference, Boston, August 1963 01 p0163 A66-10898  
Western Electronic Show and Convention, San Francisco, August 1965, Part 5, Space electronics 01 p0072 A66-11109  
Western Electronic Show and Convention, San Francisco, August 1965, Part 2, Integrated circuits 01 p0046 A66-11135



Radio astronomy - British Science Research Council Report, 1961-1964 01 p0139 A66-11155  
 Solar radiation simulation - ASTM and IES International Symposium, Los Angeles, January 1965 02 p0210 A66-11212  
 Western Electronic Show and Convention, San Francisco, August 1965, Part 3, Power electronics 02 p0179 A66-11276  
 Electronic insulation - IEEE Conference, New York, September 1965 02 p0247 A66-11284  
 Manned Space Navigation Conference, St. Petersburg, Florida, April 1964 02 p0254 A66-11314  
 Electronic packaging - SAE Conference, Los Angeles, October 1965 02 p0233 A66-11320  
 Western Electronic Show and Convention, San Francisco, August 1965, Part 6, Instruments and measurement 02 p0228 A66-11452  
 Western Electronic Show and Convention, San Francisco, August 1965, Part 1, Military electronics 02 p0197 A66-11457  
 Manned space flight - AIAA Meeting, St. Louis, October 1965 02 p0184 A66-11613  
 Nondestructive testing - Seminar, Genoa, November 1964 02 p0235 A66-11685  
 New engineering materials - IME Conference, Birmingham, England, October 1965 02 p0243 A66-11736  
 Behavior of materials under dynamic loading - ASME Colloquium, Chicago, November 1965 02 p0299 A66-11849  
 Applications of microelectronics - IEE Symposium, Southampton University, England, September 1965 02 p0201 A66-11914  
 Nuclear magnetic resonance - Preliminary Report of International Symposium, Tokyo, September 1965 02 p0276 A66-12024  
 Continental Drift Symposium, London, March 1964 03 p0360 A66-12377  
 Ionosphere and high latitude particles - COSPAR Symposium, Alpbach, Tirol, Austria, March 1964 03 p0361 A66-12639  
 Space physics - Proceedings of Summer School, Alpbach, Austria, July-August 1963 03 p0419 A66-12839  
 Physics of ionized media - French Society of Physics, National Colloquium, Toulouse, France, May 1965 03 p0401 A66-12965  
 Law of Outer Space Colloquium, Warsaw, September 1964 03 p0447 A66-13074  
 Welding technology and metal testing - Conference, Timisoara, Rumania, September 1965, Volume 1 03 p0374 A66-13116  
 Welding technology and metal testing - Conference, Timisoara, Rumania, September 1965, Volume 2 03 p0383 A66-13156  
 Rocket technology and air and space travel research - Annual Meeting, Berlin, West Germany, September 1964 04 p0581 A66-13494  
 Space electronics - IEEE International Symposium, Miami Beach, November 1965 04 p0475 A66-13575  
 Mathematical theory of optimal control - Symposium, University of Michigan, October 1964 04 p0505 A66-13987  
 Nuclear magnetic resonance and relaxation in solids - Conference, Louvain, Belgium, September 1964 04 p0548 A66-14029  
 Basic environmental problems of man in space - International Symposium, Paris, October 1962 04 p0463 A66-14063  
 Relativistic theories of gravitation - International Conference, London, July 1965, Volume 1 05 p0756 A66-14522  
 Relativistic theories of gravitation - International Conference, London, July 1965, Volume 2 05 p0757 A66-14527  
 Internal friction, damping and cyclic plasticity - ASTM Symposium, Chicago, June 1964 05 p0771 A66-14546  
 National Electronics Conference, Chicago, October 1965 05 p0639 A66-14553  
 Fiber composite materials - ASM Seminar, Metals Park, Ohio, October 1964 05 p0700 A66-14807  
 Optical and electro-optical information processing technology - Symposium, Boston, November 1964 05 p0636 A66-14818  
 Nuclear and space radiation effects - IEEE Conference, University of Michigan, Ann Arbor, July 1965 05 p0733 A66-14844  
 Switching circuit theory and logical design - IEEE Annual Symposium, University of Michigan, Ann Arbor, October 1965 05 p0637 A66-14926

New techniques in astronomy - Conference, Kazan, U.S.S.R., May 1964 05 p0679 A66-15202  
 Plasma physics - Seminar, Trieste, Italy, October 1964 05 p0724 A66-15233  
 Physics of cosmic rays - All-Union Conference, Apatity, U.S.S.R., August 1964 05 p0749 A66-15372  
 Radiation effects in electronics - ASTM and ANS Meeting, Syracuse, N.Y., October 1964 05 p0738 A66-15486  
 Thermionic electrical power generation - European Nuclear Energy Agency and IEE International Conference, London, September 1965 05 p0613 A66-15532  
 MHD - Symposium, University of Tokyo, October 1965 05 p0728 A66-15808  
 Reliability in space vehicles - Seminar, Los Angeles, April 1965 05 p0770 A66-15823  
 Military electronics - MILECON/9, Conference, Washington, D.C., September 1965 06 p0840 A66-15954  
 Atomic and molecular quantum theory - NATO and AEC International Symposium, Sanibel Island, Florida, January 1965 06 p0910 A66-16163  
 Signal transmission and processing - IEEE Symposium, New York, May 1965 06 p0829 A66-16187  
 Physiological and performance determinants in manned space systems - AAS and HFS Symposium, San Fernando Valley State College, Northridge, California, April 1965 06 p0816 A66-16234  
 Cloud physics - International Conference, Tokyo and Sapporo, Japan, May 1965 06 p0904 A66-16266  
 Insulation materials and processes for aerospace and hydrospace applications - SAMPE Symposium, San Francisco, May 1965 06 p0898 A66-16284  
 Energy conversion and storage - Conference, Oklahoma State University, October 1965 06 p0808 A66-16390  
 Dimensioning and strength calculations - Conference, Budapest, October 1965 06 p0963 A66-16472  
 Cosmic rays and problems in space physics - Conference, Yakutsk, U.S.S.R., August 1962 06 p0945 A66-16568  
 Ferroelectricity - All-Soviet Conference, Rostov, U.S.S.R., September 1964 06 p0925 A66-16712  
 V/STOL Aircraft Symposium, Wright-Patterson AFB, Ohio, November 1965 06 p0805 A66-16808  
 Manufacturing methods in space flight technology - German Symposium, Munich, November, 1964 06 p0887 A66-17068  
 Physics of semiconductors - International Conference, Paris-Royaumont, July 1964, Volume 3, Radiation damage in semiconductors 06 p0930 A66-17111  
 Aerospace - Society of Experimental Test Pilots Symposium, Beverly Hills, September 1965 07 p0985 A66-17267  
 Nuclear engineering - AICE Conference, Chicago, December 1962 07 p1079 A66-17298  
 Physics of semiconductors - International Conference, Paris, July 1964, Volume 4, Radiative recombination in semiconductors 07 p1092 A66-17310  
 Microwave theory and techniques - IEEE G-MTT Symposium, Clearwater, Florida, May 1965 07 p1006 A66-17501  
 Physics of cosmic rays - All-Union Conference, Moscow, October 1963 07 p1111 A66-17534  
 Heat transfer - AICE and ASME Conference, Cleveland, August 1964 07 p1149 A66-17576  
 Astronomical Society Conference, Eisenach, Thuringia, East Germany, September 1965 07 p1134 A66-17630  
 International Air Transport Association, Technical Conference, Miami, April 1965, Volume 1 07 p1063 A66-17667  
 Network theory - Conference, Cranfield, England, September 1965 07 p1014 A66-17744  
 International Air Transport Association, Technical Conference, Miami, April 1965, Volume 2 07 p1071 A66-17757  
 Cosmic rays - International Conference, Jaipur, India, December 1963 07 p1118 A66-17977  
 Plasma space science - Symposium, Catholic University of America, Washington, D.C., June 1963 07 p1137 A66-18072  
 Fluid dynamics - Symposium, Zakopane,

Poland, September 1963 07 p1021 A66-18101  
 Cavitation in fluid machinery - ASME Symposium, Chicago, November 1965 07 p1024 A66-18166  
 Plasma effects in solids - Conference, Paris, July 1964 07 p1100 A66-18197  
 Electron devices - IEEE Symposium, San Francisco, August 1965 07 p1011 A66-18266  
 Energetics /engineering developments in energy conversion/ - ASME International Conference, University of Rochester, August 1965 07 p0992 A66-18308  
 Civilian and Military Uses of Aerospace - Conference, New York, January 1965 08 p1299 A66-18547  
 ASTM Southeastern Engineering Conference and Tool Exposition, Atlanta, October 1965 08 p1228 A66-18685  
 Crystal-Diffusion Spectra-International Colloquium, Paris, July 1965 08 p1233 A66-19231  
 Atmospheres of Venus and Mars - Astrophysics Conference, Kiev, Ukrainian SSR, June 1964 08 p1293 A66-19322  
 ASTM conference, Purdue University, June 1965 08 p1241 A66-19713  
 Antennas in ionized medium - Colloquium, Paris, June 1965 09 p1339 A66-19841  
 Low temperature physics - International Conference, Columbus, Ohio, August-September 1964 09 p1413 A66-20004  
 Low temperature physics LT9 - International Conference, Columbus, Ohio, August 1964 09 p1424 A66-20075  
 Planetary atmospheres and surfaces - Symposium, Dorado, Puerto Rico, May 1965 09 p1448 A66-20101  
 Cosmic ray physics - All-Union Conference, Moscow, October 1963 09 p1436 A66-20201  
 Cosmic space physics - All-Union Conference, Moscow, June 1965 09 p1460 A66-20986  
 Radio astronomy, Volume 5 of Progress in radio science 1960-1963, URSI General Assembly, Tokyo, September 1963 10 p1601 A66-21058  
 Astronomical observations from space vehicles - International Astronomical Union Symposium, Liege, Belgium, August 1964 10 p1596 A66-21078  
 Scientific experiments for manned orbital flight - Goddard Memorial Symposium, Washington, D.C., March 1965 10 p1607 A66-21517  
 German Physical Society, Physics Session, Frankfurt am Main, October 1965 10 p1556 A66-22052  
 Meteorological satellite data interpretation and use - Seminar, Tokyo, November-December 1964 11 p1725 A66-22305  
 Aviation and space medicine - International Congress, Rome, October 1963 11 p1641 A66-22478  
 Radio waves and circuits - URSI Conference, Tokyo, September 1963 11 p1653 A66-22626  
 Thin ferromagnetic film physics - All-Union Symposium, Irkutsk, U.S.S.R., July 1964 11 p1751 A66-22796  
 Hypervelocity techniques - Symposium, Tullahoma, Tennessee, November 1965 11 p1683 A66-22826  
 Rarefied gas dynamics - International Symposium, Institute for Aerospace Studies, University of Toronto, July 1964, Volume 1 11 p1688 A66-22901  
 Forms of water in biologic systems - Conference, New York, October 1964 11 p1644 A66-22987  
 Automatic control - Conference, Rensselaer Polytechnic Institute, Troy, New York, June 1965 11 p1659 A66-23108  
 Optimal control - Symposium, Imperial College of Science and Technology, London, April 1964 11 p1679 A66-23271  
 Systems effectiveness - Conference, Electronic Industries Association, Washington, D.C., October 1965 11 p1788 A66-23434  
 Heat transfer information week notes - Conference, Poitiers, France, April 1963 12 p1972 A66-23522  
 Nonequilibrium thermodynamics, variational techniques and hydrodynamic stability - Symposium, University of Chicago, May 1965 12 p1974 A66-23540  
 Radiation detector, nuclear reactor, measurement, etc - Nuclear Science



Symposium, San Francisco, October 1965 12 p1910 A66-23670  
 American Federation of Information Processing Societies, Joint Computer Conference, Las Vegas, November 1965 12 p1825 A66-23824  
 Extraterrestrial civilizations - All-Union Conference, Yerevan, Armenian SSR, May 1964 12 p1813 A66-23887  
 Advances in biomedical computer applications - Conference, N.Y. Academy of Sciences, June 1965 12 p1809 A66-24227  
 Automation of control processes - International Federation on Automatic Control Congress, Basel, Switzerland, August-September 1963 12 p1850 A66-24314  
 Discrete and self-adaptive systems - International Federation on Automatic Control Congress, Basel, Switzerland, August-September 1963 12 p1851 A66-24323  
 Wire and data communication - IEEE International Convention, New York, March 1966 12 p1818 A66-24594  
 Radio communication, broadcasting and audio - IEEE International Convention, New York, March 1966 12 p1838 A66-24597  
 Aerospace and electronic systems - IEEE International Convention, New York, March 1966 12 p1818 A66-24600  
 Antennas, microwaves, electron devices - IEEE International Convention, New York, March 1966 12 p1838 A66-24613  
 Automatic control, systems science, cybernetics, biomedical engineering, human factors - IEEE International Convention, New York, March 1966 12 p1854 A66-24634  
 Circuit theory, information theory, basic sciences, electrostatic processes - IEEE International Convention, New York, March 1966 12 p1855 A66-24645  
 Power, industrial and general applications - IEEE International Convention, New York, March 1966 12 p1803 A66-24658  
 Parts, materials and packaging reliability and electric contacts - IEEE International Convention, New York, March 1966 12 p1842 A66-24663  
 Instruments, measurements, industrial electronics, nuclear science, ultrasonics - IEEE International Convention, New York, March 1966 12 p1842 A66-24672  
 Fundamental phenomena in hyperperson flow - Conference, Buffalo, June 1966 13 p2060 A66-25152  
 Stepping stones to Mars - AIAA-AAS conference, Baltimore, March 1966 13 p2177 A66-25234  
 Society of Plastics Engineers, Conference, Montreal, March 1966 13 p2111 A66-25301  
 Programming and control - International Conference, Air Force Academy, Colorado Springs, April 1965 13 p2046 A66-25339  
 Northeast Electronics Research and Engineering Meeting, Boston, November 1965 13 p2032 A66-25501  
 Stability of systems - Discussion, IME Automatic Control Group, London, May 1964 13 p2118 A66-25580  
 Electrochemical kinetics of fuel cells - Conference, Moscow, 1964 13 p1998 A66-25667  
 Circuit and system theory - Allerton Conference, University of Illinois, October 1965 13 p2049 A66-26057  
 High speed stress-strain testing of polymers - International Symposium, Boston, March 1965 13 p2114 A66-26105  
 Physics of quantum electronics - Conference, San Juan, Puerto Rico, June 1965 13 p2093 A66-26141  
 Engineering aspects of MHD - Symposium, Princeton University, March 1966 13 p2000 A66-26253  
 Stress concentration - Symposium, Kiev, Ukrainian SSR, May 1964 13 p2199 A66-26401  
 Fluid mechanics - Midwestern Mechanics Conference, Case Institute of Technology, Cleveland, April 1963 13 p2068 A66-26701  
 Cause and structure of temperature latitude sporadic E - Seminar, Swiss Village, Colorado, June 1965 14 p2279 A66-26834  
 Magnetism and magnetic materials - IEEE and AIP Conference, San Francisco, November 1965 14 p2349 A66-26875  
 Philosophical problems of Einstein theory of gravitation and relativistic cosmology - All-Union Conference, Kiev, Ukrainian SSR, May 1964 14 p2331 A66-27208  
 Photographic and spectroscopic optics -

Conference, Tokyo and Kyoto, September 1964 14 p2291 A66-27316  
 Rare earth research - Conference, Phoenix, April 1964 14 p2361 A66-27460  
 Numerical calculus and physical calculus - Colloquium, Henri Poincare Institute, Paris, May 1963  
 [PST PAPER NT-147] 14 p2323 A66-27790  
 Numerical calculus and applied mathematics - French Colloquium, Rennes, France, June 1963 14 p2324 A66-27835  
 Structures and materials - AIAA/ASME Conference, Cocoa Beach, Florida, April 1966 14 p2403 A66-27986  
 Aerospace technology, spacecraft and spacecraft systems, launching, control, recovery, etc - Space Congress, Cocoa Beach, Florida, March 1966 14 p2388 A66-28401  
 Antenna and propagation - IEEE International Symposium, Washington, D.C., August 1965 15 p2454 A66-28566  
 American Society for Quality Control - Conference, Los Angeles, May 1965 15 p2505 A66-28788  
 National Air Meeting on Clear Air Turbulence, Washington, D.C., February 1966 15 p2531 A66-28911  
 National Relay Conference, Oklahoma State University, April 1966 15 p2459 A66-28988  
 Analytical mechanics, motion stability, celestial ballistics - All-Union Conference, Moscow, January-February 1964 15 p2538 A66-29144  
 System theory - Symposium, New York, April 1965 15 p2471 A66-29367  
 Extensive air showers - International Conference on Cosmic Rays, Jaipur, India, December 1963 15 p2577 A66-29513  
 High energy interactions - International Conference on Cosmic Rays, Jaipur, India, December 1963 15 p2582 A66-29541  
 Cosmic rays, muons and neutrinos - International Conference, Jaipur, India, December 1963 15 p2586 A66-29570  
 Physics of luminescent ionic crystal - Conference, Lvov, Ukrainian SSR, January-February 1964 15 p2568 A66-29728  
 Air cargo - International Forum, Chicago, May 1966 15 p2619 A66-29788  
 Numerical solution of partial differential equations - Symposium, University of Maryland, May 1965 16 p2731 A66-30233  
 Special ceramics - Symposium, British Ceramic Research Association, Stoke-on-Trent, U.K., July 1964 16 p2728 A66-30244  
 Mars and Venus exploration - Conference, Virginia Polytechnic Institute, August 1965 16 p2796 A66-30350  
 Rarefied gas dynamics, Advances in applied mechanics - International Symposium, University of Toronto, July 1964 16 p2751 A66-30370  
 Environment and man - IES Conference, San Diego, April 1966 16 p2674 A66-30434  
 Telemetry - International Conference, Washington, D.C., May 1965 16 p2647 A66-30534  
 Physics of thin ferromagnetic films - All-Union Conference, Irkutsk, U.S.S.R., July 1964 16 p2772 A66-30680  
 Instruments and measurements, automatic control - International Conference, Stockholm, September 1964 16 p2706 A66-30879  
 AFIPS Joint Computer Conference, Boston, April 1966 16 p2656 A66-31239  
 Materials science and technology in integrated electronics - Conference, San Francisco, September 1965 16 p2781 A66-31414  
 Hall effect application - MIT Conference, Cambridge, November 1965 16 p2785 A66-31571  
 Solid Mechanics - Conference, Cleveland, April 1963 17 p3019 A66-31996  
 Transactions of International Astronomical Union, Volume 12A, Reports on astronomy 17 p2997 A66-32018  
 Circuit theory - Midwest Symposium, Oklahoma State University, May 1966 17 p2899 A66-32049  
 Origins of prebiological systems and their molecular matrices - Conference, Wakulla Springs, Florida, October 1963 17 p2849 A66-32083  
 Aerospace Medical Association, Scientific Meeting, Las Vegas, April

1966 17 p2853 A66-32134  
 Aerospace life support - Conference, American Institute of Chemical Engineers, Houston, February 1965 17 p2866 A66-32667  
 American Helicopter Society, Annual Forum, Washington, D.C., May 1966 17 p2843 A66-32723  
 Sonic boom - Symposium, Saint Louis, November 1965 17 p2846 A66-33020  
 Aviation and astronautics - Conference, Tel Aviv and Haifa, February 1966 17 p2912 A66-33063  
 Geophysical monograph on extension of gravity anomalies to unsurveyed areas 17 p2920 A66-33191  
 All-weather operations, head up displays long-range navigational aids - Conference, International Federation of Air Line Pilots Associations, Rotterdam, October 1965 17 p2953 A66-33212  
 Nature and origin of comets - International Colloquium on Astrophysics, Liege, Belgium, July 1965 17 p3008 A66-33367  
 Stress corrosion, delayed failures, fatigue corrosion and relation between these phenomena - Commissariat on Atomic Energy, Metallurgical Colloquium, Cadarache Rhone, France, June 1964 17 p2941 A66-33440  
 Physical principles of cathode electronics - All-Union Conference, Leningrad, October 1965 17 p2988 A66-33458  
 Fluid mechanics and heat transfer Conference, Santa Clara, June 1966 17 p3038 A66-33467  
 Peaceful uses of automation in outer space - Symposium, International Federation of Automatic Control, Stavanger, Norway, June 1965 18 p3240 A66-33848  
 Environmental effects on man, Volume 1 - Symposium on environmental engineering and society, London, April 1966 18 p3062 A66-34201  
 Shock and vibration - Underground, underwater and in air - Volume 2, Symposium on environmental engineering and society, London, April 1966 18 p3095 A66-34208  
 Space technology, Volume 5 - Symposium on environmental engineering and society, London, April 1966 18 p3230 A66-34208  
 Design and construction of large steerable antennas - IEE Conference, London, June 1966 18 p3079 A66-34262  
 Solar wind - Conference, California Institute of Technology, Pasadena, April 1964 18 p3166 A66-34330  
 Industrial nuclear electronic supplies - Conference, French Atomic Energy Commission, December 1965 18 p3113 A66-34411  
 Cosmic rays - International Conference, Imperial College of Science and Technology, London, September 1965, Volume 2 18 p3200 A66-35088  
 Nature of lunar surface - IAU/NASA Symposium, Goddard Space Flight Center, Greenbelt, Maryland, April 1965 19 p3456 A66-35437  
 Aerospace electronics - IEEE National Conference, Dayton, May 1966 19 p3394 A66-35501  
 Life sciences and space research, Volume 4, International Space Science Symposium, Argentina, May 1965 19 p3283 A66-35567  
 Atmospheric circulation - International Space Science Symposium, Argentina, May 1965 19 p3346 A66-35636  
 Stress-corrosion cracking of titanium - ASTM Meeting, Seattle, October-November 1965 19 p3377 A66-35647  
 Telemetry - National Conference, Boston, May 1966 19 p3297 A66-35661  
 Geometric optics - Seminar, El Paso, March 1966 19 p3399 A66-35825  
 Factors in operation of manned space chambers - ASTM Symposium, Seattle, October-November 1965 19 p3288 A66-35837  
 Serrated yielding by metals during tensile tests at temperatures near absolute zero 19 p3380 A66-35846  
 Optimization techniques - Symposium, Carnegie Institute of Technology, Pittsburgh, April 1965 19 p3307 A66-35867  
 Scintillation and semiconductor counter - Symposium, Washington, D.C., March 1966 19 p3358 A66-35906  
 Space maintenance and extravehicular activities - National Conference, Orlando, Florida, March 1966 19 p3289 A66-35946



Sensitivity methods in control theory - International Symposium on Sensitivity Analysis, Dubrovnik, Yugoslavia, August-September 1964 19 p3326 A66-36009

Refractory metals and alloys - Conference, Los Angeles, December 1963 19 p3364 A66-36104

Law of outer space - Colloquium, Athens, September 1965 19 p3480 A66-36201

Space cabin atmosphere and closed environment - ACS Symposium, Atlantic City, September 1965 19 p3292 A66-36230

Plasma physics and controlled nuclear fusion research - Conference, International Atomic Energy Agency, England, September 1965 19 p3410 A66-36494

Plasma physics and controlled nuclear fusion research - IAEA Conference, England, September 1965, Volume 2 19 p3419 A66-36539

Automatic control - Conference, University of Washington, Seattle, August 1966 19 p3330 A66-36660

Stellar evolution - International Conference, Goddard Institute for Space Studies, New York, November 1963 19 p3466 A66-36788

Microminiaturization in automatic control equipment and digital computers - Symposium, International Federation of Automatic Control and International Federation for Information Processing, Munich, October 1965 19 p3322 A66-36806

Galactic evolution and structure - Solvay Physics Conference, Brussels, September 1964 20 p3645 A66-36957

Civil aviation safety - International Symposium, Stockholm, April 1966 20 p3493 A66-36990

Cryogenic engineering, Volume II - Conference, William Marsh Rice University, Houston, August 1965 20 p3599 A66-37059

Aerospace systems - Conference, Seattle, July 1966 20 p3659 A66-37155

Metal and alloy optical properties and electronic structure - International Colloquium, Paris, September 1965 20 p3612 A66-37271

Physics of ferro- and antiferromagnetism - All-Union Conference, Sverdlovsk, U.S.S.R., July 1965 20 p3616 A66-37475

Experimental stress analysis - Conference, West Berlin, March 1966 20 p3667 A66-37496

Position of variable stars in Hertzsprung-Russell diagram - International Astronomical Union Colloquium, Bamberg, West Germany, August 1965 20 p3652 A66-37609

Fluid logic and amplification - International Conference, England, September 1965 20 p3500 A66-37642

Deformation of solids by impact of liquids and relation to rain damage in aircraft and missiles, to blade erosion in steam turbines and to cavitation erosion - Meeting, London, May 1965 20 p3546 A66-37801

Satellite observations - Symposium, Krakow, Poland, April 1965 20 p3517 A66-37834

International Union for Vacuum Science, Technique and Applications - International Congress, Stuttgart, June-July 1965 20 p3621 A66-38083

Solar terrestrial physics - Symposium, Japan, December 1965 20 p3634 A66-38211

Radiation trapped in Earth magnetic field - Conference, Christian Michelsen Institute, Bergen, Norway, August-September 1965 20 p3636 A66-38301

Progress in mechanics of linear vibrations - Symposium, Paris, April 1965 21 p3823 A66-38560

Recent progress of mechanics of linear vibrations - Symposium, Paris, April 1965 21 p3824 A66-38571

Mechanics of linear vibrations - Symposium, Paris, April 1965 21 p3824 A66-38576

Guidance and control - AIAA/JACC Conference, Seattle, August 1966 21 p3761 A66-38838

Plasma physics and problems of controlled thermonuclear fusion - Conference, Kharkov, Ukrainian SSR, May 1963 21 p3777 A66-39002

Information theory - IEEE International Symposium, University of California, Los Angeles, January-February 1966 21 p3703 A66-39134

Megagauss magnetic field generation by

explosives and related experiments - Conference, Frascati, Italy, September 1965 21 p3773 A66-39501

Structural components and applications, electronics in aeronautics and astronautics - Conference, Hanover, West Germany, May 1966 21 p3715 A66-39617

Theoretical and applied mechanics - Israel Conference, Haifa, June 1965 22 p3921 A66-39667

Electron density profiles in ionosphere and exosphere - NATO Advanced Study Institute, Finse, Norway, April 1965 22 p3903 A66-39943

Space simulation - IES/ASTM Conference, Houston, September 1966 22 p3886 A66-40204

Mediterranean cooperation for solar energy - Meeting, Marseille, May 1966 22 p3851 A66-40242

Joining of materials for aerospace systems - National Symposium, Dayton, November 1965 22 p3923 A66-40255

Information display - National Symposium, New York, September 1965 22 p3927 A66-40286

Aerodynamic deceleration systems - AIAA Conference, Houston, September 1966 22 p3848 A66-40589

Satellite communications - WESCON, Los Angeles, August 1966 22 p3867 A66-40709

Nondigital applications and interconnection aspects of integrated electronics - WESCON, Los Angeles, August 1966 22 p3878 A66-40713

State-variable techniques application to communication and radar problems - WESCON, Los Angeles, August 1966 22 p3868 A66-40715

Advances in HF solid state transmitter systems - WESCON, Los Angeles, August 1966 22 p3879 A66-40721

Advanced spaceborne computer concepts - WESCON, Los Angeles, August 1966 22 p3870 A66-40725

Millimeter wave - WESCON, Los Angeles, August 1966 22 p3879 A66-40730

Microwave receiver devices - WESCON, Los Angeles, August 1966 22 p3879 A66-40734

Power and control integrated circuits - WESCON, Los Angeles, August 1966 22 p3880 A66-40739

High availability computer systems - WESCON, Los Angeles, August 1966 22 p3871 A66-40743

HF amplifier design - WESCON, Los Angeles, August 1966 22 p3881 A66-40745

Space antenna arrays - WESCON, Los Angeles, August 1966 22 p3881 A66-40747

Solid state mechanics - All-Union Conference, Moscow, January-February 1964 23 p4134 A66-40988

Delay devices for pulse compression radar - IEE Conference, London, February 1966 23 p4033 A66-41013

Microbonding - Colloquium, Sunbury-on-Thames, Middlesex, England, January 1966 23 p4043 A66-41188

Deep submergence propulsion and marine systems - AIAA Conference, Forest Park, Illinois, February-March 1966 23 p4054 A66-41205

Advanced propellant chemistry - ACS Meeting, Detroit, April 1965 23 p4116 A66-41218

Welding and adhesion techniques in aircraft and space vehicle construction - Conference, Hanover, West Germany, May 1966 23 p4073 A66-41530

IEEE Region Six Conference, Tucson, April 1966, Volume 1 23 p4039 A66-41580

IEEE Region Six Conference, Tucson, April 1966, Volume 2 23 p4049 A66-41600

Applied mechanics - International Congress, Munich, August-September 1964 23 p4092 A66-41934

Electronic reliability - IEEE Conference, New York, May 1966 24 p4178 A66-42087

IEEE and AIAA Thermoelectric Specialists Conference, Washington, D.C., May 1966 24 p4160 A66-42106

Instrumentation in aerospace simulation facilities - International Conference, Stanford, August 1966 24 p4205 A66-42166

Double Langmuir probe measurement of turbulent structure and ionization intensity of hypervelocity projectile and spectral characteristics of probe signal fluctuation 24 p4192 A66-42198

Applied mechanics - U.S. National

Congress, University of Minnesota, Minneapolis, June 1966 24 p4287 A66-42265

Unmanned exploration of solar system - AAS Symposium, Denver, February 1965 24 p4274 A66-42653

Cosmic ray physics - All-Union Conference, Apatity, U.S.S.R., August 1964 24 p4265 A66-42901

Metrology and precision mechanics - National Conference, Warsaw, September 1966 24 p4214 A66-43011

Magnetics - International Conference, Stuttgart, April 1966, Volume 2, covering ferrite and semiconductor devices, superconductivity and magnetic logic 24 p4260 A66-43170

**CONFIDENCE LIMIT**

Relationships of hazard rate distributions to reliability growth and confidence computations 01 p0077 A66-10109

Confidence ratio for Gaussian random processes satisfying certain linear differential equations 12 p1902 A66-23769

Component testing and system reliability at various confidence limits for serially connected systems 14 p2305 A66-28428

System availability, noting lower confidence limit and estimation of time-to-failure and time-to-repair from test data 16 p2661 A66-30664

Reliability data analysis for systems, discussing confidence intervals, limits and parameters independent of mathematical models employed 16 p2714 A66-30666

Error analysis of absorbed energy flux density and ignition exposure time data, accuracy, precision and confidence limit estimates for arc image furnace ignition experiments 18 p3261 A66-34224

[AIAA PAPER 66-669] Reliability statistical confidence levels and relation to mean time between failures /MTBF/ 20 p3682 A66-37182

Reliability analysis problem involving set of 30 identical parts which had intervals to failure recorded in order to make inferences about population from which parts are random sample, noting Weibull population 20 p3592 A66-37965

Methods for finding lower confidence bounds on reliability of item, noting reliabilities for items whose lifetimes follow Weibull distribution 20 p3574 A66-37966

Bayesian statistics applied to reliability and maintainability transactions 20 p3574 A66-37967

**CONFIGURATION**

S AIRCRAFT CONFIGURATION

S HAMMERHEAD CONFIGURATION

S LAUNCH VEHICLE CONFIGURATION

S MISSILE CONFIGURATION

S PLANETARY CONFIGURATION

S SATELLITE CONFIGURATION

S SPACECRAFT CONFIGURATION

**CONFINEMENT**

SA PLASMA CONFINEMENT

SA REACTOR CONTROL

Psychological and medical aspects of human confinement, isolation and sensory deprivation 11 p1642 A66-22485

Clinical observations and tests of solitary confinement on neurotic pilots 11 p1642 A66-22486

Nervous activity increase, EEG, EKG, gas exchange, respiration, urine, blood pressure, oxygen content and morphological state of humans after prolonged pressure chamber confinement 15 p2443 A66-29444

Biological effects of confining fish in sealed aquarium with and without Chlorella 15 p2440 A66-29504

**CONFORMAL MAPPING**

Conformal mapping analysis of reflections and mode conversions in tilted millimeter circular cylindrical waveguide 03 p0344 A66-13102

Wave propagation in groove waveguide analyzed by conformal mapping 05 p0641 A66-14557

Multiple meson production analyzed by conformal mapping of Lobachevskii plane onto Euclidean strip 07 p1116 A66-17559

Open circuit voltage, inner resistance, Hall voltage and tensorial conductivity for Faraday generator, using conformal mapping for single pair of electrodes 07 p0993 A66-18309

Conformal mapping analysis of waveguide,



Limited by two parallel metallic plates with two symmetric opposite grooves of properly chosen shape 08 p1198 A66-19742

Impedances of offset parallel-coupled strip transmission lines analyzed by conformal mapping techniques 10 p1514 A66-21906

Basic biharmonic problem for any singly or doubly connected region with piecewise-smooth boundary solved by method of summary representations 11 p1778 A66-22225

Electrode size effects on performance of infinitely long MHD power generation duct calculated by conformal mapping, analyzing gas Hall parameter, electrode-insulator length ratio, etc 13 p2000 A66-25735

Conformal mapping of unit circle onto given, singly connected or multiply connected region bounded by simple closed contour 13 p2204 A66-26433

Airfoil shape construction by conformal mapping and development of analog computer program to plot two-dimensional potential flow about various airfoil sections 16 p2629 A66-31116

Critical analysis of certain conformal mappings of ellipsoid of revolution onto plane 18 p3109 A66-34739

Conformal mapping technique applied to boundary value problem of plane wave diffraction by perfectly conducting elliptical cylinder, noting integral equation 22 p3866 A66-40185

Eigenfunctions of full dislocation solution of cut annulus in plane elastostatics 23 p4144 A66-41970

Incompressible flow in two-dimensional bends treated by Rayleigh-Ritz method in Kamiyama modification of conformal mapping 24 p4157 A66-42264

Conformal mapping to determine shape and field distribution of shim used to modify field in air gap between pole faces of electromagnet 24 p4239 A66-43211

**CONFORMAL TRANSFORMATION**

Aerodynamic characteristics of arbitrary slender reentry bodies predicted by conformal mapping 10 p1481 A66-21942

Segmented electrode MHD generator performance for various electrode-insulator length ratios 13 p2000 A66-25714

Conformal transformation to determine electrical field of symmetrical air-filled strip line under static conditions 14 p2264 A66-27242

Nonrectilinear blade rows with zero thickness when produced by conformal transform 20 p3491 A66-36966

Einsteinian gravitation equations stated in terms of three-dimensional tensor analysis as applied in conformal space 23 p4091 A66-41834

New gravitation theory, noting role of Einstein equations following conformal transformation 24 p4237 A66-42540

**CONICAL FLOW**

Temperature distribution of slow incompressible viscous flow through conical tube and comparison with two inclined walls 01 p0161 A66-10435

Exact solution of conical flow equation with zero velocity and pressure 01 p0008 A66-11082

Asymptotic representation of solutions for boundary layers near weak shock waves in conical flows 02 p0176 A66-12181

Dissociation or ionization effects of air on inviscid hypersonic flow past circular cone with attached shock wave 03 p0316 A66-12928

Special cases of conical flow permitting two flows to join and predicting flow limited by conic wall 05 p0605 A66-14536

Ratio base pressure of spherical cone in turbulent flow at zero angle of attack 05 p0609 A66-15804

Compressible fluid flow, discussing simple wave supersonic flow mechanism for bodies with developable surfaces 06 p0802 A66-16352

Similarity solutions of boundary layer equations with algebraic decay for viscous incompressible fluid inside infinite circular cone 06 p0873 A66-16996

Sweeping conditions for oblique and conical shock waves and transonic flows 07 p1020 A66-17868

Quasi-conical flow to calculate pressure on wings having curved leading edges 07 p0983 A66-18229

Laminar boundary layer on cone with uniform mass transfer, discussing velocity and energy fields 08 p1161 A66-18530

Homogeneous isotropic cone with surface loadings and internal temperature distributions 08 p1309 A66-19142

Parameter estimation for laminar conical flow of viscous inelastic non-Newtonian fluids 10 p1521 A66-21056

Free-molecule flow through conical tubes noting mass transport, axial momentum, energy, flow distribution and speed ratio 11 p1635 A66-22938

Correlations of distance to downstream stagnation point and axial static pressure along axis of symmetry of near wake of cone at Mach 6 12 p1795 A66-23571

Viscous fluid motions around conical surface, using Navier-Stokes equations 12 p1797 A66-24198

Aerodynamic characteristics of shapes constructed by current surfaces of supersonic flows past cones, noting lengthwise variation of cross sections 12 p1798 A66-24438

Numerical solution of problem of supersonic flow at angle of attack past arbitrarily smooth conical bodies 12 p1798 A66-24441

Streamline flow of ideal stable gas with constant ratio of specific heats around conical body with arbitrary taper, determining flow velocity components 14 p2220 A66-27679

Flow loss in conical diffusers with boundary layer suction through single slit 16 p2629 A66-30813

Behavior of inviscid supersonic conical flow fields near crossflow stagnation points studied by constructing coordinate expansions of exact conical flow equations [AIAA PAPER 66-491] 16 p2631 A66-31494

Flow along free border of conical vortex sheet above delta wing and rolling-up conically from apex 17 p2837 A66-32274

Vortex sheets rolling-up along leading edges of delta wings, comparison with slender body theory and conical flow 17 p2837 A66-32275

Coherent conical vortex sheet formation theory in two-dimensional and three-dimensional vortex filaments 17 p2906 A66-32276

Shanks approximation of stationary shocks attached to point of cone 17 p2837 A66-32282

Wall thermal factor for supersonic flow incident on cone 17 p2838 A66-32283

Rotating vortex flow and transition phenomena in conical diffuser [AIAA PAPER 66-426] 18 p3046 A66-33643

Sources of nappe image in variable-analysis plane as related to distribution of vortices 18 p3097 A66-33909

Stability derivatives of sharp cones performing pitching oscillations in viscous hypersonic flow 21 p3693 A66-38723

Interferometric measurement of density distributions in shock layer of nonequilibrium flow field around cone 21 p3694 A66-39168

Finite difference analysis of viscous laminar converging flow in conical tubes, assuming parabolic inlet velocity profile and simplified motion equation 21 p3729 A66-39450

Supersonic flow around thin polygonal wings and polygonal wings of symmetrical thickness studied by Carafoli hydrodynamic analogy for wings in conical flow 21 p3695 A66-39603

Boundary layer transition on downstream surface of sharply pointed cones when angle of incidence is slight and boundary layer is attached throughout 23 p4007 A66-41172

Supersonic gas flow problems around lattice of conical blades solved in any approximation of perturbation theory 23 p4008 A66-41358

Surface mass transfer effect for supersonic flow over cone, examining solution of equations of motion for inviscid compressible gas with velocity field normal to surface of inner cone 23 p4011 A66-41898

Diameter and location of wake neck and trailing wake shock for pointed and blunt slender hypersonic cones 23 p4012 A66-41919

Motion equations, shear stress and skin friction for three-dimensional flow in conical

23 p4014 A66-42062

Secondary jets investigated on sharp nosed 9 degree half-angle cone at Mach 6, noting effect on ratio of jet interaction normal force coefficient to jet reaction normal force coefficient 24 p4158 A66-42791

**CONICAL INLET**

Local emissivity of vertex point of diffuse conical or V-groove cavity, noting dependence on wall material, angle factor and agreement with theoretical solution 17 p3035 A66-32613

**CONICAL NOZZLE**

Performance correlation of conical and contoured nozzles for gas-particle flows, defining differences between particle effects for such nozzles 08 p1165 A66-19157

Flow regime data for wide range of conical diffuser geometries determined from clear plastic diffuser experiments 11 p1687 A66-22331

Modification of conical plasma source of Azovskii design by replacing thin glass conical section with thick-walled neck section of glass bottle 21 p3785 A66-39039

**CONICAL SCANNING**

Antenna construction, RF system, receiver and detector, information bandwidth, target modulation and efficiency points of monopulse and conical scanning system for tracking radars 04 p0487 A66-14130

Conical beam scanning by nutating subreflector in Cassegrain antenna system, showing most favorable motion pattern from point of view of electrical performance 18 p3082 A66-34282

**CONICAL SHELL**

Plastic analysis of conical shells of revolution under axisymmetric loads based on approximate parabolic hypercylindrical yield 01 p0153 A66-10445

Axisymmetric modes and frequency vibration of thin conical shells subjected to rapid surface heating [AIAA PAPER 65-788] 03 p0434 A66-12558

Transient response of truncated conical shell due to traveling pressure front of constant velocity and amplitude approximating vibration modes 03 p0437 A66-12819

Large axisymmetric nonlinear elastic or plastic deformations of zero-moment circular conical shells 04 p0590 A66-14160

Yield point load of conical sandwich shell simply supported and loaded at vertex for material obeying Tresca yield condition [ASME PAPER 65-WA/APM-30] 05 p0779 A66-15451

Inextensional buckling of thin conical shell under axial compression [AIAA PAPER 66-125] 07 p1148 A66-18461

Unsymmetric free oscillations of conical shell of medium length and linearly variable thickness 08 p1312 A66-19432

Stress-strain state of conical shells of variable thickness loaded along generatrices and at peripheral points 08 p1312 A66-19433

Stability of thin-walled conical shells under axially symmetric loading determined from nonlinear shell theory 10 p1614 A66-21382

Elastic buckling of clamped conical shells under external pressure 10 p1617 A66-21786

Internal or external pressure effect on natural frequencies of conical shell, noting role of inertia forces, using linear shell theory 11 p1780 A66-22330

Thermal radiation from conical surfaces with nonuniform radiosity and application to nozzle design 12 p1977 A66-23598

Yield point load of conical sandwich shell simply supported and loaded at vertex for material obeying Tresca yield condition [ASME PAPER 65-WA/APM-30] 12 p1961 A66-23978

Axisymmetric configurations of oscillations of thin conical shell, solving equations for fundamental frequency 13 p2207 A66-26497

Eigenvalues of truncated cones of revolution with degenerate poles and various rigidities and geometries 14 p2400 A66-27686

Edge load solution for conical shells 14 p2408 A66-28133

Torsion of elastic cone as mixed boundary value problem, using Mellin transforms and Wiener-Hopf technique 14 p2408 A66-28395

Deformation of finned conical shell under axial load 15 p2608 A66-28781



Vibration modes of conical frustum shells with free ends  
[AIAA PAPER 66-450] 16 p2814 A66-30603

Vibration mode of conical shells measured, showing that it varies with conical angle and circumferential wave  
16 p2821 A66-31381

Stability of truncated conical thin shells under torsional load  
16 p2821 A66-31382

Longitudinal bending of elastic truncated conical shell subjected to edge loads  
17 p3020 A66-32001

Newtonian formulas for determining pitch and roll and normal force derivatives for various types of conical and spherical bodies  
17 p2838 A66-32333

Parametric vibrations determining dynamic stability of simply supported truncated conical shells under pulsating pressure  
17 p3031 A66-33075

Exact analytic solution, in confluent hypergeometric functions, to problem of stability of conical shell under uniformly distributed longitudinal compressive forces  
18 p3252 A66-33709

Limit analysis of conical shells under uniform internal pressure in correcting membrane solution  
18 p3259 A66-35017

Impact of elastic conical shell of revolution moving with constant axial velocity toward rigid obstacle  
21 p3827 A66-38692

Bend-resistant conical shells of uniform wall strength under periodic loading treated by operator method  
21 p3828 A66-38811

Effect of stiffening ribs on stressed-strained state of shallow symmetrically loaded conical shells, noting reduction of boundary value problem to integration of differential equations  
22 p3991 A66-40150

Resonant frequencies and associated mode shapes of transverse vibrations of truncated conical shells over wide range of geometrical and modal parameters  
23 p4139 A66-41691

Steady state inviscid gas flow around conical bodies solved, using stabilization method for three-dimensional supersonic flow around smooth body  
23 p4013 A66-42012

Drop bursting by surface forces such as electric fields and fluid environments with larger viscosity  
23 p4060 A66-42018

**CONJUGATED SYSTEM**

Conformal sets of aromatic and other conjugated compounds, noting that sum of combustion heat of compounds in one set equals sum of compounds in other set  
03 p0442 A66-12333

Ionospheric disturbances following geomagnetic sudden commencements propagating from two isolated locations in high latitudes which are conjugate points  
08 p1216 A66-19214

Optimal trajectory and guidance role of conjugate points in determining maximum duration of optimal control for linear and nonlinear processes  
10 p1516 A66-21076

Matrix analysis of scattering from conjugate-matched antenna  
11 p1662 A66-22541

Linear ODEs in canonical form with after-effect in functional space of continuous functions  
11 p1676 A66-22644

Data on geophysical phenomena at magnetically conjugate points on Earth including cosmic noise absorption, conjugacy of visual auroras, magnetic variations, VLF phenomena, etc  
19 p3453 A66-35981

**CONNECTOR**

**SA ELECTRIC CONNECTOR**

Cylindrical connectors, nomenclature, terminology and tables  
13 p2043 A66-26308

Table of interconnecting device for use with printed circuit board  
13 p2043 A66-26309

**CONSERVATION EQUATION**

Conservation laws in general relativity and definitions of gravitational momentum and energy  
05 p0715 A66-14531

Integral form of fluid dynamic conservation equations relative to arbitrarily moving volume  
08 p1205 A66-18677

Electron conservation equation and effects of laminar or turbulent flow on breakdown in gases  
08 p1206 A66-18933

Generalized theory of physical quantities in scalar and vector form in moving reference regions  
08 p1211 A66-19730

Mathematical model for heterogeneous

continua, discussing kinematical definitions, conservation principles, thermodynamics  
15 p2478 A66-29250

Conservation equations for cylindrical blast and radiation effect on shock layer profiles of blast wave  
16 p2686 A66-31114

Mode characteristics of solid state lasers from analytical solution of conservative equation  
18 p3118 A66-33839

Conservation equations for two-dimensional axisymmetric simultaneous turbulent mixing and supersonic combustion of hydrogen-oxygen-nitrogen-water streams solved by finite difference methods  
18 p3099 A66-34219

[AIAA PAPER 66-617] Asymptotic property derived for particular solutions of Hamilton-Jacobi equation of conservative systems with two degrees of freedom  
19 p3401 A66-36252

Approximation of nonlinear characteristics of conservative vibrations by two polygon characteristics chosen so that mechanical energy of system remains same  
21 p3833 A66-39599

Energy, linear and angular momentum conservation principles for elastic body with finite number of defects  
23 p4091 A66-41855

Separation point of laminar boundary layer before dihedral, determining conservation of momentum and mass  
23 p4013 A66-42010

**CONSERVATION LAW**

Macroscopic conservation equations for ionized dilute hydrogen plasma derived directly from Bogoliubov-Born-Green-Kirkwood-Yvon equations  
01 p0110 A66-10338

Energy function and conservation of inertial mass and three-momentum from relativity principle and conservation of energy in particle collisions  
05 p0719 A66-15530

Conservation laws involving mass, momentum and energy applied to asymptotic properties of hypersonic flow  
09 p1327 A66-20266

Conservation principle as applied to heat equation, assuming equation is one-dimensional  
12 p1974 A66-23530

Particle theory in which additive particle labels are defined in geometric terms of classical gauge theories of Yang-Mills type  
12 p1916 A66-23823

Nonlinear ordinary differential equations applicable to damped oscillatory circuits with exploding wires, obtaining conservation law and approximate solutions by Picard method  
13 p1219 A66-26667

Small-signal energy conservation theorem for one-dimensional multiveLOCITY electron beam according to Boltzmann and multistream descriptions  
15 p2467 A66-29755

Energy pulse tensor formulation of law of conservation of energy in interacting electromagnetic field, using complete inhomogeneous Lorentz group  
18 p3135 A66-34579

Komar covariant formulation of conservation laws of general relativity obtained directly from variation of scalar curvature density  
19 p3401 A66-36168

Plasma radiative processes theory with conservation principles derivation and H-theorem proof  
20 p3607 A66-37012

Field, mass, momentum and energy conservation, entropy and evolution conditions for steady MHD oblique shock discontinuities in perfectly conducting gas flow with Mach and Alfven number parameters  
21 p3795 A66-39577

**CONSTANT**

**S COUPLING CONSTANT**

**S DIELECTRIC CONSTANT**

**S ELASTIC CONSTANT**

**S GRAVITATIONAL CONSTANT**

**S GRUNEISEN CONSTANT**

**S TIME CONSTANT**

**CONSTELLATION**

**S CYGNUS CONSTELLATION**

**S ORION CONSTELLATION**

**S SCORPIO CONSTELLATION**

**CONSTITUTIONAL DIAGRAM**

Thermal, micrographic and X-ray diffraction techniques used for constitution diagram of ternary system tungsten-molybdenum-osmium at various high temperatures  
03 p0385 A66-13209

Binary boron-metal systems, except B-Cu, show large miscibility gaps in liquid state  
07 p1052 A66-18353

## CONSTRUCTION

**S AIRCRAFT CONSTRUCTION**

**S MISSILE CONSTRUCTION**

**S SANDWICH CONSTRUCTION**

**S SPACECRAFT CONSTRUCTION MATERIAL**

**S STRESSED-SKIN CONSTRUCTION**

## CONTACT

**SA ELECTRIC CONTACT**

**SA ROLLING CONTACT**

**SA SLIDING CONTACT**

Plane contact problem for circular ring and elastic or absolutely rigid disk, using method of successive approximations  
18 p3252 A66-33710

Contact problem for elastic rectangle solved by reducing problem to solution of quasi-fully regular infinite set of linear algebraic equations with bounded free terms  
19 p3476 A66-36837

## CONTACT POTENTIAL

Hot glow probe determination of plasma space potential noting disturbance due to contact potential drift and probe construction, accuracy and applicability  
01 p0113 A66-10639

Surface charges on light-induced charges in contact potential difference of semiconductors  
05 p0738 A66-15345

Contact potential difference measurements for adsorption of cesium on polycrystalline tungsten surfaces in cesium vapor  
05 p0622 A66-15582

Surface potential in high and low resistivity semiconductors determined by comparing surface and contact potentials and Fermi levels  
09 p1427 A66-20537

Contact barriers on insulating semiconductor cadmium sulfide measurements, based on pulsed light and bridge  
10 p1573 A66-21245

Stored charge storage in surface states of germanium and silicon  
10 p1581 A66-21877

Contact potential difference measurements between aged polycrystalline tungsten foil and polished single crystal disk and work function calculation for /110/ oriented surface  
10 p1582 A66-21888

Surface charge sign effect on capacitor photoelectromotive force in semiconductors and photoinduced contact potential change  
15 p2559 A66-28628

Surface charges on light-induced charges in contact potential difference of semiconductors  
15 p2569 A66-29984

Voltage and density of contact-corrosion current arising at contact surface of different metals  
18 p3124 A66-35011

Theoretical distribution of charges and potential in vicinity of metal-dielectric barrier in absence and presence of applied field  
19 p3448 A66-36753

Contact problem of half-plane inelasticity theory using Jacobi polynomials and taking into account thermal stresses and presence of adhesion and friction in contact area  
19 p3476 A66-36835

Saha-Langmuir formula applied to description of temperature dependence of positive ion current in surface ionization of silicon atoms, comparing work functions by methods using contact potential, thermionic emission and Richardson graphs  
22 p3968 A66-40942

**CONTACT RESISTANCE**

Negative resistance and oscillation generation in current voltage characteristics of indium antimonide point contacts connected with oxide layers on crystal surface  
01 p0043 A66-10764

Binary-ternary switching algebra used to analyze multiterminal two-position contact networks which include resistors and ideal rectifiers  
02 p0209 A66-11911

Mode of use and effect of precision coaxial connectors on precise methods of impedance measurement  
03 p0344 A66-13017

Thermal contact resistance between uniformly loaded thin plates in vacuum, noting hysteresis test for effect of creep [ASME PAPER 65-HT-16]  
05 p0783 A66-14740

Interfacial metallic foils effect on thermal contact resistance [ASME PAPER 65-HT-44]  
05 p0785 A66-14755

Heat transfer between two metallic cylinders in close contact, examining effect of interstitial gas on thermal contact resistances  
07 p1149 A66-17452



Contact pressure between two bodies with two contact sections in theory of creep 07 p1146 A66-18255

Steady thermal regimes in multilayer medium with perfect and imperfect contacts and varying heat 09 p1471 A66-20831

Current-controlled negative-resistance effect between nonsymmetrical ohmic contacts on opposite side of p-type indium antimonide 10 p1585 A66-22081

Negative resistance and oscillation generation in current voltage characteristics of indium antimonide point contacts connected with oxide layers on crystal surface 11 p1661 A66-22275

Surface roughness effect on boundary friction for various loads, speeds and lubricants [ASLE PREPRINT 65 AM 6AZ]

13 p2085 A66-25367

Heat transfer through contact zone of two solids which are joined 13 p2209 A66-25445

Analog computation of contact thermal resistances for two joined materials and interstitial gas 13 p2209 A66-25477

Contact bouncing in protective gas relays measured in circuit with inductive and real load 13 p2031 A66-25484

Thermal contact resistance between smooth rigid isothermal planes separated by elastically deformed smooth spheres [AIAA PAPER 66-461] 16 p2814 A66-30604

Contact resistance of sliding contact over thin film as affected by material, pressure and contact area 16 p2662 A66-30963

Effect of temperature, pressure and initial wall treatment on thermal resistance at stainless steel-liquid metal interface 17 p3036 A66-32845

Heat flux dependence and directional effect of thermal contact resistance for interface between dissimilar metals 22 p4000 A66-40921

**CONTAINER**

S CARTRIDGE

S FUEL TANK

S PACKAGING

**CONTAINMENT**

S CONFINEMENT

**CONTAMINANT**

Diffusion of heavy contaminant in turbulent atmosphere, approximating vertical wind profile and turbulent diffusion coefficient by power functions of height 01 p0096 A66-10754

Diffusion of heavy contaminant in turbulent atmosphere, approximating vertical wind profile and turbulent diffusion coefficient by power functions of height 14 p2326 A66-27853

Wettability determination and detection of organic contaminants of surface 17 p2870 A66-32206

Space simulation chamber determination of contamination causes and effects 22 p3892 A66-40238

**CONTAMINATION**

SA DECONTAMINATION

SA FUEL CONTAMINATION

SA RADIOACTIVE CONTAMINATION

SA SPACECRAFT CONTAMINATION

Contamination of carbonaceous chondrites by ordinary viable microorganisms, isolating three types of bacteria on various meteorites 03 p0325 A66-13339

LOX-compatible packaging films for maintaining cleanliness of supercleaned components 17 p2943 A66-32203

Contamination control methods used in Royal Swedish Air Force, presenting special particle counting and patch test methods in hydraulic oils 17 p2870 A66-32204

R and D clean room complex design for guidance and control systems, noting contamination control, maintenance procedures, cost factors, etc 17 p2903 A66-32209

Liquid nitrogen-cooled shield against oil vapor contamination of proton accelerator in vacuum chamber 19 p3281 A66-35814

Moisture contamination and associated water band absorption spectra recorded by balloon-borne spectrometer 20 p3554 A66-38206

Aircraft hydraulic system contamination control program under clean as you go principle 22 p3851 A66-40043

Thermal control surface contamination due to rocket exhaust plumes and effects on solar absorptance and IR emittance of protective coatings 22 p3891 A66-40231

LOX characteristics for on board breathing equipment including contaminants noxious to people, clogging of equipment, explosiveness and possible use of contaminated LOX 22 p3858 A66-40504

Gas chromatography analysis of ambient gas and vapor effects on semiconductor and solid state devices at low temperatures 24 p4179 A66-42095

Projectile-borne and gaseous impurity effects on spectroscopic turbulence and velocity measurements at reentry simulating range 24 p4190 A66-42184

**CONTINUITY EQUATION**

Stationary distribution of ozone density with height in presence of long waves in atmosphere, solving continuity equation for ozone and considering photochemical processes 01 p0062 A66-10752

Ionospheric plasma diffusion, noting electric field effect in derived equation of continuity for F region 08 p1215 A66-19206

Hollow-cylinder experiments with superconducting transition taking place while cylinders are rotating 09 p1418 A66-20040

Measurement of magnetic field produced by rotating singly and multiply-connected superconductors, formulating macroscopic electrodynamics of rotating body at low angular velocities 09 p1418 A66-20041

Solid rotating mercury cylinder, reversibly obeying London equation when cooled through superconducting transition, at given angular velocity 09 p1419 A66-20042

Coordinate systems describing portions of Friedman world and adjacent empty regions do not satisfy Liechnerovitch continuity conditions 09 p1403 A66-20595

Analytical continuation and first-order stability of short-period orbits originating at equilateral center of libration in Sun-Jupiter system 13 p2048 A66-25308

Design of composite structures of minimum weight, using flat-bottomed cylindrical tank, noting continuity condition of radial bending moment of plate and shell 14 p2395 A66-27174

Solution of continuity equation for electrons leads to high loss rate in prenoon maximum of electron density in F-2 layer 14 p2283 A66-27397

Stationary distribution of ozone density with height in presence of long waves in atmosphere, solving continuity equation for ozone and considering photochemical processes 14 p2285 A66-27851

Fluid dynamics equations of state, motion, continuity and energy stress-strain relationship and shearing stress deformations 18 p3098 A66-34120

Optimum field thicknesses of radiation-resistant drift-field solar cells obtained by continuity equation 20 p3500 A66-37492

Viscosity distribution within Moon analyzed, using Navier-Stokes and continuity equations, abnormal inertia moment explained, maria and continent distribution examined for understanding internal state of Moon 20 p3656 A66-38030

Coordinate systems describing portions of Friedman world and adjacent empty regions do not satisfy Liechnerovitch continuity conditions 20 p3603 A66-38129

Character of continuity of solutions to second-order linear elliptic equations with many independent variables 20 p3592 A66-38421

Constitutive equations for nonlinear elastic solid-linear viscous fluid mixture and for mixture of two nonlinear elastic solids 22 p3898 A66-40140

Error correction in Vlasov equations of continuity of deformations in curvilinear coordinates 22 p3948 A66-40374

Variational principles for viscous, incompressible hydromagnetic equations of flow including continuity equation, motion equations, etc 23 p4099 A66-41123

Numerical solution of continuity equation for transient compressible flow in closed vessel 24 p4193 A66-42135

Approximate steady state solutions of continuity equation containing effects of

diffusion, drift and recombination for carrier diffusion region of forward-biased p-n junction over wide range of injection 24 p4249 A66-42225

**CONTINUOUS FLOW SYSTEM**

Cantilevered continuous pipe conveying fluid at constant velocity, showing that internal and external damping and Coriolis forces may have destabilizing effect [AIAA PAPER 66-102] 05 p0774 A66-15036

Continuous flow, solid state electrochemical device for simultaneous carbon dioxide removal and oxygen generation [AICE PREPRINT 47E] 17 p2867 A66-32675

Cantilevered continuous pipe conveying fluid at constant velocity, showing that internal and external damping and Coriolis forces may have destabilizing effect [AIAA PAPER 66-102] 18 p3257 A66-34594

Continuous pneumatic mixing of liquid and solid propellant ingredients into composite type propellant 22 p3968 A66-39869

**CONTINUOUS FUNCTION**

Decomposition theory of continuous submartingales 01 p0094 A66-10728

Discrete-point series representation of continuous function 02 p0251 A66-12150

Optimal control problems considering arbitrary piecewise-continuous function with finite number of discontinuities of first kind 02 p0209 A66-12176

Continuous periodic functions approximation by Fejer and arithmetic means 03 p0388 A66-12712

Class of periodic functions for which given method of summation gives trigonometric approximation of optimal order 03 p0388 A66-12713

Algorithm determining best approximation in Chebyshev sense of continuous function on segment 04 p0540 A66-14168

Approximation of continuous function by typical mean of Fourier series 05 p0709 A66-15357

Complex variable functions, discussing boundary properties for holomorphic continuous unit disk with constant absolute value on boundary 06 p0901 A66-16007

Isoperimetric problems of controlled systems of continuous functions solved, using Lure canonical transformations 07 p1012 A66-17376

Continuation of certain classes of differentiable functions beyond limits of region 07 p1060 A66-18465

Approximation of continuous and differentiable functions by algebraic polynomials on closed interval 10 p1551 A66-21976

Linear ODEs in canonical form with after-effect in functional space of continuous functions 11 p1676 A66-22644

Linear approximation method for continuous periodic functions based on theorems concerning relation between triangular matrix and continuity modulus of subset of functions 11 p1724 A66-23365

Automatic control system relay represented by means of limit toward which continuous function tends when chosen parameter increases indefinitely 12 p1848 A66-24029

Ionospheric sounding using random diffusion of electromagnetic wave by ionospheric plasma with continuous wave through two separate antennas 16 p2653 A66-30953

Approximation of continuous and differentiable functions by algebraic polynomials on closed interval 19 p3390 A66-36186

Optimal control and dynamics of class of hybrid state continuous time systems described by differential equations combined with multistable element 19 p3337 A66-36734

Continuous system replacement by lumped parameter models, considering undamped flexural vibrations of beam systems, particularly free vibrations 21 p3825 A66-38581

Finite realization extrema of continuous time stationary stochastic processes 23 p4085 A66-41535

**CONTINUOUS NOISE**

S IMPULSE NOISE



CONTINUOUS WAVE

SA MODULATED CONTINUOUS WAVE

Planetary radar system at Venus site of NASA Deep Space Instrumentation Facility for space communications, noting continuous-wave transmitters and receivers 04 p0478 A66-13602

High power Brewster window laser with gas fills, discussing power output and efficiency parameters 04 p0531 A66-13983

Continuous recording of CW transmission frequency M.S.F. Rugby permits study of effects of traveling ionospheric disturbances on phase height of reflection levels of both magnetotonic components 04 p0488 A66-14379

Trimming microcircuit elements like evaporated thin-film and silk-screened cermet-film resistors attempted with CW and pulsed lasers 05 p0692 A66-14562

Transistor CW amplifier delivering 14 watts into 15-ohm load over frequency band from 46 to 90 mc for use with FM optical modulator 05 p0649 A66-15177

Pumping power formula for determining characteristics of continuous wave and pulsed lasers 06 p0889 A66-15900

Intensity fluctuations in output of four-level CW laser oscillators by linearized rate equations 07 p1047 A66-18434

Data pulsed transmission over electron-injection laser communication system, using continuous waves 09 p1385 A66-19934

Output power of CW laser measured by wire bolometer in form of plane single-layer spiral as sensitive element 09 p1381 A66-20364

Integrated field intensity of atmospherics analysis compared to continuous wave method for data acquisition for radio systems design 10 p1496 A66-21073

Optical second harmonic generation in focus of lowest transverse mode of continuous wave Gaussian gas laser beam 10 p1541 A66-21175

CW laser action on triple state phosphorus-sulfur transition, using hydrogen sulfide-noble gas mixtures 10 p1543 A66-21577

Short-pulse scattering by simple geometric shapes useful for heuristic models of electromagnetic scattering, illustrating creeping-wave return 10 p1500 A66-21618

CW bistatic radar design with arrival direction, distance and Doppler measurements obtained from phase comparisons and used in ionospheric wind determination from meteor trails 10 p1501 A66-21626

Floating zone technique for preparing high purity GaAs crystals for CW microwave devices 10 p1516 A66-22099

High cut-off frequency epitaxial gallium arsenide varactors generating continuous wave power when biased in avalanche region, showing dimensions, resistivities, etc 10 p1516 A66-22103

Electromagnetic propagation into cavity formed by two parallel walls, for case of continuous wave impinging perpendicularly 11 p1653 A66-22558

Current-voltage characteristics of CW X-band GaAs microwave Gunn generator 11 p1713 A66-23029

Matched filter for frequency modulated continuous wave radar signal processing system 11 p1669 A66-23110

Spurious sideband power levels for linear FM carriers encountered in FM-CW and FM pulsed radars 11 p1658 A66-23482

Continuous wave measurement of optical nonlinearity of ammonium dihydrogen phosphate, using helium-neon laser 12 p1912 A66-23716

Bulk germanium arsenide operating simultaneously as microwave amplifier, mixer and oscillator under continuous wave conditions 12 p1835 A66-24144

Radar maps of Moon and planets using bistatic continuous wave mode of radar operation between orbiting spacecraft and ground station 12 p1825 A66-24891

Radar observation of Sun, noting continuous wave transmitter, antenna, etc 13 p2022 A66-25537

Performance of two-photon laser operating in continuous wave mode, deriving formula for pulse frequency 14 p2310 A66-28166

Pulsed toroidal excitation of gas ion lasers extended to drive high power CW laser

transitions in Ar, Kr, Cl and Br, noting operating parameters and power output 15 p2513 A66-28877

CW IR laser oscillation in atomic Cl in HCl and HI gas discharges, noting use of two power supplies and energy level diagram 15 p2513 A66-28880

Receiver noise factor, discussing CW and dispersed signal source measurement techniques 16 p2649 A66-30549

Continuous wave oscillations in n-type GaAs due to voltage controlled negative conductance 17 p2983 A66-33107

High power continuous wave four-level solid neodymium glass laser showing length and host loss as dominant factors in limiting output power 17 p2937 A66-33334

Solid state CW optically pumped microwave maser, using divalent thulium doped calcium fluoride 18 p3117 A66-33614

First-and second-order sidebands due to strong CW signal intermodulation effect in 3.39 mu He-Ne laser 18 p3117 A66-33615

Continuous wave power ratings of strip transmission lines, noting temperature profile parameters, power limit curves, etc 18 p3077 A66-34062

Output power of CW laser measured by wire bolometer in form of plane single-layer spiral as sensitive element 19 p3353 A66-35321

Phase comparison telemetry consisting of passive VHF receivers and CW transmitters for satellite detection 19 p3301 A66-35692

Ionospheric absorption measurement by A3 method in which field strength of distant CW transmitter is continuously recorded 19 p3351 A66-36359

Overlay transistor used for continuous microwave power output of 6.5 watts at 1 gigacycle and over 1 watt at 2 gigacycles 20 p3524 A66-36898

Continuous wave gas laser as light source in scattered light static photoelasticity 20 p3577 A66-37443

Continuous wave UV ionized gas laser emission over four transitions in neon, krypton and argon 20 p3579 A66-37771

Self-induced divergence of continuous wave He-Ne laser beams when traversing transparent liquid, noting nonlinear effect in propagation of light 21 p3748 A66-39164

Continuous wave ultrasonic piezoelectric amplifiers at gigacycle frequencies, noting desirability of high velocity sound in active medium and unimportance of high mobility 21 p3713 A66-39467

Coupling of two avalanche diode oscillators to obtain increased continuous wave microwave power output 22 p3877 A66-40180

Frequency tuning of coherent emission over vibronic continuum of phonon-terminated optical masers by thermal tuning and wavelength-selective feedback 23 p4077 A66-41369

Competition, hysteresis and reactive Q-switching in carbon dioxide lasers at 10.6 microns, using moving mirror technique 23 p4079 A66-41631

10.6 micron output of carbon dioxide-He laser modulated, using Bragg diffraction from longitudinal acoustic waves in Te 24 p4219 A66-42251

Mode selection, relaxation oscillations, mode interaction and thermal effects in room temperature CW lasers in ellipsoidal pumping systems 24 p4221 A66-42546

Linearized population rate equations and quantum noise sources used to calculate spectra of intrinsic second moment intensity fluctuations in 3-and 4-level CW laser oscillators 24 p4221 A66-42548

Crystalline solid lasers, considering rare Earth and transition metal impurities and host materials, noting CW laser characteristics 24 p4224 A66-42799

Gas-discharge CW lasers, particularly He-Ne, carbon dioxide, argon-ion and pulsed self-terminating lasers, discussing classification, power output and gain, Doppler width, coherence and noise 24 p4224 A66-42801

**CONTINUOUS WAVE /CW/ RADAR**

CW-equivalent radar cross section measurements of reflectivity of body by short pulses 03 p0332 A66-12429

Linear homodyne mixer used to eliminate interference and extract range information

in CW radars 06 p0833 A66-16644

Satellite ionization effects, CW-reflection and pulse radar techniques in 10 to 20 mc frequency range 08 p1181 A66-18749

High resolution X-band FM/CW radar for radar cross section measurements 10 p1500 A66-21620

CW microwave oscillation in bulk GaAs, discussing harmonic content, linewidth, circuit and electronic tunability, etc 10 p1585 A66-22077

Metal wall ionized argon lasers, discussing use of water-cooled quartz discharge channels, CW lasers, development of satisfactory metal, etc 13 p2091 A66-25555

1964 results of high resolution CW radar spectral studies of Venus at NASA/JPL Deep Space Instrumentation Facility at Goldstone, California 13 p2185 A66-25812

Digital-mode FM CW laser ranging and tracking system using compound axis servomechanism 13 p2024 A66-25982

Correlations and intensity fluctuations in light from individual lasing and nonlasing modes of CW GaAs laser and threshold noise change in laser emission 13 p2102 A66-26210

Resolution of multiple target ambiguities in twin-channel frequency-modulated continuous wave radar system using fixed antenna 20 p3596 A66-37218

Coherent CW superheterodyne radar system for studying backscattering from hypersonic velocity projectile wakes 24 p4191 A66-42196

**CONTINUUM**

Small-amplitude wave propagation in incompletely ionized plasma, based on continuum theory 19 p3406 A66-35465

**CONTINUUM FLOW**

Transition regime mass flow rate and longitudinal pressure distribution along short tube with bellmouth entry 08 p1207 A66-19131

Transition from near free molecular flow at leading edge of flat plate in rarefied hypersonic flow to continuum boundary layer flow downstream 11 p1633 A66-22925

Estimates of expected relative magnitudes of convective and radiative heat transfer at stagnation point of blunt body for superorbital speeds and altitudes with continuum flow 13 p1989 A66-25154

MHD theory and experiment 13 p2156 A66-26706

Argon flow through long tube compared with Weber theoretical model, applying classical continuum equations 14 p2274 A66-27444

Mathematical model for heterogeneous continua, discussing kinematical definitions, conservation principles, thermodynamics 15 p2478 A66-29250

Low Reynolds number flow past sphere for cases involving density and temperature variations, noting compressibility, transport properties and viscous dissipation 15 p2425 A66-29740

Electro-magnetoplasma gas dynamics /EMPGD/ equations based on single fluid continuum-theory macroscopic plasma-dynamics theory 24 p4244 A66-42834

**CONTINUUM MECHANICS**

**SA DYNAMICS**

**SA FLUID MECHANICS**

**SA STATISTICAL MECHANICS**

Nonlinear elastic-plastic theory and multipolar continuum mechanics 01 p0154 A66-10482

Calculation method for natural bending pulsations of continuous medium extended to case of torsion pulsations 01 p0154 A66-10643

Pulse energy tensor and internal macroscopic interactions in gravitational field and in material media 01 p0106 A66-10656

General theory for construction of constitutive equations describing purely mechanical properties of continuous media with tensor and group theoretic concepts 01 p0106 A66-10717

Detailed account of dislocation loops according to continuum theory 04 p0590 A66-14164

Dynamic reciprocal theorem for sinusoidal oscillation of elastic medium treated as extension of static reciprocal theorem of



Betti and Rayleigh, using continuum mechanics  
[ASME PAPER 65-WA/MD-21]

05 p0779 A66-15524

Elasto-plastic matrix displacement analysis of arbitrary three-dimensional continuum under strain hardening 06 p0963 A66-16464

Heat capacity and thermal conductivity related to elastic-mechanical macroscopic physical properties, using invariance properties of tensors 06 p0971 A66-16616

Generalized theory of physical quantities in scalar and vector form in moving reference regions 08 p1211 A66-19730

Monograph on continuum mechanics principles including thermal, chemical and electrical effects 10 p1556 A66-22064

Displacement bound theorems for work hardening continua subjected to impulsive loading in inelastic continua 11 p1781 A66-22610

Kinetic theory of leading edge of plate interacting with streaming gas evaluated by Bhatnagar-Gross-Krook equation of statistical mechanics 11 p1633 A66-22924

Thermodynamics of irreversible processes applied to continuum mechanics, deriving classical rheological equations 12 p1976 A66-23546

Thermodynamics of deformation, discussing Coleman theorem 12 p1976 A66-23547

Properties of continuum determined experimentally, noting deformed shapes, displacement, strains, stresses, etc, taking advantage of grid, moire, photoelasticity and other methods 12 p1957 A66-23628

Relating general theory of elastic-plastic continuum, valid for nonisothermal deformations and explicit thermodynamic restrictions, to Drucker postulate 12 p1959 A66-23862

Uniqueness theorem for dynamically loaded rigid-plastic and rigid-viscoplastic idealizations of deformable bodies 12 p1962 A66-23999

Pulse energy tensor and internal macroscopic interactions in gravitational field and in material media 12 p1914 A66-24008

Zhukovskii and Lagally theorems for arbitrary fluid motion derivable from momentum equations of continuous medium 13 p2067 A66-26533

Fibrous continuum media theory, discussing geometrical properties, stress state, motion equations, boundary value problems, etc 14 p2397 A66-27383

Solution for free nonstationary convection in bounded region of Landau-Lifshits mechanics of continuous media 14 p2414 A66-28282

Classical analytical mechanics applied to mechanics of continua, noting relation between kinetic-stress functions and Ostrogradskii-Hamilton principle and stress tensor and finite deformation tensor 15 p2539 A66-29148

Oscillatory component in solar granulation continuum brightness fluctuations, secondary maxima in temporal autocorrelation functions and power spectra 17 p2996 A66-31920

Geometrical and kinematical conditions of compatibility associated with moving discontinuities in material media 17 p3032 A66-33501

Nonlinear material with memory defined by constitutive functional, examining fading memory theory 19 p3438 A66-35484

Weierstrass necessary condition and basic equations for optimal control of initial or boundary states of continuum mechanical MHD and hypersonic partial differential systems 20 p3535 A66-36853

Continuous media model theory and comparison with theory of many-dimensional non-Euclidean manifolds, noting kinematic characteristics of particle deformation, variational principles, thermodynamic equation, etc 21 p3756 A66-38627

Thermodynamics of irreversible processes methods applied to stress-strain relations of single-phase nonelastic continuous medium 21 p3830 A66-38986

Balance equations for heterogeneous continua - substances consisting of many distinct, possibly interacting constituents derived from classical continuum physics viewpoint 21 p3772 A66-39348

Thermoelastic wave equations in continuum mechanics model of laser-induced fracture in transparent media in terms of laser beam energy absorption 22 p3931 A66-40089

Large amplitude oscillations of cylindrical and prismatic bodies resulting from generalized shear deformation in longitudinal direction 22 p3990 A66-40141

Linear theory of micropolar elasticity, noting all components of asymmetric stress tensor are determined and motion of media is fully described when deformation and microrotation vectors are known 22 p3995 A66-40566

Continuum mechanical Cartesian tensor analysis theorem on completeness of Beltrami stress function 23 p4139 A66-41544

Energy, linear and angular momentum conservation principles for elastic body with finite number of defects 23 p4091 A66-41855

Design of models of continuum media for research in plasma physics, aerodynamics, polymeric structures, motion, creep, etc 23 p4096 A66-41935

Coupled ODE sets describing continuum wave propagation in discrete structures with and without dispersion or linearity 23 p4096 A66-41939

Thermodynamics problems when applied to continuum mechanics deformations, noting Onsager theory 23 p4096 A66-41942

Deformation theory of classical continuum in four-dimensional representation, particularly in time derivatives 23 p4144 A66-41972

Generalized strain and transition concepts for elastic-plastic deformation creep and relaxation 23 p4144 A66-41973

CONTINUUM RADIATION  
Continuous operation of gallium arsenide injection laser cooled by helium gas flow 01 p0084 A66-11190

Continuum emission from Venus, Mars, Jupiter and Saturn at 21.2 cm wavelength, measuring brightness temperature to determine source of radiation solar activity effects 11 p1776 A66-23491

Continuous operation of gallium arsenide injection laser cooled by helium gas flow 12 p1890 A66-24011

Spatial cross-correlation analyses between radial velocity and continuum brightness fluctuations of solar disk center spectrograms 17 p2996 A66-31919

Total continuum radiation from high temperature air and components for wavelength greater than 2000 angstroms, based on radiation measurements from constricted arc at atmospheric pressure 18 p3140 A66-34587

Linear polarization of continuum emission from galaxy and discrete sources, detection in radio astronomy, noting relevant synchrotron theories 21 p3815 A66-39488

XUV C, Ti, Mn, Fe, Ni, Cu, Zn and Ar line spectra and continuum radiation spectra in plasmas produced by focused ruby laser beam 22 p3954 A66-39812

CONTOUR  
Point-to-point contouring systems noting procedures, codes and cost savings [ASTME PREPRINT MS66-725] 12 p1887 A66-24423

Polynomials orthogonal with respect to contours, examining analytic function representation via Fourier series expansion of such polynomials 16 p2738 A66-31409

CONTRACT  
Alternative method of determining incentive fee schedule for government contracts, based on linear programming and system reliability 12 p1888 A66-24669

Combining R and D and follow-on production in single contract 14 p2417 A66-28434

Total value concepts applied in system effectiveness analysis are helping Contract Definition type contracts meet cost effectiveness requirements 18 p3268 A66-34251

CONTRACTION  
Length of two-dimensional contractions in terms of flow uniformity 18 p3098 A66-33952

Contraction to improve isotropy of grid-generated turbulence 22 p3899 A66-40381

CONTRACTOR  
Contractor performance on cost type contracts evaluated by comparing actual and allocated costs, using NASA PERT facilities 08 p1322 A66-19460

Relationship between military and contractors in aircraft development, noting adherence to military specifications, costs, weapons, etc 14 p2416 A66-27812

Optimal support costs of weapon systems requires contractor selection based on high order of management capability 20 p3682 A66-37238

Contractor performance evaluation program and relation to weapon system effectiveness 20 p3571 A66-37940

CONTROL  
S ADAPTIVE CONTROL

S AIRCRAFT CONTROL

S ALTITUDE CONTROL

S APPROACH CONTROL

S ATTITUDE CONTROL

S AUTOMATIC CONTROL

S AUTOMATIC GAIN CONTROL /AGC/

S BANG-BANG CONTROL

S BOUNDARY LAYER CONTROL

S COMMAND CONTROL

S CONTROLLED FUSION

S DIRECTIONAL CONTROL

S DYNAMIC CONTROL

S ELECTRIC CONTROL

S ELECTROHYDRAULIC CONTROL

S ELECTROMAGNETIC CONTROL

S ELECTRONIC CONTROL

S ENGINE CONTROL

S ENVIRONMENTAL CONTROL

S FIRE CONTROL

S FLAP CONTROL

S FLIGHT CONTROL

S FREQUENCY CONTROL

S FUEL CONTROL

S GIMBALLED CONTROL

S GROUND CONTROL

S GUIDANCE AND CONTROL

S HELICOPTER CONTROL

S HYDRAULIC CONTROL

S INVENTORY CONTROL

S LAMINAR FLOW CONTROL

S LONGITUDINAL CONTROL

S MAGNETIC CONTROL

S MANUAL CONTROL

S MISSILE CONTROL

S NUMERICAL CONTROL

S OPTIMAL CONTROL

S PHASE CONTROL

S PITCH CONTROL

S PNEUMATIC CONTROL

S PROPORTIONAL CONTROL

S QUALITY CONTROL

S RADIATION CONTROL

S RADIO CONTROL

S RANGE CONTROL

S REACTION CONTROL

S REACTOR CONTROL

S REGULATION

S REMOTE CONTROL

S ROLL CONTROL

S SATELLITE CONTROL

S SEQUENTIAL CONTROL

S SERVOCONTROL

S SERVOSTABILITY CONTROL

S SPACE VEHICLE CONTROL

S SPACECRAFT CONTROL

S STABILITY AND CONTROL

S TEMPERATURE CONTROL

S THRUST CONTROL

S TRAFFIC CONTROL

S TRAJECTORY CONTROL

S VECTOR CONTROL

S VISUAL CONTROL

S WEATHER CONTROL

S WING TIP CONTROL

CONTROL AREA  
Plotting of radius of controllability sphere for linear dynamic systems bounded with respect to control actions and having fixed time of motion 03 p0350 A66-13042

Plotting in phase space controllability region for unstable linear system of differential equations 03 p0350 A66-13043

Houston mission control center for flights from Gemini to Apollo program 14 p2272 A66-28441

Plotting of radius of controllability sphere for linear dynamic systems bounded with respect to control actions and having fixed time of motion 18 p3092 A66-35005

Plotting in phase space controllability region for unstable linear system of differential equations 18 p3092 A66-35006



CONTROL DEVICE

SA SILICON CONTROL RECTIFIER

/SCR/

Control circuit of image converter tube 01 p0071 A66-11041  
Fluid state analog-computation technology and process control computation systems [ASME PAPER 65-WA/PID-11] 05 p0624 A66-15637

Circuits for variable impedance control at centimeter-wave frequencies, using varactor semiconductors and dephasing ferrites in waveguide 07 p1002 A66-17828  
Nonlinear differential equation analysis of motion stability of plant with automatic control device 07 p1080 A66-17858

Motor controllers for DC current supply must be inverters of constant or variable frequency 08 p1168 A66-19299  
Control system of supersonic combustion, using spectral intensity ratio, monitoring combustion chamber in two wavelength regions 10 p1622 A66-21948

Control circuit of image converter tube 11 p1708 A66-23287  
Book on automatic control of linear and nonlinear systems, particularly aircraft utilization 16 p2744 A66-31058

Brake force acting on piston of constant-speed controller with fluid friction 21 p3698 A66-39330  
Comparison of Czechoslovakian human engineering standards for control pushbuttons with U.S. 22 p3859 A66-40861

High-power nanosecond commutator for control of spark chambers, laser shutters, etc 22 p3933 A66-40945

Analog and digital controls used in electron beam welding and metal working machinery including electron beam milling machine 24 p4217 A66-42345

Control PANEL

Human factors in control/indicator panel design of ground support equipment [ASME PAPER 65-WA/HUF-16] 05 p0628 A66-15696

Long-range navigation system control/display concepts and automation for airline navigation 07 p1074 A66-17779

Cockpit flight instrument display in integrated navigation system for SST, stressing smooth transition in handling from enroute navigation to terminal-area and approach procedures 07 p1078 A66-17810

Experimental testing effectiveness of sensor lines showing linkages between displays and controls 12 p1808 A66-23924

CONTROL SIMULATOR

SA COMPUTER

SA FLIGHT SIMULATOR

Mission simulation techniques for training Gemini flight controllers 02 p0186 A66-11802

Navigator sighting accuracy in midcourse guidance system for manned space flight, using simulated vehicle mounted space sextant 03 p0390 A66-12740

Navigation and control simulation portion of overall manned space cabin test program [AIAA PAPER 65-277] 03 p0328 A66-12776

Closed loop hydraulic servo system simulating flight stresses on motor case of solid propellant rocket motor in static firing test stand for calibrating stand 03 p0353 A66-13218

Simulation study of human performance in manual control tasks in orbital rendezvous and lunar landing 06 p0818 A66-16245

Manual guidance and control simulation for reentry vehicle flight and landing 08 p1203 A66-19533

Added pilot work load imposed by additional commands in compensatory display reduces tracking performance in control of simulated terrain-following aircraft 12 p1808 A66-23922

Electronic predictor instruments for dynamic control and simulation and possible application to lunar spaceship 13 p2048 A66-25896

Mechanical prediction display to improve human behavior in control system 21 p3700 A66-38454

Optimization of VTOL control concepts with and without stabilization compared with six degree of freedom motion simulator, noting system failure effects and

nonlinear concepts [ICAS PAPER 66-9] 22 p3851 A66-40675

CONTROL STABILITY

Best stabilizing control for linear system under given class of perturbations 01 p0050 A66-10354

Condition of existence of universal best stabilizing control in second order control system 01 p0050 A66-10355

Stability of control systems with tachometric feedback 01 p0067 A66-10455

Stability of automatic control system with variable structure studied for application to stabilization of linear objects whose parameters vary quite rapidly within wide limits 02 p0207 A66-11312

Frequency criteria of absolute stability of nonlinear control systems with periodically varying parameters 02 p0207 A66-11847

Stability limit on forward gain in control systems with small time delay by approximating exponential in characteristic equation 02 p0207 A66-11877

Generalizing Tsytkin stability criterion for class of time-varying nonlinear sampled data feedback systems 03 p0348 A66-12668

Current trends in nonlinear control theory 03 p0349 A66-12701

Axiomatic approach to control system theory as generalization of dynamic systems, noting weak and strong stability and Liapunov function 03 p0351 A66-13255

General dynamical system defined by contingent equation giving existence and uniqueness theorems 03 p0389 A66-13256

Stability regions of optimized modulated sample-data system determined from parametric fluctuation analysis 04 p0504 A66-13975

Relative stability of linear feedback systems noting Hurwitz, Nyquist and Mikhailov stability criteria 05 p0707 A66-14623

Limited transients for certain single-loop systems containing nonlinear amplifier and linear system 05 p0656 A66-14727

Book on structural synthesis of high-accuracy automatic control systems with large stable amplification 05 p0657 A66-15086

Boundaries of stability sector of nonlinear controlled systems with delay, deriving criterion for designing maximum boundaries 05 p0657 A66-15114

Boundedness of solutions of nonlinear functional equations for stability of feedback and electrical systems 05 p0658 A66-15182

Control mechanisms in nonlinear steady flow forces of hydraulic valves [ASME PAPER 65-WA/AUT-20] 05 p0624 A66-15616

Fundamental Theorem of Stability for systematic determination of practical stability regions for nonlinear systems [ASME PAPER 65-WA/AUT-19] 05 p0659 A66-15617

Split-path nonlinear filter /span filter/ for independent gain and phase to achieve control system compensation [ASME PAPER 65-WA/AUT-4] 05 p0659 A66-15705

Nonlinear automatic control system, discussing optimum tuning via parametric stability region construction 06 p0863 A66-16528

Automatic relay systems, describing self-oscillation induced parameter variation 06 p0863 A66-16530

Frequency condition of absolute stability of controlled systems with hysteresis nonlinearities of backlash type derived based on matrix inequalities 07 p1012 A66-17375

Principle of stabilization systems design based on sequential reduction of dimensionality of phase plane of controlled variable and derivatives 07 p1013 A66-17427

Stabilization of steady motions of nonlinear controlled system in critical case of pair of purely imaginary root 07 p1016 A66-18185

Sufficient conditions for stabilization of motion of nonstationary controlled system 07 p1016 A66-18186

Practical determination of stability region of equilibrium point of second-order nonlinear recurrence with real variables 08 p1255 A66-18639

Phase-advance stabilization of servocontrol

systems by use of limiters controlled by error signal 08 p1199 A66-18671

Attenuation factor and degree of stability of automatic control systems determined by Mikhailov criterion and Chebyshev polynomials 08 p1201 A66-19684

Stability criteria in tuned transistor amplifiers treated by feedback system theory 10 p1510 A66-21652

Absolute stability of automatic control system with allowances for external load of hydraulic servomotor 11 p1674 A66-22358

Mikhailov criterion for stability and oscillation of linear sampled data systems 11 p1674 A66-22362

Mathematical stabilization theory for dynamic systems from Liapunov motion stability theory and theory of games 11 p1736 A66-22639

Model of spectrotron with external feedback in dynamic behavior analysis, considering control pulse and transient process 11 p1677 A66-22761

Stability definitions for generalized control systems 11 p1681 A66-23450

Existence of Liapunov functions for problem of Lure with removal of complete controllability and observability 11 p1681 A66-23451

Nonlinear control systems consisting of single-loop negative feedback circuit with one isolated instantaneous type nonlinear element 12 p1850 A66-24258

Liapunov second method applied to stability of general second order bang-bang control systems 12 p1850 A66-24259

Stability and transient characteristics in single channel sinusoidal perturbation adaptive system 12 p1853 A66-24336

Generalization of parameter plane method for case when characteristic equation coefficients are nonlinear functions of system of adjustable parameters 12 p1855 A66-24642

Absolute and relative stability of linear control systems containing transport or distributed lag 12 p1855 A66-24643

Four new theorems on absolute stability of nonautonomous nonlinear control system with strongly bounded or monotonically bounded input 12 p1856 A66-24653

Automatic control system stability reserve using amplitude phase criteria with respect to modulus and phase 13 p2049 A66-26055

Stability of phase-locked loops using Fokker-Planck equation and under additive stationary white Gaussian noise linearized about some equilibrium point 13 p2025 A66-26075

Dual input describing function /DIBF/ of two-state relay with hysteresis 14 p2265 A66-27481

Stability of nonlinear control systems, noting Hermitian matrix for linear system of ordinary differential equations and analogous problem for difference equations 15 p2525 A66-28513

Dissipative gyroscopic force effects on mechanical system, noting necessary and sufficient conditions for stability and controllability 15 p2537 A66-28949

Control system stability under external forces discussing Liapunov function construction, transfer functions and matrix analysis, frequency conditions of absolute stability, etc 15 p2470 A66-29147

Self-oscillations and stability of model reference adaptive systems with constant plant parameters and control response 15 p2476 A66-29991

Stability of control systems with distributed parameters and hysteresis-curve-type nonlinearity for various critical cases of system characteristic equation 16 p2668 A66-30750

Nonlinear automatic control system, discussing optimum tuning via parametric stability region construction 16 p2670 A66-30838

Formulation and proof of theorem and lemma defining conditions of absolute stability for specified new class of control systems 17 p2901 A66-32252

Sufficient conditions for absolute stability of servosystem with backlash, taking into account plant inertia and hypothesis of absolutely inelastic collisions 17 p2901 A66-32258



Nonstationary automatic control systems design by reaction quenching method 17 p2902 A66-32580  
Dynamics of self-adaptive systems with stabilized frequency characteristics 18 p3089 A66-33735  
Attenuation factor and degree of stability of automatic control systems determined by Mikhailov criterion and Chebyshev polynomials 18 p3091 A66-34670  
Stability analysis of automatic control systems with random parameters, applying Mikhailov criterion 18 p3092 A66-34996  
Absolute stability criteria of control system with one nonlinear element, using Liapunov functions 18 p3092 A66-35016  
Stability, reproducibility and sensitivity of combined systems of automatic control with variable structure determined by presence of sliding mode region 19 p3329 A66-36025  
Stability and sensitivity of terminal linear feedback control systems 19 p3334 A66-36668  
Distributed parameter systems in discrete-time models compared with response obtained by approximating transcendental transfer function with root factor and other approximations 19 p3322 A66-36683  
Stability problems in randomly excited dynamic systems, discussing partial differential equations governing evolution of conditional probabilities and expectations 19 p3471 A66-36718  
Stability and quality of automatic control of plant with pure time delay, using regulator with constant and switching parameters 20 p3537 A66-36894  
Sufficient conditions for equilibrium stability of mixed distributed and lumped parameter feedback control system in parabolic PDE form 21 p3718 A66-38666  
Popov criterion application in determining stability of linear time-invariant systems with nonlinear feedback, using root locus 21 p3718 A66-38667  
Stability of automatic control systems with nonlinearity and nonunique equilibrium state 23 p4048 A66-40967  
Stability analysis of inertial guidance platform control system with saturation and Coulomb friction nonlinearities, using Liapunov method 23 p4089 A66-41319  
Bang-bang principle in problem of epsilon-stabilization of linear control systems extended to systems of arbitrary dimension 23 p4051 A66-41874  
Generalized Popov criterion for stability of control system with arbitrary number of memoryless nonlinearities 24 p4187 A66-42130  
Thermistor temperature sensing bridge for precision temperature control of liquid volume 24 p4214 A66-43033

## CONTROL SURFACE

SA AILERON  
SA ELEVATOR  
SA FIN  
SA STABILIZER

Response of hypersonic aircraft to abrupt control displacements, determining vehicle characteristics, design and operational parameters 09 p1330 A66-20739  
Motion equations for dynamics of aircraft control surface controlled by autopilot 14 p2328 A66-27687  
Rolling friction studies of intermetallic and zirconium oxide for control surface bearings for space reentry vehicle [ASLE PAPER 66AM 5D4] 16 p2712 A66-30413

Near UV effects on thermal control surfaces at cryogenic temperature 17 p3035 A66-32749  
Linearized motion equations for low-altitude flight pitching stability of aircraft with control surface 21 p3696 A66-38937  
Thermal control surface contamination due to rocket exhaust plumes and effects on solar absorptance and IR emittance of protective coatings 22 p3891 A66-40231  
Fluid venting effects on thermal control surfaces studied, using vacuum chamber for thermal environment simulation 22 p3891 A66-40236  
Fundamental modes of nonservo-assisted aircraft control surface 24 p4159 A66-42344

## CONTROL SYSTEM

SA ADAPTIVE CONTROL SYSTEM  
SA BIOCONTROL SYSTEM  
SA DATA CONTROL SYSTEM

## SA FEEDBACK CONTROL SYSTEM

Hydraulic gear motor and gear backlash effects on stability of hydraulic control system 01 p0014 A66-10282  
Control systems to avoid detuning effects caused by plasma in resonant cavity experiments on plasma acceleration and confinement in HF fields 01 p0040 A66-10546  
Redundancy techniques for flight control systems applied to tactical military aircraft, noting monitorless channel output selection, failures, etc 01 p0103 A66-10666  
XB-70 vehicle control system sensing, local force application, coupling and adaptability for increasing structural mode damping ratio, thus avoiding disturbing pilot accelerations and structural loads 01 p0103 A66-10672  
Difficulties in control system synthesis for launch vehicles exhibiting severe mode interaction 01 p0104 A66-10673  
Progress in constant speed drive generating systems and control equipment for constant frequency aircraft electric systems [SAE PAPER 650827] 01 p0016 A66-10827  
Turbulence amplifier system noting principles and application 02 p0180 A66-11963  
Book on systems engineering problems and tools for solution noting energy, materials, modeling, simulation, computers, control, statistics, signals, etc 02 p0307 A66-12280  
Comparison of feedback arrangements using pneumatic amplifiers for static accuracy and dynamic performance improvements of control systems 03 p0323 A66-12374  
Digital computer simulation for control system design including electrical circuits, mechanical systems and chemical processes 03 p0337 A66-12375  
Control problems associated with stable platforms using single-axis integrating gyroscopes including axes design, drift due to vibration and compensation 03 p0390 A66-12533  
Propulsion-control systems interface for V/STOL hover control in aircraft, using lift plus lift cruise propulsion concept [AIAA PAPER 65-799] 03 p0319 A66-12564  
Design and installation of antennae for airborne command and control systems, noting antenna system for SAC Airborne Command Post [AIAA PAPER 65-730] 03 p0334 A66-12581  
Flying qualities requirements related to control system complexity noting longitudinal, lateral and directional requirements [AIAA PAPER 65-794] 03 p0320 A66-12597  
Successive approximations for variational problems in control theory including pulse amplitude and pulse width modulation, using quasi-linearization techniques 03 p0349 A66-12685  
Stability of automatic control system with nonlinear elements, obtaining quadratic equations by using Liapunov method 03 p0349 A66-12707  
Spinning satellite attitude control using interaction between Earth magnetic field and onboard current carrying coils [AIAA PAPER 64-235] 03 p0430 A66-12735  
Synthesis of time-optimal control system in presence of constraints on displacement and displacement rate of steering element 03 p0350 A66-13044  
Implementation of airborne command and control systems, emphasizing communications equipment, data processing facilities, electromagnetic compatibility and aircraft configuration parameters [AIAA PAPER 65-727] 03 p0336 A66-13049  
Control system 465L used by Strategic Air Command noting automated functions, data processing, integration of human and electronic elements, etc 04 p0507 A66-13687  
Simplest system of auto-oscillatory extremal control, examining control plant output law 04 p0502 A66-13701  
Error control systems in digital communications accomplished by adding constraints to digital alphabet through coding 04 p0481 A66-13766  
Failure probability of redundant system considering dynamic and static failures of switches and control

circuit 04 p0503 A66-13770  
Algorithms for teaching open-loop optimizing control system correct recognition of situations expressed as regions of complex configuration 04 p0503 A66-13773  
Book on state variables for control theory noting transfer functions, time domain, nonlinear system stability using Liapunov method, optimization, etc 04 p0504 A66-13836  
Centralized vibration control of vibration testing noting details of automatic equalizers, switching panel, data reduction, etc 04 p0508 A66-14446  
Magnetic torquing system controlling satellite spin rate and spin axis orientation 05 p0769 A66-14521  
Global search of performance surface to find parameters optimizing performance of learning control system, using variable structure stochastic automaton 05 p0653 A66-14598  
Frequency sensor and roving notch filter for control system, discussing parasitic signals with time-varying frequencies 05 p0645 A66-14603  
Forced oscillations in nonlinear relay type control system predicted via periodic solutions to nonlinear difference equation 05 p0654 A66-14606  
V/STOL Canadair CL-84, evaluating control and lift propulsion system 05 p0609 A66-14767  
Accessory power drive, variable sweep wing actuation, hydraulic, electric and environmental control systems of Boeing SST [ASME PAPER 65-AV-13] 05 p0611 A66-15131  
Fluidic control subsystem, describing components such as electric/fluid and position transducer, operational amplifier, fluid bellows and operation characteristics [ASME PAPER 65-WA/AUT-10] 05 p0624 A66-15609  
Mathematical and control operations, utilizing fluieric components such as jet deflection type proportional fluid amplifiers, capillary-tube resistors and tank capacitors [ASME PAPER 65-WA/PID-2] 05 p0624 A66-15679  
Manual control of vehicles considering aircraft handling, human dynamics, etc [ASME PAPER 65-WA/HUF-10] 05 p0628 A66-15697  
Common framework for automata theory and control theory 06 p0863 A66-16619  
Relative stability of self-excited nonlinear oscillations subject to small amplitude perturbation 06 p0864 A66-16737  
Upper bound on dynamic/transient and steady state/quantization error in digital control systems, using direct method of Liapunov 06 p0865 A66-16741  
Criteria for reachability of subspace by trajectories of linear control system 06 p0865 A66-16744  
Nonlinear control system, discussing method to obtain estimate of region of stable initial conditions 06 p0865 A66-16747  
Sampled data control systems using z-transform method when sampling device is followed by data hold 06 p0866 A66-16749  
Control power composition and usage characterized for VTOL aircraft flight control system design 06 p0806 A66-16812  
Flight controls of tilt wing XC-142A aircraft, noting mechanization and operation of wing and flap control system 06 p0809 A66-16815  
Method of time domain analysis of nonlinear hybrid systems with first or fractional order data extrapolation 06 p0866 A66-16963  
Sensitivity of eigenvalue to changes in matrix calculated by formula used to investigate control systems 06 p0867 A66-16976  
Traffic control for space vehicles and probable flight data requirements 07 p1140 A66-17228  
Two-stage/descent and ascent/Lunar Excursion Module control system for landing gear, ascent stage, liftoff from lunar surface, etc 07 p1140 A66-17280  
Isoperimetric problems of controlled systems of continuous functions solved, using Lure canonical transformations 07 p1012 A66-17376



Synthesizing dual control in absence of a priori information concerning unknown plant parameter 07 p1012 A66-17380

Probability characteristics of distributed parameter system subjected to parametric and additive noises, obtaining mathematical expectation and correlation function expression 07 p1014 A66-17433

Graphoanalytical calculating method of statistical characteristics of step extremal control systems under steady state operation in presence of random noise 07 p1014 A66-17434

Statistical problem of control system synthesis, discussing plant algorithm 07 p1014 A66-17438

General performance indices for time and frequency response for free motion of linear discrete control systems 07 p1016 A66-18280

Frequency stabilization of gas lasers, using atomic resonance and interferometers 07 p1045 A66-18357

Techniques for synthesis of control systems, based on Liapunov second method 08 p1200 A66-19016

Charge current control circuit for nickel-cadmium cells with control electrodes 08 p1169 A66-19506

Three-axis limit cycle operation of reaction jet attitude stabilization 08 p1304 A66-19515

Reliability of automatic control systems, considering properties of controlled plant, taking error probability in control as criterion 08 p1201 A66-19691

Improvement of transient response of third order servosystems by discrete control of system parameters, noting application of switching circuit 09 p1360 A66-19859

Dynamic programming in linear vector system and application in switching system 09 p1393 A66-19909

Higher order correlation function evaluated for shot noise statistics 09 p1342 A66-19925

Carrier circuit techniques applied to fluid amplifier control systems 09 p1332 A66-20326

Book on advances in control systems, Volume 2 09 p1362 A66-20649

VTOL control power requirements under low speed flight conditions for randomly disturbed mechanical system 09 p1330 A66-20736

Fluid control system design and principles 10 p1485 A66-21511

Necessary conditions for extremum in problems of control with aftereffect 10 p1518 A66-21975

Dynamic characteristics of linear plant determined under noise conditions, allowing for error in input-signal measurement 11 p1673 A66-22202

Optimum quantization step for given distribution law of quantized signal, using minimum error distortion criteria 11 p1674 A66-22204

Optimization of five second and third-order systems with saturating and relay controllers and with random Brownian Motion input 11 p1674 A66-22222

Ambient temperature compensation in indirectly heated thermistors with negative temperature coefficients used as control elements 11 p1661 A66-22273

Control criterion for linear system with constant matrix, discussing quadratic functionals ensuring aperiodic transient 11 p1674 A66-22351

Extension of Pontryagin maximum principle for application to optimum discrete control systems 11 p1674 A66-22355

Optimum control processes in systems containing plants with distributed parameters described by ordinary or partial differential equations with initial and boundary conditions 11 p1674 A66-22356

Forced sliding regimes in automatic control systems 11 p1675 A66-22640

Optimization of systems with stepwise control constraints, using Pontryagin maximum principle to determine special features 11 p1676 A66-22753

Transient processes and periodic motions in extremal control system with higher derivative control action 11 p1677 A66-22757

Control system design capable of automatically locating malfunctioning elements and replacements from external reserve 11 p1677 A66-22762

Design of variable structure automatic control system frequency characteristics, using harmonic linearization 11 p1677 A66-22763

Optimal control systems and numerical analysis of error effect on sensitivity 11 p1680 A66-23274

Automata theory and control theory analytically compared for general and linear systems and tolerance automata 11 p1680 A66-23275

Numerical dynamic predictor for control systems disturbed by random noise, discussing Fokker-Planck equation, Crank-Nicolson difference model, etc 11 p1680 A66-23279

Adaptation, learning and self-learning in automatic systems, discussing stochastic approximation, pattern recognition, adaptive filters, etc 11 p1680 A66-23332

Complete controllability of particular plant 11 p1682 A66-23455

NERVA reactor control systems, using limiter circuits to protect nuclear subsystem from controller malfunctions and for pressure control 12 p1912 A66-23701

Quasi-optimal minimum-time controllers for high-order dynamic systems obtained by least-squares fitting points on optimal switching surface 12 p1849 A66-24253

Quadratic performance index in designing linear multivariable control systems 12 p1849 A66-24254

State variable approach for analysis of linear multivariable system with multiple eigenvalues 12 p1849 A66-24255

Automation of control processes - International Federation on Automatic Control Congress, Basel, Switzerland, August-September 1963 12 p1850 A66-24314

Rocket equipment simulation on rocket engine test facilities, describing fuel tank design for experiment with suitable flow characteristics and parameters 12 p1829 A66-24317

Orientation control of orbital astronomical observatory examined, using dynamic model consisting of three independent subsystems, each with one degree of freedom 12 p1829 A66-24318

Control of radio telescope, noting servosystem ability to keep tracking position errors and wind-caused error within certain limits 12 p1851 A66-24319

Control system of microwave antenna positioning used in communication satellite tracking, noting servosystems, converter, Leonard drive, control panel, etc 12 p1817 A66-24320

Optimum design strategies for discrete control systems with minimal time of control 12 p1852 A66-24328

Optimum dual system design for plant investigation and regime requirements 12 p1853 A66-24331

Measuring time as dynamic characteristic of performance of self-adaptive control systems 12 p1853 A66-24333

Self-adaptive control system reflecting internal and external conditions of operation 12 p1853 A66-24334

Integrated stability augmentation circuits in AN/ASW-16 automatic flight control system 12 p1837 A66-24381

Design of control deflections and structural loads of space vehicle for flight stability through atmospheric disturbances [AIAA PAPER 66-350] 12 p1954 A66-24487

Statistical characteristics of output of nonlinear sampled data control system evaluated by two methods 12 p1855 A66-24639

Stability of pulse frequency modulated closed-loop control systems determined, using state variables which define system output and error 12 p1855 A66-24640

Manual closed-loop control systems analysis, discussing operator dynamics for permanent procedural variables 12 p1855 A66-24641

Root locus methods applied to synthesis of linear multivariable control systems for noninteraction 12 p1855 A66-24644

Circuit design for high impedance amplifier for control systems, considering input and output impedance and amplifier gain 12 p1844 A66-24731

Early bird hydrogen peroxide control

system maneuvers to place satellite into final stationary position [AIAA PAPER 66-262] 12 p1954 A66-24736

Commercial communications satellite system, impact and problems [AIAA PAPER 66-273] 12 p1981 A66-24746

Satellite communications central control support system consisting of Earth stations and satellite relays accommodating different RF power, orbits and antenna orientations [AIAA PAPER 66-287] 12 p1859 A66-24758

Parameters of satellite communication system control and scheduling function, emphasising distinction between scheduling model and scheduling algorithm [AIAA PAPER 66-288] 12 p1822 A66-24759

Limitations and reliability of human operator of control systems to process information, noting importance of endurance and sensory perception 12 p1807 A66-25012

Control problems regarding space developments, considering automation, reliability, computer role, human operator, etc 13 p2056 A66-25231

Man-machine systems for interplanetary exploration, using functional analysis techniques for system design 13 p2013 A66-25281

Harmonic linearization of logic law control systems, deriving complex equivalent transmission coefficient for nonlinear part of circuit with variable structural elements 13 p2045 A66-25299

Design of multivariable control system using signal flow graph techniques and establishing optimality criteria 13 p2045 A66-25337

Programming and control - International Conference, Air Force Academy, Colorado Springs, April 1965 13 p2046 A66-25339

General theory of optimal processes, discussing general version of maximum principle 13 p2116 A66-25342

Minimizing functionals on normed linear spaces, discussing steepest descent and rendezvous problems in control theory 13 p2116 A66-25343

Control problems in operation of transport aircraft noting degrees of freedom, computer aid, human factor, etc 13 p2047 A66-25497

Circuit and system theory - Allerton Conference, University of Illinois, October 1965 13 p2049 A66-26057

Controllability of linear and nonlinear dynamical systems, using perturbation properties expressed as sensitivity functions 13 p2050 A66-26059

Sensitivity operator as extension of time-domain sensitivity function to time-varying change of elements in nonlinear dynamic system, deriving sensitivity equations 13 p2050 A66-26060

Combined optimization problem, equivalent to dual control problem, considering determination of optimal control policies for plant under random disturbances, using iterative equations 13 p2051 A66-26065

Approach to sensitivity problem of optimal control systems by introducing performance index 13 p2052 A66-26072

Stability and sensitivity requirements considered simultaneously in control system design, minimizing time domain sensitivity index and incorporating transient response characteristics 13 p2052 A66-26073

Inequality constraints in open-loop minimum time control problem 13 p2053 A66-26080

State-variable feedback decoupling of multivariable linear plants with cross coupling between various input-output pairs 13 p2053 A66-26083

Nonlinear time varying open-loop feedback system design and infinitely integrable function space boundedness condition 13 p2053 A66-26085

Sensitivity comparison of closed-loop and open-loop systems 13 p2054 A66-26092

Sensitivity of sampled data systems with finite sampling duration derived as function of pulse width 13 p2054 A66-26093

Book on unmanned aircraft and rocket control systems, flight dynamics in conjunction with control processes, design of stabilization and guidance systems 13 p2055 A66-26462

Random variable representation of errors



- in control system 14 p2263 A66-26767
- Optimal control problems described by classical boundary problems for equations of parabolic and hyperbolic type 14 p2263 A66-26768
- Probability-statistics analytic human-operator model in control systems analysis 14 p2263 A66-27108
- Control theory of nonlinear servomechanisms, based on describing function technique, provides design data for type I servomechanisms, deriving equations 14 p2264 A66-27117
- Diodes, transistors, rectifiers and inverters application to control and instrumentation systems, providing phase changing, frequency stabilization, source voltage, etc 14 p2249 A66-27118
- Spontaneous processes simulation for self-alignment of poles in recognition system 14 p2264 A66-27204
- Phase space techniques for optimization of relay control systems with plants having multivalued nonlinearities 14 p2265 A66-27482
- Synthesis of linear automatic control system with constant parameters for integral Q-factor, noting effect of small parameters on properties of optimum system 14 p2265 A66-27521
- Restrictions placed on transfer function of linear system with input and output coordinates in presence of given plant in control loop 14 p2265 A66-27522
- Solution of optimum filtering problems when input signals of automatic control system are described by different differential equations at successive time intervals 14 p2265 A66-27523
- Linearized motion equation of self-adaptive systems with stabilized frequency characteristics, considering effect of control and noise signals in basic control loop 14 p2265 A66-27525
- Coordination of integral and relay components in algorithms for adjusting control coefficients in model-reference self-adaptive control systems described by differential equations 14 p2266 A66-27526
- Transfer function of pulse amplitude modulated sampled data control systems with element generating arbitrarily shaped pulses and first order element series connected with constant parameter elements 14 p2266 A66-27527
- Approximation of variable time delays and design of constant and variable delay circuits, noting simulation of delays in automatic control systems by computers 14 p2266 A66-27528
- Minimum effort control problem in rotund reflexive Banach space and extension to Hilbert space under bounded linear transformation 14 p2266 A66-27631
- Nonsteady coordinates of linear delay system determined from observable linear combination of phase coordinates 14 p2267 A66-27671
- Autocorrelation and hypergeometric function applied in evaluating response of nonlinearities to Gaussian noise 14 p2267 A66-27726
- Money-saving technique to speed up potentiometer in control systems 14 p2267 A66-27804
- Fluid control devices 14 p2226 A66-27816
- Optimum control systems for plants described by ordinary nonlinear differential equations or differential equations with constant or variable delay 14 p2268 A66-28278
- Error coefficients and astatism estimation for controllable system in normal operation 14 p2268 A66-28353
- Dielectric-tape TV camera for panoramic scanning application in meteorological satellite, discussing subject logic and control system design 14 p2262 A66-28418
- Effect of backlash between servomotor and control element on dynamics of indirect control systems, assuming system has rigid feedback, sensitive element is inertialess and plant has positive self-regulation 14 p2269 A66-28475
- Determination for piecewise analytic F/t of what vectors can be represented by bang-bang control having finite number of discontinuities 15 p2469 A66-28514
- Simplest system of auto-oscillatory extremal control, examining control plant output law 15 p2469 A66-28542
- Functional analysis of electromechanical control systems, noting application of mathematical methods for system reliability determination 15 p2428 A66-28797
- Minimax problem for pursuit problem of two linearly controlled objects describable by identical differential equations 15 p2526 A66-28948
- Stability of variable-structure control systems, noting two-stage motion in linear system stabilization and image point impingement on switching surface 15 p2471 A66-29161
- Behavior, properties and related concepts of control systems, noting attainability function 15 p2472 A66-29373
- Synthesis of relay automatic control systems with optimum dynamic properties 15 p2476 A66-29994
- Synthesis of correcting units for automatic control systems, using quasi-invariance condition 15 p2476 A66-29995
- Averaging systems for control of sinusoidal vibration tests noting methods, crosstalk effect etc 16 p2678 A66-30463
- Vibration equipment, discussing armature and control oscillator 16 p2679 A66-30474
- Vacuum thermal environmental testing of Nimbus I control system 16 p2809 A66-30504
- Optimization of linear control systems when placing step limitations on control, using functional analysis 16 p2668 A66-30751
- Synthesis problem of optimum dynamic characteristics of multivariate linear control systems with random input signals 16 p2668 A66-30752
- Optimum control of two-dimensional oscillating system when placing limitations on control, using Butkovskii L-problem of moments 16 p2668 A66-30753
- Closed-loop automatic control system with univalued substantially nonlinear element, using approximation of characteristics by Fourier series 16 p2669 A66-30754
- Approximation method determining follow-up failure conditions for nonlinear automatic systems in presence of control and noise signals 16 p2669 A66-30755
- Optimal control problem of variable structure system, deriving necessary and sufficient conditions for existence of trajectories 16 p2669 A66-30756
- Comparison of nonoptimum and optimum strategies in dual control of inertialess plants in presence of noise in feedback loop 16 p2669 A66-30757
- Equation for conditional overshoot density of normal stationary process in centralized and positional centralized control, noting error estimate 16 p2669 A66-30767
- Solar simulation testing of thermal control systems for nuclear test detection spacecraft [AIAA PAPER 64-209] 16 p2682 A66-30890
- Hill climbing in self-optimizing control systems, noting effect of sinusoidal perturbation, application, etc 16 p2671 A66-31059
- Pneumatic control systems, discussing turbulence amplification method and system with miniaturized elements with moving parts 16 p2636 A66-31063
- Pole-zero method to determine frequency response of second-order linear control systems with phase-advance signal shaping 16 p2671 A66-31157
- Duality theory of optimal control and resulting duality correspondence between formulation of optimal control and calculus of variations, noting decomposition algorithm 16 p2671 A66-31229
- Reciprocal optimal control problem and several variations, using inequalities based on convexity assumptions 16 p2671 A66-31232
- Performance of human operators in three-state relay control system with velocity augmented displays 16 p2644 A66-31270
- Three models of constrained preview control with successive target values of nonuniform importance 16 p2644 A66-31272
- Thermostability and control of airborne electronic equipment in closed-loop forced-air cooling systems 16 p2663 A66-31325
- Simulation of fourth order type I linear system, using one-operational amplifier and two-terminal network consisting of four resistors and four capacitors 16 p2672 A66-31385
- Sensor threshold definitions applied to rate gyros, comparing old and new AIAA specifications, noting threshold definitions relation to flight control system malfunctions 16 p2708 A66-31439
- Automatic control systems with carrier frequency information transmission channel, deriving transfer functions 16 p2672 A66-31552
- Monograph on theory of ordinary delay differential equations and optimal control processes with time delay 16 p2673 A66-31749
- Text on random processes in nonlinear control systems, covering statistical analysis, nonlinear transformation with and without feedback, extremal systems, etc 16 p2673 A66-31753
- Mathematical analysis of axioms that provide local definition of generalized control systems 17 p2898 A66-31868
- Reliability of back-up system with consideration of failures in switches and automatic control systems 17 p2880 A66-31904
- R and D clean room complex design for guidance and control systems, noting contamination control, maintenance procedures, cost factors, etc 17 p2903 A66-32209
- Modern control theory applied to system design for reduction of sensitivity of system to plant-parameter variation by use of feedback 17 p2901 A66-32290
- Dynamic programming applied to synthesis of linear optimal or suboptimal multivariable control systems in which control-signal vector depends only on certain prescribed state variables 17 p2901 A66-32291
- Synthesis method for automatic control systems, examining controller design for turboprop engine 17 p2901 A66-32311
- Synthesis of control systems with minimum complexity, noting application to filter discrimination of nonstationary signals 17 p2901 A66-32568
- Optimal system determined from maximum probability criteria of target hitting 17 p2901 A66-32571
- Minimum control system optimization, noting adaptation with respect to minimum mean square error, statistical criterion calculation, etc 17 p2901 A66-32572
- Switching surface construction using one to one correspondence between points in controllability region and points on surface of n-th order system 17 p2902 A66-32575
- Accuracy problems in control systems, discussing error assessment and accuracy estimates of optimal control 17 p2902 A66-32576
- Controlling motion of object directly from accelerometer data without need of object coordinate determination 17 p3003 A66-32587
- Divergent vertical helicopter oscillations due to pilot presence in collective control loop and physiological response of pilot to oscillations 17 p2843 A66-32719
- Control forces in nonlinear integral equations solved by iteration method 17 p2902 A66-32816
- Propellant tanking computer system for monitoring and controlling Saturn IB and Saturn V vehicles [SAE PAPER 660454] 17 p2904 A66-33162
- Optimal trajectory problem solution using in-flight guidance computers for control rockets and aircraft under influence of random disturbances 17 p2956 A66-33239
- Control feel application to aircraft controls, noting man-machine system configurations, anthropometric and physical factors, sensory motor requirements, etc 17 p2869 A66-33446
- Optimal processes in sampled data control system 18 p3089 A66-33734
- Systems and operation of quantized data attitude control system for spacecraft [AIAA PAPER 64-660] 18 p3240 A66-33787
- Man-machine system in control and guidance of Saturn V launch vehicle, emphasizing participation during atmospheric phase of flight profile 18 p3242 A66-33847
- Syncom communications satellite reaction control system for spin axis precession and orbit correction, noting design and operation 18 p3242 A66-33854
- Thermal noise in internal measuring



- instruments affecting limitations on spacecraft open-loop inertial autonomous control system precision 18 p3132 A66-33872
- Trial and error method for constructing closed loop harmonic response locus of control system with one nonlinear element 18 p3089 A66-34010
- Fluid interaction devices, noting induction and turbulence amplifiers, impact modulators, logic gates, inverters, etc 18 p3054 A66-34131
- Large steerable antennas in control systems, emphasizing antennas using paraboloidal reflectors 18 p3081 A66-34267
- Accuracy limitations in control and construction of large steerable paraboloid antennas 18 p3081 A66-34273
- Aerial mount and satellite orbit effect on steerable antenna control system, noting frequency and tracking data rates 18 p3071 A66-34279
- Gust alleviation systems for transport aircraft using linkage, noninteracting and split control 18 p3052 A66-34493
- Reliability of automatic control systems, considering properties of controlled plant, taking error probability in control as criterion 18 p3091 A66-34676
- Dynamics of nonlinear control systems by constructing cross sections of parameter space 18 p3091 A66-34989
- System containing reference model with amplification factor of controller reconstructed, making system stable or auto-oscillatory 18 p3091 A66-34990
- Optimal control minimizing quadratic functional for plant, showing difference in certain phase coordinate region from linear control 18 p3092 A66-34992
- Variable-structure automatic control system with switchable phase-shifting filters for linear plants, converting error signal to control switching device 18 p3092 A66-34994
- Synthesis of time-optimal control system in presence of constraints on displacement and displacement rate of steering element 18 p3092 A66-35007
- Maintenance and inspection of air transport vehicle structures 19 p3278 A66-35399
- Flight control system design for high performance aircraft, particularly longitudinal transient response handling qualities 19 p3278 A66-35509
- Sensitivity of closed loop optimal control system to parameter variations and external perturbations 19 p3324 A66-35581
- Graphical analysis of extremal control system stepwise adapted to process with extremal characteristic located between two first-order linear operators 19 p3324 A66-35582
- Minimum-energy control law derived for attitude acquisition of satellite about single axis, using reaction-wheel control system [AIAA PAPER 65-434] 19 p3468 A66-35602
- Optimal and suboptimal design of vehicular control and proportional navigation system based on Pontryagin maximum principle 19 p3397 A66-35882
- Control moment gyroscope for angular momentum transfer with minimum power consumption, noting design and application for free body motion stabilization 19 p3360 A66-35962
- Block sensitivity coefficient analysis in application of method of transformed circuits to closed-loop control systems, noting dynamic accuracy problem 19 p3327 A66-36014
- Sensitivity analysis for relative stability of self-excited oscillations and transient response of nonlinear control systems 19 p3328 A66-36019
- Synthesis of control systems invariant to parameter changes, examining sensitivity and advantages over self-adjusting systems 19 p3328 A66-36023
- Synthesis of automatic control systems for linear plants with variable parameters satisfying specified performance criteria 19 p3328 A66-36024
- System having insensitivity to variation of plant parameters, characteristics or particular elements shown as structural problem 19 p3329 A66-36026
- Optimal control system sensitivity to inaccuracies determined in error measurement of initial state 19 p3329 A66-36028
- Synthesis of minimum sensitive open loop control system subjected to unpredictable environmental changes, discussing perturbation effects during and before process transient 19 p3329 A66-36029
- Optimal stochastic control system with control of linear plants approximating characteristics of airframes, allowing plant parameters to vary randomly 19 p3329 A66-36030
- Necessary conditions for extremum in problems of control with aftereffect 19 p3330 A66-36185
- Self-learning control system theory, discussing power yield, adaptive and extremum systems, nondeterministic systems, combined deterministic/ self-organizing systems, etc 19 p3330 A66-36433
- On-line and off-line self-organizing control systems for space vehicle application 19 p3333 A66-36661
- Learning control system design, discussing hill-climbing and pattern recognition schemes in framework of statistical decision, automata and information theory 19 p3333 A66-36662
- Coordination technique for synthesis of dynamic multilevel control systems 19 p3334 A66-36667
- Liapunov method synthesis of time variable nonlinear multivariable systems, deriving simplified control law for tracking of linear noninteracting model 19 p3335 A66-36697
- Pontryagin principle extended to control systems, computing optimal control laws 19 p3337 A66-36735
- Pneumatic control system based upon dual membrane relay permitting all fundamental logic operations 19 p3282 A66-36808
- Control algorithms for microminiaturized sampled data digital control systems 19 p3311 A66-36822
- Synthesis procedure which insures good control system performance by adding to performance index term involving sensitivity coefficients 20 p3535 A66-36854
- Mathematical model for systems comprising human operator controlling typical controlled elements, noting behavior variability and performance estimation of mean-squared error in tracking 20 p3508 A66-36861
- Closed loop control system combined with air beating technology for measurement of multicomponent microforces 20 p3555 A66-36870
- Multiloop control interaction using linearized technique, noting variable geometry intake loop 20 p3627 A66-36881
- Self-adjusting control systems with models, reviewing basic theoretical problems of analysis and synthesis 20 p3537 A66-36896
- Soviet RT-15 radio telescope control system, noting two-reflector system-telescope antennas, parabolic mainreflector and automatic and visual tracking possibilities 20 p3540 A66-37026
- Preliminary design, mission specifications and outgoing data specifications for advanced control center for vehicles in orbital flight 20 p3651 A66-37394
- General maintenance techniques for large digital controllers to achieve high order of system dependability 20 p3522 A66-37907
- Book on variational methods in control engineering covering optimal processes based on maximum principle, variational calculus and dynamic programming 20 p3539 A66-37985
- All-fluid control systems, noting achievements in vector control navigation aids and vehicle flight stabilization 20 p3503 A66-38263
- Linear dynamic system synthesis from weighting patterns 21 p3717 A66-38600
- Electromagnetic interference from pulse circuits, switches and relays produced by photo-optical control systems 21 p3709 A66-38608
- Titan II control system modification for Titan III missions involving incorporation of acceleration loop, division of autopilot, etc 21 p3819 A66-38852
- Autonomy in multiply connected variable structure automatic control systems 21 p3719 A66-39247
- Maximum transient deviation in response to step disturbance in control loop 21 p3719 A66-39398
- On-line-learning and off-line-learning self-organizing control systems 21 p3720 A66-39431
- Mathematical and control operations, utilizing flueric components such as jet deflection type proportional fluid amplifiers, capillary-tube resistors and tank capacitors [ASME PAPER 65-WA/PID-2] 21 p3699 A66-39529
- Absolute stability of distributed control system with nonlinear elements of backlash type analyzed by distributed parameters method 22 p3883 A66-39660
- High speed stable system through combination of hunting-type control system without closed cycles designed for plant optimization, with recycling type controller 22 p3883 A66-39661
- Aircraft hydraulic system contamination control program under clean as you go principle 22 p3851 A66-40043
- Flight control system providing control augmentation, self-adaptive control and self-organizing control 22 p3848 A66-40125
- Apollo environmental control system simulation chamber for suit and manned system evaluation and operational verification 22 p3892 A66-40241
- Human operator transfer function capability bounds and system stability characteristics and performance 22 p3858 A66-40252
- Adaptation, learning and self-learning in automatic systems, discussing stochastic approximation, pattern recognition, adaptive filters, etc 22 p3884 A66-40412
- Liapunov function and Meyer-Kalman-Yakubovich lemma used to obtain frequency domain stability criteria for linear plant with both monotone increasing and odd monotone increasing nonlinear feedback functions 22 p3940 A66-40529
- Optimization of linear control system by expressing quadratic performance index as quadratic functional of control functions 22 p3884 A66-40533
- Stability of nonlinear controlled systems with infinite degrees of freedom 22 p3885 A66-40692
- Differential equations with delayed argument describing laws of motion and action of control elements upon motion in problem of trajectory with moving right hand terminus 23 p3941 A66-40800
- Book on synthesis of multiloop control systems for application to automatic control and computer circuit construction 22 p3885 A66-40854
- Propulsion control systems interface for V/STOL hover control in aircraft, using lift plus lift cruise propulsion concept [AIAA PAPER 65-799] 23 p4015 A66-40985
- Control design using force as criterion, discussing effect of varying height and handle orientation of push-pull task 23 p4029 A66-41575
- Asymmetrical nonlinear oscillations of control systems analyzed by parameter plane method, considering systems with reference-perturbing and slow-varying input signals 23 p4050 A66-41610
- Propulsion control systems for Concorde aircraft, noting aero-and thermodynamic reasons for power plant variables subject to manipulation 23 p4122 A66-41776
- Averaging controls of discontinuous stochastic system with sequence of discontinuities forming Poisson flow of events 23 p4051 A66-41782
- Analog computer analysis of input signals effect on time constant, vibration frequency and overshoot ratio of nonlinear control system 23 p4051 A66-41854
- System maintainability in Back-Up Interceptor Control System /BUIC II/ using modular design of system, discussing software and failure 24 p4178 A66-42093
- Operational effectiveness and maintainability verification for surveillance and control systems influence by quantitative reliability 24 p4179 A66-42094
- Control law synthesized for limiting transient processes in second-order systems, including arbitrary functions which allow



additional requirements to be fulfilled 24 p4187 A66-42211

Analytical method based on Taylor series to substitute linear control system for nonlinear control system 24 p4188 A66-42482

Microwave transducers for measuring geometric dimensions and displacements in industrial process control 24 p4214 A66-43012

Navigation, guidance and control system instrumentation for Apollo manned lunar landing mission [AGARDOGRAPH 105] 24 p4236 A66-43124

Optimal control problem formulated for linear constant-coefficient system subjected to class of amplitude bounded load disturbances 24 p4189 A66-43205

**CONTROL VALVE**

Pulse operated bipropellant control valve design for attitude control systems of space vehicles 01 p0015 A66-10668

Four-way fluid state vortex hydraulic servovalve discussing design principles, performance and application 04 p0460 A66-13785

Electrohydraulic servovalve presenting essential characteristics of redundancy by majority choice in analog servosystem 05 p0612 A66-15413

Control valve design for cryogenic fluids, galling, seizing and stress accumulation and material-valve compatibility 12 p1885 A66-24380

Steady state characteristics and transient behavior of vortex valve, examining effect of wall friction and shearing stresses due to radial velocity gradients 20 p3501 A66-37649

Valve technology for spacecraft and rocket engine applications, discussing zero-gravity vent valve, zero leakage valve, insensitive valve seat and solenoid actuator [ASME PAPER 66-MD-61] 21 p3742 A66-38494

Temperature loop operation and transient response performance of pneumatic temperature control consisting of sensor and valve 22 p3853 A66-40540

Control valve seat leakage as function of fluid viscosity, density, pressure drop and cube function of gap between two surfaces 23 p4017 A66-41145

**CONTROLLED FUSION**

Equilibrium of plasma confined in toroid 05 p0725 A66-15240

Controlled thermonuclear fusion, international developments 10 p1555 A66-21267

Soviet high-temperature plasma physics and controlled nuclear fusion 13 p2145 A66-25736

Plasma physics and controlled nuclear fusion research - Conference, International Atomic Energy Agency, England, September 1965 19 p3410 A66-36494

Anomalous escape of ions from plasma contained in magnetic mirror into loss cone studied for evaluation feasibility of controlled thermonuclear reaction in magnetic mirror trap 19 p3415 A66-36517

Plasma physics and controlled nuclear fusion research - IAEA Conference, England, September 1965, Volume 2 19 p3419 A66-36539

Book on plasma diagnostics covering measuring devices and techniques, SHF antenna and waveguide system, emission measurements, etc 21 p3737 A66-38949

Plasma physics and problems of controlled thermonuclear fusion - Conference, Kharkov, Ukrainian SSR, May 1963 21 p3777 A66-39002

Controlled thermonuclear fusion program noting nuclear reactions, plasma production and confinement, etc 24 p4247 A66-43121

**CONTROLLED STABILITY**

Solving method for dynamic equation system describing controlled object element having distributed relationships 04 p0502 A66-13493

Analytical design of controller for stabilization of linear system with random delay in form of intermittent Markov process 04 p0504 A66-13973

Correction of motion of two degree of freedom system with one cyclic coordinate 24 p4189 A66-42837

**CONVAIR MILITARY AIRCRAFT**

S F-111 AIRCRAFT

**CONVECTION**

S ADVECTION

S FORCED CONVECTION

S FREE CONVECTION

S THERMAL CONVECTION

**CONVECTION CURRENT**

SA ELECTRON BUNCHING

Continental structure and drift from convection currents in Earth mantle indicate depth of several hundred kilometers 03 p0360 A66-12378

Cellular convection in conditionally unstable atmosphere, determining preferred areas of ascending and descending regions and current distribution 05 p0666 A66-14542

Influence of suction or injection in boundary layer flow past vertical flat porous plate in presence of uniform magnetic field 06 p0969 A66-16181

Gravity anomalies and convection currents, examining sphere and cylinder sinking beneath surface of viscous fluid 06 p0877 A66-16785

Viscous fluid model estimates of crustal thickness and free-air anomaly compared with measured free-air anomalies and seismic depths of Puerto Rico trench and mid-Atlantic rise 06 p0877 A66-16786

Synoptic interpretation of tropical land convection over Philippines 11 p1728 A66-22322

Internal wave ripples from fluid impacts on base of stably stratified fluid region, calculating particular case of single ripple in viscous fluid 11 p1693 A66-23009

Nonconducting fluid motion in infinite tube applied to violent thunderstorm dynamics, reducing current intensity to value for convection currents 14 p2346 A66-28268

Vertical wind shear effect on development and structure of convection, noting perturbation growth rate and unstable stratification 16 p2742 A66-31110

Organized convection as photographed by Gemini astronauts 18 p3129 A66-34214

Internal turbulence scale for convection jets determined, using measurements of light intensity 21 p3760 A66-39357

EHD traveling potential wave interaction inducing electroconvection in slightly conducting current without electrical contact with flow 23 p4104 A66-41496

**CONVECTIVE FLOW**

Convection pattern changes in Earth mantle and continental drift as evidence of cold origin of Earth 03 p0361 A66-12379

Solar photosphere noting radiative equilibrium theory, granules and convection observations for temperature distribution 03 p0420 A66-12840

Velocity field and wave propagation in hydrogen convective zone of Sun 03 p0425 A66-12846

Convective mass exchange in heterogeneous chemical reactions in laminar flow along wall 04 p0597 A66-14186

Rotating fluid sphere, discussing power law for dependence of Rayleigh number on Taylor number 04 p0599 A66-14471

Macrokinetics of homogeneous-heterogeneous processes in moving media and estimates of initial material concentration in core and boundary layer regions of reaction vessel flow 06 p0971 A66-16543

Initiation of precipitation in vigorous convective clouds traced to cluster of three shower cells which produce radar echo close to -30 C level [AFCLRL-SR-32-65] 07 p1062 A66-17369

Unsteady, combined free and forced convective MHD channel flow of conducting fluid through transverse magnetic field 07 p1085 A66-17580

Stability of piecewise linear velocity profile of shear flow in convectively unstable layer 07 p0980 A66-17942

Heat conduction equation for convective flow applied to gunpowder combustion under harmonic pressure variation 08 p1280 A66-19486

Analogy between eigenvalues for fluid convection and flow stability extended to rotating cylinders with corresponding temperature distribution for given angular velocities 08 p1212 A66-19821

System of equations derived for dynamics of convective atmospheric vortices for

model with unstable stratification and basic vorticity 10 p1530 A66-21274

Local boundary layer approximations of first order for steady laminar convection flow produced by nonuniform axisymmetric heating or cooling of infinite horizontal surface 10 p1620 A66-21276

Cumulus to cumulonimbus convection over mountains and dissipation of stratus and sea fog when moving inland, using Tiros photographs 11 p1728 A66-22321

Differential equations describing air movement, heat exchange and exchange of moisture 11 p1730 A66-22942

Convection and stability criteria for nonlinear steady solutions with homogeneous vertical magnetic field acting on fluid 11 p1787 A66-23420

Stability of steady finite amplitude convection determined by method of successive approximations 11 p1787 A66-23421

Nonlinear Benard convection 12 p1976 A66-23549

Axisymmetric convection between two rotating disks, noting secondary flow and viscous effects of Ekman layers 12 p1980 A66-24941

Vertical displacement rate of air particles in finite volume under effect of internal heat sources in free convection 13 p2209 A66-25318

Forced turbulent convective incompressible flow along rough plates, measuring velocity and temperature profiles 14 p2410 A66-26934

Stability to infinitesimal disturbances of plane Couette flow in presence of negative vertical temperature gradient, noting instability at critical Rayleigh number for convection without shear 15 p2481 A66-29741

Existence of convective interaction of mechanism affecting direction and stability of electric current in flowing gas, using electric arc confined in supersonic flow 15 p2481 A66-29744

Instability arising as overstability in magnetohydrodynamic Benard problem 16 p2761 A66-31104

Convective diffusion of material from single drop moving in liquid medium at low Reynolds numbers, using quasi-stationary approximation 16 p2689 A66-31516

Convective effects role in exciting axisymmetric oscillations in plasma cylinder in magnetic field with aid of radius restricted electron beam 17 p2968 A66-32538

Lunar structural lineaments as boundary conditions for convection theory 17 p3007 A66-33235

Semiconvective zone in very massive stars during hydrogen burning, noting factors leading to instability 18 p3229 A66-34142

Forced convection caused by normal and longitudinal components of flow around hot wire, noting effect of wire length 20 p3544 A66-36928

Differential equations describing air movement, heat exchange and exchange of moisture 20 p3593 A66-37855

Sturrock criteria for differentiating between absolute and convective instability and between amplification and nontransmittance of oscillations 21 p3770 A66-39028

Nonstationary convective diffusion flow toward moving droplet at small Reynolds number 22 p3902 A66-40816

Linear perturbation theory of flow due to convection of entropy and vorticity in nonuniform flow field, noting sound generation 23 p4062 A66-42051

Thermal convection in horizontally infinite layer of fluid confined between rigid heat conducting plates driven by temperature difference 23 p4151 A66-42055

**CONVECTIVE HEAT TRANSFER**

Slow motion of sphere in compressible, viscous and heat conducting fluid analyzed, using Navier-Stokes equations 01 p0006 A66-10424

Unsteady convective flow of electrically conducting fluid through vertical channel in magnetic field, using differential equations 01 p0111 A66-10426

Free convection boundary layers on horizontal flat plate 01 p0161 A66-10434

Heat transfer data obtained in combined convection regime for rotating isothermal cone, noting influence of cone vertex



angle 01 p0164 A66-10902  
 Convective heat transfer behavior of 90 percent hydrogen peroxide studied with reference to possible use as rocket propellant 01 p0164 A66-10903  
 Forced convection vaporization of Freon 113 flowing in horizontal Pyrex tube examined, using motion pictures 01 p0165 A66-10910  
 Temperature difference method of computing convective heat transfer, using flat plate laminar boundary layer equations 02 p0303 A66-11569  
 Equations of quasi-stationary mean flow of momentum and heat on spherical Earth averaged over long period, and over latitude circle 02 p0221 A66-11574  
 Natural convection at thermal leading edge on vertical wall matched with known solution immediately above this region 02 p0304 A66-12199  
 Charring ablative materials effectiveness in combined convective and radiative heating as reentry shield 03 p0444 A66-12792  
 Free convection heat transfer in partially enclosed channel flow; noting effect of vertical fin geometry and temperature [ASME PAPER 64-WA/HT-33] 04 p0595 A66-13386  
 Forced convective heat transfer from isothermal and nonisothermal uniformly spinning bodies of revolution obtained by similar flow analysis [ASME PAPER 64-WA/HT-15] 04 p0595 A66-13387  
 Heat and mass transfer rates compared with correlations for frost formation on vertical plate in free convection [ASME PAPER 65-HT-32] 04 p0595 A66-13391  
 Convective heat exchanger using air and subjected to resonant pulsating flow [ASME PAPER 65-HT-30] 04 p0595 A66-13392  
 Stationary heat sources effect on convective fluxes in unstable atmosphere 04 p0513 A66-13413  
 Heat transfer by laminar forced convection for dissipative fluid in annulus calculated, using complex variable method 04 p0598 A66-14211  
 Cellular convection in horizontal layers heated from below, noting effect of critical Rayleigh number and width-height ratio of cells 05 p0666 A66-14543  
 Heat transfer from Ar and Xe to end wall of shock tube measured, using thin film gauge monitored by IR photocell 05 p0782 A66-14705  
 Interaction of radiation and convection in laminar boundary layer of perfect gas on flat black plate [ASME PAPER 65-HT-54] 05 p0785 A66-14760  
 Convection heat transfer for turbulent flow in subsonic diffusers [ASME PAPER 65-HT-64] 05 p0605 A66-14765  
 Boundary value problem solution for composite media applied to cooling of composite cylinder by convection at outer surface [ASME PAPER 65-WA/HT-52] 05 p0792 A66-15664  
 Slug flow and film boiling of hydrogen, deriving formula for forced convective film boiling heat flux [ASME PAPER 65-WA/HT-32] 05 p0793 A66-15673  
 Convective heat transfer measurements for partially dissociated carbon monoxide and hydrogen with high Lewis number [ASME PAPER 65-WA/HT-27] 05 p0793 A66-15676  
 Interaction or coupling of radiation with conduction and convection mechanisms in nonisothermal nongray gas flowing in entrance region of tube with isothermal black walls [AIAA PAPER 66-136] 06 p0875 A66-17090  
 Ignition of ammonium perchlorate composite propellants by convective heating [AIAA PAPER 66-65] 06 p0941 A66-17101  
 Convective heat transfer in thin rectangular channels commonly found in nuclear reactor fuel assemblies 07 p1148 A66-17299  
 Empirical formula for convection coefficient of bounded space of parallelepiped shape permits determination over wide range of parameters 07 p1148 A66-17393

Dimensionless flow parameter for free convection, equivalent to Reynolds number for forced convection, used for correlating through single curve free and forced convective heat and mass transfer from single bodies 07 p1149 A66-17517  
 Combined free and forced convection flows with heat and mass transfer in laminar boundary layers on vertical surfaces 07 p1150 A66-17579  
 Convective heat transfer coefficients at rocket nozzle throat handling nonaluminaized propellant gas 07 p1151 A66-17583  
 Atmospheric argon effect on hypersonic stagnation point convective heat transfer, using arc-heated shock tube simulating flight velocities up to 34,000 fps [AIAA PAPER 66-29] 07 p1153 A66-17891  
 Variational principle generalization for elimination of simplifying assumptions in convective heat transfer model in forced incompressible flows 07 p1155 A66-18127  
 Convective and radiative heat transfer to reentry vehicles at superorbital velocities [AIAA PAPER 66-106] 07 p1155 A66-18459  
 Annular flow and two-dimensional forced convective boiling heat transfer to hydrogen in nucleate and film boiling regimes 08 p1316 A66-18832  
 Convective heat transfer and artificially turbulent flow through roughened corrugated channels 08 p1317 A66-18864  
 Prediction of solid propellant hot-gas ignition based on preignition transient convective heat transfer model [AIAA PAPER 66-67] 08 p1317 A66-18993  
 Ablation rates, surface temperature, emittances and reradiated fluxes of heat shield materials heated by irradiation [AIAA PAPER 66-44] 08 p1318 A66-19070  
 Equilibrium stability of horizontal layer of fluid in field of modulated temperature gradient when layer thickness is greater than penetration depth of heat waves 08 p1320 A66-19471  
 Heat transfer in fluids with volume heat source homogeneously distributed throughout volume of fluid 08 p1321 A66-19830  
 Free convection thermal transfer in narrow horizontal channels and infinitely wide channels 09 p1471 A66-20704  
 Temperature field in infinite plate heated simultaneously by radiation and convection 09 p1471 A66-20748  
 Heat convection in vertical annular tube filled with mechanically incompressible viscous liquid 09 p1471 A66-20823  
 Free convection heat transfer to carbon dioxide near critical point, noting free, turbulent and oscillating flow 10 p1619 A66-21271  
 Analog method for solution of unsteady radiant heat transfer problems with combined conduction and convection 10 p1622 A66-21938  
 Combined free and forced laminar convection heat transfer inside inclined circular tubes of varying position [ASME PAPER 65-WA/HT-3] 11 p1785 A66-22191  
 Convective and radiative heat transfer during atmospheric reentry examined, using double-diaphragm shock tube operated in expansion tube mode 11 p1684 A66-22828  
 Surface tension and buoyancy effects in cellular convection of electrically conducting liquid in magnetic field 12 p1978 A66-23953  
 Radiative heat transfer near stagnation point of blunt body in hypersonic flow, noting effect on convective heat transfer 12 p1978 A66-24241  
 Laboratory studies of heat balance in rocketsonde thermistors for measurement of upper air temperature, noting dissipation constant and solar radiation effect [AIAA PAPER 66-386] 12 p1883 A66-24509  
 Variational calculus methods for convective heat transfer to nonhomogeneous fluids and fluids with thermal expansion 12 p1979 A66-24817  
 Free convection film boiling heat transfer from isothermal vertical plate to subcooled stagnant liquid, using two-phase boundary layer theory 12 p1980 A66-24907  
 Estimates of expected relative magnitudes of convective and radiative heat transfer at stagnation point of blunt body for

superorbital speeds and altitudes with continuum flow 13 p1989 A66-25154  
 Engineering method for calculating distribution of convective heat transfer for continuous boundary layer gas flow past body 13 p2208 A66-25316  
 Convective heat transfer to flat plate and at stagnation point in partially ionized equilibrium air boundary layer, noting heating rates 13 p2210 A66-28720  
 Single blow transient testing of compact heat exchanger surfaces [ASME PAPER 66-GT-93] 14 p2411 A66-26997  
 Heating rates in gas mixtures of planetary atmospheres predicted by equation using transport properties of gases at lower temperatures 14 p2411 A66-27432  
 Convective heat transfer in centrifugal force field of cavity between two rotating disks in turbulent gas flow 14 p2375 A66-27692  
 Perturbation solutions in differential analysis of radiation interactions with conduction and convection 14 p2259 A66-28162  
 Transverse magnetic field applied to high Reynolds number flow of liquid mercury in pipes and ducts inhibits convective mechanism of heat transfer [AIAA PAPER 65-539] 15 p2616 A66-29279  
 Convective heat transfer to particles in shock-heated gas 15 p2617 A66-29300  
 Integral relations method for flow field calculations of blunt body entries for determining convective heat flux to reentry body 15 p2424 A66-29305  
 Forced convection heat transfer in symmetrical ducts when fluid is liquid metal, examining new prediction methods for engineering analysis and design 16 p2824 A66-30304  
 Heat transfer in radiating media and interaction of convection with radiation heat transfer, considering one-dimensional slab problem and optically thick and thin media 16 p2824 A66-30305  
 Heat transfer in liquids situated in gap between coaxial cylinders in presence of natural convection, determining effective thermal conductivity coefficient for water and ethanol 16 p2825 A66-30325  
 Convective heat transfer to and low gravity heating of liquids contained in rotating cryogenic fuel tanks in orbit [AIAA PAPER 66-432] 16 p2826 A66-30521  
 Thermal performances of radiative and convective plate fins, considering effect of mutual irradiation between surfaces, solving integro-differential equations describing process 16 p2827 A66-30816  
 Interaction of radiation and convection in laminar boundary layer of perfect gas on flat black plate [ASME PAPER 65-HT-54] 16 p2828 A66-30988  
 Thermoacoustic streaming equations, examining effect of sound on free convection from heated cylinder 16 p2828 A66-30992  
 Text on convective heat and mass transfer for first-year graduate students in mechanical, nuclear and aeronautical engineering 16 p2829 A66-31315  
 Free convective heat transfer in horizontal cylindrical interlayer with heat emitting element 17 p3034 A66-32560  
 Convective heat transfer during subsonic and supersonic gas flow in inlet section of cylindrical tube 17 p3034 A66-32561  
 Approximate calculation of free convective heat transfer in rectangular region 17 p3034 A66-32562  
 Gas-film-cooled nozzle extension application to large rocket engines, discussing operational parameters, advantages, etc [SAE PAPER 660455] 17 p2991 A66-33163  
 Forced convection heat transfer for liquid metal flow in rectangular channels with prescribed wall heat fluxes and heat sources in fluid stream 17 p3038 A66-33468  
 Frictional drag and convective heat transfer of rotating cones of arbitrary vertex angles in mixed and turbulent flow 17 p3038 A66-33469  
 Laminar boundary layer heat transfer measurements by thick-film calorimeter gauges on flat plate in dissociated and partially ionized air 17 p3039 A66-33483  
 Transverse magnetic field effects on heat



transfer in turbulent flow of mercury in circular iron tube 18 p3145 A66-34109

Transient heat transfer to liquids in cylindrical enclosures subjected to step change in wall temperature 18 p3263 A66-34384

Bench-top calorimeter for determining radiation and convection in small-scale combustion of fuel 18 p3113 A66-34425

[WSCI 66-14] Ignition pressure transient of rocket motor, discussing initial ignition event, flame spreading and final chamber filling, convective heating effect on burning rate, etc 18 p3165 A66-34449

[AIAA PAPER 66-666] Coupled radiative and convective heat fluxes in high temperature hydrogen propellant rocket nozzles with shape and temperature variations 19 p3449 A66-35612

[AIAA PAPER 65-557] Natural convective heat transfer to gas turbine rotor blade and thermal resistance of cooling system using centrifugal pump 20 p3627 A66-36926

Data correlations on forced-convective heat transfer to cryogenic fluids by nucleate, film and transition region boiling 20 p3677 A66-37098

Convective heat transfer to cryogenic nitrogen and methane from cylindrical surface by nucleate-and film-boiling at high pressures and large temperature differences 20 p3677 A66-37099

Engineering method to determine combined effects of entry and combustion heating on total char regression of ablative nozzle as function of distance from exit plane [ASME PAPER 66-MD-72] 21 p3806 A66-38500

Ignition of ammonium perchlorate composite propellants by convective heating [AIAA PAPER 66-65] 21 p3806 A66-38689

Radiative and convective heat transfer between two parallel streams of absorbing and emitting radiating gases 21 p3835 A66-38715

Free convection boundary layer along isothermal plate, using equation of laminar compressible flow and heat transfer, noting profile dependency upon wall coordinate 21 p3835 A66-38945

Unsteady convective heat transfer of incompressible fluid between two solid channel walls 21 p3728 A66-39340

Laminar forced-convective heat transfer for dissipative fluid in tube bounded by concentric circles 21 p3837 A66-39610

Regression rate for gas-solid hybrid motor described by convective heat transfer feedback mechanism through laminar sublayer [AICE PREPRINT 34B] 22 p3970 A66-39876

Heat transfer in liquid-film boiling on vertical surfaces analogous to free convection of gases in narrow vertical ducts 22 p4000 A66-40813

Free convective heat transfer in thermal boundary layer of rarefied gas 22 p3902 A66-40922

Disperse material heating by simultaneous radiative and convective energy with temperatures expressed as integral equations 23 p4148 A66-41270

Vacuum UV radiation measurement from high temperature nitrogen, detecting radiation from shock layer of ballistic model 24 p4208 A66-42182

Reentry heat flux condition transformation into specified convective coefficients and temperatures, accounting for variation of flux with wall temperature 24 p4261 A66-42795

## CONVERGENCE

Stability theorems concerning unconditionality of bases, considering Riesz theorem and Banach and Gilbert spaces 01 p0093 A66-10402

Coefficient properties and absolute convergence of Fourier series of periodic function 06 p0902 A66-16230

Proof of two theorems concerning convergence of Fourier-Lebesgue series 06 p0903 A66-16902

Convergence of nonlinear problem solutions with respect to higher derivatives 07 p1057 A66-17853

Convergence of trigonometric interpolation polynomials 07 p1058 A66-17864

Convergence of Chapman-Enskog expansion for linearized Boltzmann equation, using perturbation theory 07 p1081 A66-17935

Couette flow, Neumann-Liouville series expansion convergence for various flow regimes and related Fredholm integral equation solutions 07 p1020 A66-17964

Stability of complex moment problems determined by constructing sequence of interpolation polynomials which converge uniformly to solution in bounded region 07 p1060 A66-18099

Convergent series representation of system of measurable functions that are complete and orthonormalized 07 p1060 A66-18251

Convergence of transformations of differential equations to normal form 08 p1245 A66-19370

Convergence of numerical solutions of ODE initial value problems 09 p1394 A66-20616

Globally convergent iteration function for solution of polynomial equations according to certain algorithms 09 p1395 A66-20624

Convergence and uniqueness theorems and series convergence in difference equation theory 10 p1549 A66-21227

Convergence of solutions of finite-difference analogs of equation satisfied by generalized axially symmetric potential 11 p1723 A66-22986

Multidimensional spline theory generalized from one-dimensional spline theory and preserving minimum curvature, best approximation and convergence properties 11 p1723 A66-23182

Limit functions of sequence of solutions in nonlinear differential system of MHD, making no convergence assumptions 11 p1746 A66-23187

Limit functions of sequence of solutions in nonlinear differential system of MHD 11 p1746 A66-23188

General convergence theorem for gradient method of minimizing functions with Lipschitz continuous first partial derivatives, noting role of steepest descent algorithms 11 p1724 A66-23402

Convergence properties of exponential series expansions used as approximation in electrical network theory for real Schwartz distribution 11 p1724 A66-23423

Convergence of optimal control for denumerable system of differential equations treated by functional-space decomposition 14 p2267 A66-27672

Geometrical theory governing flow over surface of convergent spillway 14 p2277 A66-27936

Convergence of discrete analogs of Dirichlet problems for Poisson equation in two dimensions, describing finite difference method for producing algorithms 16 p2731 A66-30235

Convergence of transformations of differential equations to normal form 16 p2736 A66-30977

Limit properties of uniform process with independent increments 17 p2946 A66-32299

Aids in converging particular numerical process, noting similar technique for isotropic expansions in thermochemical equilibrium air 17 p2946 A66-32475

Fourier series of Gegenbauer function, examining convergence characteristics 18 p3126 A66-33696

Erdos and Turan theory of fine and rough convergence of interpolation and quadrature processes 18 p3127 A66-34543

Lacunary interpolatory polynomials and Mth derivatives prescribed in roots of unity, examining Dini-Lipschitz condition for convergence 18 p3127 A66-34638

Summability of independent random variables, discussing convergence properties of sequence 19 p3389 A66-35982

Class K matrices, discussing new methods and application to convergence rate of iteration procedures 19 p3391 A66-36335

Min-H Strategy in deriving two iterative methods for rapid convergence to optimum solutions for nonlinear variational two-point boundary value problems 19 p3466 A66-36677

Convergence of difference approximations in rectangular grids for general first-order quasi-linear hyperbolic initial value problems

in two independent variables 20 p3590 A66-37526

Class of nonlinear second-order differential equations with algebraic moving singular points, considering convergent series inversion and existence conditions 20 p3591 A66-37753

Asymptotic forms exhibited by powers of nonnegative matrix, discussing index of convergence and associated values 21 p3755 A66-38602

Unstable minimization problem of functional, examining construction of sequences and stability 22 p3938 A66-39899

CONVERGENT-DIVERGENT NOZZLE

Exhaust beam from colloid thruster investigated, using quadrupole mass filter [AIAA PAPER 64-874] 02 p0278 A66-11549

Analogy between gas flow through convergent/divergent nozzles and open side-contracted channel 08 p1205 A66-18628

Transonic flow in throat of convergent-divergent nozzle for continuous fluid acceleration from subsonic to supersonic velocities 23 p4013 A66-42015

CONVERGENT NOZZLE

Optimum conditions for molecular beam generation determined by measuring particle flow density and speed ratio of short beam pulses from convergent nozzle 16 p2752 A66-30384

Supersonic molecular beam apparatus, noting maximum intensity for variation of inlet stagnation pressure and nozzle-skimmer distance 16 p2746 A66-30385

Shock wave speed behind convergent and divergent ducts for different pressures and taper angles 17 p2913 A66-33072

Shock wave motion in tubes of diverging or converging cross sections 23 p4149 A66-41503

CONVERSION

SA BINARY-TO-DECIMAL CONVERSION

SA DATA CONVERSION

SA ENERGY CONVERSION

SA FREQUENCY CONVERSION

SA ISOMERIZATION

SA PHOTOVOLTAIC CONVERSION

SA POWER CONVERSION

SA THERMOELECTRIC CONVERSION

SA THERMOMAGNETIC CONVERSION

SA SYSTEM

Conversion of 2-formyl dienone III into dienone IV upon irradiation in acetic acid followed by base-catalyzed deformation of crude photoproduct 15 p2446 A66-28873

CONVERTER

SA ANALOG-TO-DIGITAL CONVERTER

SA DATA CONVERTER

SA DIGITAL-TO-ANALOG CONVERTER

SA DOWN-CONVERTER

SA ENERGY CONVERTER

SA FREQUENCY CONVERTER

SA IMAGE CONVERTER

SA SOLAR CONVERTER

SA THERMIONIC CONVERTER

SA TRANSFORMER

SA UP-CONVERTER

Airborne hyperbolic coordinate converter for Loran C signals, noting flight testing 02 p0258 A66-12047

Cryotron-type DC to AC voltage converter and measurements of cryotron circuits 04 p0494 A66-13755

Electron-optical converters in astronomy 05 p0681 A66-15212

Transistorized two-ports circuit realizing negative impedance converters with DC coupling throughout 10 p1517 A66-21654

Equivalent circuit for cycloconverter valid for AC and DC outputs, noting data on voltage drops 12 p1804 A66-24659

Thyristors for forced-commutated static converter, noting turn-on and turn-off behavior 13 p2029 A66-25115

Transistorized logarithmic amplitude converter for recording pulses of radiation detector, automatic switching of conversion scale permits amplitude measurements 13 p2077 A66-25321

Design and integrated circuit fabrication of negative impedance converter, using two transistors and two resistors 13 p2036 A66-25523

DC-to-DC nondissipatively regulated converter using inductive energy storage for voltage transformation and



- regulation 13 p2001 A66-26297  
Cryotron-type DC to AC voltage converter and measurements of cryotron circuits 15 p2454 A66-28552  
Unipolar FET converter, based on dependence of transconductance and drain current on gate bias voltage 15 p2464 A66-29124  
Negative-impedance converter design and operation 15 p2474 A66-29763  
Optimum parameters for transformation of output signal in highly sensitive DC converter when SNR for required loading source reaches maximum 17 p2887 A66-32703  
Transient processes analyzed in traveling wave converters on long-line section, taking first-order reflection into account 17 p2888 A66-32705  
Synthesizing nonlinear converter in presence of random input signals with normal distribution 18 p3092 A66-34991  
Feedback methods for conversion of electrical signals into frequencies, using oscillator with signal-current-controlled inductance 19 p3325 A66-35988
- CONVOLUTION THEORY**  
Generalized convolution theorems of periodic functions based on Fourier series formalism used to study processes in linear systems 04 p0506 A66-14402  
Analog simulation of peak smearing in spectrometers in terms of convolution transforms 13 p2084 A66-26751  
Mass forces for infinite elastic space expressed by generalized functions 15 p2615 A66-29852  
Numerical inversion of Laplace transform 18 p3127 A66-34082  
Convolution product theory applied to smoothing neutron monitor data of daily variations in cosmic ray intensity 18 p3186 A66-34808  
Space factor of linear array with isotropic sources determined, using illumination function and convolution theorem 19 p3321 A66-36414  
Complex convolution integral applied to Laplace transform expressions in sampled data theory 19 p3339 A66-36747  
Convolution type integral equation solution via reduction to Riemann problem in class of generalized functions 20 p3591 A66-37755  
Combination of probability density functions for system error analysis, using convolution or transformation methods 24 p4189 A66-42827
- CONVULSION**  
S CONTRACTION  
S EPILEPSY
- COOLANT**  
SA ENGINE COOLANT  
Coolant injection in turbulent boundary layer for protection of surfaces from effects of high temperature and high energy gas flows 08 p1320 A66-19429  
Reverse-flow film cooling of small rocket engine chamber 12 p1937 A66-24718  
Coolant passage wall temperature measurement in nuclear rocket nozzle during chemical stimulation testing by radiometry without affecting hot gas or coolant flow or disrupting heat flow 19 p3356 A66-35632  
Thermoelasticity of semiinfinite state plane with circular coolant holes 21 p3826 A66-38589  
Cryopump uses and selection of coolants 21 p3697 A66-38810
- COOLING**  
SA ABLATION  
SA AIR COOLING  
SA CRYOGENICS  
SA EVAPORATION COOLING  
SA FILM COOLING  
SA LIQUID COOLING  
SA LITHIUM COOLED REACTOR EXPERIMENT /LCRE/  
SA QUENCHING  
SA RADIATION COOLING  
SA REGENERATIVE COOLING  
SA SUBCOOLING  
SA SUPERCOOLING  
SA SURFACE COOLING  
SA THERMOELECTRIC COOLING  
SA TRANSPIRATION COOLING  
Neutrino producing cooling reaction rates indicate that discrete X-ray sources located in direction of galactic center are not neutron stars 05 p0760 A66-14895  
Quenching and slow-cooling effects on ductile-brittle bend-transition temperature of chromium wire 13 p2107 A66-25587  
Amplification of interaction of atoms and of pulsed or periodic cooling of transparent media produced by laser beam, noting changes in kinetic energy of atoms 13 p2093 A66-26021  
Free cooling of thin rod in constant temperature medium, finding temperature field for thermodynamics application 15 p2616 A66-29223  
Nozzle cooling and infiltrant loss from infiltrated refractory metal composites at high gas propellant temperature 19 p3385 A66-36157  
Experimental assembly for measuring true heat capacity of heat resistant insulating materials during natural cooling at temperatures from 1200 to 2400 degrees K 20 p3556 A66-36989  
Delayed energy produced by fission product decay when restart of nuclear rocket engine is considered, noting effects of cooldown requirements [AIAA PAPER 66-551] 22 p3946 A66-39676  
Surface properties, temperature effect, cooling and detectability of neutron stars, using pure iron and pure magnesium compositions 22 p3976 A66-39803  
Integral ratios for calculating diffusion rate of magnetic field into wall-cooled plasma 23 p4106 A66-41716  
Ion energy balance equation for ionosphere including effects of O, He, and H ions, thermoconductivity and cooling by atomic hydrogen and helium 24 p4198 A66-42431
- COOLING FIN**  
Contact effectiveness of space radiator for specific case of rectangular fin of constant thickness heated uniformly along one edge and perfectly insulated along opposite edge 03 p0444 A66-12771  
Free convection heat transfer in partially enclosed channel flow, noting effect of vertical fin geometry and temperature [ASME PAPER 64-WA/HT-33] 04 p0595 A66-13386  
Optimization of design parameters of parabolic radiating fins [ASME PAPER 65-HT-42] 05 p0784 A66-14754  
Heat rejection per unit weight of radiator with evolve type reflectors compared with radiators with rectangular fins, considering mutual irradiations of neighboring radiator parts [ASME PAPER 65-WA/HT-17] 05 p0790 A66-15647  
Grapho-analytical method of determining heat carrier parameters of cooler-radiator system in off-design operation 06 p0970 A66-16326  
Temperature distribution and efficiency of thick plate and annular fins used on heat exchangers, space radiators and nuclear fuel elements analyzed through heat conduction equation 16 p2827 A66-30815  
Thermal performances of radiative and convective plate fins, considering effect of mutual irradiation between surfaces, solving integro-differential equations describing process 16 p2827 A66-30816  
Vapor-fin heat rejection system employing boiling-condensing cycle, noting performance characteristics 18 p3055 A66-34381  
Heat transfer from gray fin-tube radiators with numerical results for diffuse surfaces, noting fin and tube emissivities 22 p3998 A66-40037
- COOLING SYSTEM**  
SA GAS COOLING SYSTEM  
SA REFRIGERATION  
SA VENTILATION  
Radiative vs active cooling systems as part of refurbishment requirements critical to economic feasibility of reusable launch vehicle systems 01 p0143 A66-10796  
XB-70A components and subsystem operation and design noting engine, electrical and cooling control systems [SAE PAPER 650841] 01 p0130 A66-10833  
Combined Peltier-Ettingshausen device evaluated for cryogenic refrigeration to 70 degrees K 02 p0272 A66-11490  
Three air-cooled and one water-cooled pressure suit evaluated in hot environments 03 p0327 A66-12360
- Cooling device for reentry vehicle windows consisting of rotating disk with radial slots placed in front of window 06 p0871 A66-16222  
Aerodynamically induced vibration in coolers, describing inclined splitter plates for noise and structural vibration elimination 07 p0991 A66-17492  
Comparison of 14 basic methods for cooling rocket engines 07 p1110 A66-17617  
Steady cooling regime of pseudoliquidified layer, determining cooling time and heat transfer coefficients of solid particles and liquid media 08 p1317 A66-18865  
Pressure drop and heat transfer to Newtonian fluids in cooled pipes for laminar flow, establishing empirical correlation 10 p1620 A66-21272  
Thermal insulation of hypersonic blunt body by central coolant injection formation of insulating layer between body and high temperature freestream 10 p1481 A66-21797  
Thermomolecular heat pump with cooling from gas diffusion through capillary material driven by external pressure difference 11 p1639 A66-22245  
Concorde fuel system in cooling application and adjustment of center of gravity through fuel distribution 11 p1637 A66-23168  
Operating characteristics of electrodeless MHD converter with primary winding cryogenically-cooled, comparing performance with one having conventional winding 12 p1803 A66-23749  
Microwave apparatus cooling system design problems 12 p1836 A66-24157  
Cooling systems for use in space, discussing specific radiator area and specific power 12 p1979 A66-24873  
Electric machines employing evaporative and universal cooling systems for aircraft use 13 p2041 A66-25902  
Low temperature techniques in satellite communications systems, noting maser, cooled parametric amplifier and trend toward closed-cycle refrigerators 13 p2042 A66-26104  
Vapor-cycle air conditioning for business aircraft, considering weight vs power consumption, compatibility with integrated system and test results [SAE PAPER 660208] 13 p2002 A66-26386  
Cooler for semiconductor lasers and photodetectors using low temperature gas 13 p2104 A66-26559  
Electron beam heating of alloy specimen and liquid-nitrogen cooled anvils for rapidly cooling it 13 p2084 A66-26560  
Noise measurement in axial flow fans for military vehicle cooling installations 14 p2220 A66-27567  
Negative effect of air countercurrents and thermal stresses on performance of cooling systems of gas turbine rotor disks with lateral air flow 15 p2570 A66-28776  
Semiconductor cooler creating hypothermia in small animals, operating on Peltier effect and employing quaternary metal alloy 15 p2444 A66-29497  
Design and laboratory tests of vapor-phase heat exchanger coupled to power generating bismuth telluride thermopile for waste heat dissipation 16 p2637 A66-31101  
Water conditioned suit performance characteristics noting cooling rate, inlet and outlet temperatures, etc 16 p2643 A66-31131  
Thermostability and control of airborne electronic equipment in closed-loop forced-air cooling systems 16 p2663 A66-31325  
Cooling of diodes, transistors and thyristors at intermediate power levels, determining heat dissipation by radiation, conduction and convection 16 p2664 A66-31346  
Cryogenic system used to remove heat from space simulator solar radiation source 20 p3541 A66-37071  
Solid cryogenics as heat sinks for cooling electronic components, particularly IR detectors in aircraft and spacecraft 20 p3676 A66-37073  
Thin insulating Teflon film bonding to internal surface of space cryopanel for increased heat transfer and faster cooling 20 p3677 A66-37100  
Fan selection for high-altitude cooling of electronic equipment 20 p3527 A66-37346  
Aircraft equipment cooling techniques and



systems, particularly natural or free convection 21 p3699 A66-39614

Materials and cooling of aircraft gas turbine engines, noting nickel and tantalum alloys, turbine-inlet temperatures, coatings, etc 23 p4122 A66-41662

**COORDINATE**

S ASTRONOMICAL COORDINATE

S CARTESIAN COORDINATE

S GEOCENTRIC COORDINATE

S LAGRANGE COORDINATE

S POLAR COORDINATE

**COORDINATE GEOMETRY**

S ANALYTIC GEOMETRY

**COORDINATE SYSTEM**

SA INERTIAL COORDINATE SYSTEM

Image translation from plate into coordinate system on another plate using homographic coordinates of object applied to astrometry 01 p0135 A66-10276

Attached coordinate system for approximate solution of compression waves emitted by expanding sphere at constant rate in ideal medium 01 p0057 A66-10420

Kinematic and physical relations for small motion superposed on initial motion defined in fixed reference frame 01 p0106 A66-10735

Tables and maps of geomagnetic coordinates corrected by higher order spherical harmonic terms 01 p0062 A66-10888

Algebraic sign of voltage field components in orbital coordinate system, using dipolar approximation of Earth magnetic field 02 p0295 A66-11655

Rotation of rigid body force affected, using matrix equations, noting coordinate system and differential equation 02 p0290 A66-11989

Quiet solar diurnal variations of geomagnetic field at middle and low latitudes during IGY to determine coordinate system and equatorial electrojet 02 p0224 A66-12118

Geometric shape of axisymmetric shock waves from point source explosion in nonhomogeneous medium 03 p0355 A66-12621

Astrometry current status, examining establishment of coordinate system and determination of astronomical constants 03 p0427 A66-12922

Establishment and plotting of suitable coordinate systems for solution of geodetic problems via satellites 03 p0367 A66-13198

Corrected tables and maps of geomagnetic coordinates, covering methods of calculation and corrected data charts 04 p0513 A66-13377

Dynamic equations in quasi-static and quasi-solenoidal approximations to describe synoptic meteorologic processes in spherical coordinate system 04 p0540 A66-13412

Lunar topographical asphericity, lunar coordinates, absolute and relative, harmonic analytical interpolation, formations, stratigraphy and optical librations 07 p1139 A66-18265

Fundamental concepts of tensor calculus essential for technological application 08 p1245 A66-18859

Pendulum motion in system of coordinates related to pendulum base, considering damping of absolute and relative angular velocity 08 p1223 A66-18892

Graph for system of currents of solar diurnal variation during IGY winter season, considering night and evening vorticity individually and using coordinate system 08 p1221 A66-19797

Coordinate systems describing portions of Friedman world and adjacent empty regions do not satisfy Liechnerovitch continuity conditions 09 p1403 A66-20595

Consistency of subtraction technique for calculating gravitational mass in nonquasi-rectangular coordinates from surface integrals provided by von Freud superpotentials 10 p1555 A66-21195

Mutual orientation of oblique aerial photographs at nadir distance greater than 50 degrees for simultaneous rotation of y and z axes of universal autograph 10 p1536 A66-21800

Integration of equations, approximating Maxwell equations, in curvilinear coordinates separating scalar Laplace equation, with vectors representing electric and magnetic fields 10 p1556 A66-21994

Geographic distribution of solar diurnal variations of magnetic field during quiet days determined by coordinate

system 11 p1696 A66-22421

Passive element analogs for linearized three-dimensional elasticity derived in rectangular, cylindrical and polar coordinates equating power dissipation and strain energy [ASME PAPER 65-AV-4] 11 p1780 A66-22467

Retarded observer time as coordinate in relativistic spherical hydrodynamic equations prevents Schwarzschild surface formation 11 p1772 A66-22779

Cylindrical coordinate system describing geomagnetic field analyzed, noting consequences in magnetic cartography when going from field to time 12 p1875 A66-24970

gradients 12 p1875 A66-24970

Stress concentration at circular hole in orthotropic cylindrical shell, using coordinates system and Bubnov-Galerkin method 13 p2206 A66-26455

Solutions of nonstationary equations of plane laminar MHD boundary layer, using transformation to specialized form of curvilinear coordinates 14 p2338 A66-26773

Astrometry current status, examining establishment of coordinate system and determination of astronomical constants 14 p2380 A66-27271

Effect of faulty compensation for accelerating force of Earth gravity on accuracy in determination by inertial navigation system of coordinate of object in flight 14 p2328 A66-27361

Reduction of order of aeroelastic and flutter motion equations while retaining purely elastic contribution of eliminated coordinates, using quasi-static assumption and matrix algebra 14 p2405 A66-27996

Quiet solar diurnal variations of geomagnetic field at middle and low latitudes during IGY to determine coordinate system and equatorial electrojet 14 p2286 A66-28077

Equivalent mass matrix for rectangular plate elements in bending, noting coordinate system 15 p2610 A66-29306

Distribution of arrival directions of muon-rich air showers, using equatorial and galactic coordinate systems 15 p2579 A66-29524

Tesseral harmonics of coordinates using Baker-Nunn data and geopotential and dynamical procedures, noting iterative cycle for correction determination 15 p2491 A66-29999

Photographing of satellites, using optical system and image converter for determining coordinates 15 p2453 A66-30002

Two-dimensional flow in fluids related to system of vortex coordinates, using Hamiltonian operator for characterization of motion studies 16 p2683 A66-30213

Evaluation of nonstereoscopic pairs of photographs obtained from vertical base by moving camera, determining spatial coordinates of points on photographs 16 p2703 A66-30512

Geometrical quality of elements of exterior orientation after double and single point resection in space, noting position determining characteristics of linear and angular parameters 16 p2704 A66-30515

Radiation coordinates for gravitational radiation in general relativity 16 p2746 A66-30528

Error determination in autonomous determination of coordinates, obtaining solution for kinematic equations of navigation in near-polar region 16 p2744 A66-31146

Nomogram construction for transformation of astronomical object position from one spherical coordinate system to another, using trigonometric functions 16 p2737 A66-31398

Book on spherical astronomy including celestial coordinate systems, parallax, diurnal motion, precession and nutation, time measurement, etc 16 p2806 A66-31738

X-Y plotter for analog computers, analog to digital converters and digital computers 17 p2925 A66-32313

Generalized vertical coordinate system for application in atmospheric dynamics 18 p3129 A66-33965

Distribution law for collective coordinates established via probability methods, noting application to Ising model and to problems of absorption 18 p3135 A66-34632

Integration of equations, approximating Maxwell equations, in curvilinear coordinates separating scalar Laplace equation, with vectors representing electric and magnetic fields 18 p3136 A66-34971

Space vehicle orientation with respect to rotating system of coordinates 19 p3467 A66-35279

Optimum radar measurement of multiple target coordinates with unknown signal amplitudes and phases 19 p3296 A66-35303

Field determination of coordinates of points of mountainous terrain from aerial photographs with known elements of external orientation 19 p3353 A66-35363

Photoelastic Wertheim law in general tensor coordinate system derived for linearly anisotropic or isotropic homogeneous matter 19 p3474 A66-36320

Coordinate control theory of self-adapting systems, considering problems of sensitivity, optimization and invariance 20 p3535 A66-36852

Divergence of gas and dust tails of comets calculated, using moving coordinate with origin at comet head 20 p3653 A66-37797

Coordinate systems describing portions of Friedman world and adjacent empty regions do not satisfy Liechnerovitch continuity conditions 20 p3603 A66-38129

Vibrations of complex structure analyzed, using coordinate system relative to displacement modes, calculating errors due to natural vibration frequencies 21 p3826 A66-38584

Graph for system of currents of solar diurnal variation during IGY winter season, considering night and evening vorticity individually, using coordinate system 21 p3733 A66-38793

General theory of stability of elastic equilibrium in three-dimensional system of orthogonal curvilinear coordinates 21 p3828 A66-38803

Elastic stability theory for second-order strain components in Cartesian, cylindrical, spherical and polar coordinates 21 p3828 A66-38804

Mixed bending problem of eccentric ring solved by coordinate system with origin at center of outer boundary of cut 21 p3831 A66-39290

Device that will conveniently, rapidly and precisely determine position of point in specific perspective from space coordinates 21 p3745 A66-39332

Approximate solution of two-dimensional boundary layer problem using Rayleigh-Ritz method, coordinate functions and interpolation 21 p3831 A66-39351

Satellite space coordinates from photographs made simultaneously from two points on Earth surface 22 p3917 A66-39739

Differential equations for stream functions of particle trajectories in unsteady three-dimensional flows in cylindrical and spherical coordinate systems 22 p3898 A66-40111

Magnetic coordinate definitions and relation to parameters of geomagnetically trapped particles 22 p3912 A66-40425

Conservative systems motion stability, generalizing precession and nutation of gyroscope with respect to noncyclic coordinate 22 p3948 A66-40681

Successive approximation method for optimization of nonlinear systems of ordinary differential equations with limitations on phase coordinates 23 p4084 A66-41352

Feedback compensated third-order control systems analysis, using coefficient plane reference system 23 p4051 A66-41703

Satellite gravitational stabilization system in orbital coordinate system, considering atmospheric resistance and damping natural oscillations 23 p4134 A66-41979

Middle surface geometry of thin shells using line coordinate system with arbitrary direction and length of base vector 24 p4291 A66-42737

**COORDINATE TRANSFORMATION**

SA SCHWARZSCHILD METRIC

Expansion of Joukowski transformation into third-degree algebraic solution for two projective planes, using certain complex function lying between two Gaussian planes 01 p0092 A66-10198



Coordinate transformation for synthesizing network functions, considering matrix equation used in Foster form realization for RC driving point impedance 02 p0207 A66-11881

Transformation and equivalence of higher than second order homogeneous linear differential equations 05 p0708 A66-15153

Boundary layer equation transformation, using special curvilinear coordinates 08 p1206 A66-18872

Trajectory analysis and Birkhoff rings in restricted three-body problem in three-dimensional coordinate system 09 p1453 A66-20251

Graphical device for transformation between horizon system of coordinates and equatorial system, noting construction techniques, operation and application 09 p1381 A66-20395

Stereographic mapping of plane Cartesian coordinate grid onto sphere for polar navigation use 09 p1401 A66-20914

Unified theory of cold plasma nonlinear oscillations /Dolph/ fails to apply to traveling wave solutions 10 p1569 A66-21921

Equations of linear automatic control systems decomposed asymptotically 10 p1518 A66-21979

Cardinal points and focal lengths of holographic system established by treating holographic imaging as projective transformation between object and image space 11 p1706 A66-22872

Relativistic rocket mechanics, considering coordinate transformation, velocity and dependence of mass on inertial reference system 11 p1775 A66-23118

Transformations for study of nonlinear systems behavior in neighborhood of phase plane infinity 13 p2054 A66-26089

Coordinate transformation of Schwarzschild metric for gravitational field of oblate Earth and equatorial satellite orbits into symmetric metric 13 p2187 A66-26137

Tensor analysis, discussing stress tensors, metric tensors, Riemann-Christoffel curvature tensor, coordinate transformations, etc 14 p2320 A66-26921

Canonical transformation in optimal steering and cut-off-relight programs for orbital transfer about central field 14 p2387 A66-28182

Motion equation of variable mass point solved, using coordinate transformation 15 p2538 A66-29048

Superpotentials in relativity theory, noting use of Freud identities and finite coordinate transformations 15 p2542 A66-29654

Moment equations from collisionless Boltzmann equation solved by transformation into polarized coordinates 15 p2555 A66-29784

Transformation equivalency of various forms of partial differential equations of motion of nonholonomic systems 16 p2747 A66-31144

Variable-parameter network analysis using z-transformation 17 p2900 A66-32199

Transformation of tesseral harmonics under rotation in elementary and self-contained method 17 p2921 A66-33225

Nonlinear transformations for solution of variational problems 18 p3089 A66-33737

Generalized vertical coordinate system for application in atmospheric dynamics 18 p3129 A66-33965

Brown lunar theory interpretation of observed lunar motion and associated rectangular-to-polar lunar coordinate transformations 18 p3234 A66-34655

Equations of linear automatic control systems decomposed asymptotically 19 p3324 A66-35857

Generalized Lur coordinates used in canonical forms for controllable systems, with applications to optimal nonlinear feedback 20 p3535 A66-36848

Congruent relativistic gravitational fields, red shift and geodetic coordinate transformations 20 p3603 A66-38011

Comparison variables transformation of linearized perturbation initial value problems for nonlinear ordinary first-order differential equation 21 p3756 A66-38817

Book on plane problems in elasticity theory for calculation of deep beams with arbitrary boundary curvilinear

coordinates 21 p3834 A66-39616

Oscillatory properties of linear matrix differential system, applying generalization of polar coordinate transformation to certain systems of second order 24 p4233 A66-43100

**COORDINATION POLYMER**

Crystal and molecular structure of chlorotetraammine /sulfur dioxide/ ruthenium chloride 06 p0820 A66-15939

Coordination of substituted pyridine N-oxides with oxovanadium /IV/ cations, noting stoichiometric variations with changes 09 p1339 A66-20878

**COPOLYMER**

Silicone copolymers lubricants containing both trifluoropropyl and halophenyl substitution to cover wide temperature range [ASLE PREPRINT 65-LC-5] 02 p0237 A66-12233

Mechanical double refraction of unsaturated copolymer polyesters of styrene subjected at different temperatures to constant tensile stress [ONERA TP 276] 04 p0538 A66-14242

Silicone copolymer lubricants containing both trifluoropropyl and halophenyl substitution to cover wide temperature range [ASLE PREPRINT 65-LC-5] 12 p1889 A66-24990

Brewster coefficient as function of temperature, number of cross-linking modes and styrene content for diethylene-glycol succinofumarates copolymerized with styrene 14 p2319 A66-28273

Superheating crystallization of ethylene-propylene and ethylene-butene-1 copolymers and extended chain morphology 17 p2943 A66-32557

**COPPER**

Van der Pauw method for measuring resistivity, Hall mobility and thickness of thin metallic film under vacuum, considering copper films 01 p0119 A66-10393

Dislocation relaxation of silver and copper and asymmetry of Bordoni internal friction peak of metals 01 p0087 A66-10603

Vibration compaction of two-component spherical copper powders, noting effects of frequency amplitude and particle sizes 01 p0087 A66-10744

Electrical properties of copper diffused p-type indium antimonide crystals 01 p0127 A66-11030

Electric properties of n-type GaAs after alloying with Cu, determining impurity concentrations 02 p0277 A66-12095

Thin copper clad laminates and problems arising in application to multilayer printed circuit boards 03 p0347 A66-13330

Total nonelastic strain recovery of copper single crystals after small prestrains, discussing parameters 04 p0535 A66-13400

Low temperature copper diffusion limits frequency range of cadmium sulfide shear mode diffusion layer transducer 06 p0851 A66-16461

Measurement of creep rate complex stress time relations for copper under loading conditions at 250 degrees 06 p0897 A66-16949

Radiotracer measurements of copper incorporated from quartz into GaAs 08 p1268 A66-18663

Copper and zinc abundances in carbonaceous, enstatite and ordinary chondrite determined by neutron activation techniques 08 p1291 A66-19093

Metallography of cadmium crystals with copper impurities obtained by sublimation from copper powder, noting that copper solubility is limited 08 p1277 A66-19623

Tensile properties of composites of tungsten or molybdenum wire uniaxially aligned in copper matrix 09 p1393 A66-20661

Cleavage characteristics of copper plate under explosive load determined and interpreted, taking finite failure time into account 10 p1613 A66-21238

Preparation and physical properties of polytetraacyanoethylene /TCNE/ copper chelate film, noting electric conductivity and heat treatment effect 10 p1574 A66-21348

Changes in fine structure of powdered copper during compression, determining dislocation density and disorientation angles, noting plastic deformation cause as packing

defect occurrence 10 p1546 A66-21505

Low energy electron diffraction study of epitaxial deposition of copper on single crystal /110/ face of tungsten under ultrahigh vacuum 12 p1894 A66-23911

Low energy electron diffraction observation of calibrated epitaxial nickel film on /111/ copper 12 p1894 A66-23912

Mechanical deformation used in fabrication of composite made of continuous columbium wires in copper matrix by drawing, noting optical inspection 12 p1895 A66-24378

Sputtering yields of copper single crystals as function of normally incident argon-ion energy 13 p2158 A66-25050

Chemical composition effect on fracture properties of Al-Zn-Mg-Cu alloys 14 p2317 A66-28009

Surface hardening of titanium alloys by copper diffusion for small-size machine parts production 15 p2522 A66-29189

Radioactive tracer technique to measure yield and angular distribution of copper sputtered from monocrystalline target subject to cesium ion bombardment [AIAA PAPER 65-379] 15 p2566 A66-29290

Free energy of aluminum alloy containing two-dimensional Guinier-Preston zones of copper atoms 16 p2722 A66-30307

Copper and Armco iron structural defects during cyclic deformation studied by electron-microscope and optical-microscope techniques 16 p2727 A66-31528

Emission spectrum of copper atom used to measure temperature and concentration of charged particles in DC-arc plasma burning under water 16 p2766 A66-31600

Metallography of cadmium crystals with copper impurities obtained by sublimation from copper powder, noting that copper solubility is limited 17 p2984 A66-33137

Elastic and plastic properties of fiber-reinforced and continuous skeleton tungsten-copper composite materials 17 p2941 A66-33425

Cleavage characteristics of copper plate under explosive load determined and interpreted, taking finite failure time into account 19 p3474 A66-35861

Fatiguing at room temperature resulting in observable diffusion of silver into copper, using precipitation reaction to analyze influence of large number of vacancies 20 p3584 A66-37618

Metal strength in pulsed magnetic fields at low temperatures, noting resistance of copper wire as function of number of pulses 21 p3750 A66-39064

Changes in fine structure of powdered copper during compression, determining dislocation density and disorientation angles, noting plastic deformation cause as packing defect occurrence 23 p4081 A66-41526

**COPPER ALLOY**

**SA BRASS**

Thermal and electrical properties of copper antimony telluride/tin telluride system as function of composition 01 p0116 A66-10190

Graphite content effect on antifriction properties of graphitized nickel-based copper and iron alloys 01 p0087 A66-10745

Effect of varying percentages of constituent elements in alumina dispersion-strengthened copper-nickel alloys, listing creep rupture properties 04 p0534 A66-13378

Aging of Cu-Ti alloy stimulated by Al additions to 2 percent and retarded by Al additions of 2 to 4 percent 12 p1892 A66-23521

X-ray study of 16 monolith and powdered brass samples with 30.07 to 40.1 percent copper, indicating two phase fields for gamma region of Cu-Zn system 12 p1896 A66-24866

Electrical resistance and thermoelectric power of Ni-Cu solid solutions near Curie point 13 p2162 A66-25407

Plastic deformation effects on preaged aluminum-copper alloy structure subjected to 40-75 percent compression 13 p2110 A66-25965

Welded beryllium-copper structures, techniques and properties 13 p2086 A66-26015

X-ray method determining diameter of Guinier-Preston I zones and fraction of copper atoms contained in such zones in Al-Cu alloys 13 p2111 A66-26583



Age hardenable nickel-copper steels with strength achieved by copper phase hardening 16 p2723 A66-30319

Kinetics of natural aging process of Al-4 percent Cu alloy, experiments indicate addition of up to 1.0 percent Mg proportionately slows down aging process 16 p2723 A66-30871

Mechanical strength, toughness, elastic modulus, relaxation stability and specific conductivity of copper-titanium alloys 16 p2727 A66-31568

Grain growth from solution precipitation and grain coalescence in liquid phase sintering of W-Ni-Fe and W-Ni-Cu alloys 17 p2939 A66-32393

Phonon-drag thermopower variation in dilute copper alloys assuming Rayleigh law for phonon scattering 17 p2984 A66-33152

Elevated temperature tensile properties of copper alloy-tungsten fiber-reinforced composites 18 p3120 A66-33724

Graphite content effect on antifriction properties of graphitized nickel-based copper and iron alloys 18 p3117 A66-34981

Grain boundary cavity growth in Al-Cu alloy during compressive creep testing 22 p3935 A66-40291

Susceptibility to cold deformation of semifinished B95-2 Al-Zn-Mg-Cu alloy products, noting machinability in manufacturing of parts 22 p3928 A66-40885

Thermoelectric power and electric resistivity of copper-gold alloy doped with 3d transition metals as function of temperature and atomic number of impurity 23 p4114 A66-41712

**COPPER COMPOUND**

Stress-strain behavior of tungsten fiber-reinforced copper composites, discussing room-temperature tensile and dynamic-modulus tests 05 p0702 A66-15324

Superhigh vacuum creation in OGRA-1 facility, using titanium sputtered liquid nitrogen-cooled copper surfaces 12 p1922 A66-24218

Resistivity and thermoelectric power of copper telluride at various temperatures, finding that it retains semiconducting properties in liquid state 13 p2162 A66-25411

Charge carrier mobility variation with temperature in copper phthalocyanin thin film 17 p2977 A66-32286

Energy spectrum of semiconductor compounds with chalcopyrite structure analyzed, using perturbation theory, noting changes resulting from crystalline and spin-orbital interactions 21 p3799 A66-38923

Superhigh vacuum creation in OGRA-1 facility, using titanium sputtered liquid nitrogen-cooled copper surfaces 22 p3957 A66-40582

Oxygen inhibition of grain boundary movement and stabilization of optical transmission in cuprous iodide thin film 23 p4110 A66-41152

Thermoelectric properties of solid solution of germanium telluride in copper antimony telluride 23 p4114 A66-41572

Liquid filter cell for telescopes, using half-saturated solution of cupric sulfate to block red leak of UG filter glass 23 p4071 A66-41927

**COPPER FLUORIDE**

Sublimation pressure of copper fluoride measured via mass spectrometry, noting dissociation energy 19 p3295 A66-36062

**COPPER OXIDE**

Cuprous oxide-cadmium sulfide junction photocells enhanced in photosensitivity and rectifying properties by exposure to periods of light and darkness 03 p0413 A66-13190

Neutron and proton bombardment effects on exciton spectrum of cuprous oxide 06 p0937 A66-17139

Film-type photocell consisting of p-n heterojunction between copper oxide and cadmium sulfide with secondary maximum in sensitivity 09 p1429 A66-20821

Cuprous oxide conductivity caused by ionization of thermal lattice defects 14 p2358 A66-27091

Temperature dependence of resistivity of zirconium oxide with copper oxide additions indicates suitability as heat sensitive resistor material in 300 to 1000 degree C range 16 p2777 A66-30872

Cuprous oxide conductivity caused by

ionization of thermal lattice defects 22 p3967 A66-40847

**CORE**

SA EARTH CORE

SA HONEYCOMB CORE

SA MAGNETIC CORE

SA REACTOR CORE

Megaton and decamegaton dynamic pressure production by blast-type compression of thick walled pipe with core subjected to internal implosion, giving theoretical foundations /Part I/ 23 p4091 A66-41859

Megaton and decamegaton dynamic pressure production by blast-type compression of thick walled pipe with core subjected to internal implosion, for case of graphite core /Part II/ 23 p4091 A66-41860

**CORE FLOW**

Secondary motion generation in vortex field, noting vortex core deformation by oscillation, radial perturbation effect on vorticity distribution, etc 13 p2070 A66-26715

**CORIOLIS EFFECT**

Atmospheric tidal oscillations, Coriolis forces dominate diurnal tide causing small scale depth 05 p0672 A66-15026

Cantilevered continuous pipe conveying fluid at constant velocity, showing that internal and external damping and Coriolis forces may have destabilizing effect [AIAA PAPER 66-102] 05 p0774 A66-15036

Comparative effects of prolonged rotation at 10 rpm on postural equilibrium in vestibular normal and vestibular defective human subjects 06 p0813 A66-16826

Perceiving undetectable rotation in semicircular canals by employing self-induced Coriolis stimulation, determining psychophysical functions for direction or rotation discrimination at different yaw velocities 09 p1337 A66-20531

Brief Vestibular Disorientation Test /BVDT/ assesses subject reaction produced by head movements in rotating chair 11 p1647 A66-22574

Coriolis interaction in first and third fundamental frequencies of ozone, noting vibration rotation spectrum and coupling of two states 13 p2016 A66-25373

Vegetative responses of human organism to angular, linear and Coriolis accelerations 13 p2011 A66-26230

Psychological and physiological reaction to Coriolis effect under artificial gravitational field simulated in rotating space station 15 p2443 A66-28682

Small Coriolis accelerations effect on functional state of human heart 15 p2437 A66-29474

Gravitational instability of magnetoplasma in radial electric field, noting resistive drift modes, stabilization criterion effect of Coriolis force, Landau damping, etc 17 p2966 A66-32425

Fluctuations in human acoustic sensitivity after 24 hours in room under effect of Coriolis accelerations of various magnitudes 17 p2861 A66-32941

Wave propagation in rarified plasma under action of Coriolis force, Hall current and self-gravitation, noting LF coupling rotation effects, etc 17 p2973 A66-33000

Cantilevered continuous pipe conveying fluid at constant velocity, showing that internal and external damping and Coriolis forces may have destabilizing effect [AIAA PAPER 66-102] 18 p3257 A66-34594

**CORK**

Sheet cork as thermal protection during vehicle launch and ascent flight [AIAA PAPER 65-356] 22 p3999 A66-40358

Internal thermal behavior of charring cork with reference to heat shield design 24 p4294 A66-42783

**CORONA**

SA AURORA

Radiative transfer equation for isothermal model of solar corona, noting radiation flux and electron density variation 01 p0131 A66-10267

Heating of solar prominence by surrounding corona, considering nonlinear dependence of thermoconductivity coefficient on temperature 01 p0131 A66-10268

Drift of magnetic fields of sunspots and bipolar areas from photosphere into corona,

coronal formations, corpuscular fluxes and nature of integral solar magnetic field 01 p0134 A66-10271

Soviet electronic telescope, indicating possibility of noneclipse observation of coronal lines in IR band 01 p0137 A66-10456

Coronal spectrum of eclipse of February 15, 1961 studied at constant height as function of heliographic latitude from circular slit spectrograph plates 02 p0286 A66-11354

Dielectronic recombination for low density plasma, estimating coefficient and ionization balance for iron and calcium ions in corona 02 p0286 A66-11357

Resonance lines of coronal ions of silicon appearing in two widely separated spectral regions 02 p0286 A66-11358

Quiet chromosphere and corona noting line intensity and coronal electron and kinetic temperature 03 p0420 A66-12841

Heating of corona and chromosphere for generating solar wind 03 p0421 A66-12848

Data on origin and effects of dust particles in interplanetary space obtained from solar corona, zodiacal light and meteor observation 03 p0425 A66-12850

Intensity of solar corona, Wolf number and biological and chemical tests conducted in Italy 04 p0577 A66-13817

Occultation of Tau A radio source by solar corona, noting interaction of radio source with corona irregularities 05 p0749 A66-15128

Achromatic coronagraph for spectrography of solar corona 07 p1030 A66-17246

Polar rays of solar corona, discussing distribution, magnetic field approximation, electron density and kinetic temperatures 07 p1133 A66-17418

Extraordinarily enhanced radial emission when radio source Taurus A was occulted by supercorona, concluding that supercorona shape is affected by intensity and direction of inclined interplanetary magnetic field 07 p1136 A66-17643

Isophotometric representation of solar corona, using photographs of equal density 07 p1136 A66-17735

Coronal and prominence phenomena accompanying solar flares noting shock wave, radio burst, ionospheric fadeouts and absorptions, coronal density and temperature increases, etc 07 p1130 A66-18075

Dynamical properties of solar wind and solar corona atmosphere with extended temperature bound strongly by gravity 07 p1132 A66-18263

Calculation of intensity and polarization of forbidden lines of Fe XIII ion in solar corona in presence of nonradial magnetic field 08 p1287 A66-18640

Green corona before birth and after death of calcium plage in intensity plot vs heliographic latitude 09 p1455 A66-20379

Stability of expanding corona against radial compressional waves 09 p1455 A66-20403

Solar wind enhancement of heavy element content in composition of solar corona relative to value for photosphere 09 p1456 A66-20415

Solar corona emission line polarization resulting from anisotropic effect of photospheric radiation 09 p1442 A66-20463

Radio brightness distribution over quiet Sun and various deductions concerning electron temperature and density of corona, including data on overdense regions radiating thermally 10 p1601 A66-21061

Thermal origin of X-ray radiation of quiet Sun possible, suggesting quasi-stable component produced in undisturbed corona and slowly varying component in active corona 10 p1598 A66-21087

Dielectronic recombination for low density plasma, estimating coefficient and ionization balance for iron and calcium ions in corona 10 p1602 A66-21088

Resonance lines of coronal ions of silicon appearing in two widely separated spectral regions 10 p1602 A66-21092

Collisional excitation of autoionizing levels in solar corona 10 p1557 A66-21093

White-light corona of Sun photographed with rocket-mounted Lyot coronagraph equipped with external occulter, noting agreement of rocket with eclipse



data 10 p1603 A66-21112  
 Exospheric model of solar wind for ionized atmosphere with velocity-dependent collision cross section 10 p1605 A66-21206  
 Solar radio bursts used to study physical properties of corona 10 p1609 A66-21853  
 Coronal spectra of solar eclipse of 1952 at Khartoum, noting spectral distribution of total corona, F corona and electron densities and separation of K and F coronas 11 p1768 A66-22364  
 Monograph on solar corona physics covering ground based, satellite and sounding rocket observation, spectral emission and absorption lines, ionization mechanism, RF and UV radiation, etc 12 p1949 A66-24069  
 Polar magnetic field variability confirmed by study of solar corona during total eclipse of May 30, 1965 in South Pacific 16 p2794 A66-30658  
 Solar activity review discussing sunspots, flares, coronal condensations, etc 17 p2997 A66-32021  
 Solar corona emission spectrum and narrow passband photography of solar disk, noting measurement of intensity variation and absorption coefficient 17 p2999 A66-32133  
 Solar supercorona wave scattering effect on position and shape of discrete radio source 17 p2999 A66-32235  
 Solar corona and interplanetary plasma noting solar wind effect on comet tails and shock wave caused by interaction of geomagnetic field and plasma 17 p3000 A66-32272  
 Theoretical transition probabilities of forbidden lines and unobserved lines of ions in solar corona 18 p3230 A66-34151  
 Radial diffusion effects on composition of solar corona and solar wind 18 p3168 A66-34344  
 Silicon, iron and nickel in solar corona determined by method of Pottasch 18 p3233 A66-34575  
 Spectral analysis methods used to calculate iron abundance in solar corona 18 p3233 A66-34577  
 Coronal scattering of radiation from solar radio source, considering angular deflections and brightness 18 p3199 A66-35044  
 LASL lens design program for Doublet Achromat, from existing Fraunhofer design, used in solar corona monochromatic photography 19 p3354 A66-35383  
 Winking filaments, prominence and coronal magnetic fields 19 p3463 A66-36171  
 Polar coronal ray form relationship to overall solar corona form 19 p3464 A66-36299  
 Brightness of white corona in vicinity of solar prominences determined by trichromatic selection from color pictures of Sun during eclipse 19 p3454 A66-36610  
 Detectability of coronal IR lines due to Mg, Al and Si ions with practicable IR spectrometers and photoconductive detectors, considering atmospheric attenuation 20 p3649 A66-37333  
 Solar magnetic field effect on solar wind, computing solar wind properties and coronal density distribution 20 p3630 A66-37334  
 Solar chromosphere observations, noting distribution of spicules and role in coronal heating 20 p3656 A66-38051  
 Primary cosmic radiation composition, discussing abundance of protons, He nuclei and heavier nuclei 20 p3632 A66-38098  
 Electron temperature of solar corona, noting radiative transfer of radio emission in corona, deriving distribution of brightness temperature over solar disk 21 p3811 A66-38638  
 Soviet papers on solar corona and corpuscular radiation in interplanetary space 21 p3812 A66-39119  
 Soviet observational data on solar corona and wind collected during solar eclipse of June 19, 1936 21 p3813 A66-39120  
 Photometry, polarization, structural peculiarities and density distribution of solar corona 21 p3813 A66-39121  
 Basic laws of variations in detailed coronal structure with solar activity phase 21 p3813 A66-39122  
 Arc shaped formations in solar corona, discussing possible existence of solar magnetic field with 22-year cycle of variations 21 p3813 A66-39123

Microparameters of solar corona as physical system, discussing Vsekhsvyatskii-Bugoslavskaja and Chapman theories 21 p3813 A66-39124  
 Polar coronal temperature inferred from density gradients and based on solar wind and latitude dependence of coronal composition 22 p3983 A66-40698  
 Scattering angle of spherical radio waves on isotropic and radially elongated inhomogeneities of supercorona of Sun 22 p3983 A66-40754  
 Transient anisotropic cosmic ray increase during recovery phase of Forbush decrease due to reflection from receding blast wave and co-rotating shock wave formed during explosive heating of solar corona 23 p4123 A66-41687  
 Solar UV emission lines for 11 elements heavier than helium analyzed, obtaining relative abundances values and relation between electron temperature and temperature gradient in chromosphere-corona transition region 23 p4130 A66-41809  
 Solar corona pictures during July 1963 eclipse, analyzing polar rays frequency distribution along Sun limb and deviation from radial direction, all linked to solar activity cycle 23 p4123 A66-41810  
 Angular velocity of solar corona determined as function of radial distance from Sun including effect of solar wind, magnetic field and viscosity 23 p4130 A66-41811  
**CORONA DISCHARGE**  
 Electron passage from surface ion into semiconductor layer interior during charging from corona discharge, estimating thermal overshoot and tunneling through potential barrier 01 p0071 A66-11025  
 Progressive modification of anode surface of negative point-to-plane system used in corona discharge with microcrystals becoming seat of luminous phenomena 03 p0395 A66-12977  
 Transition from coronal streamer discharge to spark discharge in long air gaps, noting leader role in streamer formation 06 p0919 A66-16876  
 Point-discharge currents between negative points and positive plane 11 p1695 A66-22376  
 Intensity variations of 5303 and 6374 angstrom coronal lines during last two solar cycles compared 12 p1952 A66-24931  
 Tornado dehydration and burning effects in terms of conventional hot wind mechanism, corona discharge mechanism and new ring-current mechanism 13 p2122 A66-26126  
 Correlation between clear air turbulence and aircraft electrical activity, describing corona discharges from DC-8 tail antenna 15 p2426 A66-28922  
 Siting of static discharger to control nature and occurrence positions of coronas to minimize RF noise capable of causing hazard to aircraft navigational aid systems 19 p3282 A66-36752  
 Radio wave propagation in simple plasma in presence of solar gravitational field, noting coronal and relativistic effects 21 p3771 A66-39270  
 Coronal emission-line intensities in extreme UV, calculating fluxes for resonance lines of coronal ions from rocket measurement data 21 p3816 A66-39553  
 Coronal emission lines in presence of strong sky background utilizing difference between gradients of line and sky intensities 21 p3816 A66-39554  
**CORONAGRAPH**  
 Achromatic coronagraph for spectrography of solar corona 07 p1030 A66-17246  
 White-light corona of Sun photographed with rocket-mounted Lyot coronagraph equipped with external occulter, noting agreement of rocket with eclipse data 10 p1603 A66-21112  
 Design of simplified noneclipse coronagraph, describing optical system and basic performance characteristics of instrument 22 p3921 A66-40958  
**CORONAL CONDENSATION**  
 Sunspots, plagues, coronal activity, flares, prominences and emission of coronal rays in solar center activity 03 p0420 A66-12842  
 Coronal condensation observation indicates existence of long-lived quiescent

prominences due to continuous accretion of new coronal gases 05 p0761 A66-15092  
 Current knowledge and theories of solar radio bursts and flares of various types, coronal condensation effects and quiet Sun as sources of radiation 07 p1118 A66-17631  
 Total intensities of continuum and of red, green and yellow coronal lines emitted by sporadic coronal condensation shown to yield lower limits to Fe and Ca abundances 20 p3649 A66-37332  
 Acceleration of plasma cloud from Sun producing geomagnetic storm, noting magnetic cloud squeezed out from sunspot region 24 p4262 A66-42459  
**CORONARY CIRCULATION**  
 Plane crash as result of pilots coronary disease, discussing prevention and rehabilitation 04 p0469 A66-14387  
 Electromagnetic and ultrasonic flow measurement of blood flow rate for cardiocirculatory physiology, discussing future application of nuclear resonance and laser 14 p2230 A66-27553  
 Levy hypoxia test and associated arterial oxygen desaturation and increased cardiac output 24 p4163 A66-42452  
**CORPUSCULAR RADIATION**  
 Corpuscular flux entry zone and spiral time distribution of disturbance maxima 01 p0133 A66-11165  
 Ionosphere electron content near auroral zone obtained from differential Faraday observations of multifrequency beacon satellite Explorer XXII, noting corpuscular radiation role 02 p0223 A66-12017  
 Radio emission in ionosphere during high solar activity explained as electron emission produced by particles moving as corpuscular fluxes 02 p0284 A66-12133  
 Corpuscular radiation effect on electronic components during interplanetary flight, assigning safety margins to each component 04 p0493 A66-13606  
 Quasi-stationary corpuscular streams from Sun suggesting role of active regions in formation 05 p0748 A66-14867  
 Properties of solar and geophysical phenomena analyzed, concluding that magnetic field of corpuscular fluxes has forceless structure 05 p0753 A66-15392  
 Particles in radiation belt of Earth, considering motion in dipole field, sources, loss processes, etc 05 p0756 A66-15745  
 Variations in cosmic ray intensity recorded at world network of stations during consecutive magnetic storms, noting changes in corpuscular fluxes, interplanetary medium, etc 12 p1941 A66-24167  
 Magnetic storms during IGY, assuming effect on cosmic ray intensity is associated with influence on galactic cosmic rays of magnetic fields of solar and corpuscular fluxes 12 p1941 A66-24169  
 Corpuscular intrusions into Earth magnetosphere involving entire auroral zone and occurring only on night side 12 p1871 A66-24296  
 Structure and coherency of lunar dust layer, considering corpuscular radiation such as solar wind and meteorite bombardment 12 p1952 A66-24892  
 Radio emission in ionosphere during high solar activity explained as electron emission produced by particles moving as corpuscular fluxes 14 p2241 A66-28090  
 Role of corpuscular radiation in lower ionosphere formation, noting charged particle flux, energy spectra, etc 15 p2591 A66-30024  
 Geomagnetically trapped proton and electron fluxes in immediate vicinity of Earth 18 p3186 A66-34809  
 Corpuscular radiation from UV Ceti stars assumed to be mainly protons, noting role of interstellar matter 20 p3652 A66-37611  
 Chapman-Ferraro hollows for system of parallel line currents enveloped by stratified corpuscular flux 22 p3975 A66-40806  
 Dense particle population of Van Allen belts formed by interaction of high energy corpuscular radiation with interplanetary magnetic field and geomagnetic field 23 p4123 A66-41186  
 Augmented special relativity theory to account for Einstein effects, with extension to general scalar field theory and notes on corpuscular light and galactic-centered



reference frame 23 p4090 A66-41273  
 Nighttime electron temperatures in upper F region suggest corpuscular energy input 23 p4064 A66-41682  
 Comparison of various geomagnetic variations associated with corpuscular precipitation at South Pole, noting day-night effect 23 p4064 A66-41688  
 Electromagnetic and corpuscular radiation hazards to astronauts deduced from data on dogs 24 p4166 A66-43140

**CORRELATION**  
 S ANGULAR CORRELATION  
 S AUTOCORRELATION  
 S CROSS CORRELATION  
 S DATA CORRELATION  
 S IMAGE CORRELATION  
 S STATISTICAL CORRELATION

**CORRELATION COEFFICIENT**  
 Relation between angle of attack envelopes and correlation parameter for spinning bodies entering atmosphere at large inclinations 03 p0432 A66-12811  
 Negative correlation coefficient between Izsak satellite geoid and Lee and MacDonald heat flow distribution, suggesting correlation between geoidal undulations and heat flow highs and lows 04 p0518 A66-14454  
 Change rate of pitching moment coefficient upon aerofoil correlated to deflection of flap control for application to wing reversal analysis 06 p0801 A66-16001  
 Correlation factor for induced radiation frequency shifts and crystal temperature variations in ruby laser 08 p1233 A66-19269  
 Frequency correlation in radio communication using scattering media 10 p1504 A66-21677  
 Correlation coefficients for daily ranges of horizontal component of quiet day diurnal magnetic variation 11 p1695 A66-22370  
 Coefficient of mutual correlation of noises for two-antenna phase-type direction finder 17 p2879 A66-31860  
 Spatial correlation coefficients and transverse temperature perturbation scales during turbulent nonisothermal flow of mercury in circular pipe 20 p3607 A66-36982

**CORRELATION DETECTION**  
 Correlation dependence of F-2 layer on solar wave energy entering Earth atmosphere 04 p0515 A66-13850  
 Dual-mode acquisition and tracking system using random noise as carrier signal 06 p0842 A66-15977  
 Scene correlation tracking system or sensor device measures displacement between two views of same scene 06 p0842 A66-15978  
 Correlation between strength of induced optical absorption G band and strength of features in electron spin resonance spectrum in electron irradiated diamonds 06 p0934 A66-17125  
 Fluctuation errors of analog correlation meters under time displacement of random signals 07 p1031 A66-17356  
 Transient characteristics of nanosecond-range pulse devices measured by wideband interference correlator 08 p1194 A66-19280  
 Predicting change in state of automatic control system, using correlation analysis 09 p1361 A66-20304  
 Correlation method measuring far-field patterns of large-aperture antennas, using radio star sources and auxiliary antenna for providing reference signal for cross correlation with test antenna signal 11 p1662 A66-22540  
 Vibrational analysis, discussing spectrum analyzers, correlation and autocorrelation analysis and hybrid and digital computer applications 12 p1970 A66-24722  
 Variations of zodiacal light and airglow, suggesting correlation with solar and lunar cycle 14 p2283 A66-27096  
 Quadratic integral equation solution for bandlimited signal design for binary communication, using memoryless correlation detection 19 p3296 A66-35339  
 Signal detection techniques for discrete-frequency, phase-coherent pulse frequency modulation telemetry system, using analog and digital circuits 19 p3302 A66-35698

**CORRELATION FUNCTION**  
 Scaling of near field pressure correlation patterns around jet exhaust 01 p0010 A66-10123

Turbulent motion of elastoviscous fluid degeneration when highest velocity and stress field correlation moments are neglected in comparison with second moments 02 p0217 A66-11394  
 Variance of number of zeros in narrow band normal noise of finite duration calculated from energy spectrum of phase derivative 02 p0190 A66-11406  
 Location and nature of singularity of Ising square lattice susceptibility, using Pade approximation based on Clapp spin-spin correlation function 02 p0263 A66-11887  
 Autocorrelation functions of random processes, determining parameters and amplitude of diurnal variations in cosmic ray intensity 02 p0284 A66-12129  
 Correlation of large and small scale roughness for plane wave scattering from rough surface 03 p0335 A66-12818  
 Subsystem checkout in operation termed on-line checkout, noting use of digital computer with random noise signals and role of correlation and transfer functions 04 p0493 A66-13608  
 Signal fluctuation effect on operation of electronic device, approximating empirical correlation function 04 p0504 A66-13778  
 Two-point correlation function expressed in terms of structural function of velocity field 04 p0542 A66-14305  
 Correlation equation estimating pitting fatigue life of bearings from minimal rolling contact rig data [ASME PAPER 65-WA/CF-5] 05 p0690 A66-15624  
 One-and two-dimensional superconductivity, discussing effect of thermodynamic fluctuations on off-diagonal long-range order 05 p0718 A66-15865  
 Correlation relations of output voltage of switched RC integrator 06 p0823 A66-15888  
 Transformations with correlation function unaltered, changing generalized Barker sequences 06 p0860 A66-16113  
 Multicoordinate systems, discussing control method development for plants with large number of correlated inputs and outputs 06 p0863 A66-16527  
 Ionization bursts observed in chambers used for continuous registration of intensity variations in hard component of cosmic radiation, correlating variation frequency with solar cycle 06 p0950 A66-16591  
 Correlation analysis to study reactions of human cardiovascular system during space flight of Voskhod 06 p0814 A66-17175  
 Probability characteristics of distributed parameter system subjected to parametric and additive noises, obtaining mathematical expectation and correlation function expression 07 p1014 A66-17433  
 Dimensionless flow parameter for free convection, equivalent to Reynolds number for forced convection, used for correlating through single curve free and forced convective heat and mass transfer from single bodies 07 p1149 A66-17517  
 Active regions on Sun responsible for modulation process evidenced by correlation of cosmic radiation intensity variation with solar activity features 07 p1125 A66-18002  
 Interaction between hydrogen and various titanium alloys, noting correlation between sorption capacity of alloys and type of phase diagram 07 p1050 A66-18064  
 Electronic correlator circuit yielding intercorrelation function at same rate at which signal is applied to device input 08 p1192 A66-19099  
 Performance correlation of conical and contoured nozzles for gas-particle flows, defining differences between particle effects for such nozzles 08 p1165 A66-19157  
 Spatial statistical correlation functions for normalized field of geopotential calculated for Europe and Asia 09 p1398 A66-19892  
 Higher order correlation function evaluated for shot noise statistics 09 p1342 A66-19925  
 High resolution radar correlometer measurement of spatial correlation radius of RF radiation scattered by disturbed ocean surface 09 p1343 A66-20340  
 Method determining variance and correlation function fluctuations on limiter-inertial RC circuit system 09 p1344 A66-20440  
 Errors in measuring correlation function of

two random processes represented in form of voltages 09 p1345 A66-20444  
 Auroral absorption measured, using riometers compared with energetic particle fluxes simultaneously detected by passing satellite, showing absorption and particle flux correlation 09 p1374 A66-20881  
 Cross correlation and autocorrelation functions of nonstationary signals based on optimal approximation of ensemble correlation function for one pair of signals 10 p1517 A66-21694  
 Dynamic characteristics of linear plant determined under noise conditions, allowing for error in input-signal measurement 11 p1673 A66-22202  
 Angular autocorrelation function of circular-aerial radiation pattern 11 p1662 A66-22397  
 Contribution of electron-electron correlations to longitudinal dielectric constant for case of one-component plasma, noting resonance effect and formula for plasma oscillation damping 11 p1744 A66-22446  
 Correlation function of response of multichannel electronic multiplier to Gaussian input noise 11 p1676 A66-22711  
 Radio receiver design for precisely given signal and nonsteady Gaussian noise 11 p1658 A66-23221  
 Nonstationary contributions to transport coefficients, especially bulk viscosity coefficient, combine with stationary ones yielding result equivalent to that provided by autocorrelation function theory 12 p1916 A66-23617  
 Coherent behavior of light-quantum field in quantum electrodynamics, noting explicit terms of correlation and characteristic field conditions for nth order coherence 12 p1913 A66-23727  
 Hot-wire anemometer measurement of turbulent velocity fluctuations in air flow and energy spectrum and correlation analyses 12 p1880 A66-23846  
 Time resolution error of measured correlation function, based on frequency response of hot-film and hot-wire anemometer 12 p1880 A66-23847  
 Best linear unbiased (BLU) estimator for large class of error correlation models 12 p1904 A66-24197  
 Multivariate statistical analysis of wind sounding data, applying high degree of correlation between two wind parameters and empirical density function [AIAA PAPER 66-353] 12 p1907 A66-24489  
 Properties of compressible boundary layers with heat transfer and arbitrary pressure gradients calculated, using integral equation and correlation concept for application in hypersonic flows 12 p1865 A66-24581  
 Fourier transform of time-dependent density-density correlation function calculated from linearized Boltzmann equation for Maxwell molecules 12 p1917 A66-24584  
 Transport coefficients of moderately dense gas calculated by three methods based on correlation function or generalized Boltzmann equation 12 p1979 A66-24586  
 Vertical incidence fading amplitude experiment using array of receiving antennas, obtaining data on ground diffraction pattern of reflected radio waves, noting correlation function shapes 12 p1824 A66-24840  
 Correlation functions of amplitude and intensity fluctuation for laser model near threshold obtained by using distribution functions evaluated by Fokker-Planck equation, treating amplitude as random variable 12 p1892 A66-25018  
 Effective diffusion cross section of ultrasonic and laser beam while acting on turbulent flow 13 p2062 A66-25404  
 Nonthermal microwave radiation from plasma of electrodeless induction discharge, establishing correlation between microwave and X-ray radiation 13 p2143 A66-25710  
 Triple correlative function solution for plasma system of charged particles and collision integral for pair correlative function 13 p2148 A66-25941  
 Components of gradient of performance criterion in adaptive control systems, employing correlation technique by use of



- time delay 13 p2051 A66-26067
- Extension of three-field mixing theory to include effects of convective nonlinearities on excitation in plasma, using correlation function of spectral densities for interpretation of thermally enhanced light-by-light scattering 13 p2132 A66-26151
- Correlations and intensity fluctuations in light from individual lasing and nonlasing modes of CW GaAs laser and threshold noise change in laser emission 13 p2102 A66-26210
- Photoelectron counts of photomultiplier illuminated by gas laser light source 13 p2102 A66-26211
- Quantum theory of lasers presented in terms of correlation functions of second-quantized electromagnetic and matter fields 13 p2103 A66-26214
- Coherence properties of quantized electromagnetic field and hierarchy of correlation functions for complex field operators 13 p2128 A66-26218
- Noise suppression, signal reception, and polarization measurement in cross correlated antennas as function of dipoles imbedded in random field, surrounding noise field and coherency matrix of cross correlation function 13 p2044 A66-26746
- Propagation distribution of impurity atoms in heavily doped semiconductors 14 p2356 A66-27068
- Combined frequency and space correlation of wave fields scattered by rough surfaces where conditions of applicability of Kirchhoff approximation hold true 14 p2236 A66-27144
- Correlation expressing reduced coefficient of thermal expansion as function of reduced Debye temperature for metallic solids used for predicting coefficient at any temperature 14 p2411 A66-27375
- Cross correlation of satellite signals through slab containing small anisotropic irregularities 14 p2237 A66-27398
- Integral equations derived from correlation functions, determining transport coefficients in classical fluid, formally valid to general order in density 14 p2276 A66-27635
- Chemical potential and integral equation for correlation functions of classical fluids, using Percus method when functions exhibit cluster properties 14 p2276 A66-27637
- Integral equations defining transport coefficients of moderately dense gas obtained from Boltzmann equation shown to be identical to first order in density, with results obtained by autocorrelation function method 14 p2276 A66-27639
- Autocorrelation functions of random processes, determining parameters and amplitude of diurnal variations in cosmic ray intensity 14 p2377 A66-28086
- Two-point correlation function expressed in terms of structural function of velocity field 14 p2327 A66-28218
- Equilibrium binary correlations in classical relativistic homogeneous electron gas 14 p2336 A66-28275
- Pulsed transient functions determination from control channels of multidimensional plant, assuming output signal correlation functions are determined by double averaging 15 p2469 A66-28643
- Kinetic theory of two-photon absorption from single mode of radiation field, noting dependence on coherence properties of field 15 p2544 A66-28943
- Correlation analysis technique for stochastic processes in RLCM circuits with random parameters in case of stochastic input functions 15 p2469 A66-29055
- Correlation of time variations of proton and electron intensity of outer radiation belt and dependence on geomagnetic environment 15 p2575 A66-29103
- Frequency correlation of ionospheric radio waves in inhomogeneous thin layer medium and effect of irregular horizontal ionization gradients 15 p2451 A66-29111
- Statistical properties of dispersive waves in upper atmosphere analyzed, using correlation technique 15 p2493 A66-30040
- Functional time-delay device and integration into analog correlator for analysis of autocorrelation and cross-correlation functions of measured system response signals 16 p2676 A66-30445
- Wind velocity spectra and correlation functions statistically analyzed in ULF range for lowest levels of atmosphere 16 p2742 A66-30773
- Multicordinate systems, discussing control method development for plants with large number of correlated inputs and outputs 16 p2670 A66-30837
- Hybrid analog/digital techniques for signal processing, noting performance advantages at relatively low cost and applications to linear transformation, function generation, correlation functions, etc 16 p2658 A66-31250
- Relation between output correlation functions of full-wave and half-wave linear rectifier with random inputs 16 p2664 A66-31335
- Two-dimensional correlation time relation to spectral bandwidth and corresponding one-dimensional quantities of Lampard 16 p2671 A66-31336
- Integral expression for log likelihood ratio of two Gaussian processes in signal detection 16 p2738 A66-31714
- Quantitative measurement of electron correlation spectrum for deuterium plasma in thermal equilibrium 17 p2963 A66-31885
- Mean-square response of thin elastic plate to random pressure acting normal to plate surface 17 p3021 A66-32010
- Probability distribution of phase difference between two spaced antennas excited by random fan of rays plus specular component 17 p2874 A66-32385
- Design of adaptive systems with forced oscillations, using correlation and filter methods 17 p2902 A66-32573
- Partitioning procedure for shell theory equations, using intercorrelation function 17 p3025 A66-32591
- Improved correlation function in Kirchhoff-Huygen method of solution of scattering of waves from statistically rough surfaces 18 p3068 A66-34015
- Low residue ambiguity function, using incoherently processed pulse train waveforms for application in clutter environment 18 p3070 A66-34260
- Critical heat flux for boiling water, sodium and rubidium, correlating burnout data for liquid metals only and as relation for metallic and nonmetallic fluids 18 p3262 A66-34376
- Correlation study of turbojet afterburner combustion efficiency and fuel/air ratio setting for maximization of efficiency [WSC1 66-1] 18 p3164 A66-34423
- Riometer recordings at high geomagnetic latitude of intense and sporadic absorption events correlated with occurrence of auroral and geomagnetic disturbances 18 p3108 A66-34531
- Boltzmann equation, interpreted in terms of certain correlation functions known as product densities, applied to fluctuation theorem and gases and liquids not in equilibrium 18 p3136 A66-34706
- Dynamic characteristics of unsteady feedback control system during normal operation, ascertaining signal correlation and cross correlation functions 18 p3091 A66-34987
- Noise characteristics at integrator input in nonstationary regime 19 p3311 A66-35297
- Error analysis of area correlation guidance system using parametric analysis of spatial frequency domain-equivalent power spectral density 20 p3597 A66-37237
- Moving image velocity measuring technique using parallel-slit spatial filter is treated as continuous optical correlation processing 20 p3558 A66-37288
- Linear system providing maximum signal to noise ratio for given parameters of correlation function of incoming quasi-harmonic signal mixed with white noise 20 p3515 A66-37379
- Statistical characteristics of atmospheric ozone distribution, determining autocorrelation and cross correlation functions, concentration and temperature profiles 20 p3552 A66-37751
- Correlation of magnetic fields and energetic electrons on IMP I satellite, noting depression in geomagnetic tail region, electron fluxes and diamagnetic effect 20 p3633 A66-38201
- Altitude of lower cloud boundary functional correlation with atmospheric parameters obtained from numerical weather forecast 20 p3593 A66-38366
- Distortions and errors in calculating structural and correlation functions from experimental results 20 p3594 A66-38377
- General nonequilibrium system in contact with reservoir described via correlation functions of quantized field operators, noting influence of cavity and optical pump 21 p3746 A66-38633
- Coefficients of Taylor expansion of correlation function in various velocities defined to describe space-time behavior 21 p3770 A66-38749
- Correlation formulas improvement for laminar shock tube boundary layer for air and argon 21 p3727 A66-39167
- Doppler radar measurements of wind velocity horizontal components variation in rain and snow, calculating time correlation and structural functions for neutral and unstable stratifications 21 p3760 A66-39358
- Propagation distribution of impurity atoms in heavily doped semiconductors 22 p3966 A66-40827
- Autocorrelation function and energy spectrum of radiotelegraph signal, noting channel parameter dependency on transmission speed 23 p4036 A66-41050
- First-order Markovian gyro drift numerically evaluated and square root plotted vs interval and gyro correlation time 23 p4068 A66-41318
- Quasi-stellar radio sources correlated for prediction of Lyman lines relative strengths and optical depth of nebulas beyond Lyman continuum, using simple models 23 p4130 A66-41807
- Line strengths variation in spectra of HD 124224 and HD 19832 analyzed, establishing anticorrelation of He I variations with variations in temperature 23 p4130 A66-41808
- Spectral distribution of space-time velocity correlations as function of velocity fluctuation scale in turbulent boundary layer 23 p4014 A66-42026
- Integral equations for weight function of optimum filter and correlation function of random absolute error 24 p4188 A66-42475
- Frequency characteristic and transient delta function of plant, using algorithm based on correlation functions 24 p4188 A66-42483
- Thermodynamic properties of electron plasma investigated by Bogoliubov-Born-Green-Kirkwood-Yvon hierarchy equation, calculating correlation energy 24 p4243 A66-42764
- Phase-lock servo-loop circuit for space communication providing estimate of incoming signal through correlation process 24 p4175 A66-42826
- ## CORROSION
- ### S DEGRADATION
- ### S ELECTROCHEMICAL CORROSION
- ### S EROSION
- ### S ETCHING
- ### S FRETTING CORROSION
- ### S FUEL CORROSION
- ### S METAL CORROSION
- ### S STRESS CORROSION
- ### S WEAR
- ## CORROSION PREVENTION
- Helicopter corrosion problems discussing causes, exposed surfaces, prevention and treatment 03 p0372 A66-12300
- Prevention of metallic edge corrosion of naval aircraft, evaluating surface treatments, primers, epoxy enamels, etc 03 p0380 A66-12318
- Effect of corrosive environments on various metals and anticorrosion techniques to protect metal surfaces 04 p0534 A66-13374
- Corrosion occurrence and control, noting prone areas, detection and removal 11 p1717 A66-23014
- Wear life and corrosion protection of solid film lubricants improved through substituting other lubricative pigments for graphite [ASLE PAPER 66AM 1C3] 16 p2711 A66-30405
- Voltage and density of contact-corrosion current arising at contact surface of different metals 18 p3124 A66-35011
- Throat erosion rates of carbon chokes in rocket motor nozzle predicted, using



- mathematical approach combined with experimental result  
[AIAA PAPER 65-351] 24 p4261 A66-42772
- CORROSION RESISTANCE**  
Corrosion resistance and anodic behavior of Kh18N9 steels with various nickel-manganese-carbon-titanium contents 01 p0088 A66-10987  
Heat treatment cycle effect on mechanical properties of corrosion resistant precipitation hardened steel AM 355 in terms of metallographic structure 02 p0242 A66-11304  
Nucelite, ceramic-metal composite with high mechanical strength and abrasion resistance noting crystal structure, application, properties, etc 02 p0244 A66-11742  
Explosion cladding for bonding similar and dissimilar metals without intermediate metal or externally applied heat 03 p0380 A66-12317  
Heat pipe characteristics covering performance analysis and experimental results such as heat transfer rate, life tests, working liquid selection, etc 05 p0616 A66-15544  
Measurement of surface emittance of surface coatings for selected metals, providing low-thermal emittance characteristics in IR spectrum for thermal and corrosion control [AIAA PAPER 66-18] 05 p0705 A66-15849  
Refractory alloy corrosion, discussing columbium and tantalum base tubing alloy resistance to refluxing potassium between 1800 and 2400 degrees F 06 p0894 A66-16071  
Corrosion resistance of titanium and its alloys in solutions of acetic and nitric acids as affected by aluminum additions 06 p0896 A66-16608  
Accelerated cooling of ferritic-martensitic steel and ferritic steel after sintering, combined with additional heat treatment, increases strength and corrosion resistance 06 p0896 A66-16690  
Fracture toughness and stress corrosion resistance of several heats of maraging steel compared with results for low-alloy and hot-work die steel 06 p0897 A66-16801  
Aircraft fuel tank coating corrosion resistance, discussing polyurethane and epoxy material characteristics and application 07 p1053 A66-17491  
Spark igniter that successfully operates at 50 to 120 psig chamber pressure and 2300 to 3000 degrees K without observable thermal shock or electrode erosion 08 p1281 A66-18838  
Super chromium steel survey, including applications in gas turbines and aerospace industries, physical and mechanical properties, thermal stability, corrosion resistance, etc 09 p1387 A66-19953  
Device for taking long time corrosion fatigue curves on small cross section specimens at high temperatures and pressures 09 p1388 A66-20433  
Alloying elements effect on anodic corrosion and passivation of stainless steels 09 p1390 A66-20837  
Corrosion resistance and electrochemical properties of alloys of niobium-titanium system 09 p1390 A66-20838  
Corrosion resistance, electrochemical and mechanical properties of alloys of titanium-niobium system 09 p1390 A66-20839  
Corrosion resistance of yttrium is higher at higher pH because of slower anodic process 10 p1546 A66-21747  
Corrosion of rhenium in various acids and hydroxides is electrochemical in nature and determined by kinetics of anodic and cathodic processes involved 10 p1546 A66-21748  
Chromium steel strength and corrosion resistance improvement by molybdenum and tungsten addition 11 p1716 A66-22747  
Heat treatment effect on structure, hardness, microhardness and corrosion resistance of VT1 titanium and OT4 titanium manganese-aluminum alloy sheets 12 p1897 A66-24900  
Shot peening for resistance to stress corrosion cracking of high strength steel and aluminum alloys and to improve fatigue life of landing gears, wing spars, jet engine components and other structural parts 13 p2196 A66-25771
- Composite casting as metallurgical bonding technique, noting application to weight reduction and increase of corrosion resistance 13 p2086 A66-25779  
Corrosion of magnesium in water 15 p2523 A66-29724  
Glass reinforced plastics for helicopter primary structures 18 p3124 A66-33690  
Properties of small tube Teflon heat exchangers noting corrosion resistance, smooth slippery surface, etc, and heat transfer coefficient 18 p3262 A66-34383  
Susceptibility of titanium alloys to elevated-temperature static and dynamic sea-salt stress cracking, noting operative mechanism 19 p3377 A66-35648  
Hardness, toughness, stress relaxation, corrosion resistance, etc, of niobium-aluminum alloy with stable elastic modulus 20 p3583 A66-37366  
Additive effects on jet propellants, noting corrosion and oxidation resistance 20 p3627 A66-38296  
Additives effect on antioxidant stability and antiabrasion characteristics of lubricating oils used in jet and turboprop engines 20 p3575 A66-38445  
Field cleaning of corrosion resistant steel tubing for LOX and pneumatic service 22 p3922 A66-40040  
Corrosion fatigue strength of duralumin in presence of stress concentrators, noting parameters of resistance and alloy properties 22 p3935 A66-40679  
Heat treatment effect on structure, mechanical properties and corrosion resistance of VTZ-1 alloy, noting influence of annealing 22 p3935 A66-40680  
Structural, mechanical and corrosion properties of aluminum alloy of various compositions 22 p3936 A66-40877  
Magnesium alloy components protected from corrosion by subjection to anodic oxidation 23 p4074 A66-41659
- CORROSION TEST**  
Chemical reaction between iron and extreme pressure agents like chlorine and sulfur for corrosion mechanism analysis [ASLE PREPRINT 65-LC-11] 02 p0237 A66-12254  
Corrosion control on aircraft skin, countersinks and fasteners describing tests, sealant coatings, chemical treatments, mechanical barriers, platings on fasteners and organic coatings 03 p0372 A66-12298  
Cr and Mn effects on aging mechanism and anticorrosion properties of Al-Zn-Mg alloys 03 p0381 A66-12723  
Trapezoidal stress waveforms effect on low cycle corrosion fatigue strength, clarifying mechanism of corrosion fatigue 12 p1959 A66-23849  
Chemical reaction between iron and extreme pressure agents like chlorine and sulfur for corrosion mechanism analysis [ASLE PREPRINT 65-LC-11] 12 p1889 A66-24993  
Friction corrosion caused by alternate pivoting of steel ball on plane of light alloy 14 p2302 A66-27934  
Stress corrosion testing to evaluate materials for specific application 15 p2523 A66-29723  
Stress corrosion cracking of titanium alloy in long duration and high temperature tests, using salt coating of specimens 19 p3379 A66-35657  
Stress corrosion tests on specimens of titanium alloy in contact with sodium chloride, noting crack formation and effect of argon 19 p3379 A66-35658  
Separation of gaseous, liquid and solid reaction products generated by hot salt corrosion of titanium, noting gas diffusion effect on cracking 19 p3379 A66-35659  
Corrosion tests on eight refractory metals and alloys in liquid lithium and cesium vapors 19 p3383 A66-36136  
Refractory niobium alloy corrosion tests in potassium liquid at 2000 to 2200 degrees F 19 p3383 A66-36137  
Ephemeral-corrosion tests of refractory metals in molten lithium between 2000 and 3000 degrees F 19 p3383 A66-36138  
Deformation of solids by impact of liquids and relation to rain damage in aircraft and missiles, to blade erosion in steam turbines and to cavitation erosion - Meeting, London, May 1965 20 p3546 A66-37801
- Corrosion problems with simulated fuel in launch vehicle models 21 p3750 A66-38799
- CORRUGATED PLATE**  
Characteristics of partially clamped corrugated membrane, investigating effect of forces of clamping friction 01 p0160 A66-11182  
Radiation from modulated corrugated surface excited by waveguide, noting reflection coefficient, radiation pattern, etc 19 p3302 A66-35724
- CORRUGATED SHELL**  
Exhaust mixing process in Rolls-Royce bypass jet engines, noting stream mixing in common duct with corrugated metal interface on inlet side 17 p2990 A66-32079  
Nonequilibrium flow of chemically reacting gas past infinite corrugated cylinder 21 p3724 A66-38717
- CORRUGATION**  
Corrugation growth on infinitely conducting fluid sheets, discussing acceleration induced by constant axial and linearly increasing currents 06 p0871 A66-16276
- CORTI ORGAN**  
S COCHLEA
- CORTICOSTEROID**  
Effects of 9-alpha-fluorohydrocortisone on metabolic changes occurring during six days of bed rest, including water and sodium retention, hematocrit decrease, plasma increase, etc 06 p0813 A66-16824  
Acceleration stress-induced changes in fat metabolism, level of circulating glucose and corticosterone level in rats 15 p2431 A66-28868  
Corticosterone injection in rats, assaying amino acid incorporation into liver microsomal and cell-sap protein 17 p2860 A66-32554  
Parotid fluid collection technic for determining in-flight biochemical responses for 17-OHCS levels 22 p3854 A66-39791  
Corticosteroid responses to limbic stimulation in man and localization of stimulus sites 22 p3855 A66-40487
- COSINE SERIES**  
Approximation of band-limited function by sum of cosines arising in design of phased array antennas 03 p0342 A66-12709  
Properties of sums of special trigonometric series 09 p1394 A66-20458
- COSMIC DUST**  
SA INTERPLANETARY DUST  
SA ZODIACAL DUST CLOUD  
Mariner IV Cosmic Dust Detector measurement of momentum, mass distribution, flux densities and time histories of dust particles near Earth and in space 01 p0073 A66-11113  
Interstellar obscuration of starlight suggests that vast quantities of dust spread thinly throughout galaxy differ in composition 07 p1132 A66-17254  
Extraterrestrial dust as atmospheric argon source and influx of black spherules 08 p1287 A66-18770  
Extraterrestrial dust as possible cause of background ionization and stratification in sporadic E layer 14 p2282 A66-26855  
Spatially homogeneous anisotropic irrotational solutions of Einstein field equations for cosmological dust source 14 p2330 A66-27019  
Newtonian approximation for irregularities in statistically homogeneous and isotropic dust-filled universe 14 p2386 A66-28119  
High altitude balloon top collections of cosmic dust shows evidence of absence of crystal structure in particles 15 p2604 A66-30065  
Massive central body influence on cosmic dust density distribution in Newtonian oscillating world model 19 p3464 A66-36295  
Glassy spherules found in precipitate of melted ice in Antarctica may be cosmic dust particles /microtektites/ 19 p3465 A66-36389  
Comet disintegration as basic source of interplanetary dust based on zodiacal isophots 20 p3549 A66-37037  
Singularities in Newtonian cosmology and in Friedman universes and behavior of relativistic world model with spherically symmetric distribution of matter 20 p3658 A66-38291



COSMIC GAS

Radio galaxies contribution to kinetic temperature of intergalactic gas on basis of cosmological model 03 p0426 A66-12909  
Radio galaxies contribution to kinetic temperature of intergalactic gas on basis of cosmological model 14 p2380 A66-27257  
Expanding universe theory of hot ionized intergalactic gas and blackbody radiation and X-ray emission energy spectra 21 p3817 A66-39561  
Matter traversed by low energy cosmic ray nuclei in space determined, using spallation cross sections with proton beams from accelerators and Li/M ratios 24 p4265 A66-42718

COSMIC NOISE

Electromagnetic wave absorption and cosmic noise absorption measurements useful in radio communication 01 p0072 A66-11101  
Satellite observation of solar protons from flares in September 1963, measuring impact zone effect, differential spectrum, latitude distribution of proton energies, proton fluxes, cosmic noise absorption, etc 03 p0417 A66-12649  
Multiple antenna based on corner reflector used in absorption measurements in magnetically conjugate regions 03 p0334 A66-12661  
Frequency dependence of cosmic noise levels during anomalous type II absorption, noting shielding sporadic E layer 04 p0574 A66-13859  
Response of D-region absorption of cosmic noise to passage of totality during eclipse of May 30, 1965 recorded in New Zealand 05 p0668 A66-14798  
Satellite Ariel II receiver for measuring cosmic radio noise, using dipole antenna 05 p0769 A66-15841  
Sky brightness and cosmic radio emission in satellite Ariel II 05 p0769 A66-15842  
Times of peak cosmic radio noise concentration and usefulness to forward propagation ionospheric scatter reception on DEW-Line as performance monitor, etc 06 p0825 A66-15985  
Spaceborne observations of radio noise from 0.7 to 7.0 mhz and dependence on terrestrial environment 10 p1603 A66-21115  
Satellite observation of radiation belt and absorption of cosmic noise in polar aurora during magnetic storms of February 1964 12 p1943 A66-24267  
Auroral absorption at 18-mc/s in middle latitudes, noting daily and seasonal variation 13 p2074 A66-26361  
Auroral absorption of cosmic radio noise which is not identical at magnetic conjugate point 13 p2076 A66-26743  
Auroral absorption of cosmic radio noise 18 p3238 A66-35086  
Data on geophysical phenomena at magnetically conjugate points on Earth including cosmic noise absorption, conjugacy of visual auroras, magnetic variations, VLF phenomena, etc 19 p3453 A66-35981  
Cosmic radio noise used to measure ionospheric absorption, comparing extraordinary and ordinary wave flux effect in overcoming measurement problems 19 p3351 A66-36361  
Separation of D-E and F-layer contribution to integral absorption of cosmic noise by means of combined pulse reflection and cosmic noise measurements 19 p3351 A66-36363  
Height distributions for atmospheric ionization rate and Balmer radiation resulting from precipitation of auroral protons 21 p3734 A66-39338  
Microwave background radiation field accounted for by integrated effect of population of radio sources if CN excitation is collisional in origin 22 p3978 A66-40004  
Sudden cosmic radio noise absorption, polar cap absorption and auroral absorption 24 p4202 A66-42832

**COSMIC PLASMA**  
Galactic cosmic ray intensity modulation by interplanetary plasma turbulence, noting cosmic ray and geomagnetic storm 07 p1122 A66-17987  
Plasma space science - Symposium, Catholic University of America, Washington, D.C., June 1963 07 p1137 A66-18072

Motion state of interplanetary plasma and properties of interplanetary magnetic fields, including relation to those of Sun 07 p1138 A66-18078  
Penetration of interplanetary plasma into magnetosphere, connected to aurorae and magnetic storms, noting that plasma need not behave like magnetofluid 07 p1138 A66-18081  
Electron and ion acceleration by cosmic plasma waves, examining contribution of these processes to radiation belt formation 20 p3647 A66-37033

COSMIC RADIATION

SA CERENKOV RADIATION  
SA PRIMARY COSMIC RADIATION  
Intercalibration of cosmic ray neutron monitors at nine European sea level stations and deduction of daily latitude effect in 1963 01 p0132 A66-10321  
Expected cosmic ray intensity variations on Moon from analysis of such variations on Earth 01 p0132 A66-10323  
Fine structure of energy spectra of Forbush decrease and dependence on solar cycle 01 p0132 A66-10336  
Momentum spectra of muon flux measured at various angles for production process and environmental influences 01 p0132 A66-10620  
Momentum spectrum of muons at large zenith angles and contribution of pion and kaon production 01 p0132 A66-10621  
Cosmic rays and fundamental problems in elementary particle theory 01 p0133 A66-10642  
Propagation of cosmic synchrotron radiation by individual and aggregate electrons and effect on propagation and radiation of electromagnetic waves 01 p0133 A66-10647  
Book on geo-and heliophysical effects in cosmic rays and auroras 02 p0280 A66-11329  
Forbush decrease characteristics in cosmic ray intensity 02 p0280 A66-11330  
Primary Forbush effect dependence on latitude and time from worldwide data on neutron component of cosmic rays 02 p0281 A66-11331  
Interplanetary magnetic field model developed by Elliot from data of intensity variation of low energy cosmic rays 02 p0281 A66-11332  
Seasonal variations of cosmic ray intensity in stratosphere compared with temperature variation in atmosphere 02 p0281 A66-11333  
Changes in nature of 27-day variations in cosmic ray intensity 02 p0281 A66-11334  
Stellar-diurnal variation of cosmic rays during period 1958 through 1960, on basis of meson-activity data recorder by two crossed counter telescopes 02 p0281 A66-11335  
Lunar-diurnal variation of cosmic ray intensity based on observations of neutron and meson component 02 p0281 A66-11336  
Atmospheric source of diurnal variation of cosmic radiation whose properties undergo substantial variation 02 p0281 A66-11337  
Magnetic storm accompanied by Forbush decreases taking into account atmospheric temperature, noting cyclonic storm origin 02 p0282 A66-11338  
Cosmic radiation variations during passage of cyclones agree with theory for meteorological effects based on two-meson scheme 02 p0282 A66-11339  
Diurnal and nocturnal variations in cosmic radiation intensity during period of maximum solar activity 02 p0282 A66-11340  
Compression of geomagnetic field effect on cosmic radiation at cut-off rigidities and asymptotic directions of radiation incidence 02 p0283 A66-12111  
Crossed counting telescopes used to determine distortions in cosmic ray anisotropy measurement 02 p0283 A66-12112  
Forbush decrease in cosmic radiation spectra as function of solar activity 02 p0283 A66-12113  
Effect of currents, distributed over envelope surface formed by revolution of magnetic dipole force line about its axis, on cosmic ray cut-off 02 p0284 A66-12128  
Autocorrelation functions of random processes, determining parameters and amplitude of diurnal variations in cosmic ray intensity 02 p0284 A66-12129  
Series of self-quenched Geiger counters for

visual detection in cosmic rays of unstable charged particles decaying within millisecond 03 p0417 A66-12281  
Plasma clouds, relativistic cosmic ray and subcosmic ray particle emission associated with solar flares 03 p0421 A66-12845  
Interplanetary medium observation from zodiacal light and radio wave scattering during radio source occultation and influence on galactic and solar cosmic rays 03 p0425 A66-12852  
Effects connected with auroras and magnetic storms in lower ionosphere considering radio wave attenuation, cosmic ray absorption, etc 03 p0365 A66-12854  
Cosmic ray helium nuclei along with heavier nuclei, traverse interstellar and interplanetary matter propagation in space and slope of energy spectrum 03 p0423 A66-12927  
Photon-flux measurements by high energy gamma-photon detectors onboard Explorer XI and OSO-I 03 p0423 A66-13028  
Cosmic X-ray sources in Scorpius and Crab nebula, examining creation of neutron stars from supernova explosion 03 p0423 A66-13029  
Observations of interplanetary magnetic field by Mariner and Imp spacecraft confirm predictions based on behavior of cosmic rays 03 p0429 A66-13263  
Soviet monograph on continuous measurement of cosmic ray mu component, covering experimental apparatus, data analysis, atmospheric dynamics, etc 03 p0423 A66-13287  
Geomagnetic relationship of daily variation of cosmic ray neutron intensity corrected for barometric pressure variation at various ground stations 03 p0423 A66-13360  
Excessive cosmic radiation absorption in lower nocturnal ionosphere at middle geomagnetic latitudes during Forbush effects 04 p0514 A66-13443  
Biological characteristics and physical conditions of space flights, such as low pressure, ionizing radiation, noise, acceleration, weightlessness, artificial atmosphere, feeding problems, etc 04 p0464 A66-14066  
Biological effects of cosmic radiation under laboratory and flight conditions on various craft to study measures for pharmacological and biological protection 04 p0466 A66-14077  
Diurnal variation of cosmic radiation of intermediate energies measured at Earth attributed to particle removal due to scattering by magnetic irregularities 04 p0575 A66-14181  
Cosmic ray induced lithium and calcium in iron meteorites by improved technique of potassium isotope detection 04 p0580 A66-14487  
Rocket measurements of energetic particles discussing electron fluxes, energy spectra, angular distribution and data 05 p0745 A66-14777  
Rocket measurement of energetic particles discussing proton flux, energy spectra, pitch angular distribution and data 05 p0746 A66-14778  
Secular variations of cosmic ray produced carbon 14 in 150 wood samples up to 2000 years old 05 p0747 A66-14795  
Cosmic ray contribution to background of NaI scintillation spectrometers noting counting rate, surrounding material and atomic number 05 p0678 A66-14967  
Terrestrial radiation belts, satellite data, geographical coordinate location and cosmic radiation measurement 05 p0749 A66-15230  
Cosmic radiation studies in U.S.S.R during IGY noting 11-year variations, Forbush effect, solar particle propagation, etc 05 p0749 A66-15232  
Physics of cosmic rays - All-Union Conference, Apatity, U.S.S.R., August 1964 05 p0749 A66-15372  
Stratospheric cosmic ray intensity, discussing Soviet measurements above Antarctica 05 p0751 A66-15375  
Fundamental problems in cosmic radiation astrophysics 05 p0752 A66-15379  
Cosmic radiation investigated by using meteorites 05 p0752 A66-15382  
Cosmic ray variations studied by effects on Zaisan chondrite 05 p0752 A66-15383  
Neutron-group fluxes and variations with solar activity during IYQS observed by



Elektron II 05 p0752 A66-15385  
Cosmic ray 27-day variations using  
periodograms, with measured data processed  
continuously from 1957 to 1964 05 p0753 A66-15393  
Secular changes in stratospheric cosmic ray  
intensity from 1962 to 1964 05 p0754 A66-15397  
Increase with latitude of Forbush effects  
and secular variations in cosmic ray  
intensity explained by worldwide data  
obtained with meson  
detectors 05 p0754 A66-15398  
Energy spectrum of variations in cosmic  
ray intensity and changes in spectrum with  
decreasing solar activity calculated for  
additional particle flux 05 p0754 A66-15399  
27-day changes in solar diurnal variation  
from 1957 to 1958 based on neutron  
component data, noting modulation of  
cosmic ray anisotropy 05 p0754 A66-15402  
Magnetic storm accompanied by cosmic ray  
intensity increase analyzed, considering  
Forbush effect and determining all  
peaks 05 p0755 A66-15403  
Secondary particle generation in satellite  
walls due to 0.1 to 20 beV pi-mesons and  
protons 05 p0756 A66-15411  
Series of self-quenched Geiger counters for  
visual detection in cosmic rays of unstable  
charged particles decaying within  
millisecond 05 p0756 A66-15453  
Cosmic radiation transmission at 3392  
meters through lead studied for thicknesses  
from 10 to 20 cm, measuring intensity from  
star frequency in photographic  
emulsions 06 p0944 A66-16274  
Cosmic X-ray and gamma ray astronomy in  
studying stellar evolution, cosmic ray origin  
and structure of universe 06 p0944 A66-16314  
Book on high energy particles dealing with  
concepts and techniques for studying  
properties of material through interaction  
with cosmic radiation 06 p0944 A66-16376  
Cosmic rays and problems in space physics  
- Conference, Yakutsk, U.S.S.R., August  
1962 06 p0945 A66-16568  
High energy photons from discrete sources  
of cosmic radiation, verifying radio source  
electron production through proton-nuclei-  
matter interaction 06 p0947 A66-16572  
Energy level of mu-meson at sea level in  
10 super 11 to 10 super 13 eV  
range 06 p0948 A66-16579  
Frequency distribution of time and energy  
characteristics of cosmic ray bursts used to  
construct model of interplanetary magnetic  
field 06 p0948 A66-16580  
Difference in cosmic ray intensity due to  
variations in geomagnetic  
cut-off 06 p0948 A66-16581  
Increase of cosmic ray intensity during  
Forbush decrease 06 p0948 A66-16582  
Cosmic ray behavior associated with  
sunspot activity in July 06 p0948 A66-16583  
Azimuthal measurements of cosmic ray  
variations at Yakutsk, U.S.S.R. 06 p0949 A66-16584  
Solar particle effect on daily variation in  
neutron component of cosmic  
radiation 06 p0949 A66-16585  
Anomalies in cosmic radiation during  
December 1957 accompanying geomagnetic  
storms connected with solar  
flares 06 p0949 A66-16588  
Four-year cosmic ray ionization bursts,  
using ASK-2-34 ionization  
chamber 06 p0949 A66-16589  
Secular variation of cosmic radiation  
intensity 06 p0950 A66-16590  
Ionization bursts observed in chambers  
used for continuous registration of intensity  
variations in hard component of cosmic  
radiation, correlating variation frequency  
with solar cycle 06 p0950 A66-16591  
Periodic temperature fluctuations in  
mesosphere based on underground  
measurements of cosmic ray intensity at  
Yakutsk, Siberia 06 p0950 A66-16595  
Cosmic ray intensity and geomagnetic field  
changes induced by electric current systems  
excited in ionosphere, noting seasonal  
changes in diurnal  
variations 06 p0950 A66-16596  
Instrumentation used in analysis of short-  
periodic and microvariations of cosmic ray  
intensity, noting supermonitor with

scintillation counters, photomultipliers,  
etc 06 p0951 A66-16597  
Cosmic ray spark counter operating in  
conjunction with ionization calorimeter and  
photoemulsions 06 p0880 A66-16599  
Beta-electron in nuclear photoemulsion  
study of primary cosmic ray  
properties 06 p0880 A66-16600  
Neutron monitor and mu-meson telescope  
for cosmic ray studies at Kazakh State  
University 06 p0880 A66-16601  
Automatic potentiometer for recording  
data of cosmic ray intensity obtained by  
neutron monitor 06 p0881 A66-16603  
Survey in satellite era of energetic particle  
radiations, plasmas and magnetic fields in  
space, including solar wind, solar cosmic  
rays, etc 06 p0951 A66-16612  
Measurement of cosmic radiation of  
counter telescope 06 p0882 A66-16894  
Vertical intensity and angular distributions  
of penetrating cosmic ray muons measured  
by scintillators, Geiger counters and neon  
flash tubes, underground in  
India 06 p0877 A66-17039  
Attenuation coefficients deduced in lower  
atmosphere near Rome, using IGY cosmic  
ray neutron monitor 07 p1032 A66-17465  
Physics of cosmic rays - All-Union  
Conference, Moscow, October  
1963 07 p1111 A66-17534  
Strong interactions and cosmic rays,  
discussing Regge poles, one meson  
approximation and multiperipheral model  
theory of elastic and quasi-elastic  
interactions 07 p1112 A66-17535  
Nuclear interaction at high energies,  
discussing active component structure  
ionization calorimeter application, energy  
spectrum of particles, etc 07 p1113 A66-17536  
Cosmic ray particle interaction at hundred  
beV range, discussing parameters of  
inelasticity for collision with  
nucleus 07 p1113 A66-17538  
K meson and hyperon production cross  
sections, discussing primary energy  
dependence and upper limit  
determination 07 p1113 A66-17539  
Nucleon-nucleus collisions at high energies,  
describing statistically independent  
successive interactions of incident particles  
with target nucleus 07 p1113 A66-17540  
Coefficients of inelasticity of interactions  
between cosmic ray particles with iron and  
carbon nuclei 07 p1114 A66-17544  
Fraction of energy transferred to photon-  
electron component during interactions of  
particles with graphite nuclei at energies  
exceeding 100 beV 07 p1114 A66-17545  
Ratio of energy of electron-photon  
component and energy of charged mesons in  
interaction between nucleons and iron  
nuclei 07 p1114 A66-17548  
Interaction characteristics of nuclear-active  
cosmic ray particles with carbon nuclei at  
mountain altitudes 07 p1114 A66-17549  
Nature and momentum spectra of nuclear  
active particle flux at low altitudes,  
determining root mean square  
error 07 p1115 A66-17552  
Origin of high energy pions, muons and  
photons studied from available spectral  
data 07 p1115 A66-17555  
Interaction characteristics calculated for  
Feynman diagram of nucleon-nucleon  
scattering at 300 beV 07 p1115 A66-17556  
Inelastic photonuclear process in forming  
high energy meson jets recorded by nuclear  
emulsion in stratosphere 07 p1116 A66-17557  
Polarization of cosmic ray muons with  
various residual energies, using hodoscopes  
and Wilson chamber 07 p1117 A66-17565  
Cosmic radiation measured by neutron  
monitor in Antarctic during enhanced solar  
activity in September 1963, determining  
flares connected with particles producing  
Forbush effects 07 p1118 A66-17642  
Cosmic rays - International Conference,  
Jaipur, India, December  
1963 07 p1118 A66-17977  
Orientation detector mechanism for high  
altitude cosmic ray research utilizing  
directional East-West symmetry in  
geomagnetic rigidity  
cut-off 07 p1034 A66-17980  
Solar corpuscular stream effect on  
magnetic storms and Forbush  
effect 07 p1121 A66-17985

Cosmic ray variations as affected by space  
electromagnetic  
conditions 07 p1121 A66-17986  
Galactic cosmic ray intensity modulation by  
interplanetary plasma turbulence, noting  
cosmic ray and geomagnetic  
storm 07 p1122 A66-17987  
Solar modulation and geomagnetic effects  
on cosmic rays, noting daily variation and  
rigidity spectrum 07 p1122 A66-17990  
Cosmic ray research and facilities at  
Hobart, Tasmania,  
Australia 07 p1123 A66-17992  
Intensity of cosmic ray alpha particles on  
July 16, 1959 when counting rates of  
neutron monitors were near absolute  
minimum value 07 p1124 A66-17997  
Cosmic ray modulation by interplanetary  
magnetic field indicated by dependence of  
secular, 27-day and diurnal variations on  
solar activity 07 p1124 A66-17999  
Active regions on Sun responsible for  
modulation process evidenced by correlation  
of cosmic radiation intensity variation with  
solar activity features 07 p1125 A66-18002  
Responses of cubical meson telescopes and  
neutron monitors, at equatorial and high  
latitude stations, to anisotropy with  
different assumed spectrum and latitude  
dependence 07 p1125 A66-18005  
Frequency distributions of characteristics  
of daily variation of cosmic ray intensity  
with solar activity from 1958 to  
1962 07 p1125 A66-18006  
Phase shift and amplitude computation for  
cosmic ray diurnal oscillation, using  
autocorrelation analysis  
methods 07 p1126 A66-18007  
Atmospheric diurnal variation investigated,  
using temperature controlled high-counting  
neutron and meson  
monitors 07 p1126 A66-18008  
Fluctuation of ratio of yearly average  
amplitudes of meson-to-neutron diurnal  
variation owing to variability of energy  
dependence of cosmic ray  
anisotropy 07 p1126 A66-18009  
Cosmic ray meson intensity diurnal  
variations measured, using neutron monitor  
and Geiger counter  
telescope 07 p1126 A66-18010  
Presence of genuine sidereal daily cosmic  
ray intensity variation in  
1961 07 p1126 A66-18011  
Correction of cosmic ray meson intensity  
monitor counting rates for atmospheric  
temperature variation 07 p1127 A66-18012  
Periodical and quasi-periodical cosmic ray  
variation according to data of worldwide  
network of stations, using crossed  
telescope 07 p1127 A66-18013  
Diurnal intensity time variation of cosmic  
ray neutrons compared with relative number  
of sunspots observed 07 p1127 A66-18014  
Cosmic ray diurnal variation near  
geomagnetic poles measured over declining  
phase of solar cycle, using neutron monitor  
data 07 p1127 A66-18015  
Cosmic ray threshold rigidities determined  
by trajectory calculations, noting  
disagreements between hemispheric  
data 07 p1128 A66-18017  
Empirical and experimental modulation  
functions for cosmic ray intensity variation,  
showing rigidity dependence of intensity  
changes 07 p1128 A66-18018  
Vertical cut-off rigidities of cosmic rays,  
using sixth degree simulation of  
geomagnetic field 07 p1128 A66-18019  
Galactic cosmic ray modulation by  
interplanetary plasma, deriving by method  
of best fit, direction and energy spectrum  
of anisotropy outside of geomagnetic  
field 07 p1128 A66-18020  
Sea level cosmic ray intensity and  
threshold rigidity around South African  
magnetic anomaly, noting Quenby and Wenk  
measurements 07 p1129 A66-18022  
Forbush effect and region of decreased  
cosmic ray intensity extending from Earth  
to Sun 07 p1129 A66-18024  
Temperature changes in entire atmosphere  
and effect on diurnal variation of meson  
component of cosmic rays 07 p1129 A66-18025  
Asymmetry of cosmic ray variations and  
structure of interplanetary magnetic field,  
based on data recorded at Yakutsk and  
Tiksi 07 p1130 A66-18026



- Ionospheric research from space vehicles, comparing experimental data with theoretical models of D, E and F regions 07 p1029 A66-18089
- Nottingham mu-meson spectrometer with air gap magnet replaced by magnetized iron block 07 p1036 A66-18234
- Momentum spectrum and charge ratio of mu-mesons at sea-level, noting theoretical and experimental data 07 p1131 A66-18235
- Day-to-day changes in energy spectrum of daily variation of cosmic ray intensity at middle latitude and equator for IGY 07 p1131 A66-18236
- Particle detection with electric charges of two-thirds in cosmic radiation 07 p1131 A66-18238
- Differential changes between cosmic ray intensity level inside and outside ecliptic plane by comparison of intensities recorded in polar and nonpolar regions 07 p1131 A66-18240
- Correlation relations between cosmic ray neutron intensity, horizontal magnetic field strength, critical wave frequency and terrestrial currents 08 p1283 A66-18706
- Dynamic frequency spectra of short period variations of cosmic ray intensity calculated on basis of random processes theory 08 p1283 A66-19020
- Diurnal and semidiurnal variation of cosmic ray intensity investigated with aid of selective frequency filters 08 p1283 A66-19021
- Twenty-seven-day variations of geomagnetic disturbance in aurora zone with respect to zero days of cosmic ray intensity 08 p1283 A66-19045
- Low-background gamma-ray spectrometry of induced radioactivity resulting from Bogou meteorite cosmic radiation 08 p1291 A66-19094
- Intensity variation of nucleonic component of atmospheric cosmic radiation, geomagnetic threshold rigidity and calculation of cosmic ray equator 08 p1284 A66-19398
- Interstellar and intergalactic plasma instability effects on energy distribution functions, cosmic ray diffusion and direction and interspace field interaction 08 p1285 A66-19448
- Neutrino detecting equipment located in South African mine, discussing theory of neutrino production 08 p1285 A66-19600
- Solar diurnal and semidiurnal variations in neutron component of cosmic rays obtained from worldwide network from 1959 to 1962 08 p1285 A66-19775
- Sinusoidal hydromagnetic pulsations noting morphological properties, planetary distribution and inverse dependence of amplitude, frequency and duration on solar activities 08 p1220 A66-19784
- Energy transfer mechanism in solar corpuscular flux interaction with terrestrial magnetosphere 08 p1285 A66-19786
- Solar diurnal variation data used to determine parameters of phase-amplitude modulation of periodic cosmic-ray variations 08 p1286 A66-19788
- Momentum spectrum of cosmic ray muons determined as function of zenith angle 08 p1286 A66-19834
- Construction, testing and performance of apparatus consisting of six liquid scintillation counters for underground cosmic ray analysis 08 p1286 A66-19835
- Proton I scientific space station for investigation of ultrahigh energy cosmic ray problems 09 p1463 A66-19903
- Cosmic ray physics - All-Union Conference, Moscow, October 1963 09 p1436 A66-20201
- Cosmic ray origins including galactic rays, RF radiation, metagalactic gamma radiation, etc 09 p1437 A66-20202
- Galactic and metagalactic cosmic gamma- and X-ray intensities 09 p1437 A66-20203
- Mechanisms for cosmic-radiation intensity variations, including cosmic-ray modulation effects, solar cosmic rays and variations of galactic origin 09 p1437 A66-20207
- Secular variation in intensity of cosmic rays in stratosphere and energy spectrum of primary cosmic rays correlated with solar activity 09 p1437 A66-20208
- Forbush decreases in intensity of cosmic rays analyzed from data obtained from stratospheric radiosondes at geomagnetic latitudes 51 and 41 degrees N 09 p1437 A66-20209
- Twenty-seven day modulation of galactic cosmic rays attributed to axisymmetric solar wind of magnetic inhomogeneities 09 p1438 A66-20211
- Anomalies in cosmic ray intensity increase during period of Forbush decrease 09 p1438 A66-20214
- Magnetic storms effect on cosmic rays during periods of maximum and minimum solar activity 09 p1438 A66-20215
- Spectra of solar, diurnal and secular variations, relation to modulation of cosmic rays by interplanetary magnetic field 09 p1438 A66-20216
- Specific angular sensitivity functions for investigating spatial distribution of asymmetrical cosmic ray variation 09 p1438 A66-20217
- Effect of atmospheric temperature changes on diurnal variation of meson component, using temperature coefficient and crossed telescopes methods 09 p1439 A66-20219
- Cosmic ray distribution intensity over celestial sphere determined, detecting anisotropy against background of isotropic variations, using spherical analysis 09 p1439 A66-20220
- Energy dependence of transparency of walls of transition region shell obtained from Forbush effects, in connection with cosmic ray intensity 09 p1439 A66-20221
- Latitude variation of second harmonic of diurnal variation of cosmic rays, considering curvature of particle trajectories in geomagnetic field 09 p1439 A66-20222
- Quantitative relation between strength of ionospheric effects of solar flares and amplitude of increase in cosmic radiation 09 p1439 A66-20223
- Coupling coefficient for different components of cosmic rays based on interaction of primary nucleon with air nuclei 09 p1440 A66-20224
- Cosmic radiation particle detection by nuclear emulsion aboard Sputnik V and classification according ionizing power 09 p1440 A66-20228
- Radiosonde for stratospheric cosmic ray intensity measurement, noting structure, operation and results 09 p1379 A66-20236
- Corpuscular radiation in vicinity of Earth and trapped in geomagnetic field, considering space and solar activity modulation 09 p1441 A66-20284
- Altitude and zenith angle dependences of secondary cosmic ray components in upper atmosphere 09 p1441 A66-20378
- Eight discrete cosmic X-ray sources observed by rocket techniques 09 p1442 A66-20409
- Spectra of generically related cosmic ray species 09 p1443 A66-20688
- Mean solar time from seven years data obtained by two muon telescopes at Hobart, Tasmania 09 p1443 A66-20796
- Quasi-biennial cosmic rays in tropical region estimated from results of meteorological investigation 09 p1443 A66-20860
- Cosmic space physics - All-Union Conference, Moscow, June 1965 09 p1460 A66-20986
- Cosmic rays during flights of Sputniks and Cosmos satellites investigated by analysis of charged particle fluxes obtained by gas discharge counter 10 p1595 A66-21042
- Cerenkov counter measurement of nuclear component of cosmic rays onboard Elektron II satellite as function of solar activity during IQSY 10 p1595 A66-21043
- Upper limits to cosmic ray intensity 10 p1599 A66-21104
- Collision of cosmic rays and intergalactic gas to produce neutral pions which decay into high energy gamma rays 10 p1599 A66-21106
- Transistor portable radioactivity detector utilizing self-quenching Geiger-Muller tube 11 p1703 A66-22268
- Nighttime reflection coefficient of radio wave during ionospherically disturbed period is closely correlated with cosmic-ray and solar phenomena 11 p1696 A66-22379
- Smoothing recorded tracings of cosmic ray detector 11 p1704 A66-22403
- Parameters of dynamic modulation determined from measurements of proton and alpha particle spectra, used in cosmic-ray modulation in interplanetary space 11 p1762 A66-22411
- Chromospheric flares effect on hard component of cosmic rays as function of solar coordinates during quiet and magnetically disturbed days 11 p1762 A66-22412
- Secular variation of atmospheric radiocarbon concentration, noting dependence on geomagnetic field strength 11 p1698 A66-22569
- Flux and energy spectrum of low energy cosmic ray protons, noting rocket measurement results and analogy to solar flare spectrum 11 p1764 A66-23059
- Total counting rate and detected multiplicity spectrum of standard IGY neutron monitor analyzed on basis of neutron production and cosmic radiation components 11 p1765 A66-23144
- Measurement of differential energy spectra of protons, helium nuclei and heavy nuclei by cosmic radiation telescopes mounted on POGO and Pioneer satellites 12 p1877 A66-23684
- Three parameter pulse height analyzer and coincidence system for satellite-borne scintillation telescope study of cosmic radiation 12 p1878 A66-23691
- High resolution pulse height analyzer for satellite and balloon-borne telescope 12 p1878 A66-23692
- Cosmic ray meson monitors with plastic scintillators and near cubical geometry designed for total counting rate of 1,000,000 counts/hr 12 p1879 A66-23709
- Monograph on methods and equipment used by Soviet satellites and space probes to study Earth radiation belts 12 p1938 A66-23802
- Bronzite and hypersthene chondrites, evaluating lunar or asteroidal origin 12 p1948 A66-23903
- Production rates of Cl 36 and Ar 39 in metallic and stone phases of Leedey chondrite 12 p1948 A66-23904
- Cosmic rays, collected papers on international geophysical projects 12 p1939 A66-24159
- Solar wind and geomagnetic storm effects on galactic cosmic ray 11-year variations and energy spectrum, from neutron monitor data 12 p1940 A66-24160
- Cosmic ray variations analysis based on IGY and IGC data, discussing diurnal variations, cosmic ray burst, Forbush effect and existence of interplanetary magnetic field and of solar magnetic traps 12 p1940 A66-24161
- Solar wind as radial flux of electromagnetic inhomogeneities, galactic ray modulation by solar wind and cosmic ray intensity variation with sunspot cycle 12 p1940 A66-24162
- Magnetospheric and upper atmospheric meteorological effects on cosmic ray intensity variation and solar corpuscular streams 12 p1940 A66-24163
- Cosmic ray variations and solar corpuscular stream in interplanetary space during March 1958 magnetic storm 12 p1940 A66-24164
- Forbush, geomagnetic interaction, cosmic ray variation and solar corpuscular flux effects during magnetic storms in period of maximum solar activity 12 p1940 A66-24165
- Variations in cosmic ray neutron component intensity and solar corpuscular flux with H-component of geomagnetic field during magnetic storm 12 p1941 A66-24166
- Variations in cosmic ray intensity recorded at world network of stations during consecutive magnetic storms, noting changes in corpuscular fluxes, interplanetary medium, etc 12 p1941 A66-24167
- Abrupt increase in cosmic ray intensity coinciding with presence of Forbush effects, noting dependence on geographic latitude and cut-off rigidity, obtaining energy spectra 12 p1941 A66-24168
- Magnetic storms during IGY, assuming effect on cosmic ray intensity is associated with influence on galactic cosmic rays of magnetic fields of solar and corpuscular fluxes 12 p1941 A66-24169
- Diurnal and semidiurnal variations in



cosmic-ray hard component and magnetic activity 12 p1942 A66-24176

27-day cosmic ray variations from July 1957 to December 1960 and general characteristic of electromagnetic conditions in interplanetary space 12 p1942 A66-24177

Small cosmic ray bursts effect on geomagnetic activity and nature of high-energy solar cosmic ray propagation in interplanetary space 12 p1942 A66-24179

Integral multiplicity and coupling coefficient estimation of muon-meson component of cosmic rays for case of primary particle impinging at arbitrary zenith angle 12 p1943 A66-24182

Solar-diurnal cosmic-ray variations analyzed, showing that averaging observational data over worldwide network of stations leads to large errors 12 p1943 A66-24183

Operation of scintillation and Cerenkov counters used for recording cosmic radiation, noting design, amplitude properties, collection of scintillating light from phosphor, etc 12 p1882 A66-24185

Short period variations in cosmic ray intensity, using neutron monitors, cubic telescopes, etc, analyzed with superhigh statistical precision 12 p1943 A66-24186

Al-26 and Be-10 radioactivities in cores of Pacific sediments and implications regarding low-energy proton flux in interplanetary space over last 100,000 years 12 p1943 A66-24236

Iron meteorites with low cosmic ray exposure ages examined via analysis of product of argon 39 and 13 p2177 A66-25135

Electron and proton differential velocity spectra observed for low-energy relativistic cosmic rays, noting spectral neutrality of radiation 13 p2174 A66-25570

Cosmic and UV radiation effects on breakdown of DNA and production of tumors in mice 13 p2008 A66-25642

Barometric coefficient of Leeds neutron monitor determined by method of successive differences 13 p2176 A66-26360

Solar wind parameters and geomagnetic activity determined from satellite plasma experiments and observations of magnetopause locations 13 p2075 A66-26368

Heavy ionizing particle path detection by thin dielectric sheets 13 p2084 A66-26561

Pion emission in backward hemisphere in laboratory system of cosmic ray jets 13 p2088 A66-26576

Modification of hot big-bang theory to account for helium abundance in universe and cosmic radiation temperature, noting possible variation of Newtonian gravitational constant 13 p2189 A66-26599

Production spectrum of high energy electrons from high energy cosmic ray pion decay and proton-proton collisions 13 p2176 A66-26762

High energy cosmic ray collisional pion production spectrum and pion energy and angle distributions in CMS and laboratory frames from Landau-Milekhin hydrodynamic model of very high energy nucleon 13 p2176 A66-26763

Cosmic rays and fundamental problems in elementary particle theory 14 p2377 A66-27949

Compression of geomagnetic field effect on cosmic radiation at cut-off rigidities and asymptotic directions of radiation incidence 14 p2377 A66-28070

Crossed counting telescopes used to determine distortions in cosmic ray anisotropy measurement 14 p2377 A66-28071

Forbush decrease in cosmic radiation spectra as function of solar activity 14 p2377 A66-28072

Effect of currents, distributed over envelope surface formed by revolution of magnetic dipole force line, about axis, on cosmic ray cut-off rigidity 14 p2377 A66-28085

Autocorrelation functions of random processes, determining parameters and amplitude of diurnal variations in cosmic ray intensity 14 p2377 A66-28086

Cosmic ray origin and space plasmas 14 p2377 A66-28359

Iron and stony meteorite evolution, cosmic radiation ages and space erosion

model 14 p2390 A66-28409

Cosmic radiation measurements beyond radiation belts as observed by Cosmos XVII 15 p2573 A66-28497

Measuring devices and observational methodology used in determining time variant and cyclic variations in cosmic ray occurrence 15 p2573 A66-28518

Changes in cosmic-ray rigidity spectrum during cosmic ray storms, showing correlation with magnitudes of geomagnetic disturbances 15 p2574 A66-28900

Corrected geomagnetic coordinates of Hakura compared to study of geomagnetic threshold rigidity for cosmic ray particles 15 p2484 A66-28908

Solar system geometric effect in diurnal, annual and semiannual cosmic ray variations 15 p2575 A66-29082

Energy dissipation channels of nuclear and electron components of cosmic rays in Galaxy and Metagalaxy 15 p2576 A66-29131

Biological experiments under flight conditions in Vostok spacecraft, noting reproduction of *Drosophila melanogaster* and effect of weightlessness and cosmic radiation on hereditary structures 15 p2436 A66-29465

Space flight effect on living cells examined by using higher plants as biological dosimeters 15 p2436 A66-29469

Research activities at Chacaltaya Cosmic Physics Laboratory in Bolivia 15 p2476 A66-29514

High energy interactions - International Conference on Cosmic Rays, Jaipur, India, December 1963 15 p2582 A66-29541

U.S.S.R. accelerator experiments in high energy nuclear interaction cross section and inelasticity, primary and secondary cosmic ray particle energies, charged nuclear-active particle energy spectra, momenta measurements, etc 15 p2545 A66-29549

Atmospheric fast cosmic ray neutron flux measurements, using boron fluoride recoil neutron counter 15 p2584 A66-29553

High energy mountain-altitude nuclear interactions produced by pions and nucleons, pion/proton and neutral/charged interacting particle ratios studied, using multiplate cloud chamber with air Cerenkov counter and absorption spectrometer 15 p2584 A66-29554

Interaction of nuclear active particles with atomic nuclei, using ionization chamber at 3260 m above sea level 15 p2584 A66-29558

Extremely collimated nuclear interactions in carbon induced by collisions of charged cosmic ray particles in energy region 20-100 gev 15 p2585 A66-29559

Nuclear interaction characteristics in brass and carbon, noting production by neutral and charged cosmic ray particles, observation methods, energy spectrum, etc 15 p2585 A66-29560

Peripheral inelastic encounters, complex orbital momenta and cosmic ray analyses of interactions, noting hydrodynamical model and Regge pole method 15 p2585 A66-29562

Energy and angular distribution of meson created by 22 gev protons in lithium hydride with respect to secondary cosmic radiation 15 p2585 A66-29563

Secondary cosmic radiation and meson production at high energy, noting particle flux regularities and collision 15 p2586 A66-29564

Atmospheric high-energy cosmic ray cascade, using fire ball and gev-range nucleon isobars in model 15 p2586 A66-29565

Spark emulsion chamber for balloon-borne cosmic radiation measurements 15 p2503 A66-29569

Cosmic rays, muons and neutrinos - International Conference, Jaipur, India, December 1963 15 p2586 A66-29570

Cosmic ray intensities underground and energy spectrum of cosmic ray muons at sea level, tabulating depths, operation time, angular distribution, telescope aperture, etc 15 p2587 A66-29572

Muon momentum spectrum at various zenith angles, noting pion derivation 15 p2588 A66-29577

Momentum spectra of cosmic ray muons measured at large zenith angles with improved Ashton-Wolfendale spectograph, comparing observed and predicted

intensities 15 p2588 A66-29580

Cosmic ray muons polarization at various energies and estimation of asymmetry coefficient ratio 15 p2589 A66-29581

Variation of most probable muon energy loss with momentum, noting density effect and decrease in ionization loss 15 p2589 A66-29586

Spectral energy loss rate of cosmic ray muons measured in plastic scintillator 15 p2589 A66-29587

Cosmic neutrino production and stellar evolution, prospects of observational neutrino astronomy as branch of cosmic ray physics 15 p2589 A66-29589

Cosmic ray measurements at 9000 ft underground where atmospheric muon intensity has attenuated and signal due to neutrino interactions is detectable 15 p2589 A66-29590

Large-scale underground experiment for detecting cosmic ray neutrino-induced interactions 15 p2590 A66-29591

Low energy cosmic neutrino detection with radiochemical methods, noting mass spectrometric and nuclear emulsion methods based on Pontecorvo-Davis reaction 15 p2590 A66-29592

Energy spectra of muons and neutrino production from cosmic gamma rays 15 p2547 A66-29597

Delta-electron generation by muons and fluctuations in soft cosmic ray component, assuming thick absorption layer 15 p2547 A66-29598

Energy spectra of neutrinos from secondary cosmic-ray decay in Earth atmosphere 15 p2590 A66-29646

Three types of cosmic ray measurement in commercial aircraft, using single Geiger-Muller counter 15 p2591 A66-29679

Dutch space research program noting solar and stellar research, cosmic radiation, wind measurement, rocket sounding, etc 15 p2600 A66-29910

Radiation levels on Gemini IV flight including Van Allen belt and South Atlantic Anomaly 15 p2591 A66-29997

Cosmic ray flare effects observed by Pioneer VI spacecraft 15 p2591 A66-30022

Comparison of magnetic and cosmic ray data of Pioneer VI with particle guidance properties of interplanetary magnetic field 15 p2591 A66-30023

Discrete source of cosmic gamma rays above 1 gev in balloon-borne detection 16 p2792 A66-30171

Prediction that above presently measured energy level cosmic ray spectrum will steepen abruptly and finally have cosmologically meaningful termination 16 p2793 A66-30194

Cosmic black body radiation at 2.6 mm wavelength from 2.7 to 3.4 degrees K, noting CN molecules 16 p2793 A66-30199

Cosmic microwave radiation from observations of interstellar CN rotational temperature, rotational excitation by H I region H atoms and excitation by slow electrons and slow protons in H II region 16 p2793 A66-30200

Cosmic ray storms analyzed for changes in effective integral rigidity spectrum of nucleon component, noting time dependency of spectrum exponent 16 p2793 A66-30229

Adiabatic deceleration effect on cosmic ray spectrum, noting particle momentum and energy change, diffusion coefficient independent of energy, etc 16 p2795 A66-30924

True radio-brightness distribution of cosmic radiation source by reducing spatial frequency distortions with passband radio interferometer 16 p2806 A66-31544

27-day cycle in diurnal variation of amplitude of meson component of cosmic radiation based on 20 years observation 16 p2795 A66-31692

Intergalactic matter temperature parameters such as heating by cosmic ray ionization, dissipation of hydrodynamic turbulence, inelastic electron collision with H, He and He-ions 17 p2996 A66-31912

Inverse Compton X-ray and gamma ray flux due to high energy electron interaction with cosmic blackbody radiation at 3.5 degrees K 17 p2992 A66-31914

Interstellar plasma wave damping by



relativistic suprathermal particles, noting magnetosonic and Alfvén waves 17 p2996 A66-31915

Cosmic ray neutron flux as function of altitude measured near Earth surface, using boron trifluoride detectors 17 p2992 A66-31974

Origin and propagation of cosmic radiation, discussing interplanetary magnetic fields, plasmas, Faraday rotation of polarized radiation, Zeeman splitting of hydrogen line, etc 17 p2964 A66-32029

Propagation of cosmic synchrotron radiation by individual and aggregate electrons and effect on propagation and radiation of electromagnetic waves 17 p2992 A66-32062

Cosmic neutrinos, discussing sources and forms of existence 17 p2994 A66-32835

Ionospheric electron generation formula derived, based on analysis of interaction of cosmic radiation on ionosphere 17 p2994 A66-32882

Proton I and II space stations to study cosmic ray particles of high and ultrahigh energies 17 p3004 A66-32957

Cosmic X-ray sources observed through rocket-mounted detectors, noting differences in spectra 17 p2994 A66-32970

Cosmic radio source strength, explaining spectral output from substructures of 3C-273 17 p3007 A66-33084

High altitude cosmic ray measurements by Cerenkov scintillator counter system near solar minimum 17 p2994 A66-33147

Launching balloon measurements of cosmic ray intensity as function of atmospheric depth at cosmic equator 17 p2994 A66-33150

Mass spectrometric measurement of distribution of spallation produced chromium nuclides between alloys in iron meteorite 17 p3007 A66-33282

Cometary tail phenomena interpreted, using plasma dynamics theory coupled with observed solar wind 17 p3011 A66-33390

Solar wind proton, solar flare proton and galactic ray effect on interstellar solids /comet/ 17 p3013 A66-33409

Atmospheric contribution to diurnal variation of cosmic ray meson intensity at Deep River, Canada 17 p2994 A66-33429

Proton energy density, pressure and compressibility of galactic cosmic ray gas 18 p3165 A66-34140

Mariner II data analysis on effect of magnetic field on radiation and high energy particles in interplanetary space and solar plasma 18 p3167 A66-34334

Interstellar and intergalactic plasma instability effects on energy distribution functions, cosmic ray diffusion and direction and interspace field interaction 18 p3169 A66-34477

Cosmic radiation age spectrum of chondrites by calculation based on interplanetary erosion rate, discussing asteroidal origin for meteorites 18 p3232 A66-34528

High energy X-ray spectrum from Crab Nebula at photon energies up to 90 kev 18 p3170 A66-34529

Collimation of cosmic rays by interplanetary magnetic field based on Pioneer VI measurements during flare event 18 p3170 A66-34539

Center-to-center collisions of cosmic radiation nuclei with heavy nuclei of Ag, Br plasma emulsions 18 p3170 A66-34578

HF brightness intensity of cosmic background radiation at 20.7 cm wavelength may be primordial fireball residue of big-bang cosmology 18 p3171 A66-34717

Cosmic rays - International Conference, Imperial College of Science and Technology, London, September 1965, Volume 1 18 p3171 A66-34740

Cosmic radiation, interplanetary magnetic field, solar proton propagation long-term /solar cycle/ modulation of intensity, Forbush effect and daily intensity variation 18 p3175 A66-34741

Cosmic ray modulation by solar wind fields noting transit time, energy loss and time variations 18 p3175 A66-34743

Galactic magnetic field strength and distribution determined from synchrotron emission of relativistic electrons, noting

Faraday rotation of polarized radiation from distant radio sources 18 p3235 A66-34744

Cosmic ray origin, discussing role of plasma effects in galaxies, radiogalaxies, metagalactic space, etc 18 p3175 A66-34747

X-ray and gamma ray astronomy, discussing observational methods, physical processes of generation, radiation intensity, etc 18 p3176 A66-34749

Isotopic changes in materials caused by high energy nuclear active particles and solar wind in interplanetary space and on Earth 18 p3176 A66-34750

Quasi-stellar radio source characteristics, noting methods of identification, emission of high energy particle flux, etc 18 p3176 A66-34751

Energy characteristics of 11-year cosmic ray variations, evaluating electromagnetic conditions in interplanetary space for proton, alpha particle and electron variations in energy 18 p3176 A66-34752

Explorer XVIII satellite measurements of proton energy spectra in region corotating with Sun, noting modulation of galactic cosmic radiation and source of continuous particle accelerations 18 p3177 A66-34754

Composition of cosmic rays of supernova origin, noting limited mixing and enrichment of elements of outer layer with thermonuclear synthesized core substances due to shock acceleration 18 p3177 A66-34755

Generically related cosmic ray spectrum explaining variations in abundance ratios of helium isotopes and light to medium elements in terms of solar and geomagnetic modulation 18 p3178 A66-34758

Dynamical behavior of cosmic ray gases, noting modes of hydromagnetic wave propagation and static equilibrium configurations for thermal interstellar gas and field 18 p3178 A66-34759

Galactic evolution examined, using luminosity and volume emissivity diagrams 18 p3178 A66-34760

Solar and sidereal daily variations of cosmic ray intensity at depth of 60 mwe underground in London 18 p3178 A66-34763

Two-way sidereal anisotropy vs seasonal modulation of solar daily variation 18 p3178 A66-34764

Isolation of sidereal-diurnal variations in cosmic ray intensity 18 p3179 A66-34765

Cosmic ray changes during past three solar cycles observed by balloons, noting hysteresis loop and Zurich sunspot number 18 p3179 A66-34767

Solar wind and energy modulations of cosmic rays 18 p3179 A66-34769

Galactic cosmic ray diffusion into solar system as affected by zonal distribution of solar activity, noting 11-year modulation 18 p3180 A66-34771

Cosmic ray intensity attenuation due to energy loss of particles passing through electric field in solar system 18 p3180 A66-34773

Cosmic ray nucleon and meson component intensity changes during 11-year cycle, noting asymmetry in modulating mechanism dissipation 18 p3181 A66-34776

Rigidity dependence of intensity variation of nucleonic component during solar cycle 18 p3181 A66-34778

Solar diurnal variation of cosmic ray intensity and anisotropy in interplanetary space 18 p3181 A66-34781

Semidiurnal anisotropy of cosmic radiation observed from neutron monitor data treated by numerical filter techniques 18 p3182 A66-34783

Diurnal variation of cosmic radiation in Axford-Parker model of diurnal anisotropy, noting amplitude discrepancy with prediction 18 p3182 A66-34784

Diurnal variations of cosmic ray intensity by correlating phase difference and amplitude ratio of Zugsptize and Norikura neutron monitors 18 p3182 A66-34785

Local time of maximum in diurnal variation of cosmic ray neutron intensity and relative sunspot number 18 p3182 A66-34786

Solar-diurnal and semidiurnal variation in cosmic ray neutron component during last cycle of solar activity from 1957 to 1965 18 p3182 A66-34787

Parameters of solar diurnal variation determined from neutron monitor data from 1957 to 1958 18 p3183 A66-34788

Solar diurnal variation of nucleonic component of cosmic radiation from 1957 to 1962 18 p3183 A66-34789

27-day modulation of solar diurnal variation of cosmic ray neutron component 18 p3183 A66-34790

Earth heliolatitude change and effect on cosmic ray intensity from 1963 to 1964 18 p3183 A66-34791

Spherical harmonic analysis to obtain latitude dependence of diurnal variations and changes with time during Forbush decrease 18 p3183 A66-34792

First spherical harmonic in cosmic ray distribution for different energy intervals 18 p3184 A66-34793

27-day variations of cosmic ray intensity in stratosphere from 1957 to 1963 18 p3184 A66-34794

Cosmic ray rigidity spectra during solar rotations 18 p3184 A66-34795

Twenty Forbush decreases with amplitude greater than 4 percent in neutron intensity 18 p3184 A66-34796

Rigidity dependence of Forbush decreases, using underground meson intensity measurement 18 p3184 A66-34797

Cosmic radiation and solar activity from stratosphere measurements 18 p3184 A66-34798

Cosmic ray meson intensity close to zenith, using telescopes of small solid angle 18 p3185 A66-34802

Cosmic ray anisotropy perpendicular to ecliptic plane 18 p3185 A66-34804

Frequency distribution of sudden changes of cosmic ray intensity in connection with solar activity 18 p3185 A66-34805

Convolution product theory applied to smoothing neutron monitor data of daily variations in cosmic ray intensity 18 p3186 A66-34808

First-order modulation effects of galactic cosmic radiation, considering hysteresis effect and variation of energy spectrum in 11-yr modulation 18 p3186 A66-34811

Cosmic ray electron component intensity measurements by instrument consisting of telescope made of two scintillation counters 18 p3187 A66-34815

Cosmic ray flux variation with height in stratosphere at geomagnetic latitude 47 degrees S 18 p3188 A66-34820

Activated emulsion camera detection of low energy very-heavy multiply-charged scarce cosmic ray nuclei 18 p3190 A66-34835

Balloon-borne nuclear emulsion detection of finite fluxes of low energy cosmic ray heavy nuclei and interstellar cosmic radiation propagation 18 p3191 A66-34838

Seventy-channel scintillation spectrometer high atmospheric measurement of cosmic gamma radiation of extraterrestrial origin 18 p3192 A66-34845

Spark chamber experimental investigation of flux of high energy gamma rays at high altitudes near magnetic equator 18 p3193 A66-34849

Charge ratio of cosmic ray electrons, examining excitation of baryon resonances in high energy collisions with no exchange of isospin 18 p3193 A66-34850

Balloon flight experiment to search for celestial sources of X-rays in energy range 20 to 58 kev 18 p3193 A66-34852

Energy spectrum of cosmic ray diurnal variation determined from IGY neutron monitor data by introducing upper energy cut-off parameter 18 p3195 A66-34864

Daily variations of cosmic ray distribution, examining effect of geomagnetic field, aperture, orientation and geographical position of counters 18 p3195 A66-34865

Coupling coefficients of directed muon component of cosmic rays calculated, noting higher energy displacement with increase of zenith angle 18 p3195 A66-34866

Simultaneous amplitude-phase modulation of periodic cosmic ray variations, examining properties of satellites produced by these variations for case of true waves 18 p3196 A66-34867

Smooth curves of cosmic ray neutron component intensity variations compared with H component of geomagnetic field



during IGY and IGC 18 p3196 A66-34868

Cosmic ray intensities in stratosphere over Antarctica and Murmansk, noting differences not due to low energy primary particles or temperature 18 p3196 A66-34869

Latitude distributions obtained for nucleonic and neutron components of cosmic radiation during flights from South Africa, compared with Northern Hemisphere distributions 18 p3197 A66-34878

Latitude and altitude survey in North America made by road transport carrying neutron monitor, meson telescope, mercury barometer, etc 18 p3198 A66-34879

Effect of geomagnetic cavity field on cosmic ray threshold rigidity, using model of cavity field, finding cavity shape produces amplitude in diurnal variation of cosmic ray intensity 18 p3198 A66-34882

Effect of compression and expansion of magnetosphere on cut-off rigidities and position of impact zones 18 p3198 A66-34884

Low energy fast cosmic ray neutrons, measurements of energy spectrum and primary intensity variations, using organic scintillator in field of photomultiplier tube 18 p3199 A66-34885

Cosmic ray produced lithium and calcium in iron meteorites 18 p3236 A66-34890

Coronal scattering of radiation from solar radio source, considering angular deflections and brightness 18 p3199 A66-35044

Principle source of radiative energy loss in intergalactic medium in spectral region from 2 to 18 angstroms is line emission from ions of elements oxygen, carbon, neon, magnesium and silicon 18 p3237 A66-35046

Cosmic rays - International Conference, Imperial College of Science and Technology, London, September 1965, Volume 2 18 p3200 A66-35089

Nuclear active component of cosmic rays studied with arrangement consisting of ionization calorimeter, Geiger counter hodoscope and two large spark chambers 18 p3215 A66-35156

High energy cosmic ray jets studied in large nuclear emulsion stacks at Krakow 18 p3215 A66-35161

Spectrum of nuclear active component of cosmic rays determined by nuclear calorimeter 18 p3217 A66-35171

Nucleon isobar production in photoemulsion giving rise to large energy transfer to several secondary charged particles 18 p3141 A66-35172

Particle production at superhigh energies based on composite model of particle and resonance 18 p3141 A66-35175

Two-fireball and CKP models of ultrahigh energy interactions 18 p3217 A66-35177

Mu meson charge ratio variation with energy at sea level 18 p3219 A66-35186

Positive excess of cosmic ray muons at sea level, taking into account change of ratio of proton to neutron with atmospheric depth 18 p3219 A66-35187

Positive excess of cosmic ray muons as function of energy from data collected by Nagoya spectrometer at large zenith angle 18 p3219 A66-35189

Data on energy and angular distribution of high energy muons, noting detector and structural bursts 18 p3220 A66-35193

Bursts produced by high energy muons undergoing large energy transfers analyzed for information on muon electromagnetic interactions over region where muon spectrum is known 18 p3220 A66-35195

Cosmic ray intensity measured underground by scintillation counter, noting pulse height conversion into digital form 18 p3222 A66-35206

Telescope design for detection of muons produced by neutrinos installed underground and consisting of plastic scintillators 18 p3222 A66-35212

Muons and neutrinos from energetic celestial objects, discussing charge ratio, rate and equipment used 18 p3224 A66-35226

Cosmic ray threshold rigidities examined, discussing penumbral and threshold perturbation effects produced by superimposing external magnetic fields on dipole model 18 p3096 A66-35227

High resolution magnetic hodoscope performance for charged particle analysis, measuring momentum response spectrum

and experimental error due to instrumental effects 18 p3115 A66-35228

Pulse shape discrimination technique using scintillation counter, distinguishing events of nuclear disintegration from those due to minimum ionizing particles 18 p3115 A66-35229

Quark detection in cosmic rays noting flux dependence on mass, energy loss through ionization, production spectrum threshold, etc 18 p3225 A66-35231

Flux of elementary triplets of unitary symmetry in cosmic radiation, noting production via nucleon-nucleon collision, particle interaction, etc 18 p3225 A66-35232

Secular variations of cosmic ray intensity governed by 11-year solar cycle 19 p3451 A66-35252

Cosmic radiation intensity fluctuation in stratosphere, noting absence of explanation for anomaly 19 p3451 A66-35261

Modified RK-1 radiosonde circuit for stratospheric cosmic ray measurements 19 p3352 A66-35274

Delta electrons formed in interstellar hydrogen-galactic ray collision 19 p3452 A66-35283

Red shift observed in quasi-stellar radio sources due to high gravitational potential 19 p3459 A66-35587

Biological hazard of radiation doses to which passengers of high-flying Concorde aircraft may be subjected, considering use of in-flight warning meter 19 p3452 A66-35796

Balloon measurements of cosmic ray hydrogen and helium nuclei at locations with nominal geomagnetic threshold rigidities 19 p3452 A66-35926

Maximum temperature of any substance in equilibrium with thermal radiation, considering properties of hot matter at very high densities, including gravitational interaction of photons 19 p3463 A66-36069

Sidereal variation of cosmic muon component at depth of 440 meters, attributing modulation to phenomenon linked to solar period 19 p3453 A66-36257

Geomagnetic cut-off rigidities determined for cosmic ray particles arriving at top of atmosphere over Hyderabad as function of zenith and azimuthal angles 19 p3454 A66-36642

Possible presence of relic quarks in cosmic rays 19 p3454 A66-36723

Low energy cosmic ray modulation relationship to observed interplanetary magnetic field irregularities in terms of diffusion, using space probes 19 p3454 A66-36765

Satellite instrumentation, discussing data handling systems, cosmic ray detection, signal and information processing, etc 20 p3556 A66-36963

Cosmic ray origination from extragalactic radio sources 20 p3630 A66-37252

Diurnal cosmic-ray anisotropy in studying temporal independence of small scale irregularities in interplanetary magnetic field 20 p3630 A66-37302

Intensity and spectra of cosmic ray electrons and positrons in determining mean confinement time, density and solar modulation 20 p3630 A66-37303

Astronomical model for diffusion of galactic cosmic rays in solar system, based on zonal character of solar activity 20 p3630 A66-37329

Determination of constancy of cosmic radiation and of terrestrial and cosmic ages of ferrous meteorites by radioactivity of Al 26 and Be 10 20 p3651 A66-37411

Anomalous high count of gamma rays from direction of constellation Cygnus associated with energy spectrum differing from spectrum of secondary gamma rays generated by cosmic rays 20 p3631 A66-37600

Sidereal diurnal variation of high-energy cosmic radiation, noting parameters of anisotropy coefficient, cosmic ray source distribution and air shower measurements 20 p3631 A66-37851

Gamma-spectroscopy determination of special reaction products of cosmic radiation in meteorites 20 p3656 A66-38060

Forbush decreases using meson and nucleon component records in study of sudden commencements during periods

between cosmic ray storms 20 p3632 A66-38070

Cosmic ray storms, difference in Forbush decrease recovery in nucleon and meson component 20 p3632 A66-38072

Direction response of meson telescopes with vertical and inclined axes used in recording of cosmic ray variations 20 p3632 A66-38073

Cosmic ray meson component distribution with time plots of particle flux revealed characteristic disturbances accompanying sudden commencements of geomagnetic storms associated with Forbush decreases 20 p3632 A66-38074

Magnetospheric models, discussing role of fast magnetospheric merging in connection with charged particle acceleration and magnetospheric configuration 20 p3641 A66-38330

Cosmic ray intensity recorded with scintillation counter corrected without stabilizing efficiency of counter by recording changes, using pulse height spectrum 20 p3562 A66-38433

Relativistic electron production by cosmic radiation in lower ionosphere 20 p3645 A66-38437

Sidereal anisotropy indicated for charged galactic cosmic radiation obtained by celestial scanning, using narrow angle muon telescope 21 p3808 A66-38466

Solar diurnal and semidiurnal variations in neutron component of cosmic rays obtained from worldwide network from 1959 to 1962 21 p3809 A66-38771

Sinusoidal hydromagnetic pulsations noting morphological properties, planetary distribution and inverse dependence of amplitude, frequency and duration on solar activities 21 p3733 A66-38780

Energy transfer mechanism in solar corpuscular flux interaction with terrestrial magnetosphere 21 p3809 A66-38782

Solar diurnal variation data used to determine parameters of phase-amplitude modulation of periodic cosmic-ray variations 21 p3809 A66-38784

Cosmic X-ray source near direction of north galactic pole, noting empirical results from balloon observations 21 p3810 A66-39267

Interferometric observation of cosmic emission at OH frequency, noting emission source dimensions 21 p3814 A66-39268

Cosmic radiation and space flight effects on lysogenic bacteria and human cells in culture 21 p3700 A66-39315

Cosmic-ray neutron production and flux distribution on sea level and mountain altitude measured with boron fluoride counter for Maxwellian energy distribution with shifted neutron temperature 22 p3972 A66-39680

Flare stars as sources of cosmic X-rays, spectra contain 4686-angstrom line of doubly ionized helium indicating that atmospheres contain either ionizing radiation or electrons 22 p3972 A66-39707

Cosmic microwave background radiation, considering statistically homogeneous and isotropic but nonuniform distribution of matter 22 p3978 A66-40009

Cosmic ray modulations in solar system and in interstellar space, presenting graphs of rigidity spectra of protons and helium 22 p3973 A66-40524

Dependence of diurnal cosmic ray variations on angle which is proportional to shortest distance from Earth to axis of corpuscular stream 22 p3974 A66-40757

Pulse amplitude measurement from scintillation cosmic-ray counter 22 p3920 A66-40771

Geomagnetic activity and Earth heliolatitude effect on diurnal variation of cosmic radiation, based on IGY neutron component observations 22 p3974 A66-40775

Statistical and instrumental fluctuations effect on distribution of first-harmonic amplitude and phase in harmonic analysis of cosmic radiation variation 22 p3975 A66-40776

Galactic radio sources noting disk model brightness distribution, relativistic particle energies, continuous particle acceleration and ratio between proton and electrical component of cosmic radiation 22 p3985 A66-40952

Star collapse observation by detection of



high energy neutrino fluxes produced by  
catastrophic star contraction 22 p3975 A66-40953

Penetrating radiation measurement on  
Moon surface obtained by Luna IX  
spacecraft 23 p4128 A66-41410

Transient anisotropic cosmic ray increase  
during recovery phase of Forbush decrease  
due to reflection from receding blast wave  
and co-rotating shock wave formed during  
explosive heating of solar  
corona 23 p4123 A66-41687

Shield of volatile matter acting as cosmic  
radiation barrier as possible explanation of  
contraction between radiation ages of stony  
and iron meteorites 23 p4065 A66-41832

Phosphorus 32 and 33 produced by  
interactions of secondary neutrons from  
cosmic rays with argon in atmosphere  
determined radiochemically from rainwater  
samples 23 p4124 A66-41845

Balloon-borne spark chamber observations  
of cosmic gamma rays from 30 to 500  
mev 23 p4124 A66-42066

Radiosonde for high altitude balloon  
soundings using large polyethylene balloons  
to carry payloads of electronics, cosmic ray  
and nuclei counters 23 p4087 A66-42084

Large air Cerenkov counter construction  
and performance characteristics for use in  
distinguishing protons and pions in cosmic  
radiation in 10-45 gev energy  
region 23 p4072 A66-42086

X-rays and Auger electron emission by  
krypton 81 measured, using proportional  
counter 24 p4262 A66-42430

Anisotropy of cosmic rays in N-S direction  
determined by comparison of intensity  
variations observed in Arctic and Antarctic  
regions 24 p4263 A66-42464

Cosmic ray nucleon interaction with high  
energies, estimating transition probability  
and interaction cross section of baryon in  
passive state 24 p4263 A66-42519

Cosmic ray ionization intensity  
measurement using special ion  
chamber 24 p4264 A66-42603

Pressurized Ar-filled ionization chamber  
response to charged particles in cosmic  
radiation determined as function of  
atmospheric depth 24 p4264 A66-42604

Interplanetary exploration space mission  
objectives, discussing magnetic fields,  
energetic particles, cosmic radiation,  
etc 24 p4264 A66-42660

Source spectra and composition of galactic  
cosmic rays implied by analysis of  
interstellar and interplanetary travel, noting  
solar modulation 24 p4265 A66-42716

Cosmic-ray electron flux above 4.7 BV  
measured, using lead-plate spark chamber,  
determining upper limit to primary  
flux 24 p4265 A66-42717

Solar activity variations, C 14 production  
by cosmic rays and reevaluation of C 14  
dating 24 p4265 A66-42738

Cosmic ray physics - All-Union Conference,  
Apatity, U.S.S.R., August  
1964 24 p4265 A66-42901

Satellite possibilities for measuring cosmic  
radiation in 1000 bev energy range and  
comparison of indirect and direct  
measurements 24 p4267 A66-42909

Cross section for lambda, kappa and sigma  
particle production in cosmic ray interaction  
with C, Cu and Pb nuclei dependent on  
atomic weight of target  
material 24 p4268 A66-42911

Density fluctuations of penetrating  
particles in extensive air showers at various  
distances from shower  
axis 24 p4268 A66-42916

Ratio of energy flux in nuclear active  
component to energy flux in electron  
photon component in extensive air showers  
with given numbers of  
particles 24 p4269 A66-42918

Resonance of antineutrino-electron  
interaction cross section, calculating  
electron density and velocity distribution via  
Ritz method 24 p4270 A66-42932

True and measured energy values of  
cosmic ray spectra, discussing relations and  
application of results 24 p4271 A66-42934

Polarization measurements of cosmic ray  
muons by detection of positrons from muon-  
to-positron decay 24 p4271 A66-42937

Neutron spatial asymmetry measured from

reaction of cosmic ray muons on nuclei with  
different spins 24 p4271 A66-42940

RK-1-F radiosonde for stratosphere  
measurements of X-ray photon energy  
spectrum, charged particle density and X-  
ray photon density 24 p4213 A66-42941

Multilayer wide gap spark chambers and  
application to cosmic ray  
physics 24 p4213 A66-42942

High accuracy directional recording of  
cosmic ray flux components, using counter  
telescope 24 p4213 A66-42943

Cosmic ray electron sign ratio and absolute  
flux measured by balloon-borne  
equipment 24 p4272 A66-43041

Energy spectrum of cosmic rays near  
upper limit and effect of photon-gas  
temperature 24 p4272 A66-43056

Book on space biology and medicine  
covering interplanetary trajectories,  
biological effects of prolonged and impact  
accelerations, weightlessness and cosmic  
radiation 24 p4165 A66-43130

Anisotropy of Forbush effect in  
ascertaining structure and intensity of  
interplanetary magnetic  
field 24 p4272 A66-43159

Anomalous circular polarization of hydroxyl  
radical 18-cm radiation from cosmic  
sources 24 p4272 A66-43188

Spark chamber system designed to detect  
gamma rays in cosmic radiation on high  
altitude balloon flights 24 p4215 A66-43212

**COSMIC RADIO WAVE**

Cosmic radio emission at frequencies of  
210 and 2200 kc at distances up to 8 earth  
radii measured by Zond-2 automatic  
interplanetary station 02 p0283 A66-11661

Optimum wavelength and spectral  
bandwidth for measuring polarization of  
distributed cosmic RF  
radiation 02 p0191 A66-11837

Cosmic radio-noise intensities below 5 mc  
measured by rocket  
probe 08 p1287 A66-18775

Depolarization of cosmic radio emission  
due to dispersion of Faraday rotation of  
plane of polarization of radio  
waves 09 p1441 A66-20334

Brightness distribution of cosmic radio  
noise at 4.7 mc/s 09 p1456 A66-20410

Radio emission from CTA-21 and CTA-102  
sources in cm wavelength range at  
Pulkovo 12 p1947 A66-23890

Postdetector correlation interferometry of  
size of noise burst at decimeter  
wavelengths from Jupiter 13 p2182 A66-25552

Cosmic radio emission attenuation in  
ionosphere measurements including  
characteristic period and seasonal absorption  
measurements 13 p2186 A66-26050

Auroral absorption of cosmic radio  
radiation recorded by shipboard station  
drifting in North Geographic Pole region in  
winter 1963-64 15 p2487 A66-29099

Cosmic radio wave absorption dependence  
on frequency and number of electron-ion  
collisions during atmospheric magnetic  
storms 19 p3344 A66-35267

Linear polarization of continuum emission  
from galaxy and discrete sources, detection  
in radio astronomy, noting relevant  
synchrotron theories 21 p3815 A66-39488

Cosmic radio wave, whistler and sigma  
transmitted radio wave interactions with  
ionospheric magnetoplasma in collision-  
dominated, photoequilibrium and  
photoionization-dominated  
regions 22 p3916 A66-40873

**COSMIC RAY**

**S HEAVY COSMIC RAY PRIMARY**

**S SOLAR COSMIC RAY**

**COSMIC RAY ALBEDO**

Geomagnetically trapped protons,  
examining possibility that they may be  
caused by cosmic ray albedo  
neutrons 03 p0421 A66-12868

Proton injection into radiation belts for  
large B-L space regions by cosmic ray and  
solar proton albedo neutron decay  
injection 11 p1764 A66-23130

Injection of protons into inner radiation  
belt caused by decay of fast cosmic ray  
albedo neutrons and superimposition of low-  
energy protons of unknown  
origin 20 p3639 A66-38318

**COSMIC RAY PROPAGATION**

Cosmic ray telescope /CRT/ carried on

Mariner IV Mars probe to measure flux and  
energy of protons and alpha particles in  
interplanetary space and near  
Mars 01 p0072 A66-11112

Diurnal solar variation in cosmic ray meson  
intensity recorded in southerly and  
northerly directions at high  
altitudes 04 p0574 A66-13840

Low energy spectrum of cosmic rays  
corrected for solar modulation and diffusive  
passage through interstellar  
matter 04 p0574 A66-14014

Secondary protons from interstellar cosmic-  
ray collisions, noting solar modulation  
effects on detection 05 p0747 A66-14796

Cosmic ray electromagnetic acceleration  
mechanism, calculating motion of charged  
relativistic particles in applied  
fields 05 p0753 A66-15388

Planetary distribution and interpretation of  
abrupt increases in cosmic ray intensity  
observed during periods of maximum solar  
activity but not related to visible solar  
phenomena 05 p0755 A66-15404

Solar cosmic ray propagation, discussing  
intensity time dependence in terms of  
isotropic diffusion of solar  
particles 06 p0947 A66-16571

Cosmic ray diffusion, discussing existence  
and influence of radial magnetic  
field 06 p0947 A66-16574

Contribution of spallation and ionization  
loss to operator that modulates cosmic ray  
nuclei with Z greater than or equal to 2  
during propagation 07 p1124 A66-17998

Variation spectrum stability of Forbush  
decrease and small cosmic ray flare during  
intensity recovery, noting electric field  
effect, calculation methods,  
etc 07 p1129 A66-18023

Diffusion model study of solar cosmic ray  
propagation during burst of September 28,  
1961 08 p1283 A66-19019

Propagation mechanisms of solar cosmic  
radiation in interplanetary space other than  
classical diffusion 09 p1438 A66-20212

Diffusion and regular model of motion of  
cosmic rays, noting dependence of  
applicability to cosmic ray fluxes on  
chemical composition 09 p1443 A66-20598

Lower limit of age of cosmic ray nuclei,  
flux ratio of Be nuclei to B nuclei and  
intergalactic cosmic ray  
propagation 12 p1938 A66-24092

Satellite data indicates correlations  
between cosmic ray variations and radiation  
intensity of radiation belts and related  
phenomena 12 p1941 A66-24170

Relation between Forbush decreases and  
magnetic storms, examining spatial  
distribution of predecrease moments relative  
to sudden  
commencements 12 p1941 A66-24171

Threadlike equatorial current ring and  
effect on geomagnetic cut-off rigidity of  
directed cosmic radiation 12 p1941 A66-24172

Effect of equatorial current ring  
distributed over globe on geomagnetic cut-  
off rigidity of cosmic  
rays 12 p1941 A66-24173

Stellar-diurnal variations in cosmic ray  
intensity, recording vertically falling  
particles with telescope and cross  
telescope 12 p1942 A66-24175

Effect of higher harmonics of geomagnetic  
field on cosmic ray trajectories, noting  
reception cones of Soviet  
stations 12 p1943 A66-24268

Quantum mechanics and gravitational  
effect on origin of cosmic particles,  
discussing Schrodinger wave equation,  
electric potential and alpha  
decay 12 p1944 A66-24465

Sea level energy spectrum analysis of high  
energy cosmic ray muons generated by pi-  
mu decay 15 p2589 A66-29588

Galactic acceleration and solar modulation  
of cosmic rays examined via energy  
spectrum of galactic electrons, estimating  
Fermi acceleration, low energy electron  
flux, etc 18 p3177 A66-34756

Cosmic ray friction in limiting solar wind  
cavity 18 p3180 A66-34772

Long-term modulation of cosmic ray  
intensity in interplanetary  
medium 18 p3180 A66-34774

Cosmic ray anisotropy induced by solar  
wind and magnetic field



- irregularities 18 p3181 A66-34779
- Anisotropy of cosmic ray with gradient and curvature drifts in spiral interplanetary magnetic field 18 p3181 A66-34780
- Galactic cosmic ray anisotropy behavior obtained from observations of daily variation of cosmic ray intensity 18 p3182 A66-34782
- Solar particles generated during small chromospheric flares 18 p3184 A66-34799
- Solar cosmic ray disturbances in stratosphere measured by balloon-borne radiosondes 18 p3185 A66-34800
- Degree of agreement between cosmic ray cut-offs derived from McIlwain parameter and those from numerical integration of motion equations 18 p3198 A66-34880
- Effects of deformed magnetic field on trajectories and asymptotic directions of arrival of medium energy cosmic rays at various stations, using spherical harmonics 18 p3198 A66-34883
- Cosmic ray isotropy mechanism, examining plasma beam instability and cosmic ray scattering at plasma turbulent pulsations 20 p3629 A66-37032
- Diffusion and regular model of motion of cosmic rays, noting dependence of applicability to cosmic ray fluxes on chemical composition 20 p3633 A66-38132
- ### COSMIC RAY SHOWER
- Penetrating particle detector sensitive to muons of energy greater than 700 mev and nuclear active particles of energy greater than 15 gev used to monitor extensive air shower 01 p0132 A66-10330
- Spark spectrometer for measurement of high energy cosmic ray shower particles 01 p0067 A66-10454
- Large polystyrene scintillator for cosmic shower density measurement 01 p0071 A66-11038
- High energy proton from local radio sources, using telescopic system for Cerenkov effect detection of broad atmospheric showers 05 p0753 A66-15389
- Spectrum of primary cosmic radiation determined for ultrahigh energies, based on international data on electron and meson air showers 05 p0753 A66-15390
- Primary cosmic rays of superhigh energy using extensive air shower data, noting Geiger-Muller counters, scintillation counters and muon detector 05 p0753 A66-15391
- Extensive atmospheric showers as means of gaining insight into energy spectrum and composition of primary cosmic radiation 05 p0755 A66-15405
- Atmospheric showers and high energy nuclear-active particles 05 p0756 A66-15410
- Extensive air showers of cosmic radiation, noting flux and energy distribution 06 p0947 A66-16576
- Cosmic radiation measurements in extensive air showers, recording high energy muon fluxes 06 p0947 A66-16577
- Atmospheric density effects on frequency of extensive air showers 06 p0948 A66-16578
- Extensive air showers and intensity of cosmic rays of moderate energy 06 p0949 A66-16586
- Spark chamber with air filler for cosmic ray detection 06 p0880 A66-16598
- Jet characteristics considered from viewpoint of formation of shower particles resulting from intermediate pi-pi interaction 07 p1113 A66-17542
- Energy spectra for nuclear-active particles and particle distribution in air showers indicate that pionization plays minor role relative to high energy cosmic rays 07 p1114 A66-17546
- Neutral pi-meson production in processes involved in formation of large ionization bursts by high-energy nuclear-active particles 07 p1114 A66-17547
- Energy distribution of particles produced in elementary interaction expressed in terms of shower characteristics derived from cascade theory 07 p1116 A66-17562
- Fluctuations in number of particles in electromagnetic cascade and effect on spectrum of ionization bursts produced by mu mesons 07 p1117 A66-17568
- Muon detection and energy determination in multilayer system of ionization chambers and probability of finding muon in n-electron shower at depth t 07 p1117 A66-17569
- Ultrahigh-energy primary cosmic ray particle interactions cause electron photon cascades and muon emission 07 p1117 A66-17570
- Electron-photon, mu-meson and nuclear-active components of extensive air showers 07 p1117 A66-17571
- Mu-meson flux irregularities, lateral distribution and average characteristics in extensive air showers at 200 mwe depths 07 p1118 A66-17572
- Extensive air shower high energy gamma rays in upper third of atmosphere 07 p1118 A66-17573
- Energy and density spectra of X-ray photons in extensive air showers and in stratosphere 07 p1118 A66-17574
- Mean free path for nucleon-light atom interaction changed from 75 to 90 g/sq cm affecting air shower characteristics 07 p1118 A66-17575
- Fluctuation problem in electromagnetic cascade theory analyzed, using invariant imbedding method 07 p1083 A66-17973
- Dynamical properties of solar wind and solar corona atmosphere with extended temperature bound strongly by gravity 07 p1132 A66-18263
- Model of cosmic ray shower, measuring time-integrated energy flux in radiation field 08 p1283 A66-18619
- Geomagnetic sudden-commencement storms effect on electron concentration in F-2 layer above Europe 08 p1215 A66-19082
- Earth troposphere affected by solar corpuscular fluxes, cosmic rays, atmospheric radiation, chromospheric flares and intensified radio wave absorption 08 p1285 A66-19452
- Probability of high-energy cosmic ray muon undergoing electromagnetic interaction in lead with energy transfer at various ranges 08 p1286 A66-19836
- Monte Carlo method analysis of electron photon cascade 09 p1436 A66-20134
- Primary ultrahigh energy cosmic radiation composition analyzed, using Cerenkov flash 09 p1437 A66-20205
- Ultrahigh energy primary cosmic ray energy spectrum calculated from EAS particle-number spectrum 09 p1437 A66-20206
- Geometric program for processing penetrating cosmic ray shower data consisting of individual track processing and initial point location 09 p1441 A66-20234
- Improvement of Moscow State University installation for detailed investigation of extensive air showers and high energy muons 09 p1379 A66-20237
- Sidereal component of diurnal variation of cosmic ray intensity 09 p1442 A66-20461
- Solar cosmic ray generation, interplanetary proton diffusion and stratospheric showers 10 p1595 A66-21045
- Four momentum transfer in high energy jet showers and resultant number of multifireballs 11 p1763 A66-22701
- Two-center model evaluation of four momentum transfer in high energy jet showers, noting pion or boson exchange 11 p1763 A66-22702
- Kinematic analysis of multiple pion production in high energy jet showers under asymmetric angular distribution 11 p1763 A66-22703
- Monte Carlo method test of new formulae of pion emission in high energy jet showers 11 p1763 A66-22704
- High energy cosmic ray jet showers noting energy, angular momentum, collision inelasticity, secondary meson distribution, etc 11 p1763 A66-22705
- High energy jet showers examined to obtain four momentum transfers and transverse momentum of recoil protons 11 p1763 A66-22706
- Large polystyrene scintillator for cosmic shower density measurement 11 p1708 A66-23284
- Anisotropy of weak cosmic ray bursts studied by examining diurnal variations for days with increased solar flare activity 12 p1942 A66-24178
- Scintillation counter for extensive air showers, noting time-analysis channels for determining pulse delays, monitoring unit, unit calibrating amplitude channels, etc 12 p1881 A66-24184
- Mathematical construction of extensive air shower based on hypotheses for nuclear phenomena, noting proton-proton interaction, pion generation, etc 13 p2174 A66-25454
- Separation of radio emission of extensive air showers /EAS/ polarized in East-West direction from usual Cerenkov radiation 13 p2175 A66-26023
- High energy solar cosmic ray spectrum during solar flare of February 23, 1956 15 p2575 A66-29080
- Extensive air showers - International Conference on Cosmic Rays, Jaipur, India, December 1963 15 p2577 A66-29513
- Extensive air shower generation by high energy primary rays over Bolivia studied by methods of fast timing and density sampling 15 p2577 A66-29515
- Extensive air shower studies in Australia 15 p2578 A66-29516
- Energy spectrum of high energy cosmic rays from EAS observations 15 p2578 A66-29517
- Energy spectrum and arrival directions of high energy primary cosmic rays 15 p2578 A66-29518
- Extensive air showers core structure and muon distribution 15 p2578 A66-29519
- N and muon number and lateral distribution in various air showers, noting EAS array 15 p2578 A66-29520
- Air showers size, lateral distribution and arrival direction at 5,200 m altitude 15 p2578 A66-29521
- Experimental data concerning electron, photon and muon components of extensive air showers, noting scintillation counters, Geiger-Muller counters, muon detectors, etc 15 p2579 A66-29522
- Hodoscope recordings of extensive air showers with abnormally low content of penetrating particles 15 p2579 A66-29523
- Distribution of arrival directions of muon-rich air showers, using equatorial and galactic coordinate systems 15 p2579 A66-29524
- Cosmic ray anisotropy and gamma rays in Orion analyzed, using Geiger counter and Cerenkov telescope 15 p2579 A66-29525
- High energy photons from radio sources, registering EAS with Cerenkov telescope 15 p2579 A66-29526
- Core structure and properties of extensive air showers, stressing lateral density structure of charged particles and energy of nuclear active component 15 p2579 A66-29527
- Extensive air showers at various atmospheric depths analyzed, using hodoscope counters and ionization chambers, noting differential spectra of densities 15 p2580 A66-29528
- Measurement of total number of nuclear active particles in showers with various particle numbers at 3330 m above sea level, determining size spectrum of EAS 15 p2580 A66-29529
- Structure of air showers, considering muon components and distribution of arrival directions of muon-rich EAS 15 p2580 A66-29530
- Anisotropy of arrival directions of extensive air showers /EAS/ with one or more high energy nuclear active particles 15 p2580 A66-29531
- Arrival directions of large EAS falling in 10 to 80 degree band of north declination, noting angle, azimuth and sidereal time 15 p2580 A66-29532
- Multiple muon events at sea level and association with air showers detected, using Geiger and scintillation counters 15 p2580 A66-29533
- Density spectrum of extensive air showers at very large densities from cloud chamber study 15 p2580 A66-29534
- Muon distribution and irregularities in extensive air showers, noting detector triggering 15 p2581 A66-29535
- Integral number spectrum and absorption characteristics of muons in extensive air showers 15 p2581 A66-29536
- Density fluctuation of muons in extensive air showers, obtaining minimum separation of adjacent particles 15 p2581 A66-29537
- Primary proton-air nuclei interactions leading to EAS containing very few muons, noting energy transfer fluctuation and



isobar production 15 p2581 A66-29538  
 Nucleon-initiated air shower fluctuations and random variations in FA approximation theory 15 p2581 A66-29539  
 Two large air shower studies of spectrum and isotropy of primary particles 15 p2582 A66-29540  
 Experimental data analysis of cosmic ray showers, secondary particle production by nucleon-nucleon collision at high energy, momentum distribution in pions and primary energy-inelasticity relation 15 p2583 A66-29547  
 Young air electron-photon showers at 3200 m altitude, noting average nucleon energy and inelasticity coefficient 15 p2583 A66-29552  
 Cosmic ray showers, discussing high energy interactions of nuclear active particles, intensity and energy spectra of gamma rays and muons, young air showers, ionization bursts, etc 15 p2584 A66-29555  
 Cascade theory of cosmic ray showers 15 p2586 A66-29567  
 Cosmic ray measurements, muon production from decay of charged pions and kaons, muon polarization, momentum spectra, atmospheric gamma cascades and derivation of kaon/pion ratio 15 p2587 A66-29573  
 Production rates of muons in extensive air showers determined from spatial and energy distributions 16 p2795 A66-31694  
 Muon interactions in scintillator stack analyzed for average shower development, noting agreement with theories 18 p3228 A66-33917  
 Earth troposphere affected by solar corpuscular fluxes, cosmic rays, atmospheric radiation, chromospheric flares and intensified radio wave absorption 18 p3169 A66-34481  
 Sidereal time variation of cosmic rays explained by diffusion in galactic arm for coilnear magnetic field and proximity of solar system 18 p3178 A66-34762  
 Flux limits for high energy gamma rays from quasars and other possible cosmic ray sources 18 p3186 A66-34813  
 Threshold rigidities for vertical incident cosmic ray particles derived, using trajectory computations by higher-order simulation of geomagnetic field 18 p3198 A66-34881  
 Extensive air shower research aimed at study of composition of primary cosmic rays and component properties 18 p3204 A66-35090  
 Underground scintillator stacks used to study coincidence events caused by muon extensive air showers, noting muon shower energy and grouping 18 p3204 A66-35092  
 Central part and core structure of muon extensive air shower studied by large area underground hodoscope 18 p3204 A66-35093  
 Absolute number of ultrahigh energy muons in extensive air showers estimated by using large air shower array on ground and muon detectors far below ground 18 p3205 A66-35094  
 Anisotropy of muon-rich extensive air showers examined by observation, using large area air Cerenkov detector at 60 degrees zenith angle 18 p3205 A66-35095  
 Mu-triggered extensive air showers are rich in muons and have less component energy flow than electron triggered showers 18 p3205 A66-35096  
 Decrease in distribution of arrival directions of muon-rich air showers between 15 h and 21 h in right ascension confirmed by analysis of EAS 18 p3205 A66-35097  
 Muon-poor EAS determined from 80,000 EAS recordings, representing distribution of recorded muon multiplicities over large intervals by Polya 18 p3205 A66-35098  
 Energy flow variation of high energy nuclear active particles in EAS measured by scintillation detectors in Bolivia 18 p3205 A66-35099  
 Electron-photon and nuclear active components energy of young air showers measured by ionization calorimeter, determining inelasticity coefficient 18 p3206 A66-35100  
 Ionization calorimetry of energy spectrum of leading particles in cores of EAS

compared with data from model 18 p3206 A66-35101  
 Three-dimensional Monte Carlo simulation of nuclear cascade of extensive air showers, examining nuclear particle spatial and energy distribution 18 p3206 A66-35102  
 Stationary aspects of cosmic ray propagation through atmosphere explained by model calculating high energy nuclear active and muonic components of extensive air showers, presenting energy spectra 18 p3206 A66-35103  
 Comparison of total number of nuclear active particles in cosmic ray shower measured at very high altitudes, examining discontinuities in dependence of number on shower size 18 p3206 A66-35104  
 Scintillation counter observation of EAS core structure and high energy interactions 18 p3207 A66-35106  
 Electromagnetic interactions and collisions of particles in cores of EAS studied, using GM counters, plastic scintillators and Wilson cloud chambers 18 p3207 A66-35107  
 EAS core fine structure observations using spark chamber compared with response of plastic scintillation counter 18 p3207 A66-35108  
 Neon hodoscope study of energy and production heights of high energy EAS electron-photon cascades, comparing results to nuclear emulsion study findings 18 p3207 A66-35109  
 Transition region of pulse spectrum from EAS particle density recordings by Cerenkov and scintillation detectors 18 p3207 A66-35110  
 High energy nuclear active particles in EAS discussing lateral and zenith angle distribution energy spectrum, anisotropy, etc 18 p3207 A66-35111  
 Response to EAS electron-photon cascade of plastic scintillator, cloud chamber and Geiger counter tray 18 p3208 A66-35112  
 Cerenkov and scintillation counters responses to electron-photon EAS 18 p3208 A66-35113  
 EAS mu component fluctuations in density distribution and reception spectrum recorded, using hodograph detectors 18 p3208 A66-35116  
 EAS RF emission detection, discussing enhanced Cerenkov radiation, mutual coherence effects, diffraction, Fresnel zones, Coulomb-field bremsstrahlung, etc 18 p3208 A66-35117  
 Jodrell Bank experiment testing Askarian hypothesis on radio pulses coincident with EAS under mutual coherence effects and checking coherent condition, internal reflection, shower energy, threshold and polarization 18 p3209 A66-35118  
 Air shower detection with radio receiving system, broadband band helical antenna and Cerenkov particle detector 18 p3115 A66-35119  
 Primary gamma ray production, arrival directions, particle collisions and distribution of EAS penetrating particles in intergalactic space 18 p3209 A66-35120  
 Component composition and photonuclear interactions of photon-initiated EAS 18 p3209 A66-35121  
 Heavy cosmic ray primary energy spectrum from BASJE measurements 18 p3209 A66-35122  
 Bolivian Air Shower Joint Experiment /BASJE/ fast-timing methods compared with arrival directions measured in cloud chamber pictures 18 p3210 A66-35123  
 Cloud chamber EAS density spectrum measurements at 2285 m 18 p3210 A66-35124  
 Altitude variation of EAS particle density and primary energy/nucleon spectra measured with proportional counters 18 p3210 A66-35125  
 EAS front structure and normal energy transfer determined from pulse forms recorded by Cerenkov detectors 18 p3210 A66-35126  
 Production spectra and arrival time distributions of heavy cosmic ray particles in air showers 18 p3210 A66-35127  
 High primary energy EAS composition, energy spectrum of nuclear active particles and high energy collisions 18 p3210 A66-35128

Energy spectra of muon, electron and N components of extensive air showers /EAS/ 18 p3210 A66-35129  
 Electronic data on electromagnetic core structure of extensive air showers 18 p3211 A66-35130  
 Airborne scintillation counter-spark chamber observations of particle energy flow and incident zenith angle distribution of air showers 18 p3211 A66-35131  
 Lateral distribution of high energy gamma rays, successive interactions and core structure of EAS, using emulsion chambers at mountain altitudes 18 p3211 A66-35132  
 Extensive air showers /EAS/, discussing lateral distribution function variation with atmospheric density, primary energy dissipation, shower front radius of curvature, etc 18 p3211 A66-35133  
 Muon component of vertical and inclined extensive air showers, determining energy spectrum, lateral distribution at sea level and relation of mean height of origin and sea level energy 18 p3211 A66-35134  
 Numerical calculations of lateral distribution, energy spectrum and heights of origin of muons in extensive air showers 18 p3211 A66-35135  
 Direct measurement of attenuation length of extensive air showers through water 18 p3212 A66-35136  
 Differential momentum spectrum and charge ratio of muons in EAS measured, using solid iron magnet spectrograph 18 p3212 A66-35137  
 Extensive air showers with fixed muon number and fixed electron number studied, emphasizing correlation between cascade parameter and other EAS characteristics 18 p3212 A66-35138  
 Muon component of air showers, discussing total number of muons relation to shower size 18 p3212 A66-35139  
 Comparison of various models of EAS development with experimental data and prospects of cosmological and nuclear aspects of EAS investigation 18 p3212 A66-35140  
 Monte Carlo calculations on extensive air shower development, discussing nuclear active and electromagnetic multicore frequencies in terms of particle atomic number and primary baryon 18 p3212 A66-35141  
 Mean square angular and lateral spreads of electrons and photons in cascade shower calculated over wide ranges of finite energy and observation points 18 p3213 A66-35142  
 Solar and sidereal time variations of small air showers measured by array of water Cerenkov detectors 18 p3213 A66-35143  
 Inverse problem in cascade theory of showers to derive information about nuclear interaction 18 p3213 A66-35144  
 One-dimensional cascade theory of photon-electron showers for light and heavy substances, taking into account polarization of medium upon cross section for electron bremsstrahlung 18 p3213 A66-35145  
 Bremsstrahlung and pair production processes as regarded in cascade theory of showers 18 p3213 A66-35146  
 Time lags of nuclear interacting particles in extensive air showers 18 p3214 A66-35148  
 Experimental search for heavy mass particles in air showers with total absorption spectrometer 18 p3214 A66-35149  
 Extensive air showers of energies about one trillion ev 18 p3214 A66-35151  
 Tien-Shan high altitude installation for studying strong interactions at 100-1000 gev of cosmic ray nucleons and pions 18 p3214 A66-35152  
 Balloon experiment using spark chambers and ionization spectrometer to measure flux, composition, time variation and properties of individual interactions of cosmic rays above 100 gev 18 p3115 A66-35153  
 High-energy pion generation in showers produced in carbon by cosmic ray particles 18 p3215 A66-35162  
 Azimuthal angular distributions of secondary particles in cosmic jets, discussing shower particles from fireball model 18 p3215 A66-35163  
 Shower production by pions and protons with momenta 0.1 and 20 gev/c in thin layers of matter, determining secondary



particle energies and multiplicities 18 p3216 A66-35166  
 Inelastic n-p cross section at 80 gev determined from attenuation of penetrating shower-producing cosmic ray neutrons in paraffin and graphite 18 p3216 A66-35167  
 Multiplicity of high-energy interactions causing extensive air showers determined from maximum position 18 p3217 A66-35176  
 Angular distribution of high-energy jets analyzed by kinematic approach, assuming constant transverse momentum of secondary pions 18 p3217 A66-35178  
 Relationship of neutral and charged particles generating electron-nuclear showers studied by ionization calorimeter 18 p3218 A66-35184  
 Angular distribution and energy spectrum of cosmic particle showers at large zenith angles analyzed, using ionization calorimeter 18 p3220 A66-35196  
 Electron-photon cascade showers recorded with ionization calorimeter, determining influence of value of radiation length on form of mean cascade curve 18 p3221 A66-35198  
 Electromagnetic interactions of muons analyzed underground using scintillator stack, deducing energy of cascade shower from size 18 p3221 A66-35199  
 Classification of underground electromagnetic shower events due to muon interactions in scintillator stack 18 p3221 A66-35200  
 Frequencies of secondary particles and penetrating particles, using underground scintillators, Geiger counters and flash tubes 18 p3221 A66-35202  
 Vertical intensity and angular distributions of penetrating cosmic ray muons measured underground by scintillators, Geiger counters, etc 18 p3221 A66-35205  
 Interaction between ultrahigh energy cosmic rays and neutrinos in universe, noting distortion of energy spectrum 18 p3224 A66-35220  
 Energy spectra of muons and neutrinos generated by cosmic rays in dense objects without atmosphere analyzed in connection with nebulae problems 18 p3224 A66-35221  
 Muon decays arising from neutral primary in cosmic rays, using detector built of scintillating plastic and located near sea level 18 p3224 A66-35222  
 Almost horizontal air shower observed from cloud chamber photography suggests nuclear interaction of muon 18 p3224 A66-35223  
 Angular distribution of secondaries in elementary multiple high energy production event, evaluating expected frequency of asymmetrical showers 24 p4267 A66-42905  
 Angular dependence of charged neutron-producing component of cosmic rays, using 15-channel counter telescope on rotating platform with neutral monitor 24 p4268 A66-42913  
 Distributions of extensive air showers with either fixed number of charged particles or muons, using Geiger counter and scintillation counter 24 p4268 A66-42914  
 Central region of muon shower investigated, using Geiger counter hodoscope detector 24 p4268 A66-42915  
 Monte Carlo calculations of simultaneous distribution of extensive air showers with respect to several fluctuating parameters for elementary event models 24 p4269 A66-42919  
 Extension of formalism of theory of branching random processes applied to fluctuations in development of extensive air shower cascade by Kolmogoroff method 24 p4269 A66-42920  
 Ionization calorimeter measurement of number of particles in electron photon cascade with energy transferred from ionization calorimeter 24 p4269 A66-42924  
 Computer calculation of dependence of average characteristics of extensive air showers on adopted nucleon nuclear-interaction model 24 p4270 A66-42926  
 Extent of maximum in altitude dependence curve for extensive air showers, noting energy dissipation among secondary particles 24 p4270 A66-42927  
 Calculation of rms numbers of particles in three-dimensional theory of electron-photon

showers, considering scattering 24 p4270 A66-42928  
**COSMOLOGY**  
**SA GALACTIC EVOLUTION**  
 Dimensions, form and structure of entire known universe, examining discontinuous emission of energy from stars as they cool 01 p0135 A66-10299  
 Radio astronomy contributions in solar physics, supernovas, morphology and kinematics of galaxy, etc 01 p0139 A66-11157  
 Radio astronomy research in solar system, galaxies, supernovas, radio galaxies and cosmology 01 p0139 A66-11159  
 Expanding universe theory based on equations of general theory of relativity 02 p0285 A66-11300  
 Vector tetrad in mathematical formulation of general theory of relativity and cosmological red shift 02 p0287 A66-11470  
 Friedman theory of relativistic cosmology for universe and galaxies, noting infinite and finite universe solutions for theory 04 p0578 A66-13945  
 Theory of antimatter applied to cosmology and development of metagalactic system, discussing ambiplasma 04 p0578 A66-14009  
 Background radiation density in isotropic homogeneous universe, discussing Olbers paradox 04 p0574 A66-14017  
 Structure of universe dictated by laws of physics, correlating physical with cosmological constants, particularly in atomic physics such as unit electric charge, Planck constant, etc 05 p0718 A66-15350  
 Origin of solar system, discussing monistic and dualistic theory, interstellar gas characteristics, star formation and planetary development 05 p0767 A66-15756  
 Oscillating isotropic universe without singularity with infinite density of matter 05 p0769 A66-15844  
 Cosmic space expansion in accordance with theory of universal gravitational radiation pressure 06 p0953 A66-16311  
 Derivability of cosmological equations from first law of thermodynamics and hydrodynamics equations, without using general relativity 07 p1132 A66-17207  
 Equilibrium shape of Moon, assuming homogeneity computing mean rotation configuration and pertinent single parameter equilibrium shapes 07 p1133 A66-17304  
 Combined influence of negative and positive spatially uniform pressure upon form of cosmical pulsations of isotropic world model 07 p1133 A66-17518  
 Quasi-stellar radio sources and probing of universe, discussing universe model, general relativity and Robertson solution 07 p1136 A66-17814  
 Gravitational collapse of uniform nonrotating pressure-free spheroid 08 p1255 A66-18777  
 Equation of state of matter at supernuclear density 08 p1258 A66-18783  
 Anomalous rotation of Uranus explained by deriving expressions relating random rotation component with masses of largest bodies falling on planet 08 p1297 A66-19455  
 Origin of diamonds in Canyon Diablo and Novo Urei meteorites 09 p1447 A66-19882  
 Consistency of subtraction technique for calculating gravitational mass in nonquasi-rectangular coordinates from surface integrals provided by von Freud superpotentials 10 p1555 A66-21195  
 Ionosphere formation theory, reviewing solar radiation, absorption, ionization cross section rate, electron removal in F and upper E layer, etc 10 p1533 A66-21851  
 Cosmological effects in anisotropic inhomogeneous cosmological models including Riemannian geometry, light propagation, gravitational field, etc 11 p1772 A66-22778  
 Nonconservation of baryon and cosmological theory, discussing creation of matter in discrete manner around isolated pockets with strong gravitational fields 11 p1774 A66-23067  
 Cosmological-galactic creation, steady state expansion and high energy particle production associated with radio sources 11 p1774 A66-23068  
 Elliptic galaxy formation by expansion from steady state according to Einstein-de Sitter law 11 p1775 A66-23069

Observable properties of normal relativistic world models and steady state world model defined by parameters depending on cosmological constant and present mean density of universe 12 p1946 A66-23652  
 Peculiar galaxies and associated radio sources and quasars 12 p1947 A66-23659  
 Model sequence calculations of early solar evolution extended for case of varying-G cosmology 12 p1949 A66-24118  
 First order /Jeans/ stability analysis of infinite uniform medium pervaded by magnetic field 13 p2187 A66-26138  
 Lunar origin hypothesis suggesting capture in gravitational field of Earth following storage in solar system 13 p2188 A66-26366  
 Modification of hot big-bang theory to account for helium abundance in universe and cosmic radiation temperature, noting possible variation of Newtonian gravitational constant 13 p2189 A66-26599  
 Night sky darkness explained as limitation of background radiation by various factors in static, steady state and evolving universes 13 p2075 A66-26602  
 Spatially homogeneous anisotropic irrotational solutions of Einstein field equations for cosmological dust source 14 p2330 A66-27019  
 Model of oscillating cosmos which rejuvenates during contraction 14 p2378 A66-27021  
 Philosophical problems of Einstein theory of gravitation and relativistic cosmology - All-Union Conference, Kiev, Ukrainian SSR, May 1964 14 p2331 A66-27208  
 Evolution of matter and formation of gravitational field of metagalaxy in relation to emission and aging of gravitations and interaction with nucleons 14 p2332 A66-27214  
 Existence of nonobservable things in relativistic cosmology 14 p2332 A66-27216  
 Relation between moving matter and geometrical properties of space-time 14 p2333 A66-27217  
 Gravitational field as form of matter, noting Mach inertia principle 14 p2333 A66-27218  
 Relation between gravitation and cosmological infinity 14 p2333 A66-27221  
 Conception of infinite space and time 14 p2333 A66-27222  
 Refutation of universe having infinitely increasing entropy and thus having eternal existence 14 p2333 A66-27223  
 Cosmological models for studying infinite universe 14 p2379 A66-27225  
 Infinity of universe is axiomatic character and does not depend on any mathematical or physical principle 14 p2379 A66-27226  
 Principle of matter inexhaustibility applied to construction of finite and infinite cosmological models 14 p2379 A66-27227  
 Friedmann cosmological equation for noninteracting mixture of radiation and dustlike matter 14 p2380 A66-27275  
 Dynamic evolution of clusters of galaxies 14 p2383 A66-27707  
 Cosmological theory testing with gravitational lens effect 14 p2383 A66-27710  
 Newtonian approximation for irregularities in statistically homogeneous and isotropic dust-filled universe 14 p2386 A66-28119  
 Local rather than cosmological origin of quasars analyzed, noting observational data on spectrum of 3C273B, neutral hydrogen line, etc 14 p2387 A66-28169  
 Origin and structure of quasars, suggesting cosmological and local origin, based on relation between counts of quasars and steady state model of universe 14 p2387 A66-28170  
 General cosmological problem /GCP/ based on unified field theory involving cosmological expansion, oscillation and organic evolution, discussing quadrant mechanics, entropy, ether, minimum time problem, etc 14 p2389 A66-28408  
 Red-shift law derived, using new relativity theory of Fantapple based on Lorentz group, noting relativistic cosmology and Newtonian cosmology of Milne 15 p2599 A66-29658  
 Fantapple relativity theory using elementary projective geometry and based on group theory, obtaining cosmology leading to double time scale and origin of universe from point 15 p2599 A66-29658  
 High energy photon absorption in space



due to electron-positron pair production in photon-photon collision 16 p2750 A66-30150  
 Quasi-stellar radio sources evolution as function of space-time 16 p2799 A66-30591  
 Quasars creation of matter in steady state expanding universe 16 p2800 A66-30641  
 Magnitudes and redshifts of quasi-stellar objects, supposing objects are cosmological sources in model universe 17 p2995 A66-31909  
 Quasi-stellar object origin noting spectrum, intensity distance, etc 17 p2995 A66-31910  
 Earth-like planets, theories supporting scarcity 17 p3006 A66-33016  
 Comet cosmogony of Lagrange and problems of solar system, including volcanic processes in planetary bodies, geophysical and geological arguments, etc 17 p3014 A66-33411  
 Melting of solid bodies in chondrule size, discussing accumulation mechanisms involving electrostatic acceleration and gas motions 18 p3225 A66-33622  
 Anomalous rotation of Uranus explained by deriving expressions relating random rotation component with masses of largest bodies falling on planet 18 p3232 A66-34484  
 Comparison of various models of EAS development with experimental data and prospects of cosmological and nuclear aspects of EAS investigation 18 p3212 A66-35140  
 Stationary dust-filled cosmological solution of Einstein field equations with zero lambda and without closed timelike lines 19 p3463 A66-36169  
 Massive central body influence on cosmic dust density distribution in Newtonian oscillating world model 19 p3464 A66-36295  
 Radio astronomy of quasars, discussing galactic radio source identification, luminosity, optic magnitude, gravitational effect, flux density and classification 20 p3651 A66-37438  
 Singularities in Newtonian cosmology and in Friedman universes and behavior of relativistic world model with spherically symmetric distribution of matter 20 p3658 A66-38291  
 Perturbations of spatially isotropic expanding universe in terms of small curvature variations 21 p3817 A66-39559  
 Closed universe models with two values of Hubble expansion parameter 21 p3817 A66-39560  
 Expanding universe theory of hot ionized intergalactic gas and blackbody radiation and X-ray emission energy spectra 21 p3817 A66-39561  
 Electromagnetic field of concentric rotating mass shells, noting Machian effects on cosmological models with near-Schwarzschild radius 22 p3948 A66-40525  
 Quark abundance effect on limits of anisotropy of universe determined from study of radio and quasi-stellar objects 22 p3982 A66-40539  
 Result of testing cosmological models with red shift magnitude observations of cluster galaxies and quasi-stellar radio sources 23 p4125 A66-41066  
 Cosmological evolution from red shifts of quasi-stellar radio sources 23 p4127 A66-41150  
 Evidence against steady state model of universe provided by cosmological origin of quasar red shifts 24 p4273 A66-42418  
 Singularities of cosmological solutions of gravitational equations for space filled with matter 24 p4274 A66-42521  
 Small charge asymmetry and entropy of hot universe, finding rational solution for almost-charge symmetrical case 24 p4280 A66-43057  
**COSMONAUT**  
**S ASTRONAUT**  
**COSMOS II SATELLITE**  
 Radiophysical investigations of outer ionosphere with aid of Cosmos II and Elektron I satellites and certain geophysical rockets 09 p1377 A66-21002  
 Physical experimental data collected by Cosmos II satellite dealing with ionospheric structure 09 p1377 A66-21004  
 UV solar radiation absorption in upper atmosphere determined from measurement of photoelectron currents emitted by planar metallic orthogonal photocathodes onboard Cosmos II satellite 15 p2592 A66-30051

**COSMOS III SATELLITE**  
 Radioactivity of Cosmos III satellite after U.S. thermonuclear explosion over Johnston Island 11 p1764 A66-23053  
**COSMOS IV SATELLITE**  
 Cosmic ray intensity variation with time and geographical location from single-shielded STS-5 gas counter 09 p1441 A66-20230  
**COSMOS V SATELLITE**  
 Directional intensity of electron distribution of energies larger than 40 kev with respect to pitch angles in inner belt from Cosmos V data 06 p0951 A66-17172  
 Cosmos V satellite measurement of July 9, 1962 high altitude nuclear detonation used to determine fission debris over Johnston Island 08 p1219 A66-19414  
 Soft electrons and ions study by traps on Cosmos V satellite 19 p3451 A66-35248  
**COSMOS XII SATELLITE**  
 Low energy charged particle measurements, describing satellite mounted spherical electrostatic analyzer 05 p0751 A66-15373  
**COSMOS XLI SATELLITE**  
 Cosmos XLI satellite measurements of low energy proton distribution and intensity 11 p1762 A66-22408  
**COSMOS XV SATELLITE**  
 Charged particle fluxes of 1 kev energy measured by spherical electrostatic analyzer aboard Cosmos XV 11 p1762 A66-22423  
**COSMOS SATELLITE**  
 Space studies of Cosmos and Elektron satellites including space radiation hazards, particle observation, ionosphere chemical composition, onboard equipment, etc 01 p0136 A66-10415  
 Russian Cosmos satellite series classification and description according to orbital inclination 02 p0296 A66-11889  
 Location and radiation intensity variation in upper radiation belts determined, using scintillation counters aboard Cosmos satellites 05 p0754 A66-15400  
 Characteristic distortion of Doppler curves and radio signals of artificial satellite from behind horizon 07 p1000 A66-17209  
 Radiation measurement equipment on Cosmos 41 satellite including scintillation counter, gas discharge counter, etc 08 p1228 A66-19798  
 Terrestrial radiation belt measurement with Cosmos satellite, noting launch and orbit data, instrumentation and results 09 p1441 A66-20231  
 Primary cosmic radiation and terrestrial radiation belt measurement by Cosmos XVII satellite, noting instrumentation, equipment operation and results 09 p1441 A66-20232  
 Spatial distribution of protons and electrons captured by terrestrial magnetic field, as measured by Cosmos satellites 09 p1443 A66-21011  
 Cosmic rays during flights of Sputniks and Cosmos satellites investigated by analysis of charged particle fluxes obtained by gas discharge counter 10 p1595 A66-21042  
 Geomagnetic field measurements by Cosmos satellites at 49 degrees latitude, including typical magnetograms of magnetic field intensity 10 p1526 A66-21051  
 Energy spectrum of electrons recorded by fluorescent screen indicators onboard Cosmos satellites, noting ratio of electron intensities 11 p1763 A66-23042  
 Physical pattern of high altitude fission cloud and motion of gamma and beta fission fragments captured by geomagnetic field and observed by Cosmos satellite 11 p1764 A66-23043  
 Purposes and technical details of Soviet Cosmos satellites 13 p2193 A66-25857  
 Cosmos-65 spectrophotometric measurements of atmosphere-reflected UV radiation spectra 15 p2485 A66-29076  
 Cosmos satellite observational values of atmospheric density during low solar activity 15 p2496 A66-30083  
 Telemetry data for extreme orbital deviations of Soviet satellites with orbital inclination of 65 and 51 degrees 19 p3468 A66-35722  
 Radiation measurement equipment on Cosmos XLI satellite including scintillation counter, gas discharge counter, etc 21 p3736 A66-38794

Angular, spectral and geographical distributions of outgoing fluxes of thermal radiation and Earth albedo measured, using Cosmos satellite 22 p3913 A66-40471  
 Relativistic-electron diffusion wave in outer radiation belt recorded by device mounted on Cosmos XLI satellite in high geomagnetic latitudes 22 p3974 A66-40756  
**COSPAR**  
 Space research activities in U.S. /1964 and early 1965/, condensed comprehensive report to COSPAR 09 p1458 A66-20690  
 Model atmosphere structural parameters and improvement proposals for 1964 COSPAR International Reference Atmosphere 09 p1375 A66-20989  
 Text on international cooperation in space, institutions involved and technical and political constraints 10 p1623 A66-21765  
 Catalog of sounding rocket launchings and meteorological rocket firings prepared for COSPAR 15 p2599 A66-29900  
 U.S. space science program 1965, report to COSPAR 15 p2600 A66-29903  
**COST ESTIMATE**  
 Microelectronic integrated circuits and thin films applied to inertial navigation systems to achieve cost reduction 01 p0034 A66-10011  
 Changes to improve reliability of attack aircraft, estimating cost and gains in operational effectiveness 01 p0167 A66-10049  
 Evaluation and future of cost effectiveness management 01 p0167 A66-10052  
 Maintainability and reliability cost effectiveness program /MARCEP/ for improving reliability by adding redundancy in cost-effective manner to nonredundant system 01 p0168 A66-10063  
 Product assurance in terms of cost and enhancement in reliability and quality 01 p0170 A66-10101  
 Cost factors in launch operations controlled by management techniques and tools used in other facets of research and development 01 p0141 A66-10105  
 Operational research techniques applied to procurement and capital investment programs of aviation industry 01 p0170 A66-10341  
 Economic feasibility of all-rocket approach to reusable launch system, comparing various classes of launch vehicles, noting need for payload recovery [SAE PAPER 650802] 01 p0144 A66-10817  
 Potential air freight market in next decade forecast as many-fold times present level [SAE PAPER 650782] 01 p0012 A66-10839  
 Performance operation and cost of rockets and airbreathing launch system, noting preliminary designs 02 p0295 A66-11676  
 Integrated circuit economics discussing design, construction and running costs 02 p0205 A66-11944  
 RCAF system of aircraft fleet operations management /TC-91/ for unserviceability cost estimate 02 p0178 A66-11992  
 Contractor-customer responsibilities for Model A-7 aircraft design in firm fixed price environment 03 p0320 A66-12589  
 [ATAA PAPER 65-758] 03 p0320 A66-12589  
 Cost effectiveness of VTOL short range jet airlines, discussing significance of block time [ATAA PAPER 65-797] 03 p0320 A66-12598  
 V/STOL aircraft economic and operational characteristics for commercial service over routes of 150 miles or less [SAE PAPER 650243] 03 p0446 A66-12632  
 Runway design by assessing capacity, delay of operations, costs, etc, using mathematical models 03 p0352 A66-12706  
 Flight operating techniques influence upon engine maintenance costs and new engine design, specifically Pratt and Whitney JT3C-12 on Boeing 720 aircraft [SAE PAPER 650212] 03 p0322 A66-13220  
 V/STOL transport aircraft noting productivity, flexibility, simplicity, economy of numbers, low fleet cost, high speed and turbofan propulsion 03 p0322 A66-13269  
 Ground and flight procedures of minimum cost satellite launcher noting control, range safety, reliability and orbits 04 p0586 A66-13947  
 Optimum design employing merit function of cost and weight for structural/material components and subsystems applied to space vehicles



[SAE PAPER 650785] 05 p0773 A66-15010  
Meteoroid protection weight requirements effects on space exploration costs, examining environment and hypervelocity impact penetration

[SAE PAPER 650786] 05 p0774 A66-15011  
Assault helicopter cost and system effectiveness in mission of delivering cargo from carrier to landing zone, evaluating avionics system

[AIAA PAPER 64-785] 05 p0610 A66-15079  
Energy-optimal control with cost function for bounded time and control system

[ASME PAPER 65-WA/AUT-14] 05 p0659 A66-15605  
Reliability of electronic equipment needed to increase availability and reduce maintenance cost

06 p0840 A66-15953  
Short-range aircraft design efficiency and possible reduction in operating cost

06 p0804 A66-15990  
British short-range aircraft operating cost affected by reliability, design and engines

06 p0804 A66-15991  
Short-range jet transport operating cost reduction through technical innovation, labor cost and research

06 p0804 A66-15992  
Possible cost reduction with all-wing short-range aircraft, noting ogee design

06 p0804 A66-15993  
Lowering total airline operating costs through nonaircraft

06 p0804 A66-15994  
economizing

06 p0804 A66-15994  
Price discrimination and regulation of air transportation, examining history, interplay and evolution

06 p0973 A66-16402  
Differences between inertial equipment and that in current use, emphasizing economic aspects

07 p1069 A66-17710  
Productivity and cost comparison of water-bomb forest fire fighting

07 p0989 A66-18051  
Fuel cell considered from viewpoint of fuel costs, noting hydrocarbon fuel for application with low load factor and instant starting

07 p0997 A66-18478  
Costing air traffic control deviations and relation to size of separation

09 p1401 A66-20432  
Value analysis as cost reduction factor, using production of Bulpup A and B missiles as example

11 p1711 A66-23060  
Lagrange and Mayer problems of optimal control of cost

11 p1680 A66-23277  
Systems effectiveness - Conference, Electronic Industries Association, Washington, D.C., October 1965

11 p1788 A66-23434  
Rationale for systems effectiveness in Air Force systems command

11 p1789 A66-23435  
Cost effectiveness as analytical tool for engineering and management, noting risks involved, limitations, benefits, etc

11 p1789 A66-23439  
Past and future of cost effectiveness, noting actions needed to implement growth

11 p1790 A66-23446  
Airline long-haul maintenance objectives, methods for monitoring maintenance equipment and cost

12 p1801 A66-23859  
analysis

12 p1801 A66-23860  
Cost reduction in aircraft maintenance and servicing

12 p1834 A66-24101  
Multipurpose chips for reduction of analog computer integrated circuit cost

12 p1834 A66-24101  
Estimation of manufacturing costs of low volume high-cost complex electronic subsystems

[ASTME PREPRINT MM66-701] 12 p1886 A66-24411  
Aerospace structural material machinability, cost estimating, machine tool selection, metal cutting problems, etc

[ASTME PREPRINT MM66-715] 12 p1887 A66-24419  
Point-to-point contouring systems noting procedures, codes and cost savings

[ASTME PREPRINT MS66-725] 12 p1887 A66-24423  
Digital simulation of scheduling logistic support by helicopter, using Backtrack techniques

12 p1858 A66-24683  
Effects of varying orbital parameters, including number of satellites, orbit altitude, positioning, tracking accuracy, cost effectiveness, etc, on establishment and maintenance of communications satellite

system

[AIAA PAPER 66-286] 12 p1955 A66-24757  
Minimum cost ground receiving station for synchronous satellite system

[AIAA PAPER 66-311] 12 p1859 A66-24777  
Effective radiated power /ERP/ satellite for educational TV distribution, discussing design feasibility, cost comparison, spectrum utilization and system model

[AIAA PAPER 66-320] 12 p1982 A66-24791  
Economic aspects of educational television distribution system, using comprehensive total cost model

[AIAA PAPER 66-321] 12 p1982 A66-24793  
Ground-based steerable paraboloid spherical reflector and multiplate type antennas, noting cost per unit area for unit wind speed of 30 mph and frequency of 1400 mc, performance, restrictions, etc

[AIAA PAPER 66-324] 12 p1844 A66-24794  
Silicon monolithic circuit development, discussing cost reduction and performance improvement in microcircuits

12 p1845 A66-24850  
Rotationally-symmetric intake nozzles manufactured by low cost technique for wind tunnels from glass fibers and plastics, using wooden pattern

13 p2085 A66-25080  
Reliability feasibility evaluation of Voyager spacecraft, determining launches necessary, chances of success and program cost

13 p2192 A66-25509  
Economic analysis of maintainability in selecting alternative maintenance resource allocation

13 p2210 A66-25660  
Optimum control of linear systems in presence of random disturbances, noting choice between cost design and cost variance methods

13 p2051 A66-26066  
Decision theory and dynamic programming applied to problems concerning cost and weight minimization in structural engineering

13 p2207 A66-26699  
Industrial technology and cost estimate of chemical machining metal removal process

[ASTME PAPER MR66-155] 14 p2299 A66-26953  
Machinability data for hard-to-machine materials, noting cost reductions, tool holder test program, cutting fluids, fixtures, producibility, etc

[ASTME PAPER MM66-178] 14 p2300 A66-26958  
Orbital satellite launching systems, problem of increasing percentage orbital payload at minimum cost and advantages of air breathing engines

14 p2391 A66-27010  
ATA direct operating cost formula for transport aircraft, considering flying operations, maintenance, depreciation and indirect costs

[SAE PAPER 660280] 14 p2222 A66-27289  
Cost and performance comparison of satellites, relay links, waveguides and lasers, showing line-of-sight microwave relay is best wideband data transmission medium

14 p2238 A66-27667  
Money-saving technique to speed up potentiometer in control systems

14 p2267 A66-27804  
Multimode antenna feed in radar design requiring only two hybrids for azimuth and elevation measurements

14 p2255 A66-27806  
Antenna cost, efficiency, noise, minimum detectable signal and signal temperature relationships

14 p2257 A66-27928  
Combining R and D and follow-on production in single contract

14 p2417 A66-28434  
Quality system analysis, determining structural soundness, requirements and functional relationship of components

15 p2507 A66-28794  
Small gas turbine engine controls, discussing design, development and cost factors

15 p2571 A66-28861  
Economic effects of turbulence on airline operations, considering costs on temporary grounding for repairs, passenger injuries, information dissemination on turbulence, etc

15 p2618 A66-28916  
Aircraft design for large cargo transport noting aerodynamic efficiency, wing construction, cargo loading, cost estimates, etc

15 p2426 A66-29803  
Aircraft mile cost vs seat mile cost, noting payload estimation, profit potential, productivity and other parameters

[SAE PAPER 660277] 15 p2427 A66-29823  
Helicopter capabilities in solving interurban mass transport problems, particularly cost and time considerations

[SAE PAPER 660336] 15 p2427 A66-29838  
Effect of VTOL size on operational cost per ton-mile, noting mission weight vs payload variations, comparison of fuel consumption of STOL, time savings, etc

[SAE PAPER 660316] 15 p2428 A66-29840  
V/STOL aircraft use in California corridor in next decade, considering time savings costs analysis, etc

[SAE PAPER 660317] 15 p2428 A66-29841  
Hot forming of titanium sheet structures and relation to cost

[SAE PAPER 660327] 15 p2511 A66-29848  
Selection, flow and transference of technology in large electronics aerospace firm, noting methodology, planning, market area selection, etc

16 p2830 A66-30400  
Predicting structural reliability by recent developments in statistics, reliability, cost effectiveness analysis and decision theory

[AIAA PAPER 66-503] 16 p2714 A66-30607  
Jet engine technology, including spinoffs from lift jet, propulsion systems, cost estimates, etc

16 p2791 A66-31280  
Structures cost effectiveness in optimization weight-cost design in aerospace structures

[AIAA PAPER 66-505] 16 p2831 A66-31479  
Reliability procedures in converting Thor tactical system to advanced booster in space program, noting time and costs savings

17 p3015 A66-31981  
Rules for comparing designs of aerospace transporters and selecting optimum configuration, based on overall cost criterion

17 p3040 A66-32378  
Military aircraft procurement, discussing development production cost estimate and design

17 p3040 A66-32796  
Series power switch for orientation and position computer of small lunar-orbit spacecraft designed to reduce weight and cost

17 p2878 A66-33122  
Coordinated management planning required for minimizing funding escalation and overdiversification of potential missions

[SAE PAPER 660450] 17 p3040 A66-33159  
Iterative gradient method application to trajectory optimization problems, noting feasibility to systems with continuous bang bang controls

17 p2903 A66-33259  
Practical cost reduction possibilities within aerospace industry

18 p3268 A66-33947  
Low cost approach to development of vehicle for European-based space exploration

18 p3246 A66-33972  
Algorithm for cost effectiveness comparison of aircraft tradeoffs of performance vs cost vs time of obtainability

18 p3052 A66-34163  
Total value concepts applied in system effectiveness analysis are helping Contract Definition type contracts meet cost effectiveness requirements

18 p3268 A66-34251  
Cost and performance factors of steerable parabolic reflectors, spherical reflectors and multiplate antennas

18 p3268 A66-34288  
Integrated circuit connecting and packaging discussing cost flexibility and performance characteristics

18 p3086 A66-34399  
Supersonic transport propulsion systems noting thrust requirement, noise reduction commercial feasibility, etc

[SAE PAPER 660297] 18 p3165 A66-34943  
Cost-effectiveness guidelines for designing tactical system in absence of firm specifications, noting avionics system

19 p3480 A66-35528  
Gomory all-integer linear programming algorithm based on lexicographical ordering principle and relation to cost function

19 p3309 A66-35876  
Extravehicular activities interface with data recording system and economical recovery of optimum quantity of data

19 p3291 A66-35967  
Interplanetary mission planning including energy requirements, payload definition, spacecraft design, launching, cost data, etc

19 p3470 A66-36314  
Optimization methods for preliminary cost and mass distribution assessment for multistage rocket



- vehicles 19 p3470 A66-36622
- Reusable first stages using liquid propellant compared with nonreusable stages using solid and liquid combinations, for minimum cost of loaded-and-ready-for-launch stage cost per unit of stage payload mass 19 p3470 A66-36623
- Existence of inflection points in cost vs terminal time curve for linear minimum energy regulator 19 p3339 A66-36745
- Transition matrices of ergodic finite Markov chains and readiness models in cost effectiveness systems 20 p3681 A66-37176
- Reliability requirements for spacecraft guidance and control systems, emphasizing redundancy in existing systems 20 p3596 A66-37177
- System and cost effectiveness techniques applied to procurement of military operational systems, noting need for new standards for reliability input data 20 p3682 A66-37183
- Function, method of operation, complexity and effect on weight and cost for BITE /built-in test equipment/, as applied to electric power systems for jet aircraft 20 p3499 A66-37189
- Cost-effectiveness evaluation methodology for choosing best aircraft to construct for given purpose 20 p3682 A66-37197
- Optimal support costs of weapon systems requires contractor selection based on high order of management capability 20 p3682 A66-37238
- Integrated circuits economics, discussing design, construction and running costs 20 p3531 A66-37830
- Lockheed C-5 quantitative maintainability program and application to air-vehicle utilization and cost 20 p3495 A66-37891
- effectiveness 20 p3495 A66-37891
- Spacecraft maintainance and repair cost minimization and system effectiveness increase by controlling contamination due to personnel, static electrification and bacteria 20 p3567 A66-37899
- Computerized cost-effectiveness model for large payload test vehicle system of 50-150 launch program 20 p3684 A66-37901
- Digital computer programmed optimization model of Earth-orbiting space station missions including reliability, maintainability and cost considerations 20 p3663 A66-37902
- Economics of Ownership structure and cost effectiveness in microelectronic systems 20 p3684 A66-37904
- Reliability-maintainability cost tradeoff via dynamic and linear programming, discussing states, alternatives within states, transition rates and expected costs 20 p3568 A66-37911
- Management in applying reliability and maintainability for improved cost effectiveness by first-tier supplier 20 p3685 A66-37913
- Planned inspection of hardware based on warning analysis, relation to improved cost effectiveness 20 p3569 A66-37921
- Learning curve theory used to explain tendency toward decreasing downtime observed in maintenance of many systems 20 p3569 A66-37924
- System safety concept relation to cost and system effectiveness 20 p3685 A66-37932
- Cost of turbojet engine development plans estimated in computer simulation and Monte Carlo techniques 20 p3523 A66-37935
- Project Scorpio USAF Cellular Combustion Chamber Program for cost reduction and injection pattern simplification in liquid propellant rocket engines 20 p3629 A66-38256
- SST in nonoptimum conditions, discussing cost penalties due to navigation error, air traffic conditions, sonic boom restrictions, clear air turbulence and weather 21 p3695 A66-38451
- Costing of parallel route systems for supersonic traffic, examining diurnal traffic patterns, sensitivities to fuel requirements, sonic bang avoidance and layout of track systems 21 p3761 A66-38453
- Vehicle Millemile concept in ascertaining composite mix of load and revenue needed to meet cost of operating large jet aircraft 21 p3838 A66-39244
- Castable composite high energy propellants manufacturing techniques, discussing economy based on batch mixing and continuous processing 22 p3969 A66-39870
- Optimal control synthesis for cost functionals involving convex single valued functions of state and control variables, noting steepest ascent method and evaluating gradient 22 p3885 A66-40871
- Specification and assessment of electronic equipment reliability, emphasizing statistical aspects of optimal cost/reliability estimation 22 p3883 A66-40961
- NASA management, budgetary problems, controversy of incentives system, etc 23 p4151 A66-41047
- Design characteristics and marketing prospects of Concorde SST 23 p4015 A66-41301
- New jet transports, discussing subsonic, SST and stretched versions of subsonic transports 23 p4016 A66-41302
- Short haul air transportation in Europe, noting market development with helicopter techniques and development of more efficient rotor aircraft 23 p4151 A66-41303
- Air transportation between 1980 and 2000, noting cost limitation, possible trends, management planning, etc 23 p4152 A66-41304
- Passenger and cargo aircraft development 23 p4152 A66-41647
- Manned mission design analysis, examining spacecraft electrical power requirements, weight correlation and cost estimation 23 p4021 A66-41753
- Economics of various orbital boosters from completely expendable to completely recoverable vehicles, noting concept of cost-optimum vehicle 23 p4133 A66-41775
- Factors involved in bringing propulsion system to operational status noting engine design, development, cost, testing, etc 24 p4296 A66-42243
- Launch vehicle and spacecraft cost trends including larger vehicles, post Saturn phase, performance improvement by throttling, etc [SAE PAPER 660463] 24 p4281 A66-42394
- Book on project ERIE covering techniques for analytic evaluation of space equipment designs with respect to environments and missions required in 1975 24 p4217 A66-42572
- COUETTE FLOW**
- Couette flow, unpressurized axial flow in annular gap between two cylinders and flow between two rotating cylinders, taking into account energy dissipation and dependence of viscosity on temperature 04 p0512 A66-14423
- Simultaneous radiation, conduction and convection heat transfer for steady state conditions in one-dimensional spectrally selective, emitting and scattering porous bed [ASME PAPER 65-WA/HT-23] 05 p0789 A66-15642
- Couette flow, Neumann-Liouville series expansion convergence for various flow regimes and related Fredholm integral equation solutions 07 p1020 A66-17964
- Exact solution of hydromagnetic stability of nondissipative conducting Couette flow between two coaxial cylinders in axial magnetic field 07 p1021 A66-18048
- Stability of frictionally heated Couette and Poiseuille flows, specifically Couette flow in inviscid limit 08 p1204 A66-18527
- Infinitesimal time-dependent perturbation of steady viscoelastic flows with application to Couette viscometer 08 p1208 A66-19229
- Viscosity and density variations due to imposed radial temperature gradient effects on Couette flow stability between rotating cylinders 08 p1211 A66-19681
- Accuracy of kinetic theory approximations assessed by comparison of approximate and exact solutions of Krook kinetic equation for Couette flow and shock wave structure 11 p1690 A66-22906
- Discrete ordinate technique for solution of distribution function of linearized Boltzmann equation, with application to Couette flow 11 p1692 A66-22923
- Overstability in elastico-viscous flow between rotating cylinders 11 p1693 A66-23010
- Asymptotic approximations in hydrodynamic stability problems including Couette, spiral and parallel shear flows 12 p1860 A66-23548
- Asymptotic solution, valid in physical space, obtained for kinetic layers in slip flow of linearized Couette problem 12 p1865 A66-24589
- Small gap equations for Couette flow stability considering nonaxisymmetric disturbances, solving eigenvalue problem and noting role in instability of Taylor vortices 12 p1866 A66-24946
- Stability of two-dimensional Couette-Poiseuille flow 12 p1866 A66-24951
- Heat transfer in Couette flow of radiating fluid with viscous dissipation, noting conduction coupling, effects of temperature level, profile, wall emission, fluid optical thickness, etc 13 p2210 A66-26718
- Steady state motion of Couette plasma flow in electric field, assuming transfer of collective motion is effected by ions and heat transfer by electrons 14 p2339 A66-26774
- Stability to infinitesimal disturbances of plane Couette flow in presence of negative vertical temperature gradient, noting instability at critical Rayleigh number for convection without shear 15 p2481 A66-29741
- Hydrodynamical modification of Heller treatment of mixing and unmixing of viscous fluid between two rotating cylinders 16 p2685 A66-30990
- Simultaneous radiation, conduction and convection heat transfer for steady state conditions in one-dimensional spectrally selective, emitting and scattering porous bed [ASME PAPER 65-WA/HT-23] 16 p2828 A66-30990
- Numerical solutions of Krook kinetic equation for Couette flow and plane shock wave 18 p3101 A66-34665
- Variational principle applied to boundary value problems in kinetic theory, specifically examining Kramer problem, plane Couette flow and plane Poiseuille flow 18 p3102 A66-34919
- Rotating Couette flow of miscible binary liquid mixture between two coaxial cylinders 18 p3102 A66-34924
- Couette flow and heat transfer through hard-sphere rarefied gas enclosed between parallel walls analyzed by Monte Carlo method 19 p3478 A66-35803
- Energy method applied to stability of flows governed by nonlinear Boussinesq equations, establishing universal stability region in Reynolds-Rayleigh number plane 19 p3478 A66-36199
- Couette and Poiseuille flow and temperature distribution of fluids with two viscosity ranges, including viscoplastic and dilatant fluids 19 p3341 A66-36304
- Interface propagation in mixed laminar-turbulent flow between counter-rotating concentric cylinders, noting spiral turbulence as dominant feature of Couette flow transition 20 p3547 A66-37979
- Distortion of laminar circular Couette flow measured by end effects, noting two-dimensional tangential motion near axial plane of symmetry 20 p3547 A66-37980
- Maxwell-Lorentz field equations for Couette flow birefringence of Rivlin-Ericksen viscoelastic fluid and Noll simple fluid 21 p3724 A66-38761
- Stability of viscoelastic liquid in Couette flow compared with non-Newtonian liquid of same limiting viscosity 21 p3729 A66-39451
- Pressure induced flow of elasticoviscous electrically conducting incompressible fluid between relatively moving porous walls in presence of transverse magnetic field 23 p4053 A66-41121
- Boundary layer solutions to two-dimensional stationary viscous incompressible flow past finite object under vanishing skin friction 23 p4060 A66-42009
- COULOMB COLLISION**
- Forced vibration in nonlinear system with Coulomb and combination friction 01 p0159 A66-11176
- Surface photoeffect from highly alloyed semiconductor accounting for Coulomb electron interaction 04 p0567 A66-14344
- Coulomb interaction of electrons and holes in contacts of degenerate n-and p-type semiconductors causes ground state instability relative to electron-hole pair formation 05 p0730 A66-14645
- Coulomb collision effect on transverse electron oscillations in fully ionized hot



plasma determined by Fokker-Planck equation 05 p0721 A66-14715

Particle distribution and motion in field of force, discussing density profile, energy dissipation, Coulomb charge shielding for local thermodynamic equilibrium and free orbital motion 08 p1261 A66-18743

Forced vibrations of two-degree-of-freedom system with combined Coulomb and viscous damping 09 p1469 A66-20950

Quasi-linear current instability in two-temperature plasma for Coulomb collision and free electron acceleration 10 p1569 A66-21972

Coulomb collisions and equilibrium states in fully ionized plasma, deriving kinetic equation in pairwise collision approximation 10 p1572 A66-22037

Electron Coulomb interaction in strongly alloyed semiconductor films tends to reduce all energies to constant value without changing spectrum shape 11 p1750 A66-22344

Coulomb relaxation of distribution of fast electrons or ions in Earth radiation belts 11 p1762 A66-22425

Self-consistent theory of curvilinear electron fluxes interaction with wave conducting line, taking into account space charge 11 p1655 A66-22722

Relaxation of isotropic distribution of test particles in homogeneous background gas, including nonzero temperature effects 11 p1741 A66-23390

Coulomb interaction of electrons and holes in contacts of degenerate n- and p-type semiconductors causes ground state instability relative to electron-hole pair formation 13 p2166 A66-25918

Surface photoeffect from highly alloyed semiconductor accounting for Coulomb electron interaction 14 p2367 A66-28239

Collision cross sections of ions in isoelectronic sequence of lithium, noting dipolar transitions of type 2s to np 16 p2754 A66-31261

Light absorption coefficient for indirect photon transitions during Coulomb interaction of electrons at high electron densities 16 p2787 A66-31766

Longitude dependence of distribution function of electrons for fixed value of McIlwain parameter, using kinetic equation 18 p3197 A66-34873

Galvanomagnetic effect of anisotropic electron energy spectrum on acoustical branch perturbation spectrum of system of electrons and ions in homogeneous magnetic field 20 p3618 A66-37559

Quasi-linear current instability in two-temperature plasma for Coulomb collision and free electron acceleration 21 p3794 A66-39551

Charged particle collisions effect on drift instability of low pressure plasma studies, using Landau collision integral as model collision integral 22 p3956 A66-40192

Discrepancies in electron-impact broadening of isolated ion lines due to neglect of collision-induced transitions between upper and lower levels of line and Coulomb interactions with perturbed ions 22 p3951 A66-40419

Coulomb interaction in two-zone superconductor model, noting variation of critical electron-temperature and effect on superconductivity 22 p3968 A66-40916

Self-consistent theory of curvilinear electron fluxes interaction with wave conducting line, taking into account space charge 23 p4037 A66-41460

**COULOMB POTENTIAL**

Permittivity of dielectric formed from ground state instability of semimetal, considering Coulomb attraction between electrons and holes 01 p0125 A66-10774

Tables of classical collision transport integrals for screened Coulomb potential 03 p0401 A66-12958

Radial distribution function computed for classical particles interacting with Coulomb, shielded Coulomb and truncated Coulomb forces 06 p0908 A66-16120

Permittivity of dielectric formed from ground state instability of semimetal, considering Coulomb attraction between electrons and holes 11 p1749 A66-22286

Limiting cases of screened Coulomb T matrix in complex energy

plane 15 p2547 A66-29618

Model potential consisting of Coulomb potential and linear terms in electric field potential, obtaining eigenfunctions of model and deriving optical absorption coefficient for electric field excitons 16 p2775 A66-30729

Impurity energy levels in semiconductors described by equivalent Schroedinger equation containing short-range as well as conventional terms for long-range Coulomb potential 16 p2784 A66-31446

Atomic energy levels in plasma, considering energy spectrum of hydrogen-like atom in plasma, based on cut-off Coulomb potential model 20 p3607 A66-37373

Ferromagnetic spin correlations from strong Coulomb interactions between valence electrons resulting in enhanced singlet-state repulsion 21 p3803 A66-39263

Matrix elements of Coulomb potential between Schecter functions and overlap integrals necessary in determining two-center acceptor states in p-type Ge and Si 24 p4255 A66-42497

**COULOMETER**

Quantitative coulometric analyses of water yield for thermal dehydration of solids, using electrolytic hygrometer cell 07 p1036 A66-18490

**COUNTDOWN**

Markov process model of Gemini countdown and transition probability matrix 13 p2192 A66-25505

Missile prelaunching development stage, detailing countdown and field test preparation 18 p3246 A66-34043

Alternate mode of operation for minimizing occurrence of delays caused by launch support equipment failures for Saturn manned missions 20 p3542 A66-37243

**COUNTER**

SA CERENKOV COUNTER

SA GAS DISCHARGE COUNTER

SA GEIGER COUNTER

SA IONIZATION COUNTER

SA NEUTRON COUNTER

SA PARTICLE COUNTER

SA PROPORTIONAL COUNTER

SA QUANTUM COUNTER

SA RADIATION COUNTER

SA SCINTILLATION COUNTER

Digital counter synthesis for fixed base and periodic sequence-variable base counters with various feedback loops 09 p1361 A66-20606

Counting system for use with rubidium magnetometer for ground observations of geomagnetic micropulsations with sensitivity of 1/100 gamma 13 p2085 A66-26752

Integrated circuit binary counters using majority logic current mode gate element 14 p2255 A66-27803

Realization of numerical counters with micrological elements, discussing flip-flop and memory elements 16 p2656 A66-30964

Single-chip decade counter as fuse timer and programmer for weapon system 17 p2883 A66-32125

Miniaturized no-moving-parts fluid pulse counter development for ordnance application 19 p3282 A66-36674

**COUNTERBALANCE SYSTEM**

**S COMPENSATOR**

**COUNTERMEASURE**

**S ELECTRONIC COUNTERMEASURE**

**COUNTING RATE COMPUTER**

Counting decade consisting of three ferrite-transistor triggers and fourth binary element in form of ring with rectangular hysteresis loop 02 p0232 A66-12146

Oscillograms and circuit diagrams of counter in which storage of preceding state is performed by trigger with direct coupling by means of unitrons 04 p0490 A66-13917

Correction of cosmic ray meson intensity monitor counting rates for atmospheric temperature variation 07 p1127 A66-18012

Counting decade consisting of three ferrite-transistor triggers and fourth binary element in form of ring with rectangular hysteresis loop 14 p2297 A66-28102

Oscillograms and circuit diagrams of counter in which storage of preceding state is performed by trigger with direct coupling by means of unitrons 20 p3522 A66-37875

**COUPLED MODE**

Coupled-mode equations for wave propagation through magnetized ferrite rod

with variable cross section, noting Faraday rotation 03 p0410 A66-12935

Natural modes of partitioned networks in analysis and synthesis of transfer functions, noting potential analog or root locus method 05 p0655 A66-14625

Perturbation calculation of average rate of energy transfer in random vibration of nonlinearly coupled modes 05 p0716 A66-15051

Linear dynamical systems with weak coupling solved approximately, noting examples and definition 06 p0862 A66-16362

Wave reflection and refraction across density discontinuity in two-fluid fully ionized plasma studied by coupled linearized hydrodynamic equations and Maxwell equations 07 p1088 A66-17948

Distributed-parameter systems in terms of matrices whose elements are functions of coupling parameters between modes and phase constants of modes 07 p1144 A66-18042

Decay theory of closely coupled unstable states based on Green function formulation for transition amplitude 11 p1741 A66-23189

Light coupling with phonons, magnons and plasmons, deriving wave equations and coupling constants, observing Raman effect in spin systems and in plasmas, noting second harmonic generation 13 p2132 A66-26154

Coupled wave formalism, giving unified description of parametric down conversion of light, stimulated Brillouin and Raman effects, etc, stressing exponential character of gain 13 p2132 A66-26156

Theory, basic relations and general theorems for coupled thermoelectricity 13 p2199 A66-26377

Mode selective coaxial directional couplers for measurement of unwanted harmonics effect 13 p2044 A66-26745

Coupled waveguide antenna analyzed based on coupled-mode theory 15 p2455 A66-28569

Hysteresis phenomena in He-Ne gas laser in axial magnetic field and polarization of oscillating mode within certain tuning region 15 p2516 A66-29385

Second-harmonic enhancement in nonlinear crystal by loss modulator coupling of pulsed ruby laser modes 17 p2933 A66-31939

Bandpass filter design with three coupled circuit and determination of amplitude curve and circuit constants 17 p2895 A66-33243

Self and mutual admittance of coupled dipoles in dissipative medium 18 p3065 A66-33529

Coupled waveguide circulator in which secondary waveguide is loaded with distributed nonreciprocal attenuation along coupling length 18 p3075 A66-33566

Spectral density and mean value of power flow between two stiffness coupled oscillators under white noise random excitation 18 p3251 A66-33675

Spark shadow projections in air for giant pulse synchronization from two lasers, using rotating prism to modulate quality factors 18 p3144 A66-34036

Subharmonic vibrations during resonant testing of thin walled beams for coupled torsional and bending vibrations 18 p3256 A66-34559

Laser mirror transducer decoupling from mechanical resonances of laser cavity 19 p3374 A66-35813

Coupled waveguides structure proposed as leaky-wave antenna, extending previous coupled-mode theory 19 p3320 A66-36401

Relation of kinetic theory to unstable plasmas /weak turbulence/, noting expansion parameters and extension to include discrete particle effects 19 p3418 A66-36536

Coupling between oppositely directed traveling waves in He-Ne ring laser in form of mutual backscattering of energy from each beam into direction of other 20 p3579 A66-37778

Coupling of adjacent axial modes in external Raman resonator observed as first Stokes frequency with benzene as Raman medium and Q-switched ruby laser as pump source 21 p3747 A66-39109

Support flexibility effect on natural frequency free vibrations of uniform cantilever carried by mass supported on string 21 p3833 A66-39608



- Numerical solution of full-wave equation with mode coupling governing electromagnetic wave propagation in horizontally stratified inhomogeneous anisotropic medium 22 p3863 A66-39938
- Coupled-modal equations for arbitrary vibratory system, with example for longitudinal vibrations of bar 22 p3992 A66-40298
- Large, small and infinite phased array antennas and coupling effects 22 p3881 A66-40749
- Adaptive antenna system circuitry for maximum signal to noise ratio of signals reaching ground station from deep space probe 22 p3881 A66-40750
- Electromagnetic wave scattering by stratified medium, noting Mathieu and Floquet type wave representation 24 p4171 A66-42292
- Traveling wave phototube /TWP/ theory in terms of modified TWT coupled mode theory, noting equivalent impedance concept and noise output calculation 24 p4184 A66-42746
- Electric contact design factors for shock vibration environments 24 p4186 A66-43058
- COUPLED STRESS**
- Couple stresses in problems of torsion covering prismatical bars, linear isotropic and hyperelastic bodies 04 p0591 A66-14210
- Couple-stresses in dislocated solids and effect in classical elasticity 04 p0594 A66-14292
- Static deformation of model of three-constant isotropic elastic material exhibiting phenomenon of couple stresses [ASME PAPER 65-WA/APM-3] 05 p0776 A66-15427
- Cylindrically symmetric tension field covering strain gradient effects on potential energy of elastic body [ASME PAPER 65-WA/APM-14] 05 p0777 A66-15436
- Static deformation of model of three-constant isotropic elastic material exhibiting phenomenon of couple stresses [ASME PAPER 65-WA/APM-3] 10 p1615 A66-21480
- Cylindrically symmetric tension field, covering strain gradient effects on potential energy of elastic body [ASME PAPER 65-WA/APM-14] 12 p1960 A66-23974
- Nonlinear theory for elastic surface deformation, assuming existence of strain-energy function governed mechanically by virtual work 12 p1970 A66-24564
- Stresses and coupled-stresses generated by dislocation in isotropic media treated in terms of boundary value problem for Cosserat medium 14 p2409 A66-28468
- Linearized theory of coupled stress elasticity and stress distributions around simple edge and screw dislocations 15 p2609 A66-29241
- Tensor field/vector field representation of stress functions for couple and dipolar stresses 16 p2812 A66-30261
- Couple stress theory and virtual work principle applied to thermoelasticity of Cosserat medium, including energetic, uniqueness and reciprocity theorems 17 p3031 A66-33330
- Cosserat coupled stress and effects on stress concentration factor in semiinfinite solid medium with varying elastic modulus 20 p3667 A66-37466
- Three-dimensional linear-anisotropic elasticity with inertia effects analyzed in isotropic and anisotropic Cosserat continua, deriving static and kinematic components 23 p4141 A66-41945
- COUPLING**
- SA ANTENNA COUPLER
- SA CROSS COUPLING
- SA GYROSCOPIC COUPLING
- SA MICROWAVE COUPLING
- SA OPTICAL COUPLING
- SA SPIN-SPIN COUPLING
- SA THERMOCOUPLE
- SA THERMODYNAMIC COUPLING
- Aircraft engine rotating shaft coupling design, noting splined shafts, correct lubrication, flexible members and test results 09 p1383 A66-19863
- Effect of degree of coupling between resonator system and load on generation zones and regenerative amplification of pulsed magnetron, noting characteristics 09 p1353 A66-20437
- Filter with two tuned circuits and distributed coupling based on equations for complex values of tuned circuit currents, noting formulas for mutual impedance 10 p1510 A66-21673
- Hose coupling utilized in oxygen umbilical cord for astronaut extravehicular activity 14 p2225 A66-27110
- Magnetoionic couplings and electromagnetic wave propagation in horizontally stratified layer of gyrotropic medium 14 p2283 A66-27125
- Distant-field antenna model of current sheet array used to approximate ultimate decay of mutual coupling in planar array antenna 14 p2257 A66-27926
- Asymptotic behavior of coupling coefficients of infinite array of thin walled rectangular waveguide 14 p2257 A66-27927
- Cumulative coupling and impedance mismatch and radiation pattern problems in large uniformly spaced flat phased array 15 p2456 A66-28585
- Electromagnetic and acoustic wave coupling in homogeneous compressible isotropic plasma and diffraction by half-plane due to sharp structural discontinuities in antenna configurations 15 p2448 A66-28591
- Mean probability of coupling between electrons of flame on electronegative gas and radioactive bromium tracer injected into flame, calculating electrons coupling cross section on bromium atoms 16 p2763 A66-31208
- Nonresonant coupling of, RF power to plasma during ion cyclotron resonance heating in Model C 17 p2962 A66-31822
- Numerical results of slot couplings of rectangular single mode waveguides as function of length, width, position and wavelength 19 p3311 A66-35300
- Laser action in closed molecular system with mixture of carbon dioxide, nitrogen and water vapor, noting coupling-out plate reflectivity and population inversion 19 p3373 A66-35433
- Approximate expression derived for loose coupling in turbulence theory, suggesting possible explanation for inadmissibility of Kraichnan conclusion 20 p3544 A66-36909
- Coupling phenomena in recombination processes of complex ionosphere composed of positive ions under vertical field of ionization drift applied to wind shear theory of sporadic E layers 22 p3907 A66-39962
- Tunable coupling of open waveguide type for semiconfocal Fabry-Perot cavity gives high transmission and high Q 24 p4216 A66-43221
- COUPLING CONSTANT**
- Magnetoelastic coupling constant in microwave frequency of ferrites and garnets 03 p0408 A66-12418
- Phonon interaction with iron group ions characterized by coupling constant discussing double quantum detection of phonon, propagation in dispersive medium and phonon maser 03 p0376 A66-12420
- Quantum scattering theory of hydrogen-like ions in 1-S, 3-S, 1-P and 3-P states 03 p0395 A66-13110
- High sensitivity method for measuring small phase modulations according to line width of Lissajous figures 07 p1005 A66-17346
- Coupling coefficient for different components of cosmic rays based on interaction of primary nucleon with air nuclei 09 p1440 A66-20224
- Cosmological-galactic creation, steady state expansion and high energy particle production associated with radio sources 11 p1774 A66-23068
- Integral multiplicity and coupling coefficient estimation of muon-meson component of cosmic rays for case of primary particle impinging at arbitrary zenith angle 12 p1943 A66-24182
- Radiation impedance of phased array of rectangular waveguides, noting coupling coefficient amplitude, phase difference, etc 14 p2256 A66-27910
- Dynamics of baryon-meson systems in 27-fold representation, obtaining self-consistent bound state and low lying resonant solutions with Balazs method 15 p2544 A66-28945
- Input and output coupling constants of spin-2 mesons with two pseudo-scalar mesons obtained by producing resonances at experimentally observed positions 15 p2544 A66-28947
- Dishal method, logical means of tuning multiple-resonant-circuit filters and for adjusting coupling coefficients between adjacent resonators 15 p2463 A66-29036
- Energy from hydrogen molecule interaction with magnetic field and from hyperfine interaction expressed as products of irreducible spherical tensors 15 p2548 A66-29806
- Coupling coefficient between TE 11 and TM 11 mode in tapered circular waveguides, noting behavior near cut-off frequency 17 p2895 A66-33275
- Coupling coefficients of directed muon component of cosmic rays calculated, noting higher energy displacement with increase of zenith angle 18 p3195 A66-34866
- Resonant cavity transducer for converting TE mode of rectangular waveguide into circular waveguide mode, noting coupling coefficient of cavity 22 p3918 A66-40183
- COUPLING NETWORK**
- Characteristics of balanced transistor amplifiers with symmetrical directional couplers 03 p0342 A66-12708
- Lossless multiconductor transmission line model extended for description of gyromagnetic coupling effects 06 p0846 A66-16094
- Coupled cavity slow-wave circuits, discussing equivalent circuit construction with similar current flow characteristics for behavior analysis 06 p0846 A66-16096
- Circulators from lumped circuit elements examined, calculating coil properties and analyzing construction 11 p1664 A66-22660
- Explicit relation between mutual coupling and radiation pattern of array antenna evaluated via scattering formalism, based on spherical modes 12 p1841 A66-24627
- Coupling impedance selection for Perceptron-like adaptive pattern recognition system 13 p2045 A66-25338
- Passband filters with three coupled circuits, determining circuit characteristics by method based on use of right angle triangles 13 p2043 A66-26315
- Passband filters with three coupled circuits 14 p2246 A66-26802
- Voltage-controlled switch using p-i-n diodes loop-coupled to section of WR975 waveguide for use in satellite tracking radar system 14 p2258 A66-27953
- UHF amplifier design, linear active and coupling networks, loading, admittance-impedance characteristics, etc 14 p2261 A66-28373
- Coupling efficiency evaluation in light emitting diodes 15 p2514 A66-29032
- Slot couplings of rectangular single-mode waveguides analyzed by equivalent circuit and concentrated parameter methods 17 p2879 A66-31856
- Coupling of resonators in electromechanical filter, noting application of energy trapping in piezoelectric resonators 18 p3078 A66-34090
- COVALENT BOND**
- Effect of relativistic interaction terms, mass velocity, Darwin and spin-orbit coupling upon electronic levels of covalent-bond compound semiconductors BN, SiC, AlP and GaAs 04 p0561 A66-13725
- Metal-ceramic boundary structures and reactions, considering metal-oxide and metal-glass interfaces, ionic and covalent bonds, oxidation, reduction, solution and precipitation 13 p2108 A66-25767
- COVARIANCE**
- Covariant treatment of solutions of Einstein field equations representing pure gravitational radiation propagating in fluid and electromagnetic media 15 p2542 A66-29621
- Komar covariant formulation of conservation laws of general relativity obtained directly from variation of scalar curvature density 19 p3401 A66-36168
- Weierstrass characteristic and covariant constant vector fields, noting two metric tensors with same Christoffel symbols, two



connections with same curvature tensor and Ch-equivalence class of metric tensors 22 p3941 A66-40567

**COVER**

**S CLOUD COVER**

**COWLING**

Center of pressure formulae for cowl shapes at zero incidence having profiles for which drag is minimum in Newtonian flow 01 p0006 A66-10344

**CRAB NEBULA**

Intensity of early postexplosion radiation field and high energy electron emission from supernovae 12 p1938 A66-23918

Crab Nebula X-ray spectrum from 16-120 kev by balloon 16 p2792 A66-30143

Coherent plasma radio wave emission ineffective for quasar, Crab Nebula and supernovae remnants 17 p2996 A66-31913

High energy X-ray spectrum from Crab Nebula at photon energies up to 90 kev 18 p3170 A66-34529

Spark chamber experimental investigation of flux of high energy gamma rays at high altitudes near magnetic equator 18 p3193 A66-34849

Depolarization of Crab Nebula produced by Faraday rotation in filamentary shell that surrounds nebula 20 p3648 A66-37261

**CRACK**

**SA FAILURE**

**SA FATIGUE**

**SA MICROCRACK**

**SA STRAIN**

**SA STRESS**

**SA SURFACE CRACK**

Dual trigonometric integral equations solved, then applied to determining stress field due to crack 14 p2325 A66-28391

Flat elliptical crack in infinite elastic medium under shear stress at infinity 22 p3995 A66-40457

**CRACK FORMATION**

Strength of adhesive joints showing ratio of normal and shear stress as important parameter, using crack propagation theory 01 p0152 A66-10380

Distribution of thermal stress in infinite elastic solid containing penny-shaped crack 01 p0157 A66-10960

Stress distribution in vicinity of infinite row of collinear Griffith cracks in elastic body calculated for internal pressure distribution 02 p0298 A66-11577

Varestraint test used to evaluate base metal weldability and influence of particular welding process and welding variables on hot cracking 02 p0236 A66-12227

Fracture micromechanisms of materials having regular crystalline structure, considering mechanical strength, atomic imperfections, dislocation interactions and crack growth 03 p0382 A66-13000

Stress corrosion cracking in titanium alloys in presence of salt, high temperature and sustained stress [AIAA PAPER 65-764] 03 p0383 A66-13059

Causes and development of delayed cracking in material/weld interfaces of high strength steels 03 p0375 A66-13124

Parallel grooves as surface damage in semiconductors produced by ruby laser as diffraction effect 04 p0563 A66-13753

Fractures in neodymium-doped alkaline silicates and borosilicates produced by laser beam 04 p0532 A66-14174

Microstructural alterations developing with cycling stressing in rolling contact exemplified by bearing steel parts [ASME PAPER 65-WA/CF-4] 05 p0779 A66-15623

Load cycle prediction for crack initiation and propagation in notched fatigue specimens 06 p0961 A66-15936

Ultrasonic detection of fatigue crack formation in center-notched sheets of steel and alloys of aluminum and nickel 06 p0884 A66-15938

Microscopic fatigue crack production in compressor blades, describing methods and application to ultrasonic nondestructive testing 06 p0966 A66-16799

Torsional fatigue induced slip bands and crack initiation in aluminum-zinc-magnesium alloy at room temperature to 250 degrees C 07 p1048 A66-17485

Hot cracking in Hastelloy X fusion weld as affected by microsegregation produced

during solidification 10 p1547 A66-21768

Annealing twins and twin-boundary intersections in niobium, noting invalidity of cause-and-effect relationship between twins and crack formation in bcc structures 11 p1717 A66-22998

Formation of fatigue cracks in center notched sheet specimens of various metals ultrasonically tested for axial tensile fatigue 12 p1957 A66-23630

Stress corrosion cracking test employing precracked bar stressed in bending, noting apparatus and results on martensitic steel and titanium alloy 12 p1958 A66-23647

Stress crazing mechanism for amorphous thermoplastics 13 p2112 A66-25305

Unsharpness and contrast effect on slit detection studied by radiography 13 p2086 A66-25820

Crack susceptibility of ultrahigh-strength steel welds related to thermal cycles in welding and heat treating 14 p2292 A66-27325

Heat affected zone cracking in nickel-base superalloys attributed to grain-boundary liquification 14 p2314 A66-27343

Effect of variations of seven elements on resistance of Invar production heats to weld metal cracking, using circular patch test 14 p2314 A66-27344

Crack susceptibility of ultrahigh-strength steel welds related to thermal cycles in welding and heat treating 14 p2301 A66-27345

Opening of parallel cracks by applied tensile stress in terms of dislocation distribution theory 14 p2408 A66-28389

Electron microscope investigation of dislocation effect on stress corrosion cracking in aluminum alloy 15 p2523 A66-29418

Elastic and plastic deformation of polycrystalline metals exposed to ultrasonic load and high temperatures 15 p2523 A66-29601

Stress corrosion testing to evaluate materials for specific application 15 p2523 A66-29723

Stability of two coplanar wedge-shaped cracks, showing under what conditions interaction effects are important 16 p2814 A66-30533

Plasticity problem involving plane strain and plane stress simultaneously, groove formation in machining of high temperature alloys [ASME PAPER 65-PROD-10] 16 p2714 A66-30857

Intercrystalline and transcrystalline fracture in molybdenum 16 p2727 A66-31527

Theoretical attempt to bridge gap between micro and macro crack formation, estimating plane strain transition and nominal stress for fracture 17 p2939 A66-32303

Resistance to cavitation flow erosion and cracking in metal alloys studied, using rotating disk in water [ASME PAPER 66-FE-11] 17 p2915 A66-33265

Stress level for crack initiation and propagation and delayed failures in stainless steel used for bolts 17 p2941 A66-33442

Synergistic action of dynamic stresses and fatigue corrosion in metals 17 p2942 A66-33443

Dislocation distribution and crack propagation due to stress corrosion 17 p2942 A66-33444

Stress distribution in neighborhood of crack in infinitely long elastic strip 17 p3032 A66-33503

Stress-strain state of plane containing crack in nonuniform field of compression stresses, deriving pressure at contact surface 18 p3252 A66-33714

Stress-corrosion cracking of titanium - ASTM Meeting, Seattle, October-November 1965 19 p3377 A66-35647

Susceptibility of titanium alloys to elevated-temperature static and dynamic sea-salt stress cracking, noting operative mechanism 19 p3377 A66-35648

Elevated temperature stress corrosion tests on titanium alloys, noting susceptibility in presence of hot salt 19 p3377 A66-35649

Elevated temperature stress-corrosion cracking behavior of titanium alloys, noting test variables and possible application to SST material selection 19 p3378 A66-35650

Stress corrosion in titanium alloys noting measurement techniques, crack forming

effect of chlorine and surface treatment via metal coating 19 p3378 A66-35651

Cracking and stress corrosion of titanium alloys noting test environment, temperature and measurement techniques 19 p3378 A66-35652

Hot salt cracking of titanium alloys noting stress corrosion, fracture toughness and crack propagation mechanism 19 p3378 A66-35653

Stress corrosion mechanism of titanium noting experimental conditions, results of chemical analyses, time factor, material resistance to crack formation, etc 19 p3378 A66-35654

Cracking of jet engine components made of titanium alloys results from silver chloride stress corrosion 19 p3473 A66-35655

Creep tests on titanium alloy specimens with gauge length salt-coated, noting cracking, time dependency of susceptibility degree, etc 19 p3379 A66-35656

Stress corrosion cracking of titanium alloy in long duration and high temperature tests, using salt coating of specimens 19 p3379 A66-35657

Stress corrosion tests on specimens of titanium alloy in contact with sodium chloride, noting crack formation and effect of argon 19 p3379 A66-35658

Separation of gaseous, liquid and solid reaction products generated by hot salt corrosion of titanium, noting gas diffusion effect on cracking 19 p3379 A66-35659

Thermally induced circumferential-longitudinal cracking of refractory metal inserts in solid propellant rocket engine nozzles 19 p3385 A66-36153

Formation of cleavage crack in crystalline solid, examining crack stability by study of equilibrium dislocation distribution in terms of operative stresses 19 p3475 A66-36728

High strength weldable Al alloys with good cryogenic toughness, stress-corrosion cracking resistance and tensile strength 20 p3582 A66-37091

Stress corrosion cracking of titanium alloy in sodium chloride 20 p3584 A66-37619

Crack initiation and propagation formula through fatigue process applied to interface problems, noting creep 20 p3671 A66-38105

Photomicrographs of pressure crack figures on silicon single crystals at room temperature 21 p3803 A66-39291

Double linear damage rule used in conjunction with crack initiation and propagation equations, applied to cumulative fatigue damage 22 p3989 A66-40116

Gas tungsten arc and electron beam welding for iron-base, nickel-base and cobalt-base alloys, noting use of weld filler metal to avoid cracking 22 p3924 A66-40263

Welding capacity of high-strength alloys of Al-Zn-Mg-Cu system, noting welding techniques, composition effect on mechanical properties and remedies for cracking in welds 22 p3928 A66-40882

Laser beam effect on hydrodynamic bearings, discussing microcracks and critical energy, explaining breakdowns 23 p4078 A66-41409

Stress intensity factors for single-edge cracks in rectangular sheets with end rotations, reducing stress distribution to Riemann-Hilbert problem 24 p4286 A66-42161

Stress-strain analysis of critical load-induced crack formation near elliptic or circular hole 24 p4290 A66-42438

**CRACK PROPAGATION**

Fatigue crack propagation in airframe materials under axial narrow and broadband random loading 01 p0148 A66-10139

Propagation of fatigue cracks in tensioned plate subjected to acoustic loads 01 p0148 A66-10140

Approximate stress intensity factor for embedded elliptical crack in plate subjected to uniaxial tension perpendicular to crack surface 01 p0152 A66-10377

Brittle fracture paths completely predictable and those predictable after initial random propagation 01 p0152 A66-10378

Stress field about axial crack in pressurized cylindrical shell 01 p0152 A66-10379

Stress criterion for crack growth obtained by testing aluminum sheets with transverse



machined cracks 01 p0156 A66-10919  
Crack initiation and propagation in aluminum sheets, noting ductile fracture and load limit for design 01 p0156 A66-10920  
Quantitative analysis of stress level, material characteristics or temperature level at which fracture occurs, using electron microscope 01 p0088 A66-10962  
Constant load rupture test of susceptibility of Ni-Co-Mo maraging steel to delayed hydrogen cracking 03 p0381 A66-12541  
Fracture of brittle bodies with cracks subjected to tension and compression 03 p0441 A66-13291  
Critical loads causing brittle-rupture equilibrium cracks that develop near elliptical holes in bodies that remain elastic up to fracture 03 p0441 A66-13298  
Crack propagation in tungsten single crystals with preexisting microcracks and prestraining at various temperatures 04 p0536 A66-14308  
Load cycle prediction for crack initiation and propagation in notched fatigue specimens 06 p0961 A66-15936  
Initiation and propagation of fatigue crack with reference to fish-eye pattern in ball bearing steel 06 p0965 A66-16489  
Crack propagation in quasi-brittle solid deformed by external load, using thermodynamic laws 06 p0965 A66-16491  
Brittle fracture in ceramic materials, noting Griffith theory on crack propagation, plastic deformation occurrence, stress distribution effect, etc 07 p1054 A66-18499  
Limiting equilibrium state of round infinite plate with circular arc-shaped cracks subject to plane tensile loads 08 p1305 A66-18596  
Research trends of commercial beryllium as affected by physical and alloy properties 08 p1238 A66-18853  
Stress-corrosion failure in metal alloys, discussing surface and elastic energy, adsorption, crack propagation, pits and tunneling 08 p1241 A66-19601  
Oxygen and water vapor effects on propagation of fatigue cracks in aluminum alloy sheets 10 p1614 A66-21338  
Griffith theory of brittle fracture and dependence on stress and load 10 p1614 A66-21339  
Crack opening displacement approach to fracture mechanics in yielding materials 11 p1782 A66-22693  
Field equations of elasticity theory used to solve problem of penny-shaped crack opened by unidirectional displacement in plane 12 p1969 A66-24531  
Prediction of fatigue failure of structure subjected to sinusoidal stress cycles of different amplitude and mean value [ASME PAPER 65-MET-3] 12 p1970 A66-24555  
Evaluation of model of strain hardening in fatigue with crack propagation occurring by plastic flow away from crack tip during tensile part of cycle 12 p1898 A66-24971  
Thermoplastics behavior under cyclic stress, noting failure under crack propagation or temperature due to damping capacity 13 p2112 A66-25306  
Results of crack propagation tests on polymethylmethacrylate flexed at various frequencies under cyclic loading 13 p2112 A66-25308  
Naval Ordnance Laboratory /NOL/ multiaxial fatigue test for failure mechanisms in fiber-reinforced composite materials involving cyclic stress under controlled environmental conditions 13 p2113 A66-25312  
Propagation of brittle cracks in body under compression, discussing theory of resistance of brittle bodies to compression 13 p2196 A66-25629  
Fracture surfaces of metals and alloys examined, using optical and electron microscopy, noting fracture mechanisms during crack initiation and propagation 13 p2108 A66-25768  
Production techniques for fissures in weld-deposited and wrought Ni-Cr-Fe alloy fatigue specimens and fissure effect on fatigue strength 13 p2110 A66-26017  
Equilibrium cracks in half-space and elastic layer with two rigid clamp supports 13 p2201 A66-26403

Limiting equilibrium of plate weakened by system of cracks along straight line at angle to tensile force 13 p2201 A66-26404  
Slip bands in thin plates with rectilinear cuts under tension 13 p2201 A66-26408  
Critical load under uniaxial tension for thin infinite plates with holes weakened by cracks 13 p2202 A66-26415  
Inhomogeneous elastic half-spaces examined for circular crack in plane of contact and perpendicular tensile forces, using Griffith fracture theory 13 p2203 A66-26421  
Critical load of infinite plane under tension weakened by crack evaluated by Griffith fracture theory 13 p2203 A66-26422  
Approximation method for determining limit and breaking load for infinite brittle body weakened by plane crack, noting crack propagation 13 p2203 A66-26423  
Fatigue crack propagation in low-alloy heat-treated notched steels with high yield strength [ASME PAPER 66-MET-2] 14 p2311 A66-26970  
Low cycle fatigue crack propagation characteristics of high strength steels, noting technique for life estimation of structure by numerical integration [ASME PAPER 66-MET-3] 14 p2312 A66-26971  
Fatigue crack initiation and propagation, using ultrasonic test instruments 15 p2610 A66-29316  
Low endurance fatigue properties of steel plate 15 p2615 A66-29805  
Creep fatigue, thermal cycling, vibration control, transient thermal response control, structural loads and hot part reliability relating to long-life jet engine failure [SAE PAPER 660311] 15 p2572 A66-29836  
Brittle materials failure theory for cases where presence of plane deformation or plane stressed state is assumed, using Griffith theory 16 p2822 A66-31510  
Crack formation and cleavage surfaces treated via variational principle 16 p2727 A66-31529  
Interfaces between fatigue, creep and fracture, discussing separation of fatigue process into crack initiation and crack propagation 16 p2823 A66-31711  
Growth of symmetrical plane cracks in axial symmetry and plain strain 17 p3018 A66-31927  
Photoelastic and stress quenching techniques, showing change in stress distribution with crack propagation 17 p3026 A66-32595  
Metal fatigue under randomly distributed stress noting crack propagation, computer solution of integral recurrence relations, etc 17 p3029 A66-32790  
Stress level for crack initiation and propagation and delayed failures in stainless steel used for bolts 17 p2941 A66-33442  
Stress calculation for infinite strip containing straight semiinfinite crack when clamped boundaries are displaced normal to crack 18 p3248 A66-33583  
Transverse displacement of circular plate containing radial crack examined, using small deflection theory 18 p3249 A66-33597  
Air and aqueous environments effect on mode of fracture in titanium alloys during low cycle fatigue 18 p3122 A66-33749  
Propagation of stacking faults in fcc metals, noting effect of frictional force in cutting through attractive tree and subsequent dipole formation 18 p3258 A66-34631  
Susceptibility of titanium alloys to elevated-temperature static and dynamic sea-salt stress cracking, noting operative mechanism 19 p3377 A66-35648  
Design and testing of crack-notched specimens for determination of resistance of materials to unstable opening-mode crack extension under plane strain conditions 19 p3473 A66-35805  
Singular integral equations with constant coefficients solved by Jacobi polynomials and applied to problems in fluid dynamics, crack propagation, plane elastic theory, etc 19 p3393 A66-36836  
Crack propagation, damage and fatigue fracture in plane rods with transverse cut under single step and multistep axial

load 20 p3666 A66-37307  
Metastable dislocation crack transformation into polygonal walls of edge dislocations caused by diffusion over crack surface 20 p3669 A66-37551  
Electric potential method used to study slow crack growth in center-notched plate specimens 20 p3670 A66-37794  
Stress wave, deformation and fracture caused by liquid impact, noting analogy with solid and explosive impact and loading fracture formation, propagation, etc 20 p3588 A66-37803  
Stress distribution at vertex of rapidly propagating crack in celluloid sheet of 3 mm thickness studied by polarization technique 20 p3672 A66-38114  
Plastic strain distribution near axisymmetric slit in ideally elastoplastic material described by Dugdale model 20 p3673 A66-38269  
Thin film transmission electron microscopic analysis of stress corrosion of heat-treated aluminum 21 p3749 A66-38471  
Stainless steel and aluminum alloy fracture behavior under static load and low temperatures, noting crack propagation, stress and crack-length relation, etc 21 p3830 A66-39195  
Fatigue fracture and crack propagation in ordered alloys due to plastic flow 22 p3989 A66-39891  
Double linear damage rule used in conjunction with crack initiation and propagation equations, applied to cumulative fatigue damage 22 p3989 A66-40116  
Brittle-fracture propagation tests, obtaining relations among crack propagation speed, dynamic-stress distribution, test temperature and applied stress 22 p3994 A66-40435  
Residual stress, crack propagation and fatigue fracture mechanisms in Al alloy sheets with fatigue cracks, for use in wing panels [ICAS PAPER 66-34] 23 p4137 A66-41007  
K values for crack propagation rates obtained from fatigue experiments on metals, noting correlation with tensile properties of metals 23 p4082 A66-41865  
Griffith type crack propagation due to localized thermal stress at holes, cavities, penny-shaped cracks and inclusions disturbing uniform heat flow 23 p4146 A66-41993  
Rivet attached stringer effect on stress concentration in thin elastic sheet with crack solved, using computer calculations 24 p4285 A66-42143  
Stress intensity factors, strains and rotation in infinite eccentrically cracked strip under uniform tensile stress applied at infinity 24 p4286 A66-42157  
Griffith and bond fracture with singular stresses near crack point examined via numerical analysis 24 p4288 A66-42276  
**CRASH**  
Crash and ballistic protective flight helmets, noting use of improved energy dissipating materials 17 p2863 A66-32146  
**CRASH INJURY**  
Structural design of transport aircraft to reduce fatalities, analyzing protective shell to withstand ground impact load and fuel containment [AIAA PAPER 65-773] 03 p0434 A66-12592  
Results of aircraft accidents in terms of injury and death in-flight, on impact, after impact and during escape 10 p1495 A66-22141  
Flight accident casualties, pathological changes in bodies of victims of Comet 4C SA-R7 accident in Italy 14 p2229 A66-26812  
Medical inquest of Britannia 312 crash near Innsbruck 19 p3294 A66-36441  
Air Force pathologist role in accident investigation, noting crash injuries 19 p3294 A66-36443  
**CRATER**  
SA LUNAR CRATER  
SA METEORITIC CRATER  
SA METEOROID CRATER  
Age of Martian craters investigated, based on asteroid collision and certain spatial distribution 01 p0136 A66-10439  
Lunar Lake depression explained by cryptovolcanic activity or meteorite impact 03 p0365 A66-12721  
Permanent angular displacement about vertical axis and ejecta-induced impulse



associated with Sedan crater formation 08 p1292 A66-19260  
 Age of Bosumtwi crater area, Ghana, determined by mass spectrometry of rubidium, strontium and strontium isotopic composition, compared to Ivory Coast tektite age 10 p1608 A66-21741  
 Craters on Mars from Mariner IV pictures, showing no evidence of primeval crater and analyzing aeolian erosion 16 p2800 A66-30629  
 Crestone crater morphology indicates that it is not meteoritic or cometary in origin 18 p3106 A66-34462  
 Martian surface markings, brightness along optical equator, crater erosion, asteroid collision and yellow dust clouds 22 p3981 A66-40520

## CRATERING

## SA HYPERVELOCITY CRATERING

Comparison of cratering on Earth and Moon, resulting from high velocity impact of solid objects upon planetary masses 12 p1949 A66-24199  
 Hypothesis that Luna IX rocket exhaust during soft landing caused formation of shallow crater visible in Ranger VII lunar probe photographs 15 p2593 A66-28681

## CREATIVITY

General purpose computers for solution of problems in creative design 01 p0033 A66-10863

## CREEP

## SA DEFORMATION

## SA DUCTILITY

## SA PLASTIC FLOW

## SA SHEAR CREEP

## SA STEADY STATE CREEP

## SA TENSILE CREEP

Measurement of creep rate complex stress time relations for copper under loading conditions at 250 degrees C 06 p0897 A66-16949

Approximate solution method for unsteady creep of shells within framework of theory of aging 07 p1146 A66-18254

Membrane creep and plastic deformation of annular flat plate bounded by concentric circles and subjected to evenly distributed pressure 12 p1958 A66-23710

Vaporization and creep rupture behavior of type 316 stainless steel 18 p3123 A66-33755  
 Mechanical construction materials behavior, discussing application of creep and plasticity laws 20 p3666 A66-36951

Shell stability in Euler formulation, taking into account actual redistribution of stresses that results from initial deflection and creep, noting buckling of closed cylindrical shell under axial compression 21 p3829 A66-38978

Grain boundary cavity growth in Al-Cu alloy during compressive creep testing 22 p3935 A66-40291

Creep relaxation effect on high strain fatigue in chromium and molybdenum steels 23 p4139 A66-41699

## CREEP ANALYSIS

Generalized rheological models with varying relaxation time 01 p0159 A66-11179  
 Stability of thin walled cylindrical dural shells under creep during compression and bending 02 p0297 A66-11396

Vacuum creep study of mechanical behavior of solution-hardened alloy of niobium containing tantalum, tungsten and molybdenum from 980 to 1370 degrees C 03 p0380 A66-12491

Practical data processing of stress rupture results for steels with elevated operating temperatures, tentative procedure proposed and applied 03 p0384 A66-13161

Parametric formulas for extrapolating creep and stress-rupture data for high temperature steels 03 p0439 A66-13165

Vibrational creep of polymer materials when small dynamic component resulting from heating of material due to energy dissipation of oscillations is imposed on static load 04 p0538 A66-14426

Creep damage in metal, discussing future creep rupture life, exposure, mechanical properties and heat treatment for removing damage 04 p0537 A66-14466

Norton-Hoff creep parameters by cold working tests and relaxation tests 05 p0771 A66-14534

Stress effect on negative creep in chromium-nickel-titanium steels, noting

temperature effect and specific volume change 05 p0699 A66-14684

Prior creep exposure on 1400 degrees F strength of Inco 713 cast nickel-base alloy, discussing microstructural change effects on mechanical properties [ASME PAPER 65-WA/MET-12]

05 p0703 A66-15686  
 Dimensionless parameter reliability analysis, deriving system reliability functions as applied to mechanical creep [ASME PAPER 65-WA/MET-6]

05 p0780 A66-15689  
 Elasto-creeping circular membrane, obtaining nonlinear solution for axisymmetric circular elastic creep problem 07 p1142 A66-17263

Deflections and stresses of shallow shell under creep conditions, reducing problem to system of two nonlinear integro-differential equations 07 p1143 A66-17628

Contact pressure between two bodies with two contact sections in the theory of creep 07 p1146 A66-18255

Creep problem of thin shallow shells in terms of viscoelastic theory, considering isotropic homogeneous and orthotropic quasi-homogeneous materials 08 p1311 A66-19340

Creep properties of EP-376 steel under slowly varying loads 08 p1241 A66-19590

Creep motion and hydromagnetics of ellipsoid moving in cross field 09 p1408 A66-20580

Nonlinear creep and recovery behavior of polypropylene fibers and hereditary functionals describing nonlinear viscoelastic behavior 09 p1393 A66-20663

High-temperature plastic deformation of single crystals, noting creep and dislocation 10 p1613 A66-21244

Creep analysis of close-coiled helical springs 10 p1613 A66-21319

High temperature creep measurement in helical spring 11 p1781 A66-22692

Creep behavior in Ni-Fe alloys at high temperatures, using one composition inside ordered regions and another 11 p1717 A66-22993

Diffusivity, elastic modulus and stacking fault energy effect on high temperature creep behavior of alpha brasses 11 p1717 A66-22996

Properties of moving dislocations in unstabilized creep at various temperatures analyzed by kinetic equations in Akulov theory 11 p1784 A66-23323

Vibrocreep mechanism resulting from polymeric material heating under vibrating load, noting increase of creep rate and structural changes 12 p1958 A66-23665

Circumferential creep strain of cylinders subjected to internal pressure 12 p1959 A66-23797

Russian monograph covering theory of elasticity, plasticity and creep 12 p1960 A66-23898

Creep laws in terms of generalized stress-strain rates formulated, noting secondary deformation, Tresca criterion and associated flow rule 12 p1963 A66-24037

Stress concentration in T tails of turbine blades by photoelasticity and photocreep 12 p1966 A66-24064

Axisymmetric creep of circular cylindrical shells taking into account axial forces 12 p1968 A66-24347

Dimensionless parameter reliability analysis, deriving system reliability functions as applied to mechanical creep [ASME PAPER 65-WA/MET-6]

12 p1970 A66-24540  
 Prior creep exposure on 1400 degrees F strength of Inco 713 cast nickel-base alloy, discussing microstructural change effects on mechanical properties [ASME PAPER 65-WA/MET-12]

12 p1896 A66-24542  
 Diffusion creep rate of thin foil of pure polycrystalline material 12 p1971 A66-24925

Buckling of rod with initial deflection as sinusoidal half-wave, using Bubnov-Galerkin method and Laplace transform, calculating stresses of rod when subjected to nonsteady creep 13 p2206 A66-26457

Effect of temperature on cyclic minimum creep rate and other phenomena associated with cycle dependent deformation from 77.4

to 295 degrees K [ASME PAPER 66-MET-7]

14 p2395 A66-26975  
 ASTM-ASME Joint Committee report on high temperature properties of stainless steels such as stress-temperature, yield and rupture curves, etc 14 p2313 A66-27229

Lateral creep deflection vs time relations in nonuniform thermal environments for linear polymer column described as combination of Maxwell and Voigt elements 14 p2396 A66-27355

Elastic analog for geometrically nonlinear membrane undergoing creep 14 p2396 A66-27381

Elastic analog applicability to geometrically nonlinear creep theory of circular membranes 14 p2397 A66-27390

Matrix methods for stress and deformation analysis for structures subject to plasticity and creep 14 p2402 A66-27887

Andrade creep law for metals, based on Davis law modified for variable temperature 15 p2611 A66-29420

Tensile and compressive creep behavior deduced from deflection measurements in creep bending tests on beams of trapezoidal cross section 15 p2614 A66-29666

Second-order effects in dissipative solids and their accumulation in causing rapid acceleration of tensile metal creeps 16 p2814 A66-30529

Creep and stress relaxation as function of slope of master curve in transition region 16 p2818 A66-31068

Interfaces between fatigue, creep and fracture, discussing separation of fatigue process into crack initiation and crack propagation 16 p2823 A66-31711

Creep behavior of selected polypropylene monofilament under axial loading 17 p3029 A66-32789

Nonlinear theoretical derivation of creep equations for three-dimensional processes in polymers, based on Boltzmann-Volterra creep heredity concept using stress-strain summation 17 p2943 A66-32807

Stress concentration in nonlinear creep of long thin cylindrical shell loaded at one edge by symmetrical radial shear and bending moment 18 p3248 A66-33578

Existence and uniqueness of solution in viscoelasticity theory for aging materials, considering four boundary value problems for body subjected to finite deformations 18 p3255 A66-34393

Strain-energy exposition of creep deflection theory and Ritz-Rayleigh method prediction of creep deformations of laterally loaded circular plates 18 p3256 A66-34561

Stress effects on plane creeping Newtonian flows of incompressible second-order fluids 18 p3103 A66-34929

Finite creep equations derived for circular sandwich plate under lateral pressure, considering bending moments and tensile forces 19 p3472 A66-35392

Time dependence of dislocation density in single crystal MgO undergoing plastic deformation at elevated temperatures 19 p3387 A66-35421

Hereditary theory based on stress and temperature superposition principle applied to metal creep 19 p3473 A66-35754

Creep testing of glass fiber reinforced thin plastic plates and beams under torsion and bending 19 p3473 A66-35756

Creep analysis of high temperature niobium alloys in very high vacuum 19 p3385 A66-36155

Oscillation of oscillator with elastically hereditary and weakly nonlinear characteristics, applying operational method to analysis in terms of hereditary creep theory 19 p3476 A66-36840

Tensile, creep and stress-strain behavior of high nitrogen content stainless steel quenched alloy at cryogenic temperatures 20 p3583 A66-37093

Real-order exponential function and application to describing creep process and to extrapolate time-to-rupture 20 p3669 A66-37539

Plane nonlinear creep of free boundaries in incompressible isotropic viscous fluid body 20 p3669 A66-37543

Creep design reliability criteria for creep-rupture and critical creep-strain modes of



structural element failure, both singularly and combined or bimodally 20 p3571 A66-37941

Nonsteady state zero-moment creep in shells of revolution with clamped edges under internal pressure, finding change range in stresses in time 21 p3826 A66-38612

Creep analysis at variable temperatures, noting creep rate and strain, transformed time hypothesis, temperature gradient effect, etc 21 p3826 A66-38615

Book on strength of turbine disks, analyzing material properties, design and operating conditions 21 p3743 A66-38948

Vibrational creep phenomenon occurring when small dynamic loads are superposed on static loads in thin wall steel tube 21 p3830 A66-38983

Vibrocreep mechanism resulting from polymeric material heating under vibrating load, noting increase of creep rate and structural changes 22 p3988 A66-39709

Creep analysis of stress-strain-time relation in metal with complex loading 23 p4136 A66-40998

Creep rate of polycrystalline thorium dioxide for high temperatures and pressures, examining intergranular voids formed by growth and coalescence of pores along grain boundaries 23 p4082 A66-41772

Generalized strain and transition concepts for elastic-plastic deformation creep and relaxation 23 p4144 A66-41973

Creep testing of tubular copper samples under combined tension and torsion with constant and variable loads 23 p4083 A66-41976

Steady state creep analysis of shell loads by uniform pressure for simply supported and clamped edges 23 p4145 A66-41977

Microscopic strain rate equation interpreting macroscopic creep, stress-strain and impact test results 24 p4288 A66-42274

Vibrational creep of Al alloy at normal temperature, noting plastic deformation magnitudes creep limit equations, etc 24 p4228 A66-42864

**CREEP BUCKLING**

Creep buckling, examining two-hinged H-section long column under distributed axial load and effect on buckling time, column deflection and numerical results of example 03 p0436 A66-12720

Beam deflection in creep bending for statically determinate and indeterminate cases [ASME PAPER 64-WA/MET-9] 06 p0961 A66-16208

Axisymmetric creep in cylindrical shells, noting creep buckling collapse after high temperature compression loading [AIAA PAPER 66-123] 08 p1308 A66-19002

Extensive creep deformation of thin zero-moment shell of revolution under action of internal and axial load 12 p1966 A66-24059

Creep buckling of columns under axially nonuniform temperature distribution 12 p1969 A66-24364

Creep buckling of column subjected to arbitrary temperature distribution along column, considering aluminum alloy 14 p2403 A66-27971

Creep buckling of column with nonuniform vertical temperature distribution 14 p2408 A66-28344

Instability of nonlinearly viscoelastic column under finite compression, noting boundary conditions, application to buckling problem, types of stability loss, etc 15 p2615 A66-29720

Creep bending of circular plate with temperature gradients, using iterative technique 16 p2813 A66-30269

Boundary value problems in secondary creep of circular thin shells under axisymmetric loading, giving solutions for deformation rates and stress resultants 17 p3030 A66-32891

Creep buckling of long curved sandwich panel 18 p3259 A66-35014

Load level as stability loss condition for bulging of elastoplastic rod in presence of creep 19 p3473 A66-35753

Calibration test for photorheological method of stress analysis in plastically flowing body under plastic work or creep deformation 20 p3671 A66-38101

Variational theorems for creep of shallow cylindrical shells, noting buckling and snap-through of square cylindrical panel compressed along generatrix 21 p3829 A66-38977

Stability theory methods for small elastoplastic deformations generalized to include creep effects in cylindrical shells compressed at ends 24 p4292 A66-42885

**CREEP DIAGRAM**

Sample deformation measuring device for short duration heat resistance tests 07 p1148 A66-18390

Forced oscillations of elastohereditary systems, using Rabotnov functions as kernels of integral operators, permitting description of creep curves for materials 08 p1307 A66-18884

Graphical solution to Garofalo equations describing first-and second-stage creep data 18 p3252 A66-33731

Initial nonsteady, steady and accelerated alloy creep test data surveyed and compared with phenomenological theory 19 p3473 A66-35757

Crack initiation and propagation formula through fatigue process applied to interface problems, noting creep 20 p3671 A66-38105

Strain-time curve of silver containing aligned tungsten wires at high temperatures, noting reduction of creep rate of matrix 22 p3935 A66-40200

**CREEP RESISTANCE**

Strength and heat resistance of alloys, particularly low alloy steels 01 p0084 A66-10286

Stress and temperature effects on nickel creep strength after prestressing at 4.2 and 300 degrees K 03 p0383 A66-13126

Brittle creep susceptibility of heat resistant chromium steels reduced by proper thermal treatment 03 p0384 A66-13162

Thermal contact resistance between uniformly loaded thin plates in vacuum, noting hysteresis test for effect of creep [ASME PAPER 65-HT-16] 05 p0783 A66-14740

Alloy steel fracture resistance, describing creep strain effect on gas turbine engine alloys [ASME PAPER 65-WA/MET-13] 05 p0703 A66-15685

Thorium dioxide strengthened nickel and nickel molybdenum alloys, discussing production via selective reduction, strength, creep rupture, stability and ductility characteristics 06 p0893 A66-15943

Ultrahigh-vacuum creep behavior of columbium and tantalum alloys at high temperature and over long period 06 p0894 A66-16069

Dilute tungsten rhenium alloys, determining ductility parameters, fabrication, tensile properties and creep behavior 06 p0894 A66-16070

Polyimide resins for extreme environments, discussing chemical structure, application, electrical, thermal and mechanical properties, radiation resistance, etc 06 p0899 A66-16292

Extensometer system and specimen alignment fixture for cylindrical or flat creep specimens 09 p1465 A66-19949

Alloy steel fracture resistance, describing creep strain effect on gas turbine engine alloys [ASME PAPER 65-WA/MET-13] 12 p1896 A66-24535

Scattering mechanical properties of ternary alloy creep resistant steel, emphasizing effect of heat treatment on microstructure [ASME PAPER 66-GT-112] 14 p2312 A66-27006

Temperature and creep aftereffect in high purity crystalline cadmium 15 p2523 A66-29600

Creep fatigue, thermal cycling, vibration control, transient thermal response control, structural loads and hot part reliability relating to long-life jet engine failure [SAE PAPER 660311] 15 p2572 A66-29836

Oxide-base cermets prepared by infiltration with silver and silver alloys, noting dispersion strengthening, bend creep, impact loading, etc, for gas-turbine application 16 p2730 A66-30250

Estimation of creep in Ti-Al-V alloys by high temperature bending method 16 p2724 A66-31237

Structural changes effect on creep resistance of heat resistant alloys 16 p2728 A66-31801

Creep tests on titanium alloy specimens with gauge length salt-coated, noting cracking, time dependency of susceptibility degree, etc 19 p3379 A66-35656

Creep-rupture strength and metallurgical properties of refractory Mo at 4000 degrees F 19 p3385 A66-36156

Out-of-pile thermionic power system using inert gas for heat transfer from reactor to converter, noting creep-rupture problem of materials 23 p4023 A66-41767

Cold-drawing effect on creep behavior of nickel-aluminum alloy at various temperatures through changes in fracture, precipitates and structure 24 p4227 A66-42309

Regenerative heat treatment for increasing creep life of high temperature alloys used in turbines 24 p4227 A66-42508

**CREEP TESTING MACHINE**

Creep tests to verify validity of coincident axis and constancy of volume postulates of Alcoa 1100-0 aluminum alloy 06 p0968 A66-17178

High temperature extensometer using linear variable differential transformer 07 p1030 A66-17230

Creep testing apparatus for metals, with automatic recording of longitudinal and transverse deformations at high temperatures 11 p1780 A66-22600

Apparatus for determining dynamic compressibility, creep behavior and viscoelastic properties of polymers 13 p2115 A66-26115

Creep compliance testing apparatus for surface penetration of low modulus viscoelastic plate by 1/4-inch steel sphere 13 p2115 A66-26288

Compressive creep in thermoplastic materials measured, using simple test cell apparatus 14 p2319 A66-28483

Program controlled device for applying tensile force and torque to thin walled tubular specimen during analysis of creep under stress 21 p3827 A66-38618

**CREW**

S AIRCREW

S ASTRONAUT

S FLYING PERSONNEL

S PILOT

S SPACECREW

**CRITICAL FREQUENCY**

Computer program for average values of critical frequency of F-2 layer and deviation 02 p0224 A66-12125

Correlation dependence of F-2 layer on solar wave energy entering Earth atmosphere 04 p0515 A66-13850

Comparison of diurnal variations of ionization level in F region at geographically and geomagnetically conjugate stations in Arctic and Antarctic 04 p0516 A66-13851

Critical frequency of F-2 layer at Huancayo and variation with magnetic activity at different epochs of solar activity 04 p0517 A66-14378

Transmission band and critical frequencies calculation for straight waveguides of stepped cross section 06 p0838 A66-15884

Variation in dispersion and asymmetry of F-2 layer critical frequencies, plotting particular secular variations 06 p0950 A66-16593

Harmonic analysis of diurnal changes in critical frequencies of F-2 layer as function of season and solar activity 08 p1285 A66-19777

Simplified calculation of eigenvalues of double-ridge and single-ridge waveguides from which critical frequency and wavelength are determined 11 p1656 A66-22738

Turbulence-excited atmospheric velocity, critical frequency of atmosphere, solar atmospheric power spectrum of acoustic field velocity correlation, solar convection zone, etc 11 p1772 A66-22777

Circular ring loaded by constant direction forces used to illustrate kinetic instability of elastic system under random time-dependent forces 12 p1960 A66-23950

Satellite data indicates correlations between cosmic ray variations and radiation intensity of radiation belts and related phenomena 12 p1941 A66-24170



Statistical distribution of monthly median noon critical frequency of F-2 layer from ionospheric stations at mid-latitudes, auroral regions and at polar cap 12 p1870 A66-24286

Ionospheric station simultaneous observations of sporadic E layer critical frequency variations 13 p2073 A66-26236

Lunar tidal variations in monthly median noon critical frequency in American zone during low solar activity 14 p2285 A66-27727

Computer program for average values of critical frequency of F-2 layer and deviation 14 p2287 A66-28083

Critical ionization frequencies in F-2 layer in near-polar region observed at Northern Hemisphere high latitude 15 p2487 A66-29107

Spectrum analysis of critical frequency of F-2 layer 16 p2692 A66-30330

Day-to-day variations in F-2 critical frequency 16 p2693 A66-30339

Anomalous behavior in correlating maximum electron density dependence on solar zenith distance and asymmetry in critical frequency for E layer 17 p2919 A66-32881

Contribution to dependence of variation of unperturbed ionospheric F-2 critical frequencies on season and solar activity 18 p3105 A66-34097

Phase characteristics and amplitude of correcting device ensuring closed loop mechanical system stability at critical frequency 18 p3092 A66-34995

Harmonic analysis of diurnal changes in critical frequencies of F-2 layer as function of season and solar activity 21 p3809 A66-38773

Simultaneous long term ionospheric variation in midday averages of critical frequency E and F-2 at Washington, D.C. before and after increased geomagnetic activity 22 p3914 A66-40560

Simplified calculation of eigenvalues of double-ridge and single-ridge waveguides from which critical frequency and wavelength are determined 23 p4045 A66-41476

**CRITICAL LOADING**

Efficiency of fail-safe and safe-life designs as design guideposts for static and fatigue loadings 01 p0076 A66-10065

Critical loads for anisotropic plates of various configurations and boundary conditions, detailing stability of rectangular plate and orientation of axes 01 p0154 A66-10477

Critical load of ellipsoidal end faces of cylindrical reservoir assuming deformation beyond critical load is axisymmetric 01 p0155 A66-10657

Discrete critical points of perfect structural system and three branching points in general theory of elastic stability 03 p0434 A66-12370

Critical loads causing brittle-rupture equilibrium cracks that develop near elliptical holes in bodies that remain elastic up to fracture 03 p0441 A66-13298

Equilibrium stability of rod beyond elastic limit 04 p0590 A66-14161

Nonconservative loading on linear two-degree of freedom elastic system, discussing damping effects on equilibrium stability [ASME PAPER 65-WA/APM-17] 05 p0777 A66-15439

Critical combinations of uniform pressures and concentrated loads at apex acting on shallow spherical shells determined, deriving basic differential equation [ASME PAPER 65-WA/APM-27] 05 p0778 A66-15448

Effect of torsional and lateral restraints on elastic critical load of centrally loaded simply supported beam buckling laterally 06 p0966 A66-16613

Collapse of pressurized axially stiffened thin cylinder 06 p0967 A66-16933

Elastic critical load of centrally loaded simply-supported beam which buckles laterally out of plane derived by Airy integral functions 07 p1144 A66-18049

Edge conditions effect on elastic stability of cylindrical shells extended to additional combinations of boundary conditions, considering cylinders under axial compression 08 p1310 A66-19144

Stability of thin-walled conical shells under

axially symmetric loading determined from nonlinear shell theory 10 p1614 A66-21382

Nonconservative loading on linear two-degree of freedom elastic system, discussing damping effects on equilibrium stability [ASME PAPER 65-WA/APM-17] 12 p1961 A66-23983

Critical load of ellipsoidal end faces of cylindrical reservoir, assuming deformation beyond critical load is axisymmetric 12 p1963 A66-24015

Linear creep stability of orthotropic shells, considering shear creep and lateral buckling, determining critical loads and noting errors 13 p2113 A66-25913

Critical load under uniaxial tension for thin infinite plates with holes weakened by cracks 13 p2202 A66-26415

Critical load of infinite plane under tension weakened by crack evaluated by Griffith fracture theory 13 p2203 A66-26422

Axisymmetric form of stability loss of cylindrical shell under effect of load suddenly applied along generatrix, considering inertia forces and obtaining differential equations 13 p2206 A66-26456

Imperfections and edge restraint effect on buckling of axially compressed cylinders 14 p2404 A66-27988

Destabilization of linear system with N degrees of freedom without damping subjected to nonconservative forces 15 p2609 A66-29251

Collapse loading of rotationally symmetric cylindrical shell 15 p2609 A66-29253

Critical load determination via trial and error method and transfer and stiffness matrices 17 p3023 A66-32309

Approximation method for checking stability of compression members in rigid-joint space truss or stability against out-of-plane buckling of compression members in rigid-joint plane truss 19 p3475 A66-36489

Critical buckling load at middle plane of variable-rigidity plate 21 p3832 A66-39376

Critical combinations of uniform pressures and concentrated loads at apex acting on shallow spherical shells determined, deriving basic differential equation [ASME PAPER 65-WA/AMP-27] 24 p4285 A66-42149

Stress-strain analysis of critical load-induced crack formation near elliptic or circular hole 24 p4290 A66-42438

Critical loading and stability of three-layer sloped asymmetric shells beyond elastic limit for arbitrary stress-strain diagram 24 p4290 A66-42442

**CRITICAL PATH ANALYSIS**

Reflection coefficient and critical length determination for unstable convective modes in weakly homogeneous plasmas 10 p1567 A66-21819

**CRITICAL POINT**

Electrical impurity effect on critical temperature in superconductor 03 p0413 A66-13193

Electron-phonon interaction for calculation of critical temperature for ordinary and anomalous superconductors 04 p0568 A66-14347

Paramagnetic impurity effect on critical temperature of superconductor for two-band model 05 p0738 A66-15346

Liquid-gas coexistence curve shape near critical point, allowing for volume and temperature deviations and for mathematical singularities 08 p1316 A66-18796

Magnetic and resistive superconducting transitions on bulk samples of indium-lead alloys in alpha-phase region, considering results relative to Glag theory 09 p1423 A66-20067

Asymptotic expansions of double and multiple integrals occurring in diffraction theory, using stationary phase method 10 p1550 A66-21850

Superconductivity variation in tantalum noting dependence of critical current, transition temperature and magnetic field on impurity concentration 12 p1927 A66-23856

Numerical solution of problem of supersonic flow at angle of attack past arbitrarily smooth conical bodies 12 p1798 A66-24441

Neutron irradiation effect on superconductive properties of tin and indium foils at low temperatures, noting

decrease of critical temperature and field 14 p2364 A66-27641

Critical conditions of waveguide with dielectric bushing for case of nonsymmetrical waves 14 p2259 A66-28161

Electron-phonon interaction for calculation of critical temperature for ordinary and anomalous superconductors 14 p2368 A66-28243

Betti numbers shown to be equal to binomial coefficients of torus, determining minimal set of van Hove critical points 15 p2559 A66-28624

Correlations between Lennard-Jones potential parameters and critical and boiling point constants of 28 nonpolar and 17 polar gases 15 p2618 A66-29718

Paramagnetic impurity effect on critical temperature of superconductor for two-band model 15 p2569 A66-29985

Semiautomatic potentiometer measurement of nitrogen specific heat at small intervals, noting applicability of logarithmic law for other temperature ranges 16 p2829 A66-31168

Critical temperatures and critical magnetic fields determined for superposed normal and superconducting films, noting dependence on metal thickness 19 p3443 A66-36003

Critical temperature of several bulk dilute solid solutions of transition metals in Al, Zn, In and Sn, examining effect of transition-metal impurities 21 p3796 A66-38556

Time dependent Ising-model description of binary liquid mixture near critical temperature 22 p3947 A66-39922

**CRITICAL PRESSURE**

Critical combinations of uniform pressures and concentrated loads at apex acting on shallow spherical shells determined, deriving basic differential equation [ASME PAPER 65-WA/APM-27] 05 p0778 A66-15448

Critical flow rate, critical pressure ratio and critical mass flow of dissipative adiabatic nozzle and pipeflow of ideal gas 16 p2690 A66-31635

Wall thickness requirement for cylindrical shell stability under critical radial compression derived by generalized power series 20 p3673 A66-38271

Computer analysis of cylindrical shell stability under uniform external pressure and critical pressure determination for various boundary conditions 21 p3829 A66-38979

Critical combinations of uniform pressures and concentrated loads at apex acting on shallow spherical shells determined, deriving basic differential equation [ASME PAPER 65-WA/AMP-27] 24 p4285 A66-42149

**CRITICAL REYNOLDS NUMBER**

Critical Reynolds number for pulsating Poiseuille flow determined by studying stability under harmonically and nonharmonically varying pressure gradient [ASME PAPER 66-FE-5] 17 p2914 A66-33260

Critical Reynolds number for pulsating Poiseuille flow determined by studying stability under harmonically and nonharmonically varying pressure gradient [ASME PAPER 66-FE-5] 24 p4195 A66-42578

**CRITICAL SPEED**

Effect on critical speed of thin rotating disk produced by rigid circular inclusion welded at center 19 p3363 A66-35591

**CRITICAL STRESS**

Semizero-moment shell with one edge braced by elastic support with small rigidity for deformation out of plane, noting magnitude of critical stress 04 p0588 A66-13566

Bubnov-Galerkin method extended to solution of any system of equations not associated with variational principles 08 p1306 A66-18605

Axisymmetric loss of static stability of closed circular cylindrical shell subject to longitudinal compressive stresses 08 p1312 A66-19430

Cleavage characteristics of copper plate under explosive load determined and interpreted, taking finite failure time into account 10 p1613 A66-21238

Breaking stresses in two connected elastic half-spaces determined with aid of Griffith-



- Sneddon criterion 12 p1968 A66-24349  
Effect of random distribution of point-like obstacles on dislocation movement analyzed, proving existence of critical applied stress, deriving structure of work-hardened crystal 12 p1971 A66-24924  
Melting practice, sheet thickness and thermal and mechanical treatments effect on critical stress intensity parameter and ductility of 18-nickel maraging steel 13 p2108 A66-25772  
Stability of three-layer shells or plates beyond proportionality limit, obtaining critical stress 16 p2817 A66-31054  
Critical stress, stability loss and load carrying capacity of axially compressed thin walled aluminum alloy rods 16 p2819 A66-31142  
Cleavage characteristics of copper plate under explosive load determined and interpreted, taking finite failure time into account 19 p3474 A66-35861  
Classical critical stress values for buckling of thin walled circular cylindrical shells in axial compression as function of edge conditions 23 p4143 A66-41965
- CROCCO METHOD**  
Group of transforms derived for functional in which Euler equation coincides with Crocco equation describing plane vortex gas streams 04 p0512 A66-14437  
Dorodnitsyn approximate solution method applied to Crocco forms of first and second order incompressible two-dimensional boundary layer equations 05 p0665 A66-15776
- CROSS CORRELATION**  
Transfer functions of cantilever beam and clamped-edge square plate determined by cross-correlation methods 01 p0148 A66-10136  
Wiener kernels of nonlinear system based on cross-correlation techniques 02 p0207 A66-11789  
Envelope polarity coincidence cross-correlator for detection and identification problems involving weak wideband microwave signals 05 p0646 A66-14613  
Frequency response function of lightly damped single-degree of freedom system estimated from truncated measurement of cross-correlation function of white noise excitation and response 05 p0781 A66-15788  
Cross correlation and autocorrelation functions of nonstationary signals based on optimal approximation of ensemble correlation function for one pair of signals 10 p1517 A66-21694  
VHF ionospheric radio signal cross correlation coefficients determined, using pulse counting techniques 10 p1505 A66-21731  
Cross correlation radar system for mapping of target distribution 12 p1813 A66-23789  
Cross correlation measurements of oscillator frequency stability and thermal noise and application to atomic hydrogen maser 12 p1835 A66-24128  
Power response of two-element interference frequency correlation interferometer to point source of broadband random noise 12 p1840 A66-24626  
Noise suppression, signal reception, and polarization measurement in cross correlated antennas as function of dipoles imbedded in random field, surrounding noise field and coherency matrix of cross correlation function 13 p2044 A66-26746  
Combined frequency and space correlation of wave fields scattered by rough surfaces where conditions of applicability of Kirchhoff approximation hold 14 p2236 A66-27144  
Cross correlation of satellite signals through slab containing small anisotropic irregularities 14 p2237 A66-27398  
Spatial cross-correlation analyses between radial velocity and continuum brightness fluctuations of solar disk center spectrograms 17 p2996 A66-31919  
Coherent optical system for simplifying signal processing from antenna arrays by simultaneous beam forming and cross correlation 18 p3069 A66-34248  
Noise characteristics at integrator input in nonstationary regime 19 p3311 A66-35297  
Pseudorandom binary signals as perturbation signals in simultaneous multi-input cross correlation method of obtaining linearized impulse response of system 19 p3307 A66-35730  
Ionospheric drift and radio wave dispersion determined from selective fading records and symmetry of cross correlation functions, using Fourier transforms 22 p3916 A66-40807
- CROSS COUPLING**  
Synthesis method for linear time-varying systems, discussing integral formulation and approximation functions 05 p0654 A66-14609  
Digital cross multiplication used in cross coupling and off-leveling errors in gravity measurements at sea 09 p1369 A66-19874  
Cross coupling effects in first order theories of ship motion used in measurement of gravity at sea 09 p1369 A66-19875  
State-variable feedback decoupling of multivariable linear plants with cross coupling between various input-output pairs 13 p2053 A66-26083  
Short circuited crossguide coupling used to stop oscillation of reflex klystrons and convert them into stable millimeter wave amplifiers 14 p2248 A66-27058  
Combined effect of horizontal and vertical accelerations on gravimeter readings mounted on gyroplatform or in Cardan suspension 14 p2297 A66-28111  
Gain, impedance and scan angle variation in polarization of phased radar antenna arrays constructed with hybrid-fed crossed dipole radiating elements 15 p2456 A66-28586  
Time domain method of relating cross coupling between transmission lines of multilayer structure to geometry in design of high speed digital systems 18 p3090 A66-34071  
Static stability of rolling motion of aircraft for given aileron angle when inertia cross-coupling is present, with numerical solution of nonlinear equations 22 p3848 A66-40493  
Combined effect of horizontal and vertical accelerations on gravimeter readings mounted on gyroplatform or in Cardan suspension 24 p4212 A66-42699
- CROSS LINKING**  
Equivalent transfer function of linear two-channel system of automatic control, discussing system stability dependence on cross links 20 p3537 A66-36891  
Prior gamma irradiation effect on thermal volatilization of vinyl and vinylidene fluoride polymers 20 p3587 A66-37311
- CROSS RELAXATION**  
Paramagnetic resonance spectra shift due to temperature change in cross-relaxation rutile maser 16 p2718 A66-30820  
Spectral hole burning and cross relaxation effects on steady state gain saturation of laser amplifier with inhomogeneously broadened linewidth 22 p3931 A66-40098
- CROSS SECTION**  
S ABSORPTION CROSS SECTION  
S IONIZATION CROSS SECTION  
S NEUTRON CROSS SECTION  
S RADAR CROSS SECTION  
S SCATTERING CROSS SECTION
- CROSSED FIELD**  
Laser action at 5401 angstroms in pure neon pulsed high voltage discharge 01 p0081 A66-10353  
Theory of interband magnetodispersion effects in crossed field semiconductors, obtaining expressions for Faraday and Voigt effects 02 p0272 A66-11711  
Plasma velocity field determined from glow discharge in crossed fields propagating along rectangular channel, two walls being dielectrics and other two electrodes 02 p0268 A66-11786  
Current, potential electron and atom temperature distributions between anode and cathode in low pressure crossed-field plasma accelerator 03 p0416 A66-12784  
Two-dimensional flow of inviscid nonheat-conducting gas with variable conductivity in crossed constant electric and arbitrary magnetic fields 04 p0557 A66-14422  
Fine structure of cut-off characteristic, particularly influence of emission current density in crossed-field thermionic converter 05 p0616 A66-15541  
Radiation induced during electron passage through magnetic field can be intensified and made nonrelativistic by superimposed electrostatic field 07 p1044 A66-18261  
Creep motion and hydromagnetics of ellipsoid moving in cross field 09 p1408 A66-20580  
Radiation induced during electron passage through magnetic field can be intensified and made nonrelativistic by superimposed electrostatic field 09 p1387 A66-20905  
Coherent radiation effect on stability of crossed field electron beam, noting raising of potential of space vehicle 10 p1564 A66-21544  
Plasma behavior in crossed stationary electric and magnetic fields, examining field dependence of ion velocity and ion and electron temperature 10 p1566 A66-21704  
Laminar MGD boundary layer on conducting surface in crossed electric and magnetic fields for flow core of constant temperature 11 p1745 A66-22590  
Very low phase velocity wave propagating in one direction in semiconductors in presence of crossed DC electric and magnetic fields 12 p1928 A66-24151  
Plasma acceleration in crossed magnetic and electric fields 13 p2153 A66-26520  
Electron beam analyzer for determining crossed field space charge beam analyzer 15 p2549 A66-28719  
Repetitive plasma breakdown in flat electrode accelerator, causing relatively low plasma velocity 16 p2757 A66-30107  
Interband optical absorption in germanium in crossed electric and magnetic fields, noting band perturbation theory, differential spectra, Stark broadening, experimental techniques, etc 16 p2776 A66-30736  
Self-similar solutions of two-dimensional laminar flow of incompressible electroconductive fluid in channel in crossed electric and magnetic fields, using Jacobi elliptic integrals 17 p2971 A66-32866  
Formation process of rotating plasma in homopolar-type short coaxial-electrode system in hydrogen, nitrogen or argon discharge 17 p2972 A66-32973  
Anomalous electron diffusion and ion acceleration measured in steady state low-density weakly-turbulent plasma subjected to crossed E and B fields 18 p3149 A66-34913  
Crossed-field electron beam stability for arbitrary values of Q /ratio of plasma frequency to cyclotron frequency/ 20 p3606 A66-38404  
Faraday and Voigt and dispersive magneto-optic effects in semiconductors in crossed field due to energy band transitions 21 p3800 A66-38995  
Generator of plasma with supercritical rotational velocity in crossed electric and magnetic fields 21 p3789 A66-39063  
Absorption coefficient of light in semiconductors in crossed electric and magnetic fields, examining conditions for Franz-Keldysh effect occurring in magnetic field 24 p4256 A66-42524
- CROSSED FIELD AMPLIFIER**  
Klystrons, cross field devices and traveling-wave tubes, including design and application 07 p1011 A66-18269  
Traveling wave HF crossed field photomultiplier with helical output circuit for electron multiplication at microwave modulation rates 24 p4182 A66-42567
- CROSSED FIELD GUN**  
Modified split-folded waveguide slow-wave structure for crossed field tubes that permits use of fundamental backward or first forward-wave harmonics over wide bandwidths 04 p0498 A66-14038  
MGD DC crossed field plasma accelerator capable of operating on LF AC current 08 p1262 A66-18829
- CRUSADER AIRCRAFT**  
S F-8 AIRCRAFT
- CRYOGENIC EQUIPMENT**  
SA REFRIGERATING EQUIPMENT  
Two-phase flow and heat transfer for boiling liquid nitrogen in horizontal tubes 01 p0165 A66-10909  
Cryogenic problems in temperature and level sensing discussing thermocouples, resistance sensors, vapor and gas bulb thermometers and level gauges and probes 01 p0070 A66-10955  
Equilibrium conditions for whole complex cryogenic cycle analyzed by means of Claude-Heyland cycle 05 p0786 A66-14900  
Aerodynamic analysis of cryogenic radial-inflow turbines, noting optimum velocity distribution



[ASME PAPER 65-WA/PID-6]

05 p0608 A66-15604  
Multistage cryogenic trapping system  
noting design, operation and  
application 07 p1032 A66-17665  
Low temperature physics - International  
Conference, Columbus, Ohio, August-  
September 1964 09 p1413 A66-20004  
Magnetocaloric effects in high-field  
superconductor, noting magnetic field-  
induced temperature variation effects on  
thermally isolated superconducting alloy  
specimen 09 p1420 A66-20051  
Strain measurements in cryogenic  
container, noting preparation of specimen  
surface, installation of gauges,  
etc 09 p1466 A66-20185  
Practical Philips cycle for low temperature  
refrigeration, noting equal coefficient of  
performance to that of ideal Carnot cycle  
under isothermal conditions 09 p1472 A66-20879  
Vacuum equipment selection for thin film  
processing line, comparing diffusion and ion-  
pumped evaporation systems 13 p2040 A66-25843  
Cooler for semiconductor lasers and  
photodetectors using low temperature  
gas 13 p2104 A66-26559  
Radiation efficiency of short whip antenna  
with loading coil cooled to 77 degrees K and  
4.2 degrees K at approximately 20 mc  
frequency 14 p2257 A66-27925  
Refrigerated mass spectrometer inlet  
serving also as low temperature reactor and  
rough separative device for compounds  
stable only at very low  
temperatures 16 p2645 A66-30420  
Convective heat transfer to and low  
gravity heating of liquids contained in  
rotating cryogenic fuel tanks in orbit  
[AIAA PAPER 66-432] 16 p2826 A66-30521  
Cryoelectronic integrated circuits utilizing  
superconducting storage and switching  
devices 16 p2665 A66-31417  
Irradiation system for experiments with  
Plum Brook Reactor in nuclear rocket  
program, noting cryogenic system, dynamic  
testing, etc 17 p2956 A66-32045  
Closed cycle helium refrigerator noting  
thermodynamic cycle, equipment  
arrangement and cost estimate for space  
simulator and wind tunnel application  
closed 20 p3541 A66-37070  
Cryogenic design of aluminum, titanium  
and steel alloys subjected to uniaxial, 1-to-1  
biaxial and 2-to-1 biaxial stress  
states 20 p3583 A66-37094  
Thin insulating Teflon film bonding to  
internal surface of space cryopanel for  
increased heat transfer and faster  
cooling 20 p3677 A66-37100  
Gas sorption and desorption processes at  
low pressures, discussing molecular  
adherence to cold solid surfaces, adsorption  
mechanism of isotherms, vacuum generation  
via cryotrapping effect,  
etc 20 p3605 A66-38088  
Gas flow equations for multilayer  
insulation systems for both continuum and  
free molecular flow regimes of interest in  
cryogenic space vehicle design  
[AICE PREPRINT 22A] 22 p3897 A66-39888  
Low temperature system for thermal  
conductivity measurements using Ge and Pt  
resistance thermometers and He exchange  
gas switch 24 p4215 A66-43207

**CRYOGENIC FLUID**

Control valve design for cryogenic fluids,  
galling, seizing and stress accumulation and  
material-valve  
compatibility 12 p1885 A66-24380  
Dynamic instability in undamped bellows  
face seals operating in cryogenic  
environment with torsional oscillation and  
diametrical rocking as primary motion  
[ASLE PAPER 66AM 2CE] 16 p2711 A66-30408

Radiant energy transport within cryogenic  
condensates extended to case of explicitly  
varying condensate depths and wider  
substrate temperature  
range 16 p2830 A66-31712  
Design and performance of vacuum-  
insulated pipe used to transfer cryogenic  
fluids in space program 20 p3541 A66-37069  
Cryogenic system used to remove heat  
from space simulator solar radiation

source 20 p3541 A66-37071  
Low temperature experimental apparatus  
for density determination of cryogenic  
liquids and mixtures under atmospheric and  
subatmospheric pressure 20 p3601 A66-37082  
Data correlations on forced-convective heat  
transfer to cryogenic fluids by nucleate,  
film and transition region  
boiling 20 p3677 A66-37098  
Convective heat transfer to cryogenic  
nitrogen and methane from cylindrical  
surface by nucleate-and film-boiling at high  
pressures and large temperature  
differences 20 p3677 A66-37099  
Laminar, turbulent and transition heat-  
transfer domain analysis of cryogenic fluids  
in variable reduced-gravity environment,  
with applications to space cryogen  
storage 20 p3677 A66-37103  
Dimensional and experimental analyses of  
helium bubble motion in liquid  
nitrogen 20 p3545 A66-37104  
True-mass cryogenic flowmeter for liquid  
oxygen, hydrogen and nitrogen with liquid-  
helium compatibility 21 p3740 A66-39426  
Adhesively bonded joints withstand severe  
thermal shock and have excellent bonding  
with high strength structural alloys in  
cryogenic liquids 22 p3937 A66-39778  
Cryogenic fuels evaluated for operational  
safety in space environment simulation  
laboratory /SESL/ 22 p3891 A66-40235

**CRYOGENIC MAGNET**

VGL-2 cryogenic magnetic trap, filling with  
hydrogen plasma 19 p3428 A66-36580  
High field liquid-neon-cooled  
superconducting electromagnet for cryogenic  
solid state research 20 p3601 A66-37106

**CRYOGENIC PROPELLANT**

Spaceflight application of cryogenic  
techniques including cooling magnets, noise  
reduction in parametric amplifiers and  
quantum-electronic, superconductive and IR  
sensing devices 01 p0130 A66-10789  
Model simulating energy distribution  
process /thermal stratification/ within liquid  
hydrogen stored aboard moving rocket to  
avoid pump cavitation  
[AIAA PAPER 64-426] 08 p1279 A66-18809  
Two-phase flow of evaporating cryogen in  
condensing binary mixture related to Gibbs  
potentials 08 p1318 A66-19153  
Large launch vehicle cryogenic propellant  
logistics including storage and production  
capacity optimization, cost and heat loss  
analyses by computer simulation  
[AIAA PAPER 65-259] 16 p2789 A66-30900  
Detonability of cryogenic oxidizers,  
discussing modified continuous wire  
technique analysis of detonation properties  
of trioxigen difluoride 16 p2790 A66-31194  
Propellant tanking computer system for  
monitoring and controlling Saturn IB and  
Saturn V vehicles  
[SAE PAPER 660454] 17 p2904 A66-33162  
Liquid hydrogen-oxygen cryogenic  
propulsion stages, examining structural  
material and configuration of propellant  
tank and thermal flow  
effects 18 p3246 A66-34007  
U.S. space program impact on cryogenic  
industry 20 p3624 A66-37060  
Cryogenic propellant boiloff losses in long  
duration space storage elimination by  
mechanical reliquefier, considering lunar,  
Earth-orbit and deep space application for  
hydrogen and oxygen 20 p3625 A66-37079  
Cryogenic propellant program for Saturn  
applications, discussing stringent purity  
requirements and magnitude of  
applications 20 p3541 A66-37080

**CRYOGENIC STORAGE**

Cryogenically cooled superconducting  
electromagnet design, construction and  
testing 06 p0907 A66-15935  
Tanks for cryogenic fluids on space  
vehicles noting structure, insulation,  
manufacturing techniques, materials,  
construction, etc 06 p0887 A66-17069  
Superconducting continuous film store  
evaluated, noting switching thresholds and  
functional dependence of disturb pulse  
sequences on film parameters 10 p1509 A66-21416  
Liquid hydrogen tank level in space  
measured by applying known impulse and  
determining resulting acceleration of

container 11 p1706 A66-22957  
Lightweight inflatable shadow shields for  
cryogenic space vehicles and performance in  
conjunction with  
superinsulation 16 p2810 A66-30899  
Space vehicle containers, discussing  
prolonged storage of cryogenic liquids,  
insulation requirements, container  
configuration and design, etc  
[SAE PAPER 660460] 17 p3017 A66-33165  
Test for space storability of liquid  
propellants by suitably coating storage tanks  
[AIAA PAPER 65-534] 19 p3448 A66-35613  
Weight and size optimization of flight type  
cryogenic storage supply system of oxygen  
and hydrogen for fuel cell operation and life  
support in manned  
spacecraft 19 p3292 A66-36233  
Shingle attachment of multilayer insulation  
to cryogenic flight tanks 20 p3674 A66-37061  
Lightweight superinsulation testing for  
cryogenic tank  
application 20 p3675 A66-37063  
Transient gas-flow process in multilayer  
insulation systems during evacuation  
predicted by equations in conjunction with  
measured permeabilities and diffusion  
coefficients 20 p3675 A66-37065  
Convection effect in helium charged  
insulation with partially foam-filled  
honeycomb core 20 p3675 A66-37066  
Thermal conductivity of gas-charged  
cryogenic powder  
insulation 20 p3675 A66-37067  
Saturn S-IV and S-IVB liquid hydrogen  
tank internal insulation, using polyurethane  
foam reinforced with fiberglass  
threads 20 p3675 A66-37068  
Simplifying large cryogenic research  
tankage temperature measurement methods  
including thermocouples, resistance  
thermometers, semiconductors, piezoelectric  
probes and combinations  
thereof 20 p3556 A66-37072  
Thermal analysis and weight optimization  
of low-heat-leak storage tanks, particularly  
aspects important to designers of propellant  
tanks for long-term lunar  
storage 20 p3676 A66-37078  
Lightweight titanium and inconel pressure  
vessel for Apollo cryogenic hydrogen and  
oxygen storage systems 20 p3541 A66-37092  
Childdown rate and equilibrium heat-leak  
storage loss measurements in liquid  
hydrogen storage dewars 20 p3541 A66-37101  
Laminar, turbulent and transition heat-  
transfer domain analysis of cryogenic fluids  
in variable reduced-gravity environment,  
with applications to space cryogen  
storage 20 p3677 A66-37103  
Multilayer insulating material thermal-  
mechanical environmental tests for use as  
heat shields in cryogenic storage tanks  
[AICE PREPRINT 22F] 22 p3997 A66-39889  
Liquid hydrogen tank insulation  
constructed of honeycomb core containing  
polyurethane foam for S-II  
booster 22 p3997 A66-39892  
Aircraft materials and structures for  
extreme ranges of velocity and  
temperature 22 p3990 A66-40120  
Life support systems for crew comfort and  
safety, considering thermal and radiation  
environmental control, carbon dioxide  
removal, cryogenic gas storage,  
etc 22 p3857 A66-40129

**CRYOGENICS**

SA COOLING  
SA NERNST HEAT THEOREM  
SA REFRIGERATION

Time-dependent temperature distribution  
and interface location of phase change of  
one-component systems in  
container 01 p0164 A66-10901  
Cold wall space simulating installation and  
technique for cooling wall with liquid  
nitrogen 02 p0216 A66-11895  
Materials at cryogenic temperatures  
discussing thermal lattice effects, specific  
heat, electrical and thermal conductivity,  
thermal expansion and mechanical  
properties 04 p0534 A66-13371  
Heat and mass transfer rates compared  
with correlations for frost formation on  
vertical plate in free convection  
[ASME PAPER 65-HT-32] 04 p0595 A66-13391  
Properties of neutron star at absolute zero  
temperature, discussing ground state,



particle models and energy spectrum 05 p0760 A66-14894  
 Mass spectrometer measurements of oxygen fluorides at cryogenic temperatures 06 p0821 A66-16156  
 Experimental apparatus for studying temperature dependence of electrical properties of semiconductors at low temperature 08 p1221 A66-18705  
 Platinum resistance thermometers with interchangeable characteristics for liquid hydrogen measurements, discussing standardization and calibration 08 p1226 A66-19598  
 Book on theory and measuring techniques for electrical resistance of metals at low temperatures and cryogenics 09 p1388 A66-19976  
 Discharge in germanium thin films at liquid helium temperatures, noting electrostatic ionization of impurities and shock-ionization region expansion 09 p1412 A66-19990  
 Superconducting transition temperature of SnTe samples 09 p1423 A66-20071  
 Yield strength dependence on normal to cryogenic temperatures of high strength alloys [ASME PAPER 65-PROD-14] 11 p1715 A66-22475  
 Operating characteristics of electrodeless MHD converter with primary winding cryogenically-cooled, comparing performance with one having conventional winding 12 p1803 A66-23749  
 Improvement of mechanical properties of structural adhesives and composite materials at cryogenic temperatures 12 p1899 A66-24385  
 Magnetic diffusivity measurement for cylinder of type II Nb-Zr superconductor at 4.2 degrees K, using magnetoresistance probe 14 p2350 A66-26878  
 Uniaxial permalloy film anisotropy at cryogenic temperatures and magnetization characteristics 14 p2355 A66-26914  
 Cryogenic resistance spot welding of refractory metals and conventional aerospace materials [ASTME PAPER AD66-111] 14 p2299 A66-26950  
 Reinforced plastics measured for thermal conductivity, specific heat and thermal expansion at cryogenic temperature [AIAA PAPER 65-423] 14 p2318 A66-27891  
 Electron gas electroconductivity relaxation time and energy loss in n-type InSb at cryogenic temperatures 15 p2558 A66-28611  
 Near UV effects on thermal control surfaces at cryogenic temperature 17 p3035 A66-32749  
 Materials behavior at cryogenic temperatures - ASTM meeting, Lafayette, Indiana, June 1965 19 p3380 A66-35845  
 Serrated yielding by metals during tension tests at temperatures near absolute zero 19 p3380 A66-35846  
 Factors affecting fracture characteristics of metals at cryogenic temperatures and fracture mechanics for predicting performance of defect-containing structures 19 p3380 A66-35847  
 Martensitic transformations in ferrous and nonferrous alloys, discussing kinetic and structural characteristics 19 p3380 A66-35848  
 Specific heat and thermal conductivity of metals at cryogenic temperatures 19 p3381 A66-35849  
 Absorption line between 220 and 550 mu in transmission spectra of ruby at liquid nitrogen and helium temperatures 19 p3446 A66-36342  
 Cryogenic engineering, Volume II - Conference, William Marsh Rice University, Houston, August 1965 20 p3599 A66-37059  
 Reinforced plastic materials evaluated as potential low temperature structural insulators 20 p3676 A66-37084  
 Room and cryogenic temperature mechanical properties and microstructure of electroformed nickel 20 p3582 A66-37090  
 High strength weldable Al alloys with good cryogenic toughness, stress-corrosion cracking resistance and tensile strength 20 p3582 A66-37091  
 Tensile, creep and stress-strain behavior of high nitrogen content stainless steel quenched alloy at cryogenic

temperatures 20 p3583 A66-37093  
 Cryogenic temperature effects on mechanical properties of high strength glass-reinforced plastic resins 20 p3587 A66-37095  
 Combined nuclear radiation damage and cryogenic temperature effects on tensile and shear properties of materials in outer space 20 p3583 A66-37096  
 Kapitza papers, Volume 2, 1938-1964 20 p3603 A66-37833  
 Superconducting magnets, economics, size, weight and application as devices in cryogenic environment [ASME PAPER 66-MD-22] 21 p3741 A66-38479  
 Kjeldas absorption edge in cryogenic potassium for shear magnetoacoustic wave propagation in spherical metallic Fermi surface with spin density wave ground state 21 p3800 A66-38991  
 Stainless steel and aluminum alloy fracture behavior under static load and low temperatures, noting crack propagation, stress and crack-length relation, etc 21 p3830 A66-39195  
 Fatigue fracture and crack propagation in ordered alloys due to plastic flow 22 p3989 A66-39891  
 Cell model of attractive interactions between helium atoms and effect on solid-superfluid transition in He 4 at absolute zero 23 p4090 A66-41368  
 Specific heat measurements and cryogenic thermodynamic properties of single crystal V in mixed state under 12 different magnetic fields 23 p4080 A66-41372  
 Book on low temperature techniques and common cryogenic systems 24 p4238 A66-43161  
**CRYOPUMPING**  
 Dynamic measurements of speed of pumping by activated charcoal cooled to liquid nitrogen temperatures to evaluate cryosorption 02 p0261 A66-11591  
 Spherical cryopumped chamber with test object analyzed for pumping speeds determined with gauges located in various positions, with equations relating these speeds to chamber geometry and cryopump efficiency 04 p0528 A66-14465  
 Gas capture coefficient prediction for cryopumping based on critical velocity model in space chamber simulator 10 p1520 A66-21937  
 Simulated space vacuum environment by cryosorption pumping 12 p1858 A66-24709  
 Reduction of thick boundary layers in low density wind tunnel by applying suction to nozzle, using high-speed cryopump 16 p2673 A66-30381  
 Rarefied supersonic flow condensation on cold flat plate, noting capture coefficients, shock wave behavior, etc 16 p2825 A66-30383  
 Cryosorption panels consisting of molecular sieve adsorbents bonded to refrigerated aluminum plates for pumping hydrogen at 20 degrees K 17 p2957 A66-31978  
 Energy transport within cryodeposit layer subjected to thermal radiation 20 p3676 A66-37085  
 Electrically cryopumped system for liquid helium transfer continuously at low flow rates 20 p3542 A66-37105  
 Cryopump uses and selection of coolants 21 p3697 A66-38810  
 Molecular beam chamber for cryopumping studies and capture coefficient data 22 p3890 A66-40223  
 Pumpdown characteristics and incident flux rates of ultrahigh vacuum research facility 22 p3890 A66-40224  
**CRYOSORPTION**  
 Dynamic measurements of speed of pumping by activated charcoal cooled to liquid nitrogen temperatures to evaluate cryosorption 02 p0261 A66-11591  
 Simulated space vacuum environment by cryosorption pumping 12 p1858 A66-24709  
 Cryosorption panels consisting of molecular sieve adsorbents bonded to refrigerated aluminum plates for pumping hydrogen at 20 degrees K 17 p2957 A66-31978  
**CRYOSTAT**  
**SA TEMPERATURE CONTROL**  
 Combined cryostat/oven and specimen transfer device for tensile testing, noting

design, operation and results 11 p1683 A66-22699  
 Electric contact effect and transition temperature measurement in superconducting Cu-Pb double layer films at low temperatures, using He 3 cryostat 16 p2772 A66-30322  
**CRYOTRON**  
 Cryotron-type DC to AC voltage converter and measurements of cryotron circuits 04 p0494 A66-13755  
 Cryotron-type DC to AC voltage converter and measurements of cryotron circuits 15 p2454 A66-28552  
**CRYSTAL**  
**SA BODY CENTERED CUBIC /BCC/ CRYSTAL**  
**SA CUBIC CRYSTAL**  
**SA IONIC CRYSTAL**  
**SA METAL CRYSTAL**  
**SA PIEZOELECTRIC CRYSTAL**  
**SA POLYCRYSTAL**  
**SA SINGLE CRYSTAL**  
**SA YTTRIUM-ALUMINUM GARNET /YAG/ CRYSTAL**  
**SA YTTRIUM-IRON GARNET /YIG/ CRYSTAL**  
 Specific heat, thermal expansion and conductivity and electrical conductivity of nearly perfect crystalline materials 07 p1109 A66-18497  
 Quartz crystal units and quartz crystal-controlled oscillators, discussing vibrator characteristics, trapped energy, aging, motional modes, etc 12 p1834 A66-24121  
 Load capacitance method for measurement of quartz crystal parameters 12 p1845 A66-24855  
 Current oscillation observations in photoconductive cadmium sulfide crystal 17 p2987 A66-33317  
**CRYSTAL DISLOCATION**  
 Slip-induced fracture of polycrystalline Cr, Mo and W and bcc transition metals V, Fe, Nb and Ta 01 p0085 A66-10376  
 Strain ratio measurements from uniaxial tension tests predicting metal sheet performance during pressing, considering crystal deformation 01 p0086 A66-10411  
 Prismatic slip in polycrystalline titanium diboride subjected to high hydrostatic pressure at room temperature 01 p0086 A66-10489  
 Determination methods for various types of dislocation in germanium lattice and influence on physical properties of germanium 02 p0276 A66-12066  
 Three-stage hardening in tantalum single crystals deformed in tension over limited range of orientations, temperatures and strain rates 02 p0246 A66-12194  
 Fracture micromechanisms of materials having regular crystalline structure, considering mechanical strength, atomic imperfections, dislocation interactions, and crack growth 03 p0382 A66-13000  
 Stable dislocation structures obtained by high and low temperature and precrystallization thermomechanical treatment 03 p0385 A66-13172  
 Tungsten crystal deformation and fracture analyzed as orientation function, noting tensile tests and stress-strain curves 03 p0385 A66-13208  
 Total nonelastic strain recovery of copper single crystals after small prestrains, discussing parameters 04 p0535 A66-13400  
 Macroscopic plastic strain rate relation with configuration and velocity distribution of dislocations in monocrystals with single active glide system, noting yield stress 04 p0535 A66-13731  
 Detailed account of dislocation loops according to continuum theory 04 p0590 A66-14164  
 Internal friction measurements for studying mechanical properties due to crystal dislocations 05 p0698 A66-14550  
 Four elastic constants of Laval, Raman and Viswanathan theories dynamically measured in connection with behavior data on cubic crystals 05 p0781 A66-15736  
 Contrast of dislocation near Si surface in anomalous transmission X-ray topographs 06 p0927 A66-16760  
 Four-lobed rosette stress patterns in X-ray topography of silicon bombarded by electron beam 06 p0928 A66-16761



Recombination radiation of n-type germanium with various dislocation densities, emphasizing mechanism of radiative transitions 07 p1096 A66-17324

Generation modes of dislocations in ordered alloys from Frank-Read sources 07 p1049 A66-17486

Elastic interaction energy of two infinitesimal dislocation loops in transversely isotropic medium estimated from fundamental elasticity tensor 07 p1144 A66-18044

Brittle fracture in ceramic materials, noting Griffith theory on crack propagation, plastic deformation occurrence, stress distribution effect, etc 07 p1054 A66-18499

Large dislocation loops on basal plane and rows of prismatic dislocation loops in quenched magnesium specimens 07 p1052 A66-18513

Binding energy between oxygen atom and dislocation in tantalum by measuring critical temperature at which discontinuous yield disappears on heating 07 p1052 A66-18514

Stacking faults and Burger vector dislocations in twin crystals of beryllium observed by electron microscopy 08 p1235 A66-18651

Transmission electron microscopy structural analysis of dislocations in stress-corrosion cracking of 7075 aluminum alloy 08 p1236 A66-18761

Deformation of polycrystalline MgO at elevated temperatures, with stress-strain curves for five types 08 p1243 A66-18773

Dependence of lifetime on dislocation density in vacuum-zone purified silicon single crystals 08 p1272 A66-19242

Dislocation interaction with coherent ordered zones, noting onset of plastic deformations in alloys 08 p1240 A66-19250

Interaction of dislocations with coherent ordered zones, discussing results of electron transmission and tensile test experiments 08 p1240 A66-19251

Effect of conditions of fabrication of alloyed contacts between semiconductors and metals on dislocation structure of these contacts 08 p1274 A66-19315

Stress-corrosion failure in metal alloys, discussing surface and elastic energy, adsorption, crack propagation, pits and tunneling 08 p1241 A66-19601

Dependence of expansion ratio on impurity concentration for silicon samples differing in impurity and dislocation content 09 p1412 A66-19991

Pile-up of dislocations in front of twin bands formed in crystal as result of elastic twinning 09 p1391 A66-20866

Molybdenum single crystal dislocation redistribution and subgrain boundaries formation during annealing at high temperatures 09 p1391 A66-20873

High-temperature plastic deformation of single crystals, noting creep and dislocation 10 p1613 A66-21244

Anomalous diffusion of boron parallel and perpendicular to dislocation arrays in grain boundary contained in silicon 10 p1574 A66-21356

Changes in fine structure of powdered copper during compression, determining dislocation density and disorientation angles, noting plastic deformation cause as packing defect occurrence 10 p1546 A66-21505

New parameter, dimensionless fraction of particle volume irreversibly dislocated by plastic deformation during compression, permits calculation of powder compression process and constants 10 p1540 A66-21507

Electrical properties of dislocations in artificially produced bicrystals 10 p1582 A66-21902

Spin resonance of donor electron in Ge and anisotropic line width in relation to dislocation stress 11 p1750 A66-22463

Chemical etching revealing dislocations produced by indentation on single crystals of silicon, measuring edge dislocation velocities at various shear stresses and high temperatures, determining activation energy 11 p1750 A66-22492

Effect of plastic bending on indium antimonide electrical properties, measuring crystal dislocations, Hall coefficient, etc 11 p1751 A66-22698

High-temperature deformation of magnesia

single crystals with  $\langle 110 \rangle$  tensile axis, favoring slip on systems with oblique vectors, related to observations on  $\langle 001 \rangle$  crystals 12 p1898 A66-23564

Germanium specimens with various dislocation densities quenched from high temperatures to introduce vacancies, contamination by copper atom diffusion, finding activation energy 12 p1930 A66-24801

Surface pit formation in aluminum, discussing effects of vacuum, quenching high temperature and repeated cycling 12 p1897 A66-24921

Effect of random distribution of point-like obstacles on dislocation movement analyzed, proving existence of critical applied stress, deriving structure of work-hardened crystal 12 p1971 A66-24924

Critical analysis of Hirsch linear strain hardening theory, discussing decrease of dislocation cluster radius 12 p1898 A66-24926

Plastic flow peculiarities analysis based on X-ray diffraction effects obtained by deforming single crystal molybdenum of various orientations 12 p1898 A66-25026

Plastic deformation of single crystals of titanium carbide with cube orientation in compression from 900 to 1250 degrees C 13 p1206 A66-25059

Immobile dislocation network of high density in Campo del Cielo observed by thin-film transmission electron microscopy 13 p1277 A66-25136

Transmission electron microscopic observations on preexisting dislocation as sinks for neutron-irradiation-induced point defects and dislocation reaction to subsequent deformation 13 p1207 A66-25586

Aging behavior of explosively deformed 2219 Al investigated by transmission electron microscopy 13 p2086 A66-25775

Mechanism of plastic deformation in crystalline bodies, discussing static and dynamic frictional forces in relation to dislocation structure of bodies in contact 13 p1210 A66-25887

Johnston-Gilman concept of yielding and plastic flow and strain rate effect on dynamic dislocation 13 p1297 A66-26106

Low-temperature internal friction peaks in germanium and oxygen-doped and pure silicon crystals 13 p1270 A66-26586

Amplitude probability density of random stationary signal potential and variation of free carriers in germanium semiconductor at near-ambient temperature 13 p1270 A66-26758

Domain boundaries and superdislocations of structure of Alnico V by thin film electron transmission microscopy 14 p2311 A66-26882

Diffusion of indium along sessile dislocation in silicon crystal 14 p2356 A66-27070

Dislocation structure in single crystal indium antimonide and gallium arsenide studied by X-ray diffraction 14 p2357 A66-27071

Vacuum deposited films of titanium dioxide examined, using electron microscopy and diffraction methods, noting crystal dislocation due to electron beam irradiation 14 p2359 A66-27133

Aging of aluminum alloy after quenching and strain hardening, noting Vickers hardness tests, tensile tests, precipitation phases, shearing effect, etc [PST PAPER 423] 14 p2315 A66-27468

Estimate of energy dissipation in metals, using continuous distribution of oscillating dislocations joined with Zener thermoelastic effects 14 p2315 A66-27658

Fracture mechanics, discussing crystal structure defects, particular dislocation, hardening, lattice vacancies, interstitials, etc 14 p2316 A66-27770

Effect of external forces on state of stress and dislocation density in continuous medium 14 p2402 A66-27937

Opening of parallel cracks by applied tensile stress in terms of dislocation distribution theory 14 p2408 A66-28389

Stresses and coupled-stresses generated by dislocation in isotropic media treated in terms of boundary value problem for Cosserat medium 14 p2409 A66-28468

Electron microscope investigation of dislocation structure of silicon single crystals after compressive deformation at various stages of deformation

curve 15 p2557 A66-28562

Transient and steady state photoconductivity in plastically bent germanium, noting logarithmic decay of photocurrent and logarithmic lux-ampere characteristics 15 p2558 A66-28608

Multiplication of moving dislocation in work-hardening of crystal 15 p2559 A66-28631

Acceptor nature of dislocations in p-type germanium 15 p2560 A66-28636

Electron microscope investigation of dislocation effect on stress corrosion cracking in aluminum alloy 15 p2523 A66-29418

Nonmetric connections in quasi-static plastic-elastic deformation of crystalline solid with continuous distribution of dislocations and extra-matter 16 p2746 A66-30532

Stability of two coplanar wedge-shaped cracks, showing under what conditions interaction effects are important 16 p2814 A66-30533

Schrodinger equation in semiconductor with N atoms containing dislocation, vacancy or other defect, noting phase shift and local charge neutrality 16 p2775 A66-30730

Dislocations and precipitates in GaAs injection lasers revealed by new A-B etchant 16 p2718 A66-31071

Mechanical behavior of polycrystalline iron and single crystal molybdenum in compression over various strain rate ranges, noting temperature role 16 p2724 A66-31264

LF internal friction of beryllium, noting strain amplitude dependency variation with temperature and purity, obtaining activation energies 16 p2724 A66-31265

Modes of elastic wave propagation and orientation dependence of dislocation damping in aluminum 16 p2821 A66-31452

Ultrasonic attenuation changes due to dislocation formation during yielding of magnesium, molybdenum and LiF 16 p2726 A66-31458

Annealing of lightly deformed columbium single crystals with parallel twins or parallel and intersecting twins 16 p2726 A66-31461

Dangling bonds and dislocations in semiconductors, noting existence of core charge dependent localized state in gap caused by local decrease in atom density 17 p2985 A66-33155

Dislocation distribution and crack propagation due to stress corrosion 17 p2942 A66-33444

Austenite-martensite interface dislocations in stainless steel shown as probable pinned Shockley partials 18 p3123 A66-33927

Chemical etchants for In As noting functions, rate dependence on bromine in methanol, p-n junction delineation, etc 19 p3434 A66-35349

Indentation damage and subsequent annealing effect on etch-polished Ge surfaces at room temperature examined with optical microscope, using interference contrast techniques 19 p3434 A66-35401

Time dependence of dislocation density in single crystal MgO undergoing plastic deformation at elevated temperatures 19 p3387 A66-35421

Chemical sectioning of p-type surface layers on silicon, presenting electrical and X-ray measurements of boron-induced defect distribution 19 p3436 A66-35424

Intrinsic dislocations in diffused silicon p-n junctions and effect on transient processes 19 p3437 A66-35455

Interstitial dislocation loops in beryllium oxide irradiated at high temperatures 19 p3398 A66-35495

Separation centers and dislocations during diffusion of Zn into GaAs at high temperatures, analyzing photographs of p-n junctions 19 p3445 A66-36339

Dislocation motion in silicon crystals measured by Lang X-ray technique, noting dislocation nucleation and growth with increasing stress below macroscopic yield stress 19 p3447 A66-36725

Dislocation dipoles produced by ionic bombardment of thin gold films, noting that during annealing dipoles can condense to form only one dipole 19 p3447 A66-36726

Tension and compression tests on single and polycrystalline niobium, examining twinning, slip and catastrophic



- flow 19 p3387 A66-36727
- Formation of cleavage crack in crystalline solid, examining crack stability by study of equilibrium dislocation distribution in terms of operative stresses 19 p3475 A66-36728
- Dislocation-induced relaxation in silicon single crystals by measuring internal friction and Youngs modulus at temperatures from 77 to 300 degrees K 20 p3618 A66-37561
- Chemical etch pitting techniques, determining dislocations in crystal structure caused by liquid droplet impacts, calculating stress distribution due to collision 20 p3547 A66-37806
- Fabrication methods for lithium drifted surface barrier silicon detectors, discussing lithium diffusion, stain etching, preparation for and final etch 20 p3535 A66-38417
- Photomicrographs of pressure crack figures on silicon single crystals at room temperature 21 p3803 A66-39291
- Electron energy spectrum of silicon, examining effect of screw dislocations parallel to crystallographic direction 21 p3803 A66-39296
- Crystal dislocation distribution effect on low temperature electrical transport properties in plastically deformed metals 21 p3753 A66-39587
- Silicon dioxide complexes and deposition of excess oxygen at dislocations and structural defects, examining creation of microplasma breakdown of silicon p-n junctions 22 p3965 A66-40320
- Dislocation structure in single crystal indium antimonide and gallium arsenide studied by X-ray diffraction 22 p3966 A66-40829
- Electron microscope investigation of dislocation structure of silicon single crystals after compressive deformation at various stages of deformation curve 23 p4112 A66-41283
- Changes in fine structure of powdered copper during compression, determining dislocation density and disorientation angles, noting plastic deformation cause as packing defect occurrence 23 p4081 A66-41526
- Microscopic strain rate equation interpreting macroscopic creep, stress-strain and impact test results 24 p4288 A66-42274
- Generation-recombination noise and lifetime measured using photoconductive decay in n-and p-type Ge samples doped with shallow impurities 24 p4253 A66-42357
- Dislocation arrangement and twin fault formation by quenching and tempering in titanium-tantalum alloy investigated by internal friction measurement and microscopy 24 p4228 A66-42511
- CRYSTAL FILTER**
- Bandwidth expansion of crystal filters by spacing frequency response characteristics in relay circuit at suitable distances from each other 03 p0342 A66-12895
- Ten-element band pass filter section and derivatives with classification of image-impedance functions 11 p1669 A66-23113
- Quartz crystal active filters noting design and operation of multiresonator filters 19 p3312 A66-35337
- CRYSTAL GROWTH**
- Germanium fiber single crystal growth, properties and application 01 p0116 A66-10207
- Growth of single crystal gold films in ultrahigh vacuum on clean vacuum-cleaved salt surfaces 01 p0117 A66-10242
- Thin metal film growth under applied electric field 01 p0118 A66-10246
- Crystal chemistry of nonmetallic materials prepared under moderate or high pressure and recovered and retained under ambient conditions 01 p0090 A66-10292
- Growth of ice crystals freely falling in atmosphere and form when produced by cloud element coagulation analyzed, using low pressure chamber 01 p0097 A66-11105
- Cubic beta-silicon carbide films grown on single crystal silicon substrates by heating in presence of graphite in argon atmosphere 02 p0275 A66-11871
- Ruby laser crystals grown by flame-fusion, flux and Czochralski method examined for perfection by X-ray topography and double-crystal rocking curves 04 p0529 A66-13744
- Recrystallization of bismuth films by controlled melting and resolidification 05 p0732 A66-14668
- Tungsten as thermionic emitter prepared by hydrogen reduction of tungsten fluoride, noting resistance to grain growth and properties 05 p0714 A66-15593
- Growth of absorption bands of natural and synthetic calcium fluoride crystals irradiated with protons from cyclotron at Tomsk Institute 05 p0741 A66-15857
- Yttrium effect on recrystallization and grain growth of tantalum 07 p1052 A66-18350
- Apparatus for fluoridation of hydroxyl and oxygen contaminated fluoride compounds, obtaining optically clear crystals with no Tyndall scattering for laser application 07 p1047 A66-18488
- Kinetics of reactions in iodide method of growing epitaxial germanium layers 08 p1268 A66-18797
- Epitaxial silicon layer crystal growth at low temperatures by sublimation through thin alloy zones 08 p1271 A66-19224
- Segregation processes and coefficients of effective distribution and diffusion during solidification of doped tellurium 08 p1272 A66-19247
- Crystallization kinetics of tri-alpha-naphthyl benzene in large temperature range, noting transition in morphology, crystal growth rate and viscosity 08 p1179 A66-19595
- Deposition kinetics of solid phases on electrodes of second kind, noting conditions affecting crystal growth and lattice formation 08 p1171 A66-19648
- Temperature oscillations in molten metals and relation to growth striae in melt-grown crystals 10 p1572 A66-21167
- Light emission associated with growth defects from reverse biased gallium phosphide p-n junctions 10 p1577 A66-21556
- Growth and properties of n and p type beta-silicon carbide crystals grown from pure or doped carbon-saturated silicon melts 10 p1577 A66-21563
- Floating zone technique for preparing high purity GaAs crystals for CW microwave devices 10 p1516 A66-22099
- Epitaxial growing of iron, nickel and cobalt single crystal films on sodium chloride crystals by spraying at 200 degrees C 11 p1753 A66-22805
- Electric current heating method to obtain high purity silicon epitaxial films 11 p1757 A66-23281
- Sandwich method in closed system for growing semiconductor germanium epitaxial films 11 p1757 A66-23282
- Vanadium oxide single crystal growth by flame solution and fusion, noting burner construction, crystal structure and techniques 12 p1899 A66-23565
- Doping techniques for epitaxial growth of silicon and germanium layers 12 p1832 A66-23933
- Epitaxial deposition of silicon by sublimation process at 750 degrees C, using ultrathin alloy zone crystallization 12 p1846 A66-24912
- Residual gas influence on orientation of vapor deposited NaCl crystals 13 p2159 A66-25068
- Epitaxial vapor growth of germanium from germanium iodide with hydrogen and argon atmosphere, examining various growth parameters 13 p2161 A66-25193
- Radial solution growth of GaAs single crystal layers and analysis of photoluminescence spectrum 13 p2164 A66-25488
- Moving deposition zone technique for controlling nucleation and growth of silicon films on hexagonal silicon carbide substrates 13 p2164 A66-25491
- Microscopic and electron diffractational structural analysis of epitaxial growth of PbTe by sublimation on split surface of NaCl at 150 degrees C in vacuum 13 p2170 A66-26757
- High energy Alnico alloys, discussing crystal growth, anisotropy, recrystallization, etc 14 p2311 A66-26883
- Growth kinetics and structure of evaporated tin thin films on amorphous carbon film, noting three stages after nucleation, archipelago, labyrinth and closing 14 p2359 A66-27102
- Green emission lines from solution-grown p-n junctions in GaP diodes doped with shallow donors and acceptors 14 p2251 A66-27231
- Fluorescent lifetimes of neodymium, ytterbium and samarium incorporated in ordered perovskite-type compounds determined, noting crystal structure potential for laser emission 14 p2367 A66-27976
- Structural defects arising during growth and heat treatment of CdS single crystals studied, using anomalous transmission of X-rays 15 p2557 A66-28563
- Chromium doped ruby whiskers grown by vapor phase reaction, determining chromium concentrations, noting whisker growth morphologies 15 p2561 A66-28706
- Single crystal germanium films grown on molybdenum or tungsten substrates, using electron beam zone melting process 15 p2563 A66-28726
- Concave-convex growth spirals due to screw dislocation in nickel bromide 15 p2563 A66-28730
- Fabricating perfect dendritic germanium crystals with required resistivity and dislocation density 15 p2569 A66-29787
- Growth of single crystals of rare-earth fluorides for laser application, using hydrogen fluoride atmosphere, noting ion exchange purification 16 p2779 A66-31082
- Epitaxial growth configurations of single-crystal potassium bromide on sodium chloride, using gold decoration method, showing effect of crystal orientation on growth rate 16 p2780 A66-31213
- Germanium single crystal whisker formation by iodide method of selective epitaxial growth 16 p2781 A66-31405
- X-ray diffraction analysis of single crystal silicon film grown on several natural faces of BeO by thermal decomposition of silane and hydrogen reduction of silicon tetrachloride 16 p2782 A66-31420
- Epitaxial growth techniques for silicon and germanium, discussing hydrogen reduction methods, doping and impurity control, etc 17 p2976 A66-32259
- Ice crystal size during expansion of humid air in supersonic nozzle 17 p2948 A66-32417
- Lanthanum oxide as crystal growth modifier, noting habit modifications, optical quality, etc 17 p2982 A66-33060
- Growth of single crystal and polycrystalline thin films of magnesium aluminum oxide and magnesium iron oxide, discussing techniques employed, results, etc 17 p2982 A66-33061
- Phase relations in cobalt niobate-cobalt tantalate system noting structural characteristics, solubility, phase transitions, etc 17 p2940 A66-33062
- Effect of equilibrium crystal seeds on supercooled polyethylene melt and o-xylene solution of polyethylene of same chemical nature 17 p2944 A66-33466
- Particle growth during coalescence of fine phases of metallic alloys 18 p3123 A66-34403
- Secondary mode of nucleation during sublimation growth of nickel bromide, noting formation mechanism 19 p3434 A66-35405
- Distribution of edge-type dislocations in GaAs grown from solution by traveling solvent method determined, using etching techniques 19 p3437 A66-35432
- Yttrium vanadate crystals grown and processed for optical purposes 19 p3373 A66-35434
- Hydrogen reduction techniques and layer quality measurement methods for epitaxial growth of silicon and germanium crystals 19 p3437 A66-35473
- Hexagonal crystal structure growth of CdTe thin film 19 p3438 A66-35480
- Crystal growth of rare earth tungsten bronzes using electrolytic reduction of fused mixture of rare earth tungstate and tungsten trioxide 19 p3381 A66-36037
- Measurements on physical and laser properties of vapor-grown ruby single crystals prepared by epitaxial growth 19 p3375 A66-36081
- Monograph on synthesis and properties of refractory semiconducting materials having large forbidden bandwidth and prepared from element of groups III and V 19 p3448 A66-36731
- Crystal growth, diffusion and fabrication of



gallium arsenide-phosphide junction lasers with low threshold current  
densities 20 p3577 A66-37401

Starting concentration, surface distribution of additive in alumina powder, trajectory distance and growth rate in Verneuil growth of ruby crystals 21 p3795 A66-38527

Transmission electron microscopic analysis of initial epitaxial growth stage of evaporated Au films on NaCl cleavage surfaces 21 p3798 A66-38758

Direct measurement of dispersion properties of cadmium sulfide and CdS-CdSe crystals, using Obreimov-Fresnel diffraction method, growing crystals by synthesis 21 p3799 A66-38926

Experimental molecular beam study of nucleation process in chemical-vapor growth of epitaxial silicon films 21 p3805 A66-39588

Temperature gradient-induced GaAs crystal inhomogeneity effects on electric properties 22 p3959 A66-39742

Burnout of additives for flame fusion growth of crystal 22 p3931 A66-39920

Thermal growth and deposition of silica films by silicon tetrafluoride hydrolysis 22 p3962 A66-40048

Charge distribution in thermally grown silicon dioxide and silicon n-type inversion layer 22 p3962 A66-40087

Epitaxial germanium films on gallium arsenide substrate by vacuum evaporation, considering surface preparation 22 p3963 A66-40106

Current characteristics of solution and vapor grown p-n Ge-Si and Ge-GaAs heterojunctions as function of voltage and temperature 22 p3968 A66-40963

Structural defects arising during growth and heat treatment of CdS single crystals studied, using anomalous transmission of X-rays 23 p4112 A66-41284

Potassium tantalum niobite crystal growth noting methods applied, potassium oxide evaporation and tantalum absorption rate 23 p4115 A66-41773

Transitions between phases and states of crystallographic order in films, noting conditions for preferential nucleation and analogies between two-and three-dimensional phase diagrams 24 p4251 A66-42305

Alloyed semiconductor heterojunction metallurgy and physics, noting processes of interface alloying, solution growth and vapor transport-interface alloy 24 p4252 A66-42348

MOS transistor structures with enhancement mode of operation, discussing fabrication processes via V-C characteristics, temperature effects on performance, etc 24 p4181 A66-42389

Effects of isothermal decomposition of gamma ray irradiated orthorhombic crystals of ammonium perchlorate 24 p4170 A66-42421

Heterogeneous formation of seed crystals on wettable and nonwettable condensation nucleus in supercooled water droplets 24 p4234 A66-42756

## CRYSTAL LATTICE

Friction and wear of hexagonal metals and alloys as related to crystal structure and lattice parameters in vacuum [ASLE PREPRINT 65-LC-18]

Transition temperature, critical fields, electrical resistivities and crystalline structures of technetium-tungsten alloys 03 p0411 A66-13142

Lattice and grain boundary self-diffusion coefficients of radioactive nickel 63 into high purity nickel measured over temperature range 650-475 degrees C 04 p0535 A66-13746

Energy accommodation coefficients calculated for gas particles interacting with cubic crystal lattice 04 p0548 A66-14142

Thermodynamic changes in crystal lattice on electron states of semiconductors 05 p0737 A66-15116

Radiation damage to crystalline lattices by energetic particles, discussing consequences on physical behavior of solids, particularly ceramics 05 p0738 A66-15471

Lithium transformation by plastic deformation from bcc to fcc lattice analyzed by measuring damping of free torsional oscillations of samples, noting role of internal friction 05 p0740 A66-15822

X-ray diffraction method for measuring

thermal expansion coefficient of germanium, silicon, indium antimonide and gallium arsenide 06 p0930 A66-17047

Effectiveness of measurements of X-ray diffraction intensities as probe of lattice defects introduced in perfect germanium crystals by energetic particle irradiation 06 p0933 A66-17121

Strain field calculation from linearized elasticity theory for vacancies and divacancies in diamond structure valence crystals 06 p0938 A66-17147

Quantum mechanical discussion of electron structure of crystal lattice of semiconductor as contributor to thermodynamic behavior of impurities 07 p1097 A66-17472

Imperfection formation in epitaxial gold films, observing crystal-lattice dislocations due to rotation and displacement misfits between neighboring islands of deposit film 07 p1110 A66-18517

Dielectric properties and lattice parameter dependence on temperature from X-ray studies of rubidium-potassium nitrate mixed crystals 08 p1269 A66-19008

Resonance Raman effect in crystals, discussing spontaneous and simulated scattering efficiency 08 p1259 A66-19233

Spatial dispersion of long-wave optical oscillations of lattice in polar semiconductor 08 p1276 A66-19610

Free energy calculations and crystallographic properties of vortex line lattices in type II semiconductor for square and triangular lattices in given magnetic field 09 p1421 A66-20058

Anisotropy of Snoek relaxation measured for oxygen and nitrogen in niobium 10 p1576 A66-21554

Plastic deformation effect on heat conduction of crystal lattice of sodium and potassium chlorides single crystals 10 p1587 A66-22148

Hall effect in alloyed crystals of n-type indium antimonide 10 p1589 A66-22165

Integral equations describing multiple neutron Bragg reflections in mosaic crystal 11 p1742 A66-23409

X-ray stress analysis of externally-loaded polycrystal lattice strains and residual lattice strains due to internal macro- and microstresses 12 p1957 A66-23629

Crystallization of certain aluminosilicate and gallosilicate glasses of stoichiometric composition, discussing anionic network 12 p1900 A66-24861

Maximum efficiency of power converters, using ferroelectric and nonferroelectric pyroelectrics 13 p1997 A66-25036

UV absorption and excitation spectrum of ruby and sapphire, noting structure and polarization effects, quantum efficiency, etc 13 p2162 A66-25378

Lattice parameters and constant measured in gadolinium-yttrium alloy dihydrides, using X-ray diffraction techniques 13 p2162 A66-25382

Surface orientation effect on twin accommodation in hcp metal magnesium and relation to twin boundary movement 13 p2107 A66-25585

Optical linewidth study of energy transfer between impurity ions and homogeneous broadening and lineshape changes in optical transitions 13 p2098 A66-26176

Strong electron-phonon interaction which couples electron to lattice motion in F center of alkali halide crystal by measuring temperature dependence of F center absorption and emission bands 15 p2559 A66-28629

Electron energy losses in diamond, noting correlation between plasma excitation energy and interband transition energies 15 p2564 A66-28876

Optical color center bands in amethyst quartz containing ferric ions after irradiation 16 p2767 A66-30123

Two oxycarbide phases in zirconium-carbon-oxygen compositions found in zirconia-carbon mixtures at high temperatures, giving X-ray diffraction patterns indexed as fcc at various lattice parameters 16 p2729 A66-30246

Friction and wear of hexagonal metals and alloys as related to crystal structure and lattice parameters in vacuum [ASLE PREPRINT 65-LC-18]

16 p2713 A66-30568

Intervalley scattering in III-V semiconductors, noting relation to Gunn effect, scattering in GaAs by longitudinal optic phonons, in InP by longitudinal acoustic phonons 16 p2776 A66-30733

Harmonic approximation of infinite crystal dynamics problem, noting collisional case and action of external force on atoms 16 p2820 A66-31169

Molybdenum films prepared by sputtering onto oxidized silicon substrates, analyzing resistivity, lattice parameter, orientation and grain size as function of substrate temperature and bias 16 p2783 A66-31424

Noise characteristics of solid state, X-band microwave sources, using VHF crystal oscillator, amplifier and varactor multiplier 17 p2893 A66-32924

Spatial dispersion of long-wave optical oscillations of lattice in polar semiconductor 17 p2983 A66-33124

Hardness and lattice parameter increase effect on oxidation temperature of internally oxidized Ag-Mg and Ag-Al alloys 18 p3122 A66-33750

Uniaxial stress effect on two-phonon lattice absorption bands of silicon 18 p3154 A66-33920

Dielectric constant variation in silicon single crystals, noting frequency dependence of dielectric loss, conductivity and temperature effects 19 p3436 A66-35423

Twin boundary effect on measurements of phonon momentum propagating through Ge bicrystal p-layers at liquid nitrogen temperatures 19 p3438 A66-35482

Plastic deformation effect on heat conduction of crystal lattice of sodium and potassium chlorides single crystals 19 p3440 A66-35762

Hall effect in alloyed crystals of n-type indium antimonide 19 p3441 A66-35779

Nickel aluminide structure, examining arrangement of Ti, Cr and W in lattice via X-ray spectroscopy 19 p3381 A66-35928

Effect of binding on distribution in angle of charged particles having suffered scattering with lattice atoms 19 p3403 A66-36172

Exchange interaction between f-electrons and s-electrons in atomic shells of crystal lattice of rare-earth metals, examining calculation methods for Hamiltonian of s-f exchange 20 p3617 A66-37476

Thermal conductivity of lanthanum and monochalcogenides, noting role and temperature dependence of crystal-lattice conductivity 20 p3617 A66-37556

Yield strength anisotropy due to preferred orientation estimated by Taylor model, considering cold rolled aluminum 20 p3585 A66-37784

Equilibrium diagram and existence corroboration of Ti-Rh alloy 20 p3586 A66-38093

Vacuum thermionic work function for well-outgassed polycrystalline surfaces, noting techniques for accurate measurement of current, area and temperature values 20 p3587 A66-38401

X-radiation alignment of quartz crystals for generation and detection of reverberating acoustic echoes at liquid-helium temperatures 20 p3624 A66-38409

Impurity atom behavior in diatomic InSb and GaSb crystal lattices analyzed, using nuclear gamma resonance, measuring absolute values of f, chemical displacements and line widths 21 p3799 A66-38922

Enumerating neighbors of atom in diamond-like lattices 21 p3805 A66-39584

Ruby laser-induced effect of pulsed pressure on KDP crystal surface and thermal bulk effect on excitation of ultrasonic oscillation in crystal 22 p3932 A66-40318

Vibration modes frequencies of lead telluride propagating in certain symmetric direction determined by inelastic neutron scattering 22 p3966 A66-40405

Elastic constants and interatomic interaction parameters of niobium alloyed with tantalum, titanium and vanadium 22 p3936 A66-40788

Lithium transformation by plastic deformation from bcc to fcc lattice analyzed by measuring damping of free torsional



oscillations of samples, noting role of internal friction 23 p4113 A66-41387  
Coupled ODE sets describing continuum wave propagation in discrete structures with and without dispersion or linearity 23 p4096 A66-41939  
Laue reflection method of X-ray diffraction, determining single crystal orientation 24 p4255 A66-42506

# CRYSTAL OPTICS

Light reflection by planes perpendicular to c axis in zinc sulfide crystals containing stacking faults 04 p0567 A66-14337  
Spatial structure for second harmonic generated in anisotropic medium by finite-aperture light beam 08 p1233 A66-18969  
Temperature dependence of optical birefringence on single crystals of lead zirconate-titanate solid solution measured, noting they are optically negative 08 p1269 A66-19006  
Crystal-Diffusion Spectra-International Colloquium, Paris, July 1965 08 p1233 A66-19231  
Excited ruby crystal phosphorescence noting spectral range, duration, electron excitation mechanism and upper wavelength limit 08 p1234 A66-19667  
Optical signal reception, considering use of HF subcarrier superimposed on light signal and bias-sensitive crystal detector for mixing process between subcarrier and local oscillator, deriving signal to noise ratios 09 p1346 A66-20567  
Nonlinear optical effects of third order in crystals, specifically in Hamiltonian of system containing electrons, nuclei and radiation field 09 p1387 A66-20928  
Excited ruby crystal phosphorescence noting spectral range, duration, electron excitation mechanism and upper wavelength limit 10 p1543 A66-21834  
Light beam deflection due to linear temperature gradients across electro-optic modulator crystals 11 p1737 A66-23431  
Electron beam pumped lasers, discussing energy dissipation in fast electrons passing through crystal, laser semiconductor characteristics, etc 11 p1715 A66-23433  
Absolute measurement of optical rectification coefficient in ammonium dihydrogen phosphate 12 p1912 A66-23715  
Electro-optic device with nonreciprocal properties which does not depend on Faraday magneto-optic effect 12 p1837 A66-24313  
Ruby laser experiment yielding giant pulses by separating mirrors from crystals 13 p2092 A66-25684  
Elliptic cavity design for solid state lasers, discussing multiple reflections, absorption coefficient, refraction losses, etc 13 p2092 A66-25998  
Monte Carlo technique to determine total energy and energy distribution in laser crystal due to optical pumping 13 p2093 A66-26028  
Raman diffusion spectra from crystals excited by gas laser 13 p2104 A66-26345  
UV absorption and dispersion of cadmium sulfide crystals and energy band structure 14 p2356 A66-27064  
Vector synchronism and second-harmonic light generation in focused beams 14 p2307 A66-27191  
Crystal motion effect on time behavior of laser generation mode, using high speed photography and oscillograms 15 p2518 A66-29725  
Physics of luminescent ionic crystal - Conference, Lvov, Ukrainian SSR, January-February 1964 15 p2568 A66-29728  
Impurity absorption of LiF crystals in vacuum UV 15 p2568 A66-29729  
Second harmonic generation /SHG/ by focused laser beams in nonlinear crystals 15 p2519 A66-29816  
Lattice vibrational properties of hexagonal CdSe 16 p2778 A66-31075  
Possible stabilization of AgCl crystals against solar radiation effects by addition of Cu, Ni, Zn, Cs, S or Hg 18 p3157 A66-34549  
Semiconductor technology advances in laser-energy conversion, light detection and TV transmission 20 p3534 A66-38413  
Second harmonic generation in laser crystals by Gaussian beams of finite aperture 22 p3929 A66-39657

Gallium arsenide crystal properties for use in optical filter 22 p3959 A66-39773  
UV absorption and dispersion of cadmium sulfide crystals and energy band structure 22 p3966 A66-40823  
Precision polishing technique for optical and microwave acoustical surfaces with overall flatness of one-eighth wavelength of light and parallel to 6 inches 23 p4067 A66-41248  
Single crystal wurtzite CdS luminescence as function of exciting intensity, noting shift of overlapping band structure of green-edge emission indicative of electron-hole recombination 24 p4219 A66-42250  
Surface pinned layer-like field inhomogeneities in cadmium sulfide, investigating visibility of field layer by corresponding shift of absorption edge, using Franz-Keldysh effect 24 p4254 A66-42427  
GaAs crystal as electro-optic modulator at 10.6 microns due to small carrier absorption, freedom from interband transitions and high resistivity 24 p4222 A66-42553  
Miller phenomenological rule for computing nonlinear susceptibility, determining magnitude by geometrical factor 24 p4223 A66-42568  
Split angle, total internal reflection and Wollaston prism-digital light deflection techniques 24 p4174 A66-42815  
Vector synchronism and second-harmonic light generation in focused beams 24 p4226 A66-43089

# CRYSTAL STRUCTURE

SA ANISOTROPY  
SA FACE CENTERED CUBIC /FCC/ CRYSTAL  
SA ISOTROPISM  
SA YTTRIUM-ALUMINUM GARNET /YAG/ CRYSTAL  
SA YTTRIUM-IRON GARNET /YIG/ CRYSTAL  
Domain characteristics and crystal property effects in materials and configurations for Gunn effect devices 01 p0041 A66-10571  
Structures and crystallization processes of semiconductor vanadium phosphate glasses of various composition, using electron paramagnetic resonance 01 p0091 A66-10771  
X-ray analysis of neutron irradiated quartz crystals at various temperatures, showing atomic displacements 01 p0124 A66-10772  
Laser crystals prepared economically by splitting along cleavage planes 01 p0084 A66-11046  
Present status of titanium research and development noting electronic structure, dislocation theory and alloy theory 02 p0242 A66-11525  
Nucelite, ceramic-metal composite with high mechanical strength and abrasion resistance noting crystal structure, application, properties, etc 02 p0244 A66-11742  
Crystalline structure on fatigue noting changes of body-centred metals and face-centred and hexagonal metals 02 p0245 A66-11948  
Crystal structure of hexamethylenetetramine hexahydrate determined using X-ray analysis, noting hydrogen bonding in crystalline state 03 p0330 A66-12338  
Effect of surface state of cadmium sulfide on fundamental absorption edge and fine structure obtained from gaseous phase in inert atmosphere 03 p0407 A66-12405  
Jahn-Teller effect in excited 4-T-2 state of trivalent Cr ions in ruby, discussing unilateral elastic strain effect splitting of pure electronic line 597 nm in U band 03 p0410 A66-12941  
X-ray single crystal diffraction technique determination of structure of pyridinium dicyanomethylide 04 p0472 A66-13364  
Transport effects in semimetals and narrow-gap semiconductors including nonlinear, thermomagnetic and superconductive effects and tunneling 04 p0559 A66-13451  
Thin surface films covering structure, nucleation, growth and epitaxy observation techniques such as electron and X-ray diffraction field emission, field ion microscopy, etc 04 p0559 A66-13452  
Crystal structure of porphine determined

by X-ray diffraction analysis 04 p0473 A66-13642  
Crystal structure of ammonium tricyanomethide determined by X-ray diffraction 04 p0474 A66-13833  
Hall effect of bismuth evaporated films, discussing structural dependence of sign and magnitude, effects of pathlength, impurities, gas adsorption and experimental techniques 05 p0729 A66-14510  
Impurity concentration fluctuations in silicon crystals, discussing striation visualization technique and Czochralski method 05 p0729 A66-14512  
Cadmium sulfide and cadmium selenide, discussing optical absorption, energy band structure, effective band-masses and composition changes of crystals in polarized light 05 p0731 A66-14656  
Oxygen alloyed gallium arsenide, explaining anomalous mobility distribution in crystals during fusion in presence of oxygen 05 p0731 A66-14658  
Cadmium sulfide and cadmium selenide recombination centers, discussing temperature dependence of electron capture cross sections 05 p0731 A66-14661  
Chromium nickel steel hardening as result of martensitic transformation and aging 05 p0701 A66-14861  
Anomalous scatter and energy loss of ions penetrating crystalline semiconductors 05 p0737 A66-15303  
Crystalline structure of simplest lanthanum and samarium silicates 05 p0702 A66-15337  
Semiconductor crystals, discussing dispersion property changes due to pulsed ruby laser radiation 05 p0697 A66-15354  
Behavior of aggregate under moderate loads with plastic deformation occurring in favorably oriented crystals on single active slip systems [ASME PAPER 65-WA/APM-9] 05 p0776 A66-15431  
Output characteristics of thermionic converter and improvement of performance by using emitter surfaces with particular crystallographic orientation 05 p0617 A66-15553  
Evaluation of absolute free energy of rigid-disk system at very high compression 05 p0740 A66-15772  
Physical factors determining hardening of nimonic type alloy with high niobium content, discussing formation of intermetallic phase 05 p0704 A66-15820  
Crystal and molecular structure of chlorotetraammine /sulfur dioxide/ ruthenium chloride 06 p0820 A66-15939  
Anisotropic broadening of X-ray diffraction lines and increase in lattice perimeter resulting from neutron irradiation of beryllium oxide powder 06 p0896 A66-16539  
Exciton absorption lines and long wave intrinsic edges of single-crystal CdSe and CdS at low temperatures 06 p0924 A66-16540  
Pendellosung fringes in elastically deformed silicon, observing X-ray wavefield beam interference upon superimposition on crystal exit surface 07 p1098 A66-17815  
Diamond-like semiconductors in glassy state, investigating structure and characteristics of cadmium-germanium-arsenide 07 p1106 A66-18383  
Ductility in polycrystalline single phase ceramics, noting behavior at room and high temperature of single crystal structure, dislocation, etc 07 p1054 A66-18498  
Oxidation products of thin foils of titanium carbide, noting epitaxial growth relationship between titanium carbide, transient oxides and titanium oxide 07 p1052 A66-18512  
Diffuse X-ray scattering in crystal structure of Ni-Be and Cu-Be alloys during first stage of aging due to anisotropic monoclinic lattice distortions 08 p1235 A66-18589  
Beryllium ductility in fabrication as affected by single crystal slip and fracture and improvement by grain control 08 p1238 A66-18851  
Beryllium oxide properties, fabrication and application 08 p1243 A66-18852  
Martensitic transformation in titanium alloys containing eutectoid-forming elements, noting elastic properties, shear modulus, etc 08 p1239 A66-18906  
Crystal structure and allotropic



transformation of cobalt and thermal, thermodynamic, electrical and magnetic properties 08 p1240 A66-18961

Heterojunction preparation by vacuum evaporation, describing epitaxial deposition of germanium on gallium arsenide substrate 08 p1270 A66-19058

Relation of compressibility with cohesive energy and molecular volume for dielectric solids, noting confirmation of relation for 45 crystalline compounds 08 p1244 A66-19254

Electrical capacity of galvanic cell and crystal habit and surface property effects on porous cadmium hydroxide electrode electrochemical properties 08 p1171 A66-19644

Built-in surface charge on thermally oxidized silicon as function of exposed crystal face orientation 09 p1411 A66-19929

Orientation effect on zinc diffusion rate in p-n junctions, using gallium arsenide single crystals as initial material 09 p1412 A66-19996

Anisotropy of balanced photoelectromagnetic emf in p-type germanium sample in which normal to illuminated surface coincides with crystallographic axis 09 p1413 A66-20002

Ceramic and graphite fibers and whiskers, Air Force sponsored monograph 09 p1392 A66-20475

Phase recrystallization effect on structure and mechanical properties of cast monophasic titanium alloys 09 p1389 A66-20614

Semiconductor crystals, discussing dispersion property changes due to pulsed ruby laser radiation 09 p1387 A66-20895

Structural anisotropy coefficients of crystallization in carbon-graphite materials from X-ray and linear expansion data 10 p1548 A66-21240

Vapor etching of gallium arsenide crystals with hydrogen chloride, noting usefulness in pretreatment for epitaxial substrates 10 p1575 A66-21358

Mechanical and micromechanical behavior of bulk polycrystalline boron, emphasizing fracture stress and microstrain behavior relation to materials response 10 p1548 A66-21727

Barium titanate transition front structure, noting similarity to ferroelectric and nonferroelectric crystal structure 10 p1582 A66-21881

Transition front movements in barium titanate, noting dependence of velocity on rate of heating and thermal gradients 10 p1582 A66-21882

Metal structure analysis in terms of elementary electron and ion particles 10 p1547 A66-22054

Structures and crystallization processes of semiconductor vanadium phosphate glasses of various composition, using electron paramagnetic resonance 11 p1720 A66-22282

X-ray analysis of neutron irradiated quartz crystals at various temperatures, showing atomic displacements 11 p1749 A66-22283

Energy band structure via reflection spectra of crystals of ternary zinc compound containing elements of Periodic Groups II, IV and V 11 p1750 A66-22342

Nucleation during pulse remagnetization of thin films, showing domain structure of formation, growth of nuclei, etc 11 p1752 A66-22797

Quasi-equilibrium states during pulse remagnetization of thin ferromagnetic films, discussing domain structure 11 p1752 A66-22798

Changes in domain structure of cobalt films as function of substrate temperature during sputtering and transformation from poly- to single-crystal structure 11 p1753 A66-22803

Domain structure of single-crystal epitaxial iron films as function of perfection of crystalline structure, using Lorentzian electron microscopy, noting two-axis anisotropy 11 p1753 A66-22806

Crystalline structure and magnetic properties of single-crystal films of iron-nickel alloys, for application as memory elements of computers 11 p1753 A66-22807

Domain structure and reverse magnetization of single crystal nickel films 11 p1754 A66-22816

Laser crystals prepared economically by

splitting along cleavage planes 11 p1714 A66-23293

Zeta phase in tantalum-carbon system, noting diffusionless transformation of carbon-deficient lattice under compressive stress 12 p1892 A66-23566

Microstructure viewed on several different successive parallel planes simultaneously, using multiple positive or negative transparencies, obtaining three-dimensional photomicrograph 12 p1892 A66-23626

Optical absorption and dielectric loss measurements in KCl doped SrCl sub 2 single crystals, determining involvement of impurity vacancy dipolar complexes in optical conversion of F centers to Z centers 12 p1926 A66-23718

Jump conductivity of lightly doped p-germanium single crystals, noting Hall coefficient temperature dependence and specific resistance with low donor and acceptor concentrations 12 p1927 A66-23724

Superheating of linear high polymer polyethylene crystals, evaluating time dependence of melting, differential thermal analysis and calorimeter techniques 12 p1899 A66-23937

Age hardening response correlated with structural observations of iron-nickel-cobalt alloys 12 p1895 A66-24374

Hyperfine structure of p-n junction phase boundaries in silicon according to electron microscopy data 12 p1930 A66-24461

Polarization of particle counters, noting distortion of internal fields through pre-irradiation spatial polarization 12 p1883 A66-24788

High temperature crystallization processes and physicochemical properties of lithium aluminosilicate glass 12 p1900 A66-24859

Sequence of crystallization during heat treatment of ternary system of lithium aluminosilicate glasses 12 p1900 A66-24860

Chemical durability of lithium silicate glass as result of crystallization 12 p1901 A66-24864

Grain boundary role in high temperature fracture behavior of magnesite, noting temperature and orientation dependence of shear strength 12 p1897 A66-24920

Aging effect on structure of cobalt alloys annealed at 1200 degrees C suggests formation of laminar regions 12 p1898 A66-25030

Threshold energy for avalanche multiplication in semiconductors obtained from energy band structure and crystal momentum conservation in ionization process 13 p2157 A66-25035

Length changes in electron irradiated high purity germanium at liquid helium and nitrogen temperatures, noting large initial expansion 13 p2157 A66-25047

Partial dislocation detection in silicon, using scanning electron beam technique 13 p2159 A66-25069

Photoelectric properties and relaxation time of polycrystalline layers of cadmium sulfide are highly dependent on substrate temperature 13 p2160 A66-25097

Hot wire-drawn beryllium recrystallization analyzed by hardness measurement and micrography, noting dependence on initial deformation 13 p2107 A66-25358

Iron selenides of nickel arsenide structure analyzed, noting dependence of semiconductor characteristics on iron gap arrangements 13 p2164 A66-25471

Transmission electron microscopy determination of structure and morphology of oxide films during Ti oxidation initial stages 13 p2107 A66-25584

Quenching and slow-cooling effects on ductile-brittle bend-transition temperature of chromium wire 13 p2107 A66-25587

Cadmium sulfide single crystal preparation by zone sublimation method, analyzing structure via X-ray diffraction and obtaining photosensitivity curves 13 p2165 A66-25680

X-ray analysis of molybdenum-nickel-silicon ternary crystal structure 13 p2108 A66-25683

Photoconductivity and optical transmission of cadmium-indium-telluride, noting temperature dependence 13 p2165 A66-25685

Effect of crystalline state and structural orientation of polymer on endurance of couplings with polytetrafluoroethylene components, analyzing dry friction and wear

on interfaces 13 p2113 A66-25912

Cadmium sulfide and cadmium selenide, discussing optical absorption, energy band structure, effective band-masses and composition changes of crystals in polarized light 13 p2167 A66-25931

Oxygen alloyed gallium arsenide, explaining anomalous mobility distribution in crystals during fusion in presence of oxygen 13 p2167 A66-25933

Cadmium sulfide and cadmium selenide recombination centers, discussing temperature dependence of electron capture cross sections 13 p2168 A66-25936

Morphology and structure of gallium arsenide crystals containing germanium core grown by iodine transport process in closed tube 13 p2170 A66-26587

Fine-grain structure effect on microwave power absorption thresholds of ferrimagnetic garnets and spinels 14 p2350 A66-26880

Texture and anisotropic age hardening to improve mechanical properties of AlMgSi alloys 14 p2313 A66-27011

Properties of hydrothermally grown single crystals of tetragonal lead monoxide, with contacts applied by metal evaporation 14 p2359 A66-27099

Growth kinetics and structure of evaporated tin thin films on amorphous carbon film, noting three stages after nucleation, archipelago, labyrinth and closing 14 p2359 A66-27102

Semiconductor properties of reduced barium titanate analyzed by electron spin resonance measurements at various temperatures 14 p2359 A66-27132

Chemical and physical properties of samarium dicarbide, prepared by heating samarium sesquioxide with graphite, using X-ray analysis, hydrolytic studies, etc, noting structure 14 p2362 A66-27465

Hypothesis that system sodium fluoride-yttrium trifluoride serves as model for each of binary systems of rare earth trifluorides SmF3 to LuF3 with sodium fluoride 14 p2315 A66-27466

Fluorescent lifetimes of neodymium, ytterbium and samarium incorporated in ordered perovskite-type compounds determined, noting crystal structure potential for laser emission 14 p2367 A66-27976

Electron spin resonance of gamma irradiated single crystal of barbituric acid dihydrate, noting formation and Hamiltonian parameters of free radicals 14 p2367 A66-27979

Sectorial structure effect on current carrier concentration of germanium doped indium antimonide single crystals 15 p2558 A66-28565

Martensitic transformation of Ni-Fe alloy from fcc to bcc lattice, noting stress produced by chemical free energy difference between austenite and martensite structure 15 p2520 A66-28649

Cleavage behavior of solid solution alloy Ta-Mo, noting electric resistivity, tensile properties, lattice parameters, diffraction coefficients, etc 15 p2520 A66-28650

Anisotropic vector functions of vector argument connected with crystal symmetry 15 p2526 A66-28951

Electron spin resonance saturation causing sharp decrease of DC resistance for reduced rutile crystals 15 p2567 A66-29401

Anisotropic broadening of X-ray diffraction lines and increase in lattice perimeter resulting from neutron irradiation of beryllium oxide powder 15 p2524 A66-29986

Exciton absorption lines and long wave intrinsic edges of single-crystal CdSe and CdS at low temperatures 15 p2569 A66-29987

Magnetic and structural properties of monoferrite films prepared by cathode sputtering, noting electron diffraction and micrograph patterns of films, crystal structure, etc 16 p2774 A66-30690

Effect of annealing in magnetic field on structural and magnetic properties of thin films prepared from nickel alloy 16 p2774 A66-30695

Temperature dependence of domain structure of thin ferromagnetic films prepared by thermal evaporation in vacuum 16 p2774 A66-30696



Temperature dependences of coercive force, hysteresis loops and domain structure of thin iron-gadolinium alloy films 16 p2774 A66-30698

Domain structure and hysteresis loops of thin iron-gadolinium films of different thicknesses 16 p2775 A66-30699

Lattice distortions and field gradients in alkali halide solutions, noting discrepancy in calculation of electric field gradients 16 p2775 A66-30731

Interband optical absorption in germanium in crossed electric and magnetic fields, noting band perturbation theory, differential spectra, Stark broadening, experimental techniques, etc 16 p2776 A66-30736

Thermal conductivity of polytetrafluoroethylene, noting temperature effect, crystal structure, etc 16 p2730 A66-30854

Silicon, quartz and germanium single crystal density determined via hydrostatic weighing method 16 p2777 A66-30933

Dependence of magnetostriction coefficient for diamagnetic materials on change of Fermi surface with momentum and deformation parameter 16 p2777 A66-31035

Statistical effects during generation of second harmonic in optically transparent crystals, noting coefficient of correlation between harmonic and fundamental radiation power of solid state laser 16 p2747 A66-31167

Nozzle guide vanes of ZrS-6K alloy in thermal stress induction of surface layer crystal structure changes 16 p2727 A66-31531

Semiconductor lasers with high power efficiency obtained via electron beam excitation on crystals of mixed cadmium-sulfide-selenide alloy 16 p2720 A66-31533

Epitaxial growth of single crystal, impurity free metal films using clean alkali halide surfaces in ultrahigh vacuum 16 p2784 A66-31534

Vapor growth of Ge on Ge, GaAs and Si substrates, noting preparation methods, characteristics, etc 16 p2786 A66-31686

Transverse reluctance of bismuth telluride in pulsed magnetic fields revealing fine structure of Shubnikov-De Haas oscillations interpreted as spin-splitting of Landau levels 16 p2786 A66-31695

Electron mobility in p-type indium antimonide, noting entrainment of minority carriers by majority 16 p2789 A66-31784

Epitaxial growth techniques for silicon and germanium, discussing hydrogen reduction methods, doping and impurity control, etc 17 p2976 A66-32259

Doping and firing atmosphere effects on electric resistivity of polycrystalline barium titanate, noting oxidation of small grain and positive temperature coefficient effect on large grain 17 p2978 A66-32404

Epitaxial growth of semiconductors in isothermal system approaching thermodynamic equilibrium, noting growth parameters, activation energy, etc 17 p2886 A66-32495

Electric field influence on thin metal film growth inducing coalescence of three-dimensional island-like structure 17 p2979 A66-32632

Element distribution in cermet alloys of W-Ni-Fe system determined by X-ray spectral analysis 17 p2940 A66-32848

Phase relations in cobalt niobate-cobalt tantalate system noting structural characteristics, solubility, phase transitions, etc 17 p2940 A66-33062

Gamma irradiation effects on minority carrier lifetime in germanium, noting temperature effect 17 p2987 A66-33321

Recrystallization of Ge and Si thin films and structural changes due to electron bombardment and thermal annealing 17 p2988 A66-33456

Curve equation describing ray surface cutting by arbitrary plane of symmetry in crystals 17 p2989 A66-33486

Three-dimensional X-ray diffraction data to determine structure of crystal of potassium barium hexanitrocobaltate, discussing Jahn-Teller effect 17 p2871 A66-33489

Behavior of aggregate under moderate loads with plastic deformation occurring in favorably oriented crystals on single active slip systems

## [ASME PAPER 65-WA/AMP-9]

Necessary and sufficient conditions for existence of direct and inverse piezoelectric effect in crystals and textures 18 p3153 A66-33629

Cadmium sulfide thin films as ultrasonic transducers, obtaining mixed or pure vibration modes via crystalline axis orientation 18 p3111 A66-34085

Structural chemistry of boron and compounds analyzed by X-rays, examining effects of increasing boron-to-metal ratio on boron-containing crystal structure 18 p3064 A66-34388

CW He-Ne laser measurement of light scattering in crystals noting laser output, performance and crystal imperfections 19 p3373 A66-35402

Orientation effect in GaAs injection lasers, noting emission characteristics and structural spectra 19 p3373 A66-35404

Magnetic properties and structure of ferromagnetic films obtained on single-crystal sodium chloride substrates heated to various temperatures during spray coating 19 p3438 A66-35497

Martensitic transformations in ferrous and nonferrous alloys, discussing kinetic and structural characteristics 19 p3380 A66-35848

Structural anisotropy coefficients of crystallization in carbon-graphite materials from X-ray and linear expansion data 19 p3388 A66-35863

Absorption spectra of pure and isotopic impurity crystals of naphthalene in region of first electronic and vibrational/vibron/transition 19 p3402 A66-36067

Crystal performance and mechanical noise reduction in pressure transducer in shock tube flow 20 p3558 A66-37423

Humidity effect on ferroelectric properties of barium titanate with tantalum oxide admixture, noting growth of dielectric constant and crystal polarization 20 p3617 A66-37553

Hyperfine structure of p-n junction phase boundaries in silicon according to electron microscopy data 20 p3620 A66-37693

X-ray analysis of crystal structure relationships among transition elements in binary and ternary aluminide alloys 20 p3586 A66-38092

Second-harmonic generation by focused laser beams based on experiments using He-Ne gas laser, noting SHG should be strongly peaked when focus is at either of crystal surfaces 21 p3746 A66-38554

X-ray analysis of lattice structure of terbium crystals at 120 to 300 degrees K 21 p3803 A66-39304

Existence of twins in single crystalline films of barium titanate, obtaining electron diffraction patterns 21 p3805 A66-39581

Optical spectrum of normal excitons in deformed and nondeformed n-type Ge single crystal layers for four orientations 22 p3964 A66-40306

Phase and chemical compositions of structural components forming in iron-nickel-chromium alloys with aluminum and titanium content 22 p3936 A66-40787

Heat resistance of coarse- and fine-grained D20 aluminum alloy 22 p3936 A66-40878

Angular variation of position of energy loss maxima in indium 23 p4110 A66-41180

Sectorial structure effect on current carrier concentration of germanium doped indium antimonide single crystals 23 p4112 A66-41286

Physical factors determining hardening of nimonic type alloy with high niobium content, discussing formation of intermetallic phase 23 p4080 A66-41385

Temperature homogenization effect on structure of industrial aluminum, determining mechanical properties dependency on Fe/Si ratio 23 p4081 A66-41403

Effect of manganese and zirconium additions on recrystallization temperature and grain size of aluminum alloys 23 p4081 A66-41404

Radiation, molecular orientation, crystallinity and molecular weight influences on thermoconductivity of high polymers 23 p4083 A66-41551

Zn diffusion effect on uniformly Mn-doped

GaAs wafer showing via radiotracer technique changes in impurity concentration profile 24 p4250 A66-42255

Deep /1-10 micron/ penetration of ion implanted donors in silicon, measuring density profiles via C-V method and parameter of penetrating tail section 24 p4250 A66-42256

Cs-Sb film thickness measurement method in various compositions and relation between thickness and composition 24 p4251 A66-42301

Anisotropic thermoelectric power in semiconductors as result of combined phonon and impurity scattering or in presence of carrier with anisotropic effective mass 24 p4252 A66-42352

Optical properties and energy structure parameters calculation for CdS-CdTe crystals 24 p4253 A66-42362

Magnetostriction of yttrium terbium ferrite garnets, noting absence of correlation between temperature dependences of magnetostriction and magnetization for high Tb content 24 p4256 A66-42518

Divergent-beam diffraction geometry for interpretation of Kossel diffraction patterns in space group assignment lattice parameters and structure factor evaluation 24 p4239 A66-43169

### CRYSTAL STRUCTURE DEFECT

#### SA INTERSTITIAL ATOM

#### SA LATTICE IMPERFECTION

#### SA PLASTIC DEFORMATION

Diffusion process of plasticity in metals, noting Frenkel vacancy mechanism 01 p0158 A66-11018

Combined effect of carbon impurity atoms and neutron radiation on structure of molybdenum studied by transmission electron microscopy 02 p0246 A66-12193

Equivalence of stress and electron-irradiation induced defects in degenerate p-n germanium junctions as indicated in similar voltage-anneal characteristics 04 p0562 A66-13751

Ultrapurification discussing definition, purification techniques, analytical techniques /e.g. emission and mass spectroscopy/ and role in biochemistry, metals and materials 04 p0474 A66-13867

Radiative recombination in silicon containing structural defects in lattice 04 p0569 A66-14353

German text on electronic semiconductors introducing physics of rectifiers and transistors 04 p0570 A66-14458

Boundary layer thickness responsible for anomalous lattice distortions of colloidal barium titanate 04 p0571 A66-14492

Anelasticity and relaxation time in metals and nonmetals, particularly as manifested by internal friction peak as function of frequency or temperature in study of crystalline material defects 05 p0772 A66-14548

Radiation damage of p-type silicon investigated by Hall effect, noting dislocation density and annealing behavior 05 p0735 A66-14963

Possible processes of non-radiative decay of excitons on ionized donors and acceptors in semiconducting and dielectric crystals 05 p0737 A66-15160

Radiation damage to crystalline lattices by energetic particles, discussing consequences on physical behavior of solids, particularly ceramics 05 p0738 A66-15471

Austenitic chromium-nickel-manganese steel, describing temperature effects on crystal structure and experimental techniques 05 p0704 A66-15819

Isochronal annealing from 80 to 360 degrees K of defects induced by 45-meV electrons in floating zone and pulled n-type silicon 05 p0742 A66-15873

Potential correction effect on ground states of P and ionic-S impurities in silicon discussed in terms of cavity model 06 p0930 A66-17051

Metastable defect annealing in germanium by bombardment with short pulse of high-energy electrons from Van de Graaff generator 06 p0932 A66-17115

Length change, X-ray lattice parameter, small angle X-ray scattering, electron microscopy and thermal conductivity measurements related to radiation-induced



defects in semiconductors 06 p0933 A66-17117  
 Diffusion of Li and Cu in GaAs crystals indicates reaction involving divacancies in donor-doped and undoped 06 p0935 A66-17132  
 Influence of defects introduced during fast neutron irradiation on electronic behavior of SiC, examining reasons for deterioration of SiC semiconductor 06 p0936 A66-17137  
 Point defect mobility and annealing in irradiated germanium and silicon by electron or gamma ray irradiation 06 p0937 A66-17140  
 Drift mobility of radiation induced defects in silicon between zero and 120 degrees C 06 p0937 A66-17141  
 Nature and mobility of point defects present in silicon at high temperature and interactions between them 06 p0937 A66-17142  
 Electronic states of single defects in diamond calculated by comparing electronic states of single vacancies and single interstitial carbon atoms 06 p0938 A66-17148  
 Anisotropy of electron displacement energy in silicon specimens by measuring changes in net carrier concentration caused by steady monoenergetic electron irradiations 06 p0939 A66-17152  
 Isolated vacancy interstitial pairs produced in ZnSe lattice by electron bombardment at low temperature 06 p0939 A66-17153  
 Nature and yield of photon and neutron induced defects in semiconductors determined from changes in electrical properties 06 p0939 A66-17154  
 Characteristics and properties of defects induced in silicon and germanium by 10-to 60-mev electrons and 20-to 130-mev protons 06 p0939 A66-17155  
 Oxide ceramics fabrication, with particular attention to microstructure 07 p1053 A66-18296  
 Diffraction contrast analysis, using transmission electron microscope, of two-dimensional defects present in mechanically damaged silicon after annealing 07 p1109 A66-18516  
 Imperfection formation in epitaxial gold films, observing crystal-lattice dislocations due to rotation and displacement misfits between neighboring islands of deposit film 07 p1110 A66-18517  
 Semiconductor microinhomogeneities detected by device using fluctuations of impurity concentrations during process of crystal growth 08 p1223 A66-19287  
 Influence of crystal-lattice defects on Young's modulus and damping constant of aluminum 09 p1388 A66-19980  
 Effect of electric field and crystalline dimensions on position of optical absorption edge in cadmium sulfide thin films obtained by vacuum deposition 09 p1412 A66-19995  
 Impurity-photoconductivity spectra of silicon single crystals containing lithium and arsenic impurities 09 p1413 A66-19999  
 Structure defects in silicon crystals which cause X-ray double images studied, using X-ray diffraction topography and etching technique 10 p1574 A66-21347  
 X-ray analysis of zinc diffusion induced defects in gallium 10 p1576 A66-21547  
 Boron filament tensile and flexural strength affected by surface and internal flaws with chemical polishing 10 p1548 A66-21728  
 IR absorption spectra of oxygen-defect complexes in irradiated silicon 10 p1581 A66-21737  
 Scanning electron microscope observation of electrical leakage paths due to crystal defects in silicon diodes 11 p1668 A66-23028  
 Localized enhanced diffusion in vacancy model to explain Emitter Dip Effect (EDE) in n-p-n silicon transistor 11 p1871 A66-23350  
 Oxidation rate and heat treatment effect on density of states of silicon surface potential in silicon-silicon dioxide system 12 p1932 A66-24825  
 Defect analysis by device sectioning, noting techniques, application in crystallography, electronics, etc 12 p1845 A66-24849  
 Annealing of deformed sodium, noting activation energy distribution annealing kinetics, etc 12 p1897 A66-24923  
 Defects in gallium arsenide crystals studied

by internal friction with measurements showing damping peak at 140 degrees C 13 p2157 A66-25045  
 Microstructure of epitaxial germanium films deposited on calcium fluoride substrates, noting parameters of deposition 13 p2158 A66-25063  
 Plastic deformation effects on preaged aluminum-copper alloy structure subjected to 40-75 percent compression 13 p2110 A66-25965  
 Donor impurity effect on direct-indirect transition in gallium arsenic phosphide, particularly at low temperature 13 p2170 A66-26590  
 Vacancies and agglomeration effect on integral characteristics of anomalous X-ray transmission 14 p2357 A66-27077  
 Self-compensation in electric conductivity and other properties of binary semiconductor with temperature variations 14 p2357 A66-27079  
 Dislocation-free Si crystal defects produced by fast neutron bombardment 14 p2359 A66-27092  
 Fracture mechanics, discussing crystal structure defects, particular dislocation, hardening, lattice vacancies, interstitials, etc 14 p2316 A66-27770  
 Thermal expansion coefficient of doped germanium, noting correlation between impurity used and coefficient variation 14 p2368 A66-28244  
 Radiative recombination in silicon containing structural defects in lattice 14 p2368 A66-28251  
 Electron diffraction study of structural defects in cubic phases in epitaxial tantalum oxide thin films 15 p2557 A66-28560  
 Structural defects arising during growth and heat treatment of CdS single crystals studied, using anomalous transmission of X-rays 15 p2557 A66-28563  
 Heat treatment effect on photoelectric properties of silicon with electron-induced structural defects 15 p2560 A66-28668  
 Optical inhomogeneities in n-type gallium arsenide crystals containing growth axis examined in transmission, using IR image converter, noting band gap changes 15 p2562 A66-28720  
 X-ray study of component atomic scattering and structural defects for titanium and carbide atoms in titanium carbide 15 p2520 A66-28754  
 Ion bombardment damage of molybdenum sulfide lattice studied by transmission electron microscopy, noting broadening of extinction contours and dislocation lines 15 p2567 A66-29404  
 Ionized electron centers in irradiated lithium fluoride crystals investigated by observing emission and absorption spectra 15 p2568 A66-29641  
 Magnetostriction, negative anisotropy and chainlike domain walls along line defects in thin permalloy films 16 p2776 A66-30803  
 Arsenic overpressure, obtained by including metallic arsenic along with gallium arsenide, depresses defect concentration identifying primary defect species as arsenic monovacancies 16 p2779 A66-31086  
 Copper and Armco iron structural defects during cyclic deformation studied by electron-microscope and optical-microscope techniques 16 p2727 A66-31528  
 Photo-Hall effect and photoconductivity on compensated p-InSb at low temperatures, examining temperature dependence of carrier mobility 16 p2788 A66-31773  
 Mossbauer effect and optical analog in five different recombination centers of silicon 16 p2789 A66-31785  
 Superheating crystallization of ethylene-propylene and ethylene-butene-1 copolymers and extended chain morphology 17 p2943 A66-32557  
 Structural defects in epitaxial films noting nucleation mechanism, stacking faults, growth defects, etc 17 p2985 A66-33157  
 Scanning electron microscope to examine crystal mosaic structures and lasing properties of gallium arsenide laser diodes 17 p2937 A66-33300  
 Polycrystalline nickel aluminide lightly deformed at 77, 298 and 900 degrees K exhibit fine slip band structure with mostly screw dislocations 18 p3121 A66-33747

Radiation damage in solids including crystal lattice defects, thermal migration, channeling and focusing effects, etc 18 p3155 A66-34136  
 Base drive and internal structural irregularities of transistor effect on internal current distribution and second breakdown characteristics of device 19 p3312 A66-35343  
 Planar and needle-like defects in natural quartz examined via X-ray diffraction, noting composition and diffraction contrast when observed from different Bragg planes 19 p3434 A66-35403  
 Dispersion degree of coherent scattering regions, microdeformation and packing defects probability in fcc metals determined, using approximation method 19 p3438 A66-35496  
 Factors affecting fracture characteristics of metals at cryogenic temperatures and fracture mechanics for predicting performance of defect-containing structures 19 p3380 A66-35847  
 Structural defects in infiltrated tungsten matrices related to process procedures 19 p3382 A66-36122  
 Gamma irradiation from Co 60 effect on indium antimonide, determining defect formation on dose and limiting position of Fermi level for n-and p-type material 20 p3617 A66-37552  
 Germanium damage due to low energy He, Ne, Ar and Kr ion bombardment 20 p3623 A66-38392  
 Fast-neutron irradiation effects on photoconductivity spectra and induced crystal structure defects for n-and p-type gallium arsenide single crystals 20 p3624 A66-38415  
 Relation between electrical properties and structural features of gold-and antimony-doped germanium single crystals, noting abrupt decrease in mobility 21 p3799 A66-38928  
 Steady state donor-acceptor recombination rate and effects on diode current and injection electroluminescence, using Shockley-Read-Hall semiconductor phenomenological model 21 p3800 A66-38993  
 Isochronal and isothermal stage II recovery in high energy electron irradiated n-type InSb semiconductor, based on Hall coefficient and electroconductivity 21 p3800 A66-38994  
 Heat treatment of silicon at high temperatures leads to donor centers affecting electric and photoelectric properties 21 p3802 A66-39157  
 IR radiation absorption in imperfect ionic crystals 21 p3802 A66-39158  
 Cyclotron resonance study of electron scattering by thermal acceptors in quenched Ge 21 p3805 A66-39567  
 Inhomogeneities in silicon crystal prisms studied by method of photoelectric conductivity 22 p3961 A66-39998  
 Imperfection of silicon dioxide layers caused by dust particles during thermal oxidation of silicon, measuring breakdown voltage 22 p3961 A66-39999  
 Diffusion process involving formation and subsequent migration of series of parallel shear planes within crystal for higher oxides of niobium, tungsten, molybdenum and titanium 22 p3934 A66-40011  
 Neutron irradiation-induced defects in vapor deposited niobium stannide and effects on current-carrying capacity 22 p3962 A66-40083  
 Self-compensation in electric conductivity and other properties of binary semiconductor with temperature variations 22 p3967 A66-40835  
 Dislocation-free Si crystal defects produced by fast neutron bombardment 22 p3967 A66-40848  
 Electron diffraction study of structural defects in cubic phases in epitaxial tantalum oxide thin films 23 p4112 A66-41281  
 Structural defects arising during growth and heat treatment of CdS single crystals studied, using anomalous transmission of X-rays 23 p4112 A66-41284  
 Crystal defects and performance in ruby laser, measuring coherence function of light and output energy and crystal homogeneity 23 p4077 A66-41291  
 Autoradiography used to determine



dislocation density in germanium, silicon and copper single crystals, with aid of tagged atoms 24 p4257 A66-42535

**CRYSTAL SURFACE**

Light effect on surface conductivity of gold-alloyed germanium with clean surface 01 p0125 A66-10776

Quantum-mechanical properties derived for isolated donor atom located on surface of dielectric crystal, noting hydrogenic wave function with planar nodes 02 p0271 A66-11484

Optical field effect in analyzing band structure and surface physics of silicon, noting reflectance 04 p0560 A66-13723

Current oscillations in germanium and silicon connected to compensated semiconductor, noting surface impurities 04 p0569 A66-14354

Effect of sample geometry on frequency of helicon waves in lead telluride at low temperature 07 p1101 A66-18201

Contact-making process in cadmium sulfide crystals, examining influence on plasma electron efficiency in glow discharge work 08 p1272 A66-19243

Work function of A and B faces of /111/ surface of gallium arsenide in dry and humid media 08 p1274 A66-19317

Potential distribution at germanium-electrolyte interface in iodide ion solutions 08 p1278 A66-19824

Electron microscope observation of active centers at surface of semiconductor crystals, applying to p-type Si single crystals 09 p1412 A66-19989

Extrinsic and intrinsic surface states and photoelectronic properties of insulating CdS crystals 09 p1427 A66-20256

Rapid cooling induced stress leads to separation between tin and germanium, creating pure germanium surface at plane of separation 09 p1427 A66-20366

Contact potential difference measurements between aged polycrystalline tungsten foil and polished single crystal disk and work function calculation for /110/ oriented surface 10 p1582 A66-21888

Light effect on surface conductivity of gold-alloyed germanium with clean surface 11 p1749 A66-22288

Semiconductor surface physics, with emphasis on FET electrical surface phenomena 11 p1759 A66-23462

Current oscillations in germanium and silicon connected to compensated semiconductor, noting surface impurities 14 p2368 A66-28252

Diffraction pattern study of titanium single-crystal surface 15 p2566 A66-29389

Momentum and energy accommodation for hypervelocity gas particles on crystal surface, using Lennard Jones potential and approximating lattice by system of independent forced harmonic oscillators 16 p2752 A66-30388

Pulse field effect technique investigation of electrical properties of surface states on practical Si surfaces with various surface 16 p2781 A66-31356

Electric conductivity of CdS single crystals in atmosphere, dry air, oxygen, water vapor, carbon dioxide and in transverse electric field 16 p2786 A66-31730

Vacuum thermal decomposition of InSb and GaSb surfaces, noting evaporation rates 20 p3624 A66-38411

MOS work function difference effect on surface charge density and orientation calculations for Si-silicon dioxide interfaces 22 p3962 A66-40050

Oxide film surface effect on electrophysical characteristics of Ge surface, noting potential changes and recombination rate 22 p3965 A66-40313

Adhesion force of silicates in ultrahigh vacuum as function of load force, temperature, surface roughness and crystal orientation 23 p4131 A66-41848

Electron correlation analysis method applied to interelectronic repulsion effect on localized electrons near ideal surface of seminfinit diamond-like crystal 24 p4252 A66-42349

**CRYSTALLIZATION**

**SA RECRYSTALLIZATION**

Equations describing crystallization process in low level clouds as function of ice crystal

penetration from upper clouds or from artificial seeding 02 p0254 A66-12023

Sliding friction measurements of some layer lattice compounds in ultrahigh vacuum [ASLE PREPRINT 65-LC-19] 02 p0237 A66-12251

Welding units using ultrasonic vibrations to improve crystalline structure of welds produced by automatic submerged-arc welding process 03 p0375 A66-13122

Crystallization kinetics in supercooled cloud under natural conditions 11 p1725 A66-22196

Mechanical properties of lithium silicate glasses at different stages of crystallization and relation to microstructure 12 p1900 A66-24862

Crystallization sequences in alkali aluminogermanate glass 14 p2318 A66-26947

Sliding friction measurements of some layer lattice compounds in ultrahigh vacuum [ASLE PREPRINT 65-LC-19] 16 p2713 A66-30569

Changes in massive amorphous boron filaments by heat treatments under reduced pressures and in presence of inert gases 17 p2943 A66-32852

**CRYSTALLOGRAPHY**

Laser crystals prepared economically by splitting along cleavage planes 01 p0084 A66-11046

Possible materials for second harmonic generation and laser action discussing centrosymmetric and piezoelectric crystals and single crystal plate with alternate layers of noncentrosymmetric composition 03 p0378 A66-12940

Vacuum and low temperature X-ray camera for structural analysis of oxidized materials 04 p0518 A66-13490

Molecular configuration of bis /ortho-dodecacarborane/ determined by three-dimensional X-ray crystallography 06 p0822 A66-16631

Implementation of Kossel line technique of crystallographic analysis and lattice parameter measurement in study of lattice defects in semiconductor crystals 06 p0935 A66-17133

Resistance-grown pyrolytic graphite in crystallographic, thermal and electrical measurements 08 p1244 A66-19223

Holography, X-ray crystallography and correspondence between optical image synthesis and heavy atom technique 11 p1707 A66-23194

Laser crystals prepared economically by splitting along cleavage planes 11 p1714 A66-23293

Betti numbers shown to be equal to binomial coefficients of torus, determining minimal set of van Hove critical points 15 p2559 A66-28624

Static uniaxial compression effect measurement along /100/, /110/ and /111/ on electroreflectance spectrum of gallium arsenide, using electrolyte technique 16 p2777 A66-30951

Crystallographic polarity dependent rectification in ZnS single crystals 18 p3153 A66-33610

**CUBANE**

Thermodynamic properties and appearance potentials of cubane 10 p1495 A66-21166

**CUBIC CRYSTAL**

**SA BODY CENTERED CUBIC /BCC/ CRYSTAL**

**SA FACE CENTERED CUBIC /FCC/ CRYSTAL**

**SA GRUNEISEN CONSTANT**

Energy accommodation coefficients calculated for gas particles interacting with cubic crystal lattice 04 p0548 A66-14142

Four elastic constants of Laval, Raman and Viswanathan theories dynamically measured in connection with behavior data on cubic crystals 05 p0781 A66-15736

Cubic transition-metal carbides and binding mechanism 13 p2166 A66-25835

Longitudinal Hall effect for two-band conduction and tensor relaxation times in cubic crystals 14 p2363 A66-27577

Phenomenological theory of longitudinal Hall effect in cubic crystals, assuming anisotropic dispersion law and tensorial relaxation time 20 p3618 A66-37560

**CUBIC EQUATION**

Cubic equations solved by tables compiled by Shumiagaskii and Herbert, Richards and Arsham 01 p0093 A66-10408

Approximate solution of cubic equation with real roots and applications in mechanics 17 p2947 A66-33328

**CULTURE TECHNIQUE**

Growth rate of microorganisms when rate changes with time, using continuous culture technique 02 p0183 A66-12016

Microbial contaminants evaluation for sterility in interiors of spacecraft, noting culturing technique 19 p3287 A66-35575

**CUMULUS CLOUD**

Hydrothermodynamic equations for calculating velocity, temperature and pressure fields and water content for model of stationary axisymmetric cumulus cloud 04 p0540 A66-13414

Cumuli above sea in spite of stable layer between sea surface and cloud boundary, noting condensation around salt particles penetrating ascending thermals 04 p0542 A66-14306

Numerical experiment where conditionally unstable environment was present for study of cumulus-like circulations developed from initial state 06 p0905 A66-16267

Cumulus modification experiment using station network, radiosonde and pilot balloon stations, cameras, radar data, etc 06 p0905 A66-16268

Numerical study of initiation of cumulus clouds over mountainous terrain 07 p1062 A66-17370

Stereo pairs taken at one-and two-minute intervals in photogrammetry of initiation of cumulus clouds over mountainous terrain 07 p1062 A66-17371

Probability of clear lines-of-sight estimated from sunshine and cloud cover observation 08 p1248 A66-19386

Cumulus cloud simulation by dropping solid piece of carbon dioxide into hot water 08 p1248 A66-19388

Cumulus to cumulonimbus convection over mountains and dissipation of stratus and sea fog when moving inland, using Tiros photographs 11 p1728 A66-22321

Conventional rawin, pibal and surface wind data compared with photoreconnaissance data, showing cumulus population and patterns over Florida 14 p2325 A66-26927

Entrainment problem, convective clouds and atmospheric thermal convection 14 p2325 A66-27280

Cumuli above sea in spite of stable layer between sea surface and cloud boundary, noting condensation around salt particles penetrating ascending thermals 14 p2327 A66-28219

Nonstationary models of cumuli and thermals in stratified atmosphere 18 p3130 A66-34606

**CURARE**

**S ALKALOID**

**CURIE TEMPERATURE**

Specific heat of gadolinium near Curie point, discussing measuring procedure and line drawing of calorimetric setup 01 p0118 A66-10252

Uniform compression effect on Curie temperature of ferromagnetic compound EuO 01 p0118 A66-10254

Spin wave instabilities in ferrite using parallel pumping and spin wave absorption near Curie temperature 01 p0121 A66-10539

Anomalous thermal expansion above and below Curie point as function of temperature in gadolinium single crystal 02 p0274 A66-11725

Curie temperature, static dielectric constant and electro-optic coefficient of large single crystals of barium titanate 03 p0411 A66-13007

Behavior of Ising model of ferromagnet in nonzero magnetic field, using high temperature series 04 p0563 A66-13815

Polycrystalline barium titanate ceramic with nonlinear resistance-temperature characteristic that rises steeply at ferroelectric Curie point 07 p1100 A66-18156

Ferroelectric properties of trissarcosine calcium chloride including dielectric measurement, Curie temperature region, etc 08 p1270 A66-19009



Magnetocrystal anisotropy of hexagonal ferromagnetic substances in neighborhood of Curie point 08 p1273 A66-19249  
 Uniform compression effect on Curie temperature of ferromagnetic compound EuO 13 p2168 A66-25971  
 Change in heat capacity at Curie point for ferrites 14 p2369 A66-28331  
 Flame spraying method for conversion of pure barium titanate into glass, noting dielectric Curie temperature 15 p2524 A66-29665  
 Kinetic energy causing anomalous increase in thermoelectric power in semiconducting p-type iron-chromium sulfide near Curie temperature 21 p3803 A66-39261

## CURING

## SA AGING

Curing problems of highly exothermic propellants investigated using mathematical models, detailing heat conduction and thermal properties 22 p3968 A66-39868

## CURRENT

S AIR CURRENT  
 S BEAM CURRENT  
 S CONVECTION CURRENT  
 S EARTH CURRENT  
 S EDDY CURRENT  
 S ELECTRIC CURRENT  
 S ION CURRENT  
 S IONOSPHERIC CURRENT  
 S LINE CURRENT  
 S RING CURRENT  
 S THERMAL CURRENT  
 S THRESHOLD CURRENT

## CURRENT AMPLIFIER

Pulsing technique enhances gain of silicon planar transistor low-current amplifiers 03 p0343 A66-13014  
 Current amplification factors of micropower silicon planar transistors in low current common-base and common-emitter circuits 06 p0860 A66-17196  
 High impedance semiconductor DC amplifier for use as measuring amplifier or operational amplifier 08 p1194 A66-19279  
 Electron processes in p-n-p-m transistor, relating capacitor current and emitter current and current amplification factor and emitter current 09 p1358 A66-20812  
 Backward-current amplification for transistors and effect on elements of Giacoletto equivalent circuit diagram 11 p1669 A66-23102  
 Mathematical approximation for alpha of drift transistors derived in terms of equivalent dominant pole and excess phase 11 p1671 A66-23245  
 Current amplification factor of filamentary transistor with intrinsic-conductance semiconductor base 14 p2255 A66-27751  
 Current amplification factors of micropower silicon planar transistors in low current common-base and common-emitter circuits 19 p3315 A66-35554

## CURRENT DENSITY

Release of persistent current energy by local heat injection and propagation through Nb-Zr wires 01 p0116 A66-10238  
 Microwave radiation and surface patterns formed during application of high currents and magnetic fields to n-InSb 01 p0117 A66-10244  
 Screening field and specific heat of superconductivity of sintered niobium stannide at temperatures above 4.2 degrees K 01 p0117 A66-10245  
 Current-current and current-density correlation functions for longitudinal oscillations of plasma in uniform magnetic field 01 p0109 A66-10319  
 Thermomagnetic current density in semiconductors and metals with temperature gradient 01 p0125 A66-10779  
 Germanium Esaki diode characteristics with aging, noting change in excess current after forward bias application 02 p0198 A66-11522  
 Palladium-hydrogen diffusion electrode noting current densities 04 p0460 A66-14034  
 Fluctuation-dissipation theorems for relating noise current power spectrum to first and third order conductivity tensors in thermal equilibrium and pumped Raman-active media 04 p0532 A66-14310  
 Current oscillations in germanium and silicon connected to compensated semiconductor, noting surface

impurities 04 p0569 A66-14354  
 Effects of variable ionic mobility on current collection by cylindrical body and of fringing electric field on sheath size, noting role of diffusion phenomenon 05 p0722 A66-14724  
 Third harmonic component of current density in plasma in presence of electric and magnetic fields, analyzing generation and propagation of third harmonic of electromagnetic wave in magnetoplasma 05 p0724 A66-15188  
 Current and power gain of noble gas filled converter as affected by auxiliary emitter position to electrode and geometry 05 p0618 A66-15560  
 Cylindrical receiving and scattering antennas, determining current from admittance, charge distribution and near field for incident plane wave 06 p0827 A66-16036  
 Current-convective and flute instabilities of spatially inhomogeneous current in plasma, noting effect of current density and temperature 06 p0914 A66-16140  
 Electron temperature spectroscopy for atmospheric argon plasmas, sodium vapor seeded at high temperatures, noting relationship with current density 06 p0915 A66-16178  
 Porous gas-diffusion electrodes analyzed by using four different models, comparing resulting current density-polarization characteristics 07 p0990 A66-17239  
 Electrical and electroluminescent properties of GaAs diodes at voltages below onset of negative resistance 07 p1042 A66-17330  
 Excitation of semiconductor lasers by beam of fast electrons, discussing work of Shockley, Popov, Keldysh and Krokhin 07 p1043 A66-17337  
 Polarization and Alfvén wave attenuation in Doppler-like change in transverse wave velocity when drift current is passed parallel to magnetic field in solid-bismuth plasma 07 p1102 A66-18209  
 Electrode potentials and efficiency, noting significance, types and associated equations 07 p0996 A66-18468  
 Kinetic effects in fuel cells, discussing declining efficiency with increasing output, slow electron transfer effects, concentration polarization, etc 07 p0996 A66-18469  
 Miniature Rogowski coil probes for direct measurement of current density distributions in transient plasmas 07 p1037 A66-18494  
 Current driven instabilities slowed down by increasing electron-ion collisions in configurations with sheared magnetic fields 08 p1260 A66-18539  
 Time dependent variations in current carrier density and pulse behavior of drift transistor 08 p1188 A66-18625  
 Transit time effects in space-charge-limited silicon microwave diode 08 p1188 A66-18652  
 Two-dimensional distribution of carriers in semiconductor space charge region with current flow 08 p1267 A66-18654  
 Charging current density, electrolyte concentration and temperature during charge effects on porous cadmium electrodes in nickel cadmium cells 08 p1171 A66-19645  
 Zinc-silver oxide battery for extreme temperatures, noting electrode utilization efficiencies as function of current density 08 p1173 A66-19662  
 Saturation currents of silicon multichannel field effect transistors 09 p1350 A66-19914  
 /MUCH-FET/  
 Hall effect in germanium telluride samples with various current carrier concentrations at temperatures up to 500 degrees C 09 p1413 A66-20000  
 Tunneling density of states for superconductor in tunneling junction and carrying current at zero temperature 09 p1418 A66-20035  
 High current-carrying capacity and flux trapping in homogeneous alloy single crystal type II superconductors 09 p1421 A66-20057  
 Current density distribution in MPD arc jet exhaust measured, using Hall effect sensors [AIAA PAPER 66-116] 09 p1433 A66-20089  
 Breakdown of theta pinch in helium at

high initial densities without preionization 09 p1408 A66-20422  
 Magnetic and electric field and current density distributions in propagating current sheet [AIAA PAPER 66-200] 10 p1563 A66-21442  
 Superconductivity of composite of fine niobium wire in copper, measuring critical temperature, transverse magnetic field, current density, etc 10 p1575 A66-21535  
 Perturbation technique solution for MHD flow in closed regions with symmetric flow properties and axial boundary conditions 10 p1563 A66-21543  
 Digital computer solutions to rigorous linear equations system for current density by enforcing boundary conditions at discrete points in scattering body 10 p1497 A66-21589  
 Thermomagnetic current density in semiconductors and metals with temperature gradient 11 p1749 A66-22291  
 Electron-phonon coupling in piezoelectric semiconductors, obtaining electric field and current density vectors for application to ultrasonic amplification 11 p1750 A66-22401  
 Electron beam machines for thermal milling, noting factors influencing size of heat affected zones such as current density, lens aberration, temperature rise, etc 11 p1710 A66-22700  
 Integral equations describing multiple neutron Bragg reflections in mosaic crystal 11 p1742 A66-23409  
 Transference numbers in ionized gases, contrasting current flow in electrolytes with steady state current flow in weakly ionized gases 12 p1920 A66-24097  
 Radiative recombination in gallium arsenide p-n junctions for weak currents, obtaining relation between emission spectra and current-voltage characteristics of diodes 12 p1929 A66-24456  
 Steady state structure and LF modes of infinitely long finite thickness cylindrical sheet of relativistic electrons in applied external field 12 p1873 A66-24576  
 Perturbation theory determination of third harmonic current density generated in plasma by AC field for velocity-dependent plasma 12 p1924 A66-24593  
 Boltzmann transfer equation for electrons and generation of nonlinear second harmonic of current density in inhomogeneous plasma 12 p1924 A66-24806  
 Current saturation in CdS crystals 12 p1931 A66-24814  
 Potential sweep method for organic and adsorption analyses, showing relation between galvanostatic and fast potential sweep transients, noting mathematical analysis of current-potential transients 12 p1812 A66-25000  
 Schottky and Langmuir laws verification by thermionic emission of lithium aluminosilicate with respect to current limitation caused by space charge 13 p2163 A66-25436  
 Irradiation effects by fast neutrons and gammas on collector cut-off current and base current at low current densities analyzed on silicon planar transistors 13 p2032 A66-25486  
 Current density in slightly ionized gas for arbitrary collision cross section 13 p2150 A66-26274  
 Nonlinear generation of sum and difference frequency components in current density in plasma due to two alternating electric fields 13 p2156 A66-26681  
 Gunn effect involving current oscillations higher than 1000 mc in GaAs crystal under applied electric field 14 p2355 A66-26920  
 Current dependence of recombination radiation intensity in gallium antimonide, determining radiation spectral distribution at low temperature 14 p2358 A66-27089  
 Localization conditions of high power linear HF discharge at low gas pressure, achieving localization of current and plasma density in magnetic field by using diaphragms 14 p2340 A66-27148  
 Effect of liquation inhomogeneity on superconducting properties of ternary alloy, noting enhancement of critical current density in wire prepared from this alloy 14 p2314 A66-27367  
 Zirconium-niobium alloy analyzed by oxide replica technique, noting superconductivity and tunnel effect, determining relation



between superconductivity current critical density and sample structural characteristics 14 p2314 A66-27368

Current oscillations in germanium and silicon connected to compensated semiconductor, noting surface impurities 14 p2368 A66-28252

Electric current density in semiconductor, noting harmonic mixing of microwaves by warm electrons in germanium 15 p2564 A66-28875

Current-convective and flute instabilities of spatially inhomogeneous current in plasma, noting effect of current density and temperature 15 p2556 A66-29870

Effect of temperature gradient at surface of metal on thermionic emission current 16 p2778 A66-31079

Laser cavity output optimization for maximum external quantum efficiency showing dependence on length and reflectivity for given current density 16 p2720 A66-31535

Origin of polarization of radiation from GaAs diodes, noting intensity dependence on current density and effect of anisotropic electron velocity 16 p2667 A66-31770

Undepleted current carrier effect on characteristics of inverse p-n junction 17 p2976 A66-32069

Electron velocity distribution in ionized gas under alternating electric field as function of density, temperature, etc, including effects of recombination, ionization, etc 17 p2960 A66-32426

Electric current density in ionizing discharge layer determined, using multifluid equations of conservation of momentum and gas mass 17 p2967 A66-32435

Axially symmetric or two-dimensional electrode system with emitting surface, discussing convergence and accuracy criteria of iteration methods 17 p2887 A66-32700

Harmonic series solution for electromagnetic scattering by unidirectionally conducting helical sheath when incident field is E-polarized 18 p3065 A66-33530

Nonlinear generation of combination frequencies due to strong uniform parallel electric fields in homogeneous plasma 18 p3142 A66-33918

Equation explaining polarization of solid electrolyte cell with silver plate anode, noting role of current density 18 p3056 A66-34903

Electron-phonon interaction current density, thermodynamic Green function and other electromagnetic properties of superconductors, using Froehlich-Hamilton model 19 p3438 A66-35481

Ionosphere as anisotropic dissipative medium where charged particles random thermal motion acts as thermal radiation source, noting relation between driven AC conduction current density and applied AC electric field intensity 19 p3352 A66-36630

Langmuir current-density limit derived for differing axial and radial electron beam temperatures in high-resolution image devices 20 p3524 A66-36899

Crystal growth, diffusion and fabrication of gallium arsenide-phosphide junction lasers with low threshold current densities 20 p3577 A66-37401

Space charge wave equation and impedance and stability of electron diodes, using Nyquist analysis and transit time and RF beam current 20 p3528 A66-37489

Cathode current density distribution, beam minimum radius and location and electrode current interception, using computer techniques on electron guns 20 p3528 A66-37490

Recombination radiation from Ga-Sb p-n junctions, noting spectral composition as function of current density and impurity concentration 20 p3618 A66-37563

Radiative recombination in gallium arsenide p-n junctions for weak currents, obtaining relation between emission spectra and current-voltage characteristics of diodes 20 p3619 A66-37688

Electron beams from duoplasmatron using hollow cathode arc, noting current density distributions 20 p3606 A66-38406

Optical coupling using gallium arsenide

laser for variation of frequency of diode emission through small change in current density 21 p3746 A66-38920

Radiation intensity dependence for various spectral bands of diffused gallium arsenide p-n junctions on current density 21 p3798 A66-38921

Kadomtsev current-convective instability and damping as affected by current density, wave frequency, resistivity gradient and azimuthal wave number 21 p3791 A66-39178

Current density, electron mobility, magnetoresistance, negative resistance and impact-ionization-produced solid state magnetoplasma oscillations in InSb single crystal semiconductor at high electric and magnetic fields 21 p3805 A66-39568

Recombination radiation from GaAs p-n junctions with and without Fabry-Perot resonator, noting parameter dependence on current density 22 p3932 A66-40314

Atmospheric electric field change compensation during measuring air-Earth ionic conduction and electron precipitation current densities 22 p3920 A66-40804

Current dependence of recombination radiation intensity in gallium antimonide, determining radiation spectral distribution at low temperature 22 p3967 A66-40845

Analytical expression derived for current density of arc moving extinguishing chute by force of external magnetic field 23 p4099 A66-41057

Structure effect on superconducting properties of eutectic alloys solidified under variety of growth conditions, discussing interphase boundary, current density and residual strain 24 p4250 A66-42296

Current transducer for measuring current pulses in kiloampere range and suitable for laser research applications 24 p4213 A66-42820

Localization conditions of high power linear HF discharge at low gas pressure, achieving localization of current and plasma density in magnetic field by using diaphragms 24 p4244 A66-42968

**CURRENT DISTRIBUTION**

Current and voltage distribution over length of HF discharge in helium-neon laser 01 p0082 A66-10704

Effect of currents, distributed over envelope surface formed by revolution of magnetic dipole force line about its axis, on cosmic ray cut-off 02 p0284 A66-12128

Current distribution instability elimination by HF power transistor sets prepared by microelectronic techniques 03 p0341 A66-12522

Linear antennas and characteristics regarding maximum power, directivity, height, sleeve and conical dipoles and current distribution 04 p0491 A66-13402

Current-voltage characteristics of long diodes calculated by dividing diode base into three regions 04 p0495 A66-13767

Gallium arsenide p-n junction laser diode covering injection current distribution, density and emission spectra variation 05 p0692 A66-14659

Plane electromagnetic wave scattering at rectangular conducting strips, examining front end backscattering and current distribution measurements 05 p0649 A66-15121

Current exchange between electrodes and working fluid in open-cycle MHD generators 05 p0625 A66-15814

Concentric ring antenna arrays with low sidelobes, estimating currents from Fourier-Bessel series 06 p0825 A66-16017

Current distribution for cylindrical dipole of infinite length immersed in homogeneous lossless magnetolonic anisotropic ionosphere 06 p0827 A66-16033

Electromagnetic field in current-carrying region, discussing existence criteria of improper integrals 06 p0908 A66-16130

Current distribution on L-band loop antenna composed of four quarter-circular sections 06 p0850 A66-16446

Instabilities of current and potential distribution in n-type GaAs and InP in electric field of several thousand v/cm 07 p1104 A66-18221

Open circuit voltage, inner resistance, Hall voltage and tensorial conductivity for

Faraday generator, using conformal mapping for single pair of electrodes 07 p0993 A66-18309

Electric current passage through multivalley n-germanium semiconductor plates, noting nonuniform electron distribution 08 p1273 A66-19275

Antenna radiation shows relationship to tangential component of electric field intensity along antenna 08 p1197 A66-19606

Kliatskin objections and improvements concerning integral equation describing current distribution in rectilinear antenna 08 p1197 A66-19607

Line width of semiconductor laser 08 p1234 A66-19613

Refined field effect transistors noting current, gate voltage and transconductance of proposed structures 09 p1350 A66-19918

Fredholm integral equation system for magnetic currents induced on wedge under impedance boundary condition 09 p1344 A66-20441

Morphological analysis of daily variability of geomagnetic field regular daily changes, noting current systems in polar and nonpolar regions 10 p1526 A66-21126

Current distribution along circular loop antenna, obtaining backscattering patterns as function of rotation angle 10 p1510 A66-21592

Scattering technique for measuring surface current density on cylindrical obstacles 10 p1502 A66-21637

Neutral point between two parallel line currents in highly conductive plasma, noting topological flux change and relation to solar flares 10 p1565 A66-21683

[AIAA PAPER 66-152] Current saturation from negative resistance and domain trapping in n-type gallium arsenide crystal 10 p1586 A66-22096

Current distribution and input impedance of infinite cylindrical antenna in anisotropic plasma, treating it as boundary value problem 11 p1661 A66-22396

Tube shaped and solid cylinder antennas compared, calculating surface current distribution and radiation patterns 11 p1662 A66-22543

Current distribution and input resistance of T-type, corner and bent tape vibrators powered by lumped electromotive force, using method of integro-differential equations 11 p1666 A66-22719

Space-charge-limited current in solid for field depletion of filled traps, noting current voltage characteristics 11 p1751 A66-22733

Axial current distribution in exhaust of magnetic annular arc, examining effect of entrainment on thrust measurement [AIAA PAPER 66-198] 11 p1761 A66-23084

Current and voltage distribution over length of HF discharge in helium-neon laser 11 p1714 A66-23309

Superconducting film stability under current, noting metastable state near transition point via potential analysis 12 p1930 A66-24787

Reverse current across collector-base junction in transistor 12 p1844 A66-24822

Electrode size effects on performance of infinitely long MHD power generation duct calculated by conformal mapping, analyzing gas Hall parameter, electrode-insulator length ratio, etc 13 p2000 A66-25735

Gallium arsenide p-n junction laser diode, injection current distribution, density and emission spectra variation 13 p2092 A66-25934

Distribution of current and associated field in coaxial plasma gun, noting plasmoid formation from drift 13 p2153 A66-26521

End effects in steady state MHD J x B accelerator, noting voltage and current distribution and eddy-current geometry 14 p2342 A66-27430

Microplasma breakdown in high voltage avalanche rectifiers, considering leakage current and junction impurity dislocation migration 14 p2363 A66-27583

Theoretical gains and current distribution in supergain endfire antenna arrays 14 p2256 A66-27922

Mutual impedance between two rectilinear and parallel top-loaded elements of directional antenna when elements have nonzero current at ends 14 p2257 A66-27924



Effect of currents, distributed over envelope surface formed by revolution of magnetic dipole force line about axis, on cosmic ray cut-off 14 p2377 A66-28085

Stationary phase technique synthesis of continuous linear antenna and integral equation for determining radiation pattern 14 p2259 A66-28158

Instability of current distribution related to problem of reliability in transistor electronics 15 p2468 A66-29915

Delay time and current transients occurring when thyristor is switched on by control-current pulse 15 p2468 A66-29918

Induction drag of long cylindrical satellites and Alfvén waves emitted from them determining potential and current distribution and effect on energy loss [AIAA PAPER 66-478] 16 p2799 A66-30523

O-shaped magnetic systems using unsaturated steel magnetic circuit to produce strong uniform magnetic fields for MHD machines 16 p2637 A66-31375

Frequency converters using traveling wave and backward wave tubes, noting current-wave amplitude distribution, velocity and voltage 16 p2666 A66-31550

Antenna synthesis of prescribed configuration requiring minimum current 16 p2666 A66-31555

Integral equations of current derived for TM and TE waves in excited inhomogeneous impedance band in half-plane 17 p2885 A66-32246

Two-dimensional excitation problem of circular cylinder with surface impedance varying over cylinder circumference 17 p2874 A66-32247

Infinite helical sheath antenna driven by ring delta-function generator analyzed, using Fourier transform, noting decomposition of current distribution 17 p2886 A66-32388

Line width of semiconductor laser 17 p2936 A66-33127

Local pressure effect on changes of forward current and stored charge of germanium p-n and p-s-n structures explained by change of energy gap 18 p3153 A66-33759

Cylinder magnetization in axisymmetric magnetic field, noting calculation of critical current in conductor 18 p3155 A66-34160

Kilatskin objections and improvements concerning integral equation describing current distribution in rectilinear antenna 18 p3087 A66-34963

Force-free magnetic fields generated by orthogonal current systems in unbounded conducting fluid 18 p3151 A66-35032

Base drive and internal structural irregularities of transistor effect on internal current distribution and second breakdown characteristics of device 19 p3312 A66-35343

LF common-base current transfer ratio for hot electron transport in semiconductor-metal-semiconductor point-contact-transistor structures measured as function of metal film thickness and temperature 19 p3435 A66-35410

Spatial distribution of acoustoelectric field in photoconductive CdS measurement under conditions of current saturation, determining carrier drift mobility 19 p3435 A66-35415

Normalized self and mutual admittances of two identical bare circular loop antennas in air or conducting medium evaluated, obtaining single integral equation for current distribution 19 p3321 A66-36405

Chaplygin equation solution translating current function and velocity potential from physical into hodograph plane 19 p3342 A66-36474

Two-dimensional problem of current distribution on surface of permeable electrodes adjacent to flow of conducting medium under Hall effect 20 p3611 A66-38110

Broken symmetry densities within current algebra arising in magnetic moment ratio, renormalization constants and unitary symmetry correction 20 p3606 A66-38293

Field conditions for optimal current distribution in superconducting coil 21 p3804 A66-39391

Radial current density distribution in homopolar, noting deviation of magnetic field and nature of current distribution

around anode 22 p3953 A66-39757

Experimental results of VLF dipole tests on Greenland ice cap including measurements of self-impedance, amplitude current distributions, relative efficiency and complex conductivity 22 p3874 A66-39942

Current-carrier scattering anisotropy dependence on antimony impurity concentration in n-Ge established, using measurements on Hall effect and conductivity 22 p3965 A66-40321

Pinch phenomena and current distribution in coaxial plasma gun 23 p4101 A66-41295

Current distribution and input resistance of T type, corner and bent tape vibrators powered by lumped electromotive force, using method of integro-differential equations 23 p4045 A66-41457

Space-charge-limited current in solid for field depletion of filled traps, noting current voltage characteristics 23 p4113 A66-41471

Modified Fock function for current distribution in penumbra and shadow region of plane electromagnetic wave incident upon convex cylinder, with application to backscattering 23 p4040 A66-41637

Radiation characteristics of filament with triangular current distribution situated along axis of magnetized plasma column, noting guided and space waves excited by filament 24 p4240 A66-42291

**CURRENT SHEET**

Detection of ionized gas front passage and differentiating it from current sheet in magnetically driven shock tube 07 p1020 A66-17956

Current sheet formation on plasma magnetospheric boundary at hyperbolic null point, noting possible connection with solar flare mechanism 07 p1138 A66-18082

Radiation resistance of linear current strip of finite width immersed in uniaxially anisotropic plasma 09 p1408 A66-20370

Magnetic and electric field and current density distributions in propagating current sheet [AIAA PAPER 66-200] 10 p1563 A66-21442

Distant-field antenna model of current sheet array used to approximate ultimate decay of mutual coupling in planar array antenna 14 p2257 A66-27926

Large-dimensional inverse pinch discharge study of impulsive plasma acceleration, gas dynamics and stability of unrestrained current sheet [AIAA PAPER 66-482] 18 p3141 A66-33655

Electron-ion current partitioning effects efficiency of pulsed plasma accelerators due to viscous drag caused by ions carrying current to cathode [AIAA PAPER 65-335] 18 p3147 A66-34586

**CURRENT STABILIZER**

Integrated current limiter design using transistor circuits, pn-pn switches or field effect transistors 02 p0204 A66-11935

Gunn effect n-type GaAs diode phase locked to stable frequency by injecting CW signal into circuit along with video pulse 06 p0925 A66-16671

Improved stability of field emission current at microwave frequencies in weak vacuum 06 p0854 A66-16758

Frequency synchronization of Gunn effect oscillators, frequency locking subharmonic generation, passive frequency stabilization, etc 10 p1516 A66-22095

Compound diode-transistor structure with current gain invariant with temperature 24 p4183 A66-42629

Nb-Zr strip superconductor for stabilization of critical current anisotropy and coil degradation in magnets 24 p4186 A66-43176

**CURTISS-WRIGHT MILITARY AIRCRAFT S X-19 AIRCRAFT**

**CURVE**

S HILL CURVE

S ZERO FORCE CURVE

**CURVED BEAM**

Stressed state of curved rod of rectangular cross section subject to bending, shearing, tension and compression determined from theory of elasticity 01 p0155 A66-10740

Equations of plastic interaction curves for cross section of beam subject to uniaxial stress and under simultaneous bending moment and normal force, using power

series 03 p0442 A66-13306

Out of plane free vibrations of uniform circular ring on elastic and torsional foundations producing restraints 24 p4287 A66-42165

**CURVED PANEL**

Variational formulation of equilibrium stability of nonlinear elastic circular cylindrical panel under radial stress 18 p3251 A66-33704

Creep buckling of long curved sandwich panel 18 p3259 A66-35014

**CURVED SURFACE**

Falkner-Skan similar solutions for effects of longitudinal surface curvature on incompressible laminar boundary layer flows 03 p0355 A66-12786

Solving supersonic laminar boundary layer separation by velocity profile and energy momentum concept, noting application to wedges and curved surfaces [ASME PAPER 65-APMW-19] 04 p0512 A66-14220

Stability criterion for flow in interspace between two parallel arbitrarily curved walls 07 p0980 A66-17482

Formulas for angular resilience of curvilinear surfaces of concave or convex planforms 07 p1038 A66-18060

Equations for nonshallow thin shells of arbitrary shape and variable rigidity with continuous smooth curvature 08 p1315 A66-19731

Solving supersonic laminar boundary layer separation by velocity profile and energy momentum concept, noting application to wedges and curved surfaces [ASME PAPER 65-APMW-19] 10 p1523 A66-21469

Lunar and planetary terrain roughness in terms of curvature statistics, based on Ranger VII and Bonita Lava Flow contour map analysis [AIAA PAPER 65-389] 10 p1610 A66-21955

Curvature effect on stress distribution for thin walled circular cylindrical shell with small aperture 11 p1779 A66-22237

Unsteady interaction between blunt bodies and shock wave, comparing reflected shock wave velocity decrease for plane spherically blunted cylinders 16 p2685 A66-30788

Mathematical representation of latitude-longitude point pairs for intersection of figure of Earth and plane defined by central ray of signal scattered between communications sites 18 p3068 A66-33908

Photometry of flux from surface and representation as Fourier series of time dependence of received reflected flux for torse of convex curvature 20 p3556 A66-36937

Cavitational flow past curvilinear arc constructed according to Ryabushinskii scheme 20 p3548 A66-38116

Self-preserving flow in outer part of two-dimensional curved turbulent wall jet for constant ratio of jet thickness to wall radius of curvature 22 p3844 A66-40489

Stress concentration around curvilinear holes in plate, discussing plane problem of elasticity theory and shell theory 23 p4143 A66-41960

**CUT-OFF**

Cut-off frequency in UHF transistors at high collector currents due to transition region boundary displacement 14 p2248 A66-27048

Cut-off wavelength of transverse electrostatic wave mode in ridged rectangular waveguide of arbitrary aspect ratio 14 p2257 A66-27951

Theoretical static I-V characteristics of surface gate dielectric triode and geometric factors influence on amplification factor at cut-off 22 p3872 A66-39746

Vector potential function solution to Maxwell-Minkowski equations describing cut-off phenomena for EM wave propagation in wave guide filled with homogeneous isotropic lossless moving medium 22 p3862 A66-39783

**CUT-OUT**

Photoelastic stress-concentration measurements in variously-reinforced circularly shaped cut-outs under uniaxial tension, three-dimensional effects and validity of neglecting bending stiffness 23 p4141 A66-41949



CUTTING

Selecting proper cutting tool for machining high-strength steels and alloys 08 p1229 A66-18689  
Defect analysis by device sectioning, noting techniques, application in crystallography, electronics, etc 12 p1845 A66-24849  
Durability of cutting tool alloys for producing porous cermet ball bearings, noting effect of pearlite in cermets 17 p2930 A66-32850

CW RADAR

S CONTINUOUS WAVE /CW/ RADAR

CYANATE

S ISOCYANATE

CYANIDE

Laser transition in vibrational state of ground electronic state of CN from rotational level 8 to 7 with population inversion as result 02 p0240 A66-11451  
Oscillator strength of CN violet system from shock layer by time-of-flight scanning spectrometer 03 p0393 A66-13152  
Total number of cyanide molecules and diatomic carbon free radicals and density distribution in head of Arend-Roland 1957 III comet 17 p3010 A66-33381  
Values of Morse potential for interaction of atoms in diatomic molecules carbon, CO and CN 21 p3775 A66-39072

CYANINE DYE

Desensitizer pinacryptol green effect on photographic and photoelectric properties of emulsion layers 05 p0678 A66-15157  
Stoichiometry of reaction of cyanine dye with diverse polyionic macromolecules 06 p0821 A66-16157  
Biological macromolecule detection using thiacarbocyanine dye and observation of absorption spectra changes 15 p2441 A66-29962  
Dissociation and reassociation reactions of hemocyanin mixtures analyzed by electron microscopy, noting original molecular structures 18 p3060 A66-34459  
Phthalocyanine crystal phase change effect on electric conductivity 22 p3860 A66-39921  
Stimulated emission of polymethine dyes upon pumping with Q-switched laser, noting wavelength parameters and oscillation 24 p4219 A66-42247  
Saturable dyes noting mode selection properties and absorption spectra in bleached state 24 p4220 A66-42253  
Absorber concentration effect on pulsed laser system noting performance characteristics, threshold energy, pumping dynamics and time parameters 24 p4220 A66-42254

CYANO COMPOUND

X-ray single crystal diffraction technique determination of structure of pyridinium dicyanomethylide 04 p0472 A66-13364  
Preparation and physical properties of polytricyanoethylene /TCNE/ copper chelate film, noting electric conductivity and heat treatment effect 10 p1574 A66-21348  
Series of tricyanomethyl compounds prepared in refluxing acetonitrile by alkylating potassium tricyanomethanide with alkyl iodides, alkyl, propargyl and benzyl bromides 23 p4117 A66-41229

CYANOGEN

IR and UV absorption spectra of free radical CN observed following photolysis of matrix isolated cyanogen nitride 04 p0473 A66-13644  
Kinetics of CN radicals association generated by shocking cyanogen-argon mixtures at high temperatures in reflected shock region of expansion wave 12 p1811 A66-23615  
Cosmic black body radiation at 2.6 mm wavelength from 2.7 to 3.4 degrees K, noting CN molecules 16 p2793 A66-30199  
Cosmic microwave radiation from observations of interstellar CN rotational temperature, rotational excitation by H I region H atoms and excitation by slow electrons and slow protons in H II region 16 p2793 A66-30200

CYBERNETICS

SA HUMAN ENGINEERING

Cybernetics methods suited to complex systems associated with bioastronautics 01 p0021 A66-10807  
Effect of delayed feedback in respiratory disease analyzed for behavioral cybernetic

theory, using computer-controlled delay 02 p0186 A66-11648  
Cybernetics role in space flight including control circuits for guidance and electronic equipment automation and development 04 p0469 A66-13495  
Classifying capacity of learning matrix used in cybernetics, discussing principle and application to weather forecasting and speech recognition 04 p0489 A66-13509  
Russian monograph on algorithm of machine search for logical natural derivation of investigated formulas from initial formulas via propositional calculus 07 p1004 A66-18464  
Adaptation theory concepts, examining threshold learning process, Markov chain, learning wave, feedback adaptivity, etc 11 p1647 A66-22299  
Infinite automata theory and structural logical design of digital machines 11 p1659 A66-22707  
Minimizing number of states of automaton with consideration of transition 11 p1676 A66-22708  
Abstract automata analysis based on solution of system of equations in algebra of events 11 p1676 A66-22709  
Probabilistic automata as generalization of deterministic and nondeterministic finite model, theorems and concept of definiteness 12 p1853 A66-24338  
Automatic control, systems science, cybernetics, biomedical engineering, human factors - IEEE International Convention, New York, March 1966 12 p1854 A66-24634  
Biological cybernetics applied to physiological studies during space flight, examining mathematical modeling, biological control and statistical dynamics techniques 15 p2444 A66-29460

CYCLE

S BRAYTON CYCLE  
S CLOSED CYCLE  
S RANKINE CYCLE  
S REGENERATIVE CYCLE  
S SOLAR CYCLE  
S STRESS CYCLE  
S SUNSPOT CYCLE

CYCLIC ACCELERATOR

Focused laser as accelerating cavity for cyclic particle accelerator 01 p0080 A66-10328

CYCLIC HYDROCARBON

SA ANTHRACENE

Synthesis of 1-methyl-3, 5-diphenylthiabenzenes 1-oxide suggests possibility of ylide-like character although ylene-like is not discounted 03 p0330 A66-13088  
Rates and activation parameters determined from nuclear magnetic resonance spectra for degenerate isomerizations of disubstituted benzofurazan oxides 05 p0629 A66-15155  
Heat of combustion of tricarbonylcyclopentadienylmanganese 08 p1279 A66-18798  
Methylcyclohexane dehydrogenation over platinum-alumina in absence of excess hydrogen, yielding toluene and hydrogen 11 p1650 A66-23122  
Mass spectrometric fragmentation behavior of N-n-propyl and N-n-butyl pyrrolidone and N-alkyl succinimides subsequent to electron impact 11 p1651 A66-23412  
Isolation and identification of biogenic steranes and pentacyclic triterpanes in Eocene shale 12 p1805 A66-23539  
Cyclomethylenetrinitramine-hexamethylphosphortriamide complex preparation 20 p3627 A66-38416

CYCLIC LOAD  
Optimal surface damping in two-layered cantilever for random periodic loading decreasing in symmetrical cycle 01 p0160 A66-11180  
Cyclic edge loading effect on circular reinforced cylindrical shells 04 p0589 A66-14147  
Asymptotic integration of thin elastic shell equations for design of shells of revolution subject to effect of cyclic edge loads 04 p0590 A66-14149  
Behavior of aggregate under moderate loads with plastic deformation occurring in favorably oriented crystals on single active slip systems [ASME PAPER 65-WA/APM-9]

05 p0776 A66-15431  
Plastic strain fatigue in air and vacuum, discussing strain-life relation for ductile materials and cold reweldment of fractures in vacuum [ASME PAPER 65-MET-5]

Two-parametric classification of load cycles on construction elements connected with fatigue limit tests and service life 06 p0895 A66-16203  
Plastic deformations for cyclically alternating loads, determining cycle number at which fracture occurs 06 p0965 A66-16484  
Effect of structure and volume cold-working related to structural factors on notched samples of steels subjected to cyclic stresses 07 p1048 A66-17441  
Healing of defects in steel accumulated during cyclic overloading 07 p1048 A66-17442  
Extension of Coffin formula for cyclic strength in finite regions of plastic deformation for symmetric strain cycles 07 p1143 A66-17856  
Analytical derivation of formula relating plastic deformation per cycle and number of cycles to failure for metals 07 p1050 A66-18062  
Loading frequency effects on fatigue strength of 45 and E1612 steel specimens at room temperature 07 p1147 A66-18385  
Thermomechanical response studies of solid propellants subjected to cyclic and random loading [AIAA PAPER 65-160] 10 p1590 A66-21776  
Fatigue life of aircraft gas turbine compressor disks subjected to cyclic loading 11 p1710 A66-22691  
Linear cycle set factorization, showing that uniqueness of canonical procedure is incorrect and introducing new cycle division algorithm 11 p1679 A66-23247  
Results of crack propagation tests on polymethylmethacrylate flexed at various frequencies under cyclic loading 13 p2112 A66-25308  
Soviet monograph on elastic and plastic deformation mechanism, describing stress-strain state of materials, cyclic, variable and reversed load effects, etc 13 p2206 A66-26464  
Effect of temperature on cyclic minimum creep rate and other phenomena associated with cycle dependent deformation from 77.4 to 295 degrees K [ASME PAPER 66-MET-7] 14 p2395 A66-26975

Cyclic strain fatigue tests and fatigue failure curve for age-hardened nickel based alloy K-Monel [ASME PAPER 66-MET-9] 14 p2312 A66-26977

Cyclic plastic stresses at notch roots in aluminum alloy sheet specimens under constant-amplitude repeated tension and reversed loading 17 p3023 A66-32074  
Behavior of aggregate under moderate loads with plastic deformation occurring in favorably oriented crystals on single active slip systems [ASME PAPER 65-WA/AMP-9] 18 p3248 A66-33584

Fatigue curve for one type of loading determined from stress variation during cyclic deformation and fatigue curve from other type of load application 18 p3254 A66-34231

Variable load theorem applied to alternating cyclic loads problem, based on equations of small elastoplastic deformations 21 p3830 A66-38984

Cyclically moving loads causing resonance in elastic rods, strings and torsional members having fixed ends 23 p4141 A66-41922

Time dependent stress distribution in elastoplastic cyclic deformation, emphasizing cycle hardened stainless steels 23 p4144 A66-41971

Damping mechanisms and phenomenology in materials 23 p4145 A66-41985

CYCLING

S THERMAL CYCLING

CYCLOHEXANE

Sedimentation rates of metallic particles in cyclohexane medium measured by light absorption 01 p0069 A66-10750  
Selective feedback and saturation mechanisms of Raman lasers using



secondary Raman lines, emphasizing  
cyclohexane 20 p3579 A66-37777

# CYCLONE SA ANTICYCLONE

Magnetic storm accompanied by Forbush  
decreases taking into account atmospheric  
temperature, noting cyclonic storm  
origin 02 p0282 A66-11338

Cosmic radiation variations during passage  
of cyclones agree with theory for  
meteorological effects based on two-meson  
scheme 02 p0282 A66-11339

Energy conversion from available potential  
to kinetic broken into spectral components  
permitting analysis in vicinity of  
extratropical cyclone 04 p0541 A66-13665

MHD model of cyclone, considering motion  
of type of rotating ideal compressible  
conducting fluid 08 p1213 A66-19023

Radiostrontium ratios in precipitation from  
two extratropical cyclones containing  
nuclear debris of different  
ages 23 p4124 A66-41844

# CYCLOPROPANE

Rate constants for atomic and molecular  
hydrogen ion transfer from tri- and tetra-  
atomic carbon paraffins to propylene and  
cyclopropane molecular  
ions 22 p3861 A66-40905

# CYCLOTRON

## SA ION CYCLOTRON

Cyclotron radius, magnetospheric boundary  
and Debye length scaling parameters for  
magnetospheric cavity arising from solar  
wind-induced geomagnetic storm and  
visibility of quasi-Van Allen  
belts 14 p2269 A66-27124

External injection of ions into cyclotron,  
examining case of injection of beam in  
median plane of magnet 14 p2347 A66-28310

# CYCLOTRON FREQUENCY

Dispersion characteristics of  
perpendicularly-propagating cyclotron  
harmonic wave modes in  
plasma 01 p0025 A66-10518

Cyclotron heating of electrons creating  
plasma at HF field 01 p0115 A66-11108

Space and time dependence of decaying  
resonant oscillations excited in collisionless  
plasma by infinitesimally small pulsed  
dipole 05 p0721 A66-14714

Anisotropy of scattering in tellurium,  
correlating cyclotron frequency data and  
galvanomagnetic  
measurements 05 p0738 A66-15353

Instability of plasma with spatially  
inhomogeneous current at frequencies above  
ion-cyclotron frequency, noting electron  
charge convection and wave-particle  
interaction 06 p0914 A66-16141

Cyclotron harmonic amplification of wave  
propagation in electron beams and plasmas  
with internal motions in presence of static  
magnetic field 06 p0920 A66-17013

Microwave radiation from high voltage  
plasma with oscillating electrons and  
resulting cyclotron frequency  
harmonics 08 p1264 A66-19180

Anisotropy of scattering in tellurium,  
correlating cyclotron frequency data and  
galvanomagnetic  
measurements 09 p1431 A66-20894

Coupling impedance of thin hollow electron  
beam injected into magnetic field and  
rippling at cyclotron frequency in cylindrical  
waveguide carrying E<sub>01</sub>  
mode 11 p1661 A66-22395

Longitudinal plasma oscillations excited in  
warm plasma column at microwave  
frequencies in presence of magnetic field,  
manifest themselves as absorption peaks  
near harmonics of electron cyclotron  
frequency 11 p1748 A66-23395

Plasma density drops developing when  
injecting plasma into trap with combined  
field, noting rise of HF field and  
acceleration of fraction of plasma ions with  
each drop 13 p2137 A66-25104

High refractive index at electron cyclotron  
harmonics from nonrelativistic plasma  
immersed in external magnetic  
field 13 p2145 A66-25728

Collisional effects in region of electron  
cyclotron frequency on electromagnetic  
wave propagation in  
plasma 13 p2147 A66-25752

Excitation of Alfvén waves in semimetal  
plasma at low temperature, noting wave

propagation below plasma or cyclotron  
frequency in magnetic  
field 14 p2363 A66-27516

Calculation of electromagnetic field within  
two-dimensional plasma sheath with static  
magnetic field, noting effect of electron-  
cyclotron frequency on refractive index of  
medium 15 p2549 A66-28707

Multivelocity stream effects and efficiency  
of slow-cyclotron wave amplifiers, noting  
electron velocity spread which decreases  
predicted efficiency 15 p2467 A66-29711

Instability of plasma with spatially  
inhomogeneous current at frequencies above  
ion-cyclotron frequency, noting electron  
charge convection and wave-particle  
interaction 15 p2556 A66-29871

Plasma density drops developing when  
injecting plasma into trap with combined  
field, noting rise of HF field and  
acceleration of fraction of plasma ions with  
each drop 16 p2758 A66-30283

Quasi-linear theory of plasma cyclotron  
instability for one-dimensional oscillation  
spectrum, noting energy of interaction with  
electromagnetic field, ion velocities,  
etc 16 p2762 A66-31172

HF flute unstable oscillations occurring  
when low temperature plasma is added to  
high temperature one, finding frequency and  
growth rate are of order of cyclotron  
harmonic frequency 17 p2966 A66-32423

Proton trajectories in static dipole  
magnetic field, noting effects in radiation  
belt proton pitch angle oscillation at  
cyclotron frequency, etc 17 p2993 A66-32519

Electron-cyclotron heating of plasma via  
high power oscillator, noting experimental  
setup and characteristics 18 p3151 A66-35068

Particle concentration and luminescence  
intensity correlation with electron cyclotron  
frequency in stationary SHF argon discharge  
in magnetic field 18 p3152 A66-35080

Drift instabilities calculated in beta limit,  
examining influence on electron cyclotron  
harmonic waves, Larmor radius flute,  
structure of infinite plasma in magnetic  
field, etc 19 p3418 A66-36535

Crossed-field electron beam stability for  
arbitrary values of Q /ratio of plasma  
frequency to cyclotron  
frequency/ 20 p3606 A66-38404

Linearly polarized incident electromagnetic  
waves propagated along static magnetic field  
through plasma in region of electron  
cyclotron frequency, noting wave modes  
behavior 24 p4242 A66-42400

# CYCLOTRON RADIATION

Plasma waves propagating transverse to  
uniform external magnetic field discussing  
electron motion, wavelength magnitude,  
frequencies and application of  
results 03 p0406 A66-13358

Growth of absorption bands of natural and  
synthetic calcium fluoride crystals irradiated  
with protons from cyclotron at Tomsk  
Institute 05 p0741 A66-15857

Anomalous bremsstrahlung and anomalous  
cyclotron radio emission from partially  
ionized gases in 20 to 1000 mc  
range 08 p1263 A66-19015

Excitation of backward Doppler shifted  
cyclotron radiation in magnetoactive plasma  
by electron stream 16 p2761 A66-30921

Cyclotron harmonic radiation from rare gas  
discharge in magnetic  
field 16 p2764 A66-31351

Harmonic generation in microwave  
emission from InSb, attributing resonance  
type radiation to stimulated cyclotron  
radiation and plasma wave  
excitation 17 p2978 A66-32410

Radio noise bursts from Jupiter at  
decimeter wavelengths noting Cerenkov  
emission, Doppler-shifter cyclotron emission  
and escaped-whistler  
models 18 p3225 A66-33550

Growth rate of forward-sublimous-mode  
electromagnetic wave excited in helical  
stream-plasma used to calculate Jupiter  
decametric emission 19 p3463 A66-35924

Power flow of cyclotron modes propagating  
in waveguide filled with cold collisionless  
axially magnetized plasma studied by  
Brillouin diagram 20 p3612 A66-38398

Dispersion equation for cyclotron  
electromagnetic waves for magnetoactive  
plasma injected with charged  
particles 16 p2762 A66-31173

particles 24 p4245 A66-43016

# CYCLOTRON RESONANCE

Interaction of electromagnetic fields with  
very hot plasmas using electron cyclotron  
resonance, noting microwave  
properties 01 p0026 A66-10545

Cyclotron instability dependence on  
nonmonotonic ion distribution function of  
plasma with cyclotron  
resonance 03 p0396 A66-12289

Gyroresonant interaction of electron and  
proton beam with electromagnetic waves in  
magnetosphere 03 p0419 A66-12675

Interaction of energetic electrons with  
bounded electromagnetic waves near  
cyclotron resonance, noting plasma  
diagnostics, maser and gain  
mechanism 04 p0530 A66-13953

Relationship between cyclotron resonance  
and interaction among current carriers in  
semiconductors 04 p0564 A66-14256

Cyclotron resonance in Azbel-Kaner  
geometry in n- and p-type lead telluride,  
examining anisotropy of absorption under  
anomalous skin effect  
conditions 07 p1102 A66-18205

Interaction of helicons with cyclotron  
resonance of single particles, other helicons,  
phonons, optical phonons and  
magneton 07 p1102 A66-18207

Twelve distinct mass series identified and  
mass values determined as function of  
orientation of magnetic field in Fermi  
surface of zinc at cyclotron  
resonance 10 p1581 A66-21735

Identification of mass series and mass  
values in Fermi surface of cadmium at  
cyclotron resonance compared with results  
for zinc 10 p1581 A66-21736

Plasma frequency determined by  
microwave bridge measurement of cut-off  
effect of plasma near electron cyclotron  
resonance 10 p1536 A66-21863

Generation of echo at cyclotron resonance  
in plasma provides means of measuring and  
displaying relaxation  
processes 11 p1748 A66-23393

Experiments on ion cyclotron heating of  
plasma generated by Joule heating in  
Heliotron-B 12 p1919 A66-23851

Cyclotron instabilities in hydromagnetic  
waves in magnetosphere as possible origin  
of geomagnetic micropulsations, stressing  
ion resonance mode of waves relevant to hm  
whistlers 12 p1874 A66-24842

Effect of nonlinearities on electron  
cyclotron resonance, stressing determination  
of maximum velocity of plasma under  
cyclotron resonance  
conditions 13 p2143 A66-25711

Dielectric tensor in relativistic Vlasov  
plasma in electron cyclotron harmonic  
resonance region 13 p2155 A66-26676

Relativistic plasma wave dispersion in  
cyclotron harmonic resonance  
regions 13 p2155 A66-26677

Electron cyclotron resonance plasma  
thruster for spacecraft electric propulsion  
systems 14 p2374 A66-27520

X-band electron-cyclotron resonance plasma  
accelerator 14 p2344 A66-27967

HF magnetic fields within homogeneous  
plasma sheath measured as function of  
plasma parameters and perpendicularly  
superimposed static magnetic field, noting  
resonance of electron cyclotron  
wave 15 p2549 A66-28708

Electron cyclotron resonance plasma  
accelerator design for thruster application  
and measuring techniques  
[AIAA PAPER 65-301] 15 p2572 A66-29277

HF heating of dense plasma by resonance  
excitation of cyclotron-type ion waves and  
fast magnetoacoustic  
waves 16 p2756 A66-30095

Alouette I satellite data on extraordinary  
wave resonance trace propagation along  
ionospheric magnetic field-aligned  
waveguide 16 p2697 A66-31001

Alouette I topside sounder ionograms of  
electron cyclotron harmonic resonance and  
frequency variation 16 p2697 A66-31003

Quasi-linear approximation of Cerenkov  
and cyclotron damping of electromagnetic  
waves in magnetoactive plasma, considering  
collisions of wave-absorbing resonance  
particles with plasma  
particles 16 p2762 A66-31173



- Cyclotron resonance excitation of upper level of gas-ion laser 17 p2933 A66-31937
- Steady state resonance absorption of electromagnetic wave and cyclotron heating of low-density plasma 17 p2965 A66-32321
- Alouette satellite observation of ionospheric cyclotron resonance, obtaining plasma frequency at particular height 17 p2920 A66-33085
- Magnetic beach effect on RF power transfer to ion-cyclotron waves in hydrogen and deuterium plasmas 18 p3146 A66-34463
- Semiconductor cyclotron resonance during application of constant electric field, determining carrier distribution function 19 p3437 A66-35460
- RF propagation and absorption calorimetric measurements in magnetoplasma near electron cyclotron resonance, noting power conversion 19 p3305 A66-36420
- Acceleration, reflection and accumulation of plasma by gradients of HF and static magnetic fields at electron cyclotron resonance 19 p3426 A66-36567
- Ion cyclotron resonance heating and trapping and adiabatic compression of plasma in QP machine 19 p3431 A66-36590
- Ion cyclotron resonance heating applied to C stellarator plasma formed by ohmic heating, noting Alfvén wave generation by Stix coil 19 p3432 A66-36594
- Second-harmonic electron cyclotron resonance in hydrogen plasma from HF ion source with inductive coupling situated in transverse magnetic field 20 p3607 A66-37407
- Interband microwave scattering of holes by cyclotron resonance in Ge 21 p3797 A66-38753
- Cyclotron resonance observation of electron scattering by Ga and In atoms in Ge 21 p3797 A66-38754
- Boundary behavior of plasma heated by ion cyclotron waves 21 p3780 A66-39003
- HF absorption by dense plasma in ion cyclotron resonance region 21 p3780 A66-39006
- Cyclotron resonance in nonhomogeneous plasma cylinder with HF heating 21 p3780 A66-39007
- Cyclotron resonance study of electron scattering by thermal acceptors in quenched Ge 21 p3805 A66-39567
- Ion mass spectrometry of D layer, using magnetic fields and cyclotron resonance principle 22 p3907 A66-39956
- Drift cyclotron instability observed in toroidal plasma 23 p4109 A66-42064
- Drift cyclotron oscillations of inhomogeneous collision plasma propagating across magnetic field, taking into account particle collisions with aid of Landau collision integral 24 p4243 A66-42530
- Multiple cyclotron resonance absorption lines in degenerate valence bands of Ge semiconductor studied with far IR laser submillimeter spectrometer 24 p4257 A66-42545
- CYGNUS CONSTELLATION**
- Discrete radio source scintillation, considering irregular diffraction pattern caused by ionospheric irregularities 04 p0575 A66-13380
- Electron scattering responsible for variable polarization in V444 Cygni 13 p2184 A66-25624
- Aerobee rocket measurements of cosmic X-ray sources emanating from Cygnus A, M-87 and galactic supernova remnant Cassiopeia A 13 p2174 A66-25836
- Anomalous high count of gamma rays from direction of constellation Cygnus associated with energy spectrum differing from spectrum of secondary gamma rays generated by cosmic rays 20 p3631 A66-37600
- CYLINDER**
- SA AIRYS STRESS FUNCTION
- SA CIRCULAR CYLINDER
- SA CONCENTRIC CYLINDER
- SA ELASTIC CYLINDER
- SA ELLIPTICAL CYLINDER
- SA MONOCOQUE CYLINDER
- SA ORTHOTROPIC CYLINDER
- SA OSCILLATING CYLINDER
- SA PLASMA CYLINDER
- SA ROTATING CYLINDER
- SA VISCOELASTIC CYLINDER
- Cylinders subjected to internal and external pressure and axial stress with equations for radial and tangential direction 02 p0299 A66-11706
- Induction in cylinder by field of current-carry leads, calculating input parameters and ponderomotive force 03 p0396 A66-12285
- Heat transfer and shear between coaxial cylinders of different temperatures for large Knudsen numbers 03 p0445 A66-12959
- Ion recombination effects on inhomogeneous cylinder deceleration in rarefied plasma 04 p0551 A66-13858
- Minimization of radar cross section of thin cylinder by central loading, calculating backscatter field 05 p0632 A66-14842
- Superimposed vibrations, corresponding to different propagation constants for same frequency parameter, satisfy boundary conditions at flat surfaces of cylinder 05 p0781 A66-15739
- Thermal elastohydrodynamic lubrication of rolling and sliding cylinders, noting correlation with film thickness and friction experimental data [ASLE PREPRINT 65AM 4A2]
- 07 p1040 A66-18291
- Electromagnetic field near highly conducting cylindrical antenna of finite length excited by plane electromagnetic wave 08 p1189 A66-18668
- Structural optimization of axially compressed cylinders stiffened externally with rings and/or stringers, noting effect of wall thickness on structural weight 08 p1306 A66-18806
- Field in shadow region of cylindrical wave diffraction at finite concave cylinder 08 p1257 A66-19757
- Nonstationary temperature distribution in long cylinder solved by integral transforms, giving results in form of series in Bessel and error functions 10 p1620 A66-21327
- Integral equation method solution of scattering from cylinders with arbitrarily varying anisotropic surface impedance 10 p1497 A66-21591
- Diffraction by conducting cylinder solved by approximation method, using expanded series of diffraction field of cylinder with polygonal section 11 p1662 A66-22464
- Molecular collision effect on transitional drag on cylinder traversing rarefied gas at hypersonic Mach numbers, discussing departure from free flow 11 p1632 A66-22920
- Circumferential creep strain of cylinders subjected to internal pressure 12 p1959 A66-23797
- Minimum-weight analysis of hydrostatically compressed ring-stiffened cone, showing that previous data derived for cylinders in same condition might be useful 12 p1970 A66-24702
- Heat transfer in steady flow of non-Newtonian fluid characterized by Rivlin-Ericksen constitutive equation inside wavy cylindrical tube, with momentum and energy equations solved by perturbation technique 12 p1866 A66-24960
- Resonance frequencies during longitudinal and radial oscillations of hollow cylindrical piezoelectric elements 13 p2194 A66-25086
- Flow in vicinity of right cylindrical body, considering shocks between molecules and solid 13 p1991 A66-25469
- Equations for two coupled van der Pol oscillators, Liapunov function used to find four-dimensional phase space nonperiodicity cylinder and subspace of exiting trajectories 13 p2042 A66-26088
- Computational method for cylinders under external pressure, switching from testing in plastic field to elastic field without gaps 13 p2199 A66-26328
- Solution of quasi-static problem in thermoelasticity for cylinder with time dependent boundary conditions obtained as series of Bessel functions and error functions 14 p2397 A66-27385
- Mutual conductivity of half-wave slot on conducting cylinder 14 p2398 A66-27427
- Dilatational wave resonance scattering of waterborne sound waves on hollow cylinder excited to oscillation by incident sound 14 p2401 A66-27863
- Deformation and state of stress of contiguous cylindrical rotationally symmetrical hubs and shafts of various lengths 14 p2409 A66-28459
- Perturbations caused by cylindrical body in plasma, obtaining electric field and electron and ion concentration dependences on distance 15 p2595 A66-29086
- Ponderomotive force acting on conducting cylinder in moving magnetic field of cylindrical inductor 16 p2765 A66-31408
- Two-dimensional wake in incompressible unsteady vortex flow downstream of cylindrical body 17 p2907 A66-32279
- Laminar boundary layer on cylinder with symmetric cross section bounded by two equal circular arcs treated by Pohlhausen method 17 p2911 A66-32836
- Temperature potentials in cylinder of known radius, investigating optimal heating regime and thermal kinetic factor effect on maximum potential magnitude 20 p3665 A66-36912
- Ring stringer eccentricity effects on structural optimization of stiffened axially compressed cylinders 20 p3672 A66-38166
- Electromagnetic scattering by obliquely oriented cylinders, noting extinction efficiency, propagation in cylindrical waveguides and polarization reversal 20 p3603 A66-38403
- Resonance frequencies during longitudinal and radial oscillations of hollow cylindrical piezoelectric elements 21 p3822 A66-38511
- Nonequilibrium flow of chemically reacting gas past infinite corrugated cylinder 21 p3724 A66-38717
- Radiant heat transfer between concentric spheres and coaxial cylinders, assuming isothermal inner surface to be diffuse emitter and outer surface to reflect specularly 22 p3998 A66-40030
- Asymptotic expansion of electromagnetic field scattered from convex cylinder near grazing incidence, using boundary layer theory 23 p4038 A66-41546
- Integral method derivation of thermoconductivity coefficient of cylindrical semiconductor immersed in liquid He and superheated by Joule heating 24 p4255 A66-42494
- Counterflow diffusion flame in forward stagnation region of porous cylinder with uniformly ejecting fuel gas in analysis by flame sheet model and boundary layer approximation 24 p4294 A66-42542
- CYLINDRICAL AFTERBODY**
- Supersonic gas flow past cylindrical obstacle on plate in wind tunnel at Mach number 2.5, noting separation line, pressure distribution and flow orientation 12 p1798 A66-24437
- CYLINDRICAL SHELL**
- Space-time correlation function of response of finite cylindrical shell to purely random pressure field and to subsonic boundary layer pressure fluctuations 01 p0147 A66-10131
- Damping parameters for extensional and flexural vibrations of sandwich plates and for axisymmetric vibrations of sandwich cylindrical shells 01 p0149 A66-10149
- Stress field about axial crack in pressurized cylindrical shell 01 p0152 A66-10379
- Torsional stability of elongated cylindrical shell 01 p0153 A66-10465
- Stability of cylindrical shell with elastic filler and various loadings 01 p0158 A66-11002
- Prebuckling deformation and stress-strain distributions in clamped thin cylindrical shell subjected to axial load, determining effect of boundary supports 02 p0297 A66-11557
- Ideal energy dissipating mechanisms to synthesize weight or mass index in terms of pertinent design indices, structural efficiency and material efficiency parameters 03 p0436 A66-12753
- Cylindrical shell under concentrated radial load dealt with by trigonometric series and gamma function 03 p0441 A66-13289
- Design of cylindrical shells for concentrated loads by approximate method 03 p0441 A66-13290
- Semizero-moment shell with one edge braced by elastic support with small rigidity for deformation out of plane, noting magnitude of critical stress 04 p0588 A66-13566
- Reduction of Rabotnov approximate equation describing steady creep in circular



- cylindrical shells, under axisymmetric loading, to system of integral equations 04 p0588 A66-13567
- Cyclic edge loading effect on circular reinforced cylindrical shells 04 p0589 A66-14147
- Equations for natural oscillation frequency of gas-filled cylindrical shell 04 p0590 A66-14163
- Linear small deflection theory and statistical analysis in dynamic buckling of thin cylindrical shell under axial impact [ASME PAPER 65-APMW-17] 04 p0592 A66-14218
- Increasing plastic buckling resistance of thin cylindrical /Mg and Al/ shell by means of elastic core /polyurethane foam/ [ASME PAPER 65-APMW-18] 04 p0592 A66-14219
- Statistical study of linear buckling of circular cylindrical shells under axial compression, showing preferred mode shape [ASME PAPER 65-APMW-23] 04 p0592 A66-14224
- Donnell-type nonlinear theory for instability of cylindrical shell subjected to axisymmetric moving loads with constant velocity [ASME PAPER 65-APMW-35] 04 p0594 A66-14235
- Linear elastic theory of thin shells, considering membrane and bending theories of open and closed cylindrical shell 05 p0775 A66-15083
- Steady state response of damped cylindrical sandwich shell under radially symmetric time harmonic pressure [ASME PAPER 65-WA/UNT-1] 05 p0779 A66-15601
- Cylindrical receiving and scattering antennas, determining current from admittance, charge distribution and near field for incident plane wave 06 p0827 A66-16036
- Axisymmetric dynamic response of ring supported cylinder to time dependent loads, discussing boundary conditions and differential equations of motions [AIAA PAPER 66-83] 06 p0962 A66-16265
- Corrugation growth on infinitely conducting fluid sheets, discussing acceleration induced by constant axial and linearly increasing currents 06 p0871 A66-16276
- Effect of geometry changes on carrying capacity of cylindrical shell directly after reaching plastic state 06 p0966 A66-16501
- Vibration of thin cylindrical shell giving natural frequency and mode shape 06 p0967 A66-16931
- Deleterious effect of heterogeneity on stability of composite cylindrical shells under axial compression [AIAA PAPER 66-140] 06 p0968 A66-17083
- Thermal stress of infinite closed circular cylindrical shell acted upon by concentrated heat source moving along generatrix of cylinder 07 p1142 A66-17265
- Transversely isotropic cylindrical shell vibrations solved via Bessel function for flexural, axisymmetric and torsional modes 07 p1143 A66-17499
- Steady state temperature distribution for cylindrical shells under space conditions, calculating effect of internal radiation and surface coatings 07 p1143 A66-17591
- Infinitely-long thin elastic circular cylindrical shells loaded along segment of generatrix by arbitrarily distributed loads 07 p1143 A66-17627
- Temperature distribution in infinite closed circular cylindrical shell with fixed heat source of constant intensity 07 p1154 A66-18067
- Thin shell theory to determine natural frequencies for cylindrical shells with any end conditions 07 p1146 A66-18279
- Collapse under end load of pressurized axially stiffened thin cylinders 07 p1147 A66-18282
- Linear isotropic strain-hardening applied to load-deformation characteristics of cylindrical shells under internal pressure, obtaining Tresca yield criterion and stress profiles 07 p1147 A66-18349
- Stress concentration study using third-order approximation operators for tangential stress components of cylindrical shell with elliptical, triangular and square holes 08 p1305 A66-18594
- Strain energy method used to examine stability and supercritical strains of rib-reinforced cylindrical shells under axial compression 08 p1305 A66-18595
- Asymptotic formulas derived, describing stress-strain state of circular cylindrical shell subject to concentrated heating 08 p1305 A66-18602
- Digital computer programming for design of cylindrical vessels 08 p1306 A66-18604
- Minimum rigidity of ribs ensuring cylindrical shell stability under external load determined, using matrix method 08 p1308 A66-18887
- Variational analysis of stability of infinitely long cylindrical panel under constant evenly distributed lateral loading 08 p1308 A66-18890
- Axisymmetric creep in cylindrical shells, noting creep buckling collapse after high temperature compression loading [AIAA PAPER 66-123] 08 p1308 A66-19002
- Perturbation solutions of stress and deformation problems for homogeneous anisotropic shells constructed from orthotropic material [AIAA PAPER 66-141] 08 p1309 A66-19004
- Von Karman-Donnell large-displacement equations for thin circular cylindrical shells extended by considering larger term numbers in Fourier series representing radial displacements after buckling 08 p1309 A66-19143
- Edge conditions effect on elastic stability of cylindrical shells extended to additional combinations of boundary conditions, considering cylinders under axial compression 08 p1310 A66-19144
- Imperfection maps of cylindrical shell surface measured with apparatus consisting of reference surface, rotating mounting plate, oscillograph, low pressure displacement transducer, etc 08 p1310 A66-19159
- Exact frequency solution for steady state wave propagation for plane strain vibrations of composite hollow cylinders 08 p1310 A66-19162
- Idealized cylindrical shell buckling under axial compression derived from generalized integral expression 08 p1310 A66-19166
- Inhomogeneity effect of plastic deformation distribution during torsion on locking of macroshear during alternating torsion of tubular specimens 08 p1311 A66-19313
- Axisymmetric loss of static stability of closed circular cylindrical shell subject to longitudinal compressive stresses 08 p1312 A66-19430
- Equilibrium equations in displacements for circular cylindrical shells reinforced by longitudinal and transverse ribs under arbitrary surface and edge loads 08 p1312 A66-19434
- Stress-strain state of shell having one end clamped and other under concentrated bending moments and concentrated force acting along generatrix solved by integral equation 08 p1314 A66-19579
- Equations for nonshallow thin shells of arbitrary shape and variable rigidity with continuous smooth curvature 08 p1315 A66-19731
- Nonlinear stability of orthotropic cylindrical shell under torsional stress 08 p1315 A66-19732
- Finite bending of cylindrical plates, evaluating numerical values of stress distribution in baryte sheet 09 p1465 A66-19861
- Small axisymmetric oscillations of fluid inside elastic cylindrical shell with elastic bottom determined by reducing problem to internal Neumann problem for circular cylinder 09 p1368 A66-20756
- Thermal stresses arising at high velocities in aircraft skin consisting of two load-carrying layers separated by filler 09 p1468 A66-20758
- Idealized problems concerning motion of cylindrical plasma sheets in magnetic field, noting application in geophysics 10 p1527 A66-21128
- Elastic general instability collapse pressure of ring-reinforced circular cylindrical shell subjected to uniform external pressure 10 p1613 A66-21318
- Oscillations of cylindrical shell filled with incompressible fluid of variable depth 10 p1614 A66-21328
- Buckling loads of reinforced cylindrical shells, discussing size and placement of stiffening members 10 p1614 A66-21391
- Fluid-shell interaction of infinite cylindrical shell submerged in acoustic fluid and subjected to axially propagating step wave [ASME PAPER 65-APMW-19] 10 p1615 A66-21473
- Statistical study of linear buckling of circular cylindrical shells under axial compression, showing preferred mode shape [ASME PAPER 65-APMW-23] 10 p1615 A66-21474
- Increasing plastic buckling resistance of thin cylindrical /Mg and Al/ shell by means of elastic core /polyurethane foam/ [ASME PAPER 65-APMW-18] 10 p1615 A66-21475
- Elastic behavior of ring reinforced oval cylinder subjected to uniform hydrostatic pressure 10 p1617 A66-21787
- Stressed state in medium length cylindrical shell with arbitrary closed transverse contour and method of solving it 10 p1618 A66-22178
- Frequency spectrum of natural oscillations of cylindrical shell reinforced by longitudinal ribs 11 p1779 A66-22226
- Approximate theory of shells of revolution of average thickness, using seminverse method and expansion into series in Legendre polynomials 11 p1779 A66-22229
- Stability limit of symmetric thin walled three-dimensionally loaded rods under arbitrarily distributed and concentrated conservative transverse and longitudinal loads 11 p1779 A66-22230
- Curvature effect on stress distribution for thin walled circular cylindrical shell with small aperture 11 p1779 A66-22237
- Tube shaped and solid cylinder antennas compared, calculating surface current distribution and radiation patterns 11 p1662 A66-22543
- Algorithm for computer eigenfunction solution of boundary value problem involving partial differential equations for stress functions of semimomentless cylindrical shells 11 p1782 A66-22856
- Modified first-collision model theory that agrees with experimental data on drag coefficient of cylindrical bodies in flow of rarefied gases 11 p1633 A66-22921
- Numerical analysis of thin cylindrical shell under action of external forces for small deformations, using first-order theory 11 p1783 A66-23016
- Equilibrium equations of shallow cylindrical shell of arbitrary cross section subject to arbitrary loading 11 p1783 A66-23033
- Comparison of elasticity and shell theory solutions for infinite circular cylindrical shell subjected to periodically spaced band loads [AIAA PAPER 65-139] 12 p1956 A66-23582
- Structural efficiency of orthotropic materials for cylindrical shells under axial load, including examination of fibrous composites characteristics [AIAA PAPER 65-73] 12 p1956 A66-23583
- Dynamic response of cylindrical shell subjected to time-varying load treated by explicit and implicit method of timewise integration 12 p1956 A66-23584
- Dynamic stability of cylindrical shell subjected to uniform radial pressure 12 p1956 A66-23585
- Dynamic buckling of imperfection sensitive models, specifically cylindrical shells under axial compression 12 p1957 A66-23590
- Critical impact load under which axisymmetric deformation of perfect elastic isotropic cylindrical shell becomes unstable determined, using deflection theory 12 p1959 A66-23746
- Dynamic transient response of cylindrical shell to internal pressure pulse generated by blast wave 12 p1959 A66-23799
- Linear small deflection theory and statistical analysis in dynamic buckling of thin cylindrical shell under axial impact [ASME PAPER 65-APMW-17]



Self-equilibrating bending of complete circular cylindrical shells described by first harmonic terms of Fourier series for displacement components 12 p1961 A66-23980

Creep laws in terms of generalized stress-strain rates formulated, noting secondary deformation, Tresca criterion and associated flow rule 12 p1963 A66-24037

Bending of cylindrical shell clamped at one end and reinforced by elastic ring at free end, with vertical forces uniformly distributed acting over ring 12 p1964 A66-24044

Natural oscillation frequency of smooth cylindrical shells representing combustion chambers, diffusors, etc, analyzing effect of static loads 12 p1964 A66-24045

Rarefying of dense frequency spectrum of shell-shaped elements of aircraft engines by corrugating shell surface, determining natural oscillation modes and frequencies 12 p1964 A66-24046

Approximate determination of flexural vibrations of shells of revolution with vibrations involving appearance of nodal lines along generatrix and meridional directions 12 p1964 A66-24047

Effect on long shell of circumferential and uniformly distributed load /due to explosion/ at constant rate along shell 12 p1964 A66-24048

Initial deflection effect on stability of rib-reinforced cylindrical shells under axial compression 12 p1967 A66-24109

Concentrated forces and bending moments effect on shallow cylindrical shell 12 p1967 A66-24113

Nonsymmetric strain response of simply-supported cylindrical shells to localized impact loads expressed as step, ramp and sawtooth functions and rectangular impulse 12 p1972 A66-25007

Effect of external or internal static pressure on natural frequencies of unstiffened, cross-stiffened and sandwich cylindrical shells 13 p2194 A66-25142

Stress state of weakly curved cylindrical shell analyzed, finding biharmonic function from given boundary value of partial derivatives 13 p2197 A66-25853

Stress concentration at circular hole in orthotropic cylindrical shell, using coordinates system and Bubnov-Galerkin method 13 p2206 A66-26455

Axisymmetric form of stability loss of cylindrical shell under effect of load suddenly applied along generatrix, considering inertia forces and obtaining differential equations 13 p2206 A66-26456

Oscillations of cylindrical orthotropic three-layer shell having ideal fluid flow at variable rate, establishing parametric resonance and determining limits of shell motion instability regions 13 p2206 A66-26461

Mathematical and numerical determinations of aerodynamic forces on harmonically oscillating cylindrical shell under subsonic and supersonic speeds and comparison with slender body theory results 14 p2218 A66-27405

Algorithm for analyzing transient stress waves generated in cylindrical shell by application of impulsive dynamic loads 14 p2399 A66-27609

Heated cylindrical shell with braces subjected to given compression and internal pressure, having elastic beams along edges, analyzing local deformations effect on shell strength and stability 14 p2400 A66-27684

Thermal stresses in finite cylinder with prescribed temperature distribution on curved lateral surface and with ends in contact with smooth insulating plates 14 p2400 A66-27725

Response of thin cylindrical monopole antenna to DC pulse excitation computed, using Fourier transforms, noting correlation between empirical and theoretical values 14 p2255 A66-27906

Imperfections and edge restraint effect on buckling of axially compressed cylinders 14 p2404 A66-27988

Longitudinal stiffeners eccentricity /one-sidedness/ effect on buckling strength of axially compressed cylinders 14 p2404 A66-27989

Filament overwrapped metallic cylindrical

pressure vessels show greater efficiency ratio and buckling strength 14 p2405 A66-27992

Axially loaded cylindrical structures analyzed for optimum weight construction consistent with cost constraint, emphasizing beryllium-aluminum alloys 14 p2406 A66-28023

Flutter of circular cylindrical isotropic shells 14 p2408 A66-28187

Stress analysis of cylindrical shell with reinforced and nonreinforced circular, square and rectangular cuts under tensile and torsional loads, using photoelastic coatings 15 p2607 A66-28765

Stability of cylindrical nonlinearly elastic shell under axial loads applied to shell ends 15 p2607 A66-28766

Parametric oscillations of cylindrical shell filled with liquid of variable depth 15 p2607 A66-28768

Small oscillations produced by combined action of stationary and harmonic forces in nonlinearly elastic cylindrical shell of rectangular planform 15 p2607 A66-28769

Asymptotic solutions of boundary value problems for elastic semiinfinite circular cylindrical shells by removing restriction of slow circumferential variation 15 p2609 A66-29239

Collapse loading of rotationally symmetric cylindrical shell 15 p2609 A66-29253

Supersonic flutter of circular cylindrical shells subjected to internal pressure and axial compression [AIAA PAPER 65-407] 15 p2610 A66-29281

Oscillatory pressures in idealized annular boundary layer apply to panel flutter of circular cylindrical shell in supersonic flow 15 p2610 A66-29282

Stiffener eccentricity and end moment effect on stability of cylindrical panel in axial compression 15 p2610 A66-29283

Buckling characteristics of eccentrically stiffened cylindrical shells under hydrostatic pressure loading and vibration, buckling and flutter characteristics of stiffened flat plates [AIAA PAPER 65-370] 15 p2610 A66-29285

Energy method for analysis of lowest mode symmetrical buckling of thin shell shallow spherical caps and cylindrical arches under blast loading 15 p2610 A66-29291

Stability analysis of elastic axially compressed orthotropic glass-fiber-reinforced-plastic cylindrical shell with linear heredity properties 15 p2611 A66-29341

Cylindrical thin shells with axial stringers under axial compression 15 p2614 A66-29636

Linearized unsteady supersonic potential flow theory formulation of boundary value problem of aerodynamic forces on oscillating cylinder and comparison with two-dimensional quasi-steady and slender body approximations 16 p2628 A66-30259

Bending stresses in cylindrical shell with rigid circular inclusion examined under axial tension and internal pressure [AIAA PAPER 66-525] 16 p2813 A66-30526

Optimum design of pressurized multicell cylindrical shell, noting antislosh capacity and possibility for single pass welding 16 p2816 A66-30909

Natural oscillations of three-layer circular cylindrical shells with freely supported and clamped edges 16 p2818 A66-31056

Torsion of reinforced cylindrical shell with long rectangular cutout 16 p2818 A66-31057

Equilibrium equations for closed circular cylindrical rib-reinforced shells under arbitrary loading 16 p2819 A66-31138

Liquid sloshing effect on axisymmetric vibrations of liquid-filled cylindrical shell 16 p2819 A66-31139

Linearized unsteady nonequilibrium flows produced by unsteady motion of thin foil or circular cylindrical shell in incompressible gas 16 p2687 A66-31288

Self-excited vibrations of infinitely long cylindrical shell, situated in flow of supersonic ideal gas, obtaining motion equations and analyzing stability conditions 16 p2820 A66-31333

Weight savings derived from use of contrasting ring, stringer and wall materials in J-stiffened axially compressed cylinders [AIAA PAPER 66-508] 16 p2821 A66-31480

Linearized theoretical motion equations for orthotropic cylindrical sandwich shells under initial stress, considering free

vibrations 16 p2822 A66-31490

Stressed state of cylindrical shell made of coiled glass fibers 16 p2822 A66-31625

Improved Donnell equations for concentrated load of circular cylindrical shell 16 p2823 A66-31717

Cylindrical thin shells under pressure, axial load and torque, determining plastic yield curves 17 p3021 A66-32006

Axially symmetric dynamic response of infinite, circular cylindrical shell to moving pressure load 17 p3021 A66-32009

Heterogeneity effect on multilayer composite cylindrical shell stability under axial compression 17 p3025 A66-32454

Linearized theory of free-vibratory motion of cylindrical sandwich shells under state of initial stress 17 p3025 A66-32455

Longitudinal and circumferential inertial effects on dynamic response of cylindrical shell to time-varying loads 17 p3025 A66-32470

Drag on cylinders of various height mounted on flat plate, noting dependence of compression region length on cylinder diameter during analysis of boundary layer separation phenomena 17 p2909 A66-32493

Free convective heat transfer in horizontal cylindrical interlayer with heat emitting element 17 p3034 A66-32560

Variational principle applied to formulation of stability equations of shallow shells subjected to creep 17 p3026 A66-32594

Accuracy of approximations using shell equations for predicting dynamic behavior of thin cylindrical shells, with exact solutions form Flugge shell equation [AIAA PAPER 66-447] 17 p3028 A66-32759

Propagation of elastic waves in thin cylindrical shell in terms of exact three-dimensional elastic theory 17 p3028 A66-32788

Oscillations and stability of cylindrical shell in gas flow, taking into account inertia forces 17 p3029 A66-32804

Boundary value problems in secondary creep of circular thin shells under axisymmetric loading, giving solutions for deformation rates and stress resultants 17 p3030 A66-32891

Variation equation for steady state creep applied to semimomentless cylindrical shell 17 p3030 A66-32935

Thin circular cylindrical shell behavior in axial compression, noting buckling under stress, boundary condition detail effects, etc 17 p3031 A66-33064

Donnell-type nonlinear theory for instability of cylindrical shell subjected to axisymmetric moving loads with constant velocity [ASME PAPER 65-APMW-35] 18 p3248 A66-33574

Stress concentration in nonlinear creep of long thin cylindrical shell loaded at one edge by symmetrical radial shear and bending moment 18 p3248 A66-33578

Constant external or internal pressurization effects on circular cylindrical shell under nearly uniform radial impulse 18 p3249 A66-33604

Transcendental equation describing discrete reinforcing network effect on vibrations of reinforced cylindrical shell 18 p3252 A66-33708

Solutions for large plastic deformations of cylindrical membrane shells under internal pressure 18 p3252 A66-33764

Bending characteristics of tapered cylindrical shells, discussing edge and internal influence coefficients 18 p3253 A66-33806

Theory of beams on elastic foundation used for approximate analysis of cylindrical shells with sufficient number of axial ribs 18 p3254 A66-33827

Nearly inextensional deformations of cylindrical shells, noting bending theory 18 p3256 A66-34489

Elastic stability of thin walled circular cylindrical shells in torsion, applying Galerkin method to Donnell equations for critical stresses 18 p3258 A66-34648

Forced motions of hollow cylinder encased in thin elastic shell and subjected to time-harmonic pressure at inner surface of cylinder 18 p3259 A66-35026

Thermal conductivity measurements for



hydrogen via coaxial cylindrical cell noting temperature, pressure effects, residual and conductivity values 19 p3479 A66-36290

TE wave scattering by dielectric cylinder of arbitrary cross section shape, including effects of surface wave excitation and mutual interaction 19 p3304 A66-36408

Plastic deformation in hollow metal cylinder by rapidly varying axial magnetic field, calculating time dependence assuming substance is rigid and plastic 19 p3475 A66-36602

Finite deflection and stability equations for circular cylindrical shells stiffened in longitudinal and circumferential direction 19 p3475 A66-36636

Stability of cylindrical shell of average length with elastic filler under uniform external radial pressure 20 p3665 A66-36911

In-plane stiffness matrices for composite cylinders of filament winding determined by internal pressure, axial tension and torsion tests 20 p3666 A66-37440

Cylindrical shells strengthened by stringers and formers calculated, using double trigonometric series 20 p3670 A66-37672

Wall thickness requirement for cylindrical shell stability under critical radial compression derived by generalized power series 20 p3673 A66-38271

Stress analysis of elastic cylindrical shell perforated by rectangular cut-out and governed by Donnell equation 20 p3673 A66-38272

Thermal buckling modification in large deflection equations for thin shallow cylindrical shell 20 p3673 A66-38274

Elastic stability of cylindrical shells reinforced by one or two frames and subjected to external radial pressure, noting inertia moment about skin line and frame bending stiffness optimization 21 p3828 A66-38703

Beam column supported by linear rotational and extensional springs representing elasticity of test rig, used in analog study of thermal buckling behavior of thin cylindrical shells 21 p3828 A66-38706

Stability of structurally anisotropic circular cylindrical shell under nonuniform compression 21 p3829 A66-38976

Variational theorems for creep of shallow cylindrical shells, noting buckling and snap-through of square cylindrical panel compressed along generatrix 21 p3829 A66-38977

Shell stability in Euler formulation, taking into account actual redistribution of stresses that results from initial deflection and creep, noting buckling of closed cylindrical shell under axial compression 21 p3829 A66-38978

Computer analysis of cylindrical shell stability under uniform external pressure and critical pressure determination for various boundary conditions 21 p3829 A66-38979

Axisymmetrical deformation of multilayer circular sandwich cylindrical shells, deriving governing differential equations by variational theorem 21 p3831 A66-39272

Aerodynamic resistance of cylindrical rotor determined, using method based on formulas for resistance factors of cylindrical surfaces and rotor encasement 21 p3739 A66-39328

Steady state response of damped cylindrical sandwich shell under radially symmetric time harmonic pressure [ASME PAPER 65-WA/UNT-1] 21 p3832 A66-39530

Nonlinear differential equations for cylindrically anisotropic plates, noting errors of Wolmir method 22 p3988 A66-39698

Aeroelastic stability of infinite long cylinder with outer surface exposed to inviscid flow 22 p3992 A66-40338

Postbuckled equilibrium configurations of axially compressed circular cylindrical shell determined from large deflection theory and principle of stationary potential energy 22 p3993 A66-40340

Eccentricity effect on magnitude of discontinuity stresses in unsymmetrically loaded shells of revolution, discussing results of numerical calculations 22 p3993 A66-40366

Cylindrical shell analysis for short segments of shells of revolution with

axisymmetric edge-loading and variable wall thickness, using matrix method 22 p3994 A66-40369

Progressive plastic buckling of cylindrical shells under axial compressive load, noting nonsymmetric patterns 22 p3994 A66-40432

Influence coefficients for semiinfinite and infinite circular cylindrical elastic shell subject to self-equilibrating edge loads 22 p3995 A66-40451

Characteristic equation for linear flutter problem of elastic cylindrical shell immersed in gas flow, discussing energy radiation, traveling wave propagation and discontinuity problem 22 p3995 A66-40510

Axisymmetric dynamic response of ring supported cylinder to time dependent loads, discussing boundary conditions and differential equations of motions [AIAA PAPER 66-83] 23 p4138 A66-41106

Structural efficiency of orthotropic materials for cylindrical shells under axial load, including examination of fibrous composites characteristics [AIAA PAPER 65-73] 23 p4138 A66-41107

Correct conductance and susceptance of infinite cylindrical antenna determined via asymptotic evaluation of parametric integrals 23 p4047 A66-41636

Longitudinal and tangential local and strip loads effect on magnitude of forces, moments and displacements in circular cylindrical shell 23 p4139 A66-41788

Energy method application to buckling of axially compressed cylindrical shells with ring-stiffened edges, noting upper and lower bounds and critical rigidity ratio 23 p4140 A66-41912

Stress distribution and displacements in neighborhood of circular hole in cylindrical shell subjected to load such as torsion or axial compression 23 p4142 A66-41959

Large deflection postbuckling analysis of thin walled oval cylinders under axial compression 23 p4143 A66-41961

Postbuckling behavior of circular cylindrical shell locally buckled under axial compression 23 p4143 A66-41964

Classical critical stress values for buckling of thin walled circular cylindrical shells in axial compression as function of edge conditions 23 p4143 A66-41965

Structural dynamics of axisymmetric deformation of semiinfinite plastic cylindrical shell under concentrated ring impact 23 p4147 A66-41999

Elastodynamic buckling of circular cylindrical shells, unstiffened and longitudinal stringers-stiffened 23 p4147 A66-42000

Plastic theory of structures for collapse under highly localized loading 24 p4286 A66-42152

Applied mechanics - U.S. National Congress, University of Minnesota, Minneapolis, June 1966 24 p4287 A66-42265

Prestressed circular membrane shell subjected to uniform radial line load, determining stresses and displacements from material properties, internal pressure and original size 24 p4288 A66-42272

Longitudinal and torsional plastic wave propagation in thin walled tube, governed by four quasi-linear symmetric hyperbolic PDEs of first order with two distinct wave speeds 24 p4288 A66-42277

Membrane stresses in frustum connecting two cylindrical shells with parallel axes 24 p4289 A66-42287

Stability analysis of thin two-layer shell in Gaussian coordinates with moment initially zero, including applications to stability of circular cylindrical shell 24 p4290 A66-42441

Stress concentration near circular cut in unbounded plane plate and reinforced by thin walled infinitely long cylindrical shell under tension applied at infinity 24 p4290 A66-42445

Improved central tube configuration to optimize design of pressurization multicell cylindrical shell, comparing structural efficiency with other shells 24 p4291 A66-42794

Stability theory methods for small elastoplastic deformations generalized to include creep effects in cylindrical shells compressed at ends 24 p4292 A66-42885

## CYLINDRICAL TANK

Critical load of ellipsoidal end faces of cylindrical reservoir assuming deformation beyond critical load is axisymmetric 01 p0155 A66-10657

Mechanical model for representing moment of inertia and fuel sloshing in baffled cylindrical missile tanks 08 p1205 A66-18834

Damping of liquid oscillations in cylindrical tanks, determining rigid and flexible baffle loss coefficients, baffle efficiency and maximum bending stress [AIAA PAPER 66-97] 08 p1207 A66-19000

Critical load of ellipsoidal end faces of cylindrical reservoir, assuming deformation beyond critical load is axisymmetric 12 p1963 A66-24015

Mixed flow of two gases through coaxial cylindrical tubes separated by perforated plate 14 p2273 A66-26782

Design of composite structures of minimum weight, using flat-bottomed cylindrical tank, noting continuity condition of radial bending moment of plate and shell 14 p2395 A66-27174

Space vehicle containers, discussing prolonged storage of cryogenic liquids, insulation requirements, container configuration and design, etc [SAE PAPER 660460] 17 p3017 A66-33165

Outflow of liquid from cylindrical tank through central outlet for cases where effect of gravity is small, noting distortion of liquid surface [AICE PREPRINT 17D] 22 p3897 A66-39885

## CYLINDRICAL WAVE

Spherical and cylindrical implosive waves and system of generating detonation wave that converges to given focus 03 p0445 A66-13131

Plasma resonance of cylindrical plasma in absence of magnetic field noting conductivity kernel, scattering of radiation, nonuniformity of plasma sheath and Landau damping 04 p0474 A66-13425

Nonsteady cylindrical waves propagating in cold rarefied plasma situated in strong magnetic field 04 p0557 A66-14430

Effective excitation of radial cylindrical surface waves using Green function for excitation of impedance cylinder resting on impedance plane 06 p0823 A66-15882

Dissipative effects in converging cylindrical symmetric shock wave, considering ion and electron heat conductivity, ion viscosity and energy exchange 07 p1025 A66-18180

Imploding cylindrical shock wave production through imploding detonation waves in oxygen-acetylene mixtures, using Chapman-Jouguet theory 08 p1204 A66-18523

Neutral point between two parallel line currents in highly conductive plasma, noting topological flux change and relation to solar flares [AIAA PAPER 66-152] 10 p1565 A66-21683

Variation of critical energy for direct initiation of cylindrical detonation waves as function mixture composition and initial pressure 10 p1622 A66-21830

Oscillation frequency and attenuation factor for long cylindrical waves in viscous fluid 14 p2278 A66-28068

Conservation equations for cylindrical blast and radiation effect on shock layer profiles of blast wave 16 p2686 A66-31114

Symmetrical stress wave propagation in thin plate with small, circular hole at center, noting boundary conditions and solutions via Laplace transforms and by method of characteristics 17 p3022 A66-32012

Gravitational theory based on solar observations, noting connection between gravitational eigenvalues, planetary orbit spacing and connection with cylindrical wave functions 18 p3104 A66-33757

Behavioral equations derived for caustic that envelops locally-plane cylindrical wave incident on plane surface of layered plasma wedge 19 p3296 A66-35305

Plasma convergence, structure and heating by collisionless cylindrical shock waves, discussing wave front 19 p3424 A66-36560

Propagation constants of quasi-transverse electric modes measurement in cylindrical waveguide partially filled with anisotropic plasma 20 p3525 A66-37116

Cylindrical and spherical waves propagation in weakly inhomogeneous plasma treated by



- geometrical optics, noting caustic surfaces 22 p3951 A66-39648
- Stress wave propagation analysis using exploding wire and hollow cylinder together with measurement of loading condition and response 22 p3992 A66-40203
- Energy accumulation of spherical and cylindrical shock waves in inhomogeneous gas 22 p3901 A66-40690
- Parabolic cylindrical waveguide formed by intersection of two confocal parabolic metal surfaces, determining eigenvalues of wave functions subject to boundary conditions yielding TE and TM modes 23 p4047 A66-41587
- CYSTEAMINE**
- Cystamine hydrochloride, strychnine nitrate and hexobarbital injections effect on mice subjected to vibration, noting vibration effect on swimming 15 p2431 A66-28740
- CYTIDYLIC ACID**
- Thermal condensation of cytidylic acid from mononucleotides in presence of polyphosphoric acid 17 p2852 A66-32096
- CYTCHROME**
- Molecular nitrogen photofixation relation to electron-donor respiratory system, activity of hydrogenase and dehydrogenases and photosynthesis 13 p2010 A66-25893
- Repetitions in polypeptide sequence of cytochromes 18 p3059 A66-34196
- CYTOGENESIS**
- S BIOLOGICAL CELL**
- CYTOLOGY**
- Physical state of water in living cell and model systems such as collagen and wool 11 p1645 A66-22989
- Intracellular water structure and mechanisms of cellular transport, examining plasma and intracellular membranes 11 p1645 A66-22991
- Effect of combined action of accelerations, vibration and radiation of nuclei of bone marrow cells in mice 15 p2437 A66-29478
- CZECHOSLOVAKIA**
- Czechoslovakian space research including satellite observation, radio emissions, solar activity, Doppler effect measurement, radiation hazards, etc 15 p2601 A66-29912
- Comparison of Czechoslovakian human engineering standards for control pushbuttons with U.S. standards 22 p3859 A66-40861
- D**
- D-1 SATELLITE**
- CNES D-1 satellite using Diamant launcher for study of launch systems and space environment 01 p0142 A66-10360
- D-1, D-2 and D-3 Diamant satellites developed by CNES 10 p1610 A66-21252
- D-1A satellite by Diamant for evaluating long-term performance of instrumentation, solar cell studies and geodetic experiments 10 p1612 A66-21959
- D-1 satellite thermal control while in orbit featuring heating resistance and controllable power supply, noting simulated test program 10 p1612 A66-21960
- Hammarig firing range facilities and planned launch of D-1A geodesic satellite 11 p1687 A66-23378
- French D-1 satellite, design, attitude stabilization, solar power supply, telemetry, etc 14 p2390 A66-26804
- Design, instrumentation, performance capabilities and program of D-1 satellites 16 p2812 A66-31684
- FR-1 and D-1 satellites, discussing construction principles, development, tests and supervision of CNES 18 p3094 A66-33979
- Charged particle effect in Van Allen zone on short circuit currents of photovoltaic cells on D-1A satellite 18 p3053 A66-33980
- Mobile control of FR-1 and D-1 satellites and application to integration, tests and checkout at launching 18 p3094 A66-33981
- Automatic control equipment for FR-1 and D-1 satellites 18 p3246 A66-33985
- D-1, D-2 and FR-1 satellites in French space program 24 p4296 A66-42697
- D LAYER**
- Minimum ionospheric electron density needed for radio reflection in D layer 01 p0031 A66-11037
- D-region atmospheric processes such as electron attachment, photo and other detachment processes, recombination and neutralization as studied in laboratory 03 p0362 A66-12640
- LF propagation and probe experiment yielding profile of ionospheric D region, discussing experimental techniques, computations, RF impedance probes and formulas for ionospheric data 03 p0334 A66-12643
- Electron density and collision frequency in lower D region measured by rocket sounding 03 p0366 A66-12879
- Recombination coefficient and electron production rate in lower D region during solar flare 04 p0574 A66-13444
- Response of D-region absorption of cosmic noise to passage of totality during eclipse of May 30, 1965 recorded in New Zealand 05 p0668 A66-14798
- Electron distribution in quiet D region derived from rocket measurements of wavefield generated by LF ground transmitter 05 p0670 A66-14949
- Electron energy loss rate for D region determined by Maxwellian velocity distribution of thermal component brought about by collisions with molecular nitrogen involving rotational transition 05 p0672 A66-15021
- Lower ionospheric characteristics determined by VLF radio waves propagated over long distances by multiple reflections between Earth and D region 09 p1370 A66-19973
- Electron production, density and absorption in D region as effected by X-radiation 09 p1373 A66-20484
- Motion of D region under daytime conditions 09 p1374 A66-20485
- Effect of Soviet atmospheric nuclear explosions on D and F-2 ionospheric layers, particularly observing enhancement of atmospheric noise 10 p1600 A66-22058
- Onset patterns of PCA analysis using corrected geomagnetic coordinates, with results analyzed through solar cosmic radiation, Earth magnetosphere structure and D region 12 p1944 A66-24470
- D-region electron distribution, collision frequency and amplitudes of partially reflected waves 13 p2075 A66-26739
- Plasma due to high-altitude nuclear explosion and effect on radar propagation 14 p2237 A66-27510
- Ionospheric D-region electron distributions in middle latitudes deduced from reflection of long radio waves 15 p2489 A66-29631
- Ionospheric absorption effects in D and E layers, noting refraction role and effective collision frequency 15 p2493 A66-30036
- Electron density in E- and D-regions above Kjeller, Norway, from rocket measurements of absorption and height of reflection of radio waves 16 p2692 A66-30332
- Lyman alpha ionization of nitric oxide and ion molecule reactions accounting for ionic nitric oxide content of D and E regions 16 p2694 A66-30705
- Variations in electron density with reflection of long waves in D region 17 p2918 A66-32878
- Altitude variations of frequencies and electron density with reflection in D region 17 p2919 A66-32879
- Height distribution of electron density accounting for behavior of LF and VLF radio wave propagation during sudden ionospheric disturbance /SID/ 17 p2922 A66-33349
- Nitric oxide distribution in lower ionosphere calculated from reaction coefficients and mass spectrometric measurements of density 17 p2922 A66-33354
- First-order correction to Hough theory for measuring ion density in D region, especially those involving heat transfer and compressibility 18 p3107 A66-34523
- Positive ion composition in lower ionosphere, particularly D region, considering sources for water ions, stratification of metallic ions, etc 19 p3350 A66-36354
- Comparison of magnitude of collision frequency of electrons in D and E regions obtained by satellites, rockets, etc, with cross sections measured in laboratory 19 p3352 A66-36627
- Negative ion associative detachment reaction with atomic oxygen in determination of nighttime D region electron density profiles at high latitudes 22 p3905 A66-39945
- Faraday rotation experiment for determination of electron density and collision frequency observations in arctic D region 22 p3905 A66-39946
- Gerdien-condenser rocketborne probe used to measure ion densities in D region of atmosphere 22 p3905 A66-39947
- Collision frequency in E and D regions of ionosphere for electrons and neutral molecules 22 p3906 A66-39948
- Electron density profile measurements in auroral zone D layer during quiet ionospheric conditions, using partial reflection method 22 p3906 A66-39951
- Electron density and collision frequency profiles for D region obtained through simultaneous measurement of radio wave phase and amplitude interaction 22 p3906 A66-39953
- Electron density measurements in D layer obtained, using LF radio wave propagating into ionosphere and rocketborne receivers 22 p3906 A66-39955
- Ion mass spectrometry of D layer, using magnetic fields and cyclotron resonance principle 22 p3907 A66-39956
- Electron density profiles in D layer measured through Doppler shift on VLF signal propagating from ground up and received by rocket 22 p3907 A66-39957
- Number densities of ions and electrons in D region measured, using Arcas rocket 22 p3907 A66-39958
- Long VLF path propagation measurements, determining characteristics of lower ionosphere, noting role of phase and amplitude variations during solar flares 22 p3907 A66-39959
- Ionospheric cross modulation analysis by computer-oriented simulation process, noting D region electron density and collision frequency profiles 23 p4041 A66-41641
- Ionization level of D region at middle geomagnetic latitudes as affected by fast proton flux 24 p4265 A66-42757
- Differential absorption and Faraday rotation in D region, using closed loop feedback system and two signals of different frequencies 24 p4205 A66-43218
- D-LINE**
- SA SODIUM D-LINE**
- Factors determining line reversal temperature of flame with realistic temperature cross section explained by calculation of sodium D-line contours 17 p3038 A66-33324
- DACRON**
- SA NYLON**
- DAEMO**
- S DATA ADAPTIVE EVALUATOR AND MONITOR /DAEMO/**
- DAMAGE**
- SA IMPACT DAMAGE**
- SA METEORITIC DAMAGE**
- SA PROTON DAMAGE**
- Damaged depth in germanium thin films induced by bombardment with low energy argon ions measured, using differences in sputtering yield for given energy 15 p2561 A66-28705
- Damage thresholds for various glasses exposed to laser pulses, emphasizing internal damage 15 p2524 A66-28732
- Double linear damage rule used in conjunction with crack initiation and propagation equations, applied to cumulative fatigue damage 22 p3989 A66-40116
- DAMPER**
- SA VIBRATION DAMPER**
- Stabilization system of gravity gradient test satellite and effect on damping time and steady state accuracy, noting attitude data and solar effect 21 p3819 A66-38858
- Attitude errors of inertia coupled gravity gradient satellite with solar radiation pressure as dominant disturbance, noting slot problems in stabilized package accommodating damper motion 21 p3820 A66-38861
- Control of magnetic hysteresis mechanism, increasing damping torque for use in



- gravity-oriented satellite stabilization 21 p3820 A66-38862
- Periodic symmetric two-impacts-per-cycle motion of impact damper solved, determining asymptotically stable regions 24 p4216 A66-42146
- DAMPING**
- SA DOPING
- SA ELASTIC DAMPING
- SA HYSTERESIS
- SA LANDAU DAMPING
- SA TRANSIENT OSCILLATION
- SA VIBRATION DAMPING
- SA VISCOELASTIC DAMPING
- SA VISCOUS DAMPING
- XB-70 vehicle control system sensing, local force application, coupling and adaptability for increasing structural mode damping ratio, thus avoiding disturbing pilot accelerations and structural loads 01 p0103 A66-10672
- Proportional pneumatic actuation system reliability using variable hydraulic damping, noting role of error and error rate signal 03 p0324 A66-13219
- Mathematical relation between damping and amplitude of transient process in second order system, using nomogram 03 p0351 A66-13240
- Internal friction, damping and cyclic plasticity - ASTM Symposium, Chicago, June 1964 05 p0771 A66-14546
- Damping studies concerned with stress-strain-time properties of materials and structural system 05 p0772 A66-14547
- Collisionless damping of nonlinear plasma oscillations, with exact solution of Vlasov equation for resonant electrons 08 p1260 A66-18537
- Noncollisional damping effects limiting amplitude of resonance peaks experimentally verified, using mercury plasma discharges 14 p2346 A66-28270
- Optimum parametric damping of forced oscillations when random external force operates on circuit 15 p2469 A66-28674
- LF resonances in mixed state of pure niobium, noting line shape and damping decrease 16 p2770 A66-30186
- Tolerance limits for structural components in power-filter circuit design, calculating fluctuations of damping property and phase fluctuations in multiply divided circuits 16 p2663 A66-31031
- Linear system damping while using minimum control intensity treated as functional analysis problem 16 p2672 A66-31504
- Squeeze-film method for generating high damping coefficients with limited space based on Reynolds equation and simplified Navier-Stokes equation 17 p2930 A66-32946
- Necessary and sufficient conditions for existence of classical normal and quasi-normal modes in damped linear dynamic systems [ASME PAPER 65-WA/APM-25] 18 p3134 A66-33592
- Third-order orbital gyrocompass horizontal and vertical damping techniques to eliminate gyro and bias errors in horizon sensor 18 p3110 A66-33828
- Damping coefficient measurement in transient regime by numerical integration process 20 p3599 A66-36956
- Damping by hemispheric torquing to actively control spin axis in rotor while remaining unchanged with respect to case fixed reference 21 p3737 A66-38896
- Approximate method for determining damping factors of mechanical oscillatory systems with many degrees of freedom described by linear differential equations of n-th order with constant coefficients 21 p3770 A66-38971
- Stability problems of solid body with liquid filler, noting small partial damping of liquid 21 p3770 A66-38972
- Internal nonlinear material damping effects on whirling motion of elastic shaft, noting response curves for Mentel-Fu stress-strain law 21 p3745 A66-39434
- Development of family of standard polynomials with adjustable damping, noting first-and second-degree numerators 22 p3884 A66-40514
- DARK ADAPTION**
- S NIGHT VISION

- DARK PLASMA**
- S IONIC WAVE
- DASSAULT MIRAGE III AIRCRAFT**
- Full-scale half model of GAMM Mirage III V airplane in S-1 wind tunnel of ONERA Test Center of Modane 02 p0210 A66-11202
- Pressure distribution measurement system for flow field of main turbojet intake of one-eighth scale model of Mirage III V aircraft 02 p0210 A66-11206
- DASSAULT MYSTERE XX AIRCRAFT**
- Flying characteristics of Falcon fanjet, French-built aircraft, noting landing, accommodations, soundproofing, etc 19 p3279 A66-36048
- DATA**
- S ANALOG DATA
- S BINARY DATA
- S DIGITAL DATA
- S INFORMATION
- S RADAR DATA
- S SAMPLED DATA
- S VIDEO DATA
- S WORLD DATA CENTER
- DATA ACQUISITION**
- Electronically programmable telemeter using random access multiplexing and stored program control for aerospace missions 01 p0032 A66-11130
- Information storage density reduction techniques for magnetic recording tape 01 p0034 A66-11132
- Energy spectrum of cosmic ray muons measured for data on nuclear interactions and characteristics of primary cosmic radiation 03 p0417 A66-12319
- Atmospheric model applied to fogs forming in valley bottoms and data acquisition in connection with this phenomenon 03 p0389 A66-12705
- Manned space flight program with biomedical data collection for integration of crewman into spacecraft operation 04 p0471 A66-14090
- Energy patterns from space accessible to human senses through data sensors and information acquisition 04 p0472 A66-14093
- Lunar tidal effect on oxygen green line in night airglow at Honolulu from 1961 to 1963 05 p0668 A66-14801
- Data collection system with small on-line computer that monitors stress, temperature, pressure and other physical parameters of environmental laboratory vacuum and temperature chambers [ISA PREPRINT 1.12-1-65] 05 p0638 A66-15502
- Data obtained by satellite and rocket probes on cosmic ray composition, particularly on fluxes on nuclei of elements contained in rays 06 p0946 A66-16569
- Method of time domain analysis of nonlinear hybrid systems with first or fractional order data extrapolation 06 p0866 A66-16963
- NASA Space Tracking and Data-Acquisition Network, describing command telemetry, tracking handling and recording system operations 08 p1180 A66-18587
- Data acquisition of acoustic, vibration and heat flux during static rocket testing, using balloon rigging arrangement 08 p1202 A66-18927
- Omega location and satellite reporting for worldwide observation and navigation systems 08 p1252 A66-19508
- Effectetics, informatics, control and stability in modern flight vehicle systems [AIAA PAPER 66-131] 08 p1254 A66-19565
- Device for automatically feeding experimental curve coordinates in large quantities into digital computer for high noise level photographic image 11 p1659 A66-22432
- Flight data used to determine relationship between atmospheric temperature changes and clear air turbulence occurrence at jet altitudes [AIAA PAPER 66-365] 12 p1906 A66-24477
- Lunar landing spacecraft analysis and Surveyor reliability data acquisition 13 p2192 A66-25506
- Servo tester with automatic data acquisition and reduction /STADAR/, discussing design and operational capability in Apollo program 13 p2027 A66-25661
- Computer program with data compilation, using equivalent circuit for p-i-n diode,

- employed in design of coaxial wideband variable attenuator 14 p2246 A66-26833
- Atmospheric refraction data acquisition using radiating source, receiver/transmitter and receiver/recorder 14 p2285 A66-27842
- Geoscience information acquisition by radar return studied by means of terrain target scattering coefficients 14 p2244 A66-28407
- /scatterometry/
- Space research in Hungary in 1965 including satellite tracking, ionospheric sounding, solar activity, etc, noting international data transmission 15 p2600 A66-29907
- French space program including FR-1 satellite and research in meteorology, space biology, rocket probes, electromagnetic propagation, etc 15 p2601 A66-29938
- High resolution density data from radar observations of low altitude, polar orbiting satellites reveal longitudinal and geomagnetic variation, noting regression analysis 15 p2497 A66-30085
- Optimization of data acquisition and reduction systems generated by random vibration, considering dynamic ranges 16 p2655 A66-30447
- Multisensor airborne reconnaissance mission planning and data acquisition 16 p2704 A66-30516
- Flexible commutation system for routing numerous signal-carrying leads to centrally located multiplexer for Saturn 16 p2649 A66-30540
- Sonic boom effect on people, noting ground overpressure measurement and data obtained from interviews, formal complaints, building damage, etc 17 p2868 A66-33028
- Sonic bang experience in United Kingdom from supersonic flights and explosive charges, noting intensity, waveform, damage, etc 17 p2868 A66-33029
- Effectetics, informatics, control and stability in modern flight vehicle systems [AIAA PAPER 66-131] 18 p3267 A66-33786
- CNES network of stations for FR-1 and D-1A, discussing checks of proper functioning, orbital corrections, telemetry, ground control, etc 18 p3094 A66-33978
- Eye movement data used for studying nonvisual processes involved in ocular patterns 18 p3059 A66-34198
- EOLE system consisting of balloons and satellite, interrogation for synoptic data on atmospheric circulation over Southern Hemisphere 19 p3346 A66-35638
- Receiver design and results of dual VLF transmissions for obtaining timing information 19 p3357 A66-35693
- Implementation and individual units design for DATA-CORE telemetry processing system utilized in data acquisition and processing from Saturn/Apollo 19 p3307 A66-35708
- Airborne data acquisition statistical recorder 19 p3361 A66-36669
- Real-time data gathering and flight-test technique for aircraft-carried weapons system development testing 20 p3495 A66-37207
- Data acquisition and analysis for quantitative and qualitative assessment of complex space vehicle hardware 20 p3523 A66-37975
- Soviet observational data on solar corona and wind collected during solar eclipse of June 19, 1936 21 p3813 A66-39120
- Data on unknown portions of Earth gravitational field from observations of two consecutive satellite orbits and mean orbital elements 22 p3976 A66-39693
- Radio telemetry for acquisition of Circadian rhythm data on ambulatory animal, including deep body temperature, heart rate, locomotor activity and oviposition 22 p3856 A66-39792
- Multichannel computer controlled Mobile Micrometeorological Observation System, automatic data acquisition, processing and recording system for observational analyses of turbulence of atmospheric boundary layer 22 p3943 A66-40427
- Laser technique acquisition of data on exploding-wire phenomena in explosion model, supersonic model and ablation model 23 p4091 A66-41701
- Optimal correlation of tracking data



determining Surveyor I location 23 p4129 A66-41780

Biomedical monitoring systems for crews during rest and during dynamic stress testing 24 p4167 A66-42451

Pegasus meteorite-detecting satellite design and performance and data on meteorites 24 p4283 A66-42741

**DATA ADAPTIVE EVALUATOR AND MONITOR /DAEMO/**

Adaptive data management analyzer for evaluating data compression techniques 04 p0489 A66-13620

**DATA ANALYSIS**

Dynamic data /waveforms/ analysis comparing analog with digital methods for speed, costs, flexibility, reliability, etc [SAE PAPER 650818] 01 p0033 A66-10480

Basic techniques for studying random data and distinguishing it from deterministic data [SAE PAPER 650825] 01 p0033 A66-10826

Research, development, test and operation simulating devices used in aircraft construction supply real time data, considering human factor, costs, etc 01 p0054 A66-10871

Data analysis and estimation of probability of finding sought magnitude within experimental error limits 02 p0261 A66-11810

Discrepancies in data concerning aurora type sporadic ionization in E region obtained by various high latitude stations 02 p0225 A66-12136

European Space Technology Center including upper-atmosphere scientific experiments, instrumentation, satellite control, data analysis, etc 03 p0352 A66-12481

Data analysis from film of framing camera with rotating mirrors, using frame edges as reference lines, calculating necessary corrections 05 p0677 A66-14863

Input initiation energy and potential impact energies available under processing conditions, interpreting test data 05 p0787 A66-15138

Doppler radar accuracy investigation, noting wide distribution of systematic error 07 p1064 A66-17668

Data analysis of experiments with open-cycle supersonic EGD generator for application as power source and comparison with mathematical model 07 p0993 A66-18314

Data compendium on neutral composition of atmosphere at altitudes from 100 to 200 km, noting nitrogen and oxygen concentration values from optical and mass spectroscopic studies 09 p1376 A66-20991

Data systems requirement for geographic research, noting use of orbiting sensors to obtain information on terrain, vegetation, human and animal activities, etc 10 p1532 A66-21522

Data analysis of pre-SC field intensity increases and receivable time of WWV signal at Hiraiso, Japan, and Canadian stations for 50 geomagnetic storms 12 p1872 A66-24471

DATAN, curve fitting process to approximate data and elimination of problems for programming engineer by data analysis 13 p2028 A66-26325

Machinability data for hard-to-machine materials, noting cost reductions, tool holder test program, cutting fluids, fixtures, producibility, etc [ASTME PAPER MM66-178] 14 p2300 A66-26958

Discrepancies in data concerning aurora type sporadic ionization in E region obtained by various high latitude stations 14 p2287 A66-28092

Tabular data on magnetic storms and on geomagnetic and solar data furnished by Swiss Federal Observatory 16 p2801 A66-30726

Orbital elements for Telstar communications satellites, using angle only and/or angle range data time as input information 16 p2723 A66-30898

Reevaluation of data and equations used in calculation of air viscosity coefficient and application to wind tunnel experiments 16 p2685 A66-30911

Explorer XVIII plasma flux measurement data analysis, plasma detector, map of transition zone between magnetosphere and solar wind and associated energy spectra 18 p3168 A66-34351

Amplitude analysis and statistical implications of random data analysis applied to evaluation of random signals 18 p3135 A66-34498

Solar particle propagation in magnetic fields revealing anisotropies in proton flux analyzed from Pioneer VI space probe data 18 p3170 A66-34536

Data on energy and angular distribution of high energy muons, noting detector and structural bursts 18 p3220 A66-35193

Displays of navigation data showing horizontal situation against moving map, noting use of standard charts, provision for permanent record, etc 19 p3398 A66-36733

Apollo Spacecraft Test Data Evaluation System, noting functions, operation and performance 20 p3662 A66-37247

Systems producing germanide phases noting phase diagrams of germanides of s-elements, ds-elements, fds-elements and sp-elements 20 p3616 A66-37415

Naval weapons A-7A maintainability requirement effect on management and design and analysis of early flight test data 20 p3496 A66-37920

Rocket instrumentation for galactic X-ray observation, noting scintillation counter, proportional counter and GM counter 20 p3636 A66-38237

Data statistical analysis of solar radio bursts over wide frequency range and relation to solar flares 21 p3815 A66-39372

Computer simulation experiments design for industrial systems, considering variance techniques, multiple ranking procedures, sequential sampling and spectral analysis 22 p3870 A66-40132

Statistically designed experiments in wind tunnel test programs dealing with exhaust nozzles, discussing data analysis techniques [AIAA PAPER 66-742] 23 p4052 A66-41326

Electronic reliability - IEEE Conference, New York, May 1966 24 p4178 A66-42087

Data analysis on probability papers for gamma, normal and Weibull /including exponential/ distributions 24 p4230 A66-42088

**DATA COMPRESSOR**

Redundancy reduction techniques for data compression and adaptive telemetry for aerospace application 01 p0032 A66-11131

Adaptive data management analyzer for evaluating data compression techniques 04 p0489 A66-13620

On-line computer-based aids for investigating effect of sensor data preprocessing and information compression procedures on data transmission bandwidth and reliability 19 p3307 A66-35686

Video data compression by redundancy techniques, using a posteriori curve fitting techniques to adaptively change effective resolution as function of picture detail 20 p3557 A66-37203

Data compression for TV transmission from space, using improved gray scale /IGS/ and coarse-fine PCM systems 20 p3561 A66-38262

Adaptive telemetry applied to data compression, analyzing redundancy reduction, adaptive sampling, data reconstruction, etc 21 p3708 A66-39480

Digital filtering system comprising only few integrated circuits and using addressshift register combination, compared with analog devices 23 p4067 A66-41168

Data compression feasibility for data transmission from unmanned spacecraft in deep space 24 p4282 A66-42682

**DATA CONTROL SYSTEM**

Flow of data and control information from apparatus to computer and use of microprogrammed controller 12 p1827 A66-23829

Evaluation of total square integrals arising in minimization problems of discrete data systems not requiring expansion of determinant for solution 12 p1850 A66-24265

Instrumentation simulation, discussing data system simulator facility, noting application for telemetry and instrumentation design 20 p3542 A66-37248

Logical processing units and interconnection networks design noting reliability, fault diagnosis, computer coordination of data and control processes, etc 22 p3871 A66-40728

Optimum pulse transfer functions for multivariable digital ergodic stochastic

processes 23 p4051 A66-41853

**DATA CONVERSION**

High data rate SHF communication receiver for demodulating analog or digital information, noting components 13 p2023 A66-25656

Navigational information conversion from digital readout to pictorial display 16 p2743 A66-30670

**DATA CONVERTER**

One-way microelectronic airborne digital data converter intended for use in automatic carrier landings 06 p0824 A66-15969

Data converter system for conditioning, recovery and display of aircraft position and altitude data permitting real time surveillance by ground observer 16 p2651 A66-30564

Real time cardiorespiratory rate monitor for data converter on Gemini space program 19 p3288 A66-35703

**DATA CORRELATION**

Adaptation of linear classifier without data repeating and behavior of classifier parameters 04 p0490 A66-13622

Standardization of machining criteria for aerospace materials, compiling data about tool design, planning, manufacturing, costs, etc, on simple form [ASTME PREPRINT MM66-714] 12 p1887 A66-24418

Time correlated burst retransmission PACM telemetry system, memory requirements, data time delay and bandwidth utilization efficiency 14 p2244 A66-28431

Correlation of simultaneous optical and radio auroral data showing that radio wave scattering belt includes visual auroral belt 16 p2692 A66-30329

Data correlations on forced-convective heat transfer to cryogenic fluids by nucleate, film and transition region boiling 20 p3677 A66-37098

**DATA HANDLING SYSTEM**

**SA SCIENTIFIC DATA CONDITIONING SYSTEM**

Standard Navy Maintenance and Material Management System /3M System/ detailing aviation portion of maintenance data collection program 01 p0033 A66-10118

Data control constant-bandwidth frequency system and tricom system discussed as examples of better methods of taking advantage of communication frequency spectrum 04 p0480 A66-13727

Data handling and dissemination program noting storage, retrieval, cost, automatic methods, avoidance of redundant information, etc [ISA PREPRINT 1.7-1-65] 05 p0638 A66-15515

Saturn V diphas data modem, describing computer system for prelaunch checkout 06 p0868 A66-15989

Stabilization, communication, data handling and power subsystem requirements for AOSO [AIAA PAPER 64-333] 08 p1303 A66-18817

Spaceflight data handling with emphasis on data compaction techniques based on weighted-information theory, Karhunen-Loeve theory, area recording and transmission procedure 08 p1187 A66-19536

Advanced Data Management computer programming to provide generalized routines for functions common to large class of command and management problems 10 p1623 A66-22050

Launch vehicle, spacecraft, command and data station and data utilization for meteorological satellite systems, satellite stabilization and orbit types 11 p1777 A66-22306

Digital data handling method for air traffic control system employing plan position indicators and video correlator for radar video signal analysis 11 p1732 A66-22899

Semi-automatic data system for Model C stellerator, noting oscilloscope/camera modifications 16 p2706 A66-30829

Palletized cargo systems, transit time reduction and ground support system data handling and documentation 17 p2846 A66-32844

Binary synchronous communication in additive non-Gaussian noise, discussing optimal nonlinear detector for digital data



transmission through non-Gaussian channels 18 p3067 A66-33901  
 Satellite instrumentation, discussing data handling systems, cosmic ray detection, signal and information processing, etc 20 p3556 A66-36963  
 Visual displays to aid pilot to fly, monitor and control power plant, navigational and other equipment and communicate with ATC ground stations 20 p3508 A66-36996  
 Automation of air traffic control, discussing radar, data handling and data communication 20 p3595 A66-37003  
 Data management system synthesis for acquisition, processing and transmission of data aboard manned spacecraft 20 p3514 A66-37209  
 Apollo Spacecraft Test Data Evaluation System, noting functions, operation and performance 20 p3662 A66-37247

## DATA LINK

Feedback control system in design of delta-modulation data transmission system 05 p0654 A66-14610  
 Laser communications link security against interception, examining frequency bandwidth for minimum SNR 06 p0891 A66-16650  
 Link design and transmission rates for entry and surface measurements during space exploration to Mars 13 p2021 A66-25249  
 Direct and relay link communication from Martian surface station 13 p2021 A66-25250  
 Cost and performance comparison of satellites, relay links, waveguides and lasers, showing line-of-sight microwave relay is best wideband data transmission medium 14 p2238 A66-27667  
 Computer optimization of baseband design of angle-modulated unified carrier space-ground communication link 19 p3299 A66-35664  
 Automated improvement of design /AID/ computer using nonlinear programming techniques to solve optimization problems 19 p3308 A66-35872  
 Extravehicular activities interface with data recording system and economical recovery of optimum quantity of data 19 p3291 A66-35967  
 Early Bird satellite project using proven designs in spacecraft, launch vehicle and Earth stations to provide reliable microwave link between North America and Europe for TV and telephone 22 p3865 A66-40068

## DATA PROCESSING

SA AUTOMATIC DATA PROCESSING SYSTEM  
 SA COMPUTER PROGRAM  
 SA INFORMATION  
 SA INFORMATION PROCESSING  
 SA SCIENTIFIC DATA CONDITIONING SYSTEM  
 SA VOICE DATA PROCESSING SYSTEM  
 Pulse code modulation /PCM/ for telemetry and communication between Gemini spacecraft Agena D satellite and ground stations for data processing and display 01 p0031 A66-10938  
 Data automation system /DAS/ on Mariner IV Mars probe involving real and nonreal time for experiments during cruise and encounter flights 01 p0034 A66-11119  
 Processing technique for scientific data telemetered to Earth from Mariner IV Mars probe 01 p0034 A66-11121  
 Spectral measurement of solar simulator sources using polarization interferometer spectrometer 02 p0226 A66-11219  
 Analog-to-digital conversion system for automatic meteorological data collection and transmitting system 02 p0251 A66-11259  
 Linear filtering concepts in imaging and optical data processing systems, including three-dimensional photography obtained by wave front reconstruction 02 p0240 A66-11453  
 Development in U.S. of laser application with table including government supported programs in photography, data processing, radar, etc 02 p0240 A66-11455  
 System of data processing in real time applicable to digital computer Univac 418 02 p0193 A66-11600  
 Autonomous spacecraft navigation system with data processed by optimal filtering from star/local vertical observation 02 p0255 A66-11630  
 Navigation system for supersonic transport

considering central digital computer with data processing systems with feedback 02 p0256 A66-11898  
 Numerical objective analysis for stratospheric constant pressure data at various levels 02 p0254 A66-11983  
 Computer processing of data obtained from panoramic vertical sounding of ionosphere to separate reliable portions of height-frequency characteristic from total 02 p0224 A66-12122  
 Optical data processing techniques considering storage, manipulation, holography and pattern recognition using matched filters 03 p0378 A66-12997  
 Practical data processing of stress rupture results for steels with elevated operating temperatures, tentative procedure proposed and applied 03 p0384 A66-13161  
 FM telemetry digitizing system operating on-line in real time environment results in automatic data processing 04 p0489 A66-13600  
 Content addressable memory systems promise increased computational capability for Army data processing 04 p0490 A66-13686  
 Control system 465L used by Strategic Air Command noting automated functions, data processing, integration of human and electronic elements, etc 04 p0507 A66-13687  
 Optimum satellite search equipment and procedure consisting of preliminary search and data processing 04 p0482 A66-13970  
 Data processing procedures of Apollo onboard navigation system for determination of position and velocity 05 p0712 A66-14640  
 Resampled data systems and error between output of second sampler and input signal to first sampler [ISA PREPRINT 1.12-3-65] 05 p0635 A66-15504  
 Processing satellite data at Goddard Center noting Tiros IR data, cloud pictures and Imp measurements 06 p0837 A66-15933  
 Spacecraft crew monitoring system for evaluating performance capabilities and physiological state 06 p0818 A66-16241  
 Functional requirements for computer navigational system for Concorde aircraft 07 p1065 A66-17672  
 Approximation for function calculated in N points randomly selected in region D 07 p1061 A66-18509  
 Fluid logic elements and amplifiers for data processing, signal amplification and guidance and control 08 p1199 A66-18698  
 Processing signal information from digital rate gyros and accelerometers in analytic, gimballess inertial platform 08 p1253 A66-19530  
 Multistage extremum searching process leading to development of dynamic programming system, discussing application 09 p1362 A66-20628  
 ESRO/ELDO Space Documentation Service, describing system characteristics, NASA agreement, indexing and search strategy 09 p1473 A66-20658  
 Thermospheric wind velocities computed from satellite orbital data 09 p1376 A66-20992  
 Radio telescope techniques applied to astronomy, noting data processing and antenna receiving systems including masers, parametric amplifiers, etc 10 p1602 A66-21064  
 Parallelism incorporated in large computers for increasing computational power, including internally overlapped and uniform and multiple instruction 10 p1506 A66-21212  
 Telemetering and data processing systems and sensor equipment of Mariner IV including TV camera, magnetometer, ion chamber, plasma probe, etc 11 p1778 A66-23115  
 Digitized spark chamber for balloon and satellite gamma ray astronomy, noting detector array, high voltage system and data acquisition and handling systems 12 p1877 A66-23687  
 Automatic handling of information by analog recording on magnetic tape for control, monitoring and maintenance of aircraft 12 p1880 A66-23817  
 Hybrid computer methodology and electronic data processing applied to quality evaluation of test operations 12 p1828 A66-23837  
 Data processing centers integration through ground and satellite

telecommunications networks for global information network [AIAA PAPER 66-331] 12 p1824 A66-24798  
 Deep space network /DSN/ for navigational and communications support to NASA lunar and planetary space programs 13 p2021 A66-25248  
 Ground system design, data processing, digital command and digital-human interface in flight operations problems for unmanned spacecraft on planetary exploration mission 13 p2190 A66-25257  
 Lower bounds on computation times of certain input-output transformations and tradeoff relation between computation time and dimensionality of Turing machine tapes 13 p2027 A66-25802  
 Data processing approach for management control of aircraft manufacture [SAE PAPER 660205] 13 p2211 A66-26391  
 Operations of CNES station network including work program, controlling development and data collection and verification received from satellites 14 p2270 A66-27551  
 Moire data recording and processing techniques in thermal strain fields at high temperatures, comparing experimental data with elasticity theory 14 p2400 A66-27768  
 Computer processing of data obtained from panoramic vertical sounding of ionosphere to separate reliable portions of height-frequency characteristic from total 14 p2287 A66-28081  
 Optimal scientific satellite PFM encoding system circuit design and digital data processing 14 p2244 A66-28429  
 Automatic air traffic control development in France 15 p2534 A66-29126  
 Experimental data concerning electron, photon and muon components of extensive air showers, noting scintillation counters, Geiger-Muller counters, muon detectors, etc 15 p2579 A66-29522  
 Soviet book on physiological methods in astronautics including collection, transmission and procession of medical information from long space flights 15 p2445 A66-29734  
 Updating of air cargo documentation permitting intransit control and orderly accumulation of statistical information, noting forms and teletype machines 15 p2621 A66-29800  
 Effect of modifying digital filter weights derived on least squares error basis through multiplication by certain weighting functions 16 p2659 A66-30535  
 Apollo/Saturn S-II telemetry data processing systems 16 p2652 A66-30567  
 Launching range facilities of Diamant rocket including equipment, radars, interferometers, telemetry, data processing, etc 16 p2682 A66-31233  
 Additive noise effect on SNR of decoded data, noting quantization and error role on noise composition 17 p2873 A66-31966  
 Data processing techniques for analyzing turbulence records and for estimating response of aircraft to atmospheric turbulence 17 p2843 A66-32329  
 Meteor velocity determination via diffraction method, noting instrumental errors, recording and data processing techniques, etc 17 p3000 A66-32340  
 Optimal control theory in design of aerodynamic shapes, flight paths, guidance and control logic, data processing logic, etc 17 p2950 A66-32682  
 Computer controlled digital display techniques for direct editing of research data 17 p2877 A66-32943  
 Manual methods of entering navigational data on cards for input into computer 17 p2956 A66-33447  
 Automation in flight safety, noting role of radar, flight control system reliability, data processing system used, etc 17 p2848 A66-33485  
 Improved processing of moire data by use of numerical and optical filters to eliminate noise in moire patterns 18 p3134 A66-33716  
 Capabilities of Lunar Television Image Converter system used for digital processing of Ranger and Mariner pictures 18 p3113 A66-34496  
 Flight data recording and processing system using magnetic tape for digitally



computing airborne data on flight testing of VTOL aircraft 18 p3073 A66-34679

Electronic data on electromagnetic core structure of extensive air showers 18 p3211 A66-35130

Independent research management 19 p3480 A66-35534

Data processing of PFM telemetry whereby resolution of frequency measurements is dependent upon SNR, for application to satellite parameters 19 p3301 A66-35696

Implementation and individual units design for DATA-CORE telemetry processing system utilized in data acquisition and processing from Saturn/Apollo 19 p3307 A66-35708

Microminiaturization in automatic control equipment and digital computers - Symposium, International Federation of Automatic Control and International Federation for Information Processing, Munich, October 1965 19 p3322 A66-36806

Core-memory-programmed telemetry system for aerospace vehicle with application capability for deep-space probes, orbiting spacecraft or avionics data systems 20 p3513 A66-37199

Processing of satellite observations obtained within INTEROBS program dealing with atmospheric density determination and calculation of satellite orbital elements 20 p3518 A66-37847

Systems tests coverage for data processing system 20 p3523 A66-37950

Semiautomatic mechanical system for evaluation of rocket booster test stand oscillograms 20 p3561 A66-38065

Horizon sensor data processing with compensation for statistical properties of errors, noting application of optimal filtering theory 21 p3766 A66-38882

Integrated navigation system /INS/ using stellar inertial subsystem with optimum data processing 21 p3767 A66-38891

Space modulation systems characteristics, considering data flow rate, spacecraft weight and power, antenna gain, noise figure, etc 21 p3706 A66-39477

Digital computer processing of Tiros, Nimbus and Essa vidicon cloud pictures for machine nephanalyses, discussing rectification orbital mosaics and calibration effects for future Essa flights 22 p3943 A66-40055

Automatic processing of VLF data from FR-1 satellite 22 p3870 A66-40164

Algorithm construction for processing of telemetry data in determination of space vehicle trajectories, applying dynamic filtering method 22 p3980 A66-40463

Data processing of signal reception from Soviet satellites indicates radio signals scintillation caused by diffraction of waves from ionospheric nonuniformities 22 p3866 A66-40467

Japanese air traffic control using real time computer data processing 22 p3945 A66-40617

Advanced spaceborne computer concepts - WESCON, Los Angeles, August 1966 22 p3870 A66-40725

On board computer simultaneously processing spaceborne data including life support, energy management, human performance control, etc 22 p3871 A66-40726

Associative memory organizational approaches for onboard data processing of spacecraft 22 p3871 A66-40727

Pattern recognition computer operating under automatic control and stored program control for data transfers, system operation, man-machine interface and display operations 23 p4041 A66-41056

Digital TV spectrometer for measuring optical radiation from reentry vehicles, using IR vidicon and magnetic recording for data processing 23 p4069 A66-41665

Diurnal variation of ionospheric irregularities, using differential Doppler method for analysis of data transmitted by Beacon satellite 24 p4200 A66-42596

Ground radar systems for missile defense providing faster data processing, sensor location optimization, computer control, etc 24 p4175 A66-42953

Literature survey of content-addressable and associative memory systems, noting hardware, logical operations, speed, cost, etc 24 p4177 A66-43184

## DATA PROCESSOR

Low cost airborne fixed-point data processor designed to operate with nondestructive readout instructions, constant memory and separate destructive-readout memory 08 p1184 A66-19522

Universal programming languages and processors, survey and new concepts 12 p1826 A66-23825

Associative parallel processor using word and bit logic and sequential-state-transformation mode, with application to picture processing and pattern recognition 12 p1827 A66-23830

Lockheed multiprocessor simulation system /LOMUSS I/, data processing system for computer design and analysis 12 p1827 A66-23832

Real time ground computer for Athena system and input/output data requirements in multiprocessing jobs 12 p1827 A66-23836

System approach and requirements of particular switching system of Automated Patching System /Aps/ for use on Atlantic Missile Range /AMR/ 12 p1818 A66-24596

Microminiaturized R-11 digital computer for real time computational requirements in radar data processing, fire and command control, automatic navigation, checkout, etc 21 p3707 A66-38675

Packaging monolithic integrated circuits in UNIVAC 1824 Aerospace Computer Central Processor 22 p3878 A66-40714

## DATA READOUT SYSTEM

Solid state camera system consisting of monolithic phototransistor mosaic sensor and molecular digital readout system 06 p0878 A66-15975

Graphical method by which small local users of meteorological satellite pictures can identify geographical position of features in image [AIAA PAPER 66-439] 16 p2708 A66-31467

Logic and operation principle of model of recording device for high speed readout of digital and alphabetic information from digital computer 17 p2928 A66-33494

Transfluxor program store for airborne digital computer, noting wiring pattern, economics, read amplifier, etc 18 p3072 A66-33562

Visual write-erase-nonstore and electrical readout accurate tracking display storage tube operating on principle of secondary electron emission charging of thin film dielectric 22 p3927 A66-40287

## DATA RECORDER

### SA WEATHER DATA RECORDER

Portable shock and environmental recording system 16 p2703 A66-30482

Photographic data recorder noting simultaneous event and data recording capability 22 p3917 A66-39994

Critical Data Recorder /CDR/, small autonomous instrumentation package to be carried aboard space vehicle and furnish data on series of maneuvers 24 p4212 A66-42684

## DATA RECORDING

Silicon avalanche light sources for photographic data recording 05 p0677 A66-14831

Automatic potentiometer for recording data of cosmic ray intensity obtained by neutron monitor 06 p0881 A66-16603

High data rate radar cross section measurement system for high angular precision and direct digital recording on magnetic tape 10 p1501 A66-21621

Optical techniques for satellite tracking and star identification, describing ASTRO II theodolite with photoelectric data recording 12 p1883 A66-24933

Data interpretation from ballistic and space missiles using telemetry, analog signal variation, voltage conversion systems, etc 13 p2022 A66-25494

Coherent light recording/reproducing techniques based on Debye theory of coherent light source focusing 13 p2091 A66-25541

Plasma diagnostics in terms of response times, noting conversion of phase frequency deviations of probing signal, data recording for plasma in motion and expression for waveguide frequency 14 p2298 A66-28472

Collection of information and

announcements pertaining to rocket and satellite launchings including objectives, stations, data exchange, etc 15 p2600 A66-29902

Data recording and information transfer for defects in aircraft 16 p2715 A66-31200

Data recording and telemetry system for sounding rocket, noting operation and testing results 19 p3307 A66-35680

Extravehicular activities interface with data recording system and economical recovery of optimum quantity of data 19 p3291 A66-35967

FM data systems noting design, error analysis, applications to data recording and transmission, etc 21 p3708 A66-39478

High impedance electrode technique for large-scale flight physiological data collection, emphasizing skin preparation 22 p3856 A66-39790

Automatic, multichannel system for data recording and processing obtained in studies of ionospheric structural inhomogeneities, containing magnetic-tape memory and device for digital tape memory and device for digital computer input 22 p3920 A66-40772

Medico-biological methods based on data recording on board rockets and spacecraft and telemetering information to Earth 24 p4169 A66-43141

## DATA REDUCTION

Calibration procedures and statistical analysis for error reduction in ballistic camera lead-screw type comparator 02 p0228 A66-11380

Functional characteristics of Navy Doppler tracking system and satellites used for geodesy, noting data reduction procedures and system tests 04 p0514 A66-13610

Concise numerical technique for reduction of data from thin platinum film heat transfer resistance thermometer 12 p1876 A66-23608

Servo tester with automatic data acquisition and reduction /STADAR/, discussing design and operational capability in Apollo program 13 p2027 A66-25661

Modeling and data reduction techniques for obtaining spectrum signatures of low gain LF airborne antennas 13 p2044 A66-26747

Improved gray scale and coarse-fine PCM systems for digital television bandwidth reduction, considering spacecraft application 14 p2235 A66-27036

Optimization of data acquisition and reduction systems generated by random vibration, considering dynamic ranges 16 p2655 A66-30447

Economical method of reduction of environmentally obtained shock data 16 p2703 A66-30483

Digital data compression techniques applicable in spacecraft television systems, emphasizing bandwidth reduction techniques 16 p2653 A66-30891

Downrange radar and optical data reduction used for evaluation of ejection velocities of ballistic missile penetration aids at deployment [AIAA PAPER 66-405] 16 p2804 A66-31464

Automatic reduction of recorded flight data from balloons equipped with radiation detectors and SPARMO telemetry 17 p2926 A66-33148

Large aperture millimeter wave antenna for high resolution tracking measurements and real-time data reduction 18 p3084 A66-34303

Effect of 49-, 64- and 100-term expansion of geomagnetic field on reduction of omnidirectional proton counting rate data 18 p3108 A66-34532

LEM Data Reduction System that performs concurrent data processing and telemetry conversion on computer time-shared arrangement 19 p3299 A66-35662

Data reduction techniques for vacuum measurements by mass spectrometry, emphasizing matrix algebra techniques 22 p3918 A66-40234

## DATA RETRIEVAL

### SA INFORMATION RETRIEVAL

Environmental testing, spacecraft configuration, data retrieval and flight simulation in OAO 08 p1203 A66-19517

## DATA SMOOTHING

Maximally reliable exponential prediction



equations for data rate limited tracking servomechanisms 08 p1183 A66-18931  
 Computational data smoothing by minimum mean square error  
 estimation 10 p1550 A66-21839  
 Smoothing recorded tracings of cosmic ray detector 11 p1704 A66-22403  
 Buffer storage in digital radar smoothing irregular output data flow, noting decreasing bandwidth requirements 11 p1654 A66-22656  
 Deterministic type waveform analysis techniques for noisy repetitive transient functions, noting application to hybrid computer processing of exercise ECGs 12 p1810 A66-24233  
 Optimal filter in solution of linear mean square estimation problem when process statistics are undefined 12 p1848 A66-24249  
 Mathematical model for geomagnetic field for 1965 given by internal and external spherical harmonic coefficients 16 p2695 A66-30718  
 Construction method for rms-optimal digital smoothing devices, noting case of astatic systems 16 p2670 A66-30768  
 Best straight line calculated by least squares method 16 p2736 A66-31007  
 Convolution product theory applied to smoothing neutron monitor data of daily variations in cosmic ray intensity 18 p3186 A66-34808  
 Stress-strain distribution of sharp corners effect on surface of elastic body, examining mathematical difficulties in application of Lamé equation and boundary data smoothing 23 p4135 A66-40991

## DATA STORAGE

## SA MAGNETIC TAPE

## SA MEMORY STORAGE UNIT

Two sufficient conditions for monotonic variation of signal to noise ratio of optimal filter during storage of video pulse 04 p0484 A66-14058  
 Static and dynamic characteristics of four-layer semiconductor switches as components of binary storage circuits 09 p1356 A66-20627  
 Probability distribution data analysis in real time, using delay-line time-compression storage as information source in analog and digital form 12 p1825 A66-23760  
 Two sufficient conditions for monotonic variation of signal to noise ratio of optimal filter during storage of video pulse 17 p2873 A66-32224

## DATA TRANSMISSION

## SA COMPUTER

## SA PULSE TRANSMISSION SYSTEM

## SA REDUNDANCY ENCODING

Insertion of 2 bits of specific code into frame of digital data of burst-error-correcting code for synchronism recovery 02 p0190 A66-11524  
 Maximizing flow from source to sink in lossy communication net in which flow through edge is attenuated 02 p0208 A66-11905  
 Book on channel construction for data transmission using phase-shift keying, considering relative phase telegraphy and noting subassemblies, noise effect, etc 03 p0336 A66-13285  
 Binary pulse sequence conversion to pseudoternary codes for data transmission 04 p0474 A66-13423  
 Real-time telemetry data system for linking remote tracking stations with central station near Cape Kennedy 04 p0479 A66-13615  
 Redundant data omission for reducing transmission bandwidth, associated noise vulnerability and optimum prefiltering 04 p0490 A66-13623  
 Synthesis of optimum discrete system for continuous information transmission, using statistical theory of estimates 04 p0482 A66-13971  
 Principles of data communication reviewing digital systems, modulation methods and spectral shaping of data signals to achieve maximum noise tolerance 05 p0633 A66-14991  
 Limitations of communication system transmitting data from analog source obtained, using theorem in Shannon paper on information theory 06 p0828 A66-16115  
 DECTRA long range navigational aid, DECTRA airborne receiver and Omnitrac computer 07 p1068 A66-17702  
 Time division method of multiple access to

military communications satellite by several ground stations 08 p1180 A66-18713  
 Optimization of transmitted signal and receiving filter for data transmission system with fixed channel and detection process 08 p1183 A66-18932  
 Noise rejection properties of nonmemory discrete-data transmission systems employing information feedback, decision feedback or combined 08 p1183 A66-19096  
 Optimum number of phase-quantization steps in phase-shift keying communications system for maximum data transmission rate, using binary integration method 08 p1183 A66-19097  
 Analog message transmission by optimum angle modulation system and rate distortion function deriving mean square error 09 p1360 A66-19923  
 Data pulsed transmission over electron-injection laser communication system, using continuous waves 09 p1385 A66-19934  
 Upper and lower estimates derived for Shannon reliability of information transfer in channel that is symmetrical with respect to input 09 p1397 A66-20648  
 Telemetric technique based on data modulation and coding for satellite data transfer, stressing noise suppression, operation flexibility, error correction, etc 11 p1651 A66-22366  
 Data transmission by continuously-radiating power source moving away from receiver and fluctuation noise of uniform frequency spectrum 11 p1654 A66-22633  
 Algorithm for data transmission system automatic adaptive equalization, employing change of settings during transmission in response to variation in transmission channel characteristics 11 p1656 A66-23088  
 Principle of distributed reception of information 12 p1847 A66-23737  
 Salient hardware, software, and operational features of machine for automatic graphics interface to computer /MAGIC/ operating display system 12 p1827 A66-23835  
 Brillouin principle, formulated positively to express information amount in terms of physical entropy, applied to information transmission by electromagnetic field using thermodynamics, noting quantum mechanical expressions 12 p1817 A66-24337  
 Wire and data communication - IEEE International Convention, New York, March 1966 12 p1818 A66-24594  
 Items affecting information transmitted from payload landed on remote planet to Earth via communications satellite including orbit, transmission policy and orbit injection error effect on communication capability [AIAA PAPER 66-314] 12 p1823 A66-24780  
 Social and legal questions posed by development of large-scale information grids [AIAA PAPER 66-318] 12 p1824 A66-24789  
 Asymmetric instability and charge motion in metal-silicon oxide-silicon structures 12 p1932 A66-24823  
 Optimum realizable transmitter waveforms for high-speed data transmission, noting application to low pass filter channel 13 p2019 A66-25146  
 Phase coherent digital M-ary transmission with binary waves through Gaussian channel 13 p2022 A66-25554  
 Shannon model for capacity of time-continuous and time-discrete Gaussian channel with inputs perturbed by independent noise random variable 13 p2024 A66-25938  
 Residual error probability for cyclic binary code data transmission on symmetrically random noise channels 14 p2245 A66-26795  
 Book on modulation as applied to information transmission, discussing mathematical background, linear modulation systems, FM, PM, etc 14 p2239 A66-27718  
 Error detection techniques for maximizing average rate of information transmitted through burst error channel 14 p2243 A66-28346  
 Real-time telemetry data system for linking remote tracking stations with central station near Cape Kennedy 14 p2243 A66-28348  
 Time correlated burst retransmission PACM telemetry system, memory requirements, data time delay and

bandwidth utilization 14 p2244 A66-28431  
 efficiency  
 Noise stability for wideband analog methods of information transmission based on analysis of probability distribution density, using normal rms error and anomalous error 15 p2451 A66-29119  
 probability  
 Transmission and information processing rate of human visual system 15 p2435 A66-29450  
 Binary block codes simultaneously correcting additive and synchronization errors in data transmission systems 15 p2452 A66-29660  
 Properties of Mars atmosphere analyzed by ejected capsule from spacecraft, noting communications system 16 p2650 A66-30556  
 Functioning period of remote control systems in sporadic data transmission determined using mathematical methods of queueing theory 16 p2669 A66-30766  
 Analog communication over randomly time varying channels 16 p2654 A66-31331  
 Automatic control systems with carrier frequency information transmission channel, deriving transfer functions 16 p2672 A66-31552  
 Improvements to be realized through use of single channel black coded communication system 17 p2873 A66-31967  
 Closed circuit television applied to data transfer in air traffic control, discussing accident prevention and information provision to aircraft 17 p2874 A66-32356  
 Series power switch for orientation and position computer of small lunar-orbit spacecraft designed to reduce weight and cost 17 p2878 A66-33122  
 Analog form data transmission via FM compared to digital form via phase shift keying, noting accuracy, power and bandwidth required, output signal to noise ratios, etc 18 p3067 A66-33902  
 Antisolar astronomical probe data transmission system requiring large high-gain antenna for transmission at 40 AU 19 p3300 A66-35669  
 Design of Apollo project lunar-based telemetry system for transmitting experiment data to Earth for one year 19 p3300 A66-35671  
 Instrumentation of bending moments on large space boosters, discussing ground wind restrictions, telemetry system used, data transmission link, etc 19 p3356 A66-35678  
 Integration of spacecraft tracking, telemetry and command systems using frequency multiplex subcarriers and angle modulated RF signal 19 p3300 A66-35681  
 On-line computer-based aids for investigating effect of sensor data preprocessing and information compression procedures on data transmission bandwidth and reliability 19 p3307 A66-35686  
 Phase comparison telemetry consisting of passive VHF receivers and CW transmitters for satellite detection 19 p3301 A66-35692  
 Adaptive on-off communication system for binary data transmission over noisy channel of unknown attenuation 19 p3302 A66-35709  
 Relationships among space activity, space law and intellectual property, i.e., copyright and patent law 19 p3484 A66-36223  
 Periodic burst technique for real-time retransmission of data from multiple asynchronous PCM telemetry links, providing accurate determination of individual sample time 20 p3513 A66-37200  
 Reliability design requirements for Data Transmission System for Jupiter Precursor Spacecraft 20 p3513 A66-37208  
 IBM 7094 programmed in FORTRAN IV used to determine sidebands in FM with complex periodic modulation functions 20 p3522 A66-37212  
 In-flight stress measurements on coaxial counterrotating helicopter blades, using semiconductor strain gauge with HF telemetric data transmitters 20 p3668 A66-37504  
 Noise effect on synthesis of discrete systems with and without feedback channel for transmitting continuous messages, using binary signal and criterion of minimum rms error 20 p3538 A66-37745  
 Communication design techniques for coding set of discrete memoryless channels



where transmitter and receiver have no knowledge of channels 21 p3705 A66-39144

Threshold signals and optimal modulation parameters of analog methods of transmitting information under conditions of ideal reception 21 p3705 A66-39253

FM data systems noting design, error analysis, applications to data recording and transmission, etc 21 p3708 A66-39478

Single-sideband FM for data transmission on vibration and acoustic measurements, noting SNR performance, transmission link, etc 21 p3706 A66-39479

Unmanned space vehicle on board measurements and data transmission to ground station, examining temperature and propellant measuring 21 p3741 A66-39631

Space vehicle telemetric data transmission by FM, PCM, frequency multiplex, etc 21 p3717 A66-39633

Modulation and demodulation for probabilistic coding, noting error chances and interrelations affecting performance of communications system 21 p3707 A66-39636

Plurality-count diversity combiner for fading M-ary transmission, noting nonbinary alphabets with plurality count combining for transmission of binary data 22 p3865 A66-40069

Principle of distributed reception of information 22 p3865 A66-40080

Electronic navigation system for marine applications, using communications satellite as data relay link 22 p3945 A66-40324

Narrow laser beam pointing technique in deep space-to-earth data transmission for reduction in error sources 22 p3867 A66-40496

Information and failure warnings monitoring by flight crew during autopilot operation, particularly during very low visibility landing [ICAS PAPER 66-17] 22 p3945 A66-40671

Spacecraft and Earth-terminal antennas for interplanetary communication via high power information transmission 22 p3881 A66-40748

Midpath airplane interference to digital transmission in tropospheric radio, considering scattering of radiant energy by atmospheric layers 23 p4040 A66-41594

Lasers applied to logic, memory, input-output and data transmission-linkages parts of computers 24 p4225 A66-42804

**DATING**

**SA RADIOACTIVE DATING**

Stellar evolution and evolutionary sequences, use of high speed computer methods and application to age determination of stars 09 p1448 A66-20098

Neutron activation analysis of K-Ar age for Barwell, England olive-hypersthene chondrite of December, 1965 16 p2807 A66-31760

**DAZZLE PROJECT**

**S RADAR TRACKING**

**DC**

**S DIRECT CURRENT /DC/**

**DC-8 AIRCRAFT**

**S DOUGLAS DC-8 AIRCRAFT**

**DC-9 AIRCRAFT**

**S DOUGLAS DC-9 AIRCRAFT**

**DCS**

**S DEFENSE COMMUNICATIONS SYSTEM /DCS/**

**DE HAVILLAND DH-121 AIRCRAFT**

Cockpit display correction methods used in design of Trident aircraft 03 p0328 A66-12882

Design trends in landing gear for medium- and short-range jet transports 07 p0987 A66-17286

Design criteria and operational performance of Doppler-driven map display device installed on Trident aircraft 07 p1077 A66-17802

Automatic landing development in autopilot and autoflares for Trident aircraft 10 p1553 A66-21362

Automatic landing system on trident aircraft 18 p3131 A66-33560

**DE HAVILLAND DH-125 AIRCRAFT**

HS 125 twin-jet 500-mph executive aircraft, construction, pressurization, maintenance, etc 13 p1995 A66-26282

Design, development and structural testing of DH 125 executive jet aircraft

[SAE PAPER 660216] 13 p1996 A66-26393

**DE HAVILLAND DHC-5 AIRCRAFT**

Hydraulic system of De Havilland Buffalo tactical aircraft is self-sufficient 10 p1486 A66-22033

**DE LAVAL NOZZLE**

Steady state irrotational flow of perfect gas in plane and axisymmetric Laval nozzles 01 p0008 A66-11015

Design considerations, materials and problems of De Laval nozzle as applied to liquid and solid propellant rocket engines 07 p1040 A66-18306

Inviscid flow of compressible conducting gas with aligned magnetic field through axially symmetric Laval nozzle in various transition regions 11 p1636 A66-23256

Discharge rate of multicomponent gas mixtures through de Laval nozzle from chamber containing adsorbent bed 12 p1979 A66-24587

Gas rate control of given Laval nozzle when asymptotic gas flow of unvariable type is maintained continuously near nozzle center 14 p2221 A66-28281

Expansion of supersonic flow of air with suspended solid particles during passage through Laval nozzle 14 p2279 A66-28325

Spray ejector operating in pulse rather than steady state regime, noting capability and formation of de Laval nozzle 19 p3450 A66-36603

**DEAD RECKONING**

Accuracy of navigation techniques for North Atlantic flights evaluated, based on Loran A and Doppler/GM compass automatic dead reckoning system 07 p1072 A66-17760

**DEAFNESS**

**SA HEARING LOSS**

Noise and vibration causing acoustic fatigue leading to deafness of aircrew 06 p0811 A66-16065

**DEBRIS**

**S RADIOACTIVE DEBRIS**

**S SPACE DEBRIS**

**DEBYE FUNCTION**

Diagrammatic method to obtain Helmholtz free energy of classical electron gas used to derive pair distribution function beyond Debye-Huckel result 02 p0266 A66-11478

Wing broadening in plasma of hydrogen Lyman-alpha line by local electron and quasi-static ion fields calculated, considering impact theory of electron collisions, quadrupole and dipole interactions and existent asymmetries 03 p0405 A66-13138

Complex Wentzel-Kramer-Brillouin phase integral method and low density universal instability caused by finite Debye length 07 p1088 A66-17957

Cyclotron radius, magnetospheric boundary and Debye length scaling parameters for magnetospheric cavity arising from solar wind-induced geomagnetic storm and visibility of quasi-Van Allen belts 14 p2269 A66-27124

Cross sections for sticking electrons to spherical charged particles, considering Debye screening distance of Coulomb force field 16 p2754 A66-31158

Atomic energy levels in plasma, considering energy spectrum of hydrogen-like atom in plasma, based on cut-off Coulomb potential model 20 p3607 A66-37373

**DEBYE TEMPERATURE**

Correlation expressing reduced coefficient of thermal expansion as function of reduced Debye temperature for metallic solids used for predicting coefficient at any temperature 14 p2411 A66-27375

Functional interdependence of four distinctly different parameters represented by gamma in study of thermodynamical relations for shock waves 24 p4193 A66-42270

**DECABORANE**

Friedel-Crafts methylation of decaborane, determining reactant parameters and relationship of decaborane conversion and alkylate composition 05 p0629 A66-14541

Chemistry of decaborane and structure and reactivity of stable derivatives 11 p1649 A66-22947

**DECAY**

**S DEGRADATION**

**S NEUTRON DECAY**

**S ORBIT DECAY**

**S PARTICLE DECAY**

**S PLASMA DECAY**

**S RADIOACTIVE DECAY**

**DECAY RATE**

Mean lives of 3s, 3d, 4s, 4p and 4d states in hydrogen and relative initial radiation intensities 07 p1083 A66-18420

Nonequilibrium chemical reaction effect on decay in spontaneous explosion for reactive expelled gas and inert expelling gas 08 p1179 A66-19482

Directional intensity and decay time of scintillations from anthracene and p-terphenyl single crystals under alpha particle bombardment 11 p1750 A66-22465

Bounds for decay times of pendulum damper vibrating in plane containing spin axis of space vehicle [AIAA PAPER 64-658] 12 p1954 A66-24693

Electron density and temperature in decaying hydrogen plasma determined, using monochromator 13 p2145 A66-25730

Rate of dissociative electron capture by heavy molecular ions developed in semiclassical formalism 13 p2136 A66-26271

Helium-neon laser afterglow and metastable helium atoms under long pulse excitation 14 p2307 A66-27335

Spatial distribution and time decay of intensities of geomagnetically trapped electrons from high altitude nuclear burst 20 p3643 A66-38339

Spatial distribution of trapped particles measured by Explorer XV satellite, noting decay time constants and energies 20 p3643 A66-38340

Contraction to improve isotropy of grid-generated turbulence 22 p3899 A66-40381

Generation-recombination noise and lifetime measured using photoconductive decay in n-and p-type Ge samples doped with shallow impurities 24 p4253 A66-42357

**DECELERATION**

**SA ACCELERATION**

**SA IMPACT DECELERATION**

Aerodynamic spacecraft deceleration systems examined by hydraulic analogy, noting Mach number effects on flow disturbances 04 p0507 A66-13533

Ion recombination effects on inhomogeneous cylinder deceleration in rarefied plasma 04 p0551 A66-13858

Parachute operation at high Mach numbers and dynamic pressures for reentry vehicle deceleration [AIAA PAPER 66-24] 07 p0989 A66-17888

Cardiac arrhythmias occurring during positive and negative acceleration 09 p1335 A66-20532

Deceleration of body in rarefied plasma owing to interaction with neutral and charged particles and electromagnetic fields 09 p1465 A66-21016

Computer system for control of deceleration of electrodynamic shaker during vibration test 16 p2678 A66-30465

Spacecraft longitudinal and lateral stability along reentry trajectory during deceleration period determined, using equations of motion 17 p2846 A66-32897

Plasma oscillation theory of nonlinear deceleration effect and thermal conversion of electron beams upon passage through plasma 17 p2974 A66-33284

Atmospheric reentry trajectory of space vehicle at orbital velocities and constant lift-drag ratio 18 p3244 A66-33879

Aerodynamic deceleration systems - AIAA Conference, Houston, September 1966 22 p3848 A66-40589

Limiting initial deceleration forces generated by supersonic decelerators, noting that decelerators deployed in wake region of body result in divergent wake and drag force reduction 22 p3845 A66-40595

Aerodynamic deceleration from high Mach number for ALARR project, noting rocket stage collision and deceleration systems 22 p3987 A66-40609

**DECELERATOR**

**SA ACCELERATOR**

**SA PARACHUTE**

First-stage decelerator and stabilization balloon system for payload recovery for Mach 4 and 10 flight 04 p0585 A66-13531

Interaction between hypersonic wake flow and aerodynamic deployable decelerator, predicting pressure and heat transfer of decelerator 22 p3846 A66-40605

Super- and hypersonic first-stage



- decelerators for stabilization and initial deceleration for final recovery device, noting Ballute and reefed ribbon canopy types, testing, fabrication, etc 22 p3850 A66-40606
- Dynamic characteristics of rotary wing decelerator and recovery system obtained, using frequency oscillation technique [AIAA PAPER 66-733] 22 p3893 A66-40624
- DECIMAL-TO-BINARY CONVERSION**
- S BINARY-TO-DECIMAL CONVERSION**
- DECISION ELEMENT**
- Adaptive method for synthesis of circuit of majority decision elements which realizes given logical function 14 p2268 A66-28043
- DECISION MAKING**
- Systems effectiveness through design function management, noting necessity of decision guide activities 11 p1789 A66-23441
- Asymmetric instability and charge motion in metal-silicon oxide-silicon structures 12 p1932 A66-24823
- General family of two-stage chain sampling inspection plans 15 p2506 A66-28789
- Optimum algorithm derived for making binary decisions in decision systems of hierarchic structure 15 p2469 A66-29054
- Air traffic controller performance in detecting possible conflicts among aircraft 15 p2534 A66-29125
- Images of automatic recognition system for two-dimensional patterns move in rapid nonstop manner across stationary scanning unit composed of bank of photodiodes 21 p3705 A66-39145
- Digital computer programming to evaluate designs until optimality is found in aerospace structures 22 p3922 A66-40023
- DECISION THEORY**
- SA STATISTICAL DECISION THEORY**
- Evaluation of alternatives which involve risk-taking decisions under numerous uncertainties for planning and system selection 01 p0167 A66-10050
- Operational readiness, decision-making technique for management taking into account reliability, maintainability and safety 01 p0167 A66-10051
- Search theory extremal problems, considering theorems in terms of maximum principle for finding optimal strategy 01 p0051 A66-10734
- Zero-crossing data and decision-making procedures used by computer in recognition of vowels 03 p0338 A66-13020
- Classification of unknown observations into one of two categories when decision boundary is determined from independent samples in each category 06 p0833 A66-16660
- Optimal control by random sequences, dynamic programming and Wald sequential analysis 09 p1362 A66-20644
- Signal detectability in elicited observing rate and decision processes in vigilance 11 p1646 A66-23373
- Vigilance performance in observing light flashes analyzed for effect of noise and signal rate 11 p1646 A66-23375
- Decision theory and dynamic programming applied to problems concerning cost and weight minimization in structural engineering 13 p2207 A66-26699
- Search theory extremal problems, considering theorems in terms of maximum principle for finding optimal strategy 24 p4232 A66-42750
- DECODER**
- Pulse operated miniature RF switch for space use and design from command decoder 03 p0348 A66-13343
- DECODING**
- Parallel decoding for discrete channel with statistically independent noise 02 p0189 A66-11404
- Optimum message decoding in communication systems with pulse code modulation, using minimum square-error criterion 04 p0489 A66-14415
- Adaptive decoding technique for analyzing information-carrying signals in order to control signal to noise ratio during transmission time of single compound signal 20 p3522 A66-37384
- Generalized minimum distance decoding that permits likelihood information to be used, yielding same probability of error as maximum likelihood decoding 21 p3703 A66-39137
- Communication possibility over memoryless channel with computational iterative decoding scheme that is asymptotically complex 21 p3704 A66-39141
- DECOMMUTATOR**
- Computer design of programmable decommutator for multiformat PCM telemetry data 14 p2246 A66-28432
- DECOMPOSITION**
- SA ABLATION**
- SA DEGENERATION**
- SA DEGRADATION**
- SA DISSOCIATION**
- SA ELECTROLYSIS**
- SA HYDROLYSIS**
- SA PHOTODECOMPOSITION**
- SA PHOTOLYSIS**
- SA PROPELLANT DECOMPOSITION**
- SA THERMAL DECOMPOSITION**
- Decomposition of large-scale mathematical problems in nonlinear programming 13 p2117 A66-25350
- Chemical kinetics of borane and diborane compounds, decomposition rates and molecular dissociation energy 15 p2447 A66-29237
- Radiation induced chemical decomposition in inorganic solids such as alkali metals and metallic sulfates 23 p4111 A66-41212
- DECOMPRESSION**
- SA COMPRESSION**
- SA EXPLOSIVE DECOMPRESSION**
- Explosive decompression effects on respiratory system, considering pressurized suits operating at high altitudes 06 p0816 A66-16063
- Effect of sudden intense noise and near vacuum decompression on cardiac rate of anesthetized and unanesthetized dogs 19 p3286 A66-36380
- Rapid decompression and exposure of fresh foods to near vacuum conditions 22 p3856 A66-39789
- DECOMPRESSION SICKNESS**
- Decompression sickness noting caisson and subatmospheric disease effects, symptoms, causes and prevention 10 p1488 A66-22109
- Physiological factors in decompression sickness, noting recompression, plasma replacement, etc 16 p2638 A66-30624
- Simulated orbital flights with extravehicular activities, determining incidence and severity of flyers bends due to decompression and exercise 17 p2856 A66-32148
- Task interruption and performance decrement of active pilots and flight crew personnel following rapid decompression 18 p3061 A66-33782
- Rapid decompression effects on dogs and subhuman primates, studying physical and physiological responses after loss of consciousness and recompression effects 19 p3285 A66-35839
- Physical and chemical variables of space cabin environment and effect on human body, discussing oxygen toxicity, decompression sickness, fire and blast hazards and radio protection 19 p3292 A66-36232
- Residual pathologic changes in central nervous system of dog following rapid decompression to 1 mm Hg 19 p3286 A66-36381
- DECONTAMINATION**
- SA CONTAMINATION**
- Biological burden estimation of Mars probes and capsules and various fabrication and decontamination procedures 13 p2014 A66-25287
- Microbiological decontamination of lunar spacecraft during mechanical integration and assembly 22 p3857 A66-40044
- DEEP SPACE**
- Proposal of epiatmosphere as term for outer space, noting advantages and disadvantages of terms space, upper space, cosmic space, etc 19 p3484 A66-36225
- DEEP SPACE INSTRUMENTATION FACILITY /DSIF/**
- Mission profile, operations facilities and science subsystem of Mariner IV 01 p0144 A66-11110
- Deep space tracking stations, discussing digital computers for monitoring functions such as real time measure, station performance, failure detection, etc [ISA PREPRINT 1.11-1-65]
- 05 p0635 A66-15498
- Antisolar astronomical probe data transmission system requiring large high-gain antenna for transmission at 40 AU 19 p3300 A66-35689
- Mission-dependent Deep Space Instrumentation Facility equipment designed in support of Pioneer spacecraft program including command encoder, computer buffer and demodulator synchronizer 19 p3315 A66-35670
- Narrow laser beam pointing technique in deep space-to-earth data transmission for reduction in error 22 p3867 A66-40496
- Deep space payloads, booster probes, sensors and communication systems for missions from Jupiter to Pluto 24 p4281 A66-42678
- Data compression feasibility for data transmission from unmanned spacecraft in deep space 24 p4282 A66-42682
- DEFECT**
- S CRYSTAL STRUCTURE DEFECT**
- S FLAW**
- S INHOMOGENEITY**
- S POINT DEFECT**
- DEFENSE**
- SA AIR DEFENSE SYSTEM**
- SA MILITARY TECHNOLOGY**
- SA MISSILE DEFENSE**
- SA SPACE SURVEILLANCE SYSTEM**
- Flexibility in strategic retaliatory weapons offered by bombers and missiles, discussing defense capability offered by SAC 08 p1322 A66-18558
- Polaris nuclear powered submarine defense capability, noting mobility advantages and command communications system 08 p1322 A66-18559
- U.S. military and strategic posture in aerospace, discussing intelligence and defense systems, strike capabilities and support programs 09 p1472 A66-20170
- DEFENSE COMMUNICATIONS SYSTEM /DCS/**
- Military communications satellite system noting radio frequency, TWT amplifier, synchronous altitude, etc 05 p0633 A66-15170
- [AIAA PAPER 65-323]
- Defense Communication Satellite Program for reliable worldwide military communications 08 p1179 A66-18569
- Satellite providing optimum communications to military users, noting gyroscopic stabilization of antennas, major characteristics, etc 12 p1955 A66-24740
- [AIAA PAPER 66-267]
- Characteristics and performance of synchronous satellite military communication system 12 p1859 A66-24741
- [AIAA PAPER 66-268]
- Initial Defense Communications Satellite Project /IDCSP/, current status, objectives and subsystems 12 p1820 A66-24742
- [AIAA PAPER 66-269]
- Military communications satellite developments, describing worldwide network of ground stations and 15 to 22 satellites in near-synchronous equatorial orbit 14 p2243 A66-28362
- Unclassified information concerning military communication satellite system 16 p2655 A66-31650
- U.S. strategic missile and air defense, noting Nike-X system 24 p4297 A66-42950
- DEFENSE INDUSTRY**
- Development management and cost control in British defense 07 p1156 A66-17487
- Defense equipment reliability noting specifications, field data collection, control plan, etc 12 p1833 A66-24083
- Defense Materials System control of copper, aluminum and steel and proposed program for readiness and contingency planning of external resources for aerospace industry [SAE PAPER 660286] 14 p2416 A66-27297
- DEFLAGRATION**
- Detonations in gaseous mixtures and in condensed phase, examining effects of pressure, temperature and confinement on normal detonation 12 p1980 A66-24932
- Pressure deflagration limit of high energy solid propellants increased to super atmospheric pressures by composition changes



[AIAA PAPER 66-679] 18 p3163 A66-34226  
Laboratory burners used as experimental  
analogs of actual propellant deflagration  
process, examining dependence of composite  
solid propellant deflagration on mixture  
ratio

[WSCJ 66-25] 18 p3161 A66-34417  
Solid propellant ignition, discussing  
deflagration wave propagation along gas-  
solid grain surface, flux equilibrium  
equation, etc

[AIAA PAPER 66-668] 18 p3165 A66-34441  
Propellant deflagration control for  
interaction between fluid dynamic  
disturbance and propellant combustion  
reaction 22 p3969 A66-39874  
Deflagration of hydrazine perchlorate in  
pure state and with fuel and catalyst  
additives 23 p4117 A66-41225

**DEFLECTION**  
**SA FLOW DEFLECTION**  
Large deflection analysis of circular ring  
plates under uniform transverse force along  
inner edge 02 p0298 A66-11584  
Rationalized method for beam deflection  
under concentrated loading 02 p0299 A66-11796  
Large deflection analysis of elliptical plate  
of lenticular section subjected to uniform  
temperature gradient through thickness  
03 p0440 A66-13271  
Monograph on Levy method for deflection  
of loaded simply-supported infinite plate  
strip, introducing class of real functions  
04 p0589 A66-14011  
Permanent deformations in circular plates  
subjected to uniformly distributed impulses  
compared with predictions of bending  
theory of rigid-plastic plates 11 p1781 A66-22612  
Deflection of structural members in  
Haystack antenna calculated, using framed  
structure analysis /FRAN/ program,  
obtaining improved grid analogy 15 p2614 A66-29616  
Tensile and compressive creep behavior  
deduced from deflection measurements in  
creep bending tests on beams of trapezoidal  
cross section 15 p2614 A66-29666  
Deflection of uniformly loaded circular  
plate supported at discrete points equally  
spaced along circumference of concentric  
circle 16 p2820 A66-31274  
Starting friction and kinetic friction of  
PTFE fabric-lined spherical bearings and  
deflection and permanent set under static  
loading 17 p2929 A66-31932  
Von Karman plate equations specialized to  
describe large symmetric deflections of  
circular membranes 17 p3020 A66-31999  
Dynamic characteristics of built-up plates  
analyzed with modified Reissner principle,  
obtaining natural frequencies and mode  
shapes 17 p3022 A66-32011  
Large deflections of symmetrically loaded  
shallow membrane shells of revolution,  
considering existence of boundary layer  
near edges and using asymptotic  
analysis 17 p3025 A66-32480  
Transverse displacement of circular plate  
containing radial crack examined, using  
small deflection theory 18 p3249 A66-33597  
Light deflection technique for transient  
shock wave detection by phototube  
activation based on Snell law 19 p3357 A66-35811  
Shell stability in Euler formulation, taking  
into account actual redistribution of stresses  
that results from initial deflection and  
creep, noting buckling of closed cylindrical  
shell under axial compression 21 p3829 A66-38978  
Deflection surface of structural net of any  
arbitrary shape determined by considering  
net to be portion of larger net with zero  
deflections along boundaries 21 p3833 A66-39538  
Deflection analysis of temperature  
gradient-induced buckling, curling and  
bending in thin unsupported plate with  
variable thickness 23 p4146 A66-41996  
Successive approximation analysis of large  
deflections of elastoplastic shell under  
bending deformation and load carrying  
capacity 24 p4290 A66-42440  
Linear elastic small deflection theory of  
natural frequencies of vibration of  
rectangular sandwich honeycomb plate with

mass attachment 24 p4292 A66-43046

**DEFLECTOR**  
Optical beam deflection technique using  
interferometer cavity illuminated by gas  
laser beam 15 p2512 A66-28689

**DEFORMATION**  
**SA AXISYMMETRIC DEFORMATION**  
**SA CREEP**  
**SA DISTORTION**  
**SA ELASTIC DEFORMATION**  
**SA NUCLEAR DEFORMATION**  
**SA PLASTIC DEFORMATION**  
**SA STATIC DEFORMATION**  
**SA TENSILE DEFORMATION**  
Cylinders subjected to internal and  
external pressure and axial stress with  
equations for radial and tangential  
direction 02 p0299 A66-11706  
Deformation from stress in thin walled  
pressure vessels determined by differential  
equation from boundary layer problem  
09 p1467 A66-20488  
Stress deformations in thin walled pressure  
vessels and associated nonlinear second  
order differential equation 09 p1467 A66-20490  
Creep testing apparatus for metals, with  
automatic recording of longitudinal and  
transverse deformations at high  
temperatures 11 p1780 A66-22600  
Thermodynamics of deformation, discussing  
Coleman theorem 12 p1976 A66-23547  
Longitudinal impact between cylindrical  
rods, considering local deformations and  
wave propagation in rods, showing solution  
through dimensionless equation of Sears  
theory 12 p1968 A66-24242  
Deformation of cantilever parallelogram  
box beam 12 p1969 A66-24365  
Surface-deformation measurement using  
wave front reconstruction with  
interferometry of diffusely reflecting  
bodies 13 p2080 A66-25991  
Stress relaxation dependence on heat  
deformation regime in Ti alloys VT14, VT3-1  
and VTS-1 15 p2519 A66-28537  
Fatigue curve for one type of loading  
determined from stress variation during  
cyclic deformation and fatigue curve from  
other type of load application 18 p3254 A66-34231  
Convergence of axes of plane-parallel jets  
due to reciprocal ejection effect, analyzing  
deformation of jet, rarefaction coefficient  
for air between jets, etc 20 p3544 A66-36918  
Semiconductor transducer strain gauge for  
structural deformation measurement by  
conversion to resistance variation 20 p3559 A66-37500  
Deformation modes and wrinkling of flange  
on shear spinning to determine optimum  
working conditions or spinnability of sheet  
metal 20 p3575 A66-38104  
Linear theory of micropolar elasticity,  
noting all components of asymmetric stress  
tensor are determined and motion of media  
is fully described when deformation and  
microrotation vectors are known 22 p3995 A66-40566  
Susceptibility to cold deformation of  
semifinished B95-2 Al-Zn-Mg-Cu alloy  
products, noting machinability in  
manufacturing of parts 22 p3928 A66-40885  
Deformation theory of classical continuum  
in four-dimensional representation,  
particularly in time derivatives 23 p4144 A66-41972  
Large deformation analysis of equilibrium  
of spherical momentumless shells under  
hydrostatic pressure 24 p4290 A66-42444

**DEGASSING**  
Materials under high vacuum discussing  
degassing of metals, thin film deposition,  
food dehydration, vacuum melting and  
vacuum welding 04 p0534 A66-13373

**DEGENERATION**  
**SA DECOMPOSITION**  
Volt-ampere characteristics and minority  
carrier recombination region width in  
degenerated semiconductor p-n  
junction 02 p0277 A66-12085  
Current and voltage negative feedback  
effect on distortion in common emitter  
transistor stage 03 p0340 A66-12466  
Periodically operating gate circuit with  
negative feedback for sampling in micro- and  
millisecond range 12 p1847 A66-24938  
Extension of problem of singular

perturbation for linear scalar constant  
coefficient differential-difference equation  
with single retardation to several  
retardations, noting degenerate equation  
solution 16 p2737 A66-31230  
Ideal relativistic degenerate gas in white  
dwarf star interiors, discussing state  
equations, thermodynamic relations,  
electron-ion gas mixtures, etc 21 p3775 A66-38823

**DEGRADATION**  
**SA DECOMPOSITION**  
**SA THERMAL DEGRADATION**  
Focused laser coherent radiation-induced  
degradation of solid methylene and gas  
chromatographic analysis of reaction  
products 17 p2933 A66-31870  
Feasibility of doping techniques for  
eliminating extraterrestrial solar degradation  
of ZnO used as pigment for spacecraft  
thermal control surfaces 17 p2938 A66-31961  
Electric contact design factors for shock  
vibration environments 24 p4186 A66-43058

**DEGREE OF FREEDOM**  
**SA MULTIPLE-DEGREE-OF-FREEDOM  
SYSTEM**  
Parameter and matrix solution techniques  
for analyzing forced vibrations response of  
damped multidegree of freedom systems  
[AIAA PAPER 65-786] 03 p0438 A66-13070  
Nonlinear spring-mass system with many  
degrees of freedom subjected to periodic  
exciting forces, deducing steady state forced  
vibrations equal to forcing function  
[ASME PAPER 65-APMW-30] 04 p0593 A66-14230  
Response to multiple random excitation of  
system with multiple degrees of freedom,  
connecting spectral density matrix of  
generalized coordinates with corresponding  
generalized forces 12 p1972 A66-25004  
Control problems in operation of transport  
aircraft noting degrees of freedom,  
computer aid, human factor, etc 13 p2047 A66-25497  
Excitation of vibrational degrees of  
freedom in molecular collision from  
vibrational relaxation data and molecular  
beam elastic scattering experiments 16 p2755 A66-31588  
Adiabatic invariants and third integrals of  
motion in periodic potentials in periodically  
time-dependent Hamiltonian systems of n  
degrees of freedom 17 p2945 A66-32292  
Force resonance oscillations of one degree  
of freedom system with randomly time  
varying natural frequency 17 p2959 A66-32802  
Nonlinear spring-mass system with many  
degrees of freedom subjected to periodic  
exciting forces, deducing steady state forced  
vibrations equal to forcing function  
[ASME PAPER 66-APMW-30] 18 p3249 A66-33591  
Approximate method for determining  
damping factors of mechanical oscillatory  
systems with many degrees of freedom  
described by linear differential equations of  
n-th order with constant coefficients 21 p3770 A66-38971  
Amplitude friction effect in single degree  
of freedom vibrating system by developing  
amplitude into approximate trigonometric  
series 22 p3917 A66-39669  
Theorem concerning use of instantaneous  
axis of rotation for simplification of small  
oscillation equation of angular  
momentum 22 p3992 A66-40300  
Optimization of VTOL control concepts  
with and without stabilization compared  
with six degree of freedom motion  
simulator, noting system failure effects and  
nonlinear concepts 22 p3851 A66-40675  
Stability conditions for system with two  
degrees of freedom, considering effect of  
inertial and resistance forces on inertialess  
body 23 p4137 A66-41001  
Gust design procedures based on power  
spectral techniques, considering atmospheric  
turbulence with aircraft as rigid body with  
single degree of freedom [ICAS PAPER 66-11] 23 p4017 A66-42073

**DEHYDRATION**  
Heat stress and minimal dehydration effect  
upon human tolerance to positive  
acceleration 03 p0326 A66-12353  
Effects, singly and in combination, of heat,  
exercise and hypohydration upon voluntary



dehydration in four acclimated physically-fit young men 06 p0812 A66-16533  
Quantitative coulometric analyses of water yield for thermal dehydration of solids, using electrolytic hygrometer cell 07 p1036 A66-18490  
Effects of chronic hypohydration on responses to tests of bodily functions, defining set points and mechanisms involved in changes in work performance 09 p1337 A66-20528

## DEHYDROGENATION

## SA HYDROGENATION

Comparison methods for relationship among enzymes that are same but belong to different organisms 04 p0460 A66-13367  
Catalytic dehydrogenation of hydrocarbons over chromia-alumina catalyst in absence of added hydrogen to determine heat sink capability 11 p1650 A66-23119  
Methylcyclohexane dehydrogenation over platinum-alumina in absence of excess hydrogen, yielding toluene and hydrogen 11 p1650 A66-23122

## DEICING SYSTEM

Temperature distribution of propeller heated by electric antifixer, with solutions for heater and propeller surface 09 p1328 A66-20753  
Beagle B.206 S aircraft power plant, vacuum system, air conditioning system, fire protection, hydraulics, fuel, oxygen, rain protection and deicing equipment 22 p3970 A66-39688

## DEIONIZATION

## S IONIZATION

## DELAY

## S TIME DELAY

## DELAY LINE

Delay characteristics of round and square magnetized rods of yttrium-iron garnet /YIG/ crystals compared 01 p0120 A66-10522  
Design of wideband microwave delay line using piezoelectric semiconductor transducers with acoustic gain 01 p0038 A66-10523  
Effectiveness of oscillatory circuits and delay lines for self-synchronization of polyphase multivibrators 01 p0045 A66-10992  
Effect of delayed feedback in respiratory disease analyzed for behavioral cybernetic theory, using computer-controlled delay 02 p0186 A66-11648  
Radar-pulse correlation system for discriminating between close targets at long range 02 p0191 A66-11801  
Compression of linear FM S-band pulses in axially magnetized yttrium-iron-garnet delay line 02 p0192 A66-11883  
Ultrasonic delay lines operating below 100 megacycles, particularly dispersive lines suitable for radar pulse compression systems 03 p0331 A66-12411  
Microwave acoustic delay lines made practical by low-loss propagation of microwave phonons at room temperature in single crystals 03 p0331 A66-12412  
Spin wave generation in nonuniform magnetic fields with application to magnetic delay lines 03 p0332 A66-12417  
Continuously tunable microwave delay equalizer consisting of 3-db directional coupler and two equal resonators 03 p0344 A66-13023  
Serrodyne frequency conversion determined, using sawtoothed FM of microwave oscillator and subsequent conversion with delay line in sawtoothed phase modulation, calculating phase distortion 04 p0499 A66-14052  
Synthesis of circuits containing delay lines, considering storage elements for pulsed signals 04 p0499 A66-14053  
Sweep indicator as radar feedback filter, noting double delay 04 p0501 A66-14126  
Optical ultrasonic delay lines as correlators and variable code matched filters to achieve large time-bandwidth products and high data rates 05 p0631 A66-14821  
Yttrium iron garnet /YIG/ delay line application to radar range and amplitude calibrator, altitude simulator, microwave memory and electronically steerable antenna array 06 p0842 A66-15983  
Pure spin and spin-acoustic delay modes of single crystal YIG 06 p0847 A66-16104  
Automation of equalizer consisting of delay

line with adjustable taps 06 p0831 A66-16343  
Ultrasonic delay lines, operational principles, characteristics and basic structure of traveling wave devices for communication 06 p0831 A66-16365  
Helix frequency-scanning delay line design and characteristics 06 p0849 A66-16396  
GaAs diffusion-layer transducer for VHF acoustic delay line 06 p0852 A66-16639  
Properties of helical delay line used to feed frequency scanned X-band array, noting role of ball bearing inserted in helix 06 p0854 A66-16686  
Pulse code modulation coder, using delay line as coding network 08 p1186 A66-19744  
Phase correcting circuit construction using delay line cut into adder feedback circuit 09 p1360 A66-20295  
Fluid amplifier analysis predictions for prime-element conceptual models and jet amplifier dynamic effects 09 p1333 A66-20327  
Performance and wave growth of type-M transverse-field tubes in broad delay system 09 p1352 A66-20356  
Automatic time-domain equalizer consisting of delay line with adjustable taps 10 p1503 A66-21649  
Effectiveness of oscillatory circuits and delay lines for self-synchronization of polyphase multivibrators 10 p1510 A66-21668  
Steady state oscillations in hunting system, using nonlinear amplifier and artificial delay line 11 p1681 A66-23415  
Probability distribution data analysis in real time, using delay-line time-compression storage as information source in analog and digital form 12 p1825 A66-23760  
Materials for acoustic and magnetic microwave delay lines, discussing thin film piezoelectric transducers and magnetoelastic mode of microwave propagation 13 p2165 A66-25519  
Controlled-delay circuit with flip-flop oscillators for alignment of random pulse sequences 14 p2264 A66-27207  
Reflections effect on accuracy of measuring ultrasonic group delay time during amplitude and FM by sinusoidal voltage 14 p2236 A66-27249  
Propagation and amplification of helical waves in germanium bar solid state plasma in magnetic field parallel to bar current at room temperature 14 p2363 A66-27519  
Approximation of variable time delays and design of constant and variable delay circuits, noting simulation of delays in automatic control systems by computers 14 p2266 A66-27528  
Nonsteady coordinates of linear delay system determined from observable linear combination of phase coordinates 14 p2267 A66-27671  
Serrodyne frequency conversion determined, using sawtoothed FM of microwave oscillator and subsequent conversion with delay line in sawtoothed phase modulation, calculating phase distortion 17 p2884 A66-32218  
Synthesis of circuits containing delay lines, considering storage elements for pulsed signals 17 p2884 A66-32219  
Acoustic-array microwave grating quartz transducer creates variable delay characteristic with frequency 18 p3075 A66-33608  
Properties and performance capabilities of solid state delay lines composed of materials such as quartz, sapphire and YIG having low loss acoustic propagation 19 p3319 A66-36032  
Single-wave approximation of fields of cylindrical delay system with basic E-type wave propagating at variable phase velocity 20 p3515 A66-37381  
Rake system equipment for tropospheric scatter, noting delay-resolution capabilities and circuit stability 22 p3865 A66-40067  
Delay devices for pulse compression radar - IEE Conference, London, February 1966 23 p4033 A66-41013  
Pulse compression filter synthesis using ultrasonic delay lines 23 p4034 A66-41019  
Pulsed compression network for linear FM signals using short circuited delay line and with sweep frequency corresponding to output response peak 23 p4034 A66-41020  
Inhomogeneously filled waveguides containing dielectric used as microwave delay line for pulse compression

radar 23 p4035 A66-41021  
Cascaded hybrid rings as idealized model of wideband dispersive system in stripline 23 p4035 A66-41021  
Synthesis of prescribed frequency/group delay characteristics, using passive microwave components 23 p4035 A66-41021  
Insertion loss and delay characteristics vs frequency of one-port ferrimagnetic yttrium iron garnet delay line for pulse compressor at microwave frequencies 23 p4035 A66-41021  
Delay-line content-addressed memory with information retrieval by word association 24 p4177 A66-43183

## DELAY LOCK

## SA PHASE LOCK

Performance of delay-lock discriminator nonlinear feedback device for continuous tracking of delay difference between two correlated waveforms 06 p0842 A66-15979  
Binary delay-lock tracking-loop performance for various RF implementations 18 p3069 A66-34252  
DELTA FUNCTION  
Infinite helical sheath antenna driven by ring delta-function generator analyzed, using Fourier transform, noting decomposition of current distribution 17 p2886 A66-32388  
Asymptotic inequalities to determine phase volume within given boundaries with aid of Gibbs canonical distribution 21 p3756 A66-38738  
Frequency characteristic and transient delta function of plant, using algorithm based on correlation functions 24 p4188 A66-42483

## DELTA MODULATION

Feedback control system in design of delta-modulation data transmission system 05 p0654 A66-14614  
Delta modulation compared to other systems of pulse modulation, technologically and economically, noting analysis of dynamics to which input signal is subjected 09 p1346 A66-20564  
Random and burst channel error affects output signal-to-noise ratio of delta modulation system 13 p2019 A66-25145  
Asynchronous delta-modulation system with coded pulse generation according to certain change in amplitude 13 p2030 A66-25208  
Statistical characteristics derived for delta pulse-code modulation system, in which coded quantity represents difference between two sampled signal values 15 p2452 A66-29887  
Time frequency coded pulse communication systems, noting pulse-position, pulse-code and delta modulation, signal coding, etc 16 p2647 A66-30520  
Delta modulation pictorial encoding systems analyzed to determine parameters for image communication application 19 p3299 A66-35665  
Parameter evaluation of delta modulation encoding techniques for image communication applications by computer simulation 20 p3513 A66-37201

## DELTA WING

Nature and magnitude of turbulent boundary layer pressure fluctuations over two-dimensional surfaces and narrow delta wings 01 p0005 A66-10124  
Linearized supersonic theory for favorable thickness distributions and drag reduction for wings in supersonic flow [AIAA PAPER 65-716] 03 p0314 A66-12542  
Subsonic flow near trailing edge of low aspect ratio delta wing 04 p0454 A66-13518  
Aerodynamic characteristics of fixed-geometry double delta wing SST, noting low speed handling improvement due to vortex flow [AIAA PAPER 64-591] 05 p0610 A66-15069  
Delta wing vortex breakdown in terms of theory of stability of spiraling flows 07 p0979 A66-17478  
Pressure distribution and heat transfer for laminar boundary layer flow over highly swept blunt delta wings in hypersonic free stream [AIAA PAPER 66-130] 08 p1162 A66-18953  
Angle of attack, leading edge sweep and thickness effects on hypersonic flow field of slender delta wing 08 p1164 A66-19135  
Airport suitability for delta wing commercial supersonic transport, discussing noise objectives 09 p1365 A66-20698



Griffon 02 delta-winged aircraft with composite air breathing turbofanjet engine, noting achievements and prospects 11 p1761 A66-23248

Inviscid hypersonic flow over compression side of delta wing of moderate aspect ratio 12 p1796 A66-23605

Pressure distribution over slender delta wing, considering thickness effect 12 p1796 A66-23606

Lockheed supersonic air transport design development 13 p1995 A66-25758

Double-delta supersonic air transport low-speed operational characteristics, noting wind tunnel tests and design parameters 13 p1991 A66-25760

Pressure distribution along wing and body of wing-body combination 14 p2221 A66-28185

Operation and maintenance of Lockheed L-2000 double delta SST aircraft with high thrust engine and large delta wings, designed to meet civil aviation requirements [SAE PAPER 660295] 15 p2427 A66-29832

Three-dimensional flow separation of plane boundary layer caused by half delta wing on flat plate using Cooke small cross-flow method and Maskell separation criterion [AIAA PAPER 66-428] 16 p2631 A66-31465

Three-dimensional boundary layer flow over windward side of flat delta wing in hypersonic flow at moderate angle of attack, examining viscous-inviscid interaction [AIAA PAPER 66-492] 16 p2631 A66-31477

Delta and ogee planforms with nose planes, both with and without stabilizers 17 p2837 A66-31988

Flow along free border of conical vortex sheet above delta wing and rolling-up conically from apex 17 p2837 A66-32274

Vortex sheets rolling-up along leading edges of delta wings, comparison with slender body theory and conical flow 17 p2837 A66-32275

Coherent conical vortex sheet formation theory in two-dimensional and three-dimensional vortex filaments 17 p2906 A66-32276

Gap size effect on pressure and aerodynamic heating over flap of blunt delta wing in hypersonic flow [AIAA PAPER 66-408] 17 p2840 A66-32747

Parametric study of subsonic characteristics of low-aspect-ratio delta wings, noting role of airfoil thickness and free vortices above wing surface [AIAA PAPER 66-429] 17 p2841 A66-32754

Oblique shock wave formal determination of aerodynamic forces and pressure distribution on delta wings in supersonic or moderately hypersonic flow 21 p3695 A66-39602

Theory of wings with curved leading edges in supersonic flow, including delta wings with straight leading edges in case where motion is conical 23 p4008 A66-41379

Approximate second-order supersonic delta wing theory taking into account second-order differential equation via approximate particular integral 23 p4011 A66-41897

Inviscid hypersonic flow past flat wings at large angle of attack analyzed, using homogeneous layer concept of shock layer theory 23 p4013 A66-42014

Friction and turbulent heat transfer as function of Reynolds number applied to missile rounded-off forebody, delta wings, etc, using boundary layer equations 23 p4151 A66-42056

**DEMODULATION**

Yttrium iron garnet filters, noting envelope limiting characteristics for submegacycle range modulating frequencies and response parameters 06 p0845 A66-16089

Method of time domain analysis of nonlinear hybrid systems with first or fractional order data extrapolation 06 p0866 A66-16963

Linear demodulation of AM electromagnetic wave propagating through dispersive medium 06 p0836 A66-17033

Method of demodulating frequency-modulated wave train compared to method for time-modulated wave 09 p1344 A66-20400

High data rate SHF communication receiver for demodulating analog or digital information, noting

components 13 p2023 A66-25656

Optimal demodulation of analog-type signal transmitted through randomly fading channel, assuming additive Gaussian noise and using vector space approach 15 p2474 A66-29379

Measurement of physical quantity converted to form of AC signal, noting ripple-free circuit and several clamping arrangements 21 p3709 A66-38606

Continuous nonlinear recursive filtering based on Markov processes and state-variable concepts for application to optimum analog demodulation 22 p3868 A66-40717

**DEMODULATOR**

SA PHASE DEMODULATOR

SA PHASE LOCK DEMODULATOR

Low-threshold FM demodulator with bandwidth subdivision 09 p1346 A66-20560

Equivalent transfer function determined for quadrupole inserted between ideal modulator and demodulator from frequency characteristics 17 p2928 A66-33492

Mission-dependent Deep Space Instrumentation Facility equipment designed in support of Pioneer spacecraft program including command encoder, computer buffer and demodulator synchronizer 19 p3315 A66-35670

**DENMARK**

Danish space program, emphasizing polar ionosphere and high energy primary cosmic radiation studies 15 p2601 A66-29936

**DENSITOMETER**

SA GRAVIMETER

SA MICRODENSITOMETER

Video densitometer to extract data from video display, specifically densitocardiogram 06 p0819 A66-16851

Jovian phase variations and limb-darkening of surface detail examined by scanning isodensitometer 08 p1293 A66-19266

Flat plate in hypersonic flow analysis in shock tunnel, obtaining surface pressure, using electron beam densitometer 11 p1634 A66-22931

Scanning-electron-beam densitometer for measuring density distributions in rarefied gas flow 14 p2298 A66-28342

**DENSITY**

SA ATMOSPHERIC DENSITY

SA CURRENT DENSITY

SA ELECTRON DENSITY

SA ENERGY DENSITY

SA FLUX DENSITY

SA GAS DENSITY

SA ION DENSITY

SA MAGNETOSPHERIC ELECTRON DENSITY

SA MAGNETOSPHERIC ION DENSITY

SA METEORITE DENSITY

SA OPTICAL DENSITY

SA PACKING DENSITY

SA PHOTON DENSITY

SA PLASMA DENSITY

SA POWER DENSITY

SA PROBABILITY DENSITY

SA PROTON DENSITY

SA SPACE DENSITY

Liquid oxygen density as function of temperature and pressure 08 p1280 A66-19428

Spin-free transition density matrices, using permutation group algebra 15 p2547 A66-29620

Density, viscosity, surface tension, vapor pressure and vapor liquid equilibria data of liquid ozone-fluorine mixtures considered as Newtonian fluids 23 p4119 A66-41244

**DENSITY DISTRIBUTION**

Density distribution before sphere in low density hypersonic gas flow measured with electron beam densitometer 01 p0059 A66-10635

Flow visualization technique by thin high-energy electron beam moved with respect to flow 02 p0215 A66-11550

Dispersion relation of density waves in low pressure arc discharges 02 p0269 A66-11953

Distribution of high plasma density along semiconductor rod, noting surface recombination rate and assuming existence of high level injection at one end of rod 06 p0923 A66-16176

Electromagnetic wave propagation through semiconductor with nonuniform density distribution in transverse magnetic fields 06 p0923 A66-16177

Plasma convective instability, discussing

effect of axial density gradient on weakly ionized state 06 p0917 A66-16516

Potential and charge density distributions derived for stationary charged sphere and charged body moving through plasma 08 p1261 A66-18744

Radar echo effects of satellite disturbance in plasma medium, noting electron and positive ion density distribution 08 p1302 A66-18755

Nonsteady expansion of gas into vacuum in analysis of asymptotic solutions of Sedov 08 p1210 A66-19574

Non-Einsteinian gravitation, noting that expression for invariant density of free Lagrange gravitational field holds only for slowly varying weak fields 09 p1403 A66-20769

Plasma convective instability, discussing effect of axial density gradient on weakly ionized state 09 p1409 A66-20897

Spectral distribution of light scattered by density fluctuations in dense monatomic one-component fluid 09 p1404 A66-20960

Note on paper discussing lunar shape and internal structure in connection with inhomogeneity of density distribution, showing incompatibility of hypothesis with measurements 10 p1605 A66-21210

Spatial density distribution of cold plasma probed by electromagnetic field 10 p1570 A66-22005

Initial one-dimensional density discontinuity propagation in terms of mean free time between collisions 11 p1689 A66-22905

Density variation in Ar shock waves during translational adjustment for Mach 5 to 10 velocity range, using electron beam techniques 11 p1691 A66-22915

Shock front density distributions in Ar and He determined in shock tube, using electron beam attenuation 11 p1691 A66-22916

Plasma density distribution determined from microwave beam refraction as function of angle of incidence 12 p1922 A66-24217

Atmospheric environment effects on Saturn IB launch vehicle design, showing density profiles for various altitudes and listing extremes of thermodynamic variables at specific altitudes 12 p1906 A66-24479

Multivariate statistical analysis of wind sounding data, applying high degree of correlation between two wind parameters and empirical density function [AIAA PAPER 66-353] 12 p1907 A66-24489

Carbon dioxide relaxation processes in shock waves, measuring density variation, vibrational energy, relaxation time, shock density profile, etc 13 p2061 A66-25161

Second optical harmonic generation equations for steady state laser derived from density matrix 13 p2092 A66-25682

He-Ne laser homodyne spectrometer observation of broadening of spectral profile of light scattered from carbon dioxide near critical temperature and density due to density fluctuations 13 p2133 A66-26168

Plasma wave propagation and decay processes studied from profiles of plasma density in cylindrical metal vessel and results compared to Stark effect and framing camera photographic results 13 p2149 A66-26240

Plasmoid propagation in field-free space, discussing thermal expansion, velocity distribution, charged particle density distribution, energy distribution in absence of thermodynamic equilibrium, etc 13 p2154 A66-26528

Acceleration potential method for solving linear problems of wing hydrodynamics above interface between fluids differing in density, for arbitrary Froude number 13 p2067 A66-26530

Low aspect ratio wing moving above interface of two fluids of different density, replacing value of velocity potential by value obtained at large distance downstream from wing 13 p2068 A66-26539

Superconductivity model with exact solution, determining energy levels, ground state energy, excitation spectrum, density variations, etc 14 p2360 A66-27190

Non-Einsteinian gravitation, noting that expression for invariant density of free Lagrange gravitational field holds only for



slowly varying weak fields 14 p2334 A66-27304

Density ratio and transmission probability across conical converging diffuser in free-molecule flow with selected range of speed ratios, using Monte-Carlo method 14 p2219 A66-27416

Distribution and variation of atmospheric density over thermosphere, including auroral region, noting wind motion and high altitude circulation 14 p2382 A66-27618

Density variation observed from satellites in upper atmosphere 14 p2284 A66-27619

Density distribution in exosphere, particularly Maxwellian velocity distribution disturbed by light particle escape 14 p2284 A66-27620

Mean time to failure within given time boundaries and for continuous failure density evaluated via Weibull density function 15 p2526 A66-28806

Energy spectrum of primary photoelectron, using data from atmospheric density distribution, fluxes of solar XUV radiations and absorption and ionization cross sections 15 p2574 A66-28906

Bounds on density fluctuations and electrostatic oscillation spectrum for homogeneous collisionless plasma according to Maxwell-Vlasov equation 15 p2554 A66-29749

Equation for conditional overshoot density of normal stationary process in centralized and positional centralized control, noting error estimate 16 p2669 A66-30767

Spherical semipassive probe for density/altitude and pressure/altitude profile of planetary atmospheres, notably Mars and Venus 16 p2801 A66-30889

Performance of short supersonic nozzles producing expansion and density jumps in flow, noting efficiency in obtaining maximum driving effect 16 p2630 A66-31303

Exact determination of electron density distribution in finite anisotropic plasma by integral equation relating tangential electric field and HF plasma current 16 p2767 A66-31691

State density for highly doped semiconductor in magnetic field, obtaining results at near Fermi level energies and at bottom of conduction band 16 p2788 A66-31779

Coherence conditions effects on electromagnetic field density operators and photon density distribution in single excited mode 17 p2957 A66-31975

Solar corpuscular stream density distribution and trail curvature, noting space angle of ejection and flight trajectory 17 p2992 A66-32336

Surface wave propagation along plasma column noting discharge tube properties, density distribution variation with magnetic field, attenuation due to collisional losses, etc 17 p2970 A66-32651

Elastic model for evaluating stresses in Earth induced by density variations or topographic irregularities 17 p2921 A66-33226

Total number of cyanide molecules and diatomic carbon free radicals and density distribution in head of Arend-Roland 1957 III comet 17 p3010 A66-33381

Density field calculation for collisionless expansion of moving cylindrical gas cloud, with Maxwellian random velocity distribution superimposed on uniform initial velocity 18 p3103 A66-34933

Hydrogen density in coaxial plasma injector prior to application of high voltage to electrodes, noting experimental setup and results 18 p3151 A66-35072

Plasma stabilization mechanism for electron beam caused density variation, noting use of nonlinear effects 18 p3152 A66-35082

Transition region of pulse spectrum from EAS particle density recordings by Cerenkov and scintillation detectors 18 p3207 A66-35110

High energy nuclear active particles in EAS discussing lateral and zenith angle distribution energy spectrum, anisotropy, etc 18 p3207 A66-35111

Photoproduction, lateral density distribution, energy spectrum and muon component fluctuations in electron photon cascades 18 p3208 A66-35114

Barometric effect and density spectrum of photon-initiated EAS muons 18 p3208 A66-35115

EAS mu component fluctuations in density distribution and reception spectrum recorded, using hodograph detectors 18 p3208 A66-35116

Component composition and photonuclear interactions of photon-initiated EAS 18 p3209 A66-35121

Cloud chamber EAS density spectrum measurements at 2285 m 18 p3210 A66-35124

Altitude variation of EAS particle density and primary energy/nucleon spectra measured with proportional counters 18 p3210 A66-35125

Altitude distribution of combinations of meridional gradients of pressure, temperature and density 19 p3393 A66-35394

Spatial density distribution of cold plasma probed by electromagnetic field 19 p3407 A66-36089

Divergence of third-order term in density expansion of quantum-mechanical transport coefficients analogous to that for classical systems 19 p3401 A66-36173

Thermal radiation of nonhomogeneous plasma sheath, obtaining radiation intensity formula via fluctuation theory 19 p3409 A66-36281

Aspa device designed for study of composition, energy and density distributions produced when plasma blob is injected into mirror trap with adiabatic plasma compression 19 p3423 A66-36550

Cathode current density distribution, beam minimum radius and location and electrode current interception, using computer techniques on electron guns 20 p3528 A66-37490

Field and charge density distributions in semiconductor with hot electrons, showing domain movement type oscillations due to stationary wave propagation 20 p3617 A66-37555

Trapped electrons from Russian high altitude nuclear detonation examined, noting energy spectrum and mirror point density distribution 20 p3643 A66-38342

Lunar models of figure, density distribution and gravity field from Earth telescope data 21 p3812 A66-38822

Density distribution and shock wave profile of rarefied gas slip flows past blunt bodies determined, using multibeam interferometer 21 p3724 A66-38903

Photometry, polarization, structural peculiarities and density distribution of solar corona 21 p3813 A66-39121

Interferometric measurement of density distributions in shock layer of nonequilibrium flow field around cone 21 p3694 A66-39168

Radial current density distribution in homopolar, noting deviation of magnetic field and nature of current distribution around anode 22 p3953 A66-39757

Seasonal, diurnal and latitudinal variations of electron density distributions in topside of ionosphere as revealed by Alouette I satellite 22 p3909 A66-39974

LF wave propagation in inhomogeneous plasma column, deriving normal mode of expansion and perturbed dispersion curves 22 p3955 A66-40047

Plasma density distribution determined from microwave beam refraction as function of angle of incidence 22 p3957 A66-40581

Gas ionization by fast electron beam directed along waveguide leading to longitudinal distribution of secondary electron concentration 22 p3958 A66-40938

External control of radial distribution of plasma density for magnetoplasma stabilization against helical instability 23 p4103 A66-41486

One-dimensional approximation analysis of excess carrier density distribution in illuminated semiconductor and radiative recombination effects 23 p4115 A66-41857

Resistance network analog method determination of carrier density distribution and charge constant in p-n junction for two-dimensional axisymmetric case 23 p4115 A66-41858

Neutrino energy losses from vibrating neutron stars, noting density profiles 23 p4131 A66-41863

Combination of probability density functions for system error analysis, using convolution or transformation methods 24 p4189 A66-42827

Density fluctuations of penetrating particles in extensive air showers at various distances from shower axis 24 p4268 A66-42916

Superconductivity model with exact solution, determining energy levels, ground state energy, excitation spectrum, density variations, etc 24 p4259 A66-43088

### DENSITY MEASUREMENT

#### SA X-RAY DENSITY MEASUREMENT

Gas laser interferometers for plasma low electron density measurement 01 p0069 A66-10856

Densification rates for tungsten powder compacts sintered in hydrogen/bromine atmospheres compared with those sintered in hydrogen alone at high temperatures 03 p0385 A66-13207

Gravitational potential gradient for body consisting of positive or negative masses with known density extremum value and known or unknown volumes 04 p0514 A66-13449

Mach-Zehnder interferometer for visualization and analysis of density changes in gases, liquids and solids 04 p0520 A66-13762

Instrumentation techniques for new type of gas density measuring system using light scattered from laser beam as measured quantity 05 p0698 A66-15794

Pressure, density, temperature and wind measurements in mesosphere resulted from rocket soundings to determine structure 07 p1027 A66-17361

Schlieren color photography with tri-color filter, identifying small density gradient 07 p1018 A66-17614

Densities of binary mixtures of fused alkali nitrates with alkaline earth nitrates measured by manometric densitometer and expressed as linear function of temperature 08 p1177 A66-18617

Tunneling measurements on density of states of type II semiconductor films near upper critical fields 09 p1422 A66-20060

Coaxial capacitor for measuring density of fluids in both liquid and gaseous phase over wide range of temperatures and pressures 11 p1707 A66-22961

Dissociation rate of nitrogen behind strong shock waves in nitrogen-argon mixtures determined, using time-resolved interferometric measurements of gas density 12 p1861 A66-23616

Ballistic wind and density predictions, measuring wind and D-value at 500 mb, calculating missile response to atmospheric effects [AIAA PAPER 66-359] 12 p1906 A66-24478

Design and construction of probe measuring density of neutral atoms in quiescent alkali metal magnetoplasma, noting vacuum system, electric circuitry, etc 12 p1884 A66-24984

Density of six niobium spheres which are intended for use as rotors in superconducting gyroscope 13 p2106 A66-25072

Disturbance of thermal equilibrium of weakly ionized cesium contact plasma due to wall losses measured by Langmuir probe 13 p2137 A66-25117

Electromagnetic wave propagation near missiles during hypersonic atmospheric reentry and computer program for determination of dissociated and ionized particle density in nonequilibrium nitrogen-plasma flow 13 p2150 A66-26374

Falling sphere, solar XUV radiation absorption and pressure gauge mass spectrometry for density measurements of thermosphere, comparing results and noting discrepancies 14 p2284 A66-27615

Scanning-electron-beam densitometer for measuring density distributions in rarefied gas flow 14 p2298 A66-28342

Resonance probe for plasma density measurements consisting of vacuum cylinder, noting eigenfrequency 15 p2497 A66-28711

Densities of wrought aluminum alloys computed from rule of mixtures and metallurgical phenomena and compared with



- observed densities 15 p2522 A66-29075
- Shock transition in multihead spin structure of self-sustaining gaseous detonations in oxyacetylene mixtures, including interferometric and schlieren photographic density, temperature and pressure measurements 15 p2618 A66-29607
- Shock wave thicknesses and density ratios measured in helium, argon and nitrogen, using electron beam fluorescence method at various Mach numbers in wind tunnel 15 p2480 A66-29736
- Measurement of simple and central moments of one-dimensional density function applied to pattern recognition 15 p2475 A66-29864
- High resolution density data from radar observations of low altitude, polar orbiting satellites reveal longitudinal and geomagnetic variation, noting regression analysis 15 p2497 A66-30085
- Electrical discharge probe for transient density measurements in rarefied gas flow, noting density range, flow velocity, etc 16 p2701 A66-30380
- Absolute deuterium density by energetic deuterium beam probing of plasma 16 p2759 A66-30425
- Rocket borne ionospheric direct sounding instruments to measure ion and electron density, electron temperature, thermal electron energy distribution and space electric potential versus rocket potential 16 p2705 A66-30819
- Silicon, quartz and germanium single crystal density determined via hydrostatic weighting method 16 p2777 A66-30933
- High latitude density regime in upper stratosphere inferred from Arctic and Antarctic observations 17 p2922 A66-33343
- Equidensitometric photographic isophotometry of comets and other luminous objects 17 p3011 A66-33385
- Atmospheric density measurements for altitudes up to 74 km from X-15 flights using stagnation pressure method [AIAA PAPER 66-441] 18 p3104 A66-33646
- Falling sphere experiment instrumentation for aerospace density determination including sensor, transit-time accelerometer and telemetry system 19 p3356 A66-35672
- Resistance and frequency response range of sheath surrounding electrostatic probe floating in tenuous plasma 19 p3357 A66-35808
- Density of lithium, sodium and potassium up to 1600 degrees C, using pycnometer method, showing dependence of density on temperature 20 p3582 A66-36979
- Low temperature experimental apparatus for density determination of cryogenic liquids and mixtures under atmospheric and subatmospheric pressure 20 p3601 A66-37082
- Carbon dioxide flow density in wake of shock wave front 21 p3726 A66-39091
- Plasma decay technique to measure density in discharge tubes compared to value obtained by Langmuir probe 21 p3792 A66-39182
- Vapor condensation effects on wind tunnel measurements, noting relation between air-moisture and flow field, shock wave intensity increase and density measurements on circular airfoils 22 p3843 A66-39697
- Electron beam density measurements, discussing effect of elevated rotational and vibrational temperatures 22 p3918 A66-40365
- Number densities and composition of upper atmosphere determined by rocketborne mass spectrometers, estimating temperature variation with altitude 22 p3913 A66-40553
- Deep /1-10 micron/ penetration of ion implanted donors in silicon, measuring density profiles via C-V method and parameter of penetrating tail section 24 p4250 A66-42256
- DEOXYRIBONUCLEIC ACID /DNA/**
- UV radiation effect on viscosity and optical density of DNA solutions from calf thymus and rat spleen 01 p0018 A66-11193
- Space radiation of solar and cosmic origin and biological effects, examining DNA structure and radiation induced changes 04 p0463 A66-13897
- Characteristics, fine structure and mode of functioning of bacterial cell and artificial synthesis possibility 11 p1644 A66-22713
- Amino acid genetic code in which long sequences in DNA spell out instructions transcribed into RNA and subsequently into proteins 11 p1644 A66-22714
- Cosmic and UV radiation effects on breakdown of DNA and production of tumors in mice 13 p2008 A66-25642
- Radiation damage in deoxyribonucleoproteids at molecular and supermolecular levels 13 p2010 A66-26228
- Biochemical mutation, DNA, RNA and microorganisms infecting wing tanks of jet aircraft 13 p2011 A66-26546
- Resistance transfer factor episome analyzed by measuring inactivation by cobalt gamma radiation, phosphorus and tritium, suggesting existence of DNA 14 p2228 A66-27308
- DNA synthesis in cultured mammalian cells stimulated by UV light, using radioautography and density gradient centrifugation 19 p3287 A66-36436
- Physical properties of DNA-dependent RNA polymerase from *Escherichia coli* 20 p3505 A66-37054
- Ribonuclease effect on polymerase activity in *Azotobacter vinelandii* used to verify theory that RNA polymerase is inhibited by RNA produced in reaction 20 p3510 A66-37790
- Statistical mechanics DNA molecular model, noting bonding free energy between adenine-thymine and guanine-cytosine base pairs 21 p3699 A66-38530
- Nonrandomness in base sequences of DNA 21 p3702 A66-38542
- DEPENDENT VARIABLE**
- Control feel application to aircraft controls, noting man-machine system configurations, anthropometric and physical factors, sensory motor requirements, etc 17 p2869 A66-33446
- DEPOLARIZER**
- Depolarization of cosmic radio emission due to dispersion of Faraday rotation of plane of polarization of radio waves 09 p1441 A66-20334
- DEPOSITION**
- SA ELECTRODEPOSITION
- SA EPITAXIAL DEPOSITION
- SA SEDIMENT
- SA VACUUM DEPOSITION
- SA VAPOR DEPOSITION
- Varying deposition and firing conditions effect on range of detection of chemically deposited lead sulfide IR detector cells 03 p0407 A66-12332
- Oxidation resistant pack cementation coatings for refractory metal complex structures 19 p3370 A66-36140
- DEPRESSANT**
- Halides used as burning rate depressants on combustion stability of polyurethane/ammonium perchlorate base propellants, examining acoustic instability 23 p4119 A66-41435
- DEPRIVATION**
- S CONFINEMENT
- S SENSORY DEPRIVATION
- S SLEEP DEPRIVATION
- S STARVATION
- DEPTH PERCEPTION**
- SA STEREOSCOPIC VISION
- Simulated 3-D display techniques, considering application to television, air-traffic control, scene synthesis, radar target data and signal analysis 11 p1707 A66-22960
- Schoen hypothesis concerning image arrival time at cortex, depth values, retinal input, stereopsis, etc 17 p2862 A66-33089
- DERIVATIVE**
- S NEWCOMB DERIVATIVE
- DESCENT TRAJECTORY**
- Glider reentry descent trajectories from near Earth orbit calculated, emphasizing landing accuracy and mechanical and thermal stresses 04 p0584 A66-13525
- DESCRIPTIVE GEOMETRY**
- Mayor-Mises method for solution of kinematic and kinetostatic problems of three-dimensional mechanisms [ASME PAPER 66-MD-2] 21 p3741 A66-38475
- DESERT**
- Ecological patterns of microorganisms in desert soils 15 p2441 A66-29960
- DESIGN**
- S AIRCRAFT DESIGN
- S AMPLIFIER DESIGN
- S COMPUTER DESIGN
- S ENGINE DESIGN
- S EQUIPMENT SPECIFICATIONS
- S EXPERIMENT DESIGN
- S HELICOPTER DESIGN
- S LENS DESIGN
- S LOGICAL DESIGN
- S REACTOR DESIGN
- S SPACECRAFT DESIGN
- S STRUCTURAL DESIGN
- S SYSTEMS DESIGN
- DESORPTION**
- Alkali-ion desorption energies measured on polycrystalline refractory metals at low surface coverage by electron work function 02 p0263 A66-11483
- Evolution of gases from cometary nuclei by sublimation or desorption 17 p3009 A66-33372
- DESPINNING**
- Electronically despun switched antenna using variable phase shifters to control phase of incident power to circular array of elements [AIAA PAPER 66-302] 12 p1844 A66-24769
- Implementation of electronically despun satellite antenna system considering limits of impracticability because of excessive weight, control power, etc [AIAA PAPER 66-325] 12 p1844 A66-24795
- Electronically despun antenna and electronically controlled phase shifters to increase transmitter output power for spin-stabilized communication satellites 23 p4036 A66-41142
- DESTRUCTIVE TESTING**
- SA NONDESTRUCTIVE TESTING
- Instantaneous strength determinations for exponential failure distribution are ineffective in assessing underlying failure rate 03 p0342 A66-12899
- Destructive and nondestructive testing of fiber composite materials 05 p0773 A66-14815
- High speed tensile testing of materials under destructive loads at high strain rates 13 p2197 A66-26107
- Elastic and plastic deformation of polycrystalline metals exposed to ultrasonic load and high temperatures 15 p2523 A66-29601
- DETECTION**
- SA AIRCRAFT DETECTION
- SA CORRELATION DETECTION
- SA ERROR DETECTING CODE
- SA FLAW DETECTION
- SA INSPECTION
- SA SEQUENTIAL DETECTION
- SA SIGNAL DETECTION
- SA WAVE DETECTION
- Detection of arrival of He driver gas in test section of shock tunnel 17 p2903 A66-32474
- DETECTOR**
- SA ELECTRON DETECTOR
- SA INDICATOR
- SA INFRARED DETECTOR
- SA LIFE DETECTOR
- SA MOISTURE DETECTOR
- SA NEUTRON DETECTOR
- SA PARTICLE DETECTOR
- SA PHASE DETECTOR
- SA PHOTODETECTOR
- SA RADAR DETECTOR
- SA RADIATION DETECTOR
- SA SIGNAL DETECTOR
- SA SILICON RADIATION DETECTOR
- SA SYNCHRONOUS DETECTOR
- Crystal Hall detectors prepared by gluing thin indium antimonide wafer on rectangular parallelepiped ferrite base 01 p0045 A66-11031
- DETERMINANT**
- Commutable matrices, decomposing determinant of general solution of AX equals XB into linear factors 04 p0539 A66-13869
- Commutable matrices, decomposing determinant of general solution of AX equals XB into linear factors 12 p1903 A66-24025
- Evaluation of total square integrals arising in minimization problems of discrete data systems not requiring expansion of determinant for solution 12 p1850 A66-24265
- Multidimensional matrix algebra and determinant operations [PST PAPER NT-148] 14 p2324 A66-27837
- Matrix algebra, discussing factorization, determinants, eigenvalues, polynomials,



inequalities, etc 17 p2945 A66-31869  
Theoretical interpretation of expansions in nonzero determinants formed from vertex and circuit matrices 20 p3539 A66-38283

**DETONABLE GAS MIXTURE**  
Liquid surface instability caused by sliding detonation and shock waves of gas mixture 01 p0060 A66-11192  
Nonequilibrium chemical reaction effect on decay in spontaneous explosion for reactive expelled gas and inert expelling gas 08 p1179 A66-19482  
Hydrodynamic theory relating velocity decrement and curvature of gaseous detonation to conditions at explosive inert interface [AIAA PAPER 65-39] 10 p1621 A66-21777  
Detonations in gaseous mixtures and in condensed phase, examining effects of pressure, temperature and confinement on normal detonation 12 p1980 A66-24932  
Detonation limits for binary mixtures of tetramethylsilane with oxygen, analyzing factors controlling transition from detonation to deflagration, noting condensation effects 13 p2209 A66-26303  
Detonation in gaseous mixtures and in condensed phase, reviewing aerodynamic theory 15 p2617 A66-29315  
Wall heat transfer behind plane detonation wave moving past flat plate into stationary hydrogen-oxygen mixture 17 p3033 A66-32461  
Explosion of gas mixtures noting preparation, ignition sources, equipment, detonation waves of spherical volumes, etc 21 p3834 A66-38534

**DETONATION**  
**SA EXPLOSION**  
**SA FIRING**  
Gas combustion and detonation instability 04 p0597 A66-13901  
Simple rotating drum streak camera covering principle, design, construction and application 04 p0520 A66-13940  
Performance of impact machines for testing explosive sensitivity to impact [CI PAPER WSCI-65-33] 05 p0787 A66-15137  
Theoretical detonation characteristics of ammonium perchlorate-polyurethane solid composite propellants 05 p0744 A66-15781  
Gas combustion and detonation instability 17 p3033 A66-32064  
Numerical solution of time dependent equations of one-dimensional reactive flow for idealized one-reaction detonation 17 p2908 A66-32418  
Water vapor effects on detonation reaction of H sub 2 - O sub 2 17 p3034 A66-32467  
Particle velocity in detonating gases determined by MHD principle 17 p3035 A66-32634  
Detonations in explosive gaseous mixtures and detonations in condensed phase, discussing three-dimensional vibratory phenomena, wall effects and transition between deflagration and detonation 17 p3036 A66-32846  
Limiting factors of detonation in heterogeneous systems, using one-dimensional model 18 p3265 A66-34552  
Electroexplosive devices in aerospace vehicles in two classes, propellants and high explosives, noting methods for controlling detonation desired effects 20 p3625 A66-37159  
Megaton and decamegaton dynamic pressure production by blast-type compression of thick walled pipe with core subjected to internal implosion, giving theoretical foundations /Part I/ 23 p4091 A66-41859  
Megaton and decamegaton dynamic pressure production by blast-type compression of thick walled pipe with core subjected to internal implosion, for case of graphite core /Part II/ 23 p4091 A66-41860

**DETONATION WAVE**  
Stability of plane stationary detonation wave, using detonation model of ideal perfect gas flowing in pipe at constant supersonic velocity 02 p0217 A66-11391  
Detonation theory of heterogeneous fuel mixture 02 p0217 A66-11402  
Microwave technique using oscilloscope that provides displacement-time trace of initiating shock wave as it grows to detonation in explosive 03 p0369 A66-12795  
Spherical and cylindrical implosive waves

and system of generating detonation wave that converges to given focus 03 p0445 A66-13131  
Gas temperature behind detonation front in acetylene-oxygen mixture measured by time-base photometry of hydrogen beta and gamma spectral lines 04 p0598 A66-14433  
Shock sensitivity and high-low detonation regimes in thin explosive films studied by highly instrumented two-dimensional analog of card-gap test 05 p0787 A66-15136  
[CI PAPER WSCI-65-29] 05 p0787 A66-15136  
Detonation and decompression research, comparing biological effects of explosive decompression and detonation 06 p0811 A66-16067  
Heterogeneous detonations, discussing polydisperse and monodisperse spray detonations and liquid fuel film shock-induced combustion 06 p0969 A66-16256  
[AIAA PAPER 66-109] 06 p0969 A66-16256  
Flame generation of pressure waves and wave-combustion front interactions in detonation processes treated by nonsteady gas dynamics 07 p1155 A66-18118  
Imploding cylindrical shock wave production through imploding detonation waves in oxygen-acetylene mixtures, using Chapman-Jouguet theory 08 p1204 A66-18523  
Onset of retonation, laser technology and high repetition-high resolution schlieren stroboscopic wave phenomena 08 p1318 A66-19200  
records 08 p1318 A66-19200  
One-dimensional CJ detonation existence as self-sustaining phenomenon 08 p1208 A66-19203  
Explosive wave propagation during cylindrical and plane explosions in ideal electrically conducting gas, taking account of counterpressure and magnetic field 08 p1208 A66-19372  
Nonequilibrium chemical reaction effect on decay in spontaneous explosion for reactive expelled gas and inert expelling gas 08 p1179 A66-19482  
Orifice effect on detonation wave propagation in tube, noting flame formation and detonation regeneration 10 p1523 A66-21792  
Variation of critical energy for direct initiation of cylindrical detonation waves as function mixture composition and initial pressure 10 p1622 A66-21830  
Plane shock wave compressions of cylindrical and wedge-shaped specimens used to obtain shock Hugoniot of two unreacted, composite and double-base aluminized propellants 12 p1934 A66-23589  
Chemical relaxation effects in nozzle flow by measuring high temperatures created by detonation waves in shock tube, using hydrocarbon mixtures 12 p1977 A66-23748  
Shock wave from explosion of laminar charges in air, water and vacuum 14 p2298 A66-26788  
Elastoplastic properties of copper, aluminum alloys and brass under explosive load, noting increased temperature effect on elastoplastic wave parameters 14 p2314 A66-27370  
Accelerator for jets formed by shaped charges, using principles of detonation waves 14 p2329 A66-27475  
Structure and development of detonation waves in gaseous media 14 p2399 A66-27557  
Small disturbances and effect on processes of fast combustion of inflammable compressible mixture 14 p2374 A66-27690  
Shock transition in multihead spin structure of self-sustaining gaseous detonations in oxyacetylene mixtures, including interferometric and schlieren photographic density, temperature and pressure measurements 15 p2618 A66-29607  
Ionized gas flow rate behind detonation wave used with Chapman-Jouguet condition to determine speed of sound in reaction products 16 p2687 A66-31160  
Energy release effects on unsteady gas flow in explosion 16 p2689 A66-31484  
Low velocity detonation in powder explosives 17 p3036 A66-32829  
Flow properties behind spherical detonation wave in Taylor and Zeldovich solution 17 p2913 A66-33071  
Heterogeneous detonations, discussing polydisperse and monodisperse spray detonations and liquid fuel film shock-

induced combustion [AIAA PAPER 66-109] 17 p3037 A66-33237  
Feasibility of rocket motor using detonation wave rotating in annular combustion chamber wherein propellant is injected continuously and expelled through annular nozzle 18 p3162 A66-33807  
Explosive wave propagation during cylindrical and plane explosions in ideal electrically conducting gas, taking account of counterpressure and magnetic field 18 p3099 A66-34171  
Approximate closed solutions for detonation velocity and pressure of condensed explosives 18 p3265 A66-34581  
Mach detonation wave formation conditions, noting magnitude of shock pressures in metals and possibility of obtaining steady state wave patterns 18 p3266 A66-34629  
Ideal detonation wave and Chapman-Jouguet condition, considering plane permanent and shock waves 18 p3266 A66-34721  
Continuous emission spectrum of detonation wave in nitromethane between 3800 and 8000 angstroms 19 p3477 A66-35747  
Stability limits of quasi-cylindrical diverging detonations in propane-oxygen-nitrogen mixtures 20 p3679 A66-37819  
Explosion of gas mixtures noting preparation, ignition sources, equipment, detonation waves of spherical volumes, etc 21 p3834 A66-38534  
Thermodynamic calculation of explosive properties of peracetic acid, using data from detonation wave to establish safe limits for use of acid 21 p3834 A66-38535  
Stability of one-dimensional steady detonations for periodic disturbances of small transverse wavelength 21 p3727 A66-39171  
Synchronized shadow photochronographic investigation of wire explosion shock waves in air 21 p3772 A66-39302  
Implosion experiment, discussing methods for detonation and shock wave propagation phase calculation 21 p3837 A66-39503  
Stability problem of plane steady detonation wave in ideal gas 22 p3898 A66-40156  
Detonation wave formation in flowing hydrogen-oxygen and methane-oxygen mixtures, noting induction distances and turbulence levels 23 p4057 A66-41888  
Detonation initiation behind reflected shock waves in hydrogen-oxygen-argon mixtures, noting reaction wave propagation 23 p4057 A66-41889  
Detonability of hydrogen-oxygen mixtures in large vessels at low initial pressures, using strong and weak igniters 23 p4120 A66-41890

**DETONATOR**  
Detonability of cryogenic oxydizers, discussing modified continuous wire technique analysis of detonation properties of trioxxygen difluoride 16 p2790 A66-31194

**DEUTERIUM**  
**SA HYDROGEN**  
Stable elementary particle detection of mass greater than that of proton in hydrogen, deuterium and atmospheric air samples, using mass spectrometer 01 p0060 A66-10251  
Differences in spherical intermolecular potentials of hydrogen and deuterium determined from reanalysis of second-virial-coefficient data 08 p1258 A66-18940  
Photolysis of water at 1470 angstroms in absence and presence of ethylene 09 p1338 A66-20679  
Stable elementary particle detection of mass greater than that of proton in hydrogen, deuterium and atmospheric air samples, using mass spectrometer 13 p2131 A66-25968  
Stimulated emission spectroscopy of hydrogen, nitrogen, oxygen and deuterium diatomic gases in 0.8 to 8 micron region 13 p2102 A66-26205  
Deuterium isotope effect on thresholds of europium chelate lasers, noting solvent thermal effects 13 p2105 A66-26598  
Vibrational relaxation times of deuterium in argon and krypton determined at high temperatures by shock heating gas mixtures in shock tube 13 p2136 A66-26662  
Solar wind deuterium detector and charge



- spectrum analyzer for Sunblazer probe of corona transmission 14 p2295 A66-27701
- properties 14 p2295 A66-27701
- Low temperature transport properties of hydrogen, deuterium and HD, noting quantal phase shift, intermolecular potentials, etc 14 p2414 A66-27973
- Photochemical decomposition of carbon suboxide and spectroscopic observation of carbon atom reactions with nitrogen, hydrogen and deuterium at 4.2 degrees K 14 p2233 A66-27975
- Tandem column gas-liquid chromatography labeling technique for mass spectrometry, noting ketones exchange and data on deuterium and oxygen 15 p2446 A66-28872
- compounds 15 p2446 A66-28872
- Absorption of solar neutrinos in deuterium 16 p2792 A66-30144
- Distorted wave calculation from rotational excitation of molecular hydrogen and molecular deuterium in thermal collisions with atomic hydrogen, presenting angular distributions, cross sections, etc 19 p3403 A66-36329
- Plasma production by firing giant pulse laser at solid deuterium pellet /ice/, noting strong anisotropy in plasma outburst 19 p3432 A66-36595
- Homogeneous isotopic exchange reaction between hydrogen and deuterium in single-pulse shock tube with excess argon 22 p3860 A66-40902
- Methane/deuterium exchange reaction rate measured in shock tube, using vibrational excitation mechanism to explain data 22 p3860 A66-40903
- Charge exchange cross sections for argon ions incident on hydrogen and deuterium measured over energy range of 30 to 1000 ev, taking into account ion-molecule reactions 23 p4098 A66-41267
- DEUTERIUM OXIDE**
- Isotopic exchange reactions of difluoramine with deuterium oxide and trifluoroacetic acid at low temperatures studied by NMR techniques 23 p4118 A66-41231
- DEUTERIUM PLASMA**
- Strong collisionless shock wave excitation in deuterium plasma 08 p1266 A66-19479
- Energy transfer equations for fully ionized /deuterium/ plasma including dominant and nondominant terms 13 p2143 A66-25713
- Deuterium plasma jet injection into simple biconical cusped magnetic field, noting ion energy transfer to electrons and plasma potential variations 15 p2554 A66-29748
- Absolute deuterium density by energetic deuterium beam probing of plasma 16 p2759 A66-30425
- Quantitative measurement of electron correlation spectrum for deuterium plasma in thermal equilibrium 17 p2963 A66-31885
- Plasma ion and electron temperature measurement via forward scattering spectrum of deuterium plasma 18 p3146 A66-34235
- Plasma heating and confinement in magnetic well, using deuterium plasma jet obtained by induction gun, measuring lifetimes 19 p3412 A66-36499
- Deuterium plasma containment and stability in theta pinch configuration using megajoule capacitor banks, studying density, temperature and radial distribution 19 p3413 A66-36505
- Aspa device designed for study of composition, energy and density distributions produced when plasma blob is injected into mirror trap with adiabatic plasma compression 19 p3423 A66-36550
- Electron density, temperature and other related electromagnetic effects of deuterium plasma focus formed by coaxial electrode discharge as result of Z 19 p3425 A66-36561
- pinch 19 p3425 A66-36561
- Phenomena associated with buildup of noncylindrical focused Z 19 p3425 A66-36562
- pinch 19 p3425 A66-36562
- Biconical cusp injection of dense hydrogen and deuterium plasmas by plasma gun 19 p3425 A66-36563
- Ruby laser light scattering measurements of electron and ion temperatures of hydrogen and deuterium plasmas produced in theta pinch devices 24 p4222 A66-42558
- DEUTERON**
- Plasma beam action on tritiated titanium and high energy deuteron detection in mixed-field accelerator 17 p2972 A66-32953
- DEVIATION**
- S ABERRATION
- S ECCENTRICITY
- S PHASE DEVIATION
- S STANDARD DEVIATION
- DEVICE**
- S CARTRIDGE ACTUATED DEVICE
- S COMMUNICATIONS DEVICE
- S CONTROL DEVICE
- S ELECTROEXPLOSIVE DEVICE
- S ELECTROMECHANICAL DEVICE
- S ERROR CORRECTING DEVICE
- S EXPLOSIVE DEVICE
- S FEEDING DEVICE
- S HEAT REJECTION DEVICE
- S HIGH TEMPERATURE PLASMA DEVICE
- S INSTRUMENT
- S LANDING DEVICE
- S LAUNCHING DEVICE
- S LIFT DEVICE
- S PROPELLANT ACTUATED DEVICE
- S RECOVERY DEVICE
- S RELEASE DEVICE
- S RESISTANCE DEVICE
- S SAFETY DEVICE
- S SAMPLING DEVICE
- S SCANNING DEVICE
- S SEMICONDUCTOR DEVICE
- S SOLID STATE DEVICE
- S STORAGE DEVICE
- S SUN TRACKER DEVICE
- S WARNING DEVICE
- DEWAR SYSTEM**
- Chilldown rate and equilibrium heat-leak storage loss measurements in liquid hydrogen storage dewars 20 p3541 A66-37101
- DH-121 AIRCRAFT**
- S DE HAVILLAND DH-121 AIRCRAFT
- DH-125 AIRCRAFT**
- S DE HAVILLAND DH-125 AIRCRAFT
- DIAGNOSIS**
- SA FUNCTION TEST
- Diagnostic standards for primary glaucoma in pilots, noting use of instrument tonometry and problems connected with sudden incapacitation 06 p0814 A66-16832
- German Air Force functional tests for early diagnosis of cardiovascular disease among aircrew, also discussing therapy 16 p2640 A66-31133
- DIAGRAM**
- S BENDING DIAGRAM
- S CONSTITUTIONAL DIAGRAM
- S CREEP DIAGRAM
- S ENTHALPY-ENTROPY DIAGRAM
- S EQUILIBRIUM DIAGRAM
- S EUTECTIC DIAGRAM
- S FATIGUE DIAGRAM
- S FEYNMAN DIAGRAM
- S GRAPH
- S HERTZSPRUNG-RUSSELL DIAGRAM
- S MOLLIER DIAGRAM
- S PHASE DIAGRAM
- S STRESS-STRAIN DIAGRAM
- DIAMAGNETISM**
- Dependence of magnetostriction coefficient for diamagnetic materials on change of Fermi surface with momentum and deformation parameter 16 p2777 A66-31035
- Diamagnetic properties of plasma described by extended field equations suggest existence of steady state inductive power transfer between plasma and magnetic fields 18 p3145 A66-34108
- Calculating magnetic shielding constants of diatomic HF molecules, based on gauge-invariant atomic orbitals 22 p3950 A66-39919
- DIAMANT LAUNCH VEHICLE**
- French Diamant satellite launching rocket noting design, performance, stages, propellants, instrumentation, etc 02 p0295 A66-11672
- French satellite-carrying Diamant rocket describing design, developmental testing and operating characteristics 05 p0770 A66-15201
- Design and reliability of Diamant launch vehicle 10 p1610 A66-21253
- Design and development of Diamant launch vehicle, discussing prelaunch testing 10 p1610 A66-21254
- Performance of Diamant launch vehicle including orbital considerations for planned projects 10 p1610 A66-21255
- Design and development of first liquid-fueled stage of Diamant launch vehicle 10 p1611 A66-21256
- Third stage and protective housing of Diamant launch vehicle 10 p1611 A66-21257
- Equipment located between Diamant second-stage propulsion unit and jettisonable rear skirt of third stage including antennas, auxiliary rockets, attitude changing apparatus, control and guidance, etc 10 p1518 A66-21258
- Solid propellant second stage of Diamant launch vehicle with steerable nozzles 10 p1611 A66-21259
- Diamant satellite launcher, development, launching and future 12 p1953 A66-23743
- French space program, flight tests of Diamant class rockets and A-1 satellite 12 p1981 A66-23804
- Steel for construction of propellant tank and skin of Diamant rocket 12 p1885 A66-23866
- Launching range facilities of Diamant rocket including equipment, radars, interferometers, telemetry, data processing, etc 16 p2682 A66-31233
- First two launchings of French Diamant satellite 17 p3016 A66-32378
- Diamant French satellite launching examining combustion stability during ignition, vibrations, chemical reactions between oxidizer and pressure feed system, etc 17 p3017 A66-33236
- French A1 satellite design and development, examining telecommunications equipment and monitoring diamant launcher performance 19 p3470 A66-36270
- DIAMINE**
- S ETHYLENEDIAMINE
- DIAMOND**
- SA METEORITIC DIAMOND
- Crystal chemistry of nonmetallic materials prepared under moderate or high pressure and recovered and retained under ambient conditions 01 p0090 A66-10292
- IR absorption spectra of aluminum and boron doped semiconducting synthetic diamonds 03 p0411 A66-13145
- Correlation between strength of induced optical absorption G band and strength of features in electron spin resonance spectrum in electron irradiated diamonds 06 p0934 A66-17125
- Electronic states of single defects in diamond calculated by comparing electronic states of single vacancies and single interstitial carbon atoms 06 p0938 A66-17148
- Uniaxial and hydrostatic pressure effect on absorption edge spectrum and edge excitation spectrum for visible luminescence diamond 07 p1095 A66-17320
- Ionization currents in diamond exposed to pulsed excitation and to applied pulsed electric field 10 p1586 A66-22144
- Electron energy losses in diamond, noting correlation between plasma excitation energy and interband transition energies 15 p2564 A66-28876
- Ionization currents in diamond exposed to pulsed excitation and to applied pulsed electric field 19 p3440 A66-35758
- Fine structure in direct absorption edge of cleaved type IIA diamond determined from reflectance data obtained from 5.5 to 11.5 ev at room and liquid-nitrogen temperatures 20 p3622 A66-38248
- Jahn-Teller shift reorientation in Ni impurity centers of diamond and rise of C-N pair EPR spectrum with temperature 22 p3964 A66-40307
- DIAPHRAGM**
- Thin metal diaphragms in shock tubes, discussing bursting characteristics and petalling behavior [ASME PAPER 65-WA/MET-16]
- 05 p0661 A66-15683
- Bursting shock tube diaphragms electrically, using two piezoelectric gauges 06 p0869 A66-16947
- Diaphragm-shaped external electrode used to define shape of plasma column in Tokamak machines, noting ways of maintaining plasma column equilibrium 13 p2148 A66-25755
- Annular diaphragms to produce turbulent flow in tubes 16 p2828 A66-31065
- Miniaturized piezoresistive transducer pressure diaphragm for experimental stress analysis 20 p3559 A66-37501



## DIATOMIC GAS

Vibrationally excited molecular hydrogen effect on mean 04 p0549 A66-14311

Ground state energy of charged Bose gas obtained from pair Hamiltonian and Green functions 11 p1741 A66-23392

Stimulated emission spectroscopy of hydrogen, nitrogen, oxygen and deuterium diatomic gases in 0.8 to 8 micron region 13 p2102 A66-26205

Dislocation rate magnitudes and relative collision frequencies influencing relaxation profiles in diatomic gases 14 p2274 A66-27447

Diatomic gas flow past blunt bodies, noting effect of oscillation and dissociation relaxation on mean 16 p2627 A66-30100

Quantum mechanical potential energy curve of lowest normal state of diatomic helium computed in valence bond scheme, using 17-term wave function of Slater orbitals 16 p2749 A66-30112

Numerical solution for complete Navier-Stokes equations for one-dimensional time-dependent propagation of compressible viscous thermally conducting diatomic gas, including presence of traveling shock wave 18 p3102 A66-34918

Recombination rate of diatomic gases determined from Mach number of supersonic nozzle outlet 21 p3694 A66-39090

Surface catalyticity and Reynolds number effects on nonequilibrium hypersonic stagnation flow of air or diatomic gas on highly cooled blunt body 22 p3847 A66-40919

**DIATOMIC MOLECULE**

Lifetime of radiative dissociation of excited molecular hydrogen 01 p0108 A66-10311

Potential energy curves for bound states of diatomic molecules from spectroscopic constants, using Rydberg-Klein-Rees method 01 p0108 A66-10600

Partial wave calculation of diatomic divalent molecular /HeH/ ion 04 p0547 A66-13643

Vibrational excitation cross sections of diatomic molecules calculated, using Born approximation by including polarization interaction between incident electron and molecule 06 p0912 A66-16630

Correlation energy effect on dissociation and binding energies of diatomic and polyatomic molecules 07 p1000 A66-18343

Motion yielding transition probabilities between low-lying vibrational levels of diatomic molecules 11 p1738 A66-22878

Dissociation rate of diatomic molecular fluorine 16 p2646 A66-30863

Thermal dissociation of molecular fluorine in inert gas from 1650 to 2700 degrees K in shock tube coupled to time-of-flight mass spectrometer 18 p3139 A66-34501

Electronic energy for ground state of one-electron diatomic molecule near united atom 18 p3140 A66-34512

Initial rotation effect upon vibrational excitation of diatomic molecules studied in two-dimensional collisions shows that with higher rotational energies it is increasingly difficult to excite 19 p3404 A66-36802

Sudden approximation applied to rotational transition probabilities and inelastic total cross sections for scattering of homonuclear diatomic molecules by atoms 21 p3774 A66-38526

Values of Morse potential for interaction of atoms in diatomic molecules carbon, CO and CN 21 p3775 A66-39072

Curves of attractive potential energy in diatomic molecules, noting calculations for Li-Li interactions in power series form 21 p3775 A66-39074

Absorption cross section of electron systems in bands of diatomic molecules calculated, noting effects of temperature variation 21 p3775 A66-39077

Coupled equations for open-channel components of wave function derived in total-angular-momentum representation in Feshbach approach to scattering theory for rigid rotator and atom 22 p3950 A66-39914

Dissociation energies of GaF, InF and TlF measured by high temperature mass-spectrometric techniques, noting possibility

of potential maxima in excited states 22 p3859 A66-39917

Calculating magnetic shielding constants of diatomic HF molecules, based on gauge-invariant atomic orbitals 22 p3950 A66-39919

Behavior of wave function for system of charged particles near coalescence of any two of them, noting electron-nucleus cusp conditions for diatomic molecules 22 p3861 A66-40904

Perturbation theory of heteronuclear diatomic molecules based on isoelectronic homonuclear molecules applied to carbon monoxide and nitrogen 23 p4032 A66-41646

## DIBORANE

Dichloroborane synthesized in quantitative yields by thermal hydrogenation of boron trichloride 05 p0629 A66-14540

Molecular orbitals of diborane using SCF-LCAO method, considering all electrons of molecule, calculating all integrals, with basis functions being Gaussian 06 p0940 A66-16123

Chemical kinetics of borane and diborane compounds, decomposition rates and molecular dissociation energy 15 p2447 A66-29237

Mass spectrometric analysis of contents of flow reactor in which diborane at low pressure was pyrolyzed, varying temperature, flow time, surfaces, etc 17 p2871 A66-32853

## DIBORIDE

Tungsten diboride preparation and structure 08 p1235 A66-18636

## DICKE TYPE RADIOMETER

Nomograms for radiometer sensitivity, predetection and postdetection gains and detector-output voltage used to accelerate Dicke radiometer design 11 p1666 A66-22689

Radiometric measurements of atmospheric absorption at 600 gc/s by DICKE type superheterodyne receiver, using harmonic mixing 15 p2450 A66-28999

## DICTIONARY

Dictionary of mathematical terms in English, French, Russian, German and Armenian, with English terms in alphabetical order 04 p0540 A66-14003

Russian-English Aerospace Dictionary 05 p0794 A66-15326

Chinese-English/English-Chinese astronomical and astrophysical dictionary 12 p1949 A66-24200

Dictionary of semiconductor physics and electronics, English-German, German-English 22 p3871 A66-39701

## DIE

Formulas for angular resilience of curvilinear surfaces of concave or convex planforms 07 p1038 A66-18060

Casting of plastic-ceramic dies 08 p1229 A66-18687

Contact process of linearly viscoelastic axisymmetric die, for case of noncommutative operators 15 p2611 A66-29342

Die holddown surface shape for complex forging 15 p2510 A66-29780

Hot drape forming of torus and semitoroidal bulkhead segments from aluminum alloys [SAE PAPER 660290] 15 p2511 A66-29831

Electrochemical machining techniques, noting PERA die-sinking system 20 p3562 A66-37426

Die friction effects on plane stress and plane strain in plastic bending of steel and titanium alloy beams 21 p3745 A66-39528

## DIELECTRIC CONSTANT

Electron-phonon interaction proportional to applied external electric field and sound amplification in semiconductors 01 p0118 A66-10259

Microwave permeability and permittivity measurement, knowing resonant frequency of unperturbed cavity and distribution of electric and magnetic field 01 p0025 A66-10527

Automatic measuring apparatus based on resonant cavities for measuring permittivity and permeability of ferrites as function of temperature 01 p0068 A66-10558

Permittivity of dielectric formed from ground state instability of semimetal, considering Coulomb attraction between electrons and holes 01 p0125 A66-10774

Complex permittivity of low-loss liquids measured with magic tee and variable-length

cell 03 p0368 A66-12461

Curie temperature, static dielectric constant and electro-optic coefficient of large single crystals of barium titanate 03 p0411 A66-13007

Mode guiding and gain in junction laser due to dielectric sandwich confining wave propagation 04 p0530 A66-19352

Radiation from vertical magnetic dipole in inhomogeneous stratified media above horizontal conducting plane, noting Hertz potential as contour integral 04 p0483 A66-14047

Admittance of thin long linear antenna embedded in uniaxial medium and inclined at angle theta to axis of medium 06 p0848 A66-16274

Permittivity of barium titanate single crystals with laminar domain structure 06 p0926 A66-16711

Slow polarization processes of barium titanate in weak field 06 p0927 A66-16711

Classification of ions capable of replacing Ti in barium titanate 06 p0927 A66-16711

Permittivity of barium titanate ferroceramic materials determined by various methods 06 p0927 A66-16721

Dielectric losses and permittivity of vitreous semiconductor arsenic trisulfide with silver impurity 06 p0929 A66-16921

Dielectric constants of alkali and thallium halides determined for various temperatures and frequencies, showing results obtained on sodium chloride 07 p1108 A66-18411

LF electromagnetic wave excitation in electron-ion and electron-hole plasma situated in external electrical field 08 p1262 A66-18971

Discrete spectrum of electromagnetic waves caused by excitation of dielectric layer on ideally conducting plane in homogeneous absorbing plasma 09 p1344 A66-20351

Transition radiation relative to dispersion of dielectric permittivity for charged particle passing through boundary between two media 09 p1410 A66-20930

Dielectric constant of lossy dielectric sphere determined by utilizing C band radar cross section measurement 10 p1502 A66-21631

Optical and electrical constants of beta-rhombohedral boron 10 p1379 A66-21721

Turbulent fluctuation effect on dielectric properties of weakly turbulent plasma at LF and electron plasma frequency 10 p1567 A66-21811

Permittivity of dielectric formed from ground state instability of semimetal considering Coulomb attraction between electrons and holes 11 p1749 A66-22280

Solution of two first equations of BBGKY hierarchy, obtaining dielectric constant of plasma by using Guernsey solution, giving two-particles distribution function 11 p1744 A66-22441

Contribution of electron-electron correlations to longitudinal dielectric constant for case of one-component plasma noting resonance effect and formula for plasma oscillation damping 11 p1744 A66-22441

Tensor component of dielectric permittivity of isothermal plasma derived from kinetic equation, accounting for effect of magnetic field on collision between particles 11 p1745 A66-22581

Parasitic internal oscillations in laser crystal with dielectric rod caused by total reflection from generatrix of cylindrical sample 11 p1712 A66-22731

Self-oscillations of dielectric rods between two metallic plates 11 p1669 A66-23101

Constant electric field effect on transverse dielectric constant of semiconductor 12 p1926 A66-23714

Dielectric layers of alternating low and high dielectric constant used as filters in millimeter wave, IR and optical regions 12 p1831 A66-23906

Kinetic oscillation of nonhomogeneous collision plasma, discussing drift instability ionization, longitudinal current effect etc 12 p1921 A66-24204

Complex longitudinal microwave magnetoconductivity and permittivity of n-type silicon at 77 degrees K, noting influence of DC magnetic



field 13 p2159 A66-25066  
 Capacitance transducer characteristics and applications as fuel gauge, level detector, interface detector, pressure and proximity sensors, etc 13 p2078 A66-25360  
 Electron-phonon interaction proportional to applied external electric field and sound amplification in semiconductors 13 p2168 A66-25976  
 Complex dielectric constants of lossy liquids measured by transmission measurements in X-band waveguide 13 p2082 A66-26342  
 Heavily doped semiconductor parameters determined from spectral behavior of coefficient of reflection and transmission 14 p2357 A66-27072  
 Temperature dependence of dielectric permittivity and relative expansion of bismuth ferrite in large temperature intervals, detecting phase transitions 14 p2357 A66-27078  
 Photoionization of leucocarbols and leucocyanides of malachite green, crystal violet and sunset orange dissolved in straight chain alcohols and chlorinated hydrocarbons 14 p2232 A66-27374  
 Stannic oxide ceramic formation and dielectric constant and resistivity measurements and evaluations 14 p2362 A66-27499  
 Plane wave behavior, as deduced from Mathieu function, analyzed in permittivity modulated slab immersed in medium of arbitrary constant 14 p2240 A66-27913  
 Endfire effect in dielectric foam rods and mode control by varying dielectric constant of rod 14 p2256 A66-27921  
 Dielectric constant of gold-plated rectangular parallelepiped solid at hyperfrequencies determined via resonant frequency method 14 p2366 A66-27944  
 Dielectric measurements and optical observation of potassium dihydrogen phosphate /KDP/ crystal 14 p2367 A66-27945  
 Anodic oxide film growth on sputtered tantalum films in dilute sulfuric acid, noting ionic conductivity, dielectric constant and optical properties 15 p2562 A66-28718  
 Electromagnetic propagation in weakly ionized plasma, deriving electronic distribution function and dielectric permittivity tensor 15 p2552 A66-29331  
 Dielectric constant, permeability and conductivity of random media determining electric field, current, magnetic field, etc, assuming these quantities are time harmonic plane waves 15 p2451 A66-29619  
 Flute stabilization of hot electron plasma by cold plasma which contributes to dielectric coefficient 15 p2555 A66-29759  
 Coupling and synchronization of lasers, noting field amplitudes, delayed interaction and dielectric constant 15 p2519 A66-29885  
 Dielectric constant obtained by bound electron theory is not distinguished from one obtained by warm plasma theory when considering main resonance and related phenomena 16 p2758 A66-30277  
 Optical and magneto-optical phenomena in CdSnAs sub 2, discussing reflection and absorption spectrum, optical activity, double refraction, dielectric constant, etc 16 p2788 A66-31775  
 Electrical properties of SiO films, noting independence of dielectric constant on film thickness and dependence of conductivity on applied field 17 p2978 A66-32411  
 Dominant mode perturbation theory applied to treatment of influence of imperfect waveguide contact on measured complex permittivity of semiconductors 17 p2887 A66-32643  
 Optical thickness effect on monochromatic directional transmittance and emittance of isothermal dielectric surrounded by air 18 p3134 A66-33991  
 Dielectric constant variation in silicon single crystals, noting frequency dependence of dielectric loss, conductivity and temperature effects 19 p3436 A66-35423  
 Alfven waves in bismuth for propagation along magnetic field, noting dielectric constant variation with frequency, effect on real part of refractive index, relaxation time analysis, etc 19 p3443 A66-36006

Dielectric function for homogeneous plasma calculated, using fluctuation dissipation theorem 19 p3409 A66-36289  
 Scale model of submerged VLF antenna using lossy ceramic powder to model ice and snow for submarine communication, geophysics, etc 19 p3321 A66-36416  
 Electromagnetic field analysis, determining dispersion relationship of array of identical fibers, assuming surface wave modes of each fiber are excited 19 p3305 A66-36418  
 Optical properties and complex dielectric constants of transition metals 20 p3614 A66-37276  
 Humidity effect on ferroelectric properties of barium titanate with tantalum oxide admixture, noting growth of dielectric constant and crystal polarization 20 p3617 A66-37553  
 Frequency scanned antenna with dielectric loaded waveguide, discussing experimental results 20 p3531 A66-37729  
 Double-strip H-guide structure, examining field components, characteristic equation and attenuation coefficient for each mode 20 p3533 A66-38145  
 Radio wave propagation over Earth surface, determining conductivity and dielectric constant taking into account ground effect 21 p3706 A66-39514  
 Barium titanate rods as nonlinear element of S-band resonant cavity microwave parametric amplifier, noting variation of permittivity of rods with percentage of barium titanate 22 p3872 A66-39736  
 Far-field light emission mode pattern of GaAs diode injection lasers, dielectric gradient in inversion layer and refractive index in junction 22 p3930 A66-39743  
 Kinetic oscillation of nonhomogeneous collision plasma, discussing drift instability, ionization longitudinal current effect, etc 22 p3956 A66-40568  
 Heavily doped semiconductor parameters determined from spectral behavior of coefficient of reflection and transmission 22 p3966 A66-40830  
 Temperature dependence of dielectric permittivity and relative expansion of bismuth ferrite in large temperature intervals, detecting phase transition 22 p3967 A66-40834  
 Induced microwave absorption in carbon dioxide studied at frequency of 9260 mc/sec over temperature range from 270 to 500 degrees K and pressures as high as 95 atm 22 p3985 A66-40909  
 Parasitic internal oscillations in laser crystal with dielectric rod caused by total reflection from generatrix of cylindrical sample 23 p4078 A66-41477  
 Semiconductor conductivity in strong SHF electric fields, measuring dielectric constant and Fourier component 23 p4068 A66-41620  
 Electromagnetic wave scattering by stratified medium, noting Mathieu and Floquet type wave representation 24 p4171 A66-42292  
 Electrical properties and fabrication of zinc oxide-bismuth oxide low Q capacitor with high apparent dielectric constant over wide frequency range 24 p4180 A66-42311  
 Carbon disulfide traveling wave Kerr cells with identical microwave and dielectric constants, noting light modulator construction at microwave frequencies 24 p4185 A66-42814

# DIELECTRIC MATERIAL SA CERAMICS

Zinc selenide as highly refractory substance in dielectric mirror layers for laser resonators and interference filters 02 p0238 A66-11252  
 Dielectric filler performance of silicon carbide, microsilized glass sphere and titanium dioxide at microwave frequencies 02 p0247 A66-11285  
 High-reliability microwave printed circuits using copper-clad polyethylene dielectric materials 02 p0195 A66-11288  
 Dielectric organic polymers in microcircuit communications modules 02 p0195 A66-11289  
 Rigid polyurethane foam encapsulation of high-voltage aerospace electronic systems, noting vacuum effect 02 p0248 A66-11292  
 Transformation of metal into dielectric by application of magnetic field to shift band

boundaries 02 p0274 A66-11734  
 Electrometer using temperature-autostabilizing nonlinear dielectric element as receiver 02 p0230 A66-11815  
 Microwave propagation through metallic waveguides filled with dielectrics, using field theory, network theory, Rayleigh-Ritz procedure, reaction concept, etc 02 p0206 A66-12009  
 Steps for V-I characteristic of Josephson tunnel current interaction with electromagnetic field in dielectric superconductors 03 p0407 A66-12282  
 Reflection and transmission of electromagnetic waves by dielectric medium moving parallel to and perpendicular to interface, determining coefficients 04 p0481 A66-13739  
 Waveguide containing ferrite of ferrite-dielectric insert determined by applying eigenfunction method 04 p0499 A66-14051  
 Static characteristics of field triode with gate separated from semiconductor by thin dielectric layer, considering regimes of concentration, depletion, etc 04 p0499 A66-14054  
 Impedance of dielectric oxide with uniformly distributed monoenergetic traps 04 p0501 A66-14253  
 Electrophoretic motion of dielectric particle determined from flow rate of liquid metals and semiconductors near infinite plane 05 p0733 A66-14688  
 Possible processes of non-radiative decay of excitons on ionized donors and acceptors in semiconducting and dielectric crystals 05 p0737 A66-15160  
 Steps for V-I characteristics of Josephson tunnel current interaction with electromagnetic field in dielectric superconductors 05 p0738 A66-15454  
 Dielectrics theory using average field approximation containing random concentration of ellipsoidal inclusion 06 p0908 A66-16027  
 Pole-zero analysis techniques for reflection coefficient of multiple-layer dielectric having complex permittivity 06 p0843 A66-16030  
 Long wavelength limit in scattering from homogeneous dielectric cylinder at oblique incidence 06 p0830 A66-16277  
 Optical absorption of metal films in region of transformation to dielectric, discussing valence and conduction band separation mechanism 06 p0924 A66-16518  
 Ionization under laser action extended to metals and dielectrics, noting influence on thresholds 06 p0893 A66-17065  
 Synthesis, X-ray studies and dielectric measurements of lead containing perovskites 07 p1092 A66-17220  
 Mirrors composed of multilayer stacks of dielectric films and attaining high reflectance over extended spectral range 07 p1079 A66-17290  
 Microstrip transmission on semiconductor dielectrics provide high quality interconnection between microwave functions 07 p1007 A66-17505  
 Space-charge reduction of shot noise for space-charge-limited current in solid dielectric diode 07 p1097 A66-17737  
 Solution to problem of cylindrical cavity containing ferrite and dielectric specimens in hollow cylindrical form 07 p1009 A66-17927  
 Solid-dielectrically loaded strip transmission line techniques extended to Ku-band region 08 p1192 A66-18946  
 Electric properties of passive circuit thin film components in microelectronics, discussing resistors, capacitors and microcircuit interconnections on method of preparation 08 p1192 A66-18963  
 Dielectric properties and lattice parameter dependence on temperature from X-ray studies of rubidium-potassium nitrate mixed crystals 08 p1269 A66-19008  
 Relation of compressibility with cohesive energy and molecular volume for dielectric solids, noting confirmation of relation for 45 crystalline compounds 08 p1244 A66-19254  
 Coaxial, rectangular and bandpass waveguides containing ferrite and dielectric plates in E plane, obtaining transcendental equations, determining electromagnetic wave propagation 08 p1194 A66-19312  
 True heat capacity of solid heat-resistant



dielectric or conducting materials at high temperatures 09 p1470 A66-20141

Cerenkov radiation in circularly symmetrical waveguide filled with uniform dielectric in presence of flowing modulated electron stream 09 p1351 A66-20258

Optical absorption of metal films in region of transformation to dielectric, discussing valence and conduction band separation mechanism 09 p1431 A66-20899

Boundary value problem for wave propagation on cylindrical anisotropic dielectric rod solved for hybrid modes 10 p1496 A66-21307

Frequency and temperature effects on dielectric properties of calcium, strontium and barium fluorides 10 p1577 A66-21561

Total field measurement in all directions in near zone of metallic and dielectric spheres and cones 10 p1502 A66-21635

Radar cross section of flat base dielectric cones, noting parameters such as cone angle, size, wavelength, etc 10 p1503 A66-21646

Parameters of dielectric walls of various structures with optimal radio-engineering characteristics treated by graphical method 10 p1511 A66-21676

Temperature dependence of dielectric properties of antiferroelectrics of perovskite structure in SHF range 10 p1589 A66-22168

Polar vapor effects on dielectric properties of barium titanate single crystals with metal admixtures 11 p1749 A66-22292

Wide-angle impedance matching /WAIM/ method reducing variation of reflection coefficient with scan angle and polarization by dielectric sheet located in front of array antenna face 11 p1663 A66-22547

Dipolar resonances when axially uniform warm plasma column is subjected to transverse RF electric field 12 p1815 A66-23962

Stripline cavity resonator for low microwave frequency measurements of magnetic and dielectric properties of ferrites 12 p1881 A66-24156

Secondary electron emission in zinc sulfide and magnesium fluoride thin dielectric films and semiconductor layers due to electric field stimulation 12 p1930 A66-24459

Dielectric relaxation in thermally grown silicon dioxide films 12 p1932 A66-24828

Exact mathematical solution for elastic dielectrics in controllable states, noting Rivlin and Toupin theory, cuboid deformation into rectangular block, electric field effect, etc 12 p1933 A66-24961

RF sputtering of insulators, noting effects of auxiliary magnetic field, electrode size, oxygen concentration, substrate temperature and target material on thin dielectric film formation 13 p2157 A66-25039

Current voltage characteristics of dielectric films 13 p2157 A66-25040

Nonlinear dielectric laser light absorption by neutral gas resulting in avalanche breakdown of gas due to thermal ionization 13 p2090 A66-25425

Heavy ionizing particle path detection by thin dielectric sheets 13 p2084 A66-26561

Ghost modes in open microwave resonator waveguides containing dielectric slabs of rectangular geometry with anisotropic dielectric constant 14 p2246 A66-26796

Laser frequency tuning by dielectric material interaction to produce nonlinear effects 14 p2305 A66-26867

Damping constant of electromagnetic wave in plane parallel waveguide with ferrite resonant isolator, using perturbation theory, considering dielectric and magnetic losses 14 p2250 A66-27143

Directional monochromatic emittance of isothermal diathermanous coatings on various conductors [AIAA PAPER 65-119] 14 p2411 A66-27410

Dielectric diode induction effect demonstrated through equivalent circuit 14 p2252 A66-27491

Electromagnetic wave reflection and transmission coefficients for moving dielectric slab as function of velocity of medium 14 p2239 A66-27761

Mutual and self-impedance of linear antennas in interface between dielectric layers computed, noting cases of symmetric and antisymmetric excitations 14 p2256 A66-27914

Dielectric material position effect on characteristics of ladder line slow wave structure of TW masers 14 p2258 A66-27960

Critical conditions of waveguide with dielectric bushing for case of nonsymmetrical waves 14 p2259 A66-28161

Wide angle impedance matching /WAIM/ of planar array antenna by dielectric sheet for reduction of reflection coefficient variation with scan angle and polarization 15 p2456 A66-28587

Zero magnetic field millimeter maser using trivalent iron ion in host crystalline structure of rutile /titanium dioxide/ as active material 15 p2514 A66-29018

Quasi-optical iterated-dielectric-slab rectangular waveguide filters for millimeter and submillimeter wavelengths 15 p2462 A66-29022

MHD drag of dielectric oscillating sphere in incompressible conducting fluid with uniform magnetic field aligned along axis of oscillation 15 p2553 A66-29689

MHD boundary layer flow of incompressible conducting rotational fluids over infinite dielectric disk 16 p2765 A66-31403

Dielectric properties and thermostability of glow-discharge thin organic polymer films for electronic application 16 p2783 A66-31429

Reflection and refraction of light waves at boundary of nonlinear dielectric resonator and waveguide designs using multilayer dielectric 16 p2666 A66-31557

Synthesis, X-ray studies and dielectric measurements of lead containing perovskites 17 p2976 A66-31991

Waveguide containing ferrite of ferrite-dielectric insert determined by applying eigenfunction method 17 p2884 A66-32217

Static characteristics of field triode with gate separated from semiconductor by thin dielectric layer, considering regimes of concentration, depletion, etc 17 p2884 A66-32220

Dielectric-walled vacuum vessel for space simulation testing of plasma propulsion devices 17 p2903 A66-32487

Maxwell equation solution for source currents in unbounded magnetoionic medium with uniaxial dielectric tensor, using Fourier transform technique 17 p2959 A66-32962

Photoconductivity induced in uncolored sodium chloride and aluminum oxide single crystals by radiation from ruby laser 18 p3154 A66-33939

Continuous wave power ratings of strip transmission lines, noting temperature profile parameters, power limit curves, etc 18 p3077 A66-34062

Electrical measurements of stannic oxide in ceramic form, noting forming and firing of samples, dielectric dispersion, grain boundary capacitances, etc 18 p3155 A66-34197

Method for determining temperature dependence of heat conductivity of dielectric and semiconductor materials 18 p3159 A66-35054

Calculations of energy loss of relativistic charged particles in dielectric media compared with mass operator and perturbation theory calculations and with oxygen experiment 18 p3221 A66-35201

Dielectric fiber cylindrical surface waveguide with refractive index higher than surrounding region for energy transmission at optical frequencies 19 p3302 A66-35725

Temperature dependence of dielectric properties of antiferroelectrics of perovskite structure in SHF range 19 p3441 A66-35782

Thermometer for continuous temperature measurement of dielectrics and semiconductors in electromagnetic HF fields 19 p3358 A66-35836

Laser giant pulse damage to dielectric mirror coatings immersed in nitrobenzene solution 19 p3444 A66-36075

TE wave scattering by dielectric cylinder of arbitrary cross section shape, including effects of surface wave excitation and mutual interaction 19 p3304 A66-36408

Swept frequency measurement of water-drop diameter in spherical resonator, using dielectric materials 19 p3394 A66-36417

Radiated fields for plasma external to dielectric coating surrounding biconical

antenna, equivalent circuit developed for terminating impedance 19 p3305 A66-36422

Theoretical distribution of charges and potential in vicinity of metal-dielectric barrier in absence and presence of applied field 19 p3448 A66-36753

Secondary electron emission in zinc sulfide and magnesium fluoride thin dielectric films and semiconductor layers due to electric field stimulation 20 p3620 A66-37691

Extension of equivalence principle to take into account contribution to radiation of end point of dielectric rod in dielectric antennas 20 p3531 A66-37728

Electromagnetic wave emission excited by electron stream over diffraction grating lying on boundary of semiinfinite anisotropic dielectric 20 p3519 A66-37998

Thin dielectric film wave scattering, EM interaction responses and conductivity tensor 20 p3622 A66-38385

Reflection and transmission of EM waves by dispersive dielectric cold plasma 20 p3611 A66-38394

Horn transitions from empty waveguides to dielectric surface waveguides using telegraphers equations, determining launching horn shape with minimum reflection coefficient 21 p3711 A66-38836

Tunnel current dependence on magnetic field for two superconductors with thin dielectric interface 21 p3804 A66-39314

Natural frequency equations for TEM mode oscillations of coaxial resonator with moving dielectric material 21 p3713 A66-39321

Mathematical analysis of radiation from slotted magnetic line source on conducting cylindrically capped wedge covered by dielectric layer or plasma sheath 21 p3705 A66-39349

Dielectric loss tangent measurement in pyroelectric materials for EM radiation detectors and heat transfer sensors 21 p3740 A66-39386

Theoretical static I-V characteristics of surface gate dielectric triode and geometric factors influence on amplification factor at cut-off 22 p3872 A66-39746

Equations for ionized positive plasma column of gas discharge between infinite dielectric planes under oblique magnetic field with component in direction of external electric field 22 p3953 A66-39756

Bistatic radar method for determination of permeability and permittivity of material for smooth spherical target 22 p3863 A66-39941

Growth of plane acceleration discontinuities propagating into homogeneously deformed hyperelastic dielectric material in presence of magnetic field 22 p3948 A66-40136

Wide stop bandwidths from quasi-optical filters formed from iterations of dielectric slabs demonstrated at millimeter wavelengths 22 p3877 A66-40181

Optical thickness measurement of nonabsorbing dielectric film when it is inconvenient to apply overlay film to measure thickness by Fizeau fringe shift 22 p3968 A66-40889

Electrostatic oscillations in dielectric, semiconductor and plasma in presence and absence of external magnetic field 22 p3968 A66-40947

Effectiveness parameters of spherical shield electrode surrounding negative dielectric junction of insulator in high vacuum 23 p4042 A66-41040

Diffraction of electromagnetic waves at dielectric wedge, considering skin depth and internal problem 23 p4036 A66-41134

Narrow slot antennas covered with dielectric slabs of arbitrary thickness, examining design flexibility in application as radiating elements of waveguide 23 p4046 A66-41586

Radiation in magnetoplasmas, noting correctness of infinity catastrophe theory for dielectric radiation sources in magnetoionic media 23 p4105 A66-41632

Antenna radiation theory, noting reiteration of incorrectness of infinity catastrophe theory and application to oscillating dipole in uniaxial medium 23 p4047 A66-41633

Impedance of flat strip antenna embedded in planar dielectric slab surrounded by layers of compressible isotropic electron



plasma 23 p4047 A66-41639  
Transmission coefficient and tunnel current for trapezoidal potential barrier calculated as function of applied voltage 24 p4254 A66-42385  
Nonuniform thickness of dielectric films effect on capacitance and tunnel currents of elements with metal-insulator-metal structure 24 p4254 A66-42387  
Self-trapping of laser beam due to diffraction from dielectric waveguide arising from permittivity increase of birefringent beam 24 p4222 A66-42554  
Propagation and radiation of radio waves from dielectric coated prolate spheroidal core loop antenna surrounded by plasma sheath 24 p4184 A66-42745  
Electromagnetic propagation in slowly rotating anisotropic dielectric single band waveguide modulator 24 p4175 A66-42967  
Dielectric breakdown phenomena in evaporated silicon monoxide thin film, noting electron collision effect 24 p4260 A66-43106  
Evaporation system for fabrication of multilayer dielectric films for mirrors or filters, obtaining thickness variation reduction and simultaneous deposition 24 p4218 A66-43163  
**ELECTRIC PERMEABILITY**  
Fluctuations in energy absorbed within definite periods of time by plane-surface thermal emission sensors of arbitrary dielectric permeability 01 p0069 A66-10722  
Barium titanate single crystals at infrared frequencies investigated for polarization, effective permittivity and coercive field 06 p0926 A66-16713  
Reversing permittivity of barium titanate single crystals measured, using lithium chloride solution for electrodes 06 p0926 A66-16714  
Absorption and spontaneous and stimulated emission for homogeneous isotropic nonferromagnetic Maxwellian media at rest 07 p1081 A66-18037  
Optical absorption and dielectric loss measurements in KCl doped SrCl sub 2 single crystals, determining involvement of impurity vacancy dipolar complexes in optical conversion of F centers to Z centers 12 p1926 A66-23718  
Fluctuations in energy absorbed within definite periods of time by plane-surface thermal emission sensors of arbitrary dielectric permeability 20 p3560 A66-37660  
**ELECTRIC POLARIZATION**  
Microwave scattering by dielectric slabs of finite width and hollow wedge formed by two dielectric slabs 03 p0331 A66-12306  
Wideband polarizer in circular waveguide loaded with dielectric disks 07 p1006 A66-17503  
Ferroelectric properties of trisarcosine calcium chloride including dielectric measurement, Curie temperature region, etc 08 p1270 A66-19009  
Boundary surface roughness effect on polarization of thermal electromagnetic wave emission from dielectric medium 09 p1401 A66-20115  
**ELECTRICS**  
**SA SPARK GAP**  
Testing dielectrics by direct application of two high-voltage LF electrostatic generators with long-period sinusoidal waves 03 p0340 A66-12467  
Dielectric properties of noble gases afterglows following electrodeless discharge over signal frequency and pressure ranges 04 p0551 A66-13813  
Propagation characteristics of microwaves through dielectric loaded waveguides and imperfect waveguides filled with imperfect dielectrics 04 p0498 A66-14042  
Radiation characteristics of isolated circular optical waveguides supporting low-order dielectric waveguide modes for combinations of modes, wavelength, diameter and aperture 05 p0648 A66-14910  
Theory describing ionized gas plasma in which no physical contact may occur between measuring device and plasma 06 p0843 A66-16035  
Propagation in rectangular and circular cylindrical waveguide containing inhomogeneous dielectric varying linearly and quadratically 06 p0848 A66-16108

Propagation of microwaves through circular cylindrical metallic guide filled with two different dielectrics 06 p0857 A66-16951  
Dielectric loaded waveguides, defining surface, transverse and longitudinal impedances in analogy with circuit theory definition 08 p1200 A66-19121  
Propagation of acceleration and electromagnetic waves in homogeneously deformed uniformly polarized hyperelastic dielectric 08 p1271 A66-19228  
Low loss transmission medium for optical frequencies consisting of thin wall dielectric tube separating internal high density gas from external low density gas 08 p1235 A66-19839  
Superposition and geometrical optics techniques for approximations of radar cross section of nonconducting bodies 10 p1498 A66-21598  
Radiation characteristics of dielectric coated half-wave resonant slot antenna, examining effects of improper dielectric scaling 11 p1663 A66-22553  
Design and application of dry, dielectric and water-cooled dummy loads 12 p1829 A66-23537  
Maximum dielectric strength of thin evaporated silicon oxide films, calculating breakdown processes 12 p1933 A66-24830  
Radiant energy conversion using thin dielectric films in thermoelectrostatic cycle [AIAA PAPER 64-729] 13 p2006 A66-26639  
Dielectric tensor in relativistic Vlasov plasma in electron cyclotron harmonic resonance region 13 p2155 A66-26676  
Transmission power of dielectric waveguide 14 p2251 A66-27168  
Transcendental equation derived for approximate calculation of waveguide resonators containing dielectric 14 p2251 A66-27240  
Applicability region of Mott-Gurney square law for space-charge limited currents in dielectrics 14 p2266 A66-27574  
Dispersion characteristic of stub slow-wave structure, partially filled by dielectric, of traveling wave maser 14 p2310 A66-28291  
Dielectric guide structures /Dieguides/ used for increased gain/noise ratio in low noise antennas 15 p2456 A66-28588  
Flame spraying method for conversion of pure barium titanate into glass, noting dielectric Curie temperature 15 p2524 A66-29665  
Augmented Born approximation based on variational principles applied to electromagnetic scattering from inhomogeneous dielectric spheres of finite extent 18 p3071 A66-34452  
Disintegration of alkali halide single crystals, polymers and glasses under laser radiation, noting parameters of disintegration region 18 p3119 A66-34681  
Inhomogeneously filled waveguides containing dielectric used as microwave delay line for pulse compression 23 p4035 A66-41025  
Calculation method for optimum number of thin film elements on substrate of micromodule consisting of active and passive conducting, resisting and dielectric elements 24 p4257 A66-42536  
**DIENE**  
Conversion of 2-carboxy-3-keto-9-methyl-unsaturated hexahydronaphthalene into 5/7-fused products on irradiation in aqueous and nonaqueous media, observing photochemical rearrangements 24 p4170 A66-42314  
2-carboxy-3-keto-9-methyl hexahydronaphthalene converted in high yield into 5/7 fused products on irradiation in aqueous and nonaqueous media 24 p4171 A66-43101  
**DIET**  
**S NUTRITIONAL REQUIREMENT**  
**S STARVATION**  
**DIETHYL ETHER**  
X-ray radiation effect on electrical conductivity of liquid organic semiconductors obtained on diethyl ether base with halogen derivatives of benzene, methane, etc 13 p2160 A66-25096  
**DIFFERENCE EQUATION**  
Finite difference method solving Dirichlet problem for quasi-linear elliptic equation, with results applied to calculation of

magnetic field in nonlinear media 01 p0091 A66-10165  
Solution to linear difference and differential equation with variable coefficients 01 p0092 A66-10173  
Random error in finite difference approximation of stochastic nonlinear equations in theory of random signals and noise 01 p0093 A66-10381  
Existence of explicit stable difference scheme in correct Cauchy problem for linear systems of partial differential equations with constant coefficients 01 p0094 A66-10654  
Nonlinear differential-difference equations of form  $Ly$  equals  $f(y)$  solved by using  $f(y)$  as power series in exponentials 03 p0387 A66-12614  
Nonsymmetric difference equations, examining convergence proofs 03 p0387 A66-12615  
Forced oscillations in nonlinear relay type control system predicted via periodic solutions to nonlinear difference equation 05 p0654 A66-14606  
Representation of analytical periodic Fourier transforms of difference operators by sum of squares 05 p0708 A66-15328  
Stability in small of two types of extremal systems with modulating action, using linear difference equation with periodic coefficients 07 p1013 A66-17429  
More general solution to difference equation  $y/x$  plus  $1/-y/x$  equals  $f/x$  than that derived by Euler 07 p1059 A66-17974  
Computational reduction of high speed memory requirements in solving optimization problems by dynamic programming and supersonic transport trajectory application 07 p1004 A66-17976  
Solutions in large for nonlinear hyperbolic systems of equations by difference approximation 07 p1059 A66-18032  
Fluctuations of electron numbers in general M-level system, using difference equation 08 p1279 A66-19837  
Plane nonlinear stationary problem of hill slope winds reduced to set of finite difference equations and solved by simple and matrix factorization combined with iteration by computer 09 p1398 A66-19885  
Invariant imbedding in transport process and theorems of uniqueness and existence for derived hyperbolic equation 09 p1393 A66-19906  
Asymptotic behavior, at plus infinity, of first order linear differential-difference-delay equation solutions, discussing asymptotic oscillatory number 10 p1549 A66-21224  
Conversion and uniqueness theorems and series convergence in difference equation theory 10 p1549 A66-21227  
Generalization of high accuracy alternating direction implicit /ADI/ method for solving wave equation in two space dimensions 10 p1550 A66-21845  
Difference scheme of integrated conservative type and equivalent semi-Lagrangian type for weather forecasting equation 11 p1725 A66-22195  
Existence of explicit stable difference scheme in correct Cauchy problem for linear systems of partial differential equations with constant coefficients 12 p1903 A66-24023  
Best linear unbiased /BLU/ estimator for large class of error correlation models 12 p1904 A66-24197  
Pseudorandom binary sequential digital simulation of feedback control systems subjected to random input signals 13 p2030 A66-25211  
Maximum principle for systems described by difference equations, justifying convexity assumptions for approximation of differential equations 13 p2116 A66-25344  
Dynamic programming recursive estimation of modal trajectory for nonlinear non-Gaussian noise and comparison with Bayesian estimation and case of Gaussian white noise 13 p2053 A66-26086  
State-space analysis of discretely controlled systems with finite delays 14 p2266 A66-27589  
Passage of pulse signal through distributed RC circuit with nonlinear p-n junction capacitance 14 p2254 A66-27740  
Internal regime of waveguide-slot antennas with identical resonance radiator via



- difference equations 14 p2254 A66-27743  
 Difference equations arising when one-velocity kinetic equation is solved by characteristics method, estimating error 14 p2338 A66-28280  
 Points in interior and boundary of three-dimensional supersonic gas flow determined, using characteristic method, - deriving difference equations 14 p2278 A66-28284  
 Stability of nonlinear control systems, noting Hermitian matrix for linear system of ordinary differential equations and analogous problem for difference equations 15 p2525 A66-28513  
 Generalized maximum likelihood estimators with proof of asymptotic efficiency, considering Markov chain and stochastic difference equations 15 p2525 A66-28604  
 Synthesis of linear digital recursive filters, noting application to arbitrary amplitude frequency transfer function synthesis 15 p2475 A66-29772  
 Representation of analytical periodic Fourier transform of difference operators by sum of squares 16 p2735 A66-30966  
 Extension of problem of singular perturbation for linear scalar constant coefficient differential-difference equation with single retardation to several retardations, noting degenerate equation solution 16 p2737 A66-31230  
 Book on stability, oscillation and time lags in differential and differential-difference equations, discussing Liapunov stability theorem 16 p2739 A66-31754  
 Difference analog construction for second-order elliptic differential equation in case of rectangular network 19 p3389 A66-35935  
 Maximum principle in optimization of discrete time systems described by difference equations 20 p3536 A66-36857  
 Convergence of difference approximations in rectangular grids for general first-order quasi-linear hyperbolic initial value problems in two independent variables 20 p3590 A66-37526  
 Stress analysis of difference equations for bending and shear effects in elastic grids 21 p3832 A66-39536  
 Transformation of infinite Legendre sums into finite series of Legendre polynomials by transforming sum into integral leading to difference equations 22 p3995 A66-40458
- DIFFERENTIAL ALGEBRA**  
 Bellman functional equation derived for class of optimal control problems without using Taylor series expansion or mean value theorem of differential calculus 07 p1017 A66-18347  
 Deriving interpolatory type quadrature formula by inverting linear systems of differentiation formulas 09 p1395 A66-20622  
 Differential approximation linearization technique compared with Galerkin method 16 p2732 A66-30265  
 Numerical differentiation by differential quotients, interpolations, Richardson-Romberg algorithm and other methods, including analysis of approximation errors 16 p2658 A66-31347
- DIFFERENTIAL AMPLIFIER**  
**SA SEMICONDUCTOR DEVICE**  
 Integrated sense amplifier usable with most medium to high speed coincident current memory /CCM/ systems with only two power supplies and no external components 01 p0048 A66-11144  
 Linear integrated circuits discussing differential and operational amplifiers, development, use, capabilities, new techniques, special designs and reliability 03 p0347 A66-13340  
 Thermal instability analogous to thermal runaway occurring in differential transistor amplifiers 04 p0500 A66-14097  
 Integrated DC differential instrumentation amplifier discussing drift, gain and common-mode rejection 05 p0646 A66-14641  
 Molecularized FM-FM telemetry system for providing more reliable FM subcarrier oscillators with reduced size, weight and power dissipation 06 p0824 A66-15968  
 Solid state microelectronic differential amplifier as stable high gain and high input impedance amplifier 10 p1513 A66-21903  
 Periodically operating gate circuit with negative feedback for sampling in micro-and millisecond range 12 p1847 A66-24938
- Differential amplifiers using common-collector, isolated and lateral complementary transistor structures, including frequency response, phase shift, etc 13 p2036 A66-25532  
 Transfer function for quadrature modulation single band signal generating all-pass filter, using differential operational amplifier 14 p2253 A66-27586  
 Dual transistors for noise and drift reduction in differential direct-coupled amplifier design 14 p2262 A66-28376  
 Substrate layout and deposition of all thin film differential amplifier 17 p2882 A66-32112  
 Current-mode logic gates in building differential amplifier for memory-core readout 17 p2884 A66-32127  
 Approximation technique for flow graph that eliminates nonessential equivalent circuit elements, providing for derivation of most concise model with preassigned accuracy 18 p3092 A66-35040  
 Behavior of thermally coupled transistors in differential amplifier explained in terms of empirical equation for transistor current 19 p3317 A66-35726  
 Applicability of microelectronic technique to construction of integrated wideband amplifier consisting of symmetrical differential circuit and common-emitter circuit 19 p3323 A66-36818  
 Common-mode input voltage rejection in transistor differential amplifiers by increasing collector resistance and gain of differential stage 20 p3533 A66-38280
- DIFFERENTIAL ANALYZER**  
 Surveying transistorized differentiators and integrators, giving fundamental RC and equivalent circuits 01 p0045 A66-11022  
 Accurate light-weight self-contained low-cost inertial autonavigational system including gyroscopes, accelerometer and DYDAN computer 07 p1076 A66-17793  
 Microminiature Loran-C Receiver/Indicator for analog-to-digital conversion, using integrated circuit 10 p1555 A66-22047  
 Digital differential analyzer /DDA/ design for high speed solution of differential equations common in aerospace problems 12 p1828 A66-23841  
 Digital differential analyzer for on-line studies of dynamic systems 16 p2657 A66-31245  
 Waveform analysis of electronic repetitive differential analyzer solutions of nonlinear and linear systems and describing functions evaluation using vectormeter 21 p3739 A66-39275
- DIFFERENTIAL EQUATION**  
 SA BALANCE EQUATION  
 SA BERNOULLI EQUATION  
 SA BIHARMONIC EQUATION  
 SA DUFFING EQUATION  
 SA FALKNER-SKAN EQUATION  
 SA HILL EQUATION  
 SA LAPLACE EQUATION  
 SA MATHIEU FUNCTION  
 SA PARTIAL DIFFERENTIAL EQUATION  
 SA RAYLEIGH EQUATION  
 SA REYNOLDS EQUATION  
 SA RITZ AVERAGING METHOD  
 SA RUNGE-KUTTA INTEGRATION  
 Power series expansions as solutions to differential equations, using electronic computers 01 p0091 A66-10163  
 Approximate solution for differential equations, using algorithm applied to boundary value problem involving linear equation 01 p0091 A66-10164  
 Multidimensional homogeneous difference schemata solving eigenvalue problem with elliptic operator, noting differential equation coefficients and eigenfunction error estimate 01 p0092 A66-10166  
 Numerical solution to problems with spatial variables, using partial differential equations of gas dynamics 01 p0055 A66-10169  
 Solution to linear difference and differential equation with variable coefficients 01 p0092 A66-10173  
 Error estimates for some finite difference methods of solving ordinary linear differential equations 01 p0092 A66-10315  
 Charge trapped in electron or ion beams at pressures below breakdown determined from general integro-differential equation, using approximation 01 p0111 A66-10375  
 Qualitative-quantitative analysis of solutions of second order ordinary linear homogeneous differential equations and two derivatives 01 p0093 A66-10403  
 Volterra integral equation used in alpha operational method for solution of linear differential equations 01 p0093 A66-10404  
 Unsteady convective flow of electrically conducting fluid through vertical channel in magnetic field, using differential equations 01 p0111 A66-10426  
 Parametric dependence of almost periodic solutions to nonlinear differential equations with deviating argument 01 p0094 A66-10457  
 Linear differential equation solution/nonfluctuation and boundedness estimate in connection with integral inequalities 01 p0094 A66-10650  
 Asymptotic behavior of solution to system of differential equations with random limited coefficients 01 p0095 A66-10733  
 Flexible-wall tubes flattened by fluid when velocity reaches critical value, with differential equations describing effect of stability loss 01 p0158 A66-11035  
 Exact derivative method of integrating some differential equations of nonlinear vibrations 01 p0159 A66-11173  
 Ellipsoidal wave equation /differential equation with ellipsoidal coordinates/ solution expressed as Neumann series 02 p0249 A66-11579  
 Optimal rotation of plane of circular orbit by transverse thrust force, deriving differential equations for rotational maneuver 02 p0289 A66-11653  
 Motion equation for satellite with passive and semipassive attitude control using geomagnetic field, considering elliptical and circular orbits and involving differential equations 02 p0295 A66-11670  
 Liapunov function determining sufficient conditions for stability of autonomous functional differential equations with finite time lag 02 p0249 A66-11900  
 Rotation of rigid body force affected, using matrix equations, noting coordinate system and differential equation 02 p0290 A66-11989  
 Cauchy problem for infinite order linear differential equation 02 p0250 A66-12019  
 Mixed boundary value problem in bounded region for Navier-Stokes equations and discontinuity equation 02 p0219 A66-12101  
 Analysis of equation system for constructing regularizing algorithms for optimum control determination 02 p0209 A66-12103  
 Ordinary differential equations theory yielding hydrodynamics conditions of stability with respect to finite perturbations for plane stationary curvilinear flow of ideal fluid 02 p0219 A66-12104  
 Asymptotic particular solution for linear nonhomogeneous second-order ordinary differential equation with large parameter 02 p0250 A66-12149  
 Confining annular regions for solution trajectory of relaxation oscillations described by generalized Lienard equation 02 p0261 A66-12151  
 Stability problem of steady motions, using differential equations with time delay 02 p0262 A66-12167  
 Comparison lemma for determining uniqueness of solution to Cauchy problem for ordinary differential equations 02 p0251 A66-12243  
 Singular integro-differential equations with small parameter and corresponding degenerate equations 02 p0251 A66-12244  
 Existence of stable periodic solution of Lienard equation, using asymptotic methods 03 p0392 A66-12617  
 Integral inequalities related to nonoscillation theorems for differential equations 03 p0387 A66-12618  
 Time optimization problem involving dynamic programming, boundary value problem, differential equations and optimal control 03 p0349 A66-12687  
 Stability of solution to autonomous Lienard equation, using second Liapunov method 03 p0392 A66-12688  
 Plotting in phase space controllability region for unstable linear system of differential equations 03 p0350 A66-13043



Spectral functions of generalized second-order differential equations with boundary conditions at singular end 03 p0388 A66-13115

Transformation of equivalent nth order linear differential equations 03 p0388 A66-13154

Nonlinear differential equations describing RC oscillator determining frequency, stable amplitude and transient response 03 p0345 A66-13238

Axiomatic approach to control system theory as generalization of dynamic systems, noting weak and strong stability and Liapunov function 03 p0351 A66-13255

General dynamical system defined by coupling equation giving existence and uniqueness theorems 03 p0389 A66-13256

Stochastic differential equations specifying dynamical structure of filters generating posterior probability distribution when inputs are time functions 03 p0351 A66-13259

Stability of systems of n first-order real differential equations defined over finite time interval 03 p0389 A66-13262

Resonance modes in rods for analyzing coupled oscillations in sandwich plates including differential equations for oscillations 03 p0442 A66-13303

Zeros of solutions of second-order linear differential equation, discussing Sturm comparison theorem 04 p0538 A66-13363

Nonlinear time-variant phase-lock loop differential equation for arbitrary loop voltage-controlled oscillator sweep voltages used in aerospace tracking and communication systems 04 p0502 A66-13605

Eigenvalues of free vibration equation of simply supported beam with finite number of discrete masses, using differential equation 04 p0588 A66-13823

Quadratic form as Liapunov function for linear homogeneous vector differential equation with constant coefficient matrix 04 p0539 A66-13825

Refractive index obtained from equation describing electromagnetic wave propagation in ionosphere 04 p0481 A66-13826

Differential equations of automatic tracking systems reducible to equations with constant coefficients by introducing rotating coordinates 04 p0482 A66-13977

Controllability of nonlinear processes discussing qualitative and quantitative theory and geometric properties of set of attainability 04 p0505 A66-13993

Theory of differential equations discussing extremal problems for generalization of optimal control problem 04 p0505 A66-13994

Parametric response of elastic clamped-free column, noting agreement between theory and experiments for first three spatial and first four temporal modes 04 p0594 A66-14391

Computer algorithm determination of nonlinear system dynamics, using least squares method 05 p0636 A66-14605

Existence theorem for trajectories of orionator field satisfying measurability condition 05 p0707 A66-15032

Union of and estimates for trajectories of orionator fields 05 p0707 A66-15033

Transformation and equivalence of higher than second order homogeneous linear differential equations 05 p0708 A66-15153

Existence and uniqueness of weak solution to Dirichlet problem for elliptic differential equations in Sobolev spaces with special occupancy function 05 p0708 A66-15154

Book on asymptotic expansions in powers of small parameter applied to nonsteady oscillations in nonlinear systems with one or more degrees of freedom 05 p0776 A66-15327

Duality theorems derived for problem of periodic solutions of systems of higher order differential equations 05 p0709 A66-15340

Effective transformation and asymptotic behavior of class of nonlinear differential equations 05 p0709 A66-15343

Inverse eigenvalue problem for second-order differential equation with boundary dependence on parameter 05 p0709 A66-15359

Wave propagation in elastic-plastic half-space subject to von Mises yield condition, due to combined surface pressure and shear [ASME PAPER 65-WA/APM-11] 05 p0777 A66-15433

Asymptotic solutions of second-order

ordinary differential equations in region containing irregular singularity of rank one, with application to Whittaker functions 05 p0710 A66-15475

Asymptotic solutions of second-order differential equations having irregular singularity of arbitrary rank 05 p0710 A66-15476

I-V characteristics of thermionic converters with ohmic resistance, using differential equation with boundary conditions for local potential difference between emitter and collector 05 p0619 A66-15564

Integration of differential equations governing thermal performance of spacecraft radiator [ASME PAPER 65-WA/HT-45] 05 p0792 A66-15663

Axisymmetric dynamic response of ring supported cylinder to time dependent loads, discussing boundary conditions and differential equations of motions [AIAA PAPER 66-83] 06 p0962 A66-16265

Controller analytical design for nonautonomous systems, deriving necessary and sufficient conditions for existence of optimum control 06 p0862 A66-16522

Convex programming problems, developing parametric gradient method for approximate solution 06 p0838 A66-16526

Averaging systems of integrodifferential equations for small parameter and real n vector functions 06 p0902 A66-16535

Self-similarity of solutions to motion equations for relativistic gas possessing point symmetry and nonexistence of isotropic flow 06 p0954 A66-16538

Optimal control theory for nonlinear vector differential equations containing measures 06 p0863 A66-16620

Pseudo-convex functions, discussing existence criteria, properties and application 06 p0864 A66-16621

Optimum transfer function determination, using Liapunov method and superposition theorem 06 p0864 A66-16683

Cauchy problem at infinity for certain nonlinear systems of ordinary differential equations 06 p0903 A66-16704

Nonlinear differential equation stability, describing technique for Liapunov function construction 06 p0865 A66-16743

Vector equation  $F/X/$  equals zero solved by transforming nonlinear algebraic equation into nonlinear differential equation 06 p0865 A66-16746

Equilibrium properties of system of interacting molecules calculated from differential equation of state for real gas, employing classical and thermodynamic relations 06 p0912 A66-16841

Heat conductivity problems for two-and three-layer systems solved by splitting boundary conditions and dividing system into single layers 06 p0972 A66-16842

Linear time-invariant systems, noting relation between transient response duration and differential equation coefficients 06 p0867 A66-16990

Existence and uniqueness of almost-periodic solution of system of differential equations 06 p0904 A66-17057

Discrete simulation technique using electrical circuit for finite-difference approximation of initial differential equations, noting functional potentiometers 07 p1055 A66-17201

Topological property of torus to study ergodicity of integrals of systems of periodic differential equation in absence of cyclic solutions 07 p1055 A66-17243

Elasto-creeping circular membrane, obtaining nonlinear solution for axisymmetric circular elastic creep problem 07 p1142 A66-17263

Gas flow dissipation in transonic plane-symmetric nozzle, obtaining asymptotic solutions for flow parameter 07 p0979 A66-17264

Second-order linear partial differential equation transformed to normal form, obtaining invariant representation without Ricci calculus 07 p1055 A66-17301

Analytical construction of optimal controller for solution of system of Riccati differential equations 07 p1012 A66-17377

General variational problem for system described by differential equations in which

at least one control figures linearly 07 p1012 A66-17378

Reduction of nonlinear system of differential equations to integral equation of Hammerstein type 07 p1055 A66-17421

Optimal control for systems whose behavior is described by ordinary and differential equations set with initial and boundary conditions 07 p1013 A66-17426

Differential equations defining interaction of nonlinear oscillations in certain regions of parametric space where stable periodic solutions exist 07 p1079 A66-17447

Radiant transport with isotropic scattering, evaluating approximate solutions for reflection and transmission of parallel plane radiation 07 p1152 A66-17589

Cauchy and boundary value problem for second-order nonlinear ordinary differential equations 07 p1056 A66-17607

Popov-related stability results for feedback systems proved via bounded solutions for functional equations 07 p1015 A66-17756

Discontinuous system investigated, using oscillating circuit governed by second order differential equation 07 p1015 A66-17830

Resolving matrix of normal system of ordinary linear differential equations in complex independent variable for multiply connected fields 07 p1057 A66-17835

Boundary problems concerning linear integro-differential equations with caloric operator and delayed arguments 07 p1057 A66-17842

Integral curves described by nearly homogeneous differential equation and behavior in neighborhood of singular point 07 p1057 A66-17854

Stability of quiescent point of dynamic system with random disturbance 07 p1058 A66-17907

Solution of linear differential equations with quasi-periodic coefficients by method of accelerated convergence 07 p1058 A66-17908

Two-tangents method for numerical solution of Cauchy problem for system of ordinary differential equations 07 p1058 A66-17911

Asymptotic behavior of solutions of ordinary linear differential equations involving continuous complex valued functions 07 p1058 A66-17913

Existence of logarithm for nonsingular square matrix, uniqueness for linear ordinary differential equation systems, logarithms of operators and spectral mapping 07 p1058 A66-17966

Existence and uniqueness theorems for invariant-embedding nonlinear ODE systems for absorption loss rate satisfying Lipschitz condition 07 p1059 A66-17972

Existence and uniqueness of piecewise-continuous solution to two-dimensional linear first order hyperbolic system with discontinuous coefficients 07 p1060 A66-18100

Improving estimates of solutions of linear perturbed-motion equations of mechanical systems with variable coefficients 07 p1060 A66-18188

Continuation of certain classes of differentiable functions beyond limits of region 07 p1060 A66-18465

Polymeric material deformation under harmonically varying load action, noting steady state regime temperature distribution effects 08 p1243 A66-18879

Asymptotic solution of problem of thin spherical shell free vibration for axisymmetric and general cases 08 p1308 A66-18888

Reentry guidance by threshold network storage of precomputed optimum commands, using analogy of surface approximation problem in N plus one-dimensional space [AIAA PAPER 66-52] 08 p1249 A66-19898

Extrapolation and interpolation formulas for numerical solution of differential equation 08 p1245 A66-19167

Convergence of transformations of differential equations to normal form 08 p1245 A66-19370

Discreteness and continuity conditions for spectrum of self-adjoint operator generated by differential equations system 08 p1245 A66-19371

Analog computers used in modeling of heat conduction and diffusion processes for



Fourier differential equation 08 p1319 A66-19427

Geometrical optics method for differential equations of fourth order in applications to LF plasma oscillations 08 p1265 A66-19472

Boundary problems for differential and integro-differential equations 08 p1245 A66-19631

Uniform approximation by polynomial solutions for differential equation 08 p1245 A66-19633

One type of infinite-order differential equation with polynomial coefficients of increasing power 08 p1246 A66-19707

Two uniqueness theorems for periodic solutions of second order nonlinear differential equation describing oscillatory systems 08 p1246 A66-19709

Stability analysis of multiple controls, matrix analysis, symmetry and general oscillation equation 08 p1246 A66-19832

Perturbation method for approximating solutions of nonlinear differential systems with initial conditions 09 p1393 A66-19907

Change of variables for generalization of Konyukov second-order nonlinear differential equation, using Bernoulli and Riccati equations 09 p1393 A66-19917

Two types of boundedness for components of solutions of nonlinear autonomous systems 09 p1361 A66-20501

Convergence of numerical solutions of ODE initial value problems 09 p1394 A66-20616

Numerical solution of first order first-degree two-variable for ODE for self-adjusting nonpolynomial interpolant 09 p1395 A66-20617

Runge-Kutta fourth order formula used to obtain approximate solution to differential equations 09 p1395 A66-20618

Numerical integration of coupled first order ODE of greatly differing time constant 09 p1395 A66-20619

Power series drawbacks as tool in numerical solution of differential equations 09 p1395 A66-20620

Singular solutions in optimal control problems, treating singular control surface, flooding technique and allowable switching directions 09 p1362 A66-20653

Direct method of Liapunov used to study stability of ordinary differential equation by obtaining linear bounds on vector components 09 p1363 A66-20654

Floquet form of solution to system of linear differential equations with periodic parameters 09 p1363 A66-20798

Qualitative behavior and index of trajectories in neighborhood of isolated singularity of given form 09 p1363 A66-20799

Differential equations describing boundary conditions at front of change of aggregation state, computing temperature field 09 p1471 A66-20825

Text for senior undergraduates, using Fourier series and integral transforms to discuss standard differential equations of mathematical physics 09 p1397 A66-20917

Asymptotic behavior, at plus infinity, of first order linear differential-difference-delay equation solutions, discussing asymptotic oscillatory number 10 p1549 A66-21224

Analogy between systems of differential equations in vicinity of singular point 10 p1549 A66-21234

Hypergeometric solutions of second-order linear ordinary differential equation with n-regular singular points 10 p1550 A66-21305

Influence on stability of masses which are in relative motion with respect to projectile determined, noting engine thrust effect on attitude control system performance 10 p1611 A66-21386

Large deflections of spherical shells under concentrated loads, obtaining curves for axisymmetric deformations 10 p1616 A66-21493

Chaplygin asymptotic series solution method for differential equation systems 10 p1551 A66-21915

Theorems and corollaries describing bounds for quadratic Liapunov functions 10 p1551 A66-21918

Boundedness and uniform boundedness of nonhomogeneous systems, obtaining necessary and sufficient conditions for existence of solutions 10 p1551 A66-21920

Computational solution of functional differential equations, using successive approximations 10 p1551 A66-21922

Unilateral estimates under conditions of asymptotic stability of solutions to differential equations with unbounded operators 10 p1552 A66-21985

Transcendence and algebraic independence of values of E-functions representing solution to third-order linear differential equation 10 p1552 A66-21986

Optimum control processes in systems containing plants with distributed parameters described by ordinary or partial differential equations with initial and boundary conditions 11 p1674 A66-22356

Halley comet motion during return of 1910, obtaining orbits via differential correction procedures, including perturbation by all planets but Pluto 11 p1769 A66-22531

Liapunov first method and applicability to asymptotic stability of stationary points of nonlinear differential systems 11 p1721 A66-22641

Integral curves of particular ordinary differential equation containing singularity 11 p1721 A66-22642

Sufficient conditions for asymptotic dynamic stability of linear differential system with random retardation, using Liapunov function 11 p1736 A66-22643

Current distribution and input resistance of T-type, corner and bent tape vibrators powered by lumped electromotive force, using method of integro-differential equations 11 p1666 A66-22719

Approximate solutions of second order differential equations for nonlinear electronic circuits with strong disturbance 11 p1676 A66-22735

Numerical solution to first geodesic problem of ellipsoid of rotation, using iterative application of Runge-Kutta method to differential equations of geodesic line 11 p1698 A66-22767

Global solutions of Cauchy problem for quasi-linear first-order differential equations in several space variables 11 p1722 A66-22895

Nonlinear servomechanism analyzed, using Fokker-Planck equation, discussing tracking failure 11 p1670 A66-23224

Tapered distributed RC networks with similar immittances examined for poles and zeros of two-port short circuit admittance parameters 11 p1678 A66-23241

Linear system dynamics, discussing time function vector space, spectral coefficients, orthonormal and transfer functions, parameter variation, Fourier approximation, etc 11 p1679 A66-23269

Modified phase-plane delta method for nonlinear system phase portrait 11 p1679 A66-23270

Liapunov function for case of stability with constantly acting disturbances in nonlinear spaces 11 p1723 A66-23316

Graphical-analytical method using successive approximations determines guided missile trajectory 11 p1734 A66-23344

Initial conditions determination in aircraft takeoff from mobile platform required for solution of differential equations of motions of gravity center 11 p1734 A66-23345

Limit cycles and global structure of integral curves of nonlinear system of differential equations in five-dimensional parameter space 11 p1724 A66-23364

First order wave function of helium due to one-and two-electron excitation determined by solving differential equations, noting contribution to second order energy 11 p1741 A66-23405

Stability and boundedness for solutions of class of complex differential systems obtained in terms of Liapunov-like functions 11 p1725 A66-23426

Approximate solution for differential equations and restrictive conditions with unbounded controls 11 p1681 A66-23454

Transformation of canonical system of differential equations with rapidly varying periodic coefficients into canonical system with constant coefficients 12 p1902 A66-23764

Estimates of solutions to second order differential equations generalized to include inequalities with Schwarz derivative numbers 12 p1902 A66-23768

Confidence ratio for Gaussian random processes satisfying certain linear differential equations 12 p1902 A66-2376

Stability of two-dimensional parallel flows using Orr-Sommerfeld equation and adjoint equation with asymptotic solution 12 p1861 A66-2380

Similar solution of differential equation for compressible laminar boundary layers in case of insulated walls 12 p1862 A66-2386

Monotonic two-point system for numerical integration of ordinary differential equations, for case of solutions of constant sign 12 p1902 A66-2390

Wave propagation in elastic-plastic half-space subject to von Mises yield condition due to combined surface pressure and shear [ASME PAPER 65-WA/APM-11] 12 p1961 A66-2398

Modified Ritz method for finding eigenvalues of certain nonlinear ordinary differential equations 12 p1914 A66-2400

Linear differential equation solution nonfluctuation and boundedness estimate in connection with integral inequalities 12 p1903 A66-2402

Cauchy problem for infinite order linear differential equation 12 p1903 A66-2402

Forced oscillations of coaxial multistage rotors, allowing for gyroscopic effect and rotating at different angular velocities determined by replacing differential equations with integral equations 12 p1964 A66-2405

Runge-Kutta type process of fourth, fifth and sixth orders of accuracy for numerical integration of transformed differential equations 12 p1904 A66-2418

Numerical integration of second order differential equations 12 p1904 A66-2418

Numerical integration of differential equation using exterior node quadrature formulas of Ionescu 12 p1904 A66-2419

Sufficient conditions for boundedness of solutions of nonlinear differential equation and oscillatory and asymptotically stable solutions 12 p1904 A66-2419

Boundary value problem solution constructed as expansion of particular solutions of Chaplygin equation in region bounded by parabolic line and two characteristics 12 p1904 A66-2424

Integration of equations determining location coordinates of moving object on terrestrial sphere 12 p1909 A66-2435

Deterministic optimal control, discussing Bellman dynamic programming method Pontryagin maximum principle, orbital transfer, interplanetary guidance, etc 12 p1854 A66-2463

Dynamic system stability, developments application and literature 12 p1854 A66-2463

Exact solution of ODE for plane wave diffraction on periodically rough surface after transmission through inhomogeneous layer 13 p2019 A66-2508

Mathematical programming methods for solving nonlinear state-constrained discrete optimal control problems 13 p2047 A66-2535

Stability criteria of trivial solution of rheolinear differential equation verified by calculating Liapunov function for nonlinear equations 13 p2117 A66-2539

Matrix solution of limit problems of linear system of ordinary differential equations 13 p2117 A66-2541

Existence of cycles as nonzero periodic solution to system of differential equation with one degree of freedom 13 p2117 A66-2541

Weak, strict and strict-weak Levi conditions defined in complex variables noting conditions for holomorphy and coincidence of functions 13 p2118 A66-2578

Nonlinear differential equations in theory of electrical oscillation 13 p2118 A66-2582

Averaging method for differential equations with retarded arguments 13 p2118 A66-2582

Necessary and insufficient conditions for well-posed Cauchy problems verified by Fourier analysis 13 p2118 A66-2582

Error bounds in phase-integral solution to differential equation with simple turning points 13 p2118 A66-2582

Error bounds of phase-integral method applied to wave-penetration problems 13 p2118 A66-2583



Asymptotically stable linear system  
controlled by scalar random  
input 13 p2048 A66-25849

Countable systems of differential  
equations, considering differential operator  
theory and infinite systems 13 p2119 A66-25850

Complex cycles of differential equations  
examined, deriving limit cycle of  
multiplicity, integration by quadrature,  
etc 13 p2119 A66-25851

Dynamic programming for stochastic  
systems applied in designing controller for  
transferring linear system from initial to  
final position in specified time  
interval 13 p2048 A66-25852

Equation for elliptical system in plane  
singly connected region, satisfying specified  
boundary condition 13 p2119 A66-25903

Existence and uniqueness of solution for  
first boundary value problem of system of  
specified mixed-type differential  
equations 13 p2119 A66-25905

Asymptotic solution of Cauchy problem for  
integro-differential equation with small  
parameter associated with  
derivative 13 p2119 A66-25908

Signal to noise ratio maximization using  
Pontryagin maximum principle, solving  
matched filter problem and designing signal  
with constrained energy and amplitude  
requirements 13 p2048 A66-25940

Approximate analytical solutions for  
distributed parameter networks with  
parameters as functions of spatial variable,  
using differential equation that reduces  
boundary value problem to Sturm-Liouville  
system 13 p2120 A66-26068

Bandlimited and approximately bandlimited  
signals by Fourier transforms of sampling  
function and prolate spheroidal wave  
function representing solutions of second  
order self-adjoint differential  
equations 13 p2120 A66-26077

Controllability of general class of nonlinear  
systems describable by nth order ODE with  
bounded state and control 13 p2052 A66-26079

Numerical integration methods requiring  
least computation time for truncation error  
when applied to ordinary differential  
equations, comparing Butcher with Runge-  
Kutta, Adams, etc 13 p2121 A66-26324

Diffusion-induced stress concentration near  
cavity, relating deformation diffusion and  
heat conduction via differential  
equations 13 p2203 A66-26426

Differential equilibrium equations for  
shallow shells of constant curvature under  
effect of concentrated load, using Fourier  
transform 13 p2205 A66-26440

Axisymmetric form of stability loss of  
cylindrical shell under effect of load  
suddenly applied along generatrix,  
considering inertia forces and obtaining  
differential equations 13 p2206 A66-26456

Decreasing secondary flows in spatial  
boundary layer on porous plate by boundary  
layer control /BLC/ through suction or  
blowing, using Prandtl partial differential  
equations 13 p2065 A66-26460

Text on dynamics of vibrations covering  
oscillations with variable and constant  
amplitude, damping, differential equations of  
motion, nonlinear oscillations, wave  
propagation in elastic solids, etc 13 p2207 A66-26573

Nonlinear ordinary differential equations  
applicable to damped oscillatory circuits  
with exploding wires, obtaining conservation  
law and approximate solutions by Picard  
method 13 p2129 A66-26667

Alfvén wave propagation in inhomogeneous  
magnetic fields satisfying  
magnetohydrostatic equation and allowing  
for electric currents solved, using  
differential equation 13 p2156 A66-26710

Heat transfer in Couette flow of radiating  
fluid with viscous dissipation, noting  
conduction coupling, effects of temperature  
level, profile, wall emission, fluid optical  
thickness, etc 13 p2210 A66-26718

First boundary value problem for nonlinear  
second order differential  
equations 14 p2320 A66-26942

Uniqueness of operator spectral function  
of self-adjoint boundary value problem  
involving second-order differential equation

with operator coefficients 14 p2320 A66-27158

Numerical-analytical method of obtaining  
periodic solutions to T  
systems 14 p2321 A66-27160

Green function of high degree of self-  
adjoint expansion of elliptic operator  
generated by differential expression is  
smooth inside domain and on smooth part of  
boundary 14 p2321 A66-27161

Twice continuously differentiable function  
satisfying nonlinear hyperbolic equation for  
certain initial conditions obtained, using  
averaging method 14 p2321 A66-27163

Polynomial solutions to system of  
differential equations in theory of  
elasticity 14 p2321 A66-27201

Small motion superposed on stationary  
slow deformation process of viscoelastic  
material with fading memory, based on  
Rivlin and Ericksen differential  
equation 14 p2397 A66-27384

Linear differential system for rendezvous  
with target in elliptical  
orbit 14 p2391 A66-27471

Solution of optimum filtering problems  
when input signals of automatic control  
system are described by different  
differential equations at successive time  
intervals 14 p2265 A66-27523

Coordination of integral and relay  
components in algorithms for adjusting  
control coefficients in model-reference self-  
adaptive control systems described by  
differential equations 14 p2266 A66-27526

Convergence of optimal control for  
denumerable system of differential  
equations treated by functional-space  
decomposition 14 p2267 A66-27672

Green matrix of periodic boundary value  
problem for system of linear differential  
equations 14 p2322 A66-27675

Existence of periodic solutions of  
differential equations in nonlinear mechanics  
[PST PAPER NT-147] 14 p2323 A66-27792

Linear differential equations for slowly  
rotating symmetrical satellite in circular  
orbit 14 p2392 A66-27879

Gyroscope motion on randomly shifting  
support described by linear inhomogeneous  
differential equation 14 p2297 A66-28064

Liapunov stability and instability in critical  
case of determining equation with even  
number of zero roots 14 p2336 A66-28065

Optimum control systems for plants  
described by ordinary nonlinear differential  
equations or differential equations with  
constant or variable delay 14 p2268 A66-28278

Estimation of proximity of solution for  
Cauchy problem of nonlinear differential  
equations, formulating six  
theorems 14 p2325 A66-28279

Asymptotic estimates of characteristic  
values of differential equation with periodic  
coefficients 15 p2524 A66-28507

Existence and stability of periodic motions  
in dynamic systems applied to analysis of  
uniformly asymptotically stable solutions of  
differential equations 15 p2525 A66-28508

Domains of attraction in large of periodic  
solutions of weakly nonlinear systems, using  
Liapunov function and differential  
equations 15 p2525 A66-28509

Existence, boundedness, decay and  
exponential decay of solutions of classes of  
nonlinear systems of differential equations,  
using suitable Liapunov  
functions 15 p2525 A66-28510

Linear normal form of system of real  
differential equation, noting disappearance  
of difference between Hartman and  
Sternberg hypotheses 15 p2525 A66-28511

Sufficient conditions for recurrence and  
positivity of diffusion process defined by  
stochastic differential equation, using  
Liapunov function 15 p2525 A66-28512

Stability of nonlinear control systems,  
noting Hermitian matrix for linear system of  
ordinary differential equations and  
analogous problem for difference  
equations 15 p2525 A66-28513

Numerical solution of nonlinear integro-  
differential boundary value problems with  
parabolic operators and retarded  
argument 15 p2525 A66-28519

Algorithms for numerical determination of  
asymptotically stable solutions for ordinary  
differential equations 15 p2526 A66-28734

Stability and existence of small periodic  
solutions of ordinary differential  
equations 15 p2526 A66-28735

Minimax problem for pursuit problem of  
two linearly controlled objects describable  
by identical differential  
equations 15 p2526 A66-28948

Expansion of arbitrary function of Mehler-  
Fok integral form in terms of spherical  
functions 15 p2526 A66-28952

Dynamic stability differential equations and  
stability and instability theorems derived  
from them 15 p2538 A66-29044

Parametrically analytic solution of infinite  
differential equation 15 p2527 A66-29047

Extension of dynamics to arbitrary systems  
of differential equations, proposing universal  
canonical structure generalizing Hamiltonian  
structure 15 p2539 A66-29145

Optimal control process for  
brachistochrone motion, discussing solution  
and inversion of synthesis  
problem 15 p2470 A66-29150

Asymptotic methods of nonlinear  
mechanics, involving averaging for  
differential equations, applied to motion  
equations of satellites and resonance in  
electric circuits 15 p2541 A66-29162

Periodic solutions of nonautonomous  
systems of ordinary differential equations  
and equations with delayed argument,  
examining new theoretical  
methods 15 p2527 A66-29164

Oscillating solutions of ordinary nonlinear  
nonautonomous differential equations, noting  
qualitative methods 15 p2527 A66-29168

Theory of differential equations with  
deviating argument, noting stability and  
periodic solutions 15 p2528 A66-29169

Stabilization of unstable two-point  
boundary value problems, noting field  
method for avoiding computer storage  
problems during integration of related  
differential equations 15 p2528 A66-29292

Existence theorem for nonlinear ODE  
system with continuous monotonic  
differential operators over Hilbert space and  
application to nonlinear network  
analysis 15 p2528 A66-29370

Stochastic extensions of techniques for  
using Liapunov second method in design and  
analysis of feedback controls, using  
differential equations 15 p2473 A66-29376

Differential equations describing elastic  
shells of revolution under physical  
nonlinearities, noting positive stresses in  
buckling zone 15 p2611 A66-29422

Evaluation of solution moduli of nonlinear  
contour problems pertaining to polyvibrant  
systems with delayed remainders and  
arguments 15 p2529 A66-29653

Approximate method, using power  
polynomials, for calculating distance  
between detached shock wave and  
profile 15 p2425 A66-29721

Plasma stability analysis, discussing low  
density fluid equations, variational principle  
and sufficiency condition at moderate  
densities, electric field effect,  
etc 15 p2554 A66-29746

Dynamic characteristics of automatic  
control plants determined, using term-by-  
term integration of differential  
equations 15 p2475 A66-29768

Linear initial value problems involving first  
order differential equations transformed  
into higher order systems and treated as  
boundary value problems, using numerical  
techniques 15 p2529 A66-29773

Multicategory pattern recognition, noting  
mathematical treatment, dimensional and  
correlational effects, etc 15 p2453 A66-29774

Stability of mean solution, probability  
solution and almost-everywhere solution to  
random parameter differential  
equation 15 p2529 A66-29854

Self-similarity of solutions to motion  
equations for relativistic gas possessing  
point symmetry and nonexistence of  
isentropic flow 15 p2603 A66-29978

Effective transformation and asymptotic  
behavior of class of nonlinear differential  
equations 15 p2530 A66-29979

Sandwich panel bending under thermal and  
mechanical loads, solving differential  
equations for temperature distribution,  
transverse load and uniform edge



compression with boundary conditions 16 p2812 A66-30218

Multidimensional generalized transport equations solutions and calculation by difference methods 16 p2732 A66-30240

Linear integral operators applied to singular differential equations and to computations of compressible fluid flows 16 p2683 A66-30241

Differential equation derived for cooling of infinite porous tube by gas injection through wall, determining wall temperature distribution 16 p2827 A66-30674

Unperturbed motion for follow-up systems in critical case of double zero root, noting stability and correspondence of root to solution of first approximation equation 16 p2733 A66-30738

Uniqueness and solution estimates to boundary value problems, noting solvability correlation with existence of Green function 16 p2733 A66-30739

Asymptotic behavior of solution to ordinary differential equation, noting transformation to nearly diagonal system of first order 16 p2733 A66-30741

Nonstationary problem of linear filtering in presence of additive noise solved by computer simulation 16 p2669 A66-30762

Transformation and equivalence of homogeneous linear differential equations of higher than second order, examining equivalence of regular equations with dimension 16 p2734 A66-30778

Approximate analysis of nonlinear systems similar to harmonic oscillators, using Chaplygin theory of differential inequalities 16 p2705 A66-30781

Existence theorem of recurrent solutions to differential equations defined in Banach space for dynamic and nondynamic systems 16 p2735 A66-30785

Controller analytical design for nonautonomous systems, deriving necessary and sufficient conditions for existence of optimum control 16 p2670 A66-30832

Convex programming problems, developing parametric gradient method for approximate solution 16 p2656 A66-30836

Duality theorems derived for problem of periodic solutions of systems of higher order differential equations 16 p2735 A66-30970

Averaging systems of integro-differential equations for small parameter and real  $n$  vector functions 16 p2736 A66-30973

Asymptotic behavior of solutions of ordinary linear differential equations involving continuous complex valued functions 16 p2736 A66-30976

Convergence of transformations of differential equations to normal form 16 p2736 A66-30977

Discreteness and continuity conditions for spectrum of self-adjoint operator generated by differential equations 16 p2736 A66-30979

Boundary problems for differential and integro-differential equations 16 p2736 A66-30980

Uniform approximation by polynomial solutions for differential equation 16 p2736 A66-30982

Numerical analysis of stress-strain rate of siphon bellows, using differential equations 16 p2820 A66-31145

Estimation of least distance between consecutive zeros of nontrivial solution of second order differential equation 16 p2737 A66-31228

Extension of problem of singular perturbation for linear scalar constant coefficient differential-difference equation with single retardation to several retardations, noting degenerate equation solution 16 p2737 A66-31230

Numerical problems in application of Urabe results in considering periodic nonlinear differential systems, obtaining Galerkin approximations 16 p2737 A66-31231

Analog computer technique for solving nonlinear ODE system 16 p2658 A66-31263

Volterra series analysis of aperiodic solutions to certain second order integrodifferential equations with nonlinear damping and nonlinear restoring force 16 p2737 A66-31334

Highly stable predictor-corrector methods

for solving systems of differential equations 16 p2658 A66-31348

Approximate analytical solution for pitching and rolling motion near resonance of sounding rocket, using nonlinear differential equation 16 p2811 A66-31470

[AIAA PAPER 66-463] Approximate substitution of ordinary dynamical systems for systems with retardation by increasing order of ordinary differential equations 16 p2748 A66-31505

Unsteady expansion of plane layer of ideal gas into vacuum for various laws and durations of energy release described by equations of gas dynamics 16 p2690 A66-31617

Periodic and quasi-periodic solutions to differential equations describing pulsed systems 16 p2738 A66-31709

Monograph on theory of ordinary delay differential equations and optimal control processes with time delay 16 p2673 A66-31749

Book on stability, oscillation and time lags in differential and differential-difference equations, discussing Liapunov stability theorem 16 p2739 A66-31754

Iteration methods for solution of integro-differential equations 17 p2945 A66-31807

Stability of constant solutions for second-order nonlinear differential equation which uses Hahn notations and definitions 17 p2945 A66-31837

High order Runge-Kutta formulas for systems of first and second order differential equations with small truncation error 17 p2945 A66-31877

Stochastic analysis of systems described by linear differential equations subject to random disturbances, noting application to variational behavior of optimal control systems 17 p2900 A66-32076

Propagation along rays or bicharacteristics for two equations with partial linear derivatives having two unknowns and coefficients which are indefinitely differentiable 17 p2945 A66-32280

Noise rejecting algorithms for ODE solutions with computer, using redundancy, placement of control and feedback techniques 17 p2877 A66-32569

Computer solution using Bubnov-Galerkin method to determine concentrated force effect on shallow spherical dome 17 p3026 A66-32601

Least squares method to solve linear integral and differential equations 17 p2947 A66-32608

Electron capture detector parameters in pulse sampling mode analyzed, noting kinetic processes, temperature effect, etc 17 p2961 A66-32660

Asymptotic methods of nonlinear mechanics applicable to nonlinear differential equations with random arguments 17 p2958 A66-32711

Boundedness of solutions to nearly differential equations with random arguments 17 p2947 A66-32712

Maximum error curves for Lanczos selected point method of polynomial solution to ordinary differential equations, using Chebyshev and Legendre functions 17 p2947 A66-32858

Textbook on differential equations with deviating arguments, covering existence theorems, linear equations, stability theory, boundary value problems, etc 17 p2947 A66-33188

Electromagnetic wave propagation in cylindrically stratified plasma, noting ODE describing transverse propagation of axial component 17 p2876 A66-33279

Solution method for use when linear combinations of given approximate solutions are used for representing exact solution of general ordinary linear homogeneous differential equation 18 p3125 A66-33627

Bending behavior of spherical shells through second-order differential equation with complex coefficients, noting effect of load 18 p3253 A66-33765

Bending behavior under lateral loads and stretching effects due to in-plane forces described by two uncoupled differential equations governing circular plates 18 p3253 A66-33803

Mathematical model for predicting strength and density of material from deceleration-

time history of instrumented impact probe 18 p3253 A66-33805

Thrust programming in central gravitational field, discussing reduction of Mayer-Bolza variational problem to boundary value problem for system of nonlinear differential equations 18 p3241 A66-33846

Sufficient conditions for boundedness of solutions of linear system of differential equations with variable coefficients 18 p3126 A66-33929

Discontinuity condition in optimal control problem, considering motion of points in  $n$ -dimensional space separated by hypersurface 18 p3126 A66-33930

Differential equation system describing nonsteady state motion of liquid in open channel 18 p3097 A66-33932

Approximation solution to plane bend problem in thin rod of variable rigidity 18 p3254 A66-33933

Minimal element determination for certain set related to interpolation of second-order linear ordinary differential equations 18 p3126 A66-33954

Improved Chaplygin solutions to ordinary differential equations 18 p3126 A66-33955

Infinite boundary value problem solution for third-order differential equations obtained in convergent series form 18 p3126 A66-33974

Differential inequality theorem for boundary value problem involving second-order differential equation 18 p3126 A66-33975

Topological classification of higher dimensional systems of ordinary differential equations by Liapunov functions 18 p3127 A66-33976

Existence, uniqueness and periodicity of solutions to boundary value problems for quasi-linear ODEs on topological space of continuous mappings 18 p3127 A66-34138

Heat transfer effectiveness-number of transfer unit relations determined, using differential equations to obtain temperature profile of each channel in exchanger 18 p3262 A66-34382

Square-integrable approximate solution to certain ordinary differential equations in particular function space 18 p3127 A66-34640

Solution for inhomogeneous differential linear equation in integral form obtained from Wronskian 18 p3128 A66-34701

Two physical-space and two spectral solutions of Burger equation which are exact, viscous and nonsteady 18 p3103 A66-34930

Poincare-Liapunov systems of ordinary differential equations, qualitatively investigating plane and rough systems, singular points, periodic solutions, etc 18 p3128 A66-34966

Dynamic systems described by nonlinear differential equations containing analytical functions for random initial conditions 18 p3091 A66-34984

Synthesizing time optimal control for plants described by linear differential equations with constant coefficients 18 p3092 A66-34993

Plotting in phase space controllability region for unstable linear system of differential equations 18 p3092 A66-35006

Quasi-periodic motion theory, discussing nonlinear oscillations and perturbation theory solution to differential equations 19 p3400 A66-35828

Michalov criterion for exponential polynomials, determining existence of zeros in right half-plane 19 p3388 A66-35829

Differential equations for deformations of nonuniform flat plates bent into cones 19 p3473 A66-35850

Monotonic stability of motion for neutral linear solution 19 p3400 A66-35932

Optimal control for stochastic differential equation system, noting existence and uniqueness of solution for coefficients satisfying Lipschitz condition 19 p3325 A66-35983

Solution of two-point boundary problems in optimal control syntheses in which sensitivity coefficients for differential equations satisfy jump conditions at discontinuity point 19 p3327 A66-36017

Functional derivative technique for designing self-adjusting control systems



having main part implemented by solving differential equations 19 p3328 A66-36021

Partial step integration equation for use with Adams or Adams-Bashforth method of integration of differential equations 19 p3309 A66-36045

Eigenvalue problems for systems of ordinary differential equations resolved computationally by use of quasi-linearization technique 19 p3310 A66-36046

Analogy between systems of differential equations in vicinity of singular point 19 p3389 A66-36181

Unilateral estimates under conditions of asymptotic stability of solutions to differential equations with unbounded operators 19 p3390 A66-36190

Transcendence and algebraic independence of values of E-functions representing solution to third-order linear differential equation 19 p3390 A66-36191

Homogeneous linear differential equations, examining stochastic processes for perturbations causing discontinuous solutions and for perturbations acting on entire bounded intervals 19 p3390 A66-36334

Liapunov second method and stability theory of autonomous and certain nonautonomous systems 19 p3391 A66-36438

Optimization analysis for axisymmetric rocket motor nozzle design based on assumptions for gas particle flow [AIAA PAPER 66-538] 19 p3277 A66-36598

Finite deflection and stability equations for circular cylindrical shells stiffened in longitudinal and circumferential direction 19 p3475 A66-36636

Propagation of spherically symmetric, cylindrically symmetric and plane waves examined via analytic perturbation method in solving gas dynamics equation for nonstationary compressible flow 19 p3443 A66-36638

Ordinary differential equations experimentally determined for describing performance of existing lumped-parameter time-invariant nonlinear physical systems 19 p3392 A66-36710

Optimal control and dynamics of class of hybrid state continuous time systems described by differential equations combined with multistable element 19 p3337 A66-36734

Richardson extrapolation applied to estimate accumulated truncation error for one-step method with variable step size for integrating system of ordinary differential equations 19 p3392 A66-36780

Optimum Runge-Kutta methods of orders 2, 3 and 4 for first-order differential equation with constrained minimum truncation error bounds 19 p3392 A66-36781

Step size for numerical solution of differential equation without violating stability region constraint 19 p3392 A66-36785

Relativity theory for solid-media model design, deriving equations of state and closed system of differential equations based on variational principle 19 p3401 A66-36832

Absence conditions for periodical trajectories in regions of possible existence 19 p3401 A66-36844

Transient processes in linear automatic control systems dependent on parameters which appear when differential equations of analyzing system are transformed by Laplace-Karson method 20 p3537 A66-36892

Optimal control analysis of system behavior described by linear stochastic differential equations 20 p3537 A66-36893

Subdominant solutions of linear differential equations calculated by numerical method 20 p3589 A66-36902

Asymptotic representation of systems of nonlinear differential equations, setting up lemmas and theorems 20 p3590 A66-37484

Mean value theorem for curves arising in solution of ordinary differential equation by series method 20 p3590 A66-37525

Quasi-periodic solutions of nonlinear ordinary differential equations containing parametric discontinuities 20 p3591 A66-37592

Ordinary nonlinear differential equation arising in theory of both axisymmetric and two-dimensional viscous jets falling under gravity 20 p3591 A66-37593

Linear homogeneous third-order differential equations, examining existence, uniqueness and asymptotic behavior of nontrivial nonoscillatory solutions and existence criteria for oscillatory solutions 20 p3591 A66-37608

Existence of unique periodic solution to first-order differential equation and nonautonomous system of two first-order differential equations 20 p3591 A66-37752

Class of nonlinear second-order differential equations with algebraic moving singular points, considering convergent series inversion and existence conditions 20 p3591 A66-37753

Solvability and methods of solution of boundary value problems noting uniqueness, potential theory application in solving polyharmonic equations and second-order equation 20 p3591 A66-37757

Rigorous solutions for loadings applied at apex of spherical shell, noting cases of concentrated radial and tangential force, concentrated moment about polar and planar axis, etc 20 p3670 A66-37761

Asymptotic solutions of differential equations of mass transfer with chemical reaction without assumptions concerning kinematics, showing existence of five regimes 20 p3679 A66-37789

One-dimensional inverse problem of scattering theory, noting differential equation reduction, determining traveling wave coefficient 20 p3519 A66-37993

Differential equations for quasi-homogeneous MHD flow of electrically conducting medium at low magnetic Reynolds numbers 20 p3611 A66-38109

Boundary value problems for Sturm-Liouville-type equation with asymptotic formula derived for eigenfunctions 20 p3592 A66-38420

Boundary value problems with natural boundary conditions solved by representing desired solution by finite sum 20 p3592 A66-38423

Exact solution of ODE for plane wave diffraction on periodically rough surface after transmission through inhomogeneous layer 21 p3702 A66-38514

Optimal control problem, considering system of linear differential equations subject to constraint 21 p3717 A66-38536

Functions equations with stochastic variables as initial values 21 p3755 A66-38539

Krylov-Bogoliubov method applied to linear differential equations, noting transcendental functions and error analysis 21 p3755 A66-38596

Block diagonalization theorem for linear ordinary differential equation systems and applications 21 p3755 A66-38597

Matrix quadratic equation solution derivation applied in finding steady state solutions of Riccati differential equations with constant coefficients 21 p3755 A66-38598

Envelope of parametric equations determined, using geometrical understanding for identification of singularities on envelope, noting relevance to Wankel engine design 21 p3755 A66-38599

Linear dynamic system synthesis from weighting patterns 21 p3717 A66-38600

Approximate method for solution of dynamic stability problem of shafts subjected to pulsating moment and constant axial force 21 p3743 A66-38621

Elliptic singular integro-differential operators on smooth compact manifold without and with boundary 21 p3756 A66-38626

Computer program for numerical solution of ODE systems, noting generation of symbolic solutions via Taylor series expansion 21 p3707 A66-38679

Stability and instability regions determined for third-order differential equation with periodic coefficients 21 p3756 A66-38741

Existence theorems of periodic solutions to integro-differential equation with delayed argument 21 p3756 A66-38742

Mathematical model of linear guidance law to dynamical system, noting reduction of two-point boundary value class error 21 p3765 A66-38870

Linearized motion equations for low-altitude flight pitching stability of aircraft with control surface 21 p3696 A66-38937

Approximate method for determining damping factors of mechanical oscillatory systems with many degrees of freedom described by linear differential equations of  $n$ -th order with constant coefficients 21 p3770 A66-38971

Differential inequality theorems applied to hyperbolic differential equation, discussing Riemann functions and sufficient conditions for characteristic and Cauchy problems for quasi-linear Bianchi equation 21 p3757 A66-39232

Existence conditions of solution to two-point boundary value problem for ordinary nonlinear any order differential equation 21 p3757 A66-39245

Generalized Rolle and Bernstein theorems applied to polynomial approximation of ordinary differential equations over compact linear space 21 p3758 A66-39259

Axisymmetrical deformation of multilayer circular sandwich cylindrical shells, deriving governing differential equations by variational theorem 21 p3831 A66-39272

Initial value problem solution variation linearized by simple transformation 21 p3758 A66-39273

Variation of functional determined on trajectories of differential equation systems with discontinuities, discussing application to optimal control problems 21 p3758 A66-39280

Differential equations of steady motions in perturbed nonlinear autonomous systems with one degree of freedom 21 p3772 A66-39299

Flight stability, discussing quasi-critical case in neighborhood of asymptotic stability boundary of autonomous systems and that of variable system parameters 21 p3696 A66-39594

Bending of anisotropic cylindrical bodies with curved axis under transverse force 21 p3833 A66-39595

Random acceleration theory using diffusion transformation of matrix equation into differential equation 22 p3947 A66-39664

Nonlinear differential equations for cylindrically anisotropic plates, noting errors of Wolmir method 22 p3988 A66-39698

Differential equations for stream functions of particle trajectories in unsteady three-dimensional flows in cylindrical and spherical coordinate systems 22 p3898 A66-40111

Novozhilov transformation of equation system for thin laminar shells 22 p3991 A66-40147

Effect of stiffening ribs on stressed-strained state of shallow symmetrically loaded conical shells, noting reduction of boundary value problem to integration of differential equations 22 p3991 A66-40150

Asymptotic formulas for approximate solutions of Cauchy problem by difference techniques, considering error of tabulated elements 22 p3939 A66-40154

Coupled-modal equations for arbitrary vibratory system, with example for longitudinal vibrations of bar 22 p3992 A66-40298

Algorithms for numerical determination of asymptotically stable solutions for ordinary differential equations 22 p3939 A66-40442

Stability and existence of small periodic solutions of ordinary differential equations 22 p3939 A66-40443

Existence theorem of recurrent solutions to differential equations defined in Banach space for dynamic and nondynamic systems 22 p3940 A66-40447

Dirichlet problem for elliptic system of differential equation which does not satisfy Lopatinskii condition where characteristic equation of system has simple roots 22 p3940 A66-40449

Decomposition of system of linear differential equations, using asymptotic techniques of Krylov and Bogoliubov 22 p3940 A66-40459

Liapunov function and Meyer-Kalman-Yakubovich lemma used to obtain frequency domain stability criteria for linear plant with both monotone increasing and odd monotone increasing nonlinear feedback functions 22 p3940 A66-40529

Maximum principle shown to be necessary and sufficient optimality condition for



dynamic programming method for condition of existence of regular synthesis 22 p3884 A66-40531

Book on numerical processes in differential equations including initial value and boundary value problems 22 p3941 A66-40620

Motion stability described by differential equations of perturbed motion 22 p3949 A66-40691

Taylor stability of time-dependent flow between two concentric circular cylinders, noting solution of differential equations for perturbations by Galerkin method 22 p3902 A66-40706

Generalization of differential equation of dynamo theory of geomagnetic variations to include unsteady dynamo effect in ionosphere 22 p3914 A66-40759

Stability of trivial solution to system of linear differential equation with distributed delay, determining majorant of solutions to Cauchy problems 22 p3941 A66-40797

Differential equations with delayed argument describing laws of motion and action of control elements upon motion in problem of trajectory with moving right hand terminus 22 p3941 A66-40800

Shell dynamical integral and integro-differential BVPs for linear deformable shells, examining reciprocity theorem and Kirchhoff-Love hypothesis 23 p4136 A66-40997

Periodic solutions of nonlinear differential systems, examining Galerkin procedure and method of averaging 23 p4084 A66-41054

Axisymmetric dynamic response of ring supported cylinder to time dependent loads, discussing boundary conditions and differential equations of motions [AIAA PAPER 66-83] 23 p4138 A66-41106

Successive approximation method for optimization of nonlinear systems of ordinary differential equations with limitations on phase coordinates 23 p4084 A66-41352

Automatic control system analysis via space-state method, using  $n$  first-order differential equation 23 p4049 A66-41399

Generalized function solution for ordinary differential equations 23 p4084 A66-41406

Current distribution and input resistance of  $T$  type, corner and bent tape vibrators powered by lumped electromotive force, using method of integro-differential equations 23 p4045 A66-41457

Approximate solutions of second-order differential equations for nonlinear electronic circuits with strong disturbance 23 p4049 A66-41473

Lienard type of differential equation for oscillatory system representing solution by Krylov-Bogolubov method, noting inverse problem 23 p4085 A66-41545

Trajectory stability of diffusion-type random Markov process described by Ito stochastic differential vector equations 23 p4085 A66-41554

One- and two-sided estimates for distances between two zero points of solution of nonlinear differential equation with slowly varying parameters, comparing solutions 23 p4090 A66-41563

Photoconductivity in homogeneous semiconductors when solution of second-order nonlinear differential equations with indivisible variables is obtained in elementary functions, noting light intensity effect 23 p4113 A66-41564

Impulse response of second-order time varying systems of differential equation obtained without knowledge of independent solutions of associated homogeneous equation 23 p4086 A66-41694

Numerical integration with aid of matrices for solving differential equations of structural mechanics 23 p4139 A66-41786

Approximate second-order supersonic delta wing theory taking into account second-order differential equation via approximate particular integral 23 p4011 A66-41897

Differential equations of linear theory of elastic shells derived under Kirchhoff-Love hypothesis with aid of static-geometric analog 23 p4142 A66-41956

Pressure-perturbation produced by supersonic aircraft near caustic, deriving differential equations 23 p4016 A66-42040

Existence of similar solutions for given

differential transonic equations for free stream Mach number of unity 23 p4014 A66-42049

System of differential equations describing stability of certain generalized processes in language of functional sets and distributions 24 p4230 A66-42214

Airy and Weber equations solutions and relationships in terms of exponential function in connection with hydrodynamic stability and Orr-Sommerfeld equation 24 p4193 A66-42284

Layer-like field inhomogeneities in homogeneous semiconductors occurring when conductivity decreases analyzed using Poisson and transport equations, obtaining stationary solutions for differential negative conductivity 24 p4254 A66-42424

Stability of periodic solution of nonlinear systems with coefficients dependent on amplitude and frequency 24 p4188 A66-42478

Harmonic linearization, estimating quality of oscillatory transients in nonsearching self-adjusting systems described by high order differential equations 24 p4188 A66-42480

Existence of solution of linear problems for ordinary differential equations 24 p4231 A66-42538

Book on asymptotic methods of integrating linear differential equations with varying coefficients, emphasizing equations for oscillatory processes 24 p4231 A66-42613

MOS equivalent circuit for small signal HF operation of insulated gate field effect transistor in pinch-off mode, using differential equation 24 p4183 A66-42638

Pressure, temperature, gas velocity, thrust and specific impulse of rocket combustion chambers determined, using differential equation and Runge-Kutta method 24 p4261 A66-42743

Asymptotic behavior of solution to system of differential equations with random limited coefficients 24 p4232 A66-42749

Quadratic Liapunov functional derivation for time-delay system 24 p4232 A66-42845

Oscillatory properties of linear matrix differential system, applying generalization of polar coordinate transformation to certain systems of second order 24 p4233 A66-43100

Three families of classical fifth-order Runge-Kutta formulas including Newton-Cotes, Legendre-Gauss and Lobatto and Randau types 24 p4233 A66-43206

### DIFFERENTIAL GEOMETRY

#### SA PROJECTIVE-DIFFERENTIAL GEOMETRY

Conditions of integrability for certain normal systems of equations with partial derivatives 04 p0538 A66-13469

Invariance of differential equation systems in real gas dynamics considered in affine space-time 07 p1022 A66-18104

Geometrical properties of partial differential equations with independent variables, using Cartan method 23 p4084 A66-41061

### DIFFERENTIAL INTERFEROMETRY

Holographic interferometry, advantages and operation 13 p2076 A66-25048

### DIFFERENTIAL OPERATOR

Error estimate in obtaining eigenvalues of linear self-adjoint differential operator of elliptical type by finite difference method 01 p0095 A66-11008

Stability of net method for elliptical problems investigated, using low variability of network operator 01 p0096 A66-11184

Spectral matrix of fourth-order differential operator on half-axis 02 p0250 A66-12107

Nonlinear differential-difference equations of form  $Ly$  equals  $f/y$  solved by using  $f/y$  as power series in exponentials 03 p0387 A66-12614

Poisson pseudokernel and pseudodifferential operators on manifold with boundary 05 p0708 A66-15093

Expansion in eigenfunctions of not self-conjugate boundary value problem for differential equation with singularity at zero 05 p0709 A66-15339

Traces on coordinated hyperplanes of elements of functional space 07 p1057 A66-17844

Regularization of ordinary differential operator trace in region of regular boundary conditions 07 p1057 A66-17855

Nonself-adjoint normal differential operators of second order 08 p1245 A66-19632

Projection operators applicable for rearrangement and exchange processes with full recoil effect for unified reaction theory of Feschbach 10 p1558 A66-21961

Linear ODEs in canonical form with aftereffect in functional space of continuous functions 11 p1676 A66-22644

Stability of net method for elliptical problems investigated, using low variability of network operator 12 p1903 A66-24017

Theorems associated with surface parabolic potentials 13 p2116 A66-25334

Countable systems of differential equations, considering differential operator theory and infinite systems 13 p2119 A66-25850

Second-order elliptical operator for  $m$ -dimensional Euclidian space with open region bounded by closed surface 13 p2120 A66-26010

Monograph on direct methods of qualitative spectral analysis of singular differential operators 14 p2319 A66-26873

Perturbation theorem for ordinary differential operators 14 p2321 A66-27626

Existence theorem for nonlinear ODE system with continuous monotonic differential operators over Hilbert space and application to nonlinear network analysis 15 p2528 A66-29370

Intermediate problems for eigenvalues involving self-adjoint differential operator 16 p2732 A66-30235

General boundary conditions for second-order ordinary differential operators 16 p2733 A66-30630

Analytic construction of skew derivative Green matrix for system of second order elliptic PDEs in many variables 16 p2734 A66-30749

Expansion in eigenfunctions of not self-conjugate boundary value problem for differential equation with singularity at zero 16 p2735 A66-30969

Nonself-adjoint normal differential operators of second order 16 p2736 A66-30981

Linear operators describing passage of wave beam through system of amplitude-phase converters forming quasi-optical waveguide or resonator 16 p2666 A66-31546

Discreteness conditions for spectrum of one-term differential operator, considering asymptotic distribution of eigenvalues 18 p3126 A66-33931

Graphical analysis of extremal control system stepwise adapted to process with extremal characteristic located between two first-order linear operators 19 p3324 A66-35582

Theorems associated with surface parabolic potentials 19 p3390 A66-36195

Estimation of Poisson kernels of elliptic operator with variable coefficients by using maximum principle and Fatou theorem 19 p3390 A66-36248

Discretization and differentiation of operators with commutativity proof and with application to Newton method 20 p3589 A66-36904

Eigenfunction expansion of analytic linear ordinary differential operators of boundary value problem with normalized irregular disintegrating boundary conditions 20 p3592 A66-38432

Interior regularity theorem for linear elliptic matrix differential operator 21 p3754 A66-38459

Local existence theorems for elliptic systems with linear matrix differential operator 21 p3754 A66-38460

Semiweak solutions of elliptic BVP, particularly generalized Dirichlet problem 21 p3754 A66-38461

Garding inequality and Green transformation applied to elliptic operators in eigenvalue problems 21 p3755 A66-38465

Single second-order oblique derivative problem with elliptic operator 24 p4232 A66-42830

Approximate differential operator replacing integral operator, taking ionization losses into account in electromagnetic cascade theory 24 p4269 A66-42923

### DIFFERENTIAL THERMAL ANALYSIS

#### DTA/

Superheating of linear high polymer



polyethylene crystals, evaluating time dependence of melting, differential thermal analysis and calorimeter 12 p1899 A66-23937

Heat transfer problems associated with thermal analysis, discussing influence of rate of heat transport on heat transfer process 14 p2412 A66-27494

Metallography, roentgenography and differential thermal analysis of composition temperature ranges of chromium-germanium phases 23 p4082 A66-41825

**DIFFRACTION**

SA ELECTRON DIFFRACTION

SA FRESNEL DIFFRACTION

SA LAUE DIFFRACTION

SA LIGHT TRANSMISSION

SA NEUTRON DIFFRACTION

SA PULSE DIFFRACTION

SA WAVE DIFFRACTION

SA X-RAY DIFFRACTION

Construction method for asymptotic series of given class of functions and application to diffraction theory 09 p1394 A66-20459

Asymptotic expansions of double and multiple integrals occurring in diffraction theory, using stationary phase method 10 p1550 A66-21850

**DIFFRACTION GRATING**

Automatic coordinating measuring equipment using Moire fringes used to record flight paths of rockets 01 p0070 A66-10914

Electro-optic diffraction grating for light beam modulation and diffraction 02 p0239 A66-11371

Coma-corrected, mono- and multifrequency diffraction reflector antennas, examining feed system, electronic scanner and aberrations 05 p0648 A66-14911

Rowland ghosts during movement of spectral lines in double diffraction monochromators and compensation in photoelectric spectrophotometry 05 p0681 A66-15214

Wave polarization change passing through grating 06 p0829 A66-16144

Reflection gratings as end plates in Fabry-Perot cavity, with characteristics of low absorption output coupling and wavelength-dependent alignment of end plates 09 p1385 A66-19930

Concentric circular grid method of testing for aberrations in image-forming optical system and comparison with Ronchi test 09 p1403 A66-20515

Radiated power from modulated electron beam passing near diffraction grating surface 10 p1557 A66-21567

Optical diffraction velocimeter, using backscattered laser light to measure relative velocity between light source and surface 11 p1706 A66-22958

Laser action on rotational line in carbon dioxide and nitrous oxide vibrational spectra in both P and R branches up to J values of over 50 11 p1714 A66-23357

Plane electromagnetic wave diffraction by narrow strip-grating, obtaining reflection coefficient via optical approximation method 13 p2021 A66-25395

Electromagnetic oscillation by monochromatic beam moving over diffraction grating lying on shielded dielectric 13 p2049 A66-26052

Littrow-type IR spectrometer with diffraction grating 14 p2292 A66-27322

Nonfocusing grazing incidence monochromator which utilizes planar gratings and collimating slit systems 14 p2293 A66-27326

Light transmission through optical diffraction lattice consisting of medium in EM field of laser beam 15 p2511 A66-28626

Wave polarization change passing through grating 15 p2452 A66-29874

Radiation control of ruby laser by diffraction modulator with traveling ultrasonic wave, noting computer solution of kinetic equations of population balance, radiation density, characteristic damping, etc 17 p2938 A66-33515

Acoustic-array microwave grating quartz transducer creates variable delay characteristic with frequency 18 p3075 A66-33608

Functional equation applied to wave

scattering by infinite grating of elliptic cylinders 19 p3304 A66-36409

Fourier series solution to electromagnetic wave diffraction on metallic gratings with anisotropic dielectric 20 p3512 A66-37148

Gain, efficiency, directivity and application of reflectors, considering use of passive repeaters for increased transmission efficiency 20 p3516 A66-37715

Electromagnetic wave emission excited by electron stream over diffraction grating lying on boundary of semiinfinite anisotropic dielectric 20 p3519 A66-37998

Optical properties of plane and aspherical diffraction gratings having unequal spacings of ruling, examining possible use in 50 to 500 angstrom wavelength 21 p3771 A66-39128

Pulse compression using diffraction gratings and frequency sweeps of 30 mc in quartz crystal ultrasonic transducer 23 p4034 A66-41017

Radiation control of ruby laser by diffraction modulator with traveling ultrasonic wave, noting computer solution of kinetic equations of population balance, radiation density, characteristic damping, etc 24 p4219 A66-42128

Diffraction gratings by recording laser-generated interference pattern on high resolution film as two-beam hologram 24 p4210 A66-42259

Diffraction of waves by transparent screen studied to determine what information about diffracting screen can be obtained by observing diffraction pattern 24 p4173 A66-42712

**DIFFRACTION PATH**

Radar localization deviations, examining infinitely-long conducting cylindrical obstacles 04 p0488 A66-14413

Multiple diffraction of microwaves over knife-edge obstacles, obtaining path loss 19 p3304 A66-36410

Microwave diffraction over natural obstacles, stressing variation of signal level in time, space and frequency and polarization dependence and depolarization 19 p3304 A66-36411

**DIFFRACTION PATTERN**

Laser with diffraction limited radiation pattern 01 p0082 A66-10450

Thermal, micrographic and X-ray diffraction techniques used for constitution diagram of ternary system tungsten-molybdenum-osmium at various high temperatures 03 p0385 A66-13209

Laser with diffraction limited radiation pattern 03 p0380 A66-13313

Discrete radio source scintillation, considering irregular diffraction pattern caused by ionospheric irregularities 04 p0575 A66-13380

Diffraction field determined for E-polarized plane wave incident normal to evenly spaced nonsymmetrical metallic grid 06 p0838 A66-15895

Temperature effect on diffraction curve profile for Bragg case using triple crystal spectrometer, observing intrinsic temperature effect due to thermal motion 06 p0923 A66-16186

Granularity and radial structure in circular Fraunhofer diffraction fringes produced by lycopodium powder scattering of monochromatic coherent light 06 p0891 A66-16443

Anisotropic broadening of X-ray diffraction lines and increase in lattice perimeter resulting from neutron irradiation of beryllium oxide powder 06 p0896 A66-16539

Short wave asymptotics of diffraction field at sphere for incident plane transverse waves 07 p1144 A66-18182

Diffraction contrast analysis, using transmission electron microscope, of two-dimensional defects present in mechanically damaged silicon after annealing 07 p1109 A66-18516

Multimode antennas, discussing mode and moder generation, radiation sum and difference pattern control, discontinuity reflections, monopulse antennas, etc 08 p1191 A66-18945

Small angle scattering technique with high resolution electron microscopy to determine columnar structure of thin vacuum condensed Pd films 10 p1573 A66-21247

Ground diffraction pattern caused by radio

wave reflection from F region, using array of three aerials 11 p1651 A66-22374

Diffraction by conducting cylinder solved by approximation method, using expanded series of diffraction field of cylinder with polygonal section 11 p1662 A66-22464

Optical resonator diffraction loss, noting laser oscillations in high loss arrangements, output beam power, field patterns, etc 13 p2090 A66-25195

Plane wave diffraction by infinitely conducting network representing diffracted electric field by Rayleigh expansion 13 p2021 A66-25457

Cross section method to solution of diffraction of electromagnetic wave at inhomogeneous sphere, using membrane function 14 p2239 A66-27736

Radiation characteristics of horn antennas analyzed, using edge diffraction theory, noting intensity at backlobe and far sidelobe 14 p2255 A66-27908

Production of thin copper and nickel ferrite films in inert gas plasma reveal spinel structure in electron diffraction patterns 15 p2557 A66-28564

Diffraction pattern study of titanium single-crystal surface 15 p2566 A66-29389

Anisotropic broadening of X-ray diffraction lines and increase in lattice perimeter resulting from neutron irradiation of beryllium oxide powder 15 p2524 A66-29986

Intensity distribution in Fraunhofer diffraction patterns of slit and apertures illuminated by partially coherent light 18 p3118 A66-33986

High energy measurement of neutron-proton elastic scattering, noting diffraction peak existence, differential cross section and secondary forward peak 18 p3166 A66-34163

Diffraction pattern analysis of fields generated by hoghorn-fed Cassegrain antenna operating in Fresnel zone 18 p3083 A66-34289

Optimum shape of feed patterns for paraboloidal antennas 18 p3083 A66-34293

Moire fringe precision angle transducer 19 p3355 A66-35502

Diffraction of electromagnetic plane by half-plane in uniaxially anisotropic medium solved in terms of Sommerfeld approximation 19 p3304 A66-36284

Ultrasonic light diffraction, deriving line intensity in form of quadratures with parametric dependence 20 p3601 A66-37147

Effect of emulsion thickness on optical characteristics of reconstructed images, noting sensitivity to incidence angle 20 p3558 A66-37287

Von Laue and Cowley diffraction theories of coherent diffuse X-ray scattering from random alloys, predicting diffuse intensity singularities at reciprocal lattice points 22 p3948 A66-40084

Production of thin copper and nickel ferrite films in inert gas plasma reveal spinel structure in electron diffraction patterns 23 p4112 A66-41285

Laser beams and resonators, discussing beam propagation in free space, geometrical optics application and resonator modes in view of aperture diffraction effects 24 p4225 A66-42806

Irregular diffraction analysis with ultrasonic waves, measuring air stream temperature fluctuations and velocity 24 p4176 A66-43020

Divergent-beam diffraction geometry for interpretation of Kossel diffraction patterns in space group assignment lattice parameters and structure factor evaluation 24 p4239 A66-43169

**DIFFRACTION PROPAGATION**

Diffraction losses of open resonator oscillations with plane mirrors as function of absorption band of mirror 02 p0241 A66-11772

Pendellosung fringes in elastically deformed silicon, observing X-ray wavefield beam interference upon superimposition on crystal exit surface 07 p1098 A66-17815

Diffraction velocimeter detecting and measuring transverse movement of surface by sensing light backscattered by it when laser illuminated 07 p1044 A66-18333

Random irregularities caused by mechanical distortion in lenses, reflectors or



diaphragms of optical beam waveguides and increases in diffraction  
 attenuation 09 p1345 A66-20491  
 Geometric diffraction theory to predict radar cross section of cones and disks 10 p1498 A66-21597  
 Propagation mode of harmonics and effects on reflection and transmission coefficient at plane grid 10 p1506 A66-22001  
 Fabry-Perot interferometer with mirrors in form of backed metal grid, noting changes in diffraction, reflection and transmission 11 p1704 A66-22348  
 Geometrical theory of diffraction applied to calculation of radiation pattern and impedance of monopole antenna 11 p1663 A66-22545  
 Multiple diffraction of circular or linear front acoustic wave at polygon apices 12 p1914 A66-24350  
 Phase reference beam of two-beam carrier frequency holography method used for polarization reference 12 p1883 A66-24561  
 Plane electromagnetic diffraction by wide aperture in conducting screen immersed in anisotropic medium 14 p2241 A66-27981  
 Diffraction by wide slit in uniaxially anisotropic plasma solved by multiple scattering technique 16 p2761 A66-31006  
 Propagation mode of harmonics and effects on reflection and transmission coefficient at plane grid 18 p3072 A66-34978

## DIFFRACTION TELESCOPE

Meteor velocity determination via diffraction method, noting instrumental errors, recording and data processing techniques, etc 17 p3000 A66-32340

## DIFFRACTOMETER

### SA PARTICLE SIZE

Direct measurement of dispersion properties of cadmium sulfide and CdS-CdSe crystals, using Obreimov-Fresnel diffraction method, growing crystals by synthesis 21 p3799 A66-38926

## DIFFUSION RADIATION

Angular dependence of radiation intensity scattered from plane diffuse surface illuminated by wideband collimated light 07 p1081 A66-18039  
 Stray radiation error reduction in spectral emittance measurements for diffusely reflecting materials 11 p1737 A66-23410  
 Thermal emittance and reflectance of diffuse-bottomed, specular-walled groove in solar radiant-flux environment [AIAA PAPER 66-459] 16 p2811 A66-31491  
 Shadowing effect and anomalous backscattered intensity in diffuse reflection from plane-parallel layer of random particles 18 p3068 A66-34014  
 Transfer efficiency of laser pumping cavities with diffusely reflecting wall determined, based on approximately isotropic nature of light inside cavity 19 p3372 A66-35379  
 Photometry of flux from surface and representation as Fourier series of time dependence of received reflected flux for torse of convex curvature 20 p3556 A66-36937  
 Radiant heat transfer between concentric spheres and coaxial cylinders, assuming isothermal inner surface to be diffuse emitter and outer surface to reflect specularly 22 p3998 A66-40030  
 Heat transfer from gray fin-tube radiators with numerical results for diffuse surfaces, noting fin and tube emissivities 22 p3998 A66-40037

## DIFFUSER

### SA MAGNETIC DIFFUSER

### SA NOZZLE

### SA SUPERSONIC DIFFUSER

### SA VANELESS DIFFUSER

Calculation of rotationally symmetrical turbulent boundary layer flow through straight diffusers 01 p0006 A66-10214  
 Convection heat transfer for turbulent flow in subsonic diffusers [ASME PAPER 65-HT-64] 05 p0605 A66-14765  
 Influence of inlet flow profile characteristics on diffuser static pressure efficiency, achieving pressure increase if flow has high decay rate 06 p0801 A66-16002  
 Flow regime data for wide range of conical diffuser geometries determined from clear plastic diffuser experiments 11 p1687 A66-22331  
 Radial diffuser using swirl-free

incompressible flow between narrowly spaced disks of radial channel and supply-pipe outlet [ASME PAPER 65-FE-12] 12 p1864 A66-24548  
 Density ratio and transmission probability across conical converging diffuser in free-molecule flow with selected range of speed ratios, using Monte-Carlo method 14 p2219 A66-27416  
 Conical vortex tunnel investigated for thermal efficiency and cold production 14 p2415 A66-28320  
 Flow loss in conical diffusers with boundary layer suction through single slit 16 p2629 A66-30813  
 Flow characteristics, design and performance data for subsonic two-dimensional straight centerline diffusers [ASME PAPER 66-FE-10] 17 p2915 A66-33264  
 Wall shape effects on flow regimes and performance in straight two-dimensional diffusers [ASME PAPER 66-FE-13] 17 p2915 A66-33267  
 Rotating vortex flow and transition phenomena in conical diffuser [AIAA PAPER 66-426] 18 p3046 A66-33643  
 Bell-shape diffuser for rotationally symmetrical flow 21 p3694 A66-38815  
 Velocity distribution for inlet flow in finite radial diffuser 21 p3731 A66-39591

## DIFFUSION

### SA AMBIPOLAR DIFFUSION

### SA ATMOSPHERIC DIFFUSION

### SA EDDY DIFFUSION

### SA ELECTRON DIFFUSION

### SA GASEOUS DIFFUSION

### SA IONIC DIFFUSION

### SA MOLECULAR DIFFUSION

### SA PARTICLE DIFFUSION

### SA PLASMA DIFFUSION

### SA SELF-DIFFUSION

### SA SPECIES DIFFUSION

### SA THERMAL DIFFUSION

### SA TURBULENT DIFFUSION

Optimum detection of diffusion process in white Gaussian noise, using continuous observation 02 p0190 A66-11405  
 Diffused aluminum coating for high temperature application 03 p0380 A66-12371  
 Asymptotic solution of Dirichlet problem for diffusion processes and small parameter in elliptic equations with discontinuous coefficients 03 p0388 A66-12925  
 Vacuum technique for obtaining thin layers of semiconductor material with varying impurity distribution across depth of layer 06 p0924 A66-16545  
 Resistor values in semiconductors calculated from diffusion parameters and vice versa 06 p0857 A66-16928  
 Diffusion technique preparation of GaP p-n junctions and relation of p-i-n junction electric field calculation to Baraff carrier ionization rate theory 07 p1108 A66-18415  
 Alloying technique through doped diffused layer for production of high speed silicon tunnel diodes for logic circuits and memory functions 08 p1188 A66-18653  
 Gold diffusion into silicon and formation of segregations in surface layers and crystal disturbances 08 p1268 A66-18661  
 Diffusion of selenium in cadmium telluride, using radioactive Se as tracer 10 p1574 A66-21353  
 Epitaxial, diffusion and photolithographic processes in manufacture of semiconductor component 10 p1514 A66-22056  
 Sufficient conditions for recurrence and positivity of diffusion process defined by stochastic differential equation, using Liapunov function 15 p2525 A66-28512  
 Diffusion saturation of industrial iron, molybdenum, Kh18N9T steel and ZhS6-K alloy with powdered beryllium mixture 15 p2520 A66-28538  
 Average diffusion cross section for elastic collisions of electrons with heavy particles, comparing calculated and measured values 15 p2551 A66-29225  
 Impurity conduction for arsenic diffused into p-type germanium and boron into n-type silicon 19 p3433 A66-35342  
 Diffusion process involving formation and subsequent migration of series of parallel shear planes within crystal for higher oxides of niobium, tungsten, molybdenum and titanium 22 p3934 A66-40011  
 Anodizing techniques used in diffusion

studies of TiCb system 24 p4228 A66-42616

## DIFFUSION BONDING

Roll reduction diffusion bonding for sandwich structures based on solid state diffusion process [SAE PAPER 650778] 05 p0687 A66-15006  
 Aluminum diffusion bonding for fabrication of Apollo cold plates, noting alternate bonding techniques [SAE PAPER 650779] 05 p0687 A66-15007  
 Rapid method for solid state diffusion bonding of aerospace sheet metal structures fabricated from refractory or dispersion hardened metals [SAE PAPER 650780] 05 p0688 A66-15008  
 Diffusion and regular model of motion of cosmic rays, noting dependence of applicability to cosmic ray fluxes on chemical composition 09 p1443 A66-20598  
 Joining of dissimilar metals such as molybdenum and tungsten by liquid-alloying diffusion-bonding method in which third metal is used for bonding at interface and removed by diffusion 19 p3367 A66-36116  
 Fabrication techniques for preparation of ion emitter modules requiring high-temperature leak-free bond between porous tungsten ionizer and refractory metal plenum chamber 19 p3368 A66-36118  
 Diffusion and regular model of motion of cosmic rays, noting dependence of applicability to cosmic ray fluxes on chemical composition 20 p3633 A66-38132  
 Strength of joints made in refractory metals using brazing, welding or diffusion bonding, noting role of coating 22 p3925 A66-40265  
 W-diffusion bonding in preparing segmented silicon-germanium-lead telluride thermoelements, noting properties 24 p4248 A66-42116  
 W-diffusion bonding of lead telluride base thermoelements with nonmagnetic electrodes 24 p4216 A66-42117  
 Thermal insulation and structural support for thermoelectric devices, discussing fabrication of diffusion bonded structures in conjunction with material selection 24 p4293 A66-42121  
 Tin and zinc diffusion from doped pyrolytic silicon oxide layers used to form base regions of planar n-p-n and p-n-p-GaAs transistors 24 p4254 A66-42384

## DIFFUSION COEFFICIENT

Diffusion of heavy contaminant in turbulent atmosphere, approximating vertical wind profile and turbulent diffusion coefficient by power functions of height 01 p0096 A66-10754  
 Order in equiatomic germanium silicon solid solution, using diffusion scattering of X-rays calculated by least squares method 01 p0124 A66-10768  
 Friction, diffusion, and electrical conductivity tensors obtained for plasma subjected to strong external magnetic field 01 p0114 A66-10961  
 Thermomechanical treatment and temperature on diffusion mobility and heat resistance of titanium alloys 03 p0384 A66-13170  
 Lattice and grain boundary self-diffusion coefficients of radioactive nickel 63 into high purity nickel measured over temperature range 650-475 degrees C 04 p0535 A66-13746  
 Diffusion coefficient of solar protons in steady state electromagnetic medium of interplanetary space increases with increase in proton momentum 04 p0574 A66-13839  
 Ambipolar diffusion and electron-ion recombination coefficients dependence on electron temperature in afterglow of neon plasmas 04 p0554 A66-14294  
 Internal electric field induced by ionized particles and current carriers on impurity diffusion in semiconductors, noting diffusion and Poisson equation 04 p0568 A66-14349  
 Isotopic ratios and location of light primordial rare gases in stony meteorites and correlation with diffusion coefficients 04 p0580 A66-14482  
 Base diffusion profile arising from boron redistribution in oxide, noting useful approximation 05 p0732 A66-14671  
 Retardation of gallium and arsenic or phosphorus diffusion in silicon 05 p0736 A66-14976



Holographic information of photographic plate and diffusing object 05 p0678 A66-15105  
 Variation of interdiffusion coefficient with composition for niobium-vanadium alloys determined for various diffusion temperatures 05 p0702 A66-15467  
 Determining isothermal diffusion coefficients of gases under isobaric conditions 06 p0908 A66-16154  
 Nonuniqueness of stationary solutions to system of equations in burning theory with piecewise invariable reaction rate and thermoconductivity and diffusion coefficients 06 p0970 A66-16345  
 Low temperature copper diffusion limits frequency range of cadmium sulfide shear mode diffusion layer 06 p0851 A66-16461  
 Heat transfer rate to stagnation point of catalytic surface placed in slow flow of dissociated oxygen from glow discharge tube and atom-molecule diffusion coefficient 06 p0822 A66-16632  
 Diffusion distribution of phosphorus in silicon at low surface concentration 06 p0928 A66-16893  
 High temperature oxidation of liquid yttrium and liquid lanthanides and their alloys with gold, obtaining parabolic diffusion-controlled rate constants 08 p1235 A66-18622  
 Heat capacity expression due to chemical reaction, relating composition variations and binary diffusion coefficient with Lewis number, presenting integral equation for system enthalpy 08 p1318 A66-19164  
 Electron diffusion coefficient estimated and compared with theory for case of infinite plane parallel plasma and constant electric field 08 p1264 A66-19226  
 Orientation effect on zinc diffusion rate in p-n junctions, using gallium arsenide single crystals as initial material 09 p1412 A66-19996  
 Tritium diffusion constants of stone meteorites and dependence on tritium production mechanism 09 p1456 A66-20421  
 Atmospheric structure in lower thermosphere, examining grenade clouds to determine density 09 p1375 A66-20892  
 Anomalous diffusion of boron parallel and perpendicular to dislocation arrays in grain boundary contained in silicon 10 p1574 A66-21356  
 Diffusion length dependence on energy of exciting photons for p-silicon and n-and p-germanium, using bevel-grind technique 10 p1578 A66-21666  
 Impurity atom diffusion through narrow diffusion mask opening determined by relaxation method 10 p1512 A66-21762  
 Order in equiatomic germanium silicon solid solution, using diffusion scattering of X-rays calculated by least squares method 11 p1748 A66-22279  
 Nonuniqueness of stationary solutions to system of equations in burning theory with piecewise invariable reaction rate and thermoconductivity and diffusion coefficients 11 p1785 A66-22340  
 Diffusion and propagation phenomena in air-water and water-steam emulsions in one-dimensional flow 12 p1973 A66-23524  
 Carbide formation from beta-titanium and graphite 12 p1895 A66-24377  
 Germanium specimens with various dislocation densities quenched from high temperatures to introduce vacancies, contamination by copper atom diffusion, finding activation energy 12 p1930 A66-24801  
 Diffusion coefficient measurement in fully ionized cesium plasma, using potassium plasma pulse launching techniques 13 p2155 A66-26680  
 Diffusion coefficient calculated for fluctuations due to flute instability in low pressure Penning discharge, using measured correlation times and flute amplitudes 13 p2156 A66-26688  
 Magnetic diffusivity measurement for cylinder of type II Nb-Zr superconductor at 4.2 degrees K, using magnetoresistance probe 14 p2350 A66-26878  
 Diffusion of indium along sessile dislocation in silicon crystal 14 p2356 A66-27070  
 Beryllium diffusion into gallium arsenide in /111/ plane with various electron concentrations through vacuum

deposition of heavy contaminant in turbulent atmosphere, approximating vertical wind profile and turbulent diffusion coefficient by power functions of height 14 p2358 A66-27087  
 Motion of slow positive potassium and nitrogen ions in nitrogen, measuring mobility and diffusion coefficients with apparatus whose characteristics are given 14 p2345 A66-28139  
 Motion of potassium ions in argon, using apparatus for simultaneous measurement of mobility and diffusion coefficients 14 p2345 A66-28140  
 Drift and diffusion of slow positive ions in hydrogen, using redesigned apparatus 14 p2345 A66-28141  
 Internal electric field induced by ionized particles and current carriers on impurity diffusion in semiconductors, noting diffusion and Poisson equation 14 p2368 A66-28246  
 Determining isothermal diffusion coefficients of gases under isobaric conditions 15 p2543 A66-29884  
 Isotope-dilution method in combination with chemical sectioning technique to determine self-diffusion in silicon 16 p2771 A66-30202  
 Atmospheric diffusion coefficients by measuring radial growth of chemiluminous trails deposited in upper atmosphere 16 p2695 A66-30712  
 Adiabatic deceleration effect on cosmic ray spectrum, noting particle momentum and energy change, diffusion coefficient independent of energy, etc 16 p2795 A66-30924  
 Atmospheric decay of rocket-released Li due to diffusion, wind and chemical reaction 16 p2697 A66-31008  
 Space charge polarization in glass films, discussing parameters of shift of capacitance-voltage characteristics, diffusion coefficient in metal-glass-silicon dioxide-silicon double-layer capacitor 16 p2779 A66-31089  
 Chapman-Enskog kinetic gas theory calculation of diffusion coefficient of binary gas mixture 17 p3035 A66-32694  
 Ambipolar potential in magnetoactive cold plasma applied to power generation and effects of electric field on diffusion coefficient 17 p2973 A66-32984  
 Rate of diffusion disintegration of metastable helium atoms in decaying helium plasma at very low temperatures, with excitation by electrodeless method 18 p3142 A66-33940  
 Elastic relaxation effect due to diffusion of interstitial hydrogen in tantalum and niobium 18 p3123 A66-34058  
 Diffusion of nickel in solid solution and two-phase alloys of nickel-titanium system 18 p3123 A66-34402  
 Transport properties of ionized monatomic gases, using Chapman-Enskog-Burnett approximation method for determination of thermal conductivity, diffusion coefficients and viscosity 18 p3149 A66-34927  
 Ionization and diffusion cross sections of Ca, Fe, Si and Mg atoms of disintegrated meteors 19 p3455 A66-35270  
 Stable domain propagation for case when electrons have field-independent diffusion coefficient and follow arbitrary static velocity field characteristic exhibiting negative resistivity 19 p3446 A66-36371  
 Periodic and height-dependent solutions for disturbances of concentrations of radon and thoron and decay products above Earth surface, considering turbulent diffusion and radioactive decay 19 p3453 A66-36385  
 Diffusion parameters of impurities from polycrystalline Si in hydrogen flux, noting formula for boundary conditions 19 p3321 A66-36457  
 Diffusion coefficients for transport of plasma across magnetic field calculated directly from motion of test particles 19 p3416 A66-36520  
 Low energy cosmic ray modulation relationship to observed interplanetary magnetic field irregularities in terms of diffusion, using space probes 19 p3454 A66-36765  
 Crystal growth, diffusion and fabrication of gallium arsenide-phosphide junction lasers

with low threshold current densities 20 p3577 A66-37401  
 Fatiguing at room temperature resulting in observable diffusion of silver into copper, using precipitation reaction to analyze influence of large number of vacancies 20 p3584 A66-37618  
 Chemical diffusion as affected by tungsten concentration in columbium-tungsten system measured, using couples prepared from polycrystalline pure metal 20 p3585 A66-37785  
 Sidereal diurnal variation of high-energy cosmic radiation, noting parameters of anisotropy coefficient, cosmic ray source distribution and air shower measurements 20 p3631 A66-37851  
 Integral-diffusion analysis of turbulent flow of incompressible liquid 20 p3548 A66-38111  
 Chemical equilibrium in nighttime ionosphere, estimating diffusion coefficients, noting role of transport processes 20 p3554 A66-38207  
 Diffusion coefficients in outer radiation belt, examining energy dependence on electric and magnetic disturbances contributing to transport of particles 20 p3641 A66-38327  
 Carrier motion equation in Gunn diode in terms of average drift velocity and diffusion coefficient 20 p3534 A66-38402  
 Electric field effect on donors diffusion into intrinsic semiconductor 21 p3799 A66-38927  
 Internal electric field effect on singly ionized acceptor or donor impurity diffusion in uniformly doped n-or p-type semiconductors 21 p3804 A66-39468  
 Nighttime F layer recombination and diffusion coefficients estimated from incoherent scatter measurements of electron densities and electron and ion temperatures 22 p3910 A66-39983  
 Effective diffusion cross section for meteor atoms in atmosphere, using Thomas-Fermi-Dirac and dumbbell molecule models 22 p3983 A66-40764  
 Initial radius of ionized meteor track, taking into account dependence of effective diffusion cross section of meteor atoms in atmosphere on relative velocity 22 p3984 A66-40765  
 Beryllium diffusion into gallium arsenide in /111/ plane with various electron concentrations through vacuum deposition 22 p3967 A66-40843  
 Quasi-linear theory to study turbulent diffusion of plasma caused by instabilities in oscillating discharge 23 p4100 A66-41140  
 Grain boundary self-diffusion coefficient variation with applied stress and production of lattice vacancies applied to cavity growth in high temperature fatigue of Mg 23 p4081 A66-41714  
 Integral ratios for calculating diffusion rate of magnetic field into wall-cooled plasma 23 p4106 A66-41716  
 Turbulent diffusion coefficient determined from vertical profiles of concentration of daughter products of radon 23 p4124 A66-41839  
**DIFFUSION EFFECT**  
**SA SURFACE DIFFUSION EFFECT**  
 Phosphorus diffusion production of p-type silicon for solar batteries 01 p0016 A66-11036  
 Phosphorus diffusion into silicon film and resultant defect structures 06 p0928 A66-16762  
 Built-in electric field effect on simultaneous diffusion of oppositely charged impurities in semiconductors 08 p1268 A66-18659  
 Manganese oxide effect on kinetics and mechanics of sintering of alumina powder compacts 08 p1243 A66-18774  
 Annealing and diffusion processes effect on lifetime of minority carriers in p-silicon used in production of rectifiers 08 p1272 A66-19245  
 Room temperature capacitance voltage characteristics and built-in diffusion voltages in n Ge-n Si double saturation heterojunction 09 p1411 A66-19912  
 Electrical properties, solubility and diffusion characteristics of gold in silicon, noting discrepancy between theoretical calculations and experimental measurements 09 p1432 A66-20975



Diffusivity, elastic modulus and stacking fault energy effect on high temperature creep behavior of alpha brasses 11 p1717 A66-22996

Localized enhanced diffusion in vacancy model to explain Emitter Dip Effect /EDE/ in p-n silicon transistor 11 p1671 A66-23350

Thermionic energy converter energy loss through resonance emission and excited atom diffusion, accounting for de-excitation at electrodes 12 p1922 A66-24219

Antimony ionization in p-germanium single crystals, based on diffusion of Sb into Ge 12 p1930 A66-24460

Gold or copper diffusion effect on breakdown and multiplication characteristics of high voltage silicon p-n junctions, noting presence and formation of microplasma 13 p2161 A66-25194

Zinc-antimonide with high and constant thermoelectric figure of merit obtained by solid phase diffusion 13 p2163 A66-25453

Diffusion-induced stress concentration near cavity, relating deformation diffusion and heat conduction via differential equations 13 p2203 A66-26426

Integrated circuit fabrication noting diffusion steps, temperature and time dependency, doping solid solubility, impurity distribution, etc 15 p2465 A66-29602

Occurrence of collisions between ionized and neutral particles based on analysis of spectrum diffused by E region 15 p2491 A66-30021

Ionospheric sounding using random diffusion of electromagnetic wave by ionospheric plasma with continuous wave through two separate antennas 16 p2653 A66-30953

Klystron transmitter for ionospheric diffusion soundings, noting method to obtain high stability in output power 16 p2661 A66-30954

Geometrical characteristics of framework and reflecting surface of ionospheric diffusion probe antenna, noting specifications on design, manufacture, erection, alignment and adjustment 16 p2662 A66-30956

Receiver of ionospheric diffusion probe noting radio telescope, low noise parametric amplifier, filters, signal detection, etc 16 p2662 A66-30957

Drift rate and precipitation of lithium ion in germanium as affected by resistivity, acceptors, carrier lifetime and copper diffusion 19 p3442 A66-35914

Separation centers and dislocations during diffusion of Zn into GaAs at high temperatures, analyzing photographs of p-n junctions 19 p3445 A66-36339

Antimony ionization in p-germanium single crystals, based on diffusion of Sb into Ge 20 p3620 A66-37692

Elementary gas phase reactions involving atoms and radicals by mass spectroscopic and diffusion cloud methods 21 p3702 A66-38472

Thermionic energy converter energy loss through resonance emission and excited atom diffusion, accounting for de-excitation at electrodes 22 p3957 A66-40583

Nonstationary convective diffusion flow toward moving droplet at small Reynolds number 22 p3902 A66-40816

**DIFFUSION ELECTRODE**

Palladium-hydrogen diffusion electrode noting current densities 04 p0460 A66-14034

Current voltage characteristics of four-layer structures with common diffusion p-n junction and two emitters 06 p0860 A66-17197

Apparatus for measurement of flow resistance of gas diffusion electrodes 07 p0990 A66-17233

Diffusion controlled mechanism for operation of nickel hydroxide electrode, analyzing corresponding boundary value problem and predicting electrochemical behavior 08 p1171 A66-19647

Hydrogen feeding through single-layer metallic porous electrode of fuel cell on open circuit 08 p1171 A66-19649

Hydrogen and oxygen ionization at three-phase boundary in alkaline solutions on smooth metals 08 p1171 A66-19650

Microporous metallic gas-diffusion electrodes in low temperature acid-

electrolyte fuel cells 08 p1172 A66-19651

Thermodynamic and kinetic effects of gas pressure on performance of fuel cell using one or two gas electrodes 08 p1172 A66-19654

Current voltage characteristics of four-layer structures with common diffusion p-n junction and two emitters 19 p3315 A66-35555

Photoresponse measurements of depletion capacitance and diffusion potential of GaP Schottky-Barrier diodes 20 p3534 A66-38390

**DIFFUSION FLAME**

Laminar diffusion flame occurring in mixing zone between undiluted fuel and undiluted oxidizer by process of molecular diffusion 03 p0443 A66-12489

Laminar flame speeds predicted by Spalding formulation in stoichiometric mixtures with nonnormal diffusion 03 p0443 A66-12490

Ammonium perchlorate spheres combustion in flowing gaseous fuel similar to conditions in solid rocket combustion, noting diffusion flame significance 03 p0414 A66-13225

Opposed jet diffusion flames subjected to electrostatic fields, estimating volumetric heat release rate and mass flow behavior [ASME PAPER 65-WA/ENER-3] 05 p0789 A66-15628

Aerodynamic calculations for diffusion combustion in laminar boundary layer between two plane parallel conducting gas flows in transverse magnetic field 06 p0918 A66-16844

Axial temperature variation in turbulent buoyancy-controlled diffusion flame 08 p1319 A66-19202

Flame properties as function of flame gases 14 p2414 A66-28142

Diffusion combustion in laminar boundary layer between two plane-parallel co-current streams 14 p2416 A66-28485

Laminar and turbulent diffusion flame combustion mechanisms, stabilization, flame ionization, Bunsen burner, fuel gas jet eddy diffusion, etc 15 p2616 A66-29068

Stabilization of lifted diffusion flame in turbulent methane jet flow field and measurements of gas flow velocity, turbulence and gas composition 15 p2479 A66-29608

Opposed jet diffusion flames subjected to electrostatic fields, estimating volumetric heat release rate and mass flow behavior [ASME PAPER 65-WA/ENER-3] 16 p2825 A66-30341

Diffusion flame for stagnation mixing layer created by jet fuel injected into oxidant stream at stagnation region of blunt body 17 p3033 A66-32447

LF self-vibrations of laminar diffusion flames in axial mode at frequencies corresponding to fuel system natural frequencies [WSCI 66-30] 18 p3263 A66-34414

Kinetic factors in diffusion flames, noting fuel/oxidizer ratios, equilibrium in terms of flame geometry, burning of metallic elements, etc [WSCI 66-10] 18 p3263 A66-34419

Initial broadening of diffusion flame sheet caused by nonvanishing equilibrium constant determined, using method of inner and outer expansions 23 p4148 A66-41500

Initial air-side boundary layer effect on ignition of slot injected gaseous hydrogen by hot supersonic air stream [AIAA PAPER 66-644] 23 p4149 A66-41513

Counterflow diffusion flame in forward stagnation region of porous cylinder with uniformly ejecting fuel gas in analysis by flame sheet model and boundary layer approximation 24 p4294 A66-42542

**DIFFUSION THEORY**

Error in finite difference solution of diffusion equation with impulsive end condition 01 p0093 A66-10383

Diffusion process of plasticity in metals, noting Frenkel vacancy mechanism 01 p0158 A66-11018

Physical and mathematical models in combustion theory of Zeldovich, Franck and Kamenetski 03 p0444 A66-12702

Tracer diffusion measurements in beta titanium covering Arrhenius plots, monovacancy and divacancy diffusions and new data for Sc-46, Sn-113 and P-32 03 p0382 A66-12939

Temperature distribution in flow past sphere, discussing time dependent form of Boussinesq transformation 05 p0784 A66-14752

[ASME PAPER 65-HT-38]

Carbon diffusion into titanium and zirconium nitrides, noting carbide layer parabolic growth rate and experimental techniques 05 p0704 A66-15817

Ion composition model representing conditions at low temperatures, assuming that solar cycle variation ions are distributed according to diffusive equilibrium theory 06 p0876 A66-16611

Anomalous diffusion of some group III and group V impurities in silicon 08 p1268 A66-18657

Crystal-Diffusion Spectra-International Colloquium, Paris, July 1965 08 p1233 A66-19231

Transverse diffusion theory and static and HF conductivity of plasma in strong magnetic field 09 p1406 A66-19962

Pseudoshocks in pipe flow in supersonic compressors represented as diffusion process, noting application in cascade and rotor configuration 10 p1479 A66-21363

Anomalous diffusion and instabilities of argon plasma in strong magnetic field 10 p1564 A66-21568

Sufficient conditions for optimal stochastic control of diffusion processes governed by vector equations satisfying local Lipschitz conditions 11 p1682 A66-23459

Stochastic processes in microscale relativistic fluid mechanics, discussing Dirac fluid, Klein-Gordon equation, diffusion, quantum potential, spin fluids, etc 12 p1914 A66-24093

Effective diffusion cross section of ultrasonic and laser beam while acting on turbulent flow 13 p2062 A66-25404

Relativistic hydrothermodynamics in covariant form for simple viscous fluid, omitting infinite heat conduction velocity and instantaneous diffusion flux theory from treatment of Eckart 13 p2210 A66-26333

Oscillatory phenomenon in gaseous multicomponent diffusion, noting convection caused by density inversion 15 p2481 A66-29745

Electrostatic field gradient effect in semiconductors with diffused impurities investigated, using basic diffusion theory 17 p2980 A66-32645

Drift effect on diffusion spreading of plasma inhomogeneities in magnetic field, deriving expression for Fourier component potential and magnetic field perturbations 19 p3344 A66-35265

Hydrogen combustion in air above solid noncatalytic wall heated to 800 degrees C, examining diffusion equation for slow combustion and laminar boundary layer flow over noncatalytic wall 19 p3479 A66-36249

Schottky diffusion theory applied to calculation of coefficients of homogeneous positive column in neon, using Druyvesteyn electron-energy distribution 20 p3608 A66-37462

Liquid junction cell design, noting equation integration for ideal diffusion potential and salt effects potential for heteroionic junctions of uniform ionic strength and cation concentration 20 p3502 A66-38188

Diffuse boundary scattering as possible explanation for enhanced field effect in thin metallic films through polarization reversal of ferroelectric substrates 21 p3800 A66-38990

Local structure of continuous and diffusion Markov processes compared with aid of M functionals for stochastic integrals 21 p3757 A66-39246

Random acceleration theory using diffusion transformation of matrix equation into differential equation 22 p3947 A66-39664

Thermal transient characteristics of prolate spheroidal solid, using diffusion equation for heat conduction 22 p3998 A66-40034

Carbon diffusion into titanium and zirconium nitrides, noting carbide layer parabolic growth rate and experimental techniques 23 p4083 A66-41383

Trajectory stability of diffusion-type random Markov process described by Itô stochastic differential vector equations 23 p4085 A66-41554

Diffusion current in MOS transistors



- analyzed, using three-dimensional energy band diagrams 24 p4253 A66-42383
- DIFFUSION WAVE**
- Time dependent ambipolar diffusion waves, solving electron density equation 07 p1088 A66-17951
- Shock wave structure in ionized hydrogen, using Eddington approximation to solve Rankine-Hugoniot jump 08 p1204 A66-18522
- Diffusion spectrum modifications due to positive ions collision with neutral particles observed through ionospheric probe in E layer 19 p3346 A66-35590
- Backstreamed fluid analysis via gas chromatography, using polyphenyl ether as diffusion pump fluid 24 p4239 A66-43164
- DIFFUSION WELDING**
- Brazing and diffusion bonding of titanium alloys to similar and dissimilar materials in high vacuum or inert gas [SAE PAPER 650752] 05 p0687 A66-15001
- Vacuum diffusion welding of zirconium, niobium and tantalum carbides to high-melting niobium, tantalum, molybdenum and tungsten 06 p0887 A66-16696
- High remelt temperature brazing of Ta-10W honeycomb structures by brazing with pure titanium, using diffusion sink concept 13 p2109 A66-25774
- Argon arc and resistance diffusion /vacuum/ welding of Ti and Ti alloys and protective metallic coating deposition on welded parts 13 p2110 A66-26027
- Solid state welding and brazing for surface layer bonding 22 p3925 A66-40269
- DIFLUOROAMINE**
- High temperature kinetics of difluoroamino radical decomposition in excess argon studied behind incident shock waves 03 p0413 A66-12337
- Preparation of aluminum difluoramide from trimethylamine alane and difluoroamine 13 p2018 A66-26501
- Isotopic exchange reactions of difluoroamine with deuterium oxide and trifluoroacetic acid at low temperatures studied by NMR techniques 23 p4118 A66-41231
- Difluoroamine reactions with Lewis acids studied to establish existence of difluoroammonium compounds and to obtain new oxidizers containing difluoroamino groups 23 p4031 A66-41232
- Difluoroamine chemistry for understanding nature of N-F and N-X bonds, electron distributions and existence and stabilities of N-F radicals and ions 23 p4031 A66-41233
- Thermally initiated reaction between tert-butyl iodide and tetrafluorohydrazine provides synthetic route to tert-butyl difluoroamine 23 p4118 A66-41234
- DIGESTIVE SYSTEM**
- SA GASTROINTESTINAL SYSTEM**
- SA INTESTINE**
- Physiological reactions to long periods of weightlessness beyond operational possibilities 11 p1642 A66-22484
- Nitrogen, phosphorus and calcium determination from perchloric acid digestion, process includes sample collection, preparation, digestion and determination 17 p2870 A66-32143
- DIGITAL COMMAND SYSTEM**
- Practical component packaging system for compatible use of integrated and thin film circuits in spaceborne digital command and data handling equipment 04 p0492 A66-13465
- Ground system design, data processing, digital command and digital-human interface in flight operations problems for unmanned spacecraft on planetary exploration mission 13 p2190 A66-25257
- Triple modular redundancy /TMR/ computer organization used in digital computer design for Apollo Command Module 13 p2027 A66-25258
- High reliability digital test command system for use as part of prelaunch acceptance checkout equipment for Apollo program 15 p2460 A66-28989
- High speed microwave frequency synthesizer with digital control 17 p2897 A66-33438
- Space control system using digital SUBORDINATE OR logic blocks to add optimum response capability to maneuver commands 20 p3662 A66-37229
- Acceptance checkout system for checkout assistance to Apollo CSM and LEM facilities during countdown, discussing system configuration variability, composition and operation 20 p3543 A66-37579
- DIGITAL COMMUNICATIONS SYSTEM**
- Digitally coded frequency and pulse modulation with square wave, performing spectral analysis and measuring spectral response 01 p0030 A66-10875
- Error control systems in digital communications accomplished by adding constraints to digital alphabet through coding 04 p0481 A66-13766
- Computer determination of signaling alphabet required to ensure reliable digital communication in presence of additive Gaussian noise and interchannel interference 05 p0630 A66-14588
- Principles of data communication reviewing digital systems, modulation methods and spectral shaping of data signals to achieve maximum noise tolerance 05 p0633 A66-14991
- Logical design for phase-coherent and comma-free biorthogonal telemetry system less RF carrier 06 p0823 A66-15965
- Error control over wide frequency range through adaptive dynamic channel equalization system 06 p0825 A66-15987
- Signal optimization for digital communication system over channel characterized by rational transfer function and Gaussian noise having memory 06 p0829 A66-16192
- Learning-type signal processing receivers for binary communication channels with intersymbol interference 06 p0830 A66-16196
- Simultaneous measurement of multipath and Doppler spread in real time involving fading transmission media such as HF and troposcatter [IEEE PAPER CP 65-524] 06 p0830 A66-16336
- Error probability limitations caused by multipath and Doppler smear in Kathryn modem 06 p0831 A66-16339
- Digital range measurement used in design of instantaneous communications handover system for medium altitude multisatellite system 06 p0831 A66-16340
- Optimum threshold and associated error probability for detecting binary optical signals 06 p0833 A66-16663
- Multilevel narrow-band FM digital communication system using conventional modulators and demodulators 06 p0834 A66-16856
- Component characteristic determining conversion probability of input signal to output signal allowing for random dispersion of transmission characteristics of individual components 07 p1013 A66-17385
- Noise rejection properties of nonmemory discrete-data transmission systems employing information feedback, decision feedback or combined feedback 08 p1183 A66-19096
- Optimum number of phase-quantization steps in phase-shift keying communications system for maximum data transmission rate, using binary integration method 08 p1183 A66-19097
- Digital detector for automatic radar target identification, noting design, construction and operation 11 p1654 A66-22655
- Buffer storage in digital radar smoothing irregular output data flow, noting decreasing bandwidth requirements 11 p1654 A66-22656
- Digitalization of moving target indicator signals for adaptation of digital detectors to air surveillance radars 11 p1655 A66-22657
- Algorithm for data transmission system automatic adaptive equalization, employing change of settings during transmission in response to variation in transmission channel characteristics 11 p1656 A66-23088
- Digital and RF/linear circuits compared noting monolithic, hybrid and thin film circuit limitations, phase locked loop design, etc 12 p1830 A66-23756
- Satellite ground terminal design considerations using adaptive digital communications techniques, noting analog to digital conversion [AIAA PAPER 66-290] 12 p1822 A66-24760
- Asynchronous delta-modulation system with coded pulse generation according to certain change in amplitude 13 p2030 A66-25208
- Power spectra formula of digital FM signals for phase continuous and discontinuous cases, noting results of Anderson and Saltz 13 p2020 A66-25213
- Temperature stable high power C band digital many-phased-array-radar phase shifter 13 p2035 A66-25502
- Low power long-range digital communications system based on narrow bandwidth portable transmitter and fixed station receiver 15 p2450 A66-28972
- Analog form data transmission via FM compared to digital form via phase shift keying, noting accuracy, power and bandwidth required, output signal to noise ratios, etc 18 p3067 A66-33902
- Capabilities of Lunar Television Image Converter system used for digital processing of Ranger and Mariner pictures 18 p3113 A66-34496
- Automation of air traffic control, discussing radar, data handling and data communication 20 p3595 A66-37003
- Low error probabilities in binary communication systems estimated by statistics of bivariate extreme-value theory 20 p3514 A66-37211
- Space telecommunications techniques, examining reduction of all transmissions to digital type, using current theoretical coding methods and recurrent codes and block codes for error detection 20 p3516 A66-37432
- Aircraft and spacecraft digital systems including computers for production engineering, ground telemetry and communication with aerospace vehicle and onboard equipment for tracking, guidance and simulation of inflight conditions 21 p3709 A66-39629
- Digital filtering system comprising only few integrated circuits and using addressshift register combination, compared with analog devices 23 p4067 A66-41168
- DIGITAL COMPUTER**
- SA ANALOG COMPUTER**
- SA HYBRID COMPUTER**
- Spaceborne digital computers in reliability program, using failure data in design and evaluation 01 p0033 A66-10064
- Digital computer automated X-ray diffraction method to determine residual stress to improve processing reliability 01 p0033 A66-10102
- Digital computation desirability for flight control system 01 p0104 A66-10686
- System of data processing in real time applicable to digital computer Univac 418 02 p0193 A66-11600
- Computation of values for resistances shunting sections of tapped potentiometers from data using two alternative digital computer programs 02 p0200 A66-11884
- Analog, digital and hybrid computerized systems for investigating problems in aeronautics and astronautics 02 p0193 A66-11894
- Navigation system for supersonic transport considering central digital computer with data processing systems with feedback 02 p0256 A66-11898
- MCS 920M airborne digital computer design, production processes and microelectronic techniques 02 p0193 A66-11931
- Verdan digital computer operation in aircraft noting problems of reliability 02 p0194 A66-11965
- Microvariations of Earth electromagnetic field with results recorded on tape in digital pulse code form 02 p0224 A66-12124
- Two-stage tuned amplifier design with digital computer 03 p0337 A66-12495
- Mechanization of synchronous sequential machines with minimal shift registers, using algorithm 03 p0337 A66-12572
- Automatic evaluation of echo signals from circular-scan radar using learning system 04 p0543 A66-13497
- FM telemetry digitizing system operating on-line in real time environment results in automatic data processing 04 p0489 A66-13600
- Subsystem checkout in operation termed on-line checkout, noting use of digital computer with random noise signals and role of correlation and transfer functions 04 p0493 A66-13608
- Self-repairing digital computer, discussing switching mechanism activated diagnostic procedure and failed circuitry replacement 05 p0637 A66-14930



Parallel decomposition of linear three-terminal RC network 05 p0658 A66-15124  
Deep space tracking stations, discussing digital computers for monitoring functions such as real time measure, station performance, failure detection, etc [ISA PREPRINT 1.11-1-65] 05 p0635 A66-15498

Capabilities and limitations of digital computer steady state and transient heat transfer programs [ASME PAPER 65-WA/HT-48] 05 p0638 A66-15661

Digital and numerical method solution of transient heat flow problems 07 p1150 A66-17577

Navigation equipment for civil use based on miniature inertial platform, analog and digital computers, automatic chart display, etc 07 p1067 A66-17689

Airborne computer design free of navigational functions performed by humans, using Doppler equipment 07 p1067 A66-17692

Mechanization of navigational functions for supersonic aircraft within central airborne digital computer, comparing military experience with commercial requirements 07 p1067 A66-17693

Automatic realization of reactive ladder filters by digital computer, discussing classification and removal techniques, fundamental power equation and network functions 07 p1008 A66-17752

Computational reduction of high speed memory requirements in solving optimization problems by dynamic programming and supersonic transport trajectory application 07 p1004 A66-17976

Dynamic properties of contact thermal receivers investigated with aid of digital computer 07 p1035 A66-18092

Digital computer programming for design of cylindrical vessels 08 p1306 A66-18604

Digital computers to control automatic test equipment 08 p1187 A66-18741

Power supply system of OAO consisting of solar cells, energy storage device, power controller, etc, and simulation program via digital computer 08 p1168 A66-19493

Digital computers for aerospace guidance and control, including Gemini inertial guidance and B-70 aircraft navigation systems 08 p1187 A66-19597

Digital application of fluid amplifiers, examining greater precision, accuracy and reliability of digital systems compared to speed of digital systems 09 p1349 A66-20324

Digital counter synthesis for fixed base and periodic sequence-variable base counters with various feedback loops 09 p1361 A66-20606

Matrix inversion by rank annihilation, discussing memory storage requirements, overlapping input time with computing time, number of computations, etc 09 p1395 A66-20625

Digital systems research model design containing logic gates in integrated circuit packages 09 p1356 A66-20676

Flight management by digital computers, discussing central computer, system configurations, reliability, memory, input/output, computation rates 09 p1349 A66-20683

Concorde navigation system noting inertial platform, digital computer using integrated circuits and microminiaturization 09 p1401 A66-20685

Digital computer solutions to rigorous linear equations system for current density by enforcing boundary conditions at discrete points in scattering body 10 p1497 A66-21589

Mutual dependence of interconnection and noise immunity in transistORIZED digital computer circuitry 10 p1517 A66-21692

Device for automatically feeding experimental curve coordinates in large quantities into digital computer for high noise level photographic image 11 p1659 A66-22432

Variable threshold logic, integrated logic circuits which eliminate noise effects in digital equipment 11 p1676 A66-22685

Infinite automata theory and structural logical design of digital machines 11 p1659 A66-22707

Limit behavior of closed system of automata with random input 11 p1676 A66-22710

Book on analog, digital and hybrid analog-digital computers for random process studies 11 p1659 A66-22864

SCADS, programming system for simulation of combined analog-digital systems 11 p1659 A66-23109

Automatic control systems, discussing optimal and on-line adaptive control in electricity, nuclear research, steel industry, numerical problems, etc 11 p1679 A66-23272

Digital computer determination of equilibrium conductivity effect on MHD plasma engine performance 12 p1935 A66-23604

Universal programming languages and processors, survey and new concepts 12 p1826 A66-23825

Management problems of large aerospace computer installation, considering actual costs of change and aspects of turn-around problem 12 p1827 A66-23831

Integrated modular digital computer system for ICETRAN/ICES-FORTRAN/programming of engineering problems 12 p1827 A66-23833

Real time ground computer for Athena system and input/output data requirements in multiprocessing jobs 12 p1827 A66-23836

Digital differential analyzer/DDA/ design for high speed solution of differential equations common in aerospace problems 12 p1828 A66-23841

Self-diagnosable DX-1 computer design to achieve maximum operational availability 12 p1828 A66-23843

Matrix method for partial analysis of circuits, yielding algorithm for program for automatic digital computer 12 p1828 A66-24299

Comparison of frequency shift keyed and phase shift keyed pulse compression systems via digital computer simulation 12 p1819 A66-24602

Vibrational analysis, discussing spectrum analyzers, correlation and autocorrelation analysis and hybrid and digital computer applications 12 p1970 A66-24722

Parametric analysis, penalty-effectiveness tradeoff and system selection for communications satellites, using block digital computer synthesis with subroutines for operational requirements [AIAA PAPER 66-330] 12 p1824 A66-24797

Double stream instability in finite diameter beams analyzed by numerical experiments on digital computer, showing electron trapping as cause of RF current saturation 13 p2137 A66-25044

Digital computer automatic checkout equipment for Saturn spacecraft 13 p2057 A66-25260

Space digital computer reliability laboratory testing by failure data collection from prototype equipment 13 p2027 A66-25507

Test instrumentation for threshold sensitivity and noise bandwidth measurement of narrow band phase-locked receivers, employing statistical techniques 13 p2079 A66-25659

Design and fabrication of computer subsystems for Apollo guidance and navigation systems 13 p2027 A66-25781

Digital airborne computer for navigation problem solutions including inertial navigation, flight path, time-to-go and arrival time, etc 13 p2124 A66-25839

Numerical integration method for digital computer analysis of structural frameworks 13 p2198 A66-26223

Circulation distribution over rectangular wings, based on Chushkin algorithm and lifting surface equation calculated by digital computer 13 p2068 A66-26540

Digital computer automatic checkout equipment for maintenance of avionic systems 14 p2269 A66-27157

Microvariations of Earth electromagnetic field with results recorded on tape in digital pulse code form 14 p2287 A66-28082

Digital computer application as real time telemetry processor 16 p2651 A66-30565

Iteration method of general linear programming on digital computer, using penalty functions, compared to equilibrium problem of mechanical system 16 p2669 A66-30759

Test system for n-digit combinative comparison unit realizing special, previously described algorithm 16 p2656 A66-30765

Construction method for rms-optimal digital smoothing devices, noting case of astatic systems 16 p2670 A66-30768

Time shared general-purpose digital computer with hybrid linkage to analog consoles used for determination of static and dynamic performance characteristics of rocket engines, jet engines, V/STOL aircraft, etc 16 p2658 A66-31249

Maximum increase in system error due to computer round-off errors for closed loop linear sampled data system 17 p2900 A66-32075

X-Y plotter for analog computers, analog to digital converters and digital computers 17 p2925 A66-32313

Digital computer to decode digitized or sampled PCM waveform 17 p2875 A66-32502

Feedback control system digital computer design and analysis, including frequency-domain analysis, time-domain analysis, state-space simulation program, etc 17 p2877 A66-32778

Computer controlled digital display techniques for direct editing of research data 17 p2877 A66-32943

Monograph on digital computer solution of matrix problems of elastic system vibrations 17 p2877 A66-32987

Digital computer utilization to estimate sonic boom characteristics of complex airplane configuration 17 p2847 A66-33022

Series power switch for orientation and position computer of small lunar-orbit spacecraft designed to reduce weight and cost 17 p2878 A66-33122

Manual methods of entering navigational data on cards for input into computer 17 p2956 A66-33447

Human factor aspects of digital computer programming for simulator control, discussing application and operation 17 p2869 A66-33449

Logic and operation principle of model of recording device for high speed readout of digital and alphabetic information from digital computer 17 p2928 A66-33494

Transfluxor program store for airborne digital computer, noting wiring pattern, economics, read amplifier, etc 18 p3072 A66-33562

Antenna steering system using special digital computer and precision analog power servo drive 18 p3131 A66-33867

Digital guidance and control computer used in Apollo Guidance and Navigation System 18 p3073 A66-33874

Complex component design using man-computer system with graphic input/output devices, discussing application for digital computer circuit card design [SAE PAPER 660459] 18 p3116 A66-33897

Digitally computed tables of Chebyshev approximations of Laplace shift operator transfer function enabling analog simulation of time delay systems 18 p3090 A66-34069

Time domain method of relating cross coupling between transmission lines of multilayer structure to geometry in design of high speed digital systems 18 p3090 A66-34071

Stress and deflection determination in trusses with pin or rigid joints, using digital computer 18 p3255 A66-34275

Space-frame radome design and buckling analysis for wind and deadweight static load using digital computers 18 p3095 A66-34299

Digital multiplier with incremental computing system, noting series and parallel addition system and sequential multiplication with incremental values 18 p3073 A66-34495

Flight data recording and processing system using magnetic tape for digitally computing airborne data on flight testing of VTOL aircraft 18 p3073 A66-34679

TRW Systems MARCO 4418, small high-speed lightweight reliable digital computer, for use in manned space missions 19 p3306 A66-35503

Digital simulator program /MIMIC/, discussing operation, application to parallel systems and advantages over MIDAS system 19 p3306 A66-35535

Automated improvement of design /AID/



computer using nonlinear programming techniques to solve optimization problems 19 p3308 A66-35872

Extrapolation methods for numerical integration using digital computers, comparing convergence with conventional methods 19 p3310 A66-36650

Microminiaturization in automatic control equipment and digital computers Symposium, International Federation of Automatic Control and International Federation for Information Processing, Munich, October 1965 19 p3322 A66-36806

High-speed memory units for digital computer, discussing ferrite, semiconductor and thin magnetic or ducting film memories 19 p3322 A66-36814

Design of digital computer program of Monte Carlo variety for analyses of self-contained orbital navigation systems for satellites, including error source categories 20 p3595 A66-36871

Digital computers used in error calculation in calibration curves of turboengines and other pneumatic devices 20 p3555 A66-36923

Digital computer optimization program, determining minimum weight fuel cell primary power system for MOLAB 20 p3496 A66-37156

Instrumentation simulation, discussing data system simulator facility, noting application for telemetry and instrumentation design 20 p3542 A66-37248

Digital computer analysis of kinetic equations for CO burning in presence of hydrogen 20 p3679 A66-37702

Digital computer programmed optimization model of Earth-orbiting space station missions including reliability, maintainability and cost considerations 20 p3663 A66-37902

Digital computer program for solution of space-charge-flow problem applied to design of thrusters with variable thrust vector, analyzing two ion-thruster configurations with aid of computer 20 p3629 A66-38179

Design considerations for advanced digital beam steering computer through use of geometric optics 21 p3707 A66-38674

Microminiaturized R-11 digital computer for real time computational requirements in radar data processing, fire and command control, automatic navigation, checkout, etc 21 p3707 A66-38675

High-speed multiplication for R-11 microminiaturized digital computer, using modified form of Booth Algorithm 21 p3707 A66-38676

Second-order solution for strapped-down attitude computation compared with first-order solution 21 p3763 A66-38842

Integrated navigation system /INS/ using stellar inertial subsystem with optimum data processing 21 p3767 A66-38891

Optimization of two-way space frame with single column supports for minimum weight of steel by digital language programming techniques 21 p3833 A66-39539

Magnetic memory units and memory storage unit component design for digital computer 21 p3708 A66-39626

Aircraft and spacecraft digital systems including computers for production engineering, ground telemetry and communication with aerospace vehicle and onboard equipment for tracking, guidance and simulation of inflight conditions 21 p3709 A66-39629

Digital computer programming to evaluate designs until optimality is found in aerospace structures 22 p3922 A66-40023

Heat transfer equation solution for ablating solid, assuming exponential temperature profile with numerical solution on digital computer by Runge-Kutta method 22 p3998 A66-40035

Digital computer processing of Tiros, Nimbus and Essa vidicon cloud pictures for machine nephanalyses, discussing rectification orbital mosaics and calibration effects for future Essa flights 22 p3943 A66-40055

Alphanumeric generator for display of digital computer data on TV raster and storage in memory 22 p3927 A66-40290

Digital computer program for V/STOL aircraft static propeller characteristics and optimization, based on initial wake hypothesis and trailing vortex sheet

properties 22 p3843 A66-40294

DIVIC /digital variable increment computer/ for solving hyperbolic-navigation problems, examining computational algorithms 22 p3945 A66-40335

Digital computer program for static worst case design of diode transistor logic 22 p3870 A66-40396

Automatic, multichannel system for data recording and processing obtained in studies of ionospheric structural inhomogeneities, containing magnetic-tape memory and device for digital tape memory and device for digital computer input 22 p3920 A66-40772

Digital-computer controlled receiver functions and application 23 p4044 A66-41313

Automatic detection and correction of errors in digital computers by using residue arithmetic, whether caused by arithmetic operations or data transmission 23 p4042 A66-41602

Approximate solution to digital sequential least squares estimation of eigenstates of nonlinear processes 23 p4050 A66-41614

Numerical solution via digital computer of nonlinear transient heat conduction with phase changes 23 p4149 A66-41697

Digital computer program for handling algebraic expressions in complex numbers 23 p4042 A66-41739

Digital computer program for analysis and weight optimization of thermoelectric generators for space applications 24 p4161 A66-42119

Digital computer techniques for computation of lunar disturbing function 24 p4273 A66-42204

Airborne digital computers role in electronic warfare, navigation and guidance, considering weight, power supply, costs, etc 24 p4177 A66-42245

Functional analysis applied to optimum control by reduction of variational problem to finite dimensional analysis and calculation of algorithms for use with digital computer 24 p4231 A66-42470

Maximum probability criterion on output coordinates of system for selection of parameters of optimal nonlinear control system 24 p4188 A66-42477

# DIGITAL DATA

Dynamic data /waveforms/ analysis comparing analog with digital methods for speed, costs, flexibility, reliability, etc [SAE PAPER 650818] 01 p0033 A66-10480

Insertion of 2 bits of specific code into frame of digital data of burst-error-correcting code for synchronism recovery 02 p0190 A66-11524

Digital synchronization at information levels of words, cycles and subcycles 06 p0836 A66-17027

High data rate radar cross section measurement system for high angular precision and direct digital recording on magnetic tape 10 p1501 A66-21621

Properties of metallic recording media in terms of physical properties of medium and geometrical dimensions of recording system 13 p2082 A66-26295

Optimal scientific satellite PFM encoding system circuit design and digital data processing 14 p2244 A66-28429

Digital data compression techniques applicable in spacecraft television systems, emphasizing bandwidth reduction techniques 16 p2653 A66-30891

Binary synchronous communication in additive non-Gaussian noise, discussing optimal nonlinear detector for digital data transmission through non-Gaussian channels 18 p3067 A66-33901

Upper and lower bounds on binary error probability as function of signal to noise ratio for digital data systems operating over complex Gaussian fading channel 21 p3720 A66-39638

Optimum pulse transfer functions for multivariable digital ergodic stochastic processes 23 p4051 A66-41853

# DIGITAL INTEGRATOR

Optimum design and error analysis of digital integrators for discrete system simulation via quasi-linearization 12 p1828 A66-23840

Control algorithms for microminiaturized sampled data digital control 19 p3311 A66-36822

# DIGITAL NAVIGATION SYSTEM

A-NEW MOD 1 digitally controlled navigation system for antisubmarine warfare aircraft employing Univac CP-754-8 thin film computer 01 p0098 A66-10002

Microelectronic digital system for spacecraft stabilization and control 01 p0105 A66-10689

Digital IF amplifier for thin film radar receiver 02 p0202 A66-11917

Functional requirements for computer navigational system for Concorde aircraft 07 p1065 A66-17672

DECTRA long range navigational aid, DECTRA airborne receiver and Omnitrac computer 07 p1068 A66-17702

Flight testing of FAA-Lear Siegler receiver/converter airborne system with Loran-C hyperbolic navigation system 07 p1069 A66-17706

Two automatic astronomical navigation and tracking systems compared for accuracy and performance in civil aircraft 07 p1070 A66-17722

Accurate light-weight self-contained low-cost inertial autonavigational system including gyroscopes, accelerometer and DYDAN computer 07 p1076 A66-17793

AD560 Doppler Radar sensor and computer in Boeing 707-138 aircraft 07 p1076 A66-17794

Moving map displays for navigation information portrayal, advantages and requirements for subsonic and SST airliners 07 p1076 A66-17796

A-NEW MOD 1 digitally controlled navigation system for antisubmarine warfare aircraft employing Univac CP-754-8 thin film computer 13 p2124 A66-25596

ESG strapdown inertial navigation system based on double integration of acceleration and analysis of electronic gimballing-induced errors 13 p2124 A66-25653

Digital-mode FM CW laser ranging and tracking system using compound axis servomechanism 13 p2024 A66-25982

Digital guidance and control computer used in Apollo Guidance and Navigation System 18 p3073 A66-33874

# DIGITAL SIMULATION

Two analysis methods for sequential digital servomechanism 02 p0180 A66-11683

Digital computer simulation for control system design including electrical circuits, mechanical systems and chemical processes 03 p0337 A66-12375

Magnetically oriented satellite and angular motion damping by shorted-coil and hysteresis in digital computer simulation 03 p0430 A66-12666

Digital computer simulation for phase-locked loops used as narrow-band tracking filters in space communications and radar systems 05 p0652 A66-14590

Digital computer research program for reducing bandwidth schemes and quality for picture transmission 05 p0676 A66-14820

Air traffic control simulation system based on digital computer for Eurocontrol 06 p0870 A66-16953

Discrete simulation technique using electrical circuit for finite-difference approximation of initial differential equations, noting functional potentiometers 07 p1055 A66-17201

Power supply system of OAO consisting of solar cells, energy storage device, power controller, etc, and simulation program via digital computer 08 p1168 A66-19493

Digital simulation of magnetic hysteresis, using analytic approximation of magnetic curves by seventh degree polynomials 08 p1187 A66-19513

Algorithm to automatically ascertain admissible processing sequence for all-digital simulation of analog or analog-hybrid system 10 p1507 A66-21699

American Federation of Information Processing Societies, Joint Computer Conference, Las Vegas, November 1965 12 p1825 A66-23824

Digital simulation languages, discussing history, input format, effectiveness, programming error diagnostics, etc 12 p1826 A66-23826

New block diagram compiler for sampled data system simulation 12 p1826 A66-23827

Lockheed multiprocessor simulation system /LOMUSS I/, data processing system for



- computer design and analysis 12 p1827 A66-23832
- Optimum design and error analysis of digital integrators for discrete system simulation via quasi-linearization 12 p1828 A66-23840
- Queueing model digital simulation techniques used to determine reliability of stand-by system with maintenance station 12 p1834 A66-24085
- Discrete white noise used to generate discrete colored noise by means of difference equation 12 p1850 A66-24266
- Computer program for predicting satellite long-term orbit decay and digital simulation of atmosphere and reentry conditions [ATIA PAPER 66-357] 12 p1951 A66-24491
- Digital simulation of scheduling logistic support by helicopter, using Backtrack techniques 12 p1858 A66-24683
- Digital computer analytical method for simulation of worst shock conditions for subassembly shock testing 12 p1829 A66-24726
- Pseudorandom binary sequential digital simulation of feedback control systems subjected to random input signals 13 p2030 A66-25211
- COBLOC programming system for all-digital simulation of operation of large mode-controlled hybrid computers, noting inclusion of patchable logic simulation 13 p2028 A66-25805
- Digital computer simulation of sampled data communication system using Block Diagram Compiler, B /BLODIB/ 13 p2028 A66-25937
- PCM picture transmission, pseudorandom scanning, noise, bandwidth compression and digital simulation 15 p2450 A66-28785
- High precision attitude control system using pulse width modulation evaluated by hardware fabrication and digital computer simulation 15 p2606 A66-29651
- System analyst/model designer problems in digital simulation of large-scale system 16 p2657 A66-31246
- DSL/90 digital simulation program for IBM 7090 family of computers 16 p2658 A66-31247
- Two analysis methods for sequential digital servomechanism 18 p3053 A66-34009
- Digital simulator program /MIMIC/, discussing operation, application to parallel systems and advantages over MIDAS system 19 p3306 A66-35535
- Digital simulation of guidance and control of exoatmospheric interceptor missiles for study of parameter variations effect on overall mission effectiveness 20 p3596 A66-37230
- Instrumentation simulation, discussing data system simulator facility, noting application for telemetry and instrumentation design 20 p3542 A66-37248
- Symbolic programming digital computer techniques, hardware interfacing and system errors in simulation of lunar midcourse guidance and navigation systems 20 p3543 A66-37250
- Signal simulator for testing Loran A and Loran C airborne receivers in laboratory, using digital simulator circuits to test dynamic response of tracking circuits 23 p4088 A66-41253
- SESIAC, electronic machine for statistical simulation consisting of stochastic generator, containing no equations or tabulated functions, only random pulse sources and logic networks 23 p4053 A66-41604
- Digital simulation study of acquisition capabilities of phase-locked loop in presence of noise 23 p4050 A66-41616
- DIGITAL SPACECRAFT TELEVISION**
- Improved gray scale and coarse-fine PCM systems for digital television bandwidth reduction, considering spacecraft application 14 p2235 A66-27036
- Delta modulation pictorial encoding systems analyzed to determine parameters for image communication application 19 p3299 A66-35665
- Parameter evaluation of delta modulation encoding techniques for image communication applications by computer simulation 20 p3513 A66-37201
- Digital video system for measuring broadband spectral intensity of stars and coordinates onboard OAO 20 p3557 A66-37202
- Digital TV spectrometer for measuring optical radiation from reentry vehicles, using IR vidicon and magnetic recording for data processing 23 p4069 A66-41665
- Calibration problem of using vidicon for making radiometric and spectrometric measurements, examining application to digital TV spectrometer system 23 p4069 A66-41666
- Magnetic tape and photographic film recording from video output of digital TV spectrometer system 23 p4069 A66-41667
- DIGITAL TECHNIQUE**
- Digital computer calculation of characteristics of Earth gravitational field 01 p0062 A66-10693
- Transient process of nonlinear automatic system calculated by numerical digital computer method based on convolution integral 01 p0045 A66-11021
- Solid state camera system for aerospace application incorporating monolithic phototransistor mosaic sensor, molecular digital readout system, etc 04 p0519 A66-13631
- Digital electrometric device with automatic discrete compensation 05 p0680 A66-15211
- Rapid acquisition by sequential estimation /RASE/ technique for acquisition of pseudonoise 06 p0834 A66-16859
- Thin film microcircuit for digital systems 06 p0856 A66-16927
- Fluidic closed-loop digital position-speed servocontrol system without moving parts, using pulsed air 07 p0991 A66-17878
- Channel sample-and-hold PCM telemeter, system modules, multiplexer gate groups, analog-to-digital converter, etc 08 p1184 A66-19518
- Papers on fluidics, analyzing digital and fluid amplifier design 09 p1331 A66-20316
- Fluid mechanics, fluidic devices and systems, noting design, manufacturing techniques and application 09 p1332 A66-20317
- Digital computer recomputation of stability transition curves in Hill-Meissner equation 09 p1395 A66-20623
- Digital data handling method for air traffic control system employing plan position indicators and video correlator for radar video signal analysis 11 p1732 A66-22899
- Field effect transistors in digital circuits, FET transient behavior, transistor logic and switching circuitry 11 p1673 A66-23472
- Digital techniques for identification of discrete-time and continuous-time systems from noisy input and output sample sequences via determination of transfer function model parameters 12 p1854 A66-24638
- Yield and reliability of integrated electronic devices and electronic digital systems, using redundant components by triplicating voting circuits 12 p1846 A66-24914
- Phase coherent digital M-ary transmission with binary waves through Gaussian channel 13 p2022 A66-25554
- Smith subprotonospheric whistlers and digital computation of ion effects on whistler-mode ray tracing 14 p2282 A66-26858
- Electrohydraulic digital actuator design and conversion of discrete electric input signal in binary code to linear motion 14 p2227 A66-28366
- Digital computer calculation of characteristics of Earth gravitational field 15 p2483 A66-28554
- Digital approach to gas turbine engine control based on use of pulsewidth modulated information obtained with aid of simple circuits 15 p2571 A66-28858
- Digital measurement of differential Doppler effect using transposition of phase relation of two HF signals into audiofrequency band 15 p2453 A66-30070
- Pulse rebalancing of pendulum accelerometers for digital output requirements 16 p2706 A66-30882
- Digital differential analyzer for on-line studies of dynamic systems 16 p2657 A66-31245
- Psychophysiological study of compensatory tracking on digital altimeter display and on combined digital and scale-and-pointer display 17 p2869 A66-33448
- Level quantization effect in statistical analysis of closed-loop digital automation systems 18 p3089 A66-33736
- Digital optimal control of steerable antennas using radiation lobe geometry, dynamic programming and control strategy principles 18 p3081 A66-34269
- Optimizing procedures using Fortran II FAP programming on IBM 709/7090 computers, comparing eight known techniques 19 p3308 A66-35868
- State vector determination for digital optimal control of system characterized by matrix equation 19 p3339 A66-36746
- Digital testing techniques for analog systems, describing bomb computer set for Phantom F-4D aircraft 20 p3522 A66-37246
- Transient radiation response and permanent radiation damage in monolithic silicon-junction-transistorized integrated circuit 20 p3526 A66-37318
- General maintenance techniques for large digital controllers to achieve high order of system dependability 20 p3522 A66-37907
- Digital programming and topological optimal filter design incorporating nonideal lossy elements 20 p3533 A66-38281
- Photographic data recorder noting simultaneous event and data recording capability 22 p3917 A66-39994
- Complementary symmetry flip-flop and similar transistor micropower digital logic circuit design 23 p4048 A66-41144
- Cathode ray tube device for digital video processing of Ranger pictures 23 p4071 A66-41677
- DIGITAL-TO-ANALOG CONVERTER**
- High-accuracy digital circuits producing variable pulse delay measured by timing pulse 03 p0341 A66-12521
- Digital-to-analog differential conversion using differential pulse duration modulation 07 p1009 A66-17829
- DIGITAL TO VOICE TRANSLATOR /DIVOT/ S VOCODER**
- DIGITAL TRANSDUCER**
- Linear quartz crystal temperature sensing element for digital data presentation 02 p0228 A66-11516
- Microelectronic digital chronometer and frequency meter, noting design details and thin film circuits 02 p0231 A66-11916
- Design of nonreciprocal latching ferrite devices including single toroid digital waveguide phase shifter, cut-off switch, miniaturized slow wave phase shifter, etc 12 p1839 A66-24618
- Digitization system based on photoelectron counting for scanning spectrometer 13 p2084 A66-26750
- Digital transducers utilizing magnetic recording 16 p2704 A66-30539
- DIHEDRAL EFFECT**
- Stability of fast and slow attached shocks in stationary MHD flow around dihedral 07 p1089 A66-18105
- Problems of various subsonic gas jets of finite width around dihedral obstacle solved with Chaplygin hodographic method 16 p2627 A66-30207
- Spiral instability in STOL aircraft prevented by larger wing dihedral setting, noting permissible dihedral levels and tests 16 p2634 A66-31395
- DILATATIONAL WAVE**
- Unified approach to propagation of plane, cylindrical and spherical dilation waves in elastic media, using method of characteristics [ASME PAPER 65-WA/APM-21] 05 p0778 A66-15443
- Unified approach to propagation of plane, cylindrical and spherical dilation waves in elastic media, using method of characteristics [ASME PAPER 65-WA/APM-21] 12 p1961 A66-23987
- Dilatational wave resonance scattering of waterborne sound waves on hollow cylinder excited to oscillation by incident sound 14 p2401 A66-27863
- Reflection of time-harmonic plane dilatational or shear waves from rigid or stress-free boundary of arbitrary linearly viscoelastic half-space 18 p3136 A66-35025
- DILATOMETER**
- High temperature dilatometer for shrinkage measurements in sintering of powdered metal compacts 01 p0069 A66-10748



# DILUTION

Liquid nitrogen dilution effect on LOX impact sensitivity of selected materials 10 p1590 A66-21951

# DIMENSIONAL ANALYSIS

Optimization of nonlinear control system with random input using analog computer, automatic optimizer and dimensional analysis 02 p0207 A66-11791  
Generalized dimensional analysis applied to wind distribution in planetary boundary layer, using motion equations 02 p0223 A66-11981  
High energy nuclear interaction and particle structures covering meson, baryon, composition and dimensional analysis 05 p0749 A66-15351  
Matrix methods in dimensional analysis discussing algebraic, matrix and shortcut methods [ASME PAPER 65-WA/MD-20] 05 p0710 A66-15523  
Dimensioning and strength calculations - Conference, Budapest, October 1965 06 p0963 A66-16472  
Dimensionality theory for determining failure rate of aircraft components not in operation 11 p1637 A66-22862  
Current-voltage characteristics of electric arcs approximated by dimensionless criteria 11 p1747 A66-23312  
Dimensioning heat transfer in compact plate fin heat exchangers under nonuniform temperature variation and heat conductance 12 p1978 A66-24034  
Dimensioning varactor diode frequency multipliers used in HF transmitters 14 p2259 A66-28113  
Book on similarity theory and physical interpretation, examining boundary value problems, dimensional analysis, etc 16 p2739 A66-31751  
Dimensional analysis of temperature distribution within spherical particle during nonisothermal evaporation 17 p3033 A66-32449  
Self-similarity criteria in radiative flow for unsteady one-dimensional inviscid flow of perfect gas 17 p3034 A66-32471  
Dimensional and experimental analyses of helium bubble motion in liquid nitrogen 20 p3545 A66-37104  
Laminar forced convection heat transfer to gas from circular tube, achieving boundary condition of uniform heat flux 20 p3679 A66-37508  
MHD analysis of luminescence and widening of tail of Finsler 1937 V Comet passing through solar corpuscular stream containing frozen-in magnetic field 21 p3814 A66-39277  
Dimensional filtering in IR technology for background noise elimination, discussing Fourier analysis treatment of system 21 p3768 A66-39646  
Optimization of nonlinear control systems by means of Bellman equation and dimensional analysis minimizing integral square error 23 p4051 A66-41695

**DIMENSIONAL STABILITY**  
Probability theory to calculate technological deviations in dimensions effect on strength and rigidity of thin walled structures 11 p1782 A66-22858  
Static dimensional stability of nonlinear elastic continua reduced to linear shell theory 20 p3668 A66-37527

**DIMETHYL HYDRAZINE**  
Pathological and metabolic changes due to toxicity of unsymmetrical dimethyl hydrazine /UDMH/ 22 p3858 A66-40507

# DIODE

SA CESIUM DIODE  
SA JUNCTION DIODE  
SA P-I-N DIODE  
SA PARAMETRIC DIODE  
SA PHOTODIODE  
SA THERMIONIC DIODE  
SA TUNNEL DIODE  
SA VARACTOR DIODE  
SA ZENER DIODE  
Compensating temperature effects in systems using LDG type logarithmic germanium diode 01 p0035 A66-10205  
Microplasma and avalanche diode noise pulse rate determined by carrier generation within space charge layer of breakdown region 02 p0197 A66-11431

Silver bonded diode for parametric amplifiers improves performance when cooled at liquid nitrogen temperature 02 p0198 A66-11520  
Liquid element tantalum diode characteristics 03 p0345 A66-13103  
Circuitry of diode pump integrator used for generating mean voltage which is function of repetition rate of applied pulse train 03 p0345 A66-13241  
Properties of long forward-biased diodes operating in double-injection regime 03 p0346 A66-13318  
Current-voltage characteristics of gallium arsenide diode noting temperature effect on threshold voltage and breakdown current 03 p0346 A66-13323  
Current-voltage characteristics of long diodes calculated by dividing diode base into three regions 04 p0495 A66-13767  
Metal oxide semiconductor diodes as function of semiconductor parameters considering silicon, gallium arsenide, cadmium sulfide and indium arsenide 04 p0564 A66-14040  
Properties of silicon diodes with gold alloy bases, examining anomalies in V-I characteristics 04 p0499 A66-14055  
Selective properties of gold-compensated silicon diodes, noting behavior in presence of bias currents and current voltage characteristics 04 p0499 A66-14060  
Amplification and generation properties in gold-compensated silicon diodes, noting noise spectrum and harmonic oscillations 04 p0499 A66-14061  
Q-factor of nonlinear capacitance microwave diodes determined from standing-wave ratio and phase difference for two bias voltages on diode, using passive linear quadrupole 04 p0499 A66-14062  
Methods for measuring and characterizing transistor and diode large signal parameters for use in automatic circuit analysis programs, noting radiation damage 05 p0648 A66-14848  
Correlating mean-to-surface flux ratio for highly enriched fuel rods of in-pile diodes of similar composition and geometry 05 p0620 A66-15567  
Active thin-film elements /diodes and transistors/, properties and deposition techniques 07 p1006 A66-17415  
Current-voltage characteristics of aluminum-aluminum oxide-gold diodes 08 p1188 A66-18641  
Electron transit time and impedance relation in rarefied plasma diode, considering electron and ion velocity straggling 08 p1193 A66-19193  
Piecewise linear circuit model for charge-storage or step recovery diode using conventional capacitance and resistance 09 p1350 A66-19920  
Frequency components of microwave-range oscillations from pulsed avalanche diodes of Read type driven to breakdown region 09 p1350 A66-19927  
Packageless diode fabricated by beam-lead process with no soldering or eutectic bonding 09 p1351 A66-20166  
Step-recovery diode multiplier circuit for high-order harmonic generation 09 p1359 A66-20919  
Noise suppression in solid state space charge limited diodes calculated, using open and short circuited output model 09 p1359 A66-20973  
Photovoltaic response of variously doped germanium-silicon diodes, confirming band diagram for germanium-silicon heterodiodes dominated by lattice mismatch interface states 09 p1360 A66-20978  
Worst case design of diode transistor logic inverters, considering resistor end-of-life tolerance, supply voltage variations and minimum beta of switching transistor 10 p1508 A66-21298  
Parallel-strip point-contact diode mount evaluated for video detection of millimeter waves 10 p1514 A66-21909  
Location of poles and zeros of small-signal RF impedance function of Read diode and how they affect oscillation and current tunability 10 p1516 A66-22100  
Negative-resistance avalanche diode with small space-charge layer width in small-signal admittance

measurements 10 p1516 A66-22101  
Indium antimonide diodes of various base thickness for high injection levels, results in graphical form applied to magnetic diode production 11 p1668 A66-22740  
Diode frequency converter parametric derivation incorporating capacitance of resistance converter and resistance of capacitance converter 11 p1667 A66-22794  
Computer analysis of translators using diode ring modulators and dimensioning of frequency dependent networks preceding and following modulating four-pole to obtain specific response in passband, minimizing spurious signal effect 11 p1670 A66-23197  
Miniaturized AM-diode signal detector in form of solid state circuit for frequencies in excess of 450 kc 12 p1830 A66-23735  
Diode and transistor response to ionizing radiation, describing generation of transients qualitatively and quantitatively 12 p1843 A66-24681  
Coaxial-mounted silicon point-contact diode /1 N 26/ as frequency converter for millimeter waves 12 p1846 A66-24857  
Period of constant reverse current occurring when limited-base diode is switched from forward to backward direction of current flow 13 p2028 A66-25094  
Electroluminescence and emission spectra of indium-alloyed diodes made from phosphorus doped p-type ZnTe biased in either forward or reverse direction at liquid nitrogen temperatures 13 p2029 A66-25184  
Hall reversal at negative resistance in forward biased p-Ge point contact diode 13 p2029 A66-25192  
Small-signal impedance of transferred-electron diodes, stable against domain formation 13 p2030 A66-25212  
Step-recovery diode in shunt configuration as frequency multiplier 13 p2030 A66-25215  
Exact solution, using Laplace transform, for problem of transient characteristic of semiconductor diode, challenging Nosov view 13 p2031 A66-25229  
Reversal of diode with delay between last direct pulse and first reversed pulse 13 p2031 A66-25230  
Charge measurements for transistors and diodes 13 p2040 A66-25817  
Transients in thin based semiconductor diodes to determine recombination rate on nonrectifying contact 13 p2041 A66-25942  
Improved performance in microwave Read diode oscillator with epitaxial silicon material and coaxial cavity 14 p2248 A66-27049  
Binary pulses in microwave band regenerated, using pulse regenerator with hysteresis characteristic of parametric oscillator employing variable capacitor diode 14 p2248 A66-27059  
Diodes, transistors, rectifiers and inverters application to control and instrumentation systems, providing phase changing, frequency stabilization, source voltage, etc 14 p2249 A66-27118  
Dielectric diode induction effect demonstrated through equivalent circuit 14 p2252 A66-27491  
Microwave oscillations in 4 to 31 gc/s frequency range from single Gunn diode 14 p2254 A66-27590  
Diode gate design, using bridge circuit to eliminate spurious gating signals 14 p2267 A66-27802  
Diode bridge variable attenuator used to overcome error signals and harmonic distortion in wide range AGC 14 p2267 A66-27805  
Properties of long forward-biased diodes operating in double-injection regime 14 p2260 A66-28292  
Parametric amplification in millimeter-wave range, detailing parametric amplifier with germanium epitaxial diodes for use in radiometers 14 p2260 A66-28296  
Current-voltage characteristics of gallium arsenide diode, noting temperature effect on threshold voltage and breakdown current 14 p2260 A66-28297  
Emission bands in electroluminescence from gallium arsenide diodes, noting intensity at high and low voltages and radiation and doping effect 15 p2562 A66-28714  
Backward diode application to microwave



circuit design, discussing characteristics of stripline mount with probe  
 detector 15 p2457 A66-28886  
 Controlled noise generation at high pulse rate with avalanche diodes, noting spectral voltage density and temperature coefficient 15 p2458 A66-28894  
 Conventional point-contact diodes and junction diodes with point-contact geometry, examining fabrication techniques and millimeter wave application 15 p2461 A66-29013  
 Equivalent circuit evaluation of theoretical potential and limitations of millimeter wave semiconductor diode detectors, mixers and frequency multipliers 15 p2461 A66-29015  
 Coupling efficiency evaluation in light emitting diodes 15 p2514 A66-29032  
 Capacitance variation of gold n-type gallium arsenide surface barrier diode when illuminated, applied to light detector, frequency modulation, etc 15 p2463 A66-29034  
 Complex zeros of exponential polynomial in study of stability criteria for collisionless plane vacuum diode of infinitely heavy ions in interelectrode space 15 p2464 A66-29244  
 Error estimation in diode function generator design 16 p2659 A66-30518  
 Transfer processes in steep p-n junction of long diodes with interval between forward and reverse bias 16 p2667 A66-31671  
 Electroluminescence of silicon carbide diodes 16 p2668 A66-31781  
 Secondary breakdown relaxation oscillations and I-V characteristics of point-contact n-type Ge diode 17 p2879 A66-31866  
 Passive frequency conversion utilizing nonlinear conductance, establishing lower bound for noise figure 17 p2881 A66-32060  
 Properties of silicon diodes with gold alloy bases, examining anomalies in V-I characteristics 17 p2885 A66-32221  
 Selective properties of gold-compensated silicon diodes, noting behavior in presence of bias currents and current voltage characteristics 17 p2885 A66-32226  
 Amplification and generation properties in gold-compensated silicon diodes, noting noise spectrum and harmonic oscillations 17 p2885 A66-32227  
 Q-factor of nonlinear capacitance microwave diodes determined from standing-wave ratio and phase difference for two bias voltages on diode, using passive linear quadrupole 17 p2885 A66-32228  
 Diode characteristics and application guidelines 17 p2888 A66-32782  
 Cesium ion tubes advantages over conventional tubes including ability to study electron-inertia effects 17 p2888 A66-32823  
 Germanium and silicon microwave transistor and mixer diode design for HF and low noise oscillators and amplifiers 17 p2891 A66-32912  
 Bonded backward diode fabrication and performance as microwave mixer and low-level detector 17 p2891 A66-32913  
 Resonant circuit behavior of Gunn diode, considering device as self-pumped parametric oscillator 18 p3078 A66-34086  
 Amplifier helping backward diodes as mixers and detectors in microwave systems 18 p3088 A66-35019  
 Book on analysis and design of transistor circuits including transistor parameters, emitter diode equivalent circuits, FET, amplifiers, noise, etc 18 p3089 A66-35238  
 Field and thermionic field emission responsible for excess currents in Schottky barriers formed on doped semiconductor 19 p3434 A66-35345  
 External quantum efficiency of tin doped GaAs electroluminescent diode, noting effect of zinc diffusion conditions 19 p3312 A66-35347  
 Transient processes in semiconductor diode with base having impurity concentration gradient 19 p3313 A66-35459  
 Silicon-on-sapphire batch-fabrication of computer logic and memories, describing SOS diode matrix 19 p3314 A66-35526  
 Linvill lumped models for graded semiconductor diodes considered through Beddoes notation 19 p3318 A66-35727  
 Efficiency limitation factors in radiative recombination in electroluminescent GaAs diodes, examining contribution of majority

and minority carriers injected into P region 19 p3319 A66-36264  
 Replacing heated tungsten filament and IR filter by GaAs electroluminescent diode without filter for IR illumination 19 p3320 A66-36266  
 I-V characteristic of p-n junction explained by band gap widening due to mechanical stress exerted by stylus, assuming Zener effect 19 p3323 A66-36823  
 Diode frequency converter parameter derivation incorporating capacitance of resistance converter and resistance of capacitance converter 20 p3525 A66-37131  
 Equilibrium photocurrents in silicon switching diodes from nondestructively measured electrical parameters 20 p3526 A66-37322  
 Space charge wave equation and impedance and stability of electron diodes, using Nyquist analysis and transit time and RF beam current 20 p3528 A66-37489  
 Effect of reduction of breakdown voltage by external illumination of oxide protected planar diode or by nonequilibrium carriers drifting in surface channel 20 p3528 A66-37493  
 Silicon variable capacitance diodes with high-voltage sensitivity produced by low-temperature epitaxial growth technique 20 p3528 A66-37494  
 Diode curve tracer for observing I-V characteristics of semiconductor junctions and diodes via pulse method 20 p3560 A66-37587  
 Photoreponse measurements of depletion capacitance and diffusion potential of GaP Schottky-Barrier diodes 20 p3534 A66-38390  
 Lampert double injection theory for CdS diodes with negative resistance I-V characteristic curve 20 p3535 A66-38435  
 Breakdown diodes in voltage stabilization, noting temperature effects, cascade switching, etc 21 p3710 A66-38748  
 Optical coupling using gallium arsenide laser for variation of frequency of diode emission through small change in current density 21 p3746 A66-38920  
 Recombination by tunneling in electroluminescent diodes to obtain line shape and light intensity in peak shift region 21 p3801 A66-38998  
 Parametric amplification at collector-base diode for microalloy graded-base transistor and normal mixing due to resistive nonlinearity at emitter 22 p3872 A66-39735  
 Thermal noise hypothesis applied rigorously to space charge limited diodes 22 p3872 A66-39747  
 Cesium-plasma diode effect dependence on material output of cathode in vacuum, plotting short circuit current vs vapor pressure, voltage distribution, etc 22 p3952 A66-39752  
 Dynamic characteristic theory of long diode with base containing impurity atoms producing deep energy levels in forbidden zone 22 p3873 A66-39826  
 Generation of oscillations in circuit which has long diode with base containing impurity atoms producing deep energy levels in forbidden zone 22 p3961 A66-39827  
 Miniaturized AM-diode signal detector in form of solid state circuit for frequencies in excess of 450 kc 22 p3875 A66-40078  
 Room temperature performance of GaAs laser diodes, using SCRs to achieve high pulse repetition rate 22 p3932 A66-40175  
 Noise measurement in field emission vacuum diodes, interpreting excess and shot noise spectrum in terms of work function 22 p3878 A66-40696  
 Field emission diode and triode with narrowly spaced electrodes, noting voltage and current characteristics 22 p3882 A66-40894  
 Conductance and capacitance of metal-insulator-semiconductor diodes or any two-terminal complex admittance plotted automatically as function of applied bias 22 p3882 A66-40897  
 Indium antimonide diodes of various base thickness for high injection levels results in graphical form applied to magnetic diode production 23 p4045 A66-41478  
 Volt-ampere characteristics of germanium and silicon diodes with p region formation by gold diffusion into n-type

material 23 p4046 A66-41566  
 Constant voltage avalanche breakdown state of gallium arsenide diodes after switching attributed to peak in hole generation rate 23 p4047 A66-41623  
 Proximity focused biplanar image converter diode for high speed photography, discussing basic geometries with respect to quantitative data gathering capabilities 23 p4070 A66-41673  
 Compound diode-transistor structure with current gain invariant with temperature 24 p4183 A66-42629  
 Multifunction monolithic thin film compatible diode-transistor logic circuits for data processing 24 p4178 A66-43187  
 Harmonic generation and detection in submillimeter wavelength region, emphasizing crystal point contact diode 24 p4176 A66-43191

**DIOL**  
**S GLYCOL**  
**DIOPHANTINE EQUATION**  
 Theoretical and machine aspects of ignoring singularity in approximate integration, relating uncertain cases to diophantine approximation 11 p1722 A66-22981  
 Book on ergodic problems in comparison theory and theory of diophantine, discussing residue distribution of polynomial of nth order modulo p, fractional parts of polynomial and exponential function 15 p2529 A66-29767

**DIOXIDE**  
**S CARBON DIOXIDE**  
**DIPLEXER**  
 Hybrid junction diplexer connecting transmitter and receiver to common antenna 22 p3873 A66-39784

**DIPOLE**  
**SA DIELECTRIC POLARIZATION**  
**SA ELECTRIC DIPOLE**  
**SA MAGNETIC DIPOLE**  
 LF solutions for dipoles in semiinfinite media found not to be valid for entire range of frequencies 06 p0826 A66-16032  
 Forbidden regions produced by two spatially separate point dipoles with parallel axes 14 p2361 A66-27412  
 Electron scattering by impurities in dipole form in semiconductors with anisotropic effective mass of current carriers, deriving formula for tensor of relaxation time 19 p3442 A66-35818  
 Sensitivity points method for linear systems based on structural interpretation of logarithmic sensitivity functions, introducing sensitivity dipole 19 p3327 A66-36015  
 Electromagnetic wave radiation from dipole source in thin plasma slab becoming weak outside plasma, considering total reflection 21 p3703 A66-38759  
 Polarization characteristic variations of HF signal received over short-range ionospheric path, noting phase measurement of elliptically polarized wave components, using receiving dipoles 22 p3864 A66-40065

**DIPOLE ANTENNA**  
 Electromagnetic field and radiation pattern of Hertzian electric dipole antenna in conical sheath 02 p0191 A66-11803  
 Linear antennas and characteristics regarding maximum power, directivity, height, sleeve and conical dipoles and current distribution 04 p0491 A66-13402  
 Log-periodic dipole antenna array and conical logarithmic spiral antenna design and performance 04 p0491 A66-13404  
 Admittance of short dipole antenna in ionosphere measured during rocket flights, deducing values of plasma frequency 05 p0669 A66-14945  
 Satellite Ariel II receiver for measuring cosmic radio noise, using dipole antenna 05 p0769 A66-15841  
 Cylindrical and truncated cone-type metallic dipole antennas for reception of VLF, examining theory of behavior in ionosphere 09 p1340 A66-19847  
 Design feasibility of dipole antenna for measuring electric fields at VLF from satellite moving through ionosphere 09 p1340 A66-19848  
 Plasma resonance excitation by small dipole antenna operating in pulsed mode in presence of and in absence of external



magnetic field 09 p1340 A66-19849  
 Ionospheric aerial impedance  
 measurements of wire dipole at frequency  
 of 60 kc and plasma electron and collision  
 frequency estimations 10 p1526 A66-21119  
 Variational method of computing radar  
 scattering cross sections to bistatic  
 scattering cross section for chaff  
 dipoles 10 p1503 A66-21643  
 Current distribution and input impedance  
 of infinite cylindrical antenna in anisotropic  
 plasma, treating it as boundary value  
 problem 11 p1661 A66-22396  
 Matrix analysis of scattering from  
 conjugate-matched antenna 11 p1662 A66-22541  
 Moderately superdirectional antenna with  
 directivity slightly greater than uniform-  
 current distribution of same size 11 p1664 A66-22560  
 Nonsteady radiation field of antenna  
 systems for arbitrary signals via Huygen-  
 Kirchhoff principle 11 p1670 A66-23225  
 Superdirective array of normal mode  
 helical dipoles 12 p1840 A66-24625  
 Explicit relation between mutual coupling  
 and radiation pattern of array antenna  
 evaluated via scattering formalism, based on  
 spherical modes 12 p1841 A66-24627  
 Bessel type lambda function for describing  
 properties of dipoles 12 p1841 A66-24630  
 Radiation due to axially oriented electric  
 dipole situated on axis of infinite cylindrical  
 column of insulating free space surrounded  
 by uniaxially anisotropic plasma 13 p2026 A66-26103  
 Noise suppression, signal reception, and  
 polarization measurement in cross correlated  
 antennas as function of dipoles imbedded in  
 random field, surrounding noise field and  
 coherency matrix of cross correlation  
 function 13 p2044 A66-26746  
 Radiation impedance of infinite planar  
 dipole array, phased for any angle of  
 radiation, calculated by Fourier series  
 expansion of field in plane waves 14 p2247 A66-26865  
 Plasma oscillation resonance phenomena of  
 ionospheric antenna excitation near lower  
 hybrid resonant frequency 14 p2340 A66-27127  
 Radiation characteristics of vertical dipole  
 in warm plasma, expressing vector potential  
 functions in Fourier integrals 14 p2240 A66-27916  
 Radiation from vertical dipole in warm  
 plasma determined by asymptotic series  
 expansion of integral solutions, noting  
 surface wave propagation, transformation  
 from acoustic to electromagnetic mode on  
 boundary, etc 14 p2240 A66-27917  
 Log periodic Yagi-Uda dipole antenna array  
 and extension of frequency bandwidth 14 p2256 A66-27920  
 Radiation of prescribed polarization from  
 cross-dipole antenna on aircraft carrier 15 p2447 A66-28570  
 Gain, impedance and scan angle variation  
 in polarization of phased radar antenna  
 arrays constructed with hybrid-fed crossed  
 dipole radiating elements 15 p2456 A66-28586  
 Operating principles and critical  
 dimensions of traveling wave slotted-  
 cylinder antenna with dipole elements 15 p2467 A66-29886  
 LF ionospheric measurement of  
 admittances of three orthogonal short  
 dipoles, noting impedance variation with  
 respect to frequency attitude and  
 voltage 15 p2493 A66-30038  
 Impedance measurement of 39.5 meter tip-  
 to-tip dipole antenna made during  
 ionospheric rocket flight 15 p2469 A66-30046  
 Rocket attitude determined by  
 simultaneous measurement of geomagnetic  
 field and electromagnetic field generated by  
 radio wave transmitted by rocket-mounted  
 dipole 16 p2810 A66-30958  
 Excitation of dipole wave in circular small  
 delay dielectric waveguide by sources with  
 amplitudes and phases variously distributed  
 over apertures 17 p2879 A66-31857  
 VLF dipole antenna impedance values,  
 magnetotonic and collision effects in  
 ionospheric magnetoplasma 17 p2874 A66-32386  
 Self and mutual admittance of coupled  
 dipoles in dissipative

medium 18 p3065 A66-33529  
 Antenna system for VLF radiowave  
 experiments in D region mounted on  
 Skylark rocket 19 p3321 A66-36621  
 Approximate solution for dipole radiator  
 field in space containing two conducting  
 long cylinders with parallel axes 20 p3512 A66-37146  
 Resistive and reactive components of  
 impedance of short dipole in lower  
 ionosphere 20 p3525 A66-37300  
 Input admittance, gain and noise  
 performance in dipole antennas with Esaki  
 diodes 20 p3531 A66-37731  
 Experimental results of VLF dipole tests  
 on Greenland ice cap including  
 measurements of self-impedance, amplitude  
 current distributions, relative efficiency and  
 complex conductivity 22 p3874 A66-39942  
 Borgnis U function applied to design of  
 electron tube having drift space between  
 collector and grid controlling current 22 p3876 A66-40173

# DIPOLE MOMENT

SA PYROELECTRICITY  
 Gravitational source dynamics, discussing  
 multipole structure, mass, linear momentum,  
 dipole moment and spin in axially  
 symmetric field 06 p0908 A66-16131  
 Gas adsorption on molecular sieves,  
 discussing separation caused by electrostatic  
 forces and electric fields 06 p0819 A66-16730  
 Critical Stormer pass points for quadrupole  
 field and double-ring-current field with  
 parallel or antiparallel dipole moments 09 p1404 A66-20085  
 Generalization of Keesom potential to  
 include quantum effects for adiabatic  
 interaction between two rotating dipolar  
 fields 09 p1405 A66-20677  
 Nitrogen analogs of sesquifulvalene,  
 calculating dipole moments of nitrogen  
 anhydride bases and pyridones via modified  
 Hueckel technique 11 p1651 A66-23411  
 Plasma effect on dipole magnetic field and  
 solar wind plasma-geomagnetic field  
 interaction 12 p1943 A66-24391  
 Atmospheric absorption in IR region,  
 noting effects of water vapor, ozone, carbon  
 dioxide and collision-induced dipole  
 moments 13 p2075 A66-26603  
 Dipole moment calculation for gas laser in  
 magnetic field 15 p2516 A66-29348  
 Limits to charge groups classified  
 according to structure and geometry into  
 linear dipole-type concentrated moments  
 analyzed, using generalized functions 16 p2823 A66-31713  
 Dipole phenomena in n-type GaAs caused  
 by field perturbations, showing conditions  
 for high and low field nucleation 17 p2983 A66-33106  
 Cosmic ray threshold rigidities examined,  
 discussing penumbral and threshold  
 perturbation effects produced by  
 superimposing external magnetic fields on  
 dipole model 18 p3096 A66-35227  
 Dipole moment calculation for gas laser in  
 magnetic field 20 p3576 A66-37353  
 Magnetospheric tail instabilities, auroral  
 electron acceleration and deformation due  
 to dipole magnetic field acceleration of  
 plasma particles 20 p3635 A66-38222  
 Perturbation theory of heteronuclear  
 diatomic molecules based on isoelectronic  
 homonuclear molecules applied to carbon  
 monoxide and nitrogen 23 p4032 A66-41646  
 Dipole moment of perchlorofluoride by  
 measuring absolute absorption maximum and  
 linewidth parameters in resonant  
 cavity 24 p4170 A66-43038  
 Spin-spin interaction energy for large  
 separations of two ground state hydrogen  
 atoms 24 p4239 A66-43040

# DIRAC EQUATION

Gravitational field interactions with Dirac  
 fields and electromagnetic fields studied in  
 framework of special relativity to find  
 possible C-, P-and T-violating effects 05 p0717 A66-15349  
 Stochastic processes in microscale  
 relativistic fluid mechanics, discussing Dirac  
 fluid, Klein-Gordon equation, diffusion,  
 quantum potential, spin fluids, etc 12 p1914 A66-24093  
 Dirac equation for spin-half particles in  
 curved space-time formulated by using  
 Cartan calculus, applied to treatment of

neutrinos in homogeneous nonisotropic  
 universes and plane wave geometries 12 p1905 A66-24563  
 Dirac delta function representation of  
 spark ignition, considering heat transfer  
 from reaction zone to fresh gas and flame  
 propagation 23 p4148 A66-41413  
 DIRECT CURRENT /DC/  
 SA ALTERNATING CURRENT /AC/  
 RF magnetic field effect, applied parallel  
 to external DC field, on Heisenberg  
 ferromagnet with dipolar coupling, using  
 Green function 01 p0122 A66-10579  
 DC and LF AC characteristics of silicon  
 transistor over collector current range 02 p0200 A66-11878  
 DC testers for integrated circuits  
 evaluated, emphasizing areas of application,  
 testing methods and operating characteristics 03 p0345 A66-13274  
 Aircraft and commercial application of  
 three-phase direct current resistance  
 welding, using silicon diodes 05 p0685 A66-14518  
 Thyristor equipped DC to DC regulated  
 power converter for voltage range between  
 43 and 300 v DC based on printed circuit  
 principle 06 p0857 A66-16966  
 Direct current voltage measuring and  
 recording system for laboratory use 07 p1036 A66-18486  
 Electrical properties of alpha ferric oxide  
 containing magnesium, noting temperature  
 effect, carrier concentration, conductivity  
 variations, etc 08 p1271 A66-19221  
 High impedance semiconductor DC  
 amplifier for use as measuring amplifier or  
 operational amplifier 08 p1194 A66-19279  
 Motor controllers for DC current supply  
 must be inverters of constant or variable  
 frequency 08 p1168 A66-19299  
 High efficiency lightweight DC-DC power  
 converter with step-width modulating  
 preregulator for use in Apollo Lunar  
 Excursion Module 08 p1169 A66-19496  
 Two operation modes of two-way DC  
 improved efficiency amplifier under active  
 loading 08 p1197 A66-19689  
 Phase controlled SCR circuit for variable  
 DC power application 08 p1199 A66-19807  
 Electromagnetic wave propagation in  
 plasma located in magnetic field of linear  
 direct current 10 p1506 A66-22003  
 Brushless motors of various types  
 described and compared in order of  
 increasing cost and complexity for  
 spacecraft application 11 p1640 A66-23174  
 Equivalent circuit for cycloconverter valid  
 for AC and DC outputs, noting data on  
 voltage drops 12 p1804 A66-24659  
 Precision DC potentiometer microwave test  
 set for coaxial or waveguide insertion loss  
 measurement 12 p1843 A66-24673  
 Direct current conduction of thin  
 evaporated silicon oxide films, noting  
 functional dependence on degree of  
 oxidation, composition, temperature and  
 adherence to Schottky emission law 13 p2157 A66-25034  
 DC-to-DC nondissipatively regulated  
 converter using inductive energy storage for  
 voltage transformation and regulation 13 p2001 A66-26297  
 Response of thin cylindrical monopole  
 antenna to DC pulse excitation computed,  
 using Fourier transforms, noting correlation  
 between empirical and theoretical  
 values 14 p2255 A66-27906  
 Very low DC voltage measurement using  
 chopper principle, based on resistance effect  
 and employing magnetically controlled  
 resistances 16 p2701 A66-30274  
 Model L/C water-cooled DC power supply  
 for short arc lamps, noting SCR  
 selection 16 p2635 A66-30495  
 Discrete transfer functions simulated on  
 analog computer by direct currents 16 p2656 A66-30584  
 Circuit with single externally driven  
 switch, operated at fundamental frequency  
 gives efficient conversion of DC to AC at  
 that frequency or any specified harmonic of  
 it 17 p2848 A66-31818  
 Optimum parameters for transformation of  
 output signal in highly sensitive DC  
 converter when SNR for required loading  
 source reaches maximum 17 p2887 A66-32703  
 Direct current volt-ampere characteristics



of junction gate germanium alloy FET, including field-dependent mobility effect and channel-height distribution 17 p2897 A66-33463

DC theory of unijunction transistor, calculating idealized one-dimensional model, neglecting diffusion currents but taking into account bulk recombination effects 18 p3076 A66-33934

Two operation modes of two-way DC improved efficiency amplifier under active loading 18 p3087 A66-34675

FM modulator with frequency response from DC to video while maintaining crystal stability, accommodating FM narrow-and wideband with single design 19 p3316 A66-35699

Electromagnetic wave propagation in plasma located in magnetic field of linear direct current 19 p3303 A66-36087

Plasma turbulent heating by direct current discharge in magnetic mirror trap, analyzing adiabatic compression 19 p3430 A66-36589

Brushless DC torque motor with unique position-sensing device based on variable magnetic reluctance 20 p3498 A66-37168

Circuitry of automatic surface tension measurement device 20 p3559 A66-37502

Vacuum pressure effect on separation distance for arcing of DC current between spacecraft material 21 p3771 A66-39214

Voltage control by means of Zener diode, transistor and variable-gain amplifier circuit 23 p4044 A66-41214

Thyristor circuit, basis for capacitive switching circuits, expressing switching capacitance by DC source 24 p4181 A66-42485

Precision DC potentiometer test for measuring microwave coaxial or waveguide insertion loss 24 p4182 A66-42577

Transistor theory approximation of DC and small signal I-V characteristics of p-n-p-n junction diodes and triodes 24 p4184 A66-42744

Basic considerations for DC to DC conversion networks, detailing relationship between characteristics of active resistor and maximum AC power generated by active element 24 p4189 A66-43180

**DIRECTION FINDER**

**S RADAR DIRECTION FINDER**

**S RADIO DIRECTION FINDER**

**DIRECTIONAL ANTENNA**

Directional properties of surface antennas with linear, squared and cubic phase distortions for symmetrical and asymmetrical amplitude distribution laws 01 p0035 A66-10220

Linear superdirectional antennas discussing directional properties and formulas for optimal directive gain 03 p0337 A66-13315

Design parameters of phase compensated circular arrays studied for synthesis of diametric-plane directional patterns having low sidelobes 04 p0498 A66-14043

Radiation field of single-filament logarithmic-elliptical helical antenna, assuming traveling wave along helix 04 p0501 A66-14408

Concentric ring antenna arrays with low sidelobes, estimating currents from Fourier-Bessel series 06 p0825 A66-16017

Recomputation of values of numerical approximation of integral in gain limitations of large antennas, considering sidelobe level 06 p0844 A66-16044

Symmetrical transverse electromagnetic-mode directional couplers, deriving formulas for functional parameters and insertion-loss function 06 p0844 A66-16083

TEM-mode coupled-transmission-line directional couplers, determining equal-ripple polynomials and tabulating parameters 06 p0844 A66-16084

Wideband annular-zone directional antenna, with individual radiators arranged in log-periodic concentrated groups on ring fed by conical line 08 p1190 A66-18682

Amplitude and phase direction-finding characteristics of monopulse automatic tracking system operating on sum-difference principle 08 p1190 A66-18911

Spatial radiation patterns of curved high-directivity antenna array as function of amplitude distribution and directivity 08 p1191 A66-18913

High-directional spherical antenna array,

determining shape of radiation pattern as function of orientation of individual antennas and amplitude distribution of excitation currents 08 p1197 A66-19608

Moderately superdirectional antenna with directivity slightly greater than uniform-current distribution of same size 11 p1664 A66-22560

Antenna theory, analyzing radio astronomical methods such as antenna axis, radiation pattern, gain, efficiency, etc 11 p1658 A66-23219

Nonsteady radiation field of antenna systems for arbitrary signals via Huygen-Kirchhoff principle 11 p1670 A66-23225

Superdirective array of normal mode helical dipoles 12 p1840 A66-24625

High directional antenna with variable aperture and signal processing after frequency conversion 14 p2251 A66-27237

Zonal reflectors creating fan-type radiation patterns possess structural parameters and electrical characteristics for use as high directional antennas 14 p2252 A66-27247

Mutual impedance between two rectilinear and parallel top-loaded elements of directional antenna when elements have nonzero current at ends 14 p2257 A66-27924

Linear superdirectional antennas, discussing directional properties and formulas for optimal directive gain stability 14 p2242 A66-28288

Amplitude and phase selection for maximization of directivity of scalar radiation point source 16 p2745 A66-30266

Coefficient of mutual correlation of noises for two-antenna phase-type direction finder 17 p2879 A66-31860

Directional properties of surface antennas with linear, squared and cubic phase distortions for symmetrical and asymmetrical amplitude distribution laws 17 p2880 A66-31903

High-directional spherical antenna array, determining shape of radiation pattern as function of orientation of individual antennas and amplitude distribution of excitation currents 18 p3088 A66-34964

Radio astronomy antenna theory, discussing antenna resolution, brightness distribution of celestial bodies, interferometer patterns, actual antennas, etc 20 p3530 A66-37721

Cathode ray oscillograph-directional antenna recordings of electromagnetic pulses from lightning discharges 20 p3553 A66-38081

Generalized method of calculating multielement antenna and feeder system 21 p3712 A66-39250

Waveguide directional couplers using inclined slots, considering broad-to-narrow cross and broadwall parallel guide configuration 22 p3878 A66-40546

**DIRECTIONAL CONTROL**

Effect of altitude and camera field-of-view at various degrees on geographic orientation and error in target position, using TV data 08 p1225 A66-19531

Pressure effect on cone caused by spike protruding at angles of attack may provide aerodynamic directional control at supersonic speed 16 p2629 A66-31117

**DIRECTIONAL STABILITY**

Flight experience with Ogee wing at low speed [AIAA PAPER 65-782] 03 p0318 A66-12556

Circular runway flight operations and increased directional stability [SAE PAPER 660283] 15 p2476 A66-29827

**DIRICHLET PROBLEM**

Finite difference method solving Dirichlet problem for quasi-linear elliptic equation, with results applied to calculation of magnetic field in nonlinear media 01 p0091 A66-10165

Dirichlet problem solved by probability density for Brownian particle, using Fredholm integral equation 01 p0094 A66-10730

Straight lines method applied to Dirichlet and Neumann boundary value problem for certain nonself-adjoint two-dimensional second order elliptic equations 01 p0095 A66-11014

Representation of arbitrary functions in region of convergence through Dirichlet series expansion 01 p0096 A66-11185

Dirichlet series representation of arbitrary

analytical functions in convex region of convergence with complex exponent 01 p0096 A66-11186

Fragmen-Lindelof type theorems for second-order linear elliptic equation, examining Dirichlet problem solution in infinite region 02 p0250 A66-12100

Interior and exterior Dirichlet and Neumann problems for LF acoustic oscillations 02 p0261 A66-12153

Necessary and sufficient criteria for absolute minimum of multidimensional integrals, depending on arbitrary number of real functions of real variables and partial derivatives of arbitrary maximum order 03 p0387 A66-12686

Asymptotic solution of Dirichlet problem for diffusion processes and small parameter in elliptic equations with discontinuous coefficients 03 p0388 A66-12925

Bounds for Dirichlet energy integral in terms of arbitrary vector field 04 p0539 A66-13949

Existence and uniqueness of weak solution to Dirichlet problem for elliptic differential equations in Sobolev spaces with special occupancy function 05 p0708 A66-15154

Asymptotic error estimates in solving elliptic equations of fourth order by method of finite differences 05 p0710 A66-15477

Existence and uniqueness of solutions of certain boundary value problems for degenerate elliptic equations of second kind 07 p1056 A66-17596

Twin prime problem solution depends only upon nontrivial L-zeros of Dirichlet L-functions 07 p1057 A66-17861

Representation of arbitrary integral functions by Dirichlet series in entire plane, determining number of rays on which zeros must be located 07 p1058 A66-17912

Second approximation of compressible subsonic flow over given wing profile reduced to regular Dirichlet problem 07 p0981 A66-18110

Complex perturbing potentials of constant circulation around single wing profile treated by method based on Dirichlet problem 07 p0983 A66-18341

Series expansion solutions of Dirichlet and Poincare problems for systems of elliptical PDEs 09 p1397 A66-20934

Convergence of solutions of finite-difference analogs of equation satisfied by generalized axially symmetric potential 11 p1723 A66-22986

Representation of arbitrary functions in region of convergence through Dirichlet series expansion 12 p1903 A66-24018

Dirichlet series representation of arbitrary analytical functions in convex region of convergence with complex exponent 12 p1903 A66-24019

Extended Dirichlet problem for cross section of cylindrical shell, showing asymptotic solution is valid, approximation to Dirichlet integral applied to electrostatic problem of condenser and closed tubes torsion 12 p1968 A66-24196

Majorants of solutions of first boundary problem for second order linear elliptic equations 12 p1904 A66-24238

Maximized elliptic equations, Dirichlet problem, distance function solution, maximum principle, removable singularity, etc 12 p1905 A66-24401

Dirichlet problem for degenerating elliptical equations with nonlinear lowest terms 13 p2120 A66-26007

Dirichlet problem for elliptical system, showing solvability of inhomogeneous system with uniform boundary values for half-plane and circle cases 13 p2120 A66-26008

Dirichlet problem deviation from Bitsadze system with Noetherian properties, giving Hausdorff normal solvability conditions for inhomogeneous problem 13 p2120 A66-26009

Boundary value problems for minimal surface equation 14 p2320 A66-26943

Expansion of arbitrary function of Mehler-Fok integral form in terms of spherical functions 15 p2526 A66-28952

Complex flow-perturbing potential for Joukowski profile in incompressible fluid with parabolic velocity distribution, using Jacob first order approximation to solve Dirichlet problem 16 p2627 A66-30211

Convergence of discrete analogs of



Dirichlet problems for Poisson equation in two dimensions, describing finite difference method for producing

algorithms 16 p2731 A66-30235

Certain incorrect Dirichlet and Cauchy problems of potential theory for elliptic and parabolic equations 16 p2733 A66-30744

Normal solvability of Dirichlet problem for Bitsadze elliptic system, noting conditions under which homogeneous problem has nonzero regular solutions 16 p2734 A66-30784  
Representation of arbitrary integral functions by Dirichlet series in entire plane, determining number of rays on which zeros must be located 16 p2736 A66-30975

Axiomatic theory of Dirichlet problem applicable to nonlinear PDEs and to systems of PDEs 16 p2738 A66-31704

Exactness of majorants of Dirichlet problem solution and uniqueness conditions for linear elliptic equations 17 p2947 A66-32581

General maximum principle and removable singularities, discussing case of arbitrary linear set of positive linear measure for which principle does not hold 18 p3128 A66-34661

Accuracy analysis of variable-direction diagrams for numerical solutions to heat conductivity equations 19 p3478 A66-35937

Semiweak solutions of elliptic BVP, particularly generalized Dirichlet problem 21 p3754 A66-38461

Existence and uniqueness theorems for Dirichlet problem of second-order linear elliptic equation, Neumann BVP, mixed BVP and oblique derivative problem 21 p3754 A66-38462

General theory of stability of elastic equilibrium in three-dimensional system of orthogonal curvilinear coordinates 21 p3828 A66-38803

Maximum modulus theorem extended to highly elliptic systems 21 p3758 A66-39369

Normal solvability of Dirichlet problem for Bitsadze elliptic system, noting conditions under which homogeneous problem has nonzero regular solutions 22 p3940 A66-40446

Dirichlet problem for elliptic system of differential equation which does not satisfy Lopatinski condition where characteristic equation of system has simple roots 22 p3940 A66-40449

Dirichlet problem solved by probability density for Brownian particle, using Fredholm integral equation 24 p4232 A66-42748

Electromagnetic analog computer for solving Dirichlet and Neumann equations for half-space and associated geophysical problems 24 p4202 A66-42763

# DISCHARGE

SA ARC DISCHARGE

SA CORONA DISCHARGE

SA ELECTRIC DISCHARGE

SA EXPLOSION

SA GAS DISCHARGE

SA GLOW DISCHARGE

SA PENNING DISCHARGE

SA PLASMA DISCHARGE

SA RADIO FREQUENCY DISCHARGE

SA RING DISCHARGE

SA SPARK

SA SPARK DISCHARGE

SA TOROIDAL DISCHARGE

SA TOWNSEND DISCHARGE

Geometrical theory governing flow over surface of convergent spillway 14 p2277 A66-27936

# DISCHARGE COEFFICIENT

Orifice constant discharge coefficient when Reynolds number drops below 10,000 achieved in series or parallel flow 01 p0059 A66-10958

Most probable discharge coefficient for ASME flow nozzles [ASME PAPER 65-WA/FM-1]

Discharge coefficient of quadrant-edge orifice and performance at very high Reynolds number [ASME PAPER 65-WA/FM-2]

Pressure index for predicting upstream nonnormal velocity distributions on orifice meters [ASME PAPER 65-WA/FM-3]

05 p0684 A66-15518

Book on flow measurement through pipes by square-edge orifice plate using corner tappings, including pipe layout, fluid density, temperature, pressure, orifice design, tables, graphs, etc 08 p1221 A66-18679

Relative effect of restrictive orifices, venturis or nozzles on measurement accuracy of fluid flow rates in pipes 11 p1703 A66-22207

Dynamic law for pressure variation in throttle chamber of hydraulic control booster, taking into account fluid compressibility and change in discharge coefficient 16 p2637 A66-31219

Quadrant edge orifice meter performance under cavitating conditions, noting discharge coefficient curves [ASME PAPER 66-FE-9]

Cavitation effect on discharge coefficient of standard flow nozzles [ASME PAPER 66-FE-12]

Extension of upper limit of Reynolds number for constant discharge coefficient of quadrant-edge orifice meter, noting performance in turbulent zone 21 p3724 A66-38819

Shock wave instability and mass flow accommodation for ribbon-type parachutes, noting canopy porosity and free stream Mach number 22 p3845 A66-40594

Unsteady air flow discharge coefficients compared for sharp-edged orifices with steady flow values 23 p4009 A66-41700

# DISCHARGE TUBE

SA ELECTRON TUBE

SA THYRATRON

Current and voltage distribution over length of HF discharge in helium-neon laser 01 p0082 A66-10704

Ionization potential of thulium obtained from hfs of thulium I, using discharge tube and Fabry-Perot etalon 03 p0393 A66-12322

Nonisothermic pulse discharge column in argon-cesium and helium-cesium systems with produced plasma studied for nonisothermic conductivity 03 p0398 A66-12508

Characteristics of Schuler tube with two anodes compared with one anode tube 04 p0492 A66-13472

Hydrodynamic acceleration of plasma in discharge tube into which energy is released in form of Joule heat 04 p0552 A66-14154

Precursor effects in T-tubes predominantly air-filled, using microwaves and photomultipliers, noting role of UV and plasma radiations 05 p0719 A66-14503

Heat transfer rate to stagnation point of catalytic surface placed in slow flow of dissociated oxygen from glow discharge tube and atom-molecule diffusion coefficient 06 p0822 A66-16632

Photoabsorption cross section of atomic hydrogen obtained by flowing molecular hydrogen through discharge tube 06 p0913 A66-17042

Transducers for exciting and detecting acoustic waves in discharge tube plasmas, discussing requirements, specifications and construction techniques 07 p1032 A66-17496

Potential striae determined in hollow cathode plasma 08 p1264 A66-19183

Electromagnetic behavior of shock waves and supersonic plasma fluxes generated in shock tubes, using cylindrical and conical discharge chambers 08 p1264 A66-19191

Discharge chamber with water-cooled metallic walls and HF induction 09 p1407 A66-20144

Statistical characteristics of delay time between ignition and discharge pulses of ISSh 100-3 spherical stroboscopic tube 09 p1353 A66-20363

Plasma sheath properties near discharge tube anode, noting relation of electron current distribution along discharge radius and ion energy spectrum to pressure 10 p1558 A66-21999

Low-pressure mercury vapor lamp for interferometric and spectrometric work, noting electrodes, main discharge tube, electrical circuit, etc 10 p1538 A66-22059

Current and voltage distribution over length of HF discharge in helium-neon laser 11 p1714 A66-23309

Characteristics of periodic fluctuations in voltage, current and luminous intensity of discharge through inert gases and mercury

vapor, using commercial discharge tubes 11 p1747 A66-23369

Arc discharge in cesium vapor within diode, noting plasma parameter distribution in electrode spacing during low, luminous and arc discharge phases 13 p2142 A66-25681

Magnetic probing of plasma column motion in cylindrical and toroidal discharge vessels 13 p2144 A66-25723

Helium-neon laser multibeam generation in gas discharge tube, using spherical mirrors and tapered plates 13 p2093 A66-26053

Velocities of incident and reflected shock wave colliding with plasmoid as affected by initial xenon pressure in induction discharge shock tube 13 p2153 A66-26525

Cataphoresis, moving striations and associated noise in He-Ne laser 13 p2105 A66-26591

Effect of longitudinal magnetic field on output power of gas laser operating in IR spectrum, noting gas-mixture pressure in discharge tube role 14 p2307 A66-27156

Microsecond pulsed discharges at short tube with wire electrodes containing helium gas at intermediate pressures 14 p2341 A66-27314

Radial amplification dependence over discharge cross section of He-Ne laser 15 p2515 A66-29208

Electromagnetic wave propagation in circular waveguide with axially-placed discharge tube 15 p2555 A66-29785

Simultaneous measurement of voltage, current, current derivative and X-ray output as function of time in low inductance flash X-ray discharge tube 16 p2706 A66-30935

Plasma-ion oscillations in drifted plasma effected in diode-type discharge tube by varying longitudinal magnetic field or cathode temperature 17 p2972 A66-32974

Radial amplification dependence over discharge cross section of He-Ne laser 17 p2936 A66-33057

Plasma sheath properties near discharge tube anode, noting relation of electron current distribution along discharge radius and ion energy spectrum to pressure 18 p3140 A66-34976

Alumina high temperature gas discharge tube for investigation of pulsed metal vapor laser oscillations 19 p3374 A66-35810

Low-inductance hydrogen gas discharge switch tube based on gas pressure-electrode spacing control of ionizing collisions 19 p3280 A66-35812

Conical electrode plasma source consisting of organic-glass discharge chamber with cylindrical electrode at apex, examining performance characteristics with pulsed gas admission 21 p3786 A66-39040

Plasma decay technique to measure density in discharge tubes compared to value obtained by Langmuir probe 21 p3792 A66-39182

Discharge chamber with water-cooled metallic walls and HF induction 21 p3793 A66-39415

Compact discharge lamp designed for continuous pumping of solid state laser, with integral mounts for crystals and enclosure providing cooling circuits for lamp and crystal 23 p4076 A66-41247

Effect of longitudinal magnetic field on output power of gas laser operating in IR spectrum, noting gas-mixture pressure in discharge tube 24 p4225 A66-42977

# DISCONTINUITY

SA SHOCK DISCONTINUITY

Mixed boundary value problem for second order hyperbolic equation with discontinuous coefficients having time derivatives 01 p0092 A66-10187

Discontinuous Liapunov functions applied to stability analysis of position-controlled system with symmetrically-controlled asynchronous motor 08 p1201 A66-19685

Mixed problem for general two-dimensional second-order hyperbolic equation with discontinuous coefficients solved by reduction to system of Volterra integral equations 16 p2734 A66-30747

General boundary value problems for general elliptic systems with discontinuous coefficients 16 p2735 A66-30965

Geometrical and kinematical conditions of compatibility associated with moving discontinuities in material



- media 17 p3032 A66-33501  
 Discontinuity condition in optimal control problem, considering motion of points in n-dimensional space separated by hypersurface 18 p3126 A66-33930  
 Numerical solution of problems on discontinuity at junction between homogeneous and inhomogeneous waveguides 18 p3078 A66-34094  
 Discontinuous Liapunov functions applied to stability analysis of position-controlled system with symmetrically-controlled asynchronous motor 18 p3091 A66-34671  
 Quasi-periodic solutions of nonlinear ordinary differential equations containing parametric discontinuities 20 p3591 A66-37592  
 Reflection of waves at discontinuity in refractive index gradient 22 p3866 A66-40453  
 Deformation of surface of removable wave front discontinuity in acoustically anisotropic medium with variable sound velocity 23 p4090 A66-41415  
 Stability analysis of discontinuous solution of gas dynamics PDEs for ideal fluid 23 p4055 A66-41559  
 Plasticity of bodies with abrupt surface discontinuities analyzed, based on mathematical theory of rigid-plastic nonhardenable bodies 24 p4291 A66-42736

## DISCRETE FUNCTION

- Sufficient conditions for signal reconstruction determined according to known values of that signal at discrete succession of points 04 p0483 A66-14047  
 Algorithm determining best approximation of bounded function in Chebyshev sense adapted to discrete case 04 p0540 A66-14167  
 Monitoring of discrete state discrete transition Markov source whose states are input letters to memoryless discrete noisy channel 06 p0860 A66-16189  
 Discrete simulation technique using electrical circuit for finite-difference approximation of initial differential equations, noting functional potentiometers 07 p1055 A66-17201  
 Optimal control and trajectory optimization in aperiodic discrete time functional systems 11 p1681 A66-23422  
 Directional convexity included in Halkin derivation of maximum principle, using topological and geometrical arguments related to optimal control theory 12 p1849 A66-24250  
 Digital techniques for identification of discrete-time and continuous-time systems from noisy input and output sample sequences via determination of transfer function model 12 p1854 A66-24638  
 State-space analysis of discretely controlled systems with finite delays 14 p2266 A66-27589  
 Discrete transfer functions simulated on analog computer by direct currents 16 p2656 A66-30584  
 Sufficient conditions for signal reconstruction determined according to known values of that signal at discrete succession of points 17 p2873 A66-32213  
 Discrete time signal estimation, noting minimum mean square error, minimax estimation, etc 18 p3068 A66-33905  
 Discreteness conditions for spectrum of one-term differential operator, considering asymptotic distribution of eigenvalues 18 p3126 A66-33931  
 Maximum principle in optimization of discrete time systems described by difference equations 20 p3536 A66-36857  
 Discretization and differentiation of operators with commutativity proof and with application to Newton method 20 p3589 A66-36904  
 Uniformly ergodic random processes with discrete parameters 20 p3592 A66-37816

## DISCRIMINATION

- S BRIGHTNESS DISCRIMINATION  
 S SENSORY DISCRIMINATION  
 S SPEECH DISCRIMINATION  
 S TACTILE DISCRIMINATION  
 S TIME DISCRIMINATION

## DISCRIMINATOR

- S SIGNAL DISCRIMINATOR

## DISEASE

- S EPILEPSY  
 S HEART DISEASE  
 S POLIOMYELITIS

## S RESPIRATORY DISEASE

## S VIRUS

## DISINTEGRATION

- Disintegration of alkali halide single crystals, polymers and glasses under laser radiation, noting parameters of disintegration region magnitude 18 p3119 A66-34681

## DISK

- SA LUNAR DISK  
 SA PLANETARY DISK  
 SA PLATE  
 SA ROTATING DISK  
 SA ROTOR DISK

- Pulsed pressure wave diffraction by disk at arbitrary angle 03 p0314 A66-12527  
 Amplitude distribution of ultrasonic vibrations of excited disk of barium titanate ceramic polarized perpendicularly to faces 04 p0559 A66-13471  
 Plane-strain and generalized plane-stress analysis of viscoelastic disk by comparing transient thermal stresses in disk and cylinder 04 p0591 A66-14204  
 MHD flow between torsionally oscillating disks in viscous conducting fluid subjected to uniform axial field 09 p1408 A66-20502  
 Stress-strain diagram of alloy and steel disk materials at high rates of straining and characteristic temperatures 12 p1965 A66-24054  
 Stability analysis for steady disk movement over rough horizontal plane, using Liapunov function method 16 p2715 A66-31616  
 Plane contact problem for circular ring and elastic or absolutely rigid disk, using method of successive approximations 18 p3252 A66-33710  
 Stress distribution of notched half-disk with uniform loading of bottom of notch 19 p3474 A66-36303  
 Static nodal patterns associated with normal modes of vibration disappear at large motion amplitudes due to occurrence of traveling wave component 19 p3474 A66-36344  
 Radial flow of incompressible viscous fluid between two parallel disks 20 p3548 A66-37990  
 Pressure distribution in laminar flow between parallel disks, noting inertia effects 21 p3729 A66-39439  
 Partition function for tunnel model of rigid disks evaluated in asymptotic limit of reduced volume, including close-packed value of closed systems area 22 p3949 A66-40913

## DISLOCATION

- SA CRYSTAL DISLOCATION  
 SA DISPLACEMENT  
 SA EDGE DISLOCATION  
 SA SCREW DISLOCATION

- Properties of moving dislocations in unstabilized creep at various temperatures analyzed by kinetic equations in Akulov theory 11 p1784 A66-23323  
 Dislocation problems of circular ring with simple type nonhomogeneity and of isotropic circular ring with thickness varying inversely with square of radial distance 14 p2397 A66-27392  
 Structural dislocation theory and structural distortion vector analysis 15 p2606 A66-28525

## DISPERSION

- SA MAGNETIC DISPERSION  
 SA PLASMA DISPERSION

- Dispersion of estimates of mathematical expectation and dispersion for connected meteorological time series 01 p0096 A66-10753  
 Semiconductor crystals, discussing dispersion property changes due to pulsed ruby laser radiation 05 p0697 A66-15354  
 Motion of particles of dispersed phase at inlet to sampling probe analyzed for application to two-phase medium flow 07 p1031 A66-17417  
 Semiconductor crystals, discussing dispersion property changes due to pulsed ruby laser radiation 09 p1387 A66-20895  
 Dispersion of estimates of mathematical expectation and dispersion for connected meteorological time series 14 p2326 A66-27852  
 Solution to dispersion equation of linearized Boltzmann equation in kinetic theory of rarefied gases, noting root behavior and distribution function

- structure 14 p2278 A66-28285  
 Dispersionless ballistics patterns of weapons analyzed as check on reported computer program 16 p2831 A66-31147  
 Radar return from perfectly reflecting target in presence of second medium, obtaining first approximation for return and accounting for multiple reflections and dispersion 17 p2876 A66-33104  
 Computational method for determination corridors of launch vehicle trajectory and impact dispersions [AIAA PAPER 66-483] 18 p3226 A66-33656  
 Direct measurement of dispersion properties of cadmium sulfide and CdS-CdSe crystals, using Obreilmov-Fresnel diffraction method, growing crystals by synthesis 21 p3799 A66-38926  
 Stability and surface tension of colloidal graphite dispersions in absence and presence of nonelectrolytes 21 p3754 A66-39150  
 Upper ionospheric electron density, electron gyrofrequency, ion density and ion gyrofrequency deduced from whistler-mode waves group index, energy distribution and dispersion curves 22 p3911 A66-39989  
 Optical dispersion and dispersion of birefringence, noting photoelastic methods and stress-strain optical coefficients 22 p3994 A66-40437  
 Ionospheric drift and radio wave dispersion determined from selective fading records and symmetry of cross correlation functions, using Fourier transforms 22 p3916 A66-40807  
 Dispersive device for pulse compression radar, discussing effect of signal departure from desired linear characteristics 23 p4033 A66-41014  
 Pulse compression using diffraction gratings and frequency sweeps of 30 mc in quartz crystal ultrasonic transducer 23 p4034 A66-41017  
 Random dispersive wave intensity detection and measurement in presence of noise 23 p4037 A66-41499  
 Rectangular terminal block in rectangular waveguide and dispersion equation for surface wave propagating along waveguide 23 p4046 A66-41516

## DISPERSION HARDENING

- Deformation resistance and stability dependence of strain-induced distortions in nickel alloys on various aluminum oxide distributions 01 p0087 A66-10749  
 Properties of dispersion-hardened gold, copper and platinum alloys made by chemically and vapor plating metal onto particles of metal oxides 03 p0381 A66-12550  
 Dispersion hardening of titanium carbide by boron doping from critical resolved shear stress measurements 11 p1719 A66-23399  
 Texture and anisotropic age hardening to improve mechanical properties of AlMgSi alloys 14 p2313 A66-27011  
 Heat resistance in air of dispersion hardened nickel alloys containing certain oxides prepared by powder metallurgy methods 18 p3123 A66-33785  
 Deformation resistance and stability dependence of strain-induced distortions in nickel alloys on various aluminum oxide distributions 18 p3124 A66-34983  
 Metallurgical and design characteristics of dispersion strengthened metals as function of temperature [ASME PAPER 66-MD-88] 21 p3750 A66-38505  
 Refractory metals, noting precipitation and dispersion hardening, oxygen, nitrogen and hydrogen effect, machining, coating, etc 21 p3752 A66-39240  
 Cleaning and stabilization method for dispersion strengthened materials produced from mechanically produced blends of metals plus oxide powders 22 p3935 A66-40117  
 Alloy additions of Zr, Ta, Nb, Re, Mo and Hf tendency to interact with thorium oxide particles in tungsten base alloys during exposure to greater than 2000 degrees C 23 p4079 A66-41067

## DISPLACEMENT

## SA DISLOCATION

- Two-dimensional problem of thermoelasticity involving periodic thermal effects, using Parkus thermoelastic displacement potential 01 p0155 A66-10652



Strain-displacement relations for general shell providing standard for approximate theories checking 03 p0442 A66-13305

Self-equilibrating bending of complete circular cylindrical shells described by first harmonic terms of Fourier series for displacement components 12 p1962 A66-24004

Two-dimensional problem of thermoelasticity involving periodic thermal effects, using Parkus thermoelastic displacement potential 12 p1963 A66-24014

Calculating spatial frames by procedures derived from displacement method 14 p2409 A66-28458

Two-dimensional representation of relation between stresses, displacement vector and external load for two elastic equilibrium states 15 p2608 A66-28771

Derivation of basic equations describing stresses, moment stresses and displacement of rods without torsion 15 p2608 A66-28773

Feedback-free Hall effect transducers for mechanical displacement measurement 16 p2709 A66-31578

Reaction forces calculated for system of connected solid bodies of various composition during accomplishment of given motion 20 p3598 A66-36908

Matrix displacement method applied to anisotropic plate and shell theory, including parallelogram and triangular configurations under bending, membrane forces and shear strains 21 p3831 A66-39352

Stress and displacement field of plane heat source moving at constant speed through elastic medium 21 p3837 A66-39447

Wiener-Hopf and series solutions to BVP of indentation stresses and displacements in infinite hollow elastic cylinder for axisymmetric punch of finite length and arbitrary profile 22 p3990 A66-40139

Displacement matrix analysis of three-dimensional anisotropic and inhomogeneous elastically deformable bodies represented as tetrahedral assemblies 23 p4146 A66-41989

**DISPLAY**

**S RADAR DISPLAY**

**S VISUAL DISPLAY**

**DISPLAY SYSTEM**

**SA IMAGE**

All-weather landing system for C-141 jet cargo transport using vertical navigation computer for military operations 01 p0101 A66-10035

Satellite position prediction and display /SPAD/ naval equipment that will predict, display and determine selected satellites 02 p0215 A66-11699

Aid to air navigation problem discussing reliability and accuracy, hybrid system, redundancy and credibility, display, operational environment and navigation technique 02 p0256 A66-11966

Landing task and pilot acceptance of displays for landing in reduced weather minimums [AIAA PAPER 65-722] 03 p0328 A66-12579

Cockpit display correction methods used in design of Trident aircraft 03 p0328 A66-12882

Human perceptual mechanism defined by psychological research and applied to aircraft cockpit display design 03 p0329 A66-12883

Head-up display /HUD/ developed for automatic landing in civil aircraft 03 p0329 A66-12884

Optimal control display relationships in general tracking including piloting and radar tracking operation 03 p0329 A66-13349

Fast time modeling technique for simulating predictor display for onboard orbital rendezvous 05 p0626 A66-14617

Six degree of freedom moving base simulator for testing orbital space rendezvous instrumentation 06 p0868 A66-15961

Continuous moving-scene display system for output of airborne mapping sensors such as radars, microwave radiometers and IR scanners 06 p0878 A66-15966

Video densitometer to extract data from video display, specifically densitodiagram 06 p0819 A66-16851

Automatic dynamic chart display, integrating navigation system as well as situation display and link with computer, for monitoring and updating self-contained

system 07 p1067 A66-17690

Charting for dynamic map displays preparatory to SST operations 07 p1068 A66-17705

Building blocks of pictorial navigation display for projection of servo-driven microfilm map onto rear projection screen 07 p1069 A66-17707

SST instrumentation problems, discussing reappraisal of flight deck display requirements 07 p1033 A66-17784

Head-Up Display superimposition of processed primary command or situation information for pilot eye strain reduction 07 p1076 A66-17795

Design criteria and operational performance of Doppler-driven map display device installed on Trident aircraft 07 p1077 A66-17802

Cockpit flight instrument display in integrated navigation system for SST, stressing smooth transition in handling from enroute navigation to terminal-area and approach procedures 07 p1078 A66-17810

CRT control display console models, console selection pointers, computer programming requirements, etc 07 p1003 A66-17879

Image, display and storage tube for scan conversion, digital storage and signal processing 07 p1036 A66-18270

Recognition of target on TV display as affected by target shape-smear and background clutter 08 p1226 A66-19532

Chart display methods of let-down type, roller type and optical projection for aircraft navigation 10 p1554 A66-21897

Computer controlled visual display 11 p1660 A66-22269

General purpose computers and cathode ray tube displays used in automation of air traffic control technical aids 11 p1732 A66-22900

Simulated 3-D display techniques, considering application to television, air-traffic control, scene synthesis, radar target data and signal analysis 11 p1707 A66-22960

Signal and response complexity effect on eighteen hours of visual monitoring digital display boxes 11 p1646 A66-23376

Utilization of magnetic deflection in display systems 12 p1829 A66-23536

Near-real time acquisition of aerial reconnaissance radar imagery from continuously moving and static displays 12 p1808 A66-23921

Added pilot work load imposed by additional commands in compensatory display reduces tracking performance in control of simulated terrain-following aircraft 12 p1808 A66-23922

Experimental testing effectiveness of sensor lines showing linkages between displays and controls 12 p1808 A66-23924

Faster group performance with large shared display indicates facilitating effect on group interaction process 12 p1808 A66-23926

Information assimilation from conspicuity coding of updated alphanumeric information, comparing relative effects of individual and group displays 12 p1809 A66-23927

Magnetic deflection for display systems offers improved design freedom and good frequency response 13 p2047 A66-25362

Charting for dynamic map displays preparatory to SST operations 13 p2125 A66-25869

Information display techniques for man-machine system 14 p2229 A66-26916

Man-machine systems involved in on-line man/ computer interaction, manned space systems, satellite communication and display systems 14 p2230 A66-27820

Schiphol Airport /Amsterdam/ analog computer installation for air traffic control and flight path calculations, with results displayed on automatic flight progress boards 15 p2534 A66-29311

Navigation displays for supersonic transports, discussing inductive reasoning, system performance verification, initial data verification, etc 15 p2535 A66-29625

Intensity display system similar to radar output, showing real time intensity and pattern variations created by solar lamp modules in testing of spacecraft systems in simulation facilities 16 p2680 A66-30497

Flight tests limitations, hi-fi simulation and other navigation display evaluation, detailing discontinuous simulator 16 p2743 A66-30668

Large screen real time projection display technique using Ne-He gas laser 16 p2708 A66-31412

Classification of display systems according to human sense perceptions 16 p2644 A66-31413

Target recognition performance, examining relative effect of size and smear or blur of display 17 p2864 A66-32155

British fixed-base aircraft cockpit simulator experiments, testing pilot performance when relying on windshield display as primary information source 17 p2865 A66-32182

Computer controlled digital display techniques for direct editing of research data 17 p2877 A66-32943

All-weather operations, head-up displays, long range navigational aids - Symposium, International Federation of Air Line Pilots Associations, Rotterdam, October 1965 17 p2951 A66-33198

Head-up display system as aid in bad-weather landing 17 p2951 A66-33199

Head-up display system design for civil aircraft including SST and current subsonic jets 17 p2952 A66-33200

Bendix microvision head-up display system all-weather landing aid 17 p2952 A66-33201

Head-up display systems, discussing state of the art and arguments in favor of their use 17 p2952 A66-33202

Blind landing equipment, discussing type 191 collimator unit tested on Caravelle aircraft 17 p2952 A66-33203

Head-up display used during transition from instrument to visual contact in Category II operations based on pilot sensitivity to movement and peripheral vision 17 p2953 A66-33210

All-weather operations, head up displays, long-range navigational aids - Conference, International Federation of Air Line Pilots Associations, Rotterdam, October 1965 17 p2953 A66-33212

Navigational display types and requirements for civil aircraft 17 p2956 A66-33223

Image related scanning systems for visual simulation display for space rendezvous and docking [AIAA PAPER 65-263] 18 p3093 A66-33788

Short time prediction display applicable to stabilization problems, discussing extrapolation and accelerated time scale methods 18 p3061 A66-33884

Cockpit displays associated with low altitude high-speed flight, emphasizing shift toward designing around man 19 p3287 A66-35508

Multisensor display requirements and approaches, using as example hypothetical two-man advanced tactical aircraft 19 p3396 A66-35512

On-line computer-based aids for investigating effect of sensor data preprocessing and information compression procedures on data transmission bandwidth and reliability 19 p3307 A66-35686

Displays of navigation data showing horizontal situation against moving map, noting use of standard charts, provision for permanent record, etc 19 p3398 A66-36733

Visual displays to aid pilot to fly, monitor and control power plant, navigational and other equipment and communicate with ATC ground stations 20 p3508 A66-36996

Para-Visual Detector, flight director display unit, considered by British European Airways 20 p3595 A66-37005

Mechanical prediction display to improve human behavior in control system 21 p3700 A66-38454

Information display - National Symposium, New York, September 1965 22 p3927 A66-40286

Visual write-erase-nonstore and electrical readout accurate tracking display storage tube operating on principle of secondary electron emission charging of thin film dielectric 22 p3927 A66-40287

Methodology for definition of space vehicle display system based on mission objectives and human factors 22 p3892 A66-40288

Holographic processes, uses and limitations, discussing coherent imaging, holographic



information storage and information display 22 p3918 A66-40292  
 Conductance and capacitance of metal-insulator-semiconductor diodes or any two-terminal complex admittance plotted automatically as function of applied bias 22 p3882 A66-40897  
 Pattern recognition computer operating under automatic control and stored program control for data transfers, system operation, man-machine interface and display operations 23 p4041 A66-41056  
 Head-up aircraft display systems using cathode ray tube 23 p4067 A66-41166  
 Simulator study of computing and displaying velocity in head-up display for low speed flight path control by pole track or velocity vector  
 [ICAS PAPER 66-16] 23 p4089 A66-41257

## DISSOCIATION

SA ELECTROLYSIS  
 SA GAS DISSOCIATION  
 SA MOLECULAR DISSOCIATION  
 SA PHOTODISSOCIATION  
 SA THERMAL DISSOCIATION  
 Experimental viscosity of dissociating system nitrogen tetroxide and nitrogen dioxide, obtaining force constants for Lennard-Jones potential having no effect on viscosity of gas mixture 06 p0823 A66-16635  
 Discrepancy between measured value of N-H bond dissociation energy in hydrazine and value suggested by other chemical evidence 07 p1000 A66-17463  
 Riometric data on ionospheric absorption applied to determination of dissociative recombination coefficient, noting atmospheric ionization by fragment gamma-radiation 22 p3973 A66-40468

## DISTANCE MEASURING EQUIPMENT

Microwave phase-measuring distance-determining system /SHIRAN/ enabling evaluation of slant ranges from airplane to four transponders located at ground control 02 p0227 A66-11378  
 Distance measurement by modulating linearly polarized light with respect to plane of polarization 04 p0546 A66-14393  
 Flight testing of distance measuring equipment for instrument landing system with results shown in histograms 07 p1067 A66-17691  
 Worldwide implementation of DME system feasible by removing unnecessary refinements from ground station design 07 p1068 A66-17696  
 Earth-Moon distance measurement using laser technique 09 p1453 A66-20129  
 Precise airborne geodetic survey system capable of measuring lines up to 900 nautical miles and determining nadir of aerial photographs to 24 ft 10 p1533 A66-22045  
 Measurement of distance to Moon by optical radar, discussing ruby laser/photomultiplier apparatus and procedure 16 p2647 A66-30291  
 Topocentric distance of geodetic satellite GEOS-A measured by laser telemetry from station 16 p2652 A66-30586  
 TACAN and DME navigation systems, discussing ground stations, airborne equipment and guidance 18 p3133 A66-34465  
 Generalized minimum distance decoding that permits likelihood information to be used, yielding same probability of error as maximum likelihood decoding 21 p3703 A66-39137

## DISTANCE PERCEPTION

S DEPTH PERCEPTION  
 S PERSPECTIVE

## DISTORTION

SA DEFORMATION  
 SA FLOW DISTORTION  
 SA SIGNAL DISTORTION  
 SA SURFACE DISTORTION  
 Extension of nonlinear distortion in common-emitter circuit to common-base circuit, cancelling emitter distortion and collector-loading distortion and presenting design chart independent of transistor type for CB circuit 13 p2030 A66-25217  
 Structural dislocation theory and structural distortion vector analysis 15 p2606 A66-28525

## DISTRIBUTION

S AMPLITUDE DISTRIBUTION  
 ANALYZER

S ANGULAR DISTRIBUTION  
 S BOLTZMANN DISTRIBUTION  
 S CHARGE DISTRIBUTION  
 S CURRENT DISTRIBUTION  
 S DENSITY DISTRIBUTION  
 S ELECTRON DISTRIBUTION  
 S ENERGY DISTRIBUTION  
 S FLOW DISTRIBUTION  
 S FORCE DISTRIBUTION  
 S FREQUENCY DISTRIBUTION  
 S GAUSSIAN DISTRIBUTION  
 S HOLE DISTRIBUTION  
 S ION DISTRIBUTION  
 S LIFT DISTRIBUTION  
 S LOAD DISTRIBUTION  
 S MASS DISTRIBUTION  
 S MAXWELL DISTRIBUTION  
 S MOMENT DISTRIBUTION  
 S NEUTRON DISTRIBUTION  
 S NORMAL DISTRIBUTION  
 S PATTERN DISTRIBUTION  
 S PEARSON DISTRIBUTION  
 S POISSON DISTRIBUTION  
 S PRESSURE DISTRIBUTION  
 S PROBABILITY DISTRIBUTION  
 S RADIAL DISTRIBUTION  
 S RADIATION DISTRIBUTION  
 S RANDOM DISTRIBUTION  
 S RAYLEIGH DISTRIBUTION  
 S SPATIAL DISTRIBUTION  
 S SPECTRAL ENERGY DISTRIBUTION  
 S STRESS DISTRIBUTION  
 S STRESS-STRAIN DISTRIBUTION  
 S SUBLATTICE DISTRIBUTION RATIO  
 S TEMPERATURE DISTRIBUTION  
 S VELOCITY DISTRIBUTION  
 S VERTICAL DISTRIBUTION  
 S WALL TEMPERATURE DISTRIBUTION  
 S WEIBULL DISTRIBUTION

## DISTRIBUTION FUNCTION

SA CHAPMAN-ENSKOG METHOD  
 Linear oscillations in relativistic Maxwellian plasma, detailing dispersion relations in collisionless cold electron-beam system 01 p0110 A66-10326  
 Uniform shear motion in rarefied monatomic gases in finite space, discussing distribution function of intrinsic molecular velocity 01 p0108 A66-10472  
 Effect of incomplete and inaccurate optical information on particle size distribution function, considering transparency and scattering pattern 01 p0097 A66-10758  
 Inhomogeneity distribution in single crystal semiconductor considering specific resistance and carrier lifetime and using volume gradient photoelectromotive force values 01 p0124 A66-10763  
 Plasma decay by measuring phase variation and signal amplitude with interferometer, determining distribution function and recombination coefficient 01 p0115 A66-11056  
 Electron distribution function of homogeneous Lorentzian plasma calculated by successive approximation method 01 p0115 A66-11077  
 Diagrammatic method to obtain Helmholtz free energy of classical electron gas used to derive pair distribution function beyond Debye-Huckel result 02 p0266 A66-11478  
 Nonlinear equation for distribution function of particles in plasma in electromagnetic field 02 p0267 A66-11729  
 Measurement of one- and two-dimensional distribution functions of stochastic signals, examining single channel analyzers 02 p0230 A66-11811  
 Ion direct heating in nonlinear absorption of transverse waves during scattering on plasma ions, noting equation for ion distribution function 03 p0396 A66-12283  
 Cyclotron instability dependence on nonmonotonic ion distribution function of plasma with cyclotron resonance 03 p0396 A66-12289  
 Equation for singlet distribution function as quantum-mechanical analog of Boltzmann equation 03 p0391 A66-12340  
 Nonlinear oscillations of plasma behind formation front of charged particles 03 p0397 A66-12383  
 Fodor terminal-state problem solved on basis of distribution theory without using heuristic operators 03 p0388 A66-12703  
 Distribution theory used to remove apparent contradictions observed when applying Laplace transform to discontinuous functions 03 p0388 A66-12704

Collisionless electron plasma in uniform field possessing unperturbed distribution function for electrons not considered isotropic in plane of velocity space 03 p0401 A66-12963  
 Free photon path distribution during passage through thick plane-parallel light scattering layer 04 p0541 A66-13416  
 Stability of 3-axis stabilizing platform as function of distribution of gyro units 04 p0518 A66-13568  
 Statistical characteristics of fluctuations in radio emission of atmosphere producing turbulent pulsations and displacements of hydrometeorological formations in scan field of radiotelescope, noting distribution function 04 p0517 A66-14046  
 Probability density and distribution functions associated with noise and signal plus noise in radar IF, after linear and square law detector, and after these detectors with subsequent video integration 04 p0485 A66-14115  
 High energy electron influence on electron distribution function and effect on spectra of nonthermal galactic and extragalactic radio sources 04 p0575 A66-14171  
 Impact ionization coefficient for electrons and holes in silicon determined from distribution function of hot carriers and shown to be weakly dependent on ionization cross section 04 p0565 A66-14262  
 Structure of solutions of chain of equations for deriving Boltzmann kinetic equation of gases 05 p0663 A66-15344  
 Ion direct heating in nonlinear absorption of transverse waves during scattering on plasma ions, noting equation for ion distribution function 05 p0727 A66-15455  
 Radial distribution function computed for classical particles interacting with Coulomb, shielded Coulomb and truncated Coulomb forces 06 p0908 A66-16120  
 Four conditions permitting fatigue limit obtained by Wohler curve to render consistent distribution function to mean value and deviation 06 p0965 A66-16485  
 Nonlinear stochastic system, determining distribution law for variables 06 p0862 A66-16524  
 Solution to Liouville equation, obtaining expression for singlet distribution function for system under arbitrary perturbation from equilibrium, leading to solution of linear Boltzmann equation 06 p0912 A66-16633  
 Interaction of semiconductor valence electrons with free radiation field 06 p0928 A66-16772  
 Comparison, by stochastic model, of property of distribution of centers of solar activity to form compact groups obeying differential rotation law 06 p0956 A66-17062  
 Distribution function of zeros in harmonic signals relation to frequency characteristic of latter undergoing maximum amplitude limitation 07 p1001 A66-17348  
 Angular moments of lateral-angular distribution functions in electromagnetic cascade theory calculated by method of moments 07 p1116 A66-17561  
 Effects of commensurability with mean motion of Jupiter upon distribution of mean motions of short-periodic comets 07 p1135 A66-17640  
 Phase velocity and growth coefficient of instability of plasma with discontinuous velocity distribution, noting role of ion distribution function 07 p1087 A66-17852  
 Stationary queue length Poisson distribution in single channel service system, considering reliability of device 07 p1003 A66-17862  
 Distribution function of semiconductor minority current carriers in presence of pronounced spatial inhomogeneity occurring in intensively absorbing films with intensive surface recombination 07 p1099 A66-17873  
 Partition function of hydrogen plasma derived classically and by quantum mechanics, obtaining Saha equation containing effective lowering of ionization potential 07 p1090 A66-18155  
 Anisotropy of microwave conductivity and absorption in semiconductors with hot carriers, studying distribution function of electrons 07 p1106 A66-18380  
 Magnetization using Hartree-Fock



approximation in terms of boson distribution for uniformly interacting spins 07 p1084 A66-18441

Kinetic equations, considering free and bound charges in weakly ionized hydrogen plasma, noting self-consistent approximation for second distribution function 08 p1265 A66-19375

Simple alternative derivation of conventional cluster expansion formula for matrix elements of identity and Hamiltonian for expectation value of energy of many-Fermion system 08 p1259 A66-19445

Classical statistical mechanics used to obtain expressions for density, distribution functions and other properties of fluid in equilibrium in potential 10 p1521 A66-21172

Distribution patterns of common stars in galactic plane according to spectral type, noting density gradients, main sequence, Hertzsprung-Russell diagram, etc 11 p1766 A66-22254

Inhomogeneity distribution in single crystal semiconductor, considering specific resistance and carrier lifetime by using volume gradient photoelectromotive force values 11 p1748 A66-22274

Solution of two first equations of BBGYK hierarchy, obtaining dielectric constant of plasma by using Guernsey solution, giving two-particles distribution function 11 p1744 A66-22445

Electrostatic waves in uniform plasma without collisions in linear approximation, presenting normal oscillation mode as model for damped and unstable waves 11 p1744 A66-22447

Matrix coefficient expression for film-type distributed-parameter RC circuit with arbitrary number of films and parameter distribution function 11 p1666 A66-22731

Shock structure calculations from kinetic theory, using ellipsoidal distribution function 11 p1690 A66-22912

Shock wave structure in binary gas mixtures that are monatomic and chemically inert, using Mott-Smith method 11 p1691 A66-22914

Discrete ordinate technique for solution of distribution function of linearized Boltzmann equation, with application to Couette flow 11 p1692 A66-22923

Breakdown regime of diffusion-controlled HF resonance gas discharge analyzed kinetically, solving Boltzmann equation for electron distribution function 11 p1740 A66-23081

Lagrangian for particular collisional models in fluid dynamics, considering fluctuation theory relations and stability in presence of external field 12 p1918 A66-23552

Propellant injection distribution effect on transverse modes of liquid rocket engine instability [AIAA PAPER 85-613] 12 p1977 A66-23587

N-dimensional two-sided Laplace transformation and n-dimensional Mellin transformation of distributions 12 p1904 A66-24194

Magnetic field effect on energy distribution and slowing-down times of nonequilibrium carriers in semiconductors when excitation source creates electron-hole pairs 12 p1929 A66-24451

Far field simulation of antennas with complex aperture distribution functions 12 p1840 A66-24624

Granato-Luecke frequency dependent internal friction calculated for pinning point distributions after vibration at dislocation temperature 12 p1971 A66-24922

Correlation functions of amplitude and intensity fluctuation for laser model near threshold obtained by using distribution functions evaluated by Fokker-Planck equation, treating amplitude as random variable 12 p1892 A66-25018

Likelihood detection with multiple Markov process, by expressing statistics in distribution function terms 13 p2019 A66-25060

Stabilization of drift instability in traps with magnetic field increasing toward plasma boundary, taking into account Taylor instabilities 13 p2139 A66-25335

Nonlinear oscillations of plasma behind formation front of charged

particles 13 p2139 A66-25388

Explicit approximate solution for distribution of constraints along wall of revolution assuming limiting equilibrium and for case of system with discontinuity line 13 p2195 A66-25443

Distribution, as function of azimuth, of static pressure and mass and heat transfer coefficients for case of interaction between detached shock wave on cylinder nose in hypersonic flow and turbulent boundary layer along wall 13 p1991 A66-25464

Plasma stability in magnetic field where disordered energy of particles may be liberated so as to cause collective evolution of plasma, using formalism describing particle diffusion, noting distribution function role 13 p2144 A66-25719

Microwave models of optical resonators, discussing correction of discrepancies resulting from approximations in measurements 13 p2093 A66-26006

Approximate analytical solutions for distributed parameter networks with parameters as functions of spatial variable, using differential equation that reduces boundary value problem to Sturm-Liouville system 13 p2120 A66-26068

Atmospheric distribution profiles of ozone noting formation, elimination, effect on terrestrial heat losses, UV absorption, etc 13 p2073 A66-26318

Equation of state in closed form obtained for gas composed of molecules with Lennard-Jones potential, noting compressibility factor and radial distribution function 13 p2018 A66-26446

Velocity gradient instability for monotone distribution function in guiding center plasma 13 p2154 A66-26670

Necessary conditions for stability of collisionless guiding center plasma, sufficient for stability of equilibrium configurations whose distribution functions are bell shaped 13 p2154 A66-26671

Constant current hot-wire anemometer determination of experimental time-amplitude distribution function of velocity in turbulent boundary layer 13 p2072 A66-26753

Integral equations for radial distribution functions in classical fluid 14 p2273 A66-26828

Particle distribution in low density collisionless plasma in vicinity of moving charged body smaller than Debye radius 14 p2284 A66-27556

Method of constructing particle distribution function for quasi-neutral plasma consisting of electrons and singly charged heavy ions 14 p2344 A66-27648

Estimate of energy dissipation in metals, using continuous distribution of oscillating dislocations joined with Zener thermoelastic effects 14 p2315 A66-27658

Effect of incomplete and inaccurate optical information on particle size distribution function, considering transparency and scattering pattern 14 p2326 A66-27857

Solution to dispersion equation of linearized Boltzmann equation in kinetic theory of rarefied gases, noting root behavior and distribution function structure 14 p2278 A66-28285

Fokker-Planck equation of wave propagation in medium with regular and random inhomogeneities, determining spatial angular distribution function of ray 14 p2245 A66-28474

Pearson universal random distribution generator, noting analysis of randomly chosen variables for unimodal underlying distribution 15 p2526 A66-28808

Exceedance theory application to reliability and quality control problems, noting tolerance limit and life test problem solutions 15 p2508 A66-28809

Instrument methods determining function and density of length distribution of random radio emissions 15 p2451 A66-29123

Rotational distribution function of flowing nitrogen in low density wind tunnel using electron beam fluorescence 15 p2481 A66-29737

Rotational energy distribution through shock waves in nitrogen measured, using electron beam fluorescence 15 p2481 A66-29738

Boltzmann equation for Pitot tube problem, using distribution function, deriving equations for rarefied gas flow in impact tube under hypersonic and adiabatic conditions 15 p2481 A66-29739

Magnetic effects on diffusion of ferromagnetic colloidal particles dispersed in current-carrying fluid medium, noting force effects on relaxation process 15 p2556 A66-29809

Structure of solutions of chain of equations for deriving Boltzmann kinetic equation of gases 15 p2482 A66-29972

Velocity distribution function of helium atom measured, using Doppler profile of helium line 16 p2701 A66-30377

Improved Monte Carlo method for calculating steady state monatomic rarefied-gas flows, using computer for calculating possibility of collision in given geometrical cell 16 p2753 A66-30787

Nonlinear stochastic system, determining distribution law for variables 16 p2670 A66-30834

Iterative solution to Krook-Boltzmann kinetic equation noting Navier-Stokes numerical solution, computation and analysis of distribution function within shock wave 16 p2685 A66-30945

Quasi-linear approximation of Cerenkov and cyclotron damping of electromagnetic waves in magnetoactive plasma, considering collisions of wave-absorbing resonance particles with plasma 16 p2762 A66-31173

Instability of nonlinear stationary oscillations of potential in electron-ion flows useful in distribution functions of ions and electrons 16 p2754 A66-31174

Secondary electron interaction with solid state plasma, noting energy distribution, Boltzmann equation solution, etc 16 p2789 A66-31783

Nonlinear effects in homogeneous Lorentz plasma, calculating anisotropies of electron distribution function 17 p2963 A66-31842

Lumped inertia force method for obtaining mode shape and corresponding natural frequencies 17 p3023 A66-32078

Statistical characteristics of fluctuations in radio emission of atmosphere producing turbulent pulsations and displacements of hydrometeorological formations in scan field of radiotelescope, noting distribution function 17 p2917 A66-32212

Plasma wave quasi-linear theory, noting nonlinear effect treatment via distribution function, electric field, Fourier component decay, etc 17 p2966 A66-32422

HF flute unstable oscillations occurring when low temperature plasma is added to high temperature one, finding frequency and growth rate are of order of cyclotron harmonic frequency 17 p2966 A66-32423

Convective excitation of ionic oscillations in plasma by inhomogeneous electron beam as result of spatial gradient of distribution function 17 p2968 A66-32537

Successive approximation solution to integral kinetic equation and corrections to moments of distribution function for viscous and rarefied gases 17 p2909 A66-32585

Distribution function, harmonic and statistical linearization methods applied to study forced oscillations in nonlinear oscillatory system 17 p2959 A66-32801

Distribution function and electron mobility in polar semiconductors for nonparabolic dispersion law 17 p2986 A66-33305

Nonlinear generation of combination frequencies due to strong uniform parallel electric fields in homogeneous plasma 18 p3142 A66-33918

Steady state distribution functions for photoexcited carriers in semiconductors bands determined by competition between intraband intercarrier collisions and recombination processes 18 p3154 A66-33919

Electrostatic stability of fully ionized non-Maxwellian electron-ion plasma 18 p3142 A66-33953

Kinetic equations, considering free and bound charges in weakly ionized hydrogen plasma, noting self-consistent approximation for second distribution function 18 p3146 A66-34177

Longitude dependence of distribution function of electrons for fixed value of



McIlwain parameter, using kinetic equation 18 p3197 A66-34873

Latitude distributions obtained for nucleonic and neutron components of cosmic radiation during flights from South Africa, compared with Northern Hemisphere distributions 18 p3197 A66-34878

Numerical calculations of lateral distribution, energy spectrum and heights of origin of muons in extensive air showers 18 p3211 A66-35135

Multiplicity distribution of secondary particles in photonuclear interactions of mesons, analyzing effect of intranuclear cascade 18 p3221 A66-35203

Interaction of semiconductor valence electrons with free radiation field 19 p3434 A66-35369

Silicon field effect device with AC/DC fields superimposed on gate terminals analyzed for determination of distribution of defect introduction rate with depth, especially near threshold energies 19 p3435 A66-35413

Semiconductor cyclotron resonance during application of constant electric field, determining carrier distribution function 19 p3437 A66-35460

Plateau formation mechanism for electron velocity distribution function during damping of monochromatic plasma waves 19 p3406 A66-35737

Solution of Boltzmann and rate equations for electron distribution function and state populations in nonequilibrium MHD plasmas 19 p3406 A66-35801

Exact solution of nonlinear relativistic equations of motion for electron in right circularly polarized wave propagating in whistler mode parallel to external magnetic field 19 p3303 A66-35998

Structure of hydromagnetic shockfront wherein electrostatic turbulence continuously develops, analyzed to aim at orders of magnitude for front width, electron and ion heating and magnitude of fluctuation excitation 19 p3408 A66-36278

Dipole scattering of electrons in germanium and silicon whose conduction-band structure is described by many-valley model, using distribution function and computing relaxation-time ratio 19 p3446 A66-36393

Stability of confined plasma in mirror machine depending on proper coordination of magnetic field geometry with particle distribution function 19 p3422 A66-36548

Residual gas analyzer determining qualitative distribution of gases in ultrahigh vacuums by using mass spectrometer for spatial simulation 19 p3360 A66-36614

Electron velocity distribution function in nonequilibrium plasma having spatial distribution governed by electron-electron and inelastic collisions 20 p3606 A66-36974

Distribution function for probability density of random process at output of multiplier acted upon by envelopes consisting of Gaussian noise and pulse signal 20 p3515 A66-37380

Electron energy distribution function obtained by Druyvesteyn analysis in low-current positive column neon discharge compared with theoretical distribution function 20 p3608 A66-37463

Magnetic field effect on energy distribution and slowing-down times of nonequilibrium carriers in semiconductors when excitation source creates electron-hole pairs 20 p3619 A66-37683

Statistical properties of amplitude and phase of output signal of electron beam quadrupole amplifier with superposition of regular signal plus Gaussian noise at input 20 p3519 A66-37997

Magnetic field, microscopic particle distribution function, plasma instabilities and wave-particle interactions of solar wind 20 p3632 A66-38061

Cloud and fog droplet spectra rearrangement due to external conditions calculated from distribution function of water content 20 p3594 A66-38374

Velocity distribution function of plasma in high intensity perturbation field, noting linear response for weak interaction and long wavelengths, connection formulae and

absorption of electromagnetic waves 21 p3777 A66-38760

Fokker-Planck equation applied to laser under influence of quantum fluctuations connected with dissipation, pumping and cavity thermal noise, noting distribution and correlation function 21 p3746 A66-38930

Solution to chain of kinetic gas equations, showing effect of fast reversible and slow irreversible processes on particle distribution function 21 p3771 A66-39248

Radar detection probability in presence of unknown parameters, covering pulse-to-pulse, partial and fully coherent cases 21 p3707 A66-39639

Nonsupervised sequential pattern recognition and classification, analyzing Bayes solution 21 p3720 A66-39640

Run-length encodings, determining explicit form of Huffman coding when applied to geometric distribution 21 p3758 A66-39643

Absolute stability of distributed control system with nonlinear elements of backlash type analyzed by distributed parameters method 22 p3883 A66-39660

Stabilization of drift instability in traps with magnetic field increasing toward plasma boundary, taking into account Taylor instabilities 22 p3952 A66-39712

Replacement of Poisson by Polya distribution in calculating laser intensity threshold necessary to induce ionization breakdown in gases 22 p3929 A66-39715

Field intensities and electron distribution functions in hollow cathode, graphs show potential distribution along cathode axis 22 p3953 A66-39758

Particle growth in rocket nozzle, particle size distribution, effect of channeling, determining increase of mass-median diameter of distribution 22 p3971 A66-40364

Randomly sampled random processes, discussing sampling time statistics and stationary point processes 22 p3885 A66-40869

Matrix coefficient expression for film type distributed parameter RC circuit with arbitrary number of films and parameter distribution function 23 p4045 A66-41469

Electrostatic probe in collisionless plasma wherein sheath joins region of ambipolar diffusion 23 p4104 A66-41494

Quasi-linear approximation for turbulent plasma obtained via Wiener-Hermite functional expansion for electric field and distribution function 23 p4104 A66-41504

Equilibrium distribution function of particles in phase space applicable to collisionless rarefied plasma confined by magnetic mirror, using first integrals of motion 24 p4242 A66-42399

## DISTURBANCE

## S MAGNETIC FIELD DISTURBANCE

## S SATELLITE ATTITUDE

## DISTURBANCE

## S SHEAR DISTURBANCE

## S SUDDEN IONOSPHERIC

## DISTURBANCE /SID/

## S VORTEX DISTURBANCE

## DISTURBANCE THEORY

Asymptotic solution of disturbance at large distance from source placed in flow of conducting compressible fluid in applied magnetic field 05 p0723 A66-15052

Periodic motions of simple pendulum excited by horizontal periodic disturbance 07 p1081 A66-18043

Small gap equations for Couette flow stability considering nonaxisymmetric disturbances, solving eigenvalue problem and noting role in instability of Taylor vortices 12 p1866 A66-24946

Evolution of plane switch-on and switch-off shocks in gas of finite electrical conductivity in presence of small nonlinear disturbances 12 p1866 A66-24950

Disturbance propagation in baroclinic atmosphere in presence of radiation and turbulent heat conduction 14 p2325 A66-27535

Effect of single or periodic disturbances on intermittency in pipe flow at various Reynolds numbers, noting relation of disturbance input frequency to output frequency of turbulent slugs 16 p2688 A66-31394

Bjerhammar gravimetric boundary value problem with gravity reduction defined by integral equation 19 p3345 A66-35393

Optimal control of time-varying linear systems subject to additive noises and load disturbances, based on exact plant equations 19 p3325 A66-35877

Multifactor Max-Rankine optimization technique evaluated from point of system performance, minimum mean square error, intrasystem interactions, etc 19 p3325 A66-35878

Steepest descent method extended to trajectory optimization problem for stochastically disturbed systems with application to Euler equation for white noise problem of reentering vehicle 19 p3388 A66-35879

Parameter optimization using steepest descent approximation for systems subject to worst bounded disturbance in order to provide performance index minimization 19 p3337 A66-36713

Wiener filtering theory for stationary ergodic inputs with known spectral densities and optimal control transfer functions of random-input nonlinear saturating systems with random unwanted disturbances 20 p3536 A66-36859

Parameter adaptation theory of quick-response self-adapting systems subject to parametric disturbance 20 p3536 A66-36884

Parabolic equations applied to nonlinear thermoconductivity and filtration, describing propagation of plane wave 24 p4230 A66-42219

Disturbance propagation in baroclinic atmosphere in presence of radiation and turbulent heat conduction 24 p2325 A66-42321

Chain code method of eliminating LF drift disturbance error in calculation of impulse-response function of time-invariant system 24 p4187 A66-42368

## DISTURBING FUNCTION

Disturbing function for satellite close to Earth or in resonance with Earth rotation 05 p0758 A66-14803

Resonance effects for satellites with nominally constant ground track 06 p0952 A66-15906

Soviet book on geodetic gravimetry including disturbing potential calculation methods based on Molodenskii integral equation 14 p2288 A66-28209

Digital computer techniques for computation of lunar disturbing function 24 p4273 A66-42204

## DIURESIS

Lower body negative pressure used to restore hydration after recumbency diuresis following bed rest 06 p0813 A66-16823

Combination of renal vasodilation and angiotensin infusion effect large changes in renal hemodynamics, excretion and reabsorption of sodium in anesthetized hypotensive dogs 20 p3507 A66-37607

## DIURETICS

Antidiuretic effect of positive Gz gradient acceleration 17 p2855 A66-32137

## DIURNAL RHYTHM

## S CIRCADIAN RHYTHM

## DIURNAL VARIATION

Auroral zone absorption, reporting periodic variation of sporadic E layer in Antarctica, considering magnetospheric time-of-flight spectrometer effect 01 p0061 A66-10497

Data from ion energy spectrometer mounted on Ariel I satellite indicating increased concentration of oxygen ions during afternoon at high altitudes 01 p0061 A66-10498

Electron concentration-distribution data for ten quiet days during spring 1958 in F-2 layer 01 p0063 A66-11027

Diurnal velocity variations of ionospheric wind in auroral zones and disturbance daily solar variation 01 p0064 A66-11161

Correlation of hydrogen emission and oxygen line in diffusive auroras and sporadic E layer 01 p0064 A66-11162

Relative position of solar disturbance daily variations mean flux system compared with auroral region of same period 01 p0065 A66-11169

Solar disturbance daily variations and behavior of horizontal perturbation vector based on magnetic observations at Soviet high latitude stations 01 p0065 A66-11170

Diurnal and seasonal variations in refractive index of atmosphere near Earth surface based on meteorological station data



- in Transbaikalian region 02 p0253 A66-11275
- Stellar-diurnal variation of cosmic rays during period 1958 through 1960, on basis of meson-activity data recorder by two crossed counter telescopes 02 p0281 A66-11335
- Lunar-diurnal variation of cosmic ray intensity based on observations of neutron and meson component 02 p0281 A66-11336
- Atmospheric source of diurnal variation of cosmic radiation whose properties undergo substantial variation 02 p0281 A66-11337
- Diurnal and nocturnal variations in cosmic radiation intensity during period of maximum solar activity 02 p0282 A66-11340
- Quiet solar diurnal variations of geomagnetic field at middle and low latitudes during IGY to determine coordinate system and equatorial electrojet 02 p0224 A66-12118
- Autocorrelation functions of random processes, determining parameters and amplitude of diurnal variations in cosmic ray intensity 02 p0284 A66-12129
- Relation between irregular variations in magnetic field intensity with sporadic E region containing current system responsible for quiet solar diurnal variation 02 p0225 A66-12140
- Controlling instabilities in numerical representation of diurnal and geographic variation of ionospheric data 03 p0361 A66-12501
- Magnetic activity effect on F-2 region drifts and variation with time at low latitude station 03 p0361 A66-12633
- Upper limiting rigidity of solar diurnal variation of cosmic ray primaries in free space determined by neutron monitors at sea level and meson telescopes 03 p0423 A66-13178
- Geomagnetic relationship of daily variation of cosmic ray neutron intensity corrected for barometric pressure variation at various ground stations 03 p0423 A66-13360
- Sporadic E layer characteristics over Sofia and diurnal and seasonal variations in maximum and reflection frequencies 04 p0514 A66-13447
- Harmonic analysis of solar diurnal and semidiurnal variations of wind, pressure and temperature in stratosphere, comparing observed and wind-derived heights and temperature 04 p0515 A66-13672
- Diurnal solar variation in cosmic ray meson intensity recorded in southerly and northerly directions at high altitudes 04 p0574 A66-13840
- Comparison of diurnal variations of ionization level in F region at geographically and geomagnetically conjugate stations in Arctic and Antarctic 04 p0516 A66-13851
- Quiet diurnal solar variations and relation to ionospheric parameters 04 p0516 A66-13852
- Current system of solar disturbed diurnal variations of magnetic field at high latitudes in terms of dynamo theory, taking into account forward and Hall conductivities 04 p0516 A66-13854
- Diurnal variation of cosmic radiation of intermediate energies measured at Earth attributed to particle removal due to scattering by magnetic irregularities 04 p0575 A66-14181
- Thermal maps of Murray about Venus atmosphere statistically analyzed into solar effects, latitude variations and limb darkening 04 p0579 A66-14450
- F-layer behavior over Genoa-Monte Capellino noting diurnal and seasonal variation, solar activity, nighttime concentration, spread-F, ionospheric and geomagnetic perturbations 05 p0671 A66-14982
- Increased diurnal amplitude in density of thermosphere between 200 and 300 km for decreasing solar activity 05 p0671 A66-15019
- Day-to-day variability of terrestrial magnetic daily variation, establishing morphology of different types 05 p0673 A66-15042
- Airborne ionospheric probes on both sides of magnetic equator at low African latitudes during equinoctial and solstice periods, obtaining daily behavior of F layer 05 p0674 A66-15113
- Cosmic ray 27-day variations using periodograms, with measured data processed continuously from 1957 to 1964 05 p0753 A66-15393
- Stellar diurnal variation determined during reduced solar activity from crossed-telescope and neutron monitor data 05 p0754 A66-15396
- 27-day changes in solar diurnal variation from 1957 to 1958 based on neutron component data, noting modulation of cosmic ray anisotropy 05 p0754 A66-15402
- Least squares method to determine diurnal lunar tide fluctuations from observations of Pulkovo, Greenwich and Tokyo Time Services 06 p0954 A66-16426
- Azimuthal measurements of cosmic ray variations at Yakutsk, U.S.S.R. 06 p0949 A66-16584
- Soviet and other literature on diurnal variations of cosmic ray intensity used for analysis of electromagnetic conditions in outer space 06 p0949 A66-16587
- Cosmic ray intensity and geomagnetic field changes induced by electric current systems excited in ionosphere, noting seasonal changes in diurnal variations 06 p0950 A66-16596
- Spherical harmonic analysis of diurnal surface pressure oscillation indicates that it can be represented by wave traveling westward with Sun 07 p1027 A66-17224
- Solar modulation and geomagnetic effects on cosmic rays, noting daily variation and rigidity spectrum 07 p1122 A66-17990
- Intensity variations and effective primary spectrum for mesons observed at approximate 40 mwe underground at Hobart, Tasmania, Australia 07 p1122 A66-17991
- Cosmic ray modulation by interplanetary magnetic field indicated by dependence of secular, 27-day and diurnal variations on solar activity 07 p1124 A66-17999
- Frequency distributions of characteristics of daily variation of cosmic ray intensity with solar activity from 1958 to 1962 07 p1125 A66-18006
- Phase shift and amplitude computation for cosmic ray diurnal oscillation, using autocorrelation analysis methods 07 p1126 A66-18007
- Atmospheric diurnal variation investigated, using temperature controlled high-counting neutron and meson monitors 07 p1126 A66-18008
- Fluctuation of ratio of yearly average amplitudes of meson-to-neutron diurnal variation owing to variability of energy dependence of cosmic ray anisotropy 07 p1126 A66-18009
- Cosmic ray meson intensity diurnal variations measured, using neutron monitor and Geiger counter telescope 07 p1126 A66-18010
- Periodical and quasi-periodical cosmic ray variation according to data of worldwide network of stations, using crossed telescope 07 p1127 A66-18013
- Diurnal intensity time variation of cosmic ray neutrons compared with relative number of sunspots observed 07 p1127 A66-18014
- Cosmic ray diurnal variation near geomagnetic poles measured over declining phase of solar cycle, using neutron monitor data 07 p1127 A66-18015
- Temperature changes in entire atmosphere and effect on diurnal variation of meson component of cosmic rays 07 p1129 A66-18025
- Day-to-day changes in energy spectrum of daily variation of cosmic ray intensity at middle latitude and equator for IGY 07 p1131 A66-18236
- Spherical harmonic analysis of diurnal surface pressure oscillation 08 p1246 A66-18800
- Diurnal and semidiurnal variation of cosmic ray intensity investigated with aid of selective frequency filters 08 p1283 A66-19021
- Sporadic E layer at middle and low latitudes and relation to solar quiet daily variations in ionosphere 08 p1213 A66-19027
- Space-time distribution of perturbed solar diurnal variation at high latitudes during IGY 08 p1214 A66-19033
- Scintillation observations of satellite signals noting latitude, diurnal, seasonal and sunspot cycle variations 08 p1183 A66-19208
- Diurnal variations of strength and polarization of VHF signals from synchronous Early Bird satellite 08 p1185 A66-19537
- Solar diurnal and semidiurnal variations in neutron component of cosmic rays obtained from worldwide network from 1959 to 1962 08 p1285 A66-19775
- Harmonic analysis of diurnal changes in critical frequencies of F-2 layer as function of season and solar activity 08 p1285 A66-19777
- Spatial and time variations in ionospheric absorption at long wavelengths for small elevations of Sun and at nighttime 08 p1220 A66-19778
- Earth daily diurnal rotation rate variation, assuming solar corpuscular flux composition of plasmoids possessing quasi-force-free magnetic fields 08 p1220 A66-19787
- Solar diurnal variation data used to determine parameters of phase-amplitude modulation of periodic cosmic-ray variations 08 p1286 A66-19788
- Graph for system of currents of solar diurnal variation during IGY winter season, considering night and evening vorticity individually and using coordinate system 08 p1221 A66-19797
- Spectra of solar, diurnal and secular variations, relation to modulation of cosmic rays by interplanetary magnetic field 09 p1433 A66-20216
- Effect of atmospheric temperature changes on diurnal variation of meson component, using temperature coefficient and crossed telescopes methods 09 p1439 A66-20219
- Latitude variation of second harmonic of diurnal variation of cosmic rays, considering curvature of particle trajectories in geomagnetic field 09 p1439 A66-20222
- Diurnal variation of aurora zone geophysical disturbances, examining VLF phenomena including noise, aurora and ionospheric absorption 09 p1372 A66-20375
- Geomagnetic diurnal-variation in north polar region with corrected geomagnetic latitude 09 p1373 A66-20385
- Sidereal component of diurnal variation of cosmic ray intensity 09 p1442 A66-20461
- Diurnal variation of zodiacal light at north celestial pole measured at 5300 angstroms 09 p1374 A66-20891
- Energy spectrum of auroral zone X-rays, noting electron precipitation and diurnal pattern for occurrence of bremsstrahlung 10 p1599 A66-21145
- Integrated electron content of ionosphere determined from measurements of polarization angle received from Syncom III transmissions, presenting mean diurnal variation 10 p1528 A66-21148
- Harris and Priester model used to compute amplitude of diurnally varying component of horizontal pressure acceleration, showing increase with altitude 10 p1529 A66-21150
- Diurnal properties of horizontal geomagnetic micropulsation field in New Zealand, noting variation of period, field rotation and direction of oscillating vector 10 p1529 A66-21152
- Longitudinal asymmetry of trapped energetic electron intensities attributed to lowering of mirror points in South African anomaly 10 p1599 A66-21160
- Diurnal changes in total ionospheric electron content measured, using Randle Cliff antenna 10 p1530 A66-21162
- Diurnal variation of outer radiation belt of energetic trapped electrons and relationship to magnetic activity 10 p1600 A66-21163
- Variation of IR emission from Mars surface with Mars local time in terms of diurnal temperature variations, including atmosphere effect, results suggest low thermoconductivity 10 p1604 A66-21201
- Dependence of extent of noon bite-out on geographic and magnetic coordinates on worldwide basis, noting variation of distortion parameter for diurnal variation of F-2 layer 10 p1533 A66-22061
- Correlation coefficients for daily ranges of horizontal component of quiet day diurnal magnetic variation 11 p1695 A66-22370
- Noncyclic variation during magnetically quiet days, examining seasonal changes in geomagnetic field value at night during IGY 11 p1696 A66-22420
- Geographic distribution of solar daily variations of magnetic field during quiet days determined by coordinate



system 11 p1696 A66-22421

Solar diurnal and semidiurnal variations during Forbush decreases based on neutron recordings, noting near and distant source 11 p1762 A66-22427

Ozone photochemistry in atmosphere containing hydrogen, calculating equilibrium vertical distribution, rate of formation of hydroxyl, diurnal variation, etc 11 p1700 A66-23138

Upper atmospheric diurnal tide determined via sodium vapor trail measurements 11 p1701 A66-23146

Existence of significant latitudinal variation in density from 200 to 800 km 12 p1868 A66-23556

Cosmic ray variations analysis based on IGY and IGC data, discussing diurnal variations, cosmic ray burst, Forbush effect and existence of interplanetary magnetic field and of solar magnetic traps 12 p1940 A66-24161

Cosmic ray variations and solar corpuscular stream in interplanetary space during March 1958 magnetic storm 12 p1940 A66-24164

Stellar-diurnal variations in cosmic ray intensity, recording vertically falling particles with telescope and cross telescope 12 p1942 A66-24175

Anisotropy of weak cosmic ray bursts studied by examining diurnal variations for days with increased solar flare activity 12 p1942 A66-24178

Solar-diurnal cosmic-ray variations analyzed, showing that averaging observational data over worldwide network of stations leads to large errors 12 p1943 A66-24183

Corrections of sight-line velocities for Earth diurnal rotation and annual revolution in observations of Sun 12 p1949 A66-24246

Diurnal and seasonal altitude variations of E and F layers analyzed for geomagnetic activity from rocket measurement of electron concentration 12 p1869 A66-24269

Fluctuations in diurnal variations of ionization of F-2 layer interfering with radio wave propagation determined by series expansion 12 p1869 A66-24270

Longitudinal variations of various characteristics of F-1 layer compared for periods of high and low solar activity 12 p1869 A66-24271

Vertical measurement of ionospheric absorption at continuously varying frequency, showing diurnal variation of absorption 12 p1870 A66-24289

Statistical-probability determination of lunar-solar daily and seasonal magnetic variations and geomagnetic effects 12 p1951 A66-24463

Contour maps of diurnal changes in magnetic elements provided by observatory tabulations of mean hourly values of mean monthly days 12 p1873 A66-24836

Lunar tidal effect on daily and monthly variation of polarized sky light 12 p1874 A66-24844

Mars atmosphere and ionosphere analyzed by measuring effect on radio occultation of planet, determining shape, atmosphere density profile, diurnal variations, etc 13 p2178 A66-25235

Meteorological rocket wind observations, noting diurnal oscillations and tidal characteristics 13 p2122 A66-26131

Solar radio observation at 600 mc frequency during 1961 at French station, noting flux density and solar daily variation 13 p2188 A66-26322

Correlation between amplitudes and phase angles of first two harmonics of monthly mean Sq and solar activity for period 1905-1960 14 p2376 A66-27395

Diurnal variation of average energy spectrum of auroral X-rays observed from balloon flights, assessing effect of atmospheric absorption 14 p2376 A66-27614

Density variation observed from satellites in upper atmosphere 14 p2284 A66-27619

Quiet solar diurnal variations of geomagnetic field at middle and low latitudes during IGY to determine coordinate system and equatorial electrojet 14 p2286 A66-28077

Autocorrelation functions of random processes, determining parameters and amplitude of diurnal variations in cosmic ray

intensity 14 p2377 A66-28086

Relation between irregular variations in magnetic field intensity with sporadic E region containing current system responsible for quiet solar diurnal variation 14 p2287 A66-28096

Measuring devices and observational methodology used in determining time variant and cyclic variations in cosmic ray occurrence 15 p2573 A66-28518

Solar system geometric effect in diurnal, annual and semiannual cosmic ray variations 15 p2575 A66-29082

Diurnal and seasonal variations of sporadic layer in auroral zone 15 p2487 A66-29098

Shape and location of diurnal bulge in upper atmosphere, analyzing density and temperature distribution at high latitude from satellite drag data 15 p2490 A66-29821

Winter anomaly of nondeviative ionospheric absorption of radio waves and relation to diurnal, seasonal, local and solar cycle variations 15 p2490 A66-29943

Diurnal and semidiurnal oscillations in atmospheric density, temperature, pressure and wind in subtropical Southern Hemisphere 15 p2491 A66-29964

Free sodium atom distribution in upper atmosphere related to diurnal and nocturnal variation 15 p2491 A66-30018

Rocket measurement of diurnal variation of ozone profiles above maximum concentration level 15 p2495 A66-30058

Lower atmospheric diurnal variations in air temperature, directional wind velocity and gradients during clear anticyclonic weather 16 p2742 A66-30774

Diurnal oscillation in zonal and meridional winds determined, using harmonic analysis on data obtained from meteorological rocket soundings 16 p2699 A66-31641

27-day cycle in diurnal variation of amplitude of meson component of cosmic radiation based on 20 years observation 16 p2795 A66-31692

Equatorial ionospheric drifts observed at Ibadan, Nigeria, during solar activity minimum, and relation to diurnal variation of sunspot cycle and drift velocity variations in E and F region 16 p2700 A66-31759

4-second summertime micropulsation band at College, Alaska 17 p2918 A66-32526

Diurnal variation of hydrogen atom concentration at base of exosphere, including effects of lateral flow of gas around Earth 17 p2919 A66-32996

Ionospheric electron content determined from satellite measurements, noting seasonal and diurnal variation of content and utilization of Faraday fading for measurements 17 p2920 A66-33069

Seasonal width and current intensity of equatorial electrojet at different longitudinal zones noting diurnal variations, electrojet parameters, etc 17 p2922 A66-33352

Lunar semidiurnal tides in ionosphere over Puerto Rico determined from electron density profiles for heights between 150 and 300 km 17 p2923 A66-33362

Atmospheric contribution to diurnal variation of cosmic ray meson intensity at Deep River, Canada 17 p2994 A66-33429

Contribution to dependence of variation of unperturbed ionospheric F-2 critical frequencies on season and solar activity 18 p3105 A66-34097

Vertical and horizontal structure of negative eigenvalue modes of diurnal atmospheric oscillation 18 p3107 A66-34524

Cosmic radiation, interplanetary magnetic field, solar proton propagation long-term /solar cycle/ modulation of intensity, Forbush effect and daily intensity variation 18 p3175 A66-34741

Sidereal time variation of cosmic rays explained by diffusion in galactic arm for colinear magnetic field and proximity of solar system 18 p3178 A66-34762

Solar and sidereal daily variations of cosmic ray intensity at depth of 60 mwe underground in London 18 p3178 A66-34763

Two-way sidereal anisotropy vs seasonal modulation of solar daily variation 18 p3178 A66-34764

Isolation of sidereal-diurnal variations in cosmic ray intensity 18 p3179 A66-34765

Diurnal component of solar daily variation recorded at low latitude station by east and

west pointing telescopes during periods of maximum and minimum solar activity 18 p3181 A66-34777

Cosmic ray anisotropy induced by solar wind and magnetic field irregularities 18 p3181 A66-34779

Solar diurnal variation of cosmic ray intensity and anisotropy in interplanetary space 18 p3181 A66-34781

Semidiurnal anisotropy of cosmic radiation observed from neutron monitor data treated by numerical filter techniques 18 p3182 A66-34783

Diurnal variation of cosmic radiation in Axford-Parker model of diurnal anisotropy, noting amplitude discrepancy with prediction 18 p3182 A66-34784

Diurnal variations of cosmic ray intensity by correlating phase difference and amplitude ratio of Zugspitze and Norikura neutron monitors 18 p3182 A66-34785

Local time of maximum in diurnal variation of cosmic ray neutron intensity and relative sunspot number 18 p3182 A66-34786

Solar-diurnal and semidiurnal variation in cosmic ray neutron component during last cycle of solar activity from 1957 to 1965 18 p3182 A66-34787

Parameters of solar diurnal variation determined from neutron monitor data from 1957 to 1958 18 p3183 A66-34788

Solar diurnal variation of nucleonic component of cosmic radiation from 1957 to 1962 18 p3183 A66-34789

27-day modulation of solar diurnal variation of cosmic ray neutron component 18 p3183 A66-34790

Spherical harmonic analysis to obtain latitude dependence of diurnal variations and changes with time during Forbush decrease 18 p3183 A66-34792

Convolution product theory applied to smoothing neutron monitor data of daily variations in cosmic ray intensity 18 p3186 A66-34808

First-order cosmic ray modulation, namely production by Sun, diurnal anisotropy, 11-yr cycle and Forbush decrease effect 18 p3186 A66-34810

Daily correction of meson diurnal variation for ground-level air temperature and barometric pressure effects 18 p3195 A66-34863

Energy spectrum of cosmic ray diurnal variation determined from IGY neutron monitor data by introducing upper energy cut-off parameter 18 p3195 A66-34864

Daily variations of cosmic ray distribution, examining effect of geomagnetic field, aperture, orientation and geographical position of counters 18 p3195 A66-34865

Simultaneous amplitude-phase modulation of periodic cosmic ray variations, examining properties of satellites produced by these variations for case of true waves 18 p3196 A66-34867

Effect of geomagnetic cavity field on cosmic ray threshold rigidity, using model of cavity field, finding cavity shape produces amplitude in diurnal variation of cosmic ray intensity 18 p3198 A66-34882

Solar radio activity in 1963, discussing daily flux density, mean variations, etc 19 p3458 A66-35467

Energy spectrum of auroral X-rays in range from 20 to 150 kev according to balloon measurements show remarkable diurnal variation 19 p3452 A66-35563

Turbulence coefficient and mean altitude of atmospheric boundary layer determined from diurnal temperature variations and wind profile 19 p3348 A66-35939

Ionospheric absorption measurement by A3 method in which field strength of distant CW transmitter is continuously recorded 19 p3351 A66-36359

Low and medium frequency absorption measurements at steep ionospheric incidence for demonstrating diurnal, annual and sunspot cycle changes in lower ionosphere 19 p3351 A66-36360

Diurnal and latitudinal variations in 6300 angstrom nightglow intensity determined along Pacific coast of South America, noting relation between location of antisolar point and equatorial midnight enhancement 19 p3352 A66-36628



CIRA 1965, COSPAR International Reference Atmosphere covering mean atmospheric structure variations from 30 to 100 km and from 120 to 800 km 19 p3352 A66-36796

Diurnal cosmic-ray anisotropy in studying temporal independence of small scale irregularities in interplanetary magnetic field 20 p3630 A66-37302

Meteorological rocket measurements of diurnal oscillations of pressure and density in upper stratosphere and lower mesosphere 20 p3551 A66-37515

Sidereal diurnal variation of high-energy cosmic radiation, noting parameters of anisotropy coefficient, cosmic ray source distribution and air shower measurements 20 p3631 A66-37851

Dynamical effects of liquid nucleus of Earth in diurnal terrestrial tides 20 p3553 A66-38068

Statistical analysis of diurnal variation in southern boundary of aurora, HF backscatter records and geomagnetic latitude of dayside aurora 20 p3553 A66-38193

Statistical analysis of storm-time variation and daily disturbance variation in geomagnetic storms 20 p3658 A66-38230

High energy trapped electrons in outer zone for 27-day, diurnal and storm time variations 20 p3639 A66-38317

Costing of parallel route systems for supersonic traffic, examining diurnal traffic patterns, sensitivities to fuel requirements, sonic bang avoidance and layout of track systems 21 p3761 A66-38453

Solar diurnal and semidiurnal variations in neutron component of cosmic rays obtained from worldwide network from 1959 to 1962 21 p3809 A66-38771

Harmonic analysis of diurnal changes in critical frequencies of F-2 layer as function of season and solar activity 21 p3809 A66-38773

Spatial and time variations in ionospheric absorption at long wavelengths for small elevations of Sun and at nighttime 21 p3732 A66-38774

Earth daily diurnal rotation rate variation, assuming solar corpuscular flux composition of plasmoids possessing quasi-force-free magnetic fields 21 p3733 A66-38783

Solar diurnal variation data used to determine parameters of phase-amplitude modulation of periodic cosmic-ray variations 21 p3809 A66-38784

Graph for system of currents of solar diurnal variation during IGY winter season, considering night and evening vorticity individually, using coordinate system 21 p3733 A66-38793

Winter variability of electron number density and collision frequency in lower ionosphere measured, using partial reflection method 22 p3906 A66-39950

Seasonal, diurnal and latitudinal variations of electron density distributions in topside of ionosphere as revealed by Alouette I satellite 22 p3909 A66-39974

Diurnal variation in electron densities and temperatures in F region above Puerto-Rico, using backscatter measurements 22 p3910 A66-39978

Latitudinal and diurnal variations of ionospheric electron content near auroral zone in winter from Faraday rotation data 22 p3911 A66-39985

Dependence of diurnal cosmic ray variations on angle which is proportional to shortest distance from Earth to axis of corpuscular stream 22 p3974 A66-40757

Diurnal variation in principal direction of E and H vectors of Petropavlosk-Kamchatka K index of geomagnetic field in horizon and planetary relation 22 p3914 A66-40769

Geomagnetic activity and Earth heliolatitude effect on diurnal variation of cosmic radiation, based on IGY neutron component observations 22 p3974 A66-40775

Diurnal variations in sporadic E layer parameters during solar cycle based on Moscow observations 22 p3915 A66-40781

Diurnal cyclic intensity variations of atmospheric radio noise at stations widely spaced over globe 22 p3915 A66-40782

Steady pearl type oscillations in terrestrial electromagnetic field, noting role of diurnal and seasonal variations 22 p3915 A66-40784

Measures of electron production and loss and scale height of F-1 layer during summer solar minimum 22 p3916 A66-40808

Enhanced activity in ionospheric E region at Cape Hallett and Campbell Island for information on diurnal variation and sunspot cycle changes of overhead and auroral activity 22 p3916 A66-40809

Diurnal heating of ozonosphere near stratopause level results in diurnal temperature variation of 15 degrees C and development of tidal circulation in stratospheric wind field 22 p3916 A66-40874

Time dependent behavior of temperature and density in monoconstituent atmosphere under diurnal photoheating and cooling by conduction, analyzing effect of atmosphere rotation eastward 23 p4064 A66-41678

Comparison of various geomagnetic variations associated with corpuscular precipitation at South Pole, noting day-night effect 23 p4064 A66-41688

Morning minimum of probability of existence of sporadic E layer and connection with time of sunrise 23 p4065 A66-41831

Anisotropy of cosmic rays in N-S direction determined by comparison of intensity variations observed in Arctic and Antarctic regions 24 p4263 A66-42464

Asymmetric ring current belt consisting of symmetric ring current and superimposed partial ring current system as explanation for low latitude disturbance daily variation 24 p4199 A66-42588

Diurnal behavior of topside and bottomside spread F at equatorial latitudes and association with geomagnetic activity 24 p4200 A66-42591

Diurnal variation of ionospheric irregularities, using differential Doppler method for analysis of data transmitted by Beacon satellite 24 p4200 A66-42596

Daily and seasonal variation of long distance propagation related to horizontal ionospheric gradients, particularly height of layer on wave path 24 p4174 A66-42739

Emergence and diurnal and seasonal fluctuations of sporadic E layer 24 p4201 A66-42759

Tidal circulation system induced by stratospheric wind field perturbations via diurnal ozonospheric heating 24 p4203 A66-42985

Distribution of active periods of magnetic disturbances during day and variation as affected by contact of solar magnetic flux with magnetosphere 24 p4204 A66-43151

Seasonal and diurnal fluctuation of radio wave in ionosphere in connection with fading process of reflected signal 24 p4204 A66-43155

**DIVERGENT NOZZLE**

**SA CONVERGENT-DIVERGENT NOZZLE**

Plane or axisymmetric hypersonic ideal gas flow in divergent nozzle with parabolic wall shape 14 p2221 A66-28056

Shock wave speed behind convergent and divergent ducts for different pressures and taper angles 17 p2913 A66-33072

Shock wave motion in tubes of diverging or converging cross sections 23 p4149 A66-41503

**DNA**

**S DEOXYRIBONUCLEIC ACID /DNA/**

**DO-31 AIRCRAFT**

**S DORNIER DO-31 AIRCRAFT**

**DOCKING**

Rendezvous with orbiting vehicle from launch to final docking including block diagram of homing system and techniques for matching velocities 03 p0433 A66-13284

Docking of logistics vehicle to space station investigated, using airbearing postimpact dynamic docking simulator 08 p1303 A66-18808

Full-scale prototype docking mechanism design and evaluation tests in rendezvous simulator 10 p1612 A66-21932

Rendezvous techniques and mission requirements involving space docking for transfer of personnel to and from manned space and lunar laboratories 16 p2812 A66-31683

**DODGE SATELLITE**

DODGE satellite will be capable of two- and three-axis gravity-gradient stabilization at near synchronous altitude, using moment-of-inertia distributions and libration

damping 21 p3820 A66-38860

**DOG**

Myocardiograph study of dogs leading to development of flight-rated vibrophonocardiographic system for monitoring cardiac dynamics in flight environment 17 p2924 A66-32191

**DOLPHIN**

Form and swimming characteristics of dolphin applied to design of high-speed commercial aircraft and VTOL aircraft 19 p3279 A66-36049

Dolphin body design for integrating resistance and propulsion mechanisms 19 p3279 A66-36050

**DOMAIN WALL MOTION**

High energy subdivided walls origin in silicon-iron suggested by reverse domain nucleation 10 p1582 A66-21887

Properties of high field domain in long samples of gallium arsenide, determining domain velocity and amplitude, using surface potential probe 10 p1584 A66-22074

Model technique calculation of electrostatic domains in two-valley /GaAs/ semiconductors 10 p1586 A66-22092

Coercive force for Bloch wall displacement of thin magnetic films coupled with stripe domain neon-iron films 11 p1758 A66-23359

Domain structure of partially oriented thin permalloy films analyzed through appearance of adjoining 180 degree walls of equal contrast and by electron microscopy 12 p1934 A66-25029

Approximate solution of micromagnetic equations for Neel-type domain wall in multiple films 14 p2351 A66-26887

Domain wall mobility effect on multilayer magnetic thin films consisting of permalloy layers separated by silicon oxide layers 14 p2351 A66-26888

Multilayer composite magnetic thin films used to constrain domain walls to localized region 14 p2351 A66-26889

Energy and width of domain walls in double films 14 p2351 A66-26891

Magnetostriction, negative anisotropy and chainlike domain walls along line defects in thin permalloy films 16 p2776 A66-30803

Nonuniform motion of high field domains in Gunn effect including steady and nonsteady state properties of formation stage 18 p3077 A66-34076

Field and charge density distributions in semiconductor with hot electrons, showing domain movement type oscillations due to stationary wave propagation 20 p3617 A66-37555

**DONNELL EQUATION**

Improved Donnell equations for concentrated load of circular cylindrical shell 16 p2823 A66-31717

Elastic stability of thin walled circular cylindrical shells in torsion, applying Galerkin method to Donnell equations for critical stresses 18 p3258 A66-34648

Comparison of characteristic roots arising from Fluegge and Donnell theories, when certain amount of axial prestress is imposed on circular cylinder 19 p3474 A66-36345

Stress analysis of elastic cylindrical shell perforated by rectangular cut-out and governed by Donnell equation 20 p3673 A66-38272

**DONOR**

Donor concentration in semiconductor at which hyperfine structure of spin absorption lines vanishes 04 p0564 A66-14250

Channel conductance measurements on silicon power rectifiers and midgap donor and acceptor detection on oxidized and lacquered rectifiers 08 p1189 A66-18664

Green emission lines from solution-grown p-n junctions in GaP diodes doped with shallow donors and acceptors 14 p2251 A66-27231

**DOPING**

Controlled phosphorus diffusion into silicon from phosphorus pentoxide vapor using red phosphorus as source, noting relations of resistivity-surface concentration to pressure temperature 02 p0275 A66-11872

Specific heat evidence for gapless superconductivity, examining experimental results on lanthanum doped with magnetic impurity gadolinium 09 p1420 A66-20053

Doping techniques for epitaxial growth of silicon and germanium



- layers 12 p1832 A66-23933  
Thermal expansion coefficient of doped germanium, noting correlation between impurity used and coefficient 14 p2368 A66-28244  
variation 14 p2368 A66-28244  
Controlled doping of germanium layers during evaporation, noting behavior differences for p-and n-type impurities and concentration dependence 19 p3434 A66-35344  
Photoluminescence measurements on silicon doped gallium arsenide for detection of compensation in shallow surface layers 19 p3436 A66-35430  
Electron conduction and phosphorus doping effects on room temperature and cryogenic electron spin resonance in n-type silicon 21 p3797 A66-38752  
Gold doping effects on recovery time of phosphorus, boron and arsenic impurity gaseous-diffused junction diodes and estimated gold recombination center densities 22 p3873 A66-39749  
IR absorption band growth and decay in spectra of oxygen-doped Si irradiated with fast neutron 22 p3962 A66-40085  
Neutron activation analysis of sodium dopant concentrations and distributions in lead telluride thermoelectric materials during couple operation in vacuum and argon atmosphere 24 p4247 A66-42109  
Ideal curves of metal oxide semiconductor capacity and surface potential computed for silicon and oxide thickness and doping as parameter 24 p4259 A66-43103
- DOPPLER EFFECT**  
**SA STELLAR DOPPLER SHIFT**  
Doppler effects of plasmas in semiconductors in microwave field, examining beat frequency relationship to plasma velocity 01 p0120 A66-10514  
Kinetic temperatures derived from Doppler width of airglow 5577 angstroms /OI/ line measured with Fabry-Perot interferometer 02 p0221 A66-11503  
Doppler shift and distortion of key-modulated signals in radio links with moving transmitter and receiver 02 p0191 A66-11751  
Errors in Doppler system determination of ground speed and improvement trends in wider application 02 p0258 A66-12044  
Velocity distribution in plasma jet by Doppler shift on spectral lines 03 p0403 A66-12972  
Functional characteristics of Navy Doppler tracking system and satellites used for geodesy, noting data reduction procedures and system tests 04 p0514 A66-13610  
Difference in Doppler shifts of radio waves emitted at various frequencies by satellite Elektron I radio station, plotting electron concentration dependence on altitude 04 p0515 A66-13837  
Frequency spectrum of large positive and negative Doppler shifts in VLF signals in whistler mode of propagation 04 p0517 A66-14182  
Line broadening from Stark effect and Doppler effect for plasma diagnostics 04 p0553 A66-14193  
Continuous recording of CW transmission frequency M.S.F. Rugby permits study of effects of traveling ionospheric disturbances on phase height of reflection levels of both magnetoionic components 04 p0488 A66-14379  
Doppler effect discussing relativistic form, transmission in dispersive media, broadening of spectral lines, black body radiation, rocket and satellite tracking, navigation and application 04 p0546 A66-14383  
Velocity measurements of electron front in electromagnetically generated T-tube shock waves made with microwave interferometer 04 p0558 A66-14479  
Evershed effect in inactive isolated symmetrical spot during passage across solar disk 05 p0758 A66-14773  
Electron density variation effect on Doppler shift of satellite signal reflections from ionization irregularities in ionosphere 05 p0634 A66-15265  
Simultaneous measurement of multipath and Doppler spread in real time involving fading transmission media such as HF and troposcatter [IEEE PAPER CP 65-524] 06 p0830 A66-16336  
Error probability limitations caused by multipath and Doppler smear in Kathryn modem 06 p0831 A66-16339
- Doppler broadened Cv spectral line from theta pinch and microscopic plasma velocities by reducing axial motion effect 07 p1086 A66-17654  
Doppler frequency shift and effect on single-sideband HF communication systems for supersonic transport 07 p1001 A66-17699  
Accuracy of Doppler navigational system obtained from ground information accumulated over 500 North Atlantic crossings 07 p1071 A66-17728  
Error of airborne Doppler navigation system 07 p1073 A66-17768  
Frequency-dependent ionospheric refraction effects on Doppler shift of satellite signals 08 p1181 A66-18714  
Artificial satellites detected by influences on ionosphere through 20-mc WWV bursts 08 p1181 A66-18750  
Doppler effects of injected carriers of semiconductor detected in microwave fields, used to measure semiconductor plasma drift velocity 08 p1270 A66-19060  
Thermal phase noise and VCO effects at ground receiver output of coherent two-way Doppler communication system 08 p1304 A66-19133  
Electro-optical attitude and velocity sensors for interplanetary navigation and stellar aberration and Doppler shift measurements 08 p1252 A66-19502  
Complex Doppler effect in dense cold magnetized plasma 09 p1343 A66-20339  
Accurate calibration of Doppler winds for use in computation of mesoscale wind fields 09 p1399 A66-20728  
Relation between height-time distribution of electron concentration and inhomogeneous formations of outer ionosphere 09 p1377 A66-21001  
Worldwide navigation system based on measurement of Doppler shift of stable signals transmitted from orbiting satellites, noting refraction, ship motion, air drag, timing, etc 10 p1554 A66-21512  
Doppler shift measurements using low resolution monochromator to determine mass motion in plasmas [AIAA PAPER 66-177] 11 p1735 A66-22213  
Curves of difference in Doppler shift in observations of transmitter of Elektron I satellite, noting fluctuations in electron concentration 11 p1762 A66-22409  
Critique of local ionospheric electron concentration determined by dispersion method with aid of satellite and new ionization maximum 11 p1697 A66-22428  
Substantiating possibility of determining local electron concentration by dispersion method with aid of satellites and new ionization maximum 11 p1697 A66-22429  
Observable properties of normal relativistic world models and steady state world model defined by parameters depending on cosmological constant and present mean density of universe 12 p1946 A66-23652  
Relative geodetic location by measurement of differential Doppler shift of radio signal 12 p1819 A66-24611  
Source function with large Doppler variable 13 p2174 A66-25481  
Wide angle Michelson interferometer for measuring Doppler temperature from width of 5577 angstrom atomic oxygen line in nightglow and aurora 13 p2128 A66-25799  
Spectral energy distribution and Doppler broadening of Rayleigh light scattered from hydrogen and argon gas at low density, using Fabry-Perot interferometer 13 p2133 A66-26169  
Optical- and IR-maser spectroscopy of inhomogeneously broadened resonances, using gas lasers 13 p2100 A66-26196  
Doppler frequency changes in vertically incident and reflecting sounding wave associated with geomagnetic disturbances yields information on ionospheric electric field 14 p2234 A66-26856  
Laser Doppler velocimeter for measuring localized flow velocities in liquids 14 p2306 A66-27053  
Spectral line broadening due to collisions in stimulated Raman effect 14 p2309 A66-27942  
Clear air turbulence detection with optical radar, using spectral analysis of backscattered Doppler-shifted light particle formation mapping via correlates of rough flying conditions 15 p2450 A66-28920  
CAT detection from Doppler shift in laser light backscattered from atmospheric aerosol 15 p2500 A66-28930  
Navy navigation satellite system developed by APL, using Doppler frequency measurements for navigation fix 15 p2536 A66-30001  
Beacon observations of differential Doppler and Faraday effects from analysis of signals emitted by Explorer XXII satellite 15 p2453 A66-30069  
Digital measurement of differential Doppler effect using transposition of phase relation of two HF signals into audiofrequency band 15 p2453 A66-30070  
Velocity distribution function of helium atom measured, using Doppler profile of helium line 16 p2701 A66-30377  
Total electron content of ionosphere in middle latitudes, noting results of satellite Doppler measurements, effect of solar radio noise flux, etc 16 p2694 A66-30706  
Altitude-time distribution of electron concentration, noting satellite measurements of ionospheric inhomogeneities and difference in Doppler shifts of coherent radio waves emitted by Electron I satellite 16 p2696 A66-30920  
Excitation of backward Doppler shifted cyclotron radiation in magnetoactive plasma by electron stream 16 p2761 A66-30921  
Doppler shift, velocity and line width measurements for mass motion in plasmas 17 p2925 A66-32488  
Upper atmospheric temperature measurement from Doppler line widths of atomic oxygen auroral and nightglow emission, using Michelson interferometer 17 p2919 A66-32993  
Frequency instability induced velocity error measurement in two-way coherent Doppler system 17 p2895 A66-33112  
Doppler navigation system accuracy improvement and evaluation of inertial navigator with steering computer 17 p2954 A66-33215  
Radio noise bursts from Jupiter at decimeter wavelengths noting Cerenkov emission, Doppler-shifter cyclotron emission and escaped-whistler models 18 p3225 A66-33550  
Doppler shift and high velocity mirror translation effects on mutual optical coherence function of gas laser Michelson interferometers 19 p3354 A66-35387  
Laser application for vibration measurement utilizing Doppler shift produced on wave reflected from surface vibrating normal to beam path 19 p3356 A66-35673  
Doppler shift measurements to investigate plasma rotation in theta pinch 19 p3414 A66-36512  
Total electron component of ionosphere column between satellite and Earth calculated, using differential Doppler effect 19 p3361 A66-36654  
Radio-observation station functions, observed satellite signals from beyond horizon and Doppler curve deformation 20 p3552 A66-37845  
Doppler effect on emission spectrum and energy of moving oscillator and intensity of surface wave excited by it 20 p3519 A66-37995  
Central Telecommunications Laboratory 882 P arithmetical airborne computer 20 p3523 A66-38013  
Two-dimensional time-space analysis of Doppler-effect-like phenomena in refraction and reflection of waves propagating through moving boundary between two media 21 p3706 A66-39574  
Ground state resonance, noting absence of Doppler broadening of signals in forward scattered light 22 p3931 A66-39810  
Quasi-stellar sources as local objects moving with velocities close to speed of light, noting transverse Doppler effect leads to expectation of fewer blue shifts than red shifts 22 p3981 A66-40484  
Doppler frequency shift for radio waves radiating coherently from satellite in ionosphere, considering electron concentration and angles of refraction 22 p3869 A66-40779  
Satellite application in geodetic surveys



and navigation, noting measurement and tracking techniques 22 p3915 A66-40786

Invariant imbedding and scattering of light in one-dimensional medium with moving boundary, noting relaxation of photon emission and Doppler frequency shift 23 p4087 A66-41540

Optical heterodyne receiver antenna properties, noting effective aperture of capture cross section vs directional tolerance and detection of doppler shifts in liquid scattered coherent light 24 p4174 A66-42809

**DOPPLER RADAR**

**SA PULSED DOPPLER SYSTEM**

Doppler radar for aerial navigation noting decoupling of transmitter from receiver, velocity measurement within frequency spectrum, etc 02 p0256 A66-11896

Doppler radar performance in air navigation noting calibration error, dispersion, hole-altitude phenomena, etc 02 p0256 A66-11897

Satellite-based Doppler navigation system 03 p0333 A66-12461

Doppler radar systems design, operating principles and performance characteristics 03 p0389 A66-12468

Mesoscale wind structure revealed by Doppler wind soundings taken in lower 4.5 km of atmosphere at 12-minute intervals in snowstorm 04 p0541 A66-13668

Increasing detectability of signal in noise or in other interference, noting effect and functions of radar filter, antenna scanning, pulse to pulse IF and video 04 p0486 A66-14124

Graphical comparison of Doppler-shift advantage for Chirp, Siebert and frequency hopping pulse-compression techniques 06 p0825 A66-15982

Reduction of high residual time sidelobes for phase-coded pulse compression radar systems and technique for increasing ratio of peak to residual amplitudes 06 p0833 A66-16666

Radar systems with rotating optical disks, describing optical correlation techniques 06 p0834 A66-16729

Characteristic distortion of Doppler curves and radio signals of artificial satellite from behind horizon 07 p1000 A66-17209

Doppler radar accuracy investigation, noting wide distribution of systematic error 07 p1064 A66-17668

Evaluation of four different types of Doppler radar as long range self-contained navigation aid 07 p1065 A66-17669

Serviceability and accuracy of dual Doppler installation on Boeing 707-320C aircraft 07 p1065 A66-17674

Effect of Doppler on navigation system accuracy during North Atlantic flights by Air Canada 07 p1065 A66-17677

Relationship between self-contained systems and fixing aids in light of recent subsonic jet and Doppler-system experience 07 p1066 A66-17679

Doppler equipment including planar-array antennas, varactor-multiplier sources, etc, evaluated for third generation Decca series 07 p1068 A66-17703

Up-dating of self-contained navigational aids such as Doppler, inertial and Doppler/inertial systems 07 p1070 A66-17717

Doppler-inertial system combination applied to avoid deterioration of navigational accuracy with time 07 p1070 A66-17719

MOA/BOAC Doppler/Loran A trials 1963-64, discussing navigational accuracy during transatlantic flights 07 p1072 A66-17759

Accuracy of navigation techniques for North Atlantic flights evaluated, based on Loran A and Doppler/GM compass automatic dead reckoning system 07 p1072 A66-17760

Self-contained Doppler Navigation System performance over three-year operation 07 p1074 A66-17776

Precision Doppler VOR installation in West Germany 07 p1075 A66-17781

AD560 Doppler Radar sensor and computer in Boeing 707-138 aircraft 07 p1076 A66-17794

Evaluation trials of Doppler-based primary navigation system as short-distance navigational aid 07 p1077 A66-17801

Evaluation of AD560 Doppler by Qantas, discussing ground-speed run-down problem,

radome design, along-track error and low-altitude accuracy over land and sea 07 p1078 A66-17811

Reduction of signal power in X-band CW aircraft radar echo 08 p1181 A66-18718

Dynamic Navigation System /Dynav/ for providing aircraft velocity and position-fixing information from VLF Doppler range rates 08 p1252 A66-19507

Classical spectroscopic binary star orbit determination techniques to provide orbital elements for lunar satellite tracked by Earth-based Doppler radar [AIAA PAPER 66-40] 08 p1298 A66-19727

Detectability of signal in noise of range gated MTI radars, with or without pulse lengthening in conjunction with Doppler filtering 09 p1342 A66-19951

Height measurement from Doppler navigation, examining accuracy of pressure altimeter 09 p1381 A66-20429

RADINT rocket tracking station combines Doppler and interferometer techniques, eliminating need for three or four separate ground stations 09 p1355 A66-20588

Observations of vertical motion and particle size of growing thunderstorm moving overhead, using pulsed Doppler radar 10 p1552 A66-21277

Doppler radar techniques for velocity measurement, citing military and industrial application 11 p1707 A66-23061

Short term frequency stability affecting resolution and range of Doppler radar, noting system and circuit requirements when operating under severe vibration and acoustic environment 12 p1815 A66-24133

FM and AM noise spectra of low-noise microwave tubes, solid state klystrons and solid state chains 12 p1835 A66-24135

Clear air turbulence detection with laser Doppler optical radar [AIAA PAPER 66-374] 12 p1818 A66-24498

Doppler automatic air navigation systems, discussing basic principles, operational limitations, cost/payload factor and future development 13 p2123 A66-25200

Continuous measurement of ionospheric winds based on observation of meteor trails 13 p2072 A66-25449

Effect of Doppler on navigation system accuracy during North Atlantic flights by Air Canada 13 p2125 A66-25864

Random error of drift measurements using airborne Doppler radar from observed drift output during short flight over fixed course, calculating rms values 13 p2125 A66-26449

Germanium mixer diodes encapsulated in miniature double-ended construction, examining fabrication, performance and applications 17 p2892 A66-32921

Classical spectroscopic binary star orbit determination techniques to provide orbital elements for lunar satellite tracked by Earth-based Doppler radar 18 p3234 A66-34596

Radar-updated inertial navigation of continuously-powered space vehicle during deboost phase of flight prior to lunar landing 20 p3596 A66-37221

Doppler radar measurements of wind velocity horizontal components variation in rain and snow, calculating time correlation and structural functions for neutral and unstable stratifications 21 p3760 A66-39358

Programmed oscillators to control Doppler tracking radar systems for space communications and radar astronomy 22 p3862 A66-39731

Doppler radar applied to atmospheric precipitation processes, noting drop size distribution in widespread rain, height-time sections of vertical air motion and maximum particle velocity, etc 22 p3942 A66-39737

Electron density profiles in D layer measured through Doppler shift on VLF signal propagating from ground up and received by rocket 22 p3907 A66-39957

Radar partial coherence theory for clutter construction relationship to radar cross section, waveform coding, output signal, mutual coherence function and random noise 23 p4037 A66-41312

Doppler frequency-measuring tracking system in which tracking filter or retuned heterodyne is used for definition of signal with unknown frequency 23 p4038 A66-41524

Doppler radar tracking system

measurement of impact drag coefficients for several water entry configurations 24 p4191 A66-42188

Laser Doppler velocimeter for gas and liquid flow velocity measurement 24 p4211 A66-42557

Air motion probe via Doppler radar, noting calculation of speed, direction and application to wind variance analysis 24 p4234 A66-42989

Velocity characteristics of clear-air dot angle echoes determined via Doppler radar measurements 24 p4234 A66-42990

X-band low power pulse Doppler radar and S-band weather radar for meteorological applications 24 p4176 A66-43045

**DORNIER DO-31 AIRCRAFT**

DO-31 VTOL transport design, specifications and testing, using direct jet lift for takeoff and transition to conventional flight 07 p0986 A66-17270

Do-31 V/STOL transport aircraft design including engine, wings, speed, rate of climb, etc 21 p3696 A66-39540

Do 31 system test stand including cockpit with instruments, fuselage frame, wing structure, etc 24 p4192 A66-42488

**DORNIER PARAGLIDER ROCKET**

Hot water rockets covering principle, design, advantages, testing techniques and performance capabilities 05 p0659 A66-14677

**DOSAGE**

**S RADIATION DOSE**

**DOSIMETER**

Small lightweight ion chamber dosimeter for monitoring radiation exposure to spacecraft crew members 05 p0676 A66-14632

Radiation dosimeters for SNAP-10A flight test to measure reactor leakage radiations throughout SNAPSHOT Agena orbital vehicle 12 p1876 A66-23675

Transistorized portable UV dosimeter for use in medicine, climatology, physiotherapy, meteorology and stimulated plant growth study 20 p3562 A66-38436

Polymer degradation dosimeter of polyisobutylene in heptane noting viscosity range effects, concentration change and molecular weight 21 p3739 A66-39383

**DOSIMETRY**

Book on problems in dosimetry and radiation protection 05 p0627 A66-15117

**DOUBLE BASE PROPELLANT**

Cast-double-base propellant mechanical behavior and failure during slow cooling and rapid pressurization of case-bonded rocket motors [AIAA PAPER 65-161] 12 p1934 A66-24704

**DOUBLE RESONANCE**

Lifetimes of orientation and alignment of excited atomic states examined in level crossing and optical double resonance experiments employing polarized light 11 p1740 A66-22969

Nonequilibrium population buildup and detection for IR solid state lasers and IR-optical double resonance in lanthanum chloride crystal 13 p2098 A66-26177

7P terms of excited chromium configurations examined, using level crossing and double resonance spectroscopy, noting core polarization 13 p2135 A66-26267

Double barrier transmission resonance in metal thin film triode 15 p2563 A66-28731

**DOUBLE-SIDEBAND RADIO COMMUNICATION**

Statistical properties of output of double-sideband receiver when nonlinear mechanisms at input admit unwanted double-sideband signals with Gaussian modulation 05 p0630 A66-14593

Double sideband capacitance and resistance modulation of systems and calculation of noise and amplification factors 16 p2666 A66-31561

**DOUGLAS DC-8 AIRCRAFT**

Flight testing of Phillips vertical reference inertial navigator on DC-8 aircraft 07 p1069 A66-17708

Correlation between clear air turbulence and aircraft electrical activity, describing corona discharges from DC-8 tail antenna 15 p2426 A66-28922

Douglas DC-8 super sixty series effect on airport requirements including noise level, runway problems and traffic [SAE PAPER 660281] 15 p2427 A66-29825



## DOUGLAS DC-9 AIRCRAFT

- DC-9 reliability program emphasizing simplicity improved proven components rather than completely new equipment 01 p0010 A66-10088
- DC-9 maintainability, simplicity and commonality of design with emphasis on reliability 01 p0129 A66-10092
- DC-9 aerodynamic design features and control systems [AIAA PAPER 65-738] 03 p0320 A66-12731
- Optimum operational influence on design of DC-9 cockpit 07 p0988 A66-17704
- DC-9 Douglas short-and medium-range air transport, discussing takeoff field length, fuel capacity, payload and landing-field length 12 p1800 A66-23754
- DC-9 maintainability, simplicity and commonality of design with emphasis on reliability 13 p2173 A66-26231

## DOUGLAS MILITARY AIRCRAFT

## S A-4 AIRCRAFT

## DOWN-CONVERTER

- Detection scheme for millimeter and submillimeter waves, utilizing system of quantum energy levels to down-convert HF radiation to microwave frequency 15 p2462 A66-29019

## DOWNRANGE MEASUREMENT

- Selection and development of guidance station at Gove, Australia, noting access routes, logistics problems, etc 21 p3721 A66-38643

- Requirements, functions and equipment of down-range guidance station for ELDO program in Australia 21 p3721 A66-38644

## DOWNWASH

## SA GROUND EFFECT

## SA LIFT AUGMENTATION

## SA WAKE

- Downwash corrections for wings with arbitrary sweepback in open and closed circular wind tunnels with base plate 21 p3694 A66-38936
- Rotor downwash angle and tunnel geometry effect on maximum size rotor that can be tested in closed throat wind tunnel [AIAA PAPER 66-736] 22 p3893 A66-40626
- Downwash angles behind rectangular wings of small aspect ratio calculated at subsonic velocities according to nonlinear theory 23 p4010 A66-41781

## DRAG

- SA BOUNDARY LAYER
- SA ELECTROSTATIC DRAG
- SA FRICTION DRAG
- SA INTERFERENCE DRAG
- SA MINIMUM DRAG
- SA PRESSURE DRAG
- SA SATELLITE DRAG
- SA SKIN FRICTION DRAG
- SA SUPERSONIC DRAG
- SA VISCOUS DRAG
- SA WAKE
- SA WAVE DRAG

- Drag of body of revolution with blunt base substantially reduced by mounting disk behind body with smaller diameter than body 05 p0606 A66-15059

- Contraction of satellite orbits due to atmospheric drag, extending theory to atmosphere with day-to-night sinusoidal variation with air density 07 p1132 A66-17256
- Equations of motion for Earth satellite indicate greater significance for atmospheric resistance than gravitational effect 07 p1139 A66-18190

- Long lifetime orbits about Mars affected by atmospheric drag, solar gravitational perturbations, planetary oblateness and other perturbations [AIAA PAPER 66-35] 08 p1289 A66-18987

- Probability characteristics of parameters of oscillating ellipse for satellites whose chief source of perturbation is atmospheric drag 11 p1766 A66-22232

## DRAG BALANCE

## S LIFT-DRAG RATIO

## DRAG COEFFICIENT

## SA LIFT-DRAG RATIO

- Satellite drag coefficient reevaluated in consideration of recent data on gas-surface interaction and atmospheric composition 05 p0760 A66-14941
- Pressurization effect on fuselage drag of Boeing 720 jetliner based on boundary layer measurement 05 p0606 A66-15077
- Flight test determination of parasite drag

- area and required power of Kawasaki Bell KH-4 single-rotor

- helicopter 07 p0988 A66-17525

- Parachute operation at high Mach numbers and dynamic pressures for reentry vehicle deceleration

- [AIAA PAPER 66-24] 07 p0989 A66-17888

- Flow separation, wake configuration and droplet motion in purified systems shadowgraphically analyzed 10 p1524 A66-21808

- Molecular collision effect on transitional drag on cylinder traversing rarefied gas at hypersonic Mach numbers, discussing departure from free flow 11 p1632 A66-22920

- Modified first-collision model theory that agrees with experimental data on drag coefficient of cylindrical bodies in flow of rarefied gases 11 p1633 A66-22921

- Drag force anemometer utilizing semiconductor strain gauges for measuring horizontal wind speed and direction [AIAA PAPER 66-337] 12 p1882 A66-24482

- Terminal reentry and dynamics evaluation computer program for small particles, using point-mass calculation during initial phase and determining drag coefficient [AIAA PAPER 66-380] 12 p1951 A66-24505

- Drag coefficient of gas flow in circular tube at transonic velocity 13 p2065 A66-26485

- Drag coefficient of spherical satellites at various heights, based on gas-surface interactions and atmospheric composition 14 p2382 A66-27617

- Drag coefficients and absolute atmospheric densities at high altitudes calculated, using spin and orbital decays of Explorer VI satellite conjugated with models of surface particle interaction 15 p2489 A66-29818

- Motion equations and Pontryagin maximum principle applied to space vehicle reentry trajectory optimization through independent control of lift and drag 16 p2809 A66-30884

- Flexible and rigid hinged hydrofoils noting behavior of configurations lift, drag, power input coefficients, etc 17 p2910 A66-32662

- Vekua method to solve Oseen form of Navier-Stokes equation for incompressible viscous fluid flow 18 p3097 A66-33712

- Drag coefficient of turbulent flow of electrically conducting liquid metal in MHD channels of round cross section 19 p3407 A66-36098

- Frequency of wake shedding from circular cylinder in water flow with values above critical Reynolds number, noting eddy generation and drag coefficient dependence on cavitation number 20 p3548 A66-38012

- Distance/time records, drag coefficients and Reynolds numbers of single freely-falling drops of pentane, heptane and benzene burning in cold atmosphere 20 p3626 A66-38044

- Flight performances of special small rockets with no cross wind conditions, noting drag coefficient effect 23 p4133 A66-41441

- Doppler radar tracking system measurement of impact drag coefficients for several water entry configurations 24 p4191 A66-42188

- DRAG DEVICE
- S BALLUTE

- DRAG EFFECT
- Orbital mechanics, examining problems relating to patched conics, perigee determination, eccentricity of satellite orbits and drag effect 05 p0767 A66-15754

- Conservation laws involving mass, momentum and energy applied to asymptotic properties of hypersonic flow 09 p1327 A66-20266

- Analogy between impulsive flow over circular cylinders and flat plates, and separated flow about lifting bodies moving at high angles of attack in subsonic and supersonic range [AIAA PAPER 65-395] 12 p1795 A66-23575

- Gravity turn trajectories through atmosphere including drag effects 20 p3657 A66-38181

- MEASURED aerodynamic characteristics of cone-cylinder-cone model using magnetic balance system, discussing techniques, errors and data 03 p0315 A66-12773

- Mesoscale eddies in wake of islands

- describing properties, characteristic parameters via Karman vortex street pattern, drag theory and empirical observation 07 p1061 A66-17365

- Aerodynamic drag moment of gyromotor operating in air, comparing calculated and experimental data 09 p1379 A66-20306

- Comparison of theoretical and experimental results for cylinder and flat strip models in near free molecular flow 11 p1692 A66-22926

- Drag measurement for grid of wires in rarefied gas slip flow and transition flow 11 p1633 A66-22927

- Aerodynamic drag torque on rotating sphere in transition regime, noting dependence of gas inertia on Reynolds number 11 p1635 A66-22935

- MHD drag of dielectric oscillating sphere in incompressible conducting fluid with uniform magnetic field aligned along axis of oscillation 15 p2553 A66-29689

- Aerodynamic gaseous drag torque on electromagnetically suspended isolated sphere rotating at high Mach numbers in rarefied transition regime from continuum to free molecule flow 20 p3492 A66-37473

- Drag force of flexible wire connection between aircraft and ship models and axis about which they are rotating 21 p3832 A66-39458

- Hypersonic flow, discussing heat effect on flow parameters, shock and motion equations, drag increase, etc 22 p3897 A66-39699

- DRAG REDUCTION
- Drag reduction for sailplanes, investigating adoption of laminar foil section 01 p0008 A66-11097

- Drag reduction measurements on porous cylindrical bodies with blunt nose and tail sections, using area suction [AIAA PAPER 65-561] 02 p0175 A66-11564

- Linearized supersonic theory for favorable thickness distributions and drag reduction for wings in supersonic flow [AIAA PAPER 65-716] 03 p0314 A66-12542

- Drag of body of revolution with blunt base substantially reduced by mounting disk behind body with smaller diameter than body 05 p0606 A66-15059

- Drag reduction for gliders, noting role of planform and warping of wing 05 p0607 A66-15200

- Drag decrease in glider aircraft noting wing profile, flow laminarization /boundary layer control/, landing flaps, tail, etc 05 p0607 A66-15200

- Longitudinal and transversal contours minimizing drag of slender homothetic body in hypersonic flow with Newtonian pressure distribution and constant skin-friction coefficient 06 p0802 A66-16911

- Optimum nose form determination for minimum drag in free-molecule flow of asymmetric body 11 p1635 A66-22937

- Ring wings to develop beneficial aerodynamic interference effects at supersonic speeds 13 p1995 A66-25590

- Transition delay and skin friction drag reduction by considering boundary layer flow over flexible aerodynamic surface [AIAA PAPER 66-430] 16 p2688 A66-31466

- Reynolds equations for two-dimensional uniform turbulent shear flow of Reiner-Rivlin fluid suggest drag reduction 22 p3896 A66-39671

- Limiting initial deceleration forces generated by supersonic decelerators, noting that decelerators deployed in wake region of body result in divergent wake and drag force reduction 22 p3845 A66-40595

- Pressure effects of flexible walls on boundary layer transition in turbulent pipe inlet flow 24 p4195 A66-42859

- DRAWING
- S MECHANICAL DRAWING

- DRIFT
- SA GYROSCOPIC DRIFT
- SA IONOSPHERIC DRIFT
- SA YAW

- Static drift in epitaxial planar silicon transistor choppers 01 p0035 A66-10208

- Dual transistors for noise and drift reduction in differential direct-coupled amplifier design 14 p2262 A66-28376

- Zero-level drift errors in telemetry 17 p2873 A66-31965



Temperature behavior of transistor using as reference equivalent temperature-drift sources at input of idealized drift-free transistor 18 p3088 A66-35041

Drift effect on diffusion spreading of plasma inhomogeneities in magnetic field, deriving expression for Fourier component potential and magnetic field perturbations 19 p3344 A66-35265

Fabrication methods for lithium drifted surface barrier silicon detectors, discussing lithium diffusion, stain etching, preparation for and final etch 20 p3535 A66-38417

Drift cyclotron instability observed in toroidal plasma 23 p4109 A66-42064

Chain code method of eliminating LF drift disturbance error in calculation of impulse-response function of time-invariant system 24 p4187 A66-42368

**DRIFT RATE**

Nocturnal auroral drift in meridional direction 01 p0064 A66-11163

Measuring drift velocities of mixed nitrogen ion population in nitrogen gas, noting need of ionization condition control and ion mass analysis 04 p0547 A66-13714

Soviet report on ionospheric structure variations, drift magnitude, velocity and direction 05 p0674 A66-15226

Semiconductor with dependence of drift velocity on electric field and containing region of negative differential mobility 06 p0850 A66-16444

Wentzel-Kramer-Brillouin calculation of exact solution of universal instability and drift approximation problem 07 p1089 A66-17958

Polarization and Alfvén wave attenuation in Doppler-like change in transverse wave velocity when drift current is passed parallel to magnetic field in solid-bismuth plasma 07 p1102 A66-18209

Hall current and Hall drift velocity in single crystal indium antimonide under electric and magnetic field 07 p1103 A66-18214

Ionospheric inhomogeneity movements in E and F-2 regions and height variation of drift velocity 08 p1215 A66-19052

Doppler effects of injected carriers of semiconductor detected in microwave fields, used to measure semiconductor plasma drift velocity 08 p1270 A66-19060

Vortex lines in superconductors, noting free energy of pure superconducting metal in presence of currents and fields for slowly varying drift velocities 09 p1415 A66-20007

Electric discharges in gases analyzed in terms of ion and electron drift velocity and ionization coefficient 10 p1558 A66-22057

Inhomogeneities shape effect on drift rate in ionosphere under wind and electric field effect 11 p1696 A66-22413

Kinetic oscillation of nonhomogeneous collision plasma, discussing drift instability, ionization, longitudinal current effect, etc 12 p1921 A66-24204

Motion of charged particles in rotating and fixed magnetic fields, using drift approximation equations to determine field parameters 12 p1921 A66-24209

Drift velocity of aerosol particle in field of sound wave distorted by second harmonic 13 p2127 A66-25087

Partially ionized plasma drift across toroidal magnetic field arises from collision with neutral gas molecules 13 p2146 A66-25744

Random error of drift measurements using airborne Doppler radar from observed drift output during short flight over fixed course, calculating rms values 13 p2125 A66-26449

Free hole lifetimes greater than 50 microseconds in silver bromide above 200 degrees K and measurement of drift mobility 14 p2365 A66-27756

Temperatures, Lorentzian widths and drift velocities of excited neutral and ionic species in argon-ion laser, noting thermal equilibrium achievement 15 p2512 A66-28695

Ionic drift velocity peak function for two interconverting nitrogen ion species drifting in gas in electric field 15 p2550 A66-28756

Repetitive plasma breakdown in flat electrode accelerator, causing relatively low plasma velocity 16 p2757 A66-30107

Plasma-ion oscillations in drifted plasma effected in diode-type discharge tube by

varying longitudinal magnetic field or cathode temperature 17 p2972 A66-32974

Drift rate and precipitation of lithium ion in germanium as affected by resistivity, acceptors, carrier lifetime and copper diffusion 19 p3442 A66-35914

Optimum control theory applied to shipboard inertial navigation systems with position and azimuth errors because of gyroscope drift-rate fluctuations 20 p3595 A66-36873

Electron drift velocity, ionization and attachment coefficients in water vapor and dry air measured by recording short photoelectron pulses 20 p3605 A66-38095

Nonadiabatic and adiabatic acceleration and diffusion of particles trapped in Earth magnetic field, examining particle drift, trapping boundary, auroral substorms and bounce resonances 20 p3658 A66-38326

Carrier motion equation in Gunn diode in terms of average drift velocity and diffusion coefficient 20 p3534 A66-38402

Stabilization criteria for drift instabilities in inhomogeneous plasma with external electric field derived from drift wave frequency variation 20 p3612 A66-38430

Drift velocity of aerosol particle in field of sound wave distorted by second harmonic 21 p3769 A66-38512

Stabilization criteria for drift instabilities in inhomogeneous plasma with external electric field derived from drift wave frequency variation 21 p3777 A66-38963

Equations derived for thermal drift of MOS-FET operated at drain voltages beyond pinch-off voltage 22 p3872 A66-39722

Three-dimensional electric field wave equation for homogeneous gyrotropic compressible drifting plasma derived for case having magnetostatic field and drift velocities in arbitrary directions 22 p3865 A66-40099

Nonlinear theory on effect of drifting cone plasma instability on particle drift from adiabatic trap 22 p3955 A66-40191

Charged particle collisions effect on drift instability of low pressure plasma studies, using Landau collision integral as model collision integral 22 p3956 A66-40192

Kinetic oscillation of nonhomogeneous collision plasma, discussing drift instability, ionization longitudinal current effect, etc 22 p3956 A66-40568

Motion of charged particles in rotating and fixed magnetic fields, using drift approximation equations to determine field parameters 22 p3956 A66-40573

Fluid stratification in floated gyroscope, estimating drift rate as function of time, geometry and flotation mixture 23 p4066 A66-41102

Plasma jet motion in inhomogeneous transverse magnetic field, noting drift velocity 23 p4099 A66-41130

First-order Markovian gyro drift numerically evaluated and square root plotted vs interval and gyro correlation time 23 p4068 A66-41318

Plane homogeneous wave scattering by cylindrical plasma column with glass wall placed in vacuum, noting axial drift velocity and resonance peaks 23 p4101 A66-41366

Epitaxial growth techniques used to obtain graded layers for drift field structured solar cells on Si web 23 p4019 A66-41747

**DRILL**

Production process for gun-drilling of holes in beryllium, noting filtration techniques and clamping fixture [ASTME PAPER MR66-185] 14 p2300 A66-26959

Projected rotary-percussive drilling system for obtaining lunar surface samples within specified payload and size requirements, considering drive systems 18 p3094 A66-34139

**DRIVE**

SA GEAR

SA PROPELLER DRIVE

SA ROTARY DRIVE

Peak drive power requirements, optimum drive size and torque requirements for large aperture steerable tracking antenna 18 p3055 A66-34295

**DRUGUE PARACHUTE**

Brake parachutes for high speed aircraft, considering difficulties faced by parachute designer 02 p0178 A66-12014

Aircraft escape systems design criteria established using military accident statistics, noting drogue parachute and pilot sizes 22 p3850 A66-40610

**DRONE**

Drone aircraft onboard stabilization circuit design for control signal transmission and transient response irrespective of noise background 11 p1778 A66-23348

**DROP**

**SA LIQUID DROP**

Spherical drop in electric field with equilibrium maintained through balance between electric stress and variable pressure difference between inside and outside of drop, existing only if outside and inside fluids are in motion 13 p2129 A66-26302

**DROP SIZE**

Combined effect of turbulent gravitational and electrostatic coagulation on growth rate of cloud droplets estimated by two-layer model of process 01 p0096 A66-10658

Visible and IR radiation attenuation by artificial fogs found to depend on droplet size and distribution 01 p0097 A66-10860

Effects of drop formation on rate, duration and size of welding and quality of welds in submerged-arc welding 03 p0375 A66-13123

Microstructural fluctuation in low clouds, investigating cloud droplet spectra and fluctuation of absolute total concentration 05 p0712 A66-15115

Precipitation formation considering collision efficiency of different-size droplets, noting influence of gravitational and electric fields, space charge, atmospheric turbulence, etc 06 p0905 A66-16269

Homogeneous isotropic turbulence in atmosphere model showing accretion qualities for small droplets during diffusion dissociation 08 p1212 A66-18673

Mean droplet size and dispersion of atomized liquids in industrial air determined by microscopic slides and photomicrographs 13 p2066 A66-26489

Swept frequency measurement of water-drop diameter in spherical resonator, using dielectric materials 19 p3394 A66-36417

Airborne photoelectric device for registration of cloud drops 21 p3739 A66-39365

Doppler radar applied to atmospheric precipitation processes, noting drop size distribution in widespread rain, height-time sections of vertical air motion and maximum particle velocity, etc 22 p3942 A66-39737

Atomization of water drops by high speed airstreams, noting dependency on time 23 p4016 A66-42053

**DROP TEST**

Cavitation erosion research, examining correlation between drop impact erosion and constricted tube and vibratory cavitation erosion tests 20 p3588 A66-37814

Dropping heavy stores from low altitude aircraft, considering stability of store after leaving aircraft and rebound from impact with ground 22 p3850 A66-40616

**DROP-WEIGHT TESTER**

Drop-weight sensitivity of explosive liquids tested with impact apparatus, showing increase with temperature [CI PAPER WSCI-65-28] 05 p0788 A66-15139

Drop-weight impact sensitivity testing of explosives [CI PAPER WSCI-65-27] 05 p0788 A66-15140

Drop-weight testing procedures using Olin Mathieson tester, noting mounting [CI PAPER WSCI-65-31] 05 p0788 A66-15142

Fractures in high strength low-alloy steels, discussing formation of flat and slant regions, effect of rolling direction crack reinitiation, shearing forces, etc 21 p3751 A66-39191

Drop-weight tester/photographic apparatus for studying impact initiation-explosion process in nitroglycerin 23 p4119 A66-41243

**DROSOPHILA**

Biological experiments under flight conditions in Vostok spacecraft, noting reproduction of Drosophila melanogaster and effect of weightlessness and cosmic radiation on hereditary structures 15 p2436 A66-29465

**DRUG**

S ADRENERGICS

S ALKALOID



S ANTIBIOTICS  
S MOTION SICKNESS DRUG  
S PHARMACOLOGY  
**DRY CELL BATTERY**  
SA STORAGE BATTERY  
Substitution of solid electrolytes for conventional liquid electrolytes in dry cell can enhance battery miniaturization potential without sacrifice of shelf life 08 p1167 A66-18715  
**DRY FRICTION**  
Forced vibration in nonlinear system with Coulomb and combination friction 01 p0159 A66-11176  
Dependence of dry friction force for steady state rubbing of rubberlike body on surface of crystalline elastic body 08 p1244 A66-19474  
High temperature and vacuum effects on sliding friction and surface film formation between dry lubricated and nonlubricated pair combinations of metals, carbon and ceramics, noting SNAP reactor data [ASLE PREPRINT 65AM 6A1] 10 p1540 A66-22040  
Lubrication characteristics of dry unbonded and bonded molybdenum sulfide films for varying speed, load, humidity and metal substrate [ASLE PREPRINT 65AM 5C1] 14 p2302 A66-27773  
Forced oscillations of gyroscopic tachometer with dry friction analyzed by Zhelezov theorems 17 p2928 A66-33496  
Temperature effect on dry friction coefficient in titanium alloys 19 p3376 A66-35462  
**DRY HEAT**  
Microbial contamination control of space vehicles, noting dry heat sterilization requirements 16 p2642 A66-30496  
**DSIF**  
S DEEP SPACE INSTRUMENTATION FACILITY /DSIF/  
**DTA**  
S DIFFERENTIAL THERMAL ANALYSIS /DTA/  
**DUAL CONTROL PROBLEM**  
Optimal interplanetary guidance, discussing optimization of variable observation rate and correction schedule to achieve desired terminal accuracy 04 p0544 A66-13992  
Synthesizing dual control in absence of a priori information concerning unknown plant parameter 07 p1012 A66-17380  
Optimum dual system design for plant investigation and regime requirements 12 p1853 A66-24331  
Dual quadratic programming of dynamic response of frictionless mechanical system with one-sided constraints 13 p2117 A66-25347  
Dynamic optimization and minimizing kernel function for dual control problem 13 p2117 A66-25348  
Decomposition technique by which convex control programming problem, having coupled subsystem constraints, can be decomposed into smaller subproblems 13 p2117 A66-25349  
Combined optimization problem, equivalent to dual control problem, considering determination of optimal control policies for plant under random disturbances, using iterative equations 13 p2051 A66-26065  
Comparison of nonoptimum and optimum strategies in dual control of inertialess plants in presence of noise in feedback loop 16 p2669 A66-30757  
Duality theory of optimal control and resulting duality correspondence between formulation of optimal control and calculus of variations, noting decomposition algorithm 16 p2671 A66-31229  
Dual control of plant with random amplification factor as Bayesian problem 18 p3089 A66-33738  
**DUCT**  
S ACOUSTIC DUCT  
S AIR DUCT  
S ORIFICE  
**DUCTED BODY**  
Elastic and plastic behavior of ideal materials with mechanical and thermal properties of ductile structural metals 24 p4288 A66-42275  
**DUCTED FAN**  
Acoustical fatigue study of propeller duct

designed for minimum weight to maintain specified thrust-to-weight ratio 01 p0150 A66-10155  
Ducted axial flow fan noise generation and noise spectrum 10 p1483 A66-21743  
Size and position effect, baffle effect and wake and pressure interaction effect of upstream stator on ducted axial flow fan noise 10 p1483 A66-21746  
Low speed aerodynamic loading on finite-bladed ducted propeller at zero incidence 22 p3844 A66-40394  
**DUCTED FAN ENGINE**  
Bypass engine development from conventional gas turbine to ducted-fan and aft-fan engine, noting principle of afterburning 14 p2373 A66-27014  
Ducted propeller aerodynamics in forward flight with shroud load determination 20 p3492 A66-37572  
**DUCTED FLOW**  
Thermodynamic process within combustion chamber of propulsive duct, examining potential with reference to feedback and spark discharge 11 p1761 A66-23251  
Aerodynamic characteristics of compressor entry ducts under natural and simulated conditions 13 p1992 A66-26491  
Laminar ducted flow of viscous electrically conducting fluid under uniform arbitrarily oriented magnetic field for rectangular duct with nonconducting walls 14 p2342 A66-27407  
Inverse problem of nonequilibrium dissociation and vibrational relaxation of diatomic duct flow 14 p2219 A66-27428  
Marine propellers and ducted propeller propulsive devices 16 p2688 A66-31328  
Temperature profiles and Nusselt numbers for heat transfer to MHD laminar Hartmann flow in thermal entrance region of flat duct 22 p4000 A66-40920  
Heat transfer in entrance section in rectangular duct for incompressible fluid in laminar pulsating flow with periodic pressure gradient 23 p4148 A66-41216  
**DUCTILITY**  
SA CREEP  
SA PLASTICITY  
Mechanical properties of alloys with aging martensite 05 p0701 A66-14860  
Ductile behavior of brittle material during erosive cutting [ASME PAPER 65-WA/PROD-7] 05 p0690 A66-15634  
Dilute tungsten rhenium alloys, determining ductility parameters, fabrication, tensile properties and creep behavior 06 p0894 A66-16070  
Small titanium additions effect on strength, impact ductility and structure of low-carbon low-alloy steel 06 p0895 A66-16228  
Four-point loading bend test on specimen of full plate thickness with sharp notch to 20 percent depth, with ductility criterion as fully plastic angle of bend before fracture 06 p0965 A66-16492  
Ductility in polycrystalline single phase ceramics, noting behavior at room and high temperature of single crystal structure, dislocation, etc 07 p1054 A66-18498  
Beryllium ductility in fabrication as affected by single crystal slip and fracture and improvement by grain control 08 p1238 A66-18851  
Rational compression curves and plastic deformation mechanism of cast and drawn polycrystalline beryllium 13 p2106 A66-25356  
Quenching and slow-cooling effects on ductile-brittle bend-transition temperature of chromium wire 13 p2107 A66-25587  
Ductility and production techniques of cross rolled beryllium sheet [SAE PAPER 660291] 14 p2313 A66-27287  
Ductility enhancement of tungsten by rhenium addition due to modification of grain boundary precipitate morphology 16 p2722 A66-30222  
Carbon content effect on brittle-to-ductile transition temperatures of molybdenum studied in search for high toughness propulsion system 19 p3382 A66-36106  
Welding and postheat treatment effects on bend ductility transition temperature and strength of second-generation niobium-base alloys 19 p3368 A66-36124  
Weldability of nearly 100 tantalum binary or ternary solid solution alloys and

dispersion-strengthened alloys, using room temperature bend ductility as criterion 19 p3368 A66-36125  
Mechanical properties, optical microstructure and thin foil electron microstructure of commercial pure titanium plate investigated for cause of ductility deterioration 24 p4229 A66-43105  
**DUFFING EQUATION**  
SA PROBABILITY  
Amplitude of subharmonic vibrations of even order and frequency limits of excitation for systems described by Duffing equation 01 p0159 A66-11177  
Steady states of mechanical system using perturbation method, assuming primary and secondary oscillators are tuned to single pulse, each involving Duffing type nonlinearity 04 p0545 A66-14169  
Forced solutions for Van der Pol-Duffing equation in first harmonic approximation 13 p2129 A66-26337  
**DUMBELL SPACE PROBE**  
Dumbbell librations of satellites in elliptic orbits of small eccentricity determined via WKB approximation 24 p4272 A66-42158  
**DUMMY LOAD**  
Design and application of dry, dielectric and water-cooled dummy loads 12 p1829 A66-23537  
**DUOPLASMATRON**  
Noble gas ion beams produced by duo-plasmatron magnetically analyzed while varying gas pressure in source 01 p0114 A66-10850  
Duoplasmatron with electrostatic lens decreasing ion energy while focusing ions for maximum density parallel beam 01 p0114 A66-10851  
Diagnostic work on ion sources in Germany including electrostatic drive research, duoplasmatron and porosity of tungsten emitter [DGR PAPER 66-005] 13 p2059 A66-26492  
Electrostatic ion drives technology problems, considering conversion efficiency, thrust, reliability, high voltage, mass per unit thrust, etc 17 p2991 A66-33231  
Electrostatic ion drives technology problems, discussing gaseous discharge ion sources, duoplasmatron and electron bombardment ion generator 17 p2991 A66-33234  
Electron beams from duoplasmatron using hollow cathode arc, noting current density distributions 20 p3606 A66-38406  
**DUPLEXER**  
Two basic semiconductor limiters design and performance as microwave duplexing devices 14 p2253 A66-27529  
**DUST**  
SA COSMIC DUST  
SA INTERPLANETARY DUST  
SA LUNAR DUST  
SA METEOR DUST CLOUD  
SA METEORITIC DUST  
SA TERRESTRIAL DUST BELT  
SA ZODIACAL DUST CLOUD  
Dust particles in laser cavity observed for angular stabilization and constant velocities 13 p2105 A66-26594  
Shock and ionization fronts propagation in gas-dust medium 14 p2380 A66-27255  
Metal erosion by airborne quartz dust particles, using energy values as function of material, dust size, temperature, etc, influenced by surface layer of material 16 p2813 A66-30442  
Dust cloud formation by thermal convection in Martian atmosphere 16 p2802 A66-30925  
Shock wave propagation in gas-dust medium, examining motion and velocities of gas and dust at distance approaching infinity 20 p3647 A66-37034  
**DUST COLLECTOR**  
High altitude balloon top collections of cosmic dust shows evidence of absence of crystal structure in particles 15 p2604 A66-30065  
Dust flux in upper atmosphere and on polar ice sheets 16 p2696 A66-30931  
**DYADIC**  
General relativistic dyadic formalism applied to metrics of rigid bodies moving in Einstein space of uniform space-time curvature 17 p2958 A66-32294



## DYE

- SA CYANINE DYE  
 SA METHYLENE BLUE  
 Selective saturation of organic dyes by monochromatic light for high speed switches and optical pulse amplifier 04 p0533 A66-14329  
 Photoeffect sensitization in n-and p-type semiconductors by dyes having n-or p-type photoconductivity 08 p1179 A66-19640  
 Photoionization of leucocarbinals and leucocyanides of malachite green, crystal violet and sunset orange dissolved in straight chain alcohols and chlorinated hydrocarbons 14 p2232 A66-27374  
 Blood flow measurement by indicators by taking samples in situ-dyes, thermodilution, krypton 85 14 p2230 A66-27552  
 Hole burning in bleachable absorbers used as laser Q-spoiler 15 p2517 A66-29387  
 Reversible bleachable dye-solutions for expander elements in laser 15 p2517 A66-29388  
 Q-switched ruby laser output increased by use of saturable dye solution in laser cavity 20 p3576 A66-37290

## DYNAMIC CONTROL

- Dynamic system motion control analyzed by nth order system of nonlinear differential equations 03 p0392 A66-12528  
 Solving method for dynamic equation system describing controlled object element having distributed relationships 04 p0502 A66-13493  
 Charting for dynamic map displays preparatory to SST operations 07 p1068 A66-17705  
 Dynamic Navigation System /Dynav/ for providing aircraft velocity and position-fixing information from VLF Doppler range rates 08 p1252 A66-19507  
 Optimization of terminal state of controlled system when equations of motion contain derivatives of control parameters 11 p1674 A66-22350  
 Dynamic characteristics of human operator in tracking system under spaceflight conditions onboard Voskhod II spacecraft 11 p1648 A66-23047  
 Systems design of automatic dynamic control for piloted aircraft, discussing stability, accuracy, response and behavior to external perturbations 12 p1803 A66-24090  
 Charting for dynamic map displays preparatory to SST operations 13 p2125 A66-25869  
 Electronic predictor instruments for dynamic control and simulation and possible application to lunar spaceship 13 p2048 A66-25896  
 Markov parametric algorithm for effective construction of minimal realizations of linear state-variable finite-dimensional dynamical systems from input-output data 13 p2053 A66-26084  
 Systems analysis, discussing mathematical model formulation and control 15 p2472 A66-29369  
 Matrix formulation of output controllability conditions for dynamic systems 16 p2673 A66-31587  
 Mathematical analysis of axioms that provide local definition of generalized control systems 17 p2898 A66-31868  
 Acquisition phase of attitude control function of space vehicle, using noisy measurements on one state 20 p3658 A66-36867  
 Optimal averaging theories of controls of dynamic systems 22 p3885 A66-40683

## DYNAMIC LOAD

- Aircraft crash loads and motion prediction by set of equations with results correlated by experiments on Lockheed 1649A and Curtiss C-46 01 p0009 A66-10071  
 Matrix analysis of response of geometrically nonlinear structures to prescribed dynamic loading and effects of thermomechanical midplane preload in prediction of natural frequencies and mode shapes 01 p0148 A66-10135  
 Analytical landing simulation to analyze dynamic loads and aircraft response, particularly high sink speed landing gear [SAE PAPER 650845] 01 p0011 A66-10835  
 Characteristics of partially clamped corrugated membrane, investigating effect of forces of clamping

- friction 01 p0160 A66-11182  
 Dynamic indentation of metals with conical projectiles and dynamic tip flattening of projectiles, noting inertia and strain rate effect 02 p0243 A66-11691  
 Behavior of materials under dynamic loading - ASME Colloquium, Chicago, November 1965 02 p0299 A66-11849  
 Plastic deformation of metals under wide range in strain rate 02 p0245 A66-11852  
 Structural dynamics of XC-142A tilt-wing VTOL aircraft including flutter, vibration, environmental acoustics, etc [AIAA PAPER 65-790] 03 p0318 A66-12559  
 Stress distribution measurement by vibration method, applying hand-held extensometer place by place on surface of structure subjected to dynamic load of finite amplitude [AIAA PAPER 65-785] 03 p0438 A66-13069  
 Integrated circuit testing noting dynamic test system capabilities 04 p0491 A66-13385  
 Structural dynamic load and instability problems in launch vehicles and spacecraft in lunar exploration emphasizing reliability, crew safety and mission success 04 p0585 A66-13549  
 Design analysis related to structures using materials exhibiting inelastic responses, noting deformation analysis for operational loads and instability analysis for structural failure 06 p0963 A66-16473  
 Metal powder behavior during dynamic and static pressing by energy release of high explosives 07 p1038 A66-18160  
 Dynamic buckling of circular cylindrical aluminum shells subjected to axial blast loads [AIAA PAPER 66-82] 08 p1308 A66-18996  
 High precision transient measurement of submicrosecond response of shock-loaded materials by instrumentation techniques and target alignment 08 p1226 A66-19694  
 Axisymmetric wave motion in thin walled elastic spherical shell under normal load uniformly distributed over small segment 08 p1315 A66-19763  
 Photoelastic measurement of dynamic stresses and loading of structures, examining impact stress phenomena, stress waves, vibrations, stress distribution, etc 08 p1316 A66-19805  
 Displacement bound theorems for work hardening continua subjected to impulsive loading in inelastic continua 11 p1781 A66-22610  
 Dynamic stability of cylindrical shell subjected to uniform radial pressure 12 p1956 A66-23585  
 Uniqueness theorem for dynamically loaded rigid-plastic and rigid-viscoplastic idealizations of deformable bodies 12 p1962 A66-23999  
 Motion equation for plastic deformation of simply supported beam under impulsive loading 13 p2198 A66-26113  
 Dynamic snap-through buckling of shallow spherical caps of elastic material 14 p2406 A66-27998  
 Structural design load prediction and data collected verification of methods and magnitude by Minuteman flight testing 14 p2392 A66-28000  
 Dynamic elastic deflections of shallow circular arch under dynamic pressure loading, solving nonlinear integro-differential motion equation by Galerkin method 15 p2610 A66-29284  
 Ballistic pendulum technique to measure permanent plastic deformation of shallow circular arches subject to explosive impulse loading [AIAA PAPER 65-408] 15 p2610 A66-29294  
 Response of aerospace structures to in-flight dynamic loads in HF range 16 p2813 A66-30446  
 Flight Load Survey program, written in Fortran IV, for accurate and rapid sounding of wind-induced loads on aerospace launch vehicle [AIAA PAPER 66-470] 16 p2811 A66-31473  
 Steady-state and dynamic characteristics of full circular bearing and centrally loaded arc bearing presented in design charts for turbulent lubrication analysis [ASME PAPER 66-LUBS-4] 17 p2931 A66-33178  
 Mechanical reliability research and

- development for space systems, noting effect of random dynamic loading, fatigue damage, etc 20 p3573 A66-37959  
 Inelastic buckling of rod with initial slight sinusoidal deflection subjected to short-term longitudinal compressive dynamic load 20 p3672 A66-38268  
 Dynamic buckling of circular cylindrical aluminum shells subjected to axial blast loads [AIAA PAPER 66-82] 21 p3828 A66-38728  
 Prediction characteristics of separated turbulent boundary layers in compression corners used to determine aerodynamic heating distributions and dynamic loading of supersonic vehicles 21 p3724 A66-38730  
 Vibrational creep phenomenon occurring when small dynamic loads are superposed on static loads in thin wall steel tube 21 p3830 A66-38983  
 Calculating method for parachute opening forces, system velocity, cloth pressure loading and filling time for horizontal and vertical deployment conditions 22 p3844 A66-40590  
 Steady and dynamic loads on tandem rotor, controls and airframe flight tested with Army helicopter, using automatic data processing [AIAA PAPER 66-735] 23 p4008 A66-41324  
 Energy method applied in determining upper bounds on displacements due to static and dynamic loading 24 p4288 A66-42273
- DYNAMIC MODEL**  
 Dynamic model of multistable elements noting synchrotron and spectrotron 03 p0344 A66-13046  
 Expected rigidity spectrum of variations in framework of dynamic piston model of Forbush effect 09 p1438 A66-20213  
 Numerical dynamic predictor for control systems disturbed by random noise, discussing Fokker-Planck equation, Crank-Nicolson difference model, etc 11 p1680 A66-23279  
 Orientation control of orbital astronomical observatory examined, using dynamic model consisting of three independent subsystems, each with one degree of freedom 12 p1829 A66-24318  
 Existence theorem of recurrent solutions to differential equations defined in Banach space for dynamic and nondynamic systems 16 p2735 A66-30785  
 Dynamic model of multistable elements, noting synchrotron and spectrotron 18 p3088 A66-35009  
 Dynamic system parameters substituting integral equation for differential equation of motion, noting application to nonlinear, differential and PDE systems 19 p3325 A66-35987  
 Experiments and model for adaptation of human controllers to sudden changes in plant dynamics in time-invariant situations 20 p3508 A66-36860  
 Mathematical model of linear guidance law to dynamical system, noting reduction of two-point boundary value class error 21 p3765 A66-38870  
 Existence theorem of recurrent solutions to differential equations defined in Banach space for dynamic and nondynamic systems 22 p3940 A66-40447  
 Nonlinearity and time variability dynamic models of human operators in manual control systems 23 p4029 A66-41574
- DYNAMIC MODULUS**  
 Stress-strain behavior of tungsten fiber-reinforced copper composites, discussing room-temperature tensile and dynamic-modulus tests 05 p0702 A66-15324  
 Oxygen content effect on recovery of cold worked tantalum investigated by measuring Snoek damping, electric resistivity and dynamic E modulus 11 p1717 A66-22997  
 Ultrahigh-speed photographic recording of dynamic stress-optic patterns in high photoelastic modulus materials 20 p3670 A66-37741
- DYNAMIC PRESSURE**  
 Dynamic behavior of aircrew breathing equipment considering cyclic flow response tests, stability problems, measurement techniques and human respiratory impedance 03 p0329 A66-13350  
 Fracture time for thin spherical shells subjected to internal blast



loading 04 p0586 A66-13411  
 Piston pressure gauge performance characteristics, calculating piston velocity and work and presenting viscosity coefficients for glycerine and oils 04 p0519 A66-13757  
 Dynamic environmental influences on man during space flight covering force fields, inertial forces due to acceleration and methods of protection 04 p0466 A66-14074  
 Resistance strain gauge measuring propagating dynamic strains, noting independence of waveform, effect of gauge length, time and amplitude errors, etc 13 p2198 A66-26225  
 Stress wave propagation in inhomogeneous rod applied to measurement of dynamic overpressure on moving vehicle subjected to sudden intense blast  
 loading 14 p2409 A66-28398  
 High-explosive driven shock tubes, as sources of short duration high-pressure supersonic pulses, applied in accelerating large objects 16 p2674 A66-30423  
 Control of pneumatic tire tread design parameters to limit or delay hydrodynamic pressure buildup 18 p3052 A66-34199  
 Ballistic reentry vehicle recovery via low speed water impact or air snatch after vehicle has flown unperturbed trajectory down to altitude of maximum dynamic pressure 22 p3986 A66-40597  
 Compressive strain rate testing of Al, Ti, pyrolytic graphite, lucite and micarta, noting techniques and results 24 p4227 A66-42138

**DYNAMIC PROGRAMMING**  
 Optimum control and stability of processes described by system of partial differential equations 01 p0051 A66-10705  
 State assignment effect on sequential circuit reliability represented by Markov chain, using iterative assignment method with dynamic programming 02 p0207 A66-11521  
 Time optimization problem involving dynamic programming, boundary value problem, differential equations and optimal control 03 p0349 A66-12687  
 Dynamic programming applied to numerical solution of optimization problems of flight mechanics 04 p0584 A66-13523  
 Bayes risk function of sequential games, discussing recurrence formula, decision rule and approximate computational method in pattern recognition problems 05 p0639 A66-15838  
 Accurate light-weight self-contained low-cost inertial autonavigational system including gyroscopes, accelerometer and DYDAN computer 07 p1076 A66-17793  
 Computational reduction of high speed memory requirements in solving optimization problems by dynamic programming and supersonic transport trajectory application 07 p1004 A66-17976  
 Optimum processes in systems with distributed parameters described by partial differential equations 08 p1202 A66-19710  
 Stochastic optimal control problem solution by dynamic programming and relation to interplanetary guidance 09 p1360 A66-19908  
 Dynamic programming in linear vector system and application in switching system 09 p1393 A66-19909  
 Dynamic programming approach to nonparametric problem in calculus of variations 09 p1394 A66-20131  
 Multistage extremum searching process leading to development of dynamic programming system, discussing application 09 p1362 A66-20628  
 Optimal control by random sequences, dynamic programming and Wald sequential analysis 09 p1362 A66-20644  
 Existence of optimal stationary policy in Markov decision process in study of asymptotic behavior of recurrence relations in dynamic programming 09 p1397 A66-20646  
 Dynamic programming applied to satellite intercept and rendezvous problems 09 p1362 A66-20651  
 Optimum control and stability of processes described by system of partial differential equations 11 p1675 A66-22617  
 Algorithm for optimal parameter choice in reliability control of complex systems, based on dynamic programming 11 p1675 A66-22623  
 Nonlinear circuit theory, discussing

invariant imbedding, dynamic programming and quasi-linearization 11 p1675 A66-22629  
 Black box analysis from input and output and estimation of subsystem switching by combination of differential approximation, quasi-linearization and dynamic programming technique 11 p1660 A66-23186  
 Dynamic programming method for approximate solution of gliding flight and minimum time to climb problems in boundary value theory 11 p1778 A66-23349  
 Manned space flight program management noting system efficiency, cost factors, reliability and performance reports based on Apollo project 11 p1789 A66-23437  
 Systems effectiveness through design function management, noting necessity of decision guide activities 11 p1789 A66-23441  
 Past and future of cost effectiveness, noting actions needed to implement growth 11 p1790 A66-23446  
 Monograph on continuous maximum principle covering design and control of industrial and process engineering systems, dynamic programming, process optimization, etc 12 p1901 A66-23534  
 Discrete-sample curve fitting using Chebyshev polynomials and approximate determination of optimal trajectories via dynamic programming 12 p1850 A66-24257  
 Deterministic optimal control, discussing Bellman dynamic programming method, Pontryagin maximum principle, orbital transfer, interplanetary guidance, etc 12 p1854 A66-24635  
 Adaptive utilization of communication satellite systems optimizing dynamic traffic handling of combined ground and satellite communications complex, noting network configurations 12 p1822 A66-24764  
 [AIAA PAPER 66-295] 12 p1822 A66-24764  
 Programming and control - International Conference, Air Force Academy, Colorado Springs, April 1965 13 p2046 A66-25339  
 Optimal control system geometry, discussing properties of interior points of limiting surfaces, maximum principle and separability concept 13 p2046 A66-25340  
 Duplex method applied to nonlinear programming by linearization of expressions with lambda algorithm and determining optimum point 13 p2046 A66-25345  
 Dual quadratic programming of dynamic response of frictionless mechanical system with one-sided constraints 13 p2117 A66-25347  
 Mathematical programming methods for solving nonlinear state-constrained discrete optimal control problems 13 p2047 A66-25352  
 Dynamic programming for stochastic systems applied in designing controller for transferring linear system from initial to final position in specified time interval 13 p2048 A66-25852  
 Dynamic programming recursive estimation of modal trajectory for nonlinear non-Gaussian noise and comparison with Bayesian estimation and case of Gaussian white noise 13 p2053 A66-26086  
 Synthesis of automatic control system for tracking random moving coordinate solved by dynamic programming methods 13 p2055 A66-26467  
 Decision theory and dynamic programming applied to problems concerning cost and weight minimization in structural engineering 13 p2207 A66-26699  
 Linear dynamic programming for unrestricted control, noting discrete phase function and unrestricted nonclassical function 14 p2266 A66-27591  
 Dynamic programming design of invariant multiloop feedback autostabilizers and matrix-Ricatti equation 14 p2268 A66-28184  
 Field theory, variational calculus, dynamic programming and Pontryagin maximum principle approaches to plasma optimal controllability 15 p2548 A66-28520  
 Liapunov method and dynamic programming of stability of motion of variable mass point in Oxyz coordinate reference system, allowing for Earth rotation effects 15 p2538 A66-29046  
 Dynamic system stability, control and observation, noting optimal system synthesis, application of functional analysis, Liapunov function and dynamic programming 15 p2470 A66-29149

Dynamic programming for optimum design of sampled data control systems 15 p2474 A66-29628  
 Three models of constrained preview control with successive target values of nonuniform importance 16 p2644 A66-31272  
 Text on relation between dynamic programming and variational calculus, noting application to Mayer problem, optimization and stochastic processes, etc 16 p2739 A66-31750  
 Dynamic programming applied to synthesis of linear optimal or suboptimal multivariable control systems in which control-signal vector depends only on certain prescribed state variables 17 p2901 A66-32291  
 Russian research dealing with optimal control functions of spacecraft powered by low thrust rocket engines 18 p3228 A66-33883  
 Adaptive subfield method for solution of variational problems by dynamic programming, applicable to pinpoint problem 19 p3310 A66-36651  
 Most likely trajectory estimation for dynamic system as observed through noisy measurement system, using iterative equation based on dynamic programming 19 p3334 A66-36682  
 Optimal control of dynamic systems with minimax type performance index, discussing application of proposed method of solution 19 p3334 A66-36686  
 Linear continuous time stochastic optimal control process, obtaining optimum performance achievable as function of total effort at initiation of optimization period 19 p3335 A66-36694  
 Optimal feedback control of linear discrete-time stochastic system with quadratic performance measure for bounded input 19 p3335 A66-36695  
 Liapunov method synthesis of time variable nonlinear multivariable systems, deriving simplified control law for tracking of linear noninteracting model 19 p3335 A66-36697  
 Optimization of time dependent systems in dynamic programming, using forward and backward algorithm 19 p3391 A66-36700  
 Dynamic programming for optimal algorithm for external control in presence of noise at system input and output 20 p3538 A66-37746  
 Reliability-maintainability cost tradeoff via dynamic and linear programming, discussing states, alternatives within states, transition rates and expected costs 20 p3568 A66-37911  
 Book on variational methods in control engineering covering optimal processes based on maximum principle, variational calculus and dynamic programming 20 p3539 A66-37985  
 Synthesis of control device for class of nonlinear sampled data system, obtaining processes with minimum control time 21 p3719 A66-39286  
 Computer simulation techniques, including stochastic phenomena and computer-computer applications performance evaluation 21 p3708 A66-39432  
 Linear dynamic programming for unrestricted control, noting discrete phase function and unrestricted nonclassical function 22 p3884 A66-40440  
 Maximum principle shown to be necessary and sufficient optimality condition for dynamic programming method for condition of existence of regular synthesis 22 p3884 A66-40531  
 Rational and optimal programming of electronic computers, noting application to structural mechanical problems 23 p4137 A66-41005  
 Recognition and prediction systems, developing criteria for resolvable arguments 23 p4041 A66-41395

**DYNAMIC PROPERTY**  
 Frequency dependence of dynamic properties of semiconductor small area ohmic contacts in volt-ampere characteristic regions when constant current and sinusoidal pulses are applied 06 p0838 A66-15893  
 Gravitational source dynamics, discussing multipole structure, mass, linear momentum, dipole moment and spin in axially symmetric field 06 p0908 A66-16131  
 Dynamic properties of contact thermal



- receivers investigated with aid of digital computer 07 p1035 A66-18092
- Effect of relay response time on dynamic properties of automatic system incorporating linear group and relay element with pure delay 14 p2264 A66-27358
- Dynamic characteristics of automatic control plants determined, using term-by-term integration of differential equations 15 p2475 A66-29768
- Dynamics of speed optimum control system with asynchronous two-cycle activating motor 15 p2475 A66-29990
- Synthesis problem of optimum dynamic characteristics of multivariate linear control systems with random input signals 16 p2668 A66-30752
- Dynamic characteristics of built-up plates analyzed with modified Reissner principle, obtaining natural frequencies and mode shapes 17 p3022 A66-32011
- Dynamic characteristics of unsteady feedback control system during normal operation, ascertaining signal correlation and cross correlation functions 18 p3091 A66-34987
- Missile and rocket launching with static instability, deriving approximate solution for equations of longitudinal accelerated motion 19 p3470 A66-36083
- Amplifying elements ensuring required dynamic properties of resolving amplifier without calculating entire amplifier circuitry 21 p3712 A66-39252
- DYNAMIC RESPONSE**
- Dynamic responses of panel shells and complete equipment packages to acoustic inputs to improve fabrication techniques of flight structures 01 p0149 A66-10142
- Circuit with tunnel-diode-based active element for dynamic memory used to store regenerated information 01 p0046 A66-11048
- Parameter and matrix solution techniques for analyzing forced vibrations response of damped multidegree of freedom systems [AIAA PAPER 65-786] 03 p0438 A66-13070
- Single fluid heat exchanger, using Lagrange method and thin walled stainless steel tube for theoretical and experimental dynamic response analysis [ASME PAPER 65-WA/HT-9] 05 p0791 A66-15653
- Axisymmetric dynamic response of ring supported cylinder to time dependent loads, discussing boundary conditions and differential equations of motions [AIAA PAPER 66-83] 06 p0962 A66-16265
- Measurements of dynamic behavior of rotors supported by externally pressurized gas bearings subjected to impact [ASLE PREPRINT 65AM 3A4] 07 p1039 A66-18287
- Dynamic response of supersonic transports to runway unevenness during takeoff or landing 09 p1330 A66-20692
- Response of hypersonic aircraft to abrupt control displacements, determining vehicle characteristics, design and operational parameters 09 p1330 A66-20739
- General recursion formula for dynamic response of pressure measuring systems considered as series connection of tubes and volumes 10 p1535 A66-21376
- Dynamic transient thermal response and voltage feedback in junction transistors 10 p1512 A66-21764
- Single fluid heat exchanger, using Lagrange method and thin walled stainless steel tube for theoretical and experimental dynamic response analysis [ASME PAPER 65-WA/HT-9] 11 p1785 A66-22193
- Effect of water immersion on reduction of die stresses in explosive forming, investigating dynamic response of thin elastic spherical shell surrounded by large body of fluid, employing diagrams [ASME PAPER 65-PROD-6] 11 p1709 A66-22474
- Circuit with tunnel-diode-based active element for dynamic memory used to store regenerated information 11 p1671 A66-23295
- Dynamic response of cylindrical shell subjected to time-varying load treated by explicit and implicit method of timewise integration 12 p1956 A66-23584
- Dynamic transient response of cylindrical shell to internal pressure pulse generated by blast wave 12 p1959 A66-23799
- Dynamic frequency response, noting measurement of phase and amplitude responses of active and passive devices under RF pulse conditions with very fast FM 12 p1879 A66-23814
- Dynamic stresses in infinite elastic space with circular cylindrical cavity 13 p2203 A66-26428
- Model tests for determination of structural response of Apollo command module to water impact 14 p2393 A66-28020
- Piezoelectric plate transducer for ultrasonic wave generation and detection and analysis of responses to partly periodic and partly periodic-transient inputs 15 p2497 A66-28526
- Frequency, dynamic response and jettison analyses for payload shrouds, with application to OAO 16 p2808 A66-30468
- Longitudinal and circumferential inertial effects on dynamic response of cylindrical shell to time-varying loads 17 p3025 A66-32470
- Dynamic response of clamped shallow thin elastic spherical shells under time dependent loads [AIAA PAPER 66-446] 17 p3027 A66-32758
- Load characteristics and characteristic curves for proportional and bistable fluid amplifier noting output, input and dynamic effects 18 p3054 A66-34133
- Low altitude high-speed flight from standpoint of structural loads, particularly those resulting from gust encounters 19 p3278 A66-35505
- Mathematical model of combustion instability in solid propellant rocket engines, noting system dynamic behavior, appearance of limit cycle and effect of large amplitude oscillations on burning rate 20 p3627 A66-36889
- Dynamic system response to separable nonstationary random excitation, describing statistical properties and application to launch vehicle response calculation 20 p3672 A66-38175
- Unconditional stability of Houbolt method for determining dynamic response of structures 21 p3828 A66-38713
- Statistical properties of dynamic response of structure to random load field, examining simple deterministic loadings 22 p3993 A66-40359
- Pilot dynamic response in bank angle control maneuver simulation of sidewind landing of aircraft [ICAS PAPER 66-14] 22 p3945 A66-40672
- Axisymmetric dynamic response of ring supported cylinder to time dependent loads, discussing boundary conditions and differential equations of motions [AIAA PAPER 66-83] 23 p4138 A66-41106
- Signal simulator for testing Loran A and Loran C airborne receivers in laboratory, using digital simulator circuits to test dynamic response of tracking circuits 23 p4088 A66-41253
- Wind tunnel simulation of transient state of takeoff and landing of V/STOL aircraft, noting application of electric circuit analogy to measure flow dynamic response to control valve movement 23 p4053 A66-41388
- DYNAMIC STABILITY**
- Parametric response of structures with periodic loads 01 p0152 A66-10399
- Free oscillation device for studying dynamic stability of models in hypersonic range of intermittent wind tunnels 02 p0210 A66-11210
- Proof of Hermite-Fujiwara theorem of dynamic system stability based on Liapunov-type methods 02 p0261 A66-12158
- Stability of symmetrical elastic rotor in journal bearings with flexible damped supports [ASME PAPER 65-APMW-8] 04 p0526 A66-14214
- Second order dynamical systems with time lag, negative damping coefficient and/or negative spring constant, employing Pontryagin results [ASME PAPER 65-APMW-11] 04 p0546 A66-14216
- Stability criteria for second order dynamical systems with time lag [ASME PAPER 65-APMW-12] 04 p0546 A66-14217
- Post-Newtonian hydrodynamics and stability of gaseous masses for radial and nonradial oscillations 05 p0715 A66-14523
- Stability of linear stochastic distributed parameter dynamical systems by differential integral equations [ASME PAPER 65-WA/APM-12] 05 p0717 A66-15434
- Stability concepts of physically realistic dynamical systems which are mathematically consistent, based on Liapunov, Poincare and Lagrange principles 06 p0953 A66-16077
- Linear dynamical systems with weak coupling solved approximately, noting examples and definition 06 p0862 A66-16362
- Roller-bearing design noting reliability requirements via Palmgren-Lundberg formula 06 p0886 A66-16481
- Abiation effects on static and dynamic stability of reentry vehicle [AIAA PAPER 66-51] 07 p1141 A66-17896
- Stability of quiescent point of dynamic system with random disturbance 07 p1058 A66-17907
- Dynamic stability conditions of self-acting gas lubricated journal bearings 07 p1039 A66-18231
- Stability of motion of spherically symmetric mass of compressible gas with constant space density in absence of gravitational field 08 p1298 A66-19483
- Stellar stability in region of pure hydrostatic equilibrium and local instabilities arising from superadiabatic temperature gradients or differential rotation 09 p1448 A66-20097
- Dynamic stability of circular elastic rods, noting iteration method analysis of nonlinear coupling effect between axial force and curvature in forced in-plane vibrations 09 p1467 A66-20638
- Stability of symmetrical elastic rotor in journal bearings with flexible damped supports [ASME PAPER 65-APMW-8] 10 p1539 A66-21488
- Mathematical stabilization theory for dynamic systems from Liapunov motion stability theory and theory of games 11 p1736 A66-22639
- Sufficient conditions for asymptotic dynamic stability of linear differential system with random retardation, using Liapunov function 11 p1736 A66-22643
- Young theory for rotor blade dynamic stability 11 p1638 A66-23262
- Liapunov second method applied to interconnected differential systems 11 p1682 A66-23456
- Second order dynamical systems with time lag, negative damping coefficient and/or negative spring constant, employing Pontryagin results [ASME PAPER 65-APMW-11] 12 p1913 A66-23981
- Stability criteria for second order dynamical systems with time lag [ASME PAPER 65-APMW-12] 12 p1913 A66-23982
- Stability of linear stochastic distributed parameter dynamical systems by differential integral equations [ASME PAPER 65-WA/APM-12] 12 p1914 A66-23989
- Steady state harmonic and combination response of nonlinear dynamic vibration absorber tuned to two forcing frequencies 12 p1962 A66-24001
- Dynamic stabilization of direct discharge in magnetic field 12 p1922 A66-24215
- Quasi-optimal minimum-time controllers for high-order dynamic systems obtained by least-squares fitting points on optimal switching surface 12 p1849 A66-24253
- Probabilistic stability of random processes with distributed parameters 12 p1904 A66-24340
- Inviscid equilibrium gas stability characteristics for pointed and spherically blunt bodies in unsteady supersonic flight in Mars atmosphere 13 p2191 A66-25275
- Peripheral jet ground effect machine /GEM/ stability in pitch and roll 13 p1995 A66-25591
- Trajectory prediction for moving stochastic systems 13 p2028 A66-26476
- Dynamic instability in large of elastic body



with given initial velocity and displacement, noting example of curved beam subjected to impulsive loads 14 p2408 A66-28387

Existence and stability of periodic motions in dynamic systems applied to analysis of uniformly asymptotically stable solutions of differential equations 15 p2525 A66-28508

Sufficient conditions for recurrence and positivity of diffusion process defined by stochastic differential equation, using Liapunov function 15 p2525 A66-28512

Dynamic system constructed in three-dimensional space with trajectory stable stationary point, showing construction of analogous example in any space of odd dimensionality 15 p2536 A66-28641

Singular characteristics of dynamic systems with steady state motion, noting effect of constantly acting small perturbations 15 p2537 A66-28950

Liapunov stability of motion of heavy rigid body with fixed point moving along spherical surface 15 p2537 A66-28966

Dynamic stability differential equations and stability and instability theorems derived from them 15 p2538 A66-29044

Relation between exact and approximate solutions to equations of dynamics within finite time interval, noting stability of systems with many degrees of freedom 15 p2539 A66-29146

Steady and unsteady perturbed motion effect on solid body containing cavity filled with liquid in analyzing dynamic stability of mechanical systems 15 p2539 A66-29152

Differential equations for motion stability of systems with time delay solved, using Liapunov function 15 p2540 A66-29156

Hooke law analysis of dynamic stability of closed circular cylindrical anisotropic shell compressed by longitudinal force 15 p2609 A66-29196

Behavior, properties and related concepts of control systems, noting attainability function 15 p2472 A66-29373

Prolongations and prolongational limit sets of point useful in analysis of stability and recurrence for dynamical systems 15 p2473 A66-29374

Static and dynamic stability and operation of air cushion vehicles, emphasizing advantages of flexible skirts 16 p2633 A66-30312

Dynamic instability in undamped bellows face seals operating in cryogenic environment with torsional oscillation and diametrical rocking as primary motion [ASLE PAPER 66AM 2CE] 16 p2711 A66-30408

Spiral instability in STOL aircraft prevented by larger wing dihedral setting, noting permissible dihedral levels and tests 16 p2634 A66-31395

Dynamical attitude equations for rotational motion of set of  $n$  rigid bodies interconnected by dissipative elastic joints and subjected to arbitrary forces and torques 17 p3001 A66-32345

Dynamic Antiresonant Vibration Isolator noting design, operation and capability of passively isolating VLF vibrations with high static stiffness 17 p2929 A66-32738

Mathematical problems arising in theory of optimal control in regular dynamic systems 17 p2903 A66-33096

Dynamic systems described by nonlinear differential equations containing analytical functions for random initial conditions 18 p3091 A66-34984

Theoretical and experimental analysis of Korotkoff sounds at diastole which are interpreted as dynamic instability induced by application of pressure cuff 19 p3286 A66-36431

Dynamic stabilization of plasma column by HF magnetic field 19 p3424 A66-36557

Parameter adjustment model reference adaptive control of nuclear rocket engine, noting design parameters, system performance, propellant savings estimates and dynamic stability 19 p3398 A66-36699

Gravitational contraction of stars of one solar mass examined, using Henyey method for calculating stellar evolutionary tracks 19 p3467 A66-36791

Dynamic instability of longitudinal and transverse oscillations of rod, emphasizing

fluctuation having property of white noise with unit spectral density 20 p3670 A66-37680

LF combustion oscillation analyzed by theory of dynamical stability of closed feedback loop 20 p3681 A66-38103

Continuous group and infinitesimal transformation in linear dynamic system application, considering linear network 20 p3539 A66-38148

Dynamic instability in linear vibrating system when linked to unlimited energy reservoir 21 p3825 A66-38577

Approximate method for solution of dynamic stability problem of shafts subjected to pulsating moment and constant axial force 21 p3743 A66-38621

Control of magnetic hysteresis mechanism, increasing damping torque for use in gravity-oriented satellite stabilization 21 p3820 A66-38862

Radio astronomy satellite with extendible antennas achieves gravity gradient stabilization while receiving electromagnetic radiation, analyzing dynamic behavior and effect of passive damper 21 p3820 A66-38863

Stability problems of solid body with liquid filler, noting small partial damping of liquid 21 p3770 A66-38972

Dynamical system stability examined using direct method of Liapunov, noting application to periodic solutions 21 p3718 A66-39104

Dynamic stability and transonic flow response to arbitrary perturbations of solar and stellar winds in steady state 21 p3810 A66-39556

Lateral vibration of rotating bar with circular cross section under simultaneous axial force and torque, noting eigenvalue equations and damping effects 21 p3833 A66-39598

Movchan theorem for stability of continuous systems, considering example of vibrating string and derivation of stability criterion for nonlinear elasticity 22 p3990 A66-40134

Hamilton principle, motion equations, natural boundary conditions and constitutive relations for finite deformation of one-dimensional curved elastica and radial motion and stability of circular ring 22 p3990 A66-40138

Static and dynamic stability and operation of air cushion vehicles, emphasizing advantages of flexible skirts 22 p3848 A66-40393

Dynamic stabilization of direct discharge in magnetic field 22 p3957 A66-40579

Three-dimensional parachute dynamic stability theory 22 p3845 A66-40593

Loads on bodies in wakes resulting from crossflow at submerged body or from wake translation over submerged body, noting dynamic instability 22 p3846 A66-40607

Dynamic characteristics of rotary wing decelerator and recovery system obtained, using frequency oscillation technique [AIAA PAPER 66-733] 22 p3893 A66-40624

Dynamic stability and aerodynamic damping derivative of Apollo launch escape vehicle, using wind tunnel tests [AIAA PAPER 66-757] 22 p3895 A66-40651

Wind tunnel free-flight testing of reentry vehicle dynamics, noting capability for simultaneous two-dimensional viewing of model trajectories [AIAA PAPER 66-774] 22 p3895 A66-40654

Time lag effect on dynamic stability determined, using wind tunnel tests with 10 degree cone as test body simulating ablation process by gas injection into boundary layer [AIAA PAPER 66-757] 23 p4008 A66-41330

Transcendental case of dynamical asymptotic stability of motion of autonomous system with one zero 23 p4090 A66-41553

Trajectory stability of diffusion-type random Markov process described by Ito stochastic differential vector equations 23 p4085 A66-41554

Nonlinear damping effectiveness in stabilizing time delayed systems compared to linear damping 23 p4091 A66-41692

Ablation effects on static and dynamic stability of reentry vehicle [AIAA PAPER 66-51] 24 p4283 A66-42770

**DYNAMICS**  
SA AERODYNAMICS

SA ASTRODYNAMICS  
SA BIODYNAMICS  
SA CONTINUUM MECHANICS  
SA ELASTODYNAMICS  
SA ELECTRODYNAMICS  
SA GAS DYNAMICS  
SA GEOMETRODYNAMICS  
SA HYDRODYNAMICS  
SA KINEMATICS  
SA KINETICS  
SA PLASMA DYNAMICS  
SA SPIN DYNAMICS  
SA STRUCTURAL DYNAMICS  
SA THERMODYNAMICS

General dynamical system defined by contingent equation giving existence and uniqueness theorems 03 p0389 A66-13256

Intermediate text on dynamic analysis and automatic control 08 p1200 A66-19464

Theorems on interaction of parts of mechanical system with smooth holonomic constraints 13 p2128 A66-25638

Extension of dynamics to arbitrary systems of differential equations, proposing universal canonical structure generalizing Hamiltonian structure 15 p2539 A66-29145

Investigation methods for multidimensional dynamic systems, including parametric dependence, bifurcation theory and phase-propagation separation structure 15 p2541 A66-29165

Generalized dynamics, concepts and problems, noting application in system theory 15 p2472 A66-29372

Transformation equivalency of various forms of partial differential equations of motion of nonholonomic systems 16 p2747 A66-31144

Statics and dynamics of measuring devices, deriving equation for oscillating parameters via Taylor series 16 p2709 A66-31693

Dynamic systems with impact interactions and nonlinear oscillation theory 17 p3030 A66-32812

Amplitude maxima for nonstationary oscillations of dynamic system with multiple degrees of freedom 17 p3030 A66-32813

Basic properties of pure fluid devices including operating pressure, operating power and response time 20 p3500 A66-37644

**DYNAMO THEORY**  
Current system of solar disturbed diurnal variations of magnetic field at high latitudes in terms of dynamo theory, taking into account forward and Hall conductivities 04 p0516 A66-13854

Dynamo origin of geomagnetic field, involving creation of toroidal and polar fields by nonuniform rotation 08 p1215 A66-19117

Ionospheric dynamo theory with consideration for magnetospheric current along geomagnetic force lines, noting Sq variation in solstices 09 p1372 A66-20374

Ionospheric electrodynamics, discussing conductivity, wind and dynamo theory, drift effect on ionospheric formation and wind-electromagnetic field interaction 10 p1533 A66-21852

Cowling theorem for short-circuited MHD dynamo theory 14 p2341 A66-27199

Generalization of differential equation of dynamo theory of geomagnetic variations to include unsteady dynamo effect in ionosphere 22 p3914 A66-40759

Cowling theorem for short-circuited MHD dynamo theory 24 p4246 A66-43097

Geomagnetic disturbances due to dynamo effect of ionospheric winds in lower layers of ionosphere 24 p4204 A66-43150

**DYNAVERT AIRCRAFT**  
S CANADAIR CL-84 AIRCRAFT

**DYNODE**  
S ELECTRON MULTIPLIER

**DYSPROSIUM**  
Ruby laser radiation effect on fluorescence and laser action in dysprosium doped calcium fluoride crystals 01 p0082 A66-10718

Magnetic transitions in terbium and dysprosium as affected by hydrostatic pressure at various high pressures and low temperatures 08 p1274 A66-19361

Ruby laser radiation effect on fluorescence and laser action in dysprosium doped calcium fluoride crystals 20 p3579 A66-37656



**E**

**E-2 LAYER**  
E-2 layer of atmosphere, discussing maxima, minima, variations and shielding effect of E-layer 17 p2918 A66-32877

**E-BAND**  
Modulator resulting from application of Welker effect in semiconductor and used in Q and E bands, obtaining conductivity variations 16 p2662 A66-30960

**GLASS**  
Stress corrosion on E glass fibers exposed to water vapor 11 p1720 A66-23120

**LAYER**  
**SA SPORADIC E LAYER**  
Nondeviated absorption of radio waves in intermediate region between E and F layers 01 p0031 A66-11051  
E-layer disturbances caused by particles impinging upon atmosphere during auroras noting ionization, X-rays and electrical conductivities 03 p0365 A66-12858  
Magnetoionic splitting of radio signal in E and F layers, comparing calculated and theoretical gyrofrequency values 04 p0482 A66-13861  
Dense sporadic E cloud effects on high latitude HF backscatter observation 05 p0667 A66-14792  
Electrostatic field from E region and effect on motion of electrons trapped in magnetosphere 07 p1027 A66-17252  
Ionospheric E region inhomogeneity investigated by photographic recordings of reflected signal fading 08 p1214 A66-19049  
Short wave radio transmission and reception, examining masking by E region, focusing and attenuation due to scattering at ionospheric and other nonuniformities 08 p1186 A66-19780  
Measurement of horizontal ionospheric drifts in E and F regions over magnetic equator 11 p1696 A66-22381  
Changes in current kinetic theory of NO-O reaction, based on observation of release of nitric oxide in E region 11 p1703 A66-23494  
Diurnal and seasonal altitude variations of E and F layers analyzed for geomagnetic activity from rocket measurement of electron concentration 12 p1869 A66-24269  
Spectrum analysis of nondiurnal E layer variation at Washington, D.C., show relationship of 27-day variations of sunspot number and E layer critical frequency 12 p1874 A66-24845  
Unique ionospheric electron density distribution from ionograms from valley between E and F region 14 p2283 A66-27126  
Cellular circulation in ionospheric E region 14 p2289 A66-28333  
E layer ionization and characteristic number as affected by solar X radiation in 44-60 angstrom range 15 p2487 A66-29097  
Occurrence of collisions between ionized and neutral particles based on analysis of spectrum diffused by E region 15 p2491 A66-30021  
Atomic ions of meteoric origin indicated as source of midlatitude E region in IQSY rocket measurement 15 p2492 A66-30033  
Ionospheric absorption effects in D and E layers, noting refraction role and effective collision frequency 15 p2493 A66-30036  
Ion composition and effective recombination coefficient variation of ionosphere in study of X and UV radiation ionization of E layer 15 p2495 A66-30059  
Effect of meteor activity on fading of radiowave reflected from E region 16 p2692 A66-30331  
Electron density in E-and D-regions above Kjeller, Norway, from rocket measurements of absorption and height of reflection of radio waves 16 p2692 A66-30332  
Lyman alpha ionization of nitric oxide and ion molecule reactions accounting for ionic nitric oxide content of D and E regions 16 p2694 A66-30705  
Equatorial ionospheric drifts observed at Ibadan, Nigeria, during solar activity minimum, and relation to diurnal variation of sunspot cycle and drift velocity variations in E and F region 16 p2700 A66-31759  
Dependence of electron density in E layer on Sun zenith distance, based on new

ionospheric data and ionization neutralization phenomena 17 p2919 A66-32880  
Anomalous behavior in correlating maximum electron density dependence on solar zenith distance and asymmetry in critical frequency for E layer 17 p2919 A66-32881  
Relation between optical and electrical properties of interplanetary dust in upper atmosphere and comparison with twilight-optical and ionospheric parameters 18 p3105 A66-33961  
Diffusion spectrum modifications due to positive ions collision with neutral particles observed through ionospheric probe in E layer 19 p3346 A66-35590  
Electron injection and E-layer buildup in Astron device theoretically studied by one-dimensional model, using Green functions for self-electric and self-magnetic fields 19 p3423 A66-36552  
Comparison of magnitude of collision frequency of electrons in D and E regions obtained by satellites, rockets, etc, with cross sections measured in laboratory 19 p3352 A66-36627  
E-layer critical frequency variations conditioned by solar zenith angle, taking account of transport, gradient and time variations of height scale 21 p3732 A66-38664  
Short wave radio transmission and reception, examining masking by E region, focusing and attenuation due to scattering at ionospheric and other nonuniformities 21 p3703 A66-38776  
Collision frequency in E and D regions of ionosphere for electrons and neutral molecules 22 p3906 A66-39948  
E layer properties noting role of pressure, temperature, composition and recombination coefficient when varying with height and time 22 p3907 A66-39960  
Simultaneous long term ionospheric variation in midday averages of critical frequency E and F-2 at Washington, D.C. before and after increased geomagnetic activity 22 p3914 A66-40560  
Relation between diurnal, seasonal and cyclic variations of stratifications in E layer and fine structure of sporadic E layer and E-2 layer 22 p3914 A66-40761  
Enhanced activity in ionospheric E region at Cape Hallett and Campbell Island for information on diurnal variation and sunspot cycle changes of overhead and auroral activity 22 p3916 A66-40809  
Rocket observation of upper atmospheric wind around ionospheric E layer by sodium release method, noting cloud drift 24 p4199 A66-42466

**EAR**

**SA AUDITORY PERCEPTION**  
**SA AUDITORY SENSATION AREA**  
**SA LABYRINTH**  
**SA VESTIBULAR APPARATUS**  
Perceiving undetectable rotation in semicircular canals by employing self-induced Coriolis stimulation, determining psychophysical functions for direction or rotation discrimination at different yaw velocities 09 p1337 A66-20531  
Spatial interrelations between mitochondrial apparatus of capillary cells and synapses of these cells in utricular receptor of animals at rest and after exposure to accelerations, using electron microscopy 13 p2011 A66-26250  
Effect of oxygen deficiency on acoustic organ of cats, determining content of potassium and sodium ions in perilymph, cerebrosplinal fluid and blood serum 13 p2011 A66-26251

**EAR PRESSURE TEST**

Alternobaric /pressure/ vertigo severity and frequency among Swedish RAF pilots 11 p1644 A66-22584

**EAR PROTECTOR**

Speech communications effects and temporary threshold shift reduction characteristics of British-made earplugs under quiet and high intensity impulsive noise backgrounds 24 p4168 A66-42857

**EARDRUM**

Otitic barotrauma caused by difference between atmospheric pressure and middle ear cavity pressure arising during flight, compression chamber tests, etc, and leading to deafness 10 p1488 A66-22107

**EARLY BIRD SATELLITE**

Spin-stabilization system for attitude and orbit control of synchronous Syncom and Early Bird satellites 01 p0145 A66-11133  
Early Bird satellite structures and test problems 01 p0145 A66-11134  
Early Bird satellite technology including design parameters, structure, power supply, control system and test program 06 p0958 A66-15921  
Traffic needs of communications satellites including random-passing, station-keeping /phased-passing/ and geostationary satellites 06 p0959 A66-16495  
Diurnal variations of strength and polarization of VHF signals from synchronous Early Bird satellite 08 p1185 A66-19537  
Receiving equipment for Early Bird satellite at Fucino, Italy 09 p1354 A66-20559  
Commercial communications satellite for random, phased and synchronous medium altitude, noting design, specifications and operation 11 p1777 A66-22454  
Early bird hydrogen peroxide control system maneuvers to place satellite into final stationary position [AIAA PAPER 66-262] 12 p1954 A66-24736  
Effective radiated power receiving sensitivity, bandwidth and nonlinear performance of Early Bird satellite [AIAA PAPER 66-263] 12 p1820 A66-24737  
Performance of Early Bird communications satellite and associated ground stations [AIAA PAPER 66-264] 12 p1820 A66-24738  
International Telecommunications Satellite /INTELSAT/ Consortium and COMSAT participation in program [AIAA PAPER 66-332] 12 p1982 A66-24799  
Latitudinal variations of ionospheric irregularities studied via synchronous and 1000 km satellites, noting Early Bird data, scintillation index graphs, radio star signals, etc 15 p2496 A66-30071  
Global TV communications systems utilizing Telstar and Early Bird 17 p2875 A66-32900  
Early Bird satellite project using proven designs in spacecraft, launch vehicle and Earth stations to provide reliable microwave link between North America and Europe for TV and telephone 22 p3865 A66-40068

**EARLY WARNING SYSTEM**

**SA BALLISTIC MISSILE EARLY WARNING SYSTEM /BMEWS/**  
Effective early warning system to enable pilot to cope with clear air turbulence /CAT/ 14 p2326 A66-27819  
Turbulent refractivity spectrum and optimization of airborne radar CAT detectors 22 p3944 A66-40429

**EARTH**

Color and light intensity gradient of residual light scattered and refracted into umbra of Earth shadow measured during lunar eclipse 17 p2999 A66-32068  
Source distributions of UV and X-ray emission in corona and chromosphere determined from flight of spacecraft-borne instruments into Earth shadow 17 p3001 A66-32465  
Water vapor mass below upper limit of Earth cloud cover estimated through Earth brightness measurements 21 p3735 A66-39360

**EARTH ALBEDO**

Effectiveness of albedo and Earth radiation simulation, examining fixed chamber and fixed vehicle techniques 02 p0211 A66-11216  
Basic hypothesis concerning Earth radiation belts origin, discussing neutron albedo and effects of interaction between plasma and magnetic field 02 p0283 A66-11808  
Terrestrial albedo of 40 to 190 kev X-rays measured, using directional detectors at balloon altitude 03 p0419 A66-12683  
Viewing geometry in interpretation of reflected solar radiation data from Tiros IV 04 p0515 A66-13673  
Spectral albedo of deep body of water from 4800 to 6100 angstroms by Sobolev approximate method 05 p0674 A66-15418  
Neutron albedo measurements on polar orbiting satellites 07 p1120 A66-17981  
Neutron albedo flux at 45 degree geomagnetic latitude 07 p1121 A66-17982  
Survey of U.S. and U.S.S.R. literature on processes responsible for composition and spatial distribution of radiation



- belts 08 p1285 A66-19774  
 Height dependence of albedo in Earth upper atmosphere, calculating total quantity of neutral hydrogen in 11 p1699 A66-23044  
 ionosphere  
 Solar and sky radiation and short wave albedo measured at altitudes approaching 20,000 ft in high Himalayas 11 p1765 A66-23384  
 Rocket-borne neutron detector measurements of neutron albedo and intensities at various geomagnetic latitudes 18 p3199 A66-34887  
 Earth albedo estimation, backscattered interplanetary radiation and resonance scattering of dayglow 20 p3553 A66-38194  
 Survey of U.S. and U.S.S.R. literature on processes responsible for composition and spatial distribution of radiation belts 21 p3809 A66-38770

## EARTH ATMOSPHERE

## SA IONOSPHERE

## SA LOWER ATMOSPHERE

## SA MID-LATITUDE ATMOSPHERE

## SA TROPOSPHERE

- Earth atmosphere, discussing properties of high altitude neutral atmosphere combined with measurement of solar output variations 05 p0675 A66-15743  
 Manned orbiting astronomical observatories would enable astronomer astronauts to erect large sensors in space and avoid atmospheric effects 13 p2192 A66-25689  
 Book on methods in computational physics including numerical simulation of Earth atmosphere, computation of propeller design and stellar evolution, etc 16 p2735 A66-30942  
 Thermal synthesis of amino acids from methane-ammonia-water mixture passing through Earth-crust materials 17 p2851 A66-32089  
 Thermal escape of neutral hydrogen and distribution in Earth thermosphere, noting collision in transition regions 20 p3549 A66-37292  
 Low altitude measurements of trapped electrons, noting energy spectrum and longitudinal variations of electrons, including instrumentation 20 p3638 A66-38307  
 Mechanism for connection between seismic Earth and solar activity on atmosphere and lithosphere of Earth 22 p3914 A66-40767

## EARTH CORE

- Dynamo origin of geomagnetic field, involving creation of toroidal and polar fields by nonuniform rotation 08 p1215 A66-19117  
 Toroidal fields in Earth fluid metallic core brought to surface, causing changes with time in geomagnetic field 09 p1369 A66-19877  
 Phase-change hypothesis of structure of Earth, describing liquid core as product of static pressure crushing outer electron shell in solid mantle material 09 p1375 A66-20945

## EARTH CRUST

- Probability models for Earth crustal structure applying potential field separation technique, noting role of gravitational field and Wiener filtration theory 01 p0061 A66-10479  
 Lonar Lake depression explained by cryptovolcanic activity or meteorite impact 03 p0365 A66-12721  
 Gravitational field and crust of Earth related to Earth shape 05 p0675 A66-15748  
 Viscous fluid model estimates of crustal thickness and free-air anomaly compared with measured free-air anomalies and seismic depths of Puerto Rico trench and mid-Atlantic rise 06 p0877 A66-16786  
 Relative isotopic abundance of potassium 40 in terrestrial and meteoritic samples 11 p1770 A66-22572  
 Probability models for Earth crustal structure, applying potential field separation technique, noting role of gravitational field and Wiener filtration theory 12 p1868 A66-23877  
 Electrical conductivity of Earth interior from data concerning annual geomagnetic variations for all years of solar cycle 15 p2487 A66-29101  
 Book on structural geology and tectonics for undergraduates 16 p2692 A66-30267  
 Velocity reversals in Earth crust and low velocity zone of upper lithosphere 18 p3104 A66-33913  
 Crestone crater morphology indicates that

- it is not meteoritic or cometary in origin 18 p3106 A66-34462  
 Mechanism for connection between seismic Earth and solar activity on atmosphere and lithosphere of Earth 22 p3914 A66-40767  
 Optimum filter for separation of principal geomagnetic field and magnetic field associated with Earth thin magnetoactive crust layer 22 p3915 A66-40785

## EARTH CURRENT

## SA GEOELECTRICITY

- Continental structure and drift from convection currents in Earth mantle indicate depth of several hundred kilometers 03 p0360 A66-12378  
 Convection pattern changes in Earth mantle and continental drift as evidence of cold origin of Earth 03 p0361 A66-12379  
 VLF radio wave propagation in Earth ionosphere waveguide assuming finite ground conductivity 04 p0475 A66-13429  
 Terrestrial electrical currents discussing Soviet studies on short-period fluctuations of terrestrial electromagnetic field in Arctic and Antarctic region 05 p0674 A66-15225  
 Fine structure of magnetic storm discussing prestorm, initial stage and climax of fluctuations of Pc I and Pi I 07 p1027 A66-17308  
 Natural electromagnetic field of Earth microvariational peculiarities 07 p1027 A66-17309  
 Correlation relations between cosmic ray neutron intensity, horizontal magnetic field strength, critical wave frequency and terrestrial currents 08 p1283 A66-18706  
 Threadlike equatorial current ring and effect on geomagnetic cut-off rigidity of directed cosmic radiation 12 p1941 A66-24172  
 Effect of equatorial current ring distributed over globe on geomagnetic cut-off rigidity of cosmic rays 12 p1941 A66-24173  
 Earth electrical conductivity, determined from data concerning northern and vertical components of cyclic geomagnetic variations, suggests increases with depth 12 p1871 A66-24297  
 Natural telluric currents in Arctic Ocean and relation to geomagnetic variation observed on drifting station 15 p2488 A66-29113

## EARTH MANTLE

- Velocity and density perturbation of Earth mantle in inversion of eigenperiods 05 p0673 A66-15046  
 Concept of melting within Earth, effect on thermal model of Earth and differentiation of radioactive materials within Earth 09 p1370 A66-19878  
 Phase-change hypothesis of structure of Earth, describing liquid core as product of static pressure crushing outer electron shell in solid mantle material 09 p1375 A66-20945  
 Celestial body size, composition and impact induced changes in Earth rotation from mantle data 10 p1531 A66-21286  
 Review of experimental capabilities for reaching pressure and temperature conditions prevailing in Earth mantle and core, including bibliography 17 p2918 A66-32661

## EARTH-MARS RENDEZVOUS TRAJECTORY

- Venus swingby used to decelerate manned spacecraft returning from Mars 10 p1609 A66-21928  
 Six midcourse guidance techniques, noting Earth-Mars and Earth-Venus trajectory with small and large injection error 13 p2123 A66-25252

## EARTH-MOON SYSTEM

- Zodiacal light position considering ecliptic, based on photoelectric observation 01 p0061 A66-10275  
 Solar influence on libration point satellite motion for 2500 days in vicinity of Earth-Moon system [AIAA PAPER 65-88] 02 p0288 A66-11556  
 Variation of Earth-Moon distance and inclination angle of orbital planes during period of tidal evolution 03 p0427 A66-12920  
 Approximate value of mass of Moon calculated, using noncalculus derivation of Newton modification of Kepler third law 08 p1296 A66-19380  
 Earth-Moon distance measurement using laser technique 09 p1453 A66-20129  
 Design tolerances in construction and

- operation of dual-field mechanical simulator for satellite orbits 09 p1364 A66-20589  
 Variation of Earth-Moon distance and inclination angle of orbital planes during period of tidal evolution 14 p2380 A66-27269  
 Possible origin of lunar maria, suggesting they may be scars of mechanical damage wrought on lunar hemisphere by disruptive tides of Earth 14 p2384 A66-27900  
 Variation in Earth-Moon distance as result of meteoritic impact 15 p2597 A66-29261  
 Stability of spacecraft motion in Earth-Moon system near equilateral libration point 16 p2810 A66-31252  
 Spacecraft mission to libration centers of Earth-Moon system for collecting meteoroids and photographic program carried out for establishing presence of material at centers 18 p3236 A66-34955  
 Libration point motion in restricted four-body problem and stable trajectory determination for Earth-Moon-Sun system, noting effect of initial configurations of system [AIAA PAPER 65-684] 19 p3461 A66-35891  
 Lunar origin, tidal evolution of Earth-Moon system, thermal background of lunar interior, figure and composition of Moon and radial density profile 20 p3647 A66-37038  
 Terrestrial penumbra density variation with solar activity during lunar eclipses in 11-year cycle 22 p3976 A66-39857  
 Lunar orbit evolution caused by tidal friction in Earth and Moon interiors 22 p3985 A66-40956

## EARTH-MOON TRAJECTORY

- Nonplanar trajectory originating near Earth and passing close to Moon in restricted three-body problem 08 p1292 A66-19146  
 Space probes and Earth-Moon libration points 13 p2186 A66-26012  
 Earth Moon trajectories with consecutive collisions treated, using Birkhoff transformation in planar restricted three-body problem [AIAA PAPER 65-86] 14 p2381 A66-27422  
 Cisunar libration point as place of departure, rendezvous and parking for lunar operation 14 p2390 A66-28450  
 Radiation environment in near Earth space and effect on humans during space flight to Moon 15 p2435 A66-29454  
 Three-body problem of cisunar space flight, noting effect of solar gravitational field on spacecraft trajectory 16 p2804 A66-31332  
 Earth shadow enlargement during lunar eclipse, noting contacts of lunar formations with shadow 17 p3000 A66-32341  
 Accuracy requirements for two-way spacecraft Earth-Moon orbit trajectory are greater for minimum initial velocity and in lunar proximity, considering solar gravity perturbation effect 19 p3460 A66-35721  
 Periodic motion of artificial satellite around Earth and Moon 19 p3464 A66-36369  
 Iterative guidance mode with application to three-dimensional upper stage vacuum flight 21 p3768 A66-38897

## EARTH MOTION

- Review of current knowledge and techniques for stabilizing test pads for high precision inertial guidance and control components 01 p0051 A66-10028  
 Annual motion of poles of Earth consisting of solid shell and liquid core, considering annual motion of inertia pole due to air mass displacements 08 p1220 A66-19456  
 Weak latitudinal waves observed by Orlov method at three midlatitude stations from 1924 to 1930 10 p1530 A66-21260  
 Nutation constant for absolutely solid Earth from recent astronomical unit and lunar mass measurements 12 p1867 A66-23513  
 Secular motion of Earth pole from 1900 to 1958 measured via harmonic analysis, noting rate and distance 12 p1868 A66-23669  
 Ancient solar eclipses analyzed, determining secular decrease in angular velocity of Earth by computation based on ephemeris time and astronomical constants 17 p2999 A66-32067  
 Annual motion of poles of Earth consisting of solid shell and liquid core, considering annual motion of inertia pole due to air mass displacements 18 p3106 A66-34485  
 Elastic dissipation of Earth torsional modes estimated by generalized elastodynamic



- equation 18 p3108 A66-34734
- Nutation constant for absolutely solid Earth from recent astronomical unit and lunar mass measurements 20 p3549 A66-37027
- EARTH ORBIT**
- Lunar inequality on time of perihelion passages of Earth 04 p0576 A66-13461
- Earth satellite elliptical orbit intersection point with Earth shadow determined by exact solution of fourth-power algebraic equation with respect to  $\tan$  E/2 17 p2995 A66-31848
- EARTH ORBITAL RENDEZVOUS /EOR/**
- Gemini VII star sightings analyzed, using handheld space sextant in Gemini VI, discussing effect of bias, timing, angle measurement and trajectory errors 21 p3767 A66-38893
- EARTH RADIATION**
- S TERRESTRIAL RADIATION**
- EARTH ROTATION**
- Corrections for apparent drift rate of free ideal directional gyroscope due to Earth rotation 02 p0290 A66-11986
- Time observations and variation of rotation speed of Earth 03 p0366 A66-13009
- Migration of north and south poles by angular displacement of Earth mass, explaining geographical distribution of flora and fauna, past and present 05 p0667 A66-14730
- Spherical harmonic analysis of diurnal surface pressure oscillation indicates that it can be represented by wave traveling westward with Sun 07 p1027 A66-17224
- Excitation and damping of polar motion treated as series of stochastic process in determination of damping coefficients and constants 07 p1028 A66-17420
- Coincidence of long-term variation of Chandler period of motion for Earth pole and solar activity cycles 07 p1028 A66-17524
- Fluctuations since 1956 in period of Earth rotation obtained in universal atomic time with photographic zenith tube at Neuchatel Observatory 07 p1135 A66-17633
- Earth daily diurnal rotation rate variation, assuming solar corpuscular flux composition of plasmoids possessing quasi-force-free magnetic fields 08 p1220 A66-19787
- Maximum ballistic rocket trajectory range in view of Earth rotational and curvature effects 11 p1734 A66-23346
- Corrections of sight-line velocities for Earth diurnal rotation and annual revolution in observations of Sun 12 p1949 A66-24246
- Liapunov method and dynamic programming of stability of motion of variable mass point in Oxyz coordinate reference system, allowing for Earth rotation effects 15 p2538 A66-29046
- Average rotational speed of upper atmosphere above 200 km evaluated from changes in orbital inclinations of 13 satellites 15 p2496 A66-30082
- Atomic maser clocks rotation with Earth, deriving formula for relative drift at widely separated localities arising from local gravitational potentials 16 p2745 A66-30187
- Random variation of Earth rotation relation to amplitude of free nutation 16 p2693 A66-30589
- Internal measurement of latitude, radius vectors and other geophysical properties from center of mass of astronomical system to space vehicle 16 p2698 A66-31386
- Transformation of tesseral harmonics under rotation in elementary and self-contained method 17 p2921 A66-33225
- Equatorward motions of auroras 17 p2923 A66-33356
- Solar activity and irregular variations in Earth rotational rate 19 p3345 A66-35272
- Epheermal georotational variations from deviations in quartz oscillator clocks of Paris and Greenwich observatories 19 p3351 A66-36370
- Iterative method for extracting annual and Chandlerian terms of variation of Earth rotation from experimental data of universal time 20 p3550 A66-37410
- Earth daily diurnal rotation rate variation, assuming solar corpuscular flux composition of plasmoids possessing quasi-force-free magnetic fields 21 p3733 A66-38783
- Time dependent behavior of temperature and density in monoconstituent atmosphere under diurnal photoheating and cooling by conduction, analyzing effect of atmosphere rotation eastward 23 p4064 A66-41678
- Lunar tidal variations, georotational velocity and calculation of Love number 24 p4198 A66-42246
- NASA Biosatellite Program exploring dynamic space flight effects on terrestrial organisms and Earth diurnal rotation effect on biological rhythm 24 p4168 A66-42675
- EARTH SHAPE**
- Modifying spherical harmonic analysis of surface geomagnetic field to account for Earth oblateness by two methods 01 p0061 A66-10615
- Refinement of theory for determining figure and size of Earth from observations of artificial satellites 01 p0062 A66-10692
- Orbits of artificial satellites for suitable variables, noting oblate shape of Earth and air resistance 02 p0285 A66-11256
- Uniform worldwide spatial triangulation grid for measuring Earth radius 03 p0361 A66-12532
- Comments on Volland paper about analytical model of Earth-ionosphere waveguide supposedly agreeing with Austin radio transmission formula 05 p0632 A66-14840
- Gravitational field and crust of Earth related to Earth shape 05 p0675 A66-15748
- Closed-form coordinate perturbations of elliptic orbits due to Earth oblateness, discussing four methods of deriving expressions 06 p0956 A66-16910
- Shape and gravitational field of Earth calculated by using N homogeneous incompressible fluid shells to represent distribution of terrestrial mass 07 p1028 A66-17422
- Effect of Earth oblateness on lifetime of satellite in time-varying atmospheric density [AIAA PAPER 66-63] 07 p1139 A66-18451
- Classical problem of diffraction of radio waves around spherical Earth 11 p1652 A66-22462
- Dynamic model of equilibrium figure of Earth, taking into account surface cooling and lunar gravitational effect 11 p1698 A66-22652
- Data on satellite orbits used for Earth figure, upper atmosphere density, solar radiation, etc. 12 p1868 A66-23637
- Flows and fractures as types of deformation occurring on Earth under huge loads of ice suggested by isostatic compensation of Antarctica, Arctic basin and glaciated region in North America 12 p1875 A66-24894
- Equations for translatory motion of lifting body moving at hypersonic speed, considering Earth sphericity, noting effect of centrifugal forces 13 p2193 A66-26448
- Minimum time-of-flight aircraft trajectory between two points with account of Earth sphericity 13 p2125 A66-26481
- Mass calculation for absorbing gases such as water vapor, carbon dioxide and ozone along oblique paths between two arbitrary points in atmosphere, considering vertical distribution, refraction and Earth curvature 14 p2284 A66-27541
- Horizon profile of Earth calculated from solutions of plane-parallel Rayleigh scattering atmosphere 14 p2328 A66-27880
- Effect of slope and curvature of Earth surface on disturbing potential, using Molodenskii integral equation, obtaining deflection of vertical, disturbing potential and Stokes constant 14 p2288 A66-28210
- Numerical integration principle in calculation of disturbing potential verified, using conical Earth model 14 p2288 A66-28211
- Refinement of theory for determining figure and size of Earth from observations of artificial satellites 15 p2483 A66-28553
- Flat Earth approximation of LF propagation theory 18 p3072 A66-34711
- Spheroidal-type seismogram study of wave generation, propagation, dispersion and attenuation in realistic spherical Earth models, especially Gutenberg-Bullen A-prime model 20 p3550 A66-37433
- IAU system of geocentric astronomical constants for ellipsoid Earth 20 p3653 A66-37762
- Upper wind evaluation by pilot and radiosonde balloon radar tracking for flat Earth and effects of Earth curvature 22 p3943 A66-40428
- Earth shape, moment of inertia and gravitational field determined from two nonlinear integral equations for potential of rotating incompressible fluid 23 p4063 A66-41202
- Mass calculation for absorbing gases such as water vapor, carbon dioxide and ozone along oblique paths between two arbitrary points in atmosphere, considering vertical distribution, refraction and Earth curvature 24 p4198 A66-42326
- Orbital plane precession due to ellipsoidal shape of Earth, discussing effect on meteorological and geodetic satellites 24 p4279 A66-42963
- EARTH SURFACE**
- Soviet, Swedish and Norwegian data on solar activity and barometric pressure, showing corpuscular flux effect on barometric pressure even at Earth surface 01 p0060 A66-10272
- Evaporation as molecular diffusion from large rough surface into random-lived internal scale turbulent eddies 02 p0223 A66-11960
- Climatic conditions at Earth surface, relation to long-term planetary trends in atmospheric circulation 05 p0712 A66-15221
- Airborne measurement of microwave emission from Earth surface and atmosphere for potential application of radiometry to weather satellite reconnaissance 05 p0675 A66-15765
- Reducing values of potential magnetic or gravitational field observed on Earth surface with weak profile to values on single horizontal plane in lower half-space 06 p0876 A66-16417
- Spectral distribution of direct sunlight at Earth surface at sea level, as function of air mass and concentration of aerosol, ozone and water vapor 09 p1375 A66-20962
- Nimbus I IR scanning radiometry for nocturnal imagery of clouds and other data, IR spectral returns and relation to image gray scale 10 p1531 A66-21519
- Effects of long-wave radiation exchange near Earth surface, extrapolating air temperature measurements to ground to estimate surface temperature, obtaining equivalent black body temperature of ground 11 p1702 A66-23155
- Twelve monthly world maps of daily means of total solar radiation incident on horizontal surface 11 p1702 A66-23156
- Compensated coordinates of artificial Earth satellites from synchronous observations at two given points on Earth surface 12 p1824 A66-24875
- Concentration distribution at Earth surface associated with precipitation of cloud of interacting particles forming dust source, due to turbulent scattering in time and space 13 p2122 A66-26248
- Accuracy of measuring method of vertical gradient of gravity force from gravity anomalies, using Numerov formula and Earth models 14 p2288 A66-28214
- Radar cross section of Earth surfaces as affected by wavelength, with reference to probing lunar surfaces 15 p2448 A66-28572
- VLF radio wave propagation in model Earth ionosphere waveguide with finite surface impedance and arbitrary height 15 p2449 A66-28598
- Soil investigation and geological map preparation from aerial photographs 15 p2505 A66-30014
- Aerial photography of Earth surface, discussing application in Earth and life sciences 17 p2925 A66-32609
- Earth surfaces reflecting and polarizing properties in aerial reconnaissance 17 p2918 A66-32611
- Gravity anomalies of unsurveyed areas of Earth surface and influence on satellite orbit perturbations 17 p2921 A66-33196
- Elastic model for evaluating stresses in Earth induced by density variations or topographic irregularities 17 p2921 A66-33226
- Formulas for extraterrestrial potential, anomalous gravity force gradient on Earth topographic surface, deflections of vertical, etc. 20 p3549 A66-37043
- Radio wave propagation over Earth surface, determining conductivity and dielectric constant taking into account ground



- effect 21 p3706 A66-39514  
Concentration distribution at Earth surface associated with precipitation of cloud of interacting particles forming dust source, due to turbulent scattering in time and space 22 p3942 A66-39710  
Airborne spectrozonal telephotometer used in calculation of photographic brightness coefficient of Earth surface 22 p3919 A66-40621  
Magnetic field of ring current on Earth surface according to observations during IGY 22 p3914 A66-40768  
Two-dimensional purely elastic Earth model used to study elastic equilibrium configuration between density and topographic surface irregularities 23 p4063 A66-41391
- EARTHQUAKE**  
**SA SEISMIC WAVE**  
Long-period acoustic-gravity waves launched into F region by Alaskan earthquake of March 28, 1964 08 p1219 A66-19418  
Conversion factor determination for gravity changes during Alaska earthquake, using LaCoste-Romberg geodetic meter 09 p1369 A66-19872
- EBERT SPECTROMETER**  
Mathematical design and development of balloon-borne UV Ebert-Fastie spectrometer with Sekera-type polarimeter 02 p0233 A66-12212  
Three-meter Ebert grating spectrometer with mock interferometer attachment 14 p2294 A66-27497
- EBULLITION**  
**S BOILING**
- ECCENTRICITY**  
Orbital eccentricity of balloon satellites Echo I, Echo II and Explorer XIX, discussing influence of solar radiation pressure 14 p2383 A66-27824  
Longitudinal stiffeners eccentricity /one-sidedness/ effect on buckling strength of axially compressed cylinders 14 p2404 A66-27989  
Conventional two-body orbit equations for eccentricity near unity 18 p3227 A66-33829  
Ring stringer eccentricity effects on structural optimization of stiffened axially compressed cylinders 20 p3672 A66-38166  
Eccentricity effect on magnitude of discontinuity stresses in unsymmetrically loaded shells of revolution, discussing results of numerical calculations 22 p3993 A66-40366
- ECHO**  
**SA ANECHOIC CHAMBER**  
**SA AURORAL ECHO**  
**SA LUNAR ECHO**  
**SA RADAR ECHO**  
**SA RADIO ECHO**  
Generation of echo at cyclotron resonance in plasma provides means of measuring and displaying relaxation processes 11 p1748 A66-23393  
Propagation paths between hemispheres followed by usual and unusual whistlers, giving rise to series of echoes 20 p3553 A66-38077
- ECHO I SATELLITE**  
Space communications antennas, discussing ground to space systems, satellite relay methods, etc 05 p0651 A66-15839  
Photoelectric photometry of rotation of Echo I and II satellites, discussing duration, variation with time and direction of rotation relative to revolution 11 p1769 A66-22477  
Method of closing directions used in adjustment of satellite triangulations performed on basis of results of synchronous observations of Echo I during spring of 1963 20 p3552 A66-37842  
Results of applying tetrahedron method for synchronous observations of Echo I made during May and June 1963 20 p3518 A66-37843  
Azimuth of line between Potsdam and Bucharest from Echo I satellite photographs 22 p3903 A66-39694
- ECHO II SATELLITE**  
Echo II program to launch passive communications satellite that will maintain spherical shape and surface smoothness after loss of inflatable pressure 01 p0145 A66-11122  
Full scale ground inflation tests to evaluate structural and RF backscatter characteristics of Echo II prototype spheres as function of their internal pressures 01 p0055 A66-11123  
Echo II TV system to observe deployment, inflation and injection into orbit 01 p0073 A66-11124  
Radio beacon telemetry system for measuring orbital performance of Echo II satellite, including internal pressure and skin temperature 01 p0032 A66-11125  
Experiments with Echo II satellite to determine its capability as passive communications device and study shape and surface as function of time 01 p0032 A66-11126  
Photographs of passage of Echo II into Earth shadow to determine aerosoles and atmospheric ozone height distribution 03 p0427 A66-12924  
Communication experiments with Echo II during first year in orbit, discussing reflected signals 04 p0478 A66-13594  
Radio communication between U.S.S.R. and Great Britain via passive Earth satellite Echo II and Moon signal reflection 07 p1001 A66-17345  
Photoelectric photometry of rotation of Echo I and II satellites, discussing duration, variation with time and direction of rotation relative to revolution 11 p1769 A66-22477  
Photographs of passage of Echo II into Earth shadow to determine aerosoles and atmospheric ozone height distribution 14 p2380 A66-27273  
Day-to-night and semiannual variations in exospheric density during low solar activity from observations of Echo II orbital period changes 15 p2497 A66-30084  
Photoelectric photometry of Echo II satellite and graphs of light curves giving light intensity logarithm as function of time 22 p3863 A66-39856
- ECHO PROJECT**  
Echo project objectives and results 01 p0145 A66-11127
- ECHO SATELLITE**  
Geodetic determinations from photoelectric observations of occultation of stars by satellites 03 p0428 A66-13030  
Simulation of satellite magnetic stabilization system in airbearing facility, using coils-only magnetic torquing for attitude orientation 08 p1203 A66-19514  
Forecasts of periods of brilliant visibility for satellites Echo I and II in 1966, especially for latitude of Belgium 13 p2026 A66-26321  
Photoelectric photometer used for tracking entry of artificial satellites into shadow of Earth 20 p3518 A66-37839
- ECLIPSE**  
**SA LUNAR ECLIPSE**  
**SA SOLAR ECLIPSE**  
Possible atmosphere detection on J-II and J-III satellites revealed by excess brightness on eclipse reappearance 10 p1604 A66-21202  
Mars atmospheric density determined from photoelectric measurements of eclipses of Phobos 15 p2604 A66-30049
- ECLIPSING BINARY STAR**  
Astronomical yearbook of Cracow Observatory covering ephemerides of 787 eclipsing binaries, Lagrangian points, precession coefficients, etc 11 p1768 A66-22333  
Photoelectric observations and orbital solutions of BV 267, obtaining new light elements, system light change and orbital solutions 11 p1769 A66-22533  
Photoelectric observations and orbital solutions of BV 342, obtaining light element and light curve data 11 p1769 A66-22534  
Brightness curves used to determine geometrical and physical parameters of eclipsing binary systems containing component with extended spherical atmosphere 20 p3647 A66-37031  
Tabulation of photoelectric spectrophotometric observations of eclipsing system RX Arietis 24 p4273 A66-42206  
Tabulation of photoelectric spectrophotometric observations of eclipsing system UV Leonis 24 p4273 A66-42207
- ECOLOGICAL SYSTEM**  
**S CLOSED ECOLOGICAL SYSTEM**
- ECOLOGY**  
Ecological patterns of microorganisms in desert soils 15 p2441 A66-29960
- ECONOMICS**  
Economic feasibility of all-rocket approach to reusable launch system, comparing various classes of launch vehicles, noting need for payload recovery [SAE PAPER 650802] 01 p0144 A66-10817  
Price determining factors considered in integrated circuit amplifier for AM receiver 02 p0203 A66-11925  
Runway design by assessing capacity, delay of operations, costs, etc, using mathematical models 03 p0352 A66-12706  
French aerospace industry, relationship to French economy, annual expenditures 1958 to 1964 and aircraft exports 05 p0794 A66-15189  
Government research and development inventions 06 p0972 A66-16076  
Interaction of pilot capabilities and economic factors on future air transport, noting problems with SST, V/STOL, Mach 6 transport craft, etc 07 p1156 A66-17611  
Operational problems and costs of staged solid-propellant rocket vehicles for atmosphere only, noting aerodynamic stabilization, spin motors, stage separation, jet plume, etc 07 p1140 A66-17612  
Contractor performance on cost type contracts evaluated by comparing actual and allocated costs, using NASA PERT facilities 08 p1322 A66-19460  
European and U.S. space transport models characteristics, noting possible cooperation because of costs 09 p1473 A66-20552  
U.S. nuclear rocket propulsion program costs, technology and application, noting empirical law of space nuclear program economics 11 p1734 A66-23078  
U.S. SST in competition with other SST and economic effect on airlines and U.S. economy 13 p1995 A66-25765  
Defense Materials System control of copper, aluminum and steel and proposed program for readiness and contingency planning of external resources for aerospace industry [SAE PAPER 660286] 14 p2416 A66-27297  
Economic effects of turbulence on airline operations, considering costs on temporary grounding for repairs, passenger injuries, information dissemination on turbulence, etc 15 p2618 A66-28916  
Coordinated air-surface transportation microeconomic analysis 15 p2620 A66-29796  
Factors to be considered in capital equipment and facilities for environmental testing, including management planning, work load reorientation, etc 16 p2831 A66-30441  
Transport aircraft economics of load factor and wasted seat problem 17 p2846 A66-32795  
Practical cost reduction possibilities within aerospace industry 18 p3268 A66-33947  
Economics of Ownership structure and cost effectiveness in microelectronic systems 20 p3684 A66-37904  
Management planning and profit and loss in systems design 20 p3685 A66-37918  
Economics of airport facilities and operations, noting safety and regularity problems 20 p3687 A66-38016  
Economics of various orbital boosters from completely expendable to completely recoverable vehicles, noting concept of cost-optimum vehicle 23 p4133 A66-41775  
Generalized system for project control and evaluation, considering cost, time, performance and reliability 23 p4152 A66-41777  
Hypersonic transport /HST/ evaluation noting problems in aerodynamics, economics, structures, propulsion systems, etc 24 p4159 A66-42236  
Airborne digital computers role in electronic warfare, navigation and guidance, considering weight, power supply, costs, etc 24 p4177 A66-42245
- EDDY CURRENT**  
Equation of velocity distribution of fluid in duct, evaluating effect of eddy activity on second derivative 02 p0218 A66-11759  
Tensorial character of eddy viscosity coefficient in incompressible turbulent flow 03 p0358 A66-13099  
Viscous flow eddy behavior near sharp corner, considering outer boundary conditions and stream



- function 07 p1023 A66-18115
- Viscous structure of separated eddy bounded by circular streamline and eddy in square cavity driven by moving boundary at top 08 p1166 A66-19819
- Temporal spectra of atmospheric angular momentum transfer from wind data at various tropospheric and lower stratospheric levels 11 p1697 A66-22566
- Flow parameters of incompressible ideal fluid in axisymmetric curvilinear channel, obtaining and solving nonlinear differential equation 12 p1863 A66-24243
- End effects in steady state MHD J x B accelerator, noting voltage and current distribution and eddy-current geometry 14 p2342 A66-27430
- Refractory metal tubing inspection using ultrasonic and pulsed-eddy-current methods in conjunction with X radiography 15 p2509 A66-29317
- Eddy current nondestructive test instrument for measuring magnetic permeability, electric conductivity and thickness of materials 16 p2701 A66-30320
- Scattering of electromagnetic waves in plasma, noting effect of eddy current fluctuations 16 p2654 A66-31179
- Eddy current damping effect on satellite attitude stability 17 p3016 A66-32481
- Various heat treat tempers of 2014 Al alloy and corresponding values of eddy current 17 p2940 A66-33099
- Finite amplitude disturbances in baroclinic atmosphere, considering interaction with zonal current and effect of upward eddy transport upon time change of mean static stability 21 p3759 A66-39205
- Physical principles of phase sensitive eddy-current method of detecting surface cracks in metal products 24 p4218 A66-42898
- Phase-sensitive eddy current method of detecting surface cracks in metal products, examining construction and operating principles of flaw detector 24 p4218 A66-42899
- Wind and temperature profiles for constant flux atmospheric boundary layer in lapse stratification implying relation between eddy transfer coefficient ratio and stability parameter 24 p4202 A66-42982
- Stress, eddy viscosity and viscous dissipation estimations in jet stream obtained during Project TOPCAT in Australia, using aircraft soundings 24 p4234 A66-42984
- EDDY DIFFUSION**
- Eddy conductivity, eddy viscosity and dimensionless ratio of diffusivity for mercury flowing in tube 01 p0164 A66-10904
- Karman vortex street pattern of mesoscale eddies in wake of islands [AIAA PAPER 65-16] 02 p0221 A66-11548
- Evaporation as molecular diffusion from large rough surface into random-lived internal scale turbulent eddies 02 p0223 A66-11960
- Mesoscale eddies in wake of islands describing properties, characteristic parameters via Karman vortex street pattern, drag theory and empirical observation 07 p1061 A66-17365
- Large-eddy energy equilibrium hypothesis leading to relationship between mean rate of shear strain and Reynolds shear stress involving scale of large eddies 08 p1212 A66-19817
- Ablation particulate dispersion in atmosphere estimation by calculating particle deposit concentration at Earth surface [AIAA PAPER 66-379] 12 p1951 A66-24504
- Evolution of scalar quantity spectrum in statistically stationary isotropic turbulent velocity field determined by closure approximation theory 12 p1865 A66-24583
- Lateral covariance, longitudinal eddy length-scale and vorticity-transfer-adaptation hypothesis of two-dimensional jet turbulence theory 13 p2064 A66-26123
- Effective early warning system to enable pilot to cope with clear air turbulence /CAT/ 14 p2326 A66-27819
- Average rate of eddy mixing obtained from some eddy transport problems in thermosphere, noting molecular diffusion 15 p2490 A66-29945
- Large-and small-scale atmospheric eddy velocities and scale lengths estimated, noting eddy Reynolds number ascertained from dispersion of chemical contaminants 16 p2696 A66-30927
- Atmospheric circulation and eddy diffusion based on thermal structure, oxygen transport continuity and sodium trail spreading in thermosphere 19 p3347 A66-35645
- Physical structure of upper atmosphere given by pressure and density scale heights and mean molecular mass due to diffusion 19 p3349 A66-36348
- EDGE**
- S LEADING EDGE
- S TRAILING EDGE
- EDGE DISLOCATION**
- Spectral responses of photoconductivity in plastically deformed germanium at liquid nitrogen temperature 02 p0274 A66-11720
- Couple-stresses in dislocated solids and effect in classical elasticity 04 p0594 A66-14292
- Opening of parallel cracks by applied tensile stress in terms of dislocation distribution theory 14 p2408 A66-28389
- Linearized theory of coupled stress elasticity and stress distributions around simple edge and screw dislocations 15 p2609 A66-29241
- Distribution of edge-type dislocations in GaAs grown from solution by traveling solvent method determined, using etching techniques 19 p3437 A66-35432
- Metastable dislocation crack transformation into polygonal walls of edge dislocations caused by diffusion over crack surface 20 p3669 A66-37551
- EDGE LOADING**
- Large deflection analysis of circular ring plates under uniform transverse force along inner edge 02 p0298 A66-11584
- Transverse shear displacements for orthotropic plate of constant thickness determined by iterative method 03 p0439 A66-13153
- Cyclic edge loading effect on circular reinforced cylindrical shells 04 p0589 A66-14147
- Asymptotic integration of thin elastic shell equations for design of shells of revolution subject to effect of cyclic edge loads 04 p0590 A66-14149
- Influence of edge displacements on vertical deflection of semiinfinite isotropic elastic plate 06 p0966 A66-16502
- Equilibrium equations in displacements for circular cylindrical shells reinforced by longitudinal and transverse ribs under arbitrary surface and edge loads 08 p1312 A66-19434
- Simplified calculation of axisymmetric bending of annular three-layer plates with lightweight filler by use of initial parameter method 08 p1313 A66-19437
- Edge effect in case of finite pipe under arbitrary axisymmetrical load, determining radial displacement 11 p1782 A66-22851
- Semiinfinite rectangular plate with two opposite edges clamped 12 p1962 A66-23997
- Stressed state of isotropic elastic medium with two circular holes solved, using approximation method for concentrated loads 13 p2202 A66-26417
- Imperfections and edge restraint effect on buckling of axially compressed cylinders 14 p2404 A66-27988
- Edge load solution for conical shells 14 p2408 A66-28133
- Complex variable method to solve problem of circular elastic plate elastically restrained at edge and subjected to arbitrary concentrated force 17 p3020 A66-32000
- Longitudinal bending of elastic truncated conical shell subjected to edge loads 17 p3020 A66-32001
- Dynamic elastic response of inner and outer edges of ring to distributed impact loads 18 p3247 A66-33570
- Stress concentration in nonlinear creep of long thin cylindrical shell loaded at one edge by symmetrical radial shear and bending moment 18 p3248 A66-33578
- Bending characteristics of tapered cylindrical shells, discussing edge and internal influence coefficients 18 p3253 A66-33806
- Postbuckling behavior of clamped infinite flat strip under action of shearing forces analyzed based on von Karman equations 20 p3669 A66-37531
- Elastoplastic bending of thin annular plates with free inner edge, based on Mises yield condition and Hencky stress-strain relation 20 p3671 A66-38102
- Stress-distribution in wedge-shaped plate with stiffener on one of edges loaded by axial force, reduced to difference equation solution for shear-stress transform along stiffened edge 21 p3832 A66-39460
- Influence coefficients for semiinfinite and infinite circular cylindrical elastic shell subject to self-equilibrating edge loads 22 p3995 A66-40451
- Energy method application to buckling of axially compressed cylindrical shells with ring-stiffened edges, noting upper and lower bounds and critical rigidity ratio 23 p4140 A66-41912
- Classical critical stress values for buckling of thin walled circular cylindrical shells in axial compression as function of edge conditions 23 p4143 A66-41965
- EDUCATION**
- Safety education, management process and aerospace accidents 01 p0169 A66-10073
- Astronautics education for RAF and USAF officers 06 p0972 A66-15920
- Postgraduate aviation and space medicine course at University of Rome 06 p0972 A66-16054
- Computer graphics in communication 13 p2085 A66-25364
- Apparatus for teaching and research in electron physics including emitters, cathode ray tubes, electron multipliers and mass spectrometer 18 p3088 A66-35033
- Space law education 19 p3483 A66-36217
- EDUCATIONAL TELEVISION**
- Satellite Educational and Informational Television, noting management, market and development problems in terms of profit, demand and growth potential [AIAA PAPER 66-274] 12 p1981 A66-24747
- Effective radiated power /ERP/ satellite for educational TV distribution, discussing design feasibility, cost comparison, spectrum utilization and system model [AIAA PAPER 66-320] 12 p1982 A66-24791
- Economic aspects of educational television distribution system, using comprehensive total cost model [AIAA PAPER 66-321] 12 p1982 A66-24793
- EEG**
- S ELECTROENCEPHALOGRAPH /EEG/
- EFFECT**
- S ATMOSPHERIC CONDITION EFFECT
- S BACKGROUND EFFECT
- S BARKHAUSEN EFFECT
- S BIOLOGICAL EFFECT
- S BRILLOUIN EFFECT
- S CAPTURE EFFECT
- S CERENKOV EFFECT
- S CHEMICAL EFFECT
- S COANDA EFFECT
- S COMPRESSIBILITY EFFECT
- S COMPTON EFFECT
- S CORIOLIS EFFECT
- S DIFFUSION EFFECT
- S DIHEDRAL EFFECT
- S DOPPLER EFFECT
- S DRAG EFFECT
- S ETTINGSHAUSEN EFFECT
- S ETTINGSHAUSEN-NERNST EFFECT
- S EVERSHED EFFECT
- S FARADAY EFFECT
- S FORBUSH EFFECT
- S FREE STREAM EFFECT
- S GEOMAGNETIC EFFECT
- S GRAVITATIONAL EFFECT
- S GREENHOUSE EFFECT
- S GROUND EFFECT
- S GUNN EFFECT
- S HALL EFFECT
- S HEAT EFFECT
- S JAHN-TELLER EFFECT
- S JET BLAST EFFECT
- S KERR EFFECT
- S LONG PERIOD EFFECT
- S LUNAR EFFECT
- S MAGNETIC EFFECT
- S MAGNUS EFFECT
- S MEISSNER EFFECT
- S MOSSBAUER EFFECT
- S NONOHMIC EFFECT
- S PATHOLOGICAL EFFECT



- S PELTIER EFFECT  
 S PHOTOELECTROMAGNETIC /PEM/ EFFECT  
 S PINCH EFFECT  
 S POCKEL EFFECT  
 S PRESSURE EFFECT  
 S PSYCHOLOGICAL EFFECT  
 S RADIATION EFFECT  
 S RAMAN EFFECT  
 S REENTRY EFFECT  
 S RELATIVISTIC EFFECT  
 S RESONANCE EFFECT  
 S REYNOLDS NUMBER EFFECT  
 S SCALE EFFECT  
 S SCHOTTKY EFFECT  
 S SCREEN EFFECT  
 S SEEBECK EFFECT  
 S SOLAR ACTIVITY EFFECT  
 S SOLAR EFFECT  
 S STARK EFFECT  
 S SURFACE ROUGHNESS EFFECT  
 S TAB EFFECT  
 S TEMPERATURE EFFECT  
 S THERMAL EFFECT  
 S THOMSON EFFECT  
 S THRUST EFFECT  
 S TURBULENCE EFFECT  
 S VACUUM EFFECT  
 S VESTIBULAR EFFECT  
 S VIBRATION EFFECT  
 S WIND EFFECT  
 S WING FLAP EFFECT  
 S ZEEMAN EFFECT
- EFFICIENCY**  
 S COMBUSTION EFFICIENCY  
 S COMPRESSOR EFFICIENCY  
 S ENERGY CONVERSION EFFICIENCY  
 S NOZZLE EFFICIENCY  
 S POWER EFFICIENCY  
 S PROPELLER EFFICIENCY  
 S PROPULSIVE EFFICIENCY  
 S THERMAL EFFICIENCY  
 S THERMODYNAMIC EFFICIENCY  
 S TRANSMISSION EFFICIENCY
- EFFUSION**  
 Rate of effusion for gas flow through orifice and application to fluorine gas dissociation energy 11 p1688 A66-22880  
 Vapor composition, evaporation rate and vapor pressure above chromium carbides determined by effusion method combined with mass spectrometry 14 p2310 A66-26791
- EIGENFUNCTION**  
 Eigenfunction expansions of convenient fourth order equation constructed examining convergence, method for summing various associated series and solution of boundary value plate problems 01 p0154 A66-10484  
 Waveguide containing ferrite of ferrite-dielectric insert determined by applying eigenfunction method 04 p0499 A66-14051  
 Expansion in eigenfunctions of not self-conjugate boundary value problem for differential equation with singularity at zero 05 p0709 A66-15339  
 Indirect method of estimating Green kernels, eigenvalues and eigenfunctions of operators related to elliptic problems 07 p1059 A66-18031  
 Green function-eigenvalue relationship on closed smooth boundary of open dimensional region 09 p1394 A66-20265  
 Free transverse vibrations of parabolic membranes, obtaining eigenvalues and eigenfunctions for Dirichlet conditions [ASME PAPER 65-AV-1] 11 p1780 A66-22472  
 Algorithm for computer eigenfunction solution of boundary value problem involving partial differential equations for stress functions of semimomentless cylindrical shells 11 p1782 A66-22856  
 Eigenfunction expansions and scattering theory for free-space wave equation in exterior region 12 p1912 A66-23563  
 Steady finite-amplitude motions existing for range of Taylor number, with values of Rayleigh number smaller than critical value required for overstability 12 p1866 A66-24948  
 Numerical calculation of periods of natural oscillations and corresponding eigenfunctions of planetary atmospheres as function of planets rotational speed 14 p2381 A66-27534  
 Model potential consisting of Coulomb potential and linear terms in electric field potential, obtaining eigenfunctions of model and deriving optical absorption coefficient for electric field excitons 16 p2775 A66-30729  
 Expansion in eigenfunctions of not self-conjugate boundary value problem for differential equation with singularity at zero 16 p2735 A66-30969  
 Waveguide containing ferrite of ferrite-dielectric insert determined by applying eigenfunction method 17 p2884 A66-32217  
 Perturbation-like theory for case when available starting wave function is not eigenfunction of unperturbed Hamiltonian 18 p3135 A66-34511  
 Boundary value problems for Sturm-Liouville-type equation with asymptotic formula derived for eigenfunctions 20 p3592 A66-38420  
 Eigenfunction expansion of analytic linear ordinary differential operators of boundary value problem with normalized irregular disintegrating boundary conditions 20 p3592 A66-38432  
 Multiplicative and spectral properties of nonnegative space matrices 21 p3756 A66-38740  
 Linearized potential theory for forced vibration of continuous self-exciting plate on hinged support in supersonic flow, investigating parametric resonance frequencies relation to coupling of eigenfunctions 22 p3995 A66-40508  
 Integral equation solution through Jacobi polynomials employed as eigenfunctions of certain operators 22 p3941 A66-40798  
 Eigenfunctions of full dislocation solution of cut annulus in plane elastostatics 23 p4144 A66-41970  
 Characteristic operator of Markov process on smooth manifold 24 p4230 A66-42210  
 Exact solution for eigenfrequencies of cylindrical microwave cavity partially filled with magnetized plasma 24 p4240 A66-42303  
 Numerical calculation of periods of natural oscillations and corresponding eigenfunctions of planetary atmospheres as function of planets rotational speed 24 p4273 A66-42320  
 Benard convection between free bounding surfaces for ranges of Rayleigh and Prandtl numbers achieving steady state with motion of single large cell, evaluating eigenfunction amplitudes 24 p4293 A66-42409
- EIGENVALUE**  
 Asymptotically accurate estimates of Bubnov-Galerkin method error in eigenvalue problem as applied to boundary value problem 01 p0091 A66-10162  
 Multidimensional homogeneous difference schemata solving eigenvalue problem with elliptic operator, noting differential equation coefficients and eigenfunction error estimate 01 p0092 A66-10166  
 Eigenvalues, considering losses, of modes propagating by successive reflections in infinite slab of magnetized ferrite 01 p0121 A66-10530  
 General mode structure and eigenvalues of cavities containing ferrite magnetized in axial direction 01 p0027 A66-10547  
 Error estimate in obtaining eigenvalues of linear self-adjoint differential operator of elliptical type by finite difference method 01 p0095 A66-11008  
 Spectral theory applied to elliptical boundary value problem with eigenvalue parameters 02 p0251 A66-12229  
 Nonlinear buckling of rectangular plates emphasizing calculations of thrust magnitude for boundary value problem, Von Karman equations, etc 03 p0435 A66-12612  
 Elliptic eigenvalue for reentrant region to determine vibration modes of membrane 03 p0387 A66-12620  
 Eigenvalues and norms arising in flow description represented by perturbations of Blasius solution 03 p0356 A66-12810  
 Resonances below inelastic threshold of electron hydrogen scattering using Feshbach projection-operator technique, converting to eigenvalue problem for projected Hamiltonian 04 p0547 A66-13711  
 Eigenvalues of free vibration equation of simply supported beam with finite number of discrete masses, using differential equation 04 p0588 A66-13823  
 Nonlinear eigenvalue problem for equilibrium state of rotating rod solved by perturbation procedures and Leray-Schauder degree theory 04 p0589 A66-13948  
 Inverse eigenvalue problem for second-order differential equation with boundary dependence on parameter 05 p0709 A66-15359  
 Calculation of singular values and pseudoinverse of matrix 05 p0710 A66-15474  
 Bracketing theorem applied in partitioning technique for solving Schroedinger equation to determine upper and lower bounds to energy eigenvalues, ground and excited states 06 p0911 A66-16168  
 Lower bounds to energy eigenvalues for rigid rotator in electric field /Stark effect/ 06 p0911 A66-16168  
 Sensitivity of eigenvalue to changes in matrix calculated by formula used to investigate control systems 06 p0867 A66-16976  
 Indirect method of estimating Green kernels, eigenvalues and eigenfunctions of operators related to elliptic problems 07 p1059 A66-18031  
 Analogy between eigenvalues for fluid convection and flow stability extended to rotating cylinders with corresponding temperature distribution for given angular velocities 08 p1212 A66-19821  
 Sturm-Liouville series expansion of Bessel functions and Bessel differential equation eigenvalue function 09 p1394 A66-20578  
 Eigenvalues of vibrating homogeneous membrane 09 p1396 A66-20631  
 Direct method of Liapunov used to study stability of ordinary differential equation by obtaining linear bounds on vector components 09 p1363 A66-20654  
 Heuristical method solving zeros of complex function, transcendental or algebraic, of complex variable, applicable to computation of eigenvalues of general matrix 10 p1548 A66-21214  
 Real roots of eigenvalue problem in cylindrical harmonics 10 p1550 A66-21306  
 Eigenvalues of integral equations in laser resonant cavities 10 p1542 A66-21343  
 Real eigenvalues of complex matrices, using Hermitian matrix relations 10 p1551 A66-21926  
 Calculation technique for eigenfrequencies of parallelepiped-shaped flexural mode vibrators with natural frequencies incalculable from elementary theory 11 p1705 A66-22651  
 Simplified calculation of eigenvalues of double-ridge and single-ridge waveguides from which critical frequency and wavelength are determined 11 p1656 A66-22738  
 Amplitude calculation of forced mass vibrations in damped linear mechanical system from column matrices of oscillation modes of eigenfrequencies 11 p1783 A66-23018  
 Maximum-minimum theory of eigenvalues applied to stability in Navier-Stokes equation and to incompressible elastic body vibration 11 p1694 A66-23183  
 Perturbation method approximation of eigenvalue and eigenfunction of fundamental wave propagating in H-plane bend of rectangular waveguide 12 p1815 A66-23958  
 Eigensolutions for laminar flow in porous two-dimensional channel subject to certain boundary conditions 12 p1862 A66-23994  
 Modified Ritz method for finding eigenvalues of certain nonlinear ordinary differential equations 12 p1914 A66-24003  
 State variable approach for analysis of linear multivariable system with multiple eigenvalues 12 p1849 A66-24255  
 Steady state alternating current analysis of RLC networks by computing eigenvalues and eigenvectors of corresponding matrix of coefficients 12 p1856 A66-24652  
 Small gap equations for Couette flow stability considering nonaxisymmetric disturbances, solving eigenvalue problem and noting role in instability of Taylor vortices 12 p1866 A66-24946  
 Rate of change of eigenvalues of lambda matrix and use in flutter investigation 12 p1972 A66-24978  
 Flute instability of beta and neutral plasma contained in mirror machine, considering particle motion for solution of Vlasov equation, obtaining eigenvalue equation for potential of flute-like perturbation 13 p2146 A66-25742  
 Averaging method for differential equations with retarded arguments 13 p2118 A66-25827  
 Distribution of complex eigenvalues of



three-dimensional Schroedinger equation, showing location of poles of scattering matrix and role of wave function 13 p2026 A66-26249

Eigenvalue density in vibration of elastic plates and shells, noting concentration of points for natural frequencies and influence of rotational inertia and shear strain 14 p2398 A66-27455

Eigenvalues of truncated cones of revolution with degenerate poles and various rigidities and geometries 14 p2400 A66-27686

Asymptotic estimates of characteristic values of differential equation with periodic coefficients 15 p2524 A66-28507

Convergence rate of method of least squares and some approximate Galerkin type methods in eigenvalue problems 15 p2526 A66-28696

Eigenvalues design method for nonuniformly spaced arrays that will approximate any required radiation pattern 15 p2463 A66-29026

Imaginary eigenvalue existence and zeros of modified Bessel function 15 p2528 A66-29243

Intermediate problems for eigenvalues involving self-adjoint differential operator 16 p2732 A66-30239

Stability of idealized laminar boundary flow, determining phase velocity, amplification rate and wave number of all disturbances 16 p2686 A66-30948

Shape and stability of liquid-gas interface in annular tank in force field determined by numerical integration of boundary value problem and eigenvalue [AIAA PAPER 66-425] 16 p2689 A66-31488

Sturm-Liouville eigenvalues calculated by phase function 16 p2738 A66-31715

Eigenvalue bounds for vibrating rhombical membranes 16 p2824 A66-31718

Matrix algebra, discussing factorization, determinants, eigenvalues, polynomials, inequalities, etc 17 p2945 A66-31869

Rational approximations for lower natural frequencies of uniform beam with concentrated mass or rotary inertia obtained by expanding eigenvalue equation into power series 18 p3249 A66-33599

Sensitivity of eigenvalue to changes in matrix, noting development of computational formula 18 p3127 A66-34077

Vertical and horizontal structure of negative eigenvalue modes of diurnal atmospheric oscillation 18 p3107 A66-34524

Eigenvalue problems for systems of ordinary differential equations resolved computationally by use of quasi-linearization technique 19 p3310 A66-36046

Iterative approximation method for solution of proper elements /eigenvalue/ of Sturm-Liouville equation 19 p3392 A66-36783

Application of Rayleigh principle to obtain sharp upper bounds for increase of first eigenvalue of membrane submitted to parallel and equidistant rectilinear constraints 20 p3669 A66-37544

Linear elliptic partial differential systems, eigenvalue and boundary value problems - Johns Hopkins University, Lectures, March-May 1965 21 p3754 A66-38457

Garding inequality and Green transformation applied to elliptic operators in eigenvalue problems 21 p3755 A66-38465

Algorithms for digital computation of vectors and eigenvalues of matrix 21 p3823 A66-38564

Eigenvalue problems with monotonic operators and error estimation for operator equations with continuous homogeneous operators in semilordered normalized vector space 21 p3757 A66-38942

Distribution of complex eigenvalues of three-dimensional Schroedinger equation, showing location of poles of scattering matrix and role of wave function 22 p3947 A66-39708

Eigenvalue problem for Laplace operator for two-dimensional region with boundary composed of piecewise-analytical simple closed curves solved by finite difference method 22 p3938 A66-39901

Variational methods for approximating perturbation effect on nondegenerate eigenvalue extended to degenerate case 23 p4084 A66-41390

Geometrical theory of unitary equivalence of matrices indicating successive calculation of numerical invariants 23 p4084 A66-41407

Simplified calculation of eigenvalues of double-ridge and single-ridge waveguides from which critical frequency and wavelength are determined 23 p4045 A66-41476

Orthogonality condition for eigenvalue problem of out-of-plane twist-bending vibrations of elastic ring for various sets of boundary conditions 23 p4139 A66-41693

Eigenvalue problem associated with dynamic instability of geostrophic wind 23 p4066 A66-42042

**EIGENVECTOR**

Pseudo-inverse concept extended to Hilbert space unbounded operators with arbitrary range 01 p0092 A66-10179

Two-level atom interaction with multimode gas laser cavity, obtaining stationary state and solving unique eigenvalue in special cases 12 p1891 A66-24568

Perturbation theory analyses of network matrix eigenvectors and natural frequencies 20 p3539 A66-38282

**EINSTEIN EQUATION**

**SA RELATIVITY THEORY**

Einstein gravitational equation applied to galaxies and quasars, using spherical model with spherically symmetric distribution of matter 01 p0138 A66-11033

Two general integrals of Einstein equations serviceable for obtaining certain physical quantities which are independent of choice of coordinate system 02 p0291 A66-12183

Equation of motion in relativistic gravitation theory 05 p0715 A66-14529

Exact solutions to Einstein field equations 05 p0715 A66-14532

Bianchi identity role in obtaining motion equations without infinite self-action terms in general relativity 05 p0715 A66-14893

Motion of charged finite mass in gravitational field 06 p0908 A66-16162

Einstein equations for vortical and nonvortical gravitational fields applied with relativistic approximation to Newtonian gravitational field 08 p1256 A66-19272

Non-Einsteinian gravitation, noting that expression for invariant density of free Lagrange gravitational field holds only for slowly varying weak fields 09 p1403 A66-20769

Charged particle motion determined by gravitational-electromagnetic field properties with motion equations following from integrability condition of field equations 11 p1735 A66-22343

Cosmological effects in anisotropic inhomogeneous cosmological models including Riemannian geometry, light propagation, gravitational field, etc 11 p1772 A66-22778

Freely falling point mass problem solutions for Einsteinian free space equations that also satisfy Newtonian equations in suitable coordinate system 12 p1915 A66-24889

Energy-momentum density of gravitational field according to Ozsvath-Schuecking rigorous solution to Einstein field equations 12 p1915 A66-24994

Spatially homogeneous anisotropic irrotational solutions of Einstein field equations for cosmological dust source 14 p2330 A66-27019

Philosophical problems of Einstein theory of gravitation and relativistic cosmology - All-Union Conference, Kiev, Ukrainian SSR, May 1964 14 p2331 A66-27208

Quantum gravitation theory, discussing difficulties of covariance of general relativity and nonlinearity of Einstein equation 14 p2332 A66-27215

Non-Einsteinian gravitation, noting that expression for invariant density of free Lagrange gravitational field holds only for slowly varying weak fields 14 p2334 A66-27304

Einstein spaces with gravitational wave 15 p2537 A66-28672

Covariant treatment of solutions of Einstein field equations representing pure gravitational radiation propagating in fluid and electromagnetic media 15 p2542 A66-29621

Motion of charged nongravitating test

particle in Einstein gravitational theory 15 p2542 A66-29655

Einstein field equations for perfect fluid, coupled to frozen-in magnetic field, in high-density limit of gravitational collapse 17 p2997 A66-31973

General relativistic dyadic formalism applied to metrics of rigid bodies moving in Einstein space of uniform space-time curvature 17 p2958 A66-32294

Stationary dust-filled cosmological solution of Einstein field equations with zero lambda and without closed timelike lines 19 p3463 A66-36169

Gravitational waves in presence of electromagnetic field, deriving Einstein-Maxwell equations 20 p3550 A66-37308

Singularities in universe, discussing properties of space-time continuum, matter and Einstein equations for strong fields 21 p3771 A66-39265

Singularities in closed universes, discussing closed solutions to Einstein equations and inevitability of singularity, based on Hawking theorem 21 p3771 A66-39266

General relativity theory, examining Schwarzschild surface which allows matter and light to pass through in one direction only 21 p3774 A66-39532

Rotating masses effect on inertial frames, analyzing stress energy tensor and Schwarzschild geometry 22 p3979 A66-40113

Freely falling point mass problem solutions for Einsteinian free space equations that also satisfy Newtonian equations in suitable coordinate system 23 p4090 A66-41096

Einsteinian gravitation equations stated in terms of three-dimensional tensor analysis as applied in conformal space 23 p4091 A66-41834

New gravitation theory, noting role of Einstein equations following conformal transformation 24 p4237 A66-42540

Einstein gravitation theory relation to general and special relativity, space time, unified four-dimensional continuum metric and chronogeometric theories 24 p4238 A66-43015

**EJECTION**

**SA PARACHUTING**

Downrange radar and optical data reduction used for evaluation of ejection velocities of ballistic missile penetration aids at deployment [AIAA PAPER 66-405] 16 p2804 A66-31464

Meteorite impact and ejection mechanism of tektites, examining large distances traveled by tektites 17 p3007 A66-33283

Convergence of axes of plane-parallel jets due to reciprocal ejection effect, analyzing deformation of jet, rarefaction coefficient for air between jets, etc 20 p3544 A66-36918

Rescuing men and equipment in space by manned rescue craft, unmanned craft, personal ejection capsules, etc 20 p3665 A66-38254

**EJECTION INJURY**

Causes of compression fractures of spine during large number of USAF ejections 03 p0327 A66-12361

Statistical analysis of vertebral fracture in U.S. Navy during 1959-1963 period 16 p2644 A66-31132

Emergency escape experiments using ejection seats noting rate of successful escapes, pilot injuries, minimum terrain clearance, etc 18 p3063 A66-34409

Fracture mechanism of traumatic lesion caused by seat-ejection or bail-out from F-104 G aircraft and worsened by ground impact 22 p3858 A66-40503

**EJECTION SEAT**

LW-2 Escape System for high V/STOL aircraft and outstanding recovery capabilities 06 p0806 A66-16819

Mechanical and physiological factors involved in design, testing and operation of ejection seats, examining effects of short duration acceleration 10 p1493 A66-22126

Ejection seat spin rate tests to determine temporary incapacitation possibilities 11 p1647 A66-22576

Emergency escape experiments using ejection seats noting rate of successful escapes, pilot injuries, minimum terrain clearance, etc 18 p3063 A66-34409

Fracture mechanism of traumatic lesion caused by seat-ejection or bail-out from F-



104 G aircraft and worsened by ground impact 22 p3858 A66-40503  
 Aircraft escape systems design criteria established using military accident statistics, noting drogue parachute and pilot sizes 22 p3850 A66-40610

**EJECTION TRAINING**  
**SA PILOT TRAINING**  
 Air Training Command ejection experience from 1962 to 1964 09 p1337 A66-20526

**EJECTOR**  
**SA JET PUMP**  
 Design charts for determining ejector characteristics for optimum performance of jet pump systems [ASME PAPER 65-WA/FE-32] 05 p0691 A66-15709  
 Optimum design parameters for water ejectors [ASME PAPER 65-WA/FE-31] 05 p0691 A66-15710  
 One-dimensional analysis used by Hope and Segars invalid for ejector with supersonic primary stream 18 p3100 A66-34604  
 Spray ejector operating in pulse rather than steady state regime, noting capability and formation of de Laval nozzle 19 p3450 A66-36603  
 Equation for calculating entrainment ratio of ejectors as function of velocity numbers of two frictionless one-dimensional streams flowing side by side in pressure equilibrium 22 p3899 A66-40371

**EKMAN LAYER**  
 Axisymmetric convection between two rotating disks, noting secondary flow and viscous effects of Ekman layers 12 p1980 A66-24941  
 Instability of laminar Ekman boundary layer, obtaining critical values of Reynolds numbers, perturbation growth rates and equilibrium finite amplitude solutions 24 p4197 A66-42980  
 Stability of two-dimensional boundary layer flow in rotating tank with small inflow analyzed, using perturbation theory 24 p4197 A66-42981

**ELASTIC BAR**  
 Four types of axisymmetric distribution of stresses and displacements in infinitely long rod of circular cross section with discontinuous boundary conditions 01 p0155 A66-10713  
 Central maximum loading by transverse impact on beams independent of boundary conditions calculated by simplified integral and verified by measurements 03 p0433 A66-12315  
 Equivalent networks for transversely vibrating bars under various end conditions 03 p0437 A66-12820  
 Waves in bars of mechanically unstable materials discussing differential equation of motion, jump conditions, wave velocity and application to annealed aluminum [ASME PAPER 65-WA/APM-22] 05 p0778 A66-15444  
 Transfer matrices of vibrating thin-walled open profile bars under forced, coupled bending and torsional stresses 08 p1311 A66-19342  
 Stress concentration and distribution in statically loaded tension bar with U-shaped grooves studied photoelastically 08 p1315 A66-19804  
 Free vibrations of initially straight elastic bar with free-free or clamped-free ends, undergoing inextensional motion, neglecting shearing effects and rotatory inertia 10 p1616 A66-21484  
 Laplace transform solution for small time used as complement to problem of one-dimensional propagation of stress pulse in bar with continuously nonhomogeneous elastic modulus 10 p1617 A66-21498  
 Torsion in orthotropic rod of rectangular cross section and tubular cylindrically anisotropic rod, with variable elastic moduli 12 p1966 A66-24060  
 Longitudinal oscillation frequency of rod with one end fixed and other end carrying rigid load 12 p1966 A66-24065  
 Stability of rod compressed by follow-up force created by compressed air discharge 14 p2396 A66-27179  
 Unstabilized rod buckling from impact load with longitudinal compression wave reflection 15 p2607 A66-28736

Geometrical dispersion effect on propagation of longitudinal harmonic stress waves in prestressed elastic viscoplastic bars 16 p2813 A66-30264  
 Saint Venant principle applied to dynamics of bars regarding boundary conditions and reliability problems 16 p2822 A66-31508  
 Uniformly accelerated motion stability of thin elastic bar subjected to servo force at one end 16 p2822 A66-31524  
 Waves in bars of mechanically unstable materials, discussing differential equation of motion, jump conditions, wave velocity and application to annealed aluminum [ASME PAPER 65-WA/APM-22] 18 p3247 A66-33571  
 Beam column supported by linear rotational and extensional springs representing elasticity of test rig, used in analog study of thermal buckling behavior of thin cylindrical shells 21 p3828 A66-38706  
 Optimum cross section design for thin walled bar under combined torsion and bending 21 p3832 A66-39377  
 Longitudinal, torsional and flexural free vibration of elastic slender bar of variable cross section with nonhomogeneous properties 22 p3992 A66-40299  
 Transient response characteristics of bonded strain gauges obtained by measuring elastic step wave produced in steel bar 22 p3919 A66-40436  
 Cyclically moving loads causing resonance in elastic rods, strings and torsional members having fixed ends 23 p4141 A66-41922  
 Rational one-dimensional theory of wave propagation and vibrations in elastic bars with rectangular cross section 24 p4284 A66-42137  
 Torsion of elastic rectangular bar with similarly distributed external tangential loads applied at both ends 24 p4289 A66-42436  
 Stability of rod compressed by follow-up force created by compressed air discharge 24 p4290 A66-42725

**ELASTIC BENDING**  
 Circle theorem of displacement field in elastically supported circular plate in pure bending 01 p0154 A66-10503  
 Intermediate stages of wave-type bending process in elastic plate investigated by system of approximate methods 01 p0157 A66-10983  
 Central maximum loading by transverse impact on beams independent of boundary conditions calculated by simplified integral and verified by measurements 03 p0433 A66-12315  
 Elastoplastic bending of rigid plates under transverse loading noting compressibility 03 p0441 A66-13292  
 Settling of multilayer foundation subject to normal load 03 p0441 A66-13294  
 Flexure center and semicircular cross section for shear stress distribution 04 p0586 A66-13409  
 Errors in approximation equations for dynamic bending of cylindrical rod 08 p1308 A66-18889  
 Elastic bending of isotropic plate supported by doubly periodic system of point supports under doubly periodic transverse load 08 p1311 A66-19373  
 Flexure of semiinfinite nonsymmetric three-layer plate under steady transverse compression, using state equation to determine load values impairing equilibrium of plate 09 p1468 A66-20760  
 Bending of slightly curved solid viscoelastic rod of circular cross section under effect of quasi-static and dynamic radial forces 10 p1613 A66-21324  
 Iterative procedure to obtain numerical solutions of von Karman equations for rectangular plates with finite deflections 10 p1615 A66-21477  
 Optimum study of anticlastic deformations of elastic strips with tapered edges, using Newton-Raphson iteration method 11 p1780 A66-22328  
 Bending of cylindrical shell clamped at one end and reinforced by elastic ring at free end, with vertical forces uniformly distributed acting over ring 12 p1964 A66-24044  
 Elastic bending of anisotropic plates with

stresses represented by Legendre polynomial series 12 p1968 A66-24346  
 Von Karman equations for axisymmetric nonlinear bending circular plates 12 p1969 A66-24363  
 Results of crack propagation tests on polymethylmethacrylate flexed at various frequencies under cyclic loading 13 p2112 A66-25308  
 Photoelastic intensity variations in glass beam following impact of steel ball, registering values pointwise 13 p2198 A66-26300  
 Plate deflection in own plane under moments applied to ends using elasticity theory, deriving relation between stress tensor and stress function 13 p2205 A66-26452  
 Central deflection of simply supported centrally loaded rhombic plate with formula depending on first coefficient obtained in mapping of rhombus 14 p2409 A66-28397  
 Flexure of thin elastic plate clamped to rigid columns, determining functions of complex variable 15 p2613 A66-29433  
 Tensile and compressive creep behavior deduced from deflection measurements in creep bending tests on beams of trapezoidal cross section 15 p2614 A66-29666  
 Torsion analysis of thin walled profile of bisymmetrical cross section subjected to finite twist 15 p2615 A66-29722  
 Lagrangian multiplier method applied to mixed boundary value problems such as stresses due to temperature changes in semiinfinite slab 15 p2615 A66-29733  
 Book on bending theories of sandwich plates including use of Fourier series, stress-strain state, trigonometry, deflection theory, etc 16 p2818 A66-31100  
 Boundary perturbation solution of stress concentration around curved hole in thin plate under elastic bending 16 p2819 A66-31140  
 Flexural vibration of uniform shafts treated by impedance techniques and traveling-wave concepts 17 p3022 A66-32015  
 Elastic bending of isotropic plate supported by doubly periodic system of point supports under doubly periodic transverse load 18 p3254 A66-34183  
 Subharmonic vibrations during resonant testing of thin walled beams for coupled torsional and bending vibrations 18 p3256 A66-34559  
 Elementary effects method solution of fourth-order PDEs for bending and vibration of elastic plates 20 p3671 A66-37989  
 Bending of nonorthotropic clamped plates solved, using small parameter method 21 p3826 A66-38610  
 Resonance machine design for producing torsion and bending, ensuring equality of dynamic amplification factors 21 p3827 A66-38619  
 Stress analysis of difference equations for bending and shear effects in elastic grids 21 p3832 A66-39536  
 Bending of isotropic thin plate in moment theory of elasticity, noting Kirchhoff-Love hypothesis from which relations for bending moment torque and shear force are obtained 22 p3991 A66-40151  
 Out of plane free vibrations of uniform circular ring on elastic and torsional foundations producing restraints 24 p4287 A66-42165  
 Axisymmetric bending problem of idealized elastic rigidly-plastic two-layer circular plates, deriving exact mathematically strict solutions and uniqueness conditions 24 p4290 A66-42443

**ELASTIC BODY**  
 Stress function for linear viscoelastic problems where body shape, boundary condition type or both vary with time 02 p0298 A66-11576  
 Stress distribution in vicinity of infinite row of collinear Griffith cracks in elastic body calculated for internal pressure distribution 02 p0298 A66-11577  
 Photoelastic experiment by birefringent coating method to determine stress analysis applicable for any elastic body 02 p0298 A66-11583  
 Plane-strain problems for which classical theory predicts singular stress concentrations in elastic



- solid 03 p0438 A66-13093
- Stress and deformation state in infinite solid corner of elastic body limited by three planes 03 p0442 A66-13304
- Small radial vibrations of homogeneous isotropic prestressed sphere 04 p0591 A66-14207
- Stress distribution in semiinfinite elastic media with different properties bonded along plane and containing concentric ring-shaped cavities, using Green function [ASME PAPER 65-WA/APM-2] 05 p0776 A66-15426
- Parametric response of elastic columns discussing longitudinal inertia effects, analytic stability criteria and results [ASME PAPER 65-WA/APM-13] 05 p0777 A66-15435
- Cylindrically symmetric tension field covering strain gradient effects on potential energy of elastic body [ASME PAPER 65-WA/APM-14] 05 p0777 A66-15436
- Transient wave diffraction problem solution, discussing response of elastic solid to harmonic incident pulse [ASME PAPER 65-WA/APM-16] 05 p0777 A66-15438
- Dynamic reciprocal theorem for sinusoidal oscillation of elastic medium treated as extension of static reciprocal theorem of Betti and Rayleigh, using continuum mechanics [ASME PAPER 65-WA/MD-21] 05 p0779 A66-15524
- Approximate solution method for unsteady creep of shells within framework of theory of aging 07 p1146 A66-18254
- Dependence of dry friction force for steady state rubbing of rubberlike body on surface of crystalline elastic body 08 p1244 A66-19474
- Front and zone of fractures originating in brittle elastic body under influence of high pressure arising on wall of cavity within body 08 p1313 A66-19475
- Dynamic stability of circular elastic rods, noting iteration method analysis of nonlinear coupling effect between axial force and curvature in forced in-plane vibrations 09 p1467 A66-20638
- Stress distribution in semiinfinite elastic media with different properties bonded along plane and containing concentric ring-shaped cavities, using Green function [ASME PAPER 65-WA/APM-2] 10 p1615 A66-21479
- Elastic strip and elastic annulus Differential-difference equations, using Fourier transforms and analytic continuation 11 p1780 A66-22439
- Rayleigh-Ritz method, stationary complementary and potential energy principles and Lagrange undetermined multipliers applied to free vibration of elastic body 11 p1781 A66-22611
- Transformation relation for prestress tensor in problem of indifferent equilibrium of elastic bodies derived, using approximation method 12 p1959 A66-23865
- Thermodynamics utilized to show that there is no difference between bodies defined as hypoelastic, elastic and hyperelastic 12 p1960 A66-23957
- Cylindrically symmetric tension field, covering strain gradient effects on potential energy of elastic body [ASME PAPER 65-WA/APM-14] 12 p1960 A66-23974
- Parametric response of elastic columns, discussing longitudinal inertia effects, analytic stability criteria and results [ASME PAPER 65-WA/APM-13] 12 p1961 A66-23985
- Stress function solution in dynamic linear theory of homogeneous incompressible elastic bodies 12 p1962 A66-23998
- Stress states and elastic equilibrium in semicircle pressed against rigid profile base 12 p1969 A66-24352
- Torsional stress distributed on ends and lateral face of anisotropic rod with variable elastic moduli 12 p1969 A66-24353
- Functional analysis demonstrating existence and uniqueness of displacement field, providing solution for linear viscoelasticity problem for medium having behavior satisfying coercivity condition 13 p2195 A66-25463
- Inhomogeneous elastic half-spaces examined for circular crack in plane of contact and perpendicular tensile forces, using Griffith fracture theory 13 p2203 A66-26421
- Purity effects on stress and temperature field distribution in elastic bodies, deriving equations 13 p2203 A66-26425
- Axisymmetric wave propagation in elastic body-conducting fluid system, noting parameters of motion expressed in PDE 13 p2150 A66-26427
- Stresses in concentric and eccentric compound rings 13 p2207 A66-26499
- Elastic analog applicability to geometrically nonlinear creep theory of circular membranes 14 p2397 A66-27390
- Stresses due to two equal and opposite couples applied at ends of diameter on surface of elastic sphere having concentric spherical inclusion 14 p2409 A66-28460
- Galerkin vector for elastodynamic problem of isotropic inhomogeneous body 16 p2823 A66-31707
- Axisymmetric problem in elasticity theory for infinite body weakened by system of periodically distributed coaxial slots of equal radius 17 p3026 A66-32599
- Second-order volumetric change in isotropic elastic materials without external loads 18 p3258 A66-34639
- Constitutive equations for elastic solids sustaining deformation for which displacement gradients are small but where nonlinearity is permitted, formulating plane elastostatic problem 19 p3475 A66-36429
- Impact of elastic conical shell of revolution moving with constant axial velocity toward rigid obstacle 21 p3827 A66-38692
- Optimal control of elastic flight vehicles, describing axis oscillations by equations of beam with variable cross section 21 p3768 A66-39279
- Rectangular-parallelepiped problem of restrained torsion produced by mutual rotation of two absolutely rigid diaphragms attached to opposite faces 21 p3831 A66-39292
- Dependencies of independent components of elastic compliance and rigidity tensors of elastic body reinforced in two directions 22 p3989 A66-39819
- Geometrical and statistical relations of theory of nonlinearly elastic body presented in connection with bifurcation of equilibrium of ideally elastic body 22 p3996 A66-40686
- Stress-strain distribution of sharp corners effect on surface of elastic body, examining mathematical difficulties in application of Lamé equation and boundary data smoothing 23 p4135 A66-40991
- Refined method of selecting roller contact bearing, considering parametrical resonance 23 p4072 A66-41058
- Orthogonality condition for eigenvalue problem of out-of-plane twist-bending vibrations of elastic ring for various sets of boundary conditions 23 p4139 A66-41693
- Approximate solution of certain mixed plane boundary value problems involving isotropic elastic body 23 p4140 A66-41836
- Energy, linear and angular momentum conservation principles for elastic body with finite number of defects 23 p4091 A66-41855
- Surface Rayleigh waves and resonance effects in elastic bodies, noting motion of wedge or load on surface 24 p4291 A66-42842
- ELASTIC BUCKLING**
- Prebuckling deformation and stress-strain distributions in clamped thin cylindrical shell subjected to axial load, determining effect of boundary supports 02 p0297 A66-11557
- Nonlinear buckling of rectangular plates emphasizing calculations of thrust magnitude for boundary value problem, Von Karman equations, etc 03 p0435 A66-12612
- Statistical study of linear buckling of circular cylindrical shells under axial compression, showing preferred mode shape [ASME PAPER 65-APMW-23] 04 p0592 A66-14224
- Effect of torsional and lateral restraints on elastic critical load of centrally loaded simply supported beam buckling laterally 06 p0966 A66-16613
- Elastic critical load of centrally loaded simply-supported beam which buckles laterally out of plane derived by Airy integral functions 07 p1144 A66-18049
- Collapse under end load of pressurized axially stiffened thin cylinders 07 p1147 A66-18282
- Torsional buckling of thin walled prismatic bars of arbitrary cross section, considering buckling shear resilience 08 p1311 A66-19343
- Statistical study of linear buckling of circular cylindrical shells under axial compression, showing preferred mode shape [ASME PAPER 65-APMW-23] 10 p1615 A66-21474
- Axisymmetric imperfections effect on elastic buckling of spherical caps under uniform pressure 10 p1617 A66-21785
- Elastic buckling of clamped conical shells under external pressure 10 p1617 A66-21786
- Stability and buckling of core-filled axially compressed circular cylinder 12 p1957 A66-23603
- Optimum depth, minimum area design charts for laterally supported structural beams in pure bending, discussing weight parameters, elastic buckling, material characteristics, etc 12 p1968 A66-24201
- Principle of stationary complementary energy applied to buckling of column, noting Rayleigh-Ritz method 12 p1969 A66-24362
- Collapse of spherical caps under external pressure, with data for polyvinylchloride and aluminum alloy caps 12 p1972 A66-24979
- Linear creep stability of orthotropic shells, considering shear creep and lateral buckling, determining critical loads and noting errors 13 p2113 A66-25913
- Buckling of rod with initial deflection as sinusoidal half-wave, using Bubnov-Galerkin method and Laplace transform, calculating stresses of rod when subjected to nonsteady creep 13 p2206 A66-26457
- Buckling of unstable perfectly elastic isotropic rectangular plate 14 p2396 A66-27312
- Edge restraint effects on spherical cap stability 14 p2412 A66-27435
- Newton-Kantorovic method solution of Hammerstein type nonlinear integral equation, with application to elasticity theory of buckling of thin spherical shell 14 p2322 A66-27628
- Book on stability loss of highly convex shells at supercritical strains 14 p2401 A66-27786
- Imperfections and edge restraint effect on buckling of axially compressed cylinders 14 p2404 A66-27988
- Dynamic snap-through buckling of shallow spherical caps of elastic material 14 p2406 A66-27998
- Unstabilized rod buckling from impact load with longitudinal compression wave reflection 15 p2607 A66-28736
- Dynamic elastic deflections of shallow circular arch under dynamic pressure loading, solving nonlinear integro-differential motion equation by Galerkin method 15 p2610 A66-29284
- Sandwich shell theory, including effects of transverse shear and extension and quadratic terms essential to buckling problems 17 p3021 A66-32003
- Local buckling of infinite continuous-plane elastic membrane under longitudinal load in form of concentrated forces 17 p3029 A66-32810
- Snapping of shallow simply supported sinusoidal arch under sinusoid step pressure load, using motion equations and infinitesimal stability analysis 18 p3257 A66-34591
- Stability of bending-torsional equilibrium of cantilevered bar subjected at end to follower force, as in case of wing under jet, determining critical thrust 19 p3475 A66-36432
- Book on strength, stiffness and stability of sandwich structural elements for structural designer, emphasizing practical applicability 20 p3666 A66-37010
- Postbuckling behavior of clamped infinite flat strip under action of shearing forces analyzed based on von Karman equations 20 p3669 A66-37531
- Inelastic buckling of rod with initial slight



- sinusoidal deflection subjected to short-term longitudinal compressive dynamic load 20 p3672 A66-38268
- Static perturbation technique used in analysis of stability relationship to shape of equilibrium surface for finite-dimensional problems 22 p3992 A66-40202
- Buckling of stiffened cylindrical shells under various loads and load combinations, noting optimization procedure for elastic stability [ICAS PAPER 66-13] 22 p3996 A66-40673
- Shell stability theory of current interest, noting shell with elastic filler and internal pressure 23 p4135 A66-40994
- Elastodynamic buckling of circular cylindrical shells, unstiffened and longitudinal stringers-stiffened 23 p4147 A66-42000
- ELASTIC COLLISION**
- Elastic collision effects on harmonic current amplitudes and energy conversion process in double beam and beam-plasma interactions 01 p0112 A66-10585
- Strong interactions and cosmic rays, discussing Regge poles, one meson approximation and multiperipheral model theory of elastic and quasi-elastic interactions 07 p1112 A66-17535
- Average diffusion cross section for elastic collisions of electrons with heavy particles, comparing calculated and measured values 15 p2551 A66-29225
- Fast neutrons of solar origin detected by observing protons recoiling from elastic collisions of neutrons with hydrogen nuclei in nuclear emulsion 18 p3188 A66-34824
- ELASTIC CONSTANT**
- SA YOUNGS MODULUS**
- Internal friction and elastic modulus of compressor and turbine blade materials 03 p0372 A66-12399
- Elasticity determined for axial fir-tree-type connections of turbine blade roots 03 p0440 A66-13201
- Niobium elastic constants tabulated for various temperatures, using RF pulse-echo method 04 p0536 A66-13754
- Elastic modulus and ultimate tensile strength of fibers and fiber composites 05 p0705 A66-14814
- Static deformation of model of three-constant isotropic elastic material exhibiting phenomenon of couple stresses [ASME PAPER 65-WA/APM-3] 05 p0776 A66-15427
- Four elastic constants of Laval, Raman and Viswanathan theories dynamically measured in connection with behavior data on cubic crystals 05 p0781 A66-15736
- Lateral buckling of I-beam, examining stress and strain induced change in elasticity moduli and rigidity 06 p0964 A66-16479
- High temperature extensometer using linear variable differential transformer 07 p1030 A66-17230
- Hole concentration effect on elastic constant of heavily doped p-type silicon 07 p1106 A66-18396
- Leigh theory concerning effect of electron concentration on elasticity of Al and Al alloys compared with experiment 07 p1053 A66-18520
- Aluminum-beryllium base alloys, noting problems of application as construction materials 08 p1239 A66-18904
- Infinite frequency elastic moduli of monatomic fluids related to pressure and internal energy of fluid 08 p1206 A66-18941
- Finite bending of cylindrical plates, evaluating numerical values of stress distribution in baryte sheet 09 p1465 A66-19861
- Dynamic flexural rigidity of polymer plates, measuring elastic modulus, noting variation of Youngs modulus, Poisson ratio with temperature and rate of loading 09 p1466 A66-20183
- Static deformation of model of three-constant isotropic elastic material exhibiting phenomenon of couple stresses [ASME PAPER 65-WA/APM-3] 10 p1615 A66-21480
- Elastic constants obtained from longitudinal and transverse acoustic waves propagated in single-crystal indium phosphide 10 p1578 A66-21585
- Moment stress tensor and elastic constants in statistical fluid mechanics 10 p1523 A66-21801
- X-ray determination of elastic constant of pure nickel and alloy with aluminum 10 p1547 A66-21982
- Temperature dependence of crystalline ammonia elastic moduli 10 p1589 A66-22166
- Diffusivity, elastic modulus and stacking fault energy effect on high temperature creep behavior of alpha brasses 11 p1717 A66-22996
- Glass fiber reinforcement for plastics, determining tensile strength of fibers, glass structure, elasticity modulus improvement via annealing, etc 11 p1720 A66-23126
- Elastomechanical properties of glass fibers and resins in order to determine optimum materials for reinforced glass fiber structures [ONERA TP 322] 11 p1721 A66-23200
- Structural efficiency of orthotropic materials for cylindrical shells under axial load, including examination of fibrous composites characteristics [AIAA PAPER 65-73] 12 p1956 A66-23583
- Elastic constants and thermal expansion coefficients of bodies with inhomogeneous regular structure 12 p1958 A66-23666
- Torsion in orthotropic rod of rectangular cross section and tubular cylindrically anisotropic rod, with variable elastic moduli 12 p1966 A66-24060
- Ultrasonic measurement of elastic moduli of high temperature metal 13 p2194 A66-25092
- Recording assembly for measurement of flexural and torsional moduli and internal friction at various frequencies and temperatures of small samples, using constant amplitude undamped oscillations 13 p2077 A66-25324
- Alloying effects on temperature dependence of titanium normal elastic modulus between -186 and 800 degrees C 13 p2106 A66-25329
- Stressed state of spherical shell weakened by curvilinear holes described by equation of shallow shells 13 p2202 A66-26413
- Shear relaxation time of monatomic fluids for liquid and dense gas phases calculated, using LF viscosity data and estimates of HF elastic moduli 14 p2277 A66-27977
- Effect of compression of outer layers of plate by longitudinal forces on reduced shear moduli of finned filler 16 p2816 A66-31046
- Effect of thermal population of /000/ and /100/ conduction bands on elastic constants of heavily doped n-type germanium 16 p2778 A66-31070
- Elastic field in inclusion and surrounding matrix 16 p2818 A66-31105
- Mechanical properties of solid propellants, determining elastic modulus from tensile tests via stress-strain diagram 16 p2790 A66-31193
- Laminated thin shell theory applied to calculation of elastic coefficients of fiber reinforced shells [AIAA PAPER 66-526] 16 p2822 A66-31499
- Mechanical properties of semiconductors, such as elastic modulus and internal friction determined, noting vacuum and temperature conditions 16 p2785 A66-31669
- Overall elastic moduli of inhomogeneous system composed of various solid phases firmly bonded together at arbitrary concentration 17 p3029 A66-32791
- Theoretical determination of elastic constants, Youngs moduli and Poisson ratios of filament-wound cylinders, using strain measurements in longitudinal uniaxial loading and internal pressure 19 p3472 A66-35355
- Temperature dependence of crystalline ammonia elastic moduli 19 p3441 A66-35780
- X-ray determination of elastic constant of pure nickel and alloy with aluminum 19 p3381 A66-35864
- Hardness, toughness, stress relaxation, corrosion resistance, etc, of niobium-aluminum alloy with stable elastic modulus 20 p3583 A66-37366
- Cosserat coupled stress and effects on stress concentration factor in semiinfinite solid medium with varying elastic modulus 20 p3667 A66-37466
- Ultrasonic measurement of elastic moduli of high temperature metal 21 p3823 A66-38517
- Equations for plane deformation in multimodule elasticity theory, formulating generalized Hooke law for multimodule material 21 p3826 A66-38609
- Elastic constants and thermal expansion coefficients of bodies with inhomogeneous regular structure 22 p3988 A66-39713
- Elastic constants and interatomic interaction parameters of niobium alloyed with tantalum, titanium and vanadium 22 p3936 A66-40788
- Structural efficiency of orthotropic materials for cylindrical shells under axial load, including examination of fibrous composites characteristics [AIAA PAPER 65-73] 23 p4138 A66-41107
- ELASTIC CYLINDER**
- Stresses in elliptical cross section rod subjected to elastoplastic torsion, using Legendre transforms 02 p0301 A66-12173
- Forced torsional motion of semiinfinite isotropic elastic cylinder with vibrations excited by harmonically oscillating rigid disk, using integral equation 04 p0589 A66-13829
- Stress concentration at holes to determine service life or load-carrying capacity of thick walled pressurized cylinders 06 p0966 A66-16703
- Temperature fluctuations of elastic isotropic cylinder, obtaining temperature equilibrium equations and reducing three-dimensional problems of thermoconductivity and thermoelectricity to boundary value problems 08 p1307 A66-18886
- Errors in approximation equations for dynamic bending of cylindrical rod 08 p1308 A66-18889
- Pointwise estimate for stress in uniform isotropic cylinder with zero body forces applied to Saint Venant principle 10 p1618 A66-21876
- Upper estimate of potential elastic energy of cylinder, using concept of permissible surface forces and boundary conditions 11 p1783 A66-22894
- Stresses and strains in anisotropic multilayered thick walled circular cylinder subjected to radial pressure [AIAA PAPER 65-174] 14 p2402 A66-27869
- Small oscillations produced by combined action of stationary and harmonic forces in nonlinearly elastic cylindrical shell of rectangular planform 15 p2607 A66-28769
- Frequency equations and mode displacement functions derived for plane strain free-transverse vibration of solid cylinder with elastic core bonded to thin elastic shell 16 p2823 A66-31716
- Wiener-Hopf and series solutions to BVP of indentation stresses and displacements in infinite hollow elastic cylinder for axisymmetric punch of finite length and arbitrary profile 22 p3990 A66-40139
- Two mixed boundary value problems of infinite elastic cylinder under torsion solved by dual integral equation with differentiation of boundary conditions 24 p4291 A66-42843
- ELASTIC DAMPING**
- Oscillation parameters and effects of nonlinear coupling on solid body with built-in rotating rotor 04 p0587 A66-13557
- Beam on elastic supports, determining fundamental frequency of free oscillation for one weak nonlinear boundary condition 07 p1142 A66-17260
- Harmful oscillation elimination from high rpm gyroscopic centrifuge by introducing one elastic bearing into dynamic system 08 p1307 A66-18877
- Effect of heterophase fluctuations at high and low frequencies near first order phase-transition point on elastic oscillation propagation, noting role of acoustic wave 12 p1972 A66-25020
- Boundary conditions for existence of damped solutions to plane problem in elasticity theory for half-strip with stress-free longitudinal edges 16 p2822 A66-31525
- Gyroscopic rotor vibrations excited by effect of lubrication layer in sliding bearings and stabilized with intervening elastodamping supports, taking into account moment of inertia of



- rotor 17 p3027 A66-32605
- Algorithm for rapid damping of multidimensional system 20 p3670 A66-37675
- First passage problems for lightly damped linear oscillator excited by white noise, discussing time probability distribution, densities, application of computers to obtain numerical solutions, etc 24 p4284 A66-42140
- LASTIC DEFORMATION**
- Dynamics of plate deformed symmetrically with respect to central plane treated by Lure method 01 p0157 A66-10984
- Variational theorem that is equivalent to elastic field equations for incompressible and nearly incompressible materials 02 p0297 A66-11541
- Toroidal shell stresses and displacements under internal pressure in transition range found by bending and membrane theories [AIAA PAPER 65-145] 02 p0297 A66-11542
- Equations for rotational motion of satellite and rods with end loads as stabilizer, considering rods elastic deformation caused by load bending 02 p0295 A66-11651
- Static problem of elasticity for random loads 03 p0434 A66-12529
- Finite plane stretching of neo-Hookean strip bonded at ends treated by principle of stationary potential 03 p0435 A66-12669
- Three-parameter family of nonhomogeneous deformations with strain invariants supported by surface tractions in isotropic incompressible elastic material 03 p0439 A66-13098
- Elastoplastic stressed state of plates with holes assuming Iliushin theory of deformation 04 p0587 A66-13489
- Stress concentration in semiinfinite regions occupied by elastic bodies with concentrated loads acting at region boundaries 04 p0587 A66-13563
- Semizero-moment shell with one edge braced by elastic support with small rigidity for deformation out of plane, noting magnitude of critical stress 04 p0588 A66-13566
- Maximum stress on flat plate stress corrosion strip with ends rotated 90 degrees, using nonlinear bending theory [ASME PAPER 64-WA/AV-3] 04 p0589 A66-14025
- Large axisymmetric nonlinear elastic or plastic deformations of zero-moment circular conical shells 04 p0590 A66-14160
- Small lateral deformation of shallow shells of revolution of radially varying thickness 04 p0590 A66-14165
- Linear deformation of elastic solid in which potential energy-density is function of strain and first and second gradients 04 p0591 A66-14166
- Static elastic deformation and associated change of aerodynamic characteristics of flight vehicle subject to aerodynamic and inertia loading 05 p0609 A66-15784
- Notched structure load analysis, discussing planar stress distribution in flat bar for various points of application of force 06 p0964 A66-16478
- Thermal fatigue of constrained bars made of linearly hardened material evaluated, using mathematical analysis 06 p0967 A66-16969
- Neutral-stability elastic equilibrium problems analyzed by theory of finite deformations, taking geometric and physical nonlinear deformation effects into account 06 p0967 A66-17008
- Boundary conditions producing simple waves in Green-elastic and Cauchy-elastic materials that generate three-dimensional unsteady deformations 06 p0874 A66-17010
- Tetrahedron elements with linearly varying strain for matrix displacement method, interpreting stresses at nodal points 07 p1143 A66-17493
- Karman equation for bending of flexible plate solved by Kantorovich method, taking into account geometrical nonlinear deformations 07 p1143 A66-17860
- Carrier formation due to passage of current through elastically deformed Ge, detecting nonlinearity of volt-ampere characteristics 07 p1106 A66-18381
- Polymeric material deformation under harmonically varying load action, noting steady state regime temperature distribution effects 08 p1243 A66-18879
- Deformation components of photoelastic coatings of shells affected by errors due to rotation of direction of principal deformations 08 p1307 A66-18883
- Singular solutions of concentrated force and concentrated heat source thermoelectricity 09 p1467 A66-20498
- Deformation modulus of airfield pavement materials 09 p1365 A66-20697
- Strict complementary energy theorem for finite deformation of elastic continuum established, using Lagrange strain and stress tensors as conjugate deformation and stress tensors characterizing deformation 10 p1615 A66-21478
- Rotation effect on statically rotating string-mass system determined by Eulerian formulation and prediction of critical speeds 10 p1556 A66-21495
- Wave propagation in quartz to determine third order elastic coefficients 10 p1577 A66-21557
- Ring on three-dimensional elastic foundation containing all six degrees of elastic restraint 10 p1618 A66-21956
- Transformation of sandwich plate equations and deformation of rectangular simply supported sandwich plate 10 p1618 A66-22177
- Boundary value problem for stress concentration at spherical cavity in field of isotropic tension for deformable microstructure 11 p1781 A66-22615
- Changes in microhardness, elastic modulus and shear orientation at boundary between elastic and plastic deformation in steel under tensile stress 11 p1719 A66-23387
- Minimum strain energy characterizations of Saint Venant solution to relaxed Saint Venant problem 12 p1956 A66-23561
- Dynamic strains and transient deformations on opaque body surfaces measured, using bonded birefringent strip 12 p1961 A66-23988
- Stress-strain state of shells of revolution of variable thickness and elastic parameters under effect of external loads and secondary strains obtaining strain, equilibrium and elasticity equations 12 p1963 A66-24043
- Finite deformations of rotating disk of variable thickness, consisting of elastoplastic strain-hardening material, determined from stress-strain diagram 12 p1964 A66-24051
- Nonsymmetric elasticity problem considering stress states, plane deformation and stress concentrated around circular hole 12 p1969 A66-24354
- Mechanical deformation used in fabrication of composite made of continuous columbium wires in copper matrix by drawing, noting optical inspection 12 p1895 A66-24378
- Nonlinear theory for elastic surface deformation, assuming existence of strain-energy function governed mechanically by virtual work 12 p1970 A66-24564
- Elastic problem of infinite plane in stressed state, weakened by two circular holes, solved in system of bipolar coordinates for forces applied at hole edges 12 p1970 A66-24783
- Exact mathematical solution for elastic dielectrics in controllable states, noting Rivlin and Toupin theory, cuboid deformation into rectangular block, electric field effect, etc 12 p1933 A66-24961
- Plane stress problems when yielding occurs locally, analyzing deformation using matrix notation, deriving expressions applicable with stress-strain relations 12 p1972 A66-25008
- Fracture and mechanical failure of polymeric solids at high strain rates 13 p2198 A66-26120
- Soviet monograph on elastic and plastic deformation mechanism, describing stress-strain state of materials, cyclic, variable and reversed load effects, etc 13 p2206 A66-26464
- Elastic anisotropic deformation of thin polycrystalline condensed films of Al, Ag and Ni 14 p2359 A66-27184
- Small motion superposed on stationary slow deformation process of viscoelastic material with fading memory, based on Rivlin and Ericksen differential equation 14 p2397 A66-27384
- Heated cylindrical shell with braces subjected to given compression and internal pressure, having elastic beams along edges, analyzing local deformations effect on shell strength and stability 14 p2400 A66-27684
- Stress and deformation in cross section of beam during complex loading, using steepest-descent method 14 p2400 A66-27685
- General constitutive relations for incremental deformation of metal crystals by multislip 14 p2401 A66-27784
- Derivation of approximate two-dimensional equations for thin elastic plates without resorting to Kirchhoff-type hypothesis 14 p2408 A66-28061
- Torsion of elastic cone as mixed boundary value problem, using Mellin transforms and Wiener-Hopf technique 14 p2408 A66-28395
- Elasticity of structural nonhomogeneous centro-asymmetric isotropic bodies, deriving constitutive equations and differential equations of equilibrium 14 p2409 A66-28457
- Distortion in crystals and lattices described by aeotropic model 14 p2409 A66-28467
- Stresses and coupled-stresses generated by dislocation in isotropic media treated in terms of boundary value problem for Cosserat medium 14 p2409 A66-28468
- Stress concentration near circular cavity in nonlinearly deformable material 15 p2608 A66-28780
- Boundary between applicability ranges of network and steepest descent methods in equation integration of Timoshenko theory in analysis of plate deformation 15 p2608 A66-28962
- Plate under plane stress solved in terms of stiffness properties of finite sized model element 15 p2614 A66-29611
- Second-order effects in dissipative solids and their accumulation in causing rapid acceleration of tensile metal creeps 16 p2814 A66-30529
- Nonmetric connections in quasi-static plastic-elastic deformation of crystalline solid with continuous distribution of dislocations and extra-matter 16 p2746 A66-30532
- High temperature compressive deformation equipment for ceramic materials noting loading, alignment and stress-strain measurement 16 p2682 A66-30950
- Dependence of magnetostriction coefficient for diamagnetic materials on change of Fermi surface with momentum and deformation parameter 16 p2777 A66-31035
- Asymptotic integration of three-dimensional equations of linear elasticity to analyze small deformations of plate which is initially stressed 16 p2818 A66-31106
- Thermoelastic problem for plate with prismatic inclusion of rectangular cross section discussing stress, elastic deformation, displacement potential, etc 16 p2818 A66-31108
- Elastic strain distribution in structure of quasi-isotropic polycrystalline titanium 16 p2728 A66-31787
- Linear stress-strain relation for expressing tensile stress for nonlinear large elastic deformations 17 p3018 A66-31879
- Finite rotational and inflectional deformation of incompressible homogeneous isotropic torus 17 p3018 A66-31928
- Mechanical properties of Ag, Al, Ge, Cu, Ni and Fe thin films, showing elastic deformation and strength greater in thinner films 17 p2939 A66-31971
- Elastic large-deflections of annular membrane treated by modified Foppl-von Karman equation 17 p3024 A66-32359
- Stress-strain state of annular plate made of incompressible nonlinear elastic material, noting power function describing relation between maximum tangential stress and displacement 17 p3026 A66-32596
- Structural-energetic theory of metal failure during deformation at raised temperatures 17 p3027 A66-32665
- Variational and reciprocity theorems on thermoelastic distortions in homogeneous isotropic body 17 p3032 A66-33331
- Elastic deformation of biaxially loaded columns of thin-wall open cross section with initial imperfections 17 p3032 A66-33435
- Quasi-linear hyperbolic equations governing one-dimensional longitudinal wave propagation in viscoelastic material 17 p3032 A66-33502
- Temperature range of nonlinear rigid,



elastic and viscoelastic behavior in quasi-isotropic polymeric materials and derivation of stress-strain-time relations by method of small parameters 18 p3251 A66-33701

Equations of motion for inelastic large deformations of circular membranes subjected to blast loading, useful in metal forming 18 p3252 A66-33763

Deformation and strength properties of refractory solids at temperatures up to 2000 degrees C, using indentation hardness measurements for stress-strain measurements in strength properties 18 p3254 A66-33967

Nonlinearity of relationship between stress and deformation in solids subjected to simple nonisotropic loads 18 p3258 A66-34723

Differential equations for deformations of nonuniform flat plates bent into cones 19 p3473 A66-35850

Nonlinear theory for deformation of elastic directed surface, assuming existence of strain energy function and postulating virtual work governing mechanical behavior 19 p3474 A66-36167

Constitutive equations for elastic solids sustaining deformation for which displacement gradients are small but where nonlinearity is permitted, formulating plane elastostatic problem 19 p3475 A66-36429

Elastic deformation of unbounded transversely isotropic body with internal plane-circular slot under slot surface load 19 p3476 A66-36839

Stability of cylindrical shell of average length with elastic filler under uniform external radial pressure 20 p3665 A66-36911

Spherical shell stability under external pressure for nonlinear elastic and plastic deformation 20 p3668 A66-37528

Elastic-plastic axisymmetric bending of circular cylindrical shell with constant and variable thickness 20 p3670 A66-37671

Nonisothermal deformation of viscoelastic medium analyzed on basis of thermodynamically irreversible processes 20 p3671 A66-38112

Stress and strain fields caused by straight-line dislocation located in anisotropic elastic plate 20 p3671 A66-38113

Large deflection of elastically and geometrically nonlinear circular membrane clamped along rim under uniform pressure solved by power series expressions for discontinuity and equilibrium equations 20 p3673 A66-38270

Stress analysis of elastic cylindrical shell perforated by rectangular cut-out and governed by Donnell equation 20 p3673 A66-38272

Equations for plane deformation in multimodule elasticity theory, formulating generalized Hooke law for multimodule material 21 p3826 A66-38609

Prandtl-Reuss flow law for stresses rather than stress deviators of ideally elastic-plastic bodies 21 p3829 A66-38818

Equilibrium phases of elastic materials occurring at uniform temperature and pressure and at zero deviatoric stress, examining rapid quenching and shearing effects 21 p3829 A66-38940

Stress concentration in elastically deformable bodies under effect of concentrated forces applied to boundaries, with solution of problem for two stress-concentration zones 21 p3829 A66-38975

Elasticity and thermal stress in infinite orthotropic plate exposed to distributed and concentrated heat source 21 p3830 A66-38985

Axisymmetrical deformation of multilayer circular sandwich cylindrical shells, deriving governing differential equations by variational theorem 21 p3831 A66-39272

Poynting effect theoretically analyzed, postulating tensor expression for final Green measure in general coordinates for cylindrical coordinates 22 p3988 A66-39672

Boundary value problem for isothermal unidirectional deformation of hyperelastic material applied to inflation of thick walled sphere 22 p3988 A66-39673

Elastoresistance effects in evaporated bismuth films, deposited on glass and epoxy resin substrates, used as strain gauges and transducers 22 p3962 A66-40046

Uniform magnetic field effect on plane acceleration wave propagation and growth in

homogeneously deformed perfectly electroconductive elastic material 22 p3955 A66-40135

Growth of plane acceleration discontinuities propagating into homogeneously deformed hyperelastic dielectric material in presence of magnetic field 22 p3948 A66-40136

Hamilton principle, motion equations, natural boundary conditions and constitutive relations for finite deformation of one-dimensional curved elastica and radial motion and stability of circular ring 22 p3990 A66-40138

Large amplitude oscillations of cylindrical and prismatic bodies resulting from generalized shear deformation in longitudinal direction 22 p3990 A66-40141

Method for compensating resistance of strain gauges for thermal expansion 22 p3918 A66-40155

Irreversible thermodynamics of large viscoelastic deformations, showing hidden coordinates as scalar functionals and applicability to quasi-equilibrium states 22 p3999 A66-40456

Elastic deformations in finite plane strain for which stresses are functions of polar angle as in wedge subjected to constant normal and tangential tractions on faces 22 p3996 A66-40702

Dynamic aeroelastic motion resulting from inertial and aerodynamic effects, coupled through elastic deformation, applied to jet aircraft, considering flutter, buffet, wakes and turbulence 23 p4015 A66-41035

Deformations of isotropic perfectly elastic material associated with simple shear, examining flow and collapse reactions 23 p4141 A66-41944

Laminated structure with dominant displacement from reference point for solid medium working beyond elastic limit 23 p4144 A66-41969

Generalized strain and transition concepts for elastic-plastic deformation creep and relaxation 23 p4144 A66-41973

Displacement matrix analysis of three-dimensional anisotropic and inhomogeneous elastically deformable bodies represented as tetrahedral assemblies 23 p4146 A66-41989

Elastic microstrain of polycrystalline titanium measuring device, discussing measurement error 24 p4227 A66-42222

Elastic anisotropic deformation of thin polycrystalline condensed films of Al, Ag and Ni 24 p4257 A66-42732

**ELASTIC MEDIUM**

Distribution of thermal stress in infinite elastic solid containing penny-shaped crack 01 p0157 A66-10960

Matched asymptotic expansion to derive dynamical displacements of infinite elastic space embedded with light rigid axisymmetric body 02 p0299 A66-11806

Stress distribution in elastic space reinforced by cylindrical rods 04 p0590 A66-14159

Couple-stresses in dislocated solids and effect in classical elasticity 04 p0594 A66-14292

Three-dimensional linear elasticity problems in homogeneous transversely isotropic elastic materials like infinite circular cylinder, using potential function method [ASME PAPER 65-WA/APM-26] 05 p0778 A66-15447

Poisson ratio for viscoelastic materials undergoing large strains measured, using compression test [ASME PAPER 65-WA/RP-8] 05 p0706 A66-15629

Elastic-plastic material, calculating stress concentration and deformation for planes weakened by circular holes 06 p0964 A66-16476

Flow induced structural vibrations, noting interdependence between deformation and fluid dynamic loading 06 p0872 A66-16615

Boundary conditions producing simple waves in Green-elastic and Cauchy-elastic materials that generate three-dimensional unsteady deformations 06 p0874 A66-17010

Constitutive equations for characteristic effects due to elastic behavior of continuum body expressed by stress and strain field 07 p1145 A66-18225

Thermal stress in infinite nonisotropic elastic slab with heated element on upper surface and base of slab in contact with insulating plane 07 p1145 A66-18227

Mechanical constitutive theory and methods of stress analysis for physically nonlinear solid propellants [AIAA PAPER 66-124] 07 p1110 A66-18460

Discontinuity surface propagation in linearly thermoelastic solid 08 p1311 A66-19227

Breaking stresses in two connected elastic half-spaces determined with aid of Griffith-Sneddon criterion 12 p1968 A66-24349

Stressed state of isotropic elastic medium with two circular holes solved, using approximation method for concentrated loads 13 p2202 A66-26417

Dynamic stresses in infinite elastic space with circular cylindrical cavity 13 p2203 A66-26428

Bending moment of thin nonlinearly elastic plates, noting dependence of coefficient of moment concentration on external load and material properties 13 p2203 A66-26429

Thermal field effect on stress-strain state of infinite elastic plane with circular hole examined, using Muskhelishvili principle 13 p2204 A66-26435

Stress concentration at thermally insulated holes in elastic material created by disturbance of uniform heat flow at holes 13 p2206 A66-26459

Stresses in composite spheroids of two different isotropic elastic materials under compressive forces acting along common axis of revolution 14 p2397 A66-27391

Fundamental equations for birefringence of isotropic elastic solids and isotropic viscous fluid derived from Toupin theory of photoelasticity and stress optics 14 p2408 A66-28388

Mass forces for infinite elastic space expressed by generalized functions 15 p2615 A66-29852

Stress-strain distribution near curvilinear holes in moment theory of elasticity of isotropic medium 16 p2819 A66-31143

Propagation of cylindrical shear waves in nonhomogeneous elastic bodies treated by method of characteristics [AIAA PAPER 66-444] 17 p3027 A66-32757

Plane and spherical wave propagation in locking-type of materials with viscous-type of stress-strain relationship 17 p3031 A66-33077

Three-dimensional linear elasticity problems in homogeneous transversely isotropic elastic materials like infinite circular cylinder, using potential function method [ASME PAPER 65-WA/APM-26] 18 p3248 A66-33582

Nonlinear material with memory defined by constitutive functional, examining fading memory theory 19 p3438 A66-35484

Continuous plane with circular inclusion with different elastic properties, giving solution in form of boundary equation in random variable 20 p3668 A66-37530

Complex load action on elastic-plastic structures in light of limit analysis, discussing safety criterion 21 p3826 A66-38591

Stress and displacement field of plane heat source moving at constant speed through elastic medium 21 p3837 A66-39447

Constitutive equations for nonlinear elastic solid-linear viscous fluid mixture and for mixture of two nonlinear elastic solids 22 p3998 A66-40140

Flat elliptical crack in infinite elastic medium under shear stress at infinity 22 p3995 A66-40457

Status of aircraft structural design analysis methods, examining structural elastic behavior on basis of stress analysis 23 p4138 A66-41381

Approximate solution of forced oscillation PDEs of rectangular orthotropic plate on elastic base with two characteristics 23 p4139 A66-41557

Minimum and variational principles in study of stress locking functions and stress-strain law of elastic perfectly locking materials 23 p4146 A66-41990

Wave propagation in thermoplastic media, discussing dynamic behavior, formation of



wave fronts, velocity, etc 24 p4284 A66-42139  
 Series solution to problem of spherically isotropic elastic medium bounded by concentric spherical surfaces, noting force and stress concentration 24 p4285 A66-42141  
 Circular elastic inclusion bonded to different elastic material except over arc crack, oscillation phenomena in solution indicates linear elasticity can not be used to predict stresses in this region 24 p4286 A66-42153  
 Elastic and plastic behavior of ideal materials with mechanical and thermal properties of ductile structural metals 24 p4288 A66-42275  
 Huygen principle for elastic media, comparing Kupradze formulation with formulations of Knopoff and Bollet 24 p4237 A66-42495

**ELASTIC PLATE**  
 Bending problem of circular orthotropic plate on elastic base under axisymmetric load 01 p0153 A66-10467  
 Bending of elastic rectangular plates uniformly transverse loaded along axes of symmetry 01 p0154 A66-10468  
 Intermediate stages of wave-type bending process in elastic plate investigated by system of approximate methods 01 p0157 A66-10983  
 Fundamental solutions of static and dynamic linear inextensional theories of thin elastic plates [ASME PAPER 65-WA/APM-23] 05 p0778 A66-15445  
 Influence of edge displacements on vertical deflection of semiinfinite isotropic elastic plate 06 p0966 A66-16502  
 Elasto-creeping circular membrane, obtaining nonlinear solution for axisymmetric circular elastic creep problem 07 p1142 A66-17263  
 Stress distribution due to nucleus of thermoelastic strain placed at center of elliptic insert in infinite plate of different elastic material 07 p1145 A66-18244  
 Stress-strain state of elastic space, examining circular crack for axial tensile load effects 08 p1305 A66-18597  
 Two-dimensional problem of disturbance propagation in elastic plate under concentrated load moving along boundaries at constant speed, pressure and stress-strain pattern 08 p1305 A66-18598  
 Stressed state of unbounded nonlinear isotropic plate with square hole during triaxial uniform tension 08 p1307 A66-18880  
 Small parameter method determination of pure bending and torsion of thin plate with circular hole, where material of plate obeys nonlinear elasticity law 08 p1312 A66-19435  
 Classical theory of flexural motions of elastic plates used to determine natural frequencies of uniform annular plates for nine combinations of boundary conditions 10 p1616 A66-21490  
 Natural frequencies and mode patterns for clamped and simply supported square plates of linearly variable thickness solved by finite-difference approximation, using pulsed-air vibrator 11 p1780 A66-22329  
 Exact solution of wave field of point vibrator operator on free plate in form of elastic strip, comparing theory and measurement 11 p1780 A66-22605  
 Fundamental solutions of static and dynamic linear inextensional theories of thin elastic plates [ASME PAPER 65-WA/APM-23] 12 p1960 A66-23971  
 Effect of rivet-attached stringer on stress concentrations in thin elastic sheet with circular cut-out, expressing results as correction factor 12 p1962 A66-23993  
 Inverse problem of stressed state of elastic plate reinforced by members of known rigidity under axisymmetric load 12 p1967 A66-24107  
 Plate loaded over ring-shaped zone, determining bending moment, torque and shearing force 12 p1967 A66-24111  
 Deflections, moments and shears of circular ring plate under transverse load, comparing classical and improved theory of deformation 13 p2195 A66-25180  
 Book on stress-strain analysis including photoelastic investigations of bending impact on cantilever beam 13 p2198 A66-26298

Elastic rectangular plate moment influence field calculated, using photoelastic method 13 p2198 A66-26299  
 Eigenvalue density in vibration of elastic plates and shells, noting concentration points for natural frequencies and influence of rotational inertia and shear strain 14 p2398 A66-27455  
 Stress distribution of isotropic plate with infinite row of circular holes with elastic cores or elastic ring reinforcement 15 p2612 A66-29428  
 Stability of elastic thin plate subjected to self-equilibrating stresses acting in its plane with random intensity and distribution 17 p3018 A66-31835  
 Complex variable method to solve problem of circular elastic plate elastically restrained at edge and subjected to arbitrary concentrated force 17 p3020 A66-32000  
 Mean-square response of thin elastic plate to random pressure acting normal to plate surface 17 p3021 A66-32010  
 Rotatory inertia and transverse shear effects on quasi-stationary response of elastic strip plates to uniformly moving harmonic line loads 17 p3027 A66-32663  
 Surface shear traction and torsional compliance of elastic plate pressed between identical elastic spheres 18 p3249 A66-33586  
 Forced vibrations of flexible rectangular panel backed by closed rectangular cavity under external acoustic pressure, noting sound transmission into cavity 18 p3250 A66-33674  
 Natural nonlinear oscillations of plate studied by Kirchevskii extension of work-reciprocity theorem to problems in nonlinear mechanics 18 p3252 A66-33713  
 Elementary effects method solution of fourth-order PDEs for bending and vibration of elastic plates 20 p3671 A66-37989  
 Stress and strain fields caused by straight-line dislocation located in anisotropic elastic plate 20 p3671 A66-38113  
 Successive approximation method for solving fundamental equations of nonlinear flexural vibration for rectangular elastic plate, noting effect of temperature and large amplitude 20 p3672 A66-38236  
 Stress tensor analysis of elastic plates in reference state, noting nonlinear plate theory and variational principle 20 p3673 A66-38273  
 Two-dimensional nonlinear equations of finite thermal oscillations of anisotropic thin elastic plates 20 p3673 A66-38278  
 Stress distribution in elastically nonhomogeneous rotating thin circular disk of varying thickness of anisotropic material 21 p3745 A66-39597  
 Time-dependent stress distribution in annular hereditary-elastic cylindrical-anisotropic plate 22 p3989 A66-39822  
 Instability of rectangular solid in plane strain subjected axially to constant pressure and laterally to constant hydrostatic pressure 24 p4286 A66-42150  
 Mathematical demonstration that deflection of sandwich plate can be obtained from Reissner theory of plates if deflection function is known 24 p4286 A66-42159

**ELASTIC PROPERTY**

Relation between high pressures and elastic properties of materials present in interior of Sun during process of condensation 01 p0135 A66-10297  
 Polycrystalline niobium elastic properties and effects of alloying with chromium and iron 03 p0383 A66-13128  
 Elastic properties of bearing elements of gyrotachometer and effect on frequency of oscillations 07 p1031 A66-17409  
 Elastic interaction energy of two infinitesimal dislocation loops in transversely isotropic medium estimated from fundamental elasticity tensor 07 p1144 A66-18044  
 Martensitic transformation in titanium alloys containing eutectoid-forming elements, noting elastic properties, shear modulus, etc 08 p1239 A66-18906  
 Stress-strain law and finite torsion of homogeneous circular cylinder, noting deformation and force needed to keep final state of body in equilibrium 17 p3025 A66-32499  
 Elastic and plastic properties of fiber-

reinforced and continuous skeleton tungsten-copper composite materials 17 p2941 A66-33425  
 O-O and O-N clusters in niobium detected via internal friction and elastic aftereffect measurements, noting equilibrium, kinetic properties, binding enthalpy, etc 18 p3121 A66-33728  
 Natural vibration frequencies of rocket nozzles, accounting for anisotropic elastic behavior, internal gas dynamic pressure, boundary conditions, etc 18 p3258 A66-34601  
 Oscillation of oscillator with elastically hereditary and weakly nonlinear characteristics, applying operational method to analysis in terms of hereditary creep theory 19 p3476 A66-36840  
 Approximation of elastic constants of unidirectional fiber reinforced composite material from constituent material properties, including longitudinal modulus, transverse modulus and Poisson ratio 22 p3993 A66-40342  
 Residual stress determination in elastic cylindrical orthotropic materials, using stress-strain relations and Sachs equations 22 p3994 A66-40434  
 Material strength determination based on elastoplastic and rigid-plastic theory of solid bodies 23 p4137 A66-41006

**ELASTIC SCATTERING**

**SA INELASTIC SCATTERING**

Thermal diffuse elastic electron scattering in polycrystalline Al foil, using retarding field apparatus 05 p0736 A66-14980  
 Elastic differential scattering of helium ions discussing energy analysis, geometry and target particle motion effects, and interference phenomena 05 p0719 A66-15767  
 Elastic differential scattering in low energy helium ion collisions, discussing quantal and secondary interference and two-state theory 05 p0719 A66-15768  
 Perturbation effects in differential elastic ion-atom scattering generated by crossing of molecular states from even potentials 11 p1740 A66-22972  
 Intermolecular reaction between oxygen and nitrogen at energies from 0.1 to 1.5 ev 12 p1917 A66-24222  
 Energy dependence of elastic resonance scattering of low energy electrons from He, Ne, Ar and nitrogen gases at angles ranging from 8 to 110 degrees 14 p2337 A66-27797  
 Ion beam elastic scattering cross section for proton-helium systems 14 p2337 A66-27978  
 High energy measurement of neutron-proton elastic scattering, noting diffraction peak existence, differential cross section and secondary forward peak 18 p3166 A66-34163  
 Angular distributions of elastic and inelastic alpha-particle scattering in even tin isotopes, using 40 mev alpha beam 18 p3138 A66-34166  
 Quantum effects in elastic scattering of atoms and molecules, noting classical treatment 18 p3138 A66-34458  
 Intermolecular reaction between oxygen and nitrogen at energies from 0.1 to 1.5 ev 22 p3951 A66-40584  
 Scattering of plane elastic compressional pulse by circular cylindrical cavity in infinite homogeneous isotropic linear elastic solid 23 p4145 A66-41984

**ELASTIC SHEET**

Dynamic problems of transversely isotropic half-space and elastic layer, solving contact and boundary value problems 08 p1315 A66-19708  
 Stress concentration factor for infinite plate in tension containing doubly symmetrical hole with three intersecting circles forming boundary 17 p3023 A66-32081  
 Thermoelastic stresses in elastic strips and cylinders, computing numerical value along axes and centers of elements 21 p3826 A66-38590  
 Rivet attached stringer effect on stress concentration in thin elastic sheet with crack solved, using computer calculations 24 p4285 A66-42143

**ELASTIC SHELL**

Nonlinear field equations of elastic shell in terms of reference state subjected to strain displacement 01 p0153 A66-10444  
 Free oscillations of elastic shells of



revolution 01 p0154 A66-10469  
Timoshenko-type nonlinear theory of elastic shells based on generalized Hamiltonian variational principle 01 p0157 A66-10982  
Linear elastic analysis of shells of revolution by matrix displacement method [AIAA PAPER 65-142] 03 p0437 A66-12799  
Free vibration and transient elastic response of thin shells within scope of linear theory 04 p0586 A66-13405  
Asymptotic integration of thin elastic shell equations for design of shells of revolution subject to effect of cyclic edge loads 04 p0590 A66-14149  
Deformation of circular membrane containing central rigid disk under axisymmetrically distributed load 04 p0590 A66-14150  
Linearized version for isotropic elastic plates and shells by series expansion method obtained as Euler equations 04 p0591 A66-14201  
Shell linear theory, discussing classical elasticity theory, bending equations, edge effect and asymptotic theory 06 p0962 A66-16350  
Infinitely-long thin elastic circular cylindrical shells loaded along segment of generatrix by arbitrarily distributed loads 07 p1143 A66-17627  
Extension of paper on boundary layer equations, obtaining boundary conditions on major terms of interior stresses for thin elastic shells 08 p1306 A66-18618  
Axisymmetric wave motion in thin walled elastic spherical shell under normal load uniformly distributed over small segment 08 p1315 A66-19763  
Three-dimensional linear elasticity and viscoelasticity theory to obtain axisymmetric plane-strain thickness-stretch modal response of isotropic and orthotropic thick shells 09 p1468 A66-20948  
Generalized analysis of rotationally symmetric thin elastic shells applied to cases where shell wall consists of any number of layers of isotropic or orthotropic material 10 p1617 A66-21496  
Stability analysis of freely supported thin elastic conical three-layer shell situated in potential supersonic flow 11 p1780 A66-22349  
Effect of water immersion on reduction of die stresses in explosive forming, investigating dynamic response of thin elastic spherical shell surrounded by large body of fluid, employing diagrams [ASME PAPER 65-PROD-6] 11 p1709 A66-22474  
Comparison of elasticity and shell theory solutions for infinite circular cylindrical shell subjected to periodically spaced band loads [AIAA PAPER 65-139] 12 p1956 A66-23582  
Stress-strain state of shells of revolution of variable thickness and elastic parameters under effect of external loads and secondary strains obtaining strain, equilibrium and elasticity equations 12 p1963 A66-24043  
Integrals of equations of small axisymmetrical oscillations of thin elastic shell of revolution 12 p1966 A66-24061  
Nonlinear theory of thin elastic shells, discussing surface geometry and deformation, equations of equilibrium and boundary conditions. and stress functions 13 p2196 A66-25600  
Free oscillation of thin elastic shell, using asymptotic method for integrating dynamic equations in classical linear theory 13 p2196 A66-25630  
Eigenvalue density in vibration of elastic plates and shells, noting concentration points for natural frequencies and influence of rotational inertia and shear strain 14 p2398 A66-27455  
Torsional oscillations of hollow cylinder of finite length encased in thin elastic shell 14 p2406 A66-27999  
Asymptotic solutions of boundary value problems for elastic semiinfinite circular cylindrical shells by removing restriction of slow circumferential variation 15 p2609 A66-29239  
Stress distribution in shallow logarithmic shell of revolution 15 p2609 A66-29240  
Differential equations describing elastic

shells of revolution under physical nonlinearities, noting positive stresses in buckling zone 15 p2611 A66-29422  
Computer program for axisymmetric nonlinear behavior of stiffened elastic shells of revolution with variable thickness, calculating collapse pressures [AIAA PAPER 66-529] 16 p2814 A66-30527  
Stresses and displacements in linearly elastic and toroidal shells of circular cross section determined by nonlinear numerical method [AIAA PAPER 65-144] 16 p2816 A66-30905  
Influence of relative thickness of elastic case on acoustic stability of radial modes in solid propellant rockets 16 p2791 A66-31474  
Basic theory derived for nonsymmetric elastic three-layer sandwich shells of variable rigidity 17 p3026 A66-32600  
Elastic model for evaluating stresses in Earth induced by density variations or topographic irregularities 17 p2921 A66-33226  
Stress component expressions derived for axisymmetric elastic shell problem in terms of stress resultants, moments and geometry 18 p3250 A66-33605  
Stress analysis of junction of thin elastic shells of revolution, considering axisymmetric wind and sinusoidal load distributions 18 p3253 A66-33804  
Forced motions of hollow cylinder encased in thin elastic shell and subjected to time-harmonic pressure at inner surface of cylinder 18 p3259 A66-35026  
Stiffness method for analysis of elastic-plastic shells of revolution with axisymmetric loading implemented by step-by-step method of integration in computer program 20 p3667 A66-37482  
Spherical shell stability under external pressure for nonlinear elastic and plastic deformation 20 p3668 A66-37528  
Plane contact problem for ring reinforcing junction of cylindrical and spherical shell, determining forces and displacement in ring 20 p3669 A66-37667  
Liquid instability of vibrating partially filled elastic tank, emphasizing resonant breathing mode and frequency response 20 p3672 A66-38153  
Shell theory, discussing relationship between stress function tensors and shell stress function 20 p3673 A66-38275  
Influence coefficients for semiinfinite and infinite circular cylindrical elastic shell subject to self-equilibrating edge loads 22 p3995 A66-40451  
Elastic shell theory, deriving two-dimensional theory from three-dimensional theory, noting boundary condition contraction, stress-strain relations, etc 23 p4141 A66-41936  
Membrane theory of convex shells and approaches to construction of general moment theory of elastic shells 23 p4141 A66-41938  
Differential equations of linear theory of elastic shells derived under Kirchhoff-Love hypothesis with aid of static-geometric analog 23 p4142 A66-41956  
Large deflection postbuckling analysis of thin walled oval cylinders under axial compression 23 p4143 A66-41961  
Linear thermoelastic theory of general thin shells, adopting Love-Kirchhoff assumptions and considering analogy between thermal field and fictitious body force vector 23 p4143 A66-41966

## ELASTIC STABILITY

Matrix analysis of response of geometrically nonlinear structures to prescribed dynamic loading and effects of thermomechanical midplane preload in prediction of natural frequencies and mode shapes 01 p0148 A66-10135  
Stability theory for elastomechanical systems using algebraic techniques based upon Galerkin method 01 p0153 A66-10446  
Flexible-wall tubes flattened by fluid when velocity reaches critical value, with differential equations describing effect of stability loss 01 p0158 A66-11035  
Discrete critical points of perfect structural system and three branching points in general theory of elastic stability 03 p0434 A66-12370  
Elastic equilibrium of rectangular prism with given stress-vector components at

lateral surfaces and displacements at faces 03 p0435 A66-12635  
Equilibrium stability of rod beyond elastic limit 04 p0590 A66-14161  
Increasing plastic buckling resistance of thin cylindrical /Mg and Al/ shell by means of elastic core /polyurethane foam/ [ASME PAPER 65-APMW-18] 04 p0592 A66-14219  
Elastic stability of clamped shallow spherical shells under concentrated load, noting buckling modes [ASME PAPER 65-APMW-28] 04 p0593 A66-14228  
Parametric response of elastic clamped-free column, noting agreement between theory and experiments for first three spatial and first four temporal modes 04 p0594 A66-14391  
Cantilevered continuous pipe conveying fluid at constant velocity, showing that internal and external damping and Coriolis forces may have destabilizing effect [AIAA PAPER 66-102] 05 p0774 A66-15036  
Elastic equilibrium of rectangular parallelepiped when boundary conditions on surface are given in terms of displacements 07 p1146 A66-18253  
Elastic general instability of orthotropically stiffened cylinders under axial compression [AIAA PAPER 66-139] 08 p1308 A66-19003  
Compressive strength and instability failure mechanism in uniaxial boron fiber-metal matrix composite 08 p1240 A66-19139  
Convergence of Galerkin method in nonconservative stability problems of thin elastic plates and thin elastic rods 08 p1311 A66-19339  
Stability of Al-Mg alloy spherical shells under uniform external pressure beyond elastic limit 08 p1315 A66-19591  
Book on elastic stability of plane rigid-jointed triangulated and nontriangulated frames 09 p1467 A66-20476  
Stability in elastic and aeroelastic systems analyzed by Liapunov direct method 09 p1468 A66-20800  
Elastic general instability collapse pressure of ring-reinforced circular cylindrical shell subjected to uniform external pressure 10 p1613 A66-21318  
Increasing plastic buckling resistance of thin cylindrical /Mg and Al/ shell by means of elastic core /polyurethane foam/ [ASME PAPER 65-APMW-18] 10 p1615 A66-21475  
Saint Venant principle applied to plane strain and generalized plane stress solutions of equations of linear theory of elastic equilibrium 10 p1618 A66-21875  
Maximum-minimum theory of eigenvalues applied to stability in Navier-Stokes equation and to incompressible elastic body vibration 11 p1694 A66-23183  
Transformation relation for prestress tensor in problem of indifferent equilibrium of elastic bodies derived, using approximation method 12 p1959 A66-23865  
Circular ring loaded by constant direction forces used to illustrate kinetic instability of elastic system under random time-dependent forces 12 p1960 A66-23950  
Influence of homogeneous state of initial stress on frequency of three-dimensional vibrations of plates and rods 12 p1961 A66-23984  
Fundamental frequency of four-point-supported square elastic plate 14 p2398 A66-27436  
Buckling, postbuckling and imperfection sensitivity of cylinders and shells 14 p2404 A66-27987  
Dynamic instability in large of elastic body with given initial velocity and displacement, noting example of curved beam subjected to impulsive loads 14 p2408 A66-28387  
Series in function of complex variable applied to mixed problem of elastic equilibrium of annulus 15 p2607 A66-28697  
Two-dimensional representation of relation between stresses, displacement vector and external load for two elastic equilibrium states 15 p2608 A66-28771  
Destabilization of linear system with N degrees of freedom without damping subjected to nonconservative forces 15 p2609 A66-29251



Instability of nonlinearly viscoelastic column under finite compression, noting boundary conditions, application to buckling problem, types of stability loss, etc 15 p2615 A66-29720

Stability of two coplanar wedge-shaped cracks, showing under what conditions interaction effects are important 16 p2814 A66-30533

Variational solution of simultaneous stability equations boundary value problem for transverse displacements and stress state 16 p2819 A66-31137

Free vibration of complete and incomplete rings, considering ring centerline extensibility and rotary inertia 17 p3022 A66-32016

Complex analysis of equilibrium equations in two-dimensional theory of elasticity 17 p3025 A66-32592

Elastic stability of clamped shallow spherical shells under concentrated load, noting buckling modes [ASME PAPER 65-APMW-28] 18 p3248 A66-33575

Elastic equilibrium of infinite isotropic homogeneous plate with soldered circular isotropic ring 18 p3251 A66-33703

Variational formulation of equilibrium stability of nonlinear elastic circular cylindrical panel under radial stress 18 p3251 A66-33704

Structural stability criteria of manned rotating space stations derived from elastic model experiments [AIAA PAPER 65-406] 18 p3240 A66-33822

Cantilevered continuous pipe conveying fluid at constant velocity, showing that internal and external damping and Coriolis forces may have destabilizing effect [AIAA PAPER 66-102] 18 p3257 A66-34594

Elastic stability of thin walled circular cylindrical shells in torsion, applying Galerkin method to Donnell equations for critical stresses 18 p3258 A66-34648

Sufficient condition for stability of linearly viscoelastic continuum subjected to surface tractions following partial deformation of solid are nonconservative and associated with energy source 19 p3401 A66-36302

Static dimensional stability of nonlinear elastic continua reduced to linear shell theory 20 p3668 A66-37527

Nonconservative elastic stability problems treated by Galerkin and Ritz methods 20 p3669 A66-37541

Static and dynamic stability loss of nonconservative mechanical systems describing buckling of clamped-free rod and stability loss of cantilever beam subjected to bending 20 p3672 A66-38267

Stability of circular transversely isotropic plates under various attachment conditions along contour based on Ambartsumian plate theory 21 p3826 A66-38611

Elastic stability of cylindrical shells reinforced by one or two frames and subjected to external radial pressure, noting inertia moment about skin line and frame bending stiffness 21 p3828 A66-38703

General theory of stability of elastic equilibrium in three-dimensional system of orthogonal curvilinear coordinates 21 p3828 A66-38803

Elastic stability theory for second-order strain components in Cartesian, cylindrical, spherical and polar coordinates 21 p3828 A66-38804

Moment stress effect on elastic equilibrium of plate with circular opening 22 p3991 A66-40148

Buckling, postbuckling and imperfection sensitivity of cylinders and shells 22 p3992 A66-40337

Geometrical and statistical relations of theory of nonlinearly elastic body presented in connection with bifurcation of equilibrium of ideally elastic body 22 p3996 A66-40686

Two-dimensional elastic equilibrium problems in reinforced plates with holes and bending theory problems in reinforced thin plates 23 p4137 A66-41003

Two-dimensional purely elastic Earth model used to study elastic equilibrium configuration between density and topographic surface

irregularities 23 p4063 A66-41391

Ritz method for solving elastic stability of rectangular cantilever plate in flows moving in direction perpendicular and parallel to clamped edge of plate 23 p4139 A66-41787

Galerkin based stability theory of elastic equilibrium extended to include nonconservative loads 23 p4097 A66-41983

Equilibrium of elastic sphere with pressing rigid punches 23 p4145 A66-41987

Static elastic and thermoelastic stability, discussing kinetic theory and physical interpretation of energy methods 24 p4287 A66-42271

Stability of ideal plate under compression loading beyond elastic limit 24 p4290 A66-42437

**ELASTIC STRENGTH**

Matrix application to method of initial parameters in solution of problems of elasticity and strength of materials 04 p0588 A66-13759

Elastic torsional analysis of irregular shapes, determining direct stiffness solution, shear stress and warping function distribution for shafts 06 p0966 A66-16614

Symmetrical loading of infinite plate weakened by three circular holes 08 p1306 A66-18704

Elastic problem of infinite plane in stressed state, weakened by two circular holes, solved in system of bipolar coordinates for forces applied at hole edges 12 p1970 A66-24783

Interatomic interaction effect on adsorption-induced loss of strength in metals 14 p2315 A66-27599

Oxide-base cermets prepared by infiltration with silver and silver alloys, noting dispersion strengthening, bend creep, impact loading, etc, for gas-turbine application 16 p2730 A66-30250

Monograph on nonlinear bending theory of three layer plates, covering mathematical theory of elasticity stress-strain diagrams, Galerkin method, maximum deflection criteria, etc 16 p2819 A66-31136

Whisker reinforcement of metals and effects on linear elastic stress-strain relations 21 p3752 A66-39367

Strength test results on special small rocket covering bending, stiffness and internal pressure strength of various components 23 p4133 A66-41423

**ELASTIC SYSTEM**

Parametric resonance of elastic systems with infinite number of degrees of freedom 05 p0775 A66-15310

Nonconservative loading on linear two-degree of freedom elastic system, discussing damping effects on equilibrium stability [ASME PAPER 65-WA/APM-17] 05 p0777 A66-15439

Forced oscillations of elastohydrodynamic systems, using Rabotnov functions as kernels of integral operators, permitting description of creep curves for materials 08 p1307 A66-18884

Asymptotic method of integral estimation of space-time broadband random vibrations boundary value problem for elastic systems 11 p1781 A66-22616

Lower bounds for frequencies of continuous linear elastic systems in free vibration 12 p1960 A66-23947

Nonconservative loading on linear two-degree of freedom elastic system, discussing damping effects on equilibrium stability [ASME PAPER 65-WA/APM-17] 12 p1961 A66-23983

Dual integral equation and dual series analysis and application to mixed boundary value problems in elasticity, hydrodynamics and electrostatics 15 p2526 A66-28953

Dual integral equations in elasticity theory, noting Mehler-Fok transformation of spherical functions, Fredholm equation and application to mixed boundary value problems 15 p2526 A66-28954

Monograph on digital computer solution of matrix problems of elastic system vibrations 17 p2877 A66-32987

Electric analogs construction for stability and oscillation of elastic system 20 p3670 A66-37674

Internal nonlinear material damping effects on whirling motion of elastic shaft, noting response curves for Mentel-Fu stress-strain

law 21 p3745 A66-39434

Movchan theorem for stability of continuous systems, considering example of vibrating string and derivation of stability criterion for nonlinear elasticity 22 p3990 A66-40134

Plane stressed state of nonlinear plate with opening reinforced by thin elastic rod in case of small deviations from Hooke law 22 p3991 A66-40152

Generalized constraints applied in stiffness method of structural analysis 22 p3993 A66-40341

Book on nonlinear theory of vibration absorbing systems especially elastic shock absorbers 23 p4137 A66-41053

Asymptotic solution of broadband random vibration BVP for elastic systems, based on excitation spectral width and natural frequency density 23 p4142 A66-41953

**ELASTIC WAVE**

**SA MAGNETOELASTIC WAVE**

Screen defects of various size and shape, effect on ultrasonic pulses for approximate solution of diffraction problem of elastic waves 01 p0077 A66-10419

Longitudinal elastic wave of finite amplitude propagation in isotropic solid 01 p0057 A66-10421

RF electromagnetic and elastic oscillations in ferrites 01 p0121 A66-10568

Spherical elastoplastic waves in expansion of spherical cavities in impulsively loaded thick metal spheres 02 p0300 A66-11853

Stress wave propagation in elastic-plastic solid with cylindrical or spherical symmetry and expanding core 02 p0301 A66-12166

Laser excitation in quartz of elastic modes of thick plate, suggesting energy coupling mechanisms 03 p0376 A66-12423

Unified approach to propagation of plane, cylindrical and spherical dilation waves in elastic media, using method of characteristics [ASME PAPER 65-WA/APM-21] 05 p0778 A66-15443

Longitudinal elastic-plastic pulse propagation for smooth stress-strain curves concave toward strain axis, applied to long bar loaded at end by short pressure pulse [ASME PAPER 65-WA/APM-29] 05 p0778 A66-15450

Two-dimensional problems of diffraction of weak shock or acoustic and elastic waves on obstacles of various shapes, equivalent to supersonic gas flow three-dimensional problems 06 p0909 A66-16706

Propagation of elastic disturbance in conical rod with varying elasticity 07 p1145 A66-18228

Self-excited vibrations of damped systems with traveling waves, using oscillators moving along beam resting on elastic foundation, noting flutter of plates and shells 08 p1309 A66-19116

Axisymmetric and spherical symmetric elastic stresses and deformations in cylindrical and spherical shells determined by direct numerical analysis method 08 p1309 A66-19141

Elastic wave propagation in helical springs of small helix angle, including effect of coupling between extension and rotation for large helix angle 08 p1311 A66-19293

Direct piezoelectric coupling to surface elastic waves by spatially periodic electrode, noting measurements in quartz plate and CdS film 10 p1533 A66-21068

Numerical computation verifying Forte contention in connection with relaxation phenomena associated with thermoelastic dissipation in solids 10 p1555 A66-21197

Velocity distribution of P and S waves in lunar interior, based on elastic wave propagation in rocks and P and S wave distribution in upper Earth layer 10 p1607 A66-21287

Screen defects of various size and shape, effect on ultrasonic pulses for approximate solution of diffraction problem of elastic waves 11 p1705 A66-22604

Longitudinal elastic wave of finite amplitude propagation in isotropic solid 11 p1736 A66-22606

HF elastic-wave propagation and detection in study of structural properties of condensed matter 12 p1925 A66-23658

Time-dependent variation of cross sectional



area used to generalize classical theory of elastic-plastic loading waves in thin rods 12 p1960 A66-23949

Unified approach to propagation of plane, cylindrical and spherical dilation waves in elastic media, using method of characteristics [ASME PAPER 65-WA/APM-21]

Elastic plane wave diffraction on solid strip soldered into infinite elastic medium 12 p1968 A66-24351

Phase difference due to elastic waves produced by cyclic heating of targets by impacting ions from pulsed beam 13 p2159 A66-25070

Elastic wave diffraction on rigid edge analyzed by employing acoustic analogy 13 p1991 A66-25637

Electro-optic effect and elastic wave propagation in single-domain ferroelectric lithium tantalate 13 p2170 A66-26589

Interaction between surface elastic wave and semiinfinite plasma 14 p2346 A66-28236

Stress wave propagation in inhomogeneous rod applied to measurement of dynamic overpressure on moving vehicle subjected to sudden intense blast loading 14 p2409 A66-28398

Wave propagation in elastic solids with linear stress-strain curve 15 p2607 A66-28651

Modes of elastic wave propagation and orientation dependence of dislocation damping in aluminum 16 p2821 A66-31452

Propagation of elastic waves in thin cylindrical shell in terms of exact three-dimensional elastic theory 17 p3028 A66-32788

Longitudinal elastic-plastic pulse propagation for smooth stress-strain curves concave toward strain axis, applied to long bar loaded at end by short pressure pulse [ASME PAPER 65-WA/APM-29]

Pressure distribution, surface roughness, dry friction and elastic coupling effects on wave propagation and reflection in elastic rod, using modified-Laplace transformations 18 p3259 A66-34940

Asymptotic solutions for large time obtained for predominantly mechanical mode of one-dimensional solution of coupled thermoelastic equations 19 p3400 A66-35853

Plane elastic waves of finite amplitude in Hadamard materials and harmonic materials 21 p3771 A66-39274

Elastic-plastic and stress shock wave propagation in finite-length bar with monotone decreasing cross-sectional area 22 p3995 A66-40509

Stress wave propagation, particularly dilatational waves in high polymers, rate-of-strain effects in metals and wave propagation in nonlinear time dependent solids 24 p4287 A66-42268

Plane stationary elastic wave diffraction by stress-free circular cylinder, noting cylindrical cavity case 24 p4175 A66-42841

## ELASTICITY

SA AEROELASTICITY

SA AERTHERMOELASTICITY

SA AIRYS STRESS FUNCTION

SA BIHARMONIC EQUATION

SA FLEXIBILITY

SA HUGONOT EQUATION OF STATE

SA HYPOELASTICITY

SA MAGNETOELASTICITY

SA PHOTOELASTICITY

SA PHOTOVISCOELASTICITY

SA PLASTICITY

Radiation conditions in terms of motion equations of classical elasticity and field equations show uniqueness of solution to wave scattering problems 01 p0153 A66-10431

Potential and elasticity theories for solving basic problems for hollow and compound regions 01 p0153 A66-10466

Stressed state of curved rod of rectangular cross section subject to bending, shearing, tension and compression determined from theory of elasticity 01 p0155 A66-10740

Charpy test modification using ram to deform sample, obtaining data on elastic limit corresponding to high stress rates 02 p0246 A66-12005

Shock waves in elasticity discussing upstream, downstream and Lagrange coordinate-related configurations,

propagation conditions in isotropic medium and developing equations for arbitrary shock amplitudes 03 p0392 A66-12535

Stress analysis in inelastic range at elevated temperature covering stress-strain law, point/ axially symmetric deformations of thick-walled sphere and cylinder with numerical values 03 p0436 A66-12718

Vibrational characteristics, natural frequencies and associated composite loss factor of finite-length laminated beam with alternate elastic and viscoelastic layers [ASME PAPER 65-WA/APM-1]

Book on point matching technique for solving boundary value problems of elasticity theory for multiply connected regions 06 p0962 A66-16249

Asymptotic solution to elasticity theory problem for hollow isotropic cylinder of finite dimensions and small thickness under axisymmetric load distributed over entire surface 07 p1144 A66-18183

Stability of plane Poiseuille flow between elastic boundaries 07 p1026 A66-18194

Nonlinear elasticity model for materials with partially constrained or unconstrained internal rotations 07 p1145 A66-18242

Bispherical coordinates of stresses in semiinfinite homogeneous isotropic elastic solid containing rigid spherical inclusion and subjected to point load perpendicular to plane boundary 07 p1145 A66-18243

Lower bound estimates of shakedown pressure for flush cylinder-sphere intersection, using Melan theorem and elastic analysis 07 p1146 A66-18275

Equations of motion in elasticity theory for thin-walled rod in rotating inertialess system of coordinates 08 p1307 A66-18860

Three-dimensional problem of isotropic continuous nonaxisymmetrical body of revolution, applying analytic functions of complex variable 08 p1307 A66-18885

Stress-strain state of infinite plate with two holes of different diameter solved, using integral equation derived for two-dimensional problem in elasticity theory for anisotropic medium 08 p1314 A66-19578

Asymptotic integration of equations in theory of elasticity to develop approximate theory of momentless shells 08 p1314 A66-19587

Monograph on potential methods in theory of elasticity, basing boundary value solution on theory of singular integral equations 09 p1466 A66-20332

Integration of Laplace transformed elastokinetic equations, examining stress function, displacement vector field and boundary and initial value problems 10 p1555 A66-21226

Vibrational characteristics, natural frequencies and associated composite loss factor of finite-length laminated beam with alternate elastic and viscoelastic layers [ASME PAPER 65-WA/APM-1]

Analog simulation of nonlinearly rigid systems for hard and soft elasticity by electrodynamic analogy methods 11 p1779 A66-22236

Passive element analogs for linearized three-dimensional elasticity derived in rectangular, cylindrical and polar coordinates equating power dissipation and strain energy [ASME PAPER 65-AV-4]

Russian monograph covering theory of elasticity, plasticity and creep 12 p1960 A66-23898

Russian studies of elasticity and plasticity 12 p1965 A66-24056

Two-dimensional problems in moment theory of elasticity for multiply coupled regions weakened by finite number of arbitrarily distributed circular holes 12 p1967 A66-24106

Field equations of elasticity theory used to solve problem of penny-shaped crack opened by unidirectional displacement in plane 12 p1969 A66-24531

Stress concentration methods and results, noting plane problems, holes in shells, notches, role in elasticity and plasticity, etc 13 p2195 A66-25574

State equation for rubber elasticity taking into account effect of intermolecular obstruction on configurational

entropy 13 p2116 A66-26445  
Polynomial solutions to system of differential equations in theory of elasticity 14 p2321 A66-27201

Boundary value problem of elastic/viscoplastic beams solved, using iteration method, noting wave propagation and effect of shear and inertia of axial motion of beam in motion equation 14 p2397 A66-27386

Dual trigonometric integral equations solved, then applied to determining stress field due to crack 14 p2325 A66-28391

Compatibility conditions for stress-strain and Galerkin-Papkovich representations of field equations for linear asymmetric elasticity theory 14 p2408 A66-28392

Asymptotic integration of elasticity theory equations and analysis of stressed state of anisotropic shell 15 p2609 A66-28963

Linearized theory of coupled stress elasticity and stress distributions around simple edge and screw dislocations 15 p2609 A66-29241

Soviet papers on elasticity theory problems concerning stress concentrations, equilibrium and oscillation 15 p2611 A66-29423

Harmonic approximation of infinite crystal dynamics problem, noting collisional case and action of external force on atoms 16 p2820 A66-31169

Elasticity equations for materials with different resistance to tension and compression 17 p3025 A66-32590

Two Fredholm integral equations encountered in elasticity theory solved by Wiener-Hopf method 17 p2947 A66-32783

Plane elasticity theory problem for curve with mixed boundary conditions having radial load distribution 17 p3028 A66-32784

Stress distribution in neighborhood of crack in infinitely long elastic strip 17 p3032 A66-33503

Hashin-Shtrikman theorems application in three types of boundary value problem in elasticity 18 p3249 A66-33600

Elastic-plastic antiplane problems for bonded dissimilar media containing cracks and cavities on interface and subjected to longitudinal shear loads 19 p3475 A66-36430

Contact problem of half-plane inelasticity theory using Jacobi polynomials and taking into account thermal stresses and presence of adhesion and friction in contact area 19 p3476 A66-36835

Singular integral equations with constant coefficients solved by Jacobi polynomials and applied to problems in fluid dynamics, crack propagation, plane elastic theory, etc 19 p3393 A66-36836

Contact problem for elastic rectangle solved by reducing problem to solution of quasi-fully regular infinite set of linear algebraic equations with bounded free terms 19 p3476 A66-36837

Stress concentration factors at notches, fillets and circular holes in plates under uniaxial load obtained from equations for elastic stress distribution 20 p3667 A66-37481

Elastic and elastoplastic distribution of stresses and strains around 45 degree V notch, with circular base determined by photoelastic and moire techniques 20 p3667 A66-37483

Stress function and displacement vector for linear, homogeneous, isotropic and elastic material body occupying bounded simply connected region of space 21 p3772 A66-39354

Iterative linear-elastic analysis of plane pin-jointed frames and space ball-jointed frames, accounting for temperature and geometrical changes 21 p3833 A66-39537

Classic plane problem of elasticity theory for circular beam 21 p3833 A66-39596

Book on plane problems in elasticity theory for calculation of deep beams with arbitrary boundary curvilinear coordinates 21 p3834 A66-39616

Mixed boundary value problem in elasticity of circular and quarter-plane segments 22 p3991 A66-40153

Linear theory of micropolar elasticity, noting all components of asymmetric stress tensor are determined and motion of media is fully described when deformation and microrotation vectors are



- known 22 p3995 A66-40566  
Asymptotic method for solving equations of the theory of elasticity and mathematical physics 22 p3996 A66-40687  
Three-dimensional and axisymmetric problem in elasticity theory with particular reference to photoelasticity 23 p4135 A66-40989  
Numerical analysis methods in elasticity theory for constructing models, approximate problems and analytical solutions 23 p4135 A66-40993  
Elasticity theory and passing of three-dimensional problems to two-dimensional problems 23 p4136 A66-40995  
Soviet literature survey of exact and approximate solution of two-and three-dimensional mixed boundary value problems in theory of elasticity 23 p4136 A66-40999  
Approximate solution of boundary value problems in elasticity theory as applied to thin plate theory, using homogeneous equations 23 p4136 A66-41000  
Elasticity problems solutions as related to stress distribution at holes in shells and plates 23 p4137 A66-41002  
Three-dimensional linear-anisotropic elasticity with inertia effects analyzed in isotropic and anisotropic Cosserat continua, deriving static and kinematic components 23 p4141 A66-41945  
Free and forced vibrations, static and dynamic stability and air elasticity of orthotropic shells and plates in time-alternating temperature field 23 p4142 A66-41955  
Stress concentration around curvilinear holes in plate, discussing plane problem of elasticity theory and shell theory 23 p4143 A66-41960  
Plate or shell theory analysis reduced from three-dimensional elasticity to two-dimensional problem, using power series or iterative method 23 p4143 A66-41962  
Trefftz method applied to derivation of integral for general boundary value problem in classical theory of elasticity 23 p4144 A66-41968  
Certain tensorial character of concentrated loads 24 p4289 A66-42288
- ELASTODYNAMICS**  
Saint Venant principle applied to dynamics of bars regarding boundary conditions and reliability problems 16 p2822 A66-31508  
Galerkin vector for elastodynamic problem of isotropic inhomogeneous body 16 p2823 A66-31707  
Frequency equations and mode displacement functions derived for plane strain free-transverse vibration of solid cylinder with elastic core bonded to thin elastic shell 16 p2823 A66-31716  
Elastodynamic reciprocity theorem for impulsive disturbances in linear viscoelastic medium 21 p3772 A66-39347  
Rall theorem on variational principle for linear elastodynamic BVPs on Hilbert space 23 p4138 A66-41538  
Elastodynamic buckling of circular cylindrical shells, unstiffened and longitudinal stringers-stiffened 23 p4147 A66-42000
- ELASTOHYDRODYNAMICS**  
Pressure distribution, surface temperature and deformation profile in conjunctive region of lubricated cylindrical disks rolling or sliding on their peripheral surfaces [ASLE PREPRINT 65AM 4A3] 07 p1039 A66-18290  
Thermal elastohydrodynamic lubrication of rolling and sliding cylinders, noting correlation with film thickness and friction experimental data [ASLE PREPRINT 65AM 4A2] 07 p1040 A66-18291  
Lubricant film thickness in elastohydrodynamic range measured as function of speed in rolling configuration for mineral oils and esters 07 p1040 A66-18292  
Lubrication review, 1964 24 p4217 A66-42579
- ELASTOMER**  
SA PLASTIC  
SA SYNTHETIC RUBBER  
Uniaxial tensile data for elastomers including stress-strain curve characteristics 02 p0248 A66-11428  
Fluids and elastomers for low temperature heat transfer and hydraulic systems [ASLE PREPRINT 65-LC-7] 02 p0249 A66-12256  
Oil seals such as lip seal discussing structure, performance factors and materials used 04 p0525 A66-13781  
Elastomeric silicone for aerospace electric and thermal insulation, discussing properties, application and new developments 06 p0900 A66-16297  
Properties of nonirradiated heat-shrinkable silicone and fluorosilicone rubbers for insulating and encapsulating electrical and electronic apparatus, including resistance to aging, fuels, ozone, etc 06 p0900 A66-16298  
Qualities required of materials for joint sealing, particularly elastomers, noting properties and possibilities 12 p1899 A66-23818  
Fluids and elastomers for low temperature heat transfer and hydraulic systems [ASLE PREPRINT 65-LC-7] 12 p1901 A66-24992  
Uniaxial tensile test data on stress-strain properties of polymers and elastomers as function of strain rate and temperature 13 p2115 A66-26118  
Nitroso rubbers, fully fluorinated elastomers for nitrogen tetroxide application 14 p2371 A66-28015  
Elastomeric ablative thermal shield material to meet system requirements for lifting reentry vehicles having lift-drag ratio of 0.5 to 1.5 18 p3240 A66-33801  
Complex shear modulus measuring apparatus for viscoelastic materials, including data obtained for butyl rubber and other elastomers 18 p3256 A66-34560  
Stress relaxation of gamma irradiated fluorocarbon elastomers to study radiation induced chain scissions in copolymers 20 p3587 A66-37310  
High temperature behavior of organic materials for aircraft, noting elastomers and elastomers [ICAS PAPER 66-33] 22 p3938 A66-40660
- ELASTOPLASTICITY**  
Elastoplastic matrix displacement of three-dimensional continua 01 p0152 A66-10343  
Spherical elastoplastic waves in expansion of spherical cavities in impulsively loaded thick metal spheres 02 p0300 A66-11853  
Stress wave propagation in elastic-plastic solid with cylindrical or spherical symmetry and expanding core 02 p0301 A66-12166  
Stresses in elliptical cross section rod subjected to elastoplastic torsion, using Legendre transforms 02 p0301 A66-12173  
Rigid body mechanics noting elastoplastic and ductile formation, deformation, defect appearance, etc 03 p0439 A66-13166  
Finite elastoplastic strains in thin rotating annular disk with radially varying temperature 03 p0375 A66-13293  
Generalization of Koiter theorem applied to study of adaptability of nonuniformly heated elastoplastic bodies to variable loads 04 p0594 A66-14427  
Elastic-plastic stress and strain distribution in solid or hollow shaft containing external or internal hyperbolic notches [ASME PAPER 65-WA/APM-20] 05 p0689 A66-15442  
Longitudinal elastic-plastic pulse propagation for smooth stress-strain curves concave toward strain axis, applied to long bar loaded at end by short pressure pulse [ASME PAPER 65-WA/APM-29] 05 p0778 A66-15450  
Elasto-plastic matrix displacement analysis of arbitrary three-dimensional continuum under strain hardening 06 p0963 A66-16464  
Model of elastoplastic body undergoing strain hardening, examining microstresses via internal viscosity 07 p1143 A66-17629  
Propagation of spherical waves produced by thermal shock acting on boundary of spherical cavity in infinite elastoviscoplastic body 08 p1309 A66-19115  
Transition process whereby plate approaches limiting load state under effect of transverse load that creates torques and bending moments in plate cross sections 08 p1312 A66-19436  
Approximation method solution for elastoplastic distribution of stresses in infinite plane with square hole for case of compressive force plane deformation 08 p1313 A66-19444  
Statically indeterminate elastoplastic problem under condition of complex shear 08 p1315 A66-19589  
Stability of steady state response of one degree of freedom double bilinear hysteretic model [ASME PAPER 65-WA/APM-4] 10 p1616 A66-21489  
Polarization and birefringence of photoelastoplastic medium 11 p1781 A66-22613  
Successive approximation method for elastic-plastic plane stress-strain analysis 11 p1781 A66-22690  
Crack opening displacement approach to fracture mechanics in yielding materials 11 p1782 A66-22693  
Elastoplastic deformation of bodies exposed to random forces 11 p1784 A66-23328  
Relating general theory of elastic-plastic continuum, valid for nonisothermal deformations and explicit thermodynamic restrictions, to Drucker postulate 12 p1959 A66-23862  
Time-dependent variation of cross sectional area used to generalize classical theory of elastic-plastic loading waves in thin rods 12 p1960 A66-23949  
Elastic-plastic stress-strain distribution in solid or hollow shaft containing external or internal hyperbolic notches [ASME PAPER 65-WA/APM-20] 12 p1885 A66-23977  
Finite deformations of rotating disk of variable thickness, consisting of elastoplastic strain-hardening material, determined from stress-strain diagram 12 p1964 A66-24051  
Elastoplastic behavior of anisotropic plates elastically uniform in depth, using asymptotic integration for bending problem 12 p1966 A66-24057  
Behavior of rotating solid and hollow cylinders of ideal elastoplastic material subjected to rotation and action of quasi-steady-state temperature field, considering adaptability when physicommechanical characteristics are constant 14 p2301 A66-27175  
Elastoplastic properties of copper, aluminum alloys and brass under explosive load, noting increased temperature effect on elastoplastic wave parameters 14 p2314 A66-27370  
Stress field of thermal shock on surface of spherical cavity in infinite elastic-plastic body 14 p2399 A66-27457  
Solution of plane problem of physically nonlinear bodies by method of finite differences 15 p2608 A66-28772  
Bending moment, longitudinal force, radial displacement and transverse deflection of circular plate undergoing elastoplastic bending accompanied by radial tension 16 p2822 A66-31622  
Compressibility of material in stability problems of elastoplastic plates and shells 17 p3029 A66-32809  
Longitudinal elastic-plastic pulse propagation for smooth stress-strain curves concave toward strain axis, applied to long bar loaded at end by short pressure pulse [ASME PAPER 65-WA/APM-29] 18 p3247 A66-33568  
Linear and nonlinear nonassociated flow laws analyzed for elastoplastic work-hardenable solids 18 p3255 A66-34392  
Constitutive equations for behavior of elastic/viscoplastic materials at finite strain, assuming isotropic material and isothermal processes 18 p3256 A66-34394  
Load level as stability loss condition for bulging of elastoplastic rod in presence of creep 19 p3473 A66-35753  
Complex loading problems in plastic flow theory solved by analogy with elastic solutions in elastoplastic theory 19 p3473 A66-35755  
Elastic and elastoplastic distribution of stresses and strains around 45 degree V notch, with circular base determined by photoelastic and moire techniques 20 p3667 A66-37483  
Elastoplastic bending of thin annular plates with free inner edge, based on Mises yield condition and Hencky stress-strain relation 20 p3671 A66-38102  
Inelastic buckling of rod with initial slight



sinusoidal deflection subjected to short-term longitudinal compressive dynamic load 20 p3672 A66-38268

Plastic strain distribution near axisymmetric slit in ideally elastoplastic material described by Dugdale model 20 p3673 A66-38269

Two-dimensional elastoplastic problem of stress distribution in plane with hole under compressive forces at infinity, assuming exponential yield condition controls plastic state of material 21 p3830 A66-38981

Variable load theorem applied to alternating cyclic loads problem, based on equations of small elastoplastic deformations 21 p3830 A66-38984

Thermodynamics of irreversible processes methods applied to stress-strain relations of single-phase nonelastic continuous medium 21 p3830 A66-38986

Elastic-plastic and stress shock wave propagation in finite-length bar with monotone decreasing cross-sectional area 22 p3995 A66-40509

Stress-strain determination in elastoplastic problems with aid of photoelastic epoxy resin coating 23 p4135 A66-40990

Variational techniques in solving BVPs for nonlinear plastic, elastoplastic and viscous media and in predicting existence, uniqueness and equilibrium conditions 23 p4136 A66-40996

Elastic wave radiation possible in collision of unloading wave with shock wave 23 p4054 A66-41354

Relaxation of temperature stresses in thin walled pipe under conditions of elastoplastic deformation 23 p4140 A66-41797

Membrane force in axisymmetric elastoplastic bending of clamped thin circular plate 23 p4142 A66-41951

Laminated structure with dominant displacement from reference point for solid medium working beyond elastic limit 23 p4144 A66-41969

Time dependent stress distribution in elastoplastic cyclic deformation, emphasizing cycle hardened stainless steels 23 p4144 A66-41971

Notched plates stress distribution solution under conditions of plane stress in elastoplastic domain of straining 23 p4146 A66-41994

Photoplastic method of solving plane elastoplastic problems, using celluloid as model material 24 p4287 A66-42212

Stability of ideal plate under compression loading beyond elastic limit 24 p4290 A66-42437

Successive approximation analysis of large deflections of elastoplastic shell under bending deformation and load carrying capacity 24 p4290 A66-42440

Stability analysis of thin two-layer shell in Gaussian coordinates with moment initially zero, including applications to stability of circular cylindrical shell 24 p4290 A66-42441

Critical loading and stability of three-layer sloped asymmetric shells beyond elastic limit for arbitrary stress-strain diagram 24 p4290 A66-42442

Stability theory methods for small elastoplastic deformations generalized to include creep effects in cylindrical shells compressed at ends 24 p4292 A66-42885

**ELASTOSTATICS**

Resolution of two fundamental problems of elastostatic plane into complex variables under conditions of analytical limits 05 p0775 A66-15096

Uniqueness theorem of axisymmetric exterior traction boundary value problem in linear elastostatics theory 12 p1971 A66-24818

Quantitative examination of Saint Venant principle in context of elastostatic boundary problems, i.e., axisymmetric pure torsion of bodies of revolution 19 p3473 A66-35485

Displacement boundary value problem in classical linear elastostatics, deriving ellipticity condition for uniqueness theorem 19 p3474 A66-35852

Constitutive equations for elastic solids sustaining deformation for which displacement gradients are small but where nonlinearity is permitted, formulating plane elastostatic problem 19 p3475 A66-36429

Linear elastostatic BVPs for inhomogeneous anisotropic elastic body

including existence-uniqueness theorem, based on Korn inequality 21 p3755 A66-38463

Eigenfunctions of full dislocation solution of cut annulus in plane elastostatics 23 p4144 A66-41970

**ELBOW**

Pressure losses in vaned elbows of circular cross section and possibility of gain in efficiency by splitting vanes 24 p4195 A66-42582

**ELDO LAUNCH VEHICLE**

Testing installations for third stage of ELDO rocket noting test stands, control center and fuel depot 02 p0214 A66-11247

Design and development of high energy standard engine for ELDO-B carrier rocket 02 p0279 A66-11669

Applicability of liquid hydrogen-oxygen technology to development of European launch vehicles 02 p0295 A66-11671

Research satellite projects sponsored by ELDO, ESRO and West-German Projects 625A and 625B 04 p0583 A66-13498

Shock wave frontal ionization effect on electromagnetic transmission and reception from telemetering equipment on ELDO satellite launching vehicle 09 p1406 A66-19851

European Launcher Development Organization /ELDO/ program for Europa I three-stage rocket and satellite design and testing 09 p1464 A66-20467

ELDO launch vehicle third stage configuration, propulsion system, guidance and control system and ground installations and equipment 09 p1464 A66-20468

Remote-control signaling system for ELDO satellite 09 p1345 A66-20544

CECLES/ELDO space vehicle booster program, noting design of three-stage rocket, including control and guidance system, telemetry, etc 09 p1464 A66-20655

Future programs for ELDO including launchers, guidance systems, bases, etc 09 p1464 A66-20656

Difficulties encountered in applying system of overall project management to ELDO initial program, noting PERT use, costs plans, etc 09 p1473 A66-20657

Space research in Netherlands during 1964 including work done for European Launch Development Organization 09 p1459 A66-20719

Vacuum simulation facility near Munich for testing third stage of ELDO rocket 10 p1519 A66-21374

Design and operation of test stands for ELDO rocket engines under simulated high altitude conditions 10 p1519 A66-21384

Optimization of high energy turbopump unit engine for ELDO-B carrier rocket, employing system specific impulse 10 p1591 A66-21396

European space program of launcher development 11 p1788 A66-22433

Electron beam welding of high-strength titanium alloy propellant tank for third stage of ELDO carrier rocket and determination of optimum welding parameters 12 p1885 A66-23783

Fiat design and manufacture of heat shields, satellite frame and telemetry antennas for ELDO space booster 12 p1885 A66-23914

ELDO-B program and ELDO-B 2 rocket, correlating performance of first and second stages 17 p3015 A66-32368

Performance characteristics and specifications of Coralie missile, second stage of ELDO rocket 17 p3015 A66-32369

Welding and gluing of third stage of ELDO-A rocket 23 p4073 A66-41533

**ELECTRET**

**S BARIUM TITANATE**

**ELECTRIC ANALOGY**

Temperature fields in pipe filled with Raschig rings with internal heat source during gas flow calculated by electrical analogy method 01 p0166 A66-10999

Relationship between three symbolic circuit representations of charge-capacitance effects in 4-terminal field effect transistors 04 p0500 A66-14099

Electrical analog model with distributed capacitance and resistance generates charge flow equivalent to two-dimensional transient heat conduction [ASME PAPER 65-HT-66] 05 p0786 A66-14766

Passive electrical simulation of properties of Maxwell type viscoelastic connection in

vibration absorber, noting dynamical analogy and velocity-acceleration optimization 05 p0775 A66-15300

Geometric electrical analog for two-dimensional transient heat conduction [ASME PAPER 65-WA/HT-42] 05 p0792 A66-15666

Source flow in analog solution using finite size electrode, noting potential error [ASME PAPER 65-WA/FE-6] 05 p0665 A66-15716

Equivalent h parameters for n transistors connected in cascade, establishing effect of circuit impedances 06 p0854 A66-16887

Analog method for simulating visual receptor network as model for inhibitory interaction in retina 06 p0819 A66-16849

Video densitometer to extract data from video display, specifically densitodiagram 06 p0819 A66-16851

HF analog computers for representing algebraic and differential systems and solving problems due to loop instability and drift in DC amplifiers 07 p1003 A66-17818

Torsional vibration analog computer and determination of torsional oscillation frequencies in multimass in-line systems 07 p1144 A66-18164

Equivalent circuit obtained from device charge equations for analysis of HF properties of four-terminal field effect transistors 08 p1189 A66-18669

Mathematical foundations of analog simulation proceeding from Laplace, diffusion and wave equations 08 p1187 A66-18861

Electric analogy to derive sound laboratory test specification and procedure for testing Nike-Tomahawk payload vibration 08 p1308 A66-18928

Analog computers used in modeling of heat conduction and diffusion processes for Fourier differential equation 08 p1319 A66-19427

Equivalent circuit diagram determination of change in quadrupole parameters in transistor due to current-induced heating 08 p1198 A66-19729

Circuit techniques for performing analog pulse arithmetic, using logarithmic p-n junctions on amplitudes of random nuclear pulses 09 p1356 A66-20604

Analog method for solution of unsteady radiant heat transfer problems with combined conduction and convection 10 p1622 A66-21938

Passive element analogs for linearized three-dimensional elasticity derived in rectangular, cylindrical and polar coordinates equating power dissipation and strain energy [ASME PAPER 65-AV-4] 11 p1780 A66-22467

Analog computer, programmed on digital computer, used in examination of lumped and distributed parameter models of cardiovascular system 12 p1809 A66-24230

Electrocardiogram interpretation by computer, using pattern recognition approach which permits differentiation between normal and abnormal rhythms 12 p1810 A66-24231

Source flow in analog solution using finite size electrode, noting potential error [ASME PAPER 65-WA/FE-6] 12 p1864 A66-24545

Pipeline simulation by triggered monostable multivibrator driving chopper as logarithmic function generator 13 p2027 A66-25220

Electrical analogy for wing in unsteady supersonic flow, determining distribution of lifting power for various aspect ratios 13 p1990 A66-25405

Electrical analog method used in determining potential gas flow past airfoil lattice, noting components of solution 13 p2068 A66-26541

Electrical analogy for turbulent liquid metal heat transfer in noncircular duct entrance region, solving Fourier equation, determining fluid boundary conditions, temperature distribution, etc 13 p2210 A66-26717

Tabulated data method for synthesizing third order linear transfer functions, using chain of inverted L-sections of passive resistor-capacitor elements in conjunction with single operational amplifier 16 p2671 A66-31203



- Thermal analysis of ceramic-based hybrid microcircuits, using lumped-constant electrical analog 16 p2667 A66-31594
- Waveguide-slot antenna design, considering interaction of radiators on principal wave 17 p2879 A66-31855
- Conductive sheet analogy applied to steady heat conduction problem, noting evaluation without use of potentiometers 18 p3265 A66-34491
- Critical jets of symmetrical perfect-gas flow determined by analogy between impedance network node equation and velocity potential and stream function in Tricomi plane 19 p3341 A66-36250
- Fluid circuit theory, discussing transmission lines, matching, pulse forming and definitions of current and voltage analogies 20 p3500 A66-37643
- Electric analog approximation of static and dynamic performance of Kearfott ball valve switching device, discussing application to complex circuit design 20 p3501 A66-37650
- Electric analogs construction for stability and oscillation of elastic system 20 p3670 A66-37674
- Book on boundary value problems and partial differential equations for electric circuits and other engineering problems 22 p3938 A66-39703
- RF behavior of one-dimensional plasma in electrical circuit analog with coupled resonant circuits representing normal modes 22 p3884 A66-39816
- Wind tunnel simulation of transient state of takeoff and landing of V/STOL aircraft, noting application of electric circuit analogy to measure flow dynamic response to control valve movement 23 p4053 A66-41388
- ELECTRIC ARC**
- SA SPARK
- Energy balance of cylindrically symmetric hydrogen arc immersed in axial magnetic field led to current-voltage characteristic and radial temperature distribution 04 p0554 A66-14298
- Electric arc interaction with argon flow analyzed in crossed convective and magnetic fields [ASME PAPER 65-WA/ENER-1] 05 p0728 A66-15626
- High-pressure pulse arc created by discharging capacitor bank through steadily burning argon arc 06 p0919 A66-16874
- Brightness dependence of pulse arc on power per unit length of arc, estimating charged particle density and plasma temperature 06 p0919 A66-16875
- MHD problems associated with wall-stabilized and convection-stabilized electric arcs 07 p1090 A66-18114
- Thermal shock resistant carbides, using arc-casting techniques, noting microstructure, phase diagram, mechanical properties, etc 07 p1055 A66-18504
- Parameter predicting transition from low to medium blowing rate in arc with transpiration cooled anode 08 p1168 A66-19156
- High temperature black body as spectral radiance standard for high intensity arc 09 p1471 A66-20504
- Electrical conduction behavior of laminar arc-heated flow in contact with cooled anode, noting anode current parameters [AIAA PAPER 66-188] 10 p1561 A66-21435
- Electric arc interaction with argon flow analyzed in crossed convective and magnetic fields [ASME PAPER 65-WA/ENER-1] 10 p1563 A66-21503
- Equations for electric arc column based on MHD equation 11 p1746 A66-23237
- Current-voltage characteristics of electric arcs approximated by dimensionless criteria 11 p1747 A66-23312
- Recovery of electric strength of gap after arcing related to Paschen law and measured from atmospheric pressure to vacuum by device with copper contacts 12 p1842 A66-24665
- Hydrogen arcs, sulfur hexafluoride arcs, decaying nitrogen arcs and nitrogen arcs with forced convection 13 p2137 A66-25110
- Experiments with arc jet characterized by composite electromagnetic and vortex stabilization and propelled by hydrogen or nitrogen, noting heat loss through electrodes 14 p2373 A66-27097
- Range of gas dynamic stability of arc-type electric heaters, characteristics for design and calculation of electrode diameter ensuring vortex stabilization 14 p2348 A66-28314
- Tangential electrode forces on cathode and anode electrode for arc moving in magnetic field are not negligible in plasma driving 15 p2428 A66-28687
- Existence of convective interaction mechanism affecting direction and stability of electric current in flowing gas, using electric arc confined in supersonic flow 15 p2481 A66-29744
- Electron temperature measurements in low voltage arc in saturated cesium vapor 16 p2756 A66-30105
- Electric conductivity parameters for plasma gap formed by discharge in argon and potassium mixture in electric-arc heater 16 p2766 A66-31601
- Symptomatic behavior and anode regimes of arc for electric arc with superimposed subsonic flow of argon [AIAA PAPER 66-479] 17 p2970 A66-32768
- Fastax films showing development and instability of pulsed DC arc in 30 mm Vycor tube at peak currents up to 1500 amp [AIAA PAPER 66-731] 18 p3141 A66-33667
- Composition, heat conduction and radiative energy transfer characteristics of hydrogen and argon plasmas produced by arc in cylindrical channel with cooled walls 18 p3142 A66-34023
- Thruster device using self-induced magnetic Lorentz forces to attain velocities up to 50,000 m/sec for plasma jet ejected by electric arc engines 19 p3451 A66-36637
- Low pollution electric arc air heater of CH9 and CH10 type, using metal electrodes to provide air mass flow rates at 4000 degrees K 20 p3540 A66-36950
- Field of high temperatures produced by transitional and steady state processes, using electric arcs in nonrarefied gases, obtaining existence and stability criteria for arc 20 p3606 A66-36965
- ELECTRIC BREAKDOWN**
- SA SHORT CIRCUIT
- SA VOLTAGE BREAKDOWN
- Charge trapped in electron or ion beams at pressures below breakdown determined from general integro-differential equation, using approximation method 01 p0111 A66-10375
- External electric field effects on volt-ampere characteristics and breakdown in p-n, p-n-p and p-n-p-n structures 02 p0277 A66-12090
- Multilayer circuit board defect detection and repairing using computer-controlled IR radiometer 04 p0498 A66-14016
- Atmospheric breakdown limitations to optical maser propagation 05 p0632 A66-14837
- Nonlinear microwave breakdown induced in thin high-density plasma slab when plane wave is normally incident upon it 06 p0844 A66-16038
- Second breakdown model for transistors 06 p0832 A66-16437
- Avalanche multiplication factors other than impact ionization leading to breakdown in p-n junctions 06 p0850 A66-16445
- Evolution of spark channels initiated in oxygen at 411, 680 and 950 torr by current pulses of approximately 30 amperes with durations of 30 and 40 nanoseconds 06 p0920 A66-17028
- Gas breakdown by laser can be accounted for by both microwave breakdown theory and inverse bremsstrahlung 06 p0893 A66-17040
- Origin of channel currents associated with P plus regions in silicon, discussing breakdown of field-induced junction 08 p1195 A66-19357
- Frequency components of microwave-range oscillations from pulsed avalanche diodes of Read type driven to breakdown 09 p1350 A66-19927
- Second breakdown volt-ampere characteristics in triple diffused n-p-n Si transistor 09 p1351 A66-19936
- Separation formulas of potential fields of constant currents into lower half-space with application to geomagnetic field 09 p1373 A66-20481
- Secondary breakdown in germanium alloy and diffused-alloy transistors 09 p1358 A66-20817
- Plasma instability in solids occurring in microwave frequency region 10 p1576 A66-21537
- Microplasma breakdown in reverse biased p-n junctions in epitaxial gallium arsenide 10 p1577 A66-21571
- Small-signal impedance of space-charge region of p-n junctions under avalanche breakdown conditions, using realistic physical assumptions 10 p1586 A66-22084
- Breakdown regime of diffusion-controlled HF resonance gas discharge analyzed kinetically, solving Boltzmann equation for electron distribution function 11 p1740 A66-23081
- Injection of plasma blobs into mirror trap and subsequent compression of plasma by increasing magnetic field, using longitudinal current, noting X-ray radiation 12 p1925 A66-24877
- Nonlinear dielectric laser light absorption by neutral gas resulting in avalanche breakdown of gas due to thermal ionization 13 p2090 A66-25425
- Electrical breakdown of gases by optical frequency radiation, noting laser beam attenuation and subsequent energy absorption by plasma 13 p2134 A66-26190
- Threshold data for ruby and neodymium laser pulse-induced breakdown in Xe, Ar, Kr, Ne, He, oxygen, nitrogen, air and carbon dioxide 13 p2100 A66-26191
- Plasma resonance and scattering, threshold variation and optical reflectivity in pulsed laser beam-induced gas breakdown 13 p2134 A66-26192
- Growth rate of ionization by electron impact in presence of laser beam, elastic and inelastic scattering cross sections, free-free absorption, excitation and ionization coefficients, breakdown times and thresholds 13 p2134 A66-26193
- Giant-pulse laser-induced atmospheric electric breakdown causing optical frequency discharge 13 p2134 A66-26194
- Two-dimensional analysis of flow in electrofluid dynamic generator showing effect of radial fields and viscous forces on performance, stressing effect on electrical breakdown of gas, noting basic equations 13 p2001 A66-26257
- Electric breakdown and insulation properties of vacuum and design of vacuum devices 14 p2249 A66-27105
- Breakdown of biennial oscillation of ozone and of lower stratospheric temperature of Southern Hemisphere and relation to sunspot cycle observations 14 p2286 A66-27904
- Electrical failure in solids from excess energy storage or internal disordering 15 p2568 A66-29669
- Breakdown by neodymium glass laser radiation in atomic and molecular gases, determining power densities, noting relation of pressure to breakdown power 16 p2718 A66-30938
- Avalanche breakdown voltage calculated for planar p-n junction 17 p2981 A66-32688
- Microplasma internal parameter measurement including switch-on voltage, switch-off voltage, plasma resistance, parallel capacity and internal series resistance 17 p2896 A66-33320
- Transistor testing and secondary breakdowns, featuring application of constant collector current and power with arbitrary waveform 18 p3078 A66-34087
- Separation formulas of potential fields of constant currents into lower half-space with application to geomagnetic field 19 p3346 A66-35499
- Electrical breakdown in beams of hydrogen and nitrogen produced by expanding H or N gas out of Laval nozzle cooled by liquid hydrogen or nitrogen in high vacuum 20 p3605 A66-38055
- Injection of plasma blobs into mirror trap and subsequent compression of plasma by increasing magnetic field, using longitudinal current, noting X-ray radiation 23 p4099 A66-41084
- Diffusion controlled breakdown theory applied to compute breakdown potential of helium in coaxial geometry by solving



continuity equation 23 p4105 A66-41584  
 Surge-proof silicon power diode combining  
 p-n and p-i-n structures 24 p4182 A66-42505  
 Reverse breakdown voltage increase  
 resulting from ion drift in silicon p-n  
 junctions formed by sodium ion  
 bombardment 24 p4257 A66-42621  
 Dielectric breakdown phenomena in  
 evaporated silicon monoxide thin film,  
 noting electron collision  
 effect 24 p4260 A66-43106

## ELECTRIC CELL

Gamma-electric cell, solid state device for  
 direct conversion of gamma-ray energy into  
 electrical energy 07 p1079 A66-18323  
 Oxygen regeneration in solid electrolyte  
 cell, constructed from zirconia based  
 ceramic material for space flights  
 [AICE PREPRINT 20E] 17 p2848 A66-32672

## ELECTRIC CONDUCTIVITY

## SA IONOSPHERIC CONDUCTIVITY

## SA RESISTANCE

## SA SUPERCONDUCTIVITY

Unsteady convective flow of electrically  
 conducting fluid through vertical channel in  
 magnetic field, using differential  
 equations 01 p0111 A66-10426  
 Stochastic aspects of low mobility theory  
 applied to electrical conductivity problem in  
 Wannier representation 01 p0106 A66-10723  
 Friction, diffusion, and electrical  
 conductivity tensors obtained for plasma  
 subjected to strong external magnetic  
 field 01 p0114 A66-10961  
 High temperature vacuum furnace for  
 noncontact measurements of electrical  
 conductivity of semiconductor materials in  
 liquid and solid states 01 p0071 A66-11047  
 Electric conductivity anisotropy of n-type  
 silicon in range of warm and hot  
 carriers 01 p0128 A66-11199  
 Electric conductivity of N-component gas  
 mixture containing one partially ionized  
 component 02 p0265 A66-11389  
 Fourier coefficients of tunnel diode  
 conductivity and noise current determined  
 along with conversion factor and amplitude  
 of mixer 02 p0196 A66-11424  
 Modes existing in infinite parallel-plate  
 waveguide with centrally placed  
 unidirectional conducting  
 screen 02 p0198 A66-11578  
 Semiconductor characteristics of barium  
 titanate with n-type conductivity produced  
 after heat treatment with hydrogen and  
 doping with lanthanum 02 p0273 A66-11716  
 Electrical conductivity of narrow energy  
 band semiconductors as function of electric  
 field strength 02 p0274 A66-11732  
 Electrical conductivity, Hall effect and  
 thermoelectric power as function of  
 temperature in CdSb single crystals strongly  
 doped with silver 02 p0275 A66-11968  
 Temperature dependence of surface  
 conductivity and Hall effect in germanium  
 alloyed with gold 02 p0276 A66-12078  
 Low energy nitrogen ion irradiation of  
 germanium plates resulting in conductivity  
 and inverse current  
 variation 02 p0277 A66-12081  
 Motion of medium of variable electric  
 conductivity in rectangular channel situated  
 in magnetic field 02 p0270 A66-12172  
 Germanium conductance measurement  
 when immersed in aqueous electrolyte using  
 DC and LF AC methods as polarization  
 function 03 p0407 A66-12403  
 Dielectric relaxation effects, dissipation  
 factor peak and capacitance and conductivity  
 dispersions in pure and doped sapphire  
 single crystals 03 p0409 A66-12638  
 Electric conductivity of argon  
 plasma 03 p0400 A66-12834  
 E-layer disturbances caused by particles  
 impinging upon atmosphere during auroras  
 noting ionization, X-rays and electrical  
 conductivities 03 p0365 A66-12858  
 Piezoresistance of doped n-type  
 germanium, determining nature of carrier  
 scattering mechanism in degenerate  
 materials and modification of conduction-  
 band edge resulting from impurity  
 states 03 p0412 A66-13148  
 Plasma behavior in MHD accelerators and  
 electrical nonequilibrium conductivity,  
 noting energy loss mechanisms and  
 techniques for improving cross field  
 accelerators 04 p0550 A66-13543

Temperature dependence of electric  
 conductivity in indium antimonide and  
 gallium arsenide measured by noncontact  
 method in terms of Q-factor  
 change 04 p0563 A66-13892  
 Donor and acceptor concentration on  
 electrical conductivity of n-type  
 silicon 04 p0567 A66-14341  
 Electrical conductivity of polar  
 semiconductors in electric fields, calculating  
 lattice and Coulomb electron scattering  
 mechanism by kinetic equation  
 method 04 p0568 A66-14350  
 Temperature, annealing time and radiation  
 dosage effect on electroconductivity of  
 inversion layers generated in n-type silicon  
 during bombardment with boron  
 ions 05 p0730 A66-14646  
 Electric conductivity, electrode  
 temperature and potential distribution  
 across channel in potassium seeded-argon  
 atmospheric-pressure Faraday accelerator  
 [AIAA PAPER 66-75] 05 p0723 A66-15035  
 Conduction phenomena in active base of  
 transistor and interpretation by electrical  
 model 05 p0648 A66-15103  
 Electron drift velocity and mobility of  
 indium antimonide obtained from pulsed  
 measurements of conductivity and Hall  
 effect at various  
 temperatures 06 p0922 A66-16173  
 Current voltage characteristics of cadmium  
 sulfide semiconductors showing departures  
 from Ohm law associated with ultrasonic  
 amplification, crystal length and increasing  
 conductivity 06 p0923 A66-16183  
 Low level garnet limiter with operating  
 range greater than one octave, using  
 conductivity change due to impact ionization  
 in n-type germanium, noting volt-ampere  
 characteristic 06 p0851 A66-16459  
 Various conduction mechanisms through  
 thin insulating films and relevance to  
 possible thin film devices 06 p0852 A66-16508  
 Decay of K-state in Ni-Cr, Ni-Cr-Mo and  
 Fe-Ni-Cr-Mo alloys studied in terms of  
 electric conductivity during plastic  
 deformation 06 p0896 A66-16606  
 Radial distribution of electrical  
 conductivity in ionized gas jet based on  
 value measured by induction method and  
 known temperature  
 distribution 06 p0919 A66-16880  
 Impurities effect on electrification of  
 cadmium telluride dust, specifically n and p  
 types, with electrification increasing with  
 impurity concentration 06 p0928 A66-16891  
 UV irradiation effect on electrical  
 conductivity of zinc oxide single  
 crystals 07 p1097 A66-17469  
 Electron energy levels in CdS single  
 crystals from Hall effect, conductivity and  
 space-charge-limited current  
 measurements 07 p1098 A66-17739  
 Frequency dependence of hot carrier AC  
 conductivity of covalent semiconductors,  
 considering scattering due to acoustic and  
 optical phonons 07 p1098 A66-17740  
 Piezoresistance in semiconductors, noting  
 anisotropic effect of mechanical stresses on  
 electrical conductivity 07 p1034 A66-17834  
 Mechanism of conduction in  
 pyropolysiloxanes studied for electrophysical  
 properties of vinyl  
 polymers 07 p1099 A66-17870  
 Temperature dependence of electrical  
 conductivity in organic semiconductors,  
 examining compounds during transition from  
 solid to liquid state 07 p1100 A66-17931  
 Electrical conductivity variation of low and  
 high resistance germanium due to X-ray  
 radiation absorption 07 p1100 A66-17932  
 MHD generator based on repetitive  
 injection of liquid metal slugs into head of  
 MHD channel, obtaining high  
 conductivity 07 p0993 A66-18310  
 Induced electric conductivity in germanium  
 bombarded by potassium ion in different  
 crystallographic directions 07 p1104 A66-18363  
 Volt-ampere characteristics of n-silicon in  
 strong electric field from 77 to 300 degree  
 K 07 p1105 A66-18365  
 Conductivity and Hall coefficient for zinc-  
 mercury-telluride solid  
 solution 07 p1105 A66-18366  
 Jump-conductivity surface dependence on  
 surface potential in semiconductor, based on  
 field effect basic

geometry 07 p1105 A66-18374  
 Diamond-like semiconductors in glassy  
 state, investigating structure and  
 characteristics of cadmium-germanium-  
 arsenide 07 p1106 A66-18383  
 Specific heat, thermal expansion and  
 conductivity and electrical conductivity of  
 nearly perfect crystalline  
 materials 07 p1109 A66-18497  
 Channel conductance measurements on  
 silicon power rectifiers and midgap donor  
 and acceptor detection on oxidized and  
 lacquered rectifiers 08 p1189 A66-18664  
 Electrical properties of alpha ferric oxide  
 containing magnesium, noting temperature  
 effect, carrier concentration, conductivity  
 variations, etc 08 p1271 A66-19221  
 High-field surface conductance of n-type  
 germanium observed to be negative and  
 magnitude to increase with field in high-  
 field region 08 p1271 A66-19222  
 Electrical conductivity, Hall coefficient and  
 thermoelectric power of tellurium  
 calculated, using models for anomalous sign  
 reversal of Hall  
 coefficient 08 p1271 A66-19240  
 Microwave measurement of anisotropy in  
 conductivity of semiconductor in strong  
 electrical field, using comparison of  
 absorption of two intersecting plane-  
 polarized waves 08 p1224 A66-19288  
 Contact area of boiling bubbles observed  
 through electroconductive glass/heating  
 surface/ into tank 08 p1320 A66-19556  
 Unilateral conductivity of thin high-density  
 film of refractory metal oxides, discussing  
 formation of p-i-n  
 junctions 08 p1276 A66-19568  
 P-type cadmium tin arsenide crystals,  
 plotting temperature dependences of  
 specific electroconductivity, Hall coefficient  
 and thermal electromotive  
 force 08 p1277 A66-19622  
 Hall effect, thermal emf and electrical  
 conductivity of SmS in temperature range  
 300 to 1000 degrees K 09 p1412 A66-19988  
 Dark electric conductivity, Hall effect and  
 thermally stimulated currents in gallium  
 arsenide single crystals 09 p1413 A66-19998  
 Electrical conductivity and field strength  
 in symmetrically contacted rectangular  
 samples as effected by geometrical  
 factors 09 p1425 A66-20187  
 Conductivity measurements on silver  
 bromide and silver  
 chloride 09 p1426 A66-20194  
 Variations of turbulent plasma electric  
 conductivity with input oscillation intensity  
 and with square of RF input  
 voltage 09 p1409 A66-20853  
 N-type germanium electric conductivity  
 dependence on applied electric and  
 magnetic field 09 p1430 A66-20857  
 Temperature dependence of electrical  
 conductivity in molybdenum and tungsten at  
 4.2 to 300 degrees K 09 p1391 A66-20862  
 Idealized problems concerning motion of  
 cylindrical plasma sheets in magnetic field,  
 noting application in  
 geophysics 10 p1527 A66-21128  
 Thermal and electrical conductivities of  
 molybdenum-rhenium alloys in  
 superconducting and normal  
 states 10 p1573 A66-21178  
 Preparation and physical properties of  
 polytetraacyanoethylene /TCNE/ copper  
 chelate film, noting electric conductivity and  
 heat treatment effect 10 p1574 A66-21348  
 Electric conductivity of plasma measured  
 by miniature immersed coil with RF  
 magnetic field  
 [AIAA PAPER 66-181] 10 p1561 A66-21431  
 Model for interpretation of positive column  
 two-dimensional striations of diffuse mode  
 gas discharge in uniform magnetic  
 field 10 p1564 A66-21569  
 Electrical conductivity of thin metallic  
 films with two surfaces having different  
 probabilities of specular  
 scattering 10 p1579 A66-21681  
 Electric and photoconductivity of vacuum  
 sintered and zone refined semiconductor  
 boron 10 p1579 A66-21722  
 Trap dominated conductivity changes and  
 optical absorption phenomena in near IR in  
 crystalline beta-rhombohedral  
 boron 10 p1580 A66-21723  
 Electron paramagnetic resonance, electrical



- conductivity and impurity diffusion in doped  
iron 10 p1580 A66-21724
- Electrical conductivity of single crystals of  
lithium and strontium  
oxides 10 p1581 A66-21878
- Vanadium pentoxide-boron oxide-lead oxide  
system IR absorption spectra and  
electroconductivity 10 p1582 A66-21917
- Electron excitation in germanium by alkali  
metal ions, noting effect on electrical  
conductivity 10 p1587 A66-22154
- Electroconductivity of n-type Ge in strong  
HF electrical fields 10 p1587 A66-22155
- Static instability in piezosemiconductors  
with negative differential  
conductivity 10 p1589 A66-22170
- Average electrical conductivity and state  
ionization in RF plasma flow device  
[AIAA PAPER 66-165] 11 p1742 A66-22209
- Neutron irradiation of InSb single crystals,  
noting conductivity type change in p-type  
and conductivity magnitude in n-type  
crystals 11 p1749 A66-22285
- Electrical conductance of turbulent  
magnetically active plasma, assuming  
oscillation is possible, determining width of  
peak shock wave in collisionless  
plasma 11 p1744 A66-22448
- High temperature vacuum furnace for  
noncontact measurements of electrical  
conductivity of semiconductor materials in  
liquid and solid states 11 p1709 A66-23294
- Pump conductivity of lightly doped p-  
germanium single crystals, noting Hall  
coefficient temperature dependence and  
specific resistance with low donor and  
acceptor concentrations 12 p1927 A66-23724
- Constant oil monitoring system using  
electric conductivity tester for extending oil  
life in gas turbine engines  
[SAE PAPER 650814] 12 p1935 A66-23844
- Conductivity effective-mass of holes of  
gallium arsenide crystals with various hole  
concentrations determined from frequency  
dependence of spectral reflectivity in  
12 p1928 A66-23942
- Earth electrical conductivity, determined  
from data concerning northern and vertical  
components of cyclic geomagnetic variations,  
suggests increases with  
depth 12 p1871 A66-24297
- Electric conductivity and spectral  
distribution of impurity photoconductivity of  
p- and n-silicon bombarded by fast neutrons,  
noting role of annealing 12 p1929 A66-24450
- Electric conductivity and thermal emf of  
solid solutions of silicon-germanium with  
near silicon composition and various  
current-carrier concentrations and test  
temperatures 12 p1929 A66-24454
- Evolution of plane switch-on and switch-off  
locks in gas of finite electrical  
conductivity in presence of small normal  
disturbances 12 p1866 A66-24950
- Direct current conduction of thin  
evaporated silicon oxide films, noting  
functional dependence on degree of  
oxidation, composition, temperature and  
adherence to Schottky emission  
law 13 p2157 A66-25034
- Dependence of electric properties of  
deblimited zinc telluride films on specimen  
thickness, substrate preheating temperature  
and sign of current  
carriers 13 p2160 A66-25098
- Conductivity of ionized gas in DC  
discharge in argon for various magnetic  
field intensities 13 p2139 A66-25406
- Nonstationary two-dimensional channel flow  
compressible electrically conducting fluid  
subject to traveling magnetic  
field 13 p2140 A66-25422
- Iron selenides of nickel arsenide structure  
analyzed, noting dependence of  
semiconductor characteristics on iron gap  
arrangements 13 p2164 A66-25471
- Solid electrolytes which exhibit appreciable  
electron conduction for use in galvanic  
cells 13 p1999 A66-25675
- Temperature, annealing time and radiation  
damage effect on electroconductivity of  
version layers generated in n-type silicon  
during bombardment with boron  
ions 13 p2167 A66-25921
- Electrical fluctuations in argon-potassium  
nonequilibrium plasma measured and  
correlated with theories of electrothermal  
and magnetoacoustic  
waves 13 p2149 A66-26261
- Self-compensation in electric conductivity  
and other properties of binary  
semiconductor with temperature  
variations 14 p2357 A66-27079
- Stability criteria of system with negative  
differential conductivity showing generation  
of longitudinal waves, noting amplitude  
buildup increment 14 p2358 A66-27085
- Cuprous oxide conductivity caused by  
ionization of thermal lattice  
defects 14 p2358 A66-27091
- Thallium admixture effect on electrical  
conductivity of crystalline and liquid  
selenium, noting decrease and increase in  
conductivity, determining temperature  
dependency and activation  
energy 14 p2359 A66-27177
- Effective-mass approximation of conduction  
electron scattering in very thin  
films 14 p2360 A66-27192
- Temperature dependence of Hall effect  
and conductivity of lead telluride single  
crystals containing  
bismuth 14 p2364 A66-27645
- Temperature-dependence of electric  
conductivity and Hall coefficient in  
semiconductors 14 p2364 A66-27730
- Electroconductivity, Seebeck effect and  
charge carrier mobility in Li-doped  
NiO 14 p2366 A66-27766
- Donor and acceptor concentration on  
electrical conductivity of n-type  
silicon 14 p2367 A66-28235
- Electrical conductivity of polar  
semiconductors in electric fields, calculating  
lattice and Coulomb electron scattering  
mechanism by kinetic equation  
method 14 p2368 A66-28247
- Nonconducting fluid motion in infinite  
tube applied to violent thunderstorm  
dynamics, reducing current intensity to  
value for convection  
currents 14 p2346 A66-28268
- Conductivity of n-silicon in strong  
magnetic field 14 p2370 A66-28332
- Electron gas electroconductivity relaxation  
time and energy loss in n-type InSb at  
cryogenic temperatures 15 p2558 A66-28611
- Hot electron redistribution in multivalley  
conductors in electric fields, based on  
variation under pressure of valley  
population levels, using silicon  
samples 15 p2559 A66-28622
- Electric conductivity in thin metal films  
deposited on single crystal sodium chloride  
substrates, thermally activated with negative  
temperature coefficient of  
resistance 15 p2561 A66-28704
- Pure selenium conductivity, thermal emf  
and Hall effect 15 p2563 A66-28737
- Conductivity of compressed powdered  
refractory compounds found to be  
exponential function of ratio between  
material/compact  
densities 15 p2520 A66-28749
- Electrical conductivity of Earth interior  
from data concerning annual geomagnetic  
variations for all years of solar  
cycle 15 p2487 A66-29101
- Correction of Fatkullin expressions for LF  
conductivities of homogeneous plasma in  
presence of electron-ion collisions in  
ionosphere 15 p2488 A66-29109
- Two-dimensional isothermal liquid flow  
electrically conducting in channel under  
electromagnetic fields, finding self-modeling  
solutions, using Jacobi  
functions 15 p2551 A66-29221
- Dielectric constant, permeability and  
conductivity of random media determining  
electric field, current, magnetic field, etc,  
assuming these quantities are time harmonic  
plane waves 15 p2451 A66-29619
- Temperature dependence of electric  
conductivity in indium antimonide and  
gallium arsenide measured by noncontact  
method in terms of Q-factor  
change 15 p2568 A66-29705
- Recombination rate, ionization in  
nonequilibrium electric  
prediction for dense  
plasma 15 p2554 A66-29752
- Thermal instability causes negative-  
resistance region in nonohmic point contact  
conduction in semimetals 16 p2769 A66-30155
- Thermoconductivity and electrical  
resistivity measurements with derived  
Lorentz functions for various compounds,  
using longitudinal heat  
flow 16 p2771 A66-30252
- Modulator resulting from application of  
Welker effect in semiconductor and used in  
Q and E bands, obtaining conductivity  
variations 16 p2662 A66-30960
- Ohm law for nonisothermal plasma,  
considering thermal diffusion forces,  
obtaining expressions for electric  
conductivity and Hall  
coefficient 16 p2761 A66-31085
- Thickness of gold, silver and copper thin  
films determined, using measurements of  
resistance and Hall  
voltage 16 p2780 A66-31096
- Electrical conductivity of metals,  
explaining electron scattering amplitude  
changes, phonon spectrum distortion and  
temperature effects caused by impurity  
concentration in  
conductor 16 p2780 A66-31180
- Electric conductance and capacity of  
pressed chemically-pured manganese dioxide  
powder at various  
temperatures 16 p2781 A66-31340
- Reynolds analogy computation of heat  
transfer coefficient of turbulent  
electroconducting liquids in transverse  
magnetic field 16 p2765 A66-31401
- Conduction mechanism in discontinuous  
metal films involving image forces, potential  
barrier, activation energies, saturation effect  
in conductivity, etc 16 p2783 A66-31427
- Magnetic field influence on AC surface  
field effect in germanium resulting from  
change in sample conductance and not from  
change in surface barrier  
height 16 p2784 A66-31450
- MHD wave propagation emphasizing  
viscosity, heat and electrical conductivity,  
Hall current, no nonequilibrium phenomena  
and effect of medium  
inhomogeneity 16 p2766 A66-31583
- Change in conductivity at surface of  
semiconductor due to changes in relaxation  
time and charge carrier  
densities 16 p2786 A66-31689
- Electric conductivity of CdS single crystals  
in atmosphere, dry air, oxygen, water vapor,  
carbon dioxide and in transverse electric  
field 16 p2786 A66-31730
- Dark conductivity of cadmium sulfide  
single crystals as affected by contacts,  
voltage and transverse electric  
field 16 p2786 A66-31731
- Energy levels in forbidden band of gallium  
arsenide alloyed with silver or gold,  
determining impurity levels from  
temperature dependence of electric  
conductivity and Hall  
constant 16 p2789 A66-31791
- Tunnel diode circuit stability, equivalent  
circuit and conductivity  
holograph 17 p2880 A66-31867
- Electrical conductivity and Hall mobility of  
p- and n-type semiconductors at various  
temperatures 17 p2975 A66-31900
- Electrical conductivity of concentrated  
phosphoric acid from 25-60 degrees  
C 17 p2870 A66-32042
- Decay time on sunspot magnetic fields,  
calculating conductivity of solar plasma  
while neglecting influence of negative and  
positive hydrogen ions 17 p3000 A66-32334
- Electric conductivity of multicomponent  
partially ionized gas calculated by simplified  
Chapman-Enskog method 17 p2967 A66-32446
- Electric conductivity in low voltage  
atmospheric pressure gas discharge, noting  
Maxwellian electron density  
distribution 17 p2968 A66-32484
- Quantum theory of electric conductivity of  
semiconductors with nonstandard band,  
discussing influence of spin splitting of  
Landau levels on oscillations of transverse  
magnetoresistance in  
n-InSb 17 p2978 A66-32508
- Electrical conductivity and thermoelectric  
measurements of intermediate phases in  
erbium tellurium system 17 p2979 A66-32631
- Dominant mode perturbation theory  
applied to treatment of influence of  
imperfect waveguide contact on measured  
complex permittivity of  
semiconductors 17 p2887 A66-32643
- Unsteady slip flow of electrically  
conducting viscous fluid over porous flat



plate under transverse magnetic field 17 p2973 A66-32980

P-type cadmium tin arsenide crystals, plotting temperature dependences of specific electroconductivity, Hall coefficient and thermal electromotive force 17 p2984 A66-33136

Gold and silver doping effect on Hall effect, electroconductivity thermal emf and conductivity of CdSb 17 p2984 A66-33145

Surface characteristics of semiconductors with intrinsic conductivity, determining potential distribution electric field, carrier concentrations, etc 17 p2984 A66-33146

Electron-hole conductivity effect on temperature variations of Hall coefficient and Nernst-Ettingshausen effect in semiconductor 17 p2986 A66-33309

Radiation-induced electroconductivity and secondary emission in alkali halide single crystals under positive ion bombardment 17 p2988 A66-33458

Plasma jet electrical conductivity, using inductances with different diameters as measurement device 18 p3144 A66-34101

Low temperature plasma conductivity of combustion products, particularly of exhaust gases in duct of MHD oscillator 18 p3145 A66-34107

Various experiments explaining fundamental properties of probes used in measurements of plasma arc columns 18 p3112 A66-34115

Fermi surface shape and size determination and thermoconductivity and conduction electron properties in metals 18 p3155 A66-34135

Negative temperature coefficient of electrical resistance, anomalous Hall constant and magnetoresistance constant for thin films of Be and Pb 18 p3157 A66-34627

Wyatt anomalies in tunneling conductance centered at zero bias, noting magnetic effect 18 p3159 A66-35035

Impurity conduction for arsenic diffused into p-type germanium and boron into n-type silicon 19 p3433 A66-35342

Nuclear polarization by hot carrier flow in homogeneous semiconductor, taking into account effect of strong electric field on spin lattice relaxation time 19 p3437 A66-35474

Impurities effect on electrical conductivity of air between 1000 and 10,000 degrees K 19 p3406 A66-35743

Electron excitation in germanium by alkali metal ions, noting effect on electrical conductivity 19 p3440 A66-35768

Electroconductivity of n-type Ge in strong SHF electrical fields 19 p3440 A66-35769

Sonic instability in piezosemiconductor with negative differential conductivity 19 p3441 A66-35784

Spontaneous LF conductivity fluctuations in n-type gallium arsenide samples at 77 degrees K 19 p3442 A66-35822

Texture and electric conductivity of cadmium sulfide thin films 19 p3442 A66-35865

Singularities of temperature dependence of electric resistivity of aluminum at helium temperatures 19 p3382 A66-36072

Electrical conductivities of boron trifluoride in chlorine and bromine trifluorides studied as function of temperature and concentration 19 p3295 A66-36367

Normalized self-and mutual admittances of two identical bare circular loop antennas in air or conducting medium evaluated, obtaining single integral equation for current distribution 19 p3321 A66-36405

Electric conductivity of beta and gamma phases of tantalum-carbon system as affected by temperature and composition 19 p3386 A66-36424

Anodic oxidation process for silicon, examining current flow in strong electric field as function of time, Curie-von Schweidler law and Tafel law 19 p3448 A66-36755

Electric conductivity of argon plasma 19 p3433 A66-36776

Electrical and thermal conductivity and integral degree of blackness of tantalum at temperatures above 1000 degrees C 20 p3582 A66-36977

Electromagnetic field effect on heat

transfer during laminar flow of electrically conducting incompressible fluid in flat channel 20 p3607 A66-36980

Pinch effect in InSb degenerate plasma, discussing electric conductivity and recombination emission spectra 20 p3615 A66-37371

Dependence of Hall effect and conductivity of irradiated samples on reciprocal temperature in nuclear transmutations produced in InSb by bombardment with slow neutrons 20 p3617 A66-37485

Thermoelectric device for semiconductor analysis, determining whether material is of n-or p-type conductivity 20 p3560 A66-37586

Electric conductivity and spectral distribution of impurity photoconductivity of n-and p-silicon bombarded by fast neutrons, noting role of annealing 20 p3619 A66-37682

Electric conductivity and thermal emf of solid solutions of silicon-germanium with near silicon composition and various current-carrier concentrations and test temperatures 20 p3619 A66-37686

Thin dielectric film wave scattering, EM interaction responses and conductivity tensor 20 p3622 A66-38385

Moisture content determination in liquid HF based on electroconductivity 21 p3702 A66-38519

Shubnikov-de Haas effect for transport properties of electron gas in magnetic field, noting oscillatory parts of thermal and electric conductivities 21 p3776 A66-38632

Electric conductivity of magnetically balanced arc in transverse argon flow at atmospheric pressure 21 p3777 A66-38718

Electron conduction and phosphorus doping effects on room temperature and cryogenic electron spin resonance in n-type silicon 21 p3797 A66-38752

Impurity conduction effect on electron donor recombination cross section in n-type germanium and silicon at liquid helium temperatures 21 p3801 A66-39001

Flow of strongly rarefied ionized plasma past electrically charged body solved by kinetic and Poisson equations in absence of magnetic field 21 p3795 A66-39604

Phthalocyanine crystal phase change effect on electric conductivity 22 p3860 A66-39921

Experimental results of VLF dipole tests on Greenland ice cap including measurements of self-impedance, amplitude current distributions, relative efficiency and complex conductivity 22 p3874 A66-39942

Deep centers in conducting n-type GaAs and production of Schottky layer 22 p3963 A66-40088

Taxonomy of electric charges in Si-silicon dioxide metal insulator semiconductor /MIS/ systems under presence or absence of bias 22 p3877 A66-40178

Conductivity of potassium-seeded argon plasma, assuming variable collision cross sections and Maxwellian distribution for electrons 22 p3951 A66-40363

Applications for new class of materials termed oxide-dispersion strengthened materials offering stability at high temperatures and high thermal and electrical conductivity 22 p3935 A66-40526

Self-compensation in electric conductivity and other properties of binary semiconductor with temperature variations 22 p3967 A66-40835

Stability criteria of system with negative differential conductivity showing generation of longitudinal waves, noting amplitude buildup increment 22 p3967 A66-40841

Cuprous oxide conductivity caused by ionization of thermal lattice defects 22 p3967 A66-40847

Four-point probe technique to measure conductivity of epitaxial layers on conducting substrates 23 p4110 A66-41157

Surface charge mobility measurement method applied to Si and Ge and time variation of surface conductivity 23 p4110 A66-41183

Electrical conductivity variation with temperature of chlorine and bromine trifluoride, noting maximum conductivity below freezing point of chlorine trifluoride 23 p4118 A66-41241

Spatial distributions of carrier concentration and internal field in cadmium selenide for various voltages, measuring

conductivity and Hall coefficient 23 p4112 A66-41292

Optimum seed concentrations of alkali metal in rare gas for maximum electroconductivity of slightly ionized nonequilibrium plasma 23 p4104 A66-41511

Semiconductor conductivity in strong SHF electric fields, measuring dielectric constant and Fourier component 23 p4068 A66-41620

Correct conductance and susceptance of infinite cylindrical antenna determined via asymptotic evaluation of parametric integrals 23 p4047 A66-41636

Electric and thermal conductivity effects on MHD instabilities in diffuse linear pinch 23 p4105 A66-41706

Variation of resistivity and inversion of sign of conductivity of quenched specimens of p-type silicon 23 p4115 A66-41838

Viscous electrically conducting liquid oscillating in laminar regime between parallel planes when applying magnetic field normal to planes and motion direction 23 p4108 A66-42047

Decaying free carrier concentration increase in GaAs when subjected to increased level of drive during first cycle 24 p4253 A66-42370

Hall coefficient, electrical conductivity and thermoelectric power of GaSb-Ga<sub>2</sub>Te<sub>3</sub> solid solutions as functions of composition and temperature 24 p4254 A66-42425

Effective-mass approximation of conduction electron scattering in very thin films 24 p4259 A66-43090

MHD flow, examining effects of finite electric conductivity on basic flows due to compression and shear 24 p4246 A66-43115

**ELECTRIC CONDUCTOR**

**SA DIELECTRICS**

Stability of flexible conductor in longitudinal magnetic field, using scalar potential to determine disturbed state 18 p3152 A66-35081

Plastic electric conductivity, discussing conduction by fillers in plastic matrix and conduction of polymers by virtue of molecular structure [ASME PAPER 66-MD-31] 21 p3753 A66-38486

Electrical explosion of copper wire in air and in vacuum, discussing plasma emission and I-V characteristics 21 p3791 A66-39084

**ELECTRIC CONNECTOR**

Reliability prediction and production control of electrical connection by combination of stress survival matrix test and special strength control chart 01 p0076 A66-10067

Worst case design for high reliability welded electrical connections, emphasizing encapsulation stresses and quantitative parameter 02 p0234 A66-11325

Multilayer circuit boards for interconnecting integrated circuits in computer and other large systems 04 p0498 A66-14015

Solder flow under wire insulation and effect on reliability, noting destructive and vibration test results 11 p1665 A66-22680

Intermittent connection testing for digital logic module 20 p3523 A66-37949

Microbonding difficulties in joining flat pack circuits to printed circuit boards, examining parallel gap welding connections with board material and use of dissimilar metals 23 p4043 A66-41189

Electric contact design factors for shock vibration environments 24 p4186 A66-43058

**ELECTRIC CONTACT**

Dependence of barrier height of metal-semiconductor systems on metal work function, surface states and thickness of interfacial layer 02 p0271 A66-11438

Photovoltage profiles of rhodium to p-silicon contact at high and low level injection and various temperatures 02 p0275 A66-11873

Frequency dependence of dynamic properties of semiconductor small area ohmic contacts in volt-ampere characteristic regions when constant current and sinusoidal pulses are applied 06 p0838 A66-15893

Macroscopic quantum interference effects through superconducting point contacts, with results for several superconductors 07 p1109 A66-18439



Electric Ag-CdO contacts obtained by internal high temperature oxidation method 08 p1239 A66-18900

Make-before-break contacts effect on degree of complexity of film and hybrid microelectronic nodes 08 p1191 A66-18921

Rectifying and ohmic contacts used in manufacture of gallium phosphide diodes that emit light when current is reversed 08 p1273 A66-19291

Effect of conditions of fabrication of alloyed contacts between semiconductors and metals on dislocation structure of these contacts 08 p1274 A66-19315

Electrical contact for very small planar functions and embodiment in millimeter-wave mixer diode 09 p1350 A66-19926

Schottky diode and metal-base transistor design and operation with metal-semiconductor contact 11 p1660 A66-22271

Behavior of trace elements in gallium arsenide and materials and methods used for ohmic contacts to n-and p-type specimens, stressing importance of indium 11 p1757 A66-23283

Resonance properties of germanium analyzed by passing DC and AC through samples of various specific resistance with tungsten needle contacts 11 p1759 A66-23419

Parts, materials and packaging reliability and electric contacts - IEEE International Convention, New York, March 1966 12 p1842 A66-24663

Sliding contact wear under very dry high altitude or space conditions due to lack of contact film prevented by using chemical compounds like graphite or lithium carbonate 12 p1888 A66-24664

Clad metals concept applied to low energy contact using materials system, analyzing material, mechanical and electrical properties of thin precious metal inlays 12 p1930 A66-24666

Weimer triode with contact rectifier for use as component of microminiature radio circuits, noting effect of contact rectification on current-voltage characteristics and amplifying power of such triodes 13 p2031 A66-25228

Contact bouncing in protective gas relays measured in circuit with inductive and real load 13 p2031 A66-25484

Lubricants for space environment, noting experiences with satellites and application to ball bearings and electrical contacts 13 p2086 A66-25770

Functional transformations revealing topological properties of single contact /SC/ network, simplifying task of synthesis 13 p2051 A66-26064

Properties of hydrothermally grown single crystals of tetragonal lead monoxide, with contacts applied by metal evaporation 14 p2359 A66-27099

Jet plating of gold to make ohmic contacts on silicon 14 p2361 A66-27277

High performance contactor design and development 15 p2460 A66-28993

Electric contact effect and transition temperature measurement in superconducting Cu-Pb double layer films at low temperatures, using He 3 cryostat 16 p2772 A66-30322

Dominant mode perturbation theory applied to treatment of influence of imperfect waveguide contact on measured complex permittivity of semiconductors 17 p2887 A66-32643

Excess carriers lifetime in semiconductors nonstatic measurement by photoconductive phase shift of spreading resistance under point contact 19 p3433 A66-35330

Superconducting point contact diodes for observation of microwave radiation generated by bridge with and without constant voltage steps 20 p3620 A66-37776

Voltage oscillations as function of applied magnetic field in weak contacts between superconductors in resistive region when applying currents above critical value 23 p4111 A66-41251

**ELECTRIC CONTROL**

Conversion of small-telescope mounting to electrical control 05 p0680 A66-15210

Network theory - Conference, Cranfield, England, September 1965 07 p1014 A66-17744

Circuits for variable impedance control at centimeter-wave frequencies, using varactor

semiconductors and dephasing ferrites in waveguide 07 p1002 A66-17828

Redundant electrical systems for Titan II and Gemini Titan II launch vehicles 20 p3499 A66-37193

Electrical control of boundary layer flip-flop fluidistor by disruptive discharges between electrodes producing pneumatic pressure shocks that switch output flow 20 p3501 A66-37648

Optimal discrete binary system of electrical control of beam position of phased linear antenna array 21 p3712 A66-39251

**ELECTRIC CURRENT**

SA ALTERNATING CURRENT /AC/

SA DIRECT CURRENT /DC/

SA EDDY CURRENT

SA JOSEPHSON CURRENT

SA LIGHTNING

SA PONDEROMOTIVE FORCE

SA POTENTIOMETRY

Short-circuit current change in silicon solar cell performance as function of cell thickness 01 p0014 A66-10397

Cross-sectional geometry of Nernst-Ettingshausen devices optimized for rectangular geometry and for Norwood spiral screw thread configuration 02 p0270 A66-11430

Superconducting coil degradation, noting flux jumps causing sudden decrease in series current which causes field disturbances throughout coil 02 p0271 A66-11440

Approximation method reproducing assigned time functions by using exponential polynomials in synthesis problems of electrical circuits 02 p0207 A66-11752

Coherence of Gunn oscillations enhanced by transverse magnetic field for certain applied voltages 03 p0332 A66-12427

Multicircular sector slow wave structure in millimeter wave range as modified structure of circular symmetrical circuit, noting dispersion characteristics 03 p0339 A66-12452

Beating effect of current oscillations in cadmium sulfide due to nonuniform illumination and indicating sinusoidal oscillations of different frequencies and comparable amplitude 03 p0408 A66-12453

Operation principle, design and application of coloristors which change color at predetermined temperatures determined by current passing through them 03 p0340 A66-12475

Electrochemical oxidation of p-n junctions on silicon surface in potassium nitrate solution in ethylene glycol, noting electric current 03 p0413 A66-13203

Electric current system arising from sudden enhancement of ionospheric conductivity in auroral zone 04 p0516 A66-13853

Roberts method determining accommodation coefficients of gases on bare wires leads to erroneous conclusions due to thermal inertia of experimental apparatus in vicinity of current paths 04 p0545 A66-14170

Plasma measurements including temperatures, electron density, current density, etc, noting behavior of probes in magnetic fields 05 p0726 A66-15247

Cesium filled diodes measured at various cathode temperatures, noting effect of ions generated in interelectrode space on current 05 p0728 A66-15549

Mass and energy state dependence of plasma, generated by titanium source, on electrical operating conditions of source 06 p0919 A66-16878

Magnetic-pulse working of metals based on current surge in coil inducing magnetic field to generate electric current in metal articles around coil 06 p0888 A66-17073

Transport theory based on relaxation time applied to bismuth, deriving analytic expressions for electric resistance, thermoelectricity and Hall, Seebeck and Nernst coefficients 07 p0990 A66-17237

Stimulated state, stable, lasting and reproducible, in electroluminescent cells of sublimated zinc sulfide film obtained upon passage of increasing DC voltage through them at 77 degrees K 07 p1099 A66-17914

Electric current passage through multivalley n-germanium semiconductor plates, noting nonuniform electron distribution 08 p1273 A66-19275

Batteries - International Symposium at Brighton, England in September 1964 08 p1169 A66-19641

Amplitude and phase of first harmonic of load current of differential magnetic amplifier determined, using generalized characteristics 09 p1352 A66-20303

AC current measurement to determine contribution in semiconductors, which appears as displacement current, from space charge caused by injected and alternatively modulated carriers 09 p1432 A66-20970

Current pulse measurement of thin polarized ferroelectric ceramic disks connected by short circuit under stress wave 10 p1576 A66-21546

Quasi-linear current instability in two-temperature plasma for Coulomb collision and free electron acceleration 10 p1569 A66-21972

CW microwave oscillation in bulk GaAs, discussing harmonic content, linewidth, circuit and electronic tunability, etc 10 p1585 A66-22077

Microwave oscillations in epitaxial layers of gallium arsenide 10 p1585 A66-22080

Fast coincidence circuit with high sensitivity and low recovery time, analyzing triggering and self-oscillating operation and using avalanche operating transistors 11 p1662 A66-22402

Radiation field and surface waves generated by linearly phased electric line current and electric current component oriented in plane parallel to unidirectional conducting screen, solved by modal method 11 p1652 A66-22549

Superconducting systems partitioned by thin barriers allow supercurrents to pass through, noting magnetic field penetration into barrier, AC supercurrents, structure in DC, current-voltage characteristics of barrier, etc 11 p1756 A66-22978

Density of electron states and classical effective mass of current carriers in magnetic field for semiconductor with wurtzite-type lattice 12 p1930 A66-24457

Electrical precursors in immediate vicinity of ionizing shock waves in argon analyzed, using model describing electron diffusion through shock 12 p1923 A66-24579

Capacitive probe measurements of potential fluctuation in current-oscillating CdS crystals under ultrasonic amplification conditions at room temperature 12 p1931 A66-24812

Double stream instability in finite diameter beams analyzed by numerical experiments on digital computer, showing electron trapping as cause of RF current saturation 13 p2137 A66-25044

Reversal of diode with delay between last direct pulse and first reversed pulse 13 p2031 A66-25230

Voltage drop in direction of current flow produced in superconducting alloys by current perpendicular to magnetic field explained by assuming Abrikosov filaments move under influence of Lorentz force 13 p2168 A66-26022

Precursor wave structure in electromagnetic shock tube, determining precursor velocity, electron density and current content, comparing precursor behavior with ionizing electromagnetism wave 13 p2064 A66-26259

Alfven wave propagation in inhomogeneous magnetic fields satisfying magnetohydrostatic equation and allowing for electric currents solved, using differential equation 13 p2156 A66-26710

Current changes in gas discharge as affected by laser action 14 p2306 A66-27055

Spontaneous LF current oscillations in germanium with copper, with compensated energy levels under illumination, low temperatures and electric fields, noting formation of electric domains 14 p2357 A66-27076

Stabilization of gas conductor carrying HF current with aid of steady state magnetic field, noting MHD perturbations role 14 p2341 A66-27149

Sectorial structure effect on current carrier concentration of germanium doped indium antimonide single crystals 15 p2558 A66-28565

Time variation of current, temperature and



resistance in premelt stage of wire explosion expressed in terms of initial wire and circuit data 15 p2537 A66-28722

Electric current density in semiconductor, noting harmonic mixing of microwaves by warm electrons in 15 p2564 A66-28875

Excitation of ion-acoustic waves in potassium-cesium plasma when passing current through it, finding natural frequencies of system when plasma is drifting along axis 15 p2550 A66-29214

Existence of convective interaction mechanism affecting direction and stability of electric current in flowing gas, using electric arc confined in supersonic flow 15 p2481 A66-29744

Ambipolar diffusion of plasma cloud imbedded in ionized gas with homogeneous magnetic field, assuming electric current is not vanishing 15 p2494 A66-30045

Electric potential and space charge density near Langmuir probe in hot rarefied plasma at rest, calculating current collected from plasma 16 p2759 A66-30372

Gallium arsenide and silicon solar cells under proton irradiation, noting decrease of short circuit current and open circuit voltage 16 p2636 A66-31018

Bulk oscillations in n-type Si compensated with either Au or Co deep level impurities 16 p2778 A66-31078

Effect of finite width on performance of polyphase rectangular MHD converter, showing that for isotropic fluid electric current extends in two dimensions 16 p2637 A66-31102

Efficiency criterion for semiconductors, using equations for flux density of electric current and energy for isotropic semiconductor in absence of magnetic field 16 p2789 A66-31790

Radial temperature distribution within argon plasma column determined spectroscopically at various arc currents, noting argon thermoconductivity 17 p2966 A66-32427

Space-charge-limited electron current in silicon 17 p2980 A66-32646

High-field superconductors, noting role of defects in pinning, magnetization, critical currents, applications in solenoids, etc 17 p2985 A66-33156

Critical current enhancement and degradation due to hysteresis in nonideal type II superconductors in axial magnetic fields 18 p3153 A66-33612

Stimulated state, stable, lasting and reproducible, in electroluminescent cells of sublimated zinc sulfide film obtained upon passage of increasing DC voltage through them at 77 degrees K 18 p3155 A66-34174

Current source for vacuum tube circuits delivering constant and fairly large current from cathode of pentode 18 p3079 A66-34246

Voltage and density of contact-corrosion current arising at contact surface of different metals 18 p3124 A66-35011

Energy band structure, carrier behavior and characteristic curve of p-n junction diode at high-current level, solving transport and Poisson equations 19 p3312 A66-35346

Constant current sources consisting of sealed ionization chambers for calibrating electrometers 19 p3357 A66-35809

Transient charge and discharge currents in tantalum oxide with anodic electrolyte and tantalum oxide with anodic metal 19 p3448 A66-36754

Destructive grounding system fault currents and abortive interference and elimination, using functional diagrams 20 p3542 A66-37241

Anomalous permanent changes in transistor gain after low exposure dosage of electron and/or gamma radiation related to recombination current-component buildup 20 p3526 A66-37320

Anomalous photocurrent generation in transistors, noting carrier generation and transport processes 20 p3526 A66-37321

Viscous thermoconductive model of solar wind motion, using Navier-Stokes equations 20 p3631 A66-37335

Axially oriented point source current and filament with triangular current distribution in magnetoionic medium, examining ion sheath effect on radiation

characteristics 20 p3516 A66-37624

Density of electron states and classical effective mass of current carriers in magnetic field for semiconductor with wurtzite-type lattice 20 p3620 A66-37689

Testing of silicon solar photoelectric battery when exposed to large light fluxes, noting overheating, current saturation, efficiency decrease, etc 20 p3503 A66-38439

Thermostability of germanium power transistors, noting collector leakage current 21 p3709 A66-38673

Electromagnetic wave excitation in magnetoplasma by external currents using kinetic theory, obtaining expression for energy losses, analyzing electron and ion cyclotron resonance 21 p3782 A66-39016

Quasi-linear current instability in two-temperature plasma for Coulomb collision and free electron acceleration 21 p3794 A66-39551

Negative resistance in cathode current and grid and plate current of tube in which electrodes are situated behind cathode 22 p3871 A66-39658

Cesium-plasma diode effect dependence on material output of cathode in vacuum, plotting short circuit current vs vapor pressure, voltage distribution, etc 22 p3952 A66-39752

Curve analysis of current instabilities including Gunn effect in n-type gallium arsenide 22 p3961 A66-40045

Neutron irradiation-induced defects in vapor deposited niobium stannide and effects on current-carrying capacity 22 p3962 A66-40083

Spontaneous LF current oscillations in germanium with copper, with compensated energy levels under illumination, low temperatures and electric fields, noting formation of electric domains 22 p3966 A66-40833

Domain and circuit properties effect on oscillations in GaAs 22 p3967 A66-40865

Voltage oscillations as function of applied magnetic field in weak contacts between superconductors in resistive region when applying currents above critical value 23 p4111 A66-41251

Sectorial structure effect on current carrier concentration of germanium doped indium antimonide single crystals 23 p4112 A66-41286

Sliding magnetic field effect on electric current in conducting annular channel flow, noting energy-transfer efficiency and acoustic resonance 23 p4107 A66-42030

Radiation response of low power nuxistors, noting cause of grid current and relation between grid structure and induced current 24 p4258 A66-42961

Stabilization of gas conductor carrying HF current with aid of steady state magnetic field, noting MHD perturbations 24 p4244 A66-42969

Light emission in near IR by semiconducting GaAs under current oscillations caused by electron-phonon coupling 24 p4258 A66-43000

**ELECTRIC DIPOLE**

**SA MAGNETIC DIPOLE**

**SA QUADRUPOLE**

Magnetic particle motion, analyzing effect of Earth electric dipole field 05 p0752 A66-15387

Radiation fields of moving electric dipole falling off faster than  $1/r$ , having two nonspinning point charges, variable point and moving at relativistic velocities 06 p0832 A66-16453

Radiation from axially oriented electric dipole situated at center of infinitely long axially magnetized column of uniform plasma 08 p1186 A66-19747

LF admittance measurements on orthogonal dipoles in ionosphere 09 p1341 A66-19855

Matrix formulation determination radar cross section arising when smooth conducting obstacle is illuminated by incident electromagnetic wave 10 p1497 A66-21590

Feed polarization incident upon conic reflector in antenna system specified in terms of crossed electric and magnetic dipoles 11 p1663 A66-22544

Dipolar resonances when axially uniform

warm plasma column is subjected to transverse RF electric field 12 p1815 A66-23962

MHD approach to axisymmetric perturbations in plasma permeated by static dipole field 12 p1951 A66-24574

Radiation due to axially oriented electric dipole situated on axis of infinite cylindrical column of insulating free space surrounded by uniaxially anisotropic plasma 13 p2026 A66-26103

Radiation due to time-harmonic source and field solution of electric dipole in moving uniaxial anisotropic medium by Minkowski theory 14 p2234 A66-26861

Oscillator strengths for electric dipole transitions in neutral helium 14 p2338 A66-28127

Low temperature vibronic transitions between electronic states involving destruction of photon and creation of phonon via electric dipole term of Hamiltonian 19 p3446 A66-36394

Electric dipole radiation through finite conical plasma sheath about reentry vehicle, calculating radiation pattern 19 p3304 A66-36403

Short distance expansion method used to calculate ground radio wave propagation over mixed path on spherical Earth 19 p3305 A66-36421

Electric quadrupole transition in fourth positive system of CO observed in bands of electric dipole allowed transition 19 p3404 A66-36800

Single-axis meter design and development for measuring feeble torques on massive bodies, discussing calibration, testing results, evaluation of static dipole moments and spacecraft spin-rate control moments 21 p3722 A66-38880

Light absorption by optically pumped atoms undergoing magnetic resonance, noting modulation amplitudes and modulation frequency limitation for primary interaction 22 p3930 A66-39807

Antenna radiation theory, noting reiteration of incorrectness of infinity catastrophe theory and application to oscillating dipole in uniaxial medium 23 p4047 A66-41633

Elimination of singularity in power radiated by point electric dipole in unbounded magnetoplasma within certain frequency range 24 p4241 A66-42373

Self-impedance of electric dipole immersed in plasma half-space with finite temperature 24 p4243 A66-42625

Nonlinear optics emphasizing parametric oscillation, self-focusing and trapping of laser beams and stimulated Raman, Rayleigh and Brillouin scattering, using Maxwell equations and electric dipole approximation 24 p4225 A66-42810

**ELECTRIC DISCHARGE**

**SA ARC DISCHARGE**

**SA CORONA DISCHARGE**

**SA GAS DISCHARGE**

**SA GLOW DISCHARGE**

**SA LIGHTNING**

**SA PENNING DISCHARGE**

**SA RADIO FREQUENCY DISCHARGE**

**SA SPARK**

Helium-neon laser output dependence on hollow cathode discharge conditions for electron transitions in neon 02 p0239 A66-11422

Double sheath presence in front of hot cathode in low pressure DC discharge 02 p0265 A66-11433

Excitation of ruby lasers using double-pumped high-intensity helical flash tubes, obtaining time-resolved spectra of electrical discharges and plasma temperatures 02 p0240 A66-11446

Equilibrium electron density of RF discharge excited with frequency higher than electron-neutral collision frequency and controlled by resonance from plasma dispersion 03 p0405 A66-12986

Pressure range determination where stable plasmoids exist in electric field discharge, with measurements made on rare gases 03 p0405 A66-12987

Synthesis by electrical discharge of porphine-like substances imply abiogenic possibility under primitive Earth condition 03 p0331 A66-13261



Dielectric properties of noble gases afterglows following electrodeless discharge over signal frequency and pressure ranges 04 p0551 A66-13813  
 Reflex arc in lithium vapor analyzed, using spectrographic, mass spectrometric and probe measuring techniques 04 p0554 A66-14293  
 Effect of heat removal through MHD channel walls on stability of temperature distribution during electrical discharge in gas between two planes 04 p0557 A66-14421  
 Book on theoretical and engineering problems arising in capacitor discharge technique of pulse generation 06 p0878 A66-16046  
 Preparation and properties of oxygen fluorides OF<sub>2</sub> and O<sub>6</sub>F<sub>2</sub> by electrical discharge apparatus used to prepare OF<sub>2</sub> 07 p1000 A66-18344  
 Selection, design and utilization of electrical discharge machine 08 p1229 A66-18688  
 Comparative determination of HF electrical discharge threshold in electromagnetic system 09 p1349 A66-19852  
 Discharge in germanium thin films at liquid helium temperatures, noting electrostatic ionization of impurities and shock-ionization region expansion 09 p1412 A66-19990  
 Radial distributions of number density, electron temperature and plasma potential measured in electrodeless discharge, using symmetric and asymmetric double probes [AIAA PAPER 66-194] 10 p1562 A66-21440  
 High voltage capacitor discharge from Marx circuit, using stepup transformer 10 p1486 A66-21862  
 Point-discharge currents between negative points and positive plane 11 p1695 A66-22376  
 Lightning and static electricity discharges effects on helicopter design and performance, noting blade and rotor hub protection, fuel ignition, etc 11 p1638 A66-23259  
 High speed photography determination of current cut-off and recurrent breakdowns during electrical discharges in water 12 p1922 A66-24221  
 Electrical discharge theory of cosmic atmospheric phenomena, relating lightning, novae and quasars 12 p1950 A66-24394  
 Giant-pulse laser-induced atmospheric electric breakdown causing optical frequency discharge 13 p2134 A66-26194  
 Ion pressure theory to describe steady state collisionless discharge 13 p2155 A66-26679  
 Localization conditions of high power linear HF discharge at low gas pressure, achieving localization of current and plasma density in magnetic field by using diaphragms 14 p2340 A66-27148  
 Shock tube study of high temperature gas flow around circular cylinders caused by electrical discharge 14 p2218 A66-27348  
 Measurement of plasma density generated by underwater explosions, noting modes of electrical discharge and shock front role 15 p2549 A66-28693  
 Energy balance of stationary discharges in quartz containers filled with gas at various pressures, determining relation of heat and light loss of discharge to gas pressure and discharge power 15 p2551 A66-29215  
 Electrical discharge in air, mercury vapor and nitrogen, using RF signal probe, determining electron density and temperature and random velocity in plasma 15 p2548 A66-29715  
 Electrical discharge probe for transient density measurements in rarefied gas flow, noting density range, flow velocity, etc 16 p2701 A66-30380  
 Linear electric shock tubes including segmented series-discharge driver, switchless shock tube, metal-walled driver for radiant energy conservation, etc 16 p2674 A66-30418  
 Magnetoplasma diffusion measurements in narrow discharge tube, using classical ambipolar diffusion model for weak magnetic fields 16 p2760 A66-30802  
 Discharge current, discharge voltage pressure and radius of discharge channel for filaments in water induced by tungsten filaments 18 p3142 A66-33841

Electrodeless annular discharges in argon and air 18 p3144 A66-34039  
 Electrical discharge machining of sintered aluminum powder with different alumina content 18 p3116 A66-34061  
 Plasma turbulent heating by direct current discharge in magnetic mirror trap, analyzing adiabatic compression 19 p3430 A66-36589  
 Mechanism of electrode erosion by supersonic flame jets during pulsed discharge 20 p3607 A66-36981  
 Gas pressure effect on excitation of 4.38-ev level in Pb during hollow cathode discharge in magnetic field 20 p3579 A66-37780  
 Frequency distribution of atmospheric emissions by multiple lightning discharges 20 p3553 A66-38075  
 Electric component of radiation field from same flashes recorded with histograms of product of field strength and distance, showing concentration around mean values 20 p3553 A66-38076  
 Plasmoid in shock tube with electrical discharge, measuring pressure, velocity and conductivity with magnetic probe 20 p3611 A66-38119  
 Electrochemical machining advantages over electrical discharge machining and traditional machining processes 21 p3743 A66-38669  
 Emission and absorption capacity of /zero-/ band of CN violet system at high temperatures, determining parameters of oscillator system power 21 p3775 A66-39079  
 Oscillographic studies of point discharge pulses in individual points in multiple point discharger 22 p3920 A66-40802  
 Radial distributions of number density, electron temperature and plasma potential measured in electrodeless discharge, using symmetric and asymmetric double probes [AIAA PAPER 66-194] 23 p4107 A66-41907  
 Pressure distribution in slug of shock wave excited in electrical discharge shock tube 24 p4242 A66-42405  
 Localization conditions of high power linear HF discharge at low gas pressure, achieving localization of current and plasma density in magnetic field by using diaphragms 24 p4244 A66-42968

# ELECTRIC ENERGY

Energy conversion into electrical power considering solar cells, thermoelectrics and thermionics noting advantages over fuel cells, dynamic machines and MHD 03 p0324 A66-13272  
 Utilization of microorganisms to generate electrical energy 05 p0627 A66-15478  
 Thermionic converter transforming calorific energy of flame into electric energy having protective coating of enamel-covered alumina 05 p0623 A66-15594  
 Particle detection with electric charges of two-thirds in cosmic radiation 07 p1131 A66-18238  
 IR applications to reliability assessment, stress analysis, testing, etc, of electrically energized components, thermally or by power dissipation 12 p1842 A66-24671  
 Output power and thermal efficiency of molten salt thermocell, examining applicability as generator for direct conversion of heat into electric energy 16 p2636 A66-30673  
 Transfer efficiency of theta pinch in converting capacitively stored electrical energy to plasma energy measured, using calorimeter technique 16 p2761 A66-31090  
 Electrical energy by direct conversion, noting fuel cell, thermoelectric generator, solar cell, etc 18 p3053 A66-33722  
 Frequency sensing for protection of frequency aircraft electric power systems, applying storms saturating reactor concept 20 p3499 A66-37175  
 Component reliability and failure rates in aerospace electric power systems with relays 20 p3525 A66-37180  
 Function, method of operation, complexity and effect on weight and cost for BITE /built-in test equipment/ as applied to electric power systems for jet aircraft 20 p3499 A66-37189  
 HF electric power transmission lines in aircraft noting effect of frequency, ground plane elevation and feeder configuration on impedance 20 p3499 A66-37190  
 Determination of electric power system

requirements for short-range missile 20 p3499 A66-37192  
 Electric energy from helical and coaxial explosive generators noting design, performance, limitations and loss mechanisms 21 p3699 A66-39510  
 Faraday unipolar induction in solid cylinder of nonideal type II superconductor, noting contributions to observed emf 23 p4114 A66-41629  
 Solar photovoltaic cell design for lower temperature operation, noting application to near-Sun missions 23 p4019 A66-41745

## ELECTRIC ENERGY STORAGE

Range, sensitivity and accuracy of meteorological radar improved by use of storage device 02 p0252 A66-11271  
 Fuel cells with molten carbonate electrolytes such as matrix cells and free and paste electrolyte cells, noting construction, operation, performance 07 p0996 A66-18473  
 Logarithmic pulse storage device, basic characteristics and choice of parameters as function of pulse length and measurable frequency range 09 p1356 A66-20773  
 Signal transmission factor and noise storage coefficient of two-stage pulsed-signal storage system 09 p1347 A66-20774  
 Logarithmic pulse storage device, basic characteristics and choice of parameters as function of pulse length and measurable frequency range 22 p3873 A66-39832  
 Signal transmission factor and noise storage coefficient of two-stage pulsed-signal storage system 22 p3873 A66-39833

## ELECTRIC EQUIPMENT

### SA Q-FACTOR

Progress in constant speed drive generating systems and control equipment for constant frequency aircraft electric systems [SAE PAPER 650827] 01 p0016 A66-10827  
 Comparison of inflector unmatched with line with matched one using additional capacitors, showing both devices have identical electric and time characteristics 01 p0046 A66-11057  
 Nonlinear properties of complete tunnel diode equivalent circuit emphasizing conductance, susceptance and oscillatory characteristics of barrier layer 03 p0346 A66-13317  
 Report on transistor industry covering manufacturing techniques, materials, geometries, advantages, disadvantages, etc 03 p0347 A66-13342  
 Precision coaxial standard and component designs based on constant impedance, coplanar compensation and mechanical tolerance sensitivity 10 p1514 A66-21907  
 Circulators from lumped circuit elements examined, calculating coil properties and analyzing construction 11 p1664 A66-22660  
 Mechanical-electrical components for printed circuits including rheostat with step-by-step mechanism, connectors, push buttons, etc 11 p1665 A66-22684  
 Long-term storage effects on reliability of electronic equipment, covering testing results and available data on failure rates 12 p1830 A66-23755  
 Aircraft electrical system design, power requirements, instrumentation, excess loads, etc 12 p1803 A66-24387  
 Instruments, measurements, industrial electronics, nuclear science, ultrasonics - IEEE International Convention, New York, March 1966 12 p1842 A66-24672  
 Nonlinear properties of complete tunnel diode equivalent circuit emphasizing conductance, susceptance and oscillatory characteristics of barrier layer 14 p2260 A66-28290  
 Range of gas dynamic stability of arc-type electric heaters, characteristics for design and calculation of electrode diameter ensuring vortex stabilization 14 p2348 A66-28314

## ELECTRIC FIELD

### SA ATMOSPHERIC ELECTRIC FIELD

### SA ELECTROMAGNETISM

### SA FIELD EMISSION

### SA SPARK GAP

Thin metal film growth under applied electric field 01 p0118 A66-10246  
 Spatial distribution of electrical field



obtained by focusing radiation of ruby laser 01 p0080 A66-10250

Langevin equation used to study interaction between radio wave and plasma, taking into account collisions between electrons and heavy ions and electric field caused by group displacement 01 p0022 A66-10322

Pinch effect in low pressure discharge theory, examining effect of magnetic field produced by discharge and electric field effect 01 p0110 A66-10334

Controlled bulk semiconductor amplification possible using n-type gallium arsenide with applied electric field greater than 3000 v/cm 01 p0036 A66-10351

Charged Styropor ball motions in free float between plates of perforated capacitor with alternating electric field 01 p0119 A66-10374

Tonks-Datner resonances of plasma column irradiated by RF electric field due to plasma acoustic wave propagation 01 p0025 A66-10536

Prebreakdown current in high vacuum noting field strength and field emission hypothesis 01 p0106 A66-10641

Book on satellite-caused ionospheric disturbances, particularly in particle density and electric and magnetic fields in vicinity of artificial body 01 p0138 A66-10975

Electric field configuration in oversized rectangular waveguide excited by pyramidal transition and terminated by movable short circuit 01 p0046 A66-11078

Elliptical waveguide for H-11 modes transmittance, expressed as power transmission along waveguide and square of electric field maximum value 02 p0196 A66-11417

RF electric field in electron beam/plasma interaction measurement, using nonperturbing probing technique 02 p0265 A66-11432

Penetration of electric field into metallic sphere located in stationary plasma as prototype of electric fields about Earth-Sun system 02 p0267 A66-11656

Electrical conductivity of narrow energy band semiconductors as function of electric field strength 02 p0274 A66-11732

Oscillations of electron-ion plasma in external electric field assuming uniformly accelerated motion of plasma components 02 p0268 A66-11784

External electric field effects on volt-ampere characteristics and breakdown in p-n, p-n-p and p-n-p-n structures 02 p0277 A66-12090

Self-acceleration of ionizing particles in electric field of polarized ionization trail 02 p0270 A66-12279

Polarization effects in magnetic and nonmagnetic barium plus bismuth oxide and magnesium-zinc ferrites when subjected to DC low-voltage electric fields 03 p0409 A66-12690

Wave function, polarization and decay of negative ion atoms in electric field 03 p0395 A66-12833

Spatial distribution of HF electric field in resonant discharge determined, using electron beam probing technique 03 p0404 A66-12985

Electric field effect on light absorption by silicon throughout region of phonon-assisted indirect transitions 03 p0412 A66-13150

High electric fields effect on propagation of 24-GHz microwaves along surface on n-type indium antimonide 04 p0562 A66-13749

Vortical electric field effect on inhomogeneities spreading in weakly ionized plasma /ionosphere/ in magnetic field 04 p0577 A66-13842

Electric field effect on long wave edge of extrinsic photoconductivity in zinc and mercury doped germanium 04 p0565 A66-14266

Internal electric field induced by ionized particles and current carriers on impurity diffusion in semiconductors, noting diffusion and Poisson equation 04 p0568 A66-14349

Electrical conductivity of polar semiconductors in electric fields, calculating lattice and Coulomb electron scattering mechanism by kinetic equation method 04 p0568 A66-14350

Transmission of hole-type germanium in strong electric fields, noting spectral

dependences of radiation modulation and hole absorption cross section 04 p0568 A66-14352

Penetration of external longitudinal electric field into semibounded plasma containing electron beam in absence of instabilities in system 04 p0556 A66-14416

Effects of variable ionic mobility on current collection by cylindrical body and of fringing electric field on sheath size, noting role of diffusion phenomenon 05 p0722 A66-14724

Self-acceleration of ionizing particles in electric field of polarized ionization trail 05 p0727 A66-15458

Pressurizing thrust bearings through use of ions and high electric fields [ASME PAPER 65-WA/LUB-1] 05 p0689 A66-15525

Estimation in equilibrium state surface potential and distributions of electric potential field and electron density in vicinity of object moving in ionized medium 05 p0685 A66-15795

Time dependent theory of tunneling for semiconductor junction with inhomogeneous electric field 06 p0922 A66-16174

Response of plasma in magnetic field to electric field oscillating with frequencies higher than collision frequency 06 p0915 A66-16179

Gas adsorption on molecular sieves, discussing separation caused by electrostatic forces and electric fields 06 p0819 A66-16730

Measurement of exciton absorption of gallium selenide at low temperatures in presence of electric field, noting line broadening and no splitting 06 p0929 A66-16942

Built-in electric field effect on simultaneous diffusion of oppositely charged impurities in semiconductors 08 p1268 A66-18659

Paramagnetic resonance occurring in plasma located in external electric field, noting relation between oscillation amplitude and electron frequency 08 p1262 A66-18976

Electron distribution over energy level in valence semiconductor in presence of electric field 08 p1269 A66-18977

Lorentz force maximization in continuous-flow Hall current plasma accelerators, using either axial electric field and radial magnetic field or radial electric field and slanted magnetic field 08 p1263 A66-19154

Charge density distribution, electric field strength and flow rate of turbulent flow of incompressible fluid in flat nonconducting channel 08 p1263 A66-19172

Turbulent condition in plasma beam with virtual cathode characterized by electric field oscillation spectrum, off-center plasma torch spinning into ion side and ion acceleration 08 p1264 A66-19270

Interaction of drift oscillations in homogeneous weakly turbulent plasma which tends to develop flute instability along magnetic field 08 p1264 A66-19274

Two-port network representations derived for general linear magnetic and electric field transducers, showing energy conversion leading to nonlinear relationships and applications to DC motor 08 p1224 A66-19298

Photoadsorption effect on semiconductor surfaces determined as function of various parameters, noting role of external electric field 08 p1276 A66-19378

MHD models used for analysis of stability of nonhomogeneous magnetized plasma with regard to perturbations whose electrical field is calculated from potential 08 p1265 A66-19469

Interband Faraday effect in semiconductors in strong crossed electric and magnetic fields 08 p1277 A66-19619

Electroreflectance effect on gallium arsenide surfaces at various ranges of photon energies 08 p1279 A66-19838

Kinetic equation for fast electrons in plasma in stationary electric field, taking into account electron interaction 09 p1407 A66-19963

Fluctuation of electric field distributions within germanium sample when one contact of sample is used to inject holes 09 p1412 A66-19994

Effect of electric field and crystalline

dimensions on position of optical absorption edge in cadmium sulfide thin films obtained by vacuum deposition 09 p1412 A66-19995

Electric conductivity, electric field and space charge of atmosphere under fair weather or thunderstorms 09 p1371 A66-20275

Three-centimeter wavelength frequency multiplier using gas-discharge plasma in nonuniform electric field, examining amplitude and phase instability 09 p1358 A66-20793

N-type germanium electric conductivity dependence on applied electric and magnetic field 09 p1430 A66-20857

Amplification coefficient for weak electric field arising on surface of large body in ionosphere in absence of magnetic effect, photoeffect and secondary emission 09 p1465 A66-21019

Magnetic and electric field and current density distributions in propagating current sheet [AIAA PAPER 66-200] 10 p1563 A66-21442

Plasma density instability induced by electron-hole generation in impact ionization as affected by electric field 10 p1575 A66-21536

Local magnetic field, ion density flow and electric field in plasma measured downstream of theta-pinch accelerator in presence of uniform guide field [AIAA PAPER 66-155] 10 p1565 A66-21684

Boltzmann equation for Gunn effect in GaAs, discussing scattering processes, unjustifiability of use of drifted Maxwell distribution, etc 10 p1583 A66-22067

Current oscillations and microwave emission in indium antimonide subjected to high applied parallel electric and magnetic fields at 77 degrees K 10 p1585 A66-22082

Spiraling electrons in geomagnetic field and superimposed electric field aligned with magnetic field lines 11 p1695 A66-22371

Electron-phonon coupling in piezoelectric semiconductors, obtaining electric field and current density vectors for application to ultrasonic amplification 11 p1750 A66-22401

Effect of electric field on LF oscillations of nonhomogeneous plasma contained by magnetic field, using geometrical optics approximation 11 p1744 A66-22449

Ionization charge stage for spectral lines determined by sending particle beam through field which separates components of different net charge 11 p1739 A66-22949

Thermally grown silicon dioxide layers examined, noting ionic and structural changes induced by applied electric fields at different temperatures 11 p1756 A66-23023

Space radiation shielding for space vehicles using electric and magnetic fields 11 p1778 A66-23166

Low temperature chromatographic separation of hydrogen isotopes based on interaction with alumina surface electric fields 11 p1650 A66-23209

Electric polarization field components appearing in plasmoid moving in toroidal magnetic field 11 p1747 A66-23305

Electric polarization of plasmoid moving in curvilinear magnetic fields with different signs of curvature of lines of force 11 p1747 A66-23306

Spatial variation of electric field in amplifying CdS measured, using electro-optic effect to study acoustic flux from thermal noise 11 p1758 A66-23356

Constant electric field effect on transverse dielectric constant of semiconductor 12 p1926 A66-23714

Pressurizing thrust bearings through use of ions and high electric fields [ASME PAPER 65-WA/LUB-1] 12 p1888 A66-24546

Polarization of particle counters, noting distortion of internal fields through pre-irradiation spatial polarization 12 p1883 A66-24788

Exact mathematical solution for elastic dielectrics in controllable states, noting Rivlin and Toupin theory, cuboid deformation into rectangular block, electric field effect, etc 12 p1933 A66-24961

Electroreflectance effect on gallium arsenide surfaces, noting reflectance response upon electric field modulation 13 p2158 A66-25051



- HF and LF alternating electric fields effect on weakly ionized argon, temperature modulation and production of harmonics 13 p2141 A66-25447
- Gunn effect in gallium arsenide, noting negative differential electron mobility at high electric fields in conduction band 13 p2165 A66-25546
- Photo emf of gallium arsenide determined as function of temperature, light intensity, external electric field and surface quality 13 p2165 A66-25679
- Plasma stability with plane boundary, noting effect of perturbed electric field, particle trajectory and equilibrium distribution 13 p2144 A66-25726
- Spatial distribution of electrical field obtained by focusing radiation of ruby laser 13 p2092 A66-25967
- Nonlinear optical polarization of gases and liquids, stressing second degree contribution in macroscopic electric field 13 p2132 A66-26147
- Electric fields in hydrogen plasma leading to forbidden free-bound transitions, considering photodetachment of electrons and radiative capture cross sections 13 p2135 A66-26265
- Electric field force dragging of fine jets from surface of conducting fluid in form of cylinder and hemispheroid on earthed plate 13 p2129 A66-26301
- Spherical drop in electric field with equilibrium maintained through balance between electric stress and variable pressure difference between inside and outside of drop, existing only if outside and inside fluids are in motion 13 p2129 A66-26302
- Propagation of linear polarized electromagnetic waves through helium plasma along magnetic field, measuring phase and intensity of components of electric field 13 p2155 A66-26673
- Steady state motion of Couette plasma flow in electric field, assuming transfer of collective motion is effected by ions and heat transfer by electrons 14 p2339 A66-26774
- First-order formula for component of electric field very near surface and parallel to axis of perfectly conducting center-driven cylindrical antenna 14 p2247 A66-26864
- Electromagnetic wave scattering and depolarization from rough surface, noting existence of surface current vector component pointing in direction of incident wave 14 p2235 A66-27038
- Spontaneous LF current oscillations in germanium with copper, with compensated energy levels under illumination, low temperatures and electric fields, noting formation of electric domains 14 p2357 A66-27076
- Conformal transformation to determine electrical field of symmetrical air-filled strip line under static conditions 14 p2264 A66-27242
- Microwave radiation from inductive posts of indium antimonide in broadband spectrum occurring when placed in DC magnetic field and pulsed to average electric field, results suggest solid state plasma instabilities 14 p2363 A66-27517
- Surface charge of semiconductor in strong electric field, considering quantization 14 p2364 A66-27644
- Internal electric field induced by ionized particles and current carriers on impurity diffusion in semiconductors, noting diffusion and Poisson equation 14 p2368 A66-28246
- Electrical conductivity of polar semiconductors in electric fields, calculating lattice and Coulomb electron scattering mechanism by kinetic equation 14 p2368 A66-28247
- Transmission of hole-type germanium in strong electric fields, noting spectral dependences of radiation modulation and hole absorption cross section 14 p2368 A66-28250
- Field effect measurements in n-and p-type CdTe at room temperature and pressure 15 p2558 A66-28612
- High amplitude LF current and optical transmission oscillations in CdS single crystals under high electric field and monochromatic illumination near fundamental absorption edge 15 p2558 A66-28613
- Hot electron redistribution in multivalley conductors in electric fields, based on variation under pressure of valley population levels, using silicon samples 15 p2559 A66-28622
- High field properties of gold doped germanium at liquid nitrogen temperature 15 p2560 A66-28633
- Electric field in hot plasma waveguide with infinite magnetostatic field due to harmonically varying slot and double-grid excitation 15 p2549 A66-28712
- Perturbations caused by cylindrical body in plasma, obtaining electric field and electron and ion concentration dependences on distance 15 p2595 A66-29086
- Satellite observations of primary cosmic rays compared with predictions of solar wind and electric field models of long-term intensity modulation 15 p2576 A66-29233
- Gallium arsenide absorption edge dependence on strong electric fields 16 p2769 A66-30166
- HF instabilities in plasma situated in superimposed magnetic and radial electric fields 16 p2758 A66-30293
- Ion beam velocity measurement, using radial electric and tangential magnetic field 16 p2701 A66-30347
- Absorption coefficient change due to electric field measured for indirect absorption edges of silicon and germanium, determining energies of phonons taking part in indirect optical absorption 16 p2775 A66-30728
- Model potential consisting of Coulomb potential and linear terms in electric field potential, obtaining eigenfunctions of model and deriving optical absorption coefficient for electric field excitons 16 p2775 A66-30729
- Lattice distortions and field gradients in alkali halide solutions, noting discrepancy in calculation of electric field gradients 16 p2775 A66-30731
- Change in reflectance of semiconductor induced by electric field at approximately photon energies of interband transitions 16 p2776 A66-30734
- Intrinsic electric field of rarefied ion-electron plasma in external magnetic field and plasma stability, noting use of Galerkin method to determine plasma layer slippage 16 p2760 A66-30790
- Pulse field effect technique investigation of electrical properties of surface states on practical Si surfaces with various surface 16 p2781 A66-31356
- Space charge formation and decay during passage of electric current through plasma moving in electric field, obtaining V-I characteristics 16 p2766 A66-31598
- Oxide film thickness effect on field effect silicon, noting concentration of surface electron states 16 p2787 A66-31735
- Electric field dependence of piezoresistance in germanium, noting correlation with intervalley scattering in energy balance 16 p2788 A66-31778
- Spatial periodic modulation of high field domain in cadmium sulfide 17 p2974 A66-31813
- Electric field effect for free carrier absorption, determining coefficient for acoustic phonon scattering 17 p2976 A66-32264
- Magnetoresistance effect in semiconductors applied to microwave power measurement, noting multiplying action between electric and magnetic field components of wave 17 p2885 A66-32288
- Computer-derived contour plots of electric and magnetic fields for acoustic electromagnet plane wave pulse incident on wedge 17 p2875 A66-32390
- Plasma wave quasi-linear theory, noting nonlinear effect treatment via distribution function, electric field, Fourier component decay, etc 17 p2966 A66-32422
- Gravitational instability of magnetoplasma in radial electric field, noting resistive drift modes, stabilization criterion effect of Coriolis force, Landau damping, etc 17 p2966 A66-32425
- Electron velocity distribution in ionized gas under alternating electric field as function of density, temperature, etc, including effects of recombination, ionization, etc 17 p2960 A66-32426
- Plasma heating rate in stochastic electric fields determined, using nonrelativistic collisionless lossless test particle 17 p2967 A66-32436
- Electric field influence on thin metal film growth inducing coalescence of three-dimensional island-like structure 17 p2979 A66-32632
- Stability of weakly ionized plasma in strong electric field against formation of longitudinal waves, examining hydrodynamic equations 17 p2970 A66-32715
- Sinusoidally varying HF electric field effect on glow discharge plasma, showing capability of confinement 17 p2971 A66-32785
- Longitudinal electric field effect on redistribution of emitting particles in combustion front of plane methane-air flame 17 p2870 A66-32828
- Ambipolar potential in magnetoactive cold plasma applied to power generation and effects of electric field on diffusion coefficient 17 p2973 A66-32984
- Interband Faraday effect in semiconductors in strong crossed electric and magnetic fields 17 p2983 A66-33133
- Surface characteristics of semiconductors with intrinsic conductivity, determining potential distribution electric field, carrier concentrations, etc 17 p2984 A66-33146
- Impurity concentration and electric field distribution determined in drift region of silicon p-n detectors from capacity as function of reverse voltage 17 p2986 A66-33303
- Current instability of plasma injected into germanium, noting effect of strong electric field in presence of temperature gradient 17 p2987 A66-33313
- Gas-phase heat-transfer augmentation by steady and alternating electric field in pipeflow 17 p3039 A66-33473
- Nonlinear generation of combination frequencies due to strong uniform parallel electric fields in homogeneous plasma 18 p3142 A66-33918
- X-ray irradiated MOS structure behavior, noting ionic charge motion in oxidized silicon that depends on electric field 18 p3155 A66-34083
- Ionization probability of bound state of atoms in variable electric field 18 p3140 A66-34690
- Cosmic ray intensity attenuation due to energy loss of particles passing through electric field in solar system 18 p3180 A66-34773
- Plasma instability in HF electric and constant magnetic field for sufficiently low pressure 18 p3151 A66-35067
- Operation of electron image time dissector framing camera achieving time resolution by multiple reflection in crossed magnetic and electric fields in electron image storage device 19 p3353 A66-35313
- Spatial distribution of acoustoelectric field in photoconductive CdS measurement under conditions of current saturation, determining carrier drift mobility 19 p3435 A66-35415
- Semiconductor cyclotron resonance during application of constant electric field, determining carrier distribution function 19 p3437 A66-35460
- Resonant birefringence in potassium vapor under influence of electric field of ruby laser emission 19 p3375 A66-36066
- Weak field effective mass approximation calculations of absorption coefficient in presence of electric field for transitions at normal threshold extended to arbitrary orientation of electric field in solid 19 p3447 A66-36397
- Plasma oscillation and stability in HF external electric field 19 p3417 A66-36531
- Production of hot plasma by Penning discharge in inhomogeneous magnetic field accelerating ions to high energy level by strong electric field 19 p3431 A66-36592
- Wave function, polarization and decay of negative ion atoms in electric field 19 p3404 A66-36775
- Electric field in MHD channels in presence of near-electrode potential drop 19 p3433 A66-36828
- Splitting of EPR lines of trivalent Cr ion in zinc tungstate by external electric field,



noting angular dependence and corresponding spin 20 p3615 A66-37370

Hamiltonians 20 p3615 A66-37370

Electric field in MHD generator channel under mixed boundary conditions solved by Wiener-Hopf technique, evaluating ohmic losses 20 p3500 A66-37491

Spherical coupler for fastening mirrors and plane-parallel plates at Brewster angle in gas laser 20 p3578 A66-37523

Stabilization criteria for drift instabilities in inhomogeneous plasma with external electric field derived from drift wave frequency variation 20 p3612 A66-38430

Electric field effect on donors diffusion into intrinsic semiconductor 21 p3799 A66-38927

Stabilization criteria for drift instabilities in inhomogeneous plasma with external electric field derived from drift wave frequency variation 21 p3777 A66-38963

Electric field distribution in plane-parallel layer of electron-ion plasma situated in external electric field normal to walls, deriving energy losses by kinetic theory 21 p3782 A66-39020

Longitudinal and transverse electric fields in electron beam due to interaction with plasma, showing that both fields are components of same wave 21 p3782 A66-39020

Electric field intensity of helium and argon arc column as affected by pressure and current intensity 21 p3783 A66-39021

Externally imposed oscillating electric field excites transverse electromagnetic waves propagating perpendicular to it in cold plasma 21 p3791 A66-39176

Plasma instability in HF electric field perpendicular to given magnetic field under low pressures 22 p3952 A66-39754

Equations for ionized positive plasma column of gas discharge between infinite dielectric planes under oblique magnetic field with component in direction of external electric field 22 p3953 A66-39756

Three-centimeter wavelength frequency multiplier using gas-discharge plasma in nonuniform electric field, examining amplitude and phase instability 22 p3874 A66-39852

VLF electric fields in magnetosphere surveyed with polar orbiting spacecraft 1964-45A may produce large amplitude plasma oscillations 22 p3903 A66-39937

Electric field domain motion in Ge samples with Au and Sb impurities, noting temperature and illumination effect on V-I characteristics 22 p3964 A66-40312

Infinite plate consisting of monopolar semiconductor of given thickness under effect of electric field results in change in galvanomagnetic, piezoresistance and optical properties 22 p3965 A66-40317

Spontaneous LF current oscillations in germanium with copper, with compensated energy levels under illumination, low temperatures and electric fields, noting formation of electric domains 22 p3966 A66-40833

Steady state behavior of free steadily traveling electrical domain in gallium arsenide 22 p3967 A66-40864

Parallel and transverse magnetic field effects on electric field induced optical absorption at photon energies below direct gap in Ge 23 p4109 A66-41036

Large-signal AC field effect experiments with A and B real surfaces of indium antimonide exposed to various chemical reactions and high electric field described by tunnel equation 23 p4111 A66-41185

Domain propagation with velocity of sound from negative to positive electrodes in GaAs single crystal rods under acoustoelectric oscillation 23 p4112 A66-41297

Electric microfields in plasma taken as system of charged particles moving in uniform neutralizing background, using approximations and Monte Carlo study 23 p4101 A66-41363

Electric field normally incident onto warm semimfinite plasma obtained by Wiener-Hopf technique and Vlasov equation 23 p4103 A66-41492

Quasi-linear approximation for turbulent plasma obtained via Wiener-Hermite functional expansion for electric field and

distribution function 23 p4104 A66-41504

Semiconductor conductivity in strong SHF electric fields, measuring dielectric constant and Fourier component 23 p4068 A66-41620

Constant voltage avalanche breakdown state of gallium arsenide diodes after switching attributed to peak in hole generation rate 23 p4047 A66-41623

Potential oscillations in neutral completely ionized plasma-neutral charged-particle beam system in HF electric field and growth rate of plasma instability 23 p4106 A66-41707

Electric field effects on collision efficiency of charged cloud droplets 23 p4065 A66-41846

Boundary layer control of conducting fluid by transverse magnetic field and spanwise electric field 23 p4107 A66-41904

Drop bursting by surface forces such as electric fields and fluid environments with larger viscosity 23 p4060 A66-42018

Spectral energy density of turbulent plasma determined from spatial autocorrelation functions of electric fields of HF oscillations 24 p4240 A66-42132

Surface pinned layer-like field inhomogeneities in cadmium sulfide, investigating visibility of field layer by corresponding shift of absorption edge, using Franz-Keldysh effect 24 p4254 A66-42427

Nonlinear dependence of current in electric field in thin semiconductor film in quantizing magnetic field 24 p4256 A66-42525

Mode coupling in ruby laser with reactance placed within cavity resonator with modulation frequency close to separation of axial modes, examining electric field envelope 24 p4223 A66-42565

**ELECTRIC FIELD STRENGTH**

Electric field intensity in disturbed quasi-neutral plasma homogeneity when problem is formulated as one-dimensional 01 p0115 A66-11107

Semiconductor devices at high injection levels, discussing electric fields and potential distribution in multilayer structures 04 p0495 A66-13769

Electron collision-ionization avalanches in cadmium sulfide crystal due to electric field intensities 04 p0570 A66-14489

One-dimensional plasma flow in crossed electric and magnetic fields covering subsonic, transonic and supersonic flow 05 p0720 A66-14508

Splitting of electron paramagnetic resonance lines of zinc-tungstate crystals, discussing parameters and experimental technique 05 p0738 A66-15356

Magnetic particle motion, analyzing effect of Earth electric dipole field 05 p0752 A66-15387

Opposed jet diffusion flames subjected to electrostatic fields, estimating volumetric heat release rate and mass flow behavior [ASME PAPER 65-WA/ENER-3] 05 p0789 A66-15628

Electric field effect on optical absorption edge, discussing exponential tail influence on magnitude of absorption coefficient 05 p0741 A66-15869

Hydrogen molecule multiphoton ionization, determining probability of absorption, effected by ruby laser emission 06 p0891 A66-16517

Longitudinal and transverse voltages in superconductors, noting Hall effect, resistivity and functional relation to applied magnetic field 06 p0940 A66-17162

Variation spectrum stability of Forbush decrease and small cosmic ray flare during intensity recovery, noting electric field effect, calculation methods, etc 07 p1129 A66-18023

Microwave emission from InSb, measuring energy generated at low temperatures and intense electric and magnetic fields 07 p1103 A66-18218

Instabilities of current and potential distribution in n-type GaAs and InP in electric field of several thousand v/cm 07 p1104 A66-18221

Antenna radiation shows relationship to tangential component of electric field intensity along antenna 08 p1197 A66-19606

Electric field meter /E-meter/ measurement of field strength at given point on spacecraft surface [AIAA PAPER 66-74] 08 p1227 A66-19726

Hydrogen molecule multiphoton ionization, determining probability of absorption, effected by ruby laser emission 09 p1387 A66-20898

Electric field intensity and plasma perturbation near charged infinite cylindrical body 09 p1465 A66-21018

Gradient instability of galvanomagnetic and galvanomagnetoacoustic waves in electrical fields 10 p1587 A66-22156

Field effect theory in semiconductors with capture centers, noting basic equation, quadrature expressions, etc 11 p1751 A66-22732

Uniform electric field meters for measurement at Earth surface and on aircraft and satellites 12 p1915 A66-24647

Plasma stability analysis, discussing low density fluid equations, variational principle and sufficiency condition at moderate densities, electric field effect, etc 15 p2554 A66-29746

Excitation and thermalization of plasma oscillations in stellarator 16 p2758 A66-30292

Opposed jet diffusion flames subjected to electrostatic fields, estimating volumetric heat release rate and mass flow behavior [ASME PAPER 65-WA/ENER-3] 16 p2825 A66-30341

Electric field distribution in gas discharge counters at moment radiation recorded, allowing for space charge effect 17 p2928 A66-33490

Gradient instability of galvanomagnetic and galvanomagnetoacoustic waves in electrical fields 19 p3440 A66-35770

Lightning flash mechanisms and electric field strengths in clouds 21 p3759 A66-38533

Field effect theory in semiconductors with capture centers, noting basic equation, quadrature expressions, etc 23 p4113 A66-41470

Graphical comparison of military RF interference specification limits based on electric field intensity at one meter antenna spacing 24 p4176 A66-43192

**ELECTRIC GROUNDING**

Destructive grounding system fault currents and abortive interference and elimination, using functional diagrams 20 p3542 A66-37241

**ELECTRIC IMPEDANCE**

Impedance behavior and frequency dependence of radiation pattern of wideband sheet antenna 01 p0036 A66-10366

Admittance of rectangular waveguide radiating into compressible plasma 01 p0038 A66-10517

Surface impedance of ferromagnetic metals at frequencies approaching ferromagnetic resonance, considering spatial dispersion of magnetic permeability 01 p0123 A66-10721

Surface impedance of nonhomogeneous plasma with sharply varying parameters, noting skin effect and permittivity gradient 02 p0192 A66-11840

Evaluation of AC small signal impedance of semiconductor surfaces in connection with physics of MOS structures 03 p0408 A66-12443

Impedance matrix of single three-pole and two-stage amplifier determined by Kron method 03 p0348 A66-12497

Tunable calibrated impedance for measurement of unknown terminations in millimeter range and based on reflection coefficient adjustments 03 p0371 A66-13242

Impedance cavity on radiation resistance of electromagnetic source 04 p0497 A66-13915

Impedance of dielectric oxide with uniformly distributed monoenergetic traps 04 p0501 A66-14253

Enhancement of radar cross section of cylinder by impedance loading, with determination of optimum impedance 05 p0631 A66-14636

Varactor evaluation using series resonance and determination of impedance locus of coaxially mounted varactors 07 p1008 A66-17513

Electromagnetic conductivity of superconducting alloys in critical regions in high magnetic fields 07 p1108 A66-18435

Dielectric loaded waveguides, defining surface, transverse and longitudinal impedances in analogy with circuit theory definition 08 p1200 A66-19121

Electron transit time and impedance



- relation in rarefied plasma diode, considering electron and ion velocity dragging 08 p1193 A66-19193
- Magnetic field dependence of microwave surface impedance of superconducting aluminum 09 p1416 A66-20024
- Integral equation method solution of scattering from cylinders with arbitrarily varying anisotropic surface impedance 10 p1497 A66-21591
- Electromagnetic scattering from conducting object controlled by loading portions of surface with impedances, distributed or lumped 10 p1499 A66-21610
- Filter with two tuned circuits and distributed coupling based on equations for complex values of tuned circuit currents, noting formulas for mutual impedance 10 p1510 A66-21673
- Impedance of finite slot 10 p1505 A66-21912
- Location of poles and zeros of small-signal RF impedance function of Read diode and how they affect oscillation and current tunability 10 p1516 A66-22100
- Coupling impedance of thin hollow electron beam injected into magnetic field and tripping at cyclotron frequency in cylindrical waveguide carrying E01 mode 11 p1661 A66-22395
- Geometrical theory of diffraction applied to calculation of radiation pattern and impedance of monopole antenna 11 p1663 A66-22545
- Minor lobe suppression in rectangular horn antenna through utilization of high impedance choke flange 11 p1663 A66-22556
- Ten-element band pass filter section and derivatives with classification of image-impedance functions 11 p1669 A66-23113
- Impedance of distributed surface states in MOS structures as function of frequency and bias, noting charge carrier exchange 11 p1757 A66-23206
- Reactance of gallium arsenide bulk oscillator in oscillating state, plotting values together with capacitance 12 p1835 A66-24140
- Explicit relation between mutual coupling and radiation pattern of array antenna evaluated via scattering formalism, based on spherical modes 12 p1841 A66-24627
- Approximate theory for lumped impedance loaded traveling wave linear antenna, considering possibility of nondissipative loading 12 p1841 A66-24631
- Circuit design for high impedance amplifier for control systems, considering input and output impedance and amplifier gain 12 p1844 A66-24731
- Terminal properties of Alfvén waveguides, deriving electrical input impedance of set of coaxial excitor electrodes 13 p2137 A66-25046
- Small-signal impedance of transferred-electron diodes, stable against domain formation 13 p2030 A66-25212
- Design and integrated circuit fabrication of negative impedance converter, using two transistors and two resistors 13 p2036 A66-25523
- Outer and inner bounds on driving-point impedance functions of LLFP networks with various resistance and reactance configurations 13 p2055 A66-26095
- Electromagnetic scattering by circular wire loops loaded with lumped impedances, obtaining solution to integral equation by Fourier series 14 p2247 A66-26863
- Fan-out filters giving flat response over broad bandwidths and minimization of variation of input impedance with frequency 14 p2249 A66-27106
- Characteristic admittances of comb-type and undulating waveguide filters, considering diaphragm thickness and TE propagation mode 14 p2250 A66-27147
- Inductive impedance of dynistor and relationship to positive and negative differential resistance of V-I characteristics 14 p2254 A66-27742
- Impedance integral evaluation for antenna loop immersed in conducting medium 14 p2256 A66-27923
- Mutual impedance between two rectilinear and parallel top-loaded elements of directional antenna when elements have nonzero current at ends 14 p2257 A66-27924
- Impedance transforming compensated balance to unbalanced line transformer /balun/, discussing bandwidths 14 p2258 A66-27959
- Input and output impedances and gain of hybrid-coil feedback amplifier 14 p2268 A66-28038
- High impedances obtained over wide frequency range with bipolar or unipolar transistors, noting current multiplication, bootstrapping, etc., and FET 14 p2262 A66-28377
- Input impedance of small loop of uniform electric current immersed in anisotropic cold magnetoplasma calculated by induced emf method 15 p2548 A66-28593
- Ferrite-air interface in waveguide with conducting thin film coated core solved by use of boundary condition or impedance condition 15 p2565 A66-29053
- Frequency transformations used in derivation of positive real and biquadratic immittance functions in three groups consisting of equivalent circuits 17 p2899 A66-32051
- Integral equations of current derived for TM and TE waves in excited inhomogeneous impedance band in half-plane 17 p2885 A66-32246
- Two-dimensional excitation problem of circular cylinder with surface impedance varying over cylinder circumference 17 p2874 A66-32247
- VLF dipole antenna impedance values, magnetoionic and collision effects in ionospheric magnetoplasma 17 p2874 A66-32386
- Electrophysiological patterns and cerebral impedance characteristics in orienting and discriminative behavior 17 p2860 A66-32832
- Admittance problem of cylindrical antenna in homogeneous anisotropic medium formulated and analyzed, using Fourier transforms and Wiener-Hopf technique 17 p2897 A66-33428
- Self and mutual admittance of coupled dipoles in dissipative medium 18 p3065 A66-33529
- End-fire radar echo of long thin body minimized by impedance loading technique 18 p3065 A66-33535
- Experiments of internal impedance of MHD generator show wide range of working conditions as slowly varying function of applied current 18 p3053 A66-34112
- Topological formulae for sensitivity coefficients of three-terminal-pair-network functions derived by dual procedure in terms of impedance 19 p3328 A66-36020
- Radiated fields for plasma external to dielectric coating surrounding biconical antenna, equivalent circuit developed for terminating impedance 19 p3305 A66-36422
- Attenuation, guide wavelength and characteristic impedance of rectangular waveguides with indium antimonide side wall derived for propagating modes 20 p3524 A66-37113
- Jet aircraft electric power system performance affected by transmission line impedances 20 p3499 A66-37191
- Domain velocity, stability and impedance in Gunn effect, presenting framework for analyzing space-charge waves in two-valley semiconductor 20 p3618 A66-37599
- Surface impedance of ferromagnetic metals at frequencies approaching ferromagnetic resonance, considering spatial dispersion of magnetic permeability 20 p3619 A66-37659
- Input admittance, gain and noise performance in dipole antennas with Esaki diodes 20 p3531 A66-37731
- Impedance cavity on radiation resistance of electromagnetic source 20 p3532 A66-37873
- High input impedance fluid amplifier noting electric and fluid analogs, fluid triode and mathematical model of fluid FET 21 p3697 A66-38595
- Negative resistance phenomena in metal oxide semiconductor /MOS/ diodes made from degenerate silicon substrate observed in course of investigating electrical characteristics 21 p3712 A66-39223
- Generalized method of calculating multielement antenna and feeder system 21 p3712 A66-39250
- High impedance electrode technique for large-scale flight physiological data collection, emphasizing skin preparation 22 p3856 A66-39790
- Scattering parameters for design of HF transistor circuits 22 p3877 A66-40334
- Antenna in interplanetary plasma, noting fluctuation noise in exosphere and radiation impedance when exposed to solar wind 22 p3877 A66-40466
- Impedance of flat strip antenna embedded in planar dielectric slab surrounded by layers of compressible isotropic electron plasma 23 p4047 A66-41639
- Discontinuity gas model for high pressure plasmas and application to DC confined arc and AC impedance 23 p4108 A66-42032
- Self-impedance of electric dipole immersed in plasma half-space with finite temperature 24 p4243 A66-42625
- Electric impedance measurements in hippocampus, amygdala and midbrain reticular formation during altering, orienting and discriminative responses in cat 24 p4166 A66-43167
- ELECTRIC IMPULSE**
- Impulses originating in dendrite region in most dorsal part of dorsal horn, noting correlation between membrane potential and cell firing rate 12 p1805 A66-23567
- ELECTRIC INSULATION**
- SA DIELECTRICS**
- Thin film epitaxial single crystal silicon on insulating substrate sapphire and advantages of these microelectronic devices 01 p0048 A66-11145
- Single crystal silicon films on sapphire in terms of materials properties and impact on thin film semiconductor microelectronics 01 p0048 A66-11146
- Electronic insulation - IEEE Conference, New York, September 1965 02 p0247 A66-11284
- Space environment factors in designing electrical insulation systems for space vehicles 02 p0247 A66-11290
- Simulated space environment effects on performance of silicone insulating materials 02 p0247 A66-11291
- Rigid polyurethane foam encapsulation of high-voltage aerospace electronic systems, noting vacuum effect 02 p0248 A66-11292
- Simulated nuclear power plant gamma radiation effects on magnetic film-insulated magnetic wire 02 p0248 A66-11293
- Strain gauge sensing element readiness for use dependent upon quality of base characterized by value of insulation resistance 02 p0231 A66-12000
- High temperature insulating adhesives for vacuum applications tested, including outgassing rate, mass spectra of evolved gases, electrical and mechanical properties 17 p2942 A66-31980
- High temperature, electrically insulating refractory tubes of boron carbonitride for protection of metal thermocouples 17 p2944 A66-33144
- Prebreakdown currents, conditioning rates and ultimate voltage capability of vacuum gaps and solid insulation, analyzing data on large-gap concentric cylinder configuration 23 p4042 A66-41041
- Environmental testing and evaluation of useful life of insulation material for aircraft electrical equipment operating at 280 degrees C 24 p4229 A66-43083
- ELECTRIC LEAD**
- Induction in cylinder by field of current-carry leads, calculating input parameters and ponderomotive force 03 p0396 A66-12285
- Microparallel gap welding approach for bonding fine leads to thin films 13 p2040 A66-25842
- ELECTRIC MEASUREMENT**
- SA MAGNETIC MEASUREMENT**
- Nonstationary processes measurement method in semiconductor devices by linear electron accelerator 01 p0035 A66-10189
- Microwave permeability and permittivity measurement, knowing resonant frequency of unperturbed cavity and distribution of electric and magnetic field 01 p0025 A66-10527
- Measuring equivalent circuit parameters of tunnel diode by method which forward-biased junction to valley voltage point 02 p0195 A66-11368
- Measuring properties of semiconductor grade materials, particularly resistivity, compensation and minority carrier lifetime 02 p0229 A66-11766



Multiplex measuring device and choice of analog or digital computers in electronic measurement 02 p0230 A66-11792

Measuring circuit and functional components in modern electronic measuring technique 02 p0230 A66-11793

AC technique for Hall effect measurement in low mobility semiconductor 03 p0371 A66-13249

Effective thickness of plasma sheath at cold electrode determined from electrode-plasma system capacitance 03 p0406 A66-13281

Basic techniques for measuring macroscopic plasma properties 04 p0521 A66-14189

Electric and electrostatic probes for plasma measurement 04 p0522 A66-14191

Measurement of diffusion length of excess minority carriers in semiconductors in region where carriers are generated 06 p0924 A66-16506

Reaction cavity method of measuring low-resistance semiconductors in which entire end wall of cylinder is replaced by sample being measured 06 p0881 A66-16642

Skin effect in semiconducting cylinder analyzed for electric and magnetic cases 07 p1001 A66-17350

Space-charge-limited currents and electron traps in CdS crystals thermally stimulated after electron injection 07 p1097 A66-17738

International coordination and standardization of HF quantity measurements, considering economic, psychologic and accuracy benefits 07 p1002 A66-18224

Miniature Rogowski coil probes for direct measurement of current density distributions in transient plasmas 07 p1037 A66-18494

Induction method for measuring electrical conductivity of steady plasma flow 08 p1262 A66-18858

High impedance semiconductor DC amplifier for use as measuring amplifier or operational amplifier 08 p1194 A66-19279

Hall effect measured by splitting alternating voltage produced in Hall circuit into two components, one with phase coinciding with Hall emf and other with phase departing by 90 degrees 08 p1273 A66-19289

Electric field meter /E-meter/ measurement of field strength at given point on spacecraft surface [AIAA PAPER 66-74] 08 p1227 A66-19726

Measurement of nonelectrical quantities with aid of transducers and representation of process by action diagrams 10 p1535 A66-21336

Contactless AC method for measuring small variations in resistance of highly conducting materials /zinc/ 10 p1536 A66-21703

Single probe method for measuring semiconductor resistivity, using alternating current, noting tests with germanium and silicon samples 11 p1705 A66-22598

Length changes and conductivity variations in electron irradiated n-and p-type germanium, noting methods of measurement, effects of isochronic annealing at liquid helium and nitrogen temperatures 12 p1926 A66-23717

Load capacitance method for measurement of quartz crystal parameters 12 p1845 A66-24855

Capacitance transducer characteristics and applications as fuel gauge, level detector, interface detector, pressure and proximity sensors, etc 13 p2078 A66-25360

Semiconductor diode and transistor application to various current and voltage measurement techniques 13 p2079 A66-25894

Probe measurement theory for determining thin semiconductor film electrical conductivity 13 p2168 A66-25945

Book on measurement of specific electronic parameters in circuit design 13 p2042 A66-26121

Accuracy of test device determining conductivity of semiconductor materials increased by using error calculation and design systematology 13 p2085 A66-26761

Dielectric constant of gold-plated rectangular parallelepiped solid at hyperfrequencies determined via resonant

frequency method 14 p2366 A66-27944

Semiconductor properties measurement using resonator with slit 15 p2560 A66-28639

Measuring modulus and phase angle of transistor current gain 15 p2464 A66-29058

Intermodulation effect on measurement of small Hall coefficients with double AC method 16 p2702 A66-30424

Direct measurement procedure for Hall emf semiconductor samples of circular shape 16 p2777 A66-30868

Bridge, transmission and microwave coaxial line measurement methods for evaluating high cut-off frequency varactor diode equivalent circuit 17 p2892 A66-32915

Bridge, transmission and microwave coaxial line measurement methods for evaluating high cut-off frequency varactor diode equivalent circuit 18 p3074 A66-33563

Electrical measurements of stannic oxide in ceramic form, noting forming and firing of samples, dielectric dispersion, grain boundary capacitances, etc 18 p3155 A66-34197

Capacitance transducer for measuring capacitance ratios with minimum environmental problems, noting wide application range 19 p3355 A66-35470

Dynamic resistance and derivative of superconducting tunnel junction measured by combined harmonic detection and bridge techniques 21 p3793 A66-39384

Departure phenomena of pointer type moving-coil instrument for electrical measurement with capability of torsional vibrations 23 p4071 A66-41952

Current measuring device for EHV transmission line, obtaining instantaneous magnetic field by gauging Faraday rotation angle of laser beam in flint glass rod 24 p4222 A66-42556

## ELECTRIC MOTOR

Western Electronic Show and Convention, San Francisco, August 1965, Part 3, Power electronics 02 p0179 A66-11276

Desireability of brushless DC motor when minimum size, weight, maintenance, explosive hazard and power consumption is required 02 p0179 A66-11277

Electrostatic hysteresis synchronous motor discussing development, operation characteristics, test results, advantages and limitations 04 p0459 A66-13681

Brushless induction hysteresis motor for extreme environments 07 p0991 A66-17849

Cavitation induced between rotating and stationary cylinder in vaporizing liquid within gap of simulated electric motor configuration 07 p1039 A66-18176

Two-port network representations derived for general linear magnetic and electric field transducers, showing energy conversion leading to nonlinear relationships and applications to DC motor 08 p1224 A66-19298

Motor controllers for DC current supply must be inverters of constant or variable frequency 08 p1168 A66-19299

Electronically switched DC motor commutated by light beam directed onto photodiodes 11 p1640 A66-23167

Brushless motors of various types described and compared in order of increasing cost and complexity for spacecraft application 11 p1640 A66-23174

High voltage DC brushless torpedo propulsion motor using sea water as power return and controlled by thyristors 12 p1804 A66-24660

Three-phase half-wave inverter circuit consisting of ring of three SCRs and converting DC into AC power supplied into zigzag motor load 12 p1804 A66-24662

Contactless machine with variable current and dual power supply operating with variable rotation rate, determining optimum limits of rotation speed variation 16 p2636 A66-30780

Electric or hydraulic drives for steerable satellite trackers and heightfinder radars 18 p3055 A66-34317

DC motor without commutator, run by rectified RF energy from antenna pickup probe inside waveguide 24 p4162 A66-42947

## ELECTRIC NETWORK

## SA RC NETWORK

## SA TRANSMISSION LINE

Automatic gain control circuits, discussing performance and comparing theoretical and

experimental results 04 p0501 A66-14409

Correcting network with nonlinear inductance for high voltage pulse generator noting operation, design and fabrication 08 p1194 A66-19283

Combinatorial problems in theory of application of graphs to networks, primarily trees of ladder 08 p1202 A66-19725

Circuit conveying continuously variable signals between points with large steady potential differences, having commercial resistors and capacitors and no RF coil 09 p1363 A66-20665

Automatic time-domain equalizer consisting of delay line with adjustable taps 10 p1503 A66-21649

Nonlinear circuit theory, discussing invariant imbedding, dynamic programming and quasi-linearization 11 p1675 A66-22629

Electric circuit equivalent to metal-oxide semiconductor structure 13 p2031 A66-25480

Book on electric network theory, functions and filters 14 p2263 A66-26960

Smoothing of stationary random noise by discrete smoothing network, analyzing conditions for discrete white noise, harmonic noise, etc 14 p2264 A66-27359

Transverse equalizer for reduction of time sidelobes /residues/ in phase-coded pulse compression systems 15 p2463 A66-29039

Parallel-filter automatic random equalizer for improved vibration testing 16 p2679 A66-30478

Results derived from dissipative four-terminal networks applied to varactor converter, leading to capacitance variations determination as function of polarizing potential 16 p2662 A66-30961

Computer analysis of interference in complex network resulting from common impedance coupling of signals 20 p3538 A66-37196

Continuous group and infinitesimal transformation in linear dynamic system application, considering linear network 20 p3539 A66-38148

Theoretical interpretation of expansions in nonzero determinants formed from vertex and circuit matrices 20 p3539 A66-38283

## ELECTRIC POTENTIAL

## SA BIOELECTRIC POTENTIAL

## SA VOLTAGE

Stationary germanium potentials in oxidizing media and light illumination 09 p1410 A66-19895

Electric potential and space charge density near Langmuir probe in hot rarefied plasma at rest, calculating current collected from plasma 16 p2759 A66-30372

Hill climbing in self-optimizing control systems, noting effect of sinusoidal perturbation, application, etc 16 p2671 A66-31059

Space nuclear reactor induction of positive potential and remedy by ambient plasma or positive-ion source 19 p3398 A66-35493

Optimization of MHD generating duct by varying cross-sectional area and electrical loading 19 p3281 A66-36372

Method for calculating distribution of electric potential above conducting media with parallel interfaces for general case of n layers and arbitrary resistivities of base 20 p3551 A66-37512

Electric potential method used to study slow crack growth in center-notched plate specimens 20 p3670 A66-37794

Potentials for cylindrical warm plasmas, noting anisotropic effects caused by external magnetic field 20 p3611 A66-38362

Photoresponse measurements of depletion capacitance and diffusion potential of GaP Schottky-Barrier diodes 20 p3534 A66-38390

Effectiveness parameters of spherical shield electrode surrounding negative dielectric junction of insulator in high vacuum 23 p4042 A66-41040

Spatial distributions of carrier concentration and internal field in cadmium selenide for various voltages, measuring conductivity and Hall coefficient 23 p4112 A66-41292

Oxygen electrolytic reduction using porous sintered silver electrode, noting effects of gas pressure, current and cathode thickness on potential as applied to fuel cells 24 p4161 A66-42333

Transmission coefficient and tunnel



current for trapezoidal potential barrier calculated as function of applied voltage 24 p4254 A66-42385

**ELECTRIC POWER CONVERSION**  
**SA MAGNETOHYDRODYNAMIC GENERATOR**  
 Electric power of thermionic converters, discussing electron space charge effects and relation to gas converters 05 p0615 A66-15534  
 Emitter of thermionic converter with cesium plasma heated by solar energy, determining electric power values 05 p0623 A66-15595  
 Electric power plant survey for space application, noting Rankine and Brayton cycles 10 p1485 A66-21464  
 Electrical output and conversion cycle efficiency of vortex type MHD induction generator, considering viscosity effects 13 p2156 A66-26708  
 Reservoirless thermionic energy converter developed for obtaining large quantity of electrical power in space [AIAA PAPER 65-472] 19 p3280 A66-35623  
 Ultrasonic welding uses electric power of electronic generator applied to piezomagnetic transducer for converting AC electric power into mechanical vibration 19 p3372 A66-36819  
 Electric power generator selection for Mars probe/lander 23 p4020 A66-41748  
 Isotope and solar thermoelectric generator, solar cell and battery electric power sources for unmanned scientific exploration of solar system 24 p4162 A66-42681

**ELECTRIC PROPERTY**  
**SA CAPACITANCE**  
**SA CONDUCTIVITY**  
**SA HYSTERESIS**  
**SA IMPEDANCE**  
**SA INDUCTANCE**  
**SA MAGNETIC PROPERTY**  
**SA RESISTANCE**  
 Electric properties of titanium carbide as function of number of vacancies in carbon sublattice 01 p0126 A66-10783  
 Electrical and electroluminescent properties of gallium arsenide diodes with high resistivity region flanked by low resistivity R and N regions 01 p0043 A66-10896  
 Temperature dependence of electric conductivity and Hall effect of single crystal cadmium tin arsenide 01 p0126 A66-11026  
 Electrical properties of copper diffused p-type indium antimonide 01 p0127 A66-11030  
 Transistorized LF amplifier design, determining transistor nonlinearity coefficients 02 p0199 A66-11755  
 Current gain and transconductance of silicon planar transistor for collector currents used in design of DC amplifiers 02 p0200 A66-11886  
 Electric properties of n-type GaAs after alloying with Cu, determining impurity concentrations 02 p0277 A66-12095  
 Electrical properties of cadmium selenide evaporated films prepared on substrates at various substrate temperatures 03 p0409 A66-12725  
 Electrical resistivity and Hall coefficient of undoped n-type gallium arsenide with carrier concentrations measured at various temperatures as function of uniaxial compression and hydrostatic pressure 03 p0412 A66-13149  
 Electric properties of germanium and silicon filamentary diodes in which base volume diode structure contains disintegrated region 03 p0346 A66-13319  
 Electrical and magnetic properties of cobalt telluride /gamma phase/ to verify semiconductor character 04 p0559 A66-13479  
 Magnetic and electrical transport properties of superconducting whiskers and platelets of NbC/NbN 04 p0559 A66-13716  
 Electrical, IR property measurements and annealing experiments on electron-irradiated oxygen doped germanium 04 p0562 A66-13747  
 Electrical effect of large meteorite moving in lower atmosphere 04 p0577 A66-13846  
 Complex output resistance and conductivity of electromagnetic cylindrical resonators transmitting across gaps, using variational method, noting role of incident and reflected waves 04 p0496 A66-13905  
 Influence of anisotropic stress effect on

output voltage and frequency of Colpitts oscillator with mesa NPN transistor 04 p0501 A66-14208  
 Transverse Dember effect in anisotropy of electrical and photoelectrical characteristics of indium selenide 04 p0565 A66-14259  
 Electrical properties of germanium-gallium arsenide heterojunctions of p-n and n-n structure 04 p0569 A66-14362  
 Structure, electrical properties and paramagnetic resonance absorption of barium titanate with admixtures of oxides of triple valent element 05 p0730 A66-14651  
 Dielectrics theory using average field approximation containing random concentration of ellipsoidal inclusion 06 p0908 A66-16027  
 Strain dependence of impurity conductivity measured in compensated p-type germanium, using uniaxial compression 06 p0922 A66-16171  
 Cloud physics - International Conference, Tokyo and Sapporo, Japan, May 1965 06 p0904 A66-16266  
 Radiation damage in nondegenerate germanium at low temperatures, using hot carrier technique for measuring resistivity and Hall coefficient on antimonide doped samples 06 p0932 A66-17114  
 Energy spectrum of current carriers in germanium telluride, investigating electrical properties of polycrystalline and single crystal samples 07 p1105 A66-18376  
 Experimental apparatus for studying temperature dependence of electrical properties of semiconductors at low temperature 08 p1221 A66-18705  
 Physical, thermal, electrical and optical properties of beryllium 08 p1238 A66-18849  
 Crystal structure and allotropic transformation of cobalt and thermal, thermodynamic, electrical and magnetic properties 08 p1240 A66-18961  
 Thin film microelectronics including passive and active circuit element, electric properties, vacuum apparatus and instruments 08 p1192 A66-18962  
 Electric properties of passive circuit thin film components in microelectronics, discussing resistors, capacitors and microcircuit interconnections on method of preparation 08 p1192 A66-18963  
 Resistance-grown pyrolytic graphite in crystallographic, thermal and electrical measurements 08 p1244 A66-19223  
 Electrical and magnetic properties of ten synthesized perovskite compounds of complex composition 08 p1273 A66-19268  
 Electric properties of single crystal p-type InSb, obtaining samples by zone melting, thermal processing, etc, noting hole concentration plotting 08 p1278 A66-19625  
 Metal oxide semiconductor /MOS/ transistors constructed on single crystal cadmium sulfide, noting transconductance, gate source, gate drain capacitance, etc 09 p1360 A66-20980  
 Lithium diffusion effects on electrical properties of tellurium doped n-type GaSb 10 p1578 A66-21582  
 Boron, Volume 2, Preparation, properties and application 10 p1579 A66-21718  
 Semiconductor properties including conductivity, resistivity, band gap, optical absorption, etc, analyzed on very pure and doped beta-rhombohedral boron 10 p1579 A66-21719  
 Vacuum deposited amorphous boron films, presenting structure, optical measurements and electrical properties 10 p1580 A66-21726  
 150 mc strip-line circulator using Airtron garnet material, noting isolation, insertion loss, input impedance, etc 10 p1514 A66-21910  
 Electric properties of titanium carbide as function of number of vacancies in carbon sublattice 11 p1750 A66-22296  
 Exponential resonators in filters and matching networks, determining reactance or susceptance frequency behavior by plotting curves with analog computer 11 p1661 A66-22382  
 Indium antimonide thin film preparation via vacuum deposition, noting evaporation rate effects on electrical properties of film 11 p1756 A66-23022  
 Double injection in long p-p-n diffused silicon junctions subjected to heat

treatment, noting donor density energy level and electrical properties 11 p1756 A66-23027  
 Finite size electrode effect on electrical parameter in MHD generators with segmented electrodes 12 p1802 A66-23576  
 Electric properties of antimony-doped stannic oxide in terms of optical mode lattice scattering 12 p1928 A66-23932  
 Equation relating voltage, current, ampere-hours consumed and temperature for silver oxide-zinc batteries, noting dual potential concept 12 p1804 A66-24667  
 Effects of recoil in semiconductor with thermal-neutron-absorption cross section, measuring changes in luminescence and conductive properties of CdS 13 p2166 A66-25792  
 Nonlinear differential equations in theory of electrical oscillation 13 p2118 A66-25826  
 Structure, electrical properties and paramagnetic resonance absorption of barium titanate with admixtures of oxides of triple valent element 13 p2167 A66-25926  
 Electrical characteristics of linear, segmented electrode, Hall and Faraday MHD generators operating in equilibrium and nonequilibrium ionization modes, obtaining data on loss mechanisms 13 p2001 A66-26256  
 Magnetic and electrical properties of intermetallic compound FeRh, discussing preparation of thin films 14 p2355 A66-26911  
 Electrical properties of germanium-gallium arsenide heterojunctions of p-n and n-n structure 14 p2369 A66-28260  
 Electric properties of germanium and silicon filamentary diodes in which base volume diode structure contains disintegrated region 14 p2260 A66-28293  
 Optical and electrical characteristics of n-type indium oxide films prepared by spraying, noting relation between carrier mobility and particular impurity used 15 p2559 A66-28623  
 Mercury selenide thin film transistors, measuring electric properties 15 p2560 A66-28634  
 Electrical properties of nickel ferrite in terms of Jonker model, noting magnitude of energy gap between Fe and Ni levels and mobilities of electrons and of positive holes 16 p2781 A66-31215  
 Busbar effect on interaction between conducting fluid flow and traveling wave magnetic field created by long line with concentrated inductance and capacitance, deriving line gain 16 p2765 A66-31374  
 Physical properties of thin films of CdS and CdSe formed by vacuum deposition analyzed as function of deposition and processing conditions 16 p2782 A66-31422  
 Electrical properties of impure silicon carbide obtained from Tashkent carborundum plant 16 p2786 A66-31672  
 Electrical properties of SiO films, noting independence of dielectric constant on film thickness and dependence of conductivity on applied field 17 p2978 A66-32411  
 Electric properties of single crystal p-type InSb, obtaining samples by zone melting, thermal processing, etc, noting hole concentration plotting 17 p2984 A66-33139  
 Scattering matrix properties of symmetrical octupoles 17 p2898 A66-33519  
 Relation between optical and electrical properties of interplanetary dust in upper atmosphere and comparison with twilight-optical and ionospheric parameters 18 p3105 A66-33961  
 Spatial charge region, excess electron concentration, capacitance and conductivity in semiconductor layer with Lorentz forces acting on carrier determined as functions of surface potential and applied electromagnetic field 19 p3442 A66-35819  
 Critical temperatures and critical magnetic fields determined for superposed normal and superconducting films, noting dependence on metal thickness 19 p3443 A66-36003  
 Effect of electric and magnetic properties of titanium oxide explained through Matsubara and Yokota theory extended to finite temperatures 19 p3444 A66-36175  
 Magnetic, electric and SHF properties of oxides and solid solutions of bivalent europium from 1.6 to 300 degrees K 20 p3617 A66-37478  
 Resistance and heat transfer coefficient



relation theoretically determined for flow of electrically conducting liquid in magnetic field 20 p3679 A66-37614

Electrical and photoelectrical properties of silicon photocells with different impurities, examining load characteristics, V-I forward and reverse branches plotted for silicon cells 20 p3502 A66-37734

Niobium alloys properties noting effect of molybdenum and titanium additions 20 p3585 A66-37749

Complex output resistance and conductivity of electromagnetic cylindrical resonators transmitting across gaps, using variational method, noting role of incident and reflected waves 20 p3532 A66-37863

Relation between electrical properties and structural features of gold- and antimony-doped germanium single crystals, noting abrupt decrease in mobility 21 p3799 A66-38928

Electrical properties of indium antimonide single crystals with noncompensated impurity concentration, determining position of deep-seated levels in forbidden band 21 p3799 A66-38929

Electrical and photoconductivity properties of high-resistivity gallium phosphide in intrinsic and near IR region, noting electron trap effect 21 p3800 A66-38992

Heat treatment of silicon at high temperatures leads to donor centers affecting electric and photoelectric properties 21 p3802 A66-39157

Temperature gradient-induced GaAs crystal inhomogeneity effects on electric properties 22 p3959 A66-39742

Spherical plasma probe behavior in AC potential with frequency near plasma frequency 22 p3954 A66-39811

Electric and magnetic properties in TaC systems and dependency on C-to-Ta ratio 22 p3934 A66-40091

Barium titanate semiconductors containing controlled amounts of neodymium prepared, showing dependence of electrical properties on preparative conditions and amount of rare earth 23 p4109 A66-41128

Resonance absorption of gamma-quanta by tin in germanium 23 p4110 A66-41133

Thermoelectric properties of solid solution of germanium telluride in copper antimony telluride 23 p4114 A66-41572

P-type conductivity and stored electron charge densities in high resistivity cadmium sulfide crystals 23 p4114 A66-41625

Electrical properties and fabrication of zinc oxide-bismuth oxide low Q capacitor with high apparent dielectric constant over wide frequency range 24 p4180 A66-42311

**ELECTRIC PROPULSION**

**SA IONIC PROPULSION**

**SA NUCLEAR-ELECTRIC PROPULSION**

Electric propulsion for manned interplanetary mission evaluated in light of new optimum planetary transfer trajectories of power-limited flight 02 p0289 A66-11623

Thermionic converters used in combination with core reactor for auxiliary propulsion of spacecraft 04 p0573 A66-13548

Radiation tolerant electric propulsion system to operate on SNAPSHOT satellite, permitting orbital test of ion engine and ion propulsion with nuclear power supply /SNAP-10A/ 04 p0544 A66-13630

Electric drive operating parameters and design, using exploding wire type device and electromagnetic apparatus for plasma production and acceleration 06 p0942 A66-15917

Electric and photon propulsion systems in German-American research 06 p0942 A66-15931

Electric rocket propulsion system requirements for space propulsion, comparing capabilities with chemical and electrical rockets 08 p1280 A66-18575

Electrostatic ion propulsion and electromagnetic engine experiments in Germany for application to space travel, noting nuclear energy power source 08 p1281 A66-18614

Pulsed ablating-plastic thruster in momentum and mass consumption measurements 08 p1282 A66-19138

Electric propulsion for space travel, discussing propellant consumption economics, mass energy, specific impulse

acceleration, etc 09 p1433 A66-19864

Electric propulsion in 1965, discussing electron bombardment and contact ionization thrusters, nuclear and solar-electric power systems, etc 09 p1434 A66-20246

Electric propulsion including thrusters, power systems, solar power, hybrids, etc 09 p1434 A66-20247

Vacuum arc thruster experiments in development of electric propulsion system for spacecraft [AIAA PAPER 66-202] 10 p1592 A66-21444

Microthruster power conditioning and control system design and ion propulsion [AIAA PAPER 66-215] 10 p1485 A66-21449

Geomagnetic thruster form of Alfvén wave propulsion system, using ionospheric plasma contacts [AIAA PAPER 66-257] 10 p1594 A66-21462

Electric propulsion system effective mass dependent on trajectory, vehicle parameters and thruster characteristics [AIAA PAPER 64-676] 10 p1595 A66-21936

Electrical propulsion engine performance accurately measured by thrust balance design, using flotation and flexible propellant lines [AIAA PAPER 66-228] 11 p1761 A66-23085

Performance characteristics of two-stage pulsed coaxial plasma engine [AIAA PAPER 66-240] 12 p1935 A66-24518

Lithium, ammonia and hydrogen-fueled MPD arc jets [AIAA PAPER 66-239] 12 p1936 A66-24520

Solid propellant electric thruster /SPET/ for attitude control and drift correction of space vehicles [AIAA PAPER 66-229] 12 p1937 A66-24525

Potentials of solar power electric propulsion including photovoltaic devices, array structures and weight reduction [AIAA PAPER 66-210] 12 p1937 A66-24527

Electric propulsion for space missions with regard to vehicle weight and mission cost, using manned Mars flight as example [AIAA PAPER 64-715] 13 p2173 A66-26609

Electric propulsion for spaceflights, discussing nuclear rocket technology, mission planning, payload optimization, etc 13 p2173 A66-26610

Weight criteria for integration of nuclear-electric power supply with electric thruster system as primary spacecraft propulsion [AIAA PAPER 64-765] 13 p2173 A66-26611

Experiments with arc jet characterized by composite electromagnetic and vortex stabilization and propelled by hydrogen or nitrogen, noting heat loss through electrodes 14 p2373 A66-27097

Electron cyclotron resonance plasma thruster for spacecraft electric propulsion systems 14 p2374 A66-27520

Power conditioning and ion thruster module size and number effect in terms of reliability [AIAA PAPER 65-68] 14 p2375 A66-27883

Predicted and observed calorimetric exhaust efficiencies of capacitor powered coaxial plasma guns [AIAA PAPER 65-340] 15 p2551 A66-29275

Electron cyclotron resonance plasma accelerator design for thruster application and measuring techniques [AIAA PAPER 65-301] 15 p2572 A66-29277

Test program philosophy of electric propulsion and power for planetary mission application [AIAA PAPER 65-67] 16 p2791 A66-30901

Trajectory energy requirements for low-thrust flights throughout solar system using nuclear-electric propulsion [AIAA PAPER 66-497] 16 p2805 A66-31495

Suitability of Saturn IB/Centaur and Atlas/Centaur launched solar-electric propulsion vehicles for performing 0.1-AU solar probe mission [AIAA PAPER 66-496] 17 p2991 A66-32773

Collector target complex eliminating target life time and test equipment contamination by sputtered target material, applied in testing of electrical propulsion systems [AIAA PAPER 66-500] 17 p2991 A66-32774

Electric propulsion for transfer mission between parking orbits in cislunar space under optimum payload conditions 17 p2992 A66-33238

Low-power electric propulsion systems characteristics and design

[AIAA PAPER 66-578] 18 p3165 A66-34445

Advantages of plasma propulsion include zero energy consumption when stopped and functioning by pulses, thus facilitating telecommands 20 p3628 A66-37396

Reliability consideration effect on solar-powered electric-propulsion system design 20 p3568 A66-37908

Velocity field of conducting fluid interaction with electromagnetic fields, noting applications to electric propulsion, MGD power generation and reentry 24 p4240 A66-42281

Electrical propulsion devices for space vehicles related to plasma physics, ion-beam generation and particle dynamics 24 p4262 A66-43120

**ELECTRIC PULSE**

Operational methods of semiconductor switching circuits in pulsed powered circuit /PPC/ mode for reduced power consumption 18 p3090 A66-34070

**ELECTRIC RESISTANCE**

**SA PIEZORESISTIVE DEVICE**

**SA RLC CIRCUIT**

**SA SHORT CIRCUIT**

Van der Pauw method for measuring resistivity, Hall mobility and thickness of thin metallic film under vacuum, considering copper films 01 p0119 A66-10393

Series resistance of epitaxial silicon diodes as function of bias, using transmission loss method 01 p0036 A66-10396

Electric resistivity of solid phase of lutetium hydrogen system noting action of hydrogen atom 01 p0127 A66-11090

Current amplification factor decrease and input resistance increase with current decrease in transistor circuits in microregime 02 p0207 A66-11414

Electric resistivity of carbon resistor material determined as temperature function, calculating static response characteristics of carbon bolometer 02 p0228 A66-11445

Electrical resistivity, Hall effect and magnetoresistance of bismuth antimony single crystal solid solutions 02 p0272 A66-11712

Load resistance effect on selectivity of notch filters using hyperbolically shaped RC lines 02 p0200 A66-11876

Dependence in transistorized multistage amplifiers of Q on resistances in collector loops 02 p0206 A66-12270

Variations in resistivity of silicon slices before and after irradiation 03 p0339 A66-12435

Acceptor level in iron doped Ga-As moves toward valence band with increasing temperature at approximately same rate band gap decreases 03 p0410 A66-13004

Local resistivity of semiconductor by measuring RF spreading resistance of probe on sample surface without attaching electrical contacts 03 p0371 A66-13252

Electromagnetic groundwave propagation along Earth surface, noting transmission and reflection when meeting abrupt electrical discontinuity 04 p0475 A66-13430

Resistivity and Hall coefficient vs temperature in heavily doped n-type GaSb and related semiconductors 04 p0561 A66-13734

Electrical resistivity of Nb-Zr alloys of four compositions determined as functions of temperature from 4.2 to 273.2 degrees K with nearly linear dependence 04 p0562 A66-13740

RC circuit resistance effect on characteristics of selective filters consisting of semiconductor or thin film RC circuit with range multiplier and distributed parameters 04 p0496 A66-13908

Increase in collector voltage at constant power dissipation will increase junction temperature and give apparent effect of higher thermal resistance 04 p0500 A66-14102

Pseudopotential method for determining temperature-dependent electric resistance of lithium, neglecting free electron approximation and examining electron-phonon interaction 04 p0566 A66-14316

Niobium resistivity dependence on hydrogen-impurity content at various temperature ranges 05 p0699 A66-14697

Electrical resistivity and characteristic temperature of technetium based on



thermoconductivity of pure element at and above room temperature 05 p0703 A66-15470

Metal surface structure, semiconductors and dielectric films analyzed, using image orthon technique for data on work function, electron reflection coefficient and electric resistance 05 p0621 A66-15578

Hall coefficient, electric resistance and thermoelectric power in indium-rich solid solutions measured at various pressures and at 110 degrees C 06 p0922 A66-16172

Matrix elements of electron-phonon interaction and electric resistance in nickel, using electronic structure of Fermi surfaces and phonon spectrum 06 p0894 A66-16175

Resistance across opposite vertices of n-dimensional cube with each edge at one ohm resistance expressed by equivalent circuit 06 p0851 A66-16458

Reaction cavity method of measuring low-resistance semiconductors in which entire end wall of cylinder is replaced by sample being measured 06 p0881 A66-16642

Current oscillations accompanied by mobile regions in high resistance-gallium arsenide subjected to electric field, measurement of Hall effect shows these regions are of high resistance 06 p0930 A66-17066

Hall effect and resistivity measurements on high resistance n-silicon related to formation conditions at low temperature of level placed at 160 mev from conduction band 06 p0935 A66-17128

Resistive properties of vacuum-deposited chromium films determined by grain size and impurity content 07 p1098 A66-17741

Design variables for high pressure cell with supported taper pistons that can be used for optical, electrical resistance, X-ray diffraction and Mossbauer resonance studies 07 p0997 A66-18484

Quenched-in vacancy data estimated by analysis of quenched-in resistivity in zone-refined aluminum 08 p1240 A66-19062

Electric resistivity change in Pt produced by electron bombardment 08 p1275 A66-19364

Effect of voltage and film thickness on sputtered tantalum film resistivity when used as microcircuits 09 p1411 A66-19941

Change in resistance of tin films upon destruction of superconductivity by current 09 p1411 A66-19958

Book on theory and measuring techniques for electrical resistance of metals at low temperatures and cryogenics 09 p1388 A66-19976

Sample resistance of niobium oxy-nitrides as function of temperature, using four-contact DC technique 09 p1424 A66-20073

Low temperature study of resistivity and thermoelectric power variations of silver-palladium alloys as function of concentration, caused by electron diffusion 09 p1425 A66-20079

Surface potential in high and low resistivity semiconductors determined by comparing surface and contact potentials and Fermi levels 09 p1427 A66-20537

Palladium-silver and palladium-rhodium alloys electrical resistance, Hall effect and Nernst effect as affected by temperature 09 p1389 A66-20805

Low temperature resistivity of yttrium-based alloys containing small amounts of rare earth metals, deriving exchange integrals from resistivity data 09 p1430 A66-20846

Logarithmic temperature dependence of electrical resistivity found in metallic impurity conduction in n-type germanium 09 p1430 A66-20849

Seebeck and Thomson coefficients and variable resistivity effects on thermoelectric heat pump performance 09 p1333 A66-20971

Lattice constants of ultrapure phenanthrene to determine resistivity anomaly association with polymorphic transformation 10 p1576 A66-21553

Contactless AC method for measuring small variations in resistance of highly conducting materials /zinc/ 10 p1536 A66-21703

Electrical and optical experiments performed on single crystals of beta-rhombohedral boron, noting resistivity decrease and differences between thermal and optical band gap 10 p1579 A66-21720

Neutron irradiation of InSb single crystals,

noting conductivity type change in p-type and conductivity magnitude in n-type crystals 11 p1749 A66-22285

Single probe method for measuring semiconductor resistivity, using alternating current, noting tests with germanium and silicon samples 11 p1705 A66-22598

Electrical resistivity, thermoelectric power and thermal conductivity of pseudoternary alloys in temperature range of 77 to 300 degrees K measured 11 p1750 A66-22697

Current distribution and input resistance of T-type, corner and bent tape vibrators powered by lumped electromotive force, using method of integro-differential equations 11 p1666 A66-22719

Oxygen content effect on recovery of cold worked tantalum investigated by measuring Snoek damping, electric resistivity and dynamic E modulus 11 p1717 A66-22997

Current dependence of resistivity and mobility measured in silicon epitaxial layers on control wafer 11 p1756 A66-23021

Temperature dependence of electrical resistivities of dilute binary alloys, using phenomenological approach of Krishnan and Bhatia 11 p1718 A66-23367

Dependence in transistorized multistage amplifiers of Q on resistances in collector loops 12 p1831 A66-23874

AC resistivity profiles through anodic oxide films on Al and Al alloys 12 p1895 A66-24392

Transistor base resistance measured, using input method where equivalent circuit is determined through simultaneous application of three separate frequencies to bridge 12 p1845 A66-24853

Electrical resistivities of gold-erbium alloys measured at low temperatures 12 p1933 A66-24919

Electrical resistance changes in quaternary alloy during simultaneous occurrence of phase solution coalescence and silicon spheroidization, noting effects of aging and various metal additions 12 p1898 A66-25023

Quantum size effects in thin bismuth film and specific resistance, Hall effect and reluctivity 13 p2160 A66-25107

IR emission and electrical resistivity measurements of TA 2000 plasma by interference spectrometer 13 p2138 A66-25124

Electrical resistance and thermoelectric power of Ni-Cu solid solutions near Curie point 13 p2162 A66-25407

Resistivity and thermoelectric power of copper telluride at various temperatures, finding that it retains semiconducting properties in liquid state 13 p2162 A66-25411

Instability due to coupling between compressibility and resistivity in cylindrical plasma with surface currents, noting growth rate near acoustic velocity phase 13 p2142 A66-25705

Anisotropic resistance in permalloy films based on imperfection orientation model 14 p2352 A66-26895

Semiconductor properties of reduced barium titanate analyzed by electron spin resonance measurements at various temperatures 14 p2359 A66-27132

Stannic oxide ceramic formation and dielectric constant and resistivity measurements and evaluations 14 p2362 A66-27499

Effective resistivity of metal-plate conductor with single ellipsoidal Fermi surface and specularly reflecting boundaries is independent of thickness 14 p2364 A66-27706

Series resistance of silicon microwave varactors 14 p2254 A66-27731

Instabilities occurring in tunnel diode amplifiers resulting from changes in input resistance of load circuit and method for reducing them 14 p2255 A66-27749

Resistivity and Seebeck coefficient of liquid thallium-tellurium semiconductors 14 p2366 A66-27760

Conductivity of n-silicon in strong magnetic field 14 p2370 A66-28332

Plastic deformation effect on resistivity and Hall constant of silver-palladium alloys, noting decreasing rate of change for increasing strain 15 p2560 A66-28648

Cleavage behavior of solid solution alloy Ta-Mo, noting electric resistivity, tensile

properties, lattice parameters, diffraction coefficients, etc 15 p2520 A66-28650

Temperature dependence of Hall emf and electrical resistance of Sendust type Fe-Si-Al alloys 15 p2560 A66-28678

Time variation of current, temperature and resistance in premeit stage of wire explosion expressed in terms of initial wire and circuit data 15 p2537 A66-28722

Anisotropy and annealing behavior in extrinsic single-crystal tellurium studied by measuring electric resistivity and Hall coefficient 15 p2562 A66-28725

Heat treatment effect on superconducting properties of cold-worked niobium, noting results of magnetization, critical current and resistivity measurements 15 p2564 A66-28760

Electron spin resonance saturation causing sharp decrease of DC resistance for reduced rutile crystals 15 p2567 A66-29401

Resistivity increase in Cadmium Telluride, attributed to conduction band separation due to deionization into impurity levels 16 p2768 A66-30131

Nonlinear flux flow in type II superconductor, noting resistance characteristics 16 p2768 A66-30135

RF resistance in mixed state for subcritical currents 16 p2771 A66-30193

Thermoconductivity and electrical resistivity measurements with derived Lorentz functions for various compounds, using longitudinal heat flow 16 p2771 A66-30252

Quantum size effects in thin bismuth film and specific resistance, Hall effect and reluctivity 16 p2771 A66-30286

Temperature dependence of resistivity of zirconium oxide with copper oxide additions indicates suitability as heat sensitive resistor material in 300 to 1000 degree C range 16 p2777 A66-30872

Hall effect and resistivity of Zn doped GaAs 16 p2778 A66-31069

Effect of annealing on thin gold films sandwiched between two evaporated layers of zinc sulfide, presenting resistance curves 16 p2779 A66-31083

Temperature and structure effect on hydride precipitation kinetics in titanium, using resistometric technique, noting nucleation problem 16 p2724 A66-31266

Thin silicon film deposition on amorphous fused quartz substrates by cathodic sputtering in argon atmosphere, noting resistivity data 16 p2782 A66-31421

Molybdenum films prepared by sputtering onto oxidized silicon substrates, analyzing resistivity, lattice parameter, orientation and grain size as function of substrate temperature and bias 16 p2783 A66-31424

Structure and electrical resistance as function of temperature for Nichrome-silicon monoxide cermet films on single crystal Si substrates 16 p2783 A66-31425

Effect of storage in air at high temperatures on resistance, temperature coefficient of resistance of metal alloy film resistors, noting effect of silicon oxide protective overcoating 16 p2783 A66-31426

Thermal expansion and electrical resistivity measurements below 400 degrees K on niobium and two niobium alloys containing tungsten 16 p2725 A66-31454

Proper current input for true resistivity measurements of single-crystal silicon and silicon slices 16 p2785 A66-31596

Temperature dependence of magnetization and resistivity in SHF magnesium-aluminum ferrite 16 p2786 A66-31677

Change in resistance of titanium films deposited in high vacuum from argon ion bombardment, noting dependence on energy value 16 p2789 A66-31786

Temperature dependence of electrical resistance of thin nichrome films investigated by vacuum deposition on mica base 17 p2939 A66-31969

Anisotropy of electrical resistance of indium in magnetic field shown to be nearly absent, confirming absence of open Fermi surface 17 p2977 A66-32315

Doping and firing atmosphere effects on electric resistivity of polycrystalline barium titanate, noting oxidation of small grain and positive temperature coefficient effect on large grain 17 p2978 A66-32404

Thermoelectric power and electric



resistivity measurements of n-type silver telluride at melting point and in liquid state 17 p2981 A66-32955

Low temperature resistivity, magnetic susceptibility and superconductive transition point in La containing rare earth impurities 17 p2982 A66-32972

Volt-ampere characteristics, electrical resistivity, and pressure effect on Gunn phenomena in n-type GaAs in high electric fields 17 p2985 A66-33292

Resistivity of semiconductors with periodic inhomogeneity, noting cases of surface perpendicular and surface parallel striations 18 p3155 A66-34229

Optimum aging temperatures obtained from electric resistance of beryllium alloys containing chromium and zirconium 18 p3124 A66-34406

Zero bias anomalies in normal metal tunnel junctions, noting dependence of dynamic resistance of junction on voltage and temperature 18 p3156 A66-34469

Thermal conductivity and electrical resistivity measurements on nickel alloyed steels in cast and wrought conditions 18 p3124 A66-34895

One-dimensional diode model with high resistivity n region and built-in electrical field 18 p3088 A66-35038

Thermal and electric properties of InAs-GaAs alloy as function of composition, impurity additions and temperature 19 p3436 A66-35427

Two-stage field effect transistor amplifier with high input resistance and modification of circuit enabling input resistance to be adjusted to infinity 19 p3315 A66-35560

Resistance and frequency response range of sheath surrounding electrostatic probe floating in tenuous plasma 19 p3357 A66-35808

Hardening during deformation in stoichiometric nickel manganite alloy noting temperature effect, surface characteristics and electric resistance 19 p3381 A66-35930

Microwave absorption in normal conducting films of gold plated onto superconducting tin indicates resistivity and transition temperature of gold consistent with proximity effect 19 p3443 A66-35999

Low effective resistivity of gold film plated onto tin determined by low temperature microwave absorption measurement and explained by free-electron model and superconductivity proximity effect 19 p3443 A66-36000

Minimum electric resistivity of chromium in antiferromagnetic state shows no disappearance in longitudinal magnetic field 19 p3444 A66-36071

Electrical resistance and Hall effect measurements in layer structures, confirming existence of interaction with optical relaxation vibration modes 19 p3446 A66-36343

Electric resistance and thermal expansion of Ti-Nb-Cr alloys, noting phase composition 19 p3387 A66-36450

Resistive effects in type II superconductors near upper critical field examined, using Ginzburg-Landau equations 20 p3616 A66-37374

Work function of semiconducting barium titanate as function of temperature for testing Heywang theory of polycrystalline material anomalous resistance behavior 20 p3616 A66-37404

RC circuit resistance effect on characteristics of selective filters consisting of semiconductor or thin film RC circuit with range multiplier and distributed parameters 20 p3532 A66-37866

Plasma slab resistance between juxtaposed disk electrodes, obtaining exact two- and approximate three-dimensional solution 21 p3776 A66-38546

Four-probe head sensitivity increase in measurement of volume and surface resistance of semiconductor materials by increasing separation of potential probes 21 p3709 A66-38613

Kadomtsev current-convective instability and damping as affected by current density, wave frequency, resistivity gradient and azimuthal wave number 21 p3791 A66-39178

Flux flow in type II superconductors, measuring critical current, longitudinal and

transverse voltages for varied orientation of magnetic field 21 p3802 A66-39201

Dynamic resistance and derivative of superconducting tunnel junction measured by combined harmonic detection and bridge techniques 21 p3793 A66-39384

Resistivity and Hall coefficient of Sb doped Ge at He temperatures measured as function of magnetic field and temperature to determine high field effects on impurity conduction 21 p3805 A66-39579

Input resistance of short filamental antenna in warm isotropic plasma from kinetic /Vlasov equation/ rather than hydrodynamic approach 22 p3874 A66-39939

Temperature coefficient of resistance in thin metal films, using Sondermayer analysis for vapor deposited Au, Ag and Cu films 22 p3963 A66-40105

Resistivity measurement of large number of samples of bulk-grown n-type GaAs as function of temperature near 300 degrees K 22 p3877 A66-40179

Electric resistance of amorphous iron films, noting film structure dependence on evaporation parameters 23 p4110 A66-41138

Microbonding techniques such as thermocompression bonding, soldering, electrical resistance and ultrasonic welding, noting applicability in transistor manufacture 23 p4043 A66-41190

Current distribution and input resistance of T type, corner and bent tape vibrators powered by lumped electromotive force, using method of integro-differential equations 23 p4045 A66-41457

Conversion of finite discrete frequency spectrum by n-dimensional frequency converter with nonlinear active resistance with ideal characteristics 23 p4038 A66-41519

Thermoelectric power and electric resistivity of copper-gold alloy doped with 3d transition metals as function of temperature and atomic number of impurity 23 p4114 A66-41712

Variation of resistivity and inversion of sign of conductivity of quenched specimens of p-type silicon 23 p4115 A66-41838

Sputtering voltage and current effects on resistivity of films sputtered from pure tantalum appear to be traceable to pressure and growth rate 24 p4251 A66-42297

Two-transistor circuit with output resistance of approximately 50 M ohms with improved temperature stability and high internal resistance 24 p4181 A66-42378

Electron irradiation effect on resistivity of epitaxial layers of Si and on lifetime of ordinary samples 24 p4258 A66-43008

**ELECTRIC STIMULUS**

Relaxation oscillations in n-type epitaxial silicon with point contact, discussing generation via electrical excitation of impurity centers 05 p0731 A66-14655

Electromagnetic energy transport between coils or coils external to human body and coil implanted inside body is increased by using suitable ferrite core for receiving coil 06 p0820 A66-16852

Mathematical theory relating neuronal geometry to parameters of excitation in unconditioned response of planarians to electric shock 10 p1486 A66-21296

Importance of neural site and experimental conditions in determining motivational direction /positive or negative/ produced by electrical stimulation of brain in animals 11 p1644 A66-22976

Holtzman strain experiments on rats, determining if electrical stimulation of various neural sites produce motivational consequences of appetitive or defensive behavior 13 p2009 A66-25790

Relaxation oscillations in n-type epitaxial silicon with point contact, discussing generation via electrical excitation of impurity centers 13 p2167 A66-25930

Optical art, discussing mechanism of visual perception, necessity of stimulation of visual cortex, etc 15 p2443 A66-28844

Medial forebrain bundle, lateral hypothalamic area and reinforcing brain stimulation, discussing self-stimulation 17 p2859 A66-32552

Dissociation of rhinencephalic or thalamic self-stimulation and epileptiform activity in rats 20 p3506 A66-37602

Induction and suppression of hypothalamic

self-stimulation behavior by microinjection of endogenous substances at self-stimulation site 20 p3506 A66-37603

Square-wave electropulse evaluated as more effective tactile stimulus for cross modality comparison of reaction times than more traditional stimuli 23 p4030 A66-41576

**ELECTRIC TERMINAL**

Realization of directed graph having prescribed terminal connection matrix without self-loops and minimum number of arcs 20 p3539 A66-38284

**ELECTRIC WELDING****SA PLASMA ARC WELDING**

Worst case design for high reliability welded electrical connections, emphasizing encapsulation stresses and quantitative parameter 02 p0234 A66-11325

Aircraft and commercial application of three-phase direct current resistance welding, using silicon 05 p0685 A66-14518

Relationship between metallurgy of weld and characteristics of electrical pulse producing it 05 p0686 A66-14520

Argon-arc welding of 3-mm high-strength steel sheet and molten slag arcless electric welding of 100-mm high-strength steel plate 08 p1231 A66-19168

Integrated circuit welding into electronic equipment via parallel gap method, noting military applications in forward area communications 23 p4044 A66-41198

**ELECTRIC WIRING**

Nonreactive high-voltage pulse resistors, applying transmission line principles and noting Chaperon winding 03 p0341 A66-12575

Color temperature measurement in first stage of electrical explosion of copper, silver and constantan wires as function of magnitude of energy input for various heating times 20 p3599 A66-36985

**ELECTRICALLY SUSPENDED GYROSCOPE /ESG/**

Navigation gyro design with respect to cost factors noting electrically suspended, gas bearing and other types 01 p0104 A66-10676

Development of inertial navigation system based on Electrically Suspended Gyroscopes /ESG/, with comparison to conventional inertial and hybrid systems 07 p1078 A66-17807

ESG strapdown inertial navigation system based on double integration of acceleration and analysis of electronic gimbal-induced errors 13 p2124 A66-25653

**ELECTRICITY**

**SA ANTIFERROELECTRICITY**

**SA ATMOSPHERIC ELECTRICITY**

**SA BIOELECTRICITY**

**SA GEOELECTRICITY**

**SA GYROELECTRICITY**

**SA PHOTOELECTRICITY**

**SA PIEZOELECTRICITY**

**SA PYROELECTRICITY**

**SA STATIC ELECTRICITY**

**SA THERMOELECTRICITY**

Circuit theory, information theory, basic sciences, electrostatic processes - IEEE International Convention, New York, March 1966 12 p1855 A66-24645

**ELECTRO-OPTICS**

Strain-free electro-optic effect in single crystal barium titanate as function of temperature between 10 and 120 degrees C 01 p0126 A66-10969

Mechanical and electro-optical parameters for some acetylene derivatives evaluated from IR spectra 01 p0109 A66-11004

Electro-optic diffraction grating for light beam modulation and diffraction 02 p0239 A66-11371

Switching with optical signals classifying polycrystalline noncoherent and coherent types of optoelectronic devices 02 p0200 A66-11890

Curie temperature, static dielectric constant and electro-optic coefficient of large single crystals of barium titanate 03 p0411 A66-13007

Commercial aerial camera objectives estimated with TsNIIGAIK electron-optical bench 04 p0519 A66-13662

Laser Q-switch arrangement with roof prism end reflector and electro-optical retarder 04 p0531 A66-13957

Static characteristics of gas laser internal modulation circuit, using electro-optical



crystal inserted into gas laser resonator 04 p0531 A66-14059  
Optimum receiver as ideal two-dimensional cross-correlator for any desired modulation function 04 p0486 A66-14118  
Optical and electro-optical information processing technology - Symposium, Boston, November 1964 05 p0636 A66-14818  
Standing wave read-only memory based on Lippmann color photography for information storage 05 p0636 A66-14819  
Semiconductor injection laser for use in electro-optical and optical information processing 05 p0692 A66-14823  
All-optical computer techniques, noting semiconductor laser digital devices for near future 05 p0637 A66-14824  
Electro-optical signal processors for phased linear array antennas, discussing time and spatial delay multiplexing 05 p0648 A66-14832  
Electro-optical scanning system for multiaxial strain measurements 05 p0682 A66-15302  
Systems design techniques applied to laser rangefinder and imaging devices, emphasizing relation between operational requirements and laser technology 06 p0889 A66-15967  
Transmission of large number of instrumentation channels over parallel pulse-modulated light beams, using electro-optical mosaic sources and detectors 06 p0824 A66-15970  
Practical electro-optical devices which give electrical signal in response to incident light 06 p0852 A66-16558  
Electro-optical system measuring spectral response of photosensitive material or device and output under arbitrary light spectrum as in silicon solar cell 07 p0997 A66-18485  
Vertical sweep circuit for electron-optical tubeless ferrite transformer producing nanosecond high-voltage pulses 08 p1224 A66-19290  
Mechanical and electro-optical parameters for some acetylene derivatives evaluated from IR spectra 09 p1404 A66-19942  
Electro-optic system superiority over radio and inertial techniques for space navigation determined by simulation 10 p1554 A66-21893  
Projectile detection in hyperballistics range by using electro-optics and triggering of instrumented stations with luminous and nonluminous projectiles 10 p1538 A66-22042  
Quadratic electro-optical effect in paraelectric phase of barium titanate single crystals as affected by temperature 10 p1587 A66-22153  
Spatial variation of electric field in amplifying CdS measured, using electro-optic effect to study acoustic flux from thermal noise 11 p1758 A66-23356  
Light beam deflection due to linear temperature gradients across electro-optic modulator crystals 11 p1737 A66-23431  
Absolute measurement of optical rectification coefficient in ammonium dihydrogen phosphate 12 p1912 A66-23715  
Electro-optical celestial guidance system with minaturized computer and scanning sensor 12 p1909 A66-24104  
Electro-optic device with nonreciprocal properties which does not depend on Faraday magneto-optic effect 12 p1837 A66-24313  
Optoelectronic amplitude modulator using gallium arsenide diode as carrier source and lead sulfide photoconductor as modulation element 13 p2030 A66-25207  
Electro-optical automatic celestial guidance system for spacecraft and satellites 13 p2124 A66-25643  
Electro-optic effect and elastic wave propagation in single-domain ferroelectric lithium tantalate 13 p2170 A66-26589  
Digitization system based on photoelectron counting for scanning spectrometer 13 p2084 A66-26750  
Coherent transmission of optical radar from laser source and use of RF subcarriers placed on optical beams for wideband communications purposes 14 p2244 A66-28404  
Low-cost computer design using electro-optics for information processing 16 p2657 A66-31240  
Coherent optical systems in signal

processing techniques, information theory and antenna pattern simulation 16 p2657 A66-31242  
Epitaxial-planar diffusion techniques to fabricate monolithic electro-optical mosaics of 2500 phototransistor element with internal row and surface column interconnections 16 p2665 A66-31431  
Static characteristics of gas laser internal modulation circuit, using electro-optical crystal inserted into gas laser resonator 17 p2933 A66-32225  
Retardation-type laser modulators, examining driving power, transmission and dynamic range 17 p2935 A66-32820  
Temperature autostabilizing nonlinear dielectric element /TANDEL/ to obtain desirable and optimal working temperatures of ferroelectric crystal and electro-optical devices 17 p2896 A66-33298  
Optical modulation in bulk gallium arsenide, using Gunn effect 18 p3152 A66-33606  
Quadratic electro-optical effect in paraelectric phase of barium titanate single crystals as affected by temperature 19 p3440 A66-35767  
Book on laser receivers covering noise performance, atmospheric effects, detection techniques, hardware and systems available, optical communication in visible and IR spectrum, etc 19 p3375 A66-36060  
Electroluminescent photodiodes and diode light detectors applied to microcircuit design as relays, photochoppers or multichannel couplers 19 p3320 A66-36267  
Q modulation of laser theory and application, presenting giant pulse production, phenomenological theory, output response to step function change, electro-optic and mechanical modulators 20 p3576 A66-36971  
Semiconductor optoelectronic circuits for electric signal conversion into visible light 21 p3717 A66-39627  
Semiconductor electronics, Gunn effect in optical communications, electro-optics, optoelectronics and light coupling in microminiaturization 22 p3878 A66-40623  
Dynamic laser wavelength selection by insertion of dispersive tunable electro-optic Q-spoiler within laser cavity 22 p3933 A66-40866  
Absorption coefficient of light in semiconductors in crossed electric and magnetic fields, examining conditions for Franz-Keldysh effect occurring in magnetic field 24 p4256 A66-42524  
GaAs crystal as electro-optic modulator at 10.6 microns due to small carrier absorption, freedom from interband transitions and high resistivity 24 p4222 A66-42553  
Electro-optic light modulation using Pockel and Kerr effects in crystals for communications applications, using lasers 24 p4225 A66-42811  
Split angle, total internal reflection and Wollaston prism-digital light deflection techniques 24 p4174 A66-42815  
Electro-optic modulators for IR region 0.9 to 16 microns constructed by using large single crystals of high resistivity gallium arsenide 24 p4258 A66-42957

# ELECTROACOUSTIC WAVE

Piezoelectric crystals and ceramics properties that affect application in electroacoustic transducers 03 p0408 A66-12408  
Conductivity dependence of acoustoelectric effect in cadmium sulfide samples 05 p0731 A66-14653  
Microscopic theory of electroacoustic effect for n-type Ge and Si semiconductors of many energy minima, noting electron scattering 09 p1412 A66-19986  
Influence of boundaries on wave propagation in compressible warm plasma 10 p1566 A66-21730  
Scattering of incident beam of microwaves by self-excited plasma waves in mercury arc column, deriving dispersion curve for plasma waves, identifying propagating electroacoustic waves as responsible for scattering 12 p1825 A66-24964  
Conductivity dependence of acoustoelectric effect in cadmium sulfide samples 13 p2167 A66-25928  
Influence of trapping on acousto-electric

effect in piezoelectric semiconductors, noting ultrasound absorption and experimental results in cadmium sulfide 14 p2359 A66-27101  
Acoustoelectric effects for various sound waves, using rate of energy exchange between two coupled systems in relative motion 15 p2564 A66-28970  
Excitation of electroacoustic lateral waves in compressible plasma in contact with conducting boundaries 17 p2962 A66-31817  
Slow wave interaction with drifting stream of carriers, including collision and diffusion effects, noting TWT and acoustic semiconductor amplifier cases 17 p2878 A66-31820  
Electromagnetic wave interaction with uniform isotropic plasma in cylindrical interface considered for various types of excitations, using Green functions 17 p2962 A66-31821  
Acoustic amplification in piezoelectric semiconductors, examining present state of the art 17 p2892 A66-32919  
Dispersion relations for small-amplitude electroacoustic wave propagation in dense degenerate plasma, considering ion mobility and ion gas screening effects 18 p3148 A66-34727  
Electroacoustic assembly for determining time-dependent noise frequency characteristics in recognition and identification of noise source 19 p3356 A66-35564  
Light emission from semiconducting cadmium selenide crystals when not excited with photons, electron beam or tunneling, noting association with acoustoelectric field domain 20 p3620 A66-37767

# ELECTROCARDIOGRAM

Deterministic type waveform analysis techniques for noisy repetitive transient functions, noting application to hybrid computer processing of exercise ECGs 12 p1810 A66-24233  
Electrocardiogram P wave changes relation to body position changes in space 14 p2227 A66-26810

# ELECTROCARDIOGRAPHY

Electrocardiography as related to flying personnel including case histories 01 p0019 A66-10605  
Observations on heart rates and cardiodynamics during prolonged weightlessness, discussing immersion experiment on animals 04 p0465 A66-14073  
Electrocardiogram interpretation by computer, using pattern recognition approach which permits differentiation between normal and abnormal rhythms 12 p1810 A66-24231  
ECG P wave changes due to body tilt in space of rabbits deprived of afferent impulses from pressure-receptive areas 17 p2859 A66-32230  
Space cardiology, discussing methods of biological telemetry such as ECG, seismocardiography, kinetocardiograph, arterial oscillography, etc 18 p3059 A66-34364

# ELECTROCATALYST

Platinum metal as electrocatalyst for oxidation of methanol and number of saturated hydrocarbons 02 p0188 A66-11870  
Hydrocarbon fuel cell anodes containing boron carbide as support for platinum electrocatalyst 14 p2226 A66-27902

# ELECTROCHEMICAL CELL

SA NICKEL-CADMIUM BATTERY  
Fuel cell operation utilizing liquid fuels, evaluating hydrazine and alcohol fuels and electrode materials 04 p0459 A66-13546  
New cathode and electrolyte materials for high energy electrochemical batteries 05 p0612 A66-15307  
Characteristics of electrochemical cells in which concentration of ionic species in chamber can be varied via applied electrical signal as analog of junction transistor 06 p0852 A66-16637  
Lunar and terrestrial vehicle wheels, frame, steering, suspension, electrochemical energy converters, electric traction power systems and vehicular propulsion [SAE PAPER 660150] 07 p1018 A66-17867  
Electrochemical energy conversion, discussing fuel selection, oxidants, fused salt electrolytes, liquid metal, etc 07 p0995 A66-18325



Electrode potentials and efficiency, noting significance, types and associated equations 07 p0996 A66-18468

Kinetic effects in fuel cells, measuring rate of change of electrode process characteristics 07 p0996 A66-18470

Nickel-cadmium, silver-cadmium and silver-zinc alkaline batteries for secondary spacecraft power supplies [AIAA PAPER 64-455] 08 p1168 A66-18813

Batteries - International Symposium at Brighton, England in September 1964 08 p1169 A66-19641

Photomicrographic analysis of reactions during charging and discharging of nickel-cadmium alkaline cells 08 p1170 A66-19643

Oxygen reduction in sealed nickel-cadmium cells 08 p1171 A66-19646

Microporous metallic gas-diffusion electrodes in low temperature acid-electrolyte fuel cells 08 p1172 A66-19651

Cell voltages and Coulomb efficiency in oxygen electrodes and hydrogen and hydrazine fuel cells for long duration discharges 08 p1172 A66-19652

Low temperature low pressure hydrogen/oxygen alkaline fuel cell and electrode selection 08 p1172 A66-19653

Thermodynamic and kinetic effects of gas pressure on performance of fuel cell using one or two gas electrodes 08 p1172 A66-19654

Methanol-air fuel cell with alkaline electrolyte, Ni or Pt catalysts and carbon diffusion electrode, for use in signaling devices 08 p1172 A66-19655

Power and efficiency analysis of molten salt thermocell as thermoelectrochemical energy converter 09 p1333 A66-20499

System selection for hydrogen-oxygen low temperature fuel cell with aqueous KOH electrolyte [AICE PREPRINT 13B] 10 p1484 A66-21182

Double-layer capacitance of solid silver bromide determined against platinum and gold electrodes, using electrochemical cell 12 p1933 A66-25002

Two-and three-phase boundary electrodes for fuel cells 13 p1997 A66-25113

Electrochemical kinetics of fuel cells - Conference, Moscow, 1964 13 p1998 A66-25667

Oxygen regeneration from solid electrolytic reduction of carbon dioxide for space cabin atmosphere [AICE PREPRINT 47D] 17 p2867 A66-32673

Hydrolysis under space cabin atmosphere conditions using hydrogen diffusion cathode to remedy current-blocking effect of gas between electrodes [AICE PREPRINT 47F] 17 p2867 A66-32674

Stability and lifetime of electrochemical controlled resistances depend on reading electrode material, configuration and choice of electrochemical system 17 p2878 A66-33493

Reversible light-modulated electrolytic cell for use as real-time spatial filter 18 p3077 A66-33995

Improved operating characteristics of solid-electrolyte cell at room temperature by using silver sulfur iodide 18 p3055 A66-34901

Open circuit half-cell potentials of calcium in thiocyanate-liquid ammonia solutions 18 p3055 A66-34902

Equation explaining polarization of solid electrolyte cell with silver plate anode, noting role of current density 18 p3056 A66-34903

Electrochemical power generator using silver cathode and zinc anode 21 p3698 A66-39474

Nonaqueous lithium-nickel halide batteries capabilities and limitations, explaining methods of selection and evaluation of solvent, solutes and combinations for electrolytes 23 p4021 A66-41752

High energy density Zn/O battery system, noting good low oxygen pressure and low temperature performance characteristics 23 p4022 A66-41759

Primary electrochemical power systems including gas recombination devices, sterilizable battery, fuel cells, alcohol-air units, etc 23 p4023 A66-41768

Fuel cells with ceramic electrolyte operating at high temperatures, calculating voltage and efficiency 24 p4161 A66-42503

Onboard spacecraft generation system extracts necessary breathing oxygen from ambient air, using electrochemical cell that

separates oxygen from inert gases and impurities 24 p4162 A66-42956

**ELECTROCHEMICAL CORROSION**

Corrosion rate of BT-1 titanium and 9Kh18N12MT stainless steel in manganese-ammonium sulfate solutions 01 p0089 A66-10990

Effect of corrosive environments on various metals and anticorrosion techniques to protect metal surfaces 04 p0534 A66-13374

Galvanic corrosion in panel-type couples of dissimilar metals with magnesium evaluated from tensile strength loss 08 p1241 A66-19714

Corrosion resistance and electrochemical properties of alloys of niobium-titanium system 09 p1390 A66-20838

Corrosion resistance, electrochemical and mechanical properties of alloys of titanium-niobium system 09 p1390 A66-20839

Surface hydride corrosion film effect on electrolytic corrosion and oxidation of titanium 09 p1390 A66-20841

Corrosion resistance of yttrium is higher at higher pH because of slower anodic process 10 p1546 A66-21747

Corrosion of rhenium in various acids and hydroxides is electrochemical in nature and determined by kinetics of anodic and cathodic processes 10 p1546 A66-21748

Corrosion occurrence and control, noting prone areas, detection and removal 11 p1717 A66-23014

Corrosion mechanism for eutectic or near-eutectic Mg-Zn alloys in halide solution 13 p2110 A66-26026

**ELECTROCHEMICAL MACHINING**

Electrochemical metal removal using component to be machined as anode and near mirror image of finished shape as cathode in electrolysis 01 p0079 A66-10974

Electrochemical shaped-electrode method of machining complex shapes compared to conventional method by three-dimensional copying 08 p1228 A66-18624

Structure and wear resistance of chromium-molybdenum deposits, noting parameters of electrolytic deposition, Amsler machine tests, etc [ONERA TP 319] 12 p1894 A66-24366

Electrode machining, nonliquid etchants developed for shaping metals by electrochemical milling [ASTME PREPRINT MR66-711] 12 p1886 A66-24416

Electrochemical machining at speed and control useful to shaping metal parts, analyzing electrolyte composition, temperature, pressure, voltage, penetration rate, etc [ASTME PAPER MS66-156] 14 p2299 A66-26954

Electrochemical machining of complex parts and comparison with electric discharge process [ASTME PAPER MR66-157] 14 p2299 A66-26955

Tooling and manufacturing technique and requirements for controlled removal of metal by chemical and electrochemical processes [ASTME PAPER MR66-165] 14 p2300 A66-26957

Electrochemical machining, discussing relationship between total current, applied potential, electrolyte flow rate, electrolyte conductivity and electrode gap [ASME PAPER 66-PROD-5] 14 p2300 A66-26978

Electrochemical machining techniques, noting PERA die-sinking system 20 p3562 A66-37426

Electrochemical machining advantages over electrical discharge machining and traditional machining processes 21 p3743 A66-38669

Electrochemical machining of refractory metals and complex shape 21 p3744 A66-39132

Surface alterations in manufacturing, discussing effects of electrochemical grinding and electrical discharge grinding in comparison with abrasive grinding and face milling 21 p3744 A66-39194

Manufacturing techniques for turbojets, considering metals difficult to machine and components of shapes difficult to form 23 p4074 A66-41656

Chemical and electrical energies in manufacturing noting role of numerical control, hydrostatic processes, forming, electrochemical machining, etc 24 p4217 A66-42336

**ELECTROCHEMICAL OXIDATION**

Electrochemical oxidation of p-n junctions on silicon surface in potassium nitrate solution in ethylene glycol, noting electric current 03 p0413 A66-13203

Fuel cell systems, particularly hydrogen peroxide type, noting electrochemical oxidation, water production, thermal energy, electrolyte, etc 06 p0808 A66-16391

Electrolyte-soluble fuels such as methanol, ammonia and hydrazine, noting electrochemical oxidation properties, power output, stored energy content, etc 07 p0996 A66-18472

Fuel cells oxidizing saturated and unsaturated hydrocarbons at high temperatures 07 p0996 A66-18475

Anodic luminescence in electrochemical oxidation of silicon crystal 09 p1410 A66-19897

Adsorptive phenomena effect on reaction kinetics of electrochemical oxidation involving organic materials on platinum electrode 13 p2017 A66-25676

Polarization characteristics of oxidation electrochemical oxidation-reduction processes of metallic single crystals in acid chloride solution 14 p2232 A66-27311

Solid state reduction of lanthanide ions in laser hosts, effect of presence of recombination hole-centers in photoreduced samples and elimination during electrochemical process 14 p2362 A66-27464

Performance analysis of carbon-supported platinum-ruthenium alloy catalysts with respect to anodic oxidation of methanol in acid electrolyte 17 p2870 A66-31898

Oxygen reduction on titanium nitride noting rate of electrochemical oxidation in fuel cell studies 24 p4170 A66-42422

**ELECTROCHEMISTRY**

Carbon dioxide reduction systems using chemical, electrochemical and thermal energy 02 p0185 A66-11641

Semiconductor electrochemistry and principal theoretical and experimental problems in future 03 p0331 A66-13155

Electrochemical current generator principles based on oxyhydrogen fuel cell for space travel, stressing regeneration by using solar radiation in photochemistry 04 p0459 A66-13545

Electrochemical and chemiluminescent ozonesonde performance, using analysis of comparative ascents 04 p0517 A66-14451

Selective separation of nickel titanium and nickel aluminum alloys and electrochemical behavior in various electrolytes 06 p0896 A66-16542

Potential distribution at germanium-electrolyte interface in iodide ion solutions 08 p1278 A66-19824

Electrochemical and corrosion behavior of Al-based Fe, Ni, Ti, Cu and Sb alloys and intermetallic compounds 09 p1390 A66-20840

Diffusion of electrolytic hydrogen through membranes of iron crystals as function of stress, temperature and dissolved hydrogen concentration 11 p1718 A66-23071

Potential sweep method for organic and adsorption analyses, showing relation between galvanostatic and fast potential sweep transients, noting mathematical analysis of current-potential transients 12 p1812 A66-25000

Chemiluminescent technique for flow visualization using electrochemical system and water tunnel 15 p2476 A66-29688

Chemical deposition fabrication techniques to integrate isolated thermal and electrical path into thin film substrate 17 p2883 A66-32118

Water electrolysis unit designed as flight prototype to support four-man crew for one-year mission with 90-day resupply intervals [AICE PREPRINT 47B] 17 p2867 A66-32671

Continuous flow, solid state electrochemical device for simultaneous carbon dioxide removal and oxygen generation [AICE PREPRINT 47E] 17 p2867 A66-32675

Thermodynamic properties and electromotive force of germanium telluride



used in electrochemical schemes 19 p3434 A66-35360  
Carbon dioxide decomposition and oxygen reclamation by chemical reaction with electrochemically reduced lithium 19 p3292 A66-36234  
Semiconductor electrochemistry and principal theoretical and experimental problems in future 20 p3511 A66-38134  
**ELECTROCUTANEOUS COMMUNICATION**  
Reaction time to electrocutaneous stimulation confirmed as being faster to onset than to cessation of stimulation 24 p4163 A66-42318  
**ELECTRODE**  
**SA ANODE**  
**SA CATHODE**  
**SA DIFFUSION ELECTRODE**  
**SA PLASMA ELECTRODE**  
Cobalt electrode performance in high temperature fuel cells, presenting V-I characteristics 01 p0014 A66-10358  
Focusing and accelerating electrode materials for cesium contact ion engines, noting advantages of copper, beryllium and molybdenum [AIAA PAPER 64-684] 02 p0278 A66-11537  
Two ohmic electrodes or one ohmic and one barrier electrode for current-voltage stable-negative characteristic of cadmium sulfide, noting IR radiation effects 04 p0568 A66-14351  
Low work function collector with Ba-covered thin aluminum trioxide film electrodes for high efficiency thermionic converters 05 p0621 A66-15575  
High-pressure high-temperature hydrogen-oxygen fuel cells employing nonnoble metal catalyst /porous nickel/ as electrode 06 p0808 A66-16392  
Porous gas-diffusion electrodes analyzed by using four different models, comparing resulting current density-polarization characteristics 07 p0990 A66-17239  
Hydrogen-oxygen fuel cells, using ion exchange electrolytes 07 p0996 A66-18471  
Electrode types used in low temperature fuel cells, considering porous gas-diffusion, pore-free palladium membrane and slurry electrodes 08 p1168 A66-19064  
Welding properties of high strength steels, noting electrodes and carbon diffusion 08 p1231 A66-19169  
Chemical analysis, X-ray examination, surface area determination, Tafel overvoltage and porosity measurements applied to battery electrode behavior during cycling 08 p1170 A66-19642  
Electrical capacity of galvanic cell and crystal habit and surface property effects on porous cadmium hydroxide electrode electrochemical properties 08 p1171 A66-19644  
Charging current density, electrolyte concentration and temperature during charge effects on porous cadmium electrodes in nickel cadmium cells 08 p1171 A66-19645  
Deposition kinetics of solid phases on electrodes of second kind, noting conditions affecting crystal growth and lattice formation 08 p1171 A66-19648  
Low temperature low pressure hydrogen/oxygen alkaline fuel cell and electrode selection 08 p1172 A66-19653  
Zinc-silver oxide battery for extreme temperatures, noting electrode utilization efficiencies as function of current density 08 p1173 A66-19662  
Sputtering yields of aluminum, copper and titanium measured as function of cesium ion energies for use as electrodes on cesium ion engines [AIAA PAPER 66-203] 10 p1575 A66-21445  
Electron-ion emitting characteristics of various electrode materials with cesiated surfaces for cesium contact ion thrusters [AIAA PAPER 66-208] 10 p1592 A66-21447  
Space-charge theory for steady one-dimensional current flow across evaluated space between plane electrodes 10 p1557 A66-21573  
Finite size electrode effect on electrical parameter in MHD generators with segmented electrodes 12 p1802 A66-23576  
Double-layer capacitance of solid silver bromide determined against platinum and gold electrodes, using electrochemical

cell 12 p1933 A66-25002  
Two-and three-phase boundary electrodes for fuel cells 13 p1997 A66-25113  
Functional mechanism of gas diffusion electrode 13 p1998 A66-25668  
Performance of porous gas diffusion electrode 13 p1999 A66-25669  
Theory of gas porous electrode with model 13 p1999 A66-25670  
Design of gaseous diffusion electrode 13 p1999 A66-25671  
Performance of wetted porous electrodes with reactant feed by diffusion 13 p1999 A66-25672  
Operation of porous electrodes where reactant is fed in and reaction product is removed by forced stream of electrolyte, reactant and product mixture 13 p1999 A66-25673  
Capillary equilibrium in gaseous porous electrode 13 p1999 A66-25677  
Segmented electrode MHD generator performance for various electrode-insulator length ratios 13 p2000 A66-25714  
Diaphragm-shaped external electrode used to define shape of plasma column in Tokamak machines, noting ways of maintaining plasma column equilibrium 13 p2148 A66-25755  
Electrical characteristics of linear, segmented electrode, Hall and Faraday MHD generators operating in equilibrium and nonequilibrium ionization modes, obtaining data on loss mechanisms 13 p2001 A66-26256  
Cryogenic resistance spot welding of refractory metals and conventional aerospace materials [ASTME PAPER AD66-111] 14 p2299 A66-26950  
Effect of vacuum arc remelting of air-melt electrodes on structure and elevated temperature properties of nickel base gas turbine superalloy [ASME PAPER 66-GT-113] 14 p2313 A66-27007  
Properties of second-gate electrode of MOS-FET and application as voltage-controlled integrator 14 p2248 A66-27052  
Two ohmic electrodes or one ohmic and one barrier electrode for current-voltage stable-negative characteristic of cadmium sulfide, noting IR radiation effects 14 p2368 A66-28249  
Tangential electrode forces on cathode and anode electrode for arc moving in magnetic field are not negligible in plasma driving 15 p2428 A66-28687  
Electrode implantation in dogs and detection of action currents in vegetative nerves after ten months 15 p2444 A66-29499  
Interaction of plasma jets ejected from electrode spots with accelerating magnetic field as possible cause of electrode polarity effect on flat-electrode-type plasma acceleration 16 p2757 A66-30106  
Electrode geometry, optimum configuration of hot-filament vacuum ionization gauges, and ion-collector burying technique 17 p2923 A66-31981  
Formation process of rotating plasma in homopolar-type short coaxial-electrode system in hydrogen, nitrogen or argon discharge 17 p2972 A66-32973  
Atmospheric electrode effect equations solved for case with no nuclei and convection and constant ionization 17 p2922 A66-33350  
Atmospheric electrode effect where condensation nuclei are present 17 p2922 A66-33351  
Derivative chronopotentiometry approach to measurement of transition times and study of electrode process 18 p3064 A66-34457  
Advantages and disadvantages of liquid fuels and oxidizers for direct fuel cells and electrode manufacturing techniques, noting role of nitric acid, methanol and hydrazine 18 p3056 A66-35239  
Possible measurement of current flow through electrode in plasma by inserting Rogowski coil in electrode 19 p3357 A66-35807  
Low-inductance hydrogen gas discharge switch tube based on gas pressure-electrode spacing control of ionizing collisions 19 p3280 A66-35812  
Two-dimensional problem of current

distribution on surface of permeable electrodes adjacent to flow of conducting medium under Hall effect 20 p3611 A66-38110  
High impedance electrode technique for large-scale flight physiological data collection, emphasizing skin preparation 22 p3856 A66-39790  
Output characteristics of cesium thermionic converter as function of size of electrode gap, using device with movable air-cooled stainless steel anode 22 p3853 A66-40943  
Effectiveness parameters of spherical shield electrode surrounding negative dielectric junction of insulator in high vacuum 23 p4042 A66-41040  
W-diffusion bonding of lead telluride base thermoelements with nonmagnetic electrodes 24 p4216 A66-42117  
Oxygen electrolytic reduction using porous sintered silver electrode, noting effects of gas pressure, current and cathode thickness on potential as applied to fuel cells 24 p4161 A66-42333  
Hall effect influence on characteristics of MHD generator with two pairs of electrodes with symmetrical or crosswise connections 24 p4162 A66-42873  
**ELECTRODE FILM BARRIER**  
Hall constant of semiconductors noting dependence on specimen size, film and current electrode parameters 07 p1100 A66-17933  
Ion propulsion engine with replenishable liquid-film-protected tungsten electrode, discussing construction and mass loss rate vs temperature [AIAA PAPER 65-378] 20 p3629 A66-38167  
**ELECTRODEPOSITION**  
Rhenium electrodeposition on molybdenum in study of adhesion as affected by heating, chromium codeposition and cracks 01 p0088 A66-10989  
Electroless nickel plating using hypophosphite as means of producing coatings with smooth hard surface for metal mirror blanks for solar simulation 02 p0233 A66-11235  
Iron and nickel concentrations effect on composition, quality and current yield of electrodeposition of titanium from aqueous solutions 08 p1229 A66-18794  
Deposition kinetics of solid phases on electrodes of second kind, noting conditions affecting crystal growth and lattice formation 08 p1171 A66-19648  
Electrolytic deposition of copper and gold on germanium surface 09 p1338 A66-19896  
Structure and wear resistance of chromium-molybdenum deposits, noting parameters of electrolytic deposition, Amsler machine tests, etc [ONERA TP 319] 12 p1894 A66-24366  
Structural properties correlated with magnetic characteristics of annealed electrodeposited permalloy film 14 p2354 A66-26906  
Chemically deposited thin ferrite and garnet films 14 p2249 A66-27104  
Surface structure and superconductive properties of electrodeposited tin films 15 p2564 A66-28761  
**ELECTRODYNAMICS**  
**SA QUANTUM ELECTRODYNAMICS**  
Approximate solution of principal boundary value problem of electrodynamics 02 p0262 A66-12246  
Electrodynamical jump conditions and momentum-energy laws at arbitrary moving boundary derived three-dimensionally 06 p0917 A66-16435  
Electromagnetic conductivity of superconducting alloys in critical regions in high magnetic fields 07 p1108 A66-18435  
Quantitative electrodynamical experiment on Josephson oxide tunneling junction, verifying time dependence of Josephson equation 07 p1108 A66-18438  
Extension of Ward relations to gravity, in close analogy to electrodynamics, using Gupta formulation of Einstein theory 08 p1255 A66-19078  
Text on electromagnetic force principles including Maxwell equations, electrostatics, electromagnetic waves, electron theory, relativity, etc 08 p1256 A66-19465  
Measurement of magnetic field produced by rotating singly and multiply-connected



- superconductors, formulating macroscopic electrodynamics of rotating body at low angular velocities 09 p1418 A66-20041
- Analogue simulation of nonlinearly rigid systems for hard and soft elasticity by electrodynamic analogy methods 11 p1779 A66-22236
- Friction and inertia fields induced by electromagnetic effects arising in motion of hard magnetic moment in thin circular film 11 p1753 A66-22808
- Variational formulation for linearly coupled magnetothermoelasticity, examining electrodynamics of slow moving media, equations of motion and coupled thermoconductivity equation 12 p1963 A66-24028
- Relativistic electrodynamics of moving medium, discussing Maxwell-Minkowski equations, Born equations, field vector transformations, etc 12 p1915 A66-24650
- Vibration constant of electromechanical transformation in electrodynamic vibrators 13 p1997 A66-25079
- Standard inductive energy formulas lead to error if applied to vortices in rotating fields 13 p2068 A66-26684
- Electrodynamic boundary conditions at moving boundary, determining fields in interior of semiminfinite fixed channel 14 p2235 A66-27041
- Local equations of electrodynamics for magnetic penetration and stability in London-type superconductors 16 p2784 A66-31564
- Electrodynamic properties of homogeneous magnetoactive plasmas including wave propagation, excitation, scattering, etc 20 p3608 A66-37488
- ELECTROENCEPHALOGRAM /EEG/**
- Sleep restriction effects, discussing electroencephalographic measurement results 06 p0812 A66-16733
- Experiments with rats under anesthesia subjected to acceleration, noting electroencephalograms 08 p1175 A66-19085
- EEG and cortical and subcortical responses analysis of sensory stimulation in restricted dogs and normally reared littermates 11 p1644 A66-22950
- EEGs of monkeys stimulated cyclically by whole-body vibration, plotting coherence functions relating brain records to acceleration records 12 p1806 A66-24228
- Chest-to-back accelerations effect on human electroencephalograms and work capacity 15 p2437 A66-29475
- Periodometer automatic analysis of periodic diurnal variations in EEG observations of six healthy men 15 p2440 A66-29503
- Effect of head-to-foot accelerations of up to 10 g on rabbits, noting changes in ECG, EEG, brain histology, etc, leading to ischemic conditions 18 p3060 A66-34408
- Amplitude and wave shape of averaged evoked responses in awake animals including man 20 p3505 A66-37055
- Spectral analysis of human EEG generators in posterior cerebral regions 20 p3506 A66-37604
- EEG relation to average evoked potentials and human reaction time to visual stimuli for trials with and without feedback 23 p4029 A66-41550
- Neuronal spike populations and EEG activity in chronic unrestrained cats, noting multiple unit responses of acceleration/inhibition during behavioral conditioning procedures 24 p4169 A66-43098
- ELECTROENCEPHALOGRAPHY**
- Rheographic regional method for evaluation of cerebral and ocular circulation in cardiac and cerebrovascular disease 04 p0463 A66-14002
- Heart and breathing rate and electroencephalographic responses of rats during weightlessness 04 p0467 A66-14083
- Electroencephalographic variations in albino rats, discussing transverse acceleration effects before and after splenectomy 06 p0810 A66-15908
- EEG experiments on men exposed to intermittent photic stimulation under simulated IFR conditions produced drowsiness as primary response 17 p2864 A66-32165
- Correlation of adrenal steroids and alpha frequency in EEG 17 p2860 A66-32556
- Electrophysiological patterns and cerebral impedance characteristics in orienting and discriminative behavior 17 p2860 A66-32832
- Perceptual masking and enhancements of two flashes in evoked cortical potentials recorded by electroencephalography 23 p4029 A66-41549
- ELECTROEROSION**
- S SPARK EROSION MACHINING**
- ELECTROEXPLOSIVE DEVICE**
- Mathematical evaluation of RF energy effects on electroexplosive devices, taking into account limited maximum response of circuits 03 p0334 A66-12570
- Electroexplosive device testing via pulse reflection techniques 12 p1934 A66-24674
- Electroexplosive devices in aerospace vehicles in two classes, propellants and high explosives, noting methods for controlling detonation desired 20 p3625 A66-37159
- Apollo launch escape tower electroexplosive bolts produced heat transfer to surrounding structural members, obtaining sound intensity maps 23 p4119 A66-41310
- ELECTROFORMING**
- Sintering and electroforming of complex shapes of pure chromium from hexavalent chromium bath with fluoride ions as catalyst 05 p0702 A66-15135
- Electroforming of large metal mirrors for aerospace application 15 p2509 A66-28823
- Aspheric and other irregular curve generation, using ordinary machinery 15 p2509 A66-28827
- Room and cryogenic temperature mechanical properties and microstructure of electroformed nickel 20 p3582 A66-37090
- ELECTROHYDRAULIC CONTROL**
- Electrohydraulic servovalve presenting essential characteristics of redundancy by majority choice in analog servosystem 05 p0612 A66-15413
- Static characteristics of electrohydraulic amplifier for pulse-width control drive 07 p0991 A66-17390
- Theoretical behavior and frequency response of electrohydraulic valve-controlled cylindrical vibrator capable of high thrust over wide frequency range 12 p1803 A66-23798
- Electrohydraulic digital actuator design and conversion of discrete electric input signal in binary code to linear motion 14 p2227 A66-28366
- Selection of size of hydraulic servomotor with rotary hydraulic motor controlled by electrohydraulic spool valve to reduce open-loop gain for given closed-loop stiffness 22 p3852 A66-40515
- ELECTROHYDRAULIC FORMING**
- Magnetomotive forming noting strain rate effect on material deformation, applications to aerospace technology and magnetohydraulic vs electrohydraulic forming [ASME PAPER 66-MD-19] 21 p3742 A66-38480
- ELECTROHYDRODYNAMICS**
- Growth and excitation of surface waves on capillary liquid jet stressed by electric field 07 p1087 A66-17946
- Energetics /engineering developments in energy conversion/ - ASME International Conference, University of Rochester, August 1965 07 p0992 A66-18308
- EGD power generation including functioning, coupling, broad and narrow channels, expanding momentum channel, efficiency, etc 07 p0993 A66-18313
- Data analysis of experiments with open-cycle supersonic EGD generator for application as power source and comparison with mathematical model 07 p0993 A66-18314
- Electric power generation using monopolar charged particles in fluid flow 07 p0994 A66-18315
- Mathematical models to explain parametric dependence of specific charge of liquid droplets produced by electrical spraying through metallic capillary at high potential [AIAA PAPER 66-252] 10 p1522 A66-21458
- Electrofluid dynamic power generation, high voltage generating device, direct energy conversion and supersonic electrogasdynamic generator 12 p1803 A66-24646
- Spherical drop in electric field with equilibrium maintained through balance between electric stress and variable pressure difference between inside and outside of drop, existing only if outside and inside fluids are in motion 13 p2129 A66-26302
- Laminar electrohydrodynamic flow in plane diffusor, taking into account molecular diffusion of space charge 17 p2969 A66-32544
- EHD traveling potential wave interaction inducing electroconvection in slightly conducting current without electrical contact with flow 23 p4104 A66-41496
- ELECTROJET**
- SA AURORAL ELECTROJET**
- Polar electrojet causing magnetic substorms in high latitudes flows westward along closed oval curve and is connected with auroral activity and outer radiation belt 08 p1216 A66-19216
- Occurrence frequency of midlatitude geomagnetic transition bays and relation to spatial movement of overhead electrojet current systems 08 p1218 A66-19395
- ELECTROKINETICS**
- Approximate theory for electrokinetic phenomena in capillary flows, determining interaction between mechanical and electrical energy 08 p1174 A66-19829
- Vacuum sheath effect on surface currents excited on plasma-immersed cylinder by EM and EK plane waves 22 p3954 A66-39940
- ELECTROLUMINESCENCE**
- Optical and electrical characteristics of injection electroluminescence p-n homojunctions from zinc selenium telluride crystals 01 p0119 A66-10346
- Luminous phenomena and electron emission discontinuity in aluminum thin film tunnel diodes 01 p0119 A66-10392
- Light emission in forward biased semiconductor p-n junction 03 p0409 A66-12577
- Alloy junction formation, discussing spectral characteristics of electroluminescence from forward-biased 4H SiC p-p alloy junctions as function of formation temperature 04 p0497 A66-13982
- Boron, nitrogen and gallium in photo-and electroluminescences of silicon carbide p-n junctions, noting radiative electron transitions 04 p0567 A66-14343
- Electrical and electroluminescent properties of GaAs diodes at voltages below onset of negative resistance 07 p1042 A66-17330
- Spectral distribution of luminescence excited in n-type GaAs and p-type GaP by fast-electron bombardment 07 p1096 A66-17339
- Efficiency of DC electroluminescence produced when minority carriers are injected into n-type ZnSe crystals depends on injection efficiency at contacts 07 p1097 A66-17342
- Stimulated state, stable, lasting and reproducible, in electroluminescent cells of sublimated zinc sulfide film obtained upon passage of increasing DC voltage through them at 77 degrees K 07 p1099 A66-17914
- Surface layers on ferroelectric barium-titanate crystals, noting parameters of RF induced electroluminescence 07 p1107 A66-18405
- Light activated low level switch consisting of electroluminescent GaAs p-n diode and double emitter silicon transistor 08 p1195 A66-19359
- Directional radiation from incoherent electroluminescent diodes, noting increase in refractive index for dielectric slab model 10 p1509 A66-21581
- Increased luminescence of gallium arsenide diodes by coating with titanium oxide 10 p1514 A66-22031
- Applied voltage, frequency and temperature gradient effects on ZnS /Cu/ electroluminescent cells 11 p1640 A66-22665
- Aircraft illumination utilizing electroluminescent panels 11 p1640 A66-22666
- Electroluminescence and emission spectra of indium-alloyed diodes made from phosphorus doped p-type ZnTe biased in either forward or reverse direction at liquid nitrogen temperatures 13 p2029 A66-25184
- Copper diffused gallium arsenide p-n



- p-n junctions, explaining current-voltage characteristics, light emission and capacitance of diodes at 300 and 77 degrees K 13 p2161 A66-25186
- 
- Green emission lines from solution-grown p-n junctions in GaP diodes doped with shallow donors and acceptors 14 p2251 A66-27231
- 
- Transmission spectra, electroluminescence-brightness variations with applied frequency and voltage and physical properties of ZnS thin films 14 p2361 A66-27315
- 
- Design, performance and application of multicell luminous-symbol screen with optically coupled photosemiconductive and electroluminescent films 14 p2297 A66-28112
- 
- Boron, nitrogen and gallium in photo-and electroluminescences of silicon carbide p-n junctions, noting radiative electron transitions 14 p2367 A66-28238
- 
- Emission bands in electroluminescence from gallium arsenide diodes, noting intensity at high and low voltages and radiation and doping effect 15 p2562 A66-28714
- 
- Spectral distribution of recombination radiation caused by electromagnetoluminescence /EML/ in indium antimonide 15 p2568 A66-29726
- 
- Increased luminescence of gallium arsenide diodes by coating with titanium oxide 16 p2661 A66-30851
- 
- Electroluminescence in avionic display application, noting panel design and ceramic ferroelectrics 16 p2708 A66-31411
- 
- Electroluminescence of silicon carbide diodes 16 p2668 A66-31781
- 
- Electroluminescent phenomena in injection lasers and laser diodes 17 p2985 A66-33251
- 
- Stimulated state, stable, lasting and reproducible, in electroluminescent cells of sublimated zinc sulfide film obtained upon passage of increasing DC voltage through them at 77 degrees K 18 p3155 A66-34174
- 
- External quantum efficiency of tin doped GaAs electroluminescent diode, noting effect of zinc diffusion 19 p3312 A66-35347
- 
- Efficiency limitation factors in radiative recombination in electroluminescent GaAs diodes, examining contribution of majority and minority carriers injected into P region 19 p3319 A66-36264
- 
- Replacing heated tungsten filament and IR filter by GaAs electroluminescent diode without filter for IR illumination 19 p3320 A66-36266
- 
- Electroluminescent photodiodes and diode light detectors applied to microcircuit design as relays, photochoppers or multichannel couplers 19 p3320 A66-36267
- 
- Recombination by tunneling in electroluminescent diodes to obtain line shape and light intensity in peak shift region 21 p3801 A66-38998
- 
- Injection luminescence in forward-biased CdTe p-n junction diode 23 p4112 A66-41298
- 
- Approximate steady state solutions of continuity equation containing effects of diffusion, drift and recombination for carrier diffusion region of forward-biased p-n junction over wide range of injection 24 p4249 A66-42225
- 
- Electrical and electroluminescent property of GaP diffused p-n junctions, accounting for V-I characteristics due to space-charge recombination by Sah-Noyce-Shockley theory 24 p4249 A66-42226
- 
- Injection electroluminescence in AlAs-GaAs as p-n junction diodes of graded energy gap 24 p4251 A66-42300
- 
- ELECTROLUMINESCENT LAMP**
- 
- Intensity growth and decay in Ar and Hg lines after switching on mercury vapor discharge lamps filled with Ar 15 p2542 A66-29716
- 
- ELECTROLYSIS**
- 
- Electrolytic titanium coating properties, covering porosity coating elimination by repeated electrolysis 04 p0536 A66-14005
- 
- Electrodialytical removal of reaction water from alkaline electrolyte of oxygen-hydrogen fuel cells 04 p0460 A66-14033
- 
- Flow visualization in turbomachinery, using hydrogen bubbles generated by electrolysis of working water 08 p1209 A66-19553
- 
- Transference numbers in ionized gases, contrasting current flow in electrolytes with steady state current flow in weakly ionized gases 12 p1920 A66-24097
- 
- Electrochemical machining, discussing relationship between total current, applied potential, electrolyte flow rate, electrolyte conductivity and electrode gap [ASME PAPER 66-PROD-5] 14 p2300 A66-26978
- 
- Life support subsystem for recovering breathable oxygen by water vapor electrolysis 17 p2866 A66-32194
- 
- Water electrolysis unit designed as flight prototype to support four-man crew for one-year mission with 90-day resupply intervals [AICE PREPRINT 47B] 17 p2867 A66-32671
- 
- Crystal growth of rare earth tungsten bronzes using electrolytic reduction of fused mixture of rare earth tungstate and tungsten trioxide 19 p3381 A66-36037
- 
- Widmanstätten patterns for electrolytic dissolution of iron meteorites and separation of nonmetallic portions, particularly kamacite 21 p3816 A66-39493
- 
- Electrolytic titanium coating properties, covering porosity coating elimination by repeated electrolysis 22 p3935 A66-40547
- 
- Electrolysis of wet hydrogen fluoride, noting analysis of anode products by gas chromatography and water content measurement by IR spectroscopy 23 p4118 A66-41236
- 
- ELECTROLYTE**
- 
- SA ANION
- 
- SA BATTERY
- 
- SA CATION
- 
- SA MOLTEN-SALT ELECTROLYTE
- 
- Surface recombination on interface between germanium/electrolyte boundary 05 p0738 A66-15462
- 
- Substitution of solid electrolytes for conventional liquid electrolytes in dry cell can enhance battery miniaturization potential without sacrifice of shelf life 08 p1167 A66-18715
- 
- Microporous metallic gas-diffusion electrodes in low temperature acid-electrolyte fuel cells 08 p1172 A66-19651
- 
- Stationary germanium potentials in oxidizing media and light illumination 09 p1410 A66-19895
- 
- Field effect and surface states at interface between germanium and electrolytes 10 p1586 A66-22145
- 
- AC resistivity profiles through anodic oxide films on Al and Al 12 p1895 A66-24392
- 
- Electro-oxidation of organic materials capable of functioning as fuel in fuel cells 13 p2017 A66-25674
- 
- Solid electrolytes which exhibit appreciable electron conduction for use in galvanic cells 13 p1999 A66-25675
- 
- Freezing potential for ammonia and sodium chloride solution at constant freezing rates, noting stationary nature of potential under stationary conditions 13 p2121 A66-26124
- 
- Effect of oxygen deficiency on acoustic organ of cats, determining content of potassium and sodium ions in perilymph, cerebrospinal fluid and blood serum 13 p2011 A66-26251
- 
- Electrochemical machining at speed and control useful to shaping metal parts, analyzing electrolyte composition, temperature, pressure, voltage, penetration rate, etc [ASTME PAPER MS66-156] 14 p2299 A66-26954
- 
- Increasing solubility of hydrocarbons in cesium-salt fuel cell electrolyte by replacing some of carbonate anion by fluoride 14 p2226 A66-27898
- 
- Direct and indirect oxidation fuel cell systems operating on hydrocarbon-air mixtures and using aqueous, molten and solid electrolytes, noting technological and economical problems 18 p3053 A66-33766
- 
- Improved operating characteristics of solid-electrolyte cell at room temperature by using silver sulfur iodide 18 p3055 A66-34901
- 
- Field effect and surface states at interface between germanium and electrolytes 19 p3440 A66-35759
- 
- Transient charge and discharge currents in tantalum oxide with anodic electrolyte and tantalum oxide with anodic metal 19 p3448 A66-36754
- 
- Stabilizing effect of vertical uniform magnetic field on Rayleigh-Taylor instability for electrolyte solutions 20 p3608 A66-37458
- 
- Surface recombination on interface between germanium/electrolyte boundary 20 p3622 A66-38135
- 
- Methanol-air fuel cells as long-life sources of energy for lighted buoys, TV stations, meteorological stations, etc 24 p4161 A66-42501
- 
- Mixing of gases in hydrogen-oxygen fuel cell, noting membrane allowing only electrolyte to pass through electrodes 24 p4161 A66-42502
- 
- ELECTROLYTE METABOLISM**
- 
- Electrolyte-soluble fuels such as methanol, ammonia and hydrazine, noting electrochemical oxidation properties, power output, stored energy content, etc 07 p0996 A66-18472
- 
- Mathematical model, using computer, to determine fluid and electrolyte distribution in principal body compartments of young 70-kg human male 12 p1809 A66-24229
- 
- ELECTROLYTIC MACHINING**
- 
- S SPARK EROSION MACHINING
- 
- ELECTROLYTIC POLARIZATION**
- 
- Germanium conductance measurement when immersed in aqueous electrolyte using DC and LF AC methods as polarization function 03 p0407 A66-12403
- 
- Kinetic effects in fuel cells, discussing declining efficiency with increasing output, slow electron transfer effects, concentration polarization, etc 07 p0996 A66-18469
- 
- ELECTROLYTIC POLISHING**
- 
- Structure and wear resistance of chromium-molybdenum deposits, noting parameters of electrolytic deposition, Amser machine tests, etc [ONERA TP 319] 12 p1894 A66-24366
- 
- ELECTROMAGNET**
- 
- SA COIL
- 
- SA KERR EFFECT
- 
- High field liquid-neon-cooled superconducting electromagnet for cryogenic solid state research 20 p3601 A66-37106
- 
- ELECTROMAGNETIC ABSORPTION**
- 
- Electromagnetic field absorption by electrons of semiconductor situated in quantizing magnetic field 01 p0123 A66-10725
- 
- Electromagnetic reflection characteristics of ferrite wedge absorber and lossy magnetic layers 02 p0195 A66-11253
- 
- Anisotropic absorption of electromagnetic waves by hot carriers in germanium 02 p0277 A66-12082
- 
- Anisotropic electron velocity distribution for magnetosphere assumed and complex refractive indices evaluated, using cyclotron absorption explanation of whistler cut-off 05 p0631 A66-14835
- 
- Anomalous energy absorption of electromagnetic wave impinging on semibounded plasma 06 p0915 A66-16232
- 
- Biological changes due to microwave absorption, examining energy losses due to ion conductivity and dielectric losses due to polarization relaxation in water molecules 09 p1336 A66-20931
- 
- Cerenkov electron absorption of Alfvén and magnetoacoustic waves in plasma cylinder, obtaining formula for energy absorbed by plasma and damping factor where there is no resonance layer 11 p1743 A66-22443
- 
- Steady state resonance absorption of electromagnetic wave and cyclotron heating of low-density plasma 17 p2965 A66-32321
- 
- Electromagnetic transmission and absorption in collisionless plasma slab with density gradient 17 p2876 A66-32979
- 
- Order-disorder parameter determined from HF absorption in pure superconducting films 18 p3158 A66-34687
- 
- Microwave absorption in normal conducting films of gold plated onto superconducting tin indicates resistivity and transition temperature of gold consistent with proximity effect 19 p3443 A66-35999
- 
- Low effective resistivity of gold film plated onto tin determined by low temperature microwave absorption measurement and explained by free-electron model and superconductivity proximity effect 19 p3443 A66-36000
- 
- Superconductor electromagnetic absorption in energy gap region, examining gap



- anisotropy, multiple gaps, precursor absorption and magnetic perturbation effect on optical absorption spectrum 20 p3615 A66-37281
- Electromagnetic field absorption by electrons of semiconductor situated in quantizing magnetic field 20 p3619 A66-37662
- HF absorption by dense plasma in ion cyclotron resonance region 21 p3780 A66-39006
- Collisionless heating of plasma cylinder by HF field 21 p3781 A66-39008
- Electromagnetic wave absorption in nonuniform plasma cylinder in presence of forced oscillations 21 p3781 A66-39009
- Induced microwave absorption in carbon dioxide studied at frequency of 9260 mc/sec over temperature range from 270 to 500 degrees K and pressures as high as 95 atm 22 p3985 A66-40909
- Monograph on electronic theory of heavily doped semiconductors covering energy spectrum, perturbation theory, absorption of electromagnetic waves, density states, etc 23 p4109 A66-41119
- ELECTROMAGNETIC COMPATIBILITY**
- SA ELECTRONIC EQUIPMENT TESTING**
- Output criteria function in terms of interference and performance measure 03 p0333 A66-12569
- Nomograph filter networks for control of electromagnetic interference, noting loss characteristics of element filters 03 p0341 A66-12571
- Implementation of airborne command and control systems, emphasizing communications equipment, data processing facilities, electromagnetic compatibility and aircraft configuration parameters [AIAA PAPER 65-727] 03 p0336 A66-13049
- Statistical properties of receiver output under interference conditions, obtaining first order output, probability densities, second harmonic and intermodulation interference terms 11 p1658 A66-23483
- SNAP 10a/Agema Space System, noting interrelationship of several subsystems and integration with nuclear power unit 12 p1857 A66-23677
- Radio communication, broadcasting and audio - IEEE International Convention, New York, March 1966 12 p1838 A66-24597
- Oscillator stability affecting electromagnetic compatibility during PRF generation, digital system reception, reception with phase lock, etc 12 p1838 A66-24599
- Electromagnetic compatibility tests on Minuteman weapon systems 133A and 133B 13 p2044 A66-26749
- Maximum and minimum power absorbed by antenna connected through coaxial transmission line to transmitter under unmatched conditions 18 p3078 A66-34168
- Packaging, shielding and other control techniques in formulation of grounding plan as basis of good EAGE design 20 p3542 A66-37194
- Electromagnetic compatibility of communications satellites, tropospheric scatter and line-of-sight microwave systems operating in same frequency band 23 p4040 A66-41597
- Solid state components and techniques applicable to spectrum signature measurements 23 p4047 A66-41599
- Graphical comparison of military RF interference specification limits based on electric field intensity at one meter antenna spacing 24 p4176 A66-43192
- ELECTROMAGNETIC CONTROL**
- Electromagnetic energy transport between coils or coils external to human body and coil implanted inside body is increased by using suitable ferrite core for receiving coil 06 p0820 A66-16852
- Small scale MHD fluid flywheel attitude control systems applied to deep space probes, suitable for overcoming cyclical additions of angular rate to satellite of 10 revolutions per day 16 p2811 A66-31253
- MHD theory applied to electromagnetic remote control of industrial processes and electromagnetic field effects on condensed media 18 p3142 A66-33700
- ELECTROMAGNETIC FIELD**
- Kinetic theory of Lorentz plasma in rotating magnetic fields and electromagnetic fields based on Boltzmann equation 01 p0113 A66-10640
- Linear accelerations of particles in spherical electromagnetic fluctuating field 02 p0195 A66-11254
- Achromatic electromagnetic quadrupole lens functioning for case of slight misalignment of fields 02 p0199 A66-11783
- distribution 02 p0199 A66-11783
- Electromagnetic field and radiation pattern of Hertzian electric dipole antenna in conical sheath 02 p0191 A66-11803
- Microvariations of Earth electromagnetic field with results recorded on tape in digital pulse code form 02 p0224 A66-12124
- Steps for V-I characteristic of Josephson tunnel current interaction with electromagnetic field in dielectric superconductors 03 p0407 A66-12282
- Plasma acceleration in combined constant electrical and HF field 03 p0397 A66-12386
- Model for behavior of optical maser in static magnetic field of arbitrary strength in Z direction and in electromagnetic field composed of traveling waves 03 p0379 A66-13135
- Stagnation enthalpy plasma due to propagation of electromagnetic shock wave 03 p0406 A66-13279
- Diffusion coefficient of solar protons in steady state electromagnetic medium of interplanetary space increases with increase in proton momentum 04 p0574 A66-13839
- Terrestrial electrical currents discussing Soviet studies on short-period fluctuations of terrestrial electromagnetic field in Arctic and Antarctic region 05 p0674 A66-15225
- Cosmic ray electromagnetic acceleration mechanism, calculating motion of charged relativistic particles in applied fields 05 p0753 A66-15388
- Steps for V-I characteristics of Josephson tunnel current interaction with electromagnetic field in dielectric superconductors 05 p0738 A66-15454
- Symmetrical transverse electromagnetic-mode directional couplers, deriving formulas for functional parameters and insertion-loss function 06 p0844 A66-16083
- Electromagnetic field in current-carrying region, discussing existence criteria of improper integrals 06 p0908 A66-16130
- Corrugation growth on infinitely conducting fluid sheets, discussing acceleration induced by constant axial and linearly increasing currents 06 p0871 A66-16276
- Nonradiative and stationary electromagnetic and gravitational fields 06 p0909 A66-16330
- Derivation of two equations for electromagnetic field and population inversion in solid state laser 06 p0893 A66-16773
- Image plane structure of inner and outer separatrix of asymmetric magnetic toroidal field 06 p0918 A66-16871
- Natural electromagnetic field of Earth microvariational peculiarities 07 p1027 A66-17309
- Electron diffusion in mutually perpendicular static electric and magnetic fields based on stability of laminar flow 07 p1081 A66-17953
- Aurora production via magnetic field induction during geomagnetic storms by ring current growth in Van Allen belt region 07 p1029 A66-18088
- Axisymmetric MHD flows classified by configuration of electromagnetic field 07 p1090 A66-18123
- Electromagnetic field near highly conducting cylindrical antenna of finite length excited by plane electromagnetic wave 08 p1189 A66-18668
- Rectilinear and smooth multiwave transition 08 p1191 A66-18922
- Field polarization of short-period variations /beats/ of Earth electromagnetic field investigated, using correlation analysis 08 p1214 A66-19034
- Electromagnetic field of metallic rectangular waveguide with anisotropic medium in interior 08 p1193 A66-19188
- Instability of noncollision plasma in strong external field in terms of development of nonpotential oscillations 09 p1408 A66-20599
- Antenna field calculations in Fresnel and induction regions 09 p1356 A66-20772
- Microwave emission from bulk n-type indium arsenide in presence of applied electric and magnetic fields at liquid nitrogen temperatures 10 p1572 A66-21069
- Electromagnetic field waveforms produced by transient plane waves scattering from finite objects related to those produced by impulsive plane waves 10 p1498 A66-21599
- Total field measurement in all directions in near zone of metallic and dielectric spheres and cones 10 p1502 A66-21635
- Integration of equations, approximating Maxwell equations, in curvilinear coordinates separating scalar Laplace equation, with vectors representing electric and magnetic fields 10 p1556 A66-21994
- LF plasma oscillations in constant external static electrical and magnetic fields 10 p1570 A66-22002
- Spatial density distribution of cold plasma probed by electromagnetic field 10 p1570 A66-22005
- RF electromagnetic fields to control state of flowing thermal plasma [AIAA PAPER 66-166] 11 p1742 A66-22210
- Charged particle motion determined by gravitational-electromagnetic field properties with motion equations following from integrability condition of field equations 11 p1735 A66-22343
- Radiation field and surface waves generated by linearly phased electric line current and electric current component oriented in plane parallel to unidirectional conducting screen, solved by modal method 11 p1652 A66-22549
- Surface conditions constituting front of electromagnetic field analyzed by Maxwell equations from point of view of generalized functions 11 p1654 A66-22636
- Electromagnetic induction in conducting sphere rotating in transverse field, extending results for steady state to unsteady rotation, determining magnetic moment 12 p1871 A66-24298
- Brillouin principle, formulated positively to express information amount in terms of physical entropy, applied to information transmission by electromagnetic field using thermodynamics, noting quantum mechanical expressions 12 p1817 A66-24337
- Deposition of cadmium selenide films for transducers of electromagnetic energy to acoustic energy at microwave frequencies, noting use of multiple film assemblies 12 p1839 A66-24616
- Nonrelativistic force in simple magnetizable fluid derived from thermodynamic information about energy and power 12 p1915 A66-24651
- Gravitational field effect on electromagnetic field, using rotating hollow sphere in electric and magnetic field with electric charge at center 12 p1916 A66-24995
- Wave interaction underlying diocotron effect and model of instability presentation, analyzing cylindrical wall-enclosed charge layers for application to plasmas and gas discharges 13 p2136 A66-25041
- Plasma acceleration in combined constant electrical and HF field 13 p2139 A66-25391
- Langmuir probe measurement of electromagnetic field present in cyclotron ion oscillations 13 p2140 A66-25426
- Electromagnetic fields guided by plasma walls in waveguide, determining reflection coefficients and surface impedance 13 p2148 A66-26037
- Electromagnetic oscillation by monochromatic beam moving over diffraction grating lying on shielded dielectric 13 p2049 A66-26052
- Quantum theory of lasers presented in terms of correlation functions of second-quantized electromagnetic and matter fields 13 p2103 A66-26214
- Coherence properties of quantized electromagnetic field and hierarchy of correlation functions for complex field operators 13 p2128 A66-26218
- Radiation impedance of infinite planar dipole array, phased for any angle of radiation, calculated by Fourier series expansion of field in plane waves 14 p2247 A66-26865
- Variational calculus formulation of classical electromagnetic field



- theory 14 p2330 A66-27022
- Electrodynamic boundary conditions at moving boundary, determining fields in interior of semiinfinite fixed channel 14 p2235 A66-27041
- Polarization vector in strong electromagnetic field, using two-band semiconductor, calculated from density matrix equation, relaxation times and recombination time 14 p2360 A66-27189
- Method of constructing particle distribution function for quasi-neutral plasma consisting of electrons and singly charged heavy ions 14 p2344 A66-27648
- Quasi-linear perturbation theory of transverse electromagnetic waves from instabilities in nonthermal magnetoactive plasma, using Boltzmann equation, applied to magnetospheric MHD 14 p2286 A66-27982
- Microvariations of Earth electromagnetic field with results recorded on tape in digital pulse code form 14 p2287 A66-28082
- Light transmission through optical diffraction lattice consisting of medium in EM field of laser beam 15 p2511 A66-28626
- Calculation of electromagnetic field within two-dimensional plasma sheath with static magnetic field, noting effect of electron-cyclotron frequency on refractive index of medium 15 p2549 A66-28707
- Huygen principle for electromagnetic field moving, isotropic, homogeneous and near medium, using Maxwell-Minkowski equations and Green function for field equation 15 p2537 A66-28783
- Two-dimensional isothermal liquid flow electrically conducting in channel under electromagnetic fields, finding self-modeling solutions, using Jacobi functions 15 p2551 A66-29221
- Covariant treatment of solutions of Einstein field equations representing pure gravitational radiation propagating in fluid and electromagnetic 15 p2542 A66-29621
- Media Interband optical absorption in germanium a crossed electric and magnetic fields, noting band perturbation theory, differential spectra, Stark broadening, experimental techniques, etc 16 p2776 A66-30736
- Rocket attitude determined by simultaneous measurement of geomagnetic field and electromagnetic field generated by radio wave transmitted by rocket-mounted dipole 16 p2810 A66-30958
- Coherence conditions effects on electromagnetic field density operators and photon density distribution in single excited mode 17 p2957 A66-31975
- Electric and magnetic fields effect on three-dimensional laminar boundary layer of conducting fluid near line of intersection of two surfaces 17 p2971 A66-32865
- Steady-state axially-symmetric channel flow of ionized gas in external electromagnetic field in one-dimensional approximation 17 p2971 A66-32867
- Electromagnetic field equations for plane near induction pump with secondary boundary effects 17 p2972 A66-32872
- Conducting fluid flow velocity measuring technique using properties of pulsed electromagnetic field 17 p2926 A66-32873
- Computer code study of magnetospheric trapped-particle drift under influence of magnetic field gradient, magnetic line curvature, electric rotational field and electric field across tail of magnetosphere 18 p3168 A66-34350
- Gravitational shielding and absorption, examining tidal effects induced in solid sphere by another sphere, analogy to electromagnetic fields, 18 p3135 A66-34450
- Electromagnetic cavity resonances in rotating systems investigated through covariant space-time formulation of classical electromagnetic field 18 p3119 A66-34451
- theory Green function applied to obtain alternative representations of source excite vector and scalar electromagnetic fields 18 p3071 A66-34564
- Energy characteristics of 11-year cosmic ray variations, evaluating electromagnetic conditions in interplanetary space for proton, alpha particle and electron variations in energy regions 18 p3176 A66-34752
- Hamilton principle applied to force equation for nonrelativistic and relativistic flow of compressible inviscid fluid with polarization and magnetization in connection with electromagnetic momentum 18 p3102 A66-34923
- Integration of equations, approximating Maxwell equations, in curvilinear coordinates separating scalar Laplace equation, with vectors representing electric and magnetic fields 18 p3136 A66-34971
- LF electromagnetic field behavior in cold magnetoactive plasma near resonance layer, noting condition for energy absorption increase 18 p3151 A66-35064
- Oscillations of inhomogeneous weakly ionized plasma situated in external electric and magnetic field, noting causes and conditions of plasma instability 18 p3151 A66-35066
- Derivation of two equations for electromagnetic field and population inversion in solid state laser 19 p3372 A66-35370
- Electron-phonon interaction current density, thermodynamic Green function and other electromagnetic properties of superconductors, using Froehlich-Hamilton model 19 p3438 A66-35481
- Frequency and spatially variable electric and magnetic polarizations induced in nonlinear media by electromagnetic fields 19 p3399 A66-35594
- Spatial charge region, excess electron concentration, capacitance and conductivity in semiconductor layer with Lorentz forces acting on carrier determined as functions of surface potential and applied electromagnetic field 19 p3442 A66-35819
- Thermometer for continuous temperature measurement of dielectrics and semiconductors in electromagnetic HF fields 19 p3358 A66-35836
- LF plasma oscillations in constant external static electrical and magnetic fields 19 p3407 A66-36089
- Spatial density distribution of cold plasma probed by electromagnetic field 19 p3407 A66-36089
- Common representation of electromagnetic field tensor and stress 19 p3474 A66-36319
- Governing equations for electromagnetic phenomena in lossy magnetoionic media in terms of compressivity tensor, deriving wave equations which are decoupled, giving resulting uncoupled differential equations 19 p3305 A66-36412
- Electromagnetic field analysis, determining dispersion relationship of array of identical fibers, assuming surface wave modes of each fiber are excited 19 p3305 A66-36418
- Ionospheric thermal radiation, discussing noise power per unit volume, spectral distribution, frequency, etc 19 p3352 A66-36631
- Electromagnetic field effect on heat transfer during laminar flow of electrically conducting incompressible fluid in flat channel 20 p3607 A66-36980
- Electromagnetic field penetration into magnetoactive plasma with calculation of total surface impedance of plasma 20 p3512 A66-37135
- Approximate solution for dipole radiator field in space containing two conducting long cylinders with parallel axes 20 p3512 A66-37146
- Gravitational waves in presence of electromagnetic field, deriving Einstein-Maxwell equations 20 p3550 A66-37308
- Resistive effects in type II superconductors near upper critical field examined, using Ginzburg-Landau equations 20 p3616 A66-37374
- Optical phonon production, showing existence of electric field strength range at low temperature scattering in which phonon emission results in electron stoppage 20 p3577 A66-37376
- Power transmission, gain, directivity pattern and reception between large aperture antennas in near-field region 20 p3529 A66-37709
- Electromagnetic and gas dynamic effects on magnetic compression of plasma loop 20 p3611 A66-38120
- Instability of noncollision plasma in strong external field in terms of development of nonpotential oscillations 20 p3611 A66-38133
- Antenna field calculations in Fresnel and induction regions 22 p3873 A66-39831
- Electromagnetic field of concentric rotating mass shells, noting Machian effects on cosmological models with near-Schwarzschild radius 22 p3948 A66-40525
- Adiabatic motion of auroral particles in model of electric and magnetic fields surrounding Earth, commenting on importance of higher order terms in asymptotic expansion 22 p3914 A66-40561
- Steady pearl type oscillations in terrestrial electromagnetic field, noting role of diurnal and seasonal variations 22 p3915 A66-40784
- Functioning of progressive wave plasma accelerators, discussing role of electromagnetic forces 23 p4100 A66-41177
- Energy gap and critical field rules for superconductors, discussing empirical and experimental values 23 p4113 A66-41375
- Velocity field of conducting fluid interaction with electromagnetic fields, noting applications to electric propulsion, MGD power generation and reentry 24 p4240 A66-42281
- Drift approximation of motion equations for relativistic charged particle in electromagnetic field, adiabatic trap, HF magnetic field, etc 24 p4241 A66-42332
- Book on instrumentation for high speed plasma flow including magnetic field balance, transducers, flow angle indicator, MHD profile meter, etc 24 p4211 A66-42487
- Plasma stabilization by HF electromagnetic fields, noting mode spectrum spacing along sample axis and dependence on field strength 24 p4242 A66-42517
- Maxwell field equations and constitutive equations, discussing best pedagogical formulation for electrodynamics 24 p4189 A66-42633
- Polarization vector in strong electromagnetic field, using two-band semiconductor, calculated from density matrix equation, relaxation times and recombination time 24 p4259 A66-43087
- ELECTROMAGNETIC INSTRUMENT**
- High temperature electromagnetic transducers applied as sensors for physical variables, including mechanical displacement and liquid metal flow and level 05 p0676 A66-14775
- Au continuous electromagnetic drive consisting of plasma generator and radial electric and axial magnetic fields acting as plasma accelerator 06 p0942 A66-16796
- Electromagnetic isotope separators used in nuclear physics for analysis of ion-matter interaction 08 p1257 A66-18694
- Design and operation of electromagnetic LF vibration counter, also used as tachometer when connecting electric timer into counter circuit 09 p1380 A66-20308
- Electronic components for microwave power engineering, employing electromagnetic amplifying lens, microwave rectifiers, etc 13 p2039 A66-25784
- Electromagnetic shutter for electroretinography has opening and closing times of 0.50 and 0.70 msec and range of varying controlled durations 13 p2083 A66-26552
- Problems when using RF diagnostic systems in flight test evaluation of ICBM systems, specifically when using EM systems during reentry [AIAA PAPER 66-406] 18 p3239 A66-33634
- Electromagnetic induction electrodeless plasma accelerator for thrust generation applicable to space vehicle propulsion [AIAA PAPER 66-567] 18 p3164 A66-34429
- ELECTROMAGNETIC INTERACTION**
- SA PLASMA-ELECTROMAGNETIC INTERACTION**
- Nonlinear interaction of two electromagnetic waves in infinite cold magnetoactive plasma 02 p0192 A66-11839
- Electromagnetic excitation of spherical radially laminar medium with interfaces solved rigorously by derived algorithm 03 p0331 A66-12286
- Phase angles of reflection and transmission coefficients for microwave energy of



rectangular waveguide whose electromagnetic field interacts with ferrite spheroid 04 p0496 A66-13909

Gravitational field interactions with Dirac fields and electromagnetic fields studied in framework of special relativity to find possible C-, P-and T-violating effects 05 p0717 A66-15349

Microwave induced generation of DC voltage across thin n-type germanium rod in waveguide 06 p0925 A66-16678

Nonlinear interaction between ordinary and extraordinary wave modes for collisionless cold magnetoplasma 07 p1090 A66-18203

Electromagnetic interaction between moving conducting ring and magnetic field inducing voltage in search coil 07 p1091 A66-18416

Electron temperature variation in argon MGD channel in crossed magnetic and electrical fields 08 p1263 A66-19174

Interaction of drift oscillations in homogeneous weakly turbulent plasma which tends to develop flute instability along magnetic field 08 p1264 A66-19274

Probability of high-energy cosmic ray muon undergoing electromagnetic interaction in lead with energy transfer at various ranges 08 p1286 A66-19836

Ionospheric electrodynamics, discussing conductivity, wind and dynamo theory, drift effect on ionospheric formation and wind-electromagnetic field interaction 10 p1533 A66-21852

Electromagnetic phenomena inside weak MHD shock wavefront 10 p1569 A66-21916

Thin nonrectilinear electron beam interaction with electromagnetic field of waveguide transmission line 11 p1655 A66-22723

Solar wind as radial flux of electromagnetic inhomogeneities, galactic ray modulation by solar wind and cosmic ray intensity variation with sunspot cycle 12 p1940 A66-24162

Cosmic ray variations and solar corpuscular stream in interplanetary space during March 1958 magnetic storm 12 p1940 A66-24164

Variations in cosmic ray neutron component intensity and solar corpuscular flux with H-component of geomagnetic field during magnetic storm 12 p1941 A66-24166

Kinetic theory of passage of s-and p-polarized electromagnetic waves through thin inhomogeneous plasma layer 12 p1816 A66-24225

Compensation and decompensation in ferromagnetic alloys viewed as electric interaction of spins 12 p1930 A66-24684

Nonstationary two-dimensional channel flow of compressible electrically conducting fluid subject to traveling magnetic field 13 p2140 A66-25422

Nonlinear interaction of electromagnetic waves in plasma, noting propagation of total and diffused wave 13 p2141 A66-25458

Models of matter-electromagnetic field interaction for gas lasers, using perturbation theory 13 p2103 A66-26216

Interaction of boundary layer produced by vortex flow of viscous electrically conducting fluid over disk with axial magnetic field and relation to MHD generator and hydromagnetic capacitor 13 p2156 A66-26707

Electromagnetic field interaction with accelerated material medium, considering ponderomotive forces and finiteness of deformations 14 p2335 A66-28048

Equilibrium binary correlations in classical relativistic homogeneous electron gas 14 p2336 A66-28275

Ferromagnetic microwave resonance isolators for use in waveguides 15 p2459 A66-28936

Electromagnetic form factors of electron and muon neutrinos evaluated, using intermediate vector-boson theory, noting renormalization induced by electromagnetic interactions 15 p2544 A66-28944

Electromagnetic cascades in Sydney 20-liter stack of nuclear emulsion 15 p2583 A66-29544

Nuclear radii for electromagnetic interactions of primary cosmic ray particles in nuclear emulsions 15 p2545 A66-29546

Busbar effect on interaction between conducting fluid flow and traveling wave magnetic field created by long line with

concentrated inductance and capacitance, deriving line gain 16 p2765 A66-31374

One-dimensional MHD equation solution, using calculus of variations 16 p2765 A66-31513

Slow wave interaction with drifting stream of carriers, including collision and diffusion effects, noting TWT and acoustic semiconductor amplifier cases 17 p2878 A66-31820

Energy pulse tensor formulation of law of conservation of energy in interacting electromagnetic field, using complete inhomogeneous Lorentz group 18 p3135 A66-34579

Electromagnetic interactions and collisions of particles in cores of EAS studied, using GM counters, plastic scintillators and Wilson cloud chambers 18 p3207 A66-35107

Bursts produced by high energy muons undergoing large energy transfers analyzed for information on muon electromagnetic interactions over region where muon spectrum is known 18 p3220 A66-35195

Electromagnetic interactions of muons analyzed underground using scintillator stack, deducing energy of cascade shower from size 18 p3221 A66-35199

Classification of underground electromagnetic shower events due to muon interactions in scintillator stack 18 p3221 A66-35200

Energy losses of relativistic muons in electromagnetic interactions, noting influence of atomic electrons on bremsstrahlung 18 p3222 A66-35208

Conducting nonmagnetic circular cylinder supported on magnetic field produced by alternating current 19 p3324 A66-35729

Approximation method using sum rules for energy shift in atomic system due to interaction of electrons with vacuum electromagnetic field applied to hydrogen, helium and lithium atom ground states and hydrogen molecule 19 p3402 A66-35995

Hydrodynamic stability of inhomogeneous plasma flows relative to potential electromagnetic oscillations 19 p3408 A66-36272

Phase angles of reflection and transmission coefficients for microwave energy of rectangular waveguide whose electromagnetic field interacts with ferrite spheroid 20 p3532 A66-37867

Thin dielectric film wave scattering, EM interaction responses and conductivity tensor 20 p3622 A66-38385

Electromagnetic interference from pulse circuits, switches and relays produced by photo-optical control systems 21 p3709 A66-38608

High frequency-stability EM wave source, applying thermal excitation methods to pencil quantum generator in IR region 21 p3749 A66-39336

High frequency-stability EM wave source, applying thermal excitation methods to pencil quantum generator in IR region 22 p3929 A66-39706

Kinetic theory of passage of s-and p-polarized electromagnetic waves through thin inhomogeneous plasma layer 22 p3867 A66-40587

Thin nonrectilinear electron beam interaction with electromagnetic field of waveguide transmission line 23 p4037 A66-41461

Linearly and circularly polarized fields in laser amplifier interaction with axial magnetic field, emphasizing combination tone production 23 p4079 A66-41624

Nonlinear interaction of electromagnetic waves in magnetoplasma for field-parallel wave propagation 23 p4041 A66-41642

Ultrarelativistic muon electromagnetic interaction energy loss due to bremsstrahlung and pair production 24 p4271 A66-42936

**ELECTROMAGNETIC MEASUREMENT**

Automatic measuring apparatus based on resonant cavities for measuring permittivity and permeability of ferrites as function of temperature 01 p0068 A66-10558

Transistorized proton magnetometer for observatory and field measurements, analyzing use of free-proton precession to excite electromagnetic signal 01 p0072 A66-11073

Dielectric and metallic rod equivalent circuit, examining resonant frequency change upon placement in waveguide, using perturbation techniques 05 p0649 A66-15120

Measurement of components of permeability and permittivity tensors of magnetized ferrites by cavity method 07 p1009 A66-17928

High sensitivity spinner magnetometer for remnant magnetic polarization measurement of rocks in paleomagnetic research 08 p1223 A66-19081

Absolute energy and power measurements from electromagnetic pressure in optical wavelength range 08 p1256 A66-19285

Microwave measurement of anisotropy in conductivity of semiconductor in strong electrical field, using comparison of absorption of two intersecting plane-polarized waves 08 p1224 A66-19288

High time-resolution measurement of knee position in magnetospheric ion density using whistlers 10 p1527 A66-21137

Measuring apparatus to determining amplitude and phase of components of electromagnetic wave transmitted and reflected by given propagation medium 13 p2022 A66-25465

Electromagnetic and ultrasonic flow measurement of blood flow rate for cardiocirculatory physiology, discussing future application of nuclear resonance and laser 14 p2230 A66-27553

Instantaneous electromagnetic torque measuring system developed by two-phase 60-cycle servomotor 18 p3110 A66-33834

Fast variations of electromagnetic field measured by satellites electron I and II used as indication of state of radiation belts and magnetosphere of Earth 19 p3344 A66-35257

Absolute power measurement at 1.2-mm wavelength, using gas-filled waveguide to measure rotational line absorption 22 p3921 A66-40895

**ELECTROMAGNETIC METHOD**

Magnetic storage, discussing mechanical and thermal energy conversion into magnetic field energy and electromagnetic energy transfer 05 p0717 A66-15335

Magnetic storage, discussing mechanical and thermal energy conversion into magnetic field energy and electromagnetic energy transfer 15 p2543 A66-29982

Magnetic field above surface of conductor with flaws that emerge at surface when direct current is passed through 24 p4218 A66-42897

**ELECTROMAGNETIC PROPAGATION**

**SA IONOSPHERIC PROPAGATION**

Self-field electron kinetic reaction to electromagnetic propagation in three-fluid Brownian plasma 01 p0110 A66-10335

Field structure of electromagnetic surface waves at Yagi array acting as waveguide 01 p0036 A66-10367

Electromagnetic wave propagation through multilayer isotropic and anisotropic structure 01 p0025 A66-10525

Propagation, interaction and scattering of electromagnetic waves on diffusing inhomogeneous cylindrical plasma beam 01 p0027 A66-10550

Propagation of cosmic synchrotron radiation by individual and aggregate electrons and effect on propagation and radiation of electromagnetic waves 01 p0133 A66-10647

Electromagnetic H-wave propagation of given frequency along plasma sheet surrounded by vacuum 01 p0030 A66-10697

Propagation constant of electromagnetic waves in laminated waveguide containing inhomogeneous isotropic plasma 02 p0265 A66-11410

Continuous electromagnetic radiation of two solar flares attributed to bremsstrahlung of nonrelativistic electrons and synchrotron radiation 02 p0283 A66-11660

Extension of Vladimirkii method for wave propagation in circular iris waveguide to include iris waveguides of rectangular cross section 02 p0199 A66-11787

Propagation and diffraction of electromagnetic waves in inhomogeneous magnetotonic medium, noting exoionospheric propagation and Hamiltonian optics 02 p0192 A66-12208



Electromagnetic wave propagation in plasma filled disk-loaded waveguide, obtaining plasma densities 03 p0332 A66-12426

Enhanced audiofrequency electromagnetic radiation between 500 and 1000 cps recorded in auroral zone by swept-frequency analyzer 03 p0418 A66-12659

Electromagnetic propagation in parallel strips of waveguide filled with two dielectric plates 03 p0343 A66-12936

Electromagnetic groundwave propagation along Earth surface, noting transmission and reflection when meeting abrupt electrical discontinuity 04 p0475 A66-13430

Electromagnetic wave propagation in multimode Earth waveguides of variable height 05 p0632 A66-14839

Light waveguide for general lens-like media, ideal lenses and continuous media with square-law index variation 05 p0634 A66-15178

Fundamental electromagnetic wave propagation in coaxial line filled with inhomogeneous dielectric 06 p0823 A66-15886

Propagation of electromagnetic pulses in terrestrial waveguides under transient conditions 06 p0826 A66-16023

Separation constants for finite gyromagnetic plasmas, discussing ion motion effects 06 p0826 A66-16024

Approximation technique for computing transmission and reflection coefficients for plane electromagnetic waves propagating through inhomogeneous stratified dielectric slabs 06 p0826 A66-16025

Nanosecond electromagnetic pulse dispersion in longitudinally magnetized plasma confined in coaxial transmission line 06 p0826 A66-16026

Electromagnetic wave propagation in semiconductor filled rectangular waveguide in presence of transverse magnetic field 06 p0846 A66-16092

Electric field and wave impedance in spin wave propagation in ferrimagnetic materials 06 p0847 A66-16101

Organic superconductor and dielectric IR waveguide, resonator and antenna models of insects sensory hairs, spines and pit pegs 06 p0847 A66-16103

Electromagnetic wave propagation through semiconductor with nonuniform density distribution in transverse magnetic fields 06 p0923 A66-16177

Electromagnetic propagation characteristics of Venus and Mars derived from atmospheric data 06 p0831 A66-16436

Transverse propagation of vertically polarized electromagnetic waves in horizontally stratified horizontally magnetized plasma 06 p0917 A66-16447

Asymptotic solutions of problems in wave propagation, examining electromagnetic field equations, hyperbolic equations, radiation from sources, etc 06 p0835 A66-16900

Propagation of microwaves through circular cylindrical metallic guide filled with two different dielectrics 06 p0857 A66-16951

Slab with periodically modulated refractive index, predicting short wave radiation pattern emitted 06 p0836 A66-16983

Variational method for dispersion curve of electromagnetic slow wave propagation in nonuniform plasma 06 p0836 A66-16988

Monographs on electromagnetic diffraction and propagation problems, particularly radio propagation in troposphere 06 p0836 A66-17087

Beam trajectories of electromagnetic waves in ionized toroid and effective reflecting toroidal surface 08 p1214 A66-19046

Propagation of acceleration and electromagnetic waves in homogeneously deformed uniformly polarized hyperelastic dielectric 08 p1271 A66-19228

Coaxial, rectangular and bandpass waveguides containing ferrite and dielectric plates in E plane, obtaining transcendental equations, determining electromagnetic wave propagation 08 p1194 A66-19312

Text on electromagnetic force principles including Maxwell equations, electrostatics, electromagnetic waves, electron theory, relativity, etc 08 p1256 A66-19465

Russian text on diffraction and radiation of waves 08 p1257 A66-19755

Interaction of ideally conducting sphere of

variable diameter and constant uniform magnetic field 08 p1186 A66-19760

Theory of thermal noise in ionosphere developed from Nyquist theorem expressing thermal fluctuations of current in localized resistance 09 p1340 A66-19846

Transition layer properties in reentry plasmas, examining electromagnetic propagation in plasma surrounding hypersonic missile 09 p1406 A66-19850

Quasi-linear theory of weakly turbulent plasma taking into account correlation of electric and magnetic microfields 09 p1407 A66-19966

Electromagnetic wave propagation characteristics of plasma slab on surface of arbitrary impedance, using simplified approach 09 p1342 A66-20257

Electromagnetic wave propagation in meteorology and geophysics, noting expression for refractive modulus in troposphere, considering attenuation and backscattering 09 p1343 A66-20276

Self-focusing of longitudinal electromagnetic waves in nonlinear plasma in strong magnetic field 09 p1343 A66-20343

Electromagnetic wave propagation in plasmas, surveying literature on RF field-plasma interactions [AIAA PAPER 66-170] 10 p1560 A66-21424

Influence of boundaries on wave propagation in compressible warm plasma 10 p1566 A66-21730

Propagation of quasi-TEM mode in ferrite-filled coaxial line 10 p1506 A66-21913

LF electromagnetic wave propagation peculiarities of semiconductor and negative differential conductivity effects 10 p1582 A66-21967

Electromagnetic wave propagation in plasma located in magnetic field of linear direct current 10 p1506 A66-22003

Kinetic approximation of electromagnetic surface wave propagation in infinite plasma sheath solved by Fourier method, noting resulting dispersion equation 11 p1743 A66-22441

Electromagnetic propagation into cavity formed by two parallel walls, for case of continuous wave impinging perpendicularly 11 p1653 A66-22558

Single scattering model for diffusion and propagation of waves in random media 11 p1654 A66-22635

Linear polarized plane electromagnetic wave diffraction by two pairs of parallel infinite coaxial cylinders 11 p1654 A66-22645

Beam waveguides for long distance electromagnetic wave transmission at optical wavelengths described by theory of focusing antennas 11 p1656 A66-22737

UHF ferrites as magnetically anisotropic media in which electromagnetic wave propagation rate assumes two values and magnetic permeability is of tensor nature 11 p1658 A66-23233

Electromagnetic propagation in rotating systems, classic analysis of mode-splitting phenomena caused by rotation of cavity resonator 11 p1658 A66-23266

Electromagnetic H-wave propagation of given frequency along plasma sheet surrounded by vacuum 11 p1658 A66-23299

Intense HF electromagnetic wave propagation in isothermal isotropic nonhomogeneous plasma, noting interaction with electrons of Langmuir frequency 12 p1921 A66-24212

Amplitude and phase velocity of electromagnetic waves in 1-30 kc range near Earth surface for plane and spherical Earth-ionosphere waveguide 12 p1817 A66-24278

Electromagnetic wave propagation in infinite uniform plasma medium with and without magnetic field 12 p1924 A66-24732

Collisional effects in region of electron cyclotron frequency on electromagnetic wave propagation in plasma 13 p2147 A66-25752

Reflection coefficients for electromagnetic waves in variable refractive index medium from approximate solution of linear differential equations 13 p2025 A66-26040

Propagation of circularly polarized electromagnetic waves in circular semiconductor cylinder surrounded by metal tube and immersed in DC magnetic field 13 p2169 A66-26238

Lower hybrid resonance in VLF range in satellites, noting noise emission due to trapping of electromagnetic wave propagation in transverse magnetic field 13 p2074 A66-26364

Electromagnetic wave propagation near missiles during hypersonic atmospheric reentry and computer program for determination of dissociated and ionized particle density in nonequilibrium nitrogen-plasma flow 13 p2150 A66-26374

Propagation of circularly polarized plane electromagnetic waves through helium plasma along direction of static magnetic field, determining electron density 13 p2154 A66-26672

Propagation of linear polarized electromagnetic waves through helium plasma along magnetic field, measuring phase and intensity of components of electric field 13 p2155 A66-26673

Emergence point of conical microwave beam transmission through nonuniform electron plasma 14 p2234 A66-26860

Light reflection from dielectric films of continuously varying refractive index 14 p2356 A66-26966

Magnetoionic couplings and electromagnetic wave propagation in horizontally stratified layer of gyrotropic medium 14 p2283 A66-27125

VLF electromagnetic propagation parameter determination by field strength measurements over medium distances in ionosphere 14 p2235 A66-27130

Electromagnetic wave propagation in two waveguides with different cross section connected by long continuous slot 14 p2251 A66-27169

TE surface wave determined by propagation and external magnetic field directions used in microwave circuits 14 p2363 A66-27518

Book on electromagnetic wave propagation, noting wire antenna radiation, radio astronomical antennas and plasma EM wave 14 p2239 A66-27719

Electromagnetic transmission through thin silver film on dielectrics 14 p2364 A66-27747

Plane wave behavior, as deduced from Mathieu function, analyzed in permittivity modulated slab immersed in medium of arbitrary constant permittivity 14 p2240 A66-27913

Propagation of ionizing fronts across magnetic field, examining flow behind and ahead of front 14 p2347 A66-28305

Antenna and propagation - IEEE International Symposium, Washington, D.C., August 1965 15 p2454 A66-28566

Electromagnetic and plasma wave propagation in inhomogeneous compressible isotropic collisionless electron plasma bounded by closed surface in free space 15 p2449 A66-28592

Helicon wave propagation in InSb and InAs at room temperature 15 p2559 A66-28630

Nonlinear terms of electromagnetic field in ionized gas reduced to linear system and single nonlinear equation 15 p2547 A66-29648

Propagation behavior of circular waveguide enclosing column of isotropic plasma, considering effect of glass walls for microwave device application 15 p2467 A66-29859

Frequency of arising stationary finite-amplitude waves in ferrites depends on properties of medium, angle between magnetic field and propagation direction and wave amplitude 16 p2784 A66-31548

Propagation of cosmic synchrotron radiation by individual and aggregate electrons and effect on propagation and radiation of electromagnetic waves 17 p2992 A66-32062

Parametric amplification by monochromatic pumping of electromagnetic oscillations of substance contained in resonator 17 p2885 A66-32244

Emission of electromagnetic waves by electron flux moving inside ring waveguide 17 p2874 A66-32248

Kinetic theory of electromagnetic propagation in confined magnetoactive plasma 17 p2968 A66-32539

Transverse electromagnetic wave transformation into ion-acoustic plasma oscillations with formation of intermediate



Langmuir electron wave 17 p2969 A66-32542  
 Electromagnetic wave propagation in cylindrically stratified plasma, noting ODE describing transverse propagation of axial component 17 p2876 A66-33279  
 Angular propagation constants for electromagnetic modes which may exist in continuously curved waveguide bends of rectangular cross section for microwave application 18 p3072 A66-34569  
 Time harmonic wave propagation in perfectly conducting large waveguides containing random media, emphasizing computation and physical interpretation of wave motions 18 p3072 A66-34570  
 Longitudinal propagation of superlow frequency electromagnetic waves through plane-laminar magnetoactive ionospheric plasma 19 p3296 A66-35298  
 Lunar line waveguide parameters calculated for inner conductor displacement and ratio of radii 19 p3311 A66-35301  
 Transverse propagation of electromagnetic waves in cylindrically stratified axially magnetized plasma, noting profiles of permittivity tensor 19 p3303 A66-35856  
 Configuration interaction in helium continuum between first and second quantum thresholds 19 p3402 A66-35994  
 Exact solution of nonlinear relativistic equations of motion for electron in right circularly polarized wave propagating in whistler mode parallel to external magnetic field 19 p3303 A66-35998  
 Electromagnetic wave propagation in plasma located in magnetic field of linear direct current 19 p3303 A66-36087  
 Skin-effect theory for axisymmetric plasma-field configurations 19 p3409 A66-36309  
 Incidence of cylindrical /spherical/ local-plane electromagnetic wave on weak plasma, using ray-optics methods, leading to field peculiarities 20 p3512 A66-37139  
 Self-focusing of electromagnetic waves in nonlinear anisotropic medium 20 p3513 A66-37154  
 Ionospheric electric current effects on upper atmospheric electromagnetic wave transmission and propagation, discussing magnetospheric effects, solar wind, geomagnetic field, etc 20 p3550 A66-37434  
 Behavior of transverse wave numbers /separation constant/ for electromagnetic wave propagation in anisotropic homogeneous cold plasma of arbitrary cross section 20 p3608 A66-37454  
 Antenna radiation pattern synthesis for various array distributions, noting methods applied 20 p3529 A66-37706  
 Antennas with leaky wave characteristics, noting similarities and differences with wave diffraction 20 p3529 A66-37707  
 Slot antenna research, discussing arrays and polarization characteristics 20 p3530 A66-37710  
 Formula derivation for directivity of short endfire antenna array, obtaining current amplitude and phases for maximum gain 20 p3531 A66-37725  
 Recognition and subsequent amplification of difference frequency in plasma-beam system with two electromagnetic waves propagating in opposite direction 20 p3519 A66-38006  
 Propagation paths between hemispheres followed by usual and unusual whistlers, giving rise to series of echoes 20 p3553 A66-38077  
 Cathode ray oscillograph-directional antenna recordings of electromagnetic pulses from lightning discharges 20 p3553 A66-38081  
 Book on tropospheric radiowave propagation, discussing diffraction theories, scattering phenomena, transhorizon propagation, etc 20 p3520 A66-38091  
 Microwave transmission power loss for electromagnetic propagation through bounded solid state plasma waveguide in transverse magnetic field 21 p3703 A66-38755  
 Electromagnetic wave radiation from dipole source in thin plasma slab becoming weak outside plasma, considering total reflection 21 p3703 A66-38759  
 Electromagnetic wave propagation in plasma along weakening magnetic field, considering spatial dispersion associated

with ion thermal motion 21 p3781 A66-39010  
 Longitudinal and transverse electric fields in electron beam due to interaction with plasma, showing that both fields are components of same wave 21 p3782 A66-39020  
 Electromagnetic wave propagation, excitation and dispersion in metals in magnetic field 21 p3792 A66-39300  
 Refractive index equation derived for oblique wave propagation in compressible general magnetoplasma with arbitrary directed magnetostatic field 21 p3793 A66-39350  
 LF electromagnetic wave propagation peculiarities of semiconductor and negative differential conductivity 21 p3804 A66-39546  
 Vector potential function solution to Maxwell-Minkowski equations describing cut-off phenomena for EM wave propagation in wave guide filled with homogeneous isotropic lossless moving medium 22 p3862 A66-39783  
 Numerical solution of full-wave equation with mode coupling governing electromagnetic wave propagation in horizontally stratified inhomogeneous anisotropic medium 22 p3863 A66-39938  
 Three-dimensional electric field wave equation for homogeneous gyrotropic compressible drifting plasma derived for case having magnetostatic field and drift velocities in arbitrary directions 22 p3865 A66-40099  
 Uniform magnetic field effect on plane acceleration wave propagation and growth in homogeneously deformed perfectly electroconductive elastic material 22 p3955 A66-40135  
 Growth of plane acceleration discontinuities propagating into homogeneously deformed hyperelastic dielectric material in presence of magnetic field 22 p3948 A66-40136  
 Polarized EM wave propagation and microwave Faraday rotation in solid state plasma in circular waveguide under strong magnetic field 22 p3964 A66-40170  
 Quasi-optical measurement of Faraday rotation in oversize waveguide at 2-and 1-mm wavelengths 22 p3876 A66-40172  
 Intense HF electromagnetic wave propagation in isothermal isotropic nonhomogeneous plasma, noting interaction with electrons of Langmuir frequency 22 p3956 A66-40576  
 Generalized full wave theory equations derived for EM plane wave propagation through magnetotonic medium for electron collision frequencies proportional to electron energy 22 p3869 A66-40805  
 Beam waveguides for long distance electromagnetic wave transmission at optical wavelengths described by theory of focusing antennas 23 p4037 A66-41475  
 Parabolic cylindrical waveguide formed by intersection of two confocal parabolic metal surfaces, determining eigenvalues of wave functions subject to boundary conditions yielding TE and TM modes 23 p4047 A66-41587  
 Reflection and propagation of electromagnetic pulses through dispersive media, degradation of step carrier in magnetoplasma analyzed by Laplace inversion technique 23 p4039 A66-41589  
 Radiation and propagation of electromagnetic waves, noting solution to initial value problem for moving point source in infinite homogeneous medium 23 p4040 A66-41635  
 Boundary conditions for unique solution to linearized warm plasma equations 23 p4105 A66-41640  
 Linearly polarized incident electromagnetic waves propagated along static magnetic field through plasma in region of electron cyclotron frequency, noting wave modes behavior 24 p4242 A66-42400  
 Electromagnetic propagation in semiconductor with account of nonlinear effects such as skin effects arising from electron heating by field 24 p4256 A66-42526  
 Electromagnetic wave transmission through and reflection from homogeneous nonlinear anisotropic slab between two linear isotropic media 24 p4173 A66-42706

Carbon disulfide traveling wave Kerr cells with identical microwave and dielectric constants, noting light modulator construction at microwave frequencies 24 p4185 A66-42814  
 Electromagnetic propagation in slowly rotating anisotropic dielectric single band waveguide modulator 24 p4175 A66-42967  
 Fourier analysis of Riemann-Hilbert problem of diffraction of normally incident plane electromagnetic wave by plane metallic grid above dielectric sheet and semilinear plasma 24 p4175 A66-42978  
**ELECTROMAGNETIC PROPULSION**  
 Space travel projects noting ion propulsion, electromagnetic drive and tests of flight simulation 03 p0415 A66-12483  
 Predicted and observed calorimetric exhaust efficiencies of capacitor powered coaxial plasma guns [AIAA PAPER 65-340] 15 p2551 A66-29275  
**ELECTROMAGNETIC PUMP**  
 Electric drive operating parameters and design, using exploding wire type device and electromagnetic apparatus for plasma production and acceleration 06 p0942 A66-15917  
 Experimental assembly using liquid gallium cycle for testing electromagnetic pumps and flow meters 06 p0918 A66-16847  
 Russian monograph on MHD of liquid metals, discussing application for transport and technological treatment of metals, molten salts and slags 08 p1266 A66-19566  
 Transverse magnetic field applied to high Reynolds number flow of liquid mercury in pipes and ducts inhibits convective mechanism of heat transfer [AIAA PAPER 65-539] 15 p2616 A66-29279  
**ELECTROMAGNETIC RADIATION**  
**SA ALPHA RADIATION**  
**SA BETA RADIATION**  
**SA MICROWAVE RADIATION**  
 Overall profile of ophthalmic injury associated with ionizing and nonionizing electromagnetic radiation fields based on human response to radiation exposure 01 p0018 A66-10793  
 Radio noise measurements at high altitudes using rocket probe, suggesting electromagnetic radiation from plasma waves as source mechanism 02 p0288 A66-11506  
 Effect of radiation on various types of materials and application of irradiation processes to field of industrial technology 04 p0537 A66-13375  
 Contribution of nonlinear interaction of surface oscillations in plasma to emission of electromagnetic radiation from plasma 04 p0552 A66-13882  
 Laser beam use in biology and medicine, noting interaction of electromagnetic radiation with biological systems, hazards, diagnostics, therapeutics, etc 04 p0534 A66-14455  
 Light flow amplification in inhomogeneous layer taking nonlinearity into account 05 p0692 A66-14725  
 Circular filament of electric current in unbounded magnetotonic medium, measuring radiation resistance for constant current distribution 05 p0633 A66-15122  
 Solar flares, discussing continuous electromagnetic radiation, hard X-ray radiation and microwave radio bursts 05 p0752 A66-15378  
 Expected diffraction effects on electromagnetic radiation from Mariner IV due to Martian atmosphere and occultation 06 p0827 A66-16039  
 Electromagnetic waves from plasma penetrated by pulsed electron beam in magnetic field 06 p0914 A66-16147  
 Radiation resistance of elongated conducting electromagnetic radiator in vacuum or linear dielectric 07 p1002 A66-17831  
 Mariner II solar wind measurements including data on Venus electromagnetic radiation, space magnetic fields and charged particles, energy spectra, solar plasma, etc 07 p1130 A66-18077  
 Energy sources of lunar luminescence noting effects of solar wind, corpuscular radiation, electromagnetic radiation and radioactivity 07 p1139 A66-18090  
 Model of cosmic ray shower, measuring time-integrated energy flux in radiation



- Field 08 p1283 A66-18619
- Green function method in theory of dispersion and absorption of electromagnetic radiation in semiconductors, considering resonance line shapes 09 p1411 A66-19961
- Solar electromagnetic radiation studied in terms of irradiance, UV and X-rays and radio emission 09 p1454 A66-20283
- Electromagnetic-wave radiation peculiarities in homogeneous anisotropic dispersive magnetic plasma 09 p1343 A66-20342
- Galactic X-rays, discussing soft X-rays, UV radiation, isotropic X-rays, electromagnetic radiation from X-ray sources, etc 10 p1600 A66-21854
- Continuous electromagnetic radiation from solar flares, examining X-ray bursts from synchrotron, Compton and bremsstrahlung mechanisms 11 p1762 A66-22406
- Primary cosmic ray energy spectrum, including primary flux of protons and heavier nuclei, and EM cascade pair production rates 11 p1765 A66-23192
- Interaction of electromagnetic radiation falling on plasma surface with plasma surface wave, showing that wave amplitude increases or decreases exponentially 12 p1921 A66-24211
- Nonrotating star with spherical symmetry emitting electromagnetic radiation analyzed, using gravitational field analogy 13 p2072 A66-25417
- Surface wave emission by charges passing through interface between vacuum and real dielectric, emphasizing energy loss equations 13 p2025 A66-26051
- Radiation due to time-harmonic source and field solution of electric dipole in moving uniaxial anisotropic medium by Minkowski theory 14 p2234 A66-26861
- Contribution of nonlinear interaction of surface oscillations in plasma to emission of electromagnetic radiation from plasma 14 p2343 A66-27580
- Radiation from vertical dipole in warm plasma determined by asymptotic series expansion of integral solutions, noting surface wave propagation, transformation from acoustic to electromagnetic mode on boundary, etc 14 p2240 A66-27917
- Electromagnetic waves from plasma penetrated by pulsed electron beam in magnetic field 15 p2557 A66-29877
- Naturally occurring electromagnetic radiation in audiofrequency range studied at Kiruna Geophysical Observatory 16 p2691 A66-30232
- Physical principles in plasma application for amplification and generation of electromagnetic oscillations 16 p2760 A66-30797
- Direct measurement of attenuation length of extensive air showers through water 18 p3212 A66-35136
- Light variations of flare and T Tauri stars due to surface electromagnetic activity connected with turbulence in convective zone and rotation, using Hertzprung-Russell diagram 20 p3652 A66-37610
- Electrons trapped in magnetosphere, discussing dynamo electrostatic field, energetic electron electromagnetic drift and magnetic mirror-electron orbit effects 20 p3635 A66-38226
- Equivalent circuit for pyroelectric materials used in obtaining noise equivalent power for detection of electromagnetic radiation and heat transfer measurement 20 p3562 A66-38405
- Radio astronomy satellite with extendible antennas achieves gravity gradient stabilization while receiving electromagnetic radiation, analyzing dynamic behavior and effect of passive damper 21 p3820 A66-38863
- Mathematical analysis of radiation from slotted magnetic line source on conducting cylindrically capped wedge covered by dielectric layer or plasma 21 p3705 A66-39349
- Dielectric loss tangent measurement in pyroelectric materials for EM radiation detectors and heat transfer sensors 21 p3740 A66-39386
- Chemical energy conversion to electromagnetic energy by flux compression, discussing process and obtained efficiency 21 p3698 A66-39502
- Effects of low density, temperature, proton radiation and electromagnetic radiation on thermal control materials, using synergistic testing 22 p3889 A66-40219
- Interaction of electromagnetic radiation falling on plasma surface with plasma surface wave, showing that wave amplitude increases or decreases exponentially 22 p3956 A66-40575
- Radiation in magnetoplasmas, noting correctness of infinity catastrophe theory for dielectric radiation sources in magnetotonic media 23 p4105 A66-41632
- Radiation and propagation of electromagnetic waves, noting solution to initial value problem for moving point source in infinite homogeneous medium 23 p4040 A66-41635
- Ring laser rotation rate sensor noting relation to electromagnetic radiation 24 p4223 A66-42564
- Processes for producing electromagnetic radiation including applications of spectroscopic methods, noting relation to plasma physics 24 p4238 A66-43117
- Electromagnetic and corpuscular radiation hazards to astronauts deduced from data on dogs 24 p4166 A66-43140
- ELECTROMAGNETIC SCATTERING**
- Book on satellite-caused ionospheric disturbances, particularly in particle density and electric and magnetic fields in vicinity of artificial body 01 p0138 A66-10975
- Plane wave diffraction by sinusoidal network 01 p0031 A66-11074
- Homogeneous isotropic plasma diagnosis using beam displacement in reflection of electromagnetic wave 02 p0264 A66-11240
- Interaction between electromagnetic waves and turbulent plasma 02 p0191 A66-11731
- Russian monograph on turbulent plasma theory covering turbulence formation, hysteresis, plasma oscillations, self-consistent wave interactions, etc 03 p0406 A66-13283
- Electromagnetic wave scattering discussing beam trajectories, flux density decrease and radar detection in ionized trail in form of paraboloid of revolution 03 p0337 A66-13314
- Plasma resonance of cylindrical plasma in absence of magnetic field noting conductivity kernel, scattering of radiation, nonuniformity of plasma sheath and Landau damping 04 p0474 A66-13425
- Electromagnetic wave reflection from rough surface 04 p0481 A66-13748
- Scattering of H-polarized plane waves by infinitely long axially magnetized cylinder of uniform plasma 04 p0484 A66-14100
- Electromagnetic scattering by refractive index distribution characterized by one-dimensional pressure 05 p0675 A66-14554
- Temperature dependence of Mie scattering, covering absorption and scattering of electromagnetic radiation on spherical aluminum oxide particles 05 p0718 A66-14917
- Plane electromagnetic wave scattering at rectangular conducting strips, examining front end backscattering and current distribution measurements 05 p0649 A66-15121
- Radiation absorption and scattering by small spherical solid carbon particles in wavelength range 0.2 to 40  $\mu$  calculated by classical Mie theory [AIAA PAPER 66-134] 06 p0911 A66-16261
- Long wavelength limit in scattering from homogeneous dielectric cylinder at oblique incidence 06 p0830 A66-16277
- Tonks-Dattner resonances, describing frequency modulated technique to study microwave energy irradiated plasma column 06 p0920 A66-16993
- Electromagnetic scattering by finite dense plasma sphere, discussing effects of surface wave, absorption and inhomogeneity 07 p1091 A66-18409
- Equivalence of oscillating electric field on plasma boundary, with specularly reflecting bounding wall, to unbounded plasma with planar oscillating grid at wall position 08 p1261 A66-18546
- Electromagnetic wave scattering by satellite caused by ionized coating, noting effect on echo 08 p1182 A66-18754
- Equilibrium electron density distribution in F-2 region of equatorial ionosphere, noting effects of photoionization, loss, diffusion along geomagnetic field lines and electromagnetic drift 08 p1216 A66-19210
- Comparison of signals received on two VHF scatter circuits of different geometry but viewing common scattering region 08 p1184 A66-19211
- Electromagnetic wave scattering due to plasma oscillations in plane plasma layer used as evidence of noise existence in turbulent plasma 08 p1184 A66-19273
- Interferometer for interference perturbation of electromagnetic three-cm waves 08 p1224 A66-19320
- Wave propagation equations in inhomogeneous warm plasma, emphasizing separation into quasi-electromagnetic and dynamic components 08 p1266 A66-19736
- Antennas in ionized medium - Colloquium, Paris, June 1965 09 p1339 A66-19841
- Diffraction of plane electromagnetic wave by cylinder of inhomogeneous plasma calculated by method that considers plasma as electron dipoles 09 p1406 A66-19843
- Electromagnetic wave diffraction by arbitrary shaped dielectric bodies treated by perturbation method, based on Taylor series expansion 09 p1342 A66-20086
- Relativistic mechanism of electromagnetic wave scattering at velocity fluctuations and emission from plasma in external field 09 p1344 A66-20353
- Spatial scattering of associated electromagnetic waves arising during passage of fast charged particles through semiconductors, noting role of Cerenkov radiation 09 p1428 A66-20596
- Matrix formulation determination radar cross section arising when smooth conducting obstacle is illuminated by incident electromagnetic wave 10 p1497 A66-21590
- Integral equation method solution of scattering from cylinders with arbitrarily varying anisotropic surface impedance 10 p1497 A66-21591
- Modal expansions for resonance scattering phenomena 10 p1498 A66-21595
- Saddle point, Watson transformation and residue series in survey of asymptotic methods for HF scattering 10 p1498 A66-21596
- Bistatic scattering and derivation of bistatic RCS from monostatic RCS measurements for small angles 10 p1499 A66-21608
- Electromagnetic scattering from conducting object controlled by loading portions of surface with impedances, distributed or lumped 10 p1499 A66-21610
- Scattering of electromagnetic wave by metallic sphere loaded with circumferential slot in presence of electric field 10 p1499 A66-21611
- Electromagnetic propagation and scattering in temperate plasma with dielectric regions, noting application to ionosphere and reentry condition 10 p1500 A66-21613
- Bibliography of articles on radar reflectivity and related subjects, 1957-1964 10 p1500 A66-21614
- Electromagnetic theory to determine nose-on radar cross section of perfectly conducting finite cone 10 p1500 A66-21615
- Born approximation applied to electromagnetic scattering from finite cone to determine radar cross section 10 p1500 A66-21616
- Short-pulse scattering by simple geometric shapes useful for heuristic models of electromagnetic scattering, illustrating creeping-wave return 10 p1500 A66-21618
- Electromagnetic scattering model of turbulent plasma wake behind reentry vehicle 10 p1502 A66-21634
- Anechoic chamber facility for surface field measurement in scattering studies using probes 10 p1520 A66-21638
- Electromagnetic wave scattering from 30 degree metal wedge and thick plate over wide range of bistatic angles, comparing results with Keller geometrical theory of diffraction 10 p1503 A66-21644
- Electromagnetic wave scattering from very rough surfaces, noting contribution of small and large scale roughness to scattered power 10 p1504 A66-21658



Electromagnetic scattering by cylinder with inhomogeneous sheath 11 p1652 A66-22392

Tube shaped and solid cylinder antennas compared, calculating surface current distribution and radiation patterns 11 p1662 A66-22543

Scattering theory by perfectly conducting irregular surface at very short wavelength developed, using vector field theory 11 p1652 A66-22550

Validity of two approximations for removing corners and slope discontinuities from cylindrical metallic bodies in digital approach to Maxwell equations 11 p1653 A66-22563

Plane electromagnetic wave diffraction on slot and tape having magnetic and electric fields parallel to edges of slot and tape respectively 11 p1655 A66-22717

Scattering coefficients caused by sudden change in electrical properties of narrow wall of rectangular waveguide 11 p1666 A66-22720

Plane electromagnetic wave scattering by conducting cylinder surrounded by hot magnetoplasma sheath 11 p1657 A66-23112

Backscattered and surface fields for acoustically hard and soft prolate spheroids at end-on incidence computed, using tabulation of spheroidal functions 12 p1815 A66-24119

Radar cross polarization measurements for target surface property determination, noting application to lunar studies 12 p1819 A66-24603

Maxwell equation as basis for studying multiple scattering of electromagnetic waves in inhomogeneous medium 12 p1825 A66-24886

Electromagnetic scattering by circular wire loops loaded with lumped impedances, obtaining solution to integral equation by Fourier series 14 p2247 A66-26863

Electromagnetic wave scattering and depolarization from rough surface, noting existence of surface current vector component pointing in direction of incident wave 14 p2235 A66-27038

Resonance peaks due to electromagnetic scattering by argon plasma jet observed during change in electron concentration, noting dependence of scattering on argon flow rate and electric power of arc 14 p2341 A66-27151

Electrostatic interaction effect on EM waves scattering by atmospheric aerosol particles 14 p2284 A66-27539

Normally incident plane electromagnetic wave scattering by circular cylinder coated with radially stratified sheath 14 p2238 A66-27587

Electromagnetic wave scattering by radially inhomogeneous spherical object 14 p2240 A66-27918

Plane electromagnetic diffraction by wide aperture in conducting screen immersed in anisotropic medium 14 p2241 A66-27981

Scattering of plane electromagnetic wave at infinite circular cylinder with spatially varying dielectric constant 14 p2242 A66-28155

Electromagnetic wave scattering, discussing beam trajectories, flux density decrease and radar detection in ionized trail in form of paraboloid of revolution 14 p2242 A66-28287

Omnidirectional scattering of ultrasonic waves from rough surfaces satisfying Kirchhoff theory with respect to electromagnetic scattering 15 p2536 A66-28571

Plane electromagnetic scattering by unidirectionally conducting sphere 15 p2448 A66-28573

Theoretical and experimental investigations of electromagnetic scattering by conducting cylinder coated with anisotropic ferrite sheath magnetized along axis 15 p2449 A66-28594

Electromagnetic scattering from infinite cylinder at oblique orientation 15 p2537 A66-28976

Radio wave emission due to shock wave propagation in magnetospheric boundary and electromagnetic scattering in plasma wave field 15 p2575 A66-29083

HF backscattering by plane electromagnetic wave incident on imperfectly conducting sphere covered with

concentric layers of different materials, noting refractive index value 16 p2647 A66-30224

Scattering of electromagnetic waves in plasma, noting effect of eddy current fluctuations 16 p2654 A66-31179

Electromagnetic scattering by perfectly conducting elliptical cylinder in uniaxially anisotropic medium, transforming boundary value to Helmholtz equation 16 p2654 A66-31442

Maximum beam displacement parallel to plane of incidence in plasma reflection of linear or elliptically polarized waves 17 p2974 A66-33286

Harmonic series solution for electromagnetic scattering by unidirectionally conducting helical sheath when incident field is E-polarized 18 p3065 A66-33530

Initial boundary value problems involving Maxwell equations in isotropic media solved numerically 18 p3065 A66-33533

Equivalence between scalar three-dimensional diffraction problems in homogeneous medium and two-dimensional diffraction problems in inhomogeneous medium with inverse square permittivity profile 18 p3065 A66-33534

Shadowing effect and anomalous backscattered intensity in diffuse reflection from plane-parallel layer of random particles 18 p3068 A66-34014

Improved correlation function in Kirchhoff-Huygen method of solution of scattering of waves from statistically rough surfaces 18 p3068 A66-34015

Augmented Born approximation based on variational principles applied to electromagnetic scattering from inhomogeneous dielectric spheres of finite extent 18 p3071 A66-34452

Reflection coefficient of electromagnetic wave polarized in plane normal to magnetostatic field and falling from vacuum perpendicularly on plasma boundary parallel to field 19 p3303 A66-36198

Diffraction of electromagnetic plane by half-plane in uniaxially anisotropic medium solved in terms of Sommerfeld approximation 19 p3304 A66-36284

Induced scattering of electromagnetic waves from magnetoactive plasma particles 19 p3418 A66-36533

Depolarization of electromagnetic waves backscattered from rough surface boundary 20 p3515 A66-37293

Perfectly conducting prolate spheroid illuminated by plane wave at arbitrary incidence with LF solution and expansion terms predicted from symmetries 20 p3516 A66-37622

Plane linearly polarized electromagnetic wave diffraction on several spheres forming linear system, showing solution of boundary value problems 20 p3603 A66-37754

Spatial scattering of associated electromagnetic waves arising during passage of fast charged particles through semiconductors, noting role of Cerenkov radiation 20 p3622 A66-38130

Electromagnetic scattering by obliquely oriented cylinders, noting extinction efficiency, propagation in cylindrical waveguides and polarization reversal 20 p3603 A66-38403

Microwave and optical range electromagnetic wave scattering in plasma, noting frequency and power of probing signal 21 p3789 A66-39066

Conformal mapping technique applied to boundary value problem of plane wave diffraction by perfectly conducting elliptic cylinder, noting integral equation 22 p3866 A66-40185

Uniqueness theorem for particular inverse problem of plane wave perpendicularly incident on long cylinder of complex refractive index 22 p3866 A66-40455

Resonance scattering of electromagnetic waves on arbitrary rarefied plasma region with near-zero intrinsic wave number relative to small perturbation 22 p3869 A66-40758

Phase shift from scattering by atoms with attractive potentials, predicting virtual energy states for incident energies in three-turning point range 22 p3951 A66-40906

Maxwell equation as basis for studying multiple scattering of electromagnetic waves in inhomogeneous medium 23 p4036 A66-41093

Diffraction of electromagnetic waves at dielectric wedge, considering skin depth and internal problem 23 p4036 A66-41134

Plane electromagnetic wave diffraction on slot and tape having magnetic and electric fields parallel to edges of slot and tape respectively 23 p4037 A66-41455

Scattering coefficients caused by sudden change in electrical properties of narrow wall of rectangular waveguide 23 p4045 A66-41458

Asymptotic expansion of electromagnetic field scattered from convex cylinder near grazing incidence, using boundary layer theory 23 p4038 A66-41546

Electromagnetic wave scattering by stratified medium, noting Mathieu and Floquet type wave representation 24 p4171 A66-42292

Electrostatic interaction effect on EM waves scattering by atmospheric aerosol particles 24 p4198 A66-42325

Scattering of circularly polarized electromagnetic wave in Coulomb field, noting coalescence of two-wave quanta into one quantum of double frequency 24 p4220 A66-42529

Backscatter of electromagnetic waves from rough layer simulated by acoustic backscattering from partially submerged Plexiglas layer 24 p4173 A66-42624

Diffraction of waves by transparent screen studied to determine what information about diffracting screen can be obtained by observing diffraction pattern 24 p4173 A66-42712

Resonance peaks due to electromagnetic scattering by argon plasma jet observed during change in electron concentration, noting dependence of scattering on argon flow rate and electric power of arc 24 p4244 A66-42971

**ELECTROMAGNETIC SHIELDING**

Attenuation of transient electric and magnetic fields by imperfectly conducting spherical shells 06 p0843 A66-16029

Shielding effect on modulating microwave ferrite switch in applied magnetic field and relation between inside and outside fields for thin waveguide 06 p0857 A66-16952

Plane wave shielding effectiveness of vacuum deposited thin films, using section of air-filled coaxial transmission line 12 p1835 A66-24142

Optimum antenna placement within metallic enclosure 13 p2044 A66-26748

Ground clutter shields for L-band radar using 60-ft parabolic reflector with Cassegrain geometry 15 p2457 A66-28596

Electromagnetic shielding for sensitive electronic components, noting Netic and Co-Netic magnetic alloys 15 p2465 A66-29670

Near field beyond perfectly conducting plane screen with small circular aperture 18 p3066 A66-33542

Electromagnetic interference shielding for conductors that excludes interference energy caused by both magnetic and electric fields over broad frequency range 20 p3499 A66-37195

Short wave transmission station conduction, noting shielding to prevent interference from TV transmission 20 p3543 A66-37723

Clutter shield for L-band monopulse radar employing Cassegrain parabolic reflector 24 p4173 A66-42620

**ELECTROMAGNETIC SHOCK TUBE**

Electromagnetic shock generator of high voltage nanosecond pulses with controlled length 04 p0495 A66-13885

Mach-Zehnder interferometer for electromagnetically accelerated shock waves in hydrogen 04 p0554 A66-14285

Velocity measurements of electron front in electromagnetically generated T-tube shock waves made with microwave interferometer 04 p0558 A66-14479

Electric shock tube flow modes at low pressure and conditions for shock wave detached from plasma flow 05 p0659 A66-14706

Thomson scattering measurements of magnetic annular shock tube plasmas using



Q-switched ruby laser light  
beam 05 p0660 A66-14707  
Bursting shock tube diaphragms  
electrically, using two piezoelectric  
gauges 06 p0869 A66-16947  
Detection of ionized gas front passage and  
differentiating it from current sheet in  
magnetically driven shock  
tube 07 p1020 A66-17956  
Gas and sound velocity measurements  
downstream of shock wave in  
electromagnetic tube for subsonic and  
supersonic flows 07 p1023 A66-18119  
Precursor electron front measuring  
velocity, electron temperature dependence  
on operating parameters,  
etc 08 p1259 A66-18525  
Magnetic field measurement in shock tube  
when plasma moves with respect to  
probe 08 p1226 A66-19695  
Microwave reflection measurements for  
precursor in electromagnetically driven  
shock tube, discussing axial distribution and  
electron density 09 p1409 A66-20855  
Photographic results compared with  
calculations for shock wave reflection  
velocity and wake processes in  
electromagnetic shock  
tube 12 p1921 A66-24214  
Propagation of fast shock waves in  
electromagnetic shock tube, using acoustical  
method, noting time distribution of  
pressure, wave reflection,  
etc 13 p2059 A66-25083  
Time resolved Langmuir probe  
measurements of plasma density in  
electromagnetic shock  
tubes 13 p2149 A66-26243  
Precursor wave structure in  
electromagnetic shock tube, determining  
precursor velocity, electron density and  
current content, comparing precursor  
behavior with ionizing electromagnetic  
wave 13 p2064 A66-26259  
Electromagnetic shock generator of high  
voltage nanosecond pulses with controlled  
length 15 p2466 A66-29697  
Nonstationary flow past spheres and  
cylinders in electromagnetic shock tube,  
determining time required for flow to  
become stationary 16 p2682 A66-31295  
Physical model for ionizing switch-on shock  
wave and electric field situated in  
electromagnetic shock  
tube 17 p2967 A66-32431  
Stark broadening of singly ionized argon  
lines in helium-argon plasma behind  
reflected shock wave in electromagnetic T  
tube with backstrap 18 p3138 A66-34233  
Air flow luminescence front propagation in  
electromagnetic shock tube measured, using  
phase synchronized high-speed  
photography 21 p3790 A66-39080  
Emission spectra of ionized air and H in  
electromagnetic shock tube, giving frame  
scans of spectra 21 p3726 A66-39081  
Electron density distribution in  
electromagnetic shock tube measured, using  
transverse microwave cavity and radiating  
slots in oversize plasma  
waveguide 21 p3739 A66-39382  
Photographic results compared with  
calculations for shock wave reflection  
velocity and wake processes in  
electromagnetic shock  
tube 22 p3957 A66-40578  
Electromagnetic shock generator of high  
voltage nanosecond pulses with controlled  
length  
[ASME PAPER 64-WA/FE-29]  
24 p4157 A66-42580

**ELECTROMAGNETIC WAVE**

**SA RADIO WAVE**

Microwave polarization changes during  
passage through low pressure  
plasma 01 p0110 A66-10371  
Phase shift in electromagnetic waves  
between unmagnetized and magnetized  
ferrite partially filling  
waveguide 01 p0039 A66-10538  
RF electromagnetic and elastic oscillations  
in ferrites 01 p0121 A66-10568  
Coherent nonlinear interaction of two  
electromagnetic waves in plasma, noting F  
layer radio  
communication 01 p0029 A66-10594  
Autocorrelation and spectral density of  
energy of stationary electromagnetic wave

expressed as function of same parameters of  
its component trains of  
waves 01 p1016 A66-10645  
Electromagnetic wave absorption and  
cosmic noise absorption measurements  
useful in radio  
communication 01 p0072 A66-11101  
Electromagnetic wave reflectivity  
coefficients from 1957 to 1963 statistically  
analyzed 01 p0032 A66-11102  
Diffraction of electromagnetic centimeter  
waves passing metal screen depends on  
curvature of screen edge 01 p0032 A66-11200  
Electromagnetic problems in anisotropic  
and compressible plasma solved by  
characterizing compressibility as  
compressivity tensor 02 p0266 A66-11447  
Charged particle motion in field of plane  
traveling wave and acceleration by  
transverse wave 03 p0397 A66-12387  
Reflection and transmission of  
electromagnetic waves by dielectric medium  
moving parallel to and perpendicular to  
interface, determining  
coefficients 04 p0481 A66-13739  
Refractive index obtained from equation  
describing electromagnetic wave propagation  
in ionosphere 04 p0481 A66-13826  
Ray dispersion of electromagnetic waves  
by free electrons produced in cone-shaped  
ionized wake 04 p0481 A66-13843  
Complex output resistance and  
conductivity of electromagnetic cylindrical  
resonators transmitting across gaps, using  
variational method, noting role of incident  
and reflected waves 04 p0496 A66-13905  
Interaction of energetic electrons with  
bounded electromagnetic waves near  
cyclotron resonance, noting plasma  
diagnostics, maser and gain  
mechanism 04 p0530 A66-13953  
Reflection of acoustic /electromagnetic/  
waves from geometrically complex body  
oscillating according to random  
law 04 p0483 A66-14048  
Electromagnetic wave diffraction by  
moving bodies of revolution subjected to  
pulsed radiation when spatial dimension of  
impulse may be less than linear dimension  
of body 04 p0483 A66-14050  
Distortion of electromagnetic pulse after  
propagating through dispersive channel,  
using approximate procedures and obtaining  
transient response 05 p0631 A66-14834  
Analogies of statistical electromagnetic  
wave theory to quantum field theory, noting  
probability density function of waves and  
Green function 05 p0632 A66-14843  
Dispersion theory and multilayer structure  
approximation of IR reflectivity of  
semiconductor with n on n plus stratified  
structure 05 p0736 A66-14965  
Third harmonic component of current  
density in plasma in presence of electric  
and magnetic fields, analyzing generation  
and propagation of third harmonic of  
electromagnetic wave in  
magnetoplasma 05 p0724 A66-15188  
Faraday effect in anisotropic plasma  
treated as fluid with collisions, deriving  
relations for rotation of polarization plane  
and electromagnetic wave  
ellipticity 05 p0727 A66-15531  
Book on radio wave propagation for  
aircraft radio communication including  
frequency ranges, waveguides, ionospheric  
layer influence, noise, antenna properties,  
etc 06 p0832 A66-16520  
Planar gap in plasma medium as idealized  
model for studying electromagnetic and  
plasma waves in plasma sheaths and  
ionospheric layers 06 p0920 A66-17015  
Linear demodulation of AM  
electromagnetic wave propagating through  
dispersive medium 06 p0836 A66-17033  
Intensity distribution of fringe systems  
used to verify phase inversion between two  
lobes of laser in TEM-10  
mode 07 p1043 A66-17453  
Absorption and spontaneous and stimulated  
emission for homogeneous isotropic  
nonferromagnetic Maxwellian media at  
rest 07 p1081 A66-18037  
Electromagnetic theory of waveguides  
including circular and rectangular  
waveguides, mode theory,  
etc 08 p1189 A66-18665

Electromagnetic momentum in relation to  
waveguide modes, discussing relationship  
between momentum transfer and mechanical  
forces 08 p1189 A66-18667  
Text on wavefronts and wave propagation  
in classical electromagnetic theory, general  
relativity, MHD and nonlinear  
electrodynamics 08 p1180 A66-18680  
LF electromagnetic wave excitation in  
electron-ion and electron-hole plasmas  
situated in external electrical  
field 08 p1262 A66-18975  
Electromagnetic waves in optically-inactive  
isotropic semiconducting media bounded by  
vacuum 08 p1276 A66-19609  
Quantum statistical electromagnetic wave  
propagation and relativistic damping effects  
in uniformly magnetized electron-positron  
gas 08 p1187 A66-19809  
Boundary surface roughness effect on  
polarization of thermal electromagnetic wave  
emission from dielectric  
medium 09 p1401 A66-20115  
Formation and expansion of  
electromagnetic shock waves in  
communication lines, using ferroelectric  
crystals 09 p1344 A66-20346  
Computer program for numerical solution  
of uniform hollow waveguides with  
boundaries of arbitrary  
shape 09 p1346 A66-20607  
Combination scattering of UHF  
electromagnetic waves in turbulent plasma  
in external electromagnetic  
field 09 p1347 A66-20767  
Diffraction of plane electromagnetic wave  
at planar array consisting of thin  
rectangular plates 09 p1347 A66-20787  
Inhomogeneous thick plasma layer formed  
above metallic surface, effect on reflection  
and absorption of electromagnetic  
waves 09 p1347 A66-20788  
Electromagnetic wave deflection where  
transmitted power is inherently guided by  
stored energy component, noting effect of  
Sun gravitational  
interaction 10 p1496 A66-21292  
Coherency matrix expression of  
phenomenological Stokes four-vector  
describing intensity and polarization of  
electromagnetic wave 10 p1504 A66-21651  
Electromagnetic wave diffraction around  
finite perfectly conducting  
cone 10 p1506 A66-21924  
Kinetic approximation of passage of  
electromagnetic wave through plasma layer,  
noting angle of incidence of wave on  
layer 10 p1506 A66-21993  
Kinetic theory of passage of  
electromagnetic waves through plasma  
layer 10 p1506 A66-22004  
Amplification of electromagnetic waves in  
solid state plasma in presence of carrier  
drift in external electric and magnetic  
fields 10 p1586 A66-22147  
Aperture field of leaky-wave antenna of  
finite length 11 p1661 A66-22394  
Harmonic wave generation by EM plane  
wave normally incident on collisionless  
plasma with linear density  
profile 11 p1652 A66-22548  
Coupling of ordinary and extraordinary  
electromagnetic waves in CdS induced by  
external magnetic field or  
stress 12 p1926 A66-23719  
Electromagnetic waves in isotropic laminar  
plasma waveguide 12 p1919 A66-23779  
Perturbation method approximation of  
eigenvalue and eigenfunction of fundamental  
wave propagating in H-plane bend of  
rectangular waveguide 12 p1815 A66-23958  
Boundary value problem of acoustic point  
source antenna within compressible plasma  
region with assumed rigid boundary, noting  
acoustic power conversion into  
electromagnetic waves 12 p1920 A66-24116  
Inequality of cross-polarized components of  
electromagnetic wave reflected from plane  
surface for arbitrary angle and arbitrary  
reflector properties 12 p1816 A66-24149  
Behavior of electric field of expanding  
wave in magnetically active  
plasma 12 p1921 A66-24213  
Reflection of resonance frequency  
monochromatic wave from half-space filled  
with nonlinear medium 12 p1816 A66-24226  
Electroexplosive device testing via pulse  
reflection techniques 12 p1934 A66-24674



Charged particle motion in field of plane traveling wave and acceleration by transverse wave 13 p2139 A66-25392

Plane electromagnetic wave diffraction by narrow strip-grating, obtaining reflection coefficient via optical approximation method 13 p2021 A66-25395

Decay of electron Langmuir waves in plasma in presence of magnetic field into electromagnetic waves 13 p2143 A66-25712

Plasma acceleration in circular waveguides in presence of high-power electromagnetic wave 13 p2147 A66-25746

Damping constant of electromagnetic wave in plane parallel waveguide with ferrite resonant isolator, using perturbation theory, considering dielectric and magnetic losses 14 p2250 A66-27143

Dissimilar and analogous characteristics of electromagnetic and gravitational waves 14 p2333 A66-27220

Combination scattering of UHF electromagnetic waves in turbulent plasma in external electromagnetic field 14 p2236 A66-27302

Cross section method to solution of diffraction of electromagnetic wave at inhomogeneous sphere, using membrane function 14 p2239 A66-27736

Electromagnetic wave reflection and transmission coefficients for moving dielectric slab as function of velocity of medium 14 p2239 A66-27761

Radiation characteristics of vertical dipole in warm plasma, expressing vector potential functions in Fourier integrals 14 p2240 A66-27916

Permanent magnetized ferrite antenna waveguide windows for improving EM wave transmission through plasma and reducing transmission losses during reentry 14 p2241 A66-27930

Energy propagation lines in diffraction of vertically polarized electromagnetic wave by conducting half-plane shield 14 p2241 A66-27939

Nonlinear interaction between two modulated electromagnetic waves propagating in homogeneous anisotropic Lorentz plasma 14 p2344 A66-27941

Electromagnetic waves in isotropic plasma layer and in plasma layer in magnetic field, determining second harmonics of wave and obtaining nonlinear dispersion equation 14 p2348 A66-28470

Reflection, transmission and absorption coefficients of circularly polarized electromagnetic wave incident on plasma layer situated in stationary magnetic field 14 p2348 A66-28471

Ultrasonic-electromagnetic wave interaction in metals including resonance effects from waves arising in external magnetic field, determining Fermi levels 15 p2559 A66-28621

Excitation of longitudinal electron plasma oscillations by nonlinear resonance of two TEM waves with frequencies differing by plasma frequency 16 p2757 A66-30195

Interplanetary plasma stream analysis using bistatic radar transmissions, considering wave propagation in presence of uniform magnetic field, stream velocity, Faraday rotation, etc 16 p2801 A66-30716

Diffraction of axisymmetric electromagnetic wave at surface discontinuity of impedance cylinder forming core of coaxial waveguide 16 p2861 A66-30864

Ionospheric sounding using random diffusion of electromagnetic wave by ionospheric plasma with continuous wave through two separate antennas 16 p2653 A66-30953

Electromagnetic spectrum of upper atmosphere examined, using microwave techniques, noting molecular rotation of gases with permanent electric or magnetic dipole moments 16 p2698 A66-31044

Quasi-linear approximation of Cerenkov and cyclotron damping of electromagnetic waves in magnetoactive plasma, considering collisions of wave-absorbing resonance particles with plasma 16 p2762 A66-31173

Classification of modes in electromagnetic waveguides using model solutions of source-free homogeneous wave equation 16 p2663 A66-31204

Plasma plate and cylinder oscillation

compatibility with radiation from positive argon column at four discrete frequency bands and low pressure 17 p2962 A66-31815

Density and diameter of inhomogeneous plasma cylinder determined from numerical calculation of diffraction of electromagnetic wave 17 p2963 A66-31843

Plane electromagnetic wave diffraction at two parallel circular cylinders for TM and TE polarization 17 p2879 A66-31862

Nonlinear conversion of HF transverse electromagnetic waves into plasma ion-acoustic oscillations 17 p2964 A66-31897

Reflection of acoustic /electromagnetic/ waves from geometrically complex body oscillating according to random law 17 p2873 A66-32214

Electromagnetic wave diffraction by moving bodies of revolution subjected to pulsed radiation when spatial dimension of impulse may be less than linear dimension of body 17 p2873 A66-32216

Computer-derived contour plots of electric and magnetic fields for acoustic electromagnetic plane wave pulse incident on wedge 17 p2875 A66-32390

Plasma motion and confinement in octupole magnetic field, noting electron temperature density and field fluctuation 17 p2966 A66-32428

Electromagnetic waves in optically-inactive isotropic semiconducting media bounded by vacuum 17 p2983 A66-33123

Dual mode frequency discriminator for microwave source frequency stability, discussing application of beam waveguide resonator 17 p2895 A66-33274

Diffraction of linearly polarized electromagnetic wave by coaxial cylinders, deriving approximate solution for wavelengths smaller than distance between cylinder centers 18 p3068 A66-33977

Coupled electromagnetic and electroacoustic wave propagation in inhomogeneous compressible plasma 18 p3069 A66-34089

Kinetic approximation of passage of electromagnetic wave through plasma layer, noting angle of incidence of wave on layer 18 p3072 A66-34970

Plasma half-space impedance for diffusive electron reflection from plasma vacuum boundary, noting damping decrement of surface electromagnetic wave, electric field Fourier components and absorption capacity 18 p3151 A66-35065

Amplification of electromagnetic waves in solid state plasma in presence of carrier drift in external electric and magnetic fields 19 p3440 A66-35761

Design principles of waveguide systems applicable to electromagnetic wave transmission by reflection and refraction 19 p3319 A66-36033

Bending of plane electromagnetic waves around elliptically ideally conducting cylinder of infinite length and around parallel circular dielectric cylinder, with solution as Mathieu-type series 19 p3303 A66-36064

Kinetic theory of passage of electromagnetic waves through plasma layer 19 p3303 A66-36088

Absorption of polarized electromagnetic waves at zero degrees K in n-type germanium under high uniaxial stress 19 p3446 A66-36396

Propagation constants of quasi-transverse electric modes measurement in cylindrical waveguide partially filled with anisotropic plasma 20 p3525 A66-37116

Absorption coefficients for monomers of water vapor and oxygen for various altitudes, noting seasonal variation 20 p3511 A66-37133

Electromagnetic wave propagation in plasma boundary, considering electron collision with boundary, noting role of thermal velocities of electrons 20 p3512 A66-37137

Fourier series solution to electromagnetic wave diffraction on metallic gratings with anisotropic dielectric 20 p3512 A66-37148

Radiation from open-ended circular waveguide, comparing solution for electromagnetic wave propagation with method based on Huygens principle 20 p3529 A66-37705

Absorbing materials used in construction of anechoic chambers for electromagnetic waves 20 p3543 A66-37724

Complex output resistance and conductivity of electromagnetic cylindrical resonators transmitting across gaps, using variational method, noting role of incident and reflected waves 20 p3532 A66-37863

Electromagnetic wave emission excited by electron stream over diffraction grating lying on boundary of semiinfinite anisotropic dielectric 20 p3519 A66-37998

Reflection and transmission of EM waves by dispersive dielectric cold plasma 20 p3611 A66-38394

Energy transport by electromagnetic waves, using successive approximations 21 p3770 A66-38946

Charged particle and electromagnetic wave interaction with nonequilibrium plasma, noting conversion of transverse into longitudinal waves and angular distribution of scattered radiation 21 p3781 A66-39011

Electromagnetic wave excitation in magnetoplasma by external currents using kinetic theory, obtaining expression for energy losses, analyzing electron and ion cyclotron resonance 21 p3782 A66-39016

Plasma-particle interaction in absence of magnetic field, leading to electrostatic and transverse electromagnetic waves instability 21 p3783 A66-39025

Scattering and transformation of electromagnetic waves during critical fluctuations in nonequilibrium plasma 21 p3789 A66-39065

Birefringence of certain crystals sufficiently large to allow collinear backward wave interaction of three electromagnetic waves with signal frequency tunable over large portion of IR spectrum 21 p3771 A66-39113

Externally imposed oscillating electric field excites transverse electromagnetic waves propagating perpendicular to it in cold plasma 21 p3791 A66-39176

Velocity dependent collision frequency effect on harmonic generation in ionized gas through which electromagnetic wave passes 21 p3792 A66-39180

Exact solution for transverse electromagnetic wave in plasma with diffuse boundary, noting reflection and transmission coefficients 22 p3952 A66-39719

Passage of normal plane electromagnetic wave through bi-gyrotropic plate, examining transmission and reflection components 22 p3862 A66-39828

Diffraction of plane electromagnetic wave at planar array consisting of thin rectangular plates 22 p3862 A66-39846

Inhomogeneous thick plasma layer formed above metallic surface, effect on reflection and absorption of electromagnetic waves 22 p3862 A66-39847

Vacuum sheath effect on surface currents excited on plasma-immersed cylinder by EM and EK plane waves 22 p3954 A66-39940

Behavior of electric field of expanding wave in magnetically active plasma 22 p3957 A66-40577

Reflection of resonance frequency monochromatic wave from half-space filled with nonlinear medium 22 p3867 A66-40588

Fresnel formulas for transformation of transverse electromagnetic wave into longitudinal plasma wave at dielectric-plasma interface, using Laplace transforms 22 p3869 A66-40929

Modified Fock function for current distribution in penumbra and shadow region of plane electromagnetic wave incident upon convex cylinder, with application to backscattering 23 p4040 A66-41637

Power conversion enhancement of acoustic-electromagnetic wave coupling across plasma-air boundary by suitable thickness and charged particle density 24 p4241 A66-42304

Line shape of RF dimensional effect in metals showing correlation with electromagnetic wave attenuation in skin layer 24 p4172 A66-42528

Dispersion equation for cyclotron electromagnetic waves for magnetoactive plasma injected with charged particles 24 p4245 A66-43016

Textbook reissue on diffraction of



electromagnetic and acoustic waves at open end of waveguide studied, using Wiener-Hopf-Fock factorization method 24 p4177 A66-43225

# ELECTROMAGNETISM

Intermediate text on fields and waves in communication electronics covering basic equations, oscillating systems, transmission lines, waveguides, microwave circuits, etc 01 p0031 A66-10977

Soviet and other literature on diurnal variations of cosmic ray intensity used for analysis of electromagnetic conditions in outer space 06 p0949 A66-16587

Text on electromagnetic theory for undergraduates 08 p1256 A66-19234

Comparative determination of HF electrical discharge threshold in electromagnetic system 09 p1349 A66-19852

Superfluid hydrodynamics and kinetic theory of superfluids, noting relation of macroscopic concepts of Bardeen-Cooper-Schrieffer theory to microscopic characteristics 09 p1415 A66-20006

Radio waves and circuits - URSI Conference, Tokyo, September 1963 11 p1653 A66-22626

Book on principles of antenna design, discussing fundamental laws of electromagnetism, Maxwell equations and practical forms 19 p3312 A66-35311

Book on foundations for microwave engineering 22 p3875 A66-39993

Approximate differential operator replacing integral operator, taking ionization losses into account in electromagnetic cascade theory 24 p4269 A66-42923

# ELECTROMECHANICAL DEVICE

Tape recorders of flight parameters, tabulating characteristics of ten instruments 01 p0071 A66-11072

Gyrator circuit with only three transistors designed by providing active feedback path so that circuit behaves like two-way feedback system 02 p0201 A66-11908

Reliability, life and relevance of circuit design in electromechanical switching devices 06 p0839 A66-15946

Electromechanical correction of vibrometric devices, using Lagrange-Maxwell method for refining expressions 06 p0879 A66-16421

Metal-insulator-piezoelectric semiconductor electromechanical transducer, discussing transistor and transducer operation characteristics 06 p0883 A66-16960

Capacitive biasing transducer is electromechanical analog of parametric system 06 p0860 A66-17199

Hytrol electronic/hydraulic antiskid braking system for automatic braking pressure modulation in BAC one-eleven 400 series aircraft 07 p0992 A66-18165

Two-port network representations derived for general linear magnetic and electric field transducers, showing energy conversion leading to nonlinear relationships and applications to DC motor 08 p1224 A66-19298

Reliability, life and relevance of circuit design in electromechanical switching devices 12 p1831 A66-23791

Theoretical behavior and frequency response of electrohydraulic valve-controlled cylindrical vibrator capable of high thrust over wide frequency range 12 p1803 A66-23798

Torsional-coupler mechanical filters, particularly types with higher harmonic suppression and piezoelectric material, utilized with simple structure 12 p1845 A66-24852

Frequency characteristics of bending vibrations of bounded rods with electromechanical feedback, possibility of artificially attenuating resonance vibrations and conditions for self-excitation 13 p2194 A66-25088

Characteristics and application of electromechanical switches 13 p2043 A66-26313

Nonstructural materials for space utilization including lubricants, sliding electrical contacts and dielectrics 14 p2319 A66-28006

Relay design by statistical methods 15 p2460 A66-28995

Ten-inch stroke electrodynamic thruster, noting modifications in armature guidance,

base, rotation system, trunnion lifting mechanism, etc 16 p2678 A66-30464

Computer system for control of deceleration of electrodynamic shaker during vibration test 16 p2678 A66-30465

Pulse energy and release energy dependence on electrical and mechanical parameters of magnetoelectrically driven electromechanical timing devices 17 p2928 A66-33499

Coupling of resonators in electromechanical filter, noting application of energy trapping in piezoelectric resonators 18 p3078 A66-34090

Block program testing on fatigue testing machines, noting modifications introduced and operational results 18 p3259 A66-34893

Capacitive biasing transducer is electromechanical analog of parametric system 19 p3356 A66-35557

Quasi-static processes in energy conversion statics, deriving stability criteria 19 p3281 A66-36293

Electropneumatic transducer using principle that heating moving gas increases velocity 19 p3362 A66-36811

Miniaturized piezoresistive transducer pressure diaphragm for experimental stress analysis 20 p3559 A66-37501

Strain gauge technology in U.S.A. emphasizing organization, education and performance 20 p3559 A66-37506

Frequency characteristics of bending vibrations of bounded rods with electromechanical feedback, possibility of artificially attenuating resonance vibrations and conditions for self-excitation 21 p3822 A66-38513

# ELECTROMECHANICS

Effect of poor surface finishes on existence of electromechanical effect in germanium 01 p0124 A66-10773

Effect of poor surface finishes on existence of electromechanical effect in germanium 11 p1749 A66-22284

Vibration constant of electromechanical transformation in electrodynamic vibrators 13 p1997 A66-25079

Electromechanical effects of ferroelectric crystals based on thermodynamic theory 18 p3153 A66-33630

# ELECTROMETER

SA GALVANOMETER  
Electrometer using temperature-autostabilizing nonlinear dielectric element as receiver 02 p0230 A66-11815

Constant current sources consisting of sealed ionization chambers for calibrating electrometers 19 p3357 A66-35809

# ELECTROMOTIVE FORCE

## SA PONDEROMOTIVE FORCE

Inhomogeneity distribution in single crystal semiconductor considering specific resistance and carrier lifetime and using volume gradient photoelectromotive force values 01 p0124 A66-10763

Variation in thermoelectromotive force and magnetoresistance in quantizing magnetic field in indium antimonide semiconductor, considering electron spin and conduction band nonparabolicity 01 p0124 A66-10770

Photo-emf of germanium in presence of surface recombination rate gradient 02 p0277 A66-12089

Temperature dependence of heat conductivity and thermal emf in n-type InP 02 p0277 A66-12094

Thermoelectric emf related to entropy in quantizing magnetic field in semiconductor with polyellipsoidal conduction band 04 p0564 A66-14252

Emf induced by plasma moving across constant transverse magnetic field used to determine rate of flow behind shock wave in shock tube 04 p0557 A66-14434

Photo emf effect calculated at p-n junction of crystal photodiode 08 p1268 A66-18696

Method of induced emf and integral antenna equation 08 p1197 A66-19605

P-type cadmium tin arsenide crystals, plotting temperature dependences of specific electroconductivity, Hall coefficient and thermal electromotive force 08 p1277 A66-19622

Thermal conductivity and emf of gallium arsenide at low temperatures, showing phonon drag effect 08 p1278 A66-19626

Resistance temperature dependence, Hall

constant, thermal emf and Hall mobility of silicon with phosphorus

impurities 08 p1278 A66-19772

Random nonuniformities effect on measurements of thermal emf and Nernst coefficient in strong magnetic field 09 p1412 A66-19982

Magnetophonon fluctuation of thermal emf of n-InSb in longitudinal magnetic field 09 p1412 A66-19985

Hall effect, thermal emf and electrical conductivity of SmS in temperature range 300 to 1000 degrees K 09 p1412 A66-19988

Anisotropy of balanced photoelectromagnetic emf in p-type germanium sample in which normal to illuminated surface coincides with crystallographic axis 09 p1413 A66-20002

Inhomogeneity distribution in single crystal semiconductor, considering specific resistance and carrier lifetime by using volume gradient photoelectromotive force values 11 p1748 A66-22274

Variation in thermoelectromotive force and magnetoresistance in quantizing magnetic field in indium antimonide semiconductor, considering electron spin and conduction band nonparabolicity 11 p1749 A66-22281

Electric conductivity and thermal emf of solid solutions of silicon-germanium with near silicon composition and various current-carrier concentrations and test temperatures 12 p1929 A66-24454

Thermocouple emf, noting pressure dependence and effects of contamination, plastic deformation, electrical shunting, temperature gradients, etc 13 p2076 A66-25042

Thermocouple emf pressure dependence measured for Chromel/Alumel and platinum/platinum-10 percent rhodium and platinum/platinum-13 percent rhodium 13 p2076 A66-25073

Photo emf of gallium arsenide determined as function of temperature, light intensity, external electric field and surface quality 13 p2165 A66-25679

Emf amplitude and phase for pumping and resonant circuit current calculated for inductive parametron 14 p2252 A66-27251

Entropy and heat of formation of lead telluride determined by emf temperature coefficient measurement 14 p2369 A66-28330

Input impedance of small loop of uniform electric current immersed in anisotropic cold magnetoplasma calculated by induced emf method 15 p2548 A66-28593

Surface charge sign effect on capacitor photoelectromotive force in semiconductors and photoinduced contact potential change 15 p2559 A66-28628

Direct measurement procedure for Hall emf semiconductor samples of circular shape 16 p2777 A66-30868

Thermal emf of metallic liquid couples measured as function of thermal difference between junctions and alloys composition, noting correlation between thermodynamic and thermoelectric properties of alloys 16 p2781 A66-31410

Photo emf variation with radiation power of Q-switch ruby laser incident on silicon crystal with p-n junction 17 p2978 A66-32509

Longitudinal Faraday emf, thermoelectric and Hall effects on channel flow of ionized gas 17 p2972 A66-32868

P-type cadmium tin arsenide crystals, plotting temperature dependences of specific electroconductivity, Hall coefficient and thermal electromotive force 17 p2984 A66-33136

Thermal conductivity and emf of gallium arsenide at low temperatures, showing phonon drag effect 17 p2984 A66-33140

Gold and silver doping effect on Hall effect, electroconductivity thermal emf and conductivity of CdSb 17 p2984 A66-33145

Emf expressions for substrate and gate transconductances of MOS transistor 18 p3077 A66-34074

Effect of partial substitution of silicon, germanium and lead for tin on thermal emf and thermoconductivity of solid solutions of tin telluride 20 p3612 A66-37123

Conductivity, temperature dependence, thermal emf Hall constant, thermal conductivity and resistivity of aluminides of transition metals 20 p3584 A66-37417



Quantum oscillation of transverse and longitudinal magnetothermal emf in n-type indium antimonide compared with oscillations of transverse and longitudinal magnetoresistance and Hall coefficient 20 p3618 A66-37557

Electric conductivity and thermal emf of solid solutions of silicon-germanium with near silicon composition and various current-carrier concentrations and test temperatures 20 p3619 A66-37686

Liquid junction cell design, noting equation integration for ideal diffusion potential and salt effects potential for heteroionic junctions of uniform ionic strength and cation concentration 20 p3502 A66-38188

Thermodynamics of molten lithium nitrite galvanic cell, noting emf temperature dependence 20 p3503 A66-38189

Effective electron mass dependence on pressure in InSb determined by measuring electron concentration and thermal emf 20 p3624 A66-38427

Effective electron mass dependence on pressure in InSb determined by measuring electron concentration and thermal emf 21 p3800 A66-38960

Distribution of capacitive photo-emf over surface of semiconductor determined by measuring value created by scanning surface of sample with narrow modulated-light beam 22 p3965 A66-40316

Faraday unipolar induction in solid cylinder of nonideal type II superconductor, noting contributions to observed emf 23 p4114 A66-41629

Electrical properties of barium plumbate noting conductivity, Hall field, thermoelectromotive force, magnetization, etc 24 p4253 A66-42382

**ELECTROMYOGRAM**

Electromyography signals to control external power based upon pattern recognition [ASME PAPER 65-WA/HUF-3] 05 p0628 A66-15700

**ELECTRON**

SA CONDUCTION ELECTRON

SA FAST ELECTRON

SA FREE ELECTRON

SA HIGH ENERGY ELECTRON

SA HOT ELECTRON

SA PHOTOELECTRON

SA PHOTON-ELECTRON INTERACTION

SA POSITRON

Intensity and spectra of cosmic ray electrons and positrons in determining mean confinement time, density and solar modulation 20 p3630 A66-37303

**ELECTRON ACCELERATOR**

Nonstationary processes measurement method in semiconductor devices by linear electron accelerator 01 p0035 A66-10189

Drain currents from iron and copper ion accelerator electrodes of ion engine as functions of cesium flux, temperature, voltage difference and oxygen pressure [AIAA PAPER 64-686] 03 p0416 A66-12782

Parameter perturbations of magnet and accelerating systems of electron synchrotron determined from position of center of gravity of beam 13 p2147 A66-25747

Elastic electron scattering cross sections for titanium relative to C and Be measured, using linear electron accelerator 14 p2337 A66-27795

Microtron principles, parameters and application, including comparison with other accelerators 14 p2347 A66-28308

Plasma heating rate in stochastic electric fields determined, using nonrelativistic collisionless lossless test particle 17 p2967 A66-32436

Electron-cyclotron heating of plasma via high power oscillator, noting experimental setup and characteristics 18 p3151 A66-35068

Single-wave approximation of fields of cylindrical delay system with basic E-type wave propagating at variable phase velocity 20 p3515 A66-37381

Energy distribution of trapped electrons producing solar microwave impulsive radio bursts and X-ray bursts from Sun 20 p3634 A66-38213

Magnetospheric tail instabilities, auroral electron acceleration and deformation due to dipole magnetic field acceleration of plasma particles 20 p3635 A66-38222

Acceleration of high energy electrons by means of Parker-Wentzel version of Fermi mechanism due to geometry and distorted structure of interplanetary magnetic field near magnetopause in transition region 22 p3972 A66-40003

**ELECTRON ATTACHMENT**

Ambipolar diffusion and electron attachment in photoionized nitric oxide by presence of negative ions, noting electron loss and electron density 03 p0394 A66-12326

Electron attachment and detachment coefficients for pure oxygen determined from current waveforms in drift tube 18 p2130 A66-25374

Dielectric constant obtained by bound electron theory is not distinguished from one obtained by warm plasma theory when considering main resonance and related phenomena 16 p2758 A66-30277

Gas pressure dependence of attachment and recombination coefficients for thermalized electrons in air and oxygen 18 p3143 A66-34035

Positive electron affinity of tungsten determined by evaporation of positive and negative ions from incandescent tungsten surface 20 p3605 A66-38247

**ELECTRON AVALANCHE**

HF noise from electron avalanches and relation to mechanism of cold cathode arc 04 p0502 A66-14480

Electron collision-ionization avalanches in cadmium sulfide crystal due to electric field intensities 04 p0570 A66-14489

Electron avalanches in anode and cathode directed streamers detected by high-gain image intensifier and streak shutter 08 p1263 A66-19079

One-dimensional small signal analysis of negative resistance in p-n junctions under avalanche breakdown conditions 10 p1586 A66-22083

Small-signal impedance of space-charge region of p-n junctions under avalanche breakdown conditions, using realistic physical assumptions 10 p1586 A66-22084

Metallurgical junction radius of curvature effect on avalanche breakdown voltage in Ge, Si, GaAs and GaP spherical and cylindrical p-n junctions 22 p3959 A66-39740

Avalanche breakdown voltage of quasi-planar/circular cylindrical/silicon junction and relation to increased electric field intensity in curved portion 22 p3959 A66-39741

**ELECTRON BEAM**

SA BEAM-PLASMA AMPLIFIER

SA BRILLOUIN FLOW

Electron beam pumping of noble gas ion laser 01 p0081 A66-10350

Charge trapped in electron or ion beams at pressures below breakdown determined from general integro-differential equation, using approximation 01 p0111 A66-10375

Potentialities of cylindrical plasma structures considering electron beam interaction and microwave devices, noting dispersion of waveguide containing plasma 01 p0039 A66-10526

Conventional periodically loaded waveguides with ferrimagnetic materials used in devices involving traveling wave interaction with electron beam 01 p0025 A66-10533

Electric wave growth and amplification in electron beam interaction with plasma in microwave amplifier, noting longitudinal inhomogeneity 01 p0112 A66-10588

Density distribution before sphere in low density hypersonic gas flow measured with electron beam 01 p0059 A66-10635

RF electric field in electron beam/plasma interaction measurement, using nonperturbing probing technique 02 p0265 A66-11432

Electron beam generating plasma in tube aligned with magnetic field, measuring plasma density, beam velocity distribution and RF noise spectrum 02 p0266 A66-11442

Flow visualization technique by thin high-energy electron beam moved with respect to flow 02 p0215 A66-11550

Plasma diagnostics by relativistic electron beam consisting of separate electron clusters emitting ultrashort electromagnetic

waves 03 p0396 A66-12291

Line structured pattern by vidicon tube and beam control logic 03 p0337 A66-12438

Electron beam-hot plasma interaction at low frequencies, explaining cesium discharges and gas noise 03 p0398 A66-12539

Harmonic generation in double beam system in presence of magnetic field 03 p0404 A66-12981

Harmonics in cylindrical electron beams traveling in circular drift tube and velocity-modulated by gridless buncher gap 04 p0491 A66-13421

Harmonics of electronic gyro-magnetic high-frequency in spectrum of two-electron beam collision 04 p0550 A66-13473

Electron beam-plasma interactions used to predict occurrence of amplifying waves having growth rates maximizing near to electron plasma frequency 04 p0552 A66-14036

Semiconductor and dielectrics for generation of coherent short-wave radiation, using electron beam for excitation 04 p0568 A66-14346

Penetration of external longitudinal electric field into semibounded plasma containing electron beam in absence of instabilities in system 04 p0556 A66-14416

Dispersion equation for LF electronic oscillations in electron beam Maxwell collision-free plasma 05 p0722 A66-14722

Frequency oscillation role as drift waves excited during interaction of electron beams with plasma, made impossible by ion transverse motion 05 p0722 A66-14723

Metal surface structure, semiconductors and dielectric films analyzed, using image orthicon technique for data on work function, electron reflection coefficient and electric resistance 05 p0621 A66-15578

Negative depression coefficient in traveling wave tubes at small helix parameters and different radii for helix and electron beam 06 p0838 A66-15901

Electromagnetic waves from plasma penetrated by pulsed electron beam in magnetic field 06 p0914 A66-16147

Thin film deposition by electron-beam and glow-discharge activation of various gaseous ambients 06 p0848 A66-16302

Cold quasi-neutral beams focusing in electromagnetic fields 06 p0916 A66-16347

Traveling wave characteristics of Cerenkov interaction studied by circular waveguide with electron beam flow 06 p0850 A66-16441

Space-charge wave propagation on nonuniform drifting electron beam explained, using coupled mode theory 06 p0855 A66-16767

Coupled monotron analysis of band-edge oscillations in high power traveling wave tubes, discussing electron beam interaction with coupled-cavity structure 06 p0855 A66-16768

Cyclotron harmonic amplification of wave propagation in electron beams and plasmas with internal motions in presence of static magnetic field 06 p0920 A66-17013

Energy levels and optical transitions between them which give rise to optical gain in injection lasers, examining use of PbTe and electron beam-pumping techniques 07 p1041 A66-17327

Electron beam acceleration by means of toroidal systems in which equilibrium of beam in annular orbit is achieved by image currents in metallic coating of vacuum chamber 07 p1085 A66-17648

Nonlinear effects of induced scattering of oscillations of plasma particles, examining influence on dynamics of beam instabilities 07 p1086 A66-17649

Mirror ratio is principal parameter controlling heating of plasma by electron beam in magnetic mirror system 07 p1090 A66-18260

Plasma formation during unstable electron beam passage through air, argon and hydrogen in magnetic field, determining plasma density, oscillation frequency and amplitude 08 p1263 A66-19176

Time dependent frequency spectra variations of plasma oscillations induced by electron beams during instability onset 08 p1263 A66-19177

Effective compensation of perturbation



- effects in three-turn helical magnetic field, using combinations of two-turn and perpendicular stationary magnetic fields 08 p1264 A66-19178
- Cerenkov radiation in circularly symmetrical waveguide filled with uniform dielectric in presence of flowing modulated electron stream 09 p1351 A66-20258
- Nonlinear TWT equations simplified for computing finite modulation of electron beam relative to velocity 09 p1357 A66-20778
- Mirror ratio is principal parameter controlling heating of plasma by electron beam in magnetic mirror system 09 p1409 A66-20904
- Interaction of primary unmodulated beam of electrons and plasma in magnetic field 10 p1559 A66-21349
- Coherent radiation effect on stability of crossed field electron beam, noting raising of potential of space vehicle 10 p1564 A66-21544
- Radiated power from modulated electron beam passing near diffraction grating surface 10 p1557 A66-21567
- Electron beam/nonisothermal plasma interaction and nonlinear stabilization of beam instability 10 p1569 A66-21973
- Forced emission from electron-excited cadmium selenide 10 p1544 A66-22174
- Oxidation of artificial graphitic carbon 14 oxidized to carbon 14 dioxide in presence of nonsterile soils, noting inhibition of biological activity by electron beam irradiation 11 p1649 A66-22304
- Cold quasi-neutral beams focusing in electromagnetic fields 11 p1743 A66-22346
- Coupling impedance of thin hollow electron beam injected into magnetic field and rippling at cyclotron frequency in cylindrical waveguide carrying Eo1 mode 11 p1661 A66-22395
- Thin nonrectilinear electron beam interaction with electromagnetic field of waveguide transmission line 11 p1655 A66-22723
- Raster magnification effect of moire images to observe plane deformation in specimens subjected to impact 11 p1782 A66-22857
- Density variation in Ar shock waves during translational adjustment for Mach 5 to 10 velocity range, using electron beam techniques 11 p1691 A66-22915
- Shock front density distributions in Ar and He determined in shock tube, using electron beam attenuation 11 p1691 A66-22916
- Electron beam measurement of shock wave thickness used to determine limits of validity of Navier-Stokes equations 11 p1691 A66-22917
- Flat plate in hypersonic flow analysis in shock tunnel, obtaining surface pressure, using electron beam densitometer 11 p1634 A66-22931
- Electron beam pumped lasers, discussing energy dissipation in fast electrons passing through crystal, laser semiconductor characteristics, etc 11 p1715 A66-23433
- Monograph on microwave frequency space-charge waves in electron beams including electron-wave oscillators, resonators and magnetrons 12 p1813 A66-23740
- Fresnel zone beam scanning antenna array, considering patterns, maximum scan ability and effect of interelement spacing 12 p1841 A66-24633
- Partial dislocation detection in silicon, using scanning electron beam technique 13 p2159 A66-25069
- Ion cyclotron instabilities in bounded cold beam-plasma system, noting growth rate parameters, instability conditions, etc 13 p2138 A66-25190
- Electron-beam-controlled CRT scanlaser 13 p2091 A66-25557
- Detection and analysis of oscillations excited in electron beam and plasma as result of interaction, noting frequency spectrum, phase velocities, etc 13 p2146 A66-25745
- Strength and plasticity of some electron beam melted niobium alloys in cast and annealed specimens 13 p2110 A66-25886
- Parametric amplifier design using transverse interaction and electrostatic focusing of electron beam 13 p2042 A66-26048
- Stimulated emission from electron beam excitation of tellurium and pure and n-type doped indium antimonide in semiconductor lasers 13 p2099 A66-26179
- Q-switched lasers, interaction of high power light pulse with matter and semiconductor lasers pumped with optical radiation and electron beams investigated, using quantum oscillator and amplifier 13 p2099 A66-26180
- Excitation in electron beam pumped /EBP/ GaAs lasers including electron scattering, energy dissipation pattern, phonon emission, pair production, etc 13 p2099 A66-26181
- Vacuum deposited films of titanium dioxide examined, using electron microscopy and diffraction methods, noting crystal dislocation due to electron beam irradiation 14 p2359 A66-27133
- Spurious X-band output signals observed during interaction of dual reflex klystron cavities and klystron beams 14 p2258 A66-27956
- Semiconductor and dielectrics for generation of coherent short-wave radiation, using electron beam for excitation 14 p2368 A66-28242
- Electrostatic and magnetic pinch effects in electron beam-generated plasmas 15 p2549 A66-28717
- Electron beam analyzer for determining crossed field space charge beam analyzer 15 p2549 A66-28719
- Decay of space-charge waves as due to ballistic or free-streaming process in electron beam with velocity spread 15 p2550 A66-28724
- Single crystal germanium films grown on molybdenum or tungsten substrates, using electron beam zone melting process 15 p2563 A66-28726
- Focusing of long cylindrical electron beam by means of short-period permanent magnet or long-period reversed field magnet 15 p2467 A66-29709
- Multivelocity stream effects and efficiency of slow-cyclotron wave amplifiers, noting electron velocity spread which decreases predicted efficiency 15 p2467 A66-29711
- Shock wave thicknesses and density ratios measured in helium, argon and nitrogen, using electron beam fluorescence method at various Mach numbers in wind tunnel 15 p2480 A66-29736
- Rotational distribution function of flowing nitrogen in low density wind tunnel using electron beam fluorescence 15 p2481 A66-29737
- Rotational energy distribution through shock waves in nitrogen measured, using electron beam fluorescence 15 p2481 A66-29738
- Small-signal energy conservation theorem for one-dimensional multivelocity electron beam according to Boltzmann and multistream descriptions 15 p2467 A66-29755
- Nonlinear diffusion equations in electron beam excited plasma noting two- and three-body recombination, radial distribution of electron density, light intensity, etc 15 p2555 A66-29761
- Electromagnetic waves from plasma penetrated by pulsed electron beam in magnetic field 15 p2557 A66-29877
- Injection of helical electron beams into magnetic mirror trap, examining plasma lifetime, density and electron and ion energies produced 16 p2755 A66-30092
- Energy transfer measurements in gas-sold surface interactions initiated by electron beam-excited photoemission 16 p2701 A66-30397
- Unscanned large area uniform electron beams for space /Starfish/ radiation environmental studies, using magnetic quadrupole pair and beam collimation 16 p2676 A66-30443
- Metal film preparation by electron-beam melting of metal in water-cooled crucibles 16 p2661 A66-30693
- Excitation of backward Doppler shifted cyclotron radiation in magnetoactive plasma by electron stream 16 p2761 A66-30921
- Semiconductor lasers with high power efficiency obtained via electron beam excitation on crystals of mixed cadmium-sulfide-selenide alloy 16 p2720 A66-31533
- Transport of AC disturbance /emission noise/ on electron beams magnetically compressed in microwave tubes, deriving power flow invariants 17 p2878 A66-31819
- Interaction of modulated high current pulsed electron beams with plasma in longitudinal magnetic field 17 p2963 A66-31826
- Longitudinal wave excitation in modulated electron beam interacting with plasma 17 p2963 A66-31830
- Emission of electromagnetic waves by electron flux moving inside ring waveguide 17 p2874 A66-32248
- Plasma bremsstrahlung power derived for relativistic, nonrelativistic and electron beams 17 p2965 A66-32256
- Convective excitation of ionic oscillations in plasma by inhomogeneous electron beam as result of spatial gradient of distribution function 17 p2968 A66-32537
- Response of finite relativistic beam plasma system to small disturbances analyzed, using coupled Vlasov-Maxwell equations 17 p2970 A66-32640
- Cylindrical electron beam behavior in axial, monotonically increasing magnetic field, noting compression, percentage scalloping, etc 17 p2887 A66-32696
- Ideal and perturbed focusing conditions effect on spread of immersed flow beam 17 p2971 A66-32821
- Plasma oscillation theory of nonlinear deceleration effect and thermal conversion of electron beams upon passage through plasma 17 p2974 A66-33284
- Laser based on excitation of gallium phosphorus arsenide solid solution by beam of fast electrons 17 p2937 A66-33304
- Vibrational and rotational nonequilibrium flow effects in hypersonic conical nozzle expansion of nitrogen flows and airflows 17 p2842 A66-33478
- Wave coupling and generation of gyromagnetic half-frequency harmonics in double electron-beam system 18 p3142 A66-33911
- Plasma stabilization mechanism for electron beam caused density variation, noting use of nonlinear effects 18 p3152 A66-35082
- Forced emission from electron-excited cadmium selenide 19 p3441 A66-35788
- Nonaccelerated electron beam envelope trajectory equation reformulated and solved allowing for finite emittance, space charge and self-magnetostatic forces 19 p3319 A66-36170
- Collective interactions of charged particle beams with plasma produced by electron beam, noting power loss of electron beam coincides with power of HF oscillations caused by interaction 19 p3416 A66-36524
- Plasma equilibrium in torus with HF fields and plasma heating caused by beam of escaping electrons, measuring plasma density, time-dependent plasma luminescence, etc 19 p3424 A66-36558
- Electron beam interaction with plasma in mirror magnetic fields and heating of plasma components under beam instability, noting oscillation spectrum and thermal energy 19 p3430 A66-36586
- Plasma stability, density, energy, etc, resulting from electron beam/plasma interaction which excites microwave oscillations, creating microwave discharge 19 p3430 A66-36587
- Langmuir current-density limit derived for differing axial and radial electron beam temperatures in high-resolution image devices 20 p3524 A66-36899
- Reversible property of Vlasov equation describing thermalization of electron beam in plasma and Landau damping, noting entropy is constant in nonlinear approximation 20 p3608 A66-37460
- Pulsed operation of electron-beam pumped zinc oxide laser emitting radiation in UV at very low temperatures, noting importance of use of cavity 20 p3579 A66-37768
- Electron beam rotation experiments on linear spiratron with M-type electron gun 20 p3533 A66-38005
- Electron beam scanlaser based on laser cavity directly and/or transversely degenerate having Q-spoiled for all modes but one 20 p3581 A66-38244
- Crossed-field electron beam stability for



- arbitrary values of Q /ratio of plasma frequency to cyclotron 20 p3606 A66-38404
- Electron beams from duoplasmatron using hollow cathode arc, noting current density distributions 20 p3606 A66-38406
- Electron gun with voltage drop across cathode using space charge streams for M-beam generation 21 p3710 A66-38833
- Electron beam interaction with plasma in magnetic field, obtaining stronger interaction when beam has initial modulation 21 p3782 A66-39018
- Plasma generation by electron beam with developing instability, noting plasma parameters 21 p3782 A66-39019
- Longitudinal and transverse electric fields in electron beam due to interaction with plasma, showing that both fields are components of same wave 21 p3782 A66-39020
- Characteristics of efficient semiconductor lasers in UV portion of spectrum obtained at both liquid helium and nitrogen temperatures, using pulsed electron beam excitation on ZnS 21 p3747 A66-39114
- Preferential formation of peaks of single-crystal silicon and germanium samples exposed to short-duration electron beam 21 p3801 A66-39117
- Electron beam flow visualization study of density field about skimmer entry in small free jet 21 p3727 A66-39186
- Instability of three-component plasma system studied to analyze beam-plasma interaction, noting restraining effect of electrons on instability of beam-ion coupling 21 p3792 A66-39188
- Electron beam/nonisothermal plasma interaction and nonlinear stabilization of beam instability 21 p3794 A66-39552
- RF behavior of one-dimensional plasma in electrical circuit analog with coupled resonant circuits representing normal modes 22 p3884 A66-39816
- Nonlinear TWT equations simplified for computing finite modulation of electron beam relative to velocity 22 p3873 A66-39837
- Electron beam density measurements, discussing effect of elevated rotational and vibrational temperatures 22 p3918 A66-40365
- Spectroscopic electron beam diagnostic technique, examining negligible effect elevated vibrational temperatures have on measured rotational temperatures of molecular nitrogen [AIAA PAPER 66-747] 22 p3919 A66-40633
- Gas ionization by fast electron beam directed along waveguide leading to longitudinal distribution of secondary electron concentration 22 p3958 A66-40938
- Nonsymmetric oscillations in plasma in magnetic field arising from electron beam passage through plasma, deriving dispersion equation 22 p3958 A66-40939
- Thin nonrectilinear electron beam interaction with electromagnetic field of waveguide transmission line 23 p4037 A66-41461
- Flow visualization via afterglow produced in pure low temperature nitrogen and air by electron beam projection 23 p4058 A66-41911
- Density and temperature measurement in base region flow field of clustered rocket model, using electron beam technique 24 p4210 A66-42200
- Quantitative fast response visualization technique for low density flow fields based on electron beam fluorescence probe 24 p4210 A66-42201
- ELECTRON BEAM WELDING**
- Electron beam welding as production process using Steigerwald or telefocus system, Rogowski system or special Rogowski system 02 p0236 A66-11700
- Electron beam welding with particular reference to fixture design, weld preparation, field of application, advantages and limitations 02 p0236 A66-11869
- Nonvacuum electron beam welding technique as fabricating technique for production welding 05 p0685 A66-14513
- Electron beam welding for in-space welding of spacecraft and space stations noting welding modes, power requirements, environmental influences, etc 06 p0888 A66-17072
- Electron beam machines for thermal milling, noting factors influencing size of heat affected zones such as current density, lens aberration, temperature rise, etc 11 p1710 A66-22700
- Electron beam welding of high-strength titanium alloy propellant tank for third stage of ELDO carrier rocket and determination of optimum welding parameters 12 p1885 A66-23783
- Focused energy techniques for joining, including laser welding [ASTME PREPRINT AD66-718] 12 p1886 A66-24413
- Chemical milling of columbium reentry vehicle skin panels using powdered metallurgy, vacuum processing, refractory alloy sheet rolling and electron beam welding [ASTME PREPRINT MR66-712] 12 p1886 A66-24417
- Porosity at weld fusion zone-base material interface in gas tungsten-arc and electron beam welds of tantalum 13 p2110 A66-26018
- Electron beam heating of alloy specimen and liquid-nitrogen cooled anvils for rapidly cooling it 13 p2084 A66-26560
- Vacuum and nonvacuum electron beam welding 16 p2713 A66-30593
- Welding characteristics of four advanced commercial columbium base alloys using gas tungsten arc and electron beam processes 16 p2725 A66-31437
- Electron beam welding in partial vacuum 19 p3362 A66-35325
- Applicability of electron beam welding techniques for in-space welding and maintenance, examining fabrication of typical aerospace joints 19 p3363 A66-35951
- Electron beam welding suitable for joining tungsten sheet for fabrication of solid rocket nozzles and nozzle accessories 19 p3369 A66-36128
- Electron beam welding of maraging steel, noting tensile test results on efficiency, defect formation, region of fracture nucleation, etc 19 p3371 A66-36632
- Sciaky electron beam welding equipment applications, including joining lengths of tubing for nuclear reactor 21 p3743 A66-38670
- Electron beam welding of aircraft turbine gears 21 p3744 A66-39233
- Gas turbine compressor rotor and power shaft fabrication using electron beam welding 22 p3924 A66-40258
- Electron beam welding outside of vacuum, discussing performance and tolerance parameters 22 p3924 A66-40261
- Electron beam welding and application to aerospace industry, noting basic weld joint configurations 22 p3925 A66-40268
- Plasma electron beam gun at rough vacuum pressures for welding ferrous and aluminum alloys 22 p3925 A66-40270
- Nonvacuum electron beam welding compared with vacuum process, noting effect of voltage, distance, speed, etc, in aerospace applications 22 p3925 A66-40271
- Analog and digital controls used in electron beam welding and metal working machinery including electron beam milling machine 24 p4217 A66-42345
- ELECTRON BOMBARDMENT**
- SA SECONDARY EMISSION
- Transition and bremsstrahlung spectrum from measurement of energy dependence on visible and UV radiation emitted from electron bombarded Ag targets 01 p0108 A66-10195
- Laser transition identification in electron beam pumped gallium arsenide, primarily on concentration of shallow donors and acceptors 01 p0081 A66-10348
- Equivalence of stress and electron-irradiation induced defects in degenerate p-n germanium junctions as indicated in similar voltage-anneal characteristics 04 p0562 A66-13751
- Power transistors used for stabilization of emission current of electron bombardment ion source for mass spectrograph 04 p0498 A66-14037
- Luminescence decay of electron bombarded CdS, measuring time constants 05 p0737 A66-15173
- High pressure thermionic converter, discussing current-voltage characteristics at high collector temperatures 05 p0616 A66-15545
- Elastic differential scattering of helium ions discussing energy analysis, geometry and target particle motion effects, and interference phenomena 05 p0719 A66-15767
- Optical properties of spacecraft temperature control coatings under simulated geomagnetically trapped electron bombardment [AIAA PAPER 65-137] 05 p0706 A66-15792
- Four-lobed rosette stress patterns in X-ray topography of silicon bombarded by electron beam 06 p0928 A66-16761
- Hall effect and conductivity measurements of carrier removal rate in oriented specimens of n-type Si under electron irradiation at energies from 0.3 to 2.0 mev 06 p0930 A66-17049
- Radiation damage in silicon and germanium semiconductors 06 p0932 A66-17112
- Metastable defect annealing in germanium by bombardment with short pulse of high-energy electrons from Van de Graaff generator 06 p0932 A66-17115
- Lattice vacancies and interstitials in II-VI compounds of cadmium sulfide and zinc selenide caused by electron bombardment often determine advantages or limits of material 06 p0935 A66-17130
- Proton and electron bombardment induced defects in GaAs studied by examining spectral composition and intensity of proton and cathode luminescence 06 p0936 A66-17135
- Semiconducting properties of electron irradiated silicon carbide 06 p0936 A66-17138
- Anisotropy of electron displacement energy in silicon specimens by measuring changes in net carrier concentration caused by steady monoenergetic electron irradiations 06 p0939 A66-17152
- Isolated vacancy interstitial pairs produced in ZnSe lattice by electron bombardment at low temperature 06 p0939 A66-17153
- Nature and yield of photon and neutron induced defects in semiconductors determined from changes in electrical properties 06 p0939 A66-17154
- Excitation of semiconductor lasers by beam of fast electrons, discussing work of Shockley, Popov, Keldysh and Krokhin 07 p1043 A66-17337
- Spectral distribution of luminescence excited in n-type GaAs and p-type GaP by fast-electron bombardment 07 p1096 A66-17339
- Spectral distribution of recombination radiation observed in various samples of GaAs irradiated by electron beam 07 p1043 A66-17340
- Laser action achieved in n-type indium antimonide excited by 15-kv electron beam at 20 and 4 degrees K 07 p1043 A66-17341
- Laser emission in pure cadmium sulfide crystals bombarded by electron beams 08 p1233 A66-18650
- Electric resistivity change in Pt produced by electron bombardment 08 p1275 A66-19364
- Impurity-photoconductivity spectra of silicon single crystals containing lithium and arsenic impurities 09 p1413 A66-19999
- Hysteresis nature of current-voltage characteristics observed in p-n junctions obtained by bombarding germanium crystals with fast electrons 09 p1413 A66-20001
- Electric propulsion in 1965, discussing electron bombardment and contact ionization thrusters, nuclear and solar-electric power systems, etc 09 p1434 A66-20246
- Electric propulsion systems development, discussing ion beam neutralization, nuclear power sources, contact ionization engine, etc 09 p1434 A66-20248
- Line intensities of first negative bands of nitrogen molecular ion measured as function of bombarding electron energy and gas pressure 09 p1404 A66-20377
- Plasma oscillation of electrons in Be, Mg, Al, Si, Ge, Sn, Sb and Bi studied by electron bombardment of thin foil of these solids 09 p1429 A66-20842
- Lunar X-ray detectability, noting generation by solar wind electron bombardment and flux intensity 09 p1459 A66-20885
- Ionizing role of photon radiation in gas thermionic converter, noting experimental results and application to solar energy



converters, tubular emitter converters, etc 09 p1405 A66-20923  
 Plasma measurements in cesium electron bombardment ion engine indicate that reversed cathode-anode configuration improves radial ion distribution [AIAA PAPER 66-246] 10 p1593 A66-21455  
 Ion thruster, including mercury feed system and shielded neutralizer, designed and tested for spacecraft station keeping and attitude control [AIAA PAPER 66-247] 10 p1593 A66-21456  
 Electron bombardment ion thrusters with two accelerator-grid systems for producing ion beams in directions 180 or 90 degrees apart [AIAA PAPER 66-248] 10 p1593 A66-21457  
 Life testing of electron-bombardment cesium ion engine designed for power-to-thrust ratio of 160 kw/lb [AIAA PAPER 66-233] 10 p1594 A66-21701  
 Ionization currents in diamond exposed to pulsed excitation and to applied pulsed electric field 10 p1586 A66-22144  
 Durability test of mercury electron-bombardment ion thrusters, measuring lifetime, output, power efficiency, etc [AIAA PAPER 66-231] 11 p1760 A66-22218  
 Electron impact ionization cross section of H<sup>2</sup>s/ and H<sup>2</sup>p/ in Born A, Born B, Born-Dechurk and classical approximations 11 p1738 A66-22498  
 Emission spectra of nitrogen excited by electron beam of 0.1 to 20 keV and oxygen and air bombarded by 13-keV electrons 11 p1740 A66-23040  
 Length changes and conductivity variations in electron irradiated n-and p-type germanium, noting methods of measurement, effects of isochronic annealing at liquid helium and nitrogen temperatures 12 p1926 A66-23717  
 Electron bombardment thrusters using liquid mercury cathodes, noting lifetime, propellant and power efficiency, feed system, temperature limits, etc [AIAA PAPER 66-232] 13 p2172 A66-25172  
 Design of gravity-independent force-fed liquid-metal cathode providing unlimited cathode life in gas discharge devices and mercury electron-bombardment thrusters [AIAA PAPER 66-245] 13 p2106 A66-25175  
 Measurement of total cross section for excitation of metastable atoms of helium by electron bombardment 13 p2135 A66-26266  
 Superradiance in n-type gallium arsenide at room temperature excited by electron beam 14 p2306 A66-27028  
 Laser oscillations in CdSe and CdS bombarded by fast electron beam 14 p2306 A66-27031  
 Lifetime measurement for minority carriers injected into germanium by electron bombardment 15 p2567 A66-29409  
 Model of discharge in electron bombardment thrusters noting mechanism and interplay between discharge plasma and cathode [AIAA PAPER 66-244] 16 p2791 A66-31153  
 Combination of point counting and electron microprobe techniques in mineralogical planimetric integration analysis 16 p2707 A66-31196  
 Number transmission coefficients for isotropically incident electrons determined for spacecraft shield design [AIAA PAPER 66-511] 16 p2811 A66-31497  
 Photoconductivity spectra and kinetics of p-and n-type germanium crystals bombarded by fast electrons at 5.2 and 100 degrees K 16 p2788 A66-31776  
 Additional measurements from electron-magnetic field interactions and power limitations in coaxial filament and anode geometry in electron bombardment heated thruster 17 p2990 A66-32462  
 Fluorescence bands produced by electron bombardment of ZnSe show threshold of annealing stages of radiation damage 17 p2985 A66-33154  
 Electron bombardment ion thrusters and electrostatic accelerators, discussing electrode geometry and composition and electrode erosion 17 p2991 A66-33233  
 Electrostatic ion drives technology problems, discussing gaseous discharge ion sources, duoplasmatron and electron bombardment ion

generator 17 p2991 A66-33234  
 Recrystallization of Ge and Si thin films and structural changes due to electron bombardment and thermal annealing 17 p2988 A66-33456  
 Probability of atomic excitation by electron bombardment 18 p3143 A66-34033  
 Transition radiation in optical region of spectrum for case of oblique incidence of nonrelativistic electrons on metal surface 19 p3399 A66-35593  
 Comparison of electromagnet and permanent magnet versions of electron bombardment cesium ion engine [AIAA PAPER 65-373] 19 p3450 A66-35617  
 Ionization currents in diamond exposed to pulsed excitation and to applied pulsed electric field 19 p3440 A66-35758  
 Catastrophic failures in glass diode packages and integrated circuit chips exposed to high-intensity electron pulse 19 p3318 A66-35920  
 Dissociation of hydrogen molecules by electron impact, using first-order exchange approximation and separated atoms approximation 19 p3403 A66-36328  
 Visible and UV transition radiation, bremsstrahlung and plasma due to electron bombardment of metal surfaces 20 p3604 A66-37280  
 Minority carrier trapping centers introduced by irradiation of n-type germanium analyzed, particularly effect of donor species on production, recovery and annealing of defects 20 p3623 A66-38408  
 Thermal conductivity change in single crystal InSb irradiated with electrons, noting additive thermal resistivity increases 24 p4249 A66-42228  
 Radiative recombination in annealed electron irradiated zinc doped gallium arsenide 24 p4250 A66-42229  
 Electron paramagnetic resonance and Hall effect measurements to determine properties of dominant paramagnetic defect in electron irradiated p-type silicon 24 p4250 A66-42230  
 Electron irradiation effect on resistivity of epitaxial layers of Si and on lifetime of ordinary samples 24 p4258 A66-43008  
**ELECTRON BUNCHING**  
 Electron pitch distribution anomaly as observed by Cosmos V satellite, noting possible causes of phenomenon 09 p1378 A66-21009  
 Electron injection and E-layer buildup in Astron device theoretically studied by one-dimensional model, using Green functions for self-electric and self-magnetic fields 19 p3423 A66-36552  
**ELECTRON CAPTURE**  
 Capture and recombination levels in CdS single crystals examined from photoconductivity analysis 02 p0277 A66-12087  
 Spin-orbit coupling and electron-affinity determinations from radiative capture of electrons by oxygen atoms 04 p0547 A66-13641  
 Electrical behavior of microplasmas for determination of density and energy level of capture sites induced by radiation in silicon single crystals 04 p0566 A66-14320  
 Cadmium sulfide and cadmium selenide recombination centers, discussing temperature dependence of electron capture cross sections 05 p0731 A66-14661  
 Captured electron drift from trap with spatially periodic helical magnetic field, using time variable 06 p0919 A66-16879  
 Electron capture and hole capture by impurity atoms due to radiative transitions in silicon and germanium 07 p1095 A66-17323  
 Thermal ionization of small traps in cubic piezoelectric 07 p1105 A66-18377  
 Cathodic depolarization theory of bacterial corrosion, using Desulfovibrio desulfuricans with benzyl viologen as electron acceptor 11 p1647 A66-22303  
 Injection of plasma blobs into mirror trap and subsequent compression of plasma by increasing magnetic field, using longitudinal current, noting X-ray radiation 12 p1925 A66-24877  
 Measurement of cross section for excitation of cesium atom by electron impact in prethreshold energy region, using electron trap method 12 p1925 A66-24878

Monte Carlo calculations of cross section magnitude of electron-positive-molecular-ion dissociative recombination 13 p2130 A66-25375  
 Cadmium sulfide and cadmium selenide recombination centers, discussing temperature dependence of electron capture cross sections 13 p2168 A66-25936  
 Rate of dissociative electron capture by heavy molecular ions developed in semiclassical formalism 13 p2136 A66-26271  
 Impurity photovoltaic effect in cadmium sulfide, noting radiative enhancement of spectral response upon illumination with green light 15 p2561 A66-28709  
 Static properties and interactions of neutrinos noting mass, spin, helicity, charge, lepton number, etc 15 p2546 A66-29582  
 Temporary capture of charged particles in static magnetic bottle, based on resonant perturbations and Stoermer neck 16 p2760 A66-30588  
 Electron capture detector parameters in pulse sampling mode analyzed, noting kinetic processes, temperature effect, etc 17 p2961 A66-32660  
 Electron collection from VLF receiving antennas and plasma-density probe on board FR-1 satellite, using cathode-grid device 22 p3876 A66-40162  
 Injection of plasma blobs into mirror trap and subsequent compression of plasma by increasing magnetic field, using longitudinal current, noting X-ray radiation 23 p4099 A66-41084  
 Measurement of cross section for excitation of cesium atom by electron impact in prethreshold energy region, using electron trap method 23 p4099 A66-41085  
**ELECTRON CLOUD**  
 Electron cloud drifting axially outside conducting toroidal cylinder in presence of radial electric and azimuthal magnetic fields 08 p1260 A66-18545  
**ELECTRON COLLISION**  
 Velocity dependence effect of electron collision frequency on electromagnetic wave interaction with anisotropic plasma 01 p0028 A66-10570  
 Mean electron density and collision frequency determined from radio noise absorption, average electron drift velocity and magnetic disturbance intensity observations 01 p0065 A66-11167  
 Electron recombination in monoatomic ionized gas expanding symmetrically into vacuum, particularly triple collisions with electron capture on upper atomic level 02 p0264 A66-11383  
 Electron collision cross sections of atoms and molecules of argon, helium, nitrogen and dissociation products of carbon dioxide by dual beam radiosonde methods to study low temperature plasma behind shock front 02 p0268 A66-11780  
 Third harmonic current in plasma due to velocity-dependent collision frequency of electron 03 p0401 A66-12954  
 Harmonics of electronic gyro-magnetic half-frequency in spectrum of two-electron beam collision 04 p0550 A66-13473  
 Rate of electron-ion recombination by collision of two electrons in ion field obtained by Thomson formula, noting recombination rate of three-body collision 04 p0550 A66-13710  
 Book on lower ionosphere physics noting radio wave propagation, ionospheric currents, solar radiation and flares, ion kinetics, electron collision frequencies, etc 04 p0515 A66-13835  
 Hard X-ray emission during few half-cycles of theta pinch discharge before breakdown explained by bremsstrahlung of free accelerated electrons colliding with tube wall 04 p0555 A66-14326  
 Coulomb collision effect on transverse electron oscillations in fully ionized hot plasma determined by Fokker-Planck equation 05 p0721 A66-14715  
 Consistent-field Monte Carlo method used to calculate electron and ion diode characteristics, including effect of collisions 05 p0616 A66-15539  
 Plasma conductivity as function of Larmor electron frequency and mean electron-atom collision interval in transverse magnetic field of argon and mercury



plasma 06 p0918 A66-16835  
 Scattering and conversion cross section for inhomogeneous plasma in presence of electron collision 07 p1084 A66-17529  
 Excitation cross sections of helium lines in electron-atom collisions 07 p1044 A66-17874  
 Theoretical performance of idealized infinitely segmented MHD generator with potassium-seeded argon working fluid under nonequilibrium electron heating, using energy dependent electron collision cross sections 07 p0993 A66-18312  
 Current driven instabilities slowed down by increasing electron-ion collisions in configurations with sheared magnetic fields 08 p1260 A66-18539  
 Electron loss rate dependence on internal excitation and deactivation processes in F region ion-molecule reactions 08 p1218 A66-19405  
 Field harmonics of HF plasma discharge, taking nonlinear interaction into account 09 p1407 A66-20349  
 Breakdown of theta pinch in helium at high initial densities without preionization 09 p1408 A66-20422  
 Weak collisions effect on ion waves instability in cesium plasma solved via linearized Fokker-Planck equation 10 p1568 A66-21823  
 Solid state amplifiers using streaming carriers analyzed, noting different role played by collisions when electron stream interacts with TM and TEM waves 10 p1584 A66-22072  
 Contribution of electron-electron correlations to longitudinal dielectric constant for case of one-component plasma, noting resonance effect and formula for plasma oscillation damping 11 p1744 A66-22446  
 Effective electron collision frequency from electron temperature profile for ionospheric heating in F region 11 p1697 A66-22499  
 Perturbation theory determination of third harmonic current density generated in plasma by AC field for velocity-dependent plasma 12 p1924 A66-24593  
 Electron-atom collision studied, using helium-neon laser to obtain energy transitions between excited states 13 p2137 A66-25106  
 Collisionless nonlinear coupling of electromagnetic waves near electron gyrofrequency by plasma electrons 13 p2145 A66-25734  
 Seaton formulas used to determine when gas is collision-dominated 14 p2337 A66-28115  
 Average diffusion cross section for elastic collisions of electrons with heavy particles, comparing calculated and measured values 15 p2551 A66-29225  
 Ionospheric absorption effects in D and E layers, noting refraction role and effective collision frequency 15 p2493 A66-30036  
 Electron-atom collision studied, using helium-neon laser to obtain energy transitions between excited states 16 p2758 A66-30285  
 Intergalactic matter temperature parameters such as heating by cosmic ray ionization, dissipation of hydrodynamic turbulence, inelastic electron collision with H, He and He-ions 17 p2996 A66-31912  
 Collisional Stark broadening in RF discharges, noting large ion and electron broadening contribution 17 p2960 A66-31921  
 Electric conductivity in low voltage atmospheric pressure gas discharge, noting Maxwellian electron density distribution 17 p2968 A66-32484  
 Excitation cross sections of cesium in collisions with slow electrons 17 p2989 A66-33507  
 Steady state distribution functions for photoexcited carriers in semiconductors bands determined by competition between intraband intercarrier collisions and recombination processes 18 p3154 A66-33919  
 Collision cross sections and energy scattering of atoms with slow electrons 18 p3137 A66-34024  
 Charge ratio of cosmic ray electrons, examining excitation of baryon resonances in high energy collisions with no exchange of isospin 18 p3193 A66-34850  
 Iron and nickel lines in solar UV spectrum, abundance of various metallic elements in

solar atmosphere, electron collision cross sections and oscillator f-values of electron transitions 18 p3237 A66-35050  
 Cosmic radio wave absorption dependence on frequency and number of electron-ion collisions during atmospheric magnetic storms 19 p3344 A66-35267  
 Excitation of lithium-like ions by electron impacts, with computation of cross sections for resonance and nonresonance transitions 19 p3409 A66-36326  
 High energy cross sections for electron excitations of excited hydrogen atoms in which principal quantum number is changed by 2 19 p3409 A66-36327  
 Ionosphere as anisotropic dissipative medium where charged particles random thermal motion acts as thermal radiation source, noting relation between driven AC conduction current density and applied AC electric field intensity 19 p3352 A66-36630  
 Electromagnetic wave propagation in plasma boundary, considering electron collision with boundary, noting role of thermal velocities of electrons 20 p3512 A66-37137  
 Electron concentrations and effective frequencies for electron collisions with neutral particles in atmospheric gases in shock wake 21 p3726 A66-39085  
 Electron-collision-induced magnetoplasma instability, using Boltzmann equation for wave dispersion 21 p3794 A66-39571  
 Electron-ion recombination process due to electron collision in plasma with capture electrons transferred to ground level 22 p3954 A66-39767  
 Excitation cross sections of cesium in collisions with slow electrons 24 p4249 A66-42122

## ELECTRON DECAY TIME

Effect of satellite size on electron lifetime in artificial belt, causing charged particles in radiation belts to decay at surface 10 p1596 A66-21052  
 Lifetimes of low energy electrons in outer radiation belt at magnetically quiet times 12 p1938 A66-24120  
 Decay of electron Langmuir waves in plasma in presence of magnetic field into electromagnetic waves 13 p2143 A66-25712  
 Transient behavior of energetic electrons in artificial radiation belts analyzed via satellite observations 20 p3643 A66-38341  
 Electron and neutral atom densities in helium and argon afterglow plasma obtained by two helium-neon laser interferometers, noting temporal dependence of electron decay 23 p4101 A66-41364

## ELECTRON DENSITY

SA IONOSPHERIC ELECTRON DENSITY  
 SA MAGNETOSPHERIC ELECTRON DENSITY  
 Laser interferometer to measure time and spatial variation in repetitively pulsed plasma 01 p0079 A66-10243  
 Radiative transfer equation for isothermal model of solar corona, noting radiation flux and electron density variation 01 p0131 A66-10267  
 Electron concentration, length and temperature of limb chromospheric flare, using steady state equation of hydrogen atom 01 p0131 A66-10270  
 Electron density, collision frequency and electron drift velocity obtained from plasma column interaction with electromagnetic wave on physically separated helix 01 p0025 A66-10537  
 Brush cathode used in abnormal glow region, determining features of produced plasma 02 p0196 A66-11429  
 Plasma resonance modifications in magnetic field used for electron density finding 02 p0265 A66-11434  
 Ionospheric, auroral and geomagnetic observation at Syowa Base, Antarctic 02 p0222 A66-11684  
 Transformation of metal into dielectric by application of magnetic field to shift band boundaries 02 p0274 A66-11734  
 Oscillations of electron-ion plasma in external electric field assuming uniformly accelerated motion of plasma components 02 p0268 A66-11784  
 Electron energy and momentum dissipation in n-type InSb at low temperatures, discussing collision effects on hot electron

escape 02 p0276 A66-12079  
 Plasma electron concentration measured by Fabry-Perot interferometer partially filled with gas-discharge plasma and incorporating ruby laser 03 p0375 A66-12294  
 Ambipolar diffusion and electron attachment in photoionized nitric oxide by presence of negative ions, noting electron loss and electron density 03 p0394 A66-12326  
 Electron-ion recombination in photoionized nitric oxide neon gas mixture, noting decay of electron density and correlation factors 03 p0394 A66-12327  
 X-ray spectrum of plasma electrons after passage through plane layers of obstacle immersed in plasma, setting up equations for electron energy and density 03 p0397 A66-12392  
 Fabry-Perot resonators compared with cavity resonators and microwave interferometers for plasma diagnostics, noting electron density application 03 p0398 A66-12525  
 Resonance probe noting HF voltage to excite plasma oscillation for electron density 03 p0403 A66-12971  
 Equilibrium electron density of RF discharge excited with frequency higher than electron-neutral collision frequency and controlled by resonance from plasma dispersion 03 p0405 A66-12986  
 Space shift between electron density and luminous intensity of plasma in stationary striation by microwave resonator 03 p0372 A66-13282  
 Spatial distribution and temporal decay of electron and atom concentrations in pulsed /argon afterglow/ plasma measured with laser interferometer 04 p0551 A66-13741  
 Magnetic resonance applied to semiconductors, determining electron density at nucleus sites and kinetic energy temperature of hot electrons in indium antimonide 04 p0563 A66-14030  
 Plasma electron concentration, using nonlinear light scattering on geometrical optical path 04 p0554 A66-14295  
 Quantum effects in theory of space charge layer in semiconductors, noting electron and hole density 04 p0570 A66-14366  
 Ratio of ionospheric electron to ion temperature determined independently of spectral measurements, using electron density data obtained with topside sounder 04 p0517 A66-14374  
 Finite discharge-coil length effect on axial behavior of theta pinch plasma column determined from time and space-resolved electron densities 04 p0558 A66-14496  
 Reflected shock waves in helium and argon plasmas noting electron density, Saha equations and Newtonian technique 05 p0720 A66-14505  
 Thomson scattering measurements of magnetic annular shock tube plasmas using Q-switched ruby laser light beam 05 p0660 A66-14707  
 Fractional deviation of nose whistler group delay from zero-temperature model, assuming Maxwellian magnetosphere and gyrofrequency electron density distribution 05 p0631 A66-14836  
 Computer calculation of relative populations of atomic energy levels not in thermodynamic equilibrium 05 p0718 A66-14871  
 Electron density fluctuations in turbulent wake, using stochastic analysis and statistical averaging [AIAA PAPER 65-818] 05 p0606 A66-15187  
 Plasma measurements including temperatures, electron density, current density, etc, noting behavior of probes in magnetic fields 05 p0726 A66-15247  
 Electron density variation effect on Doppler shift of satellite signal reflections from ionization irregularities in ionosphere 05 p0634 A66-15265  
 Electron density and pressure in solar atmosphere from growth curve with Stark effect of Fraunhofer lines 05 p0765 A66-15420  
 Estimation in equilibrium state surface potential and distributions of electric potential field and electron density in vicinity of object moving in ionized medium 05 p0685 A66-15795  
 Semiconductor cathode thermionic emission



- solving simultaneously Boltzmann and Poisson equations relating field intensity with electron concentration 06 p0838 A66-15892  
 Measurement of electron density of gas discharge plasma by laser interferometer 06 p0916 A66-16379  
 Electron density measurement using plasma resonance excited by swept frequency signal 06 p0917 A66-16759  
 Electron concentration and temperature distribution in argon DC arc measured with hot wire probe 06 p0918 A66-16834  
 HF electrodeless discharge in argon and krypton at high pressure noting energy adiation losses, electron density and plasma temperature 06 p0919 A66-16873  
 Time dependent ambipolar diffusion waves, solving electron density equation 07 p1088 A66-17951  
 Anomalous densities of states in normal tantalum and niobium 09 p1417 A66-20029  
 Electron density in gas-discharge attenuator with hollow cathode 09 p1358 A66-20811  
 Microwave reflection measurements for precursor in electromagnetically driven shock tube, discussing axial distribution and electron density 09 p1409 A66-20855  
 Hydrogen ion concentration, electron density and proton gyrofrequency determined from proton whistler dispersion 10 p1528 A66-21140  
 Plasma electron density as function of radius compared with ion cyclotron heating theory and stability criteria AIAA PAPER 66-158] 10 p1560 A66-21423  
 Microwave cavity techniques to measure electron precursors in shock tube AIAA PAPER 66-175] 10 p1560 A66-21427  
 Criterion of electron-heavy particle thermal nonequilibrium encountered in subsonic arc jet plasma at pressure of 1 atm AIAA PAPER 66-192] 10 p1562 A66-21438  
 Radial distributions of number density, electron temperature and plasma potential measured in electrodeless discharge, using symmetric and asymmetric double probes AIAA PAPER 66-194] 10 p1562 A66-21440  
 Single and double Langmuir probe for low density plasma, noting measurement of electron temperature and density 10 p1535 A66-21514  
 Ionization phenomena in argon due to laser radiation by measuring electron density and energy as time function after laser pulse initiation at different gas pressures and preionized conditions AIAA PAPER 66-176] 10 p1565 A66-21690  
 Electron density and temperature measured in exhaust of magnetoplasma dynamic /MPD/ source, using Langmuir probe and spectrometry AIAA PAPER 65-298] 10 p1594 A66-21780  
 Loss rates of charged particles from chemically-heated discharges in C-Stellarator, showing confinement time parameters 10 p1568 A66-21825  
 Gunn effect oscillations in high resistivity gallium arsenide cease when product of conduction electron density and sample length drops below certain level 10 p1585 A66-22076  
 Temperature and electron concentration in RF induction discharge argon plasma investigated by optical method 11 p1745 A66-22585  
 Electron concentration in AC carbon arc determined from H-beta linewidth 11 p1748 A66-23416  
 Coefficients of space charge effects for growing oxide films, derived from perturbation treatment, evaluated in terms of boundary concentrations of diffusing species 12 p1811 A66-23624  
 Computer method for determination of distribution of low lying ionization, using ordinary and extraordinary wave traces in monograms 12 p1873 A66-24838  
 Rapid electron-density oscillations on axis of imploding plasma annulus with radial oscillations 13 p2137 A66-25055  
 Silicon-silicon dioxide interface charge density in MOS structure 13 p2161 A66-25197  
 X-ray spectrum of plasma electrons after passage through plane layers of obstacle immersed in plasma, setting up equations for electron energy and density 13 p2139 A66-25398  
 Electron irregularity size and motion in interplanetary medium determined from radio source scintillation phenomena 13 p2182 A66-25571  
 Electron density and temperature in decaying hydrogen plasma determined, using monochromator 13 p2145 A66-25730  
 Electron density and temperature of hydrogen plasma determined from intensity of spectral line and continuum in region adjacent to line 13 p2145 A66-25733  
 Radiative energy losses for charge moving in magnetoactive plasma with random electron density inhomogeneities 13 p2148 A66-26038  
 Electron density at large distances from Sun determined by photoelectric measurements during total solar eclipse of July 20, 1963 13 p2187 A66-26134  
 Electron density calculations in solar corona to distance of 16 radii from center of solar disk 13 p2187 A66-26135  
 Cross section for inelastic scattering of electromagnetic radiation by electron density fluctuations in anisotropic solids, using laser sources, investigating Landau and collision damping of plasmons 13 p2132 A66-26153  
 Helium-neon gas laser used to determine electron density variation, spatial and temporal, in afterglow of Z-pinch in H at 100 mtorr 13 p2104 A66-26239  
 Surface electron density in magnetoplasmas and microwave reflection from anisotropic plasma surface 13 p2149 A66-26241  
 Precursor wave structure in electromagnetic shock tube, determining precursor velocity, electron density and current content, comparing precursor behavior with ionizing electromagnetic wave 13 p2064 A66-26259  
 Time resolved electron density measurements with microwave interferometer used in weak afterglow plasma diagnostics 13 p2083 A66-26556  
 Propagation of circularly polarized plane electromagnetic waves through helium plasma along direction of static magnetic field, determining electron density 13 p2154 A66-26672  
 Hyperfrequency interferometer measurement of plasma profile and electron density 14 p2290 A66-26821  
 Laser beam techniques for study of plasmas with high electron densities 14 p2305 A66-26822  
 Electron density in shock-produced argon plasma measured by microwave reflection probe 14 p2340 A66-27025  
 Ultrasonic flux effect on electrons in semiconductor with charged impurity centers 14 p2358 A66-27086  
 Beryllium diffusion into gallium arsenide in /111/ plane with various electron concentrations through vacuum deposition 14 p2358 A66-27087  
 Resonance peaks due to electromagnetic scattering by argon plasma jet observed during change in electron concentration, noting dependence of scattering on argon flow rate and electric power of arc 14 p2341 A66-27151  
 Laser radiation to determine electron density in dense high temperature plasma 14 p2374 A66-27507  
 Association rate between solar flares and type II bursts 14 p2376 A66-27798  
 Quantum effects in theory of space charge layer in semiconductors, noting electron and hole density 14 p2369 A66-28265  
 Electrostatic probe measurements of velocity displacement and electron density of plasma using laser compared with measurements using microwave interferometer 14 p2346 A66-28269  
 Waveguide system using Chebyshev filters for channel separation in wide frequency ranges, applied for sounding plasmas with various electron concentrations 14 p2298 A66-28473  
 Electron density in laser-induced spark in air determined, measuring simultaneously fundamental laser wavelength and second harmonic 15 p2512 A66-28685  
 HF magnetic fields within homogeneous plasma sheath measured as function of plasma parameters and perpendicularly superimposed static magnetic field, noting resonance of electron cyclotron wave 15 p2549 A66-28708  
 Outer solar corona during declining portion of solar activity cycle, noting discrepancy between radio and optical values of electron density 15 p2593 A66-28816  
 Perturbations caused by cylindrical body in plasma, obtaining electric field and electron and ion concentration dependences on distance 15 p2595 A66-29086  
 Statistical equilibrium of fundamental particles at elevated temperatures, determining degeneration parameters 15 p2618 A66-29645  
 Electrical discharge in air, mercury vapor and nitrogen, using RF signal probe, determining electron density and temperature and random velocity in plasma 15 p2548 A66-29715  
 Plasma perturbation by large probe, determining electron density and temperature and plasma potential as function of distance from probe 15 p2555 A66-29754  
 Plasma electron density and formation determined, using Fabry-Perot resonator 16 p2756 A66-30104  
 Mars atmosphere models based on Mariner IV occultation deriving electron number density, temperature, pressure, mass density, etc, noting carbon dioxide presence 16 p2800 A66-30713  
 Rocket borne ionospheric direct sounding instruments to measure ion and electron density, electron temperature, thermal electron energy distribution and space electric potential versus rocket potential 16 p2705 A66-30819  
 Activation energy and corresponding concentration of unknown donor level in n-type gallium arsenide 16 p2777 A66-31002  
 Scattering of electromagnetic waves in plasma, noting effect of eddy current fluctuations 16 p2654 A66-31179  
 Perturbation of electron density at large distances from body at high velocity in collisionless plasma under steady external magnetic field 16 p2782 A66-31181  
 Sigma-type phase occurrence in austenitic superalloys, discussing electron/atom density, residual matrix composition, etc 16 p2725 A66-31456  
 Electron density distribution in titanium carbide determined by X-ray techniques 16 p2786 A66-31678  
 Exact determination of electron density distribution in finite anisotropic plasma by integral equation relating tangential electric field and HF plasma current 16 p2787 A66-31691  
 Superconductivity of nondegenerate semiconductor thin films, dependence on current carrier concentration, impurity level positions and film thickness 16 p2787 A66-31762  
 Optical reflection, transparency and Faraday effect for indium antimonide, calculating effective electron mass, relation between energy and wave number, etc 16 p2788 A66-31777  
 Peculiarities of Hall curves of n-type alpha silicon carbide, noting concentration of conduction electrons related to temperature 16 p2789 A66-31789  
 Electron density of plasma measured by multibeam Fabry-Perot radio interferometer 17 p2963 A66-31831  
 Electronic energy of interacting atoms at short range, noting Heilmann-Feynman theorem for electron density in elliptic coordinates 17 p2961 A66-32550  
 Radiation spectra of plasma jets from IR to UV, determining electron density and argon excitation temperature, noting bremsstrahlung 18 p3144 A66-34103  
 Ionization processes in hot products of combustion processes /flame gases/ as weak plasma media, noting flame properties, mass spectroscopy, electron concentration, etc 18 p3260 A66-34106  
 Interplanetary electron number density determination by Pioneer VI radio propagation experiment 18 p3233 A66-34541  
 Electron-positron components of primary cosmic radiation, noting energy spectrum, flux, charge composition, origin, etc 18 p3176 A66-34748



Longitude dependence of distribution function of electrons for fixed value of McIlwain parameter, using kinetic equation 18 p3197 A66-34873

Shock wavefront structure in plasma, noting use of SHF diagnostics, electron concentration growth, etc 18 p3104 A66-35063

Langmuir probe curves for pulsed plasma obtained by time-sampling probe technique and compared with BBM analysis for ion saturation current 19 p3405 A66-35411

Output current characteristics of thermionic converters derived without reference to elastic and inelastic collisions and expressed as plasma electron density and temperature profile 19 p3405 A66-35428

Layer of CdS crystals photoconduction measurements suggesting change in space charge under illumination due to increase of free electron concentration in volume 19 p3438 A66-35478

Spatial charge region, excess electron concentration, capacitance and conductivity in semiconductor layer with Lorentz forces acting on carrier determined as functions of surface potential and applied electromagnetism field 19 p3442 A66-35819

Excitation and ionization of hydrogen plasma under influence of two electron groups with different temperatures and densities, using coupled system of rate equations 19 p3407 A66-36063

Stability, heating and end loss of 3.5-MJ theta pinch measured by various methods 19 p3413 A66-36507

Electron density, temperature and other related electromagnetic effects of deuterium plasma focus formed by coaxial electrode discharge as result of Z 19 p3425 A66-36561

Abnormal high electron escape rate in Tokamak-2 toroidal chamber determined by microwave probe, noting plasma-loop equilibrium breakdown as possible cause 19 p3427 A66-36575

Radio wave guiding in horizontally stratified magnetoionic medium in which electron density varies monotonically with height 19 p3305 A66-36629

Equilibrium deviation occurring in plasma with variable kinetic temperature due to radiation transport within plasma volume and outflow beyond limits of volume 20 p3606 A66-36973

Magnetization curves for two specimens of semiconducting strontium titanate of given electron density, noting magnetic hysteresis and heat capacity 21 p3796 A66-38553

Electron concentrations and effective frequencies for electron collisions with neutral particles in atmospheric gases in shock wake 21 p3726 A66-39085

Microwave cavity resonant frequency sampler for direct oscilloscope-photographic recording of electron density, recombination and diffusion time in decaying plasma 21 p3740 A66-39389

Radio electron density and magnetic field in galactic halo from primary cosmic ray and radio brightness measurements 21 p3817 A66-39563

Exact solution for transverse electromagnetic wave in plasma with diffuse boundary, noting reflection and transmission coefficients 22 p3952 A66-39719

Microwave beam incident on linearly graded plasma for electron density profile determination, using ray theory 22 p3861 A66-39723

Diurnal variation in electron densities and temperatures in F region above Puerto-Rico, using backscatter measurements 22 p3910 A66-39978

Langmuir type probe in argon arc jet, discussing surface contamination problems, causes of high electron temperature and development of automatic cleaning technique 22 p3899 A66-40368

Ultrasonic flux effect on electrons in semiconductor with charged impurity centers 22 p3967 A66-40842

Beryllium diffusion into gallium arsenide in /111/ plane with various electron concentrations through vacuum deposition 22 p3967 A66-40843

Steady state beam induced plasma parameters and behavior when affected by HF noise oscillations and effect on electron

concentration in plasma 22 p3958 A66-40933

Surface magnetoconcentration in intrinsic-conductivity semiconductors, noting space-charge region characteristics dependence on surrounding fields 23 p4110 A66-41131

Resonant frequencies of VHF Lecher line coupled to mercury arc plasma via split cylinder coupler measured as function of electron density 23 p4100 A66-41155

Multiple-pass laser interferometer used to confirm electron density inferred from Stark broadening of hydrogen beta line 23 p4101 A66-41260

Optical interferometers for low electron density measurements of transient plasmas 23 p4068 A66-41289

Spectroscopic measurements of electron densities and temperatures in argon-hydrogen plasma jet 23 p4068 A66-41290

P-type conductivity and stored electron charge densities in high resistivity cadmium sulfide crystals 23 p4114 A66-41625

Radial distributions of number density, electron temperature and plasma potential measured in electrodeless discharge, using symmetric and asymmetric double probes [AIAA PAPER 66-194] 23 p4107 A66-41907

Transmission resonant cavity measurements of electron line densities and collision frequencies in ionized wakes of hypervelocity projectiles 24 p4191 A66-42195

Electron number densities measured behind shock wave in pressure driven shock tube by microwave resonant cavity technique and by electrostatic quasi-Langmuir probe 24 p4191 A66-42197

Resonance peaks due to electromagnetic scattering by argon plasma jet observed during change in electron concentration, noting dependence of scattering on argon flow rate and electric power of arc 24 p4244 A66-42971

Allowed bands for wave generation by nonlinear effects in plasma with varying electron density 24 p4245 A66-43005

Absorption of solar energy by polar cap, noting electron concentration 24 p4204 A66-43153

**ELECTRON DENSITY PROFILE**

Electron density decay in wakes of hypervelocity aluminum and copper spheres in air and nitrogen as function of time, using transmission resonant cavity 02 p0267 A66-11529

Plasma electron density measurements, interferometric and spectroscopic techniques compared with Stark H-beta line and absolute continuum intensity method 03 p0405 A66-13136

Stark profiles of singly ionized nitrogen lines from T-tube plasma, measuring shifts and half-widths of N-ion lines, plasma temperature and electron densities 03 p0405 A66-13137

Microwave bridge to determine electron density in weakly ionized decaying plasmas 04 p0555 A66-14321

Shock wave formation in collisionless plasma investigating magnetic compression pulse, electron density and radial magnetic field profile 05 p0722 A66-14720

Rocket measurements of energetic particles discussing electron fluxes, energy spectra, angular distribution and data 05 p0745 A66-14777

Rocket measurements to investigate vertical current distribution of electrojet over India to correlate magnetic profiles with simultaneous electron density measurements 05 p0668 A66-14794

Electron density measurements in transient plasma using resolution repeater rapid-scan spectrograph 05 p0677 A66-14914

Stratospheric measurements of electrons and gamma radiation in cosmic rays, using plastic scintillator and lead sheet supplemented Geiger counters 05 p0752 A66-15386

Polar rays of solar corona, discussing distribution, magnetic field approximation, electron density and kinetic temperatures 07 p1133 A66-17418

Amplitude and duration distribution for underdense echoes from lognormally distributed meteor trails 07 p1135 A66-17638

Data analysis from Explorer XIV satellite, noting magnetic field measurements in tail of geomagnetic cavity 07 p1029 A66-18086

Ionospheric research from space vehicles, comparing experimental data with theoretical models of D, E and F regions 07 p1029 A66-18089

Radar echo effects of satellite disturbance in plasma medium, noting electron and positive ion density distribution 08 p1302 A66-18755

Electron concentration profiles above maximum of F layer calculated from measurements made on Earth surface 08 p1213 A66-19026

Messiaen theory for resonance effect in plasma electron density probe 09 p1406 A66-19856

Horizontal plate Mach-Zehnder interferometer for hypervelocity range vacuum use, high speed photography problems and electron density measurement 10 p1537 A66-21871

Microwave transmission tests in pure air plasma using hypersonic shock tunnel, obtaining electron density and collision frequency profiles, predicting propagation path signal loss and antenna radiation pattern distortion [AIAA PAPER 66-173] 11 p1742 A66-22211

Cadmium sulfide space charge limited diodes, noting current voltage characteristics and field and electron density distributions 11 p1668 A66-23026

Ionospheric effect of sudden magnetic storm eruption, noting propagation of disturbance above terrestrial surface 12 p1870 A66-24288

Transverse magnetic field effect on drifting hot plasma resonance peaks, noting oscillation mechanism and application of successive moments of Boltzmann equation 13 p1244 A66-25725

Ionospheric electron density profile and Scholmich integral equation for oblique incidence 13 p2075 A66-26740

Emergence point of conical microwave beam transmission through nonuniform electron plasma 14 p2234 A66-26860

Vertical drift of charged particles effect on electron density profile as cause of seasonal variations in ionospheric absorption 15 p2490 A66-29944

Density fluctuation effect on radar determination of total electron content in terms of recent cisunar density measurement 17 p2917 A66-32520

Lunar semidiurnal tides in ionosphere over Puerto Rico determined from electron density profiles for heights between 150 and 300 km 17 p2923 A66-33362

Instrumentation for plasma diagnostics noting electron density profile, temperature, ion-atom and electron-atom interaction, etc 20 p3556 A66-36964

Electron density distribution in electromagnetic shock tube measured, using transverse microwave cavity and radiating slots in oversize plasma waveguide 21 p3739 A66-39382

Born approximation for phase shift of microwaves scattered from underdense cylindrical plasma used to determine plasma electron density 21 p3794 A66-39572

Electron density profiles in ionosphere and exosphere - NATO Advanced Study Institute, Finse, Norway, April 1965 22 p3903 A66-39943

Negative ion associative detachment reaction with atomic oxygen in determination of nighttime D region electron density profiles at high latitudes 22 p3905 A66-39945

Winter variability of electron number density and collision frequency in lower ionosphere measured, using partial reflection method 22 p3906 A66-39950

Electron density profile measurements in auroral zone D layer during quiet ionospheric conditions, using partial reflection method 22 p3906 A66-39951

Collision frequency gradient effect on weak partial reflections from ionosphere 22 p3906 A66-39952

Electron density and collision frequency profiles for D region obtained through simultaneous measurement of radio wave phase and amplitude interaction 22 p3906 A66-39953

True height in-line computation of electron density profile from ionograms, using analog



- computer in real time 22 p3908 A66-39969  
Alouette I topside ionograms analyzed, discussing mathematical procedures and digital computer programs in use and orbit and electron density profiles 22 p3909 A66-39973  
Spectral analysis of laser discharge in pure and impure He, obtaining spectra of spark at various pressures, determining electron concentration at various stages 22 p3934 A66-40946  
Ionospheric cross modulation analysis by computer-oriented simulation process, noting D region electron density and collision frequency profiles 23 p4041 A66-41641
- ELECTRON DETECTOR**  
Wide-range automatic electron-counting frequency meter for sinusoidal and pulsed signals 02 p0230 A66-11813  
Lens technique for measuring yield and energy spectrum of secondary electrons generated by fission fragments through metal foil 12 p1916 A66-23704  
Low energy electron position detection with composite surface barrier type diode, noting design, fabrication and operation 12 p1879 A66-23705
- ELECTRON DIFFRACTION**  
Increase in extinction distance with temperature in silicon determined via high temperature electron microscopy 02 p0272 A66-11709  
Tungsten single crystal study by electron microdiffraction for distribution and effects of interstitial phases 03 p0385 A66-13194  
Thin surface films covering structure, nucleation, growth and epitaxy observation techniques such as electron and X-ray diffraction field emission, field ion microscopy, etc 04 p0559 A66-13452  
Hall effect of bismuth evaporated films, discussing structural dependence of sign and magnitude, effects of pathlength, impurities, gas adsorption and experimental techniques 05 p0729 A66-14510  
Properties of chromium particles obtained by vaporization of metal in argon at low pressure, noting cubic shape, electron diffraction pattern, etc 06 p0894 A66-16185  
Heterojunction preparation by vacuum evaporation, describing epitaxial deposition of germanium on gallium arsenide substrate 08 p1270 A66-19058  
Small angle scattering technique with high resolution electron microscopy to determine columnar structure of thin vacuum condensed Pd films 10 p1573 A66-21247  
Low-energy electron diffraction studies adsorption of cesium on Si /111/ 10 p1576 A66-21551  
Strength and structure of thin films of Al, Ag, Ge and Ni studied with electron microscope and electron diffraction technique 10 p1578 A66-21663  
Gallium arsenide whiskers on germanium structure, using electron diffraction photography and electron microscopy 11 p1757 A66-23280  
Low energy electron diffraction study of epitaxial deposition of copper on single crystal /110/ face of tungsten under ultrahigh vacuum 12 p1894 A66-23911  
Low energy electron diffraction observation of calibrated epitaxial nickel film on /111/ copper 12 p1894 A66-23912  
Effect of preparation conditions on formation of carbide phases in iron-carbon thin films, using vacuum condensation 12 p1933 A66-25025  
Domain structure of partially oriented thin permalloy films analyzed through appearance of adjoining 180 degree walls of equal contrast and by electron microscopy 12 p1934 A66-25029  
Electron diffraction study of structural defects in cubic phases in epitaxial tantalum oxide thin films 15 p2557 A66-28560  
Production of thin copper and nickel ferrite films in inert gas plasma reveal spinel structure in electron diffraction patterns 15 p2557 A66-28564  
Clean and oxygen-covered molybdenum /110/ surface analysis using low energy electron diffraction, noting various oxygen structures 16 p2721 A66-30109  
Magnetic and structural properties of monoferrite films prepared by cathode sputtering, noting electron diffraction and micrograph patterns of films, crystal structure, etc 16 p2774 A66-30690  
Existence of twins in single crystalline films of barium titanate, obtaining electron diffraction patterns 21 p3805 A66-39581  
Electron diffraction study of structural defects in cubic phases in epitaxial tantalum oxide thin films 23 p4112 A66-41281  
Production of thin copper and nickel ferrite films in inert gas plasma reveal spinel structure in electron diffraction patterns 23 p4112 A66-41285
- ELECTRON DIFFUSION**  
Electron passage from surface ion into semiconductor layer interior during charging from corona discharge, estimating thermal overshoot and tunneling through potential barrier 01 p0071 A66-11025  
Shock wave propagation phenomena including ionization relaxation, electron diffusion from shock wave front and structure of shock waves in highly rarefied gases 04 p0508 A66-13503  
Ionospheric diffusion probe determining ion and electron temperatures 05 p0674 A66-15112  
Electron diffusion in mutually perpendicular static electric and magnetic fields based on stability of laminar flow 07 p1081 A66-17953  
Hole diffusion constant dependence on electric field in n-type germanium 07 p1106 A66-18395  
Lifetime degradation rate due to cobalt gamma irradiation reduced in p-silicon due to electron injection at low temperature 07 p1106 A66-18400  
Precursor electron front measuring velocity, electron temperature dependence on operating parameters, etc 08 p1259 A66-18525  
Electron diffusion coefficient estimated and compared with theory for case of infinite plane parallel plasma and constant electric field 08 p1264 A66-19226  
Boltzmann transport equation solution for electrons in ionized gas with nonuniform electron concentration gradient 12 p1916 A66-23728  
Electrical precursors in immediate vicinity of ionizing shock waves in argon analyzed, using model describing electron diffusion through shock 12 p1923 A66-24579  
Diffusion and lifetime of plasma charged particles in magnetic field covering instability, contraction, decay, recombination, etc 13 p2138 A66-25222  
Electronic structure and Seebeck coefficient for chromium-iron alloys from 125 to 625 degrees K, emphasizing phonon drag and electron diffusion effects 14 p2310 A66-26879  
Stable domain propagation for case when electrons have field-independent diffusion coefficient and follow arbitrary static velocity field characteristic exhibiting negative resistivity 19 p3446 A66-36371  
Loss rates of trapped electrons by atmospheric collisions 20 p3640 A66-38321  
Pitch angle diffusion perturbing relativistic electrons in Van Allen zones and violating adiabatic invariants of electron motion, using Fokker-Planck equation 20 p3641 A66-38328  
RF-induced plasma shield propagation and electron diffusion 21 p3792 A66-39190  
Internal electric field effect on singly ionized acceptor or donor impurity diffusion in uniformly doped n-or p-type semiconductors 21 p3804 A66-39468  
Relativistic-electron diffusion wave in outer radiation belt recorded by device mounted on Cosmos XLI satellite in high geomagnetic latitudes 22 p3974 A66-40756  
Approximate steady state solutions of continuity equation containing effects of diffusion, drift and recombination for carrier diffusion region of forward-biased p-n junction over wide range of injection 24 p4249 A66-42225
- ELECTRON DISTRIBUTION**  
One-dimensional collisionless plasma in computer simulation with randomized electrons compared with static theory for equivalent diode 01 p0112 A66-10591  
Electron concentration-distribution data for ten quiet days during spring 1958 in F-2 layer 01 p0063 A66-11027  
Electron density distribution in linear pinch discharge with transverse rotating magnetic field 02 p0266 A66-11471  
Radiation hazard for cosmonaut inside or outside spaceship from Earth radiation belt, considering electron radiative effect, tissue sensitivity, etc 02 p0182 A66-11663  
Equatorial F-region electron density distribution is natural steady state distribution for charged fluids as shown by momentum transport equation for charged gaseous fluids 03 p0364 A66-12678  
Electron distribution function in semiconductors discussing steady state illumination effects, energy and spectral characteristics and photoconductivity oscillations at low temperatures 03 p0410 A66-12938  
High energy electron influence on electron distribution function and effect on spectra of nonthermal galactic and extragalactic radio sources 04 p0575 A66-14171  
Electron density distribution in magnetosphere inferred from dispersion characteristics of hydromagnetic wave propagating between hemispheres along geomagnetic field as in atmospheric whistlers 05 p0747 A66-14787  
Directional intensity of electron distribution of energies larger than 40 keV with respect to pitch angles in inner belt from Cosmos V data 06 p0951 A66-17172  
Photoelectron impact excitation effect on dayglow intensity, calculating energy distribution for various altitudes 07 p1028 A66-17374  
Anisotropy of microwave conductivity and absorption in semiconductors with hot carriers, studying distribution function of electrons 07 p1106 A66-18380  
Leigh theory concerning effect of electron concentration on elasticity of Al and Al alloys compared with experiment 07 p1053 A66-18520  
Electron distribution over energy level in valence semiconductor in presence of electric field 08 p1269 A66-18977  
Electric current passage through multivaleley n-germanium semiconductor plates, noting nonuniform electron distribution 08 p1273 A66-19275  
Magnetic field level in solar corona determined from generation mechanism of type II radio bursts 08 p1297 A66-19454  
Fluctuations of electron numbers in general M-level system, using difference equation 08 p1279 A66-19837  
Anisotropic effect of interelectronic scattering on semiconductor conductivity of ellipsoidal isoenergetic surface 09 p1411 A66-19981  
Electron pitch distribution anomaly as observed by Cosmos V satellite, noting possible causes of phenomenon 09 p1378 A66-21009  
Spatial distribution of protons and electrons captured by terrestrial magnetic field, as measured by Cosmos satellites 09 p1443 A66-21011  
Plasma sheath properties near discharge tube anode, noting relation of electron current distribution along discharge radius and ion energy spectrum to pressure 10 p1558 A66-21999  
Solution of two first equations of BBGYK hierarchy, obtaining dielectric constant of plasma by using Guernsey solution, giving two-particles distribution function 11 p1744 A66-22445  
Longitudinal plasma oscillations excited in warm plasma column at microwave frequencies in presence of magnetic field, manifest themselves as absorption peaks near harmonics of electron cyclotron frequency 11 p1748 A66-23395  
Boltzmann transport equation solution for electrons in ionized gas with nonuniform electron concentration gradient 12 p1916 A66-23728  
Electron distribution from 400 to 1200 km measured, using Ariel I satellite, noting latitudinal and longitudinal anomalies associated with geomagnetic field [AIAA PAPER 66-395] 12 p1872 A66-24511  
Negative conductivity, induced by nonequilibrium state in semiconductors, due to short electron lifetime in conduction band 13 p2160 A66-25101



Quasi-linear approximation method and Poisson equation used in determining static fields and electron redistribution in plasma waveguides 13 p2039 A66-25678

D-region electron distribution, collision frequency and amplitudes of partially reflected waves 13 p2075 A66-26739

Hot electron redistribution in multivalley conductors in electric fields, based on variation under pressure of valley population levels, using silicon samples 15 p2559 A66-28622

Electron concentration inhomogeneities during traveling gravity wave propagation through F layer 15 p2485 A66-29084

Plasma probe in thermal emission converter with high cesium vapor, noting parameters of diffusion, electron concentration, etc 16 p2756 A66-30103

Negative conductivity, induced by nonequilibrium state in semiconductors, due to short electron lifetime in conduction band 16 p2771 A66-30280

Trapped electron effect and stationary longitudinal wave propagation in Maxwellian hot plasma based on exact solution of nonlinear collisionless Boltzmann equation compatible with equilibrium electron distribution 16 p2761 A66-31009

Nonlinear effects in homogeneous Lorentz plasma, calculating anisotropies of electron distribution function 17 p2963 A66-31842

Electron velocity distribution in ionized gas under alternating electric field as function of density, temperature, etc, including effects of recombination, ionization, etc 17 p2960 A66-32426

Satellite observation on correlation between outer radiation zone electrons and solar activity cycle 17 p2993 A66-32518

Electron-ion emission pattern distribution obtained by pulsed laser focusing on solid target 17 p2937 A66-33256

Magnetic field level in solar corona determined from generation mechanism of type II radio bursts 18 p3232 A66-34483

Energy characteristics of 11-year cosmic ray variations, evaluating electromagnetic conditions in interplanetary space for proton, alpha particle and electron variations in energy 18 p3176 A66-34752

Plasma sheath properties near discharge tube anode, noting relation of electron current distribution along discharge radius and ion energy spectrum to pressure 18 p3140 A66-34976

Evaporated and recrystallized CdS layers, discussing electron mobility, level distribution, capture cross section and techniques of measurement 19 p3435 A66-35408

Electron levels in afterburning region of rocket exhaust plume with aluminum or alkali content 19 p3477 A66-35633

Plateau formation mechanism for electron velocity distribution function during damping of monochromatic plasma waves 19 p3406 A66-35737

Solution of Boltzmann and rate equations for electron distribution function and state populations in nonequilibrium MHD plasmas 19 p3406 A66-35801

Electron velocity distribution function in nonequilibrium plasma having spatial distribution governed by electron-electron and inelastic collisions 20 p3606 A66-36974

Energy-selective redistribution of trapped electrons in inner radiation belts associated with magnetic disturbances 20 p3630 A66-37294

Quantum oscillations of Hall effect and longitudinal and transverse reluctance in n-indium antimonide, noting spin splitting and temperature and electron concentration effect on oscillation maximum 21 p3799 A66-38924

Microwave and X radiation from plasma produced by electrodeless discharge in hydrogen, showing presence of accelerated electrons leading to plasma oscillations 21 p3783 A66-39023

Field intensities and electron distribution functions in hollow cathode, graphs show potential distribution along cathode axis 22 p3953 A66-39758

Back contact effect on distribution of current carrier concentration in

semiconductors based on diode volt-ampere characteristic 22 p3873 A66-39825

Infinite plate consisting of monolayer semiconductor of given thickness under effect of electric field results in change in galvanomagnetic, piezoresistance and optical properties 22 p3965 A66-40317

Conductivity of potassium-seeded argon plasma, assuming variable collision cross sections and Maxwellian distribution for electrons 22 p3951 A66-40363

Difluoramine chemistry for understanding nature of N-F and N-X bonds, electron distributions and existence and stabilities of N-F radicals and ions 23 p4031 A66-41233

Capture effect on I-V characteristics of junction diodes and injection coefficients in forbidden transition zone 23 p4045 A66-41444

Millimeter wave resonant interferometer capable of measuring spatial distribution of electrons in low density transient plasma column subject to perturbation 24 p4209 A66-42191

Anisotropic electron distribution in pure semiconductors near avalanche, considering indium antimonide 24 p4252 A66-42355

Numerical solution of Boltzmann kinetic equation for weakly ionized plasma in thermoelectronic converter 24 p4239 A66-42871

## ELECTRON EMISSION

SA EXO-ELECTRON EMISSION

SA PHOTOELECTRIC EMISSION

SA RADIO FREQUENCY DISCHARGE

Radiative recombination in thin film structures observing characteristic of aluminum 01 p0127 A66-11089

Radio emission in ionosphere during high solar activity explained as electron emission produced by particles moving as corpuscular fluxes 02 p0284 A66-12133

Doubly differential cross sections of electrons ejected from helium bombarded by protons 04 p0547 A66-13709

Impulsive emission of approximately 40-keV electrons from Sun observed from Mariner IV 05 p0746 A66-14779

Titanium, zirconium and hafnium, row of metals and platinum metals as new electron emitters for thermionic generators 05 p0621 A66-15576

Work function distribution of different refractory metals by Shelton method, noting dependence of electron emission of thermionic converter 05 p0621 A66-15577

Electron microscope study of emitter inhomogeneity influence on determination of electron emission constants and performance of thermionic converters 05 p0622 A66-15583

Time resolution of electron and ion emission produced by Q-switched ruby laser pulse focused on metal surface 07 p1045 A66-18358

Thermostimulated induced electron emission from samples cut from laser ruby crystals detected with open point counter 08 p1232 A66-18609

Satellite charge and sheath formation resulting from photoelectric and secondary emission 08 p1302 A66-18748

Surface physics of ion and electron emission during cesium adsorption on polycrystalline wire surfaces [AIAA PAPER 66-222] 10 p1575 A66-21450

Electron and ion emission from pulsed ruby laser illuminated metallic surface into vacuum, determining application to pulsed ion thruster [AIAA PAPER 66-230] 10 p1542 A66-21453

Hot electron emission from thin metallic films of island structure 10 p1589 A66-22171

Intensity of early postexplosion radiation field and high energy electron emission from supernovae 12 p1938 A66-23918

Secondary electron emission in zinc sulfide and magnesium fluoride thin dielectric films and semiconductor layers due to electric field stimulation 12 p1930 A66-24459

Hot-electron transistors, discussing application of Schottky-emitter transistor to VHF operation 13 p2038 A66-25561

Hot wire electron emissive probes for potential measurements in quiescent plasmas, noting plasma densities, emission levels, etc 13 p2154 A66-26554

Electron energy distribution for emission from aluminum-aluminum oxide-gold thin films 14 p2257 A66-27943

Radio emission in ionosphere during high solar activity explained as electron emission produced by particles moving as corpuscular fluxes 14 p2241 A66-28090

Rejection of Jones ionospheric model where Venus microwave emission is attributed to free-free electron emission, analyzing formation of dense Cytherean ionosphere 15 p2597 A66-29255

Electron secondary emission from interaction of ion, atom and molecular energetic beams with solids, especially when kinetic energy is significant 16 p2776 A66-30796

Time resolution of laser-induced electron emission from cesium diode at high laser power 16 p2719 A66-31135

Laser induced spontaneous electron emission from rear side of metal foils, noting electron energy vs laser energy pulse magnitude, etc 16 p2784 A66-31536

Work function of polycrystalline rhenium surface in cesium 17 p2983 A66-33103

External electron emission measurement from polished n-germanium and n-silicon surfaces 17 p2986 A66-33310

Energy distribution of electrons emitted from alkali halide films on Mo substrates during positive helium and argon ion bombardment 17 p2988 A66-33459

Solar flare electron propagation observations in interplanetary space 18 p3166 A66-34239

Increases of ionizing radiation in stratosphere correlated with recurrent magnetic storms, ionospheric perturbations in auroral zone, etc, possibly due to electrons from outer radiation belt 18 p3197 A66-34874

Zr-coated tungsten cathode in reducing divergence of electron beam emission 18 p3088 A66-35077

Various light nuclei considered as possible solar neutrino detectors, deriving cross sections and angular distributions of electrons 18 p3223 A66-35216

Direction of collapsing star determined by detecting generated neutrino front by time delay method 18 p3223 A66-35217

Hot electron emission from thin metallic films of island structure 19 p3441 A66-35785

Anisotropy of secondary electron emission in ion bombarded Si single crystals, using electron microscope 19 p3445 A66-36340

Primary and afterglow emission decay time from low temperature gaseous nitrogen excited by fast electrons explained by possible energy transfer 19 p3404 A66-36799

Energy spectrum of primary auroral electrons determined from vertical luminosity profiles of 16 auroral arcs 20 p3550 A66-37297

Secondary electron emission in zinc sulfide and magnesium fluoride thin dielectric films and semiconductor layers due to electric field stimulation 20 p3620 A66-37691

Electromagnetic wave emission excited by electron stream over diffraction grating lying on boundary of semiinfinite anisotropic dielectric 20 p3519 A66-37998

Electron drift velocity, ionization and attachment coefficients in water vapor and dry air measured by recording short photoelectron pulses 20 p3605 A66-38095

Subshell photoelectron emission in germanium at angle of 90 degrees to converting X radiation determined for two radiation sources using photographic techniques and track counting method 20 p3621 A66-38096

Electron and ion emission from polycrystalline surface of Be, Ti, Cr, Ni, Cu, Pt and type-304 stainless steel in cesium vapor 20 p3623 A66-38400

Woven and knitted electron emitters noting reliability, mechanical stability, efficiency 24 p4180 A66-42369

X-rays and Auger electron emission by krypton 81 measured, using proportional counter 24 p4282 A66-42430

## ELECTRON ENERGY

Quantum levels of electron moving in periodic field of semiconductor crystals in strong electric field 02 p0274 A66-11733

HF discharge in rectangular high vacuum waveguide in crossed magnetic and electric



- fields, calculating electron energy 02 p0268 A66-11773
- Achromatic electromagnetic quadrupole lens functioning for case of slight misalignment of fields 02 p0199 A66-11783
- distribution 02 p0199 A66-11783
- Heat capacity related to quantizing of energy levels of electron excitation of superconductor in intermediate state 02 p0277 A66-12278
- Photoelectron energy distribution in F region 03 p0364 A66-12684
- Electron energy spectrum during auroral absorption measured by Nike-Cajun analyzer 03 p0366 A66-12880
- Doubly differential cross sections of electrons ejected from helium bombarded by protons 04 p0547 A66-13709
- Interaction of energetic electrons with bounded electromagnetic waves near cyclotron resonance, noting plasma diagnostics, maser and gain mechanism 04 p0530 A66-13953
- Energy flux of electron beam absorbed by atmosphere derived from resulting intensity of first negative system of molecular nitrogen 05 p0670 A66-14948
- Radio source spectrum, discussing spectral indices, electron energy and H II density in quasi-stellar and high brightness-temperature sources 05 p0762 A66-15279
- Heat capacity related to quantization of energy levels of electron excitation of superconductor in intermediate state 05 p0738 A66-15457
- Electron energy diffusion in superconducting thin Sn and In films bombarded by alpha particles observed in terms of IR drop 06 p0927 A66-16755
- Energy dependence of threshold curve in separating collision from ionization effects and in interpreting anisotropies of electron threshold energies 06 p0938 A66-17150
- Electron energy levels in CdS single crystals from Hall effect, conductivity and space-charge-limited current measurements 07 p1098 A66-17739
- Electron energy spectra in neon, xenon and helium-neon laser discharges, calculating production and destruction rate parameters 07 p1045 A66-18354
- Measurement of energy required to form the hole-electron pair in gallium phosphide by alpha particles 07 p1107 A66-18407
- Work function of metals and semiconductors measured, using retarding potential analyzer to determine field emission electron energy distribution 08 p1228 A66-19825
- Relation of thermodynamic parameters to energy gap of superconducting elements and alloys 09 p1424 A66-20074
- Comparison between auroral effects and experimentally observed electron leakage from magnetic mirror with electron acceleration 09 p1373 A66-20471
- Thermal emf quantum oscillation and quantization of electron energy spectrum of n-InAs 09 p1429 A66-20768
- Plasma oscillation of electrons in Be, Mg, Al, Si, Ge, Sn, Sb and Bi studied by electron bombardment of thin foil of these solids 09 p1429 A66-20842
- Plasma oscillation of electrons in aluminum compound eutectoids studied, using energy analysis of electrons passed through thin foil of eutectoid, noting dependency of oscillation energy on component grain size 09 p1429 A66-20843
- Plasma oscillation of valence electrons and exciton in alkali halides, measuring differential cross section, dispersion relation and loss peak in spectrum 09 p1430 A66-20844
- Plasma oscillation of conduction electrons in sodium 09 p1430 A66-20845
- Electron excitation cross section of individual energy levels of inert gases calculated, using Born-Oppenheimer method 09 p1405 A66-20939
- Electron energy spectrum measurements by Cosmos V satellite, noting concentration and intensity at various geographic areas 09 p1378 A66-21010
- Electron excitation in germanium by alkali metal ions, noting effect on electrical conductivity 10 p1587 A66-22154
- Bremsstrahlung of nonrelativistic plasma, treating nondegenerate electron component of plasma simultaneously with degenerate component by applying Fermi-Dirac distribution 12 p1925 A66-24996
- Statistical theory of electronic energies, calculating binding energy at theoretical equilibrium separation of molecular hydrogen ion 13 p2130 A66-25370
- Photoluminescence for p-and n-type gallium arsenide as function of exciting light intensity, noting minority carrier recombination mode, electron energy spectrum, etc 13 p2169 A66-26187
- Rotational excitation of oxygen by slow electrons, calculating electron energies, quadrupole moments and energy loss rates 13 p2135 A66-26270
- Electron acceleration near Earth bow shock measured, using Explorer XVIII satellite, noting solar wind effect, energy spectrum in radiation belt and magnetospheric boundary, etc 13 p2175 A66-26355
- Polarized pyrometric probe for direct measurement of ion and electron energy in hot dense plasma 14 p2290 A66-26825
- Thermal emf quantum oscillation and quantization of electron energy spectrum of n-InAs 14 p2361 A66-27303
- Energy dependence of elastic resonance scattering of low energy electrons from He, Ne, Ar and nitrogen gases at angles ranging from 8 to 110 degrees 14 p2337 A66-27797
- Fluorescence lifetime measuring technique employing pulsed or modulated RF discharges applied to emission of second positive and first negative systems of nitrogen 14 p2337 A66-27974
- Electron excitation cross section of individual energy levels of inert gases calculated, using Born-Oppenheimer method 15 p2543 A66-28528
- Ruby phosphorescence under intense optical excitation, inferring possible recombination characteristics from initial brightness decay 15 p2558 A66-28607
- Electron energy losses in diamond, noting correlation between plasma excitation energy and interband transition energies 15 p2564 A66-28876
- Acoustoelectric effects for various sound waves, using rate of energy exchange between two coupled systems in relative motion 15 p2564 A66-28970
- Relation between frequency spectrum of pulsations in auroral luminosity and energy spectrum of auroral electrons, using photometer 15 p2489 A66-29235
- Deuterium plasma jet injection into simple biconical cusped magnetic field, noting ion energy transfer to electrons and plasma potential variations 15 p2554 A66-29748
- Single-configuration open-shell calculations for ground state of boron isoelectronic sequence, using doublet-spin-state wave function 16 p2750 A66-30122
- Electron component of plasma sheet of terrestrial magnetic trail, noting energy distribution and densities 16 p2792 A66-30142
- Energy spacing of geometrical resonance structure in very thick indium films, noting interference between electron-like states which propagate with different velocities 16 p2769 A66-30159
- Type I comet tail origin due to energetic electrons in shock structure, noting inertial slowing down of interplanetary field lines trapped in solar wind 16 p2801 A66-30919
- Laser induced spontaneous electron emission from rear side of metal foils, noting electron energy vs laser energy pulse magnitude, etc 16 p2784 A66-31536
- Ultrahigh frequency plasma oscillations, noting Maxwellian equilibrium between plasma electrons and primary, monoenergetic electrons 16 p2766 A66-31651
- Secondary electron interaction with solid state plasma, noting energy distribution, Boltzmann equation solution, etc 16 p2789 A66-31783
- Plasma injected into magnetic trap with aid of conical theta pinch investigated to determine ion and electron energy, lifetime and charged particle concentration variation 17 p2969 A66-32546
- Single donor-type randomly distributed impurity and effect on electron energy spectrum of semiconductor 17 p2982 A66-32969
- Ionization potential, dissociation energy and electron affinity for molecular oxygen 18 p3137 A66-33989
- Ion-molecular reactions of hydrogen with inert gases caused by low energy electrons in low temperature plasmas, considering energy level populations, reaction cross sections, etc 18 p3064 A66-34026
- V-I characteristics of GaAs Schottky barrier rectifiers applied in determining relation between electron energy and complex wave vector over portion of forbidden energy gap 18 p3155 A66-34161
- Electron energy loss spectra of Ge and Si in amorphous, polycrystalline and monocrystalline form 18 p3159 A66-34710
- Balloon observation of high energy primary electrons with counter system 18 p3187 A66-34816
- Electron component of primary cosmic radiation at energies greater than or equal to 15 gev studied, using nuclear emulsion stack 18 p3187 A66-34818
- X-ray spectrum produced by thermal bremsstrahlung of gas, taking Gaunt factor into account 18 p3200 A66-35049
- Electron energy quantization phenomenon in thin film studied by using dielectric barrier sandwiched between semiconductor films of same conductivity type 19 p3433 A66-35309
- RF breakdown in air studied for two electrode configurations leading to nonlinear Mathieu-like differential equations for confined electron motion 19 p3296 A66-35417
- Electron excitation in germanium by alkali metal ions, noting effect on electrical conductivity 19 p3440 A66-35768
- Buildup and confinement of plasma with high-energy electrons in PR-5 apparatus, using magnetron injection method 19 p3412 A66-36497
- Plasma with relativistic electrons in magnetic mirror trap, discussing stability and fast pulsed heating of ions 19 p3423 A66-36553
- Optical constants of silver and gold in various energy regions, measuring relative refractivities of polarized light, analyzing collective motions of conduction electrons 20 p3615 A66-37283
- Optical phonon production, showing existence of electric field strength range at low temperature scattering in which phonon emission results in electron stoppage 20 p3577 A66-37376
- Schottky diffusion theory applied to calculation of coefficients of homogeneous positive column in neon, using Druyvesteyn electron-energy distribution 20 p3608 A66-37462
- Electron energy distribution function obtained by Druyvesteyn analysis in low-current positive column neon discharge compared with theoretical distribution function 20 p3608 A66-37463
- Galvanomagnetic effect of anisotropic electron energy spectrum on acoustical branch perturbation spectrum of system of electrons and ions in homogeneous magnetic field 20 p3618 A66-37559
- Electron energy spectrum for alloyed semiconductors, determining state densities via Thomas-Fermi statistical method 20 p3618 A66-37562
- Magnetospheric boundary phenomena, noting dependence of charged particle observations on character of associated magnetic fields 20 p3641 A66-38329
- Auroral absorption analysis during geomagnetic storm, noting satellite measurement of energetic particles 20 p3642 A66-38335
- Magnetosphere tail sheet pinch model, discussing motion of particles for cases of surface crossing 20 p3642 A66-38336
- Spatial distribution of trapped particles measured by Explorer XV satellite, noting decay time constants and energies 20 p3643 A66-38340
- Electron energy spectrum of silicon, examining effect of screw dislocations parallel to crystallographic direction 21 p3803 A66-39296
- Effective mass in nuclear deformational Hamiltonian calculated by asymptotic approximation method which is two orders of magnitude better than liquid drop



- model 22 p3951 A66-40422  
Generalized full wave theory equations derived for EM plane wave propagation through magnetotonic medium for electron collision frequencies proportional to electron energy 22 p3869 A66-40805  
Mean energy required to create electron-hole pair in Si measured as function of temperature, using 23 p4111 A66-41264  
cryostat 23 p4111 A66-41264  
Instabilities resulting in loss of energetic electrons and fast electrons analyzed in electron cyclotron plasma confined by magnetic mirrors 23 p4103 A66-41490  
Electron self-energies in Fermi gas arising from coupling to optical and acoustic phonons 24 p4250 A66-42231  
Electromagnetic propagation in semiconductor with account of nonlinear effects such as skin effects arising from electron heating by field 24 p4256 A66-42526  
Temporal variations of electron energy flux in outer radiation zone measured during geomagnetic activity with instrumentation on board Explorer XII satellite 24 p4263 A66-42601
- ELECTRON FLUX**  
Rocket measurements discussing electron and proton flux, energy spectra and angular distribution in high altitudes 05 p0676 A66-14776  
Flux and energy spectrum of primary electron component measured by balloon at period near solar activity minimum 06 p0944 A66-16075  
Silicon planar transistors, noting electron flux induced surface damage mechanism 06 p0854 A66-16684  
Plasma transition from macroscopic stable state to state with virtual cathode 06 p0918 A66-16770  
Radiation tests on N/P silicon solar cells and other cover materials performed with one mev energy electrons for integrated fluxes, noting effects on physical, optical, electrical and thermal characteristics 07 p0990 A66-17238  
Explorer XV and Telstar I satellite trapped radiation measurements, noting connection between magnetospheric trapped particles and natural plasmas in space 07 p1131 A66-18084  
Explorer satellite XII, XIV and XV measurements, noting directional intensity energy flux, spatial distribution and spectra of low energy trapped protons and electrons 07 p1131 A66-18085  
Scintillation counter satellite data on low energy electron flux and particle trapping in dark magnetosphere 08 p1218 A66-19394  
Kinetic instability of terrestrial outer radiation belts calculated, using magnetospheric electron flux data 08 p1286 A66-19789  
Soft electron fluxes in upper atmosphere measured, using open type secondary electron multiplier ejected in container from rocket 09 p1443 A66-21012  
Flux of soft electrons in outer radiation belt as measured by Elektron II 09 p1445 A66-21032  
Electron flux at upper boundary of outer radiation belt measured by Elektron I and II satellites 09 p1445 A66-21034  
Auroral electrojet index and universal time variations, discussing polar disturbance statistics 10 p1528 A66-21144  
Space-charge theory for steady one-dimensional current flow across evaluated space between plane electrodes 10 p1557 A66-21573  
Auroral zone electron flux and relation to broadband radiowave absorption 11 p1703 A66-23495  
Steady state modulation by given frequency external signal of electron flow through straight waveguide, determining relation of counterradiation phase and amplitude to system parameters 12 p1921 A66-24210  
Electrons from linear accelerator directed in collimated beam at normal incidence upon thick targets of various materials, obtaining energy spectra of retrofugal electrons 13 p2136 A66-26280  
Periodic modulations of energetic electron fluxes observed throughout distant radiation zone by Geiger counters aboard satellites suggest MHD wave activity 13 p2175 A66-26354  
L-3 rocket observation of proton and electron fluxes at high altitudes, using solid state detectors 15 p2574 A66-28910  
Formation mechanism of ionospheric narrow sporadic E layers by high energy electron fluxes captured by geomagnetic field 15 p2488 A66-29110  
Rocket measurements of electron fluxes in upper atmosphere of middle latitude at altitudes of 200-500 km 15 p2592 A66-30063  
Energy spectra of electrons and protons in islands at back of magnetosphere compared with electron fluxes observed by satellites, noting similarity between particles in islands and those in aurora 16 p2695 A66-30714  
Book on electronics and electron physics advances including fast ion scattering, kinetic ejection of electrons, plasma application in microwaves, etc 16 p2747 A66-30794  
Instability of nonlinear stationary oscillations of potential in electron-ion flows useful in distribution functions of ions and electrons 16 p2754 A66-31174  
Electron flux induced excitation of magnetostatic oscillations of magnetized ferrite 16 p2784 A66-31549  
Galactic acceleration and solar modulation of cosmic rays examined via energy spectrum of galactic electrons, estimating Fermi acceleration, low energy electron flux, etc 18 p3177 A66-34756  
Flux and energy spectrum of primary electron component measured by balloon at period near solar activity minimum 18 p3187 A66-34814  
Flux and East-West asymmetry of primary electrons at geomagnetic rigidity cut-off of about 4.5 gv 18 p3187 A66-34817  
Plasma transition from macroscopic stable state to state with virtual cathode 19 p3405 A66-35367  
Correlation of magnetic fields and energetic electrons on IMP I satellite, noting depression in geomagnetic tail region, electron fluxes and diamagnetic effect 20 p3633 A66-38201  
Energetic electrons from shock heating of exosphere, discussing formation of artificial radiation belt via MHD shock wave heated and density gradient accelerated electrons 20 p3644 A66-38346  
Kinetic instability of terrestrial outer radiation belts calculated, using magnetospheric electron flux data 21 p3809 A66-38785  
Fluxes, intensities and energy distributions of magnetically trapped electrons and fluxes of magnetically trapped protons at lower edge of radiation belt 22 p3974 A66-40557  
Interplanetary electrons and associated solar flares 22 p3974 A66-40564  
Steady state modulation by given frequency external signal of electron flow through straight waveguide, determining relation of counterradiation phase and amplitude to system parameters 22 p3878 A66-40574  
Increment of constant HF electron flux in resonance probe determined for case of large constant potential, noting role of plasma 22 p3920 A66-40770  
Electron field operator derivation from dynamical rearrangement formulation applied to neutral superconductivity 23 p4112 A66-41275  
Auroral zone electron source properties deduced from electron fluxes, spectra and angular distributions measured by rocket flown into breakup phase of IBC I aurora 24 p4199 A66-42584  
Auroral zone proton-electron anticorrelations, proton angular distributions and electric fields 24 p4199 A66-42585  
Cosmic-ray electron flux above 4.7 BV measured, using lead-plate spark chamber, determining upper limit to primary flux 24 p4265 A66-42717  
Cosmic ray electron sign ratio and absolute flux measured by balloon-borne equipment 24 p4272 A66-43041
- ELECTRON GAS**  
Diagrammatic method to obtain Helmholtz free energy of classical electron gas used to derive pair distribution function beyond Debye-Huckel result 02 p0266 A66-11478

- Superconducting critical field curves for tin, indium and mercury below one degree K, with entropy difference linear in temperature for free electron gas 02 p0271 A66-11480  
Phonon field effect on plasma frequency of dense electron gas for nonzero temperatures 02 p0267 A66-11708  
Pressure dependence of initial recombination of ions in oxygen 04 p0549 A66-14287  
Isotropic photon gas interacting with electron plasma with Maxwellian distribution via Compton effect 05 p0722 A66-14721  
Radial distribution function computed for classical particles interacting with Coulomb, shielded Coulomb and truncated Coulomb forces 06 p0908 A66-16120  
Plasmon dispersion relation and damping constant derived from Green function formulation of random approximation for inverse dielectric function of electron gas 07 p1090 A66-18211  
Electron gas energy scattering in n-type indium antimonide at helium temperatures under action of DC field 07 p1104 A66-18259  
Opacity due to Compton scattering at relativistic temperatures in semidegenerate electron gas 08 p1258 A66-18779  
Electron and ion recombination coefficient in weakly ionized gas of homeopolar molecules 09 p1407 A66-19965  
Electron gas energy scattering in n-type indium antimonide at helium temperatures under action of DC field 09 p1431 A66-20903  
Extension of electron gas model to transition metals /titanium, zirconium, hafnium/, considering atom interaction up to fourth neighbor 10 p1546 A66-21664  
Injection and extraction of hot electrons in n-n heterojunctions with rapid Maxwellization of electron gas, negative resistance and semiconductor characteristics 13 p2166 A66-25920  
Electro-magnetoplasma-gas-dynamics /EMPGD/ equations for warm compressible electron gas drifting at constant velocity, finding equation for refractive index of plasma waves 14 p2339 A66-26862  
Hall coefficient and thermal emf of electron gas of PbTe in strong magnetic field 14 p2358 A66-27088  
Equilibrium binary correlations in classical relativistic homogeneous electron gas 14 p2339 A66-28275  
Electron gas electroconductivity relaxation time and energy loss in n-type InSb at cryogenic temperatures 15 p2558 A66-28611  
Meissner effect in superconducting electron gas in magnetic field 16 p2749 A66-31758  
Neutral atmosphere reduces electron gas thermal conductivity below 200 km during both day and night 20 p3552 A66-37590  
Shubnikov-de Haas effect for transport properties of electron gas in magnetic field, noting oscillatory parts of thermal and electric conductivities 21 p3776 A66-38632  
Electrical conductivity of dense plasma in strong electric field, when electron gas accelerated by field produces beam of runaway electrons 21 p3784 A66-39029  
Radiation peak formation in nonhomogeneous gas behind shock wave due to radiating atom distribution and heating of electron gas by inelastic molecular collisions 21 p3728 A66-39334  
Radiation peak formation in nonhomogeneous gas behind shock wave due to radiating atom distribution and heating of electron gas by inelastic molecular collisions 22 p3897 A66-39704  
Time dependent thermal behavior of ionospheric electron gas 22 p3913 A66-40552  
Hall coefficient and thermal emf of electron gas of PbTe in strong magnetic field 22 p3967 A66-40844  
Radiative equilibrium of electron gas in magnetic field based on quantized particle motion and perturbation theory 23 p4101 A66-41365  
Screening function of interacting electron gas at high and metallic densities by many-body perturbation theory 24 p4236 A66-42294  
Laser oscillation effect on characteristics of electron gas of helium-neon laser plasma studied in terms of wave attenuation in plasmaguide 24 p4225 A66-43006



## ELECTRON GUN

## SA CATHODE RAY TUBE

Electron image of CRT cathode formed directly on view screen, eliminating emission patchiness from oxide coated tubes 01 p0036 A66-10395

Impedance of growing wave in interaction region used to calculate minimum value of traveling wave tube noise coefficient 06 p0837 A66-17190

Low energy electron position detection with composite surface barrier type diode, noting design, fabrication and operation 12 p1879 A66-23705

Vacuum-evaporation method of fabricating thin film circuits, using resistance-heating process or electron beam 12 p1847 A66-24954

Optimum potential distribution in electron gun of low noise traveling wave tube calculated, using plasma wave number changes in accelerating portion of gun 14 p2236 A66-27236

Multistage ion gun using separate acceleration and deceleration stages and neucryptite or spodumene emitters 16 p2760 A66-30428

Axially symmetric or two-dimensional electrode system with emitting surface, discussing convergence and accuracy criteria of iteration methods 17 p2887 A66-32700

Impedance of growing wave in interaction region used to calculate minimum value of traveling wave tube noise coefficient 19 p3297 A66-35548

Cathode current density distribution, beam minimum radius and location and electrode current interception, using computer techniques on electron guns 20 p3528 A66-37490

Electron beam rotation experiments on linear spiratron with M-type electron gun 20 p3533 A66-38005

Electron gun with voltage drop across cathode using space charge streams for M-beam generation 21 p3710 A66-38833

**ELECTRON IMPACT**

Excitation and inversion method in gas lasers noting characteristics of helium-neon laser and ionized and three-level laser system 04 p0530 A66-13951

Ionization cross section of ground state helium cation by electron impact in Born exchange approximation 04 p0549 A66-14312

Vibrational excitation cross sections of diatomic molecules calculated, using Born approximation by including polarization interaction between incident electron and molecule 06 p0912 A66-16630

Quantitative comparison of systematic approaches to generation of inelastic impact cross section with aid of simple universal excitation cross section function [AIAA PAPER 66-150] 06 p0913 A66-17097

Photoelectron impact excitation effect on dayglow intensity, calculating energy distribution for various altitudes 07 p1028 A66-17374

Absolute cross section for single ionization of lithium ions by electron impact over 75.6 to 800 ev electron energy 07 p1084 A66-18425

Mass spectrometric electron impact ionization potentials rapidly obtained by electronic control and automatic data processing systems 07 p1091 A66-18489

Absolute cross section for ionization of atoms and diatomic molecules by electron impact 09 p1410 A66-20958

Born approximation of cross sections for electron and proton impact ionization of Na and Mg 11 p1737 A66-22496

Born-exchange and Ochkur approximations used to calculate electron impact ionization cross sections for He, Li, Be, Na and Mg atoms in ground states 11 p1737 A66-22497

Mass spectrometric fragmentation behavior of N-n-propyl and N-n-butyl pyrrolidone and N-alkyl succinimides subsequent to electron impact 11 p1651 A66-23412

Measurement of cross section for excitation of cesium atom by electron impact in prethreshold energy region, using electron trap method 12 p1925 A66-24878

Gas discharge by laser pulse, taking into account photoionization due to electron impact 12 p1891 A66-24887

Electron impact excitation mechanism of

argon-ion continuous and long pulse lasers 13 p2102 A66-26206

Quantitative comparison of systematic approaches to generation of inelastic impact cross section with aid of simple universal excitation cross section function [AIAA PAPER 65-150] 15 p2545 A66-29268

Fast ion molecule reaction in carbon dioxide analyzed, using mass spectrometer 16 p2645 A66-30116

Ionization of oxygen examined, using charge exchange in double mass spectrometer, noting break in electron impact ionization efficiency curve and constructing breakdown graph 20 p3605 A66-38097

Absorption spectrum of sulfur hexafluoride in far UV due to electron impact and inelastic scattering and oscillator strengths for three absorption bands 21 p3774 A66-38524

Discrepancies in electron-impact broadening of isolated ion lines due to neglect of collision-induced transitions between upper and lower levels of line and Coulomb interactions with perturbed ions 22 p3951 A66-40419

Measurement of cross section for excitation of cesium atom by electron impact in prethreshold energy region, using electron trap method 23 p4099 A66-41085

Gas discharge by laser pulse, taking into account photoionization due to electron impact 23 p4076 A66-41094

Ionization cross sections and efficiencies by electron impact and photoionization for molecular ionization at low energies 23 p4098 A66-41268

Excitation of hydrogen molecule from ground state to B and C electronic states by electron impact, using one-center wave functions of Huzinaga together with Born approximation 23 p4098 A66-41360

Small neutral hydrogen flux in total solar wind flux and electron impact and photoionization mechanisms 23 p4123 A66-41689

Windowless total radiation gauge for shock tube measurements of high temperature gas radiance 24 p4208 A66-42183

**ELECTRON INTENSITY**

Longitudinal asymmetry of trapped energetic electron intensities attributed to lowering of mirror points in South African anomaly 10 p1599 A66-21160

Energy spectrum of electrons recorded by fluorescent screen indicators onboard Cosmos satellites, noting ratio of electron intensities 11 p1763 A66-23042

Length changes in electron irradiated high purity germanium at liquid helium and nitrogen temperatures, noting large initial expansion 13 p2157 A66-25047

Data from satellite 1963 38C, showing existence of 27-day periodicity in intensities of trapped electrons undergoing two increases and linked to interplanetary magnetic field 13 p2175 A66-26353

Correlation of time variations of proton and electron intensity of outer radiation belt and dependence on geomagnetic environment 15 p2575 A66-29103

Temporal variations of outer radiation zone electron intensities at 1000 km as affected by geomagnetic storms observed by Alouette I satellite 20 p3631 A66-37623

High energy trapped electrons in outer zone for 27-day, diurnal and storm time variations 20 p3639 A66-38317

**ELECTRON INTERACTION****SA PHOTON-ELECTRON INTERACTION**

Relationship between cyclotron resonance and interaction among current carriers in semiconductors 04 p0564 A66-14256

Surface photoeffect from highly alloyed semiconductor accounting for Coulomb electron interaction 04 p0567 A66-14344

Coulomb interaction of electrons and holes in contacts of degenerate n-and p-type semiconductors causes ground state instability relative to electron-hole pair formation 05 p0730 A66-14645

Ion-electron interaction in plasma 05 p0725 A66-15243

Gorkov Ansatz in superconductivity theory exactly satisfied by system of definite number of fermions 06 p0923 A66-16273

Vector pairing in small dimensional

superconductors vanishes when pair dimensions are larger than sample or electron mean free path 06 p0930 A66-17054

Electron interaction with quadrupole pumping field, noting phase-focusing character in quadrupole region and determination of amplifier effect 06 p0859 A66-17186

Cosmic ray particle interaction at hundred bev range, discussing parameters of inelasticity for collision with nucleus 07 p1113 A66-17538

Green function/Gorkov variational procedure calculation of transition temperatures of superposed superconducting films dominated by inhomogeneous electron-electron interactions 07 p1108 A66-18436

Superimposed normal superconducting films used in conjunction with theory to investigate nature and magnitude of electron-electron interaction in normal metal 10 p1572 A66-21174

Electron Coulomb interaction in strongly alloyed semiconductor films tends to reduce all energies to constant value without changing spectrum shape 11 p1750 A66-22344

Self-consistent theory of curvilinear electron fluxes interaction with wave conducting line, taking into account space charge 11 p1655 A66-22722

Electron correlation theory in nonclosed-shell states, discussing orbital wave functions and perturbation theory 13 p2130 A66-25376

Coulomb interaction of electrons and holes in contacts of degenerate n-and p-type semiconductors causes ground state instability relative to electron-hole pair formation 13 p2166 A66-25918

Microwave amplification by interaction of electron beam with cesium plasma 14 p2345 A66-28045

Surface photoeffect from highly alloyed semiconductor accounting for Coulomb electron interaction 14 p2367 A66-28239

Ionospheric plasma movement, neutral-neutral and charged-neutral particle collisional interactions, electron-ion collision frequencies, mobility and LF Hall conductivity, irregularities, etc 15 p2495 A66-30053

Magnetization-density-wave instability of quantum plasma in random phase approximation 16 p2757 A66-30192

Book on nonlinear electron-wave interaction phenomena and application to amplifiers, oscillators and other crossed electric and magnetic field devices 16 p2653 A66-30873

Cross sections for sticking electrons to spherical charged particles, considering Debye screening distance of Coulomb force field 16 p2754 A66-31158

Light absorption coefficient for indirect photon transitions during Coulomb interaction of electrons at high electron densities 16 p2787 A66-31766

Helium plasma in confining magnetic field, noting spectral efficiency in optical region, electron temperature and density, electron ion recombination, etc 17 p2965 A66-32409

Additional measurements from electron-magnetic field interactions and power limitations in coaxial filament and anode geometry in electron bombardment heated thruster 17 p2990 A66-32462

Ferromagnetic semiconductors with exchange interaction due to conduction electrons 17 p2986 A66-33306

Suggested origin of low energy tails in radiative recombination spectra due to degenerate conduction band 19 p3437 A66-35475

Electron interaction with quadrupole pumping field, noting phase-focusing character in quadrupole region and determination of amplifier effect 19 p3314 A66-35544

Exchange interaction between f-electrons and s-electrons in atomic shells of crystal lattice of rare-earth metals, examining calculation methods for Hamiltonian of s-f exchange 20 p3617 A66-37476

Collision frequency in E and D regions of ionosphere for electrons and neutral molecules 22 p3906 A66-39948

Behavior of wave function for system of charged particles near coalescence of any



two of them, noting electron-nucleus cusp conditions for diatomic molecules 22 p3861 A66-40904

Self-consistent theory of curvilinear electron fluxes interaction with wave conducting line, taking into account space charge 23 p4037 A66-41460

Approximate ground state wave functions used in calculation of interaction energies by second-order perturbation theory 23 p4033 A66-42081

Resonance of antineutrino-electron interaction cross section, calculating electron density and velocity distribution via Ritz method 24 p4270 A66-42932

#### ELECTRON-ION RECOMBINATION

Ambipolar diffusion and electron attachment in photoionized nitric oxide by presence of negative ions, noting electron loss and electron density 03 p0394 A66-12326

Electron-ion recombination in photoionized nitric oxide neon gas mixture, noting decay of electron density and correlation factors 03 p0394 A66-12327

Optical interferometric, spectrographic and microwave techniques of electron-ion recombination in neon-spectral line 03 p0394 A66-12330

Electron-ion recombination rate and effective ionization calculated for cesium plasma by Bates method 03 p0398 A66-12510

Helium afterglow discussing stability of collisional-radiative recombination of ions with electrons and neutral particles 04 p0547 A66-13652

Rate of electron-ion recombination by collision of two electrons in ion field obtained by Thomson formula, noting recombination rate of three-body collision 04 p0550 A66-13710

Equilibrium statistical mechanics of electron-ion plasma developed in terms of Wigner distribution function 04 p0551 A66-13713

Ion-pairing process in nickel and lithium doped germanium 04 p0565 A66-14270

Electron-ion recombination processes in nonequilibrium plasma, noting validity of commonly made assumptions 05 p0625 A66-15810

Recombination rate of electrons in plasma containing ions of molecule with both repulsive and bound neutral states 05 p0729 A66-15863

Plasma formation by dissociation of molecular ions by arc discharge in apparatus for adiabatic plasma confinement 06 p0915 A66-16152

Electron and ion recombination coefficient in weakly ionized gas of homeopolar molecules 09 p1407 A66-19965

Ionosphere formation theory, reviewing solar radiation, absorption, ionization cross section rate, electron removal in F and upper E layer, etc 10 p1533 A66-21851

Monte Carlo calculations of cross section magnitude of electron-positive-molecular-ion dissociative recombination 13 p2130 A66-25375

Ionization enhancement from Van Allen electrons in South Atlantic magnetic anomaly, noting longitudinal variation of trapped electrons, electron-ion recombination, etc 13 p2176 A66-26362

Plasma formation by dissociation of molecular ions by arc discharge in apparatus for adiabatic plasma confinement 15 p2557 A66-29882

Electron-ion recombination coefficients for atmospheric ions determined in laboratory and compared with ionospheric analysis 15 p2548 A66-29947

Mean probability of coupling between electrons of flame on electronegative gas and radioactive bromine tracer injected into flame, calculating electrons coupling cross section on bromine atoms 16 p2763 A66-31208

Conductivity and electron-ion recombination coefficient in argon determined from collision cross sections of electrons with neutral particles 16 p2755 A66-31599

Gas pressure dependence of attachment and recombination coefficients for thermalized electrons in air and oxygen 18 p3143 A66-34035

Ionization outside equilibrium and

relaxation of ionization in cesium seeded argon 18 p3144 A66-34102

Steady state donor-acceptor recombination rate and effects on diode current and injection electroluminescence, using Shockley-Read-Hall semiconductor phenomenological model 21 p3800 A66-38993

Cryogenic optically excited recombination emission in single crystal InSb semiconductor and transitions involving phonon creation, acceptor impurities and band-to-band emissions 21 p3800 A66-38996

Electron-ion recombination process due to electron collision in plasma with capture electrons transferred to ground level 22 p3954 A66-39767

#### ELECTRON IONIZATION

Current discharge of helium neon laser on laser action 03 p0376 A66-12439

Thermodynamic properties of hydrogen ionized plasma in equilibrium 03 p0403 A66-12966

Spatial distributions of free electrons in near wakes of spheres in hypersonic flight [AIAA PAPER 66-55] 07 p0983 A66-18449

Intensity estimation for lunar X-rays excited by high energy terrestrial electrons from solar stream induced geomagnetic cavity 09 p1442 A66-20388

Relaxation to steady state, electron collision ionization, recombination and collision cross section uncertainties in conducting nonequilibrium plasma stream [AIAA PAPER 66-193] 10 p1562 A66-21439

Growth rate of ionization by electron impact in presence of laser beam, elastic and inelastic scattering cross sections, free-free absorption, excitation and ionization coefficients, breakdown times and thresholds 13 p2134 A66-26193

Experimental evidence of inverse bremsstrahlung and electron-impact ionization in low pressure argon ionized by giant pulse laser 15 p2544 A66-29115

Asymptotic form of wave function and threshold behavior of cross section for ionization of atomic hydrogen by electron impact 15 p2544 A66-29116

Ionized electron centers in irradiated lithium fluoride crystals investigated by observing emission and absorption spectra 15 p2568 A66-29641

Plasma ionization associated with thermal electron or nonthermal distribution of electron velocities for various gas densities 15 p2554 A66-29751

Ionization of hydrogen and hydrogenic positive ions by electron impact 19 p3409 A66-36324

Asymptotic approximation of distribution of small ionization bursts produced by high energy muon under thick layer of matter in direct electron-pair production 24 p4271 A66-42935

#### ELECTRON MASS

Temperature dependence of effective electron mass of indium antimonide 04 p0565 A66-14275

Effective mass of electrons and holes in semiconductors from magneto-optical laser emission studies 05 p0741 A66-15832

Effective mass of electrons in n-type gallium arsenide deduced from measurements of Hall coefficient and thermoelectric power 09 p1426 A66-20197

Variation and behavior of ionospheric electron concentration at altitudes of 100 to 300 km as measured by rocket probes 09 p1378 A66-21007

Composition of outer ionosphere measured, using RF mass spectrometers mounted on board Elektron I and II satellites 09 p1378 A66-21008

Effective mass in InAs and InSb from Landau shift of peak emission in laser diodes 10 p1543 A66-21579

Twelve distinct mass series identified and mass values determined as function of orientation of magnetic field in Fermi surface of zinc at cyclotron resonance 10 p1581 A66-21735

Identification of mass series and mass values in Fermi surface of cadmium at cyclotron resonance compared with results for zinc 10 p1581 A66-21736

Optical reflection, transparency and Faraday effect for indium antimonide, calculating effective electron mass, relation

between energy and wave number, etc 16 p2788 A66-31777

Effective electron mass in n-type indium arsenide at high temperatures and high carrier density, noting temperature dependence of effective electron mass 20 p3616 A66-37444

Effective electron mass dependence on pressure in InSb determined by measuring electron concentration and thermal emf 20 p3624 A66-38427

Effective electron mass dependence on pressure in InSb determined by measuring electron concentration and thermal emf 21 p3800 A66-38960

#### ELECTRON MICROSCOPE

Constructing and evaluating electrostatic filter lenses with wide image angles for low voltage electron microscope 02 p0228 A66-11498

Electron microscope filter lenses with unconventionally shaped electrodes and large image angles 02 p0228 A66-11499

Electron microscope using electrons suffering energy loss to form images for qualitative microanalysis 05 p0649 A66-15104

Improved resolution of scanning electron microscope used to define geometry of electrode areas during fabrication of solid state devices 06 p0855 A66-16769

Electron microscope observation of active centers at surface of semiconductor crystals, applying to p-type Si single crystals 09 p1412 A66-19989

Text on electron optics covering principles and application, electron lenses, cathode ray tubes, mass and beta ray spectrographs, quadrupole systems, image converters, etc 09 p1402 A66-20333

Scanning electron microscope observation of electrical leakage paths due to crystal defects in silicon diodes 11 p1668 A66-23028

Hot and cold hardening of aluminum-copper-magnesium alloys for application to missiles and aircraft skins analyzed, using electron microscope, noting metastable phases 12 p1893 A66-23747

Aluminum alloy with various metal additions analyzed for aging, using electron microscope 12 p1898 A66-25022

Electron microscope investigation of dislocation structure of silicon single crystals after compressive deformation at various stages of deformation curve 15 p2557 A66-28562

Scanning microscope for studying Si p-n junctions by electron or ion bombardment 17 p2927 A66-33454

Stroboscopic electron mirror microscope observations of Si p-n junctions in pulsed regime 17 p2928 A66-33455

Scanning electron microscope observations of p-n junctions using small periodic bias voltages 17 p2988 A66-33457

Electron microscope investigation of dislocation structure of silicon single crystals after compressive deformation at various stages of deformation curve 23 p4112 A66-41283

#### ELECTRON MICROSCOPY

Quantitative analysis of stress level, material characteristics or temperature level at which fracture occurs, using electron microscope 01 p0088 A66-10962

Aberration of width of linear image created by skew rays in composite quadrupole lens 02 p0199 A66-11782

Combined effect of carbon impurity atoms and neutron radiation on structure of molybdenum studied by transmission electron microscopy 02 p0246 A66-12193

Transmission electron microscopy to determine white etching alteration around inclusion in cyclically stressed bearing steel due to cellular grain formation [ASME PAPER 65-WA/CF-1] 05 p0703 A66-15614

Electron micrographs from fraction I protein of Chinese cabbage leaves, noting substructure in individual particle 06 p0811 A66-16119

Width of depletion region of reverse-biased silicon p-n junction 06 p0923 A66-16382

Length change, X-ray lattice parameter, small angle X-ray scattering, electron microscopy and thermal conductivity measurements related to radiation-induced



- defects in semiconductors 06 p0933 A66-17117
- Replica techniques and electron and optical microscopy to study laser irradiated metal surfaces 07 p1052 A66-18393
- Large dislocation loops on basal plane and rows of prismatic dislocation loops in quenched magnesium 07 p1052 A66-18513
- Diffraction contrast analysis, using transmission electron microscope, of two-dimensional defects present in mechanically damaged silicon after annealing 07 p1109 A66-18516
- Imperfection formation in epitaxial gold films, observing crystal-lattice dislocations due to rotation and displacement misfits between neighboring islands of deposit film 07 p1110 A66-18517
- Light and electron microscopic metallography and X-ray diffraction microanalysis of phase reaction during heat treatment of Ni-base 08 p1236 A66-18757
- Transmission electron microscopy observation of microhardness, of shock-hardened iron and bcc iron-based alloy structures 08 p1236 A66-18758
- Transmission electron microscopy structural analysis of dislocations in stress-corrosion cracking of 7075 aluminum alloy 08 p1236 A66-18761
- Martensitic transformation kinetics and maraging mechanism in Fe-Mn-Ni-Ti alloy observed by electron and X-ray diffraction 08 p1236 A66-18762
- Electron microscopic estimation of perpendicular anisotropy of magnetic thin film originating from nonmagnetic grain boundaries 08 p1270 A66-19012
- Domain structure of single-crystal epitaxial iron films as function of perfection of crystalline structure, using Lorentzian electron microscopy, noting two-axis anisotropy 11 p1753 A66-22806
- Structured water forms in biological systems, relationship to macromolecular system, detection and evaluating electron microscopy 11 p1645 A66-22992
- Domain structure of partially oriented thin permalloy films analyzed through appearance of adjoining 180 degree walls of equal contrast and by electron microscopy 12 p1934 A66-25029
- Immobile dislocation network of high density in Campo del Cielo observed by thin-film transmission electron microscopy 13 p2177 A66-25136
- Transmission electron microscopy determination of structure and morphology of oxide films during Ti oxidation initial stages 13 p2107 A66-25584
- Transmission electron microscopic observations on preexisting dislocation as sinks for neutron-irradiation-induced point defects and dislocation reaction to subsequent deformation 13 p2107 A66-25586
- Fracture surfaces of metals and alloys examined, using optical and electron microscopy, noting fracture mechanisms during crack initiation and propagation 13 p2108 A66-25768
- Aging behavior of explosively deformed 2219 Al investigated by transmission electron microscopy 13 p2086 A66-25775
- Spatial interrelations between mitochondrial apparatus of capillary cells and synapses of these cells in utricular receptor of animals at rest and after exposure to accelerations, using electron microscopy 13 p2011 A66-26250
- Domain boundaries and superdislocations of structure of Alnico V by thin film electron transmission microscopy 14 p2311 A66-26882
- Vacuum deposited films of titanium dioxide examined, using electron microscopy and diffraction methods, noting crystal dislocation due to electron beam irradiation 14 p2359 A66-27133
- Cleavage behavior of solid solution alloy Ta-Mo, noting electric resistivity, tensile properties, lattice parameters, diffraction coefficients, etc 15 p2520 A66-28650
- Structure and electrical resistance as function of temperature for Nichrome-silicon monoxide cermet films on single crystal Si substrates 16 p2783 A66-31425
- Stacking faults in titanium carbide shown by electron microscopy bounded by partial dislocations 17 p2976 A66-32263
- Dissociation and reassociation reactions of hemocyanin mixtures analyzed by electron microscopy, noting original molecular structures 18 p3060 A66-34459
- Macromolecular organization of hemocyanins and apohemocyanins as revealed by electron microscopy 18 p3060 A66-34460
- Aluminum particle combustion noting changes from preignition to burnout, flame structure, particle geometry, etc 18 p3266 A66-35021
- Optical absorption of island films of gold as function of island density obtained from electron micrographs and film thickness 19 p3435 A66-35416
- Thin film transmission electron microscopy on n-type silicon irradiated with fast neutrons, noting erratic polishing process and irregular surface 19 p3436 A66-35431
- Thin film transmission electron microscopic analysis of stress corrosion of heat-treated aluminum 21 p3749 A66-38471
- Transmission electron microscopic analysis of initial epitaxial growth stage of evaporated Au films on NaCl cleavage surfaces 21 p3798 A66-38758
- Transmission electron microscopy on polycrystalline Al, determining hardening and tensile yield stress variations as function of quenching temperature 21 p3753 A66-39586
- Transmission electron microscopic and molecular beam study of nucleation and growth in chemical vapor of epitaxial silicon films on carbon-contaminated silicon substrates 21 p3806 A66-39589
- ELECTRON MOBILITY**
- Stochastic aspects of low mobility theory applied to electrical conductivity problem in Wannier representation 01 p0106 A66-10723
- Photovoltaic response in semiconductors based on Demer effect which does not overtly depend on hole and electron mobility 02 p0275 A66-11976
- Cadmium selenide thin film transistors /TFT/ where electron mobility values exceed bulk single crystal values 02 p0276 A66-11979
- Transport effects in semimetals and narrow-gap semiconductors including nonlinear, thermomagnetic and superconductive effects and tunneling 04 p0559 A66-13451
- Transverse Demer effect in anisotropy of electrical and photoelectrical characteristics of indium selenide 04 p0565 A66-14259
- Temperature dependence of effective mass and influence of two-phonon processes on mobility in semiconductors with narrow forbidden bands 04 p0565 A66-14263
- Individual and group defect contribution to variation in carrier concentration and mobility in n-type germanium irradiated with fast neutrons 05 p0730 A66-14644
- Oxygen alloyed gallium arsenide, explaining anomalous mobility distribution in crystals during fusion in presence of oxygen 05 p0731 A66-14658
- Drift mobility induced by pulsed gamma irradiation of polystyrene 05 p0735 A66-14858
- Electron mobility in potassium and cesium DC glow discharges at low electron temperature 05 p0728 A66-15809
- Electron drift velocity and mobility of indium antimonide obtained from pulsed measurements of conductivity and Hall effect at various temperatures 06 p0922 A66-16173
- Electron mobility of gallium arsenide-phosphorus alloys 06 p0923 A66-16380
- Point defect mobility and annealing in irradiated germanium and silicon by electron or gamma ray irradiation 06 p0937 A66-17140
- Drift mobility of radiation induced defects in silicon between zero and 120 degrees C 06 p0937 A66-17141
- Electron mobility changes in GaAs single crystals due to electron irradiation interpreted in terms of ionized-scattering theory 06 p0939 A66-17151
- Coherent increase of spin wave semiconductors by electric current, if electron drift velocity exceeds spin wave phase velocity 07 p1105 A66-18368
- Mobility of hot electrons in runaway regime of n-type InSb and GaAs at low temperatures 09 p1412 A66-19987
- Three-centimeter wavelength frequency multiplier using gas-discharge plasma in nonuniform electric field, examining amplitude and phase instability 09 p1358 A66-20793
- Low temperature resistivity of yttrium-based alloys containing small amounts of rare earth metals, deriving exchange integrals from resistivity data 09 p1430 A66-20846
- Electron Hall mobility from 4 to 300 degrees K with undoped single crystals of GaAs grown in quartz boats by Bridgman method and zone-melting technique 09 p1430 A66-20848
- Plasma density instability induced by electron-hole generation in impact ionization as affected by electric field 10 p1575 A66-21536
- Nonisothermal wave motion in nondegenerate semiconductors with charge carrier possessing scalar effective mass 10 p1586 A66-22091
- Generalized equation for steady state motion of electrons in cylindrical electrostatic system with arbitrary cross section, calculating critical focusing current 11 p1735 A66-22493
- Electrophysical parameters of epitaxial p-n junction regions determined, using galvanomagnetic and photomagnetic measurements 11 p1751 A66-22734
- Indium antimonide thin film preparation via vacuum deposition, noting evaporation rate effects on electrical properties of film 11 p1756 A66-23022
- Electron attachment and detachment coefficients for pure oxygen determined from current waveforms in drift tube 13 p2130 A66-25374
- Ohm law in partially ionized inhomogeneous plasmas in presence of magnetic field derived, accounting for electron, ion and fluid motion 13 p2140 A66-25418
- Electron mobility in inversion layer on p-type silicon surface 13 p2163 A66-25439
- Consistency of Gunn effect with excitation of conduction band electrons from high mobility minimum to low mobility valleys 13 p2164 A66-25517
- Gunn effect in gallium arsenide, noting negative differential electron mobility at high electric fields in conduction band 13 p2165 A66-25546
- Effect of nonlinearities on electron cyclotron resonance, stressing determination of maximum velocity of plasma under cyclotron resonance conditions 13 p2143 A66-25711
- Individual and group defect contribution to variation in carrier concentration and mobility in n-type germanium irradiated with fast neutrons 13 p2166 A66-25917
- Oxygen alloyed gallium arsenide, explaining anomalous mobility distribution in crystals during fusion in presence of oxygen 13 p2167 A66-25933
- Equatorial electrojet cross section profile, describing longitudinal variations, current density, magnetic field produced and electron drift velocity 13 p2074 A66-26357
- Minority carrier drift mobility in p-type germanium single crystal under uniaxial lattice compression 14 p2365 A66-27758
- Transient acoustoelectric interaction in CdS and ZnS crystals during single transit, measuring electron drift 15 p2563 A66-28758
- High fields effect on negative field effect electron carrier mobility on MOS surfaces 16 p2771 A66-30196
- Radiative corrections to Thomson scattering in laser beams arising from damping of electron motion and photon density, using quantum mechanics 16 p2717 A66-30628
- Coupling of electron motion to lattice longitudinal acoustic mode in n-gallium antimonide leading to variations in sound velocity 16 p2775 A66-30732
- Structure and electron mobility of thin indium arsenide films prepared by co-evaporation technique 16 p2780 A66-31094
- Electrical properties of nickel ferrite in terms of Jonker model, noting magnitude of energy gap between Fe and Ni levels and mobilities of electrons and of positive



holes 16 p2781 A66-31215

High-mobility InSb thin film preparation by flash evaporation of elemental In and Sb in vacuum and oxidation of film surface prior to recrystallization in inert atmosphere 16 p2785 A66-31575

Origin of polarization of radiation from GaAs diodes, noting intensity dependence on current density and effect of anisotropic electron velocity distribution 16 p2667 A66-31770

Electron mobility in p-type indium antimonide, noting entrainment of minority carriers by majority carriers 16 p2789 A66-31784

Electron motion examined as major contributor to conductivity of thermally ionized gas in electrical field 17 p2964 A66-31892

Distribution function and electron mobility in polar semiconductors for nonparabolic dispersion law 17 p2986 A66-33305

Evaporated and recrystallized CdS layers, discussing electron mobility, level distribution, capture cross section and techniques of measurement 19 p3435 A66-35408

Fluid equations used in describing electron and ion motion perpendicular to field lines in slab of plasma supported against gravitational field by sheared magnetic field 19 p3417 A66-36527

Plasma electron thermal motion influence on propagation of plane oscillations of plasma which are adiabatic 21 p3781 A66-39014

Current density, electron mobility, magnetoresistance, negative resistance and impact-ionization-produced solid state magnetoplasma oscillations in InSb single crystal semiconductor at high electric and magnetic fields 21 p3805 A66-39568

Three-centimeter wavelength frequency multiplier using gas-discharge plasma in nonuniform electric field, examining amplitude and phase instability 22 p3874 A66-39852

Carrier density, mobility and space-charge-limited current in p-type silicon 22 p3962 A66-40049

Electrophysical parameters of epitaxial p-n junction regions determined, using galvanomagnetic and photomagnetic measurements 23 p4113 A66-41472

Electron effective mobility variation in AC for small signals as function of operating frequency of thin film transistors and dielectric diodes 24 p4181 A66-42392

Temperature dependence of Hall coefficient and resistivity of n-type epitaxial gallium arsenide in 4.2 to 300 degree K temperature range 24 p4254 A66-42423

Signal excitation in negatively charged antenna rod in effect of unfocused laser beam 24 p4224 A66-42753

**ELECTRON MULTIPLIER**

**SA PHOTOMULTIPLIER**

High sensitivity fast-response laser detection system, describing microwave response photoelectric detector with amplification and mixing functions 10 p1544 A66-22046

Correlation function of response of multichannel electronic multiplier to Gaussian input noise 11 p1676 A66-22711

Triaxial electron spectrometer, mounted on OGO-E spacecraft, measures flux and energy distributions of electrons, noting electron multiplier 12 p1877 A66-23689

Frequency response of avalanche photodiodes, discussing multiplication rate and extension of Townsend theory 15 p2458 A66-28889

Gain improvement to electron multiplier used in mass spectrometers 16 p2702 A66-30430

Photoelectron counter stellar photometer noting design, applicability of secondary electron multipliers, etc 18 p3113 A66-34617

Apparatus for teaching and research in electron physics including emitters, cathode ray tubes, electron multipliers and mass spectrometer 18 p3088 A66-35033

Channelled electron multiplication mechanism, discussing ionic feedback and saturation effects 19 p3359 A66-35910

Continuous channel electron multiplier operated in pulse saturated mode, noting

space charge limiting as major cause of gain saturation 19 p3359 A66-35911

Traveling wave HF crossed field photomultiplier with helical output circuit for electron multiplication at microwave modulation rates 24 p4182 A66-42567

**ELECTRON OPTICS**

TV camera, visual display and video-signal information storage tubes, noting secondary electron conduction camera tube 05 p0642 A66-14561

Nonlinear Maxwell equation for optics of many-particle system, noting Raman scattering from electron plasma 05 p0695 A66-14905

Electron-optical converters in astronomy 05 p0681 A66-15212

Text on high energy beam optics including trajectory optics in quadrupole systems and deflecting magnets, spectrometry, envelope optics and particle beams 06 p0911 A66-16306

Text on electron optics covering principles and application, electron lenses, cathode ray tubes, mass and beta ray spectrographs, quadrupole systems, image converters, etc 09 p1402 A66-20333

Electron optical method for study of metallic and semiconducting surfaces, based on low energy electron beam scanning 12 p1884 A66-24939

Quantitative observation of light modulation by electro-optic effect in reverse-biased GaAs p-n junctions at wavelength of 1.15 microns 13 p2159 A66-25067

Operation of electron image time dissector framing camera achieving time resolution by multiple reflection in crossed magnetic and electric fields in electron image storage device 19 p3353 A66-35313

**ELECTRON ORBIT**

Frequency and collisionless damping rate of electronic resonances of one-dimensional plasma in potential distribution 01 p0112 A66-10511

P super n electron configuration for systems where spin-free Hamiltonian is applicable 16 p2754 A66-30861

Core integral and electron repulsion integral for 2p-p1 Slater-type orbitals of allyl radical and benzene molecule transformed to Lowdin orthogonalized basis set of atomic orbitals 16 p2754 A66-31185

Electrons trapped in magnetosphere, discussing dynamo electrostatic field, energetic electron electromagnetic drift and magnetic mirror-electron orbit effects 20 p3635 A66-38226

**ELECTRON OSCILLATION**

Broadband tunable tunnel diode oscillator in waveguide mounting, noting role of variable capacitor 03 p0339 A66-12450

Oscillation and Maxwellian distribution of electrons in cesium plasma 03 p0403 A66-12968

Plasma waves propagating transverse to uniform external magnetic field discussing electron motion, wavelength magnitude, frequencies and application of results 03 p0406 A66-13358

Plasma ion and electron oscillation 05 p0725 A66-15235

Secondary emission ratio and multiplication constant of electron-ion oscillatory discharge 06 p0919 A66-16872

Simultaneous electron and ion oscillations on discharge gap of four-electrode chamber 06 p0919 A66-16881

HF electron oscillations in inhomogeneous plasma, noting kinetic drift instability added to hydrodynamic instability 07 p1087 A66-17915

Transformation of transverse oscillations of electron flux by short magnetic lenses studied by eigenvector concept 08 p1199 A66-18907

Paramagnetic resonance occurring in plasma located in external electric field, noting relation between oscillation amplitude and electron frequency 08 p1262 A66-18976

Gunn effect oscillators including domain formation, microwave source potentialities, power transfer, efficiency, etc 08 p1193 A66-19120

Microwave radiation from high voltage plasma with oscillating electrons and resulting cyclotron frequency

harmonics 08 p1264 A66-19180

Charged particle drift across magnetic field in plasma with oscillating electrons contained in metal chamber 08 p1264 A66-19181

Electron transit time and impedance relation in rarefied plasma diode, considering electron and ion velocity straggling 08 p1193 A66-19193

Instability of noncollision plasma in strong external field in terms of development of nonpotential oscillations 09 p1408 A66-20599

Instability of HF electron oscillations in plasma flows with nonuniform velocity profile along lines of force of external confining magnetic field 10 p1569 A66-21991

Intense HF electromagnetic wave propagation in isothermal isotropic nonhomogeneous plasma, noting interaction with electrons of Langmuir frequency 12 p1921 A66-24212

Oscillator stability affecting electromagnetism compatibility during PRF generation, digital system reception, reception with phase lock, etc 12 p1838 A66-24599

Long-wave electron oscillations excited by electron beam in rarefied plasma in presence of magnetic field 12 p1925 A66-24883

Temperature measurement in shock heated gases via spectrum line reversal method, noting connection between electronic excitation and effective vibrational temperature 13 p2208 A66-25159

Build-up oscillations in system of two identical parallel-plate capacitors flanking quadrupole capacitor in longitudinal magnetic field 13 p2044 A66-26469

Intense radiation emission at electron gyrofrequency harmonics from magnetoplasmas, discussing resonances, dispersion relations, electron trajectory perturbations, etc 13 p2155 A66-26675

Quasi-linear equations for inhomogeneous plasma in magnetic field applied to pumping of energy of Langmuir oscillations 16 p2762 A66-31176

Convective excitation of ionic oscillations in plasma by inhomogeneous electron beam as result of spatial gradient of distribution function 17 p2968 A66-32537

Convective effects role in exciting axisymmetric oscillations in plasma cylinder in magnetic field with aid of radius restricted electron beam 17 p2968 A66-32538

HF electron oscillations in inhomogeneous plasma, noting kinetic drift instability added to hydrodynamic instability 18 p3146 A66-34175

Instability of HF electron oscillations in plasma flows with nonuniform velocity profile along lines of force of external confining magnetic field 18 p3150 A66-34968

Associated nonuniform electron-nucleus oscillations in ferromagnetic substances studied to determine feasibility of maser, using magnetic-reversal nuclear magnetic resonance 20 p3577 A66-37477

Instability of noncollision plasma in strong external field in terms of development of nonpotential oscillations 20 p3611 A66-38133

Stabilization criteria for drift instabilities in inhomogeneous plasma with external electric field derived from drift wave frequency variation 20 p3612 A66-38430

Stabilization criteria for drift instabilities in inhomogeneous plasma with external electric field derived from drift wave frequency variation 21 p3777 A66-38963

Langmuir electron oscillation behavior in inhomogeneous plasma in magnetic field when applied at angle to oscillation axis 21 p3781 A66-39012

Absorption cross section of electron systems in bands of diatomic molecules calculated, noting effects of temperature variation 21 p3775 A66-39077

Intense HF electromagnetic wave propagation in isothermal isotropic nonhomogeneous plasma, noting interaction with electrons of Langmuir frequency 22 p3956 A66-40576

Collective oscillations of electron shells of atom, discussing energy, excitation and damping 22 p3959 A66-40940

Long wave electron oscillations excited by electron beam in rarefied plasma in



- presence of magnetic field 23 p4099 A66-41090
- Impurity photoconductivity spectra of p-type germanium at low temperatures, noting parameters of relative depth of equidistant minima oscillations 24 p4256 A66-42515
- ELECTRON PARAMAGNETIC RESONANCE**
- Asymmetric line near  $g$  equals 2.00 of paramagnetic resonance spectrum of MgO powder as polycrystalline spectrum of ferric ions in cubic field 01 p0123 A66-10602
- Silicon and lead sulfide electron paramagnetic resonance spectra, showing gas action and temperature effect on EPR signal amplitude and absorption lines 01 p0124 A66-10765
- Structures and crystallization processes of semiconductor vanadium phosphate glasses of various composition, using electron paramagnetic resonance 01 p0091 A66-10771
- Quantum RF physics text covering magnetic resonance theory, electron paramagnetic resonance, nuclear magnetic resonances, two-and three-level masers, RF gas spectroscopy and ammonia oscillator 01 p0108 A66-10954
- Electron paramagnetic resonance in biradicals of hydrazine series, discussing structural changes during transition from mono-to biradical state 04 p0572 A66-13877
- Compensation effect on electron paramagnetic resonance spectrum of n-type silicon 04 p0567 A66-14342
- Splitting of electron paramagnetic resonance lines of zinc-tungstate crystals, discussing parameters and experimental technique 05 p0738 A66-15356
- Electron paramagnetic resonance spectrum of carbon dioxide when absorbed on UV irradiated magnesium oxide 05 p0630 A66-15766
- Sensitized photolytic decomposition of ethanol and diethyl ether glasses analyzed at low temperature, using electron paramagnetic resonance /EPR/ spectroscopy 06 p0820 A66-16124
- Electron paramagnetic resonance analysis of low temperature irradiation effects on silicon 06 p0934 A66-17122
- Electron paramagnetic resonance, electrical conductivity and impurity diffusion in doped boron 10 p1580 A66-21724
- Potential fluctuation effect on electron paramagnetic resonance lines in compensated n-type semiconductor 10 p1587 A66-22151
- Silicon and lead sulfide electron paramagnetic resonance spectra, showing gas action and temperature effect on EPR signal amplitude and absorption lines 11 p1748 A66-22276
- Structures and crystallization processes of semiconductor vanadium phosphate glasses of various composition, using electron paramagnetic resonance 11 p1720 A66-22282
- Adsorption of CO radicals on three types of magnesium oxide using EPR techniques, noting spectrum of adsorbed radical, bonding, etc 12 p1916 A66-23619
- Compensation effect on electron paramagnetic resonance spectrum of n-type silicon 14 p2367 A66-28237
- Maser material iron doped rutile, examining theoretical and experimental disagreement in spin Hamiltonian describing paramagnetic behavior 15 p2514 A66-29027
- Hamiltonian describing EPR spectrum of trivalent chromium ion in ordered lithium-aluminum spinel and rhombic distortion causing deviation of axes in octahedron electric field 16 p2787 A66-31763
- Parametric amplification by monochromatic pumping of electromagnestic oscillations of substance contained in resonator 17 p2885 A66-32244
- Electron paramagnetic resonance study of tetraoxygen difluoride, showing existence of FOO free radical giving asymmetric spectrum 17 p2871 A66-32854
- Exchange pairs spectrum analysis based on observation of nonlinear splitting of EPR signals of pairs of exchange-coupled chromium ions in corundum 18 p3154 A66-33943
- Hydroxyl radical concentration in rarefied CO flame by EPR method 18 p3265 A66-34551
- Potential fluctuation effect on electron paramagnetic resonance lines in compensated n-type semiconductor 19 p3440 A66-35765
- EPR detection of dangling bonds at surface of silica and quartz, noting inhomogeneous expansion 19 p3445 A66-36341
- Splitting of EPR lines of trivalent Cr ion in zinc tungstate by external electric field, noting angular dependence and corresponding spin Hamiltonians 20 p3615 A66-37370
- Four electron paramagnetic resonance transitions of SO free radical generated in gas-phase discharge of sulfur dioxide 22 p3859 A66-39908
- Electron paramagnetic resonance and optical spectra of trivalent erbium in type II crystals of calcium fluoride disclose existence of cubic, tetragonal and trigonal sites 22 p3961 A66-39916
- Jahn-Teller shift reorientation in Ni impurity centers of diamond and rise of C-N pair EPR spectrum with temperature 22 p3964 A66-40307
- Optical charge exchange in silicon carbide analyzed, using electron paramagnetic resonance 22 p3964 A66-40311
- EPR spectroscopic analysis of liquid oxygen difluoride, noting photolytic dissociation into paramagnetic species 23 p4097 A66-41237
- Electron paramagnetic resonance and Hall effect measurements to determine properties of dominant paramagnetic defect in electron irradiated p-type silicon 24 p4250 A66-42230
- ELECTRON-PHONON INTERACTION**
- Electron-phonon interaction proportional to applied external electric field and sound amplification in semiconductors 01 p0118 A66-10259
- Stochastic aspects of low mobility theory applied to electrical conductivity problem in Wannier representation 01 p0106 A66-10723
- Electromagnetic field absorption by electrons of semiconductor situated in quantizing magnetic field 01 p0123 A66-10725
- Operator for electron interaction with optical phonons, noting spin-lattice relaxation and additional magnetophonic oscillations of kinetic coefficients for semiconductors 01 p0124 A66-10767
- Phonon field effect on plasma frequency of dense electron gas for nonzero temperatures 02 p0267 A66-11708
- Indirect optical transitions in semiconductors due to photons and impurities, noting absorption and emission of photons, avalanche and long wavelength radiation 02 p0273 A66-11714
- Sudden heat capacity change near electron-phonon system transition point from superconducting to normal state 02 p0277 A66-12080
- Phonon interaction with iron group ions characterized by coupling constant discussing double quantum detection of phonon, propagation in dispersive medium and phonon maser 03 p0376 A66-12420
- Acoustic-mode scattering theory obtained with tight-binding approximation of band theory and applied to narrow-band semiconduction in organic molecular crystals 04 p0560 A66-13721
- Interaction of conduction electrons with lattice vibrations in semiconductor produces additional transmission bands or disappearance of resonance absorption region 04 p0564 A66-14251
- Components of relaxation tensors associated with thermal and spontaneous phonon scattering in semiconductors 04 p0564 A66-14254
- Temperature dependence of effective mass and influence of two-phonon processes on mobility in semiconductors with narrow forbidden bands 04 p0565 A66-14263
- Pseudopotential method for determining temperature-dependent electric resistance of lithium, neglecting free electron approximation and examining electron-phonon interaction 04 p0566 A66-14316
- Electron-phonon interaction for calculation of critical temperature for ordinary and anomalous superconductors 04 p0568 A66-14347
- Electrical conductivity of polar semiconductors in electric fields, calculating lattice and Coulomb electron scattering mechanism by kinetic equation method 04 p0568 A66-14350
- Transport coefficients of n-indium arsenide to calculate electron concentration, mobility and three-band scattering mechanism 04 p0570 A66-14481
- Interaction of charge carriers with acoustic waves by deformation potential in semiconductors 05 p0732 A66-14669
- Emitter-collector current transfer ratio of electron optical phonon scattering in metal semiconductor structures 05 p0732 A66-14670
- Low temperature thermal conductivity of 2-mev electron-irradiated and annealed single-crystal silicon 05 p0741 A66-15868
- Electrically active impurities effect on germanium thermal resistivity at low temperatures measured on n-type single crystals 05 p0742 A66-15875
- Matrix elements of electron-phonon interaction and electric resistance in nickel, using electronic structure of Fermi surfaces and phonon spectrum 06 p0894 A66-16175
- Electron-phonon interaction in semiconductors, explaining electron diffusion in solid in terms of effect of electron-phonon coupling 07 p1098 A66-17824
- Superconducting transition temperatures of Cd-Hg alloys covering complete composition range, considering effect of ordering 07 p1109 A66-18444
- Thermodynamic behavior of strong coupling superconductors, with complex energy gap function and renormalization parameter for lead and mercury 09 p1423 A66-20072
- Relation of thermodynamic parameters to energy gap of superconducting elements and alloys 09 p1424 A66-20074
- Low temperature study of resistivity and thermoelectric power variations of silver-palladium alloys as function of concentration, caused by electron diffusion 09 p1425 A66-20079
- Phonon drag in p-GaAs, graphing temperature dependence of thermoelectric power 09 p1426 A66-20196
- Spin-magnetophonon interaction effect on light absorption in semiconductor 09 p1426 A66-20199
- Resonance carrier scattering and spin-magnetophonon interaction effect on semiconductor magnetic susceptibility 09 p1427 A66-20200
- Volt-ampere and current carrier mobility characteristics of semiconductors with electron-phonon bonds proportional to applied field 10 p1582 A66-21968
- Coherent excitation of optical phonons in polar semiconductors developed, using Boltzmann equations 10 p1584 A66-22071
- Hall effect in alloyed crystals of n-type indium antimonide 10 p1589 A66-22165
- Operator for electron interaction with optical phonons, noting spin-lattice relaxation and additional magnetophonic oscillations of kinetic coefficients for semiconductors 11 p1748 A66-22278
- Electron-phonon coupling in piezoelectric semiconductors, obtaining electric field and current density vectors for application to ultrasonic amplification 11 p1750 A66-22401
- Negative conductivity, induced by nonequilibrium state in semiconductors, due to short electron lifetime in conduction band 13 p2160 A66-25101
- Hot-electron transistors, discussing application of Schottky-emitter transistor to VHF operation 13 p2038 A66-25561
- Electron-phonon interaction proportional to applied external electric field and sound amplification in semiconductors 13 p2168 A66-25976
- Temperature variation and carrier concentration effects on density-of-states effective mass, polar and dipolar thermoconductivity, electron and phonon scattering and electron-phonon interaction in doped Si-Ge alloys 14 p2365 A66-27759
- Electron-phonon interaction for calculation of critical temperature for ordinary and anomalous superconductors 14 p2368 A66-28243
- Electrical conductivity of polar semiconductors in electric fields, calculating lattice and Coulomb electron scattering mechanism by kinetic equation method 14 p2368 A66-28247



Strong electron-phonon interaction which couples electron to lattice motion in F center of alkali halide crystal by measuring temperature dependence of F center absorption and emission bands 15 p2559 A66-28629

Light dispersion and absorption by impurity centers in solids calculated via two-particle Green function method, assuming weak electron-phonon interaction 15 p2559 A66-28632

Phonon spectrum of lead indium alloys noting distinctness of impurity band as inferred from electron tunneling measurements 16 p2768 A66-30130

Scattering of light from pulsed ruby laser by plasma jet, noting cross section, electron-phonon interaction, etc 16 p2716 A66-30139

Negative conductivity, induced by nonequilibrium state in semiconductors, due to short electron lifetime in conduction band 16 p2771 A66-30280

Thermoelectric power in niobium-zirconium alloys noting phonon drag peak attenuation due to Zr solute addition at very low temperatures 16 p2780 A66-31156

Electron vibration spectra of light absorption in molecular crystals, taking oscillation frequency changes as principal mechanism of exciton-phonon interaction 16 p2780 A66-31178

Hot electrons in anisotropic semiconductor, considering case of scattering by acoustic phonons within one energy valley with nondegenerate bottom 17 p2977 A66-32318

Semiconductor photoconductivity dependence on external radiation frequency, examining electron-phonon interaction 18 p3158 A66-34689

Ionization chamber to investigate distribution of energy portion transferred to photons by nuclear active particles colliding with atomic nuclei of C, Fe and Pb 18 p3215 A66-35157

Electron-phonon interaction current density, thermodynamic Green function and other electromagnetic properties of superconductors, using Froehlich-Hamilton model 19 p3438 A66-35481

Hall effect in alloyed crystals of n-type indium antimonide 19 p3441 A66-35779

Electron-phonon interaction phenomena observed in GaAs and CdS, examining current saturation, ultrasonic emission by charge carriers and acoustic amplification 19 p3445 A66-36256

Coupling between plasmons and polar phonons in degenerate semiconductor gallium antimonide analyzed, starting from electron-phonon Hamiltonian 19 p3447 A66-36400

Superconducting transition temperature of thin film, showing growth of temperature and decrease in film thickness due to phonon electron interaction 20 p3616 A66-37378

Thermal conductivity of lanthanum and monochalcogenides, noting role and temperature dependence of crystal-lattice conductivity 20 p3617 A66-37556

Ginzburg-Landau equations for local superconductors in magnetic field starting from equations of coupled electron-phonon system with treatment restricted to temperatures near critical temperature 20 p3619 A66-37641

Electromagnetic field absorption by electrons of semiconductor situated in quantizing magnetic field 20 p3619 A66-37662

Extension of pairing theory of superconductivity to electron-phonon coupling, applying Landau quasi-particle approximation 21 p3796 A66-38552

N-type Ge hot carrier Hall mobility, magnetoresistance, Maxwellian energy distribution, electron-electron and intervalley electron-phonon collisions 21 p3801 A66-38997

HF long wavelength conductivities of solid state plasmas in thermal equilibrium derived, using variational formalism 21 p3791 A66-39106

Ferromagnetic spin correlations from strong Coulomb interactions between valence electrons resulting in enhanced singlet-state repulsion 21 p3803 A66-39263

Volt-ampere and current carrier mobility characteristics of semiconductors with

electron-phonon bonds proportional to applied field 21 p3805 A66-39547

Electron attenuation of ultrasonic waves of arbitrary polarization and propagation direction for superconductors computed on BCS model, noting role of Fermi surface 22 p3960 A66-39802

Superconductivity applications in power engineering, examining properties of superconducting materials such as thin films, wires and ribbons made of ductile and brittle alloys 23 p4114 A66-41741

Electron self-energies in Fermi gas arising from coupling to optical and acoustic phonons 24 p4250 A66-42231

Light emission in near IR by semiconducting GaAs under current oscillations caused by electron-phonon coupling 24 p4258 A66-43000

### ELECTRON PHOTOGRAPHY

Silicon p-n junction analysis using electron photographic developers when space charge region is present 04 p0563 A66-13881

Silicon p-n junction analysis using electron photographic developers when space charge region is present 14 p2363 A66-27579

### ELECTRON PHOTON CASCADE

Angular distribution of secondary particles from interactions in nuclear emulsions, determining energy release ratio in electron photon cascade 07 p1113 A66-17541

Passage of high energy electrons and photons through condensed media such as photographic emulsion in cascade theory and method of moments 07 p1116 A66-17558

Angular moments of lateral-angular distribution functions in electromagnetic cascade theory calculated by method of moments 07 p1116 A66-17561

Energy distribution of particles produced in elementary interaction expressed in terms of shower characteristics derived from cascade theory 07 p1116 A66-17562

Fluctuations in number of particles in electromagnetic cascade and effect on spectrum of ionization bursts produced by mu mesons 07 p1117 A66-17568

Muon detection and energy determination in multilayer system of ionization chambers and probability of finding muon in n-electron shower at depth 07 p1117 A66-17569

Ultrahigh-energy primary cosmic ray particle interactions cause electron photon cascades and muon emission 07 p1117 A66-17570

Electron-photon, mu-meson and nuclear-active components of extensive air showers 07 p1117 A66-17571

Extensive air shower high energy gamma rays in upper third of atmosphere 07 p1118 A66-17573

Energy and density spectra of X-ray photons in extensive air showers and in stratosphere 07 p1118 A66-17574

Fluctuation problem in electromagnetic cascade theory analyzed, using invariant imbedding method 07 p1083 A66-17973

Monte Carlo method analysis of electron photon cascade 09 p1436 A66-20134

Primary cosmic ray energy spectrum, including primary flux of protons and heavier nuclei, and EM cascade pair production rates 11 p1765 A66-23192

Ionization calorimeter for measuring primary cosmic ray components, discussing nuclear interactions, energy spectra, EM cascades, etc 13 p2175 A66-26011

Young air electron-photon showers at 3200 m altitude, noting average nucleon energy and inelasticity coefficient 15 p2583 A66-29552

Electron-photon cascades caused by nuclear active component in atmosphere and on gamma rays, atmospheric absorption spectrum of primary nucleons and generation of pions 15 p2584 A66-29556

Cascade theory of cosmic ray showers 15 p2586 A66-29567

Particle number fluctuation in electron-photon shower, influence on spectrum of bursts produced by high energy mu mesons under thick filters 15 p2589 A66-29585

Delta-electron generation by muons and fluctuations in soft cosmic ray component, assuming thick absorption layer 15 p2547 A66-29598

Neon hodoscope study of energy and

production heights of high energy EAS electron-photon cascades, comparing results to nuclear emulsion study findings 18 p3207 A66-35109

Response to EAS electron-photon cascade of plastic scintillator, cloud chamber and Geiger counter tray 18 p3208 A66-35112

Compared Cerenkov and scintillation counters responses to electron-photon EAS 18 p3208 A66-35113

Photoproduction, lateral density distribution, energy spectrum and muon component fluctuations in electron photon cascades 18 p3208 A66-35114

Barometric effect and density spectrum of photon-initiated EAS 18 p3208 A66-35115

Muons Component composition and photonuclear interactions of photon-initiated EAS 18 p3209 A66-35121

Extensive air showers with fixed muon number and fixed electron number studied, emphasizing correlation between cascade parameter and other EAS characteristics 18 p3212 A66-35138

Mean square angular and lateral spreads of electrons and photons in cascade shower calculated over wide ranges of finite energy and observation points 18 p3213 A66-35142

Inverse problem in cascade theory of showers to derive information about nuclear interaction 18 p3213 A66-35144

One-dimensional cascade theory of photon-electron showers for light and heavy substances, taking into account polarization of medium upon cross section for electron bremsstrahlung 18 p3213 A66-35145

Bremsstrahlung and pair production processes as regarded in cascade theory of showers 18 p3213 A66-35146

Nuclear cascade particles ionization at various depths in iron compared with experimental data in ionization calorimeter 18 p3214 A66-35154

Energy spectra of electromagnetic cascades produced by cosmic rays observed at balloon altitudes, using composite detector 18 p3216 A66-35169

Electron-photon cascade showers recorded with ionization calorimeter, determining influence of value of radiation length on form of mean cascade curve 18 p3221 A66-35198

Counting rate statistics and energy levels of optical photons in electron photon cascade in cooled mercury atoms 22 p3951 A66-40893

Inelasticity in carbon particle nuclei interactions evaluated by variation with depth of energy of electron photon shower in thick absorber 24 p4268 A66-42910

Ratio of energy flux in nuclear active component to energy flux in electron photon component in extensive air showers with given numbers of particles 24 p4269 A66-42918

Equilibrium spectrum of photons from primary electron at photon energies close to primary energy 24 p4269 A66-42921

Ionization calorimeter measurement of number of particles in electron photon cascade with energy transferred from ionization calorimeter 24 p4269 A66-42924

Calculation of rms numbers of particles in three-dimensional theory of electron-photon showers, considering scattering 24 p4270 A66-42928

Asymptotic approximation of distribution of small ionization bursts produced by high energy muon under thick layer of matter in direct electron-pair production 24 p4271 A66-42935

### ELECTRON PLASMA

Nonlinear kinetic equation of self-similar motion of rarefied collisionless electron-ion plasma 01 p0109 A66-10260

Shear instability of spatially dependent electron current flowing in plasma 01 p0110 A66-10325

Self-field electron kinetic reaction to electromagnetic propagation in three-fluid Brownian plasma 01 p0110 A66-10335

Permittivity of dielectric formed from ground state instability of semimetal, considering Coulomb attraction between electrons and holes 01 p0125 A66-10774

Nonlinear scattering effect of Langmuir



- oscillations on electrons of plasma located in strong magnetic field 01 p0115 A66-11055
- Electron distribution function of homogeneous Lorentzian plasma calculated by successive approximation 01 p0115 A66-11077
- X-ray spectrum of plasma electrons after passage through plane layers of obstacle immersed in plasma, setting up equations for electron energy and density 03 p0397 A66-12392
- Longitudinal nonlinear traveling oscillations in hot electron plasma 03 p0401 A66-12956
- Collisionless electron plasma in uniform field possessing unperturbed distribution function for electrons not considered isotropic in plane of velocity 03 p0401 A66-12963
- Kinetic theory of unstable plasma covering growth and stabilization of spatially homogeneous electron plasma in uniform neutralizing positive charge field, Pines-Schrieffer and formally equivalent kinetic equations and Balescu 03 p0406 A66-13359
- Scattering of test particle by enhanced electric field fluctuations in plasma containing nonthermal electrons 05 p0721 A66-14713
- Temperature and electron concentration in argon and nitrogen arc plasmas by photometering plasma cross sections and comparing with reference 05 p0729 A66-15855
- Interaction between circular waves and density fluctuation in cold electron plasma filling waveguide leads to formation of overtones of HF and LF 06 p0918 A66-16869
- Charge balance in plasma formed by passage of electron beam through gas in presence of constant magnetic field 06 p0918 A66-16870
- Computer simulation of randomization of electrons in collisionless plasma 08 p1260 A66-18538
- LF electromagnetic wave excitation in electron-ion and electron-hole plasmas situated in external electrical field 08 p1262 A66-18975
- Diffraction of plane electromagnetic wave by cylinder of inhomogeneous plasma calculated by method that considers plasma as electron dipoles 09 p1406 A66-19843
- Radiation resistance of linear current strip of finite width immersed in uniaxially anisotropic plasma 09 p1408 A66-20370
- Diffusion of light by plasma electrons produced in laboratory for very small effective diffusion area 10 p1566 A66-21712
- Quasi-linear current instability in two-temperature plasma for Coulomb collision and free electron acceleration 10 p1569 A66-21972
- Permittivity of dielectric formed from ground state instability of semimetal, considering Coulomb attraction between electrons and holes 11 p1749 A66-22286
- Generation of echo at cyclotron resonance in plasma provides means of measuring and displaying relaxation 11 p1748 A66-23393
- Feasibility of using Langmuir probe for measuring statistical properties of unsteady or turbulent electron-rich plasmas [AIAA PAPER 65-544] 12 p1919 A66-23580
- Linear spatial response of electron plasma to localized one-dimensional electric field, whose frequency is low compared with electron-collision frequency 12 p1923 A66-24575
- X-ray spectrum of plasma electrons after passage through plane layers of obstacle immersed in plasma, setting up equations for electron energy and density 13 p2139 A66-25398
- Nonlinear kinetic equation of self-similar motion of rarefied collisionless electron-ion plasma 13 p2148 A66-25977
- Random phase approximation of electron conductivity of turbulent plasma and effects of random static inhomogeneities 13 p2149 A66-26245
- Transport equation for classical unstable electron plasma extended to quantum mechanical multicomponent case, rewriting kinetic equation 13 p2155 A66-26674
- Emergence point of conical microwave beam transmission through nonuniform electron plasma 14 p2234 A66-26860
- Electromagnetic and plasma wave propagation in inhomogeneous compressible isotropic collisionless electron plasma bounded by closed surface in free space 15 p2449 A66-28592
- Excited electron plasma nonlinear oscillations, beam-plasma interaction, Langmuir probe measurement of frequency and density, amplification of superimposed RF electric field, etc 15 p2552 A66-29400
- Electron-cyclotron-heated plasma stability in mirror containment systems possessing shear, minimum-B properties or both 15 p2555 A66-29760
- Effective capture of electrons in magnetic mirror trap with stationary field by pulse-type injection of helical electron beam 16 p2755 A66-30093
- Distribution of charged particles of different energies escaping from magnetic trap in which spiral moving electron fluxes are created 16 p2755 A66-30094
- Radiation belt origin, examining acceleration of solar plasma electrons to energies of 30 to 100 kev by nonlinear waves called solitons 16 p2792 A66-30156
- Excitation of longitudinal electron plasma oscillations by nonlinear resonance of two TEM waves with frequencies differing by plasma frequency 16 p2757 A66-30195
- Transverse electromagnetic wave transformation into ion-acoustic plasma oscillations with formation of intermediate Langmuir electron wave 17 p2969 A66-32542
- Strong injection in nondegenerated p-n junction producing electron-hole plasma in n region near junction 17 p2986 A66-33307
- Coupled electromagnetic and electroacoustic wave propagation in inhomogeneous compressible plasma 18 p3069 A66-34089
- Electron wave resonances in bounded plasmas, examining application to average plasma density measurement 18 p3145 A66-34113
- RF electron plasma diagnostics in magnetic field 18 p3148 A66-34730
- Oscillations of inhomogeneous weakly ionized plasma situated in external electric and magnetic field, noting causes and conditions of plasma instability 18 p3151 A66-35066
- Collision damping of transverse electron plasma oscillations 19 p3408 A66-36273
- Verification of Landau theory that longitudinal electron waves in plasma of finite temperature are damped even in absence of collisions 19 p3416 A66-36522
- Microinstability due to non-Maxwellian velocity distribution in hot electron plasma within magnetic mirror configuration 19 p3422 A66-36545
- Energetic neutral hydrogen atom injection into ECP in magnetic mirror and plasma shielding against trapped thermal neutral gas 19 p3422 A66-36547
- Plasma confinement experiments with electron injection parallel to cusped magnetic field axis in nonadiabatic regime 19 p3422 A66-36549
- Motion of plasma stream injected transverse to magnetic field, examining stream action as it crosses region where magnetic field lines reverse direction about field null line 19 p3426 A66-36568
- Beam-plasma interaction used to generate fully ionized plasma and enhance component temperature for study of plasma heating and burnout 19 p3429 A66-36585
- Temperature effect on dispersion and damping of electron plasma wave 19 p3432 A66-36762
- Simplified model of relation between electron concentration and ionization rate in steady-state inert gas discharge column leading to contraction of column 20 p3608 A66-37464
- Chemical kinetics of electron plasma reactions, discussing energy states, ion-molecule reactions, charge transfer, transport properties, phase interactions, etc 21 p3702 A66-38448
- Relativistic electron layer formation by injecting electrons into cylindrical region of Astron, using difference methods in integrating Vlasov-Maxwell equations 21 p3793 A66-39470
- Quasi-linear current instability in two-temperature plasma for Coulomb collision and free electron acceleration 21 p3794 A66-39551
- Landau damping of longitudinal electron plasma waves in finite-diameter uniform-density cylindrical plasma, assuming Maxwellian velocity distribution 22 p3955 A66-40104
- Instabilities resulting in loss of energetic electrons and fast electrons analyzed in electron cyclotron plasma confined by magnetic mirrors 23 p4103 A66-41490
- Impedance of flat strip antenna embedded in planar dielectric slab surrounded by layers of compressible isotropic electron plasma 23 p4047 A66-41639
- Thermodynamic properties of electron plasma investigated by Bogoliubov-Born-Green-Kirkwood-Yvon hierarchy equation, calculating correlation energy 24 p4243 A66-42764
- ### ELECTRON PRECIPITATION
- Particle precipitation measurements with Injun satellites, discussing space and time variations of electron precipitation, trapped Van Allen particles and auroral light emission latitude 03 p0363 A66-12648
- Relativistic electron precipitation into mesosphere at subauroral latitudes and observations of solar proton and absorption event 05 p0747 A66-14785
- Auroral phenomena in integral-invariant coordinate system, discussing pole-centered circular nature of isochasms in geomagnetic dipole coordinates 06 p0876 A66-16280
- Limit on stably trapped particle fluxes determined theoretically and compared with data from Explorer satellites 08 p1184 A66-19391
- Mechanism of electron leakage from outer radiation belt and X-ray bursts in stratosphere 09 p1446 A66-21037
- Energy spectrum of auroral zone X-rays, noting electron precipitation and diurnal pattern for occurrence of bremsstrahlung 10 p1599 A66-21145
- Energy spectrum for auroral zone X-rays, measuring simultaneously bremsstrahlung X-rays and ionospheric absorption 10 p1599 A66-21146
- Localization and motion of energetic electron precipitation regions during negative magnetic bays, noting similarity of motion to that of auroral electrojets 10 p1599 A66-21147
- VHF hiss zone morphology and correlation with particle precipitation events, from Alouette I satellite observations 11 p1700 A66-23136
- Rocketborne measurements of electron precipitation and relative brightness of ionized molecular nitrogen ion and atomic oxygen auroral emissions 11 p1764 A66-23139
- Simultaneous observations of auroral zone X-ray microbursts, using two balloon-borne radiation detectors separated by 300 km to estimate size of region of electron precipitation 12 p1944 A66-24841
- Electron precipitation onto electrodes of quadrupole amplifier and resultant impairment of output current and efficiency 13 p2043 A66-26468
- Electron precipitation in auroral zone, using observations from riometer, balloon, rocket and satellite experiments 17 p2917 A66-32363
- Precipitation flux of quasi-trapped energetic electrons near low altitude fringes of inner radiation belt as they drift into South Atlantic magnetic anomaly 18 p3170 A66-34520
- Electron precipitation in auroral zones caused by magnetospheric instability 20 p3609 A66-37820
- Method for calculating longitude dependence of geomagnetically trapped electrons at low altitude, based of scattering and energy loss due to atmospheric interactions 20 p3640 A66-38324
- Atmospheric electric field change compensation during measuring air-Earth ionic conduction and electron precipitation current densities 22 p3920 A66-40804
- Variation in energy of energetic electron precipitating into atmosphere as function of



initial energy, pitch, angle and altitude, neglecting scattering 24 p4262 A66-42463

Auroral zone microbursts associated with geomagnetic storms, negative magnetic bays and electron precipitation observed by balloon and rocket 24 p4201 A66-42600

**ELECTRON PRESSURE**

Free-free absorption coefficient of electrons in field of neutral carbon atoms calculated per unit electron pressure per carbon atom in static central field exchange approximation 18 p3233 A66-34574

**ELECTRON PROBE**

Satellite probe measurements of irregularities of electron density distribution above F-2 layer in polar region 03 p0363 A66-12642

Scanning electron beam probe for investigating nonuniformity in work function of surfaces known as patch effect 05 p0684 A66-15580

In situ probe measuring nonthermal components of electron energy distribution in ionosphere, small-scale ionization inhomogeneities and negative ion concentrations in lower ionosphere 08 p1223 A66-18745

Liquid titanium reaction with nonmetallic refractory ceramics, Ti melting behavior and electron-probe microstructural analysis 08 p1236 A66-18759

Hot wire electron emissive probes for potential measurements in quiescent plasmas, noting plasma densities, emission levels, etc 13 p2154 A66-26554

Tellurium concentration in doped GaAs correlated by electron probe microanalysis with variations in cathodoluminescence efficiency 15 p2564 A66-28878

Electron saturation current at plane probe in magnetized plasma, considering electron temperature 15 p2554 A66-29753

Spherules from Atlantic Ocean sediments studied by electron microprobe, noting terrestrial alteration and contamination of surfaces 16 p2803 A66-31222

Electron microprobe for studying thermoelectric materials and heat-resistant steel for gas-turbine blading 24 p4211 A66-42507

**ELECTRON RADIATION**

Solar flares, discussing continuous electromagnetic radiation, hard X-ray radiation and microwave radio bursts 05 p0752 A66-15378

Electric power of thermionic converters, discussing electron space charge effects and relation to gas converters 05 p0615 A66-15534

Secular conductivity changes in p-type germanium of both high and intermediate purity indicate defect annealing resulting from electron irradiation 06 p0932 A66-17116

Impurity concentration effect of electron irradiation damage in photovoltaic silicon cell with shallow p-n junction 06 p0938 A66-17145

Characteristics and properties of defects induced in silicon and germanium by 10-to 60-mev electrons and 20-to 130-mev protons 06 p0939 A66-17155

Neutron and electron irradiation damage in uniform silicon avalanche junction diode and effect on avalanche pulse rate 07 p1012 A66-18410

Radiation effects on electronic components noting sensitivity to gamma, fast neutron and electron radiation 09 p1359 A66-20969

Optical properties and thermal behavior of new absorption bands in oxygen doped silicon irradiated at low temperatures 15 p2564 A66-28874

Transmittance of optical materials between 1050 and 3000 angstroms, noting effect of simulated high energy space environment 17 p2979 A66-32615

**ELECTRON RECOMBINATION**

Dielectronic recombination for low density plasma, estimating coefficient and ionization balance for iron and calcium ions in corona 02 p0286 A66-11357

Resonance lines of coronal ions of silicon appearing in two widely separated spectral regions 02 p0286 A66-11358

Electron recombination in monoatomic ionized gas expanding symmetrically into vacuum, particularly triple collisions with electron capture on upper atomic

level 02 p0264 A66-11383

Recombination coefficient and electron production rate in lower D region during solar flare 04 p0574 A66-13444

Recombination parameters in CdS determined from kinetics and IR quenching of photocurrent relative to available illumination 04 p0564 A66-14257

Auger recombination of majority and minority carriers by low and deep-lying centers 04 p0565 A66-14261

Recombination process of electron-hole pairs in germanium irradiated with cobalt 60 gamma rays, using photovoltaic effect in p-n junctions 06 p0938 A66-17146

Distribution function of semiconductor minority current carriers in presence of pronounced spatial inhomogeneity occurring in intensively absorbing films with intensive surface recombination 07 p1099 A66-17873

Hot electron recombination peculiarities, ignoring electron temperature concept, for moderate fields and lattice temperatures 07 p1104 A66-18220

Stationary IR quenching of photocurrent in CdS, discussing recombination channels 09 p1428 A66-20538

Dielectronic recombination for low density plasma, estimating coefficient and ionization balance for iron and calcium ions in corona 10 p1602 A66-21088

Resonance lines of coronal ions of silicon appearing in two widely separated spectral regions 10 p1602 A66-21092

Cascade theory of electron recombination into ionized donors in germanium analyzed, noting several models 12 p1928 A66-23940

Electrical and gas dynamical parameters effect on length of linear constant Mach number MHD duct, assuming gas is ionized by neutron irradiation in expansion nozzle preceding duct and electron recombination takes place in duct 13 p2000 A66-25739

Optical emission from ruby induced by short pulses of relativistic electrons in which electron-hole recombination produces excitation of emission 13 p2098 A66-26173

Hot electron recombination at repulse impurity centers in germanium containing copper 14 p2357 A66-27074

Recombination radiation in semiconductor affected by strong magnetic field 14 p2363 A66-27597

Recombination rate of electron-hole pairs in anthracene determined and compared with theoretical value based on hypothesis of Coulomb capture in dielectric 14 p2369 A66-28272

Recombination centers in gamma irradiated silicon either float-zoned or melt-pulled and doped with phosphorus, arsenic or boron 15 p2562 A66-28721

Electron-hole recombination effect on semiconductor reflectivity modulation study with ruby laser 15 p2563 A66-28757

Volume recombination in transistor base for arbitrary concentrations of minority charge carriers 15 p2468 A66-29921

Formation of sporadic E layer in middle latitudes due to transport phenomenon and local production 19 p3346 A66-35589

Recombination by tunneling in electroluminescent diodes to obtain line shape and light intensity in peak shift region 21 p3801 A66-38998

Impurity conduction effect on electron donor recombination cross section in n-type germanium and silicon at liquid helium temperatures 21 p3801 A66-39001

Varying excitation intensity effects on edge emissions from pure and doped CdS powder samples, noting electron-hole recombination mechanisms 21 p3802 A66-39202

Gold doping effects on recovery time of phosphorus, boron and arsenic impurity gaseous-diffused junction diodes and estimated gold recombination center densities 22 p3873 A66-39749

Measures of electron production and loss and scale height of F-1 layer during summer solar minimum 22 p3916 A66-40808

Hot electron recombination at repulse impurity centers in germanium containing copper 22 p3966 A66-40832

Electron and neutral atom densities in helium and argon afterglow plasma obtained

by two helium-neon laser interferometers, noting temporal dependence of electron decay 23 p4101 A66-41364

Single crystal wurtzite CdS luminescence as function of exciting intensity, noting shift of overlapping band structure of green-edge emission indicative of electron-hole recombination 24 p4219 A66-42250

Generation-recombination noise and lifetime measured using photoconductive decay in n-and p-type Ge samples doped with shallow impurities 24 p4253 A66-42357

Recombination radiation in semiconductor affected by strong magnetic field 24 p4257 A66-42731

**ELECTRON SCATTERING**

Multiple scattering of medium velocity electrons in thin films of Ni, Ge, Ag and Au 01 p0116 A66-10196

Polarization and exchange effects in slow electron scattering from lithium and sodium 03 p0393 A66-12325

Phase-shift analysis of electron and hole optical scattering by high density of ionized acceptors, calculation appropriate to direct band-gap semiconductor 03 p0411 A66-13146

Oscillator strength of ruby R-1 line at liquid nitrogen temperature determined by Rozhdestvenskii hook 03 p0379 A66-13189

Resonances below inelastic threshold of electron hydrogen scattering using Feshbach projection-operator technique, converting to eigenvalue problem for projected Hamiltonian 04 p0547 A66-13711

Parameters associated with inelastic polar electron scattering in indium antimonide 04 p0565 A66-14267

Electrical conductivity of polar semiconductors in electric fields, calculating lattice and Coulomb electron scattering mechanism by kinetic equation method 04 p0568 A66-14350

Emitter-collector current transfer ratio of electron optical phonon scattering in metal semiconductor structures 05 p0732 A66-14670

Thermal diffuse elastic electron scattering in polycrystalline Al foil, using retarding field apparatus 05 p0736 A66-14980

Current-carrier scattering effect on electric and photoelectromagnetic properties of semiconductors in variable magnetic field 06 p0922 A66-16134

Electron drift velocity and mobility of indium antimonide obtained from pulsed measurements of conductivity and Hall effect at various temperatures 06 p0922 A66-16173

Conductivity and transfer coefficients calculated from electron scattering in cesium plasma 06 p0918 A66-16836

Electron distribution disruption by electric current across n-n heterojunction resulting in heating and cooling of respective electron gases in each of semiconductors, noting electron scattering 07 p1104 A66-18362

Galvanomagnetic effects in semiconductors, including Hall effect and magnetoresistivity, noting influence of carrier scattering on lattice vibrations and impurities 08 p1267 A66-18607

Zone behind reflected shock wave in shock tube using electron beam scattering, showing flow spectra and attenuation region of wave 08 p1210 A66-19586

Microscopic theory of electroacoustic effect for n-type Ge and Si semiconductors of many energy minima, noting electron scattering 09 p1412 A66-19986

Forced Mandelstam-Brillouin scattering in gases, determining hypersonic velocity for three gases 09 p1408 A66-20770

Superconductor current acceleration by application of long-wavelength magnetic field below critical temperature 10 p1573 A66-21176

Boltzmann equation for Gunn effect in GaAs, discussing scattering processes, unjustifiability of use of drifted Maxwell distribution, etc 10 p1583 A66-22067

Measurement of shift of cesium absorption lines near series edge, obtaining electron elastic scattering cross section at zero energy by extrapolation of shift 12 p1918 A66-24882

Electron scattering responsible for variable polarization in V444 Cygni 13 p2184 A66-25624



Scattering of electron beam by standing waves of photons inside laser cavity corresponds to stimulated Compton effect 13 p2096 A66-26155

Excitation in electron beam pumped /EBP/ GaAs lasers including electron scattering, energy dissipation pattern, phonon emission, air production, etc 13 p2099 A66-26181

Nearly monoenergetic electrons in collimated beam directed at normal incidence onto thick targets ranging in atomic number from Be to 13 p2136 A66-26279

Effective-mass approximation of conduction electron scattering in very thin films 14 p2360 A66-27192

Forced Mandelstam-Brillouin scattering in gases, determining hypersonic velocity for three gases 14 p2341 A66-27305

Temperature variation and carrier concentration effects on density-of-states effective mass, polar and dipolar thermoconductivity, electron and phonon scattering and electron-phonon interaction in doped Si-Ge alloys 14 p2365 A66-27759

Elastic electron scattering cross sections for titanium relative to C and Be measured, using linear electron 14 p2337 A66-27795

Energy dependence of elastic resonance scattering of low energy electrons from He, Ne, Ar and nitrogen gases at angles ranging from 8 to 110 degrees 14 p2337 A66-27797

Electrical conductivity of polar semiconductors in electric fields, calculating lattice and Coulomb electron scattering mechanism by kinetic equation method 14 p2368 A66-28247

Impurity scattering in theory of interband magneto-optical effects, noting inadequacy of first-order perturbation treatment and low and high impurity-atom concentration with weak interaction 15 p2558 A66-28610

Transmission energy spectra of 1-mev electrons with normal incidence on Al slabs measured in terms of transmission angle 15 p2543 A66-28715

Pressure effect on transition point of superconductors from Bardeen-Cooper-Schrieffer theory, perturbation theory and electron scattering near Fermi surface 15 p2568 A66-29714

Total and differential scattering cross section for slow electron calculation, using nonrelativistic quantum mechanics, shown to be erroneous 16 p2751 A66-30172

Intervalley scattering in III-V semiconductors, noting relation to Gunn effect, scattering in GaAs by longitudinal optic phonons, in InP by longitudinal acoustic phonons 16 p2776 A66-30733

Electrical conductivity of metals, explaining electron scattering amplitude changes, phonon spectrum distortion and temperature effects caused by impurity concentration in 16 p2780 A66-31180

Temperature structure of early type stellar atmospheres noting sources of opacity, electron Rayleigh scattering, etc 16 p2806 A66-31703

Secondary electron interaction with solid state plasma, noting energy distribution, Boltzmann equation solution, etc 16 p2789 A66-31783

Magnetospheric suprathermal-electron scattering in oscillating electrostatic plasma and diffusion of subthermal electrons across magnetosphere, using ion-wave propagation theory for electroconductive plasmas 17 p2993 A66-32521

Electron scattering interpretation of ionization, emission and absorption line spectra of quasi-stellar object 17 p3004 A66-32928

Electron angular distribution in copper and gold thin films attributed to individual close interaction scattering phenomena 17 p2987 A66-33314

Relativistic vs nonrelativistic scattering of slow electrons by neutral heavy atoms 18 p3137 A66-33668

Slow electron scattering on dipolar symmetrical top molecules and quadrupolar linear molecules calculated at energies below threshold for vibrational excitation 18 p3139 A66-34510

Plasma half-space impedance for diffusive

electron reflection from plasma vacuum boundary, noting damping decrement of surface electromagnetic wave, electric field Fourier components and absorption capacity 18 p3151 A66-35065

Detection of solar neutrinos for analysis of solar structure, using various detector types and recoil electrons in neutrino-electron elastic scattering process 18 p3223 A66-35214

Evaluation of predicted effect of elastic solar neutrino scattering on electrons of medium, using graph 18 p3223 A66-35215

Solution of Schroedinger equation for quantum mechanical reflection coefficient of electrons at metal semiconductor barriers 19 p3435 A66-35409

Electron scattering by impurities in dipole form in semiconductors with anisotropic effective mass of current carriers, deriving formula for tensor of relaxation time 19 p3442 A66-35818

Transitions induced by electron impact between all ground-state terms of atomic systems with computed cross sections satisfying unitarity 19 p3463 A66-35990

Phase shifts of elastic electron scattering from neutral helium, considering atomic distortion in adiabatic approximation 19 p3402 A66-35991

Electron scattering in ABO-type semiconductors by long-wave transverse-optical ferroelectric lattice mode evidenced by hydrostatic pressure measurements 19 p3444 A66-36176

Dipole scattering of electrons in germanium and silicon whose conduction-band structure is described by many-valley model, using distribution function and computing relaxation-time ratio 19 p3446 A66-36393

Thermal conductivity of lanthanum and monochalcogenides, noting role and temperature dependence of crystal-lattice conductivity 20 p3617 A66-37556

Cyclotron resonance observation of electron scattering by Ga and In atoms in Ge 21 p3797 A66-38754

Electron scattering mechanism in compensated gallium arsenide determined from Hall effect, Nernst-Ettingshausen effect and reluctance 21 p3798 A66-38914

Domain formation process during passage of current through multivalley semiconductor when electron intervalley scattering drift length exceeds diffusion length 21 p3804 A66-39313

Cyclotron resonance study of electron scattering by thermal acceptors in quenched Ge 21 p3805 A66-39567

Current-carrier scattering anisotropy dependence on antimony impurity concentration in n-Ge established, using measurements on Hall effect and conductivity 22 p3965 A66-40321

Measurement of shift of cesium absorption lines near series edge, obtaining electron elastic scattering cross section at zero energy by extrapolation of shift 23 p4097 A66-41089

Surface scattering of electrons on metallic field effect in thin layers in theory of mean-free-path influences on conductance change 23 p4110 A66-41184

Spatial distribution of hot electrons coherently scattering in thin Au film 23 p4115 A66-42063

Local density and temperature measurement in wind tunnels determined by 50-kev electron scattering, using air as test gas 24 p4192 A66-42199

Critical fields of thin superconducting films determined by specular reflection of electrons from surfaces 24 p4256 A66-42531

Calculation of rms numbers of particles in three-dimensional theory of electron-photon showers, considering scattering 24 p4270 A66-42928

Effective-mass approximation of conduction electron scattering in very thin films 24 p4259 A66-43090

# ELECTRON SOURCE

Local laser heating of cathode for electron extraction from plasmoid 06 p0889 A66-16149

Local laser heating of cathode for electron extraction from plasmoid 15 p2519 A66-29879

# ELECTRON SPECTRUM

Difference magnetic analyzer of low-energy

electrons and protons in which particles are separated before arriving at detector 02 p0284 A66-12143

Damping of electron spectrum and oscillation maximum of magneto-optical effects of semiconductor 03 p0410 A66-12943

Electron spectrum in highly alloyed gallium arsenide 05 p0730 A66-14650

Approximation of exchange operator for system of electrons, examining Slater equation for calculating atomic wave functions 06 p0910 A66-16129

Electron energy spectra in neon, xenon and helium-neon laser discharges, calculating production and destruction rate parameters 07 p1045 A66-18354

Excited ruby crystal phosphorescence noting spectral range, duration, electron excitation mechanism and upper wavelength limit 08 p1234 A66-19667

Mechanism for production of X-rays and gamma rays in galaxies, noting photon and electron spectrum 10 p1598 A66-21100

Nonequilibrium transport properties and electron relaxation at cooled surface of partially ionized argon 10 p1559 A66-21270

Excited ruby crystal phosphorescence noting spectral range, duration, electron excitation mechanism and upper wavelength limit 10 p1543 A66-21834

Continuous electromagnetic radiation from solar flares, examining X-ray bursts from synchrotron, Compton and bremsstrahlung mechanisms 11 p1762 A66-22406

Electron and proton spectrometer detector mounted on OGO-E, measurements cover seven differential energy channels 12 p1877 A66-23690

Electron and proton differential velocity spectra observed for low-energy relativistic cosmic rays, noting spectral neutrality of radiation 13 p2174 A66-25570

Electron spectrum in highly alloyed gallium arsenide 13 p2167 A66-25925

Spectrum of electron excitations with small energies compared to critical temperature of superconducting transition in absence of magnetic field 13 p2168 A66-25978

Production spectrum of high energy electrons from high energy cosmic ray pion decay and proton-proton collisions 13 p2176 A66-26762

Difference magnetic analyzer of low-energy electrons and protons in which particles are separated before arriving at detector 14 p2297 A66-28099

Electron pair production by high energy muons, noting application of Monte Carlo method for appearance of low energy with high energy partner below target plate 15 p2546 A66-29583

Differential electron spectra in radiation belt in ten energy intervals obtained by satellite spectrometer, noting soft and hard components 16 p2794 A66-30703

Hamiltonian describing EPR spectrum of trivalent chromium ion in ordered lithium-aluminum spinel and rhombic distortion causing deviation of axes in octahedron electric field 16 p2787 A66-31763

Quantitative measurement of electron correlation spectrum for deuterium plasma in thermal equilibrium 17 p2963 A66-31885

Energy spectrum change of group of electrons being convected downwind in magnetosheath and behind Earth bow shock 18 p3170 A66-34521

Energy spectra of muon, electron and N components of extensive air showers /EAS/ 18 p3210 A66-35129

Absorption spectra of pure and isotopic impurity crystals of naphthalene in region of first electronic and vibrational /vibron/ transition 19 p3402 A66-36067

Production and equilibrium spectrum of galactic cosmic ray secondary electrons arising from secondary pion and neutron decay 20 p3633 A66-38200

Integral spectrum for low-energy electrons measured with detailed definition of temperature and number density by IMP II 20 p3633 A66-38204

Electron spectra made with five-channel magnetic electron spectrometer from Star Fish explosion and from outer radiation belt 20 p3643 A66-38343

Electron, charged particle density spectrum and temperature measurements in arc jet of



partially ionized argon 21 p3790 A66-39082  
 Angular variation of position of energy loss maxima in indium 23 p4110 A66-41180  
 Equilibrium spectrum of photons from primary electron at photon energies close to primary energy 24 p4269 A66-42921

**ELECTRON SPIN**  
 Variation in thermoelectromotive force and magnetoresistance in quantizing magnetic field in indium antimonide semiconductor, considering electron spin and conduction band nonparabolicity 01 p0124 A66-10770  
 Exchange interaction of localized spins with conduction electrons leading to indirect spin-spin interactions in semiconductor 01 p0125 A66-10782  
 Electron spin effect on quantum oscillations of magnetoresistance and Hall effect in n-InSb single crystal 08 p1269 A66-18971  
 Variation in thermoelectromotive force and magnetoresistance in quantizing magnetic field in indium antimonide semiconductor, considering electron spin and conduction band nonparabolicity 11 p1749 A66-22281  
 Exchange interaction of localized spins with conduction electrons leading to indirect spin-spin interactions in semiconductor 11 p1749 A66-22295  
 Electron spin effect of oxygen and short-range static fields of hydrogen, nitrogen and oxygen molecules upon rotational excitation of these molecules by slow electrons 11 p1741 A66-23389  
 Existence of superconductivity along domain boundaries in ferromagnetic materials having domain structure when induced by nonmagnetic s-electrons or when only magnetic electrons are present 13 p2166 A66-25919  
 Electron-spin paramagnetism effect on critical field of thin aluminum superconductor films 16 p2769 A66-30169  
 Polarized-neutron scattering by tri-vanadium silicide, identifying electronic susceptibility and modification in passing through superconducting transition 16 p2770 A66-30174  
 Fulde-Ferrell effect in type II superconductors 17 p2975 A66-31887  
 Static spin susceptibility of superconductors with p-pairing and collective excitations, noting mercury and tin 24 p4257 A66-42539

**ELECTRON SPIN RESONANCE**  
 Electron spin resonance of radical cations produced by oxidation of aromatic hydrocarbons with antimony pentachloride 03 p0330 A66-12336  
 Electron spin resonance transitions involving simultaneous changes in spin states of two neighboring protons 03 p0395 A66-12343  
 Magnitude of anisotropic line broadening in ruby 03 p0413 A66-13278  
 Ground state ESR saturation effect on ruby laser output frequency at cryogenic temperature 06 p0892 A66-16753  
 Electron spin resonance center in ZnSe after electron bombardment measured with low temperature microwave cavity 06 p0934 A66-17124  
 Correlation between strength of induced optical absorption G band and strength of features in electron spin resonance spectrum in electron irradiated diamonds 06 p0934 A66-17125  
 Temperature and donor concentration of width of electron spin resonance line in center of hyperfine spectrum for phosphorus-and arsenic-doped silicon 08 p1270 A66-19014  
 Gamma irradiation intermediates of polyamide MXD-6 examined, using electron spin resonance and optical spectroscopy 08 p1243 A66-19065  
 Kinetics of hydroxyl radical in aqueous solution, examining electron spin resonance spectrum as function of flow rate, temperature and mixture composition 08 p1178 A66-19066  
 Spin resonance of donor electron in Ge and anisotropic line width in relation to dislocation stress 11 p1750 A66-22463  
 Lower hybrid resonance in VLF range in satellites, noting noise emission due to trapping of electromagnetic wave propagation in transverse magnetic

field 13 p2074 A66-26364  
 Semiconductor properties of reduced barium titanate analyzed by electron spin resonance measurements at various temperatures 14 p2359 A66-27132  
 Electron spin resonance of gamma irradiated single crystal of barbituric acid dihydrate, noting formation and Hamiltonian parameters of free radicals 14 p2367 A66-27979  
 Electron spin resonance saturation causing sharp decrease of DC resistance for reduced rutile crystals 15 p2567 A66-29401  
 High resolution ESR spectra of acyclic semidione radical anions and single aryl substituent cations 15 p2447 A66-29817  
 Electron spin resonance in rubidium and cesium observed, using selective transmission technique 16 p2750 A66-30145  
 Conduction electron spin resonance in rubidium and cesium observed, using reflection technique 16 p2750 A66-30146  
 Electron spin resonance in silicon oxide grown on Si, noting spectral line interpretation of Si-SiO sub 2 boundary 17 p2978 A66-32406  
 Spin-lattice interaction in ruby measured by electron spin resonance in uniaxially stressed crystals 17 p2981 A66-32718  
 Sb concentration and ESR linewidth of Sb donors in compensated and uncompensated n-silicon 18 p3156 A66-34475  
 Neutral-impurity scattering experiments in silicon with highly spin-polarized electrons 19 p3448 A66-36764  
 K-band superheterodyne electron spin resonance spectrometer with MO noise elimination by modified Gordon bridge with reflection cavity 20 p3559 A66-37538  
 Electron conduction and phosphorus doping effects on room temperature and cryogenic electron spin resonance in n-type silicon 21 p3797 A66-38752  
 X-band spectrometric observation of ESR of trivalent gadolinium in reduced barium titanate 21 p3797 A66-38756  
 ESR line width of phosphorus doped silicon measured, noting relation between line width and temperature in metallic impurity conduction 21 p3798 A66-38764  
 Electrical properties of barium plumbate noting conductivity, Hall field, thermoelectromotive force, magnetization, etc 24 p4253 A66-42382

**ELECTRON STATE**  
 Semiconductor superconductivity dependent on presence of different electron states in crystalline films at surface 02 p0277 A66-12277  
 Helium 3-1-P state, discussing pressure dependence of lifetime between free escape and complete blockading 03 p0395 A66-13134  
 Thermodynamic changes in crystal lattice on electron states of semiconductors 05 p0737 A66-15116  
 Potential curves and spectrum absorption of nitrogen, redetermining spectroscopic constants 05 p0763 A66-15285  
 Semiconductor superconductivity dependent on presence of different electron states in crystalline films at surface 05 p0738 A66-15456  
 Comments on radiative recombination of molecular helium ions into dissociative state 06 p0912 A66-16636  
 Population inversions promoted between electronic-excited states by fluid-mechanical techniques 07 p1083 A66-17937  
 CW laser action on triple state phosphorus-sulfur transition, using hydrogen sulfide-noble gas mixtures 10 p1543 A66-21577  
 First order wave function of helium due to one-and two-electron excitation determined by solving differential equations, noting contribution to second order energy 11 p1741 A66-23405  
 Density of electron states and classical effective mass of current carriers in magnetic field for semiconductor with wurtzite-type lattice 12 p1930 A66-24457  
 Schottky theory for metal semiconductors, noting correlation between work function and barrier height, electron affinity, etc 17 p2980 A66-32650  
 Plasma oscillations of electron shell of atom, discussing natural frequency, damping, probability and participation of plasmon in atomic reactions 17 p2962 A66-33505

Partial wave theory of two electron diatomic hydrogen molecules and calculation in zeroth order for sigma g states 18 p3139 A66-34500  
 Individual efficiency curves for excitation of two metastable electron energy states of helium by electron 18 p3139 A66-34504  
 Electron energy spectrum for alloyed semiconductors, determining state densities via Thomas-Fermi statistical method 20 p3618 A66-37562  
 Density of electron states and classical effective mass of current carriers in magnetic field for semiconductor with wurtzite-type lattice 20 p3620 A66-37689  
 Electron correlation analysis method applied to interelectronic repulsion effect on localized electrons near ideal surface of semimetallic diamond-like crystal 24 p4252 A66-42349

**ELECTRON TEMPERATURE**  
 Effect of nonzero plasma electron temperature considered in electron beam-plasma interaction wave growth computation 01 p0112 A66-10531  
 Microwave scattering from nonequilibrium plasmas where electrons have large steady drift velocity with respect to ions 02 p0266 A66-11479  
 Piezoelectric resistance of n-silicon as function of electric field intensity 02 p0273 A66-11713  
 Electron and ion temperatures determination for helium plasma produced by theta-pinch with azimuthal magnetic field, using Doppler broadening and X-ray absorption 03 p0396 A66-12292  
 Relationship between laws of electron temperature and charged particle concentration fall-off in helium plasma diffusion flow 03 p0398 A66-12520  
 Quiet chromosphere and corona noting line intensity and coronal electron and kinetic temperature 03 p0420 A66-12841  
 Ambipolar diffusion and electron-ion recombination coefficients dependence on electron temperature in afterglow of neon plasmas 04 p0554 A66-14294  
 Local electron temperature and electron density in theta pinch measured by means of scattering of laser beam 04 p0555 A66-14334  
 Ratio of ionospheric electron to ion temperature determined independently of spectral measurements, using electron density data obtained with topside sounder 04 p0517 A66-14374  
 Atomic heat of titanium, vanadium and chromium in high temperature range, discussing parameters and experimental techniques 05 p0698 A66-14511  
 Electron energy loss rate for D region determined by Maxwellian velocity distribution of thermal component brought about by collisions with molecular nitrogen involving rotational transition 05 p0672 A66-15021  
 Ionospheric diffusion probe determining ion and electron temperatures 05 p0674 A66-15112  
 Electron temperature distribution in plasma diode, discussing electron transport properties and current-voltage characteristics 05 p0615 A66-15535  
 Phenomenology of ignited cesium diode discharge noting saturation mode, obstructed mode and ball of fire 05 p0728 A66-15552  
 Electron temperature and ion density profiles across interelectrode gap of thermionic diode operating in ignited mode 05 p0621 A66-15573  
 Electron heating effect on acoustic instability of weakly ionized plasma in electric field 06 p0914 A66-16143  
 Electron temperature spectroscopy for atmospheric argon plasmas, sodium vapor seeded at high temperatures, noting relationship with current density 06 p0915 A66-16178  
 Electron concentration and temperature distribution in argon DC arc measured with hot wire probe 06 p0918 A66-16834  
 Electron temperature in plasmas measured using pressure broadening by electron impacts of isolated spectral lines, i.e., temperature dependence of shift to width



ratio 06 p0920 A66-17041  
Electron and ion temperatures in  
ionosphere show no temperature equilibrium  
in F region 06 p0877 A66-17171  
Measurements of plasma from hydrogen-  
coated titanium washer mounted at DC  
magnetic mirror 07 p1088 A66-17954  
Volt-ampere characteristics of n-silicon in  
strong electric field from 77 to 300 degree  
07 p1105 A66-18365  
Precursor electron front measuring  
velocity, electron temperature dependence  
on operating parameters,  
etc 08 p1259 A66-18525  
Water-cooled electrostatic probe capability  
of measuring local electron temperature,  
electron density, floating potential and  
saturation current ratio in dense plasmas  
[AIAA PAPER 66-73] 08 p1262 A66-18956  
Electron temperature variation in argon  
MGD channel in crossed magnetic and  
electrical fields 08 p1263 A66-19174  
Magnetic field effect on electron  
temperature, number of ionization events  
and potential gradient in argon and neon HF  
discharge 08 p1264 A66-19186  
Exchange of energy between ionosphere  
and protonosphere, noting nonlocal heating  
by photoelectrons, thermal conductivity and  
heat input by downward  
flux 08 p1215 A66-19204  
Ionospheric heating by magnetic conjugate  
point photoelectrons, showing variation of  
electron temperature with  
time 08 p1218 A66-19402  
Low pressure, high temperature and low  
values of electrical output effect on plasma  
conductivity, noting operation of MGD  
generators at high Hall  
numbers 09 p1331 A66-20137  
Hot electron emission from semiconductor  
cathode in vacuum-tube diode during  
mapping of thermoelectronic and  
photoelectronic current 09 p1429 A66-20813  
Radio brightness distribution over quiet  
sun and various deductions concerning  
electron temperature and density of corona,  
including data on overdense regions  
radiating thermally 10 p1601 A66-21061  
Nonequilibrium transport properties and  
electron relaxation at cooled surface of  
partially ionized argon 10 p1559 A66-21270  
Radial distributions of number density,  
electron temperature and plasma potential  
measured in electrodeless discharge, using  
symmetric and asymmetric double probes  
[AIAA PAPER 66-194] 10 p1562 A66-21440  
Single and double Langmuir probe for low  
density plasma, noting measurement of  
electron temperature and  
density 10 p1535 A66-21514  
Loss rates of charged particles from  
chemically-heated discharges in C-Stellarator,  
showing confinement time  
parameters 10 p1568 A66-21825  
Electron temperatures in hot argon-  
potassium discharges determined, using ratio  
of electron energy slopes from floating  
double-probe curve 10 p1568 A66-21880  
Electron temperature measurement by  
relative intensity of He I lines shown as  
inapplicable for high plasma  
densities 10 p1571 A66-22021  
Effective electron collision frequency from  
electron temperature profile for ionospheric  
heating in F region 11 p1697 A66-22499  
Electron density distributions in daytime  
F-2 layer and dependence on neutral gas,  
ion and electron  
temperatures 11 p1699 A66-23135  
Satellite observational data indicates that  
nighttime electron temperatures in upper F  
region are larger than neutral gas  
temperature 12 p1868 A66-23559  
Electron temperatures in several RF-  
generated plasmas, using air as  
medium 12 p1919 A66-23599  
Langmuir probe measurements in  
hypersonic plasma flow, evaluating  
properties of plasma jet wind tunnel,  
electron temperature and plasma  
density 12 p1920 A66-23853  
Low pressure plasma electron temperature  
inferred from Langmuir probe  
measurements differs from plasma mean  
electron energy 12 p1920 A66-23959  
Ionospheric processes and measurement of  
variations in ion temperature and

concentration using satellites, noting  
connection with 12 p1871 A66-24400  
Electron temperature determination from  
intensity ratio of singlet and triplet lines of  
neutral helium used in plasma diagnostics,  
noting complications from metastable levels  
and coupling of singlet and triplet  
systems 12 p1924 A66-24592  
Spectral line intensities variation in  
ionization of hydrogen and impurities in TA  
2000 device 13 p2138 A66-25125  
Free jet of arc heated low-density  
supersonic argon plasma examined,  
measuring radiative mechanisms, electron  
temperatures, thrust, jet structure, etc  
[AIAA PAPER 66-163] 13 p2138 A66-25167  
Langmuir probe to measure stagnation  
region shock layer ionization distribution  
under nonequilibrium hypersonic flow  
conditions [AIAA PAPER 66-167] 13 p2138 A66-25168  
Ionization phase of impurity in pulsed  
hydrogen discharge and electron  
temperature measuring  
method 13 p2141 A66-25478  
MHD instability in plasmas during pinch  
discharge, noting wave velocity dependence  
on Larmor radius, Hall effect, electron  
temperature fluctuations,  
etc 13 p2142 A66-25704  
Electron density and temperature in  
decaying hydrogen plasma determined, using  
monochromator 13 p2145 A66-25730  
Electron density and temperature of  
hydrogen plasma determined from intensity  
of spectral line and continuum in region  
adjacent to line 13 p2145 A66-25733  
Spectral characteristics of gallium arsenide  
junction luminescence, noting radiative  
recombination mechanism, energy spread of  
impurity states and line shape temperature  
dependence 13 p2168 A66-26186  
Triple-probe measurement of electron  
temperature of transient plasma from  
plasma gun 13 p2149 A66-26242  
Time behavior of 3889 and 5016 angstrom  
line helium emission during initial transient  
of RF discharge, noting pressure  
dependence and signal 13 p2104 A66-26335  
Hydrogen plasmoid density, ionization and  
electron temperature measured by fast-  
particle probing 13 p2153 A66-26526  
Spatial variations in electron temperature  
produced in steady state plasma by  
electromagnetic standing  
wave 13 p2155 A66-26678  
Pulsed type radiometer, which samples  
noise emitted by ionized medium, used to  
measure electron temperature of  
nonpermanent plasmas 14 p2290 A66-26823  
Recombination coefficient and high  
electron temperature in midlatitude sporadic  
E layer with ions of oxygen and nitrogen  
oxide 14 p2281 A66-26849  
Electron temperature in helium plasma  
determined from intensity ratios of spectral  
lines 14 p2344 A66-27643  
Law of mass action derivation of chemical  
equilibrium ionization of multitemperature  
system when electron and heavy particle  
temperature differ 15 p2551 A66-29218  
Recombination rate, ionization in  
nonequilibrium electric conductivity  
prediction for dense seeded  
plasma 15 p2554 A66-29752  
Plasma perturbation by large probe,  
determining electron density and  
temperature and plasma potential as  
function of distance from  
probe 15 p2555 A66-29754  
Electron temperature correlation with  
excitation in temperature in argon plasma  
established, using spectral analysis and  
Langmuir probe 15 p2555 A66-29762  
Electron heating effect on acoustic  
instability of weakly ionized plasma in  
electric field 15 p2556 A66-29873  
Sounding rocket measurement of  
ionospheric electron  
temperature 15 p2494 A66-30043  
Early morning ionospheric characteristics  
measured by geophysical rocket, noting  
electron concentration, solar UV emission  
intensity changes, electron temperature,  
absorption profile, etc 15 p2494 A66-30052  
Plasma electron temperature measured

from soft X-ray bremsstrahlung absorption  
by beryllium foil 16 p2756 A66-30096  
Measurement of sticking coefficient for  
thermal electrons in oxygen and air, using  
microwave circuits 16 p2756 A66-30101  
Plasma probe for dense isothermal cesium  
plasma, noting electron concentration and  
temperatures, potential  
distribution, etc 16 p2756 A66-30102  
Electron temperature measurements in low  
voltage arc in saturated cesium  
vapor 16 p2756 A66-30105  
Pressure dependent energy loss process  
determined in atomic light analysis of  
helium positive column, noting molecular-ion  
concentration relation to 3 D super 3  
population 16 p2750 A66-30114  
Spectrum of plasma fluctuations in ionized  
turbulent gas explained by statistical  
turbulence theory, noting that electron  
temperature is larger than gas  
temperature 16 p2757 A66-30173  
Electron temperature measurement by  
relative intensity of He I lines shown as  
inapplicable for high plasma  
densities 16 p2760 A66-30840  
Effect of heating of ionosphere by  
photoelectrons coming from magnetically  
conjugate point, using electron temperature  
measurements 16 p2698 A66-31214  
Double-slit spectrograph attachments for  
determining electron temperature from  
changes in linewidth and relative intensity  
of two He lines 16 p2709 A66-31614  
Plasma electron temperature measurement  
by intensity ratio of two  
lines 17 p2965 A66-32284  
Helium plasma in confining magnetic field,  
noting spectral efficiency in optical region,  
electron temperature and density, electron  
ion recombination, etc 17 p2965 A66-32409  
Plasma motion and confinement in  
octupole magnetic field, noting electron  
temperature density and field  
fluctuation 17 p2966 A66-32428  
Electron temperature determination in  
argon plasma as function of distance  
measured to axis of inductive  
windings 17 p2974 A66-33255  
Electron temperature and concentration in  
DC plasma arc determined from Thomson  
scattering of laser  
radiation 18 p3118 A66-33840  
Coupling between free electron and  
molecular vibrational temperatures in  
plasma environments, noting energy  
distribution, application to MHD generation,  
etc 18 p3145 A66-34105  
Plasma ion and electron temperature  
measurement via forward scattering  
spectrum of deuterium  
plasma 18 p3146 A66-34235  
Negative temperature coefficient of  
electrical resistance, anomalous Hall  
constant and magnetoresistance constant for  
thin films of Be and Pb 18 p3157 A66-34627  
Charged particle beam interaction with  
plasma, determining electron-ion  
temperatures and HF  
field 18 p3152 A66-35074  
Excitation and ionization of hydrogen  
plasma under influence of two electron  
groups with different temperatures and  
densities, using coupled system of rate  
equations 19 p3407 A66-36063  
Population temperatures within argon-  
calcium plasma generated by reflected  
aerodynamic shock determined by spectral  
line-reversal method 19 p3409 A66-36332  
Nonuniform plasma stability in magnetic  
field gradient 19 p3417 A66-36530  
Electron density, temperature and other  
related electromagnetic effects of deuterium  
plasma focus formed by coaxial electrode  
discharge as result of Z  
pinch 19 p3425 A66-36561  
Langmuir current-density limit derived for  
differing axial and radial electron beam  
temperatures in high-resolution image  
devices 20 p3524 A66-36899  
Instrumentation for plasma diagnostics  
noting electron density profile, temperature,  
ion-atom and electron-atom interaction,  
etc 20 p3556 A66-36964  
Electron temperatures and concentrations  
of charged particles behind strong shock  
wave in air measured, noting techniques,  
maximal values and



accuracy 20 p3545 A66-37369  
 Neutral atmosphere reduces electron gas thermal conductivity below 200 km during both day and night 20 p3552 A66-37590  
 Electron temperature of solar corona, noting radiative transfer of radio emission in corona, deriving distribution of brightness temperature over solar disk 21 p3811 A66-38638  
 Low pressure, high temperature and low values of electrical output effect on plasma conductivity, noting operation of MGD generators at high Hall numbers 21 p3698 A66-39409  
 Nonlinear modulation distortions of high power radio waves propagating in ionosphere, noting electron temperature increase from radio wave 22 p3861 A66-39647  
 Electron density, electron and ion temperature and ionic composition measurements in Peru, using incoherent scattering technique 22 p3910 A66-39977  
 Diurnal variation in electron densities and temperatures in F region above Puerto-Rico, using backscatter measurements 22 p3910 A66-39978  
 F layer electron temperature fluctuations and resultant electron density changes in daytime 22 p3910 A66-39980  
 Nighttime F layer recombination and diffusion coefficients estimated from incoherent scatter measurements of electron densities and electron and ion temperatures 22 p3910 A66-39983  
 Langmuir type probe in argon arc jet, discussing surface contamination problems, causes of high electron temperature and development of automatic cleaning technique 22 p3899 A66-40368  
 Incoherent scattering of radio waves by plasma extended to include effects of unequal ion and electron temperatures and magnetic field 22 p3867 A66-40550  
 Time dependent thermal behavior of ionospheric electron gas 22 p3913 A66-40552  
 Electron thermalization effect on semiconductor laser behavior, noting optical transition between impurity level and band, taking into account diffusion process 22 p3933 A66-40790  
 Coulomb interaction in two-zone superconductor model, noting variation of critical electron-temperature and effect on superconductivity 22 p3968 A66-40916  
 Plasmoid density, electron temperature and radius variation during propagation through magnetic field, using electric and magnetic probes 22 p3958 A66-40932  
 Singlet and triplet populations in helium and electron temperature determination from optical excitation cross sections 23 p4100 A66-41161  
 Spectroscopic measurements of electron densities and temperatures in argon-hydrogen plasma jet 23 p4068 A66-41290  
 Nighttime electron temperatures in upper F region suggest corpuscular energy input 23 p4064 A66-41682  
 Solar UV emission lines for 11 elements heavier than helium analyzed, obtaining relative abundances values and relation between electron temperature and temperature gradient in chromosphere-corona transition region 23 p4130 A66-41809  
 Radial distributions of number density, electron temperature and plasma potential measured in electrodeless discharge, using symmetric and asymmetric double probes [AIAA PAPER 66-194] 23 p4107 A66-41907  
 Ruby laser light scattering measurements of electron and ion temperatures of hydrogen and deuterium plasmas produced in theta pinch devices 24 p4222 A66-42558  
 Energy dependence of effective interaction in superconductivity, calculating critical field and specific heat 24 p4259 A66-43018  
 Automatic double probe to determine electron temperatures in ion engine exhaust 24 p4215 A66-43208

## ELECTRON TRAJECTORY

Equivalence of paramagnetic impurities in superconductor and magnetic field parallel to thin superconducting film with short mean free path 04 p0560 A66-13717  
 Radiation unit of length, calculating path-length for passage of high-energy electrons and photons through matter 06 p0912 A66-16575

Electrostatic field from E region and effect on motion of electrons trapped in magnetosphere 07 p1027 A66-17252  
 Superconductors with ferromagnetically aligned impurities, assuming electron mean free path due to spin-orbit interaction is small compared to coherence distance 07 p1108 A66-18431  
 Velocity and attenuation of ultrasonic waves in thallium when product of sound wave vector and electron mean free path is less than unity 07 p1109 A66-18445  
 Spiralling electrons in geomagnetic field and superimposed electric field aligned with magnetic field lines 11 p1695 A66-22371  
 Response of spherical plasma probe to alternating potentials determined by Boltzmann-Vlasov equation together with Maxwell equations 11 p1746 A66-23070  
 Electron trajectory equations for outer and inner flux boundaries, taking into account thermal velocities under static conditions of centrifugal electrostatic focusing 14 p2236 A66-27246  
 Multivelocity stream effects and efficiency of slow-cyclotron wave amplifiers, noting electron velocity spread which decreases predicted efficiency 15 p2467 A66-29711  
 Cylindrical electron beam behavior in axial, monotonically increasing magnetic field, noting compression, percentage scalloping, etc 17 p2887 A66-32696  
 Exact solution of nonlinear relativistic equations of motion for electron in right circularly polarized wave propagating in whistler mode parallel to external magnetic field 19 p3303 A66-35998  
 Line shape of RF dimensional effect in metals showing correlation with electromagnetic wave attenuation in skin layer 24 p4172 A66-42528

## ELECTRON TRANSFER

Vertical electron transport velocity in ionosphere 06 p0877 A66-16895  
 Hot electron transfer from light mass central valley to surrounding heavy-mass satellite valleys in n-type gallium arsenide, indium phosphide and cadmium telluride analysis based on Boltzmann equation 06 p0929 A66-17035  
 Characteristic radiation spectra emitted in process of spontaneous electron transfer from shallow donors to shallow acceptors at liquid helium temperatures in silicon 07 p1095 A66-17321  
 Kinetic effects in fuel cells, discussing declining efficiency with increasing output, slow electron transfer effects, concentration polarization, etc 07 p0996 A66-18469  
 Participation of ferredoxin of clostridium nigrificans in sulfite reduction, describing transportation of electrons for sulfide formation 08 p1177 A66-18699  
 Electron conservation equation and effects of laminar or turbulent flow on breakdown in gases 08 p1206 A66-18933  
 Interaction of dislocations with coherent ordered zones, discussing results of electron transmission and tensile test experiments 08 p1240 A66-19251  
 Binary transport of electrons and ions in equatorial ionosphere and effect on brightness of 6300 angstrom airglow at Huanayo 09 p1372 A66-20376  
 Thin-film triode devices to investigate hot-electron penetration of oxide films 10 p1509 A66-21540  
 Bipolar excitation of photoconductivity in silicon due to structural disarrangement caused by IR radiation 10 p1583 A66-22019  
 Threshold field dependence on intervalley separation in transferred electron GaAs oscillator 10 p1586 A66-22093  
 K absorption spectra of germanium and selenium in germanium selenide based on band theory of solids by assuming electrons transfer, using X-ray spectroscopy 11 p1758 A66-23368  
 Transition of group IV elements to metallic state confirmed as equivalent to generation of intrinsic current carriers 11 p1759 A66-23447  
 Thermodynamics of new generalized transport laws for liquids, gases and electrons in matter 12 p1977 A66-23557  
 Boltzmann transfer equation for electrons and generation of nonlinear second harmonic of current density in inhomogeneous

plasma 12 p1924 A66-24806  
 Gunn effect involving current oscillations higher than 1000 mc in GaAs crystal under applied electric field 14 p2355 A66-26920  
 Electron transfer from alkali metals to aromatic hydrocarbons, examining rate of chain scission in case of poly(4-vinyl biphenyl/ and poly(alpha/ vinyl naphthalene/ 17 p2870 A66-32300  
 LF common-base current transfer ratio for hot electron transport in semiconductor-metal-semiconductor point-contact-transistor structures measured as function of metal film thickness and temperature 19 p3435 A66-35410  
 Theoretical distribution of charges and potential in vicinity of metal-dielectric barrier in absence and presence of applied field 19 p3448 A66-36753  
 Recharge cross section in collisions of slow atoms or ions involving interparticle transfer of one electron 20 p3604 A66-36987  
 Electron tunneling from metal to doped indium antimonide through oxide layer measured, obtaining characteristics of conductance vs applied voltage for n-and p-type crystals 20 p3620 A66-37769  
 Crystal dislocation distribution effect on low temperature electrical transport properties in plastically deformed metals 21 p3753 A66-39587

## ELECTRON TRANSITION

Laser transition identification in electron beam pumped gallium arsenide, primarily on concentration of shallow donors and acceptors 01 p0081 A66-10348  
 Laser action at 5401 angstroms in pure neon pulsed high voltage discharge 01 p0081 A66-10353  
 Atomic beam lasers, particularly for population inversion in levels of optical transition 01 p0082 A66-10448  
 Indirect transition and temperature dependence of absorption limit in single crystal cadmium sulfide 01 p0126 A66-11006  
 Helium-neon laser output dependence on hollow cathode discharge conditions for electron transitions in neon 02 p0239 A66-11422  
 Two-and three-step laser cascades detected experimentally in helium-neon mixtures, analyzing two-step cascade starting with density matrix formulation 02 p0241 A66-11477  
 Symmetry of ground states of P, As and Sb donors in silicon determined optically 03 p0411 A66-13144  
 Atomic beam lasers, particularly for population inversion in levels of optical transition 03 p0380 A66-13311  
 Eigenvalues and eigenvectors calculated for several low-lying autoionizing levels in helium 04 p0546 A66-13365  
 Self-consistent field calculations of benzene molecule using Gaussian expansion functions, considering 42 electrons and finding interspersions of sigma and pi levels 04 p0473 A66-13648  
 Absolute band and oscillator strengths and absolute Einstein A coefficients for C-2 Swan system 04 p0549 A66-14313  
 Boron, nitrogen and gallium in photo- and electroluminescences of silicon carbide p-n junctions, noting radiative electron transitions 04 p0567 A66-14343  
 Absorption and emission spectra pertaining to electronic transitions of short-lived molecules C sub 2 and CH present in reaction zone of low-pressure oxyacetylene flames 06 p0969 A66-16126  
 Indirect and direct radiative recombination transitions in germanium and use in analysis of lifetime 07 p1094 A66-17314  
 Noncollisional damping modifies HF plasma resonance 08 p1261 A66-18644  
 Indirect transition and temperature dependence of absorption limit in single crystal cadmium sulfide 09 p1411 A66-19944  
 Numerical method of Schroedinger equation and WKB approximation compared in determination of transmission coefficients for thin insulating films 10 p1577 A66-21558  
 Spin wave sideband in absorption spectrum at low temperatures for transition of manganese ion in antiferromagnetic manganese fluoride 11 p1740 A66-22970  
 Dipole matrix elements for helium in first order shielding approximation as function of



breeding parameter 12 p1918 A66-24865  
Donor impurity effect on direct-indirect transition in gallium arsenic phosphide, particularly at low temperature 13 p2170 A66-26590  
Laser oscillator study of coherent stimulated emission of IR transitions in rare gases 14 p2308 A66-27336  
Energy level transitions in vacuum UV absorption spectrum of calcium 14 p2337 A66-27704  
Photoabsorption power due to sodium interband, using orthogonalized plane wave evaluation of matrix elements in oscillator strengths 14 p2365 A66-27753  
Oscillator strengths for electric dipole transitions in neutral helium 14 p2338 A66-28127  
Franck-Condon factors for permitted transitions in nitrogen 14 p2338 A66-28128  
Boron, nitrogen and gallium in photo- and electroluminescences of silicon carbide p-n junctions, noting radiative electron transitions 14 p2367 A66-28238  
Hall coefficient increase with temperature and electron transition to second conduction band in InSb 15 p2558 A66-28614  
Slow electron excitation cross section for solar molecule rotational and vibrational transitions based on Born approximation and point-dipole interaction 15 p2545 A66-29395  
Isotope shifts and Fermi resonance role in carbon dioxide IR laser 16 p2716 A66-30176  
Auroral excitation rates and molecular vibrational temperatures in nitrogen 2PG from Franck-Condon factors obtained from intensity measurements and high resolution absorption spectral data 16 p2692 A66-30328  
Partial differential equation solution, using small parameter method for electron hole transition 16 p2784 A66-31553  
Competition of transitions and emission in He-Ne laser, using resonator without dispersing prism 17 p2938 A66-33514  
Atomic Zeeman patterns using strong pulsed magnetic fields for electronic transitions for Si, Cu, C, O, Ca, Mg and B 18 p3137 A66-33990  
Laser action on several hyperfine transitions in Mn I 18 p3118 A66-34000  
Born cross sections for double-transition collisions of hydrogen atoms 18 p3138 A66-34150  
Derivative chronopotentiometry approach to measurement of transition times and study of electrode process 18 p3064 A66-34457  
Magnetopiezo-optical reflection in germanium observed by piezoreflection technique for direct transition 18 p3156 A66-34467  
Radiation from high-energy-level transitions excited in He-Ne laser during optical pumping with He lamp 18 p3120 A66-34697  
Iron and nickel lines in solar UV spectrum, abundance of various metallic elements in solar atmosphere, electron collision cross sections and oscillator f-values of electron transitions 18 p3237 A66-35050  
Transitions induced by electron impact between all ground-state terms of atomic systems with computed cross sections satisfying unitarity 19 p3463 A66-35990  
Lowest of UV absorption bands attributed to 4f-5d transition of trivalent rare earth ions in calcium fluoride 19 p3443 A66-36004  
Fermi surface interpretation of band structure, electron energy levels, optical properties and ferromagnetic structure of transition and noble metals 20 p3613 A66-37274  
Theoretical band structure, Fermi surface, electronic structure, magnetic and optical properties of rare earth metals 20 p3614 A66-37277  
Visible and UV transition radiation, bremsstrahlung and plasma due to electron bombardment of metal surfaces 20 p3604 A66-37280  
Direct phonon relaxation between two electronic levels in ruby and effect on temperature dependent R-line breadth 20 p3623 A66-38399  
Electron excitation of high eigenstates of hydrogen atom and convergence of total wave function expansion 21 p3774 A66-38532

Faraday and Voigt and dispersive magneto-optic effects in semiconductors in crossed field due to energy band transitions 21 p3800 A66-38995  
Cryogenic optically excited recombination emission in single crystal InSb semiconductor and transitions involving phonon creation, acceptor impurities and band-to-band emissions 21 p3800 A66-38996  
Atomic collisions, excitation transfer processes and energy level transition probabilities in plasma of gas lasers 21 p3748 A66-39305  
Gas laser frequency and emitted power dependence on resonator tuning 21 p3748 A66-39308  
Experimental excited state band locations and intensities in absorption spectrum of electron transitions in optically pumped ruby laser 21 p3749 A66-39569  
Theoretical excited state absorption spectrum of electron transitions in optically pumped ruby laser 21 p3749 A66-39570  
Degree of population inversion and inverse temperature measurement in medium 22 p3917 A66-39663  
Nonemissive multiphonon transitions and quantum yield for ruby R line 22 p3930 A66-39766  
3 cm hydrogen line from solar flares, estimating line-to-continuum ratio during flare 23 p4124 A66-41928  
Competition of transitions and emission in He-Ne laser, using resonator without dispersing prism 24 p4219 A66-42127  
Spectroscopy of IR emission and laser oscillation resulting from transient population inversions on electronic transitions in molecular nitrogen 24 p4221 A66-42550  
Electron transitions and sharp emission lines in XUV solar spectral regions with fractionally charged quarks bound to C, N and O nuclei 24 p4280 A66-43189  
**ELECTRON TUBE**  
SA CATHODE RAY TUBE  
SA DIODE  
SA DISCHARGE TUBE  
SA DUPLEXER  
SA FIBER OPTICS  
SA KLYSTRON  
SA MAGNETRON  
SA MODULATOR  
SA PHOTOTUBE  
SA RESONATOR  
SA SEMICONDUCTOR DEVICE  
SA THYRATRON  
SA TRAVELING WAVE TUBE  
SA TRIODE  
SA VACUUM TUBE  
Negative resistance in xenon planar triode due to Ramsauer effect 03 p0343 A66-12969  
Electron devices - IEEE Symposium, San Francisco, August 1965 07 p1011 A66-18266  
Wide bandwidth and high power electron tube applications in face of encroachment of solid state devices 07 p1011 A66-18271  
Performance and wave growth of type-M transverse-field tubes in broad delay system 09 p1352 A66-20356  
Electron tunneling in semiconductors with degenerate band structure 10 p1581 A66-21739  
Complex transfer admittance in quadrupole transistors from Schottky measuring principle for transconductance of electron tubes 14 p2246 A66-26797  
Cesium ion tubes advantages over conventional tubes including ability to study electron-inertia effects 17 p2888 A66-32823  
Amplitude and phase fluctuations in two-circuit quartz-crystal oscillator with crystal positioned between grid and electron tube cathode 20 p3525 A66-37152  
Electron tubes operation and performance, discussing TV, vidicon, photographic recording tubes and photoelectric devices 21 p3716 A66-39618  
Borgnis U function applied to design of electron tube having drift space between collector and grid controlling current 22 p3876 A66-40173  
**ELECTRONIC CONTROL**  
Operation and uses of triode-based electronic control device for pulse aerial cameras 03 p0368 A66-12505  
Mass spectrometric electron impact ionization potentials rapidly obtained by

electronic control and automatic data processing systems 07 p1091 A66-18489  
Electronic timer for rocket, controlling duration of burning time 08 p1188 A66-18616  
Electronic color correction during aerial photograph printing by employing specially programmed computer 10 p1534 A66-21329  
Circuit of two-state pentode resonance amplifier with electronic passband control and slightly varying amplification coefficient 11 p1667 A66-22788  
Circuit of two-state pentode resonance amplifier with electronic passband control and slightly varying amplification coefficient 20 p3525 A66-37128  
Electronically despun antenna and electronically controlled phase shifters to increase transmitter output power for spin-stabilized communication satellites 23 p4036 A66-41142  
**ELECTRONIC COUNTERMEASURE**  
Electronic compensation for phase errors in surface profile of reflecting antennas 18 p3081 A66-34277  
**ELECTRONIC EQUIPMENT**  
SA SPACECRAFT ELECTRONIC EQUIPMENT  
Predicted vs observed avionics reliability in design technique, using factual reliability data of baseline equipment and solid state component advances 01 p0035 A66-10080  
Western Electronic Show and Convention, San Francisco, August 1965, Part 6, Instruments and measurement 02 p0228 A66-11452  
Multiplex measuring device and choice of analog or digital computers in electronic measurement 02 p0230 A66-11792  
Measuring circuit and functional components in modern electronic measuring technique 02 p0230 A66-11793  
Advisability of West German electronics industry stepping into aviation electronics industry to greater extent 02 p0199 A66-11859  
Hybrid integrated-and-conventional circuit configuration in electronic equipment noting thin film circuits, encapsulation, costs, reliability, etc 02 p0204 A66-11928  
Integrated circuit economics discussing design, construction and running costs 02 p0205 A66-11944  
Operation principle, design and application of coloristors which change color at predetermined temperatures determined by current passing through them 03 p0340 A66-12475  
Avionic equipment reliability improvement through highly reliable components, noting Minuteman 03 p0343 A66-12903  
Developments in capacitor design particularly electrolytic, ceramic and mica types 03 p0347 A66-13331  
Transistorized evaporation to measure vertical water vapor and heat fluxes in lower atmosphere 04 p0519 A66-13671  
Mathematical model that takes into account factors involved in detecting faults as well as MTBF and MTTR for prediction of equipment availability 04 p0494 A66-13682  
Avionics design using integrated electronics or microelectronics, noting reduction of maintenance requirements 04 p0494 A66-13684  
Control system 465L used by Strategic Air Command noting automated functions, data processing, integration of human and electronic elements, etc 04 p0507 A66-13687  
Radar, telecommunication devices, antiraid equipment and computers for air defense system 04 p0494 A66-13693  
Design and fabrication methods of semiconductor optoelectronic devices, noting junction emitter outputs into visible spectrum 04 p0494 A66-13764  
Signal fluctuation effect on operation of electronic device, approximating empirical correlation function 04 p0504 A66-13778  
Book on electronic systems constituting space communications systems, noting orbital motions, space environment, noise, propagation, satellites, etc 04 p0481 A66-13816  
UHF voice communications system for 412L Air Weapons Control System discussing transmitter, receiver and compliance testing 04 p0497 A66-13964  
Laser beam welding electronic-component



leads 05 p0685 A66-14517  
 20-kw latching nonreciprocal X-band ferrite phase shifter design and performance 05 p0641 A66-14556  
 Electronic components, considering noise characteristics, particularly effect of gamma radiation on resistors, capacitors, diodes, etc 05 p0650 A66-15834  
 Reliability of electronic equipment needed to increase availability and reduce maintenance cost 06 p0840 A66-15953  
 Microwave filters, discussing cascaded lines of cavities, band pass and band stop filters, group delay, dissipation loss, etc 06 p0844 A66-16080  
 Properties of nonirradiated heat-shrinkable silicone and fluorosilicone rubbers for insulating and encapsulating electrical and electronic apparatus, including resistance to aging, fuels, ozone, etc 06 p0900 A66-16298  
 European Miniature Electronic Components and Assemblies Data 1965-1966, Part I, Germany and Italy 06 p0858 A66-17158  
 European Miniature Electronic Components and Assemblies Data 1965-1966, Part II, France, Netherlands, Scandinavia and Switzerland 06 p0859 A66-17159  
 Plotting oriented graph of two-stage electronic circuit with cathode coupling 08 p1200 A66-18923  
 Electronic correlator circuit yielding intercorrelation function at same rate at which signal is applied to device input 08 p1192 A66-19099  
 IEEE aerospace and navigational electronics conference at Baltimore in October 1965 08 p1250 A66-19487  
 Accessibility as factor in reducing production cost and maintenance time and increasing reliability in electronic equipment 08 p1197 A66-19526  
 Electronics methods used in laser technology and vice versa, emphasizing microwave photoelectronic devices, self-consistent gas discharges at optical frequencies, etc 09 p1386 A66-20434  
 Operation modes of electron beam generators with resonant oscillating systems and bipolar regenerative amplifiers developed from them 09 p1353 A66-20438  
 Radiation effects on electronic components noting sensitivity to gamma, fast neutron and electron radiation 09 p1359 A66-20969  
 Prediction and assessment of electronic equipment in early design, particularly that of mean time between failure 10 p1513 A66-21858  
 Moleculechron, stable molecular beam generator using pairs of resonators coupled by molecular beam 11 p1666 A66-22726  
 Interference in low-level input electronic equipment design, examining minimization methods for effects of hum, noise, etc 11 p1673 A66-23484  
 Reliability technique viewed as broad discipline encompassing entire field of traditional design, production and maintenance 12 p1832 A66-24071  
 Electronic equipment failures, which show characteristic dependence on time, divided into initial, chance and wear-out failures 12 p1832 A66-24074  
 Estimation of manufacturing costs of low volume high-cost complex electronic subsystems [ASTME PREPRINT MM66-701] 12 p1886 A66-24411  
 Aerospace and electronic systems - IEEE International Convention, New York, March 1966 12 p1818 A66-24600  
 Antennas, microwaves, electron devices - IEEE International Convention, New York, March 1966 12 p1838 A66-24613  
 Atomic origins of transient nuclear radiation effects in electronics such as neutron and gamma radiation 12 p1918 A66-24680  
 Electronic self-steering techniques applied to satellite communications systems with high gain antennas, noting transdirective array and self-phasing array [AIAA PAPER 66-326] 12 p1824 A66-24796  
 Yield and reliability of integrated electronic devices and electronic digital systems, using redundant components by triplicating voting 12 p1846 A66-24914  
 Reliability of nonelectronic components in

electronic system, noting failure modes, rates, mechanism, etc 13 p2085 A66-25655  
 Book on measurement of specific electronic parameters in circuit design 13 p2042 A66-26121  
 Reliability improvement in airborne electronic equipment 13 p2044 A66-26692  
 Electronic equipment for Iris telemetry and remote control stations for satellites 14 p2270 A66-27548  
 Air Force Avionics Laboratory and problem of transition from exploratory development to operational hardware 15 p2618 A66-28746  
 High performance contactor design and development 15 p2460 A66-28993  
 Design procedure for rotary solenoids having high unit density, low rotational inertia and inherent resistance to dynamic environments 15 p2460 A66-28994  
 Electromagnetic shielding for sensitive electronic components, noting Netic and Co-Netic magnetic alloys 15 p2465 A66-29670  
 Multichannel differential amplitude discriminator using diodes and transistors 15 p2503 A66-29694  
 Evolution and present status of electronic circuit components including manufacturing and component applications 15 p2468 A66-29890  
 Thermostability and control of airborne electronic equipment in closed-loop forced-air cooling systems 16 p2663 A66-31325  
 Basic techniques for producing thin-film electronic components 17 p2881 A66-32105  
 Mark II avionics system used in F-111A tactical fighter for navigation and weapons delivery performance 18 p3076 A66-33958  
 Electronic equipment for guided weapons design and quality evaluation 18 p3079 A66-34210  
 Industrial nuclear electronic supplies - Conference, French Atomic Energy Commission, December 1965 18 p3113 A66-34411  
 Chemical vapor deposition technique for materials for electron devices including preferred orientation, high purity material, special layer structures, etc 18 p3125 A66-34619  
 Reliability of complex electronic device incorporating great number of components 18 p3087 A66-34957  
 Apparatus for teaching and research in electron physics including emitters, cathode ray tubes, electron multipliers and mass spectrometer 18 p3088 A66-35033  
 Optical-electronic components for signal transmission, considering light emission diodes and silicon control switches 19 p3283 A66-36813  
 Fan selection for high-altitude cooling of electronic equipment 20 p3527 A66-37346  
 Forced-cooled electronic chassis development history 20 p3527 A66-37347  
 Integrated circuits economics, discussing design, construction and running costs 20 p3531 A66-37830  
 Managerial functions related to electronic component parts 20 p3683 A66-37881  
 Prediction of avionic equipment reliability in early design stage, noting equations for line replaceable unit /LRU/, classification, regression techniques, etc 20 p3573 A66-37953  
 Submillimeter wavelength electronic devices, examining development of lasers and reflected wave tubes with overlapping effective wave range 20 p3580 A66-38004  
 Geomagnetically trapped radiation effects on solid state electronic device aboard unmanned vehicles 20 p3534 A66-38349  
 Airborne electronic command device for measuring time intervals corresponding to cruising speed/ true flight altitude ratios up to 40 21 p3735 A66-38569  
 Flight electronics equipment and techniques, discussing communications devices, radio navigation apparatus, all-weather landing and onboard navigation aids 21 p3709 A66-38653  
 Electronic component, ferrite memory cores, filters and inductances adapted to integrated circuit utilization 21 p3716 A66-39622  
 Electronic navigation system for marine applications, using communications satellite

as data relay link 22 p3945 A66-40324  
 Specification and assessment of electronic equipment reliability, emphasizing statistical aspects of optimal cost/reliability estimation 22 p3883 A66-40961  
 Integrated circuit welding into electronic equipment via parallel gap method, noting military applications in forward area communications 23 p4044 A66-41198  
 Moleculechron, stable molecular beam generator using pairs of resonators coupled by molecular beam 23 p4078 A66-41464  
 Airborne digital computers role in electronic warfare, navigation and guidance, considering weight, power supply, costs, etc 24 p4177 A66-42245  
 Electronic system reliability prediction methods, comparing indices of new design with existing design 24 p4184 A66-42647  
**ELECTRONIC EQUIPMENT TESTING**  
 Air Force specification MIL-R-26667 for reliability testing of electronic equipment, commenting on MIL-STD-781 01 p0168 A66-10058  
 Military specifications MIL-HDBK-217 and MIL-R-22256, 22973 and 23094A with respect to reliability design of aircraft electronic equipment 01 p0034 A66-10059  
 Stress survival matrix test in evaluating reliability of monolithic silicon integrated circuit, measuring safety margin and performance parameter drift 01 p0035 A66-10082  
 Integrated circuit characterization by black-box analysis of interconnection parameters, noting transient response 02 p0204 A66-11937  
 Flight control by ground-based radio system discussing aerial navigation safety, operating principles, equipment for VOR and ILS and importance of calibration 03 p0390 A66-13011  
 DC testers for integrated circuits evaluated, emphasizing areas of application, testing methods and operating characteristics 03 p0345 A66-13274  
 Integrated circuit testing noting dynamic test system capabilities 04 p0491 A66-13385  
 Microelectronic amplifiers, emphasizing reliability improvement and decreased sensitivity to parameter changes 05 p0643 A66-14568  
 Accurate measurement of signal to noise ratio 05 p0634 A66-15497  
 Prediction and engineering assessment in early design, particularly mean time between failures of electronic equipment 06 p0839 A66-15948  
 Electronic component testing by methods of Advisory Group on Reliability of Electronic Equipment /AGREE/ 06 p0839 A66-15949  
 Preflight and operational status test set /PTS/ using radiating techniques for checking out aircraft electronic equipment without removal from aircraft 06 p0868 A66-15986  
 Principles and statistics behind life-test plans of MIL-STD-690 Life Test Sampling Procedures for Established Levels of Reliability and Confidence in Electronic Parts Specifications 06 p0886 A66-16332  
 Lifetime of semiconductor devices determined from noise levels 06 p0860 A66-17195  
 Reliability and accuracy testing of electronic equipment 07 p1005 A66-17357  
 Measured characteristic curves for evaluation of memory devices, specifically toroidal core 10 p1508 A66-21414  
 Continuous thermal cycling apparatus for small electronic component samples 10 p1511 A66-21751  
 Trigger functioning, failure due to grid voltage and transistor parameter changes, and reliability parameters of computer and control elements 11 p1677 A66-23032  
 SNAP-10A instrumentation and control subsystems and ground test program 12 p1911 A66-23676  
 Hybrid computer methodology and electronic data processing applied to quality evaluation of test operations 12 p1828 A66-23837  
 Forced reliability testing in electronic computers, switching circuits and digital communications systems by introducing noise or lowering input signal



level 12 p1833 A66-24077  
 Truncation method for determining life characteristics of electronic components such as transistors and vacuum tubes before testing to destruction 12 p1833 A66-24078  
 Component failure-rate testing by inspection or sampling, noting recommendations of advisory groups 12 p1833 A66-24081  
 Component reliability, especially in transistors, noting techniques, design, tests and mounting as monolithic circuits 12 p1833 A66-24082  
 Versatile avionics shop test /VAST/ system, computerized test system for carrier-based avionics 12 p1838 A66-24606  
 Fast scanning IR microscope for semiconductor evaluation used for engineering design analysis, reliability improvement, failure analysis, etc 12 p1843 A66-24676  
 Microwave component testing accuracy and analysis of error sources 12 p1883 A66-24725  
 Accelerated testing of transistors, resistors and capacitors to determine reason for certain types of component failure 12 p1844 A66-24728  
 Defect analysis by device sectioning, noting techniques, application in crystallography, electronics, etc 12 p1845 A66-24849  
 Reliability testing of electronic components at low stress levels, showing higher failure rates and different failure distributions than at maximum ratings 12 p1846 A66-24911  
 Optimum tests for check of working order of system with minimal material losses of safe or fault system 13 p2045 A66-25298  
 Secondary sensing technique for testing aerospace electronic systems by measuring side effects 13 p2079 A66-25692  
 Military and spacecraft electronic component testing, specifications and reliability programs 13 p2086 A66-25846  
 Extrapolating reliability ratings of electronic components and materials tested at high stress to low stress performance 13 p2043 A66-26220  
 Reduction of measurement error in devices for testing semiconductors, employing mechanical techniques 14 p2297 A66-28132  
 Electronic component reliability and control program 15 p2465 A66-29667  
 Silicon planar transistor design noting accelerated life test, failure data, etc 15 p2466 A66-29675  
 Test program for Gemini Attitude Control and Maneuver Electronics /ACME/ system, establishment and execution 16 p2676 A66-30438  
 Significant environmental criteria and realistic and standard test conditions for microelectronics testing 16 p2659 A66-30451  
 Monitoring device for detecting short-duration, vibration-induced electrical malfunctions, noting Gemini tests 16 p2677 A66-30454  
 Nondestructive attachment of small electronic components and integrated circuits for simulated mounting in vibration and shock testing 16 p2680 A66-30481  
 Operational test instrument for PCM bit synchronizers/signal conditioners, discussing importance of bit decision errors 16 p2659 A66-30541  
 Checkout of automatic meteorological measurement apparatus including thermograph, photoelectronic anemograph, etc, located on high tower of Institute of Applied Geophysics 16 p2704 A66-30775  
 Nomograms published in Electronic Design from 1963 to 1966 covering prototype, testing, costs, selection and avoidance of pitfalls 17 p2881 A66-32103  
 Step-stress technique to induce failures in integrated circuits to pinpoint source of reliability problems 17 p2882 A66-32114  
 Breadboard approach for integrated circuits with reduction of lost and development time, tabulating resistor and transistor parameters 17 p2884 A66-32128  
 Integrated circuit breadboarding time saving procedures 17 p2884 A66-32129  
 Integrated circuit testing by sequential, go-no-go and programming methods 17 p2884 A66-32131  
 Monogram on metrological foundations and test methods of aircraft instruments,

especially navigation instruments 18 p3111 A66-34011  
 Transistor testing and secondary breakdowns, featuring application of constant collector current and power with arbitrary waveform 18 p3078 A66-34087  
 Nondestructive testing of nonlinearities in passive electronic components, uncovering uneven film depositions, bad grindings, unreliable contacts, etc 18 p3088 A66-35020  
 Measurement of varactor diode characteristics for subsequent application in microwave low-noise parametric amplifiers 19 p3313 A66-35471  
 Built-in tests and periodic testing at field shop level applied to avionic systems operational readiness 19 p3339 A66-35504  
 Lifetime of semiconductor devices determined from noise levels 19 p3315 A66-35553  
 Electronic equipment to withstand cannon firing and extreme underwater depths 19 p3357 A66-35710  
 Indirect testing of dynamic systems involving maximum measure of parameter values from minimum test points, noting dependency of error propagation on system structure 20 p3521 A66-37210  
 Antennas for electronic navigation, discussing aircraft and ground based equipment, radiation patterns, restrictions, etc 20 p3597 A66-37719  
 Deterministic and quasi-deterministic class of electronic failure predictions as prevention strategy for use in aerospace system test or checkout program 20 p3566 A66-37887  
 Reliability testing programs applied to aircraft electronics equipment and description of development of MIL-STD-781A, exploring relation between reliability prediction and measurement techniques 20 p3570 A66-37936  
 Intermittent connection testing for digital logic module 20 p3523 A66-37949  
 Systems tests coverage for data processing system 20 p3523 A66-37950  
 Lunar Excursion Module /LEM/ reliability program, discussing engineering, manufacturing and techniques of design and qualification testing of electronic components 21 p3714 A66-39520  
 Automatic testing equipment, examining role of computer in reliability, quality of testing and time and cost savings 22 p3892 A66-40543  
 Electronic component reliability test program review including test planning, objectives and relation of types of review to projects 23 p4152 A66-41605  
 Mariner 1964 parts screening program including philosophy, program implementation, screening results and conclusions 24 p4178 A66-42089  
 Reliability prediction for electronic systems based on constant failure rate and MTBF /mean time between failures/ 24 p4185 A66-42866  
 Performance changes of various commercial types of vidicons tested in thermal chamber at practical extremes of temperature 24 p4185 A66-42959

# ELECTRONIC FILTER

## SA MICROWAVE FILTER

Constructing and evaluating electrostatic filter lenses with wide image angles for low voltage electron microscope 02 p0228 A66-11498  
 Electron microscope filter lenses with unconventionally shaped electrodes and large image angles 02 p0228 A66-11499  
 Undistorted reproduction of signal, using filter with transfer function having multiple zeros 04 p0503 A66-13706  
 Reflection and transmission coefficients of magnetically biased YIG ferrimagnetic resonator loaded in aperture of iris in coaxial transmission line 05 p0641 A66-14555  
 Frequency sensor and roving notch filter for control system, discussing parasitic signals with time-varying frequencies 05 p0645 A66-14603  
 Filtering techniques for estimating nonlinear discrete-time processes, including Bayesian estimation and weighted least squares approach 05 p0656 A66-14631  
 Band stop filters, determining advantages in high power transmission and rejection,

power capacity, Q-factor, etc 06 p0844 A66-16081  
 Symmetrical transverse electromagnetic-mode directional couplers, deriving formulas for functional parameters and insertion-loss function 06 p0844 A66-16083  
 TEM-mode coupled-transmission-line directional couplers, determining equal-ripple polynomials and tabulating parameters 06 p0844 A66-16084  
 Stable tunable RC filters with fixed capacitors, variable resistances and positive feedback 06 p0853 A66-16653  
 Dispersive network system for pulse duration modulation 06 p0866 A66-16957  
 Nonlinear characteristics of optimal inertialess filter for pulse noise to guarantee minimum rms error 07 p1014 A66-17436  
 Filtering properties of frequency-stability transport circuits of molecular beam generator, noting design considerations for high efficiency 09 p1353 A66-20442  
 Probability of signal acquisition by phase-locked oscillator system operating in frequency search mode, determining maximum admissible search rate without noise 09 p1354 A66-20443  
 Bridged-T three-terminal filter network modified to admit two same-frequency same-phase input signals of different amplitudes 09 p1361 A66-20609  
 Strip transmission line for microwave circuit design such as varactor multiplier frequency sources, filters, multiple pole diode switches, etc 09 p1356 A66-20672  
 Lumped-circuit LF general three-resonator filter in rectangular wave guide using inductive susceptances as coupling elements 10 p1514 A66-21911  
 Nonlinear filters, including system analysis optimization, realization via Volterra functionals, etc 11 p1675 A66-22630  
 Synthesizing group of parallel-input filters while minimizing insertion loss and reflection coefficient 11 p1656 A66-23065  
 Tapered distributed RC networks with similar immittances examined for poles and zeros of two-port short circuit admittance parameters 11 p1678 A66-23241  
 Digital and RF/linear circuits compared noting monolithic, hybrid and thin film circuit limitations, phase locked loop design, etc 12 p1830 A66-23756  
 Relating maximum Q-factor of second-order active filter section to Q-factor stability and to gain in active elements 13 p2030 A66-25209  
 Active transistor modulators for carrier frequency engineering, noting noise reduction, lower power requirements and modulation-filter matching 13 p2032 A66-25485  
 Radar range measurement accuracy shown to depend on receiver filter 13 p2023 A66-25666  
 Signal to noise ratio maximization using Pontryagin maximum principle, solving matched filter problem and designing signal with constrained energy and amplitude requirements 13 p2048 A66-25940  
 Electronic circuit design handbook covering control, detection, pulse and oscillator circuits, configurations, application, etc 13 p2042 A66-26056  
 Nomograph calculation for twin-T filter design 14 p2247 A66-26868  
 Redundant system reliability in aircraft design, noting amplifier and filter arrangements, diode and quadruplex circuits, etc 14 p2247 A66-27015  
 Undistorted reproduction of signal, using filter with transfer function having multiple zeros 15 p2469 A66-28549  
 Dishal method, logical means of tuning multiple-resonant-circuit filters and for adjusting coupling coefficients between adjacent resonators 15 p2463 A66-29036  
 Octave band all-pass filter with electronically tunable limiter ranges 15 p2463 A66-29037  
 Nonuniform transmission line generalization, noting application to proportional networks, exponential and Bessel lines 15 p2471 A66-29325  
 RC active filter synthesis using common-base and common-collector configurations 15 p2475 A66-29862



Transfer function characteristics of one input-two output complementary filters 17 p2880 A66-32059

Synthesis of control systems with minimum complexity, noting application to filter discrimination of nonstationary signals 17 p2901 A66-32568

Design of adaptive systems with forced oscillations, using correlation and filter methods 17 p2902 A66-32573

Design criteria for active filters using resistance and capacitance elements in feedback circuits 17 p2896 A66-33297

Half-wavelength resonators as capacitive-gap strip-line bandpass-type microwave filters, discussing parameter derivation for equivalent circuit and Cohn synthesis method 18 p3087 A66-34621

Quartz crystal active filters noting design and operation of multiresonator filters 19 p3312 A66-35337

Optimum digital filters combining position and velocity information under approximate distortionless constraint for LF navigation 20 p3596 A66-37224

Digital programming and topological optimal filter design incorporating nonideal lossy elements 20 p3533 A66-38281

Steady state and transient response characteristics of class of low pass filters noting transmission properties, frequency and time domain considerations, etc 21 p3713 A66-39271

Hybrid junction diplexer connecting transmitter and receiver to common antenna 22 p3873 A66-39784

Attenuation of single- and double-section bridge filters containing one two-winding magnetostrictive resonator and one two-winding coil 22 p3875 A66-40070

YIG resonators, oscillators and filters in microwave design 22 p3880 A66-40737

Dispersive network with attenuation equalizing network, weighting filter for control of output side lobe level with Gaussian shaped frequency response and matching system 23 p4034 A66-41016

Pulse compression filter synthesis using ultrasonic delay lines 23 p4034 A66-41019

Statistical correlation-Fourier frequency band analysis of coherent memory filter applied to pulse compression radar systems 23 p4035 A66-41023

S-band waveguide for pulse compression applications, providing cheap means of compressing wideband swept frequency pulses 23 p4035 A66-41024

Synthesis of prescribed frequency/group delay characteristics, using passive microwave components 23 p4035 A66-41027

Radar range accuracy, deriving expression for time domain calculation of accuracy degradation due to nonoptimum filtering 23 p4037 A66-41321

Optimum filtration of signals in presence of arbitrary interference, using orthogonal function series 23 p4037 A66-41514

Active and passive multiplication of RC time constants for subaudio frequency integrated filters 23 p4046 A66-41581

Horowitz minimum sensitivity decomposition does not lead to optimally sensitive networks for selected class of RC networks 24 p4181 A66-42372

Nonlinear behavior of second-order phase locked loop in presence of noise, discussing probability distribution of phase error, statistical properties of loop behavior, etc 24 p4172 A66-42618

RC filter with staggered notch frequencies for ease of adjustment and maintenance 24 p4183 A66-42628

**ELECTRONIC LEVEL**

**SA FORBIDDEN BAND**

Constants A and B of cesium superfine structure calculated from magnetic sublevel intersections 05 p0741 A66-15859

Fluctuations of electron numbers in general M-level system, using difference equation 08 p1279 A66-19837

Electron impact ionization cross section of H<sup>2</sup>s/ and H<sup>2</sup>p/ in Born A, Born B, Born-Ochkur and classical approximations 11 p1738 A66-22498

Interference of fine-structure levels in hydrogen ions passing through two successive carbon foils 11 p1740 A66-22968

Decay theory of closely coupled unstable

states based on Green function formulation for transition amplitude 11 p1741 A66-23189

Neon level broadening under effect of laser radiation studied by observing Hanle effect on fluorescent light 15 p2517 A66-29640

Electronic energy for ground state of one-electron diatomic molecule near united atom 18 p3140 A66-34512

Mean life of electronic level in O V measured by beam-foil technique 20 p3604 A66-37605

**ELECTRONIC MODULE**

Temperature cycling effect on welds of known strength which are encapsulated with several types of resins to determine internal stress in electronic modules 02 p0234 A66-11326

Producibility of electronic hardware for Pershing weapon system ground support program 02 p0198 A66-11463

Direct-immersion liquid cooling of modularized microelectronic systems on system-wide basis 06 p0841 A66-15973

Package densities and power dissipation requirements in hybrid integrated circuits solved by modular arrays 10 p1512 A66-21760

Stick module interconnection of flat packs into single-axis motherboard 11 p1665 A66-22678

Integrated modular digital computer system for ICETAN /ICES-FORTRAN/ programming of engineering problems 12 p1827 A66-23833

Solar cells for space travel, emphasizing fabrication into modules [AIAA PAPER 64-738] 13 p2007 A66-26644

Program-controlled module design using strips of nickel foil for welding of flatpack assemblies 17 p2930 A66-33121

Ground and airborne digital equipment for missile and space systems built with mass produced standardized modules interconnected by wrapped joint wiring 18 p3077 A66-34050

High-speed complementary MOS memories 19 p3314 A66-35527

Miniaturization of logic components for modular and monolithic integrated circuits in computer design 21 p3708 A66-39624

System maintainability in Back-Up Interceptor Control System /BUIC II/ using modular design of system, discussing software and failure 24 p4178 A66-42093

**ELECTRONIC PACKAGING**

Embedment stress effects on electrical characteristics of encapsulated components, presenting capacitor test results 02 p0247 A66-11287

Dielectric organic polymers in microcircuit communications modules 02 p0195 A66-11289

Electronic packaging - SAE Conference, Los Angeles, October 1965 02 p0233 A66-11320

Carrier-mother board rack approach to microcircuit interconnection and packaging 02 p0195 A66-11322

Automated flat pack welding design, discussing operational functions and major components 02 p0234 A66-11323

Reliability control in parallel gap welding used to join integrated circuit flat packs to printed circuit assemblies 02 p0234 A66-11324

Correlation of microstructure, microhardness and microchemistry in resistance welded electronic leads 02 p0234 A66-11327

Packaging tradeoffs for Pershing ground support equipment 02 p0197 A66-11459

Electronic packaging in Pershing weapon system ground support equipment 02 p0197 A66-11460

Epoxy transfer molding of high density modules for Pershing weapon system reliability and economy 02 p0234 A66-11462

Packaging techniques interrelated with design specification and manufacturing capabilities noting integrated circuit system, circuit reliability and thermal resistance 02 p0200 A66-11891

Packaging method for integrated circuits based on flow soldering components through printed wiring boards to be used in digital computer design 02 p0204 A66-11940

Practical component packaging system for compatible use of integrated and thin film circuits in spaceborne digital command and data handling equipment 04 p0492 A66-13465

Multilayer circuit boards for interconnecting integrated circuits in computer and other large systems 04 p0498 A66-14015

Thermionic converters, discussing resistant metal-bond use for collector-emitter insulation 05 p0622 A66-15590

Gas-cooled electronic equipment, discussing experimental heat transfer and pressure drop data, packaging and thermal effectiveness parameters [ASME PAPER 65-WA/HT-44] 05 p0650 A66-15665

Thermal-electrical systems for showing effect of variations in integrated circuit geometry and packaging on thermal response characteristics of simple structure 06 p0841 A66-15972

Microminiature element packaging and multilayer circuits, discussing design and production 07 p1010 A66-18247

Packageless diode fabricated by beam-lead process with no soldering or eutectic bonding 09 p1351 A66-20166

Digital systems research model design containing logic gates in integrated circuit packages 09 p1356 A66-20676

Design problems involved in transition from discrete-component circuits to integrated microelectronic circuits, noting conversion of analog and digital circuits and system packaging 10 p1512 A66-21758

Hybrid circuit rejects avoided by using ceramic channels and ultrasonic bonders during assembly of active semiconductor devices and integrated circuits to thin film network 10 p1512 A66-21759

Package densities and power dissipation requirements in hybrid integrated circuits solved by modular arrays 10 p1512 A66-21760

Electronic system packaging efficiency through reduction of passive volume of clearance, wiring and structure 11 p1665 A66-22677

Vibration and shock isolation of electronic equipment, examining isolation theory of periodic vibrations and random vibrations 11 p1667 A66-22764

Basic structure of cylindrical diode package mounted with axis normal to parallel metal surfaces extending beyond diode package 12 p1831 A66-23905

Laser welding for production microwelding, noting design, construction and application [ASTME PREPRINT MM66-707] 12 p1886 A66-24415

Parts, materials and packaging reliability and electric contacts - IEEE International Convention, New York, March 1966 12 p1842 A66-24663

Functional approach to electronic packaging of 60-mc intermediate frequency amplifier using thin film circuits 12 p1847 A66-24952

Design of electronics packaging for LEM, considering reliability, low-weight, integration, control, etc 12 p1847 A66-24956

Packaging design of electronics portion of missiles IR tracker system 13 p2040 A66-25841

Packaging VHF/UHF circuits involved in design of RF equipment used in air and spaceborne vehicles 13 p2041 A66-25844

Packaging quartz pressure transducers 13 p2084 A66-26565

Ministick packaging system for integrated circuits 14 p2249 A66-27109

Dynamic logic chassis analyzer /DLCA/, diagnostic tool for isolating faults to circuit card or component level in programmer test station /PTS/ and component test station /CTS/ ground support equipment 14 p2260 A66-28266

Thin film hybrid packaging method for series of computer logic circuits designed to operate at 100-mc clock rate 14 p2260 A66-28267

Packaging techniques for telemetry components and systems to withstand gun-launch accelerations up to 250,000 g 16 p2651 A66-30561

Electronic encapsulant thermal conductivities increased, noting dry filling potting technique, considering module reparability 16 p2664 A66-31378

Laser welding for advanced electronic packaging 16 p2715 A66-31593

Computer assemblies packaging analysis for



Optimum logic gates and inputs as function of leads 17 p2883 A66-32124  
 Printed circuit processing, state of the art 17 p2896 A66-33365  
 Embedding and encapsulating processes and design of embedding materials for electronic packaging 17 p2944 A66-33525  
 Ground and airborne digital equipment for missile and space systems built with mass produced standardized modules  
 Interconnected by wrapped joint 18 p3077 A66-34050  
 Thermoconductivity, mechanical stress, processing characteristics, etc., of various adhesives used in integrated circuits, noting neoprene cement 18 p3077 A66-34051  
 Integrated circuit connecting and packing, discussing cost flexibility and performance characteristics 18 p3086 A66-34399  
 Electronic packaging weight reduction by using magnesium-lithium 19 p3376 A66-35327  
 Packaging transistor and diode chip circuits 19 p3313 A66-35483  
 Airborne UHF telemetry receiver utilizing solid state components and high-density packaging technique 19 p3316 A66-35691  
 Microelectronics pulse code modulation PCM/multiplexer-encoder for Apollo spacecraft, emphasizing packaging techniques, discussing advance circuit design techniques 19 p3317 A66-35707  
 Integrated electronic arrays, examining fabrication, logical design, application and packaging 21 p3710 A66-38828  
 Assembly and packaging of microelectronic systems by integrated circuits, considering spatial configuration, maintainability, interconnection, thermal transfer and environmental resistance 21 p3710 A66-38830  
 Packaging technique for producing rendezvous radar and transponder noting structural design, reliability, cooling, outgassing, humidity, etc 21 p3715 A66-39527  
 Hybrid PCM telemetry system packaging for Nimbus B spacecraft 21 p3706 A66-39585  
 Packaging monolithic integrated circuits in ENVAC 1824 Aerospace Computer Central processor 22 p3878 A66-40714  
 Reliability prediction, failure rates, failure design and packaging of integrated circuit and MOS-FET microminiaturized electronic equipment 24 p4179 A66-42098  
 Systems design and packaging with integrated circuits, discussing proper circuit selection guidelines and parameters 24 p4182 A66-42499  
 Leak specifications for gas-filled electronic enclosures, discussing molecular, slow viscous, capillary and ordinary leak patterns 24 p4182 A66-42574  
 Flat-pack case for thermal resistance of integrated circuit to space environment 24 p4186 A66-43059  
**ELECTRONIC PHOTOGRAPHY**  
**SA ASTRONOMICAL PHOTOGRAPHY**  
 Image dissector for lunar observation in conjunction with Earth-based telescope, noting efficiency of resolution contrast sensitivity 12 p1883 A66-24678  
 Phase hologram generation by means of thermoplastic xerography 13 p2081 A66-26001  
 Electronic device for converting one-dimensional optical image into electronic image with subsequent conversion of electronic image into electrical image in time 16 p2709 A66-31609  
**ELECTRONIC RECORDING INSTRUMENT**  
 Performance testing, evaluation and system specification of broadband predetection recording instruments 14 p2298 A66-28430  
**ELECTRONIC SIGNAL MEASUREMENT**  
 Measuring instrument for time interval between two electrical impulses 05 p0682 A66-15311  
 Mode selective coaxial directional couplers for measurement of unwanted harmonics effect 13 p2044 A66-26745  
 Narrow band LF direct-reading random noise measurement and reduction of time requirements, using integrating RC network with time-variable components 14 p2295 A66-27716  
 Automatic recording, printing and punching of meteorological data from signals measured by automatic bridges and potentiometers on high tower of Institute of Applied Geophysics 16 p2704 A66-30776

Thermal noise in internal measuring instruments affecting limitations on spacecraft open-loop inertial autonomous control system precision 18 p3132 A66-33872  
 Operational circuits found in measuring devices and in regulation or control systems for low power signal transformation for space application 18 p3076 A66-33882  
 Possible measurement of current flow through electrode in plasma by inserting Rogowski coil in electrode 19 p3357 A66-35807  
**ELECTRONIC STRUCTURE**  
 Multiband model for monoclinic and orthorhombic rhenium dioxide exhibiting Pauli paramagnetism and metallic type conductivity 01 p0127 A66-11084  
 Electronic structure of molecules based on wave function called self-consistent field biorbital wave function 03 p0394 A66-12334  
 Plastic deformation splitting and evolution of spectral lines and excited level structure of europium ion in alkaline-earth fluoride crystals 03 p0409 A66-12717  
 Optical field effect in analyzing band structure and surface physics of silicon, noting reflectance 04 p0560 A66-13723  
 Effect of relativistic interaction terms, mass velocity, Darwin and spin-orbit coupling upon electronic levels of covalent-bond compound semiconductors BN, SiC, AlP and GaAs 04 p0561 A66-13725  
 Electronic states of single defects in diamond calculated by comparing electronic states of single vacancies and single interstitial carbon atoms 06 p0938 A66-17148  
 Low temperature alpha radiation and subsequent isothermal recovery effects on electron structure of gold, relating resulting failures to Frenkel defects 07 p1048 A66-17303  
 Quantum mechanical discussion of electron structure of crystal lattice of semiconductor as contributor to thermodynamic behavior of impurities 07 p1097 A66-17472  
 Band structure of germanium in vicinity of Brillouin zone center 07 p1097 A66-17533  
 Electronic structure of refractory compounds based on X-ray study of chromium spectra 09 p1391 A66-20871  
 Steady state structure and LF modes of infinitely long finite thickness cylindrical sheet of relativistic electrons in applied external field 12 p1873 A66-24576  
 Indium-cadmium alloy superconducting transition temperatures for varying compositions, noting electronic structure 13 p2169 A66-26278  
 Alloying real germanium surface with gold impurity and increase of fast surface states and rate of surface recombination 14 p2365 A66-27752  
 Thermionic emission from barium telluride measured by cathodes formed by direct reaction of elements and reduction of barium tellurate 19 p3436 A66-35426  
 Low temperature vibronic transitions between electronic states involving destruction of photon and creation of phonon via electric dipole term of Hamiltonian 19 p3446 A66-36394  
 Metal and alloy optical properties and electronic structure - International Colloquium, Paris, September 1965 20 p3612 A66-37271  
 Alfven wave propagation equations used to study electronic properties of semimetals 20 p3615 A66-37282  
 Electronic structures of transition metal alloys analyzed, comparing superconducting critical temperatures with H, N and O acting as electron donors 22 p3960 A66-39779  
 Indium and thallium first spectra sp<sup>2</sup> atom configurations and configuration mixing 22 p3960 A66-39801  
 Shock tube monitoring of electron-generation rate in argon-xenon ionization cross section implies that atom-atom processes in noble gases ionization cross section is independent of electronic structure 23 p4099 A66-42080  
**ELECTRONIC SWITCH**  
 Microelectronics and results achieved in relays, switches, variable capacitors and potentiometers 02 p0205 A66-11943  
 Learning matrices based on redundancy principle as nonadaptive self-correcting adjustment switches and error detectors in

electronic systems 04 p0489 A66-13510  
 Channel sample-and-hold PCM telemeter, system modules, multiplexer gate groups, analog-to-digital converter, etc 08 p1184 A66-19518  
 Electronically despun switched antenna using variable phase shifters to control phase of incident power to circular array of elements [AIAA PAPER 66-302] 12 p1844 A66-24769  
 Series power switch for orientation and position computer of small lunar-orbit spacecraft designed to reduce weight and cost 17 p2878 A66-33122  
 Textbook on transistor electronics of semiconductor switching devices in digital and some analog installations 17 p2876 A66-33190  
 Circuit functions, electrical parameters and fabrication of integrated analog switch in monolithic silicon block 19 p3320 A66-36322  
 Contactless telemetering element design, deriving equations for geometric dimensions of spring loaded oscillating system 23 p4045 A66-41398  
**ELECTRONIC TRANSDUCER**  
**SA ULTRASONIC WAVE TRANSDUCER**  
 Thin film strain gauge transducers noting temperature performance, power dissipation, metallic or ceramic construction and application to nuclear radiation testing, airborne equipment, etc 06 p0882 A66-16898  
 Transducers for exciting and detecting acoustic waves in discharge tube plasmas, discussing requirements, specifications and construction techniques 07 p1032 A66-17496  
 Groove guide, discussing development and performance of H sub 11 /low loss/ transducer 07 p1008 A66-17516  
 Ten-inch stroke electrodynamic thruster, noting modifications in armature guidance, base, rotation system, trunnion lifting mechanism, etc 16 p2678 A66-30464  
 Ferroelectric transducers, discussing feasibility of using ceramic transducers as pulsed power supplies 21 p3741 A66-39504  
 Current transducer for measuring current pulses in kiloampere range and suitable for laser research applications 24 p4213 A66-42820  
 Microwave transducers for measuring geometric dimensions and displacements in industrial process control 24 p4214 A66-43012  
**ELECTRONICS**  
**SA MEDICAL ELECTRONICS**  
**SA MICROELECTRONICS**  
**SA MOLECULAR ELECTRONICS**  
 Intermediate text on fields and waves in communication electronics covering basic equations, oscillating systems, transmission lines, waveguides, microwave circuits, etc 01 p0031 A66-10977  
 Western Electronic Show and Convention, San Francisco, August 1965, Part 5, Space electronics 01 p0072 A66-11109  
 Western Electronic Show and Convention, San Francisco, August 1965, Part 1, Military electronics 02 p0197 A66-11457  
 Pershing weapon system test stations and new microminiaturization packaging 02 p0197 A66-11458  
 Electronic systems in marine, air and space transportation noting radar, ultrasonic devices, computer techniques, etc 02 p0206 A66-12033  
 Space electronics - IEEE International Symposium, Miami Beach, November 1965 04 p0475 A66-13575  
 National Electronics Conference, Chicago, October 1965 05 p0639 A66-14553  
 Book on space communications techniques covering equipment design and components and communications subsystems, with two bibliographies 05 p0635 A66-15805  
 Military electronics - MILECON/9, Conference, Washington, D.C., September 1965 06 p0840 A66-15954  
 Aerospace electronics developments and trends toward more hybrid systems in guidance and control applications 11 p1667 A66-22954  
 Systems effectiveness - Conference, Electronic Industries Association, Washington, D.C., October 1965 11 p1788 A66-23434  
 Wire and data communication - IEEE International Convention, New York, March 1966 12 p1818 A66-24594



- Radio communication, broadcasting and audio - IEEE International Convention, New York, March 1966 12 p1838 A66-24597
- Circuit theory, information theory, basic sciences, electrostatic processes - IEEE International Convention, New York, March 1966 12 p1855 A66-24645
- Instruments, measurements, industrial electronics, nuclear science, ultrasonics - IEEE International Convention, New York, March 1966 12 p1842 A66-24672
- Northeast Electronics Research and Engineering Meeting, Boston, November 1965 13 p2032 A66-25501
- Physics of quantum electronics - Conference, San Juan, Puerto Rico, June 1965 13 p2093 A66-26141
- Adhesives and sealants in electronics, discussing resin elastomers, epoxies, polyurethanes, polysulfides, outgassing, damping, radiation effects, etc 14 p2318 A66-27103
- Text on experimental low temperature physics covering experimental techniques, liquid helium, superconductivity and electronic properties in metals 15 p2566 A66-29320
- Avionics and transportation 16 p2830 A66-30087
- Book on electronics and electron physics advances including fast ion scattering, kinetic ejection of electrons, plasma application in microwaves, etc 16 p2747 A66-30794
- Materials science and technology in integrated electronics - Conference, San Francisco, September 1965 16 p2781 A66-31414
- Integrated circuit technology, noting array trend 16 p2664 A66-31415
- Hall effect application - MIT Conference, Cambridge, November 1965 16 p2785 A66-31571
- Microwave applications of semiconductors - Symposium, London, June 1965 17 p2888 A66-32901
- Physical principles of cathode electronics - All-Union Conference, Leningrad, October 1965 17 p2988 A66-33453
- Book on glow discharge and plasma physics including collisional processes, ionization, vacuum systems, application in electronics, etc 18 p3150 A66-34946
- Aerospace electronics - IEEE National Conference, Dayton, May 1966 19 p3394 A66-35501
- Electronic theory of metals applied to study of total hemispheric thermal emission factors of polished metal bodies at temperatures below 800 degrees K 19 p3479 A66-36254
- Structural components and applications, electronics in aeronautics and astronautics - Conference, Hanover, West Germany, May 1966 21 p3715 A66-39617
- Dictionary of semiconductor physics and electronics, English-German, German-English 22 p3871 A66-39701
- Nondigital applications and interconnection aspects of integrated electronics - WESCON, Los Angeles, August 1966 22 p3878 A66-40713
- Transient radiation effects in electronics 23 p4111 A66-41211
- IEEE Region Six Conference, Tucson, April 1966, Volume 1 23 p4039 A66-41580
- IEEE Region Six Conference, Tucson, April 1966, Volume 2 23 p4049 A66-41600
- Electronic imaging technics for engineering, laboratory, astronomical and other scientific measurements - Seminar, Los Angeles, April 1965 23 p4069 A66-41664
- Electronic reliability - IEEE Conference, New York, May 1966 24 p4178 A66-42087
- ELECTROPHORESIS**
- SA COLLOID**
- Electrophoretic motion of dielectric particle determined from flow rate of liquid metals and semiconductors near infinite plane 05 p0733 A66-14688
- Electrophoretic determination on acrylamide gel of lactic dehydrogenase isozyme patterns in serum obtained from human subjects exposed to brief intense thermal impulses 06 p0814 A66-16831
- Solubility characteristics and electrophoretic and ultracentrifugal properties of human gamma globulins 09 p1334 A66-19900
- Chromatography on carboxymethyl cellulose to obtain fractions containing predominantly single bands of malate dehydrogenases 15 p2446 A66-28871
- ELECTROPHOTOMETRY**
- S PHOTOELECTRIC PHOTOMETRY**
- ELECTROPHYSIOLOGY**
- Electrophysiology of vision describing neural and photochemical processes and motor response 04 p0461 A66-13788
- Conduction velocity of single units, verified components of spinocervical tract and over-all conduction velocity determined in dorsal column of cat 06 p0810 A66-15941
- Electrophysiological study of responses of central nervous system on action of some factors of space flight 11 p1642 A66-22489
- Electrode implantation in dogs and detection of action currents in vegetative nerves after ten months 15 p2444 A66-29499
- Experimental research into olfactory code, noting psychological and physiological analysis, suggesting specific chemically sensitive molecules role 15 p2441 A66-29650
- Electrophysiological study of pituitary-adrenal axis activation during rapid eye movement /REMS/ in human urology patients 17 p2859 A66-32305
- ELECTROPLATING**
- Jet plating of gold to make ohmic contacts on silicon 14 p2361 A66-27277
- ELECTRORETINOGRAM**
- Electromagnetic shutter for electroretinography has opening and closing times of 0.50 and 0.70 msec and range of varying controlled durations 13 p2083 A66-26552
- Receptive field organization of rat retinal ganglion cells, examining maintained impulse activity with stationary spots of light 16 p2640 A66-31184
- Thresholds, b-wave latencies, stimulus intensity/b wave amplitude relationships and diffuse adaptation effects upon electroretinogram stimulation by light subtending 20 degree visual field 22 p3856 A66-40965
- ELECTROSTATIC CHARGING**
- Sources and effects of electrical charge accumulation and dissipation on spacecraft 11 p1778 A66-23485
- Electric field influence on thin metal film growth inducing coalescence of three-dimensional island-like structure 17 p2979 A66-32632
- ELECTROSTATIC DRAG**
- Electrohydrodynamic phenomena associated with motion of charged particle in plasma, showing that disturbance produced depends on particle speed 13 p2154 A66-26669
- ELECTROSTATIC FIELD**
- Mass spectrometry of positive ion beam produced by nonmagnetic emitter, using electron beam passing through electrostatic field for rare isotope analysis 03 p0397 A66-12391
- Relationship between field singularities of electrostatic theory and equations for fixed charge and dipole models, including geometrical distributions 03 p0391 A66-12404
- Electrostatic probe performance interpreted by taking into account MGD boundary layer 03 p0399 A66-12800
- Electrostatic field from E region and effect on motion of electrons trapped in magnetosphere 07 p1027 A66-17252
- Radiation induced during electron passage through magnetic field can be intensified and made nonrelativistic by superimposed electrostatic field 07 p1044 A66-18261
- Radiation induced during electron passage through magnetic field can be intensified and made nonrelativistic by superimposed electrostatic field 09 p1387 A66-20905
- Force field detection and control of objects in space, using gravitational, electrostatic or magnetostatic fields 12 p1820 A66-24677
- Mass spectrometry of positive ion beam produced by nonmagnetic emitter, using electron beam passing through electrostatic field for rare isotope analysis 13 p2139 A66-25397
- Motion equation of viscous oil flow under action of electric forces caused by surface charge 13 p2070 A66-26709
- Electrostatic interaction effect on EM wavescattering by atmospheric aerosol particles 14 p2284 A66-27539
- LF electrostatic field characteristics of clear air turbulence, noting theory and application of field sensing antennas, turbulence generated signals, etc 15 p2532 A66-28923
- MOS transistor characteristics based on model in which bulk charge due to ionized impurity in semiconductor and difference between electrostatic potential and voltage drop in channel are included 16 p2662 A66-31015
- Electrostatic field gradient effect in semiconductors with diffused impurities investigated, using basic diffusion theory 17 p2980 A66-32645
- Nonuniform motion of high field domains in Gunn effect including steady and nonsteady state properties of formation stage 18 p3077 A66-34076
- Electrostatic field influence on nucleate boiling of Freon 113, noting improvement of peak heat flux 19 p3477 A66-35407
- Surface patch electrostatic field effects on field emission single crystal plane work function determinations 21 p3770 A66-38656
- Electrostatic interaction effect on EM wavescattering by atmospheric aerosol particles 24 p4198 A66-42325
- Scattering of circularly polarized electromagnetic wave in Coulomb field, noting coalescence of two-wave quanta into one quantum of double frequency 24 p4220 A66-42529
- Scherzer theorem on aperture aberration extended to monochromatic nonrelativistic system with electrostatic or magnetic quadrupole fields with common planes of optical symmetry 24 p4239 A66-43215
- ELECTROSTATIC GENERATOR**
- Testing dielectrics by direct application of two high-voltage LF electrostatic generators with long-period sinusoidal waves 03 p0340 A66-12467
- Liquid filled electrostatic generation, noting charge transporting and insulating function of liquid helium 17 p2848 A66-31814
- ELECTROSTATIC GYROSCOPE**
- Unconventional attitude sensors required to make strapped-down gimballess inertial guidance system practical 01 p0139 A66-10004
- ELECTROSTATIC INSTRUMENT**
- Duoplasmatron with electrostatic lens decreasing ion energy while focusing ions for maximum density parallel beam 01 p0114 A66-10851
- Electrostatic spectrometers discussing deflection type, retarding-potential type and magnetic analyzers, advantages, uses, flux measurement techniques via energy selectors, etc 03 p0369 A66-12652
- Microwave amplifier, electrostatically focused klystron, for spaceborne equipment used in telecommunications of deep space 04 p0493 A66-13603
- Electrostatic fluxmeter measuring electrostatic field in atmosphere 04 p0523 A66-14307
- Low energy charged particle measurements, describing satellite mounted spherical electrostatic analyzer 05 p0751 A66-15373
- Water-cooled electrostatic probe capability of measuring local electron temperature, electron density, floating potential and saturation current ratio in dense plasmas [AIAA PAPER 66-73] 08 p1262 A66-18956
- Ion density profiles in boundary layers associated with supersonic flow of shock heated air over flat plate measured by cylindrical and flush-mounted electrostatic probes [AIAA PAPER 66-159] 10 p1565 A66-21686
- Low energy particle flux measuring circuits of spherical electrostatic analyzers aboard Elektron II and IV 11 p1704 A66-22431
- Generalized equation for steady state motion of electrons in cylindrical electrostatic system with arbitrary cross section, calculating critical focusing current 11 p1735 A66-22493
- Electrostatic double probe consisting of two parallel plates for plasma diagnostics [AIAA PAPER 65-542] 12 p1876 A66-23579
- Electrostatic fluxmeter measuring electrostatic field in atmosphere 14 p2297 A66-28220



- Electrostatic probe measurements of velocity displacement and electron density of plasma using laser compared with measurements using microwave interferometer 14 p2346 A66-28269
- Asymptotic theory of spherical electrostatic probe in collision-dominated partially ionized gas by quasi-linearization 18 p3146 A66-34583
- Electron beam rotation experiments on near spiratron with M-type electron gun 20 p3533 A66-38005
- Electron number densities measured behind shock wave in pressure driven shock tube by microwave resonant cavity technique and by electrostatic quasi-langmuir probe 24 p4191 A66-42197
- ELECTROSTATIC PLASMA**
- Ion escape from magnetic mirror trap due to nonlinear stage of plasma instability related to loss cone 01 p0109 A66-10261
- Ionic waves amplified by collective behavior in alkali plasma obtained by contact ionization of cesium or potassium vapors on surface of two coaxial tantalum cylinders 01 p0110 A66-10331
- Electrostatic ionic instability of cesium Q type machines for hot plasma-beam interactions in VLF range in sheath and plasma 03 p0404 A66-12984
- Thin electrostatic sheath near body immersed in weakly ionized flowing gas in mean free path regime for relatively small Debye length 06 p0921 A66-17102
- [AIAA PAPER 66-6] Quasi-linear theory of weakly turbulent plasma taking into account correlation of electric and magnetic microfields 09 p1407 A66-19966
- Electrostatic stability of cylindrical plasma beams composed of high velocity electrons rotating along magnetic lines of force in perpendicular direction and ions displaced along length of magnetic field 13 p2141 A66-25446
- Ion escape from magnetic mirror trap due to nonlinear stage of plasma instability related to loss cone 13 p2148 A66-25979
- Electrostatic instabilities in finite mirror-confined plasmas with loss-cone particle distributions, noting convective and nonconvective types 15 p2554 A66-29747
- Bounds on density fluctuations and electrostatic oscillation spectrum for homogeneous collisionless plasma according to Maxwell-Vlasov equation 15 p2554 A66-29749
- Magnetospheric suprathermal-electron scattering in oscillating electrostatic plasma and diffusion of subthermal electrons across magnetosphere, using ion-wave propagation theory for electroconductive plasmas 17 p2993 A66-32521
- Electrostatic stability of fully ionized non-Maxwellian electron-ion plasma 18 p3142 A66-33953
- Structure of hydromagnetic shockfront wherein electrostatic turbulence continuously develops, analyzed to aim at orders of magnitude for front width, electron and ion heating and magnitude of fluctuation excitation 19 p3408 A66-36278
- Plasma blob capture when injected perpendicular to magnetic force lines attributed to electrostatic repulsion of polarization space charge formed by interaction 20 p3610 A66-38057
- Explorer XX topside sounder observations of ionospheric irregularities in electron density and plasma wave electrostatic resonances 22 p3909 A66-39972
- Electrostatic oscillations in dielectric, semiconductor and plasma in presence and absence of external magnetic field 22 p3968 A66-40947
- Interaction models, negative energy waves and electrostatic instabilities 23 p4103 A66-41489
- Electrostatic probe in collisionless plasma wherein sheath joins region of ambipolar diffusion 23 p4104 A66-41494
- ELECTROSTATIC PRECIPITATOR**
- Gas adsorption on molecular sieves, discussing separation caused by electrostatic forces and electric fields 06 p0819 A66-18730
- ELECTROSTATIC WAVE**
- Electrostatic waves in uniform plasma without collisions in linear approximation, presenting normal oscillation mode as model for damped and unstable waves 11 p1744 A66-22447
- Cut-off wavelength of transverse electrostatic wave mode in ridged rectangular waveguide of arbitrary aspect ratio 14 p2257 A66-27951
- Unstable transverse potential oscillations in plasma with beam anisotropy and initial density modulation and analogy with known electrostatic oscillations 16 p2764 A66-31365
- Growth and propagation of electrostatic waves in medium with arbitrary mobility law, solving motion equations, emphasizing case pertinent to Gunn effect 19 p3447 A66-36399
- Electrostatic-wave propagation in collisionless plasma, noting Landau damping 19 p3432 A66-36760
- Electrostatic wave dispersion characteristics in one-dimensional plasma exhibiting Landau damping 19 p3432 A66-36761
- ELECTROSTATICS**
- SA STATIC ELECTRICITY**
- Electric resistivity of carbon resistor material determined as temperature function, calculating static response characteristics of carbon bolometer 02 p0228 A66-11445
- Electrohydrostatic boundary equations solving two-and three-dimensional axisymmetric situation and sessile drop problem 04 p0545 A66-13808
- Static characteristics of field triode with gate separated from semiconductor by thin dielectric layer, considering regimes of concentration, depletion, etc 04 p0499 A66-14054
- Static characteristics of gas laser internal modulation circuit, using electro-optical crystal inserted into gas laser resonator 04 p0531 A66-14059
- Complete resolution of concentrated load of limiting contour, determining spectrum of functional linear operator attached to interior region 06 p0967 A66-17061
- Text on electromagnetic force principles including Maxwell equations, electrostatics, electromagnetic waves, electron theory, relativity, etc 08 p1256 A66-19465
- Spherical electrostatic analyzers on Cosmos XII, Cosmos XV and Elektron II satellites 09 p1445 A66-21029
- Model technique calculation of electrostatic domains in two-valley /GaAs/ semiconductors 10 p1586 A66-22092
- Lightning and static electricity discharges effects on helicopter design and performance, noting blade and rotor hub protection, fuel ignition, etc 11 p1638 A66-23259
- Extended Dirichlet problem for cross section of cylindrical shell, showing asymptotic solution is valid, approximation to Dirichlet integral applied to electrostatic problem of condenser and closed tubes torsion 12 p1968 A66-24196
- Conformal transformation to determine electrical field of symmetrical air-filled strip line under static conditions 14 p2264 A66-27242
- Electrostatic theory of physical adsorption applied to gas-solid chromatography, discussing chromatographic inseparability of argon and oxygen at room temperature, prediction of elution order of many gases, etc 16 p2646 A66-30646
- Static characteristics of field triode with gate separated from semiconductor by thin dielectric layer, considering regimes of concentration, depletion, etc 17 p2884 A66-32220
- Static characteristics of gas laser internal modulation circuit, using electro-optical crystal inserted into gas laser resonator 17 p2933 A66-32225
- Electric field distribution in gas discharge counters at moment radiation recorded, allowing for space charge effect 17 p2928 A66-33490
- ELECTROSTRICTION**
- SA MAGNETOSTRICTION**
- Two-dimensional electrostriction to examine principal stress singularities in angular corners of plates 01 p0153 A66-10432
- Longitudinal acoustic wave generation by electrostrictive mixing of two light beams in single crystals of strontium titanate, rutile and z-cut quartz 19 p3400 A66-36073
- ELECTROTHERMAL ENGINE**
- Electrothermal propulsion system using heated gaseous nitrogen to provide Vela satellite with orbital velocity correction capability and weight savings [AIAA PAPER 66-213] 11 p1759 A66-22217
- ELEKTRON I SATELLITE**
- Difference in Doppler shifts of radio waves emitted at various frequencies by satellite Elektron I radio station, plotting electron concentration dependence on altitude 04 p0515 A66-13837
- Radiophysical investigations of outer ionosphere with aid of Cosmos II and Elektron I satellites and certain geophysical rockets 09 p1377 A66-21002
- Ionospheric parameter measurements based on ground reception of radio signals broadcast from Elektron I satellite 09 p1377 A66-21003
- Distribution and composition of particles in Earth radiation belts from data obtained by Elektron I and Elektron II satellites 09 p1445 A66-21030
- Distribution of trapped particles along orbit of Elektron I satellite 09 p1445 A66-21031
- Electron flux at upper boundary of outer radiation belt measured by Elektron I and II satellites 09 p1445 A66-21034
- Curves of difference in Doppler shift in observations of transmitter of Elektron I satellite, noting fluctuations in electron concentration 11 p1762 A66-22409
- ELEKTRON II SATELLITE**
- Neutron-group fluxes and variations with solar activity during IQYS observed by Elektron II 05 p0752 A66-15385
- Simultaneous measurements of magnetic field and positive ion fluxes in Earth magnetosphere from Elektron II satellite 09 p1444 A66-21025
- Earth magnetosphere measurements in radiation belt region from Elektron II satellite 09 p1444 A66-21026
- Distribution and composition of particles in Earth radiation belts from data obtained by Elektron I and Elektron II satellites 09 p1445 A66-21030
- Electron flux at upper boundary of outer radiation belt measured by Elektron I and II satellites 09 p1445 A66-21034
- Cerenkov counter measurement of nuclear component of cosmic rays onboard Elektron II satellite as function of solar activity during IQSY 10 p1595 A66-21043
- Solar X-radiation intensity measurement by Geiger end-window photon counters onboard Elektron II satellite 10 p1595 A66-21044
- Vertical electron density profiles determined at 725 and 1525 kc, using Elektron II satellite /1964 6B/ 10 p1600 A66-21050
- Matrix techniques for finding geomagnetic field strength in solar ecliptic coordinate system 11 p1699 A66-23052
- Metrological characteristics of three-component magnetometers with ferromagnetic probes installed in Elektron II space station 15 p2497 A66-28501
- Cerenkov counter measurements of primary cosmic ray heavy nuclei made by Elektron II satellite 18 p3199 A66-34886
- ELEKTRON IV SATELLITE**
- Primary cosmic radiation investigated by Elektron II and IV satellites 10 p1595 A66-21041
- ELEKTRON SATELLITE**
- Space studies of Cosmos and Elektron satellites including space radiation hazards, particle observation, ionosphere chemical composition, onboard equipment, etc 01 p0136 A66-10415
- RF mass spectrometer measuring ionic and neutral particle composition of outer ionosphere, mounted on Elektron satellites 02 p0229 A66-11662
- Primary cosmic radiation investigated by Elektron II and IV satellites 10 p1595 A66-21041
- Low energy particle flux measuring circuits of spherical electrostatic analyzers aboard Elektron II and IV 11 p1704 A66-22431
- Terrestrial radiation belt during solar minimum, noting results from measurement



with Elektron satellite series 18 p3175 A66-34745

**ELEMENT**

S DECISION ELEMENT

S FUEL ELEMENT

S HEAVY ELEMENT

S LIGHT ELEMENT

S NEUTRAL ELEMENT

S ORBITAL ELEMENT

S RADIOACTIVE ELEMENT

S SWITCHING ELEMENT

S TRACE ELEMENT

S TRANSITION ELEMENT

**ELEMENT ABUNDANCE**

Elemental abundances in solar atmosphere determined from intensity of absorption lines in solar spectrum 02 p0285 A66-11297

Astrophysical observation and experimental results of organic synthesis bearing on abiogenic formation of biochemical compounds formed from simple precursor in aqueous or aqueous ammonia system 02 p0181 A66-11603

Redetermination of isotopic composition of atmospheric neon resulting from measurements of neon in meteorites 04 p0517 A66-14323

Abundance of molecules, ions and atoms in late-type dwarf, giant and supergiant atmospheres 08 p1288 A66-18781

Copper and zinc abundances in carbonaceous, enstatite and ordinary chondrite determined by neutron activation techniques 08 p1291 A66-19093

Abundance and stability of major sulfur compounds in lower atmosphere of Venus calculated, assuming equilibrium between atmospheric gases and mineral phases 08 p1293 A66-19262

Abundance distribution of nuclear species in universe, examining nuclear reactions in stellar interiors as possible source 09 p1447 A66-20091

Solar wind enhancement of heavy element content in composition of solar corona relative to value for photosphere 09 p1456 A66-20415

Solar abundance of rare earths analyzed, using spectroscopy of ionized lines 10 p1605 A66-21208

Relative isotopic abundance of potassium 40 in terrestrial and meteoritic samples 11 p1770 A66-22572

High precision photoelectric scan at 8667-8668 angstrom wavelengths in solar spectrum for identification and abundance of boron 11 p1771 A66-22773

Nickel abundance in solar spectrum determined, based on atmospheric model 11 p1772 A66-22774

Interstellar molecular hydrogen abundance and possible source from giant stars 13 p2182 A66-25579

Lithium/calcium ratio of five F giant and six G giant stars 13 p2183 A66-25611

Stark broadening effect on solar atmospheric abundance determinations, with results for sodium abundance 14 p2383 A66-27709

Aerobee-borne magnetic mass spectrometric measurements of neutral composition of lower thermosphere 15 p2490 A66-29946

Telescopic measurements of primary energy spectra and abundances of He 3 and He 4 in galactic cosmic radiation 16 p2793 A66-30198

Element creating processes in interior of stars discussing combustion of carbon hydrogen, neon, neutron absorption, etc 16 p2796 A66-30271

Atmospheric decay of rocket-released Li due to diffusion, wind and chemical reaction 16 p2697 A66-31008

Mass spectrum and abundances of trapped and spallation fission xenon in Pasamonte meteorite 18 p3225 A66-33624

Silicon, iron and nickel in solar corona determined by method of Pottasch 18 p3233 A66-34575

Spectral analysis methods used to calculate iron abundance in solar corona 18 p3233 A66-34577

Composition of cosmic rays of supernova origin, noting limited mixing and enrichment of elements of outer layer with thermonuclearly synthesized core substances due to shock acceleration 18 p3177 A66-34755

Chemical abundances and energy spectra of nuclei in galactic radiation measured in interplanetary space by OGO-I satellite 18 p3190 A66-34833

Activated emulsion camera detection of low energy very-heavy multiply-charged scarce cosmic ray nuclei 18 p3190 A66-34835

Balloon-borne nuclear emulsion detection of solar cosmic ray heavy nuclei during solar burst 18 p3190 A66-34836

Balloon-borne nuclear emulsion detection of finite fluxes of low energy cosmic ray heavy nuclei and interstellar cosmic radiation propagation 18 p3191 A66-34838

Relative abundance of carbon isotopes in primary cosmic radiation estimated by separation of isotopes method in nuclear emulsion 18 p3192 A66-34843

Principle source of radiative energy loss in intergalactic medium in spectral region from 2 to 18 angstroms is line emission from ions of elements oxygen, carbon, neon, magnesium and silicon 18 p3237 A66-35046

Iron and nickel lines in solar UV spectrum, abundance of various metallic elements in solar atmosphere, electron collision cross sections and oscillator f-values of electron transitions 18 p3237 A66-35050

Boron abundance in Sun from B I lines and solar spectra 19 p3458 A66-35490

Quantitative measurement of free metallic atoms abundance and height distribution from twilight, dayglow and aurora fluorescence 19 p3349 A66-36350

Equivalent widths of spectral lines in solar spectrum used to determine strontium abundance 19 p3465 A66-36612

Total intensities of continuum and of red, green and yellow coronal lines emitted by sporadic coronal condensation shown to yield lower limits to Fe and Ca abundances 20 p3649 A66-37332

Interstellar X-ray absorption edges due to K-shell photoionization of oxygen and neon, using element abundances and atomic photoelectric cross section data 21 p3809 A66-38658

Cl, Br and I contents in carbonaceous chondrites measured by activation analysis 21 p3814 A66-39260

Rare-earth element abundance patterns in Hawaiian basalts determined by neutron activation analysis 21 p3735 A66-39492

Spectroscopic evidence on helium abundance of stars in galactic halo 21 p3817 A66-39565

Chainpur and similar, apparently primitive, chondritic meteorites may be precursors of ordinary chondrites 22 p3981 A66-40485

Solar cosmic ray multiply charged nuclei and July 18, 1961 solar event, discussing relative abundances and heavy nuclei detection 22 p3973 A66-40548

Polar coronal temperature inferred from density gradients and based on solar wind and latitude dependence of coronal composition 22 p3983 A66-40698

Isotopic composition of Xe indicates that two Ca-rich achondrites comprise group of diopside-olivine achondritic meteorites containing fission-produced Xe 24 p4264 A66-42606

Solar abundances of seven rare earths deduced for center of solar disk with weighting function method 24 p4279 A66-42711

Elemental abundances of low energy cosmic rays in July 1964 observed by sounding rocket, noting components 24 p4264 A66-42715

Hydrogen abundance in universe using gravitational effect on physical constants 24 p4279 A66-43019

**ELEMENTARY PARTICLE**

SA CHARGED PARTICLE

SA DEUTERON

SA ELECTRON

SA FAST NEUTRON

SA KAON

SA LEPTON

SA MESON

SA NEUTRINO

SA NEUTRON

SA NUCLEAR PARTICLE

SA NUCLEON

SA PHOTON

SA POSITRON

SA PROTON

Stable elementary particle detection of mass greater than that of proton in hydrogen, deuterium and atmospheric air samples, using mass spectrometer 01 p0060 A66-10251

Cosmic rays and fundamental problems in elementary particle theory 01 p0133 A66-10642

Motion equations in external gravitational field for relativistic two-point model of free elementary particle neglecting particles own field 08 p1282 A66-18606

Quantum statistical electromagnetic wave propagation and relativistic damping effects in uniformly magnetized electron-positron gas 08 p1187 A66-19809

Nature and relationship of elementary particles classified according to quark theory, for scientists lacking particle theory specialized knowledge 09 p1404 A66-20932

Distorted wave one-meson-exchange /DWOME/ for high-energy elementary particle reaction analysis, leading to different expression for transition amplitude 13 p2131 A66-25482

Stable elementary particle detection of mass greater than that of proton in hydrogen, deuterium and atmospheric air samples, using mass spectrometer 13 p2131 A66-25968

Dimensional structure and particle dynamics of metagalaxy 14 p2379 A66-27224

Cosmic rays and fundamental problems in elementary particle theory 14 p2377 A66-27949

Elementary particle theory, interactions at accelerator energies, bootstrap mechanism for generating bound states and resonances and Regge pole concept applied to high energy scattering 15 p2545 A66-29548

High energy mountain-altitude nuclear interactions produced by pions and nucleons, pion/proton and neutral/charged interacting particle ratios studied, using multiplate cloud chamber with air Cerenkov counter and absorption spectrometer 15 p2584 A66-29554

Secondary cosmic radiation and meson production at high energy, noting particle flux regularities and collision 15 p2586 A66-29564

Formula representing empirical masses of elementary particles, using two quantum numbers 15 p2546 A66-29568

Electron-muon similarities and multiple pion production by high energy muons, using accelerators and cloud chamber 15 p2546 A66-29576

High energy neutrino production in atmosphere contributed by pion, muon and kaon interactions 15 p2590 A66-29593

Angular distribution and energy loss of fast muons 15 p2547 A66-29594

Statistical approach to range and energy relationship for high energy muons 15 p2590 A66-29595

Cosmic neutrinos, discussing sources and forms of existence 17 p2994 A66-32835

Pulse shape discrimination technique using scintillation counter, distinguishing events of nuclear disintegration from those due to minimum ionizing particles 18 p3115 A66-35229

Cosmic radioastronomy, discussing radio wave emission from quasars, synchrotron effect, hydrogen emission, leptons, gravitational fields, origins of matter and antimatter, etc 20 p3651 A66-37437

Cosmic ray nucleon interaction with high energies, estimating transition probability and interaction cross section of baryon in passive state 24 p4263 A66-42519

Elementary particles interaction with atomic nuclei with energies from tens to thousands of bev 24 p4267 A66-42903

Angular distribution of secondaries in elementary multiple high energy production event, evaluating expected frequency of asymmetrical showers 24 p4267 A66-42905

**ELEVATION ANGLE**

Height finding technique using phase-in-space principle for radar system with single antenna and feed structure 17 p2872 A66-31960

Photoelectric Rotating Slit Elevation and Azimuth Sensor design, operation and performance 17 p2925 A66-32614

**ELEVATOR**

SA AILERON



- Optimal redistribution of lifting surface between wing and stabilizer-elevator unit ensuring minimum reduction of lift-drag ratio 23 p4011 A66-41796
- ELEVON**
- SAILERON**
- ELIMINATION**
- Solution of systems of polynomial equations by elimination procedure, using coding in LISP and FORMAC 21 p3707 A66-38680
- ELLIPSE**
- Large deflection analysis of elliptical plate of lenticular section subjected to uniform temperature gradient through thickness 03 p0440 A66-13271
- ELLIPSOID**
- SA OGIVE**
- Equilibrium configurations theory that rotating homogeneous fluid containing particles attracted to each other according to Newton laws and under constant pressure will form ellipsoid 01 p0056 A66-10308
- Hydrostatic problem of calculating potential on surface of nonconfocal ellipsoid from potential of simple layer on similar ellipsoid 01 p0056 A66-10309
- HF approximations for arbitrary body scattering specialized to ellipsoids and applied for source and observation points at distances large compared to scatterer size 03 p0334 A66-12817
- Ellipsoid of revolution of large aspect ratio with axis of revolution perpendicular to uniform flow at infinity analyzed for small Reynolds number 06 p0873 A66-16995
- Creep motion and hydromagnetics of ellipsoid moving in cross field 09 p1408 A66-20580
- Numerical solution to first geodetic problem of ellipsoid of rotation, using iterative application of Runge-Kutta method to differential equations of geodetic line 11 p1698 A66-22767
- Superconductivity destruction by magnetic field in type II superconductors with nonzero demagnetizing factor, especially for case of ellipsoidal body 18 p3154 A66-33942
- Critical analysis of certain conformal mappings of ellipsoid of revolution onto plane 18 p3109 A66-34739
- IAU system of geocentric astronomical constants for ellipsoid
- Earth 20 p3653 A66-37762
- Orbital plane precession due to ellipsoidal shape of Earth, discussing effect on meteorological and geodetic satellites 24 p4279 A66-42963
- ELLIPTIC EQUATION**
- Finite difference method solving Dirichlet problem for quasi-linear elliptic equation, with results applied to calculation of magnetic field in nonlinear media 01 p0091 A66-10165
- Straight lines method applied to Dirichlet and Neumann boundary value problem for certain nonself-adjoint two-dimensional second order elliptic equations 01 p0095 A66-11014
- Stability of net method for elliptical problems investigated, using low variability of network operator 01 p0096 A66-11184
- Theory of weight classes for differentiable functions of many variables, with application to boundary value problems for elliptic equations 02 p0250 A66-12099
- Fragmen-Lindelof type theorems for second-order linear elliptic equation, examining Dirichlet problem solution in infinite region 02 p0250 A66-12100
- Proof of boundary regularity connected with inhomogeneous systems of partial differential equations leading to elliptic boundary value problems 02 p0251 A66-12231
- Elliptic eigenvalue for reentrant region to determine vibration modes of membrane 03 p0387 A66-12620
- Asymptotic solution of Dirichlet problem for diffusion processes and small parameter in elliptic equations with discontinuous coefficients 03 p0388 A66-12925
- Existence and uniqueness of weak solution to Dirichlet problem for elliptic differential equations in Sobolev spaces with special occupancy function 05 p0708 A66-15154
- Asymptotic error estimates in solving elliptic equations of fourth order by method of finite differences 05 p0710 A66-15477
- Index problem for systems of singular integral equations 03 p0904 A66-17044
- A priori estimates for solutions to second order differential equation of elliptical type 06 p0904 A66-17045
- Property of solution of second-order elliptic equations 07 p1056 A66-17600
- Asymptotic behavior of solutions of boundary value problem for second-order elliptic equations 07 p1056 A66-17602
- Second order degenerate elliptic and parabolic equations, giving smoothness theorems of solutions 07 p1056 A66-17604
- Traces on coordinated hyperplanes of elements of functional space 07 p1057 A66-17844
- Indirect method of estimating Green kernels, eigenvalues and eigenfunctions of operators related to elliptic problems 07 p1059 A66-18031
- Certain inequalities for solutions of elliptic equations and derivatives near metric region 07 p1060 A66-18466
- Cauchy problem for elliptic system 09 p1396 A66-20632
- Tensor product analysis of alternating direction implicit iteration techniques for approximate solution of elliptic partial differential equations 09 p1396 A66-20637
- Series expansion solutions of Dirichlet and Poincare problems for systems of elliptical PDEs 09 p1397 A66-20934
- Nonlinear boundary value problem for elliptic PDE continuous over composite region 11 p1723 A66-23030
- Equilibrium equations of shallow cylindrical shell of arbitrary cross section subject to arbitrary loading 11 p1783 A66-23033
- Uniqueness theorems for second-order linear elliptic and parabolic equations with discontinuous boundary values 11 p1724 A66-23362
- Stability of net method for elliptical problems investigated, using low variability of network operator 12 p1903 A66-24017
- Majorants of solutions of first boundary problem for second order linear elliptic equations 12 p1904 A66-24238
- Maximized elliptic equations, Dirichlet problem, distance function solution, maximum principle, removable singularity, etc 12 p1905 A66-24401
- Analytic hyperfunction solution of elliptic equation 13 p2117 A66-25473
- Equation for elliptical system in plane singly connected region, satisfying specified boundary condition 13 p2119 A66-25903
- Boundary value problem for quasi-linear elliptic equations degenerating parabolically on boundary of region D lying in upper half-plane 13 p2119 A66-25904
- Dirichlet problem for degenerating elliptical equations with nonlinear lowest terms 13 p2120 A66-26007
- Dirichlet problem for elliptical system, showing solvability of inhomogeneous system with uniform boundary values for half-plane and circle cases 13 p2120 A66-26008
- Dirichlet problem deviation from Bitsadze system with Noetherian properties, giving Hausdorff normal solvability conditions for inhomogeneous problem 13 p2120 A66-26009
- General form of Rado-Cartan theorem for solution of second-order linear elliptic equations, using maximum principle 13 p2121 A66-26247
- Qualitative solution of even-order higher-order elliptic partial differential equations 15 p2528 A66-29335
- Finite difference method for elliptic systems of partial differential equations subjected to natural boundary conditions /generalized Neumann problems/ 16 p2731 A66-30234
- Riemann-Hilbert boundary value problem for elliptic systems of linear partial differential equations of first order 16 p2733 A66-30651
- Estimation of maximum rate of decrease in solutions to elliptic equation or system in cylinder 16 p2733 A66-30743
- Certain incorrect Dirichlet and Cauchy problems of potential theory for elliptic and parabolic equations 16 p2733 A66-30744
- Analytic construction of skew derivative Green matrix for system of second order elliptic PDEs in many variables 16 p2734 A66-30749
- Uniqueness of solution to second and third boundary value problems for second-order elliptic equation in presence of boundary singular points 16 p2734 A66-30783
- Normal solvability of Dirichlet problem for Bitsadze elliptic system, noting conditions under which homogeneous problem has nonzero regular solutions 16 p2734 A66-30784
- General boundary value problems for general elliptic systems with discontinuous coefficients 16 p2735 A66-30965
- Fractional powers of linear operators role in linear and nonlinear elliptic and parabolic equations, Fourier series in eigenfunctions of elliptic operators, etc 16 p2736 A66-30978
- First-order linear elliptic system with areolar derivatives involving n unknown complex functions 16 p2738 A66-31706
- Exactness of majorants of Dirichlet problem solution and uniqueness conditions for linear elliptic equations 17 p2947 A66-32581
- Integral representation providing one-to-one correspondence between functions of n complex variables and complex-valued harmonic functions of n plus 1 real variables 18 p3126 A66-33837
- General maximum principle and removable singularities, discussing case of arbitrary linear set of positive linear measure for which principle does not hold 18 p3128 A66-34661
- Mixed initial boundary value problem for wave equation in three space dimensions, proving existence of generalized solution 18 p3128 A66-34662
- Pointwise bounds for solutions to Cauchy problem for elliptic systems of partial differential equations, using extension of Payne and Trytten results 19 p3388 A66-35487
- Displacement boundary value problem in classical linear elastostatics, deriving ellipticity condition for uniqueness theorem 19 p3474 A66-35852
- Third boundary problem solution for two-dimensional equation of thermal conductivity in arbitrary region by locally one-dimensional method 19 p3478 A66-35934
- Difference analog construction for second-order elliptic differential equation in case of rectangular network 19 p3389 A66-35935
- General form of Rado-Cartan theorem for solution of second-order linear elliptic equations, using maximum principle 19 p3390 A66-36197
- Estimation of Poisson kernels of elliptic operator with variable coefficients by using maximum principle and Fatou theorem 19 p3390 A66-36248
- Character of continuity of solutions to second-order linear elliptic equations with many independent variables 20 p3592 A66-38421
- Linear elliptic partial differential systems, eigenvalue and boundary value problems - Johns Hopkins University, Lectures, March-May 1965 21 p3754 A66-38457
- Local existence theorems for elliptic systems with linear matrix differential operator 21 p3754 A66-38460
- Semiweak solutions of elliptic BVP, particularly generalized Dirichlet problem 21 p3754 A66-38461
- Existence and uniqueness theorems for Dirichlet problem of second-order linear elliptic equation, Neumann BVP, mixed BVP and oblique derivative problem 21 p3754 A66-38462
- Linear elastostatic BVPs for inhomogeneous anisotropic elastic body including existence-uniqueness theorem, based on Korn inequality 21 p3755 A66-38463
- Elliptic BVP in equilibrium theory of thin plates employing iterated Laplace operator 21 p3822 A66-38464
- Garding inequality and Green transformation applied to elliptic operators in eigenvalue problems 21 p3755 A66-38465
- Elliptic singular integro-differential operators on smooth compact manifold without and with boundary 21 p3756 A66-38626
- Self-induction of ellipsoidal plasmoid, deriving relevant equations 21 p3787 A66-39051
- Necessary and sufficient conditions for



matrix satisfying discrete maximum principle and difference methods for numerically solving second-order elliptic boundary value problem 21 p3757 A66-39258

Maximum modulus theorem extended to highly elliptic systems 21 p3758 A66-39369

Uniqueness of solution to second and third boundary value problems for second-order elliptic equation in presence of boundary singular points 22 p3940 A66-40445

Normal solvability of Dirichlet problem for Bitsadze elliptic system, noting conditions under which homogeneous problem has nonzero regular solutions 22 p3940 A66-40446

Dirichlet problem for elliptic system of differential equation which does not satisfy Lopatinski condition where characteristic equation of system has simple roots 22 p3940 A66-40449

Second-order quasi-linear elliptic equation with coefficients increasing over periods of time more slowly than any positive power of time 22 p3941 A66-40799

Projection method for obtaining upper and lower bound estimates of solutions to elliptic equations 22 p3942 A66-40914

Hilbert parametrix method of solving linear BVPs for second-order elliptic PDEs, using Green functions 24 p4232 A66-42740

Single second-order oblique derivative problem with elliptic operator 24 p4232 A66-42830

Linear second-order partial differential equations of elliptic type analyzed, using maximum principle and barrier functions 24 p4233 A66-43065

**ELLIPTIC FUNCTION**

Multidimensional homogeneous difference schemata solving eigenvalue problem with elliptic operator, noting differential equation coefficients and eigenfunction error estimate 01 p0092 A66-10166

Jacobi elliptic functions for designing low-pass filters whose attenuation is represented by universal normalized curve 12 p1829 A66-23661

Unsteady plane motion of pointed airfoil pair, obtaining resultant force and moment of biplane 13 p2062 A66-25400

MHD wave propagation along uniform magnetic field in cold plasma solved in terms of Jacobean elliptic functions 14 p2340 A66-27134

Regularity properties of functions from domains of definition of minimum and maximum operators for general elliptic problem with inhomogeneous boundary conditions 14 p2321 A66-27162

Topological classification of higher dimensional systems of ordinary differential equations by Liapunov functions 18 p3127 A66-33976

Elliptic boundary problem with small parameter, constructing boundary layer function 21 p3755 A66-38541

**ELLIPTIC INTEGRAL**

Staudte-Hoffmeister integral for abundance of sporadic meteoric bodies 03 p0427 A66-12921

Bounds for Dirichlet energy integral in terms of arbitrary vector field 04 p0539 A66-13949

Existence in small of fundamental solution matrices of uniformly Petrovskii-elliptic systems with coefficients having continuity modulus satisfying Dini conditions 14 p2321 A66-27159

Staudte-Hoffmeister integral for abundance of sporadic meteoric bodies 14 p2380 A66-27270

Reduction of large number of elliptic integrals, using relatively short list of formulas 14 p2322 A66-27777

Surface characteristics of semiconductors with intrinsic conductivity, determining potential distribution electric field, carrier concentrations, etc 17 p2984 A66-33146

**ELLIPTICAL CYLINDER**

Flow of non-Newtonian liquids in cylindrical pipes containing cylindrical parallel cores moving longitudinally at constant speed 03 p0358 A66-13090

Empirical expression for maximum stress and method of design for elliptic shell vessel 08 p1313 A66-19548

Elliptic cavity design for solid state lasers, discussing multiple reflections, absorption coefficient, refraction losses, etc

etc 13 p2092 A66-25998

Successive approximation method for compressibility in subsonic flow around elliptical cylinder 16 p2627 A66-30209

Electromagnetic scattering by perfectly conducting elliptical cylinder in uniaxially anisotropic medium, transforming boundary value to Helmholtz equation 16 p2654 A66-31442

Bending of plane electromagnetic waves around elliptically ideally conducting cylinder of infinite length and around parallel circular dielectric cylinder, with solution as Mathieu-type series 19 p3303 A66-36064

Functional equation applied to wave scattering by infinite grating of elliptic cylinders 19 p3304 A66-36409

Conformal mapping technique applied to boundary value problem of plane wave diffraction by perfectly conducting elliptic cylinder, noting integral equation 22 p3866 A66-40185

**ELLIPTICAL ORBIT**

**SA EULER-LAMBERT EQUATION**

Motion stability of dynamically symmetrical satellite rotating about normal to plane of elliptical orbit 02 p0295 A66-11650

Attitude stability of spinning satellite in elliptical orbit using Floquet theory [ASME PAPER 65-APMW-27] 04 p0586 A66-14227

Numerical determination of optimum two-impulse orbital transfers between inclined elliptical orbits 05 p0769 A66-15793

Molniva type communication satellite, discussing optimum orbital requirements for maximum coverage, phasing, etc 06 p0952 A66-15907

Closed-form coordinate perturbations of elliptic orbits due to Earth oblateness, discussing four methods of deriving expressions 06 p0956 A66-16910

Two-body problem applied to elliptic orbit, comparing three-impulse with single-impulse plane change applied at node 08 p1289 A66-18837

Optimum impulsive transfer between elliptic and noncoplanar circular orbits, noting paths with up to three apsidal impulses 09 p1459 A66-20884

Optimal rendezvous maneuver calculated between propelled spacecraft and unpropelled target moving in elliptical orbit of arbitrary eccentricity 11 p1768 A66-22457

Plane optimum transfer of point of variable mass between two elliptical orbits in centrally directed Newtonian force field 11 p1774 A66-23036

Linear differential system for rendezvous with target in elliptical orbit 14 p2391 A66-27471

Optimal transfer trajectories among coplanar elliptical orbits, noting application of one, two or three finite impulses 14 p2382 A66-27562

Analytical solution to linearized problem of power-off terminal rendezvous when target satellite is moving in elliptical orbit of arbitrary eccentricity 16 p2805 A66-31486

Time-dependent coverage area design parameter for Comsat systems in elliptical orbits, assuming spherical Earth and Keplerian orbits 17 p3002 A66-32472

Second-order optimal elliptical orbital transfer trajectory between two coplanar circular orbits in Newtonian force field 17 p3003 A66-32586

Attitude stability of spinning satellite in elliptical orbit, using Floquet theory [ASME PAPER 65-APMW-27] 18 p3239 A66-33590

Rendezvous between spacecraft and target flying in elliptic orbit of arbitrary eccentricity solved, using new approach [AIAA PAPER 66-537] 18 p3227 A66-33666

Minimum impulse orbital transfer between coplanar elliptical orbits with aligned axes, noting advantage of three- and two-impulse transfers 18 p3227 A66-33760

Single-impulse transition in Newtonian central force field from hyperbolic to elliptical orbit in case of radial impulse 19 p3455 A66-35276

Selection of elliptic orbit for solar probe craft without undue perihelion growth [AIAA PAPER 64-646] 19 p3459 A66-35601

Error equations of inertial navigation with special application to elliptical orbital determination and guidance [AIAA PAPER 65-691] 19 p3397 A66-35898

Simple approximations to elliptical orbits compared to predict location of planet or satellite, including linear perturbations in rectangular and curvilinear coordinates 19 p3463 A66-36246

Time of rendezvous of two satellites, one on circular and one on elliptical orbit 19 p3470 A66-36247

Minimum fuel transfer between neighboring elliptic orbits for low-thrust power-limited propulsion system, using Pontryagin maximum principle, vehicle motion and fuel consumption 20 p3645 A66-36875

Rendezvous-maneuver of thrusted space vehicle with unthrusted target flying in elliptical orbit, examining computation of rendezvous acceleration for orbital transfer 20 p3662 A66-37390

Equations describing motion of satellite in Paetzold-Zschoerner model of Earth atmosphere 20 p3654 A66-37848

Computation of impulsive and short-term perturbing forces effect on body in elliptical orbit, using Tschauner-Hempel equations 22 p3979 A66-40327

Optimum impulsive transfers between noncoplanar elliptic orbits having collinear major axes and common center of attraction, noting overlap configuration of initial and final elliptic orbits 23 p4129 A66-41686

Periodic oscillations of satellite in plane of elliptic orbit investigated to provide passive orbital stabilization of satellite 23 p4134 A66-41980

Dumbbell librations of satellites in elliptic orbits of small eccentricity determined via WKB approximation 24 p4272 A66-42158

**ELLIPTICITY**

Anisotropic transverse magnetoplasma effects in cubic semiconductors, examining reflectance and elliptic polarization 07 p1102 A66-18204

Solar eclipse coronal isotopes, noting spectrum in region of maximum visual sensitivity, ellipticity figures, Ludendorff coefficient, luminosity gradients, etc 15 p2593 A66-28867

Minimum drag bodies with elliptical cross section, using Newtonian flow theory and calculus of variations 17 p2838 A66-32346

**EMBRITTEMENT**

**SA BRITTLENESS**

Silicon and iron effects on embrittlement of cobalt-base alloy /L-605/ 01 p0085 A66-10357

Liquid metal embrittlement noting stress and intergranular corrosion, hydrogen embrittlement and behavior of silver chloride crystal 02 p0243 A66-11698

Constant load rupture test of susceptibility of Ni-Co-Mo maraging steel to delayed hydrogen cracking 03 p0381 A66-12541

Effects of nitrogen and carbon on low temperature embrittlement of vanadium, noting transition temperature increases 05 p0702 A66-15468

Hydrogen embrittlement or fatigue strength loss avoidance in overhauling and repairing of high strength aircraft steel component 13 p2087 A66-26284

Embrittlement of tantalum by room temperature deformation in presence of hydrogen 17 p2941 A66-33441

Hydrogen embrittlement reduction in springs by careful processing 19 p3362 A66-35326

Sea-water embrittlement of titanium alloy cantilever beam specimens as affected by aluminum content, aging, beta stabilizers and cooling 19 p3379 A66-35660

High temperature embrittlement of stainless steel irradiated in fast fluxes of Dounreay fast reactor at coolant temperatures of 250-350 degrees C 22 p3934 A66-40006

**EMBRYO**

**S FETUS**

**EMERGENCY BREATHING TECHNIQUE**

**S PRESSURE BREATHING**

**EMISSION**

**S AIRGLOW**

**S ATMOSPHERIC EMISSION**



- S AURORAL EMISSION  
S ELECTRON EMISSION  
S EXO-ELECTRON EMISSION  
S FIELD EMISSION  
S ION EMISSION  
S LIGHT EMISSION  
S NEUTRON EMISSION  
S OPTICAL EMISSION  
S PARTICLE EMISSION  
S PHOTOELECTRIC EMISSION  
S RADIANT ENERGY  
S RADIATION EMISSION  
S RADIO EMISSION  
S SECONDARY EMISSION  
S SPECTRAL EMISSION  
S SPONTANEOUS EMISSION  
S STEFAN-BOLTZMANN LAW  
S STIMULATED EMISSION  
S THERMAL EMISSION  
S THERMIONIC EMISSION  
S VERY LOW FREQUENCY EMISSION  
RECORDER
- EMISSION SPECTRUM**  
Chromospheric emission lines of magnesium iodine analyzed, calculating hydrogen concentration and ionization degree at 1000 km 01 p0134 A66-10269  
Metallic UV emitter producing continuous spectrum in 2000 to 500 angstrom band 01 p0071 A66-11049  
Radiative recombination of degenerate and compensated germanium indicating that emission line at low temperatures shifts to higher energies with increasing excitation 02 p0273 A66-11715  
Multiple light filter narrowing emission bands of ruby laser with multiplex resonator 03 p0378 A66-12627  
Contribution of nonlinear interaction of surface oscillations in plasma to emission of electromagnetic radiation from plasma 04 p0552 A66-13882  
Modes of emission-vs-time spectrum, optical emission spectrum and superposition spectrum of short confocal ruby laser in near field 04 p0532 A66-14290  
Gallium arsenide p-n junction laser diode covering injection current distribution, density and emission spectra variation 05 p0692 A66-14659  
Laser oscillation in calcium tungstate crystals activated with trivalent praseodymium 05 p0694 A66-14898  
Photoelectric measurements of C sub 2, C sub 3, CH and CN band strengths in near nuclear region of Comet Ikeya 1964f 05 p0762 A66-15282  
Absorption and emission spectra pertaining to electronic transitions of short-lived molecules C sub 2 and CH present in reaction zone of low-pressure oxyacetylene flames 06 p0969 A66-16126  
Emission spectrum of ruby maser calculated, using dynamics of two-level systems 06 p0891 A66-16541  
Radiative recombination emission and photoconduction in lead sulphide, emphasizing chemical deposition or vacuum evaporated layers 07 p1094 A66-17311  
Injection luminescence in InAs diodes 07 p1094 A66-17315  
Temperature dependence of emission spectrum and threshold current in GaAs lasers 07 p1042 A66-17333  
Comparison of properties of mode and nonmode GaAs diodes, discussing emission spectra oscillations and absorption constant 07 p1042 A66-17334  
Emission and absorption lines with anomalous intensity distributions indicate hydroxyl molecule concentrations in Sagittarius A 07 p1133 A66-17462  
5-cm radio emission from excited hydrogen in Omega nebula studied with quantum parametric amplifier 07 p1134 A66-17624  
Isotope shift, linewidth and precise wavelength of laser emission in ionized Hg 07 p1044 A66-18035  
Manganese X-ray emission lines in compound-oxide 07 p1105 A66-18369  
semiconductor 07 p1105 A66-18369  
Premixed flames of trimethylaluminum vapors and oxygen stabilized at reduced pressure, analyzing stability region, burning velocity and emission spectrum 08 p1318 A66-19199  
Fluorescent K-absorption and emission spectra of phosphorus in III-V semiconductor compounds 09 p1426 A66-20192  
Solar corona emission line polarization resulting from anisotropic effect of photospheric radiation 09 p1442 A66-20463  
field 09 p1442 A66-20463  
Optical spectroscopic temperature measurements in shock tubes from relative emission intensities in two wavelength regions of molecular band 09 p1382 A66-20507  
system 09 p1382 A66-20507  
Photometric monitorings of 5577 and 6300 angstrom lines during undisturbed geophysical conditions in South Atlantic 10 p1530 A66-21164  
Short wavelength wing of pure rotation emission spectrum of water vapor measured at various temperatures and nearly constant optical depth, calculating mean spectral absorption coefficient 11 p1739 A66-22952  
Emission spectra of nitrogen excited by electron beam of 0.1 to 20 kev and oxygen and air bombarded by 13-kev electrons 11 p1740 A66-23040  
X-ray produced auroral light emission in air and excitation of second positive and first negative bands in nitrogen 11 p1765 A66-23152  
Metallic UV emitter producing continuous spectrum in 2000 to 500 angstrom band 11 p1709 A66-23297  
Classification of iron VIII to XII and XIV lines in solar extreme UV spectrum and isoelectronic sequences from Ar to Ni 12 p1947 A66-23730  
Continuous emission and absorption of plasmas by calculating radiation of hydrogen plasma, deriving temperature and pressure conditions under which plasma radiates as black body 12 p1919 A66-23750  
Meteors and meteorites, discussing swarms, velocities and spectra 12 p1948 A66-23909  
Statistical study of frequency spectrum of slowly varying component of solar radio emission related to sunspots and flocculi 12 p1950 A66-24248  
Electrical discharge theory of cosmic atmospheric phenomena, relating lightning, novae and quasars 12 p1950 A66-24394  
Radiative recombination in gallium arsenide p-n junctions for weak currents, obtaining relation between emission spectra and current-voltage characteristics of diodes 12 p1929 A66-24456  
Atomic oxygen night sky emission observations with pressure scanning Fabry-Perot interferometer 12 p1873 A66-24837  
K beta 5 emission band and fundamental K-edge absorption of vanadium analyzed and results compared with vanadium spectra from other series 12 p1898 A66-25024  
Width of spontaneous emission region in degenerate gallium arsenide p-n junction, noting spectral shifts, emission, interference, etc 13 p2159 A66-25064  
Electroluminescence and emission spectra of indium-alloyed diodes made from phosphorus doped p-type ZnTe biased in either forward or reverse direction at liquid nitrogen temperatures 13 p2029 A66-25184  
Gallium arsenide p-n junction laser diode, injection current distribution, density and emission spectra variation 13 p2092 A66-25934  
Optical emission from ruby induced by short pulses of relativistic electrons in which electron-hole recombination produces excitation of emission 13 p2098 A66-26173  
High resolution piezoelectrically scanned Fabry-Perot interferometer used to study gain profiles, mode structures and emission line widths of CW Ar, Kr and Xe ion lasers and Hg-He pulsed laser 13 p2102 A66-26208  
Optical transition of manganese fluoride as function of temperature and magnetic field in both emission and absorption 14 p2351 A66-26886  
Magnetic effect on emission spectrum of negative glow plasma in hollow-cathode discharge, noting pressure effect 14 p2340 A66-27024  
LF fluctuations in emission of He-Ne gas laser measured, using Fabry-Perot resonator and ring-type resonator 14 p2307 A66-27186  
Green emission lines from solution-grown p-n junctions in GaP diodes doped with shallow donors and acceptors 14 p2251 A66-27231  
Helium-neon laser afterglow and metastable helium atoms under long pulse excitation 14 p2307 A66-27335  
Emission and absorption bands in K spectral region of titanium, using single setup 14 p2314 A66-27371  
Contribution of nonlinear interaction of surface oscillations in plasma to emission of electromagnetic radiation from plasma 14 p2343 A66-27580  
Axial and transverse mode selection, emission spectrum and transient emission behavior of confocal ruby laser operated in ellipsoidal pumping system 14 p2308 A66-27606  
Emission from hot low-density plasma due to bremsstrahlung, radiative recombination and electron collision-induced line emission 14 p2345 A66-28120  
Emission bands in electroluminescence from gallium arsenide diodes, noting intensity at high and low voltages and radiation and doping effect 15 p2562 A66-28714  
Polarization and damping rate of emission lines of ruby single crystal in strong excitation 15 p2515 A66-29207  
Absorption, excitation, and emission spectra of Ti-activated NaI single crystals at liquid helium temperatures 15 p2566 A66-29347  
Ionized electron centers in irradiated lithium fluoride crystals investigated by observing emission and absorption spectra 15 p2568 A66-29641  
Spectral variation in light polarization of Martian atmosphere for all observable phase angles 15 p2599 A66-29643  
Emission spectrum of ruby maser calculated, using dynamics of two-level systems 15 p2519 A66-29988  
Space correlation of main emission lines for night sky emission spectra and altitude distribution of sodium luminescence 15 p2495 A66-30060  
Velocity distribution function of helium atom measured, using Doppler profile of helium line 16 p2701 A66-30377  
F-layer nightglow 6300 angstrom emission intensity and electron density data, noting variations in emissions 16 p2694 A66-30708  
Emission spectroscopy of halides of carbon, silicon and boron in plasma reactor 16 p2763 A66-31190  
Reproduction of experimental and calculation of theoretical H-beta emission profile of solar flare, considering macroscopic motions inside flare 16 p2795 A66-31391  
Emission spectrum of copper atom used to measure temperature and concentration of charged particles in DC-arc plasma burning under water 16 p2766 A66-31600  
Optical pumping mechanism for anomalous excitation of OH microwave emissions from H II regions 16 p2807 A66-31756  
Solar corona emission spectrum and narrow passband photography of solar disk, noting measurement of intensity variation and absorption coefficient 17 p2999 A66-32133  
Effect of anomalous dispersion on stimulated emission spectrum of doped cadmium fluoride crystals 17 p2977 A66-32317  
Electron scattering interpretation of ionization, emission and absorption line spectra of quasi-stellar object 17 p3004 A66-32928  
Polarization and damping rate of emission lines of ruby single crystal in strong excitation 17 p2936 A66-33056  
Collisions in inner region of cometary head, structure of emission bands and formation of free radicals 17 p3010 A66-33376  
Coherent and spontaneous emission from lead-tin telluride alloys upon excitation by GaAs diode laser, noting band structure of alloy system 18 p3119 A66-34159  
Principle source of radiative energy loss in intergalactic medium in spectral region from 2 to 18 angstroms is line emission from ions of elements oxygen, carbon, neon, magnesium and silicon 18 p3237 A66-35046  
Orientation effect in GaAs injection lasers, noting emission characteristics and structural spectra 19 p3373 A66-35404  
Suggested origin of low energy tails in radiative recombination spectra due to degenerate conduction band 19 p3437 A66-35475  
Continuous emission spectrum of



detonation wave in nitromethane between 3800 and 8000 angstroms 19 p3477 A66-35747

Gallium arsenide lasers operating at room temperature investigated, based on diffusion p-n junctions, discussing emission spectrum 19 p3375 A66-36070

Pulsed laser action in visible spectrum of singly ionized Ge, Sn, Pb, In, Cd and Zn, listing temperature and pressure ranges 19 p3444 A66-36076

Quantitative measurement of free metallic atoms abundance and height distribution from twilight, dayglow and aurora fluorescence 19 p3349 A66-36330

Aerobee rocket measurement of nitric oxide in upper atmosphere, noting fluorescence in airglow layer, emission rate factors and NO densities 19 p3349 A66-36351

Absorption, excitation, and emission spectra of Ti-activated NaI single crystals at liquid helium temperatures 20 p3615 A66-37352

Radiative recombination in gallium arsenide p-n junctions for weak currents, obtaining relation between emission spectra and current-voltage characteristics of diodes 20 p3619 A66-37688

Doppler effect on emission spectrum and energy of moving oscillator and intensity of surface wave excited by it 20 p3519 A66-37995

Stimulated emission spectrum in axial-mode model of plane resonator in stationary generation regime 20 p3580 A66-38127

Scintillation counter and proportional counter spectral measurements of solar flare X-ray emissions and analogies to hot plasma 20 p3633 A66-38191

Intensity measurements on molecular oxygen Herzberg I system emitting in afterglow of microwave discharge, noting dependence of transition moment on internuclear distance 20 p3555 A66-38208

Cryogenic optically excited recombination emission in single crystal InSb semiconductor and transitions involving phonon creation, acceptor impurities and band-to-band emissions 21 p3800 A66-38996

Spectroscopic and microwave analysis plasma emission spectrum, density, electron concentration and layer velocity in electrodeless induction discharge 21 p3790 A66-39069

Emission spectrum of plasma consisting of colliding blobs, noting photographic and photoelectric recording and ion temperature measurement 21 p3790 A66-39070

Emission and absorption capacity of /zero-zero/ band of CN violet system at high temperatures, determining parameters of oscillator system power 21 p3775 A66-39079

Emission spectra of ionized air and H in electromagnetic shock tube, giving frame scans of spectra 21 p3726 A66-39081

Diameters and positions of three sources of 18-cm OH emission determined, using 90-ft steerable paraboloids 21 p3814 A66-39269

Stokes parameters measurement as function of frequency for anomalous polarized OH emission originating near thermal radio source W3 22 p3978 A66-40015

IR absorption coefficients of water vapor as function of temperature obtained from absorption and emission spectra 22 p3950 A66-40114

Room temperature performance of GaAs laser diodes, using SCRs to achieve high pulse repetition rate 22 p3932 A66-40175

Coherent radiation generation in electron-hole indium antimonide plasma, discussing emission spectrum 22 p3965 A66-40319

Upper and lower limits to expected alpha and beta hydrogen and helium line emissions due to protons and alpha particles penetrating auroral atmosphere 22 p3913 A66-40554

Emission rim formation at filaments caused by chromospheric excitation by radiation reflected from filament 23 p4126 A66-41077

Frequency tuning of coherent emission over vibronic continuum of phonon-terminated optical masers by thermal tuning and wavelength-selective feedback 23 p4077 A66-41369

Altitude profiles for dayglow emissions excited by molecular ion dissociative recombination, solar radiation fluorescence, oxygen photodissociation, electron collisions

and chemical reactions 23 p4064 A66-41680

Radiative lifetime and emission intensity measurements, determining oscillator strength and electron transition moment of first positive band system of nitrogen 23 p4033 A66-42082

Time resolved emission measurements for Cr-Ar mixtures in three spectral regions and ionization occurrence in excited state inelastic collisions 23 p4033 A66-42083

Luminescence spectra of meteorites of different classes using proton excitation, giving estimates of radiation conversion efficiency 24 p4273 A66-42363

Microwave emission from stationary plasma column measured taking into account spatial distribution of plasma density, using spectrometer 24 p4242 A66-42398

LF fluctuations in emission of He-Ne gas laser measured, using Fabry-Perot resonator and ring-type resonator 24 p4226 A66-43084

**EMITTER**

Metallic UV emitter producing continuous spectrum in 2000 to 500 angstrom band 01 p0071 A66-11049

Design and fabrication methods of semiconductor optoelectronic devices, noting junction emitter outputs into visible spectrum 04 p0494 A66-13764

Heat pipe performance, emphasizing heat carrying and waste heat dissipation functions, construction and materials testing 05 p0616 A66-15543

Output characteristics of thermionic converter and improvement of performance by using emitter surfaces with particular crystallographic orientation 05 p0617 A66-15553

Performance of thermionic converters using clad and unclad UC-ZrC emitters operated at high temperatures, noting cesium pressure effect 05 p0619 A66-15566

Emitter materials for nuclear thermionic converters, discussing /UZr/C, fuel life and performance parameters, material compatibility, etc 05 p0713 A66-15584

Emitter of thermionic converter with cesium plasma heated by solar energy, determining electric power values 05 p0623 A66-15595

Input impedance of spherical emitter in infinite homogeneous isotropic conducting medium 11 p1656 A66-23031

Metallic UV emitter producing continuous spectrum in 2000 to 500 angstrom band 11 p1709 A66-23297

Extension of nonlinear distortion in common-emitter circuit to common-base circuit, cancelling emitter distortion and collector-loading distortion and presenting design chart independent of transistor type for CB circuit 13 p2030 A66-25217

Integrated circuits with propagation delays in nanosecond range, noting emitter coupled logic circuit 13 p2036 A66-25534

Quasi-stationary distributions of potential in one-dimensional ion-electron currents near emitting surface, noting unstable regimes regarding slow variations in boundary conditions 14 p2338 A66-26772

Apparatus for teaching and research in electron physics including emitters, cathode ray tubes, electron multipliers and mass spectrometer 18 p3088 A66-35033

Measuring device for common emitter current-gain/ bandwidth product of transistors at various frequencies, noting effect of parasitic elements, assessing accidental error 21 p3737 A66-38966

Woven and knitted electron emitters noting reliability, mechanical stability, transparency and efficiency 24 p4180 A66-42369

HF transistor stability in common emitter configuration, examining performance of input admittance in circuit design and analysis 24 p4181 A66-42377

Two-transistor circuit with output resistance of approximately 50 M ohms with improved temperature stability and high internal resistance 24 p4181 A66-42378

Matrix analysis of complementary pair emitter-follower, examining overall circuit parameters, noting good DC quiescent stability 24 p4184 A66-42645

**EMOTIONAL FACTOR**

Urinary excretion of steroids and catecholamines as measure of emotional

stress of man in 56-day exposure to oxygen-helium environment 18 p3057 A66-33773

**EMPIRE MANNED INTERPLANETARY EXPEDITION**

Navigation requirements for Empire manned interplanetary missions discussing orbit determination, path corrections, sensor selection, functional systems and man-machine roles 02 p0255 A66-11317

**EMULSION**

SA COLLOID

SA NUCLEAR EMULSION

SA PHOTOGRAPHIC EMULSION

Diffusion and propagation phenomena in air-water and water-steam emulsions in one-dimensional flow 12 p1973 A66-23524

Spark emulsion chamber for balloon-borne cosmic radiation measurements 15 p2503 A66-29569

**ENCAPSULATION**

Embedment stress effects on electrical characteristics of encapsulated components, presenting capacitor test results 02 p0247 A66-11287

Temperature cycling effect on welds of known strength which are encapsulated with several types of resins to determine internal stress in electronic modules 02 p0234 A66-11326

**ENCKE METHOD**

Orbit perturbation by Encke method, using nontwo-body reference orbit, considering oblateness effects, drag, etc 15 p2598 A66-29296

**ENCODER**

Five-channel FM/FM telemetry encoder using molecular electronics, noting oscillators, delay lines and linear amplification functional blocks 04 p0493 A66-13601

Magnetic amplifier telemetry encoder circuit, using silicon controlled rectifiers /SCR/, for application in satellites and rockets 14 p2263 A66-27062

Five-channel FM/FM telemetry encoder using molecular electronics, noting oscillators, delay lines and linear amplification functional blocks 14 p2243 A66-28350

Optimal scientific satellite PFM encoding system circuit design and digital data processing 14 p2244 A66-28429

Microelectronic encoder design problems, considering stability in high gain amplifiers, resistors, capacitors and voltage reference source and low resistance in multiplex switch 17 p2883 A66-32120

Microelectronics pulse code modulation /PCM/ multiplexer-encoder for Apollo spacecraft, emphasizing packaging techniques, discussing advance circuit design techniques 19 p3317 A66-35707

Miniature shaft-angle encoder with integrated-circuit encoding matrix and built-in memory potential using single static commutation ring 20 p3558 A66-37217

**ENCODING**

SA CODING

SA DECODING

SA REDUNDANCY ENCODING

SA SIGNAL ENCODING

Delta modulation pictorial encoding systems analyzed to determine parameters for image communication application 19 p3299 A66-35665

Existence of q-ary uniform convolutional codes where q is any prime-power, noting error-correcting ability comparable to familiar maximal-length block codes 21 p3704 A66-39138

Run-length encodings, determining explicit form of Huffman coding when applied to geometric distribution 21 p3758 A66-39643

**END PLATE**

Ion drift and diffusion of magnetically confined plasma due to inclination of conducting end-plate having electron sheath which reflects ions 18 p3149 A66-34912

Cesium plasma of Q device used in study of stability of plasma devices with slanted nonconducting end plates 21 p3792 A66-39187

**ENDOCRINE SYSTEM**

SA ADRENAL GLAND

SA HORMONE

SA PITUITARY GLAND

SA THYMUS

SA THYROID

Low-gravity vibration stress effects on



weight, growth, metabolism, white blood cells and endocrine system of albino Wistar rats 11 p1643 A66-22581

**ENDOCRINOLOGY**  
Random lighting exposure effects in rats and changes caused in adrenal cortical function, circadian rhythm, endocrine system, group running activity, etc 15 p2429 A66-28487  
Corticosteroid responses to limbic stimulation in man and localization of stimulus sites 22 p3855 A66-40487

**ENDORADIOSONDE**  
Telemetering information from within body of animals and man, using tiny transmitters called endoradiosondes 04 p0469 A66-13370  
FM/AM temperature telemetering system for unrestrained intact ruminants, discussing design, fabrication and application 06 p0820 A66-16853  
Low power radio transmitters implanted to telemeter physiological information, discussing drift caused by body fluid permeability 06 p0820 A66-16854  
Microcircuit internal medical sensors with high electronic gain and lower sensitivity transducers 11 p1647 A66-22298  
Miniature long-life telemetry system for implanting in animal to study deep body temperature 11 p1649 A66-23499  
Miniaturized implantable biotelemetering transducer for study of metabolic rhythms in extraterrestrial life 24 p4167 A66-42674

**ENDOSCOPE**  
Endoscopes in aviation noting role in inspection of wing interiors, power plants, etc 07 p1040 A66-18330

**ENDOTHERMIC FUEL**  
Catalytic dehydrogenation of hydrocarbons over chromia-alumina catalyst in absence of added hydrogen to determine heat sink capability 11 p1650 A66-23119  
Methylcyclohexane dehydrogenation over platinum-alumina in absence of excess hydrogen, yielding toluene and hydrogen 11 p1650 A66-23122  
Thermal stability of endothermic hydrocarbon heat-sink fuels, noting application flying in 10 Mach speed range 11 p1759 A66-23124  
Shock tube ignition delay study of aircraft engine cooling by hydrocarbon fuels in endothermic heat sinks [AIAA PAPER 65-594] 12 p1934 A66-23588  
Kinetics of highly endothermic carbon-silica reaction for silica-reinforced resin systems 17 p2943 A66-32453

**ENERGETIC PARTICLE EXPLORER**  
S EXPLORER SATELLITE  
ENERGETIC PARTICLE EXPLORER-A  
S EXPLORER XII SATELLITE  
ENERGETIC PARTICLE EXPLORER-B  
S EXPLORER XIV SATELLITE  
ENERGETIC PARTICLE EXPLORER-C  
S EXPLORER XV SATELLITE

**ENERGY**  
SA ACTIVATION ENERGY  
SA BINDING ENERGY  
SA CHEMICAL ENERGY  
SA ELECTRIC ENERGY  
SA ELECTRON ENERGY  
SA FORMATION ENERGY  
SA FREE ENERGY  
SA INTERNAL ENERGY  
SA KINETIC ENERGY  
SA MOLECULAR ENERGY  
SA MOMENTUM ENERGY  
SA NUCLEAR ENERGY  
SA POTENTIAL ENERGY  
SA PROTON ENERGY  
SA RADIANT ENERGY  
SA SEISMIC ENERGY  
SA SOLAR ENERGY  
SA STACKING FAULT ENERGY  
SA STRAIN ENERGY  
SA SURFACE ENERGY  
SA THERMAL ENERGY  
SA THERMONUCLEAR ENERGY  
Paradoxes in thermodynamics by using imprecise terminology, citing available energy, diffusion entropy, self-mixing of gas, etc 09 p1472 A66-20907

**ENERGY ABSORPTION**  
Plasma generation by focusing laser beam in air at atmospheric pressure and room temperature indicate connection with luminous energy absorption during breakdown 05 p0692 A66-14538

Energy losses in ruby laser due to heat evolution during optical pumping, noting relation between energy absorption and population inversion 05 p0698 A66-15858  
Aircraft braking system, determining energy absorbed during landing or interrupted takeoff 06 p0807 A66-16970  
Impact dynamics of landing systems using material crushing to absorb kinetic energy of body impacting at very high velocities 14 p2402 A66-27895  
Ferromagnetic microwave resonance isolators for use in waveguides 15 p2459 A66-28936  
Most probable energy loss in silicon for pions with energies from 365 to 50 mev, examining pion beam behavior through different absorption material thicknesses 16 p2755 A66-31390  
Transmittance of optical materials between 1050 and 3000 angstroms, noting effect of simulated high energy space environment 17 p2979 A66-32615  
Acoustic wave energy absorption by superconductors in intermediate state 18 p3158 A66-34692  
LF electromagnetic field behavior in cold magnetoactive plasma near resonance layer, noting condition for energy absorption increase 18 p3151 A66-35064  
Transmission of luminous flux due to ionization of gases by high power laser, measuring energy absorption in ionized zone 19 p3403 A66-36255  
Thermoelastic wave equations in continuum mechanics model of laser-induced fracture in transparent media in terms of laser beam energy absorption 22 p3931 A66-40089  
Absorption of solar energy by polar cap, noting electron concentration 24 p4204 A66-43153

**ENERGY BAND**  
SA EXCITON  
Nonmagnetic impurity effect on critical temperature of superconductor with two energy bands overlapping near Fermi energy level 01 p0123 A66-10719  
Interband Faraday rotation at liquid-nitrogen temperature in CdS-CdSe mixed crystals 02 p0274 A66-11722  
Electrical conductivity of narrow energy band semiconductors as function of electric field strength 02 p0274 A66-11732  
Quantum levels of electron moving in periodic field of semiconductor crystals in strong electric field 02 p0274 A66-11733  
Impurity bandwidth and separation from conduction band in n-type GaAs determined from electroconductivity and Hall effect data 02 p0276 A66-12077  
Helium 3-1-P state, discussing pressure dependence of lifetime between free escape and complete blocking 03 p0395 A66-13134  
Reflectivity of n-type lead sulfide measured as function of wavelength, temperature and carrier density 03 p0412 A66-13147  
Unified model of ferromagnetism, analyzing spin-wave motion of electrons in transition metals, using atomic and energy-band features 04 p0559 A66-13450  
Integrated intensity measurements on fundamental and first overtone band systems of carbon monoxide between 2500 and 5000 degrees K 04 p0596 A66-13647  
Cadmium sulfide and cadmium selenide, discussing optical absorption, energy band structure, effective band-masses and composition changes of crystals in polarized light 05 p0731 A66-14656  
Theoretical anisotropic energy gap of superconducting lead when photon density of states is principal source of gap anisotropy 05 p0741 A66-15866  
Exponential absorption edge of gallium arsenide 05 p0742 A66-15870  
Exponential band-edge tails observed experimentally in degenerate n-type germanium tunnel diode 06 p0925 A66-16654  
Effect of fast states with discrete energy levels and quasi-continuous spectrum on capacitance of silicon dielectric film-metal structure 08 p1274 A66-19308  
Band structures and pseudopotential form factors for 14 semiconductors of diamond and zincblende structures 08 p1276 A66-19369  
Tin telluride electric properties analysis for verifying semiconductor model with two

valence bands in connection with Hall effect dependence on temperature 09 p1412 A66-19993  
Parameters of complex energy bands in semiconductors determined by free carrier Faraday rotation, Voigt effect and transport properties 09 p1426 A66-20191  
Energy band structure of germanium and silicon throughout Brillouin zone by k-p Hamiltonian 10 p1581 A66-21738  
diagonalization  
Electron tunneling in semiconductors with degenerate band structure 10 p1581 A66-21739  
Energy band structure via reflection spectra of crystals of ternary zinc compound containing elements of Periodic Groups II, IV and V 11 p1750 A66-22342  
K beta 5 emission band and fundamental K-edge absorption of vanadium analyzed and results compared with vanadium spectra from other series 12 p1898 A66-25024  
Threshold energy for avalanche multiplication in semiconductors obtained from energy band structure and crystal momentum conservation in ionization process 13 p2157 A66-25035  
Electroreflectance effect on gallium arsenide surfaces, noting reflectance response upon electric field modulation 13 p2158 A66-25051  
Cadmium sulfide and cadmium selenide, discussing optical absorption, energy band structure, effective band-masses and composition changes of crystals in polarized light 13 p2167 A66-25931  
Electronic band structure of BiSb alloy tunnel junction for various Sb concentrations 16 p2770 A66-30178  
Fundamental optical spectra theory for high energy atoms interaction with solids 17 p2977 A66-32399  
Spectral and spatial distribution of origin of injection luminescence from epitaxial gallium arsenide transistors, noting correlation between energy peak and radiation recombination 17 p2986 A66-33295  
Energy band structure, carrier behavior and characteristic curve of p-n junction diode at high-current level, solving transport and Poisson equations 19 p3312 A66-35346  
Reflection spectra of polished polycrystalline samples of various rare earth chalcogenides 19 p3442 A66-35820  
Nonmagnetic impurity effect on critical temperature of superconductor with two energy bands overlapping near Fermi energy level 20 p3619 A66-37657  
Effects of nonmagnetic impurities upon anisotropy of superconducting energy gap 21 p3797 A66-38559  
Dynamic characteristic theory of long diode with base containing impurity atoms producing deep energy levels in forbidden zone 22 p3873 A66-39826  
Theoretical model for effect of mechanical stress on generation-recombination currents in p-n junctions 22 p3963 A66-40095  
Crystal potential and correlation for energy bands in valence semiconductors evaluated on basis of orthogonalized plane wave calculations starting with Hartree-Fock equation 24 p4249 A66-42227  
Multiple energy bands effects on stress dependence of breakdown and order of magnitude in breakdown voltage of Ge and Si junction diodes 24 p4251 A66-42306  
Radiative recombination within space-charge region in germanium exposed to increasing surface field 24 p4251 A66-42308  
Diffusion current in MOS transistors analyzed, using three-dimensional energy band diagrams 24 p4253 A66-42383  
Pressure deformation of band structure of HgTe-CdTe alloys determined from measurements of Hall effect and resistivity 24 p4258 A66-43009

**ENERGY BUDGET**  
Energy balance of cylindrically symmetric hydrogen arc immersed in axial magnetic field led to current-voltage characteristic and radial temperature distribution 04 p0554 A66-14298  
Kinetic energy generation and dissipation in large-scale atmospheric circulation, using six months aerological data from North American network 11 p1731 A66-23487  
Energy balance of stationary discharges in



quartz containers filled with gas at various pressures, determining relation of heat and light loss of discharge to gas pressure and discharge power 15 p2551 A66-29215

Energy reflected from subsolar point on Moon determined, noting energy balance and radiated energy 20 p3656 A66-38052

### ENERGY CONVERSION

#### SA HEAT GENERATION

P-n transitions in gallium arsenide investigated as factor in performance of such diodes as converters of ultrasonic into electrical oscillations 01 p0036 A66-10422

Spaceflight application of cryogenic techniques including cooling magnets, noise reduction in parametric amplifiers and quantum-electronic, superconductive and IR sensing devices 01 p0130 A66-10789

Design and fabrication techniques for high voltage impulse generation by conversion of mechanical to electrical energy, using piezoelectric ceramics 01 p0016 A66-10916

Pulsating combustion compared with steady combustion as means of increasing energy conversion 01 p0166 A66-11093

Energy conversion into electrical power considering solar cells, thermoelectrics and thermionics noting advantages over fuel cells, dynamic machines and MHD 03 p0324 A66-13272

Energy conversion from available potential to kinetic broken into spectral components permitting analysis in vicinity of extratropical cyclone 04 p0541 A66-13665

Palladium-hydrogen diffusion electrode noting current densities 04 p0460 A66-14034

Various types of periodically discontinuous combustion, showing improved thermal efficiency applicable to turbine combustion chambers 05 p0787 A66-14962

Drop-weight impact sensitivity testing of explosives [CI PAPER WSCI-65-27] 05 p0788 A66-15140

Magnetic storage, discussing mechanical and thermal energy conversion into magnetic field energy and electromagnetic energy transfer 05 p0717 A66-15335

Heat transfer measured at different conditions of diode operation, obtaining data on plasma properties and electrode sheaths 05 p0616 A66-15546

Book on theoretical and engineering problems arising in capacitor discharge technique of pulse generation 06 p0878 A66-16046

Rectangular waveguide filter with trapped mode resonators, describing operation, energy handling characteristics and application 06 p0845 A66-16086

Energy conversion and storage . Conference, Oklahoma State University, October 1965 06 p0808 A66-16390

Silicon photovoltaic cells applied to solar batteries, examining efficiency with which luminous energy is converted into electrical energy 06 p0810 A66-17160

Depletion layer 1000 mc transducers for producing or detecting hypersonic waves in solids, using  $\text{CaS}$  or  $\text{GaAs}$  for high acoustoelectrical conversion 07 p1009 A66-17827

Energetics /engineering developments in energy conversion/ - ASME International Conference, University of Rochester, August 1965 07 p0992 A66-18308

Data analysis of experiments with open-cycle supersonic EGD generator for application as power source and comparison with mathematical model 07 p0993 A66-18314

Electric power generation using monopolar charged particles in fluid flow 07 p0994 A66-18315

MHD squeeze film device as energy conversion 07 p0994 A66-18316

Gamma-electric cell, solid state device for direct conversion of gamma-ray energy into electrical energy 07 p1079 A66-18323

Power plants and direct energy conversion in space vehicles 08 p1168 A66-19018

P-n transitions in gallium arsenide investigated as factor in performance of such diodes as converters of ultrasonic into electrical oscillations 11 p1664 A66-22608

Efficient conversion of electrical energy into laser radiation, using coaxial optical pump 11 p1715 A66-23479

Boundary value problem of acoustic point source antenna within compressible plasma

region with assumed rigid boundary, noting acoustic power conversion into electromagnetic waves 12 p1920 A66-24116

Electrofluid dynamic power generation, high voltage generating device, direct energy conversion and supersonic electrogasdynamic generator 12 p1803 A66-24646

Materials for producing electric energy from heat by direct conversion 13 p1997 A66-25116

Energy conversion between four different forms of kinetic energy in atmosphere 15 p2489 A66-29662

Magnetic storage, discussing mechanical and thermal energy conversion into magnetic field energy and electromagnetic energy transfer 15 p2543 A66-29982

Simplified method of evaluating thermal and ionizing energies from fission of uranium atoms 16 p2744 A66-30436

Hard superconductors as generators of strong magnetic fields to accelerate plasma in energy converters and plasma propulsion systems of spacecraft 17 p2981 A66-32898

Plasma oscillation theory of nonlinear deceleration effect and thermal conversion of electron beams upon passage through plasma 17 p2974 A66-33284

Electrical energy by direct conversion, noting fuel cell, thermoelectric generator, solar cell, etc 18 p3053 A66-33722

Book on direct energy conversion covering thermoelectric, photovoltaic, thermionic and MHD generators and fuel cell 18 p3054 A66-34164

Quasi-static processes in energy conversion statics, deriving stability criteria 19 p3281 A66-36293

Nonlinear plasma wave interaction, discussing Langmuir wave scattering on particles and energy transformation 19 p3418 A66-36532

Spacecraft power source, discussing energy conversion, processes, solar cells, radio isotopes, thermionic power converters, turbogenerators, etc 19 p3282 A66-36797

Coupling between oppositely directed traveling waves in He-Ne ring laser in form of mutual backscattering of energy from each beam into direction of other 20 p3579 A66-37778

Pulsed-mode gain characteristics in neodymium-doped silicate glass laser experimentally related to giant-pulse laser energy output 20 p3582 A66-38396

Book on plasma diagnostics covering measuring devices and techniques, SHF antenna and waveguide system, emission measurements, etc 21 p3737 A66-38949

Polarization interaction of plasma fluxes moving in transverse magnetic field, using plasma diagnostic techniques including superhigh-speed photography and double electrostatic and magnetic probes 21 p3787 A66-39053

Photoelectric devices for converting luminous to electrical energy and vice versa, considering characteristics, performance and application 21 p3716 A66-39619

Charge transfer between water drops relevance to radiation problem and efficiency of conversion of electrostatic to electromagnetic energy 22 p3942 A66-39679

Lorentz transformation of thermodynamic quantities, noting application of formalism of statistical mechanics, validity of Planck-Einstein equations for total energy and momentum 22 p3997 A66-39806

Dynamic conversion of solar and chemical energy, discussing power conditioning, Brayton-cycle system with inert gas and spacecraft batteries 22 p3851 A66-40128

Solar cell as most reliable energy conversion device for near-Earth missions, noting semiconductor material and thermal stress 23 p4017 A66-41167

Magnetic pumping heating rate for plasma, using conversion of organized energy into random energy by charged particle collisions 23 p4100 A66-41250

Intersociety Energy Conversion Engineering Conference, Los Angeles, September 1966 23 p4018 A66-41744

Laval turbine type device for starting rotors of turbojet engines, noting jet energy conversion on wheel blades and geometrical structure 23 p4122 A66-41791

Ionic reactions of gaseous methane using tandem mass spectrometer, noting translational energy 24 p4170 A66-43035

### ENERGY CONVERSION EFFICIENCY

High pressure thermionic converter, discussing current-voltage characteristics at high collector temperatures 05 p0616 A66-15545

Spontaneous radiation and nonresonant losses as dominant effects in conversion of incoherent light into coherent induced radiation 06 p0889 A66-15891

Radioisotope-photovoltaic energy conversion system, discussing principal elements, radiative exchange and efficiency calculations 07 p0990 A66-17231

Extrinsic and intrinsic epitaxially deposited single crystal gallium phosphide solar cells, noting conversion efficiencies 07 p0990 A66-17232

Electrochemical energy conversion, discussing fuel selection, oxidants, fused salt electrolytes, liquid metal, etc 07 p0995 A66-18325

Silicon photovoltaic cells in economic solar energy conversion on Earth 08 p1174 A66-19665

Solar energy for power requirement aboard satellites and spacecraft, noting thermal conversion efficiency by various methods for capturing solar radiation 08 p1174 A66-19753

Power and efficiency analysis of molten salt thermocell as thermoelectrochemical energy converter 09 p1333 A66-20499

Energy efficiency trends in two-stage repetitively pulsed coaxial plasma accelerator 12 p1935 A66-23578

Maximum efficiency of power converters, using ferroelectric and nonferroelectric pyroelectrics 13 p1997 A66-25036

Multiplier with varactor diode circuit examined, noting maximum obtainable conversion output power and efficiency 13 p2041 A66-25879

Multiple-converter thermionic module for operation from common liquid-metal heat source [AIAA PAPER 64-761] 13 p2005 A66-26628

Radiant energy conversion using thin dielectric films in thermoelectrostatic cycle [AIAA PAPER 64-729] 13 p2006 A66-26639

Molten carbonate fuel cell system performance evaluated from engineering and economic aspects [AIAA PAPER 64-747] 13 p2007 A66-26648

Performance efficiency and weight considerations for liquid MHD power conversion [AIAA PAPER 64-760] 13 p2008 A66-26660

Design and laboratory tests of vapor-phase heat exchanger coupled to power generating bismuth telluride thermopile for waste heat dissipation 16 p2637 A66-31101

Circuit with single externally driven switch, operated at fundamental frequency gives efficient conversion of DC to AC at that frequency or any specified harmonic of it 17 p2848 A66-31818

Solar energy power converter based on illumination of battery of silicon photovoltaic cells with intense light fluxes 17 p2848 A66-32856

Operating characteristics equations of energy converters constructed of anisotropic materials and subjected to physically meaningful constraints 19 p3281 A66-36292

Chemical energy conversion to electromagnetic energy by flux compression, discussing process and obtained efficiency 21 p3698 A66-39502

Thermionic energy conversion phenomena and advances, detailing  $\text{Cs}$  diode and optimum ideal performance 23 p4021 A66-41756

Pulsed energy turboalternator power generation system, discussing operation principles and performance characteristics 23 p4022 A66-41761

Conversion efficiency of  $\text{GaAs}$  solar cell at various light intensities 24 p4161 A66-42391

### ENERGY CONVERTER

#### SA FUEL CELL

#### SA PHOTOELECTRIC CELL

#### SA TRANSDUCER

Fuel cells and potential as future chemical-electric energy converters 03 p0324 A66-13234



- Gaseous heat engine cycle with gas compression from molecular effusion through capillary material 11 p1639 A66-22244
- Hysteresis effects in one-dimensional conducting gas flow through rectangular MHD converter channel with constant magnetic gap and variable electron spacing 15 p2428 A66-29219
- Output power and thermal efficiency of molten salt thermocell, examining applicability as generator for direct conversion of heat into electric energy 16 p2636 A66-30673
- Effect of finite width on performance of polyphase rectangular MHD converter, showing that for isotropic fluid electric current extends in two dimensions 16 p2637 A66-31102
- Closed magnetic trap for transverse-to-longitudinal conversion of energy of particles moving in spatially periodic magnetic field 21 p3788 A66-39059
- Ferromagnetic transducer operation principles, noting dimension optimization, energy efficiency, etc 21 p3741 A66-39505
- Plasma thermocouple and MHD generator as energy conversion devices, with bibliography 24 p4162 A66-43119
- ENERGY DENSITY**
- Fluctuation problem in electromagnetic cascade theory analyzed, using invariant imbedding method 07 p1083 A66-17973
- Fuel cells using metallic barium as fuel electrode and oxygen or chlorine as cathode, noting net energy 08 p1172 A66-19656
- Energy-momentum density of gravitational field according to Ozsvath-Schuecking rigorous solution to Einstein field equations 12 p1915 A66-24994
- General relativistic dynamics for determining place of Mach principle in relativity theory, obtaining expression for energy-momentum density of gravitational field 12 p1916 A66-25019
- Energy gap and critical field rules for superconductors, discussing empirical and experimental values 23 p4113 A66-41375
- Frequency dependence of electrostatic energy density in undamped longitudinal plasma oscillation, noting contribution of kinetic and thermal energy 23 p4104 A66-41507
- High energy density Zn/O battery system, noting good low oxygen pressure and low temperature performance characteristics 23 p4022 A66-41759
- ENERGY DISTRIBUTION**
- Scintillation hypothesis giving physical characteristics of quasars, determining energy output by star accretion 01 p0138 A66-11034
- Energy and thermal considerations during resistance weld between round wire and ribbon 02 p0233 A66-11321
- Energy distribution near jet stream and associated wave amplitude relations 05 p0711 A66-14544
- Heating process in laser welding of metal sheets, taking into account energy distribution, heat transfer and flux densities 05 p0688 A66-15347
- Solar spectrum measurement, discussing equipment design, testing and application [ISA PREPRINT 1.11-2-65] 05 p0684 A66-15511
- Estimation in equilibrium state surface potential and distributions of electric potential field and electron density in vicinity of object moving in ionized medium 05 p0685 A66-15795
- Coupling coefficients in high energy region of Earth atmosphere, considering interactions between primary nucleons and nuclei of air atoms 06 p0950 A66-16594
- Physics of spark discharges igniting gaseous mixtures, noting increase in thermal power of discharge by gas preionization resulting from energy redistribution 06 p0919 A66-16877
- Energy distribution of particles produced in elementary interaction expressed in terms of shower characteristics derived from cascade theory 07 p1116 A66-17562
- Ionization bursts in shielded spherical chambers with burst data transformed to give integral energy distribution of muon intensity at sea level 07 p1116 A66-17563
- Model simulating energy distribution process /thermal stratification/ within liquid hydrogen stored aboard moving rocket to avoid pump cavitation [AIAA PAPER 64-426] 08 p1279 A66-18809
- Work function of metals and semiconductors measured, using retarding potential analyzer to determine field emission electron energy distribution 08 p1228 A66-19825
- Energy distribution of hydrogen plasma from coaxial gun 10 p1571 A66-22013
- Temperature jump in polyatomic gases, discussing nonequilibrium energy distribution on boundary conditions 11 p1687 A66-22334
- Internal gravity wave propagation in thermally stratified atmosphere 11 p1697 A66-22567
- Input impedance of spherical emitter in infinite homogeneous isotropic conducting medium 11 p1656 A66-23031
- Kinematic computer calculations of energy distribution among products of repulsive, mixed and attractive energy release exothermic reactions 11 p1787 A66-23213
- Triaxial electron spectrometer, mounted on OGO-E spacecraft, measures flux and energy distributions of electrons, noting electron multiplier 12 p1877 A66-23689
- Magnetic field effect on energy distribution and slowing-down times of nonequilibrium carriers in semiconductors when excitation source creates electron-hole pairs 12 p1929 A66-24451
- Bremsstrahlung of nonrelativistic plasma, treating nondegenerate electron component of plasma simultaneously with degenerate component by applying Fermi-Dirac distribution 12 p1925 A66-24996
- Einstein gravitational theory in terms of orthogonal reference points, describing energy and momentum distribution by generally covariant tensors 13 p2128 A66-25946
- Discrepancy between calculated and experimental values for Raman gain in pulsed laser suggests higher energy distribution due to light trapping or Brillouin scattering 13 p2096 A66-26157
- Spectral characteristics of gallium arsenide junction luminescence, noting radiative recombination mechanism, energy spread of impurity states and line shape temperature dependence 13 p2168 A66-26186
- Self-pumping chemical laser theory and operation, noting chemical pumping 13 p2104 A66-26382
- Plasmoid propagation in field-free space, discussing thermal expansion, velocity distribution, charged particle density distribution, energy distribution in absence of thermodynamic equilibrium, etc 13 p2154 A66-26528
- Multiple scattering of energy from inhomogeneous media, comparing discrete point scatterer behavior with bulk scatterer 14 p2240 A66-27915
- Black body radiation law deduced from stochastic electrodynamics 14 p2414 A66-28173
- Energy distribution of secondary particles emitted in proton stars for tev energy range proton interactions 15 p2583 A66-29542
- Meson emission asymmetry, inelastic particle collisions and multiplicity in ultrahigh energy interactions in nuclear emulsion 15 p2545 A66-29543
- Rotational energy distribution through shock waves in nitrogen measured, using electron beam fluorescence 15 p2481 A66-29738
- Heating process in laser welding of metal sheets, taking into account energy distribution, heat transfer and flux densities 15 p2511 A66-29989
- Lewis method for obtaining thermodynamic relation between energy gap of superconductor and critical field and temperature slope 16 p2768 A66-30141
- Electron component of plasma sheet of terrestrial magnetic trail, noting energy distribution and densities 16 p2792 A66-30142
- Subharmonic structure in superconductive Pb-Pb tunneling junctions, noting energy gap values and background current temperature dependence 16 p2769 A66-30160
- Energy distribution spectrum of tungsten single crystal field emitter and shapes of Fermi surfaces 16 p2769 A66-30162
- B-L flux plots and differential energy distributions for low energy protons in nine energy intervals from 0.17 to 3.4 mev measured with satellite-mounted proton spectrometer 16 p2794 A66-30702
- Differential electron spectra in radiation belt in ten energy intervals obtained by satellite spectrometer, noting soft and hard components 16 p2794 A66-30703
- Heat-conducting gas converging spherical shock wave analysis, emphasizing energy accumulation 16 p2689 A66-31514
- Unsteady expansion of plane layer of ideal gas into vacuum for various laws and durations of energy release described by equations of gas dynamics 16 p2690 A66-31617
- Production rates of muons in extensive air showers determined from spatial and energy distributions 16 p2795 A66-31694
- Surface IR photoconductivity spectra of chemically etched p and n silicon, noting energy distribution, activation energies of centers, etc 16 p2788 A66-31774
- Electric field dependence of piezoresistance in germanium, noting correlation with intervalley scattering in energy balance 16 p2788 A66-31778
- Mars disk intensity, noting spectrophotometric measurements in search for limonite near IR spectral features 17 p2997 A66-31923
- Dangling bonds and dislocations in semiconductors, noting existence of core charge dependent localized state in gap caused by local decrease in atom density 17 p2985 A66-33155
- Energy distribution of electrons emitted from alkali halide films on Mo substrates during positive helium and argon ion bombardment 17 p2988 A66-33459
- Coupling between free electron and molecular vibrational temperatures in plasma environments, noting energy distribution, application to MHD generation, etc 18 p3145 A66-34105
- Energy flow variation of high energy nuclear active particles in EAS measured by scintillation detectors in Bolivia 18 p3205 A66-35099
- Three-dimensional Monte Carlo simulation of nuclear cascade of extensive air showers, examining nuclear particle spatial and energy distribution 18 p3206 A66-35102
- Neon hodoscope study of energy and production heights of high energy EAS electron-photon cascades, comparing results to nuclear emulsion study findings 18 p3207 A66-35109
- Airborne scintillation counter-spark chamber observations of particle energy flow and incident zenith angle distribution of air showers 18 p3211 A66-35131
- Muon component of vertical and inclined extensive air showers, determining energy spectrum, lateral distribution at sea level and relation of mean height of origin and sea level energy 18 p3211 A66-35134
- Ionization chamber to investigate distribution of energy portion transferred to photons by nuclear active particles colliding with atomic nuclei of C, Fe and Pb 18 p3215 A66-35157
- Pumping energy distribution of ruby laser, discussing existence of trapped modes and effect of partially filled water jacket surrounding ruby rods 19 p3373 A66-35389
- Energy distribution of hydrogen plasma from coaxial gun 19 p3407 A66-36097
- Magnetic field effect on energy distribution and slowing-down times of nonequilibrium carriers in semiconductors when excitation source creates electron-hole pairs 20 p3619 A66-37683
- Energy distribution of trapped electrons producing solar microwave impulsive radio bursts and X-ray bursts from Sun 20 p3634 A66-38213
- Upper atmospheric phenomena and particle precipitations noting ionization cross section, energy and spatial distribution and auroral activities 20 p3642 A66-38334
- N-type Ge hot carrier Hall mobility, magnetoresistance, Maxwellian energy distribution, electron-electron and intervalley electron-phonon



collisions 21 p3801 A66-38997  
 Nonadiabatic magnetic trap energy  
 redistribution during charged particle  
 motion in spatially periodic magnetic  
 field 21 p3788 A66-39058  
 Spectral response curves of  
 superconducting point contacts, noting  
 existence of frequency dependent Josephson  
 current amplitudes peaking in vicinity of  
 energy gap 21 p3803 A66-39262  
 Cosmic-ray neutron production and flux  
 distribution on sea level and mountain  
 altitude measured with boron fluoride  
 counter for Maxwellian energy distribution  
 with shifted neutron  
 temperature 22 p3972 A66-39680  
 Upper ionospheric electron density,  
 electron gyrofrequency, ion density and ion  
 gyrofrequency deduced from whistler-mode  
 waves group index, energy distribution and  
 dispersion curves 22 p3911 A66-39989  
 Cosmic microwave background radiation,  
 considering statistically homogeneous and  
 isotropic but nonuniform distribution of  
 matter 22 p3978 A66-40009  
 Spectral energy distributions of various  
 quasi-stellar radio sources, using  
 photoelectric spectrum  
 scanner 23 p4129 A66-41806  
 Ratio of energy flux in nuclear active  
 component to energy flux in electron  
 photon component in extensive air showers  
 with given numbers of  
 particles 24 p4269 A66-42918  
 Angular and energy distributions of muons  
 produced by interaction of atmospheric  
 neutrinos with matter  
 underground 24 p4270 A66-42933

## ENERGY EQUATION

Reduction method for high order flutter  
 systems based on energy compatibility  
 equation for normalized  
 coordinates 05 p0606 A66-15060  
 Atmospheric energetics during January-  
 February 1963 stratospheric warming  
 investigated, using spectral energy equations  
 for zonal and eddy kinetic and potential  
 energies 07 p1027 A66-17360  
 Energy integral for holonomic system of  
 points of variable mass, transforming  
 Lagrangian form via Hamiltonian  
 function 08 p1256 A66-19583  
 Rayleigh-Ritz method, stationary  
 complementary and potential energy  
 principles and Lagrange undetermined  
 multipliers applied to free vibration of  
 elastic body 11 p1781 A66-22611  
 Heat transfer in steady flow of non-  
 Newtonian fluid characterized by Rivlin-  
 Ericksen constitutive equation inside wavy  
 cylindrical tube, with momentum and energy  
 equations solved by perturbation  
 technique 12 p1866 A66-24960  
 Goedel universe analyzed, noting  
 generalized Poisson equation, angular  
 velocity in perturbed metric, equations of  
 motion in inertial frame of reference,  
 etc 13 p2183 A66-25609  
 Metal behavior during hypervelocity  
 cratering, noting momentum and energy  
 equations for impulsive loading, including  
 anisotropic stress and strain rate tensors,  
 etc 17 p3022 A66-32013  
 Velocity distribution in laminar plasma jet  
 determined from energy equation and  
 spectroscopic measurement of temperature  
 distribution 17 p2967 A66-32459  
 Arc operation under nonsteady electrical  
 inputs, noting initial conditions, energy  
 equation solution, temperature profiles,  
 application of Green function for moving  
 boundary problem, etc  
 [AIAA PAPER 66-480] 17 p2970 A66-32769  
 Discontinuous one-dimensional dissipative  
 flow of perfect liquid and gas conductor in  
 magnetic field, emphasizing case where  
 magnetohydraulic jump may  
 occur 17 p2973 A66-33070  
 Fluid dynamics equations of state, motion,  
 continuity and energy stress-strain  
 relationship and shearing stress  
 deformations 18 p3098 A66-34120  
 Supersonic MHD flow around right angle  
 bend, constructing characteristic net by  
 applying energy  
 equations 18 p3147 A66-34625  
 Properties of anisotropic continuous media  
 with energy and stresses depending on

deformation-tensor gradients and other  
 tensor magnitudes 19 p3476 A66-36833  
 Energy balance equation obtained from  
 turbulent winds from chemical release  
 studies and turbulent diffusion analysis of  
 globule expansion 20 p3554 A66-38205  
 Turbulence energy balance equation used  
 in air mass transformation  
 problem 20 p3594 A66-38369  
 Constitutive equations for nonlinear elastic  
 solid-linear viscous fluid mixture and for  
 mixture of two nonlinear elastic  
 solids 22 p3898 A66-40140  
 Linear theory of micropolar elasticity,  
 noting all components of asymmetric stress  
 tensor are determined and motion of media  
 is fully described when deformation and  
 microrotation vectors are  
 known 22 p3995 A66-40566  
 Systematizing power compaction and  
 energy compaction equations for porous  
 materials, depending on functions and  
 independent variable 23 p4075 A66-41821  
 Inviscid flow model for stagnation region  
 behind strong shock, examining inviscid  
 energy for radiating gas including self-  
 absorption effects 23 p4150 A66-41906  
 Stress-strain temperature equations and  
 energy equation with heat conduction for  
 isotropic nonlinear viscoelastic materials,  
 using irreversible  
 thermodynamics 24 p4289 A66-42280  
 Thermal emission in subsonic and  
 supersonic nozzles based on energy equation  
 solution and laws of heat  
 transfer 24 p4295 A66-42878  
 Energy equation of boundary layer in heat-  
 insulating part of flat wall used to derive  
 equations for gas heat shield efficiency,  
 demonstrating effect of nonisothermicity  
 and compressibility 24 p4196 A66-42881

## ENERGY EXCHANGE

Energy accommodation coefficients  
 calculated for gas particles interacting with  
 cubic crystal lattice 04 p0548 A66-14142  
 Rate of intercarrier energy exchange in  
 semiconductor by intraband collisions within  
 Maxwellian distribution of  
 carriers 04 p0566 A66-14314  
 Direct measurement of energy relaxation  
 time between hot electrons and lattice in n-  
 type indium antimonide in hydrogen  
 temperature range 06 p0929 A66-17036  
 Exchange of energy between ionosphere  
 and protonosphere, noting nonlocal heating  
 by photoelectrons, thermal conductivity and  
 heat input by downward  
 flux 08 p1215 A66-19204  
 Wave propagation in magnetoplasmas  
 noting momentum transfer, dispersion  
 relations, temperature relaxation effects and  
 collisional energy  
 exchange 09 p1408 A66-20372  
 Born-exchange and Ochkur approximations  
 used to calculate electron impact ionization  
 cross sections for He, Li, Be, Na and Mg  
 atoms in ground states 11 p1737 A66-22497  
 Energy exchange between beam of charged  
 particles and small amplitude  
 electromagnetic perturbation in  
 magnetosphere 11 p1700 A66-23137  
 Circumventing turbine inlet temperature  
 limitation of gas turbines by direct fluid-to-  
 fluid energy exchanger, using isentropic  
 compression waves to avoid shock losses  
 [ASME PAPER 66-GT-117] 14 p2373 A66-27009  
 Acoustoelectric effects for various sound  
 waves, using rate of energy exchange  
 between two coupled systems in relative  
 motion 15 p2564 A66-28970  
 Interaction between gas particles and solid  
 surface examined, noting idealization of  
 Morse potential and use of analog  
 computer 16 p2655 A66-30390  
 Moderately long-range relativistic  
 intermolecular forces, obtaining interaction  
 energies 17 p2960 A66-32401  
 Retarded intermolecular forces, discussing  
 Casimir and Polder retarded dipole-dipole  
 energy of interaction between two ground  
 state atoms in terms of trigonometric  
 integrals 17 p2960 A66-32402  
 Reduction of Gilchrist two-equation set for  
 free oscillations in conservative quasi-linear  
 systems with two degrees of  
 freedom 18 p3134 A66-33602  
 Plasma-electromagnetic wave interactions

during hypersonic reentry of space vehicle  
 into lower layers of atmosphere  
 [ICAS PAPER 66-37] 22 p3957 A66-40666  
 Vibrational energy exchange between  
 molecules during collision behind direct  
 shock wave front examined as function of  
 wave velocity 23 p4010 A66-41732

## ENERGY LEVEL

## SA EXCITATION

Heat capacity related to quantizing of  
 energy levels of electron excitation of  
 superconductor in intermediate  
 state 02 p0278 A66-12278  
 Total complexions for isolated assembly of  
 N quasi-independent localized systems with  
 equally spaced energy  
 levels 03 p0444 A66-12610  
 Quantum scattering theory of hydrogen-like  
 ions in 1-S, 3-S, 1-P and 3-P  
 states 03 p0395 A66-13110  
 Electrical behavior of microplasmas for  
 determination of density and energy level of  
 capture sites induced by radiation in silicon  
 single crystals 04 p0566 A66-14320  
 Computer calculation of relative  
 populations of atomic energy levels not in  
 thermodynamic  
 equilibrium 05 p0718 A66-14871  
 Heat capacity related to quantization of  
 energy levels of electron excitation of  
 superconductor in intermediate  
 state 05 p0738 A66-15457  
 Lower bounds for energy levels of  
 anharmonic oscillators 06 p0911 A66-16167  
 Lower bounds to energy eigenvalues for  
 rigid rotator in electric field /Stark  
 effect/ 06 p0911 A66-16168  
 Positions of defect energy levels in n-type  
 germanium irradiated with fast neutrons  
 analyzed by optical methods, measuring  
 spectral distribution of photoconductivity  
 and quenching curve 06 p0934 A66-17127  
 Temperature and plasma-composition  
 determination for pure thermal carbon  
 plasma 07 p1086 A66-17734  
 Fluctuation of ratio of yearly average  
 amplitudes of meson-to-neutron diurnal  
 variation owing to variability of energy  
 dependence of cosmic ray  
 anisotropy 07 p1126 A66-18009  
 Electron distribution over energy level in  
 valence semiconductor in presence of  
 electric field 08 p1269 A66-18977  
 Anomalous densities of states in normal  
 tantalum and niobium 09 p1417 A66-20029  
 Thermodynamic behavior of strong  
 coupling superconductors, with complex  
 energy gap function and renormalization  
 parameter for lead and  
 mercury 09 p1423 A66-20072  
 Boundary condition constraint method for  
 generalizing R-matrix theory, permitting use  
 of shell model as basis for nuclear-reaction  
 calculations 09 p1405 A66-20322  
 Electron excitation cross section of  
 individual energy levels of inert gases  
 calculated, using Born-Oppenheimer  
 method 09 p1405 A66-20939  
 Pressure induced change in energy gap and  
 forbidden bandwidth of lead  
 telluride 10 p1587 A66-22152  
 Perturbation effects in differential elastic  
 ion-atom scattering generated by crossing of  
 molecular states from even  
 potentials 11 p1740 A66-22972  
 Cobalt doping effects on energy level and  
 negative photoconductivity in n-type  
 silicon 12 p1926 A66-23720  
 Differences between thermodynamic  
 equilibrium of hydrogen plasma, accounting  
 for increased atomic  
 energy  
 levels 13 p2141 A66-25459  
 Spectrum of electron excitations with  
 small energies compared to critical  
 temperature of superconducting transition in  
 absence of magnetic field 13 p2168 A66-25978  
 Optical absorption, energy level structure  
 and exchange interactions of cobalt and  
 sodium cobalt fluoride  
 ions 14 p2357 A66-27075  
 Spontaneous LF current oscillations in  
 germanium with copper, with compensated  
 energy levels under illumination, low  
 temperatures and electric fields, noting  
 formation of electric  
 domains 14 p2357 A66-27076  
 Superconductivity model with exact  
 solution, determining energy levels, ground



- state energy, excitation spectrum, density variations, etc 14 p2360 A66-27190
- Energy level transitions in vacuum UV absorption spectrum of calcium vapor 14 p2337 A66-27704
- Relative vibrational transition probabilities and r centroids for 36 bands of C-X system of singly ionized nitrogen molecule 14 p2337 A66-27705
- Minimizing maximum signal energy, when signals are represented as points in N-dimensional space, by choosing origin as center of smallest hypersphere enclosing all points 14 p2243 A66-28351
- Electron excitation cross section of individual energy levels of inert gases calculated, using Born-Oppenheimer method 15 p2543 A66-28528
- Normal scalar nonet, K1 meson-2 pion decay, K1-K2 mass difference and S-wave pion scattering 15 p2544 A66-28946
- Resonance transformation of light in molecule, using Schroedinger wave equation 15 p2544 A66-29197
- Resonant absorption of monochromatic light in system with intermediate energy level 15 p2516 A66-29355
- Quantum mechanical potential energy curve of lowest normal state of diatomic helium computed in valence bond scheme, using 17-term wave function of Slater orbitals 16 p2749 A66-30112
- Pressure dependent energy loss process determined in atomic light analysis of helium positive column, noting molecular-ion concentration relation to 3 D super 3 population 16 p2750 A66-30114
- Resistivity increase in Cadmium Telluride, attributed to conduction band separation due to deionization into impurity levels 16 p2768 A66-30131
- Prediction that above presently measured energy level cosmic ray spectrum will steepen abruptly and finally have cosmologically meaningful termination 16 p2793 A66-30194
- Evaluation of energy resolution of Li-drifted Ge detectors and preamplifiers using FETs in nuclear spectrometry 16 p2660 A66-30625
- Collision cross sections of ions in isoelectronic sequence of lithium, noting dipolar transitions of type 2s to np 16 p2754 A66-31261
- Pulse field effect technique investigation of electrical properties of surface states on practical Si surfaces with various surface 16 p2781 A66-31356
- Impurity energy levels in semiconductors described by equivalent Schroedinger equation containing short-range as well as conventional terms for long-range Coulomb potential 16 p2784 A66-31446
- Kinetics of semiconductor characteristics determined from impurity photoconductivity, using circuit measuring effective cross section of current carrier capture in impurity centers 16 p2709 A66-31667
- Distribution of recombination centers over energy levels of CdS-CdSe solid solutions 16 p2787 A66-31737
- Energy levels in forbidden band of gallium arsenide alloyed with silver or gold, determining impurity levels from temperature dependence of electric conductivity and Hall constant 16 p2789 A66-31791
- Planck entropy equation and irreversibility of radiation matter interaction for stationary isothermal gas emitting resonance lines of two-level atoms 17 p2957 A66-32044
- Physical process effect on structure of H II regions, noting ionization, Lyman continuum spectral distribution and radiative transfer frequency dependence on absorptive processes 17 p3003 A66-32655
- Resonance transformation of light in molecule, using Schroedinger wave equation 17 p2961 A66-33046
- Local pressure effect on changes of forward current and stored charge of germanium p-n and p-s-n structures explained by change of energy gap 18 p3153 A66-33759
- Energy gaps of Ag-Sn, Fe-Sn and Sn film studied by electron tunneling method for various temperatures 18 p3156 A66-34474
- Energy level and crystal-field splitting of neodymium ion in yttrium oxide 18 p3157 A66-34514
- Solar neutrino detection via neutrino-chlorine reaction, discussing energy level positions and probabilities of beta transition 18 p3223 A66-35219
- Lunar figure and orbit parameters measured by optical location method 19 p3455 A66-35285
- Pressure induced change in energy gap and forbidden bandwidth of lead telluride 19 p3440 A66-35766
- Gas laser with generalized polarization characteristics, noting role of degenerate atomic energy levels 19 p3374 A66-36005
- Energy levels and interband oscillator strengths of antimony calculated in Brillouin zone by pseudopotential method, predicting polarization effects and spin-orbit splittings 19 p3446 A66-36392
- Fermi surface interpretation of band structure, electron energy levels, optical properties and ferromagnetic structure of transition and noble metals 20 p3613 A66-37274
- Resonant absorption of monochromatic light in system with intermediate energy level 20 p3604 A66-37359
- Atomic energy levels in plasma, considering energy spectrum of hydrogen-like atom in plasma, based on cut-off Coulomb potential model 20 p3607 A66-37373
- Resistive effects in type II superconductors near upper critical field examined, using Ginzburg-Landau equations 20 p3616 A66-37374
- Stimulated two quantum radiation in optical range for transitions occurring between discrete levels of impurity crystals or free atoms 20 p3577 A66-37377
- Eigenvalues and eigenfunctions of spin Hamiltonian and matrix elements of spin operator of ruby 20 p3578 A66-37584
- Gas pressure effect on excitation of 4.38-eV level in Pb during hollow cathode discharge in magnetic field 20 p3579 A66-37780
- Photodissociation laser system, discussing output energy dependence on pressure, temperature and number of successive optical pumping flashes 20 p3579 A66-37781
- Chemical kinetics of electron plasma reactions, discussing energy states, ion-molecule reactions, charge transfer, transport properties, phase interactions, etc 21 p3702 A66-38448
- Photoionization efficiency curve for sulfur hexafluoride in wavelength region 1050 to 600 angstroms with Rydberg levels from electronically excited state 21 p3774 A66-38525
- Electrical properties of indium antimonide single crystals with noncompensated impurity concentration, determining position of deep-seated levels in forbidden band 21 p3799 A66-38929
- Degree of population inversion and inverse temperature measurement in medium 22 p3917 A66-39663
- Energy levels of rotationally hindered linear molecules calculated, using variational principle based on schroedinger-like integral equation 22 p3949 A66-39665
- Effective mass in nuclear deformational Hamiltonian calculated by asymptotic approximation method which is two orders of magnitude better than liquid drop model 22 p3951 A66-40422
- Spontaneous LF current oscillations in germanium with copper, with compensated energy levels under illumination, low temperatures and electric fields, noting formation of electric domains 22 p3966 A66-40833
- Counting rate statistics and energy levels of optical photons in electron photon cascade in cooled mercury atoms 22 p3951 A66-40893
- Free-atomic pseudopotentials, sizes, s-p splittings and pseudowave functions 22 p3951 A66-40910
- Hydrogen excitation mechanism in surge prominences determined, using stationary equations for energy levels of hydrogen 23 p4126 A66-41076
- BCS model extended to intermediate and strong-coupling superconductors effective interaction strength as function of absolute-zero energy gap, phonon-frequency cut-off and Fermi surface density of states 23 p4113 A66-41376
- Hartree-Fock parameters for intermediate coupling compared with those obtained from observed energy levels for C I sequence 23 p4130 A66-41814
- 3 cm hydrogen line from solar flares, estimating line-to-continuum ratio during flare 23 p4124 A66-41928
- Energy levels and wave function of hole in field of two acceptor ions and nearest ion donor for p-type Ge and Si 24 p4255 A66-42496
- Energy levels and wave function of hole in field of two acceptor ions and nearest ion donor for p-type Ge and Si, noting numerical results 24 p4255 A66-42498
- Parametric phenomena in ferromagnetics, noting parametric excitation of quasiparticles and stationary state of excited waves 24 p4256 A66-42522
- Superconductivity model with exact solution, determining energy levels, ground state energy, excitation spectrum, density variations, etc 24 p4259 A66-43088
- Anomalous circular polarization of hydroxyl radical 18-cm radiation from cosmic sources 24 p4272 A66-43188
- ### ENERGY LOSS
- Energy dissipation of acoustic waves propagating in liquid medium and producing cavitation 01 p0106 A66-10417
- Average energy loss per ion pair of low energy nitrogen and oxygen ions in nitrogen, argon and helium 01 p0107 A66-11096
- Dissipation and stability analysis effect on limitation of energy accumulation 02 p0261 A66-11809
- Electron energy and momentum dissipation in n-type InSb at low temperatures, discussing collision effects on hot electron escape 02 p0276 A66-12079
- Ideal energy dissipating mechanisms to synthesize weight or mass index in terms of pertinent design indices, structural efficiency and material efficiency parameters 03 p0436 A66-12753
- Drain currents from iron and copper ion accelerator electrodes of ion engine as functions of cesium flux, temperature, voltage difference and oxygen pressure [AIAA PAPER 64-686] 03 p0416 A66-12782
- Forced discontinuous oscillations of fluid in pipeline, discussing energy dissipation effects in LF range 04 p0509 A66-13556
- Small amplitude LF waves in ionosphere covering momentum and energy dissipation, zero temperature plasma and waves in nonuniform plane-stratified medium 04 p0516 A66-13961
- HF electrodeless discharge in argon and krypton at high pressure noting energy radiation losses, electron density and plasma temperature 06 p0919 A66-16873
- Accuracy of calculation of energy losses by fast muons, considering cases of bremsstrahlung, direct pair production and nuclear cascades 07 p1117 A66-17567
- Muon detection and energy determination in multilayer system of ionization chambers and probability of finding muon in n-electron shower at depth t 07 p1117 A66-17569
- Slow instability caused by dissipation of negative oscillation energy in mirror-type plasma-containment device 07 p1089 A66-17959
- Energy losses at input of superconducting coil in type of magnetic flux pump designed by H. L. Laquer 08 p1268 A66-18676
- Particle distribution and motion in field of force, discussing density profile, energy dissipation, Coulomb charge shielding for local thermodynamic equilibrium and free orbital motion 08 p1261 A66-18743
- Magnitude of Compton effect of nuclear reactor operation in space 08 p1254 A66-19593
- RF losses in lead and niobium investigated for possibility of constructing superconducting linear accelerator 09 p1416 A66-20026
- Formation and expansion of electromagnetic shock waves in communication lines, using ferroelectric crystals 09 p1344 A66-20346
- Plasma oscillation of valence electrons and



exciton in alkali halides, measuring differential cross section, dispersion relation and loss peak in 09 p1430 A66-20844

Biological changes due to microwave absorption, examining energy losses due to ion conductivity and dielectric losses due to polarization relaxation in water molecules 09 p1336 A66-20931

Fluctuations effect in energy dissipation on shape of turbulence characteristics in inertial interval, using successive division of cubes 10 p1522 A66-21237

Energy dissipation of acoustic waves propagating in liquid medium and producing cavitation 11 p1735 A66-22601

Losses and overheating temperature dependences in toroidal coils with various core configurations 11 p1667 A66-22792

Rate of effusion for gas flow through orifice and application to fluorine gas dissociation energy 11 p1688 A66-22880

Electron beam pumped lasers, discussing energy dissipation in fast electrons passing through crystal, laser semiconductor characteristics, etc 11 p1715 A66-23433

Thermionic energy converter energy loss through resonance emission and excited atom diffusion, accounting for de-excitation at electrodes 12 p1922 A66-24219

Absorption of longitudinal ultrasonic waves in superconductors containing impurity atoms, noting entrainment effect role in energy dissipation of waves 12 p1929 A66-24453

Structural constant of temperature fluctuations in atmosphere determined by methods involving turbulent energy dissipation velocity and velocity distribution probability 12 p1875 A66-24871

Cooling of stellar material by thermal conduction under solar atmospheric conditions in presence and absence of magnetic field 13 p2174 A66-25618

Radiative energy losses for charge moving in magnetoactive plasma with random electron density inhomogeneities 13 p2148 A66-26038

Laser oscillation and energy losses in medium containing active molecules 13 p2093 A66-26043

Rotational excitation of oxygen by slow electrons, calculating electron energies, quadrupole moments and energy loss rates 13 p2135 A66-26270

Field separation of ground transmitter into ordinary and extraordinary modes when traversing lower boundary of anisotropic ionosphere, noting effect of incidence angle, magnetic azimuth, etc, on energy dissipation of VLF ground wave 14 p2238 A66-27613

Estimate of energy dissipation in metals, using continuous distribution of oscillating dislocations joined with Zener thermoelastic effects 14 p2315 A66-27658

Laminar flow of incompressible fluid in rectangular channel, determining temperature distribution over channel cross section and thermal flux through wall for case of energy dissipation 14 p2415 A66-28317

Electron gas electroconductivity relaxation time and energy loss in n-type InSb at cryogenic temperatures 15 p2558 A66-28611

Energy dissipation channels of nuclear and electron components of cosmic rays in Galaxy and Metagalaxy 15 p2576 A66-29131

Dynamic dissipation of magnetic field, examining mechanism by which magnetic energy is converted directly into fast particle energy 15 p2576 A66-29132

High energy muon energy spectrum, energy loss rate, primary nucleon energy spectrum and inelasticity fluctuations 15 p2587 A66-29571

Spectral energy loss rate of cosmic ray muons measured in plastic scintillator 15 p2589 A66-29587

Power dissipation in input and output matching networks of varactor doubler for calculating true input and output powers from semiconductor bulk material, noting charge storage occurrence 15 p2466 A66-29674

Induction drag of long cylindrical satellites and Alfvén waves emitted from them determining potential and current distribution and effect on energy loss [AIAA PAPER 66-478] 16 p2799 A66-30523

Servomechanism design, noting optimum response parameters, physical characteristics as functions of inertia, external force, energy dissipation, kinetic energy for operation, etc 16 p2671 A66-31062

Energy dissipation due to deformation of magnetic field in compressible conducting medium near zero field lines 16 p2762 A66-31182

Structural resonant amplitude reduction for increased fatigue life and component malfunction reduction, noting application of internal damping, and use of viscoelastic materials 16 p2715 A66-31201

Thick lithium drifted semiconductor silicon detectors for investigation of fluctuations of energy loss by high and intermediate energy particles 16 p2755 A66-31389

Crash and ballistic protective flight helmets, noting use of improved energy dissipating materials 17 p2863 A66-32146

Amplitude dependence of energy dissipation due to internal friction in metals and alloys of various lattice types under near-resonance loading 17 p2940 A66-33228

Ionization potential, dissociation energy and electron affinity for molecular oxygen 18 p3137 A66-33989

Optical frequency breakdown threshold of inert gas mixtures, using focused beam radiation from Q-spoiled neodymium laser 18 p3138 A66-34236

Electron energy loss spectra of Ge and Si in amorphous, polycrystalline and monocrystalline form 18 p3159 A66-34710

Elastic dissipation of Earth torsional modes estimated by generalized elastodynamic equation 18 p3108 A66-34734

Cosmic ray modulation by solar wind fields noting transit time, energy loss and time variations 18 p3175 A66-34743

Unifield field theory equation for energy loss rate of charged particle moving in plasma, considering screened Coulomb potential and dielectric permeability 18 p3150 A66-34937

Extensive air showers /EAS/, discussing lateral distribution function variation with atmospheric density, primary energy dissipation, shower front radius of curvature, etc 18 p3211 A66-35133

Calculations of energy loss of relativistic charged particles in dielectric media compared with mass operator and perturbation theory calculations and with oxygen experiment 18 p3221 A66-35201

Relationship between depth intensity curve and energy spectrum of muons at sea level, considering fluctuations in energy losses 18 p3222 A66-35207

Energy losses of relativistic muons in electromagnetic interactions, noting influence of atomic electrons on bremsstrahlung 18 p3222 A66-35208

Total energy loss in weakly irregular multiwave waveguide accounted for by energy losses in weakly damped waves 19 p3311 A66-35308

Fluctuations effect in energy dissipation on shape of turbulence characteristics in inertial interval, using successive division of cubes 19 p3341 A66-35859

Role of particle channeling in affecting results from crystal-line detectors used for charged particle and nuclear scattering 19 p3359 A66-35912

Self-oscillations of pulse type extremum system with plant having extremal characteristics shaped by multiplication of two coordinates 19 p3325 A66-35985

Low temperature optical fluorescence of ruby and vanadium doped magnesium oxide in which vibronic sideband intensity near sharp R line is measured as function of energy separation from no-phonon R line 19 p3446 A66-36395

Collective interactions of charged particle beams with plasma produced by electron beam, noting power loss of electron beam coincides with power of HF oscillations caused by interaction 19 p3416 A66-36524

Plasma energy loss distribution over linear surface during discharge in Tokamak TM-2 toroidal chamber measured by germanium bolometric probe 19 p3428 A66-36576

Green formula and moment functions, predicting rate of radiative energy loss from

boundaries of absorbing-emitting slab or sphere 19 p3479 A66-36597

Absorption of longitudinal ultrasonic waves in superconductors containing impurity atoms, noting entrainment effect role in energy dissipation of waves 20 p3619 A66-37685

Weak shock wave structure in viscous heat-conducting fluid, accounting for dissipation of energy during one-dimensional flow 21 p3723 A66-38587

Energy dissipation effect on panel vibration damping due to structural joints 21 p3827 A66-38693

Attitude stability of satellite composed of two elastically connected rigid bodies with energy dissipation treated by Routhian array method 21 p3818 A66-38694

Rotating spacecraft attitude changes due to energy dissipation from angular deformation treated by modal method 21 p3819 A66-38844

Electric field distribution in plane-parallel layer of electron-ion plasma situated in external electric field normal to walls, deriving energy losses by kinetic theory 21 p3782 A66-39015

Electromagnetic wave excitation in magnetoplasma by external currents using kinetic theory, obtaining expression for energy losses, analyzing electron and ion cyclotron resonance 21 p3782 A66-39016

Energy loss of charged particles during passage through weakly turbulent plasma in magnetic field with HF oscillations 22 p3952 A66-39751

Structural constant of temperature fluctuations in atmosphere determined by methods involving turbulent energy dissipation velocity and velocity distribution probability 22 p3912 A66-40332

Penetration resistance of fiberglass-reinforced plastics against small-caliber projectiles noting relations between energy loss, stopping power and plate thickness 22 p3938 A66-40433

Thermionic energy converter energy loss through resonance emission and excited atom diffusion, accounting for de-excitation at electrodes 22 p3957 A66-40583

Quantum mechanical picture of additive interrelation between signal and thermal noise, noting energy loss 23 p4035 A66-41049

Angular variation of position of energy loss maxima in indium 23 p4110 A66-41180

Vertical wind gradient variation and energy variation at height ranging from 80 to 140 km and relation to gravity waves and upper atmosphere turbulence 23 p4066 A66-41849

Neutrino energy losses from vibrating neutron stars, noting density profiles 23 p4131 A66-41863

Injection electroluminescence in AlAs-GaAs as p-n junction diodes of graded energy gap 24 p4251 A66-42300

Rotating body in vacuum, examining motion dependency on body configuration and kinetic energy distribution, noting effect of change in energy on motion 24 p4281 A66-42337

Integral equation of flat-roof resonator solved by iteration method, deriving mode patterns, phase shifts and power losses 24 p4174 A66-42807

Vanishing of sliding in mechanical systems with dry friction 24 p4218 A66-42844

Ultrarelativistic muon electromagnetic interaction energy loss due to bremsstrahlung and pair production 24 p4271 A66-42936

Focusing molecules in states losing energy with applied field, using alternate gradient technique 24 p4239 A66-43037

Spin-spin interaction energy for large separations of two ground state hydrogen atoms 24 p4239 A66-43040

Magnetic losses in superconductors at radio frequencies analyzed in terms of energy dissipation model at local flux trapping centers 24 p4260 A66-43177

**ENERGY METHOD STRESS CALCULATION**

Fracture of metals at different loading conditions by energy analysis of plastic deformation and fracture 06 p0963 A66-16465

Energy method for analysis of lowest mode symmetrical buckling of thin shell shallow spherical caps and cylindrical arches under blast loading 15 p2610 A66-29291

Plastic deformation problems for metals



- solved by energy method 15 p2510 A66-29782
- Energy method application to buckling of axially compressed cylindrical shells with ring-stiffened edges, noting upper and lower bounds and critical rigidity ratio 23 p4140 A66-41912
- Energy method applied in determining upper bounds on displacements due to static and dynamic loading 24 p4288 A66-42273
- ENERGY REQUIREMENT**
- SA METABOLISM**
- Energy calculation as time function required to switch toroidal ferrimagnetic core from one remanent state to another, considering core type used in antenna phased arrays 05 p0642 A66-14564
- Cosmic ray particle interaction at hundred bev range, discussing parameters of inelasticity for collision with nucleus 07 p1113 A66-17538
- Variation of critical energy for direct initiation of cylindrical detonation waves as function mixture composition and initial pressure 10 p1622 A66-21830
- Locomotion energy requirements for lunar surface vehicles, noting parameters affecting requirements, resistance factors, etc [SAE PAPER 660149] 12 p1858 A66-24530
- Existence of inflection points in cost vs terminal time curve for linear minimum energy regulator 19 p3339 A66-36745
- ENERGY SOURCE**
- Gas clouds in dense star clusters compared with quasar properties, analyzing possible energy sources like supernova explosions, stellar collisions and star gas interaction 01 p0137 A66-10494
- Strongly nonlinear vibrating system interaction with energy source of limited capability 01 p0159 A66-11172
- Clear air turbulence, considering energy source by transfer from large to small flow in gravity wave spectra, noting shear role and motion equations 10 p1552 A66-21289
- Reliability, durability and reduction of failure probability in radioisotope energy source design 13 p2085 A66-25285
- Possible use of IR radiation to improve visibility through fog, including atmospheric attenuation effects and radiant energy source 16 p2740 A66-30088
- Sufficient condition for stability of linearly viscoelastic continuum subjected to surface tractions following partial deformation of solid are nonconservative and associated with energy source 19 p3401 A66-36302
- Solar neutrino detection, discussing energy generation processes in Sun 19 p3454 A66-36793
- Dynamic instability in linear vibrating system when linked to unlimited energy reservoir 21 p3825 A66-38577
- Shell immersion in moving fluid under vibrations which can be damped or amplified, analyzing instability due to fluid constituting energy reservoir 21 p3825 A66-38578
- Delayed energy produced by fission product decay when restart of nuclear rocket engine is considered, noting effects of cooldown requirements [AIAA PAPER 66-551] 22 p3946 A66-39676
- Nighttime electron temperatures in upper F region suggest corpuscular energy input 23 p4064 A66-41682
- Bipolar Ni-Cd cells for ruby lasers and power sources to yield high energy pulses for firing pyrotechnic devices 23 p4022 A66-41760
- Methanol-air fuel cells as long-life sources of energy for lighted buoys, TV stations, meteorological stations, etc 24 p4161 A66-42501
- ENERGY SPECTRUM**
- Intensity and energy spectra of low energy primary cosmic ray protons determined aboard Imp-I satellite 01 p0132 A66-10601
- Energy spectrum of cosmic ray muons measured for data on nuclear interactions and characteristics of primary cosmic radiation 03 p0417 A66-12319
- Energy gap and thermoconductivity of normal and superconducting fcc lanthanum 03 p0407 A66-12320
- Injun I and III particle observations discussing methods and results on fast electrons, particle counters, energy separation, spectra, flux variation, angular distributions, etc 03 p0363 A66-12647
- Charged particles in auroral zone, measuring energy and pitch angle distribution of electrons and protons with rocket mounted solid state detectors 03 p0417 A66-12653
- Analysis of 3587 tau-meson decays in emulsion stacks, comparing experimental pion energy spectra with theory 03 p0395 A66-12697
- Cosmic ray helium nuclei along with heavier nuclei, traverse interstellar and interplanetary matter propagation in space and slope of energy spectrum 03 p0423 A66-12927
- Data concerning energy spectra of protons, alpha particles and middleweight nuclei in solar flares indicating similarity of spectra 04 p0574 A66-13838
- Diatom molecules, discussing interrelation between vibrational relaxation and thermal dissociation 04 p0597 A66-13878
- Low energy spectrum of cosmic rays corrected for solar modulation and diffusive passage through interstellar matter 04 p0574 A66-14014
- Quantum effects in theory of space charge layer in semiconductors, noting electron and hole density 04 p0570 A66-14366
- Presence of suspended particles leads to more rapid attenuation of pulsations in final stage of degeneration of isotropic turbulence 04 p0512 A66-14436
- Isotropic photon gas interacting with electron plasma with Maxwellian distribution via Compton effect 05 p0722 A66-14721
- Rocket measurements of energetic particles discussing electron fluxes, energy spectra, angular distribution and data 05 p0745 A66-14777
- Rocket measurement of energetic particles discussing proton flux, energy spectra, pitch angular distribution and data 05 p0746 A66-14778
- Solar cosmic ray generation, discussing proton energy spectrum analysis and wave propagation in interplanetary space 05 p0751 A66-15374
- Spectrum of primary cosmic radiation determined for ultrahigh energies, based on international data on electron and meson air showers 05 p0753 A66-15390
- Primary cosmic rays of superhigh energy using extensive air shower data, noting Geiger-Muller counters, scintillation counters and muon detector 05 p0753 A66-15391
- Energy spectrum of variations in cosmic ray intensity and changes in spectrum with decreasing solar activity calculated for additional particle flux 05 p0754 A66-15399
- Flux and energy spectrum of primary electron component measured by balloon at period near solar activity minimum 06 p0944 A66-16075
- Primary cosmic radiation, discussing variations of time and space of intensity, energy spectrum and chemical composition 06 p0947 A66-16573
- Nuclear emulsions exposed for several days in recoverable satellite scanned for ending tracks of cosmic ray particles, obtaining energy spectra for various nuclei 07 p1111 A66-17464
- Nuclear interaction at high energies, discussing active component structure ionization calorimeter application, energy spectrum of particles, etc 07 p1113 A66-17536
- Pl-meson momentum spectra, discussing production frequency and mechanism in hundred bev range 07 p1113 A66-17537
- Energy spectrum shape and absolute abundance of nuclear active particles at low altitude determined, using ionization calorimeter, plotting angular distribution of particles 07 p1115 A66-17551
- Nuclear active particles analysis by observing integral spectrum of ionization bursts under thick layer of dense material at low altitudes 07 p1115 A66-17554
- Polarization of cosmic ray muons with various residual energies, using hodoscopes and Wilson chamber 07 p1117 A66-17565
- Compton scattering of laser photons, noting transformation into gamma radiation photons upon collision with high energy electrons 07 p1044 A66-17816
- Responses of cubical meson telescopes and neutron monitors, at equatorial and high latitude stations, to anisotropy with different assumed spectrum and latitude dependence 07 p1125 A66-18005
- Frequency distributions of characteristics of daily variation of cosmic ray intensity with solar activity from 1958 to 1962 07 p1125 A66-18006
- Galactic cosmic ray modulation by interplanetary plasma, deriving by method of best fit, direction and energy spectrum of anisotropy outside of geomagnetic field 07 p1128 A66-18020
- Rigidity and energy spectra of primary cosmic rays in nondisturbance and disturbance periods during past 12 years 07 p1128 A66-18021
- Temperature changes in entire atmosphere and effect on diurnal variation of meson component of cosmic rays 07 p1129 A66-18025
- Mariner II solar wind measurements including data on Venus electromagnetic radiation, space magnetic fields and charged particles, energy spectra, solar plasma, etc 07 p1130 A66-18077
- Day-to-day changes in energy spectrum of daily variation of cosmic ray intensity at middle latitude and equator for IGY 07 p1131 A66-18236
- Energy spectrum of current carriers in germanium telluride, investigating electrical properties of polycrystalline and single crystal samples 07 p1105 A66-18376
- Self-consistent-field type perturbation theory for stationary and homogeneous turbulence to determine energy spectrum and response frequencies 08 p1204 A66-18531
- Effect of fast states with discrete energy levels and quasi-continuous spectrum on capacitance of silicon dielectric film-metal structure 08 p1274 A66-19308
- X-ray spectral analysis of chemical bond structure in aluminum semiconductor compounds 08 p1274 A66-19311
- Momentum spectrum of cosmic ray muons determined as function of zenith angle 08 p1286 A66-19834
- Nuclear spin relaxation in superconducting gallium measured by nuclear quadrupole resonance in zero magnetic field, using pulsed nuclear induction spectrometer 09 p1420 A66-20047
- Theoretical energy spectrum for galactic cosmic radiation based on experimental solar cosmic ray data 09 p1437 A66-20204
- Ultrahigh energy primary cosmic ray energy spectrum calculated from EAS particle-number spectrum 09 p1437 A66-20206
- Energy dependence of transparency of walls of transition region shell obtained from Forbush effects, in connection with cosmic ray intensity 09 p1439 A66-20221
- Source energy spectrum of solar XUV produced photoelectrons in ionosphere 09 p1372 A66-20382
- Thermal emf quantum oscillation and quantization of electron energy spectrum of n-InAs 09 p1429 A66-20768
- Electron energy spectrum measurements by Cosmos V satellite, noting concentration and intensity at various geographic areas 09 p1378 A66-21010
- Soft electron fluxes in upper atmosphere measured, using open type secondary electron multiplier ejected in container from rocket 09 p1443 A66-21012
- Energy spectrum of auroral zone X-rays, noting electron precipitation and diurnal pattern for occurrence of bremsstrahlung 10 p1599 A66-21145
- Optical properties of indium oxide, noting direct and indirect transitions in thin films and crystal plates, absorption coefficient as function of photon energy, etc 10 p1577 A66-21560
- Plasma sheath properties near discharge tube anode, noting relation of electron current distribution along discharge radius and ion energy spectrum to pressure 10 p1558 A66-21999
- Energy spectrum of electrons recorded by fluorescent screen indicators onboard Cosmos satellites, noting ratio of electron intensities 11 p1763 A66-23042
- Flux and energy spectrum of low energy cosmic ray protons, noting rocket measurement results and analogy to solar flare spectrum 11 p1764 A66-23059
- Total counting rate and detected



multiplicity spectrum of standard IGY neutron monitor analyzed on basis of neutron production and cosmic radiation components 11 p1765 A66-23144

Primary cosmic ray energy spectrum, including primary flux of protons and heavier nuclei, and EM cascade pair production rates 11 p1765 A66-23192

First order wave function of helium due to one-and two-electron excitation determined by solving differential equations, noting contribution to second order energy 11 p1741 A66-23405

Measurement of differential energy spectra of protons, helium nuclei and heavy nuclei by cosmic radiation telescopes mounted on POGO and Pioneer satellites 12 p1877 A66-23684

Gamma ray spark chamber with photographic recording for manned satellites, determining energy spectrum 12 p1877 A66-23688

Lens technique for measuring yield and energy spectrum of secondary electrons generated by fission fragments through metal foil 12 p1916 A66-23704

Hot-wire anemometer measurement of turbulent velocity fluctuations in air flow and energy spectrum and correlation analyses 12 p1880 A66-23846

Interaction potential of inert gases defined in terms of transport properties, noting contribution of nonadditivity to static lattice energy 12 p1917 A66-23936

Solar wind and geomagnetic storm effects on galactic cosmic ray 11-year variations and energy spectrum, from neutron monitor data 12 p1940 A66-24160

Abrupt increase in cosmic ray intensity coinciding with presence of Forbush effects, noting dependence on geographic latitude and cut-off rigidity, obtaining energy spectra 12 p1941 A66-24168

Stratospheric recordings of solar cosmic rays from chromospheric flares, calculating and comparing diffusion coefficient of cosmic rays and energy spectrum of solar protons 12 p1943 A66-24281

Energy spectra of ions emitted by beryllium, carbon and molybdenum heated by laser 13 p2131 A66-25479

Ionization calorimeter for measuring primary cosmic ray components, discussing nuclear interactions, energy spectra, EM cascades, etc 13 p2175 A66-26011

Photoluminescence for p-and n-type gallium arsenide as function of exciting light intensity, noting minority carrier recombination mode, electron energy spectrum, etc 13 p2169 A66-26187

Electrons from linear accelerator directed in collimated beam at normal incidence upon thick targets of various materials, obtaining energy spectra of retrofugal electrons 13 p2136 A66-26280

Primary cosmic ray charge and energy spectra for helium through oxygen during 1965 minimum solar modulation effect 13 p2175 A66-26348

Electron acceleration near Earth bow shock measured, using Explorer XVIII satellite, noting solar wind effect, energy spectrum in radiation belt and magnetospheric boundary, etc 13 p2175 A66-26355

Modulation theory, discussing phase-envelope relation for band limited wave in terms of Fourier series 14 p2234 A66-27032

Energy spectrum of input and output of linear multichannel summing system of delayed stochastic signals 14 p2264 A66-27243

Thermal emf quantum oscillation and quantization of electron energy spectrum of n-InAs 14 p2361 A66-27303

Diurnal variation of average energy spectrum of auroral X-rays observed from balloon flights, assessing effect of atmospheric absorption 14 p2376 A66-27614

Quantum effects in theory of space charge layer in semiconductors, noting electron and hole density 14 p2369 A66-28265

Transmission energy spectra of 1-mev electrons with normal incidence on Al slabs measured in terms of transmission angle 15 p2543 A66-28715

Electron energy losses in diamond, noting correlation between plasma excitation energy and interband transition energies 15 p2564 A66-28876

CW IR laser oscillation in atomic Cl in HCl and HI gas discharges, noting use of two power supplies and energy level diagram 15 p2513 A66-28880

Energy spectrum of primary photoelectron, using data from atmospheric density distribution, fluxes of solar XUV radiations and absorption and ionization cross sections 15 p2574 A66-28906

Relation between frequency spectrum of pulsations in auroral luminosity and energy spectrum of auroral electrons, using photometer 15 p2489 A66-29235

Extensive air showers - International Conference on Cosmic Rays, Jaipur, India, December 1963 15 p2577 A66-29513

Energy spectrum of high energy cosmic rays from EAS observations 15 p2578 A66-29517

Energy spectrum and arrival directions of high energy primary cosmic rays 15 p2578 A66-29518

Extensive air showers at various atmospheric depths analyzed, using hodoscope counters and ionization chambers, noting differential spectra of densities 15 p2580 A66-29528

Collision cross sections of high energy nucleon-nucleon interactions in nuclear emulsion 15 p2583 A66-29545

U.S.S.R. accelerator experiments in high energy nuclear interaction cross section and inelasticity, primary and secondary cosmic ray particle energies, charged nuclear-active particle energy spectra, momenta measurements, etc 15 p2545 A66-29549

High energy primary cosmic radiation research at Bristol, England, including energy spectra for nuclear interactions, nuclear emulsion stack measurements, alpha production, etc 15 p2583 A66-29550

Energy spectra of atmospheric alpha rays at balloon altitude and of alpha rays from graphite nuclear interactions 15 p2583 A66-29551

Cosmic ray showers, discussing high energy interactions of nuclear active particles, intensity and energy spectra of gamma rays and muons, young air showers, ionization bursts, etc 15 p2584 A66-29555

Nuclear interaction characteristics in brass and carbon, noting production by neutral and charged cosmic ray particles, observation methods, energy spectrum, etc 15 p2585 A66-29560

High energy muon energy spectrum, energy loss rate, primary nucleon energy spectrum and inelasticity fluctuations 15 p2587 A66-29571

Cosmic ray intensities underground and energy spectrum of cosmic ray muons at sea level, tabulating depths, operation time, angular distribution, telescope aperture, etc 15 p2587 A66-29572

Cosmic ray measurements, muon production from decay of charged pions and kaons, muon polarization, momentum spectra, atmospheric gamma cascades and derivation of kaon/pion ratio 15 p2587 A66-29573

Particle number fluctuation in electron-photon shower, influence on spectrum of bursts produced by high energy mu mesons under thick filters 15 p2589 A66-29585

Variation of most probable muon energy loss with momentum, noting density effect and decrease in ionization loss 15 p2589 A66-29586

Sea-level spectra of nuclear interactions of muons over 1000 gev compared with observed underground range spectra 15 p2590 A66-29596

Energy spectra of muons and neutrino production from cosmic gamma rays 15 p2547 A66-29597

Energy spectra of neutrinos from secondary cosmic-ray decay in Earth atmosphere 15 p2590 A66-29646

Flux and energy spectra of primary cosmic X and gamma rays between 20 kev and 1 mev from balloon-rocket measurements 15 p2591 A66-30020

Role of corpuscular radiation in lower ionosphere formation, noting charged particle flux, energy spectra, etc 15 p2591 A66-30024

Polar glow aurora, discussing optical emissions generated by solar cosmic ray protons and alpha particles, energy spectrum, atmospheric and ionospheric absorption effect, etc 15 p2492 A66-30026

Solar flare analysis by examination of high energy gamma rays, noting solar proton and solar material interaction, energy spectrum, generation of fast protons and alpha particles, etc 15 p2592 A66-30076

Flux of low energy heavy primary nuclei obtained by slicing emulsion method, using recoverable satellite during minimum solar activity period 15 p2592 A66-30077

Diatom gas flow past blunt bodies, noting effect of oscillation and dissociation relaxation on mean energy 16 p2627 A66-30100

Three quantum decay of super 1S sub zero state positronium determined via measurement of three quantum coincidence events in Al and oxygen with energy sum of 1.02 Mev 16 p2750 A66-30132

Long-range interatomic forces from thermal energy spectra, elastic scattering cross sections for atomic beams and limiting curve of dissociation 16 p2751 A66-30161

Telescopic measurements of primary energy spectra and abundances of He 3 and He 4 in galactic cosmic radiation 16 p2793 A66-30198

Energy spectra of electrons and protons in islands at back of magnetosphere compared with electron fluxes observed by satellites, noting similarity between particles in islands and those in aurora 16 p2695 A66-30714

Adiabatic deceleration effect on cosmic ray spectrum, noting particle momentum and energy change, diffusion coefficient independent of energy, etc 16 p2795 A66-30924

Quasi-linear theory of plasma cyclotron instability for one-dimensional oscillation spectrum, noting energy of interaction with electromagnetic field, ion velocities, etc 16 p2762 A66-31172

Energy spectrum of neutral hydrogen atoms from coaxial plasma gun 17 p2962 A66-31823

Laboratory work on comets, discussing spectroscopic data, incompleteness of knowledge of dissociation energies and ionization potentials, etc 17 p3012 A66-33400

Differential rigidity spectra model of nuclear component of primary cosmic radiation under various environmental influences 17 p2994 A66-33431

Theta pinch discharge study of four times ionized nitrogen /N V/ spectrum 18 p3136 A66-33628

Explorer XVIII plasma flux measurement data analysis, plasma detector, map of transition zone between magnetosphere and solar wind and associated energy spectra 18 p3168 A66-34351

High energy X-ray spectrum from Crab Nebula at photon energies up to 90 kev 18 p3170 A66-34529

Balloon experiment for measurement of secondary gamma spectrum in 100-2000 mev range, using lead scintillator sandwich spectrometer 18 p3171 A66-34708

Charged Bose gas, discussing ground-state energy, excitation spectra and plasmon-particle interactions, using Bohm-Pines and Bogoliubov approximations 18 p3140 A66-34729

Primary cosmic ray energy spectrum measurements via Proton I satellite, noting inelastic interaction cross sections, chemical composition, etc 18 p3175 A66-34746

Electron-positron components of primary cosmic radiation, noting energy spectrum, flux, charge composition, origin, etc 18 p3176 A66-34748

X-ray and gamma ray astronomy, discussing observational methods, physical processes of generation, radiation intensity, etc 18 p3176 A66-34749

Energy characteristics of 11-year cosmic ray variations, evaluating electromagnetic conditions in interplanetary space for proton, alpha particle and electron variations in energy regions 18 p3176 A66-34752

Explorer XVIII satellite measurements of proton energy spectra in region corotating with Sun, noting modulation of galactic cosmic radiation and source of continuous particle accelerations 18 p3177 A66-34754



- Composition of cosmic rays of supernova origin, noting limited mixing and enrichment of elements of outer layer with thermodynamically synthesized core substances due to shock acceleration 18 p3177 A66-34755
- Galactic acceleration and solar modulation of cosmic rays examined via energy spectrum of galactic electrons, estimating Fermi acceleration, low energy electron flux, etc 18 p3177 A66-34756
- Galactic X-ray energy spectrum noting equipment used, shape of spectra in terms of thermal radiation intensity, etc 18 p3177 A66-34757
- Generically related cosmic ray spectrum explaining variations in abundance ratios of helium isotopes and light to medium elements in terms of solar and geomagnetic modulation 18 p3178 A66-34758
- Galactic evolution examined, using luminosity and volume emissivity diagrams 18 p3178 A66-34760
- Solar and sidereal daily variations of cosmic ray intensity at depth of 60 mwe underground in London 18 p3178 A66-34763
- First-order modulation effects of galactic cosmic radiation, considering hysteresis effect and variation of energy spectrum in 1-yr modulation 18 p3186 A66-34811
- Flux and energy spectrum of primary electron component measured by balloon at period near solar activity minimum 18 p3187 A66-34814
- Electron component of primary cosmic radiation at energies greater than or equal to 15 gev studied, using nuclear emulsion stack 18 p3187 A66-34818
- Electrons, hydrogen and helium nuclei of cosmic radiation as observed in 1964 at average residual pressure of 2.4 mb compared with 1.8 mb obtained in 1963 18 p3187 A66-34819
- Rocket and balloon measurements of fast neutron intensity at high altitude from detectors flown in 1964 and 1965 18 p3188 A66-34823
- Energy spectrum of primary helium nuclei at energies greater than 6 gev 18 p3189 A66-34826
- Differential rigidity spectrum of alpha particles for R less than 2.5 gv at solar minimum 18 p3189 A66-34827
- Low energy galactic cosmic radiation studies by high altitude balloon flights carrying nuclear emulsions, including solar activity, energy and intensity spectra, etc 18 p3189 A66-34829
- Solar modulation and time variation of differential energy spectrum and flux of primary helium nuclei in 30 to 90 mev/nucleon energy range 18 p3190 A66-34832
- Chemical abundances and energy spectra of nuclei in galactic radiation measured in interplanetary space by OGO-I satellite 18 p3190 A66-34833
- Nuclear emulsion stack investigation of composition and differential energy spectra of primary cosmic ray heavy nuclei fluxes 18 p3191 A66-34837
- Balloon-borne Cerenkov scintillation counter measurements of energy spectra of primary cosmic radiation heavy nuclei at various geomagnetic latitudes 18 p3191 A66-34840
- Landau-Symon theory extension, semiconductor telescopes in primary cosmic particle charge and energy spectrometry, and capabilities of Si as cosmic particle detector 18 p3114 A66-34844
- Skyhook balloon flight Geiger counter cosmic ray monitor measurements of energy and charge spectra of galactic rays at solar minimum 18 p3192 A66-34847
- Energy spectrum of cosmic ray diurnal variation determined from IGY neutron monitor data by introducing upper energy cut-off parameter 18 p3195 A66-34864
- Plasma sheath properties near discharge tube anode, noting relation of electron current distribution along discharge radius and ion energy spectrum to pressure 18 p3140 A66-34976
- Plasmoid structure produced by coaxial plasma gun with interchangeable polarity electrodes, noting experimental setup, particle velocity, density, energy, etc 18 p3151 A66-35071
- Electron-photon and nuclear active components energy of young air showers measured by ionization calorimeter, determining inelasticity coefficient 18 p3206 A66-35100
- Ionization calorimetry of energy spectrum of leading particles in cores of EAS compared with data from model 18 p3206 A66-35101
- Stationary aspects of cosmic ray propagation through atmosphere explained by model calculating high energy nuclear active and muonic components of extensive air showers, presenting energy spectra 18 p3206 A66-35103
- High energy nuclear active particles in EAS discussing lateral and zenith angle distribution energy spectrum, anisotropy, etc 18 p3207 A66-35111
- Photoproduction, lateral density distribution, energy spectrum and muon component fluctuations in electron photon cascades 18 p3208 A66-35114
- Heavy cosmic ray primary energy spectrum from BASJE measurements 18 p3209 A66-35122
- Altitude variation of EAS particle density and primary energy/nucleon spectra measured with proportional counters 18 p3210 A66-35125
- High primary energy EAS composition, energy spectrum of nuclear active particles and high energy collisions 18 p3210 A66-35128
- Energy spectra of muon, electron and N components of extensive air showers /EAS/ 18 p3210 A66-35129
- Muon component of vertical and inclined extensive air showers, determining energy spectrum, lateral distribution at sea level and relation of mean height of origin and sea level energy 18 p3211 A66-35134
- Numerical calculations of lateral distribution, energy spectrum and heights of origin of muons in extensive air showers 18 p3211 A66-35135
- Energy spectrum, possible chemical composition and anisotropy of ultrahigh energy primary cosmic radiation 18 p3213 A66-35147
- Energy spectra of electromagnetic cascades produced by cosmic rays observed at balloon altitudes, using composite detector 18 p3216 A66-35169
- Energy spectra of nucleons, muons and gamma rays for truncated power law primary energy spectra calculated, using model for nucleon and meson production 18 p3217 A66-35174
- Relations between primary spectrum, pion multiplicity and sea level muon spectra, using integral equations 18 p3219 A66-35190
- Angular distribution and energy spectrum of cosmic particle showers at large zenith angles analyzed, using ionization calorimeter 18 p3220 A66-35196
- Relationship between depth intensity curve and energy spectrum of muons at sea level, considering fluctuations in energy losses 18 p3222 A66-35207
- Stack of nuclear emulsion exposed underground to analyze fast neutrons, obtaining energy spectrum of neutrons from measurements on hydrogen recoils 18 p3222 A66-35211
- Interaction between ultrahigh energy cosmic rays and neutrinos in universe, noting distortion of energy spectrum 18 p3224 A66-35220
- Energy spectra of muons and neutrinos generated by cosmic rays in dense objects without atmosphere analyzed in connection with nebulae problems 18 p3224 A66-35221
- Quark detection in cosmic rays noting flux dependence on mass, energy loss through ionization, production spectrum threshold, etc 18 p3225 A66-35231
- Semiempirical law for spectrum of wind velocity fluctuations and energy in lower layer of atmosphere 19 p3393 A66-35332
- Suggested origin of low energy tails in radiative recombination spectra due to degenerate conduction band 19 p3437 A66-35475
- Energy spectrum of auroral X-rays in range from 20 to 150 kev according to balloon measurements show remarkable diurnal variation 19 p3452 A66-35563
- Secondary ions energy spectra dependent on incidence angle of primary ions for varying escape angles, using molybdenum targets 19 p3403 A66-36454
- Low energy cosmic ray modulation relationship to observed interplanetary magnetic field irregularities in terms of diffusion, using space probes 19 p3454 A66-36765
- Statistical energy-and power-spectral correlation analysis of signals with nonintegrable spectra 20 p3512 A66-37149
- Energy spectrum of primary auroral electrons determined from vertical luminosity profiles of 16 auroral arcs 20 p3550 A66-37297
- Atomic energy levels in plasma, considering energy spectrum of hydrogen-like atom in plasma, based on cut-off Coulomb potential model 20 p3607 A66-37373
- Relativity theory application to space probes, discussing experimental verification, relevance to cosmological problems and utilization to particles with large energy and momentum 20 p3650 A66-37389
- Galvanomagnetic effect of anisotropic electron energy spectrum on acoustical branch perturbation spectrum of system of electrons and ions in homogeneous magnetic field 20 p3618 A66-37559
- Electron energy spectrum for alloyed semiconductors, determining state densities via Thomas-Fermi statistical method 20 p3618 A66-37562
- Anomalous high count of gamma rays from direction of constellation Cygnus associated with energy spectrum differing from spectrum of secondary gamma rays generated by cosmic rays 20 p3631 A66-37600
- Ionization due to alpha, beta and gamma radiation from ground and atmosphere in ground proximity, noting ion pair production rate and energy spectra 20 p3552 A66-37759
- Rocket instrumentation for galactic X-ray observation, noting scintillation counter, proportional counter and GM counter 20 p3636 A66-38237
- Low altitude measurements of trapped electrons, noting energy spectrum and longitudinal variations of electrons, including instrumentation 20 p3638 A66-38307
- Distribution of energetic protons in Earth radiation belt between 1962 and 1964, noting secular temporal changes, effects of magnetic storm and aspects of energy spectrum 20 p3638 A66-38312
- Vela satellite measurements of particles in solar wind and distant geomagnetosphere, noting measurement of energy spectra, flux density and directional distribution of positive ions in solar wind 20 p3639 A66-38315
- Trapped electrons from Russian high altitude nuclear detonation examined, noting energy spectrum and mirror point density distribution 20 p3643 A66-38342
- Fast-neutron irradiation effects on photoconductivity spectra and induced crystal structure defects for n-and p-type gallium arsenide single crystals 20 p3624 A66-38415
- Energy spectrum of semiconductor compounds with chalcopyrite structure analyzed, using perturbation theory, noting changes resulting from crystalline and spin-orbital interactions 21 p3799 A66-38923
- Mass and energy spectra of ions in Bostik-type plasma source studied by time-of-flight mass spectrometer 21 p3784 A66-39033
- Energy spectra of plasmoids produced in conical organic-glass plasma source, establishing various ions 21 p3786 A66-39041
- Energy spectra of fast particles of moving plasmoids obtained in Bostick plasma source examined by mass spectrometer 21 p3786 A66-39042
- Electron energy spectrum of silicon, examining effect of screw dislocations parallel to crystallographic direction 21 p3803 A66-39296
- Angular wind wave spectrum of deep ocean and variations in coastal zone, noting data on energy distribution of spectrum 21 p3760 A66-39362
- Expanding universe theory of hot ionized intergalactic gas and blackbody radiation and X-ray emission energy spectra 21 p3817 A66-39561



Energy spectrum of levels appearing in silicon single crystals irradiated by integral fluxes of fast electrons, neutrons and gamma quanta 22 p3964 A66-40193

Energy spectral density of ideal sonic boom pressure signatures and equations for HF and LF asymptotic spectral behavior 22 p3848 A66-40301

Fluxes, intensities and energy distributions of magnetically trapped electrons and fluxes of magnetically trapped protons at lower edge of radiation belt 22 p3974 A66-40557

Phase shift from scattering by atoms with attractive potentials, predicting virtual energy states for incident energies in three-turning point range 22 p3951 A66-40906

Radiation noise effect on laser optical properties, noting density vs resonator characteristics, energy spectrum, etc 22 p3933 A66-40917

Galactic radio sources noting disk model brightness distribution, relativistic particle energies, continuous particle acceleration and ratio between proton and electrical component of cosmic radiation 22 p3985 A66-40952

Parallel and transverse magnetic field effects on electric field induced optical absorption at photon energies below direct gap in Ge 23 p4109 A66-41036

Autocorrelation function and energy spectrum of radiotelegraph signal, noting channel parameter dependency on transmission speed 23 p4036 A66-41050

Monograph on electronic theory of heavily doped semiconductors covering energy spectrum, perturbation theory, absorption of electromagnetic waves, density states, etc 23 p4109 A66-41119

High energy gamma rays energy spectrum of solar flares, elucidating proton interaction with solar material 23 p4123 A66-41276

Automatic radio atmospherics recorder for simultaneous observation of waveform and energy spectrum 23 p4069 A66-41663

Spectral characteristics of turbulence in presence of mean velocity and temperature gradients 23 p4087 A66-41801

Spectral energy distributions of various quasi-stellar radio sources, using photoelectric spectrum scanner 23 p4129 A66-41806

Electron effective mobility variation in AC for small signals as function of operating frequency of thin film transistors and dielectric diodes 24 p4181 A66-42392

Pictorial representation of pulse-height energy spectra with two independent variables originating from experimental analyzer 24 p4172 A66-42490

Cosmic ray nucleon interaction with high energies, estimating transition probability and interaction cross section of baryon in passive state 24 p4263 A66-42519

Low energy proton measurements in magnetosphere using Mariner IV spacecraft 24 p4263 A66-42602

Flux and energy spectrum of low energy heavy nuclei of primary cosmic radiation measured by balloon-mounted nuclear emulsion stacks 24 p4264 A66-42608

Errors effect in determining primary energy on measurement of characteristics of nuclear interactions in cosmic radiation, considering energy spectrum 24 p4267 A66-42906

Interaction of 1000 bev particles by ionization calorimeter technique suggests free path of nuclear active particles in atmosphere decreases as particle energy increases 24 p4267 A66-42908

Soviet ground station for observation of energy spectrum, composition and anisotropy in arrival directions of primary cosmic ray particles 24 p4269 A66-42917

Stability of solutions to inverse problems in cascade theory, analyzing case when equilibrium spectrum of particles is specified 24 p4269 A66-42922

Energy spectra of muonic and electronic neutrinos in atmosphere 24 p4270 A66-42930

True and measured energy values of cosmic ray spectra, discussing relations and application of results 24 p4271 A66-42934

RK-1-F radiosonde for stratosphere measurements of X-ray photon energy spectrum, charged particle density and X-ray photon density 24 p4213 A66-42941

Energy spectrum of cosmic rays near upper limit and effect of photon-gas temperature 24 p4272 A66-43056

Plasma potential and ion energy determination via ion extraction and energy analysis 24 p4247 A66-43209

**ENERGY STORAGE**

SA ELECTRIC ENERGY STORAGE

SA THERMAL ENERGY STORAGE

Energy conversion and storage - Conference, Oklahoma State University, October 1965 06 p0808 A66-16390

Single pulse operation of lasers, noting energy storage and amplification effect for four-and three-level active medium 12 p1889 A66-23667

Ruby laser amplifier dynamics, noting amplification in energy gain regimes and correlation to theoretical equations 13 p2089 A66-25049

Solar thermionic power conversion, discussing converters, flux and temperature controls, energy storage generators, support structures, etc [AIAA PAPER 64-734] 13 p2006 A66-26641

Coupling of resonators in electromechanical filter, noting application of energy trapping in piezoelectric resonators 18 p3078 A66-34090

Optimum parameters for low-thrust propulsion system with energy storage for specific maneuver 21 p3808 A66-38974

Single pulse operation of lasers, noting energy storage and amplification effect for four-and three-level active medium 22 p3929 A66-39711

**ENERGY STORAGE DEVICE**

Text on high speed optical pulse technology, lasers and measuring techniques, emphasizing capacitor discharge application 10 p1538 A66-22063

Switch and load inductances and relation to performance reduction in superconductor energy storage systems 12 p1928 A66-24303

Solar power conversion unit consisting of thermoelectric generator, thermal storage container and waste heat radiator [AIAA PAPER 64-728] 13 p2006 A66-26638

Linear electric shock tubes including segmented series-discharge driver, switchless shock tube, metal-walled driver for radiant energy conservation, etc 16 p2674 A66-30418

Energy storage and pulse power tools for space assembly, maintenance and repair operations 19 p3364 A66-35968

Energy storage film capacitors for pulsed plasma thrusters developed for coaxial plasma gun and pulsed arc gun [AIAA PAPER 65-337] 24 p4261 A66-42780

Rapid transfer of magnetic energy via exploding foils, noting inductive storage 24 p4239 A66-43217

**ENERGY TRANSFER**

SA ANTENNA COUPLER

SA HEAT TRANSFER

SA MASS TRANSFER

SA WAVE SUPERHEATER

Laser oscillation increase in efficiency in neodymium doped glass produced through energy transfer 01 p0081 A66-10352

Argon arc stabilized by cooled walls, considering radiation calculated with aid of dependences describing transport properties of argon plasma 02 p0265 A66-11390

Wave propagation in random plasma stressing energy transfer between wave modes 03 p0404 A66-12982

Perturbation calculation of average rate of energy transfer in random vibration of nonlinearly coupled modes 05 p0716 A66-15051

Simultaneous radiation, conduction and convection heat transfer for steady state conditions in one-dimensional spectrally selective, emitting and scattering porous bed [ASME PAPER 65-WA/HT-23] 05 p0789 A66-15642

Probe for measuring energy transfer between satellite and upper atmosphere 06 p0873 A66-15922

Relative rate constants for energy transfer from excited argon atoms to various organic molecules 06 p0910 A66-16158

Traveling magnetic wave plasma accelerator, discussing representative MHD equations, force and output power

parameters and energy relations [AIAA PAPER 66-72] 06 p0942 A66-16253

Optical design of elliptical cavities and comparison of energy transfers from light source to ruby laser with cylindrical cavities 06 p0891 A66-16647

Conductivity and transfer coefficients calculated from electron scattering in cesium plasma 06 p0918 A66-16836

Electromagnetic energy transport between coils or coils external to human body and coil implanted inside body is increased by using suitable ferrite core for receiving coil 06 p0820 A66-16852

Energy transfer to small disturbances in viscous compressible heat-conductive medium defined as quantity that is monotone nonincreasing function of time 06 p0874 A66-17005

Book on determining radiative contributions to energy and momentum transport in gas under almost any density and temperature conditions 06 p0913 A66-17157

Fraction of energy transferred to photon-electron component during interactions of particles with graphite nuclei at energies exceeding 100 bev 07 p1114 A66-17545

Motion of material in solar atmosphere, analyzing horizontal inhomogeneities necessary in understanding energy transfer from granulation layer into chromosphere 07 p1138 A66-18076

Energy transfer mechanism in solar corpuscular flux interaction with terrestrial magnetosphere 08 p1285 A66-19786

Probability of high-energy cosmic ray muon undergoing electromagnetic interaction in lead with energy transfer at various ranges 08 p1286 A66-19836

Ionization effect on plasma thermoconductivity, noting expressions for conductivity due to energy transfer or dissociation 09 p1407 A66-20136

Pulse heights produced when argon, nitrogen and argon-nitrogen mixtures completely stop alpha particles 09 p1405 A66-20680

One-, two-and three-circuit systems with periodically varying inductance, capacitance and resistance influencing energy transfer, noting application to amplifier design 09 p1363 A66-20782

Dynamic transient response of fluid surrounding hot wire studied by analysis of basic transport equations for momentum and energy 10 p1521 A66-21055

Optical excitation due to impact of very slow helium ions on Ar and Kr attributed to transfer of kinetic energy into internal electron energy 11 p1740 A66-22971

Optimum energy transfer from hyperbolic orbit in Newtonian central force field in absence of transfer time limitations 11 p1774 A66-23035

Sensitized and unsensitized phosphorescence and energy transfer properties of series of aliphatic alpha diketones in fluid solution 12 p1916 A66-23620

Fluorescence behavior of gadolinium and terbium, noting nonradiative energy transfer in borate glass 13 p2158 A66-25052

Energy transfer equations for fully ionized /deuterium/ plasma including dominant and nondominant terms 13 p2143 A66-25713

Northward momentum transfer across asymmetric jet in three-dimensional atmosphere analyzed, using initial value problem, noting energy transfer and transformation 13 p2064 A66-26128

Excitation radiation transfer from trivalent chromium to neodymium examined via fluorescence spectroscopy, noting energy transfer parameters and effect on laser output 13 p2098 A66-26175

Optical linewidth study of energy transfer between impurity ions and homogeneous broadening and lineshape changes in optical transitions 13 p2098 A66-26176

Laser action on vibrational-rotational transitions and vibration energy transfer 13 p2101 A66-26204

Ionic fluorescence of europium chelates, suitability as laser materials, noting energy transfer role in population inversion 14 p2315 A66-27463

Energy-rich plasmas produced by light



- pulses from Q-switched laser, noting energy transfer from electrons to ions during expansion process 14 p2308 A66-27607
- Coherent emission from trivalent holmium ions in rare earth substituted yttrium aluminum garnet, noting three energy transfer combinations in YAG 15 p2512 A66-28690
- IR quantum counter based on energy transfer between two rare-earth ions in tungstate mixture 15 p2568 A66-29642
- Deuterium plasma jet injection into simple biconical cusped magnetic field, noting ion energy transfer to electrons and plasma potential variations 15 p2554 A66-29748
- Laser lines due to energy transfer from color centers to erbium ions in calcium fluoride crystals irradiated by gamma ray 16 p2717 A66-30278
- Thermal energy exchange between gases and solid surfaces, using realistic interaction potentials of Morse type, Maxwellian velocity distribution 16 p2825 A66-30387
- Energy transfer measurements in gas-solid surface interactions initiated by electron beam-excited photoemission 16 p2701 A66-30397
- Simultaneous radiation, conduction and convection heat transfer for steady state conditions in one-dimensional spectrally selective, emitting and scattering porous bed [ASME PAPER 65-WA/HT-23] 16 p2828 A66-30990
- Transfer efficiency of theta pinch in converting capacitively stored electrical energy to plasma energy measured, using calorimeter technique 16 p2761 A66-31090
- Radiant energy transport within cryogenic condensates extended to case of explicitly varying condensate depths and wider substrate temperature range 16 p2830 A66-31712
- Spectral density and mean value of power flow between two stiffness coupled oscillators under white noise random excitation 18 p3251 A66-33675
- EAS front structure and normal energy transfer determined from pulse forms recorded by Cerenkov detectors 18 p3210 A66-35126
- Nucleon isobar production in photoemulsion giving rise to large energy transfer to several secondary charged particles 18 p3141 A66-35172
- Bursts produced by high energy muons undergoing large energy transfers analyzed for information on muon electromagnetic interactions over region where muon spectrum is known 18 p3220 A66-35195
- Energy transfer in low velocity inelastic atomic collisions 19 p3401 A66-35464
- Analytic models of stellar evolution, describing homogeneous and inhomogeneous stages, energy conservation and transport radiative and convective transfer mechanisms, etc 19 p3467 A66-36789
- Primary and afterglow emission decay time from low temperature gaseous nitrogen excited by fast electrons explained by possible energy transfer 19 p3404 A66-36799
- Initial rotation effect upon vibrational excitation of diatomic molecules studied in two-dimensional collisions shows that with higher rotational energies it is increasingly difficult to excite vibration 19 p3404 A66-36802
- Non-Newtonian viscoelastic fluids with similarity transformations for power law fluids, noting momentum, energy and heat transfer 20 p3545 A66-37510
- Thermoconductive energy transfer from cathode of low pressure gas discharge 20 p3679 A66-38010
- Classical cross section for producing specified energy transfer in collision of two particles in laboratory system applied to atomic collision cross sections 21 p3774 A66-38544
- Energy transfer mechanism in solar corpuscular flux interaction with terrestrial magnetosphere 21 p3809 A66-38782
- Energy transport by electromagnetic waves, using successive approximations 21 p3770 A66-38946
- Instability of wave of given frequency in plasma creates waves of different frequency, velocity and oscillations and leads to energy transfer between waves 21 p3784 A66-39027
- Atomic collisions, excitation transfer processes and energy level transition probabilities in plasma of gas lasers 21 p3748 A66-39305
- Ionization effect on plasma thermoconductivity, noting expressions for conductivity due to energy transfer or dissociation 21 p3793 A66-39408
- One-, two- and three-circuit systems with periodically varying inductance, capacitance and resistance influencing energy transfer, noting application to amplifier design 22 p3884 A66-39841
- Radiant energy transfer below cloud cover in Venus atmosphere, noting greenhouse effect caused by atmosphere containing components capable of IR absorption 22 p3980 A66-40469
- Sliding magnetic field effect on electric current in conducting annular channel flow, noting energy-transfer efficiency and acoustic resonance 23 p4107 A66-42030
- Turbulence in conducting medium treated by fluid mechanical approach and kinetic theory, noting energy transfers between eddies 23 p4108 A66-42033
- Wave propagation, dispersion and energy transfer in arterial blood flow considered as fluid dynamics, noting finite amplitude effects in circulatory system and flow control mechanism 23 p4062 A66-42058
- CW laser action in holmium-doped erbium trioxide with dominant pumping by energy transfer between ions 24 p4222 A66-42555
- Glass lasers, comparing glass with crystals as hosts for laser ions, considering neodymium laser properties 24 p4224 A66-42800
- ### ENGINE
- S AIR BREATHING ENGINE
- S AIRCRAFT ENGINE
- S BY-PASS ENGINE
- S CARNOT ENGINE
- S CESIUM ENGINE
- S DUCTED FAN ENGINE
- S ELECTROTHERMAL ENGINE
- S GAS GENERATOR ENGINE
- S HEAT ENGINE
- S HELICOPTER ENGINE
- S HYDROX ENGINE
- S INTERNAL COMBUSTION ENGINE
- S ION ENGINE
- S JET ENGINE
- S LOX-HYDROGEN ENGINE
- S NUCLEAR ENGINE FOR ROCKET VEHICLE /NERVA/
- S PISTON ENGINE
- S PLASMA ENGINE
- S RAMJET ENGINE
- S RECIPROCATING ENGINE
- S RESISTOJET ENGINE
- S ROCKET ENGINE
- S SCRAMJET ENGINE
- S TURBINE ENGINE
- S TURBOFAN ENGINE
- S TURBOPROP ENGINE
- S TURBORAMJET ENGINE
- S TURBOROCKET ENGINE
- S VERNIER ENGINE
- S WANKEL ENGINE
- ### ENGINE CONTROL
- SA ROCKET ENGINE CONTROL
- Stabilization and control of Saturn S-II engine actuation system and application to other hydraulic positioning servos, reducing position errors 01 p0015 A66-10669
- XB-70A components and subsystem operation and design noting engine, electrical and cooling control systems [SAE PAPER 650841] 01 p0130 A66-10833
- Aircraft engine maintenance, discussing line, minor and major services, operating period parameters, overhaul facilities, etc 06 p0943 A66-17024
- Lucas fuel control system for Spey engine, using rotating metering valves and variable stroke fuel pump [SAE PAPER 660049] 08 p1282 A66-19389
- Isochronous and droop type governors controlling aircraft engines 08 p1282 A66-19765
- Microthruster power conditioning and control system design and ion propulsion [AIAA PAPER 66-215] 10 p1485 A66-21449
- Takeoff dynamics of VTOL aircraft, noting thrust-weight ratio, wing load, initial thrust angle, engine tilt, etc 11 p1733 A66-23339
- Control of large engine motion from soft mountings during starting and stopping [SAE PAPER 660222] 13 p2088 A66-26399
- Soviet book on automation and control of air breathing gas turbine and ramjet engines 13 p2173 A66-26463
- Dart engine controls and power monitoring instruments 14 p2225 A66-27121
- Analog computer simulation of gas turbine engines for control study, discussing steady state performance and transient response data, surge region, maximum acceleration, etc 15 p2570 A66-28852
- Electronic simulation for evaluation of control concepts and system behavior of regenerative gas turbines 15 p2571 A66-28853
- Literal acceleration limiting fuel control for gas turbine engines during speed transients 15 p2571 A66-28854
- Effect of recuperators on governing of single shaft gas turbine engines and methods used to provide satisfactory governing and overall characteristics 15 p2428 A66-28856
- Fuel flow reset and other methods of governing performance of gas turbines 15 p2571 A66-28857
- Digital approach to gas turbine engine control based on use of pulsewidth modulated information obtained with aid of simple circuits 15 p2571 A66-28858
- Lightweight universal fuel control for commercial aircraft, discussing engine requirements, design considerations, etc 15 p2571 A66-28860
- Small gas turbine engine controls, discussing design, development and cost factors 15 p2571 A66-28861
- Fluid devices for sensing, amplifying, controlling and logical functions in gas turbine control systems 15 p2572 A66-28862
- Synthesis method for automatic control systems, examining controller design for turboprop engine 17 p2901 A66-32311
- Variable geometry jet engine control using advanced hydromechanical, microelectronic and fluidic techniques 19 p3450 A66-36364
- Multiloop control interaction using linearized technique, noting variable geometry intake loop 20 p3627 A66-36881
- Attitude, translation and descent engine control for attitude and position control of LEM 21 p3308 A66-39518
- Mechanical and thermal requirements of attitude, translation and descent engine controls of Lunar Excursion Module /LEM/ 21 p3308 A66-39519
- Three-term governor for gas turbine engine system, examining effect of internally generated pressure noise on performance of different possible hydraulic systems 22 p3972 A66-40513
- ### ENGINE COOLANT
- Comparison of 14 basic methods for cooling rocket engines 07 p1110 A66-17617
- Shock tube ignition delay study of aircraft engine cooling by hydrocarbon fuels in endothermic heat sinks [AIAA PAPER 65-594] 12 p1934 A66-23588
- Specific impulse limitations of advanced nuclear rocket engines due to hydrogen transpiration coolant flows in exhaust nozzle 24 p4261 A66-42777
- ### ENGINE DESIGN
- SA ROCKET ENGINE DESIGN
- McCulloch Model 4318 Drone Target Aircraft Engine for maintainability, reliability, moderate cost and high power-to-weight ratio 01 p0129 A66-10091
- Kinematic systems and reduction gears used in turboprop engines, outlining design features 01 p0079 A66-11060
- Rolls-Royce RB 108 lift-jet engine design, characteristics and V/STOL research 05 p0745 A66-15298
- Aerodynamic analysis of cryogenic radial-inflow turbines, noting optimum velocity distribution [ASME PAPER 65-WA/PID-6] 05 p0608 A66-15604
- West Germany and international cooperation in aerospace engine development, noting VTOL aircraft and supersonic and hypersonic spacecraft 06 p0943 A66-16797
- Engine drive design for high speed VTOL aircraft, discussing thrust requirements, system type and leading area



parameters 06 p0943 A66-17018  
 V/STOL aircraft engine technology, discussing engine configuration, lift augmentation, thrust deflection, efficiency parameters, etc 06 p0943 A66-17023  
 Dimensional stability and structural integrity of labyrinth seals, considering various mechanical design criteria in application to aircraft gas turbines [SAE PAPER 660048] 09 p1383 A66-20150  
 Turbine blade and vane cooling in Rolls-Royce nonmilitary aircraft engines, noting side effects on design and development [SAE PAPER 660053] 09 p1433 A66-20151  
 High temperature turbine blade air cooling methods and cyclic and steady state endurance testing [SAE PAPER 660054] 09 p1434 A66-20152  
 Engines for supersonic and hypersonic aircraft to be used in next decade, noting suitability for cruise aircraft or boosters 09 p1435 A66-20668  
 Propulsion problems for engine of 5000 mph aircraft noting ramjet, cooling, intake, nozzle, etc 09 p1435 A66-20669  
 High temperature materials for hypersonic air-breathing engines, noting usefulness of coated refractory metals 09 p1435 A66-20670  
 Design, operating characteristics, advantages of two-cycle star configuration four-cylinder engine for general-purpose aircraft, noting crankshaft, fuel injection, cooling, etc 10 p1592 A66-21407  
 Resistojet design and fabrication, using hydrogen propellant and having 3-kw power input [AIAA PAPER 66-224] 10 p1592 A66-21451  
 Subliming materials chemistry determining parameters governing selection of subliming solids for microthrust engines [AIAA PAPER 65-595] 11 p1759 A66-22460  
 Text on fundamentals of aircraft gas turbine engine design, including component design and calculation 11 p1762 A66-23310  
 Engine reliability data for four Rolls-Royce civil aircraft engines 13 p2174 A66-26694  
 Sequential Noise Output Recording Equipment /SNORE/, aircraft engine noise test facility, for jet noise and compressor noise and acoustic absorption materials test facility [ASME PAPER 66-GT/N-41] 14 p2269 A66-26986  
 Heat transfer considerations in aircraft-engine design noting fuel, oil and icing problems 14 p2375 A66-28300  
 GE-4 turbojet engine for SST design and program development, maintenance, safety, economics, performance, noise, etc [SAE PAPER 660298] 15 p2572 A66-29833  
 Factors extending life of aircraft engine part beyond that available by in-service development of component replacement [SAE PAPER 660313] 15 p2573 A66-29838  
 Jet engine technology, including spinoff from lift jet, propulsion systems, cost estimates, etc 16 p2791 A66-31280  
 Operating stability of turbojet engines improved by use of double-rotor compressor 17 p2992 A66-33487  
 60-kw, 400-cps engine-generator system capable of providing reliable high-quality electric power at lower mission weight than presently available engine-generator sets 20 p3498 A66-37169  
 Book on aerodynamic experiment in machine building, noting self-simulation problems of machines using gas dynamics, analyzing wind tunnels 21 p3694 A66-38743  
 Factors involved in bringing propulsion system to operational status noting engine design, development, cost, testing, etc 24 p4296 A66-42243  
 Power plant development trends and effect on short and vertical takeoff aircraft design, noting improvement in thrust-weight ratio 24 p4262 A66-43051  
**ENGINE FAILURE**  
 Pratt and Whitney Aircraft system for achieving reliability assurance in gas turbine engines, discussing management, failure modes, product development and tests 01 p0128 A66-10062  
 Reliability prediction for rocket engines based on initial-failure-symptom and failure-cause estimates and uses experienced development efficiencies and effort 01 p0129 A66-10083

Machining processes effect on reliability of engine components and methods for detecting failure and failure susceptibility 01 p0077 A66-10104  
 Comparison of materials for thermal stress application based on engine operating conditions and considering metal strength 02 p0245 A66-11797  
 Creep fatigue, thermal cycling, vibration control, transient thermal response control, structural loads and hot part reliability relating to long-life jet engine failure [SAE PAPER 660311] 15 p2572 A66-29836  
 Jet engine reliability at various stages /planning, production, in-service, etc/ noting its economic aspects and global methods analyzed 16 p2790 A66-30316  
 Spectrometric oil analysis for assessing failure probability of turbojet-engine oil-wetted parts 19 p3355 A66-35524  
 Early detection of impending failure in aircraft turbines 20 p3629 A66-37828  
 Cost of turbojet engine development plans estimated in computer simulation and Monte Carlo techniques 20 p3523 A66-37935  
**ENGINE FAILURE INDICATOR**  
 Acoustic analyzer combined with modulation and pulse shape analysis for effective diagnosis of turbojet engine condition without electrical or mechanical connections 01 p0066 A66-10114  
**ENGINE MONITORING SYSTEM**  
 Dart engine controls and power monitoring instruments 14 p2225 A66-27121  
 Turbojet engine analyzer system theory and implementation for assessing current engine condition and malfunction and for predicting next mission confidence and time 19 p3355 A66-35523  
**ENGINE PART**  
 SA CLUTCH  
 SA COMBUSTION CHAMBER  
 SA FLYWHEEL  
 SA PISTON  
 SA VALVE  
 Capacitive torsional vibration transducer for measuring angular displacement of vibrations in engine shaft 12 p1880 A66-23845  
 Plasma sprayed and detonation-flame-plated protective wear-resistant coatings to extend life of aircraft jet engine parts [SAE PAPER 660310] 14 p2301 A66-27292  
**ENGINE STARTER**  
 Auxiliary power unit turbine-engine starting system analyzed to determine sufficiency of selected accumulator 16 p2637 A66-31224  
 Automatic starter for nuclear reactor rocket engine with automatic power control system 18 p3133 A66-33875  
 Aircraft gas turbine starting with automatically controlled electronic unit, noting system design, operation and performance 20 p3540 A66-38299  
 Delayed energy produced by fission product decay when restart of nuclear rocket engine is considered, noting effects of cooldown requirements [AIAA PAPER 66-551] 22 p3946 A66-39676  
**ENGINE TESTING**  
 SA ALTITUDE TEST  
 SA ENVIRONMENTAL TESTING  
 SA FLIGHT TEST  
 SA FUEL TESTING  
 SA GROUND TEST  
 SA PRELAUNCH TESTING  
 SA PROPELLANT TESTING  
 SA PULSIVE EFFICIENCY  
 SA SPACE ELECTRIC ROCKET TEST /SERT/  
 Laboratory, component and engine tests for lubricant properties of J-79 jet engine including elastomer volume swell, oxidation-corrosion, lubricity, etc [SAE PAPER 650816] 01 p0078 A66-10821  
 High altitude simulating rocket test stands including equipment and performance capabilities of several U.S. and European stands 01 p0054 A66-10880  
 Gas Dynamics Laboratory program for study of V/STOL propulsion, using NRC VTOL propulsion tunnel 01 p0008 A66-10964  
 Semiconductor based three-channel amplitude pulse analyzer for radioactive products of engine wear 01 p0046 A66-11040  
 Full-scale half model of GAMD Mirage III V airplane in S-1 wind tunnel of ONERA Test Center of Modane 02 p0210 A66-11202

JR 100 lightweight lift jet engine outline for National Aerospace Laboratory 02 p0278 A66-11306  
 Disengaging gear lubrication through heat dissipation as factor in Ryder rating of rocket lubricant [ASLE PREPRINT 65-LC-16] 02 p0237 A66-12253  
 Liquid hydrogen flow system startup of full scale simulated nuclear rocket engine 03 p0391 A66-12350  
 Flygmotor rocket engine testing facility noting unique compressed air system 04 p0506 A66-13407  
 Engine-overhaul facilities and procedures at BOAC noting use of flow principle, automatic processing and three main sections, engine dismantling, crack detection and static and dynamic balancing 07 p1111 A66-18329  
 High temperature bearing lubricant requirements for jet engine lubrication systems [SAE PAPER 660072] 09 p1383 A66-20157  
 Design and operation of test stands for ELDO rocket engines under simulated high altitude conditions 10 p1519 A66-21384  
 Semiconductor based three-channel amplitude pulse analyzer for radioactive products of engine wear 11 p1671 A66-23286  
 Aerodynamics of hangar-type engine test facilities, discussing flow stabilization, soundproofing and effect of external winds 12 p1860 A66-24973  
 First phase of thermodynamic development of compressor for 490 hp turboprop engine, test procedures and data evaluation 13 p2171 A66-25077  
 Multistrip cesium contact thrusters, integral focus life test engine and various integral focus ionizers [AIAA PAPER 66-235] 13 p2172 A66-25174  
 XB-70A propulsion system development and testing emphasizing fuel system, inlet-engine compatibility and engine installation [AIAA PAPER 65-571] 13 p2173 A66-25595  
 Reliability testing of aircraft engine components 13 p2088 A66-26689  
 Disengaging gear lubrication through heat dissipation as factor in Ryder rating of rocket lubricant [ASLE PREPRINT 65-LC-16] 16 p2713 A66-30574  
 Efficiency of two-stage repetitively pulsed coaxial plasma engine calculated from engine thrust and total mass flow [AIAA PAPER 66-342] 17 p2990 A66-32448  
 Collector target complex eliminating target life time and test equipment contamination by sputtered target material, applied in testing of electrical propulsion systems [AIAA PAPER 66-500] 17 p2991 A66-32774  
 Test equipment for Viggens motor version of Pratt and Whitney JT8D1 turbojet engine 18 p3093 A66-33938  
 Turbine engine self-excited vibrations from thermal deformation of engine components during transient operating conditions, noting vibration elimination and preventive measures 21 p3807 A66-38622  
 Small liquid propulsion systems testing in space environment simulator with high vacuum and low pumping capacity 22 p3890 A66-40226  
 Stochastic model for power transmission systems in aircraft and rocket engine testing 23 p4122 A66-41861  
**ENGINE TESTING LABORATORY**  
 Aircraft and missile engine development at Saclay Propulsion Test Center /France/ 23 p4053 A66-41648  
**ENGINEERING**  
 Computer input language for minor engineering calculation 11 p1659 A66-22712  
 Computer program for teaching senior graduate engineering course in application of matrices 12 p1828 A66-23842  
 Computer graphics in communication 13 p2085 A66-25364  
 Engineering aspects of MHD - Symposium, Princeton University, March 1966 13 p2000 A66-26253  
**ENGINEERING DEVELOPMENT**  
 Statistical development testing discussing wear rate, factorial design, random balance design, evolutionary operation and component search pattern 01 p0077 A66-10116  
 System engineering methodologies to show



w prediction of human error leads to  
 gher system performance  
 01 p0019 A66-10117  
 New engineering materials - IME  
 nference, Birmingham, England, October  
 65 02 p0243 A66-11736  
 tungsten and molybdenum as engineering  
 materials noting technology, mechanical  
 operties, application,  
 02 p0244 A66-11738  
 Light alloys for engineering application in  
 mor plates, aerospace and nuclear fields,  
 tting aluminum alloy  
 operties 02 p0244 A66-11745  
 Book on systems engineering problems and  
 ols for solution noting energy, materials,  
 odeling, simulation, computers, control,  
 atistics, signals, etc 02 p0307 A66-12280  
 Aluminum-beryllium base alloys, noting  
 problems of application as construction  
 materials 08 p1239 A66-18904  
 Effectetics, informetics, control and  
 ability in modern flight vehicle systems  
 AIAA PAPER 66-131 08 p1254 A66-19565  
 Engineering method for measuring rapidly  
 changing temperatures of gas flow with  
 steady or variable heat  
 09 p1470 A66-20142  
 Prediction and assessment of electronic  
 quipment in early design, particularly that  
 mean time between  
 10 p1513 A66-21858  
 Commercial communications satellite for  
 ndom, phased and synchronous medium  
 titude, noting design, specifications and  
 eration 11 p1777 A66-22454  
 Cost effectiveness as analytical tool for  
 engineering and management, noting risks  
 olved, limitations, benefits,  
 11 p1789 A66-23439  
 Monograph on continuous maximum  
 nicipal covering design and control of  
 ndustrial and process engineering systems,  
 namic programming, process optimization,  
 12 p1901 A66-23534  
 Maintenance and airworthiness philosophy  
 aerospace engineering 12 p1801 A66-23858  
 Standardization of machining criteria for  
 aerospace materials, compiling data about  
 bol design, planning, manufacturing, costs,  
 12 p1901 A66-23534  
 ASTM PREPRINT MM66-714  
 Selection of parts for numerically  
 ontrolled manufacturing, noting periodical  
 ecessity of intermixing with conventional  
 machining operations  
 ASTM PREPRINT MM66-724  
 12 p1887 A66-24418  
 Instruments, measurements, industrial  
 lectronics, nuclear science, ultrasonics -  
 EEE International Convention, New York,  
 arch 1966 12 p1842 A66-24672  
 Research development effectiveness  
 valuation, with computer determining  
 resource allocation 13 p2058 A66-26033  
 Effectetics, informetics, control and  
 ability in modern flight vehicle systems  
 AIAA PAPER 66-131 18 p3267 A66-33786  
 R and D problem solving and information  
 athering in engineering design, reviewing  
 I.T. research program on management of  
 science and technology 18 p3268 A66-34064  
 Book on engineering approaches to design  
 of spacecraft structures including analytical  
 echniques, materials, fabrication, launching,  
 aroute, etc 18 p3258 A66-34714  
 Systems design noting integration off all  
 eparate system-oriented  
 ctivities 20 p3682 A66-37184  
 Reliability engineering education at  
 colleges and universities 20 p3686 A66-37969  
 Reliability engineering education in U.S.  
 nd overseas, giving geographic distribution  
 of activities, trends, magnitude, government  
 upport, etc 20 p3686 A66-37970  
 Reliability education, discussing general  
 uestions, problems, levels of education,  
 ersonnel distribution,  
 20 p3686 A66-37971  
 Management role in NASA Space  
 Applications Program 20 p3687 A66-37973  
 Engineering method for measuring rapidly  
 changing temperatures of gas flow with  
 steady or variable heat  
 21 p3836 A66-39413  
 GRAVING  
 S ETCHING

ENSTROM F-28 HELICOPTER

Enstrom F-28 three-seat  
 helicopter 09 p1329 A66-20163

ENTHALPY

Plasma arc tunnel tests show  
 thermochemical heat of ablation of magnesia  
 strongly dependent on stagnation enthalpy  
 [AIAA PAPER 65-641] 01 p0089 A66-10225  
 Localized calorimetric enthalpy  
 measurements in high-energy-content gas  
 stream using evaporating liquid film to cool  
 gas sample 01 p0165 A66-10908  
 Energy balances for combustion chambers  
 of gas turbines by electronic  
 computer 03 p0416 A66-13202  
 Aluminum carbide thermodynamic  
 properties over large temperature interval  
 calculated from low-temperature heat  
 capacity and high-temperature relative  
 enthalpy 04 p0536 A66-13832  
 Equilibrium combustion products of  
 generalized hydrocarbons with oxygenated  
 air, with charts on enthalpy, entropy,  
 molecular weight, specific heat ratio, etc  
 [ASME PAPER 65-WA/ENER-2]  
 05 p0789 A66-15627  
 Effectiveness of charring ablators strongly  
 influenced by stream enthalpy level and  
 heating rate 08 p1316 A66-18812  
 Rotating bomb calorimetric technique,  
 determining accurate values of enthalpy of  
 combustion of boron and boron  
 compounds 08 p1178 A66-19068  
 Enthalpies determined from experimental  
 heat capacity and Joule-Thomson data to  
 prepare pressure-enthalpy diagrams for  
 helium-nitrogen system 08 p1320 A66-19683  
 Heat conductivity, enthalpy, entropy and  
 isobaric-isothermal potential of niobium  
 calculated from zero to 2740 degrees  
 K 09 p1388 A66-20138  
 True heat capacity of solid heat-resistant  
 dielectric or conducting materials at high  
 temperatures 09 p1470 A66-20141  
 Constant section mixture of flows with  
 different enthalpies, noting sonic blocking  
 for terminal temperature  
 differences 13 p1991 A66-25470  
 Second thermodynamic law analysis of  
 availability balance for conventional gas  
 turbine and free-piston gasifier  
 [ASME PAPER 66-GT-96] 14 p2372 A66-26999  
 Enthalpy of gas stream, calorimeter surface  
 treatment and heat transfer measurement  
 errors in arc-heated tests 14 p2411 A66-27425  
 Enthalpy and density fluctuations in high  
 speed wakes, noting typical reentry and  
 ballistic range cases 14 p2219 A66-27431  
 Elutriation diagrams in determination of  
 adsorption enthalpies from temperature  
 dependence of retention volume in band  
 maximum 14 p2232 A66-27604  
 Enthalpy and entropy of parahydrogen  
 from PVT data and from limited amount of  
 thermal data 16 p2790 A66-30907  
 Steady flow of conducting dissociating gas  
 in channel of constant cross section in  
 presence of magnetic  
 field 16 p2687 A66-31165  
 Performance calculations for propellants in  
 terms of composition and enthalpy and  
 principles of rocket  
 engines 19 p3449 A66-36287  
 Enthalpy of impure sample of niobium  
 calculated from simultaneous measurements  
 of magnetization and heat developed during  
 process of magnetizing type II  
 superconductor 20 p3616 A66-37445  
 Boundary layers with coupled heat and  
 mass transfer for large enthalpy per unit  
 mass of injected material, based on linearity  
 of perturbation equations 21 p3834 A66-38704  
 Heat conductivity, enthalpy, entropy and  
 isobaric-isothermal potential of niobium  
 calculated from zero to 2740 degrees  
 K 21 p3752 A66-39410  
 Probe design for mass flux, stagnation  
 point heat transfer and total enthalpy  
 measurements of high temperature  
 hypersonic gas flows  
 [AIAA PAPER 66-750] 22 p3919 A66-40635  
 Simulated meteor ablation tests using  
 artificial meteors of gabbro, basalt and steel  
 in ultrahigh enthalpy plasma jet  
 [ICAS PAPER 66-40] 23 p4147 A66-41009  
 Enthalpy and entropy of dissociating  
 nitrogen tetroxide, using thermodynamic  
 dependences 23 p4148 A66-41269

Gas heating in wall stabilized electric arcs  
 with axial flow applied to nitrogen arc,  
 obtaining highest enthalpy flux and  
 efficiency 24 p4295 A66-43060

ENTHALPY-ENTROPY DIAGRAM

Small charge asymmetry and entropy of  
 hot universe, finding rational solution for  
 almost-charge symmetrical  
 case 24 p4280 A66-43057

ENTROPY

SA ENTHALPY-ENTROPY DIAGRAM  
SA NERNST HEAT THEOREM

Superconducting critical field curves for  
 tin, indium and mercury below one degree  
 K, with entropy difference linear in  
 temperature for free electron  
 gas 02 p0271 A66-11480  
 Nonadditive entropy of thermal system  
 with regions of different  
 temperatures 03 p0445 A66-13188  
 Nonequilibrium thermodynamics applied to  
 problem of solid carrying electric and heat  
 currents in presence of external magnetic  
 field  
 [ASME PAPER 65-HT-1] 05 p0782 A66-14732  
 Some laser properties from viewpoint of  
 second law of thermodynamics of  
 irreversible processes 05 p0694 A66-14899  
 Equilibrium combustion products of  
 generalized hydrocarbons with oxygenated  
 air, with charts on enthalpy, entropy,  
 molecular weight, specific heat ratio, etc  
 [ASME PAPER 65-WA/ENER-2]  
 05 p0789 A66-15627  
 Heat conductivity, enthalpy, entropy and  
 isobaric-isothermal potential of niobium  
 calculated from zero to 2740 degrees  
 K 09 p1388 A66-20138  
 Paradoxes in thermodynamics by using  
 imprecise terminology, citing available  
 energy, diffusion entropy, self-mixing of gas,  
 etc 09 p1472 A66-20907  
 Thermodynamic property calculations from  
 equations of state and ideal gas properties,  
 using entropy as illustrative  
 example 10 p1619 A66-21077  
 Nonequilibrium thermodynamics applied to  
 problem of solid carrying electric and heat  
 currents in presence of external magnetic  
 field  
 [ASME PAPER 65-HT-1] 11 p1785 A66-22186  
 Generalized theorem of minimum entropy  
 production in terms of fluctuation theory  
 and variational principle, noting application  
 to heat flow in rarefied  
 gases 12 p1974 A66-23541  
 Mechanical flow processes and variational  
 methods based on fluctuation theory, noting  
 relations on minimum entropy production,  
 two-dimensional laminar flow of  
 incompressible fluid, etc 12 p1975 A66-23543  
 Blast wave theory with and without  
 entropy layer effect, determining asymptotic  
 flow, far downstream of blunted nose, past  
 given body 12 p1861 A66-23808  
 Brillouin principle, formulated positively to  
 express information amount in terms of  
 physical entropy, applied to information  
 transmission by electromagnetic field using  
 thermodynamics, noting quantum mechanical  
 expressions 12 p1817 A66-24337  
 Second thermodynamic law analysis of  
 availability balance for conventional gas  
 turbine and free-piston gasifier  
 [ASME PAPER 66-GT-96] 14 p2372 A66-26999  
 Refutation of universe having infinitely  
 increasing entropy and thus having eternal  
 existence 14 p2333 A66-27223  
 Macroscopic equations for nonequilibrium  
 processes in rarefied gases by disrupting  
 moment equations infinite chain, using  
 function of maximum entropy  
 distribution 14 p2336 A66-28059  
 Entropy and heat of formation of lead  
 telluride determined by emf temperature  
 coefficient measurement 14 p2369 A66-28330  
 General cosmological problem /GCP/ based  
 on unified field theory involving  
 cosmological expansion, oscillation and  
 organic evolution, discussing quadrant  
 mechanics, entropy, ether, minimum time  
 problem, etc 14 p2389 A66-28408  
 Second law of thermodynamics, discussing  
 Clausius and Boltzmann mathematical  
 expressions of entropy, role of  
 irreversibility and relationship between  
 increase of entropy and increase of  
 disorder 15 p2616 A66-29062



Enthalpy and entropy of parahydrogen from PVT data and from limited amount of thermal data 16 p2790 A66-30907

Statistical entropy of nonequilibrium plasma, assuming binary correlations remain small and neglecting higher order correlations, analyzing irreversible evolution of simple density 16 p2763 A66-31210

Hypersonic flow past blunt body near stagnation point examined, noting surface layer, characterized by increased density and decreased entropy of

gas 16 p2630 A66-31305  
Planck entropy equation and irreversibility of radiation matter interaction for stationary isothermal gas emitting resonance lines of two-level atoms 17 p2957 A66-32044

Physicochemical quantitative analysis of cometary nucleus-coma buildup relationship, discussing gas liberation, entropy and enthalpy variation, change of state and gross energy balance 17 p3010 A66-33374

Wall term in Boltzmann H relationship leads to increase in entropy for solutions to Boltzmann equations 19 p3401 A66-35584

Operational reliability of finite automatic systems in terms of entropy in individual components 20 p3538 A66-37486

Maximum entropy in estimating damage distribution of single degree of freedom system subjected to random loading, noting reliability 20 p3571 A66-37942

Heat conductivity, enthalpy, entropy and isobaric-isothermal potential of niobium calculated from zero to 2740 degrees K 21 p3752 A66-39410

Enthalpy and entropy of dissociating nitrogen tetroxide, using thermodynamic dependences 23 p4148 A66-41269

Linear perturbation theory of flow due to convection of entropy and vorticity in nonuniform flow field, noting sound generation 23 p4062 A66-42051

Argon entropy diagram calculation from sound velocity data and P-V-T relation 24 p4238 A66-42887

## ENVIRONMENT

SA EXTRATERRESTRIAL ENVIRONMENT

SA FRICTIONLESS ENVIRONMENT

SA HIGH ALTITUDE ENVIRONMENT

SA HIGH GRAVITY ENVIRONMENT

SA HIGH TEMPERATURE ENVIRONMENT

SA LOW TEMPERATURE ENVIRONMENT

SA LUNAR ENVIRONMENT

SA PLANETARY ENVIRONMENT

SA ROTATING ENVIRONMENT

SA SPACE ENVIRONMENT

SA SPACECRAFT ENVIRONMENT

SA THERMAL ENVIRONMENT

Operational environment formulation for airborne navigation radar 19 p3397 A66-35521

## ENVIRONMENT SIMULATION

SA SPACE SIMULATION

Effectiveness of albedo and Earth radiation simulation, examining fixed chamber and fixed vehicle techniques 02 p0211 A66-11216

Albedo and planetary radiation simulation to provide field angle and uniformity of intensity for thermal testing 02 p0211 A66-11217

Design of radiation source system simulating albedo and planetary emission energy flux to space vehicle in any planetary orbit 02 p0212 A66-11218

Survival of Earth organisms under environment simulated low pressure, low oxygen, low temperature and low extraterrestrial conditions 02 p0181 A66-11605

Low friction environment effects on maintenance operations in simulator noting torquing-force capability, hand-eye coordination, etc 02 p0186 A66-11645

Artificial environment in manned spacecraft for preserving human life, comparing physical, chemical and biological processes 04 p0470 A66-14079

Animal exposure to low pressure-high oxygen environment noting pressure control, electronic watering device and constant environmental temperature 06 p0815 A66-15942

Three-axis acceleration control task designed to detect space flight-induced decrements in piloting skills 06 p0818 A66-16246

Scale model testing of lunar surface vehicles in simulated low gravity field [SAE PAPER 660148] 07 p1017 A66-17251

Mathematical model of thermal simulation of manned spacecraft in space chamber [AIAA PAPER 66-22] 07 p1140 A66-17887

Simulator design for inclusion of man/machine interactions and human behavioral and performance considerations in system design 08 p1203 A66-19534

Engineering problems in SNAP reactor component irradiation program, including material compatibility, vacuum equipment selection and operation and contaminants within chamber 12 p1857 A66-23674

Laboratory instrumentation for testing and calibration of in situ probes for lower ionosphere, mesosphere and stratosphere 13 p2059 A66-26549

Laboratory simulation of solar radiation under varying atmospheric conditions 14 p2327 A66-28135

Hypoxemia induced in man by sustained forward acceleration while breathing pure oxygen in five pounds per square inch absolute environment 15 p2430 A66-28659

Simulation of solar flare radiation effects on white mice in spacecraft along circumlunar trajectory 15 p2445 A66-29512

Unique free-floating externally ballasted system for obtaining static flotation characteristics 16 p2677 A66-30450

Environment simulation for space vehicle explosive separation system testing, noting equipment, performance, etc 16 p2679 A66-30470

Fast rise programmed centrifuge, noting acceleration testing capabilities, power speed control, etc 16 p2679 A66-30473

Simulation of aircraft crashes to evaluate seating and restraint systems 16 p2680 A66-30480

Blast environment simulation developing high pressures of relatively long duration, noting helical winding of cord explosive 16 p2681 A66-30501

Low atmospheric pressure and oxygen-rich environment effect on characteristics of uninterrupted long-term exposure to toxic gases of space cabin atmospheres, noting animal testing 16 p2642 A66-30623

Visual simulation device for aircraft pilot and astronaut 16 p2643 A66-30952

Human renal response to 56-day exposure to oxygen-helium atmosphere at 258 mm Hg total pressure 18 p3057 A66-33770

Human blood enzyme response to 56-day exposure to oxygen-helium atmosphere at 258 mm Hg total pressure 18 p3057 A66-33771

Bite-size foods included in feeding study of man exposed for 56 days to oxygen-helium atmosphere 18 p3061 A66-33775

Nutritional evaluation of feeding bite-size foods to man exposed for 56 days to oxygen-helium atmosphere 18 p3061 A66-33776

Space molecular sink design to create vacuum environment, emphasizing pumping and test chamber instrumentation 18 p3093 A66-33797

Low friction environment effects on maintenance operations in simulator noting torquing-force capability, hand-eye coordination, etc 18 p3061 A66-33821

Temperature, time and loading conditions for adhesion or cohesion of structural metals in vacuum 18 p3117 A66-34651

Total simulation system mass effect on certain human force outputs in tractionless environments 19 p3293 A66-36243

Laboratory environment simulation of multipath propagation interference effects on low channel capacity FM systems 22 p3865 A66-40066

Environmental simulation of aerospace missions including solar radiation, high vacuum, zero g, micrometeorites, etc 22 p3886 A66-40131

Interplanetary space environment effect on surface thermal radiative properties, noting results of exposure to simulated solar plasma, solar UV, solar wind, etc 22 p3889 A66-40218

McDonnell Martian Environmental Simulation Facility, analyzing sand and dust storm behavior at low pressures 22 p3891 A66-40227

Hypoxia of simulated high altitude exposure prolongs synaptic delay and conduction time in brain system of rats 22 p3855 A66-40403

Simulation role in automatic testing system for missiles and rocket stages 23 p4052 A66-41135

Micrometeoroid environment effect on metal surface thermal properties, using simulated space vehicle placed in solar space environment chamber [AIAA PAPER 65-138] 23 p4140 A66-41894

ENVIRONMENTAL CHAMBER

Correlating heat flux from quartz envelope tungsten filament lamps in Aerospace Research Chamber to simulate solar irradiated surfaces 02 p0302 A66-11214

Space environment simulation vacuum chamber design and operation in terms of manned testing 03 p0352 A66-12757

Vibration temperature chamber design considering access to top of shaker head, fast stabilization time and reduced downtime for maintenance and adaptability 04 p0508 A66-14449

Ultrahigh vacuum chamber with liquid-helium-cooled liner for space environment simulation 08 p1202 A66-18926

French CNES space simulation chamber for satellite testing 10 p1520 A66-21756

Simulated space vacuum environment by cryosorption pumping system 12 p1858 A66-24709

Fail-safe system used in temperature environment testing chambers functioning independently of control system and reacting to valve failure, power loss, etc 14 p2270 A66-27666

Space simulation facility, based on ion-getter pump system, using ion and titanium sublimation pumps and stainless steel shrouds for thermal conditioning 16 p2677 A66-30453

Oxygen compatibility environmental test chambers noting design, performance and results of operation 16 p2679 A66-30471

Test chamber to simulate vacuum and heat sink characteristics of space, measuring optical constants of coatings 16 p2680 A66-30491

ONERA space environment simulating chambers, giving function and characteristics of each apparatus 18 p3094 A66-34008

Factors in operation of manned space chambers - ASTM Symposium, Seattle, October-November 1965 19 p3288 A66-35837

Man-rating Douglas space simulator, 39-ft-diam sphere with pumping speed adequate for manned operation while maintaining simulated space vacuum 19 p3340 A66-35844

Rapid repressurization of space simulation chamber reliably affected by use of commercially available muffler 19 p3340 A66-35844

High vacuum pumping system techniques to meet requirements for space simulation chambers 19 p3371 A66-36649

Stability of precision gravity sensing tiltmeter determined, noting test facility used, results and performance characteristics 21 p3721 A66-38871

Ground tilt isolation platform construction and performance noting design features, performance characteristics and efficiency 21 p3722 A66-38872

Vibration measurement results on air supported isolation platforms, noting effects of heavy vehicle passing sound pressure 21 p3722 A66-38874

Rescue teams for manned testing in environmental chamber for Gemini spacecraft noting personnel, chamber and personal equipment, test operations and rescue function and drill 22 p3857 A66-40240

Apollo environmental control system simulation chamber for suit and manned system evaluation and operational verification 22 p3892 A66-40241

ENVIRONMENTAL CONTROL

SA CLEAN ROOM

Spacecraft Thermal environment control to insulate cryogenics in bulk for space use 01 p0161 A66-10290

Animal and human test of manned spacecraft life support system consisting of closed system with recirculating air loop, examining potassium superoxide-potassium hydroxide chemistry 02 p0183 A66-11492

Tests of advanced life support and



environmental control systems in manned space laboratory  
 02 p0186 A66-11646  
 Bioinstrumentation and monitoring device which relates complex environmental variables to development of psychophysiological stress evaluation for controlling environment of space capsules  
 06 p0878 A66-15963  
 Polyimide resins for extreme environments, discussing chemical structure, application, electrical, thermal and mechanical properties, radiation resistance, etc  
 06 p0899 A66-16292  
 Measuring temperature coefficient and drift for small capacitors, noting design and environmental control  
 09 p1359 A66-20921  
 Self-contained environmental control system for biosatellite study of prolonged effects of weightlessness and radiation [AICE PREPRINT 19D]  
 10 p1491 A66-21186  
 Personnel comfort and protection from thermal stress, discussing clothing, environmental temperature, metabolic heat production, solar radiation, etc  
 10 p1492 A66-22120  
 Equipment, techniques and principles of human survival in hostile environment  
 10 p1493 A66-22121  
 Long duration manned spacecraft material and structural requirements in radiation and meteoroid shielding, thermal control, cabin sealing, etc  
 11 p1778 A66-23074  
 Reliability of fatigue test results, noting calibration method and frequency, specimen preparation, alignment and environmental factors  
 12 p1958 A66-23656  
 Microbial accumulation on sterile steel, glass and Lucite strips in industrial clean rooms  
 13 p2013 A66-25286  
 Thermal and fluid mechanics problems in Gemini spacecraft environment control system development  
 14 p2226 A66-27813  
 Environmental parameters affecting spacecraft comfort during weightlessness and optimization of comfort  
 14 p2231 A66-28412  
 Environmental conditions in space station noting optimum pressure, gas concentrations and temperatures  
 16 p2641 A66-30346  
 Full pressure suit design for high altitude and space missions, discussing material selection, physiological requirements, etc  
 16 p2642 A66-30462  
 Centrifuge performance, noting angular velocity constancy vibration levels in terms of acceleration, temperature effects, etc  
 16 p2679 A66-30476  
 Centralization of environmental control equipment for cost reduction, improved tolerances and test  
 16 p2680 A66-30479  
 Particle and droplet contamination of spacecraft cabin atmosphere, examining exogenous and endogenous sources, medical aspects of inhalation and exhalation, effect of weightlessness, etc  
 17 p2866 A66-32207  
 Environmental control manufacture discussing cleaning, design and maintenance problems, historical background, etc  
 17 p2903 A66-32208  
 Contamination problems in space program, discussing clean room equipment, maintenance, cleaning problems, etc  
 17 p2866 A66-32210  
 Contamination control of manned spacecraft, noting problem of biological interactions and methods of monitoring  
 17 p2866 A66-32211  
 Bosch process closed cycle oxygen production unit for space application [AICE PREPRINT 47A]  
 17 p2867 A66-32670  
 Trace contaminant control in closed environments as requirement for safe air in habitable areas of manned spacecraft [AICE PREPRINT 26A]  
 17 p2867 A66-32676  
 Contamination control and space program, objectives, achievements, NASA courses, etc  
 17 p2868 A66-32894  
 Apollo LEM ECS and main subsystems design emphasizing maintenance of pressure, temperature, relative humidity and oxygen at safe levels  
 18 p3062 A66-33956  
 Instrument unit analysis for Saturn IB/V program, noting environmental, guidance and flight control, electrical systems and countdown procedure  
 19 p3354 A66-35469  
 Synthesis of minimum sensitive open loop

control system subjected to unpredictable environmental changes, discussing perturbation effects during and before process transient  
 19 p3329 A66-36029  
 Chemical methods for carbon dioxide conversion for oxygen recovery, including relationship to biological processes  
 19 p3293 A66-36235  
 Spacecraft trace contamination control requirements quantitatively defined, emphasizing physical and chemical sorbents and combustion catalysts  
 19 p3293 A66-36237  
 Integrated program approach for contamination control of space cabin atmospheres based on identification, estimation of concentration and system specifications  
 19 p3293 A66-36238  
 Carbon dioxide control by enzymatic reaction in spacecraft atmosphere by hydrolyase and multienzyme  
 19 p3293 A66-36240  
 Air ionization effect on vigilance task performance, noting smaller decrement for environment containing negative ions  
 20 p3504 A66-36933  
 Spacecraft maintainance and repair cost minimization and system effectiveness increase by controlling contamination due to personnel, static electrification and bacteria  
 20 p3567 A66-37899  
 Equipment design and weight estimates for lunar production of oxygen and water  
 22 p3977 A66-39896  
 Cleaning techniques for zip gun or hand-held maneuvering unit and environmental life support system or ventilation control module used for astronaut White walk in space  
 22 p3886 A66-40039  
 Life support systems for crew comfort and safety, considering thermal and radiation environmental control, carbon dioxide removal, cryogenic gas storage, etc  
 22 p3857 A66-40129  
 Tests of advanced life support and environmental control systems in manned space laboratory simulator  
 24 p4168 A66-42779  
**ENVIRONMENTAL LABORATORY**  
 Data collection system with small on-line computer that monitors stress, temperature, pressure and other physical parameters of environmental laboratory vacuum and temperature chambers  
 [ISA PREPRINT 1.12-1-65]  
 05 p0638 A66-15502  
 Chronic exposure of rats to gaseous environments of varied composition and pressure, noting exposure capsules, gas flow system, respiratory gas analyzer, etc  
 16 p2643 A66-30650  
**ENVIRONMENTAL SCIENCE**  
 Human factors engineering, discussing man-machine allocation of system functions, task equipment analysis, model and mock-up analysis and environmental analysis  
 11 p1647 A66-22301  
 Origin, setting and evolution of human factors engineering and man-made environment  
 11 p1648 A66-23100  
 Environment and man - IES Conference, San Diego, April 1966  
 16 p2674 A66-30434  
 Space medicine and biology studies of space flight environmental factors based on experiments with animals and manned spacecraft  
 18 p3056 A66-33699  
 Environmental effects on man, Volume 1 - Symposium on environmental engineering and society, London, April 1966  
 18 p3062 A66-34201  
 Shock and vibration - Underground, under water and in air - Volume 2, Symposium on environmental engineering and society, London, April 1966  
 18 p3095 A66-34205  
 Space technology, Volume 5 - Symposium on environmental engineering and society, London, April 1966  
 18 p3230 A66-34208  
 Space cabin atmosphere and closed environment - ACS Symposium, Atlantic City, September 1965  
 19 p3292 A66-36230  
 Book on physiological responses of healthy mammals to natural changes or extremes of physical environment, considering heat, cold, light, atmospheric pressure and water  
 20 p3505 A66-37253  
 Detection of extraterrestrial biological systems, noting criteria such as radiant energy requirements for life evolution, molecular characteristics,

etc  
 24 p4164 A66-42669  
 Experimental biology in space, discussing goals, contributions and future potentials  
 24 p4164 A66-42670  
**ENVIRONMENTAL SURVEY SATELLITE /ESSA/**  
**S ESSA SATELLITE**  
**ENVIRONMENTAL TEMPERATURE**  
 Thermological aspects of Martian surface environment based on radiometric temperature measurements  
 16 p2799 A66-30435  
**ENVIRONMENTAL TESTING**  
**SA ERIE PROJECT**  
**SA MATERIAL TESTING**  
 Protective coatings for extreme temperature environment discussing types, application, performance in oxidizing atmospheres, tests and industrial problems  
 01 p0084 A66-10090  
 Full scale ground inflation tests to evaluate structural and RF backscatter characteristics of Echo II prototype spheres as function of their internal pressures  
 01 p0055 A66-11123  
 Spectral match tolerance selection for solar simulator with respect to various test specimens  
 02 p0214 A66-11237  
 LF and infrasonic noise effects on mans cardiac rhythm, hearing, vision, motor control, spatial orientation, speech and subjective tolerance  
 07 p0999 A66-17656  
 Metabolic rates in pressurized pressure suit, affecting heat balance of subjects metabolic heat with heat removed by environmental control  
 07 p0997 A66-17657  
 Rats exposed to space cabin atmosphere for two weeks, noting mortality rate, organism functioning, growth rate, etc  
 07 p0998 A66-17663  
 Multistage cryogenic trapping system noting design, operation and application  
 07 p1032 A66-17665  
 Effect of environmental extremes on Miniature Inertial Navigation System, showing vibration and centrifuge testing data  
 08 p1251 A66-19491  
 Environmental testing, spacecraft configuration, data retrieval and flight simulation in OAO  
 08 p1203 A66-19517  
 SNAP-15A radioisotope thermoelectric generator with power output of about 1 mw, design, development and potential uses  
 12 p1911 A66-23680  
 Equipment and methods for simulating natural or induced environments for reliability testing  
 12 p1833 A66-24079  
 Test program evaluating protective clothing and safety equipment for personnel working in Saturn booster at minus 100 F in oxygen-rich or deficient environment, noting problems with communications, visibility, breathing, etc  
 12 p1810 A66-24958  
 Environment-simulation testing effectiveness for unmanned space systems  
 13 p2057 A66-25282  
 Time, pressure and temperature effects on adhesion of structural metals in vacuum and space environment  
 14 p2316 A66-28005  
 Graphite composites suitability for use on hypersonic entry vehicle components  
 14 p2319 A66-28014  
 Environmental test criteria for lunar and planetary soils, discussing particle size, clay, hydrothermal alteration, cohesion, adhesion, vacuum and temperature effects, etc  
 14 p2387 A66-28179  
 Ariel II /UK-2/ international satellite environmental test  
 14 p2394 A66-28426  
 Psychological and physiological reaction to Coriolis effect under artificial gravitational field simulated in rotating space station  
 15 p2443 A66-28682  
 Lubricant selection for lunar missions and manned spacecraft based on compatibility with oxygen-rich environment, propellant, anodic coatings and sliding friction behavior in vacuum  
 [ASLE PAPER 66AM 7A2]  
 16 p2712 A66-30415  
 Performance of SNAP-10A instrumentation during component qualification, ground system and flight system tests, noting environmental conditions  
 16 p2744 A66-30439  
 Factors to be considered in capital equipment and facilities for environmental



testing, including management planning, work load reorientation, etc 16 p2831 A66-30441

Test facility for combined sonic and mechanical excitation of flight-and surface-vehicle hardware, using electropneumatic transducers 16 p2676 A66-30444

Significant environmental criteria and realistic and standard test conditions for microelectronics testing 16 p2659 A66-30451

Monitoring device for detecting short-duration, vibration-induced electrical malfunctions, noting Gemini tests 16 p2677 A66-30454

Structural mounting of large diameter cylindrical missile section in centrifuge for high acceleration environmental testing 16 p2677 A66-30458

Design concepts and requirements for combined acceleration-vibration testing 16 p2678 A66-30459

Averaging systems for control of sinusoidal vibration tests noting methods, crosstalk effect etc 16 p2678 A66-30463

Long term solar simulation test, noting spacecraft performance, equipment design, instrumentation, etc 16 p2678 A66-30469

Hostile long term storage environments, discussing aircraft component condition following extensive exposure 16 p2635 A66-30472

Interaction effects of combined environment testing for aerospace systems 16 p2679 A66-30477

Portable shock and environmental recording system 16 p2703 A66-30482

Economical method of reduction of environmentally obtained shock data 16 p2703 A66-30483

Test program for thermal-vacuum testing of Centaur vehicle components 16 p2808 A66-30485

Errors inherent in specification of shock motions by shock spectra 16 p2813 A66-30488

Shock spectrum analyzer for space vehicle structures, etc, noting galvanometer selection 16 p2703 A66-30489

Environmental testing associated with sterilization of planetary capsule, discussing time vs temperature cycles and flight acceptance 16 p2642 A66-30493

Design of test facility capable of producing eight environments either singly or in combination 16 p2681 A66-30506

Feasibility of oxygen-helium atmosphere at 380 mm Hg total pressure proven by two-week exposure of four men 16 p2639 A66-31120

Pulmonary effects of two-week exposure of four men to helium-oxygen atmosphere at total pressure of 380 mm Hg 16 p2639 A66-31121

Thermal balance and heat exchange between four men exposed to helium-oxygen atmosphere at 380 mm Hg total pressure 16 p2639 A66-31122

Hamsters, mice and rats exposed to elevated oxygen tensions for 60-day periods with nitrogen at high or minimal levels 16 p2640 A66-31129

Thermal similarity study of models in space environmental chambers for deducing characteristics of typical space vehicle element [AIAA PAPER 66-460] 16 p2683 A66-31469

Electric conductivity of CdS single crystals in atmosphere, dry air, oxygen, water vapor, carbon dioxide and in transverse electric field 16 p2786 A66-31730

Regenerative life support system for four-man crew on long duration tests, noting biological constraint parameters 17 p2862 A66-32138

Gravitational environment, effect of change on frogs measured using gravitoceptors in vestibular apparatus 17 p2865 A66-32183

Tracer dilution technique for measuring quantity of urine voided by crew members in manned spacecraft environment 17 p2870 A66-32192

Thermal comfort zones for helium-oxygen and helium-nitrogen atmospheres at reduced pressures 17 p2865 A66-32193

Adaptive responses of adrenal cortex to some environmental stressors, exercise and acceleration 17 p2862 A66-33093

Vibration effects on chromosomes of *Tradescantia paludosa* and other microspores

subjected to Vostok satellite conditions 18 p3058 A66-33781

Environment influence on design and development of Black Knight rocket engine 18 p3163 A66-34211

Capacitance transducer for measuring capacitance ratios with minimum environmental problems, noting wide application range 19 p3355 A66-35470

Human performance in space simulation chambers and physiological limitations 19 p3288 A66-35838

Instrumentation for biophysical data acquisition for pressure-suited test subjects in space environment simulation testing 19 p3289 A66-35840

Physical and psychological aspects of man in space, examining oxygen supply, temperature extremes, meteorites, radiation and effects of confinement, isolation and sensory impoverishment 19 p3287 A66-36645

Nuclear radiation and liquid hydrogen effect on environmental mechanical properties of phenolic asbestos, glass and linen resins 20 p3587 A66-37097

Man rating requirements of space environment simulation laboratory, consisting of two large chambers with floors which can be cooled by liquid nitrogen down to 92 degrees K 22 p3892 A66-40239

Graphite, molybdenum and tungsten sulfides and calcium fluoride effective as solid lubricants in extreme environments 23 p4075 A66-41870

Polymeric materials, metals and lubricant compatibility with vacuum environment, considering radiation damage and thermal control effects 24 p4226 A66-42096

Book on project ERIE covering techniques for analytic evaluation of space equipment designs with respect to environments and missions required in 1975 24 p4217 A66-42572

Environment influence on design and development of Black Knight rocket engine 24 p4261 A66-42573

Bourdon-helix pressure-sensitive switch for air vehicle hydraulic system of XB-70A aircraft and other instruments operating in severe environment 24 p4213 A66-42824

Environmental testing and evaluation of useful life of insulation material for aircraft electrical equipment operating at 280 degrees C 24 p4229 A66-43083

ENZYME

SA AMIDASE

SA CARBONIC ANHYDRASE

Comparison methods for relationship among enzymes that are same but belong to different organisms 04 p0460 A66-13367

Substrate specificity of proteolytic enzyme thermolysin /Thermolase/ isolated from bacterial cultures 09 p1338 A66-20582

Purification of enzyme responsible for degradation of nicotine to 6-hydroxynicotine 09 p1339 A66-20877

Dipeptidyl-beta-naphthylamidase activated by chloride in extracts of rat and bovine anterior pituitary glands 13 p2010 A66-25900

Human blood enzyme response to 56-day exposure to oxygen-helium atmosphere at 258 mm Hg total pressure 18 p3057 A66-33771

Physical properties of DNA-dependent RNA polymerase from *Escherichia coli* 20 p3505 A66-37054

Metabolic correlates of glucocorticoid induction of enzymes in man studied in terms of ACTH induced changes in tryptophan turnover along inducible pathways 24 p4166 A66-43168

ENZYME ACTIVITY

Mechanism, prevention and treatment of oxygen toxicity in central nervous system, noting acetylcholinesterase activity 03 p0326 A66-13346

Mechanism of in vivo rbc damage by oxygen, noting effect on canine erythrocytes 03 p0326 A66-13348

Nature of particles involved in lipid synthesis in yeast 06 p0822 A66-16566

Participation of ferredoxin of clostridium nigrificans in sulfite reduction, describing transportation of electrons for sulfide formation 08 p1177 A66-18699

Crystalline lactic dehydrogenases in reaction with p-hydroxymercuribenzoate in urea 13 p2009 A66-25796

Molecular nitrogen photofixation relation to electron-donor respiratory system,

activity of hydrogenase and dehydrogenases and photosynthesis 13 p2010 A66-25893

Effects of alpha glycerophosphate and of palmityl-coenzyme A on lipid synthesis in yeast extracts 15 p2429 A66-28616

Structural and functional properties of heart and muscle type subunits of lactic dehydrogenases investigated, using comparative amino acid analysis 15 p2446 A66-28864

Stereospecific hydrolytic action of acylase studied by gas-liquid chromatography 17 p2869 A66-31871

Lysosomal enzymes in rats exposed to 100 percent oxygen to determine possibility of accelerated in vivo lipid peroxidation 17 p2857 A66-32169

Ribonucleoside triphosphatase in rabbit reticulocytes, discussing distribution in extracts, behavior in purification of amino acid and properties 17 p2859 A66-32553

Dipeptidyl arylamidase I of bovine pituitary tissue and chloride and sulphydryl activation of seryltyrosyl-beta-naphthylamide hydrolysis 17 p2861 A66-32899

Carbon dioxide control by enzymatic reaction in spacecraft atmosphere by hydrolyase and multienzyme system 19 p3293 A66-36240

Semiquantitative spot test detection of peroxide in low concentrations of hydrogen peroxide 20 p3510 A66-37056

Synthesis of peptides related to active site of esterase enzymes 20 p3510 A66-37633

Chloride requirement for cathepsin C 24 p4165 A66-43099

EOR

S EARTH ORBITAL RENDEZVOUS /EOR/

EPE-A

S EXPLORER XII SATELLITE

EPE-B

S EXPLORER XIV SATELLITE

EPE-C

S EXPLORER XV SATELLITE

EPHEMERIS

Computation of approximate coordinates of Moon with estimation of accuracy over time interval of 50 years 02 p0292 A66-12235

Minor planets and ephemeris calculations with bibliography 02 p0292 A66-12262

System of astronomical constants adopted in 1965 by International Astronomical Union for introduction in 1968, discussing difficulties in consistency, compatibility and durability 03 p0429 A66-13195

Annual astronomical almanac compiled by Madrid Observatory 11 p1770 A66-22638

Minor planets, comets and satellites motions and positions in outline of present research 17 p2998 A66-32025

Two-star implementation by stellar inertial guidance system 18 p3133 A66-34047

Brown lunar theory interpretation of observed lunar motion and associated rectangular-to-polar lunar coordinate transformations 18 p3234 A66-34655

EPHEMERIS TIME

SA UNIVERSAL TIME

Lunar inequality on time of perihelion passages of Earth 04 p0576 A66-13461

Ephemeris time determined by photographic observation of Moon 10 p1606 A66-21261

Astronomical yearbook of Cracow Observatory covering ephemerides of 787 eclipsing binaries, Lagrangian points, precession coefficients, etc 11 p1768 A66-22333

Atomic standards of frequency and second of ephemeris time, discussing frequency of Cs 133 transition at zero field 14 p2296 A66-27899

EPILEPSY

Dissociation of rhinencephalic or thalamic self-stimulation and epileptiform activity in rats 20 p3506 A66-37602

EPINEPHRINE

Degree of mental stress correlated with excretion of catecholamine, free adrenaline and noradrenaline in urine 04 p0470 A66-14081

Protective effect of adrenaline, subgaleally injected, on survival time of rats subjected to acute hypoxia 06 p0811 A66-16064

EPITAXIAL DEPOSITION

Thin film epitaxial single crystal silicon on insulating substrate sapphire and advantages



of these microelectronic devices 01 p0048 A66-11145

Single crystal silicon films on sapphire in terms of materials properties and impact on thin film semiconductor microelectronics 01 p0048 A66-11146

Semiconductor diodes discussing germanium and silicon diode structures, ultrasonic chip bonding and epitaxial material effects on 03 p0348 A66-13344

Thin surface films covering structure, nucleation, growth and epitaxy observation techniques such as electron and X-ray diffraction field emission, field ion microscopy, etc 04 p0559 A66-13452

Relaxation oscillations in n-type epitaxial silicon with point contact, discussing generation via electrical excitation of impurity centers 05 p0731 A66-14655

Residual stress in epitaxial silicon film on sapphire measured by cantilever beam technique 05 p0733 A66-14673

Extrinsic and intrinsic epitaxially deposited single crystal gallium phosphide solar cells, noting conversion efficiencies 07 p0990 A66-17232

Potential distribution in epitaxial p-n semiconductor measured via moving light spot, determining deposition depth 07 p1106 A66-18382

Oxidation products of thin foils of titanium carbide, noting epitaxial growth relationship between titanium carbide, transient oxides and titanium oxide 07 p1052 A66-18512

Imperfection formation in epitaxial gold films, observing crystal-lattice dislocations due to rotation and displacement misfits between neighboring islands of deposit film 07 p1110 A66-18517

Kinetics of reactions in iodide method of growing epitaxial germanium layers 08 p1268 A66-18797

Heterojunction preparation by vacuum evaporation, describing epitaxial deposition of germanium on gallium arsenide substrate 08 p1270 A66-19058

Epitaxial silicon layer crystal growth at low temperatures by sublimation through thin alloy zones 08 p1271 A66-19224

Vapor etching of gallium arsenide crystals with hydrogen chloride, noting usefulness in pretreatment for epitaxial substrates 10 p1575 A66-21358

Microplasma breakdown in reverse biased p-n junctions in epitaxial gallium arsenide 10 p1577 A66-21571

Stacking-fault defects in epitaxial silicon layers grown on chemically polished substrates 10 p1578 A66-21576

Epitaxial, diffusion and photolithographic processes in manufacture of semiconductor component 10 p1514 A66-22056

Microwave oscillations in epitaxial layers of gallium arsenide 10 p1585 A66-22080

Electrophysical parameters of epitaxial p-n junction regions determined, using galvanomagnetic and photomagnetic measurements 11 p1751 A66-22734

Epitaxial growing of iron, nickel and cobalt single crystal films on sodium chloride crystals by spraying at 200 degrees C 11 p1753 A66-22805

Domain structure of single-crystal epitaxial iron films as function of perfection of crystalline structure, using Lorentzian electron microscopy, noting two-axis anisotropy 11 p1753 A66-22806

Anisotropy of films deposited on cylindrical substrate 11 p1754 A66-22812

Current dependence of resistivity and mobility measured in silicon epitaxial layers on control wafer 11 p1756 A66-23021

Electric current heating method to obtain high purity silicon epitaxial films 11 p1757 A66-23281

Sandwich method in closed system for growing semiconductor germanium epitaxial films 11 p1757 A66-23282

Low energy electron diffraction study of epitaxial deposition of copper on single crystal /110/ face of tungsten under ultrahigh vacuum 12 p1894 A66-23911

Low energy electron diffraction observation of calibrated epitaxial nickel film on /111/ copper 12 p1894 A66-23912

Doping techniques for epitaxial growth of silicon and germanium

layers 12 p1832 A66-23933

Growth and structure of evaporated silicon layers, noting defects due to stacking disorders 12 p1928 A66-23938

Polysilicon insulated gate field effect transistor having active element fabricated in epitaxially deposited film on oxidized single crystal silicon substrate 12 p1845 A66-24831

Epitaxial deposition of silicon by sublimation process at 750 degrees C, using ultrathin alloy zone crystallization 12 p1846 A66-24912

Single crystal silicon on spinel, achieving epitaxy on magnesia aluminate by Spilane pyrolysis and silicon chloride reduction in hydrogen atmosphere 13 p2158 A66-25053

Microstructure of epitaxial germanium films deposited on calcium fluoride substrates, noting parameters of deposition 13 p2158 A66-25063

Transport equation for germanium-gallium arsenide-iodine system and epitaxial vapor growth preparation of GaAs-Ge heterojunction by closed tube process 13 p2161 A66-25185

Epitaxial vapor growth of germanium from germanium iodide with hydrogen and argon atmosphere, examining various growth parameters 13 p2161 A66-25193

Moving deposition zone technique for controlling nucleation and growth of silicon films on hexagonal silicon carbide substrates 13 p2164 A66-25491

P-n-p and n-p-n silicon epitaxial power transistors, noting geometry vs output for interdigitated structures 13 p2037 A66-25542

Single crystal silicon epitaxy growth on foreign substrates by chemical vapor deposition techniques, noting epitaxial geometry 13 p2113 A66-25648

Relaxation oscillations in n-type epitaxial silicon with point contact, discussing generation via electrical excitation of impurity centers 13 p2167 A66-25930

Microscopic and electron diffraction structural analysis of epitaxial growth of PbTe by sublimation on split surface of NaCl at 150 degrees C in vacuum 13 p2170 A66-26757

Improved performance in microwave Read diode oscillator with epitaxial silicon material and coaxial cavity 14 p2248 A66-27049

Electron diffraction study of structural defects in cubic phases in epitaxial tantalum oxide thin films 15 p2557 A66-28560

Degree of perfection of Ge and GaAs single crystals and epitaxial films effect on integral intensity jump at K absorption edge seen in Bragg diffraction 15 p2557 A66-28561

Epitaxial growth of silicon on basal plane of hexagonal silicon carbide substrates analyzed, using silane pyrolysis in flow system, evaluating effects of deposition variables on grown film properties 15 p2561 A66-28703

Preparation, X-ray measurements and photovoltaic properties of Ge-epitaxial-PbS heterojunctions 15 p2562 A66-28710

Electric characteristics of epitaxial Ge films vacuum deposited on seminsulating GaAs substrates with thicknesses near one million angstroms 15 p2566 A66-29386

Pump modulation factor of various GaAs and Si varactor diodes under operating conditions, noting experimental bandwidth gain via increased shot noise 16 p2663 A66-31017

Epitaxial growth configurations of single-crystal potassium bromide on sodium chloride, using gold decoration method, showing effect of crystal orientation on growth rate 16 p2780 A66-31213

Germanium single crystal whisker formation by iodide method of selective epitaxial growth 16 p2781 A66-31405

Selective epitaxial deposition of seminsulating GaAs for p-n junction and integrated circuit application 16 p2665 A66-31418

Deposition of single-crystal silicon films on sapphire substrates by pyrolytic decomposition, noting properties 16 p2782 A66-31419

Epitaxial growth of low pressure sputtered-silver films, noting dependence of growth on kinetic energy distribution of

sputtered atoms 16 p2784 A66-31532

Epitaxial growth of single crystal, impurity free metal films using clean alkali halide surfaces in ultrahigh vacuum 16 p2784 A66-31534

Vapor growth of Ge on Ge, GaAs and Si substrates, noting preparation methods, characteristics, etc 16 p2786 A66-31686

Epitaxial growth techniques for silicon and germanium, discussing hydrogen reduction methods, doping and impurity control, etc 17 p2976 A66-32259

Surface state density of MOS structure, noting difference between gas deposited and thermally grown samples 17 p2978 A66-32405

Epitaxial growth of semiconductors in isothermal system approaching thermodynamic equilibrium, noting growth parameters, activation energy, etc 17 p2886 A66-32495

Structural defects in epitaxial films noting nucleation mechanism, stacking faults, growth defects, etc 17 p2985 A66-33157

Spectral and spatial distribution of origin of injection luminescence from epitaxial gallium arsenide transistors, noting correlation between energy peak and radiation recombination 17 p2986 A66-33295

Nickel, nickel-zinc and magnesium-zinc ferrite thin films, using chemical deposition on alumina substrates for millimeter wave application 18 p3153 A66-33732

Hydrogen reduction techniques and layer quality measurement methods for epitaxial growth of silicon and germanium crystals 19 p3437 A66-35473

Carrier mobility and concentration in epitaxial silicon layers obtained by vacuum sublimation 19 p3442 A66-35866

Measurements on physical and laser properties of vapor-grown ruby single crystals prepared by epitaxial growth 19 p3375 A66-36081

Isolated GaAs transistors on high resistivity GaAs substrate, noting production via epitaxial etch-refill technique, performance and isolation 20 p3616 A66-37405

Silicon variable capacitance diodes with high-voltage sensitivity produced by low-temperature epitaxial growth technique 20 p3528 A66-37494

Normal incidence reflectivity and transmissivity coefficient measurements in Ge thin epitaxial films 20 p3623 A66-38397

Model estimate of oxygen concentration captured from residual gases by epitaxial germanium and silicon films prepared by vacuum deposition 21 p3795 A66-38521

Transmission electron microscopic analysis of initial epitaxial growth stage of evaporated Au films on NaCl cleavage surfaces 21 p3798 A66-38758

Heteroepitaxial deposition of films of germanium in single-crystal form on sapphire by vapor growth techniques 21 p3802 A66-39163

Experimental molecular beam study of nucleation process in chemical-vapor growth of epitaxial silicon films 21 p3805 A66-39588

Transmission electron microscopic and molecular beam study of nucleation and growth in chemical vapor of epitaxial silicon films on carbon-contaminated silicon substrates 21 p3806 A66-39589

1.60 micron stimulated and spontaneous emissions from epitaxial single crystals in quasi-binary III-V compound semiconductor diodes of injection lasers at 77 degrees K 22 p3930 A66-39750

Change in temperature conditions during growth of epitaxial germanium films from molecular beam in vacuum 22 p3961 A66-39928

Effect of donor Zn and Cd additions and acceptor Se and Te additions on rate of growth and morphology of epitaxial GaAs films grown from gas phase by chemical reaction 22 p3961 A66-39929

Epitaxial germanium films on gallium arsenide substrate by vacuum evaporation, considering surface preparation 22 p3963 A66-40106

Four-point probe technique to measure conductivity of epitaxial layers on conducting substrates 23 p4110 A66-41157

Electron diffraction study of structural defects in cubic phases in epitaxial tantalum



- oxide thin films 23 p4112 A66-41281
- Degree of perfection of Ge and GaAs single crystals and epitaxial films effect on integral intensity jump at K absorption edge seen in Bragg diffraction 23 p4112 A66-41282
- Electrophysical parameters of epitaxial p-n junction regions determined, using galvanomagnetic and photomagnetic measurements 23 p4113 A66-41472
- Epitaxial growth techniques used to obtain graded layers for drift field structured solar cells on Si web 23 p4019 A66-41747
- Sputtering voltage and current effects on resistivity of films sputtered from pure tantalum appear to be traceable to pressure and growth rate 24 p4251 A66-42297
- Epitaxial growth of bulk quality GaAs on GaAs and Ge substrates, using hydrogen stream saturated at room temperature with arsenic chloride 24 p4251 A66-42307
- Tin and zinc diffusion from doped pyrolytic silicon oxide layers used to form base regions of planar n-p-n and p-n-p-GaAs transistors 24 p4254 A66-42384
- Contour epitaxial deposition for semiconductor devices and integrated circuits, producing regions with well defined doping and geometry in crystal with flat surface 24 p4181 A66-42386
- MOS transistor structures with enhancement mode of operation, discussing fabrication processes via V-C characteristics, temperature effects on performance, etc 24 p4181 A66-42389
- Temperature dependence of Hall coefficient and resistivity of n-type epitaxial gallium arsenide in 4.2 to 300 degree K temperature range 24 p4254 A66-42423
- Evaporation system for fabrication of multilayer dielectric films for mirrors or filters, obtaining thickness variation reduction and simultaneous deposition 24 p4218 A66-43163
- EPOXY RESIN**
- Use of monofilament composites of S-glass fibers and epoxy-resin in primary aircraft structure [AIAA PAPER 65-761] 05 p0772 A66-14729
- Griffith flaw theory in analyzing failures in epoxy castings [ASME PAPER 65-WA/RP-6] 05 p0779 A66-15631
- Aircraft fuel tank coating corrosion resistance, discussing polyurethane and epoxy material characteristics and application 07 p1053 A66-17491
- Printed circuit laminate measling, definition, origin, effects and control 11 p1664 A66-22673
- Multilayer circuit laminate fabrication and comparison of glass-base laminates with phenolic-paper-base and epoxy-paper-base grades 11 p1664 A66-22675
- Thermal properties, tensile strength and uses of combination of glass fiber and epoxy resin material, Fiberglass S/994/, in space vehicles 12 p1899 A66-23966
- Surface area, complexes and water effect on properties of carbon fiber resin composites 13 p2111 A66-25166
- 24-channel recorder for stress-strain states due to thermal effects of operating epoxy-resin machine components 13 p2080 A66-25914
- Embedding and encapsulating processes and design of embedding materials for electronic packaging 17 p2944 A66-33525
- Microwave energy attenuation by dissipative material consisting of epoxy resin loaded with fine powder of iron carbonyl 20 p3587 A66-37585
- Use of monofilament composites of S-glass fibers and epoxy-resin in primary aircraft structure [AIAA PAPER 65-761] 23 p4083 A66-40979
- Stress-strain determination in elastoplastic problems with aid of photoelastic epoxy resin coating 23 p4135 A66-40990
- EQUATION**
- S ADIABATIC EQUATION
- S BALANCE EQUATION
- S BERNOULLI EQUATION
- S BETHE-SALPETER EQUATION
- S BIHARMONIC EQUATION
- S BOLTZMANN EQUATION
- S BOLTZMANN-VLASOV EQUATION
- S BOOTSTRAP EQUATION
- S BRAGG EQUATION
- S BURGER EQUATION
- S CHANDRASEKHAR EQUATION
- S CHAPLYGIN EQUATION
- S CHARACTERISTIC EQUATION
- S CONSERVATION EQUATION
- S CONTINUITY EQUATION
- S CUBIC EQUATION
- S DIFFERENCE EQUATION
- S DIFFERENTIAL EQUATION
- S DIOPHANTINE EQUATION
- S DIRAC EQUATION
- S DONNELL EQUATION
- S DUFFING EQUATION
- S EINSTEIN EQUATION
- S ELLIPTIC EQUATION
- S ENERGY EQUATION
- S EULER EQUATION
- S EULER-LAGRANGE EQUATION
- S EULER-LAMBERT EQUATION
- S FALKNER-SKAN EQUATION
- S FIRST ORDER EQUATION
- S FLOW EQUATION
- S FOKKER-PLANCK EQUATION
- S GIBBS EQUATION
- S HAMILTON-JACOBI EQUATION
- S HEAT EQUATION
- S HELMHOLTZ EQUATION
- S HILL EQUATION
- S HYDRODYNAMIC EQUATION
- S HYPERBOLIC EQUATION
- S INTEGRAL EQUATION
- S KINEMATIC EQUATION
- S KINETIC EQUATION
- S KLEIN-GORDON EQUATION
- S KROOK EQUATION
- S LAGRANGE EQUATION
- S LAME WAVE EQUATION
- S LAPLACE EQUATION
- S LINEAR EQUATION
- S LIOUVILLE EQUATION
- S MACROSCOPIC EQUATION
- S MAXWELL EQUATION
- S MILNE EQUATION
- S MOMENT EQUATION
- S MOTION EQUATION
- S NAVIER-STOKES EQUATION
- S NONLINEAR EQUATION
- S ORBIT EQUATION
- S PARABOLIC EQUATION
- S PERIOD EQUATION
- S PLANCK EQUATION
- S POISSON EQUATION
- S QUADRATIC EQUATION
- S RAYLEIGH EQUATION
- S REISSNER EQUATION
- S REYNOLDS EQUATION
- S SAHA EQUATION
- S SCHROEDINGER EQUATION
- S SHALLOW SHELL EQUATION
- S STATE EQUATION
- S STOKES-BELTRAMI EQUATION
- S TRANSPORT EQUATION
- S TREFFTZ EQUATION
- S VLASOV EQUATION
- S VOLTERRA EQUATION
- S VON KARMAN EQUATION
- S VORTICITY EQUATION
- S WAVE EQUATION
- S WIENER-HOPF EQUATION

**EQUATOR**

- SA GEOMAGNETIC EQUATOR
- SA MAGNETIC EQUATOR
- SA TRANSEQUATORIAL PROPAGATION
- Wave solutions to linearized quasi-hydrostatic equations for adiabatic nonviscous flow on equatorially oriented beta plane 02 p0254 A66-11982

**EQUATORIAL ELECTROJET**

- Quiet solar diurnal variations of geomagnetic field at middle and low latitudes during IGY to determine coordinate system and equatorial electrojet 02 p0224 A66-12118
- Rocket measurements to investigate vertical current distribution of electrojet over India to correlate magnetic profiles with simultaneous electron density measurements 05 p0668 A66-14794
- Electric currents in ionosphere measured by sounding rockets equipped with nuclear free precession magnetometers and Langmuir probes launched near Peru 05 p0668 A66-14800
- Geomagnetic cut-off rigidity variations calculated relative to disturbed field models represented by equatorial current 09 p1438 A66-20210
- Equatorial sporadic E layer instability

- explained by ion inertia and plasma inhomogeneities 10 p1527 A66-21129
- Enhancement of amplitude of sudden commencement of magnetic storms in horizontal component of geomagnetic field 11 p1696 A66-22380
- Threadlike equatorial current ring and effect on geomagnetic cut-off rigidity of directed cosmic radiation 12 p1941 A66-24172
- Effect of equatorial current ring distributed over globe on geomagnetic cut-off rigidity of cosmic rays 12 p1941 A66-24173
- Equatorial electrojet cross section profile, describing longitudinal variations, current density, magnetic field produced and electron drift velocity 13 p2074 A66-26357
- Cross sections of geomagnetic field intensity and ionospheric characteristics obtained by airborne equipment crossings of geomagnetic dip equator 13 p2074 A66-26358
- Horizontal geomagnetic fluctuations during nighttime magnetic storms studied at equatorial stations 13 p2075 A66-26738
- Quiet solar diurnal variations of geomagnetic field at middle and low latitudes during IGY to determine coordinate system and equatorial electrojet 14 p2286 A66-28077
- Nike-Cajun rocket investigation of equatorial D and E region parameters and effect on electrojet 15 p2493 A66-30035
- Seasonal width and current intensity of equatorial electrojet at different longitudinal zones noting diurnal variations, electrojet parameters, etc 17 p2922 A66-33352
- Hydrodynamic and thermodynamic equations for biennial variations of zonal atmospheric circulation in equatorial area 19 p3346 A66-35640
- Equatorial electrojet model construction to fit direct measurements 19 p3348 A66-35927
- Long-term variation in equatorial sporadic E and electrojet caused by sunspot cycle 20 p3549 A66-37291

**EQUATORIAL ORBIT**

- Diagram for determination of topocentric equatorial coordinates of satellites 20 p3518 A66-37837
- Coverage and overlap of communications satellites in circular equatorial orbits for multiple-access intercommunication 22 p3870 A66-40964
- Van Allen belt study using equatorially orbiting satellite, examining trapped particle origin and energies 23 p4123 A66-41038

**EQUATORIAL SATELLITE**

- Military communications satellite system noting radio frequency, TWT amplifier, synchronous altitude, etc [AIAA PAPER 65-323] 05 p0633 A66-15170
- Diagram for determination of topocentric equatorial coordinates of satellites 20 p3518 A66-37837

**EQUILIBRIUM**

- SA BODY SWAY TEST
- SA CHEMICAL EQUILIBRIUM
- SA LIQUID-VAPOR EQUILIBRIUM
- SA NONEQUILIBRIUM
- SA STABILIZATION
- SA STEADY STATE
- SA THERMODYNAMIC EQUILIBRIUM
- Practical determination of stability region of equilibrium point of second-order nonlinear recurrence with real variables 08 p1255 A66-18639
- Equilibrium equations of shallow cylindrical shell of arbitrary cross section subject to arbitrary loading 11 p1783 A66-23033
- Spherical drop in electric field with equilibrium maintained through balance between electric stress and variable pressure difference between inside and outside of drop, existing only if outside and inside fluids are in motion 13 p2129 A66-26302
- Critical plasma pressure for equilibrium in toroidal system, noting close relationship between equilibrium and stability problems 14 p2347 A66-28303
- Mitchell structure design of lightest framework to equilibrate system of given forces 23 p4147 A66-41998
- Equilibrium theory of plasma stability in EM field, applying virial theorem and variational principle to random infinitesimal plasma perturbations 24 p4241 A66-42330



**EQUILIBRIUM DIAGRAM**

Gas-filled closed ring-current surface with continuum of equilibrium figures in external magnetic field in case of surface tension 03 p0354 A66-12388

Measurement of equilibrium fractions of helium ions present in helium beams scattered at zero degrees through carbon foils 06 p0912 A66-17038

Equilibrium stability of horizontal layer of fluid in field of modulated temperature gradient when layer thickness is greater than penetration depth of heat waves 08 p1320 A66-19471

Ozone photochemistry in atmosphere containing hydrogen, calculating equilibrium vertical distribution, rate of formation of hydroxyl, diurnal variation, etc 11 p1700 A66-23138

Gas-filled closed ring-current surface with continuum of equilibrium figures in external magnetic field in case of surface tension 13 p2062 A66-25393

Equilibrium structure of magnetic fields in stars analyzed, employing perturbation theory for assumed polytropic configuration 17 p3005 A66-33001

Phase equilibrium of Nb-Al binary system determined via metallographic, X-ray diffraction hardness and thermal analysis techniques, noting solubility, structure, nucleation growth, etc 18 p3120 A66-33723

Stability of low pressure confined plasma taking into account effect of particle collisions, analyzing equilibrium configuration stability 19 p3417 A66-36529

Equilibrium diagram and existence corroboration of Ti-Rh alloy 20 p3586 A66-38093

Titanium-rich end of Ti-Al solid solution equilibrium diagram 22 p3934 A66-39781

**EQUILIBRIUM FLOW**

**SA NONEQUILIBRIUM FLOW**

Liapunov work on equilibrium configuration of inhomogeneous rotating fluid 01 p0056 A66-10305

Series of equilibrium configurations for homogeneous rotating fluid in monograph of Liapunov 01 p0056 A66-10306

Liapunov monograph on equations for surfaces of equilibrium configurations of rotating fluid deriving from ellipsoids 01 p0056 A66-10307

Equilibrium configurations theory that rotating homogeneous fluid containing particles attracted to each other according to Newton laws and under constant pressure will form ellipsoid 01 p0056 A66-10308

Photochemical studies of oxygen-ozone and carbon dioxide equilibria with bromine UV lamp 04 p0473 A66-13397

Boundary layer relation between viscosity laws of perfect gas and equilibrium dissociating air 04 p0456 A66-14158

Book on physical gas dynamics including transport theory, kinetic theory, thermodynamics, equilibrium, fluid flow, radiative transfer, etc 05 p0666 A66-15848

Experimental data compared to theory for expansion of high temperature air in equilibrium and nonequilibrium flow through Mach number 10 contoured nozzle [AIAA PAPER 66-2] 06 p0803 A66-17089

Inviscid supersonic nozzle flow of ideal dissociating gas, sudden freezing, equilibrium-recombination mechanism and velocity distribution 08 p1163 A66-18983

Equilibrium air total radiation mechanism, vacuum UV radiation and relation to hypervelocity entry studied, using shock tube blunt model test flow [AIAA PAPER 66-103] 09 p1469 A66-20087

Surface boundary layer charge of isothermal atmosphere of fully ionized equilibrium plasma in gravitational field 10 p1609 A66-21813

Velocity defect profiles in equilibrium turbulent boundary layers and eddy viscosity hypotheses 11 p1693 A66-23005

Hypersonic flow of equilibrium dissociating air around sphere numerically analyzed by Lunev method 12 p1796 A66-23901

Parametric method of solving equations of laminar boundary layer with longitudinal pressure gradient during equilibrium gas dissociation 12 p1863 A66-24367

Equilibrium flow of ideal gas and

condensing vapor mixture from nozzle, using basic equations to describe process 12 p1863 A66-24368

Supersonic air flow past blunt bodies and equilibrium physicochemical conversion effects 12 p1797 A66-24426

Airfoil equilibrium stability under elastic force and uniform wind action 13 p2062 A66-25402

State equation and equilibrium correlations for hydrogen type plasma 13 p2157 A66-26756

Natural modes and eigenfunctions of low amplitude oscillation determined by Ritz averaging method for ideal fluid with equilibrium surface in weak force field 16 p2687 A66-31297

Hypersonic laminar boundary layer flow of equilibrium dissociating gas 16 p2630 A66-31306

Plastic equilibrium flow equations of thin walled shells 21 p3830 A66-38982

Integration of near equilibrium flows in propulsive nozzles, estimating length of transition region from equilibrium condition to kinetic solution [AICE PREPRINT 28C] 22 p3971 A66-39884

**EQUIPMENT**

S AIRBORNE EQUIPMENT

S AUDIO EQUIPMENT

S CHECKOUT EQUIPMENT

S CRYOGENIC EQUIPMENT

S DISTANCE MEASURING EQUIPMENT

S ELECTRIC EQUIPMENT

S ELECTRONIC EQUIPMENT

S ELECTRONIC EQUIPMENT TESTING

S GROUND SUPPORT EQUIPMENT

S HEATING EQUIPMENT

S HYDRAULIC EQUIPMENT

S MEDICAL EQUIPMENT

S OPTICAL EQUIPMENT

S PNEUMATIC EQUIPMENT

S POSITIONING EQUIPMENT

S RADAR EQUIPMENT

S RADIO EQUIPMENT

S REFRIGERATING EQUIPMENT

S TELEVISION EQUIPMENT

S TEST EQUIPMENT

S THERMONUCLEAR EQUIPMENT

S TRAINING EQUIPMENT

S VACUUM EQUIPMENT

S VIDEO EQUIPMENT

S X-RAY EQUIPMENT

**EQUIPMENT SPECIFICATIONS**

Satellite position prediction and display /SPAD/ naval equipment that will predict, display and determine selected satellites 02 p0215 A66-11699

Effect of thermal instability in shop areas, static and dynamic loading and floor movement on precision fabrication and assembly [SAE PAPER 650759] 05 p0688 A66-15274

Long-term storage effects on reliability of electronic equipment, covering testing results and available data on failure rates 12 p1830 A66-23755

Defense equipment reliability noting specifications, field data collection, control plan, etc 12 p1833 A66-24083

Book on project ERIE covering techniques for analytic evaluation of space equipment designs with respect to environments and missions required in 1975 24 p4217 A66-42572

**ERBIUM**

Laser characteristics of and coherent oscillations from trivalent Tm, Ho, Yb and Er ions in yttrium aluminum garnet 01 p0079 A66-10241

Laser lines due to energy transfer from color centers to erbium ions in calcium fluoride crystals irradiated by gamma ray 16 p2717 A66-30278

Electrical conductivity and thermoelectric measurements of intermediate phases in erbium tellurium system 17 p2979 A66-32631

Electron paramagnetic resonance and optical spectra of trivalent erbium in type II crystals of calcium fluoride disclose existence of cubic, tetragonal and trigonal sites 22 p3961 A66-39916

**ERBIUM ALLOY**

Electrical resistivities of gold-erbium alloys measured at low temperatures 12 p1933 A66-24919

**ERBIUM COMPOUND**

Electric conductivity and thermoelectric power measurements in Er-Se system indicates degenerate

semiconductors 04 p0562 A66-13736

CW laser action in holmium-doped erbium trioxide with dominant pumping by energy transfer between ions 24 p4222 A66-42555

**ERGODIC PROCESS**

Markov chains, skew products and ergodic theorems for general dynamic systems 01 p0095 A66-10731

Coding theorems for almost-periodic channels 05 p0638 A66-15362

Topological property of torus to study ergodicity of integrals of systems of periodic differential equation in absence of cyclic solutions 07 p1055 A66-17243

Markov chains with discrete accident intervention forming semi-Markov process, considering application to single-line mass servicing system with queue 12 p1902 A66-23766

Book on ergodic problems in comparison theory and theory of diophantine, discussing residue distribution of polynomial of nth order modulo p, fractional parts of polynomial and exponential function 15 p2529 A66-29767

Statistical structure of meteorological field, with attention to ergodic properties 18 p3129 A66-34100

Wiener filtering theory for stationary ergodic inputs with known spectral densities and optimal control transfer functions of random-input nonlinear saturating systems with random unwanted disturbances 20 p3536 A66-36859

Transition matrices of ergodic finite Markov chains and readiness models in cost effectiveness systems analysis 20 p3681 A66-37176

Ergodicity of trajectories in systems with two periodic differential equations and two sets of unknowns 20 p3591 A66-37815

Uniformly ergodic random processes with discrete parameters 20 p3592 A66-37816

Noncollision ergodic shock wave propagating in plasma situated in magnetic field and thermal oscillation effect on thermonuclear kinetics 21 p3787 A66-39052

Optimum pulse transfer functions for multivariable digital ergodic stochastic processes 23 p4051 A66-41853

**ERGONOMICS**

**S BIOTECHNOLOGY**

**ERIE PROJECT**

Book on project ERIE covering techniques for analytic evaluation of space equipment designs with respect to environments and missions required in 1975 24 p4217 A66-42572

**EROS ASTEROID**

Technical feasibility of 1975 manned flyby mission to Eros and examination of lesser bodies of solar system 14 p2390 A66-28411

**EROSION**

**SA ETCHING**

**SA MATERIALS EROSION**

**SA RAIN EROSION**

**SA SPARK EROSION MACHINING**

**SA SURFACE EROSION**

**SA WEAR**

Ductile behavior of brittle material during erosive cutting [ASME PAPER 65-WA/PROD-7] 05 p0690 A66-15634

Erosive cutting of brittle material by normal impact of stream of solid particles [ASME PAPER 65-WA/PROD-8] 05 p0690 A66-15635

Elimination of turbine erosion in T56 turboprop engine [ASME PAPER 65-WA/GTP-9] 05 p0745 A66-15724

Helicopter rotor blade and engine erosion by sand and seawater 06 p0804 A66-15997

Iron and stony meteorite evolution, cosmic radiation ages and space erosion model 14 p2390 A66-28409

Insulation surface regression mechanism in rocket motors, examining ablation corrosion and erosion effects 22 p3970 A66-39872

**ERROR**

**SA INSTRUMENT ERROR**

**SA PHASE ERROR**

**SA PILOT ERROR**

**SA POSITION ERROR**

**SA RANDOM ERROR**

**SA RANGE ERROR**

**SA ROOT-MEAN-SQUARE ERROR**

**SA TRUNCATION ERROR**

**SA VELOCITY ERROR**



Error estimates for some finite difference methods of solving ordinary linear differential equations 01 p0092 A66-10315

Covariance matrix approximation and conservative error volume estimate 02 p0249 A66-11568

Distance-and velocity-measurement errors in coherent-pulse systems with periodic modulation law 06 p0837 A66-17180

Errors in approximation equations for dynamic bending of cylindrical rod 08 p1308 A66-18889

Reabsorption of synchrotron radiation as error source in discrete radio emission source parameter determination 08 p1297 A66-19450

First order error analysis, radar antenna calibration technique and polarization scattering matrix 10 p1501 A66-21627

Computational data smoothing by minimum mean square error estimation 10 p1550 A66-21839

Incorrect input-induced errors in meteorological satellite photogrids 11 p1704 A66-22318

Component tolerance and measuring error effects on noise measurements 11 p1652 A66-22384

Systematic error in processing series of analog data 11 p1707 A66-23058

Error propagation at above information limits postulated by Shannon sampling theorem and Gabor expansion theorem 11 p1657 A66-23105

Differences in MHD emission occurrence times, considering ionospheric penetration propagation toward equator and error sources 11 p1701 A66-23150

Modified phase-plane delta method for nonlinear system phase portrait 11 p1679 A66-23270

Optimal control systems and numerical analysis of error effect on sensitivity 11 p1680 A66-23274

Stray radiation error reduction in spectral emittance measurements for diffusely reflecting materials 11 p1737 A66-23410

Error analysis for statorscope or radar altimeter phototriangulation readings and radio geodetic coordinate photography phototriangulation 12 p1867 A66-23517

Optimum design and error analysis of digital integrators for discrete system simulation via quasi-linearization 12 p1828 A66-23840

Time resolution error of measured correlation function, based on frequency response of hot-film and hot-wire anemometer 12 p1880 A66-23847

Dynamic range bounds of error detection circuits of tracking radars, minimizing probability of excluding Rayleigh distributed signal 12 p1817 A66-24302

Calibration problem of load-measuring instruments solved, using automatic digital voltmeter [ASTME PREPRINT IQ66-705] 12 p1882 A66-24412

Microwave component testing accuracy and analysis of error sources 12 p1883 A66-24725

Error bounds in phase-integral solution to differential equation with simple turning points 13 p2118 A66-25829

Error bounds of phase-integral methods applied to wave-penetration problems 13 p2118 A66-25830

Iterative approximation of rational transfer function in Laplace transform variable  $s$ , optimal with respect to given input and output time functions, and deviation from desired output-input-time functional relation 13 p2054 A66-26087

Residual error probability for cyclic binary code data transmission on symmetrically random noise channels 14 p2245 A66-26795

Enthalpy of gas stream, calorimeter surface treatment and heat transfer measurement errors in arc-heated tests 14 p2411 A66-27425

Error in tracking loops as satellite passes over tracking system 14 p2265 A66-27480

Theoretical and experimental study of accuracy of Diane interferometric tracking network 14 p2238 A66-27545

Averaging error of system of nonlinear differential equations with time periodic right-hand sides 14 p2322 A66-27674

Atmospheric noise FSK error probabilities for envelope detection

receiver 14 p2243 A66-28352

Error coefficients and astatism estimation for controllable system in normal operation 14 p2268 A66-28353

Critical Human Performance and Evaluation /CHPAE/ Program methods for evaluating and predicting human performance and potential error probabilities 14 p2231 A66-28422

Error bounds based on a priori inequalities for solutions of boundary value problems for linear elliptic partial differential equations 16 p2731 A66-30236

A posteriori error bounds in iterative matrix inversion 16 p2732 A66-30238

Error estimation in diode function generator design 16 p2659 A66-30518

Effect of modifying digital filter weights derived on least squares error basis through multiplication by certain weighting functions 16 p2659 A66-30535

Errors in state vector arising from impulse representation of finite pulse width sampled data system 16 p2672 A66-31338

Numerical differentiation by differential quotients, interpolations, Richardson-Romberg algorithm and other methods, including analysis of approximation errors 16 p2658 A66-31347

Finite difference estimation of boundary value problem errors 17 p2945 A66-31878

Zero-level drift errors in telemetry 17 p2873 A66-31965

Assessment of error of method of successive approximations in determination of circular plate deflections 17 p3026 A66-32598

Checkout procedure for automatic test systems, checkout error probability and relation to tolerance limits 17 p2888 A66-32777

Maximum error curves for Lanczos selected point method of polynomial solution to ordinary differential equations, using Chebyshev and Legendre functions 17 p2947 A66-32858

Error analysis of absorbed energy flux density and ignition exposure time data, accuracy, precision and confidence limit estimates for arc image furnace ignition experiments 18 p3261 A66-34224

[AIAA PAPER 66-669] Reabsorption of synchrotron radiation as error source in discrete radio emission source parameter determination 18 p3169 A66-34479

Inertial navigation technique based on least squares criteria of optimality with filter providing estimates of system errors 19 p3396 A66-35517

Distance-and velocity-measurement errors in coherent-pulse systems with periodic modulation law 19 p3297 A66-35538

Extreme value statistics estimation of low error probabilities in binary communication systems 19 p3301 A66-35688

Multifactor Max-Rankine optimization technique evaluated from point of system performance, minimum mean square error, intrasystem interactions, etc 19 p3325 A66-35878

Error estimates for difference methods in forced vibration problems 20 p3589 A66-36901

Low error probabilities in binary communication systems estimated by statistics of bivariate extreme-value theory 20 p3514 A66-37211

Critical Human Performance and Evaluation /CHPAE/ Program 20 p3509 A66-37893

Radar target tracking error induced by ground reflection of radar echo from static beam split autotracking radar 20 p3520 A66-38142

Integral criterion based on absolute value of error, integral-square-ideal error, used as measure of distortion of communication system 20 p3539 A66-38285

Distortions and errors in calculating structural and correlation functions from experimental results 20 p3594 A66-38377

Distortions and errors in calculating spectral densities from finite series of random function values 20 p3594 A66-38378

Error analysis for statorscope or radar altimeter phototriangulation readings and radio geodetic coordinate photography phototriangulation 21 p3732 A66-38661

Waveform analysis of electronic repetitive differential analyzer solutions of nonlinear and linear systems and describing functions evaluation using vectormeter 21 p3739 A66-39275

Sampling theorem for Fourier transform reconstruction of band-limited signals, applications to stationary stochastic processes and analysis of round-off, truncation and random errors 22 p3884 A66-40168

Chain code method of eliminating LF drift disturbance error in calculation of impulse-response function of time-invariant system 24 p4187 A66-42368

Errors effect in determining primary energy on measurement of characteristics of nuclear interactions in cosmic radiation, considering energy spectrum 24 p4267 A66-42906

Error free recovery of signals from irregularly spaced samples in terms of completeness of sets of nonharmonic exponentials 24 p4189 A66-43202

**ERROR BAND**

Improvement on Montgomery prediction of error probability in intermittent system operating during short intervals when SNR is above certain threshold level 12 p1816 A66-24138

Control of radio telescope, noting servosystem ability to keep tracking position errors and wind-caused error within certain limits 12 p1851 A66-24319

Radiolocation theory compared with communication theory, noting trading of frequency bandwidth of radar signal for error suppression 15 p2535 A66-29860

Inertial components and systems evaluation with figures of merit for requirements, noting accelerometer errors, limiting response, etc 16 p2707 A66-31148

Maximum permissible error in radiation patterns calculated by Fourier analysis of near field measurements of antennas 22 p3861 A66-39716

**ERROR CORRECTING DEVICE**

Recognition procedure identifying given star constellation despite erroneous scanning, for application in celestial navigation 01 p0102 A66-10619

Shock and vibration measurement system with error correcting techniques including dynamic calibration data, noise detection, etc [SAE PAPER 650820] 01 p0069 A66-10822

Reseau techniques application to cartographic photography to improve analytical procedures, reduce mensuration errors and aid in automating systematic corrections 02 p0228 A66-11382

Learning matrices based on redundancy principle as nonadaptive self-correcting adjustment switches and error detectors in electronic systems 04 p0489 A66-13510

Optimum signal shape for transmission of discrete information, discussing signal-noise characteristics 04 p0488 A66-14414

Error correcting learning machines application to unknown linear dynamic systems 05 p0653 A66-14602

Resampled data systems and error between output of second sampler and input signal to first sampler [ISA PREPRINT 1.12-3-65] 05 p0635 A66-15504

Phase-correcting circuit design methods for equalizing phase characteristics of high sensitivity communication channels 07 p1001 A66-17343

Compass performance improvement, discussing Sperry C-12 compass system accuracy, operational features, etc 07 p1033 A66-17721

Horizontal and vertical control system for determining three-dimensional coordinates in lunar charting by aeronautical chart and information center 08 p1293 A66-19263

Error damping procedures for gimballless inertial navigational systems 08 p1253 A66-19528

Feedback method for reducing errors of counter telescopes due to missed counts and accidental coincidences 09 p1379 A66-20235

Elimination of coupling error between gyroscope and platform, considering rate-integrating gyros with inertial platform 09 p1382 A66-20563



Halley comet motion during return of 1910, obtaining orbits via differential correction procedures, including perturbation by all planets but Pluto 11 p1769 A66-22531

Recognition procedure identifying given star constellation despite erroneous scanning, for application in celestial navigation 13 p2123 A66-25179

Combined automatic control systems with automatic adjustment of amplification coefficient of disturbance controller for error reduction 13 p2045 A66-25300

Accuracy of test device determining conductivity of semiconductor materials increased by using error calculation and design systematology 13 p2085 A66-26761

Reduction of measurement error in devices for testing semiconductors, employing mechanical techniques 14 p2297 A66-28132

Errors in wind speed measurements under conditions of turbulence, noting quantitative aspects of lateral, vertical and data processing errors 15 p2533 A66-28940

Aircraft navigational error parameters combined statistically and used to evaluate wander expected in transport aircraft operating in transoceanic environment 15 p2535 A66-29624

Binary block codes simultaneously correcting additive and synchronization errors in data transmission systems 15 p2452 A66-29660

Synthesis of correcting units for automatic control systems, using quasi-invariance condition 15 p2476 A66-29995

Minimum time control systems with servoloop relay for optimal error correction, employing matrix analysis 16 p2671 A66-31061

Communications system design consisting of sequential encoder-decoder in conjunction with modulation detection 18 p3067 A66-33903

Phase characteristics and amplitude of correcting device ensuring closed loop mechanical system stability at critical frequency 18 p3092 A66-34995

Automatic failure detection, location and correction system for failures in unmanned spacecraft using frequency-shift-keyed subcarrier 19 p3316 A66-35679

Feedback methods for conversion of electrical signals into frequencies, using oscillator with signal-current-controlled inductance 19 p3325 A66-35988

Flame temperature measurement using response time of Wolfram-rhenium thermocouples to correct radiation errors in optical pyrometer readings 19 p3360 A66-36160

Digital computers used in error calculation in calibration curves of turboengines and other pneumatic devices 20 p3555 A66-36923

Fourier transform used in correction of instrument contour error when observing solar spectral line profile 20 p3647 A66-37042

Existence of q-ary uniform convolutional codes where q is any prime-power, noting error-correcting ability comparable to familiar maximal-length block codes 21 p3704 A66-39138

Self-synchronizing codes derived from binary cyclic codes 21 p3720 A66-39635

Error correcting problem in space trajectory of continuous powered space vehicle, discussing optimal terminal guidance [AIAA PAPER 65-696] 22 p3945 A66-40367

Integral monitor development for ILS localizer, predicting changes in track position and width, noting principles of operation and performance 23 p4044 A66-41322

Automatic detection and correction of errors in digital computers by using residue arithmetic, whether caused by arithmetic operations or data transmission operations 23 p4042 A66-41602

**ERROR DETECTING CODE**

Parallel decoding for discrete channel with statistically independent noise 02 p0189 A66-11404

Optimum detection of diffusion process in white Gaussian noise, using continuous observation 02 p0190 A66-11405

Insertion of 2 bits of specific code into frame of digital data of burst-error-correcting code for synchronism recovery 02 p0190 A66-11524

Mathematical structure and characteristics

of codes used in transmission over nonsymmetric channels 02 p0209 A66-12020

Error control systems in digital communications accomplished by adding constraints to digital alphabet through coding 04 p0481 A66-13766

Error control over wide frequency range through adaptive dynamic channel equalization system 06 p0825 A66-15987

Extension, modification and analysis of Gorenstein-Zierler decoding algorithm for binary codes of Bose, Ray-Chaudhuri and Hocquenghem /BCH/ correcting erasures and errors 06 p0837 A66-16114

Codes with variable parameter based on use of properties of magic squares 06 p0837 A66-16510

Jittered sampling obtaining error bounds for sample independent and correlated jitter and bandpass sampling 06 p0865 A66-16742

Nonbinary codes used to improve noise rejection and reliability of telemechanical systems 09 p1361 A66-20315

Simultaneous error correction and burst error detection, using binary linear cyclic codes 09 p1347 A66-20643

Upper and lower estimates derived for Shannon reliability of information transfer in channel that is symmetrical with respect to input 09 p1397 A66-20648

Generation, selection and implementation of burst-error-detecting and -correcting Fire code, using computed tables 10 p1496 A66-21513

Telemetric technique based on data modulation and coding for satellite data transfer, stressing noise suppression, operation flexibility, error correction, etc 11 p1651 A66-22366

Influence coefficients for computation of atmospheric components of reentry vehicle circular error probable /CEP/, using Bliss adjoint method, noting effects of certain inadequacies on system performance [AIAA PAPER 66-358] 12 p1908 A66-24517

Errors by mutual interference in frequency-time coding in satellite communications systems, deriving expressions relating commissive and omissive error rates, simultaneous users per unit bandwidth, etc 12 p1821 A66-24752

Phase shift keying with transmitted reference, obtaining probability of error for m-phase receiver system in presence of additive Gaussian noise 13 p2019 A66-25147

Near minimal set of tests detecting all single faults in combinational logic net, using shortcut methods 13 p2040 A66-25804

Codes with variable parameter based on use of properties of magic squares 13 p2028 A66-25950

Mathematical structure and characteristics of codes used in transmission over nonsymmetric channels 14 p2266 A66-27571

Shortened cyclic codes for multiple burst error detection 14 p2245 A66-28041

Error detection techniques for maximizing average rate of information transmitted through burst error channel 14 p2243 A66-28346

FM error calculation via comparison of demodulated output with input 16 p2649 A66-30544

Visual and tactile display for compensatory tracking, noting conditions for minimum error, mean square error, etc 16 p2644 A66-31271

Accuracy problems in control systems, discussing error assessment and accuracy estimates of optimal control 17 p2902 A66-32576

Vibration analysis of CSIRO 210-ft radio telescope, discussing natural frequencies, structure resonance effects, error detection, etc 18 p3083 A66-34297

Cyclic product codes operating in variable redundancy modes used in communications systems, noting protection against errors 19 p3296 A66-35336

Auxiliary autonomous piggyback detector and recorder system for spacecraft failure detection following touchdown 19 p3315 A66-35676

Noise immunity of summation codes that enable all errors of one polarity to be detected in code 20 p3511 A66-37126

Zero defects program, discussing principles, operation and results [ASME PAPER 66-MD-26] 21 p3837 A66-38482

Generalized minimum distance decoding that permits likelihood information to be used, yielding same probability of error as maximum likelihood decoding 21 p3703 A66-39137

Coded and phase-modulated signals detected by receiver containing phase detector and decoder operating algebraically on quantized phase values, using polynomial representation 21 p3704 A66-39139

Upper and lower bounds on binary error probability as function of signal to noise ratio for digital data systems operating over complex Gaussian fading channel 21 p3720 A66-39638

Nonsupervised sequential pattern recognition and classification, analyzing Bayes solution 21 p3720 A66-39640

Error probabilities in binary transmission of signals over selectively fading diversity channels containing specular and scatter type components 22 p3864 A66-40058

Theoretical methods for reliable machine design, comparing redundant residue number system code with linear codes and majority voting techniques 23 p4042 A66-41603

**ERROR FUNCTION**

Asymptotically accurate estimates of Bubnov-Galerkin method error in eigenvalue problem as applied to boundary value problem 01 p0091 A66-10162

Multidimensional homogeneous difference schemata solving eigenvalue problem with elliptic operator, noting differential equation coefficients and eigenfunction error estimate 01 p0092 A66-10166

Rational approximations to generalized hypergeometric functions and error function proven to converge to desired limit 01 p0093 A66-10384

Statistical determination of error variance and application to variance analysis of electrical or mechanical components 01 p0095 A66-10872

Error estimate in obtaining eigenvalues of linear self-adjoint differential operator of elliptical type by finite difference method 01 p0095 A66-11008

Data analysis and estimation of probability of finding sought magnitude within experimental error limits 02 p0261 A66-11810

Function for which error functional attains its maximum value as sphere constitutes solution of polyharmonic equation 02 p0250 A66-12109

Prediction error of time series from finite past 03 p0387 A66-12619

Behavior store, memory store and experience store of learning automation 04 p0489 A66-13483

Radar localization deviations, examining infinitely-long conducting cylindrical obstacles 04 p0488 A66-14413

Optimum message decoding in communication systems with pulse code modulation, using minimum square-error criterion 04 p0489 A66-14415

Evaluation of methods for estimating circular error probable /CEP/ or system accuracy of ballistic missiles employing inertial navigation systems 04 p0544 A66-14444

Error effect in a priori information on sequential estimate variance of linear system states, noting optimal filter synthesis 05 p0653 A66-14601

Worst case error analysis for systems with bounds on forcing function and time derivatives, using Pontryagin maximum principle 05 p0636 A66-14612

Probability of error for quadratic digital detectors contaminated by Gaussian noise 05 p0649 A66-15184

Optimum reception of M-ary Gaussian signals in Gaussian noise in terms of waveform with minimum error probability 05 p0634 A66-15185

Theory of errors when principal stresses are separated in photoelasticity for higher accuracy 05 p0775 A66-15301

Atmospheric noise effect on performance of noncoherent frequency shift keying /NCSKF/ under fading conditions compared



with that obtained when noise is Gaussian 06 p0830 A66-16335

Communication through unknown or random channel, using part of transmission energy to identify channel parameters by receiver 06 p0830 A66-16337

Error probability limitations caused by multipath and Doppler smear in Kathryn modem 06 p0831 A66-16339

Classification of unknown observations into one of two categories when decision boundary is determined from independent samples in each category 06 p0833 A66-16660

Optimum distribution of correcting pulses in single parameter correction 06 p0957 A66-17168

Maximum accuracies of parameter estimates for complex signals reflected from several points 06 p0837 A66-17191

Fluctuation errors of analog correlation meters under time displacement of random signals 07 p1031 A66-17356

Calculation of integrals of infinitely differentiable functions, showing error estimate by network method for periodic functions 07 p1056 A66-17597

Doppler radar accuracy investigation, noting wide distribution of systematic error 07 p1064 A66-17668

Route structure and navigation system error over North Atlantic and advantages of SST inertial navigation system 07 p1068 A66-17701

Error effects in forecasting wind speed and direction on equivalent headwinds and flight times 07 p1063 A66-18338

Rounding off effects on mathematical expectation of random error in measurements involving n-dimensional quantity given in vector form 07 p1061 A66-18508

Error estimates in application of linear plate theory to deflection and stress determination as function of boundary conditions, correlation between geometric plate parameters and load distribution 08 p1305 A66-18599

Reliability of automatic control systems, considering properties of controlled plant, taking error probability in control as criterion 08 p1201 A66-19691

Accuracy of Iaryshev equation for determining errors in surface temperature measurements due to heat losses in sensor 09 p1380 A66-20314

Errors in measuring correlation function of two random processes represented in form of voltages 09 p1345 A66-20444

Summation of errors with variable distribution parameters in finishing and assembling of batches of parts 09 p1384 A66-20766

Error assessment in antenna radiation patterns at small distances by means of collimator which shapes plane wave region 09 p1358 A66-20807

Error bounds in best approximation of given function in Banach space constrained by inequality relationships 11 p1722 A66-22984

Tabulation of constants in two types of error estimates for Romberg quadrature formulas 11 p1722 A66-22985

Computer calculation of depletion layer properties of simultaneously-diffused, double-diffused and triple-diffused transistors 12 p1832 A66-23964

Atmospheric vertical temperature profile determined from outgoing radiation spectrum, evaluating error probability and accuracy 12 p1874 A66-24869

Optical system correction through coefficient selection of aspheric surface, computing vector sums of all aberration orders to give spot diagrams and light distribution in image 14 p2334 A66-27317

Solution of quasi-static problem in thermoelasticity for cylinder with time dependent boundary conditions obtained as series of Bessel functions and error functions 14 p2397 A66-27385

Stability analysis of symmetrically loaded thin walled spherical shell, noting construction of asymptotic expansion, error estimation and application of elasticity theory 15 p2608 A66-28955

Error estimates for approximation formulas for Bessel functions and Hankel functions

obtained, using Luke trapezoidal rule 16 p2736 A66-31021

Error determination in autonomous determination of coordinates, obtaining solution for kinematic equations of navigation in near-polar region 16 p2744 A66-31146

Absorbance and emittance of metal surfaces determined via cyclic incident radiation, noting error computation and method accuracy parameters 16 p2829 A66-31487

[AIAA PAPER 66-416] Integrating error equations of inertial navigation system for objects in Keplerian motion 16 p2744 A66-31507

Maximum increase in system error due to computer round-off errors for closed loop linear sampled data system 17 p2900 A66-32075

Reliability of automatic control systems, considering properties of controlled plant, taking error probability in control as criterion 18 p3091 A66-34676

Maximum accuracies of parameter estimates for complex signals reflected from several points 19 p3297 A66-35549

Error equations of inertial navigation with special application to elliptical orbital determination and guidance [AIAA PAPER 65-691] 19 p3397 A66-35898

Sensitivity analysis and Liapunov stability, discussing correctly set problem and parametric imbedding within theory of partial differential equations 19 p3326 A66-36010

Sensitivity theory of nonlinear sampled data control system, establishing conditions for stability of equilibrium positions 19 p3327 A66-36012

Optimal control system sensitivity to inaccuracies determined in error measurement of initial state 19 p3329 A66-36028

Vibrations of complex structure analyzed, using coordinate system relative to displacement modes, calculating errors due to natural vibration frequencies 21 p3826 A66-38584

Atmospheric vertical temperature profile determined from outgoing radiation spectrum, evaluating error probability and accuracy 22 p3912 A66-40330

Error correction in Vlasov equations of continuity of deformations in curvilinear coordinates 22 p3948 A66-40374

Prediction of rocket engine flight performance with less than 2 percent error in specific impulse data measured at sea level 23 p4120 A66-41111

Combination of probability density functions for system error analysis, using convolution or transformation methods 24 p4189 A66-42827

Optical measurements and navigation during midcourse and orbital phases of space mission, deriving linear equations for propagation of time dependent navigation errors [AGARDOGRAPH 105] 24 p4176 A66-43127

## ERROR SIGNAL

Proportional pneumatic actuation system reliability using variable hydraulic damping, noting role of error and error rate signal 03 p0324 A66-13219

Linear smoothing method minimizing mean-square error in time series where signal statistics are unknown and noise is additive, deriving filter 05 p0653 A66-14600

Transfer function identification of linear time-varying system with input and output signals available in sampled data form [ASME PAPER 65-WA/AUT-16] 05 p0659 A66-15620

Error probability computation for incoherent diversity reception in multichannel communications 06 p0828 A66-16111

Finite wide-sense stationary sequence followed by another sequence corresponding to linear filtering without delay, minimizing mean square error 06 p0828 A66-16116

Series analysis of closed-loop system containing loaded hydraulic valve, with equations of motion and response of system to ramp input and Coulomb load 06 p0810 A66-16915

Error in checkout systems for space or weapon systems 08 p1223 A66-18740

Optimum quantization step for given distribution law of quantized signal, using minimum error distortion criteria 11 p1674 A66-2220

Error analysis in dynamic measurement rotation rate when converting mechanical to electrical quantities 11 p1708 A66-2323

Hybrid PCM-FM communication system noting quantization error and threshold characteristics 13 p2020 A66-2521

Optimum systems with limited processing information, analyzing class of input signal and minimizing amplitude of error signals 13 p2048 A66-2588

Scintillating target intensity effect on performance of PPM optical tracker used as error sensor in various guidance systems 13 p2125 A66-2598

Effect of faulty compensation for accelerating force of Earth gravity on accuracy in determination by inertial navigation system of coordinate of object in flight 14 p2328 A66-2736

Filter design minimizing maximum value of estimation error over all admissible signal waveforms 15 p2474 A66-2938

LF drift reduction for integrators of repetitive signals 15 p2475 A66-2986

Variable-structure automatic control system with switchable phase-shifting filters for linear plants, converting error signal to control switching device 18 p3092 A66-3499

Frequency stabilization of gas laser to lock output to center of atomic resonance, using error signal 20 p3580 A66-3824

Statistical communication theory, examining problem of selecting set of multipowered finite duration waveforms to minimize error rate for coherent channel perturbed by white Gaussian noise 21 p3704 A66-3914

External lock NMR spectrometer conversion to field lock-frequency lock type by polarity inversion of error signal 21 p3740 A66-3939

Error probability in PCM/FM with phase lock loop discriminators, noting role of input SNR 23 p4037 A66-4132

Absolute stability of specific class of nonlinear pulsed automatic systems, noting error signal and amplitude modulation 24 p4189 A66-4294

## ERYTHROCYTE

Respiratory activity and hematological factors of avian blood cells, discussing oxygen consumption, thermal effects, tissue and erythrocyte metabolism 23 p4024 A66-4104

## ESCAPE CAPSULE

Nose-down pitching of capsule crew escape system observed during track test after separation from test vehicle and due to change in capsule pressure distribution 22 p3850 A66-4060

Emergency escape from multicrew orbital vehicles during launch, orbit, reentry and landing by lifting reentry module [ICAS PAPER 66-35] 22 p3988 A66-4066

## ESCAPE VELOCITY

Orbital transfer takeoff spirals with maximum momentum change 02 p0290 A66-1198

Earth departure plane change, interplanetary mission launches and launch windows 10 p1609 A66-2192

## ESCHERICHIA

Proton tunneling and mutation rate of Escherichia coli B To T1 and T2 phage resistance in water 13 p2008 A66-2578

Physical properties of DNA-dependent RNA polymerase from Escherichia coli 20 p3505 A66-3705

Space diet effect on aerobic and anaerobic microflora of human feces 22 p3854 A66-3979

## ESG

## S ELECTRICALLY SUSPENDED GYROSCOPE /ESG/

## ESRO I SATELLITE

Devices on ESRO satellite to be launched in 1967 by NASA rocket, noting photometers for auroral measurements, plasma probe for electron density, scintillation counter etc 03 p0430 A66-1248

ESRO-I satellite design and auroral activity study 16 p2810 A66-3100

European Space Research Organization origins, aims and present state of



- organization 17 p3040 A66-32371
- RO II SATELLITE**
- ESRO projects include sounding rocket experiments, small satellites launched by scout, small space probes and Astronomical satellite 04 p0599 A66-13500
- Experiments in measurement of solar, cosmic and geomagnetically trapped /Van Allen/ radiation to be undertaken by ESRO I satellite 06 p0879 A66-16507
- Space simulator design for testing of ESRO I satellite, noting three-level operating concept, independent control of main shroud sections, etc 18 p3096 A66-34620
- PCM telemetry system for satellites based on projected requirements and subsystems currently available, noting satellite ESRO II as example of digital telemetry application 20 p3519 A66-38062
- SSA SATELLITE**
- Digital computer processing of Tiros, Nimbus and Essa vidicon cloud pictures for machine nephalanyses, discussing rectification orbital mosaics and calibration effects for future Essa flights 22 p3943 A66-40055
- STER**
- SA NITRATE ESTER**
- SA POLYESTER**
- Gas chromatography for resolution and separation of racemic amino acids as TFA-sec-butanol ester derivatives applied to protein analysis 15 p2446 A66-28866
- Synthesis of alpha-amino acid l-menthyl esters under mild conditions, using alpha-amino acid N-carboxy anhydride /NCA/ and l-menthol 16 p2646 A66-31186
- Resolution method for DL-amino-acids via menthyl ester derivatives and gas-liquid chromatographic analysis of crystalline products 17 p2869 A66-31872
- Nucleosides and polynucleotides synthesis from sugars and heterocyclic bases by metaphosphate esters 17 p2852 A66-32095
- Synthesis of peptides related to active site of esteratic enzymes 20 p3510 A66-37633
- Stereoselective synthesis of optically active amino acids from menthyl esters and alpha-keto acids 23 p4032 A66-41378
- Synthetic fire-resistant hydraulic fluids based on phosphate esters must be provided with continuous removal of dissociation products for constant regeneration and protection of unaltered fluid from accelerated decomposition 24 p4229 A66-42509
- ETCHING**
- Vacuum thermal etching of nickel and etch figure development by boron addition 03 p0383 A66-13127
- Stain film of chemical species formed by gas phase reaction on silicon 05 p0736 A66-14978
- Dissolution kinetics of iron filamentary single crystals in dilute acidic environments shown to obey Frank topographical theorems describing etch-rate anisotropy 07 p1107 A66-18412
- High resolution molybdenum evaporation mask fabrication by scribing and etching for use in semiconductor devices 08 p1189 A66-18662
- Dimensional control of oxide films on n- and p-type silicon by thermal oxidation and chemical etching in HF 08 p1230 A66-18870
- Methods for producing microcircuits from vacuum deposited thin film elements, discussing layout, masking and etching 08 p1192 A66-18968
- Semiconductor microinhomogeneities detected by device using fluctuations of impurity concentrations during process of crystal growth 08 p1223 A66-19287
- Structure defects in silicon crystals which cause X-ray double images studied, using X-ray diffraction topography and etching technique 10 p1574 A66-21347
- Chemical etching revealing dislocations produced by indentation on single crystals of silicon, measuring edge dislocation velocities at various shear stresses and high temperatures, determining activation energy 11 p1750 A66-22492
- Epitaxial vapor growth of germanium from germanium iodide with hydrogen and argon atmosphere, examining various growth parameters 13 p2161 A66-25193
- Silver salts effect on etching of germanium single crystals, noting photomicrographs of structural changes 13 p2169 A66-26584
- Surface states on Si crystal as affected by chemical etching and thermal oxidation studied by pulsed field effect 15 p2567 A66-29403
- Dislocations and precipitates in GaAs injection lasers revealed by new A-B etchant 16 p2718 A66-31071
- Chemical etchants for In As noting functions, rate dependence on bromine in methanol, p-n junction delineation, etc 19 p3434 A66-35349
- Chemical blanking and vibratory radiusing of Mo alloys 19 p3370 A66-36134
- Fabrication methods for lithium drifted surface barrier silicon detectors, discussing lithium diffusion, stain etching, preparation for and final etch 20 p3535 A66-38417
- ETHANOL**
- S ETHYL ALCOHOL**
- ETHER**
- SA DIETHYL ETHER**
- SA POLYPHENYL ETHER**
- Sensitized photolytic decomposition of ethanol and diethyl ether glasses analyzed at low temperature, using electron paramagnetic resonance /EPR/ spectroscopy 06 p0820 A66-16124
- Temperature and oxygen effect on aromatic solute sensitized photo-decomposition of ethanol and ether glasses 06 p0821 A66-16125
- ETHYL ALCOHOL**
- Sensitized photolytic decomposition of ethanol and diethyl ether glasses analyzed at low temperature, using electron paramagnetic resonance /EPR/ spectroscopy 06 p0820 A66-16124
- Temperature and oxygen effect on aromatic solute sensitized photo-decomposition of ethanol and ether glasses 06 p0821 A66-16125
- Cavitation flow of water and ethyl alcohol in venturi tube, noting effect of varying vapor concentration and thermodynamic properties 20 p3544 A66-36924
- ETHYLENE**
- S POLYETHYLENE**
- S TRICHLOROETHYLENE**
- ETHYLENE COMPOUND**
- Carbon and ethylene tetrachloride ultrasonic modulators applied to IR laser heterodyne experiments on InAs photodiode 11 p1714 A66-23353
- Pipe flow turbulent temperature fluctuation measurements in mercury and ethylene glycol with fast response thermocouple 14 p2410 A66-26936
- Remission factor of nonradiating /ethylene polyterephthalate/ cellular structure and transparency to visible radiation 22 p3852 A66-40246
- Series of tricyanomethyl compounds prepared in refluxing acetonitrile by alkylating potassium tricyanomethanide with alkyl iodides, alkyl, propargyl and benzyl bromides 23 p4117 A66-41229
- ETHYLENEDIAMINE**
- Proton magnetic resonance studies of linewidth, second moment and spin-lattice relaxation time of solid triethylenediamine /TEDA/ 08 p1177 A66-18934
- ETTINGSHAUSEN EFFECT**
- Combined Peltier-Ettingshausen device evaluated for cryogenic refrigeration to 70 degrees K 02 p0272 A66-11490
- Thermoelectric and thermomagnetic properties of semiconductors applied to refrigeration, discussing Peltier and Ettingshausen effects 21 p3798 A66-38767
- ETTINGSHAUSEN-NERNST EFFECT**
- Cross-sectional geometry of Nernst-Ettingshausen devices optimized for rectangular geometry and for Norwood spiral screw thread configuration 02 p0270 A66-11430
- Specific conductivity, Hall, Nernst-Ettingshausen and other transfer effects in InAs-CdTe and InAs-ZnTe alloys 09 p1428 A66-20539
- Palladium-silver and palladium-rhodium alloys electrical resistance, Hall effect and Nernst effect as affected by temperature 09 p1389 A66-20805
- Direct measurement of Nernst-Ettingshausen dimensionless figure of merit as ratio of two voltages 10 p1576 A66-21542
- Ettingshausen-Nernst effects in InAs-InP solid solutions, discussing differential thermal emf, scattering at acoustical and thermal oscillations of lattice, ionic impurities, etc 12 p1930 A66-24685
- Electron-hole conductivity effect on temperature variations of Hall coefficient and Nernst-Ettingshausen effect in semiconductor 17 p2986 A66-33309
- Electron scattering mechanism in compensated gallium arsenide determined from Hall effect, Nernst-Ettingshausen effect and reluctance 21 p3798 A66-38914
- EUCLIDEAN SPACE**
- Reduction of nonlinear system of differential equations to integral equation of Hammerstein type 07 p1055 A66-17421
- Euclidean nature of relativistic rotating disk in conclusions of Eddington and Lorentz 08 p1255 A66-18857
- Global solutions of Navier-Stokes equations, analyzing solution vector for nonnegative time values in three-dimensional Euclidean space for continuous initial data 12 p1867 A66-24962
- Second-order elliptical operator for m-dimensional Euclidian space with open region bounded by closed surface 13 p2120 A66-26010
- Small parameter problem for parabolic differential equations examining motion of Markov-type random point in Euclidean space 16 p2733 A66-30737
- Partial differential solutions related to concave and quadratic nonlinear programming problems over Euclidean N-space 19 p3308 A66-35870
- EULER BUCKLING**
- Thermal deformation of flat plate considering temperature gradient effect through thickness, showing that plate is not exhibiting Euler buckling 03 p0442 A66-13301
- Shell stability in Euler formulation, taking into account actual redistribution of stresses that results from initial deflection and creep, noting buckling of closed cylindrical shell under axial compression 21 p3829 A66-38978
- EULER EQUATION**
- Linearized version for isotropic elastic plates and shells by series expansion method obtained as Euler equations 04 p0591 A66-14201
- Group of transforms derived for functional in which Euler equation coincides with Crocco equation describing plane vortex gas streams 04 p0512 A66-14437
- Uniform motion of vortex system in inviscid fluid, examining effect of compressibility on motion of vortex singularities 08 p1204 A66-18528
- Rotation effect on statically rotating string-mass system determined by Eulerian formulation and prediction of critical speeds 10 p1556 A66-21495
- Scalar formulation of ideal charged adiabatic gas flow in presence of gravitational and electromagnetic fields 10 p1524 A66-21814
- Bi-linear expansions treating Euler transform of special integrand, reviewing properties of Jacobi function for application in quantum mechanics or plasma physics 12 p1905 A66-24566
- Lagrange theorem extended for solution of three-body problem to regular configurations of more than three particles 16 p2804 A66-31393
- Stationary, two-dimensional solutions of Euler equation which contain closed regions of constant vorticity 17 p2907 A66-32414
- Phase-plane analysis of motion of self-excited asymmetric rigid body, examining periodic solutions of Euler equations 19 p3399 A66-35486
- Motion equations of rigid body, discussing transformation from Lagrange equation to Euler equation 19 p3400 A66-35831
- Steepest descent method extended to trajectory optimization problem for stochastically disturbed systems with application to Euler equation for white noise problem of reentering vehicle 19 p3388 A66-35879
- Eulerian finite difference method for solving time-dependent equations of motion for compressible fluid flow, noting shock wave diffraction, supersonic blunt body



interaction with shock wave, etc 21 p3730 A66-39472

Intermediate-thrust arcs in central force field satisfying optimality conditions, noting that motions are degenerate solutions of Euler equations 22 p3980 A66-40460

Navier-Stokes equations solutions for coefficient of viscosity tending to zero become solution to Euler equations in Cauchy problem for equations of hydrodynamics 24 p4193 A66-42232

**EULER-LAGRANGE EQUATION**

Characteristics of linear optimal systems whose performance criterion is defined by minimum of infinite integral of quadratic function of outputs and inputs of system 01 p0049 A66-10016

Successive approximation methods of solving optimal control problems, based on variational calculus and Euler-Lagrange equation 11 p1679 A66-23273

**EULER-LAMBERT EQUATION**

SA ELLIPTICAL ORBIT

Euler-Lambert equation for orbital transfer in Newtonian field solved by approximate method 22 p3981 A66-40475

Lambert theorem for orbital transfer in elliptic, parabolic and hyperbolic cases 23 p4127 A66-41117

**EUROPE**

SA DENMARK

SA FRANCE

SA GERMANY

SA GREAT BRITAIN

SA ITALY

SA NORWAY

SA SWEDEN

SA SWITZERLAND

SA USSR

Eurocontrol efforts in optimum safe spacing of aircraft in flight with minimum restrictions by radar observations and pilot reports 01 p0102 A66-10180

Bretigny experimental control center for studying air traffic control for Eurocontrol 01 p0053 A66-10181

Problems of spatial triangulation of Europe by means of satellites 03 p0446 A66-12458

Air traffic control simulation system based on digital computer for Eurocontrol 06 p0870 A66-16953

European Miniature Electronic Components and Assemblies Data 1965-1966, Part II, France, Netherlands, Scandinavia and Switzerland 06 p0859 A66-17159

European air cargo marketing and air freight industry 15 p2620 A66-29795

Aviation safety research in Europe, considering military and civil sectors 20 p3540 A66-36993

**EUROPEAN I SPACECRAFT**

Europa I rocket stage-separation conditions simulated by Modane wind tunnel facilities 02 p0210 A66-11211

European Launcher Development Organization /ELDO/ program for Europa I three-stage rocket and satellite design and testing 09 p1464 A66-20467

**EUROPEAN SPACE PROGRAM**

European Space Research Organization /ESRO/ objectives and program including sounding rockets, satellite payloads and astronomical satellite 01 p0170 A66-10248

French space program and projects under development 01 p0170 A66-10359

Proposals for television satellite in Europe noting direct transmission of TV programs, design principles and power supply 01 p0030 A66-10797

San Marco project, joint effort of NASA and Italian Space Commission to launch satellite for atmospheric and ionospheric measurements 01 p0143 A66-10809

European space program and establishment of space agency to study and explore space 02 p0305 A66-11248

European industry suggestions concerning space projects 02 p0305 A66-11249

German participation in aerospace technology noting space transporter design and development 02 p0177 A66-11667

Applicability of liquid hydrogen-oxygen technology to development of European launch vehicles 02 p0295 A66-11671

Objectives, nature, origin and organization of Eurospace, noting communications satellite and space transport committees 02 p0306 A66-11674

CNES and ESRO station network duties including satellite signal transmission recording, follow vehicle trajectory, telecommand onboard operations, etc 03 p0333 A66-12477

Diane, European interferometric tracking station noting antenna system, calibration operations, angular measurement, etc 03 p0333 A66-12478

Station network designed for CNES using Doppler frequency tracking, coherent systems of demodulation, polarization, etc 03 p0351 A66-12479

European Space Technology Center including upper-atmosphere scientific experiments, instrumentation, satellite control, data analysis, etc 03 p0352 A66-12481

Devices on ESRO satellite to be launched in 1967 by NASA rocket, noting photometers for auroral measurements, plasma probe for electron density, scintillation counter, etc 03 p0430 A66-12484

Nickel-cadmium battery development for use in D-I satellite undertaken by French CNES /National Center of Space Research/ 03 p0323 A66-13025

Research satellite projects sponsored by ELDO, ESRO and West-German Projects 625A and 625B 04 p0583 A66-13498

ESRO projects include sounding rocket experiments, small satellites launched by Scout, small space probes and Astronomical Satellite 04 p0599 A66-13500

Instrumentation for testing first stage lox-kerosene rocket engines of ELDO satellite launcher, noting pressure transducer and computer data system [ISA PREPRINT 1.12-5-65] 05 p0684 A66-15514

Spacecraft for studying space radiation and ionosphere by ESRO 06 p0958 A66-15995

Design, manufacture and testing procedures for satellites in UK-3 program 06 p0959 A66-16307

Planning European space projects in industry 06 p0973 A66-16497

French National Center of Space Studies, facilities and functions 06 p0973 A66-16934

French space program since creation of CNES in 1961 09 p1472 A66-19862

European Launcher Development Organization /ELDO/ program for Europa I three-stage rocket and satellite design and testing 09 p1464 A66-20467

CECLES/ELDO space vehicle booster program, noting design of three-stage rocket, including control and guidance system, telemetry, etc 09 p1464 A66-20655

Future programs for ELDO including launchers, guidance systems, bases, etc 09 p1464 A66-20656

Difficulties encountered in applying system of overall project management to ELDO initial program, noting PERT use, costs plans, etc 09 p1473 A66-20657

ESRO/ELDO Space Documentation Service, describing system characteristics, NASA agreement, indexing and search strategy 09 p1473 A66-20658

United Kingdom space projects, detailing Skylark, Blue Streak, Black Knight and Black Arrow rockets 09 p1464 A66-20684

Aerospace related research activities in Austria during 1964 09 p1458 A66-20708

Czechoslovakia space research noting satellite tracking, solar research, upper atmosphere, meteoritic studies, satellite dynamics and life sciences 09 p1458 A66-20711

Space research activity in Denmark, discussing international cooperation and ionospheric sounding 09 p1458 A66-20712

Aerospace research in France during 1964 09 p1458 A66-20714

Aerospace research in Italy including San Marco project, ionospheric measurements, cooperation with NASA, rocket experiments, etc 09 p1458 A66-20717

Space research in Netherlands during 1964 including work done for European Launch Development Organization 09 p1459 A66-20719

Aerospace research in Poland using satellite observations for geodesy, geophysics and atmospheric dynamics 09 p1459 A66-20721

Optical observations of artificial satellites used for geodetic and geophysical purposes in Rumanian Peoples

Republic 09 p1458 A66-20721

Space research in Sweden including cosm, rays, aurora, radio astronomy, rock, sounding, etc 09 p1459 A66-20722

Space research activities in United Kingdom during 1964 and early 1965 09 p1459 A66-20723

Design and reliability of Diamant launch vehicle 10 p1610 A66-21251

Design and operation of test stands for ELDO rocket engines under simulated high altitude conditions 10 p1519 A66-21368

European space program of launcher development 11 p1788 A66-22421

European space organizations, particular ESRO and ELDO 11 p1788 A66-23111

French space program, flight tests of Diamant class rockets and A-1 satellite 12 p1981 A66-23800

Fiat design and manufacture of heat shields, satellite frame and telemetry antennas for ELDO space booster 12 p1885 A66-23921

Scientific and technical program of ESRO including launching of sounding rocket satellites, space probes, astronomical observatory and scientific interplanetary probe 13 p2211 A66-26221

British space research for 1965-66 including rocket development, satellite tracking, solar radiation, ionospheric sounding, etc 15 p2599 A66-29811

Dutch space research program noting solar and stellar research, cosmic radiation, wind measurement, rocket sounding, etc 15 p2600 A66-29911

German Democratic Republic space program noting equipment for satellite observation, geodesy, aeronomy, etc 15 p2600 A66-29912

Czechoslovakian space research including satellite observation, radio emissions, solar activity, Doppler effect measurement, radiation hazards, etc 15 p2601 A66-29911

Polish space program noting international cooperation, satellite observation, radio astronomy, rocket sounding, etc 15 p2601 A66-29912

National report on space research in Sweden 15 p2601 A66-29913

Danish space program, emphasizing polar ionosphere and high energy primary cosmic radiation studies 15 p2601 A66-29913

French space program including FR- satellite and research in meteorology, space biology, rocket probes, electromagnetic propagation, etc 15 p2601 A66-29913

Propulsion systems for European launch vehicles for scientific satellites, interplanetary probes and orbiting astronomical observatories 17 p2990 A66-32371

European Space Research Organization origins, aims and present state of organization 17 p3040 A66-32371

Great Britain, future in space, discussing propulsion, nuclear power, satellite orbit guidance, stabilization and attitude control 18 p3268 A66-33941

Low cost approach to development of vehicle for European-based space exploration 18 p3246 A66-33971

Space simulator design for testing of ESRO II satellite, noting three-level operating concept, independent control of main shroud sections, etc 18 p3096 A66-34621

European Space Research Organization /ESRO/ history, objectives, organization and activities 18 p3269 A66-34731

EOLE system consisting of balloons and satellite, interrogation for synoptic data on atmospheric circulation over Southern Hemisphere 19 p3346 A66-35631

French booster projects for orbiting stationary communication satellites, noting SEREB /solid propellant/ and LRBA /liquid propellant/ 19 p3469 A66-36041

French A1 satellite design and development, examining telecommunication equipment and monitoring diamant launch performance 19 p3470 A66-36271

Instrumentation of ESRO telemetry receiving stations noting receiver, recording monitoring and demodulation equipment 21 p3702 A66-38601

ESRO mission, organizational structure, plans and programs 23 p4151 A66-41041

EUROSPACE-supported research carried



out by Germany and England on space-shuttle system between Earth and orbiting station  
[ICAS PAPER 66-3] 23 p4134 A66-42067  
D-1, D-2 and FR-1 satellites in French space program 24 p4296 A66-42697  
National Research Council and San Marco project in Italian space program 24 p4297 A66-42698  
**EUROPEAN SPACE RESEARCH ORGANIZATION SATELLITE**  
**S ESRO II SATELLITE**  
**EUROPIUM**  
Uniform compression effect on Curie temperature of ferromagnetic compound  
EuO 01 p0118 A66-10254  
Emission current density and effective work function of samarium, europium and gadolinium hexaborides 02 p0270 A66-11426  
Plastic deformation splitting and evolution of spectral lines and excited level structure of europium ion in alkaline-earth fluoride crystals 03 p0409 A66-12717  
Uniform compression effect on Curie temperature of ferromagnetic compound  
EuO 13 p2168 A66-25971  
Deuterium isotope effect on thresholds of europium chelate lasers, noting solvent thermal effects 13 p2105 A66-26598  
Ionic fluorescence of europium chelates, suitability as laser materials, noting energy transfer role in population inversion 14 p2315 A66-27463  
Fluorescence quantum efficiencies of octa-coordinated europium homogeneous and mixed chelates in organic solvents, noting effect of oxygen removal 23 p4030 A66-41153  
Spectroscopic, chemical and laser properties of piperidinium salt of europium tetrakis 24 p4226 A66-43034  
**EUROPIUM COMPOUND**  
Organic cations effect on laser threshold of solutions of tetrakis form of europium benzoyletrifluoroacetate 07 p1046 A66-18418  
**EUTECTIC ALLOY**  
Solubility and concentration curves for elements in solid solutions of alpha and beta titanium at eutectic and peritectic temperatures 01 p0087 A66-10660  
Superconducting transition temperatures measured for various tin-gallium compositions in quenched and annealed states 02 p0271 A66-11482  
Unidirectional solidified eutectic alloys as reinforced composites 05 p0700 A66-14811  
Plasma oscillation of electrons in aluminum compound eutectoids studied, using energy analysis of electrons passed through thin foil of eutectoid, noting dependency of oscillation energy on component grain size 09 p1429 A66-20843  
Corrosion mechanism for eutectic or near-eutectic Mg-Zn alloys in halide solution 13 p2110 A66-26026  
Cobalt and nickel eutectic alloys modification with selected elements for high temperature application, noting microstructure and tensile behavior 16 p2726 A66-31460  
Ti-Be system phase diagram, noting solubility and formation of eutectoid and eutectic 18 p3121 A66-33725  
Melting point and microhardness of carbon-saturated TiC-VC solid solutions, noting temperature of eutectic of TiC-VC with graphite 22 p3934 A66-39866  
Structure effect on superconducting properties of eutectic alloys solidified under variety of growth conditions, discussing interphase boundary, current density and residual strain 24 p4250 A66-42296  
**EUTECTIC DIAGRAM**  
Au-Sn-Pb section of Au-Pb-Sn phase diagram, examining solderability of gold coatings of electronic components 16 p2722 A66-30223  
Carbon solubility in Ta, Nb and V at temperatures from 1500 degrees C to eutectic temperatures 24 p4228 A66-43062  
**EVACUATION**  
**S GAS EVACUATION**  
**EVAPORATION**  
**SA BOILING**  
**SA TRANSPIRATION**  
**SA VAPORIZATION**  
Evaporation as molecular diffusion from large rough surface into random-lived internal scale turbulent

eddies 02 p0223 A66-11960  
Transistorized evaporation to measure vertical water vapor and heat fluxes in lower atmosphere 04 p0519 A66-13671  
Thin film transistors using evaporated silicon films on sapphire 09 p1351 A66-19939  
Vapor composition, evaporation rate and vapor pressure above chromium carbides determined by effusion method combined with mass spectrometry 14 p2310 A66-26791  
Spherical substrate converted to parabolic mirror by selective evaporation of aluminum, using silver as nonuniform thickness layer 15 p2499 A66-28841  
Dimensional analysis of temperature distribution within spherical particle during nonisothermal evaporation 17 p3033 A66-32449  
Lanthanum hexaboride evaporation from Knudsen cell studied by mass spectrography for composition, sublimation heat and ion current 17 p2981 A66-32849  
Winds caused by synoptic situations and strong local turbulence effect on evaporation measurements at Adriatic seaboard of Central Italy 18 p3130 A66-34720  
Evaporation system for fabrication of multilayer dielectric films for mirrors or filters, obtaining thickness variation reduction and simultaneous deposition 24 p4218 A66-43163  
**EVAPORATION COOLING**  
Electric machines employing evaporative and universal cooling systems for aircraft use 13 p2041 A66-25902  
**EVAPORATION RATE**  
Lubricant testing for supersonic aircraft, examining temperature requirements, viscosity, evaporation characteristics, etc 10 p1539 A66-21399  
Thickness of laminar liquid film draining from vertical surface analytically determined by assuming evaporation rate is known constant [ASME PAPER 65-HT-39] 11 p1785 A66-22189  
Vacuum effects on lubricants and bearing materials due to reduced ambient pressure and low concentration of oxidizing gases 12 p1885 A66-24383  
Mass evaporation rate and heat transfer coefficients for water drops supported by own superheated vapor over flat plate 16 p2830 A66-31680  
Vaporization and creep rupture behavior of type 316 stainless steel 18 p3123 A66-33755  
Mass evaporation rate and heat transfer coefficients for water drops supported by own superheated vapor over flat plate 18 p3262 A66-34378  
Reaction rates of decomposition burning of small spheres of liquid hydrazine 20 p3626 A66-38043  
Vacuum thermal decomposition of InSb and GaSb surfaces, noting evaporation rates 20 p3624 A66-38411  
Coverage dependent evaporative lifetimes of various metals and oxygenated W ribbon filaments at high temperatures 22 p3934 A66-40097  
Potassium tantalum niobate crystal growth noting methods applied, potassium oxide evaporation and tantalum absorption rate 23 p4115 A66-41773  
Evaporation rates of lead telluride and lead tin telluride in pressed and sintered thermoelement form 24 p4247 A66-42108  
**EVERSHED EFFECT**  
Evershed effect in inactive isolated symmetrical spot during passage across solar disk 05 p0758 A66-14773  
Interpretation of Evershed effect by material streaming in penumbral fine structure 05 p0758 A66-14774  
**EVOLUTION**  
**SA BIOGENY**  
**SA GALACTIC EVOLUTION**  
**SA GAS EVOLUTION**  
**SA LUNAR EVOLUTION**  
**SA PLANETARY EVOLUTION**  
**SA STELLAR EVOLUTION**  
Chemical evolution studied by finding and reconstructing chemical reactions that might have occurred among primeval molecules on surface of Earth 05 p0629 A66-15017  
**EXCHANGE**  
**S CHARGE EXCHANGE**  
**S ENERGY EXCHANGE**  
**S GAS EXCHANGE**

**S ION EXCHANGE**  
**EXCHANGER**  
**S HEAT EXCHANGER**  
**EXCITATION**  
**SA ACOUSTIC EXCITATION**  
**SA ATOMIC EXCITATION**  
**SA ENERGY LEVEL**  
**SA HARMONIC EXCITATION**  
**SA IONIZATION**  
**SA SELF-EXCITATION**  
Optical spectrum of normal excitons in deformed and nondeformed n-type Ge single crystal layers for four orientations 22 p3964 A66-40306  
**EXCITED STATE**  
Mercury photosensitized oxidation of perfluoropropene to study postulated excited molecule mechanism 02 p0188 A66-11596  
Jahn-Teller effect in excited 4-T-2 state of trivalent Cr ions in ruby, discussing unilateral elastic strain effect splitting of pure electronic line 597 nm in U band 03 p0410 A66-12941  
Unified model of ferromagnetism, analyzing spin-wave motion of electrons in transition metals, using atomic and energy-band features 04 p0559 A66-13450  
Vibrationally excited molecular hydrogen effect on mean polarizability 04 p0549 A66-14311  
Barrat theory of multiple scattering of magnetic resonance radiation, accounting for vapor dispersion and photon propagation time 05 p0697 A66-15172  
Low temperature excitation spectrum for ferro- and antiferromagnets with large crystalline field splittings 05 p0741 A66-15867  
Internal and vibrational partition functions of carbon dioxide and rotational line intensities arising from transitions from ground and first excited states 06 p0907 A66-15945  
Bracketing theorem applied in partitioning technique for solving Schroedinger equation to determine upper and lower bounds to energy eigenvalues, ground and excited states 06 p0911 A66-16166  
Bethe approximation of ionization cross sections of excited states of atomic hydrogen by high energy electrons 06 p0912 A66-17037  
Population inversions promoted between electronic-excited states by fluid-mechanical techniques 07 p1083 A66-17937  
Decay of F-center excitations in alkali halides induced by short intense pulse of Q-switched ruby laser 08 p1275 A66-19367  
Electron excitation cross section of individual energy levels of inert gases calculated, using Born-Oppenheimer method 09 p1405 A66-20939  
Excited state of cesium lifetime determined from double magnetic resonance experiments 09 p1406 A66-20944  
Departures from local thermal equilibrium in helium plasma produced by magnetically-driven shock wave in T-tube 10 p1566 A66-21811  
Kinetics and gas dynamics equations derived to determine state of gas behind strong shock waves, accounting for all excited states of neutral atoms 11 p1688 A66-22586  
Cascade theory of electron recombination into ionized donors in germanium analyzed, noting several models 12 p1928 A66-23940  
Electron-atom collision studied, using helium-neon laser to obtain energy transitions between excited states 13 p2137 A66-25106  
Excited-singlet even parity states of anthracene in near UV, noting role of absorption spectroscopy 13 p2132 A66-26143  
Absorption behavior of optically pumped ruby rod, noting amplification at room temperature and absorption at cryogenic temperature 13 p2098 A66-26174  
Steady state variation of light intensity with distance for monochromatic light, noting dependence of absorption coefficient on degree of excitation of electronic system 13 p2099 A66-26183  
Helium-neon gas laser used to study pressure effect on line shape of 2s-2p optical transitions of neon excited states 13 p2100 A66-26198  
Radiative recombination lifetimes in laser-



excited silicon, correlating emission with photoconductivity 13 p2105 A66-26597

Effective lifetime of excited state of gas laser, with account of near photon transfer 14 p2306 A66-27135

Electron excitation cross section of individual energy levels of inert gases calculated, using Born-Oppenheimer method 15 p2543 A66-28528

Excited state of cesium lifetime determined from double magnetic resonance experiments 15 p2543 A66-28532

Radiative cascade patterns in helium-neon gas system using idealized model, computing spontaneous decays which are compared with laser experiments 15 p2512 A66-28699

Resonance signal inversion in Rb optical pumping and relation of mixing of excited state sublevels 15 p2517 A66-29410

Electron-atom collision studied, using helium-neon laser to obtain energy transitions between excited states 16 p2758 A66-30285

Auroral excitation rates and molecular vibrational temperatures in nitrogen 2PG from Franck-Condon factors obtained from intensity measurements and high resolution absorption spectral data 16 p2692 A66-30328

Energy transfer measurements in gas-solid surface interactions initiated by electron beam-excited photoemission 16 p2701 A66-30397

Color centers in alkali metal azides, noting change of ion from linear to bent configuration 16 p2777 A66-31023

Dynamic Jahn-Teller effect in excited state vanadium doped aluminum oxide 17 p2981 A66-32717

Spectra and intensity vs excitation level and spatial distribution vs current density determined for optical radiation by electron excited cadmium sulfide 17 p2937 A66-33308

Excitation cross sections of cesium in collisions with slow electrons 17 p2989 A66-33507

Intermediate state peculiarities effect on Raman scattering spectra of excited gas molecules 17 p2960 A66-33508

Excitation of 3S sub 2 neon level by metastable helium atoms during He-Ne discharge 17 p2938 A66-33513

Long-lived impact excitation states of particles measured from cross section of nonelastic collision with second particle 18 p3137 A66-34025

Molecular orbital studies of ground and low lying excited states of HeH molecular ion 18 p3139 A66-34509

Charged Bose gas, discussing ground-state energy, excitation spectra and plasmon-particle interactions, using Bohm-Pines and Bogoliubov approximations 18 p3140 A66-34729

Excitation of ground state hydrogen atoms by fast protons, evaluating total Born cross section in limit of infinitely massive protons 19 p3403 A66-36333

Detection of three radio lines arising from transitions between highly excited states of neutral helium 20 p3652 A66-37615

Chemical kinetics of electron plasma reactions, discussing energy states, ion-molecule reactions, charge transfer, transport properties, phase interactions, etc 21 p3702 A66-38448

Photoionization efficiency curve for sulfur hexafluoride in wavelength region 1050 to 600 angstroms with Rydberg levels from electronically excited state 21 p3774 A66-38525

Photoionization cross sections for N and O atoms and ions in state of excitation, using quantum defect method 21 p3775 A66-39076

Atomic collisions, excitation transfer processes and energy level transition probabilities in plasma of gas lasers 21 p3748 A66-39305

Experimental excited state band locations and intensities in absorption spectrum of electron transitions in optically pumped ruby laser 21 p3749 A66-39569

Theoretical excited state absorption spectrum of electron transitions in optically pumped ruby laser 21 p3749 A66-39570

Dissociation energies of GaF, InF and TiF measured by high temperature mass-spectrometric techniques, noting possibility of potential maxima in excited

states 22 p3859 A66-39917

Precise measurement of excited-state lifetimes for radiative and collision-induced relaxation in fine structure levels of atomic neon, noting optical transitions 23 p4098 A66-41361

Time resolved emission measurements for Cr-Ar mixtures in three spectral regions and ionization occurrence in excited state inelastic collisions 23 p4033 A66-42083

Excitation cross sections of cesium in collisions with slow electrons 24 p4249 A66-42122

Excitation of 3S sub 2 neon level by metastable helium atoms during He-Ne discharge 24 p4219 A66-42126

**EXCITON**

SA ENERGY BAND

SA POSITRONIUM

Mean free path influence on transverse collective excitations in strong coupling superconducting alloys 02 p0271 A66-11481

Semiconductor excitation-level spitting for shallow impurity state due to spin orbital shifts 04 p0565 A66-14260

Possible processes of non-radiative decay of excitons on ionized donors and acceptors in semiconducting and dielectric crystals 05 p0737 A66-15160

Exciton absorption lines and long wave intrinsic edges of single-crystal CdSe and CdS at low temperatures 06 p0924 A66-16540

Measurement of exciton absorption of gallium selenide at low temperatures in presence of electric field, noting line broadening and no splitting 06 p0929 A66-16942

Neutron and proton bombardment effects on exciton spectrum of cuprous oxide 06 p0937 A66-17139

Group II-VI semiconductors, examining theory of bound exciton complexes, lattice vibrations, phonon-assisted edge emission and higher energy bands 08 p1271 A66-19239

Exciton absorption lines and long wave intrinsic edges of single-crystal CdSe and CdS at low temperatures 15 p2569 A66-29987

Free current carrier formation in molecular crystal, examining dependence of photoconductivity on magnetic field intensity 18 p3158 A66-34683

Optical spectrum of normal excitons in deformed and nondeformed n-type Ge single crystal layers for four orientations 22 p3964 A66-40306

**EXCRETION**

Light effect on rhythmic excretion of water and electrolytes in humans 09 p1335 A66-20534

Sodium excretion during extracellular volume expansion and associated changes in renal blood flow and intrarenal blood distribution during natriuresis accompanying saline loading in dogs 13 p2012 A66-26582

Indolyiacroyl glycine excretion in man 16 p2638 A66-30634

Combination of renal vasodilation and angiotensin infusion effect large changes in renal hemodynamics, excretion and reabsorption of sodium in anesthetized hydropenic dogs 20 p3507 A66-37607

PAH transport mechanism in dogs with hydrazine-depressed para-aminohippurate treated with acetate, 6,8-epidithioctanate and 6,8-epidithioctanoamide 22 p3854 A66-39795

**EXECUTIVE AIRCRAFT**

SA BEAGLE B-206 AIRCRAFT

Design and market research aspects of Hamburger HFB 320 jet executive aircraft 10 p1482 A66-21360

Oxygen storage and distributions systems development trends for business aircraft [SAE PAPER 660207] 13 p2002 A66-26387

Air conditioning development in Beech aircraft [SAE PAPER 660209] 13 p2002 A66-26388

Defining fatigue load environment for business aircraft [SAE PAPER 660215] 13 p2199 A66-26392

FAA research, development and airworthiness compliance for general aviation aircraft [SAE PAPER 660217] 13 p1996 A66-26394

Flying qualities of six late-model personal-owner aircraft in visual and instrument flight [SAE PAPER 660219] 13 p1996 A66-26396

High by-pass turbofan for business aircraft,

comparing jet propulsion system efficiency with fan engines, cost factors and market potentials [SAE PAPER 660221] 13 p2173 A66-264

British Executive and General Aviation/BEAGLE/ and development of Beagle B.2 S twin-engine executive aircraft 22 p3847 A66-398

**EXERCISE**

Maximum exercise tolerance in healthy aircrew members limited by cardiac output 24 p4163 A66-424

**EXHAUST**

S ROCKET EXHAUST

EXHAUST GAS

SA JET STREAM

Exhaust of pinched plasma from axial orifice involves electromagnetic current profile diffraction and thermal expansion of gas column [AIAA PAPER 65-92] 02 p0267 A66-115

Expression derived for vibrational relaxation in recombining expanding nozzle exhaust gas, assessing effect of chemical reactions on this mechanism 16 p2687 A66-311

Exhaust mixing process in Rolls-Royce bypass jet engines, noting stream mixing common duct with corrugated metal interface on inlet side 17 p2990 A66-320

Short duration technique providing simulation of thermodynamic properties and composition of exhaust products of liquid and solid propellant rocket engines [AIAA PAPER 66-760] 22 p3894 A66-406

**EXHAUST JET**

Exhaust beam from conoid thruster investigated, using quadrupole mass filter [AIAA PAPER 64-674] 02 p0278 A66-115

Response of Langmuir probes in rocket exhaust jets, noting sensitivity to chamber temperature and pressure and alkali metal concentration 14 p2294 A66-274

Accelerating particulate flow studied, using blowdown system for component velocities and friction 17 p2916 A66-334

Microwave attenuation magnitude associated with exhaust plasma of nonauminized and aluminized composite propellant 21 p3807 A66-386

**EXHAUST NOZZLE**

SA ROCKET NOZZLE

Form rolling used to form L-shaped struts from L605 alloy for economical fabrication of supports for jet engine exhaust nozzles 10 p1545 A66-212

Exhaust nozzle performance noting testing techniques, cruise engine installations, data accuracy, etc [AIAA PAPER 66-641] 18 p3048 A66-342

Heating from Saturn solid propellant S- and S-IVB stage motor exhausts and S-IVB Centaur retro motor exhaust theoretically and experimentally analyzed [AIAA PAPER 66-653] 19 p3479 A66-366

Statistically designed experiments in wind tunnel test programs dealing with exhaust nozzles, discussing data analysis techniques [AIAA PAPER 66-742] 23 p4052 A66-413

Specific impulse limitations of advanced nuclear rocket engines due to hydrodynamic transpiration coolant flows in exhaust nozzle 24 p4261 A66-427

**EXHAUST SIMULATOR**

Scaling of near field pressure correlation patterns around jet exhaust 01 p0010 A66-101

Highly underexpanded sonic jet in wind tunnel study of stagnation temperature pressure and shock profiles 08 p1164 A66-191

Wind tunnel test program for simulation of gas-particle rocket exhaust plume, separate flow around nozzle and base recirculation [AIAA PAPER 66-767] 22 p3895 A66-406

**EXHAUST VELOCITY**

Velocity and momentum of high current steady state coaxial plasma noting mass flow, exhaust velocity, thrust, arc voltage and power 02 p0267 A66-115

**EXISTENCE THEOREM**

Condition of existence of universal stabilizing control in second order control system 01 p0050 A66-103

Existence and formal uniqueness theorems of partial linear differential equations with Cauchy conditions on characteristic multiplicity hyperplane 01 p0095 A66-110



Existence theorem for trajectories of priorior field satisfying measurability condition 05 p0707 A66-15032

Cauchy problem for first-order nonlinear equation 05 p0709 A66-15360

Sufficient condition for existence of admissible control for optimization systems [ASME PAPER 65-WA/AUT-12] 05 p0710 A66-15607

Electromagnetic field in current-carrying region, discussing existence criteria of improper integrals 06 p0908 A66-16130

Controller analytical design for nonautonomous systems, deriving necessary and sufficient conditions for existence of optimum control 06 p0862 A66-16522

Existence in large of periodic solutions of hyperbolic partial differential equations 06 p0903 A66-16899

Existence and uniqueness of solutions of certain boundary value problems for degenerate elliptic equations of second kind 07 p1056 A66-17596

Cauchy and boundary value problem for second-order nonlinear ordinary differential equations 07 p1056 A66-17607

Regularization of ordinary differential operator trace in region of regular boundary conditions 07 p1057 A66-17855

Existence and uniqueness theorems for invariant-imbedding nonlinear ODE systems for absorption loss rate satisfying Lipschitz condition 07 p1059 A66-17972

Existence and uniqueness of piecewise-continuous solution to two-dimensional linear first order hyperbolic system with discontinuous coefficients 07 p1060 A66-18100

Convergent series representation of system of measurable functions that are complete and orthonormalized 07 p1060 A66-18251

Necessary conditions for existence of univalent integrals in equations of motion of heavy gyrost at fixed at one point 08 p1227 A66-19762

Invariant imbedding in transport process and theorems of uniqueness and existence for derived hyperbolic equation 09 p1393 A66-19906

Proof, by degenerate kernel method of existence and uniqueness of solution for one class of nonlinear integral equations 09 p1394 A66-20455

Existence of relationship between slope of servosystem functions with limited bandwidth and bandwidth magnitude 09 p1346 A66-20575

Stochastic linear programming as activity analysis model for determination of maximal profit operations for companies 09 p1349 A66-20635

Second-order linear equations with nonnegative characteristic form in analysis of first boundary value problem 09 p1397 A66-20734

Boundedness and uniform boundedness of nonhomogeneous systems, obtaining necessary and sufficient conditions for existence of solutions 10 p1551 A66-21920

Computational solution of functional differential equations, using successive approximations 10 p1551 A66-21922

Existence theorems for nonlinear equations having indefinite and potential operators 10 p1551 A66-21977

Existence and convergence theorems for minimizing sequences for extremum problems in presence of constraints 10 p1551 A66-21978

Existence of optimal stochastic controls 11 p1682 A66-23457

Existence theorems for optimal control solutions of Pontryagin and Lagrange problems 11 p1725 A66-23458

Boundary value problem solutions in meteorology 12 p1905 A66-23664

Quasi-linear boundary value problems solved with Galerkin convergence method 12 p1902 A66-23863

Existence of cycles as nonzero periodic solution to system of differential equations with one degree of freedom 13 p2117 A66-25415

Initial value problem for Navier-Stokes equation 14 p2273 A66-26939

Existence of periodic solutions of differential equations in nonlinear mechanics [PST PAPER NT-147] 14 p2323 A66-27792

Existence and stability theorems for almost

periodic solutions of nearly Liapunov systems 15 p2527 A66-29050

Uniqueness and existence theorems for parabolic partial differential equations for case of free boundary 15 p2528 A66-29334

Existence theorem for nonlinear ODE system with continuous monotonic differential operators over Hilbert space and application to nonlinear network analysis 15 p2528 A66-29370

Uniqueness and solution estimates to boundary value problems, noting solvability correlation with existence of Green function 16 p2733 A66-30739

Existence theorem of recurrent solutions to differential equations defined in Banach space for dynamic and nondynamic systems 16 p2735 A66-30785

Controller analytical design for nonautonomous systems, deriving necessary and sufficient conditions for existence of optimum control 16 p2670 A66-30832

Nonlinear parabolic equations, considering existence, uniqueness theorems, abstract Cauchy problem, etc 17 p2946 A66-32307

Textbook on differential equations with deviating arguments, covering existence theorems, linear equations, stability theory, boundary value problems, etc 17 p2947 A66-33188

Differential inequality theorem for boundary value problem involving second-order differential equation 18 p3126 A66-33975

Optimal control for stochastic differential equation system, noting existence and uniqueness of solution for coefficients satisfying Lipschitz condition 19 p3325 A66-35983

Existence theorems for nonlinear equations having indefinite and potential operators 19 p3390 A66-36187

Existence and convergence theorems for minimizing sequences for extremum problems in presence of constraints 19 p3390 A66-36188

Boundary value problem solutions in meteorology 19 p3394 A66-36194

Existence of inflection points in cost vs terminal time curve for linear minimum energy regulator 19 p3339 A66-36745

Absence conditions for periodical trajectories in regions of possible existence 19 p3401 A66-36844

Axisymmetric viscous flow with electric conductivity around barrier, deriving existence theorem for zero Reynolds number 20 p3609 A66-37568

Linear homogeneous third-order differential equations, examining existence, uniqueness and asymptotic behavior of nontrivial nonoscillatory solutions and existence criteria for oscillatory solutions 20 p3591 A66-37608

Existence of unique periodic solution to first-order differential equation and nonautonomous system of two first-order differential equations 20 p3591 A66-37752

Local existence theorems for elliptic systems with linear matrix differential operator 21 p3754 A66-38460

Existence and uniqueness theorems for Dirichlet problem of second-order linear elliptic equation, Neumann BVP, mixed BVP and oblique derivative problem 21 p3754 A66-38462

Linear elastostatic BVPs for inhomogeneous anisotropic elastic body including existence-uniqueness theorem, based on Korn inequality 21 p3755 A66-38463

Existence theorems of periodic solutions to integro-differential equation with delayed argument 21 p3756 A66-38742

Existence of angular boundary values of harmonic function in sphere 21 p3757 A66-38909

Existence conditions of solution to two-point boundary value problem for ordinary nonlinear any order differential equation 21 p3757 A66-39245

Existence of smooth solution for system of equations describing nonlinear oscillations of thin plate and shallow shell 22 p3989 A66-39905

Existence theorem of recurrent solutions to differential equations defined in Banach space for dynamic and nondynamic systems 22 p3940 A66-40447

Variational techniques in solving BVPs for nonlinear plastic, elastoplastic and viscous media and in predicting existence, uniqueness and equilibrium conditions 23 p4136 A66-40996

Existence theorem for stationary flow in magnetic field of incompressible viscous fluid electrically conductive around solid electrically conducting obstacle 23 p4100 A66-41173

Existence and uniqueness theorems in Poincare-Liapunov theory for multipoint control boundary value problems 23 p4085 A66-41539

Existence of solution of linear problems for ordinary differential equations 24 p4231 A66-42538

Weak and strict solution existence theorem for initial-boundary value problem for nonlinear hyperbolic equation in relativistic quantum mechanics 24 p4237 A66-42829

**EXO-ELECTRON EMISSION**

External electron emission measurement from polished n-germanium and n-silicon surfaces 17 p2986 A66-33310

**EXOBIOLOGY**

**S BIOASTRONAUTICS**

**S EXTRATERRESTRIAL LIFE**

**EXOSPHERE**

Density distribution in exosphere, particularly Maxwellian velocity distribution disturbed by light particle escape 14 p2284 A66-27620

Exospheric temperature, scale heights and mean molecular weight up to 3500 km derived from satellite accelerations in 1964 15 p2484 A66-28819

Day-to-night and semiannual variations in exospheric density during low solar activity from observations of Echo II orbital period changes 15 p2497 A66-30084

Diurnal variation of hydrogen atom concentration at base of exosphere, including effects of lateral flow of gas around Earth 17 p2919 A66-32996

Electron density profiles in ionosphere and exosphere - NATO Advanced Study Institute, Finse, Norway, April 1965 22 p3903 A66-39943

Antenna in interplanetary plasma, noting fluctuation noise in exosphere and radiation impedance when exposed to solar wind 22 p3877 A66-40466

Plasma concentration diagnostics in exosphere from delay time of forward frequency as function of parameter of whistler trajectory 22 p3915 A66-40774

Guiding of whistlers due to exospheric anisotropy, electron density and geomagnetic field effects 22 p3915 A66-40803

**EXOTHERMIC REACTION**

Pyrotechnics for efficient preheating of space power systems by simple lightweight chemical blends that produce heat pyrotechnically 04 p0460 A66-13926

Computed high temperature rate constants for hydrogen atom transfers involving light elements, noting activation energies for exothermic reactions [CI PAPER WSCI-65-24] 05 p0629 A66-15148

Kinematic computer calculations of energy distribution among products of repulsive, mixed and attractive energy release exothermic reactions 11 p1787 A66-23213

Phase determination by electron-probe X-ray microanalysis of nickel aluminide self-bonding coating produced by flame-spraying 12 p1892 A66-23560

Exothermal discontinuities propagation in conducting media without restricting magnetic field orientation, noting velocity and energy released, showing that existence of propagation velocities leads to two detonation modes 13 p2149 A66-26260

Polystyrene exposure to oxygen, causing ignition in shock tube but failing to ignite under surface exposure 14 p2370 A66-27476

Ignition model for condensed thermally unstable propellant by exothermal processes taking place in condensed phase 18 p3260 A66-33719

Small perturbation method applied to combustion stability of high explosives taking into account heat release in K phase 19 p3477 A66-35740

Exothermic brazing of refractory metals, tabulating braze filler metals that formed acceptable joints with molybdenum,



- tungsten and TZM alloy 19 p3367 A66-36117  
Curing problems of highly exothermic propellants investigated using mathematical models, detailing heat conduction and thermal properties 22 p3968 A66-39868
- EXPANDING UNIVERSE THEORY**  
**S COSMOLOGY**  
**EXPANSION**  
**S GAS EXPANSION**  
**S KARHUNEN-LOEVE EXPANSION**  
**S NOZZLE EXPANSION**  
**S PRANDTL-MEYER EXPANSION**  
**S SERIES EXPANSION**  
**S THERMAL EXPANSION**  
**S WIENER-HERMITE EXPANSION**  
**EXPANSION WAVE**  
Decomposition of expanding wave into amplifying and attenuating components 09 p1347 A66-20781  
General solution for class of initial value problems for systems of aerodynamic equations, constructing reference solution to Cauchy problem involving shock and expansion waves 11 p1694 A66-23363  
Kinetics of CN radicals association generated by shocking cyanogen-argon mixtures at high temperatures in reflected shock region of expansion wave 12 p1811 A66-23615  
Stress expansion-wave propagation from circular hole in thin infinite plate under abrupt permanent load 13 p2202 A66-26419  
Shock waves from empty cavity collapsing with spherical symmetry on small solid sphere 13 p2071 A66-26723  
Exact solutions for unsteady two-dimensional gas dynamics equations for self-similar flow behind shocks and expansion waves 14 p2278 A66-28143  
Decomposition of expanding wave into amplifying and attenuating components 22 p3862 A66-39840  
Recombination of carbon monoxide and atomic oxygen in expansion wave at high temperature in single pulse shock tube 22 p3860 A66-40527
- EXPERIMENT**  
**S LITHIUM COOLED REACTOR**  
**EXPERIMENT /LCRE/**  
**EXPERIMENT DESIGN**  
Design charts for determining ejector characteristics for optimum performance of jet pump systems [ASME PAPER 65-WA/FE-32] 05 p0691 A66-15709  
Optimum design parameters for water ejectors [ASME PAPER 65-WA/FE-31] 05 p0691 A66-15710  
Aircraft, missile and space systems flight test programs using statistical experimental design techniques [AIAA PAPER 65-221] 09 p1330 A66-20745  
Post-Apollo experiments for space 11 p1775 A66-23075  
Interaction effects of combined environment testing for aerospace systems 16 p2679 A66-30477
- EXPLODING CONDUCTOR**  
Hard X-rays from exploding wires, noting high penetrating power after current dip 13 p2127 A66-25573  
Exploding bridgewire systems, discussing theory of wire explosion and various applications 18 p3135 A66-34191  
Color temperature measurement in first stage of electrical explosion of copper, silver and constantan wires as function of magnitude of energy input for various heating times 20 p3599 A66-36985  
Spectral distribution of light emission of exploding wire systems measured by high-speed drum camera and rotating shutter 20 p3603 A66-37742  
Electrical explosion of copper wire in air and in vacuum, discussing plasma emission and I-V characteristics 21 p3791 A66-39084  
Synchronized shadow photochronographic investigation of wire explosion shock waves in air 21 p3772 A66-39302  
Electric energy from helical and coaxial explosive generators noting design, performance, limitations and loss mechanisms 21 p3699 A66-39510  
Spectral distribution of light from exploding wire sources noting environment, pressure, energy and material effects 22 p3948 A66-40197

- Stress wave propagation analysis using exploding wire and hollow cylinder together with measurement of loading condition and response 22 p3992 A66-40203  
Laser technique acquisition of data on exploding-wire phenomena in explosion model, supersonic model and ablation model 23 p4091 A66-41701  
Kinetics of heating and evaporation of exploding copper and brass wires in air and polyethylene tubes studied by X-ray techniques 24 p4238 A66-42976  
Rapid transfer of magnetic energy via exploding foils, noting inductive storage 24 p4239 A66-43217
- EXPLODING CONDUCTOR CIRCUIT**  
Electric drive operating parameters and design, using exploding wire type device and electromagnetic apparatus for plasma production and acceleration 06 p0942 A66-15917  
Nonlinear ordinary differential equations applicable to damped oscillatory circuits with exploding wires, obtaining conservation law and approximate solutions by Picard method 13 p2129 A66-26667  
Time variation of current, temperature and resistance in premelt stage of wire explosion expressed in terms of initial wire and circuit data 15 p2537 A66-28722
- EXPLORATION**  
**S LUNAR EXPLORATION**  
**S PLANETARY EXPLORATION**  
**S SPACE EXPLORATION**  
**EXPLORER VI SATELLITE**  
Drag coefficients and absolute atmospheric densities at high altitudes calculated, using spin and orbital decays of Explorer VI satellite conjugated with models of surface particle interaction 15 p2489 A66-29818
- EXPLORER VII SATELLITE**  
Composition and energy spectra of primary cosmic radiation in low energy regions from observations of Mariner II and Explorer VII 05 p0752 A66-15384  
Inhomogeneities of ionospheric electron concentration in Pacific Ocean region obtained with aid of signals from Explorer VII satellite 08 p1213 A66-19025
- EXPLORER X SATELLITE**  
Plasma and magnetic field data from Explorer X, emphasizing correlation with multiple crossings of geomagnetic cavity boundary on dark hemisphere of Earth 07 p1029 A66-18087
- EXPLORER XI SATELLITE**  
Photon-flux measurements by high energy gamma-photon detectors onboard Explorer XI and OSO-I 03 p0423 A66-13028
- EXPLORER XII SATELLITE**  
Explorer satellite XII, XIV and XV measurements, noting directional intensity energy flux, spatial distribution and spectra of low energy trapped protons and electrons 07 p1131 A66-18085  
Transition region magnetic field and polar magnetic disturbances, comparing Explorer XII data with ground measurements from Arctic observatories 08 p1218 A66-19399  
Bit-plane encoding technique used for reducing redundancy in data gathered in space probes 18 p3073 A66-34249  
Solar wind observations with Explorer XII and IMP, noting periodic fluctuations in solar proton flux and detection of 3 mev electrons of interplanetary origin 18 p3167 A66-34335  
Temporal variations of electron energy flux in outer radiation zone measured during geomagnetic activity with instrumentation on board Explorer XII satellite 24 p4263 A66-42601
- EXPLORER XIV SATELLITE**  
Data analysis from Explorer XIV satellite, noting magnetic field measurements in tail of geomagnetic cavity 07 p1029 A66-18086
- EXPLORER XV SATELLITE**  
Explorer XV and Telstar I satellite trapped radiation measurements, noting connection between magnetospheric trapped particles and natural plasmas in space 07 p1131 A66-18084
- EXPLORER XVII SATELLITE**  
Intensity and energy spectra of low energy primary cosmic ray protons determined aboard Imp-I satellite 01 p0132 A66-10601
- EXPLORER XVIII SATELLITE**  
Interplanetary magnetic effects of solar

- flares recorded by Explorer XVIII and Pioneer V 03 p0419 A66-12681  
Explorer XVIII continuous monitoring of vector field data deemed plausible correlation with noncontinuous data coverage of Pioneer V 03 p0419 A66-12681  
Quasi-stationary corotating structure in interplanetary magnetic field observed with Imp I satellite during three solar rotations noting data on solar wind 05 p0746 A66-1478  
Correlated magnetic tail and radiation belt observations from Explorer 18 /Imp I satellite and APL satellite 1963 38C in April 1964 08 p1284 A66-19413  
Imp-I observation of magnetic wake of Moon or Earth 11 p1697 A66-22424  
Imp-I observations of solar wind properties, including interaction with geomagnetic field and flow characteristics of positive ion component 11 p1775 A66-23131  
Electron acceleration near Earth bow shock measured, using Explorer XVIII satellite noting solar wind effect, energy spectrum of radiation belt and magnetospheric boundary etc 13 p2175 A66-26313  
Criticism of Ivanov assumption regarding IMP-I observation of lunar wake in solar wind by magnetic field and plasma measurements 15 p2575 A66-29103  
Measurements of geomagnetic field at various distances using IMP-I satellite noting magnetically neutral sheet in tail and observation of five magnetic storms 16 p2695 A66-30713  
Interplanetary magnetic-field measurements taken by Interplanetary Monitoring Platform /IMP-I/ 18 p3231 A66-34372  
Explorer XVIII plasma flux measurements data analysis, plasma detector, map of transition zone between magnetosphere and solar wind and associated energy spectra 18 p3168 A66-34331  
Magnetopause boundaries and geomagnetic field at magnetopause and interaction region by IMP I 18 p3106 A66-34331  
Explorer XVIII satellite measurements of proton energy spectra in region corotating with Sun, noting modulation of galactic cosmic radiation and source of continuous particle accelerations 18 p3177 A66-34717
- EXPLORER XX SATELLITE**  
Communications system of Explorer X ionospheric satellite 04 p0481 A66-13803  
Explorer XX satellite observations of plasma resonances at fixed frequencies in topside ionosphere, noting patterns, effects of geomagnetic field, electron concentration etc 13 p2074 A66-26313  
Topside ionosphere, emphasizing experiments with incoherent scatter radar and topside sounder 22 p3908 A66-39913  
Explorer XX topside sounder observation of ionospheric irregularities in electron density and plasma wave electrostatic resonances 22 p3909 A66-39913
- EXPLORER XXII SATELLITE**  
Ionosphere electron content near auroral zone obtained from differential Faraday observations of multifrequency beacon satellite Explorer XXII, noting corpuscular radiation role 02 p0223 A66-12033  
Electrostatic probe, discussing Explorer XXII measurements of electron concentration and temperature at 1000 km altitude 05 p0746 A66-14772  
F-layer structure at subauroral and auroral latitudes measured by multifrequency beacon satellite Explorer XXII 08 p1212 A66-18613  
Beacon observations of differential Doppler and Faraday effects from analysis of signals emitted by Explorer XXII satellite 15 p2453 A66-30003  
Ground-reflected wave effects and regular fading superposed on Faraday fading observed in signal strength recordings from Transit IVA and Explorer XXII 16 p2692 A66-30313
- EXPLORER XXX SATELLITE**  
**SA INTERNATIONAL QUIET SUN YEAR /IQSY/**  
Solrad VIII observation of May 20, 1964 solar eclipse penumbral zone in X-ray and UV bands 21 p3810 A66-38448
- EXPLORER XXXIII SATELLITE**  
AIMP-D spacecraft mission analysis determining launch conditions and trajectory



shaping for attaining lunar orbit, noting errors, flight path angle, etc  
[AIAA PAPER 66-535] 18 p3226 A66-33665

**EXPLODER SATELLITE**  
SA RADIO ASTRONOMY EXPLORER /RAE/ SATELLITE  
Attitude control system, using magnetic interaction with geomagnetic field to check spin rate and spin axis orientation of spin-stabilized Explorer A  
satellite 08 p1304 A66-19512

Accurate tracking of Beacon-Explorer orbiting optical reflectors, using pulsed ruby laser beams 09 p1341 A66-19902

Ruby laser energy reflected off Explorer XXII satellite 14 p2306 A66-27054

DME-A satellite attitude control, discussing performance of spin control system 21 p3821 A66-38879

Hydromagnetic wave propagation in magnetosphere, using Explorer satellite observations 24 p4198 A66-42434

**EXPLOSION**  
SA BLAST  
SA CHEMICAL EXPLOSION  
SA DETONATION  
SA DISCHARGE  
SA GAS EXPLOSION  
SA IMPLOSION  
SA LAMINAR FLAME  
SA METAL COMBUSTION  
SA NUCLEAR EXPLOSION  
SA THERMONUCLEAR EXPLOSION  
SA UNDERWATER EXPLOSION  
Theory of localized explosions in inhomogeneous atmosphere applied to initial phase of development of chromospheric flare 03 p0422 A66-12916

Test method evaluating explosive sensitivity, due to shock, of materials immersed in oxygen difluoride for application to rocket propulsion systems [CI PAPER WSCI-65-34] 05 p0743 A66-15150

Hypersonic perfect gas flow around slightly blunted plate, discussing analogy between asymptotic shock behavior and explosion theory 07 p0981 A66-18109

Effect on long shell of circumferential and uniformly distributed load /due to explosion/ at constant rate along shell 12 p1964 A66-24048

Theory of localized explosions in inhomogeneous atmosphere applied to initial phase of development of chromospheric flare 14 p2376 A66-27265

Elastoplastic properties of copper, aluminum alloys and brass under explosive load, noting increased temperature effect on elastoplastic wave parameters 14 p2314 A66-27370

Overpressure of liquid propellant explosion in vacuum and atmosphere 14 p2370 A66-27451

Internal fracture of spheroids caused by focusing explosive waves 17 p3027 A66-32636

Thermal self-ignition theory employing general functions of temperature characterizing reaction rate of explosive 19 p3477 A66-35741

Lead stearate effect on heat of explosion in nitro-cellulose propellant combustion at various pressure levels 20 p3626 A66-38041

Critical parameters in Poisson-Boltzmann equation of steady state thermal explosion theory, noting temperature gradient 20 p3680 A66-38047

Thermodynamic calculation of explosive properties of peracetic acid, using data from detonation wave to establish safe limits for use of acid 21 p3834 A66-38535

Explosive nature of chromospheric flares, effect of magnetic fields and thermoconductivity calculated, using mathematical model 22 p3975 A66-40852

Drop-weight tester/photographic apparatus for studying impact initiation-explosion process in nitroglycerin 23 p4119 A66-41243

Extended explosive charge giving rise to pressure waveform for analysis of sonic boom 24 p4159 A66-42417

**EXPLOSIVE**  
SA CHARGE  
SA HIGH EXPLOSIVE  
SA NITROCELLULOSE  
SA NITROGLYCERIN  
SA PENTOLITE  
SA PROPELLANT  
Drop-weight sensitivity of explosive liquids

tested with impact apparatus, showing increase with temperature  
[CI PAPER WSCI-65-28] 05 p0788 A66-15139

Drop-weight impact sensitivity testing of explosives  
[CI PAPER WSCI-65-27] 05 p0788 A66-15140

Gas compression-conduction mechanism contribution to shock initiation of granular explosives, analyzing surface temperature of interstitial gas and grain distribution  
[CI PAPER WSCI-65-30] 05 p0788 A66-15141

Combustion temperatures of explosives PETN, hexogyn and tetryl in constant pressure bomb in nitrogen atmosphere 08 p1316 A66-18795

Safety requirements for handling and testing unstable materials, particularly hydrazinium diperchlorate /HP sub 2/ solid propellant oxidizer 12 p1812 A66-24469

Explosive compaction of ceramic materials 12 p1900 A66-24720

Hugoniot equations of stage derived for several unreacted explosives and propellants from optical measurements of shock wave and particle velocities 13 p2171 A66-25377

Decomposition times of liquid nitromethane, liquid tetranitromethane and hexogen single crystals in shock waves 14 p2275 A66-27598

Blast environment simulation developing high pressures of relatively long duration, noting helical winding of cord explosive 16 p2681 A66-30501

Low velocity detonation in powder explosives 17 p3036 A66-32829

Approximate closed solutions for detonation velocity and pressure of condensed explosives 18 p3265 A66-34581

Explosive sensitivity of dust or sprays ignited behind reflected shock simulated by shock tube, measuring ignition delay dependence on shock temperature 20 p3680 A66-38039

Megagauss magnetic field generation by explosives and related experiments - Conference, Frascati, Italy, September 1965 21 p3773 A66-39501

**EXPLOSIVE DECOMPRESSION**  
Detonation and decompression research, comparing biological effects of explosive decompression and detonation 06 p0811 A66-16067

Biological effects of explosive decompression noting parameters such as altitude, pressure differential, compartment volume and rate of pressure loss 10 p1492 A66-22111

**EXPLOSIVE DEVICE**  
SA DETONATOR  
SA ELECTROEXPLOSIVE DEVICE  
Launching of beryllium, aluminum and steel projectiles up to 54,100 ft/sec 11 p1685 A66-22838

Behavior of pyrotechnic devices and explosives studied when heated to 145 degrees C for 36 hours /three separate times/ for development of dry-heat sterilizable equipment for space vehicles 13 p2014 A66-25288

Detonability of cryogenic oxidizers, discussing modified continuous wire technique analysis of detonation properties of trioxxygen difluoride 16 p2790 A66-31194

Explosive driven magnetic generator applied to investigate electric, optical and elastic properties of various substances, plasma physics and charged particle accelerator 16 p2637 A66-31585

Aerospace ordnance handbook intended as up-to-date reference on design and methodology of explosive systems used in space technology 18 p3159 A66-34184

Exploding bridgewire systems, discussing theory of wire explosion and various applications 18 p3135 A66-34191

Explosive separation systems for spacecraft compared with spring mechanism 20 p3665 A66-38264

Single explosive train for simpler safer shroud separation from spacecraft 20 p3665 A66-38265

Pulsed electrical power generation from detonation-driven linear MHD channels with magnetically located explosive 21 p3699 A66-39509

Behavior of pyrotechnic devices and explosives studied when heated to 145 degrees C for 36 hours /three separate

times/ for development of dry heat sterilizable equipment for space vehicles 24 p4260 A66-42784

**EXPLOSIVE FORMING**  
Explosion cladding for bonding similar and dissimilar metals without intermediate metal or externally applied heat 03 p0380 A66-12317

Safety measures in working with beryllium, discussing berylliosis prevention, dust reduction, protective suits, etc 05 p0687 A66-14862

Explosive welding of dissimilar alloy sheets 06 p0886 A66-16366

Critique of paper by Carter and Kennedy regarding origin of diamonds in Canyon Diablo and Novo Urei meteorite 09 p1447 A66-19881

Effect of water immersion on reduction of die stresses in explosive forming, investigating dynamic response of thin elastic spherical shell surrounded by large body of fluid, employing diagrams [ASME PAPER 65-PROD-6] 11 p1709 A66-22474

Aging behavior of explosively deformed 2219 Al investigated by transmission electron microscopy 13 p2086 A66-25775

Shock wave from explosion of laminar charges in air, water and vacuum 14 p2298 A66-26788

Explosive cladding for strong metal-metal bonds [ASTME PAPER AD66-112] 14 p2299 A66-26951

Metal hardening by explosive loading under near triaxial compression determined by charged power and independent of plastic deformation magnitude 15 p2523 A66-29599

Explosive technique for shaping low plasticity sheet metals by heating blanks with pyrotechnic agent in sand, with reference to Mo and Mg alloys 15 p2511 A66-29783

Underwater explosive stretch forming of clamped circular mild-steel blanks as affected by clamping ring and reflecting plate 16 p2709 A66-30268

Explosive forming process for deep aluminum shells, discussing limits and failure 17 p2930 A66-33091

Chemical energy conversion to electromagnet energy by flux compression, discussing process and obtained efficiency 21 p3698 A66-39502

**EXPLOSIVE GAS**  
SA GAS EXPLOSION  
Explosive hazard of gases generated by transformer potting materials of styrene-polyester copolymer, epoxy resin and polyimide resin when subjected to overloads 02 p0247 A66-11286

Asymptotic expansion applied to strong explosion in heat-conducting gas 07 p1025 A66-18181

Nonequilibrium chemical reaction effect on decay in spontaneous explosion for reactive expelled gas and inert expelling gas 08 p1179 A66-19482

Glass tube containing pressurized helium progressively imploded by coaxial explosive charge, considering application to hypervelocity guns 11 p1686 A66-22840

Explosive gas guns for hypervelocity acceleration 11 p1686 A66-22841

Detonation in gaseous mixtures and in condensed phase, reviewing aerodynamic theory 15 p2617 A66-29315

Exact analytic solution for propagation of spherical explosion waves in self-gravitating gas sphere 17 p3004 A66-32839

**EXPONENTIAL FUNCTION**  
Systematics of fission based on exponential mass formula, discussing neutron capture 02 p0263 A66-11835

Electric field effect on optical absorption edge, discussing exponential tail influence on magnitude of absorption coefficient 05 p0741 A66-15869

Noise rejection properties of time discrimination method of pulsed signals improved by using exponential rather than selecting function 08 p1182 A66-18916

Maximally reliable exponential prediction equations for data rate limited tracking servomechanisms 08 p1183 A66-18931

Large displacement bending of rods for



constant deformation cross section, negligible shearing forces and exponential stress-strain relation 08 p1314 A66-19580  
 Numerical integration of coupled first order ODE of greatly differing time constant 09 p1395 A66-20619  
 Convergence properties of exponential series expansions used as approximation in electrical network theory for real Schwartz distribution 11 p1724 A66-23423  
 Statistical distribution of first occurrence and recurrence of crossing of given level in continuous random process determined, using approximate forms and exponential distribution 13 p2116 A66-25141  
 Error bounds in phase-integral solution to differential equation with simple turning points 13 p2118 A66-25829  
 Functional integration analysis of exponential behavior of nonlinear feedback control systems 13 p2052 A66-26076  
 Calculus of functional differences particularly for case of exponential function 14 p2323 A66-27778  
 Thermal stratification and thermostability effects on turbulent diffusion approximated by Swinbank exponential wind profile 15 p2530 A66-28603  
 Reliability growth measurement via exponential smoothing, noting prediction of successive elements from given time series 15 p2508 A66-28805  
 Iterative derivation of approximation of real function by exponential series 15 p2527 A66-29056  
 Complex zeros of exponential polynomial in study of stability criteria for collisionless plane vacuum diode of infinitely heavy ions in interelectrode space 15 p2464 A66-29244  
 Book on ergodic problems in comparison theory and theory of diophantine, discussing residue distribution of polynomial of  $n$ th order modulo  $p$ , fractional parts of polynomial and exponential function 15 p2529 A66-29767  
 Necessary and sufficient condition for growth of solution to second order PDE with delayed arguments 16 p2733 A66-30742  
 Partial totals method of estimation for one parameter exponential model, comparing procedure with maximum likelihood, least squares and weighted least squares estimators 16 p2737 A66-31384  
 Integral representation providing one-to-one correspondence between functions of  $n$  complex variables and complex-valued harmonic functions of  $n$  plus 1 real variables 18 p3126 A66-33837  
 Real-order exponential function and application to describing creep process and to extrapolate 20 p3669 A66-37539  
 Unified approach to synthesis of orthonormal exponential functions with elements whose asymptotic order may be chosen arbitrarily and poles that may be real, complex or both 20 p3522 A66-37665  
 Methods for finding lower confidence bounds on reliability of item, noting reliabilities for items whose lifetimes follow Weibull distribution 20 p3574 A66-37966  
 Truncated sequential life acceptance tests of AGREE Task Group Three type, noting that such tests while useful are not optimum 20 p3574 A66-37968  
 Nonsteady helical flow of viscoelastic liquid contained in circular cylinder, noting occurrence of oscillations in fluid decaying exponentially with time 21 p3723 A66-38588  
 Heat transfer equation solution for ablating solid, assuming exponential temperature profile with numerical solution on digital computer by Runge-Kutta method 22 p3998 A66-40035  
 Airy and Weber equations solutions and relationships in terms of exponential function in connection with hydrodynamic stability and Orr-Sommerfeld equation 24 p4193 A66-42284

## EXPOSURE S RADIATION EXPOSURE EXPULSION

Computer-simulated mathematical model of thermal environmental effects on expulsion system design parameters for liquid-propellant gas-generator rocket engine [AIAA PAPER 66-686] 18 p3163 A66-34228

## EXTENSOMETER

Stress distribution measurement by vibration method, applying hand-held extensometer place by place on surface of structure subjected to dynamic load of finite amplitude [AIAA PAPER 65-785] 03 p0438 A66-13069  
 High temperature extensometer using linear variable differential transformer 07 p1030 A66-17230  
 Extensometer system and specimen alignment fixture for cylindrical or flat creep specimens 09 p1465 A66-19949  
 Longitudinal and transverse resistance-coefficients of thin film supporting materials, noting deformation resistance 13 p2107 A66-25460  
 Calibration method for tensile testing apparatus for testing elongated high modulus fibers and graphing of typical load elongation curves 17 p2943 A66-32400

## EXTERNAL STORE

### S NACELLE

## EXTINGUISHER

### S FIRE EXTINGUISHER

## EXTRACTION

S HYDROLYSIS  
 S ION EXTRACTION  
 S SEPARATION  
 S SOLVENT EXTRACTION

## EXTRAGALACTIC LIGHT

Radio and optical observations of discrete radio sources, evaluating flux density measurement, position, brightness distribution and polarization 20 p3645 A66-36959  
 Line-of-sight velocities in gas in peculiar extragalactic radio source NGC 4038-39 measured in orientations across object 23 p4129 A66-41805  
 Coordinates, flux densities and spectral indices of various radio sources believed to be extragalactic 24 p4273 A66-42416

## EXTRATERRESTRIAL ENVIRONMENT

### SA LUNAR ENVIRONMENT

### SA PLANETARY ENVIRONMENT

### SA SPACE ENVIRONMENT

Establishing absolute value for total wavelength integration of solar irradiance at Earth upper atmospheric limit and spectral distribution of this radiation 02 p0279 A66-11220  
 Survival of Earth organisms under environment simulated low pressure, low oxygen, low temperature and low extraterrestrial conditions 02 p0181 A66-11605  
 Physiological problems of weightlessness discussing motion sickness, fluid volume control and chronic effects on circulatory system 04 p0465 A66-14071  
 Dynamic environmental influences on man during space flight covering force fields, inertial forces due to acceleration and methods of protection 04 p0466 A66-14074  
 Solar spectrum measurement, discussing equipment design, testing and application [ISA PREPRINT 1.11-2-65] 05 p0684 A66-15511  
 Comet atmosphere analyzed for neutral particle distribution, acceleration and velocity variations relative to Sun, brightness, etc 10 p1605 A66-21207  
 Text on life into space covering space biology, extraterrestrial environment, temperature, pressure, acceleration, radiation effects, etc 10 p1492 A66-22062  
 Extraterrestrial environment and calculation of realistic metabolic requirements for astronauts 11 p1648 A66-23003  
 Space probe sterilization problems, noting methods employed, development requirements, monitoring of contamination, etc 13 p2012 A66-25266  
 Physiological study and instrumentation of pigtail Macaque under extended exposure to near-zero gravity environment 13 p2014 A66-25514  
 Meteoroid environment, meteoroid impact hazard on spacecraft structure and meteoroid shields 13 p2193 A66-25845  
 Penetration and absorption of solar optical, UV and EUV radiation in upper atmosphere /ionosphere, exosphere and ozone layer upper boundary/ 15 p2573 A66-28683  
 Microbiological and cytological experiments in Vostok spacecraft, noting behavior of

lysogenic E coli K-12 culture and normal and cancerous human cells 15 p2436 A66-294

Physiological reactions of Russian astronauts under prolonged weightlessness noting motor activity, heart and pulse breathing rates, arterial pressure, etc 15 p2436 A66-294

Immunological reactions of Russian spacemen before and after space flight 15 p2436 A66-294

Space flight effect on living cells examined by using higher plants as biological dosimeters 15 p2436 A66-294

Monograph on manned space flight discussing environment, crew, spacecraft navigation, guidance, control, communications, etc 16 p2809 A66-308

Oxygen reclamation for manned spacecraft considering stored, nonregenerative and molten carbonate systems 17 p2864 A66-321

Stress in spacecraft crew member measured using parotid fluid, noting relationship between biochemical variables under stress and nonstress conditions 17 p2866 A66-321

Attitude control system for OGC discussing design principles, space environment effects, reliability, etc 18 p3242 A66-338

Extravehicular maneuvering technique research, discussing manual locomotion methods, powered units, computer simulation, zero-g flight and space tests 19 p3291 A66-358

Automated biological laboratory with initial missions to Mars, noting functions operational and necessary instrumentation 24 p4167 A66-426

## EXTRATERRESTRIAL LIFE

### SA LIFE DETECTOR

Life on small extinct stars and large planets 01 p0133 A66-101

Possibility of life originating in different forms in various parts of universe response to changing environmental conditions 01 p0017 A66-103

Prevalence and diversity of life in Cosmos tracing divergent evolution in response variety of environment 01 p0017 A66-103

Extraterrestrial life or exobiology noting life possibility on Mars, Moon as possible information source, continuous generation matter in universe, etc 01 p0017 A66-104  
 Papers on experimental and theoretical aspects of exobiology 02 p0181 A66-116

Exobiology concepts suggest that apparent inherent limitations on temperature pressure or chemical environment for life matter are geocentric myths 02 p0181 A66-116

Astrophysical observation and experimental results of organic synthesis bearing abiogenic formation of biochemical compounds formed from simple precursor aqueous or aqueous ammonia system 02 p0181 A66-116

Lunar atmosphere and hydrosphere predicting dimensional correlation of craters and maria of primordial lunar life noting dark and smooth appearance 02 p0181 A66-116

Martian life possibilities discussing atmosphere, clouds, violet layer, temperature and biological interpretation dark areas 02 p0181 A66-116

Martian life-detection instruments and experiments, examining biological criteria and visual, organic, chemical and metabolic tests 02 p0183 A66-116

Radio search for intelligent extraterrestrial life, estimating civilization distribution frequency of best sensitivity and aggregate signal detection 02 p0191 A66-116

Exobiological trend and problems indicating types of organic matter on planet and origin and transfer of organisms in solar system 02 p0182 A66-116

Space travel and exploration covering biological and technical difficulties such as radiation, meteor impact, vehicle sterilization, etc 04 p0469 A66-138

Neurophysiological aspects of manned extraterrestrial space flights such as motor responses by sensory inputs, cortical responses, etc 04 p0464 A66-140

Biological characteristics and physical



conditions of space flights, such as low pressure, ionizing radiation, noise, acceleration, weightlessness, artificial atmosphere, feeding problems, etc 04 p0464 A66-14066

Future of environmental biology, discussing space research on living organisms in extraterrestrial environment 04 p0470 A66-14069

Heat loss in space, discussing temperature regulation during space walk via heat exchangers in air ventilated space suit 04 p0470 A66-14070

Telemetric Universal Sensor /TELUS/ describing measurement, processing and control of biological data from terrestrial and aerospace sources

ISA PREPRINT 1.2-2-65 05 p0683 A66-15506

Detection of microbial life on near planets by measuring physical parameters 06 p0810 A66-15909

Biosytlektes, device for collecting microorganisms in interplanetary space or upper atmospheric layers 06 p0814 A66-15914

Electrolysis-Hydrogenomonas bacterial bioregenerative life support system for manned space flight of long duration 06 p0815 A66-15929

Origination of organic matter and distribution of invisible bodies capable of supporting life 06 p0811 A66-16322

Extraterrestrial life detection and life support systems in manned space travel, noting electronic equipment necessary for it 08 p1175 A66-18727

Chemical composition of meteorites and micropaleontological evidence of existing meteoric biological carbonaceous chondrites 08 p1287 A66-18767

Spectral reflectance of selected vegetation, animal integuments and minerals for life detection on Mars 10 p1608 A66-21520

Martian life in light of Mariner IV data on adverse atmospheric composition, temperature and radiation 10 p1486 A66-21740

Mars environmental conditions, life organism detection, evaluation and limiting effects 11 p1771 A66-22715

Mineralogical, chemical and microscopic analyses of carbonaceous chondrites reveal presence of substances usually synthesized by living cells on Earth 11 p1771 A66-22744

Space travel and exploration and relationship to scientific research, with comments on exobiology 12 p1946 A66-23635

Space travel and exploration, biological and technical difficulties, radiation, meteor impact, vehicle sterilization, etc 12 p1807 A66-23640

Extraterrestrial life in solar system, discussing equipment for Mars exploration, noting Gulliver program, Multivator automatic biochemical testing apparatus and TV microscope 12 p1805 A66-23794

Extraterrestrial civilizations - All-Union Conference, Yerevan, Armenian SSR, May 1964 12 p1813 A66-23887

Communication with extraterrestrial civilizations 12 p1947 A66-23888

Detection of information transmitted by extraterrestrial civilizations 12 p1814 A66-23889

Information-bearing artificial signal from extraterrestrial civilizations is indistinguishable from natural noise 12 p1814 A66-23892

Possibility of detection of extraterrestrial civilizations by radio communications 12 p1814 A66-23893

Communication with extraterrestrial civilizations in radio wavelength range 12 p1814 A66-23895

Information theory techniques for search and analysis of radio signals from extraterrestrial civilizations 12 p1814 A66-23896

Approaches for analyzing possible life forms on other planets, noting detection of microorganisms or enzymes, radio contact and retracing life in laboratory 13 p2009 A66-25798

Nontechnical book on extraterrestrial life including origin of life, life signs in meteorites, Moon and Mars, man-machine combinations for space purposes, etc 13 p2011 A66-26317

Automatic chemical processing systems for

extraterrestrial biochemical investigations 14 p2233 A66-28414

Extraterrestrial life detection based on catalysis of oxygen exchange between labeled oxyanions and water, noting equipment 15 p2441 A66-29961

Pasteur Probe assay of asymmetry of D, L amino acids in detection of Martian life 15 p2447 A66-30025

Possible existence of plant life on Mars, judging from Mariner photograph data on Mars atmosphere and surface 16 p2798 A66-30356

Biogenesis, chemical evolution, detection of extraterrestrial life and future automated biological laboratory to explore Mars 16 p2798 A66-30361

Book on extraterrestrial biology covering origin processes of life, planets, life detection, etc 16 p2639 A66-30874

Engineering constraints involved in selection of Martian landing site for lander vehicles 18 p3232 A66-34367

Automated Biological Laboratory for Mars mission exobiological experiments controlled by computer routines 18 p3062 A66-34369

Processing of planetary soil samples for detection of extraterrestrial life 18 p3062 A66-34370

Mass spectrometry and gas chromatography in analysis of organic compounds present in extraterrestrial bodies to provide information on existence of life 18 p3059 A66-34373

Chemical composition of meteorites and micropaleontological evidence of existing meteoric biological carbonaceous chondrites 19 p3459 A66-35570

Mars probe instrument package design for biological exploration 19 p3287 A66-35572

Microorganism changes under extreme environmental factors, noting possible Martian life and meteoritic organic compounds 19 p3284 A66-35574

Possible adaptation of asteroids to support human life for indefinite periods of time 19 p3285 A66-36241

Book on possibility of extrasolar intelligence covering origin of planetary systems, development of life and terrestrial biological evolution 20 p3506 A66-37305

Book on natural evolution including origins of universe, stellar and planetary evolution, beginnings of life on Earth and development of intelligence and technical civilizations among galactic communities 24 p4163 A66-42347

Unmanned exploration of solar system - AAS Symposium, Denver, February 1965 24 p4274 A66-42653

Detection of extraterrestrial biological systems, noting criteria such as radiant energy requirements for life evolution, molecular characteristics, etc 24 p4164 A66-42669

Experimental biology in space, discussing goals, contributions and future potentials 24 p4164 A66-42670

Extraterrestrial life detection on Mars and limitations on terrestrial observations and flyby and landing missions 24 p4167 A66-42673

Wolf Trap Mars microorganism detection, assuming photosynthetic and respiration cycles in inorganic biochemical compounds 24 p4168 A66-42676

**EXTRATERRESTRIAL MATTER**

Terrestrial origin of pseudometeoritic Igast objects 08 p1298 A66-19596

Deposition of black magnetic spherules from atmosphere at two stations in New Mexico believed to be of extraterrestrial origin 09 p1370 A66-19879

Friedmann cosmological equation for noninteracting mixture of radiation and dustlike matter 14 p2380 A66-27275

Origin of tektites with Moon considered most likely extraterrestrial source 20 p3656 A66-38059

Sporadic E layer formation at night, noting ionization sources and intensity 23 p4064 A66-41645

**EXTRATERRESTRIAL RADIATION**

**S PLANETARY RADIATION**

**S SPACE RADIATION**

**EXTRAVEHICULAR OPERATION**

**SA ASTRONAUT LOCOMOTION**

DOD Gemini experiment D-12 astronaut

maneuvering unit /AMU/ design, detailing propulsion, flight control, oxygen and power supply, abort-alarm and communications 02 p0294 A66-11643

Extravehicular mobility unit /EMU/ to be worn by astronauts on Apollo lunar landing mission 08 p1176 A66-18584

Orbital flight of cosmonauts Beliaev and Leonov on March 18, 1965 includes description of spacecraft and extravehicular activity 09 p1464 A66-20460

Integrated space suit, suit loop and backpack system for intravehicular operation on interplanetary missions 13 p2013 A66-25277

Mathematical model study of three-mass retrieval technique using anchor mass in space for future Gemini extravehicular operation 16 p2812 A66-31538

Simulated orbital flights with extravehicular activities, determining incidence and severity of flyers bends due to decompression and exercise 17 p2856 A66-32148

Ideal operation of portable life support system /PLSS/ requires anticipatory response to astronauts changing heat dissipation needs 17 p2863 A66-32152

Space maintenance and extravehicular activities - National Conference, Orlando, Florida, March 1966 19 p3289 A66-35946

Extravehicular space activities related to assembly and maintenance of large space stations, antennas and solar collectors 19 p3290 A66-35947

Very rapid-curing capsular adhesive developed for use in astronaut-to-space vehicle attachment device 19 p3363 A66-35949

Applicability of electron beam welding techniques for in-space welding and maintenance, examining fabrication of typical aerospace joints 19 p3363 A66-35951

Tool fastener interface problems peculiar to extravehicular environment examined by measurement of torque and linear /or push-pull/ forces 19 p3363 A66-35952

Extravehicular astronaut maneuvering and retrieval using thrusting devices and tether lines 19 p3290 A66-35956

Low-thrust jet fitted shoe for zero-gravity movement 19 p3290 A66-35957

Astronaut maneuvering unit, discussing experiments, performance requirements, design concepts, system tradeoffs, packaging and configuration 19 p3290 A66-35958

Remote maneuvering unit, discussing principle, functions, feasibility, composition and application 19 p3469 A66-35959

Extravehicular maneuvering techniques research, discussing manual locomotion methods, powered units, computer simulation, zero-g flight and space tests 19 p3291 A66-35960

Modular maneuvering unit for crew members providing independent propulsion, life support, power supply and communication capability 19 p3450 A66-35961

Computer simulation and performance prediction of MMU astronaut maneuvering system, discussing acceleration, velocity, displacement, fuel consumption, propulsion efficiency 19 p3291 A66-35964

Gemini extravehicular spacecraft maintenance experiments under simulated conditions 19 p3364 A66-35965

T-27 Space Flight Simulator, for extravehicular activity training, utilizing closed-circuit TV system 19 p3291 A66-35966

Extravehicular activities interface with data recording system and economical recovery of optimum quantity of data 19 p3291 A66-35967

Extravehicular activity /EVA/ mission simulation, discussing design parameters effect on operating characteristics 19 p3469 A66-35969

Hard shell constant-volume pressure suit affords secure self-contained extravehicular environment capable of fulfilling variety of space maintenance roles 19 p3291 A66-35971

Extravehicular environment and mobility constraints affecting design of anthropomorphic space suit for working astronaut 19 p3291 A66-35972

Controller, employing voice recognition principle, for attitude control system of astronaut maneuvering unit in various space tasks 19 p3291 A66-35973



Spacecraft in-flight interior and exterior maintenance problems for long missions 19 p3469 A66-35975  
Extravehicular activity during Voskhod II flight, discussing motion and orientation of Soviet cosmonaut in space 21 p3701 A66-39337

## EXTREMUM VALUE

## SA GUMBEL THEORY

Search theory extremal problems, considering theorems in terms of maximum principle for finding optimal strategy 01 p0051 A66-10734  
Gravitational potential gradient for body consisting of positive or negative masses with known density extremum value and known or unknown volumes 04 p0514 A66-13449

Simplest system of auto-oscillatory extremal control, examining control plant output law 04 p0502 A66-13701

Theory of differential equations discussing extremal problems for generalization of optimal control problem 04 p0505 A66-13994

Extremal problems in aerodynamics, discussing mathematical and physical models for optimum aerodynamic shape 04 p0455 A66-13995

Extremum problem connected with simultaneous approximations of some functions analyzed by polynomials and derivatives 04 p0540 A66-14467

Extremum problems with asymmetrical supplementary conditions in certain classes of analytical functions 04 p0540 A66-14468

Solution of extremal problems of celestial mechanics 05 p0764 A66-15318

Extreme properties of operator which degenerates to trigonometric polynomials in case of periodic functions 05 p0709 A66-15358

Necessary conditions for extremum in problems of control with aftereffect 10 p1518 A66-21975

Existence and convergence theorems for minimizing sequences for extremum problems in presence of constraints 10 p1551 A66-21978

Asymptotic conditions of extremum as function of small parameter in calculus of variation 11 p1723 A66-23327

Gumbel theory of extreme values as statistical technique in reliability problems, with emphasis on double exponential distribution 12 p1833 A66-24084

Maximum information principle applied to search for minimum of function 13 p2028 A66-26475

Simplest system of auto-oscillatory extremal control, examining control plant output law 15 p2469 A66-28542

Variational problem in Banach space including optimal control problems, deriving conditions for extremality and Pontryagin maximum principle 15 p2473 A66-29378

Graphic analysis of behavior of stepwise extremal control system adapted to process showing inertia after static characteristic 16 p2668 A66-30585

Graphical analysis of extremal control system stepwise adapted to process with extremal characteristic located between two first-order linear operators 19 p3324 A66-35582

Extreme value statistics estimation of low error probabilities in binary communication systems 19 p3301 A66-35688

Self-oscillations of pulse type extremum system with plant having extremal characteristics shaped by multiplication of two coordinates 19 p3325 A66-35985

Invariance effect for finite number of coordinates in infinite dimensional automatic control system 19 p3325 A66-35986

Necessary conditions for extremum in problems of control with aftereffect 19 p3330 A66-36185

Existence and convergence theorems for minimizing sequences for extremum problems in presence of constraints 19 p3390 A66-36188

Existence and properties determined for most effective sequential method of seeking argument value at which continuous function of one variable assumes extremum value 19 p3391 A66-36659

Absolute extremum existence in boltz-mayer-type variational problem established by optimality principle 19 p3472 A66-36843

Low error probabilities in binary communication systems estimated by statistics of bivariate extreme-value theory 20 p3514 A66-37211

Dynamic programming for optimal algorithm for external control in presence of noise at system input and output 20 p3538 A66-37746

Relationship of earliest failures to fleet size and parent population 20 p3573 A66-37956

Extension of extremum principles concerned with velocity fields for boundary value problems of incompressible rigid viscoplastic /Bingham/ solid 21 p3832 A66-39440

Optimizer for shaping control signal of hunting-type system with plant in form of nonlinear inertialess element, examining inadequacy for system operation 22 p3883 A66-39659

Successive approximation method for optimization of nonlinear systems of ordinary differential equations with limitations on phase coordinates 23 p4084 A66-41352

Search theory extremal problems, considering theorems in terms of maximum principle for finding optimal strategy 24 p4232 A66-42750

## EXTRUSION

## SA COLD WORKING

Extrusion, reextrusion and drawing of tungsten and tungsten-rhenium alloy tubing 05 p0688 A66-15067

Extrusion process for complex beryllium structures, noting die-wear problem 08 p1230 A66-18843

Stress rupture of double extruded wrought alloy of cast nickel-base superalloys 12 p1895 A66-24373

Extrusion of refractory metal alloys at 5000 degrees F [ASTME PAPER MF66-108] 14 p2299 A66-26949

Extruded tungsten composites containing fibered or reacted additives examined, noting stress rupture life, temperature effect, creep properties, density, hardness, etc 16 p2723 A66-30639

Extrusion spinning method for fabricating refractory metals such as tungsten provides maximum material yield compared to normal tube extrusion processes 19 p3369 A66-36129

Extrusion of viscous incompressible substance through round hole in infinite wall, obtaining pressure and velocity fields 23 p4057 A66-41738

Extrusion of viscous incompressible substance through round hole in infinite wall, obtaining pressure and velocity fields 23 p4057 A66-41738

SA LENS  
SA OCULAR CIRCULATION  
SA RETINA  
SA VISION

Schoen hypothesis concerning image arrival time at cortex, depth values, retinal input, stereopsis, etc 17 p2862 A66-33089

Computer ray tracing study of image-forming in eyes as affected by pupil size, refractive indices and curvatures of cornea and lens 23 p4025 A66-41149

EYE DISEASE  
S GLAUCOMA  
EYE MOVEMENT

Basic physiological oculomotor mechanisms that make human image stabilization possible, examining flight disturbance effect on system stability 01 p0019 A66-10607

Oculomotor responses to vestibular and optokinetic stimuli during eight-turn spins in jet trainer aircraft 01 p0020 A66-10612

Visual acuity definition and clinical measurement of relevant factors 04 p0462 A66-13793

Influence of eye lid movement upon electro-oculographic recording of vertical saccadic eye movements 07 p0999 A66-17662

Contribution of accommodation and eye movements to effectiveness of visual observation and tracking of objects by aircraft personnel 10 p1490 A66-22133

Interaction between optokinetic and vestibulo-ocular responses during head rotation in various planes 11 p1643 A66-22583

Eye control in relation to visual process, showing derivation of position information from pointing of eyeball 12 p1807 A66-23645

Neuron network model of oculomotor system to understand human eye movement 13 p2008 A66-25336

Human eye, capabilities as optical instrument, particularly spatial filtering effects, visual acuity, eye movement and light receptors 14 p2228 A66-27650

Otolith organ activity within Earth standard, one-half standard and zero gravity environments and effect of extralabyrinthine factors effect upon counterrolling 15 p2431 A66-28664

Prolonged optokinetic stimulation effect on rabbits studied by corneoretinal potential changes during eyeball motion 15 p2437 A66-29471

Urinary excretion of 3-methoxy-4-hydroxymandelic acid during dreaming sleep in man 16 p2638 A66-30633

Pilot eye movement data by recording eye fixations on flight instruments 16 p2644 A66-31273

Biochemical experiments aimed at explaining rapid eye movement sleep /REMS/ 16 p2641 A66-31391

Gaze direction lead during slow patterns of head movement 17 p2865 A66-32179

Electrophysiological study of pituitary adrenal axis activation during rapid eye movement /REMS/ in human urology patients 17 p2859 A66-32303

Eye movement data used for studying nonvisual processes involved in oculomotor patterns 18 p3059 A66-34191

Pulse stimulated eye response cancellation due to information contained in subsequent pulse with longer duration 20 p3504 A66-36944

Illusion theory to explain differences between true motion of figure and apparent motion, emphasizing geometric effect in changes in retinal images 20 p3504 A66-36944

EYE PROTECTION  
Protection devices against vision impairment occurring during exposure of airmen and military personnel to intense visible radiation 01 p0019 A66-10482

Overall profile of ophthalmic injury associated with ionizing and nonionizing electromagnetic radiation fields based on human response to radiation exposure 01 p0018 A66-10793

Hazards, effect, safety and precaution for prevention of physical injuries from laser radiation 04 p0529 A66-13694

High altitude visual flight environment discussing sky brightness, instrument and runway lighting, visual fields, eye protection, etc 10 p1494 A66-22133

Protection and hazard to eyes of uninformed operators and bystanders from laser light 14 p2309 A66-27668

Eye patch and flashblindness protection 22 p3857 A66-39794

Explosive lens flash blindness protection system consisting of flight helmet to support goggle lens, sensing device and discriminator unit 24 p4168 A66-42853

## F

## F-1 LAYER

Improved F-1 layer prediction system that can be used to predict maximum usable frequency /MUF/ for northern latitudes 07 p1000 A66-17213

Longitudinal variations of various characteristics of F-1 layer compared for periods of high and low solar activity 12 p1869 A66-24271

Dependence of electron concentration in F-1 layer on zenith angle of Sun 15 p2486 A66-29092

Measures of electron production and loss and scale height of F-1 layer during summer solar minimum 22 p3916 A66-40806

F-1 layer formation as affected by solar activity, seasons and time of day 24 p4202 A66-42761

F-2 LAYER  
Electron concentration-distribution data for ten quiet days during spring 1958 in F-2 layer 01 p0063 A66-11027

Computer program for average values of critical frequency of F-2 layer and deviation 02 p0224 A66-12125

Magnetic activity effect on F-2 region drifts and variation with time at low



latitude station 03 p0361 A66-12633  
 Correlation dependence of F-2 layer on solar wave energy entering Earth atmosphere 04 p0515 A66-13850  
 Comparison of diurnal variations of ionization level in F region at geographically and geomagnetically conjugate stations in Arctic and Antarctic 04 p0516 A66-13851  
 Critical frequency of F-2 layer at Huancayo and variation with magnetic activity at different epochs of solar activity 04 p0517 A66-14378  
 Ambipolar diffusion in magnetic field showing plasma equations of momentum-transfer yield unambiguous steady state solutions 05 p0669 A66-14943  
 Variation in dispersion and asymmetry of F-2 layer critical frequencies, plotting particular secular variations 06 p0950 A66-16593  
 Geomagnetic sudden-commencement storms effect on electron concentration in F-2 layer above Europe 08 p1215 A66-19082  
 True height variations of F-2 layer for bay disturbances of geomagnetic field obtained from ionograms, assuming they are caused by horizontal electric field 08 p1216 A66-19213  
 Power series solution of F-2 layer diffusion equation, calculating equilibrium electron density from equatorial profile 08 p1216 A66-19215  
 Ionospheric F-2 region equatorial anomaly may not be caused by geomagnetic field 08 p1217 A66-19217  
 Improved HF prediction using ray tracing techniques to determine F-2 layer scale heights and scale height h for alpha-Chapman electron density distribution 08 p1217 A66-19218  
 Harmonic analysis of diurnal changes in critical frequencies of F-2 layer as function of season and solar activity 08 p1285 A66-19777  
 Dependence of variations in critical F-2 ionization on solar activity 08 p1220 A66-19791  
 Electron density distributions in daytime F-2 layer and dependence on neutral gas, ion and electron temperatures 11 p1699 A66-23135  
 Satellite data indicates correlations between cosmic ray variations and radiation intensity of radiation belts and related phenomena 12 p1941 A66-24170  
 Fluctuations in diurnal variations of ionization of F-2 layer interfering with radio wave propagation determined by series expansion 12 p1869 A66-24270  
 Relation between magnetic activity and ionospheric disturbances in F-2 layer studied on basis of 30-year data 12 p1870 A66-24285  
 Statistical distribution of monthly median noon critical frequency of F-2 layer from ionospheric stations at mid-latitudes, auroral regions and at polar cap 12 p1870 A66-24286  
 Effects of solar flare radiation on electron density of F-2 layer at maximum level in and near equatorial anomalous zone 12 p1944 A66-24834  
 Solution of continuity equation for electrons leads to high loss rate in prenoon maximum of electron density in F-2 layer 14 p2283 A66-27397  
 Lunar tidal variations in monthly median noon critical frequency in American zone during low solar activity 14 p2285 A66-27727  
 Computer program for average values of critical frequency of F-2 layer and deviation 14 p2287 A66-28083  
 Cyclic variations in maximum electron concentration of F-2 layer with solar activity explained by upper atmosphere temperature variations 15 p2486 A66-29093  
 Fast phase fluctuations of signal reflected from F-2 layer 15 p2451 A66-29094  
 Critical ionization frequencies in F-2 layer in near-polar region observed at Northern Hemisphere high latitude stations 15 p2487 A66-29107  
 Cyclic curves of F-2 layer critical frequencies based on seasonal phase variations in solar cycle 15 p2488 A66-29108  
 Spectrum analysis of critical frequency of F-2 layer 16 p2692 A66-30330  
 Day-to-day variations in F-2 critical frequency 16 p2693 A66-30339  
 Microbarographic analysis of troposphere-

ionospheric storm relationship, ground level pressure fluctuations and polar region traveling pressure waves 17 p2920 A66-33088  
 Initial disturbances in F-2 layer at middle latitudes during magnetic storms which begin with sudden commencement and relation to magnetic field changes 17 p2922 A66-33353  
 Contribution to dependence of variation of unperturbed ionospheric F-2 critical frequencies on season and solar activity 18 p3105 A66-34097  
 Nature of middle-latitude ionospheric perturbations 19 p3344 A66-35262  
 Anomalous enhancement of F-2 ionization in high latitude around geomagnetic noon due to formation of irregularity or new layer around locality 20 p3658 A66-38234  
 Harmonic analysis of diurnal changes in critical frequencies of F-2 layer as function of season and solar activity 21 p3809 A66-38773  
 Dependence of variations in critical F-2 ionization on solar activity 21 p3733 A66-38787  
 Mean variation of electron density profile of ionosphere above Lindau/Harz, noting semiannual variation of F-2 layer peak height related to solar activity 22 p3908 A66-39965  
 Seasonal anomaly of F-2 layer critical frequency partially explained by assumed electron-ion flux flowing between magnetically conjugate points from summer to winter hemisphere 22 p3908 A66-39966  
 Lunar tidal effects on noon real-height F-2 electron density profile data from two-year interval 22 p3908 A66-39967  
 Simultaneous long term ionospheric variation in midday averages of critical frequency E and F-2 at Washington, D.C. before and after increased geomagnetic activity 22 p3914 A66-40560  
 Anomalous enhancement of ionospheric F-2 region electron density at post-sunset time in low and equatorial latitudes 24 p4198 A66-42462  
 Optimum communications working frequencies for F-2 layer reflection selected with aid of communications reliability function 24 p4176 A66-43160

#### F-4 AIRCRAFT

General Electric self-adaptive control effect on airframe handling quality characteristics in F-4A aircraft 01 p0098 A66-10006  
 Automatic and semiautomatic vectoring and landing capability of U.S. Navy carrier-based aircraft F-4G Phantom II 01 p0099 A66-10009  
 Boundary layer control/BLC/ high lift system used as integral part in design of F-4 Mach 2 plus Navy interceptor [AIAA PAPER 65-714] 01 p0013 A66-10951  
 Boundary layer control/BLC/ high lift system used as integral part in design of F-4 Mach 2 plus Navy interceptor [AIAA PAPER 65-714] 12 p1801 A66-24095  
 Digital testing techniques for analog systems, describing bomb computer set for Phantom F-4D aircraft 20 p3522 A66-37246  
 General Electric self-adaptive control effect on airframe handling quality characteristics in F-4A aircraft 23 p4088 A66-40982

#### F-5 AIRCRAFT

F-5/T-38 design philosophy to meet rigorous operational and maintenance requirements 01 p0010 A66-10094  
 Northrop F-5 as supersonic tactical fighter [AIAA PAPER 65-778] 03 p0320 A66-12593

#### F-8 AIRCRAFT

Glide slope direct lift control of carrier landings, discussing trim change with actuation and longitudinal stability and control 07 p0986 A66-17272  
 Investment cast 17-4PH incorporated into actuating and supporting mechanism double droop leading edge of wing of F-8E/FN/ French Crusader 17 p2929 A66-32693

#### F-27 AIRCRAFT

S FOKKER F-27 AIRCRAFT

#### F-28 AIRCRAFT

S ENSTROM F-28 HELICOPTER  
 S FOKKER F-28 AIRCRAFT

#### F CENTER

Decay of F-center excitations in alkali halides induced by short intense pulse of Q-switched ruby laser 08 p1275 A66-19367

Strong electron-phonon interaction which couples electron to lattice motion in F center of alkali halide crystal by measuring temperature dependence of F center absorption and emission bands 15 p2559 A66-28629

#### F LAYER

Nondeviated absorption of radio waves in intermediate region between E and F layers 01 p0031 A66-11051  
 MHD absorption of internal gravitational waves in ionospheric F layer in terms of traveling disturbances 02 p0283 A66-12116  
 Equatorial F-region electron density distribution is natural steady state distribution for charged fluids as shown by momentum transport equation for charged gaseous fluids 03 p0364 A66-12678  
 Radar echoes explained in terms of backscatter from field-aligned irregularities in F region 03 p0334 A66-12679  
 Photoelectron energy distribution in F region 03 p0364 A66-12684  
 Magnetoionic splitting of radio signal in E and F layers, comparing calculated and theoretical gyrofrequency values 04 p0482 A66-13861  
 Dense sporadic E cloud effects on high latitude HF backscatter observation 05 p0667 A66-14792  
 Ionospheric F region electron density and electron and ion temperatures measured by ground-based radar backscatter 05 p0670 A66-14950  
 F-layer behavior over Genoa-Monte Capellino noting diurnal and seasonal variation, solar activity, nighttime concentration, spread-F, ionospheric and geomagnetic perturbations 05 p0671 A66-14982  
 Airborne ionospheric probes on both sides of magnetic equator at low African latitudes during equinoctial and solstice periods, obtaining daily behavior of F layer 05 p0674 A66-15113  
 F-layer structure at subauroral and auroral latitudes measured by multifrequency beacon satellite Explorer XXII 08 p1212 A66-18610  
 Electron concentration profiles above maximum of F layer calculated from measurements made on Earth surface 08 p1213 A66-19026  
 Ionograms showing satellite traces interpreted as inverted trough disturbance traveling in F region 08 p1216 A66-19212  
 Thermospheric heating effect on F-region ionization and electron density in daily basis study 08 p1218 A66-19404  
 Long-period acoustic-gravity waves launched into F region by Alaskan earthquake of March 28, 1964 08 p1219 A66-19418  
 Upper atmospheric parameters that control daytime electron density distributions in F-1 region determined with use of N/h/ profiles 09 p1372 A66-20369  
 Latitudinal dependence of sunrise effect in F region determined from Schermerling data for four ground stations 09 p1373 A66-20383  
 Effect of Soviet atmospheric nuclear explosions on D and F-2 ionospheric layers, particularly observing enhancement of atmospheric noise 10 p1600 A66-22058  
 Seasonal variation of F-region parameters at sunspot minimum, noting effects of ionospheric disturbances 11 p1695 A66-22368  
 Ground diffraction pattern caused by radio wave reflection from F region, using array of three aerias 11 p1651 A66-22374  
 Measurement of horizontal ionospheric drifts in E and F regions over magnetic equator 11 p1696 A66-22381  
 Effective electron collision frequency from electron temperature profile for ionospheric heating in F region 11 p1697 A66-22499  
 Midlatitude trough in F-region ionization of night ionosphere revealed by ion trap on polar-orbiting satellite 11 p1699 A66-23134  
 Diurnal and seasonable altitude variations of E and F layers analyzed for geomagnetic activity from rocket measurement of electron concentration 12 p1869 A66-24269  
 Ionograms made at Australian ionosonde stations during magnetically quiet world day interval, obtaining information on F region ionization, noting existence of universal time control of ionization 12 p1873 A66-24835



Unique ionospheric electron density distribution from ionograms from valley between E and F region 14 p2283 A66-27126

MHD absorption of internal gravitational waves in ionospheric F layer in terms of traveling disturbances 14 p2286 A66-28075

Electron concentration inhomogeneities during traveling gravity wave propagation through F layer 15 p2485 A66-29084

Electron-concentration distribution in ionospheric F-2 layer with vertical distribution of electron-ion gas 15 p2486 A66-29096

Relation between solar radiation and electron concentration up to F layer analyzed in winter and summer 15 p2487 A66-29106

Nightglow emission from atomic oxygen caused by dissociative recombination in F region 16 p2694 A66-30707

F-layer nightglow 6300 angstrom emission intensity and electron density data, noting variations in emissions 16 p2694 A66-30708

Maximum ionization in ionospheric F region around geomagnetic equator, noting instruments and observed variations 16 p2697 A66-30995

Equatorial ionospheric drifts observed at Ibadan, Nigeria, during solar activity minimum, and relation to diurnal variation of sunspot cycle and drift velocity variations in E and F region 16 p2700 A66-31759

Spread F and ionospheric F region irregularities relation to magnetic field alignment, discussing radio star scintillations 17 p2923 A66-33433

Temporal variations in temperature and drift velocity in ionosphere determined from nighttime variations of F-region electron density profiles at Puerto Rico 18 p3107 A66-34522

Magnitude of vertical drifts in F-region during high and low sunspot years, considering effect of ambipolar diffusion along geomagnetic lines of force 19 p3347 A66-35923

Separation of D-E and F-layer contribution to integral absorption of cosmic noise by means of combined pulse reflection and cosmic noise measurements 19 p3351 A66-36363

Pressure gradients in F region from model atmosphere, estimating from motion equations variation of magnitude and direction of wind with local time, season and epoch of solar cycle 19 p3352 A66-36626

Very steep latitudinal electron density gradients in topside F layer at high altitudes 20 p3554 A66-38197

Latitudinal variation of Pc-1 micropulsation propagation, examining attenuation by ionospheric F region duct that acts as waveguide for hydromagnetic waves 20 p3554 A66-38203

Successive hourly variations of equivalent current systems of magnetic bay disturbance patterns and F layer minimum frequency increases 20 p3658 A66-38232

Attachment coefficient and temperature dependence of ionic reactions in F layer for various activation energies 22 p3908 A66-39968

Electron density and electron and ion temperatures in F region studied by ground-based radar observations at Millstone Hill 22 p3909 A66-39976

Diurnal variation in electron densities and temperatures in F region above Puerto-Rico, using backscatter measurements 22 p3910 A66-39978

F layer electron temperature fluctuations and resultant electron density changes in daytime 22 p3910 A66-39980

Dependence of seasonal occurrence probability of F-zero layer on level of geomagnetic activity and ionospheric activity observed above Ashkhabad 22 p3914 A66-40760

Nighttime electron temperatures in upper F region suggest corpuscular energy input 23 p4064 A66-41682

Ionospheric electron content at temperature latitudes during declining phase of sunspot cycle determined by observation of Faraday effect 24 p4200 A66-42595

Decrease in electron density of ionospheric F region following passage of powered rocket 24 p4201 A66-42609

Magnetospheric phenomena related to geomagnetic tail noting F region, polar auroras and solar Lyman alpha radiation scattering in night sky 24 p4203 A66-43029

**F-104 AIRCRAFT**

F-104J production program from Japanese standpoint [AIAA PAPER 65-804] 03 p0446 A66-12600

Worldwide F-104 program, discussing licensing agreements and weapons system management [AIAA PAPER 65-776] 03 p0447 A66-13065

NASARR international program concerning F-15 fire-control systems for F-104 Starfighter [AIAA PAPER 65-777] 03 p0447 A66-13066

**F-110 AIRCRAFT**

**S F-4 AIRCRAFT**

**F-111 AIRCRAFT**

Flight development of F-111 swing wing fighter in A strike and B interceptor versions for Air Force and Navy 03 p0317 A66-12534

General Dynamics/Grumman multimission variable-sweep fighter for Navy and Air Force 04 p0458 A66-13930

Flight test report of F-111 aircraft, considering variable wing sweep, stability augmentation in automatic gains, high performance with slow speed takeoff and landing 07 p0986 A66-17273

F-111 swing-wing /variable-sweep/ aircraft program 11 p1637 A66-23101

Systems effectiveness and F-111, concept, cost, applicability, reliability, performance, etc, and use during F-111 aircraft development 11 p1789 A66-23440

Mark II avionics system used in F-111A tactical fighter for navigation and weapons delivery performance 18 p3076 A66-33958

Program management at subsystem subcontractor level for product reliability and maintainability in developing AN/APQ-110 terrain following radar for F-111A 20 p3685 A66-37914

Maintainability program of F-111B aircraft 20 p3574 A66-37961

**FABRIC**

**SA PARACHUTE FABRIC**

Glass, quartz, mineral and ceramic fibers woven into fabric provide thermal insulation, reinforced plastic, filtration, friction materials and electrical insulation 01 p0091 A66-10356

**FABRY-PEROT INTERFEROMETER**

Multichannel Fabry-Perot interferometer noting design, application, construction, calibration and measurements on plasma 02 p0232 A66-12201

Fabry-Perot interferometric modulator for laser beam, noting error of precise alignment of reflecting surfaces and Gaussian type of imperfections 02 p0232 A66-12202

Plasma electron concentration measured by Fabry-Perot interferometer partially filled with gas-discharge plasma and incorporating ruby laser 03 p0375 A66-12294

Optical interferometric, spectrographic and microwave techniques of electron-ion recombination in neon-spectral line 03 p0394 A66-12330

Fabry-Perot resonators compared with cavity resonators and microwave interferometers for plasma diagnostics, noting electron density application 03 p0398 A66-12525

Intensity distribution in Fabry-Perot interferometer producing resonant waves for large Fresnel number applied in model for filament-form laser mechanism 03 p0379 A66-13097

UHF Fabry-Perot interferometer for measuring low plasma electron density 04 p0518 A66-13475

Fabry-Perot interferometer and confocal and spherical resonator, calculating integral equations for eigenvalue and eigenfunction of lowest order TW eigenmode 04 p0523 A66-14277

Fabry-Perot fine etalon in astronomical use such as H-alpha emission line profile measurement 05 p0681 A66-15213

Fabry-Perot interferometer using wire grids instead of glass plates, covering operation, advantages and bandwidth characteristics 05 p0682 A66-15355

Mode losses of single iteration in confocal

beam waveguide resonator and transmission systems with circular lenses separated by twice focal length 06 p0848 A66-1610

Coherent amplification coefficients of neon lines in helium-neon 08 p1234 A66-1931

mixture Isotope shift measurement for 632 angstroms helium-neon laser transition 10 p1540 A66-2107

Estimation of incidence angles for which resolution limit of real Fabry-Perot etalon approaches value of ideal etalon 10 p1537 A66-2203

Fabry-Perot interferometer with mirrors in form of metallic strips to facilitate use in far IR and microwave spectral regions 11 p1704 A66-2234

Fabry-Perot interferometer with mirrors in form of backed metal grid, noting change in diffraction, reflection and transmission 11 p1704 A66-2234

Interferometer apparatus used in combination with Fabry-Perot etalon to study properties of low density atomic streams 11 p1709 A66-2329

Atomic oxygen night sky emission observations with pressure scanning Fabry-Perot interferometer 12 p1873 A66-2483

Fabry-Perot interferometer adjustment for reflectance of narrow-band dielectric reflection coating peaked in UV spectral region 13 p2081 A66-2600

Spectral energy distribution and Doppler broadening of Rayleigh light scattered from hydrogen and argon gas at low density using Fabry-Perot interferometer 13 p2133 A66-2610

High resolution piezoelectrically scanned Fabry-Perot interferometer used to study gain profiles, mode structures and emission line widths of CW Ar, Kr and Xe ion laser and Hg-He pulsed laser 13 p2102 A66-2620

Ruby laser monochromatic radiation separation by tapered multiplex interferometer with opposition dispersion 13 p2082 A66-2643

High Q Fabry-Perot interferometer for measurement of atmospheric gas losses, particularly water vapor absorption, using coherent light source in 100-300 frequency range 15 p2501 A66-2900

Laser oscillation with totally reflecting roof prism as cavity, noting output mirror alignment for two rotation axes 15 p2517 A66-2943

Estimation of incidence angles for which resolution limit of real Fabry-Perot etalon approaches value of ideal etalon 16 p2706 A66-3083

Multiple beam interferometer theory noting discrepancy between intensity distribution and Airy formula determination of theoretical resolving power 16 p2706 A66-3093

K-band Fabry-Perot resonator using planar and concave mirrors, determining overvoltage factors in interferometer, noting diffraction losses 16 p2707 A66-3123

Particle velocity in gas particle two-phase nozzle expansion using gas laser and Fabry-Perot interferometer for rocket engine propulsion [AIAA PAPER 66-522] 16 p2708 A66-3153

Electron density of plasma measured by multibeam Fabry-Perot radio interferometer 17 p2963 A66-3183

Transmission characteristics of Fabry-Perot aluminum-magnesium fluoride-aluminum interference filters in far UV region, noting preparation methods, optical properties etc 17 p2958 A66-3263

Fabry-Perot etalon use for interferometry and laser control, noting low angle scattering, laser oscillation, thermal tuning sensitivity, etc 17 p2925 A66-3263

Methane content of upper atmosphere determined by Fabry-Perot interferometer measurement of radiation transmission methane absorption band 17 p2926 A66-3293

Solar radiation and lunar observations at submillimeter wavelengths using Fabry-Perot interferometer 17 p3005 A66-3303

Stability of Fabry-Perot etalons with larboss areas 18 p3111 A66-3393

Automatic control of spacing of Fabry-Perot interferometers to transmit at given wavelength 20 p3558 A66-3723

Tunable birefringent Fabry-Perot



- interferometer used in study of solar magnetic fields, using Zeeman effect 20 p3558 A66-37289
- Laser emission interferograms obtained with Fabry-Perot cross-grating interferometer in submillimeter wavelength range 20 p3559 A66-37546
- Optical spectra of ultrashort optical pulses generated by mode-locked glass-doped neodymium lasers, considering saturable absorber cell placed parallel to Fabry-Perot reflector 21 p3747 A66-39115
- Laser amplifier theory using Fabry-Perot interferometer and Laplace transform for obtaining transient solutions in addition to steady state solutions 21 p3748 A66-39224
- Fabry-Perot interferometer in spectroscopy using satellites and 22 p3920 A66-40793
- rockets
- Interference filter of Fabry-Perot interferometer-type for studying millimeter and submillimeter plasma radiation 22 p3958 A66-40936
- Ruby laser giant pulse off-axial modes detected with high resolution spherical Fabry-Perot interferometer 23 p4079 A66-41627
- Edser-Butler band amplitude dependence on modulating effect of interference grating 24 p4212 A66-42819
- Tunable coupling of open waveguide type for semiconfocal Fabry-Perot cavity gives high transmission and high Q 24 p4216 A66-43221
- FABRY-PEROT LASER**
- Multireflector Fabry-Perot laser resonators, discussing suppression effect against unwanted modes 03 p0380 A66-13325
- Microwave models used to measure frequency and quality factors of Fabry-Perot resonator with plane square mirrors operating in X-band 05 p0695 A66-14909
- Modulation of laser light with composite Fabry-Perot resonator, using more than three multiple reflecting plates 05 p0698 A66-15836
- Threshold pumping energies compared to determine losses in Fabry-Perot resonators due to mirror misalignment 05 p0685 A66-15856
- Multiple internal-reflection folded-path rectangular laser configuration for obtaining length of active media between Fabry-Perot reflectors 06 p0891 A66-16652
- Reflection gratings as end plates in Fabry-Perot cavity, with characteristics of low absorption output coupling and wavelength-dependent alignment of end plates 09 p1385 A66-19930
- Solid state laser output exhibiting regular and irregular spikes analyzed through relaxation oscillations and classical physics 09 p1387 A66-20568
- Laser induced gas breakdown at high pressures, noting effect of plasma density on index of refraction via optical frequency resonance measurement 10 p1542 A66-21564
- Pressure effects in Fabry-Perot lossy-cavity gas laser output 13 p2101 A66-26199
- Mode theory of spherical mirror resonators, discussing diffraction losses, resonant conditions, mode patterns, internal focusing elements, mode selection, etc 20 p3599 A66-36972
- Spectral and time-dependent characteristics of stimulated radiation from ruby pulse laser, using Fabry-Perot etalon in fine-structure observation 22 p3931 A66-39823
- Recombination radiation from GaAs p-n junctions with and without Fabry-Perot resonator, noting parameter dependence on current density 22 p3932 A66-40314
- Theory of steady multimode oscillation of solid state laser extended to cavities with inefficient end mirrors or losses dependent on frequency 23 p4077 A66-41274
- FABRY-PEROT SPECTROMETER**
- Plasma electron density and formation determined, using Fabry-Perot resonator 16 p2756 A66-30104
- Grille spectrometer, noting greater signal to noise ratio than that of scanning Fabry-Perot spectrometer for airglow observations 19 p3353 A66-35378
- FACE CENTERED CUBIC /FCC/ CRYSTAL**
- Crystalline structure on fatigue noting changes of body-centred metals and face-centred and hexagonal metals 02 p0245 A66-11948
- Energy gap and thermoconductivity of normal and superconducting fcc lanthanum 03 p0407 A66-12320
- Hydrogen effect on strength, plasticity and brittleness of metals with fcc lattice at various temperatures and hydrogen concentrations 12 p1894 A66-23763
- Martensitic transformation of Ni-Fe alloy from fcc to bcc lattice, noting stress produced by chemical free energy difference between austenite and martensite structure 15 p2520 A66-28649
- Momentum and energy accommodation for hypervelocity gas particles on crystal surface, using Lennard Jones potential and approximating lattice by system of independent forced harmonic oscillators 16 p2752 A66-30388
- Upper and lower bounds on partition functions for finite systems of rigid disks and spheres for high density limit 18 p3139 A66-34503
- Propagation of stacking faults in fcc metals, noting effect of frictional force in cutting through attractive tree and subsequent dipole formation 18 p3258 A66-34631
- Enumerating neighbors of atom in diamond-like lattices 21 p3805 A66-39584
- FACILITY**
- S DEEP SPACE INSTRUMENTATION FACILITY /DSIF/
- S GROUND HANDLING FACILITY
- S HIGH FIELD MAGNET FACILITY
- S LAUNCHING FACILITY
- S RESEARCH FACILITY
- S TEST FACILITY
- FACSIMILE TRANSMISSION**
- Panoramic facsimile camera providing IR and visible spectrum imagery designed for unmanned space operation, noting construction, weight, etc 13 p2077 A66-25236
- FACTOR**
- S AGE FACTOR
- S AMPLIFICATION FACTOR
- S EMOTIONAL FACTOR
- S FORM FACTOR
- S FRANCK-CONDON FACTOR
- S GEOMETRIC FACTOR
- S HUMAN FACTOR
- S LOAD FACTOR
- S MASS FLOW FACTOR
- S PH FACTOR
- S PHYSICAL FACTOR
- S PHYSIOLOGICAL FACTOR
- S PSYCHOLOGICAL FACTOR
- S Q-FACTOR
- S SAFETY FACTOR
- S SEX FACTOR
- S SOCIAL FACTOR
- S TIME FACTOR
- S WEIGHT FACTOR
- FACTOR ANALYSIS**
- Matrix algebra, discussing factorization, determinants, eigenvalues, polynomials, inequalities, etc 17 p2945 A66-31869
- Symbolic factoring of multivariate polynomial with integer coefficients, noting application of Kronecker method and techniques of implementation 21 p3708 A66-38681
- Synthesis of linear multivariable control systems in statistical dynamics, using method of factorization of spectral matrices 23 p4048 A66-41394
- Textbook reissue on diffraction of electromagnetic and acoustic waves at open end of waveguide studied, using Wiener-Hopf-Fock factorization method 24 p4177 A66-43225
- FADING**
- SA RAYLEIGH FADING
- SA SELECTIVE FADING
- SA SIGNAL FADING
- Fading and multipath propagation mechanism for communication links involving satellites and aircraft with antenna beams, assuming fading models and estimating marging required for FSK teletype transmission [AIAA PAPER 66-294] 12 p1822 A66-24763
- FAI**
- S FIELD-ALIGNED IRREGULARITY /FAI/
- FAIL-SAFE SYSTEM**
- Fail-safe system used in temperature environment testing chambers functioning independently of control system and reacting to valve failure, power loss, etc 14 p2270 A66-27666
- Numerical analysis of safety level of fail-safe structure with method applicable to multiloop path structures with discrete elements 20 p3666 A66-37001
- FAILURE**
- SA ABORT
- SA CRACK
- SA ENGINE FAILURE
- SA FATIGUE
- SA FRACTURE
- SA SHORT CIRCUIT
- SA STRAIN
- SA STRESS
- SA STRUCTURAL FAILURE
- SA SYSTEM FAILURE
- Linear estimation for log Weibull distribution from random sample of ordered failure time 01 p0091 A66-10120
- Reliability in optimal control problems in terms of probability of faultless operation 13 p2047 A66-25626
- Frequency of maintenance evaluation in maintainability analysis by substituting failure rate for frequency of corrective maintenance or frequency of interruption 20 p3569 A66-37923
- FAILURE MODE**
- Pratt and Whitney Aircraft system for achieving reliability assurance in gas turbine engines, discussing management, failure modes, product development and tests 01 p0128 A66-10062
- Spaceborne digital computers in reliability program, using failure data in design and evaluation 01 p0033 A66-10064
- DC-9 reliability program emphasizing simplicity improved proven components rather than completely new equipment 01 p0010 A66-10088
- Parameter dependent approach mechanization for in-flight testing of aircraft system, considering electronic subsystems 01 p0010 A66-10096
- Relationships of hazard rate distributions to reliability growth and confidence computations 01 p0077 A66-10109
- Statistical engineering aspects of probe testing for achieving mature designs earlier in product life cycle 01 p0077 A66-10115
- Metallographic polishing procedures used to reveal failure modes in gold-aluminum thermocompression bonds 01 p0049 A66-11153
- Reliability and design factors for space power conditioning equipment examining peak power, component part specifications, integrated circuits and failure analysis 02 p0180 A66-11283
- Reliability of photogrammetric equipment discussing formulation of criteria, contractor requirements and testing 02 p0227 A66-11377
- Instantaneous strength determinations for exponential failure distribution are ineffective in assessing underlying failure rate 03 p0342 A66-12899
- Mathematical model that takes into account factors involved in detecting faults as well as MTBF and MTTR for prediction of equipment availability 04 p0494 A66-13682
- Assured performance calibration discussing statistical quality control, instrument variability, vacuum tube and digital voltmeter histories, calibration costs, etc 04 p0520 A66-13941
- Strength of fiber reinforced metals, examining fracture mode 05 p0700 A66-14813
- Fatigue test of 1000 aluminum specimens in order to assess accuracy with which lower tail of probability distribution of failure curve fits experimental results 05 p0774 A66-15056
- Reliability of integrated circuits noting stress test schedules, failure rates and sources 05 p0650 A66-15369
- Modes of contact fatigue failure classified after appearance and factors promoting initiation and propagation, noting fatigue life of roller bearings subjected to cyclic contact stress [ASME PAPER 65-WA/CF-2]
- 05 p0690 A66-15621
- Spacecraft microelectronic device failure modes and mechanisms 05 p0650 A66-15830
- Capacitor reliability as function of voltage and temperature of dielectric and environmental conditions 06 p0839 A66-15951



Beach and ratchet marks plus component geometry information and stresses to pinpoint fatigue failure in service 08 p1306 A66-18634

Compression instability of unidirectional composites consisting of regularly spaced arrays of axially loaded columns supported by elastic filler [AIAA PAPER 66-143] 08 p1309 A66-19005

Reliability and failure mechanisms of integrated circuits 11 p1669 A66-23158

Accelerated testing of transistors, resistors and capacitors to determine reason for certain types of component failure 12 p1844 A66-24728

Defect analysis by device sectioning, noting techniques, application in crystallography, electronics, etc 12 p1845 A66-24849

Failure mode effect, block redundancy, functional redundancy and cooperative multichannel design for system reliability in Mariner spacecraft 13 p2191 A66-25284

Naval Ordnance Laboratory /NOL/ multiaxial fatigue test for failure mechanisms in fiber-reinforced composite materials involving cyclic stress under controlled environmental conditions 13 p2113 A66-25312

Space digital computer reliability laboratory testing by failure data collection from prototype equipment 13 p2027 A66-25507

Reliability of nonelectronic components in electronic system, noting failure modes, rates, mechanism, etc 13 p2085 A66-25655

Component failure examples of Gemini rendezvous radar, emphasizing need for closed loop reliability program 13 p2039 A66-25786

Causes of failure and guidelines for design of solid state lasers 14 p2309 A66-27669

Probability of survival of system consisting of one active and m redundant elements 15 p2454 A66-28546

Statistical failure detection, employing distribution analysis of parameter changes which removes artificial constraints imposed by arbitrary specification limits 15 p2507 A66-28799

Mean time to failure within given time boundaries and for continuous failure density evaluated via Weibull density function 15 p2526 A66-28806

Application of escape probability concept to systems development for quality control, noting minimization of system failure 15 p2508 A66-28812

Failure effect on phased array radar systems, noting treatment of outage threshold on probabilistic ground and interdependence of system parts 16 p2652 A66-30663

Step-stress technique to induce failures in integrated circuits to pinpoint source of reliability problems 17 p2882 A66-32114

Allotment of probability shares method applied to improving safety in design by diagnosing failure and probability of accident 20 p3494 A66-36999

Failure mode and effect analysis /FMEA/ application to each stage of system design and development oriented reliability program 20 p3568 A66-37915

Identifying critical elements /parts and components/ as criteria for system design tradeoff at system and circuit levels 20 p3568 A66-37916

System effectiveness through reliability prediction, reviewing fundamentals of prediction techniques including time-to-failure, variables data and physics of failure 20 p3572 A66-37952

Apollo spacecraft parts screening program, showing dependence on reliability for mission success 24 p4216 A66-42090

Failure mechanisms of CdS and CdSe thin film FETs noting volt-ampere characteristics, temperature, electrical stress and humidity effects 24 p4181 A66-42381

Reliability estimate methods for equipment using data independent of time to failure factor contrasted with one-or two-sided assigned specification limits 24 p4218 A66-42713

**FAIRING**

**SA LANDING GEAR**

Requirements, materials, fabrication and testing of exit nose fairing for A3 Polaris

missile, noting use of laminated wood as optimum material 06 p0885 A66-16300

**FALKNER-SKAN EQUATION**

Falkner-Skan similar solutions for effects of longitudinal surface curvature on incompressible laminar boundary layer flows 03 p0355 A66-12786

Approximate solution of second-order incompressible boundary layer equations, using mathematical model reformulated for application in vicinity of separation point 23 p4058 A66-41924

**FALLOUT**

**SA RADIOACTIVE FALLOUT**

Formula for average rate of atmospheric particle fallout in terms of height-averaged values of density and viscosity of atmosphere 01 p0097 A66-10760

Formula for average rate of atmospheric particle fallout in terms of height-averaged values of density and viscosity of atmosphere 14 p2327 A66-27859

**FAN**

**SA COMPRESSOR**

**SA DUCTED FAN**

**SA LIFT FAN**

**SA VENTILATOR**

Noise measurement in axial flow fans for military vehicle cooling installations 14 p2220 A66-27567

Fan selection for high-altitude cooling of electronic equipment 20 p3527 A66-37346

**FAN-IN-WING AIRCRAFT**

Fan-wing combinations for three-dimensional flow solutions investigated to determine V/STOL aerodynamic characteristics [AIAA PAPER 65-85] 05 p0606 A66-15076

Fan-wing combinations for three-dimensional flow solutions investigated to determine V/STOL aerodynamic characteristics [AIAA PAPER 65-85] 14 p2274 A66-27415

V/STOL aircraft for commercial short-haul transports, considering turboprops, fan-in-wing and propulsion wings 24 p4159 A66-42891

Aerodynamic coefficients of large-aspect-ratio fan-in-wing airfoil, noting that velocity field consists of inflow to fan, parallel flow and circulation flow 24 p4158 A66-43050

**FAP**

**S FORTRAN II ASSEMBLY PROGRAM**

/FAP/

**FAR FIELD**

Far field simulation of antennas with complex aperture distribution functions 12 p1840 A66-24624

Beam divergence and far field patterns in ruby lasers 16 p2719 A66-31098

Radiation fields of center-fed cylindrical antenna surrounded by plasma sheath, graphically presenting far-field patterns and surface wave fields 18 p3141 A66-33538

Composition in far field of rocket jet mixing with air 18 p3260 A66-33808

Confocal resonator theory instead of diffraction as explanation of 90 degree rotation between near and far fields of ruby lasers 20 p3581 A66-38243

Cialdea-Bagolini optometer investigation of far point in scotopic vision and nocturnal myopia 22 p3856 A66-40501

**FAR INFRARED**

IR spectroscopic instrument modifications and innovations, noting filter grating permitting measurement in far IR 02 p0230 A66-11794

High detectivity gallium doped germanium detector for far IR radiation 02 p0231 A66-12062

Far IR observation of plasma emitted radiation and observation of plasma effect on propagation of externally generated radiation 04 p0522 A66-14196

Modes of tilt-mirror optical resonator, using spillover radiation to extract coherent far IR 16 p2747 A66-31134

Lunar mapping in far IR, including hot spots during total eclipse of December 19, 1964 16 p2698 A66-31225

Multiple cyclotron resonance absorption lines in degenerate valence bands of Ge semiconductor studied with far IR laser spectrometer 24 p4257 A66-42545

**FAR ULTRAVIOLET**

Manned Orbiting Laboratory experiments

such as airglow, solar corona, cosmic ray plasma, far UV image orthicon, etc 04 p0585 A66-136

Optical absorption and reflectivity of single crystals of strontium fluoride and cadmium fluoride in far UV 17 p2974 A66-318

Solar XUV spectrum, discussing spectral lines, variations, structure of chromosphere and corona 18 p3229 A66-341

Optical constants in far UV, using reflectometer permitting measurement of various incidence angles 19 p3361 A66-366

X-ray absorption edge observation of transmittance measurements through thin unbacked metal films in XUV as function of wavelength 20 p3613 A66-372

Aerobee rocket instrumentation and rocket sounding techniques for investigating far UV auroral emission 20 p3552 A66-375

Absorption spectrum of sulfur hexafluoride in far UV due to electron impact at inelastic scattering and oscillator strength for three absorption bands 21 p3774 A66-385

XUV C, Ti, Mn, Fe, Ni, Cu, Zn and Ar L<sub>II</sub> spectra and continuum radiation spectra of plasmas produced by focused ruby laser beam 22 p3954 A66-395

Fabry-Perot interferometer in spectroscopy using satellites and rockets 22 p3920 A66-402

Electron transitions and sharp emission lines in XUV solar spectral regions with fractionally charged quarks bound to C, N and O nuclei 24 p4280 A66-431

**FARADAY DARK SPACE**

Formulas relating detector current to average UHF power obtained for position plasma column and dark Faraday region glow discharge 02 p0269 A66-111

Approximate equality of drift and random currents at boundary between Faraday dark space and head of striated positive column in discharges through neon 12 p1920 A66-234

**FARADAY-DOPPLER TECHNIQUE**

Combined Faraday polarization and Doppler frequency measurements of lunar radio echoes of Earth magnetospheric wake 08 p1296 A66-194

**FARADAY EFFECT**

Theory of interband magnetodispersion effects in crossed field semiconductor obtaining expressions for Faraday and Voigt effects 02 p0272 A66-111

Interband Faraday rotation at liquid nitrogen temperature in CdS-CdSe mixed crystals 02 p0274 A66-111

Transmission and attenuation of elastic and magnetoelastic waves in yttrium iron garnet 03 p0408 A66-121

Faraday type MHD accelerator with series connected electrodes investigated by employing external jumpers 03 p0399 A66-121

Measuring rapidly changing microwave phase and attenuation, using switch frequency bridge circuit 05 p0644 A66-141

Electric conductivity, electrode temperature and potential distribution across channel in potassium seeded argon atmospheric-pressure Faraday accelerator [AIAA PAPER 66-75] 05 p0723 A66-151

Faraday effect in anisotropic plasma treated as fluid with collisions, deriving relations for rotation of polarization plane and electromagnetic wave ellipticity 05 p0727 A66-151

Orientation of satellite-borne dipole emitter and influence on ground-based recording of Faraday effect 07 p1028 A66-171

Faraday effect on hot electrons in germanium and silicon 07 p1105 A66-181

Faraday rotation analysis of simple frequency radio transmission from satellite to determine local electron density 08 p1181 A66-181

Faraday polarization rotation of linearly polarized lunar-reflected radio waves used to measure ionospheric electron content during July 20, 1963 solar eclipse 08 p1284 A66-191

Interband Faraday effect in semiconductors in strong crossed electric and magnetic fields 08 p1277 A66-191

Simultaneous observations of Jupiter at three frequencies, noting phase consistency



- of flux variations, Faraday rotation and flux density 09 p1450 A66-20108
- Parameters of complex energy bands in semiconductors determined by free carrier Faraday rotation, Voigt effect and transport properties 09 p1426 A66-20191
- Depolarization of cosmic radio emission due to dispersion of Faraday rotation of plane of polarization of radio waves 09 p1441 A66-20334
- Diurnal changes in total ionospheric electron content measured, using Randle Cliff antenna 10 p1530 A66-21162
- Radar polarization scattering matrix invariance properties of elliptic and circular polarized antenna 10 p1500 A66-21619
- Central Italy ionospheric electron density, examining Faraday rotation of 54 mc signals from Transit IVA 11 p1695 A66-22377
- Coupling of ordinary and extraordinary electromagnetic waves in CdS induced by external magnetic field or stress 12 p1926 A66-23719
- Longitudinal magnetic field effect upon gas discharge, Zeeman effect and Faraday effect in He-Ne gas laser 12 p1890 A66-24224
- Magnetization induced by circularly polarized laser light incident on nonabsorbing material, in absence of external magnetic field, in doped calcium fluoride proportional to light intensity and Verdet constant 13 p2131 A66-26142
- Resonator cavity measurement of microwave Faraday effect in low resistivity semiconductors 14 p2349 A66-26799
- Faraday effect method for measuring magnetic fields of extremely short duration and device for observing slightly luminous phenomena 14 p2290 A66-26824
- Microwave Faraday effect in n-type germanium, discussing Faraday rotation, ellipticity, magnetoabsorption, complex conductivity tensor elements and measurement of microwave polarization anisotropy 14 p2349 A66-26826
- IR and visible helium-neon laser modulation using Faraday rotation in YIG 14 p2305 A66-26881
- Faraday effect in rare earth garnet ferrites and metallic ion g values in IR spectrum 14 p2364 A66-27703
- Total ionospheric electron content measurements at Delhi using Faraday fading of satellite beacon transmissions during solar minimum 15 p2495 A66-30067
- Beacon observations of differential Doppler and Faraday effects from analysis of signals emitted by Explorer XXII satellite 15 p2453 A66-30069
- Electron content for ionospheric station located 47 degrees N determined from observation of Faraday polarization rotation 15 p2496 A66-30073
- Interplanetary plasma stream analysis using bistatic radar transmissions, considering wave propagation in presence of uniform magnetic field, stream velocity, Faraday rotation, etc 16 p2801 A66-30716
- Multiple reflection effects in Faraday rotation in thin film semiconductors 16 p2778 A66-31073
- Origin and propagation of cosmic radiation, discussing interplanetary magnetic fields, plasmas, Faraday rotation of polarized radiation, Zeeman splitting of hydrogen line, etc 17 p2964 A66-32029
- Complex refractive index of Earth surface and ionospheric Faraday effect measurements 17 p2873 A66-32200
- Longitudinal Faraday emf, thermoelectric and Hall effects on channel flow of ionized gas 17 p2972 A66-32868
- Ionospheric electron content determined from satellite measurements, noting seasonal and diurnal variation of content and utilization of Faraday fading for measurements 17 p2920 A66-33069
- Interband Faraday effect in semiconductors in strong crossed electric and magnetic fields 17 p2983 A66-33133
- Ionospheric electron content determined by closely spaced frequency and rotation rate methods, using satellite transmission 18 p3104 A66-33547
- Faraday rotation from 24-hr satellite at high frequencies provides means of studying electron content of ionosphere and fluctuations 18 p3106 A66-34200
- Galactic magnetic field strength and distribution determined from synchrotron emission of relativistic electrons, noting Faraday rotation of polarized radiation from distant radio sources 18 p3235 A66-34744
- Ionospheric Faraday effect and determination of total electron content in ionosphere 18 p3109 A66-35042
- Faraday rotation variation with galactic coordinates studied for emission from 86 linearly polarized radio sources 18 p3238 A66-35236
- Faraday rotation obtained with pulsed high-field magnets for controlling laser cavities 19 p3372 A66-35380
- Operation of Q-switching device based on Faraday effect and used with ruby laser for application to plasma diagnostics 19 p3375 A66-36079
- Depolarization of Crab Nebula produced by Faraday rotation in filamentary shell that surrounds nebula 20 p3648 A66-37261
- Ionospheric electron content variation with solar radio flux from Faraday rotation data at magnetic equator 20 p3633 A66-38198
- Faraday and Voigt and dispersive magneto-optic effects in semiconductors in crossed field due to energy band transitions 21 p3800 A66-38995
- Ionospheric electron content over Ahmedabad and Bombay from differential Faraday rotations of plane polarized radio waves from Beacon satellite 21 p3734 A66-39229
- Faraday rotation experiment for determination of electron density and collision frequency observations in arctic D region 22 p3905 A66-39946
- Latitudinal and diurnal variations of ionospheric electron content near auroral zone in winter from Faraday rotation data 22 p3911 A66-39985
- Faraday rotation measurements of decameter wavelength radiation from Jupiter, calculating ionospheric electron content 22 p3977 A66-39987
- Polarized EM wave propagation and microwave Faraday rotation in solid state plasma in circular waveguide under strong magnetic field 22 p3964 A66-40170
- Quasi-optical measurement of Faraday rotation in oversize waveguide at 2-and 1-mm wavelengths 22 p3876 A66-40172
- Observed Faraday polarization variation of satellite transmission radio signals due to ionospheric irregularities, latitudinal electron density variations and antenna geometry readout error 22 p3867 A66-40556
- Longitudinal magnetic field effect upon gas discharge, Zeeman effect and Faraday effect in He-Ne gas laser 22 p3933 A66-40586
- Faraday unipolar induction in solid cylinder of nonideal type II superconductor, noting contributions to observed emf 23 p4114 A66-41629
- Saturation induced optical nonreciprocity in He-Ne ring laser plasma, eliminating frequency locking by using Faraday effect 24 p4221 A66-42552
- Current measuring device for EHV transmission line, obtaining instantaneous magnetic field by gauging Faraday rotation angle of laser beam in flint glass rod 24 p4222 A66-42556
- Ionospheric electron content at temperature latitudes during declining phase of sunspot cycle determined by observation of Faraday effect 24 p4200 A66-42595
- Differential absorption and Faraday rotation in D region, using closed loop feedback system and two signals of different frequencies 24 p4205 A66-43218
- FAST ELECTRON**
- Injun I and III particle observations discussing methods and results on fast electrons, particle counters, energy separation, spectra, flux variation, angular distributions, etc 03 p0363 A66-12647
- Semiconducting properties of electron irradiated silicon carbide 06 p0936 A66-17138
- Kinetic equation for fast electrons in plasma in stationary electric field, taking into account electron interaction 09 p1407 A66-19963
- Plasma oscillations in metallic single crystal films induced by fast electrons 13 p2139 A66-25330
- Photoconductivity spectra and kinetics of p-and n-type germanium crystals bombarded by fast electrons at 5.2 and 100 degrees K 16 p2788 A66-31776
- Laser based on excitation of gallium phosphorus arsenide solid solution by beam of fast electrons 17 p2937 A66-33304
- Spectra and intensity vs excitation level and spatial distribution vs current density determined for optical radiation by electron excited cadmium sulfide 17 p2937 A66-33308
- Primary and afterglow emission decay time from low temperature gaseous nitrogen excited by fast electrons explained by possible energy transfer 19 p3404 A66-36799
- Instabilities resulting in loss of energetic electrons and fast electrons analyzed in electron cyclotron plasma confined by magnetic mirrors 23 p4103 A66-41490
- FAST NEUTRON**
- SA THERMAL NEUTRON**
- Fast and slow neutrons detected by proportional and scintillation counters 05 p0755 A66-15408
- Rapid neutrons irradiation effect on thermal conductivity of ternary semiconducting arsenide compounds 06 p0933 A66-17119
- Positions of defect energy levels in n-type germanium irradiated with fast neutrons analyzed by optical methods, measuring spectral distribution of photoconductivity and quenching curve 06 p0934 A66-17127
- Influence of defects introduced during fast neutron irradiation on electronic behavior of SiC, examining reasons for deterioration of SiC semiconductor devices 06 p0936 A66-17137
- Ripening of defects induced by fast neutrons in germanium in course of low temperature annealing 06 p0937 A66-17143
- Effect of irradiation of silicon by fast neutrons on switching time of alloy diode synthesized on silicon base 07 p1099 A66-17929
- Fast neutrons effects on operating characteristics of silicon controlled rectifiers 07 p1010 A66-18149
- Irradiation effects by fast neutrons and gammas on collector cut-off current and base current at low current densities analyzed on silicon planar transistors 13 p2032 A66-25486
- Dislocation-free Si crystal defects produced by fast neutron bombardment 14 p2359 A66-27092
- Atmospheric fast cosmic ray neutron flux measurements, using boron fluoride recoil neutron counter 15 p2584 A66-29553
- Gamma radiation and fast neutron effects on dark resistance, photoconductivity, majority carrier mobility, recombination kinetics, etc, in CdS single crystal 16 p2787 A66-31765
- Fast neutron effect on conductivity and thermoelectric power of germanium, noting decrease of conductivity due to phonon scattering 18 p3157 A66-34626
- Rocket and balloon measurements of fast neutron intensity at high altitude from detectors flown in 1964 and 1965 18 p3188 A66-34823
- Fast neutrons of solar origin detected by observing protons recoiling from elastic collisions of neutrons with hydrogen nuclei in nuclear emulsion 18 p3188 A66-34824
- Low energy fast cosmic ray neutrons, measurements of energy spectrum and primary intensity variations, using organic scintillator in field of photomultiplier tube 18 p3199 A66-34885
- Stack of nuclear emulsion exposed underground to analyze fast neutrons, obtaining energy spectrum of neutrons from measurements on hydrogen recoils 18 p3222 A66-35211
- Fast-neutron irradiation effects on photoconductivity spectra and induced crystal structure defects for n-and p-type gallium arsenide single crystals 20 p3624 A66-38415
- Fast neutron effect on electrical properties of boron-doped n-type silicon samples with resistance, noting decrease in hole concentration and mobility 22 p3961 A66-39829
- IR absorption band growth and decay in spectra of oxygen-doped Si irradiated with



fast neutron 22 p3962 A66-40085  
Dislocation-free Si crystal defects produced by fast neutron bombardment 22 p3967 A66-40848

**FAST REACTOR**  
High temperature embrittlement of stainless steel irradiated in fast fluxes of Dounreay fast reactor at coolant temperatures of 250-350 degrees C 22 p3934 A66-40006

**FASTENER**  
SA BOLT  
SA CLAMP  
SA FITTING  
SA JOINT  
SA RIVET  
Increased aluminum panel acoustic resistance due to combination of surface treatment and mylar gasket-universal head mounting technique 01 p0149 A66-10144  
Stress distribution in bolted fastenings noting effects of internal and external forces on deformation, energy and screw mechanism and methods of calculation 06 p0964 A66-16480  
Stress analysis of rim-straddling fastenings for axial compressor and turbine blades 13 p2171 A66-25081  
Tool fastener interface problems peculiar to extravehicular environment examined by measurement of torque and linear /or push-pull/ forces 19 p3363 A66-35952

**FAT**  
S LIPID

**FATIGUE**  
SA ACOUSTIC FATIGUE  
SA BENDING FATIGUE  
SA CRACK  
SA FAILURE  
SA FLIGHT FATIGUE  
SA FRACTURE  
SA METAL FATIGUE  
SA SHEAR FATIGUE  
SA STRAIN  
SA STRAIN FATIGUE  
SA STRESS  
SA STRUCTURAL FATIGUE  
SA THERMAL FATIGUE  
Cyclic plastic stresses at notch roots in aluminum alloy sheet specimens under constant-amplitude repeated tension and reversed loading 17 p3023 A66-32074  
Double linear damage rule used in conjunction with crack initiation and propagation equations, applied to cumulative fatigue damage 22 p3989 A66-40116

**FATIGUE /BIOL/**  
Industrial alertness management in relation to production rate, quality control and operator safety 12 p1810 A66-24957  
Human factors in B-58 aircraft accidents, considering nose-high landing requirement, pilot fatigue and evaluation of ejection facilities 17 p2864 A66-32166

**FATIGUE DIAGRAM**  
Crystalline structure on fatigue noting changes of body-centred metals and face-centred and hexagonal metals 02 p0245 A66-11948  
Healing of defects in steel accumulated during cyclic overloading 07 p1048 A66-17442  
Formation of fatigue cracks in center notched sheet specimens of various metals ultrasonically tested for axial tensile fatigue 12 p1957 A66-23630  
Sintered aluminum powder endurance under bending stresses and cladding effect on fatigue resistance 14 p2318 A66-28198  
Monte Carlo simulation studies for fatigue data analysis of rolling-contact bearings, using Weibull equation [ASLE PAPER 66AM 1B2] 16 p2710 A66-30401  
Curves as quantitative criteria of corrosion fatigue of metals 18 p3259 A66-35010  
Fatigue behavior of aluminum reinforced with stainless steel wires, considering effects of fiber volume fraction and interfacial bond 23 p4081 A66-41661

**FATIGUE LIFE**  
Efficiency of fail-safe and safe-life designs as design guideposts for static and fatigue loadings 01 p0076 A66-10065  
Fatigue life and reliability calculations for fail-safe redundant structure 01 p0146 A66-10119  
Linear estimation for log Weibull distribution from random sample of ordered

failure time 01 p0091 A66-10120  
Structural response theory and acoustic fatigue aspects contributing to estimation of fatigue life of aerodynamic structures 01 p0147 A66-10122  
Fatigue analysis calculations of systems with non-Gaussian output, using crest and extremal statistics of 01 p0147 A66-10127  
Strain 01 p0147 A66-10127  
Statistical aspects of height of rise and fall in continuous random loading relevant to fatigue failure 01 p0147 A66-10128  
Fatigue failure in aircraft panels studied by determining spectral densities of response of continuous skin stringer panels under random noise 01 p0147 A66-10130  
Excitation 01 p0147 A66-10130  
Stress response and fatigue life of acoustically excited brazed steel honeycomb panels for variations in thickness 01 p0147 A66-10133  
Analog computer application to prediction of nonlinear response of panel structure to random forcing function 01 p0148 A66-10134  
Fatigue crack propagation in airframe materials under axial narrow and broadband random loading 01 p0148 A66-10139  
Displacement response prediction and fatigue life of honeycomb sandwich panels subjected to acoustic excitation 01 p0149 A66-10141  
Interface discontinuities from improper heat balance and effects on fatigue life of spot welded joint in austenitic stainless steel 02 p0235 A66-11469  
Component hardness differences of SAE 52100 steel effect on bearing fatigue, using five-ball fatigue tester and rolling element bearings 03 p0372 A66-12349  
Instantaneous strength determinations for exponential failure distribution are ineffective in assessing underlying failure rate 03 p0342 A66-12899  
Optimizing fatigue life of flexibly mounted rolling bearings, discussing shaft and housing structure 03 p0373 A66-12929  
Ausforming effect on rolling contact fatigue life of M-50 bearing steel [ASME PAPER 65-LUB-9] 04 p0536 A66-14243  
Probability method for fatigue strength, assessing damage from random values, time variation of stress range and statistical relationships of addition 04 p0594 A66-14400  
Surface film effects on fatigue life of steels 05 p0703 A66-15483  
Modes of contact fatigue failure classified after appearance and factors promoting initiation and propagation, noting fatigue life of roller bearings subjected to cyclic contact stress [ASME PAPER 65-WA/CF-2] 05 p0690 A66-15621  
Lubricant effect on fatigue life of stationary ball on flat contact subjected to oscillatory normal load [ASME PAPER 65-WA/CF-3] 05 p0690 A66-15622  
Correlation equation estimating pitting fatigue life of bearings from minimal rolling contact rig data [ASME PAPER 65-WA/CF-5] 05 p0690 A66-15624  
Compressive residual stress effects on surface layers of through-hardened bearing steels produced by prenitriding before hardening [ASME PAPER 65-WA/CF-7] 05 p0690 A66-15625  
Mean strain cumulative damage and effect in low cycle fatigue of 2024-T351 aluminum alloy, covering strain cycling, fatigue life, residual ductility, etc [ASME PAPER 65-WA/MET-5] 05 p0703 A66-15690  
Principles and statistics behind life-test plans of MIL-STD-690 Life Test Sampling Procedures for Established Levels of Reliability and Confidence in Electronic Parts Specifications 06 p0886 A66-16332  
Dimensioning and strength calculations - Conference, Budapest, October 1965 06 p0963 A66-16472  
Rubber-compound fatigue resistance, examining effects of preliminary prolonged heating and cooling 06 p0901 A66-16482  
Service life of antifriction bearings represented by Weibull distribution law,

with computer method for parameters at density function 06 p0886 A66-16472  
Stress cycle shape effect on fatigue strength of metals, noting graphical method for predicting fatigue life 06 p0965 A66-16472  
Resonance-type fatigue testing machine for variable stress ranges and frequencies from 100 to 400 cps 07 p1147 A66-18332  
Effect of residual stresses /tensional pressure/ on fatigue limit of welded parts and structures 08 p1310 A66-19147  
Effect of plastic coatings on fatigue strength of steel and welded steel samples subjected to concentrated stress 08 p1231 A66-19147  
S/N fatigue life gauge for direct measurement of cumulative fatigue damage to predict structural failure 08 p1316 A66-19816  
Life testing of electron-bombarded cesium ion engine designed for power-thrust ratio of 160 kw/lb [AIAA PAPER 66-233] 10 p1594 A66-21706  
Fatigue life of aircraft gas turbine compressor disks subjected to cyclic loading 11 p1710 A66-22615  
Vacuum effect on fatigue life of aluminum under constant stress cyclic bending deformation 11 p1717 A66-22998  
Truncation method for determining characteristics of electronic components such as transistors and vacuum tubes before testing to destruction 12 p1833 A66-24088  
Tabulated reliability data on communications systems components for possible application to other fields 12 p1833 A66-24088  
Statistical interpretation of fatigue fracture phenomena in metals, relating development of successive damage to external loading processes 12 p1968 A66-24398  
Prediction of fatigue failure of structures subjected to sinusoidal stress cycles of different amplitude and mean value [ASME PAPER 65-MET-3] 12 p1970 A66-24598  
Cumulative damage and fatigue applicability to solid propellant-liner bond failure, noting useful life and stress-time relationship [AIAA PAPER 65-191] 12 p1937 A66-24706  
Properly controlled high-stress life testing used to evaluate failure rate of high reliability solid state components integrated circuits 12 p1846 A66-24938  
Thermoplastics behavior under cyclic stress, noting failure under cyclic propagation or temperature due to damping capacity 13 p2112 A66-25338  
Production techniques for fissures in welds deposited and wrought Ni-Cr-Fe alloy fatigue specimens and fissure effect on fatigue strength 13 p2110 A66-26010  
Hydrogen embrittlement or fatigue strength loss avoidance in overhauling and repairing of high strength aircraft steel component 13 p2087 A66-26228  
SNAP-8 turboelectric nuclear space power system including component tests, corrosion program and status of systems [AIAA PAPER 64-758] 13 p2126 A66-26666  
Low cycle fatigue crack propagation characteristics of high strength steels noting technique for life estimation of structure by numerical integration [ASME PAPER 66-MET-3] 14 p2312 A66-26998  
Plastic strain effect on fatigue strength of aircraft skin sheets with hole subjected to constant loading, noting stress concentration at hole 16 p2815 A66-30606  
Transverse cut-out effect on fatigue strength of rotating shaft under constant bending load, noting fatigue stress concentration factor 16 p2815 A66-30606  
Structural resonant amplitude reduction for increased fatigue life and component malfunction reduction, noting application of internal damping, and use of viscoelastic materials 16 p2715 A66-31206  
Fatigue damage accumulation in materials at high temperatures under variable load noting calculation of fatigue life 18 p3254 A66-34226  
Streak test excellent acceptance technique for assurance of reproducibility of service life for ablative thrust chamber of M150A variable thrust rocket engine [AIAA PAPER 65-608] 19 p3449 A66-35606



Optimum number of test aircraft in test program to predetermine endurance and service life of same aircraft in serial production 20 p3493 A66-36921

Cobalt addition to titanium alloy, discussing effect on tensile strength, thermal stability fatigue strength, ductility and notch sensitivity 20 p3582 A66-37049

Crack propagation, damage and fatigue fracture in plane rods with transverse cut under single step and multistep axial load 20 p3666 A66-37307

Lifting aircraft structures subjected to acoustic pressures, noting estimation of panel joint rms stress 20 p3666 A66-37422

Fatiguing at room temperature resulting in observable diffusion of silver into copper, using precipitation reaction to analyze influence of large number of vacancies 20 p3584 A66-37618

Water and mercury cavitation damage on solids in cavitating venturi tunnels consisting of single event symmetrical craters and irregular fatigue-type failures 20 p3586 A66-37813

System effectiveness through reliability prediction, reviewing fundamentals of prediction techniques including time-to-failure, variables data and physics of failure 20 p3572 A66-37952

Crack initiation and propagation formula through fatigue process applied to interface problems, noting creep 20 p3671 A66-38105

Maraging steel properties, discussing composition, strengthening mechanism, tensile and impact toughness, mechanical and fatigue properties, etc 20 p3587 A66-38431

Fatigue endurance limits for sintered alloys in various density ranges [ASME PAPER 66-MD-77] 21 p3822 A66-38502

Rolling-element bearing material technology, examining fatigue effect of material properties and processing variables 21 p3750 A66-38624

Reliability handbook covering system effectiveness, fatigue life patterns, reliability testing, malfunction and failure analysis, etc 21 p3744 A66-39215

Fatigue fracture and crack propagation in ordered alloys due to plastic flow 22 p3989 A66-39891

Measuring wear life and friction coefficient of dry film and solid film lubricants and plastic materials in ultrahigh vacuum 22 p3923 A66-40216

Corrosion fatigue strength of duralumin in presence of stress concentrators, noting parameters of resistance and alloy properties 22 p3935 A66-40679

High cycle fatigue strength of titanium, Cb and Al alloys correlated with constants of logarithmic true stress-strain curve 24 p4229 A66-43080

Environmental testing and evaluation of useful life of insulation material for aircraft electrical equipment operating at 280 degrees C 24 p4229 A66-43083

### FATIGUE TEST

Fatigue tests of optimized structural configurations consisting of sandwich panels containing core layers 01 p0150 A66-10152

Acoustic fatigue testing of 20 fuselage panels of XC-142A VTOL/STOL transport aircraft, using simulated propeller noise 01 p0151 A66-10158

Size effect of bending and twisting fatigue strength by calculating probability of flaws on surface 02 p0243 A66-11581

Component hardness differences of SAE 52100 steel effect on bearing fatigue, using five-ball fatigue tester and rolling element bearings 03 p0372 A66-12349

Fatigue strength of heat-treatable alloyed steels 03 p0384 A66-13168

Mechanical testing methods, discussing quasi-static and fatigue fracture due to tensile compressive load and cyclic deformation characteristics of materials 04 p0537 A66-14399

Fatigue test of 1000 aluminum specimens in order to assess accuracy with which lower tail of probability distribution of failure curve fits experimental results 05 p0774 A66-15056

Nonhazardous and nondestructive method for testing pressure regulating valves, using

simulated gas flow and pressure [ASME PAPER 65-WA/AUT-7] 05 p0661 A66-15707

Roller-bearing design noting reliability requirements via Palmgren-Lundberg formula 06 p0886 A66-16481

Two-parametric classification of load cycles on construction elements connected with fatigue limit tests and service life 06 p0964 A66-16483

Four conditions permitting fatigue limit obtained by Wohler curve to render consistent distribution function to mean value and deviation 06 p0965 A66-16485

Effect of structure and volume cold-working related to structural factors on notched samples of steels subjected to cyclic stresses 07 p1048 A66-17441

Fatigue stress analysis, using graphical technique for complex problem of bending and torsional out-of-phase variable frequency vibrations 07 p1147 A66-18342

Loading frequency effects on fatigue strength of 45 and E1612 steel specimens at room temperature 07 p1147 A66-18385

Similarity criteria, showing that scale effect in fatigue fracture is caused by distortion of similarity 07 p1147 A66-18386

Beach and ratchet marks plus component geometry information and stresses to pinpoint fatigue failure in service 08 p1306 A66-18634

Nickel alloy testing for thermal fatigue and bow evaluation, using miniature airfoil specimens, in aircraft gas turbine application [SAE PAPER 660056] 09 p1388 A66-20154

Oxygen and water vapor effects on propagation of fatigue cracks in aluminum alloy sheets 10 p1614 A66-21338

Reliability of fatigue test results, noting calibration method and frequency, specimen preparation, alignment and environmental factors 12 p1958 A66-23656

Rest period effect on fatigue testing of polyester fiberglass and polymethylmethacrylate plastics under static and intermittent tensile loads 12 p1899 A66-24039

Evaluation of model of strain hardening in fatigue with crack propagation occurring by plastic flow away from crack tip during tensile part of cycle 12 p1898 A66-24971

Results of crack propagation tests on polymethylmethacrylate flexed at various frequencies under cyclic loading 13 p2112 A66-25308

Naval Ordnance Laboratory /NOL/ multiaxial fatigue test for failure mechanisms in fiber-reinforced composite materials involving cyclic stress under controlled environmental conditions 13 p2113 A66-25312

Cyclic residual plastic deformation method for determining metal fatigue which is independent of stress 13 p2195 A66-25442

YS-11 transport aircraft fatigue testing, noting wing fatigue damage and equipment used 13 p2197 A66-26099

Cyclic strain fatigue tests and fatigue failure curve for age-hardened nickel based alloy K-Monel [ASME PAPER 66-MET-9] 14 p2312 A66-26977

Strength of adhesive-bonded lap joints as affected by changes in temperature and fatigue 14 p2401 A66-27772

Full-scale and model test for dynamic effects of LEM landing 14 p2393 A66-28019

Precleaning treatment and coating effect on fatigue strengths of aluminum alloys 15 p2521 A66-29071

Fatigue crack initiation and propagation, using ultrasonic test instruments 15 p2610 A66-29316

Low endurance fatigue properties of steel plate 15 p2615 A66-29805

Fatigue tests at high stress levels under rotating bending of carbon steel and roll material, analyzing stress-strain behavior in plastic fatigue process 16 p2815 A66-30809

Standard prolonged work test using treadmill for evaluation of fatigue and stress in man 17 p2863 A66-32150

Fatigue concept application to rotorcraft noting fatigue requirements, accident prevention methods, etc 17 p2843 A66-32721

Hughes OH-6A helicopter fail-safe structural composition noting design, fatigue testing, application of redundant design features, etc 17 p2845 A66-32736

Stress corrosion, delayed failures, fatigue corrosion and relation between these phenomena - Commissariat on Atomic Energy, Metallurgical Colloquium, Cadarache, Rhone, France, June 1964 17 p2941 A66-33440

Air and aqueous environments effect on mode of fracture in titanium alloys during low cycle fatigue 18 p3122 A66-33749

Fatigue curve for one type of loading determined from stress variation during cyclic deformation and fatigue curve from other type of load application 18 p3254 A66-34231

Algorithm used in circuit design, evaluating equivalent strain at critical point of airframe structure, verifying it during fatigue tests 20 p3665 A66-36880

Aircraft structures strength and longevity obtained by applying standards and criteria to design and manufacture including static, fatigue and fail-safe tests 20 p3666 A66-37000

Maraging steels for landing gear forgings, noting fabrication, distortion and fatigue tests 21 p3751 A66-39237

SH-3A airframe fatigue test facility for automatic simulation of helicopter flight and landing loads 22 p3992 A66-40251

Brittle-fracture propagation tests, obtaining relations among crack propagation speed, dynamic-stress distribution, test temperature and applied stress 22 p3994 A66-40435

Grain boundary self-diffusion coefficient variation with applied stress and production of lattice vacancies applied to cavity growth in high temperature fatigue of Mg 23 p4081 A66-41714

K values for crack propagation rates obtained from fatigue experiments on metals, noting correlation with tensile properties of metals 23 p4082 A66-41865

Full-scale and model test for dynamic effects of LEM landing 24 p4283 A66-42771

### FATIGUE TESTING MACHINE

Constrained stress-strain test of Ni-Cr-Mo steel carried out on plane bending plastic fatigue testing machine 02 p0243 A66-11580

Fatigue testing machine for loads in rotating beam 03 p0440 A66-13167

Fatigue testing of structure, using machines producing loads by centrifugal forces 06 p0965 A66-16488

Microscopic fatigue crack production in compressor blades, describing methods and application to ultrasonic nondestructive testing 06 p0966 A66-16799

Fatigue testing machine with two shaft-rotation speeds for HF and LF testing 07 p1147 A66-18388

Device for taking long time corrosion fatigue curves on small cross section specimens at high temperatures and pressures 09 p1388 A66-20433

Heating unit of device for testing small samples of sintered materials for thermal fatigue 11 p1709 A66-23475

Trapezoidal stress waveforms effect on low cycle corrosion fatigue strength, clarifying mechanism of corrosion fatigue 12 p1959 A66-23849

Fatigue testing metal rods in rotating beam machines without machining as-produced specimen surface 14 p2318 A66-28481

Helicopter airframe fatigue testing noting fail-safe design, crack detection, loads applied, test facilities and techniques, etc 17 p3027 A66-32737

Variable stress measurement using wire type resistance strain gauges in measuring bridge circuit 18 p3112 A66-34232

Block program testing on fatigue testing machines, noting modifications introduced and operational results 18 p3259 A66-34893

High temperature fatigue in pure lead and aluminum observed continuously by microscopic cinecamera combined with fatigue machine 19 p3386 A66-36366

Fatigue testing machine shear strain measurements near cracks on Al flat plate surfaces by observing birefringence 23 p4147 A66-41997

### FATTY ACID

Nature of particles involved in lipid synthesis in yeast 06 p0822 A66-16566



Effects of alpha glycerophosphate and of palmitoyl-coenzyme A on lipid synthesis in yeast extracts 15 p2429 A66-28616  
Acceleration stress-induced changes in fat metabolism, level of circulating glucose and corticosterone level in rats 15 p2431 A66-28868  
Sympathetic nervous system integrity following water immersion evaluated by measuring plasma-free fatty acid responses to passive tilting 16 p2639 A66-30649  
Serum glucose and free fatty acids in man during prolonged exercise 17 p2859 A66-32366  
Amino-acid-sequence determination in peptides using N-fatty acids, mass spectra of peptide derivatives and computer techniques 20 p3510 A66-37057  
Fatty acid synthesis by *Saccharomyces cerevisiae* crude particles 23 p4029 A66-41377

**FAULT MECHANICS**  
**SA STACKING FAULT**  
Weapon subsystem safety estimation by fault-tree method alone or in combination with Karnaugh maps 01 p0168 A66-10069  
Fault location in modern airborne radar, discussing maintenance reduction techniques and reliability improvement 07 p1006 A66-17495  
Optimization of quality control procedures in searching for faults, using mathematical models 08 p1232 A66-19767  
Scanning electron microscope observation of electrical leakage paths due to crystal defects in silicon diodes 11 p1668 A66-23028  
Unattended weapons systems operation from rural power systems, emphasizing sensing to determine transfer from primary commercial to alternate source and fault patterns 20 p3542 A66-37242  
Alternate mode of operation for minimizing occurrence of delays caused by launch support equipment failures for Saturn manned missions 20 p3542 A66-37243  
Minuteman weapon system maintainability, discussing fault detection and isolation, ground system, standardization, tools and system requirements analysis 24 p4281 A66-42092

**FBFM**  
**S FEEDBACK FREQUENCY MODULATION /FBFM/**

**FCC**  
**S FACE CENTERED CUBIC /FCC/ CRYSTAL**

**FECES**  
Enteric microbial flora changes in man exposed 56 days to oxygen-helium atmosphere 18 p3058 A66-33777

**FEED SYSTEM**  
Multipurpose feed system for 60-ft paraboloid antennas 04 p0493 A66-13616  
Linking monopulse radar antennas in aircraft tracking system 04 p0497 A66-13965  
Coma-corrected, mono-and multifrequency diffraction reflector antennas, examining feed system, electronic scanner and aberrations 05 p0648 A66-14911  
Multiple-feed system for microwave focusing objective, discussing array factors 06 p0827 A66-16042  
Helix frequency-scanning delay line design and characteristics 06 p0849 A66-16396  
Circularly polarized monopulse feed system for use with parabolic reflectors generates response independent of return-signal polarization 06 p0851 A66-16448  
Ion thruster, including mercury feed system and shielded neutralizer, designed and tested for spacecraft station keeping and attitude control [AIAA PAPER 66-247] 10 p1593 A66-21456  
Device for automatically feeding experimental curve coordinates in large quantities into digital computer for high noise level photographic image 11 p1659 A66-22432  
Feed polarization incident upon conic reflector in antenna system specified in terms of crossed electric and magnetic dipoles 11 p1663 A66-22544  
Zero-g vapor feed system with no moving parts, noting ion engine testing, propellant use efficiency and surface tension storage [AIAA PAPER 66-249] 11 p1761 A66-23083  
Design of gravity-independent force-fed liquid-metal cathode providing unlimited cathode life in gas discharge devices and

mercury electron-bombardment thrusters [AIAA PAPER 66-245] 13 p2106 A66-25175  
Zero-gravity mercury feed system for mercury-electron bombardment spacecraft engines [AIAA PAPER 66-250] 13 p2172 A66-25176  
Circularly polarized tracking feed in Haystack antenna 13 p2035 A66-25504  
Multimode antenna feed in radar design requiring only two hybrids for azimuth and elevation measurements 14 p2255 A66-27806  
Dielectric guide structures /Dieguides/ used for increased gain/noise ratio in low noise antennas 15 p2456 A66-28588  
Monopulse channel phase measurement by composite radiation pattern of feed 15 p2456 A66-28589  
Dual polarized high-power synthetic conical scan tracking system at various frequency ranges for parabolic reflector used in communication link 16 p2650 A66-30552  
Design and testing of cross polarized feed for 10 ft diameter parabolic dish, noting coincidence of focal and aperture plane 16 p2666 A66-31565  
Rear feeds for paraboloidal reflectors 18 p3075 A66-33618  
Improved feed synthesis using multimodes for large circular paraboloids at Parkes 18 p3084 A66-34310  
Reflector surface and feed-support structure for center-fed paraboloidal aerial system for satellite communication 18 p3085 A66-34315  
High-power feed for satellite tracking radar using four-way static split system with Cassegrain antenna and four symmetrical horns, noting phase shift errors 18 p3086 A66-34324  
Surface tension propellant storage and feed systems for zero-g ion engines 19 p3450 A66-35615  
Multipurpose feed system for large paraboloid antennas operable in S band 19 p3316 A66-35685  
Ultralow-noise planetary radar receiving system with high-performance feed and maser preamplifiers, noting aperture utilization 19 p3301 A66-35690  
Japanese ground antennas for use with communications satellites Teistar, Relay and Syncom 20 p3530 A66-37718  
Effect of random fluctuations of voltage and frequency of gyrorotor feed current on change in rotor angular velocity, noting gyro drift 21 p3738 A66-38970  
Generalized method of calculating multielement antenna and feeder system 21 p3712 A66-39250

**FEEDBACK**  
**SA DEGENERATION**  
**SA NONLINEAR FEEDBACK**  
**SA REGENERATION**  
**SA SENSORY FEEDBACK**  
Sweep indicator as radar feedback filter, noting double delay 04 p0501 A66-14126  
Operation of FM microwave generator with external feedback connected to mismatched long line 06 p0852 A66-16512  
Phase correcting circuit construction using delay line cut into adder feedback circuit 09 p1360 A66-20295  
Natural frequency and self-excitation of transistor-operated autogenerator with open-loop feedback 09 p1354 A66-20453  
Digital counter synthesis for fixed base and periodic sequence-variable base counters with various feedback loops 09 p1361 A66-20606  
Comparison of sequential and nonsequential detection systems with uncertainty feedback, showing performance as function of peak-to-average power ratio 10 p1518 A66-21838  
Adaptation theory concepts, examining threshold learning process, Markov chain, learning wave, feedback adaptivity, etc 11 p1647 A66-22299  
Feedback to quadrupole that incorporates device for converting voltage into time parameter of periodic sequence of pulses and vice versa 11 p1671 A66-23334  
Frequency characteristics of bending vibrations of bounded rods with electromechanical feedback, possibility of artificially attenuating resonance vibrations

and conditions for self-excitation 13 p2194 A66-25088  
Operation of FM microwave generator with external feedback connected to mismatched long line 13 p2041 A66-25952  
Monotone feedback shift register /MFSR/, enumerating closed cycles and stable MFSRs 13 p2050 A66-26063  
State-variable feedback decoupling of multivariable linear plants with cross coupling between various input-output pairs 13 p2053 A66-26083  
Frequency oscillations in oscillator with double-loop delayed feedback 14 p2259 A66-28165  
Feedback effect on current voltage characteristic of device with negative feedback and reactivity of device in negative resistance 15 p2464 A66-29121  
Laser action with nonresonant feedback using high gain ruby crystals 16 p2717 A66-30297  
Design criteria for active filters using resistance and capacitance elements in feedback circuits 17 p2896 A66-33297  
Minimum feedback loop realizations of synchronous sequential switching circuits 18 p3090 A66-34072  
Information feedback and psychophysical variables in two-alternative temporal forced-choice auditory-signal-detection task 18 p3063 A66-35023  
Lightweight power-conditioning system for ion engines using energy-storage transformers for conversion, nondissipative regulation and protection 20 p3628 A66-37172  
LF combustion oscillation analyzed by theory of dynamical stability of closed feedback loop 20 p3681 A66-38103  
Frequency characteristics of bending vibrations of bounded rods with electromechanical feedback, possibility of artificially attenuating resonance vibrations and conditions for self-excitation 21 p3822 A66-38513  
Feedback to quadrupole that incorporates device for converting voltage into time parameter of periodic sequence of pulses and vice versa 22 p3877 A66-40414  
Signal and receiver-parameter optimization for additive noise channels with feedback link 22 p3868 A66-40719

**FEEDBACK AMPLIFIER**  
Magnetic semiconductor amplifier behavior with internal feedback and negative control currents 01 p0045 A66-11023  
Operation mode instability of transistorized amplifier with constant current feedback treated as autonomous quadrupole 02 p0198 A66-11750  
Comparison of feedback arrangements using pneumatic amplifiers for static accuracy and dynamic performance improvements of control systems 03 p0323 A66-12374  
Fast analog comparator for hybrid computation using wideband DC amplifier with regenerative feedback circuit providing digital output 03 p0337 A66-12573  
Loop gain and return difference defined in the theoretical study of transistor feedback amplifiers 03 p0349 A66-13012  
Operational amplifier design using normal feedback equations with grounded output voltage for input, discussing frequency response and determination of open-loop gain magnitude 03 p0351 A66-13276  
Automatic gain control circuits, discussing performance and comparing theoretical and experimental results 04 p0501 A66-14409  
Cascode configuration using two interconnected field effect transistors to reduce reverse feedback capacitance for better suitability for VHF communications circuits 05 p0645 A66-14585  
Amplitude response curves for HF circuits in transistorized feedback amplifier determined, using polar-diagram method 05 p0647 A66-14680  
Active RC filters employing operational amplifier to obtain biquadratic rational functions 05 p0658 A66-15125  
Synthesis of RC active filters with prescribed pole sensitivity, noting shunt feedback solution of complex conjugate phantom zeros 05 p0658 A66-15126



Aerial radiation patterns, discussing determination through near field pattern processing 06 p0858 A66-16994

Closed loop gain of multiple feedback circuit determined, using return-difference matrix analysis 07 p1015 A66-17754

High gain HF transistor amplifier design, considering deviations of device parameters and variations with temperature and bias 08 p1197 A66-19561

Schuessler-elliptic low pass filters, discussing solution of approximation problem for low pass filters with good transient response 08 p1198 A66-19748

Feedback used in increasing passband and gain of tuned amplifier, achieving compensation for input reactance when deviating from resonant frequency 09 p1353 A66-20439

Sensitivity of transistor multiple loop feedback amplifier to parameter variations evaluated via replacement with equivalent circuit systems 09 p1355 A66-20603

Feedback amplifier noise characteristics based on noisy quadrupole theory 11 p1664 A66-22650

Onset of unstable modes in paramagnetic quantum amplifier in which feedback is due to energy of active particles in resonator or by external pumping 11 p1712 A66-22729

Seven-stage RL feedback amplifier with 500-mc low-pass bandwidth and 52 db gain, employing frequency compensation technique 11 p1671 A66-23244

Matrix algebra applications to circuit analysis, deriving transistor matrix for use in feedback amplifier 12 p1847 A66-23758

Linearity of phase vs input signal characteristics of phase modulators improved through feedback 13 p2036 A66-25524

Redundant system reliability in aircraft design, noting amplifier and filter arrangements, diode and quadruplex circuits, etc. 14 p2247 A66-27015

Spectral features of stable generation of oscillation in delayed-feedback microwave oscillator consisting of TW amplifier and waveguide delay line 14 p2267 A66-27738

Input and output impedances and gain of hybrid-coil feedback amplifier 14 p2268 A66-28038

Solid state communications devices, discussing HF small signal amplifiers, transistor circuits, varactor diodes for frequency multiplier chains, etc. 14 p2261 A66-28368

Closed loop active networks with distributed RC elements, noting circuit composition, parameters and application 15 p2471 A66-29327

RC active filter synthesis using common-base and common-collector configurations 15 p2475 A66-29862

Step response of saturating feedback amplifier with single time constant, noting design graph for amplifier 16 p2660 A66-30580

Feasibility of solid state negative feedback amplifiers based on use of RC networks meeting requirements of frequency stability, high tolerance and long shelf life 17 p2880 A66-31955

Oscillation conditions for feedback lasers, superradiant directionally coherent emission lasers and coherence brightened emission lasers 17 p2934 A66-32628

Noise figure and optimum source impedance single and double stage transistor amplifiers with negative feedback 17 p2897 A66-33452

Optimum complementary feedback amplifier design having high input and low output impedances, low noise and stable gain over wide frequency range 18 p3074 A66-33556

Relative circuit gain of common-emitter antisaturation feedback circuit configurations as function of circuit parameters 18 p3090 A66-34088

Flueric feedback integration and computation with design by root locus method 19 p3282 A66-36675

Multiloop flight control system root sensitivity to open loop parameter variation, describing method of analysis 19 p3335 A66-36690

Book on feedback circuit analysis covering circuit stability, closed loop transient response, frequency response, compensating networks, etc. 20 p3537 A66-37047

Multiloop flight control system root sensitivity to open-loop parameter variation, describing method of analysis 22 p3884 A66-40360

Onset of unstable modes in paramagnetic quantum amplifier in which feedback is due to energy of active particles in resonator or by external pumping 23 p4078 A66-41467

Three amplifier and oscillator configurations analyzed for controlling location of dominant poles of feedback circuit within possible realizable region 23 p4050 A66-41612

## FEEDBACK CONTROL SYSTEM

### SA SCHULER TUNING

### SA SERVOMECHANISM

Evolution of Honeywell first generation adaptive autopilot inner loop and application to F-94, F-101, X-15 and X-20 vehicles 01 p0099 A66-10008

Optimum guidance in two dimensions of constant acceleration low-thrust vehicle spiraling away from and in toward planet 01 p0100 A66-10026

Stability of control systems with tachometric feedback 01 p0067 A66-10455

Effect of delayed feedback in respiratory disease analyzed for behavioral cybernetic theory, using computer-controlled delay 02 p0186 A66-11648

Generalizing Tsytkin stability criterion for class of time-varying nonlinear sampled data feedback systems 03 p0348 A66-12668

Optimal control approach and uncertainties to feedback control problems 03 p0349 A66-12995

Graphical method for determining closed-loop frequency response of nonlinear feedback control systems 03 p0349 A66-13021

Optimal control process with stochastic feedback for automatic control system 04 p0502 A66-13699

Systems malfunction emphasizing parameter choice for automatic detection 04 p0503 A66-13705

Sampled-data control system introduction, discussing representation of real continuous time functions by impulse trains via transform methods 04 p0506 A66-14184

Feedback control system in design of delta-modulation data transmission system 05 p0654 A66-14610

Optimization theory and converse of circle criterion for simple time-varying feedback system 05 p0655 A66-14620

Relative stability of linear feedback systems noting Hurwitz, Nyquist and Mikhailov stability criteria 05 p0707 A66-14623

Graphical display of transfer function of loaded and null-adjusted symmetrical parallel-tee network 05 p0656 A66-14628

Design of optimal servocontrol system with feedback, using variational calculus method 05 p0657 A66-15099

Boundedness of solutions of nonlinear functional equations for stability of feedback and electrical systems 05 p0658 A66-15182

Transient behavior of feedback stabilized phase-angle-pickup system 06 p0861 A66-16358

Nonsymmetric self-oscillations in relay system, discussing sliding mode of operation of controller with feedback 06 p0863 A66-16529

Optimal control system terminal condition sensitivity, examining parameter variation effects on open loop, feedback and optimal open loop adjacent to closed loop control 06 p0864 A66-16738

Liapunov function construction, using stochastic analog of deterministic method of partial integration 06 p0865 A66-16745

Feedback shift register connection using chain, discussing pseudorandom noise generator 06 p0867 A66-16987

Popov-related stability results for feedback systems proved via bounded solutions for functional equations 07 p1015 A66-17756

Fluidic closed-loop digital position-speed servocontrol system without moving parts, using pulsed air 07 p0991 A66-17878

Feedback method for reducing errors of

counter telescopes due to missed counts and accidental coincidences 09 p1379 A66-20235

Low operating speed of pure fluid digital operating elements is chief limiting factor to application of pure fluid amplifier to feedback control system 09 p1361 A66-20325

Automatic control systems commutable rigid feedback to create astaticism in variable structured systems 09 p1364 A66-20912

Feedback control design analysis using circuit determinants for active and passive elements 10 p1516 A66-21233

Matrix form of Routh algorithm and invariance principle used in digital computer construction of root locus of system 11 p1679 A66-23268

Stability inequality for class of nonlinear feedback systems partially answered by taking into account slope of nonlinear function 12 p1849 A66-24252

Nonlinear control systems consisting of single-loop negative feedback circuit with one isolated instantaneous type nonlinear element 12 p1850 A66-24258

Stable self-adjusting system with single adjustable parameter designed, using inverse model of desired transfer function of closed-loop system in feedback control circuit with large amplification factor 12 p1851 A66-24315

Algebraic conditions of controllability and observability and relation between two Riccati-type matrix equations, deriving one from optimal regulation and second from optimal linear filtering 12 p1854 A66-24339

Dynamic system stability, developments, application and literature 12 p1854 A66-24636

Generalization of parameter plane method for case when characteristic equation coefficients are nonlinear functions of system of adjustable parameters 12 p1855 A66-24642

Pseudorandom binary sequential digital simulation of feedback control systems subjected to random input signals 13 p2030 A66-25211

Antenna drive with feedback control system for radio telescope, noting design, construction and operation 13 p2038 A66-25640

Equalization systems for stochastic processes, discussing automatic adaptive servocontrol, feedback control and vibration simulation equipment 13 p2048 A66-25848

Control system design, analyzing sensitivity of system performance to parameter variations by obtaining time domain measure of sensitivity 13 p2050 A66-26062

Synthesis problem solution for performance criteria defined by time domain sensitivity function, noting controller structure, parametric minimization and operative adjustment of parameters 13 p2051 A66-26071

Sufficient conditions of stability of single-loop nonlinear feedback systems 13 p2052 A66-26074

Functional integration analysis of exponential behavior of nonlinear feedback control systems 13 p2052 A66-26076

Multiparameter sensitivity matrix analysis of linear feedback multiloop systems 13 p2053 A66-26082

Nonlinear time varying open-loop feedback system design and infinitely integrable function space boundedness condition 13 p2053 A66-26085

Nonlinear signal comparators in feedback structures used for input-output invariance of single piecewise constant parameter 13 p2054 A66-26090

Sensitivity comparison of closed-loop and open-loop systems 13 p2054 A66-26092

Optimum guidance in two dimensions of constant acceleration low-thrust vehicle spiraling away from and in toward planet 14 p2328 A66-27419

Dual input describing function /DIDF/ of two-state relay with hysteresis 14 p2265 A66-27481

Adaptive servocontrol equalization system using true integrator instead of RC averager in feedback loop and memory circuit 14 p2267 A66-27664

Automatic control of wideband vibration testing of nonrigid structure with wide range of acceleration levels requiring



computation of feedback signal 14 p2267 A66-27665

Solid propellant rocket engine omnialaxis liquid injection thrust vector control system, using function generator in signal-summing feedback loop to control flow in servovalves and increase motor reliability 14 p2226 A66-27700

Diode bridge variable attenuator used to overcome error signals and harmonic distortion in wide range AGC 14 p2267 A66-27805

Dynamic programming design of invariant multiloop feedback autostabilizers and matrix-Ricatti equation 14 p2268 A66-28184

Optimal control process with stochastic feedback for automatic control system 15 p2469 A66-28540

Systems malfunction emphasizing parameter choice for automatic detection 15 p2469 A66-28547

Conceptual model for industrial quality control problem, noting adequacy in satisfying management goals and customer requirements 15 p2506 A66-28793

Stochastic extensions of techniques for using Liapunov second method in design and analysis of feedback controls, using differential equations 15 p2473 A66-29376

Comparison of nonoptimum and optimum strategies in dual control of inertialess plants in presence of noise in feedback loop 16 p2669 A66-30757

Energy feedback adaptive control system for elimination of effects of load inertia variations in servomechanisms 16 p2670 A66-30812

Model reference adaptive techniques applied to feedback attitude control system to minimize instrumentation 16 p2809 A66-30830

Nonlinear feedback composed of combination of nonlinear functions of state variables separately to stabilize amplitude response and provide time optimal control 16 p2670 A66-30831

Analytical design method for synthesis of feedback controller for multivariable linear control systems, considering transfer function 16 p2671 A66-31111

Parameterized feedback control of nonlinear dynamic system 16 p2672 A66-31337

Gas tungsten arc welding process automation based on feedback control concept 16 p2715 A66-31435

Modern control theory applied to system design for reduction of sensitivity of system to plant-parameter variation by use of feedback 17 p2901 A66-32290

Maximum principle application to optimal control procedure, minimizing transient response and decreasing effect of random changes in system parameters 17 p2902 A66-32577

Feedback control system digital computer design and analysis, including frequency-domain analysis, time-domain analysis, state-space simulation program, etc 17 p2877 A66-32778

Exact evaluation of responses of feedback control system with time delay to deterministic input 18 p3090 A66-34081

Dynamic characteristics of unsteady feedback control system during normal operation, ascertaining signal correlation and cross correlation functions 18 p3091 A66-34987

Feedback methods for conversion of electrical signals into frequencies, using oscillator with signal-current-controlled inductance 19 p3325 A66-35988

Sensitivity theory of nonlinear sampled data control system, establishing conditions for stability of equilibrium positions 19 p3327 A66-36012

Sensitivity analysis of time varying systems, comparing vector output errors of feedback and open loop system with same nominal transfer characteristics 19 p3327 A66-36013

Laser output energy controller having eight-to-one improvement in pulse repeatability in solid state lasers 19 p3374 A66-36034

Evolution of Honeywell first generations adaptive autopilot inner loop and application to F-94, F-101, X-15 and X-20 vehicles 19 p3397 A66-36483

Estimation method of learning time of time-varying threshold learning processes /TLP/ 19 p3333 A66-36664

Stability and sensitivity of terminal linear feedback control systems 19 p3334 A66-36668

Linear optimal control techniques for design of control system for short-range stationkeeping of large assault helicopter 19 p3280 A66-36688

Linear optimal control in systems with uncertain parameters, noting application to design of compensating network for flexible booster for uncertain value of first bending mode 19 p3471 A66-36696

Describing function for analysis of feedback control systems with time-invariant nonlinear elements, simplifying derivation by taking derivative of output of nonlinear element with respect to input 19 p3336 A66-36705

Optimum design of piecewise-linear switching functions for linear, constant, lumped systems with single ideal relay controller 19 p3336 A66-36708

Optimization criterion capable of simultaneously considering different performance aspects applied to linear second-order control system with acceleration, velocity and displacement feedback loops 19 p3337 A66-36714

Explicit method for calculating closed-loop gains defining stability boundary and subsequent phase margin boundaries of two-loop linear feedback system 19 p3337 A66-36716

Input-output stability conditions of time-varying nonlinear feedback systems obtained, using concepts of loop gain, concity and positivity 19 p3338 A66-36739

Parameter-plane method analysis of nonlinear equations of asymmetric oscillations in adaptive feedback control systems 19 p3338 A66-36740

Horowitz root-locus compensation method extended to analysis and design of high-gain linear control systems with variable coefficients 19 p3338 A66-36741

Generalized Lur coordinates used in canonical forms for controllable systems, with applications to optimal nonlinear feedback 20 p3535 A66-36848

Suboptimal adjoint-vector control theory for linearization of feedback control systems independent of nominal trajectory 20 p3535 A66-36849

Optimum control laws for bilinear system, using distributed parameter model with optimizing procedures including bang-bang control and optimum feedback control 20 p3598 A66-36856

Synthesis parametry of ensemble-averaged second-order polynomial approximation to performance index of optimal guidance linear feedback control system 20 p3589 A66-36858

Synthesis of constant or time-varying linear feedback control laws for application in multiple input systems with frequency symmetry 20 p3645 A66-36864

Automatic tracking radar control via nonstationary filter, noting design principle and operation 20 p3536 A66-36866

General adaptive approach based upon minimizing moments of power density spectrum of system error in feedback control system 20 p3536 A66-36877

Block diagram of closed loop automatic control system and conditional feedback control system, both with passive adaptation 20 p3536 A66-36883

Continuous time multivariate optimal filter for feedback realization applied to augmentation and rapid alignment of inertial systems 20 p3596 A66-37231

Monograph on approximate analysis of randomly excited nonlinear controls, discussing feedback system performance, functional and quasi-functional representation, zero mean systems, etc 20 p3538 A66-37577

Noise effect on synthesis of discrete systems with and without feedback channel for transmitting continuous messages, using binary signal and criterion of minimum rms error 20 p3538 A66-37745

Design of integrating and position servomechanisms having tachometer-generator feedback, noting role of inertia

moments effect 20 p3540 A66-38444

Sufficient conditions for equilibrium stability of mixed distributed and lumped parameter feedback control system in parabolic PDE form 21 p3718 A66-38666

Popov criterion application in determining stability of linear time-invariant systems with nonlinear feedback, using root locus 21 p3718 A66-38667

Feedback control system behavior, examining influence of values of structural parameters and variations in domain of complex variable 21 p3718 A66-38806

Feedback control system performance indexes used to characterize response precision, analyzing parameter dependence of integral square error /ISE/, integral time square error /ITSE/ and Feldbaum index 21 p3718 A66-38807

Parameter change effect on feedback control system magnitudes directly measurable on step and frequency response diagram, including delay time, overshoot and passband 21 p3718 A66-38808

Pneumatic servomotor synthesis by root loci technique providing direct insight into effects of parameter changes on system response 21 p3697 A66-39216

Liapunov function and Meyer-Kaiman-Yakubovich lemma used to obtain frequency domain stability criteria for linear plant with both monotone increasing and odd monotone increasing nonlinear feedback functions 22 p3940 A66-40529

Linear dynamic analysis of angular motion of spinning axisymmetrical rocket or spacecraft, emphasizing rigid body with thrust misalignment and another motion caused by deflection of control surfaces or jets 22 p3988 A66-40618

Optimal feedback control of random discrete-time system using Pontryagin maximum principle 23 p4049 A66-41543

IEEE Region Six Conference, Tucson, April 1966, Volume 2 23 p4049 A66-41600

Feedback compensated third-order control systems analysis, using coefficient plane reference system 23 p4051 A66-41703

**FEEDBACK FREQUENCY MODULATION**

**/FBFM/**

Threshold performance of frequency demodulator using feedback compared to phase locked loop 04 p0492 A66-13587

Optimized hybrid unidigit pulse code modulation system, noting use of secondary feedback loop and equalization of gain/frequency characteristic of coder 08 p1186 A66-19740

Rheostat-capacitance generators of FM oscillators with multiobe feedback 09 p1354 A66-20452

**FEEDING DEVICE**

Feeding paraboloidal reflectors by stacked horns, using 45 degree polarization and double stacking of horns 18 p3081 A66-34270

Diffraction pattern analysis of fields generated by hoghorn-fed Cassegrain antenna operating in Fresnel zone 18 p3083 A66-34289

Four-and five-horn tracking feeds for large antennas, emphasizing sum channel gain in five-horn feed 18 p3083 A66-34292

Optimum shape of feed patterns for paraboloidal antennas 18 p3083 A66-34293

Feed horn for large parabolic reflectors has low spillover, nearly uniform aperture illumination, equal F and H plane patterns and wide frequency bandwidth 18 p3084 A66-34302

Millimeter wavelength parabolic reflector with Cassegrain feed system 18 p3095 A66-34325

**FELLOWSHIP AIRCRAFT**

**S FOKKER F-28 AIRCRAFT**

**FERMAT PRINCIPLE**

Radar beam trajectory as function of refractive index lapse rate on basis of Fermat principle, assuming isotropic atmosphere with homogeneous stratification 18 p3130 A66-34719

**FERMI-DIRAC STATISTICS**

Semiconductor surface plasma density and conductivity, calculating distribution and variation via energy band curvature 06 p0929 A66-16981

Bremsstrahlung of nonrelativistic plasma, treating nondegenerate electron component of plasma simultaneously with degenerate



component by applying Fermi-Dirac distribution 12 p1925 A66-24996

**FERRI STATISTICS**

Properties of dense matter in nuclear statistical equilibrium analyzed at high densities and temperatures in connection with stellar evolution 04 p0549 A66-14372

Photoluminescence for p-and n-type gallium arsenide as function of exciting light intensity, noting minority carrier recombination mode, electron energy spectrum, etc 13 p2169 A66-26187

Static equations for characteristic parameter in superfluid Fermi gas 18 p3147 A66-34688

Statistical thermodynamics of Fermi and Bose gases 20 p3674 A66-36905

Gamma irradiation from Co 60 effect on indium antimonide, determining defect formation on dose and limiting position of Fermi level for n-and p-type material 20 p3617 A66-37552

Pitch-angle dependence of first-order Fermi acceleration of particles trapped between shock front and moving magnetic mirror 21 p3776 A66-39564

Acceleration of high energy electrons by means of Parker-Wentzel version of Fermi mechanism due to geometry and distorted structure of interplanetary magnetic field near magnetopause in transition region 22 p3972 A66-40003

**FERRI SURFACE**

Mean free path influence on transverse collective excitations in strong coupling superconducting alloys 02 p0271 A66-11481

Matrix elements of electron-phonon interaction and electric resistance in nickel, using electronic structure of Fermi surfaces and phonon spectrum 06 p0894 A66-16175

Angular correlation of photons measured for positrons annihilating in normal and superconducting lead without observing any effect on Fermi surface 07 p1109 A66-18440

Superconductivity inhibition by normal polarization, noting mechanism of second order suppressive effect 08 p1255 A66-18631

Change in Fermi surface topology, induced in superconductor by external pressure, leads to nonlinear variation of transition temperature with pressure 08 p1269 A66-18978

Anomalies in low temperature properties of noble metal alloys such as thermoelectric power and nonmonotonic behavior of resistivity with temperature 08 p1274 A66-19362

Photoadsorption effect on semiconductor surfaces determined as function of various parameters, noting role of external electric field 08 p1276 A66-19378

Positron annihilation of single oriented crystals of vanadium silicide, measuring angular correlation between gamma rays for calculation of Fermi surface 09 p1419 A66-20046

Surface potential in high and low resistivity semiconductors determined by comparing surface and contact potentials and Fermi levels 09 p1427 A66-20537

Diamagnetic impurity effect on temperature of superconducting transition for Fermi surface topology sensitive to impurity additions 09 p1428 A66-20594

Twelve distinct mass series identified and mass values determined as function of orientation of magnetic field in Fermi surface of zinc at cyclotron resonance 10 p1581 A66-21735

Identification of mass series and mass values in Fermi surface of cadmium at cyclotron resonance compared with results for zinc 10 p1581 A66-21736

Metal structure analysis in terms of elementary electron and ion particles 10 p1547 A66-22054

Effective resistivity of metal-plate conductor with single ellipsoidal Fermi surface and specularly reflecting boundaries is independent of thickness 14 p2364 A66-27706

Fermi surface of metals and semimetals and quantum oscillations in ultrasonic attenuation and magnetic susceptibility of InBi 14 p2366 A66-27763

Ultrasonic-electromagnetic wave interaction in metals including resonance effects from waves arising in external magnetic field,

determining Fermi levels 15 p2559 A66-28621

Pressure effect on transition point of superconductors from Bardeen-Cooper-Schrieffer theory, perturbation theory and electron scattering near Fermi surface 15 p2568 A66-29714

Energy distribution spectrum of tungsten single crystal field emitter and shapes of Fermi surfaces 16 p2769 A66-30162

Valence-band bending to Fermi level and radiative recombination in zinc sulfide with liquid electrodes 16 p2771 A66-30201

RF size effect on ineffective electrons in magnetic field parallel to surface of cadmium plates studied by observing harmonic oscillations of impedance 16 p2772 A66-30289

Dependence of magnetostriction coefficient for diamagnetic materials on change of Fermi surface with momentum and deformation parameter 16 p2777 A66-31035

State density for highly doped semiconductor in magnetic field, obtaining results at near Fermi level energies and at bottom of conduction band 16 p2788 A66-31779

Fermi surface of indium investigated by means of RF size effect at 3 Mc 17 p2977 A66-32316

Ultrasonic attenuation in superconductors, extending BCS theory to include electron scattering effects, effect of anisotropy of Fermi surface, etc 17 p2981 A66-32960

Fermi surface shape and size determination and thermoconductivity and conduction electron properties in metals 18 p3155 A66-34135

Localized magnetic states and Fermi surface anomalies in tunneling 18 p3159 A66-35036

Fermi surface interpretation of band structure, electron energy levels, optical properties and ferromagnetic structure of transition and noble metals 20 p3613 A66-37274

Theoretical band structure, Fermi surface, electronic structure, magnetic and optical properties of rare earth metals 20 p3614 A66-37277

Diamagnetic impurity effect on temperature of superconducting transition for Fermi surface topology sensitive to impurity additions 20 p3622 A66-38128

Kjeldaa absorption edge in cryogenic potassium for shear magnetoacoustic wave propagation in spherical metallic Fermi surface with spin density wave ground state 21 p3800 A66-38991

Electron attenuation of ultrasonic waves of arbitrary polarization and propagation direction for superconductors computed on BCS model, noting role of Fermi surface 22 p3960 A66-39802

BCS model extended to intermediate and strong-coupling superconductors effective interaction strength as function of absolute-zero energy gap, phonon-frequency cut-off and Fermi surface density of states 23 p4113 A66-41376

Thermoelectric power and electric resistivity of copper-gold alloy doped with 3d transition metals as function of temperature and atomic number of impurity 23 p4114 A66-41712

Magnetic breakdown on usual effective Hamiltonian theory for Bloch electrons in magnetic field, using simple two-dimensional rectangular model 24 p4249 A66-42223

Electron self-energies in Fermi gas arising from coupling to optical and acoustic phonons 24 p4250 A66-42231

**FERRIION**

Gorkov Ansatz in superconductivity theory exactly satisfied by system of definite number of fermions 06 p0923 A66-16273

Simple alternative derivation of conventional cluster expansion formula for matrix elements of identity and Hamiltonian for expectation value of energy of many-Fermion system 08 p1259 A66-19445

First-order density matrix corresponding to nondegenerate eigenstate be N-representable for time-reversal invariant Hamiltonian and quantum-mechanical system of N identical fermions 20 p3606 A66-38290

**FERRIC ION**

Properties of ferrous ion in iron germanium oxide studied in terms of

Mossbauer effect and susceptibility measurements 20 p3621 A66-37823

Solid state maser oscillator operating in zero field configuration, using ferric ion substituted as impurity in aluminum nitrate host crystal 24 p4221 A66-42551

**FERRIMAGNET**

Energy calculation as time function required to switch toroidal ferrimagnetic core from one remanent state to another, considering core type used in antenna phased arrays 05 p0642 A66-14564

Approximate molecular-field and quantum mechanical methods used to describe temperature dependence of saturation magnetization in ferrites and ferrimagnets 19 p3445 A66-36317

Resonance curve analysis from microwave absorption measurements on polycrystalline ferrimagnetic doped and undoped garnets at room and low temperatures, with application to low noise receivers 24 p4260 A66-43172

Geometry and magnetic parameters effect on magnetically tunable filters consisting of rectangular waveguide and containing thin magnetized ferrite slab against one wall 24 p4186 A66-43173

**FERRIMAGNETISM**

Microwave behavior of ferrimagnetics and plasmas - IEE Conference, London, September 1965 01 p0022 A66-10507

Energy considerations for transverse electric modes in ferrite loaded rectangular waveguides and associated thermodynamic paradox 01 p0037 A66-10510

Electric field and wave impedance in spin wave propagation in ferrimagnetic materials 06 p0847 A66-16101

YIG resonator tuning for low noise parametric amplifier 07 p1006 A66-17504

High power phase shifter for phased array systems, using temperature compensated garnet along with dielectric liquid cooling technique 07 p1007 A66-17507

Fine-grain structure effect on microwave power absorption thresholds of ferrimagnetic garnets and spinels 14 p2350 A66-26880

High speed ferrimagnetic microtransducer capable of embedding in wide variety of materials and sensors to explore stress characteristics and pressure profiles 20 p3555 A66-36851

Nonlinear inductance effect on leading edge of high voltage nanosecond pulses during passage through ferrite magnetic field 21 p3801 A66-39156

Magnetics - International Conference, Stuttgart, April 1966, Volume 2, covering ferrite and semiconductor devices, superconductivity and magnetic logic 24 p4260 A66-43170

**FERRITE**

**SA BARIUM FERRITE**

**SA STEEL**

Flat transversely magnetized ferrites in traveling wave amplifier 01 p0037 A66-10515

Parametric excitation of first order magnon/phonon instabilities in ferrimagnet or antiferromagnet by photon or phonon parallel-pump 01 p0120 A66-10519

Three-port waveguide circulator design analyzed with X-band, using magnesium manganese ferrite 01 p0038 A66-10524

Eigenvalues, considering losses, of modes propagating by successive reflections in infinite slab of magnetized ferrite 01 p0121 A66-10530

4-port E-plane cross junction ferrite circulator analyzed in X-band 01 p0039 A66-10532

Phase shift in electromagnetic waves between unmagnetized and magnetized ferrite partially filling waveguide 01 p0039 A66-10538

Spin wave instabilities in ferrite using parallel pumping and spin wave absorption near Curie temperature 01 p0121 A66-10539

Thermodynamic paradox consisting of boundary value problem with mathematical inconsistency observed in rectangular waveguides loaded with magnetized ferrite 01 p0121 A66-10540

General mode structure and eigenvalues of cavities containing ferrite magnetized in axial direction 01 p0027 A66-10547

Differential phase shifts in circularly cylindrical waveguides partially filled with



- circumferentially magnetized ferrite compared with theoretic 01 p0027 A66-10553
- computation 01 p0027 A66-10553
- Uniform ferrite slow wave structure analysis of parameters, discussing three applications 01 p0040 A66-10554
- Hysteresis-free UHF ferrite phase modulator using remanent field in rotating ferrite disk as modulating feature 01 p0040 A66-10556
- Dispersion curves and field component computations for longitudinally magnetized ferrite slab in rectangular waveguide 01 p0027 A66-10557
- Automatic measuring apparatus based on resonant cavities for measuring permittivity and permeability of ferrites as function of temperature 01 p0068 A66-10558
- Solution of ferrite boundary value problem in rectangular waveguide and resolution of Lewin paradox 01 p0028 A66-10560
- RF electromagnetic and elastic oscillations in ferrites 01 p0121 A66-10568
- Rectangular waveguide with diaphragm method for ferrimagnetic resonance measurements in ferrites 01 p0041 A66-10573
- Configuration of broadband waveguide Y circulator 01 p0041 A66-10578
- Figure of merit characterizing performance of ferrite slabs in two high power microwave waveguide 01 p0042 A66-10586
- Four passive power limiters based on waveguide devices employing effect of reradiation by ferrites 01 p0042 A66-10587
- Complex permittivity and permeability of lithium aluminium ferrite in cavity resonator determined, using perturbation theory 01 p0123 A66-10590
- Remanent ferrite phase shifter as beam steering elements in phased array radars 01 p0042 A66-10592
- Crystal Hall detectors prepared by gluing thin indium antimonide wafer on rectangular parallelepiped ferrite base 01 p0045 A66-11031
- Electromagnetic reflection characteristics of ferrite wedge absorber and lossy magnetic layers combination 02 p0195 A66-11253
- Relations for interaction between waveguide field and ferrite obtained from reflection and transmission coefficients, using perturbation method 02 p0196 A66-11416
- Anomalous heat conductivity in ferrites at Neel temperature due to corresponding anomalous heat capacity 02 p0277 A66-12088
- Counting decade consisting of three ferrite-transistor triggers and fourth binary element in form of ring with rectangular hysteresis loop 02 p0232 A66-12146
- Polarization effects in magnetic and nonmagnetic barium plus bismuth oxide and magnesium-zinc ferrites when subjected to DC low-voltage electric fields 03 p0409 A66-12690
- Coupled-mode equations for wave propagation through magnetized ferrite rod with variable cross section, noting Faraday rotation 03 p0410 A66-12935
- Phase angles of reflection and transmission coefficients for microwave energy of rectangular waveguide whose electromagnetic field interacts with ferrite spheroid 04 p0496 A66-13909
- Waveguide containing ferrite of ferrite-dielectric insert determined by applying eigenfunction method 04 p0499 A66-14051
- High speed microwave ferrite amplitude and phase modulators in standard rectangular waveguide 06 p0841 A66-15959
- Shielding effect on modulating microwave ferrite switch in applied magnetic field and relation between inside and outside fields for thin waveguide 06 p0857 A66-16952
- Q-factor of ferrite-core networks measured by nonlinear inductance 07 p1031 A66-17400
- Admissible bounds of ambient temperature and supply voltage fluctuations from stable operation conditions of ferrite transistor elements 07 p1005 A66-17406
- Digital latching phase shifter which combines submicrosecond switching with compact ferrite strip transmission line structure 07 p1007 A66-17506
- Circuits for variable impedance control at centimeter-wave frequencies, using varactor semiconductors and dephasing ferrites in waveguide 07 p1002 A66-17828
- Solution to problem of cylindrical cavity containing ferrite specimen in form of hollow cylinder 07 p1009 A66-17926
- Solution to problem of cylindrical cavity containing ferrite and dielectric specimens in hollow cylindrical form 07 p1009 A66-17927
- Ferrite-based microelements as quasi-resonant RC circuits 08 p1191 A66-18914
- Coaxial, rectangular and bandpass waveguides containing ferrite and dielectric plates in E plane, obtaining transcendental equations, determining electromagnetic wave propagation 08 p1194 A66-19312
- Effect of thermal and thermomagnetic treatment of nickel-cobalt ferrite single crystal on rotational magnetic hysteresis losses 09 p1412 A66-19983
- Design, construction and electrical performance of 20-kw 8.5 to 9.5 gc nonreciprocal latching X-band ferrite phase shifter 09 p1352 A66-20259
- So-called thermodynamic paradox associated with magnetized ferrite-loaded rectangular waveguide 09 p1347 A66-20608
- Doubling frequency in ferrites in presence of constant magnetic field not equal to resonance field at frequency being doubled 09 p1348 A66-20791
- Switching properties of partially set square-loop ferrite core, noting flux level influence, measurement techniques, etc 10 p1508 A66-21413
- Ferrite component for radio relay equipment such as antenna insulator, waveguide and coaxial equipment insulator and circulator 11 p1664 A66-22658
- Ferrites for resonance-directional insulators and circulators, noting properties at microwave frequencies and applicability 11 p1664 A66-22659
- Stripline cavity resonator for low microwave frequency measurements of magnetic and dielectric properties of ferrites 12 p1881 A66-24156
- Exact equation for phase constant obtained for rectangular waveguides partially filled with ferrite, using ABCD matrix, eliminating writing of field equations and matching boundary conditions 12 p1839 A66-24617
- Design of nonreciprocal latching ferrite devices including single toroid digital waveguide phase shifter, cut-off switch, miniaturized slow wave phase shifter, etc 12 p1839 A66-24618
- Hardening temperature effect on saturation magnetization and distribution of cations over sublattices in magnesium-base ferrites 13 p2160 A66-25100
- Chemically deposited thin ferrite and garnet films 14 p2249 A66-27104
- Approximate engineering method of calculating coaxial and artificial ferrite containing lines and artificial ferrite containing lines shaping high power video pulses with fronts of nanosecond duration 14 p2236 A66-27238
- Capacitance type ferrite transducers consisting of polycrystalline yttrium garnet of high resistivity 14 p2252 A66-27248
- Ferrite controlled polarization of slot radiator by rectangular waveguide excited by H<sub>10</sub> wave 14 p2252 A66-27252
- Experimental verification of theoretical behavior of ferrite structural discontinuity between rectangular waveguide filled with homogeneous dielectric and waveguide filled with transverse magnetized ferrite 14 p2253 A66-27585
- Faraday effect in rare earth garnet ferrites and metallic ion g values in IR spectrum 14 p2364 A66-27703
- Permanent magnetized ferrite antenna waveguide windows for improving EM wave transmission through plasma and reducing transmission losses during reentry 14 p2241 A66-27930
- Design and operation of ferrite rectangular waveguide modulator in 5 to 7 gc/s range 14 p2258 A66-27963
- Counting decade consisting of three ferrite-transistor triggers and fourth binary element in form of ring with rectangular hysteresis loop 14 p2297 A66-28102
- Change in heat capacity at Curie point for ferrites 14 p2369 A66-28331
- Production of thin copper and nickel ferrite films in inert gas plasma reveal spinel structure in electron diffraction patterns 15 p2557 A66-28564
- Beam scan at millimeter wavelengths obtained from ferrite antenna aperture 15 p2455 A66-28574
- Theoretical and experimental investigations of electromagnetic scattering by conducting cylinder coated with anisotropic ferrite sheath magnetized along axis 15 p2449 A66-28594
- Nonlinear losses in ferrite phase inverter in relation to natural ferromagnetic resonance 15 p2560 A66-28671
- Temperature dependence of line width anisotropy field in Mn substituted ZnY 15 p2565 A66-29028
- Magnetic relaxation and high temperature effect of Bloch wall stabilization in ferrite Mn-Fe 15 p2565 A66-29058
- Ferrite-air interface in waveguide with conducting thin film coated core solved by use of boundary condition or impedance condition 15 p2565 A66-29058
- Change in ferrite transverse dimensions examining effect on variable-field isolator performance in X-band 15 p2565 A66-29058
- HF oscillations in single-crystal magnesian manganese ferrite 16 p2772 A66-30229
- Electrical properties of nickel ferrite in terms of Jonker model, noting magnitude of energy gap between Fe and Ni levels and mobilities of electrons and of positive holes 16 p2781 A66-31211
- Frequency of arising stationary finite amplitude waves in ferrites depends on properties of medium, angle between magnetic field and propagation direction and wave amplitude 16 p2784 A66-31544
- Electron flux induced excitation of magnetostatic oscillations of magnetized ferrite 16 p2784 A66-31544
- Temperature dependence of magnetization and resistivity in SHF magnesium-aluminum ferrite 16 p2786 A66-31677
- Handbook of microwave ferrite materials 16 p2787 A66-31750
- Waveguide containing ferrite of ferrite dielectric insert determined by applying eigenfunction method 17 p2884 A66-32211
- Batch fabrication of large-capacity memory stacks, using integration of monolithic ferrite stack with integrated MOS circuitry 17 p2886 A66-32511
- Developmental memory using monolithic ferrite integrated arrays of magnetic storage elements provides cost and power savings 17 p2886 A66-32511
- Nickel, nickel-zinc and magnesium-zinc ferrite thin films, using chemical deposition on alumina substrates for millimeter wave application 18 p3153 A66-33737
- High-speed memory units for digital computer, discussing ferrite, semiconductor and thin magnetic or ducting film memories 19 p3322 A66-36817
- Phase angles of reflection and transmission coefficients for microwave energy of rectangular waveguide whose electromagnetic field interacts with ferrite spheroid 20 p3532 A66-37864
- Electronic component, ferrite memory cores, filters and inductances adapted to integrated circuit utilization 21 p3716 A66-39627
- Doubling frequency in ferrites in presence of constant magnetic field not equal to resonance field at frequency being doubled 22 p3874 A66-39817
- Ultraminiature ferrite device design parameters for application in microwave receiver systems 22 p3880 A66-40778
- HF magnetic susceptibility of ferrites with two magnetic sublattices 23 p4110 A66-41119
- Production of thin copper and nickel ferrite films in inert gas plasma reveal spinel structure in electron diffraction patterns 23 p4112 A66-41228
- Induced uniaxial anisotropy energy of manganese-bearing ferrites, noting effect of metal additives 24 p4253 A66-42364
- Material selection for linear ferrite device including determination of internal biasing field, estimate of required saturation magnetization, etc 24 p4280 A66-43177
- Latching phase modulator in standard rectangular waveguide, using square loop magnetic properties of toroidal ferrite



materials to obtain digital increments of reciprocal phase shift 24 p4186 A66-43174

Ferrite core memory system organization for lower cost and higher performance, noting diode decoded drive system 24 p4177 A66-43182

## FERROELECTRICS

### SA ANTIFERROELECTRICITY

Optical phase modulator using ferroelectric barium titanate crystal plate 01 p0117 A66-10240

Nuclear magnetic resonance study of ferroelectric phase transition in  $\text{NaNO}_2$  02 p0276 A66-12027

Electrostatic hysteresis synchronous motor discussing development, operation characteristics, test results, advantages and limitations 04 p0459 A66-13681

Ferroelectricity - All-Soviet Conference, Rostov, U.S.S.R., September 1964 06 p0925 A66-16712

UHF dispersion in barium titanate ferroelectric crystals explained as microwave scattering 06 p0926 A66-16717

Ferroelectric properties and morphotropic phase boundary in phase diagram of ternary system of compounds of lead, titanium and nickel 06 p0927 A66-16720

Electric properties of thin ferroelectric films of barium titanate compound 06 p0927 A66-16724

Polarization and volt-ampere characteristics of ferroelectrics simultaneously under static and alternating fields 06 p0854 A66-16726

Phase transitions in lithium niobate and tantalate, discussing ferroelectricity 07 p1092 A66-17221

Polycrystalline barium titanate ceramic with nonlinear resistance-temperature characteristic that rises steeply at ferroelectric Curie point 07 p1100 A66-18156

Ferroelectric properties of trisarcosine calcium chloride including dielectric measurement, Curie temperature region, etc 08 p1270 A66-19009

Current pulse measurement of thin polarized ferroelectric ceramic disks connected by short circuit under stress wave 10 p1576 A66-21546

Barium titanate transition front structure, noting similarity to ferroelectric and nonferroelectric crystal structure 10 p1582 A66-21881

Gadolinium molybdenate as ferroelectric host in pulsed laser, noting light modulation and crystal domain 11 p1713 A66-23207

Ultrasonic piezoelectric investigation of asymmetric polarizability of barium titanate crystal 11 p1757 A66-23252

Maximum efficiency of power converters, using ferroelectric and nonferroelectric pyroelectrics 13 p1997 A66-25036

Piezoelectric constants of polycrystalline ferroelectrics of barium titanate type, noting dependence on ceramic sintering temperature and applied constant voltage 13 p2160 A66-25099

Temperature dependent soft-mode lattice vibration in perovskite-type ferroelectric crystal single-oscillator 15 p2567 A66-29394

Phase transitions in lithium niobate and tantalate, discussing ferroelectricity 17 p2976 A66-31992

Temperature autostabilizing nonlinear dielectric element /TANDEL/ to obtain desirable and optimal working temperatures of ferroelectric crystal and electro-optical devices 17 p2896 A66-33298

Effect of ferroelectric polarization interacting with space charge on insulated-gate thin-film transistor parameters 17 p2896 A66-33299

Electromechanical effects of ferroelectric crystals based on thermodynamic theory 18 p3153 A66-33630

Proper mechanical vibrations effect on some properties of triglycine sulfate TANDEL /temperature autostabilizing nonlinear dielectric element/ 18 p3075 A66-33632

Electron scattering in ABO-type semiconductors by long-wave transverse-optical ferroelectric lattice mode evidenced by hydrostatic pressure measurements 19 p3444 A66-36176

Diffuse boundary scattering as possible explanation for enhanced field effect in thin metallic films through polarization reversal

of ferroelectric substrates 21 p3800 A66-38990

Applications for ferroelectric cold conductors and GaAs light-sensitive diodes, examining supersonic amplification in CdS 21 p3716 A66-39620

## FERROMAGNETIC FILM

Pulse transmission through cavity, observing if instability or bistable response is present, in connection with behavior of ferromagnetic thin films of permalloy 01 p0120 A66-10529

Thin ferromagnetic Fe-Ni films, discussing elastic tensile stresses on structure of interdomain boundaries and distribution of magnetization vectors 04 p0563 A66-13876

Electron microscopic estimation of perpendicular anisotropy of magnetic thin film originating from nonmagnetic grain boundaries 08 p1270 A66-19012

Magnetic measurements and exchange interactions in thin anisotropic ferromagnetic films 09 p1410 A66-19905

Hysteresis properties of thin ferromagnetic films of nickel-iron and of nickel-iron-molybdenum compositions, noting anisotropic dispersion 09 p1431 A66-20868

Ferromagnetic film behavior near hard direction of magnetization 09 p1431 A66-20869

Elastic tensile stress effect on domain structure of thin ferromagnetic films composed of iron and nickel 09 p1431 A66-20870

Thin ferromagnetic film physics - All-Union Symposium, Irkutsk, U.S.S.R., July 1964 11 p1751 A66-22796

Nucleation during pulse remagnetization of thin films, showing domain structure of formation, growth of nuclei, etc 11 p1752 A66-22797

Quasi-equilibrium states during pulse remagnetization of thin ferromagnetic films, discussing domain structure 11 p1752 A66-22798

Motion of magnetic moment of thin ferromagnetic films in rotating magnetic field, determining signals of first and second harmonics as function of field intensity 11 p1752 A66-22800

Transverse galvanomagnetic effect in single-domain ferromagnetic film, noting role of Hall effect 11 p1752 A66-22801

SHF susceptibility of ferromagnetic thin films for constant magnetic fields far from electromagnet resonance 11 p1753 A66-22809

Multifilm absorption spectrum dependence on magnetic interaction, deposition, thickness and quality of ferromagnetic and insulating films 11 p1753 A66-22810

Ferromagnetic multifilm systems effect on SHF power transmission and variation of resonator parameter 11 p1754 A66-22811

Reverse magnetization and energy of anisotropy of single crystal ferromagnetic films 11 p1754 A66-22815

Induced anisotropy of ferromagnetic atom pairs and magnetostriction stresses in Fe-Ni thin films subject to annealing 11 p1755 A66-22818

Quasi-static reverse magnetization of thin ferromagnetic films under action of SHF field 11 p1755 A66-22823

Incoherent rotation of reverse magnetization in thin ferromagnetic films, allowing for internal magnetostriction and exchange interaction 11 p1755 A66-22824

Interaction between layers of ferromagnetic films of different composition and coercivity separated by insulating quartz layer, obtaining films by vacuum deposition 12 p1933 A66-25028

Nonuniform rotation of local magnetization vectors in thin nickel-iron films, measuring contribution of time-dependent variations in torque during magnetic field reversal 12 p1934 A66-25031

Magnetostatic model for perpendicular anisotropy in polycrystalline nickel-iron thin films 14 p2352 A66-26893

Thin ferromagnetic Fe-Ni films, discussing elastic tensile stresses on structure of interdomain boundaries and distribution of magnetization vectors 14 p2363 A66-27581

Physics of thin ferromagnetic films - All-

Union Conference, Irkutsk, U.S.S.R., July 1964 16 p2772 A66-30680

Pulse switching of thin ferromagnetic films in nanosecond range and operation characteristics of measuring circuit 16 p2773 A66-30681

Planar Hall /galvanomagnetic/ effect in thin iron or nickel ferromagnetic films 16 p2773 A66-30684

Planar Hall effect used to determine magnetic properties of ferromagnetic films such as anisotropy field and coercive force 16 p2773 A66-30685

Static properties of vacuum deposited thin permalloy films 16 p2773 A66-30687

Technology, preparation and properties of multilayer ferromagnetic films, including influence of composition and deposition conditions on coercive force values, shape of hysteresis loops, etc 16 p2773 A66-30688

Magnetic interaction between layers of two-layer ferromagnetic film, discussing inhomogeneity effects, Barkhausen jumps, reverse magnetization nuclei, etc 16 p2774 A66-30689

Magnetic and structural properties of monoferrite films prepared by cathode sputtering, noting electron diffraction and micrograph patterns of films, crystal structure, etc 16 p2774 A66-30690

Effect of annealing in magnetic field on structural and magnetic properties of thin films prepared from nickel alloy 16 p2774 A66-30695

Temperature dependence of domain structure of thin ferromagnetic films prepared by thermal evaporation in vacuum 16 p2774 A66-30696

Apparatus for analysis and preparation of magnetic properties of thin ferromagnetic films in vacuo, noting hysteresis loop, thermal evaporation, etc 16 p2661 A66-30697

Magnetic properties and structure of ferromagnetic films obtained on single-crystal sodium chloride substrates heated to various temperatures during spray coating 19 p3438 A66-35497

Associated nonuniform electron-nucleus oscillations in ferromagnetic substances studied to determine feasibility of maser, using magnetic-reversal nuclear magnetic resonance 20 p3577 A66-37477

## FERROMAGNETIC RESONANCE

Saturation characteristics of ferromagnetic amplifiers 01 p0041 A66-10567

Rectangular waveguide with diaphragm method for ferrimagnetic resonance measurements in ferrites 01 p0041 A66-10573

Surface impedance of ferromagnetic metals at frequencies approaching ferromagnetic resonance, considering spatial dispersion of magnetic permeability 01 p0123 A66-10721

Nuclear magnetic resonance - Preliminary Report of International Symposium, Tokyo, September 1965 02 p0276 A66-12024

Nuclear magnetic resonance measured and tabulated for many impurity nuclei in ferromagnetic alloys Fe, Co and Ni 02 p0276 A66-12025

Microwave acoustic waves generated by ferromagnetic resonance and spin-wave resonance modes in magnetic film 03 p0331 A66-12409

Measurement of components of permeability and permittivity tensors of magnetized ferrites by cavity method 07 p1009 A66-17928

Narrow voltage pulse open core ferromagnetic oscillator generation with high off-duty factor 11 p1667 A66-22791

Multifilm absorption spectrum dependence on magnetic interaction, deposition, thickness and quality of ferromagnetic and insulating films 11 p1753 A66-22810

Electron and nuclear magnetic system interaction in ferromagnetic crystals, effect on basic characteristics of nuclear magnetic resonance in ferromagnetics 11 p1754 A66-22813

Ferromagnetic resonance in thin magnetic permalloy films, examining laws governing spin-wave spectrum for parallel orientation of magnetic field 11 p1755 A66-22822

Forced oscillations of ferrite core circuit, showing phase characteristics and parameters of inductance and amplitude 12 p1958 A66-23725

Nonlinear losses in ferrite phase inverter



in relation to natural ferromagnetic resonance 15 p2560 A66-28677  
 Ferromagnetic microwave resonance isolators for use in waveguides 15 p2459 A66-28936  
 Temperature dependence of line width and anisotropy field in Mn substituted ZnY 15 p2565 A66-29028  
 HF oscillations in single-crystal magnesium manganese ferrite 16 p2772 A66-30294  
 Electron flux induced excitation of magnetostatic oscillations of magnetized ferrite 16 p2784 A66-31549  
 Surface impedance of ferromagnetic metals at frequencies approaching ferromagnetic resonance, considering spatial dispersion of magnetic permeability 20 p3619 A66-37659  
 Spin wave excitation by ferromagnetic resonance, measuring coercive field as function of temperature by Kerr effect method and determining magnetic properties of thin films 20 p3621 A66-38085  
 Ferromagnetic spin correlations from strong Coulomb interactions between valence electrons resulting in enhanced singlet-state repulsion 21 p3803 A66-39263  
 Simultaneous existence /triple resonance/ of spin, helical and acoustic waves in ferromagnetic conductor in strong magnetic field 22 p3964 A66-40310

## FERROMAGNETISM

## SA ANTIFERROMAGNETISM

## SA BARKHAUSEN EFFECT

## SA BLOCH WALL

Mechanical energy dispersion by internal friction mechanism of ferromagnetic metals in alternating magnetic field 01 p0116 A66-10193  
 Anomalous Barkhausen effect in ferromagnetic alloys 01 p0117 A66-10239  
 Uniform compression effect on Curie temperature of ferromagnetic compound EuO 01 p0118 A66-10254  
 Loaded linewidth measured for given value of circuit coupling, determining unloaded linewidth, noting ferromagnetic parametric amplification and harmonic generation 01 p0039 A66-10528  
 Conventional periodically loaded waveguides with ferrimagnetic materials used in devices involving traveling wave interaction with electron beam 01 p0025 A66-10533  
 RF magnetic field effect, applied parallel to external DC field, on Heisenberg ferromagnet with dipolar coupling, using Green function 01 p0122 A66-10579  
 Unified model of ferromagnetism, analyzing spin-wave motion of electrons in transition metals, using atomic and energy-band features 04 p0559 A66-13450  
 Behavior of Ising model of ferromagnet in nonzero magnetic field, using high temperature series 04 p0563 A66-13815  
 Complex susceptibility measured, using voltage induced in loop around ferromagnetic core situated at short-circuit end of coaxial line 05 p0716 A66-15028  
 Low temperature excitation spectrum for ferro- and antiferromagnets with large crystalline field splittings 05 p0741 A66-15867  
 Superconductors with ferromagnetically aligned impurities, assuming electron mean free path due to spin-orbit interaction is small compared to coherence distance 07 p1108 A66-18431  
 Magnetocrystal anisotropy of hexagonal ferromagnetic substances in neighborhood of Curie point 08 p1273 A66-19249  
 Electrical and magnetic properties of ten synthesized perovskite compounds of complex composition 08 p1273 A66-19268  
 Phase transitions theory analyzed by simple self-consistent equations including ferromagnetism, antiferromagnetism, liquid-gas condensations and melting and freezing 09 p1424 A66-20076  
 Thermoelectric power of actual ferromagnetic metals over wide temperature range, examining effect of alloying and solute magnetic ions 09 p1425 A66-20080  
 So-called thermodynamic paradox associated with magnetized ferrite-loaded rectangular waveguide 09 p1347 A66-20608  
 Conduction electron interaction with spin wave in ferromagnetic superconductor, noting decay and

damping 09 p1430 A66-20867  
 Stability theory of magnetic phases for simplified quasi-particle band model of transition metals and alloys 10 p1580 A66-21734  
 UHF ferrites as magnetically anisotropic media in which electromagnetic wave propagation rate assumes two values and magnetic permeability is of tensor nature 11 p1658 A66-23233  
 Green function random phase decoupling scheme investigation of magnetic impurities effect on thermal properties of cubic spin-1/2 Heisenberg ferromagnet 11 p1758 A66-23394  
 Compensation and decompensation in ferromagnetic alloys viewed as electric interaction of spins 12 p1930 A66-24684  
 Existence of superconductivity along domain boundaries in ferromagnetic materials having domain structure when induced by nonmagnetic s-electrons or when only magnetic electrons are present 13 p2166 A66-25919  
 Uniform compression effect on Curie temperature of ferromagnetic compound EuO 13 p2168 A66-25971  
 Coexistence of superconductivity and ferromagnetism in alloy containing paramagnetic impurities explained by spin-orbit interaction of conduction electrons 13 p2169 A66-26566  
 Plasma-spin wave interaction in ferromagnetic semiconductors and metals with easy-plane and easy-axis magnetic anisotropy 14 p2360 A66-27188  
 Superconductivity and origin of magnetic field at nucleus and ferromagnetism problems analyzed in rare earth metals and alloys 14 p2362 A66-27461  
 Metrological characteristics of three-component magnetometers with ferromagnetic probes installed in Elektron II space station 15 p2497 A66-28501  
 Pressure effect on magnetic moment of solids, noting magnetic transition point, ferromagnetic anomalies, etc 15 p2565 A66-29067  
 Magnetic effects on diffusion of ferromagnetic colloidal particles dispersed in current-carrying fluid medium, noting force effects on relaxation process 15 p2556 A66-29809  
 Electronic density of states of superconducting ferromagnetic alloys determined by static electron-impurity exchange interaction 16 p2768 A66-30148  
 Heat magnetization in simple model applied to thulium intermetallic compounds 16 p2745 A66-30177  
 Ferromagnetic semiconductors with exchange interaction due to conduction electrons 17 p2986 A66-33306  
 Galvanomagnetic effect in ferromagnetic metals, developing theory of planar Hall effect in terms of spin-orbit interaction of electrons 18 p3158 A66-34682  
 German papers on metal physics, chemical bonds in crystals and ferromagnetism 19 p3439 A66-35712  
 Quantum theoretical ferromagnetic behavior of chemical bonds in transition metals and Hartree-Fock calculation of atomic orbitals 19 p3439 A66-35713  
 Micromagnetic theory of ferromagnetics, discussing magnetization curve, saturation and hysteresis effects 19 p3439 A66-35714  
 Magnetization curve and magnetic hysteresis of ferromagnetic single crystals 19 p3439 A66-35715  
 Effect of electric and magnetic properties of titanium oxide explained through Matsubara and Yokota theory extended to finite temperatures 19 p3444 A66-36175  
 Ferromagnetic fluid developing body force under magnetic field influence, noting changes in internal pressure, velocity, etc, applied to attitude control devices, accelerometers, etc 19 p3445 A66-36178  
 Fermi surface interpretation of band structure, electron energy levels, optical properties and ferromagnetic structure of transition and noble metals 20 p3613 A66-37274  
 Physics of ferro- and antiferromagnetism - All-Union Conference, Sverdlovsk, U.S.S.R., July 1965 20 p3616 A66-37475  
 Contrast formation of coupled walls

studied by electron microscope with variable defocusing 20 p3620 A66-37321  
 Magnetic properties of ferromagnetic zinc-zirconium alloy between 120 degrees and 0.1 degrees K, suggesting possible indication of superconductivity 21 p3801 A66-39000  
 Fluidmagnetic buoyancy effects in ferrohydrodynamic /FHD/ flows and implications of Earnshaw levitation theorem 23 p4057 A66-41885  
 Parametric phenomena in ferromagnetics, noting parametric excitation of quasi-particles and stationary state of excited waves 24 p4256 A66-42522  
 Plasma-spin wave interaction in ferromagnetic semiconductors and metals with easy plane and easy axis magnetic anisotropy 24 p4259 A66-43086

## FERRY SPACECRAFT

Relative advantages of ballistic missiles and orbital ferries for placing payloads in orbit 02 p0306 A66-11862  
 Orbital space station development based on multimission space station module for six persons and multipurpose logistics vehicles for ferry resupply 03 p0432 A66-12904  
 Titan III as ferry-resupply system with analysis of performance as affected by orbit altitude and inclination parameters [SAE PAPER 660446] 18 p3245 A66-33892

## FET

## S FIELD EFFECT TRANSISTOR /FET/

## FETUS

Biosatellite for TV monitoring of development of opossum embryonic fetus in space environment 08 p1174 A66-18583

## FEYNMAN DIAGRAM

Interaction characteristics calculated for Feynman diagram of nucleon-nucleon scattering at 300 bev 07 p1115 A66-17556  
 Electromagnetic form factors of electron and muon neutrinos evaluated, using intermediate vector-boson theory, noting renormalization induced by electromagnetic interactions 15 p2544 A66-28944  
 Semiempirical theory based on virial and Feynman theorems relating physical parameters and mechanical behavior of metals with structural characteristics 22 p3937 A66-40927  
 Gauge transformations of third kind and operator gauge transformations of first and second kinds, relating electron and photon propagators to quantum electrodynamical vertex function 23 p4098 A66-41392

## FIAT G-222 AIRCRAFT

Controls, systems and equipment of five different configurations of FIAT G 222 V/STOL transport aircraft for Italian Air Force 02 p0177 A66-11868

## FIBER

## SA GLASS FIBER

## SA REINFORCING FIBER

## SA SYNTHETIC FIBER

Ceramic and graphite fibers and whiskers, Air Force sponsored monograph 09 p1392 A66-20475  
 Fiber orientation effect on ultimate tensile strength of aluminum-steel-silica fiber-reinforced metals 12 p1896 A66-24533  
 Fibrous continuum media theory, discussing geometrical properties, stress state, motion equations, boundary value problems, etc 14 p2397 A66-27383  
 Heat transfer, thermal conductivity and thermal diffusivity of loose fibrous materials under vacuum 20 p3587 A66-36978  
 Macroscopic viscoelastic properties of fiber reinforced materials analyzed on basis of composite cylinder assemblage model and correspondence principle 21 p3827 A66-38697

## FIBER OPTICS

## SA VIDICON

Light interaction effects potentially useful in optical logic functions, emphasizing fiber lasers 05 p0693 A66-14825  
 Waveguide coupling between adjacent parallel fibers as means of transferring radiation from one element to another 05 p0693 A66-14827  
 Fraunhofer pattern of laser light transmitted through optical fiber, noting spatial frequency of interference fringes between light waves 05 p0696 A66-14972  
 Fiber optics assemblies for high resolution photographic application 14 p2292 A66-27321  
 Transient fiber optics probe for space resolved diagnostics of dense plasmas,



noting adaptation to temperature measurements by line intensity and line ratio method 23 p4107 A66-41887  
Fiber optics application to wave guidance of X-rays 24 p4236 A66-42252

**FIBER STRENGTH**  
Glass, quartz, mineral and ceramic fibers woven into fabric provide thermal insulation, reinforced plastic, filtration, friction materials and electrical insulation 01 p0091 A66-10356  
Origin and properties of fiber composite materials 05 p0705 A66-14808  
Strength of whiskers in fiber composite materials 05 p0705 A66-14809  
Influence of fiber and matrix characteristics on mechanics of deformation and fracture of fibrous composite 05 p0773 A66-14810  
Structural mechanics and critical conditions of fiber composite materials 05 p0773 A66-14907  
Compressive strength and instability failure mechanism in uniaxial boron fiber-metal matrix composite 08 p1240 A66-19139  
Elastomechanical properties of glass fibers and resins in order to determine optimum materials for reinforced glass fiber structures  
[ONERA TP 322] 11 p1721 A66-23200  
Two-dimensional fibrous media theory, noting stress-strain states, bodies with microstructures, fibrous representation of bar structures, etc 15 p2614 A66-29719  
Calibration method for tensile testing apparatus for testing elongated high modulus fibers and graphing of typical load elongation curves 17 p2943 A66-32400  
Mechanical properties of metallic and ceramic fibers in metallic matrices and refractory fibers in ceramic matrices 21 p3751 A66-39231  
Fatigue behavior of aluminum reinforced with stainless steel wires, considering effects of fiber volume fraction and interfacial bond 23 p4081 A66-41661  
Fiber geometry effect on shear stress distribution in composite materials 24 p4292 A66-42861

**FIBERGLASS**  
S GLASS FIBER  
**FIELD**  
S ANTENNA FIELD  
S BOSON FIELD  
S CROSSED FIELD  
S ELECTRIC FIELD  
S ELECTROMAGNETIC FIELD  
S ELECTROSTATIC FIELD  
S FAR FIELD  
S FLOW FIELD  
S FORCE FIELD  
S GEOMAGNETIC FIELD  
S GRAVITATIONAL FIELD  
S INTERSTELLAR MAGNETIC FIELD  
S MAGNETIC FIELD  
S MAGNETOSTATIC FIELD  
S MULTIPOLAR FIELD  
S POTENTIAL FIELD  
S PRESSURE FIELD  
S RADIATION FIELD  
S SELF-CONSISTENT FIELD /SCF/  
S SOUND FIELD  
S STAR FIELD  
S STELLAR FIELD  
S STRAIN FIELD  
S TEMPERATURE FIELD  
S TENSOR FIELD  
S VISUAL FIELD  
Space-time correlation function of response of finite cylindrical shell to purely random pressure field and to subsonic boundary layer pressure fluctuations 01 p0147 A66-10131

**FIELD-ALIGNED IRREGULARITY /FAI/**  
Achromatic electromagnetic quadrupole lens functioning for case of slight misalignment of fields 02 p0199 A66-11783  
Radar echoes explained in terms of backscatter from field-aligned irregularities in F region 03 p0334 A66-12679  
Correlation of peak occurrence of HF radar echoes and high-latitude spread-F measurements near time of local sunset 18 p3107 A66-34525

**FIELD EFFECT TRANSISTOR /FET/**  
**SA METAL OXIDE SEMICONDUCTOR /MOS/**  
Surface conductivity of germanium gold alloyed at liquid nitrogen temperature, considering field effect 01 p0127 A66-11059  
Transient gamma radiation pulse effects on MOS field effect transistors 01 p0049 A66-11151  
Integrated current limiter design using transistor circuits, pn-pn switches or field effect transistors 02 p0204 A66-11935  
Transmission-line model of insulated-gate field effect transistor /MOS transistor/ in pre-pinchoff mode, determining small signal response 02 p0205 A66-11980  
Curve tracer adapter for junction field effect transistors and manufacturing operations system, discussing basic circuitry and uses 03 p0348 A66-13345  
Integrated circuit for time division multiplexers having flexible integrated gate driver circuit for field effect transistor analog gates 04 p0492 A66-13598  
Simple derivation of small-signal equivalent circuit for arbitrarily doped 4-terminal field effect transistors 04 p0500 A66-14098  
Relationship between three symbolic circuit representations of charge-capacitance effects in 4-terminal field effect transistors 04 p0500 A66-14099  
Comparing VHF cascade circuits with double diffusion silicon planar transistors and metal oxide field effect planar transistors 04 p0501 A66-14133  
Metal oxide semiconductor structures in integrated circuits as high and low resistances, inverters and AC amplifiers 05 p0643 A66-14569  
Noise in metal oxide semiconductor field effect transistors, using thermal noise activity in conducting channel 05 p0644 A66-14580  
Cascode configuration using two interconnected field effect transistors to reduce reverse feedback capacitance for better suitability for VHF communications circuits 05 p0645 A66-14585  
Conditioning and isolation of Apollo stabilization and control system signals, using field effect transistors 05 p0646 A66-14638  
Current flow, charge distribution and transient response equations derived for insulated-gate field effect transistors 05 p0647 A66-14666  
Neutron radiation effects on silicon field effect transistors 05 p0739 A66-15489  
Instability of metal oxide silicon field effect transistors found due to sodium-ion migration 06 p0842 A66-16010  
Width of depletion region of reverse-biased silicon p-n junction 06 p0923 A66-16382  
Thermal noise effects in field effect transistors at LF 06 p0850 A66-16440  
Lead telluride single crystal grown on cleaved rock-salt substrates for thin-film field effect transistors 06 p0854 A66-16679  
Improved resolution of scanning electron microscope used to define geometry of electrode areas during fabrication of solid state devices 06 p0855 A66-16769  
Field effect transistor circuits used to replace bipolar transistors or thermionic devices and action as variable ohmic resistor 06 p0856 A66-16867  
Field effect transistors applied in circuit design including triggers, gates, impedance adapters, etc 06 p0856 A66-16919  
Field effect transistors and unijunction transistors in sawtooth generator, cascade amplifier, voltage regulator, etc 06 p0856 A66-16920  
Epitaxial metal-oxide-semiconductor transistor with tunable high-pass filter-type response characteristics with insertion gain in passband 06 p0857 A66-16959  
Radiation-induced leakage current across gate-to-substrate and drain-to-substrate semiconductor junction dominates behavior of MOS field effect transistors for small gate impedances 07 p1009 A66-18146  
Jump-conductivity surface dependence on surface potential in semiconductor, based on field effect basic geometry 07 p1105 A66-18374  
Equivalent circuit and DC characteristics

derivation for MOS transistor in common-gate electrode arrangement 08 p1188 A66-18656  
Equivalent circuit and gain in single lumped approximation for MOS field effect transistor 08 p1189 A66-18660  
Equivalent circuit obtained from device charge equations for analysis of HF properties of four-terminal field effect transistors 08 p1189 A66-18669  
Fabrication of active thin film elements, considering bipolar and unipolar transistor, hot electron devices, field effect transistors and single crystal semiconductor films 08 p1192 A66-18964  
Unitron, junction-type unipolar field transistor, design, operation, parameter, production technology and uses in electronic circuitry 08 p1193 A66-19277  
Small signal properties of field effect devices, junction and MOS 08 p1195 A66-19356  
Transient response of MOS-FET transistor investigated by exposing p-and n-channel devices to 600 kev flash X-ray machine 08 p1196 A66-19498  
Saturation currents of silicon multichannel field effect transistors 09 p1350 A66-19914  
Refined field effect transistors noting current, gate voltage and transconductance of proposed structures 09 p1350 A66-19918  
Thin film transistors using evaporated silicon films on sapphire 09 p1351 A66-19939  
Galvanomagnetic and field effect measurements on Ge double crystals 09 p1427 A66-20419  
Field effect transistor used in analog switching circuits 09 p1355 A66-20571  
Static characteristics of insulated gate field effect transistor with gate electrodes at both sides of semiconducting channel, including space charge limited currents analysis 09 p1359 A66-20974  
Metal oxide semiconductor /MOS/ transistors constructed on single crystal cadmium sulfide, noting transconductance, gate source, gate drain capacitance, etc 09 p1360 A66-20980  
Inversion layers of MOS field effect transistors observed by scanning-electron microscope and current measured 10 p1574 A66-21355  
Field effect transistor input capacitance in pinch-off region derived by using two parallel coupled condensers as equivalent 10 p1510 A66-21657  
Gridistor, semiconductor device with form of field-effect triode and application as amplifier or oscillator for wide range of frequencies and powers 10 p1511 A66-21714  
Advances in discrete semiconductor devices, parametrically evaluating device performance 10 p1513 A66-21901  
Operating principles and application of field effect transistor 11 p1665 A66-22686  
Monographs on field effect transistors 11 p1671 A66-23460  
Field effect transistors, principles, design and application 11 p1672 A66-23461  
Semiconductor surface physics, with emphasis on FET electrical surface phenomena 11 p1759 A66-23462  
Conduction through insulating layers in insulated-gate FET, noting tunneling and breakdown 11 p1672 A66-23463  
Thin silicon-dioxide film properties and growth for insulating gate electrode and semiconductor of MOS field effect device 11 p1759 A66-23464  
Carrier drift mobility and characteristics of field effect transistor, noting drain saturation resistance and surface scattering 11 p1672 A66-23465  
Thermal noise, shot noise and 1/f noise in field effect transistors 11 p1672 A66-23466  
Radiation damage in bipolar, insulated gate, field effect, gallium arsenide and thin film transistors 11 p1672 A66-23467  
Fabrication, ladder geometry, diffusion depth, oxide thickness, etc, of MOS FETs 11 p1672 A66-23468  
Thin film FETs including structural analysis, operating parameters, MOS transistors, carrier mobility in polycrystalline films, etc 11 p1672 A66-23469  
Field effect transistor application to linear amplifier and attenuator



circuits 11 p1673 A66-23470  
 Insulated gate field effect transistors in HF-UHF linear amplifiers 11 p1673 A66-23471  
 Field effect transistors in digital circuits, FET transient behavior, transistor logic and switching circuitry 11 p1673 A66-23472  
 Existence of limitation on properties and diffusion mode in junction and insulated gate field effect transistors 12 p1837 A66-24306  
 Planar silicon insulated-gate field-effect transistor using silicon nitride as diffusion mask, passivating layer and gate insulator 12 p1837 A66-24310  
 Polysilicon insulated gate field effect transistor having active element fabricated in epitaxially deposited film on oxidized single crystal silicon 12 p1845 A66-24847  
 MOS FETs in microelectronics, including digital arrays and logic gates 12 p1845 A66-24847  
 FET amplifier driving common-emitter bipolar-transistor second stage operated with channel not pinched off 13 p2029 A66-25206  
 Surface photovoltage measured in vapor-deposited cadmium sulfide using metal-insulator-semiconductor-structures, noting surface potential analysis as applied to thin film field effect transistor 13 p2164 A66-25487  
 Effect of magnetic field on field effect at germanium surface, determining rate of surface recombination 13 p2166 A66-25697  
 High gain low-noise electronic amplifier with field effect transistor at UHF range, noting design parameters and performance 13 p2040 A66-25832  
 AC, DC and pulse amplifiers including FET amplifiers, using semiconductor components and employed in measuring devices 13 p2079 A66-25895  
 Properties of second-gate electrode of MOS-FET and application as voltage-controlled integrator 14 p2248 A66-27052  
 Low noise preamplifier with field effect transistors for use with IR detectors 14 p2249 A66-27116  
 Junction field effect transistor used for switching 14 p2252 A66-27459  
 FET in biased p-n junction controlled electric field applied to low level circuit design 14 p2261 A66-28374  
 Temperature dependence of FET drain characteristics, square wave behavior, carrier mobility transfer characteristics and contact potential 14 p2261 A66-28375  
 High impedances obtained over wide frequency range with bipolar or unipolar transistors, noting current multiplication, bootstrapping, etc., and FET 14 p2262 A66-28377  
 Causes of noise in semiconductor amplifiers, noting FET, tunnel diode and varactor 14 p2268 A66-28383  
 Thermal noise of input conductance and gate-drain conductance in junction-gate FET 15 p2458 A66-28892  
 Unipolar FET converter, based on dependence of transconductance and drain current on gate bias voltage 15 p2464 A66-29124  
 Annealing effects of gamma ray irradiation on MOS FET increase donor surface state density 15 p2567 A66-29413  
 Graph-analytical method of calculating channel transistors of arbitrary geometrical shape 15 p2469 A66-29928  
 Frequency dependence of transconductance of unistrons 15 p2469 A66-29929  
 Evaluation of energy resolution of Li-drifted Ge detectors and preamplifiers using FETs in nuclear spectrometry 16 p2660 A66-30625  
 Semiconductor device development with emphasis on field transistors, transistor with metallic base and controlled diode 16 p2660 A66-30631  
 Thermal noise theory extended for insulated gate /MOS/ FET with gate voltage induced channel structure by including bulk charge from ionized impurities in semiconductor substrate 16 p2663 A66-31016  
 Thin film transistors and use in integrated circuits 16 p2664 A66-31416  
 Physical properties of thin films of CdS and CdSe formed by vacuum deposition analyzed as function of deposition and

processing conditions 16 p2782 A66-31422  
 Magnetic field influence on AC surface field effect in germanium resulting from change in sample conductance and not from change in surface barrier height 16 p2784 A66-31450  
 Metal oxide semiconductor transistors use in integrated circuits, discussing field effect devices, analog circuits configurations and applications 17 p2882 A66-32108  
 MOS transistors in integrated switching circuits to obtain desirable characteristics of pentode vacuum tubes and bipolar transistors 17 p2882 A66-32109  
 Thin film transistor design and performance 17 p2885 A66-32380  
 Very high input impedance buffer circuit using field effect transistors for voltage sensing in high impedance analog simulator 17 p2886 A66-32381  
 Junction field-effect transistor parameters and application guidelines compared to metal oxide semiconductor 17 p2888 A66-32779  
 Ionizing radiation effect on FET with silicon nitride as insulating layer, noting reduction of shift in gate turn-on voltage 17 p2983 A66-33105  
 FET structures with linearly graded junctions noting maximum gain configuration, transconductance expression, etc 17 p2895 A66-33116  
 Enhancement mode MOS-FET HF thermal noise in drain and gate analyzed, using channel transmission line model 17 p2897 A66-33462  
 Direct current volt-ampere characteristics of junction gate germanium alloy FET, including field-dependent mobility effect and channel-height distribution 17 p2897 A66-33463  
 Time and space dependent voltage variations in differential channel zone of field effect transistor with insulated gate 18 p3088 A66-35039  
 Book on analysis and design of transistor circuits including transistor parameters, emitter diode equivalent circuits, FET, amplifiers, noise, etc 18 p3089 A66-35238  
 Silicon field effect device with AC/DC fields superimposed on gate terminals analyzed for determination of distribution of defect introduction rate with depth, especially near threshold energies 19 p3435 A66-35413  
 Two-stage field effect transistor amplifier with high input resistance and modification of circuit enabling input resistance to be adjusted to infinity 19 p3315 A66-35560  
 Ultrahigh speed PCM telemetry systems using high-speed FET circuits 19 p3302 A66-35701  
 Differential low level junction field effect transistor commutators performance and characteristics for design 19 p3317 A66-35702  
 Wideband low-noise charge-sensitive preamplifier with n-channel field-effect-transistor input, giving experimental characteristics 19 p3318 A66-35916  
 Low-noise charge sensitive preamplifier for semiconductor detectors using paralleled field effect transistors 19 p3318 A66-35917  
 Miniature shaft-angle encoder with integrated-circuit encoding matrix and built-in memory potential using single static commutation ring 20 p3558 A66-37217  
 High input impedance fluid amplifier noting electric and fluid analogs, fluid triode and mathematical model of fluid FET 21 p3697 A66-38595  
 Silicon nitride as possible replacement for silicon dioxide in highly stable and reliable semiconductor devices, especially insulated-gate field effect transistor circuits 21 p3710 A66-38827  
 Barrier height determination in thin film sandwich tunnel diodes, using value of internal electric field and electric tunnel method 22 p3959 A66-39720  
 Equations derived for thermal drift of MOS-FET operated at drain voltages beyond pinchoff voltage 22 p3872 A66-39722  
 Large-signal AC field effect experiments with A and B real surfaces of indium antimonide exposed to various chemical reactions and high electric field described by tunnel equation 23 p4111 A66-41185

Reliability prediction, failure rates, fail-safe design and packaging of integrated circuit and MOS-FET microminiaturized electronic equipment 24 p4179 A66-42098  
 Field effect transistors in shock tunnel instrumentation circuitry associated with piezoelectric transducers operating in environment of widely ranging pressures, temperatures and testing times 24 p4207 A66-42170  
 Small and low cost voltage-tunable audio filter using field effect transistors as tuning element in place of inductors for space communications 24 p4180 A66-42331  
 Failure mechanisms of CdS and CdSe thin film FETs noting volt-ampere characteristics, temperature, electrical stress, and humidity effects 24 p4181 A66-42388  
 Electron effective mobility variation in AC for small signals as function of operating frequency of thin film transistors and dielectric diodes 24 p4181 A66-42392  
 FET characteristics in chopping and analog switching applications 24 p4182 A66-42504  
 MOS equivalent circuit for small signal HF operation of insulated gate field effect transistor in pinch-off mode, using differential equation 24 p4183 A66-42638  
 Small signal forward and reverse transfer parameters derived for metal oxide semiconductor and junction-gate field effect transistors from simple unified charge control analysis 24 p4185 A66-43037  
 Amplifiers using field effect device in first stage and bipolar transistor in second with limited drain-source voltage 24 p4185 A66-43037

## FIELD EMISSION

Prebreakdown current in high vacuum noting field strength and field emission hypothesis 01 p0106 A66-10641  
 Field-emission current voltage behavior of p-type germanium crystals whose surfaces were prepared by high field evaporation 02 p0271 A66-11432  
 Nonequilibrium field effect on silicon in region of high majority carrier depletion and nonequilibrium between energy bands 03 p0410 A66-12941  
 Propagation between Earth and ionosphere up to 100 km of VLF radio waves sent by ground transmitter, calculating field pattern 05 p0672 A66-15042  
 Harmonic microwave generation by field emission cathode in superconducting cavity 06 p0854 A66-16752  
 Improved stability of field emission current at microwave frequencies in weak vacuum 06 p0854 A66-16752  
 Work function of metals and semiconductors measured, using retarding potential analyzer to determine field emission electron energy distribution 08 p1228 A66-19824  
 Field effect and surface states at interface between germanium and electrolytes 10 p1586 A66-22141  
 Differences in MHD emission occurrence times, considering ionospheric penetration propagation toward equator and error sources 11 p1701 A66-23158  
 Field emission of germanium alloyed with silver and irradiated with IR 13 p2160 A66-25103  
 Dielectric field cathode model of field and photofield emission from high resistivity Si and Ge at low temperatures 15 p2558 A66-28602  
 Semiconductor properties measurement using resonator with slit 15 p2580 A66-28663  
 Energy distribution spectrum of tungsten single crystal field emitter and shapes of Fermi surfaces 16 p2769 A66-30162  
 Field emission of germanium alloyed with silver and irradiated with IR 16 p2771 A66-30287  
 Field emission in thin semiconductor layers upon metallic substrate, noting V-I characteristics dependence on Si layer thickness, tunnel effects, etc 17 p2977 A66-32261  
 Zr-coated tungsten cathode in reducing divergence of electron beam emission 18 p3088 A66-35074  
 Field and thermionic field emission responsible for excess currents in Schottky barriers formed on doped semiconductors 19 p3434 A66-35341



Field effect and surface states at interface between germanium and electrolytes 19 p3440 A66-35759  
 Adsorption of lithium on /110/, /111/ and /112/ planes of single-crystal tungsten in field-emission projector, measuring work function dependence on concentration 20 p3618 A66-37558  
 GaAs field emission cathode microscopy patterns prepared by chemical etching and low temperature field desorption 20 p3623 A66-38393  
 Surface patch electrostatic field effects on field emission single crystal plane work function determinations 21 p3770 A66-38656  
 Noise measurement in field emission vacuum diodes, interpreting excess and shot noise spectrum in terms of work function 22 p3878 A66-40696  
 Field emission diode and triode with narrowly spaced electrodes, noting voltage and current characteristics 22 p3882 A66-40894  
 Surface scattering of electrons on metallic field effect in thin layers -in theory of mean-free-path influences on conductance change 23 p4110 A66-41184

**FIELD INTENSITY METER**  
 Anechoic chamber facility for surface field measurement in scattering studies using probes 10 p1520 A66-21638  
 Uniform electric field meters for measurement at Earth surface and on aircraft and satellites 12 p1915 A66-24647  
 Ultrasonic field intensity in liquid measured with microradiometer, discussing instrument design concepts, advantages and operation 21 p3735 A66-38518  
 Field intensities and electron distribution functions in hollow cathode, graphs show potential distribution along cathode axis 22 p3953 A66-39758

**FIELD MODE THEORY**  
 Space-charge-limited current in solid for field depletion of filled traps, noting current voltage characteristics 11 p1751 A66-22733  
 Gravitational theory developed by generalizing Newtonian and special relativistic concepts 13 p2129 A66-26332  
 Field separation of ground transmitter into ordinary and extraordinary modes when traversing lower boundary of anisotropic ionosphere, noting effect of incidence angle, magnetic azimuth, etc, on energy dissipation of VLF ground wave 14 p2238 A66-27613  
 Gas laser with generalized polarization characteristics, noting role of degenerate atomic energy levels 19 p3374 A66-36005  
 Space-charge-limited current in solid for field depletion of filled traps, noting current voltage characteristics 23 p4113 A66-41471

**FIELD STRENGTH**  
**SA ELECTRIC FIELD STRENGTH**  
**SA MAGNETIC FIELD INTENSITY**  
 Prebreakdown current in high vacuum noting field strength and field emission hypothesis 01 p0106 A66-10641  
 Total vector modulus measurements from absolute field element observations and proton magnetometer 04 p0516 A66-13866  
 Simultaneous long distance tropospheric propagation measurements at 560 and 774 mc/s over North Sea 04 p0483 A66-14045  
 Semiconductor cathode thermionic emission by solving simultaneously Boltzmann and Poisson equations relating field intensity with electron concentration 06 p0838 A66-15892  
 Received field strength dependence on maximum and minimum usable carrier frequency range for ionospheric scattering 06 p0836 A66-17034  
 Gravitational irregularities in Santa Barbara channel, California 09 p1369 A66-19873  
 Long-term geomagnetic influence on medium frequency nighttime sky wave field strength 09 p1341 A66-19916  
 Electrical conductivity and field strength in symmetrically contacted rectangular samples as effected by geometrical factors 09 p1425 A66-20187  
 VLF electromagnetic propagation parameter determination by field strength measurements over medium distances in ionosphere 14 p2235 A66-27130

Causes giving rise to or influencing change of integral field strength of atmospherics during solar flare in VLF region brought to quantitative stage 14 p2237 A66-27400  
 Satellite-emitted short radio wave field intensity and ionospheric parameters 15 p2447 A66-28493  
 Ionospheric absorption measurement by A3 method in which field strength of distant CW transmitter is continuously recorded 19 p3351 A66-36359  
 Electric component of radiation field from same flashes recorded with histograms of product of field strength and distance, showing concentration around mean values 20 p3553 A66-38076  
 Tropospheric radio wave propagation field strength measurements and attenuation differences among various mixed land and sea transmission paths 20 p3520 A66-38144  
 Layer-like field inhomogeneities in homogeneous semiconductors occurring when conductivity decreases analyzed using Poisson and transport equations, obtaining stationary solutions for differential negative conductivity 24 p4254 A66-42424

**FIELD THEORY**  
**SA FUNCTION SPACE**  
**SA QUANTUM ELECTRODYNAMICS**  
**SA QUANTUM THEORY**  
**SA RELATIVITY THEORY**  
**SA UNIFIED FIELD THEORY**  
 General theory for construction of constitutive equations describing purely mechanical properties of continuous media with tensor and group theoretic concepts 01 p0106 A66-10717  
 Microwave propagation through metallic waveguides filled with dielectrics, using field theory, network theory, Rayleigh-Ritz procedure, reaction concept, etc 02 p0206 A66-12009  
 Particle-field interaction in magnetosphere discussing categories, properties, scale model experiments, etc 03 p0363 A66-12646  
 Local gravity anomalies for circular cylinder with vertical axis, discussing solution to direct and inverse problems of quantitative interpretation of fields 04 p0516 A66-13960  
 Exact solutions to Einstein field equations 05 p0715 A66-14532  
 Nonradiative and stationary electromagnetic and gravitational fields 06 p0909 A66-16330  
 Resolving matrix of normal system of ordinary linear differential equations in complex independent variable for multiply connected fields 07 p1057 A66-17835  
 Temperature dependence of Ginzburg-Landau coefficient in type I superconductors 09 p1420 A66-20048  
 Field penetration in superconductors with surface layers, describing LF low field AC susceptibility measurements in swept DC fields 09 p1420 A66-20049  
 Nonconservation of baryon and cosmological theory, discussing creation of matter in discrete manner around isolated pockets with strong gravitational fields 11 p1774 A66-23067  
 Operational calculus for finite rings employing Galois fields for periodic sequences via transfer function application 11 p1678 A66-23242  
 One-boson Lee model of solvable field theory with nontrivial charge and mass renormalization as example of Lehmann-Symanzik-Zimmermann formalism 12 p1917 A66-24098  
 Relativistic electrodynamics of moving medium, discussing Maxwell-Minkowski equations, Born equations, field vector transformations, etc 12 p1915 A66-24650  
 Nonrelativistic force in simple magnetizable fluid derived from thermodynamic information about energy and power 12 p1915 A66-24651  
 Models of matter-electromagnetic field interaction for gas lasers, using perturbation theory 13 p2103 A66-26216  
 Coherence properties of quantized electromagnetic field and hierarchy of correlation functions for complex field operators 13 p2128 A66-26218  
 Partial-wave dispersion in N/D form used to analyze superconductivity 13 p2136 A66-26331

Spatially homogeneous anisotropic irrotational solutions of Einstein field equations for cosmological dust source 14 p2330 A66-27019  
 Variational calculus formulation of classical electromagnetic field theory 14 p2330 A66-27022  
 Text on traveling wave antenna design and field equations in terms of TW sources 14 p2254 A66-27720  
 Field theory, variational calculus, dynamic programming and Pontryagin maximum principle approaches to plasma optimal controllability 15 p2548 A66-28520  
 Space-time correlation tensor of turbulent fields by phase space functional Lebesgue-Stieltjes integration, statistical hydromechanics and probability measure theory 15 p2479 A66-29398  
 Lorentz invariant space-time gravitational field theory, Maxwellian gravitokinetic field of potential and kinetic components and precession of orbit of Mercury analyzed by Einstein restricted theory of relativity 16 p2802 A66-31011  
 Angular dependence of spin-lattice relaxation times in ruby evaluated, using second order perturbation wave function and field coupling representation 16 p2781 A66-31220  
 Einstein field equations for perfect fluid, coupled to frozen-in magnetic field, in high-density limit of gravitational collapse 17 p2997 A66-31973  
 Stationary dust-filled cosmological solution of Einstein field equations with zero lambda and without closed timelike lines 19 p3463 A66-36169  
 General relativistic field equations of compressible fluid sphere with variable polytropic index 20 p3545 A66-37465  
 Covariant gravitational field equations in de Sitter space and quantum mechanical equations of motion associated with particles of given spin, employing gauge principle 21 p3769 A66-38645  
 Flux flow in type II superconductors, measuring critical current, longitudinal and transverse voltages for varied orientation of magnetic field 21 p3802 A66-39201  
 Time-mass dependent events during motion of material particle, using Hamilton-Jacobi equation of relativistic mechanics in Minkowski continuum 21 p3772 A66-39276  
 Augmented special relativity theory to account for Einstein effects, with extension to general scalar field theory and notes on corpuscular light and galactic-centered reference frame 23 p4090 A66-41273

**FIGHTER AIRCRAFT**  
 Optimization of terrain following performance for supersonic fighter aircraft, developing usable command signal 01 p0102 A66-10045  
 Lift fans for advanced V/STOL aircraft, describing performance improvement parameters 06 p0807 A66-17020  
 Man-machine conflict in high performance tactical fighter 07 p0998 A66-17282  
 Cost-effectiveness guidelines for designing tactical system in absence of firm specifications, noting avionics system 19 p3480 A66-35529  
 Optimization of terrain following performance for supersonic fighter aircraft, developing usable command signal 19 p3397 A66-36484  
 Dive flight behavior of propeller-driven and jet fighters 21 p3696 A66-38652

**FIGURE OF MERIT**  
 Universal definition of figure of merit associated with variable parameter one-port for RF switching and modulation 02 p0201 A66-11903  
 Figure of merit and methods of finding optimal filters for pulse-forming networks, taking into account frequency response as well as time response 02 p0208 A66-11910  
 Direct measurement of Nernst-Ettingshausen dimensionless figure of merit as ratio of two voltages 10 p1576 A66-21542  
 Correction to theory of Harman method of determining thermoelectric figure of merit 12 p1928 A66-23963  
 Zinc-antimonide with high and constant thermoelectric figure of merit obtained by solid phase diffusion 13 p2163 A66-25453  
 Figure of merit for reflection type



varactor phase shifter 13 p2037 A66-25545  
 Photometric figures of merit for various shaped semiconductor luminescent sources operating in spontaneous mode 14 p2362 A66-27495  
 Intermodulation elimination in transistors, determining figure of merit and sensitivity as function of operating current 17 p2895 A66-33115  
 L-band traveling wave maser using chromium doped rutile, discussing inverted susceptibility as figure of merit 20 p3580 A66-38239  
 Maximum figure of merit for broadband semiconductors, using theory of mobility due to acoustic mode and optical mode scattering 24 p4248 A66-42114

**FILAMENT**  
 SA HEATING EQUIPMENT  
 Boron filament tensile and flexural strength affected by surface and internal flaws with chemical polishing 10 p1548 A66-21728  
 Flame initiated filament oscillations, noting photographic measurement of oscillation frequencies 15 p2573 A66-28646  
 Continuous silicon carbide filaments prepared using chemical vapor-deposition techniques, analyzing cross sections, x-ray diffraction and tensile strength 20 p3588 A66-37772  
 Radiation characteristics of filament with triangular current distribution situated along axis of magnetized plasma column, noting guided and space waves excited by filament 24 p4240 A66-42291

**FILAMENT WINDING**  
 Continuous bias tape wrapping of ablative components 06 p0885 A66-16288  
 Large diameter filament-wound structure fabrication and testing for deep submersibles 06 p0886 A66-16304  
 Stiffness properties of filament wound structures derived from idealization based on structural and geometric properties [AIAA PAPER 66-144] 06 p0962 A66-16409  
 Composite materials manufacture and application to high temperatures, with evaluation of various binders and filaments 06 p0898 A66-17110  
 Glass-resin interaction of filament-wound composites, determining material properties and application to high performance pressure vessels 11 p1783 A66-23121  
 Composite materials, noting fibrous composites using whiskers, fabrication including spray-up, filament winding, etc, mechanical properties, application for rocket nozzles, heat shields, etc 14 p2318 A66-27228  
 Stresses and strains in anisotropic multilayered thick walled circular cylinder subjected to radial pressure [AIAA PAPER 65-174] 14 p2402 A66-27869  
 Filament overwrapped metallic cylindrical pressure vessels show greater efficiency ratio and buckling strength 14 p2405 A66-27992  
 Tension string structure of high strength filaments for ultralightweight planetary entry vehicle 14 p2407 A66-28028  
 Stressed state of cylindrical shell made of coiled glass fibers 16 p2822 A66-31625  
 Change in tensile strength during winding of prestressed oriented glass fiber filaments 17 p2942 A66-32047  
 Wound fiber structures with reference to solid propellant motors, discussing optimum angle of winding 18 p3254 A66-34005  
 Theoretical determination of elastic constants, Youngs moduli and Poisson ratios of filament-wound cylinders, using strain measurements in longitudinal uniaxial loading and internal pressure loading 19 p3472 A66-35355  
 Burst hoop test and new ISAS ring test methods for rapid evaluation of hoop strength of filament-wound fiberglass reinforced plastic cylindrical specimens 19 p3472 A66-35356  
 In-plane stiffness matrices for composite cylinders of filament winding determined by internal pressure, axial tension and torsion tests 20 p3666 A66-37440  
 Radiographic examination of large filament-wound solid propellant motor cases 21 p3744 A66-39152  
 Equations for analysis of prestressed cylindrical shells made of fiberglass

reinforced plastics with hollow fibers, longitudinally and transversely wound 22 p3990 A66-40143  
 Wound glass-fiber material used in reinforced plastic construction for production of solid fuel heavy missiles 23 p4074 A66-41653

**FILIER**  
 SA RESIN  
 Effect of compression of outer layers of plate by longitudinal forces on reduced shear moduli of finned filler 16 p2816 A66-31046

**FILM**  
 SA COATING  
 SA FERROMAGNETIC FILM  
 SA HELIUM FILM  
 SA MAGNETIC FILM  
 SA METAL FILM  
 SA OXIDE FILM  
 SA PHOTOGRAPHIC EMULSION  
 SA PHOTOGRAPHIC FILM  
 SA PLASTIC FILM  
 SA SILICON FILM  
 SA THIN FILM  
 Volt-ampere characteristics of variable Josephson current interaction with resonance oscillations in superconducting film tunnel structure 03 p0413 A66-13312  
 Mirrors composed of multilayer stacks of dielectric films and attaining high reflectance over extended spectral range 07 p1079 A66-17290  
 Simplified formulas relating parameters and geometry of film-type two-terminal RC networks with distributed parameters 12 p1830 A66-23736  
 Taylor stability of liquid film on body surface and flow stabilization relative to two-dimensional perturbations 12 p1863 A66-24434  
 Reflection measurements of RbI film in UV to observe optical property differences between films and single crystals 12 p1931 A66-24813  
 Design, performance and application of multicell luminous-symbol screen with optically coupled photosemiconductive and electroluminescent films 14 p2297 A66-28112  
 Determination of refractive index of polyethylene terephthalate film necessary in calculations of surface shape of film concentrators 20 p3603 A66-37738  
 Dynamic behavior of soap film stretched between two coaxial rings, assuming potential energy of this surface to be proportional to surface area 21 p3772 A66-39353

**FILM BOILING**  
 Disruption of thin liquid film flowing over heating surface, investigating boiling, evaporation and thermocapillary effects 01 p0165 A66-10906  
 Heat transfer to two-phase film-boiling nitrogen, discussing straight and swirl flow experimental apparatus [ASME PAPER 65-HT-37] 05 p0773 A66-14751  
 Transient quenching method of determining critical heat flux and transfer coefficients in film and nucleate boiling liquid metals, specifically magnesium [ASME PAPER 65-HT-49] 05 p0785 A66-14757  
 Slug flow and film boiling of hydrogen, deriving formula for forced convective film boiling heat flux [ASME PAPER 65-WA/HT-32] 05 p0793 A66-15673  
 Film boiling of saturated nitrogen flowing upward in vertical heated tube, noting annular-flow regime change to vapor matrix [ASME PAPER 65-WA/HT-26] 05 p0793 A66-15677  
 Thermal conditions in boiling liquids including container wall damage-flux density relationship, stable and unstable boiling in bubble evaporation region and film vaporization 07 p1154 A66-18066  
 Annular flow and two-dimensional forced convective boiling heat transfer to hydrogen in nucleate and film boiling regimes 08 p1316 A66-18832  
 Saturated film-boiling heat transfer coefficient measurements of ethanol, pentane and Freon 113 at atmospheric pressure [ASME PAPER 65-AV-37] 11 p1788 A66-22468  
 Thermionic energy-conversion diode using liquid metal as electron

oscillator 11 p1640 A66-23404  
 Free convection film boiling heat transfer from isothermal vertical plate to subcooled stagnant liquid, using two-phase boundary layer theory 12 p1980 A66-24907  
 Saturated and surface film boiling from horizontal isothermal plate in longitudinal flow field analysis, based on two-phase boundary layer theory, correlating heat transfer and skin friction characteristics 12 p1980 A66-24908  
 Mass evaporation rate and heat transfer coefficients for water drops supported by own superheated vapor over flat plate 16 p2830 A66-31680  
 Mass evaporation rate and heat transfer coefficients for water drops supported by own superheated vapor over flat plate 18 p3262 A66-34376  
 Data correlations on forced-convective heat transfer to cryogenic fluids by nucleate film and transition region boiling 20 p3677 A66-37098  
 Convective heat transfer to cryogenic nitrogen and methane from cylindrical surface by nucleate-and film-boiling at high pressures and large temperature differences 20 p3677 A66-37099  
 Heat transfer in liquid-film boiling on vertical surfaces analogous to free convection of gases in narrow vertical ducts 22 p4000 A66-408130

**FILM CONDENSATION**  
 Physical mechanisms of instabilities altering two-phase flow pattern of liquid film 01 p0165 A66-10906  
 Stoichiometric thin films of Al<sub>2</sub>S<sub>3</sub> prepared by coevaporation of elements onto glass substrates held at 550 degrees C 02 p0270 A66-11436  
 Condensation in variable acceleration fields especially linear variation occurring in constant cross section rotating thermosyphon [ASME PAPER 64-WA/GTP-2] 02 p0304 A66-11764  
 Heat transfer during film condensation of liquid metal vapor, discussing thermal resistance effect of condensation coefficient [ASME PAPER 65-HT-29] 05 p0784 A66-14748  
 RF sputtering for deposition of wide variety of thin films, discussing basic theory and apparatus 06 p0924 A66-16431  
 Active thin-film elements /diodes and transistors/, properties and deposition techniques 07 p1006 A66-17418  
 Monitoring techniques for thin film deposition in passive microcircuit networks 08 p1192 A66-18967  
 Heat transfer during film condensation of liquid metal vapor, discussing thermal resistance effect of condensation coefficient [ASME PAPER 65-HT-29] 11 p1784 A66-22182  
 Asymptotic series solution to problem of laminar film condensation on nonisothermal vertical plate, considering inertia and convection effects 12 p1978 A66-23998  
 Passive thin-film component materials vacuum evaporation and sputtering processes 13 p2039 A66-25645  
 Vacuum deposited films of titanium dioxide examined, using electron microscopy and diffraction methods, noting crystal dislocation due to electron beam irradiation 14 p2359 A66-27135  
 Metal film preparation by electron-beam melting of metal in water-cooled crucibles 16 p2661 A66-30698  
 Boron film characteristics and preparation by direct resistance heating of elemental boron filaments 16 p2778 A66-31074  
 Epitaxial growth techniques for silicon and germanium, discussing hydrogen reduction methods, doping and impurity control, etc 17 p2976 A66-32259  
 Laminar film condensation of vapor flow along flat plate and cylindrical surface 18 p3261 A66-34362  
 Integral solution of laminar film condensation with combined gravitational-type body force and forced convection concurrent and parallel to surface 20 p3678 A66-37118  
 Effect of donor Zn and Cd additions and acceptor Se and Te additions on rate of growth and morphology of epitaxial GaAs films grown from gas phase by chemical reaction 22 p3961 A66-39929



Microwave discharge technique for depositing noncrystalline oxide films of silicon, germanium, boron, titanium and selenium on substrates by decomposing compounds by oxygen 23 p4109 A66-41129  
 Electric resistance of amorphous iron films, noting film structure dependence on evaporation parameters 23 p4110 A66-41138  
 Recrystallization of evaporated CdS layers in environment containing various elements, obtaining oxygen enhanced crystal growth 24 p4253 A66-42356  
 Mechanical system for monitored deposition of sequential thin films on any one of five substrates from any of five independent sources and through any of five masks 24 p4218 A66-43216

# FILM COOLING

Localized calorimetric enthalpy measurements in high-energy-content gas stream using evaporating liquid film to cool gas sample 01 p0165 A66-10908  
 Effect of various factors in film-cooling phenomena obtained by vertically injecting air into turbulent boundary layer on flat plate 02 p0303 A66-11586  
 Crystallites of CdS in obliquely evaporated film on relative intensity of X-ray diffraction peaks 05 p0736 A66-14975  
 High strain sensitivity in CdS evaporated films, noting effects of tension and/or compression on film resistance 05 p0736 A66-14977  
 Cooling effect of secondary fluid injection on heat transfer between shrouded rotating disk and radially inward main flow stream [ASME PAPER 65-WA/HT-20] 05 p0789 A66-15644  
 Cooling effect of secondary fluid injection on heat transfer between shrouded rotating disk and radially inward main flow stream [ASME PAPER 65-WA/HT-20] 11 p1785 A66-22194  
 Reverse-flow film cooling of small rocket engine chamber 12 p1937 A66-24718  
 Electric machines employing evaporative and universal cooling systems for aircraft use 13 p2041 A66-25902  
 Gas film for protective cooling of surface having regular macroroughness 14 p2410 A66-26783  
 Film cooling in supersonic free stream flowing along flat plate in Mach 3 wind tunnel, using air as secondary fluid 17 p2839 A66-32441  
 Gas-film-cooled nozzle extension application to large rocket engines, discussing operational parameters, advantages, etc [SAE PAPER 660455] 17 p2991 A66-33163  
 Mach 16 hot shot wind tunnel testing of film cooling techniques 17 p3039 A66-33482  
 Liquid film cooling of small diameter throat tubes 18 p3263 A66-34385  
 Liquid film cooling by dual slot injection, determining film coolant injection rate and effects of two different mainstream Reynolds numbers 24 p4295 A66-42787

FILM THICKNESS  
 Thin metal film growth under applied electric field 01 p0118 A66-10246  
 Zero-bias capacitance of thin intrinsic semiconductor film sandwiched between identical electron-injecting contacts compared with value for noninjecting contacts 02 p0270 A66-11437  
 Transition temperature dependence on thickness of superimposed films of iron and tin 03 p0407 A66-12323  
 Boundary layer thickness responsible for anomalous lattice distortions of colloidal barium titanate 04 p0571 A66-14492  
 Monolithic silicon integrated circuit technology noting thin film, insulating and conducting layers, microelectronics, MOS systems, etc 05 p0642 A66-14559  
 Helium II film free-convection heat transfer, discussing mathematical analysis for vertical flat plate and horizontal circular cylinder [ASME PAPER 65-WA/HT-10] 05 p0791 A66-15652  
 Film thickness measurements on printed circuit-board material plated with gold over copper, using X-ray emission and absorption and beta ray backscatter test methods 06 p0886 A66-16429  
 Distribution function of semiconductor

minority current carriers in presence of pronounced spatial inhomogeneity occurring in intensively absorbing films with intensive surface recombination 07 p1099 A66-17873  
 Thermal elastohydrodynamic lubrication of rolling and sliding cylinders, noting correlation with film thickness and friction experimental data [ASLE PREPRINT 65AM 4A2] 07 p1040 A66-18291  
 Lubricant film thickness in elastohydrodynamic range measured as function of speed in rolling configuration for mineral oils and esters 07 p1040 A66-18292  
 Imperfection formation in epitaxial gold films, observing crystal-lattice dislocations due to rotation and displacement misfits between neighboring islands of deposit film 07 p1110 A66-18517  
 Effect of voltage and film thickness on sputtered tantalum film resistivity when used as microcircuits 09 p1411 A66-19941  
 Tunnel effect measurements of superimposed aluminum and lead films used to determine effect of normal metal on superconductor 10 p1573 A66-21179  
 Variation in coercivity of magnetization loops of multilayer films of nickel as function of rate of rise in applied magnetic field 10 p1575 A66-21412  
 Superconducting continuous film store evaluated, noting switching thresholds and functional dependence of disturb pulse sequences on film parameters 10 p1509 A66-21416  
 Strength and structure of thin films of Al, Ag, Ge and Ni studied with electron microscope and electron diffraction technique 10 p1578 A66-21663  
 Thickness of laminar liquid film draining from vertical surface analytically determined by assuming evaporation rate is known constant [ASME PAPER 65-HT-39] 11 p1785 A66-22189  
 Domain structure of single-crystal epitaxial iron films as function of perfection of crystalline structure, using Lorentzian electron microscopy, noting two-axis anisotropy 11 p1753 A66-22806  
 Multifilm absorption spectrum dependence on magnetic interaction, deposition, thickness and quality of ferromagnetic and insulating films 11 p1753 A66-22810  
 Ferromagnetic multifilm systems effect on SHF power transmission and variation of resonator parameter 11 p1754 A66-22811  
 Anisotropy of films deposited on cylindrical substrate 11 p1754 A66-22812  
 Ferromagnetic resonance in thin magnetic permalloy films, examining laws governing spin-wave spectrum for parallel orientation of magnetic field 11 p1755 A66-22822  
 Formation of oxide films on metals using polarized light to measure film thickness and vibrating capacitor measurements of changes in Volta potential, noting extension of Mott theory 11 p1718 A66-23211  
 Parabolic growth deviations in thermal oxidation of silicon 11 p1758 A66-23351  
 Microstructure of epitaxial germanium films deposited on calcium fluoride substrates, noting parameters of deposition 13 p2158 A66-25063  
 Magnetoresistance effect applied to Rotatable Initial Susceptibility II films, explaining resulting hysteresis loops and torque curves 13 p2161 A66-25183  
 Approximate solution of micromagnetic equations for Neel-type domain wall in multiple films 14 p2351 A66-26887  
 Magnetic properties of vacuum deposited iron nickel films 14 p2354 A66-26908  
 Hall coefficient and mobility in thin evaporated gold films on glass substrates 15 p2563 A66-28733  
 Spherical substrate converted to parabolic mirror by selective evaporation of aluminum, using silver as nonuniform thickness layer 15 p2499 A66-28841  
 Electric characteristics of epitaxial Ge films vacuum deposited on seminsulating GaAs substrates with thicknesses near one million angstroms 15 p2566 A66-29386  
 Effects of angular dispersion of anisotropy and film thickness on thin permalloy ferromagnetic film pulse switching 16 p2773 A66-30682

Technology, preparation and properties of multilayer ferromagnetic films, including influence of composition and deposition conditions on coercive force values, shape of hysteresis loops, etc 16 p2773 A66-30688  
 Domain structure and hysteresis loops of thin iron-gadolinium films of different thicknesses 16 p2775 A66-30699  
 Thickness of gold, silver and copper thin films determined, using measurements of resistance and Hall voltage 16 p2780 A66-31096  
 Variation in photoelectric output of thin metal layers calculated as function of thickness, determining output for two light polarizations 16 p2780 A66-31211  
 Temperature effect on color of thin layers of gold of various thicknesses connected with anomalous absorption phenomenon in gold layers 16 p2780 A66-31212  
 Device for controlling thickness of thin films prepared by sputtering in vacuum 16 p2708 A66-31362  
 Oxide film thickness effect on field effect silicon, noting concentration of surface electron states 16 p2787 A66-31735  
 Superconductivity of nondegenerate semiconductor thin films, dependence on current carrier concentration, impurity level positions and film thickness 16 p2787 A66-31762  
 Mechanical properties of Ag, Al, Ge, Cu, Ni and Fe thin films, showing elastic deformation and strength greater in thinner films 17 p2939 A66-31971  
 Thick film techniques, discussing applications, limitations, passive elements and design characteristics of cermet element 17 p2882 A66-32107  
 Recrystallization of Ge and Si thin films and structural changes due to electron bombardment and thermal annealing 17 p2988 A66-33456  
 LF common-base current transfer ratio for hot electron transport in semiconductor-metal-semiconductor point-contact-transistor structures measured as function of metal film thickness and temperature 19 p3435 A66-35410  
 Optical absorption of island films of gold as function of island density obtained from electron micrographs and film thickness 19 p3435 A66-35416  
 Oxide films grown on GaAs in oxygen plasma 19 p3437 A66-35435  
 Critical temperatures and critical magnetic fields determined for superposed normal and superconducting films, noting dependence on metal thickness 19 p3443 A66-36003  
 Integrated circuits, examining thin film evolution, noting advantages of size reduction, reliability and functional value 19 p3322 A66-36817  
 Normal incidence reflectivity and transmissivity coefficient measurements in Ge thin epitaxial films 20 p3623 A66-38397  
 Resistance decrease in vacuum-evaporated gold films from 150 to 250 degrees C when environment is cycled from inert to oxidizing 21 p3802 A66-39161  
 Change in temperature conditions during growth of epitaxial germanium films from molecular beam in vacuum 22 p3961 A66-39928  
 Elastoresistance effects in evaporated bismuth films, deposited on glass and epoxy resin substrates, used as strain gauges and transducers 22 p3962 A66-40046  
 Optical thickness measurement of nonabsorbing dielectric film when it is inconvenient to apply overlay film to measure thickness by Fizeau fringe shift 22 p3968 A66-40889  
 Cs-Sb film thickness measurement method in various compositions and relation between thickness and composition 24 p4251 A66-42301  
 Optical constants of triple, symmetrical and absorbing thin film used with layer thickness to determine complex transmission factor 24 p4258 A66-42994  
 Transition temperature for superconductivity in superimposed films of silver and tin in which alloying between two metals is minimized 24 p4259 A66-43068  
 Evaporation system for fabrication of multilayer dielectric films for mirrors or



filters, obtaining thickness variation reduction and simultaneous deposition 24 p4218 A66-43163

Rain effect on satellite communications Earth terminal rigid radomes, determining transmission loss and water film thickness 24 p4192 A66-43195

**FILTER**

SA ADAPTIVE FILTER

SA BAND PASS FILTER

SA CRYSTAL FILTER

SA ELECTRONIC FILTER

SA FLUIDIZED BED

SA HIGH PASS FILTER

SA IMAGE FILTER

SA INFRARED FILTER

SA KALMAN-SCHMIDT FILTER

SA LINEAR FILTER

SA LOW PASS FILTER

SA MASS FILTER

SA MICROWAVE FILTER

SA NONLINEAR FILTER

SA OPTICAL FILTER

SA RADAR FILTER

SA RADIO FILTER

SA SEPARATOR

SA TRACKING FILTER

SA WAVEGUIDE FILTER

SA WIENER FILTER

RC circuit filter properties during operation under complex load in form of parallel connection of resistance and capacitance 01 p0036 A66-10224

Exhaust beam from colloid thruster investigated, using quadrupole mass filter [AIAA PAPER 64-674] 02 p0278 A66-11549

Load resistance effect on selectivity of notch filters using hyperbolically shaped RC lines 02 p0200 A66-11876

Nomograph filter networks for control of electromagnetic interference, noting loss characteristics of element filters 03 p0341 A66-12571

RC circuit resistance effect on characteristics of selective filters consisting of semiconductor or thin film RC circuit with range multiplier and distributed parameters 04 p0496 A66-13908

Two sufficient conditions for monotonic variation of signal to noise ratio of optimal filter during storage of video pulse 04 p0484 A66-14058

Design of microwave filters 06 p0844 A66-16079

Degradation of matched filter receiver operating in non-Gaussian noise, considering performance in presence of ideal impulse noise 06 p0856 A66-16864

Optimum filters for signal detection in clutter 08 p1190 A66-18716

Optimization of transmitted signal and receiving filter for data transmission system with fixed channel and detection process 08 p1183 A66-18932

Acquisition behavior of phase-locked loops analyzed by treating loop as first-order loop with slowly varying dependent bias 12 p1856 A66-24648

Torsional-coupler mechanical filters, particularly types with higher harmonic suppression and piezoelectric material, utilized with simple structure 12 p1845 A66-24852

Pulse forming networks whose step responses have ripples of equal height 13 p2029 A66-25205

Book on electric network theory, functions and filters 14 p2263 A66-26960

Characteristic admittances of comb-type and undulating waveguide filters, considering diaphragm thickness and TE propagation mode 14 p2250 A66-27147

Pulse shape formed during discharge of chain-type artificial line 14 p2251 A66-27171

Two active parallel-T circuit variations of RC networks in filter design 14 p2264 A66-27458

Waveguide system using Chebyshev filters for channel separation in wide frequency ranges, applied for sounding plasmas with various electron concentrations 14 p2298 A66-28473

Filter design minimizing maximum value of estimation error over all admissible signal waveforms 15 p2474 A66-29380

Bit error rate improvement without source coding, using matched filters 16 p2659 A66-30548

Tolerance limits for structural components in power-filter circuit design, calculating fluctuations of damping property and phase fluctuations in multiply divided circuits 16 p2663 A66-31031

RC circuit filter properties during operation under complex load in form of parallel connection of resistance and capacitance 17 p2880 A66-31908

Two sufficient conditions for monotonic variation of signal to noise ratio of optimal filter during storage of video pulse 17 p2873 A66-32224

Quality of digital smoothing filters with finite transient time improved by rational choice of delay 17 p2878 A66-33491

Modulators with constant input resistance applied to FDM communications systems for simplification or elimination of filters 18 p3066 A66-33565

Use of balanced filter pairs for nondispersive analysis of aluminum and silicon in aluminum-silicon mixtures 18 p3063 A66-33693

Coupling of resonators in electromechanical filter, noting application of energy trapping in piezoelectric resonators 18 p3078 A66-34090

Inductorless filters, noting increased sensitivity of RC active networks to component tolerances 18 p3078 A66-34092

Inertial navigation technique based on least squares criteria of optimality with filter providing estimates of system errors 19 p3396 A66-35517

Nonlinear filtering theory based on invariant imbedding for orbit determination and adaptive control problems 19 p3303 A66-36244

RC circuit resistance effect on characteristics of selective filters consisting of semiconductor or thin film RC circuit with range multiplier and distributed parameters 20 p3532 A66-37866

Flight tests on aircraft and analysis by automatic filter, noting structural and aerodynamic problems resulting from use of transient method 21 p3824 A66-38574

Optimum filtering when signals and noises are incoming on different channels, defining filtering by rectangular matrix of filters 21 p3711 A66-39149

Mechanical-type filters used in electronic circuits including quartz filters, piezoelectric materials, metallic resonators, ceramic converters, torsion resonators and miniaturized filters 21 p3717 A66-39628

Digital filtering system comprising only few integrated circuits and using addressshift register combination, compared with analog devices 23 p4067 A66-41168

HF transmitter multicoupler for connecting several transmitters to single antenna 23 p4046 A66-41548

Signal and filter waveshape deviations for binary correlator receivers, noting degradation in performance of matched filter systems 23 p4040 A66-41592

Integral equations for weight function of optimum filter and correlation function of random absolute error 24 p4188 A66-42475

**FILTRATION**

Statistical description of signal filtration 13 p2045 A66-25295

Solution of optimum filtering problems when input signals of automatic control system are described by different differential equations at successive time intervals 14 p2265 A66-27523

Filter cake growth and filtration rate on circular leaf in three dimensions, noting Lucite-sugar water runs 15 p2480 A66-29671

**FIN**

SA COOLING FIN

Temperature distribution along thin fins with temperature-dependent thermal properties and internal heat generation [ASME PAPER 65-WA/HT-50] 05 p0791 A66-15657

Dimensioning heat transfer in compact plate fin heat exchangers under nonuniform temperature variation and heat conductance 12 p1978 A66-24034

Heat dissipated inside compartments by internal structural members on high speed aircraft 14 p2414 A66-28188

**FINE STRUCTURE**

Semiconductor excitation-level splitting for

shallow impurity state due to spin orbital shifts 04 p0565 A66-14260

Interpretation of Evershed effect by material streaming in penumbral fine structure 05 p0758 A66-14774

Fine structure of cut-off characteristic, particularly influence of emission current density in crossed-field thermionic converter 05 p0616 A66-15541

Fine structure of vibrational-rotational spectrum of difluoroborane and difluoroborane-d 08 p1178 A66-18932

Interference of fine-structure levels in hydrogen ions passing through two successive carbon foils 11 p1740 A66-22961

Pressure effects of argon on fine structure components of first two members of cesium principal series 13 p2135 A66-26263

Pressure effects of helium on fine structure components of first two members of cesium principal series, noting changes in shift curves 13 p2135 A66-26263

Angular distribution of outgoing gamma radiation associated with giant dipole resonance in Si super 28 nucleus 16 p2750 A66-30149

EAS core fine structure observations using spark chamber compared with response of plastic scintillation counter 18 p3207 A66-35102

Fine and hyperfine structure of term in 3p level of lithium studied by level-crossing spectroscopy technique, determining fine structure separation value 19 p3443 A66-35981

Fine structure in direct absorption edge of cleaved type IIA diamond determined from reflectance data obtained from 5.5 to 11.5 eV at room and liquid-nitrogen temperatures 20 p3622 A66-38246

Precise measurement of excited-state lifetimes for radiative and collision-induced relaxation in fine structure levels of atomic neon, noting optical transitions 23 p4098 A66-41361

Stark splitting effect on fine structure level probabilities for hydrogen lines, taking account of spontaneous transition probabilities and Lamb shift 23 p4098 A66-41361

**FINISH**

SA COATING

SA MACHINING

SA PAINT

SA PLATING

SA SURFACE FINISH

Precleaning treatment and coating effect on fatigue strengths of aluminum alloys 15 p2521 A66-29079

Chemical blanking and vibratory tumbling of Mo alloys 19 p3370 A66-36134

**FINITE DIFFERENCE METHOD**

Finite difference method solving Dirichlet problem for quasi-linear elliptic equation with results applied to calculation of magnetic field in nonlinear media 01 p0091 A66-10164

Error estimates for some finite difference methods of solving ordinary linear differential equations 01 p0092 A66-10311

Random error in finite difference approximation of stochastic nonlinear equations in theory of random signals and noise 01 p0093 A66-10384

Error in finite difference solution of diffusion equation with impulsive end condition 01 p0093 A66-10384

Simplified leading-edge flow boundary value problem of Bhatnager-Gross-Krook equation solved by finite difference method 01 p0058 A66-10634

Error estimate in obtaining eigenvalues of linear self-adjoint differential operator of elliptical type by finite difference method 01 p0095 A66-11009

Economical difference scheme of continuous computation for numerical solution to Stefan problem having multiple spatial dimensional variables and phases 01 p0166 A66-11004

Difference method with smoothing of coefficients for numerical solution of Stefan problem with multidimensional phase fronts and any number of independent variables 01 p0166 A66-11011

Nonlinear difference schemes for hyperbolic equation applied to solution of one-and multidimensional transport and



quasi-linear equations 01 p0095 A66-11013  
 Temperature difference method of  
 computing convective heat transfer, using  
 flat plate laminar boundary layer  
 equations 02 p0303 A66-11569  
 Transient analysis of matrix equations of  
 complex structural system, using finite  
 difference method 03 p0437 A66-12815  
 Nonlinear inverse heat conduction problem  
 solved by finite difference method, using  
 least squares and future temperatures  
 [ASME PAPER 65-HT-40] 05 p0784 A66-14753  
 Finite-difference equations derived and  
 applied at or near flexural discontinuities in  
 plates subjected to bending 05 p0774 A66-15063  
 Asymptotic error estimates in solving  
 elliptic equations of fourth order by method  
 of finite differences 05 p0710 A66-15477  
 Conversion of gravity reduction problem  
 into internal boundary value problem which  
 is solved by finite difference  
 methods 06 p0876 A66-16416  
 Numerical attempts to estimate  
 determination accuracy of finite difference  
 method for geopotential field 06 p0905 A66-16551  
 Digital and numerical method solution of  
 transient heat flow problems 07 p1150 A66-17577  
 Exact numerical solution of time-dependent  
 compressible Navier-Stokes equations  
 describing transient compressible viscous  
 heat-conducting flow [AIAA PAPER 66-30] 08 p1207 A66-18986  
 Exact frequency solution for steady state  
 wave propagation for plane strain vibrations  
 of composite hollow cylinders 08 p1310 A66-19162  
 Natural frequencies and node patterns for  
 clamped and simply supported square plates  
 of linearly variable thickness solved by  
 finite-difference approximation, using  
 pulsed-air vibrator 11 p1780 A66-22329  
 Modified Elliassen finite difference grid  
 solution of primitive hydrostatic equations  
 system for barotropic and baroclinic model  
 of atmosphere 11 p1730 A66-22946  
 Convergence of solutions of finite-  
 difference analogs of equation satisfied by  
 generalized axially symmetric  
 potential 11 p1723 A66-22986  
 Numerical dynamic predictor for control  
 systems disturbed by random noise,  
 discussing Fokker-Planck equation, Crank-  
 Nicolson difference model, etc 11 p1680 A66-23279  
 Finite-difference scheme for short-term  
 operational weather forecasts from two-level  
 model atmosphere equations 12 p1909 A66-24870  
 Equations describing motion of barotropic  
 fluid with free surface solved, using finite  
 difference methods based on two-step Lax-  
 Wendroff scheme 13 p2121 A66-25814  
 Finite difference equations for two-  
 dimensional rod-lattice structures 13 p2199 A66-26379  
 Net-point method determination of two  
 finite-difference systems for systems of  
 Navier-Stokes equations 13 p2066 A66-26504  
 Finite-difference method for computing  
 transient velocity profiles in laminar  
 boundary layer around two-dimensional  
 cylinder, noting Blasius flow oscillations 14 p2274 A66-27434  
 State-space analysis of discretely controlled  
 systems with finite delays 14 p2266 A66-27589  
 Finite difference solution of nonlinear  
 boundary value problem of Landau-Vlasov  
 equation for charged particle for Maxwellian  
 distribution function 14 p2344 A66-27625  
 Calculus of functional differences  
 particularly for case of exponential  
 function 14 p2323 A66-27778  
 Finite difference method solution of  
 parabolic and hyperbolic partial differential  
 equations in one space variable 14 p2324 A66-28146  
 Numerical attempts to estimate  
 determination accuracy of finite difference  
 method for geopotential field 14 p2327 A66-28223  
 Ideal gas flow past infinite circular cone at  
 angle of attack, noting finite-difference  
 method for self-similar solution of Prandtl  
 boundary layer equation 14 p2222 A66-28283

Solution of plane problem of physically  
 nonlinear bodies by method of finite  
 differences 15 p2608 A66-28772  
 Finite difference method for elliptic  
 systems of partial differential equations  
 subjected to natural boundary conditions  
 /generalized Neumann problems/ 16 p2731 A66-30234  
 Convergence of discrete analogs of  
 Dirichlet problems for Poisson equation in  
 two dimensions, describing finite difference  
 method for producing algorithms 16 p2731 A66-30235  
 Multidimensional generalized transport  
 equations solutions and calculation by  
 difference methods 16 p2732 A66-30240  
 Laminar viscous wake interaction with  
 supersonic external inviscid flow  
 downstream treated by implicit finite  
 difference method [AIAA PAPER 66-454] 16 p2689 A66-31468  
 General numerical method of  
 characteristics for three-dimensional  
 unsteady magnetofluid dynamics of multi-  
 component medium 16 p2690 A66-31653  
 Unified treatment of nonlinear partial  
 differential equations, considering solution  
 technique in engineering application 16 p2739 A66-31740  
 Finite difference estimation of boundary  
 value problem errors 17 p2945 A66-31878  
 Acoustic problems formulated and solved  
 by finite element method of variational  
 calculus, using both force and displacement  
 procedures 17 p2957 A66-31945  
 Vibration analysis of static plates and  
 shells by finite element method 17 p3019 A66-31950  
 Finite element method using stability  
 coefficient matrices in conjunction with  
 stiffness matrices for problem of stability of  
 plates 17 p3024 A66-32360  
 Longitudinal and circumferential inertial  
 effects on dynamic response of cylindrical  
 shell to time-varying loads 17 p3025 A66-32470  
 Finite-difference calculation of MHD flow  
 of conducting fluid past circular cylinder in  
 transverse magnetic field based on Navier-  
 Stokes equation 17 p2971 A66-32862  
 Finite difference method for uniform  
 nonpermanent laminar flow of non-  
 Newtonian fluids between plane, parallel  
 fixed walls, for case of variable pressure  
 gradients 17 p2911 A66-32951  
 Implicit finite difference method applied  
 to plane hypersonic flow over blunt circular  
 cylinder 17 p2842 A66-33170  
 Noniterative finite-difference method for  
 solution of Poisson and Laplace equations  
 for linear boundary conditions, discussing  
 slow viscous flow results [ASME PAPER 66-FE-1] 17 p2914 A66-33258  
 Finite difference method for shock wave  
 propagation into supersonic crossflow 17 p2916 A66-33479  
 Conservation equations for two-dimensional  
 axisymmetric simultaneous turbulent mixing  
 and supersonic combustion of hydrogen-  
 oxygen-nitrogen-water streams solved by  
 finite difference methods [AIAA PAPER 66-617] 18 p3099 A66-34219  
 Multiple rocket engine exhaust plumes  
 calculated by method of characteristics and  
 finite difference and compared with  
 schlieren data [AIAA PAPER 66-651] 18 p3264 A66-34448  
 Numerical integration of primitive  
 equations by simulated backward difference  
 method, using two-step iteration for  
 divergent barotropic model of  
 atmosphere 19 p3393 A66-36057  
 Numerical integration scheme for  
 oscillatory equations with second-order  
 accuracy and sharp cut-off for high  
 frequencies 19 p3389 A66-36058  
 Finite difference method approach to  
 discontinuity in parabolic equations for  
 shear laminar boundary layer flow of  
 injected gas past wall 19 p3342 A66-36477  
 Functional polynomial fitting of continuous  
 functional, using Laplace transforms to  
 reduce number of measured records for  
 identifying kernels of second-degree  
 approximation 19 p3391 A66-36703  
 Error estimates for difference methods in  
 forced vibration problems 20 p3589 A66-36901  
 Modified Elliassen finite difference grid

solution of primitive hydrostatic equations  
 system for barotropic and baroclinic model  
 of atmosphere 20 p3593 A66-37859  
 Optimization of efficiency of gas turbine  
 cycles with heat recovery by finite  
 difference method using digital  
 computer 21 p3807 A66-38805  
 RC network model applied to study of  
 transient response of semiconductor diode,  
 obtaining accuracy estimates for finite-  
 difference representation of one-dimensional  
 diffusion equation 21 p3713 A66-39298  
 Finite difference analysis of viscous  
 laminar converging flow in conical tubes,  
 assuming parabolic inlet velocity profile and  
 simplified motion equation 21 p3729 A66-39450  
 Relativistic electron layer formation by  
 injecting electrons into cylindrical region of  
 Astron, using difference methods in  
 integrating Vlasov-Maxwell  
 equations 21 p3793 A66-39470  
 Eulerian finite difference method for  
 solving time-dependent equations of motion  
 for compressible fluid flow, noting shock  
 wave diffraction, supersonic blunt body  
 interaction with shock wave, etc 21 p3730 A66-39472  
 Communication network response to  
 arbitrary transients calculated by digital  
 computer, permitting replacement of  
 analytic-function wave forms by lists of  
 equi-interval sample values 22 p3883 A66-39724  
 Eigenvalue problem for Laplace operator  
 for two-dimensional region with boundary  
 composed of piecewise-analytical simple  
 closed curves solved by finite difference  
 method 22 p3938 A66-39901  
 Heat equation solution by use of Crandall  
 optimum finite difference method with  
 boundary discontinuity 22 p3997 A66-40029  
 Finite-difference scheme for short-term  
 operational weather forecasts from two-level  
 model atmosphere equations 22 p3943 A66-40331  
 Compressible turbulent boundary layer on  
 flat plate, noting correspondence between  
 compressible and incompressible flow,  
 numerical results on skin friction and heat  
 transfer, etc 22 p3899 A66-40344  
 Pseudoviscosity method using finite  
 difference equations for calculating two-  
 dimensional flow fields for supersonic  
 motion of inviscid gas 22 p3901 A66-40494  
 Finite difference method solution of  
 Navier-Stokes equations and applicability to  
 cylindrical-channel viscous flow at small  
 Reynolds numbers 23 p4062 A66-42061  
 Net point method determination of two  
 finite difference systems for systems of  
 Navier-Stokes equations 24 p4195 A66-42724  
**FINITE-STATE MACHINE**  
 Moore and Mealy diagrams in analysis and  
 synthesis of finite automations 03 p0337 A66-12376  
 Algorithm used for synthesis of regular  
 events in asynchronous automatic  
 machines 07 p1014 A66-17437  
 Automata theory and control theory  
 analytically compared for general and linear  
 systems and tolerance automata 11 p1680 A66-23275  
 Probabilistic automata as generalization of  
 deterministic and nondeterministic finite  
 model, theorems and concept of  
 definiteness 12 p1853 A66-24338  
 Reliability of finite automata determined  
 from analysis of elements capable of  
 misalignment, input errors and structural  
 design 16 p2669 A66-30761  
**FINLAND**  
 Finnish space research program in 1965,  
 outlining optical satellite tracking  
 experiments by various  
 observatories 15 p2600 A66-29906  
**FINNED BODY**  
 Optimization of fin geometry to maximize  
 free-convection heat transfer in air at  
 atmospheric pressure [ASME PAPER 65-HT-12] 05 p0783 A66-14738  
 Deformation of finned conical shell under  
 axial load 15 p2608 A66-28781  
 Effect of compression of outer layers of  
 plate by longitudinal forces on reduced  
 shear moduli of finned  
 filler 16 p2816 A66-31046



## FIRE

Determining whether aircraft was on fire before crash by examination of wreckage fragments 09 p1329 A66-20241

## FIRE CONTROL

NASARR international program concerning F-15 fire-control systems for F-104 Starfighter [AIAA PAPER 65-777] 03 p0447 A66-13066  
Physiological stress and fatigue in aerial missions for forest fire control, noting in-flight and postflight exercise heart rate 12 p1810 A66-25009

## FIRE EXTINGUISHER

Chemical inhibition of pentaborane-oxygen reaction in development of improved fire protection systems 03 p0413 A66-12487  
Productivity and cost comparison of water-bomb forest fire fighting aircraft 07 p0989 A66-18051

## FIRE PREVENTION

Comparison of rheological properties and fire resistance of hydraulic fluids for aerospace vehicles [ASLE PREPRINT 65-LC-6] 02 p0249 A66-12257  
Fire resistant hydraulic fluids for commercial and military application including siloxanes, silicones, esters and superrefined mineral oil [ASME PAPER 64-WA/LUB-14] 10 p1547 A66-21171

Comparison of rheological properties and fire resistance of hydraulic fluids for aerospace vehicles [ASLE PREPRINT 65-LC-6] 12 p1901 A66-24991

Electronic hydrogen leak and fire detector systems installed on Saturn S-IVB static test firing stands, discussing installation and operational problems 20 p3557 A66-37216  
Prevention and control of Ti machining fires 21 p3744 A66-39198  
Synthetic fire-resistant hydraulic fluids based on phosphate esters must be provided with continuous removal of dissociation products for constant regeneration and protection of unaltered fluid from accelerated decomposition 24 p4229 A66-42509

## FIREBRIGADE PROCEDURE

Semiautomatic digital data processing system used in ground control of interceptor aircraft, noting track marking on PPI display, control of height radar, radio message transmission, etc 14 p2271 A66-28299

## FIRING

SA DETONATION  
SA ROCKET FIRING  
SA STATIC FIRING  
SA TEST FIRING  
Varying deposition and firing conditions effect on range of detection of chemically deposited lead sulfide IR detector cells 03 p0407 A66-12332  
Doping and firing atmosphere effects on electric resistivity of polycrystalline barium titanate, noting oxidation of small grain and positive temperature coefficient effect on large grain 17 p2978 A66-32404

## FIRST ORDER EQUATION

SA REYNOLDS EQUATION  
Global solutions of Cauchy problem for quasi-linear first-order differential equations in several space variables 11 p1722 A66-22895  
Cauchy problem of first-order nonlinear partial differential equations 13 p2121 A66-26503  
Canonical form for two-terminal nonlinear RLC network first-order ordinary differential equations 15 p2472 A66-29371  
Graphical analysis of extremal control system stepwise adapted to process with extremal characteristic located between two first-order linear operators 19 p3324 A66-35582  
Optimum Runge-Kutta methods of orders 2, 3 and 4 for first-order differential equation with constrained minimum truncation error bounds 19 p3392 A66-36781  
Runge-Kutta fourth-order method for solution of N simultaneous first-order differential equations economically evaluated 19 p3392 A66-36782  
Existence of unique periodic solution to first-order differential equation and nonautonomous system of two first-order differential equations 20 p3591 A66-37752

Comparison variables transformation of linearized perturbation initial value problems for nonlinear ordinary first-order differential equation 21 p3756 A66-38817  
Cauchy problem of first-order nonlinear partial differential equations 22 p3939 A66-40439  
Stability of solution obtained in first approximation, introducing concept of quantity gamma for n-dimensional systems 24 p4230 A66-42216  
Numerical solution of linear boundary value problems 24 p4233 A66-43201

## FISH

Relative specific energy capabilities of fish and birds and body structure relative to environment 01 p0017 A66-10200  
Simulated fish propulsion analysis of boundary layer transition and vortex chain shedding 13 p2071 A66-26725  
Biological effects of confining fish in sealed aquarium with and without Chlorella 15 p2440 A66-29504

## FISSION

Systematics of fission based on exponential mass formula, discussing neutron capture 02 p0263 A66-11835  
Fission method to study uranium distribution in natural minerals 09 p1460 A66-20963  
Liquid water and nitrogen drops vibrating in natural frequencies above hot plate on vapor cushion analyzed by photographic techniques and used to simulate atomic nuclei fission 18 p3262 A66-34377

## FISSION PRODUCT

In-pile pumping system tested on thermionic converter SIRENE 56 for gaseous fission products 05 p0619 A66-15565  
Plasma generation by fission fragment ionization of noble gases, discussing theory, ionization tube and data 10 p1564 A66-21545  
Lens technique for measuring yield and energy spectrum of secondary electrons generated by fission fragments through metal foil 12 p1916 A66-23704  
Pressure wave generation in fissioning gas, examining amplification of pressure pulse with helium 3 as driver 15 p2555 A66-29756  
Delayed energy produced by fission product decay when restart of nuclear rocket engine is required, noting effects of cooldown requirements [AIAA PAPER 66-551] 22 p3946 A66-39676

## FITNESS

S FLIGHT FITNESS  
S PHYSICAL FITNESS

## FITTING

SA FASTENER  
DATAN, curve fitting process to approximate data and elimination of problems for programming engineer by data analysis 13 p2028 A66-26325

## FIXED FREQUENCY TOPSIDE SOUNDER

## S TOPSIDE PROGRAM

## FIXED POINT

Book on motion theory of several coupled rigid bodies about fixed point, particularly gyroscope and gyrost at Cardan suspension 06 p0910 A66-17067  
Uniform structure for Lipschitz condition on functions between sets, extensions to nonmetric spaces and fixed point theorem for uniform spaces 07 p1059 A66-17969  
Proof of theorem, let  $X$ ,  $T$ ,  $\pi$  be transformation group, where  $X$  is Peano continuum with end point fixed under  $T$  10 p1551 A66-21927

## FIXED-WING AIRCRAFT

Propeller control at low airspeed on turboprop engines in any fixed-wing aircraft, with special reference to thrust or drag in approach and landing [AIAA PAPER 65-709] 01 p0013 A66-10946  
British and French VTOL landing gear design, describing unique Scone fixed-wing VTOL aircraft 08 p1167 A66-18627  
Propeller control at low airspeed on turboprop engines in any fixed-wing aircraft, with special reference to thrust or drag in approach and landing [AIAA PAPER 65-709] 09 p1329 A66-20242

## FLAME

SA CHAPMAN-JOUGET FLAME  
SA COMBUSTION  
SA DIFFUSION FLAME  
SA FLARE

## SA JET FLAME

## SA LAMINAR FLAME

## SA PREMIXED FLAME

Weightlessness effect on flame ignition, burning rate, self-extinguishment, etc 16 p2825 A66-30487  
Emission of Auer-Weisbach mixture in flames 16 p2827 A66-30852  
Heat transfer rates and two-color temperature measurements for propane-oxygen flame seeded with aluminum powder [WSCI 66-2] 18 p3264 A66-34422  
Hydroxyl radical concentration in rarefied CO flame by EPR method 18 p3265 A66-34551

## FLAME FRONT

Droplet combustion fronts in hydrazine-nitrogen tetroxide system determined from kinetics of vapor decomposition, noting two-flame front model [CI PAPER WSCI-65-21] 05 p0743 A66-15146  
Flame generation of pressure waves and wave-combustion front interactions in detonation processes treated by nonsteady gas dynamics 07 p1155 A66-18118  
Longitudinal electric field effect on redistribution of emitting particles in combustion front of plane methane-air flame 17 p2870 A66-32828  
Transfer process effect on stability of plane flame front, deriving revised, approximate solution for large finite Reynolds numbers 19 p3479 A66-36828  
Gas flow formation ahead of flame front in circular and rectangular shock tubes analyzed, based on high speed photographs and method of characteristics 21 p3836 A66-39097

## FLAME INTERACTION

Rarefied hydrogen flame interaction between hydrogen atoms and molecules of certain organic, aliphatic and cyclic compounds 01 p0161 A66-10414  
Shock wave/flame front interaction in cylindrical chamber 14 p2412 A66-27438  
Mean probability of coupling between electrons of flame on electronegative gas and radioactive bromium tracer injected into flame, calculating electrons coupling cross section on bromium atoms 16 p2763 A66-31208

## FLAME IONIZATION

Microwave molecular resonance and bremsstrahlung continuum from flames measured with maser radiometer at various pressures [AIAA PAPER 65-106] 05 p0793 A66-15780  
Flame as source of emission of visible UV and IR radiation and ionization source for certain combinations of fuels and oxidants 08 p1317 A66-18856  
Quantitative determination of impurities in organic compounds using flame ionization detector 14 p2232 A66-27610  
Laminar and turbulent diffusion flame combustion mechanisms, stabilization, flame ionization, Bunsen burner, fuel gas jet eddy diffusion, etc 15 p2616 A66-29068  
Dissociation layer heights on Venus, Mars and Jupiter, noting CO flame airglow intensities 15 p2604 A66-30050  
Profile of ionized calcium resonance lines radiated from arc plasma jet observed by Fabry-Perot etalon 17 p2970 A66-32714  
Longitudinal electric field effect on redistribution of emitting particles in combustion front of plane methane-air flame 17 p2870 A66-32828  
Ionization processes in hot products of combustion processes /flame gases/ as weak plasma media, noting flame properties, mass spectroscopy, electron concentration, etc 18 p3260 A66-34106  
Hot flame gases ionization by electron reactions at atmospheric pressure 18 p3137 A66-34116  
Hydrogen-air flame with sodium traces studied by quadrupole mass spectrometric analyzer 19 p3476 A66-35323  
Solid-vapor equilibrium in helium-methane system from triple point equilibrium temperature of methane down to low temperature within limits of flame ionization technique 20 p3676 A66-37086  
Correlation between chemi-ionization in flames containing organic fuels and heat of oxidation of carbon in fuel molecule 23 p4147 A66-41154



# FLAME PLATING

S ACETYLENE  
S ALUMINUM OXIDE  
S TUNGSTEN CARBIDE  
S WELDING

## FLAME PROBE

Methane-rich premixed flames of perchloric acid analysis noting burning velocities, temperatures and burnt gas composition required for stoichiometric mixtures 02 p0304 A66-12018

Absorption and emission spectra pertaining to electronic transitions of short-lived molecules C sub 2 and CH present in reaction zone of low-pressure oxyacetylene flames 06 p0969 A66-16126

Book on foundation of analytical flame spectroscopy technique, emphasizing excitation sources and radiation processes 06 p0822 A66-16521  
Vanadium oxide single crystal growth by flame solution and fusion, noting burner construction, crystal structure and techniques 12 p1899 A66-23565

Spectral analysis of organic flames, noting band intensity variation of different radicals with air-fuel composition and influence of diluents 14 p2413 A66-27722

FORTTRAN program for calculation of approximate total half-intensity line widths of several spectral lines for atoms in common analytical flames 20 p3605 A66-37758

## FLAME PROPAGATION

### SA BURNING RATE

Equation solution for flame propagation in gas mixture with first-order exothermic chemical reaction 02 p0302 A66-11392

Steady state flame propagation regimes, taking into account effect of heat losses through pipe walls on fuel mixture combustion 02 p0302 A66-11401

Laminar flame speeds predicted by Spalding formulation in stoichiometric mixtures with nonnormal diffusion 03 p0443 A66-12490

Algorithm determining end product concentration of mixture for chain isothermal propagation of plane flame 06 p0971 A66-16710

Flow field of two-dimensional Bunsen flame according to source sheet approximation 07 p1154 A66-17940

Linear pyrolysis velocity measuring device for ammonium perchlorate in one-dimensional flow 08 p1279 A66-18723

Flame spreading velocity over surface of igniting solid rocket propellants as function of atmospheric pressure and chemistry and specimen surface condition

[AIAA PAPER 66-68] 08 p1317 A66-18949  
Transmission of IR radiation from flames through various carbon dioxide

pathlengths 09 p1471 A66-20509  
Mathematical model of flame propagation in laminar and turbulent

flow 10 p1619 A66-21072  
Propagation stability of spherical flame in gas dynamic configuration of Landau and Markstein, showing that flame is stable relative to first spherical

harmonics 14 p2410 A66-26779  
Flame wavelength during vibrational combustion of gas mixtures in

tubes 14 p2415 A66-28327  
Complex variable theory of flame surface interaction and flow field of two-dimensional V-shaped flame simulated by source and sink sheets 15 p2617 A66-29605

Flame propagation theory using one-dimensional model and radial temperature variation to obtain dependence of propagation velocity on thermal-diffusivity coefficient 16 p2830 A66-31515

Five halogenated hydrocarbons and effect on flame speed of 17 p3032 A66-31881

methane 17 p3032 A66-31881  
Chlorine-fluorine mixture combustion, examining flame speeds, temperatures and burned gas composition

[WSCI 66-31] 18 p3263 A66-34415  
Overall structure of combustion process in jet flow of hydrocarbon-air mixtures

stressing conditions for ramjet engines, noting flame propagation angles, flow computation, etc 18 p3264 A66-34444

[AIAA PAPER 66-573] 18 p3264 A66-34444  
Ignition pressure transient of rocket motor, discussing initial ignition event,

flame spreading and final chamber filling, convective heating effect on burning rate, etc

[AIAA PAPER 66-666] 18 p3165 A66-34449

Stability analysis of one-dimensional steady laminar flame propagation with conductive heat loss 20 p3680 A66-38045

Chemical-ionization in reaction zones of hydrocarbon-oxygen or hydrocarbon air flames, noting association with abnormal excitation of hydroxyl

radical 20 p3626 A66-38046  
Boundary conditions of downstream singularity in nonadiabatic

flames 20 p3680 A66-38048  
Methane flames formed in long, horizontal column of methane-air mixture caused by interdiffusion, using wind

tunnel 20 p3681 A66-38246  
Unstable combustion products, of glow discharge, discussing effect of propagation rate of hydrogen-oxygen

flame 21 p3834 A66-38473  
Explosion of gas mixtures noting preparation, ignition sources, equipment, detonation waves of spherical volumes, etc 21 p3834 A66-38534

Dirac delta function representation of spark ignition, considering heat transfer from reaction zone to fresh gas and flame propagation 23 p4148 A66-41413

Flame propagation velocity parameters in turbulent flow as function of flow pulsation velocity, normal burning velocity and relative heating 23 p4149 A66-41792

Detonation wave formation in flowing hydrogen-oxygen and methane-oxygen mixtures, noting induction distances and turbulence levels 23 p4057 A66-41888

Flame of homogeneous gas mixture in terms of similarity criteria applied to combustion process 24 p4295 A66-42883

SA BURNING RATE 24 p4295 A66-42883

SA BURNING RATE 24 p4295 A66-42883

SA BURNING RATE 24 p4295 A66-42883

SA BURNING RATE 24 p4295 A66-42883

SA BURNING RATE 24 p4295 A66-42883

SA BURNING RATE 24 p4295 A66-42883

SA BURNING RATE 24 p4295 A66-42883

SA BURNING RATE 24 p4295 A66-42883

SA BURNING RATE 24 p4295 A66-42883

SA BURNING RATE 24 p4295 A66-42883

SA BURNING RATE 24 p4295 A66-42883

SA BURNING RATE 24 p4295 A66-42883

SA BURNING RATE 24 p4295 A66-42883

SA BURNING RATE 24 p4295 A66-42883

SA BURNING RATE 24 p4295 A66-42883

SA BURNING RATE 24 p4295 A66-42883

SA BURNING RATE 24 p4295 A66-42883

SA BURNING RATE 24 p4295 A66-42883

SA BURNING RATE 24 p4295 A66-42883

SA BURNING RATE 24 p4295 A66-42883

SA BURNING RATE 24 p4295 A66-42883

SA BURNING RATE 24 p4295 A66-42883

SA BURNING RATE 24 p4295 A66-42883

measurements of gas flow velocity, turbulence and gas

composition 15 p2479 A66-29608

Opposed jet diffusion flames subjected to electrostatic fields, estimating volumetric heat release rate and mass flow behavior [ASME PAPER 65-WA/ENER-3]

16 p2825 A66-30341  
Discontinuity characteristics of trough-shaped flame stabilizers for combustion in wake of poorly streamlined body during period of ignition arrest 20 p3674 A66-36915

FLAME TEMPERATURE 20 p3674 A66-36915

Temperature inhomogeneities in flame jet in condensed system as affected by flow agitation, carbon particles and metal particles 04 p0597 A66-13697

Calculation of mean temperature of mixture burning in flame tube of annular combustion chamber 04 p0597 A66-13760

Thermionic converter transforming calorific energy of flame into electric energy having protective coating of enamel-covered alumina 05 p0623 A66-15594

Axial temperature variation in turbulent buoyancy-controlled diffusion flame 08 p1319 A66-19202

Flame expansion rate in turbulent flow of homogeneous inflammable mixture at ignition temperatures from 423 to 823 degrees K 14 p2374 A66-27691

Organic flame temperatures and burning velocities at various fuel-air ratios measured, noting band intensity, effect of diluents, etc 14 p2413 A66-27723

Liquid hydrazine decomposition process to determine what chemical or physical changes may be occurring that cause breaks in burning rate/ pressure curves, measuring flame temperature and light emission 15 p2570 A66-29610

Factors determining line reversal temperature of flame with realistic temperature cross section explained by calculation of sodium D-line contours 17 p3038 A66-33324

Direct measuring radiation calorimeter developed for determining radiant heat flux of solid propellant gas flame in rocket combustion chambers

[AIAA PAPER 65-358] 18 p3159 A66-33814  
Flame temperature measurement using response time of Wolfram-rhenium thermocouples to correct radiation errors in optical pyrometer

readings 19 p3360 A66-36160  
Hydrogen/oxygen and hydrogen/air flame temperature experiments on porous flat flame burner 20 p3680 A66-38042

Initial broadening of diffusion flame sheet caused by nonvanishing equilibrium constant determined, using method of inner and outer expansions 23 p4148 A66-41500

Flame temperature measurements by thermal neutron probe providing data on measured and computed transmission vs Cd foil thickness 23 p4148 A66-41501

Temperature of fluorine-hydrogen flame from 1/3, 0/ band of FH vibration-rotation experimentally determined to be in agreement with theoretical figure of 3994 degrees K for stoichiometric mixture 24 p4295 A66-42992

FLANGE 24 p4295 A66-42992

SA METAL PLATE 24 p4295 A66-42992

Critical bending angles of rollers used in shaping profiled rings and casings with titanium alloy flanges 23 p4075 A66-41794

FLANGE WRINKLING 23 p4075 A66-41794

Design and construction of 10 ft diameter bakeable UHV all metal seal, taking into account thermal stresses and effect on flanges 16 p2712 A66-30455

Deformation modes and wrinkling of flange on shear spinning to determine optimum working conditions or spinnability of sheet metal 20 p3575 A66-38104

FLAP 20 p3575 A66-38104

S JET FLAP 20 p3575 A66-38104

S SPLIT FLAP 20 p3575 A66-38104

S STABILIZATION 20 p3575 A66-38104

S WING FLAP 20 p3575 A66-38104

FLAP CONTROL 20 p3575 A66-38104

Change rate of pitching moment coefficient upon aerofoil correlated to deflection of flap control for application to wing reversal analysis 06 p0801 A66-16001

Short-periodic motion of tailless glider



analyzed to determine degree of overcompensation of flap required for good stability 23 p4016 A66-41784

#### FLARE SA ILLUMINATION SA PYROTECHNICS SA SOLAR FLARE

Square flare for stabilizing upper stages of multistage ballistic missiles, discussing test results and aerodynamic advantages over conical flare 03 p0432 A66-12770  
Comet flares and cometary nuclear structure, specifically considering Schwassman-Wachmann I 17 p3009 A66-33371  
IR emitting flares, examining major parameters governing methods of analysis and performance 18 p3135 A66-34192

#### FLARED BODY

Static and dynamic stability and drag of blunt-nosed flare-stabilized bodies at velocities up to 8.2 km per second [AIAA PAPER 65-44] 12 p1799 A66-24699  
Laminar, transitional and turbulent boundary layer flows with adverse pressure gradient on axisymmetric blunted conical flared body at Mach 10 [AIAA PAPER 66-493] 18 p3047 A66-33658  
Light variations of flare and T Tauri stars due to surface electromagnetic activity connected with turbulence in convective zone and rotation, using Hertzprung-Russell diagram 20 p3652 A66-37610  
Corpuscular radiation from UV Ceti stars assumed to be mainly protons, noting role of interstellar matter 20 p3652 A66-37611  
Flare stars as sources of cosmic X-rays, spectra contain 4686-angstrom line of doubly ionized helium indicating that atmospheres contain either ionizing radiation or electrons 22 p3972 A66-39707

#### FLASH BLINDNESS

SA VISION  
Protection devices against vision impairment occurring during exposure of airmen and military personnel to intense visible radiation 01 p0019 A66-10481  
Decay time of positive afterimage following high intensity flashes measured by monocular and binocular brightness matching 18 p3062 A66-33993  
Eye patch and flashblindness protection 22 p3857 A66-39794  
Explosive lens flash blindness protection system consisting of flight helmet to support goggle lens, sensing device and discriminator unit 24 p4168 A66-42853

#### FLASH TUBE

Excitation of ruby lasers using double-pumped high-intensity helical flash tubes, obtaining time-resolved spectra of electrical discharges and plasma temperatures 02 p0240 A66-11446  
Xenon flashtube design and operating capabilities 10 p1537 A66-21870  
Dismountable flash lamp for laser, including cross sectional scale drawing and wiring diagram 11 p1714 A66-23296  
Efficient conversion of electrical energy into laser radiation, using coaxial optical pump 11 p1715 A66-23479  
Simultaneous measurement of voltage, current, current derivative and X-ray output as function of time in low inductance flash X-ray discharge tube 16 p2706 A66-30935  
Ruby laser pumping system and low cost mercury flash tube with high repetition rates used for micromachining process 22 p3933 A66-40336

#### FLAT LAYER

Radiative heat transfer in flat layer of absorbing, reradiating and nonscattering gray medium with optical properties independent of temperature 04 p0598 A66-14425  
Photoelastic determination of stress concentration factor for flat strips notched on both sides under tension 23 p4140 A66-41852

#### FLAT PLATE

Two-phase flow over flat plate analyzing velocity profile, shear coefficient and heat transfer of laminar boundary layer formed over plate 01 p0006 A66-10423  
Free convection boundary layers on horizontal flat plate 01 p0161 A66-10434  
Square plate vibration patterns determined, using stereophotogrammetry 01 p0157 A66-10921

High subsonic flow passing choked flat plate cascade with comparatively small pitch chord ratio 02 p0175 A66-11305

Effect of various factors in film-cooling phenomena obtained by vertically injecting air into turbulent boundary layer on flat plate 02 p0303 A66-11586

Vortex streets behind circular cylinders and flat plates analyzed, using photography and hot wire techniques, noting role of walls and wakes 03 p0354 A66-12321

Hypersonic flow separation over simple geometries and aerodynamic controls, noting pressure gradients and heating-rate distributions

[AIAA PAPER 65-753] 03 p0314 A66-12587  
Thermal deformation of flat plate considering temperature gradient effect through thickness, showing that plate is not exhibiting Euler buckling 03 p0442 A66-13301

Boundary layer control by blowing, analyzing turbulent boundary layer for flow about flat plate of incompressible fluid with intense cross flows 04 p0509 A66-13573

Monograph on Levy method for deflection of loaded simply-supported infinite plate strip, introducing class of real functions 04 p0589 A66-14011

Aerodynamic characteristics of flat rectangular plate placed normal to flow of highly rarefied gas 04 p0456 A66-14141

Interaction of radiation and convection in laminar boundary layer of perfect gas on flat black plate

[ASME PAPER 65-HT-54] 05 p0785 A66-14760  
Heat transfer and equilibrium temperature on flat plate in region of strong interaction in hypersonic flow 05 p0607 A66-15465

Heat and mass transfer from vertical plates boundary layer in convection at low Reynolds number by interferometry [ASME PAPER 65-WA/HT-39] 05 p0664 A66-15669

Turbulent velocity profile produced by controlling boundary layer thickness, using wires placed parallel to plate and normal to flow direction [ASME PAPER 65-WA/FE-29] 05 p0664 A66-15711

Influence of suction or injection in boundary layer flow past vertical flat porous plate in presence of uniform magnetic field 06 p0969 A66-16181

Thermal stress concentration factors for rectangular flat plates penetrated by holes [AIAA PAPER 66-120] 06 p0962 A66-16262

Temperature distribution of fluid in laminar boundary layer of flat plate and heat flow from fluid to plate wall 06 p0872 A66-16467

Four-point loading bend test on specimen of full plate thickness with sharp notch to 20 percent depth, with ductility criterion as fully plastic angle of bend before fracture 06 p0965 A66-16492

Flow field study of shock wave and boundary layer development at leading edge of sharp flat plate in rarefied hypersonic flow

[AIAA PAPER 66-31] 06 p0803 A66-17082  
Nonsimilar solution of incompressible boundary layer over flat plate in presence of shear flow, using approximate method 08 p1204 A66-18529

Shock wave shapes on cold flat plate in rarefied hypersonic flow tunnel measured by optical-flow techniques 08 p1165 A66-19165

Increased mass transfer from flat plate caused by wake from cylinders located near boundary layer edge 08 p1211 A66-19682

Small transverse flow effect on spanwise perturbation of two-dimensional boundary layer of flat plate 08 p1166 A66-19820

Ion density profiles in boundary layers associated with supersonic flow of shock heated air over flat plate measured by cylindrical and flush-mounted electrostatic probes

[AIAA PAPER 66-159] 10 p1565 A66-21686  
Compressibility effect on flow in MHD boundary layer of semiinfinite thermally insulated flat plate 10 p1525 A66-21847

Combined loads minimum weight analysis of stiffened truss-core sandwich flat plate and cylinder 10 p1618 A66-21940

Transition from near free molecular flow at leading edge of flat plate in rarefied hypersonic flow to continuum boundary

layer flow downstream 11 p1633 A66-2292

Flow over sharp and blunt flat plates at zero angle of attack in hypersonic shock tunnel, measuring surface skin friction, heat transfer, static pressure and shock layer pitot pressure 11 p1633 A66-2292

Pressure distribution and low density effects on sharp flat plates and sharp and blunt cones measured in hypersonic wind tunnel 11 p1634 A66-2293

Flat plate in hypersonic flow analysis in shock tunnel, obtaining surface pressure using electron beam densitometer 11 p1634 A66-2293

Thick laminar boundary layer influence a supersonic speeds and low Reynolds numbers 11 p1634 A66-2293

Flow field near leading edge of heated flat plate in Mach 0.5 airflow 11 p1634 A66-2293

Equation for laminar boundary layer of flat plate in viscous compressible gas flow under chemical relaxation, solved by approximate method in series form 12 p1863 A66-2424

Nonlinear two-dimensional cavity theory for choked unsymmetric flow over flat plate at arbitrary attack angle, noting variation of lift and drag coefficients [ASME PAPER 65-FE-13] 12 p1864 A66-2454

Free convection film boiling heat transfer from isothermal vertical plate to subcooled stagnant liquid, using two-phase boundary layer theory 12 p1980 A66-2490

Heat-transfer coefficients calculated for forced convection from heated flat plate at zero incidence to stream of viscous fluid noting role of Reynolds number 12 p1981 A66-2494

Numerical analysis of steady two-dimensional motion of viscous fluid past flat plate at zero incidence to uniform stream with solutions for Navier-Stokes equations 12 p1866 A66-2494

Rarefied flow transition at leading edge of flat plate examined, using Navier-Stokes equation, noting new low density jump conditions, viscous layer characteristics effect of normal pressure gradient etc 13 p2061 A66-2516

Turbulent flow intensity measured in turbulent wake of small fence along flat plate covered with flabby skin, for analysis of drag reduction in aerodynamics 13 p2063 A66-2559

Hot-wire analysis of permanent sound fields during varied flow velocity around flat plate boundary layer, noting resonance effect of sound amplitude 13 p2063 A66-2590

Stress concentration for cylindrical bending of plates with holes, deriving equations and evaluating errors in classical theory 13 p2203 A66-2642

Approximate methods of computing heat transfer through laminar boundary layer considering boundary layer along flat plate and second order effects 13 p1993 A66-2671

Convective heat transfer to flat plate at stagnation point in partially ionized equilibrium air boundary layer, noting heating rates 13 p2210 A66-2672

First-collision process at sharp leading edge of flat plate aligned with hypersonic free stream 13 p1993 A66-2672

Analytical methods for studying turbulent boundary layers at high Mach numbers, comparing theory and experiments for flat plate flow, predicting boundary layer properties around hypersonic configurations 14 p2217 A66-2709

Coupled parametric and self-excited vibration of plate with supersonic flow past one side, assuming periodically varying forces act in plane of plate, noting degeneration of parametric resonance main region 14 p2398 A66-2745

Periodically excited boundary layer disturbances above flat plate in water flow scanned by hot-wire anemometer under various conditions 14 p2275 A66-2747

Central deflection of simply supported centrally loaded rhombic plate with formula depending on first coefficient obtained in mapping of rhombus 14 p2409 A66-28397

Effect of unsteady longitudinal vortices on Blasius profile in traditional boundary layer of flat plate 14 p2279 A66-28461

Rarefied supersonic flow condensation on cold flat plate, noting capture coefficients



- shock wave behavior, etc 16 p2825 A66-30383
- Interaction of radiation and convection in laminar boundary layer of perfect gas on flat black plate
- ASME PAPER 65-HT-54] 16 p2828 A66-30988
- Design, fabrication and testing of flat plate solar thermoelectric generator for near-Earth orbits, including comparison with photovoltaic cell 16 p2636 A66-31019
- Flat plate solar thermoelectric generator panels for near-Earth orbits, comparing design, fabrication and testing to photovoltaic cells 16 p2637 A66-31103
- Skin friction methods compared for problem of turbulent compressible boundary layer on flat plate at hypersonic Mach numbers 16 p2686 A66-31118
- Three-dimensional flow separation of plane boundary layer caused by half delta wing on flat plate using Cooke small cross-flow method and Maskell separation criterion [AIAA PAPER 66-428] 16 p2631 A66-31465
- Transition delay and skin friction drag reduction by considering boundary layer flow over flexible aerodynamic surface [AIAA PAPER 66-430] 16 p2688 A66-31466
- Hypersonic strong-interaction similarity solutions for viscous compressible flow past plate analyzed using Navier-Stokes equations 16 p2632 A66-31655
- Turbulent heat transfer measurements on transpiring flat plate in Mach 8 tunnel using nitrogen, helium and argon as injection gases 17 p2838 A66-32439
- Film cooling in supersonic free stream flowing along flat plate in Mach 3 wind tunnel, using air as secondary fluid 17 p2839 A66-32441
- Wall heat transfer behind plane detonation wave moving past flat plate into stationary hydrogen-oxygen mixture 17 p3033 A66-32461
- Secondary flow for supersonic boundary layers with or without swept edges, noting effect of compressibility and heat transfer on reverse flow 17 p2840 A66-32485
- Drag on cylinders of various height mounted on flat plate, noting dependence of compression region length on cylinder diameter during analysis of boundary layer separation phenomena 17 p2909 A66-32493
- Photoelastic and stress quenching techniques, showing change in stress distribution with crack propagation 17 p3026 A66-32595
- Separated unsteady flow about flat plate rotating impulsively from rest to uniform angular velocity about axis along leading edge, noting torsional oscillations [AIAA PAPER 66-427] 17 p2910 A66-32753
- Three-dimensional boundary layer for accelerating flow over semiinfinite flat plate with or without suction 17 p2911 A66-32838
- Unsteady slip flow of electrically conducting viscous fluid over porous flat plate under transverse magnetic field 17 p2973 A66-32980
- Elasticoviscosity and cross viscosity of second-order fluid effects on advancement over infinite flat plate 17 p2912 A66-32981
- Heat transfer resulting from normal impingement of turbulent high temperature jet on infinitely large flat plate 17 p3039 A66-33470
- Laminar boundary layer heat transfer measurements by thick-film calorimeter gauges on flat plate in dissociated and partially ionized air 17 p3039 A66-33483
- Boundary layer problem concerned with effects of radiation absorption and emission for flow of high speed gas over flat plate [AIAA PAPER 66-521] 18 p3047 A66-33662
- Free vibrations of two flat plates fixed at right angle with cross-sectional distortion 18 p3251 A66-33678
- Heat transfer caused by combustion of triethylaluminum on flat plate in Mach 3 flow, noting significance of lag at stagnation pressure 18 p3260 A66-33817
- Temperature distribution in rectangular flat plate during heat application and cooling periods in spot welding procedure 18 p3260 A66-34066
- Step function distribution of heat transfer for laminar supersonic boundary layer described as function of decay factor 18 p3261 A66-34363
- Lift and drag of supercavitating isolated hydrofoil or hydrofoils in cascade, noting characteristics of flat plate and circular arc foils 18 p3100 A66-34642
- Boundary layer of steady incompressible plane crossed fields MHD flow at large Reynolds number 18 p3147 A66-34663
- Differential equations for deformations of nonuniform flat plates bent into cones 19 p3473 A66-35850
- Bismuth telluride alloy solar thermoelectric flat plate generators applied to auxiliary power systems for exploratory missions toward Sun 20 p3497 A66-37166
- Skin friction drag of power law fluids in turbulent flow over flat plate shown as function of non-Newtonian Reynolds number and shear rate exponent 20 p3545 A66-37507
- Postbuckling behavior of clamped infinite flat strip under action of shearing forces analyzed based on von Karman equations 20 p3669 A66-37531
- Asymmetric shear flow of viscous fluid past flat plate, justifying constant pressure assumption and examining flow patterns at lower surface in plate proximity 20 p3547 A66-37978
- Figure that results from disintegration of package of plates during fall through atmosphere, deriving equations for rotational motion of plates 20 p3493 A66-38118
- Heat transfer between turbulent flow of air and isothermal wall plate and constant thermal flux at surface 21 p3835 A66-38907
- Thermal stresses in flat rectangular isotropic plate of constant thickness under arbitrary and no temperature variation in terms of Fourier series and integrals 21 p3832 A66-39443
- Velocity profile, induced magnetic field, shear stresses and skin friction on plates for viscoelastic liquid flow between nonconducting oscillating infinite flat plates in uniform TM field 21 p3794 A66-39575
- Viscous drag on flat plate in supersonic flow injected with gas in boundary layer, examining exit cone of rocket nozzle 22 p3970 A66-39875
- Integral equation for heat flux in inverse heat conduction for infinite flat plate as in solid rocket igniters 22 p3998 A66-40031
- Mass transfer from cone in supersonic flow in tests performed at zero angle of attack, preserving Mangler transformation which transforms flat plate solution to cone 22 p3843 A66-40036
- Compressible turbulent boundary layer on flat plate, noting correspondence between compressible and incompressible flow, numerical results on skin friction and heat transfer, etc 22 p3899 A66-40344
- Flow field study of shock wave and boundary layer development at leading edge of sharp flat plate in rarefied hypersonic flow [AIAA PAPER 66-31] 22 p3844 A66-40349
- Flow of unsteady compressible boundary layer over semiinfinite flat plate whose temperature exceeds free stream temperature 22 p3902 A66-40707
- Nongray radiation effects on laminar boundary layer of absorbing gas over flat plate, using absorption coefficient with stepwise frequency 23 p4012 A66-41903
- Approximate integral method for determining thermal boundary layer and heat transfer on flat plate with insulated surface 23 p4150 A66-41920
- Potential energy and conservativeness of normal pressure field acting on flat plates 23 p4141 A66-41926
- Fatigue testing machine shear strain measurements near cracks on Al flat plate surfaces by observing birefringence 23 p4147 A66-41997
- Approximate Navier-Stokes equations for viscous flow conditions near trailing edge of flat plate 23 p4059 A66-42001
- Similar solutions for laminar boundary layer under forced convection of mixture of fluids with constant mass density and temperature and composition dependent parameters for flat plate analysis 23 p4059 A66-42007
- Two-dimensional roughness element effect on boundary layer transition, noting free stream turbulence level influence on amplification rate of disturbance 23 p4060 A66-42020
- Turbulent boundary layer at flat plate in extremely turbulent flow, noting effect on shearing stress and velocity distribution 23 p4061 A66-42028
- Flat plate laminar boundary layer in supersonic wind tunnel, measuring pressure distribution and profiles and heat transfer rates, noting dissociation fraction effects 24 p4194 A66-42411
- Closed form relationship for estimation of flat plate turbulent heating rates at hypervelocities 24 p4158 A66-42788
- FLAT SURFACE**
- Discharge in large radius cylindrical hollow cathodes with uniform plasma layer above flat end face investigated experimentally 02 p0199 A66-11812
- Extremization of products of powers of functionals as applied to flat top wings for maximizing lift drag ratio in hypersonic flow 17 p2842 A66-33242
- Flat Earth approximation of LF propagation theory 18 p3072 A66-34711
- Propagation of turbulent jet colliding with flat surface at certain incidence angle analyzed for applications to V/STOL aircraft, ventilation equipment, etc 23 p4056 A66-41737
- Round turbulent low speed airjet impingement on flat surface and application to theoretical analysis of inviscid rotational flow 23 p4012 A66-42002
- Inviscid hypersonic flow past flat wings at large angle of attack analyzed, using homogeneous layer concept of shock layer theory 23 p4013 A66-42014
- FLAW**
- Silicon field effect device with AC/DC fields superimposed on gate terminals analyzed for determination of distribution of defect introduction rate with depth, especially near threshold energies 19 p3435 A66-35413
- FLAW DETECTION**
- SA NONDESTRUCTIVE TESTING**
- SA X-RAY INSPECTION**
- Size effect of bending and twisting fatigue strength by calculating probability of flaws on surface 02 p0243 A66-11581
- Pattern recognition applied to fault detection in equipment testing procedure 06 p0868 A66-15984
- Nondestructive test method using fluorescent penetrant techniques for detecting intergranular surface attack on Inconel-X thrust chamber tubing 07 p1040 A66-18392
- Design of Malfunction Detection System used on board orbiting laboratory type vehicles to monitor and evaluate critical signals 10 p1538 A66-22043
- Statistical failure detection, employing distribution analysis of parameter changes which removes artificial constraints imposed by arbitrary specification limits 15 p2507 A66-28799
- Part failure detection methods, noting interrelationship between part sampling and reliability, destructive and nondestructive component testing, etc 15 p2507 A66-28800
- Nondestructive ultrasonic testing in machine and boiler construction engineering, noting material properties and behavior of parts, flaw detection, etc 21 p3743 A66-38939
- Magnetic field above surface of conductor with flaws that emerge at surface when direct current is passed through 24 p4218 A66-42897
- Physical principles of phase sensitive eddy-current method of detecting surface cracks in metal products 24 p4218 A66-42898
- Phase-sensitive eddy current method of detecting surface cracks in metal products, examining construction and operating principles of flaw detector 24 p4218 A66-42899
- FLEET BALLISTIC MISSILE /FBM/ WEAPON SYSTEM**
- S POLARIS MISSILE**
- FLEXIBILITY**
- SA ELASTICITY**
- SA PLASTICITY**
- Stiffness, carry-over factor and fixed-end moment of axially loaded nonuniform members under tension or compression 17 p3024 A66-32397



## FLEXIBLE BODY

Flexible satellite attitude control, analyzing satellite as thin circular plate with application to radio telescopes, noting vibration modes and nonlinear gyroscopic coupling terms 01 p0142 A66-10674

Characteristics of flexible circular plate, considering stress and strain in friction zone at clamped section 01 p0160 A66-11181

Nonlinear dynamics of free rotating flexibly connected double-mass space station 03 p0431 A66-12744

Generalized method for predicting pressure loss of straight and bent flexible sections of metal hose 04 p0459 A66-13640

Karman equation for bending of flexible plate solved by Kantorovich method, taking into account geometrical nonlinear deformations 07 p1143 A66-17860

Pressure wave propagation velocity in horizontal liquid-filled flexible tubes 07 p1146 A66-18277

AMRA high speed tensile testing analysis of dynamic stress-strain behavior in beryllium oxide in flexure and in compression 13 p2115 A66-26114

Flexible baffle effect on nature and magnitude of damping and sloshing motions of liquid propellants over wide range of conditions 16 p2685 A66-30915

## FLEXIBLE WING

Paraglider wing analysis based on assumption that flexibility allows it to take shape that aerodynamic pressure and internal stresses dictate [ASME PAPER 64-WA-AV-4] 10 p1483 A66-21472

Recoverable and reusable radio controlled sounding rocket equipped with deployable flexible wings attached to paraglider beams 24 p4284 A66-43071

## FLEXOWRITER

User-oriented computer programming system using Flexowriter modified to construct new two-dimensional programming language 12 p1826 A66-23828

## FLICKER FUSION FREQUENCY

Review of data on visual flicker fusion and intermittent stimulation 04 p0462 A66-13792

Effect of extremes in magnetic environment on physiological behavior 08 p1174 A66-18585

## FLIGHT

S BALLOON FLIGHT

S BUFFETING

S FREE FLIGHT

S HYPERSONIC FLIGHT

S INTERPLANETARY FLIGHT

S JET FLIGHT

S LUNAR FLIGHT

S MAN POWERED FLIGHT

S METEOROLOGICAL FLIGHT

S OVER-WATER FLIGHT

S PARABOLIC FLIGHT

S PREFLIGHT ANALYSIS

S PREFLIGHT OPERATION

S ROCKET FLIGHT

S SPACE FLIGHT

S SUPERSONIC FLIGHT

S VERTICAL FLIGHT

S VISUAL FLIGHT

## FLIGHT ALTITUDE

Altitude measurement requirements for supersonic transport including flight profile, air traffic control, climb, etc 09 p1400 A66-20426

Airborne electronic command device for measuring time intervals corresponding to cruising speed/ true flight altitude ratios up to 40 21 p3735 A66-38569

## FLIGHT CHARACTERISTICS

SA AIR SPEED

Measuring Meteor 1 rocket flight parameters from ground using phototeodolites and astronomical and optical-acoustic methods 01 p0031 A66-11067

Tape recorders of flight parameters, tabulating characteristics of ten instruments 01 p0071 A66-11072

Effect of canard foreplane on longitudinal long-period perturbed motion of aircraft depends on change in hinge moments with Mach number change 04 p0458 A66-14152

Flight characteristics and test program of CL-84 light tilt-wing V/STOL Army support vehicle 07 p0986 A66-17271

Book on aircraft testing techniques for aeronautical technical school

students 08 p1167 A66-18590

Dragon rocket probe, launch history and flight modifications 10 p1611 A66-21397

Aircraft vibration in transonic region caused by aileron oscillations, eliminated by friction dampers 12 p1801 A66-24035

Annual report, 1964-65 /Aeronautical Research Laboratories, Australian Defence Scientific Service/ on aerodynamics, guided weapons and systems and flight research 13 p2056 A66-25120

Flight characteristics of compound helicopter with fixed rotor and jet engine 13 p1995 A66-25761

Scramjet aircraft performance capabilities, noting operating parameters such as thrust coefficient, flight velocity, acceleration, fuel consumption, etc 13 p2173 A66-26032

Wind tunnels to predict flight characteristics based on models and test probes 14 p2270 A66-27564

Data processing techniques for analyzing turbulence records and for estimating response of aircraft to atmospheric turbulence 17 p2843 A66-32329

Approximate atmospheric entry trajectories on cylindrical planet, noting minor circle turn maneuver and bank angle schedule 21 p3811 A66-38705

Prediction of rocket engine flight performance with less than 2 percent error in specific impulse data measured at sea level 23 p4120 A66-41111

## FLIGHT CLOTHING

SA PRESSURIZED SUIT

SA PROTECTIVE CLOTHING

Sport-type knit suit indicated as most suitable astronaut clothing in small-volume cabin during comfortable microclimatic conditions 15 p2443 A66-29458

Comparative insulative properties of wet and dry type immersion protection flight clothing 16 p2643 A66-31127

## FLIGHT CONDITION

Atmospheric temperature changes as factor in detection of clear air turbulence, especially above 25,000 ft, noting aircraft instrumentation used 15 p2532 A66-28918

Takeoff and landings by periscope under various flight conditions, noting effect of variations in image magnification 22 p3946 A66-40859

## FLIGHT CONTROL

SA ATTITUDE CONTROL

SA IN-FLIGHT MONITORING

Adaptive flight control system, using sampled data to identify aircraft parameter, for high performance aircraft 01 p0009 A66-10005

Automatic flight control system for A-7A featuring high fixed gain dual channels, series servos and control augmentation in addition to normal attitude and path control functions 01 p0098 A66-10007

Automatic and semiautomatic vectoring and landing capability of U.S. Navy carrier-based aircraft F-4G Phantom II 01 p0099 A66-10009

Research and development progress toward synthesis of pure fluid flight control system 01 p0140 A66-10021

Aerospace vehicle flight control - SAE and NASA Conference, Los Angeles, July 1965 01 p0102 A66-10661

Outer loop control mechanization for automatic landing systems associated with flight control, noting series servo concept as compared to parallel servo mechanization 01 p0014 A66-10664

Triple redundancy with majority logic voting in application for increased safety and reliability of aircraft stability augmentation and/or automatic flight control 01 p0103 A66-10665

Redundancy techniques for flight control systems applied to tactical military aircraft, noting monitorless channel output selection, failures, etc 01 p0103 A66-10666

Hydrologic redundant systems for overall flight control systems 01 p0015 A66-10667

Balanced power concept for weight savings in aircraft actuation system consisting of mechanically actuated flight control surface, mechanical servo, flywheel and motor 01 p0015 A66-10670

Mechanical servoactuator for all-mechanical flight control system for aerospace vehicles, noting traction transmission effect on toroidal actuator, cascading for power

amplification, etc 01 p0015 A66-10677

Difficulties in control system synthesis for launch vehicles exhibiting severe mode interaction 01 p0104 A66-10677

Future sensing and information requirements and system ideas applicable to flight control 01 p0104 A66-10677

Drift of coordinate transformation matrix of quantized attitude reference system of aerospace vehicle undergoing coning motions 01 p0142 A66-10677

Float-cocking phenomenon in single-axis floated gyroscopes caused by impressed angular velocity on sensible radial compliance 01 p0068 A66-10677

Gemini flight control system performance during second unmanned flight 01 p0104 A66-10677

Digital computation desirability for flight control system 01 p0104 A66-10677

Fluid control and guidance systems summary of available hardware 01 p0015 A66-10677

Microelectronic digital system for spacecraft stabilization and control 01 p0105 A66-10677

Reliability factors in flight control, particularly automatic landing systems and controls for VTOL aircraft in transition regime 02 p0231 A66-11867

Human pilot behavior compared with automatic pilots in terms of adaptability response time and reliability 02 p0187 A66-11867

Optimum control synthesis review theory and practice, especially for flight mechanics and control 03 p0349 A66-12777

Mathematical model based on control and queueing theory for human controller for turn-round operations on airport apron 03 p0329 A66-12877

In-flight monitoring of advanced aircraft discussing system requirements and constraints [ISA PREPRINT 1.3-2-65] 05 p0684 A66-15517

Airborne navigation and flight-control equipment for reducing weather minimum to lowest possible level 06 p0907 A66-16427

XB-70 hydraulic system, describing characteristics, operation-mechanism of fluid power system, power generation, utilization and distribution 06 p0809 A66-16777

Probability state variable device /neutronron/, operation, functions and application 06 p0819 A66-16867

Control power composition and usage characterized for VTOL aircraft flight control system design 06 p0806 A66-16877

Flight controls of tilt wing X-142 aircraft, noting mechanization and operation of wing and flap control system 06 p0809 A66-16877

X-15 flight problems not encountered during simulation, particularly differences in aerodynamics, control systems, cockpit equipment, etc 07 p1017 A66-17277

XB-70A, high Mach number handling qualities and suggested improvements through addition of better instruments presentation, automatic flight control etc 07 p0986 A66-17277

Visual aid in detection, recognition and acquisition of targets at different altitudes and speeds 07 p0998 A66-17277

Functional requirements for computer navigational system for Concorde aircraft 07 p1065 A66-17677

Navigation and flight instrument, discussing deficiencies of panel-mounted navigational command system 07 p1033 A66-17677

Location of flight control system for simplifying crew procedure and reducing navigation error in areas of high traffic density 07 p1068 A66-17677

DECTRA long range navigational aircraft DECTRA airborne receiver and Omnitron computer 07 p1068 A66-17777

Building blocks of pictorial navigational display for projection of servo-driven microfilm map onto rear projection screen 07 p1069 A66-17777

Flight testing of Philips vertical reference inertial navigator on DC-8 aircraft 07 p1069 A66-17777

Advanced airborne computer double system applied to fault detection, location flight management and



navigation 07 p1003 A66-17715  
 Position-attitude-true-heading-steering  
 navigation system noting accuracy,  
 reliability, maintenance, operational  
 requirements and functional  
 features 07 p1070 A66-17720  
 Two automatic astronomical navigation and  
 tracking systems compared for accuracy and  
 performance in civil  
 aircraft 07 p1070 A66-17722  
 Schuler tuned inertial system as flight  
 sensor and control of VTOL aircraft  
 translational velocity during hover phase  
 and landing 07 p1070 A66-17724  
 MOA/BOAC Doppler/Loran A trials 1963-64,  
 discussing navigational accuracy during  
 transatlantic flights 07 p1072 A66-17759  
 Operational factors in automated  
 navigational computations, with  
 consideration of self-contained aids, ground-  
 based systems and astrosatellite  
 navigation 07 p1075 A66-17780  
 FAA regulation of civilian use of U.S.  
 airspace 08 p1321 A66-18548  
 Manual guidance and control simulation for  
 reentry vehicle flight and  
 landing 08 p1203 A66-19533  
 Visual display system providing instrument  
 data in one-to-one correspondence with real  
 world, using cathode ray tube images of  
 horizon and runway projected on aircraft  
 windshield 08 p1203 A66-19764  
 Aerospace technology including past  
 progress, predictions, minimum and  
 maximum speeds for safe flight control,  
 economics, propulsion,  
 etc 09 p1472 A66-20164  
 Thermal management /heat-sink and  
 pressurization and cooling systems/, fuel,  
 flying control and hydraulic and electrical  
 systems of Lockheed L-2000 SST  
 project 09 p1329 A66-20391  
 Book on flight dynamics, covering optimum  
 control, multistage rocket trajectory  
 optimization, VTOL aircraft dynamics,  
 autopilot design, etc 11 p1732 A66-23335  
 Automatic pilot consisting of guidance  
 system for flight trajectory control and  
 stabilization system for angular acceleration  
 control 12 p1909 A66-23815  
 Integrated stability augmentation circuits  
 in AN/ASW-16 automatic flight control  
 system 12 p1837 A66-24381  
 Aeronautical stability problems, discussing  
 background, rigid and elastic stability and  
 adaptive control 13 p1994 A66-25582  
 Book on unmanned aircraft and rocket  
 control systems, flight dynamics in  
 conjunction with control processes, design  
 of stabilization and guidance  
 systems 13 p2055 A66-26462  
 Fixed shaft turboprop flight control system  
 for business and utility aircraft  
 [SAE PAPER 660218] 14 p2225 A66-27119  
 Effect of faulty compensation for  
 accelerating force of Earth gravity on  
 accuracy in determination by inertial  
 navigation system of coordinate of object in  
 flight 14 p2328 A66-27361  
 Duplex pitch channel in Hawker Siddeley  
 Trident autopilot for glide path extension  
 and flareout control 14 p2328 A66-28229  
 Saturn launch vehicle flight control system  
 model based on rigid-body control  
 law 15 p2605 A66-28747  
 Flight control systems, automatic landing  
 devices and inertial navigation with  
 gyros 15 p2534 A66-29365  
 Sensor threshold definitions applied to rate  
 gyros, comparing old and new AIAA  
 specifications, noting threshold definitions  
 relation to flight control system  
 malfunctions 16 p2708 A66-31439  
 Low-altitude control of U.S. Army rotary  
 wing aircraft 17 p2950 A66-32722  
 USAF CH-3C helicopter V/STOL in flight  
 refueling, discussing requirements, system  
 characteristics and flight  
 tests 17 p2844 A66-32724  
 Integrated Helicopter Avionics System  
 flight control, noting stability augmentation,  
 long-term motion control, outer and inner  
 loop function separation and fail-safe  
 capability 17 p2951 A66-32730  
 Lift engine technology, noting effect on  
 operational transport aircraft design, VTOL  
 capabilities, low speed control,  
 etc 17 p2844 A66-32732

Flight control design parameters and  
 performance effects on VTOL aircraft  
 handling qualities, noting manufacture and  
 flight test results 17 p2845 A66-32733  
 Centrifugal pump for liquid metal power-  
 transmission in flight control systems  
 [ASME PAPER 66-FE-20] 17 p2932 A66-33273  
 Vertical-track free-fall rocket sled system,  
 discussing design principles, operation and  
 performance  
 characteristics 18 p3093 A66-33796  
 Optimized spacecraft control process  
 eliminates gravitational field-caused  
 nonlinearities by taking as control  
 parameters osculating characteristics of  
 planetocentric motion 18 p3242 A66-33851  
 Position and flight-path control techniques  
 for satellites and space  
 probes 18 p3246 A66-34677  
 Instrument unit analysis for Saturn IB/V  
 program, noting environmental, guidance and  
 flight control, electrical systems and  
 countdown procedure 19 p3354 A66-35469  
 Flight control for low altitude high-speed  
 mission, discussing applicable requirements,  
 analysis and design  
 techniques 19 p3396 A66-35506  
 Flight control system design for high  
 performance aircraft, particularly longitudinal  
 transient response handling  
 qualities 19 p3278 A66-35509  
 Short period longitudinal aerodynamics of  
 reentry vehicle flight control system, using  
 sensitivity techniques 19 p3396 A66-35510  
 Multiloop flight control system root  
 sensitivity to open loop parameter variation,  
 describing method of  
 analysis 19 p3335 A66-36690  
 Visual displays to aid pilot to fly, monitor  
 and control power plant, navigational and  
 other equipment and communicate with ATC  
 ground stations 20 p3508 A66-36996  
 Dive flight behavior of propeller-driven  
 and jet fighters 21 p3696 A66-38652  
 Flight control system for low weather  
 minima for use in small business craft and  
 large air transports 21 p3761 A66-38655  
 Flight control system providing control  
 augmentation, self-adaptive control and self-  
 organizing control 22 p3848 A66-40125  
 Multiloop flight control system root  
 sensitivity to open-loop parameter variation,  
 describing method of  
 analysis 22 p3884 A66-40360  
 NaK-77 suitability for 1000-F liquid-metal  
 hydraulic flight control  
 systems 22 p3852 A66-40498  
 Wind tunnel flight data correlation  
 program, considering tunnel wall effects,  
 measurement and control of thrust and  
 propeller blade angle  
 [AIAA PAPER 66-737] 22 p3893 A66-40627  
 Automatic flight control system for A-7A  
 featuring high fixed gain dual channels,  
 series servos and control augmentation in  
 addition to normal attitude and path control  
 functions 23 p4088 A66-40983  
 Duplicate monitored system for automatic  
 landing control of VC10 and  
 Concorde 23 p4088 A66-41163  
 Simulator study of computing and  
 displaying velocity in head-up display for  
 low speed flight path control by pole track  
 or velocity vector  
 [ICAS PAPER 66-16] 23 p4089 A66-41257  
 Automatic flight control for VJ 101C VTOL  
 aircraft, noting autopilot  
 function 23 p4016 A66-41931  
 Skin temperature rate reentry guidance  
 and control system using thermocouple  
 sensors and operating in manual or  
 automatic mode  
 [AIAA PAPER 65-47] 24 p4235 A66-42765  
**FLIGHT FATIGUE**  
 Flight fatigue studies, discussing  
 parametric evaluation of crew performance  
 on overseas flights 06 p0816 A66-16057  
 Aircraft crew fatigue on long distance jet  
 flights, measuring flight safety parameters  
 such as heartbeat, pulse rate and  
 temperature 12 p1808 A66-23753  
 Flight fatigue treatment by acetyl-aspartic  
 acid and citrulline, noting improved reaction  
 to acoustic and visual  
 stimuli 17 p2859 A66-32232  
 Aviation fatigue noting flight-time  
 limitations, indicators of excessive fatigue,  
 new developments related to international

flights and Forest Service  
 flights 19 p3294 A66-36383  
**FLIGHT FITNESS**  
 Profile of pattern of airsickness obtained  
 for 1067 naval aviators in pre-solo and basic  
 acrobatic phase of primary flight  
 training 06 p0814 A66-16833  
 Otitic barotrauma caused by difference  
 between atmospheric pressure and middle  
 ear cavity pressure arising during flight,  
 compression chamber tests, etc, and leading  
 to deafness 10 p1488 A66-22107  
 Effects and causes of sinus barotrauma  
 /pressure differential between sinuses and  
 outside atmosphere/ noting prevention,  
 treatment and  
 aftereffects 10 p1488 A66-22108  
**FLIGHT HAZARD**  
 Task interruption and performance  
 decrement of active pilots and flight crew  
 personnel following rapid  
 decompression 18 p3061 A66-33782  
 Promotion of aviation safety, discussing  
 adoption of new accident statistics,  
 elimination of catastrophes and STOL  
 design extension to medium and long-range  
 aircraft 23 p4152 A66-41305  
**FLIGHT INSTRUMENT**  
**SA HORIZON SCANNER**  
**SA POSITION INDICATOR**  
 Manned aircraft self-contained checkout  
 and fault isolation systems, discussing  
 characteristics and operational concepts  
 [ISA PREPRINT 1.3-3-65] 05 p0684 A66-15513  
 SST instrumentation problems, discussing  
 reappraisal of flight deck display  
 requirements 07 p1033 A66-17784  
 Flight deck display for future aircraft  
 projects, emphasizing vertical scale director  
 instruments for cockpit  
 display 11 p1649 A66-23250  
 In-flight pilot responses to new  
 nongyroscopic blind flight Kenyon  
 instrument 15 p2442 A66-28662  
**FLIGHT LOAD RECORDER**  
 Flight Load Survey program, written in  
 Fortran IV, for accurate and rapid sounding  
 of wind-induced loads on aerospace launch  
 vehicle  
 [AIAA PAPER 66-470] 16 p2811 A66-31473  
**FLIGHT MECHANICS**  
 Successive linearization for variational  
 problems of flight  
 mechanics 04 p0458 A66-13698  
 Aerodynamic penetration and radius in  
 drag and lift during atmospheric entry  
 process  
 [AIAA PAPER 66-16] 07 p0983 A66-18447  
 Optimum sliding regimes in variational  
 problems of atmospheric flight dynamics  
 with smooth trajectory and continuous  
 controls 11 p1733 A66-23343  
 Direct and orbit flight modes considered  
 for unmanned lander on Mars, noting  
 ballistic coefficients, flight path angles,  
 targeting capability, etc 13 p2180 A66-25243  
 Successive linearization for variational  
 problems of flight  
 mechanics 15 p2425 A66-28539  
 Control-engineering and flight-mechanics  
 problem of rendezvous guidance, considering  
 target body without guidance and second  
 body in gravitational field without  
 atmosphere 20 p3595 A66-36874  
 Unmanned spacecraft trajectories,  
 discussing flight mechanics of solar system  
 exploration 22 p3983 A66-40700  
**FLIGHT OPTIMIZATION**  
**SA OPTIMUM THRUST PROGRAMMING**  
 Shortest time air routes determined by  
 method based on law of refraction, assuming  
 quasi-continuous wind  
 field 02 p0260 A66-12055  
 Dynamic programming applied to numerical  
 solution of optimization problems of flight  
 mechanics 04 p0584 A66-13523  
 Computer method calculation of minimum  
 time track, using quasi-optical law of  
 refraction 07 p1066 A66-17681  
 Grid navigation method, employing  
 Mercator chart, is suitable for high latitudes  
 and supersonic aircraft 07 p1066 A66-17683  
 Economy of body traveling over given  
 distance at certain velocity and constant air  
 density 07 p0983 A66-18161  
 Optimum gliding regime using Krotov  
 generalized theory and linear partial  
 differential equations 11 p1732 A66-22354



Multistage rocket acceleration by explosive separation of individual stages, solving optimization problems connected with problem 11 p1777 A66-22456

Dynamic programming method for approximate solution of gliding flight and minimum time to climb problems in boundary value theory 11 p1778 A66-23349

Aerospacecraft performance optimization and design evaluation for airbreathing-rocket propulsive systems by variational calculus [AIAA PAPER 65-18] 12 p1954 A66-24694

Flight path optimization methods for given aircraft performance objectives 13 p1995 A66-25764

Circular runway flight operations and increased directional stability [SAE PAPER 660283] 15 p2476 A66-29827

## FLIGHT PATH

Shortest time air routes determined by method based on law of refraction, assuming quasi-continuous wind field 02 p0260 A66-12055

Mathematical formulation of lateral and longitudinal separation standards for subsonic and supersonic aircraft operation 07 p1066 A66-17680

Aircraft separation criteria applied to supersonic transport, describing standards and parameters of air traffic safety 07 p1066 A66-17682

Vertime, navigation system for vertical plane control 07 p1069 A66-17716

Approximate reentry velocity and heating equations applied to any atmosphere satisfying hydrostatic equilibrium, noting motion equations for flight path 08 p1303 A66-18836

Vertical separation effect on safety of civil jet aircraft with type II or III altimeter over North Atlantic 10 p1553 A66-21334

Frequency distribution of route temperature at supersonic flight levels, noting effect on payload during extended trips [AIAA PAPER 66-371] 12 p1802 A66-24499

Digital airborne computer for navigation problem solutions including inertial navigation, flight path, time-to-go and arrival time, etc 13 p2124 A66-25839

Vertime, navigation system for vertical plane control 13 p2125 A66-25863

Minimum time-of-flight aircraft trajectory between two points with account of Earth sphericity 13 p2125 A66-26481

CAT detection by photometric star tracking system from moving aircraft 15 p2500 A66-28931

Schiphol Airport /Amsterdam/ analog computer installation for air traffic control and flight path calculations, with results displayed on automatic flight progress boards 15 p2534 A66-29311

Optimum model route structure for North Atlantic subsonic jet traffic 15 p2535 A66-29713

Optimal control theory in design of aerodynamic shapes, flight paths, guidance and control logic, data processing logic, etc 17 p2950 A66-32682

Atmospheric turbulence determined from velocity fluctuations in flight path direction measured by wing-tip mounted hot-wire anemometer 20 p3593 A66-37470

Simulator study of computing and displaying velocity in head-up display for low speed flight path control by pole track or velocity vector 23 p4089 A66-41257

Cross wind effect on special small rocket during powered flight, calculating flight path angle at burnout for launching angle determination 23 p4133 A66-41442

Flight path dispersion of special small rocket /SSR/ due to thrust misalignment, stabilizing effects of spin during powered flight by canting control vane in nozzle 23 p4133 A66-41443

Single air flow acceleration and deviation for propulsion and lift of high speed aircraft, analyzing long-range flight paths [ICAS PAPER 66-41] 23 p4122 A66-42070

## FLIGHT PLAN

Flight management by digital computers, discussing central computer, system configurations, reliability, memory, input/output, computation rates 09 p1349 A66-20683

Text on theory of automated air navigation, examining methods of flight preparation and precision 22 p3946 A66-40855

**FLIGHT RECORDER**

Automatic handling of information by analog recording on magnetic tape for control, monitoring and maintenance of aircraft 12 p1880 A66-23817

Flight recorder utilization in British civilian jet and turboprop aircraft 21 p3696 A66-38603

Digital filtering system comprising only few integrated circuits and using addershift register combination, compared with analog devices 23 p4067 A66-41168

## FLIGHT SAFETY

Plane crash as result of pilots coronary disease, discussing prevention and rehabilitation 04 p0469 A66-14387

Problems in pilot fitness evaluation, especially physical and emotional capability assessment for flight safety 09 p1335 A66-20533

Protection standards for population around missile launching sites, noting missile malfunctions, particularly breakdowns of guidance and control systems 09 p1457 A66-20554

Airmen exposure and safety at high altitude with reference to SST 13 p2015 A66-25762

Economic effects of turbulence on airline operations, considering costs on temporary grounding for repairs, passenger injuries, information dissemination on turbulence, etc 15 p2618 A66-28916

Automation in flight safety, noting role of radar, flight control system reliability, data processing system used, etc 17 p2848 A66-33485

Coronary diseases and flight safety 19 p3295 A66-36445

Flight safety and experiences with pilots treated in West Germany military hospital 19 p3295 A66-36446

Civil aviation safety - International Symposium, Stockholm, April 1966 20 p3493 A66-36990

Flight safety in Soviet civil aviation including takeoff and landing, cruising in airport vicinity, meteorology and medicine 20 p3494 A66-36991

Aviation safety research in Europe, considering military and civil sectors 20 p3540 A66-36993

Human errors in flight safety and need for automation 20 p3508 A66-36994

Allotment of probability shares /APS/, statistical approach for guiding safety measures to improve aviation 20 p3494 A66-36998

National and international trends in ATC from standpoint of pilot and operator safety 20 p3595 A66-37004

Missile and space system accident potential evaluated numerically 20 p3685 A66-37931

## FLIGHT SIMULATION

Simulation testing of modular maneuvering unit for stabilized and untethered maneuvers in free space 02 p0215 A66-11625

Task loading effect on pilot performance in computer simulated low altitude high speed flight 02 p0187 A66-11829

Simulation techniques in aeronautics and astronautics, discussing role in development of desirable control and flight characteristics 02 p0215 A66-11892

Space travel projects noting ion propulsion, electromagnetic drive and tests of flight simulation 03 p0415 A66-12483

T tail aircraft in deep stall conditions in fixed-base cockpit simulation at large angle of attack [AIAA PAPER 65-781] 03 p0322 A66-13068

Carrier landing improvements in Fresnel lens optical landing system, emphasizing compensated-meatball stabilization [AIAA PAPER 65-791] 03 p0322 A66-13228

Royal Aircraft Establishment facilities in England for aircraft structure testing under supersonic conditions, simulating aircraft takeoff, flight and landing 04 p0508 A66-14021

Monitoring human performance during manned orbital flight for assessment of central nervous system function, noting animal studies during simulated stresses of space flight 04 p0468 A66-14088

Role of ground and flight simulation test facility on past, current and future developments in aerospace propulsion 06 p0867 A66-15932

V/STOL Aircraft Symposium, Wright-Patterson AFB, Ohio, November 1965 06 p0805 A66-16808

Flight simulation developments for V/STOL visual device requirements including mirrors focusing images at infinity, transparency image storage techniques, optical probes, etc 06 p0869 A66-16814

Control and lift-propulsion systems and model testing of Canadair CL-84 V/STOL tilt-wing aircraft 06 p0806 A66-16811

Simulated flights evaluating verbal communication intelligibility in oxygen breathing mixtures at low atmospheric pressures compared with results obtained in room air at ground level 06 p0813 A66-16822

X-15 flight problems not encountered during simulation, particularly differences in aerodynamics, control systems, cockpit equipment, etc 07 p1017 A66-17272

NAE helium hypersonic wind tunnel for hypersonic flight simulation and boundary layer studies 07 p1018 A66-18051

Environmental testing, spacecraft configuration, data retrieval and flight simulation in OAO experiments 08 p1203 A66-19511

Manual guidance and control simulation for reentry vehicle flight and landing 08 p1203 A66-19533

Vestibular system response of pilot and nonpilot to banking and turning in USAFSAM biaxial simulator 09 p1335 A66-20533

Thrust stand simulation for determining space vehicle rocket motor attach-point motion 10 p1520 A66-21933

DC-9 flight simulator using monolithic integrated-circuit GP-4 computer 11 p1683 A66-22683

Rocket equipment simulation on rocket engine test facilities, describing fuel tank design for experiment with suitable flow characteristics and parameters 12 p1829 A66-24311

Aerospace and space simulation including rendezvous and docking, lunar landing and operation of supersonic transports 12 p1858 A66-24603

Flight simulation of SST transport using hybrid computer 13 p2028 A66-26333

Simulated Martian entry conditions in Earth test program showing requirements for launch vehicle, tracking, cost and schedule [AIAA PAPER 65-219] 14 p2392 A66-27873

SST air traffic control and arrival and departure simulation 15 p2425 A66-28743

Mechanism having six degrees of freedom for flight simulation in pilot training 15 p2476 A66-29633

Ionospheric flight simulation in which ion distribution of neutral gas expanding into rarefied ionized gas under magnetic field is measured 16 p2759 A66-30373

Simulation testing pilot performance in orbiting Gemini spacecraft based on tracking rate errors and fuel consumption 17 p2872 A66-31963

Myocardiograph study of dogs leading to development of flight-rated vibrophonocardiographic system for monitoring cardiac dynamics in flight environment 17 p2924 A66-32153

Flight simulator techniques applied to all weather landing problems 17 p2869 A66-33203

Low altitude-high speed flight simulation experiment in air-to-ground target recognition via closed-circuit TV, determining effects of camera view field and target size 17 p2927 A66-33483

High speed hybrid computer simulation of aerospace vehicle motion 18 p3094 A66-34063

Aircraft and spacecraft digital systems including computers for production engineering, ground telemetry and communication with aerospace vehicle and onboard equipment for tracking, guidance and simulation of inflight conditions 21 p3709 A66-39623

SH-3A airframe fatigue test facility for automatic simulation of helicopter flight and landing loads 22 p3992 A66-40213



CL-84 V/STOL flight simulation at Canadair through design, development and flight testing of flapped tilt-wing prototype [ICAS PAPER 66-18] 24 p4159 A66-42493

**LIGHT SIMULATOR**

Research, development, test and operation simulating devices used in aircraft construction supply real time data, considering human factor, costs, etc 01 p0054 A66-10871

Airborne V/STOL simulators used for handling qualities research at National Aeronautical Establishment, Ottawa, Canada [AIAA PAPER 65-705] 01 p0054 A66-10943

Computer flight simulators at Langley discussing Boeing 707 jet, helicopter, air traffic control, orbital rendezvous and docking, lunar navigation and landing 01 p0055 A66-10957

Carrier landing characteristics of vectored-thrust aircraft obtained in piloted fixed-base flight simulator studies [AIAA PAPER 65-792] 03 p0390 A66-12560

Experimental fixed and moving-base flight simulator investigation of generalized aircraft longitudinal pilot induced oscillations [AIAA PAPER 65-793] 03 p0352 A66-12596

Marine pilot training to develop visual habit patterns as aid in reducing mid-air collision hazards 07 p0999 A66-17712

Climb profiles by SST pilot evaluated by simulator study using instrument, Mach altitude display and flight director 07 p0988 A66-17783

Apollo and LEM mission simulators, noting computer complex providing real time simulation, mathematical models, telemetry, display equipment, aural effects, etc 07 p1018 A66-18331

Flight simulator for telescopic observation of Earth from orbit, discussing configuration of optical system 10 p1518 A66-21230

Operational space flight simulator using closed-circuit TV with pinhole optics 10 p1518 A66-21231

Flight environmental simulation of control loading, fuselage movement and visual systems 10 p1520 A66-21855

Flight simulators in reducing cost of flight training 11 p1687 A66-23169

Supersonic transport operations, particularly analog computer facility at Langley Research Center and ATC simulator at National Aviation Facilities Experimental Center 15 p2443 A66-28744

Flight tests limitations, hi-fi simulation and other navigation display evaluation, detailing discontinuous simulator 16 p2743 A66-30668

T-27 space flight simulator design, system performance and use for training and research at USAF Aerospace Research Pilot School [AIAA PAPER 65-265] 18 p3093 A66-33789

T-27 Space Flight Simulator, for extravehicular activity training, utilizing closed-circuit TV system 19 p3291 A66-35966

Space flight simulator including performance requirements, facility design, applications, etc 21 p3721 A66-38856

Azimuth reference system design and stability, noting flight simulator installation 21 p3723 A66-38888

Flight simulation laboratory layout and construction using hybrid computer systems, noting cost estimation 23 p4052 A66-41136

Simulator study of computing and displaying velocity in head-up display for low speed flight path control by pole track or velocity vector 23 p4089 A66-41257

**FLIGHT STABILITY TEST**

Sounding rocket instability, covering exact and approximate solution and Magnus moment coefficient for hypersonic rolling vehicle /Sandia Nitehawk rocket system/ [AIAA PAPER 66-62] 06 p0958 A66-16252

Flight test report of F-111 aircraft, considering variable wing sweep, stability augmentation in automatic gains, high performance with slow speed takeoff and landing 07 p0986 A66-17273

Flight stability, discussing quasi-critical case in neighborhood of asymptotic stability boundary of autonomous systems and that of variable system 21 p3696 A66-39594

FLIGHT STRESS

SA SPACE FLIGHT STRESS

Closed loop hydraulic servo system simulating flight stresses on motor case of solid propellant rocket motor in static firing test stand for calibrating 03 p0353 A66-13218

Effects on man of direct /escape/ and indirect /aircraft flight/ movement through atmosphere, considering moderate and high-speed aerodynamic forces 10 p1488 A66-22106

Aircraft crew fatigue on long distance jet flights, measuring flight safety parameters such as heartbeat, pulse rate and temperature 12 p1808 A66-23753

Physiological stress and fatigue in aerial missions for forest fire control, noting in-flight and postflight exercise heart rate 12 p1810 A66-25009

Stress in spacecraft crew members measured using parotid fluid, noting relationship between biochemical variables under stress and nonstress conditions 17 p2866 A66-32196

Primary shift of phase of circadian periodicity effected by time displacement for physiological functions 19 p3285 A66-36374

Labyrinthine nystagmus and sensation of turning evoked by impulsive stimuli in yaw, pitch and roll compared for subjects in plane of rotation and in tilted position 24 p4163 A66-42448

FLIGHT TEST

Central Inertial Guidance Test Facility /CIGTF/ at Holloman AFB, outlining tradeoff between operational and analytical considerations 01 p0102 A66-10047

Parameter dependent approach mechanization for in-flight testing of aircraft system, considering electronic subsystems 01 p0010 A66-10096

Flight testing of Litton LN-12 inertial navigation system consisting of four-gimbal two-gyro platform and analog computer 02 p0259 A66-12049

Flight development of F-111 swing wing fighter in A strike and B interceptor versions for Air Force and Navy 03 p0317 A66-12534

Design considerations in Lockheed rigid rotor application to compound helicopter, noting wind tunnel and flight test with XH-51A helicopter [AIAA PAPER 65-757] 03 p0318 A66-12552

Autoland, stalling and jet V/STOL systems for flight testing of aircraft [AIAA PAPER 65-783] 03 p0318 A66-12557

Analytical tool for computer flight testing of VTOL designs, evaluating effects of steady state flight, maneuvers, gust response and weapon recoil 04 p0490 A66-14137

F5D-1 aircraft delta wing modification, describing wind tunnel and flight test results with ogee wing 06 p0802 A66-16805

XC-142A Flight Test Program, program statistics, aircraft instrumentation and flying qualities in hover and transition flight regimes 06 p0807 A66-16820

Aerospace - Society of Experimental Test Pilots Symposium, Beverly Hills, September 1965 07 p0985 A66-17267

Aircraft erect and inverted spinning characteristics, discussing Hawker-Siddeley Hunter T.Mk. 7 spin properties and application of controls for recovery 07 p0987 A66-17489

Flight test determination of parasite drag area and required power of Kawasaki Bell KH-4 single-rotor helicopter 07 p0988 A66-17525

Flight testing of distance measuring equipment for instrument landing system with results shown in histograms 07 p1067 A66-17691

Flight testing of Phillips vertical reference inertial navigator on DC-8 aircraft 07 p1069 A66-17708

Flight tests of navigation systems including hyperbolic system, Doppler system, radio altimeter testing, deviation in gyromagnetic compasses, etc 07 p1073 A66-17770

Book on aircraft testing techniques for aeronautical technical school students 08 p1167 A66-18590

Stagnation point velocity and pressure distribution over heat-sink shielded reentry

vehicle to test boundary layer heat transfer theories 08 p1161 A66-18811

Military aircraft from design stage through service life, emphasizing flight testing 08 p1322 A66-19017

Aircraft, missile and space systems flight test programs using statistical experimental design techniques [AIAA PAPER 65-221] 09 p1330 A66-20745

Reliability engineering concepts for manned spacecraft development and test program to achieve operational readiness with minimum flight tests 12 p1884 A66-23742

Text on longitudinal static stability of low-speed aircraft including effect on pilot, flight test, pitch maneuverability, etc 14 p2222 A66-26792

Handling and operation of XB-70 aircraft, noting flight testing, folding wing tips, weight, speed, etc 14 p2222 A66-27284

[SAE PAPER 660273] 14 p2222 A66-27284

Structural design load prediction and data collected verification of methods and magnitude by Minuteman flight testing 14 p2392 A66-28000

Structure and thermal protection system of start program including load paths, heat shield, materials, etc 14 p2407 A66-28024

Hydraulic system supporting Apollo/Saturn V space vehicle tested to determine bending and flexuring in flight 14 p2226 A66-28031

Flight tests limitations, hi-fi simulation and other navigation display evaluation, detailing discontinuous simulator 16 p2743 A66-30668

High speed computer technique for simulating test design parameters for evaluation of ballistic-weapon system accuracy [AIAA PAPER 65-222] 16 p2809 A66-30888

Thermal model for performance of cork insulation on Minuteman missile in launch environment 16 p2827 A66-30893

Test program philosophy of electric propulsion and power for planetary mission application [AIAA PAPER 65-67] 16 p2791 A66-30901

Flight tests on various agricultural aircraft noting safety record data 16 p2634 A66-31284

S-61F helicopter flight test program, noting design modifications for high speed performance 17 p2844 A66-32726

Helicopter rotor blade applied as scanning radar antenna, noting performance during flight tests, feasibility, etc 17 p2875 A66-32727

XV-5A V/STOL aircraft flight testing, noting handling qualities and sequential diversion capability 17 p2844 A66-32731

Problems when using RF diagnostic systems in flight test evaluation of ICBM systems, specifically when using EM systems during reentry [AIAA PAPER 66-406] 18 p3239 A66-33634

Flight performance of small diameter folding fin aircraft rocket using particle trajectory shows large dispersion magnitudes 18 p3240 A66-33819

Test pilot training, discussing syllabus, instrumentation, schools, etc 18 p3062 A66-33948

XB-70A research aircraft and flight tests to aid SST 18 p3051 A66-33957

XB-70A flight testing, examining effect of aerodynamic lift, gross weight, altitude, temperature and similar parameters on sonic boom signatures 18 p3052 A66-33959

Staff flight test design velocity comparison technique for estimating in-flight inertial platform attitude 18 p3132 A66-34044

Special missile flight test equipment, detailing velocity accumulator, elevation programmer, telemetry system, junction box and illumination measurement 18 p3111 A66-34049

VTOL aircraft performance characteristics noting flying qualities, hover dynamics, transition flight and variable stability system 18 p3052 A66-34623

Flight data recording and processing system using magnetic tape for digitally computing airborne data on flight testing of VTOL aircraft 18 p3073 A66-34679

Flight testing of laminar flow control on X-21 aircraft, noting degradation of laminar performance in proximity of clouds or atmospheric turbulence, feasibility, handling,



- etc 18 p3050 A66-34949  
 Temperature rate measurement for design of control and guidance system in reentry vehicles, using Temperature Rate Flight Control System /TRFCS/ 19 p3396 A66-35511  
 Navigation satellite system providing precise position information of aircraft, noting flight tests 19 p3396 A66-35516  
 Experimental maneuver demand aircraft control system, noting design considerations, operation and performance characteristics 20 p3493 A66-36887  
 XB-70 aircraft safety program developed during flight tests applied to future SST civil aircraft 20 p3494 A66-37006  
 Predelivery reflight policies role in airplane system reliability, noting failures during various test and retest flights 20 p3495 A66-37178  
 Real-time data gathering and flight-test technique for aircraft-carried weapons system development testing 20 p3495 A66-37207  
 Nitrogen powered hydraulic attitude control system of Little Joe II solid propellant launch vehicle for flight testing escape mechanism used on Apollo 20 p3499 A66-37314  
 Lifing aircraft structures subjected to acoustic pressures, noting estimation of panel joint rms stress 20 p3666 A66-37422  
 XB-70A reliability program applied to initial system design stage from inception to present flight test program 20 p3568 A66-37917  
 Naval weapons A-7A maintainability requirement effect on management and design and analysis of early flight test data 20 p3496 A66-37920  
 Flight tests on aircraft and analysis by automatic filter, noting structural and aerodynamic problems resulting from use of transient method 21 p3824 A66-38574  
 Multiplexer coder unit for AC carrier transducers and DC signals used in PCM flight trials system 21 p3709 A66-38605  
 No-gimbal system mechanizations evaluated by flight test and compared for advantages, noting system error 21 p3764 A66-38851  
 Langley Lunar Landing Research Facility for flight tests of landing vehicle and simulation of lunar gravity field 21 p3821 A66-38900  
 Flight testing of Beagle B.206 S aircraft revealed need for forward shift of CG in series II model due to more powerful engines 22 p3848 A66-39690  
 Coordinated laboratory and flight test program, determining stability of solar concentrator reflective surfaces in orbital environment 22 p3889 A66-40220  
 Flight testing of laminar flow control on full-scale swept wings, examining total pressure probes, wing wake drag and boundary layer stability utilizing pressure transducer [AIAA PAPER 66-734] 22 p3846 A66-40625  
 Lift fan propulsion system using 62.5-inch lift fans flight tested in XV-5A aircraft from hover to subsonic flight regions [AIAA PAPER 66-739] 22 p3972 A66-40628  
 Pulse and harmonic techniques used in flight flutter testing, emphasizing natural turbulent excitation and limitations [ICAS PAPER 66-10] 23 p4015 A66-41256  
 Steady and dynamic loads on tandem rotor, controls and airframe flight tested with Army helicopter, using automatic data processing [AIAA PAPER 66-735] 23 p4008 A66-41324  
 Flight performances of special small rockets with no cross wind conditions, noting drag coefficient effect 23 p4133 A66-41441  
 Preflight consideration of astronaut performance testing program for Gemini XI flight, noting manual operations and devices used 24 p4168 A66-42742
- FLIGHT TEST INSTRUMENT**  
 Microwave phase-measuring distance-determining system /SHIRAN/ enabling evaluation of slant ranges from airplane to four transponders located at ground control 02 p0227 A66-11378  
 Flight testing instruments used in control programs, treating airborne installations and ground stations 09 p1380 A66-20330  
 Radiation dosimeters for SNAP-10A flight test to measure reactor leakage radiations throughout SNAPSHOT Agena orbital vehicle 12 p1876 A66-23675
- FLIGHT TEST VEHICLE**  
 Man-rated booster design provides alternate manual propulsion and guidance control enabling astronaut participation in mission success [AIAA PAPER 65-251] 10 p1612 A66-21949
- FLIGHT TIME**  
 Evaluation of minimum-time courses for aircraft and inherent error 02 p0257 A66-12035  
 Air traffic control system capacity and navigational requirements for North Atlantic and continental transition areas, discussing relationship to accuracy and flight time economy 07 p1069 A66-17713  
 Error effects in forecasting wind speed and direction on equivalent headwinds and flight times 07 p1063 A66-18338  
 Minimum time-of-flight aircraft trajectory between two points with account of Earth sphericity 13 p2125 A66-26481  
 Results of approximate computation of rocket apogee from data on flight duration between different trajectory points 14 p2383 A66-27815
- FLIGHT TRAINING**  
**SA EJECTION TRAINING**  
**SA PILOT TRAINING**  
 Criteria for aircrew selection, describing aptitude and performance tests used by RAF 10 p1494 A66-22137  
 Procurement source and military rank as predictors of success in flight training 15 p2442 A66-28660  
 Preflight planning and training stages for Gemini V, considering spacecraft test, mission simulators, planetarium, survival and parachute training, etc 17 p2868 A66-32686  
 Voluntary withdrawal from primary flight training as function of individual flight instructor 22 p3856 A66-39793  
 Helicopter trainee performance following synthetic flight training, noting flyable aircraft attached to ground effects machine 22 p3857 A66-40250  
 Functional subsystem analysis in Instructional System Approach to transition training of flight crews 23 p4030 A66-41579
- FLIGHT VEHICLE**  
 Optimal control of elastic flight vehicles, describing axis oscillations by equations of beam with variable cross section 21 p3768 A66-39279  
 Book on aeromechanics of flight vehicles including structure and physical properties of atmosphere, wing characteristics, research methods, aerodynamic characteristics of principal units of aircraft and rockets, etc 21 p3695 A66-39288  
 Vibration test specifications for flight vehicle components developed from broad engineering viewpoint 21 p3822 A66-39609  
 Angular stabilization of flight vehicle by introduction of cubic terms of variable parameters into control law 23 p4088 A66-40968  
 Movable platform and differential throttle control configurations for lunar manned flying vehicle 24 p4284 A66-42954
- FLIP-FLOP**  
 Low power consumption, high reliability and fully integrated silicon monolithic complementary flip-flop circuit 01 p0047 A66-11139  
 Tunnel diode and transistor circuit controlled by trigger pulses operating as oscillator, univibrator and flip-flop 02 p0199 A66-11819  
 Solid state flip-flop store element arranged on multilayer printed circuit board 02 p0193 A66-11929  
 Fluidic devices, discussing design, equivalence to logic circuits, fluid amplifier application to build flip-flops, etc 06 p0809 A66-16794  
 Transistor-tunnel diode flip-flop with built-in gating 11 p1669 A66-23159  
 Integrated circuit gate ring counters, noting flip-flop variety comparison 11 p1677 A66-23178  
 Realization of numerical counters with micrological elements, discussing flip-flop and memory elements 16 p2656 A66-30964  
 Electric parameters of components and resultant properties of transistorized flip-flop circuits 16 p2663 A66-3102
- Electrical control of boundary layer flip-flop fluidistor by disruptive discharge between electrodes producing pneumatic pressure shocks that switch output flow 20 p3501 A66-3764  
 Operation principles of turbulence amplifiers, considering application to low cost automation, using conventional pneumatic valves and cylinders 20 p3502 A66-3765  
 Frequency meter for measuring center frequency of random pulses distributed according to Poisson law, consisting of integrating circuit with high time constant 22 p3918 A66-4040  
 Complementary symmetry flip-flop an similar transistor micropower digital logic circuit design 23 p4048 A66-4114
- FLOTATION SYSTEM**  
 Floated inertial platform, gimballess attitude device utilizing floated sphere to isolate inertial components from acceleration and vibration environments 01 p0099 A66-1001  
 Unique free-floating externally ballasted system for obtaining static flotation characteristics 16 p2677 A66-3045  
 Apparent additive mass coefficient for three-dimensional hydrodynamic impacts problem of floating sphere in incompressible fluid 20 p3548 A66-38118  
 Floating vibratory gyroscope having enhanced sensitivity to angular velocity 21 p3739 A66-3932  
 Tests for obtaining water trajectory data and underwater flow field photographs used in determining deployment sequence of water recovery system flotation bag for reentry vehicle 22 p3987 A66-40600
- FLOW**  
**S AIRFLOW**  
**S ANNULAR FLOW**  
**S AXIAL FLOW**  
**S AXISYMMETRIC FLOW**  
**S BAROTROPIC FLOW**  
**S BASE FLOW**  
**S BELTRAMI FLOW**  
**S BLASIUS FLOW**  
**S BLOOD FLOW**  
**S BRILLOUIN FLOW**  
**S CARTAN SPACE**  
**S CASCADE FLOW**  
**S CAVITATION FLOW**  
**S CHANNEL FLOW**  
**S COAXIAL FLOW**  
**S COMBUSTIBLE FLOW**  
**S COMPRESSIBLE FLOW**  
**S CONICAL FLOW**  
**S CONTINUUM FLOW**  
**S CONVECTIVE FLOW**  
**S CORE FLOW**  
**S COUETTE FLOW**  
**S DUCTED FLOW**  
**S EQUILIBRIUM FLOW**  
**S FREE FLOW**  
**S FROZEN FLOW**  
**S FUEL FLOW**  
**S GAS FLOW**  
**S HARTMANN FLOW**  
**S HEAD FLOW**  
**S HEAT FLOW**  
**S HELICAL FLOW**  
**S HYPERSONIC FLOW**  
**S HYPERVELOCITY FLOW**  
**S INCOMPRESSIBLE FLOW**  
**S INDUCED FLUID FLOW**  
**S INLET FLOW**  
**S INVISCID FLOW**  
**S IRROTATIONAL FLOW**  
**S ISOTHERMAL FLOW**  
**S JET FLOW**  
**S KARMAN-BODEWADT FLOW**  
**S KNUDSEN FLOW**  
**S LAMINAR FLOW**  
**S LIQUID FLOW**  
**S MAGNETOHYDRODYNAMIC FLOW**  
**S MASS FLOW**  
**S MERIDIONAL FLOW**  
**S MIXED FLOW**  
**S MOLECULAR FLOW**  
**S MULTIPHASE FLOW**  
**S NON-NEWTONIAN FLOW**  
**S NONEQUILIBRIUM FLOW**  
**S NONVISCOUS FLOW**  
**S NOZZLE FLOW**  
**S ONE-DIMENSIONAL FLOW**  
**S OSCILLATING FLOW**



S PLASMA FLOW  
 S PLASTIC FLOW  
 S POISEUILLE FLOW  
 S POTENTIAL FLOW  
 S PULSATING FLOW  
 S RADIAL FLOW  
 S RAYLEIGH NUMBER  
 S REATTACHED FLOW  
 S REVERSED FLOW  
 S ROTATIONAL FLOW  
 S SECONDARY FLOW  
 S SEPARATED FLOW  
 S SHEAR FLOW  
 S SLIP FLOW  
 S SMALL PERTURBATION FLOW  
 S SONIC FLOW  
 S STAGNATION FLOW  
 S STEADY FLOW  
 S STEADY STATE FLOW  
 S STRATIFIED FLOW  
 S STREAMLINE FLOW  
 S SUBSONIC FLOW  
 S SUPERCavitating FLOW  
 S SUPERFLUID FLOW  
 S SUPERSONIC FLOW  
 S THREE-DIMENSIONAL FLOW  
 S TRANSONIC FLOW  
 S TURBULENT FLOW  
 S TWO-DIMENSIONAL FLOW  
 S TWO-PHASE FLOW  
 S UNIFORM FLOW  
 S UNSTEADY FLOW  
 S VISCOELASTIC FLOW  
 S VISCOUS FLOW  
 S VORTEX FLOW  
 S WALL FLOW  
 S WATER FLOW  
 S WEDGE FLOW  
 S WING FLOW METHOD TEST

**FLOW CHAMBER**  
 Low speed flow visualization technique using light-pulse illuminated plastic particles suspended in revolving bowl of brine 09 p1364 A66-20399

**FLOW CHARACTERISTICS**  
 Approximate determination of flow characteristics around multistage nonstationary blade configuration, using singularity method 01 p0006 A66-10442  
 Tangential velocity profile and flow temperature in vortex chamber of vortex tube and dimensions of tube, nozzle and cold-end orifice 02 p0217 A66-11589  
 Discrete gas-into-liquid flow process, compensating absence of mass forces and unfavorable load directions with motion of liquid 02 p0218 A66-11657  
 Pohlhausen method applied to shock wave/boundary layer interaction, calculating flow characteristics of laminar separation region 04 p0455 A66-14138  
 Heat transfer and flow friction characteristics of matrices of high porosity with radiation heat source [ASME PAPER 65-HT-6] 05 p0782 A66-14734  
 Flow properties in turbulent near wake of circular and elliptic cones at zero angle of attack in Mach 6 flow [AIAA PAPER 66-54] 07 p0980 A66-17897  
 Restatement of physical definition of Reynolds number, making it valid for all types of flow 08 p1206 A66-18855  
 Heat transfer and flow friction characteristics of matrices of high porosity with radiation heat source [ASME PAPER 65-HT-6] 11 p1785 A66-22188  
 Imp-I observations of solar wind properties, including interaction with geomagnetic field and flow characteristics of positive ion component 11 p1775 A66-23132  
 Rocket equipment simulation on rocket engine test facilities, describing fuel tank design for experiment with suitable flow characteristics and parameters 12 p1829 A66-24317  
 Flow past elliptic cones in wind tunnels at varying Mach and Reynolds numbers, noting surface pressure distribution, shock wave shapes and flow parameters at supersonic speeds 12 p1798 A66-24439  
 Prediction of local flow conditions at crest of aerofoil section in sonic stream 13 p1992 A66-26697  
 Quasi-linearization applied in boundary layer calculations, noting simple flow over solid surface 15 p2479 A66-29299  
 Two-dimensional flow of incompressible conducting viscous liquid in inlet region of

straight channel under magnetic field, obtaining flow characteristics 15 p2553 A66-29742  
 Flow characteristics of pneumatic resistors determined by three-point method 16 p2636 A66-30633  
 Nonstationary flow past spheres and cylinders in electromagnetic shock tube, determining time required for flow to become stationary 16 p2682 A66-31295  
 Effect of oscillatory relaxation of air boundary layer on flow characteristics around wedge 16 p2632 A66-31629  
 Approximation for moment equations of kinetic theory which describe source flow expansion with application to free jet 17 p2907 A66-32412  
 Primary and secondary flow interaction in plug nozzle, obtaining solutions by iteration and isentropic relation 17 p2839 A66-32476  
 Flow characteristics, design and performance data for subsonic two-dimensional straight centerline diffusers [ASME PAPER 66-FE-10] 17 p2915 A66-33264  
 Beam deflection type proportional fluid amplifier, noting pressure and flow gain parameters, transfer characteristics, etc 18 p3054 A66-34129  
 Critical parameters and flow characteristics of swept wings with full-chord laminar flow, noting boundary layer disturbance effects 18 p3050 A66-34950  
 High temperature flow characteristics in free piston shock tube measured by means of pulsed light of He-Ne gas laser 19 p3339 A66-35353  
 Ferromagnetic fluid developing body force under magnetic field influence, noting changes in internal pressure, velocity, etc, applied to attitude control devices, accelerometers, etc 19 p3445 A66-36178  
 Degree of similarity of turbulent flow characteristics in geometrically similar flows 24 p4197 A66-42949

**FLOW COEFFICIENT**  
 Flow coefficient through nozzle with circular cross section and elliptical cylindrical profile supplied from container with static pressure equal to stagnation pressure 03 p0314 A66-12695  
 Losses when compressible and constant density fluids flow across abrupt enlargements and contractions [ASME PAPER 65-WA/PTC-1] 05 p0663 A66-15603  
 Thrust measurement for calibrating nozzle flow coefficients by direct primary method [ASME PAPER 64-WA/FM-3] 06 p0871 A66-16220  
 Flow loss in conical diffusers with boundary layer suction through single slit 16 p2629 A66-30813  
 Flow coefficient of nozzle calculated by thickness of quantity of motion of laminar boundary layer at nozzle exit 20 p3545 A66-37412  
 Unsteady air flow discharge coefficients compared for sharp-edged orifices with steady flow values 23 p4009 A66-41700  
 Flow coefficient of elliptical cylindrical pipe, analyzing boundary layer at exit for various Reynolds numbers, noting velocity profile 23 p4014 A66-42057

**FLOW DEFLECTION**  
 Axial deviation of gas flow resulting from mixing turbulent gas jets 07 p1019 A66-17395  
 Rotation vector increase derived for secondary incompressible fluid flow in curved channels 07 p1023 A66-18134  
 Flow induction by rotary jets, involving isentropic flow deflection followed by constant-area mixing 09 p1327 A66-20737  
 Crosswind effect on turbulent jet parameters for submerged jet propagation at angle to unrestricted flow 12 p1864 A66-24445  
 Displacement and heat transfer effects of laminar and turbulent boundary layers far downstream in slowly expanding hypersonic nozzle, determining inviscid core flow 15 p2424 A66-29273  
 Nonisothermal axisymmetrical turbulent jet curved by gravity and inertial forces 19 p3342 A66-36465  
 Rotary jet flow induction studied with analytical flow model, noting mutual deflection of primary and secondary flow and jet dissipation 19 p3277 A66-36488

Plasma jet deflection in magnetic field set up by current flowing through four bars so that directions of flow were opposite in adjacent bars 19 p3426 A66-36569  
 Low thrust divergent flow cesium-on-tungsten contact ionization electrostatic thruster for satellite attitude control and stationkeeping missions [AIAA PAPER 66-569] 20 p3628 A66-37051  
 Incompressible flow in two-dimensional bends treated by Rayleigh-Ritz method in Kamiyama modification of conformal mapping 24 p4157 A66-42264  
 Maximum wave drag in supersonic flow deflection 24 p4158 A66-42852  
 Inhomogeneity of axial velocity component in or near blades forming impeller intake of radial compressor attributed to flow deflection 24 p4158 A66-43067

**FLOW DIRECTION INDICATOR**  
 Special cases of conical flow permitting two flows to join and predicting flow limited by conic wall 05 p0605 A66-14536

**FLOW DISTORTION**  
 Velocity and pressure fields caused by slow rotation of sphere in slightly viscoelastic fluid contained in infinite cylinder 01 p0057 A66-10428  
 Transonic test section of S-2 wind tunnel and qualification test to prove good quality of flow 02 p0210 A66-11205  
 Hypersonic wakes, effects of turbulent fluctuations on air ionization reaction rates measured by averaging and regrouping perturbed source terms of chemical rate equations [AIAA PAPER 65-819] 03 p0359 A66-13230  
 Asymptotic solution of disturbance at large distance from source placed in flow of conducting compressible fluid in applied magnetic field 05 p0723 A66-15052  
 Pressure coefficient criterion for transition between two- and three-dimensional turbulent cavity flow 10 p1523 A66-21791  
 Shape of plane and circular jet deformed by gas flow impinging at angle of incidence determined from head drag of jet relative to flow 13 p2062 A66-25320  
 Cold forming of metals, noting thin tube flow boundary variation with permanent deformation due to torsion and tension 13 p2195 A66-25455  
 Perturbation spectra and decrements of plane parallel flows at small Reynolds numbers with even and odd velocity profiles 14 p2278 A66-28055  
 Aerodynamic interference between helicopter rotor blade and fuselage and wing in hovering and forward flight, describing method of converting two-dimensional analysis to three-dimensional case 18 p3047 A66-33681  
 Distortion of laminar circular Couette flow measured by end effects, noting two-dimensional tangential motion near axial plane of symmetry 20 p3547 A66-37980

**FLOW DISTRIBUTION**  
**SA CHAPMAN-ENSKOG METHOD**  
 Flow rate distribution and mixing ratio of two impinging jets in simulation of bipropellant liquid rocket system, using hypergolic propellants 02 p0278 A66-11590  
 Extremal concentrations in laminar flow of incompressible viscous liquid along tube of constant cross section, noting recombination reactions 04 p0597 A66-13695  
 Negative correlation coefficient between Izsak satellite geoid and Lee and MacDonald heat flow distribution, suggesting correlation between geoidal undulations and heat flow highs and lows 04 p0518 A66-14454  
 Arbitrary quasi-orthogonals for calculating flow distribution in turbomachine, noting digital computer calculations 05 p0662 A66-14989  
 Molten carbonate fuel cell module featuring flexibility of construction, electrical simplicity and effective gas distribution characteristics [AICE PREPRINT 20D] 10 p1484 A66-21187  
 Free-molecule flow through conical tubes noting mass transport, axial momentum, energy, flow distribution and speed ratio 11 p1635 A66-22938  
 Arbitrary quasi-orthogonals for calculating flow distribution in turbomachine, noting digital computer calculations [ASME PAPER 65-WA/GTP-2]



Concentration profile of heavy species for binary fluid mixture under body force from uniformly mixed upstream condition, considering inviscid hydrodynamical model 18 p3103 A66-34925  
 Atmospheric turbulence coefficient determination from flow fluctuations, measuring error as function of observation duration 20 p3594 A66-38379

## FLOW EQUATION

Plane adiabatic motion of ideal gas determined by separating variables of motion equations in curvilinear coordinates 01 p0006 A66-10471  
 Exaction solution of conical flow equation with zero velocity and pressure 01 p0008 A66-11082  
 Existence and uniqueness of Cauchy problem for Boltzmann equation describing flow past convex body of rarefied gas of structureless particles 02 p0261 A66-12022  
 Hydromagnetic flow against rotating disk noting magnetic field effect on torque, boundary layer thickness and velocity profile, applying motion equation 03 p0399 A66-12689  
 Turbulence and pressure verification of equations for particular class of non-Newtonian fluids 03 p0359 A66-13245  
 Statistical derivation of equations for fully ionized plasma 05 p0725 A66-15239  
 Equations of motion of turbulent gas and formulation of simple model of turbulence from classical Liouville equation and aerodynamics of rarefied gas 06 p0802 A66-16537  
 Self-similarity of solutions to motion equations for relativistic gas possessing point symmetry and nonexistence of isentropic flow 06 p0954 A66-16538  
 Rotationally symmetric flow of non-Newtonian fluid in presence of infinite rotating disk, solving Navier-stokes equation and determining velocity profiles 07 p1019 A66-17258  
 Flow function equations for transonic flow past closed profile 07 p0982 A66-18121  
 Analogy between gas flow through convergent/divergent nozzles and open side-contracted channel 08 p1205 A66-18628  
 Numerical method applied to inviscid compressible two-dimensional or axisymmetrical fluid flows for problems involving subsonic, transonic and supersonic flow regions 08 p1207 A66-19127  
 Newtonian flow over fixed two-dimensional body in unsteady flow, emphasizing shock layer 08 p1164 A66-19129  
 Acceleration of two-dimensional MGD source flow through sonic velocity, simplifying flow equations 08 p1263 A66-19151  
 Equations of inviscid flow of perfect gas over cusped concave bodies, noting dependency of shock wave slope on infinite Mach number 08 p1166 A66-19818  
 Radiation effect on hydrodynamic shock wave parameter distribution for bodies entering dense atmospheric layers at supersonic velocities 11 p1635 A66-23051  
 Convection and stability criteria for nonlinear steady solutions with homogeneous vertical magnetic field acting on fluid 11 p1787 A66-23420  
 Stability of steady finite amplitude convection determined by method of successive approximations 11 p1787 A66-23421  
 Flow parameters of incompressible ideal fluid in axisymmetric curvilinear channel, obtaining and solving nonlinear differential equation 12 p1863 A66-24243  
 Viscosity and thermoconductivity effects on asymptotic sonic flow structure near profiles and bodies of revolution 12 p1863 A66-24342  
 Initial flow in entrance of straight circular pipe computed as refinement of Atkinson and Goldstein solution 12 p1867 A66-24980  
 Two-dimensional analysis of flow in electrofluid dynamic generator showing effect of radial fields and viscous forces on performance, stressing effect on electrical breakdown of gas, noting basic equations 13 p2001 A66-26257  
 Zhukovskii and Lagally theorems for arbitrary fluid motion derivable from

momentum equations of continuous medium 13 p2067 A66-26533  
 MHD theory and experiment 13 p2156 A66-26706  
 Motion equation of viscous oil flow under action of electric forces caused by surface charge 13 p2070 A66-26709  
 Solutions of nonstationary equations of plane laminar MHD boundary layer, using transformation to specialized form of curvilinear coordinates 14 p2338 A66-26773  
 Invariant rheological equation for flow of fluid whose viscosity varies independent of time 14 p2272 A66-26776  
 Existence and uniqueness of Cauchy problem for Boltzmann equation describing flow past convex body of rarefied gas of structureless particles 14 p2334 A66-27573  
 Modified MGD equations describing plane nonstationary flow in magnetic field perpendicular to flow 14 p2345 A66-28067  
 Points in interior and boundary of three-dimensional supersonic gas flow determined, using characteristic method, deriving difference equations 14 p2278 A66-28284  
 Integration of third-order differential equation of laminar boundary layer on porous surface 15 p2477 A66-28777  
 Mathematical model for heterogeneous continua, discussing kinematical definitions, conservation principles, thermodynamics 15 p2478 A66-29250  
 Double unsteady laminar boundary layers on solid bodies in presence of oscillating external flow of small amplitude 15 p2480 A66-29686  
 Equations of motion of turbulent gas and formulation of simple model of turbulence from classical Liouville equation and aerodynamics of rarefied gas 15 p2482 A66-29973  
 Self-similarity of solutions to motion equations for relativistic gas possessing point symmetry and nonexistence of isentropic flow 15 p2603 A66-29978  
 Flow in viscous incompressible conducting fluid subjected to magnetic field in concentric cylinders rotating at different angular velocities, assuming planar motion, using differential equations 16 p2757 A66-30214  
 Hydrodynamical modification of Heller treatment of mixing and unmixing of viscous fluid between two rotating cylinders 16 p2685 A66-30940  
 Approximation of Chaplygin plane motion equations of gas flow at high supersonic velocities 16 p2688 A66-31304  
 MHD first-order partial differential equations used to investigate wave front between perturbed and unperturbed flow regions in magnetosonic propagation through homogeneous medium 16 p2764 A66-31363  
 Optimum operation modes of MHD converter 16 p2637 A66-31368  
 Three-dimensional MHD flow near forward stagnation point magnetic fields with large induction values described by differential equations, showing tendency towards two-dimensional flow 16 p2765 A66-31373  
 Self-similarity criteria in radiative flow for unsteady one-dimensional inviscid flow of perfect gas 17 p3034 A66-32471  
 Self-similar solutions of two-dimensional laminar flow of incompressible electroconductive fluid in channel in crossed electric and magnetic fields, using Jacobi elliptic integrals 17 p2971 A66-32866  
 Prediction of hydrostatic gas journal bearing performance by solving simultaneous flow equations with Fortran II computer program [ASME PAPER 66-LUBS-16] 17 p2932 A66-33187  
 Channel flow general equations including nonviscous uniform flow, steady flow, stagnation state and speed of sound in ideal gas 18 p3098 A66-34121  
 Vorticity and vortex flows, discussing free and forced vortices, circular vortex, spiral vortex, compressible fluids and incompressible flows 18 p3099 A66-34126  
 Boundary layer equations for nonstationary plane flow of viscous incompressible fluid 18 p3100 A66-34545  
 Two physical-space and two spectral solutions of Burger equation which are

exact, viscous and nonsteady 18 p3103 A66-3493  
 Classical/quantum views of nonequilibrium gas flow equations with arbitrary number of relaxation times 19 p3340 A66-3573  
 One-dimensional heat flow equation for liquid nitrogen end-cooled ruby laser rod 20 p3581 A66-3838  
 Transonic flow in axisymmetric nozzle with nearly sharp wall curvatures, extending Friedrich equations 21 p3693 A66-3868  
 Modified Poiseuille equation for gas flow through capillaries, applicable to flow regimes extending from molecular to viscous flow 21 p3725 A66-3894  
 Periodic flows of orientable anisotropic fluids tending to be unoriented at resonance considered through linear equations which predict resonance phenomenon 21 p3727 A66-3917  
 Vector equations of steady incompressible viscous flow in absence of extraneous forces, discussing Beltrami flow, double laminar flow and plane flow 21 p3728 A66-3943  
 Vector equations of steady inviscid thermally nonconducting gas flows from geometric theory of triply orthogonal spatial curves 21 p3729 A66-3944  
 Linear flow equation motion of fluid with suspended impurities, noting that under certain assumptions velocity fields can be described by family of potential functions 21 p3729 A66-3944  
 Nonlinear computational instability in long-term numerical integration of two-dimensional incompressible flow equation 21 p3730 A66-3947  
 Gas flow equations for multilayer insulation systems for both continuum and free molecular flow regimes of interest in cryogenic space vehicle design [AICE PREPRINT 22A] 22 p3897 A66-3988  
 Longitudinal viscosity effect in equations for plane transonic flow for initial stages of shock formation downstream in nozzle 22 p3844 A66-4036  
 Variational principles for viscous, incompressible hydromagnetic equations of flow including continuity equation, motion equations, etc 23 p4099 A66-4112  
 Surface mass transfer effect for supersonic flow over cone, examining solution of equations of motion for inviscid compressible gas with velocity field normal to surface of inner cone 23 p4011 A66-4181  
 Constitutive equations of plastic and elastoviscoplastic flow theory for nonstationary yield conditions and strain hardening 23 p4146 A66-4199  
 Existence of similar solutions for given differential transonic equations for free stream Mach number of unity 23 p4014 A66-4204  
 Radiation fronts in gas dynamics examining flow through or behind aerodynamic shock 23 p4062 A66-4205  
 Motion equations, shear stress and skin friction for three-dimensional flow in conical pipes 23 p4014 A66-4206  
 Similarity solutions of boundary layer equations for blowing through porous surface, obtaining skin friction 24 p4194 A66-4254  
 Velocity gradient on blunt axisymmetric bodies in stagnation region if pressure distribution is known, using isentropic flow equations 24 p4158 A66-4277  
 Invariant solution classification for equations of two-dimensional steady stagnation motion of gas 24 p4196 A66-4286  
 Laminar flow of fluid with varying viscosity in tube with walls at constant temperature, analyzing equations of motion and equations for conservation of energy 24 p4197 A66-4299

**FLOW FIELD**  
 Steady nonviscous flow in field with sources of energy, force and mass investigated under assumption of small perturbations 01 p0057 A66-1043  
 Hypersonic flow field about slender cone derived from heat-pressure-wake survey 01 p0007 A66-1067  
 Flow field about subsonic jet exhausting into quiescent and low velocity air stream [AIAA PAPER 65-704] 01 p0008 A66-1099  
 Pressure distribution measurement systems



for flow field of main turbojet intake of one-eighth scale model of Mirage III V aircraft 02 p0210 A66-11206

Turbulent mixing of axisymmetric jet of partially dissociated nitrogen with ambient air, establishing mixing and decay characteristics [AIAA PAPER 65-823] 03 p0359 A66-13231

Supersonic and hypersonic flow fields around plane and axisymmetric bodies and inlets obtained by nonlinear characteristics method 04 p0454 A66-13519

Flow field in centrifugal compressor impeller [ASME PAPER 65-WA/GTP-7] 05 p0608 A66-15722

Closed form solution of axisymmetric transonic flow about obstacle 05 p0665 A66-15796

Oscillating disk induced flow, discussing mathematical formulation of flow field produced by finite-amplitude rotational oscillations 06 p0872 A66-16354

Flow field of two-dimensional Bunsen flame according to source sheet approximation 07 p1154 A66-17940

Flow field in rectangular cavities at low Reynolds number 07 p1020 A66-17941

Asymmetric hypersonic blunt body problem of determining two-dimensional steady rotational flow field between profile and detached shock 07 p0982 A66-18132

Spatial distributions of free electrons in near wakes of spheres in hypersonic flight [AIAA PAPER 66-55] 07 p0983 A66-18449

Two-dimensional probability distribution for simultaneous turbulent velocities at two points in plane perpendicular to mean velocity of wind tunnel 08 p1205 A66-18542

Thrust-vector control and flow field produced by secondary gas injection into supersonic stream 08 p1162 A66-18831

Predicting wake-induced nonuniform flow field in plane of rotor disk [AIAA PAPER 66-17] 08 p1162 A66-18951

Inviscid supersonic flow fields of reacting gas mixture around pointed bodies calculated, using characteristics method 08 p1164 A66-19128

Nonstationary supersonic flow in near sonic range, calculating pressure distribution in oscillating profile 09 p1328 A66-20875

Entry flight, relation between laboratory flows, in-flight conditions and MGD effects on flow field, drag and heat transfer [AIAA PAPER 66-161] 10 p1611 A66-21682

Approximate method for analyzing chemically reacting turbulent flow fields having initial homogeneities [AIAA PAPER 65-37] 10 p1523 A66-21770

Flow field around minimal-drag slender body examined by Newton-Busemann theory and gas dynamic theory 11 p1632 A66-22524

Expansion tube for interferometric observation of hypersonic flow fields 11 p1684 A66-22830

Flow field near leading edge of heated flat plate in Mach 0.5 airflow 11 p1634 A66-22934

Hypersonic flow field about slender cone derived from heat-pressure-wake survey 13 p1990 A66-25182

Nonequilibrium inviscid flow about arbitrarily shaped body with detached shock waves, using method with time derivative and bypassing boundary conditions [AIAA PAPER 65-24] 14 p2218 A66-27404

Longitudinal wave histories in liquid rocket motor 14 p2374 A66-27450

Stream function coordinates for flow in shock layer around axisymmetric blunt-nosed body in hypersonic stream 14 p2221 A66-28145

Complex variable theory of flame surface interaction and flow field of two-dimensional V-shaped flame simulated by source and sink sheets 15 p2617 A66-29605

Linearized unsteady nonequilibrium flows produced by unsteady motion of thin foil or circular cylindrical shell in incompressible gas 16 p2687 A66-31288

Behavior of inviscid supersonic conical flow fields near crossflow stagnation points studied by constructing coordinate expansions of exact conical flow equations [AIAA PAPER 66-491] 16 p2631 A66-31494

Relation between shock expansion method and Whitham rule to examine shock wave motion in nonuniform

region 16 p2691 A66-31661

Source type hypersonic free stream effects on flow field about axisymmetric cone, obtaining properties in shock layer, boundary layer, pressure gradient, etc 17 p2837 A66-32080

Stationary or slowly moving nonconducting sphere in current carrying incompressible fluid 17 p2908 A66-32421

Effect of sudden enlargements and contractions in flow area on single pressure waves in gases in pipes, covering incident waves of various pressure amplitudes 17 p2841 A66-32890

Turbulent swirling jets issuing from round orifice studied experimentally and theoretically, based on continuity equations and Reynolds equations of motion 17 p2913 A66-33067

Loading of thin ring airfoil in unbounded spherical source flow field, calculating vortex distribution, strength, etc [ASME PAPER 66-FE-3] 17 p2914 A66-33259

Short duration simulation of rocket exhaust products, flow duration through nozzle and effect on recirculation flow fields 17 p2904 A66-33475

Finite difference method for shock wave propagation into supersonic crossflow 17 p2916 A66-33479

Aerodynamic stability of slender cone under ablation effect including pressure distribution measurement, ablation-flow field interaction, flow analysis during oscillation, etc [AIAA PAPER 66-410] 18 p3045 A66-33635

Method of characteristics computer code applied to partial differential equations of inviscid fluid, calculating flow fields [AIAA PAPER 66-412] 18 p3097 A66-33637

Partial differential equations for three-dimensional inviscid flow solved for flow field over blunt body shapes at various angles of attack, for application to Apollo spacecraft [AIAA PAPER 66-413] 18 p3045 A66-33638

Surface friction induced vertical motions for nonaccelerated flow calculated from surface pressure pattern 18 p3129 A66-33963

Static enthalpy and velocity profile within viscous wake of circular cylinder at Mach 20 18 p3049 A66-34582

Flow field of highly underexpanded axisymmetric jet impinging on flat convex or concave surface calculated by modified inverse method 18 p3100 A66-34600

Two-dimensional solution of Laplace equation for vortex formations in incompressible fluid 18 p3100 A66-34634

Approximation theory for calculating linearized subsonic and supersonic flow over pulsating bodies with low aspect ratio, noting structure of flow field 19 p3277 A66-36641

Interferometric measurement of density distributions in shock layer of nonequilibrium flow field around cone 21 p3694 A66-39168

Hypersonic flow, discussing heat effect on flow parameters, shock and motion equations, drag increase, etc 22 p3897 A66-39699

Generation of pressure wave by explosion of condensed phase fuel particles dispersed in gaseous oxidizer [AIAA PAPER 65-357] 22 p3999 A66-40357

Pseudoviscosity method using finite difference equations for calculating two-dimensional flow fields for supersonic motion of inviscid gas 22 p3901 A66-40494

Aerodynamic problem of steady potential flow and added mass in unsteady motion of idealized hemispherical parachute 22 p3845 A66-40591

Tests for obtaining water trajectory data and underwater flow field photographs used in determining deployment sequence of water recovery system flotation bag for reentry vehicle 22 p3987 A66-40601

Bluntness and boundary layer displacement effects on air breathing engine hypersonic inlet flow fields [AIAA PAPER 65-617] 23 p4007 A66-41109

Electrostatic probe in collisionless plasma wherein sheath joins region of ambipolar diffusion 23 p4104 A66-41494

Liquid drop flow in twisted fan-shaped nonisothermal jet allowing change in

viscosity coefficient in flow field, using boundary layer equations 23 p4055 A66-41567

Extrusion of viscous incompressible substance through round hole in infinite wall, obtaining pressure and velocity fields 23 p4057 A66-41738

Mass transfer into aerodynamic body flow fields, examining model shear flow in Rayleigh problem for blowing current across gas-solid interface 23 p4058 A66-41900

Hydrodynamic phenomena in rotating fluid systems, characterizing flow of fluid whose viscosities, thermal conductivity and specific heats are constant 23 p4058 A66-41940

Radiometer system with photomultiplier tube for measuring absolute radiation from hypervelocity projectile flow fields 24 p4208 A66-42181

## FLOW GEOMETRY

Cross-sectional geometry of Nernst-Ettingshausen devices optimized for rectangular geometry and for Norwood spiral screw thread configuration 02 p0270 A66-11430

Ringleb theory on snow cornice-like flows analyzed, including arguments on representation of real fluid flows and model of step-sink flow [ASME PAPER 65-WA/FE-11] 05 p0664 A66-15678

Geometrical theory governing flow over surface of convergent spillway 14 p2277 A66-27936

Linearized problem of oblique incidence of weightless flow of ideal gas on surface of heavy liquid, using eigenvalues and eigenfunctions of integral equation 19 p3342 A66-36470

Multistep axisymmetrical supersonic exit cones optimum geometry design diagram based on external oblique and normal compression shock 20 p3628 A66-36927

Rotor downwash angle and tunnel geometry effect on maximum size rotor that can be tested in closed throat wind tunnel [AIAA PAPER 66-736] 22 p3893 A66-40626

## FLOW GRAPH

SA SIGNAL FLOW GRAPH

Plotting and analysis of oriented graphs of electrical circuits of any complexity by considering them as N poles 19 p0050 A66-10218

Digital computer determination of coefficients of transfer function from impulse response in time domain 07 p1060 A66-18334

Columbium and tantalum alloy tubing production for space power systems including extruding, rocking, annealing, flow diagram, etc 12 p1893 A66-23627

Flow graph in model of jet curtain in ideal incompressible weightless fluid with isolated vortex 12 p1798 A66-24433

Flow diagram for dimensioning of jet compressors to plot irreversible mixing, noting shape of mixing channel, design guidelines, etc 16 p2632 A66-31645

Plotting and analysis of oriented graphs of electrical circuits of any complexity by considering them as N poles 17 p2898 A66-31901

Flowgraph techniques for closed systems, discussing properties, approximation method, topology equation, frequency response, constraints, oscillatory and stochastic processes, etc 17 p2898 A66-31954

Flow graph analysis of lossless nonideal 3- and 4-port junction circulators for visualizing scattering matrices and calculating coefficients of combined networks 17 p2896 A66-33277

Piecewise linear system modeling via topological techniques, using flowgraph method for network synthesis 18 p3090 A66-34247

Approximation technique for flow graph that eliminates nonessential equivalent circuit elements, providing for derivation of most concise model with preassigned accuracy 18 p3092 A66-35040

## FLOW MEASUREMENT

Density distribution before sphere in low density hypersonic gas flow measured with electron beam densitometer 01 p0059 A66-10635

Rotating arm apparatus at National Aerospace Laboratory in Japan for pressure-distribution and heat-transfer flow



measurement 01 p0053 A66-10636  
 Relationship of laminar wake width to wake transition distance for cones 02 p0175 A66-11561  
 Rheology of liquids discussing viscometers, models for prediction and industrial and biological application 03 p0355 A66-12601  
 Book on vacuum science and engineering covering properties of gases at low pressure, vacuum measurements and vacuum pump and system design 04 p0545 A66-13934  
 SNAP-8 instrumentation, emphasizing selection and installation of aerospace type transducers for liquid metal service [ISA PREPRINT 1.11-4-65] 05 p0683 A66-15510

Coupled flow problem, comparing flow induced by steady rotation of permeable and impermeable disks 06 p0871 A66-16353  
 Compressible subsonic flow with symmetric Zhukovskii profile calculated by correspondence principle 07 p1023 A66-18112  
 Book on flow measurement through pipes by square-edge orifice plate using corner tappings, including pipe layout, fluid density, temperature, pressure, orifice design, tables, graphs, etc 08 p1221 A66-18679  
 Relative effect of restrictive orifices, venturis or nozzles on measurement accuracy of fluid flow rates in pipes 11 p1703 A66-22207

Mean and dynamic skin friction, separation and transition in low-speed laminar and turbulent flow measured by thin-film heated element 11 p1693 A66-23013

Fluid dynamic behavior of system predicted by performing measurements on model of system 11 p1693 A66-23173

Liquid hydrogen flow system performance during startup transient of nuclear rocket measured in full-scale simulated engine system, approximating in-flight exhaust conditions 12 p1911 A66-23699

Cavitation delay time variation with velocity, size, dissolved air content, liquid tension, flow history and surface characteristics [ASME PAPER 65-FE-9] 12 p1864 A66-24552

Blood flow measurement by indicators by taking samples in situ-dyes, thermomodulation, krypton 85 14 p2230 A66-27552

Electromagnetic and ultrasonic flow measurement of blood flow rate for cardiocirculatory physiology, discussing future application of nuclear resonance and laser 14 p2230 A66-27553

Dynamic and steady state flow disturbances encountered by aircraft during carrier landing approach in water tunnel simulation study [AIAA PAPER 65-332] 16 p2634 A66-31319

Cavitation effect on discharge coefficient of standard flow nozzles [ASME PAPER 66-FE-12] 17 p2915 A66-33266

Dynamic pressure and flow measurements on small integrated high speed systems, using high speed pressure transducing equipment in integrated circuits and hot-wire anemometry 20 p3560 A66-37652

Hot-wire anemometer design with linear characteristics for measurement of velocity fluctuations of flow 20 p3560 A66-37760

Carbon dioxide flow density in wake of shock wave front 21 p3726 A66-39091

## FLOW METER

Transverse-field induction flowmeter to monitor shock tube gas velocity 03 p0353 A66-13250

Thermal flow meter incorporating effect of axial conduction [ASME PAPER 65-HT-19] 05 p0676 A66-14741

Discharge coefficient of quadrant-edge orifice and performance at very high Reynolds number [ASME PAPER 65-WA/FM-2] 05 p0663 A66-15517

Pressure index for predicting upstream nonnormal velocity distributions on orifice meters [ASME PAPER 65-WA/FM-3] 05 p0684 A66-15518

Nonstandard approach section effects on flow coefficients for venturi and orifice meters [ASME PAPER 65-WA/FM-5] 05 p0684 A66-15519

Density and Reynolds number effects on turbine meter performance in gas flow

## measurement

[ASME PAPER 64-WA/FM-1] 06 p0879 A66-16219

Experimental assembly using liquid gallium cycle for testing electromagnetic pumps and flow meters 06 p0918 A66-16847

Piston-type flowmeter for automatic recording fuel consumption 09 p1380 A66-20310

Thermal flow meter incorporating effect of axial conduction [ASME PAPER 65-HT-19] 11 p1703 A66-22187

Laser Doppler velocimeter for measuring localized flow velocities in liquids 14 p2306 A66-27053

Maintaining of flow similarity in calibration of nozzle type water meters for study of working processes of pumps 14 p2225 A66-27698

Time constant of turbine-flow meter sensor 14 p2295 A66-27712

Fringing effect on sensitivity of magnetic flow meter 17 p2926 A66-32874

Quadrant edge orifice meter performance under cavitating conditions, noting discharge coefficient curves [ASME PAPER 66-FE-9] 17 p2915 A66-33263

Viscosity effect on performance of turbine type flow meters calculated to meet accuracy requirement for complete use of propellants in rocket propelled vehicles 19 p3361 A66-36646

Calibration of turbine flow meter on air against pitot tube traverse, considering random scatter 19 p3362 A66-36750

Leak-rate transducers capable of aerospace flight detection of small gas flow rates in critical joints of Saturn engine systems 20 p3557 A66-37215

Calibration device for flow and volume meters for liquid rocket engine propellant 20 p3561 A66-38066

True-mass cryogenic flowmeter for liquid oxygen, hydrogen and nitrogen with liquid-helium compatibility 21 p3740 A66-39426

## FLOW PATTERN

Physical mechanisms of instabilities altering two-phase flow pattern of liquid film 01 p0165 A66-10907

Convection pattern changes in Earth mantle and continental drift as evidence of cold origin of Earth 03 p0361 A66-12379

Flow past fluid film-covered sphere and cylinder of given radius in different fluid, discussing external and film flow conditions 04 p0509 A66-13555

Dimensionless flow parameter for free convection, equivalent to Reynolds number for forced convection, used for correlating through single curve free and forced convective heat and mass transfer from single bodies 07 p1149 A66-17517

Critical condition for aerosol deposition from symmetrical flow past solid body, considering case of circular cylinder 08 p1247 A66-19304

MHD flow patterns 12 p1920 A66-23955

Mixing of laminar viscous incompressible jets expelled from equally spaced holes in vertical wall, obtaining solution by using Navier-Stokes equation 12 p1864 A66-24444

Constant section mixture of flows with different enthalpies, noting sonic blocking for terminal temperature differences 13 p1991 A66-25470

Potential double waves at interface between two-dimensional nonsteady barotropic gas flow and region of undisturbed gas 13 p2063 A66-25633

Simultaneous diffusion of momentum and energy in turbulent mixing, noting static and stagnation properties, density and temperature variations, flow pattern, etc 13 p2070 A66-26721

Pressure drop as function of flow rate for helical flow of non-Newtonian polyisobutylene solution 15 p2477 A66-28615

Flow pattern and heat transfer distribution in regions of adverse pressure gradient and separated flow over two-dimensional models in Mach 10 airflow 15 p2424 A66-29271

Performance of short supersonic nozzles producing expansion and density jumps in flow, noting efficiency in obtaining maximum driving effect 16 p2630 A66-31303

Bergman integral operator to generate families of transonic flow patterns which yield Ringleb pattern as special

## case

Geometrically different volutes effect on impeller of centrifugal pump performance, discussing radial thrust, head and runout capacity [ASME PAPER 66-FE-14] 17 p2932 A66-33268

Critical condition for aerosol depositor from symmetrical flow past solid body, considering case of circular cylinder 19 p3393 A66-36043

Asymmetric shear flow of viscous fluid past flat plate, justifying constant pressure assumption and examining flow patterns at lower surface in plate proximity 20 p3547 A66-37979

Flow transition from propeller in free stream to axial pump in cylindrical shroud for impeller clearance between zero and infinity 21 p3695 A66-39499

Aerodynamic breakup of liquid drops in flow behind plane shock wave analyzed via high speed photography, noting experimental setup, parameter variation, etc 22 p3899 A66-40199

Flow pattern of three-dimensional interaction of oblique shock with boundary layer obtained when shock generated by wedge spanning supersonic wind tunnel interacts with side wall 22 p3901 A66-40499

Annular nozzle shapes established via method of straight line characteristics, noting flow patterns at various regions 23 p4009 A66-4173

Analytical method for studying pattern of flow from nozzle into vacuum used to calculate plume shape for rocket exhausting into hypersonic stream 24 p4158 A66-42799

Low level atmospheric flow structure resolution, noting equipment and results of wind speed variations 24 p4235 A66-43079

## FLOW REGULATOR

Regenerative heat exchangers, covering heat transfer and pressure loss characteristics of glass ceramic matrix materials [ASME PAPER 65-HT-35] 05 p0784 A66-14759

Supersonic retardation cascades for losses, reduction of supersonic flow to subsonic in turbines and compressors 10 p1591 A66-21389

Gas flow regulator system conforming to prescribed time-dependent program, based on mass flow limitation properties of sonic orifices and polynomial approximation to exponential 12 p1859 A66-24719

Flexible baffle effect on nature and magnitude of damping and sloshing motion of liquid propellants over wide range of conditions 16 p2685 A66-30919

## FLOW RESISTANCE

Calculation of rotationally symmetric turbulent boundary layer flow through straight diffusers 01 p0006 A66-10219

Drag reduction for sailplanes, investigating adoption of laminar foil section 01 p0008 A66-11099

Sphere drag measurements at low Reynolds number 02 p0219 A66-11959

Drag of sphere moving along axis of rotating viscous fluid 02 p0219 A66-11959

Flow resistance of partially permeable wedge to incompressible fluid incident on base or vertex 03 p0359 A66-13189

Peripheral friction stresses and friction resistance moments in flow around rotating disk in closed housing 04 p0508 A66-13449

Air flow resistance and effective porosity of round wire parachute fabrics with varying wire thickness and mesh width 04 p0538 A66-13539

Solid bodies in plane parallel flow of ideal fluid, discussing one-parameter family of ablation bodies with steady shape 04 p0596 A66-13559

Quasi-steady flow relations to study wave action in duct with gauze 06 p0873 A66-16939

Apparatus for measurement of flow resistance of gas diffusion electrodes 07 p0990 A66-17239

Quantitative estimation of effect of hydrodynamic resistance of adding surface active additives to turbulent fluid flow 07 p1023 A66-18159

Aerodynamic pressure and resistance calculated from gas flow past circular cylinders with piecewise constant diameters 08 p1232 A66-19339

Pressure distribution on star-shaped bodies in wind tunnel at Mach 4 and Reynolds



number .000006 08 p1165 A66-19480  
 Fluid resistance of rough disk rotating in closed vessel, noting dependence on flow Reynolds number of plate moment coefficient, axial clearance, etc 08 p1210 A66-19554  
 Resistance due to viscous shear on circular cylinder in oscillating stream calculated by boundary layer equations formulated in polar coordinates 09 p1367 A66-20262  
 One-dimensional adiabatic compressible gas flow in cylindrical tube taking into account Reynolds number variations along tube and compressibility effect on friction factor 09 p1368 A66-20827  
 Hydraulic resistance coefficient dependence on Reynolds and Hartmann numbers in turbulent flow of conducting fluid through tube in magnetic field 11 p1743 A66-22337  
 Friction resistance of compressible turbulent gas flow through initial section of cooled pipe with large gas-wall temperature gradients 11 p1688 A66-22597  
 Variable mass plasma blob acceleration due to eroding electrodes, taking into account motion resistance of unperturbed gas 11 p1745 A66-22850  
 Clamping conditions effect on critical flow rate of fluid moving through pipe, taking into account direction and friction forces on stability 11 p1782 A66-22853  
 Fluid flow impedance parameters and properties, discussing nonlinear orifice resistors in fluidic circuitry, tube resistance and fluid capacity 12 p1803 A66-24384  
 Hydraulic resistance of air flow through porous steel plate 13 p2065 A66-26483  
 Hydraulic resistance and heat transfer in laminar-turbulent transition region in tube with heating and cooling of water 14 p2414 A66-27830  
 Liquid flow with viscosity changing under effect of nonisothermicity 15 p2478 A66-29222  
 Hydraulic resistance, heat and mass transfer in vortical flow, noting power optimal conditions of operation 16 p2825 A66-30323  
 Orifice increases resistance coefficient when edge of wedge is facing incident flow and decreases it when wedge is turned around 16 p2689 A66-31518  
 Critical flow rate, critical pressure ratio and critical mass flow of dissipative adiabatic nozzle and pipeflow of ideal gas 16 p2690 A66-31635  
 Dolphin body design for integrating resistance and propulsion mechanisms 19 p3279 A66-36050  
 Brake force acting on piston of constant-speed controller with fluid friction 21 p3698 A66-39330  
 Nearly free molecular flow in rarefied gas dynamics in comparison of theoretical and experimental results with reference to drag 23 p4060 A66-42025  
 Pressure losses in vanned elbows of circular cross section and possibility of gain in efficiency by splitting vanes 24 p4195 A66-42582

**FLOW SEPARATION**  
 Edge suction effect occurring in steady subsonic flow along one of legs of convex corner directed toward edge 02 p0175 A66-11558  
 Hypersonic flow separation over simple geometries and aerodynamic controls, noting pressure gradients and heating-rate distributions [AIAA PAPER 65-753] 03 p0314 A66-12587  
 Centripetal gas turbine interblade channel without diffuser regions in rotor eliminates pressure gradient buildup in flow core 03 p0315 A66-12698  
 Jet deflection by curvilinear walls in VTOL takeoff, examining parameters affecting flow separation 04 p0572 A66-13512  
 Flow separation effect on heat transfer characteristics of turbulent pipe flow [ASME PAPER 65-WA/HT-12] 05 p0790 A66-15651  
 Outlet angle in axial compressor cascades, accounting for effect of shear flows, Bernoulli surface rotation and flow separation [ASME PAPER 65-WA/FE-2] 05 p0608 A66-15714

Separation of gases from isotopes in compression shock produced in expanding gas flow past obstruction, dependent on gas density and hydrokinetic properties of components 06 p0875 A66-17052  
 Modified Karman-Pohlhausen pulse integral equation for calculating boundary layers is more accurate when seeking flow separation point 07 p1019 A66-17391  
 Effect of wake of flow past body on pressure distribution over body 07 p0979 A66-17477  
 Clearance loss in rectilinear cascade, emphasizing flow separation and vortices shed at blade tips 07 p0880 A66-17483  
 Ablation effects on static and dynamic stability of reentry vehicle [AIAA PAPER 66-51] 07 p1141 A66-17896  
 Lip shock strength in flow behind backward facing step 08 p1207 A66-19155  
 Friction of rotating disk in revolving housing, noting parameters of dimensionless momentum coefficient, separation of fluid flow into core and secondary flow 09 p1384 A66-20486  
 Laplace transform and analog computation applied to simulation of heat transfer between wall separated fluids, determining transfer functions and frequency responses 09 p1472 A66-20908  
 Flow separation, wake configuration and droplet motion in purified systems shadowgraphically analyzed 10 p1524 A66-21808  
 Flow separation effect on heat transfer characteristics of turbulent pipe flow [ASME PAPER 65-WA/HT-12] 11 p1785 A66-22192  
 Mean and dynamic skin friction, separation and transition in low-speed laminar and turbulent flow measured by thin-film heated element 11 p1693 A66-23013  
 Supersonic gas flow past cylindrical obstacle on plate in wind tunnel at Mach number 2.5, noting separation line, pressure distribution and flow orientation 12 p1798 A66-24437  
 Pressure effect on cone caused by spike protruding at angles of attack may provide aerodynamic directional control at supersonic speed 16 p2629 A66-31117  
 Three-dimensional flow separation of plane boundary layer caused by half delta wing on flat plate using Cooke small cross-flow method and Maskell separation criterion [AIAA PAPER 66-428] 16 p2631 A66-31465  
 Position and dimension of separation zone and bottom pressure calculation for supersonic gas flow around body 16 p2632 A66-31619  
 Turbulent gas flow in wake of flow separation from solid surface 17 p2909 A66-32563  
 Laminar separation in supersonic and hypersonic flow analyzed in gun tunnel, noting concept of incipient separation and free interaction principle [AIAA PAPER 66-455] 17 p2910 A66-32761  
 Terminal shock-boundary layer interaction on slender cone-cylinder payloads at supersonic speeds and resulting flow separation [AIAA PAPER 66-471] 18 p3250 A66-33653  
 Three-dimensional flow separation about immersed surfaces 18 p3098 A66-34019  
 Shock wave boundary layer interactions and shear flow regimes in hypersonic inlet flows [AIAA PAPER 66-606] 18 p3049 A66-34447  
 Boundary and shock layer separation visualization, using nitric oxide in flows with massive blowing 18 p3100 A66-34602  
 Fluidic electro-fluid converter development from study of jet separation from curved surface as affected by geometry, Reynolds number and wall temperature 19 p3282 A66-36673  
 Probabilistic model equations relating column height, feed location, degree of separation and flow rates for continuous chromatographic column 20 p3510 A66-37363  
 Strouhal number effect on sound-excited laminar-turbulent transition in separated boundary layers formed by round or plane nozzle 22 p3899 A66-40382  
 Pressure gradient elution technique for rapid and quantitative chromatographic separation of purine and pyrimidine

bases 22 p3860 A66-40402  
 Lifting wings in supersonic regime, analyzing flow separation at leading edges [ICAS PAPER 66-20] 22 p3847 A66-40670  
 Wind tunnel tests determining plume induced flow separation pattern on missile configurations as ratio of nozzle to ambient pressure 23 p4012 A66-41914  
 Ablation effects on static and dynamic stability of reentry vehicle [AIAA PAPER 66-51] 24 p4283 A66-42770

**FLOW STABILITY**  
 Nonuniqueness and low stability of solutions to hydromechanical problems demonstrated by steady motion of viscous fluid 01 p0055 A66-10168  
 Flow stability theorem for viscous homogeneous and incompressible fluid through infinitely long cylindrical pipe of arbitrary cross section 01 p0058 A66-10504  
 Inviscid stability of laminar mixing of two parallel streams of compressible fluid with respect to three-dimensional wavy disturbances 02 p0218 A66-11955  
 Orr-Sommerfeld equation of shear layer between parallel uniform streams in Hermite function series, noting wave number 02 p0219 A66-12074  
 Steady flow possessing extremal kinetic energy compared to equivortex flow for stability analysis 02 p0219 A66-12169  
 Stability analysis of adiabatic flow of incompressible fluid without equation linearization and by constructing functional from hydrodynamic fields 02 p0220 A66-12170  
 Stabilization of inviscid pure-vortex flow with finite conductivity, using axially applied magnetic field [AIAA PAPER 64-435] 03 p0399 A66-12787  
 Hypersonic wake transition map noting far wake, near wake and interpolation phenomena 03 p0356 A66-12814  
 Stabilization of laminar conducting fluid flowing down inclined plane in transverse magnetic field 03 p0356 A66-12946  
 Stability of parallel flows with frequency-dependent viscosity 03 p0357 A66-12960  
 Laminar stability of incompressible and stationary flows with curved streamlines, applying integral method and noting time dependence of flow 03 p0357 A66-13089  
 Flow of non-Newtonian liquids in cylindrical pipes containing cylindrical parallel cores moving longitudinally at constant speed 03 p0358 A66-13090  
 Plasma flow discussing flow mode stabilization in channel formed by two electrodes, flow parameters and plasma conductivity 04 p0529 A66-13553  
 Non-Newtonian media, parallel flow, discussing effects of two- and three-dimensional perturbations on flow stability 04 p0510 A66-13872  
 Entrance region Newtonian flow analysis in tube of circular cross section for possible use in viscometry and flow stability studies [AICE PREPRINT 19D] 04 p0511 A66-13935  
 Laminar flow stability of layer of viscoelastic fluid flowing down infinite inclined plane under action of gravity 04 p0512 A66-14428  
 Hydrodynamic stability of parallel dusty gas flows, discussing energy balance and viscous sublayer structure 05 p0662 A66-14703  
 Flow stability in multitube forced convection vaporizers, using Freon 113 in closed test loop with five-tube boiler [ASME PAPER 65-HT-61] 05 p0786 A66-14762  
 Nonlinear stability of zonal flows in two-dimensional quasi-solenoidal model when absolute eddy is monotonic function of width 06 p0905 A66-16549  
 Flow induced structural vibrations, noting interdependence between deformation and fluid dynamic loading 06 p0872 A66-16615  
 Similarity solutions of boundary layer equations with algebraic decay for viscous incompressible fluid inside infinite circular cone 06 p0873 A66-16996  
 Pressure gradient effect on stability of laminar boundary layer when skin friction at wall vanishes, noting Reynolds number of flow 06 p0874 A66-16999  
 Delta wing vortex breakdown in terms of theory of stability of spiraling flows 07 p0979 A66-17478  
 Stability criterion for flow in interspace



between two parallel arbitrarily curved walls 07 p0980 A66-17482

Stability of piecewise linear velocity profile of shear flow in convectively unstable layer 07 p0980 A66-17942

Electron diffusion in mutually perpendicular static electric and magnetic fields based on stability of laminar flow 07 p1081 A66-17953

Exact solution of hydromagnetic stability of nondissipative conducting Couette flow between two coaxial cylinders in axial magnetic field 07 p1021 A66-18048

Heat transfer and stability of laminar hypersonic separated flow around annular cavity conical model 07 p0981 A66-18117

Stability of plane Poiseuille flow between elastic boundaries 07 p1026 A66-18194

Stability of frictionally heated Couette and Poiseuille flows, specifically Couette flow in inviscid limit 08 p1204 A66-18527

Equilibrium stability of horizontal layer of fluid in field of modulated temperature gradient when layer thickness is greater than penetration depth of heat waves 08 p1320 A66-19471

Viscosity and density variations due to imposed radial temperature gradient effects on Couette flow stability between rotating cylinders 08 p1211 A66-19681

Analogy between eigenvalues for fluid convection and flow stability extended to rotating cylinders with corresponding temperature distribution for given angular velocities 08 p1212 A66-19821

Stability of set of Jeffery-Hamel profiles, approximating profiles in two-dimensional divergent channels, investigated by numerical solution of Orr-Sommerfeld problem 08 p1212 A66-19823

Stability of plane motion of fluid subject to continuous perturbations distributed over volume and boundary of flow 09 p1368 A66-20755

Instability of hypersonic shock layer flow over blunt bodies with surface cavities coupled to dynamic stability of body 10 p1619 A66-21156

Hydromagnetic stability of current-carrying fluid between two coaxial cylinders with radii ratio 0.05 to 0.9 10 p1568 A66-21829

Clamping conditions effect on critical flow rate of fluid moving through pipe, taking into account direction and friction forces on stability 11 p1782 A66-22853

Overstability in elastico-viscous flow between rotating cylinders 11 p1693 A66-23010

Stability of forward and rearward slug flows due to motion of body through perfectly conducting liquid with embedded magnetic field 11 p1746 A66-23011

MGD stability treated by transfer function method for lumped-parameter dynamic systems 11 p1677 A66-23114

Stability of vortex-free incompressible fluid flow 11 p1694 A66-23331

Plasma burner in which heating of gas is effected in jet discharge stabilized by vortex or flow methods 11 p1748 A66-23417

Stability of steady finite amplitude convection determined by method of successive approximations 11 p1787 A66-23421

Nonlinear Benard convection 12 p1976 A66-23549

Stability of two-dimensional parallel flows, using Orr-Sommerfeld equation and adjoint equation with asymptotic solution 12 p1861 A66-23809

Liquid film flow stability, considering two-dimensional perturbations, hydrodynamic friction with allowance for finite curvature radius of bounding surface 12 p1864 A66-24435

Stability of plane inviscid jet and wake studied for possible growth in downstream spatial direction 12 p1865 A66-24582

Instability criterion in air, argon and carbon dioxide at various pressures and layer depths, detecting convection and determining Rayleigh number for application in transport properties of gases 12 p1980 A66-24942

Orr-Sommerfeld equation regarding stability of parallel flows solved for large Reynolds number, using inner and outer expansion theory 12 p1866 A66-24944

Small gap equations for Couette flow

stability considering nonaxisymmetric disturbances, solving eigenvalue problem and noting role in instability of Taylor vortices 12 p1866 A66-24946

Steady finite-amplitude motions existing for range of Taylor number, with values of Rayleigh number smaller than critical value required for overstability 12 p1866 A66-24948

Stability of two-dimensional Couette-Poiseuille flow 12 p1866 A66-24951

Potential stabilized two-component supersonic flow of thin body and surface form for given pressure distribution and component separation 13 p1994 A66-26765

Stability of cylindrical sheet of fluid during motion through motionless gas ambient 14 p2273 A66-26778

Non-Newtonian media, parallel flow, discussing effects of two- and three-dimensional perturbations on flow stability 14 p2275 A66-27572

Perturbation equations solved for viscous flow stability over concave cylindrical surface 14 p2276 A66-27729

Nonlinear stability of zonal flows in two-dimensional quasi-solenoidal model when absolute eddy is monotonic function of width 14 p2327 A66-28221

Range of gas dynamic stability of arc-type electric heaters, characteristics for design and calculation of electrode diameter ensuring vortex stabilization 14 p2348 A66-28314

Temperature effect on motion stability of fluid between rotating cylinders 14 p2415 A66-28323

Variational problem solved, giving lower stability bounds for finite disturbances of viscous incompressible flow 15 p2478 A66-29245

Stability to infinitesimal disturbances of plane Couette flow in presence of negative vertical temperature gradient, noting instability at critical Rayleigh number for convection without shear 15 p2481 A66-29741

Natural frequency of fluid oscillations in complex pipelines 16 p2687 A66-31296

Flow instability of incompressible nonconducting fluid in thin cylindrical conducting elastic pipe in constant uniform magnetic field 16 p2764 A66-31367

Laminar-turbulent transition conditions in MHD channel flow 16 p2764 A66-31370

Effect of radiative and photochemical processes on stability of two level baroclinic flow, noting low and high shear instability, wavelength, phase speed, etc 16 p2700 A66-31644

Structure of axisymmetric core of spiraling fluid with high vorticity 17 p2907 A66-32277

Absolute stability of some plane parallel flows at high Reynolds number 17 p2907 A66-32322

Numerical solution of time dependent equations of one-dimensional reactive flow for idealized one-reaction detonation 17 p2908 A66-32418

Jet disintegration into large drops in Vivdenko and Shabalin paper 17 p2909 A66-32566

Three-dimensional boundary layer for accelerating flow over semiinfinite flat plate with or without suction 17 p2911 A66-32838

Variational principle for steady flows of ideal liquid and sufficient conditions for nonlinear stability under finite perturbations 17 p2913 A66-33168

Spiral flow stability of idealized viscoelastic liquid between two rotating concentric cylinders with axial pressure gradient 17 p2914 A66-33171

Gravitational stability of laminar liquid layer flowing down inclined plane and heated from below 17 p2914 A66-33172

Critical Reynolds number for pulsating Poiseuille flow determined by studying stability under harmonically and nonharmonically varying pressure gradient [ASME PAPER 66-FE-5] 17 p2914 A66-33260

Boundary value problem of Stokes equations proving branching for flow between two rotating concentric cylinders and nonexistence of singular flow 18 p3101 A66-34659

Instability of free laminar boundary layer between parallel streams analyzed for incompressible fluid, noting values of

Reynolds number 18 p3102 A66-34949

Stability of swirling flow of viscous conducting fluid in presence of circular magnetic field 18 p3150 A66-34949

Energy method applied to stability of flow governed by nonlinear Boussinesq equation establishing universal stability region Reynolds-Rayleigh number plane 19 p3478 A66-361

Space charge wave equation and impedance and stability of electron diodes, using Nyquist analysis and transit time and beam current 20 p3528 A66-374

Sufficient conditions for instability against small oscillations of symmetric laminar flow of inviscid incompressible perfect magnetofluid 21 p3791 A66-391

Stability of viscoelastic liquid in Couette flow compared with non-Newtonian liquid same limiting viscosity 21 p3729 A66-394

Laminar mixing of two parallel streams of compressible fluid stability with respect to supersonic disturbances 22 p3900 A66-403

Rayleigh turning-point criterion in velocity profile extended to spatially increasing flow disturbance 22 p3900 A66-403

Oscillation of tubular cantilevers conveying fluid, discussing theoretical conditions of stability 22 p3994 A66-404

Oscillation of tubular cantilevers conveying fluid, checking stability aspects of theory and accounting for internal and viscous damping 22 p3994 A66-404

Aerodynamic problem of steady potential flow and added mass in unsteady motion idealized hemispherical parachute 22 p3845 A66-405

Stability analysis of discontinuous solutions of gas dynamics PDEs for ideal fluid 23 p4055 A66-415

Hydraulic loss decrease in complex pipeline owing to wire grating 23 p4024 A66-417

Nonstationary flows around vibrational obstacles with application to wing flutter and to interactions of various aircraft components 23 p4012 A66-419

Shear flow transition to turbulence and instability phenomena, discussing parallel and laminar flows 23 p4060 A66-422

Taylor vortices growth and instability using mathematical model 23 p4062 A66-422

Experimental verification of stability criteria for incompressible inviscid flow with helical streamlines, using rotating cylinders 23 p4062 A66-422

Thermal convection in horizontally infinite layer of fluid confined between rigid heat conducting plates driven by temperature difference 23 p4151 A66-426

Critical Reynolds number for pulsating Poiseuille flow determined by studying stability under harmonically and nonharmonically varying pressure gradient [ASME PAPER 66-FE-5] 24 p4195 A66-428

Secondary steady or periodic flow generation from stability loss by laminar flow of viscous incompressible fluid, noting nonuniqueness of solution 24 p4195 A66-428

### FLOW THEORY

#### SA FLUID MECHANICS

#### SA HYDRODYNAMICS

#### SA MIXING LENGTH FLOW THEORY

Approximation of strains in plastic plates and shells on basis of nonassociated flow law 01 p0155 A66-107

Existence and uniqueness of solution to second boundary value Neumann problem for linear flow theory 02 p0296 A66-112

Flow past slender bodies of revolution of low aspect ratio wings with finite span cross-sectional area 04 p0454 A66-135

Tube gas flow theory applicable to laminar flow, slip flow, transition region of flow at free molecular flow 07 p1023 A66-181

Limiting equilibrium of shallow spherical shell of circular planform, using Tresca yield condition and related flow law 08 p1312 A66-194

Cross flow relation to force distribution on circular cylinders curved in plane containing wind vector at subcritical Reynolds number 09 p1328 A66-207

Flow theory hardening function at inversion of relation between strain rate and stress rate 11 p1784 A66-233

Approximate hypersonic stagnation point flow analysis of thermal conduction a



- radiative transport in shock layer 12 p1860 A66-23595
- Complex flow-perturbing potential for Joukowski profile in incompressible fluid with parabolic velocity distribution, using Jacob first order approximation to solve Dirichlet problem 16 p2627 A66-30211
- Theory of unsteady one-dimensional motion of ideal incompressible fluid, discussing equation of state 16 p2688 A66-31300
- Book on jet theory in ideal fluids, covering compressible flow, steady jet flow, infinite flow past polygonal obstacle, unsteady flow, etc 16 p2632 A66-31746
- Physical and mathematical point of view on flow and fracture 17 p3021 A66-32004
- Temperature and pressure distribution for fluid flow through porous matrix, noting chemical reaction, heat transfer, boundary layer flow, etc [AIAA PAPER 66-423] 17 p2910 A66-32752
- Flow structure and heat transfer for rearward facing step in supersonic flow, discussing critical Reynolds number, flow through lip shock, etc 17 p2913 A66-33068
- Fluid flow analysis of solar wind interaction with magnetosphere 18 p3168 A66-34346
- Linear and nonlinear nonassociated flow laws analyzed for elastoplastic work-hardenable solids 18 p3255 A66-34392
- Cavitation behavior of Herschel-type venturi tube, noting constant flow for varying venturi profile 18 p3114 A66-34646
- Linearized calculation of subsonic wings with rounded leading edge 20 p3491 A66-36949
- Quantities and relations for describing two-phase flows, kinematics and kinetics of both phases of laminar pipeflow 21 p3724 A66-38933
- Propagation of turbulent jet colliding with flat surface at certain incidence angle analyzed for applications to V/STOL aircraft, ventilation equipment, etc 23 p4056 A66-41737
- Parametric method in laminar boundary layer theory, noting reduction of equations for incompressible fluid 23 p4059 A66-42008
- ### FLOW VELOCITY
- #### SA MASS FLOW RATE
- Conformal mapping to calculate exit flow velocity of compressible frictionless subsonic flow through plane blade cascade 01 p0005 A66-10212
- Velocity changes and concomitant losses in rotating transonic blade cascade 01 p0005 A66-10213
- Masses attached to body of revolution estimated by Vandrey method of calculating disturbed velocity potential of flow of ideal fluid 01 p0058 A66-10462
- Homogeneous turbulent flow merging with turbulent or laminar flow of equal velocity 01 p0058 A66-10475
- Flexible-wall tubes flattened by fluid when velocity reaches critical value, with differential equations describing effect of stability loss 01 p0158 A66-11035
- Dynamic equations for two-point double correlations of fluid pulsation velocities and particles suspended in it, noting isotropic turbulence degeneration 02 p0217 A66-11393
- Collisionless plasma flow over cone when flow velocity is greater than ion wave speed [AIAA PAPER 65-125] 02 p0267 A66-11534
- Equation of velocity distribution of fluid in duct, evaluating effect of eddy activity on second derivative 02 p0218 A66-11759
- Oseen flow in plane studied, using approach having velocity field expressed in terms of four auxiliary functions 02 p0218 A66-11805
- Numerical solution of two-dimensional Navier-Stokes equations for confined wake formed by merging of two-plane Poiseuille flow streams 04 p0511 A66-13936
- Emf induced by plasma moving across constant transverse magnetic field used to determine rate of flow behind shock wave in shock tube 04 p0557 A66-14434
- Electrophoretic motion of dielectric particle determined from flow rate of liquid metals and semiconductors near infinite plane 05 p0733 A66-14688
- Viscous fluid flow, examining effect of time dependent suction applied at wall of infinite extent 06 p0871 A66-16351
- Hybrid fuel regression rate, discussing oxidizer flow rate and burner pressure interdependence [AIAA PAPER 66-113] 06 p0941 A66-16407
- Mean flow pattern of round air jet in ambient airstream parallel to jet axis 06 p0802 A66-16504
- Heat transfer rate to stagnation point of catalytic surface placed in slow flow of dissociated oxygen from glow discharge tube and atom-molecule diffusion coefficient 06 p0822 A66-16632
- MHD traveling wave converter, determining frictional fluid losses due to boundary flow and calculating performance 07 p0990 A66-17240
- Rotationally symmetric flow of non-Newtonian fluid in presence of infinite rotating disk, solving Navier-stokes equation and determining velocity profiles 07 p1019 A66-17258
- Thermal diffusion coefficient and composition of gas mixtures by measuring gas flow rate in capillary tube as function of viscosity 07 p1148 A66-17394
- Decay of scalar quantity fluctuations in stationary isotropic turbulent velocity field studied by direct interaction approximation 07 p1020 A66-17944
- Loss in pressure of perforated bottoms as function of resistance parameter of single boreholes 07 p1021 A66-18058
- Gas and sound velocity measurements downstream of shock wave in electromagnetic tube for subsonic and supersonic flows 07 p1023 A66-18119
- Plane rotational motions of perfect fluid in presence of elliptical and circular cylinders and flat plates 07 p1026 A66-18340
- Kinetics of hydroxyl radical in aqueous solution, examining electron spin resonance spectrum as function of flow rate, temperature and mixture composition 08 p1178 A66-19066
- Charge density distribution, electric field strength and flow rate of turbulent flow of incompressible fluid in flat nonconducting channel 08 p1263 A66-19172
- Initial stage of motion in Rayleigh problem, calculating time variable velocity of tangential stress on and velocity of gas near plate 08 p1209 A66-19477
- Transverse magnetic field effect on velocity profile of turbulent mercury flow most pronounced in suddenly expanding flow 09 p1409 A66-20834
- Taylor relation between velocity partial time and space derivatives in high Reynolds number turbulent shear flow 10 p1522 A66-21467
- Flow velocity, static pressure and test-section pitot pressure of expansion tube, using unheated /room temperature/ hydrogen driver 11 p1683 A66-22827
- Velocity variation along two types of confined jets, with and without lateral flow, in presence of transverse magnetic field 13 p2140 A66-25444
- Steady flow of anisotropic conducting medium in half-space under influence of magnetic field 13 p2142 A66-25632
- Text on high velocity hydrodynamics including wing flow, compressible fluids, motion of slender profile, etc 13 p2066 A66-26529
- Low aspect ratio wing moving above interface of two fluids of different density, replacing value of velocity potential by value obtained at large distance downstream from wing 13 p2068 A66-26539
- Velocity profile within boundary layer region for flow of second-order fluid past symmetrical cylinder determined for nondimensional parameter formed by velocity and material constants 13 p2068 A66-26666
- Lift, drag and inertial forces due to uniform unsteady flow with constant acceleration past fixed circular cylinder, determining vorticity flux 13 p1993 A66-26705
- Laser Doppler velocimeter for measuring localized flow velocities in liquids 14 p2306 A66-27053
- Enthalpy and density fluctuations in high speed wakes, noting typical reentry and ballistic range cases 14 p2219 A66-27431
- Streamline flow of ideal stable gas with constant ratio of specific heats around conical body with arbitrary taper, determining flow velocity components 14 p2220 A66-27679
- Velocity field in turbulent flow based on momentum transfer, determining velocity distribution for flow near solid surface 14 p2276 A66-27681
- Acoustical control of atmospheric boundary layer investigated in wind tunnel for flow velocity range from 5 to 40 m/sec 14 p2277 A66-27862
- Laminar adiabatic gas flow in parallel plane channel taking place up to 3/4 of critical velocity 14 p2278 A66-28315
- Concentration waves excited by internal modulation of charged particle concentrations in cross section of plasma flow analyzed for various velocities of flow 15 p2550 A66-29212
- Stabilization of lifted diffusion flame in turbulent methane jet flow field and measurements of gas flow velocity, turbulence and gas composition 15 p2479 A66-29608
- Critical injection parameter on porous plate with turbulent boundary layer, noting conditions of neutralization reaction 16 p2684 A66-30324
- High-velocity subsonic flow past wedge in wind tunnel with perforated walls, applying solution to optimum parameter determination of suction system 16 p2630 A66-31291
- Nonstationary aerodynamic load for harmonically oscillating body in fluid flow with constant mean velocity measured, determining errors as functions of system parameters 16 p2630 A66-31302
- Velocity profiles in outer region of turbulent boundary layer in porous part of floor of wind tunnel for various mass transfer rates 17 p2905 A66-31841
- Stress in spacecraft crew members measured using parotid fluid, noting relationship between biochemical variables under stress and nonstress conditions 17 p2866 A66-32196
- Burning velocity in turbulent stream of homogeneous mixture 17 p3036 A66-32826
- Conducting fluid flow velocity measuring technique using properties of pulsed electromagnetic field 17 p2926 A66-32873
- Laminar flow velocity field and pressure distribution in inlet region of rectangular ducts [ASME PAPER 66-FE-7] 17 p2914 A66-33261
- Fluid dynamics equations of state, motion, continuity and energy stress-strain relationship and shearing stress deformations 18 p3098 A66-34120
- Flow of incompressible viscous fluid subject to conditions governed by Navier-Stokes equation, examining fluid velocity as time tends to infinity 18 p3101 A66-34660
- Structure of flow past bodies with radial cross section in wind tunnel at various Mach numbers and angles of attack, noting position of shock waves 19 p3276 A66-36473
- Open air welding of titanium, noting nozzle design for optimum shielding, argon gas flow rate and magnitude of electrode extension 19 p3371 A66-36633
- Electrically cryopumped system for liquid helium transfer continuously at low flow rates 20 p3542 A66-37105
- Plasma velocity measurements in and outside plasmatron nozzle and free stream from combustion chamber as function of flow rate of stabilizing gas and combustion chamber 20 p3609 A66-37567
- Plasma flow velocity profile measurement by electrostatic probe detection of plasma drop caused by gas breakdown due to focused giant pulse laser 20 p3612 A66-38395
- Flow velocity effect on thermometer reading and consequences for measuring thermodynamic efficiency of hydraulic machines 21 p3737 A66-38935
- Magnetic field effect on stability of fluid in motion of plane parallel flows, determining critical flow velocity and critical Reynolds number 21 p3777 A66-38944
- Book on flow and thermal boundary layers including laminar and turbulent flow velocity profiles, Prandtl equation, heat transfer problems, etc 22 p3897 A66-39702
- Viscosity, surface tension and inclination angle effect on motion of long bubbles in



- closed tubes 22 p3900 A66-40388
- Dual path ultrasonic measurement of fluid flow and speed of sound, using two sound-speed meters in opposition to produce sum and difference frequencies 22 p3921 A66-40896
- Main parameters of two-stage hydraulic amplifier-actuator system determined with aid of pressure and flow-rate amplification factors 23 p4017 A66-40970
- Detonation wave formation in flowing hydrogen-oxygen and methane-oxygen mixtures, noting induction distances and turbulence levels 23 p4057 A66-41888
- Laser Doppler velocimeter for gas and liquid flow velocity measurement 24 p4211 A66-42557
- Temperature compensated thermoanemometer using bead shaped thermistor, for use in nonisothermal boundary layers 24 p4212 A66-42704
- Metrology and precision mechanics - National Conference, Warsaw, September 1966 24 p4214 A66-43011
- Measuring devices for velocity of fluid in undefined motion, noting fluid dynamic transducers 24 p4214 A66-43013
- FLOW VISUALIZATION**
- Acceleration and dynamics of argon plasma in inductive hydrodynamic shock tube 01 p0113 A66-10638
- Critical and limit roughnesses and techniques of visualization and transition fixing in Modane wind tunnel 02 p0216 A66-11207
- Flow visualization technique by thin high-energy electron beam moved with respect to flow 02 p0215 A66-11550
- Nonreturn circuit V/STOL wind tunnel to reduce external wind effects 02 p0216 A66-11964
- Aerodynamic spacecraft deceleration systems examined by hydraulic analogy, noting Mach number effects on flow disturbances 04 p0507 A66-13533
- Tests of obstacle-induced flow recirculation using flow visualization technique and making power measurements 04 p0455 A66-14135
- Advantages of gas lasers as light sources in aerodynamic research 06 p0893 A66-16944
- Conventional flow visualization using laser light source [AIAA PAPER 66-127] 06 p0870 A66-17104
- Behavior of individual cavitation bubbles in cavitating flows of water and liquid Mercury, using two-dimensional Plexiglas venturi 07 p1025 A66-18177
- Motion picture on cavitation hysteresis, details on test apparatus, noting cavitation delay time 07 p1025 A66-18178
- Flow visualization in turbomachinery, using hydrogen bubbles generated by electrolysis of working water 08 p1209 A66-19553
- Temperature-velocity phase lag of vibrations of air columns excited by heat supply 08 p1320 A66-19555
- Low speed flow visualization technique using light-pulse illuminated plastic particles suspended in revolving bowl of brine 09 p1364 A66-20399
- Visualization of flow in transverse plane across main stream past cylinder 09 p1364 A66-20600
- Wave front reconstruction /holography/, hologram production, interferometry, schlieren photography and shadowgrams applied to fluid mechanics 10 p1536 A66-21750
- Laser application to streak photography methods of time resolved flow visualization for transient flows 10 p1536 A66-21752
- Visualization technique for solving three-dimensional liquid flow problems, using small particles suspended in and moving with liquid 11 p1682 A66-22206
- Wind tunnel apparatus for flow visualizations at Mach 14 by glow discharge method 13 p2059 A66-26376
- Aerodynamic smoke tunnels for flow visualization 13 p2059 A66-26543
- Three-dimensional flow visualization approach to complex flow characteristics in centrifugal impeller [ASME PAPER 66-GT-83] 14 p2274 A66-26989
- Schlieren system for flow visualization 14 p2270 A66-27817
- Chemiluminescent technique for flow visualization using electrochemical system and water tunnel 15 p2476 A66-29688
- Coherent gas laser light to meet requirements of streak photography for time-resolved flow visualization 17 p2935 A66-32959
- Hydraulic analogy to compressible gas flow, discussing application to aerodynamic motions, flow visualization, measuring techniques and instrumentation [ASME PAPER 66-FE-16] 17 p2915 A66-33269
- Fastax films showing development and instability of pulsed DC arc in 30 mm Vycor tube at peak currents up to 1500 amp [AIAA PAPER 66-731] 18 p3141 A66-33667
- Flow visualization in compressible fluids, examining optical techniques and Toepler schlieren system 18 p3094 A66-34134
- Boundary and shock layer separation visualization, using nitric oxide in flows with massive blowing 18 p3100 A66-34602
- Primary and afterglow emission decay time from low temperature gaseous nitrogen excited by fast electrons explained by possible energy transfer 19 p3404 A66-36799
- Density distribution and shock wave profile of rarefied gas slip flows past blunt bodies determined, using multibeam interferometer 21 p3724 A66-38903
- Electron beam flow visualization study of density field about skimmer entry in small free jet 21 p3727 A66-39186
- Lateral fluid jet visualization for spanwise launching on wing model with low aspect ratio in subsonic flow 21 p3731 A66-39593
- Flow visualization via afterglow produced in pure low temperature nitrogen and air by electron beam projection 23 p4058 A66-41911
- Magnetically driven shock tube as tool for aerodynamic studies of high velocity high enthalpy flows 24 p4190 A66-42172
- Quantitative fast response visualization technique for low density flow fields based on electron beam fluorescence probe 24 p4210 A66-42201
- High sensitivity method of visualization of supersonic flow of rarefied gas, using glow from cathode parts of glow discharge 24 p4196 A66-42876
- FLOW**
- S FLUORINE-LIQUID OXYGEN /FLOX/ FLUCTUATION THEORY /STAT MECH/**
- Fluctuation errors of analog correlation meters under time displacement of random signals 07 p1031 A66-17356
- Fluctuation problem in electromagnetic cascade theory analyzed, using invariant imbedding method 07 p1083 A66-17973
- Time-space spectral analysis of meteorological fields based on time-dependent spectra of wind velocity, temperature, pressure and turbulent pulse and heat fluxes 09 p1397 A66-19883
- Statistical theory of inert particle fluctuations applied to fine structure of clouds and formation of cloud-particle spectrum 09 p1398 A66-19890
- Fluctuations effect in energy dissipation on shape of turbulence characteristics in inertial interval, using successive division of cubes 10 p1522 A66-21237
- Generalized theorem of minimum entropy production in terms of fluctuation theory and variational principle, noting application to heat flow in rarefied gases 12 p1974 A66-23541
- Mechanical flow processes and variational methods based on fluctuation theory, noting relations on minimum entropy production, two-dimensional laminar flow of incompressible fluid, etc 12 p1975 A66-23543
- Two branches of fluctuation theory, conventional thermostatics or equilibrium statistical mechanics and time-dependent correlation functions 12 p1976 A66-23553
- Two-time probability distribution function, autocorrelation function, Liouville equation and fluctuation theory of plasma kinetics 13 p2156 A66-26685
- Cosmic radiation intensity fluctuation in stratosphere, noting absence of explanation for anomaly 19 p3451 A66-35261
- Fluctuations effect in energy dissipation on shape of turbulence characteristics in inertial interval, using successive division of cubes 19 p3341 A66-35859
- Thermal radiation of nonhomogeneous plasma sheath, obtaining radiation intensity formula via fluctuation theory 19 p3409 A66-36
- Dielectric function for homogeneous plasma calculated, using fluctuation dissipation theorem 19 p3409 A66-36
- Atmospheric turbulence coefficient determination from flow fluctuation measuring error as function of observation duration 20 p3594 A66-38
- Chemico-physical and biological fluctuation and causality dependence on space phenomena 21 p3811 A66-38
- Necessity of fitting causality concept new experimental techniques 21 p3769 A66-38
- FLUID**
- SA ANISOTROPIC FLUID
- SA BINARY FLUID
- SA BODY FLUID
- SA COMPRESSIBLE FLUID
- SA CRYOGENIC FLUID
- SA GAS
- SA HIGH TEMPERATURE FLUID
- SA HYDRAULIC FLUID
- SA IDEAL FLUID
- SA INCOMPRESSIBLE FLUID
- SA LIQUID
- SA MAXWELL FLUID
- SA NEWTONIAN FLUID
- SA NON-NEWTONIAN FLUID
- SA REINER-RIVLIN FLUID
- SA ROTATING FLUID
- SA SUPERFLUIDITY
- SA THREE-FLUID MODEL
- SA TWO-FLUID MODEL
- SA VISCOUS FLUID
- SA WEIGHTLESS FLUID
- SA WORKING FLUID
- Spectral distribution of light scattered density fluctuations in dense monatomic one-component fluid 09 p1404 A66-20
- Free energy of pure fluids as function of thermodynamic temperature determined from measurements of internal energy noting case of carbon dioxide 12 p1981 A66-24
- Linear instability of laser propagation in fluid with coupling between light and medium 18 p3120 A66-35
- FLUID AMPLIFICATION**
- Proportional axisymmetric fluid-amplifier element, noting operation of three-term modulator and application to various amplifiers 07 p0992 A66-180
- Fluid logic and amplification - International Conference, England, September 1965 20 p3500 A66-376
- FLUID AMPLIFIER**
- Research and development progress toward synthesis of pure fluid flight control system 01 p0140 A66-100
- Fluid control and guidance system summary of available hardware 01 p0015 A66-106
- Fluid state power amplifier discussion, design, construction, operation, advantages and limitations 04 p0460 A66-137
- Fluid amplifier technology noting details on materials, uses and types, especially wa effect oscillator type 04 p0460 A66-139
- Active two-input pure fluid OR-NOR gate fabrication by logic binary-to-decimal converter [ASME PAPER 65-WA/AUT-13] 05 p0624 A66-156
- Fluidic control subsystem, describing components such as electric/fluid actuator, position transducer, operational amplifier, fluid bellows and operation characteristics [ASME PAPER 65-WA/AUT-10] 05 p0624 A66-156
- Fluidic control devices physical mechanisms, including jet-on-jet and turbulence amplifiers, vortex and boundary layer control devices [ASME PAPER 65-WA/AUT-21] 05 p0624 A66-156
- Transfer function of pneumatic capacitance of fixed gas mass in rigid walled container taking into account heat transfer during compression and expansion [ASME PAPER 65-WA/AUT-18] 05 p0624 A66-156
- Fluid state analog-computation technology and process control computation system [ASME PAPER 65-WA/PID-11] 05 p0624 A66-156



- Mathematical and control operations, utilizing fluieric components such as jet deflection type proportional fluid amplifiers, capillary-tube resistors and tank capacitors [ASME PAPER 65-WA/PID-2]
- 05 p0624 A66-15679
- Survey of fluid amplifier
- 06 p0808 A66-16226
- Fluidic devices, discussing design, equivalence to logic circuits, fluid amplifier application to build flip-flops, etc
- 06 p0809 A66-16794
- Fluidic closed-loop digital position-speed servocontrol system without moving parts, using pulsed air
- 07 p0991 A66-17878
- Fluid logic elements and amplifiers for data processing, signal amplification and guidance and control
- 08 p1199 A66-18698
- Pure-fluid amplifier in automatic control
- 09 p1331 A66-20299
- Papers on fluidics, analyzing digital and fluid amplifier design
- 09 p1331 A66-20316
- Fluid mechanics, fluidic devices and systems, noting design, manufacturing techniques and application
- 09 p1332 A66-20317
- Operation, design, application and technology of vortex devices
- 09 p1332 A66-20318
- Performance characteristics of jet deflection type proportional fluid amplifier
- 09 p1332 A66-20319
- Operational pure-fluid amplifier with negative and positive gain designed by electronic principles
- 09 p1332 A66-20320
- Digital fluid amplifiers and application, noting breadboard miniaturization
- 09 p1332 A66-20321
- Fluid digital amplifiers of axisymmetric focused jet design, based on focused-jet stabilizing effect known in ground effect vehicle aerodynamics
- 09 p1332 A66-20322
- Fluid flow and design of fluidic amplifiers, considering flow as two-dimensional and using mathematical solutions
- 09 p1367 A66-20323
- Digital application of fluid amplifiers, examining greater precision, accuracy and reliability of digital systems compared to speed of digital systems
- 09 p1349 A66-20324
- Low operating speed of pure fluid digital operating elements is chief limiting factor to application of pure fluid amplifier to feedback control system
- 09 p1361 A66-20325
- Carrier circuit techniques applied to fluid amplifier control systems
- 09 p1332 A66-20326
- Fluid amplifier analysis predictions for prime-element conceptual models and jet amplifier dynamic effects
- 09 p1333 A66-20327
- Fluid control system design and principles
- 10 p1485 A66-21511
- Fluid devices as affected by delay for signal transmission in lines, jet behavior and Coanda effect
- 13 p2062 A66-25366
- Fluid control devices
- 14 p2226 A66-27816
- Fluid devices for sensing, amplifying, controlling and logical functions in gas turbine control systems
- 15 p2572 A66-28862
- Pneumatic control systems, discussing turbulence amplification method and system with miniaturized elements with moving parts
- 16 p2636 A66-31063
- Pressure vs flow plots of orifice, tube, porous-metal and variable resistors used in fluid amplifier and logic circuit design
- 17 p2849 A66-33524
- Stream-interaction amplifiers and uses in fluidic circuits, discussing momentum exchange, pressure differential and Coanda effect
- 18 p3053 A66-33898
- Papers on fluid interaction devices
- 18 p3098 A66-34117
- Physical phenomena occurring within fluid devices, particularly pneumatic devices, considering Maxwellian distribution of velocities, ideal gas law and mean free path
- 18 p3098 A66-34118
- Fluid circuit theory, discussing setting up of electrical analogs, transfer functions, transmission line equations, wave propagation speed, etc
- 18 p3099 A66-34127
- Fluid amplifier operation characteristics, noting gain, switching circuits, power jet pressure effects, etc
- 18 p3054 A66-34128
- Beam deflection type proportional fluid amplifier, noting pressure and flow gain parameters, transfer characteristics, etc
- 18 p3054 A66-34129
- Vortex devices, describing Hillsch tube, vortex diode, triode, oscillator, pressure ratio sensor, etc
- 18 p3054 A66-34130
- Fluid interaction devices, noting induction and turbulence amplifiers, impact modulators, logic gates, inverters, etc
- 18 p3054 A66-34131
- Acoustic output, turbulence in jets and noise sources in fluid amplifiers noting design, noise reduction by jet edge, input nozzle design, forced secondary flow, etc
- 18 p3054 A66-34132
- Load characteristics and characteristic curves for proportional and bistable fluid amplifier noting output, input and dynamic effects
- 18 p3054 A66-34133
- Acoustic sensitivity and logic circuitry of fluidic turbulence amplifiers for application to laminar jet streams
- 18 p3056 A66-35012
- Variable geometry jet engine control using advanced hydromechanical, microelectronic and fluidic techniques
- 19 p3450 A66-36364
- Amplifiers using properties of vortex flow confined within flattened cylindrical chamber, considering velocity distribution
- 19 p3281 A66-36634
- Temperature sensing and control by fluidic devices, using FM and phase discrimination for gas turbine engine application
- 19 p3361 A66-36672
- Fluidic electro-fluid converter development from study of jet separation from curved surface as affected by geometry, Reynolds number and wall temperature
- 19 p3282 A66-36673
- Miniaturized no-moving-parts fluid pulse counter development for ordnance application
- 19 p3282 A66-36674
- Fluieric feedback integration and computation with design by root locus method
- 19 p3282 A66-36675
- Wall interaction digital stream amplifier with increased flow gain, impedance matching, outputs decoupled and noise reduction
- 19 p3283 A66-36812
- Steady state characteristics and transient behavior of vortex valve, examining effect of wall friction and shearing stresses due to radial velocity gradients
- 20 p3501 A66-37649
- Turbulence amplifier developed as pure fluid amplifier and logic element in which laminar jet is directed at mouth of collector tube and pressure at any input causes turbulence, reducing output to zero
- 20 p3501 A66-37653
- Operation principles of turbulence amplifiers, considering application to low cost automation, using conventional pneumatic valves and cylinders
- 20 p3502 A66-37655
- All-fluid control systems, noting achievements in vector control navigation aids and vehicle flight stabilization
- 20 p3503 A66-38263
- Fluid amplifier application to process control including turbulence amplifiers, logic function performance, etc
- 21 p3697 A66-38477
- [ASME PAPER 66-MD-8]
- High-pressure supersonic fluid amplifier design and performance, noting effect of nozzle expansion ratio on design operating pressures
- 21 p3697 A66-38485
- [ASME PAPER 66-MD-29]
- High input impedance fluid amplifier noting electric and fluid analogs, fluid triode and mathematical model of fluid FET
- 21 p3697 A66-38595
- Attitude control system/engine control system for hover control of turbojet VTOL aircraft
- 21 p3697 A66-38902
- Impact modulators using two impacting fluid jets for fluidic system design
- 21 p3698 A66-39463
- Fluidic system design of single and double airfoil amplifiers based on airfoil surface characteristics
- 21 p3698 A66-39464
- Mathematical and control operations, utilizing fluieric components such as jet deflection type proportional fluid amplifiers, capillary-tube resistors and tank capacitors [ASME PAPER 65-WA/PID-2]
- 21 p3699 A66-39529
- Main parameters of two-stage hydraulic amplifier-actuator system determined with aid of pressure and flow-rate amplification factors
- 23 p4017 A66-40970
- FLUID BOUNDARY**
- Flow of orientable fluid between coaxial cones, discussing fluid behavior for low and moderate velocity gradients
- 04 p0512 A66-14473
- Temperature distribution in fluid spherical layer enveloping gravitating sphere
- 08 p1320 A66-19485
- Free convection thermal transfer in narrow horizontal channels and infinitely wide channels
- 09 p1471 A66-20704
- Torsional oscillations of fluid sphere with rigid boundary in uniform magnetic field
- 11 p1745 A66-23007
- Behavior of system of infinite compressible fluids under gravity and magnetic field action, with MGD equations showing instability at plasma boundaries
- 11 p1748 A66-23418
- Nonsteady motion of slender body near interface between fluids of different densities
- 13 p2067 A66-26536
- Cavity depth for waterdrop impacts against water, discussing apparatus, equation for cavity depth, effect of gravitational potential energy, liquid surface behavior, etc
- 15 p2477 A66-28716
- Fluid loading effect on acoustic radiation from point-driven infinite orthotropic plate
- 18 p3251 A66-33677
- Two-dimensional non-Newtonian nonisothermal viscous liquid boundary layer flow in stagnation point proximity and flow deviations due to pressure gradient and shearing stress
- 18 p3266 A66-34637
- FLUID FLOW**
- S GAS FLOW**
- S INDUCED FLUID FLOW**
- S LIQUID FLOW**
- S RECIRCULATIVE FLUID FLOW**
- FLUID INJECTION**
- SA GAS INJECTION**
- SA LIQUID INJECTION**
- Laminar flow in two-dimensional channel with uniformly porous walls through which fluid is uniformly injected
- 05 p0662 A66-15057
- Shielding of surface from parallel thermal radiation beams by distributed injection of fluid containing absorbing particles into boundary layer flow over surface near stagnation point
- [ASME PAPER 65-WA/HT-21]
- 05 p0789 A66-15643
- Influence of suction or injection in boundary layer flow past vertical flat porous plate in presence of uniform magnetic field
- 06 p0969 A66-16181
- Surface pressure distribution on high-velocity body with large injection rate or ablation rate
- [AIAA PAPER 66-89]
- 07 p0984 A66-18455
- Axisymmetric stagnation-point boundary layer with constant shear inner layer solution
- 08 p1207 A66-19150
- Coolant injection in turbulent boundary layer for protection of surfaces from effects of high temperature and high energy gas flows
- 08 p1320 A66-19429
- Split-stream chromatographic injection parameters including optimum component velocity, column flow, mixing tube cross section, etc
- 10 p1534 A66-21294
- Thermal insulation of hypersonic blunt body by central coolant injection formation of insulating layer between body and high temperature freestream
- 10 p1481 A66-21797
- Turbulent flow process in transpiration cooling through study of uniform fluid injection along porous tube
- [ASME PAPER 65-APM-29]
- 12 p1862 A66-23969
- Velocity defect law for turbulent incompressible boundary layer with wall injection or suction
- 13 p2063 A66-25430
- Critical injection parameter on porous plate with turbulent boundary layer, noting conditions of neutralization reaction
- 16 p2684 A66-30324
- Separation streamline for massive blowing in free stream for model injected into arc tunnel flow
- [AIAA PAPER 66-457]
- 18 p3046 A66-33650
- Increasing mass flow through gas turbine without additional work from compressor and consequently increasing thermal efficiency, noting combustion problem [WSCI 66-17]
- 18 p3164 A66-34424



Tangential fluid injection for control of shock-boundary layer interaction [AIAA PAPER 66-656] 18 p3048 A66-34439

Thrust magnitude control for solid rocket by fluid injection just upstream of throat 21 p3818 A66-38699

Effect of mass injection into cavity on hypersonic boundary layer transition and on heating downstream 21 p3835 A66-38734

Shielding of surface from parallel thermal radiation beams by distributed injection of fluid containing absorbing particles into boundary layer flow over surface near stagnation point [ASME PAPER 65-WA/HT-21] 22 p3997 A66-40026

Surface pressure distribution on high velocity body with large injection rate or ablation rate [AIAA PAPER 66-89] 22 p3844 A66-40348

Secondary injection induced shock shape and vertex location solved by equivalent blunt body in supersonic flow 23 p4058 A66-41899

**FLUID JET**

SA AIR JET

SA GAS JET

SA VAPOR JET

SA WATER JET

Expansion parameters of liquids expelled into vacuum as related to orbital perturbations arising from liquid venting and impingement on adjacent hardware 10 p1481 A66-21947

Collision of opposed supersonic jets in pulse discharges, noting formation of shock-constricted plasma regions between electrodes 15 p2551 A66-29216

Convergence of axes of plane-parallel jets due to reciprocal ejection effect, analyzing deformation of jet, rarefaction coefficient for air between jets, etc 20 p3544 A66-36918

Stability of liquid Newtonian jets ejected from circular capillary tubing into stagnant air, noting influencing factors such as nozzle turbulence, velocity profile development and ambient medium properties 20 p3545 A66-37509

Munroe jet formation when small cavity or bubble in liquid is subjected to impact or shock 20 p3546 A66-37804

Hydrodynamic implosion mechanism and impact of liquid jets formed by collapsing cavitation bubbles, examining damage to solid boundaries 20 p3547 A66-37811

Impact modulators using two impacting fluid jets for fluidic system design 21 p3698 A66-39463

Lateral fluid jet visualization for spanwise launching on wing model with low aspect ratio in subsonic flow 21 p3731 A66-39593

**FLUID LOGIC**

Fluid logic elements and amplifiers for data processing, signal amplification and guidance and control 08 p1199 A66-18698

**FLUID MECHANICS**

SA AERODYNAMICS

SA CONTINUUM MECHANICS

SA GAS DYNAMICS

SA HYDRAULICS

SA HYDRODYNAMICS

SA HYDROSTATICS

SA MAGNETOHYDROSTATICS

SA THERMODYNAMICS

Collected works of Liapunov on equilibrium configurations of fluids 01 p0056 A66-10304

Fluid control and guidance systems summary of available hardwares 01 p0015 A66-10688

Book on fluid flow and heat transfer for designing, selecting, testing and installing various heat exchangers 02 p0305 A66-12240

Definition, equations, static and dynamic problems and normal and shear stress functions of subfluids 03 p0354 A66-12531

Surface instabilities discussing stability of movement of nonrigorous planar surface of liquid layer when subjected to motion in direction perpendicular to its face 03 p0354 A66-12537

Flow past fluid film-covered sphere and cylinder of given radius in different fluid, discussing external and film flow conditions 04 p0509 A66-13555

German book on theoretical fluid dynamics covering potential flow of ideal fluids and gases, viscous fluids, boundary layer theory,

hydrodynamic stability and turbulent flow 05 p0662 A66-15085

Compressibility charts for nonpolar and slightly polar substances in gaseous and liquid states and in two-phase region, using four independent parameters [ASME PAPER 65-WA/PID-1] 05 p0793 A66-15680

Physical properties of dense supercritical fluids composed of spherical molecules, noting spatial correlation 06 p0909 A66-16700

Population inversions promoted between electronic-excited states by fluid-mechanical techniques 07 p1083 A66-17937

Fluid dynamics - Symposium, Zakopane, Poland, September 1963 07 p1021 A66-18101

Class of uniform motions of continuous media and rarefied gases 08 p1210 A66-19575

Asymptotic solutions of Grad system of kinetic moments in Maxwell gas and gas consisting of molecules repelling mutually to inverse of distance 08 p1210 A66-19576

Generalized theory of physical quantities in scalar and vector form in moving reference regions 08 p1211 A66-19730

Fluid mechanics, fluidic devices and systems, noting design, manufacturing techniques and application 09 p1332 A66-20317

Flow properties of fluid through slots of micron dimension 09 p1384 A66-20752

Initial velocity and density conditions for three-dimensional boundary layer equations, noting wakes and jets 10 p1522 A66-21303

Moment stress tensor and elastic constants in statistical fluid mechanics 10 p1523 A66-21801

Turbulent vortices in quantum and classical fluid and time dependent meniscus depth of water, He I and He II 10 p1525 A66-21965

Structure of conducting and insulating liquids as affected by interatomic forces 11 p1693 A66-22979

Fluid dynamic behavior of system predicted by performing measurements on model of system 11 p1693 A66-23173

Book on basic developments in fluid dynamics including numerical solution of problems in gas dynamics, stability of parallel flows, blast wave theory, etc 12 p1861 A66-23806

Fluid flow impedance parameters and properties, discussing nonlinear orifice resistors in fluidic circuitry, tube resistance and fluid capacity 12 p1803 A66-24384

Unsteady plane motion of pointed airfoil pair, obtaining resultant force and moment of biplane 13 p2062 A66-25400

Soviet papers on fluid and gas flows 13 p2065 A66-26482

Laminar boundary layer characteristics determined by Howarth and Kochin-Loitianskii methods, using simple quadratures 13 p2066 A66-26487

Velocity profile within boundary layer region for flow of second-order fluid past symmetrical cylinder determined for nondimensional parameter formed by velocity and material constants 13 p2068 A66-26666

Fluid mechanics - Midwestern Mechanics Conference, Case Institute of Technology, Cleveland, April 1963 13 p2068 A66-26701

Forces on hovering slender body of revolution submerged under waves of moderate wavelength, considering beam seas and head seas 13 p2071 A66-26724

Constant vorticity of fluid in discontinuity region checked by method based on temperature analog 14 p2273 A66-26784

Integral equations for radial distribution functions in classical fluid 14 p2273 A66-26828

Mechanics of contained fluids in subgravity 14 p2275 A66-27558

Equiaffine geometry of double field and application to steady fluid flow theory 14 p2275 A66-27592

Integral equations derived from correlation functions, determining transport coefficients in classical fluid, formally valid to general order in density 14 p2276 A66-27635

Chemical potential and integral equation for correlation functions of classical fluids, using Percus method when functions exhibit cluster properties 14 p2276 A66-27637

Ideal conducting fluid in electromagnetic

and gravitational fields treated relativistic mechanics, using variational principles 14 p2277 A66-28101

Oscillations, gyroscopes, theory of mechanisms, fluid and gas mechanics - Union Conference, Moscow, January-February 1964 15 p2540 A66-28101

Turbulent fluid flow with consideration of structure and statistical and functional formulations 15 p2478 A66-28101

Emerson and impulse ring wave examining rigorous solution of Cauchy-Poisson problem with finite energy 15 p2480 A66-28101

Theory of transversely isotropic fluids, fluid having rigid microstructure 15 p2480 A66-28101

Asymmetrical hydromechanical fluid motion equation solutions including capillary discharge, sphere in fluid motion and suspension viscosity 16 p2689 A66-31011

Dynamic influence of orography on atmospheric motion examined, using fluid mechanics analogy with periodicity boundary condition 16 p2699 A66-31011

Progress in aeronautical sciences, noting delta wing vortex sheets, rotating flow boundary layer flows, etc 17 p2906 A66-33011

Method and equipment effects on stability measurements of hydraulic using mechanical and sonic methods 17 p2943 A66-33011

Book on theory of steady viscometric flow of non-Newtonian fluids, discussing deformation and interpretation of experiments 17 p2912 A66-33011

Discontinuous one-dimensional dissipation of perfect liquid and gas conduction magnetic field, emphasizing case where magnetohydraulic jump may occur 17 p2973 A66-33011

Fluid mechanics and heat transfer Conference, Santa Clara, June 1966 17 p3038 A66-33011

Fluid mechanical analysis of tektite origin based on hypothesis of material ejection from Earth surface in liquid jet form under meteoritic impact 18 p3227 A66-33011

Differential equation system describing nonsteady state motion of liquid in channel 18 p3097 A66-33011

Fluid dynamic field determined for growth effect machines 18 p3098 A66-33011

Fluid dynamics equations of state, motion continuity and energy stress-strain relationship and shearing stress deformations 18 p3098 A66-33011

MHD and fluid dynamics interpretation of solar wind-comet interaction 18 p3169 A66-33011

Fluid dynamic characteristics of propeller pumps in presence of oscillatory cavitation noting performance of J-2 rocket engine system [AIAA PAPER 66-559] 18 p3246 A66-33011

Book on mechanics of liquids and gases 18 p3102 A66-33011

Arbitrary motion of circular cylinders in ideal fluid near wall, using Fourier series 19 p3342 A66-33011

Fluid equations used in describing electric and ion motion perpendicular to field in slab of plasma supported against gravitational field by sheared magnetic field 19 p3417 A66-33011

Singular integral equations with constant coefficients solved by Jacobi polynomial and applied to problems in fluid dynamics crack propagation, plane elastic theory etc 19 p3393 A66-33011

Ordinary nonlinear differential equations arising in theory of both axisymmetric two-dimensional viscous jets falling under gravity 20 p3591 A66-33011

Basic properties of pure fluid development including operating pressure, operational power and response time 20 p3500 A66-33011

Kapitza papers, Volume 2, 1938-1964 20 p3603 A66-33011

Fluid mechanics model representation of solar wind and geomagnetic field interaction, noting flow parameters in shock layer and application of MHD equations 20 p3642 A66-33011

Shell immersion in moving fluid under vibrations which can be damped or amplified, analyzing instability due to constituting energy



reservoir 21 p3825 A66-38578  
 Difference approximations to PDEs of fluid dynamics used to determine necessary condition for stability, examining advective, diffusive and inertial terms 21 p3730 A66-39471  
 Flow mechanics and flow 21 p3730 A66-39498  
 Machinery 21 p3730 A66-39498  
 Turbulent vortices in quantum and classical fluid and time dependent meniscus depth of water, He I and He II 21 p3731 A66-39544  
 Equiaffine geometry of double field and application to steady fluid flow theory 22 p3900 A66-40441  
 Spontaneous ignition of inflammable fluids by hot surfaces, discussing static hot plate and wind tunnel rigs 23 p4083 A66-41278  
 Fluidmagnetic buoyancy effects in ferrohydrodynamic /FHD/ flows and implications of Ernschaw levitation theorem 23 p4057 A66-41885  
 Drop bursting by surface forces such as electric fields and fluid environments with larger viscosity 23 p4060 A66-42018  
 Turbulence in conducting medium treated by fluid mechanical approach and kinetic theory, noting energy transfers between eddies 23 p4108 A66-42033  
 Numerical solution of Bhatnagar-Gross-Krook model for shock wave structure problem, noting Chapman-Enskog approximation 23 p4061 A66-42037  
 Wave propagation, dispersion and energy transfer in arterial blood flow considered as fluid dynamics, noting finite amplitude effects in circulatory system and flow control mechanism 23 p4062 A66-42058  
 Navier-Stokes equations solutions for coefficient of viscosity tending to zero become solution to Euler equations in Cauchy problem for equations of hydrodynamics 24 p4193 A66-42232  
 Nonlinearity of governing equations of fluid mechanics, assuming fluid fluctuations are nearly normally distributed 24 p4193 A66-42283  
 Micropolar fluid theory with derivation of motion equation, constitutive equations and boundary conditions, noting channel flow 24 p4195 A66-42288  
**FLUID POWER**  
 Forced discontinuous oscillations of fluid in pipeline, discussing energy dissipation effects in LF range 04 p0509 A66-13556  
 Fluid squeeze-film damping, presenting linear analysis and approximate design equations for several damper configurations [ASME PAPER 65-WA/AUT-6] 05 p0664 A66-15706  
 XB-70 hydraulic system, describing characteristics, operation-mechanism of fluid power system, power generation, utilization and distribution 06 p0809 A66-16790  
 Fluid power, Reference 23 p4018 A66-41715  
**FLUID ROTOR GYROSCOPE**  
 Fluid stratification in floated gyroscope, estimating drift rate as function of time, geometry and flotation 23 p4066 A66-41102  
**FLUID SWITCHING ELEMENT**  
 Effectiveness of split cross-flow heat exchangers, emphasizing uniform exit temperature distribution for unmixed fluids [ASME PAPER 65-HT-24] 05 p0783 A66-14745  
 Leakage detection system for monitoring component test stand hydraulic circuit 06 p0869 A66-16792  
 Fluidic devices, discussing design, equivalence to logic circuits, fluid amplifier application to build flip-flops, etc 06 p0809 A66-16794  
 Pressure vs flow plots of orifice, tube, porous-metal and variable resistors used in fluid amplifier and logic circuit design 17 p2849 A66-33524  
 Problems of miniaturization of fluid mechanic components 19 p3343 A66-36807  
 Bistable fluid elements without moving parts for switching fluid currents show stability against load and supply pressure fluctuation 19 p3283 A66-36810  
 Binary adder and other pneumatic logic elements producing any two-valued function of three two-valued input parameter by proper arrangement of input jet nozzles 20 p3496 A66-36862

Cascade free jet logical element interactions and application to multiple-parameter logical function 20 p3496 A66-36863  
 Electrical control of boundary layer flip-flop fluidistor by disruptive discharges between electrodes producing pneumatic pressure shocks that switch output flow 20 p3501 A66-37648  
 Operation principles of fluid switches and oscillators, examining possible practical application to temperature measurement 20 p3560 A66-37651  
 AEI Airlog system for exploiting pneumatic techniques for sequential control and interlock protection of process plant and machinery 20 p3502 A66-37654  
 Operating characteristics of pneumatic bistable element using Coanda effect, examining correlation between outlet flow and pressure and feed 21 p3697 A66-38802  
 Fluidics problems involved in design and manufacturing individual elements and power consumption 21 p3697 A66-38967  
 Electric-to-fluidic and mechanical-to-fluidic transducers and sensors in fluidic system design 22 p3852 A66-40423  
**FLUID TRANSMISSION LINE**  
 Turbulent heat transport coefficient of various fluids in pipes measured, obtaining formula from experimental data 09 p1367 A66-20702  
 Turbulent heat transport coefficient of various fluids in pipes measured, obtaining formula from experimental data 11 p1688 A66-22592  
 Natural frequency of fluid oscillations in complex pipelines 16 p2687 A66-31296  
 Amplitude frequency response of blocked pneumatic lines used in fluidic systems, noting correlation to electric-pneumatic analogy prediction 19 p3372 A66-36684  
 Fluid circuit theory, discussing transmission lines, matching, pulse forming and definitions of current and voltage analogies 20 p3500 A66-37643  
 Oscillation of tubular cantilevers conveying fluid, discussing theoretical conditions of stability 22 p3994 A66-40408  
 Oscillation of tubular cantilevers conveying fluid, checking stability aspects of theory and accounting for internal and viscous damping 22 p3994 A66-40409  
**FLUID TRANSPIRATION**  
 Fluid-transpiration plasma source and liquid-cooled mechanically sealed short arc source for solar simulation 02 p0213 A66-11229  
**FLUIDIZED BED**  
 Heat transfer between fluidized bed and submerged cylinder 18 p3267 A66-35056  
 Mean absolute particle velocity in fluidized bed calculated by radioactive isotope method 18 p3267 A66-35058  
**FLUORESCENCE**  
**SA PHOSPHOR**  
**SA PHOTOLUMINESCENCE**  
 Ruby laser radiation effect on fluorescence and laser action in dysprosium doped calcium fluoride crystals 01 p0082 A66-10718  
 Optical whispering mode of polished cylinders and implication in laser technology, noting trapped fluorescent light 02 p0262 A66-12203  
 Zeeman effects in fluorescent edge emission and absorption spectra of zinc oxide platelets, noting magnetic splitting 04 p0561 A66-13724  
 Mid-day daylight intensities arising from solar ionizing radiation 05 p0748 A66-14942  
 Electron spin resonance center in ZnSe after electron bombardment measured with low temperature microwave 06 p0934 A66-17124  
 Affinity and stoichiometry of binding of 1-anilino-8-naphthalene sulfonate /ANS/ to apomyoglobin and 08 p1177 A66-18701  
 Fluorescent K-absorption and emission spectra of phosphorus in III-V semiconductor compounds 09 p1426 A66-20192  
 Fluorescence behavior of gadolinium and terbium, noting nonradiative energy transfer in borate glass 13 p2158 A66-25052  
 Spectroscopy of lithium fluoride crystals

activated with uranium trioxide for laser action, showing anomalous fluorescent decay under high intensity 13 p2092 A66-25997  
 Ionic fluorescence of europium chelates, suitability as laser materials, noting energy transfer role in population inversion 14 p2315 A66-27463  
 Fluorescence lifetime measuring technique employing pulsed or modulated RF discharges applied to emission of second positive and first negative systems of nitrogen 14 p2337 A66-27974  
 Fluorescent lifetimes of neodymium, ytterbium and samarium incorporated in ordered perovskite-type compounds determined, noting crystal structure potential for laser 14 p2367 A66-27976  
 Fluorescence of NO during photodissociation of nitrous oxide due to vacuum UV radiation 15 p2542 A66-29351  
 Absorption, photoionization and fluorescence of carbon dioxide measured in regions of strong band and continuous absorption in various spectral ranges 16 p2749 A66-30111  
 Visible spectrum of radiation release from type I supernova 16 p2796 A66-30163  
 Fluorescence bands produced by electron bombardment of ZnSe show threshold of annealing stages of radiation damage 17 p2985 A66-33154  
 Fluorescent-solid lasers design and performance noting materials 17 p2937 A66-33250  
 Two-step excitation quantum counter fluorescence in trivalent thulium ion at room temperature 18 p3152 A66-33607  
 Quantitative measurement of free metallic atoms abundance and height distribution from twilight, dayglow and aurora fluorescence 19 p3349 A66-36350  
 Low temperature optical fluorescence of ruby and vanadium doped magnesium oxide in which vibronic sideband intensity near sharp R line is measured as function of energy separation from no-phonon R line 19 p3446 A66-36395  
 Fluorescence of rare earth, actinide and transition metal ions in insulating crystals as result of optical excitation, discussing spectroscopic properties and operating characteristics 20 p3575 A66-36969  
 Fluorescence of NO during photodissociation of nitrous oxide due to vacuum UV radiation 20 p3602 A66-37356  
 Vibrational relaxation measurements in carbon dioxide, using induced-fluorescence technique 20 p3578 A66-37595  
 Ruby laser radiation effect on fluorescence and laser action in dysprosium doped calcium fluoride crystals 20 p3579 A66-37656  
 Optical properties of cryptocyanine noting transient decay of fluorescence, using ruby laser and transmission of methanol solution 22 p3932 A66-40103  
**FLUORIDE**  
**SA ALUMINUM FLUORIDE**  
**SA BARIUM FLUORIDE**  
**SA BORON FLUORIDE**  
**SA CADMIUM FLUORIDE**  
**SA CALCIUM FLUORIDE**  
**SA CESIUM FLUORIDE**  
**SA COPPER FLUORIDE**  
**SA HYDROGEN FLUORIDE**  
**SA LITHIUM FLUORIDE**  
**SA MAGNESIUM FLUORIDE**  
**SA NITROGEN FLUORIDE**  
**SA OXYGEN FLUORIDE**  
**SA PERCHLORYL FLUORIDE**  
**SA SODIUM FLUORIDE**  
**SA STRONTIUM FLUORIDE**  
**SA SULFUR FLUORIDE**  
 Recombination effects in nozzle flows of hydrogen/ fluorine rocket engines 08 p1279 A66-19152  
 Sublimation rate of iron fluoride and identification of vapor species by Knudsen technique, using mass spectrometer 11 p1651 A66-23413  
 Increasing solubility of hydrocarbons in cesium-salt fuel cell electrolyte by replacing some of carbonate anion by fluoride 14 p2226 A66-27898  
 Growth of single crystals of rare-earth fluorides for laser application, using



hydrogen fluoride atmosphere, noting ion exchange purification 16 p2779 A66-31082

FLUORINATION

Apparatus for fluoridation of hydroxyl and oxygen contaminated fluoride compounds, obtaining optically clear crystals with no Tyndall scattering for laser application 07 p1047 A66-18488

High temperature equilibria among vapor species produced by fluorination of beryllium in Knudsen effusion cell, using mass spectrometer, deriving dissociation energy 12 p1811 A66-23621

FLUORINE

Upper ignition limit for reaction of fluorine with hydrogen 09 p1338 A66-20394  
Rate of effusion for gas flow through orifice and application to fluorine gas dissociation energy 11 p1688 A66-22880

Nuclear magnetic resonance classification of alcohols and hydroxyl groups from FL-19 spectra of trifluoroacetates 15 p2447 A66-29238

Spin-rotation interaction and relaxation time of fluorine nuclei in benzotrifluoride calculated, using time-dependent perturbation theory 16 p2645 A66-30110  
Dissociation rate of diatomic molecular fluorine 16 p2646 A66-30863

Spectrum of singly ionized fluorine, tabulating forbidden transitions 18 p3064 A66-33994  
Chlorine-fluorine mixture combustion, examining flame speeds, temperatures and burned gas composition [WSCI 66-31] 18 p3263 A66-34415

Thermal dissociation of molecular fluorine in inert gas from 1650 to 2700 degrees K in shock tube coupled to time-of-flight mass spectrometer 18 p3139 A66-34501

Fluorine concentration in oxygen monitored by instrument with nickel thermoconductivity cell 20 p3511 A66-38173  
RL10 pump-fed rocket engine modified for fluorine-hydrogen application [ASME PAPER 66-MD-74] 21 p3806 A66-38501

Nonequilibrium dissociation losses in hydrogen-fluorine propellant system, indicating rate control of recombination steps [AICE PREPRINT 28A] 22 p3969 A66-39882

Radioanalysis applied to effects of ionizing radiation on volatile inorganic compounds of fluorine, oxygen and nitrogen, noting mass spectrometric peaks 23 p4032 A66-41235

Heat of formation of oxygen difluoride for reaction with hydrogen, using Parr fluorine combustion bomb containing metal ampoule employing burst diaphragm 23 p4118 A66-41238

Density, viscosity, surface tension, vapor pressure and vapor liquid equilibria data of liquid ozone-fluorine mixtures considered as Newtonian fluids 23 p4119 A66-41244

Fluorine, chlorine and other trace elements determined through differentiated photoelectric detection from Tasmania using statistical techniques, showing hydroxyl lattice sites by chlorine and fluorine 24 p4198 A66-42364

Temperature of fluorine-hydrogen flame from  $\gamma$ ,  $\theta$  band of FH vibration-rotation experimentally determined to be in agreement with theoretical figure of 3994 degrees K for stoichiometric mixture 24 p4295 A66-42992

FLUORINE COMPOUND

SA NITROGEN-FLUORINE COMPOUND  
SA ORGANIC FLUORINE COMPOUND  
Mass spectrometer measurements of oxygen fluorides at cryogenic temperatures 06 p0821 A66-16156

Photolysis of trifluoronitrosomethane in gas phase, using red light above 6000 angstroms 06 p0821 A66-16159

Photolysis of fluorotrichloromethane, using 2138 angstrom zinc lamp 06 p0822 A66-16160

Apparatus for fluoridation of hydroxyl and oxygen contaminated fluoride compounds, obtaining optically clear crystals with no Tyndall scattering for laser application 07 p1047 A66-18488

Thermal decomposition of difluorocarbene radical diluted in argon analyzed behind incident shock waves at high temperatures 12 p1811 A66-23623

Preparation of aluminum difluoramide from trimethylamine and 12 p1811 A66-23621

difluoramine 13 p2018 A66-26501  
Advanced propellant chemistry - ACS Meeting, Detroit, April 1965 23 p4116 A66-41218

FLUORINE-LIQUID OXYGEN /FLOX/

Flox-light hydrocarbon combinations desirable as liquid rocket propellants due to high specific impulse, hypergolicity and cooling properties [AIAA PAPER 66-581] 18 p3159 A66-33809

FLUORO COMPOUND

SA POLYTETRAFLUOROETHYLENE  
Gas laser output and threshold in population inversion from photodissociation of methyl iodide and fluoro iodo methylidyne 06 p0892 A66-16771

Fine structure of vibrational-rotational spectrum of difluoroborane and difluoroborane-d 08 p1178 A66-18935

Photolysis of trifluoroethylene iodide in presence of nitric oxide and oxygen 12 p1812 A66-25001  
Calorimeter bomb combustion of hydrocarbons and fluoro-substituted hydrocarbons with nitrogen trifluoride and nitrogen trifluoride-oxygen mixtures and mass spectrometric analysis 15 p2570 A66-29609

Gas laser output and threshold in population inversion from photodissociation of methyl iodide and fluoroiodo methylidyne 19 p3372 A66-35368

Isotopic exchange reactions of difluoramine with deuterium oxide and trifluoroacetic acid at low temperatures studied by NMR techniques 23 p4118 A66-41231

FLUOROCARBON

Mercury photosensitized decomposition of perfluoropropene to gain information about reactive species produced 02 p0188 A66-11595  
Mercury photosensitized oxidation of perfluoropropene to study postulated excited molecule mechanism 02 p0188 A66-11596

Silicone copolymers lubricants containing both trifluoropropyl and halophenyl substitution to cover wide temperature range [ASLE PREPRINT 65-LC-5] 02 p0237 A66-12233

Fluorocarbon oxidation and photolysis of mixtures of trifluoroiodomethane, oxygen, nitric oxide and hydroiodic acid 08 p1178 A66-19069

Silicone copolymer lubricants containing both trifluoropropyl and halophenyl substitution to cover wide temperature range [ASLE PREPRINT 65-LC-5] 12 p1889 A66-24990

Cardiovascular deconditioning from weightlessness treated by 9-alpha-fluorohydrocortisone 17 p2858 A66-32180

Fluorine wide line nuclear magnetic resonance spectrum to determine sign of spin-spin coupling constant for anisotropy of chemical shift 18 p3063 A66-33916

Stress relaxation of gamma irradiated fluorocarbon elastomers to study radiation induced chain scissions in copolymers 20 p3587 A66-37310

Prior gamma irradiation effect on thermal volatilization of vinyl and vinylidene fluoride polymers 20 p3587 A66-37311

Polymer chemistry for solid propellant binder development, examining attempts to introduce oxidants into binder structure 23 p4117 A66-41228

FLUORSPAR

S CALCIUM FLUORIDE

FLUTTER

SA BOUNDARY LAYER CONTROL

SA PANEL FLUTTER

SA SUBSONIC FLUTTER

SA SUPERSONIC FLUTTER

SA TRANSONIC FLUTTER

SA VIBRATION

Flutter, time base error and jitter analyzed in multichannel magnetic recorder, noting measurement techniques 13 p2079 A66-25662

FLUTTER ANALYSIS

Nonmathematical notes on propeller whirl flutter 02 p0300 A66-11993  
Aerodynamic damping effect on cascading double circular arc blades vibrating in transitory mode 03 p0313 A66-12397

subsonic flow at Mach numbers up to 0.7 [AIAA PAPER 65-772] 03 p0434 A66-12

Reduced stiffness responses of airplane longitudinal control, noting elevator flutter and stick-fixed dynamic longitudinal stability [AIAA PAPER 65-784] 03 p0320 A66-12

Two- and three-dimensional plates undergoing limit cycle oscillations supersonic flow treated by Von Karman large deflection theory and quasi-steady aerodynamic theory [AIAA PAPER 66-79] 05 p0774 A66-15

Reduction method for high order flutter systems based on energy compatibility equation for normalized coordinates 05 p0606 A66-15

Supersonic panel flutter using small deflection plate theory and three dimensional unsteady aerodynamic theory [AIAA PAPER 64-491] 05 p0609 A66-15

Improved numerical procedure for harmonically deforming lifting surfaces for supersonic kernel function method [AIAA PAPER 66-78] 08 p1163 A66-18

Self-excited vibrations of damped systems with traveling waves, using oscillation moving along beam resting on elastic foundation, noting flutter of plates and shells 08 p1309 A66-18

Liapunov stability criterion for panel flutter in supersonic flow derived from second method of Liapunov 08 p1310 A66-18

Stability of three-layer cylindrical shell gas stream, analyzing oscillation mode critical flutter dependence on flow resistance to transverse shear 08 p1314 A66-18

Modified strip analysis method predicting finite-span, swept or unswept wing flutter at subsonic to hypersonic speeds 09 p1328 A66-20

Stability in elastic and aeroelastic systems analyzed by Liapunov direct method 09 p1468 A66-20

Forced vibrations of two-degree-of-freedom system with combined Coulomb and viscous damping 09 p1469 A66-20

Mistuning effect on vibration of turbomachine blades induced by wakes 12 p1959 A66-23

Rate of change of eigenvalues of laminated matrix and use in flutter investigation 12 p1972 A66-24

Turbine blade vibration damping, expressing mechanical forces via method of concentrated masses 12 p1938 A66-24

Taper ratio effects on transonic flutter characteristics of series of thin cantilever wings with 45 degree sweepback and aspect ratio 4 13 p2199 A66-26

Reduction of order of aeroelastic flutter motion equations while retaining purely elastic contribution of elimination coordinates, using quasi-static assumption and matrix algebra 14 p2405 A66-27

Flutter of circular cylindrical isotropic shells 14 p2408 A66-28

Flutter conditions for finite-span hydrofoil under partial cavitation or supercavitation 16 p2688 A66-31

Flow instability of incompressible nonconducting fluid in thin cylindrical conducting elastic pipe in constant uniform magnetic field 16 p2764 A66-31

Aeroelastic stability of light aircraft examining appearance of structural nonlinearities in global vibration test determining critical flutter speed 17 p3023 A66-32

Longitudinal acceleration and angular velocity of rotation effect on flexural vibration of elongated body of revolution supersonic flow applied to critical flutter calculation 17 p3027 A66-32

Flexible and rigid hinged hydrofoils not behavior of configurations lift, drag, power input coefficients, etc 17 p2910 A66-32

Flutter of simply supported thin isotropic parallelogrammatic flat panels in supersonic flow [AIAA PAPER 66-474] 17 p3028 A66-32

Bending-torsional flutter of uniform swept wing with velocity component aerodynamic strip theory [AIAA PAPER 66-475] 17 p3028 A66-32

Supersonic flutter from vibration characteristics of trapezoidal wing with



- aspect ratio 17 p3031 A66-33073
- Flutter of rectangular orthotropic panel supported by defelectional spring along two edges in supersonic 18 p3257 A66-34590
- airflow 18 p3257 A66-34590
- Two- and three-dimensional plates in high supersonic flow undergoing limit cycle oscillations analyzed, using aerodynamic theory and von Karman large deflection plate theory 18 p3257 A66-34593
- Binary flutter of wedges in hypersonic flow according to piston theory and McIntosh derivatives 19 p3473 A66-35625
- Reduced stiffness responses of airplane to longitudinal control, noting elevator flutter and stick-fixed dynamic longitudinal stability [AIAA PAPER 65-784] 19 p3279 A66-36485
- Linearized equilibrium conditions for force densities of aircraft oscillating in flight, determining Rayleigh-Ritz equations, measuring elastomechanical parameters by vibration tests 21 p3825 A66-38579
- Common electronic techniques for studying aeroelasticity in high performance aircraft 21 p3827 A66-38654
- Flutter of infinitely long panel of finite width with upper surface exposed to inviscid flow, noting critical wavelength and flutter velocity 21 p3827 A66-38691
- Aeroelastic stability of infinite long cylinder with outer surface exposed to inviscid flow 22 p3992 A66-40338
- Characteristic equation for linear flutter problem of elastic cylindrical shell immersed in gas flow, discussing energy radiation, traveling wave propagation and discontinuity problem 22 p3995 A66-40510
- Flutter of variable geometry aircraft models as affected by airfoil sweep, pivot and wing-empennage coupling [ICAS PAPER 66-12] 22 p3996 A66-40674
- Airfoil pitching motion and flap rotational motion in two-dimensional low supersonic flow in wind tunnels 23 p4053 A66-40975
- Pulse and harmonic techniques used in flight flutter testing, emphasizing natural turbulent excitation and limitations [ICAS PAPER 66-10] 23 p4015 A66-41256
- Nonstationary flows around vibrating obstacles with application to wing flutter and to interactions of various aircraft components 23 p4012 A66-41937
- FLUX
- S ELECTRON FLUX
- S HEAT FLUX
- S NEUTRON FLUX
- S PARTICLE FLUX
- S SCALAR MAGNETIC FLUX
- S SOLAR FLUX
- FLUX DENSITY
- Luminosity distribution of radio galaxies in terms of flux density 02 p0292 A66-12189
- Electromagnetic wave scattering discussing beam trajectories, flux density decrease and radar detection in ionized trail in form of paraboloid of revolution 03 p0337 A66-13314
- Radiation of finite volume of nonequilibrium plasma, discussing integral flux parameters 04 p0552 A66-13873
- Flux density of Cas A measured, using horn-reflector antenna, response compared with output of reference-noise source 05 p0762 A66-15278
- Quasi-stellar radio source 3C 273 observed with on-off and dual-beam techniques at millimeter wavelength, noting flux variation 05 p0764 A66-15292
- Quasi-stellar radio sources 3C 273 and 3C 279 observed, using on-off and dual-beam techniques at 1 mm wavelength, computing flux densities 05 p0764 A66-15293
- Heating process in laser welding of metal sheets, taking into account energy distribution, heat transfer and flux densities 05 p0688 A66-15347
- Radio sources at 612 and 1400 mc/s and flux density for spectral index and spectral curvature parameter 05 p0769 A66-15843
- Instrument measuring field index of DC magnetic fields, particularly circular accelerators using two identical vibrating measuring coils 06 p0883 A66-16946
- Catalog of radio sources and description of Bologna radio telescope 07 p1134 A66-17527
- Jupiter microwave emission, noting brightness distribution, Van Allen belt flux density and polarization 09 p1450 A66-20105
- Simultaneous observations of Jupiter on three frequencies, noting phase consistency of flux variations, Faraday rotation and flux density 09 p1450 A66-20108
- Lunar X-ray detectability, noting generation by solar wind electron bombardment and flux intensity 09 p1459 A66-20885
- Radio galaxies luminosity, size, shape, distribution in space, and continuum flux densities from normal galaxies 10 p1601 A66-21060
- Switching properties of partially set square-loop ferrite core, noting flux level influence, measurement techniques, etc 10 p1508 A66-21413
- Revised equation for thermokinetic phenomena under Fourier relationship, considering certain finite time is required for development, noting role of flux density 12 p1973 A66-23526
- Observable properties of normal relativistic world models and steady state world model defined by parameters depending on cosmological constant and present mean density of universe 12 p1946 A66-23652
- High resolving power interferometric observations of angular diameters of anomalous high flux density HF radio sources 12 p1950 A66-24390
- Solar radio observation at 600 mc frequency during 1961 at French station, noting flux density and solar daily variation 13 p2188 A66-26322
- Absolute calibration of solar radio flux density at 1000, 2000 and 3750 mc, using newly constructed standard horns 13 p2189 A66-26568
- Flux density, polarization characteristics and position measurements for type IV bursts in meter and microwave range 14 p2378 A66-26933
- Radiation of finite volume of nonequilibrium plasma, discussing integral flux parameters 14 p2343 A66-27575
- LF spectrum measurements of radio source 3C84, including plot of flux density vs frequency 14 p2384 A66-27846
- Electromagnetic wave scattering, discussing beam trajectories, flux density decrease and radar detection in ionized trail in form of paraboloid of revolution 14 p2242 A66-28287
- Heating process in laser welding of metal sheets, taking into account energy distribution, heat transfer and flux densities 15 p2511 A66-29989
- Potential difference across type II superconductor in intermediate state attributed to fields produced by quantized flux lines moving through material 16 p2768 A66-30129
- Jupiter decametric radio emission spectrum noting power at various frequencies, mean flux density, magnetic pole locations, etc 16 p2801 A66-30922
- Flux density variations in quasi-stellar radio source CTA 102 16 p2807 A66-31755
- Efficiency criterion for flux density of electric current and energy for isotropic semiconductor in absence of magnetic field 16 p2789 A66-31790
- Flux density of nonthermal radio sources at 8000 mc noting measurement correction, correlation between curvature index spectral index and component separation 17 p2995 A66-31911
- Solar magnetic field measurements noting magnetic flux, development of bipolar magnetic region, etc 17 p2996 A66-31918
- Limb darkening measurements of Venus at 8-14 microns with 200 inch Hale telescope 17 p3002 A66-32517
- Error analysis of absorbed energy flux density and ignition exposure time data, accuracy, precision and confidence limit estimates for arc image furnace ignition experiments [AIAA PAPER 66-669] 18 p3261 A66-34224
- Primary cosmic ray energy spectrum measurements via Proton I satellite, noting inelastic interaction cross sections, chemical composition, etc 18 p3175 A66-34746
- Solar radio activity in 1963, discussing daily flux density, mean variations, etc 19 p3458 A66-35467
- Spectra of nine discrete radio sources in 20-40 mc/s range 19 p3459 A66-35491
- Dual beam technique and antenna used to observe variations in flux of radiomsource 3C 273 20 p3650 A66-37344
- Interferometric observation of flux densities of solar radio emission at 4000 mc/sec and relationship to 27-day recurrence tendency of summation of planetary 3-hour indices 20 p3634 A66-38214
- Vela satellite measurements of particles in solar wind and distant geomagnetosphere, noting measurement of energy spectra, flux density and directional distribution of positive ions in solar wind 20 p3639 A66-38315
- Radio astronomy measurements requiring absolute intensity calibrations, noting flux densities and measurements of very dark areas of sky 21 p3815 A66-39484
- Radio source flux density relation to antenna temperature studied, using antenna integral and convolute integral 22 p3862 A66-39814
- Conformal mapping to determine shape and field distribution of shim used to modify field in air gap between pole faces of electromagnet 24 p4239 A66-43211
- FLUX MAPPING
- SA FLOW MEASUREMENT
- Heat-transfer coefficient for annular dispersed flows in absence of vaporization, explaining high values obtained by flux profile effect 12 p1973 A66-23523
- Spectral and vertical distribution of atmospheric IR radiation flux divergence for five model atmospheres, noting dependence on sighting angle 12 p1874 A66-24868
- Magnetization of synthetic filamentary superconductors, discussing sample preparation, critical field and transition temperature effect on flux jumping and magnetic hysteresis loop 13 p2157 A66-25037
- Electron-positron components of primary cosmic radiation, noting energy spectrum, flux, charge composition, origin, etc 18 p3176 A66-34748
- Flux gate magnetometer for interplanetary magnetic field measurements 19 p3356 A66-35674
- Superconducting properties of Nb-Zr alloy, discussing resistive transition, ultrasonic attenuation, flux jump magnetic instabilities, etc 21 p3796 A66-38550
- Flux flow in type II superconductors, measuring critical current, longitudinal and transverse voltages for varied orientation of magnetic field 21 p3802 A66-39201
- Spectral and vertical distribution of atmospheric IR radiation flux divergence for five model atmospheres, noting dependence on sighting angle 22 p3912 A66-40329
- Interference between deformed plane wave and reference wave in coherence, obtaining transfer function of objective, using holography 23 p4067 A66-41178
- FLYBY MISSION
- Manned Venus and Mars flybys and Mars landings using only Saturn-Apollo hardware 02 p0290 A66-12067
- Flyby landing excursion mode compared with standard manned planetary stopover missions [AIAA PAPER 66-36] 06 p0953 A66-16414
- Manned interplanetary flight, emphasizing nonstop flybys past Mars and Venus, reviewing launch and departure modes, energy requirements, environmental control, navigation spacecraft power source, etc 08 p1286 A66-18561
- Conceptual unmanned spacecraft designs for Jupiter exploration including flyby and orbiter missions [AIAA PAPER 65-388] 14 p2394 A66-28176
- Technical feasibility of 1975 manned flyby mission to Eros and examination of lesser bodies of solar system 14 p2390 A66-28411
- Mars and Venus manned interplanetary flyby missions 16 p2808 A66-30368
- Jupiter swingby missions to outer planets [AIAA PAPER 66-536] 16 p2805 A66-31502
- Matched asymptotic expansions and patched conics used to simplify flyby interplanetary trajectories [AIAA PAPER 65-689] 19 p3462 A66-35895
- Interplanetary manned spacecraft maneuvers including perihelion brake, off-perihelion acceleration and retromaneuvers and heliocentric planet-approach maneuvers [AIAA PAPER 65-695] 19 p3462 A66-35902
- Guidance, navigation, propulsion and course



correction specifications for Mars or Venus  
manned flyby missions 20 p3596 A66-37226  
Transfer paths to Mars via Venus  
compared with direct flight, discussing  
direct free fall transfer, flyby and free fall  
transfer 20 p3651 A66-37392  
Mars data transmission difficulty in long-  
life Mars flyby and orbiter and Earth-return  
mission 24 p4277 A66-42666  
Repeated close Venus flybys and several  
close solar approaches incorporated in same  
mission 24 p4278 A66-42687  
Conceptual design and parametric  
evaluation of advanced Mariner flyby  
bus/lander mission to Mars in 1969 and 1971  
launch opportunities 24 p4282 A66-42690  
Jupiter swingby missions to outer planets  
[AIAA PAPER 66-536] 24 p4279 A66-42797

## FLYING

## S HIGH ALTITUDE FLYING

## S HIGH SPEED FLYING

## FLYING PERSONNEL

## SA AIRCREW

## SA ASTRONAUT

## SA PILOT

Electrocardiography as related to flying  
personnel including case  
histories 01 p0019 A66-10605

Functional subsystem analysis in  
Instructional System Approach to transition  
training of flight crews 23 p4030 A66-41579

## FLYING PLATFORM

## SA GROUND EFFECT MACHINE

One-man lunar Rover craft design and  
performance, considering bipropellant rocket  
powered platform kinesthetically controlled  
by astronaut 08 p1303 A66-18822

Aircraft as platform for solar eclipse  
observation, discussing history, project  
APEQS, navigation problems, aircraft used,  
etc 16 p2705 A66-30822

Movable platform and differential throttle  
control configurations for lunar manned  
flying vehicle 24 p4284 A66-42954

## FLYING PLATFORM STABILITY

Aircraft stabilization for solar eclipse  
observation, emphasizing use of autopilot for  
maximum control 16 p2743 A66-30823

## FLYWHEEL

Small scale MHD fluid flywheel attitude  
control systems applied to deep space  
probes, suitable for overcoming cyclical  
additions of angular rate to satellite of 10  
revolutions per day 16 p2811 A66-31253

Control system and loading of magnetically  
driven flywheels for three-dimensional  
satellite orientation 18 p3243 A66-33857

Motion of solid body with rotating  
flywheels rotating at constant velocities  
relative to inertial space and  
body 22 p3948 A66-40682

## FOAM

## SA COLLOID

## SA POLYURETHANE FOAM

Gaseous diffusion in polymeric foam and  
experimental results, using closed cell  
polyurethane foam 13 p2112 A66-25304

## FOAMED MATERIAL

Rigid polyurethane foam encapsulation of  
high-voltage aerospace electronic systems,  
noting vacuum effect 02 p0248 A66-11292

Structural analysis and experimental  
verification of sandwich panels with thin  
plastic-film facings and foam-plastic cores  
under compression and bending  
loads 03 p0437 A66-12769

Thermal conductivity of formed-plastic  
composite insulation systems for liquid  
hydrogen storage tank  
[AICE PREPRINT 22D] 22 p3997 A66-39893

## FOCUS

## S IMAGE CONTRAST

## FOCUSING

Focusing effects estimated for radio  
propagation along ricochet trajectory,  
considering ionospheric  
refraction 04 p0482 A66-13860

Self-focusing of longitudinal  
electromagnetic waves in nonlinear plasma  
in strong magnetic field 09 p1343 A66-20343

Generalized equation for steady state  
motion of electrons in cylindrical  
electrostatic system with arbitrary cross  
section, calculating critical focusing  
current 11 p1735 A66-22493

Weakly focusing transparent media  
properties and guided transmission of  
coherent light beams with relatively small

loss 11 p1657 A66-23091

Self-focusing of light from Kerr effect and  
changes in density of  
matter 13 p2167 A66-25109

Optical ray tracing to predict focusing  
characteristics of laser light in refractive  
targets, calculating heating effects in target,  
noting target geometry, refractive index,  
thickness of skin layers,  
etc 13 p2090 A66-25531

Coherent light recording/reproducing  
techniques based on Debye theory of  
coherent light source  
focusing 13 p2091 A66-25541

Fringe field double focusing magnetic  
spectrograph, noting resolution, solid angle,  
energy range, astigmatic lens,  
etc 13 p2083 A66-26551

Vector synchronism and second-harmonic  
light generation in focused  
beams 14 p2307 A66-27191

Accelerator with nonlinear spiral focusing,  
approximating size of stability region,  
adiabatic damping, transverse phase stability  
and perturbations effect 14 p2347 A66-28309

Focusing of long cylindrical electron beam  
by means of short-period permanent magnet  
or long-period reversed field  
magnet 15 p2467 A66-29709

Self-focusing of light from Kerr effect and  
changes in density of  
matter 16 p2745 A66-30288

Ideal and perturbed focusing conditions  
effect on spread of immersed flow  
beam 17 p2971 A66-32821

Focusing molecules in states losing energy  
with applied field, using alternate gradient  
technique 24 p4239 A66-43037

Vector synchronism and second-harmonic  
light generation in focused  
beams 24 p4226 A66-43089

Refraction due to acoustic focusing of  
sound waves in lower troposphere, noting  
effect of wind profile 24 p4203 A66-43108

## FOG

Visible and IR radiation attenuation by  
artificial fogs found to depend on droplet  
size and distribution 01 p0097 A66-10860

Effectiveness of meteorological radar in  
determination of range of meteorological  
visibility in fog 02 p0252 A66-11272

Angular volume-scattering functions  
measured as function of scattering angle for  
natural fogs in atmosphere, using coherent  
and incoherent radiation 02 p0262 A66-12211

Atmospheric model applied to fogs forming  
in valley bottoms and data acquisition in  
connection with this  
phenomenon 03 p0389 A66-12705

Kennington method tested for forecasting  
time of clearance of radiation  
fog 03 p0389 A66-12890

Occurrence of supernumerary fogbows at  
subfreezing temperatures, noting interval of  
appearance and possible formation  
mechanism 09 p1400 A66-20733

Fog and low stratus clouds studied, using  
Tiroso VII photographs of North Pacific  
fog 11 p1728 A66-22323

Possible use of IR radiation to improve  
visibility through fog, including atmospheric  
attenuation effects and radiant energy  
source 16 p2740 A66-30088

Readout technique for laser fog  
disdrometer 17 p2927 A66-33346

Cloud and fog droplet spectra  
rearrangement due to external conditions  
calculated from distribution function of  
water content 20 p3594 A66-38374

Blowing system effect on fog dispersion  
over limited area 20 p3595 A66-38380

Fog transmittance attenuation factor,  
comparing photometric values and values  
calculated from microstructural observations,  
using flow trap 21 p3759 A66-38917

Dispersion of supercooled fogs over airports  
by seeding with dry ice  
[ICAS PAPER 66-7] 23 p4086 A66-41255

## FOIL

## SA METAL FOIL

Diffusion creep rate of thin foil of pure  
polycrystalline material 12 p1971 A66-24925

## FOIL BEARING

Externally pressurized foil gas bearings,  
employing successive approximations method  
to solve Reynolds equation for fluid and  
equilibrium equation for foil  
[ASME PAPER 65-LUB-1]

04 p0526 A66-142

## FOKKER F-27 AIRCRAFT

Netherlands Nationaal Lucht-en  
Ruimtevaartlaboratorium /NLR/ activities  
discussing production of Fokker F-27 and  
28 aircraft and other  
projects 07 p1017 A66-17

## FOKKER F-28 AIRCRAFT

Fokker F-28 Fellowship shorthaul  
passenger aircraft 06 p0807 A66-17

Netherlands Nationaal Lucht-en  
Ruimtevaartlaboratorium /NLR/ activities  
discussing production of Fokker F-27 and  
28 aircraft and other  
projects 07 p1017 A66-17

## FOKKER-PLANCK EQUATION

General 13-moment approximation  
Fokker-Planck equation for  
plasma 04 p0558 A66-14

Scattering of test particle by enhanced  
electric field fluctuations in plasma  
containing nonthermal  
electrons 05 p0721 A66-14

Coulomb collision effect on transverse  
electron oscillations in fully ionized  
plasma determined by Fokker-Planck  
equation 05 p0721 A66-14

Transient processes in vacuum tube  
oscillator synchronized by small harmonic  
signal with random initial phase in presence  
of noise 09 p1357 A66-20

Weak collisions effect on ion wave  
instability in cesium plasma solved by  
linearized Fokker-Planck  
equation 10 p1568 A66-21

Linear and nonlinear oscillators randomly  
perturbed, using Fokker-Planck equation  
with application to nuclear  
reactors 11 p1721 A66-22

Nonlinear servomechanism analyzed, using  
Fokker-Planck equation, discussing tracking  
failure 11 p1670 A66-23

Numerical dynamic predictor for complex  
systems disturbed by random noise  
discussing Fokker-Planck equation, Crank-  
Nicolson difference model,  
etc 11 p1680 A66-23

Relaxation of isotropic distribution of  
particles in homogeneous background  
including nonzero temperature  
effects 11 p1741 A66-23

Correlation functions of amplitude and  
intensity fluctuation for laser model near  
threshold obtained by using distribution  
functions evaluated by Fokker-Planck  
equation, treating amplitude as random  
variable 12 p1892 A66-24

Stability of phase-locked loops using  
Fokker-Planck equation and under additive  
stationary white Gaussian noise linearized  
about some equilibrium  
point 13 p2025 A66-24

Tracking interruption probability in second-  
order astatic system, obtaining solution from  
Fokker-Planck equation and computer  
simulation 14 p2265 A66-25

Solution of stochastic differential equation  
with Markov coefficients by reduction to  
nonrandom PDE of Fokker-Planck  
type 14 p2324 A66-25

Fokker-Planck equation of wave  
propagation in medium with regular  
random inhomogeneities, determining spatial  
angular distribution function of  
ray 14 p2245 A66-25

High energy solar proton propagation in  
interplanetary magnetic field by Fokker-  
Planck equation 15 p2575 A66-26

Hydromagnetic, resistive and  
microinstabilities in plasmas, noting parametric  
collisions and effect and validity of Maxwell  
Vlasov equations with Fokker-Planck  
collision term 19 p3417 A66-30

Diffusion of protons in outer radiation belt  
due to violation of third adiabatic invariant  
for trapped particles 20 p3640 A66-31

Pitch angle diffusion perturbing relativistic  
electrons in Van Allen zones and violating  
adiabatic invariants of electron motion  
using Fokker-Planck  
equation 20 p3641 A66-31

Fokker-Planck equation applied to electron  
under influence of quantum fluctuations  
connected with dissipation, pumping in  
cavity thermal noise, noting distribution  
correlation function 21 p3746 A66-31

Langevin treatment for linear, nonlinear  
stationary and nonstationary random noise



processes compared with Markov methods 21 p3771 A66-39107

Transient processes in vacuum tube oscillator synchronized by small harmonic signal with random initial phase in presence of noise 22 p3873 A66-39834

**FOLDING STRUCTURE**

SA BALLOON

SA PARACHUTE

SA PARAGLIDER

Advances attributable to XB-70 program including aerodynamic concepts, structural material, design, systems and equipment development [SAE PAPER 650798] 01 p0012 A66-10844

Folded antennas, discussing Franklin array and current distribution via equivalent circuit analysis and application for TV transmission and reception 20 p3530 A66-37712

**FOOD**

**S NUTRITION**

**S SPACE FOOD**

**FOOD INTAKE**

Bite-size foods included in feeding study of man exposed for 56 days to oxygen-helium atmosphere 18 p3061 A66-33775

Nutritional evaluation of feeding bite-size foods to man exposed for 56 days to oxygen-helium atmosphere 18 p3061 A66-33776

**FORBIDDEN BAND**

Thermoelectricity decrease of bismuth-telluride based solid solutions due to forbidden bandwidth and majority and minority carrier mobility 01 p0127 A66-11029

Temperature dependence of effective mass and influence of two-phonon processes on mobility in semiconductors with narrow forbidden bands 04 p0565 A66-14263

Radiative recombination in silicon containing structural defects in lattice 04 p0569 A66-14353

Quantum effects in theory of space charge layer in semiconductors, noting electron and hole density 04 p0570 A66-14366

Electron spectrum in highly alloyed gallium arsenide 05 p0730 A66-14650

Gallium arsenide recombination-radiation spectrum discussing effects of impurities on short wave radiation band energy 05 p0731 A66-14657

Enhanced intensity of forbidden lines of neutral oxygen in 28 planetary nebula spectra linked to lower ionization levels 05 p0759 A66-14874

High resolution absorption spectrum of nitrogen in fourth and fifth orders from 1060 to 1520 angstroms 05 p0763 A66-15284

Mechanism for indirect phototransition in semiconductors near natural absorption edge when interacting with current carriers 07 p1105 A66-18373

Calculation of intensity and polarization of forbidden lines of Fe XIII ion in solar corona in presence of nonradial magnetic field 08 p1287 A66-18640

Efficiency of drift-type semiconductor photocell 09 p1358 A66-20816

Bipolar excitation of photoconductivity in silicon due to structural disarrangement caused by IR radiation 10 p1583 A66-22019

Indium antimonide optical absorption shift, forbidden band narrowing and tin alloying induced by neutron bombardment 10 p1587 A66-22150

Pressure induced change in energy gap and forbidden bandwidth of lead telluride 10 p1587 A66-22152

Width variation of forbidden band of Si in electric field of p-n junction 10 p1588 A66-22160

Transition of group IV elements to metallic state confirmed as equivalent to generation of intrinsic current carriers 11 p1759 A66-23447

Electron spectrum in highly alloyed gallium arsenide 13 p2167 A66-25925

Gallium arsenide recombination-radiation spectrum, discussing effects of impurities on short wave radiation band energy 13 p2167 A66-25932

Electric fields in hydrogen plasma leading to forbidden free-bound transitions, considering photodetachment of electrons and radiative capture cross sections 13 p2135 A66-26265

Recombination radiation of strongly

arsenic-doped germanium, noting narrowing of forbidden band 14 p2358 A66-27080

Radiative recombination in silicon containing structural defects in lattice 14 p2368 A66-28251

Quantum effects in theory of space charge layer in semiconductors, noting electron and hole density 14 p2369 A66-28265

Temperature dependence of mean ionization energy changes in germanium and silicon samples exposed to X-rays caused by changes in forbidden bandwidth 16 p2788 A66-31782

Energy levels in forbidden band of gallium arsenide alloyed with silver or gold, determining impurity levels from temperature dependence of electric conductivity and Hall constant 16 p2789 A66-31791

Spectroscopic measurements of cold plasma charged particle concentrations, specifically spectral broadening due to Stark effect, forbidden-line intensities affected by internal electric fields and autoionization line intensities 18 p3143 A66-34032

Theoretical transition probabilities of forbidden lines and unobserved lines of ions in solar corona 18 p3230 A66-34151

Iron and nickel lines in solar UV spectrum, abundance of various metallic elements in solar atmosphere, electron collision cross sections and oscillator f-values of electron transitions 18 p3237 A66-35050

Twin boundary effect on measurements of phonon momentum propagating through Ge bicrystal p-layers at liquid nitrogen temperatures 19 p3438 A66-35482

Indium antimonide optical absorption shift, forbidden band narrowing and tin alloying induced by neutron bombardment 19 p3440 A66-35764

Pressure induced change in energy gap and forbidden bandwidth of lead telluride 19 p3440 A66-35766

Width variation of forbidden band of Si in electric field of p-n junction 19 p3440 A66-35774

Monograph on synthesis and properties of refractory semiconducting materials having large forbidden bandwidth and prepared from element of groups III and V 19 p3448 A66-36731

Electrical properties of indium antimonide single crystals with noncompensated impurity concentration, determining position of deep-seated levels in forbidden band 21 p3799 A66-38929

Dynamic characteristic theory of long diode with base containing impurity atoms producing deep energy levels in forbidden zone 22 p3961 A66-39827

Recombination radiation of strongly arsenic-doped germanium, noting narrowing of forbidden band 22 p3967 A66-40836

Behavior of lambda 6300 angstrom Fraunhofer absorption line in solar spectrum 22 p3984 A66-40850

Hartree-Fock parameters for intermediate coupling compared with those obtained from observed energy levels for C I sequence 23 p4130 A66-41814

**FORBIDDEN TRANSITION**

Forbidden absorption spectrum of ionized iron in solar absorption ascertained with high resolution direct intensity recordings 02 p0286 A66-11353

Forbidden regions produced by two spatially separate point dipoles with parallel axes 14 p2361 A66-27412

Forbidden transitions in atomic systems induced by uniform and nonuniform intermolecular electrical fields in plasma 16 p2786 A66-31562

Spectrum of singly ionized fluorine, tabulating forbidden transitions 18 p3064 A66-33994

Electric quadrupole transition in fourth positive system of CO observed in bands of electric dipole allowed transition 19 p3404 A66-36800

Capture effect on I-V characteristics of junction diodes and injection coefficients in forbidden transition zone 23 p4045 A66-41444

**FORBUSH DECREASE**

Intercalibration of cosmic ray neutron monitors at nine European sea level stations and deduction of daily latitude effect in 1963 01 p0132 A66-10321

Fine structure of energy spectra of Forbush decrease and dependence on solar cycle 01 p0132 A66-10336

Primary Forbush effect dependence on latitude and time from worldwide data on neutron component of cosmic rays 02 p0281 A66-11331

Magnetic storm accompanied by Forbush decreases taking into account atmospheric temperature, noting cyclonic storm origin 02 p0282 A66-11338

Forbush decrease in cosmic radiation spectra as function of solar activity 02 p0283 A66-12113

Increase of cosmic ray intensity during Forbush decrease 06 p0948 A66-16582

Primary cosmic ray variations and Forbush decrease in solar-cycle change 07 p1122 A66-17988

Secular trend of cosmic ray intensity in stratosphere and primary cosmic ray energy spectrum based on 3000 radiosonde measurements 07 p1123 A66-17993

Intensity variation of heavy nuclei in primary cosmic radiation during times of solar disturbances 07 p1123 A66-17996

Changes in rigidity spectra of primary cosmic radiation during Forbush decreases and 27-day variations 07 p1125 A66-18003

Hysteresis effect in long term variation in cosmic radiation, investigating whether such effect appears during short term /Forbush/ decreases 07 p1125 A66-18004

Variation spectrum stability of Forbush decrease and small cosmic ray flare during intensity recovery, noting electric field effect, calculation methods, etc 07 p1129 A66-18023

Forbush decreases in intensity of cosmic rays analyzed from data obtained from stratospheric radiosondes at geomagnetic latitudes 51 and 41 degrees N 09 p1437 A66-20209

Anomalies in cosmic ray intensity increase during period of Forbush decrease 09 p1438 A66-20214

Solar diurnal and semidiurnal variations during Forbush decreases based on neutron recordings, noting near and distant source 11 p1762 A66-22427

Cosmic ray variations and solar corpuscular stream in interplanetary space during March 1958 magnetic storm 12 p1940 A66-24164

Relation between Forbush decreases and magnetic storms, examining spatial distribution of predecrease moments relative to sudden commencements 12 p1941 A66-24171

Forbush decrease in cosmic radiation spectra as function of solar activity 14 p2377 A66-28072

Astronomical model study of physics of penetration of interstellar cosmic rays into solar system 18 p3168 A66-34342

Spherical harmonic analysis to obtain latitude dependence of diurnal variations and changes with time during Forbush decrease 18 p3183 A66-34792

Twenty Forbush decreases with amplitude greater than 4 percent in neutron intensity 18 p3184 A66-34796

Rigidity dependence of Forbush decreases, using underground meson intensity measurement 18 p3184 A66-34797

Solar cosmic ray disturbances in stratosphere measured by balloon-borne radiosondes 18 p3185 A66-34800

First-order cosmic ray modulation, namely production by Sun, diurnal anisotropy, 11-yr cycle and Forbush decrease 18 p3186 A66-34810

Modulation data for primary cosmic ray spectrum at low rigidities determined from daily latitude curves of cosmic ray nucleonic component obtained from IGY neutron monitors 18 p3194 A66-34860

Forbush decreases using meson and nucleon component records in study of sudden commencements during periods between cosmic ray storms 20 p3632 A66-38070

Forbush decreases associated with magnetic events not definitely accepted as



storm sudden  
 commencements 20 p3632 A66-38071  
 Cosmic ray storms, difference in Forbush decrease recovery in nucleon and meson component 20 p3632 A66-38072  
 Cosmic ray meson component distribution with time plots of particle flux revealed characteristic disturbances accompanying sudden commencements of geomagnetic storms associated with Forbush decreases 20 p3632 A66-38074  
 Uppsala IGY-neutron monitor multiplicity measurements indicate increase of attenuation coefficient with increasing multiplicity 20 p3632 A66-38079  
 Transient anisotropic cosmic ray increase during recovery phase of Forbush decrease due to reflection from receding blast wave and co-rotating shock wave formed during explosive heating of solar corona 23 p4123 A66-41687

**FORBUSH EFFECT**  
 Book on geo- and heliophysical effects in cosmic rays and auroras 02 p0280 A66-11329  
 Forbush decrease characteristics in cosmic ray intensity 02 p0280 A66-11330  
 Excessive cosmic radiation absorption in lower nocturnal ionosphere at middle geomagnetic latitudes during Forbush effects 04 p0514 A66-13443  
 Cosmic radiation studies in U.S.S.R during IGY noting 11-year variations, Forbush effect, solar particle propagation, etc 05 p0749 A66-15232  
 Relation between Forbush decreases and chromospheric flares, obtaining longitudinal distributions before and after onset, using statistics 05 p0753 A66-15394  
 Changes in solar cosmic ray and geomagnetic field intensities during magnetic storms accompanied by decrease in galactic cosmic ray intensity, using moving averages method 05 p0753 A66-15395  
 Increase with latitude of Forbush effects and secular variations in cosmic ray intensity explained by worldwide data obtained with meson detectors 05 p0754 A66-15398  
 Magnetic storm accompanied by cosmic ray intensity increase analyzed, considering Forbush effect and determining all peaks 05 p0755 A66-15403  
 Cosmic radiation measured by neutron monitor in Antarctic during enhanced solar activity in September 1963, determining flares connected with particles producing Forbush effects 07 p1118 A66-17642  
 Solar corpuscular stream effect on magnetic storms and Forbush effect 07 p1121 A66-17985  
 Cosmic ray intensity measured during geomagnetically quiet and active days from 1959 to 1963 by using balloon flights, noting role of ionization, Forbush effect, etc 07 p1124 A66-18000  
 Forbush effect and region of decreased cosmic ray intensity extending from Earth to Sun 07 p1129 A66-18024  
 Expected rigidity spectrum of variations in framework of dynamic piston model of Forbush effect 09 p1438 A66-20213  
 Energy dependence of transparency of walls of transition region shell obtained from Forbush effects, in connection with cosmic ray intensity 09 p1439 A66-20221  
 Cosmic ray variations analysis based on IGY and IGC data, discussing diurnal variations, cosmic ray burst, Forbush effect and existence of interplanetary magnetic field and of solar magnetic traps 12 p1940 A66-24161  
 Forbush, geomagnetic interaction, cosmic ray variation and solar corpuscular flux effects during magnetic storms in period of maximum solar activity 12 p1940 A66-24165  
 Abrupt increase in cosmic ray intensity coinciding with presence of Forbush effects, noting dependence on geographic latitude and cut-off rigidity, obtaining energy spectra 12 p1941 A66-24168  
 Forbush effect and solar cosmic ray manifestation of effect of compression of Earth magnetosphere 12 p1941 A66-24174  
 Cosmic radiation, interplanetary magnetic field, solar proton propagation long-term /solar cycle/ modulation of intensity, Forbush effect and daily intensity variation 18 p3175 A66-34741

Solar particles generated during small chromospheric flares 18 p3184 A66-34799  
 Anisotropy of Forbush effect in ascertaining structure and intensity of interplanetary magnetic field 24 p4272 A66-43159

**FORCE**  
 SA AERODYNAMIC FORCE  
 SA CENTRIFUGAL FORCE  
 SA CENTRIPETAL FORCE  
 SA ELECTROMOTIVE FORCE  
 SA G FORCE  
 SA INERTIAL FORCE  
 SA LIFT FORCE  
 SA LORENTZ FORCE  
 SA MEMBRANE FORCE  
 SA PONDEROMOTIVE FORCE  
 SA STRAIN  
 SA STRESS  
 SA TORQUE  
 SA TORSION  
 SA VAN DER WAALS FORCE  
 Matrix force analysis for calculating stresses and deflections in partitioned complex structures 16 p2820 A66-31324  
 Closed loop control system combined with air beating technology for measurement of multicomponent microforces 20 p3555 A66-36870

**FORCE DISPLACEMENT INDICATOR**  
 Calibration problem of load-measuring instruments solved, using automatic digital voltmeter [ASTME PREPRINT IQ66-705] 12 p1882 A66-24412  
 Design and function of air bearings, measuring displacement force of system checking by autocollimation method 13 p2085 A66-25074

**FORCE DISTRIBUTION**  
 SA NORMAL FORCE DISTRIBUTION  
 Simplified method for verifying previously calculated bar forces in plane trusses extended to three-dimensional structures 10 p1616 A66-21492  
 Lifting body with controllable radial force, examining acceleration and deceleration, equation of motion, target hitting accuracy improvement via force variation, etc 11 p1733 A66-23338  
 Three-dimensional statically indeterminate frame with rigid modes, noting effect of bending moments for shifting forces 13 p2207 A66-26498  
 Tangential electrode forces on cathode and anode electrode for arc moving in magnetic field are not negligible in plasma driving 15 p2428 A66-28687  
 Concentrated forces on shells, discussing load distributions and pressure variations 23 p4142 A66-41957  
 Series solution to problem of spherically isotropic elastic medium bounded by concentric spherical surfaces, noting force and stress concentration 24 p4285 A66-42141

**FORCE FIELD**  
 Finite collision time for artificial celestial body moving under influence of Newtonian force from attractive center 01 p0137 A66-10794  
 Terrestrial gravitational potential determined by observation of satellite motion, assuming trajectory is determined solely by force field 03 p0428 A66-13027  
 Motion stability of linear continuous systems noting influence of various forces 03 p0438 A66-13094  
 Experimental viscosity of dissociating system nitrogen tetroxide and nitrogen dioxide, obtaining force constants for Lennard-Jones potential having no effect on viscosity of gas mixture 06 p0823 A66-16635  
 Particle distribution and motion in field of force, discussing density profile, energy dissipation, Coulomb charge shielding for local thermodynamic equilibrium and free orbital motion 08 p1261 A66-18743  
 Satellite orbit evolution under effect of small perturbing force with constant magnitude and direction 08 p1298 A66-19570  
 Motion stability of gyroscope in universal suspension with spring restraints and damper in gravitational field extended to include Newtonian central force field 08 p1226 A66-19582  
 Vehicle motion parameters in Newtonian central force field determined, using geometrical structures devised from

properties of velocity  
 hodograph 08 p1226 A66-19584  
 Equations of motion of gyrost at having fixed point and gyrost at rotating about fixed point in Newtonian force field 08 p1227 A66-19761  
 Plane optimum transfer of point of variable mass between two elliptical orbits in centrally directed Newtonian force field 11 p1774 A66-23036  
 Turbulent heat transfer effect on gas stratification in field of Archimedes forces 12 p1979 A66-24429  
 Nonrelativistic force in simple magnetizable fluid derived from thermodynamic information about energy and power 12 p1915 A66-24655  
 Force field detection and control of objects in space, using gravitational electrostatic or magnetostatic fields 12 p1820 A66-24677  
 Relations among vibrational frequencies of isotopically substituted molecules when only one Cartesian coordinate of any atom is involved in motion, obtaining general valence-force-constant matrix 14 p2336 A66-27377  
 Motion of material point in central force field, reducing problem to solution of boundary value problem based on Pontryagin maximum principle, using analog computers 14 p2245 A66-28282  
 Differential equation of motion of two variable-mass points in central force field 15 p2538 A66-29042  
 Motion of constant relative kinetic motion gyrost at through force field 15 p2502 A66-29333  
 Integrability of motion equations for rigid body motion about fixed point in Newtonian force field 15 p2542 A66-29333  
 Servomechanism design, noting optimum response parameters, physical characteristics as functions of inertia, external force, energy dissipation, kinetic energy, operation, etc 16 p2671 A66-31061  
 Shape and stability of liquid-gas interface in annular tank in force field determined by numerical integration of boundary value problem and eigenvalue [AIAA PAPER 66-425] 16 p2689 A66-31481  
 Second-order optimal elliptical orbital transfer trajectory between two coplanar circular orbits in Newtonian force field 17 p3003 A66-32583  
 Inertial navigation system theory that uses increased numbers of newtonometers/force measuring devices/ in place of gyroscopic sensitive elements 17 p2926 A66-32803  
 Single-impulse transition in Newtonian central force field from hyperbolic to elliptical orbit in case of radial impulse 19 p3455 A66-35277  
 Stability of bending-torsional equilibrium of cantilevered bar subjected at end to follower force, as in case of wing under jet determining critical thrust 19 p3475 A66-36433  
 Motion of arbitrary gyrostabilizer in central Newtonian force field, applying Liapunov stability conditions for regular precession 19 p3362 A66-36843  
 Rarefied gas motion instability, constructing general solution for effect of various force fields 19 p3343 A66-36843  
 Nonlinear ODE of radial motion of body in nonlinear central force fields, considering drag effects 21 p3773 A66-39433  
 Intermediate-thrust arcs in central force field satisfying optimality conditions, noting that motions are degenerate solutions of Euler equations 22 p3980 A66-40466  
 Optimum trajectory of pulsed coplanar orbital transfer in central Newtonian force field with restrictions placed on distance to attracting center 22 p3980 A66-40466

**FORCE-FREE MAGNETIC FIELD**  
 Force-free paramagnetic model and force-free Bessel function model of stability of feeble pinch, presenting numerical calculations using Newcomb criterion 13 p2144 A66-25722  
 Force-free magnetic fields generated by orthogonal current systems in unbounded conducting fluid 18 p3151 A66-35033  
 Motion of isolated energetic charge particle in simple force-free magnetic field with rectilinear lines of



- Force 19 p3400 A66-35925
- FORCE LINE**
- Reconnection of magnetic lines of force to form closed loops during transient phase of rotation of spheres and cylinders from rest 12 p1868 A66-23857
- FORCED CONVECTION**
- Forced convection vaporization of Freon 113 flowing in horizontal Pyrex tube examined, using motion pictures 01 p0165 A66-10910
- Liquid cooling on semiconductor devices noting natural convection, nucleated boiling, forced convection and forced convection with boiling 02 p0203 A66-11922
- Forced motion of viscous liquid heated nonuniformly from below and subject to nonlinear basic temperature profile 02 p0219 A66-11958
- Forced convective heat transfer from isothermal and nonisothermal uniformly spinning bodies of revolution obtained by similar flow analysis [ASME PAPER 64-WA/HT-15] 04 p0595 A66-13387
- Free convection on laminar forced flow heat transfer in horizontal circular tube [ASME PAPER 65-HT-23] 05 p0783 A66-14744
- Flow stability in multitube forced convection vaporizers, using Freon 113 in closed test loop with five-tube boiler [ASME PAPER 65-HT-61] 05 p0786 A66-14762
- Combined free and forced convection flows with heat and mass transfer in laminar boundary layers on vertical surfaces 07 p1150 A66-17579
- Unsteady, combined free and forced convective MHD channel flow of conducting fluid through transverse magnetic field 07 p1085 A66-17580
- Annular flow and two-dimensional forced convective boiling heat transfer to hydrogen in nucleate and film boiling regimes 08 p1316 A66-18832
- Increased mass transfer from flat plate caused by wake from cylinders located near boundary layer edge 08 p1211 A66-19682
- Forced convection problem for steady fully-developed laminar flow in straight channel when fluid properties are functions of temperature 09 p1366 A66-20175
- Saturated and surface film boiling from horizontal isothermal plate in longitudinal flow field analysis, based on two-phase boundary layer theory, correlating heat transfer and skin friction characteristics 12 p1980 A66-24908
- Heat-transfer coefficients calculated for forced convection from heated flat plate at zero incidence to stream of viscous fluid, noting role of Reynolds number 12 p1981 A66-24945
- Unsteady laminar forced and free convection in coaxial sector tubes in presence of constant axial temperature gradient, accounting for oscillation and resonance 13 p2210 A66-26719
- Forced convection heat transfer in symmetrical ducts when fluid is liquid metal, examining new prediction methods for engineering analysis and design 16 p2824 A66-30304
- Pressure and temperature measurements obtained from closed loop, forced convection boiling and condensing processes under zero gravity 16 p2826 A66-30490
- Free convection on laminar forced flow heat transfer in horizontal circular tube [ASME PAPER 65-HT-23] 16 p2828 A66-30983
- Heat transfer of forced laminar convection in multiply connected regions 16 p2830 A66-31708
- Forced convection heat transfer for liquid metal flow in rectangular channels with prescribed wall heat fluxes and heat sources in fluid stream 17 p3038 A66-33468
- Forced convection heat transfer coefficient of single pin fixed on plate, deriving expression for case corresponding to infinite circular cylinder 18 p3266 A66-34647
- Forced convection caused by normal and longitudinal components of flow around hot wire, noting effect of wire length 20 p3544 A66-36928
- Data correlations on forced-convective heat transfer to cryogenic fluids by nucleate, film and transition region boiling 20 p3677 A66-37098
- Integral solution of laminar film condensation with combined gravitational-type body force and forced convection concurrent and parallel to surface 20 p3678 A66-37118
- Laminar forced convection heat transfer to gas from circular tube, achieving boundary condition of uniform heat flux 20 p3679 A66-37508
- Laminar forced-convective heat transfer for dissipative fluid in tube bounded by concentric circles 21 p3837 A66-39610
- Similar solutions for laminar boundary layer under forced convection of mixture of fluids with constant mass density and temperature and composition dependent parameters for flat plate analysis 23 p4059 A66-42007
- FORCED OSCILLATION**
- Laboratory vibratory stand for calibrating sensors of oscillatory motion 01 p0070 A66-11020
- Graphical method for investigating forced oscillations in nonlinear systems with piecewise linear characteristics 01 p0159 A66-11175
- Forced discontinuous oscillations of fluid in pipeline, discussing energy dissipation effects in LF range 04 p0509 A66-13556
- Steady states of mechanical system using perturbation method, assuming primary and secondary oscillators are tuned to single pulse, each involving Duffing type nonlinearity 04 p0545 A66-14169
- Pressure response to forced oscillation of shallow cylindrical porous chamber [ASME PAPER 65-WA/FE-9] 05 p0780 A66-15730
- Pressure phase angle and frequency for forced oscillations of small porous chamber [ASME PAPER 65-WA/FE-8] 05 p0685 A66-15731
- Nonlinear forced oscillations in phase automatic frequency control system, accounting for nonlinearity of system 07 p1001 A66-17353
- Forced oscillations of elastohydrodynamic systems, using Rabotnov functions as kernels of integral operators, permitting description of creep curves for materials 08 p1307 A66-18884
- Steady state sound disturbances induced in monatomic gas by oscillating plane boundary 11 p1737 A66-22904
- Forced oscillations of ferrite core circuit, showing phase characteristics and parameters of inductance and amplitude 12 p1958 A66-23725
- Forced oscillations of coaxial multidisk rotors, allowing for gyroscopic effect and rotating at different angular velocities determined by replacing differential equations with integral equations 12 p1964 A66-24050
- Transition probabilities of nitrogen-nitrogen collision obtained with time-dependent wave functions of forced harmonic oscillator and by numerical methods 13 p2131 A66-25384
- Secondary motion generation in vortex field, noting vortex core deformation by oscillation, radial perturbation effect on vorticity distribution, etc 13 p2070 A66-26715
- Forced oscillations of three-layer plate used as vibration dampers for engine components 14 p2400 A66-27696
- Optimum parametric damping of forced oscillations when random external force operates on circuit 15 p2469 A66-28674
- Numerical problems in application of Urabe results in considering periodic nonlinear differential systems, obtaining Galerkin approximations 16 p2737 A66-31231
- Design of adaptive systems with forced oscillations, using correlation and filter methods 17 p2902 A66-32573
- Distribution function, harmonic and statistical linearization methods applied to study forced oscillations in nonlinear oscillatory system 17 p2959 A66-32801
- Force resonance oscillations of one degree of freedom system with randomly time varying natural frequency 17 p2959 A66-32802
- Forced oscillations of gyroscopic tachometer with dry friction analyzed by Zhelyazkov theorems 17 p2928 A66-33496
- Gyrochamber radial rigidity effect on amplitudes of forced oscillations of gyroscope with dynamically unbalanced rotor 17 p2928 A66-33497
- Traveling waves interaction in gas laser, explaining forcing-of-oscillations and traveling wave suppression effect 18 p3119 A66-34685
- Parameter-plane method analysis of nonlinear equations of asymmetric oscillations in adaptive feedback control systems 19 p3338 A66-36740
- Electromagnetic wave absorption in nonuniform plasma cylinder in presence of forced oscillations 21 p3781 A66-39009
- Necessary conditions for subharmonic and superharmonic synchronization in weakly nonlinear systems that permit energy exchange between response at excitation frequency and close to resonance frequency 21 p3772 A66-39355
- Haag general synchronization theory for oscillating systems with one degree of freedom applied to boundary value problems for multivibrating systems 21 p3774 A66-39607
- Approximate solution of forced oscillation PDEs of rectangular orthotropic plate on elastic base with two characteristics 23 p4139 A66-41557
- Nearly-periodic oscillations in nonlinear systems having periodic coefficients and subject to external periodic force 23 p4141 A66-41947
- Oscillations of nonlinear system with one degree of freedom caused by periodic force and with random variation in natural frequency 24 p4237 A66-42446
- FORCED VIBRATION**
- Beam forced vibration with harmonically time-variant motion produced by uniformly distributed load, assuming one boundary condition is nonlinear 01 p0157 A66-10926
- Transverse vibrations of viscoelastic shaft fixed at one end and supporting mass subjected to sinusoidal force at other 01 p0158 A66-11080
- Forced vibration of system with polygonal hysteresis loops in presence of constant force 01 p0159 A66-11174
- Forced vibration in nonlinear system with Coulomb and combination friction 01 p0159 A66-11176
- Parameter and matrix solution techniques for analyzing forced vibrations response of damped multidegree of freedom systems [AIAA PAPER 65-786] 03 p0438 A66-13070
- Steady state response of damped cylindrical sandwich shell under radially symmetric time harmonic pressure [ASME PAPER 65-WA/UNT-1] 05 p0779 A66-15601
- Forced vibrations of two-degree-of-freedom system with combined Coulomb and viscous damping 09 p1469 A66-20950
- Forced vibration function for stresses and displacements in viscoelastic thick-walled cylinder case-bonded to thin shell, noting pressure and strain effect [AIAA PAPER 65-173] 10 p1617 A66-21784
- Mechanical forced vibrations encountered in aviation, assessing physiological and neurophysiological effects including visual acuity 10 p1493 A66-22128
- Exact solution of wave field of point vibrator operator on free plate in form of elastic strip, comparing theory and measurement 11 p1780 A66-22605
- Mistuning effect on vibration of turbomachine blades induced by wakes 12 p1959 A66-23796
- Transient motion of simple mechanical systems using vectors as alternative to finding equivalent control system and solution by root locus method 12 p1971 A66-24975
- Multiple force generator for vibration testing large packages which minimizes problems of mobility, isolation and alignment 16 p2677 A66-30457
- Forced aperiodic vibrations in idealized viscously damped system, subjected to parametric excitation by forcing function with uniformly accelerating frequency and constant displacement amplitude 16 p2678 A66-30460
- Small transverse vibrations of linearly viscoelastic Timoshenko beam of incompressible material, detailing free and forced vibration 17 p3024 A66-32361



Forced motions of hollow cylinder encased in thin elastic shell and subjected to time-harmonic pressure at inner surface of cylinder 18 p3259 A66-35026

Error estimates for difference methods in forced vibration problems 20 p3589 A66-36901

Characteristic phase-lag method for analyzing forced response of damped systems used in optimal multipoint excitation 21 p3824 A66-38568

Steady state response of damped cylindrical sandwich shell under radially symmetric time harmonic pressure [ASME PAPER 65-WA/UNT-1] 21 p3832 A66-39530

Linearized potential theory for forced vibration of continuous self-exciting plate on hinged support in supersonic flow, investigating parametric resonance frequencies relation to coupling of eigenfunctions 22 p3995 A66-40508

Panel flutter analysis via forced vibration technique noting frequency coalescence, flutter boundary and experimental technique [AIAA PAPER 66-769] 22 p3895 A66-40650

Transient response of lightly coupled nonlinear two degree of freedom systems subject to forcing 23 p4091 A66-41696

Steady state free and forced vibration response of beams supported on nonlinear springs of Duffing type 23 p4140 A66-41913

Free and forced vibration effect on drift of gyroscope supported in gimbals 23 p4071 A66-41981

Input signal level for stability loss or self-oscillations in automatic control system, using analysis for nonlinear systems with forced vibrations 24 p4188 A66-42476

**FORCED VIBRATORY MOTION EQUATION**

Forced oscillations in nonlinear relay type control system predicted via periodic solutions to nonlinear difference equation 05 p0654 A66-14606

Forcing function acting upon rigid body rotating about fixed point replaced by motion of axis of rotation and another forcing function 08 p1310 A66-19158

Amplitude calculation of forced mass vibrations in damped linear mechanical system from column matrices of oscillation modes of eigenfrequencies 11 p1783 A66-23018

Forced solutions for Van der Pol-Duffing equation in first harmonic approximation 13 p2129 A66-26337

Amplitude ratio of two forced vibrations for asymmetric shaft rotor excited by periodic external force 16 p2714 A66-30811

**FORECASTING**

**S PREDICTION THEORY**

**S STATISTICAL FORECASTING PROJECT**

**S WEATHER FORECASTING**

**FORGING**

Estimation of die loads in impact forging of axially symmetric disks and flat slabs [ASME PAPER 65-WA/PROD-1] 05 p0691 A66-15636

Forging techniques for vacuum hot-pressed unclad beryllium metal billets, noting temperature effect 08 p1230 A66-18845

Ausforging, process of plastically deforming austenitic steel at high temperatures, without recrystallization and prior to transformation 13 p2107 A66-25639

Newer titanium alloys compared with present production alloys from closed die forgings in typical airframe and engine configuration 14 p2317 A66-28011

Forging methods for reliably producing unalloyed molybdenum forgings with high impact strength for rocket nozzle application 19 p3366 A66-36107

Evolution of tungsten forging processes, discussing warm-forming, ring-rolling and combination forging methods 19 p3366 A66-36108

Fabrication process for turning cast Cb-10W-10Ta alloy ingots into large-diameter rings by forging and ring rolling 19 p3366 A66-36111

**FORM FACTOR**

Electromagnetic form factors of electron and muon neutrinos evaluated, using intermediate vector-boson theory, noting renormalization induced by electromagnetic interactions 15 p2544 A66-28944

**FORM PERCEPTION**

**SA PERSPECTIVE**

Visual perception of forms and relevant factors 04 p0462 A66-13796

**FORMALDEHYDE**

**SA PHENOL FORMALDEHYDE**

Molecule reorientation and transition probability in molecular beam maser using formaldehyde 22 p3929 A66-39662

**FORMAMIDE**

**S AMIDE**

**FORMATION**

**S CRACK FORMATION**

**FORMATION ENERGY**

Concentration dependence of thermodynamical functions of interstitial solid solutions, calculating energy of formation 08 p1258 A66-18897

Devitrification of glass around collapsed bubbles in tektites, noting formation mechanism 11 p1773 A66-22962

Thermodynamic and physical properties of beryllium hydroxide at four temperatures in 1567-1808 degrees K range, with computation of free energy of formation 14 p2370 A66-27372

**FORMATION HEAT**

Alloy junction formation, discussing spectral characteristics of electroluminescence from forward-biased 4H SiC p-p alloy junctions as function of formation temperature 04 p0497 A66-13982

Composition and combustion products of boron at 300 to 3200 degrees K and heat of formation of boron oxide 16 p2830 A66-31604

Nitrate heat of formation value revised by re-evaluating lattice energy of cesium nitrate, considering charge distribution in anion 23 p4031 A66-41221

Heat of formation of perfluoroammonium ion estimated from thermochemical correlations and compared with estimates by means of Kapustinskii approximation for lattice energies 23 p4031 A66-41222

Heat of formation of oxygen difluoride for reaction with hydrogen, using Parr fluorine combustion bomb containing metal ampoule employing burst diaphragm 23 p4118 A66-41238

Heat of pyrolysis of resin in silica-phenolic ablator determined from combustion calorimetry measurements of heats of formation 23 p4150 A66-41892

**FORMING**

**SA COLD FORMING**

**SA ELECTROFORMING**

**SA ELECTROHYDRAULIC FORMING**

**SA EXPLOSIVE FORMING**

**SA HOT FORMING**

**SA MAGNETIC FORMING**

**SA METAL FORMING**

**SA MOLECULAR FORMING**

**SA ROLL FORMING**

**SA STRETCH FORMING**

Silicone alumina low temperature low-pressure plastic molding technique for precision forming of ceramic materials for aerospace structural application 10 p1538 A66-21130

Chemical and electrical energies in manufacturing noting role of numerical control, hydrostatic processes, forming, electrochemical machining, etc 24 p4217 A66-42336

**FORMULA**

**S BETHE-HEITLER FORMULA**

**S RECURSION FORMULA**

**FORSTERITE**

**S SILICATE**

**FORTRAN**

Integrated modular digital computer system for ICETRAN/ICES-FORTRAN/programming of engineering problems 12 p1827 A66-23833

Subroutines and functions of BE VISION, package of FORTRAN programs for drawing orthographic views of combinations of plane and quadric surfaces 15 p2510 A66-29770

Flight Load Survey program, written in Fortran IV, for accurate and rapid sounding of wind-induced loads on aerospace launch vehicle [AIAA PAPER 66-470] 16 p2811 A66-31473

Fortran program for finding minimum value of monotonic function defined on ordered sets of positive integers 19 p3309 A66-36044

**FORTRAN II ASSEMBLY PROGRAM /FAP**

Optimizing procedures using Fortran FAP programming on IBM 709/70 computers, comparing eight known techniques 19 p3308 A66-3580

**FORWARD SCATTER**

Plasma ion and electron temperature measurement via forward scattering spectrum of deuterium plasma 18 p3146 A66-3420

Tropopause detection by radar, examining detection of high altitude clear-air turbulence by radar and forward-scatter techniques 22 p3912 A66-4030

**FOSTER THEORY**

Coordinate transformation for synthesis network functions, considering matrix equation used in Foster form realization RC driving point impedance 02 p0207 A66-1140

Distributed RC network synthesis determining necessary and sufficient conditions for driving point impedance frequency response of transfer function and Foster type realizations 11 p1678 A66-2370

**FOUNDATION**

**S STRUCTURAL FOUNDATION**

**FOUR-BODY METHOD**

Solar influence on libration point satellite motion for 2500 days in vicinity of Earth-Moon system [AIAA PAPER 65-88] 02 p0288 A66-1140

Intermolecular forces for two-, three- and four-bodies and those in liquid or condensed medium 06 p0911 A66-1610

Stability of spacecraft motion in Earth-Moon system near equatorial libration point 16 p2810 A66-3150

Libration point motion in restricted four-body problem and stable trajectories determination for Earth-Moon-Sun system noting effect of initial configurations system [AIAA PAPER 65-684] 19 p3461 A66-3580

**FOURIER ANALYSIS**

Invalidity of Walkinshaw method for calculating periodically loaded waveguide under certain conditions 04 p0496 A66-13982

Sufficient conditions for containing modulus of Fourier indices of almost periodic solution of nonlinear almost periodic system 05 p0709 A66-1500

Jittered sampling obtaining error bounds for sample independent and correlated jitter and bandpass sampling 06 p0865 A66-1610

Harmonic analysis of periodic sequence of pulses, using Fourier analysis 07 p1001 A66-1700

Fourier analysis, used to determine particle size, strains and faulting, applied to silver films evaporated onto glass substrates at different residual gas pressures 09 p1383 A66-2020

Transient behavior of varactor bridge doubler examined, using direct digital integration of circuit equations 10 p1513 A66-2140

Kinetic approximation of electromagnetic surface wave propagation in infinite plasma sheath solved by Fourier method, noting resulting dispersion equation 11 p1743 A66-2240

Conditions on Fourier coefficients of function  $f(x)$  sufficient to be of bounded variation 11 p1723 A66-2300

Necessary and insufficient conditions for well-posed Cauchy problems verified by Fourier analysis 13 p2118 A66-2500

Sufficient conditions for containing modulus of Fourier indices of almost periodic solution of nonlinear almost periodic system 16 p2735 A66-3000

Plasma wave quasi-linear theory, noting nonlinear effect treatment via distribution function, electric field, Fourier components, decay, etc 17 p2966 A66-3200

Fourier analysis determination of optimum efficiency of cavity-controlled Gunn-effect oscillator when bias voltage is almost constant times voltage 20 p3527 A66-3700

Sidereal diurnal variation of high-energy cosmic radiation, noting parameters of anisotropy coefficient, cosmic ray source distribution and air shower measurements 20 p3631 A66-3700

Invalidity of Walkinshaw method for calculating periodically loaded waveguide



- under certain conditions 20 p3532 A66-37869  
 Modulation and demodulation for probabilistic coding, noting error chances and interrelations affecting performance of communications system 21 p3707 A66-39636  
 Dimensional filtering in IR technology for background noise elimination, discussing Fourier analysis treatment of system 21 p3768 A66-39646  
 Maximum permissible error in radiation patterns calculated by Fourier analysis of near field measurements of antennas 22 p3861 A66-39716  
 Semiconductor conductivity in strong SHF electric fields, measuring dielectric constant and Fourier component 23 p4068 A66-41620  
 Line shape of RF dimensional effect in metals showing correlation with electromagnetic wave attenuation in skin layer 24 p4172 A66-42528
- FOURIER-BESSEL SERIES**  
 Concentric ring antenna arrays with low sidelobes, estimating currents from Fourier-Bessel series 06 p0825 A66-16017
- FOURIER LAW**  
 Revised equation for thermokinetic phenomena under Fourier relationship, considering certain finite time is required for development, noting role of flux density 12 p1973 A66-23526  
 Electrical analogy for turbulent liquid metal heat transfer in noncircular duct entrance region, solving Fourier equation, determining fluid boundary conditions, temperature distribution, etc 13 p2210 A66-26717
- FOURIER SERIES**  
**SA GIBBS PHENOMENON**  
 Kinetic theory of Lorentz plasma in rotating magnetic fields and electromagnetic fields based on Boltzmann equation 01 p0113 A66-10640  
 Estimates in Stepanov metric of deviation of uniform almost periodic function with bounded spectra from S-almost periodic functions 01 p0094 A66-10649  
 Sufficient conditions for transformation sequence exhibiting Gibbs phenomenon when using triangular methods of Fourier series summability 02 p0250 A66-12106  
 Class of periodic functions for which given method of summation gives trigonometric approximation of optimal order 03 p0388 A66-12713  
 Generalized convolution theorems of periodic functions based on Fourier series formalism used to study processes in linear systems 04 p0506 A66-14402  
 Synthesis method for linear time-varying systems, discussing integral formulation and approximation functions 05 p0654 A66-14609  
 Approximation of continuous function by typical mean of Fourier series 05 p0709 A66-15357  
 Extreme properties of operator which degenerates to trigonometric polynomials in case of periodic functions 05 p0709 A66-15358  
 Sampling representations of band limited deterministic signals obtained, using nonharmonic Fourier series 06 p0861 A66-16194  
 Linear methods of summation of Fourier-Laplace series 06 p0902 A66-16229  
 Coefficient properties and absolute convergence of Fourier series of periodic function 06 p0902 A66-16230  
 Proof of two theorems concerning convergence of Fourier-Lebesgue series 06 p0903 A66-16902  
 Approximation theorem and uniqueness theorem for abstract equations with almost periodic coefficients 07 p1056 A66-17603  
 Convergent series representation of system of measurable functions that are complete and orthonormalized 07 p1060 A66-18251  
 Von Karman-Donnell large-displacement equations for thin circular cylindrical shells extended by considering larger term numbers in Fourier series representing radial displacements after buckling 08 p1309 A66-19143  
 Fourier analysis of modulation products in nonlinear device output and optimum frequency conversion for n-frequency input 09 p1396 A66-20639  
 Necessary and sufficient condition for matrix distribution to have positive-real Laplace transform 09 p1396 A66-20641
- Floquet form of solution to system of linear differential equations with periodic parameters 09 p1363 A66-20798  
 Text for senior undergraduates, using Fourier series and integral transforms to discuss standard differential equations of mathematical physics 09 p1397 A66-20917  
 Short-pulse scattering by simple geometric shapes useful for heuristic models of electromagnetic scattering, illustrating creeping-wave return 10 p1500 A66-21618  
 Secondary flows in turbine cascades, obtaining correlations between velocity distributions and circulations along span by expanding Fourier series 11 p1632 A66-22664  
 Linear system dynamics, discussing time function vector space, spectral coefficients, orthonormal and transfer functions, parameter variation, Fourier approximation, etc 11 p1679 A66-23269  
 Spherical summability of Fourier series of function integrable on unitary group 11 p1723 A66-23360  
 Self-equilibrating bending of complete circular cylindrical shells described by first harmonic terms of Fourier series for displacement components 12 p1962 A66-24004  
 Estimates in Stepanov metric of deviation of uniform almost periodic function with bounded spectra from S-almost periodic functions 12 p1903 A66-24020  
 Inverse Laplace transformations in terms of Laguerre functions 12 p1905 A66-24654  
 Fourier representation for Markov chains and strong ratio theorem 12 p1905 A66-24820  
 Digital calculation of transient one-dimensional heat flow confirms accuracy of small and large Fourier number approximations 12 p1981 A66-24998  
 Electromagnetic scattering by circular wire loops loaded with lumped impedances, obtaining solution to integral equation by Fourier series 14 p2247 A66-26863  
 Radiation impedance of infinite planar dipole array, phased for any angle of radiation, calculated by Fourier series expansion of field in plane waves 14 p2247 A66-26865  
 Modulation theory, discussing phase-envelope relation for band limited wave in terms of Fourier series 14 p2234 A66-27032  
 Thermal stresses in finite cylinder with prescribed temperature distribution on curved lateral surface and with ends in contact with smooth insulating plates 14 p2400 A66-27725  
 Radiation characteristics of vertical dipole in warm plasma, expressing vector potential functions in Fourier integrals 14 p2240 A66-27916  
 Summation of Fourier series associated with integrable function  $f(x)$ , using weighted averages of partial sums 15 p2529 A66-29848  
 Integral expression for coefficients of Fourier series attached to nonintegrable function 15 p2529 A66-29853  
 Closed-loop automatic control system with unvalued substantially nonlinear element, using approximation of characteristics by Fourier series 16 p2669 A66-30754  
 Fractional powers of linear operators role in linear and nonlinear elliptic and parabolic equations, Fourier series in eigenfunctions of elliptic operators, etc 16 p2736 A66-30978  
 Book on bending theories of sandwich plates including use of Fourier series, stress-strain state, trigonometry, deflection theory, etc 16 p2818 A66-31100  
 Polynomials orthogonal with respect to contours, examining analytic function representation via Fourier series expansion of such polynomials 16 p2738 A66-31409  
 Continuous functions with given differential properties on perfect measure set and application to Fourier series 16 p2740 A66-31799  
 Fourier series convergence domain of perturbation function in restricted three-body problem representing planetary configuration 17 p2995 A66-31845  
 Uniform harmonic summability of Fourier series and conjugate series 17 p2947 A66-32840  
 Fourier series of Gegenbauer function, examining convergence characteristics 18 p3126 A66-33696  
 Asymptotic expression for difference between continuous periodic function and typical mean of Fourier series 18 p3128 A66-35013  
 Arbitrary motion of circular cylinder in ideal fluid near wall, using Fourier series 19 p3342 A66-36468  
 Photometry of flux from surface and representation as Fourier series of time dependence of received reflected flux for torse of convex curvature 20 p3556 A66-36937  
 Fourier series solution to electromagnetic wave diffraction on metallic gratings with anisotropic dielectric 20 p3512 A66-37148  
 Exact solution of thermoelastic problems in two dimensions, using doubly infinite Fourier series 20 p3673 A66-38276  
 Thermal stresses in flat rectangular isotropic plate of constant thickness under arbitrary and no temperature variation in terms of Fourier series and integrals 21 p3832 A66-39443  
 Local approximation of continuous periodic function by Fourier series 24 p4231 A66-42513  
 Fourier analysis of Riemann-Hilbert problem of diffraction of normally incident plane electromagnetic wave by plane metallic grid above dielectric sheet and semiminfinite plasma 24 p4175 A66-42978
- FOURIER TRANSFORM**  
 Elements of eclipsing binary spherical stars determined from Fourier transforms of their light curves by defining characteristic functions of system 02 p0285 A66-11298  
 Steady state problems in orthotropic slabs subjected to forces and temperature distribution on faces solved by Fourier transform [ASME PAPER 65-APMW-33] 04 p0593 A66-14233  
 Representation of analytical periodic Fourier transforms of difference operators by sum of squares 05 p0708 A66-15328  
 Effect produced on pulse by manipulating transform zeros 06 p0861 A66-16191  
 Book on Fourier transform spectrometry detailing interferometers and programming procedures 06 p0908 A66-16225  
 Length of compact function estimated from noisy measurement of modulus of Fourier transform 06 p0867 A66-16977  
 Linear time-invariant systems, noting relation between transient response duration and differential equation coefficients 06 p0867 A66-16990  
 Time-normalized Fourier transform of sampling function of stationary random process as bounded nonstationary random function of frequency 08 p1200 A66-18908  
 Statistics of product of Gaussian noise process and pseudorandom binary code 09 p1342 A66-19919  
 Geomagnetic micropulsations, noting diurnal patterns of phase difference, propagation medium dispersive characteristics, signal velocities, etc 10 p1529 A66-21151  
 Harmonic suppression ratios in RF amplifiers calculated, using circuit parameters and applying Fourier transformations 10 p1508 A66-21299  
 Landau damping and velocity Fourier transform of initial perturbation in longitudinal plasma oscillations 10 p1567 A66-21817  
 Elastic strip and elastic annulus differential-difference equations, using Fourier transforms and analytic continuation 11 p1780 A66-22439  
 Resolution and noise in Fourier transform spectrometer, considering mechanical limitations and diffraction effects 11 p1705 A66-22869  
 Steady state problems in orthotropic slabs subjected to forces and temperature distribution on faces, solved by Fourier transform [ASME PAPER 65-APMW-33] 12 p1960 A66-23973  
 Fourier transform of time-dependent density-density correlation function calculated from linearized Boltzmann equation for Maxwell molecules 12 p1917 A66-24584  
 Pattern synthesis method for linear array using integral mean of Fourier approximation 12 p1841 A66-24628  
 Cesaro summability and Fourier transform



for evaluating divergent series and integrals occurring in circuit design and analysis 12 p1856 A66-24730

Bandlimited and approximately bandlimited signals by Fourier transforms of sampling function and prolate spheroidal wave function representing solutions of second order self-adjoint differential equations 13 p2120 A66-26077

Differential equilibrium equations for shallow shells of constant curvature under effect of concentrated load, using Fourier transform 13 p2205 A66-26440

Temperature field of infinite plate with variable temperature at one edge determined, using double Fourier integral transform 14 p2411 A66-27166

Response of thin cylindrical monopole antenna to DC pulse excitation computed, using Fourier transforms, noting correlation between empirical and theoretical values 14 p2255 A66-27906

Equilibrium binary correlations in classical relativistic homogeneous electron gas 14 p2336 A66-28275

Fourier transform spectroscopy, history and current status 15 p2498 A66-28838

Time jitter due to inherent noise when sampling intervals in Fourier transform spectroscopy by interferometer, examining effects and elimination methods 15 p2499 A66-28849

Representation of analytical periodic Fourier transform of difference operators by sum of squares 16 p2735 A66-30966

Two-dimensional correlation time relation to spectral bandwidth and corresponding one-dimensional quantities of Lampard 16 p2671 A66-31336

Anisotropic nonhomogeneous linear viscoelasticity analogy with thermal stresses in terms of Fourier transform 17 p3020 A66-31998

Infinite helical sheath antenna driven by ring delta-function generator analyzed, using Fourier transform, noting decomposition of current distribution 17 p2886 A66-32388

Hertzian contact of anisotropic bodies, reducing problem to one of evaluating contour integrals by Fourier transform method 17 p3029 A66-32792

Maxwell equation solution for source currents in unbounded magnetoionic medium with uniaxial dielectric tensor, using Fourier transform technique 17 p2959 A66-32962

Admittance problem of cylindrical antenna in homogeneous anisotropic medium formulated and analyzed, using Fourier transforms and Wiener-Hopf technique 17 p2897 A66-33428

Source distribution determination from radiation pattern and field amplitudes expressed as Fourier transform pair 18 p3066 A66-33545

Numerical inversion of Laplace transform 18 p3127 A66-34082

Solar cycle period determined by Fourier transform as applied to truncated sinusoids 18 p3232 A66-34535

Holography principles, discussing basic equation, Fourier transform holograms and hologram interferometry 20 p3556 A66-36929

Near IR two-beam interferometer built for astronomical observations by Fourier transform spectroscopy, noting resolution of spectra of Venus and Mars 20 p3556 A66-36939

Fourier transform used in correction of instrument contour error when observing solar spectral line profile 20 p3647 A66-37042

Filter theory method applied in solving analytical construction problems for optimal controllers, noting existence of Fourier transform and Pally-Wiener condition 21 p3719 A66-39282

Sampling theorem for Fourier transform reconstruction of band-limited signals, applications to stationary stochastic processes and analysis of round-off, truncation and random errors 22 p3884 A66-40168

Finite Fourier sine transform method of obtaining closed-form solution, calculating eigenfrequencies for free vibrations of partially fixed beam carrying concentrated masses 22 p3992 A66-40296

Ionospheric drift and radio wave dispersion determined from selective fading records

and symmetry of cross correlation functions, using Fourier transforms 22 p3916 A66-40807

Correction method for instrumental astigmatism to determine center-to-limb variation of solar UV continuum 22 p3984 A66-40891

Photon time-of-arrival distribution measured in highly monochromatic and spatially coherent light beam from low pressure Hg discharge lamp 23 p4076 A66-41265

LF pulse propagation, describing measurement technique and Fourier transform of signal 23 p4039 A66-41588

Combination of probability density functions for system error analysis, using convolution or transformation methods 24 p4189 A66-42827

Visual perception threshold based on Wiener or power spectrum of noise in relation to Fourier transform of relevant image detail 24 p4165 A66-43025

#### FOURTH STAGE

##### S SATURN S-IV STAGE

##### FR-1 SATELLITE

French FR-1 satellite for observation of ionized layers of atmosphere by propagation of VLF waves in ionosphere 04 p0586 A66-14385

FR-1 French satellite, functions, structure and performance 13 p2192 A66-25493

Scientific satellite FR-1 and VLF radio transmission 13 p2193 A66-26232

Design, objectives and equipment of French FR-1 satellite 14 p2390 A66-26800

French space program including FR-1 satellite and research in meteorology, space biology, rocket probes, electromagnetic propagation, etc 15 p2601 A66-29938

FR-1 and D-1 satellites, discussing construction principles, development, tests and supervision of CNES 18 p3094 A66-33979

Mobile control of FR-1 and D-1 satellites and application to integration, tests and checkout at launching ramp 18 p3094 A66-33981

Automatic control equipment for FR-1 and D-1 satellites 18 p3246 A66-33985

FR-1 satellite components and antennas for VLF signals 22 p3986 A66-40158

FR-1 satellite component reliability program 22 p3876 A66-40159

Aerobee rocket preliminary tests and FR-1 project 22 p3986 A66-40160

FR-1 satellite receiving antennas and adaptation for measuring circuits 22 p3876 A66-40161

Electron collection from VLF receiving antennas and plasma-density probe on board FR-1 satellite, using cathode-grid device 22 p3876 A66-40162

FR-1 satellite contact with surrounding plasma ensured by cathode device tested on Aerobee rocket 22 p3876 A66-40163

Automatic processing of VLF data from FR-1 satellite 22 p3870 A66-40164

VLF signal phase and amplitude from FR-1 satellite measured by phase-locked filter 22 p3866 A66-40165

D-1, D-2 and FR-1 satellites in French space program 24 p4296 A66-42697

##### FRACTIONATION

Complete fractionation of bacteriochlorophyll and degradation products by two rapid methods, using small amount of Rhodospirillum rubrum 17 p2859 A66-32308

##### FRACTOGRAPHY

Quantitative analysis of stress level, material characteristics or temperature level at which fracture occurs, using electron microscope 01 p0088 A66-10962

Plastic deformation preceding fracture in tungsten carbide-cobalt alloys 11 p1717 A66-22994

Ductility enhancement of tungsten by rhenium addition due to modification of grain boundary precipitate morphology 16 p2722 A66-30222

Air and aqueous environments effect on mode of fracture in titanium alloys during low cycle fatigue 18 p3122 A66-33749

##### FRACTURE

Mechanical and micromechanical behavior of bulk polycrystalline boron, emphasizing fracture stress and microstrain behavior relation to materials response 10 p1548 A66-21727

Diffraction of scalar surface waves impinging at arbitrary angle on fracture impedance plane 13 p2024 A66-2599

Internal fracture of spheroids caused by focusing explosive waves 17 p3027 A66-3286

##### FRACTURE MECHANICS

SA GRIFFITH FRACTURE THEORY

Statistical aspects of height of rise and fall in continuous random loading relevant to fatigue failure 01 p0147 A66-1016

Slip-induced fracture of polycrystalline Cu, Mo and W and bcc transition metals V, H, Nb and Ta 01 p0085 A66-1032

Fractography and optical metallography analysis of fracture mode of thorium tungsten-rhenium alloy showing ductility 01 p0085 A66-1032

Hypervelocity impact force per crack surface area correlated to stress-to-fracture of target, experimenting with aluminum and copper as targets and projectiles 01 p0154 A66-1032

Fracture micromechanisms of materials having regular crystalline structure, considering mechanical strength, atomic imperfections, dislocation interactions at crack growth 03 p0382 A66-1306

Fracture propagation in steels discussing macrostructure analysis, differences in intercrystalline and transcrystalline mechanism, plastic surface stresses and strains, etc 03 p0384 A66-1306

Rigid body mechanics noting elastoplastic and ductile formation, deformation, ductility appearance, etc 03 p0439 A66-1306

Fractures in neodymium-doped alkali silicates and borosilicates produced by laser beam 04 p0532 A66-1434

Mechanical testing methods, discussing quasi-static and fatigue fracture due to tensile compressive load and cyclic deformation characteristics of materials 04 p0537 A66-1434

Influence of fiber and matrix characteristics on mechanics of deformation and fracture of fibrous composite 05 p0773 A66-1434

Griffith flaw theory in analyzing failures of epoxy castings [ASME PAPER 65-WA/RP-6] 05 p0779 A66-1506

Plastic deformations for cyclically alternating loads, determining cycle number at which fracture occurs 06 p0965 A66-1606

Initiation and propagation of fatigue crack with reference to fish-eye pattern in bearing steel 06 p0965 A66-1606

Delayed fracture in high strength steel due to hydrogen penetration 06 p0895 A66-1606

Crack propagation in quasi-brittle solid deformed by external load, using thermodynamic laws 06 p0965 A66-1606

Four-point loading bend test on specimens of full plate thickness with sharp notch 20 percent depth, with ductility criterions fully plastic angle of bend before fracture 06 p0965 A66-1606

Brittle fracture in ceramic materials noting Griffith theory on crack propagation plastic deformation occurrence, stress distribution effect, etc 07 p1054 A66-1806

Fracture mechanics and amount of deformation metals can withstand subjected to forming procedures 08 p1235 A66-1806

Front and zone of fractures originating in brittle elastic body under influence of high pressure arising on wall of cavity with body 08 p1313 A66-1906

Gaudin-Meloy distribution parameter estimation from fracture data, based on moments about origin [AICE PREPRINT 17E] 10 p1613 A66-2106

Crack opening displacement approach to fracture mechanics in yielding materials 11 p1782 A66-2206

Statistical interpretation of fatigue fracture phenomena in metals, relating development of successive damage to external load processes 12 p1968 A66-2406

Plastic deformation of Charpy specimen under plane stress-strain conditions, noting low temperature brittle fracture behavior effects of notch geometry and loading etc 12 p1969 A66-2406

Flows and fractures as types of deformation occurring on Earth under high loads of ice suggested by isostatic compensation of Antarctica, Arctic basin etc



- glaciated region in North America 12 p1875 A66-24894
- Fracture surfaces of metals and alloys examined, using optical and electron microscopy, noting fracture mechanisms during crack initiation and propagation 13 p2108 A66-25768
- Fracture and mechanical failure of polymeric solids at high strain rates 13 p2198 A66-26120
- Monte Carlo model of elementary fracture process, noting role of energy in comminution, uneven distribution of energy vs frequency, etc 13 p2207 A66-26600
- Self-sustained fracture of stressed brittle body with assessment of fragment mean dimension 14 p2399 A66-27594
- Fracture mechanics, discussing crystal structure defects, particular dislocation, hardening, lattice vacancies, interstitials, etc 14 p2316 A66-27770
- Stability of two coplanar wedge-shaped cracks, showing under what conditions interaction effects are important 16 p2814 A66-30533
- Rupture strength increase in tungsten and molybdenum chopped wires silicide coated by pack diffusion and incorporated in mullite matrix by vacuum hot pressing [ACS PAPER 7-C-65F] 16 p2723 A66-30949
- Intercrystalline and transcrystalline fracture in molybdenum 16 p2727 A66-31527
- Physical and mathematical point of view on flow and fracture 17 p3021 A66-32004
- Theoretical attempt to bridge gap between micro and macro crack formation, estimating plane strain transition and nominal stress for fracture 17 p2939 A66-32303
- Fracture initiation and growth in linearly viscoelastic materials using energy formulation, establishing extension of Griffith initiation criterion 17 p2939 A66-32304
- Multiple fracturing caused by putting intense radiation into solid in time short compared with elastic relaxation time 17 p2979 A66-32637
- Stress calculation for infinite strip containing straight semiinfinite crack when clamped boundaries are displaced normal to crack 18 p3248 A66-33583
- Elastic-plastic antiplane problems for bonded dissimilar media containing cracks and cavities on interface and subjected to longitudinal shear loads 19 p3475 A66-36430
- Stress wave, deformation and fracture caused by liquid impact, noting analogy with solid and explosive impact and loading fracture formation, propagation, etc 20 p3588 A66-37803
- Crack initiation and propagation formula through fatigue process applied to interface problems, noting creep 20 p3671 A66-38105
- Strength of ceramic specimens with parallel cylindrical holes, noting strength/weight characteristics during compression loading 21 p3753 A66-38677
- Fractures in high strength low-alloy steels, discussing formation of flat and slant regions, effect of rolling direction crack reinitiation, shearing forces, etc 21 p3751 A66-39191
- Stainless steel and aluminum alloy fracture behavior under static load and low temperatures, noting crack propagation, stress and crack-length relation, etc 21 p3830 A66-39195
- Thermoelastic wave equations in continuum mechanics model of laser-induced fracture in transparent media in terms of laser beam energy absorption 22 p3931 A66-40089
- Brittle-fracture propagation tests, obtaining relations among crack propagation speed, dynamic-stress distribution, test temperature and applied stress 22 p3994 A66-40435
- Fracture mechanism of traumatic lesion caused by seat-ejection or bail-out from F-104 G aircraft and worsened by ground impact 22 p3858 A66-40503
- Stress distribution analysis on contracted section of cylindrical tensile test pieces based on Stassi plasticity condition 23 p4142 A66-41950
- Three-dimensional stresses near border of discontinuity plane under arbitrary loading, obtaining solution for uniform shear applied to surface of crack 24 p4285 A66-42148
- Griffith and bond fracture with singular stresses near crack point examined via numerical analysis 24 p4288 A66-42276
- Self-sustained fracture of stressed brittle body with assessment of fragment mean dimension 24 p4291 A66-42734
- Vacuum furnace for studying high temperature fracture of ceramic materials, noting tests on polycrystalline aluminum oxide 24 p4192 A66-43220
- FRACTURE RESISTANCE**
- SA SHOT PEENING**
- Crack initiation and propagation in aluminum sheets, noting ductile fracture and load limit for design purposes 01 p0156 A66-10920
- Mechanical proof test used to reduce variability and screen out weaker elements of brittle materials with widely scattered strength values 03 p0436 A66-12754
- Fracture of brittle bodies with cracks subjected to tension and compression 03 p0441 A66-13291
- Breaking strength of plastic metals under impulse loading by measuring axial tensile stresses 05 p0699 A66-14685
- Fracture of metals at different loading conditions by energy analysis of plastic deformation and fracture 06 p0963 A66-16465
- Synthesis and fabrication methods for intermetallic carbides, borides, beryllides, nitrides and silicides, decreasing susceptibility to brittle fracture 07 p1051 A66-18298
- Brittle fracture characteristics and fine structure parameters in steel 09 p1391 A66-20864
- Grain boundary role in high temperature fracture behavior of magnesium, noting temperature and orientation dependence of shear strength 12 p1897 A66-24920
- Specimen anisotropy during tensile elongation to rupture of composite solid propellants, based on analysis of dilatational behavior 17 p2989 A66-32451
- Residual stress, crack propagation and fatigue fracture mechanisms in Al alloy sheets with fatigue cracks, for use in wing panels [ICAS PAPER 66-34] 23 p4137 A66-41007
- FRACTURE TOUGHNESS**
- Fracture strength of two rocket-nozzle-grade graphites under ten biaxial stress states at room temperature 03 p0435 A66-12637
- Fracture toughness of X7000-series aluminum alloy plate weldments 05 p0686 A66-14695
- Alloy steel fracture resistance, describing creep strain effect on gas turbine engine alloys [ASME PAPER 65-WA/MET-13] 05 p0703 A66-15685
- Plastic deformation effect on strain energy release rate, examining axial rigidity of plate with central propagating crack under uniaxial tension [ASME PAPER 65-WA/MET-9] 05 p0780 A66-15687
- Plane strain fracture toughness of high strength aluminum alloys measuring techniques and relevant metallurgical factors [ASME PAPER 64-WA/MET-11] 06 p0895 A66-16209
- Fracture toughness and stress corrosion resistance of several heats of maraging steel compared with results for low-alloy and hot-work die steel 06 p0897 A66-16801
- Low-temperature mechanical properties and fracture toughness of commercial and extra-low-interstitial grade Ti-6Al-6V-2Sn 08 p1242 A66-19719
- Alloy steel fracture resistance, describing creep strain effect on gas turbine engine alloys [ASME PAPER 65-WA/MET-13] 12 p1896 A66-24535
- Plastic deformation effect on strain energy release rate, examining axial rigidity of plate with central propagating crack under uniaxial tension [ASME PAPER 65-WA/MET-9] 12 p1970 A66-24539
- Fracture characteristics of welds in aluminum alloys evaluated by tear and notch tensile tests 13 p2197 A66-25776
- Fracture toughness of notched A-302B and Ni-Mo-V steels with various size specimens [ASME PAPER 66-MET-1] 14 p2311 A66-26969
- Stress-corrosion susceptibility of high-strength steel at various levels of tensile yield strength and fracture toughness [ASME PAPER 66-MET-5] 14 p2300 A66-26973
- Biaxial fracture strength of textured titanium alloy for design of liquid fuel tankage 14 p2405 A66-27994
- Chemical composition effect on fracture properties of Al-Zn-Mg-Cu alloys 14 p2317 A66-28009
- Neutron irradiation effect on fracture toughness of several structural and pressure vessel steels studied by Charpy V-notch impact test and tensile test 15 p2521 A66-29074
- Interfaces between fatigue, creep and fracture, discussing separation of fatigue process into crack initiation and crack propagation 16 p2823 A66-31711
- Impact fracture toughness of brazed laminates of maraging steels and titanium alloys found to be 2 to 7.8 times greater than homogeneous specimens of like size [AIAA PAPER 65-566] 19 p3377 A66-35620
- Hot salt cracking of titanium alloys noting stress corrosion, fracture toughness and crack propagation mechanism 19 p3378 A66-35653
- Design and testing of crack-notched specimens for determination of resistance of materials to unstable opening-mode crack extension under plane strain conditions 19 p3473 A66-35805
- Factors affecting fracture characteristics of metals at cryogenic temperatures and fracture mechanics for predicting performance of defect-containing structures 19 p3380 A66-35847
- Quenching, annealing and high temperature treatment effect on transverse rupture strength of sintered tungsten carbide [ASME PAPER 66-MD-17] 21 p3750 A66-38478
- FRAGMENTATION**
- Mass spectrometric fragmentation behavior of N-n-propyl and N-n-butyl pyrrolidone and N-alkyl succinimides subsequent to electron impact 11 p1651 A66-23412
- Fragmentation probabilities, charge spectrum and interaction mean free paths of relativistic heavy nuclei in primary cosmic radiation investigated in stack of nuclear emulsions 16 p2795 A66-31010
- FRAME**
- SA AIRFRAME**
- SA GRID**
- Calculating spatial frames by procedures derived from displacement method 14 p2409 A66-28458
- Pseudorandom scanning of uniformly dense rectangular frame 18 p3078 A66-34080
- Iterative linear-elastic analysis of plane pin-jointed frames and space ball-jointed frames, accounting for temperature and geometrical changes 21 p3833 A66-39537
- Surface contour and structural requirements of reflecting panels of multiplate antenna, examining manufacturing, installation and cost advantages 23 p4138 A66-41259
- Micell structure design of lightest framework to equilibrate system of given forces 23 p4147 A66-41998
- FRAME PHOTOGRAPHY**
- Multistrip transformation of aerial photographs using rigid special masking frames in accordance with contour line 02 p0231 A66-11971
- FRAMING CAMERA**
- Automatic frame photometer with modified circuit 02 p0227 A66-11349
- Device for marking and standardizing askafilms 02 p0227 A66-11351
- Image motion and corresponding loss of resolution from rotational motions of airborne vehicle and camera parameters 02 p0228 A66-11381
- Data analysis from film of framing camera with rotating mirrors, using frame edges as reference lines, calculating necessary corrections 05 p0677 A66-14863
- FRANCE**
- French space program and projects under development 01 p0170 A66-10359
- CNES D-1 satellite using Diamant launcher for study of launch systems and space



environment 01 p0142 A66-10360  
 French aerospace industry, relationship to French economy, annual expenditures 1958 to 1964 and aircraft  
 exports 05 p0794 A66-15189  
 French National Center of Space Studies, facilities and functions 06 p0973 A66-16934  
 French space program since creation of CNES in 1961 09 p1472 A66-19862  
 French space program, flight tests of Diamant class rockets and A-1 satellite 12 p1981 A66-23804  
 French commercial aircraft accident investigation 13 p1994 A66-25232  
 Automatic air traffic control development in France 15 p2534 A66-29126  
 French space program including FR-1 satellite and research in meteorology, space biology, rocket probes, electromagnetic propagation, etc 15 p2601 A66-29938  
 French booster projects for orbiting stationary communication satellites, noting SEREB /solid propellant/ and LRBA /liquid propellant/ 19 p3469 A66-36047  
 French A1 satellite design and development, examining telecommunications equipment and monitoring diamant launcher performance 19 p3470 A66-36270

**FRANCK-CONDON FACTOR**  
 Franck-Condon factors to high quantum numbers covering methods, results and tabulation 04 p0548 A66-13830  
 Wave functions and Franck-Condon factors for transitions in molecular nitrogen obtained by Numerov integration of Schroedinger equation 09 p1404 A66-20411  
 Relative intensity measurements of 50 major bands of Lyman-Birge-Hopfield /LBH/ system of nitrogen 12 p1869 A66-23919  
 Franck-Condon factors for ionization of hydrogen and deuterium, noting vibrational eigenenergies of D sub 2 14 p2337 A66-27972  
 Franck-Condon factors for permitted transitions in nitrogen 14 p2338 A66-28128  
 Auroral excitation rates and molecular vibrational temperatures in nitrogen 2PG from Franck-Condon factors obtained from intensity measurements and high resolution absorption spectral data 16 p2692 A66-30328  
 Vibration-rotation interaction effect on Franck-Condon factors for band system of RbH molecule 18 p3137 A66-33923  
 Radiative lifetime and emission intensity measurements, determining oscillator strength and electron transition moment of first positive band system of nitrogen 23 p4033 A66-42082

**FRAUNHOFER LINE**  
**SA PHOTOSPHERE**  
 Profiles of intense resonance lines and variation from center of limb of solar disk 03 p0427 A66-12917  
 Radiation characteristics of isolated circular optical waveguides supporting low-order dielectric waveguide modes for combinations of modes, wavelength, diameter and aperture 05 p0648 A66-14910  
 Fraunhofer pattern of laser light transmitted through optical fiber, noting spatial frequency of interference fringes between light waves 05 p0696 A66-14972  
 Electron density and pressure in solar atmosphere from growth curve with Stark effect of Fraunhofer lines 05 p0765 A66-15420  
 Granularity and radial structure in circular Fraunhofer diffraction fringes produced by lycopodium powder scattering of monochromatic coherent light 06 p0891 A66-16443  
 Fresnel and Fraunhofer patterns of overmoded feeds and reflector antennas 12 p1841 A66-24632  
 Profiles of intense resonance lines and variation from center of limb of solar disk 14 p2380 A66-27266  
 Broadening of Fraunhofer hydrogen lines in solar spectrum, noting Stark effect 14 p2380 A66-27274  
 Image reconstruction with Fraunhofer holograms formed from opaque or transparent diffracting objects in aperture with coherent illumination 15 p2500 A66-28973  
 Absence of temperature difference between solar equatorial and polar limb near minimum, employing photoelectric comparison of Fraunhofer line

strengths 16 p2800 A66-30643  
 Magnesium I lines in solar spectrum searched on basis of multiplet table of wavelengths, intensities, excitation potentials of magnesium spectrum 16 p2802 A66-30939  
 Spatial cross-correlation analyses between radial velocity and continuum brightness fluctuations of solar disk center spectrograms 17 p2996 A66-31919  
 Intensity distribution in Fraunhofer diffraction patterns of slit and apertures illuminated by partially coherent light 18 p3118 A66-33986  
 Fraunhofer spectrum of singly ionized yttrium extended in IR solar spectrum 18 p3236 A66-34892  
 LASL lens design program for Doublet Achromat, from existing Fraunhofer design, used in solar corona monochromatic photography 19 p3354 A66-35383  
 Macroscopic velocity field in solar atmosphere and physical nature of motion, analyzing radiative transfer in spectral lines 19 p3465 A66-36604  
 Ultrasonic light diffraction, deriving line intensity in form of quadratures with parametric dependence 20 p3601 A66-37147  
 Total intensities of continuum and of red, green and yellow coronal lines emitted by sporadic coronal condensation shown to yield lower limits to Fe and Ca abundances 20 p3649 A66-37332  
 Power transmission, gain, directivity pattern and reception between large aperture antennas in near-field region 20 p3529 A66-37709  
 Behavior of lambda 6300 angstrom Fraunhofer absorption line in solar spectrum 22 p3984 A66-40850

**FREDHOLM INTEGRAL EQUATION**  
 Exactness of mechanical quadrature approximation of eigenvalues and eigenfunctions of Fredholm integral equation 01 p0092 A66-10316  
 Dirichlet problem solved by probability density for Brownian particle, using Fredholm integral equation 01 p0094 A66-10730  
 Modes in optical resonator formed by two reflectors of dissimilar spherical curvature and circular shape 03 p0391 A66-12305  
 Couette flow, Neumann-Liouville series expansion convergence for various flow regimes and related Fredholm integral equation solutions 07 p1020 A66-17964  
 Stress-strain state of elastic space, examining circular crack for axial tensile load effects 08 p1305 A66-18597  
 Fredholm integral equation system for magnetic currents induced on wedge under impedance boundary condition 09 p1344 A66-20441  
 Numerical solution of Fredholm integral equation with singularities and application to annular airfoil theory 09 p1396 A66-20626  
 Formalism of regular perturbation theory similar to Fredholm resolvent and having infinite radius of convergence 11 p1740 A66-23184  
 Axisymmetric problems of heat conductivity theory for layer with one constant boundary and one circular boundary solved by paired integral equations method 12 p1978 A66-24207  
 Plane stationary problem of heat conduction for mixed boundary conditions solved, using Fredholm integral equation with symmetrical kernel 12 p1979 A66-24372  
 Lifting systems and motion of slender profile at arbitrary distance from liquid or solid boundary, using kernel degeneration method to reduce singular equation to Fredholm equation 13 p2067 A66-26531  
 Numerical analysis of infinite phased array of open rectangular waveguides, noting use of Fredholm integral equation, effects of wall thickness and reflection coefficient 14 p2255 A66-27909  
 Radiative energy transfer between concentric spheres separated by absorbing and emitting gas, noting analogy to atmosphere with spherical symmetry 15 p2615 A66-28620  
 Dual integral equation and dual series analysis and application to mixed boundary value problems in elasticity, hydrodynamics and electrostatics 15 p2526 A66-28953

Dual integral equations in elasticity theory noting Mehler-Fok transformation of spherical functions, Fredholm equation and application to mixed boundary value problems 15 p2526 A66-28953  
 Axisymmetric problem in elasticity theory for infinite body weakened by system of periodically distributed coaxial slots of equal radius 17 p3026 A66-32599  
 Two Fredholm integral equations encountered in elasticity theory solved by Wiener-Hopf method 17 p2947 A66-32788  
 Axisymmetric problems of heat conductivity theory for layer with one constant boundary and one circular boundary solved by paired integral equations method 22 p4000 A66-40571  
 Two-dimensional problem for layer with mixed boundary conditions, obtaining solutions for Fredholm integral equations and relations for temperature distribution 22 p4001 A66-40930  
 Fredholm integral equations obtained in study of boundary value problem occurring in thin shallow shell theory 23 p4140 A66-41830  
 Dirichlet problem solved by probability density for Brownian particle, using Fredholm integral equation 24 p4232 A66-42747

**FREE ATMOSPHERE**  
 Equations for reflecting effect of underlying surfaces on long wave radiation fluxes in free atmosphere 01 p0062 A66-10767  
 Equations for reflecting effect of underlying surfaces on long wave radiation fluxes in free atmosphere 14 p2285 A66-27867  
 Aircraft bumpiness conditions in free atmosphere relation to turbulence and other aerological data 18 p3049 A66-34619  
 Long-wave radiative heat transfer between clouds and free atmosphere as basic factor in weather forecasting 20 p3594 A66-38373

**FREE BOUNDARY**  
 Homogeneous turbulent flow merging with turbulent or laminar flow of equal velocity 01 p0058 A66-10470  
 Free-boundary nonlinear problem of smooth curve drawn in single circle so that doubly connected region formed by curve and circle satisfies specific existence conditions 02 p0250 A66-12107  
 Two-dimensional problems of gas dynamics with free boundaries, discussing existence and uniqueness of subsonic potential gas flow 04 p0510 A66-13877  
 Hydrodynamic instability of shear layers using inviscid linearized stability theory of spatially growing disturbances 04 p0513 A66-14477  
 Approximate solution of magnetospheric free boundary for steady state interaction between field-free streaming plasma and magnetic dipole 07 p1088 A66-17955  
 Free boundary problem for heat equation with heat input at melting interface 09 p1470 A66-20267  
 Two-dimensional problems of gas dynamics with free boundaries, discussing existence and uniqueness of subsonic potential gas flow 12 p1863 A66-24027  
 Uniqueness and existence theorems for parabolic partial differential equations for case of free boundary 15 p2528 A66-29333  
 Linearized three-dimensional potential flow equations for response of liquids in cylindrical containers to slightly off-axis acceleration 17 p2916 A66-33477

**FREE CONVECTION**  
 Free convection boundary layers on horizontal flat plate 01 p0161 A66-10433  
 Natural convection at thermal leading edge on vertical wall matched with known solution immediately above this region 02 p0304 A66-12119  
 Nonisothermal wall problem for vertical right circular cone in laminar free convection for fluids with low Prandtl numbers 02 p0305 A66-12207  
 Free convection heat transfer in partially enclosed channel flow, noting effect of vertical fin geometry and temperature [ASME PAPER 64-WA/HT-33] 04 p0595 A66-13338  
 Laminar to turbulent transition along aluminum plate in free convection measured, using hot-wire probes 04 p0596 A66-13511



Porous blowing and suction for laminar boundary layer during free convection at vertical surface 04 p0597 A66-13820

Optimization of fin geometry to maximize free-convection heat transfer in air at atmospheric pressure [ASME PAPER 65-HT-12] 05 p0783 A66-14738

Free convection on laminar forced flow heat transfer in horizontal circular tube [ASME PAPER 65-HT-23] 05 p0783 A66-14744

Reversed heat conduction in natural convection at thermal leading edge on vertical wall [ASME PAPER 65-WA/HT-34] 05 p0792 A66-15672

Unsteady, combined free and forced convective MHD channel flow of conducting fluid through transverse magnetic field 07 p1085 A66-17580

Particle velocity distribution in free convection in air for flat velocity field 08 p1321 A66-19733

First-order perturbation analysis of free convection of liquid metal from isothermal vertical finite plate extended to uniform heat flux 10 p1619 A66-21054

Free convection heat transfer to carbon dioxide near critical point, noting free, turbulent and oscillating flow 10 p1619 A66-21271

Laminar free convection flow and velocity and temperature distributions in air above thin horizontal electrically heated wire 12 p1980 A66-24906

Free convection film boiling heat transfer from isothermal vertical plate to subcooled stagnant liquid, using two-phase boundary layer theory 12 p1980 A66-24907

Interferometric determination of temperature field compared with exact analytical solutions for laminar boundary layer in case of free convection 13 p2208 A66-25314

Interferometric determination of temperature field in two-dimensional finite space in conditions of free convection with internal heat sources 13 p2209 A66-25317

Vertical displacement rate of air particles in finite volume under effect of internal heat sources in free convection 13 p2209 A66-25318

Porous blowing and suction for laminar boundary layer during free convection at vertical surface 13 p2209 A66-25319

Solution for free nonstationary convection in bounded region of Landau-Lifshits mechanics of continuous media 14 p2414 A66-28282

Boussinesq approximation for hydrodynamic stability of natural thermal convection of fluid between two parallel vertical planes and calculation of critical Reynolds number 15 p2617 A66-29399

Steady free convection in vertical slot, noting growth of boundary layers and temperature gradient 15 p2618 A66-29693

Free convection on laminar forced flow heat transfer in horizontal circular tube [ASME PAPER 65-HT-23] 16 p2828 A66-30983

Approximate calculation of free convective heat transfer in rectangular region 17 p3034 A66-32562

Sound field parameter dependence of coefficient of heat transfer from horizontal cylinder at near zero Grashof numbers 19 p3478 A66-35751

Boundary layer equations of MHD free convection from heated horizontal plate in vertical uniform magnetic field 21 p3776 A66-38707

Free convection boundary layer along isothermal plate, using equation of laminar compressible flow and heat transfer, noting profile dependency upon wall coordinate 21 p3835 A66-38945

Free convective heat transfer in thermal boundary layer of rarefied gas 22 p3902 A66-40922

**FREE ELECTRON**

Ray dispersion of electromagnetic waves by free electrons produced in cone-shaped ionized wake 04 p0481 A66-13843

Plasma oscillation of conduction electrons in sodium 09 p1430 A66-20845

Van Hove diagonal singularity condition for free electrons in periodic lattice impurity field 17 p2959 A66-33291

Layer of CdS crystals photoconduction

measurements suggesting change in space charge under illumination due to increase of free electron concentration in volume 19 p3438 A66-35478

Time dependent Schrodinger equation for Bloch electron in presence of laser field, using WKB approximation method, compared with perturbation theory 23 p4077 A66-41266

**FREE ENERGY**

Diagrammatic method to obtain Helmholtz free energy of classical electron gas used to derive pair distribution function beyond Debye-Huckel result 02 p0266 A66-11478

Evaluation of absolute free energy of rigid-disk system at very high compression 05 p0740 A66-15772

Extension, for heterogeneous sphere, of previous work which gave expressions for mean strain and rupture as functions of hydrostatic and nonhydrostatic components of free energy 08 p1212 A66-18638

Equation for entropy of formation of interstitial solid solution with two interstitial sublattices, using phase diagram for constants in free energy and activity equations 08 p1258 A66-18903

Vortex lines in superconductors, noting free energy of pure superconducting metal in presence of currents and fields for slowly varying drift velocities 09 p1415 A66-20007

Free energy calculations and crystallographic properties of vortex line lattices in type II semiconductor for square and triangular lattices in given magnetic field 09 p1421 A66-20058

Complete behavior of mixed state type II semiconductor in sufficiently large magnetic field 09 p1421 A66-20059

Linear free energy relationship between benzoyl and acetyl ion intensities in mass spectra of benzo- and acetophenones explained by kinetic argument 10 p1495 A66-21165

Free energy functional of superconducting alloys based on Green function decomposition 10 p1573 A66-21241

Free energy of pure fluids as function of thermodynamic temperature determined from measurements of internal energy, noting case of carbon dioxide 12 p1981 A66-24997

Single sample chamber determining magnetothermodynamic characteristics including magnetic moment, heat capacity in magnetic fields, entropy change, free energy, etc 13 p2083 A66-26558

Stability limits and Gibbs free energy for type II superconductor in magnetic field as functional of ordering parameter, using Bardeen-Cooper-Schrieffer theory 14 p2360 A66-27193

Thermodynamic and physical properties of beryllium hydroxide at four temperatures in 1587-1808 degrees K range, with computation of free energy of formation 14 p2370 A66-27372

Free energy of single and multicomponent plasmas in particle number density determined, using quantum mechanical perturbation expansion of partition function 15 p2552 A66-29617

Free energy of aluminum alloy containing two-dimensional Guinier-Preston zones of copper atoms 16 p2722 A66-30307

Generalized model of ideal compressible anisotropic fluid, determining dependence of free energy on density 16 p2689 A66-31517

Gradient 16 p2689 A66-31517

Virial expansions for plasma free energy in method of collective variables 16 p2767 A66-31728

Text on thermodynamics of refractory compounds covering thermodynamic properties of borides, carbides, nitrides and oxides of 31 elements 16 p2728 A66-31748

Radial plasma transport in magnetic wells, emphasizing LF instabilities not stabilized by positive gradient and employing free energy arguments 19 p3415 A66-36516

Partition function for tunnel model of rigid disks evaluated in asymptotic limit of reduced volume, including close-packed value of closed systems 22 p3949 A66-40913

Stability limits and Gibbs free energy for type II superconductor in magnetic field as functional of ordering parameter, using Bardeen-Cooper-Schrieffer

theory 24 p4259 A66-43091

**FREE FALL**

**SA WEIGHTLESSNESS**

Interaction of two identical spheres falling freely in viscous fluid under laminar flow conditions 01 p0058 A66-10487

Interaction of two identical spheres falling freely in viscous fluid under laminar flow conditions 09 p1367 A66-20701

Effects on man of direct /escape/ and indirect /aircraft flight/ movement through atmosphere, considering moderate and high-speed aerodynamic forces 10 p1488 A66-22106

Freely falling point mass problem solutions for Einsteinian free space equations that also satisfy Newtonian equations in suitable coordinate system 12 p1915 A66-24889

Vertical-track free-fall rocket sled system, discussing design principles, operation and performance characteristics 18 p3093 A66-33796

Transfer paths to Mars via Venus compared with direct flight, discussing direct free fall transfer, flyby and free fall transfer 20 p3651 A66-37392

Freely falling point mass problem solutions for Einsteinian free space equations that also satisfy Newtonian equations in suitable coordinate system 23 p4090 A66-41096

Free fall test of Surveyor test vehicle unaided by recovery parachutes to radar-controlled soft landing on ground 24 p4284 A66-42896

**FREE FLIGHT**

Psychophysical orientation mechanisms of man under weightlessness simulation, gravity conditions encountered on Earth, in orbital flight and during free floating in space 06 p0814 A66-17177

Book on dynamics of elastic structures in free flight 16 p2815 A66-30612

Separated shock wave distance from free flying blunt body influence by real gas oscillation excitation 19 p3341 A66-35746

Onboard miniaturized telemetry system for stagnation point temperature measurements on free-flight models in ballistic ranges 24 p4209 A66-42189

Simultaneous FM telemetry measurement of four aerodynamic forces acting on free flying models in wind tunnel 24 p4209 A66-42190

Interplanetary trajectories, considering gravity effect, free flight trajectory and forces acting on space vehicle 24 p4280 A66-43132

**FREE FLIGHT TEST APPARATUS**

Free flight dynamic stability measurements indicate that boundary layer transition has no perceptible effect [AIAA PAPER 64-427] 08 p1161 A66-18810

Refinements of hypersonic testing techniques in 100-inch tunnel F of von Karman gas dynamics facility 11 p1686 A66-22842

Free flight model technique in hypervelocity shock tunnel for aerodynamic force and moment measurement by optical instrumentation [AIAA PAPER 66-771] 22 p3847 A66-40652

Free flight multibody test techniques, discussing drogue body testing, mechanized free flight models and salvo launches [AIAA PAPER 66-772] 22 p3895 A66-40653

Wind tunnel free-flight testing of reentry vehicle dynamics, noting capability for simultaneous two-dimensional viewing of model trajectories [AIAA PAPER 66-774] 22 p3895 A66-40654

Total aerodynamic forces and moments of free flying body in wind tunnel determined from accelerations measured and telemetered by onboard instruments [AIAA PAPER 66-775] 22 p3896 A66-40655

Launch and recovery system for large instrumented free flight models in high speed wind tunnel, using miniaturized telemetry and recording equipment [AIAA PAPER 66-776] 22 p3896 A66-40656

Launching device for free flying models in conventional wind tunnels consisting of split hollow shell enclosing model [AIAA PAPER 66-773] 23 p4052 A66-41332

Rapid opening mechanical gate valve consisting of blade assembly, blade catcher and primer holder used in conjunction with hypervelocity free flight range experiments 24 p4162 A66-43219



## FREE FLOW

Free convection thermal transfer in narrow horizontal channels and infinitely wide channels 09 p1471 A66-20704

Molecular collision effect on transitional drag on cylinder traversing rarefied gas at hypersonic Mach numbers, discussing departure from free flow 11 p1632 A66-22920

Free laminar boundary layer flow between parallel streams of different magnetic fields and temperatures for incompressible viscous fluid 21 p3776 A66-38682

Laminar incompressible axisymmetric free jet with swirl, examining perturbation scheme for stream function and asymptotic series 21 p3729 A66-39453

**FREE JET**

Turbulent mixing of axisymmetric jet of partially dissociated nitrogen with ambient air, establishing mixing and decay characteristics [AIAA PAPER 65-823] 03 p0359 A66-13231

Two sets of Tollmein and Goertler equations derived for two-dimensional compressible free jet mixing layer, using similarity assumption [AIAA PAPER 65-821] 04 p0510 A66-13692

Velocity distributions in molecular beams of argon produced by supersonic nozzle sources, using time of flight method 04 p0548 A66-14012

Free steady state jet subject to axial tension applied to Newtonian liquids, noting effect of flow variables on dimensionless criterion 04 p0512 A66-14209

Qualitative and quantitative solution of linearized approximations to boundary layer equations, noting free jet and wall-slot injection into moving stream [ASME PAPER 65-APMW-6] 04 p0512 A66-14212

Laminar and turbulent MHD free jet, using Peskin analysis 05 p0721 A66-14719

Inner and outer expansions method applied to source flow model involving viscous effects in hypersonic axisymmetric free jets at large Reynolds numbers 07 p0982 A66-18122

Qualitative and quantitative solution of linearized approximations to boundary layer equations, noting free jet and wall-slot injection into moving stream [ASME PAPER 65-APMW-6] 10 p1523 A66-21470

Performance of simple diffusers of fixed geometry in flow regimes with viscous and compressibility influence involving free-jet test sections, conical and contoured nozzles and gas flows at high Mach numbers 11 p1686 A66-22844

Three-dimensional viscous free mixing, describing numerical and experimental solutions for wake and jet flows [AIAA PAPER 65-49] 15 p2424 A66-29272

Spread and decay of turbulent free jets and shear-stress analysis of turbulent mixing zones 15 p2424 A66-29295

Laminar to turbulent transition in free jets 15 p2424 A66-29303

Inviscid and viscous flow in central core of supersonic free jet in wind tunnel, noting shock wave location at high Reynolds number 16 p2628 A66-30375

Structure and properties of free supersonic jets including impact pressure and velocity distribution measurements, condensation, etc 16 p2628 A66-30376

Mixing of free jet boundary which includes laminar and turbulent flow region in tandem 16 p2685 A66-30805

Approximation for moment equations of kinetic theory which describe source flow expansion with application to free jet 17 p2907 A66-32412

Hypersonic self-similarity of barrel shock in source-type free jets at high pressure ratio 17 p2839 A66-32468

Acoustic output, turbulence in jets and noise sources in fluid amplifiers noting design, noise reduction by jet edge, input nozzle design, forced secondary flow, etc 18 p3054 A66-34132

Similarity solutions of heated two-dimensional laminar free jets with arbitrary Prandtl number and nonlinear viscosity-temperature energy dissipation relationships 18 p3103 A66-34932

Cascade free jet logical element

interactions and application to multiple-parameter logical function 20 p3496 A66-36863

Electron beam flow visualization study of density field about skimmer entry in small free jet 21 p3727 A66-39186

Free jet MHD accelerator for determining minimum length of crossed field accelerators, noting operation and solution in closed form 21 p3699 A66-39645

Model tests on free jet scramjet facility configurations at high Mach numbers, obtaining data on bypass flow pressure recovery and diffusion process [AIAA PAPER 66-745] 22 p3846 A66-40632

Free and confined turbulent and free laminar plane jets in highly diffused magnetic fluid 23 p4107 A66-42005

**FREE MOLECULAR FLOW**

Simplified leading-edge flow boundary value problem of Bhatnager-Gross-Krook equation solved by finite difference method 01 p0058 A66-10633

Rotating arm apparatus at National Aerospace Laboratory in Japan for pressure-distribution and heat-transfer flow measurement 01 p0053 A66-10636

Solid surface interaction of atoms and molecules of wedge cavity in rarefied free molecular gas stream 04 p0456 A66-14143

Shrello approximation used to derive formulas for moment characteristics of axisymmetric bodies rotating in hypersonic free molecular flow 04 p0456 A66-14155

Satellite drag coefficient reevaluated in consideration of recent data on gas-surface interaction and atmospheric composition 05 p0760 A66-14941

Theory of highly rarefied cascade flow and proposal for new axial flow molecular pump in free molecule range 06 p0803 A66-16945

Aerodynamic and heat transfer characteristics of cross-stream wedge in low density aerodynamics, investigating transition from continuum to free molecular flow 07 p0982 A66-18126

Heat transfer and mass flux expressions for recombination interactions at solid-gas interface due to transport of atomic and ionized particles to spacecraft in ionosphere 08 p1161 A66-18747

Shock tunnel heat transfer measurement and hypersonic viscous flow over pointed cones, particularly viscous-layer regime at low Reynolds numbers [AIAA PAPER 66-34] 08 p1163 A66-18957

Transition regime mass flow rate and longitudinal pressure distribution along short tube with bellmouth entry 08 p1207 A66-19131

Heat transfer to wedge in nearly free-molecular hypersonic flow of strongly rarefied gas 08 p1165 A66-19484

Gas flow in free-molecular regime with negligible collision approached by diffuse reflection model 11 p1688 A66-22525

Optimum minimal-drag shape of slender axisymmetric body in free molecular flow 11 p1632 A66-22526

Minimal-drag shape of nonslender body of revolution in diffuse free molecular flow 11 p1632 A66-22527

Boltzmann equation behavior, at large Knudsen numbers, for free molecular interactions with infinite collision cross section 11 p1691 A66-22918

Asymptotic solution of rarefied gas flow, using free molecular approximations 11 p1692 A66-22919

Transition from near free molecular flow at leading edge of flat plate in rarefied hypersonic flow to continuum boundary layer flow downstream 11 p1633 A66-22925

Comparison of theoretical and experimental results for cylinder and flat strip models in near free molecular flow 11 p1692 A66-22926

Heat transfer and pressure data extended from classical thin boundary layer regime to near-free-molecule flow in study of low density effects in hypersonic wedge flows 11 p1633 A66-22928

Mass flow of nitrogen gas through circular orifice at five Knudsen number values from 0.13 to 1.78 and range of upstream to downstream pressure ratios 11 p1692 A66-22936

Optimum nose form determination for

minimum drag in free-molecule flow of asymmetric body 11 p1635 A66-22937

Free-molecule flow through conical tubes noting mass transport, axial momentum, energy, flow distribution and speed ratio 11 p1635 A66-22938

Impact tube pressure probe response to free molecular rarefied gas flow for arbitrary angle of attack 11 p1692 A66-22939

Internal flow problems in free, nearly free, molecular regimes and higher transition flows, using Boltzmann equation and series expansion to solve integral equation for surface collision density 11 p1693 A66-22940

Terminal reentry and dynamics evaluation computer program for small particles, using point-mass calculation during initial phase and determining drag coefficient [AIAA PAPER 66-380] 12 p1951 A66-24505

Flow in vicinity of right cylindrical body, considering shocks between molecules and solid 13 p1991 A66-25469

Rarefied gas mechanics based on Boltzmann equation with prescribed boundary conditions 13 p2071 A66-26726

Density ratio and transmission probability across conical converging diffuser in free-molecule flow with selected range of speed ratios, using Monte-Carlo method 14 p2219 A66-27416

Similarity law for longitudinal contours of optimum bodies minimizing drag in hypersonic and low subsonic free molecular flows constrained on length, base width, wetted area, etc 14 p2221 A66-28183

Boltzmann equation for Pitot tube problem, using distribution function, deriving equations for rarefied gas flow in impact tube under hypersonic and adiabatic conditions 15 p2481 A66-29738

Surface protrusions and holes, Maxwell kinetic gas theory and surface interaction of current of free molecules and rigid body 16 p2686 A66-31042

Book on radiation gas dynamics including radiative heat transfer, waves and shock waves, kinetic theory, relativistic mechanics, free-molecule flow, etc 16 p2829 A66-31314

Monte Carlo calculation of probability of free molecular conductance of cylindrical tube with wall sorption 17 p2906 A66-31977

Free-molecular flow of rarefied gas in plane channels or through cells of heat-conducting grid whose cells are smaller than mean free path of gas molecules 19 p3277 A66-36480

Heat conduction in rarefied gases between concentric spheres by moment method, considering accommodation coefficients at inner sphere surface 21 p3834 A66-38708

Free molecular flow as Markov chain, describing motion via probability function in multireflection system 22 p3951 A66-40454

Nearly free molecular flow in rarefied gas dynamics in comparison of theoretical and experimental results with reference to drag 23 p4060 A66-42025

**FREE OSCILLATION**

Free oscillations of elastic shells of revolution 01 p0154 A66-10469

Coupling method for determining natural oscillations of ideal incompressible liquid in vessel consisting of two regions 01 p0059 A66-11017

Large amplitude-free oscillations of beams and plates by means of Ritz-Galerkin technique 02 p0297 A66-11554

Form, period and spectrum of free oscillations in LC circuits with nonlinear capacitive p-n alloy junctions, 02 p0198 A66-11704

Large amplitude oscillation of anisotropic triangular plates 04 p0591 A66-14202

Longitudinal oscillations of Voigt body bar whose characteristics vary with time and are bounded 06 p0964 A66-16475

Behavior of fluids under weightlessness and in weak gravitational fields, formulating small linear oscillations of ideal fluid under surface tension 06 p0873 A66-16708

Beam on elastic supports, determining fundamental frequency of free oscillation for one weak nonlinear boundary condition 07 p1142 A66-17260

Unsymmetric free oscillations of conical shell of medium length and linearly variable thickness 08 p1312 A66-19432

Variational principle for free oscillations of



gravitating elastic compressible sphere 09 p1456 A66-20412  
Hamel and Cypkin methods, used to determine free oscillation of plus-or-minus servomechanism, applied to transfer function of certain type 10 p1517 A66-21283  
Frequency of free oscillations of beam when two of four boundary conditions for elastic clamping at both ends contain nonlinear terms 10 p1613 A66-21325  
Free oscillation stability of closed-loop self-adjusting system with several parameters, noting two methods of measuring relative damping 11 p1677 A66-22760  
Free oscillation of thin elastic shell, using asymptotic method for integrating dynamic equations in classical linear theory 13 p2196 A66-25630  
Free oscillation amplitude increase from resonance traversal occurring when perturbation frequency passes through resonant value in weakly nonlinear system 13 p2146 A66-25740  
Free gyroscope motion as affected by dry friction and free and forced oscillation 15 p2541 A66-29170  
Approximate solution of free axisymmetric oscillations of circular structurally orthotropic plate of specific laws of variable thickness 15 p2613 A66-29436  
Random variation of Earth rotation relation to amplitude of free nutation 16 p2693 A66-30589  
Periodic and quasi-periodic solutions to differential equations describing pulsed systems 16 p2738 A66-31709  
Reduction of Gilchrist two-equation set for free oscillations in conservative quasi-linear systems with two degrees of freedom 18 p3134 A66-33602  
Matrix methods of forces and displacements applied to free oscillations of aircraft structures, proposing procedure yielding coherent mass matrix 21 p3825 A66-38582  
Approximation of nonlinear characteristics of conservative vibrations by two polygon characteristics chosen so that mechanical energy of system remains same 21 p3833 A66-39599  
Cylindrical functions for calculating free oscillations of Saturn rings and estimation of upper limit to mass of ring if motion is stable against axisymmetric perturbations 23 p4125 A66-41063  
Free longitudinal oscillations of finite viscoelastic rod, neglecting relaxation 23 p4139 A66-41555  
**FREE RADICAL**  
IR and UV absorption spectra of free radical NCN observed following photolysis of matrix isolated cyanogen nitride 04 p0473 A66-13644  
Superhigh speed IR spectrometers used in detection and study of free radicals and photochemical reaction, pulse discharges in gases, etc 05 p0685 A66-15862  
Free radical CCO spectroscopy when produced by vacuum UV photolysis of matrix isolated carbon suboxide 06 p0821 A66-16128  
Hydroquinone and oxygen effects on photovoltaic characteristics of optically excited chlorophyll 06 p0812 A66-16357  
Paramagnetic resonance spectra of free radicals in hydrogen peroxide and alcohols during intense UV irradiation 11 p1650 A66-23216  
Free radical reactions in irradiation of model systems and role of radicals in radiation damage 13 p2010 A66-26227  
Electron spin resonance of gamma irradiated single crystal of barbituric acid dihydrate, noting formation and Hamiltonian parameters of free radicals 14 p2367 A66-27979  
Control of abundance of neutral hydroxyl radical in unionized interstellar gas 17 p3003 A66-32658  
Electron paramagnetic resonance study of tetraoxygen difluoride, showing existence of FOO free radical giving asymmetric spectrum 17 p2871 A66-32854  
Collisions in inner region of cometary head, structure of emission bands and formation of free radicals 17 p3010 A66-33376  
Rotational line intensities of lambda 4300

band of CH in spectrum of comet Ikeya 17 p3010 A66-33379  
Rotational and vibrational temperature of diatomic C in comets derived from high resolution spectra, considering transition probabilities in R and P branches 17 p3010 A66-33380  
Total number of cyanide molecules and diatomic carbon free radicals and density distribution in head of Arend-Roland 1957 III comet 17 p3010 A66-33381  
Triatomic carbon spectrum transition bands based on available photographic and densitometric data 17 p3013 A66-33401  
Microwave absorption spectrometer for measuring absolute concentrations of free radicals at any point in conventional gas flow reaction system [AIAA PAPER 66-677] 18 p3112 A66-34245  
Hydrogen bonding kinetics in free radical liquid-phase reactions 21 p3702 A66-38520  
Free radicals and metastable molecules produced by short-duration pulsed electrical discharges studied by mass spectrometer, using collision-free molecular-beam sampling system 22 p3949 A66-39909  
Qualitative detection of alkyl-free radicals generated by pyrolyzing certain organic compounds, using modified commercial mass spectrometer 23 p4067 A66-41246  
**FREE SPACE**  
Impedance cavity on radiation resistance of electromagnetic source 04 p0497 A66-13915  
General theory of minimum fuel free space trajectories 06 p0954 A66-16624  
Optimal free-space fixed thrust trajectories using impulsive trajectories as starting iteratives [AIAA PAPER 66-96] 06 p0956 A66-17094  
Eigenfunction expansions and scattering theory for free-space wave equation in exterior region 12 p1912 A66-23563  
Freely falling point mass problem solutions for Einsteinian free space equations that also satisfy Newtonian equations in suitable coordinate system 12 p1915 A66-24889  
Electromagnetic and plasma wave propagation in inhomogeneous compressible isotropic collisionless electron plasma bounded by closed surface in free space 15 p2449 A66-28592  
Optimal free-space fixed thrust trajectories using impulsive trajectories as starting iteratives [AIAA PAPER 66-96] 17 p3001 A66-32457  
Impedance cavity on radiation resistance of electromagnetic source 20 p3532 A66-37873  
Freely falling point mass problem solutions for Einsteinian free space equations that also satisfy Newtonian equations in suitable coordinate system 23 p4090 A66-41096  
**FREE STREAM**  
Oscillating laminar separated flow formed ahead of forward facing step oscillating transversely to hypersonic free stream, noting phase differences between separation point movement and that of step 14 p2221 A66-28110  
Series expansion solutions for shock tube laminar wall boundary layer, taking into account mutual interaction between boundary layer and free stream 15 p2479 A66-29270  
Source type hypersonic free stream effects on flow field about axisymmetric cone, obtaining properties in shock layer, boundary layer, pressure gradient, etc 17 p2837 A66-32080  
Shock wave instability and mass flow accommodation for ribbon-type parachutes, noting canopy porosity and free stream Mach number 22 p3845 A66-40594  
Flow of unsteady compressible boundary layer over semiinfinite flat plate whose temperature exceeds free stream temperature 22 p3902 A66-40707  
Laminar turbulent transition in freestream boundary layer behind axisymmetric and plane nozzle 23 p4061 A66-42036  
**FREE STREAM EFFECT**  
Near wake of slender cone at free stream Mach numbers of 8 and 12 08 p1164 A66-19130  
Plasma pulses free-streaming from source plate into vacuum along magnetic field 10 p1567 A66-21821  
Molecular beam approximation for plane normal shock in free stream monatomic gas

flow at large Mach numbers 11 p1690 A66-22911  
Free stream turbulence effects on heat transfer rates evaluated by boundary layer approximation 16 p2824 A66-30302  
Film cooling in supersonic free stream flowing along flat plate in Mach 3 wind tunnel, using air as secondary fluid 17 p2839 A66-32441  
Response of two-dimensional laminar boundary layer to fluctuating free stream or surface oscillation 17 p2908 A66-32443  
Relaxation processes behind shock wave in free stream partially dissociated and vibrationally excited by monitoring time history of radiative emission in shock tube [AIAA PAPER 66-519] 17 p2911 A66-32775  
Separation streamline for massive blowing in free stream for model injected into arc tunnel flow [AIAA PAPER 66-457] 18 p3046 A66-33650  
Spark discharge generated blast wave application to shock on shock simulation, free-stream sound speed determination and hypervelocity flow measurements [AIAA PAPER 66-763] 22 p3894 A66-40645  
**FREE VIBRATION**  
Free vibration and transient elastic response of thin shells within scope of linear theory 04 p0586 A66-13405  
Dynamic matrices for natural vibrations of missile considered as beam and as thin walled shell under given boundary conditions 04 p0587 A66-13534  
Eigenvalues of free vibration equation of simply supported beam with finite number of discrete masses, using differential equation 04 p0588 A66-13823  
Asymptotic analysis for equations of axisymmetric vibrations of thin shells [ASME PAPER 65-WA/APM-15] 05 p0777 A66-15437  
Vibration in aircraft jet engine rotating compressor disks of small and large blades [ASME PAPER 65-WA/GTP-11] 05 p0780 A66-15726  
Computer analysis of axisymmetric free vibrations of orthotropic shells of revolution and elastic rings [AIAA PAPER 65-109] 05 p0781 A66-15790  
Displaced frequency technique to determine generalized masses of freely vibrating structure 06 p0967 A66-16930  
Free flexural fundamental vibrations of simply supported isosceles triangular, rhombic and parallelogram plates using special adaptations of point-matching method 06 p0967 A66-16950  
Asymptotic solution of problem of thin spherical shell free vibration for axisymmetric and general cases 08 p1308 A66-18888  
Galerkin method to solve free vibration problem of thin oblate spheroidal shells 09 p1468 A66-20949  
Free vibrations of initially straight elastic bar with free-free or clamped-free ends, undergoing inextensional motion, neglecting shearing effects and rotatory inertia 10 p1616 A66-21484  
Classical theory of flexural motions of elastic plates used to determine natural frequencies of uniform annular plates for nine combinations of boundary conditions 10 p1616 A66-21490  
Frequencies of free lateral resonant vibration of conical beams and truncated wedges for all combinations of simply supported, clamped and free end conditions 10 p1616 A66-21491  
Generalized analysis of rotationally symmetric thin elastic shells applied to cases where shell wall consists of any number of layers of isotropic or orthotropic material 10 p1617 A66-21496  
Internal or external pressure effect on natural frequencies of conical shell, noting role of inertia forces, using linear shell theory 11 p1780 A66-22330  
Free transverse vibrations of parabolic membranes, obtaining eigenvalues and eigenfunctions for Dirichlet conditions [ASME PAPER 65-AV-1] 11 p1780 A66-22472  
Rayleigh-Ritz method, stationary complementary and potential energy principles and Lagrange undetermined multipliers applied to free vibration of elastic body 11 p1781 A66-22611



Lower bounds for frequencies of continuous linear elastic systems in free vibration 12 p1960 A66-23947

Vibration modes of conical frustum shells with free ends [AIAA PAPER 66-450] 16 p2814 A66-30603

Linearized theoretical motion equations for orthotropic cylindrical sandwich shells under initial stress, considering free vibrations 16 p2822 A66-31490

Free vibration of trapezoidal cantilever plates with swept-back leading edge 16 p2823 A66-31666

Frequency equations and mode displacement functions derived for plane strain free-transverse vibration of solid cylinder with elastic core bonded to thin elastic shell 16 p2823 A66-31716

Free vibration of complete and incomplete rings, considering ring centerline extensibility and rotary inertia 17 p3022 A66-32016

Small transverse vibrations of linearly viscoelastic Timoshenko beam of incompressible material, detailing free and forced vibration 17 p3024 A66-32361

Linearized theory of free-vibratory motion of cylindrical sandwich shells under state of initial stress 17 p3025 A66-32455

Frequency equation for free vibration of uniform cantilever beam carrying concentrated mass and moment of inertia at tip 17 p3030 A66-32966

Stability of unsymmetrical rigid rotor supported in axially unsymmetrical bearings, noting three methods of solution 18 p3116 A66-33672

Free flexural vibration of cylindrical shells stiffened by equidistant ring frames treated by finite difference calculus 18 p3250 A66-33673

Free vibrations of two flat plates fixed at right angle with cross-sectional distortion 18 p3251 A66-33678

Free vibrations and stability of rectangular orthotropic plates reinforced by network of ribs 18 p3252 A66-33705

Successive approximation method for solving fundamental equations of nonlinear flexural vibration for rectangular elastic plate, noting effect of temperature and large amplitude 20 p3672 A66-38236

Free vibration analysis techniques for computers and derivation from past methods 21 p3823 A66-38561

Two-dimensional vibration problems treated by Bolotin edge-effect procedure 21 p3823 A66-38565

Continuous system replacement by lumped parameter models, considering undamped flexural vibrations of beam systems, particularly free vibrations 21 p3825 A66-38581

Free vibration of composite system analyzed, using Rayleigh-Ritz method 21 p3825 A66-38583

Support flexibility effect on natural frequency free vibrations of uniform cantilever carried by mass supported on string 21 p3833 A66-39608

Finite Fourier sine transform method of obtaining closed-form solution, calculating eigenfrequencies for free vibrations of partially fixed beam carrying concentrated masses 22 p3992 A66-40296

Longitudinal, torsional and flexural free vibration of elastic slender bar of variable cross section with nonhomogeneous properties 22 p3992 A66-40299

Steady state free and forced vibration response of beams supported on nonlinear springs of Duffing type 23 p4140 A66-41913

Free and forced vibration effect on drift of gyroscope supported in gimbal 23 p4071 A66-41981

Out of plane free vibrations of uniform circular ring on elastic and torsional foundations producing restraints 24 p4287 A66-42165

**FREEDOM FIGHTER AIRCRAFT**

**S F-5 AIRCRAFT**

**FREEZING**

**SA FROST**

Melting and freezing of finite and semiinfinite bodies, discussing variational, heat balance integral, Riemann-Mellin contour integral, etc 06 p0971 A66-16728

Carbon dioxide effect on shattering of

freezing water drops, using methanol-cooled chamber with variable temperature control 10 p1552 A66-21290

Mathematical analysis of thermal wave technique for linear kinetics from viewpoint of solid-liquid interface 18 p3265 A66-34508

Freezing of supercooled water drops to determine dependence of heterogeneous nucleation on temperature and on duration of supercooling 19 p3394 A66-36384

**FREEZING POINT**

Freezing potential for ammonia and sodium chloride solution at constant freezing rates, noting stationary nature of potential under stationary conditions 13 p2121 A66-26124

Electrical conductivity variation with temperature of chlorine and bromine trifluoride, noting maximum conductivity below freezing point of chlorine trifluoride 23 p4118 A66-41241

**FREIGHT COST**

Specialized services provided by air freight forwarding industry to shipper and carrier 15 p2619 A66-29790

Transportation needs of business in small shipment category, discussing role of air freight 15 p2619 A66-29791

Outlook for air cargo handling indicates reduction of cost and increased efficiency by use of intermodel containers 15 p2620 A66-29799

**FRENCH SATELLITE**  
**S FR-1 SATELLITE****FREON**

Low thrust cold gas reaction jet system for small spacecraft with nitrogen, ammonia, Freon-12 and Freon-14, analyzing thrust chamber pressure history [ASME PAPER 65-WA/AUT-11] 05 p0624 A66-15608

Electrostatic field influence on nucleate boiling of Freon 113, noting improvement of peak heat flux 19 p3477 A66-35407

**FREON 12**

VECO 32A11 thermistor element for temperature and liquid level sensing in hazardous gases such as Freon 12 21 p3740 A66-39388

**FREQUENCY**

**SA AUDIOFREQUENCY**

**SA CARRIER FREQUENCY**

**SA CRITICAL FREQUENCY**

**SA CYCLOTRON FREQUENCY**

**SA HIGH FREQUENCY**

**SA INFRASONIC FREQUENCY**

**SA IONIZATION FREQUENCY**

**SA LOW FREQUENCY**

**SA MAXIMUM USABLE FREQUENCY**

**SA MICROWAVE FREQUENCY**

**SA NATURAL FREQUENCY**

**SA OSCILLATION FREQUENCY**

**SA PLASMA FREQUENCY**

**SA RADIO FREQUENCY**

**SA RESONANT FREQUENCY**

**SA SWEEP FREQUENCY**

**SA ULTRAHIGH FREQUENCY**

**SA ULTRALOW FREQUENCY**

**SA VERY HIGH FREQUENCY**

**SA VERY LOW FREQUENCY**

**SA VIBRATIONAL FREQUENCY**

Spectrum of spatial frequencies of object analyzed through Michelson method 21 p3738 A66-39130

**FREQUENCY AMPLIFIER**

**SA INTERMEDIATE FREQUENCY AMPLIFIER**

Parameters of tunnel diode mixer with RF amplifier measured, using tunnel diode as calibrated shot noise generator 02 p0196 A66-11423

Field effect transistors and unijunction transistors in sawtooth generator, cascade amplifier, voltage regulator, etc 06 p0856 A66-16920

Maximum gain condition of resonance amplifier for given passband, determining amplification coefficient 07 p1005 A66-17351

Output signal and noise components determination from difference-frequency amplifier of two-channel receiver 10 p1504 A66-21671

Microwave circuit design for HF amplifiers and radar systems using either hybrid approach with germanium transistors or monolithic one with silicon transistors 10 p1512 A66-21761

Bulk germanium arsenide operating

simultaneously as microwave amplifier mixer and oscillator under continuous wave conditions 12 p1835 A66-24144

5 kw LF power amplifier with improved frequency response, noting design and operation 12 p1843 A66-24688

Bandwidth of nonoverdriven abrupt-junction varactor-frequency doubler, deriving upper bounds for minimum constant T for lossless case 15 p2465 A66-29326

Recognition and subsequent amplification of difference frequency in plasma-beam system with two electromagnetic waves propagating in opposite direction 20 p3519 A66-38000

Block diagrams and frequency characteristics of resistance capacitance resonance amplifier 21 p3713 A66-39253

**FREQUENCY ANALYSIS****SA OSCILLOSCOPE**

RC circuit filter properties during operation under complex load in form of parallel connection of resistance and capacitance 01 p0036 A66-10220

Stability of single-frequency solutions to quasi-linear autonomous systems with two degrees of freedom 02 p0262 A66-12178

Forced discontinuous oscillations of fluid in pipeline, discussing energy dissipation effects in LF range 04 p0509 A66-13555

Frequency characteristics of pulse automatic control systems determined by auxiliary pulse system 04 p0502 A66-13700

Determination of spectral curves, using electrical frequency analyzers 04 p0520 A66-13760

Keying phase-sensitive loop with capacitive loading in selection circuits for frequency separation of telemetry signals 04 p0504 A66-13770

Frequency characteristics of single coordinate inversion photodiode in presence of low signal level, using equivalent circuit 04 p0499 A66-14050

Frequency analysis of wideband RL and RLC phase shifters, using Chebyshev polynomials 04 p0501 A66-14400

Distribution function of zeros in harmonic signals relation to frequency characteristics of latter undergoing maximum amplitude limitation 07 p1001 A66-17340

Short-pulse shaping of high repetition rate with transistorized blocking oscillator 07 p1001 A66-17350

Relay correlator for determining frequency characteristics in searchless self-adjusting systems under steady noise 07 p1012 A66-17370

Distortions of linear system reactions with change in amplitude-frequency and phase frequency characteristics 08 p1183 A66-19100

Exact frequency solution for steady state wave propagation for plane strain vibration of composite hollow cylinders 08 p1310 A66-19180

Resonance Raman effect in crystal, discussing spontaneous and stimulated scattering efficiency 08 p1259 A66-19230

Possible amplitude-frequency and phase frequency characteristics of selective systems with smooth passband control and nonminimal phase 09 p1352 A66-20290

Linear system induced amplitude-frequency and phase-frequency distortions 09 p1361 A66-20290

Radiation resistance of linear current strip of finite width immersed in uniaxial anisotropic plasma medium 09 p1408 A66-20370

Frequency stabilization method for reflex klystrons and other self-excited microwave oscillators 09 p1357 A66-20780

Operation of nonlinear servosystem with autocorrelator as measuring element in presence of noise 11 p1677 A66-22750

Model of spectrometer with external feedback in dynamic behavior analysis, considering control pulse and transfer process 11 p1677 A66-22760

Response of logarithmic frequency characteristics of dynamic linear systems to small parameter variations 12 p1848 A66-23780

Internal gravity waves in stratified liquid for two-dimensional case, noting relation between oscillation frequency and



wavelength 13 p2062 A66-25177  
 Coriolis interaction in first and third  
 fundamental frequencies of ozone, noting  
 vibration rotation spectrum and coupling of  
 two states 13 p2016 A66-25373  
 Microwave transmission and scattering  
 measured in laboratory plasma, noting  
 moving regions occulting microwave beam,  
 existence of turbulence elements and  
 frequency spectrum of uniformly scattered  
 component 13 p2143 A66-25709  
 Axisymmetric configurations of oscillations  
 of thin conical shell, solving equations for  
 fundamental frequency 13 p2207 A66-26497  
 Spectral features of stable generation of  
 oscillation in delayed-feedback microwave  
 oscillator consisting of TW amplifier and  
 waveguide delay line 14 p2267 A66-27738  
 Automatic speech analyzer capable of  
 detecting frequencies of three primary voice  
 formants 14 p2296 A66-27864  
 Frequency characteristics of pulse  
 automatic control systems determined by  
 auxiliary pulse system 15 p2469 A66-28544  
 Frequency spectrum of FM signal for  
 carrier modulation by any number of  
 subcarriers 16 p2649 A66-30547  
 Frequency of strong ionospheric  
 disturbances, noting effect of high and low  
 solar activity, deviations from monthly  
 median, use of statistical analysis,  
 etc 16 p2699 A66-31387  
 RC circuit filter properties during  
 operation under complex load in form of  
 parallel connection of resistance and  
 capacitance 17 p2880 A66-31908  
 Frequency characteristics of single  
 coordinate inversion photodiode in presence  
 of low signal level, using equivalent  
 circuit 17 p2885 A66-32222  
 Frequency analysis of simplex signals using  
 closed loop magnetic tape  
 recorder 17 p2925 A66-32312  
 Feedback control system digital computer  
 design and analysis, including frequency-  
 domain analysis, time-domain analysis, state-  
 space simulation program, etc 17 p2877 A66-32778  
 Aircraft mass and stiffness estimations by  
 displaced frequency 18 p3254 A66-33949  
 Possible amplitude-frequency and phase-  
 frequency characteristics of selective  
 systems with smooth passband control and  
 nonminimal phase 18 p3087 A66-34958  
 Linear system induced amplitude-frequency  
 and phase-frequency 18 p3091 A66-34959  
 Distortions Equivalent systems with identical accuracy  
 at fixed moment of time through transfer  
 function of steady state correcting  
 device 18 p3091 A66-34988  
 Conventional equivalent circuit of tunnel  
 diode with inverse frequency stability  
 characteristics 19 p3312 A66-35348  
 Frequency stabilization method for reflex  
 klystrons and other self-excited microwave  
 oscillators 22 p3874 A66-39839  
 Cut-off frequency of high voltage GaAs  
 varactors, comparing theoretical and  
 experimental values 24 p4183 A66-42632

**FREQUENCY ASSIGNMENT**  
 Synchronous stationary satellite system for  
 networking television and radio material to  
 broadcast stations, noting frequency  
 requirements and constraints  
 [AIAA PAPER 66-284] 12 p1821 A66-24755  
 Role of International Telecommunication  
 Union in satellite communication  
 development, noting history, organization,  
 operation  
 [AIAA PAPER 66-443] 12 p1983 A66-24800  
 International RF space allocation for  
 astronomical purposes 15 p2449 A66-28743

**FREQUENCY BAND**  
 SA C-BAND  
 SA K-BAND  
 SA KU-BAND  
 SA L-BAND  
 SA P-BAND  
 SA RADIO SPECTRUM  
 SA S-BAND  
 SA X-BAND

Wideband junction circulator design with  
 maximum product of isolation and frequency  
 bandwidth but maintaining minimum  
 temperature and DC magnetic field  
 variation 01 p0040 A66-10548

Radio search for intelligent extraterrestrial  
 life, estimating civilization distribution,  
 frequency of best sensitivity and aggregate  
 signal detection 02 p0191 A66-11610  
 Widening of frequency bands of frequency  
 multipliers and dividers by shifting spectra  
 to higher ranges 02 p0206 A66-12271  
 Bandwidth expansion of crystal filters by  
 spacing frequency response characteristics  
 in relay circuit at suitable distances from  
 each other 03 p0342 A66-12895  
 Harmonic structure and band splitting of  
 type II solar radio bursts 03 p0429 A66-13179  
 Transmission band and critical frequencies  
 calculation for straight waveguides of  
 stepped cross section 06 p0838 A66-15884  
 Quadrature modulation single-sideband  
 circuit as frequency translating two-port,  
 comparing performance with conventional  
 modulator-with-SSB filter 07 p1015 A66-17746  
 Existence of relationship between slope of  
 servo-system functions with limited  
 bandwidth and bandwidth  
 magnitude 09 p1346 A66-20575  
 Frequency spectrum of microwave emission  
 from n-type gallium arsenide 10 p1574 A66-21354  
 Data transmission by continuously-radiating  
 power source moving away from receiver  
 and fluctuation noise of uniform frequency  
 spectrum 11 p1654 A66-22633  
 Amplitudes and linewidth of discrete  
 spectrum of natural frequencies of thin  
 magnetic films, noting motion equations,  
 dispersion ratio and resonance  
 peaks 11 p1752 A66-22799  
 Widening of frequency bands of frequency  
 multipliers and dividers by shifting spectra  
 to higher ranges 12 p1831 A66-23875  
 Rarefying of dense frequency spectrum of  
 shell-shaped elements of aircraft engines by  
 corrugating shell surface, determining  
 natural oscillation modes and  
 frequencies 12 p1964 A66-24046  
 Models of hybrid AM-PM signal modulated  
 by single sinusoid and having one-sided  
 frequency spectrum described by using  
 MacLaurin series expansions, noting phase  
 relation of sidebands to  
 carrier 14 p2235 A66-27061  
 Log periodic Yagi-Uda dipole antenna array  
 and extension of frequency  
 bandwidth 14 p2256 A66-27920  
 Plasma diagnostics in terms of response  
 times, noting conversion of phase frequency  
 deviations of probing signal, data recording  
 for plasma in motion and expression for  
 waveguide frequency 14 p2298 A66-28472  
 Relation between frequency spectrum of  
 pulsations in auroral luminosity and energy  
 spectrum of auroral electrons, using  
 photometer 15 p2489 A66-29235  
 True radio-brightness distribution of  
 cosmic radiation source by reducing spatial  
 frequency distortions with passband radio  
 interferometer 16 p2806 A66-31544  
 Frequencies of secondary particles and  
 penetrating particles, using underground  
 scintillators, Geiger counters and flash  
 tubes 18 p3221 A66-35202  
 PCM bandwidth halving and twin working  
 method of superimposing two PCM channels  
 in frequency band occupied by one PCM  
 channel 19 p3305 A66-36625  
 Pulse-shaping networks with frequency-  
 band limitation, noting approximation of  
 idealized networks with echo  
 equalizers 19 p3306 A66-36656  
 Frequency spectrum of laser impulse in Q-  
 switching regime wider than that of single  
 impulse radiated by laser in ordinary  
 regime 20 p3576 A66-37141  
 Frequency sensing for protection of  
 frequency aircraft electric power systems,  
 applying storms saturating reactor  
 concept 20 p3499 A66-37175  
 Broadening frequency bandwidth of full-  
 wave directive loop antennas employing  
 reflectors and directors 20 p3531 A66-37727  
 Stepped structure of sunrise fall observed  
 at various frequency bands of atmospheric  
 activity suggest it is due to wave  
 propagation between Earth and E and D  
 layers 21 p3706 A66-39374  
 Statistical correlation-Fourier frequency  
 band analysis of coherent memory filter

applied to pulse compression radar  
 systems 23 p4035 A66-41023  
 Wide frequency bandwidth properties of  
 arrays of shunt slots in ridged  
 waveguide 24 p4187 A66-43194

**FREQUENCY CONTROL**  
 SA AUTOMATIC FREQUENCY CONTROL  
 Quartz crystals in frequency stabilization at  
 present and in future 01 p0045 A66-10991  
 Frequency stabilization for narrow band  
 microwave oscillators, using supplementary  
 resonator connected by transmission line  
 with basic resonator of  
 oscillator 04 p0496 A66-13904  
 Gunn effect n-type GaAs diode phase  
 locked to stable frequency by injecting CW  
 signal into circuit along with video  
 pulse 06 p0925 A66-16671  
 Tuning multicircuit resonant systems to  
 given frequency passband by graphical  
 resonance curves 07 p1005 A66-17401  
 Numerical representation of controlled  
 quantity expressed by linear frequency  
 signal 07 p1005 A66-17405  
 Stable single-frequency output from laser  
 cavity obtained by filter method and  
 resonance suppression 07 p1045 A66-18356  
 Frequency stabilization of gas lasers, using  
 atomic resonance and  
 interferometers 07 p1045 A66-18357  
 Motor controllers for DC current supply  
 must be inverters of constant or variable  
 frequency 08 p1168 A66-19299  
 Quartz crystals in frequency stabilization at  
 present and in future 10 p1510 A66-21667  
 Frequency correlation in radio  
 communication using scattering  
 media 10 p1504 A66-21677  
 Pulse-phase locked automatic frequency  
 control for multiplication  
 conversion 10 p1504 A66-21678  
 Interference ratios in space telecasting,  
 considering methods of control for  
 cochannel broadcasting  
 [AIAA PAPER 66-283] 12 p1821 A66-24754  
 Random vibration testing, discussing  
 Derritron vibration control oscillator and  
 frequency measurement by splitting into  
 narrow bands 16 p2715 A66-31202  
 Frequency agility theory and application  
 for improved radar, range and angle  
 detection 16 p2655 A66-31649  
 Tunnel diode application to tunable  
 microwave oscillators, noting coupling to  
 high Q factor resonator for frequency  
 stability 17 p2885 A66-32287  
 Frequency stabilization of gas laser by  
 servomechanism and Lamb dip  
 method 17 p2937 A66-33252  
 Dual mode frequency discriminator for  
 microwave source frequency stability,  
 discussing application of beam waveguide  
 resonator 17 p2895 A66-33274  
 Collision frequency control application to  
 control plasma-electromagnetic interaction  
 [IEEE PAPER CP-65-444] 18 p3068 A66-33907  
 Frequency control accuracy measured for  
 hydromechanical constant speed drive with  
 precise speed trim 20 p3499 A66-37174  
 Frequency stabilization for narrow band  
 microwave oscillators, using supplementary  
 resonator connected by transmission line  
 with basic resonator of  
 oscillator 20 p3532 A66-37862  
 Frequency stabilization of gas laser to lock  
 output to center of atomic resonance, using  
 error signal 20 p3580 A66-38241  
 Frequency distortions correction for  
 pulsation amplifier of  
 thermoanemometer 21 p3739 A66-39331  
 Programmed oscillators to control Doppler  
 tracking radar systems for space  
 communications and radar  
 astronomy 22 p3862 A66-39731  
 Frequency variations of pi-equivalent  
 circuit parameters of junction transistor,  
 noting expansion of hyperbolic function into  
 Taylor series 22 p3873 A66-39815  
 Four-layer p-n-p-n diodes having two  
 separate capacitance modes enables use as  
 controlled element in frequency keying  
 circuits 22 p3875 A66-40074  
 Pontryagin maximum principle  
 minimization of time frequency transition in  
 white noise driven phase-locked  
 loop 23 p4048 A66-41316  
 Frequency dependence of electrostatic



energy density in undamped longitudinal plasma oscillation, noting contribution of kinetic and thermal energy 23 p4104 A66-41507

RC filter with staggered notch frequencies for ease of adjustment and maintenance 24 p4183 A66-42628

## FREQUENCY CONVERSION

Serrrodyne frequency conversion determined, using sawtoothed FM of microwave oscillator and subsequent conversion with delay line in sawtoothed phase modulation, calculating phase distortion 04 p0499 A66-14052

Fourier analysis of modulation products in nonlinear device output and optimum frequency conversion for n-frequency input 09 p1396 A66-20639

Laser frequency tuning by dielectric material interaction to produce nonlinear effects 14 p2305 A66-26867

High directional antenna with variable aperture and signal processing after frequency conversion 14 p2251 A66-27237

Passive frequency conversion utilizing nonlinear conductance, establishing lower bound for noise figure 17 p2881 A66-32060

Serrrodyne frequency conversion determined, using sawtoothed FM of microwave oscillator and subsequent conversion with delay line in sawtoothed phase modulation, calculating phase distortion 17 p2884 A66-32218

Optical frequency breakdown threshold of inert gas mixtures, using focused beam radiation from Q-spoiled neodymium laser 18 p3138 A66-34236

Frequency doubling of laser light with variable Q-switched resonator 22 p3929 A66-39654

Convex programming procedure yielding algorithm for tuning out system from possible resonance zone 23 p4090 A66-41408

Frequency up-conversion technique with signal mixing, noting equipment and results 24 p4183 A66-42630

## FREQUENCY CONVERTER

### SA PARAMETRIC FREQUENCY CONVERTER

Design problem of transistorized frequency converters 01 p0045 A66-10993

Regenerative frequency converters used as signal limiters, determining characteristics from equivalent circuit of semiconductor diode 02 p0199 A66-11758

Nonlinear distortion and truncation errors in frequency converters and parametric amplifiers 02 p0201 A66-11902

Instability of tunnel diode frequency converter, discussing effects of temperature and instability 04 p0501 A66-14411

Linear voltage-to-frequency converter provides constant-amplitude output with varying frequencies and constant-frequency output with varying amplitudes 05 p0649 A66-15263

Tunnel diode mixer operation expressed as bias and local oscillator voltages available gain, minimum noise figure and output conductance, carrying out numerical analysis 06 p0846 A66-16095

Amplification factors and optimum matching conditions calculated for complex capacitive diode frequency converters 07 p1005 A66-17347

Gain-bandwidth limitations and optimum design of noninverting frequency converters comprised of parametric conductance in parallel with parametric capacitance pumped in time-quadrature 07 p1017 A66-18348

Design problem of transistorized frequency converters 10 p1510 A66-21669

Diode frequency converter parameter derivation incorporating capacitance of resistance converter and resistance of capacitance converter 11 p1667 A66-22794

Solid state UHF telemetry converter using microwave interdigital multiplexing filter containing integrated semiconductor elements 12 p1840 A66-24622

Coaxial-mounted silicon point-contact diode /1 N 26/ as frequency converter for millimeter waves 12 p1846 A66-24857

Noise factor of linear receiving systems in quantum and classical regions, noting role of dual push-pull amplifier and frequency converter 13 p2020 A66-25226

Variable speed constant frequency /VSCF/

generating system for helicopters 16 p2636 A66-30600

Results derived from dissipative four-terminal networks applied to varactor convertor, leading to capacitance variations determination as function of polarizing potential 16 p2662 A66-30961

Frequency converters using traveling wave and backward wave tubes, noting current-wave amplitude distribution, velocity and voltage 16 p2666 A66-31550

Analog computer and logic circuitry combination for variable frequency signal production, noting application to adaptive control systems 18 p3089 A66-33561

Transfer functions, optimum impedance matching conditions, input and output admittances and voltage spectra of transistorized frequency converters 20 p3525 A66-37125

Diode frequency converter parameter derivation incorporating capacitance of resistance converter and resistance of capacitance converter 20 p3525 A66-37131

Electrical power control and conditioning subsystem for Manned Orbital Research Laboratory /MORL/, noting Brayton cycle, system optimization, alternator and frequency converter selection 20 p3497 A66-37157

Varactor-diode frequency converter properties and operation at L-band 21 p3713 A66-39379

Parametric amplification at collector-base diode for microalloy graded-base transistor and normal mixing due to resistive nonlinearity at emitter 22 p3872 A66-39735

Conversion of finite discrete frequency spectrum by n-dimensional frequency converter with nonlinear active resistance with ideal characteristics 23 p4038 A66-41519

Three-circuit system with circuits connected by nonlinear capacitance applied to frequency converters, amplifiers, etc 23 p4049 A66-41565

## FREQUENCY DISTRIBUTION

### SA POISSON DISTRIBUTION

### SA WEIGHTING /MATH/

Wing broadening in plasma of hydrogen Lyman-alpha line by local electron and quasi-static ion fields calculated, considering impact theory of electron collisions, quadrupole and dipole interactions and existent asymmetries 03 p0405 A66-13138

Solutions for integral equation associated with equation of radiative transfer for isotropic scattering and complete redistribution in frequency cases 05 p0762 A66-15276

Nonsymmetric self-oscillations in relay system, discussing sliding mode of operation of controller with feedback loop 06 p0863 A66-16529

Frequency pattern for transmission from ground stations providing worldwide unambiguous navigation aid for civil aircraft, noting airborne equipment 07 p1073 A66-17769

Frequency distributions of characteristics of daily variation of cosmic ray intensity with solar activity from 1958 to 1962 07 p1125 A66-18006

Frequency distribution of route temperature at supersonic flight levels, noting effect on payload during extended trips [AIAA PAPER 66-371] 12 p1802 A66-24499

Band pass characteristics realized by four-layer distributed RC network without series resistance and amplifier scheme used as model for integrated circuits, noting frequency characteristics variation 13 p2051 A66-26069

Monte Carlo model of elementary fracture process, noting role of energy in comminution, uneven distribution of energy vs frequency, etc 13 p2207 A66-26600

Combined frequency and space correlation of wave fields scattered by rough surfaces where conditions of applicability of Kirchhoff approximation hold true 14 p2236 A66-27144

Dependence of frequency distribution of auroral displays in zenith on latitude and local time in magnetically quiet and disturbed periods analyzed by all-sky camera network in Northern Hemisphere 15 p2488 A66-29227

Circularity index of lunar craters indicating two populations as shown by frequency distribution curve 15 p2597 A66-29252

Frequency distribution of secondary lunar craters determined from Ranger VI photographs, hypothesizing that part of these depressions are subsidence formations 15 p2598 A66-29252

Atmospheric density statistics from cumulative frequencies for seasons a function of altitude for design of booster vehicles 16 p2741 A66-30600

Frequency distribution of atmospheric emissions by multiple lightning discharges 20 p3553 A66-38007

Energy spectral density of ideal sonoboom pressure signatures and equations for HF and LF asymptotic spectral behavior 22 p3848 A66-40300

Atmospheric turbulence effect on frequency spectra of light intensity fluctuations examined, using He-Ne laser 23 p4035 A66-41032

Solar corona pictures during July 1962 eclipse, analyzing polar rays frequency distribution along Sun limb and deviation from radial direction, all linked to solar activity cycle 23 p4123 A66-41831

## FREQUENCY DIVIDER

Phase shifter which includes ring potentiometer and passive network, noting possible frequency division application 01 p0043 A66-10870

Widening of frequency bands of frequency multipliers and dividers by shifting spectra to higher ranges 02 p0206 A66-12270

UHF quarter-wave frequency divider with parametric diode placed transversely in rectangular waveguide resonator 06 p0839 A66-15900

Economical frequency divider with arbitrary coefficient of division 06 p0849 A66-16360

Single tunnel diode multivibrator producing stable frequency division by factors to ten 06 p0852 A66-16510

Pulse-frequency division using parallel connected dividers 07 p1005 A66-17350

Harmonic frequency divider by using inertialess nonlinear element and inertialess nonlinear element such as thermistor 09 p1353 A66-20449

Synthesizing group of parallel-input filter while minimizing insertion loss and reflection coefficient 11 p1656 A66-23060

Widening of frequency bands of frequency multipliers and dividers by shifting spectra to higher ranges 12 p1831 A66-23870

Stability of automatic phase control system for output generation from voltage controlled oscillator 12 p1836 A66-24300

Multiple access modulation techniques /frequency-division, time-division, spread spectrum and pulse-address/ for use in communications satellites [AIAA PAPER 66-278] 12 p1821 A66-24750

Communications satellite system efficiency enhanced by using automatic adaptive voice multiplexer in ground terminal equipment [AIAA PAPER 66-291] 12 p1822 A66-24760

Single tunnel diode multivibrator producing stable frequency division by factors to ten 13 p2041 A66-25955

Economical frequency divider with arbitrary coefficient of division 13 p2042 A66-25955

Frequency division by various factors in magnetic frequency divider with gate excitation winding circuit 16 p2666 A66-31550

Frequency dividers for sequence of pulses using relaxation generators with rectangular timing voltage 17 p2887 A66-32700

Multiple-access systems and characteristics in communications satellite applications, specifically frequency-division multiplex and spread-spectrum modes 20 p3511 A66-36889

## FREQUENCY-DIVISION MULTIPLEXING

Circuit analysis of reduction of intermodulation distortion generated in high power coupled cavity traveling-wave tube for single sideband frequency division multiplex transmitters 04 p0498 A66-14030

Integration of spacecraft tracking, telemetry and command systems using frequency multiplex subcarriers and angle modulated RF signal 19 p3300 A66-35680

## FREQUENCY MEASUREMENT

Wide-range automatic electron-counting



frequency meter for sinusoidal and pulsed signals 02 p0230 A66-11813

Microelectronic digital chronometer and frequency meter, noting design details and thin film circuits 02 p0231 A66-11916

Frequency deviation measurement by digital circuit 03 p0372 A66-13332

Comparison of PCM and PFM telemetry systems in terms of transmission rate, bandwidth, error rate and power 04 p0477 A66-13584

Superimposed vibrations, corresponding to different propagation constants for same frequency parameter, satisfy boundary conditions at flat surfaces of cylinder 05 p0781 A66-15739

Helical oscillations of plasma immersed in time-varying static magnetic field, measuring frequency, amplitude and transition modes 07 p1103 A66-18216

Microwave emission from InSb in magnetic fields, explaining experimental results via modified traveling wave helicon model 07 p1104 A66-18219

Phase-locked marker for rapid identification and accurate measurement of arbitrary frequency in spectrum under analysis 09 p1382 A66-20673

Absolute wavelength stability of helium-neon laser measured by direct interferometric comparison with Hg 198 standard lamp 11 p1712 A66-22868

Instrumentation for measurement of short-term frequency stability of microwave sources 12 p1816 A66-24134

Direct frequency comparison of atomic hydrogen masers in different places and conditions by simultaneous monitoring of Loran C signals 12 p1890 A66-24145

Measuring system for analyzing performance of oscillators of moderate short-term stability, using readily available equipment 12 p1835 A66-24146

Mossbauer effect, frequency measurement and red shift in relativistic gravitational field 12 p1914 A66-24404

Computation method of damped resonance frequencies for system of equal masses, spring constants and viscous damping coefficients 13 p2194 A66-25140

Small frequency shift measurement method for X-band plasma-loaded cavities 13 p2084 A66-26562

Plasma frequency measurement based on Hall effect proportional to electron concentration 15 p2453 A66-29931

Navy navigation satellite system developed by APL, using Doppler frequency measurements for navigation fix 15 p2536 A66-30001

Digital measurement of differential Doppler effect using transposition of phase relation of two HF signals into audiofrequency band 15 p2453 A66-30070

Precision phase meter, discussing principle of operation, design, circuit description and uses 18 p3075 A66-33832

Rise and fall times of transistors in switching operation, comparing variation of lifetime of minority carriers with results obtained from cut-off frequency measurements 19 p3313 A66-35350

Data processing of PFM telemetry whereby resolution of frequency measurements is dependent upon SNR, for application to satellite parameters 19 p3301 A66-35696

One-port log-periodic circuits, determining conditions for which phase of input reflection coefficient varies linearly with logarithm of frequency 19 p3324 A66-35717

Feasibility of improved accuracy in light velocity measurement in vacuum by using superconducting parallelepiped hyperfrequency cavity 19 p3360 A66-36253

Frequency measurement using autocorrelator as frequency discriminator, noting technique and high-noise sensitivity 19 p3306 A66-36657

Frequency of wake shedding from circular cylinder in water flow with values above critical Reynolds number, noting eddy generation and drag coefficient dependence on cavitation number 20 p3548 A66-38012

Erosion destruction mechanism in polycrystalline graphite, noting effect of gas flow over surfaces, flow pulsation frequency and generated aerodynamic loads 21 p3754 A66-38957

Inverse transfer function of pulse-forming network for binary code transmission with small intersymbol interference in time domain and narrow bandwidth in frequency domain 22 p3866 A66-40182

Frequency meter for measuring center frequency of random pulses distributed according to Poisson law, consisting of integrating circuit with high time constant 22 p3918 A66-40404

Bridge circuit measurement of phase at UHF and microwave frequencies, examining amplitude modulation and mixer types 24 p4171 A66-42101

Increase in standard deviation of VLF propagation over very long paths 24 p4172 A66-42420

Frequency characteristic and transient delta function of plant, using algorithm based on correlation functions 24 p4188 A66-42483

Frequency temperature dependence of longitudinal and transverse hypersonic wave absorption coefficients in quartz and artificial ruby crystal 24 p4255 A66-42514

## FREQUENCY MODULATION

SA FEEDBACK FREQUENCY MODULATION /FBFM/

SA PULSE AMPLITUDE MODULATION /PAM/

SA PULSE FREQUENCY MODULATION /PFM/

SA PULSE MODULATION

Digitally coded frequency and pulse modulation with square wave, performing spectral analysis and measuring spectral response 01 p0030 A66-10875

Carrier frequency stabilization of FM laser with respect to center of atomic gain profile, using small distortion present in laser oscillation 01 p0083 A66-10966

Wideband FM transmitters and RF-to-RF repeaters for space application in S- and X-band frequency ranges 01 p0032 A66-11129

Compression of linear FM S-band pulses in axially magnetized yttrium-iron-garnet delay line 02 p0192 A66-11883

Collector modulation class C transistor amplifiers analyzed theoretically, revealing certain parameters influence on efficiency and modulation linearity 02 p0201 A66-11912

FM by mechanical tuning of cavity setting in gallium arsenide crystals for application to communication system 03 p0332 A66-12428

Synthesis of all-pass networks noting uses in signal expansion in time domain, signal phase-splitting, signal delay without FM, etc 03 p0345 A66-13273

Signal to noise ratios for band-limited signals and filtering processes, using simultaneously noise and modulated carrier, noting limiter, summation and bias noise 04 p0477 A66-13586

FM telemetry digitizing system operating on-line in real time environment results in automatic data processing 04 p0489 A66-13600

Five-channel FM/FM telemetry encoder using molecular electronics, noting oscillators, delay lines and linear amplification functional blocks 04 p0493 A66-13601

Data control constant-bandwidth frequency system and tricom system discussed as examples of better methods of taking advantage of communication frequency spectrum 04 p0480 A66-13727

Frequency manipulated signal spectrum for case of modulating function with arbitrary off-duty factor 04 p0482 A66-13912

FM laser oscillation theory discussing effect of arbitrary atomic line shape, saturation, mode pulling, power output, sideband amplitude, distortion, etc 04 p0530 A66-13954

Experiments on helium-neon FM lasers covering phase-locked and FM region power output, modulation index and distortion experiments 04 p0530 A66-13955

Zero conversion loss obtained for certain frequency change using second-order ideal ring modulator with reactive idler circuit at normal output terminals 04 p0500 A66-14094

Comparison of matched-filter analysis and quasi-matched filter analysis of linear FM pulse compression 04 p0486 A66-14117

Performance comparison of cascade two-transistor amplifier configuration with single high-performance transistor used in FM RF

application 05 p0645 A66-14586

Transistor CW amplifier delivering 14 watts into 15-ohm load over frequency band from 46 to 90 mc for use with FM optical modulator 05 p0649 A66-15177

Spectral density of FM baseband wave when it is quantized random facsimile signal 05 p0634 A66-15183

Operating principles of pulse and frequency modulation, using step-recovery diodes as circuit elements 05 p0651 A66-15835

Molecularized FM-FM telemetry system for providing more reliable FM subcarrier oscillators with reduced size, weight and power dissipation 06 p0824 A66-15968

Yttrium iron garnet filters, noting envelope limiting characteristics for submegacycle range modulating frequencies and response parameters 06 p0845 A66-16089

Frequency-selective transmission etalon replaces end mirror of FM laser so that total power is obtained as single optical frequency 06 p0890 A66-16381

Operation of FM microwave generator with external feedback connected to mismatched long line 06 p0852 A66-16512

Linear homodyne mixer used to eliminate interference and extract range information in CW radars 06 p0833 A66-16644

Reflex klystron as subcarrier detector for microwave signals modulated by RF carriers in 100 to 500 kc range 06 p0853 A66-16651

Multilevel narrow-band FM digital communication system using conventional modulators and demodulators 06 p0834 A66-16856

Suppression of FM in parallel signal channels, using Mix-On-Self /MOS/ loop 06 p0834 A66-16858

Binary FM signal originating from single frequency source 06 p0835 A66-16861

Tonks-Dattner resonances, describing frequency modulated technique to study microwave energy irradiated plasma column 06 p0920 A66-16993

Predicting and measuring FM of reflex klystron noise performance when subjected to random acoustical and mechanical vibration 07 p1008 A66-17512

Radar observations of Venus in Soviet Union in June 1964 using frequency keying and linear frequency modulation techniques 07 p1134 A66-17619

Tunnel diode voltage-controlled oscillator to expand FM system channel capacity 07 p1010 A66-18246

Phase-locking effect and phase sum of LF and HF oscillating modes in laser 07 p1046 A66-18413

Medium-capacity satellite receiving system for multiplex FM telephony transmission 08 p1183 A66-18947

Signal to noise ratios of AM, FM and PM systems applied to FM-FM receiver 08 p1185 A66-19563

Complex signal coding with on-off pulses of varying width and repetition period, using equal-slope approximation of signal waveforms 08 p1186 A66-19739

Plasma permittivity modulation by ion waves for thermally ionized alkali plasma in microwave resonator 08 p1266 A66-19811

Semiconductor lasers, FM techniques and multiple-scatter paths used to overcome modulation noise under varying weather conditions 09 p1385 A66-19915

Low-threshold FM demodulator with bandwidth subdivision 09 p1346 A66-20560

High resolution X-band FM/CW radar for radar cross section measurements 10 p1500 A66-21620

Spectral method of determining bandwidth requirement for FM signals based on amount of tolerable distortion at discriminator output 10 p1504 A66-21653

Nonstationary processes and destabilizing factors effect on nonlinear distortion in frequency detector with detuned circuits 10 p1510 A66-21672

Optimal amplitude modulations for radar signal design subject to simultaneous peak and average power constraints 10 p1505 A66-21840

Pressure and heat transfer measurement by FM telemetry for models flying freely in hypersonic wind tunnel streams 10 p1538 A66-22041



AM and FM of transferred electron microwave generators, noting voltage dependence 10 p1515 A66-22094

Small peak phase deviation measured from required characteristics in linear frequency-modulated and pulse-compression radar system 11 p1652 A66-22386

Matched filter for frequency modulated continuous wave radar signal processing system 11 p1669 A66-23110

Reflex klystrons as microwave FM detector and theoretical circuit predictions 11 p1670 A66-23160

Computer analysis of translators using diode ring modulators and dimensioning of frequency dependent networks preceding and following modulating four-pole to obtain specific response in passband, minimizing spurious signal effect 11 p1670 A66-23197

VHF power modulation receivers using germanium injection modulators produce no additional noise at frequencies around 25 cps 11 p1670 A66-23228

Spurious sideband power levels for linear FM carriers encountered in FM-CW and FM pulsed radars 11 p1658 A66-23482

Dynamic frequency response, noting measurement of phase and amplitude responses of active and passive devices under RF pulse conditions with very fast FM 12 p1879 A66-23814

Nomograph for FM/FM telemetry system design 12 p1815 A66-24103

Instrumentation for measurement of short-term frequency stability of microwave sources 12 p1816 A66-24134

Steady state modulation by given frequency external signal of electron flow through straight waveguide, determining relation of counterradiation phase and amplitude to system parameters 12 p1921 A66-24210

Clear air turbulence types at high altitude identified and intensity and wavelength measured by FM instrument, using vane gust probe installed in U-2 aircraft [AIAA PAPER 66-362] 12 p1907 A66-24494

Transverse wave FM phototube system for detection of microwave-frequency modulated light, noting design, operation and application 12 p1838 A66-24558

Power spectra formula of digital FM signals for phase continuous and discontinuous cases, noting results of Anderson and Saltz 13 p2020 A66-25213

Hybrid PCM-FM communication system, noting quantization error and threshold characteristics 13 p2020 A66-25218

Pulse frequency multistable devices whose states differ, along with output voltage, by generated pulse rate 13 p2045 A66-25297

Microwave varactor diode efficiency as waveguide frequency modulator and multiplier 13 p2039 A66-25641

Flutter, time base error and jitter analyzed in multichannel magnetic recorder, noting measurement techniques 13 p2079 A66-25662

Operation of FM microwave generator with external feedback connected to mismatched long line 13 p2041 A66-25952

Atmospheric turbulence effects on laser beam propagation, noting beam cross section, phase variation, AM and FM, etc 14 p2235 A66-27035

Book on modulation as applied to information transmission, discussing mathematical background, linear modulation systems, FM, PM, etc 14 p2239 A66-27718

Desensitization in FM or PM transistorized receivers 14 p2259 A66-28042

Five-channel FM/FM telemetry encoder using molecular electronics, noting oscillators, delay lines and linear amplification functional blocks 14 p2243 A66-28350

Relation between RF of Jovian decametric emission bursts and modulation by Io searching for modulation by three outer Galilean satellites 15 p2597 A66-29232

Effect of harmonic distortion on Bessel-zero technique for FM deviation measurement used in calibration of carrier deviation and FM signal generator instruments 15 p2467 A66-29857

Radiolocation theory compared with communication theory, noting trading of frequency bandwidth of radar signal for error suppression 15 p2535 A66-29860

Comparison of frequency-modulated tunnel diode oscillators 15 p2468 A66-29924

Propagation velocity and attenuation variation effect in coaxial cables on frequency modulated carrier evaluated, using IBM 1620 computer 16 p2649 A66-30542

FM telemetry Rf link performance evaluated by constructing model of subcarrier multiplex, based on predicted noise power spectrum at Rf demodulator output 16 p2649 A66-30543

FM error calculation via comparison of demodulated output with input 16 p2649 A66-30544

Expansion of Inter-Range Instrumentation Group FM/FM baseband, noting maintenance of system performance with added channels 16 p2649 A66-30545

Frequency spectrum of FM signal for carrier modulation by any number of subcarriers 16 p2649 A66-30547

FM 10 watt S-band transmitter for space telemetry and data application 16 p2651 A66-30560

FM/FM and PAM/PM integrated telemetry systems with MDI for missile evaluation system 16 p2651 A66-30562

Communication effectiveness over VLF paths impaired by variability of VLF field strength due to modal interference effects 16 p2653 A66-30723

Digital computer to decode digitized or sampled PCM waveform 17 p2875 A66-32502

Signal transmission through double FM regaining LF signal by two-stage frequency demodulation at receiving end 17 p2876 A66-33451

Spectrum broadening of long-duration high-frequency pulses by FM 17 p2877 A66-33521

Multilevel narrow-band digital FM modem noting design principles, signal to noise ratio vs error rates, etc 18 p3067 A66-33900

Ultrasonic cell which modulates intensity of He-Ne laser beam for communication of intelligence 18 p3118 A66-34059

Plasma jet electrical conductivity, using inductances with different diameters as measurement device 18 p3144 A66-34101

Interference in passband of FM or PM channel due to adjacent FM or PM channel in telemetry system 19 p3300 A66-35687

Optimization of control loop type for minimum threshold which is function of modulation index, obtaining results using sine wave modulation 19 p3301 A66-35695

FM modulator with frequency response from DC to video while maintaining crystal stability, accommodating FM narrow-and wideband with single design 19 p3316 A66-35699

Temperature sensing and control by fluidic devices, using FM and phase discrimination for gas turbine engine application 19 p3361 A66-36672

IBM 7094 programmed in FORTRAN IV used to determine sidebands in FM with complex periodic modulation functions 20 p3522 A66-37212

Resolution of multiple target ambiguities in twin-channel frequency-modulated continuous wave radar system using fixed antenna 20 p3596 A66-37218

Frequency modulation in quartz oscillators, deriving nonlinear distortion and frequency deviation factors and analyzing effect of destabilizing factors 20 p3516 A66-37383

Medium frequency, FM, VHF and UHF TV broadcasting and receiving antennas 20 p3530 A66-37717

Frequency manipulated signal spectrum for case of modulating function with arbitrary off-duty factor 20 p3518 A66-37870

Stationarity conditions for FM oscillations with noise-modulated frequency 20 p3519 A66-38003

FM data systems noting design, error analysis, applications to data recording and transmission, etc 21 p3708 A66-39478

Single-sideband FM for data transmission on vibration and acoustic measurements, noting SNR performance, transmission link, etc 21 p3706 A66-39479

Space vehicle telemetric data transmission by FM, PCM, frequency multiplex, etc 21 p3717 A66-39633

Light absorption by optically pumped atoms undergoing magnetic resonance, noting modulation amplitudes and

modulation frequency limitation for primary interaction 22 p3930 A66-39807

Distortion of FM signals after being processed through time-invariant channels with nonlinear phase characteristic and fluctuating amplitude function 22 p3864 A66-40061

Laboratory environment simulation of multipath propagation interference effects on low channel capacity FM systems 22 p3865 A66-40066

Steady state modulation by given frequency external signal of electron flow through straight waveguide, determining relation of counterradiation phase and amplitude to system parameters 22 p3878 A66-40574

Pulsed compression network for linear FM signals using short circuited delay line and with sweep frequency corresponding to output response peak 23 p4034 A66-41020

Adjustable time domain equalizer for reduction of distortion caused by paired echoes in pulse compression radar system 23 p4034 A66-41021

Error probability in PCM/FM with phase-locked loop discriminators, noting role of input SNR 23 p4037 A66-41326

Ballistic range blast-traversal testing technique using scale models containing fast response FM telemetry system modulated by capacitance type pressure transducer [AIAA PAPER 66-777] 23 p4053 A66-41333

Simultaneous FM telemetry measurement of four aerodynamic forces acting on free flying models in wind tunnel 24 p4209 A66-42190

Phase-lock servo-loop circuit for space communication providing estimate of incoming signal through correlation process 24 p4175 A66-42820

Square-law detection system for multiple FM signals with noise 24 p4175 A66-42963

**FREQUENCY MODULATION**

**PHOTOMULTIPLIER**

Traveling wave HF crossed field photomultiplier with helical output circuit for electron multiplication at microwave modulation rates 24 p4182 A66-42561

**FREQUENCY MULTIPLIER**

Frequency multiplication mechanism using microwave gas discharge of air, argon or neon 01 p0029 A66-10583

Increased efficiency and power-handling capability of high order idlerless frequency multipliers by using hyperabrupt varactors 02 p0195 A66-11363

Widening of frequency bands of frequency multipliers and dividers by shifting spectra to higher ranges 02 p0206 A66-12273

Two-cavity klystron frequency multiplier for generating waves less than 1 mm 03 p0342 A66-12881

Harmonics in cylindrical electron beams traveling in circular drift tube and velocity modulated by gridless buncher gap 04 p0491 A66-13420

CW klystron frequency multiplier for generating submillimeter waves 04 p0492 A66-13422

Varactors for frequency multiplication 05 p0649 A66-15363

Measurement results on frequency doublers in millimeter wave region, using unencapsulated silicon varactor diodes and gallium arsenide/ phosphor bronze point contact varactor 08 p1198 A66-19747

Gallium arsenide phosphide heterojunction diode used to triple from X band to Ka band 09 p1350 A66-19922

Pulse repetition rate of magnetic pulse generators increased by transforming generator power supply frequency, using static frequency multipliers 09 p1352 A66-20307

Strip transmission line for microwave circuit design such as varactor multiplier frequency sources, filters, multiple pole diode switches, etc 09 p1356 A66-20672

Three-centimeter wavelength frequency multiplier using gas-discharge plasma in nonuniform electric field, examining amplitude and phase instability 09 p1358 A66-20795

Step-recovery diode multiplier circuit for high-order harmonic generation 09 p1359 A66-20919

Signal to noise ratio at output of



frequency doubler performing nonlinear transformation by quadrature circuit 10 p1510 A66-21670

High-efficiency microwave frequency doublers using varactor diode design by technique based on Manley and Rowe energy relations 10 p1512 A66-21763

Transient behavior of varactor bridge doubler examined, using direct digital integration of circuit equations 10 p1513 A66-21859

Frequency multiplication circuits, examining effects of short-term stability on oscillator system 10 p1514 A66-22044

Effect of amplitude noise or spurious signals in varactor frequency multiplier 11 p1661 A66-22383

High-ratio multipliers and tunnel diode generators as solid state microwave sources considered in analysis of varactor circuits 11 p1670 A66-23196

Widening of frequency bands of frequency multipliers and dividers by shifting spectra to higher ranges 12 p1831 A66-23875

Broadband X to K band varactor frequency doubler, noting efficiency increase by replacing variable resistance element with varactor 12 p1832 A66-23908

Nonlinear systems including oscillators, frequency multipliers, limiters, etc, driven by periodic carrier, deriving circuit theory for small perturbations propagated throughout system 12 p1848 A66-24136

Output signal of harmonic generator with noise sources in circuit, using perturbation analysis and assuming noise effect on signal in transducer is band-limited 12 p1835 A66-24137

Additive phase noise measurement in step-recovery-diode in frequency multiplier compared to ideal multiplier 12 p1835 A66-24141

Step-recovery diode in shunt configuration as frequency multiplier 13 p2030 A66-25215

Varactor diode as frequency multiplication element, discussing design parameters and noise characteristics 13 p2039 A66-25699

Multiplier with varactor diode circuit examined, noting maximum obtainable conversion output power and efficiency 13 p2041 A66-25879

Light frequency multipliers for nonlinear optical effects at various wavelengths, considering focusing, laser beam finite divergence, air breakdown, stimulated Raman emission, etc 13 p2096 A66-26146

Modified series model for abrupt-junction varactor diode used as harmonic frequency doubler 14 p2257 A66-27952

Exact circuit analysis of abrupt-junction varactor diode frequency doubler 14 p2268 A66-27957

Dimensioning varactor diode frequency multipliers used in HF transmitters 14 p2259 A66-28113

Directivity diagram of N-antenna radio interferometer when interferometer is in frequency-multiplication regime, noting role of SNR 15 p2449 A66-28640

Developments in varactor technology, noting large-area step-recovery varactor with nearly twice power-handling capacity of step junction devices 15 p2457 A66-28654

Equivalent circuit evaluation of theoretical potential and limitations of millimeter wave semiconductor diode detectors, mixers and frequency multipliers 15 p2461 A66-29015

Gallium arsenide varactor diode design for parametric amplifiers and multipliers, noting efficient harmonic generation at higher microwave frequency 15 p2466 A66-29677

Varactor frequency doubler response to amplitude and phase modulated signals 17 p2878 A66-31811

Design of adaptive systems with forced oscillations, using correlation and filter methods 17 p2902 A66-32573

Series connection of varactor wafers for higher breakdown voltages without loss of cut-off frequency, noting power output 17 p2867 A66-32698

Broadband semiconductor diode frequency multipliers, examining performance, noise theory, realization and frequency multiplication mechanism 17 p2890 A66-32904

Varactor diode harmonic generators for S-band with VHF input and microwave output 17 p2892 A66-32916

Signal analysis of abrupt and graded junction varactor harmonic generators with idlers, showing how load and source resistances may be optimized 17 p2893 A66-32922

X-band solid state source using chain of frequency multiplier stages and driven by transistor crystal controlled driver unit 17 p2893 A66-32923

Signal to noise ratio in frequency multipliers with varactor diodes, noting relaxation oscillation type instability and techniques for minimizing noise effect on signal 17 p2894 A66-32988

Phase-jitter spectrum of oscillators and frequency multipliers, noting additive nature of output 17 p2894 A66-33111

Iterative solution of large signal abrupt junction varactor doubler as input frequency is varied, given power of source and load impedance 17 p2895 A66-33276

Broadband semiconductor diode frequency multipliers, examining performance, noise theory, realization and frequency multiplication mechanism 18 p3075 A66-33564

Signal analysis of abrupt and graded junction varactor harmonic generators with idlers, showing how load and source resistances may be optimized 20 p3531 A66-37831

Frequency multiplication using diffusion capacitance with derivation of efficiency expression 20 p3519 A66-38001

Possibility of realization of multicascade tunnel diode frequency doublers without intercascade amplification 20 p3533 A66-38009

Varactor frequency multipliers, discussing application in low-power ultra-short-wave devices in moving objects for communication purposes 21 p3709 A66-38623

J-band multiplier design noting extension of frequency coverage, components, noise performance, frequency stability, tuning range, etc 21 p3711 A66-38837

Multiplier with nonlinear capacitance and resistance showing improvement in conversion efficiency, allowable input power and converted output power 21 p3712 A66-39227

Solid state frequency multipliers for LEM landing and rendezvous 21 p3715 A66-39525

Three-centimeter wavelength frequency multiplier using gas-discharge plasma in nonuniform electric field, examining amplitude and phase instability 22 p3874 A66-39852

Four-layer p-n-p-n diodes having two separate capacitance modes enables use as controlled element in frequency keying circuits 22 p3875 A66-40074

Overlay transistors at microwave frequencies for amplifiers, oscillators, etc, used in telemetry 22 p3879 A66-40722

High power microwave frequency multiplier matching very low varactor impedances 22 p3879 A66-40723

Microwave solid state multiplier for space use noting temperature variations, vibration-induced noise, outgassing, etc 22 p3879 A66-40724

AC background in phase of output oscillation of multistage frequency multipliers attributed to presence of HF harmonics in automatic bias circuit 23 p4038 A66-41520

# FREQUENCY RANGE

Data control constant-bandwidth frequency system and tricom system discussed as examples of better methods of taking advantage of communication frequency spectrum 04 p0480 A66-13727

Measurement of small coefficients of nonlinear distortions from ratio between effective voltages of first harmonic and total signal 04 p0497 A66-13916

Practical technique for performing transformations between time and frequency domains applied to synthesis of four-terminal RLC networks 05 p0657 A66-14995

Frequency range of more than 60 gc obtained by introducing microwave absorber into last stage of multishaft absorber, improving reflection coefficient 05 p0648 A66-15029

Frequency dependence of dynamic properties of semiconductor small area ohmic contacts in volt-ampere characteristic regions when constant current and

sinusoidal pulses are applied 06 p0833 A66-15893

Received field strength dependence on maximum and minimum usable carrier frequency range for ionospheric scattering 06 p0836 A66-17034

Dynamic flexural rigidity of polymer plates, measuring elastic modulus, noting variation of Youngs modulus, Poisson ratio with temperature and rate of loading 09 p1466 A66-20183

Probability of signal acquisition by phase-locked oscillator system operating in frequency search mode, determining maximum admissible search rate without noise 09 p1345 A66-20443

Short-wave frequency range spacecraft communications, discussing Earth signal reception, signal trajectories from orbits above and below F-2 layer, etc 09 p1348 A66-21013

P-i-n diode modulators for K and Q frequency bands, extending operation from 18 to 40 gc 10 p1513 A66-21856

Atomic frequency standard fluctuation, instability due to noise and atomic beam frequency stability 12 p1881 A66-24125

Statistical analysis of circuit noise effect on oscillators according to perturbation theory, discussing power spectrum, power and signal phase spectral densities, frequency stability, etc 12 p1834 A66-24127

Cross correlation measurements of oscillator frequency stability and thermal noise and application to atomic hydrogen maser 12 p1835 A66-24128

Dependence of beat frequency of neodymium laser axial modes on distance between mirrors and neodymium rod position within resonator 12 p1891 A66-24881

Direct-coupled multistage integrated amplifier design for optimum performance under arbitrary cascade configuration, noting power gain and frequency range 13 p2040 A66-25831

Parameter indeterminacy in system identification for mathematical model with adjustable parameters matched to system output by feedback 13 p2054 A66-26091

Junction filters for eight channels in SHF range with provision for 1800 paths, noting bandpass width signal mixing for antenna feed, attenuation, capability, etc 14 p2252 A66-27351

Circuits incorporating varactor diodes, pumped at IF, as mixers, analyzing circuit characteristics 14 p2236 A66-27352

Orthotropic-elasticity solutions applied to wave propagation in infinite cylindrical shell, obtaining asymptotic solutions for HF range 14 p2400 A66-27662

High impedances obtained over wide frequency range with bipolar or unipolar transistors, noting current multiplication, bootstrapping, etc, and FET 14 p2262 A66-28377

Waveguide system using Chebyshev filters for channel separation in wide frequency ranges, applied for sounding plasmas with various electron concentrations 14 p2298 A66-28473

Response of aerospace structures to in-flight dynamic loads in HF range 16 p2813 A66-30446

Ten-inch stroke electrodynamic thruster, noting modifications in armature guidance, base, rotation system, trunnion lifting mechanism, etc 16 p2678 A66-30464

Vibration equipment, discussing armature and control oscillator 16 p2679 A66-30474

Dual polarized high-power synthetic conical scan tracking system at various frequency ranges for parabolic reflector used in communication link 16 p2650 A66-30552

Wind velocity spectra and correlation functions statistically analyzed in ULF range for lowest levels of atmosphere 16 p2742 A66-30773

Transistorized wideband and pulse type amplifiers for nanosecond frequency range 16 p2664 A66-31357

Noise behavior of X-band microwave mixer over range of intermediate frequencies and local oscillator powers, noting variation of mixer conversion gain, etc 17 p2892 A66-32920

Coupling coefficient between TE 11 and TM 11 mode in tapered circular waveguides,



noting behavior near cut-off frequency 17 p2895 A66-33275  
 Frequency spectrum of continuous thermal radiation emission of plasma layer 17 p2974 A66-33285  
 Transformation coefficient and secondary radiation pattern when doubling frequency of focused coherent light beam in approximation of given primary-beam field 20 p3576 A66-37145  
 Measurement of small coefficients of nonlinear distortions from ratio between effective voltages of first harmonic and total signal 20 p3532 A66-37874  
 Flux trapping of RF fields in superconductors from measurements on superconductive resonant circuits in frequency range of 10-1000 mc 21 p3796 A66-38555  
 Data statistical analysis of solar radio bursts over wide frequency range and relation to solar flares 21 p3815 A66-39372  
 Dependence of beat frequency of neodymium laser axial modes on distance between mirrors and neodymium rod position within resonator 23 p4076 A66-41088  
 Viscoelastic properties of liquids under steady flow determined experimentally in frequency range 5-75 mc/s, using internal reflection of pulse of shear wave at surface of fused quartz bar 23 p4066 A66-41159  
 Electrical properties and fabrication of zinc oxide-bismuth oxide low Q capacitor with high apparent dielectric constant over wide frequency range 24 p4180 A66-42311  
 Elimination of singularity in power radiated by point electric dipole in unbounded magnetoplasma within certain frequency range 24 p4241 A66-42373

**FREQUENCY REGULATOR**  
 Seven-stage RL feedback amplifier with 500-mc low-pass bandwidth and 52 db gain, employing frequency compensation technique 11 p1671 A66-23244  
 Coherent laser-type light generators with capability of adjusting frequency over visible spectrum 19 p3375 A66-36265  
 Synthesis of constant or time-varying linear feedback control laws for application in multiple input systems with frequency symmetry 20 p3645 A66-36864

**FREQUENCY RESPONSE**  
 Graphical method for determining closed-loop frequency response of nonlinear feedback control systems 03 p0349 A66-13021  
 Wind tunnel technique for measuring frequency response of flexible airplane to vertical sinusoidal gusts [AIAA PAPER 65-787] 03 p0438 A66-13071  
 Operational amplifier design using normal feedback equations with grounded output voltage for input, discussing frequency response and determination of open-loop gain magnitude 03 p0351 A66-13276  
 Parametric response of elastic clamped-free column, noting agreement between theory and experiments for first three spatial and first four temporal modes 04 p0594 A66-14391  
 Instability of tunnel diode frequency converter, discussing effects of temperature and instability 04 p0501 A66-14411  
 Frequency response function of lightly damped single-degree of freedom system estimated from truncated measurement of cross-correlation function of white noise excitation and response 05 p0781 A66-15788  
 Approximate methods for plotting logarithmic frequency responses of discrete systems with and without time lag, noting PAM systems 07 p1012 A66-17382  
 General performance indices for time and frequency response for free motion of linear discrete control systems 07 p1016 A66-18280  
 Loading frequency effects on fatigue strength of 45 and E1612 steel specimens at room temperature 07 p1147 A66-18385  
 Self-consistent-field type perturbation theory for stationary and homogeneous turbulence to determine energy spectrum and response frequencies 08 p1204 A66-18531  
 Root hodograph method for determining amplitude and phase frequency characteristics of dynamic linear systems 08 p1202 A66-19692  
 HF pulse decay in input of slightly detuned multistage synchronous single-circuit amplifier 08 p1198 A66-19737

Intrinsic noise effect on synchronization of self-excited oscillators, determining phase diffusion coefficient, frequency fluctuation spectra and spectral line 09 p1344 A66-20345  
 Weighting function and frequency response determination of linear system with N degrees of freedom, using convergent series solution 09 p1396 A66-20636  
 Circuit conveying continuously variable signals between points with large steady potential differences, having commercial resistors and capacitors and no RF coil 09 p1363 A66-20665  
 Laplace transform and analog computation applied to simulation of heat transfer between wall separated fluids, determining transfer functions and frequency responses 09 p1472 A66-20908  
 Hamel and Cypkin methods, used to determine free oscillation of plus-or-minus servomechanism, applied to transfer function of certain type 10 p1517 A66-21283  
 Spiking behavior of multimode ruby laser in spherical resonator, interpreting near-field patterns, frequency spectrum, etc 10 p1542 A66-21311  
 Resolving power and microphotometric granularity of IR films measured with resolvometer, noting dependence on frequency of incident light 10 p1534 A66-21332  
 Two-terminal current-controlled negative resistance devices examined, using equivalent circuit, noting stability criterion, frequency response, etc 10 p1513 A66-21860  
 Transient and frequency response of distributed resistance-conductance-capacitance network 11 p1675 A66-22389  
 Force and moment response of pneumatic tires undergoing nonstationary lateral motions, using motion equations [ASME PAPER 65-AV-2] 11 p1636 A66-22471  
 Distributed RC network synthesis, determining necessary and sufficient conditions for driving point impedance frequency response of transfer functions and Foster type 11 p1678 A66-23240  
 Surface roughness and tolerances in model scattering experiments, noting shape perturbation consequences, frequency characteristics wave behavior, etc 11 p1658 A66-23406  
 Forced oscillations of ferrite core circuit, showing phase characteristics and parameters of inductance and amplitude 12 p1958 A66-23725  
 Dynamic frequency response, noting measurement of phase and amplitude responses of active and passive devices under RF pulse conditions with very fast FM 12 p1879 A66-23814  
 Time resolution error of measured correlation function, based on frequency response of hot-film and hot-wire anemometer 12 p1880 A66-23847  
 Alteration of antenna spatial frequency response due to time constant of radiometer and scan velocity 12 p1837 A66-24311  
 Deviations from BCS behavior in temperature dependence of ultrasonic absorption in superconducting tin 13 p2158 A66-25056  
 Pulse forming networks whose step responses have ripples of equal height 13 p2029 A66-25205  
 Magnetic deflection for display systems offers improved design freedom and good frequency response 13 p2047 A66-25362  
 Differential amplifiers using common-collector, isolated and lateral complementary transistor structures, including frequency response, phase shift, etc 13 p2036 A66-25532  
 Unbounded isothermal atmosphere response to time harmonic point disturbances, exact solutions obtained for frequency ranges of acoustic waves, trapped oscillations and gravity 13 p2183 A66-25613  
 Fan-out filters giving flat response over broad bandwidths and minimization of variation of input impedance with frequency 14 p2249 A66-27106  
 Linearized motion equation of self-adaptive systems with stabilized frequency characteristics, considering effect of control and noise signals in basic control loop 14 p2265 A66-27525

HF transistor circuit design, noting effect of bias frequency and temperature on y and h parameters 14 p2261 A66-28368  
 HF amplifier design, using two-port theory, measurement of Si epitaxial mesa transistor y-parameters, discussing power gain, sensitivity and inherent stability 14 p2261 A66-28370  
 Modulus of loop-gain frequency responses and mean-square error in transistor operational amplifier 15 p2454 A66-28544  
 Frequency response of avalanche photodiodes, discussing multiplication ratio and extension of Townsend theory 15 p2458 A66-28888  
 Transfer function realization using R network and control source, noting constraints such as multiplicative factors, poles, boundary frequencies, etc 15 p2471 A66-29322  
 Output power frequency response of single mode helium neon laser, determining effect of atomic collisions on frequency responses of individual atoms 15 p2518 A66-29818  
 Transverse and axial magnetic field effects on gas lasers, deriving expression for atomic and macroscopic polarization, determining oscillation mode characteristics, frequency responses, etc 15 p2518 A66-29819  
 Mechanical shutter with time resolution 0.1 msec designed for spectroscopic observation of decaying plasmas 16 p2701 A66-30270  
 Forced aperiodic vibrations in idealized viscously damped system, subjected to parametric excitation by forcing function with uniformly accelerating frequency and constant displacement amplitude 16 p2678 A66-30468  
 International specification for shock pulse shapes and magnitudes, noting duration, tolerance, etc 16 p2712 A66-30470  
 Network analysis and amplitude frequency response characteristic of operational amplifier for DC analog computer 16 p2659 A66-30512  
 Physiological telemetry, using pulse duration approach for acceptable frequency response 16 p2642 A66-30544  
 Polarization characteristics of type IV solar radio bursts noting position, direction and frequency range 16 p2793 A66-30655  
 Pole-zero method to determine frequency response of second-order linear control systems with phase-advance signal shaping 16 p2671 A66-31157  
 Flowgraph techniques for closed systems, discussing properties, approximation methods, topology equation, frequency response constraints, oscillatory and stochastic processes, etc 17 p2898 A66-31957  
 Physical process effect on structure of F II regions, noting ionization, Lyman continuum spectral distribution and radiative transfer frequency dependence of absorptive processes 17 p3003 A66-32655  
 Simple diode parametric amplifier, discussing bandwidth and noise measurements, compensating circuits for gain-frequency response improvement 17 p2892 A66-32918  
 Parametric and tunnel diode amplifiers for radio astronomy, noting diode quality, operating frequency range, noise, temperatures, etc 17 p2892 A66-32919  
 Solid state microwave source for severe vibration environment and 20 mw of power, discussing circuit design, noise performance, frequency stability 17 p2893 A66-32922  
 Sonic boom measurement instrumentation, noting use of frequency response, vibration isolation, wind screening, etc 17 p2926 A66-33022  
 FM modulator with frequency response from DC to video while maintaining crystal stability, accommodating FM narrow-and wideband with single design 19 p3316 A66-35699  
 Sampling techniques for conversion of broadband signal into multiple narrow bandwidth and reconversion back to original signal 19 p3302 A66-35700  
 Normal modes and mode coefficients of lossless circular multimode waveguide determined from boundary conditions, noting frequency dependence of mode conversion 19 p3317 A66-35718  
 Resistance and frequency response range



of sheath surrounding electrostatic probe floating in tenuous plasma 19 p3357 A66-35808

Photographic process role in holography, noting relationship of exposure and transmittance by highly nonlinear inverse power law 19 p3357 A66-35815

Surface roughness effect on radar backscattering cross section of conducting spherical target examined by applying Kirchhoff method 19 p3304 A66-36407

Amplitude frequency response of blocked pneumatic lines used in fluidic systems, noting correlation to electric-pneumatic analogy prediction 19 p3372 A66-36684

Linear system with given structure identified from measured input and output time histories of frequency responses including curve-fitting, equation of motion and set of equations of motion methods 20 p3537 A66-36885

Analog computer method for reconstruction of data distorted by physical system response noise 20 p3627 A66-36888

Resistive effects in  $\gamma$ -type II superconductors near upper critical field examined, using Ginzburg-Landau equations 20 p3616 A66-37374

Phosphate glass effect on frequency behavior of n-inversion layers on silicon MOS diodes 20 p3529 A66-37545

Liquid instability of vibrating partially filled elastic tank, emphasizing resonant breathing mode and frequency response 20 p3672 A66-38153

Parameter change effect on feedback control system magnitudes directly measurable on step and frequency response diagram, including delay time, overshoot and passband 21 p3718 A66-38808

Electronic test method for determining ultrasonic transducer frequency response involving actual signal transmission and reception 21 p3738 A66-39151

Spectral response curves of superconducting point contacts, noting existence of frequency dependent Josephson current amplitudes peaking in vicinity of energy gap 21 p3803 A66-39262

Nonlinear automatic system with logical device analyzed in presence of external action, obtaining harmonic linearization coefficients 21 p3719 A66-39284

Dispersive network with attenuation equalizing network, weighting filter for control of output side lobe level with Gaussian shaped frequency response and matching system 23 p4034 A66-41016

Photodetectors capable of microwave modulation frequency response operating in visible or near IR portion of optical spectrum 24 p4212 A66-42808

Transistor parameters in integrated circuits including saturation resistance, voltage breakdown and frequency response and optimization of operation dependence on impurity concentration, geometry, etc 24 p4186 A66-43079

**FREQUENCY SCANNING**

Frequency sensor and roving notch filter for control system, discussing parasitic signals with time-varying frequencies 05 p0645 A66-14603

Properties of helical delay line used to feed frequency scanned X-band array, noting role of ball bearing inserted in helix 06 p0854 A66-16686

Frequency scanned antenna with dielectric loaded waveguide, discussing experimental results 20 p3531 A66-37729

Reception of signals reflected from ionosphere in vertical radar probing, examining frequency-difference combinations 22 p3869 A66-40780

Equations of motion of continuous single loop adaptive control system with scan modulated parameters, noting stability analysis method 24 p4188 A66-42479

**FREQUENCY SHIFT**

Linear accelerator for micrometeoroids operated in radially stable mode and variable frequency for hypervelocity impact studies 01 p0053 A66-10852

Real and theoretical accuracy of direction finding discussing phase, frequency and amplitude fluctuation of signal 04 p0544 A66-14412

Shifts in output frequency of cesium vapor

magnetometer due to temperature, light intensity and orientation, noting Zeeman component and geomagnetic field 05 p0678 A66-14968

Plasma conductivity measurement in terms of frequency shifts and Q-factor variation in RF oscillatory circuit produced by presence of plasma sample in induction coil 08 p1264 A66-19190

Raman laser materials selection, emphasizing frequency shifts and excitation power threshold 11 p1721 A66-23477

Frequency shift in resonance transition induced in potassium vapor by ruby laser pulse 13 p2089 A66-25103

Small frequency shift measurement method for X-band plasma-loaded cavities 13 p2084 A66-26562

Atmospheric noise FSK error probabilities for envelope detection receiver 14 p2243 A66-28352

Measurement of single line in P branch of carbon dioxide vibro-rotational absorption band using tuned optical maser spectroscopy, noting presence of shifted frequencies 15 p2512 A66-28691

Frequency shift in resonance transition induced in potassium vapor by ruby laser pulse 16 p2717 A66-30282

Tuning of ammonia beam maser resonator based on frequency shift method, noting hysteresis appearance and elimination 16 p2720 A66-31696

Frequency variation of ionospherically propagated radio waves by spectrum analysis of received signal 17 p2874 A66-32384

Automatic failure detection, location and correction system for failures in unmanned spacecraft using frequency-shift-keyed subcarrier 19 p3316 A66-35679

Nonstationary flicker-type frequency fluctuations effect on form and width of spectral line 20 p3513 A66-37153

Microwave emission frequency shift during uniaxial stress on Si epitaxial planar and diffused mesa type diodes 23 p4044 A66-41299

Pressure- and gain-dependent frequency shift measurements in stabilized 6328 angstrom He-Ne laser 24 p4224 A66-42803

**FREQUENCY-SHIFT KEYING**

Atmospheric noise effect on performance of noncoherent frequency shift keying /NCFSK/ under fading conditions compared with that obtained when noise is Gaussian 06 p0830 A66-16335

Nonorthogonal coding in communicating through dispersive or multipath fading channels for increased data rate without increased bandwidth 06 p0835 A66-16866

Radar observations of Venus in Soviet Union in June 1964 using frequency keying and linear frequency modulation techniques 07 p1134 A66-17619

Soviet radar observations of Venus in 1964 using frequency-shift keying and periodic linear FM of transmitter 09 p1452 A66-20123

Design of parallel frequency-shift keying system for use in multipath channels 10 p1504 A66-21661

Comparison of frequency shift keyed and phase shift keyed pulse compression systems via digital computer simulation 12 p1819 A66-24602

Upper and lower bounds on binary error probability as function of signal to noise ratio for digital data systems operating over complex Gaussian fading channel 21 p3720 A66-39638

**FREQUENCY STANDARD**

Flying clock experiment with traveling cesium beam clocks 11 p1703 A66-22251

History and development of atomic frequency standard, discussing newest atomic oscillators 12 p1880 A66-24122

Frequency fluctuations in frequency standards, analyzing noise and finite observation time effects and atomic standard characteristics, using servocontrolled oscillator 12 p1881 A66-24123

Optically pumped rubidium 87 maser oscillator 12 p1890 A66-24124

Atomic frequency standard fluctuation, instability due to noise and atomic beam frequency stability 12 p1881 A66-24125

Quartz crystal oscillators and effect on precise time measurements by atomic clocks 12 p1881 A66-24129

Statistical analysis of noise quality of atomic frequency standards including masers 12 p1881 A66-24130

Cesium beam atomic time and frequency standards 13 p2079 A66-25874

Atomic standards of frequency and second of ephemeris time, discussing frequency of Cs 133 transition at zero field 14 p2296 A66-27899

Atomic and molecular frequency standards, considering use of cesium 17 p2927 A66-33244

Frequency comparison by beat-frequency comparators, harmonic generators and permanent phase observation devices 17 p2927 A66-33245

Atomic clocks, frequency standards of atomic beam resonators, masers and gas cells and application to space research 18 p3110 A66-33982

Accelerometer standard designed for reciprocity and comparison calibrations of vibration transducers 18 p3112 A66-34207

Frequency standard system using quartz servo-oscillators for design and testing of high-stability frequency sources 18 p3087 A66-34705

Atomic time standards, describing cesium beam standard, ammonia maser and gas-cell type clocks 19 p3354 A66-35468

Atomic clocks and synchronization for space research 22 p3920 A66-40794

**FREQUENCY SYNCHRONIZATION**

Frequency synchronization of Gunn effect oscillators, frequency locking subharmonic generation, passive frequency stabilization, etc 10 p1516 A66-22095

Frequency stability and spectral purity of p-n junction laser output improved by synchronization with gas laser beam 15 p2518 A66-29717

Receiver design and results of dual VLF transmissions for obtaining timing information 19 p3357 A66-35693

Wave synchronization in gas laser with ring resonator cavity 21 p3748 A66-39301

Synchronized shadow photochronographic investigation of wire explosion shock waves in air 21 p3772 A66-39302

Photographic integration process using Loran-C pulses for precise synchronization of timing signals at any point in continental U.S. 22 p3862 A66-39733

**FREQUENCY SYNTHESIS**

Applications of microelectronics - IEE Symposium, Southampton University, England, September 1965 02 p0201 A66-11914

Frequency synthesizer producing or deriving any required channel frequency from small number of crystal references 02 p0203 A66-11927

LF transfer functions synthesized with microelectronic circuits 05 p0644 A66-14575

Design of variable structure automatic control system frequency characteristics, using harmonic linearization 11 p1677 A66-22763

Errors by mutual interference in frequency-time coding in satellite communications systems, deriving expressions relating commissive and omissive error rates, simultaneous users per unit bandwidth, etc 12 p1821 A66-24752

Aperture synthesis technique for increasing information rate to radio astronomy array by rejecting restriction of fractional bandwidths 13 p2037 A66-25553

Mixer cross products of mixer frequency charts to determine spurious responses with respect to desired output frequency 13 p2040 A66-25825

Tunable precision frequency source using phase locked variable frequency oscillator for mobile radio sets 15 p2451 A66-29313

High speed microwave frequency synthesizer with digital control 17 p2897 A66-33438

Higher harmonics generation of ion cyclotron frequency in longitudinally magnetized plasmas, noting experimental setup and pressure effects 21 p3777 A66-38766

**FREQUENCY TRANSLATION SYSTEM**

Serrodyne system using either TWT or solid state phase shift for frequency translation 01 p0044 A66-10933

Communications satellite transponder discussing system requirements for RF



conversion and amplification 04 p0492 A66-13595

Computer analysis of translators using diode ring modulators and dimensioning of frequency dependent networks preceding and following modulating four-pole to obtain specific response in passband, minimizing spurious signal effect 11 p1670 A66-23197

YIG magnetostatic mode serrodyne capable of milliwatt modulation power levels through 30 mc/s 15 p2463 A66-29029

Receiving and predetection recording system with frequency translation and wideband FM for Atlantic Missile Range 16 p2648 A66-30536

Device for frequency translations in microwave range employing latching ferrite phase shifter and digital switching driver to obtain multiple step approximation 19 p3314 A66-35520

**FRESNEL DIFFRACTION**

Fresnel diffraction laws for calculation of light amplitude distribution in image spot of point as function of aperture dimensions used on hologram, source function, etc 04 p0532 A66-14173

Hologram imaging process in which Fresnel diffraction pattern of object is recorded by scanning at X-band 06 p0881 A66-16638

Image luminance of paraxial rays, image formation and ray tracing in holography, using Fresnel-Kirchhoff diffraction formula 15 p2501 A66-28975

Near-field diffraction of helium-neon laser at circular apertures 16 p2720 A66-31727

EAS RF emission detection, discussing enhanced Cerenkov radiation, mutual coherence effects, diffraction, Fresnel zones, Coulomb-field bremsstrahlung, etc 18 p3208 A66-35117

Power transmission, gain, directivity pattern and reception between large aperture antennas in near-field region 20 p3529 A66-37709

**FRESNEL INTEGRAL**

Fresnel formulas for transformation of transverse electromagnetic wave into longitudinal plasma wave at dielectric-plasma interface, using Laplace transforms 22 p3869 A66-40929

**FRESNEL REFLECTOR**

Ground reflection effect on polarization of radiation scattered from top of Rayleigh atmosphere, using Fresnel and Lambert models [AIAA PAPER 66-514] 16 p2699 A66-31498

Modification to theory of differential absorption experiment involving Fresnel reflection coefficient of ionospheric irregularities 20 p3555 A66-38209

Passage of normal plane electromagnetic wave through bi-gyrotropic plate, examining transmission and reflection components 22 p3862 A66-39828

Optical thickness measurement of nonabsorbing dielectric film when it is inconvenient to apply overlay film to measure thickness by Fizeau fringe shift 22 p3968 A66-40889

**FRESNEL REGION**

Path-loss equation derived for two parabolic antennas with aperture illumination of form of second-order exponential function 03 p0336 A66-13101

Fresnel gain of aperture antenna, developing rigorous analytical formula for circular aperture antennas with parabolic tapered illumination 05 p0651 A66-15837

Engineering method of calculating Fresnel coefficients based on use of nomograms 08 p1182 A66-18917

Antenna field calculations in Fresnel and induction regions 09 p1356 A66-20772

Range requirements in radar cross section measurements in terms of permissible variations in amplitude and phase of incident field at target 10 p1498 A66-21601

Fresnel and Fraunhofer patterns of overmoded feeds and reflector antennas 12 p1841 A66-24632

Fresnel zone beam scanning antenna array, considering patterns, maximum scan ability and effect of interelement spacing 12 p1841 A66-24633

Diffraction pattern analysis of fields generated by hoghorn-fed Cassegrain antenna operating in Fresnel zone 18 p3083 A66-34289

Antenna field calculations in Fresnel and induction regions 22 p3873 A66-39831

Soret Zone Plate simulation by longitudinally distributed coaxial aperture system, noting system activation and operation 23 p4068 A66-41622

**FRETTING**

Wear and grease lubrication effects in matched aircraft spline specimens subjected to oscillatory motion 16 p2713 A66-30572

Surface shear traction and torsional compliance of elastic plate pressed between identical elastic spheres 18 p3249 A66-33586

**FRETTING CORROSION**

**SA WEAR**

Detection and causes of fretting corrosion, discussing prevention via lubrication, effects of load, surface finish, material hardness, friction coefficient, vibration, etc 18 p3117 A66-34400

Molybdenum bisulfide as lubricant in aircraft construction to combat fretting corrosion, facilitate assembly and dismantling of parts and reduce frequency of maintenance 23 p4074 A66-41658

**FRICITION**

**SA ABRASION**

**SA DRY FRICTION**

**SA INTERNAL FRICTION**

**SA KINETIC FRICTION**

**SA SKIN FRICTION**

**SA SLIDING FRICTION**

**SA STATIC FRICTION**

**SA WEAR**

Friction welding technique using heat produced by friction between two surfaces 03 p0374 A66-13117

Book on friction and wear covering nature of interaction between solid surfaces, general concepts and engineering and design calculations 04 p0526 A66-13834

Friction corrosion caused by alternate pivoting of steel ball on plane of light alloy 14 p2302 A66-27934

Starting friction and kinetic friction of PTFE fabric-lined spherical bearings and deflection and permanent set under static loading 17 p2929 A66-31932

Quadratic and linear friction effects on time-weighted fuel-optimal singular control of nonlinear systems 19 p3338 A66-36744

Friction and imbalance moments relative to gimbal axes and effects on gyrovertical motion under starting conditions 21 p3739 A66-39325

Die friction effects on plane stress and plane strain in plastic bending of steel and titanium alloy beams 21 p3745 A66-39528

**FRICITION COEFFICIENT**

Friction induced vibration to determine existence of critical velocity of driven surface [ASME PAPER 65-LUB-5] 04 p0527 A66-14241

Frictional and viscoelastic properties of plastics and rubber show relationship to sliding speed and temperature [ASME PAPER 65-LUB-15] 04 p0528 A66-14247

Limiting relative laws of friction and heat transfer applicable to nonisothermal gas flow with finite Reynolds numbers 04 p0598 A66-14440

Heat transfer and wall friction for low velocity flow of gases in downstream region of smooth electrically heated tubes, considering transition region [ASME PAPER 65-WA/HT-18] 05 p0790 A66-15646

Friction corrections introduced in results obtained by differential pendulum method in measuring acceleration of gravity at sea, noting motion equations 06 p0879 A66-16418

Dependence of dry friction force for steady state rubbing of rubberlike body on surface of crystalline elastic body 08 p1244 A66-19474

Approximate solutions with error estimate for stationary boundary layer with desired distribution of pressure and mass transfer along wall 08 p1166 A66-19828

Friction of rotating disk in revolving housing, noting parameters of dimensionless momentum coefficient, separation of fluid flow into core and secondary flow 09 p1384 A66-20486

Optimum slender body with variable skin friction coefficient, noting minimal drag

design for hypersonic flow under Newtonian pressure distribution 11 p1631 A66-22513

Shape of nonslender body of revolution for minimum total drag in viscous hypersonic flow at Newtonian pressure distribution and constant friction coefficient 11 p1631 A66-22516

Transversal contour of minimum pressure drag for body with noncircular cross section 11 p1631 A66-22517

Transversal contour of minimum total drag of body in Newtonian flow 11 p1631 A66-22518

Friction and inertia fields induced by electromagnetic effects arising in motion of hard magnetic moment in thin circular film 11 p1753 A66-22808

Solid and dry-film lubricants, tabulating kinetic coefficients of friction, noting particle size, viscosity, costs, wear life, application, etc 12 p1885 A66-24099

Effect of crystalline state and structural orientation of polymer on endurance of couplings with polytetrafluoroethylene components, analyzing dry friction and wear on interfaces 13 p2113 A66-25912

Friction and lubrication of polymers 13 p2087 A66-26304

Lubrication characteristics of dry, unbonded and bonded molybdenum sulfide films for varying speed, load, humidity and metal substrate [ASLE PREPRINT 65AM 5C1] 14 p2302 A66-27773

Metal flow, friction and lubricant performance during stamping of thin titanium alloy blanks 14 p2304 A66-28202

Experimental friction and lubrication system parameters including load coefficient, oil volume, friction coefficient and bearing temperature characteristics, in mathematical terms 15 p2505 A66-28523

Heat transfer and wall friction for low velocity flow of gases in downstream region of smooth electrically heated tubes, considering transition region [ASME PAPER 65-WA/HT-18] 16 p2828 A66-30991

Nitrogen tetroxide dissociation effect on surface friction in turbulent boundary layer 16 p2686 A66-31064

Graphite lubricant physical and chemical combinations with other materials for improved high temperature friction and wear, discussing nuclear irradiation for graphite lattice modification 17 p2929 A66-31933

Lift-to-drag ratio attainable by slender, homothetic body at hypersonic speeds, assuming Newtonian pressure distribution and constant skin-friction coefficient 17 p2838 A66-32348

Velocity and temperature profiles, hydrodynamic elements, heat transfer and friction coefficients of turbulent incompressible flow through circular and flat tube 17 p2909 A66-32583

Detection and causes of fretting corrosion, discussing prevention via lubrication, effects of load, surface finish, material hardness, friction coefficient, vibration, etc 18 p3117 A66-34400

Parameter variation effect on self-excited torsional oscillations and sustained frictional vibrations in mechanical systems, comparing results with analog computer predictions 18 p3256 A66-34558

Skin friction coefficient predictions in turbulent compressible flow, using design nomograph based on Spaiding-Chi method 18 p3100 A66-34603

Temperature effect on dry friction coefficient in titanium alloys 19 p3376 A66-35462

Wind profiles obtained from meteorological tower plotting wind velocity, normalized by value of friction velocity, as function of measurement heights 21 p3759 A66-39356

Frictional resistance of finite disks and cones rotating in power law non-Newtonian fluids 21 p3730 A66-39456

Friction moment of rotating ellipsoids in infinite medium, calculating turbulent boundary layer for rotating sphere 21 p3731 A66-39500

Two-wedge system analyzed by Coulomb friction law and applied to simple screw and worm gears and screw



- combination 22 p3922 A66-39668  
Measuring wear life and friction coefficient of dry film and solid film lubricants and plastic materials in ultrahigh vacuum 22 p3923 A66-40216  
Carrying capacity and moment of friction calculated for cylindrical MHD bearing for small magnitude of radial clearance 23 p4074 A66-41736  
Approximation of self-similar plane and axisymmetric problems for high temperature laminar boundary layer, based on equations for boundary layer of finite thickness for high temperature gas 23 p4149 A66-41783  
Friction and turbulent heat transfer as function of Reynolds number applied to missile rounded-off forebody, delta wings, etc, using boundary layer equations 23 p4151 A66-42056
- FRICITION DRAG**  
SA SKIN FRICITION DRAG  
Friction-drag and heat-transfer coefficients of plate in turbulent gas flow, estimating effect of turbulent Prandtl number 06 p0872 A66-16469  
Minimization of total drag /pressure and friction/ of two-dimensional wing with unspecified chord, finding extremal solutions which include one, two or three subarcs 11 p1630 A66-22504  
Friction resistance of compressible turbulent gas flow through initial section of cooled pipe with large gas-wall temperature gradients 11 p1688 A66-22597  
Maximum friction along jet path in mixing zone at constant pressure applied in finding irrotational wall velocity 13 p2063 A66-25468  
Classical and quantum mechanical turbulence in Helium 2 heat flow, noting transition from laminar turbulent flow of normal and superfluid component, Reynolds number dependence on mutual friction coupling, etc 13 p2128 A66-26275  
Stationary viscous incompressible fluid flow past rough surface, noting solution stability and friction stress determination for given pressure gradient 16 p2688 A66-31301  
Frictional drag and convective heat transfer of rotating cones of arbitrary vertex angles in mixed and turbulent flow 17 p3038 A66-33469
- FRICITION-LOSS COEFFICIENT**  
Losses in vaneless diffusers of centrifugal compressors and pumps due to wall friction and sudden expansion mixing at entrance [ASME PAPER 65-FE-1] 10 p1540 A66-21504
- FRICITION MEASUREMENT**  
Characteristics of flexible circular plate, considering stress and strain in friction zone at clamped section 01 p0160 A66-11181  
Characteristics of partially clamped corrugated membrane, investigating effect of forces of clamping friction 01 p0160 A66-11182  
Sliding friction tests at ultrahigh load of eight greases and 18 dry lubricants and various base materials [ASLE PREPRINT 65-LC-23] 02 p0237 A66-12249  
Friction and wear of hexagonal metals and alloys as related to crystal structure and lattice parameters in vacuum [ASLE PREPRINT 65-LC-18] 02 p0237 A66-12252  
Internal friction measurements for studying mechanical properties due to crystal dislocations 05 p0698 A66-14550  
Measurement of friction of materials sliding in JP-4 fluid to predict performance of hydraulic pump 06 p0884 A66-16136  
MHD traveling wave converter, determining frictional fluid losses due to boundary flow and calculating performance 07 p0990 A66-17240  
Friction stresses in turbulent lubrication film and dependence on Reynolds number and pressure distribution studied, using mixing-length hypothesis [ASLE PREPRINT 65AM 3A1] 07 p1039 A66-18289  
Thermal elastohydrodynamic lubrication of rolling and sliding cylinders, noting correlation with film thickness and friction experimental data [ASLE PREPRINT 65AM 4A2] 07 p1040 A66-18291  
Heat exchange, friction and mass exchange in laminar multicomponent boundary layer during injection of extraneous gases 09 p1368 A66-20705  
Heat exchange, friction and mass exchange in laminar multicomponent boundary layer during injection of extraneous gases 11 p1688 A66-22591  
Operation, maintenance and installation of friction and nonfriction bearings, noting characteristics, problems, etc 11 p1711 A66-22951  
Liquid film flow stability, considering two-dimensional perturbations, hydrodynamic friction with allowance for finite curvature radius of bounding surface 12 p1864 A66-24435  
Test rig for gas-lubricated journal bearings measuring frictional torque, gas film pressure distribution, static and dynamic eccentricity changes, etc 12 p1859 A66-24929  
Surface roughness effect on boundary friction for various loads, speeds and lubricants [ASLE PREPRINT 65 AM 6AZ] 13 p2085 A66-25367  
Mechanism of plastic deformation in crystalline bodies, discussing static and dynamic frictional forces in relation to dislocation structure of bodies in contact 13 p2110 A66-25887  
Friction and wear of hexagonal metals and alloys as related to crystal structure and lattice parameters in vacuum [ASLE PREPRINT 65-LC-18] 16 p2713 A66-30568  
Sliding friction tests at ultrahigh load of eight greases and 18 dry lubricants and various base materials [ASLE PREPRINT 65-LC-23] 16 p2713 A66-30571  
Turbulent flow of dilute viscoelastic non-Newtonian fluids in pipes, noting frictional characteristics, elastic fluid parameters, etc 17 p2906 A66-32036  
Displacement detector to provide direct measurement of shear forces in aerodynamics on small surface elements in hotshot wind tunnels 24 p4207 A66-42169
- FRICITION REDUCTION**  
Operation, maintenance and installation of friction and nonfriction bearings, noting characteristics, problems, etc 11 p1711 A66-22951  
Aircraft vibration in transonic region caused by aileron oscillations, eliminated by friction dampers 12 p1801 A66-24035  
Structural changes in metal surface layers under boundary friction conditions in presence of surface active lubricant additives 13 p2086 A66-25884  
SNAP-8 reactor oscillating bearings to provide low friction self-lubrication at 1150 degrees F 16 p2712 A66-30414  
Reduction of friction forces in radial thrust bearings and three-point-contact bearings when compulsory oscillations of outer and inner races have same direction in both bearings 21 p3745 A66-39333
- FRICITIONLESS ENVIRONMENT**  
Low friction environment effects on maintenance operations in simulator noting torquing-force capability, hand-eye coordination, etc 02 p0186 A66-11645  
Low friction environment effects on maintenance operations in simulator noting torquing-force capability, hand-eye coordination, etc 18 p3061 A66-33821
- FRIEDEL-CRAFT REACTION**  
Friedel-Crafts methylation of decaborane, determining reactant parameters and relationship of decaborane conversion and alkylate composition 05 p0629 A66-14541
- FRINGE**  
Fringing effect on sensitivity of magnetic flow meter 17 p2926 A66-32874
- FROG**  
Gravitational environment, effect of change on frogs measured using gravitoceptors in vestibular apparatus 17 p2865 A66-32183
- FRONT**  
S FLAME FRONT  
S SHOCK FRONT  
S WAVE FRONT  
S WEATHER FRONT
- FROST**  
Heat and mass transfer rates compared with correlations for frost formation on vertical plate in free convection [ASME PAPER 65-HT-32] 04 p0595 A66-13391  
Carbon dioxide frost as thermal insulation for hypersonic spacecraft, noting conductivity 06 p0969 A66-16301  
IR spectral reflectance of water frost and solid carbon dioxide 15 p2501 A66-28977  
Martian wave of darkening attributed to soil frost phenomena 22 p3981 A66-40478
- FROUDE NUMBER**  
Acceleration potentials applied to motion, at arbitrary Froud numbers, of high-aspect-ratio wing immersed in incompressible ideal fluid 08 p1205 A66-18601  
Acceleration potential method for solving linear problems of wing hydrodynamics above interface between fluids differing in density, for arbitrary Froude number 13 p2067 A66-26530  
Two-layer model of pressure jump produced by mountains 22 p3944 A66-40966
- FROZEN FLOW**  
Isentropic expansion of argon plasma in Laval nozzle, discussing parallel flow parameters, frozen flow, thermodynamic equilibrium, energy balance, etc 05 p0720 A66-14509  
Stagnation point heat transfer for binary air diffusion model including dissociation and ionization 05 p0665 A66-15775  
Numerical calculations of axially symmetric two-dimensional steady expansions of monatomic gas, using approximate Boltzmann equation with Krook collision term 11 p1690 A66-22908  
Species diffusion in frozen hypersonic boundary layer with Falkner-Skan velocity profiles, where surface is linear, given as Mellin transform, constructing series and asymptotic expansion of surface concentration 13 p2060 A66-25158  
Transonic nonequilibrium approximations for reacting gas mixture flow 17 p2913 A66-33080
- FUEL**  
S AIRCRAFT FUEL  
S CARBON  
S CHEMICAL FUEL  
S ENDOTHERMIC FUEL  
S FLAME  
S HYDROCARBON FUEL  
S HYDROGEN FUEL  
S JET FUEL  
S KEROSENE  
S METAL FUEL  
S NUCLEAR FUEL  
S OIL  
S PROPELLANT  
S REACTOR FUEL
- FUEL-AIR RATIO**  
Impact-induced combustion in hypersonic ramjet engines, determining hypersonic fuel-air mixing from hydrogen concentration at Laval nozzle outlet 10 p1591 A66-21359  
JP-5 fuel-air mixture ignition by platinum catalytic igniters, using ramjet engine baffle combustors 13 p2171 A66-25594  
Two-phase self-ignition of isooctane-air mixture, considering preignition phase and temperature zones 13 p2209 A66-25695  
Spectral analysis of organic flames, noting band intensity variation of different radicals with air-fuel composition and influence of diluents 14 p2413 A66-27722  
Organic flame temperatures and burning velocities at various fuel-air ratios measured, noting band intensity, effect of diluents, etc 14 p2413 A66-27723  
Correlation study of turbojet afterburner combustion efficiency and fuel/air ratio setting for maximization of efficiency [WSCI 66-1] 18 p3164 A66-34423
- FUEL CELL**  
SA BIOCHEMICAL FUEL CELL  
SA REGENERATIVE FUEL CELL  
Cobalt electrode performance in high temperature fuel cells, presenting V-I characteristics 01 p0014 A66-10358  
Static moisture removal system developed for space power application from tests determining vapor-pressure characteristics of capillary fuel cell 01 p0012 A66-10912  
Platinum metal as electrocatalyst for oxidation of methanol and number of saturated hydrocarbons 02 p0188 A66-11870  
Hydrogen fuel cells for space use noting Bacon cells, membrane cells and Gemini and Apollo fuel cells 03 p0323 A66-12482  
Fuel cells and potential as future chemical-



electric energy converters 03 p0324 A66-13234

Electrochemical current generator principles based on oxyhydrogen fuel cell for space travel, stressing regeneration by using solar radiation in photochemistry 04 p0459 A66-13545

Fuel cell operation utilizing liquid fuels, evaluating hydrazine and alcohol fuels and electrode materials 04 p0459 A66-13546

Electrodialytical removal of reaction water from alkaline electrolyte of oxygen-hydrogen fuel cells 04 p0460 A66-14033

Gas permeation measurements on ion exchange fuel cell membranes using chromatography 05 p0611 A66-14539

Energy conversion and storage . Conference, Oklahoma State University, October 1965 06 p0808 A66-16390

Fuel cell systems, particularly hydrogen peroxide type, noting electrochemical oxidation, water production, thermal energy, electrolyte, etc 06 p0808 A66-16391

High-pressure high-temperature hydrogen-oxygen fuel cells employing nonnoble metal catalyst /porous nickel/ as electrode 06 p0808 A66-16392

Auxiliary power devices using solar, chemical and nuclear sources 07 p0992 A66-18305

Fuel cell development, detailing Gemini, Apollo and asbestos systems 07 p0995 A66-18324

Electrochemical energy conversion, discussing fuel selection, oxidants, fused salt electrolytes, liquid metal, etc 07 p0995 A66-18325

Heat and mass transfer in ion exchange membrane fuel cells 07 p0995 A66-18326

Introduction to fuel cells 07 p0995 A66-18467

Kinetic effects in fuel cells, discussing declining efficiency with increasing output, slow electron transfer effects, concentration polarization, etc 07 p0996 A66-18469

Kinetic effects in fuel cells, measuring rate of change of electrode process characteristics 07 p0996 A66-18470

Hydrogen-oxygen fuel cells, using ion exchange electrolytes 07 p0996 A66-18471

Electrolyte-soluble fuels such as methanol, ammonia and hydrazine, noting electrochemical oxidation properties, power output, stored energy content, etc 07 p0996 A66-18472

Fuel cells with molten carbonate electrolytes such as matrix cells and free and paste electrolyte cells, noting construction, operation, performance 07 p0996 A66-18473

Solid oxide electrolyte with hydrogen fuel, discussing cell thermodynamics, application limitations, etc 07 p0996 A66-18474

Fuel cells oxidizing saturated and unsaturated hydrocarbons at high temperatures 07 p0996 A66-18475

Fuel cell economics connected with vehicle applications as power sources 07 p0997 A66-18477

Fuel cell considered from viewpoint of fuel costs, noting hydrocarbon fuel for application with low load factor and instant starting 07 p0997 A66-18478

Electrode types used in low temperature fuel cells, considering porous gas-diffusion, pore-free palladium membrane and slurry electrodes 08 p1168 A66-19064

Hydrogen feeding through single-layer metallic porous electrode of fuel cell on open circuit 08 p1171 A66-19649

Hydrogen and oxygen ionization at three-phase boundary in alkaline solutions on smooth metals 08 p1171 A66-19650

Microporous metallic gas-diffusion electrodes in low temperature acid-electrolyte fuel cells 08 p1172 A66-19651

Cell voltages and Coulomb efficiency in oxygen electrodes and hydrogen and hydrazine fuel cells for long duration discharges 08 p1172 A66-19652

Low temperature low pressure hydrogen/oxygen alkaline fuel cell and electrode selection 08 p1172 A66-19653

Thermodynamic and kinetic effects of gas pressure on performance of fuel cell using one or two gas electrodes 08 p1172 A66-19654

Methanol-air fuel cell with alkaline electrolyte, Ni or Pt catalysts and carbon

diffusion electrode, for use in signaling devices 08 p1172 A66-19655

Fuel cells using metallic barium as fuel electrode and oxygen or chlorine as cathode, noting net energy densities 08 p1172 A66-19656

Geometrically ordered gas-diffusion electrodes for fuel cells consisting of platinum steel with funnel-shaped cavities 09 p1333 A66-20424

System selection for hydrogen-oxygen low temperature fuel cell with aqueous KOH electrolyte [AICE PREPRINT 13B] 10 p1484 A66-21182

Molten carbonate fuel cell module featuring flexibility of construction, electrical simplicity and effective gas distribution characteristics [AICE PREPRINT 20D] 10 p1484 A66-21187

Fuel cell systems operating at low temperatures, noting control loops, hydrogen/oxygen, nickel electrode, asbestos systems, etc [AICE PREPRINT 15D] 10 p1484 A66-21192

Hydrogen-oxygen fuel cell for spacecraft power system 10 p1485 A66-21465

Application perspectives for dissolved fuel cells, particularly methanol and hydrazine cells 11 p1639 A66-22242

Carbon deposition boundaries and other constant parameter curves in triangular representation of C-H-O equilibria, with application to fuel cells 11 p1639 A66-22243

Fuel cell development in U.S., Europe and Great Britain, noting design, performance and problems 11 p1639 A66-22247

Two-and three-phase boundary electrodes for fuel cells 13 p1997 A66-25113

Electrochemical kinetics of fuel cells - Conference, Moscow, 1964 13 p1998 A66-25667

Functional mechanism of gas diffusion electrode 13 p1998 A66-25668

Performance of porous gas diffusion electrode 13 p1999 A66-25669

Theory of gas porous electrode with model 13 p1999 A66-25670

Design of gaseous diffusion electrode 13 p1999 A66-25671

Performance of wetted porous electrodes with reactant feed by diffusion 13 p1999 A66-25672

Operation of porous electrodes where reactant is fed in and reaction product is removed by forced stream of electrolyte, reactant and product mixture 13 p1999 A66-25673

Electro-oxidation of organic materials capable of functioning as fuel in fuel cells 13 p2017 A66-25674

Capillary equilibrium in gaseous porous electrode 13 p1999 A66-25677

Fuel cells compared with other power systems for space application [AIAA PAPER 64-723] 13 p2005 A66-26618

Engineering problems in design of fuel cell systems including complicated duty cycles, response time, high power density and efficiency [AIAA PAPER 64-743] 13 p2007 A66-26645

Hydrocarbon-air fuel cell power source using reformer to supply hydrogen and producing net output of 5 kw at 110 v and 60 cps [AIAA PAPER 64-745] 13 p2007 A66-26646

Fuel cell reliability maximized and weight minimized for space mission power requirement [AIAA PAPER 64-746] 13 p2007 A66-26647

Molten carbonate fuel cell system performance evaluated from engineering and economic aspects [AIAA PAPER 64-747] 13 p2007 A66-26648

Fuel cell power plant for Apollo command and service module from engineering viewpoint [AIAA PAPER 64-748] 13 p2007 A66-26649

Increasing solubility of hydrocarbons in cesium-salt fuel cell electrolyte by replacing some of carbonate anion by flouride 14 p2226 A66-27898

Hydrocarbon fuel cell anodes containing boron carbide as support for platinum electrocatalyst 14 p2226 A66-27902

Boron carbide as potential substitute for platinum as catalyst for fuel cell cathodes 14 p2227 A66-28174

Performance analysis of carbon-supported platinum-ruthenium alloy catalysts with

respect to anodic oxidation of methanol in acid electrolyte 17 p2870 A66-31898

Fuel cell systems for generating electricity 17 p2849 A66-33173

Electrical energy by direct conversion, noting fuel cell, thermoelectric generator, solar cell, etc 18 p3053 A66-33722

Direct and indirect oxidation fuel cell systems operating on hydrocarbon-air mixtures and using aqueous, molten and solid electrolytes, noting technological and economical problems 18 p3053 A66-33766

Book on direct energy conversion covering thermoelectric, photovoltaic, thermionic and MHD generators and fuel cell 18 p3054 A66-34164

Temperature profile and design parameters in adiabatic fuel cell with stationary electrolyte where cooling takes place by convection and conduction 18 p3263 A66-34386

Advantages and disadvantages of liquid fuels and oxidizers for direct fuel cells and electrode manufacturing techniques, noting role of nitric acid, methanol and hydrazine 18 p3056 A66-35239

Digital computer optimization program, determining minimum weight fuel cell primary power system for MOLAB 20 p3496 A66-37156

Effect of variations in mission and vehicle constraints on hydrogen-oxygen fuel cell system optimization 20 p3497 A66-37160

Fuel cell power conversion by AC link type static inverter 20 p3498 A66-37173

Lithium chloride power plant theory and technology, noting application to critical weapons systems 23 p4021 A66-41758

Primary electrochemical power systems including gas recombination devices, sterilizable battery, fuel cells, alcohol-air units, etc 23 p4023 A66-41768

Performance characteristics of sintered plate nickel-cadmium, silver-cadmium and silver-zinc batteries regarding energy output, discharge voltage, charging cycle life, etc 23 p4023 A66-41769

Oxygen electrolytic reduction using porous sintered silver electrode, noting effects of gas pressure, current and cathode thickness on potential as applied to fuel cells 24 p4161 A66-42333

Oxygen reduction on titanium nitride noting rate of electrochemical oxidation in fuel cell studies 24 p4170 A66-42422

Methanol-air fuel cells as long-life sources of energy for lighted buoys, TV stations, meteorological stations, etc 24 p4161 A66-42501

Mixing of gases in hydrogen-oxygen fuel cell, noting membrane allowing only electrolyte to pass through electrodes 24 p4161 A66-42502

Fuel cells with ceramic electrolyte operating at high temperatures, calculating voltage and efficiency 24 p4161 A66-42503

### FUEL COMBUSTION

#### SA METAL COMBUSTION

Steady state flame propagation regimes, taking into account effect of heat losses through pipe walls on fuel mixture combustion 02 p0302 A66-11401

Detonation theory of heterogeneous fuel mixture 02 p0217 A66-11402

Chemical kinetics of nonequilibrium combustion of propane-air and ethane-air mixtures in one-dimensional flow, including ignition delay and reaction time [CI PAPER WSCI-65-19] 05 p0788 A66-15143

Burning modes in initially unmixed reactants, describing stagnation region formation by interaction of opposed flows of fuel and oxidant [AIAA PAPER 66-71] 06 p0969 A66-16258

Mixing processes for isothermal and nonisothermal simulation of flows in combustion chambers 13 p2210 A66-26490

Spectral analysis of organic flames, noting band intensity variation of different radicals with air-fuel composition and influence of diluents 14 p2413 A66-27722

Automatic ignition in methane-chlorine mixture, investigating photochemical and thermal chlorination of methane in gas phase 17 p2989 A66-32824

Pressure dependence of burning rate of stoichiometric fuel-oxidizer mixtures 17 p3036 A66-32825



- Diffusion combustion in turbulent compressible gas flow 17 p3036 A66-32827
- Heat transfer caused by combustion of triethylaluminum on flat plate in Mach 3 flow, noting significance of lag at stagnation pressure 18 p3260 A66-33817
- Bench-top calorimeter for determining radiation and convection in small-scale combustion of fuel [WSCJ 66-14] 18 p3113 A66-34425
- Ignition analysis of condensed phase fuel suddenly exposed to stationary hot oxidizing gas, noting strong pressure effect due to feedback mechanism 20 p3626 A66-37386
- Polymer flammability measured in terms of minimum oxygen content needed for burning, noting effect of various agents for reducing flammability 20 p3680 A66-38040
- Book on fuel behavior in piston-engine, jet and rocket 21 p3806 A66-38950
- Correlation between chemi-ionization in flames containing organic fuels and heat of oxidation of carbon in fuel molecule 23 p4147 A66-41154
- Pressure variation induced by ignition of air-hydrocarbon mixtures - studied by stroboscopic cinematography and simultaneous pressure measurement 23 p4148 A66-41176
- Supersonic combustion simulation facility and duplicable static parameters for hydrogen fuel [AIAA PAPER 66-743] 23 p4052 A66-41327
- Combustion of atomized liquid fuels, noting optimum value of atomization fineness affecting completeness of combustion 24 p4293 A66-42208
- Model determination of effects of injecting and mixing fuel in inlet diffuser of two-shock inlet hypersonic ramjet or scramjet [AIAA PAPER 66-648] 24 p4261 A66-42641
- FUEL CONSUMPTION**
- Hybrid propulsion application to advanced missions covering fuel consumption, combustion efficiency and throttling performance [ATAA PAPER 64-226] 03 p0415 A66-12748
- Thrust modulation with minimum limit cycle in bang-bang system, reducing fuel consumption for spacecraft attitude control system 03 p0432 A66-13206
- General theory of minimum fuel free space trajectories 06 p0954 A66-16624
- Dual flow engines with high by-pass ratios, considering engine process parameter effects, fuel consumption, efficiency, etc 06 p0944 A66-17025
- Minimum fuel transfer solution of Lawden problem involving finite number of impulse thrusts separated by coasting arcs [ATAA PAPER 66-7] 07 p1136 A66-17881
- First-order perturbation solution to problem of minimum-fuel orbit transfer in form of equal slope guidance constraint [ATAA PAPER 66-11] 07 p1137 A66-17883
- Piston-type flowmeter for automatic recording fuel consumption 09 p1380 A66-20310
- Intake requirements and cold efflux of high-bypass turbofan engines can be turned to advantage by integrated installation arrangements which reduce long-haul operating costs 09 p1434 A66-20392
- Comparison of piston engine with turbojet engine, noting power-weight ratio, specific fuel consumption, performance characteristics, etc 10 p1591 A66-21392
- DC-9 Douglas short-and medium-range air transport, discussing takeoff field length, fuel capacity, payload and landing-field length 12 p1800 A66-23754
- Scramjet aircraft performance capabilities, noting operating parameters such as thrust coefficient, flight velocity, acceleration, fuel consumption, etc 13 p2173 A66-26032
- SST air traffic control and fuel consumption dependence on wind drift and atmospheric temperature 14 p2328 A66-28231
- Turbofan engine fuel consumption, noting high cycle pressure ratio compressor, regenerator, etc [SAE PAPER 660322] 15 p2573 A66-29842
- Analytic solution in terms of modified Bessel functions of synergetic turn in exponential atmosphere, using spacecraft engines only for drag cancellation and orbit trimming [AIAA PAPER 66-487] 16 p2811 A66-31493
- Optimum stabilization problem for axisymmetric satellite, considering fuel consumption 19 p3467 A66-35277
- Viscosity effect on performance of turbine type flow meters calculated to meet accuracy requirement for complete use of propellants in rocket propelled vehicles 19 p3361 A66-36646
- Trajectory corrections of space vehicle launched toward planet, noting fuel consumption 20 p3595 A66-36872
- FUEL CONTAMINATION**
- Microbiological attack in aircraft fuel systems and protective measures 06 p0940 A66-15996
- Contamination control in missile systems, considering rocket engine cleanliness as quality control parameter 09 p1432 A66-19954
- Contamination, viscosity, shear stability, breakdown and foaming of MIL-H-5606 hydraulic fluid and swelling effect on synthetic rubber 18 p3125 A66-34652
- FUEL CONTROL**
- Lucas fuel control system for Spey engine, using rotating metering valves and variable stroke fuel pump [SAE PAPER 660049] 08 p1282 A66-19389
- Fuel requirements for high altitude high-Mach number aircraft, noting thermal stability, autooxidation, self-ignition, specific heat, etc 10 p1590 A66-21400
- Gas turbine fuel controls, analysis and design 15 p2570 A66-28851
- Literal acceleration limiting fuel control for gas turbine engines during speed transients 15 p2571 A66-28854
- Gas turbine engine analog simulation for acceleration sensing fuel control studies, comparing results with actual engine performance 15 p2571 A66-28855
- Effect of recuperators on governing of single shaft gas turbine engines and methods used to provide satisfactory governing and overall characteristics 15 p2428 A66-28856
- Fuel flow reset and other methods of governing performance of gas turbines 15 p2571 A66-28857
- Microelectronic fuel control for gas turbine engines, discussing mechanical flow and microelectronic packages and component fabrication and assembly 15 p2571 A66-28859
- Lightweight universal fuel control for commercial aircraft, discussing engine requirements, design considerations, etc 15 p2571 A66-28860
- Random balance statistical method of identifying major causes of performance variations in jet engine fuel control units 15 p2572 A66-28863
- Pontryagin principle extended to control systems, computing optimal control laws 19 p3337 A66-36735
- Time-fuel optimal regulator for third-order model of reaction jet-controlled spacecraft with time delay 19 p3338 A66-36743
- Quadratic and linear friction effects on time-weighted fuel-optimal singular control of nonlinear systems 19 p3338 A66-36744
- Iterative computational procedures applicable to optimal control problems including treatment of minimum-error regulator, minimum-error rendezvous and minimum-fuel terminal control 20 p3536 A66-36855
- Analog computation of minimum fuel trajectories with soft landings in uniform gravitational field, using Pontryagin maximum principle to reduce two-point BVP with optimal controllers 23 p4133 A66-41618
- FUEL CORROSION**
- Corrosion problems with simulated fuel in launch vehicle models 21 p3750 A66-38799
- Throat erosion rates of carbon chokes in rocket motor nozzle predicted, using mathematical approach combined with experimental result [AIAA PAPER 65-351] 24 p4261 A66-42772
- FUEL ECONOMY**
- Analytical solution to determine rocket design for maximum payload 02 p0294 A66-11634
- Propellant extraction from lunar material, giving cost analysis of manufacture and use in Earth-Moon space flight with expendable and reusable tankers 10 p1610 A66-21943
- Fuel and energy minimization in three-dimensional attitude control by reaction jet or reaction wheel in orbiting satellite 18 p3244 A66-33865
- FUEL ELEMENT**
- Refractory materials properties used in nuclear fuel element 07 p1079 A66-18302
- FUEL FLOW**
- Quasi-linear partial differential equations of transients in liquid rocket engine propellant feed system solved, determining transient pressure ratio [ASME PAPER 65-FE-23] 06 p0942 A66-16217
- Molten carbonate fuel cell module featuring flexibility of construction, electrical simplicity and effective gas distribution characteristics [AICE PREPRINT 20D] 10 p1484 A66-21187
- Limiting factors of detonation in heterogeneous systems, using one-dimensional model 18 p3265 A66-34552
- FUEL GAUGE**
- SA CAPACITIVE FUEL GAUGE**
- Fluid content measurement in storage tanks under zero-g conditions discussing gas law system, trace material, capacitive panel and RF methods [AIAA PAPER 65-365] 19 p3340 A66-35611
- FUEL INJECTION**
- SA GAS INJECTION**
- SA LIQUID INJECTION**
- Combustion and heat transfer in rocket combustion chamber burning liquid oxygen and gaseous hydrogen 02 p0279 A66-11668
- Supersonic ramjet fuel injection, fuel-air mixing and combustion in turbulent air stream, noting mixing and combustion time 09 p1434 A66-20473
- Propellant injection distribution effect on transverse modes of liquid rocket engine instability [AIAA PAPER 65-613] 12 p1977 A66-23587
- Laminar air flow past porous plate through which fuel and oxidizer mixture is injected, deriving diffusion combustion processes that develop in laminar boundary layer 14 p2371 A66-28318
- Diffusion flame for stagnation mixing layer created by jet fuel injected into oxidant stream at stagnation region of blunt body 17 p3033 A66-32447
- Underwater thermal propulsion system powered by closed-cycle steam power plant fed by high-temperature variable gas flow from oxygen-hydrocarbon combustion apparatus [AIAA PAPER 65-481] 19 p3479 A66-36492
- Penetration distance for secondary liquid injection into supersonic airstream, emphasizing jet flow far from injection orifice 20 p3548 A66-38151
- Project Scorpio USAF Cellular Combustion Chamber Program for cost reduction and injection pattern simplification in liquid propellant rocket engines 20 p3629 A66-38256
- Shock tunnel external burning experiments to investigate effects of reactive fuel injection into air stream flowing around body [AIAA PAPER 66-744] 22 p3893 A66-40631
- FUEL PUMP**
- Jet pump development and testing on Lear Jet Model 24 and Model 40, noting fuel pump system performance, requirements and configuration [SAE PAPER 660223] 13 p2002 A66-26398
- Fluid dynamic characteristics of propellant pumps in presence of oscillatory cavitation, noting performance of J-2 rocket engine system [AIAA PAPER 66-559] 18 p3246 A66-34428
- FUEL SPRAY**
- Thermal radiation absorption by droplet or spray during ignition and combustion of atomized liquid fuels 01 p0164 A66-10899
- Combustion of hydrazine droplets burning in hydrazine vapor investigated via suspended droplet technique [AIAA PAPER 65-355] 14 p2370 A66-27413
- Compressed-gas dispersion effect on gas turbine engine operation, deriving spraying law, jet stream, penetration depth, etc 21 p3808 A66-38934
- FUEL SYSTEM**
- SA AIRCRAFT FUEL SYSTEM**
- Rocket equipment simulation on rocket engine test facilities, describing fuel tank design for experiment with suitable flow characteristics and parameters 12 p1829 A66-24317
- Relation between pressure-type fuel supply



system and pressure variation in combustion chamber of rocket engine 14 p2373 A66-27382  
Regression rates of metalized hybrid fuel systems applied to lithium hydride butyl rubber-fluorine-oxygen system, oxidizer flow, etc 15 p2569 A66-29289  
LF self-vibrations of laminar diffusion flames in axial mode at frequencies corresponding to fuel system natural frequencies [WSCI 66-30] 18 p3263 A66-34414

## FUEL TANK

SA PROPELLANT TANK  
SA STORAGE TANK

Structural design of transport aircraft to reduce fatalities, analyzing protective shell to withstand ground impact load and fuel containment

[AIAA PAPER 65-773] 03 p0434 A66-12592

Mechanical model for representing moment of inertia and fuel sloshing in baffled cylindrical missile tanks 08 p1205 A66-18834

Reactivity of titanium alloy oxidizer tank with nitrogen tetroxide oxidizer under vibration analyzed for LEM when subjected to impact 13 p2111 A66-26222

Tank design, optimization program and testing for effect on storage penalties associated with liquid hydrogen for hypersonic aircraft application 14 p2394 A66-28026

Convective heat transfer to and low gravity heating of liquids contained in rotating cryogenic fuel tanks in orbit [AIAA PAPER 66-432] 16 p2826 A66-30521

Flexible baffle effect on nature and magnitude of damping and sloshing motions of liquid propellants over wide range of conditions 16 p2685 A66-30915

Laminated reinforced plastics used in construction of jettisonable fuel tank, aircraft equipment components, radomes, missiles and satellite parts 23 p4074 A66-41654

## FUEL TANK PRESSURIZATION SYSTEM

Reliability design concepts in cryogenic fluid systems in Saturn S-IV stage propulsion system, noting hydrogen and LOX tank pressurization systems 01 p0129 A66-10079

## FUEL TESTING

Air conditions, flight altitude and fuel composition effects on ramjet engine, specific impulse and efficiency 01 p0130 A66-10925

Refractory material cermet fabrication, discussing techniques of preparation, fuel-metal compatibility and fuel canning 05 p0713 A66-15585

1965 supplement to 1958 ASTM manual for rating aviation fuels by supercharge and aviation methods 14 p2370 A66-27230

Cryogenic fuels evaluated for operational safety in space environment simulation laboratory /SESL/ 22 p3891 A66-40235

## FUEL VALVE

Four-way fluid state vortex hydraulic servovalve discussing design principles, performance and application 04 p0460 A66-13785

## FUME

## S GAS

## FUNCTION

S ANALYTIC FUNCTION  
S APERIODIC FUNCTION  
S ASYMPTOTIC FUNCTION  
S BESSEL FUNCTION  
S CHARACTERISTIC FUNCTION  
S COMPOSITE FUNCTION  
S CONTINUOUS FUNCTION  
S CORRELATION FUNCTION  
S DEBYE FUNCTION  
S DELTA FUNCTION  
S DISCRETE FUNCTION  
S DISTRIBUTION FUNCTION  
S DISTURBING FUNCTION  
S ELLIPTIC FUNCTION  
S ERROR FUNCTION  
S EXPONENTIAL FUNCTION  
S GAMMA FUNCTION  
S GAUSS FUNCTION  
S GREEN FUNCTION  
S HANKEL FUNCTION  
S HARMONIC FUNCTION  
S HEART FUNCTION  
S HYPERGEOMETRIC FUNCTION  
S INTEGRAL FUNCTION  
S KERNEL FUNCTION

S LAGUERRE FUNCTION  
S LEGENDRE FUNCTION SERIES  
S LIAPUNOV FUNCTION  
S LOMMEL FUNCTION  
S MATHIEU FUNCTION  
S MUSCULAR FUNCTION  
S ORTHOGONAL FUNCTION  
S PERIODIC FUNCTION  
S PROLATE SPHEROID FUNCTION  
S PULMONARY FUNCTION  
S RADIATION FUNCTION  
S RATIONAL FUNCTION  
S RENAL FUNCTION  
S SCATTERING FUNCTION  
S SPACE-TIME FUNCTION  
S SPALDING FUNCTION  
S SPLINE FUNCTION  
S STEP FUNCTION  
S STREAM FUNCTION  
S STRESS FUNCTION  
S SWITCHING FUNCTION  
S TIME FUNCTION  
S TRANSCENDENTAL FUNCTION  
S TRANSFER FUNCTION  
S TRIGONOMETRIC FUNCTION  
S VERTEX FUNCTION  
S WAVE FUNCTION  
S WHITTAKER FUNCTION  
S WORK FUNCTION

## FUNCTION GENERATOR

Electronic analog computer nonlinear function generation by using silicon carbide varistors 11 p1660 A66-23254

Nonohmic-resistor analog function generator, using output voltage summation of nonlinear combination channels for input range 11 p1660 A66-23255

Solid propellant rocket engine omniaxis liquid injection thrust vector control system, using function generator in signal-summing feedback loop to control flow in servovalves and increase motor reliability 14 p2226 A66-27700

Error estimation in diode function generator design 16 p2659 A66-30518

Infinite helical sheath antenna driven by ring delta-function generator analyzed, using Fourier transform, noting decomposition of current distribution 17 p2886 A66-32388

Sensitivity to variations in parameter of signals in networks of linear transfer functions and instantaneous function generators, noting relay characteristics 19 p3327 A66-36018

Trainable nonlinear function generator using threshold logic elements for pattern classifiers 19 p3338 A66-36737

## FUNCTION SPACE

## SA EUCLIDEAN SPACE

## SA HILBERT SPACE

Traces on coordinated hyperplanes of elements of functional space 07 p1057 A66-17844

Synthesis of adaptive control systems by function space methods 09 p1362 A66-20652

Nonlinear time varying open-loop feedback system design and infinitely integrable function space boundedness condition 13 p2053 A66-26085

Theory of physical systems governed by nonlinear functional equations such as vector nonlinear Volterra integral equation [AIAA PAPER 64-680] 14 p2375 A66-27884

Generalized measures and integration in function spaces, giving problems and application 17 p2946 A66-32298

Square-integrable approximate solution to certain ordinary differential equations in particular function space 18 p3127 A66-34640

Nonlinear transformations of probability measures in functional spaces, noting application of random-process theory 21 p3757 A66-38952

Spline theory methods of interpolating linear functional containing Peano kernel 21 p3757 A66-39257

## FUNCTION TEST

## SA DIAGNOSIS

Qualitative analytic function-test maintainability prediction equations from regression analyses on hardware 20 p3569 A66-37922

Functional subsystem analysis in Instructional System Approach to transition training of flight crews 23 p4030 A66-41579

## FUNCTIONAL ANALYSIS

## SA BANACH SPACE

## SA SERIES EXPANSION

Inverse problem of Khavinson and Khavir approximated for complex plane sets 02 p0250 A66-12096

Analysis of equation system for constructing regularizing algorithms for optimum control determination 02 p0209 A66-12103

Free-boundary nonlinear problem of smooth curve drawn in single circle so that doubly connected region formed by curve and circle satisfies specific existence conditions 02 p0250 A66-12103

Uniqueness of optimum approximation sums of single variable functions for multivariable functions in Lebesgue space 04 p0538 A66-13481

Monograph on Levy method for deflection of loaded simply-supported infinite plate strip, introducing class of real functions 04 p0589 A66-14013

System requirements analysis provides orderly identification of hardware, facilities personnel and procedures necessary for system mission success [ASME PAPER 65-WA/AV-2]

Optimal control, discussing fundamental general necessary conditions for Mayer problem solution 06 p0864 A66-16628

Direct method of calculus of variations for finding minimum point for scalar function on functional space 06 p0904 A66-17003

Calculation of integrals of infinitesimal differentiable functions, showing error estimate by network method for periodic functions 07 p1056 A66-17593

Estimates of Taylor coefficients in theory of regular function of several complex variables 07 p1056 A66-17603

Removable singularities in multidimensional minimal hypersurfaces in compact space 07 p1057 A66-17833

Wentzel-Kramer-Brillouin calculation of exact solution of universal instability and drift approximation 07 p1089 A66-17953

Existence of logarithm for nonsingular square matrix, uniqueness for linear ordinary differential equation systems logarithms of operators and spectral mapping 07 p1058 A66-17963

Uniform structure for Lipschitz condition on functions between sets, extensions to nonmetric spaces and fixed point theorems for uniform spaces 07 p1059 A66-17963

Boundaries of convexity of star-shaped functions, order alpha, in open circular region /0, 1/ 07 p1059 A66-18093

Bellman functional equation derived for class of optimal control problems without using Taylor series expansion or mean value theorem of differential calculus 07 p1017 A66-18343

Certain inequalities for solutions of elliptic equations and derivatives near metric region 07 p1060 A66-18463

Nearly ideal cartographic projections of variable type and reduction of certain functional to minimum 08 p1217 A66-19343

Interpolation function of real variable investigating process constructed for given system of points 09 p1394 A66-20453

Nonlinear creep and recovery behavior of polypropylene fibers and hereditary functionals describing nonlinear viscoelastic behavior 09 p1393 A66-20663

Matrix inequality theorems, discussing Krasnoselskii and Krein inequality and Kantorovich inequality 10 p1549 A66-21223

Random errors of derivatives obtained from least squares approximations to empirical functions 10 p1550 A66-21343

Boundedness and uniform boundedness of nonhomogeneous systems, obtaining necessary and sufficient conditions for existence of solutions 10 p1551 A66-21923

Theorems for uniform approximations by algebraic and trigonometric rational functions, noting application in determining functional properties 10 p1552 A66-21983

Nonlinear filters, including system analysis optimization, realization via Volterra functionals, etc 11 p1675 A66-22633

Linear ODEs in canonical form with aftereffect in functional space of continuous functions 11 p1676 A66-22643

Hypergeometric mean value, showing expression for mean of order t of series of



positive values with positive weights as limiting case 11 p1722 A66-22953

Simple inequality involving expectations of convex functions and 11 p1723 A66-23185

Majorization 11 p1723 A66-23185

Approximation of function of many variables by linear 11 p1723 A66-23313

Methods 11 p1723 A66-23313

Spectral analysis of bounded functions and method for constructing them either continuous or 11 p1724 A66-23403

Noncontinuous 11 p1724 A66-23403

Mathematical analysis of analogies between theory of heat conduction and theory of functions of complex 12 p1977 A66-23562

Approximate solution of equation with normally distributed 12 p1902 A66-23899

Operators 12 p1902 A66-23899

General vector notation for multiple integrals 12 p1903 A66-24091

Maximized elliptic equations, Dirichlet problem, distance function solution, maximum principle, removable singularity, etc 12 p1905 A66-24401

Man-machine systems for interplanetary exploration, using functional analysis techniques for system 13 p2013 A66-25281

Design 13 p2013 A66-25281

Minimizing functionals on normed linear spaces, discussing steepest descent and rendezvous problems in control theory 13 p2116 A66-25343

Functional analysis demonstrating existence and uniqueness of displacement field, providing solution for linear viscoelasticity problem for medium having behavior satisfying coercivity condition 13 p2195 A66-25463

Sensitivity operator as extension of time-domain sensitivity function to time-varying change of elements in nonlinear dynamic system, deriving sensitivity equations 13 p2050 A66-26060

Functional transformations revealing topological properties of single contact /SC/ network, simplifying task of synthesis 13 p2051 A66-26064

Bandlimited and approximately bandlimited signals by Fourier transforms of sampling function and prolate spheroidal wave function representing solutions of second order self-adjoint differential equations 13 p2120 A66-26077

Locating zeros of complex functions by computing topological 13 p2121 A66-26326

Index 13 p2121 A66-26326

Maximum information principle applied to search for minimum of function 13 p2028 A66-26475

Functional analysis of electromechanical control systems, noting application of mathematical methods for system reliability determination 15 p2428 A66-28797

Pearson universal random distribution generator, noting analysis of randomly chosen variables for unimodal underlying distribution 15 p2526 A66-28808

Expansion of arbitrary function of Mehler-Fok integral form in terms of spherical functions 15 p2526 A66-28952

Dynamic system stability, control and observation, noting optimal system synthesis, application of functional analysis, Liapunov function and dynamic programming 15 p2470 A66-29149

Formula involving two impedances leads to equations for positive real functions, for application to power gain of symmetric and antisymmetric filters 15 p2464 A66-29322

Uniqueness, existence and stability of solutions to polyvibrant systems with delayed remainder and arguments 15 p2528 A66-29652

Evaluation of solution moduli of nonlinear contour problems pertaining to polyvibrant systems with delayed remainders and arguments 15 p2529 A66-29653

Modified sprindzuk theorem, discussing transcendental functional analysis 16 p2732 A66-30531

Necessary and sufficient condition for growth of solution to second order PDE with delayed arguments 16 p2733 A66-30742

Analytic construction of skew derivative Green matrix for system of second order elliptic PDEs in many variables 16 p2734 A66-30749

Optimization of linear control systems when placing step limitations on control, using functional analysis 16 p2668 A66-30751

Function approximation from finite number of arbitrary points, using iteration methods 16 p2734 A66-30760

Solution of heat-conduction equation over functional spaces possessing fractional derivatives with respect to time, applied as solution to first boundary value problem 16 p2827 A66-30779

Uniqueness of solution to second and third boundary value problems for second-order elliptic equation in presence of boundary singular points 16 p2734 A66-30783

Functional analysis methods applied to optimal control system sensitivity problem 16 p2671 A66-31060

Volterra series analysis of aperiodic solutions to certain second order integrodifferential equations with nonlinear damping and nonlinear restoring force 16 p2737 A66-31334

Linear system damping while using minimum control intensity treated as functional analysis problem 16 p2672 A66-31504

Multipole analysis of acoustic radiation to explore dependence of mass density on functional character of source distribution 17 p2957 A66-31951

Limit properties of uniform process with independent increments 17 p2946 A66-32299

Necessary condition for optimal control in nonlinear automatic control system determined, using method of successive approximations 17 p2902 A66-32574

Accuracy problems in control systems, discussing error assessment and accuracy estimates of optimal control 17 p2902 A66-32576

Stochastic processes, formulation and solution using characteristic functionals, transformations, and measure theory 17 p2947 A66-33095

Torsion of nonlinear viscoelastic circular cylinder in terms of stress tensors prescribed by time-functionals of finite strains 17 p3032 A66-33332

Sufficient conditions for boundedness of solutions of linear system of differential equations with variable coefficients 18 p3126 A66-33929

Existence, uniqueness and periodicity of solutions to boundary value problems for quasi-linear ODEs on topological space of continuous mappings 18 p3127 A66-34138

Invariance effect for finite number of coordinates in infinite dimensional automatic control system 19 p3325 A66-35986

Functional derivative technique for designing self-adjusting control systems having main part implemented by solving differential equations 19 p3328 A66-36021

Nearly ideal cartographic projections of variable type and reduction of certain functional to minimum 19 p3348 A66-36054

Theorems for uniform approximations by algebraic and trigonometric rational functions, noting application in determining functional properties 19 p3390 A66-36189

Random variable-dependent probability measures induced in Borel body from uniform catenaries and related to Lebesgue measures 19 p3391 A66-36434

Optimal control of dynamic systems with minimax type performance index, discussing application of proposed method of solution 19 p3334 A66-36686

Functional polynomial fitting of continuous functional, using Laplace transforms to reduce number of measured records for identifying kernels of second-degree approximation 19 p3391 A66-36703

Generalizations of functional Lagrange expansion to multivariable nonlinear systems such as state space and functional equations in s domain for control problems application 19 p3391 A66-36704

Describing function for analysis of feedback control systems with time-invariant nonlinear elements, simplifying derivation by taking derivative of output of nonlinear element with respect to input 19 p3336 A66-36705

Input-output stability conditions of time-varying nonlinear feedback systems

obtained, using concepts of loop gain, concity and positivity 19 p3338 A66-36739

Weierstrass necessary condition and basic equations for optimal control of initial or boundary states of continuum mechanical MHD and hypersonic partial differential systems 20 p3535 A66-36853

Optimum transformation of linear system with minimal rms error from given point to fixed delta-environment of another given point 20 p3537 A66-36890

Subadditive functional expectations and inequality of variables 20 p3590 A66-37111

Monograph on approximate analysis of randomly excited nonlinear controls, discussing feedback system performance, functional and quasi-functional representation, zero mean systems, etc 20 p3538 A66-37577

Convolution type integral equation solution via reduction to Riemann problem in class of generalized functions 20 p3591 A66-37755

Abstract machine design with recursive function programming language, showing simulator construction in Fortran 20 p3523 A66-38018

Block diagonalization theorem for linear ordinary differential equation systems and applications 21 p3755 A66-38597

Asymptotic forms exhibited by powers of nonnegative matrix, discussing index of convergence and associated values 21 p3755 A66-38602

Computer program for numerical solution of ODE systems, noting generation of symbolic solutions via Taylor series expansion 21 p3707 A66-38679

Local structure of continuous and diffusion Markov processes compared with aid of M functionals for stochastic integrals 21 p3757 A66-39246

Spline theory methods of interpolating linear functional containing Peano kernel 21 p3757 A66-39257

Synthesis of optimal Liapunov-Bellman function, noting sequential solution method for independent variables and method using first-order partial differential equation 21 p3758 A66-39281

Uniqueness of solution to second and third boundary value problems for second-order elliptic equation in presence of boundary singular points 22 p3940 A66-40445

Optimal control synthesis for cost functionals involving convex single valued functions of state and control variables, noting steepest ascent method and evaluating gradient 22 p3885 A66-40871

Gauge transformations of third kind and operator gauge transformations of first and second kinds, relating electron and photon propagators to quantum electrodynamical vertex function 23 p4098 A66-41392

Parameters of dynamic systems described by PDEs determined by replacing PDE with integral equation and eliminating via recursion process terms resulting from initial and boundary conditions 23 p4084 A66-41396

Generalized function solution for ordinary differential equations 23 p4084 A66-41406

Finite realization extrema of continuous time stationary stochastic processes 23 p4085 A66-41535

Existence and uniqueness theorems in Poincare-Liapunov theory for multipoint control boundary value problems 23 p4085 A66-41539

System of differential equations describing stability of certain generalized processes in language of functional sets and distributions 24 p4230 A66-42214

Functional analysis applied to optimum control by reduction of variational problem to finite dimensional analysis and calculation of algorithms for use with digital computer 24 p4231 A66-42470

**FUNCTIONAL INTEGRATION**

Functional system integration as means of displaying complex electrical and electronic systems to minimize initial design, equipment checkout and trouble shooting problems 02 p0306 A66-11637

Control criterion for linear system with constant matrix, discussing quadratic functionals ensuring aperiodic transient 11 p1674 A66-22351

Averaging method for differential



equations with retarded arguments 13 p2118 A66-25827  
 Functional integration analysis of exponential behavior of nonlinear feedback control systems 13 p2052 A66-26076  
 Space-time correlation tensor of turbulent fields by phase space functional Lebesgue-Stieltjes integration, statistical hydromechanics and probability measure theory 15 p2479 A66-29398  
 Maximum error curves for Lanczos selected point method of polynomial solution to ordinary differential equations, using Chebyshev and Legendre functions 17 p2947 A66-32858  
 Payload integration in space experimentation, discussing commonality, flight and load matrices, experiment-spacecraft-ground system interfaces, computer methods, etc 20 p3662 A66-37186

## FUNGUS

SA SPORE  
 SA YEAST  
 Genetic control of gibberellin production in fungus *Gibberella fujikuroi* 23 p4025 A66-41307

## FURNACE

SA IMAGE FURNACE  
 SA SOLAR FURNACE  
 SA VACUUM FURNACE  
 Cylindrical black body furnace with graphite resistance built in France, attaining 1600 degrees C, for calibration of radiation pyrometers 09 p1383 A66-20909  
 Apparatus for melting boron carbide inductively on water-cooled hearth, noting application to other refractory materials 13 p2088 A66-26563

## FUSE

Fuse evaluation for spacecraft power system 08 p1196 A66-19504  
 Circuit overloading protection using automatic reset, breakers and fuses 14 p2249 A66-27120

## FUSELAGE

SA AIRFRAME  
 SA WING-FUSELAGE COMBINATION  
 Aircraft fuselage design in region of center section for case of asymmetric bending 11 p1782 A66-22854

## FUSION

SA CONTROLLED FUSION  
 SA NUCLEAR FUSION  
 Closed-form solution for constant velocity solidification of spheres initially at fusion temperature 10 p1622 A66-21889  
 Vanadium oxide single crystal growth by flame solution and fusion, noting burner construction, crystal structure and techniques 12 p1899 A66-23565  
 Space thermal control using fusible materials, with analysis of one-dimensional adiabatic system 18 p2826 A66-30505

## FUSION WELDING

Laser beam welding electronic-component leads 05 p0685 A66-14517  
 Laser welding evaluated with regard to performance and production application 05 p0686 A66-14692  
 Transverse weld shrinkage and distortion in aluminum butt welds due to lack of stress equilibrium about neutral planes of plate thickness 05 p0686 A66-14696  
 Aluminum alloy butt fusion welds, discussing ghost lack of fusion phenomenon mechanism, characteristics and causes 06 p0887 A66-16800  
 Pulsed laser welding, wire-to-wire, sheet-to-sheet, circuit board, vacuum tube, etc 07 p1038 A66-18153  
 Fusion welding processes dependent upon electric heat source 09 p1384 A66-20610  
 Hot cracking in Hastelloy X fusion weld as affected by microsegregation produced during solidification 10 p1547 A66-21768  
 Orbit arc automatic tungsten inert gas fusion welding and application to joining tubular systems in aerospace industry [ASTME PREPRINT AD66-719] 12 p1886 A66-24410  
 Porosity at weld fusion zone-base material interface in gas tungsten-arc and electron beam welds of tantalum 13 p2110 A66-26018  
 Laser welding of aerospace structural alloys and resultant joint properties 13 p2087 A66-26019  
 Metal welding technology, including problems of thermal deformation and heat

effect on properties of welded materials 14 p2298 A66-26945  
 Residual stress control in welded structure noting stress reduction by preheat, prestressing by fusion welding and spot weld impact treatment 22 p3924 A66-40262  
 Solid state laser application to fusion welding 22 p3926 A66-40274  
 Welding, thermal flux control and contamination prevention of Saturn rockets, particularly fusion 23 p4073 A66-41534

## F4H AIRCRAFT

## S F-4 AIRCRAFT

## F8U AIRCRAFT

## S F-8 AIRCRAFT

## G

## G FORCE

## SA ACCELERATION STRESS

## SA GRAVITY

Perception of apparent vertical without visual cues depending on longitudinal axes of body and head to direction of resultant acceleration above 1 g 04 p0468 A66-14086  
 Otolith organ activity within Earth standard, one-half standard and zero gravity environments and effect of extralabyrinthine factors effect upon counterrolling 15 p2431 A66-28664  
 Centrifugal acceleration effect on sexual apparatus, cardiovascular system and respiratory organs of female monkey 15 p2437 A66-29472  
 Prolonged hypokinesia effect on human resistance to transverse g-forces, detailing respiratory and circulatory systems, motor response and visual acuity 15 p2437 A66-29473  
 Model of vestibular apparatus emphasizing function of otolithic part, noting reactions of receptor-neuron system to g forces 15 p2444 A66-29496  
 Condensation tests in smooth and porous coated tubes in multi-g centripetal acceleration fields for increasing heat transfer coefficient of condensing nitrogen 18 p3262 A66-34379  
 Effect of head-to-foot accelerations of up to 10 g on rabbits, noting changes in ECG, EEG, brain histology, etc, leading to ischemic conditions 18 p3060 A66-34408  
 Origin of chest pains associated with G force sinusoidal vibration, noting effect of anterior chest wall anesthetization, results suggest pain originates in chest wall 19 p3286 A66-36375

## G-222 AIRCRAFT

## S FIAT G-222 AIRCRAFT

## GADOLINIUM

Specific heat of gadolinium near Curie point, discussing measuring procedure and line drawing of calorimetric setup 01 p0118 A66-10252  
 Emission current density and effective work function of samarium, europium and gadolinium hexaborides 02 p0270 A66-11426  
 Anomalous thermal expansion above and below Curie point as function of temperature in gadolinium single crystal 02 p0274 A66-11725  
 Specific heat evidence for gapless superconductivity, examining experimental results on lanthanum doped with magnetic impurity gadolinium 09 p1420 A66-20053  
 Gadolinium molybdenate as ferroelectric host in pulsed laser, noting light modulation and crystal domain 11 p1713 A66-23207  
 Fluorescence behavior of gadolinium and terbium, noting nonradiative energy transfer in borate glass 13 p2158 A66-25052  
 Lattice parameters and constant measured in gadolinium-yttrium alloy dihydrides, using X-ray diffraction techniques 13 p2162 A66-25382  
 Vapor pressures of solid samarium and liquid gadolinium at high temperatures using Knudsen effusion method, noting sublimation heats for samarium 14 p2314 A66-27462  
 Magnetic state of gadolinium impurities in superconducting lanthanum 16 p2768 A66-30134  
 Temperature dependences of coercive force, hysteresis loops and domain structure of thin iron-gadolinium alloy

films 16 p2774 A66-3064  
 Domain structure and hysteresis loops thin iron-gadolinium films of different thicknesses 16 p2775 A66-3064  
 X-band spectrometric observation of ES of trivalent gadolinium in reduced barium titanate 21 p3797 A66-3877

## GAIN

## SA POWER GAIN

Gain-bandwidth limitations for physical realizable systems obtained in integral form by employing generalized representation theorem for bounded-real functions 02 p0208 A66-1193  
 Predicting transistor gain degradation from neutron radiation environment from variation of radiation damage constant as function of temperature and current 05 p0735 A66-1481  
 Random error effect on directional gain of sectional parabolic antenna with automatic phasing, setting sections effectively by three control points method 14 p2250 A66-2710  
 Harmonic analysis of current gains of internal slope of nonuniform base transistors 14 p2254 A66-2766  
 Controlling gain of individual transistor amplifier stages to enable amplifier to handle input signals with wide dynamic ranges 14 p2262 A66-2833  
 Communication satellite design noting use for educational and commercial purposes instrumentation applied, etc 17 p2872 A66-3191  
 FET structures with linearly graded junctions noting maximum gain configuration, transconductance expressions etc 17 p2895 A66-3311  
 Relative circuit gain of common-emitter antisaturation feedback circuit configurations as function of circuit parameters 18 p3090 A66-3408  
 Approximate theory for estimating effect of manufacturing tolerances on design of parabolic reflector performance 18 p3082 A66-3428  
 Tolerance theory for parabolic reflector antenna, noting gain and radiation-pattern distortion 18 p3082 A66-3428  
 Reduced gain and increased sidelobe caused by errors in surface of parabolic reflector 18 p3085 A66-3439  
 Modified Goonhilly No. 1 aerial noise temperature, gain and figure of merit 18 p3085 A66-3439  
 Gain loss ratio between one antenna and two antennas used to analyze antenna gain loss for long-range tropospheric propagation of ultrashort waves 20 p3525 A66-3711  
 Antenna measurement for input impedance, gain and directivity characteristics 20 p3531 A66-3777

**GALACTIC EVOLUTION**  
**SA STELLAR EVOLUTION**  
 Galactic X-ray astronomy discussing neutron stars, thermal bremsstrahlung at synchrotron radiation 02 p0290 A66-1189  
 Origin of primary cosmic rays discussing galactic theory, propagation characteristics and measurement results 04 p0574 A66-1381  
 Origin of solar system, discussing monistic and dualistic theory, interstellar characteristics, star formation and planetary development 05 p0767 A66-1577  
 Book on galactic structure including distribution of common stars, solar motion, interstellar hydrogen distribution, galactic radio emission, planetary nebulae, etc 11 p1766 A66-2222  
 Distribution patterns of common stars in galactic plane according to spectral type noting density gradients, main sequence Hertzsprung-Russell diagram, etc 11 p1766 A66-2222  
 Statistical determination of stellar motion compounded of radial velocity in line of sight and transverse velocity perpendicular to it, considering galactic orbits of near stars, velocity ellipsoids, etc 11 p1766 A66-2222  
 Cosmological-galactic creation, steady state expansion and high energy particle production associated with radio sources 11 p1774 A66-2306  
 Elliptical galaxy formation by expansion from steady state according to Einstein-Sitter law 11 p1775 A66-2306  
 Dynamic evolution of clusters of



- galaxies 14 p2383 A66-27707
- Galactic evolutionary patterns in neighborhood of solar system, assuming rate of star formation depends on time parametrically 15 p2594 A66-28985
- Rapid mass ejection from highly evolved stars as explanation for observation of high abundance of galactic helium 15 p2599 A66-29680
- gas 15 p2599 A66-29680
- Metagalactic existence of type of hypothetical particles representing stable closed Einstein microcosms 18 p3233 A66-34547
- HF brightness intensity of cosmic background radiation at 20.7 cm wavelength may be primordial fireball residue of big-bang cosmology 18 p3171 A66-34717
- Galactic evolution examined, using luminosity and volume emissivity diagrams 18 p3178 A66-34760
- Galactic evolution and structure - Solvay Physics Conference, Brussels, September 1964 20 p3645 A66-36957
- Synchrotron theory to calculate energy content of radio sources as function of relativistic electrons and magnetic flux 20 p3645 A66-36961
- Perturbations of spatially isotropic expanding universe in terms of small curvature variations 21 p3817 A66-39559
- Forms of red shift magnitude relation for Friedmann type relativistic model universes 23 p4125 A66-41046
- Cosmological evolution from red shifts of quasi-stellar radio sources 23 p4127 A66-41150
- Dynamical requirements for existence of interstellar magnetic field in solar neighborhood 23 p4124 A66-41812
- Suggestion that quasar red shifts result from inflow of matter at relativistic velocity in gravitational field of highly condensed white dwarf 24 p4274 A66-42419
- GALACTIC MAGNETIC FIELD**
- Solar magnetic field may have originated during process of Sun formation from galactic magnetic field which pervaded interstellar gas from which Sun condensed 08 p1292 A66-19261
- Large-scale aspects of gaseous components of our Galaxy, noting dynamics of gaseous systems with magnetic fields, virial theory, angular momentum, spiral structure of galactic disk, etc 11 p1767 A66-22263
- IR radiation from interstellar grains, measuring intensity as wavelength function and radiation polarization for information on grain temperature and composition and galactic magnetic fields 14 p2377 A66-28122
- Irregularity of galactic magnetic field structure in vicinity of Sun indicated by starlight polarization, interstellar cloud motion and Milky Way photography 15 p2595 A66-29130
- Galactic magnetic field strength and distribution determined from synchrotron emission of relativistic electrons, noting Faraday rotation of polarized radiation from distant radio sources 18 p3235 A66-34744
- Dynamical behavior of cosmic ray gases, noting modes of hydromagnetic wave propagation and static equilibrium configurations for thermal interstellar gas and field 18 p3178 A66-34759
- Galactic model for studying hydromagnetic stability of spiral arm in which field lines are helices around axis 18 p3237 A66-35043
- Faraday rotation variation with galactic coordinates studied for emission from 86 linearly polarized radio sources 18 p3238 A66-35236
- Galactic magnetic fields, considering magnetic flux, frequency of fields in radio galaxy, disk, interstellar gas dynamics and spiral structure 20 p3645 A66-36958
- Radio electron density and magnetic field in galactic halo from primary cosmic ray and radio brightness measurements 21 p3817 A66-39563
- Underground telescopes confirm two-way sidereal anisotropy in charged primary cosmic radiation 22 p3973 A66-40534
- Theoretical model for quasars characterizes them as galactic flares, based on study of high energy phenomena associated with solar flares 22 p3982 A66-40536
- GALACTIC RADIATION**
- Expected cosmic ray intensity variations on Moon from analysis of such variations on Earth 01 p0132 A66-10323
- Radio astronomy research in solar system, galaxies, supernovas, radio galaxies and cosmology 01 p0139 A66-11159
- Solar modulation of low-energy galactic helium spectrum as observed on IMP I satellite 03 p0418 A66-12671
- High energy electron influence on electron distribution function and effect on spectra of nonthermal galactic and extragalactic radio sources 04 p0575 A66-14171
- Neutrino producing cooling reaction rates indicate that discrete X-ray sources located in direction of galactic center are not neutron stars 05 p0760 A66-14895
- Radio source spectrum, discussing spectral indices, electron energy and H II density in quasi-stellar and high brightness-temperature sources 05 p0762 A66-15279
- Solar and galactic cosmic ray characteristics, origin and flux-time variations, examining relation between solar flares and geomagnetic storms 05 p0756 A66-15751
- Galactic cosmic ray intensity modulation by interplanetary plasma turbulence, noting cosmic ray and geomagnetic storm 07 p1122 A66-17987
- Spectral variation of low energy galactic cosmic ray protons and helium nuclei measured by balloon flights 07 p1123 A66-17995
- Cosmic ray origins including galactic rays, RF radiation, metagalactic gamma radiation, etc 09 p1437 A66-20202
- Galactic and metagalactic cosmic gamma- and X-ray intensities 09 p1437 A66-20203
- Theoretical energy spectrum for galactic cosmic radiation based on experimental solar cosmic ray data 09 p1437 A66-20204
- Ultrahigh energy primary cosmic ray energy spectrum calculated from EAS particle-number spectrum 09 p1437 A66-20206
- Mechanisms for cosmic-radiation intensity variations, including cosmic-ray modulation effects, solar cosmic rays and variations of galactic origin 09 p1437 A66-20207
- Twenty-seven day modulation of galactic cosmic rays attributed to axisymmetric solar wind of magnetic inhomogeneities 09 p1438 A66-20211
- Galactical distribution of X-ray sources, noting concentration toward galactic plane 09 p1442 A66-20414
- Probable relation between OB associations, runaway stars, supernovas and X-ray sources 09 p1443 A66-20469
- Spectra of generically related cosmic ray species 09 p1443 A66-20688
- UV radiation from galaxies, radio sources, quasi-stellar objects and Seyfert galaxies, examining Lyman alpha fluxes 10 p1598 A66-21098
- Mechanism for production of X-rays and gamma rays in galaxies, noting photon and electron spectrum 10 p1598 A66-21100
- IR emission lines possibly originating from galactic, interstellar and stellar hydrogen regions 10 p1599 A66-21113
- Galactic X-rays, discussing soft X-rays, UV radiation, isotropic X-rays, electromagnetic radiation from X-ray sources, etc 10 p1600 A66-21854
- Lower limit of age of cosmic ray nuclei, flux ratio of Be nuclei to B nuclei and intergalactic cosmic ray propagation 12 p1938 A66-24092
- Solar wind and geomagnetic storm effects on galactic cosmic ray 11-year variations and energy spectrum, from neutron monitor data 12 p1940 A66-24160
- Solar wind as radial flux of electromagnetic inhomogeneities, galactic ray modulation by solar wind and cosmic ray intensity variation with sunspot cycle 12 p1940 A66-24162
- Electrical discharge theory of cosmic atmospheric phenomena, relating lightning, novae and quasars 12 p1950 A66-24394
- Quantum mechanics and gravitational effect on origin of cosmic particles, discussing Schroedinger wave equation, electric potential and alpha decay 12 p1944 A66-24465
- Shielding of manned Mars vehicles from solar and galactic cosmic radiation and radiobiological tolerance criteria 13 p2190 A66-25261
- Aerobee rocket measurements of cosmic X-ray sources emanating from Cygnus A, M-87 and galactic supernova remnant Cassiopeia A 13 p2174 A66-25836
- Galactic plane emission at 408 mc/s using Australian 210 ft radio telescope 13 p2186 A66-26030
- Solar radio burst at night during recording of 18-mc galactic noise by globally located antennas 13 p2176 A66-26367
- Galactic low RF background radiation spectrum and measurements of sky brightness temperature 14 p2383 A66-27708
- Telescopic measurements of primary energy spectra and abundances of He 3 and He 4 in galactic cosmic radiation 16 p2793 A66-30198
- Inverse Compton X-ray and gamma ray flux due to high energy electron interaction with cosmic blackbody radiation at 3.5 degrees K 17 p2992 A66-31914
- Free-free galactic X-ray emission from hot fully-ionized hydrogenic plasma 17 p2992 A66-31916
- Crystal spectra and broadband measurements of solar and galactic UV, X-rays, gamma rays, etc, outside Earth atmosphere 17 p2998 A66-32030
- Solar protons and neutrons shown not to play important part in production of radiation belt protons 17 p2993 A66-32529
- Proton energy density, pressure and compressibility of galactic cosmic ray gas 18 p3165 A66-34140
- Astronomical model study of physics of penetration of interstellar cosmic rays into solar system 18 p3168 A66-34342
- Galactic acceleration and solar modulation of cosmic rays examined via energy spectrum of galactic electrons, estimating Fermi acceleration, low energy electron flux, etc 18 p3177 A66-34756
- Galactic X-ray energy spectrum noting equipment used, shape of spectra in terms of thermal radiation intensity, etc 18 p3177 A66-34757
- Sidereal time variation of cosmic rays explained by diffusion in galactic arm for colinear magnetic field and proximity of solar system 18 p3178 A66-34762
- Galactic cosmic ray diffusion into solar system as affected by zonal distribution of solar activity, noting 11-year modulation 18 p3180 A66-34771
- Long-term modulation of cosmic ray intensity in interplanetary medium 18 p3180 A66-34774
- Galactic cosmic ray anisotropy behavior obtained from observations of daily variation of cosmic ray intensity 18 p3182 A66-34782
- Modulation effects in galactic and solar cosmic rays in interplanetary space 18 p3185 A66-34806
- First-order modulation effects of galactic cosmic radiation, considering hysteresis effect and variation of energy spectrum in 11-yr modulation 18 p3186 A66-34811
- Solar modulation of galactic protons and helium nuclei from 1963 to 1965 18 p3188 A66-34821
- Low energy galactic cosmic radiation studies by high altitude balloon flights carrying nuclear emulsions, including solar activity, energy and intensity spectra, etc 18 p3189 A66-34829
- Balloon flight data obtained at 50 and 65 degrees N geomagnetic latitude on spectra of primary cosmic ray hydrogen and helium nuclei, using Cerenkov scintillator technique 18 p3190 A66-34831
- Solar modulation and time variation of differential energy spectrum and flux of primary helium nuclei in 30 to 90 mev/nucleon energy range 18 p3190 A66-34832
- Chemical abundances and energy spectra of nuclei in galactic radiation measured in interplanetary space by OGO-I satellite 18 p3190 A66-34833
- Seventy-channel scintillation spectrometer high atmospheric measurement of cosmic gamma radiation of extraterrestrial origin 18 p3192 A66-34845
- Skyhook balloon flight Geiger counter cosmic ray monitor measurements of energy and charge spectra of galactic rays at solar minimum 18 p3192 A66-34847
- Energy spectrum of primary galactic X-rays



- between 20 and 50 kev observed during night with NaI crystal 50-channel spectrometer 18 p3193 A66-34851
- Delta electrons formed in interstellar hydrogen-galactic ray collision 19 p3452 A66-35283
- Galactic and atmospheric X-ray characteristics determined by two scintillation counters borne on sounding rocket booster 19 p3452 A66-35354
- Balloon measurements of cosmic ray hydrogen and helium nuclei at locations with nominal geomagnetic threshold rigidities 19 p3452 A66-35926
- Low energy cosmic ray modulation relationship to observed interplanetary magnetic field irregularities in terms of diffusion, using space probes 19 p3454 A66-36765
- Astronomical model for diffusion of galactic cosmic rays in solar system, based on zonal character of solar activity 20 p3630 A66-37329
- Cosmic radiation theories and experimental supporting evidence, origin of cosmic ray particles and relation between cosmic ray sources and radio wave 20 p3631 A66-37436
- Production and equilibrium spectrum of galactic cosmic ray secondary electrons arising from secondary pion and neutron decay 20 p3633 A66-38200
- Rocket instrumentation for galactic X-ray observation, noting scintillation counter, proportional counter and GM counter 20 p3636 A66-38237
- Sidereal anisotropy indicated for charged galactic cosmic radiation obtained by celestial scanning, using narrow angle moon telescope 21 p3808 A66-38466
- Radio electron density and magnetic field in galactic halo from primary cosmic ray and radio brightness measurements 21 p3817 A66-39563
- Spectroscopic evidence on helium abundance of stars in galactic halo 21 p3817 A66-39565
- Galactic radio sources noting disk model brightness distribution, relativistic particle energies, continuous particle acceleration and ratio between proton and electrical component of cosmic radiation 22 p3985 A66-40952
- Celestial X-ray sources at low galactic longitude located by rocket observation 23 p4123 A66-41148
- Rocketborne instruments for observing galactic X-rays including scintillation and proportional and GM counters 23 p4067 A66-41287
- Sporadic E layer formation at night, noting ionization sources and intensity 23 p4064 A66-41645
- Source spectra and composition of galactic cosmic rays implied by analysis of interstellar and interplanetary travel, noting solar modulation 24 p4265 A66-42716
- Shielding of manned Mars vehicles from solar and galactic cosmic radiation and radiobiological tolerance criteria 24 p4283 A66-42785
- GALACTIC RADIO WAVE**
- Preponderance of negative velocity hydrogen, found equally in north and south galactic polar caps, surveyed with Harvard 60-ft antenna 02 p0292 A66-12187
- Ionospheric effect on spectrum of general background galactic radio emission below 10 mc/s 02 p0284 A66-12192
- Comparison of optical and radio observations of spiral structure of galaxies 03 p0423 A66-12454
- Polarized OH emission near W3 region 04 p0579 A66-14175
- OH emission in direction of source W49, comparing earlier observations 04 p0579 A66-14176
- Survey of radio emission fluxes from eight Sb-type, ten Sc-type, two Ir-type and one Pec-type galaxy 05 p0759 A66-14873
- Galactic cluster radio emission 05 p0759 A66-14887
- Galaxy M82, analyzing continuous optical magnetobremssstrahlung and relativistic electrons 05 p0752 A66-15380
- Origin of continuum radio emission in directions away from Milky Way 05 p0766 A66-15480
- Times of peak cosmic radio noise concentration and usefulness to forward propagation ionospheric scatter reception on DEW-Line as performance monitor, etc 06 p0825 A66-15985
- Galactic center dynamics revealed by hydroxyl radicals present in interstellar medium, noting detection of radio emissions caused by star-excited atoms and molecules 09 p1453 A66-20239
- Galactic radio astronomy developments including 21-cm line studies, galactic discrete sources, background radiation and polarization 10 p1601 A66-21059
- Galactic radio noise between 1.5 and 10 mc observed by Alouette I satellite 10 p1604 A66-21121
- Continuous radio emission in our Galaxy, discussing radio stars, background features, corona, emission mechanisms, etc 11 p1767 A66-22259
- RF spectrum of OH radiation in interstellar space, including emission intensity and linear polarization 11 p1774 A66-22963
- OH emission and narrow spectral features made with circularly polarized field horn on 140-ft radio telescope in November 1965 14 p2384 A66-27901
- Radio astronomy applications, noting solar and galactical emissions, planetary radiation measurement, instrumentation, etc 17 p2998 A66-32028
- Empirical decision-making techniques, determining nature of quasi-stellar source or galaxy 18 p3234 A66-34616
- Brightness distribution of 3C444 radio source obtained from lunar occultation 18 p3235 A66-34658
- First spectral observation at 21-cm line with radiotelescope at Nancy, France 20 p3654 A66-37825
- Direction, frequency and polarization of radio emission from galactic OH determined by hypothesis of stimulated emission 21 p3814 A66-39213
- Linear polarization of continuum emission from galaxy and discrete sources, detection in radio astronomy, noting relevant synchrotron theories 21 p3815 A66-39488
- Millimeter wave radio astronomy, discussing solar system, galaxy and extragalactic sources 22 p3983 A66-40732
- GALAXY**
- SA MILKY WAY
- SA RADIO GALAXY
- SA SPIRAL GALAXY
- SA STAR
- SA SUPERNOVA
- Einstein gravitational equation applied to galaxies and quasars, using spherical model with spherically symmetric distribution of matter 01 p0138 A66-11033
- Ring of ionized hydrogen in region 3.5 to 4.5 kpc from galactic center 03 p0426 A66-12908
- Resonance cases and small divisors in third integral of motion used to calculate galactic orbits on plane of symmetry of nonaxisymmetric galaxy 08 p1296 A66-19353
- Data on large-scale distribution of interstellar hydrogen important for studies of spiral arms and galactic disk 11 p1766 A66-22257
- Optical interstellar absorption lines and galactic structure, noting observational data and comparison with 21 cm studies 11 p1767 A66-22258
- Stellar dynamics of Galactic system, discussing relations between density and velocity distributions of stars 11 p1767 A66-22262
- Elliptic galaxy formation by expansion from steady state according to Einstein-de Sitter law 11 p1775 A66-23069
- Peculiar galaxies and associated radio sources and quasars 12 p1947 A66-23659
- Dimensional structure and particle dynamics of metagalaxy 14 p2379 A66-27224
- Ring of ionized hydrogen in region 3.5 to 4.5 kpc from galactic center 14 p2380 A66-27256
- Gravitational theory for dynamical basis of quasi-stationary spiral structure of stars 14 p2381 A66-27500
- Galactic structure observational aspects - NATO International Summer Course, Athens September 1964 15 p2593 A66-28980

- Formula derivation for stellar motion and analysis of stellar spatial distribution using Kapteyn scheme and Schalen-Lindblad method 15 p2593 A66-28980
- Radio astronomy measurement of galactic structure, using thermal and nonthermal radiation and neutral hydrogen line emission 15 p2594 A66-28980
- Density and velocity distributions of steady state stellar systems in Galaxy, examining relation between spiral structure and composition 15 p2594 A66-28980
- Observational needs for galactic research, discussing stellar luminosity, interstellar absorption, etc 15 p2594 A66-28980
- Energy dissipation channels of nuclear and electron components of cosmic rays in Galaxy and Metagalaxy 15 p2576 A66-29130
- Cometary motion in outer solar system, region, taking galactic nucleus as perturbing body 15 p2596 A66-29130
- Interstellar medium survey including cloud structure and velocity field of interstellar gas, galactic magnetic field, etc 16 p2799 A66-30520
- Presence and detectability of hydrogen molecular form in galaxy 17 p3001 A66-32230
- Identification of radio source 05 21-36 with N-galaxy, noting high optical luminosity and tabulated spectrogram data 20 p3650 A66-37329
- Spiral patterns of disk-like galaxies explained in terms of density waves that are collective modes of stellar system analogous to plasma waves 24 p4273 A66-42220
- GALERKIN METHOD**
- Asymptotically accurate estimates
- Bubnov-Galerkin method error in eigenvalue problem as applied to boundary value problem 01 p0091 A66-10101
- Stability theory for elastomechanics systems using algebraic techniques based upon Galerkin method 01 p0153 A66-10401
- Amplitude of subharmonic vibrations at even order and frequency limits
- excitation for systems described by Duffing equation 01 p0159 A66-11101
- Large amplitude-free oscillations of beams and plates by means of Ritz-Galerkin technique 02 p0297 A66-11501
- Solution to nonlinear periodic system using Galerkin approximation method of generated trigonometric polynomials 04 p0539 A66-13901
- Bubnov-Galerkin method extended
- solution of any system of equations not associated with variational principles 08 p1306 A66-18601
- Convergence of Galerkin method
- nonconservative stability problems of thin elastic plates and thin elastic rods 08 p1311 A66-19301
- Galerkin method to solve free vibration problem of thin oblate spheroidal shells 09 p1468 A66-20901
- Quasi-linear boundary value problem solved with Galerkin convergence method 12 p1902 A66-23801
- Stress concentration at circular hole in orthotropic cylindrical shell, using coordinates system and Bubnov-Galerkin method 13 p2206 A66-26401
- Compatibility conditions for stress-strain and Galerkin-Papkovich representations of field equations for linear asymmetric elasticity theory 14 p2408 A66-28301
- Convergence rate of method of least squares and some approximate Galerkin type methods in eigenvalue problems 15 p2526 A66-28601
- Differential approximation linearization technique compared with Galerkin method 16 p2732 A66-30201
- Intrinsic electric field of rarefied ion electron plasma in external magnetic field and plasma stability, noting use of Galerkin method to determine plasma layer slippage 16 p2760 A66-30701
- Monograph on nonlinear bending theory of three layer plates, covering mathematical theory of elasticity stress-strain diagram Galerkin method, maximum deflection criteria, etc 16 p2819 A66-31101
- Numerical problems in application of Urabe results in considering periodic nonlinear differential systems, obtaining Galerkin approximations 16 p2737 A66-31201
- Stationary viscous incompressible fluid



Flow past rough surface, noting solution stability and friction stress determination for given pressure 16 p2688 A66-31301

Gradient Galerkin vector for elastodynamic problem of isotropic inhomogeneous body 16 p2823 A66-31707

Computer solution using Bubnov-Galerkin method to determine concentrated force effect on shallow spherical dome 17 p3026 A66-32601

Nonconservative elastic stability problems treated by Galerkin and Ritz methods 20 p3669 A66-37541

Taylor stability of time-dependent flow between two concentric circular cylinders, noting solution of differential equations for perturbations by Galerkin method 22 p3902 A66-40706

Periodic solutions of nonlinear differential systems, examining Galerkin procedure and method of averaging 23 p4084 A66-41054

Analogue of Galerkin method for solving boundary value problems and quasi-linear operator equations 23 p4086 A66-41569

Steady fully developed MHD channel flow of viscous electrically conducting fluid studied by Galerkin method under applied magnetic and electric fields 23 p4107 A66-41886

Galerkin based stability theory of elastic equilibrium extended to include nonconservative loads 23 p4097 A66-41983

Nonlinear flexural vibrations of thin circular rings analyzed, using Galerkin procedure on motion equations 24 p4285 A66-42142

Method of weighted residuals /MWR/, Galerkin method and variational method compared for approximate solution of differential equations 24 p4232 A66-42836

Flow behind shock wave in long tube analyzed by time effect and integrating equations, using Galerkin method 24 p4197 A66-42997

**GALLIUM**

Radiation damage to germanium, silicon, indium and gallium antimonides and arsenides 01 p0119 A66-10373

Gallium concentrations in iron phases of several chondritic meteorites 02 p0290 A66-11962

Retardation of gallium and arsenic or phosphorus diffusion in silicon 05 p0736 A66-14976

Experimental assembly using liquid gallium cycle for testing electromagnetic pumps and flow meters 06 p0918 A66-16847

Superconductivity of gallium metastable phase, noting transition temperature and critical field 08 p1267 A66-18649

Thermoconductivity of germanium alloyed with arsenic and gallium depends on impurity type starting from certain impurity concentration 14 p2359 A66-27178

Cyclotron resonance observation of electron scattering by Ga and In atoms in Ge 21 p3797 A66-38754

Butler iron meteorite composition, noting very high concentration of germanium, gallium and nickel exhibiting Widmanstätten pattern 22 p3978 A66-40014

**GALLIUM ALLOY**

Superconducting properties of niobium-gallium alloys at high temperatures, high current densities and high magnetic field intensities 01 p0123 A66-10703

Solubility range of 75 atomic percent vanadium-gallium system to determine phases in equilibrium and ascertain presence or absence of superconductivity 07 p1052 A66-18352

Superconducting properties and phase composition of silver-gallium alloys 09 p1411 A66-19960

Superconducting properties of niobium-gallium alloys at high temperatures, high current densities and high magnetic field intensities 11 p1758 A66-23308

Semiconducting properties of several gallium and indium antimony tellurides systems and their metallurgical aspects 17 p2986 A66-33296

**GALLIUM ANTIMONIDE**

Microstructural and X-ray studies of solid solutions of Ga-Sb-Te system to determine solubility region in gallium antimonide section of phase diagram 01 p0120 A66-10458

Resistivity and Hall coefficient vs temperature in heavily doped n-type GaSb and related semiconductors 04 p0561 A66-13734

Stimulated radiation from zinc diffusion p-n junctions in gallium antimonide crystals 04 p0569 A66-14355

Recombination radiation spectra of n-type gallium antimonide on concentration of tellurium base region 04 p0570 A66-14364

Galvanic and thermomagnetic coefficients of undoped polycrystalline p-type GaSb sample in weak magnetic field, emphasizing hole mobility 04 p0571 A66-14499

Stimulated emission in GaSb diodes made from crystals prepared by Czochralski method 07 p1096 A66-17336

Structural formation and electrical properties of polycrystalline thin films of GaSb obtained by discrete vacuum evaporation method 08 p1267 A66-18588

Lithium diffusion effects on electrical properties of tellurium doped n-type GaSb 10 p1578 A66-21582

Thermoconductivity measurements of p-type gallium antimonide in solid and liquid state 10 p1590 A66-22176

Optical excitation in indium arsenide and gallium antimonide yielding laser radiation 13 p2090 A66-25438

Laser action in gallium antimonide diodes, examining emitted light spectrum vs injected current, temperature effect, radiative efficiency, etc 13 p2100 A66-26184

Current dependence of recombination radiation intensity in gallium antimonide, determining radiation spectral distribution at low temperature 14 p2358 A66-27089

Shubnikov-de Haas oscillations in magnetoresistance of Li-diffused Te-doped n-type GaSb 14 p2366 A66-27764

Stimulated radiation from zinc diffusion p-n junctions in gallium antimonide crystals 14 p2368 A66-28253

Recombination radiation spectra of n-type gallium antimonide on concentration of tellurium base region 14 p2369 A66-28263

Coupling of electron motion to lattice longitudinal acoustic mode in n-gallium antimonide leading to variations in sound velocity 16 p2775 A66-30732

Minimum spectral line width, threshold current density, radiation-peak displacement and possible recombination mechanism for GaSb laser diode p-n junctions in coherent radiation 16 p2721 A66-31764

Thermoconductivity measurements of p-type gallium antimonide in solid and liquid state 19 p3441 A66-35790

Coupling between plasmons and polar phonons in degenerate semiconductor gallium antimonide analyzed, starting from electron-phonon Hamiltonian 19 p3447 A66-36400

Recombination radiation from Ga-Sb p-n junctions, noting spectral composition as function of current density and impurity concentration 20 p3618 A66-37563

Quasi-localized states associated with high-energy conduction-band minima in semiconductors, particularly Se-doped GaSb, plotting pressure-dependence of photoluminescence 20 p3618 A66-37598

Impurity atom behavior in diatomic InSb and GaSb crystal lattices analyzed, using nuclear gamma resonance, measuring absolute values of  $f$ , chemical displacements and line widths 21 p3799 A66-38922

I-V characteristics of p-gallium antimonide based tunnel junction at various temperatures analyzed, finding secondary peaks exhibited by inverted diodes 21 p3799 A66-38925

Current dependence of recombination radiation intensity in gallium antimonide, determining radiation spectral distribution at low temperature 22 p3967 A66-40845

Ultrasonic wave absorption in GaAs and GaSb compounds at temperatures from 95 to 300 degrees K 23 p4113 A66-41417

Hall coefficient, electrical conductivity and thermoelectric power of GaSb-Ga<sub>2</sub>Te<sub>3</sub> solid solutions as functions of composition and temperature 24 p4254 A66-42425

**GALLIUM ARSENIDE**

Laser transition identification in electron beam pumped gallium arsenide, primarily on concentration of shallow donors and

acceptors 01 p0081 A66-10348

Controlled bulk semiconductor amplification possible using n-type gallium arsenide with applied electric field greater than 3000 v/cm 01 p0036 A66-10351

Gallium arsenide injection laser for prolonged operation at liquid nitrogen temperatures 01 p0081 A66-10369

P-n transitions in gallium arsenide investigated as factor in performance of such diodes as converters of ultrasonic into electrical oscillations 01 p0036 A66-10422

Domain characteristics and crystal property effects in materials and configurations for Gunn effect devices 01 p0041 A66-10571

Growth and propagation of space charge waves in presence of differential negative resistance in n-GaAs 01 p0122 A66-10577

Thermal limitations on capabilities of gallium arsenide p-n junction lasers 01 p0082 A66-10895

Electrical and electroluminescent properties of gallium arsenide diodes with high resistivity region flanked by low resistivity R and N regions 01 p0043 A66-10896

Laser-action threshold in electron-beam excited gallium arsenide and effect of temperature and doping 01 p0083 A66-10971

Continuous operation of gallium arsenide injection laser cooled by helium gas flow 01 p0084 A66-11190

Impurity bandwidth and separation from conduction band in n-type GaAs determined from electroconductivity and Hall effect data 02 p0276 A66-12077

Electric properties of n-type GaAs after alloying with Cu, determining impurity concentrations 02 p0277 A66-12095

FM by mechanical tuning of cavity setting in gallium arsenide crystals for application to communication system 03 p0332 A66-12428

GaAs optically coupled transistor structure with lasing emitter 03 p0377 A66-12442

Synchronization of microwave oscillations in n-type GaAs, noting pulse spectrum 03 p0377 A66-12444

Acceptor level in iron doped Ga-As moves toward valence band with increasing temperature at approximately same rate band gap decreases 03 p0410 A66-13004

Lasing in p-type GaAs in which population inversion is brought about by avalanche breakdown of high resistivity region in material 03 p0378 A66-13008

Electrical resistivity and Hall coefficient of undoped n-type gallium arsenide with carrier concentrations measured at various temperatures as function of uniaxial compression and hydrostatic pressure 03 p0412 A66-13149

Current-voltage characteristics of gallium arsenide diode noting temperature effect on threshold voltage and breakdown current 03 p0346 A66-13323

Current-voltage characteristics of zinc-diffused gallium arsenide diodes measured between 4.2 and 300 degrees K with varying carrier concentrations in n-type region 04 p0494 A66-13733

Temperature dependence of electric conductivity in indium antimonide and gallium arsenide measured by noncontact method in terms of Q-factor change 04 p0563 A66-13892

Thermometric characteristics of gallium arsenide and germanium diodes 04 p0495 A66-13894

Semiconductor maser design and principles tabulating indium phosphide, gallium and indium arsenide types 04 p0532 A66-14183

Recombination radiation in gallium arsenide due to alpha particles 04 p0565 A66-14269

Semiconductor p-n junction laser consisting of gallium arsenide-phosphorus solid solution 04 p0532 A66-14274

Thermoconductivity of gallium arsenide from 300 to 470 degrees K 04 p0566 A66-14299

Laser excitation in gallium arsenide anode by slow electrons, taking into account diffraction and absorption losses 04 p0533 A66-14319

Tellurium alloyed impurity on IR absorption spectrum in n-type gallium arsenide 04 p0569 A66-14360

Electric oscillation by monochromatic light



in high resistivity gallium arsenide, noting temperature dependence 04 p0569 A66-14361

Electrical properties of germanium-gallium arsenide heterojunctions of p-n and n-n structure 04 p0569 A66-14362

Optically connected laser constructed on gallium arsenide p-n junction, noting coherent radiation 04 p0533 A66-14363

Electron spectrum in highly alloyed gallium arsenide 05 p0730 A66-14650

Gallium arsenide recombination-radiation spectrum discussing effects of impurities on short wave radiation band energy 05 p0731 A66-14657

Oxygen alloyed gallium arsenide, explaining anomalous mobility distribution in crystals during fusion in presence of oxygen 05 p0731 A66-14658

Gallium arsenide p-n junction laser diode covering injection current distribution, density and emission spectra variation 05 p0692 A66-14659

Diffusion rate of silicon from sputtered film of silicon into gallium arsenide as function of ambient arsenic pressure at 900 and 1000 degrees C 05 p0732 A66-14665

Thermal diffusion of impurity atoms suggested as possible cause of GaAs Esaki diode deterioration by Weisberg and Gold 05 p0733 A66-14672

Recombination emission process in direct semiconductor devices for realization of high speed nondestructive readout from tunnel diodes without direct measurement or perturbation 05 p0647 A66-14828

Shift of emission spectrum in pulsed GaAs laser, noting waveform characteristics 05 p0696 A66-14974

Radiation damage and annealing of gallium arsenide laser diode 05 p0696 A66-14979

Exponential absorption edge of gallium arsenide 05 p0742 A66-15870

Lattice thermal conductivity of GaAs and InSb calculated for 2 to 300 degrees K, considering separate contributions of longitudinal and transverse phonons 05 p0742 A66-15872

Electron mobility of gallium arsenide-phosphorus alloys 06 p0923 A66-16380

GaAs diffusion-layer transducer for VHF acoustic delay line 06 p0852 A66-16639

Gallium arsenide tunnel diode oscillator tuned with 5-10 GHz YIG 06 p0853 A66-16648

Gunn effect n-type GaAs diode phase locked to stable frequency by injecting CW signal into circuit along with video pulse 06 p0925 A66-16671

Current instabilities in gallium arsenide, noting oscillation frequency and volt-ampere characteristics 06 p0925 A66-16688

Characteristics of spontaneous IR source for which external quantum efficiency of forward-biased GaAs p-n junction measures 40 percent at 20 degrees K 06 p0855 A66-16766

X-ray diffraction method for measuring thermal expansion coefficient of germanium, silicon, indium antimonide and gallium arsenide 06 p0930 A66-17047

Current oscillations accompanied by mobile regions in high resistance gallium arsenide subjected to electric field, measurement of Hall effect shows these regions are of high resistance 06 p0930 A66-17066

Semiconductor radiation damage in III-V compounds indium antimonide, gallium arsenide and indium arsenide, including values of threshold displacement energies, post-irradiation recovery, etc 06 p0935 A66-17129

Diffusion of Li and Cu in GaAs crystals indicates reaction involving divacancies in donor-doped and undoped crystals 06 p0935 A66-17132

Implementation of Kossel line technique of crystallographic analysis and lattice parameter measurement in study of lattice defects in semiconductor crystals 06 p0935 A66-17133

Proton and electron bombardment induced defects in GaAs studied by examining spectral composition and intensity of proton and cathode luminescence 06 p0936 A66-17135

Electron mobility changes in GaAs single crystals due to electron irradiation interpreted in terms of ionized-scattering theory 06 p0939 A66-17151

Radiative recombination in p-n junctions

produced by diffusion of beryllium into GaAs with very high electron concentration 07 p1096 A66-17325

Energy spectrum of recombination radiation from forward-biased heavily doped GaAs diodes at 4.2, 77 and 290 degrees K as function of current 07 p1096 A66-17326

Optical model for refractive index variation of zinc-diffused GaAs injection laser at 77 degrees K and 8400 angstroms 07 p1041 A66-17328

Temperature dependence of loss and gain factor of GaAs diode and threshold current density of GaAs laser and junction luminescence of GaAs 07 p1042 A66-17332

Temperature dependence of emission spectrum and threshold current in GaAs lasers 07 p1042 A66-17333

Uniaxial strain effects in /100/ junction orientation GaAs laser diodes, discussing photon polarization 07 p1042 A66-17335

Optical emission induced in gallium arsenide samples by bombardment with high energy electron pulses 07 p1096 A66-17338

Spectral distribution of luminescence excited in n-type GaAs and p-type GaP by fast-electron bombardment 07 p1096 A66-17339

Spectral distribution of recombination radiation observed in various samples of GaAs irradiated by electron beam 07 p1043 A66-17340

Depletion layer 1000 mc transducers for producing or detecting hypersonic waves in solids, using CaS or GaAs for high acoustoelectrical conversion efficiency 07 p1009 A66-17827

Time dependent fluctuations in photoconductivity of Cu doped low ohmic n-type gallium arsenide exposed to IR radiation 07 p1099 A66-17876

Instabilities of current and potential distribution in n-type GaAs and InP in electric field of several thousand v/cm 07 p1104 A66-18221

Continuous-wave operation of laser diode at room temperature 07 p1044 A66-18245

Coherent radiation from gallium arsenide p-n junction formed by beryllium diffusion, noting radiative recombination with zinc 07 p1105 A66-18378

Current-voltage relationship of Au on GaAs Schottky barrier, examining introduction of single temperature independent parameter 07 p1106 A66-18399

Formed point contact gallium arsenide backward diodes compared with conventional millimeter-wave diodes show advantage as low level baseband current detectors 08 p1189 A66-18658

Radiotracer measurements of copper incorporated from quartz into GaAs 08 p1268 A66-18663

Photoelectric behavior of n-type Ga-As wafers having shallow zinc diffused surface layers 08 p1269 A66-18869

Behavior of high field instabilities in n-type gallium arsenide, examining device prospects related to phenomenological model for Gunn effect 08 p1270 A66-19122

Gallium arsenide luminescent diodes with triangular resonator producing coherent emission at high density current 08 p1193 A66-19195

Work function of A and B faces of /111/ surface of gallium arsenide in dry and humid media 08 p1274 A66-19317

Mossbauer effect in polycrystalline indium phosphide and gallium arsenide 08 p1277 A66-19618

Fe, Ni and Co in gallium arsenide determined by tunnel spectroscopy 08 p1278 A66-19624

Thermal conductivity and emf of gallium arsenide at low temperatures, showing phonon drag effect 08 p1278 A66-19626

Measurement results on frequency doublers in millimeter wave region, using unencapsulated silicon varactor diodes and gallium arsenide/phosphor bronze point-contact varactor 08 p1198 A66-19745

Electroreflectance effect on gallium arsenide surfaces at various ranges of photon energies 08 p1279 A66-19838

Gallium arsenide phosphide heterojunction diode used to triple from X band to Ka band 09 p1350 A66-19924

Recombination-radiation spectra of GaP-GaAs p-n heterojunctions 09 p1412 A66-19984

Mobility of hot electrons in runaway regime of n-type InSb and GaAs at low temperatures 09 p1412 A66-19987

Orientation effect on zinc diffusion rate in p-n junctions, using gallium arsenide single crystals as initial material 09 p1412 A66-19996

Change in photoconductivity and photoelectromagnetic effect of gallium arsenide single crystals caused by constant illumination of spectral compositions 09 p1412 A66-19997

Dark electric conductivity, Hall effect and thermally stimulated currents in gallium arsenide single crystals 09 p1413 A66-19998

Phonon drag in p-GaAs, graphing temperature dependence of thermoelectric power 09 p1426 A66-20196

Effective mass of electrons in n-type gallium arsenide deduced from measurements of Hall coefficient and thermoelectric power 09 p1426 A66-20197

Electron Hall mobility from 4 to 300 degrees K with undoped single crystals of GaAs grown in quartz boats by Bridgman method and zone-melting technique 09 p1430 A66-20848

Frequency spectrum of microwave emission from n-type gallium arsenide 10 p1574 A66-21357

Vapor etching of gallium arsenide crystals with hydrogen chloride, noting usefulness in pretreatment for epitaxial substrates 10 p1575 A66-21358

X-ray analysis of zinc diffusion induced defects in gallium arsenide 10 p1576 A66-21547

Microplasma breakdown in reverse biased p-n junctions in epitaxial gallium arsenide 10 p1577 A66-21571

Directional radiation from incoherent electroluminescent diodes, noting increase in refractive index for dielectric slab model 10 p1509 A66-21583

Silicon and selenium doping effects on gallium arsenide laser characteristics 10 p1543 A66-21879

Increased luminescence of gallium arsenide diodes by coating with titanium oxide 10 p1514 A66-22031

Boltzmann equation for Gunn effect in GaAs, discussing scattering processes, unjustifiability of use of drifted Maxwell distribution, etc 10 p1583 A66-22067

Growth and propagation of infinitesimal space charge waves under differential negative resistance and inhibition of dipole waves and domains in gallium arsenide, estimating thermoelectric effects 10 p1584 A66-22068

Dependence of threshold field for Gunn oscillations on energy minima separation, noting decrease under uniaxial stress 10 p1584 A66-22073

Properties of high field domain in long samples of gallium arsenide, determining domain velocity and amplitude, using surface potential probe 10 p1584 A66-22074

Gunn effect in polar semiconductors described by transferred electron model, that predicts bulk differential negative resistance and domain formation 10 p1585 A66-22075

Gunn effect oscillations in high resistivity gallium arsenide cease when product of conduction electron density and sample length drops below certain level 10 p1585 A66-22076

CW microwave oscillation in bulk GaAs, discussing harmonic content, linewidth, circuit and electronic tunability, etc 10 p1585 A66-22077

Device fabricating techniques and circuit configurations for high peak power gallium arsenide oscillators 10 p1585 A66-22078

Linear microwave amplification in n-type gallium arsenide bulk semiconductor at room temperature, noting negative conductance and peak gain 10 p1515 A66-22079

Microwave oscillations in epitaxial layers of gallium arsenide 10 p1585 A66-22080

Model technique calculation of electrostatic domains in two-valley /GaAs/ semiconductors 10 p1586 A66-22092

Threshold field dependence on intervalley separation in transferred electron GaAs



- oscillator 10 p1586 A66-22093
- Current saturation from negative resistance and domain trapping in n-type gallium arsenide crystal 10 p1586 A66-22096
- Phase locking of two gallium arsenide oscillators at 2 to 4 gc under CW operation 10 p1516 A66-22097
- Microwave amplification in n-type germanium arsenide 10 p1516 A66-22098
- Floating zone technique for preparing high purity GaAs crystals for CW microwave devices 10 p1516 A66-22099
- Microwave oscillations from reverse-biased gallium arsenide diodes of diffused p-n junctions and surface barrier structures 10 p1516 A66-22102
- High cut-off frequency epitaxial gallium arsenide varactors generating continuous wave power when biased in avalanche region, showing dimensions, resistivities, etc 10 p1516 A66-22103
- Gallium arsenide laser excitation by fast electrons 10 p1544 A66-22146
- Retention of semiconductor properties by gallium arsenide after irradiation by fast-neutron flux 10 p1589 A66-22167
- P-n transitions in gallium arsenide investigated as factor in performance of such diodes as converters of ultrasonic into electrical oscillations 11 p1664 A66-22608
- Current-voltage characteristics of CW X-band GaAs microwave Gunn generator 11 p1713 A66-23029
- Gallium arsenide whiskers on germanium structure, using electron diffraction photography and electron microscopy 11 p1757 A66-23280
- Behavior of trace elements in gallium arsenide and materials and methods used for ohmic contacts to n-and p-type specimens, stressing importance of indium 11 p1757 A66-23283
- Film scanning system using GaAs light-emitting diode and phototransistor light detector 11 p1709 A66-23476
- Hole and electron smearing and p-type absorption influence on threshold current 11 p1715 A66-23478
- Conductivity effective-mass of holes of gallium arsenide crystals with various hole concentrations determined from frequency dependence of spectral reflectivity in IR 12 p1928 A66-23942
- Parameter dependence of intermediate frequency voltage indicated during establishment of optimum conditions for optical receivers and merit of subcarrier mixing 12 p1832 A66-23960
- Continuous operation of gallium arsenide injection laser cooled by helium gas flow 12 p1890 A66-24011
- Reactance of gallium arsenide bulk oscillator in oscillating state, plotting values together with capacitance 12 p1835 A66-24140
- Differential equation for prediction of output spectra of unlocked driven bulk-GaAs and tunnel diode 12 p1836 A66-24147
- Oscillators in gallium arsenide p-n junctions for weak currents, obtaining relation between emission spectra and current-voltage characteristics of diodes 12 p1929 A66-24456
- Threshold energy for avalanche multiplication in semiconductors obtained from energy band structure and crystal momentum conservation in ionization process 13 p2157 A66-25035
- Defects in gallium arsenide crystals studied by internal friction with measurements showing damping peak at 140 degrees C 13 p2157 A66-25045
- Electroreflectance effect on gallium arsenide surfaces, noting reflectance response upon electric field modulation 13 p2158 A66-25051
- Width of spontaneous emission region in degenerate gallium arsenide p-n junction, noting spectral shifts, emission, interference, etc 13 p2159 A66-25064
- Quantitative observation of light modulation by electro-optic effect in reverse-biased GaAs p-n junctions at wavelength of 1.15 microns 13 p2159 A66-25067
- Gallium arsenide laser diode characteristics 13 p2089 A66-25112
- Transport equation for germanium-gallium arsenide-iodine system and epitaxial vapor growth preparation of GaAs-Ge heterojunction by closed tube process 13 p2161 A66-25185
- Copper diffused gallium arsenide p-n junctions, explaining current-voltage characteristics, light emission and capacitance of diodes at 300 and 77 degrees K 13 p2161 A66-25186
- Radial solution growth of GaAs single crystal layers and analysis of photoluminescence spectrum 13 p2164 A66-25488
- Consistency of Gunn effect with excitation of conduction band electrons from high mobility minimum to low mobility valleys 13 p2164 A66-25517
- Optically coupled linear circuit techniques, discussing GaAs p-n junction diode, noncoherent light emitters and silicon p-n junction photosensors 13 p2036 A66-25521
- Gunn effect in gallium arsenide, noting negative differential electron mobility at high electric fields in conduction band 13 p2165 A66-25546
- Photo emf of gallium arsenide determined as function of temperature, light intensity, external electric field and surface quality 13 p2165 A66-25679
- Solar noise in optical communications, background radiation dependence on detector aperture, noise power and application to GaAs diodes and gas lasers 13 p2024 A66-25833
- Electron spectrum in highly alloyed gallium arsenide 13 p2167 A66-25925
- Gallium arsenide recombination-radiation spectrum, discussing effects of impurities on short wave radiation band energy 13 p2167 A66-25932
- Oxygen alloyed gallium arsenide, explaining anomalous mobility distribution in crystals during fusion in presence of oxygen 13 p2167 A66-25933
- Gallium arsenide p-n junction laser diode, injection current distribution, density and emission spectra variation 13 p2092 A66-25934
- Photoluminescence and stimulated emission of gallium arsenide and indium antimonide obtained by optical pumping, noting effect of applied magnetic field on laser and diode emissions 13 p2099 A66-26182
- Spectral characteristics of gallium arsenide junction luminescence, noting radiative recombination mechanism, energy spread of impurity states and line shape temperature dependence 13 p2168 A66-26186
- Photoluminescence for p-and n-type gallium arsenide as function of exciting light intensity, noting minority carrier recombination mode, electron energy spectrum, etc 13 p2169 A66-26187
- Correlations and intensity fluctuations in light from individual lasing and nonlasing modes of CW GaAs laser and threshold noise change in laser emission 13 p2102 A66-26210
- Cooler for semiconductor lasers and photodetectors using low temperature gas 13 p2104 A66-26559
- Inverse variation of external efficiency of incoherent radiation in GaAs diode with temperature due to increased absorption, noting constancy of quantum efficiency 13 p2105 A66-26570
- Mathematical model of GaAs injection laser applied in determining maximum obtainable power output, using rate equations of electron and photon densities and thermal resistance for optimum value 13 p2105 A66-26572
- Morphology and structure of gallium arsenide crystals containing germanium core grown by iodine transport process in closed tube 13 p2170 A66-26587
- Gunn effect involving current oscillations higher than 1000 mc in GaAs crystal under applied electric field 14 p2355 A66-26920
- Superradiance in n-type gallium arsenide at room temperature excited by electron beam 14 p2306 A66-27028
- Gunn oscillators fabricated from ultra-thin gallium arsenide chips 14 p2248 A66-27050
- Spectral distribution of photosensitivity of gallium arsenide p-n junctions in near UV region 14 p2356 A66-27067
- Dislocation structure in single crystal indium antimonide and gallium arsenide studied by X-ray diffraction 14 p2357 A66-27071
- Tunnel effect in gallium arsenide diodes at low temperatures 14 p2248 A66-27081
- Injection-current dependence of intensity of recombination radiation of separate bands in gallium arsenide 14 p2249 A66-27084
- Beryllium diffusion into gallium arsenide in /111/ plane with various electron concentrations through vacuum deposition 14 p2358 A66-27087
- Semiconductor GaAs quantum generator with two-photon absorption of neodymium laser emission 14 p2307 A66-27187
- Time parameters of powerful laser measured with GaAs photodiode, noting time constant and time resolution of photodiode 14 p2309 A66-27750
- Tellurium alloyed impurity on IR absorption spectrum in n-type gallium arsenide 14 p2369 A66-28258
- Electric oscillation by monochromatic light in high resistivity gallium arsenide, noting temperature dependence 14 p2369 A66-28259
- Electrical properties of germanium-gallium arsenide heterojunctions of p-n and n-n structure 14 p2369 A66-28260
- Optically connected laser constructed on gallium arsenide p-n junction, noting coherent radiation 14 p2310 A66-28262
- Current-voltage characteristics of gallium arsenide diode, noting temperature effect on threshold voltage and breakdown current 14 p2260 A66-28297
- Degree of perfection of Ge and GaAs single crystals and epitaxial films effect on integral intensity jump at K absorption edge seen in Bragg diffraction 15 p2557 A66-28561
- Spontaneous emission and transverse gain measurements in GaAs injection laser at 80 degrees K and for 8466 angstrom wavelength 15 p2511 A66-28627
- IR radiation from gallium arsenide prepared with ohmic contacts and excited by various nanosecond pulses, noting radiation above Gunn effect instability region 15 p2561 A66-28688
- Free carrier absorption on GaAs films which exhibit absorption edge shift to lower energies 15 p2561 A66-28698
- Emission bands in electroluminescence from gallium arsenide diodes, noting intensity at high and low voltages and radiation and doping effect 15 p2562 A66-28714
- Optical inhomogeneities in n-type gallium arsenide crystals containing growth axis examined in transmission, using IR image converter, noting band gap changes 15 p2562 A66-28720
- Measurement of ultrasonic attenuation vs temperature for longitudinal and transverse phonons in semiinsulating gallium arsenide 15 p2563 A66-28729
- Tellurium concentration in doped GaAs correlated by electron probe microanalysis with variations in cathodoluminescence efficiency 15 p2564 A66-28878
- Capacitance variation of gold n-type gallium arsenide surface barrier diode when illuminated, applied to light detector, frequency modulation, etc 15 p2463 A66-29034
- Oscillations in power generation of n-type GaAs at frequencies far in excess of intrinsic Gunn frequency 15 p2565 A66-29041
- Gallium arsenide laser design using p-n junction obtained by diffusion of zinc in tellurium doped n-GaAs single crystal 15 p2514 A66-29057
- Electric characteristics of epitaxial Ge films vacuum deposited on semiinsulating GaAs substrates with thicknesses near one million angstroms 15 p2566 A66-29386
- Spontaneous and coherent photoluminescence in cadmium mercury telluride crystals excited optically by GaAs diode laser 15 p2517 A66-29390
- Gallium arsenide varactor diode design for parametric amplifiers and multipliers, noting efficient harmonic generation at higher microwave frequency 15 p2466 A66-29677
- Temperature dependence of electric conductivity in indium antimonide and gallium arsenide measured by noncontact method in terms of Q-factor change 15 p2568 A66-29705
- Thermometric characteristics of gallium



arsenide and germanium diodes 15 p2467 A66-29708

Gallium arsenide absorption edge dependence on strong electric fields 16 p2769 A66-30166

Intervalley scattering in III-V semiconductors, noting relation to Gunn effect, scattering in GaAs by longitudinal optic phonons, in InP by longitudinal acoustic phonons 16 p2776 A66-30733

Increased luminescence of gallium arsenide diodes by coating with titanium oxide 16 p2661 A66-30851

Static uniaxial compression effect measurement along /100/, /110/ and /111/ on electroreflectance spectrum of gallium arsenide, using electrolyte technique 16 p2777 A66-30951

Activation energy and corresponding concentration of unknown donor level in n-type gallium arsenide 16 p2777 A66-31002

Pump modulation factor of various GaAs and Si varactor diodes under operating conditions, noting experimental bandwidth gain via increased shot noise 16 p2663 A66-31017

Gallium arsenide and silicon solar cells under proton irradiation, noting decrease of short circuit current and open circuit voltage 16 p2636 A66-31018

Hall effect and resistivity of Zn doped GaAs 16 p2778 A66-31069

Dislocations and precipitates in GaAs injection lasers revealed by new A-B etchant 16 p2718 A66-31071

Arsenic overpressure, obtained by including metallic arsenic along with gallium arsenide, depresses defect concentration identifying primary defect species as arsenic monovacancies 16 p2779 A66-31086

Selective epitaxial deposition of semiinsulating GaAs for p-n junction and integrated circuit application 16 p2665 A66-31418

Laser cavity output optimization for maximum external quantum efficiency showing dependence on length and reflectivity for given current density 16 p2720 A66-31535

Vapor growth of Ge on Ge, GaAs and Si substrates, noting preparation methods, characteristics, etc 16 p2786 A66-31686

Origin of polarization of radiation from GaAs diodes, noting intensity dependence on current density and effect of anisotropic electron velocity distribution 16 p2667 A66-31770

Temperature dependence of lifetime of electrons and holes in GaAs, noting trapping effect of recombination centers and capture levels 16 p2787 A66-31771

Energy levels in forbidden band of gallium arsenide alloyed with silver or gold, determining impurity levels from temperature dependence of electric conductivity and Hall constant 16 p2789 A66-31791

Conduction-electron plasmons interaction with longitudinal optical phonon in Raman spectrum of gallium arsenide 17 p2975 A66-31888

P-n junction lasers for short range communications, examining design, technological problems and performance 17 p2933 A66-31956

High field V-I characteristics of n-type GaAs, noting critical field current saturation, field distribution, trapping, hysteresis, etc 17 p2978 A66-32403

Selective diffused junction laser, discussing GaAs laser used for quenching experiment 17 p2934 A66-32408

Large wavelength changes in gallium arsenide injection lasers due to changes in cavity Q 17 p2935 A66-32635

Schottky theory for metal semiconductors, noting correlation between work function and barrier height, electron affinity, etc 17 p2980 A66-32650

Intensity noise in multimode GaAs laser emission 17 p2935 A66-32689

Series connection of varactor wafers for higher breakdown voltages without loss of cut-off frequency, noting power output 17 p2887 A66-32698

Dipole phenomena in n-type GaAs caused by field perturbations, showing conditions for high and low field

nucleation 17 p2983 A66-33106

Continuous wave oscillations in n-type GaAs due to voltage controlled negative conductance 17 p2983 A66-33107

Current wave form observation in GaAs, using transmission line concept and pulse splitting technique 17 p2983 A66-33109

Self-modulation in gallium arsenide oscillators, noting material and field characteristics, Gunn effect, etc 17 p2895 A66-33114

Mossbauer effect in polycrystalline indium phosphide and gallium arsenide 17 p2983 A66-33132

Fe, Ni and Co in gallium arsenide determined by tunnel spectroscopy 17 p2984 A66-33138

Thermal conductivity and emf of gallium arsenide at low temperatures, showing phonon drag effect 17 p2984 A66-33140

Electroluminescent phenomena in injection lasers and laser diodes 17 p2985 A66-33251

Volt-ampere characteristics, electrical resistivity, and pressure effect on Gunn phenomena in n-type GaAs in high electric fields 17 p2985 A66-33292

Spectral and spatial distribution of origin of injection luminescence from epitaxial gallium arsenide transistors, noting correlation between energy peak and radiation recombination 17 p2986 A66-33295

Scanning electron microscope to examine crystal mosaic structures and lasing properties of gallium arsenide laser diodes 17 p2937 A66-33300

Gallium arsenide four-layer device doped with selenium fabricated by triple diffusion 17 p2896 A66-33302

Photocurrent and leakage current in zinc diffused GaAs junction diodes in terms of channel effect 17 p2987 A66-33319

Optical modulation in bulk gallium arsenide, using Gunn effect 18 p3152 A66-33606

Gallium arsenide diode laser as pulsed IR source for experiment and design considerations for radar indication of cloud height and visibility 18 p3066 A66-33616

Thermodynamic and optical properties of Ge, Si, diamond and GaAs, obtained by inelastic neutron scattering technique, used to measure vibrational spectrum 18 p3154 A66-33922

Coherent and spontaneous emission from lead-tin telluride alloys upon excitation by GaAs diode laser, noting band structure of alloy system 18 p3119 A66-34159

V-I characteristics of GaAs Schottky barrier rectifiers applied in determining relation between electron energy and complex wave vector over portion of forbidden energy gap 18 p3155 A66-34161

External quantum efficiency of tin doped GaAs electroluminescent diode, noting effect of zinc diffusion conditions 19 p3312 A66-35347

Reproducible ohmic contact preparation for high resistivity n-type GaAs in fabrication of Gunn oscillators 19 p3313 A66-35351

Orientation effect in GaAs injection lasers, noting emission characteristics and structural spectra 19 p3373 A66-35404

Thermal and electric properties of InAs-GaAs alloy as function of composition, impurity additions and temperature 19 p3436 A66-35427

Photoluminescence measurements on silicon doped gallium arsenide for detection of compensation in shallow surface layers 19 p3436 A66-35430

Distribution of edge-type dislocations in GaAs grown from solution by traveling solvent method determined, using etching techniques 19 p3437 A66-35432

Oxide films grown on GaAs in oxygen plasma 19 p3437 A66-35435

Gallium arsenide laser excitation by fast electrons 19 p3374 A66-35760

Retention of semiconductor properties by gallium arsenide after irradiation by fast-neutron flux 19 p3441 A66-35781

Spontaneous LF conductivity fluctuations in n-type gallium arsenide samples at 77 degrees K 19 p3442 A66-35822

Gallium arsenide lasers operating at room temperature investigated, based on diffusion p-n junctions, discussing emission spectrum 19 p3375 A66-36070

Enhancement of optical second-harmon generation by reflection phase matching ZnS and GaAs 19 p3375 A66-360

Varactor characteristics, applications, equivalent circuits, measurement problem etc 19 p3319 A66-361

Electron-phonon interaction phenomenon observed in GaAs and CdS, examining current saturation, ultrasonic emission charge carriers and acoustic amplification 19 p3445 A66-362

Replacing heated tungsten filament and filter by GaAs electroluminescent diode without filter for IR illumination 19 p3320 A66-362

Separation centers and dislocations during diffusion of Zn into GaAs at high temperatures, analyzing photographs of p-n junctions 19 p3445 A66-363

Microwaves from gallium arsenide excited by impressed voltage 20 p3612 A66-372

Crystal growth, diffusion and fabrication of gallium arsenide-phosphide junction laser with low threshold current densities 20 p3577 A66-374

Isolated GaAs transistors on high resistivity GaAs substrate, noting production via epitaxial etch-refill technique, performance and isolation properties 20 p3616 A66-374

Fourier analysis determination of optimum efficiency of cavity-controlled Gunn-effect oscillator when bias voltage is almost twice times voltage 20 p3527 A66-374

Avalanche transistor generation of jitter free nanosecond current pulses for driving GaAs laser diodes at low temperatures 20 p3528 A66-374

Space-charge-limited current voltage-dependent behavior in gallium arsenide 20 p3616 A66-374

Polarization of pulsed radiation from GaAs laser diode to determine origin of natural oscillations of resonator 20 p3578 A66-375

Reflectivity of heavily doped samples of n-type gallium arsenide of known carrier concentration and determination of dependence of effective mass upon carrier concentration 20 p3619 A66-376

Radiative recombination in gallium arsenide p-n junctions for weak current obtaining relation between emission spectrum and current-voltage characteristics of diodes 20 p3619 A66-376

Impurity concentration effect on maximum continuous wave power from gallium arsenide lasers at 77 degrees K 20 p3580 A66-377

Temperature dependence of absorption bands by localized vibration mode associated with substitutional impurities in phosphorus-doped gallium arsenide 20 p3622 A66-382

Gain factor variation with threshold current in reflective and antireflective film of GaAs laser with photon and current densities 20 p3581 A66-383

GaAs field emission cathode microscope patterns prepared by chemical etching at low temperature field desorption 20 p3623 A66-383

Vacuum thermal decomposition of InSb and GaSb surfaces, noting evaporation rates 20 p3624 A66-384

Fast-neutron irradiation effects on photoconductivity spectra and induced crystal structure defects for n- and p-type gallium arsenide single crystals 20 p3624 A66-384

Electron scattering mechanism in compensated gallium arsenide determined from Hall effect, Nernst-Ettingshausen effect and reluctance 21 p3798 A66-389

Optical coupling using gallium arsenide laser for variation of frequency of diode emission through small change in current density 21 p3746 A66-389

Radiation intensity dependence for various spectral bands of diffused gallium arsenide p-n junctions on current density 21 p3798 A66-389

Performance of GaAs semiconductor laser with resonator, noting dependence of forbidden zone width and absorption coefficient on free carrier concentration and incident photon energy 21 p3746 A66-389

Modulation by ultrasonic diffraction of 10 micron laser radiation in photoelastic Cd



GaAs and Si crystals 21 p3747 A66-39112  
 IR and microwave radiations associated with current controlled instability /negative resistance/ in GaAs, noting Gunn threshold and V-I characteristics 21 p3802 A66-39162  
 IR absorption, reflectivity and transmission in n-type gallium arsenide single crystals at room temperature due to impurities and high carrier concentration 21 p3805 A66-39580  
 Applications for ferroelectric cold conductors and GaAs light-sensitive diodes, examining supersonic amplification in CdS 21 p3716 A66-39620  
 High power Gunn-effect oscillators constructed from thin epitaxial layers of GaAs, noting relation of drive voltage to frequency, efficiency and power output 22 p3959 A66-39725  
 Temperature gradient-induced GaAs crystal inhomogeneity effects on electric properties 22 p3959 A66-39742  
 Far-field light emission mode pattern of GaAs diode injection lasers, dielectric gradient in inversion layer and refractive index in junction 22 p3930 A66-39743  
 Separation method for two components of excess and thermal currents in gallium arsenide tunnel diodes 22 p3873 A66-39748  
 Gallium arsenide crystal properties for use in optical filter 22 p3959 A66-39773  
 Photovoltaic response of p-n Ge-Si and Ge-GaAs heterojunctions dominated by carrier generation in narrow or wide gap material 22 p3960 A66-39813  
 Effect of donor Zn and Cd additions and acceptor Se and Te additions on rate of growth and morphology of epitaxial GaAs films grown from gas phase by chemical reaction 22 p3961 A66-39929  
 Performance characteristics of avalanche-breakdown transit-time GaAs varactor diodes for miniaturized microwave circuits 22 p3874 A66-39991  
 Curve analysis of current instabilities including Gunn effect in n-type gallium arsenide 22 p3961 A66-40045  
 Thermal conductivity of InP-GaAs solid solutions in vacuum 22 p3962 A66-40051  
 Deep centers in conducting n-type GaAs and production of Schottky layer 22 p3963 A66-40088  
 Stable space-charge layers in two-valley semiconductors 22 p3963 A66-40101  
 Spontaneous and stimulated emission from GaAs diodes with three-layer structures consisting of n-n-p, n-i-p or n-p-p diodes 22 p3932 A66-40102  
 Epitaxial germanium films on gallium arsenide substrate by vacuum evaporation, considering surface preparation 22 p3963 A66-40106  
 Resistivity measurement of large number of samples of bulk-grown n-type GaAs as function of temperature near 300 degrees K 22 p3877 A66-40179  
 Recombination radiation from GaAs p-n junctions with and without Fabry-Perot resonator, noting parameter dependence on current density 22 p3932 A66-40314  
 Solid state millimeter wave receivers for space vehicle environments, discussing integral mixer IF amplifiers, oscillators and varactor multipliers 22 p3879 A66-40733  
 Spectral distribution of photosensitivity of gallium arsenide p-n junctions in near UV region 22 p3966 A66-40826  
 Dislocation structure in single crystal indium antimonide and gallium arsenide studied by X-ray diffraction 22 p3966 A66-40829  
 Tunnel effect in gallium arsenide diodes at low temperatures 22 p3882 A66-40837  
 Injection-current dependence of intensity of recombination radiation of separate bands in gallium arsenide 22 p3882 A66-40840  
 Beryllium diffusion into gallium arsenide in /111/ plane with various electron concentrations through vacuum deposition 22 p3967 A66-40843  
 Steady state behavior of free steadily traveling electrical domain in gallium arsenide 22 p3967 A66-40864  
 Domain and circuit properties effect on oscillations in GaAs 22 p3967 A66-40865  
 Current characteristics of solution and vapor grown p-n Ge-Si and Ge-GaAs heterojunctions as function of voltage and

temperature 22 p3968 A66-40963  
 Degree of perfection of Ge and GaAs single crystals and epitaxial films effect on integral intensity jump at K absorption edge seen in Bragg diffraction 23 p4112 A66-41282  
 Continuous current oscillation in GaAs caused by acoustoelectric effect 23 p4112 A66-41296  
 Domain propagation with velocity of sound from negative to positive electrodes in GaAs single crystal rods under acoustoelectric oscillation 23 p4112 A66-41297  
 Ultrasonic wave absorption in GaAs and GaSb compounds at temperatures from 95 to 300 degrees K 23 p4113 A66-41417  
 GaAs semiconductor quantum generator heating during injection pulse, analyzing temperature effect on external quantum output and generator efficiency 23 p4078 A66-41621  
 Radiative recombination in annealed electron irradiated zinc doped gallium arsenide 24 p4250 A66-42229  
 Zn diffusion effect on uniformly Mn-doped GaAs wafer showing via radiotracer technique changes in impurity concentration profile 24 p4250 A66-42255  
 IR active localized vibrational modes absorption in lithium and copper compensated silicon doped gallium arsenide 24 p4251 A66-42298  
 Epitaxial growth of bulk quality GaAs on GaAs and Ge substrates, using hydrogen stream saturated at room temperature with arsenic chloride 24 p4251 A66-42307  
 Decaying free carrier concentration increase in GaAs when subjected to increased level of drive during first cycle 24 p4253 A66-42370  
 Tin and zinc diffusion from doped pyrolytic silicon oxide layers used to form base regions of planar n-p-n and p-n-p-GaAs transistors 24 p4254 A66-42384  
 Conversion efficiency of GaAs solar cell at various light intensities 24 p4161 A66-42391  
 Temperature dependence of Hall coefficient and resistivity of n-type epitaxial gallium arsenide in 4.2 to 300 degree K temperature range 24 p4254 A66-42423  
 GaAs crystal as electro-optic modulator at 10.6 microns due to small carrier absorption, freedom from interband transitions and high resistivity 24 p4222 A66-42553  
 Transverse gain and spontaneous and stimulated emission at 8466 angstroms in GaAs structures 24 p4222 A66-42561  
 IR GaAs laser amplifier with gains as high as 2000, output powers of 150 mw and saturation occurring with current increase at low light levels 24 p4223 A66-42562  
 Cut-off frequency of high voltage GaAs varactors, comparing theoretical and experimental values 24 p4183 A66-42632  
 Semiconductor laser technology, operating principles, material properties and performance, with emphasis on GaAs junction lasers 24 p4224 A66-42802  
 Electro-optic modulators for IR region 0.9 to 16 microns constructed by using large single crystals of high resistivity gallium arsenide 24 p4258 A66-42957  
 Curves computed for avalanche multiplication and Zener tunneling for gallium arsenide specimens of various thicknesses 24 p4258 A66-42958  
 Light emission in near IR by semiconducting GaAs under current oscillations caused by electron-phonon coupling 24 p4258 A66-43000  
 Semiconductor GaAs quantum generator with two-photon absorption of neodymium laser emission 24 p4226 A66-43085  
**GALLIUM COMPOUND**  
 Superconducting transition temperatures measured for various tin-gallium compositions in quenched and annealed states 02 p0271 A66-11482  
 Changes in ordinary refractive index and birefringence of gallium sulfide and gallium selenide as function of wavelength for visible and near IR at low temperatures 06 p0929 A66-16940  
 Donor impurity effect on direct-indirect transition in gallium arsenic phosphide, particularly at low temperature 13 p2170 A66-26590  
 Optical reflection of gallium sulfide and gallium selenide single

crystal 15 p2566 A66-29206  
 Optical reflection of gallium sulfide and gallium selenide single crystals 17 p2982 A66-33055  
 Hall coefficient, electrical conductivity and thermoelectric power of GaSb-Ga<sub>2</sub>Te<sub>3</sub> solid solutions as functions of composition and temperature 24 p4254 A66-42425  
**GALLIUM PHOSPHIDE**  
 Photoluminescent time decay of red band in gallium phosphide doped with shallow acceptor Zn and deep donor O 04 p0560 A66-13722  
 Extrinsic and intrinsic epitaxially deposited single crystal gallium phosphide solar cells, noting conversion efficiencies 07 p0990 A66-17232  
 Light emission and photovoltaic effect of GaP diodes near bandgap 07 p1004 A66-17319  
 Spectral distribution of luminescence excited in n-type GaAs and p-type GaP by fast-electron bombardment 07 p1096 A66-17339  
 Measurement of energy required to form one hole-electron pair in gallium phosphide by alpha particles 07 p1107 A66-18407  
 Diffusion technique preparation of GaP p-n junctions and relation of p-i-n junction electric field calculation to Baraff carrier ionization rate theory 07 p1108 A66-18415  
 Rectifying and ohmic contacts used in manufacture of gallium phosphide diodes that emit light when current is reversed 08 p1273 A66-19291  
 Gallium arsenide phosphide heterojunction diode used to triple from X band to Ka band 09 p1350 A66-19924  
 Recombination-radiation spectra of GaP-GaAs p-n heterojunctions 09 p1412 A66-19984  
 Light emission associated with growth defects from reverse biased gallium phosphide p-n junctions 10 p1577 A66-21556  
 Direct-indirect transition effect on Hall effect in gallium /arsenic phosphide/ 10 p1543 A66-21570  
 Green emission lines from solution-grown p-n junctions in GaP diodes doped with shallow donors and acceptors 14 p2251 A66-27231  
 Photoreponse measurements of depletion capacitance and diffusion potential of GaP Schottky-Barrier diodes 20 p3534 A66-38390  
 Electrical and photoconductivity properties of high-resistivity gallium phosphide in intrinsic and near IR region, noting electron trap effect 21 p3800 A66-38992  
 Electrical and electroluminescent property of GaP diffused p-n junctions, accounting for V-I characteristics due to space-charge recombination by Sah-Noyce-Shockley theory 24 p4249 A66-42226  
**GALLIUM SELENIDE**  
 Measurement of exciton absorption of gallium selenide at low temperatures in presence of electric field, noting line broadening and no splitting 06 p0929 A66-16942  
 Optical reflection of gallium sulfide and gallium selenide single crystal 15 p2566 A66-29206  
 Optical reflection of gallium sulfide and gallium selenide single crystals 17 p2982 A66-33055  
 Absorption and dispersion spectrum of laminar gallium selenide crystal 21 p3802 A66-39159  
**GALVANIC CELL**  
 Electrical capacity of galvanic cell and crystal habit and surface property effects on porous cadmium hydroxide electrode electrochemical properties 08 p1171 A66-19644  
 Solid electrolytes which exhibit appreciable electron conduction for use in galvanic cells 13 p1999 A66-25675  
 Thermodynamics of molten lithium nitride galvanic cell, noting emf temperature dependence 20 p3503 A66-38189  
**GALVANOMAGNETISM**  
 Anisotropy of scattering in tellurium, correlating cyclotron frequency data and galvanomagnetic measurements 05 p0738 A66-15353  
 Anisotropy axes dispersion relation to plane galvanomagnetic effect in thin permalloy films to obtain Gaussian directional distribution 07 p1092 A66-17222  
 Galvanomagnetic effects in semiconductors,



including Hall effect and magnetoresistivity, noting influence of carrier scattering on lattice vibrations and impurities 08 p1267 A66-18607

Magnetoresistance measurements of germanium in strong magnetic field 08 p1277 A66-19616

Variable impedance device using galvanomagnetic effects in semiconductors 09 p1351 A66-19932

Galvanomagnetic and field effect measurements on Ge double crystals 09 p1427 A66-20419

Anisotropy of scattering in tellurium, correlating cyclotron frequency data and galvanomagnetic measurements 09 p1431 A66-20894

Transport properties of III-V and II-VI semiconducting compounds with zincblende structure under uniaxial stress, calculating galvanomagnetic coefficients, Faraday effect, plasma frequency, etc 10 p1578 A66-21665

Gradient instability of galvanomagnetic and galvanomagnetoacoustic waves in electrical fields 10 p1587 A66-22156

Electrophysical parameters of epitaxial p-n junction regions determined, using galvanomagnetic and photomagnetic measurements 11 p1751 A66-22734

Transverse galvanomagnetic effect in single-domain ferromagnetic film, noting role of Hall effect equation 11 p1752 A66-22801

Hall effect and galvanic magnetoresistance measurements in single crystal /mercuric manganese/ telluride solid solutions 12 p1927 A66-23729

Nonlinear galvanomagnetic effects in n-type InSb in quantum limit, using uncompensated and compensated samples 14 p2366 A66-27762

Galvanomagnetic and thermomagnetic effects in mixed state of type II superconductor 16 p2771 A66-30197

Anisotropy axes dispersion relation to plane galvanomagnetic effect in thin permalloy films to obtain Gaussian directional distribution 17 p2976 A66-31993

Magnetoresistance measurements of germanium in strong magnetic field 17 p2983 A66-33130

Galvanomagnetic effect in ferromagnetic metals, developing theory of planar Hall effect in terms of spin-orbit interaction of electrons 18 p3158 A66-34682

Gradient instability of galvanomagnetic and galvanomagnetoacoustic waves in electrical fields 19 p3440 A66-35770

Galvanomagnetic effect of anisotropic electron energy spectrum on acoustical branch perturbation spectrum of system of electrons and ions in homogeneous magnetic field 20 p3618 A66-37559

Relation between surface grain structure and galvanomagnetic properties of polycrystalline mercury telluride thin films with high current-carrier mobility 20 p3624 A66-38434

Galvanomagnetic effects in p-type aluminum antimonide, discussing field dependence of Hall effect and magnetoresistance 21 p3801 A66-38999

Infinite plate consisting of monopolar semiconductor of given thickness under effect of electric field results in change in galvanomagnetic, piezoresistance and optical properties 22 p3965 A66-40317

Electrophysical parameters of epitaxial p-n junction regions determined, using galvanomagnetic and photomagnetic measurements 23 p4113 A66-41472

Nonlinear dependence of current in electric field in thin semiconductor film in quantizing magnetic field 24 p4256 A66-42525

**GALVANOMETER**

**SA ELECTROMETER**

Shock spectrum analyzer for space vehicle structures, etc, noting galvanometer selection 16 p2703 A66-30489

**GAME THEORY**

**SA ARTIFICIAL INTELLIGENCE**

Decomposition theory of continuous submartingales 01 p0094 A66-10728

Differential games, theorem and analysis, discussing controlled object pursuits and computation of minimal time of termination 04 p0539 A66-13989

Optimal program control for minimization

of finite state vector norm of linear system with two types of sets of permissible controls 07 p1013 A66-17425

Mathematical stabilization theory for dynamic systems from Liapunov motion stability theory and theory of games 11 p1736 A66-22639

Sensitivity design of systems with optimal controller structures, using game theory 13 p2050 A66-26061

Communication design techniques for coding set of discrete memoryless channels where transmitter and receiver have no knowledge of channels selected 21 p3705 A66-39144

Continuous sequential decision for derivation of minimum search time for determining one nonzero mean process in presence of finite number of hypotheses 21 p3705 A66-39148

**GAMMA FUNCTION**

Reliability of system, with recovery, consisting of n plus m elements, m elements being in redundant system 08 p1200 A66-19670

Handbook of generalized gas dynamics including one-dimensional gas dynamics, compressible flow tables, gamma function, isentropic flow, etc 13 p2063 A66-25694

Mean time to failure within given time boundaries and for continuous failure density evaluated via Weibull density function 15 p2526 A66-28806

Reliability of system with recovery consisting of n plus m elements, m elements being in redundant system 20 p3538 A66-37262

Iterative algorithms for calculating sum of some series, considering gamma and theta functions 21 p3758 A66-39368

Data analysis on probability papers for gamma, normal and Weibull /including exponential/ distributions 24 p4230 A66-42088

**GAMMA GLOBULIN**

Solubility characteristics and electrophoretic and ultracentrifugal properties of human gamma globulins 09 p1334 A66-19900

Ultrasonic wave splitting of individual fragments and isolated polypeptide chains of human gamma globulin molecule 16 p2639 A66-30793

**GAMMA RADIATION**

**SA BREMSSTRAHLUNG**

**SA CERENKOV RADIATION**

**SA NUCLEAR RADIATION**

**SA SPACE RADIATION**

Transient gamma radiation pulse effects on MOS field effect transistors 01 p0049 A66-11151

Simulated nuclear power plant gamma radiation effects on magnetic film-insulated magnetic wire 02 p0248 A66-11293

Photon-flux measurements by high energy gamma-photon detectors onboard Explorer XI and OSO-I 03 p0423 A66-13028

Silicon surface damage, discussing low energy gamma irradiation effect on bulk lifetime and recombination velocity 05 p0729 A66-14565

Neutron and gamma sensitivities of nine detectors tested at Sandia Pulsed Reactor 05 p0734 A66-14854

Drift mobility induced by pulsed gamma irradiation of polystyrene 05 p0735 A66-14858

Stratospheric measurements of electrons and gamma radiation in cosmic rays, using plastic scintillator and lead sheet supplemented Geiger counters 05 p0752 A66-15386

Electronic components, considering noise characteristics, particularly effect of gamma radiation on resistors, capacitors, diodes, etc 05 p0650 A66-15834

Cosmic X-ray and gamma ray astronomy in studying stellar evolution, cosmic ray origin and structure of universe 06 p0944 A66-16314

Surface state density variations on metal oxide semiconductor capacitors due to gamma radiation 06 p0925 A66-16646

Gamma irradiated germanium at zero degrees C, studying annealing of recombination center, obtaining life times from transient decay of photoconductivity 06 p0934 A66-17126

In-pile neutron and gamma-ray irradiation of n-type indium antimonide, isochronous annealing indicating existence of five

recovery stages 06 p0936 A66-17126

Gamma irradiation effects on float-zone single-crystal p-type boron-doped silicon, using lithium drifted p-i-n junctions 06 p0937 A66-17126

Nucleon passage through atmosphere as meson production data including nuclear cascade intensity, gamma ray production, etc, and mean free path values for nuclear interaction 07 p1115 A66-17512

Extensive air shower high energy gamma rays in upper third of atmosphere 07 p1118 A66-17512

USAF whole body gamma spectrometry support of Air Force aerospace mission 07 p0999 A66-17606

Compton scattering of laser photon noting transformation into gamma radiative photons upon collision with high energy electrons 07 p1044 A66-17812

Gamma-electric cell, solid state device for direct conversion of gamma-ray energy into electrical energy 07 p1079 A66-18332

Lifetime degradation rate due to cobalt gamma irradiation reduced in p-silicon due to electron injection at low temperature 07 p1106 A66-18406

Gamma irradiation intermediates of polyamide MXD-6 examined, using electron spin resonance and optical spectroscopy 08 p1243 A66-19066

Low-background gamma-ray spectrometry of induced radioactivity resulting from Bogov meteorite cosmic radiation 08 p1291 A66-19066

Positron annihilation of single oriented crystals of vanadium silicide, measuring angular correlation between gamma rays for calculation of Fermi surface 09 p1419 A66-20042

Cosmic ray origins including galactic ray, RF radiation, metagalactic gamma radiation, etc 09 p1437 A66-20202

Galactic and metagalactic cosmic gamma and X-ray intensities 09 p1437 A66-20202

Radiation effects on electronic component noting sensitivity to gamma, fast neutron and electron radiation 09 p1359 A66-20966

Proton-nuclear and electron-positron component of primary cosmic rays 09 p1446 A66-21042

Mechanism for production of X-rays and gamma rays in galaxies, noting photon an electron spectrum 10 p1598 A66-21102

Upper limits to cosmic ray intensity 10 p1599 A66-21102

Cerenkov measurements of high energy gamma ray flux from quasi-stellar radiation sources in mountains near Dublin 10 p1599 A66-21102

Collision of cosmic rays and intergalactic gas to produce neutral pions which decay into high energy gamma rays 10 p1599 A66-21102

Transistor portable radioactivity detector utilizing self-quenching Geiger-Muller tube 11 p1703 A66-22226

Physical pattern of high altitude fission cloud and motion of gamma and beta fission fragments captured by geomagnetic field and observed by Cosmos satellite 11 p1764 A66-23042

Spark chamber with vidicon readout for balloon-and satellite-borne high energy gamma ray astronomy analysis, noting Cerenkov counter 12 p1877 A66-23688

Digitized spark chamber for balloon and satellite gamma ray astronomy, noting detector array, high voltage system and data acquisition and handling systems 12 p1877 A66-23688

Gamma ray spark chamber with photographic recording for manned satellites, determining energy spectrum 12 p1877 A66-23688

Nuclear instrumentation for lunar surface and subsurface measurements in Apollo Extensions System 12 p1878 A66-23699

Gamma radiating debris cloud of high altitude nuclear explosions scanned by gamma scintillation detector assembled into directional uranium shield 12 p1878 A66-23699

Neutron and gamma radiation measurements during low and high power NERVA reactor tests, determining leakage and radiation environment 12 p1911 A66-23704



- Atomic origins of transient nuclear radiation effects in electronics such as neutron and gamma 12 p1918 A66-24680
- Irradiation effects by fast neutrons and gammas on collector cut-off current and base current at low current densities analyzed on silicon planar 13 p2032 A66-25486
- Resistance transfer factor episode analyzed by measuring inactivation by cobalt gamma radiation, phosphorus and tritium, suggesting existence of 14 p2228 A66-27308
- DNA Electron spin resonance of gamma irradiated single crystal of barbituric acid dihydrate, noting formation and Hamiltonian parameters of free 14 p2367 A66-27979
- Radicals Neutron analysis techniques for determining hydrogen presence on lunar or planetary surfaces, based on measurement of gamma radiation 14 p2233 A66-28105
- Recombination centers in gamma irradiated silicon either float-zoned or melt-pulled and doped with phosphorus, arsenic or boron 15 p2562 A66-28721
- Annealing effects of gamma ray irradiation on MOS FET increase donor surface state density 15 p2567 A66-29413
- Injurious effect of gamma radiation and 660 and 120 mev protons on white mice and protective action of certain pharmacologicals 15 p2438 A66-29480
- Effect of shielding individual parts of rats on variations in reaction to radiation during exposure to gamma rays and high energy protons 15 p2438 A66-29481
- Extensive air shower generation by high energy primary rays over Bolivia studied by methods of fast timing and density sampling 15 p2577 A66-29515
- Cosmic ray anisotropy and gamma rays in Orion analyzed, using Geiger counter and Cerenkov telescope 15 p2579 A66-29525
- Cosmic ray showers, discussing high energy interactions of nuclear active particles, intensity and energy spectra of gamma rays and muons, young air showers, ionization bursts, etc 15 p2584 A66-29555
- Flux and energy spectra of primary cosmic X and gamma rays between 20 kev and 1 mev from balloon-rocket measurements 15 p2591 A66-30020
- Solar flare analysis by examination of high energy gamma rays, noting solar proton and solar material interaction, energy spectrum, generation of fast protons and alpha particles, etc 15 p2592 A66-30076
- Discrete source of cosmic gamma rays above 1 gev in balloon-borne detection 16 p2792 A66-30171
- Gamma radiation and fast neutron effects on dark resistance, photoconductivity, majority carrier mobility, recombination kinetics, etc, in CdS single crystal 16 p2787 A66-31765
- Thermal conductivity cell measurements of depolymerization rate of polytetrafluoroethylene exposed to gamma radiation in flowing helium atmosphere 17 p2942 A66-31880
- Inverse Compton X-ray and gamma ray flux due to high energy electron interaction with cosmic blackbody radiation at 3.5 degrees K 17 p2992 A66-31914
- Crystal spectra and broadband measurements of solar and galactic UV, X-rays, gamma rays, etc, outside Earth atmosphere 17 p2998 A66-32030
- Hazards of macrofractionated gamma ray irradiation hazards upon Rhesus monkeys 17 p2858 A66-32189
- Gamma irradiation effects on minority carrier lifetime in germanium, noting temperature effect 17 p2987 A66-33321
- Current decay in anthracene irradiated by gamma ray 18 p3157 A66-34476
- Balloon flight near peak of solar cycle in search for solar and cosmic gamma rays 18 p3169 A66-34515
- Balloon experiment for measurement of secondary gamma spectrum in 100-2000 mev range, using lead scintillator sandwich spectrometer 18 p3171 A66-34708
- X-ray and gamma ray astronomy, discussing observational methods, physical processes of generation, radiation intensity, etc 18 p3176 A66-34749
- Flux limits for high energy gamma rays from quasars and other possible cosmic ray sources 18 p3186 A66-34813
- Seventy-channel scintillation spectrometer high atmospheric measurement of cosmic gamma radiation of extraterrestrial origin 18 p3192 A66-34845
- Spark chamber experimental investigation of flux of high energy gamma rays at high altitudes near magnetic equator 18 p3193 A66-34849
- Extensive air shower research aimed at study of composition of primary cosmic rays and component properties 18 p3204 A66-35090
- Decrease in distribution of arrival directions of muon-rich air showers between 15 h and 21 h in right ascension confirmed by analysis of EAS 18 p3205 A66-35097
- Primary gamma ray production, arrival directions, particle collisions and distribution of EAS penetrating particles in intergalactic space 18 p3209 A66-35120
- Lateral distribution of high energy gamma rays, successive interactions and core structure of EAS, using emulsion chambers at mountain altitudes 18 p3211 A66-35132
- High energy nuclear interactions in graphite 18 p3140 A66-35159
- High energy interaction studied on Norikura Mountain and Mount Chacaltaya, using large area emulsion chamber 18 p3216 A66-35170
- Energy spectra of nucleons, muons and gamma rays for truncated power law primary energy spectra calculated, using model for nucleon and meson production 18 p3217 A66-35174
- Planar and needle-like defects in natural quartz examined via X-ray diffraction, noting composition and diffraction contrast when observed from different Bragg planes 19 p3434 A66-35403
- Absorption spectra modification in silica ceramics after gamma irradiation from Co-60 19 p3388 A66-35463
- Lithium-drifted germanium detector resolution and efficiency as function of temperature for gamma rays 19 p3359 A66-35915
- Range of atoms recoiling from photonuclear reactions in solids measured by foil-sandwich irradiations followed by radiochemical detection methods 19 p3402 A66-36002
- Stress relaxation of gamma irradiated fluorocarbon elastomers to study radiation induced chain scissions in copolymers 20 p3587 A66-37310
- Prior gamma irradiation effect on thermal volatilization of vinyl and vinylidene fluoride polymers 20 p3587 A66-37311
- Anomalous permanent changes in transistor gain after low exposure dosage of electron and/or gamma radiation related to recombination current-component buildup 20 p3528 A66-37320
- Gamma irradiation from Co 60 effect on indium antimonide, determining defect formation on dose and limiting position of Fermi level for n-and p-type material 20 p3617 A66-37552
- Anomalous high count of gamma rays from direction of constellation Cygnus associated with energy spectrum differing from spectrum of secondary gamma rays generated by cosmic rays 20 p3631 A66-37600
- Ionization due to alpha, beta and gamma radiation from ground and atmosphere in ground proximity, noting ion pair production rate and energy spectra 20 p3552 A66-37759
- Gamma-spectroscopy determination of special reaction products of cosmic radiation in meteorites 20 p3656 A66-38060
- High-energy gamma-ray absorption in photon field between sources and Earth and within radio sources themselves 21 p3809 A66-39210
- Fission spectrum neutron damage and gamma ray damage in n-type Si, comparing results of measurements by degradation of minority carrier lifetimes 22 p3962 A66-40086
- Riometric data on ionospheric absorption applied to determination of dissociative recombination coefficient, noting atmospheric ionization by fragment gamma-radiation 22 p3973 A66-40468
- Upper limits resulting from search for solar photons in 100-kev to 2-mev range from balloon observations 22 p3973 A66-40549
- Resonance absorption of gamma-quanta by tin in germanium 23 p4110 A66-41133
- High energy gamma rays energy spectrum of solar flares, elucidating proton interaction with solar material 23 p4123 A66-41276
- Neutron, proton and gamma radiation effect on small animals examined, using conditioned response drinking method 23 p4027 A66-41345
- Gamma and fast neutron radiation effect on nervous activity of mice examined, using conditioned reflex drinking method 23 p4028 A66-41346
- Gamma radiation, fast neutron and proton effect on conditioned and motor responses, nervous activity, excitation and inhibitory processes of white rats 23 p4028 A66-41347
- Effect of total chronic and acute gamma radiation on higher nervous activity of white rats 23 p4028 A66-41348
- Prolonged gamma-radiation induced electromiographic characteristics of vestibular reflex guinea pig hind-leg muscle 23 p4028 A66-41349
- Balloon-borne spark chamber observations of cosmic gamma rays from 30 to 500 mev 23 p4124 A66-42066
- Effects of isothermal decomposition of gamma ray irradiated orthorhombic crystals of ammonium perchlorate 24 p4170 A66-42421
- Spark chamber system designed to detect gamma rays in cosmic radiation on high altitude balloon flights 24 p4215 A66-43212
- GAMMA RAY ASTRONOMY EXPLORER S EXPLORER XI SATELLITE**
- GAMMA RAY BEAM**
- Monopole antenna signal produced via bombardment by flux of gamma rays from nuclear explosion 11 p1663 A66-22546
- Gamma photon flux from solar Na 22 disintegration emitted by Sun after chromospheric eruption 13 p2176 A66-26760
- Cosmic ray measurements, muon production from decay of charged pions and kaons, muon polarization, momentum spectra, atmospheric gamma cascades and derivation of kaon/pion ratio 15 p2587 A66-29573
- GAP**
- SA SPARK GAP**
- Gap size effect on pressure and aerodynamic heating over flap of blunt delta wing in hypersonic flow [AIAA PAPER 66-408] 17 p2840 A66-32747
- Half-wavelength resonators as capacitive-gap strip-line bandpass-type microwave filters, discussing parameter derivation for equivalent circuit and Cohn synthesis method 18 p3087 A66-34621
- GARNET**
- SA YTTRIUM-ALUMINUM GARNET /YAG/ CRYSTAL**
- SA YTTRIUM-IRON GARNET /YIG/ CRYSTAL**
- Fine-grain structure effect on microwave power absorption thresholds of ferrimagnetic garnets and spinels 14 p2350 A66-26880
- Chemically deposited thin ferrite and garnet films 14 p2249 A66-27104
- Faraday effect in rare earth garnet ferrites and metallic ion g values in IR spectrum 14 p2364 A66-27703
- GAS**
- SA AIR**
- SA ATMOSPHERE**
- SA ATOMIC GAS**
- SA COSMIC GAS**
- SA DIATOMIC GAS**
- SA ELECTRON GAS**
- SA EXHAUST GAS**
- SA EXPLOSIVE GAS**
- SA GRAY GAS**
- SA HIGH TEMPERATURE GAS**
- SA HOT GAS**
- SA IDEAL GAS**
- SA INTERPLANETARY GAS**
- SA INTERSTELLAR GAS**
- SA IONIZED GAS**
- SA LIQUID GAS**
- SA LORENTZ GAS**
- SA MOLECULAR GAS**
- SA MONATOMIC GAS**
- SA NONPOLAR GAS**
- SA PERFECT GAS**



SA POLAR GAS  
SA POLYATOMIC GAS  
SA RARE GAS  
SA RAREFIED GAS  
SA REAL GAS  
SA RESIDUAL GAS  
Nonlinear optical polarization of gases and liquids, stressing second degree contribution in macroscopic electric field 13 p2132 A66-26147

## GAS ANALYZER

Portable photoelectric instrument for determining oxygen admixture in hydrogen, nitrogen and inert gases with low sensitivity 02 p0231 A66-11999  
Miniature proportional counters with low background level for determining ultrasmall quantities of Ar 37 and H 10 p1610 A66-22017  
Interferometric measurement of ultrasonic velocity in gases at frequencies around 100 kc/s to determine vibrational relaxation 12 p1913 A66-23821  
Automatic electroanalytical equipment for determination of gas traces by conductometry, potentiometry, coulometry and galvanometry 14 p2296 A66-27734  
Cryopumping, titanium-sublimation and ion-pumping mechanisms studied for exhausting vacuum chambers to simulate outer space 16 p2677 A66-30456  
Efficiency of radiation sources in IR gas analyzer 16 p2706 A66-30849  
Photoionization mass spectrometer with 180-degree magnetic analyzer with inclined pole faces, applicability to gas analysis 19 p3354 A66-35419  
Miniature proportional counters with low background level for determining ultrasmall quantities of Ar 37 and H 19 p3453 A66-36103  
Residual gas analyzer determining qualitative distribution of gases in ultrahigh vacuums by using mass spectrometer for spatial simulation 19 p3360 A66-36614  
Fluorine concentration in oxygen monitored by instrument with nickel thermoconductivity cell 20 p3511 A66-38173

## GAS BEARING

Gas lubricated bearing principles and application problems 01 p0077 A66-10217  
Navigation gyro design with respect to cost factors noting electrically suspended, gas bearing and other types 01 p0104 A66-10676  
Opposed hydrostatic pad proportions and flow restriction in affecting load capacity, flow and pad stiffness 03 p0373 A66-12930  
Gas-lubricated bearing equations derived that are valid for wide range of temperature and Mach numbers 04 p0526 A66-14156  
Stability of symmetrical elastic rotor in journal bearings with flexible damped supports [ASME PAPER 65-APMW-8] 04 p0526 A66-14214  
Externally pressurized foil gas bearings, employing successive approximations method to solve Reynolds equation for fluid and equilibrium equation for foil [ASME PAPER 65-LUB-1] 04 p0526 A66-14237  
Whirl instability and pneumatic hammer for rigid rotor in pressurized gas journal bearings [ASME PAPER 65-LUB-12] 04 p0527 A66-14245  
Cylindrical squeeze-film gas journal bearing, noting load deflection experiments [ASME PAPER 65-LUB-13] 04 p0527 A66-14246  
Reynolds equation for compressible and incompressible lubrication for load coefficients and attitude angles of axial groove cylindrical bearings [ASME PAPER 65-LUB-16] 04 p0528 A66-14248  
Stability bounds for externally pressurized gas-lubricated thrust bearing [ASME PAPER 65-WA/APM-31] 05 p0689 A66-15452  
Exponential thermodynamic path function to predict pressure distribution and load-carrying capacity of infinite gas-lubricated slider bearing 06 p0885 A66-16223  
Load capacity and attitude angle of gas lubricated short journal bearing 06 p0885 A66-16224

Dynamic stability conditions of self-acting gas lubricated journal bearings 07 p1039 A66-18231  
Measurements of dynamic behavior of rotors supported by externally pressurized gas bearings subjected to impact [ASLE PREPRINT 65AM 3A4] 07 p1039 A66-18287  
Lift in spherical ball bearings with air lubrication calculated, taking into account inertial term in general equations of aerodynamics, gap variability and air compressibility 08 p1232 A66-19693  
Gas-bearing facilities for determining axial stress-strain and lateral strain of brittle materials to high temperature 08 p1242 A66-19722  
Modern gas bearings of self-acting and externally pressurized types in turbomachinery 09 p1384 A66-20297  
Gas bearing analysis and design, presenting specifications of European and American turbomachinery 10 p1539 A66-21170  
Stability of symmetrical elastic rotor in journal bearings with flexible damped supports [ASME PAPER 65-APMW-8] 10 p1539 A66-21488  
Stability bounds for externally pressurized gas-lubricated thrust bearing [ASME PAPER 65-WA/APM-31] 12 p1885 A66-23970  
Cylindrical squeeze-film gas journal bearing, noting load deflection experiments [ASME PAPER 65-LUB-13] 12 p1888 A66-24551  
Test rig for gas-lubricated journal bearings measuring frictional torque, gas film pressure distribution, static and dynamic eccentricity changes, etc 12 p1859 A66-24929  
Design and function of air bearings, measuring displacement force of system checking by autocollimation 13 p2085 A66-25074  
Designing hydrostatic journal-and thrust-gas bearings 13 p2085 A66-25365  
Brayton-cycle space power system, describing solar collector, heat receiver/storage unit, recuperator, radiator and gas bearings [AIAA PAPER 64-726] 13 p2006 A66-26635  
Gas lubricated bearings used in Brayton cycle closed-loop system turbomachinery in design of two-shaft power plant [ASME PAPER 66-GT/CLC-9] 14 p2300 A66-26982  
Design of 500-kwe closed Brayton cycle power conversion system, analyzing various turbomachinery configurations hermetically sealed and operating on gas bearings [ASME PAPER 66-GT/CLC-15] 14 p2225 A66-26985  
Differential equation for lubrication layer pressure in gas lubrication of sliding bearings at large transverse temperature drops 15 p2505 A66-28524  
Externally pressurized gas journal bearings, evaluating various design parameters for operating at high temperatures and high speeds [ASLE PAPER 66AM 4B2] 16 p2711 A66-30410  
Rotor-tilting pad gas lubricated journal bearing system performance determined by solving dynamic equations together with time-transient Reynolds equation [ASME PAPER 66-LUBS-3] 17 p2931 A66-33177  
Spherical squeeze-film hybrid bearing with small steady-state radial displacement treated by perturbation method [ASME PAPER 66-LUBS-5] 17 p2931 A66-33179  
Surface roughness effects in hydromagnetically lubricated externally pressurized bearings and hydromagnetic squeeze film between two circular plates [ASME PAPER 66-LUBS-9] 17 p2931 A66-33182  
Turbulent hydrodynamic lubrication theories and solution of Constantinescu equation for finite-length journal bearing [ASME PAPER 66-LUBS-11] 17 p2931 A66-33184  
Performance of hydrodynamic, hydrostatic or hybrid bearings determined by numerical solution of Reynolds lubrication equation for incompressible fluid films

## [ASME PAPER 66-LUBS-4]

17 p2932 A66-3318  
Prediction of hydrostatic gas journal bearing performance by solving simultaneous flow equations with Fortran II computer program [ASME PAPER 66-LUBS-16] 17 p2932 A66-3318  
Closed loop control system combined with air heating technology for measurement of multicomponent microforces 20 p3555 A66-3687  
Carrying capacity and moment of friction calculated for cylindrical MHD bearing of small magnitude of radial clearance 23 p4074 A66-417

**GAS CELL**  
Relaxing gas in cylindrical heat conductivity cell showing homogeneous phase maintained in thermal equilibrium with surface effects and exhibiting characteristics of monatomic gas 12 p1980 A66-2490  
Atomic time standards, describing cesium beam standard, ammonia maser and gas-cell type clocks 19 p3354 A66-3541  
Gaseous diffusion cells to remove carbon dioxide from spacecraft life support systems discussing construction material in terms of permeability coefficients substrate porosity 19 p3293 A66-3628

**GAS CHROMATOGRAPHY**  
Thermal stability to racemization at resolution of several racemic amino acid diastereomeric derivatives by gas chromatography 01 p0021 A66-106  
Pyrolysis of diol succino-maleates copolymerized with styrene at various temperatures, using gas chromatography [ONERA TP 251] 02 p0188 A66-116  
Gas phase nonideality and mean column pressure effects on sample retention in gas-solid partition chromatographic systems with real carrier gases 04 p0472 A66-133  
Gas permeation measurements on 1 exchange fuel cell membranes using chromatography 05 p0611 A66-145  
Quantitative interpretation of gas chromatograms, discussing separation process and identification of mixture components 08 p1179 A66-192  
Isolation and identification of bioglyceranes and pentacyclic triterpanes Eocene shale 12 p1805 A66-235  
Hydrocarbons synthesized abiogenically at those found in terrestrial samples, using gas chromatography and mass spectrometry connection with terrestrial life 12 p1806 A66-249  
Chemical analysis of permanent and trace organic gases in 30-day manned experiments using gas chromatography 12 p1811 A66-250  
Micro gas chromatographic system for Mars atmosphere analysis during capsule descent 14 p2232 A66-272  
Elutriation diagrams in determination of adsorption enthalpies from temperature dependence of retention volume in bar maximum 14 p2232 A66-276  
Gas chromatography for resolution of a separation of racemic amino acids as TF sec-butanol ester derivatives applied to protein analysis 15 p2446 A66-286  
Optical scanning and resolution of D, amino acids by gas-liquid chromatography and mass spectrometry 15 p2446 A66-286  
Tandem column gas-liquid chromatography labeling technique for mass spectrometry noting ketones exchange and data deuterium and oxygen compounds 15 p2446 A66-286  
Focused laser coherent radiation-induced degradation of solid methylene and gas chromatographic analysis of reaction products 17 p2933 A66-3317  
Stereospecific hydrolytic action of acyls studied by gas-liquid chromatography 17 p2869 A66-316  
Resolution method for DL-amino-acids menthyl ester derivatives and gas-liquid chromatographic analysis of crystalline products 17 p2869 A66-316  
High sensitivity optical resolution of amino diastereoisomers by gas liquid chromatography 17 p2869 A66-316  
Space cabin contamination control discussing temperature effects, analysis of IR gas chromatography and chemical methods 17 p2863 A66-320



Liquid oxygen purity control for onboard breathing equipment by IR absorption spectrophotometry and gas chromatography 17 p2866 A66-32233

Alpha-chloro alkanoyl valine methyl esters analyzed, finding that diastereoisomeric pairs separation by gas-liquid chromatography can assess steric conditions around amide bond 17 p2871 A66-32932

GLC-mass spectrometric stereoisomer discrimination as means of detecting biological processes 18 p3059 A66-34372

Mass spectrometry and gas chromatography in analysis of organic compounds present in extraterrestrial bodies to provide information on existence of life 18 p3059 A66-34373

Paraffinic hydrocarbons composition in Orgueil, Murray, Mokoia and other meteorites identified by gas chromatography 19 p3459 A66-35571

Probabilistic model equations relating column height, feed location, degree of separation and flow rates for continuous chromatographic column 20 p3510 A66-37363

Gas liquid chromatography resolution of racemic hydroxy and beta-mercapto-amino acids involving suitable derivation of functional group 20 p3510 A66-37606

Gaseous dispersion in laminar flow through circular tube with mass transfer to retentive layer 22 p3900 A66-40411

Electrolysis of wet hydrogen fluoride, noting analysis of anode products by gas chromatography and water content measurement by IR spectroscopy 23 p4118 A66-41236

Chlorine trifluoride analysis using combination of gas chromatography and IR spectrophotometry, noting column containing trichloroethylene 23 p4032 A66-41239

Nuclear magnetic resonance techniques applied to nitrogen tetroxide for determining proton content, noting gas chromatograph with two stainless steel columns packed with porous glass 23 p4032 A66-41240

Gas chromatography analysis of ambient gas and vapor effects on semiconductor and solid state devices at low temperatures 24 p4179 A66-42095

Backstreamed fluid analysis via gas chromatography, using polyphenyl ether as diffusion pump fluid 24 p4239 A66-43164

**GAS COMPOSITION**

Methane-rich premixed flames of perchloric acid analysis noting burning velocities, temperatures and burnt gas composition required for stoichiometric mixtures 02 p0304 A66-12018

Stagnation point viscous shock layer equations for three-component gas model in chemical nonequilibrium and binary gas model in vibrational and chemical nonequilibrium, noting heat transfer rates 08 p1164 A66-19125

Quantitative interpretation of gas chromatograms, discussing separation process and identification of mixture components 08 p1179 A66-19383

Equation of state in closed form obtained for gas composed of molecules with Lennard-Jones potential, noting compressibility factor and radial distribution function 13 p2018 A66-26446

Approximate and characteristics methods to predict effect of gas composition on forces and static stability of planetary entry configurations in air and assumed Martian atmospheres [AIAA PAPER 65-318] 19 p3275 A66-35605

**GAS COOLED REACTOR /GCR/**

Nonconventional application of electric power-generating closed-cycle gas turbines [ASME PAPER 66-GT/CLC-8] 14 p2224 A66-26981

**GAS COOLING SYSTEM**

Injection method for coolant has no substantial effect on efficiency of gas curtain used to shield machine parts 04 p0598 A66-14438

Gas film for protective cooling of surface having regular macroroughness 14 p2410 A66-26783

Differential equation derived for cooling of infinite porous tube by gas injection through wall, determining wall temperature distribution 16 p2827 A66-30674

Mathematical solution for expressing comfort level of man in gas-cooled space suit and space cabin, noting environmental parameters 17 p2863 A66-32142

Gas-film-cooled nozzle extension application to large rocket engines, discussing operational parameters, advantages, etc [SAE PAPER 660455] 17 p2991 A66-33163

Cryogenic propellant boiloff losses in long duration space storage elimination by mechanical reliquifier, considering lunar, Earth-orbit and deep space application for hydrogen and oxygen 20 p3625 A66-37079

Ranque tube application for gas cooling, discussing performance characteristics of vortex tube with and without heat exchanger 21 p3834 A66-38625

Adiabatic exponents in equations for gas cooling by vaporization 21 p3835 A66-38905

**GAS DENSITY**

Boltzmann-Landau equation to calculate transport coefficients of moderately dense quantum gases 04 p0549 A66-14478

Instrumentation techniques for new type of gas density measuring system using light scattered from laser beam as measured quantity 05 p0698 A66-15794

Initial value problem of converging shock wave propagation in quiescent gas of variable density 10 p1521 A66-21228

Dissociation rate of nitrogen behind strong shock waves in nitrogen-argon mixtures determined, using time-resolved interferometric measurements of gas density 12 p1861 A66-23616

Vacuum effects on lubricants and bearing materials due to reduced ambient pressure and low concentration of oxidizing gases 12 p1885 A66-24383

Kinetic theory of dense gases generalized for all orders, deriving integral equations for transport coefficients and showing temperature dependence of bulk viscosity 12 p1979 A66-24565

Enthalpy and density fluctuations in high speed wakes, noting typical reentry and ballistic range cases 14 p2219 A66-27431

Mass calculation for absorbing gases such as water vapor, carbon dioxide and ozone along oblique paths between two arbitrary points in atmosphere, considering vertical distribution, refraction and Earth curvature 14 p2284 A66-27541

Integral equations derived from correlation functions, determining transport coefficients in classical fluid, formally valid to general order in density 14 p2276 A66-27635

First order in density corrections to transport coefficients of moderately dense gas /viscosity and thermoconductivity/, using Boltzmann equation 14 p2276 A66-27636

Integral equations defining transport coefficients of moderately dense gas obtained from Boltzmann equation shown to be identical to first order in density, with results obtained by autocorrelation function method 14 p2276 A66-27639

Seaton formulas used to determine when gas is collision-dominated 14 p2337 A66-28115

Shock wave thicknesses and density ratios measured in helium, argon and nitrogen, using electron beam fluorescence method at various Mach numbers in wind tunnel 15 p2480 A66-29736

Hypersonic flow past blunt body near stagnation point examined, noting surface layer, characterized by increased density and decreased entropy of gas 16 p2630 A66-31305

Local density and temperature measurement in wind tunnels determined by 50-kev electron scattering, using air as test gas 24 p4192 A66-42199

Mass calculation for absorbing gases such as water vapor, carbon dioxide and ozone along oblique paths between two arbitrary points in atmosphere, considering vertical distribution, refraction and Earth curvature 24 p4198 A66-42326

**GAS DISCHARGE**

**SA ELECTRIC DISCHARGE**

**SA GLOW DISCHARGE**

Cold cathode gas discharge controlled by magnetic field in design of plasma switch 01 p0042 A66-10582

Frequency multiplication mechanism using microwave gas discharge of air, argon or neon 01 p0029 A66-10583

HF discharge in rectangular high vacuum waveguide in crossed magnetic and electric fields, calculating electron energy 02 p0268 A66-11773

Positive gas discharge column equilibrium and instability factors, noting increase in ionization and plasma conductivity from decreased electron heating 03 p0398 A66-12509

Electron beam-hot plasma interaction at low frequencies, explaining cesium discharges and gas noise 03 p0398 A66-12539

Intense laser beam focusing effect in gas to study light-induced discharges by time-resolved spectroscopy and photography 03 p0378 A66-12978

Characteristics of Schuler tube with two anodes compared with one anode tube 04 p0492 A66-13472

Temperature in toroidal theta pinch discharge with image converter camera 04 p0553 A66-14284

Effect of heat removal through MHD channel walls on stability of temperature distribution during electrical discharge in gas between two planes 04 p0557 A66-14421

Z-pinch discharge in rare gases and light phenomena as described by model of converging cylindrical shock waves impelled by magnetic piston 04 p0558 A66-14495

Laser oscillations of silicon tetrachloride, silicon tetrafluoride and ethyl silicate in gaseous discharge 05 p0696 A66-14973

Inert gas-filled controllable thermionic generator in form of gas triodes based on gas discharge phenomena 05 p0618 A66-15556

Superhigh speed IR spectrometers used in detection and study of free radicals and photochemical reaction, pulse discharges in gases, etc 05 p0685 A66-15862

CW IR laser oscillation in HBr and HI gas discharge 06 p0892 A66-16756

HF electrodeless discharge in argon and krypton at high pressure noting energy radiation losses, electron density and plasma temperature 06 p0919 A66-16873

Evolution of spark channels initiated in oxygen at 411, 680 and 950 torr by current pulses of approximately 30 amperes with durations of 30 and 40 nanoseconds 06 p0920 A66-17028

Current noise of gas-discharge plasma reduced by adding grid with negative bias 06 p0837 A66-17200

Magnetic field effect on electron temperature, number of ionization events and potential gradient in argon and neon HF discharge 08 p1264 A66-19186

Plasma conductivity measurement in terms of frequency shifts and Q-factor variation in RF oscillatory circuit produced by presence of plasma sample in induction coil 08 p1264 A66-19190

Cell voltages and Coulomb efficiency in oxygen electrodes and hydrogen and hydrazine fuel cells for long duration discharges 08 p1172 A66-19652

Three-centimeter wavelength frequency multiplier using gas-discharge plasma in nonuniform electric field, examining amplitude and phase 09 p1358 A66-20793

Instability Electron density in gas-discharge attenuator with hollow cathode 09 p1358 A66-20811

Guarding probes in hot-cathode mercury vapor discharge 10 p1564 A66-21552

Excitation of neon levels in hollow-cathode discharge in neon-hydrogen mixture as result possibly from recombination processes involving dissociation and triple collisions 10 p1558 A66-22023

Electric discharges in gases analyzed in terms of ion and electron drift velocity and ionization coefficient 10 p1558 A66-22057

Faust 1, hardcore discharge stability experiment with final configuration obtained from radial inward collapse of plasma sheath from tube wall 11 p1744 A66-22451

Conductance and susceptance of neon plasma measured by Q-meter method in frequency range from 0.5 to 25 mc 11 p1745 A66-22587

Breakdown regime of diffusion-controlled HF resonance gas discharge analyzed kinetically, solving Boltzmann equation for electron distribution 11 p1740 A66-23081



Characteristics of periodic fluctuations in voltage, current and luminous intensity of discharge through inert gases and mercury vapor, using commercial discharge tubes 11 p1747 A66-23369

Electron temperatures in several RF-generated plasmas, using air as medium 12 p1919 A66-23599

Nonlinear phenomena in HF plasma discharge, establishing qualitative relation between gas pressure, consumed microwave power and harmonic generation efficiency 12 p1919 A66-23711

Discharge rate of multicomponent gas mixtures through de Laval nozzle from chamber containing adsorbent bed 12 p1979 A66-24587

Gas discharge by laser pulse, taking into account photoionization due to electron impact 12 p1891 A66-24887

Wave interaction underlying diocotron effect and model of instability presentation, analyzing cylindrical wall-enclosed charge layers for application to plasmas and gas discharges 13 p2136 A66-25041

Design of gravity-independent force-fed liquid-metal cathode providing unlimited cathode life in gas discharge devices and mercury electron-bombardment thrusters [AIAA PAPER 66-245] 13 p2106 A66-25175

Conductivity of ionized gas in DC discharge in argon for various magnetic field intensities 13 p2139 A66-25406

Ionization phase of impurity in pulsed hydrogen discharge and electron temperature measuring method 13 p2141 A66-25478

Gabor type auxiliary discharge thermionic converter producing ions for space charge neutralization by impact, noting critical converter equation 13 p1998 A66-25530

Cold cathode magnetron gauge characteristics and striking characteristics of gaseous discharge 13 p2078 A66-25647

Laser pumping by intense noble gas discharge in zeta-pinch geometry 13 p2092 A66-25995

Plasma resonance and scattering, threshold variation and optical reflectivity in pulsed laser beam-induced gas breakdown 13 p2134 A66-26192

Growth rate of ionization by electron impact in presence of laser beam, elastic and inelastic scattering cross sections, free-free absorption, excitation and ionization coefficients, breakdown times and thresholds 13 p2134 A66-26193

Current changes in gas discharge as affected by lasing action 14 p2306 A66-27055

Microsecond pulsed discharges at short tube with wire electrodes containing helium gas at intermediate pressures 14 p2341 A66-27314

Radiative cascade patterns in helium-neon gas system using idealized model, computing spontaneous decays which are compared with laser experiments 15 p2512 A66-28699

CW IR laser oscillation in atomic Cl in HCl and HI gas discharges, noting use of two power supplies and energy level diagram 15 p2513 A66-28880

Coefficient of light amplification in gas discharge 15 p2515 A66-29203

Current voltage characteristic of gas discharge for one-dimensional stationary case with fixed temperatures at conductor end, noting voltage saturation 15 p2551 A66-29224

Normal atom concentration in cesium and mercury vapors during pulse discharge 15 p2545 A66-29343

Electrical discharge in air, mercury vapor and nitrogen, using RF signal probe, determining electron density and temperature and random velocity in plasma 15 p2548 A66-29715

Intensity growth and decay in Ar and Hg lines after switching on mercury vapor discharge lamps filled with Ar 15 p2542 A66-29716

Excitation of neon levels in hollow-cathode discharge in neon-hydrogen mixture as result possibly from recombination processes involving dissociation and triple collisions 16 p2753 A66-30842

Cyclotron harmonic radiation from rare gas discharge in magnetic field 16 p2764 A66-31351

High voltage pulsed electrodeless discharge in rare gas as light source for ruby and Nd glass laser excitation and observation of output characteristics 16 p2720 A66-31448

Electric current density in ionizing discharge layer determined, using multifluid equations of conservation of momentum and gas mass 17 p2967 A66-32435

Electric conductivity in low voltage atmospheric pressure gas discharge, noting Maxwellian electron density distribution 17 p2968 A66-32484

Formation process of rotating plasma in homopolar-type short coaxial-electrode system in hydrogen, nitrogen or argon discharge 17 p2972 A66-32973

Coefficient of light amplification in gas discharge 17 p2935 A66-33052

Electrostatic ion drives technology problems, discussing gaseous discharge ion sources, duoplasmatron and electron bombardment ion generator 17 p2991 A66-33234

Type II collision roles in population buildup in zinc vapor and in zinc mercury vapor mixture 17 p2960 A66-33511

Excitation of 3S sub 2 neon level by metastable helium atoms during He-Ne discharge 17 p2938 A66-33513

Electrodeless annular discharges in argon and air 18 p3144 A66-34039

Atomic concentration measurement in discharged nitrogen, oxygen and hydrogen 18 p3139 A66-34507

Current noise of gas-discharge plasma reduced by adding grid with negative bias 19 p3297 A66-35558

Alumina high temperature gas discharge tube for investigation of pulsed metal vapor laser oscillations 19 p3374 A66-35810

Hot cathode-gas discharge in equipotential space of magnetic field, noting formation of plasma column with opposite charge and discharge instability 19 p3408 A66-36275

Numerical calculations of parameters of steady state HF high pressure vortical discharge of argon in air 20 p3607 A66-36975

Geometry of steady state annular electrodeless discharge in argon and xenon as function of discharge power, type of gas, gas pressure, etc 20 p3607 A66-36976

Normal atom concentration in cesium and mercury vapors during pulse discharge 20 p3604 A66-37348

Thermoconductive energy transfer from cathode of low pressure gas discharge 20 p3679 A66-38010

Discharge current and laser light noise measurements effect in gas discharge helium-neon laser, using equivalent circuit 20 p3580 A66-38240

Conical electrode plasma source consisting of organic-glass discharge chamber with cylindrical electrode at apex, examining performance characteristics with pulsed gas admission 21 p3786 A66-39040

Equations for ionized positive plasma column of gas discharge between infinite dielectric planes under oblique magnetic field with component in direction of external electric field 22 p3953 A66-39756

Radial current density distribution in homopolar, noting deviation of magnetic field and nature of current distribution around anode 22 p3953 A66-39757

Magnetic resonance in He 3 ground states examined through interaction with metastable atoms in gas discharge, observing transfer of transverse magnetization by collision 22 p3931 A66-39809

Three-centimeter wavelength frequency multiplier using gas-discharge plasma in nonuniform electric field, examining amplitude and phase 22 p3874 A66-39852

Four electron paramagnetic resonance transitions of SO free radical generated in gas-phase discharge of sulfur dioxide 22 p3859 A66-39908

High temperature high density carbon plasma production in arc chamber of shock tube 22 p3955 A66-40092

Paschen series laser lines in atomic and molecular hydrogen 22 p3933 A66-40892

Spectral analysis of laser discharge in pure and impure He, obtaining spectra of spark at various pressures, determining electron concentration at various

stages 22 p3934 A66-40909

Gas discharge by laser pulse, taking into account photoionization due to electron impact 23 p4076 A66-41009

Microwave discharge technique for depositing noncrystalline oxide films of silicon, germanium, boron, titanium or selenium on substrates by decomposition compounds by oxygen 23 p4109 A66-41109

Diffusion controlled breakdown theory applied to compute breakdown potential of helium in coaxial geometry by solving continuity equation 23 p4105 A66-41589

Excitation of 3S sub 2 neon level by metastable helium atoms during He-Ne discharge 24 p4219 A66-42219

Gas-discharge CW lasers, particularly H, Ne, carbon dioxide, argon-ion and pulse self-terminating lasers, discussing classification, power output and gain Doppler width, coherence and noise 24 p4224 A66-42289

### GAS DISCHARGE COUNTER

Radiation measurement equipment 24 p4224 A66-42289

Cosmos 41 satellite including scintillation counter, gas discharge counter, etc 08 p1228 A66-19708

Cosmic rays during flights of Sputniks and Cosmos satellites investigated by analysis of charged particle fluxes obtained by gas discharge counter 10 p1595 A66-21095

Electric field distribution in gas discharge counters at moment radiation recorded allowing for space charge effect 17 p2928 A66-33428

Radiation measurement equipment 24 p4224 A66-42289

Cosmos XLI satellite including scintillation counter, gas discharge counter, etc 21 p3736 A66-38736

Penetrating radiation measurement of Moon surface obtained by Luna 1 spacecraft 23 p4128 A66-41428

### GAS DISSOCIATION

Convective heat transfer measurements from partially dissociated carbon monoxide and hydrogen with high Lewis number [ASME PAPER 65-WA/HT-27] 05 p0793 A66-15693

Comments on radiative recombination of molecular helium ions into dissociative state 06 p0912 A66-16692

Microinstability limitations of DCX energetic plasma from gas dissociation at Lorentz force dissociation 10 p1568 A66-21838

Iodine evaluated as working fluid in supersonic wind tunnel through study of iodine dissociation process 11 p1683 A66-22583

Nonsteady isentropic compression wave generate high-velocity air flows with very low ambient dissociation levels 11 p1684 A66-22584

Rate of effusion for gas flow through orifice and application to fluorine gas dissociation energy 11 p1688 A66-22838

Dissociation rate of nitrogen behind strong shock waves in nitrogen-argon mixture determined, using time-resolved interferometric measurements of gas density 12 p1861 A66-23681

Microwave plasma torch noting design, operation and application 12 p1857 A66-23857

Parametric method of solving equations of laminar boundary layer with longitudinal pressure gradient during equilibrium gas dissociation 12 p1863 A66-24383

Ionization cross section for rare gases and hydrogen atoms calculated from perturbation theory, noting ruby laser photon absorption 13 p2133 A66-26133

Electrical breakdown of gases by optical frequency radiation, noting laser beam attenuation and subsequent energy absorption by plasma 13 p2134 A66-26134

Nonequilibrium laminar boundary layer binary dissociating gas determined by solving nonlinear partial differential equations governing system [AIAA PAPER 65-129] 14 p2274 A66-27474

Inverse problem of nonequilibrium dissociation and vibrational relaxation in diatomic duct flow 14 p2219 A66-27479

Viscosity of equilibrium dissociating nitrogen tetroxide calculated from compressibility and critical parameters 14 p2371 A66-27871

Thermal conductivity of equilibrium



- dissociating nitrogen 14 p2371 A66-27828  
 tetraoxide dissociation 14 p2371 A66-27829  
 equations 14 p2371 A66-27829  
 Hypersonic laminar boundary layer flow of equilibrium dissociating 16 p2630 A66-31306  
 Dissociation rate of undiluted carbon monoxide behind strong shock waves produced in arc discharge shock tube AIAA PAPER 66-518] 18 p3063 A66-33660  
 Dissociational rate constants and vibrational relaxation times modifications, considering coupling of vibrational and dissociational nonequilibrium of expanding gas in nozzle 18 p3047 A66-33661  
 Buoyancy in convecting ideal dissociating gas analyzed, obtaining solution for one-dimensional unsteady free mixing 18 p3103 A66-34931  
 General theorems for dissociated and chemically reacting compressible laminar unsteady two-component boundary layers derived, based on Nirenberg maximum principle 20 p3510 A66-37524  
 Supersonic nozzle flow of dissociated oxygen, nitrogen and carbon dioxide 21 p3694 A66-39089  
 Recombination rate of diatomic gases determined from Mach number of supersonic nozzle outlet 21 p3694 A66-39090  
 Restoration rate of equilibrium dissociation disturbed by shock reflection 21 p3726 A66-39093  
 Nonequilibrium dissociation losses in hydrogen-fluorine propellant system, indicating rate control of recombination steps AICE PREPRINT 28A] 22 p3969 A66-39882  
 Carbon dioxide dissociation rate measured from 3000 to 5000 degrees K, considering decrease in temperature and increase in density caused by endothermic dissociation 22 p3859 A66-39915
- AS DYNAMICS**  
**SA AERODYNAMICS**  
**SA FLUID MECHANICS**  
**SA MAGNETOHYDRODYNAMICS**  
**SA RAREFIED GAS DYNAMICS**  
 Numerical solution to problems with spatial variables, using partial differential equations of gas dynamics 01 p0055 A66-10169  
 Dynamic pressure and temperature measurements of forward gas expulsion during high speed stall of jet engines [SAE PAPER 650840] 01 p0130 A66-10832  
 Cauchy problem for linearized Boltzmann equation in kinetic theory of gases 01 p0107 A66-11011  
 Transformation of unknown functions and independent variables entering into differential equations for motion of nonviscous nonheat-conducting gas 02 p0220 A66-12178  
 Two-dimensional problems of gas dynamics with free boundaries, discussing existence and uniqueness of subsonic potential gas flow 04 p0510 A66-13870  
 Post-Newtonian hydrodynamics and stability of gaseous masses for radial and nonradial oscillations 05 p0715 A66-14523  
 Book on physical gas dynamics including transport theory, kinetic theory, thermodynamics, equilibrium, fluid flow, radiative transfer, etc 05 p0666 A66-15848  
 Self-similarity of solutions to motion equations for relativistic gas possessing point symmetry and nonexistence of isentropic flow 06 p0954 A66-16538  
 One-dimensional unsteady motions of heat conducting gas in which heat conduction has significant role, formulating boundary value problems with self-similar solutions 06 p0917 A66-16709  
 Gas dynamics equation for wing of zero-thickness with two subsonic leading edges in supersonic flow reduced to wave equation 06 p0803 A66-17006  
 Rarefied gas dynamics in space flight and hypersonic low density wind tunnel of Goettingen Aerodynamics Research Facility 07 p1017 A66-17479  
 Variational problems in gas dynamics, examining vortex and vortex free motion, minimum drag conditions, etc 07 p0983 A66-18144  
 Analogy between gas flow through convergent/divergent nozzles and open side-contracted channel 08 p1205 A66-18628  
 Stability of motion of spherically symmetric mass of compressible gas with constant space density in absence of gravitational field 08 p1298 A66-19483  
 Supersonic gas dynamics variational problems concerning determination of axisymmetric minimum drag 08 p1166 A66-19573  
 Book on thin wing and aerodynamic characteristics in subsonic gas flow 09 p1327 A66-19975  
 Group properties of short wave equations in gas dynamics 10 p1522 A66-21315  
 Chemical reaction kinetics and gas dynamics combined to analyze processes occurring in combustion chambers and nozzles of jet and rocket engines 10 p1620 A66-21367  
 Ballistic performance change in spinning rocket motors attributed to internal gas dynamics and combustion effects, noting grain geometry influence 10 p1590 A66-21945  
 Large-scale aspects of gaseous components of our Galaxy, noting dynamics of gaseous systems with magnetic fields, virial theory, angular momentum, spiral structure of galactic disk, etc 11 p1767 A66-22263  
 Numerical solution of heat conduction and gas dynamics equations by sifting over separate regions 11 p1785 A66-22339  
 Gas dynamic problems in low pressure microthrust engines, noting parameters such as type of nozzle flow, pressure drop causes, etc 11 p1761 A66-22461  
 Kinetics and gas dynamics equations derived to determine state of gas behind strong shock waves, accounting for all excited states of neutral atoms 11 p1688 A66-22586  
 Aerodynamic drag torque on rotating sphere in transition regime, noting dependence of gas inertia on Reynolds number 11 p1635 A66-22935  
 Book on basic developments in fluid dynamics including numerical solution of problems in gas dynamics, stability of parallel flows, blast wave theory, etc 12 p1861 A66-23806  
 Numerical solutions of problems in gas dynamics in U.S.S.R., using computers stressing methods for solving systems of nonlinear partial differential equations 12 p1861 A66-23807  
 Two-dimensional problems of gas dynamics with free boundaries, discussing existence and uniqueness of subsonic potential gas flow 12 p1863 A66-24026  
 Handbook of generalized gas dynamics including one-dimensional gas dynamics, compressible flow tables, gamma function, isentropic flow, etc 13 p2063 A66-25694  
 Electrical and gas dynamical parameters effect on length of linear constant Mach number MHD duct, assuming gas is ionized by neutron irradiation in expansion nozzle preceding duct and electron recombination takes place in duct 13 p2000 A66-25739  
 Soviet text on gas dynamics including thermodynamics, gas motion equations, aerodynamic heating, rarefied and supersonic gas flow, etc 13 p2064 A66-26252  
 Experimental analysis of regression rates in hybrid rocket engines for both chemical kinetics and gas dynamics domains 13 p2173 A66-26369  
 Propagation stability of spherical flame in gas dynamic configuration of Landau and Markstein, showing that flame is stable relative to first spherical harmonics 14 p2410 A66-26779  
 Book on interstellar gas dynamics 14 p2378 A66-26807  
 Electro-magnetoplasma-gas-dynamics /EMPGD/ equations for warm compressible electron gas drifting at constant velocity, finding equation for refractive index of plasma waves 14 p2339 A66-26862  
 Text on vacuum science and technology including kinetic theory of gases, gas flow, pumps, vacuum measurements and equipment, etc 14 p2335 A66-27721  
 Book on shock wave relaxation processes, discussing laws governing statistical equilibrium, thermal dislocation and ionization, nonequilibrium zones behind shock wavefront, plasma shock propagation, etc 14 p2277 A66-27788  
 Book on uniform steady motion of ideal gas and gas dynamics of supersonic wind tunnels 14 p2220 A66-27789  
 Adiabatic dispersion into empty space of triaxial gaseous ellipsoid studied by Ovsinnikov exact solution of equations of gasdynamics 14 p2278 A66-28060  
 Range of gas dynamic stability of arc-type electric heaters, characteristics for design and calculation of electrode diameter ensuring vortex stabilization 14 p2348 A66-28314  
 MHD equations applied to hypersonic flow of solar plasma around magnetosphere and approximation with simpler equations of gas dynamics 15 p2483 A66-28815  
 Variation problem solution in hypersonic gas dynamics, noting intake portion construction for body with minimum resistance for limited length and flat end 15 p2477 A66-28956  
 Spatial problems in gas dynamics solved by difference methods, discussing supersonic flow 15 p2423 A66-29174  
 Oscillatory behavior in rocket engines, analyzing interaction between shock wave and burning solid propellant surface and stressing gas dynamics 15 p2572 A66-29298  
 Book on dynamics and thermodynamics of gases, emphasizing modern theory of gas behavior at hypersonic velocities and extremely high altitudes 15 p2482 A66-29914  
 Self-similarity of solutions to motion equations for relativistic gas possessing point symmetry and nonexistence of isentropic flow 15 p2603 A66-29978  
 Book on radiation gas dynamics including radiative heat transfer, waves and shock waves, kinetic theory, relativistic mechanics, free-molecule flow, etc 16 p2829 A66-31314  
 Heat-conducting gas converging spherical shock wave analysis, emphasizing energy accumulation 16 p2689 A66-31514  
 Oblique condensation discontinuities calculated during flow of supercooled water vapor in supersonic jets 16 p2690 A66-31608  
 Unsteady expansion of plane layer of ideal gas into vacuum for various laws and durations of energy release described by equations of gas dynamics 16 p2690 A66-31617  
 Shock wave excited by pulsed current flowing between two plane parallel electrodes in rarefied air 16 p2690 A66-31621  
 Relaxation and evaporation zones behind normal shock in mixture of air, water vapor and water droplets 17 p2908 A66-32445  
 Primary and secondary flow interaction in plug nozzle, obtaining solutions by iteration and isentropic relation 17 p2839 A66-32476  
 Successive approximation solution to integral kinetic equation and corrections to moments of distribution function for viscous and rarefied gases 17 p2909 A66-32585  
 Virial theorem study of magnetic field effect on gravitational instability of primeval gas cloud, noting possibility of collapse upon change in magnetic flux 17 p3005 A66-33002  
 Melting of solid bodies in chondrule size, discussing accumulation mechanisms involving electrostatic acceleration and gas motions 18 p3225 A66-33622  
 Large-dimensional inverse pinch discharge study of impulsive plasma acceleration, gas dynamics and stability of unrestrained current sheet [AIAA PAPER 66-482] 18 p3141 A66-33655  
 Equilibrium thermodynamic and gas dynamic parameter calculation for low temperature plasma, using electromagnetic and diaphragm-type shock tubes 18 p3144 A66-34037  
 Book on mechanics of liquids and gases 18 p3102 A66-34731  
 Shock front and current sheet separation predicted in magnetically driven shock tube with axial magnetic field and hydrogen as test gas 18 p3149 A66-34917  
 Asymptotic solution of nonlinear hyperbolic equation in gas dynamics, with applications in explosion theory, astrophysics, etc 19 p3390 A66-36200  
 Book on physics of shock waves and high temperature hydrodynamic



- phenomena 19 p3341 A66-36316  
Optimum thrust nozzle contours for chemically reacting gas flows, obtaining set of partial differential equations for gas dynamic properties [AIAA PAPER 66-638] 19 p3277 A66-36599  
Propagation of spherically symmetric, cylindrically symmetric and plane waves examined via analytic perturbation method in solving gas dynamics equation for nonstationary compressible flow 19 p3343 A66-36638  
Galactic magnetic fields, considering magnetic flux, frequency of fields in radio galaxy, disk, interstellar gas dynamics and spiral structure 20 p3645 A66-36958  
Steady state oscillations in semiinfinite gas excited by harmonically oscillating wall, using single-collision time kinetic model 20 p3605 A66-37635  
Internal ballistic considerations in hybrid rocket design, noting throttling and regimes of operation involving effects of surface-or gas-phase reaction kinetics [AIAA PAPER 66-628] 20 p3663 A66-38035  
Supersonic gas flow states in transition regime, discussing change from dynamical to molecular flow, velocity and pressure distribution and conditions for freezing of translational degrees of freedom 20 p3548 A66-38084  
Gas sorption and desorption processes at low pressures, discussing molecular adherence to cold solid surfaces, adsorption mechanism of isotherms, vacuum generation via cryotrapping effect, etc 20 p3605 A66-38088  
Electromagnetic and gas dynamic effects on magnetic compression of plasma loop 20 p3611 A66-38120  
Nonisentropic two-dimensional MHD flow 21 p3777 A66-38725  
Book on aerodynamic experiment in machine building, noting self-simulation problems of machines using gas dynamics, analyzing wind tunnels 21 p3694 A66-38743  
Gas molecule excitation in shock wave analysis based on behavior of gas flow past obstacle in shock tube 21 p3726 A66-39092  
Quantum corrections to second virial coefficient for low-temperature gas 21 p3836 A66-39175  
Free jet MHD accelerator for determining minimum length of crossed field accelerators, noting operation and solution in closed form 21 p3699 A66-39645  
Carbon dioxide dissociation rate measured from 3000 to 5000 degrees K, considering decrease in temperature and increase in density caused by endothermic dissociation 22 p3859 A66-39915  
Weak plane shock waves formation by impulsive motion of piston for viscous heat conducting gas 22 p3900 A66-40383  
Shallow water theory of formation and decay of hydraulic shock waves in nonsteady homentropic gas flow 23 p4055 A66-41541  
Stability analysis of discontinuous solution of gas dynamics PDEs for ideal fluid 23 p4055 A66-41559  
Gas dynamic calculations of power generator with closed circulation of fissionable gas supported by nuclear reaction behind supersonic diffuser 23 p4022 A66-41763  
Three-dimensional supersonic gas flow past smooth blunt bodies, considering gas dynamic equations for mixed and purely supersonic regions 23 p4013 A66-42016  
Partly invariant solutions of equations admitting Lie group and application to gas dynamics 23 p4086 A66-42024  
Radiation fronts in gas dynamics, examining flow through or behind aerodynamic shock 23 p4062 A66-42052  
Static elastic and thermoelastic stability, discussing kinetic theory and physical interpretation of energy methods 24 p4287 A66-42271  
Invariant solution classification for equations of two-dimensional steady state motion of gas 24 p4196 A66-42867
- GAS EVACUATION**  
Gas capture coefficient prediction for cryopumping based on critical velocity model in space chamber simulator 10 p1520 A66-21937  
Ultrahigh-vacuum mercury-vapor unit design, noting performance characteristics 15 p2429 A66-29700
- GAS EVOLUTION**  
Mass flow rate of gas evolution from burning solid rocket propellant during transient depressurization of combustion chamber [AIAA PAPER 65-104] 08 p1282 A66-19163  
Porosity in titanium arc welds, noting sources of gas evolution and probable causative gases, particularly molecular hydrogen and oxygen 14 p2302 A66-27346  
Thermal conductivity cell measurements of depolymerization rate of polytetrafluoroethylene exposed to gamma radiation in flowing helium atmosphere 17 p2942 A66-31880  
Evolution of gases from cometary nuclei by sublimation or desorption 17 p3009 A66-33372  
OH production by sublimation and gas hydrate occurrence in cometary nuclei 17 p3009 A66-33373  
Graphite and C-H-O gas phase equilibrium at high temperatures and pressures in implication of Earth ocean and atmosphere development 17 p3015 A66-33432
- GAS EXCHANGE**  
**SA OXYGEN PRODUCTION**  
Alveolar nitrogen concentration and environmental pressure influence upon rate of gas absorption from nonventilated lung in dog 03 p0324 A66-12357  
Vibrational excitation effect in hydrogen-deuterium exchange 05 p0718 A66-15156  
Apparatus for measurement of flow resistance of gas diffusion electrodes 07 p0990 A66-17233  
Nonequilibrium internal distributions effect on rates of chemical gas-phase exchange reactions 11 p1650 A66-23212  
Algal bioregenerative photosynthetic gas exchange system 19 p3293 A66-36239
- GAS EXPANSION**  
Nonequilibrium expansion of air through hypersonic nozzle extended to higher reservoir temperatures and pressures 02 p0303 A66-11565  
Water-vapor condensation zones of moist air expansions in Laval type nozzles with thermal choking 03 p0317 A66-12948  
Velocity distributions in molecular beams of argon produced by supersonic nozzle sources, using time of flight method 04 p0548 A66-14012  
Nonsteady expansion of gas into vacuum in analysis of asymptotic solutions of Sedov 08 p1210 A66-19574  
Device for generation of strong shock waves in air 10 p1525 A66-22014  
Numerical calculations of axially symmetric two-dimensional steady expansions of monatomic gas, using approximate Boltzmann equation with Krook collision term 11 p1690 A66-22908  
Steady state expansion of gas into vacuum, considering continuum inviscid analysis, collision-free analysis, supersonic flow and hypersonic limits, etc, for spherical and cylindrical symmetry 12 p1860 A66-23607  
Adiabatic dispersion into empty space of triaxial gaseous ellipsoid studied by Ovsinnikov exact solution of equations of gasdynamics 14 p2278 A66-28060  
Steady nonisentropic jet expansion in vacuum with pressure tensor approximated by second-order moment technique and BGK model 16 p2684 A66-30605  
Unsteady expansion of plane layer of ideal gas into vacuum for various laws and durations of energy release described by equations of gas dynamics 16 p2690 A66-31617  
Relativistic gas expansion into intergalactic space noting energy content, modes of expansion and radio source distribution 18 p3236 A66-34761  
Density field calculation for collisionless expansion of moving cylindrical gas cloud, with Maxwellian random velocity distribution superimposed on uniform initial velocity 18 p3103 A66-34933  
Shock wave and glow cloud of nitrogen dioxide released at 110 km altitude 19 p3345 A66-35492  
Population inversion in adiabatic expansion of molecular gas mixture with three vibrational levels 19 p3402 A66-36068  
Device for generation of strong shock waves in air 19 p3341 A66-36316  
Laval points in ideal gas expansion with energy losses in nozzle or turbine-blade cascade 19 p3276 A66-36316  
Rarefied gas motion instability, constructing general solution for effect of various force fields 19 p3343 A66-36316  
Pneumatic vernier engines in aircraft spacecraft, discussing weight, gas expansions and gas temperature 20 p3627 A66-36316  
Kaufman assumption regarding universe expansion considered untenable because requires intergalactic hydrogen temperature to remain constant while hydrogen expanded in volume 22 p3978 A66-40316
- GAS EXPLOSION**  
**SA EXPLOSIVE GAS**  
Stability of gas expelled by piston considering velocity, temperature and time represented as explosion with shock wave 03 p0355 A66-12357  
Gas combustion and detonation instability 04 p0597 A66-12357  
Gas temperature behind detonation front in acetylene-oxygen mixture measured by time-base photometry of hydrogen beta gamma spectral lines 04 p0598 A66-12357  
Gas compression-conduction mechanism contribution to shock initiation of granular explosives, analyzing surface temperature interstitial gas and grain distribution [CI PAPER WSCI-65-30] 05 p0788 A66-12357  
Energy distribution in cavitation bubble collapsing at interface between liquid and solid approximated by localized explosion ideal gas 06 p0870 A66-12357  
Explosive wave propagation during cylindrical and plane explosions in electrically conducting gas, taking account of counterpressure and magnetic field 08 p1208 A66-12357  
Hydrodynamic theory relating velocity decrement and curvature of gas detonation to conditions at explosive interface [AIAA PAPER 65-39] 10 p1621 A66-12357  
Nonstationary problem of thermal explosion, taking into account temperature dependence on induction time coordinate 10 p1622 A66-12357  
Energy distribution in cavitation bubble collapsing at interface between liquid and solid approximated by localized explosion ideal gas 13 p2064 A66-12357  
Detonation in gaseous mixtures and condensed phase, reviewing aerodynamic theory 15 p2617 A66-12357  
Energy release effects on unsteady flow in explosion 16 p2689 A66-12357  
Gas combustion and detonation instability 17 p3033 A66-12357  
Explosive wave propagation during cylindrical and plane explosions in electrically conducting gas, taking account of counterpressure and magnetic field 18 p3099 A66-12357
- GAS FLOW**  
**SA AIRFLOW**  
**SA CHEMICAL RELAXATION**  
**SA KNUDSEN FLOW**  
**SA MAGNETOHYDRODYNAMIC FLOW**  
**SA PLASMA FLOW**  
Throttle devices to control compressible gas flow, using gas dynamics laws 01 p0006 A66-12357  
Simple wave interaction in polytropic rarefied gases flowing from parallel channel 01 p0006 A66-12357  
Density distribution before sphere in density hypersonic gas flow measured by electron beam densitometer 01 p0059 A66-12357  
Near electrode layers of potential change on hot electrodes in weakly ionized flow 02 p0264 A66-12357  
Stability of plane stationary detonation wave, using detonation model of perfect gas flowing in pipe at conical supersonic velocity 02 p0217 A66-12357  
Statistics of locally-isotropic turbulent flow for gas with density sensitive heat mechanism [AIAA PAPER 65-38] 02 p0302 A66-12357  
Speed of carburized gas in immediate vicinity of flame front and wake as related to flame stabilization in subsonic flow 02 p0304 A66-12357  
Hartmann problem solved for isothermal



- motion of heavy neutral viscous gas containing small impurities of light ions and electrons in crossed electric and magnetic fields 02 p0269 A66-12131
- Plane transonic gas flow past symmetrical convex profile at zero angle of attack along axis of channel with parallel walls 02 p0176 A66-12171
- Three-dimensional unsteady flow in uniformly expanding layer and dispersion of gas in vacuum 02 p0220 A66-12177
- Interference between plane surfaces in supersonic gas flow between two rectangular parallelepipeds 02 p0220 A66-12180
- Asymptotic representation of solutions for boundary layers near weak shock waves in conical flows 02 p0176 A66-12181
- Heat transfer and friction for laminar flow of gas in circular tube at high heating rate, using finite difference method 02 p0304 A66-12198
- Performance of vortex-stabilized arc radiation source in which arc current, gas pressure, gas flow rate and nozzle diameter are prime variables 02 p0270 A66-12209
- Local heat transfer during turbulent gas flow in pipe for large temperature differences, describing test apparatus and results 03 p0443 A66-12517
- Difference in properties of constituents of stratified multicomponent ideal gas and effect on nozzle flow [AIAA PAPER 64-266] 03 p0315 A66-12747
- Mutual effects of vaporization, combustion and coking processes during material decomposition in high temperature gas flow 03 p0445 A66-12828
- Pulse transmitter for measuring heat transfer in ionized gas 03 p0370 A66-12830
- Numerical solutions for inviscid nitrogen gas flows over circular cylinder where nonequilibrium prevails through nose region 03 p0317 A66-13211
- MHD experiments with high enthalpy flow of argon 03 p0445 A66-13214
- Transverse-field induction flowmeter to monitor shock tube gas velocity 03 p0353 A66-13250
- Thermocouple and inertialess temperature sensor for velocity fluctuations in gas flow 04 p0519 A66-13657
- Temperature of gas moving in frame of reference with respect to rest frame 04 p0597 A66-13814
- Hydrodynamic systems expressed by kinetic equations, deriving equations of aerodynamics without knowledge of interaction of gas molecules 04 p0510 A66-13879
- Book on vacuum science and engineering covering properties of gases at low pressure, vacuum measurements and vacuum pump and system design 04 p0545 A66-13934
- Aerodynamic characteristics of flat rectangular plate placed normal to flow of highly rarefied gas 04 p0456 A66-14141
- Potential distribution over arc in vortex-type plasmatron determined from voltage data and direct measurement by electrostatic voltmeters 04 p0557 A66-14435
- Limiting relative laws of friction and heat transfer applicable to nonisothermal gas flow with finite Reynolds numbers 04 p0598 A66-14440
- Adherence of gas to wall, investigating Boltzmann equations for perfect fluid, Prandtl-type flow and state of rest fluid 05 p0661 A66-14535
- Hydrodynamic stability of parallel dusty gas flows, discussing energy balance and viscous sublayer structure 05 p0662 A66-14703
- Transition flow of nitrogen through short circular tubes with length-to-diameter ratios from 0.005 to 1 and pressure ratios from 1 to 20 05 p0605 A66-14704
- Thermometric transducer and RC loop for measuring rapidly changing temperature in pulsed gas flow 05 p0682 A66-15312
- Pressure drop in entrance region of abrupt inlet circular tube for continuum laminar flow conditions [ASME PAPER 65-WA/APM-5] 05 p0663 A66-15428
- Electric arc interaction with argon flow analyzed in crossed convective and magnetic fields [ASME PAPER 65-WA/ENER-1] 05 p0728 A66-15626
- Shift of gas mass from high pressure to low pressure sides of divided vessel, with communication by bursting diaphragm and by-pass valve [ASME PAPER 65-WA/PID-3] 05 p0664 A66-15638
- Heat transfer and wall friction for low velocity flow of gases in downstream region of smooth electrically heated tubes, considering transition region [ASME PAPER 65-WA/HT-18] 05 p0790 A66-15646
- Heat losses from turbulent gas flowing through poorly insulated pipe where heat lost from outer surface is by free convection and radiation, solving heat equation [ASME PAPER 65-WA/HT-16] 05 p0790 A66-15648
- Pressure response to forced oscillation of shallow cylindrical porous chamber [ASME PAPER 65-WA/FE-9] 05 p0780 A66-15730
- Asymptotic solutions for viscous flow of transparent radiating gas in stagnation region, using method of matched inner and outer expansions [AIAA PAPER 66-105] 06 p0871 A66-16254
- Propagation of shock wave of gas flow from axisymmetric nozzle 06 p0802 A66-16422
- Separation of gases from isotopes in compression shock produced in expanding gas flow past obstruction, dependent on gas density and hydrokinetic properties of components 06 p0875 A66-17052
- Interaction or coupling of radiation with conduction and convection mechanisms in nonisothermal nongray gas flowing in entrance region of tube with isothermal black walls [AIAA PAPER 66-136] 06 p0875 A66-17090
- Gas flow dissipation in transonic plane-symmetric nozzle, obtaining asymptotic solutions for flow parameter equations 07 p0979 A66-17264
- Heat transfer coefficients for helium and hydrogen gas flowing through electrically heated Inconel tube 07 p1148 A66-17300
- Axial deviation of gas flow resulting from mixing turbulent gas jets 07 p1019 A66-17395
- Heat transfer between body and gas flow near stagnation point 07 p1019 A66-17396
- Detached shock wave created by rectilinear uniform translation of obstacle placed in perfect gas in adiabatic flow 07 p0979 A66-17448
- Group properties of PDE system for one-dimensional gas flows with plane waves, using external Cartan forms 07 p1019 A66-17859
- Gas and sound velocity measurements downstream of shock wave in electromagnetic tube for subsonic and supersonic flows 07 p1023 A66-18119
- Method of characteristics applied to three-dimensional supersonic flow equations for compressible inviscid gas 07 p0982 A66-18130
- Tube gas flow theory applicable to laminar flow, slip flow, transition region of flow and free molecular flow 07 p1023 A66-18131
- Numerical computer solutions for several nonlinear gas flow problems in high speed aerodynamics 07 p0983 A66-18143
- Two-dimensional steady MGD flow of ideal thermally nonconducting fluid with infinite conductivity, when magnetic intensity and velocity are orthogonal 08 p1261 A66-18675
- Thrust-vector control and flow field produced by secondary gas injection into supersonic stream 08 p1162 A66-18831
- Inviscid supersonic nozzle flow of ideal dissociating gas, sudden freezing, equilibrium-recombination mechanism and velocity distribution [AIAA PAPER 66-1] 08 p1163 A66-18983
- Large-scale expansion nozzle control by heterogeneous nucleation and mercury vapor and drop growth processes in nitrogen flow [AIAA PAPER 66-85] 08 p1318 A66-18997
- Performance correlation of conical and contoured nozzles for gas-particle flows, defining differences between particle effects for such nozzles 08 p1165 A66-19157
- Aerodynamic pressure and resistance calculated from gas flow past circular cylinders with piecewise constant diameters 08 p1232 A66-19338
- Atomization of liquid-spray particles in Venturi scrubber, investigating acceleration by high-speed photography 08 p1208 A66-19422
- Laminar boundary layer in gas flow with arbitrary external velocity and temperature gradient solved by single-parameter approximation 08 p1319 A66-19424
- Coolant injection in turbulent boundary layer for protection of surfaces from effects of high temperature and high energy gas flows 08 p1320 A66-19429
- Exact partial solutions to transonic gas flow equations used to describe flow around shape streamlined by supersonic flow with additional shock wave 08 p1209 A66-19473
- Peculiarities of aerodynamic characteristics of flow past plate and pointed and blunt slender cones in viscous hypersonic thermodynamically ideal gas 08 p1165 A66-19571
- Approximate methods for integration of equations of plane isentropic motion of gas at supersonic velocities 08 p1165 A66-19572
- Nonisentropic simple waves in two-dimensional steady flow of ideal gas 08 p1210 A66-19585
- Engineering method for measuring rapidly changing temperatures of gas flow with steady or variable heat transfer 09 p1470 A66-20142
- Conducting gas flow in Hall MHD generator reduced to quasi-one-dimensional problem 09 p1331 A66-20145
- Asymptotic steady state solution to problem of thermal separation of components across shear layer between cold jet mixture and hot ambient gas 09 p1470 A66-20178
- One-dimensional adiabatic compressible gas flow in cylindrical tube taking into account Reynolds number variations along tube and compressibility effect on friction factor 09 p1368 A66-20827
- Pressure drop in entrance region of abrupt inlet circular tube for continuum laminar flow conditions [ASME PAPER 65-WA/APM-5] 10 p1523 A66-21471
- Electric arc interaction with argon flow analyzed in crossed convective and magnetic fields [ASME PAPER 65-WA/ENER-1] 10 p1563 A66-21503
- Scalar formulation of ideal charged adiabatic gas flow in presence of gravitational and electromagnetic fields 10 p1524 A66-21814
- Relative effect of restrictive orifices, venturils or nozzles on measurement accuracy of fluid flow rates in pipes 11 p1703 A66-22207
- Three-dimensional supersonic gas flow past truncated cone with shock separation calculated by method of characteristics 11 p1629 A66-22336
- Gas flow in free-molecular regime with negligible collision approached by diffuse reflection model 11 p1688 A66-22525
- Rate of effusion for gas flow through orifice and application to fluorine gas dissociation energy 11 p1688 A66-22880
- Molecular beam approximation for plane normal shock in free stream monatomic gas flow at large Mach numbers 11 p1690 A66-22911
- Coaxial capacitor for measuring density of fluids in both liquid and gaseous phase over wide range of temperatures and pressures 11 p1707 A66-22961
- Thermal transpiration analysis with various gases, testing relation between translation component of thermoconductivity coefficient and maximum transpiration effect for particular gas, obtaining rotational collision numbers 11 p1787 A66-23214
- Secondary flows influence on concentration distribution of heavy species in vortex comprised primarily of lightweight gas [AIAA PAPER 65-582] 12 p1860 A66-23573
- Rugged micromanometer capable of reliably measuring pressure differences as low as 10 mtorr in flow of gaseous media 12 p1876 A66-23601
- Blast wave theory with and without entropy layer effect, determining asymptotic flow, far downstream of blunted nose, past



given body 12 p1861 A66-23808  
 Supersonic viscous gas flow near blunt body numerically determined by equations similar to Navier-Stokes 12 p1796 A66-23900  
 Two-dimensional potential flow of polytropic gas with stationary streamlines 12 p1862 A66-24007  
 Equation for laminar boundary layer on flat plate in viscous compressible gas flow under chemical relaxation, solved by approximate method in series 12 p1863 A66-24244  
 Exact solutions for triple wave type hydrodynamic equations for confined isothermal gas flow and polytropic gas efflux into vacuum 12 p1863 A66-24360  
 Airfoil cascade oscillation in near-sonic gas flow 12 p1798 A66-24432  
 Aerodynamic forces on system of N thin slightly twisted profiles in subsonic unsteady flow for small angle of attack, examining acoustic resonance for arbitrary small harmonic oscillations 12 p1798 A66-24436  
 Supersonic gas flow past cylindrical obstacle on plate in wind tunnel at Mach number 2.5, noting separation line, pressure distribution and flow orientation 12 p1798 A66-24437  
 Hypersonic flow of inviscid gas past cone, obtaining solution for entire flow including turbulent boundary layer and velocity field, using zero approximation method 12 p1798 A66-24440  
 Gas flow regulator system conforming to prescribed time-dependent program, based on mass flow limitation properties of sonic orifices and polynomial approximation for exponential 12 p1859 A66-24713  
 Nonequilibrium effect in two-dimensional steady flow of ionizing gas past magnetized wall, calculating velocity distribution along wall 12 p1924 A66-24809  
 Evolution of plane switch-on and switch-off shocks in gas of finite electrical conductivity in presence of small normal disturbances 12 p1866 A66-24950  
 Chemical reactions in gas flows including relation between dissociation and recombination kinetics, thermal decomposition of hydrazine, kinetics of high temperature air, etc, analyzed, using shock tube 13 p2016 A66-25160  
 Rarefied gas flow problems solved by hydrodynamic equations and representations of stress tensor and heat flux reproducing Navier-Stokes continuum limit and free molecule limit, noting velocity distribution interpolation 13 p2061 A66-25163  
 Shape of plane and circular jet deformed by gas flow impinging at angle of incidence determined from head drag of jet relative to flow 13 p2062 A66-25320  
 Potential double waves at interface between two-dimensional nonsteady barotropic gas flow and region of undisturbed gas 13 p2063 A66-25633  
 Drag coefficient of gas flow in circular tube at transonic velocity 13 p2065 A66-26485  
 One-dimensional gas flow in tube with heat transfer 13 p2066 A66-26488  
 Electrical analog method used in determining potential gas flow past airfoil lattice, noting components of solution 13 p2068 A66-26541  
 Properties of laminar boundary layer undergoing surface catalysis with two reactants and two products obeying Langmuir-Hinshelwood mechanism, solving concentration field by integral equation 13 p2019 A66-26663  
 Mixed flow of two gases through coaxial cylindrical tubes separated by perforated plate 14 p2273 A66-26782  
 Shock tube study of high temperature gas flow around circular cylinders caused by electrical discharge 14 p2218 A66-27348  
 Argon flow through long tube compared with Weber theoretical model, applying classical continuum 14 p2274 A66-27444  
 Measurement of temperature profile in gas stream by moving thermocouple at constant rate in both directions across cross section of stream 14 p2294 A66-27485  
 Dynamic method of measuring gas temperature up to 2500 degrees C by short-

term exposure of thermocouple to gas stream 14 p2294 A66-27486  
 Hydrodynamic systems expressed by kinetic equations, deriving equations of aerodynamics without knowledge of interaction of gas molecules 14 p2275 A66-27569  
 Streamline flow of ideal stable gas with constant ratio of specific heats around conical body with arbitrary taper, determining flow velocity components 14 p2220 A66-27679  
 Convective heat transfer in centrifugal force field of cavity between two rotating disks in turbulent gas flow 14 p2375 A66-27692  
 Trails arising in wake of fan-type jets in transverse gas flow during uniform fuel-air mixture combustion 14 p2413 A66-27693  
 Gas-particle flow, particle velocity distributions and lag loss reduction for rocket nozzles 14 p2375 A66-27893  
 Dorodnitsyn-Belotserkovskii method for nonuniform supersonic gas flow past sphere 14 p2221 A66-28066  
 Hartmann problem solved for isothermal motion of heavy neutral viscous gas containing small impurities of light ions and electrons in crossed electric and magnetic fields 14 p2345 A66-28088  
 Arc cathodes as heat sources in low pressure gas flows, noting loss of material and other effects 14 p2346 A66-28178  
 Gas rate control of given Laval nozzle when asymptotic gas flow of unvariable type is maintained continuously near nozzle center 14 p2221 A66-28281  
 Ideal gas flow past infinite circular cone at angle of attack, noting finite-difference method for self-similar solution of Prandtl boundary layer equation 14 p2222 A66-28283  
 Points in interior and boundary of three-dimensional supersonic gas flow determined, using characteristic method, deriving difference equations 14 p2278 A66-28284  
 Laminar adiabatic gas flow in parallel plane channel taking place up to 3/4 of critical velocity 14 p2278 A66-28315  
 Stimulated interphase heat transfer in nonuniform gas flow with suspended particles and periodic motion variations 14 p2415 A66-28322  
 Scanning-electron-beam densitometer for measuring density distributions in rarefied gas flow 14 p2298 A66-28342  
 Heat and mass transfer process in reacting boundary layer of compressible gas in laminar flow along semiinfinite porous plate 14 p2416 A66-28484  
 Approximate iterative calculation of non-Newtonian supersonic gas flow past highly blunt bodies 15 p2423 A66-28959  
 Characteristic for partially invariant solutions of hydrodynamic equations, specifically adiabatic plane-parallel gas motion 15 p2478 A66-29177  
 Rotational distribution function of flowing nitrogen in low density wind tunnel using electron beam fluorescence 15 p2481 A66-29737  
 Existence of convective interaction mechanism affecting direction and stability of electric current in flowing gas, using electric arc confined in supersonic flow 15 p2481 A66-29744  
 Exact solution derived for gas jet flow with three characteristic high subsonic velocities, using Falkovich extension of Chaplygin hodographic method 15 p2425 A66-29850  
 Steady flow of highly rarefied ionized gas through channel with magnetic field solved by Monte Carlo method obtaining density, energies, wall shear stress, etc 16 p2759 A66-30371  
 Response of impact and static pressure probes in rarefied high speed gas flow 16 p2628 A66-30378  
 Chronic exposure of rats to gaseous environments of varied composition and pressure, noting exposure capsules, gas flow system, respiratory gas analyzer, etc 16 p2643 A66-30650  
 High accuracy variable area meter calibrations with multiple gases 16 p2704 A66-30672  
 Limiting conditions of temperature, gas flow rate and heat removal for combustion

of methane in atomic oxygen, calculating heat balance of process 16 p2827 A66-30  
 Heat transfer and wall friction for velocity flow of gases in downstream region of smooth electrically heated tube considering transition region [ASME PAPER 65-WA/HT-18] 16 p2828 A66-30  
 Surface protrusions and holes, Maxwell kinetic gas theory and surface interaction current of free molecules and radiation body 16 p2686 A66-31  
 Axially flowing gas through arc discharge examining effect on I-V characteristic radial temperature distribution in column 16 p2762 A66-31  
 Ionized gas flow rate behind detonation wave used with Chapman-Jouguet condition to determine speed of sound in reaction products 16 p2687 A66-31  
 Steady flow of conducting dissociating in channel of constant cross section in presence of magnetic field 16 p2687 A66-31  
 Mixed sub-and supersonic gas flow in pressure nozzle free of vortex neglecting viscosity and heat conduction 16 p2630 A66-31  
 Approximation of Chaplygin plane motion equations of gas flow at high supersonic velocities 16 p2688 A66-31  
 Self-excited vibrations of infinitely cylindrical shell, situated in flow supersonic ideal gas, obtaining motion equations and analyzing stability conditions 16 p2820 A66-31  
 General solutions of MHD equations of linear nonsteady and plane steady motion of ideally conducting gas 16 p2764 A66-31  
 Flow of compressible conducting around symmetrical wing in longitudinal magnetic field 16 p2766 A66-31  
 Thermodynamic parameters of gas behind strong shock wave in helium 16 p2690 A66-31  
 Fully ionized gas flow over wedge of finite angle for applied magnetic field aligned with incident stream 16 p2767 A66-31  
 Approximation for moment equations of kinetic theory which describe source expansion with application to free jet 17 p2907 A66-31  
 Convective heat transfer during subsonic and supersonic gas flow in inlet section of cylindrical tube 17 p3034 A66-31  
 Velocity of arc wind measured for various magnetic fields and distances above path, using temperature probe dragmeter 17 p2969 A66-31  
 Gas flow and self-diffusion in capillaries 17 p2909 A66-31  
 Capillary gas flow and self-diffusion affected by pressure ranging from free molecule to continuum regimes 17 p2910 A66-31  
 Oscillations and stability of cylindrical shell in gas flow, taking into account internal forces 17 p3029 A66-31  
 Diffusion combustion in turbulent compressible gas flow 17 p3036 A66-31  
 Effect of sudden enlargements and contractions in flow area on single pressure waves in gases in pipes, covering incident waves of various pressure amplitudes 17 p2841 A66-31  
 Diurnal variation of hydrogen concentration at base of exosphere including effects of lateral flow of gas around Earth 17 p2919 A66-31  
 Hydraulic analogy to compressible gas flow discussing application to aerodynamic motions, flow visualization, measurement techniques and instrumentation [ASME PAPER 66-FE-16] 17 p2915 A66-31  
 Theoretical and physical limitations restricting hydraulic analogy to compressible gas flow [ASME PAPER 66-FE-17] 17 p2915 A66-31  
 Accelerating particulate flow studied, using blowdown system for component velocities and friction 17 p2916 A66-31  
 Gas-phase heat-transfer augmentation in steady and alternating electric field pipeflow 17 p3039 A66-31  
 Boundary layer problem concerned with effects of radiation absorption and emission for flow of high speed gas over flat plate [AIAA PAPER 66-521] 18 p3047 A66-31



- Fastax films showing development and instability of pulsed DC arc in 30 mm Vycor tube at peak currents up to 1500 amp [AIAA PAPER 66-731] 18 p3141 A66-33667
- Friction and heat exchange effects on one-dimensional flow profile of ideal gases 18 p3098 A66-34122
- Hollow electric collector probe for measuring ion density in rapidly flowing slightly ionized gas 18 p3112 A66-34244
- Fluid flow analysis of solar wind interaction with magnetosphere 18 p3168 A66-34346
- Lagrange equation for symmetric, nonhomotropic, spherical, cylindrical and one-dimensional unsteady flow of perfectly conducting gas behind normal shock wave of variable strength 18 p3102 A66-34728
- Classical/quantum views of nonequilibrium gas flow equations with arbitrary number of relaxation times 19 p3340 A66-35738
- Numerical integration of boundary layer equations for dissociating gas flows, determining heat flow near stagnation point 19 p3341 A66-35739
- Critical jets of symmetrical perfect-gas flow determined by analogy between impedance network node equation and velocity potential and stream function in Tricomi plane 19 p3341 A66-36250
- Diffusion parameters of impurities from polycrystalline Si in hydrogen flux, noting formula for boundary conditions 19 p3321 A66-36457
- Linearized problem of oblique incidence of weightless flow of ideal gas on surface of heavy liquid, using eigenvalues and eigenfunctions of integral equation 19 p3342 A66-36470
- Numerical approximation of Riemann integration for plane gas flow at supersonic speeds 19 p3276 A66-36475
- Finite difference method approach to discontinuity in parabolic equations for shear laminar boundary layer flow of injected gas past wall 19 p3342 A66-36477
- Separation of laminar boundary layer of gas flow from cone as function of angle of attack, Mach number, etc 19 p3277 A66-36478
- Free-molecular flow of rarefied gas in plane channels or through cells of heat conducting grid whose cells are smaller than mean free path of gas 19 p3277 A66-36480
- Steady isothermal motion of viscous gas between outer fixed sphere and eccentrically located rotating inner sphere 19 p3371 A66-36481
- Optimization analysis for axisymmetric rocket motor nozzle design based on assumptions for gas particle flow [AIAA PAPER 66-538] 19 p3277 A66-36598
- Mutual effects of vaporization, combustion and coking processes during material decomposition in high temperature gas flow 19 p3479 A66-36770
- Pulse transmitter for measuring heat transfer in ionized gas 19 p3362 A66-36772
- Plane viscous problem of gas motion through weak straight line discontinuity of acceleration, noting formation of boundary layer 19 p3278 A66-36845
- Simultaneous passage of two unmixed gas flows through joint two-circuit turbojet nozzle into ambient medium 20 p3627 A66-36917
- Jet deflection in drifting subsonic gas flow 20 p3491 A66-36919
- Field of high temperatures produced by transitional and steady state processes, using electric arcs in nonrarefied gases, obtaining existence and stability criteria for arc 20 p3606 A66-36965
- Transient gas-flow process in multilayer insulation systems during evacuation predicted by equations in conjunction with measured permeabilities and diffusion coefficients 20 p3675 A66-37065
- Laminar forced convection heat transfer to gas from circular tube, achieving boundary condition of uniform heat flux 20 p3679 A66-37508
- Compressibility law corresponding to Tomotika and Tamada generalized approximation for transonic flow, noting Tomotika and Tamada gas 20 p3492 A66-37574
- Second approximation of transonic theory gas laws for thin bodies 20 p3493 A66-37988
- Vacuum technique application to space research, discussing partial pressure measurements, space simulation procedures and rarefied gas flow 20 p3544 A66-38089
- Radiative heat transfer effect on propagation of plane pressure waves in inviscid nonheat-conducting gas applied in theory of angular intensity distribution of integral radiation 20 p3548 A66-38107
- Semiinfinite flow of axisymmetric flow of viscous thermoelectric gas around blunt body with ablation shield, noting magnetic field effect 20 p3611 A66-38108
- Density of steady state gas flow expanding from viscous to molecular flow regime approximately calculated 21 p3723 A66-38507
- Inviscid hypersonic nonequilibrium flow of three-component gas past circular cone, using exact reaction-rate equations to correct solution first obtained from approximate equations 21 p3693 A66-38711
- Modified Poiseuille equation for gas flow through capillaries, applicable to flow regimes extending from molecular to viscous flow 21 p3725 A66-38943
- Erosion destruction mechanism in polycrystalline graphite, noting effect of gas flow over surfaces, flow pulsation frequency and generated aerodynamic loads 21 p3754 A66-38957
- Gas molecule excitation in shock wake analysis based on behavior of gas flow past obstacle in shock tube 21 p3726 A66-39092
- Gas flow formation ahead of flame front in circular and rectangular shock tubes analyzed, based on high speed photographs and method of characteristics 21 p3836 A66-39097
- Temperature associated with longitudinal thermal velocities overshoots for Mach numbers slightly higher than 1 for monatomic gases in rarefied gas flows 21 p3727 A66-39184
- Aerodynamic effect of free transverse gas flow on propagation of turbulent gas jet, analyzing jet mixing process and jet axis curvature 21 p3727 A66-39255
- Engineering method for measuring rapidly changing temperatures of gas flow with steady or variable heat transfer 21 p3836 A66-39413
- Conducting gas flow in Hall MHD generator reduced to quasi-one-dimensional problem 21 p3698 A66-39416
- Vector equations of steady inviscid thermally nonconducting gas flows from geometric theory of triply orthogonal spatial curves 21 p3729 A66-39446
- Close binary systems involving transfer of angular momentum, considering circulatory patterns of gaseous flow and axial rotation of component stars 21 p3815 A66-39483
- Field, mass, momentum and energy conservation, entropy and evolution conditions for steady MHD oblique shock discontinuities in perfectly conducting gas flow with Mach and Alfvén number parameters 21 p3795 A66-39577
- Gas flow equations for multilayer insulation systems for both continuum and free molecular flow regimes of interest in cryogenic space vehicle design [AICE PREPRINT 22A] 22 p3897 A66-39888
- Hypersonic gas flow past blunt body problem solved by integral correlation method, taking into account radiation effects and gas dynamic parameter distribution in shock wave layer 22 p3897 A66-39902
- Heat losses from turbulent gas flowing through poorly insulated pipe where heat lost from outer surface is by free convection and radiation, solving heat equation [ASME PAPER 65-WA/HT-16] 22 p3997 A66-40027
- Gas flow in supersonic wind tunnel measured with high speed photography, noting experimental techniques and applications 22 p3886 A66-40199
- Langmuir type probe in argon arc jet, discussing surface contamination problems, causes of high electron temperature and development of automatic cleaning technique 22 p3899 A66-40368
- Hydraulic analogy methods for simulation of internal gas flows containing combination zone 22 p3901 A66-40500
- Characteristic equation for linear flutter problem of elastic cylindrical shell immersed in gas flow, discussing energy radiation, traveling wave propagation and discontinuity problem 22 p3995 A66-40510
- Probe design for mass flux, stagnation point heat transfer and total enthalpy measurements of high temperature hypersonic gas flows [AIAA PAPER 66-750] 22 p3919 A66-40635
- Wind tunnel test program for simulation of gas-particle rocket exhaust plume, separated flow around nozzle and base recirculation [AIAA PAPER 66-767] 22 p3895 A66-40648
- Reentry aerodynamics research in Japan including sounding rocket program, optimum reentry trajectory, nonequilibrium flow in nose region of blunt body, wind tunnels, etc [ICAS PAPER 66-36] 22 p3847 A66-40659
- Adiabatic gas flow pattern in plane parallel channel near critical point 22 p3902 A66-40815
- Particle-in-cell /PIC/ method for approximate solution of propagation and reflection of plane shock waves in dusty gases 23 p4054 A66-41158
- Moment method in hypersonic flow of rarefied gas around bodies of arbitrary shape 23 p4054 A66-41357
- Supersonic gas flow problems around lattice of conical blades solved in any approximation of perturbation theory 23 p4008 A66-41358
- Supersonic unsteady gas flow around bodies at low Strouhal numbers, noting angle of attack amplitude and leading edge shock wave 23 p4009 A66-41719
- Unsteady supersonic gas flow around lattice of thinly curved plates for calculation of aerodynamic forces and moments acting on oscillating profile 23 p4009 A66-41722
- Thermal transport in channel-gas flow, discussing integral equation and power series solution 23 p4150 A66-41869
- Asymptotic solutions for viscous flow of transparent radiating gas in stagnation region, using method of matched inner and outer expansions [AIAA PAPER 66-105] 23 p4057 A66-41881
- Radiative cooling of uniform gas flow to determine reduction of heat flux incident on space vehicle surface, considering nose cap radiation during reentry 23 p4150 A66-41905
- Steady state inviscid gas flow around conical bodies solved, using stabilization method for three-dimensional supersonic flow around smooth body 23 p4013 A66-42012
- Unification of various small-epsilon theories of real gas flows based on assumption of specific-heat ratio near unity 23 p4151 A66-42050
- Magnetically driven shock tube as tool for aerodynamic studies of high velocity high enthalpy flows 24 p4190 A66-42172
- High density highly ionized nitrogen flow in plasma wind tunnel 24 p4191 A66-42192
- Electrostatic probe and VHF microwave reflectometry study of nitrogen flow around models in hotshot wind tunnels, determining plasma sheath physical characteristics 24 p4191 A66-42193
- Leak specifications for gas-filled electronic enclosures, discussing molecular, slow viscous, capillary and ordinary leak patterns 24 p4182 A66-42574
- Isentropic two-dimensional nonstationary flow of polytropic gas adjoining region with quiescent gas, constructing approximate picture of motion near arbitrary discontinuities 24 p4195 A66-42723
- Motion of continuous medium with solid or liquid particles treated by two-velocity model 24 p4195 A66-42839
- GAS-GAS INTERACTION**  
Phase behavior in helium-xenon system exhibiting gas-gas equilibria 13 p2018 A66-26444
- GAS GENERATOR**  
Oxygen regeneration in solid electrolyte cell, constructed from zirconia based ceramic material for space flights [AICE PREPRINT 20E] 17 p2848 A66-32672
- Gas generator systems, discussing applications such as auxiliary power units, servosystem power sources and pressurization devices 18 p3054 A66-34189



Sea level and high altitude ignition of fuel-rich gas generator/turbine manifold assembly 24 p4294 A66-42640

## GAS GENERATOR ENGINE

Analog design technique for pellet motors, gas-generating devices in which propellant is in form of numerous small individual grains [AIAA PAPER 65-193] 03 p0415 A66-12759

Hypersonic wind tunnel, noting hot gas generation by piston drive in gun barrel, stagnation temperatures and other operating parameters 17 p2904 A66-32895

Computer-simulated mathematical model of thermal environmental effects on expulsion system design parameters for liquid-propellant gas-generator rocket engine [AIAA PAPER 66-686] 18 p3163 A66-34228

## GAS GUN

High precision transient measurement of submicrosecond response of shock-loaded materials by instrumentation techniques and target alignment 08 p1226 A66-19694

Glass tube containing pressurized helium progressively imploded by coaxial explosive charge, considering application to hypervelocity guns 11 p1686 A66-22840

Explosive gas guns for hypervelocity acceleration 11 p1686 A66-22841

Helium gas gun for studying penetration and shock reflection from hypervelocity impact 11 p1687 A66-23263

Projectile-borne and gaseous impurity effects on spectroscopic turbulence and velocity measurements at reentry simulating range 24 p4190 A66-42184

Microwave reflectometer instrumentation for Ames light-gas guns, measuring time-distance values of projectiles during acceleration 24 p4209 A66-42185

## GAS HEATING

Gas clouds in dense star clusters compared with quasar properties, analyzing possible energy sources like supernova explosions, stellar collisions and star gas interaction 01 p0137 A66-10494

Breakdown of gases under influence of laser spark phenomena with subsequent absorption of laser radiation and gas heating 01 p0082 A66-10646

Applicability of Pascal law in nonuniformly heated gases verified by measuring pressure anisotropy vs temperature gradient in gas sample 03 p0393 A66-13187

Light pulse absorption in gas and measurement of temperatures attained noting hydrodynamic, breakdown and radiative transfer mechanisms and wave velocities 08 p1319 A66-19276

Time duration and length of compressed region and heated gas behind shock wave front determined by thermal probe 11 p1682 A66-22593

Internal resistance shock tube driver gas heating system to heat helium driver gas to 1000 degrees F at 15,000 psia 11 p1685 A66-22836

MHD power generation by pulsating preheated gas with shock waves, noting thermodynamic cycle composition, efficiency and parameters 13 p2001 A66-26258

Breakdown of gases under influence of laser spark phenomena with subsequent absorption of laser radiation and gas heating 17 p2933 A66-32061

Electropneumatic transducer using principle that heating moving gas increases velocity 19 p3362 A66-36811

Spectral characteristics of gases heated by shock waves, noting absorption capacity distribution as function of wavelength 21 p3726 A66-39078

Pressure distribution in slug of shock wave excited in electrical discharge shock tube 24 p4242 A66-42405

Gas heating in wall stabilized electric arcs with axial flow applied to nitrogen arc, obtaining highest enthalpy flux and efficiency 24 p4295 A66-43060

## GAS INJECTION

Dynamic measurements of speed of pumping by activated charcoal cooled to liquid nitrogen temperatures to evaluate cryosorption 02 p0261 A66-11591

Vortex effect in rotating flow of compressed gas injected into vortex tube, noting role of turbulent heat transfer 03 p0354 A66-12390

Qualitative and quantitative solution of

linearized approximations to boundary layer equations, noting free jet and wall-slot injection into moving stream [ASME PAPER 65-APMW-6]

Motion, temperature distribution, concentration and change in electric conductivity of ionized gas in initial section of plane channel 04 p0512 A66-14212

Heat exchange, friction and mass exchange in laminar multicomponent boundary layer during injection of extraneous gases 04 p0557 A66-14432

Qualitative and quantitative solution of linearized approximations to boundary layer equations, noting free jet and wall-slot injection into moving stream [ASME PAPER 65-APMW-6]

Heat exchange, friction and mass exchange in laminar multicomponent boundary layer during injection of extraneous gases 10 p1523 A66-21470

Pressure distribution and air injection effects in transitional separated flow over spiked hemisphere at supersonic speed 11 p1688 A66-22591

Heat transfer and mass transfer near stagnation point during injection and suction of various gases through blunt body surface 11 p1635 A66-23004

Vortex effect in rotating flow of compressed gas injected into vortex tube, noting role of turbulent heat transfer 12 p1979 A66-24427

Thermal insulation of surfaces by cold gas injection into laminar compressible boundary layer of air in chemical equilibrium 13 p1993 A66-26730

Tests on rocket thrust vector control using hot injectant gas from same fuel and oxidizer as main engine, tabulating data 16 p2810 A66-30902

Effect of injected plasma on curvilinear magnetic field, noting polarization effect 17 p2962 A66-31825

Plasma injection into programmed magnetic field 17 p2963 A66-31828

Turbulent heat transfer measurements on transpiring flat plate in Mach 8 tunnel using nitrogen, helium and argon as injection gases 17 p2838 A66-32439

Turbulent boundary layer in gas flow past curvilinear permeable surface with gas injection into flow kernel 19 p3342 A66-36464

Plasma generating gun using coaxial electrodes, gas injection and preionization device for regulation with plasma purification by injection into magnetic field with double curvature 19 p3427 A66-36572

Protective cooling of insulated plane surface by multislot and network type gas injection into turbulent boundary layer of incident flow 20 p3681 A66-38123

Viscous drag on flat plate in supersonic flow injected with gas in boundary layer, examining exit cone of rocket nozzle 22 p3970 A66-39875

Time lag effect on dynamic stability determined, using wind tunnel tests with 10 degree cone as test body simulating ablation process by gas injection into boundary layer [AIAA PAPER 66-757] 23 p4008 A66-41330

Dispersion equation for cyclotron electromagnetic waves for magnetoactive plasma injected with charged particles 24 p4245 A66-43016

## GAS-ION INTERACTION

Average energy loss per ion pair of low energy nitrogen and oxygen ions in nitrogen, argon and helium 01 p0107 A66-11096

Neutral atomic beam used to measure total ionization cross section of argon atoms incident on low density argon gas 07 p1083 A66-18421

## GAS JET

Measuring thermal fluxes in solid bodies by high temperature gas jets, noting Kastelin-Bronskiy method 04 p0596 A66-13653

Radial distribution of electrical conductivity in ionized gas jet based on value measured by induction method and known temperature distribution 06 p0919 A66-16880

Axial deviation of gas flow resulting from mixing turbulent gas jets 07 p1019 A66-17395

Rotating satellite stability assuming inertia

axis is oriented toward Sun, noting dependency on jets of cold gas and nozzle calibration 09 p1401 A66-200

Axisymmetric liquid nitrogen turbulent propagating under supercritical pressure gaseous nitrogen medium 12 p1864 A66-24

Stabilization of lifted diffusion flame turbulent methane jet flow field measurements of gas flow velocity turbulence and gas composition 15 p2479 A66-290

Problems of various subsonic gas jets finite width around dihedral obstacle solved with Chaplygin hodographic method 16 p2627 A66-30

Expansion of axisymmetrical heated gas in homogeneous slipstream experiments, studied and compared with equivalent problem in theory of heat conduction 19 p3342 A66-36

Spray ejector operating in pulse rather than steady state regime, noting capabilities and formation of de Laval nozzle 19 p3450 A66-36

Mass transfer and hydrodynamics of gas injection into liquid surface, deriving empirical equations for hollow truncated point formed around injection point 21 p3336 A66-38

Laminar gas jet mixing as affected by periodic vorticity produced by mechanical vibration of orifice 23 p4055 A66-41

Line-of-sight velocities in gas in peculiar extragalactic radio source NGC 4038 measured in orientations across object 23 p4129 A66-41

Acceleration of gas during compression conditions of acute angled geometry, using collapsing chamber rather than shay charge 24 p4196 A66-42

## GAS LASER

Peak power transients of near confocal helium-neon laser working at 6328 angstrom on pulsed discharge basis 01 p0080 A66-10

Coherence properties of helium-neon laser with superimposed modes examined interference pattern 01 p0081 A66-10

Self-locked gas laser mode dependence cavity length and position of laser medium in cavity 01 p0081 A66-10

Electron beam pumping of noble gas laser 01 p0081 A66-10

Laser action at 5401 angstroms in neon pulsed high voltage discharge 01 p0081 A66-10

Laser with diffraction limited radiation pattern 01 p0082 A66-10

Current and voltage distribution on length of HF discharge in helium-neon laser 01 p0082 A66-10

Phase relations of longitudinal modes of gas laser with annular resonator 01 p0082 A66-10

Aluminum cold cathodes with single 6328 angstrom helium-neon gas laser lifetimes exceeding 3000 hours 01 p0043 A66-10

Gas laser interferometers for plasma electron density measurement 01 p0069 A66-10

Plasma ring discharge excitation used drive high current density electrodeless for exciting gas ion laser transitions 01 p0083 A66-10

UV and visible laser oscillations fluorine, phosphorus and chlorine atoms pulsed chlorine, phosphorus fluoride and sulfur fluoride gas discharges 01 p0083 A66-10

Ruby crystal optical properties investigated by interference rings from reflecting He laser beam from crystal face 01 p0083 A66-10

Metallic plasma tube for ion lasers allowed them to run at higher current densities than with ceramic tubes 02 p0239 A66-11

Pressure dependence of output of helium-neon gaseous laser in high pressure range 02 p0239 A66-11

Laser with hollow cathode discharge neon-hydrogen mixture and cavity formed by cylindrical mirrors 02 p0239 A66-11

Helium-neon laser output dependence hollow cathode discharge conditions electron transitions in neon 02 p0239 A66-11

Laser transition in vibrational state ground electronic state of CN from



rotational level 8 to 7 with population inversion as result 02 p0240 A66-11451  
Helium-neon laser amplifier as function of mixture ratio, gas pressure, input signal level and electrical power input to amplifier tube 02 p0242 A66-12206  
Width of decay quanta in gas lasers depends on energies and lifetimes of atomic levels involved in stimulated transitions and nonlinear response of 03 p0376 A66-12303  
Gain and bandwidth narrowing in regenerative helium-xenon laser amplifier 03 p0376 A66-12308  
Current discharge of helium neon laser on laser action 03 p0376 A66-12439  
Laser with diffraction limited radiation pattern 03 p0380 A66-13313  
Multireflector Fabry-Perot laser resonators, discussing suppression effect against unwanted modes 03 p0380 A66-13325  
Periodic variation of quality factor of He-Ne gas laser cavity by vibrating quartz-modulation of light beam 04 p0529 A66-13477  
Excitation and inversion method in gas lasers noting characteristics of helium-neon laser and ionized and three-level laser system 04 p0530 A66-13951  
Experiments on helium-neon FM lasers covering phase-locked and FM region power output, modulation index and distortion experiments 04 p0530 A66-13955  
High power Brewster window laser with gas fills, discussing power output and efficiency parameters 04 p0531 A66-13983  
CW gas laser, measuring vibrational rotational translation frequencies of carbon monoxide 04 p0531 A66-13984  
Static characteristics of gas laser internal modulation circuit, using electro-optical crystal inserted into gas laser resonator 04 p0531 A66-14059  
Rise time and output power of single pulse in He-Ne laser measured by method of changing Q-factor by plate located in resonant cavity 04 p0533 A66-14332  
Small particle detection capability of low-gain helium-neon gas laser enhanced by use of Stokes settling law and layered sedimentation technique 05 p0692 A66-14583  
Helium-neon laser output characteristics as function of laser parameters 05 p0694 A66-14897  
Traveling wave oscillations of ion ring laser in mirror-ring resonator 05 p0694 A66-14903  
Two lenses with focal ratios of  $f/4$  and  $f/2.65$  used to collimate light from helium-neon laser 05 p0695 A66-14921  
Microwave beats identified between modes in bromine-argon mixture 05 p0695 A66-14923  
Electrodeless excitation of discharge in helium-neon gas laser tube applied to voice transmission 05 p0696 A66-14924  
CW laser oscillation between 11.48 and 11.55 microns from nitrogen-carbon disulfide system 06 p0890 A66-16384  
Wavelength of  $3s2-2p4$  transition of neon measured, using helium-neon laser 06 p0890 A66-16387  
Helium-neon gas lasers, discussing amplitude variation suppression technique 06 p0892 A66-16670  
CW high-power carbon dioxide-nitrogen-helium laser operation, noting helium addition 06 p0892 A66-16754  
Gas laser output and threshold in population inversion from photodissociation of methyl iodide and fluoro iodo methylidyne 06 p0892 A66-16771  
Advantages of gas lasers as light sources in aerodynamic research 06 p0893 A66-16944  
Interferometers 06 p0893 A66-16944  
Interference phenomenon of serrated system of rings surrounding central beam of gas laser analyzed, using helium neon tube placed between two exterior mirrors 06 p0893 A66-17064  
Intensity of polarized light transmitted through laser amplifier and linear polarizer, as function of axial magnetic field strength 07 p1041 A66-17292  
Intensity distribution of fringe systems used to verify phase inversion between two lobes of laser in TEM-10 mode 07 p1043 A66-17453  
Electron energy spectra in neon, xenon and helium-neon laser discharges, calculating

production and destruction rate parameters 07 p1045 A66-18354  
Gas laser direct modulation 07 p1045 A66-18355  
Frequency stabilization of gas lasers, using atomic resonance and interferometers 07 p1045 A66-18357  
Beat frequencies and coherence properties in circularly polarized atomic transitions of gaseous lasers with axial magnetic fields 07 p1046 A66-18429  
Beat frequency and rotation of polarization plane in He-Ne laser with axial magnetic field 07 p1046 A66-18430  
Anode-current spectrum of photomultiplier illuminated by light of time-varying intensity and derivation of moments of photoelectron counts 07 p1047 A66-18432  
Helium-neon gas discharge intensification for 6328A laser wavelength, discussing measurement techniques, gain parameters and results 08 p1232 A66-18632  
Laser development, discussing basic theory, pumping methods and laser types 08 p1233 A66-18700  
Higher order calculation of laser output, noting approximation method for linewidth parameter and Lamb dip shape accuracy 08 p1233 A66-19063  
Helium-neon gas laser used in Raman spectroscopy 08 p1233 A66-19232  
Gas laser emission solution by determining emission field density dependence on resonator parameters, relaxation characteristics and atom excitation in gas discharge plasma 08 p1234 A66-19271  
Nonlinear Zeeman effect for gas laser 08 p1234 A66-19638  
Micromachining with pulsed helium-neon gas laser, noting experimental techniques, operation and application 08 p1232 A66-19734  
Isolation of 1.0621 line in He-Ne gas laser by multilayer dielectric-coated mirrors with sharp spectral cut-off characteristics 09 p1386 A66-20517  
Gas laser end reflector using Pellin-Broca prism for spectral line selection 09 p1386 A66-20518  
Isotope shift measurement for 6328 angstroms helium-neon laser transition 10 p1540 A66-21070  
Optical second harmonic generation in focus of lowest transverse mode of continuous wave Gaussian gas laser beam 10 p1541 A66-21175  
Simultaneous action of RF perturbation between Zeeman sublevels of atomic transition which is also producing laser oscillation 10 p1541 A66-21177  
Laser induced gas breakdown at high pressures, noting effect of plasma density on index of refraction via optical frequency resonance measurement 10 p1542 A66-21564  
CW laser action on triple state phosphorus-sulfur transition, using hydrogen sulfide-noble gas mixtures 10 p1543 A66-21577  
Microwave antenna simulation at optical frequency, using neon-helium continuous gas laser 11 p1662 A66-22539  
Absolute wavelength stability of helium-neon laser measured by direct interferometric comparison with Hg 198 standard lamp 11 p1712 A66-22868  
Wavelength measurement of helium-neon laser emission by double-channel recording interferometer, using krypton-86 primary standard 11 p1712 A66-22874  
Design and operation of helium-neon laser noting radiation, frequency structure, power density, external magnetic field effect, application, etc 11 p1713 A66-22980  
Mode suppression techniques for gas laser single axial mode operation for large mirror separations 11 p1713 A66-23093  
Ruby crystal optical properties investigated by interference rings from reflecting He-Ne laser beam from crystal face 11 p1714 A66-23292  
Current and voltage distribution over length of HF discharge in helium-neon laser 11 p1714 A66-23309  
Q-switching of carbon dioxide and nitrous oxide gas laser transitions 11 p1714 A66-23354  
Vibrational and rotational relaxations in carbon dioxide and nitrous oxide laser systems, using Q-switching techniques 11 p1714 A66-23355

Laser action on rotational line in carbon dioxide and nitrous oxide vibrational spectra in both P and R branches up to J values of over 50 11 p1714 A66-23357  
Continuous wave measurement of optical nonlinearity of ammonium dihydrogen phosphate, using helium-neon laser 12 p1912 A66-23716  
Polish-made He-Ne red gas lasers, describing power outputs, gas pressure, He/Ne ratio, mirror transmission coefficient and interferometric application 12 p1889 A66-23946  
Balanced mixer action for optical heterodyning, using Magic-T optical mixer 12 p1890 A66-24153  
Longitudinal magnetic field effect upon gas discharge, Zeeman effect and Faraday effect in He-Ne gas laser 12 p1890 A66-24224  
Two-level atom interaction with multimode gas laser cavity, obtaining stationary state and solving unique eigenvalue in special cases 12 p1891 A66-24568  
Dependence of emission intensity of gas laser on longitudinal and transverse magnetic fields, using simplified model 12 p1891 A66-24885  
Optical resonator diffraction loss, noting laser oscillations in high loss arrangements, output beam power, field patterns, etc 13 p2090 A66-25195  
Nonlinear dielectric laser light absorption by neutral gas resulting in avalanche breakdown of gas due to thermal ionization 13 p2090 A66-25425  
Metal wall ionized argon lasers, discussing use of water-cooled quartz discharge channels, CW lasers, development of satisfactory metal, etc 13 p2091 A66-25555  
Output power of 6328 angstrom He-Ne gas laser as function of laser gain, cavity loss and output coupling 13 p2091 A66-25651  
Alignment of laser mirrors using gas laser with highly collimated beam of small diameter 13 p2092 A66-25824  
Solar noise in optical communications, background radiation dependence on detector aperture, noise power and application to GaAs diodes and gas lasers 13 p2024 A66-25833  
Helium-neon laser multibeam generation in gas discharge tube, using spherical mirrors and tapered plates 13 p2093 A66-26053  
He-Ne laser homodyne spectrometer observation of broadening of spectral profile of light scattered from carbon dioxide near critical temperature and density due to density fluctuations 13 p2133 A66-26168  
Far-IR laser molecular spectroscopy including IR laser oscillators, photon noise, detectors and nuclear optics 13 p2100 A66-26195  
Optical and IR-maser spectroscopy of inhomogeneously broadened resonances, using gas lasers 13 p2100 A66-26196  
Organic gas magnetically tuned laser spectroscopy, discussing resolution, absorption spectra and vibrational deactivation 13 p2100 A66-26197  
Helium-neon gas laser used to study pressure effect on line shape of  $2s-2p$  optical transitions of neon excited states 13 p2100 A66-26198  
Pressure effects in Fabry-Perot lossy-cavity gas laser output 13 p2101 A66-26199  
Dependence of Zeeman beat frequency on interferometer tuning in single-mode He-Ne laser with various gas pressures and magnetic field strengths 13 p2101 A66-26201  
Laser action on vibrational-rotational transitions and vibration energy transfer 13 p2101 A66-26204  
Electron impact excitation mechanism of argon-ion continuous and long pulse lasers 13 p2102 A66-26206  
Transition probabilities and lifetimes in ionized argon gas lasers 13 p2102 A66-26207  
High resolution piezoelectrically scanned Fabry-Perot interferometer used to study gain profiles, mode structures and emission line widths of CW Ar, Kr and Xe ion lasers and Hg-He pulsed laser 13 p2102 A66-26208  
Photoelectron counts of photomultiplier illuminated by gas laser light source 13 p2102 A66-26211  
Models of matter-electromagnetic field interaction for gas lasers, using perturbation theory 13 p2103 A66-26216



Helium-neon gas laser used to determine electron density variation, spatial and temporal, in afterglow of Z-pinch in H at 100 torr 13 p2104 A66-26239

Magnitude and phase of complex spatial coherence of He-Ne laser 13 p2104 A66-26334

Helium-neon laser emission on 6401 angstrom line, noting intensity vs mirror shift and optical cavity 13 p2104 A66-26336

instability 13 p2104 A66-26336

Raman diffusion spectra from crystals excited by gas laser 13 p2104 A66-26345

Alignment of angular positions of spherical mirror and grating of Fastie-Ebert spectrometer, using bright collimated monochromatic beam of He-Ne laser 13 p2084 A66-26564

Maximum output power approximated for 6328 angstrom He-Ne gas laser, noting optimum mirror transmission and laser geometry 13 p2105 A66-26571

Cataphoresis, moving striations and associated noise in He-Ne laser 13 p2105 A66-26591

Dust particles in laser cavity observed for angular stabilization and constant velocities 13 p2105 A66-26594

IR and visible helium-neon laser modulation using Faraday rotation in YIG 14 p2305 A66-26881

Vibrational-rotational line strengths and widths in carbon dioxide, using carbon dioxide-neon laser 14 p2306 A66-27030

Current changes in gas discharge as affected by lasing action 14 p2306 A66-27055

Effective lifetime of excited state of gas laser, with account of near photon transfer 14 p2306 A66-27135

Effect of longitudinal magnetic field on output power of gas laser operating in IR spectrum, noting gas-mixture pressure in discharge tube role 14 p2307 A66-27156

LF fluctuations in emission of He-Ne gas laser measured, using Fabry-Perot resonator and ring-type resonator 14 p2307 A66-27186

Lateral shearing interferometer with gas-laser light source for testing large optical systems 14 p2307 A66-27320

Helium-neon laser afterglow and metastable helium atoms under long pulse excitation 14 p2307 A66-27335

Laser oscillator study of coherent stimulated emission of IR transitions in rare gases 14 p2308 A66-27336

Oscillation types for gas-laser semiconcentric resonator 14 p2310 A66-28160

Precision automatic tracking using CW He-Ne laser, noting performance and application 14 p2245 A66-28448

Optical beam deflection technique using interferometer cavity illuminated by gas laser beam 15 p2512 A66-28689

Optical beam scattering of gas laser for measurement of photoelastic constants and application to lithium niobate 15 p2512 A66-28692

Temperatures, Lorentzian widths and drift velocities of excited neutral and ionic species in argon-ion laser, noting thermal equilibrium achievement 15 p2512 A66-28695

Gas laser output wavelength stabilization by use of external passive optical interferometer 15 p2513 A66-28835

Pulsed toroidal excitation of gas ion lasers extended to drive high power CW laser transitions in Ar, Kr, Cl and Br, noting operating parameters and power output 15 p2513 A66-28877

Mark I SMASER design, submillimeter wave gas laser capable of continuous wave or pulse operation 15 p2514 A66-29009

118-micron wavelength water vapor gas laser with 4-inch diameter two-meter focal length mirror resonator 15 p2514 A66-29010

Experimental evidence of inverse bremsstrahlung and electron-impact ionization in low pressure argon ionized by giant pulse laser 15 p2544 A66-29115

Dipole moment calculation for gas laser in magnetic field 15 p2516 A66-29348

Relation between laser parameters and cathode diameter in excitation of He-Ne mixture by discharge of hollow cylinder 15 p2516 A66-29357

Pulsed nitrogen laser action in wind tunnel-simulated supersonic

flow 15 p2516 A66-29384

Hysteresis phenomena in He-Ne gas laser in axial magnetic field and polarization of oscillating mode within certain tuning region 15 p2516 A66-29385

Frequency stability and spectral purity of p-n junction laser output improved by synchronization with gas laser beam 15 p2518 A66-29717

Output power frequency response of single mode helium neon laser, determining effects of atomic collisions on frequency response of individual atoms 15 p2518 A66-29812

Transverse and axial magnetic field effects on gas lasers, deriving expression for atomic and macroscopic polarization, determining oscillation mode characteristics, frequency responses, etc 15 p2518 A66-29813

Isotope shifts and Fermi resonance role in carbon dioxide IR laser 16 p2716 A66-30176

Actual line shape expected from accelerating radiating ion, errors due to Lorentzian approximation and results for ion laser transition in rare gas lasers 16 p2716 A66-30181

Optical harmonic generation in IR in zinc blende, hexagonal and trigonal crystals, using unfocused carbon dioxide laser in CW and Q-switched operation 16 p2716 A66-30182

Unmodulated laser output at controlled frequency, using correcting beats from reference laser 16 p2717 A66-30205

Demodulation method in which phase modulation of laser beam is converted to amplitude modulation by autocorrelation 16 p2717 A66-30616

Near-Bose-Einstein probability distribution of photoelectron counts produced by He-Ne gas laser narrow band Gaussian light source operating slightly below oscillation threshold 16 p2717 A66-30645

Semiclassical theory of quantum generators, examining laser system response to effect of monochromatic standing wave based on kinetic equation for density matrix 16 p2718 A66-30865

Collision broadened linewidth and saturation parameters for 6328 angstrom transition of Ne in He-Ne laser 16 p2718 A66-31084

Mode locking in gaseous laser whose cavity is length modulated at mode separation frequency 16 p2719 A66-31095

Small signal modulation effect on photoelectron counting of He-Ne laser intensity fluctuations 16 p2719 A66-31097

Large screen real time projection display technique using Ne-He gas laser 16 p2708 A66-31412

Particle velocity in gas particle two-phase nozzle expansion using gas laser and Fabry-Perot interferometer for rocket engine propulsion [AIAA PAPER 66-522] 16 p2708 A66-31500

Helium-neon laser modulation by positive and negative voltage pulses 16 p2720 A66-31559

Gas lasers for interferometric measurements of lengths, noting methods that stabilize wavelengths of lasers 16 p2720 A66-31697

Near-field diffraction of helium-neon laser at circular apertures 16 p2720 A66-31727

Multiphoton plasma production and stimulated recombination radiation in lead telluride, considering electron-hole pair production rate 17 p2975 A66-31884

Cyclotron resonance excitation of upper level of gas-ion laser 17 p2933 A66-31937

Static characteristics of gas laser internal modulation circuit, using electro-optical crystal inserted into gas laser resonator 17 p2933 A66-32225

Gas laser emission in weak longitudinal magnetic field assuming Zeeman splitting is much smaller than Doppler linewidth 17 p2934 A66-32319

Laser and maser development, discussing design improvements and application for television, space communications, etc 17 p2934 A66-32353

Fluctuations in mean refractive index over long path through turbulent atmosphere examined, using Michelson interferometer with He-Ne laser source 17 p2948 A66-32618

Internal phase modulation in He-Ne laser using electro-optic effect in crystal quartz, observing spectrum and RF mode

beats 17 p2934 A66-32618

Coherent gas laser light to microscopy requirements of streak photography time-resolved flow 17 p2935 A66-32619

visualization 17 p2935 A66-32619

Power enhancement in pulsed He-lasers, noting overshooting for RF discharge modulation with square wave 17 p2935 A66-32619

Carbon dioxide laser principle of performance 17 p2936 A66-32620

High-power molecular laser based vibrational-rotational energy level, not carbon dioxide-neon-helium laser design 17 p2936 A66-32620

Ion lasers involving electron transitions, atoms or molecules with lost electrons 17 p2937 A66-32621

Frequency stabilization of gas laser servomechanism and Lamb dip method 17 p2937 A66-32621

Michelson interferometer used to study modes of red He-Ne laser 17 p2937 A66-32621

Measuring amplification of coherent optical radiation in neon-helium filled tube 17 p2938 A66-32622

Competition of transitions and emission, He-Ne laser, using resonator with dispersing prism 17 p2938 A66-32622

Laser radar ranging system using pseudorandom code modulation, considering application to pulse and digital circuit, statistical communication theory and electrical engineering 18 p3117 A66-33017

First- and second-order sidebands due to strong CW signal intermodulation effects, 3.39 mu He-Ne laser 18 p3117 A66-33017

Vibrational excitation, population inversion and coupling out of carbon dioxide-nitrogen water vapor laser 18 p3118 A66-33018

Ionized noble gas lasers, considering problems at higher powers, especially those of inversion mechanism and magnetic field effects 18 p3118 A66-33018

Ultrasonic cell which modulates intensity of He-Ne laser beam for communication, intelligence 18 p3118 A66-33018

Nonlinear Zeeman effect for gas laser 18 p3119 A66-33019

Traveling waves interaction in gas laser, explaining forcing-of-oscillations and traveling wave suppression effect 18 p3119 A66-33019

Decay cross section of pumped metastable He atoms in He-Ne laser 18 p3119 A66-33019

Ne-He laser output dependence on pressure and nonexcited atom concentration 18 p3119 A66-33019

Radiation from high-energy-level transitions excited in He-Ne laser during optical pumping with He lamp 18 p3120 A66-33020

High temperature flow characteristics of free piston shock tube measured by means of pulsed light of He-Ne gas laser 19 p3339 A66-33539

Helium-neon laser assessment as source of high precision range measurements 19 p3372 A66-33632

Gas laser output and threshold population inversion from photodissociation of methyl iodide and fluoriodoacetylene 19 p3372 A66-33632

Gas laser used to determine residue wedge angle in optical flats and display of relief maps 19 p3373 A66-33633

CW He-Ne laser measurement of light scattering in crystals noting laser output performance and crystal imperfections 19 p3373 A66-33633

Atomic time standards, describing cesium beam standard, ammonia maser and gas type clocks 19 p3354 A66-33634

Spatial coherence measurement of He laser output 19 p3373 A66-33633

Gas laser with generalized polarization characteristics, noting role of degenerate atomic energy levels 19 p3374 A66-33634

Pulsed discharges of OCS molecular laser 19 p3375 A66-33635

Dipole moment calculation for gas laser magnetic field 20 p3576 A66-33636

Relation between laser parameters and cathode diameter in excitation of He mixture by discharge of hollow cylinder 20 p3576 A66-33636

Nonreciprocal effects associated with excitation current observed in DC-excited He-Ne ring laser, noting coupling



- phenomena between right and left waves 20 p3577 A66-37408
- Magnitude of Hanle effect of neon atoms emitted by laser dependence on excitation discharge intensity explained by multiple coherent diffusion at metastable level 20 p3577 A66-37409
- Continuous wave gas laser as light source in scattered light static photoelasticity 20 p3577 A66-37443
- Spherical coupler for fastening mirrors and plane-parallel plates at Brewster angle in gas laser 20 p3578 A66-37523
- Identification of number of lines at 11 microns emitted from pulsed carbon dioxide laser as P branch of carbon dioxide vibrational transition 20 p3579 A66-37629
- Phase relations of longitudinal modes in gas laser with annular resonator 20 p3579 A66-37663
- Upper laser states deriving population through cascade transitions from higher laser states of argon ion noting consistency of laser output current dependence with current dependence of cascade rate 20 p3579 A66-37774
- Coupling between oppositely directed traveling waves in He-Ne ring laser in form of mutual backscattering of energy from each beam into direction of other 20 p3579 A66-37778
- Degradation of continuous argon laser performance when positioned in axial magnetic field, noting role of quenching, radiation trapping and excitation mechanisms 20 p3579 A66-37779
- Discharge current and laser light noise measurements effect in gas discharge helium-neon laser, using equivalent circuit 20 p3580 A66-38240
- Frequency stabilization of gas laser to lock output to center of atomic resonance, using error signal 20 p3580 A66-38241
- Pulsed nitrogen laser delivering high average power without complications of conventional Q-switching 20 p3581 A66-38266
- Spontaneous emission noise power added to amplified signal in laser amplifier in He-Xe gas discharge and saturation relation to population inversion 20 p3581 A66-38387
- Laser machining, discussing hole drilling, microwelding metal removal and application to hard brittle materials [ASME PAPER 66-MD-28] 21 p3742 A66-38484
- Second-harmonic generation by focused laser beams based on experiments using He-Ne gas laser, noting SHG should be strongly peaked when focus is at either of crystal surfaces 21 p3746 A66-38554
- General nonequilibrium system in contact with reservoir described via correlation functions of quantized field operators, noting influence of cavity and optical pump 21 p3746 A66-38633
- Hyperfine spectrum of xenon in 3.5 mm maser transition noting experimental setup, gain profiles for various input power levels and structural properties 21 p3746 A66-38763
- Self-induced divergence of continuous wave He-Ne laser beams when traversing transparent liquid, noting nonlinear effect in propagation of light 21 p3748 A66-39164
- Wave synchronization in gas laser with ring resonator cavity 21 p3748 A66-39301
- Atomic collisions, excitation transfer processes and energy level transition probabilities in plasma of gas lasers 21 p3748 A66-39305
- Gas laser frequency and emitted power dependence on resonator tuning 21 p3748 A66-39308
- Gas laser alignment, obtaining oscillation on three lines of He-Ne laser 22 p3930 A66-39718
- Atomic degeneracy influence on mode interactions in gas laser 22 p3931 A66-39930
- Light reflection from shock waves clarified through propagation in shock tubes, using gas laser 22 p3898 A66-40012
- Pulsed coaxial transmission line nitrogen gas laser, noting pressure effect 22 p3932 A66-40107
- Intracavity interferometer laser measurements of power gain and output in single-frequency Ar laser and 6328-angstrom Ne isotope shift 22 p3932 A66-40110
- Longitudinal magnetic field effect upon gas discharge, Zeeman effect and Faraday effect in He-Ne gas laser 22 p3933 A66-40586
- Dependence of emission intensity of gas laser on longitudinal and transverse magnetic fields, using simplified model 23 p4076 A66-41092
- Plasma fluctuation effect on gas laser noise, noting relation between modulation amplitude of light output and frequency noise and oscillation spectrum 23 p4077 A66-41294
- Electron and neutral atom densities in helium and argon afterglow plasma obtained by two helium-neon laser interferometers, noting temporal dependence of electron decay 23 p4101 A66-41364
- Performance characteristics for pulse type Ar laser with external interferential system of quasi-confocal spherical mirrors 23 p4078 A66-41452
- Radiative power amplification of He-Ne laser with nearly confocal resonators 23 p4078 A66-41453
- Competition, hysteresis and reactive Q-switching in carbon dioxide lasers at 10.6 microns, using moving mirror technique 23 p4079 A66-41631
- Resonator misalignment effect on output of neon-helium laser with spherical mirrors 23 p4079 A66-41830
- Measuring amplification of coherent optical radiation in neon-helium filled tube 24 p4219 A66-42125
- Competition of transitions and emission in He-Ne laser, using resonator without dispersing prism 24 p4219 A66-42127
- Zeeman laser interferometer, using axial magnetic field to obtain simultaneous left- and right-hand circularly polarized oscillation modes at upper and lower cavity resonances 24 p4219 A66-42248
- Conductivity modulation by heavy-to-light hole transitions in p-type germanium noting carrier lifetime and ringing of laser pulse 24 p4219 A66-42249
- 10.6 micron output of carbon dioxide-He laser modulated, using Bragg diffraction from longitudinal acoustic waves in Te 24 p4219 A66-42251
- Book on lasers covering optical cavities, gas lasers, solid state lasers, optical pumping, Q-switching, population inversion, etc 24 p4220 A66-42319
- Saturation induced optical nonreciprocity in He-Ne ring laser plasma, eliminating frequency locking by using Faraday effect 24 p4221 A66-42552
- Laser Doppler velocimeter for gas and liquid flow velocity measurement 24 p4211 A66-42557
- Scattering matrix analysis of single frequency Michelson type He-Ne gas laser, including frequency and amplitude stability analysis of oscillation spectrum 24 p4223 A66-42566
- Gas-discharge CW lasers, particularly He-Ne, carbon dioxide, argon-ion and pulsed self-terminating lasers, discussing classification, power output and gain, Doppler width, coherence and noise 24 p4224 A66-42801
- Pressure- and gain-dependent frequency shift measurements in stabilized 6328 angstrom He-Ne laser 24 p4224 A66-42803
- Optical heterodyne receiver antenna properties, noting effective aperture of capture cross section vs directional tolerance and detection of doppler shifts in liquid scattered coherent light 24 p4174 A66-42809
- Effect of longitudinal magnetic field on output power of gas laser operating in IR spectrum, noting gas-mixture pressure in discharge tube 24 p4225 A66-42977
- Laser oscillation effect on characteristics of electron gas of helium-neon laser plasma studied in terms of wave attenuation in plasmaguide 24 p4225 A66-43006
- Beating of oscillating frequencies corresponding to two directions of travel of annular cavity laser with active gas medium in movement 24 p4225 A66-43007
- LF fluctuations in emission of He-Ne gas laser measured, using Fabry-Perot resonator and ring-type resonator 24 p4226 A66-43084
- GAS-LIQUID INTERACTION**
- Discrete gas-into-liquid flow process, compensating absence of mass forces and unfavorable load directions with motion of liquid 02 p0218 A66-11657
- Equilibrium flow of ideal gas and condensing vapor mixture from nozzle, using basic equations to describe process 12 p1863 A66-24368
- Motion of gas bubble in weightless viscous fluid with temperature gradient 14 p2273 A66-26786
- Localization of gas-liquid interface by capillary effects, noting error in adverse acceleration equation 16 p2685 A66-30917
- Mass transfer in gas-liquid dispersions, noting effect of flow rate, bubble size, etc 18 p3266 A66-34736
- High speed photographic investigation of propagation and disintegration of interaction of two-phase gas-liquid flow in venturi scrubber 18 p3114 A66-35059
- Thermodynamic properties and solubilities of He molecular nitrogen, molecular oxygen, Ar and nitrogen trioxide in liquid nitrogen tetroxide 19 p3449 A66-36368
- GAS LUBRICANT**
- Ball bearing lubrication with vapor from volatile organic compounds for wide temperature range and long term operation [ASLE PREPRINT 65-LC-24] 02 p0237 A66-12248
- Gas-lubricated bearing equations derived that are valid for wide range of temperature and Mach numbers 04 p0526 A66-14156
- Continuous fluid film self-acting cylindrical journal bearing theory and design data, introducing isothermal bulk modulus into lubrication equations [ASLE PREPRINT 65AM 3A2] 07 p1039 A66-18285
- Externally pressurized nonrotating porous wall air lubricated journal bearing properties, taking into account surface roughness effects [ASLE PREPRINT 65AM 3A5] 07 p1039 A66-18286
- Lift in spherical ball bearings with air lubrication calculated, taking into account inertial term in general equations of aerodynamics, gap variability and air compressibility 08 p1232 A66-19693
- Modern gas bearings of self-acting and externally pressurized types in turbomachinery 09 p1384 A66-20297
- Pressure distribution of gas-lubricated spiral-groove thrust bearing or compressor [ASME PAPER 66-LUBS-1] 17 p2931 A66-33176
- GAS MASER**
- Light output from helium-neon gas maser photographed with and without intracavity modulation at locking frequency, using high speed rotating mirror 07 p1040 A66-17205
- Pulse excitation of volume of gas to coherently radiating state applied to beam maser spectrometer 12 p1879 A66-23731
- Hydrogen atom beam characteristics, discussing signal power, generating frequency, radiation signal damping and hydrogen atom relaxation time 14 p2310 A66-28289
- Very fine-beamed maser oscillation produced in atomic hydrogen by HF discharge observed by double focusing technique 24 p4225 A66-42993
- GAS-METAL INTERACTION**
- Hot plastic deformation effect on gas content, structure and mechanical properties of industrial molybdenum, niobium and titanium 01 p0086 A66-10451
- Heat resistance in air of four industrial austenitic-ferrite steels with low nickel content at 750-1050 degrees C, noting oxide scale formation 01 p0088 A66-10988
- Metallized propellant and gas-solid suspension flow through nozzle in high energy systems 06 p0803 A66-16912
- Interaction between hydrogen and various titanium alloys, noting correlation between sorption capacity of alloys and type of phase diagram 07 p1050 A66-18064
- GAS METER**
- Vertical distribution of atmospheric ozone measured by balloon-borne Sun-seeking guidance system and light-scattering gypsum screen 01 p0071 A66-11044
- Vertical distribution of atmospheric ozone measured by balloon-borne Sun-seeking guidance system and light-scattering gypsum screen 11 p1709 A66-23291



High accuracy variable area meter calibrations with multiple gases 16 p2704 A66-30672

**GAS MIXTURE**

**SA DETONABLE GAS MIXTURE**

Reference point in thermodynamic similarity for investigating binary gas mixtures 01 p0163 A66-10627

Electric conductivity of N-component gas mixture containing one partially ionized component 02 p0265 A66-11389

Equation solution for flame propagation in gas mixture with first-order exothermic chemical reaction 02 p0302 A66-11392

Two-and three-step laser cascades detected experimentally in helium-neon mixtures, analyzing two-step cascade starting with density matrix formulation 02 p0241 A66-11477

Helium-neon laser amplifier as function of mixture ratio, gas pressure, input signal level and electrical power input to amplifier tube 02 p0242 A66-12206

Electron-ion recombination in photoionized nitric oxide neon gas mixture, noting decay of electron density and correlation factors 03 p0394 A66-12327

Unsteady boundary layer flow of multicomponent gas mixtures, investigating combustion instability in liquid and hybrid rocket motors [AIAA PAPER 65-41] 03 p0444 A66-12796

Temperature overshoot in monatomic gas shock wave 03 p0357 A66-12957

Warren momentum integral method for predicting compressible free mixing of two dissimilar gases [AIAA PAPER 65-822] 03 p0357 A66-13083

Kinetic studies of hydroxyl radicals in shock waves, considering recombination via particular reaction in lean hydrogen-oxygen mixtures 04 p0596 A66-13646

High temperature analysis of mechanism and kinetics of tetrafluoroethylene decomposition and oxidation in excess argon behind shock waves, using UV absorption and mass spectrometry 04 p0571 A66-13650

Vibrational relaxation model of high temperature gas to determine dissipative coefficients in highly nonequilibrium gas mixtures with binary collisions 04 p0455 A66-14140

Performance of thermal diffusion columns studied for limits of validity of theory of isotopic mixtures in case of mixtures of gases 04 p0598 A66-14325

Interaction virial coefficient of binary gas mixtures by Guggenheim-McGlashan method 05 p0718 A66-15527

Nonuniqueness of stationary solutions to system of equations in burning theory with piecewise invariable reaction rate and thermoconductivity and diffusion coefficients 06 p0970 A66-16345

Ignition of hydrogen-oxygen-argon mixtures containing small amounts of hydrocarbons and bromine substituted hydrocarbons in shock tubes 06 p0822 A66-16634

Experimental viscosity of dissociating system nitrogen tetroxide and nitrogen dioxide, obtaining force constants for Lennard-Jones potential having no effect on viscosity of gas mixture 06 p0823 A66-16635

Porous cermet of iron, bronze and stainless steel efficiently arrest flame of burning gas mixtures 06 p0897 A66-16694

Simulated flights evaluating verbal communication intelligibility in oxygen breathing mixtures at low atmospheric pressures compared with results obtained in room air at ground level 06 p0813 A66-16827

Physics of spark discharges igniting gaseous mixtures, noting increase in thermal power of discharge by gas preionization resulting from energy redistribution 06 p0919 A66-16877

Linearized wave equation of supersonic flow with single relaxation process, using model gas mixture 06 p0874 A66-17003

Separation of gases from isotopes in compression shock produced in expanding gas flow past obstruction, dependent on gas density and hydrokinetic properties of components 06 p0875 A66-17052

Thermal diffusion coefficient and composition of gas mixtures by measuring gas flow rate in capillary tube as function of viscosity 07 p1148 A66-17394

Velocity potential equation for linearized steady motion of gas mixture with multiple reactions 07 p1023 A66-18116

Heat conductivity of binary gas mixtures compared with theoretical and experimental results 07 p1155 A66-18159

Time dependence of electron density during afterglow of plasma in helium-hydrogen, neon-hydrogen and argon-hydrogen mixtures measured by microwave cavity 07 p1091 A66-18398

Methane concentration relation to relaxation frequency and vibrational specific heat of mixtures of oxygen and methane 08 p1178 A66-18938

Inviscid supersonic flow fields of reacting gas mixture around pointed bodies calculated, using characteristics method 08 p1164 A66-19128

Theoretical formulae for thermal diffusion of binary gas mixtures 08 p1320 A66-19569

Thermodynamic parameters of carbon dioxide and argon mixture behind straight shock wavefront 09 p1470 A66-20146

Separation of gas mixture in curved supersonic flow, noting parameters of concentration gradient profile variation 10 p1522 A66-21269

Nonuniqueness of stationary solutions to system of equations in burning theory with piecewise invariable reaction rate and thermoconductivity and diffusion coefficients 11 p1785 A66-22340

Thermal conduction of hydrogen-helium gas mixtures and dependence on hydrogen concentration 11 p1786 A66-22500

Thermal properties of gaseous mixtures measured with experimental apparatus containing differential manometer 11 p1704 A66-22595

Shock wave structure in binary gas mixtures that are monatomic and chemically inert, using Mott-Smith method 11 p1691 A66-22914

Accuracy and applicability of approximate formulas describing heat conductivity of binary gas mixture 11 p1787 A66-23318

Kinetics of CN radicals association generated by shocking cyanogen-argon mixtures at high temperatures in reflected shock region of expansion wave 12 p1811 A66-23615

Book on thermodynamic properties of combustion gases 12 p1978 A66-24192

Interferogram interpretation to determine carbon dioxide concentration in air mixture 13 p2208 A66-25315

Vibrational relaxation times of deuterium in argon and krypton determined at high temperatures by shock heating gas mixtures in shock tube 13 p2136 A66-26662

Laminar air flow past porous plate through which fuel and oxidizer mixture is injected, deriving diffusion combustion processes that develop in laminar boundary layer 14 p2371 A66-28318

Thermodynamic characteristics of two volumes of binary gas mixture connected through capillary tube 14 p2415 A66-28324

Flame wavelength during vibrational combustion of gas mixtures in tubes 14 p2415 A66-28327

Viscosity coefficients of gas mixtures at atmospheric pressure and various temperatures 14 p2415 A66-28328

Nonlinear system of partial differential equations describing one-dimensional combustion process of gas mixture 15 p2616 A66-28961

Schlieren photographs of spark ignition in turbulent gas mixture flows and analysis of ignition delay and burning velocity 15 p2616 A66-29069

Electroconductivity of combustion products of propane-air mixture determined by double Langmuir probes 15 p2617 A66-29312

Oscillatory phenomenon in gaseous multicomponent diffusion, noting convection caused by density inversion 15 p2481 A66-29745

Approximation method for thermal diffusion factor of almost Lorentzian gas mixture with better convergence properties than Chapman-Enskog approximation 16 p2824 A66-30119

Effect of air mixture application on optimum ascent trajectories and ratio of payload to takeoff weight of carrier rocket

configurations 16 p2790 A66-30030

Environmental conditions in space stationing optimum pressure, gas concentration and temperatures 16 p2641 A66-30030

Thermal diffusion in isotopic gas mixtures 16 p2826 A66-30030

Thermal ignition of flowing gas mixture at nonreactive noncatalytic hot surfaces 16 p2830 A66-310

Thermal diffusion factor of binary mixtures, discussing some relatively unknown characteristics 17 p3033 A66-320

Thermal comfort zones for helium-oxygen and helium-nitrogen atmospheres at reduced pressures 17 p2865 A66-320

Chapman-Enskog kinetic gas theory calculation of diffusion coefficient of binary gas mixture 17 p3035 A66-320

Automatic ignition in methane-chlorine mixture, investigating photochemical and thermal chlorination of methane in phase 17 p2989 A66-320

Transonic nonequilibrium approximation for reacting gas mixture flow 17 p2913 A66-330

Direct and indirect oxidation fuel systems operating on hydrocarbon mixtures and using aqueous, molten solid electrolytes, noting technological and economical problems 18 p3053 A66-330

Computer programs for combustion rate of hydrogen-air mixture 18 p3063 A66-330

Overall structure of combustion process, jet flow of hydrocarbon-air mixture, stressing conditions for ramjet engine, noting flame propagation angles, computation, etc [AIAA PAPER 66-573] 18 p3264 A66-340

Shock formation in mixture of chemically reacting ideal gases due to piston action 18 p3100 A66-340

Correlation method of law of corresponding states for calculating thermodynamic properties of real gases and their mixtures 18 p3267 A66-350

Vibrational relaxation of carbon dioxide mixtures with noble gases 19 p3295 A66-350

One-dimensional problem of sound propagation in two-component reactive gas mixture 19 p3341 A66-350

Population inversion in adiabatic expansion of molecular gas mixture with vibrational levels 19 p3402 A66-350

Liquid-vapor phase equilibria of neon normal hydrogen system 20 p3676 A66-370

Low temperature liquid-vapor equilibria in neon-oxygen system at pressures up to 5000 psi from 63 to 152 degrees K 20 p3601 A66-370

P-V-T behavior of argon, nitrogen, argon-nitrogen gas mixtures 20 p3677 A66-370

Stability limits of quasi-cylindrical diverging detonations in propane-oxygen nitrogen mixtures 20 p3679 A66-370

Hydrogen/oxygen and hydrogen/air flame temperature experiments on porous flame burner 20 p3680 A66-370

Fluorine concentration in oxygen monitored by instrument with nickel thermoconductivity cell 20 p3511 A66-380

Methane flames formed in long, horizontal column of methane-air mixture caused by interdiffusion, using wind tunnel 20 p3681 A66-380

Ideal relativistic degenerate gas in white dwarf star interiors, discussing stability equations, thermodynamic relations, electron-ion gas mixtures, etc 21 p3775 A66-380

Thermal conductivity and accommodation coefficient measurements in gas mixtures of atomic and molecular oxygen 21 p3836 A66-380

Thermodynamic parameters of carbon dioxide and argon mixture behind straight shock wavefront 21 p3836 A66-380

Thermal conductivity of carbon dioxide critical region interpreted, considering as mixture of clusters and heat transfer to formation and breaking of clusters 21 p3837 A66-380

Stability problem of plane steady detonation wave in ideal gas 22 p3898 A66-400

Gas mixtures evaluation for MIG weld aluminum alloy noting nondestructive



- mechanical and stress corrosion testing 22 p3925 A66-40266
- Transverse separation of rare gas-metal vapor mixture components in positive nonisothermal plasma column in plain-symmetric glow discharge 22 p3958 A66-40934
- Pressure variation induced by ignition of air-hydrocarbon mixtures studied by stioscopic cinematography and simultaneous pressure measurement 23 p4148 A66-41176
- Compressibility factor chart for hydrocarbon-hydrogen and nitrogen-hydrogen gas mixtures, correlating pressure and temperature, using state equation 23 p4150 A66-41866
- Detonation wave formation in flowing hydrogen-oxygen and methane-oxygen mixtures, noting induction distances and turbulence levels 23 p4057 A66-41888
- Detonation initiation behind reflected shock waves in hydrogen-oxygen-argon mixtures, noting reaction wave propagation 23 p4057 A66-41889
- Detonability of hydrogen-oxygen mixtures in large vessels at low initial pressures, using strong and weak igniters 23 p4120 A66-41890
- Homogeneous gas phase and surface reactions based on mass transfer mechanism during quenching of oxygen-nitrogen mixtures from high temperatures 24 p4170 A66-42134
- Mixing of gases in hydrogen-oxygen fuel cell, noting membrane allowing only electrolyte to pass through electrodes 24 p4161 A66-42502
- Flame of homogeneous gas mixture in terms of similarity criteria applied to combustion process analysis 24 p4295 A66-42883
- Regenerative air conditioning systems of spacecraft cabins for long missions, analyzing principal parameters of gas mixtures for life requirements 24 p4169 A66-43142
- GAS PHASE**
- Effect of surface state of cadmium sulfide on fundamental absorption edge and fine structure obtained from gaseous phase in inert atmosphere 03 p0407 A66-12405
- Stain film of chemical species formed by gas phase reaction on silicon 05 p0736 A66-14978
- Stable aerosol formation from vapor pressure of hot lava of volcanic eruptions, causing evaporation and condensation from gas phase 10 p1607 A66-21288
- Phase behavior in helium-xenon system exhibiting gas-gas equilibria 13 p2018 A66-26444
- Correlations between Lennard-Jones potential parameters and critical and boiling point constants of 28 nonpolar and 17 polar gases 15 p2618 A66-29718
- Solid-vapor equilibrium in helium-methane system from triple point equilibrium temperature of methane down to low temperature within limits of flame ionization technique 20 p3676 A66-37086
- Ignition analysis of condensed phase fuel suddenly exposed to stationary hot oxidizing gas, noting strong pressure effect due to feedback mechanism 20 p3626 A66-37386
- Elementary gas phase reactions involving atoms and radicals by mass spectroscopic and diffusion cloud methods 21 p3702 A66-38472
- High temperature rate constants for H-atom transfers involving light atoms evaluated, using hard sphere collision theory 22 p3950 A66-39924
- Low pressure low temperature ignition of hypergolic propellants, particularly hydrazine-nitrogen tetroxide systems, in space environment simulator and conclusions on gas phase reactions 22 p3892 A66-40237
- Homogeneous gas phase and surface reactions based on mass transfer mechanism during quenching of oxygen-nitrogen mixtures from high temperatures 24 p4170 A66-42134
- GAS PRESSURE**
- Noble gas ion beams produced by duoplasmatron magnetically analyzed while varying gas pressure in source 01 p0114 A66-10850
- Pulse ionization manometer based on open 6Zh2P pentode with oxide cathode for measuring fluctuating inactive-gas pressure 04 p0520 A66-13893
- Roberts method determining accommodation coefficients of gases on bare wires leads to erroneous conclusions due to thermal inertia of experimental apparatus in vicinity of current paths 04 p0545 A66-14170
- Pressure dependence of Townsend second coefficient for sparking potential in gases at constant E/p 06 p0911 A66-16283
- Compensation magnetic probe and plasmascopie study of plasmoid motion in uniform axisymmetrical magnetic field 08 p1264 A66-19182
- Temperature and gas pressure in sunspots determined by measuring equivalent width and intensity of damped wings of spectral lines 09 p1457 A66-20465
- Ionization phenomena in argon due to laser radiation by measuring electron density and energy as time function after laser pulse initiation at different gas pressures and preionized conditions [AIAA PAPER 66-176] 10 p1565 A66-21690
- Laboratory instrumentation for testing and calibration of in situ probes for lower ionosphere, mesosphere and stratosphere 13 p2059 A66-26549
- Localization conditions of high power linear HF discharge at low gas pressure, achieving localization of current and plasma density in magnetic field by using diaphragms 14 p2340 A66-27148
- Static pressure distributions in supersonic nozzle flows of dissociated hydrogen plus argon 14 p2219 A66-27442
- Fluorescence lifetime measuring technique employing pulsed or modulated RF discharges applied to emission of second positive and first negative systems of nitrogen 14 p2337 A66-27974
- Energy balance of stationary discharges in quartz containers filled with gas at various pressures, determining relation of heat and light loss of discharge to gas pressure and discharge power 15 p2551 A66-29215
- Shock transition in multihead spin structure of self-sustaining gaseous detonations in oxyacetylene mixtures, including interferometric and schlieren photographic density, temperature and pressure measurements 15 p2618 A66-29607
- Pulse ionization manometer based on open 6Zh2P pentode with oxide cathode for measuring fluctuating inactive-gas pressure 15 p2503 A66-29706
- Pressure rise in inner region of hydrogen arc discharge in axial magnetic field 16 p2764 A66-31352
- Manometer for measuring gas pressure from current required to heat platinum wire to certain temperature 16 p2708 A66-31359
- Detection of arrival of He driver gas in test section of shock tunnel 17 p2903 A66-32474
- Gas pressure dependence of attachment and recombination coefficients for thermalized electrons in air and oxygen 18 p3143 A66-34035
- Natural vibration frequencies of rocket nozzles, accounting for anisotropic elastic behavior, internal gas dynamic pressure, boundary conditions, etc 18 p3258 A66-34601
- Low-inductance hydrogen gas discharge switch tube based on gas pressure-electrode spacing control of ionizing collisions 19 p3280 A66-35812
- Tungsten and tungsten composite fabrication by gas-pressure-bonding process 19 p3368 A66-36123
- Residual gases total and partial pressures measured, using pressure gauges incorporating hot or cold cathodes, noting omegatron 19 p3361 A66-36616
- Gas pressure effect on excitation of 4.38-ev level in Pb during hollow cathode discharge in magnetic field 20 p3579 A66-37780
- Continuous in vivo recording of partial pressure of arterial carbon dioxide and oxygen by mass spectrography 21 p3701 A66-39494
- Hydrogen, nitrogen, oxygen and helium gas pumping by ionization pressure gauges in space simulators 22 p3891 A66-40233
- Pressure- and gain-dependent frequency shift measurements in stabilized 6328 angstrom He-Ne laser 24 p4224 A66-42803
- Localization conditions of high power linear HF discharge at low gas pressure, achieving localization of current and plasma density in magnetic field by using diaphragms 24 p4244 A66-42968
- Ionization gauge for transient gas pressure measurement 24 p4215 A66-43210
- GAS PROPELLANT**
- Wall friction, heat transfer and real-gas propellant effects in two-stage light gas guns 11 p1685 A66-22837
- Reverse-flow film cooling of small rocket engine chamber 12 p1937 A66-24718
- Particle size distribution, aging effects, terminal velocity measurements and production techniques of slush hydrogen investigated as potential upgraded spacecraft fuel 20 p3676 A66-37075
- GAS-SOLID INTERFACE**
- Quantum theoretic probability of trapping inert gas atom on solid surface with linear lattice 01 p0108 A66-10634
- Multiphase flow system with regard to chemical and nuclear processes, rocketry and air pollution control noting adiabatic potential, laminar and electrodynamic flow 03 p0354 A66-12312
- Turbulent boundary layer interaction with graphite heat shield noting boundary layer velocity, temperature and chemical composition profiles [AIAA PAPER 65-824] 03 p0446 A66-13232
- Gas phase nonideality and mean column pressure effects on sample retention in gas-solid partition chromatographic systems with real carrier gases 04 p0472 A66-13396
- Satellite drag coefficient reevaluated in consideration of recent data on gas-surface interaction and atmospheric composition 05 p0760 A66-14941
- Gas mean and solid mean velocity profiles of small particles suspended in turbulent air, noting effect of solid motion on laminar structure and shear stress at wall [ASME PAPER 65-WA/FE-24] 05 p0665 A66-15713
- Momentum and energy accommodation coefficients for moving gas interaction with solid surface, with attention to molecular mass and velocity flux distribution 07 p1083 A66-18135
- Nonequilibrium ionization of suspension of solid particles expanding supersonically in nozzle, particularly lowering of ionization due to injection in flow of high work function 15 p2615 A66-28762
- Thermal energy exchange between gases and solid surfaces, using realistic interaction potentials of Morse type, Maxwellian velocity distribution 16 p2825 A66-30387
- Momentum and energy accommodation for hypervelocity gas particles on crystal surface, using Lennard Jones potential and approximating lattice by system of independent forced harmonic oscillators 16 p2752 A66-30388
- Interaction between gas particles and solid surface examined, noting idealization of Morse potential and use of analog computer 16 p2655 A66-30390
- Energy accommodation coefficient variation with energy of gas molecules impinging on clean surfaces or adsorbed monolayers 16 p2645 A66-30391
- Hydrogen, He, Ne and Xe high energy molecular beam scattering from gold film surfaces during evaporative deposition 16 p2752 A66-30392
- Energy transfer measurements in gas-solid surface interactions initiated by electron beam-excited photoemission 16 p2701 A66-30397
- Electrostatic theory of physical adsorption applied to gas-solid chromatography, discussing chromatographic inseparability of argon and oxygen at room temperature, prediction of elution order of many gases, etc 16 p2646 A66-30646
- Heat shield and rocket nozzle chemical reactions based on equilibrium thermodynamics of high temperature materials at gas-solid interface 18 p3260 A66-33825
- Solid propellant ignition, discussing deflagration wave propagation along gas-solid grain surface, flux equilibrium equation, etc [AIAA PAPER 66-668] 18 p3165 A66-34441
- Mass transfer across gas-solid interface



associated with semiconductor solids 18 p3087 A66-34737

Mass transfer into aerodynamic body flow fields, examining model shear flow in Rayleigh problem for blowing current across gas-solid interface 23 p4058 A66-41900

Thermal accommodation coefficients of He on tungsten and hydrogen on hydrogen-covered tungsten at temperatures of 325, 403 and 473 degrees K 23 p4033 A66-42078

Arc image stagnation-flow reactor for measuring gas-solid reaction rates between 2000 and 3000 degrees K 24 p4216 A66-43214

### GAS SPECTROSCOPY

Absorption coefficient for lines with combined Doppler and Lorentz broadening calculated, using Runge-Kutta method, continued fraction expansion and Hermite-Gauss quadrature 03 p0393 A66-13267

Photochemical studies of oxygen-ozone and carbon dioxide equilibria with bromine UV lamp 04 p0473 A66-13397

Forced Mandelstam-Brillouin scattering in gases, determining hypersonic velocity for three gases 09 p1408 A66-20770

Gas spectroscopy of laser-induced stimulated Brillouin effect in high pressure oxygen 11 p1715 A66-23432

Temperature measurement in shock heated gases via spectrum line reversal method, noting connection between electronic excitation and effective vibrational temperature 13 p2208 A66-25159

High-temperature gas radiance in simulated planetary atmosphere at various entry velocities [AIAA PAPER 66-183] 13 p1990 A66-25169

Empirical curve of growth on S/I/ line of 1-0 hydrogen quadrupole band obtained, laboratory and planetary hydrogen quadrupole spectra corrected for saturation 13 p2184 A66-25621

Organic gas magnetically tuned laser spectroscopy, discussing resolution, absorption spectra and vibrational deactivation 13 p2100 A66-26197

Vibrational-rotational line strengths and widths in carbon dioxide, using carbon dioxide-neon laser 14 p2306 A66-27030

Forced Mandelstam-Brillouin scattering in gases, determining hypersonic velocity for three gases 14 p2341 A66-27305

Energy dependence of elastic resonance scattering of low energy electrons from He, Ne, Ar and nitrogen gases at angles ranging from 8 to 110 degrees 14 p2337 A66-27797

Shock tube techniques used in measurement of temperature and absolute line intensities for neutral atoms of iron, lead and tin 18 p3109 A66-33695

Book on microwave spectroscopy of gases 18 p3065 A66-35237

Single continuous correlation for total band absorbance of radiating gases 20 p3678 A66-37121

Spectroscopic electron beam diagnostic technique, examining negligible effect elevated vibrational temperatures have on measured rotational temperatures of molecular nitrogen [AIAA PAPER 66-747] 22 p3919 A66-40633

Spectrum of three-times ionized nitrogen analyzed in wavelength region 300-8000 angstroms, using theta pinch discharge, connecting singlets and triplets 24 p4240 A66-43104

### GAS STREAM

Evaluating temperature measuring methods for hot gas stream in thermal-to electric-energy converters 01 p0066 A66-10204

Localized calorimetric enthalpy measurements in high-energy-content gas stream using evaporating liquid film to cool gas sample 01 p0165 A66-10908

Group of transforms derived for functional in which Euler equation coincides with Crocco equation describing plane vortex gas streams 04 p0512 A66-14437

Gas stream behind shock wave in contracting channel, discussing flow parameters during discharge from supersonic and divergent nozzle 05 p0607 A66-15321

Stability of three-layer cylindrical shell in gas stream, analyzing oscillation mode and critical flutter dependence on filler resistance to transverse shear 08 p1314 A66-19581

Nonuniform thermal flux for fuel elements and core of nuclear heat exchangers, determining heat transfer coefficient between adjacent fluid streams by mass transfer 12 p1973 A66-23527

Mixing zone of two wakes, studying cooling effect of gas stream directed tangentially or at small angle to container 16 p2689 A66-31607

Critical lengths in subsonic and supersonic gas-particle flow in vertical constant area tube, considering effect of governing variables and inlet conditions of system [ASME PAPER 66-FE-19] 17 p2915 A66-33272

Radiative and convective heat transfer between two parallel streams of absorbing and emitting radiating gases 21 p3835 A66-38715

### GAS TRANSPORT

Laminar boundary layer of nitrogen flow over helium cooled sphere with porous wall 01 p0162 A66-10463

Aircraft control power requirements provided by lift fan propulsion system for V/STOL flight, noting gas power transfer [SAE PAPER 650831] 01 p0130 A66-10830

Approximation formulas for certain collision integrals of gas transport 03 p0395 A66-12836

Monte Carlo method solution of heat transfer in rarefied gas between infinite flat plates 05 p0787 A66-14987

Book on determining radiative contributions to energy and momentum transport in gas under almost any density and temperature conditions 06 p0913 A66-17157

Monte Carlo method to reveal properties of hydrogen transport near critical level of escape of Earth upper atmosphere 07 p1028 A66-17362

Radiant flux to base region of axisymmetric real gas system with nonisothermal temperature distribution 07 p1151 A66-17588

Second and third virial coefficient for exponential repulsive potential by accurate numerical integration and by asymptotic formula 07 p1083 A66-17934

Nonisothermal gaseous transport of hot injected plasma in semiconductor 07 p1103 A66-18213

Hydrogen feeding through single-layer metallic porous electrode of fuel cell on open circuit 08 p1171 A66-19649

Arc plasma generator for anode research, noting design operation techniques and results [AIAA PAPER 66-162] 10 p1485 A66-21687

Multidimensional radiation transport equations for nonscattering quasi-equilibrium gray gas obtained by spherical harmonic approximation [AIAA PAPER 65-81] 10 p1621 A66-21774

Instability criterion in air, argon and carbon dioxide at various pressures and layer depths, detecting convection and determining Rayleigh number for application in transport properties of gases 12 p1980 A66-24942

Conditions under which gas bubbles arise in organs and physiological fluids of living organism during pressure drop 13 p2011 A66-26577

Mathematical representation for transport phenomena in living organism 13 p2011 A66-26578

Book on heat transfer covering new instrumentation and analytical techniques for definitive solution to classical and complex problems 16 p2824 A66-30301

Measuring and calculating methods for dilute gas transport properties independent of fluid dynamic environment in which they operate 16 p2825 A66-30306

Approximation formulas for certain collision integrals of gas transport 19 p3404 A66-36778

Thermal conductivity of gases measured, using thermal diffusion columns 23 p4149 A66-41502

Mixing of gases in hydrogen-oxygen fuel cell, noting membrane allowing only electrolyte to pass through electrodes 24 p4161 A66-42502

### GAS TURBINE

#### SA AFTERBURNER

#### SA AIRCRAFT ENGINE

## SA TURBINE ENGINE

Nickel-chromium base alloys considering aircraft and industrial gas turbine application 02 p0244 A66-1174

Refractory metals for gas turbine an ramjet aircraft engines, noting niobium an tantalum alloys 02 p0245 A66-1174

Operating performance of deep groove ball bearing used for gas turbine at high d values 03 p0372 A66-1246

Centripetal gas turbine interblade channel without diffuser regions in rotor eliminate pressure gradient buildup in flow core 03 p0315 A66-1264

Casting technique based on directional solidification for nickel and cobalt alloy used in gas turbine blades [AIAA PAPER 65-742] 03 p0382 A66-1304

Energy balances for combustion chamber of gas turbines by electronic computer 03 p0416 A66-1320

Book on matched parameters of gas turbine engines for aircraft including rpm and peripheral speed, calculating parameters for axial-flow compressors, centrifugal compressors, turbojet, turboprop, etc 04 p0573 A66-1400

Regenerative heat exchangers, covering heat transfer and pressure loss characteristics of glass ceramic materials [ASME PAPER 65-HT-35] 05 p0784 A66-1474

Arbitrary quasi-orthogonals for calculating flow distribution in turbomachine, noting digital computer calculations 05 p0662 A66-1494

Aerodynamic analysis of cryogenic radial inflow turbines, noting optimum velocity distribution [ASME PAPER 65-WA/PID-6] 05 p0608 A66-1560

Cooling effect of secondary fluid injection on heat transfer between shrouded rotating disk and radially inward main flow stream [ASME PAPER 65-WA/HT-20] 05 p0789 A66-1566

Alloy steel fracture resistance, describing creep strain effect on gas turbine engine alloys [ASME PAPER 65-WA/MET-13] 05 p0703 A66-1561

Traveling wave vibration in stationary and rotating cylindrical shells in gas turbine engines [ASME PAPER 65-WA/GTP-3] 05 p0780 A66-1573

Supersonic cascade tunnel to evaluate compressor blade performance [ASME PAPER 65-WA/GTP-4] 05 p0661 A66-1573

Pulse jet engine where hot gas discharge rather than developing thrust is used to obtain shaft power [ASME PAPER 65-WA/GTP-6] 05 p0745 A66-1572

Air cooled gas turbine rotor and stator airfoils, presenting problem definition analysis techniques, material application and cascade and engine testing [ASME PAPER 65-WA/GTP-10] 05 p0691 A66-1573

Vibration in aircraft jet engine rotating compressor disks of small and large blades [ASME PAPER 65-WA/GTP-11] 05 p0780 A66-1573

Density and Reynolds number effects on turbine meter performance in gas flow measurement [ASME PAPER 64-WA/FM-1] 06 p0879 A66-1621

Production and recent developments in gas turbines and propulsive engines in West Germany 06 p0942 A66-1678

High temperature alloys for gas turbine examining advances in creep strength, low cycle fatigue and wrought and cast turbine blading alloys [SAE PAPER 650708] 06 p0898 A66-1707

Capability of investment casting process for production of integrally cast turbine wheels and nozzles for high temperature gas turbine application [SAE PAPER 650706] 07 p1037 A66-1724

Temperature indicating paints applied to high-temperature and high-velocity gas streams in gas turbine design [SAE PAPER 650705] 07 p1110 A66-1786

Gas temperature effect on therm



- condition of vanes during acceleration of gas turbine engine 08 p1281 A66-18866
- Carbon seals for gas turbine evaluated in statistically designed test 08 p1232 A66-19381
- Method 08 p1232 A66-19381
- Dimensional stability and structural integrity of labyrinth seals, considering various mechanical design criteria in application to aircraft gas turbines [SAE PAPER 660048] 09 p1383 A66-20150
- Precision casting based on directional solidification resulting in longitudinal columnar grains with preferred orientation, eliminating transverse grain boundaries in gas turbine elements 09 p1388 A66-20153
- [SAE PAPER 660055] 09 p1388 A66-20153
- Aircraft turbine engine oil drain practices, discussing engine design and materials and minimum and maximum drain time [SAE PAPER 660073] 09 p1434 A66-20158
- Polytropic technique for gas turbine performance, prediction and evaluation, noting use of sophistication factor [SAE PAPER 660161] 09 p1434 A66-20161
- Auxiliary turbine power generator using gas from solid propellant 09 p1333 A66-20331
- BMW model 6012 gas turbine for helicopter application weighs 50 kg but develops 100 hp 10 p1591 A66-21402
- Cooling effect of secondary fluid injection on heat transfer between shrouded rotating disk and radially inward main flow stream [ASME PAPER 65-WA/HT-20] 11 p1785 A66-22194
- Fatigue life of aircraft gas turbine compressor disks subjected to cyclic loading 11 p1710 A66-22691
- Heat resistant nickel-based alloys for gas turbine blades and disks 11 p1716 A66-22752
- Text on fundamentals of aircraft gas turbine engine design, including component design and calculation 11 p1762 A66-23310
- Constant oil monitoring system using electric conductivity tester for extending oil life in gas turbine engines [SAE PAPER 650814] 12 p1935 A66-23844
- Alloy steel fracture resistance, describing creep strain effect on gas turbine engine alloys [ASME PAPER 65-WA/MET-13] 12 p1896 A66-24535
- Superalloy coatings for gas turbine components assessed, criticizing lack of objective comparative data, noting pack-cementation and spray diffusion processes 13 p2108 A66-25652
- Soviet book on automation and control of air breathing gas turbine and ramjet engines 13 p2173 A66-26463
- Intermittent propellant flow gas turbine for spacecraft power supply [AIAA PAPER 64-754] 13 p2008 A66-26655
- Nonconventional application of electric power-generating closed-cycle gas turbines [ASME PAPER 66-GT/CLC-8] 14 p2224 A66-26981
- Graphical matching solution for gas turbine power plant closed cycle systems [ASME PAPER 66-GT/CLC-14] 14 p2224 A66-26984
- Blade noise generation in gas turbine engines [ASME PAPER 66-GT/N-43] 14 p2372 A66-26988
- New cycle concepts in development of gas turbine and turbomachinery [ASME PAPER 66-GT-85] 14 p2372 A66-26991
- Shaft-power turbine design, including rotor vibration problems, computer high speed testing, application as auxiliary power supply in turbojets, etc [ASME PAPER 66-GT-87] 14 p2225 A66-26992
- Inlet guide vane system for control of small single-shaft gas turbines [ASME PAPER 66-GT-89] 14 p2372 A66-26993
- Small gas turbines, market, technical problems, etc [ASME PAPER 66-GT-90] 14 p2372 A66-26994
- U.S. Army program for small gas turbine, noting turbine specific horsepower, component, payload-range curve, etc [ASME PAPER 66-GT-91] 14 p2372 A66-26995
- Overrunning clutches in gas turbines, design, performance characteristics and application to A-4D Skyhawk aircraft, UH-2 helicopter and Curtiss-Wright X-19 VTOL drive systems [ASME PAPER 66-GT-92] 14 p2300 A66-26996
- Second thermodynamic law analysis of availability balance for conventional gas turbine and free-piston gasifier [ASME PAPER 66-GT-96] 14 p2372 A66-26999
- Long-life base load service at 1600 F turbine inlet temperature, noting fuel-air and temperature controls [ASME PAPER 66-GT-98] 14 p2372 A66-27000
- Cold work and precipitation hardening effect on tensile and thermal characteristics of gas turbine alloys [ASME PAPER 66-GT-102] 14 p2312 A66-27002
- CERCOR glass-ceramic axial flow rotary regenerator as inexpensive component for gas turbine regeneration [ASME PAPER 66-GT/107] 14 p2301 A66-27004
- Liquid phase compression in closed cycle gas turbine by using particular working fluids for application to nuclear power stations [ASME PAPER 66-GT-111] 14 p2411 A66-27005
- Effect of vacuum arc remelting of airmelt electrodes on structure and elevated temperature properties of nickel base gas turbine superalloy [ASME PAPER 66-GT-113] 14 p2313 A66-27007
- Circumventing turbine inlet temperature limitation of gas turbines by direct fluid-to-fluid energy exchanger, using isentropic compression waves to avoid shock losses [ASME PAPER 66-GT-117] 14 p2373 A66-27009
- Bypass engine development from conventional gas turbine to ducted-fan and aft-fan engine, noting principle of afterburning 14 p2373 A66-27014
- Negative effect of air countercurrents and thermal stresses on performance of cooling systems of gas turbine rotor disks with lateral air flow 15 p2570 A66-28776
- Gas turbine fuel controls, analysis and design 15 p2570 A66-28851
- Analog computer simulation of gas turbine engines for control study, discussing steady state performance and transient response data, surge region, maximum acceleration, etc 15 p2570 A66-28852
- Electronic simulation for evaluation of control concepts and system behavior of regenerative gas turbines 15 p2571 A66-28853
- Literary acceleration limiting fuel control for gas turbine engines during speed transients 15 p2571 A66-28854
- Gas turbine engine analog simulation for acceleration sensing fuel control studies, comparing results with actual engine performance 15 p2571 A66-28855
- Effect of recuperators on governing of single shaft gas turbine engines and methods used to provide satisfactory governing and overall characteristics 15 p2428 A66-28856
- Fuel flow reset and other methods of governing performance of gas turbines 15 p2571 A66-28857
- Digital approach to gas turbine engine control based on use of pulsewidth modulated information obtained with aid of simple circuits 15 p2571 A66-28858
- Microelectronic fuel control for gas turbine engines, discussing mechanical flow and microelectronic packages and component fabrication and assembly 15 p2571 A66-28859
- Lightweight universal fuel control for commercial aircraft, discussing engine requirements, design 15 p2571 A66-28860
- Small gas turbine engine controls, discussing design, development and cost factors 15 p2571 A66-28861
- Fluid devices for sensing, amplifying, controlling and logical functions in gas turbine control systems 15 p2572 A66-28862
- Factors affecting useful life of subsonic gas turbine engine components including metallurgical variances, stress-cycle relationships, surface coating, etc [SAE PAPER 660312] 15 p2573 A66-29837
- Oxide-base cermets prepared by infiltration with silver and silver alloys, noting dispersion strengthening, bend creep, impact loading, etc, for gas-turbine application 16 p2730 A66-30250
- Ceramic materials selection for principal high temperature components of gas turbines 16 p2790 A66-30256
- Supersonic cascade tunnel used to evaluate compressor blade performance [ASME PAPER 65-WA/GTP-4] 16 p2673 A66-30340
- Traveling wave vibration in stationary and rotating cylindrical shells in gas turbine engines [ASME PAPER 65-WA-GTP-3] 16 p2813 A66-30342
- Arbitrary quasi-orthogonals for calculating flow distribution in turbomachine, noting digital computer calculations [ASME PAPER 65-WA/GTP-2] 16 p2684 A66-30344
- Split-inner-race ball bearings design for use as thrust bearings on aircraft gas turbines [ASME PAPER 66-LUBS-10] 17 p2931 A66-33183
- Gas turbine theory operating principle analyzed by Teodorescu-Coanda networks, including definition of depressive blade and fluid flow analysis 17 p2992 A66-33488
- Increasing mass flow through gas turbine without additional work from compressor and consequently increasing thermal efficiency, noting combustion problem [WSCI 66-17] 18 p3164 A66-34424
- Calibration of turbine flow meter on air against pitot tube traverse, considering random scatter 19 p3362 A66-36750
- Discharge of cooling air from blades into flow-through part of gas turbine, examining mixing of gas behind blade array with air from blade edges and effect of injected air on turbine efficiency 20 p3627 A66-36913
- Natural convective heat transfer to gas turbine rotor blade and thermal resistance of cooling system using centrifugal pump 20 p3627 A66-36926
- Aircraft turbine engine oil drain practices, discussing engine design and materials and minimum and maximum drain time [SAE PAPER 660073] 20 p3628 A66-37255
- Aircraft gas turbine starting with automatically controlled electronic unit, noting system design, operation and performance 20 p3540 A66-38299
- Optimization of efficiency of gas turbine cycles with heat recovery by finite difference method using digital computer 21 p3807 A66-38805
- Compressed-gas dispersion effect on gas turbine engine operation, deriving spraying law, jet stream, penetration depth, etc 21 p3808 A66-38934
- Gas turbine compressor rotor and power shaft fabrication using electron beam welding 22 p3924 A66-40258
- Cooled blades in gas turbines allowing use of higher gas temperatures and necessitating calculation of heat transfer and skin friction coefficients 22 p3999 A66-40492
- Three-term governor for gas turbine engine system, examining effect of internally generated pressure noise on performance of different possible hydraulic systems 22 p3972 A66-40513
- Casting technique based on directional solidification for nickel and cobalt alloys used in gas turbine blades [AIAA PAPER 65-742] 23 p4079 A66-40973
- Gas turbine blades fabricated from various alloys tested in stationary turbine burning diesel fuel 23 p4121 A66-41401
- Materials and cooling of aircraft gas turbine engines, noting nickel and tantalum alloys, turbine-inlet temperatures, coatings, etc 23 p4122 A66-41662
- ## GAS VALVE
- Combustion chamber of propulsive duct including duct potential, feedback, reed-type valve, aerodynamic valve, Venturi design, fuel control, etc 07 p1110 A66-18162
- Low temperature system for thermal conductivity measurements using Ge and Pt resistance thermometers and He exchange gas switch 24 p4215 A66-43207
- ## GAS VISCOSITY
- Shock wave structure for gas with discrete velocity distribution, examining compression and reflection from plane surface, Broadwell model and increase in specific mass 03 p0354 A66-12538
- Terminal rise velocity of small distorted gas bubbles in liquid of small



viscosity 06 p0874 A66-17000  
 Temperature and density dependence of viscosity of parahydrogen determined by Welber torsional crystal method 09 p1392 A66-20082  
 Morse potential functions for nonpolar gases determined from experimental viscosity and second virial coefficient 12 p1917 A66-23934  
 Binary-collision expansion for viscosity of two-dimensional gas of hard disks, showing dynamical origin of divergence appearing in first correction of Boltzmann equation 13 p2136 A66-26276  
 Viscosity of equilibrium dissociating nitrogen tetroxide calculated from compressibility and critical parameters 14 p2371 A66-27827  
 Viscosity coefficients of gas mixtures at atmospheric pressure and various temperatures 14 p2415 A66-28328  
 Reevaluation of data and equations used in calculation of air viscosity coefficient and application to wind tunnel experiments 16 p2685 A66-30911  
 Collision integrals calculated for interactions Li-H, Li-Li, H-H and H-H plus in LiH system 16 p2766 A66-31612

**GAS WELDING**  
**SA TUNGSTEN INERT GAS /TIG/ WELDING**  
 Short-circuiting gas metal-arc welding of high nickel alloys for manufacture of liquid rocket engine components with aerospace quality 05 p0686 A66-14691  
 Electrode tip geometry effect on characteristics of gas tungsten arc welding operating in cathode spot mode 05 p0686 A66-14693  
 Spray transfer gas metal-arc welding of titanium plate, using flux backing technique 13 p2087 A66-26016  
 Porosity at weld fusion zone-base material interface in gas tungsten-arc and electron beam welds of tantalum 13 p2110 A66-26018  
 Gas mixtures evaluation for MIG welding aluminum alloy noting nondestructive, mechanical and stress corrosion testing 22 p3925 A66-40266

**GASEOUS DIFFUSION**  
 Diffusivities of oxygen in polycrystalline niobium at 600 and 815 degrees C 02 p0243 A66-11721  
 Probes in atmospheric pressure argon plasma where ion diffusion is function of temperature 03 p0406 A66-13280  
 Gaseous impurity distribution /oxygen/ between scale and diffusion layer after heat treatment of various titanium alloys 05 p0699 A66-14700  
 Diffusion in supersonic duct flow composed of boundary layers, with application to hypersonic inlet with internal compression [AIAA PAPER 64-245] 05 p0806 A66-15071  
 Determining isothermal diffusion coefficients of gases under isobaric conditions 06 p0908 A66-16154  
 Porous gas-diffusion electrodes analyzed by using four different models, comparing resulting current density-polarization characteristics 07 p0990 A66-17239  
 Pressure dependency in oxidation of platinum above 800 degrees C explained by boundary layer diffusion mechanism 07 p1000 A66-17476  
 Electron conservation equation and effects of laminar or turbulent flow on breakdown in gases 08 p1206 A66-18933  
 Geometrically ordered gas-diffusion electrodes for fuel cells consisting of platinum steel with funnel-shaped cavities 09 p1333 A66-20424  
 Gaseous heat engine cycle with gas compression from molecular effusion through capillary material 11 p1639 A66-22244  
 Thermomolecular heat pump with cooling from gas diffusion through capillary material driven by external pressure difference 11 p1639 A66-22245  
 Gaseous diffusion in polymeric foam and experimental results, using closed cell polyurethane foam 13 p2112 A66-25304  
 Functional mechanism of gas diffusion electrode 13 p1998 A66-25668  
 Performance of porous gas diffusion electrode 13 p1999 A66-25669  
 Theory of gas porous electrode with model 13 p1999 A66-25670

Design of gaseous diffusion electrode 13 p1999 A66-25671  
 Stability of cylindrical sheet of fluid during motion through motionless gas ambient 14 p2273 A66-26778  
 Mass spectrometry of composition and density of neutral atmosphere, noting diffuse separation of gases 14 p2285 A66-27621  
 Argon diffusion from biotite of mica schist due to intrusion of dyke analyzed on basis of thermal metamorphism and isotope migration 14 p2384 A66-27848  
 Mobility of various ions in nitrogen and argon and mobility and diffusion of ions in hydrogen 14 p2345 A66-28138  
 Diffusion combustion in laminar boundary layer between two plane-parallel co-current streams 14 p2416 A66-28485  
 Oscillatory phenomenon in gaseous multicomponent diffusion, noting convection caused by density inversion 15 p2481 A66-29745  
 Determining isothermal diffusion coefficients of gases under isobaric conditions 15 p2543 A66-29884  
 Separation of gaseous, liquid and solid reaction products generated by hot salt corrosion of titanium, noting gas diffusion effect on cracking 19 p3379 A66-35659  
 Gaseous diffusion cells to remove carbon dioxide from spacecraft life support system, discussing construction material in terms of permeability coefficients substrate porosity 19 p3293 A66-36236  
 Molecular diffusion coefficient calculated in 130-200 km region from time variation of radiance distribution from glow clouds produced by grenade detonation 21 p3734 A66-39339  
 Gold doping effects on recovery time of phosphorus, boron and arsenic impurity gaseous-diffused junction diodes and estimated gold recombination center densities 22 p3873 A66-39749  
 Gaseous dispersion in laminar flow through circular tube with mass transfer to retentive layer 22 p3900 A66-40411

**GASEOUS FISSION REACTOR**  
 In-pile pumping system tested on thermionic converter SIRENE 56 for gaseous fission products 05 p0619 A66-15565  
 Plasma core nuclear rocket utilizing MHD driven vortex [AIAA PAPER 65-583] 14 p2329 A66-27409  
 MHD species separation of U 235 from hydrogen in gaseous nuclear rocket using time varying traveling wave electromagnetic field [AIAA PAPER 66-499] 16 p2745 A66-30606

**GASEOUS IONIZATION**  
**SA PENNING DISCHARGE**  
 Electron collision cross sections of atoms and molecules of argon, helium, nitrogen and dissociation products of carbon dioxide by dual beam radiosonde methods to study low temperature plasma behind shock front 02 p0288 A66-11780  
 Inverted ion magnetron principle of gas ionization based on velocity of rotation of electron sheet on anode 05 p0723 A66-15162  
 Ionization of inert-gas atoms and of hydrogen and nitrogen molecules by alkali metal ions of energies greater than 1 to 30 kev 06 p0915 A66-16151  
 Pressure dependence of Townsend second coefficient for sparking potential in gases at constant E/p 06 p0911 A66-16283  
 Ionization rate behind shock waves in argon, allowing for excitation and ionization by atom-atom collisions 07 p1020 A66-17938  
 Hydrogen and oxygen ionization at three-phase boundary in alkaline solutions on smooth metals 08 p1171 A66-19650  
 Line intensities of first negative bands of nitrogen molecular ion measured as function of bombarding electron energy and gas pressure 09 p1404 A66-20377  
 Plasma generation by fission fragment ionization of noble gases, discussing theory, ionization tube and data analysis 10 p1564 A66-21545  
 Plasma production by optical irradiation of gases and by solids, considering interaction of laser radiation with surfaces and irradiation of particles of solid material in vacuum [AIAA PAPER 66-174] 11 p1742 A66-22212

Growth rate of ionization by electron impact in presence of laser beam, elastic and inelastic scattering cross sections, free absorption, excitation and ionization coefficients, breakdown times and thresholds 13 p2134 A66-26276  
 Ionic drift velocity peak function for the interconverting nitrogen ion species drift in gas in electric field 15 p2550 A66-28328  
 Plasma ionization associated with thermal electron or nonthermal distribution of electron velocities for various gas densities 15 p2554 A66-29884  
 Ionization of inert-gas atoms and hydrogen and nitrogen molecules by alkali metal ions of energies greater than 1 to 30 kev 15 p2548 A66-29884  
 Effective ionization and charge exchange areas of certain gases undergoing collision ionization by accelerated ions 17 p2961 A66-32961  
 Ionization of low temperature supersonic plasma jets, noting kinetics of elementary processes, gas dynamic parameters and effects of combustion and alkali metal admixtures 18 p3143 A66-34443  
 Ionization processes in hot products of combustion processes /flame gases/ as well as plasma media, noting flame properties, mass spectroscopy, electron concentration, etc 18 p3260 A66-34443  
 Transmission of luminous flux due to ionization of gases by high power laser measuring energy absorption in ionization zone 19 p3403 A66-36236  
 Initial phase of shock produced ionization in argon, krypton and xenon to elucidate atom-atom ionization reaction to determine cross section 23 p4098 A66-42698

**GASTROINTESTINAL SYSTEM**  
**SA DIGESTIVE SYSTEM**  
**SA INTESTINE**  
 Gastric secretion after simultaneous action of radiation and hypoxia 06 p0810 A66-16154  
 Short-term starvation effect on gastric mucosa of weanling vs post-weanling rats 16 p2638 A66-30606

**GAUGE**  
**SA FUEL GAUGE**  
**SA ION GAUGE**  
**SA IONIZATION GAUGE**  
**SA PRESSURE GAUGE**  
**SA SPUTTERING GAUGE**  
**SA STRAIN GAUGE**  
**SA THERMOCOUPLE GAUGE**  
**SA VACUUM GAUGE**  
 Gauge transformations of third kind operator gauge transformations of first and second kinds, relating electron and photon propagators to quantum electrodynamics vertex function 23 p4098 A66-42698

**GAUGE INVARIANCE**  
 Covariant gravitational field equations in de Sitter space and quantum mechanical equations of motion associated with particles of given spin, employing gauge principle 21 p3769 A66-38669

**GAUSS FUNCTION**  
 Self-consistent field calculations of benzene molecule using Gaussian expansion functions, considering 42 electrons and finding interspersions of sigma and pi levels 04 p0473 A66-12673  
 Set theory applied to zero-memory nonlinear stochastic problems to determine Gauss function properties 05 p0707 A66-16154  
 Molecular orbitals of diborane using the LCAO method, considering all electrons in molecule, calculating all integrals, with basis functions being Gaussian 06 p0940 A66-16154  
 Relationship between geometric optics autocorrelation approach to lunar planetary radar echoes for Gauss autocorrelation function 09 p1341 A66-17938  
 Radar range measurement accuracy shown to depend on receiver filter 13 p2023 A66-25669

**GAUSS-MARKOV THEOREM**  
 Optimal adaptive estimation of sample stochastic process described by initially unknown parameter vector 06 p0865 A66-16154

**GAUSSIAN DISTRIBUTION**  
 Fatigue analysis calculations of systems with non-Gaussian output, using crest and extremal statistics of strain 01 p0147 A66-10147  
 Homogeneous turbulent flow merging with



- turbulent or laminar flow of equal velocity 01 p0058 A66-10475
- Gaussian probability distribution of bilinear single-degree of freedom system response to impulse excitation [ASME PAPER 65-APMW-29] 04 p0593 A66-14229
- Quasi-stellar radio source 3C 279 observed with on-off technique, noting antenna recorded temperatures to resemble Gaussian distribution 05 p0763 A66-15291
- Anisotropy axes dispersion relation to plane galvanomagnetic effect in thin permalloy films to obtain Gaussian directional distribution 07 p1092 A66-17222
- Localized diffusion of phosphorus in silicon used to produce deep p-n junctions with Gaussian P distribution 08 p1268 A66-18678
- Optimum quantization step for given distribution law of quantized signal, using minimum error distortion criteria 11 p1674 A66-22204
- Equation governing properties encountered in Gaussian beam propagation represented graphically on impedance chart, showing relation between Gaussian mode and geometrical optics 11 p1656 A66-23089
- Computer calculation of depletion layer properties of simultaneously-diffused, double-diffused and triple-diffused transistors 12 p1832 A66-23964
- Emitter capacity in double diffused transistors by integrating Gaussian expression for base impurity concentration 12 p1837 A66-24309
- K emission band of graphite examined, using grazing incidence spectrometer and Gaussian window function 12 p1931 A66-24802
- Statistical distribution of first occurrence and recurrence of crossing of given level in continuous random process determined, using approximate forms and exponential distribution 13 p2116 A66-25141
- Potential energy surfaces on triatomic hydrogen molecule ion computed with generalized Gaussian orbitals 13 p2130 A66-25371
- Density of Gaussian distributions and Wiener-Hopf integral equation 15 p2526 A66-28606
- Integral expression for log likelihood ratio of two Gaussian processes in signal detection 16 p2738 A66-31714
- Anisotropy axes dispersion relation to plane galvanomagnetic effect in thin permalloy films to obtain Gaussian directional distribution 17 p2976 A66-31993
- Asymmetrical property of binary pseudorandom noise generators, noting Gaussian probability density function in output of low pass filter 17 p2894 A66-33110
- Gaussian probability distribution of bilinear single-degree of freedom system response to impulse excitation [ASME PAPER 65-APMW-29] 18 p3249 A66-33587
- Precipitation model explaining formation of rain drops from clouds less than several kilometers thick, assuming Gaussian frequency distribution of vertical currents 18 p3130 A66-35015
- Stimulated emission of radiation in semiconductors, calculating dependence on temperature and impurity concentration, using Kane model with Gaussian band tail for density of states and optical model 21 p3795 A66-38547
- Addition of uniform and Gaussian distributions, exact and approximate solutions 22 p3939 A66-40171
- Dispersive network with attenuation equalizing network, weighting filter for control of output side lobe level with Gaussian shaped frequency response and matching system 23 p4034 A66-41016
- GAUSSIAN NOISE**
- Programming method for determining modulation parameters required to change siren sine wave output to random Gaussian noise 01 p0053 A66-10147
- Optimum detection of diffusion process in white Gaussian noise, using continuous observation 02 p0190 A66-11405
- Wiener kernels of nonlinear system based on cross-correlation techniques 02 p0207 A66-11789
- Statistical description of noise waves including moments, probability distribution and density, spectral density, correlation and covariance and characteristic function 04 p0485 A66-14109
- Numerical characteristics of signal-noise mixture at output of autocorrelation device for sinusoidal signal and Gaussian noise 04 p0501 A66-14407
- Computer determination of signaling alphabet required to ensure reliable digital communication in presence of additive Gaussian noise and interchannel interference 05 p0630 A66-14588
- Probability of error for quadratic digital detectors contaminated by Gaussian noise 05 p0649 A66-15184
- Optimum reception of M-ary Gaussian signals in Gaussian noise in terms of waveform with minimum error probability 05 p0634 A66-15185
- Clutter rejection in radar systems using mismatched filter when Gaussian noise is present, giving results for decaying RF signal and rectangular RF pulse 06 p0828 A66-16137
- Signal optimization for digital communication system over channel characterized by rational transfer function and Gaussian noise having memory 06 p0829 A66-16192
- Maximum likelihood detection of band limited binary signals perturbed by Gaussian noise and intersymbol interference 06 p0829 A66-16193
- Atmospheric noise effect on performance of noncoherent frequency shift keying /NCSFK/ under fading conditions compared with that obtained when noise is Gaussian 06 p0830 A66-16335
- State of continuous nonlinear dynamical system driven by white Gaussian noise from discrete nonlinear observations corrupted by white Gaussian noise [AIAA PAPER 66-38] 06 p0862 A66-16412
- Optimum rate allocation for encoding sets of analog messages when allocation total is fixed by channel capacity 06 p0833 A66-16667
- Degradation of matched filter receiver operating in non-Gaussian noise, considering performance in presence of ideal impulse noise 06 p0856 A66-16864
- Information matrices for estimating range parameters of moving targets obtained by combining a priori information with reflected radar signals with additive white Gaussian noise 08 p1180 A66-18711
- Statistics of product of Gaussian noise process and pseudorandom binary code 09 p1342 A66-19919
- Correlation function of response of multichannel electronic multiplier to Gaussian input noise 11 p1676 A66-22711
- Radio receiver design for precisely given signal and nonsteady Gaussian noise 11 p1658 A66-23221
- One-dimensional probability density of phase derivative of mixture of radio signal and Gaussian noise 11 p1658 A66-23222
- Statistical properties of receiver output under interference conditions, obtaining first order output, probability densities, second harmonic and intermodulation interference terms 11 p1658 A66-23483
- Detection and false alarm probabilities for number of sinusoidal pulses in Gaussian noise subjected to amplitude limiting of arbitrary hardness 12 p1820 A66-24649
- Phase shift keying with transmitted reference, obtaining probability of error for m-phase receiver system in presence of additive Gaussian noise 13 p2019 A66-25147
- Phase coherent digital M-ary transmission with binary waves through Gaussian channel 13 p2022 A66-25554
- Shannon model for capacity of time-continuous and time-discrete Gaussian channel with inputs perturbed by independent noise random variable 13 p2024 A66-25938
- Frequency domain design of time-limited binary signals imbedded in colored Gaussian noise 13 p2052 A66-26078
- Dynamic programming recursive estimation of modal trajectory for nonlinear non-Gaussian noise and comparison with Bayesian estimation and case of Gaussian white noise 13 p2053 A66-26086
- Autocorrelation and hypergeometric function applied in evaluating response of nonlinearities to Gaussian noise 14 p2267 A66-27726
- Number of intersections of level by Gaussian stochastic process 15 p2525 A66-28605
- Controlled noise generation at high pulse rate with avalanche diodes, noting spectral voltage density and temperature coefficient 15 p2458 A66-28894
- Optimal demodulation of analog-type signal transmitted through randomly fading channel, assuming additive Gaussian noise and using vector space approach 15 p2474 A66-29379
- Polyphase coding modulation system with additive white Gaussian noise, finding channel capacity bounds on maximum rate and error exponent 15 p2452 A66-29659
- Analog communication over randomly time varying channels 16 p2654 A66-31331
- Theoretical probability densities of amplitude-comparison, and phase-comparison monopulse radars excited by Gaussian signals and Gaussian noises 17 p2872 A66-31962
- Joint maximum likelihood estimator for signal amplitude and noise power density in coherent PCM channel with white Gaussian noise 18 p3070 A66-34256
- Response of phase-locked loop near threshold to input consisting of modulated carrier and white Gaussian noise, noting role of SNR 18 p3070 A66-34259
- Singular detection of known signals in additive Gaussian noise for application to mathematical models 19 p3296 A66-35334
- Optimum estimate of nonlinear process in presence of non-Gaussian noise and disturbances, deriving algorithm for correcting approximation 19 p3323 A66-35340
- Dependent sampling effect on performance of nonparametric coincidence or median detector, considering constant signal detection in stationary additive noise 19 p3324 A66-35513
- Graph techniques used in connection with nonharmonic series representation of stationary Gaussian signals for analysis of nonlinear systems 19 p3392 A66-36706
- Digital computer synthesis of simulated ground clutter of radar signals produced by noise generator and characterized by power spectral density and probability density functions 20 p3514 A66-37222
- Distribution function for probability density of random process at output of multiplier acted upon by envelopes consisting of Gaussian noise and pulse signal 20 p3515 A66-37380
- Statistical properties of amplitude and phase of output signal of electron beam quadrupole amplifier with superposition of regular signal plus Gaussian noise at input 20 p3519 A66-37997
- Binaural unmasking of tones masked by broadband Gaussian noise including theoretical work on equalization and cancellation model 21 p3702 A66-38646
- Statistical communication theory, examining problem of selecting set of M equipowered finite duration waveforms to minimize error rate for coherent channel perturbed by white Gaussian noise 21 p3704 A66-39140
- Coding scheme using noiseless feedback link to improve communication over noisy forward link, assuming no bandwidth constraint 21 p3704 A66-39142
- Coding scheme using noiseless feedback link to improve communication over noisy forward link, assuming band-limited signals 21 p3704 A66-39143
- Message estimation of sample function from continuous Gaussian random process, establishing and evaluating optimal bounds for procedure 21 p3720 A66-39637
- Approximately minimax detection of vector signal on Gaussian background 22 p3939 A66-40188
- Colored noise under conditions where noise sources produce white Gaussian noise and physical system is modelled by linear finite-dimensional dynamical systems 22 p3884 A66-40397
- S-band waveguide for pulse compression applications, providing cheap means of compressing wideband swept frequency pulses 23 p4035 A66-41024



Neyman-Pearson detector performance in detecting constant signal in additive Gaussian noise 24 p4173 A66-42623

**GCR**  
**S GAS COOLED REACTOR /GCR/**  
**GEAR**  
**SA LANDING GEAR**  
 Hydraulic gear motor and gear backlash effects on stability of hydraulic control system 01 p0014 A66-10282  
 Kinematic systems and reduction gears used in turboprop engines, outlining design features 01 p0079 A66-11060  
 Disengaging gear lubrication through heat dissipation as factor in Ryder rating of rocket lubricant  
 [ASLE PREPRINT 65-LC-16] 02 p0237 A66-12253  
 Shaft deflection at any point determined by geometric method for shaft diameter selection 05 p0687 A66-14994  
 Gears evaluation testing under vacuum chamber space simulation  
 [ASLE PAPER 66AM 7A4] 16 p2712 A66-30417  
 Disengaging gear lubrication through heat dissipation as factor in Ryder rating of rocket lubricant  
 [ASLE PREPRINT 65-LC-16] 16 p2713 A66-30574  
 Electron beam welding of aircraft turbine gears 21 p3744 A66-39233  
 Machining of gear train made of titanium alloy, discussing surface treatment 23 p4074 A66-41650

**GEAR TOOTH**  
 Effect of engagement angle and tooth distribution on spur gear alignment, establishing relation between rotation diagrams and engagement angle error 01 p0077 A66-10284

**GEGENSCHNEIN**  
 Gegenschnein brightness near 5300 angstroms deduced from photoelectric measurements finding no long period variations, no correlation with airglow, solar flares, etc 16 p2800 A66-30655

**GEIGER COUNTER**  
**SA NEUTRON COUNTER**  
 Primary cosmic rays of superhigh energy using extensive air shower data, noting Geiger-Muller counters, scintillation counters and muon detector 05 p0753 A66-15391  
 Vertical intensity and angular distributions of penetrating cosmic ray muons measured by scintillators, Geiger counters and neon flash tubes, underground in India 06 p0877 A66-17039  
 South latitude cosmic-ray plateau determined by measuring cosmic radiation-caused charged particle and neutron fluxes 08 p1284 A66-19415  
 Primary cosmic radiation and terrestrial radiation belt measurement by Cosmos XVII satellite, noting instrumentation, equipment operation and results 09 p1441 A66-20232  
 Particle localization in spark chamber and ion drift in Wilson cloud chamber, noting experimental result of simultaneous observation of identical particles 09 p1379 A66-20233  
 Transistor portable radioactivity detector utilizing self-quenching Geiger-Muller tube 11 p1703 A66-22268  
 Periodic modulations of energetic electron fluxes observed throughout distant radiation zone by Geiger counters aboard satellites suggest MHD wave activity 13 p2175 A66-26354  
 Counting characteristics of SI-5G counters in pre-Geiger region, measuring voltage dependence of dead time 15 p2502 A66-29114  
 Hodoscope recordings of extensive air showers with abnormally low content of penetrating particles 15 p2579 A66-29523  
 Cosmic ray anisotropy and gamma rays in Orion analyzed, using Geiger counter and Cerenkov telescope 15 p2579 A66-29525  
 Extensive air showers at various atmospheric depths analyzed, using hodoscope counters and ionization chambers, noting differential spectra of densities 15 p2580 A66-29528  
 Multiple muon events at sea level and association with air showers detected, using Geiger and scintillation counters 15 p2580 A66-29533  
 AFCL grazing incidence grating

monochromator used with thin window flow Geiger detector on Aerobee rocket for solar spectrum recordings between 30 and 130 angstroms 15 p2605 A66-30079  
 High energy electron acceleration detected in shock transition region of terrestrial magnetosphere, using Au-Si surface barrier solid state detector and IMP-I satellite mounted GM counter 18 p3177 A66-34753  
 Electromagnetic interactions and collisions of particles in cores of EAS studied, using GM counters, plastic scintillators and Wilson cloud chambers 18 p3207 A66-35107  
 Response to EAS electron-photon cascade of plastic scintillator, cloud chamber and Geiger counter tray compared 18 p3208 A66-35112  
 Meson properties analyzed underground by spark calorimeter operated by telescope of Geiger counters 18 p3220 A66-35194  
 Rocket instrumentation for galactic X-ray observation, noting scintillation counter, proportional counter and GM counter 20 p3636 A66-38237  
 Latitude and longitude variation of count rate and intensity-time dependence of proton flux in inner radiation belt measured by Anton 302 G-M counter in Ariel I satellite 20 p3638 A66-38306  
 Angular dependence of charged neutron-producing component of cosmic rays, using 15-channel counter telescope on rotating platform with neutral monitor 24 p4268 A66-42913  
 Distributions of extensive air showers with either fixed number of charged particles or muons, using Geiger counter and scintillation counter 24 p4268 A66-42914  
 Central region of muon shower investigated, using Geiger counter hodoscope detector 24 p4268 A66-42915

**GEL**  
 Adsorption at semiconductor and gel surfaces discussing chemisorption theory, ionizing radiation effect and structural parameters 04 p0563 A66-13768  
 Nonelectrolytes and hydroxy and fluorobenzoates behavior on elution through columns of tightly cross-linked dextran gels 11 p1645 A66-22990

**GEMINI 4 MISSION**  
 Radiation levels on Gemini IV flight including Van Allen belt and South Atlantic Anomaly 15 p2591 A66-29997

**GEMINI 5 MISSION**  
 Preflight planning and training stages for Gemini V, considering spacecraft test, mission simulators, planetarium, survival and parachute training, etc 17 p2868 A66-32686  
 Astronaut observation in Gemini and Mercury space flights that stars cannot be seen in daytime, noting first-magnitude stars and background illumination 22 p3982 A66-40523

**GEMINI 6 MISSION**  
 Gemini VI rendezvous procedure and results, showing success dependence on presentation to flight crew of sufficient information developed on board 17 p3016 A66-32687

**GEMINI PROJECT**  
**SA MERCURY PROJECT**  
 Reliability program for Gemini Launch Vehicle examining hardware changes, hydraulic redundancy, guidance, power distribution and addition of malfunction detection system 01 p0141 A66-10111  
 Gemini navigation problems considering launch vehicle standby guidance, post insertion orbit correction, catch-up maneuvers, rendezvous terminal guidance, orbit navigation and reentry guidance 02 p0254 A66-11315  
 USAF manned space navigation experiment on Gemini and implications on MOL 02 p0255 A66-11318  
 Gemini and Apollo Earth-orbital programs 02 p0185 A66-11615  
 DOD Gemini experiment D-12 astronaut maneuvering unit /AMU/ design, detailing propulsion, flight control, oxygen and power supply, abort-alarm and communications 02 p0294 A66-11643  
 Mission simulation techniques for training Gemini flight controllers 02 p0186 A66-11802  
 Gemini V failures and successes, evaluating spacecraft and rendezvous guidance and

navigation systems performances and prolonged exposure to space environment 02 p0296 A66-12000  
 USAF manned space navigation experiment on Gemini and implications for MOL 02 p0257 A66-12000  
 Gemini System Interference Monitor /SIM/ for simultaneous monitoring and removal of control of many widely separated test points from central location 05 p0645 A66-14550  
 Gemini guidance and control, discussing design, ground monitoring, launch and flight guidance, spacecraft instrumentation, maneuvering, etc 06 p0906 A66-15900  
 Gemini manned flight program date 07 p1140 A66-17200  
 Astronaut selection and crew preparation procedures for Gemini and Apollo programs 08 p1176 A66-18500  
 Gemini and Apollo space programs, present status, future plans and development trends 09 p1453 A66-20100  
 Gemini and Apollo Earth Orbital flights precursors to Apollo extension and other Earth Orbital missions 10 p1611 A66-21500  
 Logbook account of Gemini VI and V missions 11 p1777 A66-22200  
 Spectrometer for measuring electron flux and energy at Gemini orbital altitudes 12 p1876 A66-23600  
 Weather support problems in Gemini and Apollo programs [AIAA PAPER 66-334] 12 p1953 A66-24400  
 Markov process model of Gemini countdown and transition probability matrix 13 p2192 A66-25500  
 Gemini noncoherent pulse radar system using interferometer methods for angle information, noting failures of diode capacitor combination and methods of reliability improvement 13 p2035 A66-25500  
 Gemini Voice Recording System, MRS 25 for voice-time tape recording during manned space flights 13 p2081 A66-28000  
 Structural dynamics of Gemini program, discussing environmental prediction, component testing, docking system, stability, etc 14 p2393 A66-28000  
 Gemini rendezvous launch operation planning for simultaneous launch countdown 14 p2394 A66-28400  
 Gemini experiments program, examining crew integration, mission planning and prelaunch operations 15 p2606 A66-30000  
 Telemetry tracking acquisition aid system /TELTRAC/ applied to Gemini project, noting antenna, receiver, error analysis, etc 16 p2650 A66-30500  
 Proton energy spectrum of fluxes penetrating packs of passive radiating sensors on Gemini IV and V missions 17 p2865 A66-32700  
 Real time cardiorespiratory rate monitoring for data converter on Gemini space program 19 p3288 A66-35700  
 First half of Gemini program noting design, prelaunch operations, astronaut training, EVA, etc 19 p3469 A66-35800  
 Telemetry system design for astronaut maneuvering unit /AMU/ involving digital combination and filtering of serial PCM pulse train used to modulate FM transmitter 20 p3513 A66-37200  
 Preflight consideration of astronaut performance testing program for Gemini flight, noting manual operations and devices used 24 p4168 A66-42200

**GEMINI SPACECRAFT**  
 Gemini spacecraft rendezvous radar device noting angle measurements, astronaut display, command link and design problems 01 p0105 A66-10800  
 Pulse code modulation /PCM/ for telemetry and communication between Gemini spacecraft Agena D satellite and ground stations for data processing and display 01 p0031 A66-10900  
 Coordinated program for airborne and ground support equipment testing of Gemini spacecraft and launch vehicle by different manufacturers 02 p0294 A66-11600  
 Gemini spacecraft and launch vehicle interface design, development and configuration control 02 p0294 A66-11600  
 Gemini ablative heat shield, noting nonmetallic honeycomb reinforcement and insulative char 02 p0294 A66-11600  
 Gemini spacecraft reentry guidance scheme



with onboard computations of reference trajectory and guidance coefficients [AIAA PAPER 65-48] 03 p0390 A66-12758

Voice communication in space discussing Gemini subsystem, Apollo Command Module system and laser communication techniques 04 p0477 A66-13588

MOL program noting design requirements, operation, functions, etc 08 p1300 A66-18556

Solid state transmitters for Gemini spacecraft telemetry system, noting PCM system operation and design 08 p1181 A66-18728

High reliability system for sensing excessive and potentially dangerous turning rates of Gemini launch vehicle 08 p1225 A66-19525

Digital computers for aerospace guidance and control, including Gemini inertial guidance and B-70 aircraft navigation systems 08 p1187 A66-19597

Gemini rendezvous radar using interferometric angle measuring system, digital range data readout, analog range display and target vehicle command link 09 p1346 A66-20583

Gemini Systems Interference Monitor /SIM/ including signal conditioner having simultaneous monitoring and remote control from central location 11 p1687 A66-23480

Component failure examples of Gemini rendezvous radar, emphasizing need for closed loop reliability program 13 p2039 A66-25786

Thermal and fluid mechanics problems in Gemini spacecraft environment control system development 14 p2226 A66-27813

Materials for manned spacecraft with emphasis on Gemini spacecraft 14 p2406 A66-28003

Launch vehicle testing and hardware reliability in Gemini launch vehicle and Titan II 14 p2394 A66-28427

Monitoring device for detecting short-duration, vibration-induced electrical malfunctions, noting Gemini tests 16 p2677 A66-30454

Mathematical model study of three-mass retrieval technique using anchor mass in space for future Gemini extravehicular operations 16 p2812 A66-31538

Simulation testing pilot performance in orbiting Gemini spacecraft based on tracking rate errors and fuel consumption 17 p2872 A66-31963

Lifting reentry test phases and effect of pilot performance on miss distance in first manned Gemini flight, discussing spacecraft control 17 p3016 A66-32685

Errors in Gemini rendezvous radar interferometer due to antenna ellipticity and coupling of adjacent antennas 17 p2876 A66-33437

Capability, calibration and testing of linear variable differential transformers /LVDT/ for Gemini rendezvous radar 18 p3096 A66-34497

Gemini reentry guidance and control system consisting of inertial guidance and attitude control systems 19 p3470 A66-36679

Data management system synthesis for acquisition, processing and transmission of data aboard manned spacecraft 20 p3514 A66-37209

High speed technique for automatically testing spacecraft PCM telemetry systems 20 p3514 A66-37213

Gemini VII star sightings analyzed, using handheld space sextant in Gemini VI, discussing effect of bias, timing, angle measurement and trajectory errors 21 p3767 A66-38893

Rescue teams for manned testing in environmental chamber for Gemini spacecraft noting personnel, chamber and personal equipment, test operations and rescue function and drill 22 p3857 A66-40240

UV photography quantitative analysis of stellar spectra from Gemini X spacecraft 24 p4273 A66-42209

Gemini ablative heat shield, noting nonmetallic honeycomb reinforcement of insulative char 24 p4283 A66-42773

Stellar extinction measurements made in Gemini IX flight, determining existence and location of Link layer from airglow study 24 p4280 A66-43026

# GENERAL DYNAMICS MILITARY AIRCRAFT

S B-58 AIRCRAFT  
S F-111 AIRCRAFT

## GENERATION

SA HARMONIC GENERATION  
SA HEAT GENERATION  
SA PLASMA GENERATION  
SA REGENERATION  
SA VORTEX GENERATION

Generation recombination noise in Ge single crystals under fast neutron irradiation, using reversible technique to vary noise parameters 16 p2778 A66-31072

## GENERATOR

SA ACOUSTIC GENERATOR  
SA ALTERNATING CURRENT GENERATOR  
SA ARC GENERATOR  
SA COLLOIDAL GENERATOR  
SA COMMUTATOR  
SA ELECTROSTATIC GENERATOR  
SA FUNCTION GENERATOR  
SA GAS GENERATOR  
SA HALL GENERATOR  
SA HARMONIC GENERATOR  
SA IMPULSE GENERATOR  
SA INDUCTOR  
SA MAGNETOHYDRODYNAMIC GENERATOR  
SA MAGNETOSOLIDMECHANIC GENERATOR  
SA NERNST GENERATOR  
SA OPTICAL GENERATOR  
SA PLASMA GENERATOR  
SA POWER GENERATOR  
SA PULSED GENERATOR  
SA QUANTUM GENERATOR  
SA SHOCK WAVE GENERATOR  
SA SIGNAL GENERATOR  
SA SOLAR GENERATOR  
SA STATOR  
SA STEAM GENERATOR  
SA TURBOGENERATOR  
SA VAPOR GENERATOR  
SA VOLTAGE GENERATOR  
SA VORTEX GENERATOR  
SA WAKE GENERATOR

Progress in constant speed drive generating systems and control equipment for constant frequency aircraft electric systems [SAE PAPER 650827] 01 p0016 A66-10827

Operation modes of electron beam generators with resonant oscillating systems and bipolar regenerative amplifiers developed from them 09 p1353 A66-20438

Order-sequence generator for Iris remote control system and telemetry of satellites 14 p2253 A66-27549

Electric energy from helical and coaxial explosive generators noting design, performance, limitations and loss mechanisms 21 p3699 A66-39510

## GENETIC CODE

Amino acid genetic code in which long sequences in DNA spell out instructions transcribed into RNA and subsequently into proteins 11 p1644 A66-22714

Paleogenetic study of ferredoxin structure, reconstructing evolution from amino acid sequence 14 p2228 A66-27810

Physicochemical processes in memory, learning, consciousness and other mental processes in man 15 p2431 A66-28671

Molecular biology noting hemoglobin and enzyme cytochrome evolution, amino acid code, ribonucleic acid, etc 17 p2853 A66-32101

## GENETICS

SA CHROMOSOME  
SA CYTOCHROME  
SA MUTATION

Chemical protection from radiation exposure-induced genetic changes 15 p2438 A66-29484

Postirradiation restitutive capacity of yeast cell suspensions in wort-agar and water after exposure to 1300 rad/min ionizing radiation 15 p2438 A66-29485

Radiosensitivity differences in yeast cells in terms of differences in chromosome-replication and genetic-structure-restitution intensities 15 p2438 A66-29486

Genetic control of gibberellin production in fungus *Gibberella fujikuroi* 23 p4025 A66-41307

## GEOCENTRIC COORDINATE

Assumption of spatial system parallel to mean geocentric system in compensation of triangulation grid 03 p0424 A66-12459

Photographic determination of dependence of topocentric coordinates of Moon on geocentric coordinates 03 p0366 A66-13031

Geocentric pendular control for detection of direction of terrestrial field 05 p0713 A66-15414

Directional accuracy of chords and angles in geocentric equatorial coordinate system in stellar triangulation 12 p1867 A66-23515

Error analysis for statorscope or radar altimeter phototriangulation readings and radio geodetic coordinate photography phototriangulation 12 p1867 A66-23517

Electronic trispheration, three-dimensional analog of triangulation, for long distance geodetic surveys 12 p1875 A66-24936

Influence of parallax of near cosmic bodies on equatorial coordinates 14 p2388 A66-28339

Liapunov method and dynamic programming of stability of motion of variable mass point in Oxyz coordinate reference system, allowing for Earth rotation effects 15 p2538 A66-29046

IAU system of geocentric astronomical constants for ellipsoid Earth 20 p3653 A66-37762

Observational method for determining topocentric and geocentric coordinates of satellite consisting in identification of plane of local meridian or prime vertical on photographic plate 20 p3654 A66-37838

Influence of errors on geocentric position of satellite calculated in accordance with INTEROBS program 20 p3654 A66-37844

Directional accuracy of chords and angles in geocentric equatorial coordinate system in stellar triangulation 21 p3732 A66-38659

Error analysis for statorscope or radar altimeter phototriangulation readings and radio geodetic coordinate photography phototriangulation 21 p3732 A66-38661

## GEOCHEMISTRY

### SA GEOPHYSICS

Biologic-type alkanes of indigenous origin more than 2.7 billion years old present in Precambrian rocks of Sudan formation 03 p0325 A66-12366

Convection pattern changes in Earth mantle and continental drift as evidence of cold origin of Earth 03 p0361 A66-12379

Origin of atypical meteorites from Arizona meteorite crater 05 p0761 A66-15264

Alkali and titanite analyses of tektites before and after G-1 precision monitoring 08 p1291 A66-19076

Terrestrial origin of pseudometeoritic Igast objects 08 p1298 A66-19596

Remote measurement of trace amounts of vapors in lunar and planetary atmospheres as indicator of biologic and geologic surface conditions 10 p1608 A66-21532

Age of Bosumtwi crater area, Ghana, determined by mass spectrometry of rubidium, strontium and strontium isotopic composition, compared to Ivory Coast tektite age 10 p1608 A66-21741

Relative isotopic abundance of potassium 40 in terrestrial and meteoritic samples 11 p1770 A66-22572

Isolation and identification of biogenic steranes and pentacyclic triterpanes in Eocene shale 12 p1805 A66-23539

Nondispersive X-ray spectrometer for remote geochemical analysis of lunar or planetary surfaces 12 p1878 A66-23694

Hydrocarbons synthesized abiogenically and those found in terrestrial samples, using gas chromatography and mass spectrometry in connection with terrestrial life 12 p1806 A66-24965

Chemical composition and origin of moldavites, noting densities, refractive indices, oxide content, rubidium-strontium ratio, etc 13 p2187 A66-26234

Goldschmidt geochemical classification of elements into siderophile, chalcophile, lithophile and atophile groups and pertinence to meteorite research 15 p2598 A66-29632

Spherules from Atlantic Ocean sediments studied by electron microprobe, noting terrestrial alteration and contamination of surfaces 16 p2803 A66-31222

Sulfur compounds analysis in lipid extracts



from Orgueil meteorite support concept of low temperature environment on parent body and differ from petroleum 20 p3648 A66-37304  
Cl, Br and I contents in carbonaceous chondrites measured by activation analysis 21 p3814 A66-39260  
Stratigraphic distribution of carbohydrate residues in middle Devonian Onondaga beds of Pennsylvania and western New York and application to paleontology and paleoecology 22 p3912 A66-40133

GEODESY

SA CELESTIAL GEODESY  
SA TOPOGRAPHY

Geodetic instruments for measurement of angles and lines in large spaces 04 p0524 A66-14397  
Asymptotic behavior of gravitational field studied by Peeling theorem for case where curvature tensor of space-time has direction that can be demonstrated as geodesic trajectory 07 p1080 A66-17451  
Geodesy and gravity 09 p1371 A66-20268  
Numerical solution to first geodetic problem of ellipsoid of rotation, using iterative application of Runge-Kutta method to differential equations of geodetic line 11 p1698 A66-22767  
Soviet book on geodetic gravimetry including disturbing potential calculation methods based on Molodenskii integral equation 14 p2288 A66-28209  
Geophysical monograph on extension of gravity anomalies to unsurveyed areas 17 p2920 A66-33191  
External gravity field and geodetic boundary value problem 17 p2921 A66-33195  
Critical analysis of /Earth/ spheroidal equilibrium configuration 18 p3109 A66-34738

GEODETIC POSITION

Position of artificial Earth satellite determined, using geodetic coordinate system with origin at center of reference ellipsoid 04 p0516 A66-13959  
Determining coordinates of astrogeodetic grid points by Molodenskii integral formulas and accuracy estimation by astrogravimetric interpolation of deviations 08 p1217 A66-19345  
Directional accuracy of chords and angles in geocentric equatorial coordinate system in stellar triangulation 12 p1867 A66-23515  
Error analysis for statorscope or radar altimeter phototriangulation readings and radio geodetic coordinate photography phototriangulation 12 p1867 A66-23517  
Relative geodetic location by measurement of differential Doppler shift of radio signal 12 p1819 A66-24611  
Compensated coordinates of artificial Earth satellites from synchronous observations at two given points on Earth surface 12 p1824 A66-24875  
Electronic trispheration, three-dimensional analog of triangulation, for long distance geodetic surveys 12 p1875 A66-24936  
Determining coordinates of astrogeodetic grid points by Molodenskii integral formulas and accuracy estimation by astrogravimetric interpolation of deviations 19 p3348 A66-36053  
Congruent relativistic gravitational fields, red shift and geodetic coordinate transformations 20 p3603 A66-38011  
Directional accuracy of chords and angles in geocentric equatorial coordinate system in stellar triangulation 21 p3732 A66-38659  
Error analysis for statorscope or radar altimeter phototriangulation readings and radio geodetic coordinate photography phototriangulation 21 p3732 A66-38661

GEODETIC SATELLITE

Satellite geodesy noting gravitational and geometric use, current national program, orbit perturbations, etc 02 p0225 A66-12236  
Problems of spatial triangulation of Europe by means of satellites 03 p0446 A66-12458  
Cosmic triangulation systems assessing polar method for determining geodetic satellite coordinates and inherent error estimation and correction 03 p0361 A66-12502  
Tracking network of Smithsonian Observatory and geodetic results 03 p0336 A66-13026  
Geodetic determinations from photoelectric observations of occultation of stars by satellites 03 p0428 A66-13030

Position of satellite traveling along perpendicular bisector of line joining two fixed points determined by simultaneous observations with accuracy of one inch 03 p0366 A66-13196  
Kepler method in determining length of satellite radius vector independent of linear measurements from Earth, discussing accuracy in geodetic measurement 03 p0366 A66-13197  
Establishment and plotting of suitable coordinate systems for solution of geodetic problems via satellites 03 p0367 A66-13198  
Functional characteristics of Navy Doppler tracking system and satellites used for geodesy, noting data reduction procedures and system tests 04 p0514 A66-13610  
Accuracy in geodetic measurement, discussing contribution of satellite observations 09 p1374 A66-20629  
Hyperaltitude photography, applications and advantages 10 p1535 A66-21523  
Earth atlas based on high altitude photography, Nimbus and IR imagery and high altitude radar 10 p1532 A66-21527  
Absolute direction in space and control of stellar triangulation equations 12 p1875 A66-24874  
Tracking record of synchronous satellites over two-year period revealing effects of second and third order longitude components in Earth gravity - potential field 12 p1875 A66-24893  
Topocentric distance of geodetic satellite GEOS-A measured by laser telemetry from station 16 p2652 A66-30586  
Satellite properties for geodetic application, noting inclination angle, orbit calculation, eccentricity, etc 16 p2700 A66-31794  
Orbital plane precession due to ellipsoidal shape of Earth, discussing effect on meteorological and geodetic satellites 24 p4279 A66-42963

GEODETIC SURVEYING

Information theory applications to angle and line measuring devices with description of use in geodetic instruments 03 p0368 A66-12506  
Radiogeodetic plotting device for piloting aircraft on assigned track 03 p0389 A66-12507  
Establishment and plotting of suitable coordinate systems for solution of geodetic problems via satellites 03 p0367 A66-13198  
Conversion factor determination for gravity changes during Alaska earthquake, using LaCoste-Romberg geodetic meter 09 p1369 A66-19872  
Accuracy in geodetic measurement, discussing contribution of satellite observations 09 p1374 A66-20629  
Data systems requirement for geographic research, noting use of orbiting sensors to obtain information on terrain, vegetation, human and animal activities, etc 10 p1532 A66-21522  
Precise airborne geodetic survey system capable of measuring lines up to 900 nautical miles and determining nadir of aerial photographs to 24 ft 10 p1533 A66-22045  
Celestial mechanics covering two-body problem, planetary and asteroid theory, interplanetary trajectories, lunar probe, spherical harmonics, etc 17 p2997 A66-32019  
Limitations of method of least squares in terms of quality of estimates it provides in geodetic measurements 20 p3590 A66-37471  
Satellite application in geodetic surveys and navigation, noting measurement and tracking techniques 22 p3915 A66-40786  
Satellite radius vector as measure of length in geodesy, noting satellite perturbation factors 23 p4063 A66-41070

GEOELECTRICITY  
SA GEOPOTENTIAL  
Relation between solar activity and geoelectrical phenomena 05 p0761 A66-15229  
Geomagnetic storms employed in determining geoelectrical parameters via magnetotelluric sounding 12 p1868 A66-23668  
Spread in values of vertical magnetic field component during sudden commencements of magnetic storms attributed to local geoelectric conditions 12 p1871 A66-24295  
Earth electrical conductivity, determined from data concerning northern and vertical

components of cyclic geomagnetic variations suggests increases with depth 12 p1871 A66-24299  
Uniform electric field meters for measurement at Earth surface and on aircraft and satellites 12 p1915 A66-24642  
Radio wave propagation over Earth surface determining conductivity and dielectric constant taking into account ground effect 21 p3706 A66-39513

GEOGRAPHY

S ANTARCTICA  
S ARCTIC  
S EUROPE  
S NORTH AMERICA

GEOD

Mutual dependence of harmonic coefficients of gravitational potential derived from satellite observations as source of computed geoid height distortions at Earth surface 16 p2700 A66-31802  
Geoid undulation steady at density discontinuity surface whereas gradient shows instability 18 p3105 A66-34099  
Formulas for extraterrestrial potential anomalous gravity force gradient on Earth topographic surface, deflections of vertical etc 20 p3549 A66-37042

GEOLOGY

SA GEOCHEMISTRY  
SA GEOPHYSICS  
SA LITHOLOGY  
SA LUNAR GEOLOGY  
SA MINERAL  
SA OROGRAPHY  
SA PETROGRAPHY  
SA STRATIGRAPHY

Probable interior structure of planets in solar system and Moon, based on data relative to terrestrial theory 05 p0768 A66-15761  
Fission method to study uranium distribution in natural minerals 09 p1460 A66-20968  
Nimbus I IR scanning radiometry for nocturnal imagery of clouds and other data IR spectral returns and relation to image gray scale 10 p1531 A66-21518  
Geological data on Mars, noting effect of wind 13 p2189 A66-26588  
Geoscience information acquisition by radar return studied by means of terrain target scattering coefficients /scatrometry/ 14 p2244 A66-28408  
Soil investigation and geological map preparation from aerial photographs 15 p2505 A66-30016  
Book on structural geology and tectonics for undergraduates 16 p2692 A66-30261  
Graphite and C-H-O gas phase equilibrium at high temperatures and pressures in implication of Earth ocean and atmospheric development 17 p3015 A66-33432  
Physiographic and geologic features revealed through analysis of pictures from Tiros satellites, useful for terrain information 18 p3104 A66-33742  
Terrestrial calderas, defined as basins of subsidence larger than volcanic crater, associated pyroclastic deposits and possible lunar application 19 p3458 A66-35458  
Geologic evaluation of simultaneous produced like-and cross-polarized radar imagery 19 p3351 A66-36332  
Correlation of like and cross polarized side-looking radar images with geologic features for terrain discrimination 24 p4173 A66-42623

GEOMAGNETIC ANOMALY

Progressive change in worldwide current systems and auroral zone electrojets on geomagnetic bays examined with magnetic data during IGY 01 p0063 A66-10859  
Ionospheric, auroral and geomagnetic observation at Syowa Base, Antarctica 02 p0222 A66-11682  
Sea level cosmic ray intensity and threshold rigidity around South Africa magnetic anomaly, noting Quenby and Wen measurements 07 p1129 A66-18020  
Ionospheric F-2 region equatorial anomaly may not be caused by geomagnetic field 08 p1217 A66-19211  
Annual variations of ionospheric absorption at medium and long wavelengths measured by A3 method at midlatitudes 08 p1220 A66-19777  
Anomalies in cosmic ray intensity increases



- during period of Forbush decrease 09 p1438 A66-20214
- Upper atmosphere physics including heating, circulation, ionization, composition, emissions, geomagnetic variations, polar auroras, etc 09 p1375 A66-20987
- Longitudinal asymmetry of trapped energetic electron intensities attributed to lowering of mirror points in South African anomaly 10 p1599 A66-21160
- Photometric monitorings of 5577 and 6300 angstrom lines during undisturbed geophysical conditions in South Atlantic 10 p1530 A66-21164
- Dependence of extent of noon bite-out on geographic and magnetic coordinates on worldwide basis, noting variation of distortion parameter for diurnal variation of F-2 layer 10 p1533 A66-22061
- Cross sections of geomagnetic field intensity and ionospheric characteristics obtained by airborne equipment crossings of geomagnetic dip equator 13 p2074 A66-26358
- Ionization enhancement from Van Allen electrons in South Atlantic magnetic anomaly, noting longitudinal variation of trapped electrons, electron-ion recombination, etc 13 p2176 A66-26362
- VLF anomalies on midlatitude paths during local nighttime not caused by solar flares, nuclear detonations or magnetic storms 13 p2074 A66-26365
- Changes in cosmic-ray rigidity spectrum during cosmic ray storms, showing correlation with magnitudes of geomagnetic disturbances 15 p2574 A66-28900
- Dependence of frequency distribution of auroral displays in zenith on latitude and local time in magnetically quiet and disturbed periods analyzed by all-sky camera network in Northern Hemisphere 15 p2488 A66-29227
- Precipitation flux of quasi-trapped energetic electrons near low altitude fringes of inner radiation belt as they drift into South Atlantic magnetic anomaly 18 p3170 A66-34520
- Riometer recordings at high geomagnetic latitude of intense and sporadic absorption events correlated with occurrence of auroral and geomagnetic disturbances 18 p3108 A66-34531
- Longitude dependence of distribution function of electrons for fixed value of McIlwain parameter, using kinetic equation 18 p3197 A66-34873
- Butare crater, showing existence of nonnegligible anomalies, noting hypothesis of oblique penetration 20 p3657 A66-38067
- Anomalous enhancement of F-2 ionization in high latitude around geomagnetic noon due to formation of irregularity or new layer around locality 20 p3658 A66-38234
- Acceleration of electrons in inner radiation belt by magnetic field variations over slope of geomagnetic anomaly in resonance with longitudinal drift frequencies of electrons 20 p3638 A66-38308
- Changes in 1 to 4 mev electron population during solar quiet periods and 55-mev protons near South Atlantic anomaly measured by various geophysical satellites 20 p3638 A66-38310
- Temporal stability of inner zone protons determined by Injun I satellite measurements in vicinity of South Atlantic magnetic anomaly 20 p3638 A66-38311
- Ionospheric ionization produced by precipitation of particles from Van Allen belts, examining influence of magnetic anomalies, longitudinal drift and local effects during magnetically quiet periods 20 p3641 A66-38325
- Phase anomaly detected by chemical test D during decreasing phase of last solar cycle 21 p3732 A66-38629
- Semiannual variation in geomagnetic disturbance amplitudes consisting of one-to-one correspondence between average daily amplitude index and solar declination 21 p3732 A66-38635
- Annual variations of ionospheric absorption at medium and long wavelengths measured by A3 method at midlatitudes 21 p3732 A66-38775
- Geomagnetic disturbances due to dynamo effect of ionospheric winds in lower layers of ionosphere 24 p4204 A66-43150
- Distribution of active periods of magnetic disturbances during day and variation as affected by contact of solar magnetic flux with magnetosphere 24 p4204 A66-43151
- GEOMAGNETIC CROTCHET**
- S IONOSPHERIC CURRENT**
- GEOMAGNETIC EFFECT**
- Magnetic activity effect on F-2 region drifts and variation with time at low latitude station 03 p0361 A66-12633
- Relationships between VLF phase fluctuations, radio signal fading and natural geomagnetic background observed in British Columbia 04 p0487 A66-14367
- Dense sporadic E cloud effects on high latitude HF backscatter observation 05 p0667 A66-14792
- Polar cap absorption riometer data compared for Thule, Greenland and College, Alaska for determining geomagnetic activity influence 05 p0670 A66-14951
- Difference in cosmic ray intensity due to variations in geomagnetic cut-off 06 p0948 A66-16581
- Solar modulation and geomagnetic effects on cosmic rays, noting daily variation and rigidity spectrum 07 p1122 A66-17990
- Plasma and magnetic field data from Explorer X, emphasizing correlation with multiple crossings of geomagnetic cavity boundary on dark hemisphere of Earth 07 p1029 A66-18087
- Equilibrium electron density distribution in F-2 region of equatorial ionosphere, noting effects of photoionization, loss, diffusion along geomagnetic field lines and electromagnetic drift 08 p1216 A66-19210
- Transition region magnetic field and polar magnetic disturbances, comparing Explorer XII data with ground measurements from Arctic observatories 08 p1218 A66-19399
- Long-term geomagnetic influence on medium frequency nighttime sky wave field strength 09 p1341 A66-19916
- Terrestrial radiation belt measurement with Cosmos satellite, noting launch and orbit data, instrumentation and results 09 p1441 A66-20231
- Procession of UK-3 satellite perturbed by geomagnetic torque 09 p1464 A66-20474
- High time-resolution measurement of knee position in magnetospheric ion density using whistlers 10 p1527 A66-21137
- Electron density and total electron content in force tubes near knee in magnetospheric ionization studied, using whistlers 10 p1527 A66-21138
- Geomagnetic activity corresponding to 11-year sunspot cycle shown to occur in double sunspot cycle /22 years/ 10 p1604 A66-21159
- Differences in MHD emission occurrence times, considering ionospheric penetration propagation toward equator and error sources 11 p1701 A66-23150
- HF noise signals and association with auroral disturbances analyzed, using data from IGY network of backscatter sounders 11 p1701 A66-23154
- Statistical-probability determination of lunar-solar daily and seasonal magnetic variations and geomagnetic effects 12 p1951 A66-24463
- Cylindrical coordinate system describing geomagnetic field analyzed, noting consequences in magnetic cartography when going from field to time gradients 12 p1875 A66-24970
- Spacecraft magnetic testing, discussing geomagnetic effects on orbiting satellites, magnetic dipole moment, etc 13 p2058 A66-25847
- Rotation in polarization ellipse of hydromagnetic oscillations type Pc 1 from observations at magnetically conjugate stations 13 p2073 A66-26347
- Solar wind parameters and geomagnetic activity determined from satellite plasma experiments and observations of magnetopause locations 13 p2075 A66-26368
- Sporadic E layer formation by wind motion in conjunction with geomagnetic and electric fields 14 p2281 A66-26848
- Auroral zone position changes as function of magnetic activity and time of day 15 p2486 A66-29091
- Total ionospheric electron content measurements at Delhi using Faraday fading of satellite beacon transmissions during solar minimum 15 p2495 A66-30067
- High resolution power spectrum of international magnetic character, showing two subsidiary peaks on both sides of 27-day period 16 p2695 A66-30719
- Direct phase technique for studying polarization phenomena associated with reflections of radio waves from meteor trails 16 p2655 A66-31543
- Worldwide geomagnetic disturbances generated by Starfish high altitude nuclear detonation, July 9, 1962 17 p2918 A66-32527
- Daily variations of cosmic ray distribution, examining effect of geomagnetic field, aperture, orientation and geographical position of counters 18 p3195 A66-34865
- Ground magnetogram-IMP I data comparison and geomagnetic field effects on interplanetary magnetic field sector structure 20 p3657 A66-38219
- Electron concentration data obtained by rocket probes in quiet ionosphere with solar and geomagnetic activity, as function of time of day, season and altitude 21 p3809 A66-38772
- Variation of geomagnetic activity with phase of Moon tested for statistical significance, noting fluctuations at lunar period 22 p3982 A66-40555
- Equatorial measurement of intensity of protons with energies greater than 400 kev and electrons with energies greater than 2 mev in outer radiation belt center in 1964 22 p3974 A66-40755
- Dependence of seasonal occurrence probability of F-zero layer on level of geomagnetic activity and ionospheric activity observed above 22 p3914 A66-40760
- Ashkhabad Guiding of whistlers due to exospheric anisotropy, electron density and geomagnetic field effects 22 p3915 A66-40803
- Diurnal behavior of topside and bottomside spread F at equatorial latitudes and association with geomagnetic activity 24 p4200 A66-42591
- Subsidiary peaks in power spectra of CI and Kp /magnetic indices/ attributed to amplitude modulation of 27-day components 24 p4201 A66-42607
- GEOMAGNETIC EQUATOR**
- Electrostatic probe, discussing Explorer XXII measurements of electron concentration and temperature at 1000 km altitude 05 p0746 A66-14782
- Flux of alpha component of primary cosmic radiation determined at top of atmosphere, using nuclear emulsion stack exposed near geomagnetic equator 05 p0756 A66-15529
- Intensities and ratios of intensities of Be, B and S nuclei determined near geomagnetic equator in India, using nuclear emulsion stack 10 p1600 A66-21844
- Photometric measurements of tracks of heavy primary particles found in emulsion stack near geomagnetic equator, noting ratio of C and N nuclei to O nuclei 11 p1762 A66-22654
- Effects of solar flare radiation on electron density of F-2 layer at maximum level in and near equatorial anomalous zone 12 p1944 A66-24834
- Primary proton and helium nuclei flux and East-West and North-South asymmetries measured near geomagnetic equator 18 p3193 A66-34854
- Synchrotron radiation measurements near magnetic equator, noting radio spectrum radiation due to injection of relativistic electrons into trapped orbits of geomagnetic field 20 p3644 A66-38347
- GEOMAGNETIC FIELD**
- SA MAGNETOSPHERE**
- Vertical continuation of two-dimensional geomagnetic and gravitational fields from given contour line on Earth surface by two methods 01 p0060 A66-10161
- Geomagnetic field fluctuations corresponding to solar wind intensity changes as related to change in phase of solar activity cycle 01 p0061 A66-10279
- Modifying spherical harmonic analysis of surface geomagnetic field to account for Earth oblateness by two methods 01 p0061 A66-10615
- Geomagnetic field represented as dipoles located by least squares gradient



method 01 p0063 A66-11052  
 Geomagnetic activity forecasting method based on investigation of solar chromospheric structure and filaments as indicative of magnetic conditions in layers 01 p0064 A66-11100  
 Ocean current effects on geomagnetic field and aurora borealis 02 p0221 A66-11344  
 Algebraic sign of voltage field components in orbital coordinate system, using dipolar approximation of Earth magnetic field 02 p0295 A66-11655  
 Motion equation for satellite with passive and semipassive attitude control using geomagnetic field, considering elliptical and circular orbits and involving differential equations 02 p0295 A66-11670  
 Compression of geomagnetic field effect on cosmic radiation at cut-off rigidities and asymptotic directions of radiation incidence 02 p0283 A66-12111  
 Quiet solar diurnal variations of geomagnetic field at middle and low latitudes during IGY to determine coordinate system and equatorial electrojet 02 p0224 A66-12118  
 Structural design and equipment of three-component mobile field station Izmiran-4 that uses quartz sensitive elements for magnetic variation 02 p0232 A66-12123  
 Excitation of magnetic field in spherical conductor for case where vortex concentration is assumed to be constant for entire core 02 p0225 A66-12141  
 Earth magnetic field represented as dipole field to study secular variations of field 02 p0225 A66-12142  
 Propagation and diffraction of electromagnetic waves in inhomogeneous magnetoionic medium, noting exoionospheric propagation and Hamiltonian optics 02 p0192 A66-12208  
 Interplanetary medium observation from zodiacal light and radio wave scattering during radio source occultation and influence on galactic and solar cosmic rays 03 p0425 A66-12852  
 Corrected tables and maps of geomagnetic coordinates, covering methods of calculation and corrected data charts 04 p0513 A66-13377  
 Terrestrial magnetic field and secular variations 04 p0514 A66-13448  
 Quiet diurnal solar variations and relation to ionospheric parameters 04 p0516 A66-13852  
 Total vector modulus measurements from absolute field element observations and proton magnetometer 04 p0516 A66-13866  
 Electron density distribution in magnetosphere inferred from dispersion characteristics of hydromagnetic wave propagating between hemispheres along geomagnetic field as in atmospheric whistlers 05 p0747 A66-14787  
 Electric currents in ionosphere measured by sounding rockets equipped with nuclear free precession magnetometers and Langmuir probes launched near Peru 05 p0668 A66-14800  
 Quasi-stationary corpuscular streams from Sun suggesting role of active regions in formation 05 p0748 A66-14867  
 Lower ionospheric wind effect on geomagnetic field 05 p0668 A66-14935  
 Geomagnetic secular variation data analyzed at five observatories indicates high significance for amplitudes obtained for 50-year cycle by harmonic analysis 05 p0670 A66-14952  
 Shifts in output frequency of cesium vapor magnetometer due to temperature, light intensity and orientation, noting Zeeman component and geomagnetic field 05 p0678 A66-14968  
 Day-to-day variability of terrestrial magnetic daily variation, establishing morphology of different types 05 p0673 A66-15042  
 Oscillations of geomagnetic field recorded at two high-latitude conjugate points, noting frequency spectra and amplitude relationships 05 p0673 A66-15049  
 Earth magnetic field including mathematical descriptions, origin, daily magnetic variations, polar and auroral disturbances, magnetic storms, activity

indices and whistlers 05 p0675 A66-15742  
 Cosmic ray intensity and geomagnetic field changes induced by electric current systems excited in ionosphere, noting seasonal changes in diurnal variations 06 p0950 A66-16596  
 Structure and variation of radiation belts during magnetic storm, including configuration of forbidden region in connection with magnetic field 06 p0951 A66-17048  
 Magnetospheric boundaries formation, noting neutral points on day and night sides and possible penetration of solar flux particles 06 p0877 A66-17170  
 Westward drift of secular variations in inclination and alteration of terrestrial magnetic moment estimated from archeomagnetic data 07 p1027 A66-17307  
 Vertical cut-off rigidities of cosmic rays, using sixth degree simulation of geomagnetic field 07 p1128 A66-18019  
 Data analysis from Explorer XIV satellite, noting magnetic field measurements in tail of geomagnetic cavity 07 p1029 A66-18086  
 Correlation relations between cosmic ray neutron intensity, horizontal magnetic field strength, critical wave frequency and terrestrial currents 08 p1283 A66-18706  
 Spherical harmonic analysis of main part of Earth magnetic field from standpoint of probability theory 08 p1214 A66-19037  
 Statistical analysis of worldwide magnetic charts of epoch 1955.0 for main part of Earth magnetic field 08 p1214 A66-19038  
 Distribution of Z-component of geomagnetic field at high altitude calculated by integral and spherical analysis methods 08 p1214 A66-19039  
 Comparison of magnetic observations aboard Zaria and aeromagnetic surveying according to magnet plan 08 p1214 A66-19040  
 Geomagnetic and ionospheric observations of 1964 expedition of Zaria 08 p1214 A66-19041  
 Towed Z magnetometer with pendulum supported by Cardan suspension, comparing measurements with those obtained on Zaria 08 p1223 A66-19055  
 Dynamo origin of geomagnetic field, involving creation of toroidal and polar fields by nonuniform rotation 08 p1215 A66-19117  
 Interplanetary medium properties considered in scaling of observed effects of interaction of solar wind with Earth dipolar magnetic field 08 p1292 A66-19123  
 Appleton anomaly of F-2 layer examined, assuming ionization induced horizontal motion of neutral air 08 p1215 A66-19207  
 True height variations of F-2 layer for bay disturbances of geomagnetic field obtained from ionograms, assuming they are caused by horizontal electric field 08 p1216 A66-19213  
 Ionospheric disturbances following geomagnetic sudden commencements propagating from two isolated locations in high latitudes which are conjugate points 08 p1216 A66-19214  
 Correlated magnetic tail and radiation belt observations from Explorer 18 /Imp I/ satellite and APL satellite 1963 38C in April 1964 08 p1284 A66-19411  
 Tabulation of spherical harmonic coefficients of geomagnetic field data for trapped-particle evaluation 08 p1219 A66-19419  
 Spinning rocket attitude measured from geomagnetic field and solar cell data, using digital computer technique, noting instrumentation 08 p1225 A66-19492  
 Attitude control system, using magnetic interaction with geomagnetic field to check spin rate and spin axis orientation of spin-stabilized Explorer A 08 p1304 A66-19512  
 Digital simulation of magnetic hysteresis, using analytic approximation of magnetic curves by seventh degree polynomials 08 p1187 A66-19513  
 Hourly distribution and variation of perturbed geomagnetic field, using instantaneous synoptic charts in geomagnetic coordinates 08 p1220 A66-19783  
 Energy transfer mechanism in solar corpuscular flux interaction with terrestrial magnetosphere 08 p1285 A66-19786

Earth daily diurnal rotation rate variation assuming solar corpuscular flux composition of plasmoids possessing quasi-force-free magnetic fields 08 p1220 A66-19788  
 Design and operation of telemagnetograph for visual observation of geomagnetic field 08 p1228 A66-19798  
 Total geomagnetic field intensity measurements made over last ten years facilitate preliminary magnetic anomaly map of Gulf of Mexico 09 p1369 A66-19877  
 Toroidal fields in Earth fluid metallic core brought to surface, causing changes with time in geomagnetic field 09 p1369 A66-19877  
 Geomagnetic cut-off rigidity variation calculated relative to disturbed field model, represented by equatorial current 09 p1438 A66-20211  
 Latitude variation of second harmonic of diurnal variation of cosmic rays, considering curvature of particle trajectories in geomagnetic field 09 p1439 A66-20222  
 Magnetic fields in magnetosphere, using electrostatic and electromagnetism units, noting Earth field, high altitude and distant fields, etc 09 p1371 A66-20277  
 Ionospheric dynamo theory with consideration for magnetospheric current along geomagnetic force lines, noting S variation in solstices 09 p1372 A66-20370  
 Nocturnal electrical conductivity of equatorial ionosphere 09 p1373 A66-20387  
 Satellite emission of variable frequency signal guided by ionization irregularities existing along force line of geomagnetic field 09 p1374 A66-20388  
 Geomagnetic field measurements by Cosmos satellites at 49 degrees latitude including typical magnetograms of magnetic field intensity 10 p1526 A66-21051  
 Role of coupling phenomena in recombination processes of complex ionosphere composed of two types of positive ions examined via wind-shear theory 10 p1526 A66-21128  
 Morphological analysis of daily variability of geomagnetic field regular daily changes, noting current systems in polar and nonpolar regions 10 p1526 A66-21127  
 Effect of Moon phase and celestial latitude on lunar modulation of geomagnetic activity 10 p1529 A66-21157  
 Vlasov equation of particle orbits in planar magnetic fields, with application to shock wave at geomagnetopause 10 p1606 A66-21241  
 Ionospheric electrodynamics, discussing conductivity, wind and dynamo theory, drift effect on ionospheric formation and wind-electromagnetic field interaction 10 p1533 A66-21857  
 Correlation coefficients for daily ranges of horizontal component of quiet day diurnal magnetic variation 11 p1695 A66-22377  
 Interaction of solar corpuscular stream with geomagnetic field forming Earth's magnetosphere and particle penetration within magnetosphere in neutral point region 11 p1696 A66-22407  
 Noncyclic variation during magnetically quiet days, examining seasonal changes in geomagnetic field value at night during IGY 11 p1696 A66-22420  
 Geographic distribution of solar daily variations of magnetic field during quiet days determined by coordinate system 11 p1696 A66-22422  
 Analytical representation of secular variation of geomagnetic field between 1850 and 1950 11 p1696 A66-22422  
 Imp-I observation of magnetic wake of Moon or Earth 11 p1697 A66-22422  
 Secular variation of atmospheric radiocarbon concentration, noting dependence on geomagnetic field strength 11 p1698 A66-22568  
 Matrix techniques for finding geomagnetic field strength in solar ecliptic coordinate system 11 p1699 A66-23052  
 Geomagnetic field confinement by solar wind to form magnetosphere and magnetic tail 11 p1699 A66-23127  
 Imp-I observations of solar wind properties, including interaction with geomagnetic field and flow characteristics of positive ion component 11 p1775 A66-23132  
 Solar wind particle diffusion into geomagnetic tail and then down field lines to polar cap 11 p1700 A66-23142



Propagation of MHD emissions in Alfvén mode along high latitude geomagnetic field lines, auroral zone signal energy penetration and isotropic wave mode  
11 p1701 A66-23151

Monograph on methods and equipment used by Soviet satellites and space probes to study Earth radiation belts  
12 p1938 A66-23802

Reconnection of magnetic lines of force to form closed loops during transient phase of rotation of spheres and cylinders from rest  
12 p1868 A66-23857

Magnetic fields of terrestrial planets, considering Mariner II measurements of magnetic field of Venus and motions in Earth core  
12 p1948 A66-24032

Satellite data indicates correlations between cosmic ray variations and radiation intensity of radiation belts and related phenomena  
12 p1941 A66-24170

Forbush effect and solar cosmic ray manifestation of effect of compression of Earth magnetosphere  
12 p1941 A66-24174

Diurnal and semidiurnal variations in cosmic-ray hard component and magnetic activity  
12 p1942 A66-24176

Motion of magnetically charged neutrino in cosmic magnetic fields  
12 p1942 A66-24181

Effect of higher harmonics of geomagnetic field on cosmic ray trajectories, noting reception cones of Soviet stations  
12 p1943 A66-24268

Diurnal and seasonal altitude variations of E and F layers analyzed for geomagnetic activity from rocket measurement of electron concentration  
12 p1869 A66-24269

Structure of main geomagnetic field over Eurasia, noting difference in spectra over oceans and continents  
12 p1870 A66-24280

Relation between magnetic activity and ionospheric disturbances in F-2 layer studied on basis of 30-year data  
12 p1870 A66-24285

Ionization structure of polar auroras from spatial distribution of radar-reflecting zones, taking into account magnetic field variations  
12 p1871 A66-24293

Earth electrical conductivity, determined from data concerning northern and vertical components of cyclic geomagnetic variations, suggests increases with depth  
12 p1871 A66-24297

Plasma effect on dipole magnetic field and solar wind plasma-geomagnetic field interaction  
12 p1943 A66-24391

Electron distribution from 400 to 1200 km measured, using Ariel I satellite, noting latitudinal and longitudinal anomalies associated with geomagnetic field  
12 p1872 A66-24511

[ATAA PAPER 66-395]

Ionograms made at Australian ionosonde stations during magnetically quiet world day interval, obtaining information on F region ionization, noting existence of universal time control of ionization  
12 p1873 A66-24835

Contour maps of diurnal changes in magnetic elements provided by observatory tabulations of mean hourly values of mean monthly days  
12 p1873 A66-24836

Cylindrical coordinate system describing geomagnetic field analyzed, noting consequences in magnetic cartography when going from field to time  
12 p1875 A66-24970

Explorer XX satellite observations of plasma resonances at fixed frequencies in topside ionosphere, noting patterns, effect of geomagnetic field, electron concentration, etc  
13 p2074 A66-26352

Equatorial electrojet cross section profile, describing longitudinal variations, current density, magnetic field produced and electron drift velocity  
13 p2074 A66-26357

Cross sections of geomagnetic field intensity and ionospheric characteristics obtained by airborne equipment crossings of geomagnetic dip equator  
13 p2074 A66-26358

Magnetic toroidal resonances and vibrating field lines, using basic toroidal equation in determining validity of heuristic vibrating string model  
13 p2074 A66-26359

Lower hybrid resonance in VLF range in satellites, noting noise emission due to trapping of electromagnetic wave propagation in transverse magnetic field  
13 p2074 A66-26364

Auroral absorption of cosmic radio noise which is not identical at magnetic conjugate

point  
13 p2076 A66-26743

Doppler frequency changes in vertically incident and reflecting sounding wave associated with geomagnetic disturbances yields information on ionospheric electric field  
14 p2234 A66-26856

Orbit precession effect on gyroscopic stabilization of satellite in geomagnetic field  
14 p2391 A66-27473

Generalization of measurement of vertical and horizontal components of terrestrial magnetic field intensity with proton magnetometer  
14 p2295 A66-27624

Compression of geomagnetic field effect on cosmic radiation at cut-off rigidities and asymptotic directions of radiation incidence  
14 p2377 A66-28070

Quiet solar diurnal variations of geomagnetic field at middle and low latitudes during IGY to determine coordinate system and equatorial electrojet  
14 p2286 A66-28077

Excitation of magnetic field in spherical conductor for case where vortex concentration is assumed to be constant for entire core  
14 p2287 A66-28097

Earth magnetic field represented as dipole field to study secular variations of field  
14 p2287 A66-28098

Pioneer I observations of geomagnetic field, discussing amplitude and polarization of oblique pulses, existence of collisionless oblique magnetic shock waves, soft electron acceleration, etc  
15 p2482 A66-28500

Metrological characteristics of three-component magnetometers with ferromagnetic probes installed in Elektron II space station  
15 p2497 A66-28501

Auroras, frequency, geographical distribution, types, evolutionary processes and auroral phenomena  
15 p2482 A66-28517

Elementary geomagnetic polar disturbances, lip-shaped auroral ionization patterns and existence of energetic electrons on night side of magnetosphere  
15 p2485 A66-28909

Solar wind magnetic field as medium for plasma-magnetosphere interaction  
15 p2575 A66-29078

Electrical conductivity of Earth interior from data concerning annual geomagnetic variations for all years of solar cycle  
15 p2487 A66-29101

Solar corpuscular stream magnetic field effect on change in orientation of geomagnetic field related to change in stream geoeffectiveness  
15 p2575 A66-29102

Correlation of time variations of proton and electron intensity of outer radiation belt and dependence on geomagnetic environment  
15 p2575 A66-29103

Overhead ionospheric current function corresponding to Sq field, examining assumption of rotation of quiet day horizontal component  
15 p2488 A66-29231

High incidence and erraticism of sporadic E occurrence in temperate zones where horizontal component of geomagnetic field is greatest, attributed to horizontal wind shear  
15 p2490 A66-29949

Electron component of plasma sheet of terrestrial magnetic trail, noting energy distribution and densities  
16 p2792 A66-30142

Radiation belt origin, examining acceleration of solar plasma electrons to energies of 30 to 100 kev by nonlinear waves called solitons  
16 p2792 A66-30156

MHD model of interface between solar wind and geomagnetic field on Earth tail, showing existence of unstable waves  
16 p2695 A66-30717

Mathematical model for geomagnetic field for 1965 given by internal and external spherical harmonic coefficients  
16 p2695 A66-30718

Rocket attitude determined by simultaneous measurement of geomagnetic field and electromagnetic field generated by radio wave transmitted by rocket-mounted dipole  
16 p2810 A66-30958

Solar corona and interplanetary plasma noting solar wind effect on comet tails and shock wave caused by interaction of geomagnetic field and plasma  
17 p3000 A66-32272

Type I comet trail relation to interaction of solar wind with geomagnetic field, noting tail ray formation mechanism, interplanetary

plasma measurements, etc  
17 p3012 A66-33396

Dynamics of geomagnetic tail, noting transformation of magnetic energy into kinetic energy due to pinch instability and auroral activity  
18 p3106 A66-34162

Reconnection mechanism for geomagnetic and interplanetary field lines, estimating field-cutting efficiency at magnetopause  
18 p3231 A66-34348

Magnetopause boundaries and geomagnetic field at magnetopause and interaction region by IMP I  
18 p3106 A66-34352

Magnetosphere shape and distortion of magnetic field within magnetosphere  
18 p3106 A66-34353

Effect of 49-, 64- and 100-term expansion of geomagnetic field on reduction of omnidirectional proton counting rate data  
18 p3108 A66-34532

Geomagnetic field intensity in India over past 4,000 years determined from ancient remanent magnetization in bricks, pots and potsherds  
18 p3108 A66-34716

Satellite and space probe measurements indicate continual confinement of geomagnetic field by solar wind forming magnetosphere and Earth magnetic tail  
18 p3235 A66-34742

Generically related cosmic ray spectrum explaining variations in abundance ratios of helium isotopes and light to medium elements in terms of solar and geomagnetic modulation  
18 p3178 A66-34758

Smooth curves of cosmic ray neutron component intensity variations compared with H component of geomagnetic field during IGY and IGC  
18 p3196 A66-34868

Threshold rigidities for vertical incident cosmic ray particles derived, using trajectory computations by higher-order simulation of geomagnetic field  
18 p3198 A66-34881

Effect of geomagnetic cavity field on cosmic ray threshold rigidity, using model of cavity field, finding cavity shape produces amplitude in diurnal variation of cosmic ray intensity  
18 p3198 A66-34882

Effects of deformed magnetic field on trajectories and asymptotic directions of arrival of medium energy cosmic rays at various stations, using spherical harmonics  
18 p3198 A66-34883

Cosmic ray threshold rigidities examined, discussing penumbral and threshold perturbation effects produced by superimposing external magnetic fields on dipole model  
18 p3096 A66-35227

Multipole parameters for series of spherical analysis of geomagnetic field from 1829 to 1958  
19 p3344 A66-35258

Secular variations of geomagnetic field before our era studied by method using archeological objects  
19 p3345 A66-35273

Device for visible recording of H component of geomagnetic field  
19 p3352 A66-35275

Data on geophysical phenomena at magnetically conjugate points on Earth including cosmic noise absorption, conjugacy of visual auroras, magnetic variations, VLF phenomena, etc  
19 p3453 A66-35981

Geomagnetic cut-off rigidities determined for cosmic ray particles arriving at top of atmosphere over Hyderabad as function of zenith and azimuthal angles  
19 p3454 A66-36642

Planetary magnetic fields noting Earth magnetic field  
20 p3648 A66-37295

Tropospheric and ionospheric refraction, aspect sensitivity and height of radio aurora, backscatter radar aurora observation and geomagnetic field anomalies  
20 p3520 A66-38199

Polar geomagnetic and solar terrestrial disturbances related to PCA and solar flare  
20 p3636 A66-38228

Magnetosphere tail, annual magnetospheric configurative variation and seasonal variation in polar cap magnetic intensity  
20 p3657 A66-38229

Geomagnetic field model based on definition of core field, crustal field, ionospheric currents and plasma pressures, examining trapped particle behavior  
20 p3555 A66-38302

Definitions and properties of magnetic



coordinates B, L, K, R, lambda and A, discussing role of these parameters in study of geomagnetically trapped particles 20 p3555 A66-38304

Charged particles and plasma in geomagnetic field, noting diffusion of trapped particles and acceleration by Fermi mechanism and wave acceleration 20 p3640 A66-38319

Magnetospheric boundary phenomena, noting dependence of charged particle observations on character of associated magnetic fields 20 p3641 A66-38329

Adiabatic theory of distorted motion of charged particles in geomagnetic field, showing dependence on equatorial pitch angle 20 p3642 A66-38332

Magnetosphere tail sheet pinch model, discussing motion of particles for cases of surface crossing 20 p3642 A66-38336

Fluid mechanics model representation of solar wind and geomagnetic field interaction, noting flow parameters in shock layer and application of MHD equations 20 p3642 A66-38337

Synchrotron radiation measurements near magnetic equator, noting radio spectrum radiation due to injection of relativistic electrons into trapped orbits of geomagnetic field 20 p3644 A66-38347

Principal geomagnetic field approximation by centered dipole field and eccentric dipole field 21 p3732 A66-38663

Hourly distribution and variation of perturbed geomagnetic field, using instantaneous synoptic charts in geomagnetic coordinates 21 p3732 A66-38779

Energy transfer mechanism in solar corpuscular flux interaction with terrestrial magnetosphere 21 p3809 A66-38782

Earth daily diurnal rotation rate variation, assuming solar corpuscular flux composition of plasmoids possessing quasi-force-free magnetic fields 21 p3733 A66-38783

Design and operation of telemagnetograph for visual observation of geomagnetic field 21 p3736 A66-38795

Stabilization and control system of Tiros-wheel satellite, using current-carrying coil interaction with geomagnetic field 21 p3821 A66-38878

Magnetic field-aligned ionization detected during minimum sunspot activity, using radio telescopes of radio interferometer 22 p3908 A66-39964

Vacuum conditions in space based on data obtained by Earth-orbiting satellites, noting shock front and magnetopause caused by interaction of solar wind with geomagnetic field 22 p3979 A66-40205

Field boundary of two line currents immersed in streaming plasma treated by conformal transformation 22 p3956 A66-40386

Magnetic field of ring current on Earth surface according to observations during IGY 22 p3914 A66-40768

Diurnal variation in principal direction of E and H vectors of Petropavlovsk-Kamchatka K index of geomagnetic field in horizon and planetary relation 22 p3914 A66-40769

Steady pearl type oscillations in terrestrial electromagnetic field, noting role of diurnal and seasonal variations 22 p3915 A66-40784

Optimum filter for separation of principal geomagnetic field and magnetic field associated with Earth thin magnetoactive crust layer 22 p3915 A66-40785

Dense particle population of Van Allen belts formed by interaction of high energy corpuscular radiation with interplanetary magnetic field and geomagnetic field 23 p4123 A66-41186

Cusp configuration of neutral point on boundary of geomagnetic cavity in solar wind 23 p4123 A66-41508

Comparison of various geomagnetic variations associated with corpuscular precipitation at South Pole, noting day-night effect 23 p4064 A66-41688

Equinoxes, having highest solar corpuscular radiation hitting probability, as observation periods for geomagnetic activity, aurora, etc 24 p4274 A66-42433

Lunar modulation of geomagnetic activity from 1884 to 1959 analyzed using magnetic character figure, noting relation to solar activity 24 p4201 A66-42598

Angular dependence of charged neutron

producing component of cosmic rays, using 15-channel counter telescope on rotating platform with neutral monitor 24 p4268 A66-42913

Magnetospheric phenomena related to geomagnetic tail noting F region, polar auroras and solar Lyman alpha radiation scattering in night sky 24 p4203 A66-43029

Adiabatic theory and lowest order invariants applied to Van Allen radiation indicate that without collisions particles would remain in geomagnetic field 24 p4240 A66-43110

## GEOMAGNETIC HOLLOW

Intensity estimation for lunar X-rays excited by high energy terrestrial electrons from solar stream induced geomagnetic cavity 09 p1442 A66-20388

Solar plasma flow around geomagnetic cavity studied by numerical blunt body analog, proposing MGD boundary pressure as condition for self-consistent solution [AIAA PAPER 65-121] 10 p1533 A66-21775

Magnetohydrostatic cavity formed around system of line currents in infinitely conducting atmosphere 14 p2279 A66-28394

## GEOMAGNETIC LATITUDE

Tables and maps of geomagnetic coordinates corrected by higher order spherical harmonic terms 01 p0062 A66-10888

Catalog of observations on auroral phenomena in Western Europe below geomagnetic latitude of 55 degrees for years 1601 to 1700 01 p0139 A66-11104

Excessive cosmic radiation absorption in lower nocturnal ionosphere at middle geomagnetic latitudes during Forbush effects 04 p0514 A66-13443

Neutron albedo flux at 45 degree geomagnetic latitude 07 p1121 A66-17982

Time variation of primary cosmic ray rigidity spectrum over solar cycle derived by measuring latitude effect of nucleonic components 07 p1127 A66-18016

Scintillation counter satellite data on low energy electron flux and particle trapping in dark magnetosphere 08 p1218 A66-19394

Intensity variation of nucleonic component of atmospheric cosmic radiation, geomagnetic threshold rigidity and calculation of cosmic ray equator 08 p1284 A66-19398

Geomagnetic diurnal-variation in north polar region with corrected geomagnetic latitude 09 p1373 A66-20385

Latitudinal dependence of geomagnetic disturbance magnitude along noon and midnight meridians for different seasons, noting effect on auroral zone 09 p1373 A66-20386

Gradual variation observed in time of occurrence of spread-F peak with geomagnetic latitude 11 p1702 A66-23370

Onset patterns of PCA analysis using corrected geomagnetic coordinates, with results analyzed through solar cosmic radiation, Earth magnetosphere structure and D region 12 p1944 A66-24470

Corrected geomagnetic coordinates of Hakura compared to study of geomagnetic threshold rigidity for cosmic ray particles 15 p2484 A66-28908

Latitude distribution curves of two quasi-circular zones of maximum magnetic activity along 12 consecutive meridians of local geomagnetic time 15 p2487 A66-29100

Anderson hypothesis on semiannual variation in upper atmosphere density and relation to geomagnetic latitude effects, analyzing Samos II 17 p2920 A66-33087

Balloon flight data obtained at 50 and 65 degrees N geomagnetic latitude on spectra of primary cosmic ray hydrogen and helium nuclei, using Cerenkov scintillator technique 18 p3190 A66-34831

Balloon-borne Cerenkov scintillation counter measurements of energy spectra of primary cosmic radiation heavy nuclei at various geomagnetic latitudes 18 p3191 A66-34840

Rocket-borne neutron detector measurements of neutron albedo and intensities at various geomagnetic latitudes 18 p3199 A66-34887

Latitude dependence of neutron multiplicity detected by shipborne neutron monitor, examining threshold rigidity

dependence on intensity of events 20 p3632 A66-38077

Statistical analysis of diurnal variation of southern boundary of aurora, HF backscatter records and geomagnetic latitude of dayside aurora 20 p3553 A66-38119

Very steep latitudinal electron density gradients in topside F layer at high altitudes 20 p3554 A66-38119

Latitudinal variation of Pc-1 micropulsation propagation, examining attenuation by ionospheric F region duct that acts as waveguide for hydromagnetic waves 20 p3554 A66-38200

Solar cosmic ray alpha particle relation to PCA and lowest latitude of enhancement 20 p3635 A66-38222

Non-Stoermer cut-off variation with geomagnetic latitude of PCA during quiet Sun period 20 p3635 A66-38222

Enhanced activity in ionospheric E region at Cape Hallett and Campbell Island for information on diurnal variation and sunspot cycle changes of overhead and auroral activity 22 p3916 A66-40800

## GEOMAGNETIC PULSATION

Pc-type pulsation variations with geomagnetic activity and latitude from records of Wingst, Gottingen and Furstenfeldbruck observatories 01 p0060 A66-10189

Analog-digital transformations in detection of microvariations in geomagnetic field 01 p0061 A66-10655

Geomagnetic pulsation pc-5 in and near auroral zones based on data collected during IGY period, noting local time dependence 01 p0062 A66-10688

Short period fluctuations in intensity of auroral luminescence and relation to geomagnetic fluctuations 01 p0065 A66-11166

Geomagnetic micropulsation periods relation to dimensions of magnetosphere considering inverse dependence on level of magnetic activity 02 p0224 A66-12111

Pulsations of aurora luminescence and irregular quasi-periodic oscillations of geomagnetic field 02 p0224 A66-12122

Microvariations of Earth electromagnetic field with results recorded on tape in digital pulse code form 02 p0224 A66-12122

Short-period geomagnetic micropulsations and observing apparatus 03 p0360 A66-12344

Spectral density functions of hydromagnetic emissions at high latitude 03 p0367 A66-13268

Micropulsations of Earth magnetic field and relation to various types of auroras 04 p0515 A66-13844

Small amplitude LF waves in ionosphere covering momentum and energy dissipation zero temperature plasma and waves in nonuniform plane-stratified medium 04 p0516 A66-13968

Pearl micropulsations in auroral zone at Flin Flon, Manitoba 05 p0667 A66-14799

Whistler and VLF emissions recorded in northern Italy, noting daily occurrence and positive correlation with geomagnetic activity 05 p0671 A66-14988

ELF emission from electron and proton beams injected into magnetospheric plasma 05 p0748 A66-15044

Time-agreement of sudden commencement indicated by geomagnetic micropulsation results from Byrd Station and Great Whale river 06 p0875 A66-16278

Fine structure of magnetic storm discussing prestorm, initial stage and climatology of fluctuations of Pc I and Pc II 07 p1027 A66-17300

Natural electromagnetic field of Earth microvariational peculiarities 07 p1027 A66-17300

Geomagnetic micropulsation properties and nature with periods ranging from 10 seconds to several minutes 08 p1214 A66-19033

Excitation features and amplitude-period relation of magnetic Pc1 oscillations magnetically conjugate regions 08 p1214 A66-19033

Spatial properties of rapid geomagnetic fluctuations, noting correlation and epoch differences between distant stations azimuthal distributions and Parkinson plane effects 08 p1219 A66-19411

Sinusoidal hydromagnetic pulsations noting morphological properties, planetary



- distribution and inverse dependence of amplitude, frequency and duration on solar activities 08 p1220 A66-19784
- Geomagnetic micropulsations, noting diurnal patterns of phase difference, propagation medium dispersive characteristics, signal velocities, etc 10 p1529 A66-21151
- Diurnal properties of horizontal geomagnetic micropulsation field in New Zealand, noting variation of period, field rotation and direction of oscillating vector 10 p1529 A66-21152
- Fast variation of geomagnetic field in polar region 11 p1698 A66-22896
- Characteristic periods of pearl-type variations in geomagnetic field 11 p1698 A66-22897
- VHF hiss zone morphology and correlation with particle precipitation events, from Alouette I satellite observations 11 p1700 A66-23136
- High-altitude nuclear explosion-induced geomagnetic micropulsations in analysis of sudden commencement data and Alfvén velocity-altitude profile 11 p1700 A66-23143
- Schumann-ELF natural background samples recorded in three components at separated points resolved by analog and digital methods into constituent modes for comparison 12 p1815 A66-24115
- Time variation of preferential-polarization vector of pearl-type oscillations during course of observations at Lovozero station, U.S.S.R. 12 p1871 A66-24294
- Cyclotron instabilities in hydromagnetic waves in magnetosphere as possible origin of geomagnetic micropulsations, stressing ion resonance mode of waves relevant to hm whistlers 12 p1874 A66-24842
- Magnetic toroidal resonances and vibrating field lines, using basic toroidal equation in determining validity of heuristic vibrating string model 13 p2074 A66-26359
- Counting system for use with rubidium magnetometer for ground observations of geomagnetic micropulsations with sensitivity of 1/100 gamma 13 p2085 A66-26752
- Simultaneous appearance of in-phase ULF geomagnetic pulses at two conjugate points 13 p2076 A66-26759
- Analog-digital transformations in detection of microvariations in geomagnetic field 14 p2286 A66-28035
- Geomagnetic micropulsation periods relation to dimensions of magnetosphere, considering inverse dependence on level of magnetic activity 14 p2287 A66-28078
- Pulsations of aurora luminescence and irregular quasi-periodic oscillations of geomagnetic field 14 p2287 A66-28079
- Microvariations of Earth electromagnetic field with results recorded on tape in digital pulse code form 14 p2287 A66-28082
- Power spectra computation for testing geomagnetic micropulsation period dependency on latitude 14 p2287 A66-28171
- Dynamic spectrum of geomagnetic pulsations at low latitude studied by magnetic tape recording 15 p2484 A66-28904
- Space-time variations in frequency and amplitude of Pc1 oscillations observed during April 1964 15 p2488 A66-29112
- Natural telluric currents in Arctic Ocean and relation to geomagnetic variation observed on drifting station 15 p2488 A66-29113
- Scintillation height measurement, noting irregularity distribution during various ionospheric conditions 16 p2691 A66-30230
- Micropulsations generated by low-energy proton via cyclotron instability in outer radiation belt, noting pitch angle scattering 16 p2794 A66-30700
- Semiannual wave in recurrence tendency of geomagnetic activity, noting correlation with sunspot cycle 16 p2696 A66-30722
- 4-second summertime micropulsation band at College, Alaska 17 p2918 A66-32526
- Geomagnetic micropulsations observed, using five-station array of three-component induction variometers 17 p2923 A66-33360
- Abundance of individual effects /pt, bp, bps/ of geomagnetic pulsations and variations at Goettingen and Fuerstenfeldbruck stations 18 p3105 A66-34096
- Equatorial transmission of geomagnetic micropulsations through ionosphere and lower exosphere below 2000 km altitude 18 p3107 A66-34526
- Three-dimensional polarizations of high-latitude micropulsations derived for conjugate point observatories from hydromagnetic wave-ionospheric current model 18 p3107 A66-34527
- Fast variations of electromagnetic field measured by satellites electron I and II used as indication of state of radiation belts and magnetosphere of Earth 19 p3344 A66-35257
- Latitudinal variation of Pc-1 micropulsation propagation, examining attenuation by ionospheric F region duct that acts as waveguide for hydromagnetic waves 20 p3554 A66-38203
- Sudden impulses and pc5 variations resulting from magnetospheric deformations and solar wind pressure changes 20 p3657 A66-38223
- Sinusoidal hydromagnetic pulsations noting morphological properties, planetary distribution and inverse dependence of amplitude, frequency and duration on solar activities 21 p3733 A66-38780
- Fast variation of geomagnetic field in polar region 21 p3733 A66-38964
- Characteristic periods of pearl-type variations in geomagnetic field 21 p3733 A66-38965
- Transmission and coupling resonance of hydromagnetic disturbances in nonuniform model magnetosphere calculated by approximate dipole coordinates valid near equatorial plane 21 p3734 A66-39217
- Generalization of differential equation of dynamo theory of geomagnetic variations to include unsteady dynamo effect in ionosphere 22 p3914 A66-40759
- GEOMAGNETIC STORM**
- SA IONOSPHERIC STORM**
- SA SUDDEN IONOSPHERIC DISTURBANCE /SID/**
- Solar flare characteristics interrelation with magnitude of resultant blast wave, examining sudden commencement of geomagnetic storms 01 p0063 A66-10891
- Monographs on auroras, geomagnetic disturbances and ionosphere at high latitudes 01 p0064 A66-11160
- Magnetic storm accompanied by Forbush decreases taking into account atmospheric temperature, noting cyclonic storm origin 02 p0282 A66-11338
- Chromospheric and coronal propagation of disturbing agents generating changes in intensity of solar radio emission 02 p0287 A66-11489
- Transfer and acceleration of particles in Earth magnetosphere effect on origin of radiation belt 02 p0283 A66-12110
- Energy characteristics of ionospheric disturbances and nature of geomagnetic and ionospheric disturbances 02 p0284 A66-12117
- Location of latitude over which aurora current passes as function of geomagnetic storm intensity 02 p0225 A66-12139
- Ionospheric and polar-geomagnetic disturbance and PCA event on February 11, 1958 caused by solar flare 03 p0360 A66-12345
- 27-day recurrence tendencies of solar plasma velocity and magnetic index from Mariner II 03 p0417 A66-12346
- Sudden commencements of magnetic storms and sudden impulses in study of vector changes and equivalent current systems 03 p0360 A66-12347
- Inverted SC in low latitude regions and classification as magnetic sudden impulse 03 p0360 A66-12348
- Solar flares, solar wind, particle emission from activity regions, flare-associated particles and nuclear reactions in flare regions 03 p0418 A66-12665
- Shock waves in solar wind and magnetic storms, deriving equations governing shock, ambient and driver gas velocities 03 p0418 A66-12672
- Recurrent geomagnetic storms and structure of solar wind consisting of fast M-region stream embedded in slower ambient wind 03 p0418 A66-12673
- Tabulated data on principal magnetic storms from April through October 1965 and selected geomagnetic and solar data for June 1965 03 p0424 A66-12680
- Effects connected with auroras and magnetic storms in lower ionosphere considering radio wave attenuation, cosmic ray absorption, etc 03 p0365 A66-12854
- Auroras and magnetic storm models including those of Chapman and Ferraro, Alfvén, and Axford and Hines, noting magnetization of solar plasma 03 p0365 A66-12856
- Geomagnetic disturbances and related visual auroras noting pulsations, excitation processes, etc 03 p0365 A66-12857
- Auroral zone X-ray bursts and polar magnetic substorms 03 p0422 A66-12873
- Geomagnetic relationship of daily variation of cosmic ray neutron intensity corrected for barometric pressure variation at various ground stations 03 p0423 A66-13360
- Current system of solar disturbed diurnal variations of magnetic field at high latitudes in terms of dynamo theory, taking into account forward and Hall conductivities 04 p0516 A66-13854
- Recurrent magnetic perturbations after flocculus passage through central solar meridian, examining activity decrease between solar maxima 04 p0516 A66-13865
- Diurnal variation of cosmic radiation of intermediate energies measured at Earth attributed to particle removal due to scattering by magnetic irregularities 04 p0575 A66-14181
- Dipole latitude of auroral activity during periods of zero and very weak magnetic disturbance 04 p0517 A66-14375
- Critical frequency of F-2 layer at Huanqiao and variation with magnetic activity at different epochs of solar activity 04 p0517 A66-14378
- Worldwide positive-negative impulse pair observed on geomagnetic records found to be recurrent and associated with M-region disturbances 05 p0670 A66-14953
- IGY geomagnetic observations, notably magnetic storms in Soviet Union and Antarctic 05 p0674 A66-15224
- Relation between solar activity and geoelectrical phenomena 05 p0761 A66-15229
- Electromagnetic disturbances effects on particles trapped in radiation belts 05 p0749 A66-15251
- Changes in solar cosmic ray and geomagnetic field intensities during magnetic storms accompanied by decrease in galactic cosmic ray intensity, using moving averages method 05 p0753 A66-15395
- Magnetic storm accompanied by cosmic ray intensity increase analyzed, considering Forbush effect and determining all peaks 05 p0755 A66-15403
- Solar and galactic cosmic ray characteristics, origin and flux-time variations, examining relation between solar flares and geomagnetic storms 05 p0756 A66-15751
- Rocket and satellite data contribution to new physical description of aurora in which Earth magnetosphere acts like gigantic cathode ray tube 06 p0875 A66-16015
- Anomalies in cosmic radiation during December 1957 accompanying geomagnetic storms connected with solar flares 06 p0949 A66-16588
- Secular variation of cosmic radiation intensity 06 p0950 A66-16590
- Structure and variation of radiation belts during magnetic storm, including configuration of forbidden region in connection with magnetic field 06 p0951 A66-17048
- Magnetospheric perturbations to probe interplanetary plasma, noting sudden and gradual commencement of geomagnetic storms 07 p1121 A66-17984
- Solar corpuscular stream effect on magnetic storms and Forbush effect 07 p1121 A66-17985
- Periodical and quasi-periodical cosmic ray variation according to data of worldwide network of stations, using crossed telescope 07 p1127 A66-18013
- Aurora production via magnetic field induction during geomagnetic storms by ring current growth in Van Allen belt region 07 p1029 A66-18088
- Dynamical properties of solar wind and solar corona atmosphere with extended temperature bound strongly by



gravity 07 p1132 A66-18263  
 Ionospheric magnetic perturbations at high latitudes of northern hemisphere during years of maximum solar activity 08 p1213 A66-19028  
 Twenty-seven-day variations of geomagnetic disturbance in aurora zone with respect to zero days of cosmic ray intensity 08 p1283 A66-19045  
 Aurora relations with ionospheric currents responsible for magnetic disturbance, noting sign of bay 08 p1215 A66-19054  
 Geomagnetic sudden-commencement storms effect on electron concentration in F-2 layer above Europe 08 p1215 A66-19082  
 Radio auroral echoes and correlation to geomagnetic disturbance 08 p1215 A66-19205  
 Polar electrojet causing magnetic substorms in high latitudes flows westward along closed oval curve and is connected with auroral activity and outer radiation belt 08 p1216 A66-19216  
 Occurrence frequency of midlatitude geomagnetic transition bays and relation to spatial movement of overhead electrojet current systems 08 p1218 A66-19395  
 Ring current growth tendency prior to sudden magnetospheric compression 08 p1219 A66-19406  
 Correlated magnetic tail and radiation belt observations from Explorer 18 /Imp I/ satellite and APL satellite 1963 38C in April 1964 08 p1284 A66-19411  
 Anomalies in cosmic ray intensity increase during period of Forbush decrease 09 p1438 A66-20214  
 Magnetic storms effect on cosmic rays during periods of maximum and minimum solar activity 09 p1438 A66-20215  
 Diurnal variation of aurora zone geophysical disturbances, examining VLF phenomena including noise, aurora and ionospheric absorption 09 p1372 A66-20375  
 Magnetospheric electric fields, noting implications of magnetic storm theories 10 p1528 A66-21149  
 Annual variation of auroral absorption attributed to frictional interaction between streaming plasma and geomagnetic field 10 p1530 A66-21161  
 Enhancement of amplitude of sudden commencement of magnetic storms in horizontal component of geomagnetic field 11 p1696 A66-22380  
 Chromospheric flares effect on hard component of cosmic rays as function of solar coordinates during quiet and magnetically disturbed days 11 p1762 A66-22412  
 Anomalous ionization of lower ionosphere at medium latitudes during worldwide geomagnetic storm result in increased radio wave absorption in ionosphere 11 p1696 A66-22416  
 Correlation between unipolar magnetic regions and recurrent geomagnetic storms 11 p1773 A66-22784  
 Objections to idea of solar ejection of neutral hydrogen and responsibility for geomagnetic storm 11 p1776 A66-23496  
 Geomagnetic storms employed in determining geoelectrical parameters via magnetotelluric sounding 12 p1868 A66-23668  
 Solar wind and geomagnetic storm effects on galactic cosmic ray 11-year variations and energy spectrum, from neutron monitor data 12 p1940 A66-24160  
 Cosmic ray variations and solar corpuscular stream in interplanetary space during March 1958 magnetic storm 12 p1940 A66-24164  
 Forbush, geomagnetic interaction, cosmic ray variation and solar corpuscular flux effects during magnetic storms in period of maximum solar activity 12 p1940 A66-24165  
 Variations in cosmic ray neutron component intensity and solar corpuscular flux with H-component of geomagnetic field during magnetic storm 12 p1941 A66-24166  
 Abrupt increase in cosmic ray intensity coinciding with presence of Forbush effects, noting dependence on geographic latitude and cut-off rigidity, obtaining energy spectra 12 p1941 A66-24168  
 Magnetic storms during IGY, assuming effect on cosmic ray intensity is associated with influence on galactic cosmic rays of magnetic fields of solar and corpuscular fluxes 12 p1941 A66-24169

Relation between Forbush decreases and magnetic storms, examining spatial distribution of predecrease moments relative to sudden commencements 12 p1941 A66-24171  
 Satellite observation of radiation belt and absorption of cosmic noise in polar aurora during magnetic storms of February 1964 12 p1943 A66-24267  
 Statistical distribution of monthly median noon critical frequency of F-2 layer from ionospheric stations at mid-latitudes, auroral regions and at polar cap 12 p1870 A66-24286  
 Ionospheric effect of sudden magnetic storm eruption, noting propagation of disturbance above terrestrial surface 12 p1870 A66-24288  
 Spread in values of vertical magnetic field component during sudden commencements of magnetic storms attributed to local geoelectric conditions 12 p1871 A66-24295  
 Corpuscular intrusions into Earth magnetosphere involving entire auroral zone and occurring only on night 12 p1871 A66-24296  
 Data analysis of pre-SC field intensity increases and receivable time of WWV signal at Hiraiso, Japan, and Canadian stations for 50 geomagnetic storms 12 p1872 A66-24471  
 Enhanced ionization along midnight auroral zone during elementary geomagnetic disturbances 12 p1872 A66-24472  
 Horizontal geomagnetic fluctuations during nighttime magnetic storms studied at equatorial stations 13 p2075 A66-26738  
 Cyclotron radius, magnetospheric boundary and Debye length scaling parameters for magnetospheric cavity arising from solar wind-induced geomagnetic storm and visibility of quasi-Van Allen belts 14 p2269 A66-27124  
 Transfer and acceleration of particles in Earth magnetosphere effect on origin of radiation belt 14 p2377 A66-28069  
 Energy characteristics of ionospheric disturbances and nature of geomagnetic and ionospheric disturbances 14 p2377 A66-28076  
 Location of latitude over which aurora current passes as function of geomagnetic storm intensity 14 p2287 A66-28095  
 Solar wind parameter variation, magnetosphere flux interaction and dependence of geomagnetic storm on magnetospheric conditions and geomagnetic field increase 15 p2575 A66-29079  
 Auroral occurrence rate at zenith as function of latitude for magnetically quiet and magnetically disturbed periods 15 p2486 A66-29092  
 High resolution density data from radar observations of low altitude, polar orbiting satellites reveal longitudinal and geomagnetic variation, noting regression analysis 15 p2497 A66-30085  
 Polar magnetic substorms associated with westward traveling surge 16 p2693 A66-30334  
 Poleward motion of auroral bands in midnight sector during early phase of auroral substorm and cause of planetary scale auroral displays 16 p2693 A66-30335  
 Patches and irregular bands and eastward motions in morning sector of auroras 16 p2693 A66-30336  
 Measurements of geomagnetic field at various distances using IMP-I satellite, noting magnetically neutral sheet in tail and observation of five magnetic storms 16 p2695 A66-30715  
 Tabular data on magnetic storms and on geomagnetic and solar data furnished by Swiss Federal Observatory 16 p2801 A66-30726  
 Solar corpuscular stream density distribution and trail curvature, noting space angle of ejection and flight trajectory 17 p2992 A66-32336  
 Initial disturbances in F-2 layer at middle latitudes during magnetic storms which begin with sudden commencement and relation to magnetic field changes 17 p2922 A66-33353  
 Mariner II space probe measurements of solar wind including velocity, temperature, time dependence of proton velocity, temperature and density 18 p3167 A66-34331  
 Magnetosphere topology changes due to solar wind interactions, geomagnetic storms

and interactions with interplanetary magnetic field outside magnetosphere 18 p3106 A66-343  
 Increases of ionizing radiation in stratosphere correlated with recurrent magnetic storms, ionospheric perturbation in auroral zone, etc, possibly due electrons from outer radiation belt 18 p3197 A66-348  
 Radial displacement of particles excited by solar-wind-induced current at boundary and ring current within magnetosphere 19 p3451 A66-352  
 Cosmic radio wave absorption dependence on frequency and number of electron-ion collisions during atmospheric magnetic storms 19 p3344 A66-352  
 Sudden commencements of magnetic storms on basis of observations made at H Observatory, with classification into several types and distribution in geomagnetic time established 20 p3551 A66-375  
 Temporal variations of outer radiation zone electron intensities at 1000 km as affected by geomagnetic storms observed by Alouette I satellite 20 p3631 A66-376  
 Cosmic ray meson component distribution with time plots of particle flux reveal characteristic disturbances accompanying sudden commencements of geomagnetic storms associated with Forbush decreases 20 p3632 A66-380  
 Solar terrestrial physics - Symposium Japan, December 1965 20 p3634 A66-382  
 SID-AND terrestrial disturbance-causing enhanced solar particle emissions associated with intense solar flares and plasma streams 20 p3634 A66-382  
 Optical emission energy of solar flare at plasma cloud acceleration producing geomagnetic storm 20 p3635 A66-382  
 Polar cap absorption and upper atmospheric solar-terrestrial disturbances due to solar flare and type IV outburst 20 p3636 A66-382  
 Statistical analysis of storm-time variations and daily disturbance variation in geomagnetic storms 20 p3658 A66-382  
 Statistical correlation analysis of isolated geomagnetic bay occurrence and relation to solar cycle variation 20 p3658 A66-382  
 Successive hourly variations of equivalent current systems of magnetic bay disturbance patterns and F layer minimum frequency increases 20 p3658 A66-382  
 Geomagnetic storms occurrence, three types of calm periods and intermittent periods of atmospheric disturbances 20 p3658 A66-382  
 Distribution of energetic protons in Earth radiation belt between 1962 and 1964, noting secular temporal changes, effects of magnetic storm and aspects of energy spectrum 20 p3638 A66-383  
 High energy trapped electrons in outer zone for 27-day, diurnal and storm time variations 20 p3639 A66-383  
 Nonadiabatic and adiabatic acceleration and diffusion of particles trapped in Earth magnetic field, examining particle drift trapping boundary, auroral substorms and bounce resonances 20 p3658 A66-383  
 Diffusion coefficients in outer radiation belt, examining energy dependence of electric and magnetic disturbances contributing to transport of particles 20 p3641 A66-383  
 Auroral absorption analysis during geomagnetic storm, noting satellite measurement of energetic particles 20 p3642 A66-383  
 Thermospheric energetics characterized as series of superposed and interconnected atmospheric heat engines and refrigerators 22 p3913 A66-4053  
 Simultaneous long term ionospheric variation in midday averages of critical frequency E and F-2 at Washington, D.C. before and after increased geomagnetic activity 22 p3914 A66-4056  
 Growth and decay of ring current in polar electrojet, using magnetic storm examples 22 p3974 A66-4056  
 Dependence of diurnal cosmic ray variations on angle which is proportional to shortest distance from Earth to axis of corpuscular stream 22 p3974 A66-4075  
 Magnetic field of ring current on Earth



- surface according to observations during IGY 22 p3914 A66-40768
- Geomagnetic activity and Earth heliolatitude effect on diurnal variation of cosmic radiation, based on IGY neutron component observations 22 p3974 A66-40775
- Measures of electron production and loss and scale height of F-1 layer during summer solar minimum 22 p3916 A66-40808
- Acceleration of plasma cloud from Sun producing geomagnetic storm, noting magnetic cloud squeezed out from sunspot region 24 p4262 A66-42459
- Nonsymmetric inflation of dipole magnetic field by ionized gas, noting nonsymmetric gas dissipation 24 p4199 A66-42587
- Asymmetric ring current belt consisting of symmetric ring current and superimposed partial ring current system as explanation for low latitude disturbance daily variation 24 p4199 A66-42588
- Inner magnetosphere inflation during geomagnetic storm observed by Explorer XXVI, noting relation of various phases to charged particles 24 p4200 A66-42589
- Power spectrum analysis of mean daily values of magnetic data for 27 observatories 24 p4201 A66-42597
- Auroral zone microbursts associated with geomagnetic storms, negative magnetic bays and electron precipitation observed by balloon and rocket 24 p4201 A66-42600
- Temporal variations of electron energy flux in outer radiation zone measured during geomagnetic activity with instrumentation on board Explorer XII satellite 24 p4263 A66-42601
- Quiet and disturbed conditions of magnetosphere, noting dynamo theory and various geomagnetic storms 24 p4202 A66-42831
- GEOMAGNETICALLY TRAPPED PARTICLE**
- SA PROTON BELT**
- Motions of geomagnetically trapped particles and asymmetric configuration of magnetospheric trapping region caused by solar wind 01 p0060 A66-10159
- Optical damage of spacecraft thermal control coatings in simulated space radiation environment of geomagnetically trapped particles [AIAA PAPER 65-646] 01 p0089 A66-10227
- Extension of measurements in Van Allen belt concerning particle equator crossing at given pitch angle between magnetic mirrors, suggesting repulsing force from equator 01 p0132 A66-10495
- Average atmosphere encountered by geomagnetically trapped protons 03 p0364 A66-12676
- Geomagnetically trapped protons, examining possibility that they may be caused by cosmic ray albedo neutrons 03 p0421 A66-12868
- Time and altitude dependence of 55-mev trapped protons in South Atlantic region detected by nuclear emulsions onboard satellites 05 p0747 A66-14784
- Average steady-state omnidirectional trapped electron flux due to beta decay from orbiting leakage reactor neutrons 05 p0747 A66-14786
- Electromagnetic disturbances effects on particles trapped in radiation belts 05 p0749 A66-15251
- Particles in radiation belt of Earth, considering motion in dipole field, sources, loss processes, etc 05 p0756 A66-15745
- Optical properties of spacecraft temperature control coatings under simulated geomagnetically trapped electron bombardment [AIAA PAPER 65-137] 05 p0706 A66-15792
- Magnetospheric boundaries formation, noting neutral points on day and night sides and possible penetration of solar flux particles 06 p0877 A66-17170
- Electrostatic field from E region and effect on motion of electrons trapped in magnetosphere 07 p1027 A66-17252
- Scintillation counter satellite data on low energy electron flux and particle trapping in dark magnetosphere 08 p1218 A66-19394
- Fermi acceleration of charged particles in shock transition region beyond magnetosphere 08 p1219 A66-19407
- Approximation error on interchange stability of Van Allen belt corrected 08 p1284 A66-19421
- Survey of U.S. and U.S.S.R. literature on processes responsible for composition and spatial distribution of radiation belts 08 p1285 A66-19774
- Critical Stormer pass points for quadrupole field and double-ring-current field with parallel or antiparallel dipole moments 09 p1404 A66-20085
- Radiation belt formation from neutron decay and geomagnetic trapping as affected by Coulomb encounters and particle diffusion 09 p1440 A66-20226
- Fast particle trapping by separatrix displacement in asymmetric outer boundary of magnetosphere 09 p1440 A66-20227
- Corpuscular radiation in vicinity of Earth and trapped in geomagnetic field, considering space and solar activity modulation 09 p1441 A66-20284
- Spatial distribution of protons and electrons captured by terrestrial magnetic field, as measured by Cosmos satellites 09 p1443 A66-21011
- Radiation belts theorized as resulting from penetration of charged particles into magnetosphere, accelerated by reversed phase of magnetic storm 09 p1444 A66-21022
- VLF phase perturbations produced by Soviet high altitude nuclear explosion of November 1, 1962 10 p1496 A66-21153
- Longitudinal asymmetry of trapped energetic electron intensities attributed to lowering of mirror points in South African anomaly 10 p1599 A66-21160
- Diurnal variation of outer radiation belt of energetic trapped electrons and relationship to magnetic activity 10 p1600 A66-21163
- Spiralling electrons in geomagnetic field and superimposed electric field aligned with magnetic field lines 11 p1695 A66-22371
- Interaction of solar corpuscular stream with geomagnetic field forming Earth magnetosphere and particle penetration within magnetosphere in neutral point region 11 p1696 A66-22407
- Van Allen radiation belt noting composition, charged particle motion in dipolar magnetic field, particle origins, etc 11 p1763 A66-22769
- Physical pattern of high altitude fission cloud and motion of gamma and beta fission fragments captured by geomagnetic field and observed by Cosmos satellite 11 p1764 A66-23043
- Mean radial particle displacement per unit time due to magnetic impulses for two-dimensional transport motion of magnetospheric trapped particle 11 p1765 A66-23149
- Lifetimes of low energy electrons in outer radiation belt at magnetically quiet times 12 p1938 A66-24120
- Threadlike equatorial current ring and effect on geomagnetic cut-off rigidity of directed cosmic radiation 12 p1941 A66-24172
- Effect of equatorial current ring distributed over globe on geomagnetic cut-off rigidity of cosmic rays 12 p1941 A66-24173
- Pitch-angle distribution and differential energy spectrum of polar aurora protons penetrating Earth atmosphere 12 p1870 A66-24283
- Data from satellite 1963 38C, showing existence of 27-day periodicity in intensities of trapped electrons undergoing two increases and linked to interplanetary magnetic field 13 p2175 A66-26353
- Ionization enhancement from Van Allen electrons in South Atlantic magnetic anomaly, noting longitudinal variation of trapped electrons, electron-ion recombination, etc 13 p2176 A66-26362
- Formation mechanism of ionospheric narrow sporadic E layers by high energy electron fluxes captured by geomagnetic field 15 p2488 A66-29110
- Micropulsations generated by low-energy proton via cyclotron instability in outer radiation belt, noting pitch angle scattering 16 p2794 A66-30700
- Orbit calculations used to evaluate effective atmospheric densities traversed by geomagnetically trapped 125-mev protons in South Atlantic anomaly 17 p2993 A66-32528
- Solar protons and neutrons shown not to play important part in production of radiation belt protons 17 p2993 A66-32529
- Computer code study of magnetospheric trapped-particle drift under influence of magnetic field gradient, magnetic line curvature, electric rotational field and electric field across tail of magnetosphere 18 p3168 A66-34350
- Relation between energy of geomagnetically trapped particles and disturbance field near Earth 18 p3169 A66-34516
- Precipitation flux of quasi-trapped energetic electrons near low altitude fringes of inner radiation belt as they drift into South Atlantic magnetic anomaly 18 p3170 A66-34520
- Star Fish radiation belt discrepancy between theoretical and experimental values may be due to explosion in belt of naturally trapped protons 18 p3170 A66-34530
- Particle acceleration in neutral sheet of geomagnetic tail in two models and implications for auroral and solar activities 18 p3179 A66-34766
- Geomagnetically trapped proton and electron fluxes in immediate vicinity of Earth 18 p3186 A66-34809
- Flux and East-West asymmetry of primary electrons at geomagnetic rigidity cut-off of about 4.5 gv 18 p3187 A66-34817
- Transfer coefficients of charged particles trapped in magnetic field of Earth studied, examining concept of sudden pulses as basic mechanism 19 p3451 A66-35260
- Energy-selective redistribution of trapped electrons in inner radiation belts associated with magnetic disturbances 20 p3630 A66-37294
- Van Allen radiation belt particle motion in spherically confined magnetosphere 20 p3630 A66-37301
- Ring current-induced variations in geomagnetically trapped particle fluxes 20 p3633 A66-38192
- Correlation of magnetic fields and energetic electrons on IMP I satellite, noting depression in geomagnetic tail region, electron fluxes and diamagnetic effect 20 p3633 A66-38201
- Magnetospheric tail instabilities, auroral electron acceleration and deformation due to dipole magnetic field acceleration of plasma particles 20 p3635 A66-38222
- Electrons trapped in magnetosphere, discussing dynamo electrostatic field, energetic electron electromagnetic drift and magnetic mirror-electron orbit effects 20 p3635 A66-38226
- Radiation trapped in Earth magnetic field - Conference, Christian Michelsen Institute, Bergen, Norway, August-September 1965 20 p3636 A66-38301
- Geomagnetic field model based on definition of core field, crustal field, ionospheric currents and plasma pressures, examining trapped particle behavior 20 p3555 A66-38302
- Definitions and properties of magnetic coordinates B, L, K, R, lambda and A, discussing role of these parameters in study of geomagnetically trapped particles 20 p3555 A66-38304
- Physical principles of radiation belts and geomagnetically trapped radiation 20 p3637 A66-38305
- Low altitude measurements of trapped electrons, noting energy spectrum and longitudinal variations of electrons, including instrumentation 20 p3638 A66-38307
- Changes in 1 to 4 mev electron population during solar quiet periods and 55-mev protons near South Atlantic anomaly measured by various geophysical satellites 20 p3638 A66-38310
- High energy trapped electrons in outer zone for 27-day, diurnal and storm time variations 20 p3639 A66-38317
- Loss rates of trapped electrons by atmospheric collisions 20 p3640 A66-38321
- Acceleration processes of outer zone protons investigated, using Kellogg hypothesis of radiation belt formation through magnetic disturbances where third adiabatic invariant is violated 20 p3640 A66-38322
- Method for calculating longitude dependence of geomagnetically trapped electrons at low altitude, based of scattering



and energy loss due to atmospheric interactions 20 p3640 A66-38324

Nonadiabatic and adiabatic acceleration and diffusion of particles trapped in Earth magnetic field, examining particle drift, trapping boundary, auroral substorms and bounce resonances 20 p3658 A66-38326

Shape of magnetopause determined by solving equations for boundary of geomagnetic field with trapped particles 20 p3641 A66-38331

Adiabatic theory of distorted motion of charged particles in geomagnetic field, showing dependence on equatorial pitch angle 20 p3642 A66-38332

Artificial radiation belt sources, noting positrons and alpha particles, nuclear explosion, etc 20 p3643 A66-38338

Spatial distribution and time decay of intensities of geomagnetically trapped electrons from high altitude nuclear burst 20 p3643 A66-38339

Spatial distribution of trapped particles measured by Explorer XV satellite, noting decay time constants and energies 20 p3643 A66-38340

Trapped electrons from Russian high altitude nuclear detonation examined, noting energy spectrum and mirror point density distribution 20 p3643 A66-38342

Electron spectra made with five-channel magnetic electron spectrometer from Star Fish explosion and from outer radiation belt 20 p3643 A66-38343

High altitude nuclear detonations, discussing data on trapped radiation, values of empirical and theoretical spectra and artificial radiation belts 20 p3643 A66-38344

Geomagnetically trapped radiation effects on solid state electronic device aboard unmanned vehicles 20 p3634 A66-38349

Geomagnetically trapped radiation damage to orbiting solar cells and transistors both before and after Operation Star Fish 20 p3503 A66-38350

Average radiation fluxes on satellites in lower radiation belt 20 p3644 A66-38351

Proton environment above 4 mev in model constructed by using exponential energy spectrum 20 p3644 A66-38354

Survey of U.S. and U.S.S.R. literature on processes responsible for composition and spatial distribution of radiation belts 21 p3809 A66-38770

Ionospheric heating by photoelectrons streaming from sunlit magnetic conjugate point established from incoherent backscatter spectra data 22 p3910 A66-39979

Magnetic coordinate definitions and relation to parameters of geomagnetically trapped particles 22 p3912 A66-40425

Fluxes, intensities and energy distributions of magnetically trapped electrons and fluxes of magnetically trapped protons at lower edge of radiation belt 22 p3974 A66-40557

Van Allen belt study using equatorially orbiting satellite, examining trapped particle origin and energies 23 p4123 A66-41038

**GEOMAGNETISM**

**SA M-REGION**

**SA SPHERICAL HARMONICS**

High sensitivity spinner magnetometer for remnant magnetic polarization measurement of rocks in paleomagnetic research 08 p1223 A66-19081

Space research in West Germany including upper atmosphere time-dependent structure, geomagnetism, space radiation, artificial ion cloud, etc 09 p1458 A66-20713

Soviet book on high latitude research in field of geomagnetism and aeronomy including ionospheric storm, atmospheric absorption, etc 24 p4203 A66-43149

**GEOMETRIC FACTOR**

Delay characteristics of round and square magnetized rods of yttrium-iron garnet /YIG/ crystals compared 01 p0120 A66-10522

Relationship between field singularities of electrostatic theory and equations for fixed charge and dipole models, including geometrical distributions 03 p0391 A66-12404

Geometric shape of axisymmetric shock waves from point source explosion in nonhomogeneous medium 03 p0355 A66-12621

Spherical cryopumped chamber with test object analyzed for pumping speeds determined with gauges located in various positions, with equations relating these

speeds to chamber geometry and cryopump efficiency 04 p0528 A66-14465

Maximum range of ballistic missile with given burnout speed and altitude, optimum angle obtained by geometrical means 05 p0760 A66-14891

Effect of geometry changes on carrying capacity of cylindrical shell directly after reaching plastic state 06 p0966 A66-16501

Effect of various geometries on performance and characteristics of helical antennas, considering input impedance and radiation pattern 07 p1006 A66-17474

Sine of angle of incidence of solar radiation graphically represented as geometrical factor of irradiation intensity 08 p1283 A66-18626

Electrical conductivity and field strength in symmetrically contacted rectangular samples as effected by geometrical factors 09 p1425 A66-20187

Turbine vanes of aircraft engines and experimental plants, determining structural angle of outlet, maximum thickness and area of profile, setting angle, etc 09 p1328 A66-20761

Optimal control system geometry, discussing properties of interior points of limiting surfaces, maximum principle and separability concept 13 p2046 A66-25340

Analysis of antenna parameters for determining equivalent radius of noncircular antennas 14 p2253 A66-27531

Geometric dimensional, plasma temperature and pressure effects on capillary discharge with evaporating wall /CDEW/ 18 p3143 A66-34028

Envelope of parametric equations determined, using geometrical understanding for identification of singularities on envelope, noting relevance to Wankel engine design 21 p3755 A66-38599

Popov criterion application in determining stability of linear time-invariant systems with nonlinear feedback, using root locus 21 p3718 A66-38667

Run-length encodings, determining explicit form of Huffman coding when applied to geometric distribution 21 p3758 A66-39643

Metallurgical junction radius of curvature effect on avalanche breakdown voltage in Ge, Si, GaAs and GaP spherical and cylindrical p-n junctions 22 p3959 A66-39740

Avalanche breakdown voltage of quasi-planar /circular cylindrical/ silicon junction and relation to increased electric field intensity in curved portion 22 p3959 A66-39741

Theoretical static I-V characteristics of surface gate dielectric triode and geometric factors influence on amplification factor at cut-off 22 p3872 A66-39746

Microwave-frequency waveguide losses minimized by controlling effects of geometry, propagation mode, construction materials, surface finish and surface contamination 22 p3874 A66-39992

Mach number and body geometry effects on stability characteristics of oscillation in supersonic regime of bodies of revolution 22 p3844 A66-40373

Contactless telemetering element design, deriving equations for geometric dimensions of spring loaded, oscillating system 23 p4045 A66-41398

Geometrical theory of unitary equivalence of matrices indicating successive calculation of numerical invariants 23 p4084 A66-41407

Static firing tests on special small rockets /SSR/ with different igniter cases and combustion instabilities 23 p4119 A66-41436

Perron theorem, Liapunov functions and stability analysis of certain perturbed systems 23 p4085 A66-41552

Generalization and extension of Perron theorem to behavior of solutions of certain perturbed systems 24 p4230 A66-42215

Contour epitaxial deposition for semiconductor devices and integrated circuits, producing regions with well defined doping and geometry in crystal with flat surface 24 p4181 A66-42386

Incompressible viscous flow around right angle corner, noting effect of geometry on boundary layer and cross flow 24 p4194 A66-42410

Miller phenomenological rule for computing nonlinear susceptibility, determining

magnitude by geometrical factor 24 p4223 A66-42561

Fiber geometry effect on shear stress distribution in composite materials 24 p4292 A66-42861

Microwave transducers for measuring geometric dimensions and displacements in industrial process control 24 p4214 A66-43014

**GEOMETRICAL HYDROMAGNETIC**

LF drift waves observed in thermally ionized cesium plasma in magnetic field with variable curvature 23 p4106 A66-41711

**GEOMETRICAL OPTICS**

Confocal multimode resonator with open walled structure formed by two spherical reflectors spaced by their common radius of curvature 01 p0081 A66-10370

Geometrical acoustics in magnetic materials, examining control of direction and shape of beam by introducing inhomogeneities in medium 01 p0120 A66-10500

Huygens principle in geometrical optics to solve certain time problems in calculus of variations, particularly airplane minimum time [SAE PAPER 650784] 01 p0105 A66-10841

Jupiter photoelectric spectral scan in U.S. reproduced as geometric reflectivity vs wavelength, using Aerobee rocket 02 p0286 A66-11351

Dielectric prism in bend of plane waveguide, considering geometrical optics and calculation electrostatically with power series solution 02 p0196 A66-11411

Book on modern optics including laser and coherent light, geometrical optics, lens systems, instruments, etc 03 p0392 A66-12623

HF approximations for arbitrary body scattering specialized to ellipsoids and applied for source and observation points at distances large compared to scatterer size 03 p0334 A66-12813

Ray dispersion of electromagnetic waves by free electrons produced in cone-shaped ionized wake 04 p0481 A66-13841

Plasma electron concentration, using nonlinear light scattering on geometrical optical path 04 p0554 A66-14221

Wave propagation for LF radio waves analogous to geometrical optics with path integral describing effects of Earth's conductivity, curvature and reflection height 05 p0632 A66-14841

Periodic gas lenses, discussing structural ray optics properties of alternating gradient focusing systems 05 p0717 A66-15181

Lens primary aberration evaluation using Twyman interferometer, developing exact equations for high-order lens defects 06 p0879 A66-16111

Geometrical distortions of Tiros satellite television pictures, estimating loss of contiguity and photogrammetry 07 p1036 A66-18481

Geometrical optics method for differential equations of fourth order in applications to LF plasma oscillations 08 p1265 A66-19471

Relationship between geometric optics and autocorrelation approach to lunar and planetary radar echoes for Gaussian autocorrelation function 09 p1341 A66-19870

Combination of geometrical and physical optics with modern system design such as computers, cameras for aerial use, space tracking, etc 09 p1403 A66-20911

Jupiter photoelectric spectral scan in U.S. reproduced as geometric reflectivity vs wavelength, using Aerobee rocket 10 p1603 A66-21091

Superposition and geometrical optical techniques for approximations of radar cross section of nonconducting bodies 10 p1498 A66-21591

Electromagnetic wave scattering from 3 degree metal wedge and thick plate over wide range of bistatic angles, comparing results with Keller geometrical theory of diffraction 10 p1503 A66-21641

Effect of electric field on LF oscillation of nonhomogeneous plasma contained by magnetic field, using geometrical optical approximation 11 p1744 A66-22441

Geometrical theory of diffraction applied to calculation of radiation pattern and impedance of monopole antenna 11 p1663 A66-22541

Rotation rule added to construction rule



for rays determining geometrical optics field, noting that polarization trihedral is not rotational about ray 11 p1735 A66-22554

Equation governing properties encountered in Gaussian beam propagation represented graphically on impedance chart, showing relation between Gaussian mode and geometrical optics 11 p1656 A66-23089

Weakly focusing transparent media properties and guided transmission of coherent light beams with relatively small loss 11 p1657 A66-23091

Radio wave propagation in artificial ionized cloud in upper atmosphere determined, using geometrical optics 12 p1817 A66-24274

Laser pumping by intense noble gas discharge in zeta-pinch geometry 13 p2092 A66-25995

Field intensity of ultrashort radio waves in superrefraction 14 p2242 A66-28154

Transmission loss in whistler mode of propagation of VLF radio waves for path portion underneath ionosphere, using geometrical optics 16 p2652 A66-30709

Geometric diffraction theory, and radar cross section estimation from rectangular flat plate scattering measurements 18 p3065 A66-33537

Geometric optics - Seminar, El Paso, March 1966 19 p3399 A66-35823

Self-focusing and self-trapping of intense light beams in nonlinear medium examined, using approximations of geometrical optics and accounting for diffraction effects 20 p3602 A66-37372

Geometric diffraction theory for scalar wave incident on plane screen, emphasizing normally and nonnormally incident plane waves and spherical waves 21 p3769 A66-38601

Design considerations for advanced digital beam steering computer through use of geometric optics 21 p3707 A66-38674

Two-dimensional reflector with large angular field theoretically and experimentally studied, using geometrical optics 21 p3710 A66-38745

Cylindrical and spherical waves propagation in weakly inhomogeneous plasma treated by geometrical optics, noting caustic surfaces 22 p3951 A66-39648

Far-field light emission mode pattern of GaAs diode injection lasers, dielectric gradient in inversion layer and refractive index in junction 22 p3930 A66-39743

HF and VHF guided propagation in ionospheric whispering gallery treated by geometrical optics, emphasizing long-range paths between two terminals in ionosphere 22 p3863 A66-39933

Laser beams and resonators, discussing beam propagation in free space, geometrical optics application and resonator modes in view of aperture diffraction effects 24 p4225 A66-42806

**GEOMETRODYNAMICS**

Conditions for presence of constant center of pressure in geometrically-complex body immersed in fluid of variable density in stable equilibrium 07 p1031 A66-17408

Particle theory in which additive particle labels are defined in geometric terms of classical gauge theories of Yang-Mills type 12 p1916 A66-23823

Relation between moving matter and geometrical properties of space-time 14 p2333 A66-27217

Gravitational field evaluated as physical field and as strictly geometrical field 14 p2333 A66-27219

Classical analytical mechanics applied to mechanics of continua, noting relation between kinetic-stress functions and Ostrogradskii-Hamilton principle and stress tensor and finite deformation tensor 15 p2539 A66-29148

Rotating masses effect on inertial frames, analyzing stress energy tensor and Schwarzschild geometry 22 p3979 A66-40113

**GEOMETRY**

SA ANALYTIC GEOMETRY

SA DESCRIPTIVE GEOMETRY

SA DIFFERENTIAL GEOMETRY

SA FLOW GEOMETRY

SA HYPERGEOMETRIC FUNCTION

SA NONEUCLIDEAN GEOMETRY

SA NOZZLE GEOMETRY

SA PROJECTIVE-DIFFERENTIAL GEOMETRY

SA SURFACE GEOMETRY

SA TANK GEOMETRY

SA TOPOLOGY

SA VARIABLE GEOMETRY STRUCTURE

Book on space, time and relativity for nonmathematicians noting geometry, kinematics, dynamics and Einstein theory 08 p1255 A66-18893

Computer algorithm for geometric programming methods 19 p3309 A66-35874

Logical element geometry effect on fluid flow in turbulent reattachment device 20 p3501 A66-37645

Monograph on solving shell stability dynamic problems by geometric approximation 20 p3671 A66-37983

Vector equations of steady inviscid thermally nonconducting gas flows from geometric theory of triply orthogonal spatial curves 21 p3729 A66-39446

Geometric analysis of recordings by IR scanners, emphasizing significance of stereo imagery 24 p4210 A66-42289

**GEOPHYSICAL OBSERVATORY**

SA OGO

Corrected tables and maps of geomagnetic coordinates, covering methods of calculation and corrected data charts 04 p0513 A66-13377

Atmospheric whistler activity, discussing anomaly of low geographic latitude detection and various propagation modes at Rabat, Morocco from 1956 to 1958 05 p0673 A66-15048

Planetary distribution and interpretation of abrupt increases in cosmic ray intensity observed during periods of maximum solar activity but not related to visible solar phenomena 05 p0755 A66-15404

Improvement of Moscow State University installation for detailed investigation of extensive air showers and high energy muons 09 p1379 A66-20237

Weak latitudinal waves observed by Orlov method at three midlatitude stations from 1924 to 1930 10 p1530 A66-21260

Research activities at Chacaltaya Cosmic Physics Laboratory in Bolivia 15 p2476 A66-29514

National report on space research in Sweden 15 p2601 A66-29933

Power spectrum analysis of mean daily values of magnetic data for 27 observatories 24 p4201 A66-42597

**GEOPHYSICAL SATELLITE**

Evaluation of satellite radar altimetry for geophysical and oceanographic measurement 01 p0137 A66-10801

Auroral absorption height obtained from statistical satellite data on average precipitation rate of electrons in auroral zone as function of energy 03 p0364 A66-12663

Soviet report on ionospheric structure variations, drift magnitude, velocity and direction 05 p0674 A66-15226

Space research activities in U.S. /1964 and early 1965/, condensed comprehensive report to COSPAR 09 p1458 A66-20690

Upper atmosphere temperature and pressure measured with manometers mounted on rockets, using method of successive approximations 09 p1375 A66-20988

Soviet monograph on atmospheric exploration using rockets and satellites, covering meteorological and geophysical instrumentation, measurement parameters, etc 13 p2083 A66-26502

Geophysical rocket determination of aerosol scattering coefficient variation from brightness values at 70-450 km heights 15 p2495 A66-30057

**GEOPHYSICS**

SA GEOCHEMISTRY

SA INTERNATIONAL GEOPHYSICAL YEAR /IGY/

SA PETROGRAPHY

Continental Drift Symposium, London, March 1964 03 p0360 A66-12377

International Satellite Bibliography including orbital theory, lunar-satellite motion, artificial asteroids, geomagnetic field, geodesy, navigation, etc 03 p0424 A66-12457

Ionosphere and high latitude particles - COSPAR Symposium, Alpbach, Tirol, Austria, March 1964 03 p0361 A66-12639

International Geophysical Calendar for 1966 prepared by International Ursigram and World Days Service with advice of IQSY reporters 08 p1219 A66-19410

Concept of melting within Earth, effect on thermal model of Earth and differentiation of radioactive materials within Earth 09 p1370 A66-19878

Handbook of geophysics and space environments, 1965 09 p1370 A66-20267

Aerospace research in Poland using satellite observations for geodesy, geophysics and atmospheric dynamics 09 p1459 A66-20721

Statistical analysis of geophysical data 14 p2283 A66-26932

Encyclopedia of physics, Volume 49, Part I - Geophysics III 15 p2482 A66-28516

Book on advances in geophysics including astrogeology, atmospheric ozone, fluctuations of ground-water levels, etc 16 p2700 A66-31742

Celestial mechanics covering two-body problem, planetary and asteroid theory, interplanetary trajectories, lunar probe, spherical harmonics, etc 17 p2997 A66-32019

Review of experimental capabilities for reaching pressure and temperature conditions prevailing in Earth mantle and core, including bibliography 17 p2918 A66-32661

Data on geophysical phenomena at magnetically conjugate points on Earth including cosmic noise absorption, conjugacy of visual auroras, magnetic variations, VLF phenomena, etc 19 p3453 A66-35981

Temporary series representing evolution vs time of natural fluctuating phenomena /geophysical, climatic, biologic/ and relation to sunspot cycle 21 p3733 A66-39133

Depth estimation for buried anomalous mass from vertical gravity observation 23 p4063 A66-41203

Electromagnetic analog computer for solving Dirichlet and Neumann equations for half-space and associated geophysical problems 24 p4202 A66-42763

**GEOPOTENTIAL**

Vorticity equation describing properties of large-scale atmospheric motions 04 p0542 A66-14304

Numerical attempts to estimate determination accuracy of finite difference method for geopotential field 06 p0905 A66-16551

Artificial satellite theory extended to include long-periodic variations due to solid tesseral harmonics of geopotential 08 p1295 A66-19351

Spatial statistical correlation functions for normalized field of geopotential calculated for Europe and Asia 09 p1398 A66-19892

Separation formulas of potential fields of constant currents into lower half-space with application to geomagnetic field 09 p1373 A66-20481

Numerical attempts to estimate determination accuracy of finite difference method for geopotential field 14 p2327 A66-28223

Tesseral harmonics of coordinates using Baker-Nunn data and geopotential and dynamical procedures, noting iterative cycle for correction determination 15 p2491 A66-29999

Even zonal harmonic coefficients of Earth gravitational potential evaluated by analyzing precessions of satellite orbital planes 16 p2694 A66-30618

Pizzetti theory formulas for space normal gravity field of Earth extended to space surrounding Earth 17 p2921 A66-33194

Gravity anomalies of unsurveyed areas of Earth surface and influence on satellite orbit perturbations 17 p2921 A66-33196

Objective analysis of wind and temperature distribution in vertical cross section through atmosphere derived from radiosonde and rawinsonde data 17 p2949 A66-33336

Separation formulas of potential fields of constant currents into lower half-space with application to geomagnetic field 19 p3346 A66-35499

Satellite motion under influence of longitude-dependent terms of geopotential in reference frame rotating with satellite mean motion, noting tesseral harmonics effect and dynamical and librational



- resonances 19 p3470 A66-36388  
 Energy integral study of geopotential harmonic variation effects on satellite motion near critical inclination 20 p3653 A66-37763  
 Coefficients associated with near-resonance conditions with geopotential harmonics of order 12 in data obtained by tracking satellite 1965 89A 22 p3903 A66-39685  
 Geopotential variations related to five-day mean in Central Mediterranean and derivation of regression equations for forecasting 22 p3943 A66-40389  
 Numerical analysis of meteorological fields investigated statistically 22 p3943 A66-40390

## GEOPOTENTIAL HEIGHT

- Mutual dependence of harmonic coefficients of gravitational potential derived from satellite observations as source of computed geoid height distortions at Earth surface 16 p2700 A66-31804  
 Vertical wind gradient variation and energy variation at height ranging from 80 to 140 km and relation to gravity waves and upper atmosphere turbulence 23 p4066 A66-41849

## GEOSTROPHIC WIND

- Quasi-Lagrangian study of inviscid barotropic fluid for analysis of certain ageostrophic jet flows 02 p0222 A66-11825  
 Geostrophic coefficient of friction dependence on stratification from wind profile measurements at lower atmospheric layer 06 p0906 A66-16555  
 Kinetic energy variations in different parts of baric centers during atmospheric motion 08 p1217 A66-19301  
 Earth troposphere affected by solar corpuscular fluxes, cosmic rays, atmospheric radiation, chromospheric flares and intensified radio wave absorption 08 p1285 A66-19452  
 Estimated 10-mb geostrophic winds compared with winds measured by rocketsondes 11 p1731 A66-23385  
 Geostrophic coefficient of friction dependence on stratification from wind profile measurements at lower atmospheric layer 14 p2328 A66-28227  
 Numerical analysis of wind velocity profile measurements and theoretical calculation of profile by numerical methods, based on geostrophic friction coefficient 16 p2741 A66-30771  
 Computation of theoretical maximum probabilities of geostrophic wind components using network sampling theory 17 p2949 A66-33347  
 Earth troposphere affected by solar corpuscular fluxes, cosmic rays, atmospheric radiation, chromospheric flares and intensified radio wave absorption 18 p3169 A66-34481  
 Kinetic energy variations in different parts of baric centers during atmospheric motion 19 p3348 A66-36038  
 Baroclinic instability of quasi-geostrophic perturbation to zonal wind in two-layer inviscid model, examining short wavelength cut-off in terms of potential vorticity 20 p3550 A66-37468  
 Eigenvalue problem associated with dynamic instability of geostrophic wind 23 p4066 A66-42042

## GEOTROPISM

- Gravitational influence on living organisms studied by klinostate principle 06 p0811 A66-16061  
 Gravity effect on basipetal transport of auxin studied by growing plants both erect and on horizontal clinostats 06 p0812 A66-16564  
 Gravitational force perception thresholds of plants in weightless conditions measured in terms of growth and development 19 p3284 A66-35569

## GERDIEN CONDENSER

- Probe techniques in polar ionosphere covering cylindrical Langmuir, RF and mobility probes, Gerdien condensers, error sources, techniques, etc 03 p0362 A66-12641  
 Gerdien type chamber for measurements of ion mobility spectrum in terrestrial mesosphere and Mars atmosphere 18 p3114 A66-34712  
 Gerdien-condenser rocketborne probe used to measure ion densities in D region of atmosphere 22 p3905 A66-39947

## GERMANIUM

- Compensating temperature effects in systems using LDG type logarithmic germanium diode 01 p0035 A66-10205  
 Germanium fiber single crystal growth, properties and application 01 p0116 A66-10207  
 Radiation damage to germanium, silicon, indium and gallium antimonides and arsenides 01 p0119 A66-10373  
 Effect of poor surface finishes on existence of electromechanical effect in germanium 01 p0124 A66-10773  
 Light effect on surface conductivity of gold-alloyed germanium with clean surface 01 p0125 A66-10776  
 Electric current oscillations in germanium semiconductors having carriers in nonthermal equilibrium state 01 p0128 A66-11197  
 Oxygen impurity atom interaction with radiation-induced defects in germanium over wide temperature range, producing optically active oxygen defect complexes 02 p0272 A66-11486  
 Germanium Esaki diode characteristics with aging, noting change in excess current after forward bias application 02 p0198 A66-11522  
 Radiative recombination of degenerate and compensated germanium indicating that emission line at low temperatures shifts to higher energies with increasing excitation 02 p0273 A66-11715  
 Spectral distribution of carrier lifetime obtained from photomagnetoelectric effect and photoconductivity 02 p0273 A66-11719  
 Spectral responses of photoconductivity in plastically deformed germanium at liquid nitrogen temperature 02 p0274 A66-11720  
 Determination methods for various types of dislocation in germanium lattice and influence on physical properties of germanium 02 p0276 A66-12066  
 Temperature dependence of surface conductivity and Hall effect in germanium alloyed with gold 02 p0276 A66-12078  
 Anisotropic absorption of electromagnetic waves by hot carriers in germanium 02 p0277 A66-12082  
 Photo-emf of germanium in presence of surface recombination rate gradient 02 p0277 A66-12089  
 Impurity concentration dependence of difference between heat capacities at constant pressure and at constant volume in Ge 02 p0277 A66-12093  
 Germanium conductance measurement when immersed in aqueous electrolyte using DC and LF AC methods as polarization function 03 p0407 A66-12403  
 Uniaxial stress effect on minority carrier concentration, mobility and lifetime in germanium p-n junction 03 p0409 A66-12726  
 Piezoresistance of doped n-type germanium, determining nature of carrier scattering mechanism in degenerate materials and modification of conduction-band edge resulting from impurity states 03 p0412 A66-13148  
 Parametric amplification in millimeter-wave range, detailing parametric amplifier with germanium epitaxial diodes for use in radiometers 03 p0346 A66-13322  
 Chemical etching method useful for electron microscope observation of damage regions of high-energy neutron irradiated n-type germanium 04 p0562 A66-13738  
 Electrical, IR property measurements and annealing experiments on electron-irradiated oxygen doped germanium 04 p0562 A66-13747  
 Thermometric characteristics of gallium arsenide and germanium diodes 04 p0495 A66-13894  
 Electric field effect on long wave edge of extrinsic photoconductivity in zinc and mercury doped germanium 04 p0565 A66-14266  
 Ion-pairing process in nickel and lithium doped germanium 04 p0565 A66-14270  
 Temperature dependence of hole-capture cross section in germanium 04 p0565 A66-14271  
 Transmission of hole-type germanium in strong electric fields, noting spectral dependences of radiation modulation and hole absorption cross section 04 p0568 A66-14352

- Current oscillations in germanium and silicon connected to compensated semiconductor, noting surface impurities 04 p0569 A66-14355  
 Temperature dependent component in low temperature thermoelectric power of doped n-germanium observed in liquid helium region, noting negative magnetoresistance 04 p0570 A66-14369  
 Roentgen characteristic temperature of germanium and silicon calculated from elastic oscillation spectra 05 p0730 A66-14644  
 Germanium films deposited on heated crystal calcium fluoride substrates in vacuum system 05 p0732 A66-14666  
 Semiconductor thin film p-n junction thermocouples consisting of germanium crystal deposit in vacuum 05 p0736 A66-14974  
 Surface recombination on interface between germanium/electrolyte boundary 05 p0738 A66-15466  
 Electrically active impurities effect on germanium thermal resistivity at low temperatures measured on n-type single crystals 05 p0742 A66-15877  
 Compensation dependence of impurity conduction in n-type germanium containing antimony atoms 05 p0743 A66-15877  
 Strain dependence of impurity conductivity measured in compensated p-type germanium using uniaxial compression 06 p0922 A66-16177  
 Helicons in n-type silicon and germanium calculating collective modes of electrons in external magnetic field from frequency and wavelength-dependent conductivity tensor 06 p0923 A66-16279  
 Microwave switching and pulse modulation by impact ionization, using DC electric field to break down n-type germanium 06 p0851 A66-16455  
 Low level garnet limiter with operating range greater than one octave, using conductivity change due to impact ionization in n-type germanium, noting volt-ampere characteristic 06 p0851 A66-16455  
 Exponential band-edge tails observed experimentally in degenerate n-type germanium tunnel diode 06 p0925 A66-16665  
 Microwave induced generation of DC voltage across thin n-type germanium rod in waveguide 06 p0925 A66-16677  
 HF response of copper doped p-type germanium IR detectors 06 p0882 A66-16768  
 X-ray diffraction method for measuring thermal expansion coefficient of germanium, silicon, indium antimonide and gallium arsenide 06 p0930 A66-17047  
 Radiation damage in silicon and germanium semiconductors 06 p0932 A66-17111  
 Radiation damage in nondegenerate germanium at low temperatures, using hot carrier technique for measuring resistivity and Hall coefficient on antimonide doped samples 06 p0932 A66-17111  
 Metastable defect annealing in germanium by bombardment with short pulse of high energy electrons from Van de Graaf generator 06 p0932 A66-17111  
 Effectiveness of measurements of X-ray diffraction intensities as probe of lattice defects introduced in perfect germanium crystals by energetic particle irradiation 06 p0933 A66-17127  
 Gamma irradiated germanium at zero degrees C, studying annealing of recombination center, obtaining life time from transient decay of photoconductivity 06 p0934 A66-17127  
 Positions of defect energy levels in n-type germanium irradiated with fast neutrons analyzed by optical methods, measuring spectral distribution of photoconductivity and quenching curve 06 p0934 A66-17127  
 Point defect mobility and annealing in irradiated germanium and silicon by electron or gamma ray irradiation 06 p0937 A66-17140  
 Ripening of defects induced by fast neutrons in germanium in course of low temperature annealing 06 p0937 A66-17144  
 Characteristics and properties of defects induced in silicon and germanium by 10-to 60-mev electrons and 20-to 130-mev protons 06 p0939 A66-17156  
 Indirect and direct radiative recombination transitions in germanium and use in analysis of lifetime 07 p1094 A66-17314  
 Radiative recombination in germanium



- doped with As, Sb or In, using optical or electrical injection at 10 to 20 degrees K 07 p1095 A66-17322
- Electron capture and hole capture by impurity atoms due to radiative transitions in silicon and germanium 07 p1095 A66-17323
- Recombination radiation of n-type germanium with various dislocation densities, emphasizing mechanism of radiative transitions 07 p1096 A66-17324
- Ion damage and successive annealing of germanium observed by electron microscope 07 p1097 A66-17528
- Band structure of germanium in vicinity of Brillouin zone center 07 p1097 A66-17533
- Vacuum fusion and IR absorption determination of bulk oxygen content of germanium crystals 07 p1098 A66-17743
- Silicon-germanium thermoelectric power-generating devices 07 p0994 A66-18318
- Induced electric conductivity in germanium bombarded by potassium ion in different crystallographic directions 07 p1104 A66-18363
- Faraday effect on hot electrons in germanium and silicon 07 p1105 A66-18370
- X-ray characteristic temperature of germanium-silicon solid solution of equiatomic composition 07 p1106 A66-18379
- Carrier formation due to passage of current through elastically deformed Ge, detecting nonlinearity of volt-ampere characteristics 07 p1106 A66-18381
- Hole diffusion constant dependence on electric field in n-type germanium 07 p1106 A66-18395
- Stress-volume results between 20 and 140 kbar for germanium shock loaded in one-dimensional strain 07 p1108 A66-18419
- 600-mev proton irradiation effects on density and mobility of majority carriers in n-type germanium 08 p1267 A66-18647
- Kinetics of reactions in iodide method of growing epitaxial germanium 08 p1268 A66-18797
- Oscillations in impurity photoconductivity and absorption spectra of p-germanium samples 08 p1269 A66-18973
- Corrections to effective mass theory of shallow impurity states in germanium, using perturbation theory and wave functions 08 p1269 A66-19007
- High-field surface conductance of n-type germanium observed to be negative and magnitude to increase with field in high-field region 08 p1271 A66-19222
- Grid dispersion mobility dependence on temperature in p-type Ge, noting discrepancy of theoretical and experimental results 08 p1273 A66-19257
- Electric current passage through multivalley n-germanium semiconductor plates, noting nonuniform electron distribution 08 p1273 A66-19275
- Hall effect measured by splitting alternating voltage produced in Hall circuit into two components, one with phase coinciding with Hall emf and other with phase departing by 90 degrees 08 p1273 A66-19289
- Optical absorption in germanium in region of forward transition with spectral transmission curve having structure in form of two minima 08 p1274 A66-19316
- Recombination of hot current carriers via recombination center on germanium surface 08 p1276 A66-19611
- Magnetoresistance measurements of germanium in strong magnetic field 08 p1277 A66-19616
- Ionization energy in silicon carbide and germanium irradiated by electrons 08 p1278 A66-19628
- Potential distribution at germanium-electrolyte interface in iodide ion solutions 08 p1278 A66-19824
- Stationary germanium potentials in oxidizing media and light illumination 09 p1410 A66-19895
- Electrolytic deposition of copper and gold on germanium surface 09 p1338 A66-19896
- Microscopic theory of electroacoustic effect for n-type Ge and Si semiconductors of many energy minima, noting electron scattering 09 p1412 A66-19986
- Discharge in germanium thin films at liquid helium temperatures, noting electrostatic ionization of impurities and shock-ionization region 09 p1412 A66-19990
- Fluctuation of electric field distributions within germanium sample when one contact of sample is used to inject holes 09 p1412 A66-19994
- Hysteresis nature of current-voltage characteristics observed in p-n junctions obtained by bombarding germanium crystals with fast electrons 09 p1413 A66-20001
- Anisotropy of balanced photoelectromagnetic emf in p-type germanium sample in which normal to illuminated surface coincides with crystallographic axis 09 p1413 A66-20002
- Balanced anisotropic photoelectromagnetic effect in germanium 09 p1413 A66-20003
- Rapid cooling induced stress leads to separation between tin and germanium, creating pure germanium surface at plane of separation 09 p1427 A66-20366
- Galvanomagnetic and field effect measurements on Ge double crystals 09 p1427 A66-20419
- Characteristics of cadmium sulfide photocells and p-n junction photocells, using germanium or silicon 09 p1355 A66-20573
- Logarithmic temperature dependence of electrical resistivity found in metallic impurity conduction in n-type germanium 09 p1430 A66-20849
- N-type germanium electric conductivity dependence on applied electric and magnetic field 09 p1430 A66-20857
- Photovoltaic response of variously doped germanium-silicon diodes, confirming band diagram for germanium-silicon heterodiodes dominated by lattice mismatch interface states 09 p1360 A66-20978
- Diffusion length dependence on energy of exciting photons for p-silicon and n-and p-germanium, using bevel-grind technique 10 p1578 A66-21666
- Polarization of helicons in n-type silicon and germanium 10 p1580 A66-21733
- Energy band structure of germanium and silicon throughout Brillouin zone by k-p Hamiltonian 10 p1581 A66-21738
- Diagonalization 10 p1581 A66-21738
- Stored charge storage in surface states of germanium and silicon 10 p1581 A66-21877
- Field effect and surface states at interface between germanium and electrolytes 10 p1586 A66-22145
- Electron excitation in germanium by alkali metal ions, noting effect on electrical conductivity 10 p1587 A66-22154
- Electroconductivity of n-type Ge in strong SHF electrical fields 10 p1587 A66-22155
- Disappearance of impurity levels in germanium containing arsenic in presence of large injection level 10 p1588 A66-22161
- Effect of poor surface finishes on existence of electromechanical effect in germanium 11 p1749 A66-22284
- Light effect on surface conductivity of gold-alloyed germanium with clean surface 11 p1749 A66-22288
- Spin resonance of donor electron in Ge and anisotropic line width in relation to dislocation stress 11 p1750 A66-22463
- VHF power modulation receivers using germanium injection modulators produce no additional noise at frequencies around 25 cps 11 p1670 A66-23228
- Gallium arsenide whiskers on germanium structure, using electron diffraction photography and electron microscopy 11 p1757 A66-23280
- Sandwich method in closed system for growing semiconductor germanium epitaxial films 11 p1757 A66-23282
- Resonance properties of germanium analyzed by passing DC and AC through samples of various specific resistance with tungsten needle contacts 11 p1759 A66-23419
- Splitting in indirect absorption edge spectrum dependent on direction and magnitude of applied stress and light polarization with respect to stress axis 12 p1927 A66-23721
- Doping techniques for epitaxial growth of silicon and germanium layers 12 p1832 A66-23933
- Cascade theory of electron recombination into ionized donors in germanium analyzed, noting several models 12 p1928 A66-23940
- Accelerated life tests of germanium transistors, with failure percentage plotted against time 12 p1834 A66-24086
- Absorption spectrum of germanium at various temperatures and wavelengths and of heavily doped germanium at room temperature, obtaining agreement for both cases with theory of structural absorption of holes 12 p1929 A66-24452
- Electric conductivity and thermal emf of solid solutions of silicon-germanium with near silicon composition and various current-carrier concentrations and test temperatures 12 p1929 A66-24454
- Antimony ionization in p-germanium single crystals, based on diffusion of Sb into Ge 12 p1930 A66-24460
- Germanium specimens with various dislocation densities quenched from high temperatures to introduce vacancies, contamination by copper atom diffusion, finding activation energy 12 p1930 A66-24801
- High field magnetoresistance and random inhomogeneities in arsenic-or antimony-doped n-type germanium 12 p1931 A66-24805
- Length changes in electron irradiated high purity germanium at liquid helium and nitrogen temperatures, noting large initial expansion 13 p2157 A66-25047
- Microstructure of epitaxial germanium films deposited on calcium fluoride substrates, noting parameters of deposition 13 p2158 A66-25063
- Field emission of germanium alloyed with silver and irradiated with IR 13 p2160 A66-25108
- Transport equation for germanium-gallium arsenide-iodine system and epitaxial vapor growth preparation of GaAs-Ge heterojunction by closed tube process 13 p2161 A66-25185
- Uniaxial stress effect on Ge inclined p-n junctions 13 p2161 A66-25191
- Hall reversal at negative resistance in forward biased p-Ge point contact diode 13 p2029 A66-25192
- Diffused-base alloyed-emitter p-n-p type planar germanium microwave transistor 13 p2038 A66-25558
- Effect of magnetic field on field effect at germanium surface, determining rate of surface recombination 13 p2166 A66-25697
- Individual and group defect contribution to variation in carrier concentration and mobility in n-type germanium irradiated with fast neutrons 13 p2166 A66-25917
- Roentgen characteristic temperature of germanium and silicon calculated from elastic oscillation spectra 13 p2167 A66-25922
- Silver salts effect on etching of germanium single crystals, noting photomicrographs of structural changes 13 p2169 A66-26584
- Low-temperature internal friction peaks in germanium and oxygen-doped and pure silicon crystals 13 p2170 A66-26586
- Morphology and structure of gallium arsenide crystals containing germanium core grown by iodine transport process in closed tube 13 p2170 A66-26587
- Amplitude probability density of random stationary signal potential and variation of free carriers in germanium semiconductor at near-ambient temperature 13 p2170 A66-26758
- Microwave Faraday effect in n-type germanium, discussing Faraday rotation, ellipticity, magnetoabsorption, complex conductivity tensor elements and measurement of microwave polarization anisotropy 14 p2349 A66-26826
- Crystallization sequences in alkali aluminogermanate glass 14 p2318 A66-26947
- Microwave rotator using hot carrier property of n-type germanium 14 p2248 A66-27056
- Surface photoconductivity dependence on thermal and spectral state and time lag of germanium 14 p2357 A66-27073
- Hot electron recombination at repulse impurity centers in germanium containing copper 14 p2357 A66-27074
- Spontaneous LF current oscillations in germanium with copper, with compensated energy levels under illumination, low temperatures and electric fields, noting formation of electric domains 14 p2357 A66-27076
- Recombination radiation of strongly arsenic-doped germanium, noting narrowing of forbidden band 14 p2358 A66-27080
- Thermoconductivity of germanium alloyed



with arsenic and gallium depends on impurity type starting from certain impurity concentration 14 p2359 A66-27178

Influence of p and n doping on electrification of dust of Ge monocrystals grown from zone-melted material 14 p2364 A66-27717

Alloying real germanium surface with gold impurity and increase of fast surface states and rate of surface recombination 14 p2365 A66-27752

Photoelectric yield and energy distribution for clean-cleaved cesium-covered /111/ surfaces of silicon and germanium 14 p2365 A66-27755

Minority carrier drift mobility in p-type germanium single crystal under uniaxial lattice compression 14 p2365 A66-27758

Field-effect-modulated optical absorption spectrum for various values of Ge surface potential 14 p2366 A66-27765

Transmission of hole-type germanium in strong electric fields, noting spectral dependences of radiation modulation and hole absorption cross section 14 p2368 A66-28250

Current oscillations in germanium and silicon connected to compensated semiconductor, noting impurities 14 p2368 A66-28252

Electrical properties of germanium-gallium arsenide heterojunctions of p-n and n-n structure 14 p2369 A66-28260

Parametric amplification in millimeter-wave range, detailing parametric amplifier with germanium epitaxial diodes for use in radiometers 14 p2260 A66-28296

Degree of perfection of Ge and GaAs single crystals and epitaxial films effect on integral intensity jump at K absorption edge seen in Bragg diffraction 15 p2557 A66-28561

Transient and steady state photoconductivity in plastically bent germanium, noting logarithmic decay of photocurrent and logarithmic lux-ampere characteristics 15 p2558 A66-28608

Dielectric field cathode model of field and photofield emission from high resistivity Si and Ge at low temperatures 15 p2558 A66-28609

Effect of impurity atoms or neutron irradiation on X-ray diffraction intensities of silicon and germanium crystals 15 p2559 A66-28625

High field properties of gold doped germanium at liquid nitrogen temperature 15 p2560 A66-28633

Acceptor nature of dislocations in p-type germanium 15 p2560 A66-28636

Damaged depth in germanium thin films induced by bombardment with low energy argon ions measured, using differences in sputtering yield for given energy 15 p2561 A66-28705

Seebeck coefficient of germanium films vacuum-deposited on Vycor substrate 15 p2562 A66-28723

Electric characteristics of epitaxial Ge films vacuum deposited on seminsulating GaAs substrates with thicknesses near one million angstroms 15 p2566 A66-29386

Lifetime measurement for minority carriers injected into germanium by electron bombardment 15 p2567 A66-29409

Thermometric characteristics of gallium arsenide and germanium diodes 15 p2467 A66-29708

Fabricating perfect dendritic germanium crystals with required resistivity and dislocation density 15 p2569 A66-29787

Field emission of germanium alloyed with silver and irradiated with IR 16 p2771 A66-30287

Evaluation of energy resolution of Li-drifted Ge detectors and preamplifiers using FETs in nuclear spectrometry 16 p2660 A66-30625

Absorption coefficient change due to electric field measured for indirect absorption edges of silicon and germanium, determining energies of phonons taking part in indirect optical absorption 16 p2775 A66-30728

Magnetic field effect on direct band-to-band tunnel current in doped germanium, noting decreases in reverse current and current-voltage characteristics 16 p2776 A66-30735

Effect of thermal population of /000/ and /100/ conduction bands on elastic constants of heavily doped n-type germanium 16 p2778 A66-31070

Generation recombination noise in Ge single crystals under fast neutron irradiation, using reversible technique to vary noise parameters 16 p2778 A66-31072

Local pressure effect on forward and reverse current in germanium p-n junction 16 p2779 A66-31081

Germanium single crystal whisker formation by iodide method of selective epitaxial growth 16 p2781 A66-31405

Magnetic field influence on AC surface field effect in germanium resulting from change in sample conductance and not from change in surface barrier height 16 p2784 A66-31450

Photoconductivity spectra and kinetics of p-and n-type germanium crystals bombarded by fast electrons at 5.2 and 100 degrees K 16 p2788 A66-31776

Electric field dependence of piezoresistance in germanium, noting correlation with intervalley scattering in energy balance 16 p2788 A66-31778

Temperature dependence of mean ionization energy changes in germanium and silicon samples exposed to X-rays caused by changes in forbidden bandwidth 16 p2788 A66-31782

Instability of Sb and Au-doped n-type germanium during carrier injection, examining current-voltage and frequency characteristics and illumination effects 17 p2974 A66-31858

Secondary breakdown relaxation oscillations and I-V characteristics of point-contact n-type Ge diode 17 p2879 A66-31866

Epitaxial growth techniques for silicon and germanium, discussing hydrogen reduction methods, doping and impurity control, etc 17 p2976 A66-32259

Longitudinal Hall effect in n-type germanium measured on basis of anisotropic scattering theory, taking into account tensor character 17 p2976 A66-32260

Oxygen defect complexes in neutron irradiated germanium 17 p2980 A66-32847

Structure and batch fabrication of beam lead planar Ge Esaki diode 17 p2895 A66-33119

Recombination of hot current carriers via recombination center on germanium surface 17 p2983 A66-33125

Magnetoresistance measurements of germanium in strong magnetic field 17 p2983 A66-33130

Ionization energy in silicon carbide and germanium irradiated by electrons 17 p2984 A66-33142

Negative photoconductivity in germanium at temperature and doping levels important with impurity conduction 17 p2985 A66-33293

Damaged germanium surface epitaxial layer influence on resistivity and mobility of thin semiconductor sheets 17 p2986 A66-33294

External electron emission measurement from polished n-germanium and n-silicon surfaces 17 p2986 A66-33310

Current instability of plasma injected into germanium, noting effect of strong electric field in presence of temperature gradient 17 p2987 A66-33313

Negative photoconductivity in germanium, noting breakdown and negative conductivity in In region, volt-ampere characteristics, etc 17 p2987 A66-33315

Recrystallization of Ge and Si thin films and structural changes due to electron bombardment and thermal annealing 17 p2988 A66-33456

Thermodynamic and optical properties of Ge, Si, diamond and GaAs, obtained by inelastic neutron scattering technique, used to measure vibrational spectrum 18 p3154 A66-33922

Magnetopiezo-optical reflection in germanium observed by piezoreflection technique for direct transition 18 p3156 A66-34467

Electron energy loss spectra of Ge and Si in amorphous, polycrystalline and monocrystalline form 18 p3159 A66-34710

Impurity conduction for arsenic diffused into p-type germanium and boron into n-type silicon 19 p3433 A66-35342

Controlled doping of germanium layers during evaporation, noting behavior differences for p-and n-type impurities and concentration dependence 19 p3434 A66-35344

Hydrogen reduction techniques and layer quality measurement methods for epitaxial growth of silicon and germanium crystals 19 p3437 A66-35477

Twin boundary effect on measurements of phonon momentum propagating through Ge bicrystal p-layers at liquid nitrogen temperatures 19 p3438 A66-35481

Field effect and surface states at interface between germanium and electrolytes 19 p3440 A66-35755

Electron excitation in germanium by alkali metal ions, noting effect on electrical conductivity 19 p3440 A66-35761

Electroconductivity of n-type Ge in strong SHF electrical fields 19 p3440 A66-35761

Disappearance of impurity levels in germanium containing arsenic in presence of large injection level 19 p3441 A66-35777

Drift rate and precipitation of lithium ions in germanium as affected by resistivity acceptors, carrier lifetime and copper diffusion 19 p3442 A66-35911

Lithium-drifted germanium detector resolution and efficiency as function of temperature for gamma rays 19 p3359 A66-35911

Splitting of ground state of neutral mercury two-hole acceptor in unstressed silicon or germanium evidenced by intensity decrease of photoabsorption peaks 19 p3444 A66-36174

Dipole scattering of electrons in germanium and silicon whose conduction band structure is described by many-valley model, using distribution function and computing relaxation-time ratio 19 p3446 A66-36339

Absorption of polarized electromagnetic waves at zero degrees K in n-type germanium under high uniaxial stress 19 p3446 A66-36339

Photomagnetic anomaly in germanium in induction coil subject to variations in magnetic moment 20 p3618 A66-37581

Absorption spectrum of germanium at various temperatures and wavelengths and of heavily doped germanium at room temperature, obtaining agreement for both cases with theory of structural absorption of holes 20 p3619 A66-37681

Electric conductivity and thermal emf of solid solutions of silicon-germanium with near silicon composition and various current-carrier concentrations and temperatures 20 p3619 A66-37681

Antimony ionization in p-germanium single crystals, based on diffusion of Sb into Ge 20 p3620 A66-37691

Subshell photoelectron emission in germanium at angle of 90 degrees to converting X radiation determined for two radiation sources using photographic techniques and track counting method 20 p3621 A66-38091

Surface recombination on interface between germanium/electrolyte boundary 20 p3622 A66-38131

Germanium damage due to low energy He, Ne, Ar and Kr ion bombardment 20 p3623 A66-38339

Normal incidence reflectivity and transmissivity coefficient measurements in Ge thin epitaxial films 20 p3623 A66-38339

Model estimate of oxygen concentration captured from residual gases by epitaxial germanium and silicon films prepared by vacuum deposition 21 p3795 A66-38521

Thermostability of germanium power transistors, noting collector leakage current 21 p3709 A66-38671

Interband microwave scattering of holes by cyclotron resonance in Ge 21 p3797 A66-38751

Cyclotron resonance observation of electron scattering by Ga and In atoms in Ge 21 p3797 A66-38751

Spiral instabilities in semiconducting germanium plasma in radial electric and axial magnetic fields 21 p3797 A66-38751

Relation between electrical properties and structural features of gold-and antimony-doped germanium single crystals, noting abrupt decrease in



- mobility 21 p3799 A66-38928  
N-type Ge hot carrier Hall mobility, magnetoresistance, Maxwellian energy distribution, electron-electron and intervalley electron-phonon collisions 21 p3801 A66-38997  
Preferential formation of peaks of single-crystal silicon and germanium samples exposed to short-duration electron beam 21 p3801 A66-39117  
Heteroepitaxial deposition of films of germanium in single-crystal form on sapphire by vapor growth techniques 21 p3802 A66-39163  
Cyclotron resonance study of electron scattering by thermal acceptors in quenched Ge 21 p3805 A66-39567  
Energy and wave functions of singly charged donor impurity centers in silicon and germanium 22 p3959 A66-39772  
Predicted plasma mode in microwave frequency range for magnetoplasma excitations in germanium, applying theory to n-type and p-type lead telluride 22 p3960 A66-39805  
Photovoltaic response of p-n Ge-Si and Ge-GaAs heterojunctions dominated by carrier generation in narrow or wide gap material 22 p3960 A66-39813  
Change in temperature conditions during growth of epitaxial germanium films from molecular beam in vacuum 22 p3961 A66-39928  
Butler iron meteorite composition, noting unusually high cobalt and germanium content and low cooling rate 22 p3978 A66-40013  
Butler iron meteorite composition, noting very high concentration of germanium, gallium and nickel exhibiting Widmanstätten pattern 22 p3978 A66-40014  
Optical spectrum of normal excitons in deformed and nondeformed n-type Ge single crystal layers for four orientations 22 p3964 A66-40306  
Current-carrier scattering anisotropy dependence on antimony impurity concentration in n-Ge established, using measurements on Hall effect and conductivity 22 p3965 A66-40321  
Method of characterization for germanium microwave transistors and circuit design principles for low noise performance 22 p3881 A66-40746  
Surface photoconductivity dependence on thermal and spectral state and time lag of germanium 22 p3966 A66-40831  
Hot electron recombination at repulse impurity centers in germanium containing copper 22 p3966 A66-40832  
Spontaneous LF current oscillations in germanium with copper, with compensated energy levels under illumination, low temperatures and electric fields, noting formation of electric domains 22 p3966 A66-40833  
Recombination radiation of strongly arsenic-doped germanium, noting narrowing of forbidden band 22 p3967 A66-40836  
Parallel and transverse magnetic field effects on electric field induced optical absorption at photon energies below direct gap in Ge 23 p4109 A66-41036  
Resonance absorption of gamma-quanta by tin in germanium 23 p4110 A66-41133  
Surface charge mobility measurement method applied to Si and Ge and time variation of surface conductivity 23 p4110 A66-41183  
Degree of perfection of Ge and GaAs single crystals and epitaxial films effect on integral intensity jump at K absorption edge seen in Bragg diffraction 23 p4112 A66-41282  
Resistance meters for heavily doped silicon and germanium 23 p4068 A66-41571  
X-ray K-absorption spectra of titanium, vanadium and germanium in germanides 23 p4082 A66-41826  
Silicon-germanium lead-telluride segmenting for improved thermoelectric efficiency, noting sequential fabrication process difficulties 24 p4248 A66-42115  
W-diffusion bonding in preparing segmented silicon-germanium-lead telluride thermoelements, noting properties 24 p4248 A66-42116  
Radiative recombination within space-charge region in germanium exposed to increasing surface field 24 p4251 A66-42308  
Generation-recombination noise and lifetime measured using photoconductive decay in n-and p-type Ge samples doped with shallow impurities 24 p4253 A66-42357  
Surface photovoltage theory for small signals in Si and Ge, considering photocarrier trapping on surface and conductivity in space charge region 24 p4253 A66-42358  
Energy levels and wave function of hole in field of two acceptor ions and nearest ion donor for p-type Ge and Si 24 p4255 A66-42496  
Matrix elements of Coulomb potential between Schechter functions and overlap integrals necessary in determining two-center acceptor states in p-type Ge and Si 24 p4255 A66-42497  
Energy levels and wave function of hole in field of two acceptor ions and nearest ion donor for p-type Ge and Si, noting numerical results 24 p4255 A66-42498  
Multiple cyclotron resonance absorption lines in degenerate valence bands of Ge semiconductor studied with far IR laser submillimeter spectrometer 24 p4257 A66-42545
- GERMANIUM ALLOY**  
Surface conductivity of germanium gold alloyed at liquid nitrogen temperature, considering field effect 01 p0127 A66-11059  
Thermal and magnetic properties of GeTe and PbTe semiconductors containing transition elements in solution 01 p0127 A66-11079  
Nonlinear electrical effects and recombination of hot electrons in compensated germanium, studying steady and transient I-V characteristics 02 p0273 A66-11717  
Uniaxial stress effect on germanium-silicon alloyed heterojunction 03 p0410 A66-12729  
Piezomagnetoresistance on compressive stress for antimony-alloyed germanium, observing magnetic field induction 04 p0569 A66-14358  
Thermoconductivity of alloyed solid silicon-germanium solutions 05 p0731 A66-14652  
Secondary breakdown in germanium alloy and diffused-alloy transistors 09 p1358 A66-20817  
N-type germanium alloyed with gold shows negative photoconductivity in strong electric fields 10 p1589 A66-22173  
Germanium alloy transistor for high current and low saturation voltage requirements, noting high efficiency, physical properties, application, etc 13 p2037 A66-25543  
Thermoconductivity of alloyed solid silicon-germanium solutions 13 p2167 A66-25927  
Temperature variation and carrier concentration effects on density-of-states effective mass, polar and dipolar thermoconductivity, electron and phonon scattering and electron-phonon interaction in doped Si-Ge alloys 14 p2365 A66-27759  
Piezomagnetoresistance on compressive stress for antimony-alloyed germanium, observing magnetic field induction 14 p2368 A66-28256  
Stable microwave oscillations in single crystal Ge alloy p-n junction diodes 15 p2567 A66-29402  
Tunnel diode capacitance relation to displacement interpreted in terms of impurity drift in nonuniform field of p-n junction in highly doped germanium diodes 19 p3433 A66-35302  
N-type germanium alloyed with gold shows negative photoconductivity in strong electric fields 19 p3441 A66-35787  
Metallography, roentgenography and differential thermal analysis of composition temperature ranges of chromium-germanium phases 23 p4082 A66-41825
- GERMANIUM COMPOUND**  
Order in equiatomic germanium silicon solid solution, using diffusion scattering of X-rays calculated by least squares method 01 p0124 A66-10768  
Microwave rotation spectrum for GeS in frequency ranges from 10.7 to 11.4 and 32.1 to 34.1 gc at temperatures between 450 and 650 degrees C 04 p0567 A66-14336  
Mercury and zinc ions in germanium, discussing hole capture cross section in comparison to standard white noise source 05 p0731 A66-14660  
Structure of sulfide films deposited on silicon and germanium single crystals 07 p1092 A66-17223  
Electrical conductivity variation of low and high resistance germanium due to X-ray radiation absorption 07 p1100 A66-17932  
Energy spectrum of current carriers in germanium telluride, investigating electrical properties of polycrystalline and single crystal samples 07 p1105 A66-18376  
Optical modulation of current in germanium-silicon n-n heterojunctions, noting consistency of I-V, C-V and photocurrent spectra characteristics with depletion region model of material 08 p1273 A66-19253  
Hall effect in germanium telluride samples with various current carrier concentrations at temperatures up to 500 degrees C 09 p1413 A66-20000  
Superconductivity in Ag doped GeTe and monoxides of Ti and Nb 09 p1423 A66-20070  
Order in equiatomic germanium silicon solid solution, using diffusion scattering of X-rays calculated by least squares method 11 p1748 A66-22279  
K absorption spectra of germanium and selenium in germanium selenide based on band theory of solids by assuming electrons transfer, using X-ray spectroscopy 11 p1758 A66-23368  
Length changes and conductivity variations in electron irradiated n-and p-type germanium, noting methods of measurement, effects of isochronic annealing at liquid helium and nitrogen temperatures 12 p1926 A66-23717  
Bulk germanium arsenide operating simultaneously as microwave amplifier, mixer and oscillator under continuous wave conditions 12 p1835 A66-24144  
Epitaxial vapor growth of germanium from germanium iodide with hydrogen and argon atmosphere, examining various growth parameters 13 p2161 A66-25193  
Mercury and zinc ions in germanium, discussing hole capture cross section in comparison to standard white noise source 13 p2167 A66-25935  
Hydrazine hydrate interaction with halogenides of tetravalent germanium in aqueous organic solvents 14 p2231 A66-27137  
Cadmium and indium thiogermanates, properties and synthesis 14 p2361 A66-27339  
Thermal expansion coefficient of doped germanium, noting correlation between impurity used and coefficient variation 14 p2368 A66-28244  
Current voltage characteristic of three layer germanium semiconductors, noting quadratic dependence of current on voltage 16 p2785 A66-31668  
Vapor growth of Ge on Ge, GaAs and Si substrates, noting preparation methods, characteristics, etc 16 p2786 A66-31686  
Current-carrier scattering in germanium telluride 16 p2788 A66-31780  
Structure of sulfide films deposited on silicon and germanium single crystals 17 p2976 A66-31994  
Gamma irradiation effects on minority carrier lifetime in germanium, noting temperature effect 17 p2987 A66-33321  
Thermodynamic properties and electromotive force of germanium telluride used in electrochemical schemes 19 p3434 A66-35360  
Indentation damage and subsequent annealing effect on etch-polished Ge surfaces at room temperature examined with optical microscope, using interference contrast techniques 19 p3434 A66-35401  
Systems producing germanide phases noting phase diagrams of germanides of s-elements, ds-elements, fds-elements and sp-elements 20 p3616 A66-37415  
Properties of ferrous ion in iron germanium oxide studied in terms of Mossbauer effect and susceptibility measurements 20 p3621 A66-37823  
Thermoelectric properties of solid solution of germanium telluride in copper antimony telluride 23 p4114 A66-41572  
Equiatomic rare earth germanide magnetic structural characteristics 24 p4252 A66-42353



Impurity photoconductivity spectra of p-type germanium at low temperatures, noting parameters of relative depth of equidistant minima oscillations 24 p4256 A66-42515

## GERMANIUM OXIDE

Germanium dioxide surface adsorption characteristics with respect to water vapor 10 p1583 A66-21983

Structure and properties of intermediate components of iron-oxide-germanium-oxide system analyzed, using heat treatment 13 p2162 A66-25355

## GERMANIUM RECTIFIER

Electric properties of germanium and silicon filamentary diodes in which base volume diode structure contains disintegrated region 03 p0346 A66-13319

Electric properties of germanium and silicon filamentary diodes in which base volume diode structure contains disintegrated region 14 p2260 A66-28293

Bonded backward diode fabrication and performance as microwave mixer and low-level detector 17 p2891 A66-32913

Germanium mixer diodes encapsulated in miniature double-ended construction, examining fabrication, performance and applications 17 p2892 A66-32921

Tunnel effect current in esaki diodes calculated for operation at low temperatures, examining WKB wave functions for steady state 18 p3086 A66-34390

## GERMANY

## SA WEST GERMANY

Max Planck Institute activities in space and atmospheric artificial ion cloud production and radiation measurement 01 p0170 A66-10362

Development of air transport in East Germany after World War II including route charts of Lufthansa 01 p0170 A66-11071

German participation in aerospace technology noting space transporter design and development 02 p0177 A66-11667

Production and recent developments in gas turbines and propulsive engines in West Germany 06 p0942 A66-16795

West Germany and international cooperation in aerospace engine development, noting VTOL aircraft and supersonic and hypersonic spacecraft 06 p0943 A66-16797

European Miniature Electronic Components and Assemblies Data 1965-1966, Part I, Germany and Italy 06 p0858 A66-17158

German and Austrian astronomical observatories reports on personnel, equipment, projects and publications 13 p2189 A66-26736

Space research in Federal Republic of Germany during 1965 15 p2599 A66-29901

German Democratic Republic space program noting equipment for satellite observation, geodesy, aeronomy, etc 15 p2600 A66-29911

Interrelation between lunar phase and occurrence of precipitation larger than 10.0 mm per day in northern Germany 16 p2742 A66-31113

## GERMINATION

Seed germination and seedling growth dependence on oxygen, noting microaerobic capabilities among vascular plants, water effect, etc 18 p3059 A66-34204

## GERONTOLOGY

## S AGING

## GETOL AIRCRAFT

Ground effect takeoff and landing /GETOL/ aircraft, noting problems in controlling it and configurations of annular jet 16 p2635 A66-31396

## GETTER

Molybdenum and titanium cathodes applied in getter ion pump, noting improvement of initial and average performance 13 p2078 A66-25649

## GIANT STAR

Solar system formation theory that planets were formed from gigantic gaseous suns as result of tidal action and loss of mass by suns 01 p0135 A66-10298

Magnetoturbulent kinetic energy instrumental in removal of general relativistic instability of supermassive stars 01 p0138 A66-10882

Evolution of 15 solar masses star from main sequence through helium core burning, comparing with evolution of less massive

stars 11 p1773 A66-22782

Interstellar molecular hydrogen abundance and possible source from giant stars 13 p2182 A66-25579

Lithium/calcium ratio of five F giant and six G giant stars 13 p2183 A66-25611

Dynamic stability of supermassive stars with nuclear-energy generation, noting rotation and limiting mass for hydrogen burning 14 p2385 A66-28117

Arguments inferring that all population II red giant stars become planetary nebulae 20 p3656 A66-38050

## GIBBS EQUATION

Thermodynamic functions determined for nonequilibrium system using Gibbs local equilibrium ensembles to incorporate temperature inhomogeneity 03 p0445 A66-13191

Shift of gas mass from high pressure to low pressure sides of divided vessel, with communication by bursting diaphragm and by-pass valve 05 p0664 A66-15638

Asymptotic inequalities to determine phase volume within given boundaries with aid of Gibbs canonical distribution 21 p3756 A66-38738

## GIBBS PHENOMENON

## SA FOURIER SERIES

Sufficient conditions for transformation sequence exhibiting Gibbs phenomenon when using triangular methods of Fourier series summability 02 p0250 A66-12106

Equilibrium phases of elastic materials occurring at uniform temperature and pressure and at zero deviatoric stress, examining rapid quenching and shearing effects 21 p3829 A66-38940

Gibbs-DiMarzio theory of glass transition used to derive Simba-Boyer parameter, which is function only of fractional unoccupied volume 22 p3938 A66-40911

## GIMBAL

Free and forced vibration effect on drift of gyroscope supported in gimbal 23 p4071 A66-41981

## GIMBALLED CONTROL

Terminal prediction guidance for rocket vehicles in terms of strapped-down and gimbaled platform 01 p0101 A66-10042

Tests of airborne, gimbal and stabilized mounts of LaCoste-Romberg and Askania-Graf gravity meters conducted in 1962 04 p0524 A66-14452

Gimballed jet engine development, noting application to V/STOL aircraft and design of plenum chamber burning engine 10 p1591 A66-21366

ESG strapdown inertial navigation system based on double integration of acceleration and analysis of electronic gimbaling-induced errors 13 p2124 A66-25653

Inertial guidance systems using three-gimbal, four-gimbal and ball-type platforms, operative control of aircraft, ships and ballistic missiles 13 p2125 A66-26140

Motion of gyroscope in gimbal suspension 17 p2958 A66-32589

Mechanization of vectorial equations by means of four-gimbal platform and speed sensor for automatic setting of hybrid inertial systems 20 p3597 A66-37395

Friction and imbalance moments relative to gimbal axes and effects on gyrovertical motion under starting conditions 21 p3739 A66-39325

Inertial measurement unit and pulse torquing of Apollo spacecraft, noting components and operation [GIMBALDOGRAPH 105] 24 p4215 A66-43126

GIMBALESS INERTIAL REFERENCE SYSTEM

No-gimbal system mechanizations evaluated by flight test and compared for advantages, noting system error 21 p3764 A66-38851

## GLAND

## S ADRENAL GLAND

## S ENDOCRINE SYSTEM

## S PAROTID

## S PITUITARY GLAND

## S THYMUS

## S THYROID

## GLARE

Visual effects produced by factors of so-called glare from stationary and moving

targets 16 p2641 A66-31388

## GLASS

## SA E GLASS

## SA SILICA GLASS

Structures and crystallization processes of semiconductor vanadium phosphate glasses of various composition, using electron paramagnetic resonance 01 p0091 A66-10771

Physical properties of uncommon noncrystalline amorphous silica, alumina, magnesium fluoride and gold-silicon alloy examined for identification as glasses [ACS PAPER 20-G-64F] 02 p0248 A66-11295

Polarization of light from glass laser doped with two percent positive trivalent neodymium measured with time resolution of less than microsecond 03 p0378 A66-13006

Sensitized photolytic decomposition of ethanol and diethyl ether glasses analyzed at low temperature, using electron paramagnetic resonance /EPR/ spectroscopy 06 p0820 A66-16124

Temperature and oxygen effect on aromatic solute sensitized photo-decomposition of ethanol and ether glasses 06 p0821 A66-16125

Glass properties, formation and application to aerospace systems 07 p1054 A66-18301

Glass as component of metal-based materials in powder metallurgy noting properties, interaction of molten glass with metals, etc 10 p1548 A66-21510

Structures and crystallization processes of semiconductor vanadium phosphate glasses of various composition, using electron paramagnetic resonance 11 p1720 A66-22282

Glass transition temperature of polymethyl methacrylate as affected by low concentrations of monomer and diethyl phthalate plasticizers 11 p1720 A66-22977

High temperature crystallization processes and physicochemical properties of lithium/aluminosilicate glass 12 p1900 A66-24855

Chemical durability of lithium silicate glass as result of crystallization 12 p1901 A66-24864

Fluorescence behavior of gadolinium and terbium, noting nonradiative energy transfer in borate glass 13 p2158 A66-25055

Thermal optical behavior of glasses and other potential laser materials and thermal distortion in air, water, benzene, ethanol and toluene 13 p2092 A66-25996

Crystallization sequences in alkali aluminogermanate glass 14 p2318 A66-26947

CERCOR glass-ceramic axial flow rotary regenerator as inexpensive component for gas turbine regeneration [ASME PAPER 66-GT/107] 14 p2301 A66-27004

Rubidium-strontium isotopic study of five types of glass from Bosumtwi crater in Ghana and Ivory Coast 14 p2284 A66-27602

Damage thresholds for various glasses exposed to laser pulses, emphasizing internal damage 15 p2524 A66-28732

Low threshold neodymium glass laser oscillator with high repetition 17 p2937 A66-33325

Critical magnetic field and transition temperature measurements of superconducting indium in porous glass, using LF mutual inductance technique 21 p3796 A66-38549

Optical spectra of ultrashort optical pulses generated by mode-locked glass-doped neodymium lasers, considering saturable absorber cell placed parallel to Fabry-Perot reflector 21 p3747 A66-39115

Gibbs-DiMarzio theory of glass transition used to derive Simba-Boyer parameter, which is function only of fractional unoccupied volume 22 p3938 A66-40911

Glass lasers, comparing glass with crystals as hosts for laser ions, considering neodymium laser properties 24 p4224 A66-42800

GLASS COATING

Transient resistance and time delay of protective glass coatings on film resistance thermometer 06 p0882 A66-16845

Particle size and heat treatment effects on stability and reflectance of thermal control glass pigment coatings under UV radiation [ATAA PAPER 65-136] 15 p2616 A66-29288

Increasing sturdiness of glass-to-metal seals in cesium vapors 15 p2429 A66-29707



- Space charge polarization in glass films, discussing parameters of shift of capacitance-voltage characteristics, diffusion coefficient in metal-glass-silicon dioxide-silicon double-layer capacitor 16 p2779 A66-31089
- GLASS FIBER**
- Glass, quartz, mineral and ceramic fibers woven into fabric provide thermal insulation, reinforced plastic, filtration, friction materials and electrical insulation 01 p0091 A66-10356
- Interference effects at thin transparent cylindrical glass fibers exposed to coherent light from He-Ne laser 01 p0081 A66-10368
- Physical properties of 181 glass cloth laminates of diallyl orthophthalate and isophthalate in high temperature range 02 p0248 A66-11689
- Engineering exploitation of glass fiber reinforced plastics for aircraft structures [AIAA PAPER 65-762] 03 p0386 A66-12590
- Use of monofilament composites of S-glass fibers and epoxy-resin in primary aircraft structure [AIAA PAPER 65-761] 05 p0772 A66-14729
- Fiber composite materials - ASM Seminar, Metals Park, Ohio, October 1964 05 p0700 A66-14807
- Origin and properties of fiber composite materials 05 p0705 A66-14808
- Manufacturing glass-fiber-reinforced plastic container for high pressure helium gas in European launcher rockets 06 p0889 A66-17076
- Optimum reinforced composite strength of glass-reinforced plastics depends on filament geometry factors such as filament content, orientation and dimensions [AIAA PAPER 66-142] 06 p0901 A66-17081
- Symmetrical negative resistance in valence-exchange reaction in semiconductor pnp-type glass junctions 09 p1430 A66-20847
- Glass-resin interaction of filament-wound composites, determining material properties and application to high performance pressure vessels 11 p1783 A66-23121
- Glass fiber reinforcement for plastics, determining tensile strength of fibers, glass structure, elasticity modulus improvement via annealing, etc 11 p1720 A66-23126
- Elastomechanical properties of glass fibers and resins in order to determine optimum materials for reinforced glass fiber structures [ONERA TP 322] 11 p1721 A66-23200
- Thermal properties, tensile strength and uses of combination of glass fiber and epoxy resin material, Fiberglass S /994/, in space vehicles 12 p1899 A66-23966
- Rest period effect on fatigue testing of polyester fiberglass and polymethylmethacrylate plastics under static and intermittent tensile loads 12 p1899 A66-24039
- Tensile testing of fiberglass plastic anisotropic specimens with axis at angle to reinforcing fiber direction 12 p1899 A66-24040
- Strain gauge load measuring transducer operating in bending mode and based on elastic properties of epoxide glass fabric laminate 12 p1884 A66-24985
- Magnetization of synthetic filamentary superconductors, discussing sample preparation, critical field and transition temperature effect on flux jumping and magnetic hysteresis loop 13 p2157 A66-25037
- Rotationally-symmetric intake nozzles manufactured by low cost technique for wind tunnels from glass fibers and plastics, using wooden pattern 13 p2085 A66-25080
- Role of discontinuous fibers /whiskers/ in forming composites and how reinforcing parameters and processing vary from those used in continuous fibers systems, noting differences between boron and fiberglass whisker characteristics 13 p2113 A66-25310
- High temperature structural properties of polybenzimidazole, polyimide and phenolic laminates under different loading conditions 13 p2113 A66-25311
- Stress concentration in glass-fiber reinforced plastic with spatial irregularities 13 p2115 A66-26406
- Resin fiberglass sandwich materials for reinforcement of plastic laminated space structures 14 p2402 A66-27876
- Stressed state of cylindrical shell made of coiled glass fibers 16 p2822 A66-31625
- Axisymmetric deformation of cylindrical shell consisting of many layers of glass fabric connected by polymer mass 16 p2823 A66-31626
- Models for producing glass-fiber-reinforced plastic structural components 17 p2929 A66-31968
- Change in tensile strength during winding of prestressed oriented glass fiber filaments 17 p2942 A66-32047
- Prestressing effect on strength of glass fiber reinforced metal shells 17 p2939 A66-32048
- Glass reinforced plastics for helicopter primary structures 18 p3124 A66-33690
- Burst hoop test and new ISAS ring test methods for rapid evaluation of hoop strength of filament-wound fiberglass reinforced plastic cylindrical specimens 19 p3472 A66-35356
- Creep testing of glass fiber reinforced thin plastic plates and beams under torsion and bending 19 p3473 A66-35756
- Composite structures of glass-fiber reinforced resin and other materials for launch shell structures [AIAA PAPER 65-286] 20 p3672 A66-38165
- Equations for analysis of prestressed cylindrical shells made of fiberglass reinforced plastics with hollow fibers, longitudinally and transversely wound 22 p3990 A66-40143
- Penetration resistance of fiberglass-reinforced plastics against small-caliber projectiles noting relations between energy loss, stopping power and plate thickness 22 p3938 A66-40433
- Use of monofilament composites of S-glass fibers and epoxy-resin in primary aircraft structure [AIAA PAPER 65-761] 23 p4083 A66-40979
- High temperature structural properties of glass fabric-reinforced polybenzimidazole, polyimide and phenolic laminates for aerospace application 23 p4083 A66-41389
- Temperature and heat resistant properties of fiberglass-reinforced plastic nose cone in supersonic flight 23 p4132 A66-41421
- Prestressing effect on fiber alignment and strength of glass fiber laminates 24 p4289 A66-42338
- GLAUCOMA**
- Diagnostic standards for primary glaucoma in pilots, noting use of instrument tonometry and problems connected with sudden incapacitation 06 p0814 A66-16832
- GLIDE LANDING**
- Parachute and cushion landing system for specific payload geometry for touchdown with gliding descent, considering minimum weight design 19 p3278 A66-35626
- GLIDE PATH**
- Optimum gliding regime using Krotov generalized theory and linear partial differential equations 11 p1732 A66-22354
- Oscillatory trajectories in atmospheric entry of lifting vehicles at subcircular speeds and constant angles of attack with initial conditions deviating from equilibrium glide 17 p3016 A66-33065
- Glide range with variable lift drag ratio expressed in power series of speed 20 p3492 A66-37428
- GLIDE SLOPE**
- Adaptive coupler providing extended automatic glide slope beam following by compensating for beam convergence 01 p0101 A66-10036
- Visual segment vs glide slope geometry 12 p1810 A66-24959
- GLIDER**
- SA HYPERSONIC GLIDER**
- SA PARAGLIDER**
- SA SPACE GLIDER**
- Drag reduction for gliders, noting role of planform and warping of wing 05 p0607 A66-15198
- Drag decrease in glider aircraft noting wing profile, flow laminarization /boundary layer control/, landing flaps, tail, etc 05 p0607 A66-15200
- Glider performance including sink speeds, climb speed, absolute thermal strength, etc 07 p0989 A66-18057
- Longitudinal stability and controllability characteristics of glider, considering effect of elastic warp of wing 09 p1331 A66-20757
- Statistical research on g-loadings and atmospheric turbulence in field of structural strength limits for sporting gliders 12 p1801 A66-23855
- Instrumentation of Polish gliders including altimeters, rate-of-climb, turn and air speed indicators, magnetic compasses, artificial horizon, etc 12 p1882 A66-24386
- Safety-factor problem in glider design, discussing limiting load concept in form of extreme load in exceptional cases of operation 21 p3696 A66-38620
- Short-periodic motion of tailless glider analyzed to determine degree of overcompensation of flap required for good stability 23 p4016 A66-41784
- GLOBAL TRACKING NETWORK**
- /GLOTRAC/**
- Global maximum for particle idealization of rocket propelled vehicle moving in calculus of variations, noting Lagrange equation 04 p0538 A66-13462
- GLOBULIN**
- SA GAMMA GLOBULIN**
- Antibody globulin coupled to diazotized aminoaryl derivative of carboxymethyl-cellulose to form immunoadsorbent for extracting antigens 12 p1805 A66-23568
- GLOSSARY**
- European Miniature Electronic Components and Assemblies Data 1965-1966, Part I, Germany and Italy 06 p0858 A66-17158
- European Miniature Electronic Components and Assemblies Data 1965-1966, Part II, France, Netherlands, Scandinavia and Switzerland 06 p0859 A66-17159
- Space technology jargon, noting language used, origin and formation of words, acronyms, etc 16 p2831 A66-31151
- Glossary of gravimetric and celestial geodesy 23 p4063 A66-41525
- GLOTRAC**
- S GLOBAL TRACKING NETWORK**
- /GLOTRAC/**
- GLOW DISCHARGE**
- SA ELECTRIC DISCHARGE**
- Hot glow probe determination of plasma space potential noting disturbance due to contact potential drift and probe construction, accuracy and applicability 01 p0113 A66-10639
- Effect produced by nonhomogeneous HF field on distributed plasma parameters 01 p0115 A66-11050
- Brush cathode used in abnormal glow region, determining features of produced plasma 02 p0196 A66-11429
- Plasma velocity field determined from glow discharge in crossed fields propagating along rectangular channel, two walls being dielectrics and other two electrodes 02 p0268 A66-11786
- Formulas relating detector current to average UHF power obtained for positive plasma column and dark Faraday region of glow discharge 02 p0269 A66-11844
- Photochemical studies of oxygen-ozone and carbon dioxide equilibria with bromine UV lamp 04 p0473 A66-13397
- Electron mobility in potassium and cesium DC glow discharges at low electron temperature 05 p0728 A66-15809
- Thin film deposition by electron-beam and glow-discharge activation of various gaseous ambients 06 p0848 A66-16302
- Radio noise emission from Venus surface explained in terms of glow discharge 06 p0957 A66-17174
- Contact-making process in cadmium sulfide crystals, examining influence on plasma electron efficiency in glow discharge effect 08 p1272 A66-19243
- Stable plasma belt trapped in permanent dipolar magnetic field, measuring floating potential, electric and magnetic drifts, etc 08 p1265 A66-19408
- Silicon dioxide glass films by decomposing tetraethoxysilane in AC-induced glow discharge in which water is chemically incorporated into oxide films 09 p1432 A66-20979
- Time- and space-resolved measurements on self-excited moving striations and on low pressure glow discharge to externally excited pulses 10 p1564 A66-21565
- Model for interpretation of positive column two-dimensional striations of diffuse mode



gas discharge in uniform magnetic field 10 p1564 A66-21569

Plasma behavior in crossed stationary electric and magnetic fields, examining field dependence of ion velocity and ion and electron temperature 10 p1566 A66-21704

Glow-discharge shock tube examination of chemiluminescent, surface-catalytic and gas-phase reaction rates, noting temperature dependence of NO-O and CO-O chemiluminescent reactions 13 p2016 A66-25368

Wind tunnel apparatus for flow visualizations at Mach 14 by glow discharge method 13 p2059 A66-26376

Discharge afterglow in low pressure tube studied by photomultiplier 13 p2150 A66-26473

Magnetic effect on emission spectrum of negative glow plasma in hollow-cathode discharge, noting pressure effect 14 p2340 A66-27024

Inverse brush cathode design that functions like brush cathode in producing negative glow plasma 15 p2550 A66-28728

CW IR laser oscillation in atomic Cl in HCl and HI gas discharges, noting use of two power supplies and energy level diagram 15 p2513 A66-28880

Catalytic efficiency of noncatalysts interferes with accuracy of measurement, noting necessity of oxygen treatment of noncatalytic surfaces 15 p2502 A66-29310

Acoustic wave generation and amplification in weakly ionized plasma, explaining sound emission in glow discharge and modulation in plasma afterglow 15 p2556 A66-29808

Dielectric properties and thermostability of glow-discharge thin organic polymer films for electronic application 16 p2783 A66-31429

Microwave switching tube for rapid pulse transmission on microwave communication channel, utilizing glow discharge 16 p2666 A66-31445

Detection of centimeter waves in glow discharge plasma feasible as result of processes generated in cathode irradiated by UHF field 16 p2765 A66-31560

Sinusoidally varying HF electric field effect on glow discharge plasma, showing capability of confinement 17 p2971 A66-32785

Book on glow discharge and plasma physics including collisional processes, ionization, vacuum systems, application in electronics, etc 18 p3150 A66-34946

Glowing high-voltage discharge produced with hollow anode in discharge gap of various configurations 18 p3152 A66-35079

Hydrogen ions detected near anode of glow discharge at various pressures, using mass spectrometer 19 p3410 A66-36455

Positive plasma column produced by hydrogen glow discharge studied by mass spectrometer for various pressures and currents 20 p3608 A66-37459

Electron energy distribution function obtained by Druyvesteyn analysis in low-current positive column neon discharge compared with theoretical distribution function 20 p3608 A66-37463

Unstable combustion products of glow discharge, discussing effect of propagation rate of hydrogen-oxygen flame 21 p3834 A66-38473

Transverse separation of rare gas-metal vapor mixture components in positive nonisothermal plasma column in plain-symmetric glow discharge 22 p3958 A66-40934

Inorganic thin film surface finish for boron filaments, noting improved adhesion to organic resins and high temperature oxidation resistance 23 p4082 A66-41895

High sensitivity method of visualization of supersonic flow of rarefied gas, using glow from cathode parts of glow discharge 24 p4196 A66-42876

**GLUCOSE**

Nonelectrolytes and hydroxy and fluorobenzoates behavior on elution through columns of tightly cross-linked dextran gels 11 p1645 A66-22990

Acceleration stress-induced changes in fat metabolism, level of circulating glucose and corticosterone level in rats 15 p2431 A66-28868

Serum glucose and free fatty acids in man during prolonged exercise 17 p2859 A66-32366

Difference spectra of glucose cultures of *Chlorella vulgaris* beyernick indicate increased pigmentation in white light and monochromatic light over dark controls 20 p3507 A66-37791

**GLYCINE**

Ferroelectric properties of trissarcosine calcium chloride including dielectric measurement, Curie temperature region, etc 08 p1270 A66-19009

Indolylacryl glycine excretion in man 16 p2638 A66-30634

Stimulated Brillouin scattering in ferroelectric triglycine sulphate crystals and Rochelle salt exhibiting second-order phase transition, measuring scattering threshold as temperature function 20 p3620 A66-37770

**GLYCOGEN**

Age effect on liver glycogenesis in rats exposed to acceleration stress 17 p2860 A66-32555

Myocardial glycogenolysis in rat ventricle and relation to severity of exercise 20 p3505 A66-37058

**GLYCOL**

Oscillographic polarography to determine relation between adsorption characteristics and molecular weight of polyethylene glycol 14 p2295 A66-27655

**GNOTOBIOTICS**

Spacecraft sterilization problem using gnotobiotic techniques and isolators, noting peracetic acid role and hot wire techniques for insertions 13 p2014 A66-25289

**GOLD**

Growth of single crystal gold films in ultrahigh vacuum on clean vacuum-cleaved salt surfaces 01 p0117 A66-10242

Low temperature alpha radiation and subsequent isothermal recovery effects on electron structure of gold, relating resulting failures to Frenkel defects 07 p1048 A66-17303

Current-voltage relationship of Au on GaAs Schottky barrier, examining introduction of single temperature independent parameter 07 p1106 A66-18399

Gold diffusion into silicon and formation of segregations in surface layers and crystal disturbances 08 p1268 A66-18861

Time-temperature total hemispherical emittance study of gold-plated 304 stainless steel in temperature range of 1000-1800 degrees F 12 p1895 A66-24376

Transmission factor of rectilinearly polarized light as affected by plasma oscillations in granular films of gold 13 p2163 A66-25440

Jet plating of gold to make ohmic contacts on silicon 14 p2361 A66-27277

Photoemission of electrons from Si and Au valence bands into thermally grown silicon dioxide conduction band 14 p2365 A66-27757

Electron energy distribution for emission from aluminum-aluminum oxide-gold thin films 14 p2257 A66-27943

Precipitation effects in phosphorus-diffused silicon after gold diffusion, using transmission X-ray diffraction microscopy 15 p2561 A66-28700

Effect of electrical charge on surface of glass substrate on nucleation density and initial growth structure of thin films of gold prepared by evaporation under ultrahigh vacuum 15 p2466 A66-29683

Hydrogen, He, Ne and Xe high energy molecular beam scattering from gold film surfaces during evaporative deposition 16 p2752 A66-30392

Effect of annealing on thin gold films sandwiched between two evaporated layers of zinc sulfide, presenting resistance curves 16 p2779 A66-31083

Temperature effect on color of thin layers of gold of various thicknesses connected with anomalous absorption phenomenon in gold layers 16 p2780 A66-31212

Epitaxial growth configurations of single-crystal potassium bromide on sodium chloride, using gold decoration method, showing effect of crystal orientation on growth rate 16 p2780 A66-31213

Vapor deposited gold thin films to obtain adhesion and durability between film and substrate essential as lubricants in high vacuum 17 p2929 A66-31979

Gold distribution and precipitation in phosphorus-diffused silicon

wafers 17 p2980 A66-3264

Gold and silver doping effect on Hall effect, electroconductivity thermal emf and conductivity of CdSb 17 p2984 A66-3314

Low effective resistivity of gold film plated onto tin determined by low temperature microwave absorption measurement and explained by free-electron model and superconductivity proximity effect 19 p3443 A66-3601

Dislocation dipoles produced by ion bombardment of thin gold films, noting that during annealing dipoles can condense form only one dipole 19 p3447 A66-3671

Vectorial photoelectric effect and quantum efficiency measurement in thin gold film for two light polarizations, using Lallemand electronic camera 20 p3614 A66-3721

Optical constants of silver and gold various energy regions, measuring relative refractivities of polarized light, analyzing collective motions of conduction electrons 20 p3615 A66-3721

Transmission electron microscopic analysis of initial epitaxial growth stage evaporated Au films on NaCl cleavage surfaces 21 p3798 A66-3871

Gold doping effects on recovery time of phosphorus, boron and arsenic impurity gaseous-diffused junction diodes and estimated gold recombination center densities 22 p3873 A66-3971

Spatial distribution of hot electron coherently scattering in thin Au film 23 p4115 A66-4201

**GOLD ALLOY**

Properties of dispersion-hardened gold-copper and platinum alloys made chemically and vapor plating metal or particles of metal oxides 03 p0381 A66-1251

Properties of silicon diodes with gold all bases, examining anomalies in V-characteristics 04 p0499 A66-1401

Selective properties of gold-compensated silicon diodes, noting behavior in presence of bias currents and current voltage characteristics 04 p0499 A66-1401

Amplification and generation properties of gold-compensated silicon diodes, noting noise spectrum and harmonic oscillations 04 p0499 A66-1401

Conditions for formation of barium and gold compound for semiconductor 04 p0570 A66-1431

High temperature oxidation of liquid yttrium and liquid lanthanides and their alloys with gold, obtaining parabolic diffusion-controlled rate constants 08 p1235 A66-1861

N-type germanium alloyed with gold showing negative photoconductivity in strong electric fields 10 p1589 A66-2221

Electrical resistivities of gold-erbium alloys measured at low temperatures 12 p1933 A66-2411

Alloying real germanium surface with gold impurity and increase of fast surface state and rate of surface recombination 14 p2365 A66-2771

Charging effect of Ag-Au alloys and other properties determined by perturbation theory 14 p2365 A66-2771

Conditions for formation of barium and gold compound for semiconductor 14 p2369 A66-2811

AuSn-Pb section of Au-Pb-Sn phase diagram, examining solderability of gold coatings of electronic components 16 p2722 A66-3031

Properties of silicon diodes with gold all bases, examining anomalies in V-characteristics 17 p2885 A66-3211

Selective properties of gold-compensated silicon diodes, noting behavior in presence of bias currents and current voltage characteristics 17 p2885 A66-3211

Amplification and generation properties of gold-compensated silicon diodes, noting noise spectrum and harmonic oscillations 17 p2885 A66-3211

N-type germanium alloyed with gold showing negative photoconductivity in strong electric fields 19 p3441 A66-3511

Thermoelectric power and electrical resistivity of copper-gold alloy doped with 3d transition metals as function of temperature and atomic number impurity 23 p4114 A66-4111



**LD PLATE**  
Resistance decrease in vacuum-evaporated  
old films from 150 to 250 degrees C when  
environment is cycled from inert to  
oxidizing 21 p3802 A66-39161

**NDOLA**  
Fiberglass balloon gondola used to eliminate  
environmental problems in photomultipliers  
and spark chambers carried by high altitude  
balloons 10 p1618 A66-21866

**ONIOMETER**  
Electronic solid state goniometer for  
producing navigation information for  
transmission from VHF omnirange /VOR/  
ground station 05 p0645 A66-14582

**OURSAT PROBLEM**  
Goursat problem for hyperbolic systems of  
two first-order equations solved by integral  
relation method 13 p2119 A66-25855  
Plate fixed on two opposite sides and  
simply supported on other two sides treated  
by method based on generalized Goursat  
theorem to lattice 20 p3674 A66-38295

**RADIANT**  
SA POTENTIAL GRADIENT  
SA PRESSURE GRADIENT  
SA TEMPERATURE GRADIENT  
Steepest descent, covering iterative  
methods for driving support mapping  
gradient to zero in convex  
programming 04 p0540 A66-13997

**RAIN**  
SA PROPELLANT GRAIN  
Variation of LN 29546 test for  
determination of susceptibility of aluminum  
alloy sheet to coarse grain  
formation 14 p2313 A66-27013  
Kh16N15M2B steel properties and effects  
of grain size and Nb/C  
ratio 15 p2519 A66-28536  
Heat conductivity coefficients of granular  
materials calculated by cylindrical and  
spherical models with porosity of 0.215 and  
0.476 respectively 20 p3678 A66-37421  
Thermal conductivity of finely divided and  
granular materials through solid phase and  
interstitial gas or by radiation between  
granules 21 p3835 A66-38768

**RAIN BOUNDARY**  
Lattice and grain boundary self-diffusion  
coefficients of radioactive nickel 63 into  
high purity nickel measured over  
temperature range 650-475 degrees  
C 04 p0535 A66-13746  
Exact measurement of local temperature,  
determining grain boundary temperature  
gradient, describing  
probe 06 p0882 A66-16938  
Precision casting based on directional  
solidification resulting in longitudinal  
columnar grains with preferred orientation,  
eliminating transverse grain boundaries in  
gas turbine elements  
[SAE PAPER 660055] 09 p1388 A66-20153  
Anomalous diffusion of boron parallel and  
perpendicular to dislocation arrays in grain  
boundary contained in  
silicon 10 p1574 A66-21356  
Electrical properties of dislocations in  
artificially produced  
polycrystals 10 p1582 A66-21902  
Annealing twins and twin-boundary  
intersections in niobium, noting invalidity of  
cause-and-effect relationship between twins  
and crack formation in bcc  
structures 11 p1717 A66-22998  
Initial yielding characteristics of vacuum-  
melted iron as function of thermal history  
after slow cooling or quenching, noting  
interstitial segregation into grain  
boundaries 11 p1719 A66-23398  
Grain boundary role in high temperature  
fracture behavior of magnesia, noting  
temperature and orientation dependence of  
shear strength 12 p1897 A66-24920  
Surface pit formation in aluminum,  
discussing effects of vacuum, quenching  
high temperature and repeated  
cycling 12 p1897 A66-24921  
Diffusion creep rate of thin foil of pure  
polycrystalline material 12 p1971 A66-24925  
Heat affected zone cracking in nickel-base  
superalloys attributed to grain-boundary  
liquitation 14 p2314 A66-27343  
Ductility enhancement of tungsten by  
rhenium addition due to modification of  
grain boundary precipitate

morphology 16 p2722 A66-30222  
Rhenium effect on interface energies of  
Cr, Mo and W, noting liquid surface tension,  
solid surface energy and grain-boundary  
grooving 18 p3121 A66-33726  
Grain boundary grooving in Cr, Mo and W,  
noting formation mechanism, effect of  
carbon on activation energy for surface  
diffusion, etc 18 p3121 A66-33727  
Electrical measurements of stannic oxide  
in ceramic form, noting forming and firing  
of samples, dielectric dispersion, grain  
boundary capacitances,  
etc 18 p3155 A66-34197  
Grain boundary precipitation and  
intermediate phase in polycrystalline oxide  
systems after annealing 19 p3387 A66-35414  
Improved thermal shock resistance of  
zirconia upon addition of 15 mole percent  
titanium attributed to metal in grain  
boundary 19 p3381 A66-35979  
Grain boundary migration in pure  
aluminum and lead under reversed torsional  
and bending stresses at elevated  
temperatures 19 p3386 A66-36365  
Relation between surface grain structure  
and galvanomagnetic properties of  
polycrystalline mercury telluride thin films  
with high current-carrier  
mobility 20 p3624 A66-38434  
High temperature tensile deformation of  
polycrystalline magnesia prepared by single-  
crystal recrystallization and hot  
pressing 21 p3753 A66-38592  
Deformation of aluminum single crystals  
during constant load tensile  
test 22 p3935 A66-40201  
Grain boundary cavity growth in Al-Cu  
alloy during compressive creep  
testing 22 p3935 A66-40291  
Oxygen inhibition of grain boundary  
movement and stabilization of optical  
transmission in cuprous iodide thin  
film 23 p4110 A66-41152  
Grain boundary self-diffusion coefficient  
variation with applied stress and production  
of lattice vacancies applied to cavity growth  
in high temperature fatigue of  
Mg 23 p4081 A66-41714  
Creep rate of polycrystalline thorium  
dioxide for high temperatures and  
pressures, examining intergranular voids  
formed by growth and coalescence of pores  
along grain boundaries 23 p4082 A66-41772  
Anodizing techniques used in diffusion  
studies of TiC system 24 p4228 A66-42616

**GRAPH**  
SA CHART  
SA FLOW GRAPH  
SA NOMOGRAPH  
SA OSCILLOGRAPH  
SA SPECTROGRAPH  
Graphs for problems of computing system  
design automation, specifically finding  
algorithm for graph scheme  
construction 02 p0250 A66-12102  
Graphical method for motions of nonlinear  
systems with several degrees of freedom  
based on expansion of graphic construction  
of phase-plane  
trajectories 03 p0436 A66-12693  
Kinetic equations of complex reactions  
derived, using conical graphs, reducing  
reversible reaction problems to problems of  
irreversible kinetics 06 p0822 A66-18544  
Synthesis of automation elements and  
finite automata in graphical  
form 07 p1012 A66-17383  
Properties, symmetries, code matrices and  
Euler paths for linear graphs used as  
models for physical systems, considering  
planar triply connected  
graphs 07 p1057 A66-17747  
Plotting oriented graph of two-stage  
electronic circuit with cathode  
coupling 08 p1200 A66-18923  
Evolutionary graphs to solve systems of  
linear equations 08 p1246 A66-19635  
Graphical analysis of recurring and  
periodic waveforms to determine  
fundamental frequency and major harmonic  
components 10 p1549 A66-21232  
Parameters of dielectric walls of various  
structures with optimal radio-engineering  
characteristics treated by graphical  
method 10 p1511 A66-21676  
Linear graphs theory as part of topology  
solving problems in circuitry, psychology,

linear programming, matrices, network  
theory, etc 11 p1875 A66-22627  
Indium antimonide diodes of various base  
thickness for high injection levels, results in  
graphical form applied to magnetic diode  
production 11 p1666 A66-22740  
Graphical analysis of tunnel diode  
monostable circuits described by high order  
nonlinear differential  
equations 11 p1677 A66-22766  
Algebraic and graphical methods for  
evaluating system stability and parameter  
sensitivity 12 p1854 A66-24382  
Carpet plotting technique for increased  
interpolation accuracy 13 p2031 A66-25363  
Graphical determination of phase  
trajectories and oscillation limits of  
nonlinear sampled system 13 p2056 A66-26755  
Graphical matching solution for gas turbine  
power plant closed cycle systems  
[ASME PAPER 66-GT/CLC-14] 14 p2224 A66-26984  
Graph analysis by connectivity  
considerations, based on generating and  
characteristic functions, noting application  
to sampled data systems, discrete Markov  
processes, computer programs,  
etc 15 p2453 A66-29771  
Graphic analysis of behavior of stepwise  
extremal control system adapted to process  
showing inertia after static  
characteristic 16 p2668 A66-30585  
Synchro system transfer functions  
comprising synchro and resolver cascades of  
nonidentical units, giving graphs for system  
transformation ratio and phase  
shift 16 p2672 A66-31440  
Generalized star-mesh transformation in  
network theory obtained using fact that  
Kirchoff rules, Maxwell rules, Mason rules  
and Coates formulas can be obtained from  
each other 17 p2899 A66-32053  
Graph-theoretic concepts for relating Reed  
segs and their duals to two classes of  
subgraphs 17 p2900 A66-32054  
Evolutionary graphs to solve systems of  
linear equations 18 p3127 A66-34173  
Graph and derivation of performance  
characteristics of phase-shift-keyed  
communication systems where receiver  
phase reference is noisy 18 p3069 A66-34250  
Graph techniques used in connection with  
nonharmonic series representation of  
stationary Gaussian signals for analysis of  
nonlinear systems 19 p3392 A66-36706  
Computer algorithm for recognition and  
extraction of planar graph from incidence  
matrix 20 p3523 A66-38279  
Realization of directed graph having  
prescribed terminal connection matrix  
without self-loops and minimum number of  
arcs 20 p3539 A66-38284  
Mayor-Mises method for solution of  
kinematic and kinetostatic problems of  
three-dimensional mechanisms  
[ASME PAPER 66-MD-2] 21 p3741 A66-38475  
Graphic solution for factoring higher-order  
polynomials of response function resulting  
from analysis of linear filter  
networks 21 p3756 A66-38672  
Thermal growth and deposition of silica  
films by silicon tetrafluoride  
hydrolysis 22 p3962 A66-40048  
Graphical determination of atmospheric  
pressure from rocketsonde temperature  
measurements 22 p3943 A66-40056  
Indium antimonide diodes of various base  
thickness for high injection levels results in  
graphical form applied to magnetic diode  
production 23 p4045 A66-41478  
Graph theory and enumeration of basic  
kinematic chains and  
mechanisms 23 p4097 A66-41978  
Pictorial representation of pulse-height  
energy spectra with two independent  
variables originating from experimental  
analyzer 24 p4172 A66-42490

**GRAPHIC ARTS**  
Computer graphics in  
communication 13 p2085 A66-25364  
Complex component design using man-  
computer system with graphic input/output  
devices, discussing application for digital  
computer circuit card design  
[SAE PAPER 660459] 18 p3116 A66-33897  
Adhesive backed birefringent tape for  
separation of thin film and printed circuit  
master drawings with near perfect



registration for microelectronic production  
masking purposes 24 p4180 A66-42312

## GRAPHITE

## SA PYROLYTIC GRAPHITE

Graphite content effect on antifriction  
properties of graphitized nickel-based  
copper and iron alloys 01 p0087 A66-10745

Temperature control of graphite nuclear  
furnace, using 02 p0228 A66-11517

Fracture strength of two rocket-nozzle-  
grade graphites under ten biaxial stress  
states at room 03 p0435 A66-12637

temperature 03 p0435 A66-12637

Turbulent boundary layer interaction with  
graphite heat shield noting boundary layer  
velocity, temperature and chemical  
composition profiles [AIAA PAPER 65-824] 03 p0446 A66-13232

Graphite and carbon steel case hardening  
by chromium 05 p0702 A66-15111

Growth and destruction of ice mantles on  
interstellar graphite grains by sputtering,  
thermal evaporation and cloud  
collisions 05 p0765 A66-15845

Mineral content and structure of graphite  
and sulfide inclusions in iron meteorites  
measured by reflected light and  
microprobe 06 p0952 A66-15940

Interaction characteristics of nuclear-active  
cosmic ray particles with carbon nuclei at  
mountain altitudes 07 p1114 A66-17549

Graphite properties relationship to  
microstructure and control by fabrication  
techniques and material  
selection 07 p1053 A66-18295

Graphite protection against high-  
temperature oxidation by making composites  
with high-resistant metal  
powders 07 p1055 A66-18505

Mie scattering calculation to support  
theory that interstellar extinction is caused  
by graphite particles 08 p1288 A66-18786

Resistance-grown pyrolytic graphite in  
crystallographic, thermal and electrical  
measurements 08 p1244 A66-19223

Aluminum nitride coatings on graphite  
deposited by introduction of plasma-  
generating gas into electric arc between  
tungsten cathode and aluminum filament  
anode 09 p1392 A66-20149

Ceramic and graphite fibers and whiskers,  
Air Force sponsored  
monograph 09 p1392 A66-20475

Plasma and carbide coatings for protecting  
graphite surfaces at high temperatures  
obtained by sputtering or deposition and  
thermal treatment to induce  
diffusion 10 p1548 A66-21508

Sliding contact wear under very dry high  
altitude or space conditions due to lack of  
contact film prevented by using chemical  
compounds like graphite or lithium  
carbonate 12 p1888 A66-24664

K emission band of graphite examined,  
using grazing incidence spectrometer and  
Gaussian window function 12 p1931 A66-24802

Graphite composites suitability for use on  
hypersonic entry vehicle  
components 14 p2319 A66-28014

Carbide-graphite skeleton materials  
prepared by sintering compressed graphite  
powder during thermochemical treatment  
with carbide-forming  
elements 15 p2524 A66-28751

Graphite lubricant physical and chemical  
combinations with other materials for  
improved high temperature friction and  
wear, discussing nuclear irradiation for  
graphite lattice  
modification 17 p2929 A66-31933

Graphite and C-H-O gas phase equilibrium  
at high temperatures and pressures in  
implication of Earth ocean and atmosphere  
development 17 p3015 A66-33432

Mie computations made possible by precise  
data experimentally determined for  
wavelength dependence of refractive index  
of graphite 18 p3233 A66-34576

Carbon/graphite material /carbitex/,  
physical, thermal, mechanical and chemical  
properties 18 p3125 A66-34618

Graphite content effect on antifriction  
properties of graphitized nickel-based  
copper and iron alloys 18 p3117 A66-34981

High energy nuclear interactions in  
graphite 18 p3140 A66-35159

Wavelength dependence of polarization by

small graphite flakes with anisotropic  
dielectric constant 20 p3649 A66-37324

Shock propagation and attenuation in  
porous graphite and aluminum foams, noting  
effects of particle shape and size on  
materials response to shock  
loading 20 p3588 A66-38407

Reactions between silica and graphite  
studied in vacuum from 1445 to 1765  
degrees C by continuously measuring  
amount of carbon monoxide  
formed 21 p3753 A66-38593

Stability and surface tension of colloidal  
graphite dispersions in absence and  
presence of  
nonelectrolytes 21 p3754 A66-39150

Aluminum nitride coatings on graphite  
deposited by introduction of plasma-  
generating gas into electric arc between  
tungsten cathode and aluminum filament  
anode 21 p3754 A66-39419

Melting point and microhardness of carbon-  
saturated TiC-VC solid solutions, noting  
temperature of eutectic of TiC-VC with  
graphite 22 p3934 A66-39866

Plasma and carbide coatings for protecting  
graphite surfaces at high temperatures  
obtained by sputtering or deposition and  
thermal treatment to induce  
diffusion 23 p4083 A66-41528

High temperature testing and evaluation of  
graphite helical-screw expanders and  
compressors for use with inert gas Brayton  
cycle 23 p4075 A66-41755

Megaton and decamegaton dynamic  
pressure production by blast-type  
compression of thick walled pipe with core  
subjected to internal implosion, for case of  
graphite core /Part II/ 23 p4091 A66-41860

Iridium coating for graphite oxidation  
protection at temperatures over 2000  
degrees C 23 p4083 A66-41891

Ceylon and artificial graphite behavior  
under very high pressure, examining  
problem of metallic phase of  
carbon 24 p4229 A66-42751

## GRATING

## SA DIFFRACTION GRATING

## SA INTERFERENCE GRATING

Techniques for rocket solar UV and for  
UV spectroscopy 13 p2081 A66-26013

Hydraulic loss decrease in complex  
pipeline owing to wire  
grating 23 p4024 A66-41798

## GRAVIMETER

## SA DENSITOMETER

Tests of airborne, gimbal and stabilized  
mounts of LaCoste-Romberg and Askania-  
Graf gravity meters conducted in  
1962 04 p0524 A66-14452

Gravimeter monitoring S dilational mode of  
Earth, consisting of fused quartz operating  
in high vacuum incorporated into  
electrostatic null-seeking  
servo 04 p0524 A66-14453

Gravitational irregularities in Santa Barbara  
channel, California 09 p1369 A66-19873

Combined effect of horizontal and vertical  
accelerations on gravimeter readings  
mounted on gyroplatform or in Cardan  
suspension 14 p2297 A66-28111

Gravimeter error in recording of Earth  
tides, examining leveling and calibration  
problems 14 p2298 A66-28400

Combined effect of horizontal and vertical  
accelerations on gravimeter readings  
mounted on gyroplatform or in Cardan  
suspension 24 p4212 A66-42699

## GRAVIMETRY

## SA THERMOGRAVIMETRY

Graphic calculation of gravimetric effect of  
three-dimensional masses of arbitrary  
form 07 p1028 A66-17423

Determining coordinates of astrogeodetic  
grid points by Molodenskii integral formulas  
and accuracy estimation by astrogravimetric  
interpolation of  
deviations 08 p1217 A66-19345

Digital cross multiplication used in cross  
coupling and off-leveling errors in gravity  
measurements at sea 09 p1369 A66-19874

Cross coupling effects in first order  
theories of ship motion used in  
measurement of gravity at  
sea 09 p1369 A66-19875

Soviet book on geodetic gravimetry  
including disturbing potential calculation  
methods based on Molodenskii integral

equation 14 p2288 A66-2828

Global harmonic and statistical analysis  
gravimetry 17 p2920 A66-33

Earth gravity vector calculation at group  
level and various elevations in  
space 17 p2921 A66-33

Bjerhammar gravimetric boundary value  
problem with gravity reduction defined by  
integral equation 19 p3345 A66-35

Determining coordinates of astrogeodetic  
grid points by Molodenskii integral formulas  
and accuracy estimation by astrogravimetric  
interpolation of  
deviations 19 p3348 A66-36

Depth estimation for buried anomalies  
mass from vertical gravity  
observation 23 p4063 A66-41

Glossary of gravimetric and celestial  
geodesy 23 p4063 A66-41

Discrimination capability of second and  
third derivatives of gravitational potential  
used in gravimetric  
investigation 24 p4202 A66-42

## GRAVITATION THEORY

Gravitation viewed as source of universal  
energy produced by condensation of  
from rarefied nebula to dense  
mass 01 p0135 A66-10

Uniqueness of gravitation theory developed  
by method of classical Lorentz covariance  
field theory 01 p0107 A66-11

Semigenerally covariant motion equations  
of particles moving in external gravitational  
field 03 p0392 A66-12

Evolution of system of gravitation  
interacting point particles noting quasi-  
equilibrium states and particle evaporation  
and radiation 03 p0427 A66-12

Relativistic theories of gravitation  
International Conference, London, July 1965  
Volume 1 05 p0756 A66-14

Gravitational waves and radiation, relativistic  
waves and null elements in  
space-time 05 p0757 A66-14

Relativistic theories of gravitation  
International Conference, London, July 1965  
Volume 2 05 p0757 A66-14

New theory of gravitation by Hoyle and  
Narlikar, noting transformation of equations  
to Einstein equations 05 p0757 A66-14

Equation of motion in relativistic  
gravitation theory 05 p0715 A66-14

Quantum theory of gravitation with respect  
to classical theories and Einsteinian  
theory 05 p0757 A66-14

Conservation laws in general relativity and  
definitions of gravitational momentum and  
energy 05 p0715 A66-14

Bianchi identity role in obtaining motion  
equations without infinite self-action terms  
in general relativity 05 p0715 A66-14

Lorentz-invariant theories of gravitation  
analyzed, using astronomical tests and  
comparing results predicted by theories  
with general relativity 05 p0716 A66-15

formulas 05 p0716 A66-15

Cosmic space expansion in accordance with  
theory of universal gravitational radiation  
pressure 06 p0953 A66-16

Extension of Ward relations to gravity,  
close analogy to electrodynamics, using  
Gupta formulation of Einstein  
theory 08 p1255 A66-19

General theory of relativity, application to  
isolated system relative to slow moving  
too-dense structure and empirical proofs  
theory 10 p1556 A66-22

Charged particle motion determined by  
gravitational-electromagnetic field properties  
with motion equations following from  
integrability condition of field  
equations 11 p1735 A66-22

Nonconservation of baryon and  
cosmological theory, discussing creation of  
matter in discrete manner around isolated  
pockets with strong gravitational  
fields 11 p1774 A66-23

Gravitation theory and new principle of  
equivalence of inertial and gravitational  
energies 12 p1913 A66-23

Energy-momentum density of gravitation  
field according to Ozsvath-Schueckel  
rigorous solution to Einstein field  
equations 12 p1915 A66-24

General relativistic dynamics for  
determining place of Mach principle in  
relativity theory, obtaining expression for  
energy-momentum density of gravitation



- field 12 p1916 A66-25019
- Einstein gravitational theory in terms of orthogonal reference points, describing energy and momentum distribution by generally covariant tensors 13 p2128 A66-25946
- Gravitational theory developed by generalizing Newtonian and special relativistic concepts 13 p2129 A66-26332
- Multipole moments in Einstein gravitational theory 14 p2330 A66-27020
- Philosophical problems of Einstein theory of gravitation and relativistic cosmology - All-Union Conference, Kiev, Ukrainian SSR, May 1964 14 p2331 A66-27208
- Composition, state and evolution of gravitational theory, noting Newtonian, Einstein and unified field stages 14 p2331 A66-27209
- Matter and gravitation role in unified gravitational field theory, including Einstein general theory of relativity 14 p2332 A66-27210
- Identity between inertial and gravitational fields in infinitesimally small region of space-time, discussing equivalence and Mach principle 14 p2332 A66-27211
- Quantum gravitation theory, discussing difficulties of covariance of general relativity and nonlinearity of Einstein equation 14 p2332 A66-27215
- Evolution of system of gravitational interacting point particles, noting quasi-equilibrium states and particle evaporation and radiation 14 p2380 A66-27258
- Gravitational theory for dynamical basis of quasi-stationary spiral structure of stars 14 p2381 A66-27500
- Lorentz-covariant theory of gravitation constructed with linear field equations 15 p2542 A66-29332
- Simplified method for derivation of universal gravitation law from Kepler law of planetary orbits 16 p2747 A66-30870
- Theory of relativity, discussing Einstein theory of gravitation, evolution of stars, equations of motion, etc 16 p2748 A66-31267
- General theory of relativity, emphasizing works discussed at London and Tbilisi conferences on gravitation theory 17 p2960 A66-33504
- Gravitational theory based on solar observations, noting connection between gravitational eigenvalues, planetary orbit spacing and connection with cylindrical wave functions 18 p3104 A66-33757
- Empirical decision-making techniques, determining nature of quasi-stellar source or galaxy 18 p3234 A66-34616
- Mass-energy relationship in gravitation, correlating Newton and Einstein concepts via acceptance of positive and negative masses and energies 18 p3136 A66-34633
- Maximum temperature of any substance in equilibrium with thermal radiation, considering properties of hot matter at very high densities, including gravitational interaction of photons 19 p3463 A66-36069
- Covariant gravitational field equations in de Sitter space and quantum mechanical equations of motion associated with particles of given spin, employing gauge principle 21 p3769 A66-38645
- Rylov concept of relative gravitational field applied to calculation of energy of Synge plane gravitational waves with respect to separate reference points 21 p3772 A66-39294
- General relativity theory, examining Schwarzschild surface which allows matter and light to pass through in one direction only 21 p3774 A66-39532
- Einsteinian gravitation equations stated in terms of three-dimensional tensor analysis as applied in conformal space 23 p4091 A66-41834
- Singularities of cosmological solutions of gravitational equations for space filled with matter 24 p4274 A66-42521
- New gravitation theory, noting role of Einstein equations following conformal transformation 24 p4237 A66-42540
- Einstein gravitation theory relation to general and special relativity, space time, unified four-dimensional continuum metric and chronogeometric theories 24 p4238 A66-43015
- GRAVITATIONAL COLLAPSE**
- Kinematics of collapse and discussion of observable properties of baryons and collapsing stars 05 p0757 A66-14524
- Gravitational collapse of uniform nonrotating pressure-free spheroid 08 p1255 A66-18777
- Equation of state of matter at supernuclear density 08 p1258 A66-18783
- Retarded observer time as coordinate in relativistic spherical hydrodynamic equations prevents Schwarzschild surface formation 11 p1772 A66-22779
- Newtonian and relativistic analysis of orbits of electromagnetically neutral test particles in magnetic universe 12 p1914 A66-24567
- Relativistic astrophysics covering evolution of moderate to supermassive stars, radiation and gravitational field and stellar collapse 14 p2385 A66-27948
- Strong radio sources as accounted for by repulsive effect of relativistic origin 16 p2796 A66-30149
- Einstein field equations for perfect fluid, coupled to frozen-in magnetic field, in high-density limit of gravitational collapse 17 p2997 A66-31973
- Virial theorem study of magnetic field effect on gravitational instability of primeval gas cloud, noting possibility of collapse upon change in magnetic flux 17 p3005 A66-33002
- Elliptic Kruskal-Schwarzschild space, discussing identification of points which limit Kruskal space into Minkowski space 19 p3389 A66-35942
- Gravitational contraction of stars of one solar mass examined, using Henyey method for calculating stellar evolutionary tracks 19 p3467 A66-36791
- Stellar evolution for high temperature, predominantly neutrino processes, noting breakdown of homology relation between density and temperature 19 p3467 A66-36795
- Relativity theory application to space probes, discussing experimental verification, relevance to cosmological problems and utilization to particles with large energy and momentum 20 p3650 A66-37389
- Irreversible gravitational collapse as consequence of Postulate X and application to quasars 21 p3813 A66-39208
- Star collapse observation by detection of high energy neutrino fluxes produced by catastrophic star contraction 22 p3975 A66-40953
- Star formation and gravitational instability in nonrotating medium permeated by strong magnetic field 23 p4125 A66-41012
- Thermal instabilities role in star formation, discussing intercloud medium, magnetic pressure and gravitational collapse 23 p4125 A66-41062
- GRAVITATIONAL CONSTANT**
- Theory of aircraft measurement of gravity using gyroplatform, ideal gimbal suspension and three orthogonal string sensors, deriving formula for unperturbed gravity value, discussing perturbation measurement errors 03 p0366 A66-12991
- Kepler method in determining length of satellite radius vector independent of linear measurements from Earth, discussing accuracy in geodetic measurement 03 p0366 A66-13197
- Modification of hot big-bang theory to account for helium abundance in universe and cosmic radiation temperature, noting possible variation of Newtonian gravitational constant 13 p2189 A66-26599
- Theory of aircraft measurement of gravity using gyroplatform, ideal gimbal suspension and three orthogonal string sensors, deriving formula for unperturbed gravity value, discussing perturbation measurement errors 15 p2483 A66-28666
- Sundman variable for regularization of three-body problem motion 17 p3004 A66-32952
- GRAVITATIONAL EFFECT**
- SA LUNAR GRAVITATIONAL EFFECT
- SA SOLAR GRAVITATIONAL EFFECT
- SA WEIGHTLESSNESS
- Gravitational effects of photons or neutrinos radiated from point mass as accurately treated by Newtonian approximation 02 p0263 A66-11867
- Gravity effect on hemodynamic factors and sodium and water excretion in two dogs subjected to change from supine to erect position and water immersion 03 p0324 A66-12352
- Turbulent jet axis under crossflow of different density assuming static pressure, excess heat content and projection of mean jet velocity 04 p0509 A66-13856
- MHD equations for inhomogeneous rotation of medium about Z-axis in presence of gravitational force 04 p0516 A66-13857
- Non-Newtonian media, parallel flow, discussing effects of two- and three-dimensional perturbations on flow stability 04 p0510 A66-13872
- Deflection of light rays by gravitational lenses 05 p0757 A66-14526
- Gravitational effects not consistent with relativity theory, showing statistical correlation between solar activity and variations in Earth rotational velocity 05 p0757 A66-14533
- Gravitational influence on living organisms studied by klinostate principle 06 p0811 A66-16061
- Simulation and environment effect on astronaut performance in space to understand work-task effort 06 p0817 A66-16239
- Gravity effect on basipetal transport of auxin studied by growing plants both erect and on horizontal clinostats 06 p0812 A66-16564
- Scale model testing of lunar surface vehicles in simulated low gravity field [SAE PAPER 660148] 07 p1017 A66-17251
- Neurologic adaptations and audiogenic responses in mice exposed to chronic 2X gravity field, noting development of more efficient circulatory system, growth pattern alterations, etc 07 p0998 A66-17660
- Experiments with anesthetized dogs subjected to g accelerations, observing behavior of arterial oxygen saturation and pulmonary ventilation during short periods 08 p1175 A66-19083
- Experiments with rats under anesthesia subjected to acceleration, noting electroencephalograms 08 p1175 A66-19085
- Stability of motion of spherically symmetric mass of compressible gas with constant space density in absence of gravitational field 08 p1298 A66-19483
- Temperature distribution in fluid spherical layer enveloping gravitating sphere 08 p1320 A66-19485
- Finite strength spherical shock wave propagation due to explosion into inhomogeneous nongravitating and self-gravitating systems 08 p1211 A66-19810
- Superfluid critical velocity in He 2 isothermal gravitational flow in narrow channels 09 p1366 A66-20018
- Superconducting persistent magnets, cryogenic pumping and other low temperature techniques for measuring gravitational forces on charged particles 09 p1379 A66-20083
- Mechanical interpretation of problem of passage of light through curved light conductor 09 p1387 A66-20790
- Marginal convection in self-gravitating sphere of uniform incompressible fluid with uniform heat sources distribution 11 p1785 A66-22437
- Saturn ring stability examined, using model stabilized by gravitational dilution and random particle motions 11 p1769 A66-22530
- Dispersion equation for cylindrical plasma with finite electrical conductivity under influence of applied magnetic field and own gravitational field 12 p1920 A66-24191
- Quantum mechanics and gravitational effect on origin of cosmic particles, discussing Schrodinger wave equation, electric potential and alpha decay 12 p1944 A66-24465
- Force field detection and control of objects in space, using gravitational, electrostatic or magnetostatic fields 12 p1820 A66-24677
- Clear air turbulence structure, noting measurement results obtained by Canberra aircraft and TOPCAT project, energy yield of gravitational shearing waves, etc 13 p2122 A66-26127
- Effect of faulty compensation for accelerating force of Earth gravity on accuracy in determination by inertial



navigation system of coordinate of object in flight 14 p2328 A66-27361

Gravitational perturbations of circular satellite orbit [AIAA PAPER 65-550] 14 p2381 A66-27418

Non-Newtonian media, parallel flow, discussing effects of two- and three-dimensional perturbations on flow stability 14 p2275 A66-27572

Cosmological theory testing with gravitational lens effect 14 p2383 A66-27710

Possible origin of lunar maria, suggesting they may be scars of mechanical damage wrought on lunar hemisphere by disruptive tides of Earth 14 p2384 A66-27900

Cavity depth for waterdrop impacts against water, discussing apparatus, equation for cavity depth, effect of gravitational potential energy, liquid surface behavior, etc 15 p2477 A66-28716

Semianalytical solution of motion of satellite in lunar orbit, considering perturbations due to lunar and Earth gravity and solar attraction 15 p2604 A66-30016

Gravity effect on nucleate boiling heat transfer 16 p2825 A66-30486

Gravitational perturbation effect on MHD stability of helical magnetic field in spiral arm 16 p2800 A66-30652

Light propagation through Schwarzschild singular sphere, solving problem of visual image of emitting surface of gravitating sphere as seen by observer 16 p2748 A66-31171

Gravitationally induced uniform rotation of body having stationary point and supporting rotating masses 16 p2748 A66-31521

Gravitational environment, effect of change on frogs measured using gravitoceptors in vestibular apparatus 17 p2865 A66-32183

Exact analytic solution for propagation of spherical explosion waves in self-gravitating gas sphere 17 p3004 A66-32839

Gravitational stability of laminar liquid layer flowing down inclined plane and heated from below 17 p2914 A66-33172

Vertical-track free-fall rocket sled system, discussing design principles, operation and performance characteristics 18 p3093 A66-33796

Gravitational shielding and absorption, examining tidal effects induced in solid sphere by another sphere, analogy to electromagnetic fields, etc 18 p3135 A66-34450

Light deflection by solar activity 19 p3455 A66-35249

Weightlessness effects on man with data from Voskhod flights 19 p3284 A66-35568

Gravitational force perception thresholds of plants in weightless conditions measured in terms of growth and development 19 p3284 A66-35569

Dynamic effects on satellite motion of mechanical deformations in stabilizing system, deriving equations for rotational motion about center of inertia 19 p3472 A66-36831

Ordinary nonlinear differential equation arising in theory of both axisymmetric and two-dimensional viscous jets falling under gravity 20 p3591 A66-37593

Gravity turn trajectories through atmosphere including drag effects 20 p3657 A66-38181

Mechanical interpretation of problem of passage of light through curved light conductor 22 p3931 A66-39849

Structural integrity studies of gravitational and inertial loading effects on British solid propellant grains 23 p4115 A66-41112

Finite resistivity instabilities of sheet pinch examined, using numerical analysis in terms of normal modes 23 p4106 A66-41709

Satellite gravitational stabilization system in orbital coordinate system, considering atmospheric resistance and damping natural oscillations 23 p4134 A66-41979

Hydrogen abundance in universe using gravitational effect on physical constants 24 p4279 A66-43019

Interplanetary trajectories, considering gravity effect, free flight trajectory and forces acting on space vehicle 24 p4280 A66-43132

## GRAVITATIONAL FIELD

Vertical continuation of two-dimensional geomagnetic and gravitational fields from

given contour line on Earth surface by two methods 01 p0060 A66-10161

Probability models for Earth crustal structure applying potential field separation technique, noting role of gravitational field and Wiener filtration theory 01 p0061 A66-10479

Pulse energy tensor and internal macroscopic interactions in gravitational field and in material media 01 p0106 A66-10656

Digital computer calculation of characteristics of Earth gravitational field 01 p0062 A66-10693

Einstein gravitational equation applied to galaxies and quasars, using spherical model with spherically symmetric distribution of matter 01 p0138 A66-11033

Laws of motion for monopolar particle in given gravitational field 01 p0107 A66-11076

Second derivatives of gravity calculated from interdependencies between coefficients of formulas, using least squares method, weight coefficients being variable 01 p0063 A66-11098

Satellite geodesy noting gravitational and geometric use, current national program, orbit perturbations, etc 02 p0225 A66-12236

Charge separation into film about symmetrically gravitating body at high temperatures and small Debye radius 03 p0396 A66-12290

Local gravity anomalies for circular cylinder with vertical axis, discussing solution to direct and inverse problems of quantitative interpretation of fields 04 p0516 A66-13960

Gravitational field interactions with Dirac fields and electromagnetic fields studied in framework of special relativity to find possible C-, P- and T-violating effects 05 p0717 A66-15349

Transfer of point over ellipse between two coplanar circular orbits in Newtonian gravitational field determined by method of variations 05 p0765 A66-15423

Gravitational field and crust of Earth related to Earth shape 05 p0675 A66-15748

Gravitational source dynamics, discussing multipole structure, mass, linear momentum, dipole moment and spin in axially symmetric field 06 p0908 A66-16131

Motion of charged finite mass in gravitational field 06 p0908 A66-16162

Gravitational compass in analysis of gravitational field in general relativity 06 p0909 A66-16329

Nonradiative and stationary electromagnetic and gravitational fields 06 p0909 A66-16330

Conversion of gravity reduction problem into internal boundary value problem which is solved by finite difference methods 06 p0876 A66-16416

Friction corrections introduced in results obtained by differential pendulum method in measuring acceleration of gravity at sea, noting motion equations 06 p0879 A66-16418

Behavior of fluids under weightlessness and in weak gravitational fields, formulating small linear oscillations of ideal fluid under surface tension 06 p0873 A66-16708

Shape and gravitational field of Earth calculated by using N homogeneous incompressible fluid shells to represent distribution of terrestrial mass 07 p1028 A66-17422

Asymptotic behavior of gravitational field studied by Peeling theorem for case where curvature tensor of space-time has direction that can be demonstrated as geodesic trajectory 07 p1080 A66-17451

Motion equation for system of n bodies assuming half retarded and half advanced mass-distribution 07 p1137 A66-18053

Motion equations in external gravitational field for relativistic two-point model of free elementary particle neglecting particles own field 08 p1282 A66-18606

Einstein equations for vortical and nonvortical gravitational fields applied with relativistic approximation to Newtonian gravitational field 08 p1256 A66-19272

Motion stability of gyroscope in universal suspension with spring restraints and damper in gravitational field extended to include Newtonian central force

field 08 p1226 A66-19561

Conversion factor determination for gravity changes during Alaska earthquake, using LaCoste-Romberg geodetic meter 09 p1369 A66-19821

Gravitational irregularities in Santa Barbara channel, California 09 p1369 A66-19821

Geodesy and gravity 09 p1371 A66-20201

Coordinate systems describing portions of Friedman world and adjacent empty region do not satisfy Liechnerovitch continuity conditions 09 p1403 A66-20581

Non-Einsteinian gravitation, noting the expression for invariant density of free Lagrange gravitational field holds only for slowly varying weak fields 09 p1403 A66-20711

Consistency of subtraction technique for calculating gravitational mass in nonquasirectangular coordinates from surface integrals provided by von Freud superpotentials 10 p1555 A66-21111

Gravity gradient sensor application manned orbital spacecraft, noting instrumentation for various functions 10 p1535 A66-21511

Effect of incompressibility of substance on gravitational instability, deriving dispersive equation and comparing results with problem of incompressible fluids 11 p1735 A66-22411

Human and animal study of physiologic and neurophysiological responses at different intensity levels and short periods of gravitational field 11 p1641 A66-22411

Cosmological effects in anisotropic inhomogeneous cosmological models including Riemannian geometry, light propagation, gravitational field, etc 11 p1772 A66-22711

Behavior of system of infinite compressible fluids under gravity and magnetic field action, with MGD equations showing instabilities at plasma boundaries 11 p1748 A66-23411

Probability models for Earth crustal structure, applying potential field separation technique, noting role of gravitational field and Wiener filtration theory 12 p1868 A66-23811

Pulse energy tensor and internal macroscopic interactions in gravitational field and in material media 12 p1914 A66-24011

Model sequence calculations of early solar evolution extended for case of varying cosmology 12 p1949 A66-24111

Necessary condition for motion stability of particle moving in gravitational field of axisymmetric planet 12 p1949 A66-24211

Mossbauer effect, frequency measurement and red shift in relativistic gravitational field 12 p1914 A66-24411

Freely falling point mass problem solution for Einsteinian free space equations that also satisfy Newtonian equations in suitable coordinate system 12 p1915 A66-24811

Gravitational field effect on electromagnetic field, using rotating hollow sphere in electric and magnetic field with electric charge at center 12 p1916 A66-24911

Nonrotating star with spherical symmetry emitting electromagnetic radiation analyzed using gravitational field analogy 13 p2072 A66-25411

Periodic solutions for sputnik motion in gravitational field of two other bodies of finite mass 13 p2186 A66-25811

Coordinate transformation of Schwarzschild metric for gravitational field of oblate Earth and equatorial satellite orbits into symmetric metric 13 p2187 A66-26111

First order /Jeans/ stability analysis of infinite uniform medium pervaded by magnetic field 13 p2187 A66-26111

Evolution of matter and formation of gravitational field of metagalaxy in relation to emission and aging of gravitations interaction with nucleons 14 p2332 A66-27211

Gravitational field as form of matter noting Mach inertia principle 14 p2333 A66-27211

Gravitational field evaluated as physical field and as strictly geometrical field 14 p2333 A66-27211

Relation between gravitation and cosmological infinity 14 p2333 A66-27211

Non-Einsteinian gravitation, noting the



expression for invariant density of free  
Lagrange gravitational field holds only for  
slowly varying weak  
Fields 14 p2334 A66-27304  
Soviet book on geodetic gravimetry  
including disturbing potential calculation  
methods based on Molodenskii integral  
equation 14 p2288 A66-28209  
Molodenskii first approximation equations  
used in determination of characteristics of  
terrestrial gravitational field, noting  
techniques to average  
corrections 14 p2288 A66-28213  
Digital computer calculation of  
characteristics of Earth gravitational  
field 15 p2483 A66-28554  
Psychological and physiological reaction to  
Coriolis effect under artificial gravitational  
field simulated in rotating space  
station 15 p2443 A66-28682  
Stokes problem solution for intensity of  
regularized gravity field around Earth and  
at surface in form of rapidly converging  
series 15 p2527 A66-28965  
Covariant treatment of solutions of  
Einstein field equations representing pure  
gravitational radiation propagating in fluid  
and electromagnetic  
media 15 p2542 A66-29621  
Lorentz invariant space-time gravitational  
field theory, Maxwellian gravitokinetic field  
of potential and kinetic components and  
precession of orbit of Mercury analyzed by  
Einstein restricted theory of  
relativity 16 p2802 A66-31011  
Geophysical monograph on extension of  
gravity anomalies to unsurveyed  
areas 17 p2920 A66-33191  
Earth gravity vector calculation at ground  
level and various elevations in  
space 17 p2921 A66-33193  
Pizzetti theory formulas for space normal  
gravity field of Earth extended to space  
surrounding Earth 17 p2921 A66-33194  
External gravity field and geodetic  
boundary value problem 17 p2921 A66-33195  
Gravity anomalies of unsurveyed areas of  
Earth surface and influence on satellite  
orbit perturbations 17 p2921 A66-33196  
Maximum payload delivery with restricted-  
power propulsion system, noting trajectory  
optimization course-correction-time  
distribution, etc 18 p3242 A66-33849  
Potential energy in gravitational field,  
considering relativistic concept of negative  
mass, two-body motion and gravity effects  
on atomic nucleus 18 p3136 A66-34722  
Torque on rigid body in circular orbit in  
gravitational central field derived, using  
body-centered coordinate system aligned  
with gravity gradient  
vector 18 p3237 A66-35030  
Bjerhammar gravimetric boundary value  
problem with gravity reduction defined by  
integral equation 19 p3345 A66-35393  
Guidance equations including first-order  
effects of Earth oblate gravitational field,  
solving motion equations and evaluating  
downrange and crossrange miss distance and  
time-of-flight errors 19 p3397 A66-35599  
Controller synthesis for three-axis reaction-  
wheel control of space vehicle in negligible  
gravitational field, using optimization theory  
and Pontryagin maximum  
principle 19 p3468 A66-35883  
Control-engineering and flight-mechanics  
problem of rendezvous guidance, considering  
target body without guidance and second  
body in gravitational field without  
atmosphere 20 p3595 A66-36874  
Formulas for extraterrestrial potential,  
anomalous gravity force gradient on Earth  
topographic surface, deflections of vertical,  
etc 20 p3549 A66-37043  
Laminar, turbulent and transition heat-  
transfer domain analysis of cryogenic fluids  
in variable reduced-gravity environment,  
with applications to space cryogen  
storage 20 p3677 A66-37103  
Congruent relativistic gravitational fields,  
red shift and geodetic coordinate  
transformations 20 p3603 A66-38011  
Coordinate systems describing portions of  
Friedman world and adjacent empty regions  
do not satisfy Liechnerovitch continuity  
conditions 20 p3603 A66-38129  
Data on unknown portions of Earth  
gravitational field from observations of two

consecutive satellite orbits and mean orbital  
elements 22 p3976 A66-39693  
Optimum trajectories between material  
points moving along same orbit in  
gravitational field of spherically symmetric  
central body, obtaining numerical solutions  
for circular initial orbit 22 p3980 A66-40462  
Freely falling point mass problem solutions  
for Einsteinian free space equations that  
also satisfy Newtonian equations in suitable  
coordinate system 23 p4090 A66-41096  
Earth shape, moment of inertia and  
gravitational field determined from two  
nonlinear integral equations for potential of  
rotating incompressible  
fluid 23 p4063 A66-41202  
Non-Markovian evolution equation for  
velocities distribution in homogeneous  
gravitational system 23 p4100 A66-41249  
Augmented special relativity theory to  
account for Einstein effects, with extension  
to general scalar field theory and notes on  
corpuscular light and galactic-centered  
reference frame 23 p4090 A66-41273  
Resistive ballooning mode relation to  
universal instability in gravitational field  
and role in toroidal plasma with rotational  
transform 23 p4102 A66-41483  
Analog computation of minimum fuel  
trajectories with soft landings in uniform  
gravitational field, using Pontryagin  
maximum principle to reduce two-point BVP  
with optimal controllers 23 p4133 A66-41618  
Wave motions of liquid extended to case  
where derivative functions describing free  
surface are present in boundary conditions  
of problem 23 p4057 A66-41833  
Tesseral harmonics of Earth gravitational  
field camera tracking of five  
satellites 23 p4066 A66-41847  
Rotation of rigid bodies in Newtonian  
central gravitational field, with applications  
to navigation and satellite  
motion 23 p4096 A66-41941  
Shape and motion of cavities in steady  
planar supercavitating flows, noting  
transverse gravity field effect on Helmholtz  
flow past forebody experiencing drag  
alone 23 p4062 A66-42059  
Suggestion that quasar red shifts result  
from inflow of matter at relativistic velocity  
in gravitational field of highly condensed  
white dwarf 24 p4274 A66-42419

# GRAVITATIONAL POTENTIAL

Solving potentialities of third vertical  
derivative method for gravity  
potential 01 p0061 A66-10690  
Terrestrial gravitational potential  
determined by observation of satellite  
motion, assuming trajectory is determined  
solely by force field 03 p0428 A66-13027  
Gravitational potential gradient for body  
consisting of positive or negative masses  
with known density extremum value and  
known or unknown  
volumes 04 p0514 A66-13449  
Negative correlation coefficient between  
Izsak satellite geoid and Lee and MacDonald  
heat flow distribution, suggesting correlation  
between geoidal undulations and heat flow  
highs and lows 04 p0518 A66-14454  
Even harmonics in Earth gravitational  
potential function estimated from motions  
of orbital planes of seven  
satellites 05 p0671 A66-14956  
Reducing values of potential magnetic or  
gravitational field observed on Earth surface  
with weak profile to values on single  
horizontal plane in lower  
half-space 06 p0876 A66-16417  
Odd zonal harmonics in Earth gravitational  
potential determined by analyzing changes  
in eccentricities of satellites, with orbital  
inclinations spaced  
uniformly 09 p1374 A66-20883  
Celestial body size, composition and impact  
induced changes in Earth rotation from  
mantle data 10 p1531 A66-21286  
Second degree sectorial harmonic of Earth  
gravitational potential based on 338-day  
variation in revolution period of  
Syncom 11 p1697 A66-22436  
Even zonal harmonics in terrestrial  
gravitational potential, noting agreement  
between coefficients obtained from satellite  
measurements 11 p1702 A66-23493  
Gravitational and satellite data  
determination of spherical-function series

coefficients for expansion of Earth  
gravitational potential 12 p1867 A66-23516  
Hamiltonian mechanics applied to planetary  
and artificial satellite motion  
problems 12 p1950 A66-24402  
Tracking record of synchronous satellites  
over two-year period revealing effects of  
second and third order longitude  
components in Earth gravity potential  
field 12 p1875 A66-24893  
Gravitational potential effects on physical  
properties of mass far from other mass or  
energy, noting Planck equation, Planck  
constant, etc 14 p2335 A66-27940  
Solving potentialities of third vertical  
derivative method for gravity  
potential 14 p2286 A66-28034  
Effect of slope and curvature of Earth  
surface on disturbing potential, using  
Molodenskii integral equation, obtaining  
deflection of vertical, disturbing potential  
and Stokes constant 14 p2288 A66-28210  
Numerical integration principle in  
calculation of disturbing potential verified,  
using conical Earth model 14 p2288 A66-28211  
Corrections to individual terms of Stokes  
approximation for disturbing potential given  
in series expansion of spherical functions,  
using Earth model 14 p2288 A66-28212  
Accuracy of measuring method of vertical  
gradient of gravity force from gravity  
anomalies, using Numerov formula and Earth  
models 14 p2288 A66-28214  
Motion of charged nongravitating test  
particle in Einstein gravitational  
theory 15 p2542 A66-29655  
Atomic maser clocks rotation with Earth,  
deriving formula for relative drift at widely  
separated localities arising from local  
gravitational potentials 16 p2745 A66-30187  
Mutual dependence of harmonic  
coefficients of gravitational potential  
derived from satellite observations as source  
of computed geoid height distortions at  
Earth surface 16 p2700 A66-31804  
Perturbation of near circular orbits by  
Earth gravitational  
potential 17 p3005 A66-32997  
Zonal harmonics in external potential of  
Earth determined from secular motion of  
satellite orbits 17 p2921 A66-33227  
Tesseral perturbations of repeating ground  
track synchronous satellite orbits in  
gravitational potential 18 p3233 A66-34595  
Red shift observed in quasi-stellar radio  
sources due to high gravitational  
potential 19 p3459 A66-35587  
Gravity on planets explored by reference  
system expressing gradient magnitudes, data  
on equipotential and application to system  
with continuous rotation in  
space 19 p3346 A66-35627  
Formulas for extraterrestrial potential,  
anomalous gravity force gradient on Earth  
topographic surface, deflections of vertical,  
etc 20 p3549 A66-37043  
Gravitational and satellite data  
determination of spherical-function series  
coefficients for expansion of Earth  
gravitational potential 21 p3732 A66-38660  
Discrimination capability of second and  
third derivatives of gravitational potential  
used in gravimetric  
investigation 24 p4202 A66-42762  
Earth gravitational potential derived from  
satellite motion 24 p4202 A66-42833

# GRAVITATIONAL RADIATION

Motion of finite mass particles in external  
gravitational field determined by comparison  
of relativity and Minkowsky theories,  
considering gravitational  
radiation 04 p0545 A66-14172  
Gravitational interaction and gravitational  
waves discussing Schwarzschild metric, weak  
interaction, spinor field and free neutrino  
wave 04 p0546 A66-14315  
Gravitational waves and radiation, relating  
waves and null elements in  
space-time 05 p0757 A66-14525  
Gravitational emission from double star  
systems 06 p0955 A66-16779  
General relativity for study of emission of  
gravitational waves from isolated  
axisymmetric sources vibrating smoothly for  
finite period 08 p1254 A66-18621  
Gravitational radiation and possible  
experimental detection 14 p2335 A66-27947  
Radiation coordinates for gravitational



radiation in general 16 p2746 A66-30528  
 relativity 19 p3456 A66-35376  
 Gravitational emission from double star systems 19 p3456 A66-35376  
 Perturbations of spatially isotropic expanding universe in terms of small curvature variations 21 p3817 A66-39559

## GRAVITY

SA ARTIFICIAL GRAVITY  
 SA HIGH GRAVITY ENVIRONMENT  
 SA LUNAR GRAVITATION  
 SA PLANETARY GRAVITATION  
 SA SUBGRAVITY  
 Theory of aircraft measurement of gravity using gyroplatform, ideal gimbal suspension and three orthogonal string sensors, deriving formula for unperturbed gravity value, discussing perturbation measurement errors 03 p0366 A66-12991  
 Gravity anomalies and convection currents, examining sphere and cylinder sinking beneath surface of viscous fluid 06 p0877 A66-16785  
 Viscous fluid model estimates of crustal thickness and free-air anomaly compared with measured free-air anomalies and seismic depths of Puerto Rico trench and mid-Atlantic rise 06 p0877 A66-16786  
 Psychophysical orientation mechanisms of man under weightlessness simulation, gravity conditions encountered on Earth, in orbital flight and during free floating in space 06 p0814 A66-17177  
 Temperature distribution in fluid spherical layer enveloping gravitating sphere 08 p1320 A66-19485  
 Planetary perturbation effect on solar surface 13 p2180 A66-25427  
 Gravitational theory developed by generalizing Newtonian and special relativistic concepts 13 p2129 A66-26332  
 Quantum gravitation theory, discussing difficulties of covariance of general relativity and nonlinearity of Einstein equation 14 p2332 A66-27215  
 Theory of aircraft measurement of gravity using gyroplatform, ideal gimbal suspension and three orthogonal string sensors, deriving formula for unperturbed gravity value, discussing perturbation measurement errors 15 p2483 A66-28666  
 Human otolith and cupula system behavior under anomalous gravity conditions 15 p2434 A66-29446  
 Nonisothermal axisymmetrical turbulent jet curved by gravity and inertial forces 19 p3342 A66-36465

## GRAVITY CENTER

Simulation method for confirming computations of space vehicle motions continuing after firing around gravity center of vehicle 02 p0215 A66-11673  
 Classification of all nonplanar motions in problem of two fixed gravitation centers of arbitrary masses corresponding to real potential 02 p0292 A66-12234  
 Properties of linearized system of equations of perturbed motion and application to motion of center of mass of space vehicle 06 p0957 A66-17169  
 Initial conditions determination in aircraft takeoff from mobile platform required for solution of differential equations of motions of gravity center 11 p1734 A66-23345  
 Parameter perturbations of magnet and accelerating systems of electron synchrotron determined from position of center of gravity of beam 13 p2147 A66-25747  
 Book on artificial satellite motion relative to center of mass and effects on measurements, observation and system performance 14 p2379 A66-27200  
 Compensation for error resulting from inclination of frame of gyrocompass with elastic recovery moment, based on shifting of gravity center along major axis 14 p2294 A66-27363  
 Orbit design problems and spacecraft motion about center of mass 15 p2596 A66-29159  
 Stability of vehicle passing from water to air as function of neutral point, maneuver point and center of gravity 23 p4015 A66-40987

GRAVITY GRADIENT SATELLITE  
 SA DODGE SATELLITE  
 Attitude stabilization of radio telescope satellite by passive gravity gradient

control 01 p0142 A66-10685  
 Gravity gradient stabilization systems for orientation of spacecraft and for damping of associated librations 01 p0143 A66-10798  
 Nonlinear resonance effect on attitude librations of undamped rigid gravity gradient stabilized satellite in circular Earth orbit 01 p0143 A66-10811  
 Material elasticity effects on planar librational motion of rigid satellite under action of gravity 01 p0144 A66-10812  
 Expected frequency with which gravitationally-oriented Earth-pointing satellite will undergo angular deflection due to micrometeorite impact 03 p0430 A66-12737  
 Communications satellite technology problems discussing synchronization of orbit, attitude stabilization, lifetime and power supply 04 p0475 A66-13499  
 Minimization of solar radiation pressure effects for gravity-gradient stabilized satellites, primarily attitude errors of pressure torques [ASME PAPER 65-WA/AUT-2] 05 p0770 A66-15703  
 Gravity gradient sensor application to manned orbital spacecraft, noting instrumentation for various functions 10 p1535 A66-21533  
 Requirements for gravity gradient stabilization of medium and synchronous altitude communication satellite systems using zero gain antennas, noting stabilization accuracy, stationkeeping effects, etc [AIAA PAPER 66-303] 12 p1955 A66-24770  
 Gravitational stabilization systems achieving passive satellite orientation, using gravitational field 15 p2606 A66-29158  
 Dynamical attitude equations for rotational motion of set of  $n$  rigid bodies interconnected by dissipative elastic joints and subjected to arbitrary forces and torques 17 p3001 A66-32345  
 Earth gravity vector calculation at ground level and various elevations in space 17 p2921 A66-33193  
 Gravity gradient torques and stabilization conditions in calculation method for satellites 17 p3017 A66-33240  
 Damping technique effect on performance of gravity-gradient satellite stabilization, noting means of creating restoring torques 18 p3243 A66-33861  
 Gravity gradient stabilization of near-Earth satellite with extensible boom and libration damping with combined lossy spring and magnetic hysteresis rods 18 p3244 A66-33862  
 Passive stabilization of space vehicles with asymmetric mass distribution, using coupled system with optimum damping 20 p3659 A66-36869  
 Dynamical formalism for arbitrary number of interconnected rigid bodies analyzed with reference to passive attitude stabilization of satellites 20 p3659 A66-36886  
 Gravity torque effects on spinning satellite 21 p3818 A66-38714  
 Gravity gradient satellite stabilization and performance analyzed, using computer simulation of motion equations, including eddy current dampers, solar effect, orbital eccentricity, etc 21 p3819 A66-38857  
 Stabilization system of gravity gradient test satellite and effect on damping time and steady state accuracy, noting attitude data and solar effect 21 p3819 A66-38858  
 Gravity gradient stabilization system and sensor subsystem for attitude determination and flight test data on gravity gradient components of applications technology satellite /ATS/ 21 p3820 A66-38859  
 DODGE satellite will be capable of two- and three-axis gravity-gradient stabilization at near synchronous altitude, using moment-of-inertia distributions and libration damping 21 p3820 A66-38860  
 Attitude errors of inertially coupled gravity gradient satellite with solar radiation pressure as dominant disturbance, noting slot problems in stabilized package accommodating damper 21 p3820 A66-38861  
 Control of magnetic hysteresis mechanism, increasing damping torque for use in gravity-oriented satellite stabilization 21 p3820 A66-38862

Radio astronomy satellite with extendible antennas achieves gravity gradient stabilization while receiving electromagnetic radiation, analyzing dynamic behavior and effect of passive damper 21 p3820 A66-38860  
 Inertia product terms effect on satellite gravitational torques 24 p4283 A66-42789

GRAVITY WAVE  
 Acoustic, gravitational and gyroscopic oscillation spectra of baroclinic atmosphere over rotating spherical Earth with emphasis on energy composition 01 p0062 A66-10855  
 MHD absorption of internal gravitational waves in ionospheric F layer in terms of traveling disturbances 02 p0283 A66-12111  
 Reflection and ducting of atmospheric acoustic-gravity waves whose temperature and horizontal wind velocity vary arbitrarily with height 06 p0876 A66-16279  
 Long-period acoustic-gravity waves launched into F region by Alaska earthquake of March 28, 1964 08 p1219 A66-19418  
 Mesoscale disturbance observed in vicinity of cold vortex center, emphasizing gravity waves 09 p1400 A66-20855  
 Clear air turbulence, considering energy source by transfer from large to small flow in gravity wave spectra, noting shear roll and motion equations 10 p1552 A66-21282  
 Internal gravity wave propagation in thermally stratified atmosphere 11 p1697 A66-22569  
 Internal gravity waves in stratified liquid for two-dimensional case, noting relation between oscillation frequency and wavelength 13 p2062 A66-25177  
 Interaction mechanism between internal gravity waves and radiative photochemical processes, noting solar radiation absorption, heat of atomic oxygen recombination, etc 13 p2073 A66-26128  
 Justification for multiple isothermal layer approximation to real atmospheric acoustic gravity wave propagation 14 p2234 A66-26851  
 Dissimilar and analogous characteristics of electromagnetic and gravitational waves 14 p2333 A66-27222  
 MHD absorption of internal gravitational waves in ionospheric F layer in terms of traveling disturbances 14 p2286 A66-28077  
 Response of atmosphere to impulsive point disturbances 14 p2386 A66-28122  
 Cellular circulation in ionospheric region 14 p2289 A66-28833  
 Head-on collision between two pressure jumps in two-layer atmospheric Einstein spaces with gravitational wave 15 p2537 A66-28679  
 Local energy of weak gravitational wave 15 p2537 A66-28679  
 Wind shear, gravity waves and Richardson number in relation to clear air turbulence /CAT/ 15 p2425 A66-28911  
 Electron concentration inhomogeneities during traveling gravity wave propagation through F layer 15 p2485 A66-29087  
 Long finite amplitude wave motions and interactions in inviscid fluid flows 15 p2478 A66-29241  
 Atmospheric motions from sodium cloud firings in 80 to 200 km height region, noting internal gravity waves, atmospheric tide and drift 15 p2489 A66-29669  
 Quasi-geostrophic wave motions of inertial gravity wave type and Rossby wave type in equatorial area 19 p3348 A66-36055  
 Gravitational waves in presence of electromagnetic field, deriving Einstein-Maxwell equations 20 p3550 A66-37300  
 Internal atmospheric gravity waves in isothermal medium, solving hydrodynamic equations, determining wave propagation in realistic atmosphere for range of wave parameters, wind amplitude, reflectance, etc 20 p3554 A66-38200  
 Vertical wind gradient variation and energy variation at height ranging from 80 to 14 km and relation to gravity waves and upper atmosphere turbulence 23 p4066 A66-4184  
 Traveling disturbance in ionosphere due to nuclear detonation detected as acoustic gravity wave modes, noting range-time diagrams 24 p4200 A66-42599

GRAY GAS  
 SA NONGRAY ATMOSPHERE  
 Radiative heat transfer in flat layer of



- absorbing, reradiating and nonscattering  
ray medium with optical properties  
dependent of  
temperature 04 p0598 A66-14425
- Unattainability of detailed balancing in  
thermodynamic equilibrium of gray  
atmosphere 11 p1772 A66-22776
- Radiative heat-flux potential for nongray  
as derived, noting origins of vector  
differential equation for gray  
gas 12 p1977 A66-23596
- Error in plane-layer approximation of  
boundary layer emission associated with  
gray gas flow past plane  
19 p3341 A66-35752
- SEASE
- Grease lubricants for aerospace application,  
determining physical properties and testing  
them at 400 degrees F and under high  
vacuum  
[ASME PAPER 66AM 3C2] 16 p2711 A66-30409
- Wear and grease lubrication effects in  
mated aircraft spline specimens subjected  
to oscillatory motion 16 p2713 A66-30572
- REAT BRITAIN
- Royal Aircraft Establishment facilities in  
England for aircraft structure testing under  
supersonic conditions, simulating aircraft  
takeoff, flight and  
landing 04 p0508 A66-14021
- United Kingdom space projects, detailing  
Skylark, Blue Streak, Black Knight and  
Black Arrow rockets 09 p1464 A66-20684
- Space research activities in United  
Kingdom during 1964 and early  
1965 09 p1459 A66-20725
- British Air Registration Board approach to  
safety of advanced complex aircraft and  
assessment of aircraft  
reliability 13 p2088 A66-26690
- British space research for 1965-66 including  
rocket development, satellite tracking, solar  
radiation, ionospheric  
sounding, etc 15 p2599 A66-29898
- Sonic bang experience in United Kingdom  
from supersonic flights and explosive  
charges, noting intensity, waveform, damage,  
etc 17 p2868 A66-33029
- Great Britain, future in space, discussing  
propulsion, nuclear power, satellite orbit,  
guidance, stabilization and attitude  
control 18 p3268 A66-33945
- Chondrite meteorite that fell in Barwell,  
England, December 24, 1965, may have  
weighed 200 pounds before fragmentation,  
breakup occurred at extremely low  
altitude 18 p3228 A66-34053
- British influence on world aviation, past,  
present and future 23 p4151 A66-41258
- Aeronautical research in U.K. by  
government establishments, industry and  
universities 23 p4017 A66-42072
- REEN FUNCTION
- RF magnetic field effect, applied parallel  
to external DC field, on Heisenberg  
ferromagnet with dipolar coupling, using  
Green function 01 p0122 A66-10579
- Nonmagnetic impurity effect on critical  
temperature of superconductor with two  
energy bands overlapping near Fermi energy  
level 01 p0123 A66-10719
- Derivation of asymptotic form of Green  
function, using hydrodynamic approximation  
method 04 p0510 A66-13875
- Green functions for coupled problem of  
thermoelasticity obtained from solutions of  
thermal stresses theory 04 p0591 A66-14206
- Analogies of statistical electromagnetic  
wave theory to quantum field theory, noting  
probability density function of waves and  
Green function 05 p0632 A66-14843
- Stress distribution in semiinfinite elastic  
media with different properties bonded  
along plane and containing concentric ring-  
shaped cavities, using Green function  
[ASME PAPER 65-WA/APM-2] 05 p0776 A66-15426
- Fundamental solutions of static and  
dynamic linear inextensional theories of thin  
elastic plates  
[ASME PAPER 65-WA/APM-23] 05 p0778 A66-15445
- Exact solution for Green function of open  
spherical shell subjected to harmonically  
oscillating concentrated load and any  
consistent boundary conditions  
[ASME PAPER 65-WA/APM-24] 05 p0778 A66-15446
- Effective excitation of radial cylindrical  
surface waves using Green function for  
excitation of impedance cylinder resting on  
impedance plane 06 p0823 A66-15882
- Surface wave diffraction by wedge as  
determined by Chu and Kouyoumjian  
compared with results using simpler Green  
function 06 p0827 A66-16043
- Scattering of TM surface wave by metallic  
strip above dielectric-clad ground plane,  
developing expression for Green function  
and formula for reflection  
coefficient 06 p0845 A66-16091
- Dyadic Green function for anisotropic and  
compressible media based on reformulation  
of governing equations for electromagnetic  
phenomena in compressible anisotropic  
plasma 06 p0832 A66-16455
- Displacements and temperatures  
accompanying deformation in unbounded  
thermoelastic semispace with concentrated  
force and heat source 06 p0966 A66-16505
- Behavior of Green function for Helmholtz  
equation external to bounded convex region,  
obtaining integral  
representation 06 p0903 A66-16705
- Indirect method of estimating Green  
kernels, eigenvalues and eigenfunctions of  
operators related to elliptic  
problems 07 p1059 A66-18031
- Plasmon dispersion relation and damping  
constant derived from Green function  
formulation of random approximation for  
inverse dielectric function of electron  
gas 07 p1090 A66-18211
- Green function/Gorkov variational  
procedure calculation of transition  
temperatures of superposed superconducting  
films dominated by inhomogeneous electron-  
electron interactions 07 p1108 A66-18436
- Series solution for deflection of  
rectangular plate subjected to concentrated  
load at arbitrary location, using Green  
function 08 p1310 A66-19161
- Interband Faraday effect in semiconductors  
in strong crossed electric and magnetic  
fields 08 p1277 A66-19619
- Optimum processes in systems with  
distributed parameters described by partial  
differential equations 08 p1202 A66-19710
- Green function method in theory of  
dispersion and absorption of electromagnetic  
radiation in semiconductors, considering  
resonance line shapes  
theory 09 p1411 A66-19961
- Green function-eigenvalue relationship on  
closed smooth boundary of open dimensional  
region 09 p1394 A66-20265
- Series solution for average wave field in  
medium with random inhomogeneities by  
using Green function for wave  
equation 09 p1343 A66-20335
- Bounds for two-dimensional discrete  
harmonic Green function used in boundary  
problems 09 p1395 A66-20621
- Temperature and environment effect on  
absorption spectra of two-level system,  
using stochastic model and Green  
function 09 p1348 A66-20959
- Free energy functional of superconducting  
alloys based on Green function  
decomposition 10 p1573 A66-21241
- Stress distribution in semiinfinite elastic  
media with different properties bonded  
along plane and containing concentric ring-  
shaped cavities, using Green function  
[ASME PAPER 65-WA/APM-2] 10 p1615 A66-21479
- Decay theory of closely coupled unstable  
states based on Green function formulation  
for transition amplitude 11 p1741 A66-23189
- Ground state energy of charged Bose gas  
obtained from pair Hamiltonian and Green  
functions 11 p1741 A66-23392
- Green function random phase decoupling  
scheme investigation of magnetic impurities  
effect on thermal properties of cubic spin-  
1/2 Heisenberg  
ferromagnet 11 p1758 A66-23394
- Fundamental solutions of static and  
dynamic linear inextensional theories of thin  
elastic plates  
[ASME PAPER 65-WA/APM-23] 12 p1960 A66-23971
- Second-order elliptical operator for m-  
dimensional Euclidean space with open  
region bounded by closed  
surface 13 p2120 A66-26010
- Green function of high degree of self-  
adjoint expansion of elliptic operator  
generated by differential expression is  
smooth inside domain and on smooth part of  
boundary 14 p2321 A66-27161
- Derivation of asymptotic form of Green  
function, using hydrodynamic approximation  
method 14 p2275 A66-27578
- Light dispersion and absorption by  
impurity centers in solids calculated via  
two-particle Green function method,  
assuming weak electron-phonon  
interaction 15 p2559 A66-28632
- Huygen principle for electromagnetic field  
in moving, isotropic, homogeneous and  
linear medium, using Maxwell-Minkowski  
equations and Green function for field  
equation 15 p2537 A66-28783
- Green-Hadamard functions of Tricomi  
singular problems for generalized wave  
equation, expressing equation integrals as  
hypergeometric Humbert and Horn  
series 15 p2530 A66-29855
- Convergence of discrete analogs of  
Dirichlet problems for Poisson equation in  
two dimensions, describing finite difference  
method for producing  
algorithms 16 p2731 A66-30235
- Analytic construction of skew derivative  
Green matrix for system of second order  
elliptic PDEs in many  
variables 16 p2734 A66-30749
- Generalized matrix inverse and differential  
operator with generalized Green function as  
kernel 16 p2738 A66-31719
- Electromagnetic wave interaction with  
uniform isotropic plasma in cylindrical  
interface considered for various types of  
excitations, using Green  
functions 17 p2962 A66-31821
- Green functions for heat source and  
concentrated force acting in unbounded  
thermoelastic space, applying perturbation  
method and Laplace  
transforms 17 p3018 A66-31836
- Integral equations of current derived for  
TM and TE waves in excited inhomogeneous  
impedance band in  
half-plane 17 p2885 A66-32246
- Arc operation under nonsteady electrical  
inputs, noting initial conditions, energy  
equation solution, temperature profiles,  
application of Green function for moving  
boundary problem, etc  
[AIAA PAPER 66-480] 17 p2970 A66-32769
- Interband Faraday effect in semiconductors  
in strong crossed electric and magnetic  
fields 17 p2983 A66-33133
- Exact solution for Green function of open  
spherical shell subjected to harmonically  
oscillating concentrated load and any  
consistent boundary conditions  
[ASME PAPER 65-WA/APM-24] 18 p3248 A66-33576
- Differential inequality theorem for  
boundary value problem involving second-  
order differential  
equation 18 p3126 A66-33975
- Torsion of prismatic rods of triangular or  
trapezoidal cross section, using Green  
function to obtain exact  
solution 18 p3256 A66-34395
- Green function applied to obtain  
alternative representations of source excite  
vector and scalar electromagnetic  
fields 18 p3071 A66-34564
- Electron-phonon interaction current  
density, thermodynamic Green function and  
other electromagnetic properties of  
superconductors, using Froehlich-Hamilton  
model 19 p3438 A66-35481
- Green formula and moment functions,  
predicting rate of radiative energy loss from  
boundaries of absorbing-emitting slab or  
sphere 19 p3479 A66-36597
- Nonmagnetic impurity effect on critical  
temperature of superconductor with two  
energy bands overlapping near Fermi energy  
level 20 p3619 A66-37657
- Garding inequality and Green  
transformation applied to elliptic operators  
in eigenvalue problems 21 p3755 A66-38465
- Longitudinal sound waves attenuation in  
superconductor with spatially dependent  
energy gap by Green function method  
applied to ultrasonic attenuation in type II  
superconductor 21 p3795 A66-38548



Kinetic equations in hydrodynamic approximation for weakly reacting and excited Bose systems, finding asymptotic expressions for Green function 23 p4055 A66-41412

Volterra equation and Green function to solve MHD problem of unsteady flow of viscous incompressible conducting fluid with time dependency 23 p4106 A66-41837

Hilbert parametric method of solving linear BVPs for second-order elliptic PDEs, using Green functions 24 p4232 A66-42740

**GREEN THEOREM**

Free-boundary nonlinear problem of smooth curve drawn in single circle so that doubly connected region formed by curve and circle satisfies specific existence conditions 02 p0250 A66-12105

Boundary condition constraint method for generalizing R-matrix theory, permitting use of shell model as basis for nuclear-reaction calculations 09 p1405 A66-20822

Uniqueness and solution estimates to boundary value problems, noting solvability correlation with existence of Green function 16 p2733 A66-30739

Poynting effect theoretically analyzed, postulating tensor expression for final Green measure in general coordinates for cylindrical coordinates 22 p3988 A66-39672

Mean viscous dissipation and bulk temperature variation in incompressible fully developed duct heat transfer, using Green theorem 22 p3998 A66-40033

**GREENHOUSE EFFECT**

Microwave radar observations of Venus, discussing surface thermometric temperatures, greenhouse effect, etc 09 p1451 A66-20113

Hopf analytical solution for values of ratio of gray absorption coefficients for insulating and escaping radiation /greenhouse parameter/ assumed constant at all depths, presenting temperature distribution graphs 10 p1605 A66-21204

Radiant energy transfer below cloud cover in Venus atmosphere, noting greenhouse effect caused by atmosphere containing components capable of IR absorption 22 p3980 A66-40469

**GREENWICH MEAN TIME**

**S UNIVERSAL TIME**

**GRENADE**

Rocket grenade measurement of temperature, pressure, density and wind velocity in upper atmosphere 10 p1533 A66-21832

**GRID**

**SA GRATING**

**SA LATTICE**

**SA MATRIX**

Reflection coefficients of plane wave field in grid-earth system, using averaged boundary conditions 04 p0482 A66-13907

Diffraction field determined for E-polarized plane wave incident normal to evenly spaced nonsymmetrical metallic grid 06 p0838 A66-15895

Operational geographic correlation /gridding/ of Nimbus meteorological data [AIAA PAPER 66-438] 18 p3128 A66-33645

Reflection coefficients of plane wave field in grid-Earth system, using averaged boundary conditions 20 p3518 A66-37865

Multielement antenna scanning grid-phasing method having random function distribution at aperture 20 p3533 A66-37994

Contraction to improve isotropy of grid-generated turbulence 22 p3899 A66-40381

Grid turbulence for large Reynolds numbers, noting consistency of power spectra values with Kolmogoroff scaling, decay law and Reynolds number effect on turbulence 24 p4194 A66-42408

Radiation response of low power nixistors, noting cause of grid current and relation between grid structure and induced current 24 p4258 A66-42961

**GRIFFITH FRACTURE THEORY**

Approximate stress intensity factor for embedded elliptical crack in plate subjected to uniaxial tension perpendicular to crack surface 01 p0152 A66-10377

Stress distribution in vicinity of infinite row of collinear Griffith cracks in elastic body calculated for internal pressure distribution 02 p0298 A66-11577

Griffith flaw theory in analyzing failures in

epoxy castings [ASME PAPER 65-WA/RP-6] 05 p0779 A66-15631

Griffith theory of brittle fracture and dependence on stress and load 10 p1614 A66-21339

Breaking stresses in two connected elastic half-spaces determined with aid of Griffith-Sneddon criterion 12 p1968 A66-24349

Inhomogeneous elastic half-spaces examined for circular crack in plane of contact and perpendicular tensile forces, using Griffith fracture theory 13 p2203 A66-26421

Critical load of infinite plane under tension weakened by crack evaluated by Griffith fracture theory 13 p2203 A66-26422

Brittle materials failure theory for cases where presence of plane deformation or plane stressed state is assumed, using Griffith theory 16 p2822 A66-31510

Fracture initiation and growth in linearly viscoelastic materials using energy formulation, establishing extension of Griffith initiation criterion 17 p2939 A66-32304

Elastic-plastic antiplane problems for bonded dissimilar media containing cracks and cavities on interface and subjected to longitudinal shear loads 19 p3475 A66-36430

Griffith type crack propagation due to localized thermal stress at holes, cavities, penny-shaped cracks and inclusions disturbing uniform heat flow 23 p4146 A66-41993

**GRIFFON AIRCRAFT**

**S NORD 1500 AIRCRAFT**

**GRINDING**

Grinding technique for accurate and proportional subdivision of chondritic meteoritic specimen and separation of metallic and silicate components for chemical analysis 08 p1179 A66-19095

Spherical aberration correction by grinding concave mirror to generate aspheric contour 15 p2498 A66-28826

**GROOVE**

Effective emittance of machined surfaces determined through groove models numerically analyzed 14 p2334 A66-27429

Thermal emittance and reflectance of diffuse-bottomed, specular-walled groove in solar radiant-flux environment [AIAA PAPER 66-459] 16 p2811 A66-31491

Grain boundary grooving in Cr, Mo and W, noting formation mechanism, effect of carbon on activation energy for surface diffusion, etc 18 p3121 A66-33727

**GROUND**

**S EARTH**

**GROUND-AIR-GROUND COMMUNICATION**

Space communications antennas, discussing ground to space systems, satellite relay methods, etc 05 p0651 A66-15839

VHF aircraft-satellite relay /VASR/ as means of improving long-range communications, with flight test results 06 p0825 A66-15988

Listening and two-way communication tests to study satellite as active relay for communications between aircraft in-flight and ground terminal, using Syncom III 08 p1185 A66-19538

Antenna requirements for satellite communications system ground stations, discussing antenna and mount designs 13 p2038 A66-25575

Monopulse radar air-to-surface slant range measurement 17 p2872 A66-31958

Ground radar systems for missile defense providing faster data processing, sensor location optimization, computer control, etc 24 p4175 A66-42953

**GROUND CONTROL**

Ground-based Minuteman pulse code modulation telemetry system, discussing routine and novel applications [ISA PREPRINT 1.12-4-65] 05 p0635 A66-15507

Ground-based steerable paraboloid spherical reflector and multiplate type antennas, noting cost per unit area for unit wind speed of 30 mph and frequency of 1400 mc, performance, restrictions, etc [AIAA PAPER 66-324] 12 p1844 A66-24794

CNES network of stations for FR-1 and D-1A, discussing checks of proper functioning, orbital corrections, telemetry, ground

control, etc 18 p3094 A66-3392

Preliminary design, mission specification and outgoing data specifications for advanced control center for vehicles orbital flight 20 p3651 A66-373

Air traffic control problems posed advent of supersonic transport may be eased by pictorial navigation display 20 p3598 A66-381

**GROUND EFFECT**

**SA DOWNWASH**

**SA LIFT**

**SA WAKE**

Ground effect on pressure distribution a lift coefficient of jet-flap wing tested wind tunnel 07 p0981 A66-186

Ground proximity effect on maximum lift drag ratio for wing with uniform spanwise circulation, considering vortex model 11 p1636 A66-233

Measurement accuracy of antenna to range evaluated for gain, elliptical polarization angle, boresight axis and ground reflected energy 12 p1836 A66-243

Ground reflection shock, compression and expansion waves caused by supersonic aircraft examined, noting correlations between wave intensity, incidence and pressure jump 13 p2062 A66-253

Vortex flow of ideal incompressible fluid past plate or slender wing near so wall 13 p2067 A66-262

**GROUND EFFECT MACHINE**

**SA AIR CUSHION VEHICLE**

**SA FLYING PLATFORM**

**SA GETOL AIRCRAFT**

**SA WESTLAND SR-N5 GROUND EFFECT MACHINE**

Theoretical and experimental analysis of structural, functional and design characteristics of air cushion vehicles at zero speed, examining lift coefficient viscosity effect, static tests, etc 01 p0011 A66-104

Economic indices of passenger-carrying air cushion vehicles and fundamental characteristics with reference to hydrodynamic vessels 02 p0177 A66-114

Hovercraft noise due to propeller, engine and transmission, examining reduction techniques, comparing with aircraft as surface transport 04 p0457 A66-133

SR-N5 hovercraft accidents analyzed prevention of future overturnings or plough-ins 05 p0609 A66-144

Flexible skirts and performance of ground effect machine 06 p0805 A66-163

Air cushion vehicle transport potential discussing attitudes and regulatory policies interurban, offshore, transoceanic, off-road agricultural, search and rescue operations 06 p0805 A66-163

Performance capabilities, cost characteristics and development costs of high-velocity GEM ocean carriers designed to compete with air transport 06 p0807 A66-163

Fluid digital amplifiers of axisymmetric focused jet design, based on focused-stalling effect known in ground effect vehicle aerodynamics 09 p1332 A66-203

Navigational problems arising from use of hovercraft 09 p1401 A66-204

Bertin-type air cushion vehicles, examining power supply and refinements required for over-water application 10 p1483 A66-216

New lift and propulsion techniques for development of V/STOL aircraft, helicopter and ground effect machines 11 p1636 A66-226

Comparison of air cushion vehicles supported by peripheral jets or by cushion contained in bell-shaped structure stressing simplicity of latter 12 p1862 A66-238

Hovercraft wavemaking resistance, discussing theory and experimental model 12 p1802 A66-242

Calculation of pressure beneath hovercraft indicating cushion pressure could be up to 10 percent higher than previous values 12 p1971 A66-244

Idealized ground effect wing, with close to ground, assumed to be semicircular lifting line in transverse plane, considering minimum induced drag 12 p1800 A66-250

Peripheral jet ground effect machine /GEM/ stability in pitch and



oll 13 p1995 A66-25591  
Terraplane, air-cushion vehicle for varied terrain, design, performance characteristics, etc 13 p1997 A66-26735  
Static and dynamic stability and operation of air cushion vehicles, emphasizing advantages of flexible skirts 16 p2633 A66-30312  
Ground effect takeoff and landing GETOL/ aircraft, noting problems in controlling it and configurations of annular jet 16 p2635 A66-31396  
Dynamics of noise and loading actions on helicopters, V/STOL aircraft and ground effect machines 18 p3050 A66-33679  
Noise generation due to mass introduction, applied force and stress in helicopters, V/STOL aircraft and ground effect machine 18 p3051 A66-33687  
External noise associated with hovercraft propeller 18 p3051 A66-33689  
Design study of two-seat road-going air cushion vehicle 18 p3052 A66-33973  
Fluid dynamic field determined for ground effect machines 18 p3098 A66-34060  
Hovering performance of plenum chamber type of ground effect machine over land and water, showing single nondimensional parameter controlling phenomena of overwater operation 19 p3279 A66-36487  
Transmission systems selection for high-speed lightweight applications, including air-cushion vehicles and Bell X-22A V/STOL aircraft ASME PAPER 66-MD-71] 21 p3743 A66-38499  
Propulsion systems for air cushion craft SKIP-I in marine environment AIAA PAPER 66-731A] 21 p3808 A66-39100  
Base surface and dimensional characteristics of peripheral gap minimize total force absorbed by ground effect machine with given weight, speed and altitude 21 p3696 A66-39601  
Helicopter trainee performance following synthetic flight training, noting flyable aircraft attached to ground effects machine 22 p3857 A66-40250  
Static and dynamic stability and operation of air cushion vehicles, emphasizing advantages of flexible skirts 22 p3848 A66-40393  
Performance of two-dimensional curtain jets of air cushion vehicles based on incompressible flow theory, noting stability criteria 22 p3844 A66-40499  
Hovercraft difficulty in accelerating through hump, noting wave resistance increase for pressure differential between two compartments of cushion with transverse stability skirt 22 p3901 A66-40678  
Peripheral jet theory in design of air cushion vehicles 23 p4013 A66-42004  
**GROUND HANDLING**  
Airline safety maintenance, noting British system of classification of parts into chapter numbers, ground equipment used and testing methods 12 p1857 A66-24038  
Outlook for air cargo handling indicates reduction of cost and increased efficiency by use of intermodel containers 15 p2620 A66-29799  
**GROUND HANDLING FACILITY**  
Terminal facilities, support equipment and operational characteristics of V/STOL aircraft 09 p1330 A66-20696  
Houston mission control center for flights from Gemini to Apollo program 14 p2272 A66-28441  
**GROUND SPEED**  
SA AIR SPEED  
SA VELOCITY  
Evaluation of AD560 Doppler by Qantas, discussing ground-speed run-down problem, radome design, along-track error and low-altitude accuracy over land and sea 07 p1078 A66-17811  
**GROUND STATE**  
Permittivity of dielectric formed from ground state instability of semimetal, considering Coulomb attraction between electrons and holes 01 p0125 A66-10774  
Symmetry of ground states of P, As and Sb donors in silicon determined optically 03 p0411 A66-13144  
Guillemin-Zener energy of ionized hydrogen molecule 04 p0546 A66-13455  
Internal and vibrational partition functions

of carbon dioxide and rotational line intensities arising from transitions from ground and first excited states 06 p0907 A66-15945  
Bracketing theorem applied in partitioning technique for solving Schroedinger equation to determine upper and lower bounds to energy eigenvalues, ground and excited states 06 p0911 A66-16166  
Potential correction effect on ground states of P and ionic-S impurities in silicon discussed in terms of cavity model 06 p0930 A66-17051  
Perturbation expansions for ground state function of helium atom, using Hartree or Hartree-Fock model Hamiltonian, based on Weiss-Martin variation-perturbation calculation 07 p1083 A66-18422  
Permittivity of dielectric formed from ground state instability of semimetal, considering Coulomb attraction between electrons and holes 11 p1749 A66-22286  
Zero-field splitting in ground state of ruby, considering effect of spin-spin interaction, using L gamma representation 11 p1750 A66-22491  
Ground state of hydrogen molecule treated by perturbation theory through second order, noting energy and wave function 11 p1738 A66-22882  
Excitation mechanism and rate of nitrogen ions in shock-heated atomic-molecular nitrogen mixtures, noting vibrational relaxation 11 p1739 A66-22885  
Product of oscillator strength, stark width and ground state density measured in T tube plasmas, using neutral helium resonance line 11 p1747 A66-23391  
Ground state energy of charged Bose gas obtained from pair Hamiltonian and Green functions 11 p1741 A66-23392  
Depopulation of ground state chromium ions in ruby under optical pumping explained via rate equations 13 p2089 A66-25188  
Optical pumping in ground states and metastable atomic states 14 p2305 A66-26963  
Superconductivity model with exact solution, determining energy levels, ground state energy, excitation spectrum, density variations, etc 14 p2360 A66-27190  
Single-configuration open-shell calculations for ground state of boron isoelectronic sequence, using doublet-spin-state wave function 16 p2750 A66-30122  
Momentum eigenfunction for ground state of hydrogen molecule ion 18 p3106 A66-34506  
Molecular orbital studies of ground and low lying excited states of HeH molecular ion 18 p3139 A66-34509  
Electronic energy for ground state of one-electron diatomic molecule near united atom 18 p3140 A66-34512  
Transitions induced by electron impact between all ground-state terms of atomic systems with computed cross sections satisfying unitarity 19 p3463 A66-35990  
Approximation method using sum rules for energy shift in atomic system due to interaction of electrons with vacuum electromagnetic field applied to hydrogen, helium and lithium atom ground states and hydrogen molecule 19 p3402 A66-35995  
Splitting of ground state of neutral mercury two-hole acceptor in unstressed silicon or germanium evidenced by intensity decrease of photoabsorption peaks 19 p3444 A66-36174  
Excitation of ground state hydrogen atoms by fast protons, evaluating total Born cross section in limit of infinitely massive protons 19 p3403 A66-36333  
Ground-state spin memory in excited state of ruby under broadband optical pumping, observing change in relative populations of Zeeman components 20 p3578 A66-37596  
Second-order WKB corrections to Rydberg-Klein-Rees potential curve for hydrogen 22 p3949 A66-39911  
Fractional metastable-state population measurements of Cr ions in ruby crystal under Q-switching operation 23 p4077 A66-41288  
Excitation of hydrogen molecule from ground state to B and C electronic states by electron impact, using one-center wave functions of Huzinaga together with Born

approximation 23 p4098 A66-41360  
Superconductivity model with exact solution, determining energy levels, ground state energy, excitation spectrum, density variations, etc 24 p4259 A66-43088  
**GROUND STATION**  
**SA TRACKING STATION**  
Advanced integrated landing system /AALS/ consisting of azimuth and elevation ground station, ground display site and airborne unit, emphasizing scanning-beam technique 01 p0101 A66-10034  
Satellite communication, noting satellite and ground terminal design performance criteria 01 p0030 A66-10804  
Pulse code modulation /PCM/ for telemetry and communication between Gemini spacecraft Agena D satellite and ground stations for data processing and display 01 p0031 A66-10938  
85-ft paraboloid antenna with new type of Cassegrainian feed system for satellite communication ground station at Nova Scotia 02 p0189 A66-11362  
Loran C system and technique of ground stations for giving ships fixes 02 p0257 A66-12037  
Worldwide navigation system using existing ground and airborne equipment and limited number of navigation satellites 02 p0259 A66-12054  
Modifying ground station deployment, transmitted frequencies and bandwidths for Dectra 2 Navigation system in North Atlantic area 02 p0260 A66-12057  
Discrepancies in data concerning aurora type sporadic ionization in E region obtained by various high latitude stations 02 p0225 A66-12136  
CNES and ESRO station network duties including satellite signal transmission recording, follow vehicle trajectory, telecommand onboard operations, etc 03 p0333 A66-12477  
Diane, European interferometric tracking station noting antenna system, calibration operations, angular measurement, etc 03 p0333 A66-12478  
Station network designed for CNES using Doppler frequency tracking, coherent systems of demodulation, polarization, etc 03 p0351 A66-12479  
Electronic solid state goniometer for producing navigation information for transmission from VHF omnirange /VOR/ ground station 05 p0645 A66-14582  
Satellite telecommunication principles and equipment 06 p0835 A66-16935  
Worldwide implementation of DME system feasible by removing unnecessary refinements from ground station design 07 p1068 A66-17696  
Design and electrical properties of 25-meter Cassegrainian antenna installed at Raisting ground station for radio communications via satellites 08 p1190 A66-18681  
Medium-capacity satellite receiving system for multiplex FM telemetry transmission 08 p1183 A66-18947  
Automated ground station, with computer controlled telemetry system, for Saturn launch vehicle checkout 09 p1347 A66-20675  
Ground station characteristics and requirements in fields of tracking, telemetry and remote control 10 p1520 A66-21706  
Diane ground station interferometry antenna, examining choice of polarization and use of slots for precise measurements 10 p1511 A66-21708  
Self-compensation of phase angle of Diane station coaxial cable of discontinuous disk structure throughout wide temperature range 10 p1511 A66-21709  
Diane tracking station electronic equipment accomplishes variable and selective amplification of signals and coherent demodulation of phase information 10 p1520 A66-21710  
Ground station installations for observation in ionosphere of noncoherent diffusion of plasma by electrons 10 p1532 A66-21711  
Variations in cosmic ray intensity recorded at world network of stations during consecutive magnetic storms, noting changes in corpuscular fluxes, interplanetary medium, etc 12 p1941 A66-24167  
Solar-diurnal cosmic-ray variations



analyzed, showing that averaging observational data over worldwide network of stations leads to large errors 12 p1943 A66-24183

Effect of higher harmonics of geomagnetic field on cosmic ray trajectories, noting reception cones of Soviet stations 12 p1943 A66-24268

Effects of technical parameters of station on results of observations of sporadic E layer, noting that frequencies depend weakly on receiver and transmitter 12 p1869 A66-24272

Satellite communications central control support system consisting of Earth stations and satellite relays accommodating different RF power, orbits and antenna orientations [AIAA PAPER 66-287] 12 p1859 A66-24758

Satellite ground terminal design considerations using adaptive digital communications techniques, noting analog to digital conversion [AIAA PAPER 66-290] 12 p1822 A66-24760

Minimum cost ground receiving station for synchronous satellite system [AIAA PAPER 66-311] 12 p1859 A66-24777

Antenna requirements for satellite communications system ground stations, discussing antenna and mount designs 13 p2038 A66-25575

Discrepancies in data concerning aurora type sporadic ionization in E region obtained by various high latitude stations 14 p2287 A66-28092

Transportable satellite communications ground station design [AIAA PAPER 66-289] 15 p2477 A66-29865

Australian space program noting rocket soundings, Beacon satellites, station development, etc 15 p2600 A66-29909

Varactor diode parametric amplifiers compared for various applications in satellite communication ground stations including FM reception, tracking and radio noise reception 17 p2890 A66-32908

Low-cost ground station design for satellite communications, with emphasis on Cassegrain reflector antenna and drive system 18 p3093 A66-33868

Multiple-element steerable Earth-station antenna for communicating with communications satellite 18 p3080 A66-34264

TACAN and DME navigation systems, discussing ground stations, airborne equipment and guidance systems 18 p3133 A66-34465

Ground stations used in telemetry, tracking and remote control of French satellites 18 p3071 A66-34466

System consisting of communications satellites distributed in nonsynchronous orbits and set of ground stations, formulating link scheduling problem as optimum control 19 p3303 A66-35884

Coverage of satellite passes from ground station for combined satellite-ground base studies of upper atmosphere 20 p3515 A66-37298

Selection and development of guidance station at Gove, Australia, noting access routes, logistics problems, etc 21 p3721 A66-38643

Requirements, functions and equipment of down-range guidance station for ELDO program in Australia 21 p3721 A66-38644

High resolution IR scanning system and vidicon automatic picture transmission of Nimbus II and ground station printout instrumentation 21 p3821 A66-39497

Unmanned space vehicle on board measurements and data transmission to ground station, examining temperature and propellant measuring techniques 21 p3741 A66-39631

Comsat Operations Center for support of International Telecommunications Satellites 22 p3867 A66-40710

Military air-transportable satellite communications terminal design, noting parabolic antenna and amplifier 22 p3896 A66-40712

Antenna systems for deep space communication emphasizing ground station, balancing of ground antenna aperture with spacecraft performance, arrays, etc 24 p4171 A66-42244

Soviet ground station for observation of energy spectrum, composition and

anisotropy in arrival directions of primary cosmic ray particles 24 p4269 A66-42917

Electromagnetic structure of radioelectric whistlers, considering wavefront curvature in D layer, noting signal reception at two distant ground stations 24 p4176 A66-43001

Interplanetary space and celestial observations from ground stations, satellites and space rockets 24 p4280 A66-43133

### GROUND SUPPORT EQUIPMENT

Real time ground computer for Athena system and input/output data requirements in multiprocessing jobs 12 p1827 A66-23836

Advanced avionics systems for improved surveillance and communications for Army ground-support aircraft 13 p2023 A66-25644

Ground support equipment for Pershing weapon system 20 p3542 A66-37239

U.S. Lunar Orbiter program 20 p3663 A66-38063

Aircraft and spacecraft digital systems including computers for production engineering, ground telemetry and communication with aerospace vehicle and onboard equipment for tracking, guidance and simulation of inflight conditions 21 p3709 A66-39629

### GROUND SUPPORT SYSTEM

#### SA SATELLITE GROUND SUPPORT NETWORK

Electronic packaging in Pershing weapon system ground support equipment 02 p0197 A66-11460

Producibility of electronic hardware for Pershing weapon system ground support program 02 p0198 A66-11463

Ground support equipment and launch installations for Apollo launch operation and testing 02 p0215 A66-11614

Coordinated program for airborne and ground support equipment testing of Gemini spacecraft and launch vehicle by two different manufacturers 02 p0294 A66-11635

Operational and maintenance ground equipment, electronics and systems test concepts of Minuteman II ICBM weapons systems 02 p0216 A66-12239

Spacecraft and ground equipment design of lunar orbiter telecommunications system 04 p0477 A66-13580

Human factors in control/indicator panel design of ground support equipment [ASME PAPER 65-WA/HUF-16] 05 p0628 A66-15696

XB-70 fluid power ground support system, describing functions of hydraulic ground power unit, fluid servicing trailer and filtration cart 06 p0869 A66-16791

Universal long range radio navigational system, discussing purpose and function of ground-based system 07 p1065 A66-17671

Design and program for Apollo Lunar Excursion Module, noting propulsion, guidance, control, ground support, etc 08 p1300 A66-18554

Ground support equipment /GSE/ concept, onboard checkout system for large space boosters [AIAA PAPER 64-298] 10 p1612 A66-21935

Hydraulic and pneumatic power equipment for ground support of space vehicles and support in space environment [AIAA PAPER 65-524] 12 p1804 A66-24717

Lincoln Experimental Terminal /LET/ system, ground antenna, RF and signal processing equipment for communications via several satellites [AIAA PAPER 66-272] 12 p1821 A66-24745

Ground system design, data processing, digital command and digital-human interface in flight operations problems for unmanned spacecraft on planetary exploration mission 13 p2190 A66-25257

Satellite tracking telemetry system used by Diane network of ground stations 14 p2233 A66-26803

Ground-based test setup using p-n-p-n controlled switches, logic circuitry and sensitive relays to analyze telemetered pulse signals from four lines of airborne electronic system 14 p2255 A66-27807

Palletized cargo systems, transit time reduction and ground support system data handling and documentation 17 p2846 A66-32844

Checkout criteria and requirements for manned spacecraft, specifically Apollo [AIAA PAPER 65-284] 18 p3093 A66-33791

Interface between aerospace systems with man, spacecraft and supporting ground stations 20 p3662 A66-371

Payload integration in space experimentation, discussing commonality of flight and load matrices, experimental spacecraft-ground system interfaces, computer methods, etc 20 p3662 A66-371

Packaging, shielding and other containment techniques in formulation of grounding plan as basis of good EAGE design 20 p3542 A66-371

Minuteman weapon system maintainability discussing fault detection and isolation ground system, standardization, tools and system requirements analysis 24 p4281 A66-42917

### GROUND TEST

Measuring Meteor 1 rocket flight parameters from ground using phototeodolites and astronomical optical-acoustic methods 01 p0031 A66-116

Full scale ground inflation tests evaluate structural and RF backscatter characteristics of Echo II prototype sphere as function of their internal pressures 01 p0055 A66-117

SNAP-10A instrumentation and control subsystems and ground test program 12 p1911 A66-234

Ground testing of large nuclear rocket discussing decontamination requirements maintain safety level with longer runtimes and higher reactor levels 19 p3398 A66-366

### GROUND TRACK

Computation capability onboard manned spacecraft of out-of-plane maneuver, achieving specified ground track 02 p0256 A66-116

Apollo Manned Space Flight Network /MSFN/ tracking and communications systems for tracking lunar spacecraft 15 p2450 A66-287

Tesseral perturbations of repeating ground track synchronous satellite orbits gravitational potential 18 p3233 A66-344

Satellite space coordinates from photographs made simultaneously from two points on Earth surface 22 p3917 A66-396

### GROUND WAVE

Electromagnetic groundwave propagation along Earth surface, noting transmission a reflection when meeting abrupt electrical discontinuity 04 p0475 A66-134

Field separation of ground transmitter in ordinary and extraordinary modes when traversing lower boundary of anisotropic ionosphere, noting effect of incidence angle magnetic azimuth, etc, on energy dissipation of VLF ground wave 14 p2238 A66-276

Extension of work on ground wave propagation along two-section mixed path to three-section paths, using microwave frequency, water and aluminum plates 15 p2452 A66-294

Sonic boom shape distortion due to reflection and scattering by ground surface with finite acoustic impedance 17 p2905 A66-311

Short distance expansion method used to calculate ground radio wave propagation over mixed path on spherical Earth 19 p3305 A66-366

### GROUP BEHAVIOR

Solution for group properties of equation for monoenergetic charged-particle beam extended to beam in presence of stationary background and multivelocity and multicomponent beams 04 p0556 A66-14

Faster group performance with large shared display indicates facilitating effect on group interaction process 12 p1808 A66-234

Model for social system for extended duration spaceship crews subject to isolation, confinement and/or stress 13 p2013 A66-256

### GROUP THEORY

General theory for construction of constitutive equations describing pure mechanical properties of continuous media with tensor and group theoretic concepts 01 p0106 A66-10

Simple semigroup treatment of problems involving powers of nonnegative matrices 02 p0249 A66-11

Probabilistic model for analyzing change



through time in binary dyadic relation on finite set of points 04 p0540 A66-14001

Group properties of PDE system for one-dimensional gas flows with plane waves, using external Cartan 07 p1019 A66-17859

Group classification of solutions to Hopf equation according to type of viscosity coefficient 08 p1209 A66-19476

Group properties of short wave equations in gas dynamics 10 p1522 A66-21315

Fantapple relativity theory using elementary projective geometry and based on group theory, obtaining cosmology leading to double time scale and origin of universe from point 15 p2599 A66-29658

P super n electron configuration for systems where spin-free Hamiltonian is applicable 16 p2754 A66-30861

Integral equivalence of two given systems of square integral matrices, reducing problem to determination of principal ideal ring 16 p2738 A66-31563

Nonnegative matrix analysis, discussing summation and multiplication 19 p3391 A66-36337

Group theory of invariance of finite linear state-variable transformations generating new linear dynamic system and application to electric network 20 p3539 A66-38147

Continuous group and infinitesimal transformation in linear dynamic system application, considering linear network 20 p3539 A66-38148

Conditional stability and boundedness of conditionally invariant sets derived from vector Liapunov function 21 p3755 A66-38538

Covariant gravitational field equations in de Sitter space and quantum mechanical equations of motion associated with particles of given spin, employing gauge principle 21 p3769 A66-38645

Existence of similar solutions for given differential transonic equations for free stream Mach number of unity 23 p4014 A66-42049

Decompositions induced in completely o-simple rectangular semigroup by matrix congruence 24 p4232 A66-42900

**GROUP VELOCITY**

Group velocity measurements in delay systems of quantum paramagnetic amplifiers 09 p1380 A66-20361

Correctors for variations in group propagation time of AM wave transmitted by radio carrier wave, noting circuit analysis for matched and unmatched all-pass IF filters 14 p2252 A66-27353

Group velocity and power flow relations for surface waves in plane-stratified anisotropic media 18 p3066 A66-33539

Group velocity and power flow of surface waves on uniaxial plasma slab 18 p3066 A66-33540

Group velocity measurements in delay systems of quantum paramagnetic amplifiers 19 p3353 A66-35319

Group velocity of wave packet propagating radially across plasma immersed in static axial magnetic field, examining ringing phenomena due to pulsed transmission 23 p4101 A66-41261

**GROWTH**

**SA CRYSTAL GROWTH**

**SA GERMINATION**

Growth rate of microorganisms when rate changes with time, using continuous culture technique 02 p0183 A66-12016

Photolumination effect on growth rate of *Chlorella vulgaris*, discussing action spectrum and mechanism of light requirement for heterotrophic growth 20 p3507 A66-37792

**GRUMAN MILITARY AIRCRAFT**

**S A-6 AIRCRAFT**

**S F-111 AIRCRAFT**

**GRUNEISEN CONSTANT**

Thermal expansion of complex semiconductors from 20 to 340 degrees K, calculating Gruneisen constant for diamond, silicon, germanium, tin, etc 01 p0124 A66-10769

Pressure dependent critical temperature and magnetic field of superconducting transitions in metals 09 p1429 A66-20597

Thermal expansion of complex semiconductors from 20 to 340 degrees K, calculating Gruneisen constant for diamond,

silicon, germanium, tin, etc 11 p1749 A66-22280

Lindemann, Grueneisen and melting laws in theory of normal properties of high pressure solids 18 p3135 A66-34237

Pressure dependent critical temperature and magnetic field of superconducting transitions in metals 20 p3622 A66-38131

Functional interdependence of four distinctly different parameters represented by gamma in study of thermodynamical relations for shock waves 24 p4193 A66-42270

**GUIDANCE**

**S AIRCRAFT GUIDANCE**

**S HOMING**

**S INERTIAL GUIDANCE**

**S MAP-MATCHING GUIDANCE**

**S MIDCOURSE GUIDANCE**

**S NAVIGATION AND GUIDANCE**

**S REENTRY GUIDANCE**

**S SATELLITE GUIDANCE**

**S SPACECRAFT GUIDANCE**

**S TERMINAL GUIDANCE**

**GUIDANCE AND CONTROL**

Ion guidance and control - AIAA Conference, Minneapolis, August 1965 01 p0097 A66-10001

Navigation, guidance and control systems to meet basic trajectory and crew safety requirements of LEM 01 p0102 A66-10043

Synthesis of optimal linear control system coupled with vehicle configuration design technique for guidance parameters and temperature accumulation along optimum entry trajectories 01 p0105 A66-10787

Computer logical gates for characteristics of large systems as local guidance control and regulation systems of plants 03 p0348 A66-12603

Linear expression for constraints to obtain general solution to impulsive guidance laws 03 p0390 A66-12801

LEM mission and pilot role in spacecraft control including guidance and control systems, retromaneuvering, landing-site inspection, etc 05 p0713 A66-15166

Gemini guidance and control, discussing design, ground monitoring, launch and flight guidance, spacecraft instrumentation, maneuvering, etc 06 p0906 A66-15924

Fuel optimum guidance law to achieve required velocity 06 p0906 A66-15928

Direct and analytical solution of polynomial-type guidance functions for optimal space flight [AIAA PAPER 66-94] 06 p0907 A66-17093

Fluid logic elements and amplifiers for data processing, signal amplification and guidance and control 08 p1199 A66-18698

Dimensionless differential corrections and proper coordinate system for generalized preflight guidance analysis 08 p1249 A66-18819

Multimission standardized guidance and control system and evaluation of cost effectiveness 08 p1253 A66-19540

Digital computers for aerospace guidance and control, including Gemini inertial guidance and B-70 aircraft navigation systems 08 p1187 A66-19597

Protection standards for population around missile launching sites, noting missile malfunctions, particularly breakdowns of guidance and control systems 09 p1457 A66-20554

CECLES/ELDO space vehicle booster program, noting design of three-stage rocket, including control and guidance system, telemetry, etc 09 p1464 A66-20655

Optimal trajectory and guidance role of conjugate points in determining maximum duration of optimal control for linear and nonlinear processes 10 p1516 A66-21076

Theoretical and engineering aspects of applying predicting systems to automatic guidance and control 11 p1673 A66-22201

Guidance by parabolic extrapolation of short-range missile toward pre-established target controlling it aerodynamically, noting finder, computer and navigational errors 11 p1734 A66-23500

Guidance and control of Mars orbiter-lander mission 13 p2123 A66-25254

Guidance control technique for soft automatic lunar landing 16 p2743 A66-30887

Optimal control theory in design of aerodynamic shapes, flight paths, guidance and control logic, data processing logic,

etc 17 p2950 A66-32682

Guidance and control systems of Mariner planetary spacecraft, noting requirements, flight performance, systems configuration, etc 18 p3242 A66-33852

Single-axis Sun-tracking system for satellite orientation, noting operation modes and system performance 18 p3243 A66-33855

Advanced control and guidance research at NASA 18 p3131 A66-33866

Digital guidance and control computer used in Apollo Guidance and Navigation System 18 p3073 A66-33874

Simulator results on guidance and control during supercircular atmospheric entry maneuvers 18 p3244 A66-33878

Short time prediction display applicable to stabilization problems, discussing extrapolation and accelerated time scale methods 18 p3061 A66-33884

Temperature rate measurement for design of control and guidance system in reentry vehicles, using Temperature Rate Flight Control System /TRFCS/ 19 p3396 A66-35511

Guidance equations including first-order effects of Earth oblate gravitational field, solving motion equations and evaluating downrange and crossrange miss distance and time-of-flight errors 19 p3397 A66-35599

Gemini reentry guidance and control system consisting of inertial guidance and attitude control systems 19 p3470 A66-36679

Control-engineering and flight-mechanics problem of rendezvous guidance, considering target body without guidance and second body in gravitational field without atmosphere 20 p3595 A66-36874

Reliability requirements for spacecraft guidance and control systems, emphasizing redundancy in existing systems 20 p3596 A66-37177

Redundant electrical systems for Titan II and Gemini Titan II launch vehicles 20 p3499 A66-37193

Digital simulation of guidance and control of exoatmospheric interceptor missiles for study of parameter variations effect on overall mission effectiveness 20 p3596 A66-37230

Guidance scheme for control of multistage rocket vehicle through ascent phase of complex space mission [AIAA PAPER 64-640] 20 p3597 A66-38156

Steering philosophy for rocket booster, using position and/or velocity profiles until desired injection speed is attained [AIAA PAPER 64-639] 20 p3597 A66-38157

Requirements, functions and equipment of down-range guidance station for ELDO program in Australia 21 p3721 A66-38644

Guidance and control - AIAA/JACC Conference, Seattle, August 1966 21 p3761 A66-38838

Computational errors and requirements evaluated for free and restrained strapdown sensor mechanization, based on analytic models 21 p3763 A66-38841

Stationkeeping problems and guidance technique for control of stationkeeping maneuver between orbiting vehicles 21 p3765 A66-38865

Modulation of L/D and bank angle to achieved heading, range and trajectory stabilization, using closed form equations 21 p3765 A66-38868

Airborne guidance computations using prescribed-h method, representing two-body motion in inertial space, presenting equations for target hitting, circular orbit, etc 21 p3765 A66-38869

Mathematical model of linear guidance law to dynamical system, noting reduction of two-point boundary value class error 21 p3765 A66-38870

Inertial and electromagnetic guidance and navigation systems for vehicular and global application 22 p3944 A66-40124

**GUIDANCE SENSOR**

**SA IMAGE DISSECTOR TUBE**

Satellite guidance system using star-field locating sensor with gyration masses controlled by centrifugal and gravitational force interaction 02 p0256 A66-11984

Automatic star trackers for long range aircraft navigation, discussing instrumentation methods and use of pulse code modulation for sensor design 02 p0257 A66-12029



- Schuler tuned inertial system as flight sensor and control of VTOL aircraft translational velocity during hover phase and landing 07 p1070 A66-17724
- Inertial reference unit to provide attitude and thrust maneuver measurements for Lunar Orbiter spacecraft 08 p1253 A66-19529
- Electro-optical celestial guidance system with miniaturized computer and scanning sensor 12 p1909 A66-24104
- Electro-optical automatic celestial guidance system for spacecraft and satellites 13 p2124 A66-25643
- Bore-sighted scanning star tracker for precise attitude sensing and control of sounding rocket 14 p2329 A66-28452
- Sensors for Earth satellite orientation to solve general problem of space vehicle orientation 18 p3245 A66-33888
- Star tracking tests to achieve accurate stellar sensor positioning prior to missile launching, considering calibration of critical hardware 18 p3132 A66-34045
- Preflight and in-flight testing of stellar sensor subsystem for guidance of ballistic missiles 18 p3111 A66-34046
- Control signal generator and output characteristics of angular position and velocity sensors used in single-axis Sun-oriented system of Vostok spacecraft 19 p3394 A66-35280
- V-gyro pair as dual-rate sensor, examining gimbal equations for gyros 21 p3736 A66-38712
- Strapdown inertial sensor configuration based on time modulated torquing approach in gyro and accelerometer 21 p3764 A66-38849
- Strapped-down inertial sensor loops design criterion for desired total system performance, noting loop dynamic error 21 p3764 A66-38850
- Automatic feedback table leveling system, noting tilt to simulate aerodynamic drag 21 p3722 A66-38887
- Book on spacecraft navigation systems covering sensors operation and construction, with emphasis on astronomical, inertial and complex navigation systems 21 p3768 A66-39289
- Apollo mission evolution, with particular reference to lunar descent, landing, takeoff and rendezvous performed by LEM 21 p3822 A66-39517
- Analytic axes alignment for strapdown inertial system, describing computational procedures for ground-based and in-flight correction of attitude parameters 23 p4088 A66-41115
- Microwave radiometry feasibility as technique for navigation data-sensing in Army aircraft 23 p4089 A66-41317
- GUIDANCE SYSTEM**
- SA MIDCOURSE GUIDANCE**
- SA RENDEZVOUS GUIDANCE SYSTEM**
- Thermal compression bond failures in internal electric interconnects on circuit boards of advanced Minuteman guidance system 01 p0049 A66-11152
- Gemini spacecraft reentry guidance scheme with onboard computations of reference trajectory and guidance coefficients [AIAA PAPER 65-48] 03 p0390 A66-12758
- Intercepting moving completed powered-flight of ICBM missile 04 p0581 A66-13458
- Automatic testing and evaluation system for launch-vehicle digital computer and data adapter of Saturn IB/Saturn V guidance system 04 p0507 A66-13612
- Future missile guidance capability would permit usage against broad spectrum of tactical targets by use of multimode sensor array 04 p0585 A66-13923
- Longitudinal photoelements examined for guidance and homing 04 p0524 A66-14398
- Guidance system for British Navy anti-aircraft missile Seaslug using Cartesian control beam-riding, noting simulation testing 07 p1079 A66-18327
- Processing signal information from digital rate gyros and accelerometers in analytic, gimballess inertial platform 08 p1253 A66-19530
- Iterative guidance law for Saturn launch vehicle for lunar landing, examining trajectory optimization 08 p1253 A66-19539
- Computer-controlled vidicon terminal guidance system 08 p1253 A66-19541
- Optimum antenna requirements for radio-slope guidance system and vertical control in blind landing 08 p1254 A66-19833
- Future programs for ELDO including launchers, guidance systems, bases, etc 09 p1464 A66-20656
- Manual guidance system for atmospheric entry of lifting reentry vehicles 10 p1554 A66-21930
- Automatic pilot consisting of guidance system for flight trajectory control and stabilization system for angular acceleration control 12 p1909 A66-23815
- Missile guidance systems based on p-matrix guidance methods [AIAA PAPER 64-667] 12 p1910 A66-24711
- Onboard guidance scheme as backup to Earth-based orbit determination techniques and for approach navigation and orbit correction in planetary capture maneuver 13 p2123 A66-25253
- Design and fabrication of computer subsystems for Apollo guidance and navigation systems 13 p2027 A66-25781
- Titan III guidance and navigation system modification for lunar mission application 14 p2329 A66-28451
- R and D clean room complex design for guidance and control systems, noting contamination control, maintenance procedures, cost factors, etc 17 p2903 A66-32209
- Nuclear radiation anticollision instrumentation for guidance systems of helicopters and other vehicles, both air and surface 17 p2926 A66-33097
- Analytic solutions for predicting motion of high-thrust rockets applied in guidance and real-time targeting [AIAA PAPER 66-452] 18 p3226 A66-33648
- Man-machine system in control and guidance of Saturn V launch vehicle, emphasizing participation during atmospheric phase of flight profile 18 p3242 A66-33847
- Satellite orbiting via radio command guidance, discussing results with communications and weather satellites, guidance system used, control methods, etc 18 p3131 A66-33848
- Solar alignment system for Skylark rocket attitude control, describing system composition, operation and results 18 p3243 A66-33856
- Guidance and navigational system hardware for Apollo Command Module and LEM 18 p3132 A66-33877
- Terminal guidance system instrumentation for Surveyor project lunar soft-landing spacecraft 18 p3132 A66-33881
- TACAN and DME navigation systems, discussing ground stations, airborne equipment and guidance systems 18 p3133 A66-34465
- Closed loop control system for space vehicle guidance, formulating efficient steering algorithm 19 p3471 A66-36685
- Error analysis of area correlation guidance system using parametric analysis of spatial frequency domain-equivalent power spectral density 20 p3597 A66-37237
- Manual steering, hybrid guidance system, in-flight computations and trajectory for automatic descent and landing system for LEM 21 p3768 A66-38899
- Monograph on theory of gyroscopic instruments and devices 23 p4066 A66-41052
- GUIDE VANE**
- Parametric analysis of supersonic compressors, determining relative efficiencies of various leading and trailing guide vane configurations 10 p1479 A66-21365
- Inlet guide vane system for control of small single-shaft gas turbines [ASME PAPER 66-GT-89] 14 p2372 A66-26993
- Nozzle guide vanes of ZHS-6K alloy in thermal stress induction of surface layer crystal structure changes 16 p2727 A66-31531
- GUIDED MISSILE**
- Graphical-analytical method using successive approximations determines guided missile trajectory 11 p1734 A66-23344
- Annual report, 1964-65 / Aeronautical Research Laboratories, Australian Defence Scientific Service/ on aerodynamics, guided weapons and systems and flight research 13 p2056 A66-25120
- Textbook on automatic guidance missiles and space vehicles 17 p2951 A66-33033
- Text on radio remote control a telemetry and missile application, including modulation and multiplex techniques 17 p2876 A66-33033
- Stellar inertial guidance system composed of integral inertial platform-stellar sensor combination, airborne digital computer and power supply for Polaris missile 18 p3132 A66-34045
- Preflight and in-flight testing of stellar sensor subsystem for guidance of ballistic missiles 18 p3111 A66-34046
- Electronic equipment for guided weapon design and quality evaluation 18 p3079 A66-34046
- Book on ballistics of long-range guided missiles and practical methods 20 p3664 A66-38033
- Propellant sloshing in tanks of guided missile, giving mathematical description of numerical and experimental results Coralie stage 21 p3818 A66-38033
- Dither and sinusoidal incidence variation effect on control wing hinge moments of transonic-supersonic rolling maneuver guided missile [AIAA PAPER 66-755] 22 p3846 A66-40033
- GULF STREAM**
- Aerial observation of sea surface measuring wind direction, speed, wind direction and period of Gulf Stream along coast 10 p1532 A66-21033
- GULLIVER PROGRAM**
- Future of environmental biology, discussing space research on living organisms extraterrestrial environment 04 p0470 A66-14033
- Extraterrestrial life in solar system discussing equipment for Mars exploration noting Gulliver program, Multivator automatic biochemical testing apparatus and TV microscope 12 p1805 A66-23033
- GUMBEL THEORY**
- SA EXTREMUM VALUE**
- Gumbel theory of extreme values a statistical technique in reliability problems with emphasis on double exponential distribution 12 p1833 A66-24033
- GUN**
- SA CROSSED FIELD GUN**
- SA ELECTRON GUN**
- SA GAS GUN**
- SA HYPERVELOCITY GUN**
- SA PLASMA GUN**
- Production process for gun-drilling of holes in beryllium, noting filtration technique and clamping fixture [ASTME PAPER MR66-185] 14 p2300 A66-26033
- GUN LAUNCHING DEVICE**
- Gun-launched meteorological sounding system, describing launcher, vehicle, sensor systems and sensitivity [AIAA PAPER 66-382] 12 p1954 A66-24033
- Upper atmospheric wind measurement by gun launched projectiles, computing wind component contour parameters [AIAA PAPER 66-403] 12 p1908 A66-24033
- Large bore gun launched rockets, design and performance 14 p2270 A66-27033
- UHF telemetry system to withstand shock of gun launched vertical sounding probes 16 p2650 A66-30033
- Electronic equipment to withstand cannon firing and extreme underwater depths 19 p3357 A66-35033
- High altitude research project using inch gun for measurement of upper atmospheric wind shear patterns 19 p3340 A66-36033
- Ionospheric winds measurement by luminous trimethyl aluminum trails produced by gun-launched projectiles 24 p4200 A66-42033
- GUNN EFFECT**
- Domain characteristics and crystal properties in materials and configurations Gunn effect devices 01 p0041 A66-10033
- Coherence of Gunn oscillations enhanced by transverse magnetic field for certain applied voltages 03 p0332 A66-12033
- FM by mechanical tuning of cavity setting in gallium arsenide crystals for application to communication system 03 p0332 A66-12033
- Semiconducting materials noting bo



- model, band theory model, uses and Gunn effect 05 p0737 A66-15065
- Coherent current oscillations observed in dark conductive In-doped CdS at 77 and 300 degrees K 06 p0925 A66-16659
- Gunn effect n-type GaAs diode phase locked to stable frequency by injecting CW signal into circuit along with video pulse 06 p0925 A66-16671
- Current instabilities in gallium arsenide, noting oscillation frequency and volt-ampere characteristics 06 p0925 A66-16688
- Gunn effect oscillators including domain formation, microwave source potentialities, power transfer, efficiency, etc 08 p1193 A66-19120
- Behavior of high field instabilities in n-type gallium arsenide, examining device prospects related to phenomenological model for Gunn effect 08 p1270 A66-19122
- Current-voltage characteristics of CW X- and GaAs microwave Gunn generator 11 p1713 A66-23029
- Small-signal impedance of transferred-electron diodes, stable against domain formation 13 p2030 A66-25212
- Noise performance of Gunn microwave generator and noise-power measurements made on Gunn oscillator in X and J band 13 p2030 A66-25221
- Consistency of Gunn effect with excitation of conduction band electrons from high mobility minimum to low mobility valleys 13 p2164 A66-25517
- Gunn effect in gallium arsenide, noting negative differential electron mobility at high electric fields in conduction band 13 p2165 A66-25546
- Gunn effect involving current oscillations higher than 1000 mc in GaAs crystal under applied electric field 14 p2355 A66-26920
- Microwave oscillations in 4 to 31 gc/s frequency range from single Gunn diode 14 p2254 A66-27590
- Intervalley scattering in III-V semiconductors, noting relation to Gunn effect, scattering in GaAs by longitudinal optic phonons, in InP by longitudinal acoustic phonons 16 p2776 A66-30733
- Single trapping center effect on growth of small amplitude space charge waves and propagation velocity, deriving dispersion relations 16 p2781 A66-31216
- Dipole phenomena in n-type GaAs caused by field perturbations, showing conditions for high and low field nucleation 17 p2983 A66-33106
- Current wave form observation in GaAs, using transmission line concept and pulse splitting technique 17 p2983 A66-33109
- Volt-ampere characteristics, electrical resistivity, and pressure effect on Gunn phenomena in n-type GaAs in high electric fields 17 p2985 A66-33292
- Optical modulation in bulk gallium arsenide, using Gunn effect 18 p3152 A66-33606
- Nonuniform motion of high field domains in Gunn effect including steady and nonsteady state properties of formation stage 18 p3077 A66-34076
- Resonant circuit behavior of Gunn diode, considering device as self-pumped parametric oscillator 18 p3078 A66-34086
- Reproducible ohmic contact preparation for high resistivity n-type GaAs in fabrication of Gunn oscillators 19 p3313 A66-35351
- Stable domain propagation for case when electrons have field-independent diffusion coefficient and follow arbitrary static velocity field characteristic exhibiting negative resistivity 19 p3446 A66-36371
- Growth and propagation of electrostatic waves in medium with arbitrary mobility law, solving motion equations, emphasizing case pertinent to Gunn effect 19 p3447 A66-36399
- Microwaves from gallium arsenide excited by impressed voltage 20 p3612 A66-37251
- Upper oscillation frequency limit for Gunn oscillator imposed by finite energy-relaxation time of heated carriers 20 p3527 A66-37449
- Fourier analysis determination of optimum efficiency of cavity-controlled Gunn-effect oscillator when bias voltage is almost two times voltage 20 p3527 A66-37450
- Domain velocity, stability and impedance in Gunn effect, presenting framework for analyzing space-charge waves in two-valley semiconductor 20 p3618 A66-37599
- Gunn oscillations in indium arsenide, measuring electrical properties of diodes, noting current voltage characteristics as function of applied stress 20 p3620 A66-37773
- Carrier motion equation in Gunn diode in terms of average drift velocity and diffusion coefficient 20 p3534 A66-38402
- IR and microwave radiations associated with current controlled instability /negative resistance/ in GaAs, noting Gunn threshold and V-I characteristics 21 p3802 A66-39162
- High power Gunn-effect oscillators constructed from thin epitaxial layers of GaAs, noting relation of drive voltage to frequency, efficiency and power output 22 p3959 A66-39725
- Curve analysis of current instabilities including Gunn effect in n-type gallium arsenide 22 p3961 A66-40045
- Resistivity measurement of large number of samples of bulk-grown n-type GaAs as function of temperature near 300 degrees K 22 p3877 A66-40179
- Semiconductor electronics, Gunn effect in optical communications, electro-optics, optoelectronics and light coupling in microminiaturization 22 p3878 A66-40623
- Continuous current oscillation in GaAs caused by acoustoelectric effect 23 p4112 A66-41296
- Decaying free carrier concentration increase in GaAs when subjected to increased level of drive during first cycle 24 p4253 A66-42370
- Surface pinned layer-like field inhomogeneities in cadmium sulfide, investigating visibility of field layer by corresponding shift of absorption edge, using Franz-Keldysh effect 24 p4254 A66-42427
- GUNNERY TRAINING**
- Instructional System model for meeting USAF maintenance technical training requirements for complying with weapon system requirements 23 p4030 A66-41578
- GUST**
- SA STORM
- SA TURBULENCE
- SA WIND
- Approximate formula for probability density of time lapse between wind gusts 08 p1247 A66-18803
- Gust design procedures based on power spectral techniques, considering atmospheric turbulence with aircraft as rigid body with single degree of freedom [ICAS PAPER 66-11] 23 p4017 A66-42073
- GUST ALLEVIATOR**
- Gust alleviation systems for transport aircraft using linkage, noninteracting and split control 18 p3052 A66-34493
- Pilot protection from aircraft vibration caused by atmospheric turbulence 20 p3508 A66-36997
- GUST LOAD**
- Wind tunnel technique for measuring frequency response of flexible airplane to vertical sinusoidal gusts [AIAA PAPER 65-787] 03 p0438 A66-13071
- Vibration exposure with varying peak and rms acceleration and frequency in low altitude high-speed flight 03 p0329 A66-13355
- French Air Regulation 2054 applicable to sailplanes, considering effect on design speed and gust loads 07 p0989 A66-17822
- Spectral density of vertical wind gusts in clouds calculated, including turbulent energy dissipation rates in cloud strata 09 p1398 A66-19884
- Low altitude turbulence model for aircraft gust load estimation related to meteorological parameters, terrain conditions and height [AIAA PAPER 65-14] 09 p1400 A66-20741
- Load factor estimation for flights in turbulent conditions by replacing exact transfer function with equivalent statistical model 10 p1482 A66-21385
- Statistical research on g-loadings and atmospheric turbulence in field of structural strength limits for sporting gliders 12 p1801 A66-23855
- Relationship between atmospheric gust criteria and performance of supersonic inlet and propulsion [AIAA PAPER 66-367] 12 p1801 A66-24495
- YS-11 transport aircraft fatigue testing, noting wing fatigue damage and equipment used 13 p2197 A66-26099
- Defining fatigue load environment for business aircraft [SAE PAPER 660215] 13 p2199 A66-26392
- Aircraft design for gust loads encounter based on power spectral results 14 p2405 A66-27995
- Wing penetration into zone of sharply localized gust, deriving equations for forces and moments acting on wing 16 p2630 A66-31292
- Low altitude high-speed flight from standpoint of structural loads, particularly those resulting from gust encounters 19 p3278 A66-35505
- FAA safety research on aircraft reliability, discussing power spectral gust design, structural strength, turbine performance and lightning strike effects 20 p3540 A66-36992
- GUTENBERG MODEL**
- Spheroidal-type seismogram study of wave generation, propagation, dispersion and attenuation in realistic spherical Earth models, especially Gutenberg-Bullen A-prime model 20 p3550 A66-37433
- GYRATION**
- S ROTATION**
- GYRATOR**
- Gyrator circuit with only three transistors designed by providing active feedback path so that circuit behaves like two-way feedback system 02 p0201 A66-11908
- Network containing only two gyrators and two capacitors sufficient to synthesize given positive real driving-point function 02 p0209 A66-11913
- Gyrator realization, discussing impedance/frequency characteristics of transistor circuit used 18 p3078 A66-34079
- Direct-coupled gyrator suitable for integrated circuits and time variation 20 p3527 A66-37447
- High-quality transistorized gyrator for integration 20 p3528 A66-37455
- GYRO**
- S GYROSCOPE**
- GYRO HORIZON**
- Error of two-rotor gyrohorizon compass caused by hydraulic damper during stop or steady motion 24 p4210 A66-42447
- GYRO-STABILIZED**
- Comparison of differentiating and integrating correction circuits for stability of forced gyrostabilizers for high value of amplification coefficient 02 p0226 A66-11313
- Permanent axes of rotation for gyrostabilizer under influence of forces depending only on position of gyrostabilizer 07 p1035 A66-18191
- Stabilization of gyrostabilizer using motion equations as given by Volterra 07 p1035 A66-18193
- Operation and structural components of inertial navigation system, noting accelerometers, gyroscopic platform stabilizers, error effect, etc 13 p2123 A66-25138
- Optimum stability of body with fixed point, using stabilizing gyros 13 p2127 A66-25627
- Motion of constant relative kinetic motion gyrostabilizer through force field 15 p2502 A66-29337
- Gyro-stabilized heliostat for airborne astronomy noting design principles, achieved stability, servoloop and mechanical system 16 p2705 A66-30824
- Gyro-stabilized airborne solar eclipse spectrograph, noting wavelength range, dispersion accuracy, guidance mechanism, etc 16 p2705 A66-30825
- Russian monograph on gyroscopic stabilizer theory and error assessment 17 p2925 A66-32567
- Stability of particular solution to gyrostabilizer motion in Newtonian central force field 20 p3604 A66-38424
- GYROCOMPASS**
- Response of inertial platform in orbital gyrocompass mode studied for satellite vehicle [AIAA PAPER 64-238] 03 p0369 A66-12736
- Single rotor correctable gyrocompass in form of astatic gyroscope 07 p1032 A66-17622
- Serviceability and accuracy of Sperry C-12



compass system on Boeing 707-320C aircraft from June to October 07 p1065 A66-17673

Grid navigation method, employing Mercator chart, is suitable for high latitudes and supersonic aircraft 07 p1066 A66-17683

Position-attitude-true-heading-steering navigation system noting accuracy, reliability, maintenance, operational requirements and functional features 07 p1070 A66-17720

Compass performance improvement, discussing Sperry C-12 compass system accuracy, operational features, etc 07 p1033 A66-17721

Flight trials of Bendix/Elliott Polar Path compass, discussing accuracy, stability, performance and weakness 07 p1033 A66-17758

Interplanetary trajectory adaptive gyrocompass system, discussing orbital angular velocity, angular acceleration, error sensitivity coefficients, error sources, etc 13 p2124 A66-25256

Compensation for error resulting from inclination of frame of gyrocompass with elastic recovery moment, based on shifting of gravity center along major axis 14 p2294 A66-27363

Stability of gyrocompass investigated by linear mechanics methods 17 p2958 A66-32606

Third-order orbital gyrocompass horizontal and vertical damping techniques to eliminate gyro and bias errors in horizon sensor 18 p3110 A66-33828

Linear filtering technique for estimation of azimuth alignment of inertial guidance system in presence of disturbances with no measurement noise 19 p3398 A66-36689

Mechanization of vectorial equations by means of four-gimbal platform and speed sensor for automatic setting of hybrid inertial systems 20 p3597 A66-37395

Effect of vibration of base on indications of gyrocompass extended to include LF sinusoidal displacements of base corresponding to rocking motion, noting free play effect, gyro drift and vertical moment 21 p3738 A66-38989

Inertial navigation for civil airline operations, noting azimuth alignment made by automatic gyrocompassing [ICAS PAPER 66-6] 22 p3946 A66-40677

Error of two-rotor gyrohorizon compass caused by hydraulic damper during stop or steady motion 24 p4210 A66-42447

IMU/inertial measurement unit/gyrocompass as attitude reference in space 24 p4214 A66-42955

## GYROELECTRICITY

Gyroelectric and gyromagnetic rectangular waveguides compared for cases of electrostatic and magnetostatic fields transverse to EM wave propagation direction 19 p3317 A66-35719

## GYROINTERACTION

Plasma and electron gyroresonance effects on admittance of RF plasma probe surrounded by ion sheath 09 p1381 A66-20373

Wave propagation during gyroresonance interaction, noting nonlongitudinal characteristics of waves generated in magnetosphere between beams of charged particles 13 p2072 A66-25462

## GYROMAGNETISM

Lossless multiconductor transmission line model extended for description of gyromagnetic coupling effects 06 p0846 A66-16094

Flight trials of Bendix/Elliott Polar Path compass, discussing accuracy, stability, performance and weakness 07 p1033 A66-17758

Optical pumping of rubidium atoms, treating oriented atoms as magnetized macroscopic gyroscope 18 p3120 A66-35029

Gyroelectric and gyromagnetic rectangular waveguides compared for cases of electrostatic and magnetostatic fields transverse to EM wave propagation direction 19 p3317 A66-35719

Behavior of transverse wave numbers/separation constant/ for electromagnetic wave propagation in anisotropic homogeneous cold plasma of arbitrary cross section 20 p3608 A66-37454

## GYROSCOPE

## SA ATTITUDE GYRO

## SA ELECTRICALLY SUSPENDED GYROSCOPE /ESG/

## SA ELECTROSTATIC GYROSCOPE

## SA FLUID ROTOR GYROSCOPE

## SA ROTOR GYROSCOPE

Accelerometers and gyroscopes tested underground, discussing ground motion attenuation with depth investigated in Deep-Hole program 01 p0051 A66-10038

Inertial-grade gyroscope theory and application, noting two-degree and single degree of freedom gyros, reference frames and gyrocompasses 01 p0067 A66-10488

Navigation gyro design with respect to cost factors noting electrically suspended, gas bearing and other types 01 p0104 A66-10676

North-seeking rate gyroscope design with variable gain amplifier control of housing 01 p0070 A66-10877

Satellite guidance system using star-field locating sensor with gyrating masses controlled by centrifugal and gravitational force interaction 02 p0256 A66-11984

Rate gyros with various vibrating shafts and frequencies 03 p0368 A66-12499

Theory of aircraft measurement of gravity using gyroplatform, ideal gimbal suspension and three orthogonal string sensors, deriving formula for unperturbed gravity value, discussing perturbation measurement errors 03 p0366 A66-12991

Inertial navigation and accelerometers deriving law of gyroscopics, noting design of gyroscopes like ball and gas bearings, gimbal suspension, electrostatic, laser, etc 04 p0543 A66-13362

Geocentric pendular control for detection of direction of terrestrial field 05 p0713 A66-15414

Book on motion theory of several coupled rigid bodies about fixed point, particularly gyroscope and gyrostat in Cardan suspension 06 p0910 A66-17067

Gyroscopes, accelerometers and error sources in inertial navigation systems 08 p1249 A66-19056

Pulsed-torqued gyroscopes with nonlinear characteristics and quantized sampled-data signals, determining theoretical performance 08 p1224 A66-19489

Accelerated coincidence of gyro servocontrol system at discrete moments of time with values of target coordinates 08 p1254 A66-19678

Aerodynamic drag moment of gyromotor operating in air, comparing calculated and experimental data 09 p1379 A66-20306

Motion of suspension axis of integrating gyro with dry friction, mounted on oscillating base 09 p1379 A66-20307

Book on dynamic and static balancing of rotating machine parts and devices, particularly gyroscopes, noting effect on bearings, vibration causes, etc 09 p1383 A66-20915

Spin axis orientation of spherical free gyroscope determined by using phosphorescent coating on rotor 10 p1536 A66-21861

Operational characteristics of LC tuned solid state static inverter used as power supply in autopilot gyros of Titan rockets, noting power oscillator circuit 12 p1804 A66-24661

Inertial gyroscope and accelerometer design and components 13 p2076 A66-25127

Orion Inertial Navigation System, detailing accelerometers, gyroscopes, computers, components, maintenance, operation, etc 13 p2125 A66-26575

Motion of gyroscope with variable moments of inertia on movable base, deriving motion equations 14 p2291 A66-27165

Nonlinear gyroscopic system equations solved by analog computer and verified through method of harmonic linearization 14 p2294 A66-27362

Gyroscopic device design for determining integral direction of aerodynamic moment vector, noting system and block diagrams 14 p2294 A66-27365

Theory of aircraft measurement of gravity using gyroplatform, ideal gimbal suspension and three orthogonal string sensors, deriving formula for unperturbed gravity value, discussing perturbation measurement errors 15 p2483 A66-28666

Free gyroscope motion as affected by dry

friction and free and forced oscillation 15 p2541 A66-29101

Development of theory of gyrocompass, gyrohorizons and gyroverticals 15 p2502 A66-29101

Orbital rendezvous, stressing necessity measuring absolute angular velocity of line of sight connecting two vehicles, noting details on gyroscopes, coupling, optimization, etc 16 p2743 A66-30303

Sensor threshold definitions applied to gyros, comparing old and new AIA specifications, noting threshold definition, relation to flight control system malfunctions 16 p2708 A66-31401

Motion of gyroscope in gimbal suspension 17 p2958 A66-32606

Natural oscillation frequency of gyro mounted in torsional suspension, taking into account moments of inertia of sensitive element 17 p2926 A66-32606

Inertial navigation system theory that uses increased numbers of newtonometers for measuring devices/ in place of gyroscopic sensitive elements 17 p2926 A66-32606

Forced oscillations of gyroscopic tachometer with dry friction analyzed Zhelezov theorems 17 p2928 A66-33401

Gyrochamber radial rigidity effect amplitudes of forced oscillations gyroscope with dynamically unbalanced rotor 17 p2928 A66-33401

Slew plane technique for locating two gyro input axes without removing platform from test vehicle and with limited optical access 18 p3133 A66-34001

Optimum control theory applied shipboard inertial navigation systems with position and azimuth errors because gyroscope drift-rate fluctuations 20 p3595 A66-36689

Accelerated coincidence of gyro servocontrol system at discrete moments of time with values of target coordinates 20 p3597 A66-37395

V-gyro pair as dual-rate sensor, examining gimbal equations for gyros 21 p3736 A66-38989

Strapdown inertial sensor configuration based on time modulated torquing approach in gyro and accelerometer readout 21 p3764 A66-38989

Elimination of rate gyro angular acceleration error and scale factor sensitivity to wheel speed by integration output signal 21 p3767 A66-38989

Navigation gyroscopes design principles examining effects of friction in suspension system and other gyroscopic drift causes 22 p3917 A66-40677

Monograph on theory of gyroscopic instruments and devices 23 p4066 A66-41001

Magnetic field rapidly reversed in short superconducting coil by subjecting coil to increasing external reverse field 24 p4216 A66-42955

## GYROSCOPE FLOTATION

Floated inertial platform, gimballess attitude device utilizing floated sphere to isolate inertial components from acceleration and vibration environments 01 p0099 A66-10038

Float-cocking phenomenon in single-axis floated gyroscopes caused by impressing angular velocity on sensible radial compliance 01 p0068 A66-10038

Statistical characteristics of angular drift velocity of gyrostabilizer employing floated gyroscopes 01 p0068 A66-10038

Statistical characteristics of angular drift velocity of gyrostabilizer employing floated gyroscopes 11 p1705 A66-22401

Stable equilibrium position of axis of rotation of cylinder in rotating chamber filled with one or two liquids 17 p2928 A66-32606

Floating vibratory gyroscope having enhanced sensitivity to angular velocity 21 p3739 A66-39001

Analysis of perfect frictionless suspension of rotating body with two degrees of freedom mounted on rotating shaft of spin axis deflection [AIAA PAPER 65-435] 23 p4066 A66-41001

Gyroscopic dynamics for obliquity in gimbal axes noting free motion, nutation and drift rate 23 p4071 A66-41001



# GYROSCOPIC COUPLING

Elimination of coupling error between gyroscope and platform, considering rate-integrating gyros with inertial platform 09 p1382 A66-20563  
Circuit theory reciprocity theorem for dynamic linear systems with gyroscopic coupling for steady state response 12 p1912 A66-23611  
Combined effect of horizontal and vertical accelerations on gravimeter readings mounted on gyroplatform or in Cardan suspension 14 p2297 A66-28111  
Combined effect of horizontal and vertical accelerations on gravimeter readings mounted on gyroplatform or in Cardan suspension 24 p4212 A66-42699

# GYROSCOPIC DRIFT

Statistical characteristics of angular drift velocity of gyrostabilizer employing floating gyroscopes 01 p0068 A66-10710  
Preflight checking of aircraft gyroscopes and accelerometers noting built-in spin detection, torque generator and gimbal check 01 p0070 A66-10956  
Corrections for apparent drift rate of free ideal directional gyroscope due to Earth rotation 02 p0290 A66-11986  
Drift of free gyro with variable kinetic moment under constant overloads, noting gyro departure from initial position relative to inner and outer gimbal axes when gravity center shifts along axis 09 p1379 A66-20305  
Statistical characteristics of angular drift velocity of gyrostabilizer employing floating gyroscopes 11 p1705 A66-22625  
Effect of small periodic moment applied to axis of inner gimbal on gyro drift when gyro is mounted on base fluctuating about two mutually perpendicular axes 13 p2082 A66-26458  
Gyro drifts in Cardan suspension with mobile base, determining angle of rotation 17 p2926 A66-32798  
Inertial navigation system performance and self-test capability, noting errors from gyro drift 17 p2954 A66-33217  
Inertial sensor performance degradation in strapped-down environment, noting gyro drift error and accelerometer bias 21 p3763 A66-38839  
Spacecraft attitude reference system using passive temperature control device and four gyros in skewed position 21 p3764 A66-38853  
Inertial platform test station for shipboard maintenance and calibration of platform used in A6A and E2A aircraft, examining accelerometer bias and gyro drift tests 21 p3723 A66-38889  
Astatic gyroscope in rotating Cardan suspension and drifts due to angular oscillations of base 21 p3737 A66-38969  
Effect of random fluctuations of voltage and frequency of gyrorotor feed current on change in rotor angular velocity, noting gyro drift 21 p3738 A66-38970  
Effect of vibration of base on indications of gyrocompass extended to include LF sinusoidal displacements of base corresponding to rocking motion, noting free play effect, gyro drift and vertical moment 21 p3738 A66-38989  
First-order Markovian gyro drift numerically evaluated and square root plotted vs interval and gyro correlation time 23 p4068 A66-41318  
Free and forced vibration effect on drift of gyroscope supported in gimbals 23 p4071 A66-41981

# GYROSCOPIC PENDULUM

Nonperturbability of direction of axis of gyropendulum toward center of attraction with respect to motion of bearing point 07 p1031 A66-17407  
Oscillatory motion of pendulum-gyroscope system near given position of relative stability 07 p1035 A66-18192

# GYROSCOPIC STABILITY

Motion stability of gyroscopic and physical pendulums on unstable base 01 p0067 A66-10459  
Inertial system using gyros and accelerometers, determining autonomously plant curvilinear coordinates and plant space orientation parameter 02 p0260 A66-12168  
Three-phase supply stable in amplitude and frequency as wheel power supply for inertial quality gyroscope 03 p0340 A66-12494

Control problems associated with stable platforms using single-axis integrating gyroscopes including axes design, drift due to vibration and compensation 03 p0390 A66-12533  
High stability control circuit operating tuning fork in constant amplitude self-excitation circuit, using mechanical oscillator excited by fundamental wave of amplified feedback voltage 03 p0371 A66-13243  
Stability of 3-axis stabilizing platform as function of distribution of gyro units 04 p0518 A66-13568  
Stability of two-rotor gyrocompass with properties differing from those of Geckeler-Anschutz compass 04 p0518 A66-13569  
Two-gyro platforms are less stable than single-gyro platforms 06 p0879 A66-16344  
Elastic properties of bearing elements of gyrotachometer and effect on frequency of oscillations 07 p1031 A66-17409  
Harmful oscillation elimination from high rpm gyroscopic centrifuge by introducing one elastic bearing into dynamic system 08 p1307 A66-18877  
Motion stability of gyroscope in universal suspension with spring restraints and damper in gravitational field extended to include Newtonian central force field 08 p1226 A66-19582  
Equations of motion of gyrostabilizer having fixed point and gyrostabilizer rotating about fixed point in Newtonian force field 08 p1227 A66-19761  
Necessary conditions for existence of univalent integrals in equations of motion of heavy gyrostabilizer fixed at one point 08 p1227 A66-19762  
Two-gyro platforms are less stable than single-gyro platforms 11 p1704 A66-22341  
Satellite providing optimum communications to military users, noting gyroscopic stabilization of antennas, major characteristics, etc [ATAA PAPER 66-267] 12 p1955 A66-24740  
Orbit precession effect on gyroscopic stabilization of satellite in geomagnetic field 14 p2391 A66-27473  
Motion equations and simulation of spin-stabilized interplanetary spacecraft closed-loop pitch control system, using low-thrust gas jet torquers with rate gyro sensors 14 p2392 A66-27881  
Spin angular velocity stability of gyroscope with incompressible fluid-filled cavity as function of three degrees of freedom 14 p2277 A66-28051  
Routh theorem describing motion stability of holonomic systems applied to nonholonomic systems, specifically Bobylov spherical gyroscope 14 p2297 A66-28062  
Gyroscope motion on randomly shifting support described by linear inhomogeneous differential equation 14 p2297 A66-28064  
Gyroscopic stabilization of relative equilibrium of satellite 15 p2605 A66-28489  
Dissipative gyroscopic force effects on mechanical system, noting necessary and sufficient conditions for stability and controllability 15 p2537 A66-28949  
Oscillations, gyroscopes, theory of mechanisms, fluid and gas mechanics - All-Union Conference, Moscow, January-February 1964 15 p2540 A66-29160  
Gyroscopic system motion under random forces effect 15 p2541 A66-29172  
Stability of gyroscopes, gyrostabilizers and gyroscopic systems treated by methods of Liapunov and Chetaev 15 p2542 A66-29173  
Relativistic precession measurement using satellite as precise orbiting gyroscope [ATAA PAPER 65-36] 17 p3001 A66-32450  
Gyroscopic rotor vibrations excited by effect of lubrication layer in sliding bearings and stabilized with intervening elastodamping supports, taking into account moment of inertia of rotor 17 p3027 A66-32605  
Stability of gyrocompass investigated by linear mechanics methods 17 p2958 A66-32606  
Rotational motion analysis, considering two distinct laws governing behavior of spinning body and obtaining total motion by superposition of vectorial movements due to laws 18 p3134 A66-33588  
Twin-gyro system for satellite stabilization, eliminating disruptive cross-coupling effects

and changing gyro speed without distributing satellite attitude 19 p3468 A66-35628  
Control moment gyroscope for angular momentum transfer with minimum power consumption, noting design and application for free body motion stabilization 19 p3360 A66-35962  
Motion of arbitrary gyrostabilizer in central Newtonian force field, applying Liapunov stability conditions for regular precession 19 p3362 A66-36841  
Semipassive two-gyroscope damper for countering high angular rates of Earth-pointing satellites 20 p3659 A66-36868  
Gyro and accelerometer errors in ternary torqued inertial components mounted on surface to surface missile, noting angular vibration environment 21 p3764 A66-38848  
Motion stability of version of Cardan suspension gyro 21 p3738 A66-38988  
Friction and imbalance moments relative to gimbal axes and effects on gyrovertical motion under starting conditions 21 p3739 A66-39325  
Gyro in Cardan suspension, discussing stability criteria for rotations about largest or smallest moment of inertia 22 p3947 A66-39695  
Conservative systems motion stability, generalizing precession and nutation of gyroscope with respect to noncyclic coordinate 22 p3948 A66-40681  
Inertial measurement unit and pulse torquing of Apollo spacecraft, noting components and operation [AGARDOGRAPH 105] 24 p4215 A66-43126  
**GYROTROPIC MEDIUM**  
Gyrotropic properties in simple and canted two-sublattice antiferromagnetics in small static magnetic field 01 p0122 A66-10569  
Nanosecond electromagnetic pulse dispersion in longitudinally magnetized plasma confined in coaxial transmission line 06 p0826 A66-16026  
Oblique incidence on plane boundary between two general gyrotropic plasma media, evaluating reflection and transmission coefficients 06 p0913 A66-16132  
Coupled wave equation for homogeneous gyrotropic compressible warm plasma derived, using partial differential equations 14 p2340 A66-27037  
Wave equation for inhomogeneous isotropic hot plasma 14 p2340 A66-27044  
Magnetoionic couplings and electromagnetic wave propagation in horizontally stratified layer of gyrotropic medium 14 p2283 A66-27125  
Passage of normal plane electromagnetic wave through bi-gyrotropic plate, examining transmission and reflection components 22 p3862 A66-39828

# H

# H-ALPHA LINE

Ratio of average transmission coefficients of L-beta and H-alpha and reabsorption in hydrogen pulsed discharge 01 p0111 A66-10390  
Spicules of solar chromospheric disk identified in H-alpha line 02 p0292 A66-12190  
Fabry-Perot fine etalon in astronomical use such as H-alpha emission line profile measurement 05 p0681 A66-15213  
H-alpha double limb observed in spectroheliograms is instrumental and not solar phenomenon 09 p1455 A66-20404  
Hydrogen-alpha solar limb patrol providing photographic record of observable prominences 11 p1776 A66-23427  
Photometric measurements of solar flares and prominences for central intensities in hydrogen alpha 16 p2804 A66-31397  
Flare observations in H-alpha line, line and continuous spectra of flares, and optical characteristics of proton flares 17 p2993 A66-32364  
Grid computations of model atmospheres for A-type stars, considering effects of Balmer-line blanketing 18 p3227 A66-33762  
Diffusion emission of solar prominences in hydrogen alpha Balmer line, noting luminescence due to resonance scattering of solar emission 23 p4126 A66-41073



## H-BETA LINE

Electron concentration in AC carbon arc determined from H-beta linewidth 11 p1748 A66-23416  
 Reproduction of experimental and calculation of theoretical H-beta emission profile of solar flare, considering macroscopic motions inside flare 16 p2795 A66-31391

## H-WAVE

Electromagnetic H-wave propagation of given frequency along plasma sheet surrounded by vacuum 01 p0030 A66-10697  
 Elliptical waveguide for H-11 modes transmittance, expressed as power transmission along waveguide and square of electric field maximum value 02 p0196 A66-11417  
 Propagation in anisotropic radially stratified circular waveguides 08 p1198 A66-19749  
 Coefficient of reflection of H-11 mode shock wave emitted from aperture of circular waveguide with infinite flange 09 p1344 A66-20347  
 Reflection factors and wave amplitudes of diffraction spectra for incidence of H-p, 0 waves onto inductive obstacles in rectangular waveguides 09 p1358 A66-20808  
 Eigenvalues and dispersion equations for magnetic and electric symmetric waves in circular multislot waveguides 09 p1358 A66-20809  
 Charged particle radial distribution determination as function of amplitude of HF magnetic field, using diffusion in discharge induced by HF traveling H-wave 10 p1570 A66-21998  
 Electromagnetic H-wave propagation of given frequency along plasma sheet surrounded by vacuum 11 p1658 A66-23299  
 Ferrite controlled polarization of slot radiator by rectangular waveguide excited by H10 wave 14 p2252 A66-27252  
 H-plane bifurcation of parallel plate waveguide filled with anisotropic plasma 15 p2457 A66-28597  
 Reflection of aperiodically damped H-01 and E-01 waves of tapered waveguide used in Vernier autotracking 15 p2467 A66-29764  
 Slot filters for H waves in circular waveguide 17 p2879 A66-31863  
 Charged particle radial distribution determination as function of amplitude of HF magnetic field, using diffusion in discharge induced by HF traveling H-wave 18 p3151 A66-34975  
 H-type surface wave propagation in rectangular waveguide having wall consisting of transversely magnetized ferrite plate 19 p3313 A66-35456

## HAFNIUM

Hall effect on hafnium paramagnetic susceptibility at room and cryogenic temperature 05 p0699 A66-14687  
 Extension of electron gas model to transition metals /titanium, zirconium, hafnium/, considering atom interaction up to fourth neighbor 10 p1548 A66-21664  
 Depressing effect of hafnium and zirconium on work function of tungsten, tantalum, niobium and rhenium 14 p2314 A66-27369  
 Oxidation of powdered titanium, zirconium, hafnium, vanadium, niobium and tantalum 16 p2724 A66-31355

## HAFNIUM ALLOY

Decrease in work function of W-Hf system caused by formation of alloy with better emission properties than those of hafnium 02 p0270 A66-11425  
 High temperature oxidation-resistant hafnium tantalum alloys, noting phase composition 14 p2315 A66-27501

## HAFNIUM CARBIDE

X-ray measurements of thermal expansion of arc-cast carbides of titanium, zirconium and hafnium 03 p0381 A66-12636

## HALF-PLANE

Energy propagation lines in diffraction of vertically polarized electromagnetic wave by conducting half-plane shield 14 p2241 A66-27939  
 Diffraction by conducting half-plane in plasma 17 p2876 A66-33427

## HALF-SPACE

Five-year measurements of circumglobal radiation and of short wave radiation from

lateral half-spaces 02 p0220 A66-11258  
 Poisson pseudokernel and pseudodifferential operators on manifold with boundary 05 p0708 A66-15093  
 Reducing values of potential magnetic or gravitational field observed on Earth surface with weak profile to values on single horizontal plane in lower half-space 06 p0876 A66-16417  
 Shock wave propagation in lower half-space filled with compressible fluid 07 p1026 A66-18256  
 Dynamic problems of transversely isotropic half-space and elastic layer, solving contact and boundary value problems 08 p1315 A66-19708  
 Nonseparated flow of finite conductivity fluid past half-body with flow branching 13 p2067 A66-26534  
 Unique absolutely continuous extensions of strict solutions to first-order nonlinear partial differential equations, satisfying these equations at almost all points of half-space 15 p2527 A66-29060  
 Viscoelastic half-space problems with noncommutative operators including solution for equilibrium equation 22 p3989 A66-39821  
 Axisymmetric problems of heat conductivity theory for layer with one constant boundary and one circular boundary solved by paired integral equations method 22 p4000 A66-40571

## HALIDE

SA ALKALI HALIDE  
 SA BROMIDE  
 SA CHLORIDE  
 SA FLUORIDE  
 SA IODIDE  
 SA METAL HALIDE  
 SA OXYHALIDE  
 CW IR laser oscillation in HBr and HI gas discharge 06 p0892 A66-16756  
 Corrosion mechanism for eutectic or near-eutectic Mg-Zn alloys in halide solution 13 p2110 A66-26026  
 Emission spectroscopy of halides of carbon, silicon and boron in plasma reactor 16 p2763 A66-31190  
 Halides used as burning rate depressants on combustion stability of polyurethane/ammonium perchlorate base propellants, examining acoustic instability 23 p4119 A66-41435

## HALL ACCELERATOR

Faraday type MHD accelerator with series connected electrodes investigated by employing external jumpers 03 p0399 A66-12808  
 Variation of electron temperature and number density, ion current density and plasma potential through low density Hall current ion accelerator as function of magnetic field strength [AIAA PAPER 66-76] 08 p1262 A66-18994  
 Varying instability frequency in simulated arc jet-Hall accelerator [AIAA PAPER 66-156] 10 p1559 A66-21422  
 Langmuir probe velocity and acceleration measurements for coaxial Hall accelerators [AIAA PAPER 66-196] 10 p1562 A66-21441  
 Performance capabilities of Hall current accelerators determined from parameters influencing anode power loss [AIAA PAPER 66-201] 10 p1563 A66-21443  
 Effect of mass entrainment from vacuum tank and electrode erosion on plasma velocity determined from mass flow and thrust of Hall accelerator [AIAA PAPER 65-297] 18 p3147 A66-34585  
 High performance annular Hall-current accelerator using radial magnetic field and axial electric field with cesium as propellant [AIAA PAPER 65-300] 19 p3450 A66-35614

## HALL EFFECT

Van der Pauw method for measuring resistivity, Hall mobility and thickness of thin metallic film under vacuum, considering copper films 01 p0119 A66-10393  
 Temperature dependence of electric conductivity and Hall effect of single crystal cadmium tin arsenide 01 p0126 A66-11026  
 Plasma flow described by dimensionless similarity parameter characterized by relative independence of ion and electron components 01 p0116 A66-11191  
 N-type conductive cadmium selenide single crystals investigated for heat treatment and Hall effects in selenium

vapor 01 p0127 A66-111  
 Hall currents effect during acceleration plasma intrinsic magnetic field 02 p0264 A66-113  
 Electrical resistivity, Hall effect a magnetoresistance of bismuth antimony single crystal solid solutions 02 p0272 A66-117  
 Electrical conductivity, Hall effect a thermoelectric power as function temperature in CdSb single crystals strongly doped with silver 02 p0275 A66-118  
 Temperature dependence of surface conductivity and Hall effect in germanium alloyed with gold 02 p0276 A66-120  
 Motion of vortex lines in superconductors noting dissipation and viscosity, Hall effect and effective mass 03 p0411 A66-131  
 AC technique for Hall effect measurements in low mobility semiconductor 03 p0371 A66-132  
 Hall effect in thin polycrystalline evaporated bismuth films obtained sublimation under very hard vacuum 04 p0567 A66-143  
 Hall effect of bismuth evaporated film discussing structural dependence of sign a magnitude, effects of pathlength, impurity, gas adsorption and experimental techniques 05 p0729 A66-145  
 Hall effect on hafnium paramagnetic susceptibility at room and cryogenic temperature 05 p0699 A66-146  
 Radiation damage of p-type silicon investigated by Hall effect, noting dislocation density and annealing behavior 05 p0735 A66-148  
 Optimum electrode arrangement in MIM channel, taking into account Hall effect 05 p0722 A66-145  
 Boundary layer solutions for Rayleigh problem in MGD with Hall effect, using Karman-Pohlhausen technique 05 p0728 A66-157  
 Electron drift velocity and mobility in indium antimonide obtained from pulse measurements of conductivity and Hall effect at various temperatures 06 p0922 A66-161  
 Hall effect and conductivity measurements of carrier removal rate in oriented specimens of n-type Si under electron irradiation at energies from 0.3 to 1.0 mev 06 p0930 A66-170  
 Current oscillations accompanied by mobility regions in high resistance gallium arsenide subjected to electric field, measurement of Hall effect shows these regions are of high resistance 06 p0930 A66-170  
 Radiation damage in nondegenerate germanium at low temperatures, using Hall carrier technique for measuring resistivity and Hall coefficient on antimonide dopants 06 p0932 A66-171  
 Hall effect and resistivity measurements on high resistance n-silicon related formation conditions at low temperature level placed at 160 mev from conductivity band 06 p0935 A66-171  
 Longitudinal and transverse voltages superconductors, noting Hall effect, resistivity and functional relation to applied magnetic field 06 p0940 A66-171  
 Electron energy levels in CdS single crystals from Hall effect, conductivity and space-charge-limited current measurements 07 p1098 A66-177  
 Hall constant of semiconductors noting dependence on specimen size, film area, current electrode parameters 07 p1100 A66-179  
 Hall current and Hall drift velocity single crystal indium antimonide under electric and magnetic field 07 p1103 A66-182  
 Open circuit voltage, inner resistance, Hall voltage and tensorial conductivity of Faraday generator, using conformal mapping for single pair of electrodes 07 p0993 A66-183  
 Hall effect in two-dimensional flow conducting gas interacting with external inhomogeneous magnetic field along insulating plane 08 p1205 A66-185  
 Galvanomagnetic effects in semiconductor including Hall effect and magnetoresistivity noting influence of carrier scattering lattice vibrations and



- impurities 08 p1267 A66-18607
- Power characteristics of linear 08 p1267 A66-18607
- Axisymmetric flow of ideal incompressible 08 p1267 A66-18607
- conducting gas with Hall effect in two- 08 p1267 A66-18607
- component magnetic field 08 p1168 A66-18863
- Electron spin effect on quantum 08 p1267 A66-18607
- oscillations of magnetoresistance and Hall 08 p1267 A66-18607
- effect in n-InSb single 08 p1267 A66-18607
- crystal 08 p1269 A66-18971
- Lorentz force maximization in continuous- 08 p1269 A66-18971
- flow Hall current plasma accelerators, using 08 p1269 A66-18971
- other axial electric field and radial 08 p1269 A66-18971
- magnetic field or radial electric field and 08 p1269 A66-18971
- lanted magnetic field 08 p1263 A66-19154
- Hall effect measured by splitting 08 p1263 A66-19154
- alternating voltage produced in Hall circuit 08 p1263 A66-19154
- into two components, one with phase 08 p1263 A66-19154
- inciding with Hall emf and other with 08 p1263 A66-19154
- phase departing by 90 08 p1263 A66-19154
- degrees 08 p1273 A66-19289
- Hall effect B-H loop recorder for thin 08 p1273 A66-19289
- magnetic films 08 p1224 A66-19297
- P-type cadmium tin arsenide crystals, 08 p1224 A66-19297
- plotting temperature dependences of 08 p1224 A66-19297
- specific electroconductivity, Hall coefficient 08 p1224 A66-19297
- and thermal electromotive 08 p1224 A66-19297
- force 08 p1277 A66-19622
- Computation and measurement of Hall 08 p1277 A66-19622
- potentials and flow field perturbations in 08 p1277 A66-19622
- GD flow of axisymmetric free 08 p1277 A66-19622
- jet 08 p1266 A66-19815
- Hall effect, thermal emf and electrical 08 p1266 A66-19815
- conductivity of SmS in temperature range 08 p1266 A66-19815
- 00 to 1000 degrees K 09 p1412 A66-19988
- Tin telluride electric properties analysis 09 p1412 A66-19988
- for verifying semiconductor model with two 09 p1412 A66-19988
- valence bands in connection with Hall effect 09 p1412 A66-19988
- dependence on 09 p1412 A66-19988
- temperature 09 p1412 A66-19988
- Dark electric conductivity, Hall effect and 09 p1412 A66-19988
- thermally stimulated currents in gallium 09 p1412 A66-19988
- arsenide single crystals 09 p1413 A66-19998
- Hall effect in germanium telluride samples 09 p1413 A66-19998
- with various current carrier concentrations 09 p1413 A66-19998
- at temperatures up to 500 degrees 09 p1413 A66-19998
- 09 p1413 A66-20000
- Current density distribution in MPD arc 09 p1413 A66-20000
- jet exhaust measured, using Hall effect 09 p1413 A66-20000
- sensors 09 p1433 A66-20089
- AIAA PAPER 66-116] 09 p1433 A66-20089
- Stationary nonviscous plane flow of 09 p1433 A66-20089
- conducting plasma in narrow channel subject 09 p1433 A66-20089
- to transverse magnetic field and Hall effect, 09 p1433 A66-20089
- using sectionized electrodes, noting 09 p1433 A66-20089
- boundary layer near 09 p1407 A66-20135
- mode 09 p1407 A66-20135
- Effective mass of electrons in n-type 09 p1407 A66-20135
- gallium arsenide deduced from 09 p1407 A66-20135
- measurements of Hall coefficient and 09 p1428 A66-20197
- thermoelectric power 09 p1428 A66-20197
- Specific conductivity, Hall, Nernst- 09 p1428 A66-20197
- Thomson and other transfer effects in 09 p1428 A66-20197
- InAs-CdTe and InAs-ZnTe 09 p1428 A66-20197
- alloys 09 p1428 A66-20539
- Palladium-silver and palladium-rhodium 09 p1428 A66-20539
- films electrical resistance, Hall effect and 09 p1428 A66-20539
- Nernst effect as affected by 09 p1389 A66-20805
- temperature 09 p1389 A66-20805
- Electron Hall mobility from 4 to 300 09 p1389 A66-20805
- degrees K with undoped single crystals of 09 p1389 A66-20805
- GaAs grown in quartz boats by Bridgman 09 p1389 A66-20805
- method and zone-melting 09 p1389 A66-20805
- technique 09 p1430 A66-20848
- n-type germanium electric conductivity 09 p1430 A66-20848
- dependence on applied electric and 09 p1430 A66-20848
- magnetic field 09 p1430 A66-20857
- Direct-indirect transition effect on Hall 09 p1430 A66-20857
- effect in gallium /arsenic 09 p1430 A66-20857
- phosphide/ 10 p1543 A66-21570
- Hall effect in alloyed crystals of n-type 10 p1543 A66-21570
- indium antimonide 10 p1589 A66-22165
- Transverse galvanomagnetic effect in 10 p1589 A66-22165
- angle-domain ferromagnetic film, noting 10 p1589 A66-22165
- able of Hall effect 10 p1589 A66-22165
- equation 11 p1752 A66-22801
- Current dependence of resistivity and 11 p1752 A66-22801
- mobility measured in silicon epitaxial layers 11 p1752 A66-22801
- in control wafer 11 p1756 A66-23021
- Quantum mechanical formula for low-field 11 p1756 A66-23021
- Hall effect in density matrix approach, 11 p1756 A66-23021
- treating this effect in disordered 11 p1756 A66-23021
- systems 12 p1927 A66-23723
- Jump conductivity of lightly doped p- 12 p1927 A66-23723
- ermanium single crystals, noting Hall 12 p1927 A66-23723
- coefficient temperature dependence and 12 p1927 A66-23723
- specific resistance with low donor and 12 p1927 A66-23723
- acceptor concentrations 12 p1927 A66-23723
- Hall effect and galvanic magnetoresistance 12 p1927 A66-23723
- measurements in single crystal /mercuric 12 p1927 A66-23723
- manganese/ telluride solid 12 p1927 A66-23723
- solutions 12 p1927 A66-23723
- Plasma flow described by dimensionless 12 p1927 A66-23723
- similarity parameter characterized by 12 p1927 A66-23723
- relative independence of ion and electron 12 p1927 A66-23723
- components 12 p1920 A66-24012
- Spectral equations of homogeneous MHD 12 p1920 A66-24012
- turbulence in strong uniform magnetic field 12 p1920 A66-24012
- in presence of Hall effect 12 p1924 A66-24807
- Hall reversal at negative resistance in 12 p1924 A66-24807
- forward biased p-Ge point contact 12 p1924 A66-24807
- diode 13 p2029 A66-25192
- Temperature dependence on Hall effect of 13 p2029 A66-25192
- thin iron layers 13 p2162 A66-25412
- Hall mobility and Hall constant variation 13 p2162 A66-25412
- for lead telluride-tin telluride polycrystals at 13 p2162 A66-25412
- high temperatures 13 p2163 A66-25419
- Magnetic semiconductor efficiency 13 p2163 A66-25419
- determined from product of majority carrier 13 p2163 A66-25419
- mobility and effective magnetic 13 p2163 A66-25419
- permeability 13 p2163 A66-25420
- MHD instability in plasmas during pinch 13 p2163 A66-25420
- discharge, noting wave velocity dependence 13 p2163 A66-25420
- on Larmor radius, Hall effect, electron 13 p2163 A66-25420
- temperature fluctuations, 13 p2163 A66-25420
- etc 13 p2142 A66-25704
- Electrode size effects on performance of 13 p2142 A66-25704
- infinitely long MHD power generation duct 13 p2142 A66-25704
- calculated by conformal mapping, analyzing 13 p2142 A66-25704
- gas Hall parameter, electrode-insulator 13 p2142 A66-25704
- length ratio, etc 13 p2000 A66-25735
- Longitudinal Hall effect for two-band 13 p2000 A66-25735
- conduction and tensor relaxation times in 13 p2000 A66-25735
- cubic crystals 14 p2363 A66-27577
- Temperature dependence of Hall effect 14 p2363 A66-27577
- and conductivity of lead telluride single 14 p2363 A66-27577
- crystals containing 14 p2364 A66-27645
- bismuth 14 p2364 A66-27645
- Temperature-dependence of electric 14 p2364 A66-27645
- conductivity and Hall coefficient in 14 p2364 A66-27645
- semiconductors 14 p2364 A66-27730
- Electroconductivity, Seebeck effect and 14 p2364 A66-27730
- charge carrier mobility in Li-doped 14 p2364 A66-27730
- NiO 14 p2366 A66-27766
- Basic equations and methods for transverse 14 p2366 A66-27766
- MHD flow analysis when Hall currents are 14 p2366 A66-27766
- not suppressed, noting set of suitable 14 p2366 A66-27766
- simplifications, restrictive conditions and 14 p2366 A66-27766
- boundary value 14 p2346 A66-28301
- considerations 14 p2346 A66-28301
- Hall coefficient increase with temperature 14 p2346 A66-28301
- and electron transition to second conduction 14 p2346 A66-28301
- band in InSb 15 p2558 A66-28614
- Plastic deformation effect on resistivity 15 p2558 A66-28614
- and Hall constant of silver-palladium alloys, 15 p2558 A66-28614
- noting decreasing rate of change for 15 p2558 A66-28614
- increasing strain 15 p2560 A66-28648
- Temperature dependence of Hall emf and 15 p2560 A66-28648
- electrical resistance of Sendust type Fe-Si- 15 p2560 A66-28648
- Al alloys 15 p2560 A66-28678
- Anisotropy and annealing behavior in 15 p2560 A66-28678
- extrinsic single-crystal tellurium studied by 15 p2560 A66-28678
- measuring electric resistivity and Hall 15 p2560 A66-28678
- coefficient 15 p2562 A66-28725
- Hall coefficient and mobility in thin 15 p2562 A66-28725
- evaporated gold films on glass 15 p2562 A66-28725
- substrates 15 p2563 A66-28733
- Pure selenium conductivity, thermal emf 15 p2563 A66-28733
- and Hall effect 15 p2563 A66-28737
- One-dimensional flow through nozzle and 15 p2563 A66-28737
- stability of weakly ionized plasma with 15 p2563 A66-28737
- induced Hall current 15 p2550 A66-28958
- Plasma frequency measurement based on 15 p2550 A66-28958
- Hall effect proportional to electron 15 p2550 A66-28958
- concentration 15 p2453 A66-29931
- Peltier effect analogy of heat absorption 15 p2453 A66-29931
- and emission at junction in superconductor 15 p2453 A66-29931
- between region in flux-flow state and region 15 p2453 A66-29931
- with no flux flow 16 p2769 A66-30154
- Intermodulation effect on measurement of 16 p2769 A66-30154
- small Hall coefficients with double AC 16 p2769 A66-30154
- method 16 p2702 A66-30424
- Planar Hall /galvanomagnetic/ effect in 16 p2702 A66-30424
- thin iron or nickel ferromagnetic 16 p2702 A66-30424
- films 16 p2773 A66-30684
- Planar Hall effect used to determine 16 p2773 A66-30684
- magnetic properties of ferromagnetic films 16 p2773 A66-30684
- such as anisotropy field and coercive 16 p2773 A66-30684
- force 16 p2773 A66-30685
- Direct measurement procedure for Hall 16 p2773 A66-30685
- emf semiconductor samples of circular 16 p2773 A66-30685
- shape 16 p2777 A66-30868
- Hall constant of semiconductor films 16 p2777 A66-30868
- deposited on electrically conducting 16 p2777 A66-30868
- substrates calculated by formula derived 16 p2777 A66-30868
- from Konkov phenomenological 16 p2777 A66-30868
- theory 16 p2777 A66-30869
- Hall effect and resistivity of Zn doped 16 p2777 A66-30869
- GaAs 16 p2778 A66-31069
- Ohm law for nonisothermal plasma, 16 p2778 A66-31069
- considering thermal diffusion forces, 16 p2778 A66-31069
- obtaining expressions for electric 16 p2778 A66-31069
- conductivity and Hall 16 p2778 A66-31069
- coefficient 16 p2761 A66-31085
- Thickness of gold, silver and copper thin 16 p2761 A66-31085
- films determined, using measurements of 16 p2761 A66-31085
- resistance and Hall 16 p2761 A66-31085
- voltage 16 p2780 A66-31096
- Hall effect application - MIT Conference, 16 p2780 A66-31096
- Cambridge, November 16 p2780 A66-31096
- 1965 16 p2785 A66-31571
- Hall effect and related phenomena, noting 16 p2785 A66-31571
- magnetic-temperature-impurity 16 p2785 A66-31571
- effect 16 p2785 A66-31572
- Gain-bandwidth product of Hall magnetic 16 p2785 A66-31572
- amplifier circuits design 16 p2866 A66-31573
- Hall devices and multipliers, characteristics 16 p2866 A66-31573
- and types 16 p2866 A66-31574
- Hall effect of homogeneous semiconductors 16 p2866 A66-31574
- in nonuniform magnetic fields and of thin 16 p2866 A66-31574
- inhomogeneous films in uniform 16 p2866 A66-31574
- field 16 p2866 A66-31576
- Angular transducer using Hall effect, 16 p2866 A66-31576
- noting errors due to distortions in magnetic 16 p2866 A66-31576
- circuit and temperature 16 p2866 A66-31576
- effects 16 p2709 A66-31577
- Feedback-free Hall effect transducers for 16 p2709 A66-31577
- mechanical displacement 16 p2709 A66-31577
- measurement 16 p2709 A66-31578
- Hall effect multiplier for noise 16 p2709 A66-31578
- measurement, generation of single sideband 16 p2709 A66-31578
- and phase-modulated signals, 16 p2709 A66-31578
- etc 16 p2866 A66-31579
- Static errors in Hall effect multiplying 16 p2866 A66-31579
- devices 16 p2867 A66-31580
- Hall voltages in silicon obtained by 16 p2867 A66-31580
- combining MOS transistor structure with 16 p2867 A66-31580
- Hall effect of material, noting experimental 16 p2867 A66-31580
- results, design criteria, 16 p2867 A66-31580
- etc 16 p2867 A66-31581
- MHD wave propagation emphasizing 16 p2867 A66-31581
- viscosity, heat and electrical conductivity, 16 p2867 A66-31581
- Hall current, no nonequilibrium phenomena 16 p2867 A66-31581
- and effect of medium 16 p2867 A66-31581
- inhomogeneity 16 p2766 A66-31583
- Photo-Hall effect and photoconductivity on 16 p2766 A66-31583
- compensated p-InSb at low temperatures, 16 p2766 A66-31583
- examining temperature dependence of 16 p2766 A66-31583
- carrier mobility 16 p2788 A66-31773
- Peculiarities of Hall curves of n-type alpha 16 p2788 A66-31773
- silicon carbide, noting concentration of 16 p2788 A66-31773
- conduction electrons related to 16 p2788 A66-31773
- temperature 16 p2789 A66-31789
- Energy levels in forbidden band of gallium 16 p2789 A66-31789
- arsenide alloyed with silver or gold, 16 p2789 A66-31789
- determining impurity levels from 16 p2789 A66-31789
- temperature dependence of electric 16 p2789 A66-31789
- conductivity and Hall 16 p2789 A66-31789
- constant 16 p2789 A66-31791
- Electrical conductivity and Hall mobility of 16 p2789 A66-31791
- p- and n-type semiconductors at various 16 p2789 A66-31791
- temperatures 17 p2975 A66-31900
- Longitudinal Hall effect in n-type 17 p2975 A66-31900
- germanium measured on basis of anisotropic 17 p2975 A66-31900
- scattering theory, taking into account tensor 17 p2975 A66-31900
- character 17 p2976 A66-32260
- Steady state structure of MHD shock 17 p2976 A66-32260
- waves, taking Hall current effect into 17 p2976 A66-32260
- account 17 p2965 A66-32419
- Hall current effect on capillary instability 17 p2965 A66-32419
- of finitely conducting liquid jet carrying 17 p2965 A66-32419
- axial volume current 17 p2908 A66-32432
- Hall effect in collision dominated gaseous 17 p2908 A66-32432
- plasma immersed in uniform magnetic 17 p2908 A66-32432
- field 17 p2969 A66-32629
- Longitudinal Faraday emf, thermoelectric 17 p2969 A66-32629
- and Hall effects on channel flow of ionized 17 p2969 A66-32629
- gas 17 p2972 A66-32868
- Geometric, gasdynamic and electromagnetic 17 p2972 A66-32868
- parameters of one-dimensional flow of 17 p2972 A66-32868
- conducting gas with Hall effect for 17 p2972 A66-32868
- maximum power tapping from channel 17 p2972 A66-32868
- electrodes 17 p2972 A66-32869
- P-type cadmium tin arsenide crystals, 17 p2984 A66-33136
- plotting temperature dependences of 17 p2984 A66-33136
- specific electroconductivity, Hall coefficient 17 p2984 A66-33136
- and thermal electromotive 17 p2984 A66-33136
- force 17 p2984 A66-33136
- Gold and silver doping effect on Hall 17 p2984 A66-33136
- effect, electroconductivity thermal emf and 17 p2984 A66-33136
- conductivity of CdSb 17 p2984 A66-33145
- Uniaxial compression and hydrostatic 17 p2984 A66-33145
- pressure effect on piezoresistance and piezo- 17 p2984 A66-33145
- Hall effects in n- and p-type 17 p2984 A66-33145
- AlSb 17 p2984 A66-33153



Electron-hole conductivity effect on temperature variations of Hall coefficient and Nernst-Ettingshausen effect in semiconductor 17 p2986 A66-33309

Negative temperature coefficient of electrical resistance, anomalous Hall constant and magnetoresistance constant for thin films of Be and Pb 18 p3157 A66-34627

Galvanomagnetic effect in ferromagnetic metals, developing theory of planar Hall effect in terms of spin-orbit interaction of electrons 18 p3158 A66-34682

Optimum MHD generators using anisotropic plasma, discussing conducting-gas MHD flow, Hall effect, ion slip effect, etc 18 p3152 A66-35075

Quantum oscillations in magnetoresistance, Hall coefficient and thermoelectric power in strong transverse and longitudinal magnetic fields for n-InAs polycrystals at liquid helium temperature 19 p3438 A66-35479

Hall effect influence on steady hypersonic flow of inviscid compressible gas past wedge 19 p3275 A66-35736

Hall effect in alloyed crystals of n-type indium antimonide 19 p3441 A66-35779

Resonant frequency of helicon waves in indium, deriving high field Hall coefficient 19 p3445 A66-36331

Electrical resistance and Hall effect measurements in layer structures, confirming existence of interaction with optical relaxation vibration modes 19 p3446 A66-36343

Conductivity, temperature dependence, thermal emf Hall constant, thermal conductivity and resistivity of aluminides of transition metals 20 p3584 A66-37417

Dependence of Hall effect and conductivity of irradiated samples on reciprocal temperature in nuclear transmutations produced in InSb by bombardment with slow neutrons 20 p3617 A66-37485

Quantum oscillation of transverse and longitudinal magnetothermal emf in n-type indium antimonide compared with oscillations of transverse and longitudinal magnetoresistance and Hall coefficient 20 p3618 A66-37557

Phenomenological theory of longitudinal Hall effect in cubic crystals, assuming anisotropic dispersion law and tensorial relaxation time 20 p3618 A66-37560

Nonequilibrium ionization phenomena interaction with nonuniform flow of plasma, reviewing nonequilibrium characteristics for uniform flow with electric and magnetic fields 20 p3610 A66-37982

Two-dimensional problem of current distribution on surface of permeable electrodes adjacent to flow of conducting medium under Hall effect 20 p3611 A66-38110

Effective electron mass dependence on pressure in InSb determined by measuring electron concentration and thermal emf 20 p3624 A66-38427

Electron scattering mechanism in compensated gallium arsenide determined from Hall effect, Nernst-Ettingshausen effect and reluctance 21 p3798 A66-38914

Quantum oscillations of Hall effect and longitudinal and transverse reluctance in n-indium antimonide, noting spin splitting and temperature and electron concentration effect on oscillation maximum 21 p3799 A66-38924

Effective electron mass dependence on pressure in InSb determined by measuring electron concentration and thermal emf 21 p3800 A66-38960

N-type Ge hot carrier Hall mobility, magnetoresistance, Maxwellian energy distribution, electron-electron and intervalley electron-phonon collisions 21 p3801 A66-38997

Galvanomagnetic effects in p-type aluminum antimonide, discussing field dependence of Hall effect and magnetoresistance 21 p3801 A66-38999

Stationary nonviscous plane flow of conducting plasma in narrow channel subject to transverse magnetic field and Hall effect, using sectionized electrodes, noting boundary layer near anode 21 p3793 A66-39407

Resistivity and Hall coefficient of Sb doped Ge at He temperatures measured as function of magnetic field and temperature

to determine high field effects on impurity conduction 21 p3805 A66-39579

Hall effect in poly-n-vinylcarbazole-iodine charge-transfer complex, noting sign discrepancy of majority carrier 22 p3963 A66-40109

Rayleigh-Taylor instability of plasma is unaffected by inclusion of Hall current and electron-inertia terms in generalized Ohm law 22 p3956 A66-40420

Spatial distributions of carrier concentration and internal field in cadmium selenide for various voltages, measuring conductivity and Hall coefficient 23 p4112 A66-41292

Axial pressure asymmetry produced by Hall effect in linear pinch discharge 23 p4104 A66-41512

Steady fully developed MHD channel flow of viscous electrically conducting fluid studied by Galerkin method under applied magnetic and electric fields 23 p4107 A66-41886

Hall effect in MHD generator using partially ionized gas 23 p4108 A66-42031

Electron paramagnetic resonance and Hall effect measurements to determine properties of dominant paramagnetic defect in electron irradiated p-type silicon 24 p4250 A66-42230

Electrical properties of barium plumbate noting conductivity, Hall field, thermoelectromotive force, magnetization, etc 24 p4253 A66-42382

Temperature dependence of Hall coefficient and resistivity of n-type epitaxial gallium arsenide in 4.2 to 300 degree K temperature range 24 p4254 A66-42423

Hall coefficient, electrical conductivity and thermoelectric power of GaSb-Ga<sub>2</sub>Te<sub>3</sub> solid solutions as functions of composition and temperature 24 p4254 A66-42425

Plane laminar jet of incompressible conducting fluid propagating homogeneous magnetic field at magnetic Reynolds number 24 p4196 A66-42872

Hall effect influence on characteristics of MHD generator with two pairs of electrodes with symmetrical or crosswise connections 24 p4162 A66-42873

Pressure deformation of band structure of HgTe-CdTe alloys determined from measurements of Hall effect and resistivity 24 p4258 A66-43009

## HALL GENERATOR

Conducting gas flow in Hall MHD generator reduced to quasi-one-dimensional problem 09 p1331 A66-20145

One-dimensional model for constant-area rectangular and coaxial Hall-current generator geometries, estimating MHD characteristics for nonequilibrium plasma 12 p1802 A66-23609

Hall generator constructed by vapor deposition of thin films of indium arsenide from 4 to 500 degrees K 12 p1838 A66-24407

Electrical characteristics of linear, segmented electrode, Hall and Faraday MHD generators operating in equilibrium and nonequilibrium ionization modes, obtaining data on loss mechanisms 13 p2001 A66-26256

Electrical power dependence of ideally sectioned Faraday MHD generator on nonequilibrium plasma flow Mach number 16 p2637 A66-31606

Conducting gas flow in Hall MHD generator reduced to quasi-one-dimensional problem 21 p3698 A66-39416

Stability of one-dimensional magnetoacoustic waves traveling in axial direction in Hall type MHD generator analyzed by steady state flow equations 23 p4024 A66-41884

## HALOGEN

SA BROMINE

SA CHLORINE

SA FLUORINE

SA IODINE

Cl, Br and I contents in carbonaceous chondrites measured by activation analysis 21 p3814 A66-39260

## HALOGEN COMPOUND

SA HALIDE

Fluorocarbon oxidation and photolysis of mixtures of trifluoriodomethane, oxygen, nitric oxide and hydroiodic acid 08 p1178 A66-19069

Electrical conductivities of boron

trifluoride in chlorine and bromine trifluorides studied as function of temperature and concentration 19 p3295 A66-3637

**HAMBURGER HFB 320 AIRCRAFT**

British Lockheed undercarriage and hydraulic system for German HFB 320 Harb aircraft 04 p0458 A66-1391

Design and market research aspects of Hamburger HFB 320 jet executive aircraft 10 p1482 A66-2121

Sandwich panel composed of plastic turbular cells in parts of Hansa aircraft 13 p1994 A66-2561

**HAMILTON-JACOBI EQUATION**

Optimum stabilization of tumbling satellite using Hamilton-Jacobi method 04 p0585 A66-1391

Book on mathematics underlying celestial mechanics, including central force problem, n-body problem, Hamilton-Jacobi and perturbation theories 11 p1776 A66-2391

Hamiltonian mechanics applied to planetary and artificial satellite motion problems 12 p1950 A66-2461

Newtonian and relativistic analysis of orbits of electromagnetically neutral particles in magnetic universe 12 p1914 A66-2461

Reducing optimal control variation problems to limit problem associated with Hamilton-Jacobi equation 13 p2047 A66-2561

Stabilization of unstable two-point boundary value problems, noting first method for avoiding computer storage problems during integration of related differential equations 15 p2528 A66-2961

Synthesis of specific optimum control for optimum stabilization problem of tumbling satellite via Hamilton-Jacobi theory, comparing results with optimum solution 18 p3246 A66-3461

Asymptotic property derived for particular solutions of Hamilton-Jacobi equation for conservative systems with two degrees of freedom 19 p3401 A66-3636

Time-mass dependent events during motion of material particle, using Hamilton-Jacobi equation of relativistic mechanics 21 p3772 A66-3941

**HAMILTONIAN**

Resonances below inelastic threshold for electron hydrogen scattering using Feshbach projection-operator technique, converting eigenvalue problem for projected Hamiltonian 04 p0547 A66-1391

Bracketing theorem applied in partitioning technique for solving Schrodinger equation to determine upper and lower bounds to energy eigenvalues, ground state excited states 06 p0911 A66-1616

Signal propagation on infinite lossless transmission line in quantum field theory finding total Hamiltonian of system 07 p1046 A66-1836

Perturbation expansions for ground state function of helium atom, using Hartree-Fock Hartree-Fock model Hamiltonian, based on Weiss-Martin variation-perturbation calculation 07 p1083 A66-1836

Stability of bodies with holonomic constrained moving parts, using method of Liapunov to demonstrate dependence on motion stability on potential function generalized coordinates [AIAA PAPER 66-101] 07 p1082 A66-1836

Spectrum and eigenstates of Barden Cooper-Schrieffer /BCS/ reduced Hamiltonian in theory of superconductivity 08 p1276 A66-1916

Energy integral for holonomic system of points of variable mass, transformed Lagrangian form via Hamiltonian function 08 p1256 A66-1916

Nonlinear optical effects of third order crystals, specifically in Hamiltonian system containing electrons, nuclei, radiation field 09 p1387 A66-2061

Energy band structure of germanium on silicon throughout Brillouin zone by Hamiltonian diagonalization 10 p1581 A66-2161

Optimal cooperative state rendezvous Pontryagin maximum principle for independently controlled systems having common goal 11 p1765 A66-2261

Equations obtained from Hamiltonian coupling, first Stokes line, first anti-Stokes



line and coherent field for Raman laser 11 p1711 A66-22490  
Ground state energy of charged Bose gas obtained from pair Hamiltonian and Green functions 11 p1741 A66-23392  
Text on dynamics of vibrations covering oscillations with variable and constant amplitude, damping, differential equations of motion, nonlinear oscillations, wave propagation in elastic solids, etc 13 p2207 A66-26573  
Maser material iron doped rutile, examining theoretical and experimental disagreement in spin Hamiltonian describing paramagnetic behavior 15 p2514 A66-29027  
Extension of dynamics to arbitrary systems of differential equations, proposing universal canonical structure generalizing Hamiltonian structure 15 p2539 A66-29145  
Two-dimensional flow in fluids related to system of vortex coordinates, using Hamiltonian operator for characterization of motion studies 16 p2683 A66-30213  
Spin-free derivation of Pauling rules for evaluating matrix elements for spin-free Hamiltonian over anti-symmetric Slater bond functions 16 p2754 A66-30860  
Hamiltonian describing EPR spectrum of trivalent chromium ion in ordered lithium-aluminum spinel and rhombic distortion causing deviation of axes in octahedron electric field 16 p2787 A66-31763  
Adiabatic invariants and third integrals of motion in periodic potentials in periodically time-dependent Hamiltonian systems of  $n$  degrees of freedom 17 p2945 A66-32292  
Normal ordering method of solving boson equations leading to closed solutions of Schrodinger and density operator equations in certain cases only 17 p2945 A66-32293  
Perturbation-like theory for case when available starting wave function is not eigenfunction of unperturbed Hamiltonian 18 p3135 A66-34511  
Newton law for simple inviscid fluid using Hamilton principle, emphasizing physical interpretation of Lin constraint 18 p3102 A66-34922  
Hamilton principle applied to force equation for nonrelativistic and relativistic flow of compressible inviscid fluid with polarization and magnetization in connection with electromagnetic momentum 18 p3102 A66-34923  
Electron-phonon interaction current density, thermodynamic Green function and other electromagnetic properties of superconductors, using Froehlich-Hamilton model 19 p3438 A66-35481  
Generalized method of averaging and von Zelpel method as applied to perturbed Hamiltonian system of appropriate form [AIAA PAPER 65-687] 19 p3462 A66-35893  
Low temperature vibronic transitions between electronic states involving destruction of photon and creation of phonon via electric dipole term of Hamiltonian 19 p3446 A66-36394  
Coupling between plasmons and polar phonons in degenerate semiconductor gallium antimonide analyzed, starting from electron-phonon Hamiltonian 19 p3447 A66-36400  
Min-H Strategy in deriving two iterative methods for rapid convergence to optimum solutions for nonlinear variational two-point boundary value problems 19 p3466 A66-36677  
Generalization of Sternheimer potential to include wave functions involving spin in nonfactorable way, exhibiting approximate Hamiltonian 19 p3405 A66-36803  
First-order density matrix corresponding to nondegenerate eigenstate be  $N$ -representable for time-reversal invariant Hamiltonian and quantum-mechanical system of  $N$  identical fermions 20 p3606 A66-38290  
Stability of bodies with holonomically constrained moving parts, using method of Liapunov to demonstrate dependence of motion stability on potential function of generalized coordinates [AIAA PAPER 66-101] 21 p3827 A66-38695  
Effective mass in nuclear deformational Hamiltonian calculated by asymptotic approximation method which is two orders of magnitude better than liquid drop model 22 p3951 A66-40422  
Feynman integral for classical waves

evaluated, using Hamiltonian approach to summation 23 p4086 A66-41867  
Magnetic breakdown on usual effective Hamiltonian theory for Bloch electrons in magnetic field, using simple two-dimensional rectangular model 24 p4249 A66-42223  
**HAMMERHEAD CONFIGURATION**  
Transonic buffeting effects on hammerhead shaped payloads analyzed, using power spectral techniques and wind tunnel tests 20 p3672 A66-38170  
**HANDBOOK**  
**SA MANUAL**  
SAE handbook, 1966, supplies definitions, testing methods, measurement methods and data for engineering materials, machine elements and vehicle components 10 p1540 A66-21700  
Encyclopedia of physics, Volume 49, Part I - Geophysics III 15 p2482 A66-28516  
Handbook of microwave ferrite materials 16 p2787 A66-31752  
Reliability handbook covering system effectiveness, fatigue life patterns, reliability testing, malfunction and failure analysis, etc 21 p3744 A66-39215  
**HANDLEY PAGE HP-137 AIRCRAFT**  
VC10 test flight of autoflare and automatic landing instrumentation 23 p4015 A66-41165  
**HANDLING**  
**S AIR CARGO HANDLING**  
**S DATA HANDLING SYSTEM**  
**S GROUND HANDLING**  
**S LOW SPEED HANDLING**  
**HANDLING EQUIPMENT**  
**S STORAGE**  
**S TRANSPORTATION**  
**HANDLING QUALITY**  
General Electric self-adaptive control effect on airframe handling quality characteristics in F-4A 01 p0098 A66-10006  
Lateral-directional handling qualities of large transport, examining factors involved in pilot maneuvers 01 p0101 A66-10037  
Flight program and performance of X-15 research aircraft noting aerodynamic heating, cockpit, controls and handling qualities 01 p0011 A66-10340  
Airborne V/STOL simulators used for handling qualities research at National Aeronautical Establishment, Ottawa, Canada [AIAA PAPER 65-705] 01 p0054 A66-10943  
Variable stability system /VSS/ incorporated into X-22A aircraft to obtain flight data on VTOL aircraft [AIAA PAPER 65-706] 01 p0013 A66-10944  
Handling stability and control research in development of STOL utility transport aircraft [AIAA PAPER 65-713] 01 p0013 A66-10950  
Stability and control characteristics of STOL aircraft in low speed landing approach portion of flight regime [AIAA PAPER 65-715] 01 p0013 A66-10952  
Handling qualities research for C-5A, noting inconsistencies in magnitudes of parameters and parameters to be specified [AIAA PAPER 65-740] 03 p0317 A66-12548  
Flying qualities requirements related to control system complexity noting longitudinal, lateral and directional requirements [AIAA PAPER 65-794] 03 p0320 A66-12597  
Three independent systems of matrix equations for solving transfer function of multiparameter linear system handling by human operator 03 p0328 A66-12699  
Flight evaluation of various longitudinal handling qualities involving parameters and region of pilot acceptance [AIAA PAPER 65-780] 03 p0322 A66-13067  
Size effect on VTOL aircraft hover and low speed handling qualities for helicopter and jet VTOL 06 p0806 A66-16813  
**XC-142A Flight Test Program**, program statistics, aircraft instrumentation and flying qualities in hover and transition flight regimes 06 p0807 A66-16820  
Design recommendations to offset greater momenta and sensitivity to gust winds of jointless helicopter rotor 10 p1483 A66-21388  
Handling stability and control research in development of STOL utility transport aircraft [AIAA PAPER 65-713] 12 p1801 A66-24094  
Flying qualities of six late-model personal-owner aircraft in visual and instrument

flight [SAE PAPER 660219] 13 p1996 A66-26396  
Simulated lunar landing maneuver of Apollo spacecraft, determining pilot control problems and handling qualities 16 p2743 A66-30886  
Lateral-directional handling qualities of large transport, examining factors involved in pilot maneuvers 16 p2634 A66-31318  
Stability and control characteristics of STOL aircraft in low speed landing approach portion of flight regime [AIAA PAPER 65-715] 16 p2635 A66-31591  
XV-5A V/STOL aircraft flight testing, noting handling qualities and sequential diversion capability 17 p2844 A66-32731  
Lift engine technology, noting effect on operational transport aircraft design, VTOL capabilities, low speed control, etc 17 p2844 A66-32732  
Flight control design parameters and performance effects on VTOL aircraft handling qualities, noting manufacture and flight test results 17 p2845 A66-32733  
Helicopter handling qualities during hover noting pilot performance, position control tasks with and without gusts, effects of stability derivatives, etc 17 p2845 A66-32734  
Flight control for low altitude high-speed mission, discussing applicable requirements, analysis and design techniques 19 p3396 A66-35506  
Flight control system design for high performance aircraft, particularly longitudinal transient response handling qualities 19 p3278 A66-35509  
Handling in hovering mode of Dornier VTOL transport aircraft with and without autostabilizer, obtaining moments about roll, pitch and yaw axis 20 p3493 A66-36879  
General Electric self-adaptive control effect on airframe handling quality characteristics in F-4A aircraft 23 p4088 A66-40982  
**HANDS**  
**S HIGH ALTITUDE NUCLEAR DETECTION STUDIES /HANDS/**  
**HANKEL FUNCTION**  
Nonuniformly spaced antenna array synthesis using lambda function via Chebyshev-Gauss quadrature and Hankel transform 12 p1841 A66-24629  
Solution of set of  $n$  dual integral equations with Hankel kernel 14 p2321 A66-27377  
Error estimates for approximation formulas for Bessel functions and Hankel functions obtained, using Luke trapezoidal rule 16 p2736 A66-31021  
**HARDENING**  
**SA AGE HARDENING**  
**SA COLD HARDENING**  
**SA DISPERSION HARDENING**  
**SA PRECIPITATION HARDENING**  
**SA STRAIN HARDENING**  
**SA WORK HARDENING**  
Graphite and carbon steel case hardening by chromium 05 p0702 A66-15111  
Physical factors determining hardening of nimonic type alloy with high niobium content, discussing formation of intermetallic phase 05 p0704 A66-15820  
Hot and cold hardening of aluminum-copper-magnesium alloys for application to missiles and aircraft skins analyzed, using electron microscope, noting metastable phases 12 p1893 A66-23747  
Strain rate and temperature changes in solution hardened niobium alloy, emphasizing behavioral difference between pure niobium and alloy, noting flow stress 12 p1894 A66-23941  
Hardening temperature effect on saturation magnetization and distribution of cations over sublattices in magnesium-base ferrites 13 p2160 A66-25100  
Aging of aluminum alloy after quenching and strain hardening, noting Vickers hardness tests, tensile tests, precipitation phases, shearing effect, etc [PST PAPER 423] 14 p2315 A66-27468  
Fracture mechanics, discussing crystal structure defects, particular dislocation, hardening, lattice vacancies, interstitials, etc 14 p2316 A66-27770  
Hardening and softening of nickel-alumina alloys 15 p2519 A66-28533  
Various factors affecting hardening of KhN35VT1u /EI787/ alloy 15 p2519 A66-28535



Laser beam effect on hardening of steel 16 p2721 A66-31802  
 Hardening during deformation in stoichiometric nickel manganite alloy noting temperature effect, surface characteristics and electric resistance 19 p3381 A66-35930  
 Mechanical and physical effects of metastable phases arising during hardening of titanium alloys containing transition elements 20 p3585 A66-37699  
 Manufacturing of semifinished pressed products of AD31 Al-Mg-Si alloy, examining coarse-grained structure occurring after hardening and machining 22 p3928 A66-40886

**HARDNESS****SA BRITTLENESS**

Maximum error in high-temperature hardness determination for tungsten and molybdenum with known measurement errors 02 p0233 A66-12275  
 Component hardness differences of SAE 52100 steel effect on bearing fatigue, using five-ball fatigue tester and rolling element bearings 03 p0372 A66-12349  
 Rockwell hardness test discussing standardization by cycle control and equipment modification 03 p0439 A66-13158  
 Regularities in hardness variations in niobium binary alloy 05 p0704 A66-15821  
 Relation between hardness and ultimate strength of tungsten and molybdenum over wide temperature range 06 p0897 A66-16698  
 Microhardness changes in polycrystalline aluminum irradiated by alpha, beta and neutron particles 07 p1092 A66-17305  
 Binary, ternary and quaternary niobium alloy mechanical properties such as resistance to heat, plastic deformation, relation between hardness and rupture strength, etc 08 p1239 A66-18905  
 Residual stress-strain state of WC-Co alloys by changing sample size during process 09 p1389 A66-20806  
 Templugs, temperature-sensitive metal inserts that function on basis that certain alloys undergo permanent hardness changes upon heating 12 p1880 A66-24070  
 Hardness and lattice parameter increase effect on oxidation temperature of internally oxidized Ag-Mg and Ag-Al alloys 18 p3122 A66-33750  
 Deformation and strength properties of refractory solids at temperatures up to 2000 degrees C, using indentation hardness measurements for stress-strain measurements in strength 18 p3254 A66-33967  
 Plastic deformation effect on physical and mechanical properties of hard cylindrical samples of tungsten-cobalt alloy 21 p3752 A66-39405  
 Regularities in hardness variations in niobium binary alloy 23 p4081 A66-41386  
 Anisotropy in mechanical properties of lamellar solids due to abrasiveness, examining wear and surface damage produced by laminar solid on metal during slipping and hardness 24 p4229 A66-42701

**HARDWARE**

Test facility for combined sonic and mechanical excitation of flight-and surface-vehicle hardware, using electropneumatic transducers 16 p2676 A66-30444

**HARMONIC ANALYSIS**

Modifying spherical harmonic analysis of surface geomagnetic field to account for Earth oblateness by two methods 01 p0061 A66-10615  
 Harmonic analysis on analog computer by method giving very high Q modeling filters 01 p0034 A66-11024  
 Analysis and harmonic synthesis of periodic signals of any form by successive steps 05 p0657 A66-14728  
 Distribution function of zeros in harmonic signals relation to frequency characteristic of latter undergoing maximum amplitude limitation 07 p1001 A66-17348  
 Harmonic analysis of periodic sequence of pulses, using Fourier analysis 07 p1001 A66-17349  
 Lunar topographical asphericity, lunar coordinates, absolute and relative, harmonic analytical interpolation, formations, stratigraphy and optical librations 07 p1139 A66-18265  
 Polymeric material deformation under harmonically varying load action, noting

steady state regime temperature distribution effects 08 p1243 A66-18879

Intermediate text on dynamic analysis and automatic control 08 p1200 A66-19464

Green function-eigenvalue relationship on closed smooth boundary of open dimensional region 09 p1394 A66-20265

Transient processes in vacuum tube oscillator synchronized by small harmonic signal with random initial phase in presence of noise 09 p1357 A66-20775

Graphical analysis of recurring and periodic waveforms to determine fundamental frequency and major harmonic components 10 p1549 A66-21232

Real roots of eigenvalue problem in cylindrical harmonics 10 p1550 A66-21306

Nonlinear transfer characteristics derived from measured harmonic levels in output when input is sinusoidal wave 11 p1661 A66-22393

Second degree sectorial harmonic of Earth gravitational potential based on 338-day variation in revolution period of Syncom 11 p1697 A66-22436

Cauchy problem for two-dimensional Laplace equation in infinite strip 11 p1722 A66-22646

Statistical properties of receiver output under interference conditions, obtaining first order output, probability densities, second harmonic and intermodulation interference terms 11 p1658 A66-23483

Secular motion of Earth pole from 1900 to 1958 measured via harmonic analysis, noting rate and distance 12 p1868 A66-23669

Self-equilibrating bending of complete circular cylindrical shells described by first harmonic terms of Fourier series for displacement components 12 p1962 A66-24004

Nonlinear gyroscopic system equations solved by analog computer and verified through method of harmonic linearization 14 p2294 A66-27362

Harmonic analysis of current gains and internal slope of nonuniform base transistors 14 p2254 A66-27601

Harmonic analysis of accuracy of reproduction in digital form of operators selecting period of time quantization, duration of analog-to-digital conversion, etc 16 p2669 A66-30758

Harmonic approximation of infinite crystal dynamics problem, noting collisional case and action of external force on atoms 16 p2820 A66-31169

Diurnal oscillation in zonal and meridional winds determined, using harmonic analysis on data obtained from meteorological rocket soundings 16 p2699 A66-31641

Global harmonic and statistical analysis of gravimetry 17 p2920 A66-33192

Trial and error method for constructing closed loop harmonic response locus of control system with one nonlinear element 18 p3089 A66-34010

Critical analysis of /Earth/ spherical equilibrium configuration 18 p3109 A66-34738

Sputnik III data application to plotting of total magnetic field intensity chart above U.S.S.R., using spherical harmonic analysis 19 p3345 A66-35290

Dynamical effects of liquid nucleus of Earth in diurnal terrestrial tides 20 p3553 A66-38068

Transient processes in vacuum tube oscillator synchronized by small harmonic signal with random initial phase in presence of noise 22 p3873 A66-39834

Statistical and instrumental fluctuations effect on distribution of first-harmonic amplitude and phase in harmonic analysis of cosmic radiation variation 22 p3975 A66-40776

Stability of periodic solution of nonlinear systems with coefficients dependent on amplitude and frequency 24 p4188 A66-42478

**HARMONIC EXCITATION**

Overall structural vibration behavior based on determination of structural parameters from harmonic vibration tests 03 p0440 A66-13227

Parametric excitation of nonlinear system with hardening springs, showing existence of higher order subharmonics [ASME PAPER 65-WA/APM-7]

05 p0717 A66-15429

Spatial structure for second harmonic generated in anisotropic medium by finite-

aperture light beam 08 p1233 A66-18896

Parametric excitation of nonlinear system with hardening springs, showing existence of higher order subharmonics [ASME PAPER 65-WA/APM-7]

10 p1616 A66-21446

Plasma oscillation resonance phenomena of ionospheric antenna excitation near lower hybrid resonant

frequency 14 p2340 A66-27121

Alouette I satellite data on extraordinary wave resonance trace propagation along ionospheric magnetic field-aligned waveguide 16 p2697 A66-31010

Alouette I topside sounder ionograms electron cyclotron harmonic resonance at frequency variation 16 p2697 A66-31010

Second-harmonic enhancement in nonlinear crystal by loss modulator coupling of pulsed ruby laser modes 17 p2933 A66-31919

True natural frequencies and modes determined from harmonic vibration test using not exactly appropriate excitation 17 p3024 A66-32310

Periodic solutions of nonlinear mechanical oscillator under harmonic excitation and plot of resonance curves 18 p3259 A66-34986

Steady state oscillations in semiinfinite gas excited by harmonically oscillating wave using single-collision time kinetic model 20 p3605 A66-37610

Single point excitation techniques for resonance testing of structural inert stiffness and damping matrices 21 p3824 A66-38510

**HARMONIC FUNCTION**

**SA AIRYS STRESS FUNCTION**

**SA BIHARMONIC EQUATION**

Extension of Broman theorem stating that if function that is harmonic in unit circle belongs to special class its complete radial variation is bounded 03 p0387 A66-12610

Growth index and support function for plurisubharmonic functions in convex tubular radial regions 03 p0388 A66-12610

Existence and uniqueness of optimal algorithms proven for application transformation of potential fields 06 p0875 A66-16110

Fellerian character invariant by passage product of kernels, noting separately excessive and separately superharmonic functions 06 p0904 A66-17010

Boundary properties of Cauchy integrals and harmonically conjugate functions of regions having rectifiable boundary 07 p1059 A66-18010

Separation of harmonic components of function E/t/ by double differentiation with subsequent integration 08 p1185 A66-19010

Limiting rate of decrease of harmonic function in three variables 08 p1246 A66-19010

Bounds for two-dimensional discrete harmonic Green function used in boundary problems 09 p1395 A66-20610

Design of variable structure automatic control system frequency characteristics using harmonic linearization 11 p1677 A66-22310

Series expansion of harmonic function of closed unit circle with center at pole 14 p2321 A66-27210

Existence and uniqueness of optimal algorithms proven for application transformation of potential fields 15 p2483 A66-28610

Approximate continuation of harmonic and parabolic functions as solutions of Laplace and heat equations 16 p2732 A66-30310

Axiomatic theory of Dirichlet problem applicable to nonlinear PDEs and to systems of PDEs 16 p2738 A66-31110

Integral representation providing one-to-one correspondence between functions of complex variables and complex-valued harmonic functions of  $n$  plus 1 real variables 18 p3126 A66-33410

Separation of harmonic components of function E/t/ by double differentiation with subsequent integration 18 p3128 A66-34410

Existence of angular boundary values of harmonic function in sphere 21 p3757 A66-38810

Waveform analysis of electronic repetitive differential analyzer solutions of nonlinear and linear systems and describing functions



evaluation using  
 vector meter 21 p3739 A66-39275  
 Nonlinear automatic system with logical  
 device analyzed in presence of external  
 action, obtaining harmonic linearization  
 coefficients 21 p3719 A66-39284  
 Properties of functions of metamaterials  
 and metacoloric equations, using Liouville-  
 Picard theories together with Harnack  
 theory for solutions 21 p3837 A66-39611  
 Harmonic linearization, estimating quality  
 of oscillatory transients in nonsearching  
 self-adjusting systems described by high  
 order differential  
 equations 24 p4188 A66-42480  
**HARMONIC GENERATION**  
 Loaded linewidth measured for given value  
 of circuit coupling, determining unloaded  
 linewidth, noting ferromagnetic parametric  
 amplification and harmonic  
 generation 01 p0039 A66-10528  
 Reflection of second harmonic waves  
 created in nonlinear interaction of waves at  
 plasma boundary for case of oblique  
 incidence and weak spatial  
 dispersion 01 p0030 A66-10698  
 Second harmonic light generation, stressing  
 saturation effects occurring at high laser  
 power levels, solving nonlinear coupled  
 Maxwell equations 02 p0239 A66-11443  
 Second harmonic power up to 8 gc from  
 YIG-tuned transistor 03 p0339 A66-12440  
 Spurious signals in wideband S-to X-band  
 varactor tripler suggesting they were caused  
 by pumped-up LF resonances in input  
 circuit 03 p0339 A66-12451  
 Possible materials for second harmonic  
 generation and laser action discussing  
 centrosymmetric and piezoelectric crystals  
 and single crystal plate with alternate layers  
 of noncentrosymmetric  
 composition 03 p0378 A66-12940  
 Third harmonic current in plasma due to  
 velocity-dependent collision frequency of  
 electron 03 p0401 A66-12954  
 Harmonic generation in double beam  
 system in presence of magnetic  
 field 03 p0404 A66-12981  
 Harmonics in cylindrical electron beams  
 traveling in circular drift tube and velocity-  
 modulated by gridless buncher  
 gap 04 p0491 A66-13421  
 Harmonics of electronic gyromagnetic half-  
 frequency in spectrum of two-electron beam  
 collision 04 p0550 A66-13473  
 Light scattering theory and generation of  
 second harmonic in plasma in external  
 magnetic field 04 p0555 A66-13433  
 Third harmonic component of current  
 density in plasma in presence of electric  
 and magnetic fields, analyzing generation  
 and propagation of third harmonic of  
 electromagnetic wave in  
 magnetoplasma 05 p0724 A66-15188  
 Nonlinear harmonic generation by plasma  
 cylinder 06 p0916 A66-16377  
 Continuous optical second-harmonic  
 generation using ND/YAG laser and crystal  
 of single-domain lithium  
 niobate 06 p0889 A66-16378  
 Harmonic microwave generation by field-  
 emission cathode in superconducting  
 cavity 06 p0854 A66-16757  
 First-order approximation for second-  
 harmonic distortion in sinusoidal voltage  
 generator connected through resistor to  
 base-emitter circuit of  
 transistor 06 p0858 A66-16984  
 Bailey and Martyn theories concerning  
 ionospheric cross-modulation extended to  
 cover simple cases of heterodyne and  
 harmonic generation by electromagnetic  
 fields in plasma 06 p0920 A66-17031  
 Frequency dependence of hot carrier AC  
 conductivity of covalent semiconductors,  
 considering scattering due to acoustic and  
 optical phonons 07 p1098 A66-17740  
 Optical nonlinearities of plasma, including  
 second-harmonic generation and stimulated  
 Raman effects 07 p1091 A66-18433  
 Piecewise linear circuit model for charge-  
 storage or step recovery diode using  
 conventional capacitance and  
 resistance 09 p1350 A66-19920  
 Step-recovery diode multiplier circuit for  
 high-order harmonic  
 generation 09 p1359 A66-20919  
 Optical second harmonic generation in

focus of lowest transverse mode of  
 continuous wave Gaussian gas laser  
 beam 10 p1541 A66-21175  
 Gamma-level ring-core magnetometer  
 sensitivity parameters, noting frequency,  
 dynamic differential permeability, number of  
 pickup turns, etc 10 p1508 A66-21415  
 Second harmonic generation by laser  
 beams of finite spectral width, using  
 quantum transitions and kinetic equations,  
 noting shape of pumping line at  
 fundamental frequency 10 p1544 A66-22026  
 Harmonic wave generation by EM plane  
 wave normally incident on collisionless  
 plasma with linear density  
 profile 11 p1652 A66-22548  
 Reflection of second harmonic waves  
 created in nonlinear interaction of waves at  
 plasma boundary for case of oblique  
 incidence and weak spatial  
 dispersion 11 p1658 A66-23300  
 Continuous wave measurement of optical  
 nonlinearity of ammonium dihydrogen  
 phosphate, using helium-neon  
 laser 12 p1912 A66-23716  
 Perturbation theory determination of third  
 harmonic current density generated in  
 plasma by AC field for velocity-dependent  
 plasma 12 p1924 A66-24593  
 Boltzmann transfer equation for electrons  
 and generation of nonlinear second harmonic  
 of current density in inhomogeneous  
 plasma 12 p1924 A66-24806  
 Harmonic generation in short magnetized  
 plasma column from helical oscillation near  
 critical magnetic field for helical  
 instability 12 p1925 A66-24815  
 Consistent theory of nonlinear optical  
 effects in bounded light beams by extending  
 parabolic equations to nonlinear  
 problems 12 p1891 A66-24888  
 Second harmonic generated by transmitting  
 laser radiation through tellurium  
 monocrystal, while filtering out fundamental  
 frequency 13 p2090 A66-25437  
 HF and LF alternating electric fields  
 effect on weakly ionized argon, temperature  
 modulation and production of  
 harmonics 13 p2141 A66-25447  
 Second optical harmonic generation  
 equations for steady state laser derived  
 from density matrix 13 p2092 A66-25682  
 Varactor diode as frequency multiplication  
 element, discussing design parameters and  
 noise characteristics 13 p2039 A66-25699  
 Physics of quantum electronics -  
 Conference, San Juan, Puerto Rico, June  
 1965 13 p2093 A66-26141  
 Second harmonic generation of light  
 analyzed, stressing saturation effects  
 occurring at high laser power, solving  
 nonlinear Maxwell  
 equations 13 p2096 A66-26144  
 Nonlinear susceptibility describing second  
 harmonic generation of light measured in  
 semiconductors with zinc-blende symmetry,  
 using quantum mechanics and laser  
 wavelength 13 p2168 A66-26149  
 Second harmonic generation by Q-switched  
 laser pulse from silicon and germanium  
 surfaces 13 p2096 A66-26150  
 Light coupling with phonons, magnons and  
 plasmons, deriving wave equations and  
 coupling constants, observing Raman effect  
 in spin systems and in plasmas, noting  
 second harmonic  
 generation 13 p2132 A66-26154  
 Vector synchronism and second-harmonic  
 light generation in focused  
 beams 14 p2307 A66-27191  
 Electromagnetic waves in isotropic plasma  
 layer and in plasma layer in magnetic field,  
 determining second harmonics of wave and  
 obtaining nonlinear dispersion  
 equation 14 p2348 A66-28470  
 Electron density in laser-induced spark in  
 air determined, measuring simultaneously  
 fundamental laser wavelength and second  
 harmonic 15 p2512 A66-28685  
 Power dissipation in input and output  
 matching networks of varactor doubler for  
 calculating true input and output powers  
 from semiconductor bulk material, noting  
 charge storage  
 occurrence 15 p2466 A66-29674  
 Gallium arsenide varactor diode design for  
 parametric amplifiers and multipliers, noting  
 efficient harmonic generation at higher

microwave frequency 15 p2466 A66-29677  
 Second harmonic generation /SHG/ by  
 focused laser beams in nonlinear  
 crystals 15 p2519 A66-29816  
 Optical harmonic generation in IR in zinc  
 blende, hexagonal and trigonal crystals,  
 using unfocused carbon dioxide laser in CW  
 and Q-switched operation 16 p2716 A66-30182  
 Second harmonic generation by laser  
 beams of finite spectral width, using  
 quantum transitions and kinetic equations,  
 noting shape of pumping line at  
 fundamental frequency 16 p2718 A66-30845  
 Statistical effects during generation of  
 second harmonic in optically transparent  
 crystals, noting coefficient of correlation  
 between harmonic and fundamental radiation  
 power of solid state laser 16 p2747 A66-31167  
 Plasma plate and cylinder oscillation  
 compatibility with radiation from positive  
 argon column at four discrete frequency  
 bands and low pressure 17 p2962 A66-31815  
 Circuit with single externally driven  
 switch, operated at fundamental frequency  
 gives efficient conversion of DC to AC at  
 that frequency or any specified harmonic of  
 it 17 p2848 A66-31818  
 Harmonic generation in microwave  
 emission from InSb, attributing resonance  
 type radiation to stimulated cyclotron  
 radiation and plasma wave  
 excitation 17 p2978 A66-32410  
 Wave coupling and generation of  
 gyromagnetic half-frequency harmonics in  
 double electron-beam  
 system 18 p3142 A66-33911  
 Enhancement of optical second-harmonic  
 generation by reflection phase matching in  
 ZnS and GaAs 19 p3375 A66-36074  
 Frequency doubling in resonance laser,  
 obtaining second harmonic field for laser  
 radiation by giant pulses 20 p3576 A66-37144  
 Second-harmonic electron cyclotron  
 resonance in hydrogen plasma from HF ion  
 source with inductive coupling situated in  
 transverse magnetic field 20 p3607 A66-37407  
 Second harmonic frequency generation  
 obtained in process of optical mixing of  
 collinear neodymium laser beams in  
 potassium dihydrogen  
 phosphate 20 p3578 A66-37550  
 High-speed rotor operation in bearing  
 clearances, discussing induction of nonlinear  
 vibration, harmonic generation and computer  
 simulation results  
 [ASME PAPER 66-MD-1] 21 p3741 A66-38474  
 Second-harmonic generation by focused  
 laser beams based on experiments using He-  
 Ne gas laser, noting SHG should be strongly  
 peaked when focus is at either of crystal  
 surfaces 21 p3746 A66-38554  
 Higher harmonics generation of ion  
 cyclotron frequency in longitudinally  
 magnetized plasmas, noting experimental  
 setup and pressure  
 effects 21 p3777 A66-38766  
 Velocity dependent collision frequency  
 effect on harmonic generation in ionized gas  
 through which electromagnetic wave  
 passes 21 p3792 A66-39180  
 Second harmonic generation in laser  
 crystals by Gaussian beams of finite  
 aperture 22 p3929 A66-39657  
 Consistent theory of nonlinear optical  
 effects in bounded light beams by extending  
 parabolic equations to nonlinear  
 problems 23 p4076 A66-41095  
 Nonlinear interaction of electromagnetic  
 waves in magnetoplasma for field-parallel  
 wave propagation 23 p4041 A66-41642  
 Miller phenomenological rule for computing  
 nonlinear susceptibility, determining  
 magnitude by geometrical  
 factor 24 p4223 A66-42568  
 Stability criteria derived for horizon  
 sensors which track point on horizon where  
 second harmonic of signal generated by scan  
 motion of field of view is  
 zero 24 p4175 A66-42821  
 Vector synchronism and second-harmonic  
 light generation in focused  
 beams 24 p4226 A66-43089  
 Harmonic generation and detection in  
 submillimeter wavelength region,  
 emphasizing crystal point contact  
 diode 24 p4176 A66-43191  
**HARMONIC GENERATOR**  
 Difference frequency between harmonics



of millimeter wave oscillators at submillimeter wavelength, using crossed waveguide harmonic generator as harmonic mixer 07 p1008 A66-17514

Nonlinear phenomena in HF plasma discharge, establishing qualitative relation between gas pressure, consumed microwave power and harmonic generation 12 p1919 A66-23711

Output signal of harmonic generator with noise sources in circuit, using perturbation analysis and assuming noise effect on signal in transducer is 12 p1835 A66-24137

Submillimeter spectroscopy using Froome plasma metal junction harmonic generator 15 p2501 A66-29007

Equivalent circuit evaluation of theoretical potential and limitations of millimeter wave semiconductor diode detectors, mixers and frequency multipliers 15 p2461 A66-29015

Current-voltage characteristic for tunnel-diode millimeter wave harmonic generator in 24 to 72 gc region 15 p2462 A66-29024

Submillimeter wave mixing of output of carcinotron and output of klystron in crossed-waveguide harmonic generator 15 p2463 A66-29025

Varactor diode harmonic generators for S-band with VHF input and microwave output 17 p2892 A66-32916

Signal analysis of abrupt and graded junction varactor harmonic generators with idlers, showing how load and source resistances may be optimized 17 p2893 A66-32922

Wide tuning range solid state microwave source consisting of transistor oscillator and varactor diode harmonic generator chain 17 p2893 A66-32926

Frequency comparison by beat-frequency comparators, harmonic generators and permanent phase observation devices 17 p2927 A66-33245

Signal analysis of abrupt and graded junction varactor harmonic generators with idlers, showing how load and source resistances may be optimized 20 p3531 A66-37831

J-band multiplier design noting extension of frequency coverage, components, noise performance, frequency stability, tuning range, etc 21 p3711 A66-38837

## HARMONIC MOTION

Forced solutions for Van der Pol-Duffing equation in first harmonic approximation 13 p2129 A66-26337

Energy integral study of geopotential harmonic variation effects on satellite motion near critical inclination 20 p3653 A66-37763

## HARMONIC OSCILLATION

Forced torsional motion of semiinfinite isotropic elastic cylinder with vibrations excited by harmonically oscillating rigid disk, using integral equation 04 p0589 A66-13829

Amplification and generation properties in gold-compensated silicon diodes, noting noise spectrum and harmonic oscillations 04 p0499 A66-14061

Nonlinear spring-mass system with many degrees of freedom subjected to periodic exciting forces, deducing steady state forced vibrations equal to forcing function [ASME PAPER 65-APMW-30] 04 p0593 A66-14230

Exact solution for Green function of open spherical shell subjected to harmonically oscillating concentrated load and any consistent boundary conditions [ASME PAPER 65-WA/APM-24] 05 p0778 A66-15446

Dynamic reciprocal theorem for sinusoidal oscillation of elastic medium treated as extension of static reciprocal theorem of Betti and Rayleigh, using continuum mechanics [ASME PAPER 65-WA/MD-21] 05 p0779 A66-15524

Three-dimensional motion of rigid system turning about fixed axis and simultaneously oscillating along same axis 07 p1079 A66-17302

Multimode antennas, discussing mode and mode generation, radiation sum and difference pattern control, discontinuity reflections, monopulse antennas, etc 08 p1191 A66-18945

Formal variance of measurement error in frequency and phase of harmonic signal in narrow-band noise background 08 p1201 A66-19688

Weak harmonic signal effect on synchronized oscillator analyzed, based on van der Pol equation 11 p1667 A66-22790

Formula for numerical values of propagation rates of flexural harmonic waves of various lengths 11 p1784 A66-23315

One-boson Lee model of solvable field theory with nontrivial charge and mass renormalization as example of Lehmann-Symanzik-Zimmermann formalism 12 p1917 A66-24098

Aerodynamic forces on system of N thin slightly twisted profiles in subsonic unsteady flow for small angle of attack, examining acoustic resonance for arbitrary small harmonic oscillations 12 p1798 A66-24436

IR maser action on vibrational transitions of thermally pumped polyatomic molecules 13 p2101 A66-26203

Mathematical and numerical determinations of aerodynamic forces on harmonically oscillating cylindrical shell under subsonic and supersonic speeds and comparison with slender body theory results 14 p2218 A66-27405

Aerodynamic forces acting on harmonically oscillating thin profile in stalled plane parallel flow of ideal incompressible fluid 14 p2220 A66-27695

Accelerator with nonlinear spiral focusing, approximating size of stability region, adiabatic damping, transverse phase stability and perturbations effect 14 p2347 A66-28309

Thermoelasticity equations describing harmonic vibrations of medium solved via singular integral equation 14 p2408 A66-28390

Oscillating solutions of ordinary nonlinear nonautonomous differential equations, noting qualitative methods 15 p2527 A66-29168

Singular integral equations for thermoelasticity equations describing harmonic oscillations of medium, applied in boundary value problems 15 p2611 A66-29419

RF size effect on ineffective electrons in magnetic field parallel to surface of cadmium plates studied by observing harmonic oscillations of impedance 16 p2772 A66-30289

Nonstationary aerodynamic load for harmonically oscillating body in fluid flow with constant mean velocity measured, determining errors as functions of system parameters 16 p2630 A66-31302

Amplification and generation properties in gold-compensated silicon diodes, noting noise spectrum and harmonic oscillations 17 p2885 A66-32227

Exact solution for Green function of open spherical shell subjected to harmonically oscillating concentrated load and any consistent boundary conditions [ASME PAPER 65-WA/APM-24/] 18 p3248 A66-33576

Nonlinear spring-mass system with many degrees of freedom subjected to periodic exciting forces, deducing steady state forced vibrations equal to forcing function [ASME PAPER 66-APMW-30] 18 p3249 A66-33591

Formal variance of measurement error in frequency and phase of harmonic signal in narrow-band noise background 18 p3091 A66-34674

Weak harmonic signal effect on synchronized oscillator analyzed, based on van der Pol equation 20 p3525 A66-37130

Steady state oscillations in semiinfinite gas excited by harmonically oscillating wall, using single-collision time kinetic model 20 p3605 A66-37635

Nearly-periodic oscillations in nonlinear systems having periodic coefficients and subject to external periodic force 23 p4141 A66-41947

Reverse flow and deformation optimization theories applied to subsonic aeroelasticity of lifting surface in harmonic oscillation, using numerical integration and computer programs 24 p4157 A66-42343

## HARMONIC OSCILLATOR

Amplitude and phase of anharmonic oscillator, using relativistic Schroedinger

equation in magnetic field 05 p0695 A66-1490

Random model for classical electrodynamics presents properties of quantum electrodynamics as extension of work on harmonic oscillator under magnetic field 06 p0867 A66-1706

Forcing function acting upon rigid body rotating about fixed point replaced by motion of axis of rotation and another forcing function 08 p1310 A66-1918

Black body radiation law deduced from stochastic electrodynamics 14 p2414 A66-2817

RF harmonic oscillator design, using characteristic equations for natural oscillation frequency expressions, analyzing changing load effects, changing passive parameters, etc 14 p2282 A66-2838

Momentum and energy accommodation for hypervelocity gas particles on crystal surface, using Lennard Jones potential and approximating lattice by system of independent forced harmonic oscillators 16 p2752 A66-3038

Approximate analysis of nonlinear systems similar to harmonic oscillators, using Chaplygin theory of differential inequalities 16 p2705 A66-3079

Flowgraph techniques for closed systems discussing properties, approximation methodology equation, frequency response constraints, oscillatory and stochastic processes, etc 17 p2898 A66-3198

## HARMONIC RADIATION

Harmonic structure and band splitting in type II solar radio bursts 03 p0429 A66-1317

Plasma waves propagating transverse to uniform external magnetic field discussing electron motion, wavelength magnitude frequencies and application of results 03 p0406 A66-1337

L-band waffle-iron filter fabrication and modifications for high power characteristics 06 p0847 A66-1617

Field polarization of short-period variations/beats/ of Earth electromagnetic field investigated, using correlation analysis 08 p1214 A66-1903

Harmonic suppression ratios in RF amplifiers calculated, using circuit parameters and applying Fourier transformations 10 p1508 A66-2129

Intense radiation emission at gyrofrequency harmonics from magnetoplasmas, discussing resonances dispersion relations, electron trajectory perturbations, etc 13 p2155 A66-2669

Mode selective coaxial directional coupler for measurement of unwanted harmonic effect 13 p2044 A66-2678

Electric current density in semiconductor noting harmonic mixing of microwaves in warm electrons in germanium 15 p2564 A66-2887

## HARMONICS

SA SPHERICAL HARMONICS

SA TESSERAL HARMONICS

SA ZONAL HARMONICS

Drift velocity of aerosol particle in field sound wave distorted by second harmonic 13 p2127 A66-2508

Drift velocity of aerosol particle in field sound wave distorted by second harmonic 21 p3769 A66-3858

## HARTMANN FLOW

Hartmann problem solved for isothermal motion of heavy neutral viscous gas containing small impurities of light ions and electrons in crossed electric and magnetic fields 02 p0269 A66-1217

Hydraulic resistance coefficient dependence on Reynolds and Hartmann numbers in turbulent flow of conducting fluid through tube in magnetic field 11 p1743 A66-2237

Hartmann problem solved for isothermal motion of heavy neutral viscous gas containing small impurities of light ions and electrons in crossed electric and magnetic fields 14 p2345 A66-2808

Nonequilibrium ionization phenomena interaction with nonuniform flow of plasma reviewing nonequilibrium characteristics of uniform flow with electric and magnetic fields 20 p3610 A66-3798

Wall conductance effect on stability of Hartmann flow in curved channel, solving



eigenvalue problem via Galerkin method 21 p3777 A66-38762  
 Temperature profiles and Nusselt numbers for heat transfer to MHD laminar Hartmann flow in thermal entrance region of flat duct 22 p4000 A66-40920  
**HARTREE-FOCK CALCULATION**  
 Perturbation expansions for ground state function of helium atom, using Hartree or Hartree-Fock model Hamiltonian, based on Weiss-Martin variation-perturbation calculation 07 p1083 A66-18422  
 Magnetization using Hartree-Fock approximation in terms of boson distribution or uniformly interacting spins 07 p1084 A66-18441  
 Hartree-Fock approximation method for calculating efficiencies of multiple-photon processes 11 p1737 A66-22495  
 Improving uncoupled Hartree-Fock expectation values for atomic and molecular properties 11 p1738 A66-22877  
 Collective oscillations of atoms in Hartree-Fock approximation 16 p2751 A66-30191  
 Quantum theoretical ferromagnetic behavior of chemical bonds in transition metals and Hartree-Fock calculation of atomic orbitals 19 p3439 A66-35713  
 Photoionization cross sections calculated for carbon, nitrogen and oxygen ions, using Hartree-Fock approximation for final transition stages 19 p3405 A66-36805  
 Hartree-Fock parameters for intermediate coupling compared with those obtained from observed energy levels for C I sequence 23 p4130 A66-41814  
 Crystal potential and correlation for energy bands in valence semiconductors evaluated on basis of orthogonalized plane wave calculations starting with Hartree-Fock equation 24 p4249 A66-42227  
**HASP**  
**HIGH ALTITUDE SOUNDING PROJECTILE /HASP/**  
**HASTELLOY**  
 Hot cracking in Hastelloy X fusion weld as affected by microsegregation produced during solidification 10 p1547 A66-21768  
 Creep design reliability criteria for creep-rupture and critical creep-strain modes of structural element failure, both singularly and combined or 20 p3571 A66-37941  
**HAWKER P 1127 AIRCRAFT**  
 Kestrel P-1127 V/STOL strike/reconnaissance aircraft evaluation trials with reference to background, aircraft description, organization, pilot training and major tasks 07 p0985 A66-17268  
 Kestrel P-1127/ Tripartite V/STOL Operational Trials, describing aircraft performance, test unit organization, results, etc 18 p3052 A66-34945  
 Unit for centralizing AC-carrier measurements onboard VTOL Hawker Siddeley P 1127 aircraft 21 p3741 A66-39475  
**HAYSTACK PROJECT**  
 Circularly polarized tracking feed in haystack antenna 13 p2035 A66-25504  
 Deflection of structural members in haystack antenna calculated, using framed structure analysis /FRAN/ program, obtaining improved grid analogy 15 p2614 A66-29616  
**HAZARD**  
 AIRCRAFT HAZARD  
 FLIGHT HAZARD  
 METEOROID HAZARD  
 NOISE HAZARD  
 OPERATIONAL HAZARD  
 RADIATION HAZARD  
 SAFETY  
 SAFETY HAZARD  
 TOXICITY AND SAFETY HAZARD  
 Relationships of hazard rate distributions to reliability growth and confidence computations 01 p0077 A66-10109  
 Hazards associated with ignition of various condensed phase hydrogen-oxygen systems 20 p3625 A66-37083  
**HAZE**  
 FOG  
 VISIBILITY  
 Spectral brightness of haze and effect on interpretation of aerial photographs 15 p2504 A66-30006

**HD-1 GROUND EFFECT MACHINE**  
 S HOVERCRAFT HD.1 GROUND EFFECT MACHINE  
**HEAD FLOW**  
 Shape of head wave in linearized supersonic flow past finite span wing, considering waves with convex and concave leading edge 16 p2632 A66-31792  
**HEAD MOVEMENT**  
 Brief Vestibular Disorientation Test /BVDT/ assesses subject reaction produced by head movements in rotating chair 11 p1647 A66-22574  
 Gaze direction lead during slow patterns of head movement 17 p2865 A66-32179  
 Slow waveform of eye position change relative to head oscillating sinusoidally about vertical axis 24 p4163 A66-42449  
**HEALTH**  
 SA HYGIENE  
 SA SANITATION  
 Health hazards in handling and processing beryllium and its compounds, noting effect on lungs and reviewing AEC recommendations 08 p1177 A66-18854  
**HEARING**  
 SA BINAURAL HEARING  
 SA SOUND LOCALIZATION  
 Human engineering of acoustic fatigue for optimum data processing performance [ASME PAPER 66-MD-25] 21 p3700 A66-38481  
 Increased ambient pressure effect on hearing function in divers 22 p3853 A66-39787  
 Sound pressure in external auditory meatus and near center of cat head in absence of animal as function of frequency 22 p3854 A66-40166  
**HEARING LOSS**  
 SA DEAFNESS  
 Monolithic silicon class B hearing aid push-pull amplifier with low idling current and low current drain 01 p0047 A66-11140  
 High noise levels effect on hearing damage of technical personnel of military airfield 04 p0472 A66-14386  
 Noise and vibration causing acoustic fatigue leading to deafness of aircrew 06 p0811 A66-16065  
 Relative contribution of stapedial reflex to remote and contralateral remote masking 09 p1337 A66-20953  
 Noise exposure duration indicator, recording cumulative time exceeding one of five preset sound pressure levels of noise, noting amplifier, rectifier, etc 10 p1536 A66-21742  
 Hearing acuity requirements of aircraft personnel, examining discrimination from background noise and acoustic trauma causative factors 10 p1493 A66-22130  
 Speech audiometry in observing hearing loss with aid of live voice 13 p2015 A66-26700  
 Damage-risk criteria for exposure to sound, including graphs of maximum steady-sound pressures and durations of exposures that can be tolerable 14 p2230 A66-27657  
 Hearing impairment from overexposure to impulsive noise, noting relationship between temporary threshold shift and peak level and duration of impulsive noise 17 p2862 A66-31948  
**HEART**  
 S CARDIOGRAPHY  
 S CARDIOVASCULAR SYSTEM  
**HEART DISEASE**  
 Plane crash as result of pilots coronary disease, discussing prevention and rehabilitation 04 p0469 A66-14387  
 Clinical and medicolegal considerations on fatal case of myocardial infarct involving military pilot in flight 14 p2229 A66-26813  
 Coronary diseases and flight safety 19 p3295 A66-36445  
**HEART FUNCTION**  
 SA MUSCULAR FUNCTION  
 Small Coriolis accelerations effect on functional state of human heart 15 p2437 A66-29474  
 Myocardial glycogenolysis in rat ventricle and relation to severity of exercise 20 p3505 A66-37058  
**HEART RATE**  
 SA PULSE RATE /BIOL/  
 Psychophysiological effects of low friction on man, particularly rotation on visual

reaction time, heart rate and spatial orientation 06 p0868 A66-16240  
 Cardiac arrhythmias occurring during positive and negative acceleration 09 p1335 A66-20532  
 Effects of water immersion, recumbency and activity without negative breathing pressures, measuring heart rate and blood pressure with and without tilting 11 p1642 A66-22573  
 Electrocardiogram interpretation by computer, using pattern recognition approach which permits differentiation between normal and abnormal rhythms 12 p1810 A66-24231  
 Physiological stress and fatigue in aerial missions for forest fire control, noting in-flight and postflight exercise heart rate 12 p1810 A66-25009  
 Physiological reactions of Russian astronauts under prolonged weightlessness, noting motor activity, heart and pulse beat, breathing rates, arterial pressure, etc 15 p2436 A66-29467  
 Daily physiological rhythm changes associated with light intensity and color, noting body temperature oscillations vs light intensity, heart rate changes, etc 15 p2441 A66-29959  
 Sympathetic nervous system integrity following water immersion evaluated by measuring plasma-free fatty acid responses to passive tilting 16 p2639 A66-30649  
 Blood pressure and heart rate during hypothalamic self-simulation in dogs, discussing experimental methods and results, physiological response, etc 16 p2640 A66-31154  
 Impedance plethysmographic system for monitoring right ventricular output to obtain cardiac output 17 p2924 A66-32149  
 Parasympathetic control of heart rate in monkeys under acceleration stress, noting ECG changes and effect of atropine sulfate on change of rate 17 p2857 A66-32176  
 Effect of sudden intense noise and near vacuum decompression on cardiac rate of anesthetized and unanesthetized dogs 19 p3286 A66-36380  
 Tilt table response and blood volume changes associated with 30 days of bed rest, evaluating time required to recover from cardiovascular deconditioning 22 p3853 A66-39785  
 Radio telemetry for acquisition of Circadian rhythm data on ambulatory animal, including deep body temperature, heart rate, locomotor activity and oviposition 22 p3856 A66-39792  
 Flack Test for cardiorespiratory integrity, noting heart rate 24 p4164 A66-42454  
 Tilt table orthostatic tolerance test, noting heart rate change and mechanical systole shortening 24 p4164 A66-42455  
**HEAT**  
 S CALORIMETER  
 S COMBUSTION HEAT  
 S DRY HEAT  
 S ENTHALPY  
 S ENTROPY  
 S FORMATION HEAT  
 S NERNST HEAT THEOREM  
 S NUCLEAR HEAT  
 S SOLAR HEAT  
 S SOLUTION HEAT  
 S SPECIFIC HEAT  
 S THERMAL FATIGUE  
 S THERMAL NOISE  
 S VAPORIZATION HEAT  
**HEAT ACCLIMATIZATION**  
 SA THERMAL COMFORT  
 Effects, singly and in combination, of heat, exercise and hypohydration upon voluntary dehydration in four acclimated physically-fit young men 06 p0812 A66-16533  
 Thermal responses of man during rest and exercise in helium oxygen environment for various temperatures 24 p4163 A66-42317  
**HEAT BALANCE**  
 Energy balances for combustion chambers of gas turbines by electronic computer 03 p0416 A66-13202  
 Experimental apparatus and procedure for thorough testing of satellite heat balance 05 p0659 A66-14682  
 Metabolic rates in pressurized pressure suit, affecting heat balance of subjects



metabolic heat with heat removed by environmental control 07 p0997 A66-17657  
Thermal balance and electric resistance of vacuum-heated wire for thermoconductivity measurements 09 p1390 A66-20830  
Thermal events in diurnal breathing cycle and vapor loss reduction in volatile liquid storage [AICE PREPRINT 11C] 10 p1521 A66-21181  
Limiting conditions of temperature, gas flow rate and heat removal for combustion of methane in atomic oxygen, calculating heat balance of process 16 p2827 A66-30792  
Thermal balance and heat exchange between four men exposed to helium-oxygen atmosphere at 380 mm Hg total pressure 16 p2639 A66-31122  
Calorimetric study of effects of hydrazine on heat balance, source of metabolic energy and rate of protein catabolism of rats 17 p2856 A66-32158

## HEAT BUDGET

## S ATMOSPHERIC HEAT BUDGET

## HEAT CAPACITY

Heat potential theories applied to boundary value problem for heat conduction equation 01 p0160 A66-10167  
Sudden heat capacity change near electron-phonon system transition point from superconducting to normal state 02 p0277 A66-12080  
Anomalous heat conductivity in ferrites at Neel temperature due to corresponding anomalous heat capacity 02 p0277 A66-12088  
Impurity concentration dependence of difference between heat capacities at constant pressure and at constant volume in Ge 02 p0277 A66-12093  
Heat capacity related to quantizing of energy levels of electron excitation of superconductor in intermediate state 02 p0277 A66-12278  
Aluminum carbide thermodynamic properties over large temperature interval calculated from low-temperature heat capacity and high-temperature relative enthalpy 04 p0536 A66-13832  
Heat capacity related to quantization of energy levels of electron excitation of superconductor in intermediate state 05 p0738 A66-15457  
Heat capacity and thermal conductivity related to elastic-mechanical macroscopic physical properties, using invariance properties of tensors 06 p0971 A66-16616  
Heat capacity expression due to chemical reaction, relating composition variations and binary diffusion coefficient with Lewis number, presenting integral equation for system enthalpy 08 p1318 A66-19164  
Strong coupling cell theory of liquid helium, noting heat capacity 09 p1391 A66-20011  
Heat capacity measurements of liquid He 3 to improve precision in determination of effective mass ratio 09 p1392 A66-20014  
Heat capacity of adsorbed He 3 films at temperatures from 0.1 to 4 degrees K, with adsorption surfaces made of monolayers of argon preadsorbed on copper 09 p1392 A66-20020  
True heat capacity of solid heat-resistant dielectric or conducting materials at high temperatures 09 p1470 A66-20141  
Change in heat capacity at Curie point for ferrites 14 p2369 A66-28331  
Heat capacity of high purity beryllium measured at temperatures below 30 degrees K 16 p2775 A66-30727  
Text on thermodynamics of refractory compounds covering thermodynamic properties of borides, carbides, nitrides and oxides of 31 elements 16 p2728 A66-31748  
Thermodynamics including first and second laws, differential and state variables, heat capacity and specific heat 18 p3260 A66-34119  
Experimental assembly for measuring true heat capacity of heat resistant insulating materials during natural cooling at temperatures from 1200 to 2400 degrees K 20 p3556 A66-36989  
Simultaneous measurement of heat conductivity, heat capacity and thermal diffusivity of solid and liquid metals at high temperature 20 p3678 A66-37120  
Magnetization curves for two specimens of semiconducting strontium titanate of given electron density, noting magnetic hysteresis

and heat capacity 21 p3796 A66-38553  
**HEAT DISSIPATION**  
Heat dissipation values for spacecraft silver oxide-zinc primary and nickel oxide-cadmium secondary batteries determined with calorimeter 03 p0323 A66-12772  
Construction problems of continuous-duty DC excited ion lasers 04 p0530 A66-13956  
Thermistor for measuring rate of liquid-phase exothermal and endothermal reactions in terms of heat loss, considering condensation polymerization of terephthalyl chloride with ethylene glycol in dioxane solution 05 p0787 A66-14959  
Dissipative effects in converging cylindrical symmetric shock wave, considering ion and electron heat conductivity, ion viscosity and energy exchange 07 p1025 A66-18180  
Design and application of dry, dielectric and water-cooled dummy loads 12 p1829 A66-23537  
Heat dissipated inside compartments by internal structural members on high speed aircraft 14 p2414 A66-28188  
Thermal models for microwave dissipation within p-i-n diode for forward and reverse biased states 15 p2458 A66-28890  
Cooling of diodes, transistors and thyristors at intermediate power levels, determining heat dissipation by radiation, conduction and convection 16 p2664 A66-31346  
Design and test flying of transistorized sonde used with Suomi-Kuhn radiometer for measurement of heat loss by long wave radiation from atmosphere 19 p3353 A66-35316  
Physical limits of miniaturization, noting element size, packing density, heat dissipation, etc, in connection with integrated circuits 19 p3323 A66-36825  
Cryogenic system used to remove heat from space simulator solar radiation source 20 p3541 A66-37071  
Forced-cooled electronic chassis development history 20 p3527 A66-37347  
Water-circulation-cooled space suit, discussing heat dissipation mechanism, body temperature maintenance, metabolic rates, astronaut comfort, etc 20 p3509 A66-38164  
Thermal loss measurement at tube end during reflection of shock waves, using platinum thermometers and high speed photography 21 p3727 A66-39096  
Dissipation of sheet of heated air in turbulent air flow in pipe 21 p3836 A66-39445

## HEAT EFFECT

## SA ABLATION

## SA PELTIER EFFECT

## SA THERMAL DEGRADATION

Heated cylindrical shell with braces subjected to given compression and internal pressure, having elastic beams along edges, analyzing local deformations effect on shell strength and stability 14 p2400 A66-27684  
Heat magnetization in simple model applied to thulium intermetallic compounds 16 p2745 A66-30177  
Hypersonic flow, discussing heat effect on flow parameters, shock and motion equations, drag increase, etc 22 p3897 A66-39699  
Heating environment for space vehicle, examining wind and incident radiation effects on heat transfer to liquid hydrogen, insulation surface thermal properties and optimization of insulation system 22 p3986 A66-39777

## HEAT ENGINE

## SA AFTERBURNER

## SA CARNOT ENGINE

## SA ELECTROTHERMAL ENGINE

## SA GAS GENERATOR ENGINE

## SA INTERNAL COMBUSTION ENGINE

## SA POWER PLANT

## SA TURBINE

Brayton cycle nuclear space power systems and heat transfer components 01 p0016 A66-10913  
Gaseous heat engine cycle with gas compression from molecular effusion through capillary material 11 p1639 A66-22244

## HEAT EQUATION

Partial-region method for solving nonsteady heat conduction problems in which region considered is divided into several subregions 01 p0163 A66-10739  
Reduction of quasi-linear partial

differential equations to single linear heat equation 02 p0251 A66-12157  
Cauchy problem of heat conduction equation and inversion of Weierstrass transform on certain symmetrical Riemann spaces 03 p0444 A66-12771  
Contact effectiveness of space radiator for specific case of rectangular fin of constant thickness heated uniformly along one edge and perfectly insulated along opposite edge 03 p0444 A66-12771  
Hydrothermodynamic equations for calculating velocity, temperature and pressure fields and water content for model of stationary axisymmetric cumulus cloud 04 p0540 A66-13416  
Method for steady state heat conduction bodies of revolution 04 p0596 A66-13416  
Heat equation of temperature field for monotonic heating or cooling of thin plate 04 p0596 A66-13416  
Numerical integration of heat propagating equation, calculating temperature field for fluid flow with variable physical parameters 04 p0596 A66-13416  
Charged fluid in presence of electromagnetic induction and thermodynamic exchange, noting Cauchy problem, thermodynamic and heat equations 05 p0787 A66-15160  
Derivation of wave-type heat equation satisfying second law of thermodynamics and modified Onsager symmetry relations 06 p0971 A66-16616  
Unsteady heat conduction in finite homogeneous region of arbitrary geometry and initial conditions with inhomogeneous boundary conditions 07 p1150 A66-17516  
Uniqueness theorem for Cauchy problem for heat equation, using Poisson representation 07 p1153 A66-17516  
Poisson representation and Cauchy problem for heat equation, with improved results over previous paper 07 p1153 A66-17516  
Networks method applied to approximate solution of heat conduction equation for spatial boundary conditions with aid of theory of hypermatrices 07 p1153 A66-17516  
Approximate reentry velocity and heating equations applied to any atmosphere satisfying hydrostatic equilibrium, noting motion equations for flight path 08 p1303 A66-18887  
Analog computers used in modeling of heat conduction and diffusion processes for Fourier differential equation 08 p1319 A66-19422  
Heat conduction equation for convective flow applied to gunpowder combustion under harmonic pressure variation 08 p1280 A66-19422  
Free boundary problem for heat equation with heat input at melting interface 09 p1470 A66-20202  
Steady thermal regimes in multilayered medium with perfect and imperfect contact and varying heat conductivity 09 p1471 A66-20202  
Mathematical model of flame propagation in laminar and turbulent flow 10 p1619 A66-21077  
Approximate solution of initial boundary value problems involving heat conduction in inhomogeneous and anisotropic media 10 p1620 A66-21322  
Heat conduction equation for axisymmetric pulse heating of cylindrical sample with constant surface conditions 10 p1622 A66-21887  
Closed-form solution for constant velocity solidification of spheres initially at fusion temperature 10 p1622 A66-21887  
Numerical solution of heat conduction in gas dynamics equations by sifting over separate regions 11 p1785 A66-22333  
Alternating direction schemes for heat equation in general cross sections with 1 space dimensions and nonlinear equations 11 p1722 A66-22996  
Linear heat conduction in metals with temperature-dependent physical properties and constant illumination 11 p1787 A66-23262  
Revised equation for thermokinetic phenomena under Fourier relationship considering certain finite time is required for development, noting role of fluid density 12 p1973 A66-23552  
Conservation principle as applied to heat



equation, assuming equation is one-dimensional 12 p1974 A66-23530

Variational principle application to heat conduction in solids, noting temperature dependence, physical meaning of Lagrangian heat flow between parallel plates, etc 12 p1975 A66-23542

Heat conduction problem simulation, using moving interfaces, solving Stefan and Verigin problems 12 p1978 A66-24371

Plane stationary problem of heat conduction for mixed boundary conditions solved, using Fredholm integral equation with symmetrical kernel 12 p1979 A66-24372

Heat transfer equations for rocketborne stratospheric temperature sensor in form of spherical bead thermistor and experimental analysis of physical, thermodynamic and electrical characteristics of rocketsonde [AIAA PAPER 66-385] 12 p1882 A66-24508

Generalized heat equation solution expansion in terms of radial heat polynomials, Appel transforms and Laguerre polynomials 13 p2118 A66-25793

Solution of quasi-static problem in thermoelasticity for cylinder with time dependent boundary conditions obtained as series of Bessel functions and error functions 14 p2397 A66-27385

Uniqueness theorems of Cauchy problem for parabolic equations of heat conduction 14 p2322 A66-27630

Motion equations for beam with lateral surface thermally insulated, including effects of shear deformation and rotatory inertia and thermoelastic coupling in heat conduction equation 14 p2399 A66-27661

Approximate continuation of harmonic and parabolic functions as solutions of Laplace and heat equations 16 p2732 A66-30242

Propagation theory of chaotic movements in connection with propagation of heat 16 p2693 A66-30581

Asymptotic behavior of solutions to equations for laminar boundary layer far from wall 16 p2684 A66-30582

Solution of heat-conduction equation over functional spaces possessing fractional derivatives with respect to time, applied as solution to first boundary value problem 16 p2827 A66-30779

Temperature distribution and efficiency of thick plate and annular fins used on heat exchangers, space radiators and nuclear fuel elements analyzed through heat conduction equation 16 p2827 A66-30815

Radiant energy transport within cryogenic condensates extended to case of explicitly varying condensate depths and wider substrate temperature range 16 p2830 A66-31712

Floating random walk and use in Monte Carlo solutions to partial differential equation of heat conduction 16 p2739 A66-31720

Stationary heat conduction problems with internal heat sources treated by Kontorovich variational method 17 p3034 A66-32565

Partial differential equation describing transient conduction in multidimensional inhomogeneous media solved by method based on use of known boundary conditions 18 p3262 A66-34380

Additional conditions for boundary value problem with directional derivative in heat conduction 18 p3127 A66-34544

Temperature at wedge under action of heat source of variable dimensions and intensity 18 p3266 A66-35052

Plane steady state problem solved in thermoconductivity theory in case of boundary conditions of third kind for regions of special shape 18 p3267 A66-35055

Heat equation solution in form of series in time derivatives of boundary functions arranged in ascending order 18 p3267 A66-35057

Third boundary problem solution for two-dimensional equation of thermal conductivity in arbitrary region by locally one-dimensional method 19 p3478 A66-35934

Accuracy analysis of variable-direction diagrams for numerical solutions to heat conductivity equations 19 p3478 A66-35937

Thermal conductivity equation solved for four combinations of concentration of radioactive elements in lunar crust, using result for crust thickness

estimate 20 p3648 A66-37151

Properties of functions of metaharmonic and metacaloric equations, using Liouville-Picard theories together with Harnack theory for solutions 21 p3837 A66-39611

Poisson representation of solutions to Cauchy problem for heat equation, showing applicability of Nicolescu method of imaginary reflection 21 p3837 A66-39612

Heat equation solution by use of Crandall optimum finite difference method with boundary discontinuity 22 p3997 A66-40029

Integral equation for heat flux in inverse heat conduction for infinite flat plate as in solid rocket igniters 22 p3998 A66-40031

Thermal transient characteristics of prolate spheroidal solid, using diffusion equation for heat conduction 22 p3998 A66-40034

Heat transfer equation solution for ablating solid, assuming exponential temperature profile with numerical solution on digital computer by Runge-Kutta method 22 p3998 A66-40035

Transient heat conduction problems solved by high capacity computers 22 p3999 A66-40379

Simultaneous one-dimensional heat conduction equations solved by means of matrix similarity transformations in direct computational procedure 22 p3940 A66-40488

Reduction of PDE system of heat transfer, using Hermitian approximating polynomials to obtain solution to initial system 23 p4041 A66-40971

Numerical solution via digital computer of nonlinear transient heat conduction with phase changes 23 p4149 A66-41697

# HEAT EXCHANGER

## SA REGENERATOR

## SA TUBE HEAT EXCHANGER

Heat transfer unit, operational method and data relating heat exchanger performance to deposit forming tendencies of jet fuel for supersonic aircraft [SAE PAPER 650803] 01 p0128 A66-10845

Book on fluid flow and heat transfer for designing, selecting, testing and installing various heat exchangers 02 p0305 A66-12240

Convective heat exchanger using air and subjected to resonant pulsating flow [ASME PAPER 65-HT-30] 04 p0595 A66-13392

Heat loss in space, discussing temperature regulation during space walk via heat exchangers in air ventilated space suit 04 p0470 A66-14070

Effectiveness of split cross-flow heat exchangers, emphasizing uniform exit temperature distribution for unmixed fluids [ASME PAPER 65-HT-24] 05 p0783 A66-14745

Regenerative heat exchangers, covering heat transfer and pressure loss characteristics of glass ceramic matrix materials [ASME PAPER 65-HT-35] 05 p0784 A66-14750

Exact solution for wall and fluid temperature distributions for counterflow heat exchanger with effect of longitudinal heat conduction [ASME PAPER 65-HT-63] 05 p0786 A66-14764

Equilibrium conditions for whole complex cryogenic cycle analyzed by means of Claude-Heyland cycle 05 p0786 A66-14900

Liquid-metal heat transport fluid circulation, discussing molten lithium pump development and testing for high performance mobile nuclear plants [ASME PAPER 65-WA/FE-18] 05 p0689 A66-15611

Single fluid heat exchanger, using Lagrange method and thin walled stainless steel tube for theoretical and experimental dynamic response analysis [ASME PAPER 65-WA/HT-9] 05 p0791 A66-15653

Aerodynamically induced vibration in coolers, describing inclined splitter plates for noise and structural vibration elimination 07 p0991 A66-17492

Heat transfer coefficients in liquid metal concurrent flow double pipe heat exchangers 07 p1150 A66-17582

Heat exchange through absorbing media, determining combined modes of radiation and conduction via exchange factor approximation 07 p1152 A66-17590

Polytropic technique for gas turbine performance, prediction and evaluation, noting use of sophistication factor

[SAE PAPER 660161] 09 p1434 A66-20161

Stagnation temperature control of high-pressure supersonic wind tunnel, using regenerative heat exchangers with porous packing 09 p1471 A66-20802

Liquid-metal heat transport fluid circulation, discussing molten lithium pump development and testing for high performance mobile nuclear plants [ASME PAPER 65-WA/FE-18] 10 p1539 A66-21502

Single fluid heat exchanger, using Lagrange method and thin walled stainless steel tube for theoretical and experimental dynamic response analysis [ASME PAPER 65-WA/HT-9] 11 p1785 A66-22193

Formula determining tubing length in heat exchanger required for steady state heat-transfer coefficient, noting role of Prandtl number 12 p1973 A66-23525

Nonuniform thermal flux for fuel elements and core of nuclear heat exchangers, determining heat transfer coefficient between adjacent fluid streams by mass transfer 12 p1973 A66-23527

Dimensioning heat transfer in compact plate fin heat exchangers under nonuniform temperature variation and heat conductance 12 p1978 A66-24034

Single blow transient testing of compact heat exchanger surfaces [ASME PAPER 66-GT-93] 14 p2411 A66-26997

CERCOR glass-ceramic axial flow rotary regenerator as inexpensive component for gas turbine regeneration [ASME PAPER 66-GT/107] 14 p2301 A66-27004

Incompressible fluid static thrust augmentation devices for aircraft propulsion for cases of presence and absence of heat and work exchange [ASME PAPER 66-GT-116] 14 p2373 A66-27008

Forced convection heat transfer in symmetrical ducts when fluid is liquid metal, examining new prediction methods for engineering analysis and design 16 p2824 A66-30304

Temperature distribution and efficiency of thick plate and annular fins used on heat exchangers, space radiators and nuclear fuel elements analyzed through heat conduction equation 16 p2827 A66-30815

Design and laboratory tests of vapor-phase heat exchanger coupled to power generating bismuth telluride thermopile for waste heat dissipation 16 p2637 A66-31101

Water conditioned suit performance characteristics noting cooling rate, inlet and outlet temperatures, etc 16 p2643 A66-31131

Nonstationary heat-transfer coefficient dependence on thermal stress variation in heat exchanging surface 17 p3034 A66-32559

Aerodynamic noise in wind tunnel heat exchanger 18 p3094 A66-34020

Unidirectional regenerator problem analytically solved, presenting local effectiveness graphs 18 p3261 A66-34361

Vapor-fin heat rejection system employing boiling-condensing cycle, noting performance characteristics 18 p3055 A66-34381

Heat transfer effectiveness-number of transfer unit relations determined, using differential equations to obtain temperature profile of each channel in exchanger 18 p3262 A66-34382

Feasibility analysis of very high temperature uranium-bearing liquid alloy heat exchanger for hydrogen gas, considering several ternary component liquid alloy systems [AIAA PAPER 66-622] 19 p3476 A66-35358

Feasibility of using water condensates recovered from heat exchangers of pressure suits as emergency drinking water source 19 p3294 A66-36379

Indirectly heated PTC resistor for measurements of low pressures and high air velocities, noting basic circuit and application to heat exchangers 19 p3362 A66-36824

Heat exchangers for liquid hydrogen conversion to ambient temperature hydrogen gas, using water heat source 20 p3677 A66-37102

Equilibrium control and burning rate control of solid propellant in heat



exchanger 20 p3629 A66-38155  
 Ranque tube application for gas cooling, discussing performance characteristics of vortex tube with and without heat exchanger 21 p3334 A66-38625  
 Recirculation of liquid through cell and external heat exchanger to solve problem of repeated flashing in europium chelate lasers 21 p3747 A66-39108

## HEAT FLOW

## SA SOLAR HEAT FLOW

Natural convection at thermal leading edge on vertical wall matched with known solution immediately above this region 02 p0304 A66-12199  
 Biot variational method applied to transient heating of porous half-space from which gas escapes [AIAA PAPER 65-118] 03 p0444 A66-12766  
 Negative correlation coefficient between Izsak satellite geoid and Lee and MacDonald heat flow distribution, suggesting correlation between geoidal undulations and heat flow highs and lows 04 p0518 A66-14454  
 Electrical analog model with distributed capacitance and resistance generates charge flow equivalent to two-dimensional transient heat conduction [ASME PAPER 65-HT-66] 05 p0786 A66-14766  
 Macrokinetics of homogeneous-heterogeneous processes in moving media and estimates of initial material concentration in core and boundary layer regions of reaction vessel flow 06 p0971 A66-16543  
 Digital and numerical method solution of transient heat flow problems 07 p1150 A66-17577  
 Thermal stresses due to axisymmetric heat flow past spherical cavity inside long circular cylinder solved by stress functions and thermoelastic displacement potentials 08 p1313 A66-19547  
 Damping of small amplitude vibrations of fine wire as probe of onset and development of critical flow phenomena in He 2 at moderate Reynolds numbers 09 p1365 A66-20016  
 Time dependent stability of one-dimensional laminar flames with distributed heat losses 10 p1621 A66-21809  
 Generalized theorem of minimum entropy production in terms of fluctuation theory and variational principle, noting application to heat flow in rarefied gases 12 p1974 A66-23541  
 Classical and quantum mechanical turbulence in Helium 2 heat flow, noting transition from laminar turbulent flow of normal and superfluid component, Reynolds number dependence on mutual friction coupling, etc 13 p2128 A66-26275  
 Stress concentration at thermally insulated holes in elastic material created by disturbance of uniform heat flow at holes 13 p2206 A66-26459  
 Thermoconductivity and electrical resistivity measurements with derived Lorentz functions for various compounds, using longitudinal heat flow 16 p2771 A66-30252  
 Radiometric temperature measurement of Mars surface microclimate, examining heat flow balance, taking into account solar and planetary radiation effects [AIAA PAPER 66-436] 16 p2799 A66-30522  
 Evolution of two different homogeneous media separated by straight wall with arbitrary transmission and reflection properties, noting heat flow, vibration, diffusion coupled vibration, etc 17 p3036 A66-32842  
 Numerical methods applied to class of flowing fluid thermal problems in space radiators for life support and auxiliary power systems [AIAA PAPER 66-431] 18 p3097 A66-33644  
 Coolant passage wall temperature measurement in nuclear rocket nozzle during chemical stimulation testing by radiometry without affecting hot gas or coolant flow or disrupting heat flow 19 p3356 A66-35632  
 Numerical integration of boundary layer equations for dissociating gas flows, determining heat flow near stagnation point 19 p3341 A66-35739  
 Two-dimensional problems in which heat

flow is predominantly in one direction solved by approximate methods, noting constant profile of temperature 19 p3478 A66-35854  
 Thermal analysis and weight optimization of low-heat-leak storage tanks, particularly aspects important to designers of propellant tanks for long-term lunar storage 20 p3676 A66-37078  
 Role of radiative transfer in mechanism of heat flow in lunar surface, noting magnitude of contribution to transfer 20 p3648 A66-37260  
 One-dimensional heat flow equation for liquid nitrogen end-cooled ruby laser rod 20 p3581 A66-38386  
 Griffith type crack propagation due to localized thermal stress at holes, cavities, penny-shaped cracks and inclusions disturbing uniform heat flow 23 p4146 A66-41993

## HEAT FLUX

Release of persistent current energy by local heat injection and propagation through Nb-Zr wires 01 p0116 A66-10238  
 Heat flux measurements and electrode temperature estimation in pulse electromagnetic plasma accelerator 02 p0265 A66-11398  
 Heat flux from lunar emission incident on surface in circular orbit as function of orbital parameters [AIAA PAPER 64-336] 03 p0425 A66-12756  
 Direct measurements of turbulent thermal flux using airborne pulse type system 04 p0513 A66-13418  
 Measuring thermal fluxes in solid bodies by high temperature gas jets, noting Kastelin-Bronsky method 04 p0596 A66-13653  
 Radiant heat fluxes on surface of heating body with varying temperature 04 p0597 A66-13822  
 Spectral dynamics of laminar convection, discussing transformation of Benard convection problem into spectral domain 04 p0599 A66-14472  
 Nucleate boiling instability of alkali metals noting effects of surface material, chemical treatment, heat flux and cavity geometry [ASME PAPER 65-HT-22] 05 p0783 A66-14743  
 Nonlinear inverse heat conduction problem solved by finite difference method, using least squares and future temperatures [ASME PAPER 65-HT-40] 05 p0784 A66-14753  
 Commercial grade sodium boiling from horizontal disk at various pressures and temperatures attaining high heat fluxes, noting surface finish effects [ASME PAPER 65-HT-51] 05 p0785 A66-14758  
 Pool boiling potassium, discussing heat flux behavior, experimental setup and results for burnout heat flux 07 p1152 A66-17593  
 Discrete bubble regime to merging bubble regime transition in nucleate boiling of methanol and water 07 p1152 A66-17594  
 Thermal conditions in boiling liquids including container wall damage-flux density relationship, stable and unstable boiling in bubble evaporation region and film vaporization 07 p1154 A66-18066  
 Exchange of energy between ionosphere and protonosphere, noting nonlocal heating by photoelectrons, thermal conductivity and heat input by downward flux 08 p1215 A66-19204  
 Distribution of specific thermal flux on body surface heated by plasma jet 09 p1407 A66-20139  
 Measuring thermal flux produced in reflection of shock waves from plane heat-conducting wall 09 p1469 A66-20140  
 First-order perturbation analysis of free convection of liquid metal from isothermal vertical finite plate extended to uniform heat flux 10 p1619 A66-21054  
 Nonuniform thermal flux for fuel elements and core of nuclear heat exchangers, determining heat transfer coefficient between adjacent fluid streams by mass transfer 12 p1973 A66-23527  
 Rarefied gas flow problems solved by hydrodynamic equations and representations of stress tensor and heat flux reproducing Navier-Stokes continuum limit and free molecule limit, noting velocity distribution interpolation 13 p2061 A66-25163  
 Pressure distribution and heat flux on surface of nose cone 14 p2217 A66-27337

Thermokinetic transcendental equation for heat flux through three juxtaposed walls and handling of singularity difficulties [PST PAPER NT-148] 14 p2414 A66-27839  
 Solution for free nonstationary convection in bounded region of Landau-Lifshitz mechanics of continuous media 14 p2414 A66-28282  
 Heat pipe exhibiting very high effective thermal conductivity, showing temperature distribution, boiling heat transfer coefficients, vapor temperature and pressure drop 16 p2827 A66-30910  
 Nucleate boiling instability of alkali metal noting effects of surface material, chemical treatment, heat flux and cavity geometry [ASME PAPER 65-HT-22] 16 p2828 A66-30988  
 Commercial grade sodium boiling from horizontal disk at various pressures and temperatures attaining high heat fluxes, noting surface finish effects [ASME PAPER 65-HT-51] 16 p2828 A66-30988  
 Surface heating rates for metals, semiconductors and insulators subject to high irradiance produced by carbon-arc image furnace 16 p2829 A66-31088  
 Direct measuring radiation calorimeter developed for determining radiant heat flux of solid propellant gas flame in rocket combustion chambers [AIAA PAPER 65-358] 18 p3159 A66-33819  
 Fluid dynamics equations of state, motion continuity and energy stress-strain relationship and shearing stress deformations 18 p3098 A66-34121  
 Conservation equations for two-dimensional axisymmetric simultaneous turbulent mixing and supersonic combustion of hydrogen-oxygen-nitrogen-water streams solved by finite difference methods [AIAA PAPER 66-617] 18 p3099 A66-34211  
 Critical heat flux for boiling water, sodium and rubidium, correlating burnout data for liquid metals only and as relation to metallic and nonmetallic fluids 18 p3262 A66-34374  
 Solid propellant ignition, discussing deflagration wave propagation along gas-solid grain surface, flux equilibrium equation, etc [AIAA PAPER 66-668] 18 p3165 A66-34440  
 Electrostatic field influence on nucleate boiling of Freon 113, noting improvement of peak heat flux 19 p3477 A66-35400  
 Stratification with bottom heating analysis using approximate integral approach 19 p3477 A66-35633  
 Compressive load effects on heat flux through multilayer insulation 20 p3675 A66-37068  
 Surface temperature of seminfinitesimal solid exposed to one-dimensional heat flux calculated with method allowing accuracy at long time intervals 20 p3678 A66-37388  
 Heat-flux density transmitted by relatively broad low-velocity argon plasma jet to vertical cold plate 20 p3608 A66-37466  
 Laminar forced convection heat transfer to gas from circular tube, achieving boundary condition of uniform heat flux 20 p3679 A66-37500  
 Ablation analysis in cylindrical coordinate for axisymmetrical configuration of wall materials with temperature-dependent properties and nonlinear heat flux conditions at boundaries [AIAA PAPER 66-542] 20 p3680 A66-38039  
 Hydrogen/oxygen and hydrogen/air flame temperature experiments on porous flame burner 20 p3680 A66-38044  
 Stability analysis of one-dimensional steady laminar flame propagation with conductive heat loss 20 p3680 A66-38044  
 Turbulence energy balance equation used in air mass transformation problem 20 p3594 A66-38366  
 Atmospheric stratification effect on radiative thermal flux, including diagram for flux estimate from temperature gradient 20 p3594 A66-38377  
 Heat transfer between turbulent flow of air and isothermal wall plate and constant thermal flux at surface 21 p3835 A66-38990  
 Thermal loss measurement at tube end during reflection of shock waves, using platinum thermometers and high speed photography 21 p3727 A66-39093  
 Distribution of specific thermal flux of



- body surface heated by plasma  
 et 21 p3793 A66-39411
- Measuring thermal flux produced in  
 reflection of shock waves from plane heat-  
 conducting wall 21 p3836 A66-39412
- Hypergolic ignition of composite solid  
 propellants, examining oxidizer  
 concentration, heat flux and exothermic  
 reactions 22 p3969 A66-39871
- Integral equation for heat flux in inverse  
 heat conduction for infinite flat plate as in  
 solid rocket igniters 22 p3998 A66-40031
- Nonlinear boundary value problem for  
 temperature distribution in convex solid  
 with radiation boundary  
 condition 22 p3999 A66-40565
- Heat flux dependence and directional  
 effect of thermal contact resistance for  
 interface between dissimilar  
 metals 22 p4006 A66-40921
- Welding, thermal flux control and  
 contamination prevention of Saturn rockets,  
 particularly fusion  
 welding 23 p4073 A66-41534
- Reentry heat flux condition transformation  
 into specified convective coefficients and  
 temperatures, accounting for variation of  
 flux with wall 24 p4261 A66-42795
- Upward heat flux with vanishing counter  
 potential temperature gradient in lower  
 atmosphere and in laboratory  
 experiments 24 p4202 A66-42983
- HEAT GENERATION**
- Heat transfer of internal heat generating  
 fluid in turbulent regime, using electrical  
 dissipation and measuring wall to bulk  
 temperature differences  
 [ASME PAPER 65-WA/HT-15] 05 p0790 A66-15649
- Behavior of current carrying  
 superconducting coil with heat generation in  
 windings, noting voltage-current  
 characteristics 10 p1509 A66-21562
- Plasma oscillation theory of nonlinear  
 acceleration effect and thermal conversion  
 of electron beams upon passage through  
 plasma 17 p2974 A66-33284
- Heat transfer of internal heat generating  
 fluid in turbulent regime, using electrical  
 dissipation and measuring wall to bulk  
 temperature differences  
 [ASME PAPER 65-WA/HT-15] 22 p3997 A66-40028
- Approximate solution of variation problems  
 in heat explosion theory, noting difficulty  
 resulting from heat liberation dependence on  
 temperature 24 p4295 A66-42884
- HEAT PUMP**
- Seebeck and Thomson coefficients and  
 variable resistivity effects on thermoelectric  
 heat pump performance 09 p1333 A66-20971
- Thermomolecular heat pump with cooling  
 from gas diffusion through capillary material  
 driven by external pressure  
 difference 11 p1639 A66-22245
- HEAT REGULATION**
- Personal thermal conditioning system  
 emphasizing heat exchange between body  
 and environment to provide comfort with  
 water-cooled protective  
 clothing 02 p0188 A66-12012
- Thermal management of Lockheed L-2000  
 supersonic transport heat sources and sinks,  
 considering flight profile, aircraft  
 configuration and heat transfer modes  
 [ASME PAPER 65-AV-40] 09 p1329 A66-20298
- Heat regulation, acclimatization and human  
 tolerance upon exposure to moderate, hot  
 and cold temperatures 10 p1489 A66-22119
- HEAT REJECTION DEVICE**
- SA RADIATOR**
- Heat rejection from space radiator of  
 power system used as energy source when  
 integrated with life support  
 system 02 p0186 A66-11642
- Potassium condensing tests of horizontal  
 multitube convective and radiative  
 condensers operating at vapor temperatures  
 from 1250 to 1500 degrees  
 05 p0786 A66-14932
- Heat pipes as heat removal systems in  
 space thermionic power supplies, discussing  
 laminar, turbulent flow and heat transfer  
 efficiency 05 p0789 A66-15542
- Heat pipe performance, emphasizing heat  
 carrying and waste heat dissipation  
 functions, construction and materials  
 testing 05 p0616 A66-15543
- Heat pipe characteristics covering  
 performance analysis and experimental  
 results such as heat transfer rate, life tests,  
 working liquid selection,  
 etc 05 p0616 A66-15544
- Refractory material cermet fabrication,  
 discussing techniques of preparation, fuel-  
 metal compatibility and fuel  
 canning 05 p0713 A66-15585
- Heat rejection per unit weight of radiator  
 with evolve type reflectors compared with  
 radiators with rectangular fins, considering  
 mutual irradiations of neighboring radiator  
 parts  
 [ASME PAPER 65-WA/HT-17] 05 p0790 A66-15647
- Vapor-fin heat rejection system employing  
 boiling-condensing cycle, noting performance  
 characteristics 18 p3055 A66-34381
- HEAT RESISTANCE**
- Strength and heat resistance of alloys,  
 particularly low alloy  
 steels 01 p0084 A66-10286
- Heat transfer between metallic surfaces in  
 contact  
 [AIAA PAPER 65-661] 01 p0086 A66-10599
- Heat resistance in air of four industrial  
 austenitic-ferrite steels with low nickel  
 content at 750-1050 degrees C, noting oxide  
 scale formation 01 p0088 A66-10988
- Packaging techniques interrelated with  
 design specification and manufacturing  
 capabilities noting integrated circuit system,  
 circuit reliability and thermal  
 resistance 02 p0200 A66-11891
- Thermomechanical treatment and  
 temperature on diffusion mobility and heat  
 resistance of titanium  
 alloys 03 p0384 A66-13170
- Temperature effect of plastic deformation  
 on aging kinetics of heat resistant austenitic  
 steels 03 p0385 A66-13171
- Stable dislocation structures obtained by  
 high and low temperature and  
 precrystallization thermomechanical  
 treatment 03 p0385 A66-13172
- Improvement of heat resistance of nickel  
 by high temperature thermomechanical  
 treatment 03 p0385 A66-13173
- Boron addition induced nickel heat  
 resistance measured by internal friction as  
 function of elastic  
 oscillations 05 p0699 A66-14690
- Electrically active impurities effect on  
 germanium thermal resistivity at low  
 temperatures measured on n-type single  
 crystals 05 p0742 A66-15875
- Heat resistant chromium carbide coating  
 with silicate binder applied to  
 steel 06 p0896 A66-18609
- Thermal fatigue of constrained bars made  
 of linearly hardened material evaluated,  
 using mathematical  
 analysis 06 p0967 A66-16969
- Heat resistance and tensile strength of  
 aluminum filament wire compared to  
 ordinary wire 07 p1049 A66-17869
- Sample deformation measuring device for  
 short duration heat resistance  
 tests 07 p1148 A66-18390
- Steady cooling regime of pseudoliquefied  
 layer, determining cooling time and heat  
 transfer coefficients of solid particles and  
 liquid media 08 p1317 A66-18865
- Binary, ternary and quaternary niobium  
 alloy mechanical properties such as  
 resistance to heat, plastic deformation,  
 relation between hardness and rupture  
 strength, etc 08 p1239 A66-18905
- Supersonic aircraft finishes resisting  
 corrosion and high temperatures, including  
 epoxy-amine cured primers, acrylic paints,  
 silicone, synthetic enamels,  
 etc 10 p1547 A66-21136
- Endurance and creep of chromium steels  
 with extended thermal  
 treatment 11 p1716 A66-22746
- Heat resistant nickel-based alloys for gas  
 turbine blades and disks 11 p1716 A66-22752
- Destruction of heat resistant alloys by  
 repeated heating and cooling, deriving  
 formulas which are applied to thermocyclic  
 loads under conditions of stressed  
 state 14 p2310 A66-26790
- Heat resistance, bending and tensile creep  
 of multicomponent Ti  
 alloys 15 p2519 A66-28534
- Trace element effect on lifetime of iron-  
 chromium-aluminum heat-resisting  
 alloy 16 p2723 A66-30311
- Mechanical strength, toughness, elastic  
 modulus, relaxation stability and specific  
 conductivity of copper-titanium  
 alloys 16 p2727 A66-31568
- Structural changes effect on creep  
 resistance of heat resistant  
 alloys 16 p2728 A66-31801
- Effect of temperature, pressure and initial  
 wall treatment on thermal resistance at  
 stainless steel-liquid metal  
 interface 17 p3036 A66-32845
- Heat resistance in air of dispersion  
 hardened nickel alloys containing certain  
 oxides prepared by powder metallurgy  
 methods 18 p3123 A66-33785
- Natural convective heat transfer to gas  
 turbine rotor blade and thermal resistance  
 of cooling system using centrifugal  
 pump 20 p3627 A66-36926
- Experimental assembly for measuring true  
 heat capacity of heat resistant insulating  
 materials during natural cooling at  
 temperatures from 1200 to 2400 degrees  
 K 20 p3556 A66-36989
- Heat sink construction for semiconductor  
 devices 20 p3526 A66-37345
- Nitrogen addition effect on heat resistance  
 of chromium-manganese-austenitic  
 alloys 20 p3584 A66-37695
- Heat resistance of coarse- and fine-grained  
 D20 aluminum alloy 22 p3936 A66-40878
- Alloying principles for refractory metals  
 based on softening mechanism, examining  
 increased heat resistance of rhenium  
 softened by  
 recrystallization 23 p4082 A66-41822
- Thermal conductivity change in single  
 crystal InSb irradiated with electrons,  
 noting additive thermal resistivity  
 increases 24 p4249 A66-42228
- Electron microprobe for studying  
 thermoelectric materials and heat-resistant  
 steel for gas-turbine  
 blading 24 p4211 A66-42507
- Heat resistance of refractory alloys  
 containing nickel, cobalt, tungsten, niobium,  
 etc, and cermets, noting application in  
 rocket engines 24 p4228 A66-43049
- Flat-pack case for thermal resistance of  
 integrated circuit to space  
 environment 24 p4186 A66-43059
- HEAT SHIELD**
- SA RADIATION SHIELDING**
- SA SPACECRAFT SHIELDING**
- SA THERMAL PROTECTION**
- Maximum temperature profile in phenolic  
 resin-siliceous fiber heat shields on ICBM  
 and Mercury spacecraft  
 [AIAA PAPER 65-638] 01 p0162 A66-10596
- Cermet ablatives for thermal shields in  
 fabrication of nozzles and nose cones  
 [SAE PAPER 650767] 01 p0078 A66-10838
- Gemini ablative heat shield, noting  
 nonmetallic honeycomb reinforcement of  
 insulative char 02 p0294 A66-11639
- Turbulent boundary layer interaction with  
 graphite heat shield noting boundary layer  
 velocity, temperature and chemical  
 composition profiles  
 [AIAA PAPER 65-824] 03 p0446 A66-13232
- Make wire, light pipe and spring wire  
 ablation sensors development for measuring  
 parameters of heat shield materials for  
 reentry vehicles 03 p0372 A66-13257
- Stagnation point velocity and pressure  
 distribution over heat-sink shielded reentry  
 vehicle to test boundary layer heat transfer  
 theories 08 p1181 A66-18811
- Ablation rates, surface temperature,  
 emittances and reradiated fluxes of heat  
 shield materials heated by irradiation  
 [AIAA PAPER 66-44] 08 p1318 A66-19070
- Photographic spectra of ablating plastics in  
 thermodynamic environments related to  
 species and temperatures in boundary layers  
 [AIAA PAPER 66-132] 08 p1318 A66-19071
- Flat design and manufacture of heat  
 shields, satellite frame and telemetry  
 antennas for ELDO space  
 booster 12 p1885 A66-23914
- Thermal radiation parameter measurements  
 of coating materials, using steady state heat  
 balance method  
 [AIAA PAPER 64-256] 12 p1979 A66-24701
- Evaluation of polyimide impregnated resins



- for application as heat shield binder when combined with silica and carbon fibers, noting thermostability characteristics 13 p2112 A66-25309
- Composite materials, noting fibrous composites using whiskers, fabrication including spray-up, filament winding, etc, mechanical properties, application for rocket nozzles, heat shields, etc 14 p2318 A66-27228
- Split Teflon shield to delay exposure of plasma arc probe to air jet until equilibrium conditions have been attained 14 p2412 A66-27448
- Ablation of reentry heat shields, discussing fiberglass reinforced phenolic resin, charring, graphite, radiation, etc 14 p2412 A66-27484
- Base thermal environment measured on flight tests of eight-engine LOX/RP-1 propelled Saturn I booster [AIAA PAPER 65-212] 14 p2391 A66-27873
- Structure and thermal protection system of start program including load paths, heat shield, materials, etc 14 p2407 A66-28024
- Structural and heat shield designs for lifting entry vehicles for orbital missions analyzed for effects of wall thickness and weight on vehicle size and total weight 14 p2393 A66-28025
- Radiative-type heat shields using backface cooling in analysis, including thermal effects and structural heat short effects [AIAA PAPER 66-507] 16 p2826 A66-30525
- Material properties and thermal inputs on heat shields for Mars entry, noting importance of insulation vs ablation due to uncertainties in radiant heating inputs 16 p2809 A66-30895
- Double wall ablative heat shield panels for manned lifting entry vehicles, noting nylon phenolic and elastomeric silicone ablators [AIAA PAPER 66-506] 16 p2822 A66-31496
- Definitions of adiabatic shield and amount of heat, discussing inconsistencies 17 p3036 A66-32786
- Char-layer structural integrity limits application of charring-ablator heat-protection materials to advanced ballistic reentry [AIAA PAPER 66-424] 18 p3239 A66-33642
- Optimum entry vehicle design using aerobreaking for manned Earth entry at hypersonic speeds, examining blunted conic, biconic and tetrahedral configurations [AIAA PAPER 66-489] 18 p3239 A66-33657
- Elastomeric ablative thermal shield material to meet system requirements for lifting reentry vehicles having lift-drag ratio of 0.5 to 1.5 18 p3240 A66-33801
- Heat shield and rocket nozzle chemical reactions based on equilibrium thermodynamics of high temperature materials at gas-solid interface 18 p3260 A66-33825
- Refractory metal honeycomb structure fabrication for heat shield panels, using D-36 columbium alloys 19 p3371 A66-36161
- Mariner IV temperature control subsystem hardware, examining thermal shields, thermally actuated louver system and flexible multilayer shields [ASME PAPER 66-MD-64] 21 p3818 A66-38496
- Calculating specific heat and conductivity of ablating specimens exposed to radiant heat fluxes 22 p3998 A66-40032
- Plastic laminates use for ablation shields, noting importance of heat flow and comparison of thermal screens 22 p3938 A66-40417
- Composite thermal coating consisting of refractory facing and slightly heat-conducting decomposing lining 22 p4000 A66-40818
- Gemini ablative heat shield, noting nonmetallic honeycomb reinforcement of insulative char 24 p4283 A66-42773
- Internal thermal behavior of charring cork with reference to heat shield design 24 p4294 A66-42783
- Energy equation of boundary layer in heat-insulating part of flat wall used to derive equations for gas heat shield efficiency, demonstrating effect of nonisothermicity and compressibility 24 p4196 A66-42881
- HEAT SINK**
- Catalytic dehydrogenation of hydrocarbons over chromia-alumina catalyst in absence of added hydrogen to determine heat sink capability 11 p1650 A66-23119
- Thermal stability of endothermic hydrocarbon heat-sink fuels, noting application flying in 10 Mach speed range 11 p1759 A66-23124
- SCR circuit design operating under transient loads higher than steady state rating, using transient capabilities and heat sink 12 p1848 A66-24088
- Solid cryogenics as heat sinks for cooling electronic components, particularly IR detectors in aircraft and spacecraft 20 p3676 A66-37073
- Heat sink construction for semiconductor devices 20 p3526 A66-37345
- HEAT SOURCE**
- Steady nonviscous flow in field with sources of energy, force and mass investigated under assumption of small perturbations 01 p0057 A66-10430
- Stationary heat sources effect on convective fluxes in unstable atmosphere 04 p0513 A66-13413
- Use of point and line heat sources for measuring thermophysical quantities of plane-parallel plates and thin films 07 p1149 A66-17530
- Temperature distribution in infinite closed circular cylindrical shell with fixed heat source of constant intensity 07 p1154 A66-18067
- Heat transfer in fluids with volume heat source homogeneously distributed throughout volume of fluid 08 p1321 A66-19830
- Fusion welding processes dependent upon electric heat source 09 p1384 A66-20610
- Characteristics of two high-power high-intensity radiation heat sources developed by Ames Research Center [AIAA PAPER 66-185] 11 p1638 A66-22214
- Marginal convection in self-gravitating sphere of uniform incompressible fluid with uniform heat sources 11 p1785 A66-22437
- Unsteady temperature field in infinite cylinder in presence of internal heat source 11 p1786 A66-22852
- Interferometric determination of temperature field in two-dimensional finite space in conditions of free convection with internal heat sources 13 p2209 A66-25317
- Vertical displacement rate of air particles in finite volume under effect of internal heat sources in free convection 13 p2209 A66-25318
- Design of isotopic heat sources for space missions, noting atmospheric contamination when source burns on reentry, source and shield weights, sealing of alpha emitters, etc 16 p2745 A66-31710
- Argon arc torch as compact heat source for thermophysical studies 17 p2928 A66-33500
- Temperature at wedge under action of heat source of variable dimensions and intensity 18 p2266 A66-35052
- Stress and displacement field of plane heat source moving at constant speed through elastic medium 21 p3837 A66-39447
- HEAT STROKE**
- Hematological and metabolic effects of short intense thermal stress 09 p1334 A66-20523
- HEAT TEST**
- Book on metal testing at high temperatures including tension, relaxation, compression, impact, nonsteady conditions, hardness, etc 06 p0966 A66-16561
- Single blow transient testing of compact heat exchanger surfaces [ASME PAPER 66-GT-93] 14 p2411 A66-26997
- Heat affected zone cracking in nickel-base superalloys attributed to grain-boundary liquation 14 p2314 A66-27343
- Thermally induced circumferential-longitudinal cracking of refractory metal inserts in solid propellant rocket engine nozzles 19 p3385 A66-36153
- Creep-rupture strength and metallurgical properties of refractory Mo at 4000 degrees F 19 p3385 A66-36156
- HEAT TOLERANCE**
- Hematological changes in seven healthy young males subjected to intense heating transients 01 p0017 A66-10611
- Upper thermal tolerance limits for
- unimpaired mental performance 03 p0325 A66-12313
- Electrophoretic determination on acrylamide gel of lactic dehydrogenase isozyme patterns in serum obtained from human subjects exposed to brief intense thermal impulses 06 p0814 A66-16818
- HEAT TRANSFER**
- SA AERODYNAMIC HEAT TRANSFER
- SA CONVECTIVE HEAT TRANSFER
- SA HYPERSONIC HEAT TRANSFER
- SA LAMINAR HEAT TRANSFER
- SA NUCLEATE BOILING
- SA RADIATIVE HEAT TRANSFER
- SA STEFAN-BOLTZMANN LAW
- SA SUPERSONIC HEAT TRANSFER
- SA THERMAL DIFFUSION
- SA THERMAL EXPANSION
- SA THERMAL RADIATION
- SA THERMODYNAMICS
- SA TRANSPORT PROPERTY
- SA TURBULENT HEAT TRANSFER
- Thermal and electric properties of indium antimonide/indium telluride alloys
- function of composition and anneal temperature 01 p0116 A66-10116
- Text on theory of heat and mass transfer from viewpoint of thermodynamics irreversible processes 01 p0161 A66-10216
- Two-phase flow over flat plate analyzed velocity profile, shear coefficient and heat transfer of laminar boundary layer from over plate 01 p0006 A66-10416
- Heat and mass transfer treated thermodynamically of irreversible processes 01 p0162 A66-10616
- Parameters of internal heat and mass transfer determined from temperature and moisture content measurements and use characteristic function of irreversible thermodynamics 01 p0162 A66-10616
- Heat and mass transfer in nonuniform gas suspension flow treated by irreversible thermodynamics 01 p0163 A66-10616
- Heat transfer in porous solids with gas filling 01 p0163 A66-10616
- Aerodynamic and heat transfer measurements using interferometer with continuous wave laser as source 01 p0069 A66-10816
- Heat transfer - National Conference Boston, August 1963 01 p0163 A66-10816
- Analytical prediction of transient heat transfer performance of thermal energy storage devices 01 p0016 A66-10916
- Surface coating of lyophobic films affecting surface interactions at phase interfaces of heterogeneous systems during transfer process 01 p0166 A66-10916
- Oxygen and combustion, examining mechanisms of flame combustion and study of heat transmission 01 p0166 A66-11016
- Combustion and heat transfer in rocket combustion chamber burning liquid oxygen and gaseous hydrogen 02 p0279 A66-11616
- Heat transfer and friction for laminar flow of gas in circular tube at high heating rate using finite difference method 02 p0304 A66-12116
- Fluids and elastomers for low temperature heat transfer and hydraulic systems [ASLE PREPRINT 65-LC-7] 02 p0249 A66-12216
- Local heat transfer during turbulent gas flow in pipe for large temperature differences, describing test apparatus and results 03 p0443 A66-12516
- Radiative and convective transient heat transfer for photographic windows hypersonic reentry vehicles [AIAA PAPER 64-251] 03 p0444 A66-12716
- Mathematical model for predicting heat transfer in vicinity of protuberances 03 p0444 A66-12716
- Pulse transmitter for measuring heat transfer in ionized gas flow 03 p0370 A66-12816
- Heat transfer and shear between coaxial cylinders of different temperatures for large Knudsen numbers 03 p0445 A66-12916
- Viscous dissipation effect on temperature profile in thermal entrance region between parallel plates, considering flow laminar velocity profile developed 03 p0358 A66-13016
- Heat transfer from shrouded rotating disk to single radial inflow determined, using a turbine model test facility [ASME PAPER 64-WA/HT-49]



- Pressure distribution and heat transfer for flow over simulated cylindrical parachutes  
[ASME PAPER 64-WA/HT-7] 04 p0595 A66-13389
- Base heating of launch vehicles examined by studying heat transfer processes in two-dimensional recirculation zone behind blunt trailing edge in Mach 3 wind tunnel  
[AIAA PAPER 65-825] 04 p0454 A66-13690
- Phase change across interface of suddenly pressurized binary liquid-vapor system  
[ASME PAPER 64-WA/AV-1] 04 p0597 A66-14026
- Unsteady state heat transfer with flowing fluid through porous solids  
[ASME PAPER 65-HT-10] 05 p0782 A66-14736
- Thermal flow meter incorporating effect of axial conduction  
[ASME PAPER 65-HT-19] 05 p0676 A66-14741
- Heat transfer during film condensation of liquid metal vapor, discussing thermal resistance effect of condensation coefficient  
[ASME PAPER 65-HT-29] 05 p0784 A66-14748
- Heat transfer rate to simulated skin, discussing power input determination from temperature rise  
[ASME PAPER 65-HT-33] 05 p0627 A66-14749
- Space-time temperature distribution in one-dimensional systems with heat transfer across contacts  
[ASME PAPER 65-HT-59] 05 p0785 A66-14761
- Monte Carlo method solution of heat transfer in rarefied gas between infinite flat plates  
05 p0787 A66-14987
- One-dimensional transient heat flow through honeycomb sandwich panels  
[AIAA PAPER 64-258] 05 p0775 A66-15080
- Heat conduction in thermocouples with lateral heat leakages applied to calibration microcalorimeters of Calvet type  
05 p0679 A66-15174
- Heating process in laser welding of metal sheets, taking into account energy distribution, heat transfer and flux densities  
05 p0688 A66-15347
- Heat transfer measured at different conditions of diode operation, obtaining data on plasma properties and electrode sheaths  
05 p0616 A66-15546
- Simultaneous radiation, conduction and convection heat transfer for steady state conditions in one-dimensional spectrally selective, emitting and scattering porous media  
[ASME PAPER 65-WA/HT-23] 05 p0789 A66-15642
- Cooling effect of secondary fluid injection on heat transfer between shrouded rotating disk and radially inward main flow stream  
[ASME PAPER 65-WA/HT-20] 05 p0789 A66-15644
- Heat losses from turbulent gas flowing through poorly insulated pipe where heat lost from outer surface is by free convection and radiation, solving heat equation  
[ASME PAPER 65-WA/HT-16] 05 p0790 A66-15648
- Cylinders in reciprocating harmonic vibration, calculating momentum, heat and mass transfer in forced convective field via perturbation technique  
[ASME PAPER 65-WA/HT-6] 05 p0791 A66-15654
- Heat transfer and flow in turbulent separated airflow over downward step in plate surface with suction and injection  
[ASME PAPER 65-WA/HT-2] 05 p0664 A66-15656
- Capabilities and limitations of digital computer steady state and transient heat transfer programs  
[ASME PAPER 65-WA/HT-48] 05 p0638 A66-15661
- Gas-cooled electronic equipment, discussing experimental heat transfer and pressure drop data, packaging and thermal effectiveness parameters  
[ASME PAPER 65-WA/HT-44] 05 p0650 A66-15665
- Axial thermal gradient stresses in finite length thin cylinders, evaluating distinct boundary conditions  
[ASME PAPER 65-WA/MET-17] 05 p0780 A66-15682
- Heat transfer to blunt bodies with catalytic and noncatalytic surfaces in nonequilibrium dissociated hypersonic flow  
[AIAA PAPER 66-3] 05 p0609 A66-15850
- Base heating scaling criteria for four-engine rocket cluster operating at high altitude  
[AIAA PAPER 65-826] 05 p0771 A66-15851
- Energy losses in ruby laser due to heat evolution during optical pumping, noting relation between energy absorption and population inversion  
05 p0698 A66-15858
- Heat transfer at low temperatures, discussing thermal conduction parameters of powdered alumina in helium gas  
06 p0969 A66-16282
- Heat transfer in base flow region, determining parameter of correlation for hydrogen injection and combustion, adiabatic flame temperature, heating rates and recovery temperature  
[AIAA PAPER 66-108] 06 p0970 A66-16408
- Heat transfer from plasmas to water-cooled tubes, using nitrogen, hydrogen and argon with Reynolds number range of 400 to 3500 and various power levels  
06 p0971 A66-16432
- Temperature distribution of fluid in laminar boundary layer of flat plate and heat flow from fluid to plate wall  
06 p0872 A66-16467
- Book on boiling heat transfer and two-phase flow  
06 p0971 A66-16610
- Minimum heat transfer levels and vapor formation in boiling liquid metals  
06 p0972 A66-16843
- Interaction or coupling of radiation with conduction and convection mechanisms in nonisothermal nongray gas flowing in entrance region of tube with isothermal black walls  
[AIAA PAPER 66-136] 06 p0875 A66-17090
- Heat transfer between body and gas flow near stagnation point  
07 p1019 A66-17396
- Heat transfer between two metallic cylinders in close contact, examining effect of interstitial gas on thermal contact resistances  
07 p1149 A66-17452
- Heat transfer - AICE and ASME Conference, Cleveland, August 1964  
07 p1149 A66-17576
- Transient heat transfer from liquid sodium spray impinging on vertical plate  
07 p1151 A66-17587
- Ozone decomposition effect upon heat transfer determined, using differential energy and material balance equations  
07 p1152 A66-17595
- Nucleation and boiling liquids phenomena, using Clapeyron equation in expressing saturation curve  
07 p1154 A66-18029
- Heat transfer and stability of laminar hypersonic separated flow around annular cavity conical model  
07 p0981 A66-18117
- Heat and mass transfer in ion exchange membrane fuel cells  
07 p0995 A66-18326
- Boiling heat transfer in liquid metals including boiling instability, superheats, two-phase flow, forced convection, heat flux, etc  
08 p1316 A66-18684
- Papers on interactions of space vehicles with ionized atmosphere  
08 p1302 A66-18742
- Heat transfer and mass flux expressions for recombination interactions at solid-gas interface due to transport of atomic and ionized particles to spacecraft in ionosphere  
08 p1161 A66-18747
- Stagnation point velocity and pressure distribution over heat-sink shielded reentry vehicle to test boundary layer heat transfer theories  
08 p1161 A66-18811
- Pressure distribution and heat transfer for laminar boundary layer flow over highly swept blunt delta wings in hypersonic free stream  
[AIAA PAPER 66-130] 08 p1162 A66-18953
- Shock tunnel heat transfer measurement and hypersonic viscous flow over pointed cones, particularly viscous-layer regime at low Reynolds numbers  
[AIAA PAPER 66-34] 08 p1163 A66-18957
- Heat transfer processes during ignition of solid propellant rockets, considering radiative and convective components  
[AIAA PAPER 66-66] 08 p1279 A66-18992
- Stagnation point viscous shock layer equations for three-component gas model in chemical nonequilibrium and binary gas model in vibrational and chemical nonequilibrium, noting heat transfer rates  
08 p1164 A66-19125
- Compressible turbulent boundary layer as momentum integral and moment-of-momentum integral equations for arbitrary pressure gradient, noting surface heat-transfer effects  
08 p1207 A66-19126
- Heat transfer in 20-inch hypersonic wind tunnel to two-dimensional inlet ramp at various angles of attack  
08 p1318 A66-19147
- Light pulse absorption in gas and measurement of temperatures attained noting hydrodynamic, breakdown and radiative transfer mechanisms and wave velocities  
08 p1319 A66-19276
- Coolant injection in turbulent boundary layer for protection of surfaces from effects of high temperature and high energy gas flows  
08 p1320 A66-19429
- Time variation in boiling heat transfer caused by bubble generation  
08 p1320 A66-19557
- Momentum, heat and mass transfer in turbulent boundary layer flow of power law fluids over smooth flat plate  
08 p1210 A66-19679
- Hypersonic shock tunnel study, examining effects of roughness, bluntness and angle of attack on boundary layer transition  
08 p1166 A66-19813
- Modified Cochran method giving valid expansions for singular perturbation problems in heat transfer  
09 p1469 A66-20084
- Soviet and foreign papers on physics of boiling including heat transfer, heat release, bubbling processes, kinetics and sonic aspects of boiling and bibliography  
09 p1469 A66-20100
- Measuring thermal flux produced in reflection of shock waves from plane heat-conducting wall  
09 p1469 A66-20140
- Engineering method for measuring rapidly changing temperatures of gas flow with steady or variable heat transfer  
09 p1470 A66-20142
- Critical heat flux under forced motion of underheated alcoholic aqueous solutions  
09 p1470 A66-20148
- Heat transfer through turbulent incompressible boundary layer in presence of moderate pressure gradient  
09 p1366 A66-20174
- Forced convection problem for steady fully-developed laminar flow in straight channel when fluid properties are functions of temperature  
09 p1366 A66-20175
- Heat transfer in laminar flow between parallel porous walls with discontinuous change in wall temperature  
09 p1470 A66-20176
- Heat Transfer Bibliography  
09 p1470 A66-20180
- Boundary layer theory applied to solution of problems of combined heat and mass transfer, using approximate single-parameter integral method  
09 p1367 A66-20703
- Differential equations describing boundary conditions at front of change of aggregation state, computing temperature field  
09 p1471 A66-20825
- Laplace transform and analog computation applied to simulation of heat transfer between wall separated fluids, determining transfer functions and frequency responses  
09 p1472 A66-20908
- Numerical solution of laminar boundary layer momentum, energy and diffusion differential equations for heat and mass transfer on moving continuous flat surface with injection or suction  
10 p1619 A66-21053
- Relativistic transformation laws of thermodynamic variables, including temperature and heat transfer  
10 p1619 A66-21198
- Separation of gas mixture in curved supersonic flow, noting parameters of concentration gradient profile variation  
10 p1522 A66-21269
- Pressure drop and heat transfer to Newtonian fluids in cooled pipes for laminar flow, establishing empirical correlation  
10 p1620 A66-21272
- Heat transfer and distribution of velocity, temperature and concentration in laminar supersonic boundary layers with blowing of light gas with desired pressure and heat distribution  
10 p1620 A66-21394
- Heat transfer measurement to side wall of shock tube behind incident shock wave in argon and xenon



[AIAA PAPER 66-160] 10 p1560 A66-21428  
Entry flight, relation between laboratory flows, in-flight conditions and MGD effects on flow field, drag and heat transfer [AIAA PAPER 66-161] 10 p1611 A66-21682  
MHD natural convection in cylinder, noting independence of thermodynamic profile from magnetic field 10 p1566 A66-21794  
Pressure and heat transfer measurement by FM telemetry for models flying freely in hypersonic wind tunnel  
streams 10 p1538 A66-22041  
Heat transfer during film condensation of liquid metal vapor, discussing thermal resistance effect of condensation coefficient [ASME PAPER 65-HT-29] 11 p1784 A66-22182  
Radiative heat exchange between conducting plates with specular reflection, discussing internal conduction, surface radiation and application to radiating fins [ASME PAPER 65-HT-28] 11 p1784 A66-22183  
Thermal flow meter incorporating effect of axial conduction [ASME PAPER 65-HT-19] 11 p1703 A66-22187  
Cooling effect of secondary fluid injection on heat transfer between shrouded rotating disk and radially inward main flow stream [ASME PAPER 65-WA/HT-20] 11 p1785 A66-22194  
Mass and energy transfer characteristics of cathode attachment zone in high intensity arcs [AIAA PAPER 66-187] 11 p1742 A66-22215  
Temperature jump in polyatomic gases, discussing nonequilibrium energy distribution on boundary conditions 11 p1687 A66-22334  
Wall friction, heat transfer and real-gas propellant effects in two-stage light gas guns 11 p1685 A66-22837  
Differential equations describing air movement, heat exchange and exchange of moisture 11 p1730 A66-22942  
Heat transfer between longitudinal flow of air and staggered cluster of tubes 11 p1787 A66-23311  
Heat transfer information week notes - Conference, Poitiers, France, April 1963 12 p1972 A66-23522  
Nucleate saturated pool boiling over horizontal plate, noting bubble development relation to boiling through heat exchange 12 p1973 A66-23528  
Maxwellian theory, within classical mechanics of fluids, adapted to material and thermal conductivity in turbulent flows, calculating mass and heat transfer 12 p1973 A66-23529  
Wire recovery temperature in steady state wind tunnels determined without detailed knowledge of convective heat transfer rate to wire 12 p1860 A66-23612  
Dimensioning heat transfer in compact plate fin heat exchangers under nonuniform temperature variation and heat conductance 12 p1978 A66-24034  
Transient processes in thermistor circuits during pulsation-type variations in heat transfer 12 p1978 A66-24369  
Heat transfer and mass transfer near stagnation point during injection and suction of various gases through blunt body surface 12 p1979 A66-24427  
Properties of compressible boundary layers with heat transfer and arbitrary pressure gradients calculated, using integral equation and correlation concept for application in hypersonic flows 12 p1865 A66-24581  
Correlation for boundary layer transition on sharp slender cones with heat transfer, using wind tunnel and free flight data 12 p1799 A66-24708  
Nonequilibrium heat transfer distributions around blunt-nosed aerodynamic bodies, using analytical method, for design analyses of hypervelocity flight vehicles 12 p1799 A66-24715  
Heat and mass transfer phenomena analyzed, using thermodynamics of irreversible processes and incorporating certain particular data of kinetic and statistical theories 12 p1980 A66-24910  
Heat transfer in steady flow of non-Newtonian fluid characterized by Rivlin-Ericksen constitutive equation inside wavy cylindrical tube, with momentum and energy equations solved by perturbation technique 12 p1866 A66-24960

Fluids and elastomers for low temperature heat transfer and hydraulic systems [ASLE PREPRINT 65-LC-7] 12 p1901 A66-24992  
Viscous hypersonic blunt body problem examined, using Newtonian thin-shock-layer theory, slp effect, Navier-Stokes shock structure, etc 13 p1990 A66-25157  
Heat exchange between axisymmetric jet flow and plate situated normal to flow 13 p2208 A66-25313  
Analog computation of contact thermal resistances for two joined materials and interstitial gas 13 p2209 A66-25477  
Heat transfer measurement in solid cylindrical isotropic probes, considering isothermal heat transmission under steady state conditions 13 p2209 A66-25566  
Temperature stresses and heat transfer at thin plate edges reinforced with thin rods under nonstationary thermal conditions 13 p2202 A66-26416  
Variation of mean thermal conductivity of nickel-cadmium cell determined as function of overcharge current and environmental temperature [AIAA PAPER 64-751] 13 p2007 A66-26652  
Fluid mechanics - Midwestern Mechanics Conference, Case Institute of Technology, Cleveland, April 1963 13 p2068 A66-26701  
Approximate methods of computing heat transfer through laminar boundary layer, considering boundary layer along flat plate and second order effects 13 p1993 A66-26712  
Electrical analogy for turbulent liquid metal heat transfer in noncircular duct entrance region, solving Fourier equation, determining fluid boundary conditions, temperature distribution, etc 13 p2210 A66-26717  
Steady state motion of Couette plasma flow in electric field, assuming transfer of collective motion is effected by ions and heat transfer by electrons 14 p2339 A66-26774  
Critical heat flow for propagated heat exchange crises during boiling of liquid 14 p2410 A66-26787  
Heat transfer bibliography of 32 Japanese works including heat transfer application, phase change, separated flow, radiation, transpiration and mass transfer 14 p2410 A66-26937  
Heat transfer bibliography of Russian works including conductive, convective and radiant heat transfer, phase and chemical conversions, mass transfer, etc 14 p2410 A66-26938  
Heat transfer rate in thermal inlet of circular tube, describing experimental apparatus and observational results 14 p2411 A66-27313  
Heat transfer equation to find temperature distribution in two-dimensional and circular jets 14 p2274 A66-27378  
Laminar separated hypersonic flow over spiked bodies in gun tunnel for analyzing parameters influencing heat transfer rates in reattachment region 14 p2218 A66-27403  
Nonequilibrium laminar boundary layer of binary dissociating gas determined by solving nonlinear partial differential equations governing system [AIAA PAPER 65-129] 14 p2274 A66-27406  
Enthalpy of gas stream, calorimeter surface treatment and heat transfer measurement errors in arc-heated tests 14 p2411 A66-27425  
Heat transfer problems associated with thermal analysis, discussing influence of rate of heat transport on heat transfer process 14 p2412 A66-27494  
Hydraulic resistance and heat transfer in laminar-turbulent transition region in tube with heating and cooling of water 14 p2414 A66-27830  
Heat transfer considerations in aircraft-engine design noting fuel, oil and icing problems 14 p2375 A66-28300  
Stimulated interphase heat transfer in nonuniform gas flow with suspended particles and periodic motion variations 14 p2415 A66-28322  
Heat and mass transfer treated by thermodynamics of irreversible processes 14 p2416 A66-28486  
Heat and mass transfer in radial flow between two fixed or co-rotating parallel disks, obtaining series expansion of Navier-

Stokes equation 15 p2615 A66-2860  
Flow pattern and heat transfer distribution in regions of adverse pressure gradient at separated flow over two-dimensional model in Mach 10 airflow 15 p2424 A66-2920  
Displacement and heat transfer effects in laminar and turbulent boundary layers downstream in slowly expanding hypersonic nozzle, determining inviscid core flow 15 p2424 A66-2920  
Catalytic efficiency of noncatalyst interferes with accuracy of measurement noting necessity of oxygen treatment on noncatalytic surfaces 15 p2502 A66-2990  
Heating process in laser welding of metal sheets, taking into account energy distribution, heat transfer and fluid densities 15 p2511 A66-2990  
Book on heat transfer covering instrumentation and analytical techniques for definitive solution to classical and complex problems 16 p2824 A66-3000  
Free stream turbulence effects on heat transfer rates evaluated by boundary layer approximation 16 p2824 A66-3000  
Mass transfer, friction and heat transfer analyzed and calculated for turbulent boundary layers in compressible flow 16 p2824 A66-3000  
Hydraulic resistance, heat and mass transfer in vortical flow, noting possible optimal conditions of operation 16 p2825 A66-3000  
Effect of orifice dimensions and heat transfer to surface with orifice on pressure measured in low density gases 16 p2628 A66-3000  
Gravity effect on nucleate boiling heat transfer 16 p2825 A66-3000  
Thermal contact resistance between smooth rigid isothermal planes separated by elastically deformed smooth spheres [AIAA PAPER 66-461] 16 p2814 A66-3000  
Monte Carlo solutions to two molecular flow problems, heat transfer between parallel walls and shock wave profile computer programmed in Boltzmann equation analysis 16 p2686 A66-3000  
Heat transfer rate to simulated skin discussing power input determination from temperature rise [ASME PAPER 65-HT-33] 16 p2643 A66-3000  
Simultaneous radiation, conduction and convection heat transfer for steady state conditions in one-dimensional spectral selective, emitting and scattering porous bed [ASME PAPER 65-WA/HT-23] 16 p2828 A66-3000  
Intensification of heat transfer in bundle of tubes with transverse ribs in longitudinal flow 16 p2828 A66-3100  
Local heat transfer rates and pressure distributions over windward half of yawed circular cylinder at Mach 8 16 p2630 A66-3100  
Wire-to-surface heat transfer and error in hot-wire anemometer measurements 16 p2708 A66-3100  
Diffusive corrosion processes caused by circular tubes by reactive fluid simulated rotating disk electrodes 16 p2728 A66-3100  
ONERA research on use of magnetic suspension systems in hypersonic wind tunnels and measurement of base pressure and heat transfer rates 16 p2683 A66-3100  
Ribbon ablative thermocouples for 3000 to 5000 degree F range 17 p2924 A66-3200  
Pressure distribution, skin friction and heat transfer for sharp and blunt-nosed slender bodies in hypersonic air flow 17 p2837 A66-3200  
Base, recompression and laminar near wall regions of cones in hypersonic air flow 17 p2838 A66-3200  
Dimensional analysis of temperature distribution within spherical particle during nonisothermal evaporation 17 p3033 A66-3200  
Wall heat transfer behind plane detonation wave moving past flat plate into stationary hydrogen-oxygen mixture 17 p3033 A66-3200  
Hypersonic wind-tunnel test program giving data on turbulent boundary layer with mass addition including Mach number effect on heat transfer and skin friction reduction and massive flow blowing 17 p2839 A66-3200



- Secondary flow for supersonic boundary layers with or without swept edges, noting effect of compressibility and heat transfer on reverse flow 17 p2840 A66-32485
- Heat transfer problems solved, using Pohlhausen solution for phase-space trajectory, noting effect of boundary conditions and application of analog computer 17 p3034 A66-32497
- Heat transfer and stress wave evolution prior to ablation and thermal equilibrium in exposure of solid and liquid materials to laser sources 17 p2979 A66-32638
- Temperature and pressure distribution for fluid flow through porous matrix, noting chemical reaction, heat transfer, boundary layer flow, etc 17 p2910 A66-32752
- [AIAA PAPER 66-423] 17 p2910 A66-32752
- Series solution to parabolic PDE for heat transfer from smooth wall to turbulent boundary layer 17 p3037 A66-33041
- Heat transfer bibliography including listing of works on boundary layer flow, phase change, channel flow, MHD conduction, etc 17 p3037 A66-33043
- Heat transfer bibliography of Russian works, including listing of works on thermodynamics, heat conduction, radiant and convective heat transfer processes, phase change, mass transfer, drying processes, etc 17 p3037 A66-33044
- Flow structure and heat transfer for rearward facing step in supersonic flow, discussing critical Reynolds number, flow through lip shock, etc 17 p2913 A66-33068
- Fluid mechanics and heat transfer - Conference, Santa Clara, June 1966 17 p3038 A66-33467
- Gas-phase heat-transfer augmentation by steady and alternating electric field in pipeflow 17 p3039 A66-33473
- Stagnation-point heat-transfer measurements in partially dissociated supersonic air arc tunnel 17 p3040 A66-33484
- Turbulent boundary layers in compressible and incompressible flow, examining pressure gradients, temperature distribution and heat transfer effects 18 p3097 A66-33595
- Heat transfer caused by combustion of triethylaluminum on flat plate in Mach 3 flow, noting significance of lag at stagnation pressure 18 p3260 A66-33817
- Heat transfer - AICE and ASME Conference, Los Angeles, August 1965 18 p3261 A66-34375
- Heat transfer effectiveness-number of transfer unit relations determined, using differential equations to obtain temperature profile of each channel in exchanger 18 p3262 A66-34382
- Temperature profile and design parameters in adiabatic fuel cell with stationary electrolyte where cooling takes place by convection and conduction 18 p3263 A66-34386
- Heat transfer rates and two-color temperature measurements for propane-oxygen flame seeded with aluminum powder [WSCI 66-2] 18 p3264 A66-34422
- First-order correction to Houtt theory for measuring ion density in D region, respectively those involving heat transfer and compressibility 18 p3107 A66-34523
- Temperature distribution and propagation of periodic temperature fluctuations in damped semiinfinite rod 18 p3267 A66-35061
- Soviet bibliography on heat and mass transfer 18 p3267 A66-35062
- Stagnation point heat transfer in dissociating or ionizing real gases for case of discontinuous Prandtl numbers 19 p3478 A66-35749
- Couette flow and heat transfer through hard-sphere rarefied gas enclosed between parallel walls analyzed by Monte Carlo method 19 p3478 A66-35803
- Linearizer for constant temperature hot-wire anemometer, detailing linearization circuit 19 p3357 A66-35806
- Heat release mechanism of developed nucleate boiling process 19 p3478 A66-35940
- Molecular-kinetic resistance effect on heat exchange in Nusselt-type vapor condensation on vertical plate and in vapor-bubble growth in superheated liquid 19 p3479 A66-36310
- Pulse transmitter for measuring heat transfer in ionized gas 19 p3362 A66-36772
- Heat transfer, thermal conductivity and thermal diffusivity of loose fibrous materials under vacuum 20 p3587 A66-36978
- Heat transfer in turbulent carbon dioxide pipeflow at supercritical region 20 p3674 A66-36983
- Thin Insulating Teflon film bonding to internal surface of space cryopanels for increased heat transfer and faster cooling 20 p3677 A66-37100
- Laminar, turbulent and transition heat-transfer domain analysis of cryogenic fluids in variable reduced-gravity environment, with applications to space cryogen storage 20 p3677 A66-37103
- Heat transfer literature published in 1965 on conduction, channel flow, boundary layer flow, separated flow, transfer mechanism, etc 20 p3678 A66-37117
- Analytical expressions for maximum slope of fluid temperature transient response, based on Hansen mathematical model, and for reduced time slope 20 p3678 A66-37119
- Blasius series for heat and mass transfer in two-dimensional boundary layers, discussing velocity and concentration profiles 20 p3678 A66-37122
- Sealed nickel-cadmium batteries for space power systems, noting 100 amp-hr cell with adhydrode and systems considerations relating to heat transfer and charge control 20 p3497 A66-37161
- Non-Newtonian viscoelastic fluids with similarity transformations for power law fluids, noting momentum, energy and heat transfer 20 p3545 A66-37510
- Differential equations describing air movement, heat exchange and exchange of moisture 20 p3593 A66-37855
- Thermodynamics of combustion and concepts of aerothermochemistry using Newton-Raphson iteration process, noting transfer phenomena of matter, heat and momentum 20 p3680 A66-38090
- Equivalent circuit for pyroelectric materials used in obtaining noise equivalent power for detection of electromagnetic radiation and heat transfer measurement 20 p3562 A66-38405
- Soviet and foreign papers on physics of boiling covering heat transfer, heat release, bubbling processes, kinetics and sonic aspects of boiling, including bibliography 21 p3834 A66-38509
- Boundary layers with coupled heat and mass transfer for large enthalpy per unit mass of injected material, based on linearity of perturbation equations 21 p3834 A66-38704
- Assembly and packaging of microelectronic systems by integrated circuits, considering spatial configuration, maintainability, interconnection, thermal transfer and environmental resistance 21 p3710 A66-38830
- HF pressure fluctuations in heat transfer of diisopropyl hexane seen as caused by shock waves produced by collapsing bubbles 21 p3835 A66-38906
- Heat transfer between turbulent flow of air and isothermal wall plate and constant thermal flux at surface 21 p3835 A66-38907
- Nonisentropic nonequilibrium lithium plasma flow through nozzle with allowance for friction and heat transfer 21 p3694 A66-39088
- Heat transfer in wake of reflected shock wave in reacting gases, using calorimetry and shock tube technique 21 p3727 A66-39095
- Thermal conductivity and accommodation coefficient measurements in gas mixture of atomic and molecular oxygen 21 p3836 A66-39174
- Nondestructive testing for material evaluation, noting color radiography, ultrasonic imaging, transmission, attenuation, heat transfer and residual stress measurement 21 p3830 A66-39192
- Measuring thermal flux produced in reflection of shock waves from plane heat-conducting wall 21 p3836 A66-39412
- Engineering method for measuring rapidly changing temperatures of gas flow with steady or variable heat transfer 21 p3836 A66-39413
- Heat transfer in conducting, absorbing, emitting, scattering and heat generating medium 21 p3836 A66-39438
- Heat transfer in laminar flow of Bingham material through circular pipe, taking into account dissipation effect 21 p3836 A66-39441
- Thermal conductivity of carbon dioxide in critical region interpreted, considering gas as mixture of clusters and heat transfer due to formation and breaking of clusters 21 p3837 A66-39454
- Boundary layer equation solution along vertical hot plate for constant plate temperature, noting use of Blasius technique 21 p3837 A66-39590
- Photography of small freely moving particles undergoing heat and mass transfer, using beam splitter to align two cameras on drop 22 p3917 A66-39675
- Book on flow and thermal boundary layers including laminar and turbulent flow velocity profiles, Prandtl equation, heat transfer problems, etc 22 p3897 A66-39702
- Heating environment for space vehicle, examining wind and incident radiation effects on heat transfer to liquid hydrogen, insulation surface thermal properties and optimization of insulation system 22 p3986 A66-39777
- Gas flow equations for multilayer insulation systems for both continuum and free molecular flow regimes of interest in cryogenic space vehicle design [AICE PREPRINT 22A] 22 p3897 A66-39888
- Heat transfer and flow in turbulent separated airflow over downward step in plate surface with suction and injection [ASME PAPER 65-WA/HT-2] 22 p3898 A66-40025
- Heat losses from turbulent gas flowing through poorly insulated pipe where heat lost from outer surface is by free convection and radiation, solving heat equation [ASME PAPER 65-WA/HT-16] 22 p3997 A66-40027
- Mean viscous dissipation and bulk temperature variation in incompressible fully developed duct heat transfer, using Green theorem 22 p3998 A66-40033
- Heat transfer from gray fin-tube radiators with numerical results for diffuse surfaces, noting fin and tube emissivities 22 p3998 A66-40037
- Semi-diurnal oscillation in surface pressure as result of strong resonance amplification of small oscillations due to surface heating and gravitational tidal force of Sun 22 p3942 A66-40052
- Marangoni flow, motion of liquid surfaces under influence of surface tension gradients, explaining high fluxes obtained in boiling heat transfer 22 p3999 A66-40303
- Interaction between hypersonic wake flow and aerodynamic deployable decelerator, predicting pressure and heat transfer of decelerator 22 p3846 A66-40605
- Probe design for mass flux, stagnation point heat transfer and total enthalpy measurements of high temperature hypersonic gas flows [AIAA PAPER 66-750] 22 p3919 A66-40635
- Shock impingement on blunt body in hypersonic flow, noting alteration of flow and local heat transfer rate near impingement point [AIAA PAPER 66-756] 22 p3846 A66-40641
- Short duration technique providing simulation of thermodynamic properties and composition of exhaust products of liquid and solid propellant rocket engines [AIAA PAPER 66-760] 22 p3894 A66-40643
- Nonaxisymmetric temperature fields for orthotropic hollow cylinder and sphere solved using Bessel functions, noting heat transfer between external and internal surfaces 22 p4000 A66-40693
- Matrix functions and use in problems of heat and mass transfer 22 p4000 A66-40820
- Heat transfer in nonisothermal plate with laminar boundary layer 22 p4000 A66-40822
- Mechanism of nucleate boiling from superheated surface studied fluid-dynamically and thermodynamically 22 p4000 A66-40918
- Temperature profiles and Nusselt numbers for heat transfer to MHD laminar Hartmann flow in thermal entrance region of flat duct 22 p4000 A66-40920
- Approximate solution of PDE for heat transfer in uniform-property universal turbulent boundary layer 22 p4001 A66-40923



Heat transfer through turbulent boundary layer, using velocity and temperature profiles as phenomenological relations 23 p4147 A66-41120

Heat transfer in entrance section in rectangular duct for incompressible fluid in laminar pulsating flow with periodic pressure gradient 23 p4148 A66-41216

Spontaneous ignition of inflammable fluids by hot surfaces, discussing static hot plate and wind tunnel rigs 23 p4083 A66-41278

Apollo launch escape tower electroexplosive bolts produced heat transfer to surrounding structural members, obtaining sound intensity maps 23 p4119 A66-41310

Monograph on kinetic theory of plasmas, deriving state equation, Maxwell equation for plasma-magnetic field interaction and boundary layer heat transfer expressions 23 p4102 A66-41400

Dirac delta function representation of spark ignition, considering heat transfer from reaction zone to fresh gas and flame propagation 23 p4148 A66-41413

Initial broadening of diffusion flame sheet caused by nonvanishing equilibrium constant determined, using method of inner and outer expansions 23 p4148 A66-41500

Out-of-pile thermionic power system using inert gas for heat transfer from reactor to converter, noting creep-rupture problem of materials 23 p4023 A66-41767

Thermal transport in channel-gas flow, discussing integral equation and power series solution 23 p4150 A66-41869

Heat transfer to blunt bodies with catalytic and noncatalytic surfaces in nonequilibrium dissociated hypersonic flow [AIAA PAPER 66-3] 23 p4150 A66-41878

Approximate integral method for determining thermal boundary layer and heat transfer on flat plate with insulated surface 23 p4150 A66-41920

Heat transfer in incompressible viscous fluid between two nearly parallel walls with harmonically varying distance, determining velocity field and temperature distribution 23 p4150 A66-42029

Network for compensating electrical output of thin film resistance thermometers for deviations due to large heat-transfer rates 24 p4207 A66-42176

Pyroelectric heat-transfer sensor performance compared with thin skin thermocouple heat sensors, noting discrepancy in measurement results in severe environment 24 p4207 A66-42177

Semiconductor surface thermocouples, determining heat-transfer rates associated with wind tunnel testing 24 p4208 A66-42178

Characteristics of plasma generator with transpiration-cooled porous electrode, noting related heat transfer studies 24 p4161 A66-42263

Benard convection between free bounding surfaces for ranges of Rayleigh and Prandtl numbers achieving steady state with motion of single large cell, evaluating eigenfunction amplitudes 24 p4293 A66-42409

Flat plate laminar boundary layer in supersonic wind tunnel, measuring pressure distribution and profiles and heat transfer rates, noting dissociation fraction effects 24 p4194 A66-42411

Heat transfer from enclosed rotating disk, analyzing effects of radial outflow and inflow on temperature profile and Nusselt numbers on rotor and stator 24 p4294 A66-42705

Ordered state theory and application to technological and theoretical heat transfer problems 24 p4294 A66-42735

Thermal emission in subsonic and supersonic nozzles based on energy equation solution and laws of heat transfer 24 p4295 A66-42878

**HEAT-TRANSFER COEFFICIENT**

Variation of local heat-transfer coefficients produced by impinging jets reexamined in light of velocity and turbulence distributions effects 02 p0304 A66-12197

Surface cooling effect on accuracy of black body coefficient determination for highly heated materials 03 p0444 A66-12518

Free convection heat transfer in partially enclosed channel flow, noting effect of vertical fin geometry and temperature

[ASME PAPER 64-WA/HT-33] 04 p0595 A66-13386

Thermal energy transfer in base portion of stagnant region obtained from plane and axisymmetric flow 04 p0454 A66-13570

Heat transfer and flow friction characteristics of matrices of high porosity with radiation heat source [ASME PAPER 65-HT-6] 05 p0782 A66-14734

Heat transfer coefficient by impingement of two-dimensional air jets [ASME PAPER 65-HT-20] 05 p0605 A66-14742

Heat transfer to two-phase film-boiling nitrogen, discussing straight and swirl flow experimental apparatus [ASME PAPER 65-HT-37] 05 p0773 A66-14751

Transient quenching method of determining critical heat flux and transfer coefficients in film and nucleate boiling liquid metals, specifically magnesium [ASME PAPER 65-HT-49] 05 p0785 A66-14757

Relation between flow in separated region and heat transfer for shallow rectangular cavity in subsonic turbulent airflow 05 p0607 A66-15463

Heat transfer and equilibrium temperature on flat plate in region of strong interaction in hypersonic flow 05 p0607 A66-15465

Heat transfer and wall friction for low velocity flow of gases in downstream region of smooth electrically heated tubes, considering transition region [ASME PAPER 65-WA/HT-18] 05 p0790 A66-15646

Heat transfer and velocity characteristics of thermal and hydrodynamic laminar flow in ducts of arbitrary cross section, considering boundary conditions at wall [ASME PAPER 65-WA/HT-13] 05 p0790 A66-15650

Flow separation effect on heat transfer characteristics of turbulent pipe flow [ASME PAPER 65-WA/HT-12] 05 p0790 A66-15651

Helium II film free-convection heat transfer, discussing mathematical analysis for vertical flat plate and horizontal circular cylinder [ASME PAPER 65-WA/HT-10] 05 p0791 A66-15652

Laminar heat transfer and pressure distribution in open cavity supersonic flow, noting heat-transfer coefficient [ASME PAPER 65-WA/HT-37] 05 p0608 A66-15670

Local heat transfer coefficients in nozzle under conditions of cold-wall low density high speed laminar flow 05 p0609 A66-15774

Nonuniqueness of stationary solutions to system of equations in burning theory with piecewise invariable reaction rate and thermoconductivity and diffusion coefficients 06 p0970 A66-16345

System of adjustable parameters for measuring fast varying temperatures in bounded space, using thermocouple with compensating circuit 06 p0879 A66-16420

Friction-drag and heat-transfer coefficients of plate in turbulent gas flow, estimating effect of turbulent Prandtl number 06 p0872 A66-16469

Heat transfer rate to stagnation point of catalytic surface placed in slow flow of dissociated oxygen from glow discharge tube and atom-molecule diffusion coefficient 06 p0822 A66-16632

Heat transfer coefficients for helium and hydrogen gas flowing through electrically heated Inconel tube 07 p1148 A66-17300

Empirical formula for convection coefficient of bounded space of parallelepiped shape permits determination over wide range of parameters 07 p1148 A66-17393

Local heat transfer to immersed cylinder in transonic cross flow for gaseous stream 07 p1150 A66-17581

Heat transfer coefficients in liquid metal concurrent flow double pipe heat exchangers 07 p1150 A66-17582

Convective heat transfer coefficients at rocket nozzle throat handling nonaluminized propellant gas 07 p1151 A66-17583

Liquid metal condensation, noting two-phase turbulent condensation mechanism and determining heat transfer coefficients 07 p1152 A66-17592

Steady state thermal conductance coefficient at interface formed by nominally flat rough contacting surface placed in vacuum environment 07 p1153 A66-17893

[AIAA PAPER 66-42] 07 p1153 A66-17893

Surface pressure, heat transfer coefficient, wave structure and shock disturbances of inviscid supersonic flow field along corner of intersecting wedges [AIAA PAPER 66-128] 07 p0984 A66-18462

Steady cooling regime of pseudoliquefied layer, determining cooling time and heat transfer coefficients of solid particles and liquid media 08 p1317 A66-18865

Stationary heat transfer through wall with longitudinal rectangular ribs and variable coefficient of thermal conductivity 08 p1319 A66-19426

Effectiveness and heat transfer coefficients with transpiration of distilled water and air examined across porous plate 08 p1320 A66-19558

Turbulent heat transport coefficient of various fluids in pipes measured, obtaining formula from experimental data 09 p1367 A66-20702

Slender profile of infinitely thin supersonic wing that provides minimum mean heat transfer coefficient at given lift-drag ratio 09 p1328 A66-20750

Local and average heat-transfer coefficients for encased rotating disk cooled by radial flow 09 p1471 A66-20820

Heat transfer and flow friction characteristics of matrices of high porosity with radiation heat source [ASME PAPER 65-HT-6] 11 p1785 A66-22188

Heat transfer coefficient by impingement of two-dimensional air jets [ASME PAPER 65-HT-20] 11 p1629 A66-22196

Flow separation effect on heat transfer characteristics of turbulent pipe flow [ASME PAPER 65-WA/HT-12] 11 p1785 A66-22199

Nonuniqueness of stationary solutions to system of equations in burning theory with piecewise invariable reaction rate and thermoconductivity and diffusion coefficients 11 p1785 A66-22341

Saturated film-boiling heat transfer coefficient measurements of ethanol, pentane and Freon 113 at atmospheric pressure [ASME PAPER 65-AV-37] 11 p1786 A66-22468

Turbulent heat transport coefficient of various fluids in pipes measured, obtaining formula from experimental data 11 p1688 A66-22593

Heat transfer in turbulent flow of incompressible fluid in plane curved channel 11 p1694 A66-23318

Single observation method for determining coefficient of heat transfer as function of temperature in stationary regime 11 p1787 A66-23318

Heat-transfer coefficient for annular dispersed flows in absence of vaporization explaining high values obtained by flux profile effect 12 p1973 A66-23522

Formula determining tubing length in heat exchanger required for steady state heat transfer coefficient, noting role of Prandtl number 12 p1973 A66-23522

Nonuniform thermal flux for fuel element and core of nuclear heat exchangers determining heat transfer coefficient between adjacent fluid streams by mass transfer 12 p1973 A66-23522

Thin body temperature during periodic variations of heat transfer coefficient in ambient medium 12 p1978 A66-24372

Surface temperature of solid bodies measured by crayons, thermography, hardness, etc, particularly heat transfer tubes, current-carrying bodies, etc 12 p1882 A66-24400

Saturated and surface film boiling from horizontal isothermal plate in longitudinal flow field analysis, based on two-phase boundary layer theory, correlating heat transfer and skin friction characteristics 12 p1980 A66-24900

Heat-transfer coefficients calculated for forced convection from heated flat plate at zero incidence to stream of viscous fluid noting role of Reynolds number 12 p1981 A66-24940



- Engineering method for calculating distribution of convective heat transfer for continuous boundary layer gas flow past body 13 p2208 A66-25316
- Heat transfer through contact zone of two solids which are joined 13 p2209 A66-25445
- Distribution, as function of azimuth, of static pressure and mass and heat transfer coefficients for case of interaction between detached shock wave on cylinder nose in supersonic flow and turbulent boundary layer along wall 13 p1991 A66-25464
- Forced turbulent convective incompressible flow along rough plates, measuring velocity and temperature profiles 14 p2410 A66-26934
- Measurement of heat exchange coefficient for heated cylindrical copper wire immersed in sand particles or glass beads at various low pressures 14 p2415 A66-28319
- Heat transfer coefficients between layers of thin film structure on niobium and aluminum substrates at liquid helium temperature 15 p2616 A66-28763
- Convective heat transfer to particles in shock-heated gas 15 p2617 A66-29300
- Heat transfer in liquids situated in gap between coaxial cylinders in presence of natural convection, determining effective thermal conductivity coefficient for water and ethanol 16 p2825 A66-30325
- Heat pipe exhibiting very high effective thermal conductivity, showing temperature distribution, boiling heat transfer coefficients, vapor temperature and pressure drop 16 p2827 A66-30914
- Heat transfer and wall friction for low velocity flow of gases in downstream region of smooth electrically heated tubes, considering transition region ASME PAPER 65-WA/HT-18 16 p2828 A66-30991
- Reynolds analogy computation of heat transfer coefficient of turbulent electroconducting liquids in transverse magnetic field 16 p2765 A66-31401
- Mass evaporation rate and heat transfer coefficients for water drops supported by own superheated vapor over flat plate 16 p2830 A66-31680
- Nonstationary heat-transfer coefficient dependence on thermal stress variation in heat exchanging surface 17 p3034 A66-32559
- Velocity and temperature profiles, hydrodynamic elements, heat transfer and friction coefficients of turbulent incompressible flow through circular and flat tube 17 p2909 A66-32583
- Turbulent flow near boundary and equations for mass- or heat-transfer coefficient in terms of turbulent diffusion coefficient and thermal diffusivity 17 p3037 A66-33042
- Heat transfer resulting from normal impingement of turbulent high temperature jet on infinitely large flat plate 17 p3039 A66-33470
- Local and mean heat transfer coefficients determined in tubes with high heat flux densities 18 p3261 A66-34360
- Mass evaporation rate and heat transfer coefficients for water drops supported by own superheated vapor over flat plate 18 p3262 A66-34378
- Condensation tests in smooth and porous coated tubes in multi-g centripetal acceleration fields for increasing heat transfer coefficient of condensing nitrogen 18 p3262 A66-34379
- Properties of small tube Teflon heat exchangers noting corrosion resistance, smooth slippery surface, etc, and heat transfer coefficient 18 p3262 A66-34383
- Forced convection heat transfer coefficient of single pin fixed on plate, deriving expression for case corresponding to infinite circular cylinder 18 p3266 A66-34647
- Method for determining temperature dependence of heat conductivity of dielectric and semiconductor materials 18 p3159 A66-35054
- Heat transfer between fluidized bed and submerged cylinder 18 p3267 A66-35056
- Nonequilibrium thermoconductivity coefficient for heat transfer in dissociating gas system at low pressure 19 p3477 A66-35366
- Sound field parameter dependence of coefficient of heat transfer from horizontal cylinder at near zero Grashof numbers 19 p3478 A66-35751
- Heat transfer coefficients over range of Reynolds numbers for solid-vapor mixture of parahydrogen discharge below triple point pressure 20 p3679 A66-37511
- Resistance and heat transfer coefficient relation theoretically determined for flow of electrically conducting liquid in magnetic field 20 p3679 A66-37614
- Heat transfer between copper sphere and air flow at normal and reduced pressure for various Reynolds numbers 21 p3835 A66-38904
- Heat transfer dependence on pressure and thermal loads in bubble boiling of mercury and Hg-Mg alloys 22 p3999 A66-40295
- Cooled blades in gas turbines allowing use of higher gas temperatures and necessitating calculation of heat transfer and skin friction coefficients 22 p3999 A66-40492
- Equilibrium temperature and heat transfer of sphere in supersonic flow of rarefied air 23 p4010 A66-41733
- Approximation of self-similar plane and axisymmetric problems for high temperature laminar boundary layer, based on equations for boundary layer of finite thickness for high temperature gas 23 p4149 A66-41783
- Measuring devices and techniques for heat-transfer rate, pressure and force in hotshot tunnels 24 p4206 A66-42168
- Diffusion thermo effect on temperature field in combined heat and mass transfer processes, noting experiments with stagnation flow, turbulent boundary layer, etc 24 p4293 A66-42282
- Upward heat flux with vanishing counter potential temperature gradient in lower atmosphere and in laboratory experiments 24 p4202 A66-42983
- Approximation method for calculating transient temperature field in solid for case where heat-transfer coefficient varies 24 p4296 A66-43224
- HEAT TREATMENT**
- SA HARDENING**
- SA QUENCHING**
- Coil spring alloys for temperatures above 400 degrees F noting design stresses, heat treatments and relaxation 01 p0079 A66-10959
- N-type conductive cadmium selenide single crystals investigated for heat treatment and Hall effects in selenium vapor 01 p0127 A66-11194
- Heat treatment cycle effect on mechanical properties of corrosion resistant precipitation hardened steel AM 355 in terms of metallographic structure 02 p0242 A66-11304
- Brittle creep susceptibility of heat resistant chromium steels reduced by proper thermal treatment 03 p0384 A66-13162
- Fatigue strength of heat-treatable alloyed steels 03 p0384 A66-13168
- Vacancy concentration favorable for structural polygonization due to effect of cyclic heat treatment in lattice of steel 03 p0385 A66-13174
- Creep damage in metal, discussing future creep rupture life, exposure, mechanical properties and heat treatment for removing damage 04 p0537 A66-14466
- Postweld heat treatment on nickel alloy weld deposit noting metallography, microhardness and room temperature tests 05 p0698 A66-14515
- Gaseous impurity distribution /oxygen/ between scale and diffusion layer after heat treatment of various titanium alloys 05 p0699 A66-14700
- Healing of defects in steel accumulated during cyclic overloading 07 p1048 A66-17442
- Nature and properties of white band in welded steels, occurring also as result of heating, noting role of critical temperature range and gradient 07 p1037 A66-17443
- Maraging steel response to heat treatment including formability, machinability, stress-corrosion resistance and cold-working behavior of austenitic and martensitic phases 08 p1239 A66-18959
- Thermal stress of unbounded plate and cylinder heated under variation of medium temperature 08 p1313 A66-19442
- Critical heat flux under forced motion of underheated alcoholic aqueous solutions 09 p1470 A66-20148
- Quench aging, heat treatment which rationalizes role of vacancy-solute atom association and effect on precipitation hardening aluminum alloys 10 p1545 A66-21218
- Aus-bay quenching, heat treatment process which minimizes distortion and increases tensile strength 10 p1545 A66-21219
- Preparation and physical properties of polytriacetylene /TCNE/ copper chelate film, noting electric conductivity and heat treatment effect 10 p1574 A66-21348
- Lithium diffusion effects on electrical properties of tellurium doped n-type GaSb 10 p1578 A66-21582
- Phase composition effect on relaxation stability of chromium steel used for helical spring 11 p1716 A66-22750
- Double injection in long p-p-n diffused silicon junctions subjected to heat treatment, noting donor density energy level and electrical properties 11 p1756 A66-23027
- Changes in mechanical and electrical properties of thin Zn, Cd and Cu films during machining and thermal treatment 11 p1758 A66-23322
- Initial yielding characteristics of vacuum-melted iron as function of thermal history after slow cooling or quenching, noting interstitial segregation into grain boundaries 11 p1719 A66-23398
- Tensile, static notch, stress rupture, creep and salt stress corrosion tests at appropriate temperatures, evaluating effect of solution annealing temperatures of Ti-8Al-1Mo-IV 12 p1892 A66-23625
- Instantaneous strength, rigidity and strain characteristics of reinforced plastics surface-heated on one side 12 p1899 A66-24041
- Heat treatment and ionizing irradiations effect on charge distribution and number of surface states in silicon-silicon dioxide system 12 p1932 A66-24824
- Oxidation rate and heat treatment effect on density of states of silicon surface potential in silicon-silicon dioxide system 12 p1932 A66-24825
- Sequence of crystallization during heat treatment of ternary system of lithium aluminosilicate glasses 12 p1900 A66-24860
- Density, microhardness, elastic constants and surface strength relation to microstructure of lithium aluminosilicate glass crystallized under various conditions of heat treatment 12 p1901 A66-24863
- Heat treatment effect on structure, hardness, microhardness and corrosion resistance of VT1 titanium and OT4 titanium manganese-aluminum alloy sheets 12 p1897 A66-24900
- Phase difference due to elastic waves produced by cyclic heating of targets by impacting ions from pulsed beam 13 p2159 A66-25070
- High temperature plastic deformation and hardening effects on brittleness, strength and viscosity of austenitic steel and alloys 13 p2106 A66-25328
- Structure and properties of intermediate components of iron-oxide-germanium-oxide system analyzed, using heat treatment 13 p2162 A66-25355
- Melting practice, sheet thickness and thermal and mechanical treatments effect on critical stress intensity parameter and ductility of 18-nickel maraging steel 13 p2108 A66-25772
- Aging behavior of rods produced by extrusion of manganese-containing aluminum alloy subjected to solution heat treatment, noting microstructure and mechanical properties 13 p2111 A66-26585
- High-temperature nickel sheet alloys as affected by composition, production methods and heat treatment [ASME PAPER 66-GT-104] 14 p2312 A66-27003
- Scattering mechanical properties of ternary alloy creep resistant steel, emphasizing effect of heat treatment on microstructure [ASME PAPER 66-GT-112] 14 p2312 A66-27006
- Crack susceptibility of ultrahigh-strength steel welds related to thermal cycles in welding and heat treating 14 p2292 A66-27325
- Crack susceptibility of ultrahigh-strength steel welds related to thermal cycles in welding and heat treating 14 p2301 A66-27345



Structural defects arising during growth and heat treatment of CdS single crystals studied, using anomalous transmission of X-rays 15 p2557 A66-28563

Heat treatment effect on photoelectric properties of silicon with electron-induced structural defects 15 p2560 A66-28668

Molybdenum recrystallization as affected by La and Y additions under various types of heat treatment 15 p2520 A66-28670

Heat treatment effect on superconducting properties of cold-worked niobium, noting results of magnetization, critical current and resistivity measurements 15 p2564 A66-28760

Surface temperature determination procedure for laser heated metals based on heat conduction equations and ion emission from surface 15 p2514 A66-29035

Microstructure and cooling rate effect on tensile and impact properties of titanium alloy Ti-6Al-6V-2Sn 15 p2521 A66-29072

Effects of heat treatment and aging on phase composition, strength and plasticity of industrial titanium alloys 15 p2522 A66-29178

Phase transformations in titanium alloys annealed at high temperatures and subjected to aging processes 15 p2522 A66-29181

Linear expansion at various temperatures of titanium alloys and effect of alpha grain size and heat treatment on expansion coefficient 15 p2522 A66-29182

Weldable titanium alloys hardened by heat treatment and with structure immune to high temperatures 15 p2522 A66-29186

VT14-16 titanium alloys strength and plasticity with cold working and heat treatment 15 p2522 A66-29188

Hardenability /ratio between phase transformation and cooling rates at given point of sample cross section/ in several titanium alloys after annealing 15 p2522 A66-29190

Heat treatment of titanium alloy sheets clad with industrial trial-grade titanium for preventing surface oxidation and hydrogen absorption 15 p2522 A66-29191

Effect of annealing and aging on structure, hardness, strength and plasticity of VT15 alloy welds 15 p2523 A66-29192

Mechanical properties of Ti-Al-Mo-Zr-Sn alloy as affected by varying cooling rate in heat treatment 15 p2523 A66-29194

Welded joints in sheets of two-phase titanium alloys in study of heat treatment effects on structure and mechanical properties 15 p2523 A66-29195

Particle size and heat treatment effects on stability and reflectance of thermal control glass pigment coatings under UV radiation [AIAA PAPER 65-136] 15 p2616 A66-29288

Explosive technique for shaping low plasticity sheet metals by heating blanks with pyrotechnic agent in sand, with reference to Mo and Mg alloys 15 p2511 A66-29783

Hot drape forming of torus and semitoroidal bulkhead segments from aluminum alloys [SAE PAPER 660290] 15 p2511 A66-29831

Biological and engineering problems in spacecraft sterilization, noting heat treatment 15 p2445 A66-29996

Temperature dependence of magnetization and resistivity in SHF magnesium-aluminum ferrite 16 p2786 A66-31677

Silver oxide films by cathodic sputtering, discussing changes in sample preparation and material characteristics due to aging and heat treatment 17 p2976 A66-32262

Changes in massive amorphous boron filaments by heat treatments under reduced pressures and in presence of inert gases 17 p2943 A66-32852

Various heat treat temps of 2014 Al alloy and corresponding values of eddy current 17 p2940 A66-33099

Heat treatment effect on IR reflectivities of heavily doped n-type silicon 17 p2988 A66-33327

Thermal conversion mechanism in heat treatment of InSb indicates hydrogen dissolved plays role of donor while behavior of oxygen is not yet known 19 p3433 A66-35331

Maraging steel properties, discussing composition, strengthening mechanism, tensile and impact toughness, mechanical

and fatigue properties, 20 p3587 A66-38431

Thin film transmission electron microscopic analysis of stress corrosion of heat-treated aluminum 21 p3749 A66-38471

Quenching, annealing and high temperature treatment effect on transverse rupture strength of sintered tungsten carbide [ASME PAPER 66-MD-17] 21 p3750 A66-38478

Starting concentration, surface distribution of additive in alumina powder, trajectory distance and growth rate in Verneuil growth of ruby crystals 21 p3795 A66-38527

Recirculation of liquid through cell and external heat exchanger to solve problem of repeated flashing in europium chelate lasers 21 p3747 A66-39108

Heat treatment of silicon at high temperatures leads to donor centers affecting electric and photoelectric properties 21 p3802 A66-39157

100-200 ksi yield-strength notched steels for high-toughness weldments, discussing quenched and tempered steels, maraging steels, heat treatment effects, etc 21 p3751 A66-39193

Cyclotron resonance study of electron scattering by thermal acceptors in quenched Ge 21 p3805 A66-39567

Microstructural and superconductivity analyses of Nb-Ti-O compound as function of thermomechanical processing treatment, plotting critical current density against transverse magnetic field 22 p3960 A66-39780

Utilization tests of nonradiating Francia cellular structures placed on spiral insulator and heated to low and medium temperatures 22 p3852 A66-40247

Gas tungsten arc and electron beam welding for iron-base, nickel-base and cobalt-base alloys, noting use of weld filler metal to avoid cracking 22 p3924 A66-40263

Heat treatment effect on structure, mechanical properties and corrosion resistance of VTZ-1 alloy, noting influence of annealing 22 p3935 A66-40680

Effect of titanium, zirconium, vanadium and cerium additions on properties and macrostructure of aluminum alloy tested in cast and heat treated states 23 p4080 A66-41271

Structural defects arising during growth and heat treatment of CdS single crystals studied, using anomalous transmission of X-rays 23 p4112 A66-41284

Surface layer of heat-treated steel alloy after work hardening 23 p4081 A66-41405

Regenerative heat treatment for increasing creep life of high temperature alloys used in turbines 24 p4227 A66-42508

Notch and heat treatment effect on compressive buckling of WC/Co alloys 24 p4228 A66-43063

**HEATER**

**SA FURNACE**

Range of gas dynamic stability of arc-type electric heaters, characteristics for design and calculation of electrode diameter ensuring vortex stabilization 14 p2348 A66-28314

**HEATING**

**SA AERODYNAMIC HEATING**

**SA ARC HEATING**

**SA ATMOSPHERIC HEATING**

**SA BASE HEATING**

**SA GAS HEATING**

**SA INDUCTION HEATING**

**SA IONOSPHERIC HEATING**

**SA JOULE HEATING**

**SA KINETIC HEATING**

**SA MAGNETOHYDRODYNAMIC SHEAR HEATING**

**SA PLASMA HEATING**

**SA PULSE HEATING**

**SA RADIANT HEATING**

**SA RESISTANCE HEATING**

**SA SHOCK HEATING**

**SA STRUCTURAL HEATING**

**SA SUPERHEATING**

**SA TRANSIENT HEATING**

Substrate temperature measurement and control showing desirability of large-area low temperature radiation source for glass substrate heating 24 p4218 A66-43165

**HEATING EQUIPMENT**

**SA FILAMENT**

**SA FURNACE**

Contact effectiveness of space radiator specific case of rectangular fin of constant thickness heated uniformly along one edge and perfectly insulated along opposite edge 03 p0444 A66-1270

Heating by laser beam with application of lithium, noting use for high temperature plasma production 08 p1233 A66-1884

Heating unit of device for testing small samples of sintered materials for thermal fatigue 11 p1709 A66-2347

**HEAVY COSMIC RAY PRIMARY**

Intensity variation of heavy nuclei in primary cosmic radiation during times of solar disturbances 07 p1123 A66-1793

Chemical abundances and energy spectra of nuclei in galactic radiation measured interplanetary space byOGO-I satellite 18 p3190 A66-3484

Detection of low energy multiply charged primary cosmic ray nuclei in nuclear emulsions and relation of nuclei to solar cycle 18 p3190 A66-3484

Activated emulsion camera detection of low energy very-heavy multiply-charged scarce cosmic ray nuclei 18 p3190 A66-3484

Balloon-borne nuclear emulsion detection of solar cosmic ray heavy nuclei during solar burst 18 p3190 A66-3484

Nuclear emulsion stack investigation of composition and differential energy spectra of primary cosmic ray heavy nuclei fluxes 18 p3191 A66-3484

Balloon-borne nuclear emulsion detection of finite fluxes of low energy cosmic ray heavy nuclei and interstellar cosmic radiation propagation 18 p3191 A66-3484

Differential spectra of charge components of primary cosmic ray heavy nuclei at different solar modulation levels and effect of interstellar propagation 18 p3191 A66-3484

Balloon-borne Cerenkov scintillation counter measurements of energy spectra of primary cosmic radiation heavy nuclei at various geomagnetic latitudes 18 p3191 A66-3484

Tracks of nuclei of primary cosmic ray that ended within nuclear emulsions and possibility of separating isotopes 18 p3192 A66-3484

Relative abundance of carbon isotopes in primary cosmic radiation estimated by separation of isotopes method in nuclear emulsion 18 p3192 A66-3484

COSPAR research on heavy primary cosmic ions in nuclear emulsions exposed in polar satellite 18 p3192 A66-3484

Cerenkov counter measurements of primary cosmic ray heavy nuclei made by Elektron II satellite 18 p3199 A66-3488

Heavy cosmic ray primary energy spectrum from BASJE measurements 18 p3209 A66-3512

Search for long-lived particle fluxes with masses larger than about five nucleon masses created by cosmic radiation 18 p3214 A66-3515

High energy jets produced by heavy primary nuclei of cosmic origin and fragmentation products 18 p3215 A66-3516

Solar cosmic ray multiply charged nuclei and July 18, 1961 solar event, discussing relative abundances and heavy nuclei detection 22 p3973 A66-4054

**HEAVY ELEMENT**

Heavy metal derivative solid lubricants properties and application [ASLE PAPER 66AM 2B3] 16 p2711 A66-3040

Solar UV emission lines for 11 elements heavier than helium analyzed, obtaining relative abundances values and relation between electron temperature and temperature gradient in chromosphere corona transition region 23 p4130 A66-4180

**HEAVY ION**

Atomic scattering contribution to pulse height defect and energy dispersion of heavy ions in semiconductor detectors 10 p1558 A66-2186

COSPAR research on heavy primary cosmic ions in nuclear emulsions exposed in polar satellite 18 p3192 A66-3484

**HEAVY NUCLEUS**

Cosmic ray helium nuclei along with heavier nuclei, traverse interstellar and interplanetary matter propagation in space



and slope of energy spectrum 03 p0423 A66-12927  
 Flux of low energy heavy primary nuclei obtained by slicing emulsion method, using recoverable satellite during minimum solar activity period 15 p2592 A66-30077  
 Flux of primary cosmic ray heavy nuclei measured with sandwich of C.2 and G.5 emulsions at magnetic latitude 42 degrees N, noting solar modulation as shown by neutron monitor data 16 p2794 A66-30720  
 Fragmentation probabilities, charge spectrum and interaction mean free paths of relativistic heavy nuclei in primary cosmic radiation investigated in stack of nuclear emulsions 16 p2795 A66-31010  
 Chemical abundances and energy spectra of nuclei in galactic radiation measured in interplanetary space by OGO-I satellite 18 p3190 A66-34833  
 Detection of low energy multiply charged primary cosmic ray nuclei in nuclear emulsions and relation of nuclei to solar cycle 18 p3190 A66-34834  
 Activated emulsion camera detection of low energy very-heavy multiply-charged scarce cosmic ray nuclei 18 p3190 A66-34835  
 Balloon-borne nuclear emulsion detection of solar cosmic ray heavy nuclei during solar burst 18 p3190 A66-34836  
 Nuclear emulsion stack investigation of composition and differential energy spectra of primary cosmic ray heavy nuclei fluxes 18 p3191 A66-34837  
 Balloon-borne nuclear emulsion detection of finite fluxes of low energy cosmic ray heavy nuclei and interstellar cosmic radiation propagation 18 p3191 A66-34838  
 Differential spectra of charge components of primary cosmic ray heavy nuclei at different solar modulation levels and effects of interstellar propagation 18 p3191 A66-34839  
 Balloon-borne Cerenkov scintillation counter measurements of energy spectra of primary cosmic radiation heavy nuclei at various geomagnetic latitudes 18 p3191 A66-34840  
 Relative abundance of carbon isotopes in primary cosmic radiation estimated by separation of isotopes method in nuclear emulsion 18 p3192 A66-34843  
 Cerenkov counter measurements of primary cosmic ray heavy nuclei made by Elektron II satellite 18 p3199 A66-34886  
 Experimental search for heavy mass particles in air showers with total absorption spectrometer 18 p3214 A66-35149  
 High energy jets produced by heavy primary nuclei of cosmic origin and fragmentation products 18 p3215 A66-35160  
 Primary cosmic radiation composition, discussing abundance of protons, He nuclei and heavier nuclei 20 p3632 A66-38098  
 Flux and energy spectrum of low energy heavy nuclei of primary cosmic radiation measured by balloon-mounted nuclear emulsion stacks 24 p4264 A66-42608  
**HEAVY WATER**  
 S DEUTERIUM OXIDE  
**HEIGHT**  
 S GEOPOTENTIAL HEIGHT  
 S SCALE HEIGHT  
**HEISENBERG THEORY**  
 Gravitational interaction and gravitational waves discussing Schwarzschild metric, weak interaction, spinor field and free neutrino wave 04 p0546 A66-14315  
 Solid state laser system, describing quantum mechanical treatment of self-sustained oscillation for one mode 07 p1044 A66-17817  
 Green function random phase decoupling scheme investigation of magnetic impurities effect on thermal properties of cubic spin-1/2 Heisenberg ferromagnet 11 p1758 A66-23394  
**HELICAL ANTENNA**  
 Radiation field of single-filament logarithmic-elliptical helical antenna, assuming traveling wave along helix 04 p0501 A66-14408  
 Propagation conditions for nonsymmetric parasitic waves and filtering properties in helical waveguide with dielectric coating and metallic casing 06 p0838 A66-15887  
 Helix frequency-scanning delay line design and characteristics 06 p0849 A66-16396  
 Effect of various geometries on performance and characteristics of helical antennas, considering input impedance and radiation pattern 07 p1006 A66-17474  
 Power flux distribution of symmetrical wave outside and inside antenna septum with anisotropic medium 08 p1193 A66-19189  
 Moderately superdirective antenna with directivity slightly greater than uniform-current distribution of same size 11 p1664 A66-22560  
 Superdirective array of normal mode helical dipoles 12 p1840 A66-24625  
 Infinite helical sheath antenna driven by ring delta-function generator analyzed, using Fourier transform, noting decomposition of current distribution 17 p2886 A66-32388  
 Air shower detection with radio receiving system, broadband band helical antenna and Cerenkov particle detector 18 p3115 A66-35119  
 Contrawound helical antenna with independent control of polarization bandwidth and gain used for receiving or low-power transmitting 21 p3714 A66-39496  
**HELICAL FLOW**  
 Oscillation modes on oscillators in locally concentrated magnetic field determined by simultaneous study of predominant and helical modes 01 p0116 A66-11195  
 Delta wing vortex breakdown in terms of theory of stability of spiraling flows 07 p0979 A66-17478  
 Stability and dissipation in second and third-order fluid approximations of boundary value problems for unsteady simple shear flow  
 [AICE PREPRINT 21F] 10 p1521 A66-21188  
 Pressure drop as function of flow rate for helical flow of non-Newtonian polyisobutylene solution 15 p2477 A66-28615  
 Helical flows of viscous compressible fluids for homogeneous and inhomogeneous flows 18 p3103 A66-34942  
 Nonsteady helical flow of viscoelastic liquid contained in circular cylinder, noting occurrence of oscillations in fluid decaying exponentially with time 21 p3723 A66-38588  
 High temperature testing and evaluation of graphite helical-screw expanders and compressors for use with inert gas Brayton cycle 23 p4075 A66-41755  
 Experimental verification of stability criteria for incompressible inviscid flow with helical streamlines, using rotating cylinders 23 p4062 A66-42046  
**HELICAL INDUCER**  
 Plasmoid motion and purification in helical magnetic field and mass spectrograms of pure dense hydrogen  
 plasmoids 21 p3787 A66-39048  
**HELICAL WINDING**  
 Negative depression coefficient in traveling wave tubes at small helix parameters and different radii for helix and electron beam 06 p0838 A66-15901  
 Elastic wave propagation in helical springs of small helix angle, including effect of coupling between extension and rotation for large helix angle 08 p1311 A66-19293  
 Creep analysis of close-coiled helical springs 10 p1613 A66-21319  
 Direction and magnitudes of electric polarization vectors for plasma moving through helical and toroidal magnetic fields 11 p1747 A66-23304  
 Blast environment simulation developing high pressures of relatively long duration, noting helical winding of cord explosive 16 p2681 A66-30501  
 Gravitational perturbation effect on MHD stability of helical magnetic field in spiral arm 16 p2800 A66-30652  
 Harmonic series solution for electromagnetic scattering by unidirectionally conducting helical sheath when incident field is E-polarized 18 p3065 A66-33530  
 Helical fields possessing mean magnetic wells treated by stream function formalism, calculating field shape 19 p3413 A66-36503  
 Spurious mode effects on performance of helix type traveling wave amplifier 21 p3712 A66-39222  
**HELICOPTER**  
 SA CH-3 HELICOPTER  
 SA CH-53 HELICOPTER  
 SA ENSTROM F-28 HELICOPTER

SA KAWASAKI KH-4 HELICOPTER  
 SA MILITARY HELICOPTER  
 SA ROTARY WING AIRCRAFT  
 SA SH-3 HELICOPTER  
 SA SIKORSKY S-61 HELICOPTER  
 SA TANDEM-ROTOR HELICOPTER  
 SA UH-2 HELICOPTER  
 Helicopter navigation requirements for low altitude sea missions at beyond-horizon distance from supporting ship or shore base 04 p0544 A66-14442  
 Disturbed helicopter motions and family of stability derivatives in longitudinal and lateral modes 05 p0609 A66-14998  
 Light passenger helicopter similar to Fayrey Rotodyne craft and combining principles of autogyro and rotor helicopter 10 p1483 A66-21389  
 Flight characteristics of compound helicopter with fixed rotor and jet engine 13 p1995 A66-25761  
 LF navigation and secondary surveillance radar /SSR/ used in commercial helicopters of New York airways  
 [SAE PAPER 660319] 14 p2223 A66-27299  
 Helicopter capabilities in solving interurban mass transport problems, particularly cost and time considerations [SAE PAPER 660336] 15 p2427 A66-29835  
 Variable speed constant frequency /VSCF/ generating system for helicopters 16 p2636 A66-30600  
 Helicopter simulation system for avionic evaluation 16 p2682 A66-31248  
 American Helicopter Society, Annual Forum, Washington, D.C., May 1966 17 p2843 A66-32723  
 Military vertical replenishment and utility helicopter operational requirements and load carrying capacity 17 p2845 A66-32740  
 Noise generation due to mass introduction, applied force and stress in helicopters, V/STOL aircraft and ground effect machine 18 p3051 A66-33687  
 Djinn, Alouette II and III, Super-Frelon and SA 330 helicopters 18 p3052 A66-34464  
 Canadian labor market for commercial helicopter pilots 18 p3268 A66-34624  
 Low speed wind tunnel design and testing including V/STOL aircraft, helicopters, reentry vehicles, etc 20 p3540 A66-37009  
 UH-1D helicopter reliability determination and maintenance through planned data acquisition, analysis and corrective action program 20 p3572 A66-37946  
 Helicopter trainee performance following synthetic flight training, noting flyable aircraft attached to ground effects machine 22 p3857 A66-40250  
**HELICOPTER CONTROL**  
 Spatial disorientation experiences of Army helicopter pilots, noting accident and incident statistics, methods of correction, etc 11 p1648 A66-22578  
 Automatic stabilization of helicopters by using autopilots 12 p1801 A66-24388  
 Helicopter pilot performance evaluation method based on ability to precisely control rotor rotational velocity 17 p2864 A66-32163  
 Low-altitude control of U.S. Army rotary wing aircraft 17 p2950 A66-32722  
 Helicopter handling qualities during hover noting pilot performance, position control tasks with and without gusts, effects of stability derivatives, etc 17 p2845 A66-32734  
 Nuclear radiation anticollision instrumentation for guidance systems of helicopters and other vehicles, both air and surface 17 p2926 A66-33097  
 Linear optimal control techniques for design of control system for short-range stationkeeping of large assault helicopter 19 p3280 A66-36688  
 Hover augmentation system /HAS/ design for analog computer helicopter simulation and flight control 21 p3696 A66-38901  
**HELICOPTER DESIGN**  
 Helicopter corrosion problems discussing causes, exposed surfaces, prevention and treatment 03 p0372 A66-12300  
 Design considerations in Lockheed rigid rotor application to compound helicopter, noting wind tunnel and flight test with XH-51A helicopter  
 [AIAA PAPER 65-757] 03 p0318 A66-12552  
 New lift and propulsion techniques in development of V/STOL aircraft, helicopters and ground effect



machines 11 p1636 A66-22695  
Lightning and static electricity discharges effects on helicopter design and performance, noting blade and rotor hub protection, fuel ignition, etc 11 p1636 A66-23259  
Microwave power transmission, noting theoretical loss, power transfer, helicopter operation, etc 13 p2024 A66-25783  
High performance rotary wing VTOL aircraft, noting results from High Performance Helicopter Program and Exploratory Development Compound Program [SAE PAPER 660314] 14 p2223 A66-27293  
Helicopter design and application to common carrier transportation, particularly between airport and city [SAE PAPER 660335] 15 p2428 A66-29846  
Helicopter airfoils, discussing design improvement by proper choice of camber and leading edge 17 p2840 A66-32725  
Systems integration in helicopters, discussing design history, equipment used, operational features, etc 17 p3040 A66-32729  
Integrated Helicopter Avionics System flight control, noting stability augmentation, long-term motion control, outer and inner loop function separation and fail-safe capability 17 p2951 A66-32730  
Loss of power effects on helicopter at high speeds, noting combination of blade analysis with motion equations, application of computer simulation, etc 17 p2845 A66-32735  
Hughes OH-6A helicopter fail-safe structural composition noting design, fatigue testing, application of redundant design features, etc 17 p2845 A66-32736  
Helicopter airframe fatigue testing noting fail-safe design, crack detection, loads applied, test facilities and techniques, etc 17 p3027 A66-32737  
Loading considerations in design of large helicopters for transport of externally suspended cargo 17 p2845 A66-32741  
SA 330 tactical helicopter technical development discussing design, test equipment and methods employed 17 p2846 A66-32743  
Twin engine UH-2 Seasprite helicopter, noting increased power availability, advantages and performance characteristics 20 p3495 A66-37046  
VTOL operational availability computer simulation model, studying initial and tradeoff design, maintenance, logistics, manpower and flight operational requirements 20 p3543 A66-37909

**HELICOPTER ENGINE**  
Propulsion systems for helicopters, stressing variable area turbine for turboshaft engines 04 p0573 A66-14134  
BMW model 6012 gas turbine for helicopter application weighs 50 kg but develops 100 hp 10 p1591 A66-21402  
Overrunning clutches in gas turbines, design, performance characteristics and application to A-4D Skyhawk aircraft, UH-2 helicopter and Curtiss-Wright X-19 VTOL drive systems [ASME PAPER 66-GT-92] 14 p2300 A66-26996

**HELICOPTER PERFORMANCE**  
Assault helicopter cost and system effectiveness in mission of delivering cargo from carrier to landing zone, evaluating avionics system [AIAA PAPER 64-785] 05 p0610 A66-15079  
CH-53A helicopter design, testing, reliability and flight characteristics 07 p0988 A66-17494  
Flight test determination of parasite drag area and required power of Kawasaki Bell KH-4 single-rotor helicopter 07 p0988 A66-17525  
Aircraft design parameter development, discussing supersonic air transport, helicopter and V/STOL design problems, metal fatigue, etc 08 p1167 A66-18707  
Digital simulation of scheduling logistic support by helicopter, using Backtrack techniques 12 p1858 A66-24683  
High performance rotary wing VTOL aircraft, noting results from High Performance Helicopter Program and Exploratory Development Compound Program [SAE PAPER 660314] 14 p2223 A66-27293  
Divergent vertical helicopter oscillations

due to pilot presence in collective control loop and physiological response of pilot to oscillations 17 p2843 A66-32719  
Advanced heavy lift helicopters performance with hot cycle propulsion 17 p2843 A66-32720  
USAF CH-3C helicopter V/STOL in flight refueling, discussing requirements, system characteristics and flight tests 17 p2844 A66-32724  
S-61F helicopter flight test program, noting design modifications for high speed performance 17 p2844 A66-32726  
Helicopter landing in zero-zero weather, describing experiment in England involving landing in dense fog 17 p2844 A66-32728  
Heavy equipment short-range transportation with crane-type helicopters, noting correlation between lift capacity and aircraft weight 17 p2845 A66-32739  
Dynamics of noise and loading actions on helicopters, V/STOL aircraft and ground effect machines 18 p3050 A66-33679  
Use of wing to unload helicopter rotor for cases with and without auxiliary propulsion, noting wing effect on performance, stability, maneuvers, etc 19 p3279 A66-36486  
SH-3A airframe fatigue test facility for automatic simulation of helicopter flight and landing loads 22 p3992 A66-40251  
Short haul air transportation in Europe, noting market development with helicopter techniques and development of more efficient rotor aircraft 23 p4151 A66-41303  
Steady and dynamic loads on tandem rotor, controls and airframe flight tested with Army helicopter, using automatic data processing [AIAA PAPER 66-735] 23 p4008 A66-41324

**HELICOPTER PROPELLER DRIVE**  
Ureka, vibration balancing device capable of reducing helicopter shaft eccentricity to zero 11 p1638 A66-23260

**HELICOPTER ROTOR**  
Stopped and slow rotor aircraft configuration for fundamental limitations on forward flight speed of compound helicopters [SAE PAPER 650806] 01 p0012 A66-10847  
Helicopter rotor blade and engine erosion by sand and seawater 06 p0804 A66-15997  
Design recommendations to offset greater momenta and sensitivity to gust winds of jointless helicopter rotor 10 p1483 A66-21388  
Young theory of rotor blade motion stability in powered flight 11 p1638 A66-23261  
Rigid rotor structural design and testing 13 p2196 A66-25763  
Blade vibration simulation in helicopter trainer by applying amplitude motion to trainer 14 p2271 A66-28030  
Static thrust experiments on single degree-of-freedom torsional vibration of helicopter rotor blades due to stall, and amplitude dependence on blade mean pitch angle and reduced vibrational frequency 16 p2634 A66-31321  
Unsteady aerodynamic characteristics of model helicopter rotor operating in vortex ring state, considering thrust and torque fluctuation 16 p2634 A66-31322  
Fail-safe concept application to rotorcraft noting fatigue requirements, accident prevention methods, etc 17 p2843 A66-32721  
Helicopter rotor blade applied as scanning radar antenna, noting performance during flight tests, feasibility, etc 17 p2875 A66-32727  
Flying qualities and aircraft control during tandem rotor helicopter external sling drag operations 17 p2846 A66-32742  
Aerodynamic interference between helicopter rotor blade and fuselage and wing in hovering and forward flight, describing method of converting two-dimensional analysis to three-dimensional case 18 p3047 A66-33681  
Measurement method for aerodynamic damping of helicopter rotors in forward flight 18 p3047 A66-33684  
Helicopter rotor performance limitations theoretically analyzed 18 p3051 A66-33685  
Use of wing to unload helicopter rotor for cases with and without auxiliary propulsion, noting wing effect on performance, stability, maneuvers, etc 19 p3279 A66-36486  
In-flight stress measurements on coaxial

counterrotating helicopter blades, using semiconductor strain gauge with HF telemetric data 20 p3668 A66-37504  
transmitters 20 p3668 A66-37504  
Radial flow effects on helicopter rotor blades, noting minimum drag variation 22 p3843 A66-40248  
Rotor downwash angle and tunnel geometry effect on maximum size rotor that can be tested in closed throat wind tunnel [AIAA PAPER 66-736] 22 p3893 A66-40626  
Reentry and recovery of space vehicles in reliable shock free landings, using modified helicopter rotor for hypersonic flow and thermal problems 24 p4284 A66-43073

**HELICOPTER WING**  
Use of wing to unload helicopter rotor for cases with and without auxiliary propulsion, noting wing effect on performance, stability, maneuvers, etc 19 p3279 A66-36486

**HELIOCENTRIC ORBIT**  
Spectroscopic observations of Sun-grazing Ikeya-Seki Comet /1965/ at minimum possible heliocentric distance 05 p0761 A66-15100  
Past and future comet orbits, examining value of auxiliary anomaly in Makover's method as function of heliocentric distance of perihelion 17 p3000 A66-32337  
Interplanetary manned spacecraft maneuvers including perihelion brake, off-perihelion acceleration and retromaneuvers and heliocentric planet-approach maneuvers [AIAA PAPER 65-695] 19 p3462 A66-35902

**HELIOGRAPHY**  
**SA SPECTROHELIOGRAPH**  
Time-marking during high speed cinematography of details on Sun with SKS-1M camera 05 p0681 A66-15216  
Polarization photography of solar corona, noting apparatus used for separation of K from F component 16 p2705 A66-30827  
Rocketborne filter heliograms in Mg II line at 2802.7 angstroms including tabulated data 17 p2997 A66-31925  
Photospheric bridges over sunspots studied by meniscus photoheliograph at Tashkent Astronomical Observatory 20 p3646 A66-37030

**HELIOS**  
**S SUN**  
**HELITRON**  
**S BACKWARD WAVE OSCILLATOR**  
**HELIUM**  
**SA LIQUID HELIUM**  
Continuous operation of gallium arsenide injection laser cooled by helium gas flow 01 p0084 A66-11190  
Helium 3-1-P state, discussing pressure dependence of lifetime between free escape and complete blockading 03 p0395 A66-13134  
Eigenvalues and eigenvectors calculated for several low-lying autoionizing levels in helium 04 p0546 A66-13365  
Doubly differential cross sections of electrons ejected from helium bombarded by protons 04 p0547 A66-13709  
Ionization cross section of ground state helium cation by electron impact in Born exchange approximation 04 p0549 A66-14312  
Radiogenic, spallogenic and primordial noble gases in stone meteorites, determining helium and neon content 05 p0756 A66-14506  
Electrons, hydrogen nuclei and helium nuclei observed in primary cosmic radiation by balloon in 1963, discussing integral intensity and differential energy spectrums 05 p0746 A66-14780  
Elastic differential scattering of helium ions discussing energy analysis, geometry and target particle motion effects, and interference phenomena 05 p0719 A66-15767  
CW laser action in carbon dioxide-helium mixtures 06 p0890 A66-16385  
Comments on radiative recombination of molecular helium ions into dissociative state 06 p0912 A66-16636  
Measurement of equilibrium fractions of helium ions present in helium beams scattered at zero degrees through carbon foils 06 p0912 A66-17038  
Manufacturing glass-fiber-reinforced plastic container for high pressure helium gas in European launcher rockets 06 p0889 A66-17076  
Light output from helium-neon gas maser photographed with and without intracavity modulation at locking frequency, using high speed rotating mirror 07 p1040 A66-17205



Heat transfer coefficients for helium and hydrogen gas flowing through electrically heated Inconel tube 07 p1148 A66-17300  
Excitation cross sections of helium lines in electron/atom collisions 07 p1044 A66-17874  
Enthalpies determined from experimental heat capacity and Joule-Thomson data to prepare pressure-enthalpy diagrams for helium-nitrogen system 08 p1320 A66-19683  
Motion and properties of quantized vortex rings in superfluid helium at low temperatures 09 p1415 A66-20009  
Detection by coincidence counting techniques of two-photon decay of metastable state of singly ionized helium 09 p1404 A66-20290  
Stellar evolution for star of 30 solar masses during helium ignition, depletion and exhaustion 09 p1455 A66-20406  
Quasi-statistical pressure broadening of diffuse helium lines 10 p1606 A66-21243  
Electron impact ionization cross section of  $H/2s/$  and  $H/2p/$  in Born A, Born B, Born-Cochran and classical approximations 11 p1738 A66-22498  
Thermal conduction of hydrogen-helium gas mixtures and dependence on hydrogen concentration 11 p1786 A66-22500  
Glass tube containing pressurized helium progressively imploded by coaxial explosive charge, considering application to hypervelocity guns 11 p1686 A66-22840  
Upper atmospheric helium ion chemical loss process, distribution of nitrogen ion and rate coefficient of helium ion-molecular nitrogen reaction 11 p1701 A66-23153  
Helium gas gun for studying penetration and shock reflection from hypervelocity impact 11 p1687 A66-23263  
Continuous operation of gallium arsenide injection laser cooled by helium gas flow 12 p1890 A66-24011  
Hydrogen and helium spectra of gaseous nebulae in theory and observation 13 p2183 A66-25610  
Output power of 6328 angstrom He-Ne gas laser as function of laser gain, cavity loss and output coupling 13 p2091 A66-25651  
Helium-neon gas laser used to determine electron density variation, spatial and temporal, in afterglow of Z-pinch in H at 100 mtorr 13 p2104 A66-26239  
Positron-helium scattering below positronium threshold, using adiabatic method previously tested in positron hydrogen scattering, presenting phase shifts and momentum transfer cross section computations 13 p2134 A66-26262  
Pressure effects of helium on fine structure components of first two members of cesium principal series, noting changes in shift curves 13 p2135 A66-26264  
Measurement of total cross section for excitation of metastable atoms of helium by electron bombardment 13 p2135 A66-26266  
Differential scattering of ionized helium on neon and argon and ionized argon on argon measured at various relative energies and scattering angles 13 p2135 A66-26269  
Microsecond pulsed discharges at short tube with wire electrodes containing helium gas at intermediate pressures 14 p2341 A66-27314  
Helium whistler detection by VLF receiver aboard Canadian satellite Alouette II, noting application to composition and electron density measurement of ionosphere 14 p2285 A66-27847  
Oscillator strengths for electric dipole transitions in neutral helium 14 p2338 A66-28127  
Rapid mass ejection from highly evolved stars as explanation for observation of high abundance of galactic helium gas 15 p2599 A66-29680  
Quantum mechanical potential energy curve of lowest normal state of diatomic helium computed in valence bond scheme, using 17-term wave function of Slater orbitals 16 p2749 A66-30112  
Isotopic composition of low-energy helium nuclei in primary cosmic radiation at solar minimum 16 p2792 A66-30138  
Telescopic measurements of primary energy spectra and abundances of He 3 and He 4 in galactic cosmic radiation 16 p2793 A66-30198  
Photoelectric yields of alkali halides

measured, using rare gas ion chamber to determine flux distribution of helium continuum and obtain absorption coefficients 16 p2754 A66-30855  
Pulmonary effects of two-week exposure of four men to helium-oxygen atmosphere at total pressure of 380 mm Hg 16 p2639 A66-31121  
Thermal balance and heat exchange between four men exposed to helium-oxygen atmosphere at 380 mm Hg total pressure 16 p2639 A66-31122  
Thermodynamic parameters of gas behind strong shock wave in helium 16 p2690 A66-31630  
High-power molecular laser based on vibrational-rotational energy level, noting carbon dioxide-neon-helium laser design 17 p2936 A66-33248  
Measuring amplification of coherent optical radiation in neon-helium filled tube 17 p2938 A66-33512  
Excitation of 35 sub 2 neon level by metastable helium atoms during He-Ne discharge 17 p2938 A66-33513  
Suitability of oxygen-helium atmosphere for manned space missions proven by 56-day human exposure at 258 mm Hg total pressure 18 p3057 A66-33768  
Major and minor constituents of oxygen-helium atmosphere to which humans were exposed for 56 days 18 p3057 A66-33769  
Human renal response to 56-day exposure to oxygen-helium atmosphere at 258 mm Hg total pressure 18 p3057 A66-33770  
Human blood enzyme response to 56-day exposure to oxygen-helium atmosphere at 258 mm Hg total pressure 18 p3057 A66-33771  
Exercise performance and cardiovascular response of man exposed for 56 days to oxygen-helium atmosphere 18 p3057 A66-33772  
Urinary excretion of steroids and catecholamines as measure of emotional stress of man in 56-day exposure to oxygen-helium environment 18 p3057 A66-33773  
Respiratory effects of 56-day human exposure to oxygen-helium atmosphere 18 p3058 A66-33774  
Enteric microbial flora changes in man exposed 56 days to oxygen-helium atmosphere 18 p3058 A66-33777  
Oral, cutaneous and aerosol bacteriological evaluation of astronaut exposed to oxygen-helium atmosphere at low pressure 18 p3058 A66-33778  
Clinical findings of effect on man during 56-day exposure to oxygen-helium atmosphere at 258 mm Hg total pressure 18 p3058 A66-33779  
Individual efficiency curves for excitation of two metastable electron energy states of helium by electron impact 18 p3139 A66-34504  
Retarding potential measurement of kinetic energy of electrons released in Penning ionization by excited helium atoms in metastable electron states 18 p3139 A66-34505  
Balloon flight data obtained at 50 and 65 degrees N geomagnetic latitude on spectra of primary cosmic ray hydrogen and helium nuclei, using Cerenkov scintillator technique 18 p3190 A66-34831  
Solar modulation and time variation of differential energy spectrum and flux of primary helium nuclei in 30 to 90 mev/nucleon energy range 18 p3190 A66-34832  
He-3-He-4 isotopic composition of primary cosmic ray helium flux in terms of energy, rigidity and solar modulation 18 p3192 A66-34841  
Balloon-borne scintillation counter measurements of isotopic composition, energy/nucleon and rigidity spectra of primary cosmic helium nuclei 18 p3193 A66-34848  
Cerenkov counter using sulfur hexafluoride gas as radiator developed for study of isotopic composition of helium nuclei in primary cosmic radiation 18 p3193 A66-34853  
Phase shifts of elastic electron scattering from neutral helium, considering atomic distortion in adiabatic approximation 19 p3402 A66-35991  
Atomic hydrogen and helium emissions in upper atmosphere determined by diffraction

spectrophotometer measurement of twilight airglow and aurora 19 p3350 A66-36352  
Hydrogen and helium ions formation and destruction, charge transfer, diffusion, role during solar activity, using mass spectrometry, ground radar, etc 19 p3350 A66-36356  
Convection effect in helium charged insulation with partially foam-filled honeycomb core 20 p3675 A66-37066  
Closed cycle helium refrigerator noting thermodynamic cycle, equipment arrangement and cost estimate for space simulator and wind tunnel application closed 20 p3541 A66-37070  
Dimensional and experimental analyses of helium bubble motion in liquid nitrogen 20 p3545 A66-37104  
Nonreciprocal effects associated with excitation current observed in DC-excited He-Ne ring laser, noting coupling phenomena between right and left waves 20 p3577 A66-37408  
Detection of three radio lines arising from transitions between highly excited states of neutral helium 20 p3652 A66-37615  
Spectroscopic evidence on helium abundance of stars in galactic halo 21 p3817 A66-39565  
Flare stars as sources of cosmic X-rays, spectra contain 4686-angstrom line of doubly ionized helium indicating that atmospheres contain either ionizing radiation or electrons 22 p3972 A66-39707  
Prolonged exposures to acute anoxia cause reductions in viability of hydrated rye seeds, findings suggest helium may be harmful as atmospheric component in manned space capsules 22 p3855 A66-40480  
D-3 helium absorption line on solar disk connected to chromospheric flare origin 22 p3984 A66-40851  
Singlet and triplet populations in helium and electron temperature determination from optical excitation cross sections 23 p4100 A66-41161  
Line strengths variation in spectra of HD 124224 and HD 19832 analyzed, establishing anticorrelation of He I variations with variations in temperature 23 p4130 A66-41808  
Intrinsic rotation of Orion B stars with weak He lines, discussing color-magnitude diagram 23 p4130 A66-41815  
Thermal accommodation coefficients of He on tungsten and hydrogen on hydrogen-covered tungsten at temperatures of 325, 403 and 473 degrees K 23 p4033 A66-42078  
Measuring amplification of coherent optical radiation in neon-helium filled tube 24 p4219 A66-42125  
Excitation of 3S sub 2 neon level by metastable helium atoms during He-Ne discharge 24 p4219 A66-42126  
Thermal responses of man during rest and exercise in helium oxygen environment for various temperatures 24 p4163 A66-42317  
**HELIUM AFTERGLOW**  
Time-resolved spectroscopic measurement of absolute intensity, spectral profiles and self-absorption for He I lines in early helium afterglow 03 p0396 A66-12307  
Helium afterglow discussing stability of collisional-radiative recombination of ions with electrons and neutral particles 04 p0547 A66-13652  
Charge transfer between helium ions and molecules of nitrogen and oxygen in crossed-beam experiment within energy range 3 to 600 ev 05 p0671 A66-14954  
Helium afterglow in HF pulse-discharge plasma at 77 K from dissociative recombination of molecular helium ion with thermal electron 10 p1572 A66-22022  
Helium-neon laser afterglow and metastable helium atoms under long pulse excitation 14 p2307 A66-27335  
Helium afterglow in HF pulse-discharge plasma at 77 degrees K from dissociative recombination of molecular helium ion with thermal electron 16 p2760 A66-30841  
Electron and neutral atom densities in helium and argon afterglow plasma obtained by two helium-neon laser interferometers, noting temporal dependence of electron decay 23 p4101 A66-41364  
**HELIUM ATOM**  
Cosmic ray helium nuclei along with heavier nuclei, traverse interstellar and



- interplanetary matter propagation in space and slope of energy spectrum 03 p0423 A66-12927
- Terrestrial helium loss by speculated reaction between helium metastables and oxygen atoms 05 p0669 A66-14940
- Elastic differential scattering in low energy helium ion collisions, discussing quantal and secondary interference and two-state theory 05 p0719 A66-15768
- Solar cosmic ray particle composition, charge and energy spectra of nuclear components and isotopic composition of H and He 07 p1132 A66-18264
- Perturbation expansions for ground state function of helium atom, using Hartree or Hartree-Fock model Hamiltonian, based on Weiss-Martin variation-perturbation calculation 07 p1083 A66-18422
- First order wave function of helium due to one-and two-electron excitation determined by solving differential equations, noting contribution to second order energy 11 p1741 A66-23405
- Velocity distribution function of helium atom measured, using Doppler profile of helium line 16 p2701 A66-30377
- Electrons, hydrogen and helium nuclei of cosmic radiation as observed in 1964 at average residual pressure of 2.4 mb compared with 1.8 mb obtained in 1963 18 p3187 A66-34819
- Solar modulation of galactic protons and helium nuclei from 1963 to 1965 18 p3188 A66-34821
- Balloon-borne Cerenkov scintillation counter for measurements of primary proton and helium spectra and modulations 18 p3188 A66-34822
- Helium nuclei flux at top of atmosphere shows independence of solar activity 18 p3189 A66-34825
- Energy spectrum of primary helium nuclei at energies greater than 6 gev 18 p3189 A66-34826
- Differential rigidity spectrum of alpha particles for R less than 2.5 gv at solar minimum 18 p3189 A66-34827
- Optical pumping on He 4 atom in metastable level, examining modulation of light in absorption in longitudinal and transverse beams and obtaining magnetic resonance curves 22 p3930 A66-39808
- Helium atoms in 2P level contribute to formation of excited helium molecules in positive column of DC discharge, noting IR portion of pumping radiation is responsible for enhancement of molecular population 22 p3950 A66-39918
- Cell model of attractive interactions between helium atoms and effect on solid-superfluid transition in He 4 at absolute zero 23 p4090 A66-41368
- ### HELIUM COMPOUND
- Helium-neon laser amplifier as function of mixture ratio, gas pressure, input signal level and electrical power input to amplifier tube 02 p0242 A66-12206
- ### HELIUM FILM
- Heat capacity of adsorbed He 3 films at temperatures from 0.1 to 4 degrees K, with adsorption surfaces made of monolayers of argon preadsorbed on copper 09 p1392 A66-20020
- ### HELIUM PLASMA
- Electron and ion temperatures determination for helium plasma produced by theta-pinch with azimuthal magnetic field, using Doppler broadening and X-ray absorption 03 p0396 A66-12292
- Current discharge of helium neon laser on laser action 03 p0376 A66-12439
- Relationship between laws of electron temperature and charged particle concentration fall-off in helium plasma diffusion flow 03 p0398 A66-12520
- Spectral line intensities of hydrogen and helium plasma in P.I.G. discharge 04 p0553 A66-14283
- Reflected shock waves in helium and argon plasmas noting electron density, Saha equations and Newtonian technique 05 p0720 A66-14505
- High uncertainty in measurement of helium plasma temperature by two-line relative intensity method 05 p0722 A66-14913
- Helium-plasma decay in spherical balloon and volume removal by electron-ion recombination 06 p0914 A66-16146
- Heat transfer at low temperatures, discussing thermal conduction parameters of powdered alumina in helium 06 p0969 A66-16282
- Effect of ion drift from discharge on ionization state of helium-plasma model 08 p1265 A66-19374
- Breakdown of theta pinch in helium at high initial densities without preionization 09 p1408 A66-20422
- Microwave scattering theory applied to underdense cylindrical plasma measurements 09 p1409 A66-20851
- Spectroscopic analysis of helium plasma heated by reflected shock in T-tube, discussing luminous front and preceding shock 09 p1409 A66-20854
- Ion temperature measurement of streaming helium plasma by Langmuir double probe method, discussing effect of stream velocity 10 p1558 A66-21071
- Departures from local thermal equilibrium in helium plasma produced by magnetically-driven shock wave in T-tube 10 p1566 A66-21811
- Microinstability limitations of DCX-1 energetic plasma from gas dissociation and Lorentz force dissociation 10 p1568 A66-21826
- Electron temperature measurement by relative intensity of He I lines shown as inapplicable for high plasma densities 10 p1571 A66-22021
- Electric output and gas conductivity of cesium-seeded helium closed-loop MPD generator with auxiliary ionization 11 p1639 A66-22246
- Evolution of 5 solar masses star model from main sequence through core helium burning compared to 3 solar masses model, noting Hertzsprung-Russell diagram 11 p1772 A66-22780
- Evolution of 9 solar masses stellar model of population I initial composition from main sequence through core helium burning 11 p1773 A66-22781
- Nonlinear phenomena in HF plasma discharge, establishing qualitative relation between gas pressure, consumed microwave power and harmonic generation efficiency 12 p1919 A66-23711
- Hot-wire anemometer determination of electron and ion temperature, neutral particle temperature, concentration and velocity and potential of partially ionized helium plasma 12 p1882 A66-24223
- Electron temperature determination from intensity ratio of singlet and triplet lines of neutral helium used in plasma diagnostics, noting complications from metastable levels and coupling of singlet and triplet systems 12 p1924 A66-24592
- Collisional effects in region of electron cyclotron frequency on electromagnetic wave propagation in plasma 13 p2147 A66-25752
- Plasma wave propagation and decay processes studied from profiles of plasma density in cylindrical metal vessel and results compared to Stark effect and framing camera photographic results 13 p2149 A66-26240
- Helium-neon laser emission on 6401 angstrom line, noting intensity vs mirror shift and optical cavity instability 13 p2104 A66-26336
- Modification of hot big-bang theory to account for helium abundance in universe and cosmic radiation temperature, noting possible variation of Newtonian gravitational constant 13 p2189 A66-26599
- Excitation of azimuthal wave number equals 2 mode by helical instability for helium plasma 13 p2156 A66-26686
- Spectroscopic analysis of helium plasma shock waves, produced by annular discharge type conical coll shock tube 14 p2341 A66-27310
- Microwave measurement techniques for helium afterglow plasma 14 p2342 A66-27504
- Electron temperature in helium plasma determined from intensity ratios of spectral lines 14 p2344 A66-27643
- Production of thin copper and nickel ferrite films in inert gas plasma reveal spinel structure in electron diffraction patterns 15 p2557 A66-28564
- Helium-plasma decay in spherical balloon and volume removal by electron-ion recombination 15 p2556 A66-29873
- Modes of Kadomtsev plasma instability in helium positive column, noting diffusional loss 16 p2757 A66-30181
- Electron temperature measurement by relative intensity of He I lines shown as inapplicable for high plasma densities 16 p2760 A66-30841
- Emission line profiles of helium plasma formed by laser heating 17 p2933 A66-32228
- Helium plasma in confining magnetic field noting spectral efficiency in optical region electron temperature and density, electron ion recombination, etc 17 p2965 A66-32401
- Rate of diffusion disintegration of metastable helium atoms in decaying helium plasma at very low temperatures, with excitation by electrodeless method 18 p3142 A66-33941
- Effect of ion drift from discharge on ionization state of helium-plasma model 18 p3146 A66-34171
- Stark broadening of singly ionized argon lines in helium-argon plasma behind reflected shock wave in electromagnetic tube with backstrap 18 p3138 A66-34231
- Configuration interaction in helium continuum between first and second quantum thresholds 19 p3402 A66-35991
- Power balance measurements and particle loss rate of ohmically heated helium and hydrogen discharges in C stellarator 19 p3428 A66-36571
- Electric field intensity of helium and argon arc column as affected by pressure and current intensity 21 p3783 A66-39021
- Hot-wire anemometer determination of electron and ion temperature, neutral particle temperature, concentration and velocity and potential of partially ionized helium plasma 22 p3919 A66-40581
- Plasmoid-like RF helium plasma, noting molecular ion formation and destruction leading to evaluation of lower limit for molecular collisional-radiative recombination coefficient 22 p3957 A66-40901
- Production of thin copper and nickel ferrite films in inert gas plasma reveal spinel structure in electron diffraction patterns 23 p4112 A66-41281
- Saturation induced optical nonreciprocity in He-Ne ring laser plasma, eliminating frequency locking by using Faraday effect 24 p4221 A66-42552
- Low temperature system for thermal conductivity measurements using Ge and Pt resistance thermometers and He exchange gas switch 24 p4215 A66-43207
- ### HELIUM 2
- Thermal counterflow of He 2 in wide channels of rectangular cross section investigated in terms of damping of small-amplitude transverse vibration of fine wire 04 p0510 A66-13712
- Helium II film free-convection heat transfer, discussing mathematical analysis for vertical flat plate and horizontal circular cylinder [ASME PAPER 65-WA/HT-10] 05 p0791 A66-15652
- Vortices disintegration in rotating helium 2 in presence of oscillating disk when container stops rotating, noting role of helium angular velocity 12 p1865 A66-24880
- Ginzburg-Pitaevskii two-fluid formulation of superfluidity problem describing behavior of helium 2 in rotating annular cylinder, considering constant angular velocity and angular momentum 13 p2128 A66-26272
- Classical and quantum mechanical turbulence in Helium 2 heat flow, noting transition from laminar turbulent flow of normal and superfluid component, Reynolds number dependence on mutual friction coupling, etc 13 p2128 A66-26275
- Production of He I and He II spectral lines excited by helium ions from van de Graaff accelerator 20 p3604 A66-37628
- Vortices disintegration in rotating helium 2 in presence of oscillating disk when container stops rotating, noting role of helium angular velocity 23 p4053 A66-41087
- ### HELIUM 3
- Transition to superfluid state in He 3, measuring behavior of specific heat with three-stage adiabatic demagnetization apparatus 09 p1391 A66-20010



Acoustic impedance of liquid He 3 under vapor pressure 09 p1391 A66-20012  
 Acoustic impedance of liquid He 3 under pressure of up to 12.5 atm 09 p1391 A66-20013  
 Heat capacity measurements of liquid He 3 to improve precision in determination of effective mass ratio 09 p1392 A66-20014  
 Diffusion and regular model of motion of cosmic rays, noting dependence of applicability to cosmic ray fluxes on chemical composition 09 p1443 A66-20598  
 Pressure wave generation in fissioning gas, examining amplification of pressure pulse with helium 3 as driver 15 p2555 A66-29756  
 Abundance of isotopic helium 3 nuclei in primary cosmic radiation, using nuclear emulsion stack 18 p3189 A66-34828  
 Diffusion and regular model of motion of cosmic rays, noting dependence of applicability to cosmic ray fluxes on chemical composition 20 p3633 A66-38132  
**HELLMANN-FEYNMAN THEOREM**  
 New force theorem for determining molecular energy derivatives with respect to internuclear distance derived from Hellmann-Feynman expression 11 p1741 A66-23217  
 Electronic energy of interacting atoms at short range, noting Hellman-Feynman theorem for electron density in elliptic coordinates 17 p2961 A66-32550  
 Conditions under which optimal wave functions satisfy various time-dependent Hellmann-Feynman theorems 22 p3947 A66-39923  
**HELMET**  
 Crash and ballistic protective flight helmets, noting use of improved energy dissipating materials 17 p2863 A66-32146  
 Aircrew helmet design for protection against buffeting and against crash impacts 17 p2865 A66-32188  
**HELMHOLTZ EQUATION**  
**SA WAVE EQUATION**  
 Behavior of Green function for Helmholtz equation external to bounded convex region, obtaining integral representation 06 p0903 A66-16705  
 Separation of electromagnetic and plasma modes in two-fluid lossy compressible plasma, deriving field qualities from two Helmholtz equations 11 p1653 A66-22561  
 Wave diffraction problems in wedge-shaped regions solved, using Wiener-Hopf and Helmholtz equations and superposition principle 12 p1915 A66-24819  
**HELMHOLTZ-KELVIN TIME SCALE**  
 Rayleigh-Taylor nonconfined and Kelvin-Helmholtz confined interchange instabilities obtained from nonlinear computer models 17 p2967 A66-32434  
**HEMATOCRIT RATIO**  
 Hematocrit index and arterial-blood gas composition in white rats during artificial hypothermia 15 p2440 A66-29511  
**HEMATOLOGY**  
**SA BLOOD**  
 Hematological changes in seven healthy young males subjected to intense heating transients 01 p0017 A66-10611  
 Continuous exposure of rats to 100 percent oxygen at 450 mm Hg for 64 days shows no physiological effects 12 p1807 A66-25013  
 Liquid breathing effects on dogs in hyperbaric chamber 21 p3699 A66-38447  
 Respiratory activity and hematological factors of avian blood cells, discussing oxygen consumption, thermal effects, tissue and erythrocyte metabolism 23 p4024 A66-41043  
**HEMATOPOIETIC SYSTEM**  
 Pulsed microwave irradiation of dogs noting body weight, rectal temperature and hematologic response 03 p0326 A66-13351  
 Partial canine body exposure to ionization radiation noting anorexia, weight loss, vomiting and hypersialosis due to 1000 kVp X-ray exposure 03 p0326 A66-13352  
 Pathomorphological changes in hemopoietic organs of mice after irradiation with high energy protons 15 p2438 A66-29482  
**HEMATURIA**  
**S URINE**  
**HEMISPHERE**  
**S NORTHERN HEMISPHERE**  
**S SOUTHERN HEMISPHERE**

# HEMODYNAMIC RESPONSE

Gravity effect on hemodynamic factors and sodium and water excretion in two dogs subjected to change from supine to erect position and water immersion 03 p0324 A66-12352  
 Acute hemodynamic effects of G-suit inflation, noting elevation of central venous pressure, cardiac output falling due to depressor reflexes and role of ganglionic blockade 12 p1811 A66-25014  
 Combination of renal vasodilation and angiotensin infusion effect large changes in renal hemodynamics, excretion and reabsorption of sodium in anesthetized hypotensive dogs 20 p3507 A66-37607  
 Cardiopulmonary hemodynamics in dogs under transverse acceleration studied in terms of changes in heart and lungs 24 p4163 A66-42450

# HEMOGLOBIN

Affinity and stoichiometry of binding of 1-anilino-8-naphthalene sulfonate /ANS/ to apomoglobin and apohemoglobin 08 p1177 A66-18701  
 Immunochemical studies on interspecies molecular hybrids of hemoglobin 13 p2010 A66-25898

# HEMOLYSIS

Mechanism of in vivo rbc damage by oxygen, noting effect on canine erythrocytes 03 p0326 A66-13348

# HEPTANE

Polymer degradation dosimeter of polyisobutylene in heptane noting viscosity range effects, concentration change and molecular weight 21 p3739 A66-39383

# HERMETIC SEAL

Cycle life and energy yield of hermetically sealed secondary silver-zinc batteries for aerospace application [AIAA PAPER 64-749] 13 p2007 A66-26650  
 Seal performance optimization, noting alignment, lubrication, gasketing, balance, etc [ASLE PAPER 66AM 2C2] 16 p2711 A66-30407

Dynamic instability in undamped bellows face seals operating in cryogenic environment with torsional oscillation and diametrical rocking as primary motion [ASLE PAPER 66AM 2CE] 16 p2711 A66-30408

Shaft sealing systems on centrifugal compressors, noting labyrinth, restrictive ring shaft, liquid film and mechanical and special seals [ASME PAPER 66-MD-42] 21 p3742 A66-38490

Psychological effects of velocity and hermetic compartments on astronaut performance 24 p4166 A66-43146

# HERMITIAN POLYNOMIAL

Absorption coefficient for lines with combined Doppler and Lorentz broadening calculated, using Runge-Kutta method, continued fraction expansion and Hermite-Gauss quadrature 03 p0393 A66-13267  
 Real eigenvalues of complex matrices, using Hermitian matrix relations 10 p1551 A66-21926

Hermite interpolation combined with Ritz method for numerical approximation of solution of two-point boundary value problems 16 p2732 A66-30243  
 Maximization of second-degree polynomial on unit sphere 19 p3392 A66-36787  
 Reduction of PDE system of heat transfer, using Hermitian approximating polynomials to obtain solution to initial system 23 p4041 A66-40971

# HERTZSPRUNG-RUSSELL DIAGRAM

Distribution patterns of common stars in galactic plane according to spectral type, noting density gradients, main sequence, Hertzsprung-Russell diagram, etc 11 p1766 A66-22254  
 Evolution of 5 solar masses star model from main sequence through core helium burning compared to 3 solar masses model, noting Hertzsprung-Russell diagram 11 p1772 A66-22780

Analytic models of stellar evolution, describing homogeneous and inhomogeneous stages, energy conservation and transport radiative and convective transfer mechanisms, etc 19 p3467 A66-36789  
 Position of variable stars in Hertzsprung-Russell diagram - International Astronomical

Union Colloquium, Bamberg, West Germany, August 1965 20 p3652 A66-37609

Light variations of flare and T Tauri stars due to surface electromagnetic activity connected with turbulence in convective zone and rotation, using Hertzsprung-Russell diagram 20 p3652 A66-37610

Pulsation in cepheid instability strip in H-R diagram, giving equations for spherically symmetric motion 21 p3816 A66-39489

# HETERODYNE

## SA OPTICAL HETERODYNE

## SA SUPERHETERODYNE RECEIVER

Bailey and Martyn theories concerning ionospheric cross-modulation extended to cover simple cases of heterodyne and harmonic generation by electromagnetic fields in plasma 06 p0920 A66-17031

Heterodyne detection at millimeter wavelengths shown in distributed structure of bulk indium antimonide, noting conversion loss and noise properties 15 p2462 A66-29017

Engineering analysis of heterodyne modulation method of checking heterodyne receivers, considering input-signal circuits having minimum effects on heterodyne characteristics 23 p4043 A66-41060

Doppler frequency-measuring tracking system in which tracking filter or retuned heterodyne is used for definition of signal with unknown frequency 23 p4038 A66-41524

# HETEROGENEITY

Heterogeneity effect on multilayer composite cylindrical shell stability under axial compression 17 p3025 A66-32454

Limiting factors of detonation in heterogeneous systems, using one-dimensional model 18 p3265 A66-34552

# HETEROTROPIA

Difference spectra of glucose cultures of *Chlorella vulgaris* beyernick indicate increased pigmentation in white light and monochromatic light over dark controls 20 p3507 A66-37791

# HEXABORIDE

X-ray L band absorption spectra of rare earth atoms in hexaborides, collecting evidence on valence state 01 p0126 A66-10980  
 Lanthanum hexaboride evaporation from Knudsen cell studied by mass spectrography for composition, sublimation heat and ion current 17 p2981 A66-32849

# HEXAGONAL CELL

Crystalline structure on fatigue noting changes of body-centred metals and face-centred and hexagonal metals 02 p0245 A66-11948

Hexagonal crystal structure growth of CdTe thin film 19 p3438 A66-35480

# HEXAMETHYLENETETRAMINE

Crystal structure of hexamethylenetetramine hexahydrate determined using X-ray analysis, noting hydrogen bonding in crystalline state 03 p0330 A66-12338

# HEXANE

## SA CYCLOHEXANE

HF pressure fluctuations in heat transfer of diisopropyl hexane seen as caused by shock waves produced by collapsing bubbles 21 p3835 A66-38906

# HEXOGENE

Decomposition times of liquid nitromethane, liquid tetranitromethane and hexogen single crystals in shock waves 14 p2275 A66-27598

# HFB 320 AIRCRAFT

## S HAMBURGER HFB 320 AIRCRAFT

## HXX HELICOPTER

## S CH-53 HELICOPTER

# HIGH ALTITUDE

Diurnal solar variation in cosmic ray meson intensity recorded in southerly and northerly directions at high altitudes 04 p0574 A66-13840

Externally caused radio frequency interference /RFI/ in electronic subsystems of ballistic vehicles at orbital altitudes 13 p2027 A66-26744

# HIGH ALTITUDE BALLOON PROGRAM

High altitude balloons for scientific research noting zero-pressure balloon 05 p0611 A66-15271

Fiberglass balloon gondola used to eliminate environmental problems in photomultipliers and spark chambers carried by high altitude balloons 10 p1618 A66-21866



High altitude balloons used to carry scientific instruments 14 p2222 A66-26926  
 Simultaneous IR emission and auroral X-ray observations from high altitude balloon flights 14 p2376 A66-27399  
 High altitude balloon top collections of cosmic dust shows evidence of absence of crystal structure in particles 15 p2604 A66-30065

**HIGH ALTITUDE BREATHING**

Human evaluation and testing requirements for physiological protective efficiency of civil aviation oxygen equipment 17 p2863 A66-32151

**HIGH ALTITUDE ENVIRONMENT**

Atmospheric mixing time and lifetime of atomic and molecular oxygen at high altitude, noting agreement with barometric distribution law, concentration pattern, etc 15 p2486 A66-29088  
 Lifetime high altitude environment effect on man, noting Peruvian natives adaptation to constant hypoxia 22 p3854 A66-40112  
 Hypoxia of simulated high altitude exposure prolongs synaptic delay and conduction time in brain system of rats 22 p3855 A66-40403

**HIGH ALTITUDE FLYING**

Internal friction and vertical separation effects on airways and traffic control and high altitude deviation in barometric altimeters 08 p1249 A66-18693  
 Thin section bearings used to solve spatial needs and temperature problems of high altitude flying 08 p1229 A66-18827  
 Utilitarian space applications, discussing communications, weather, geodetic and navigation satellites and high speed aircraft 09 p1453 A66-20169  
 High altitude visual flight environment, discussing sky brightness, instrument and runway lighting, visual fields, eye protection, etc 10 p1494 A66-22131

**HIGH ALTITUDE NUCLEAR DETECTION**

STUDIES /HANDS/  
 High-altitude nuclear explosion detector design for Vela project 09 p1463 A66-19968

**HIGH ALTITUDE PRESSURE**

Physiological effects of pressure breathing and aveolar oxygen tension at high altitude 10 p1489 A66-22117  
 History, design configurations, construction and materials of pressure suits for human protection at high altitudes 10 p1492 A66-22118

**HIGH ALTITUDE SOUNDING PROJECTILE /HASP/**

Gun-launched meteorological sounding system, describing launcher, vehicle, sensor systems and sensitivity [AIAA PAPER 66-382] 12 p1954 A66-24506  
 Upper atmospheric wind measurement with gun launched projectiles, computing wind component contour parameters [AIAA PAPER 66-403] 12 p1908 A66-24515  
 High altitude research project using 16-inch gun for measurement of upper atmospheric wind shear patterns 19 p3340 A66-36644

**HIGH ALTITUDE TESTING**

Rocket measurements discussing electron and proton flux, energy spectra and angular distribution in high altitudes 05 p0676 A66-14776  
 Average steady-state omnidirectional trapped electron flux due to beta decay from orbiting leakage reactor neutrons 05 p0747 A66-14786  
 High altitude aircraft for calibration of solar cells and extrapolation of data to obtain outer space short circuit current 06 p0808 A66-16013  
 Cosmos V satellite measurement of July 9, 1962 high altitude nuclear detonation used to determine fission debris over Johnston Island 08 p1219 A66-19414  
 Radioactivity of Cosmos III satellite after U.S. thermonuclear explosion over Johnston Island 11 p1764 A66-23053  
 High-altitude nuclear explosion-induced geomagnetic micropulsations in analysis of sudden commencement data and Alfvén velocity-altitude profile 11 p1700 A66-23143  
 Gamma radiating debris cloud of high-altitude nuclear explosions scanned by gamma scintillation detector assembled into directional uranium shield 12 p1878 A66-23696

Parachute for meteorological rockets, noting design, testing, high altitude performance, etc 12 p1802 A66-24514  
 [AIAA PAPER 66-399]  
 Plasma due to high-altitude nuclear explosion and effect on radar propagation 14 p2237 A66-27510  
 Ionospheric effects over Delhi of Russian high altitude nuclear explosions in Central Asia and of U.S.A. explosions at Johnston Island, autumn 1962 17 p2918 A66-32695  
 Lift, drag and static pitching measurements on lifting bodies at simulated hypersonic cold-wall conditions [AIAA PAPER 66-467] 18 p3046 A66-33651  
 Latitude and longitude variation of count rate and intensity-time dependence of proton flux in inner radiation belt measured by Anton 302 G-M counter in Ariel I satellite 20 p3638 A66-38306  
 Trapped electrons from Russian high altitude nuclear detonation examined, noting energy spectrum and mirror point density distribution 20 p3643 A66-38342  
 High altitude nuclear detonations, discussing data on trapped radiation, values of empirical and theoretical spectra and artificial radiation belts 20 p3643 A66-38344  
 High altitude parachute systems test techniques for analysis of inflation, stability variations, porosity, effects at low dynamic pressure, etc 22 p3849 A66-40602  
 Sea level and high altitude ignition of fuel-rich gas generator/turbine manifold assembly 24 p4294 A66-42640

**HIGH ENERGY ELECTRON**

High energy protons in synchrocyclotron testing of polyethylene, aluminum, lead and titanium hydride 05 p0627 A66-15118  
 Radiation unit of length, calculating path-length for passage of high-energy electrons and photons through matter 06 p0912 A66-16575  
 Bethe approximation of ionization cross sections of excited states of atomic hydrogen by high energy electrons 06 p0912 A66-17037  
 Dependence of lifetime on injected level in high-energy electron-irradiated silicon with production of total displacements per primary recoil event 06 p0939 A66-17156  
 Optical emission induced in gallium arsenide samples by bombardment with high energy electron pulses 07 p1096 A66-17338  
 Fraction of energy transferred to photon-electron component during interactions of particles with graphite nuclei at energies exceeding 100 bev 07 p1114 A66-17545  
 Passage of high energy electrons and photons through condensed media such as photographic emulsion in cascade theory and method of moments 07 p1116 A66-17558  
 Bethe-Born approximation and partial ionization cross sections of singly and doubly charged helium and neon ions 14 p2336 A66-26830  
 Bethe-Born approximation and partial ionization cross sections of argon, krypton and xenon ions 14 p2336 A66-26831  
 Formation mechanism of ionospheric narrow sporadic E layers by high energy electron fluxes captured by geomagnetic field 15 p2488 A66-29110  
 Inverse Compton X-ray and gamma ray flux due to high energy electron interaction with cosmic blackbody radiation at 3.5 degrees K 17 p2992 A66-31914  
 High energy electron acceleration detected in shock transition region of terrestrial magnetosphere, using Au-Si surface barrier solid state detector and IMP-I satellite mounted GM counter 18 p3177 A66-34753  
 Synchrotron radiation from high-energy electrons spiraling in magnetic field, noting parameter effects and computation of numerical results 20 p3644 A66-38348  
 Isochronal and isothermal stage II recovery in high energy electron irradiated n-type InSb semiconductor, based on Hall coefficient and electroconductivity 21 p3800 A66-38994  
 Acceleration of high energy electrons by means of Parker-Wentzel version of Fermi mechanism due to geometry and distorted structure of interplanetary magnetic field near magnetopause in transition region 22 p3972 A66-40003

**HIGH ENERGY INTERACTION**

High energy nuclear interaction and particle structures covering meson, baryon composition and dimensional analysis 05 p0749 A66-15151  
 High energy interaction of nucleons with complex nuclei described by model cascade-type nucleon and pion multiplication within nucleus 05 p0755 A66-15152  
 Book on high energy particles dealing with concepts and techniques for study of properties of material through interaction with cosmic radiation 06 p0944 A66-16013  
 Nucleon-nucleus collisions at high energy, describing statistically independent successive interactions of incident particles with target nucleus 07 p1113 A66-17515  
 Energy spectra for nuclear-active particles and particle distribution in air show indicate that pionization plays minor role relative to high energy cosmic rays 07 p1114 A66-17516  
 Origin of high energy pions, muons and photons studied from available spectral data 07 p1115 A66-17517  
 Ultrahigh-energy primary cosmic ray particle interactions cause electron phot cascades and muon emission 07 p1117 A66-17518  
 Extensive air shower high energy gamma rays in upper third of atmosphere 07 p1118 A66-17519  
 Probability of high-energy cosmic ray muons undergoing electromagnetic interaction lead with energy transfer at various ranges 08 p1286 A66-19813  
 Four momentum transfer in high energy jet showers and resultant number multireballs 11 p1763 A66-22715  
 Cosmological-galactic creation, steady state expansion and high energy particle production associated with radio sources 11 p1774 A66-23003  
 Distorted wave one-meson-exchange /DWOME/ for high-energy elementary particle reaction analysis, leading to different expression for transition amplitude 13 p2131 A66-25418  
 High energy solar cosmic ray spectrum during solar flare of February 2, 1956 15 p2575 A66-29068  
 High energy interactions - International Conference on Cosmic Rays, Jaipur, India, December 1963 15 p2582 A66-29558  
 Meson emission asymmetry, inelastic particle collisions and multiplicity in ultrahigh energy interactions in nuclear emulsion 15 p2545 A66-29554  
 Collision cross sections of high energy nucleon-nucleon interactions in nuclear emulsion 15 p2583 A66-29554  
 Elementary particle theory, interactions at accelerator energies, bootstrap mechanism for generating bound states and resonance, and Regge pole concept applied to high energy scattering 15 p2545 A66-29554  
 U.S.S.R. accelerator experiments in high energy nuclear interaction cross section and inelasticity, primary and secondary cosmic ray particle energies, charged nuclear-active particle energy spectra, momenta measurements, etc 15 p2545 A66-29554  
 High energy primary cosmic radiation research at Bristol, England, including energy spectra for nuclear interactions nuclear emulsion stack measurements, alpha production, etc 15 p2583 A66-29554  
 High energy mountain-altitude nuclear interactions produced by pions and nucleons, pion/proton and neutral/charged interacting particle ratios studied, using multiplate cloud chamber with air Cerenkov counter and absorption spectrometer 15 p2584 A66-29554  
 Cosmic ray showers, discussing high energy interactions of nuclear active particles, intensity and energy spectra of gamma rays and muons, young air showers, ionization bursts, etc 15 p2584 A66-29555  
 Electron-photon cascades caused by nuclear active component in atmosphere and on gamma rays, atmospheric absorption spectrum of primary nucleons and generation of pions 15 p2584 A66-29556  
 Particle energy measurements in high energy jets with large stacks of nuclear emulsion 15 p2584 A66-29557  
 Extremely collimated nuclear interactions



## SUBJECT INDEX

in carbon induced by collisions of charged cosmic ray particles in energy region 20-100 gev 15 p2585 A66-29559

Secondary cosmic radiation and meson production at high energy, noting particle flux regularities and 15 p2586 A66-29564

Electron pair production by high energy muons, noting application of Monte Carlo method for appearance of low energy with high energy partner below target plate 15 p2546 A66-29583

Multiple penetrating particles underground, noting interaction of muons with matter at 148 meters water 15 p2546 A66-29584

Particle number fluctuation in electron-photon shower, influence on spectrum of bursts produced by high energy mu mesons under thick filters 15 p2589 A66-29585

Hydrogen, He, Ne and Xe high energy molecular beam scattering from gold film surfaces during evaporative deposition 16 p2752 A66-30392

High energy argon atom interactions with surfaces and variations in accommodation coefficient 16 p2702 A66-30399

Developments in study of high energy particles of 25 to 30 gev 16 p2795 A66-31268

Plasma beam action on tritiated titanium and high energy deuteron detection in mixed-field accelerator 17 p2972 A66-32953

Balloon observation of high energy primary electrons with counter system 18 p3187 A66-34816

Charge ratio of cosmic ray electrons, examining excitation of baryon resonances in high energy collisions with no exchange of isospin 18 p3193 A66-34850

High energy particle interaction research, noting that within eight years accelerators will be capable of beams of 28 plus 28 bev protons 18 p3204 A66-35091

Scintillation counter observation of EAS core structure and high energy interactions 18 p3207 A66-35106

High primary energy EAS composition, energy spectrum of nuclear active particles and high energy 18 p3210 A66-35128

Extremely high energy nuclear interactions observed by emulsion chamber, deriving inelasticity of nucleons and mesons and transverse momentum of 18 p3215 A66-35158

High energy nuclear interactions in graphite 18 p3140 A66-35159

Energy measurement errors effect on characteristics of elementary interactions 18 p3140 A66-35168

Energy spectra of electromagnetic cascades produced by cosmic rays observed at balloon altitudes, using composite detector 18 p3216 A66-35169

High energy interaction studied on Norikura Mountain and Mount Chacaltaya, using large area emulsion chamber 18 p3216 A66-35170

Multiplicity of high-energy interactions causing extensive air showers determined from maximum position 18 p3217 A66-35176

Two-fireball and CKP models of ultrahigh energy interactions 18 p3217 A66-35177

Energy estimation of high-energy interactions by quartile angle of emitted tracks, estimating fireball mass and elasticities 18 p3218 A66-35179

Nucleon interaction with complex nuclei at high energy in terms of multiple collision model 18 p3218 A66-35180

Angular distribution of secondary particles in multiple production at high energy, noting multiplicity and inelasticity dependence on primary energy 18 p3218 A66-35181

Tskhra-Tskaro installation for study of high-energy cosmic particle interaction with matter 18 p3218 A66-35182

Bremsstrahlung of electron impinging on fixed center of force and subsequent anomalous interaction, noting similar effect in strong interactions 18 p3218 A66-35183

High energy interaction calculation and experimental techniques 18 p3219 A66-35185

Interaction between ultrahigh energy cosmic rays and neutrinos in universe, noting distortion of energy spectrum 18 p3224 A66-35220

Phenomenological picture of production of secondary particles in nucleon interactions at energies of hundreds and thousands of bev 24 p4267 A66-42902

Elementary particles interaction with atomic nuclei with energies from tens to thousands of bev 24 p4267 A66-42903

High energy inelastic interactions, discussing necessity of statistical methods, secondary particle composition and angular distribution, etc 24 p4267 A66-42904

High energy particle interactions initiate large ionization bursts, noting pion production 24 p4267 A66-42907

Interaction of 1000 bev particles by ionization calorimeter technique suggests free path of nuclear active particles in atmosphere decreases as particle energy increases 24 p4267 A66-42908

Inelastic interactions at ultrahigh energies, discussing secondary particle jets production moving in same direction as colliding particles 24 p4268 A66-42912

Stability of solutions to inverse problems in cascade theory, analyzing case when equilibrium spectrum of particles is specified 24 p4269 A66-42922

### HIGH ENERGY OXIDIZER

### S PROPELLANT OXIDIZER

### HIGH ENERGY PROPELLANT

Design and development of high energy standard engine for ELDO-B carrier rocket 02 p0279 A66-11669

Machine computation of thermodynamic properties of hydrazine from 32 degrees F to 1.02 times critical density 03 p0414 A66-12760

Design criteria for launch-vehicle high-energy stage, emphasizing operational reliability, mission range and low development effort 06 p0959 A66-16494

Nonequilibrium dissociation losses in hydrogen-fluorine propellant system, indicating rate control of recombination steps 22 p3969 A66-39882

### HIGH EXPLOSIVE

Spherical and cylindrical implosive waves and system of generating detonation wave that converges to given focus 03 p0445 A66-13131

Nature and rate of linear surface regression of TNT, RDX, Tetryl and PETN, using hot-plane pyrolysis technique over surface temperatures to 500 degrees C 04 p0571 A66-13645

Metal powder behavior during dynamic and static pressing by energy release of high explosives 07 p1038 A66-18160

High-explosive driven shock tubes, as sources of short duration high-pressure supersonic pulses, applied in accelerating large objects 16 p2674 A66-30423

Small perturbation method applied to combustion stability of high explosives taking into account heat release in K phase 19 p3477 A66-35740

Electroexplosive devices in aerospace vehicles in two classes, propellants and high explosives, noting methods for controlling detonation desired 20 p3625 A66-37159

### HIGH FIELD MAGNET FACILITY

High critical magnetic field, high current superconductors, degradation and practical magnet systems 14 p2364 A66-27649

High field liquid-neon-cooled superconducting electromagnet for cryogenic solid state research 20 p3601 A66-37106

AC losses and magnetic field aberrations associated with use of high-field superconducting wire in adiabatic demagnetization apparatus 21 p3804 A66-39381

High density thermonuclear plasma confinement by multimegagauss magnetic fields 21 p3793 A66-39508

Superconductivity of Ta-Ti solid solution alloy wires subject to steady magnetic high field 22 p3960 A66-39782

Iterative design procedure for optimum placement of vapor deposited Nb-Sn ribbon superconductors in high field large bore modular magnets 24 p4186 A66-43175

### HIGH FREQUENCY

Effect produced by nonhomogeneous HF field on distributed plasma parameters 01 p0115 A66-11050

## HIGH GRAVITY ENVIRONMENT

Linear coefficient of amplification of carbon dioxide subjected to HF excitation field for laser emission 02 p0241 A66-12003

Ionization potential of thulium obtained from hfs of thulium I, using discharge tube and Fabry-Perot etalon 03 p0393 A66-12322

HF behavior of transistors, using Giacomello equivalent circuit 06 p0856 A66-16918

HF pulse rise in high-Q synchronous amplifier with one circuit per stage by approximation method 07 p1009 A66-18069

International coordination and standardization of HF quantity measurements, considering economic, psychologic and accuracy benefits 07 p1002 A66-18224

Instability of noncollision plasma in strong external field in terms of development of nonpotential oscillations 09 p1408 A66-20599

Selection of minimum noise temperature for HF amplifiers in SHF receivers 11 p1667 A66-22795

HF technique for surveillance and tracking of reentry capsule, in departure from planned reentry corridors 12 p1819 A66-24608

HF power transistor delivering 40 watts of RF power at 175 mc at 8 db gain and 75 percent efficiency, noting design and operation 13 p2035 A66-25511

Y-parameter graphs and data for HF circuits obtained from General Radio transfer function and immittance bridge 14 p2261 A66-28370

Spectral analysis of HF oscillations with phase-modulated fluctuations as functions of phase dispersion and spectral form of modulating fluctuations 17 p2898 A66-31854

Sinusoidally varying HF electric field effect on glow discharge plasma, showing capability of confinement 17 p2971 A66-32785

Electron temperature determination in argon plasma as function of distance measured to axis of inductive windings 17 p2974 A66-33255

Spectrum broadening of long-duration high-frequency pulses by FM 17 p2877 A66-33521

Faraday rotation from 24-hr satellite at high frequencies provides means of studying electron content of ionosphere and fluctuations 18 p3106 A66-34200

Thermometer for continuous temperature measurement of dielectrics and semiconductors in electromagnetic HF fields 19 p3358 A66-35836

Selection of minimum noise temperature for HF amplifiers in SHF receivers 20 p3525 A66-37132

Instability of noncollision plasma in strong external field in terms of development of nonpotential oscillations 20 p3611 A66-38133

HF long-distance radio signal transmission and high and low antenna sighting 20 p3521 A66-38358

Polarization characteristic variations of HF signal received over short-range ionospheric path, noting phase measurement of elliptically polarized wave components, using receiving dipoles 22 p3864 A66-40065

Scattering parameters for design of HF transistor circuits 22 p3877 A66-40334

HF conductivity of quasi-equilibrium isotropic fully ionized two-temperature plasma 23 p4102 A66-41367

HF transmitter multicoupler for connecting several transmitters to single antenna 23 p4046 A66-41548

Semiconductor conductivity in strong SHF electric fields, measuring dielectric constant and Fourier component 23 p4068 A66-41620

Potential oscillations in neutral completely ionized plasma-neutral charged-particle beam system in HF electric field and growth rate of plasma instability 23 p4106 A66-41707

HF transistor stability in common emitter configuration, examining performance of input admittance in circuit design and analysis 24 p4181 A66-42377

Transmissibility, isolator mass effects, vibration source and receiver characteristics for HF vibration isolation problem 24 p4291 A66-42860

### HIGH GRAVITY ENVIRONMENT

Feasibility of solid state negative feedback amplifiers based on use of RC networks meeting requirements of frequency stability, high tolerance and long shelf life 17 p2880 A66-31955



## HIGH LIFT DEVICE

Boundary layer control /BLC/ high lift system used as integral part in design of F-4 Mach 2 plus Navy interceptor [AIAA PAPER 65-714] 01 p0013 A66-10951  
Flight experiments to assess stalling behavior and handling problems arising in design, maintenance and operation of suction wing for high lift [AIAA PAPER 65-750] 03 p0319 A66-12586  
Boundary layer control high lift system for high speed aircraft, using ejector for momentum augmentation and air bleed from propulsion system [AIAA PAPER 64-589] 05 p0610 A66-15070  
Boundary layer control /BLC/ high lift system used as integral part in design of F-4 Mach 2 plus Navy interceptor [AIAA PAPER 65-714] 12 p1801 A66-24095

## HIGH PASS FILTER

Epitaxial metal-oxide-semiconductor transistor with tunable high-pass filter-type response characteristics with insertion gain in passband 06 p0857 A66-16959  
Logarithmic amplifier with pulse-length discrimination followed by high-pass filter for reducing adverse effects of distributed clutter in radar receivers 08 p1180 A66-18712  
Active filters and oscillators using simulated inductance 11 p1661 A66-22387  
Dielectric layers of alternating low and high dielectric constant used as filters in millimeter wave, IR and optical regions 12 p1831 A66-23906

## HIGH SPEED CAMERA

Camera timing marker blocks with dual spark and neon light sources for high speed camera 03 p0367 A66-12310  
High speed camera survey 03 p0367 A66-12311  
Cinematographic system in which capacitor-discharge pulses are substitutes for high speed shutter 03 p0368 A66-12465  
Laser technique to photograph hypervelocity projectiles in free-flight range 03 p0379 A66-13248  
Time-marking during high speed cinematography of details on Sun with SKS-1M camera 05 p0681 A66-15216  
High-speed stereoscopic photography development, noting application of frequency wobbling method to photography of explosions 10 p1534 A66-21330  
High speed photography equipment, light sources, shutters and special cameras 10 p1536 A66-21867  
Ultrahigh speed photographic instruments, discussing camera characteristics, shuttering, illumination, film transport and selection 10 p1537 A66-21868  
Kerr cell as shutters and laser modulators in high speed photography 10 p1537 A66-21869  
Horizontal plate Mach-Zehnder interferometer for hypervelocity range vacuum use, high speed photography problems and electron density measurement 10 p1537 A66-21871  
Five-stage transmission secondary-emission image intensifier tube as high speed shutter for moment and streak photography 12 p1883 A66-24937  
RKD-2 high speed raster camera with two rotating disks 14 p2295 A66-27653  
Crystal motion effect on time behavior of laser generation mode, using high speed photography and oscillograms 15 p2518 A66-29725  
High speed stroboscopic photography using Kerr cell modulated laser source 16 p2705 A66-30828  
Fast lens component for SFR high speed photographic recorder with asymmetric objectives 17 p2927 A66-33439  
Operation of electron image time dissector framing camera achieving time resolution by multiple reflection in crossed magnetic and electric fields in electron image storage device 19 p3353 A66-35313  
High-speed photographic techniques, recording impact and postimpact phenomena, used in prediction of flow resulting from hypervelocity impact of pellet with thin plate 20 p3560 A66-37740  
Gas flow in supersonic wind tunnel measured with high speed photography, noting experimental techniques and applications 22 p3886 A66-40199

Proximity focused biplanar image converter diode for high speed photography, discussing basic geometries with respect to quantitative data gathering capabilities 23 p4070 A66-41673  
Photographic equipment using image converter tube as electronic shutter with exposure times from 0.5 to 5000 microseconds 23 p4070 A66-41674  
Multipurpose ultrahigh speed camera system, noting use as monosecond Kerr cell, image converter and giant laser pulse generator 23 p4071 A66-41675  
High speed photograph analysis of compressed volumes of plasma formed in reaction of colliding supersonic flares of high power pulsed discharge 24 p4244 A66-42875  
Thermoanemometric and high speed motion-picture photographic experimental analysis of air vortex ring structure 24 p4196 A66-42879

## HIGH SPEED FLYING

Laminar and turbulent boundary layer flow in ablating cones in hypervelocity flight [AIAA PAPER 66-27] 07 p1020 A66-17889  
STOL for high speed aircraft, discussing aerodynamic parameters, lift coefficient, increase methods, etc 09 p1327 A66-20245  
Text on high velocity aerodynamics, including subsonic, supersonic and hypersonic flows, rarefied gases, boundary layer theory and MHD 10 p1479 A66-21057  
Young theory of rotor blade motion stability in powered flight 11 p1638 A66-23261  
Decreased flying ability of pilots in simulated low altitude high speed flight from 0.4 to 0.9 Mach 12 p1809 A66-23928  
Heat dissipated inside compartments by internal structural members on high speed aircraft 14 p2414 A66-28188  
S-61F helicopter flight test program, noting design modifications for high speed performance 17 p2844 A66-32726  
Short takeoff and landing for high speed aircraft, discussing aerodynamic parameters of lift coefficient of flap system, lift-drag ratio and thrust 18 p3052 A66-33971  
Low altitude high-speed flight from standpoint of structural loads, particularly those resulting from gust encounters 19 p3278 A66-35505  
Flight control for low altitude high-speed mission, discussing applicable requirements, analysis and design techniques 19 p3396 A66-35506  
Aircrew response effects to prolonged low altitude high-speed flight vibration 19 p3287 A66-35507  
Cockpit displays associated with low altitude high-speed flight, emphasizing shift toward designing around man 19 p3287 A66-35508  
Laminar and turbulent boundary layer flow in ablating cones in hypervelocity flight [AIAA PAPER 66-27] 21 p3723 A66-38686  
Single air flow acceleration and deviation for propulsion and lift of high speed aircraft, analyzing long-range flight paths [ICAS PAPER 66-41] 23 p4122 A66-42070

## HIGH STRENGTH ALLOY

Zinc effect on mechanical properties and microstructure of Al-Si-Cr-Mg alloy 03 p0382 A66-12724  
Plane strain fracture toughness of high strength aluminum alloys measuring techniques and relevant metallurgical factors [ASME PAPER 64-WA/MET-11] 06 p0895 A66-16209  
Saturn Launch Vehicle Program technical equipment and engineering techniques for solving structural, propulsion, launch and control problems 06 p0959 A66-16496  
Yield strength dependence on normal to cryogenic temperatures of high strength alloys [ASME PAPER 65-PROD-14] 11 p1715 A66-22475  
Sintered W and W plus additive billets used to test feasibility of producing fiber-bearing composites by elongation during extrusion 11 p1715 A66-22537  
Yield and flow stress reduction in high strength metals during ultrasonic vibration 16 p2821 A66-31462  
Microquenched age-formed titanium alloys

and titanium Bi-alloy composites, discussing production process using spherical particles produced by rotating electrode [SAE PAPER 660458] 17 p2940 A66-33164  
Air and aqueous environments effect on mode of fracture in titanium alloys during low cycle fatigue 18 p3122 A66-33749  
Aging behavior and mechanical properties of three wrought high-strength magnesium alloys 18 p3122 A66-33751  
Heat resistance in air of dispersion hardened nickel alloys containing certain oxides prepared by powder metallurgy methods 18 p3123 A66-33781  
Carbon content effect on brittle-to-ductile transition temperatures of molybdenum studied in search for high toughness, propulsion system material 19 p3382 A66-36106  
High strength weldable Al alloys with good cryogenic toughness, stress-corrosion cracking resistance and tensile strength 20 p3582 A66-37091  
Adhesively bonded joints withstand severe thermal shock and have excellent bonding with high strength structural alloys in cryogenic liquids 22 p3937 A66-39778  
Welding capacity of high-strength alloys of Al-Zn-Mg-Cu system, noting welding techniques, composition effect on mechanical properties and remedies for cracking in welds 22 p3928 A66-40882

**HIGH STRENGTH STEEL**  
Causes and development of delayed cracking in material/weld interfaces of high strength steels 03 p0375 A66-13124  
Design properties, application and fabricability of super 12-Cr steels 04 p0535 A66-13630  
Ausforming effect on rolling contact fatigue life of M-50 bearing steel [ASME PAPER 65-LUB-9] 04 p0536 A66-14243  
Argon-arc welding of 3-mm high-strength steel sheet and molten slag arcless electric welding of 100-mm high-strength steel plate 08 p1231 A66-1916  
Aus-bay quenching, heat treatment process which minimizes distortion and increases tensile strength 10 p1545 A66-21213  
Diffusion of electrolytic hydrogen through membranes of iron crystals as function of stress, temperature and dissolved hydrogen concentration 11 p1718 A66-23071  
Shot peening for resistance to stress corrosion cracking of high strength steel and aluminum alloys and to improve fatigue life of landing gears, wing spars, jet engine components and other structural parts 13 p2196 A66-25773  
Mechanical properties of structural steel subjected to thermomechanical strengthening treatment 13 p2109 A66-25881  
Hydrogen embrittlement or fatigue strength loss avoidance in overhauling and repairing of high strength aircraft steel component 13 p2087 A66-26221  
Low cycle fatigue crack propagative characteristics of high strength steel, noting technique for life estimation structure by numerical integration [ASME PAPER 66-MET-3] 14 p2312 A66-26929  
Stress-corrosion susceptibility of high strength steel at various levels of tensile yield strength and fracture toughness [ASME PAPER 66-MET-5] 14 p2300 A66-26928  
Crack susceptibility of ultrahigh-strength steel welds related to thermal cycles of welding and heat treating 14 p2292 A66-27336  
Crack susceptibility of ultrahigh-strength steel welds related to thermal cycles of welding and heat treating 14 p2301 A66-27336  
Fractures in high strength low-alloy steel, discussing formation of flat and slag regions, effect of rolling direction crack reinitiation, shearing forces, etc 21 p3751 A66-39139

**HIGH TEMPERATURE AIR**  
Equilibrium radiative transport properties of high temperature air coupled with aerodynamic flow field generated by planetary reentry vehicles 01 p0163 A66-10768  
Boundary layer relation between viscous laws of perfect gas and equilibrium dissociating air 04 p0456 A66-14356



## SUBJECT INDEX

Experimental data compared to theory for expansion of high temperature air in equilibrium and nonequilibrium flow through Mach number 10 contoured nozzle [AIAA PAPER 66-2] 06 p0803 A66-17089

High resolution equilibrium radiation spectra for shock layer of blunt bodies at reentry velocities and radiative recombination of N and O ions [AIAA PAPER 66-104] 07 p0984 A66-18458

Equilibrium air total radiation mechanism, vacuum UV radiation and relation to hypervelocity entry studied, using shock tube blunt model test flow [AIAA PAPER 66-103] 09 p1469 A66-20087

Book on thermodynamic functions and shock adiabats of air at high temperature and pressure 14 p2413 A66-27787

Absorption coefficients for nitrogen and oxygen ion in air at temperatures of 150,000 to 800,000 degrees K 15 p2617 A66-29345

Oxidizability in air of three titanium alloys at temperatures from 700 to 1100 degrees C 16 p2727 A66-31570

Inviscid hypersonic flow past circular cone at finite angle of attack with attached shock wave in presence of dissociation air behind shock wave 17 p2837 A66-32033

Black body radiation, pressure and temperature dependences of equilibrium composition, enthalpy, specific heat and electron density of air-carbon plasmas 18 p3144 A66-34040

Total continuum radiation from high temperature air and components for wavelength greater than 2000 angstroms, based on radiation measurements from constricted arc at atmospheric pressure 18 p3140 A66-34587

Impurities effect on electrical conductivity of air between 1000 and 10,000 degrees K 19 p3406 A66-35743

Sound propagation characteristics in isotropic gas, considering acoustic absorption and relaxation effects 19 p3341 A66-36288

Absorption coefficients for nitrogen and oxygen ions in air at temperatures of 150,000 to 800,000 degrees K 20 p3604 A66-37350

Vacuum UV radiation in equilibrium air measured by photoelectric gauge 21 p3835 A66-38732

Brightness temperature of shock waves dependence on wave amplitude in xenon and air at high temperature 22 p3898 A66-40190

### HIGH TEMPERATURE ALLOY

#### SA REFRACTORY ALLOY

Polythermal and isothermal cross sections of phase diagram of titanium-niobium-chromium system at high temperatures 01 p0086 A66-10453

Coil spring alloys for temperatures above 300 degrees F noting design stresses, heat treatments and relaxation 01 p0079 A66-10959

Diffused aluminum coating for high temperature application 03 p0380 A66-12371

Internal friction and elastic modulus of compressor and turbine blade materials 03 p0372 A66-12399

Nonconservative motion of jogged screw dislocations in high temperature deformation of Al-Mg alloys 03 p0382 A66-12937

High temperature oxidation resistance of zirconium boride/molybdenum disilicide alloys 04 p0535 A66-13435

Heat and fatigue-resistant metal alloys for construction of jet aircraft combustion chambers, including 18 NiCoMo alloy suitable for temperatures up to 650 degrees 05 p0704 A66-15806

Austenitic chromium-nickel-manganese steel, describing temperature effects on crystal structure and experimental techniques 05 p0704 A66-15819

Regularities in hardness variations in niobium binary alloy 05 p0704 A66-15821

Rupture life prediction for several high temperature alloys under linearly increasing stress in nuclear reactors [ASME PAPER 65-MET-1] 06 p0895 A66-16205

Processing, testing and application of refractory metals to various high temperature environments 06 p0895 A66-16500

High temperature alloys for gas turbine, examining advances in creep strength, low

cycle fatigue and wrought and cast turbine blading alloys [SAE PAPER 650708] 06 p0898 A66-17079

Oxidation kinetics of pure tungsten and tungsten alloys with various niobium content at high test temperatures 07 p1050 A66-18065

Precision casting based on directional solidification resulting in longitudinal columnar grains with preferred orientation, eliminating transverse grain boundaries in gas turbine elements [SAE PAPER 660055] 09 p1388 A66-20153

Construction and design of Apollo spacecraft, examining high temperature aluminum and titanium alloys and fabricating methods 10 p1545 A66-21217

Form rolling used to form L-shaped strips from L605 alloy for economical fabrication of supports for jet engine exhaust nozzles 10 p1545 A66-21220

Heat treatable alpha-beta titanium alloy, Ti-679, with excellent creep and yield strength in 600 to 900 degrees F range 10 p1545 A66-21221

Creep behavior in Ni-Fe alloys at high temperatures, using one composition inside ordered regions and another outside 11 p1717 A66-22993

Diffusivity, elastic modulus and stacking fault energy effect on high temperature creep behavior of alpha brasses 11 p1717 A66-22996

High temperature plastic deformation and hardening effects on brittleness, strength and viscosity of austenitic steel and alloys 13 p2106 A66-25328

Structural effect on DC magnetic behavior of high temperature alloys 14 p2311 A66-26884

High-temperature nickel sheet alloys as affected by composition, production methods and heat treatment [ASME PAPER 66-GT-104] 14 p2312 A66-27003

High temperature oxidation-resistant hafnium tantalum alloys, noting phase composition 14 p2315 A66-27501

Newer titanium alloys compared with present production alloys from closed die forgings in typical airframe and engine configuration 14 p2317 A66-28011

Structural changes and variations in hardness at high temperatures in titanium alloys, determining aging temperatures producing maximum hardness 15 p2522 A66-29183

Weldable titanium alloys hardened by heat treatment and with structure immune to high temperatures 15 p2522 A66-29186

High temperature oxidation of two ductile Cr-Ru alloys with composition near bcc alpha-phase solubility limit analyzed by four different techniques 16 p2721 A66-30220

Plasticity problem involving plane strain and plane stress simultaneously, groove formation in machining of high temperature alloys [ASME PAPER 65-PROD-10] 16 p2714 A66-30857

Estimation of creep in Ti-Al-V alloys by high temperature bending method 16 p2724 A66-31237

Cobalt and nickel eutectic alloys modification with selected elements for high temperature application, noting microstructure and tensile behavior 16 p2726 A66-31460

Strain hardening of high temperature titanium multiphase solid solution by deformation and subsequent rapid cooling 17 p2940 A66-33229

High temperature properties and recrystallization of heat-resistant alloy A-286 experimentally studied, noting faster occurrence of overaging with increased cold working 19 p3376 A66-35357

Reactive brazing alloys evaluated for columbium alloy foil brazing in order to avoid erosion and embrittlement of conventional brazing alloys 19 p3367 A66-36115

Protective coatings for titanium and tantalum refractory alloy brazing envelopes, offering ephemeral protection from oxidation at ultrahigh temperatures 19 p3384 A66-36143

Creep analysis of high temperature niobium alloys in very high

## HIGH TEMPERATURE FLUID

vacuum 19 p3385 A66-36155

High temperature refractory alloy fabrication for microwave antennas in hypersonic glide reentry vehicles 19 p3370 A66-36158

Particle size effects in age hardening of high temperature Ni-based alloys 20 p3586 A66-38094

High temperature oxidation resistance of zirconium boride/molybdenum disilicide alloys 20 p3586 A66-38137

Gas tungsten arc and electron beam welding for iron-base, nickel-base and cobalt-base alloys, noting use of weld filler metal to avoid cracking 22 p3924 A66-40263

Self-diffusion parameters of Nb in solid solutions with beta-Ti and beta-Zr at high temperatures 22 p3937 A66-40925

Alloy additions of Zr, Ta, Nb, Re, Mo and Hf tendency to interact with thorium oxide particles in tungsten base alloys during exposure to greater than 2000 degrees C 23 p4079 A66-41067

Structural materials for oxidizing environments at high temperature analyzed including nickel, cobalt and chromium alloys 23 p4080 A66-41125

Regularities in hardness variations in niobium binary alloy 23 p4081 A66-41386

Regenerative heat treatment for increasing creep life of high temperature alloys used in turbines 24 p4227 A66-42508

### HIGH TEMPERATURE ENVIRONMENT

#### SA THERMAL ENVIRONMENT

Temperature distribution in porous tube, examining transpiration cooling as thermal protection to surfaces exposed to high temperatures 03 p0445 A66-12806

Spark igniter that successfully operates at 50 to 120 psig chamber pressure and 2300 to 3000 degrees K without observable thermal shock or electrode erosion 08 p1281 A66-18838

Electric Ag-CdO contacts obtained by internal high temperature oxidation method 08 p1239 A66-18900

Acoustic and optical phonon drag of pure ionic n-type semiconductors having NaCl structure, calculating kinetic coefficients 08 p1273 A66-19252

Specific heat of iron, cobalt and nickel in high temperature range measured, using quasi-adiabatic operating calorimeter 08 p1240 A66-19255

Device for taking long time corrosion fatigue curves on small cross section specimens at high temperatures and pressures 09 p1388 A66-20433

High temperature thermocouples as in-core sensors provide NRX and KIWI reactor temperature control [AIAA PAPER 65-598] 10 p1555 A66-21944

Three-day battery capable of operation at temperature of 425 degrees C for use on lunar and planetary probes 13 p1999 A66-25691

High temperature strain gauge design 17 p2926 A66-32985

Tensile properties of protectively coated refractory metals for structural components in high temperature oxidizing environments 19 p3385 A66-36151

Stress rupture properties of tungsten wire at high temperatures, noting effect of primary recrystallization on microhardness, ductility and grain size 21 p3751 A66-39196

### HIGH TEMPERATURE FLUID

High temperature fluids, designated PR-143, suitable for hydraulic systems in range -50 to 700 degrees F [ASLE PREPRINT 65-LC-3] 02 p0238 A66-12258

Fire resistant hydraulic fluids for commercial and military application including siloxanes, silicones, esters and superrefined mineral oil [ASME PAPER 64-WA/LUB-14] 10 p1547 A66-21171

High temperature fluids, designated PR-143, suitable for hydraulic systems in range minus 50 to 700 degrees F [ASLE PREPRINT 65-LC-3] 12 p1889 A66-24988

High temperature flow characteristics in free piston shock tube measured by means of pulsed light of He-Ne gas laser 19 p3339 A66-35353

Criteria for hydraulic fluids for supersonic



aircraft noting fluid toxicity, fire hazards, compatibility with elastomeric materials, etc 24 p4229 A66-42380

## HIGH TEMPERATURE GAS

Vibrational relaxation model of high temperature gas to determine dissipative coefficients in highly nonequilibrium gas mixtures with binary collisions 04 p0455 A66-14140

Thermal conductivity of Ar, Ne and Kr from 1500 to 5000 degrees K [ASME PAPER 65-HT-3] 05 p0782 A66-14733

Computed high temperature rate constants for hydrogen atom transfers involving light elements, noting activation energies for exothermic reactions [CI PAPER WSCI-65-24] 05 p0629 A66-15148

High gas temperature measurement using colliding shock waves 10 p1622 A66-21883

Thermal conductivity of Ar, Ne and Kr from 1500 to 5000 degrees K [ASME PAPER 65-HT-3] 11 p1785 A66-22185

Homogeneous dissociation kinetics of gas examined by means of adiabatic compression apparatus attached to mass spectrometer 13 p2079 A66-25821

Shock tube study of high temperature gas flow around circular cylinders caused by electrical discharge 14 p2218 A66-27348

Thermal conductivity of hydrogen at temperatures up to 4700 degrees F determined indirectly from effective conductivity of porous tungsten specimens filled with pressurized hydrogen 18 p3125 A66-34387

Carbon dioxide dissociation rate measured from 3000 to 5000 degrees K, considering decrease in temperature and increase in density caused by endothermic dissociation 22 p3859 A66-39915

Methane/deuterium exchange reaction rate measured in shock tube, using vibrational excitation mechanism to explain data 22 p3860 A66-40903

Approximation of self-similar plane and axisymmetric problems for high temperature laminar boundary layer, based on equations for boundary layer of finite thickness for high temperature gas 23 p4149 A66-41783

Vacuum UV radiation measurement from high temperature nitrogen, detecting radiation from shock layer of ballistic model 24 p4208 A66-42182

Windowless total radiation gauge for shock tube measurements of high temperature gas radiance 24 p4208 A66-42183

Thermodynamic properties of high temperature gas deviating widely from ideal gas, considering acetylene combustion products 24 p4295 A66-43107

## HIGH TEMPERATURE LUBRICANT

Polyolefin fluids with wide viscosity range compared with petroleum oils and existing synthetic lubricants for extreme temperature application [ASLE PREPRINT 65-LC-1] 02 p0238 A66-12259

Properties of polyaromatic C-ethers for use as high temperature lubricants with outstanding gear load-carrying capability [ASLE PREPRINT 65-LC-2] 02 p0238 A66-12260

High temperature bearing lubricant requirements for jet engine lubrication systems [SAE PAPER 660072] 09 p1383 A66-20157

High temperature and vacuum effects on sliding friction and surface film formation between dry lubricated and nonlubricated pair combinations of metals, carbon and ceramics, noting SNAP reactor data [ASLE PREPRINT 65AM 6A1] 10 p1540 A66-22040

Polyolefin fluids with wide viscosity range compared with petroleum oils and existing synthetic lubricants for extreme temperature application [ASLE PREPRINT 65-LC-1] 12 p1888 A66-24986

Properties of polyaromatic C-ethers for use as high temperature lubricants with outstanding gear load-carrying capability [ASLE PREPRINT 65-LC-2] 12 p1889 A66-24987

Graphite lubricant physical and chemical combinations with other materials for improved high temperature friction and wear, discussing nuclear irradiation for

graphite lattice modification 17 p2929 A66-31933

## HIGH TEMPERATURE MATERIAL

Probabilistic method of reliability prediction of high temperature highly stressed structural parts in optimization of engineering design 01 p0145 A66-10081

Reliability and reproducibility of SIL-TEMP 84 fabric used as reinforced filler in ablative components and high temperature insulating material in rockets and missiles 01 p0089 A66-10089

Materials - ASTM International Conference, Philadelphia, February 01 p0085 A66-10291

Physical properties of 181 glass cloth laminates of diallyl orthophthalate and isophthalate in high temperature range 02 p0248 A66-11689

Erosion, oxidation, loss of strength and reduction of ductility resulting from long-time elevated temperature stressed exposure of nickel alloy used in jet engine design [AIAA PAPER 65-744] 03 p0381 A66-12583

Mutual effects of vaporization, combustion and coking processes during material decomposition in high temperature gas flow 03 p0445 A66-12828

Testing and application of hard facing methods used on turbine engine components to provide wear resistance at high temperature 03 p0373 A66-13085

High temperature behavior and properties of refractory materials such as molybdenum, tungsten, silicides, aluminides and carbides 04 p0534 A66-13372

Design properties, application and fabricability of super 12-Cr steels 04 p0535 A66-13638

Oxidation kinetics of tantalum-iron and tantalum-cobalt alloys and iron and cobalt at 500-900 degrees C 04 p0535 A66-13696

High temperature electromagnetic transducers applied as sensors for physical variables, including mechanical displacement and liquid metal flow and level 05 p0676 A66-14775

Kinetic studies of high temperature carbon-silica reactions in charred silica-reinforced phenolic resins [CI PAPER WSCI-65-25] 05 p0788 A66-15149

Carbon and graphite textiles use as ablative reinforcements for high temperature phenolic resin systems 06 p0899 A66-16285

Quantitative determination of Nb in large amounts of Zr and Ti in large amounts of Nb and Zr at high temperature, using oscillographic polarography 06 p0823 A66-16840

Capability of investment casting process in production of integrally cast turbine wheels and nozzles for high temperature gas turbine application [SAE PAPER 650706] 07 p1037 A66-17249

Three-angle method of measuring optical constants of metals at high temperatures, detailing instrumentation, precision and physical basis 07 p1081 A66-18038

BeO properties and relationship to microstructure and fabrication variable 07 p1051 A66-18297

Materials for extreme temperature and g loading during suborbital, manned and superorbital reentry 07 p1051 A66-18303

Thermodynamic stability and reaction kinetics of solids at high temperature 07 p1054 A66-18496

MAR-M 509, new cast cobalt-base superalloy for high temperature service, noting creep strength, aging, microstructure, oxidation resistance, etc 08 p1239 A66-18958

Thermal expansion of tungsten and tantalum in high temperature range 09 p1388 A66-20147

Metallurgical factors for materials in jet engines, considering ductility, strength loss, strain-cycling criteria, etc [SAE PAPER 660057] 09 p1388 A66-20155

Supersonic aircraft finishes resisting corrosion and high temperatures, including epoxy-amine cured primers, acrylic paints, silicone, synthetic enamels, etc 10 p1547 A66-21136

Plasma and carbide coatings for protecting graphite surfaces at high temperatures obtained by sputtering or deposition and

thermal treatment to induce diffusion 10 p1548 A66-21508

Refractory properties and resistance to thermal shock of sintered tantalum carbide impregnated with copper or silver at high temperature [ONERA TP 323] 11 p1718 A66-23201

High-temperature deformation of magnesium single crystals with /110/ tensile axis, favoring slip on systems with oblique vectors, related to observations on /001/ crystals 12 p1898 A66-23564

High temperature crystallization processes and physicochemical properties of lithium aluminosilicate glass 12 p1900 A66-24855

Grain boundary role in high temperature fracture behavior of magnesia, noting temperature and orientation dependence of shear strength 12 p1897 A66-24920

Materials for producing electric energy from heat by direct conversion 13 p1997 A66-25110

High remelt temperature brazing of Tai 10W honeycomb structures by brazing with pure titanium, using diffusion sink concept 13 p2109 A66-25770

Permanent compressive deformation of pyrolytic graphite rapidly heated to very high temperatures and loaded in compression direction 14 p2318 A66-27870

High temperature polyimide and polybenzimidazole honeycomb material, measuring shear and compressive strength and moduli 14 p2319 A66-28011

Temperature measurement above 1000 degrees K, using disappearing filament and line reversal optical pyrometers 15 p2502 A66-29080

Elastic and plastic deformation of polycrystalline metals exposed to ultrasonic load and high temperatures 15 p2523 A66-29600

Ceramic materials selection for principal high temperature components of gas turbines 16 p2790 A66-30200

Preferred orientation of pyrolytic carbon, noting relationships and equivalence of parameters 16 p2780 A66-31000

Behavior of ceramic insulating materials under nonisothermal conditions at high temperatures 16 p2731 A66-31600

Polytriphenylene synthesis at high temperatures using fused salts 17 p2869 A66-31800

High temperature insulating adhesives for vacuum applications tested, including outgassing rate, mass spectra of evolved gases, electrical and mechanical properties 17 p2942 A66-31900

High temperature, electrically insulating refractory tubes of boron carbonitride for protection of metal thermocouples 17 p2944 A66-33100

Heat shield and rocket nozzle chemical reactions based on equilibrium thermodynamics of high temperature materials at gas-solid interface 18 p3260 A66-33800

Tungsten heat conductivity between 1500 and 3000 degrees K and Lorentz number temperature dependence 19 p3350 A66-35500

Mutual effects of vaporization, combustion and coking processes during material decomposition in high temperature gas flow 19 p3479 A66-36700

Electrical and thermal conductivity at integral degree of blackness of tantalum at temperatures above 1000 degrees C 20 p3582 A66-36500

Simultaneous measurement of heat conductivity, heat capacity and thermal diffusivity of solid and liquid metals at high temperature 20 p3678 A66-37100

Honeycomb structure, examining assembly skin delamination at spars or terminus fitting, glasscloth radome and inspection techniques 20 p3671 A66-37400

Mechanical properties of metallic and ceramic fibers in metallic matrices and refractory fibers in ceramic matrices 21 p3751 A66-39300

Thermal expansion of tungsten and tantalum in high temperature range 21 p3753 A66-39300

Critical high temperature structural problems in missiles and manned lift reentry vehicles, considering meteoric impact and pressure vessel flaws



- growth 22 p3989 A66-40119
- Aircraft materials and structures for extreme ranges of velocity and temperature 22 p3990 A66-40120
- High temperature adhesive properties of epoxy, epoxy-phenolic, polybenzimidazole and polyimide 22 p3937 A66-40278
- Oxidation and mechanical performance of tungsten and composite tungsten systems at high temperatures and pressures, determining surface recession rate up to 750 degrees R AIAA PAPER 65-293] 22 p3935 A66-40343
- Applications for new class of materials termed oxide-dispersion strengthened materials offering stability at high temperatures and high thermal and electrical conductivity 22 p3935 A66-40526
- High temperature behavior of organic materials for aircraft, noting elastomers and elastomers ICAS PAPER 66-33] 22 p3938 A66-40660
- High temperature structural properties of glass fabric-reinforced polybenzimidazole, polyimide and phenolic laminates for aerospace application 23 p4083 A66-41389
- Plasma and carbide coatings for protecting graphite surfaces at high temperatures obtained by sputtering or deposition and thermal treatment to induce diffusion 23 p4083 A66-41528
- Protective coating problems of superrefractory alloys for use in space sleds at temperatures above 1000 degrees C 23 p4081 A66-41655
- Materials and cooling of aircraft gas turbine engines, noting nickel and tantalum alloys, turbine-inlet temperatures, coatings, etc 23 p4122 A66-41662
- Structural design problems of hypersonic air vehicles with air breathing propulsion, discussing relation to future hypersonic commercial air transport ICAS PAPER 66-31] 24 p4281 A66-42491
- Fuel cells with ceramic electrolyte operating at high temperatures, calculating voltage and efficiency 24 p4161 A66-42503
- Pure titanium tensile property, hardness and impact value at high temperatures, noting structural change from annealing 24 p4228 A66-42510
- HIGH TEMPERATURE PLASMA**
- High temperature air-carbon plasma noting black body radiation, atomic constants and thermodynamic equilibrium 04 p0599 A66-14460
- Heating by laser beam with application to lithium, noting use for high temperature plasma production 08 p1233 A66-18972
- Bremsstrahlung, recombination radiation and electromagnetic emission from high-temperature high density plasmas 10 p1566 A66-21705
- Hot plasma probed with atomic beam in presence of intense self-radiation flux and magnetic field impulse 10 p1571 A66-22011
- Kinetic equation with collision frequency operator used to represent high-temperature plasma instabilities induced by particle collisions 12 p1918 A66-23555
- Soviet high-temperature plasma physics and controlled nuclear fusion 13 p2145 A66-25736
- Laser radiation to determine electron density in dense high temperature plasma 14 p2374 A66-27507
- Magnetic mirror trapping of hot-electron plasma heated in quartz discharge tube 14 p2343 A66-27596
- Shock tube in studying high temperature plasma, noting other experimental devices 17 p2904 A66-33038
- Hot plasma probed with atomic beam in presence of intense self-radiation flux and magnetic field impulse 19 p3407 A66-36095
- Collisionless heating of plasma cylinder by RF field 21 p3781 A66-39008
- High temperature high density carbon plasma production in arc chamber of shock tube 22 p3955 A66-40092
- Ion oscillations in high temperature electron-ion plasma with HF perturbations 23 p4102 A66-41485
- High temperature physicochemical characteristics of thermoelectric plasma, examining operating principles of several versions of plasma generator 24 p4243 A66-42537
- Magnetic mirror trapping of hot-electron plasma heated in quartz discharge tube 24 p4243 A66-42730
- HIGH TEMPERATURE PLASMA DEVICE**
- Electron temperature measurement by relative intensity of He I lines shown as inapplicable for high plasma densities 10 p1571 A66-22021
- Electron temperature measurement by relative intensity of He I lines shown as inapplicable for high plasma densities 16 p2760 A66-30840
- HIGH TEMPERATURE RESEARCH**
- Thermal, micrographic and X-ray diffraction techniques used for constitution diagram of ternary system tungsten-molybdenum-osmium at various high temperatures 03 p0385 A66-13209
- High temperature measurement in combustion chambers of air breathing engines discussing optical, pneumatic, acoustic and calorimeter methods 04 p0518 A66-13537
- Variation of interdiffusion coefficient with composition for niobium-vanadium alloys determined for various diffusion temperatures 05 p0702 A66-15467
- Book on metal testing at high temperatures including tension, relaxation, compression, impact, nonsteady conditions, hardness, etc 06 p0966 A66-16561
- High temperature extensometer using linear variable differential transformer 07 p1030 A66-17230
- High temperature materials for hypersonic air-breathing engines, noting usefulness of coated refractory metals 09 p1435 A66-20670
- Cylindrical black body furnace with graphite resistance built in France, attaining 1600 degrees C, for calibration of radiation pyrometers 09 p1383 A66-20909
- Phase equilibria in Zr-Co-C and Nb-Fe-C ternary systems at high temperatures, using X-ray and microscopic analyses 10 p1546 A66-21509
- Creep testing apparatus for metals, with automatic recording of longitudinal and transverse deformations at high temperatures 11 p1780 A66-22600
- Thermal decomposition of difluorocarbene radical diluted in argon analyzed behind incident shock waves at high temperatures 12 p1811 A66-23623
- High temperature compacted-ceramic insulated, metal sheathed and hermetically sealed thermocouples for use in nuclear reactors and nonnuclear environment 12 p1879 A66-23698
- Ultrasonic measurement of elastic modulus of high temperature metal 13 p2194 A66-25092
- Vibrational relaxation times of deuterium in argon and krypton determined at high temperatures by shock heating gas mixtures in shock tube 13 p2136 A66-26662
- Moire data recording and processing techniques in thermal strain fields at high temperatures, comparing experimental data with elasticity theory 14 p2400 A66-27768
- Effect of high temperature thermomechanical condition on structure and phase composition of titanium alloys, noting deformation role in hardening 15 p2522 A66-29184
- Thermal diffusivity and specific heat of molybdenum at high temperatures measured, using variable heating in induction furnace 15 p2523 A66-29226
- High temperature compressive deformation equipment for ceramic materials noting loading, alignment and stress-strain measurement 16 p2682 A66-30950
- Slip in single crystal tungsten deformed in tension at temperatures from 2500 to 5000 degrees F 16 p2725 A66-31453
- Review of experimental capabilities for reaching pressure and temperature conditions prevailing in Earth mantle and core, including bibliography 17 p2918 A66-32661
- Deformation and strength properties of refractory solids at temperatures up to 2000 degrees C, using indentation hardness measurements for stress-strain measurements in strength properties 18 p3254 A66-33967
- Book on physics of shock waves and high temperature hydrodynamic phenomena 19 p3341 A66-36316
- Grain boundary migration in pure aluminum and lead under reversed torsional and bending stresses at elevated temperatures 19 p3386 A66-36365
- Applications of plasma jets with enclosed flames in space industry, noting design of burners 19 p3281 A66-36601
- Testing of adhesive bonding at high temperatures for use in reentry vehicles, using IR energy on specimen preloaded in shear [ASME PAPER 66-MD-38] 21 p3742 A66-38488
- Ultrasonic measurement of elastic modulus of high temperature metal 21 p3823 A66-38517
- Imaging techniques to obtain temperature and emissivity measurements and phase diagrams of high melting point ceramic oxides with aid of solar furnace 21 p3738 A66-39102
- Phase equilibria in Zr-Co-C and Nb-Fe-C ternary systems at high temperatures, using X-ray and microscopic analyses 23 p4081 A66-41529
- Grain boundary self-diffusion coefficient variation with applied stress and production of lattice vacancies applied to cavity growth in high temperature fatigue of Mg 23 p4081 A66-41714
- High temperature testing and evaluation of graphite helical-screw expanders and compressors for use with inert gas Brayton cycle 23 p4075 A66-41755
- HIGH VACUUM**
- Prebreakdown current in high vacuum noting field strength and field emission hypothesis 01 p0106 A66-10641
- Materials under high vacuum discussing degassing of metals, thin film deposition, food dehydration, vacuum melting and vacuum welding 04 p0534 A66-13373
- Thermionic emission properties of rhenium tape coated with lanthanum hexaboride, examining usefulness as low temperature emitter 06 p0883 A66-17029
- Diffusion, getter-ion and cryogenic high vacuum pumping methods, showing relationship of pressure vs gas load, operating efficiency and cost as function of system size 17 p2930 A66-32945
- Creep analysis of high temperature niobium alloys in very high vacuum 19 p3385 A66-36155
- Gauges and systems applicable to measurement of extremely high vacuums, considering ion gauges with modulators, suppressor gauges, extractor gauges and cold cathode type gauges 24 p4215 A66-43066
- HIGH WATER PROJECT**
- Two Project High Water experiments producing optical, ELF, RF, and radar data on ionospheric abort of large water quantities and expansion process 14 p2289 A66-28417
- HILBERT SPACE**
- Pseudo-inverse concept extended to Hilbert space unbounded operators with arbitrary range 01 p0092 A66-10179
- Steepest descent, covering iterative methods for driving support mapping gradient to zero in convex programming 04 p0540 A66-13997
- Generalized extensions of operators for mapping everywhere dense linear set onto generalized set of Hilbert space elements 05 p0708 A66-15329
- Algebra of singular integral operators, discussing action on Hilbert space and homomorphism 06 p0901 A66-16008
- Optimal control, discussing fundamental general necessary conditions for Mayer problem solution 06 p0864 A66-16623
- Perturbation method in theory of dynamic stability of systems with distributed parameters, discussing linear Hamiltonian equation in separable Hilbert space 07 p1056 A66-17606
- Linear and antilinear transformations for real and complex Hilbert space 07 p1058 A66-17963
- Convergence of Galerkin method in nonconservative stability problems of thin elastic plates and thin elastic rods 08 p1311 A66-19339



- Spectrum and eigenstates of Bardeen-Cooper-Schrieffer /BCS/ reduced Hamiltonian in theory of superconductivity 08 p1276 A66-19446
- Approximate solution for elasticity problems, noting mathematical determination of stress distribution in any homogeneous isotropic body 09 p1468 A66-20642
- Boundary condition constraint method for generalizing R-matrix theory, permitting use of shell model as basis for nuclear-reaction calculations 09 p1405 A66-20822
- Minimizing functionals on normed linear spaces, discussing steepest descent and rendezvous problems in control theory 13 p2116 A66-25343
- Minimum effort control problem in rotund reflexive Banach space and extension to Hilbert space under bounded linear transformation 14 p2266 A66-27631
- Existence theorem for nonlinear ODE system with continuous monotonic differential operators over Hilbert space and application to nonlinear network analysis 15 p2528 A66-29370
- Generalized extensions of operators for mapping everywhere dense linear set onto generalized set of Hilbert space elements 16 p2735 A66-30967
- Rall theorem on variational principle for linear elastodynamic BVPs on Hilbert space 23 p4138 A66-41538
- HILBERT TRANSFORM**
- Length of compact function estimated from noisy measurement of modulus of Fourier transform 06 p0867 A66-16977
- Fourier analysis of Riemann-Hilbert problem of diffraction of normally incident plane electromagnetic wave by plane metallic grid above dielectric sheet and semilinear plasma 24 p4175 A66-42978
- HILL CURVE**
- Markov chain hill-climbing scheme for probable fast-time learning absorbing model 19 p3333 A66-36663
- HILL EQUATION**
- Solution to two equations for wave propagation in periodic media expressed as solution to Hill equation 06 p0848 A66-16106
- Digital computer recomputation of stability transition curves in Hill-Meissner equation 09 p1395 A66-20623
- Eigenvalues and eigenvectors obtained by numerical solution of special Hill equation in lubrication theory [ASME PAPER 66-LUBS-13] 17 p2932 A66-33185
- HILL LUNAR THEORY**
- Book on celestial mechanics considering Laplace-Newcombe method, Hill planet and lunar methods, periodic orbits methods, etc., using differential equations 09 p1459 A66-20916
- HILL REACTION**
- Photoreduction of viologen dyes analyzed with chloroplasts, noting oxygen evolution and photophosphorylation efficiency, reduction potentials, etc 16 p2638 A66-30647
- Isolation of morphologically intact and photochemically functional chloroplasts from marine chrysomonad *Hymenomonas* sp 16 p2638 A66-30648
- HINGE**
- Design equations and curves for calculating critical spring rates of single-axis and two-axis flexure hinges 04 p0525 A66-13637
- HINGE MOMENT**
- Dither and sinusoidal incidence variations effect on control wing hinge moments of transonic-supersonic rolling maneuvering guided missile [AIAA PAPER 66-755] 22 p3846 A66-40639
- HISTOGRAM**
- Electric component of radiation field from same flashes recorded with histograms of product of field strength and distance, showing concentration around mean values 20 p3553 A66-38076
- HISTOLOGY**
- Continuous exposure of rats to 100 percent oxygen at 450 mm Hg for 64 days shows no physiological effects 12 p1807 A66-25013
- Response of tissue culture cells to low magnetic fields, noting no quantitative growth differences 12 p1807 A66-25015
- Structural and functional properties of heart and muscle type subunits of lactic dehydrogenases investigated, using

- comparative amino acid analysis 15 p2446 A66-28864
- HODOGRAPH METHOD**
- Compressible fluid flow, discussing simple wave supersonic flow mechanism for bodies with developable surfaces 06 p0802 A66-16352
- Flow function equations for transonic flow past closed profile contours 07 p0982 A66-18121
- Vehicle motion parameters in Newtonian central force field determined, using geometrical structures devised from properties of velocity hodograph 08 p1226 A66-19584
- Root hodograph method for determining amplitude and phase frequency characteristics of dynamic linear systems 08 p1202 A66-19692
- Navigational inertial system dynamic property analysis at high flight speeds, using hodographic characteristic equation for longitudinal and lateral aircraft motion error determination 09 p1401 A66-20913
- Exact solution derived for gas jet flow with three characteristic high subsonic velocities, using Falkovich extension of Chaplygin hodographic method 15 p2425 A66-29850
- Problems of various subsonic gas jets of finite width around dihedral obstacle solved with Chaplygin hodographic method 16 p2627 A66-30207
- Subsonic flow around circular cylinders using three alternate hodographic approximations to Chaplygin law 16 p2627 A66-30208
- Principle function tabulation for plane transonic flows study by hodographic method 16 p2686 A66-31034
- Tunnel diode circuit stability, equivalent circuit and conductivity hodograph 17 p2880 A66-31867
- Shock-induced boundary layer separation on supersonic intake, using hodograph technique for flow structure analysis 17 p2841 A66-32896
- Equivalent transfer function determined for quadrupole inserted between ideal modulator and demodulator from frequency characteristics 17 p2928 A66-33492
- Neon hodoscope study of energy and production heights of high energy EAS electron-photon cascades, comparing results to nuclear emulsion study findings 18 p3207 A66-35109
- EAS mu component fluctuations in density distribution and reception spectrum recorded, using hodograph detectors 18 p3208 A66-35116
- Chaplygin equation solution translating current function and velocity potential from physical into hodograph plane 19 p3342 A66-36474
- Book on transonic and hypersonic flow theory covering motion and shock equations, application of Newtonian theory, temperature effect, behavior of minimum drag bodies, etc 20 p3492 A66-37495
- HODOGRAPH THEORY**
- Lighthill integral transform methods in hodograph transformation theory of plane compressible transonic shock-free potential flows around airfoil sections in solution space of Chaplygin equation [ICAS PAPER 66-26] 23 p4007 A66-41008
- HOHMANN ORBITAL TRANSFER**
- Optimum transfer between Kepler ellipses, noting Hohmann orbital transfer method and geodesics and metric tensors in phase space 04 p0579 A66-14459
- Optimum orbital transfer from circular to nonintersecting elliptical orbit with use of two impulses of unequal specific impulses 14 p2387 A66-28181
- Minimum impulse orbital transfer between coplanar elliptical orbits with aligned axes, noting advantage of three- and two-impulse transfers 18 p3227 A66-33760
- Low thrust trajectory optimization, using Newton-Raphson method to solve nonlinear two-point boundary value problem [AIAA PAPER 65-698] 19 p3462 A66-35904
- Orbital transfer and rendezvous maneuvers between inclined circular orbits, particularly bielliptic transfer with plane change, Hohmann transfer with plane change and in-plane modified Hohmann transfer 20 p3657 A66-38158

## HOLE DISTRIBUTION

- Hole current and electron current affected by local pressure applied on emitter surface of planar-diffused n-p-n silicon transistor 04 p0558 A66-13420
- Mercury and zinc ions in germanium discussing hole capture cross section in comparison to standard white noise source 05 p0731 A66-14660
- Measurement of diffusion length of excess minority carriers in semiconductors in region where carriers are generated 06 p0924 A66-16506
- Hole diffusion constant dependence on electric field in n-type germanium 07 p1106 A66-18395
- Hole concentration effect on elastic constant of heavily doped p-type silicon 07 p1106 A66-18396
- Measurement of energy required to form one hole-electron pair in gallium phosphide by alpha particles 07 p1107 A66-18407
- Electric properties of single crystal p-type InSb, obtaining samples by zone melting, thermal processing, etc., noting hole concentration plotting 08 p1278 A66-19625
- Electrophysical parameters of epitaxial p-n junction regions determined, using galvanomagnetic and photomagnetic measurements 11 p1751 A66-22734
- Conductivity effective-mass of holes of gallium arsenide crystals with various hole concentrations determined from frequency dependence of spectral reflectivity in IR 12 p1928 A66-23994
- Two-dimensional problems in moment theory of elasticity for multiply coupled regions weakened by finite number of arbitrarily distributed circular holes 12 p1967 A66-24109
- Mercury and zinc ions in germanium discussing hole capture cross section in comparison to standard white noise source 13 p2167 A66-25933
- Transient and steady state photoconductivity in plastically bent germanium, noting logarithmic decay of photocurrent and logarithmic lux-ampere characteristics 15 p2558 A66-28860
- Spherical shell weakened by several circular holes translated into infinity systems of quasi-regular algebraic equation in canonical form 15 p2608 A66-28776
- Stress distribution around reinforced circular holes spaced equally on infinite sheets 16 p2815 A66-30808
- Stress-strain distribution near curvilinear holes in moment theory of elasticity in isotropic medium 16 p2819 A66-31111
- Electric properties of single crystal p-type InSb, obtaining samples by zone melting, thermal processing, etc., noting hole concentration plotting 17 p2984 A66-33134
- Concentration and lifetime of minority carriers in cadmium sulfide determined by method based on optically induced changes in concentration 19 p3437 A66-35437
- Thermoelasticity of semilinear state plane with circular coolant holes 21 p3826 A66-38535
- Optical determination of hole concentration dependence in p-type silicon semiconductor by measuring absorption coefficients 21 p3798 A66-38798
- Crystal dislocation distribution effect on low temperature electrical transport properties in plastically deformed 3B metals 21 p3753 A66-39340
- Infinite plate consisting of monocrystalline semiconductor of given thickness under effect of electric field results in changes in galvanomagnetic, piezoresistance and optical properties 22 p3965 A66-40000
- Capture effect on I-V characteristics of junction diodes and injection coefficients in forbidden transition zone 23 p4045 A66-41000
- Electrophysical parameters of epitaxial p-n junction regions determined, using galvanomagnetic and photomagnetic measurements 23 p4113 A66-41000
- Griffith type crack propagation due to localized thermal stress at holes, causing penny-shaped cracks and inclusions disturbing uniform heat flow 23 p4146 A66-41000
- HOLE MOBILITY**
- Acceptor level in iron doped Ga-As material toward valence band with increasing



temperature at approximately same rate band gap decreases 03 p0410 A66-13004

Transport effects in semimetals and narrow-gap semiconductors including nonlinear, thermomagnetic and superconductive effects and tunneling 04 p0559 A66-13451

Transverse Dember effect in anisotropy of electrical and photoelectrical characteristics of indium selenide 04 p0565 A66-14259

Temperature dependence of effective mass and influence of two-phonon processes on mobility in semiconductors with narrow forbidden bands 04 p0565 A66-14263

Hole-type superconductivity in semiconductors 04 p0565 A66-14265

Transmission of hole-type germanium in strong electric fields, noting spectral dependences of radiation modulation and hole absorption cross section 04 p0568 A66-14352

Galvanic and thermomagnetic coefficients of undoped polycrystalline p-type GaSb sample in weak magnetic field, emphasizing hole mobility 04 p0571 A66-14499

Charge-carrier concentration and mobility in thin silicon specimens 10 p1589 A66-22172

Free hole lifetimes greater than 50 microseconds in silver bromide above 200 degrees K and measurement of drift mobility 14 p2365 A66-27756

Transmission of hole-type germanium in strong electric fields, noting spectral dependences of radiation modulation and hole absorption cross section 14 p2368 A66-28250

Electrical properties of nickel ferrite in terms of Jonker model, noting magnitude of energy gap between Fe and Ni levels and mobilities of electrons and of positive holes 16 p2781 A66-31215

Electron-hole conductivity effect on temperature variations of Hall coefficient and Nernst-Ettingshausen effect in semiconductor 17 p2986 A66-33309

Charge-carrier concentration and mobility in thin silicon specimens 19 p3441 A66-35786

Interband microwave scattering of holes by cyclotron resonance in Ge 21 p3797 A66-38753

Varying excitation intensity effects on edge emissions from pure and doped CdS powder samples, noting electron-hole recombination mechanisms 21 p3802 A66-39202

Fast neutron effect on electrical properties of boron-doped n-type silicon samples with resistance, noting decrease in hole concentration and mobility 22 p3961 A66-39829

Mean energy required to create electron-hole pair in Si measured as function of temperature, using cryostat 23 p4111 A66-41264

Magnetic pinch formation in indium antimonide and possibility of population inversion in pinch, using strong current supported by electron-hole plasma 24 p4249 A66-42224

Conductivity modulation by heavy-to-light hole transitions in p-type germanium noting carrier lifetime and ringing of laser pulse 24 p4219 A66-42249

Charge carrier mobility by combining conductance with thermogravimetric measurements 24 p4250 A66-42295

Energy levels and wave function of hole in field of two acceptor ions and nearest ion donor for p-type Ge and Si 24 p4255 A66-42496

Energy levels and wave function of hole in field of two acceptor ions and nearest ion donor for p-type Ge and Si, noting numerical results 24 p4255 A66-42498

**HOLMIUM**

Laser characteristics of and coherent oscillations from trivalent Tm, Ho, Yb and Er ions in yttrium aluminum garnet 01 p0079 A66-10241

Coherent emission from trivalent holmium ions in rare earth substituted yttrium aluminum garnet, noting three energy transfer combinations in YAG 15 p2512 A66-28690

CW laser action in holmium-doped erbium trioxide with dominant pumping by energy transfer between ions 24 p4222 A66-42555

HOLOGRAPHY

Linear filtering concepts in imaging and optical data processing systems, including three-dimensional photography obtained by wave front reconstruction 02 p0240 A66-11453

Laser application problems in interferometry, radar and holography including mechanical stability, noise suppression, dirty laser beam restoration, etc 02 p0240 A66-11454

Mode-controlled giant pulse laser used to produce two-beam hologram in short exposure time of 30 nsec 02 p0233 A66-12215

Optical data processing techniques considering storage, manipulation, holography and pattern recognition using matched filters 03 p0378 A66-12997

Interferometry with holographically reconstructed comparison beam discussing principles, techniques and error sources 04 p0521 A66-13985

Fresnel diffraction laws for calculation of light amplitude distribution in image spot of point as function of aperture dimensions used on hologram, source, function, etc 04 p0532 A66-14173

Progress in wavefront reconstruction imaging, using laser and X-ray 05 p0677 A66-14833

Holographic information of photographic plate and diffusing object 05 p0678 A66-15105

Hologram imaging process in which Fresnel diffraction pattern of object is recorded by scanning at X-band 06 p0881 A66-16638

Effect obtained by rotating holograms, noting image inversion when rotating hologram 180 degrees about vertical axis in hologram plane 06 p0881 A66-16676

Reconstruction of phase objects by holographic imaging as three-dimensional lensless photography 07 p1032 A66-17461

Holographic study of time average of coherent wavefronts scattered from vibrating object 07 p1144 A66-18034

Interferometric hologram evaluation and real time vibration analysis of diffuse objects 07 p1144 A66-18040

Hologram-generated ghost image experiments to verify fragment displacement theory and diffuse light waveforms 10 p1534 A66-21249

Photography providing complete illusion of reality of object represented, noting holographic and interference techniques 10 p1534 A66-21331

Laser application in photography, noting interferometric and holographic techniques 10 p1535 A66-21333

Wave front reconstruction /holography/, hologram production, interferometry, schlieren photography and shadowgrams applied to fluid mechanics 10 p1536 A66-21750

Hologram photography, principles, techniques and application 11 p1705 A66-22669

Cardinal points and focal lengths of holographic system established by treating holographic imaging as projective transformation between object and image space 11 p1706 A66-22872

Television transmission of Fresnel type hologram for originally transparent object 11 p1707 A66-23092

Holography, X-ray crystallography and correspondence between optical image synthesis and heavy atom technique 11 p1707 A66-23194

Two-beam interferometry by wavefront reconstruction from hologram recorded with coherent background successively interfere in same latent image 11 p1708 A66-23204

Ghost imaging of solid objects by holograms formed in near field without using Fourier transforming lenses 11 p1708 A66-23205

Hologram television transmission using microwave wavelength, yielding aperture-limited resolution and aperture-size reduction method for low resolution 12 p1881 A66-24152

Phase reference beam of two-beam carrier frequency holography method used for polarization reference 12 p1883 A66-24561

Radar maps of Moon and planets using bistatic continuous wave mode of radar operation between orbiting spacecraft and ground station 12 p1825 A66-24891

Dual-and multiple-beam interferometry by wave front reconstruction from surfaces of standard engineering components, applicable to structural dilatation problems 12 p1884 A66-24967

Holographic interferometry, advantages and operation 13 p2076 A66-25048

Holograms and wavefront reconstruction techniques involving prismatic refraction of monochromatic and coherent laser light causing interference pattern on photographic emulsion 13 p2076 A66-25144

Lens aberration correction using Gabor wavefront reconstruction method to produce hologram of spherically aberrated wavefront emerging from lens 13 p2080 A66-25990

Photographic copies of holograms taken with laser light noting film, light source, directional effect, processing, etc 13 p2081 A66-26000

Phase hologram generation by means of thermoplastic xerography 13 p2081 A66-26001

Moving target hologram generation using modified Michelson interferometer 13 p2081 A66-26003

Reconstitution in space of curve recorded photographically by displacement of luminous point illuminated by coherent light 13 p2082 A66-26343

Hologram quality as affected by illumination of stationary objects through moving scatterer while maintaining stationary coherent background 13 p2084 A66-26588

Holography process and application 14 p2290 A66-26870

Holograms of object illuminated with spatially incoherent light from low pressure mercury lamp, using afocal lens in interferometer for wavefront splitting 15 p2497 A66-28694

Absence of phase-recording or twin-image separation in Gabor holography 15 p2498 A66-28759

Hologram construction for real three-dimensional scene without visual anomalies, noting technique and results 15 p2499 A66-28879

Image reconstruction with Fraunhofer holograms formed from opaque or transparent diffracting objects in aperture with coherent illumination 15 p2500 A66-28973

Photographic recording of spatially modulated coherent light 15 p2501 A66-28974

Image luminance of paraxial rays, image formation and ray tracing in holography, using Fresnel-Kirchhoff diffraction formula 15 p2501 A66-28975

Hologram reconstruction obtained by illuminating hologram plate with common two-cell flashlight 15 p2502 A66-29033

Holography of pure phase objects, considering incoherent viewing 16 p2700 A66-30206

Image distortion within cinematographic process as related to photography, noting quality estimation, visual perception criteria, etc 16 p2702 A66-30432

Bibliography of holograms 16 p2702 A66-30433

Schlieren photographs from holograms, apparatus and method 16 p2707 A66-31092

Hologram construction and sources of image degradation including random vibrations, film transfer characteristics, etc 16 p2707 A66-31243

Complex spatial filter produced by inserting Fourier hologram into Fraunhofer plane of coherent image-forming system 17 p2925 A66-32616

Readout technique for laser fog disdrometer 17 p2927 A66-33346

Color hologram for white light reconstruction constructed from three-dimensional diffusely reflecting objects 18 p3109 A66-33611

Polarization-induced crossed polarization figure in hologram 18 p3111 A66-33997

Coherent optical reconstruction from microwave holograms in two-step Gabor image-formation technique 18 p3111 A66-33999

Holography principles and development, considering wave front reconstruction, Lippmann photography, laser light, application to TV, etc 18 p3115 A66-35244

Shadowgrams, schlieren photographs and



interferograms produced from reconstructed wavefront 19 p3354 A66-35386

Photographic process role in holography, noting relationship of exposure and transmittance by highly nonlinear inverse power law 19 p3357 A66-35815

Holography principles, discussing basic equation, Fourier transform holograms and hologram interferometry 20 p3556 A66-36929

Analytical and geometric relationships between hologram scene and reconstructed images 20 p3556 A66-36934

Effect of emulsion thickness on optical characteristics of reconstructed images, noting sensitivity to incidence angle 20 p3558 A66-37287

Holography theory and construction methods including experiments with thick or three-dimensional recording media, considering applications to microscopy, X-ray holography and TV 20 p3560 A66-37620

Holography, discussing potential uses, frozen wave fields, holograms at X-ray wavelength and stress analysis 21 p3739 A66-39199

Finite grain size of photographic film effect on holography for cylindrical wavefronts 21 p3740 A66-39393

Laser bibliography July-December 1965, including references to holograms 21 p3749 A66-39541

Holographic processes, uses and limitations, discussing coherent imaging, holographic information storage and information display 22 p3918 A66-40292

Hologram recording system as interferometer 22 p3920 A66-40887

Spatial phase modulation of wavefronts used in spatial filtering and holography, examining means of preventing or reducing noise and distortion 22 p3920 A66-40888

Interference between deformed plane wave and reference wave in coherence, obtaining transfer function of objective, using holography 23 p4067 A66-41178

Image restoration via phase holograms, noting applications to deteriorated photographic negatives and positives 23 p4068 A66-41411

Wave front scattering and refraction by laser spark studied by holograms of air plasma formed by giant ruby laser pulse 24 p4219 A66-42131

Diffraction gratings by recording laser-generated interference pattern on high resolution film as two-beam hologram 24 p4210 A66-42259

White light reflection holography extended to recording of volume holograms in emulsions on sheet film 24 p4220 A66-42260

Pulsed laser holograph and problem of overcoming limited coherence 24 p4211 A66-42560

Achromatization of holograms using two-lens configuration 24 p4211 A66-42626

Noise limitations in obtaining three-dimensional images by holographic techniques, considering graininess of photographic emulsion 24 p4212 A66-42752

Reconstruction of hologram in nonmonochromatic light as constituting incoherent addition of images reconstructed from hologram area elements 24 p4215 A66-43053

Compressible and incompressible flows made visible by optical method sensitive to density variations, shadowgraph, schlieren system, Mach-Zehnder interferometer and holographic interferometry with lasers 24 p4192 A66-43196

**HOMING**

Homing by steepest descent method rather than proportional navigation 12 p1909 A66-24262

**HOMING DEVICE**

**S GUIDANCE SYSTEM**

**HOMODYNE**

Coherent interference rejection, discussing noise and modulator-leakage pickup rejection in laser communications experiments 07 p1001 A66-17217

**HOMOGENEOUS TURBULENCE**

Existence and uniqueness of solution for second boundary value Neumann problem in linear flow theory 02 p0296 A66-11242

Turbulence in hydrodynamics and plasma physics 05 p0727 A66-15260

Decaying second-order isothermal reaction

in limit of homogeneous turbulence in final period of decay 10 p1496 A66-21828

Inertia and pressure effects on energy potential of homogeneous and isotropic turbulence in weakly compressible medium 18 p3100 A66-34608

**HOMOLOGY**

Stellar evolution for high temperature, predominantly neutrino processes, noting breakdown of homology relation between density and temperature 19 p3467 A66-36795

**HONEYCOMB**

**SA MULTILAYER STRUCTURE**

Aluminum honeycomb sandwich structures under axial compressive loading in reliability safety margin analysis, using derived statistical strength data 01 p0145 A66-10086

Honeycomb design, structures, developments and advantages, discussing materials and sandwich construction [ASME PAPER 65-AV-17] 02 p0236 A66-11795

One-dimensional transient heat flow through honeycomb sandwich panels [AIAA PAPER 64-258] 05 p0775 A66-15080

Microwave scattering system for detection of voids in fiberglass-honeycomb ablative materials causing drop in receiver signal strength 09 p1385 A66-20966

Effect of conventional ammunition on aluminum honeycomb paneling, noting reduction of load-bearing and peel-strength properties 13 p2196 A66-25599

High remelt temperature brazing of Ta-10W honeycomb structures by brazing with pure titanium, using diffusion sink concept 13 p2109 A66-25774

High temperature polyimide and polybenzazole honeycomb material, measuring shear and compressive strengths and modul 14 p2319 A66-28012

Radiant-interchange configuration factors between various selected plane surfaces with common contact 16 p2826 A66-30530

Mechanical behavior of three-layer plates with honeycomb filler under longitudinal compression 16 p2817 A66-31049

Bending problem of three-layer plates with fillers 16 p2817 A66-31050

Design equations for three-layer plate with rigid filler 16 p2817 A66-31051

Shear flow generated in rotational flow, noting honeycomb structure satisfactory in rotational flow about thin airfoils 21 p3724 A66-38735

**HONEYCOMB CORE**

Displacement response prediction and fatigue life of honeycomb sandwich panels subjected to acoustic excitation 01 p0149 A66-10141

Synthetic spherulites in plastic foam and synthetic tube segments in honeycomb form as fillers in sandwich construction 10 p1614 A66-21390

Sandwich cores consisting of tubes arranged in honeycomb configuration with tube axes normal to sandwich surface 12 p1959 A66-23782

Manufacturing methods and equipment to sculpture aluminum honeycomb core, discussing tracer control, airfoil mill, traversing router, etc [SAE PAPER 660326] 14 p2301 A66-27294

Refractory metal honeycomb structure fabrication for heat shield panels, using D-36 columbium alloys 19 p3371 A66-36161

Honeycomb structure, examining assembly, skin delamination at spars or terminal fitting, glasscloth radome and inspection techniques 20 p3671 A66-37827

Linear elastic small deflection theory of natural frequencies of vibration of rectangular sandwich honeycomb plate with mass attachment 24 p4292 A66-43046

**HOOKE LAW**

Elastic-plastic material, calculating stress concentration and deformation for planes weakened by circular holes 06 p0964 A66-16476

Hooke law extension to include term expressing dependence of stress on spatial variation of strain, noting rotation of polarization plane in sound wave propagation in isotropic medium 14 p2334 A66-27478

Hooke law analysis of dynamic stability of closed circular cylindrical anisotropic shell compressed by longitudinal force 15 p2609 A66-29196

Variational solution of simultaneous stability equations boundary value problem for transverse displacements and stress state 16 p2819 A66-31137

Linearity, stress, strain, time and birefringence relations in plastic model materials, using Hooke law 20 p3668 A66-37498

Equations for plane deformation in multimodule elasticity theory, formulating generalized Hooke law for multimodule material 21 p3826 A66-38609

Plane stressed state of nonlinear plate with opening reinforced by thin elastic rod in case of small deviations from Hooke law 22 p3991 A66-40152

**HOPE SPACECRAFT**

**S HYDROGEN OXYGEN /HOPE/ SPACECRAFT**

**HORIZON**

**S GYRO HORIZON**

**S RADIO HORIZON**

**HORIZON SCANNER**

**SA INFRARED HORIZON SCANNER**

Transhorizon propagation using ORBIS, noting burst propagation and quasi-sinusoidal fading 15 p2451 A66-29230

Sunfollower assembly for maintaining horizon scanner in Sun vertical 21 p3740 A66-39387

**HORIZON SENSING**

**SA ATTITUDE CONTROL**

Self-contained orbital navigation system using Earth-horizon measurements in 14-16 mu carbon dioxide absorption band, using Kalman linear filter theory 01 p0100 A66-10024

Response of inertial platform in orbital gyrocompass mode studied for satellite vehicle [AIAA PAPER 64-238] 03 p0369 A66-12730

Propellant rocket exhaust plume effect on error calculation for radiation balance II tracker 18 p3240 A66-33791

TACITE rocket sounding of characteristic of IR contrast between Earth and space 20 p3663 A66-38033

Horizon sensor data processing with compensation for statistical properties of errors, noting application of optimum filtering theory 21 p3766 A66-38888

Kalman filter divergence control, noting analytical and empirical modification methods 21 p3766 A66-38888

Stability criteria derived for horizon sensors which track point on horizon where second harmonic of signal generated by scan motion of field of view is zero 24 p4175 A66-42811

Horizon sensing problems for application to spacecraft stabilization techniques, including sensors using Earth brightness, conic scanners and interference caused by cloud haze and other atmospheric phenomena 24 p4235 A66-42811

**HORIZONTAL ATTITUDE**

Combined effect of horizontal and vertical accelerations on gravimeter reading, mounted on gyroplatform or in Card suspension 14 p2297 A66-28111

Combined effect of horizontal and vertical accelerations on gravimeter reading, mounted on gyroplatform or in Card suspension 24 p4212 A66-42611

**HORIZONTAL TAIL**

Large transport aircraft design, examining effect of high horizontal stabilizer location on vertical fin [AIAA PAPER 65-331] 13 p1994 A66-25511

**HORMONE**

**SA ADRENOCORTICOTROPIN /ACTH/ SA INSULIN**

Gravity effect on basipetal transport auxin studied by growing plants both erect and on horizontal clinostats 06 p0812 A66-16411

Adrenocorticotrophin-releasing hormone appears in peripheral blood of rats under physiological stress, noting role of pituitary gland 14 p2228 A66-27211

Urinary excretion of steroids as catecholamines as measure of emotional stress of man in 56-day exposure to oxygen-helium environment 18 p3057 A66-33111

**HORMONE METABOLISM**

Degree of mental stress correlated with excretion of catecholamine, free adrenaline and noradrenaline in



- horn antenna 04 p0470 A66-14081
- Radiation patterns of transversely polarized horn reflector antenna, using image method 01 p0044 A66-10937
- Flux density of Cas A measured, using horn-reflector antenna, response compared with output of reference-noise source 05 p0762 A66-15278
- Circular horn radiators with annular seal connections to antenna for simultaneous transmission of dual waves decoupled by polarization 09 p1354 A66-20493
- Radio telescope techniques applied to astronomy, noting data processing and antenna receiving systems including masers, parametric amplifiers, etc 10 p1602 A66-21064
- Minor lobe suppression in rectangular horn antenna through utilization of high impedance choke flange 11 p1663 A66-22556
- Radiating mechanisms in reflector antenna system including aperture radiation, direct feed radiation and diffracted radiation 11 p1673 A66-23481
- Radiation characteristics of horn antennas analyzed, using edge diffraction theory, noting intensity at backlobe and far sidelobe 14 p2255 A66-27908
- Modification of horn antennas for low sidelobes, emphasizing reduction of backlobes of pyramidal horn antenna 15 p2457 A66-28595
- Horn radiators with high attenuation capabilities, noting design features, application to parabolic antennas, etc 17 p2894 A66-32989
- Rear feeds for paraboloidal reflectors 18 p3075 A66-33618
- Four-horn and five-horn monopulse antenna system properties including illumination apertures, gain factor, temperature, etc 18 p3080 A66-34265
- Feeding paraboloidal reflectors by stacked horns, using 45 degree polarization and double stacking of horns 18 p3081 A66-34270
- Diffraction pattern analysis of fields generated by hoghorn-fed Cassegrain antenna operating in Fresnel zone 18 p3083 A66-34289
- Four-and five-horn tracking feeds for large antennas, emphasizing sum channel gain in five-horn feed 18 p3083 A66-34292
- Radiation pattern synthesis for circular aperture horn antennas, assuming aperture distribution consisting of fields of cylindrical waveguide modes and by linear combination of radiation pattern functions 19 p3320 A66-36404
- Large reflector shape measured by method using horn antenna illumination and small auxiliary reflecting device 20 p3527 A66-37448
- Horn transitions from empty waveguides to dielectric surface waveguides using telegraphers equations, determining launching horn shape with minimum reflection coefficient 21 p3711 A66-38836
- OT CATHODE**
- Double sheath presence in front of hot cathode in low pressure DC discharge 02 p0265 A66-11433
- Cesium filled diodes measured at various cathode temperatures, noting effect of ions generated in interelectrode space on current 05 p0728 A66-15549
- Colloidal thruster with hot cathode charged colloidal particle source [AIAA PAPER 66-255] 10 p1593 A66-21460
- OT CYCLE PROPULSION SYSTEM**
- Hot cycle rotor/wing aircraft for high speed VTOL, embodying lightweight lift/propulsion system and high payload capability with economic benefits 06 p0805 A66-16810
- Advanced heavy lift helicopters performance with hot cycle propulsion 17 p2843 A66-32720
- OT ELECTRON**
- Nonlinear electrical effects and recombination of hot electrons in compensated germanium, studying steady and transient I-V characteristics 02 p0273 A66-11717
- Electron energy and momentum dissipation in n-type InSb at low temperatures, discussing collision effects on hot electron escape 02 p0276 A66-12079
- Longitudinal nonlinear traveling oscillations in hot electron plasma 03 p0401 A66-12956
- Impact ionization coefficient for electrons and holes in silicon determined from distribution function of hot carriers and shown to be weakly dependent on ionization cross section 04 p0565 A66-14262
- Plasma instability in oscillating discharge, with linear analysis of several types 05 p0723 A66-15161
- Direct measurement of energy relaxation time between hot electrons and lattice in n-type indium antimonide in hydrogen temperature range 06 p0929 A66-17036
- Radiation damage in nondegenerate germanium at low temperatures, using hot carrier technique for measuring resistivity and Hall coefficient on antimonide doped samples 06 p0932 A66-17114
- Hot electron recombination peculiarities, ignoring electron temperature concept, for moderate fields and lattice temperatures 07 p1104 A66-18220
- Mirror ratio is principal parameter controlling heating of plasma by electron beam in magnetic mirror system 07 p1090 A66-18260
- Faraday effect on hot electrons in germanium and silicon 07 p1105 A66-18370
- Instability initiating plasma transport across magnetic field in plasma discharge occurring after plasma decayed for some time, damping loss by addition of cold electrons to discharge 08 p1260 A66-18544
- Mobility of hot electrons in runaway regime of n-type InSb and GaAs at low temperatures 09 p1412 A66-19987
- Hot electron emission from semiconductor cathode in vacuum-tube diode during tapping of thermoelectronic and autoelectronic current 09 p1429 A66-20813
- Mirror ratio is principal parameter controlling heating of plasma by electron beam in magnetic mirror system 09 p1409 A66-20904
- Hot electron emission from thin metallic films of island structure 10 p1589 A66-22171
- Hot-electron transistors, discussing application of Schottky-emitter transistor to VHF operation 13 p2038 A66-25561
- Injection and extraction of hot electrons in n-n heterojunctions with rapid Maxwellization of electron gas, negative resistance and semiconductor characteristics 13 p2166 A66-25920
- Gunn effect involving current oscillations higher than 1000 mc in GaAs crystal under applied electric field 14 p2355 A66-26920
- Microwave rotator using hot carrier property of n-type germanium 14 p2248 A66-27056
- Hot electron recombination at repulse impurity centers in germanium containing copper 14 p2357 A66-27074
- Large annular steady state stable hot-electron plasma blanket formed by magnetically trapping electrons originating in intense arc gas discharge 14 p2347 A66-28304
- Hot electron redistribution in multivalley conductors in electric fields, based on variation under pressure of valley population levels, using silicon samples 15 p2559 A66-28622
- Electric current density in semiconductor, noting harmonic mixing of microwaves by warm electrons in germanium 15 p2564 A66-28875
- Acoustoelectric effects for various sound waves, using rate of energy exchange between two coupled systems in relative motion 15 p2564 A66-28970
- Hot carrier microwave detector based on thermoelectric effect of warm carriers in bulk semiconductor and assuming Maxwell-Boltzmann distribution for heated carriers 15 p2461 A66-29014
- Flute stabilization of hot electron plasma by cold plasma which contributes to dielectric coefficient 15 p2555 A66-29759
- Electron-cyclotron-heated plasma stability in mirror containment systems possessing shear, minimum-B properties or both 15 p2555 A66-29760
- Hot electrons in anisotropic semiconductor, considering case of scattering by acoustic phonons within one energy valley with nondegenerate bottom 17 p2977 A66-32318
- Magnetospheric suprathermal-electron scattering in oscillating electrostatic plasma and diffusion of subthermal electrons across magnetosphere, using ion-wave propagation theory for electroconductive plasmas 17 p2993 A66-32521
- Nonlinear ionic-acoustic wave propagation in collisionless hot electron plasma with at least one cold ion stream 17 p2973 A66-32976
- LF common-base current transfer ratio for hot electron transport in semiconductor-metal-semiconductor point-contact-transistor structures measured as function of metal film thickness and temperature 19 p3435 A66-35410
- Hot electron emission from thin metallic films of island structure 19 p3441 A66-35785
- Beam-plasma interaction used to generate fully ionized plasma and enhance component temperature for study of plasma heating and burnout 19 p3429 A66-36585
- Field and charge density distributions in semiconductor with hot electrons, showing domain movement type oscillations due to stationary wave propagation 20 p3617 A66-37555
- Hot electron recombination at repulse impurity centers in germanium containing copper 22 p3966 A66-40832
- Spatial distribution of hot electrons coherently scattering in thin Au film 23 p4115 A66-42063
- HOT FORMING**
- Construction of hot forming tool made of fused silica ceramic 08 p1229 A66-18691
- Thermal stability, adhesion prevention, stress and die wear reduction and air pollution of industrial lubricants 14 p2304 A66-28207
- Hot forming of titanium sheet structures and relation to cost [SAE PAPER 660327] 15 p2511 A66-29845
- HOT GAS**
- Transient cooling of spherical mass of high temperature gas by thermal radiation, neglecting ionization and dissociation effects [ASME PAPER 65-APMW-22] 04 p0598 A66-14223
- Prediction of solid propellant hot-gas ignition based on preignition transient convective heat transfer model [AIAA PAPER 66-67] 08 p1317 A66-18993
- Line-of-sight IR spectral temperature profile measurements in inhomogeneous hot gas 09 p1382 A66-20505
- Spectroradiometric pyrometry of shock heated gases by IR emission and absorption measurements 09 p1382 A66-20508
- Transient cooling of spherical mass of high temperature gas by thermal radiation, neglecting ionization and dissociation effects [ASME PAPER 65-APMW-22] 10 p1621 A66-21468
- Electrothermal propulsion system using heated gaseous nitrogen to provide Vela satellite with orbital velocity correction capability and weight savings [AIAA PAPER 66-213] 11 p1759 A66-22217
- Adiabatic dispersion into empty space of triaxial gaseous ellipsoid studied by Ovsliannikov exact solution of equations of gasdynamics 14 p2278 A66-28060
- Hot flame gases ionization by electron reactions at atmospheric pressure 18 p3137 A66-34116
- HOT GAS SYSTEM**
- Underwater thermal propulsion system powered by closed-cycle steam power plant fed by high-temperature variable gas flow from oxygen-hydrocarbon combustion apparatus [AIAA PAPER 65-481] 19 p3479 A66-36492
- HOT PRESSING**
- Fabrication and properties of translucent bodies of hot-pressed alumina, beryllia and magnesite with data on density, microstructure, thermoconductivity, etc 07 p1054 A66-18502
- Hot-pressed high-purity polycrystalline MgO 12 p1900 A66-24721
- Recrystallization in titanium alloy strips subjected to various levels of hot rolling 15 p2522 A66-29185
- Laboratory press for high temperatures and pressures analyses of hard material powders, noting carbon dies and measurements of densification vs time 16 p2673 A66-30254
- Continuous hot pressing apparatus design,



operation, production economy and results with oxidic materials and metals 16 p2709 A66-30255

Hot pressing technology applied to various metal alloys, noting physical, thermal and electrical properties 16 p2714 A66-30626

Rupture strength increase in tungsten and molybdenum chopped wires silicide coated by pack diffusion and incorporated in mullite matrix by vacuum hot pressing [ACS PAPER 7-C-65F] 16 p2723 A66-30949

Fine particle size pure tungsten and thoriated tungsten powder produced by hot pressing in graphite dies at temperatures from 1500 to 1800 degrees C 19 p3382 A66-36120

High temperature tensile deformation of polycrystalline magnesla prepared by single-crystal recrystallization and hot pressing 21 p3753 A66-38592

**HOT SPOT**

IR measurements on eclipsed Moon, discovering hot spots on lunar surface 19 p3457 A66-35448

**HOT WATER ROCKET**

Hot water rockets covering principle, design, advantages, testing techniques and performance capabilities 05 p0659 A66-14677

**HOT WIRE**

Roberts method determining accommodation coefficients of gases on bare wires leads to erroneous conclusions due to thermal inertia of experimental apparatus in vicinity of current paths 04 p0545 A66-14170

Measurement of heat exchange coefficient for heated cylindrical copper wire immersed in sand particles or glass beads at various low pressures 14 p2415 A66-28319

Forced convection caused by normal and longitudinal components of flow around hot wire, noting effect of wire length 20 p3544 A66-36928

**HOT-WIRE ANEMOMETER**

Hot wire Wheatstone bridge used in automatic control and method to obtain linear response in large speed fields 02 p0229 A66-11760

Parametric analogies used to obtain design characteristics of thermal and viscosity vacuum meters and hot-wire anemometers 07 p1031 A66-17412

Dynamic transient response of fluid surrounding hot wire studied by analysis of basic transport equations for momentum and energy 10 p1521 A66-21055

Thermistor hot-wire anemometer with feedback bridge circuit for measuring air flow rates to 20 m/sec from zero to 50 degrees C 11 p1709 A66-23320

Hot-wire anemometer measurement of turbulent velocity fluctuations in air flow and energy spectrum and correlation analyses 12 p1880 A66-23846

Time resolution error of measured correlation function, based on frequency response of hot-film and hot-wire anemometer 12 p1880 A66-23847

Hot-wire anemometer applications to turbulence measurements in conducting liquids and vacuum deposition of quartz film on coated hot-film probe 12 p1880 A66-23848

Hot-wire anemometer determination of electron and ion temperature, neutral particle temperature, concentration and velocity and potential of partially ionized helium plasma 12 p1882 A66-24223

Wake dimensions growth and turbulent energy decay in incompressible axisymmetric wakes surveyed, using hot-wire anemometer in low speed wind tunnel [ASME PAPER 65-FE-8] 12 p1799 A66-24556

Constant current hot-wire anemometer determination of experimental time-amplitude distribution function of velocity in turbulent boundary layer 13 p2072 A66-26753

Wire-to-surface heat transfer and error in hot-wire anemometer measurements 16 p2708 A66-31256

Three dimensional character of wake of circular cylinder at three Reynolds numbers utilizing hot wire anemometers 16 p2632 A66-31659

Linearizer for constant temperature hot-wire anemometer, detailing linearization circuit 19 p3357 A66-35806

Dynamic pressure and flow measurements on small integrated high speed systems,

using high speed pressure transducing equipment in integrated circuits and hot-wire anemometry 20 p3560 A66-37652

Hot-wire anemometer design with linear characteristics for measurement of velocity fluctuations of flow 20 p3560 A66-37760

Frequency distortions correction for pulsation amplifier of thermoanemometer 21 p3739 A66-39331

Experimental boundary layer study on hovering rotors using evaporative chemical films, pressure probes and hot wire anemometers 22 p3843 A66-40249

Hot-wire anemometer determination of electron and ion temperature, neutral particle temperature, concentration and velocity and potential of partially ionized helium plasma 22 p3919 A66-40585

Instantaneous shear stress at liquid flow boundary, measuring turbulence and velocity fluctuation in close proximity of pipe wall 24 p4194 A66-42415

Wake motion through moving blade row, demonstrating chopping phenomenon via hot-wire anemometer traces taken downstream of rotor 24 p4157 A66-42583

**HOT-WIRE MEASUREMENT**

Laminar to turbulent transition along aluminum plate in free convection measured, using hot-wire probes 04 p0596 A66-13515

Hot-wire measurements in plane turbulent jet of air 10 p1480 A66-21466

Wire recovery temperature in steady state wind tunnels determined without detailed knowledge of convective heat transfer rate to wire 12 p1860 A66-23612

Laminar free convection flow and velocity and temperature distributions in air above thin horizontal electrically heated wire 12 p1980 A66-24906

Hot wire-drawn beryllium recrystallization analyzed by hardness measurement and micrography, noting dependence on initial deformation 13 p2107 A66-25358

Hot-wire analysis of permanent sound fields during varied flow velocity around flat plate boundary layer, noting resonance effect of sound amplitude 13 p2063 A66-25901

Hot wire electron emissive probes for potential measurements in quiescent plasmas, noting plasma densities, emission levels, etc 13 p2154 A66-26554

Hot wire measurements in radial turbulent incompressible air jet 18 p3045 A66-33593

Heat conductivity coefficient of cesium vapor at temperatures from 1000 to 1600 degrees K and 1 to 5 torr measured by hot tungsten filament method 18 p3142 A66-34022

**HOT-WIRE TURBULENCE MEASURING APPARATUS**

Hot-wire turbulence spectral analyzer for measuring power spectrum of wind tunnel fluctuation flow 11 p1703 A66-22197

Atmospheric turbulence determined from velocity fluctuations in flight path direction measured by wing-tip mounted hot-wire anemometer 20 p3593 A66-37470

Microwave airflow simulator measurements of hot-film and hot-wire turbulence transisor 24 p4211 A66-42576

**HOTSHOT TUNNEL**

Six-component balance equipped with semiconductor strain gauges and inertia compensated for hotshot wind tunnels 24 p4206 A66-42167

Measuring devices and techniques for heat-transfer rate, pressure and force in hotshot tunnels 24 p4206 A66-42168

Displacement detector to provide direct measurement of shear forces in aerodynamics on small surface elements in hotshot wind tunnels 24 p4207 A66-42169

Electrostatic probe and VHF microwave reflectometry study of nitrogen flow around models in hotshot wind tunnels, determining plasma sheath physical characteristics 24 p4191 A66-42193

**HOVERCRAFT HD.1 GROUND EFFECT MACHINE**

Empirical estimation of hovercraft propeller noise level, correction curves for blade number and noise correlation 10 p1484 A66-21799

**HOVERING**

Hovering performance of plenum chamber type of ground effect machine over land and water, showing single nondimensional

parameter controlling phenomena of overwater operation 19 p3279 A66-36446

Hover augmentation system /HAS/ design for analog computer helicopter simulation and flight control 21 p3696 A66-38900

Attitude control system/engine control system for hover control of turbojet VTO aircraft 21 p3697 A66-38900

**HOVERING STABILITY**

Propulsion-control systems interface for V/STOL hover control in aircraft, using plus lift cruise propulsion concept [AIAA PAPER 65-799] 03 p0319 A66-12500

Altitude control for VTOL aircraft facilitates control of hovering flight, noting construction, operation principles and performance 10 p1484 A66-21370

Efficiency factors such as roll scanning methods and pitch control effectiveness in hover control system for VTOL aircraft 11 p1638 A66-23220

Helicopter handling qualities during hovering, noting pilot performance, position control tasks with and without gusts, effects of stability derivatives, etc 17 p2845 A66-32700

Handling in hovering mode of Dornier VTOL transport aircraft with and without autostabilizer, obtaining moments about roll, pitch and yaw axis 20 p3493 A66-36800

Experimental boundary layer study of hovering rotors using evaporative chemical films, pressure probes and hot wire anemometers 22 p3843 A66-40249

Propulsion control systems interface for V/STOL hover control in aircraft, using plus lift cruise propulsion concept [AIAA PAPER 65-799] 23 p4015 A66-40900

**HP-137 AIRCRAFT**

S HANDLEY PAGE HP-137 AIRCRAFT

**HS-125 AIRCRAFT**

S DE HAVILLAND DH-125 AIRCRAFT

**HSS-2 HELICOPTER**

S SH-3 HELICOPTER

**HUB**

Deformation and state of stress in contiguous cylindrical rotationally symmetrical hubs and shafts of various lengths 14 p2409 A66-28400

**HUECKEL TECHNIQUE**

Nitrogen analogs of sesquifulvalene, calculating dipole moments of nitro, anhydro bases and pyridones via modified Hueckel technique 11 p1651 A66-23400

Extended Hueckel method calculations of bonding in N, F oxidizers 23 p4030 A66-41200

Three-dimensional Hueckel molecular orbital calculations performed on series of molecules made from atoms of H, C, N, O, and Cl 23 p4031 A66-41200

**HUGONIOT EQUATION OF STATE SA PLASTICITY**

Shock compression of liquid argon at very high pressures and temperatures reflecting shock wave from tungsten wall for testing interatomic potential 11 p1694 A66-23200

Hugoniot equations of state derived from several unreacted explosives and propellants from optical measurements of shock wave and particle velocities 13 p2171 A66-25300

Two-dimensional radiation-coupled wedge flow analyzed, using integral relations method and Rankine-Hugoniot relations 18 p3100 A66-34500

**HUMAN BEHAVIOR**

Human pilot behavior compared with automatic pilots in terms of adaptability, response time and reliability 02 p0187 A66-11800

Effect of weightlessness on cardiovascular neuromuscular and autonomic nervous systems 06 p0810 A66-15500

Simulator design for inclusion of man/machine interactions and human behavioral and performance considerations in system design 08 p1203 A66-19800

Experimental psychological testing and results in choice and training of cosmonauts 15 p2434 A66-29400

Physiological and biochemical tests on man subjected to isolation and hypokinesia 15 p2434 A66-29400

Human behavioral effects during 56-day exposure to oxygen-helium atmosphere 258 mm Hg total pressure, present temperature, psychomotor and sleep performances 18 p3061 A66-33700

Human dreaming sleep and correlation



- changes in urine volume and osmolality 19 p3285 A66-36065
- Personality development, application of theory to problems of aerospace selection 19 p3294 A66-36378
- Book on human spatial orientation and effect on behavior 20 p3508 A66-37011
- Psychological effects of velocity and hermetic compartments on astronaut performance 24 p4166 A66-43146
- HUMAN BODY**
- Stress-strain relationships for tension, compression and shear of femoral bone loaded longitudinally and transversely [ASME PAPER 65-WA/HUF-7] 05 p0626 A66-15698
- Electrophoretic determination on acrylamide gel of lactic dehydrogenase isozyme patterns in serum obtained from human subjects exposed to brief intense thermal impulses 06 p0814 A66-16831
- Electromagnetic energy transport between coils or coils external to human body and coil implanted inside body is increased by using suitable ferrite core for receiving coil 06 p0820 A66-16852
- Bone calcium loss during two weeks of simulated weightlessness, using X-ray wedge technique 11 p1643 A66-22577
- Mathematical model of human body predicting inertial properties in any fixed body position, including location of mass center [AIAA PAPER 65-498] 12 p1810 A66-24719
- Electrocardiogram P wave changes relation to body position changes in space 14 p2227 A66-26810
- Human eye, capabilities as optical instrument, particularly spatial filtering effects, visual acuity, eye movement and light receptors 14 p2228 A66-27650
- Long-term lower body negative pressure in supine position effect on deterioration in cardiovascular function of man during prolonged bed rest 15 p2430 A66-28657
- Human response to predicted Apollo landing impacts in selected body orientations 15 p2430 A66-28663
- Human otolith and cupula system behavior under anomalous gravity conditions 15 p2434 A66-29446
- Mechanical impedance of human body subjected to vibration combined with various magnitudes of linear acceleration 17 p2863 A66-32154
- Mass measurement of man in zero gravity environment, discussing laboratory device using linear harmonic motion 17 p2924 A66-32171
- HUMAN CENTRIFUGE**
- Short radius onboard centrifugation for simulated gravity during prolonged space flight, providing zero G at eye level and maximum G at feet 09 p1334 A66-20524
- Physical and physiological nomenclature for acceleration, noting weightlessness, human centrifuge, etc 10 p1493 A66-22122
- Physiological reactions of human body to transverse acceleration, examining means of increasing organism resistance to these effects 11 p1643 A66-22575
- Cardiovascular stress resulting from radial acceleration gradient impeding venous return analyzed by rotation of seated subject about Z axis /Rz/ 12 p1807 A66-25016
- Effectiveness of antimotion sickness drugs compared by using recommended and larger than recommended doses as tested in slow rotation room 12 p1807 A66-25017
- X-ray motion picture recording of change in A-P chest diameter and heart position of five human subjects during transverse centrifuge accelerations of 5G and 10G 16 p2639 A66-31119
- HUMAN ENGINEERING**
- SA ANTHROPOMETRY**
- SA CYBERNETICS**
- SA MAN-MACHINE SYSTEM**
- Problem areas in long duration manned space flight noting vehicle maintenance, extravehicular activities, visual skill performance, spacecraft control, etc [SAE PAPER 650809] 01 p0021 A66-10818
- Comparative merits of visual, audible and composite aircraft warning systems for optimum human response to causal condition 01 p0021 A66-10939
- Man-machine relationship during space flight 04 p0471 A66-14085
- Psychological research relevant to human factors engineering of man-machine systems, discussing information processing 05 p0626 A66-14616
- Rigid articulated pressure suits, discussing design, construction and operation for low external pressure, mobility requirements, etc 06 p0815 A66-15927
- Optimum operational influence on design of DC-9 cockpit 07 p0988 A66-17704
- Human factor in design of controls and instrumentation in aircraft, discussing man-machine dynamics 10 p1494 A66-22135
- RCA life sciences paper on microscale medical sensors, adaptation theory, logic techniques and human factors engineering 11 p1647 A66-22297
- Human factors engineering, discussing man-machine allocation of system functions, task equipment analysis, model and mock-up analysis and environmental analysis 11 p1647 A66-22301
- Origin, setting and evolution of human factors engineering and man-made environment 11 p1648 A66-23100
- Man-machine systems involved in on-line man/ computer interaction, manned space systems, satellite communication and display systems 14 p2230 A66-27820
- Present status of human engineering field, considering relationship of specific human functions constituting subsystem to system as whole 17 p2868 A66-32875
- Human physiological and psychological characteristics effects on design of mobile lunar laboratory 17 p2904 A66-32944
- Mechanical prediction display to improve human behavior in control system 21 p3700 A66-38454
- Human engineering of acoustic fatigue for optimum data processing performance [ASME PAPER 66-MD-25] 21 p3700 A66-38481
- Airliner seat and galley design, investigating loading and safety, comfort, convertible seats, upholstery, quick-change seating, etc 21 p3696 A66-39344
- Comparison of Czechoslovakian human engineering standards for control pushbuttons with U.S. standards 22 p3859 A66-40861
- Psychomotor test equipment, describing Two-hand Device, Reaction Sensing Device and Rudder Control Test 23 p4029 A66-41042
- Control design using force as criterion, discussing effect of varying height and handle orientation of push-pull task 23 p4029 A66-41575
- Text evaluating application of human body size and mechanical capabilities to equipment design for man-machine integration 23 p4030 A66-41619
- HUMAN FACTOR**
- Human factors in design criteria for maintainability and reliability 01 p0018 A66-10077
- Human factors in Concorde SST program 03 p0329 A66-13357
- Energy patterns from space accessible to human senses through data sensors and information acquisition 04 p0472 A66-14093
- Human factors in control/indicator panel design of ground support equipment [ASME PAPER 65-WA/HUF-16] 05 p0628 A66-15696
- Book on human factors evaluation in man-machine system design 06 p0972 A66-16250
- Aeromedical factors of Titan II ICBM support, discussing human factors in missile crew and propellant transfer 11 p1648 A66-22582
- Dynamic characteristics of human operator in tracking system under spaceflight conditions onboard Voskhod II spacecraft 11 p1648 A66-23047
- Human factors and system effectiveness, noting role of customer project officer, contractor engineering manager and human factor specialist 11 p1790 A66-23445
- Telesensors, teleoperators and telecontrols for remote operations 12 p1876 A66-23672
- Automatic control, systems science, cybernetics, biomedical engineering, human factors - IEEE International Convention, New York, March 1966 12 p1854 A66-24634
- Limitations and reliability of human operator of control systems to process information, noting importance of endurance and sensory perception 12 p1807 A66-25012
- Ground system design, data processing, digital command and digital-human interface in flight operations problems for unmanned spacecraft on planetary exploration mission 13 p2190 A66-25257
- Control problems in operation of transport aircraft noting degrees of freedom, computer aid, human factor, etc 13 p2047 A66-25497
- Vertical vibration simulator for low-altitude high-speed /LAHS/ aircraft systems human factor research 13 p2059 A66-26547
- Human factor tests in large-scale operational system testing techniques [ASME PAPER 66-HUF-11] 14 p2229 A66-26967
- Effective thermal radiation surface of humans subjected to omnidirectional radiation 16 p2645 A66-31806
- Control feel application to aircraft controls, noting man-machine system configurations, anthropometric and physical factors, sensory motor requirements, etc 17 p2869 A66-33446
- Human factor aspects of digital computer programming for simulator control, discussing application and operation 17 p2869 A66-33449
- Accidents involving human error evaluated from medical point of view 18 p3053 A66-34947
- Aircrew response effects to prolonged low altitude high-speed flight vibration 19 p3287 A66-35507
- Cockpit displays associated with low altitude high-speed flight, emphasizing shift toward designing around man 19 p3287 A66-35508
- Factors in operation of manned space chambers - ASTM Symposium, Seattle, October-November 1965 19 p3288 A66-35837
- Man-rating criteria in Boeing space environmental simulation chamber, discussing structural design, vacuum chambers, repressurization, manlock pumping systems, aerospace medical training, etc 19 p3289 A66-35841
- Possible adaptation of asteroids to support human life for indefinite periods of time 19 p3285 A66-36241
- PERT-type network, mathematical model and human factor approaches to maintainability and availability predictions for man-machine systems 20 p3684 A66-37892
- Human factor relation to system effectiveness and human performance relation to operational reliability and maintainability 20 p3509 A66-37894
- V/STOL aircraft human reliability factors and requirements for displays and controls in various operational modes under low altitude, high speed and all-weather conditions 20 p3509 A66-37895
- Human operator behavior following step change in controlled element, determining limitations on operator descriptions and measurement methods which might be employed 22 p3858 A66-40253
- Connection between equivalent time-delay and LF phase lag in neuromuscular system data 22 p3854 A66-40254
- Methodology for definition of space vehicle display system based on mission objectives and human factors 22 p3892 A66-40288
- HUMAN PATHOLOGY**
- Origin of chest pains associated with G force sinusoidal vibration, noting effect of anterior chest wall anesthetization, results suggest pain originates in chest wall 19 p3286 A66-36375
- Cosmic radiation and space flight effects on lysogenic bacteria and human cells in culture 21 p3700 A66-39315
- Physiopathological phenomena of space flight stresses, especially weightlessness 22 p3856 A66-40506
- Pathological and metabolic changes due to toxicity of unsymmetrical dimethyl hydrazine /UDMH/ 22 p3858 A66-40507
- HUMAN PERFORMANCE**
- SA ASTRONAUT PERFORMANCE**
- SA OPERATOR PERFORMANCE**
- SA PILOT ERROR**
- Reliability estimation procedure combines task ratings with empirically based data in



derivation of regression equation 01 p0018 A66-10076

System engineering methodologies to show how prediction of human error leads to higher system performance

reliabilities 01 p0019 A66-10117

Similarity concept applied to study of work done by living creatures in various situations 01 p0017 A66-10302

Time sharing and vigilance study by Wiener reanalyzed from signal detection theory viewpoint 01 p0020 A66-10613

Decision interval effect on signal detectability in vigilance task involving clock 01 p0020 A66-10614

Effect of amphetamine on signal detectability in vigilance task 01 p0020 A66-10616

Human motor performance activities in simulated weightless environment 02 p0185 A66-11626

Physiological testing under simulated reduced gravity conditions with subject suspended and performing exercises on inclined treadmill 02 p0186 A66-11644

Low friction environment effects on maintenance operations in simulator noting torquing-force capability, hand-eye coordination, etc 02 p0186 A66-11645

Effects of physical location of visual stimuli on intentional response time /IRT/ 02 p0183 A66-12075

Light and noise level, stimulus intensity and background shade variation effect on reaction time 02 p0183 A66-12076

Upper thermal tolerance limits for unimpaired mental performance 03 p0325 A66-12359

Space environment simulation vacuum chamber design and operation in terms of manned testing 03 p0352 A66-12757

Human perceptual mechanism defined by psychological research and applied to aircraft cockpit display design 03 p0329 A66-12883

Mathematical model based on control and queueing theory for human controller for turn-round operations on airport apron 03 p0329 A66-12886

Monitoring human performance during manned orbital flight for assessment of central nervous system function, noting animal studies during simulated stresses of space flight 04 p0468 A66-14088

Threshold of feeling data by generating sensation of rotation and nystagmic reaction by rotating subject and abruptly halting rotation 06 p0811 A66-16066

Physiological and performance determinants in manned space systems - AAS and HFS Symposium, San Fernando Valley State College, Northridge, California, April 1965 06 p0816 A66-16234

Simulation study of human performance in manual control tasks in orbital rendezvous and lunar landing 06 p0818 A66-16245

Minimum field of view required for rapid accurate navigation star identification-acquisition established between 25 and 30 degrees 06 p0906 A66-16247

Spacecraft design influenced by man in capacity as designer and crew member 06 p0818 A66-16248

Simulated flights evaluating verbal communication intelligibility in oxygen breathing mixtures at low atmospheric pressures compared with results obtained in room air at ground level 06 p0813 A66-16827

Performance and physiological effects of adrenalin or insulin in human subjects 06 p0813 A66-16829

Human accommodative system, investigating absence of odd-error signal mechanism under restricted monocular viewing conditions 06 p0819 A66-16850

Airborne computer design free of navigational functions performed by humans, using Doppler equipment 07 p1067 A66-17692

Criteria for quality of aerial camera systems including allowances for ground scene properties, photographic grain and human observer, noting role of resolving power and transfer function 07 p1035 A66-18154

Effects of chronic hypohydration on responses to tests of bodily functions, defining set points and mechanisms involved in changes in work

performance 09 p1337 A66-20528

Perceiving undetectable rotation in semicircular canals by employing self-induced Coriolis stimulation, determining psychophysical functions for direction or rotation discrimination at different yaw velocities 09 p1337 A66-20531

Human efficiency measured in producing power by tramping, hand cranking and lateral pumping modes 11 p1648 A66-23082

Added pilot work load imposed by additional commands in compensatory display reduces tracking performance in control of simulated terrain-following aircraft 12 p1808 A66-23922

Experimental testing effectiveness of sensor lines showing linkages between displays and controls 12 p1808 A66-23924

Industrial alertness management in relation to production rate, quality control and operator safety 12 p1810 A66-24957

Acute hemodynamic effects of G-suit inflation, noting elevation of central venous pressure, cardiac output falling due to depressor reflexes and role of ganglionic blockade 12 p1811 A66-25014

Human subjects making comparisons of duration of two tones in forced choice situation for signal with same or different intensities 14 p2229 A66-27309

Critical Human Performance and Evaluation /CHPAE/ Program methods for evaluating and predicting human performance and potential error probabilities 14 p2231 A66-28422

Individual differences in performance of vigilance task 14 p2228 A66-28480

Reliability-maintenance relationship including accessibility, design, crew duty cycle, and equipment failure rates, number of restorations, etc, in long-duration manned missions 15 p2606 A66-28804

Application of escape probability concept to systems development for quality control, noting minimization of system failure 15 p2508 A66-28812

Weapon system design, noting variables for manning and skill requirements, parameters of operational readiness, etc 15 p2618 A66-28813

Physiological, psychological and biochemical effects on humans after 8-hr inhalation of low carbon monoxide concentration 15 p2435 A66-29448

Transmission and information processing rate of human visual system 15 p2435 A66-29450

Chest-to-back accelerations effect on human electroencephalograms and work capacity 15 p2437 A66-29475

Means of formulation by humans of sequence of actions, noting error distribution and clustering of responses 15 p2445 A66-29502

Work output characteristics and capabilities of undersea work crews during extended missions 16 p2642 A66-30507

German Air Force functional tests for early diagnosis of cardiovascular disease among aircrew, also discussing therapy 16 p2640 A66-31133

Visual monitoring of multichannel displays, noting number of channels used, operator performance characteristics, etc 16 p2644 A66-31269

Visual and tactile display for compensatory tracking, noting conditions for minimum error, mean square error, etc 16 p2644 A66-31271

Standard prolonged work test using treadmill for evaluation of fatigue and stress in man 17 p2863 A66-32150

Target recognition performance, examining relative effect of size and smear or blur of display 17 p2864 A66-32155

Abstract higher mental functioning of human operator during exposure to transverse acceleration stress 17 p2857 A66-32161

Stress in spacecraft crew members measured using parotid fluid, noting relationship between biochemical variables under stress and nonstress conditions 17 p2866 A66-32196

Fluctuations in human acoustic sensitivity after 24 hours in room under effect of Coriolis accelerations of various magnitudes 17 p2861 A66-32941

Exercise performance and cardiovascular response of man exposed for 56 days to oxygen-helium atmosphere 18 p3057 A66-3377

Low friction environment effects on maintenance operations in simulator noting torquing-force capability, hand-eye coordination, etc 18 p3061 A66-3382

Information feedback and psychophysical variables in two-alternative temporal forced choice auditory-signal-detection task 18 p3063 A66-3502

Limits of human performance and interaction of man and machine 19 p3292 A66-361

Total simulation system mass effects on certain human force outputs in tractionless environments 19 p3293 A66-3624

Mathematical evaluation of human visual performance, discussing functions in machine systems, application of TV for systems monitoring, etc 19 p3294 A66-3628

Experiments and model for adaptation of human controllers to sudden changes in plant dynamics in time-invariant situations 20 p3508 A66-3686

Noise effect on human performance 20 p3504 A66-3693

Air ionization effect on vigilance task performance, noting smaller decrement for environment containing negative ions 20 p3504 A66-3693

Human errors in flight safety and need for automation 20 p3508 A66-3693

Critical Human Performance and Evaluation /CHPAE/ Program 20 p3509 A66-3788

Human factor relation to system effectiveness and human performance relation to operational reliability and maintainability 20 p3509 A66-3788

Legibility analysis to investigate effects of scale factors, graduation marks, etc, on speed and accuracy of reading moving target instruments 21 p3701 A66-3942

Human performance analysis based on two criteria, zero and 100 percent legibility of moving targets consisting of black alphanumeric symbols, finding mean angular velocities 21 p3701 A66-3942

Competing visual tasks used in psychological stress testing of special mission personnel 21 p3701 A66-3942

Adaptation to prolonged exposures in revolving space station simulator 22 p3853 A66-3978

Telescope field of view requirements for human recognition of navigation stars 22 p3946 A66-4086

Target conspicuity for predicting level of search performance as function of spatial and temporal variables 22 p3859 A66-4086

Distortion, fill and noise effects on pattern discrimination 23 p4030 A66-4157

Maximum exercise tolerance in health aircrew members limited by cardiac output 24 p4163 A66-4245

### HUMAN REACTION

Human transfer function for pilot response for multiaxis and multiloop problems 02 p0185 A66-1163

Lower body negative pressure used to restore hydration after recumbency diuresis following bed rest 06 p0813 A66-1682

Effects of 9-alpha-fluorohydrocortisone on metabolic changes occurring during six days of bed rest, including water and sodium retention, hematocrit decrease, plasma increase, etc 06 p0813 A66-1682

Measurement of oculogravic illusion in subjects with or without labyrinthine defects, showing validity as specific response to stimulation of otolith organs 06 p0813 A66-1682

Effect of environmental stress on aircrew performance including failure, distraction, fear, discomfort, speed and load and combat conditions 10 p1494 A66-2213

Subgravity tower and axis results obtained on man and animals, discussing transition from acceleration to weightlessness and vice versa 11 p1641 A66-2248

Occipital evoked potential correlated with visual anomaly under stimulus of incoherent succession of randomly patterned optical images 12 p1806 A66-2438

Neuron network model of oculomotor system to understand human eye



- movement 13 p2008 A66-25336
- Psychological testing of military pilots, discussing apprehensiveness under adverse conditions such as bad weather or fatigue 14 p2229 A66-27493
- Environmental parameters affecting spacecrew comfort during weightlessness and optimization of comfort 14 p2231 A66-28412
- Human response to predicted Apollo landing impacts in selected body orientations 15 p2430 A66-28663
- Psychological and physiological reaction to Coriolis effect under artificial gravitational field simulated in rotating space station 15 p2443 A66-28682
- Nervous activity increase, EEG, EKG, gas exchange, respiration, urine, blood pressure, oxygen content and morphological state of humans after prolonged pressure chamber confinement 15 p2443 A66-29444
- Human reaction to simulated landing impact overload, including analysis of EKG, kinetocardiogram, blood pressure and respiration data 15 p2443 A66-29445
- Human physiological and hygienic problems when confined in closed system of circulating biological substances 15 p2443 A66-29457
- Prolonged hypokinesia effect on human resistance to transverse g-forces, detailing respiratory and circulatory systems, motor response and visual acuity 15 p2437 A66-29473
- Lowering of psychic tone, absentmindedness and vigilance decline during astronaut weightlessness on long space flights 15 p2442 A66-30003
- Anticipatory psychological stress determiners include perceived probability of occurrence, proximity and unpleasantness associated with occurrence of threatening event 16 p2640 A66-31130
- Human reaction to pure oxygen inhalation interrupting previous hypoxia 17 p2849 A66-31832
- Windshield scratches and effect on depth perception, visual acuity and fatigue 17 p2862 A66-31833
- Human reaction to sonic boom 17 p2868 A66-33027
- Sonic boom effect on people, noting ground overpressure measurement and data obtained from interviews, formal complaints, building damage, etc 17 p2868 A66-33028
- Sonic bang experience in United Kingdom from supersonic flights and explosive charges, noting intensity, waveform, damage, etc 17 p2868 A66-33029
- Laboratory physiological-psychological responses to impulsive acoustic stimuli and sonic booms from supersonic aircraft 17 p2868 A66-33030
- Change pattern in human cerebral blood flow during time immediately following initiation of carbon dioxide inhalation 18 p3056 A66-33691
- Environmental effects on man, Volume 1 - Symposium on environmental engineering and society, London, April 1966 18 p3062 A66-34201
- Laboratory measurement of psychological, pathological and physiological effects of LF vibration on man 18 p3062 A66-34202
- Consequences of heart-to-foot acceleration gradients on tolerance to positive acceleration determined on variable radius centrifuge 19 p3285 A66-36373
- Primary shift of phase of circadian periodicity effected by time displacement for physiological functions 19 p3285 A66-36374
- Manually imposed angular accelerations during weightlessness period of parabolic flight, obtaining electrooculographic recordings for analyzing nystagmic response 19 p3286 A66-36382
- Square root of time effect on human perception of stimulus pattern unvarying over time 20 p3505 A66-37108
- Induction and suppression of hypothalamic self-stimulation behavior by microinjection of endogenous substances at self-stimulation site 20 p3506 A66-37603
- Spectral analysis of human EEG generators in posterior cerebral regions 20 p3506 A66-37604
- Radiation dose measurements and predictions for space vehicle, noting human response 20 p3665 A66-38352
- Parotid fluid collection technic for determining in-flight biochemical responses for 17-OHCS levels 22 p3854 A66-39791
- Corticosteroid responses to limbic stimulation in man and localization of stimulus sites 22 p3855 A66-40487
- Fracture mechanism of traumatic lesion caused by seat-ejection or bail-out from F-104 G aircraft and worsened by ground impact 22 p3858 A66-40503
- Thresholds, b-wave latencies, stimulus intensity/b wave amplitude relationships and diffuse adaptation effects upon electroretinogram stimulation by light subtending 20 degree visual field 22 p3856 A66-40965
- EEG relation to average evoked potentials and human reaction time to visual stimuli for trials with and without feedback 23 p4029 A66-41550
- Thermal responses of man during rest and exercise in helium oxygen environment for various temperatures 24 p4163 A66-42317
- Reaction time to electrocutaneous stimulation confirmed as being faster to onset than to cessation of stimulation 24 p4163 A66-42318
- Laboratory measurement of psychological, pathological and physiological effects of LF vibration on man 24 p4167 A66-42575
- Physiological disturbances caused by action of prolonged accelerations on human organism, examining methods of increasing maximum g force tolerance levels 24 p4166 A66-43136
- Physiological and biomechanical reactions of humans exposed to action of g forces, examining effects of impact acceleration 24 p4166 A66-43137
- Sensory, motor and vegetative reactions of human organisms under conditions of weightlessness in orbiting spacecraft or aircraft 24 p4166 A66-43138
- HUMAN TOLERANCE**
- Personal thermal conditioning system emphasizing heat exchange between body and environment to provide comfort with water-cooled protective clothing 02 p0188 A66-12012
- Heat stress and minimal dehydration effect upon human tolerance to positive acceleration 03 p0326 A66-12353
- Human tolerance limits in water impact, identifying environmental and trauma characteristics 03 p0327 A66-12356
- Biological stresses of manned space flight in limiting flight duration, noting isolation effect 04 p0469 A66-13507
- Breathing mechanics during transverse acceleration, discussing experiments and measurements made on man 04 p0466 A66-14075
- Human stress reactions to three-day march, sleep deprivation, food and oxygen starvation, noting changes in central nervous system functions 04 p0467 A66-14080
- High noise levels effect on hearing damage of technical personnel of military airfield 04 p0472 A66-14386
- Human response to sinusoidal and random vibrations [ASME PAPER 65-WA/HUF-19] 05 p0625 A66-15693
- Psychophysiological effects of low friction on man, particularly rotation on visual reaction time, heart rate and spatial orientation 06 p0868 A66-16240
- Effects, singly and in combination, of heat, exercise and hypohydration upon voluntary dehydration in four acclimated physically-fit young men 06 p0812 A66-16533
- LF and infrasonic noise effects on mans cardiac rhythm, hearing, vision, motor control, spatial orientation, speech and subjective tolerance 07 p0999 A66-17656
- Hematological and metabolic effects of short intense thermal stress 09 p1334 A66-20523
- Decompression sickness noting caisson and subatmospheric disease effects, symptoms, causes and prevention 10 p1488 A66-22109
- Biological effects of explosive decompression noting parameters such as altitude, pressure differential, compartment volume and rate of pressure loss 10 p1492 A66-22111
- History, design configurations, construction and materials of pressure suits for human protection at high altitudes 10 p1492 A66-22118
- Heat regulation, acclimatization and human tolerance upon exposure to moderate, hot and cold temperatures 10 p1489 A66-22119
- Equipment, techniques and principles of human survival in hostile environment 10 p1493 A66-22121
- Physiological and psychological effects on man during U.S. suborbital and orbital flights from Project Mercury 11 p1642 A66-22483
- Shielding of manned Mars vehicles from solar and galactic cosmic radiation and radiobiological tolerance criteria 13 p2190 A66-25261
- Hypoxemia induced in man by sustained forward acceleration while breathing pure oxygen in five pounds per square inch absolute environment 15 p2430 A66-28659
- Abrupt angular acceleration effect on man, noting physiological responses such as blood pressure, EKG, EEG, cardiovascular, respiratory and nervous reactions, etc 15 p2434 A66-29447
- Resistance to hypoxia by individuals at height of 1650 m trained for high altitude climbing, noting equipment 15 p2435 A66-29449
- Small Coriolis accelerations effect on functional state of human heart 15 p2437 A66-29474
- Physical and biological blast effects from explosive fragmentation of gaseous nitrogen flight pressurized Atlas missile without propellants [AIAA PAPER 65-195] 16 p2810 A66-30897
- Feasibility of oxygen-helium atmosphere at 380 mm Hg total pressure proven by two-week exposure of four men 16 p2639 A66-31120
- Physical conditioning found to have no effect on human tolerance of positive Gs during gradual or rapid onset centrifuge runs 16 p2640 A66-31123
- Dose-equivalent plastic manikin simulates interaction of all types of radiation with human body geometry for space radiation research 16 p2643 A66-31126
- Adaptive responses of adrenal cortex to some environmental stressors, exercise and acceleration 17 p2862 A66-33093
- Human tolerance of short-term transverse seat vibration, noting visual effects 18 p3060 A66-33682
- Clinical findings of effect on man during 56-day exposure to oxygen-helium atmosphere at 258 mm Hg total pressure 18 p3058 A66-33779
- Aviation fatigue noting flight-time limitations, indicators of excessive fatigue, new developments related to international flights and Forest Service flights 19 p3294 A66-36383
- Shielding of manned Mars vehicles from solar and galactic cosmic radiation and radiobiological tolerance criteria 24 p4283 A66-42785
- HUMAN WASTE**
- SA FECES
- SA URINE
- Human water consumption in warm environment examined by linear regression analysis of 22 metabolic variables 13 p2015 A66-26733
- Biological procession of human secretions and water regeneration by Chlorella in bacterial colony 15 p2440 A66-29501
- Human waste nutrient assimilation by Chinese cabbage plants grown in air-moisture medium in closed system 15 p2440 A66-29507
- Indolylacryl glycine excretion in man 16 p2638 A66-30634
- Urinary excretion of 3-methoxy-4-hydroxymandelic acid during dreaming sleep in man 16 p2638 A66-30635
- Microbial profiles of 20 men under simulated space conditions indicates that certain men can go unwashed six weeks 17 p2856 A66-32160
- Human waste products water reclamation systems render space crew independent of stored water requirements [AICE PREPRINT 54A] 17 p2867 A66-32668
- Enteric microbial flora changes in man



exposed 56 days to oxygen-helium atmosphere 18 p3058 A66-33777  
Space diet effect on aerobic and anaerobic microflora of human feces 22 p3854 A66-39796

## HUMIDITY

## SA WATER VAPOR

Interpretation of inverse relationship between long-lasting radioactivity and relative humidity in near-ground layer of atmosphere 02 p0279 A66-11261  
Dependence of vertical structure parameters of atmospheric temperature and humidity fields on atmospheric long-wave radiation field, noting transport equation 04 p0542 A66-14303  
Heat transfer and vaporization factors incorporated in diffusion equations for thermal and humidity fluxes over bodies of water 08 p1247 A66-19306  
Malkevich atmospheric transfer function calculation for Northern Hemisphere in order to correct satellite radiation measurements 09 p1435 A66-19887  
Variations in vertical temperature and humidity profiles used to determine underlying terrestrial surface temperature from outgoing radiation 09 p1398 A66-19888  
Low humidity and dehydration in jet fuselage, noting water metabolism and effect of various beverages 10 p1491 A66-21335  
Heat and humidity transfer effects and turbulent exchange influence on cloud formation 11 p1730 A66-22941  
Differential equations describing air movement, heat exchange and exchange of moisture 11 p1730 A66-22942  
Fields of outgoing radiation in 8-12 micron region, calculating surface temperature and effective water vapor content 11 p1698 A66-22943  
Time and height variations of temperature, wind speed and moisture content during dissipation of low level jet on May 14, 1962 before sunrise near Dallas 11 p1730 A66-23379  
Alpha radiation frost point hygrometer obtains stratosphere moisture profiles [AIAA PAPER 66-368] 12 p1872 A66-24496  
Dependence of vertical structure parameters of atmospheric temperature and humidity fields on atmospheric long-wave radiation field, noting transport equation 14 p2327 A66-28217  
Low atmospheric temperature and humidity changes beneath subsidence inversion above Southern England 15 p2530 A66-28599  
Humidity attenuation in 8 to 13 micron IR window used in radiance measurement from orbiting satellite 15 p2531 A66-28848  
Vacuum spectrometer measurement of absorption band of atmospheric water vapor 15 p2542 A66-29346  
Radiation data measured by Tiros IV satellite for determination of global distribution of atmospheric water vapor 15 p2533 A66-30029  
Solar radiation absorption by atmospheric water vapor, deriving formulas that include scattering and absorption by aerosol as additional parameter 16 p2691 A66-30228  
Atmospheric moisture from balloon radiometer measurements of atmospheric profiles of long wave irradiance [AIAA PAPER 65-461] 16 p2706 A66-30910  
Numerical model of Earth atmosphere used to compute hydro-and thermodynamic evolution of global moist atmosphere, considering solar heating, evaporation, etc 16 p2697 A66-30943  
Radar image edges sharpness relationship to relative humidity near ground 17 p2948 A66-32270  
Spectral composition of direct solar radiation variation with height of Sun and relation between aerosol absorption band and humidity 17 p2994 A66-32857  
Heat transfer and vaporization factors incorporated in diffusion equations for thermal and humidity fluxes over bodies of water 19 p3393 A66-36042  
Vacuum spectrometer measurement of absorption band of atmospheric water vapor 20 p3602 A66-37351  
Heat and humidity transfer effects and turbulent exchange influence on cloud

formation 20 p3593 A66-37854  
Differential equations describing air movement, heat exchange and exchange of moisture 20 p3593 A66-37855  
Fields of outgoing radiation in 8-12 micron region, calculating surface temperature and effective water vapor content 20 p3553 A66-37856  
Temperature automatic control system in photographic laboratory compensating for humidity changes by using semiwet bulb controller 20 p3561 A66-38049  
Sound absorption in air at 1/3-octave frequency intervals as function of humidity and temperature at normal atmospheric pressure for studies in room acoustics 21 p3769 A66-38648  
Vertical motion of moisture fields and saturation deficit determination from nephelanalysis of Tiros cloud photographs for operational quantitative precipitation forecasting /QPF/ 22 p3943 A66-40054  
Short-range weather forecasting based on principles of fluid dynamics 23 p4087 A66-42017

## HUMIDITY MEASUREMENT

## SA HYGROMETER

Vertical temperature and humidity distributions of atmosphere determined from satellite measurements of carbon dioxide and water-vapor absorption bands 09 p1376 A66-20999  
Balloon-borne instrument for measuring downward flux of thermal radiation from atmospheric water vapor, using gold doped germanium detector 11 p1706 A66-22888  
Moisture contamination effects at altitude by package, balloon and associated train 15 p2492 A66-30032  
Morning humidity variation relation to dew content and visibility of atmosphere, noting role of water vapor 19 p3393 A66-35395  
Tiros IV atmospheric IR radiation measurements and application to weather analysis, using quasi-global synoptic maps of troposphere relative humidity 19 p3393 A66-35637  
Absorption and brightness temperature variations of atmosphere on basis of statistical characteristics of vertical temperature and humidity structures 23 p4087 A66-41802  
Temperature and humidity variations in weak convection over England, noting measurement techniques and results 24 p4235 A66-43076

## HUNGARY

Space research in Hungary in 1965 including satellite tracking, ionospheric sounding, solar activity, etc, noting international data transmission 15 p2600 A66-29907

## HUSTLER AIRCRAFT

## S B-58 AIRCRAFT

## HUYGEN PRINCIPLE

Huygens principle in geometrical optics to solve certain time problems in calculus of variations, particularly airplane minimum time [SAE PAPER 650784] 01 p0105 A66-10841  
Computer method calculation of minimum time track, using quasi-optical law of refraction 07 p1066 A66-17681  
Nonsteady radiation field of antenna systems for arbitrary signals via Huygen-Kirchhoff principle 11 p1670 A66-23225  
Misinterpretation of theories of light, noting no clear-cut and simple distinction or opposition between theories of Newton and Huygens 16 p2749 A66-31722  
Improved correlation function in Kirchhoff-Huygen method of solution of scattering of waves from statistically rough surfaces 18 p3068 A66-34015  
Huygen principle for elastic media, comparing Kupradze formulation with formulations of Knopoff and Bollet 24 p4237 A66-42495

## HU2K-1 HELICOPTER

## S UH-2 HELICOPTER

## HYBRID COMBUSTION

Unsteady boundary layer flow of multicomponent gas mixtures, investigating combustion instability in liquid and hybrid rocket motors [AIAA PAPER 65-41] 03 p0444 A66-12796  
Hypergolic ignition and restart in Plexiglas window hybrid rocket motor, including

oxidizer flow transient, flame propagation chamber pressurization rates, etc [AIAA PAPER 66-69] 07 p1111 A66-18441  
Hybrid rocket combustion regression rate and turbulent boundary layer mass transfer 14 p2412 A66-27441

## HYBRID COMPUTER

Hybrid computer simulation system for aeronautical and astronautical test work 02 p0215 A66-11841  
Analog, digital and hybrid computerized systems for investigating problems in aeronautics and astronautics 02 p0193 A66-11841  
Fast analog comparator for hybrid computation using wideband DC amplifier with regenerative feedback circuit providing digital output 03 p0337 A66-12515  
Heuristic approach to reinforcement learning control systems, describing operation and simulation on IBM 1710-GED hybrid computer 06 p0864 A66-16741  
Hybrid computer methodology and electronic data processing applied to quality evaluation of test operations 12 p1828 A66-23841  
Hybrid computer simulation of lunar excursion module and maneuvers with orbiting command service module 12 p1828 A66-23841  
Advances in biomedical computer applications - Conference, N.Y. Academy Sciences, June 1965 12 p1809 A66-24241  
Electrocardiogram interpretation by computer, using pattern recognition approach which permits differentiation between normal and abnormal rhythms 12 p1810 A66-24241  
Deterministic type waveform analysis techniques for noisy repetitive transfer functions, noting application to hybrid computer processing of exercise ECGs 12 p1810 A66-24241  
COBLOC programming system for a digital simulation of operation of large mode-controlled hybrid computers, noting inclusion of patchable logic simulation 13 p2028 A66-25841  
Flight simulation of SST transport using hybrid computer 13 p2028 A66-25841  
System measuring various respiratory parameters using hybrid computer for monitoring and instrumentation 16 p2643 A66-31141  
Hybrid analog/digital techniques for signal processing, noting performance advantage at relatively low cost and applications in linear transformation, function generation, correlation functions, etc 16 p2658 A66-31241  
High speed hybrid computer simulation of aerospace vehicle motion 18 p3094 A66-34041  
Control algorithms synthesis for analytic adaptive control systems with nonlinear plants investigated with hybrid computer 20 p3536 A66-36841  
Multichannel computer controlled Mobile Micrometeorological Observation System automatic data acquisition, processing and recording system for observational analysis of turbulence of atmospheric boundary layer 22 p3943 A66-40441  
Flight simulation laboratory layout and construction using hybrid computer system noting cost estimation 23 p4052 A66-41141  
Pontryagin maximum principle applied to solution of optimal control problems with hybrid computer, using digital parameter optimizer to solve two-point boundary value problem 23 p4042 A66-41641

## HYBRID PROPELLANT

Hybrid fuel regression rate, discussing oxidizer flow rate and burner pressure interdependence [AIAA PAPER 66-113] 06 p0941 A66-16441  
Data on combustion of pyrolyzing solids applicable to combustion chambers of hybrid propulsion devices, placing emphasis on coal 07 p1154 A66-18041  
Hybrid rocket engine performance noting stable fuel burning, burning rate, thrust modulation, ignition delay and use of tricomponent fuels 10 p1594 A66-21741  
Tagaform synthetic hypergolic fuel for hybrid rockets, discussing polymerization ignition delay, etc 11 p1760 A66-22241  
Plane shock wave compressions cylindrical and wedge-shaped specimens used to obtain shock Hugoniot of two



reacted, composite and double-base  
 unimized propellants 12 p1934 A66-23589  
 Swedish hypergolic propellant for rocket  
 motors consisting of fuming nitric acid as  
 oxidizer and condensation product of liquid  
 aromatic amines and aldehydes as solid  
 fuel 14 p2374 A66-27566  
 Regression rates of metalized hybrid fuel  
 systems applied to lithium hydride butyl  
 rubber-fluorine-oxygen system, oxidizer  
 flow, etc 15 p2569 A66-29289  
 Combustion of solid or hybrid propellants  
 with one or more solid phases, noting  
 properties, erosive and hybrid combustion,  
 etc 18 p3165 A66-35240  
 Laplace transform analysis of solid or  
 hybrid propellant ignition by exothermic  
 heterogeneous reactions in presence of  
 radiant energy flux 21 p3806 A66-38688  
 Regression rate for gas-solid hybrid motor  
 described by convective heat transfer  
 feedback mechanism through laminar  
 boundary layer  
 [ASME PREPRINT 34B] 22 p3970 A66-39876  
**HYBRID PROPULSION**  
 Hybrid propulsion application to advanced  
 missions covering fuel consumption,  
 combustion efficiency and throttling  
 performance  
 [AIAA PAPER 64-226] 03 p0415 A66-12748  
 Hybrid type two- or three-stage aerospace  
 vehicle design to place payload in orbit,  
 discussing recoverable stages, drives and air  
 breathing engines 16 p2635 A66-31682  
**HYBRID ROCKET**  
 Hybrid rocket motor HR 4, using fuming  
 nitric acid as oxidizer and mixture of  
 polyesters and acrylic plastics as other solid  
 propellant 12 p1935 A66-23867  
 Experimental analysis of regression rates  
 of hybrid rocket engines for both chemical  
 kinetics and gas dynamics  
 13 p2173 A66-26369  
 Internal ballistic considerations in hybrid  
 rocket design, noting throttling and regimes  
 of operation involving effects of surface- or  
 gas-phase reaction kinetics  
 [AIAA PAPER 66-628] 20 p3663 A66-38035  
 Hybrid rocket combustion mechanism,  
 burning rate, mass transfer coefficient,  
 throttling effects and grain design  
 [ASME PREPRINT 34C] 22 p3970 A66-39877  
 Combustion and performance  
 characteristics of lithium aluminum  
 hydride/hydrogen peroxide hybrid rocket  
 [ASME PREPRINT 34D] 22 p3969 A66-39878  
 HR-4 research engine development and  
 hybrid engine in terms of construction and  
 variable thrust, noting polymerized amino  
 acid compound fuel 23 p4121 A66-41170  
 Ablation velocity, rocket motor working  
 conditions and combustion instabilities for  
 hybrid rockets, using solid fuel and liquid  
 or gaseous oxidizer 24 p4261 A66-42695  
**HYDRATE**  
 OH production by sublimation and gas  
 hydrate occurrence in cometary  
 nuclei 17 p3009 A66-33373  
**HYDRATION**  
**WATER DEHYDRATION**  
 Lower body negative pressure used to  
 restore hydration after recumbency diuresis  
 following bed rest 06 p0813 A66-16823  
 Effects of 9-alpha-fluorohydrocortisone on  
 metabolic changes occurring during six days  
 of bed rest, including water and sodium  
 retention, hematocrit decrease, plasma  
 increase, etc 06 p0813 A66-16824  
**HYDRAULIC ACTUATOR**  
 Balanced power concept for weight savings  
 in aircraft actuation system consisting of  
 mechanically actuated flight control surface,  
 mechanical servo, flywheel and  
 motor 01 p0015 A66-10670  
 Pressure peaks in hydraulic actuator  
 inertia load aggravated in presence of valve  
 overlap, noting cavitation damage  
 [ASME PAPER 65-FE-4] 06 p0808 A66-16213  
 Self-oscillating hydraulic vibration  
 apparatus capable of generating high cyclic  
 actuating power for testing  
 purposes 07 p1147 A66-18389  
 Transient response of valve-controlled  
 actuator with inertial loading to step input  
 excitation, considering fluid  
 compressibility 11 p1640 A66-22622  
 Electrohydraulic digital actuator design and  
 conversion of discrete electric input signal

in binary code to linear  
 motion 14 p2227 A66-28366  
 Main parameters of two-stage hydraulic  
 amplifier-actuator system determined with  
 aid of pressure and flow-rate amplification  
 factors 23 p4017 A66-40970  
**HYDRAULIC ANALOGY**  
 Hydraulic analogy experiments at optimum  
 depths obtained analytically, noting surface  
 waves in liquid 02 p0217 A66-11555  
 Aerodynamic spacecraft deceleration  
 systems examined by hydraulic analogy,  
 noting Mach number effects on flow  
 disturbances 04 p0507 A66-13533  
 Hydraulic analogy to compressible gas flow,  
 discussing application to aerodynamic  
 motions, flow visualization, measuring  
 techniques and instrumentation  
 [ASME PAPER 66-FE-16] 17 p2915 A66-33269  
 Theoretical and physical limitations  
 restricting hydraulic analogy to compressible  
 gas flow  
 [ASME PAPER 66-FE-17] 17 p2915 A66-33270  
 Hydraulic analogy methods for simulation  
 of internal gas flows containing combination  
 zone 22 p3901 A66-40500  
**HYDRAULIC CONTROL**  
**SA ELECTROHYDRAULIC CONTROL**  
 Feasibility of pure-fluid missile control  
 system demonstrated by systems analyses,  
 preflight tests and flight  
 tests 01 p0140 A66-10020  
 Research and development progress toward  
 synthesis of pure fluid flight control  
 system 01 p0140 A66-10021  
 Two-axis fluid control system for artillery  
 type missile performs best with spinning  
 attitude system when wind and thrust  
 misalignment disturbances are  
 considered 01 p0140 A66-10022  
 Hydraulic gear motor and gear backlash  
 effects on stability of hydraulic control  
 system 01 p0014 A66-10282  
 Operating characteristics of torque motors  
 and application to actuating pneumatic and  
 hydraulic control  
 mechanisms 03 p0323 A66-12906  
 Four-way fluid state vortex hydraulic  
 servovalve discussing design principles,  
 performance and  
 application 04 p0460 A66-13785  
 Leakage detection system for monitoring  
 component test stand hydraulic  
 circuit 06 p0869 A66-16792  
 Altitude control for VTOL aircraft  
 facilitates control of hovering flight, noting  
 construction, operation principles and  
 performance 10 p1484 A66-21379  
 Hydraulic servocontrol system performance  
 improvement by eliminating turbulent flow  
 and regulating servomotor pressure  
 drop 13 p1997 A66-25130  
 Dynamic law for pressure variation in  
 throttle chamber of hydraulic control  
 booster, taking into account fluid  
 compressibility and change in discharge  
 coefficient 16 p2637 A66-31219  
 Large tracking antenna opposed torque  
 pump motor analysis 18 p3055 A66-34294  
 Electric or hydraulic drives for steerable  
 satellite trackers and heightfinder  
 radars 18 p3055 A66-34317  
 Variable fluid-transformer control of fluid  
 flow in increasing efficiency of hydraulic  
 control systems 19 p3281 A66-36671  
 Fluidics problems involved in design and  
 manufacturing individual elements and  
 power consumption  
 reduction 21 p3697 A66-38967  
 Control valve seat leakage as function of  
 fluid viscosity, density, pressure drop and  
 cube function of gap between two  
 surfaces 23 p4017 A66-41145  
**HYDRAULIC EQUIPMENT**  
 Closed loop hydraulic servo system  
 simulating flight stresses on motor case of  
 solid propellant rocket motor in static firing  
 test stand for calibrating  
 stand 03 p0353 A66-13218  
 XB-70 fluid power ground support system,  
 describing functions of hydraulic ground  
 power unit, fluid servicing trailer and  
 filtration cart 06 p0869 A66-16791  
 XB-70 landing gear inspection, describing  
 hydraulic jack used 06 p0869 A66-16793  
 Cavitation in fluid machinery - ASME  
 Symposium, Chicago, November  
 1965 07 p1024 A66-18166

Miniature hydraulic power  
 units 08 p1174 A66-19808  
 Hydraulic and pneumatic power equipment  
 for ground support of space vehicles and  
 support in space environment  
 [AIAA PAPER 65-524] 12 p1804 A66-24717  
 Extremal values of stress resulting from  
 fluctuating pressure in hydraulic  
 cylinder 13 p2196 A66-25757  
 Closed loop hydraulic high-speed universal  
 testing machine and simulation of high  
 strain rate conditions 13 p2197 A66-26108  
 Pressure in sealing groove and increase  
 time due to pumping action of moving wall  
 applied to force cylinder of translational  
 motion, considering liquid in groove  
 laminar 14 p2225 A66-27688  
 Oscillation amplitude of rotor with  
 hydraulic dampers on elastic  
 supports 14 p2374 A66-27689  
 Basic properties of pure fluid devices  
 including operating pressure, operating  
 power and response time 20 p3500 A66-37644  
 Flow velocity effect on thermometer  
 reading and consequences for measuring  
 thermodynamic efficiency of hydraulic  
 machines 21 p3737 A66-38935  
**HYDRAULIC FLUID**  
**SA OIL**  
 Fluids and elastomers for low temperature  
 heat transfer and hydraulic systems  
 [ASLE PREPRINT 65-LC-7] 02 p0249 A66-12256  
 Comparison of rheological properties and  
 fire resistance of hydraulic fluids for  
 aerospace vehicles  
 [ASLE PREPRINT 65-LC-6] 02 p0249 A66-12257  
 High temperature fluids, designated PR-  
 143, suitable for hydraulic systems in range  
 -50 to 700 degrees F  
 [ASLE PREPRINT 65-LC-3] 02 p0238 A66-12258  
 Canned motor pump for nitrogen tetroxide  
 or hazardous liquids, noting ball bearings,  
 chemical materials, balancing drum and  
 helium leak tested motor parts  
 [ASME PAPER 65-WA/FE-3] 05 p0691 A66-15715  
 Fire resistant hydraulic fluids for  
 commercial and military application  
 including siloxanes, silicones, esters and  
 superrefined mineral oil  
 [ASME PAPER 64-WA/LUB-14] 10 p1547 A66-21171  
 High temperature fluids, designated PR-  
 143, suitable for hydraulic systems in range  
 minus 50 to 700 degrees F  
 [ASLE PREPRINT 65-LC-3] 12 p1889 A66-24988  
 Comparison of rheological properties and  
 fire resistance of hydraulic fluids for  
 aerospace vehicles  
 [ASLE PREPRINT 65-LC-6] 12 p1901 A66-24991  
 Fluids and elastomers for low temperature  
 heat transfer and hydraulic systems  
 [ASLE PREPRINT 65-LC-7] 12 p1901 A66-24992  
 Contamination control methods used in  
 Royal Swedish Air Force, presenting special  
 particle counting and patch test methods in  
 hydraulic oils 17 p2870 A66-32204  
 Method and equipment effects on shear  
 stability measurements of hydraulic oils,  
 using mechanical and sonic  
 methods 17 p2943 A66-32830  
 Contamination, viscosity, shear stability,  
 breakdown and foaming of MIL-H-5606  
 hydraulic fluid and swelling effect on  
 synthetic rubber 18 p3125 A66-34652  
 Criteria for hydraulic fluids for supersonic  
 aircraft noting fluid toxicity, fire hazards,  
 compatibility with elastomeric materials,  
 etc 24 p4229 A66-42380  
 Synthetic fire-resistant hydraulic fluids  
 based on phosphate esters must be provided  
 with continuous removal of dissociation  
 products for constant regeneration and  
 protection of unaltered fluid from  
 accelerated  
 decomposition 24 p4229 A66-42509  
**HYDRAULIC PUMP**  
 Measurement of friction of materials  
 sliding in JP-4 fluid to predict performance  
 of hydraulic pump 06 p0884 A66-16136  
 Hydraulic performance and sensitivity of  
 various configurations of centrifugal pumps



- to tip clearance effects  
[ASME PAPER 64-WA/FE-17] 06 p0884 A66-16211
- SST aircraft fluid power systems and performance, discussing power requirements, materials, maintenance, configuration, surface temperature distribution, etc [ASME PAPER 66-MD-35] 21 p3697 A66-38487
- Backstreamed fluid analysis via gas chromatography, using polyphenyl ether as diffusion pump fluid 24 p4239 A66-43164
- HYDRAULIC SHOCK**  
Shallow water theory of formation and decay of hydraulic shock waves in nonsteady homentropic gas flow 23 p4055 A66-41541
- HYDRAULIC SYSTEM**  
**SA AIRCRAFT HYDRAULIC SYSTEM**  
High dosage nuclear radiation tests of hydraulic systems and components for space vehicle use 01 p0014 A66-10113  
Proportional pneumatic actuation system reliability using variable hydraulic damping, noting role of error and error rate signal 03 p0324 A66-13219  
Resonant characteristics of hydraulic systems, particularly water or oil-supply lines, using impedance approach [ASME PAPER 65-FE-6] 06 p0885 A66-16214  
XB-70 hydraulic system, describing characteristics, operation-mechanism of fluid power system, power generation, utilization and distribution 06 p0809 A66-16790  
Hytrol electronic/hydraulic antiskid braking system for automatic braking pressure modulation in BAC one-eleven 400 series aircraft 07 p0992 A66-18165  
Auxiliary turbine power generator using gas from solid propellant 09 p1333 A66-20331  
Flow properties of fluid through slots of micron dimension 09 p1384 A66-20752  
Pressure surges, surge accumulators and relief valves studied on Titan I launch vehicle simulator 13 p2056 A66-25131  
Hydraulic system supporting Apollo/Saturn V space vehicle tested to determine bending and flexuring in flight 14 p2226 A66-28031  
Nitrogen powered hydraulic attitude control system of Little Joe II solid propellant launch vehicle for flight testing escape mechanism used on Apollo 20 p3499 A66-37314  
Hydraulic support system for free-flight simulation with Saturn V-Apollo vehicle, discussing stability requirements, upper bounds of system design, conversion from nonlinear to linear model, etc 21 p3722 A66-38876  
NaK-77 suitability for 1000-F liquid-metal hydraulic flight control systems 22 p3852 A66-40498  
Three-term governor for gas turbine engine system, examining effect of internally generated pressure noise on performance of different possible hydraulic systems 22 p3972 A66-40513  
Selection of size of hydraulic servometer with rotary hydraulic motor controlled by electrohydraulic spool valve to reduce open-loop gain for given closed-loop stiffness 22 p3852 A66-40515  
Hydraulic loss decrease in complex pipeline owing to wire grating 23 p4024 A66-41798
- HYDRAULIC VALVE**  
Control mechanisms in nonlinear steady flow forces of hydraulic valves [ASME PAPER 65-WA/AUT-20] 05 p0624 A66-15616  
Series analysis of closed-loop system containing loaded hydraulic valve, with equations of motion and response of system to ramp input and Coulomb load 06 p0810 A66-16915  
Multiple quick-disconnect valve used in auxiliary power unit /APU/ of aircraft and serving several systems at once while preventing fluid leakage from one system to another 14 p2226 A66-28032
- HYDRAULICS**  
**SA FLUID MECHANICS**  
Hydraulic jump as plane turbulent wall jet under adverse pressure gradient and finite depth of flow 01 p0056 A66-10314  
Mechanical strength of plastic buckling of sheet metals under lateral hydraulic loads 15 p2510 A66-29778  
Fluid power, Reference
- issue 23 p4018 A66-41715
- HYDRAZINE**  
**SA DIMETHYL HYDRAZINE**  
**SA TETRAFLUOROHYDRAZINE**  
Machine computation of thermodynamic properties of hydrazine from 32 degrees F to 1.02 times critical density 03 p0414 A66-12760  
Electron paramagnetic resonance in biradicals of hydrazine series, discussing structural changes during transition from mono- to biradical state 04 p0572 A66-13877  
Toxicological effect of hydrazine and monomethylhydrazine in blood serum of rats 05 p0626 A66-14642  
Immiscibility and rapid interface reaction rate as cause of disruption in nitrogen tetroxide-hydrazine impinging jets [CI PAPER WSCI-65-20] 05 p0743 A66-15145  
Droplet combustion fronts in hydrazine-nitrogen tetroxide system determined from kinetics of vapor decomposition, noting two-flame front model 05 p0743 A66-15146  
Discrepancy between measured value of N-H bond dissociation energy in hydrazine and value suggested by other chemical evidence 07 p1000 A66-17463  
Electrolyte-soluble fuels such as methanol, ammonia and hydrazine, noting electrochemical oxidation properties, power output, stored energy content, etc 07 p0996 A66-18472  
Application perspectives for dissolved fuel cells, particularly methanol and hydrazine cells 11 p1639 A66-22242  
Hydrazine hydrate interaction with halogenides of tetravalent germanium in aqueous organic solvents 14 p2231 A66-27137  
Combustion of hydrazine droplets burning in hydrazine vapor investigated via suspended droplet technique [AIAA PAPER 65-355] 14 p2370 A66-27413  
Liquid hydrazine decomposition process to determine what chemical or physical changes may be occurring that cause breaks in burning rate/ pressure curves, measuring flame temperature and light emission 15 p2570 A66-29610  
Increase of arterial lactate and pyruvate in blood glucose of fasted anesthetized dog after hydrazine injection 17 p2856 A66-32157  
Calorimetric study of effects of hydrazine on heat balance, source of metabolic energy and rate of protein catabolism of rats 17 p2856 A66-32158  
Toxic effects of hydrazine derivatives tested in dogs, producing methemoglobin and pigmentation in blood 17 p2856 A66-32159  
Effect of 0.6 LD/50 intraperitoneal dose of hydrazine on coagulation mechanism in rats, comparing results with saline injected controls 17 p2857 A66-32167  
Hydrazine/nitrogen tetroxide propellant system, examining reaction mechanisms at rocket chamber conditions [AIAA PAPER 66-662] 18 p3160 A66-34223  
Vibrational spectrum of liquid, solid and gaseous tetradeuterated hydrazine and Raman study of hydrogen bonding in hydrazine 19 p3295 A66-36801  
Reaction rates of decomposition burning of small spheres of liquid hydrazine 20 p3626 A66-38043  
Molecular elimination of nitrogen from hydrazine from single molecule and not radical-radical combination 21 p3806 A66-38531  
PAH transport mechanism in dogs with hydrazine-depressed para-aminohippurate treated with acetate, 6,8-epidithioctanate and 6,8-epidithioctanoamide 22 p3854 A66-39795  
Ultimate energy achievable in propellants, evaluating oxidizing group as propellant with model fuel, hydrazine 23 p4116 A66-41219
- HYDRAZINE PERCHLORATE**  
T-burner tests for combustion stability evaluation of hydrazine diperchlorate [AIAA PAPER 66-599] 18 p3264 A66-34430  
Deflagration of hydrazine perchlorate in pure state and with fuel and catalyst additives 23 p4117 A66-41225  
Manometric measurement of pressure rise as measure of formation rate of volatile products of thermal decomposition of hydrazinium monoperchlorate and
- hydrazinium diperchlorate 23 p4117 A66-41225
- HYDRIDE**  
**SA ALUMINUM HYDRIDE**  
**SA ANHYDRIDE**  
**SA BORON HYDRIDE**  
**SA LITHIUM HYDRIDE**  
**SA NITROGEN HYDRIDE**  
**SA ZIRCONIUM HYDRIDE**  
Schlesinger reaction and chemical composition of mixed hydride reagents 11 p1649 A66-22242  
Comparative calculation used in computation of physicochemical properties of hydrides, including densities of beryllium hydride, entropy of cesium hydride, crystal lattice energy of rubidium deuteride, etc 13 p2018 A66-26262  
Temperature and structure effect on hydride precipitation kinetics in titanium using resistometric technique, noting nucleation problem 16 p2724 A66-31316
- HYDROCARBON**  
**SA CYCLIC HYDROCARBON**  
Ball bearing lubrication with vapor from volatile organic compounds for wide temperature range and long term operation [ASLE PREPRINT 65-LC-24] 02 p0237 A66-12237  
Physical properties of new class lubricants, methyl alkyl silicones, illustrating exceptional lubricating ability [ASLE PREPRINT 65-LC-4] 02 p0238 A66-12238  
Potential parameters used to calculate thermophysical characteristics of solid hydrocarbons at high temperatures 03 p0330 A66-12230  
Hydrocarbons synthesized abiotically, those found in terrestrial samples, using chromatography and mass spectrometry connection with terrestrial life 12 p1806 A66-24246  
Physical properties of new class lubricants, methyl alkyl silicones, illustrating exceptional lubricating ability [ASLE PREPRINT 65-LC-4] 12 p1889 A66-24249  
Thermal decomposition of tert-butyl hydroperoxide with oxygen and acetone addition studied by isotopic tracer 13 p2017 A66-26267  
Proton transfer between hydrogen methane, ethane, propane and butanes, using high-pressure mass spectrometry, employing ion source with beta rays as ionization medium 13 p2018 A66-26268  
Photoionization of leucocarbinoles, leucocyanides of malachite green, crystal violet and sunset orange dissolved straight chain alcohols and chlorinated hydrocarbons 14 p2232 A66-27138  
Thermal degradation of mesoporphy, obtaining various alkylpyrroles and hydrocarbons, noting role of controlled pyrolysis as adjunct to mass spectrometry 15 p2446 A66-28046  
Five halogenated hydrocarbons and effect on flame speed of methane 17 p3032 A66-31312  
Electron transfer from alkali metals aromatic hydrocarbons, examining rate of chain scission in case of poly(4-vinyl biphenyl) and poly(alpha-methyl naphthalene) 17 p2870 A66-32160  
Direct and indirect oxidation fuel systems operating on hydrocarbon-mixtures and using aqueous, molten solid electrolytes, noting technological economic problems 18 p3053 A66-33333  
Paraffinic hydrocarbons composition Orgeuil, Murray, Mokola and other meteorites identified by gas chromatography 19 p3459 A66-35359  
Potential parameters used to calculate thermophysical characteristics of solid hydrocarbons at high temperatures 19 p3295 A66-36801  
Morse potential function determined from viscosity and second virial coefficient, used to approximate pair interaction potential hydrocarbons 20 p3605 A66-37055  
Distance/time records, drag coefficient and Reynolds numbers of single free falling drops of pentane, heptane, benzene burning in cold atmosphere 20 p3626 A66-38043  
Pyrolytic graphite production by thermal decomposition of hydrocarbon gas on heated



surface, noting annealing, alloying and residual stresses  
[ASME PAPER 66-MD-54] 21 p3753 A66-38493

Rate constants for atomic and molecular hydrogen ion transfer from tri- and tetra-atomic carbon paraffins to propylene and cyclopropane molecular ions 22 p3861 A66-40905

Aromatic hydrocarbon synthesis by passing ethane through silica gel at high temperature 23 p4032 A66-41306

Compressibility factor chart for hydrocarbon-hydrogen and nitrogen-hydrogen gas mixtures, correlating pressure and temperature, using state equation 23 p4150 A66-41866

Column chromatography used to determine hydrocarbons present in Moonie crude oil from Queensland, Australia, that is two hundred million years old 24 p4170 A66-43024

**HYDROCARBON COMBUSTION**

Rarefied hydrogen flame interaction between hydrogen atoms and molecules of certain organic, aliphatic and cyclic compounds 01 p0101 A66-10414

Behavior of excess radical concentrations, H, OH and O as function of height above reaction zone in premixed acetylene-air flames 03 p0414 A66-12488

Chemical kinetics of nonequilibrium combustion of propane-air and ethane-air mixtures in one-dimensional flow, including ignition delay and reaction time [ASME PAPER WSCI-65-19] 05 p0788 A66-15143

Equilibrium combustion products of generalized hydrocarbons with oxygenated air, with charts on enthalpy, entropy, molecular weight, specific heat ratio, etc [ASME PAPER 65-WA/ENER-2] 05 p0789 A66-15627

Ignition of hydrogen-oxygen-argon mixtures containing small amounts of hydrocarbons and bromine substituted hydrocarbons in shock tubes 06 p0822 A66-16634

Catalytic dehydrogenation of hydrocarbons over chromia-alumina catalyst in absence of added hydrogen to determine heat sink capability 11 p1650 A66-23119

Calorimeter bomb combustion of hydrocarbons and fluoro-substituted hydrocarbons with nitrogen trifluoride and nitrogen trifluoride-oxygen mixtures and mass spectrometric analysis 15 p2570 A66-29609

Cometary and hydrocarbon flame spectra compared, discussing Swan, HCO and other band systems 17 p3013 A66-33404

Heat transfer caused by combustion of triethylaluminum on flat plate in Mach 3 flow, noting significance of lag at stagnation pressure 18 p3260 A66-33817

Plasma behavior in laminar and turbulent hydrocarbon-air flames, discussing flame ionization, electron concentration and recombination, detonation wave ionization data, ignition, etc 18 p3143 A66-34027

Overall structure of combustion process in jet flow of hydrocarbon-air mixtures stressing conditions for ramjet engines, noting flame propagation angles, flow computation, etc [AIAA PAPER 66-573] 18 p3264 A66-34444

Chemical-ionization in reaction zones of hydrocarbon-oxygen or hydrocarbon air flames, noting association with abnormal excitation of hydroxyl radical 20 p3626 A66-38046

**HYDROCARBON FUEL**

Lead oxides formed from tetraethyl lead (TEL) in combustion zone identified in analysis of antiknock properties 03 p0413 A66-12486

Flammability hazards of aircraft hydrocarbon fuels as function of temperature and pressure based on equilibrium conditions [AIAA PAPER 65-801] 03 p0414 A66-12565

Hypergolic ignition of light hydrocarbon fuels with fluorine-oxygen (flox) mixtures [ASME PAPER WSCI-65-23] 05 p0743 A66-15147

Introduction to fuel cells 07 p0995 A66-18467

Fuel cells oxidizing saturated and unsaturated hydrocarbons at high temperatures 07 p0996 A66-18475

Prediction of failure behavior in composite hydrocarbon fuel binder propellants

[AIAA PAPER 65-156] 10 p1590 A66-21946

Thermal stability of endothermic hydrocarbon heat-sink fuels, noting application flying in 10 Mach speed range 11 p1759 A66-23124

Shock tube ignition delay study of aircraft engine cooling by hydrocarbon fuels in endothermic heat sinks [AIAA PAPER 65-594] 12 p1934 A66-23588

Engineering problems in design of fuel cell systems including complicated duty cycles, response time, high power density and efficiency [AIAA PAPER 64-743] 13 p2007 A66-26645

Increasing solubility of hydrocarbons in cesium-salt fuel cell electrolyte by replacing some of carbonate anion by fluoride 14 p2226 A66-27898

Flox-light hydrocarbon combinations desirable as liquid rocket propellants due to high specific impulse, hypergolicity and cooling properties [AIAA PAPER 66-581] 18 p3159 A66-33809

**HYDROCHLORIC ACID**

Biological content of 17 known specimens of type I and type II meteorites, noting indigenous objects are mineralized with limonite and contain residues insoluble in hydrochloric and hydrofluoric acid 24 p4275 A66-42655

**HYDRODYNAMIC EQUATION**

Nonuniqueness and low stability of solutions to hydromechanical problems demonstrated by steady motion of viscous fluid 01 p0055 A66-10168

Nonlinear equations of atmospheric hydrodynamics solved, using numerical algorithm 01 p0096 A66-10751

Hydrodynamic equations for one-dimensional, adiabatic, frictionless, ideal-gas flow and general matrix form equations for coupled chemical reaction kinetics of C-H-O/N systems 02 p0303 A66-11533

Derivation of asymptotic form of Green function, using hydrodynamic approximation method 04 p0510 A66-13875

Hydrodynamic systems expressed by kinetic equations, deriving equations of aerodynamics without knowledge of interaction of gas molecules 04 p0510 A66-13879

Spectral dynamics of laminar convection, discussing transformation of Benard convection problem into spectral domain 04 p0599 A66-14472

Short-term weather forecasting equation solved exactly 06 p0904 A66-16233

Interaction between circular waves and density fluctuation in cold electron plasma filling waveguide leads to formation of overtones of HF and LF 06 p0918 A66-16869

Derivability of cosmological equations from first law of thermodynamics and hydrodynamics equations, without using general relativity 07 p1132 A66-17207

Short-range forecasting of baric and kinematic atmospheric fields from complete system of thermohydrodynamic equations 07 p1062 A66-17918

Wave reflection and refraction across density discontinuity in two-fluid fully ionized plasma studied by coupled linearized hydrodynamic equations and Maxwell equations 07 p1088 A66-17948

Simple waves in one-dimensional nonsteady nonmagnetic relaxation hydrodynamic flows of chemically reacting compressible gases 07 p1020 A66-17965

Dissipative effects in converging cylindrical symmetric shock wave, considering ion and electron heat conductivity, ion viscosity and energy exchange 07 p1025 A66-18180

Uniform motion of vortex system in inviscid fluid, examining effect of compressibility on motion of vortex singularities 08 p1204 A66-18528

Integral form of fluid dynamic conservation equations relative to arbitrarily moving volume 08 p1205 A66-18677

Approximation method of calculating axisymmetric oscillations of shells of revolution filled with liquid 08 p1308 A66-18891

Neutral disparate mass mixtures, replacing Boltzmann collision integrals by relaxation-type kinetic models with model equation terms ordered according to mass ratio, deriving two-fluid transport

equations 10 p1523 A66-21802

Hydrodynamic problem of nonviscous liquid flow past two spheres solved, using new method of solution 10 p1525 A66-21919

Hydrodynamic equations describing strongly rarefied collisionless plasma 10 p1572 A66-22035

Radiation effect on hydrodynamic shock wave parameter distribution for bodies entering dense atmospheric layers at supersonic velocities 11 p1635 A66-23051

Mechanical flow processes and variational methods based on fluctuation theory, noting relations on minimum entropy production, two-dimensional laminar flow of incompressible fluid, etc 12 p1975 A66-23543

Short-range forecasting of baric and kinematic atmospheric fields from complete system of thermohydrodynamic equations 12 p1905 A66-23879

Statistical derivation of linear viscoelastic equations, relating stresses to minor deformation 12 p1969 A66-24355

Exact solutions for triple wave type hydrodynamic equations for confined isothermal gas flow and polytropic gas efflux into vacuum 12 p1863 A66-24360

Velocity field excitation due to thin wing motion in vicinity of finite length pressure wave with variable gas parameters 12 p1797 A66-24431

Liquid film flow stability, considering two-dimensional perturbations, hydrodynamic friction with allowance for finite curvature radius of bounding surface 12 p1864 A66-24435

Factors connected with atmospheric dynamic processes, applying hydrodynamic equations to wind field and pressure field variations 12 p1909 A66-24786

Hydrodynamic equation for ideal compressible fluid in case of steady three-dimensional vortex motion solved via two second order PDEs 12 p1865 A66-24867

Rarefied gas flow problems solved by hydrodynamic equations and representations of stress tensor and heat flux reproducing Navier-Stokes continuum limit and free molecule limit, noting velocity distribution interpolation 13 p2061 A66-25163

Zhukovskii and Lagally theorems for arbitrary fluid motion derivable from momentum equations of continuous medium 13 p2067 A66-26533

Equations from hydrodynamic equations, determining steady state fields and currents in plasma caused by microwave field, using quasi-linear approximation 14 p2341 A66-27153

Hydrodynamic systems expressed by kinetic equations, deriving equations of aerodynamics without knowledge of interaction of gas molecules 14 p2275 A66-27569

Derivation of asymptotic form of Green function, using hydrodynamic approximation method 14 p2275 A66-27578

Nonlinear equations of atmospheric hydrodynamics solved, using numerical algorithm 14 p2285 A66-27850

MHD approximation of solar plasma fluxes observed by Mariner II as free rotating jets 15 p2574 A66-29077

Characteristic for partially invariant solutions of hydrodynamic equations, specifically adiabatic plane-parallel gas motion 15 p2478 A66-29177

Shock wave strengthening of metals studied by hydrodynamic conservation equations, noting microstructure changes 16 p2723 A66-30318

Statistical analysis of solar atmospheric motion, noting three dimensional geometry of subjacent turbulent convection 16 p2803 A66-31257

Laminar steady motion transition to turbulent flow in systems described by hydrodynamic equations, including small amplitude steady periodic motion analysis 16 p2689 A66-31512

Book on jet theory in ideal fluids, covering compressible flow, steady jet flow, infinite flow past polygonal obstacle, unsteady flow, etc 16 p2632 A66-31746

Stability of weakly ionized plasma in strong electric field against formation of longitudinal waves, examining hydrodynamic equations 17 p2970 A66-32715



Stationary boundary value problem of Navier-Stokes equation for incompressible viscous fluids 17 p2911 A66-32817

Hydrodynamic and thermodynamic equations for biennial variations of zonal atmospheric circulation in equatorial area 19 p3346 A66-35640

Apparent additive mass coefficient for three-dimensional hydrodynamic impact problem of floating sphere in incompressible fluid 20 p3548 A66-38117

Internal atmospheric gravity waves in isothermal medium, solving hydrodynamic equations, determining wave propagation in realistic atmosphere for range of wave parameters, wind amplitude, reflected energy, etc 20 p3554 A66-38202

False reflection of computational mode waves at boundary due to use of finite differences 21 p3759 A66-39207

Hydrodynamic equations derived for classical multicomponent ideal fluid, using expansions in small parameter  $\mu$  21 p3728 A66-39297

Hydrodynamic equations for liquid with intrinsic rotation applicable to suspensions and liquid/vapor systems 21 p3728 A66-39312

Stress velocities and numbers and use in hydrodynamic distorted and undistorted models 22 p3897 A66-39674

Shock wave propagation in plasma across magnetic field, solving problem via two-component hydrodynamic equation 22 p3953 A66-39765

Hydrodynamic equation for ideal compressible fluid in case of steady three-dimensional vortex motion solved via two second order PDEs 22 p3899 A66-40328

Planar and rotary sloshing motion of liquid, using analytic mechanical model that consists of mass point constraint to parabolic surface 22 p3993 A66-40361

Nonsymmetric oscillations in plasma in magnetic field arising from electron beam passage through plasma, deriving dispersion equation 22 p3958 A66-40939

Kinetic equations in hydrodynamic approximation for weakly reacting and excited Bose systems, finding asymptotic expressions for Green function 23 p4055 A66-41412

Higher order corrections to Chew-Goldberger-Low theory, with attention to Vlasov equation 23 p4103 A66-41487

Four-plasmon hydrodynamic equations describing weak turbulence spectrum in universal equilibrium region of plasma without magnetic field 24 p4243 A66-42532

Equations from hydrodynamic equations, determining steady state fields and currents in plasma caused by microwave field, using quasi-linear approximation 24 p4244 A66-42973

**HYDRODYNAMIC STABILITY**

Stability of rod clamped at one end and situated in parallel fluid flow, considering head resistance and lateral forces 01 p0007 A66-10736

Disruption of thin liquid film flowing over heating surface, investigating boiling, evaporation and thermocapillary effects 01 p0165 A66-10906

Physical mechanisms of instabilities altering two-phase flow pattern of liquid film 01 p0165 A66-10907

Forced convection vaporization of Freon 113 flowing in horizontal Pyrex tube examined, using motion pictures 01 p0165 A66-10910

Ordinary differential equations theory yielding hydrodynamics conditions of stability with respect to finite perturbations for plane stationary curvilinear flow of ideal fluid 02 p0219 A66-12104

Stability analysis of adiabatic flow of incompressible fluid without equation linearization and by constructing functional from hydrodynamic fields 02 p0220 A66-12170

Liquid-phase viscosity effect on disruption of hydrodynamic stability of bubble boiling in large liquid volume 04 p0599 A66-14441

Hydrodynamic instability of shear layers, using inviscid linearized stability theory of spatially growing disturbances 04 p0513 A66-14474

Stability of two-phase unidimensional flow, relating hydrodynamic response to that of servomechanism 05 p0723 A66-15098

Linearized equation and energy principle for plasma stability 05 p0726 A66-15254

Asymptotic methods for hydrodynamic stability of slightly nonuniform plasma 05 p0727 A66-15261

Hydromagnetic stabilization of periodic magnetic fields composed of mirrors and quadrupole fields 07 p1088 A66-17949

Phased oscillator stability solved, using hydrodynamic approximation 08 p1266 A66-19668

Hypersonic shock tunnel study, examining effects of roughness, bluntness and angle of attack on boundary layer transition 08 p1166 A66-19813

Stellar stability in region of pure hydrostatic equilibrium and local instabilities arising from superadiabatic temperature gradients or differential rotation 09 p1448 A66-20097

Stability of plane motion of fluid subject to continuous perturbations distributed over volume and boundary of flow 09 p1368 A66-20755

Oscillation stability criteria for simple surge tank obtained from second method of Liapunov 10 p1523 A66-21497

Approximate method for analyzing chemically reacting turbulent flow fields having initial homogeneities [AIAA PAPER 65-37] 10 p1523 A66-21770

Phased oscillator stability solved, using hydrodynamic approximation 10 p1568 A66-21835

Effect of incompressibility of substance on gravitational instability, deriving dispersion equation and comparing results with problem of incompressible fluids 11 p1735 A66-22410

Nonequilibrium thermodynamics, variational techniques and hydrodynamic stability - Symposium, University of Chicago, May 1965 12 p1974 A66-23540

Asymptotic approximations in hydrodynamic stability problems including Couette, spiral and parallel shear flows 12 p1860 A66-23548

Nonlinear hydrodynamic stability theory, considering application to thermal convection and curved flows 12 p1976 A66-23551

Lagrangian for particular collisional models in fluid dynamics, considering fluctuation theory relations and stability in presence of external field 12 p1918 A66-23552

Statistical aspects of plasma oscillation, examining plasma evolution in terms of Landau theory, particularly after instability onset 12 p1918 A66-23554

Kinetic equation with collision frequency operator used to represent high-temperature plasma instabilities induced by particle collisions 12 p1918 A66-23555

Transverse flow velocity effect on laminar flow shape stability 12 p1863 A66-24428

Stability of vertical water jet examined by imposing audiofrequency disturbances 13 p2060 A66-25133

Internal gravity waves in stratified liquid for two-dimensional case, noting relation between oscillation frequency and wavelength 13 p2062 A66-25177

Boussinesq approximation for hydrodynamic stability of natural thermal convection of fluid between two parallel vertical planes and calculation of critical Reynolds number 15 p2617 A66-29399

Large-dimensional inverse pinch discharge study of impulsive plasma acceleration, gas dynamics and stability of unrestrained current sheet [AIAA PAPER 66-482] 18 p3141 A66-33655

Navier-Stokes equations, differences for laminar jets and turbulent jets, submerged jets and transition layer stability 18 p3099 A66-34123

Frequency and wave-vector-dependent dielectric tensor of drifting plasma in magnetic field calculated, based on macroscopic diffusion equation 18 p3146 A66-34473

Boltzmann equation, interpreted in terms of certain correlation functions known as product densities, applied to fluctuation theorem and gases and liquids not in equilibrium 18 p3136 A66-34706

Vibration spectrum of lattice of rectilinear

vortices in charged and neutral superfluid systems studied in terms of Landau superfluid hydrodynamics 19 p3400 A66-358

Hydrodynamic stability of inhomogeneous plasma flows relative to potential electromagnetic oscillations 19 p3408 A66-362

Quasi-geostrophic instability of disturbance of small amplitude in baroclinic zonal flow caused by barotropic, baroclinic or critical layer instabilities 20 p3550 A66-374

Baroclinic instability of quasi-geostrophic perturbation to zonal wind in two-layer inviscid model, examining short wavelength cut-off in terms of potential vorticity 20 p3550 A66-374

Liquid instability of vibrating partially filled elastic tank, emphasizing resonance breathing mode and frequency response 20 p3672 A66-381

Stability of one-dimensional steady detonations for periodic disturbances of small transverse wavelength 21 p3727 A66-392

Monograph on dynamics of body within liquid-filled cavities associated with practical problems of rocket technology such as seismic stability of liquid propelled tank 21 p3831 A66-393

Difference approximations to PDEs of fluid dynamics used to determine necessary condition for stability, examining advective diffusive and inertial terms 21 p3730 A66-394

Plaint coatings applied to streamlines bodies to reduce hydrodynamic drag against stabilizing laminar boundary layer against transition to turbulence 23 p4059 A66-414

Hydrodynamic stability of incompressible fluid based on Navier-Stokes equation including numerical calculations of boundary layer disturbances and temperature dependent material constants 23 p4060 A66-421

Eigenvalue problem associated with dynamic instability of geostrophic wind 23 p4066 A66-421

Alry and Weber equations solutions and relationships in terms of exponential function in connection with hydrodynamic stability and Orr-Sommerfeld equation 24 p4193 A66-422

Laminar boundary layer characteristics of continuous moving surface, noting hydrodynamic critical Reynolds number, disturbance amplitude function and energy criterion stability 24 p4194 A66-422

**HYDRODYNAMIC TUNNEL**

Acceleration and dynamics of argon plasma in inductive hydrodynamic shock tube 01 p0113 A66-100

**HYDRODYNAMICS**

SA ELASTOHYDRODYNAMICS

SA ELECTROHYDRODYNAMICS

SA FLOW THEORY

SA FLUID MECHANICS

SA HYDRAULICS

SA KROOK EQUATION

SA MAGNETOHYDRODYNAMICS

Flexible-wall tubes flattened by fluid flow velocity reaches critical value, wave differential equations describing effect on stability loss 01 p0158 A66-111

Hydrodynamic behavior of mercury in laminar and turbulent flow in tube discussing effect of vacuum and protective gas 04 p0511 A66-141

Post-Newtonian hydrodynamics and stability of gaseous masses for radial and nonradial oscillations 05 p0715 A66-141

German book on theoretical fluid dynamics covering potential flow of ideal fluids and gases, viscous fluids, boundary layer theory, hydrodynamic stability and turbulence flow 05 p0662 A66-150

Motion of solid body with cavity filled with viscous incompressible fluid at small Reynolds number, reducing hydrodynamic problem to solution of stationary linear boundary value problems 06 p0873 A66-161

Relativistic hydrodynamics of relativistic gas discussing limiting cases depending on chemical reaction and annihilation rates at pair growth 08 p1206 A66-189

Hydrodynamic theory relating velocity decrement and curvature of gas flow from detonation to conditions at explosive interface



- IAA PAPER 65-39] 10 p1621 A66-21777  
Retarded observer time as coordinate in  
relativistic spherical hydrodynamic equations  
events Schwarzschild surface  
formation 11 p1772 A66-22779  
Dynamics of pump rotor allowing for  
hydrodynamic forces arising in seals,  
determining region of unstable rotor motion  
and amplitude of  
oscillations 12 p1964 A66-24049  
ONERA laboratory weightlessness  
simulation tests on liquids, accelerometers,  
hydrodynamic braking, etc 13 p2058 A66-26371  
Liquid behavior under simulated  
weightlessness 13 p2065 A66-26372  
Text on high velocity hydrodynamics  
including wing flow, compressible fluids,  
motion of slender profile,  
etc 13 p2066 A66-26529  
Standard inductive energy formulas lead to  
error if applied to vortices in rotating  
fields 13 p2068 A66-26684  
Fluid mechanics - Midwestern Mechanics  
conference, Case Institute of Technology,  
Cleveland, April 1963 13 p2068 A66-26701  
Stability of cylindrical sheet of fluid  
during motion through motionless gas  
ambient 14 p2273 A66-26778  
Boundary layer generation for viscous  
incompressible fluid flow past rigid wall or  
obstacle to which fluid  
adheres 14 p2274 A66-26940  
Peripheral inelastic encounters, complex  
orbital momenta and cosmic ray analyses of  
interactions, noting hydrodynamical model  
and Regge pole method 15 p2585 A66-29562  
Book on methods in computational physics  
including numerical simulation of Earth  
atmosphere, computation of propeller design  
and stellar evolution, etc 16 p2735 A66-30942  
Numerical model of Earth atmosphere used  
to compute hydro- and thermodynamic  
evolution of global moist atmosphere,  
considering solar heating, evaporation,  
etc 16 p2697 A66-30943  
Flexible and rigid hinged hydrofoils noting  
behavior of configurations lift, drag, power  
input coefficients, etc 17 p2910 A66-32662  
Separated unsteady flow about flat plate  
rotating impulsively from rest to uniform  
angular velocity about axis along leading  
edge, noting torsional oscillations  
IAA PAPER 66-427] 17 p2910 A66-32753  
Bernoulli theorem development and  
extension 17 p2911 A66-32819  
Experimental analysis of Taylor columns  
likely to bear on processes occurring in  
Jupiter atmosphere 17 p3006 A66-33013  
Concentration profile of heavy species for  
binary fluid mixture under body force from  
uniformly mixed upstream condition,  
considering inviscid hydrodynamical  
model 18 p3103 A66-34925  
Book on physics of shock waves and high  
temperature hydrodynamic  
phenomena 19 p3341 A66-36316  
Hydrodynamic implosion mechanism and  
impact of liquid jets formed by collapsing  
cavitation bubbles, examining damage to  
solid boundaries 20 p3547 A66-37811  
Rheology theories of material deformation  
and flow including classical theories of  
elasticity and hydrodynamics covered by  
nonlinear viscoelasticity 22 p3898 A66-40019  
Planetary scale atmospheric circulations of  
Jupiter and Saturn using fluid dynamics,  
noting rotation effects 23 p4129 A66-41679  
Hydrodynamic phenomena in rotating fluid  
systems, characterizing flow of fluid whose  
viscosities, thermal conductivity and specific  
heats are constant 23 p4058 A66-41940  
Similar solutions for laminar boundary  
layer under forced convection of mixture of  
fluids with constant mass density and  
temperature and composition dependent  
parameters for flat plate  
analysis 23 p4059 A66-42007  
Short-range weather forecasting based on  
principles of fluid  
dynamics 23 p4087 A66-42017  
Nonstationary Navier-Stokes equations  
solved, using implicit difference scheme,  
demonstrating convergence with aid of  
difference analog of energy equality of  
hydrodynamics 24 p4231 A66-42234  
Measuring devices for velocity of fluid in  
undefined motion, noting fluid dynamic  
transducers 24 p4214 A66-43013  
**HYDROFLUORIC ACID**  
Dimensional control of oxide films on n-  
and p-type silicon by thermal oxidation and  
chemical etching in HF 08 p1230 A66-18870  
Biological content of 17 known specimens  
of type I and type II meteorites, noting  
indigenous objects are mineralized with  
limonite and contain residues insoluble in  
hydrochloric and hydrofluoric  
acid 24 p4275 A66-42655  
**HYDROFOIL**  
**SA AIRFOIL**  
Hydrofoil profile and surface roughness  
effect on cavitation  
performance 07 p1024 A66-18168  
Supercavitating flow past straight cascade  
of arbitrary hydrofoils 07 p1024 A66-18169  
Cavitating and noncavitating flows past  
plano-convex hydrofoil, noting oscillation  
frequency dependence on attack angle,  
tunnel velocity and cavitation number  
[ASME PAPER 65-FE-3] 12 p1865 A66-24557  
Marine propellers and ducted propeller  
propulsive devices 16 p2688 A66-31328  
Wall effect removal on supercavitating  
flow, estimating effects due to tunnel ducts  
and boundary layer  
blocking 18 p3101 A66-34643  
Optimum fully cavitating hydrofoils having  
analytic profiles at zero cavitation number  
investigated by Levi-Civita  
method 19 p3342 A66-36493  
**HYDROFOIL OSCILLATION**  
Flutter conditions for finite-span hydrofoils  
under partial cavitation or  
supercavitation 16 p2688 A66-31329  
Flexible and rigid hinged hydrofoils noting  
behavior of configurations lift, drag, power  
input coefficients, etc 17 p2910 A66-32662  
Lift and drag of supercavitating isolated  
hydrofoil or hydrofoils in cascade, noting  
characteristics of flat plate and circular arc  
foils 18 p3100 A66-34642  
**HYDROGEN**  
**SA DEUTERIUM**  
**SA LIQUID HYDROGEN**  
**SA LOX-HYDROGEN ENGINE**  
**SA PARA HYDROGEN**  
**SA TRITIUM**  
Charge exchange and ionization cross  
sections for hydrogen ions passing through  
ordinary and heavy  
hydrogen 01 p0107 A66-10194  
Stable elementary particle detection of mass  
greater than that of proton in hydrogen,  
deuterium and atmospheric air samples,  
using mass spectrometer 01 p0060 A66-10251  
Lifetime of radiative dissociation of  
excited molecular  
hydrogen 01 p0108 A66-10311  
Correlation of hydrogen emission and  
oxygen line in diffusive auroras and  
sporadic E layer 01 p0064 A66-11162  
Ring of ionized hydrogen in region 3.5 to  
4.5 kpc from galactic  
center 03 p0426 A66-12908  
Densification rates for tungsten powder  
compacts sintered in hydrogen/bromine  
atmospheres compared with those sintered  
in hydrogen alone at high  
temperatures 03 p0385 A66-13207  
Reaction of molecular hydrogen with  
oxygen in absence of molecular oxygen at  
various temperatures, using stirred reactor  
with mass spectrometer 04 p0473 A66-13649  
Electromagnetically driven ionizing shock  
waves propagating in hydrogen at speeds to  
relativistic conditions 04 p0511 A66-14010  
Palladium-hydrogen diffusion electrode  
noting current densities 04 p0460 A66-14034  
Vibrationally excited molecular hydrogen  
effect on mean  
polarizability 04 p0549 A66-14311  
Homeopolar semiconductors, discussing  
radiation recombination parameters on  
impurity centers with phonon  
participation 05 p0731 A66-14654  
Niobium resistivity dependence on  
hydrogen-impurity content at various  
temperature ranges 05 p0699 A66-14697  
Electrons, hydrogen nuclei and helium  
nuclei observed in primary cosmic radiation  
by balloon in 1963, discussing integral  
intensity and differential energy  
spectrums 05 p0746 A66-14780  
Electron density measurements in transient  
plasma using resolution repeater rapid-scan  
spectrograph 05 p0677 A66-14914  
Tensile tests and strain rates at various  
temperatures on palladium hydrogen alloys,  
noting plastic deformation and strain  
aging 05 p0701 A66-14966  
Slug flow and film boiling of hydrogen,  
deriving formula for forced convective film  
boiling heat flux  
[ASME PAPER 65-WA/HT-32]  
05 p0793 A66-15673  
Delayed fracture in high strength steel due  
to hydrogen penetration 06 p0895 A66-16490  
Heat transfer coefficients for helium and  
hydrogen gas flowing through electrically  
heated Inconel tube 07 p1148 A66-17300  
Monte Carlo method to reveal properties  
of hydrogen transport near critical level of  
escape of Earth upper  
atmosphere 07 p1028 A66-17362  
5-cm radio emission from excited hydrogen  
in Omega nebula studied with quantum  
parametric amplifier 07 p1134 A66-17624  
Interaction between hydrogen and various  
titanium alloys, noting correlation between  
sorption capacity of alloys and type of phase  
diagram 07 p1050 A66-18064  
Annular flow and two-dimensional forced  
convective boiling heat transfer to hydrogen  
in nucleate and film boiling  
regimes 08 p1316 A66-18832  
Hydrogen solubility in liquid niobium at  
high temperatures and partial  
pressures 08 p1241 A66-19377  
Flow visualization in turbomachinery, using  
hydrogen bubbles generated by electrolysis  
of working water 08 p1209 A66-19553  
Hydrogen feeding through single-layer  
metallic porous electrode of fuel cell on  
open circuit 08 p1171 A66-19649  
Upper ignition limit for reaction of  
fluorine with hydrogen 09 p1338 A66-20394  
Data on large-scale distribution of  
interstellar hydrogen important for studies  
of spiral arms and galactic  
disk 11 p1766 A66-22257  
Thermal conduction of hydrogen-helium gas  
mixtures and dependence on hydrogen  
concentration 11 p1786 A66-22500  
Cross sections of inelastic collisions of  
hydrogen and nitrogen molecular ions with  
hydrogen molecules 11 p1738 A66-22879  
Ground state of hydrogen molecule treated  
by perturbation theory through second  
order, noting energy and wave  
function 11 p1738 A66-22882  
Vibrational relaxation of hydrogen mixed  
with argon in shock tube studied by  
schlieren technique 11 p1739 A66-22886  
Diffusion of electrolytic hydrogen through  
membranes of iron crystals as function of  
stress, temperature and dissolved hydrogen  
concentration 11 p1718 A66-23071  
Low temperature chromatographic  
separation of hydrogen isotopes based on  
interaction with alumina surface electric  
fields 11 p1650 A66-23209  
Receiver of hydrogen line interferometer  
at California Institute of  
Technology 13 p2182 A66-25551  
Interstellar molecular hydrogen abundance  
and possible source from giant  
stars 13 p2182 A66-25579  
Hydrogen and helium spectra of gaseous  
nebulae in theory and  
observation 13 p2183 A66-25610  
Empirical curve of growth on S/I line of  
1-0 hydrogen quadrupole band obtained,  
laboratory and planetary hydrogen  
quadrupole spectra corrected for  
saturation 13 p2184 A66-25621  
Homeopolar semiconductors, discussing  
radiation recombination parameters on  
impurity centers with phonon  
participation 13 p2167 A66-25929  
Stable elementary particle detection of  
mass greater than that of proton in  
hydrogen, deuterium and atmospheric air  
samples, using mass  
spectrometer 13 p2131 A66-25968  
Capillary viscosity meter measurements of  
hydrogen-deuterium  
solutions 13 p2114 A66-25970  
Auroral hydrogen emission in night sky,  
noting variance with sunspot cycle and  
magnetic activity 13 p2073 A66-26029  
Ionization cross section for rare gases and  
hydrogen atoms calculated from  
perturbation theory, noting ruby laser



photon absorption 13 p2133 A66-26188  
 Stimulated emission spectroscopy of hydrogen, nitrogen, oxygen and deuterium diatomic gases in 0.8 to 8 micron region 13 p2102 A66-26205  
 Helium-neon gas laser used to determine electron density variation, spatial and temporal, in afterglow of Z-pinch in H at 100 mtorr 13 p2104 A66-26239  
 Analytical solution to rate equations for branching chain reactions of hydrogen-oxygen reaction under shock tube conditions, for application to ignition problems 13 p2018 A66-26442  
 Proton transfer between hydrogen and methane, ethane, propane and butanes, using high-pressure mass spectrometry, employing ion source with beta rays as ionizing medium 13 p2018 A66-26443  
 Numerical solution of steady state jump equations for normal ionizing shock waves in hydrogen, assuming upstream and downstream states at chemical equilibrium 13 p2154 A66-26661  
 Ring of ionized hydrogen in region 3.5 to 4.5 kpc from galactic center 14 p2380 A66-27256  
 Broadening of Fraunhofer hydrogen lines in solar spectrum, noting Stark effect 14 p2380 A66-27274  
 Porosity in titanium arc welds, noting sources of gas evolution and probable causative gases, particularly molecular hydrogen and oxygen 14 p2302 A66-27346  
 Static pressure distributions in supersonic nozzle flows of dissociated hydrogen plus argon 14 p2219 A66-27442  
 Formulae relating 21-cm emission intensity to density of interstellar hydrogen gas 14 p2383 A66-27799  
 Low temperature transport properties of hydrogen, deuterium and HD, noting quantal phase shift, intermolecular potentials, etc 14 p2414 A66-27973  
 Photochemical decomposition of carbon suboxide and spectroscopic observation of carbon atom reactions with nitrogen, hydrogen and deuterium at 4.2 degrees K 14 p2233 A66-27975  
 Neutron analysis techniques for determining hydrogen presence on lunar or planetary surfaces, based on measurement of gamma radiation 14 p2233 A66-28105  
 Drift and diffusion of slow positive ions in hydrogen, using redesigned apparatus 14 p2345 A66-28141  
 Hydrogen effect on strength, plastic deformation and microstructure of hardened titanium alloys 15 p2522 A66-29179  
 Oxygen and hydrogen effect on microstructure, tensile and impact strength and hardness of titanium alloys 15 p2522 A66-29180  
 Enthalpy and entropy of parahydrogen from PVT data and from limited amount of thermal data 16 p2790 A66-30907  
 Solubility of hydrogen in titanium 16 p2724 A66-31238  
 Cryosorption panels consisting of molecular sieve adsorbents bonded to refrigerated aluminum plates for pumping hydrogen at 20 degrees K 17 p2957 A66-31978  
 Presence and detectability of hydrogen in molecular form in galaxy 17 p3001 A66-32365  
 Water vapor effects on detonation reaction of H sub 2 - O sub 2 17 p3034 A66-32467  
 Embrittlement of tantalum by room temperature deformation in presence of hydrogen 17 p2941 A66-33441  
 Computer programs for combustion rates of hydrogen-air mixture 18 p3063 A66-33830  
 Elastic relaxation effect due to diffusion of interstitial hydrogen in tantalum and niobium 18 p3123 A66-34058  
 Semiconvective zone in very massive stars during hydrogen burning, noting factors leading to instability 18 p3229 A66-34142  
 Thermal conductivity of hydrogen at temperatures up to 4700 degrees F determined indirectly from effective conductivity of porous tungsten specimens filled with pressurized hydrogen 18 p3125 A66-34387  
 Balloon flight data obtained at 50 and 65 degrees N geomagnetic latitude on spectra of primary cosmic ray hydrogen and helium nuclei, using Cerenkov scintillator technique 18 p3190 A66-34831

Hydrogen embrittlement reduction in springs by careful processing 19 p3362 A66-35326  
 Feasibility analysis of very high temperature uranium-bearing liquid alloy heat exchanger for hydrogen gas, considering several ternary component liquid alloy systems [AIAA PAPER 66-622] 19 p3476 A66-35358  
 Hydrogen pumping by means of phenomenon of hydrogen absorption by solid layer of carbon dioxide condensed at temperature of 20.4-14 degrees K 19 p3400 A66-36099  
 Spectral receiver of Nancy radiotelescope of correlation type, for extragalactic observations on 21-cm neutral hydrogen band 19 p3319 A66-36259  
 Ionization of hydrogen and hydrogenic positive ions by electron impact 19 p3409 A66-36324  
 Dissociation of hydrogen molecules by electron impact, using first-order exchange approximation and separated atoms approximation 19 p3403 A66-36328  
 Cross sections for vibrational excitation of water by collision with water and molecular hydrogen calculated, using radial scattering equations 19 p3403 A66-36330  
 Diffusion parameters of impurities from polycrystalline Si in hydrogen flux, noting formula for boundary conditions 19 p3321 A66-36457  
 Hydrogen line profile in Paschen series of solar spectrum, taking into account Stark effect and line broadening 20 p3648 A66-37045  
 Particle size distribution, aging effects, terminal velocity measurements and production techniques of slush hydrogen investigated as potential upgraded spacecraft fuel 20 p3676 A66-37075  
 Three superconducting niobium stannide liquid level sensors tested in triple point slush or liquid hydrogen for capability of detecting liquid-vapor interface 20 p3557 A66-37076  
 Hazards associated with ignition of various condensed phase hydrogen-oxygen systems 20 p3625 A66-37083  
 Effect of variations in mission and vehicle constraints on hydrogen-oxygen fuel cell system optimization 20 p3497 A66-37160  
 Thermal escape of neutral hydrogen and distribution in Earth thermosphere, noting collision in transition 20 p3549 A66-37292  
 Digital computer analysis of kinetic equations for CO burning in presence of hydrogen 20 p3679 A66-37702  
 Phase diagram of titanium-oxygen-hydrogen system, plotting isotherms and isobars for equilibrium hydrogen pressure, noting oxygen effect 20 p3585 A66-37748  
 Molecular hydrogen structure, considering planetary and stellar atmospheres and interstellar space 21 p3815 A66-39487  
 Solid solutions of titanium, tungsten, chromium prepared by carbidization of mixtures in hydrogen medium and obtained as fine-grained carbide 22 p3934 A66-39865  
 Nonequilibrium dissociation losses in hydrogen-fluorine propellant system, indicating rate control of recombination steps [AICE PREPRINT 28A] 22 p3969 A66-39882  
 Second-order WKB corrections to Rydberg-Klein-Rees potential curve for hydrogen 22 p3949 A66-39911  
 Paschen series laser lines in atomic and molecular hydrogen 22 p3933 A66-40892  
 Homogeneous isotopic exchange reaction between hydrogen and deuterium in single-pulse shock tube with excess argon 22 p3860 A66-40902  
 Hydrogen excitation mechanism in surge prominences determined, using stationary equations for energy levels of hydrogen 23 p4126 A66-41076  
 Excitation of H-alpha lines in solar chromosphere from internal and external sources, noting theoretical and empiric results 23 p4127 A66-41080  
 Heat of formation of oxygen difluoride for reaction with hydrogen, using Parr fluorine combustion bomb containing metal ampoule employing burst 23 p4118 A66-41080

diaphragm 23 p4118 A66-41080  
 Charge exchange cross sections for argon incident on hydrogen and deuterium measured over energy range of 30 to 100 eV, taking into account ion-molecule reactions 23 p4098 A66-41080  
 Excitation of hydrogen molecule from ground state to B and C electronic states by electron impact, using one-center wave functions of Huzinaga together with Brueckner approximation 23 p4098 A66-41080  
 Height-luminosity distribution of auroral hydrogen beta emission measured with rocket mounted photometer 23 p4065 A66-41080  
 Optical hydrogen-line profiles in Orion nebula compared to radio profile obtained from antenna response and weight factors of brightness temperature 23 p4131 A66-41080  
 Compressibility factor chart for hydrocarbon-hydrogen and nitrogen-hydrogen gas mixtures, correlating pressure, temperature, using state equation 23 p4150 A66-41080  
 Detonability of hydrogen-oxygen mixture in large vessels at low initial pressure using strong and weak igniters 23 p4120 A66-41080  
 Thermal accommodation coefficients of hydrogen on tungsten and hydrogen on hydrogen covered tungsten at temperatures of 300, 403 and 473 degrees K 23 p4033 A66-42080  
 Ion energy balance equation for ionospheric including effects of O, He, and H ion thermoconductivity and cooling by atomic hydrogen and helium 24 p4198 A66-42080  
 Temperature of fluorine-hydrogen flame from 3, 0/ band of FH vibration-rotation experimentally determined to be in agreement with theoretical figure of 3000 degrees K for stoichiometric mixture 24 p4295 A66-42080  
 Hydrogen abundance in universe using gravitational effect on physical constants 24 p4279 A66-43080

**HYDROGEN ATOM**  
 Electron concentration, length and temperature of limb chromospheric flare using steady state equation of hydrogen atom 01 p0131 A66-10080  
 Rarefied hydrogen flame interaction between hydrogen atoms and molecules of certain organic, aliphatic and cyclic compounds 01 p0161 A66-10080  
 Electric resistivity of solid phase lutetium hydrogen system noting action of hydrogen atom 01 p0127 A66-11080  
 Positron scattering by atomic hydrogen at various incident energies 02 p0262 A66-11080  
 Atomic hydrogen reaction with HO-2 source of hydrogen molecules in lower thermosphere 02 p0221 A66-11080  
 Angular distribution of fast H and H<sup>+</sup> ion dissociation fragments on hydrogen gas noting transverse velocity distribution 03 p0394 A66-12080  
 Design, operation and performance capability of hydrogen maser 03 p0377 A66-12080  
 Stereospecificity in hydrogen transfer reaction characteristic of 6-keto steroids studied by mass spectrometry 03 p0330 A66-13080  
 Hydrogen atom beam characteristics: discussing signal power, generating frequency, radiation signal damping of hydrogen atom relaxation time 03 p0380 A66-13080  
 Mach-Zehnder interferometer for electromagnetically accelerated shock waves in hydrogen 04 p0554 A66-14080  
 Computed high temperature rate constants for hydrogen atom transfers involving hydrogen elements, noting activation energies of exothermic reactions [CI PAPER WSCI-65-24] 05 p0629 A66-15080  
 Variation of scattering cross section with beam intensity for ruby laser light in atomic hydrogen 05 p0698 A66-15080  
 Bethe approximation of ionization cross sections of excited states of atomic hydrogen by high energy electrons 06 p0912 A66-17080  
 Photoabsorption cross section of atomic hydrogen obtained by flowing molecular hydrogen through discharge tube 06 p0913 A66-17080



- Solar cosmic ray particle composition, large and energy spectra of nuclear components and isotopic composition of H and He 07 p1132 A66-18264
- Mean lives of 3s, 3d, 4s, 4p and 4d states of hydrogen and relative initial radiation intensities 07 p1083 A66-18420
- Beam source producing atomic and molecular hydrogen by molecular association at high temperatures 07 p1084 A66-18492
- Density of neutral hydrogen in intergalactic space, using spectroscopic examination of quasi-stellar source 3C 08 p1288 A66-18782
- Perturbation theory of ionization of hydrogen and rare-gas atoms by simultaneous absorption of several photons 11 p1715 A66-23388
- Cross correlation measurements of oscillator frequency stability and thermal noise and application to atomic hydrogen maser 12 p1835 A66-24128
- Hydrogen atom beam characteristics, discussing signal power, generating frequency, radiation signal damping and hydrogen atom relaxation 14 p2310 A66-28289
- AMO method applied to bcc crystal of hydrogen atoms, taking into account all many-center integrals 15 p2543 A66-28784
- Calculation of effective excitation cross sections of hydrogen atoms for collisions with nitrogen molecules and hydrogen atoms 15 p2545 A66-29211
- Energy from hydrogen molecule interaction with magnetic field and from hyperfine interaction expressed as products of irreducible spherical tensors 15 p2548 A66-29806
- Diurnal variation of hydrogen atom concentration at base of exosphere, including effects of lateral flow of gas around Earth 17 p2919 A66-32996
- Born cross sections for double-transition collisions of hydrogen atoms 18 p3138 A66-34150
- Partial wave theory of two electron Rlatomic hydrogen molecules and calculation in zeroth order for sigma g states 18 p3139 A66-34500
- Atomic concentration measurement in discharged nitrogen, oxygen and hydrogen 18 p3139 A66-34507
- Approximation method using sum rules for energy shift in atomic system due to interaction of electrons with vacuum electromagnetic field applied to hydrogen, helium and lithium atom ground states and hydrogen molecule 19 p3402 A66-35995
- High energy cross sections for electron excitations of excited hydrogen atoms in which principal quantum number is changed by 2 19 p3409 A66-36327
- Distorted wave calculation from rotational excitation of molecular hydrogen and molecular deuterium in thermal collisions with atomic hydrogen, presenting angular distributions, cross sections, etc 19 p3403 A66-36329
- Excitation of ground state hydrogen atoms by fast protons, evaluating total Born cross section in limit of infinitely massive protons 19 p3403 A66-36333
- Lyman alpha airglow observations indicate diurnal variation of atomic hydrogen in thermosphere and exosphere with abundance change with solar activity 19 p3349 A66-36349
- Atomic hydrogen and helium emissions in upper atmosphere determined by diffraction spectrophotometer measurement of twilight airglow and aurora 19 p3350 A66-36352
- Energetic neutral hydrogen atom injection into ECP in magnetic mirror and plasma shielding against trapped thermal neutral gas 19 p3422 A66-36547
- Neutral-impurity scattering and scaled electron-hydrogen-atom collision problem for hydrogenic-type impurities in semiconductor studied by method using highly spin-polarized carriers 19 p3448 A66-36763
- Electron excitation of high eigenstates of hydrogen atom and convergence of total wave function expansion 21 p3774 A66-38532
- Fast neutral hydrogen atom beams used to probe plasma density and time- and space-dependent plasma distribution in longitudinal magnetic field 21 p3786 A66-39046
- Intense beams of fast neutral hydrogen atoms injected into magnetic trap by ionization in strong magnetic field 21 p3789 A66-39060
- Charge exchange of protons in alkali metal vapors with formation of highly excited hydrogen atoms, noting cross section, reaction mechanism, etc 22 p3953 A66-39762
- High temperature rate constants for H-atom transfers involving light atoms evaluated, using hard sphere collision theory 22 p3950 A66-39924
- Photoabsorption cross section of atomic hydrogen by molecular hydrogen flow through discharge tube 23 p4098 A66-41245
- Stark splitting effect on fine structure level probabilities for hydrogen lines, taking account of spontaneous transition probabilities and Lamb shift 23 p4098 A66-41362
- 3 cm hydrogen line from solar flares, estimating line-to-continuum ratio during flare 23 p4124 A66-41928
- Very fine-beamed maser oscillation produced in atomic hydrogen by HF discharge observed by double focusing technique 24 p4225 A66-42993
- Spin-spin interaction energy for large separations of two ground state hydrogen atoms 24 p4239 A66-43040
- HYDROGEN BOND**
- Crystal structure of hexamethylenetetramine hexahydrate determined using X-ray analysis, noting hydrogen bonding in crystalline state 03 p0330 A66-12338
- Vibrational spectrum of liquid, solid and gaseous tetradeuterated hydrazine and Raman study of hydrogen bonding in hydrazine 19 p3295 A66-36801
- Hydrogen bonding kinetics in free radical liquid-phase reactions 21 p3702 A66-38520
- HYDROGEN COMPOUND**
- CW IR laser oscillation in HBr and HI gas discharge 06 p0892 A66-16756
- IR and UV absorption spectra of solid HN sub 3 film after photolysis with unfiltered radiation from Hg lamp 18 p3064 A66-34455
- HYDROGEN FLUORIDE**
- Kinetics of HF decomposition in HF mixtures behind incident shock waves over various temperature ranges, using IR emission 06 p0941 A66-16127
- Measurement of hydrogen-fluorine kinetics at high temperatures [AIAA PAPER 66-637] 18 p3064 A66-34437
- Moisture content determination in liquid HF based on electroconductivity 21 p3702 A66-38519
- Electrolysis of wet hydrogen fluoride, noting analysis of anode products by gas chromatography and water content measurement by IR spectroscopy 23 p4118 A66-41236
- HYDROGEN FUEL**
- Hydrogen fuel cells for space use noting Bacon cells, membrane cells and Gemini and Apollo fuel cells 03 p0323 A66-12482
- Heat transfer in base flow region, determining parameter of correlation for hydrogen injection and combustion, adiabatic flame temperature, heating rates and recovery temperature [AIAA PAPER 66-108] 06 p0970 A66-16408
- Electrode potentials and efficiency, noting significance, types and associated equations 07 p0996 A66-18468
- Hydrogen-oxygen fuel cells, using ion exchange electrolytes 07 p0996 A66-18471
- Commercial fuel cells, noting biochemical, regenerative and low temperature carbon monoxide fuel cell 07 p0996 A66-18476
- Fuel cell economics connected with vehicle applications as power sources 07 p0997 A66-18477
- Resistojet design and fabrication, using hydrogen propellant and having 3-kw power input [AIAA PAPER 66-224] 10 p1592 A66-21451
- Feasibility of using columbium alloy B-66 and Ta-10W as regeneratively cooled nozzle materials in hydrogen fuel engine 10 p1547 A66-21782
- Hydrocarbon-air fuel cell power source using reformer to supply hydrogen and producing net output of 5 kw at 110 v and 60 cps [AIAA PAPER 64-745] 13 p2007 A66-26646
- Tank design, optimization program and testing for effect on storage penalties associated with liquid hydrogen for hypersonic aircraft 14 p2394 A66-28026
- Centaur project with assessment of reliability of explosive one-shot devices 14 p2394 A66-28444
- MHD species separation of U 235 from hydrogen in gaseous nuclear rocket using time varying traveling wave electromagnet field [AIAA PAPER 66-499] 16 p2745 A66-30606
- Coupled radiative and convective heat fluxes in high temperature hydrogen propellant rocket nozzles with shape and temperature variations [AIAA PAPER 65-557] 19 p3449 A66-35612
- Hydrogen/oxygen and hydrogen/air flame temperature experiments on porous flat flame burner 20 p3680 A66-38042
- Supersonic combustion simulation facility and duplicable static parameters for hydrogen fuel [AIAA PAPER 66-743] 23 p4052 A66-41327
- Initial air-side boundary layer effect on ignition of slot injected gaseous hydrogen by hot supersonic air stream [AIAA PAPER 66-644] 23 p4149 A66-41513
- HYDROGEN ION**
- Quantum scattering theory of hydrogen-like ions in 1-S, 3-S, 1-P and 3-P states 03 p0395 A66-13110
- Guillemin-Zener energy of ionized hydrogen molecule 04 p0546 A66-13455
- Resonances below inelastic threshold of electron hydrogen scattering using Feshbach projection-operator technique, converting to eigenvalue problem for projected Hamiltonian 04 p0547 A66-13711
- Spectroscopic measurements using membrane-type shock tube for absolute determination of continuous absorption coefficients of negative hydrogen ions 04 p0553 A66-14279
- Hydrogen molecule multiphoton ionization, determining probability of absorption, effected by ruby laser emission 06 p0891 A66-16517
- Mass and energy state dependence of plasma, generated by titanium source, on electrical operating conditions of source 06 p0919 A66-16878
- Shock wave structure in ionized hydrogen, using Eddington approximation to solve Rankine-Hugoniot jump equation 08 p1204 A66-18522
- Hydrogen molecule multiphoton ionization, determining probability of absorption, effected by ruby laser emission 09 p1387 A66-20898
- Hydrogen ion concentration, electron density and proton gyrofrequency determined from proton whistler dispersion 10 p1528 A66-21140
- IR absorption spectrum of local H-ion oscillations in KCl crystals doped with Na, Rb, Cs, I, Br and F 10 p1588 A66-22158
- Interference of fine-structure levels in hydrogen ions passing through two successive carbon foils 11 p1740 A66-22968
- Statistical theory of electronic energies, calculating binding energy at theoretical equilibrium separation of molecular hydrogen ion 13 p2130 A66-25370
- Potential energy surfaces on triatomic hydrogen molecule ion computed with generalized Gaussian orbitals 13 p2130 A66-25371
- Hydrogen ion intrusion into stainless steel surface measured with apparatus in which hydrogen and helium condensation pumps provide ultrahigh vacuum 13 p2108 A66-25754
- Franck-Condon factors for ionization of hydrogen and deuterium, noting vibrational eigenenergies of D sub 2 14 p2337 A66-27972
- Surface blistering of metals due to low energy hydrogen ion bombardment, determining solar absorptance change in gold-plated specimens 14 p2316 A66-28007
- Asymptotic form of wave function and threshold behavior of cross section for ionization of atomic hydrogen by electron impact 15 p2544 A66-29116
- Absorption coefficients for nitrogen and oxygen ion in air at temperatures of 150,000



to 800,000 degrees K 15 p2617 A66-29345  
 Intensities of optically thick lines emitted by hydrogen-like ions in steady state plasma for various electron temperatures and densities 16 p2758 A66-30276  
 Ion-molecular reactions of hydrogen with inert gases caused by low energy electrons in low temperature plasmas, considering energy level populations, reaction cross sections, etc 18 p3064 A66-34026  
 Momentum eigenfunction for ground state of hydrogen molecule ion 18 p3106 A66-34506  
 IR absorption spectrum of local H-ion oscillations in KCl crystals doped with Na, Rb, Cs, I, Br and F 19 p3440 A66-35772  
 Negative hydrogen ions as cause of continuous emission in solar flares 19 p3453 A66-36297  
 Hydrogen and helium ions formation and destruction, charge transfer, diffusion, role during solar activity, using mass spectrometry, ground radar, etc 19 p3350 A66-36356  
 Chemical composition of ionized components of outer ionosphere above main ionization maximum region measured by satellites 19 p3350 A66-36357  
 Hydrogen ions detected near anode of glow discharge at various pressures, using mass spectrometer 19 p3410 A66-36455  
 Absorption coefficients for nitrogen and oxygen ions in air at temperatures of 150,000 to 800,000 degrees K 20 p3604 A66-37350  
 Beam foil excitation technique application in measuring mean lives of 2p and 3p levels of hydrogen 21 p3774 A66-38543  
 Rate constants for atomic and molecular hydrogen ion transfer from tri- and tetra-atomic carbon paraffins to propylene and cyclopropane molecular ions 22 p3861 A66-40905

**HYDROGEN OXYGEN /HOPE/ SPACECRAFT**  
 Gaseous hydrogen and liquid oxygen combustion and heat transfer in small rocket chamber 14 p2375 A66-28104

**HYDROGEN PEROXIDE**  
 Convective heat transfer behavior of 90 percent hydrogen peroxide studied with reference to possible use as rocket propellant 01 p0164 A66-10903  
 Fuel cell systems, particularly hydrogen peroxide type, noting electrochemical oxidation, water production, thermal energy, electrolyte, etc 06 p0808 A66-16391  
 Kinetics of hydroxyl radical in aqueous solution, examining electron spin resonance spectrum as function of flow rate, temperature and mixture composition 08 p1178 A66-19066  
 Paramagnetic resonance spectra of free radicals in hydrogen peroxide and alcohols during intense UV irradiation 11 p1650 A66-23216  
 Early bird hydrogen peroxide control system maneuvers to place satellite into final stationary position [AIAA PAPER 66-262] 12 p1954 A66-24736  
 Semiquantitative spot test detection of peroxide in low concentrations of hydrogen peroxide 20 p3510 A66-37056  
 Combustion and performance characteristics of lithium aluminum hydride/hydrogen peroxide hybrid rocket [AICE PREPRINT 34D] 22 p3969 A66-39878

**HYDROGEN PLASMA**  
 Macroscopic conservation equations for ionized dilute hydrogen plasma derived directly from Bogoliubov-Born-Green-Kirkwood-Yvon equations 01 p0110 A66-10338  
 Ratio of average transmission coefficients of L-beta and H-alpha and reabsorption in hydrogen pulsed discharge 01 p0111 A66-10390  
 Stabilization of pinch discharge in hydrogen 02 p0267 A66-11726  
 Stark broadening of Balmer lines in hydrogen plasma produced by alternating axial magnetic field induced by coil surrounding discharge 03 p0400 A66-12934  
 Thermodynamic properties of hydrogen ionized plasma in equilibrium 03 p0403 A66-12966  
 Temperature of hydrogen plasma jet at atmospheric pressure by measuring electric field on profile of Stark broadened

line 03 p0403 A66-12973  
 Velocity and attenuation of Alfvén waves in hydrogenous plasma at LF and HF by experiment 03 p0406 A66-13177  
 Spectral line intensities of hydrogen and helium plasma in P.I.G. discharge 04 p0553 A66-14283  
 Measurements of plasma from hydrogen-loaded titanium washer mounted at DC magnetic mirror 07 p1088 A66-17954  
 Partition function of hydrogen plasma derived classically and by quantum mechanics, obtaining Saha equation containing effective lowering of ionization potential 07 p1090 A66-18155  
 Time dependence of electron density during afterglow of plasma in helium-hydrogen, neon-hydrogen and argon-hydrogen mixtures measured by microwave cavity 07 p1091 A66-18398  
 Supersonic hydrogen jet production in vacuum 08 p1207 A66-19196  
 Kinetic equations, considering free and bound charges in weakly ionized hydrogen plasma, noting self-consistent approximation for second distribution function 08 p1265 A66-19375  
 Nonpotential Alfvén drift waves and magnetic noise in magnetosonic stationary hydrogen plasma 10 p1569 A66-21964  
 Proton concentration of hydrogen plasma in alpha apparatus by probe with fast-atom beams 10 p1571 A66-22012  
 Energy distribution of hydrogen plasma from coaxial gun 10 p1571 A66-22013  
 Hydromagnetic waves in partially ionized cylindrical hydrogen plasma 11 p1745 A66-22453  
 Solar wind particle diffusion into geomagnetic tail and then down field lines to polar cap 11 p1700 A66-23142  
 Hydrogen plasma ionization density calculation by three methods 11 p1747 A66-23265  
 Objections to idea of solar ejection of neutral hydrogen and responsibility for geomagnetic storm 11 p1776 A66-23496  
 Continuous emission and absorption of plasmas by calculating radiation of hydrogen plasma, deriving temperature and pressure conditions under which plasma radiates as black body 12 p1919 A66-23750  
 Superhigh vacuum creation in OGRA-1 facility, using titanium sputtered liquid nitrogen-cooled copper surfaces 12 p1922 A66-24218  
 Hydrogen arcs, sulfur hexafluoride arcs, decaying nitrogen arcs and nitrogen arcs with forced convection 13 p2137 A66-25110  
 Spectral line intensities variation in ionization of hydrogen and impurities in TA 2000 device 13 p2138 A66-25125  
 Differences between thermodynamic equilibrium of hydrogen plasma, accounting for increased atomic energy levels 13 p2141 A66-25459  
 Ionization phase of impurity in pulsed hydrogen discharge and electron temperature measuring method 13 p2141 A66-25478  
 Electrostatic instabilities of hydrogen discharge in strong electric field and effects on ohmic heating and electric conductivity 13 p2144 A66-25721  
 Electron density and temperature in decaying hydrogen plasma determined, using monochromator 13 p2145 A66-25730  
 Electron density and temperature of hydrogen plasma determined from intensity of spectral line and continuum in region adjacent to line 13 p2145 A66-25733  
 Tenuous hydrogen plasma injection into axial magnetic cusp field at entrance of long solenoid 13 p2147 A66-25749  
 Delays effect on performance of coaxial plasma guns with about 20 kv applied, shown to produce fast burst of clean plasma containing pure hydrogen ion 13 p2000 A66-25750  
 Plasma wave propagation and decay processes studied from profiles of plasma density in cylindrical metal vessel and results compared to Stark effect and framing camera photographic results 13 p2149 A66-26240  
 Electric fields in hydrogen plasma leading to forbidden free-bound transitions, considering photodetachment of electrons

and radiative capture cross sections 13 p2135 A66-26240  
 Hydrogen plasmoid density, ionization at electron temperature measured by fast particle probing 13 p2153 A66-26240  
 State equation and equilibrium correlations for hydrogen type plasma 13 p2157 A66-26240  
 Pressure rise in inner region of hydrogen arc discharge in axial magnetic field 16 p2764 A66-31100  
 Energy spectrum of neutral hydrogen atoms from coaxial plasma gun 17 p2962 A66-31100  
 Free-free galactic X-ray emission from fully-ionized hydrogenic plasma 17 p2992 A66-31100  
 Kinetic equations, considering free and bound charges in weakly ionized hydrogen plasma, noting self-consistent approximation for second distribution function 18 p3146 A66-34026  
 Magnetic beach effect on RF power transfer to ion-cyclotron waves in hydrogen and deuterium plasmas 18 p3146 A66-34026  
 Excitation and ionization of hydrogen plasma under influence of two electron groups with different temperatures and densities, using coupled system of rate equations 19 p3407 A66-36100  
 Proton concentration of hydrogen plasma in alpha apparatus by probe with fast-atom beams 19 p3407 A66-36100  
 Energy distribution of hydrogen plasma from coaxial gun 19 p3407 A66-36100  
 Stable and unstable behavior of preheated hydrogen plasma in linear and cusped theta pinches 19 p3414 A66-36100  
 Livermore neutral-injection experiment studying stability of steady state 20-hydrogen plasma in various confinement magnetic fields 19 p3421 A66-36100  
 Hot plasma production in OGRA-II injection of fast hydrogen atoms in magnetic mirror trap with stabilized hexagonal field 19 p3421 A66-36100  
 Biconical cusp injection of dense hydrogen and deuterium plasmas by plasma gun 19 p3425 A66-36100  
 Joule heating of hydrogen plasma in toroidal Tokamak-3 device by annular electric current, noting stability and plasma interacting with diaphragm 19 p3427 A66-36100  
 Power balance measurements and partial loss rate of ohmically heated helium in hydrogen discharges in C stellarator 19 p3428 A66-36100  
 VGL-2 cryogenic magnetic trap, filling with hydrogen plasma 19 p3428 A66-36100  
 Second-harmonic electron cyclotron resonance in hydrogen plasma from HF source with inductive coupling situated transverse magnetic field 20 p3607 A66-37400  
 Positive plasma column produced by hydrogen glow discharge studied by mass spectrometer for various pressures and currents 20 p3608 A66-37400  
 Electrical breakdown in beams of hydrogen and nitrogen produced by expanding H or gas out of Laval nozzle cooled by liquid hydrogen or nitrogen in high vacuum 20 p3605 A66-38000  
 Increasing plasma density in OGRA 1 20 p3610 A66-38000  
 Plasma diagnostics method, measuring parameters of hydrogen plasma with beams of fast hydrogen atoms and ions 21 p3784 A66-39000  
 Plasmoid motion and purification in heli magnetic field and mass spectrograms of pure dense hydrogen 21 p3787 A66-39000  
 Nonpotential Alfvén drift waves and magnetic noise in magnetosonic stationary hydrogen plasma 21 p3794 A66-39000  
 Superhigh vacuum creation in OGRA facility, using titanium sputtered liquid nitrogen-cooled copper surfaces 22 p3957 A66-40905  
 Spectroscopic measurements of electron densities and temperatures in argon hydrogen plasma jet 23 p4068 A66-41200  
 Ruby laser light scattering measurements of electron and ion temperatures of hydrogen and deuterium plasmas produced in theta pinch devices 24 p4222 A66-42200  
 Ambiplasma sources of positronium, protonium and muonium radiation, etc



theorizing that quasars may be ambiplasmas containing admixtures of matter and antimatter 24 p4280 A66-43027

**HYDROGEN RECOMBINATION**  
Thermal sulfur equilibrium in burnt gas of hydrogen-oxygen flames 02 p0303 A66-11594  
Recombination effects in nozzle flows of hydrogen/fluorine rocket engines 08 p1279 A66-19152  
Altitude distribution of atmospheric molecular and atomic hydrogen, showing results of Lyman alpha absorption measurements 17 p2919 A66-32995

**HYDROGENATION**  
**HA DEHYDROGENATION**  
Dichloroborane synthesized in quantitative yields by thermal hydrogenation of boron trichloride 05 p0629 A66-14540  
Thermochemical deposition of refractory metals, alloys and compounds, discussing tungsten, rhenium and molybdenum impurity, grain orientation and application to thermionic devices 05 p0622 A66-15591  
Thorium dioxide strengthened nickel and nickel molybdenum alloys, discussing production via selective reduction, strength, creep rupture, stability and ductility characteristics 06 p0893 A66-15943  
Hydrogen effect on strength, plasticity and brittleness of metals with fcc lattice at various temperatures and hydrogen concentrations 12 p1894 A66-23763  
Purification of turbine oil by hydrogenation, using Al-Co-Mo catalyst 20 p3575 A66-38382

**HYDROGENOMONAS**  
Electrolysis-Hydrogenomonas bacterial bioregenerative life support system for manned space flight of long duration 06 p0815 A66-15929

**HYDROKINETICS**  
Separation of gases from isotopes in compression shock produced in expanding gas flow past obstruction, dependent on gas density and hydrokinetic properties of components 06 p0875 A66-17052

**HYDROLOGY**  
**SA METEOROLOGY**  
Hypersaturation photography, applications and advantages 10 p1535 A66-21523

**HYDROLYSIS**  
**SA HYDRATION**  
Chemical and physical properties of samarium dicarbide, prepared by heating samarium sesquioxide with graphite, using X-ray analysis, hydrolytic studies, etc, noting structure 14 p2362 A66-27465  
Thermal growth and deposition of silica films by silicon tetrafluoride hydrolysis 22 p3962 A66-40048  
Hydrolytic reactions of nitrogen fluorides, noting inertness of nitrogen trifluoride to pure water and reaction with aqueous base to give nitrite and fluoride 23 p4118 A66-41242

**HYDROMAGNETIC FLOW**  
**SA MAGNETOHYDRODYNAMIC FLOW**  
**HYDROMAGNETIC STABILITY**  
**SA MAGNETOHYDRODYNAMIC STABILITY**  
**HYDROMAGNETIC WAVE**  
**SA MAGNETOHYDRODYNAMIC WAVE**  
**HYDROMAGNETISM**  
**SA GEOMETRICAL HYDROMAGNETIC**  
**SA MAGNETOHYDRODYNAMICS**  
**SA MAGNETOHYDROSTATICS**  
**SA PLASMA**  
**HYDROMETEOROLOGY**  
Statistical characteristics of fluctuations in radio emission of atmosphere producing turbulent pulsations and displacements of hydrometeorological formations in scan field of radiotelescope, noting distribution function 04 p0517 A66-14046  
Statistical characteristics of fluctuations in radio emission of atmosphere producing turbulent pulsations and displacements of hydrometeorological formations in scan field of radiotelescope, noting distribution function 17 p2917 A66-32212

**HYDROSTATIC PRESSURE**  
Linear and nonlinear stability and critical strains of closed thin walled circular cylindrical shell under hydrostatic pressure 01 p0155 A66-10738  
Wave solutions to linearized quasi-hydrostatic equations for adiabatic nonviscous flow on equatorially oriented

beta plane 02 p0254 A66-11982  
Electrical resistivity and Hall coefficient of undoped n-type gallium arsenide with carrier concentrations measured at various temperatures as function of uniaxial compression and hydrostatic pressure 03 p0412 A66-13149  
Whirl instability and pneumatic hammer for rigid rotor in pressurized gas journal bearings [ASME PAPER 65-LUB-12] 04 p0527 A66-14245  
Plastic deformation in body under uniform pressure, establishing necessary condition for existence of uniform stressed state in inhomogeneous body 07 p1142 A66-17261  
Uniaxial and hydrostatic pressure effect on absorption edge spectrum and edge excitation spectrum for visible luminescence diamond 07 p1095 A66-17320  
Plastic properties of brittle materials analyzed by hydrostatic pressure, using double ring, calculating radial pressure on sample, between rings, etc 08 p1305 A66-18600  
Magnetic transitions in terbium and dysprosium as affected by hydrostatic pressure at various high pressures and low temperatures 08 p1274 A66-19361  
Origin of diamonds in Canyon Diablo and Novo Urei meteorites 09 p1447 A66-19882  
Elastic behavior of ring reinforced oval cylinder subjected to uniform hydrostatic pressure 10 p1617 A66-21787  
Modified Ellissen finite difference grid solution of primitive hydrostatic equations system for barotropic and baroclinic model of atmosphere 11 p1730 A66-22946  
Minimum-weight analysis of hydrostatically compressed ring-stiffened cone, showing that previous data derived for cylinders in same condition might be useful 12 p1970 A66-24702  
Magnetohydrostatic theory of sunspots combined with optical approach to obtain hydrostatic pressure difference 13 p2184 A66-25622  
Pressure effect on magnetic moment of solids, noting magnetic transition point, ferromagnetic anomalies, etc 15 p2565 A66-29067  
Hydrostatic pressure effect on energy gap, carrier concentration and electron and hole mobilities of indium antimonide 16 p2784 A66-31447  
Buoyancy and magnetohydrostatic stability of magnetic body immersed in magnetizable fluid 16 p2749 A66-31757  
Uniaxial compression and hydrostatic pressure effect on piezoresistance and piezo-Hall effects in n-and p-type AlSb 17 p2984 A66-33153  
Rotating speed effect on design of dynamic seals for rocket engine turbopumps, presenting aspects of design of hydrostatic seal [ASME PAPER 66-FE-18] 17 p2932 A66-33271  
Electron scattering in ABO-type semiconductors by long-wave transverse-optical ferroelectric lattice mode evidenced by hydrostatic pressure measurements 19 p3444 A66-36176  
Compressional wave velocity in limestones, marbles and single crystal of calcite under hydrostatic pressure to 20 kbar 19 p3351 A66-36387  
Modified Ellissen finite difference grid solution of primitive hydrostatic equations system for barotropic and baroclinic model of atmosphere 20 p3593 A66-37859  
Instability of rectangular solid in plane strain subjected axially to constant pressure and laterally to constant hydrostatic pressure 24 p4286 A66-42150  
Large deformation analysis of equilibrium of spherical momentumless shells under hydrostatic pressure 24 p4290 A66-42444

**HYDROSTATICS**  
**SA MAGNETOHYDROSTATICS**  
Hydrostatic problem of calculating potential on surface of nonconfocal ellipsoid from potential of simple layer on similar ellipsoid 01 p0056 A66-10309  
Electrohydrostatic boundary equations solving two-and three-dimensional axisymmetric situation and sessile drop problem 04 p0545 A66-13808  
Equilibrium shape of Moon, assuming

homogeneity computing mean rotation configuration and pertinent single parameter equilibrium shapes 07 p1133 A66-17304  
Extension, for heterogeneous sphere, of previous work which gave expressions for mean strain and rupture as functions of hydrostatic and nonhydrostatic components of free energy 08 p1212 A66-18638  
Approximate reentry velocity and heating equations applied to any atmosphere satisfying hydrostatic equilibrium, noting motion equations for flight path 08 p1303 A66-18836  
Curve fitting technique for integration of hydrostatic equilibrium equations of planetary constitution simplified by introduction of homology-invariant variables 16 p2799 A66-30619  
Silicon, quartz and germanium single crystal density determined via hydrostatic weighing method 16 p2777 A66-30933  
Analytic models of stellar evolution, describing homogeneous and inhomogeneous stages, energy conservation and transport radiative and convective transfer mechanisms, etc 19 p3467 A66-36789

**HYDROX ENGINE**  
Liquid hydrogen-oxygen cryogenic propulsion stages, examining structural material and configuration of propellant tank and thermal flow effects 18 p3246 A66-34007

**HYDROXYL**  
Kinetic studies of hydroxyl radicals in shock waves, considering recombination via particular reaction in lean hydrogen-oxygen mixtures 04 p0596 A66-13646  
Polarized OH emission near W3 region 04 p0579 A66-14175  
OH emission in direction of source W49, comparing earlier observations 04 p0579 A66-14176  
Emission and absorption lines with anomalous intensity distributions indicate hydroxyl molecule concentrations in Sagittarius A 07 p1133 A66-17462  
Kinetics of hydroxyl radical in aqueous solution, examining electron spin resonance spectrum as function of flow rate, temperature and mixture composition 08 p1178 A66-19066  
Galactic center dynamics revealed by hydroxyl radicals present in interstellar medium, noting detection of radio emissions caused by star-excited atoms and molecules 09 p1453 A66-20239  
RF spectrum of OH radiation in interstellar space, including emission intensity and linear polarization 11 p1774 A66-22963  
Nuclear magnetic resonance classification of alcohols and hydroxyl groups from FI-19 spectra of trifluoroacetates 15 p2447 A66-29238  
Optical pumping mechanism for anomalous excitation of OH microwave emissions from H II regions 16 p2807 A66-31756  
Control of abundance of neutral hydroxyl radical in unionized interstellar gas 17 p3003 A66-32658  
Polymer molecular structure, discussing concentration of primary and secondary hydroxyl groups, use of NMR to establish stereo and positional isomeric configuration, etc 17 p2871 A66-33003  
Hydroxyl radical concentration in rarefied CO flame by EPR method 18 p3265 A66-34551  
Stimulated emission processes interpreting OH microwave emission from points in sky, using anisotropic UV radiation which leads to molecule alignment and population inversion 20 p3650 A66-37343  
Direction, frequency and polarization of radio emission from galactic OH determined by hypothesis of stimulated emission 21 p3814 A66-39213  
Dimensions and positions of three sources of 18-cm OH emission determined, using 90-ft steerable paraboloids 21 p3814 A66-39269  
Stokes parameters measurement as function of frequency for anomalous polarized OH emission originating near thermal radio source W3 22 p3978 A66-40015  
Anomalous circular polarization of hydroxyl radical 18-cm radiation from cosmic sources 24 p4272 A66-43188

**HYGIENE**  
**SA HEALTH**



## SA SANITATION

- Space flight problems in maintaining personal hygiene 15 p2435 A66-29456  
Microbial profiles of 20 men under simulated space conditions indicates that certain men can go unwashed six weeks 17 p2856 A66-32160

## HYGROMETER

- Transistorized evaporation to measure vertical water vapor and heat fluxes in lower atmosphere 04 p0519 A66-13671  
Quantitative coulometric analyses of water yield for thermal dehydration of solids, using electrolytic hygrometer cell 07 p1036 A66-18490

## HYPERBOLIC EQUATION

- Mixed boundary value problem for second order hyperbolic equation with discontinuous coefficients having time derivatives 01 p0092 A66-10187  
Recurrence formula for Riemann function for certain operator in  $n$ -dimensional analog of hyperbolic differential equation 01 p0093 A66-10382  
Perturbation of boundary value problem for second order hyperbolic equation 01 p0095 A66-10927  
Nonlinear difference schemes for hyperbolic equation applied to solution of one- and multidimensional transport and quasi-linear equations 01 p0095 A66-11013  
Singular perturbation for mixed Cauchy problem relative to equation with second-order partial linear hyperbolic derivatives 05 p0708 A66-15094  
Cauchy problem for hyperbolic singular convolution-type integral equation 05 p0708 A66-15320  
Existence in large of periodic solutions of hyperbolic partial differential equations 06 p0903 A66-16899  
Asymptotic solutions of problems in wave propagation, examining electromagnetic field equations, hyperbolic equations, radiation from sources, etc 06 p0835 A66-16900  
Criterion of nonrigorous hyperbolicity for equation system with nondiagonal quasi-linear partial derivatives after putting system in diagonal quasi-linear form for relativistic MHD 06 p0921 A66-17058  
Solvability of general mixed boundary value problems for multidimensional hyperbolic integro-differential equation of arbitrary order with analytic coefficients 07 p1056 A66-17608  
Stability of solutions of Cauchy problem for linear hyperbolic differential equations 07 p1056 A66-17609  
Jump discontinuities in nonlinear hyperbolic systems of equations applied to formation of magnetoacoustic shocks from simple waves 07 p1089 A66-17967  
Solutions in large for nonlinear hyperbolic systems of equations by difference approximation 07 p1059 A66-18032  
Modification of Fourier law used to obtain hyperbolic wave equations of thermomagnetoelasticity for conductors and wave equations of thermopiezoelectricity 08 p1270 A66-19113  
Invariant imbedding in transport process and theorems of uniqueness and existence for derived hyperbolic equation 09 p1393 A66-19906  
Dependence of hyperbolic equations in apex of characteristic cone on initial functions 10 p1551 A66-21974  
Relations between coefficients of characteristic equation of automatic systems and parameters of root loci with hyperbolic branches 11 p1680 A66-23325  
Integral relations method to reduce by approximation PDEs to ODEs or to algebraic or transcendental equations 13 p2119 A66-25854  
Protter criterion for correctness of Cauchy problem for second-order degenerate hyperbolic equation 13 p2120 A66-26246  
Optimal control problems described by classical boundary problems for equations of parabolic and hyperbolic type 14 p2263 A66-26768  
Twice continuously differentiable function satisfying nonlinear hyperbolic equation for certain initial conditions obtained, using averaging method 14 p2321 A66-27163  
Decay of solutions of initial boundary value

- problem for hyperbolic equations in unbounded regions 14 p2322 A66-27629  
Finite difference method solution of parabolic and hyperbolic partial differential equations in one space variable 14 p2324 A66-28146  
Mixed problem for general two-dimensional second-order hyperbolic equation with discontinuous coefficients solved by reduction to system of Volterra integral equations 16 p2734 A66-30747  
Multidimensional hyperbolic equations of any order with discontinuous coefficients, noting conditions for analytic or continuous solution 16 p2734 A66-30782  
General numerical method of characteristics for three-dimensional unsteady magnetofluid dynamics of multi-component medium 16 p2690 A66-31653  
Singularities of solutions of nonlinear hyperbolic equations of order greater than unity 17 p2946 A66-32379  
Dependence of hyperbolic equations in apex of characteristic cone on initial functions 19 p3389 A66-36184  
Protter criterion for correctness of Cauchy problem for second-order degenerate hyperbolic equation 19 p3390 A66-36196  
Asymptotic solution of nonlinear hyperbolic equation in gas dynamics, with applications in explosion theory, astrophysics, etc 19 p3390 A66-36200  
Powers of integral operator generated by Cauchy problem for second-order hyperbolic equation solved by Riesz method of analytical continuation 21 p3756 A66-38739  
Riemann representation method in viscoelasticity extended to functional partial differential equations of hyperbolic type 21 p3829 A66-38941  
Differential inequality theorems applied to hyperbolic differential equation, discussing Riemann functions and sufficient conditions for characteristic and Cauchy problems for quasi-linear Blanchi equation 21 p3757 A66-39232  
Frequency variations of piezoelectric circuit parameters of junction transistor, noting expansion of hyperbolic function into Taylor series 22 p3873 A66-39815  
Cauchy and boundary value problems for second-order hyperbolic equations degenerating within and on boundary of region 22 p3939 A66-40189  
Multidimensional hyperbolic equations of any order with discontinuous coefficients, noting conditions for analytic or continuous solution 22 p3939 A66-40444  
Progressing wave formalism method of obtaining approximate solution of suitable problems of wave equation and other linear hyperbolic partial differential equations 23 p4036 A66-41055  
Weak and strict solution existence theorem for initial-boundary value problem for nonlinear hyperbolic equation in relativistic quantum mechanics 24 p4237 A66-42829
- HYPERBOLIC ORBIT**  
Axisymmetric cluster of hyperbolic trajectories of material particle near planet, for space navigation application 02 p0289 A66-11652  
Powered manned Mars flyby departing Earth near minimum velocity point, considering required maneuver within Mars influence for valid return legs 11 p1768 A66-22455  
Optimum energy transfer from hyperbolic orbit in Newtonian central force field in absence of transfer time limitations 11 p1774 A66-23035  
Onboard guidance scheme as backup to Earth-based orbit determination techniques and for approach navigation and orbit correction in planetary capture maneuver 13 p2123 A66-25253  
Hyperbolic comets and Oort hypothesis of cometary cloud, discussing probability distribution and existence of interstellar source 17 p3013 A66-33406  
Single-impulse transition in Newtonian central force field from hyperbolic to elliptical orbit in case of radial impulse 19 p3455 A66-35276  
Computer iteration scheme for calculating arbitrary hyperbolic transfer orbit in field of attracting center, based on Gauss equations 19 p3455 A66-35278

## HYPERBOLIC REENTRY

- Reentry flight corridor depth reduction result of inadequate flight data hyperbolic speeds, noting overshoot limit and inverted attitude [AIAA PAPER 65-19] 12 p1952 A66-24619  
Optimum entry vehicle design using aerobreaking for manned Earth entry hyperbolic speeds, examining blunted conic and tetrahedral configurations [AIAA PAPER 66-489] 18 p3239 A66-33619  
Aerothermodynamic characteristics of Apollo command module at hyperbolic Earth entry velocities [AIAA PAPER 65-491] 20 p3664 A66-38119
- HYPERBOLIC SPACE**  
Aberration, Thomas precession and for relativistic collision invariants Lobachevsky or hyperbolic space simplified relativistic kinematics 03 p0392 A66-12619
- HYPERBOLIC SYSTEM**  
Bergeron and first approximation method for solving problems of unsteady fluid flow in pipeline 04 p0511 A66-14119  
Flight testing of FAA-Lear Siegler receiver/converter airborne system with Loran-C hyperbolic navigation system 07 p1069 A66-17719  
Existence and uniqueness of piecewise continuous solution to two-dimensional linear first order hyperbolic system with discontinuous coefficients 07 p1060 A66-18119  
Omega location and satellite reporting for worldwide observation and navigation systems 08 p1252 A66-19519  
Convergence of difference approximation in rectangular grids for general first-order quasi-linear hyperbolic initial value problem in two independent variables 20 p3590 A66-37519  
DIVIC /digital variable increment computer/ for solving hyperbolic navigation problems, examining computational algorithms 22 p3945 A66-40319  
Optimal regulation of linear symmetric hyperbolic systems of partial differential equations with finite dimensional control 22 p3884 A66-40519  
General theory of mixed problems for two-dimensional hyperbolic system of any order with continuous and discontinuous coefficients 24 p4230 A66-42219
- HYPERCAPNIA**  
Effects of cold and abnormal atmosphere, discussing tolerance limits to hypercapnia, anoxia induced hypothermia and hypoxia 04 p0464 A66-14019
- HYPERFINE STRUCTURE**  
Electron paramagnetic resonance in biradicals of hydrazine series, discussing structural changes during transition from mono- to biradical state 04 p0572 A66-13819  
Donor concentration in semiconductor which hyperfine structure of spin absorption lines vanishes 04 p0564 A66-14219  
Polarization of nuclear spins in semiconductor in strong electric and magnetic fields, noting relaxation mechanisms, and hyperfine relaxation frequency 04 p0567 A66-14319  
Constants A and B of cesium superfluid structure calculated from magnetic sublevel intersections 05 p0741 A66-15819  
Temperature and donor concentration width of electron spin resonance line center of hyperfine spectrum for phosphorus- and arsenic-doped silicon 08 p1270 A66-19113  
Hyperfine structure of p-n junction phase boundaries in silicon according to electron microscopy data 12 p1930 A66-24419  
7P terms of excited chromium configurations examined, using level crossing and double resonance spectroscopy noting core polarization 13 p2135 A66-26219  
Values for contribution of core polarization to hyperfine structure of excited states of chromium compared theoretically and experimentally, extracting core contribution to magnetic field 13 p2135 A66-26219  
Polarization of nuclear spins in semiconductor in strong electric and magnetic fields, noting relaxation mechanisms, and hyperfine relaxation frequency 14 p2367 A66-28219  
Energy from hydrogen molecule interaction with magnetic field and from hyperfine interaction expressed as products



- irreducible spherical  
sensors 15 p2548 A66-29806
- Fine and hyperfine structure of term in 3p level of lithium studied by level-crossing spectroscopy technique, determining fine structure separation  
value 19 p3443 A66-35989
- Hyperfine structure of p-n junction phase boundaries in silicon according to electron microscopy data 20 p3620 A66-37693
- Hyperfine spectrum of xenon in 3.5 mm maser transition noting experimental setup, gain profiles for various input power levels and structural properties 21 p3746 A66-38763
- Anomalous circular polarization of hydroxyl radical 18-cm radiation from cosmic sources 24 p4272 A66-43188
- HYPERGEOMETRIC FUNCTION**
- Rational approximations to generalized hypergeometric functions and error function proven to converge to desired limit 01 p0093 A66-10384
- Atomic integral obtained with magnetic dipole-dipole operator in form of finite sum of integrals over hypergeometric functions 11 p1739 A66-22887
- Hypergeometric mean value, showing expression for mean of order t of series of positive values with positive weights as limiting case 11 p1722 A66-22953
- Analytic hyperfunction solution of elliptic equation 13 p2117 A66-25473
- Generalized heat equation solution expansion in terms of radial heat polynomials, Appel transforms and Laguerre polynomials 13 p2118 A66-25793
- Autocorrelation and hypergeometric function applied in evaluating response of nonlinearities to Gaussian noise 14 p2267 A66-27726
- Fourier series of Gegenbauer function, examining convergence characteristics 18 p3126 A66-33696
- Exact analytic solution, in confluent hypergeometric functions, to problem of stability of conical shell under uniformly distributed longitudinal compressive forces 18 p3252 A66-33709
- HYPERGOLIC PROPELLANT**
- Flow rate distribution and mixing ratio of two impinging jets in simulation of bipropellant liquid rocket system, using hypergolic propellants 02 p0278 A66-11590
- Hypergolic ignition of light hydrocarbon fuels with fluorine-oxygen /flox/ mixtures [AIAA PAPER WSCI-65-23] 05 p0743 A66-15147
- Hypergolic ignition and restart in Plexiglas window hybrid rocket motor, including oxidizer flow transient, flame propagation, chamber pressurization rates, etc [AIAA PAPER 66-69] 07 p1111 A66-18452
- Flame spreading velocity over surface of igniting solid rocket propellants as function of atmospheric pressure and chemistry and specimen surface condition [AIAA PAPER 66-68] 08 p1317 A66-18949
- Tagaform synthetic hypergolic fuel for hybrid rockets, discussing polymerization, ignition delay, etc 11 p1760 A66-22249
- Hybrid rocket motor HR 4, using fuming nitric acid as oxidizer and mixture of polyesters and acrylic plastics as other solid propellant 12 p1935 A66-23867
- Swedish hypergolic propellant for rocket motors consisting of fuming nitric acid as oxidizer and condensation product of liquid aromatic amines and aldehydes as solid fuel 14 p2374 A66-27566
- Flox-light hydrocarbon combinations desirable as liquid rocket propellants due to high specific impulse, hypergolicity and cooling properties [AIAA PAPER 66-581] 18 p3159 A66-33809
- Stability of various plastics toward hypergolic rocket fuel components aeroline and nitrogen tetroxide 18 p3125 A66-35242
- Hypergolic liquid propellant combinations, noting effect of feed pressure, injection tube diameter and fluid free path on ignition process in combustion chamber 20 p3626 A66-38140
- Hypergolic ignition of composite solid propellants, examining oxidizer concentration, heat flux and exothermic reactions 22 p3969 A66-39871
- Low pressure low temperature ignition of hypergolic propellants, particularly hydrazine-nitrogen tetroxide systems, in space environment simulator and conclusions on gas phase reactions 22 p3892 A66-40237
- HYPERON**
- K meson and hyperon production cross sections, discussing primary energy dependence and upper limit determination 07 p1113 A66-17539
- Dynamics and symmetries of nonleptonic hyperon decay based on assumptions of parity-violating and parity-conserving amplitudes and SU symmetry 20 p3606 A66-38292
- HYPEROXIA**
- Preference of mice for oxygen-poor atmosphere after removal from 60 and 90 percent oxygen atmospheres 15 p2439 A66-29489
- HYPERPLANE**
- Invariant hyperplanes for linear dynamical systems, discussing geometric properties and relation to controllability and observability 12 p1849 A66-24256
- HYPERSONIC AIRCRAFT**
- Turboramjet-powered hypersonic aircraft evaluated for cruise and boost mission for orbital launching [AIAA PAPER 65-759] 03 p0318 A66-12553
- Hypersonic aircraft and aerodynamic aspects for global transport operation noting shock waves, Mach number and gas dynamics 04 p0453 A66-13504
- Engines for supersonic and hypersonic aircraft to be used in next decade, noting suitability for cruise aircraft or boosters 09 p1435 A66-20668
- Propulsion problems for engine of 5000 mph aircraft noting ramjet, cooling, intake, nozzle, etc 09 p1435 A66-20669
- Response of hypersonic aircraft to abrupt control displacements, determining vehicle characteristics, design and operational parameters 09 p1330 A66-20739
- Boundary layer effect on lift and drag characteristics of hypersonic lifting bodies 10 p1480 A66-21409
- Stabilizing methods for hypersonic aircraft, noting effect of aircraft characteristic parameters on magnitude of balancing coefficients of lifting force 14 p2223 A66-27680
- Tank design, optimization program and testing for effect on storage penalties associated with liquid hydrogen for hypersonic aircraft 14 p2394 A66-28026
- Refractory ceramics for air breathing engine for Mach 7 aircraft, noting zirconia properties 16 p2790 A66-30257
- High performance aerodynamic vehicle design, noting configuration variables, optimum performance parameters, vehicle force characteristics, optimization of hypersonic aircraft performance, etc [AIAA PAPER 66-486] 16 p2635 A66-31476
- Turboramjet powered hypersonic aircraft evaluated for cruise and boost mission for orbital launching [AIAA PAPER 65-759] 23 p4015 A66-40974
- Hypersonic transport /HST/ evaluation noting problems in aerodynamics, economics, structures, propulsion systems, etc 24 p4159 A66-42236
- Aircraft flying up to 6000 miles at Mach numbers up to 8, noting problems in aerodynamics, propulsion, structural weight, cooling, etc 24 p4157 A66-42237
- Hypersonic transport technology, considering designs for Mach numbers up to 14, altitude up to 140,000 ft and 150 passengers 24 p4159 A66-42238
- Stability, control, navigation, guidance and air traffic control of hypersonic vehicles noting inertial technology, flight planning and optimal control 24 p4235 A66-42239
- HYPERSONIC BOUNDARY LAYER**
- Introductory book on hypersonic aerodynamics covering continuum flow of inviscid nonheat-conducting perfect gas and real gas, viscous and low density effects in hypersonic flow 02 p0176 A66-11875
- Laminar boundary layer transition on highly cooled 10 degree cone in hypersonic flow, using heat gauges to study turbulent burst propagation 03 p0315 A66-12788
- Controlled three-dimensional roughness effect on hypersonic laminar boundary layer transition
- [AIAA PAPER 66-26] 06 p0804 A66-17092
- NAE helium hypersonic wind tunnel for hypersonic flight simulation and boundary layer studies 07 p1018 A66-18050
- Asymmetric hypersonic blunt body problem of determining two-dimensional steady rotational flow field between profile and detached shock 07 p0982 A66-18132
- Species diffusion in frozen hypersonic boundary layer with Falkner-Skan velocity profiles, where surface is linear, given as Mellin transform, constructing series and asymptotic expansion of surface concentration 13 p2060 A66-25158
- Hypersonic viscous interaction on very slender body of revolution having thick boundary layer and surface mass transfer 13 p1992 A66-26447
- Analytical methods for studying turbulent boundary layers at high Mach numbers, comparing theory and experiments for flat plate flow, predicting boundary layer properties around hypersonic configurations 14 p2217 A66-27098
- Laminar boundary layer transition in hypersonic shock tunnel of cone, noting effect of high Mach numbers and tip surface roughness, using surface heat transfer gauges [AIAA PAPER 66-494] 17 p2841 A66-32772
- Hypersonic boundary layer separation and expansion at shoulder of blunt based body 21 p3693 A66-38683
- Bluntness and boundary layer displacement effects on air breathing engine hypersonic inlet flow fields [AIAA PAPER 65-617] 23 p4007 A66-41109
- HYPERSONIC COMBUSTION**
- Impact-induced combustion in hypersonic ramjet engines, determining hypersonic fuel-air mixing from hydrogen concentration at Laval nozzle outlet 10 p1591 A66-21359
- Model determination of effects of injecting and mixing fuel in inlet diffuser of two-shock inlet hypersonic ramjet or scramjet [AIAA PAPER 66-648] 24 p4261 A66-42641
- HYPERSONIC FLIGHT**
- Base flow and near wake problem at very low Reynolds numbers, using general solution of Stokes equation of motion for two-dimensional and axisymmetric flows 04 p0456 A66-14469
- Supersonic combustion ramjet engine /scramjet/ for hypersonic flight noting fuel injection, chemical kinetics, combustor cooling, mixing processes and measurements 05 p0745 A66-15272
- High temperature materials for hypersonic air-breathing engines, noting usefulness of coated refractory metals 09 p1435 A66-20670
- Scramjet performance at high hypersonic speeds noting integration with waverider vehicle, hydrogen fuel, drag forces effect, test program, etc 09 p1435 A66-20671
- Ablative materials for thermal protection and minimum mass transfer of aircraft flying at hypersonic speeds 10 p1620 A66-21404
- X-15 as tool for progress in hypersonic flight, examining problems of transmitting and reducing wealth of telemetry data 16 p2634 A66-31285
- HYPERSONIC FLOW**
- Hypersonic flow field about slender cone derived from heat-pressure-wake survey 01 p0007 A66-10618
- Density distribution before sphere in low density hypersonic gas flow measured with electron beam densitometer 01 p0059 A66-10635
- Introductory book on hypersonic aerodynamics covering continuum flow of inviscid nonheat-conducting perfect gas and real gas, viscous and low density effects in hypersonic flow 02 p0176 A66-11875
- Hypersonic flow separation over simple geometries and aerodynamic controls, noting pressure gradients and heating-rate distributions [AIAA PAPER 65-753] 03 p0314 A66-12587
- Rarefied hypersonic flow at high Mach numbers and stagnation temperatures encountered by ballistic missiles and satellites, noting air plasma with magnetic field [AIAA PAPER 65-754] 03 p0354 A66-12588
- Combustion and sublimation in aerothermochemical interaction between



dissociated air stream and graphite surface in hypersonic laminar viscous flow [AIAA PAPER 65-42] 03 p0444 A66-12797

Dissociation or ionization effects of air on inviscid hypersonic flow past circular cone with attached shock wave 03 p0316 A66-12928

Numerical solutions for inviscid nitrogen gas flows over circular cylinder where nonequilibrium prevails through nose region 03 p0317 A66-13211

Gun-shock tunnel for hypersonic aerodynamics experiments 03 p0353 A66-13213

Laboratory test methods for hypersonic flow simulation past reentry vehicle, ICBM and meteorite 04 p0506 A66-13502

Supersonic and hypersonic flow fields around plane and axisymmetric bodies and inlets obtained by nonlinear characteristics method 04 p0454 A66-13519

Wing-fuselage interaction effects on static and dynamic stability at low and moderate hypersonic Mach numbers by small-disturbance approximation to shock-expansion method [AIAA PAPER 65-719] 04 p0454 A66-13552

Hypersonic airflow at alpha angle of attack about flat wing with shock wave on upstream side attached 04 p0454 A66-13572

Extremal problems in aerodynamics, discussing mathematical and physical models for optimum aerodynamic shape 04 p0455 A66-13995

Shrello approximation used to derive formulas for moment characteristics of axisymmetric bodies rotating in hypersonic free molecular flow 04 p0456 A66-14155

Effect of interaction of dissipating and isentropic currents on flow at base region of bodies moving with hypersonic velocity 05 p0607 A66-15314

Heat transfer and equilibrium temperature on flat plate in region of strong interaction in hypersonic flow 05 p0607 A66-15465

Heat transfer to blunt bodies with, catalytic and noncatalytic surfaces in nonequilibrium dissociated hypersonic flow [AIAA PAPER 66-3] 05 p0609 A66-15850

Longitudinal and transversal contours minimizing drag of slender homothetic body in hypersonic flow with Newtonian pressure distribution and constant skin-friction coefficient 06 p0802 A66-16911

Flow field study of shock wave and boundary layer development at leading edge of sharp flat plate in rarefied hypersonic flow [AIAA PAPER 66-31] 06 p0803 A66-17082

Atmospheric argon effect on hypersonic stagnation point convective heat transfer, using arc-heated shock tube simulating flight velocities up to 34,000 fps [AIAA PAPER 66-29] 07 p1153 A66-17891

Hypersonic perfect gas flow around slightly blunted plate, discussing analogy between asymptotic shock behavior and explosion theory 07 p0981 A66-18109

Heat transfer and stability of laminar hypersonic separated flow around annular cavity conical model 07 p0981 A66-18117

Inner and outer expansions method applied to source flow model involving viscous effects in hypersonic axisymmetric free jets at large Reynolds numbers 07 p0982 A66-18122

Hypersonic gas flow near blunt body, examining entropy effects 07 p0983 A66-18140

Hypersonic gas flow past axisymmetric slender blunt body by Chernyi approximate method 07 p0983 A66-18142

Hypersonic collisionless source flow analysis of comet dust tail model, assuming composition consists of small dust particles acted upon by solar radiation pressure [AIAA PAPER 66-32] 08 p1289 A66-18948

Pressure distribution and heat transfer for laminar boundary layer flow over highly swept blunt delta wings in hypersonic free stream [AIAA PAPER 66-130] 08 p1162 A66-18953

Shock tunnel heat transfer measurement and hypersonic viscous flow over pointed cones, particularly viscous-layer regime at low Reynolds numbers [AIAA PAPER 66-34] 08 p1163 A66-18957

Inviscid supersonic nozzle flow of ideal dissociating gas, sudden freezing,

equilibrium-recombination mechanism and velocity distribution [AIAA PAPER 66-1] 08 p1163 A66-18983

Exact numerical solution of time-dependent compressible Navier-Stokes equations describing transient compressible viscous heat-conducting flow [AIAA PAPER 66-30] 08 p1207 A66-18986

Aerodynamic properties of simple bodies in hypersonic transition regime 08 p1164 A66-19132

Angle of attack, leading edge sweep and thicknesses effects on hypersonic flow field of slender delta wing 08 p1164 A66-19135

Shock wave shapes on cold flat plate in rarefied hypersonic flow tunnel measured by optical-flow techniques 08 p1165 A66-19165

Heat transfer to wedge in nearly free-molecular hypersonic flow of strongly rarefied gas 08 p1165 A66-19484

Peculiarities of aerodynamic characteristics of flow past plate and pointed and blunt slender cones in viscous hypersonic thermodynamically ideal gas 08 p1165 A66-19571

Equations of inviscid flow of perfect gas over cusped concave bodies, noting dependency of shock wave slope on infinite Mach number 08 p1166 A66-19818

Conservation laws involving mass, momentum and energy applied to asymptotic properties of hypersonic flow 09 p1327 A66-20266

Hypersonic flow of air past circular cylinder with nonequilibrium oxygen dissociation, including dissociation of free stream 10 p1479 A66-21375

Newtonian pressure law and minimum resistance body in hypersonic aerodynamics 11 p1688 A66-22510

Drag minimization in slender bodies of revolution in hypersonic flow with Newtonian pressure distribution 11 p1631 A66-22512

Optimum slender body with variable skin friction coefficient, noting minimal drag design for hypersonic flow under Newtonian pressure distribution 11 p1631 A66-22513

Minimum pressure drag for nonslender hypersonic body calculated, using normalized coordinates 11 p1631 A66-22515

Shape of nonslender body of revolution for minimum total drag in viscous hypersonic flow at Newtonian pressure distribution and constant friction coefficient 11 p1631 A66-22516

Transversal contour of minimum pressure drag for body with noncircular cross section 11 p1631 A66-22517

Starlike solutions of optimum transversal contour problem treated by Young inequality 11 p1631 A66-22519

Total drag minimization for three-dimensional body in Newtonian flow, assuming two planes of symmetry and constant skin-friction coefficient 11 p1632 A66-22520

Slender shapes of minimum pressure drag in hypersonic inviscid flow characterized by Newton-Busemann law 11 p1632 A66-22522

Nonslender shapes of minimum pressure drag in flow characterized by Newton-Busemann pressure law 11 p1632 A66-22523

Expansion tube for interferometric observation of hypersonic flow fields 11 p1684 A66-22830

Arc-driven vortex type heater-accelerator for possible use in reentry flight simulation 11 p1684 A66-22832

Performance of simple diffusers of fixed geometry in flow regimes with viscous and compressibility influence involving free-jet test sections, conical and contoured nozzles and gas flows at high Mach numbers 11 p1686 A66-22844

Molecular collision effect on transitional drag on cylinder traversing rarefied gas at hypersonic Mach numbers, discussing departure from free flow 11 p1632 A66-22920

Transition from near free molecular flow at leading edge of flat plate in rarefied hypersonic flow to continuum boundary layer flow downstream 11 p1633 A66-22925

Heat transfer and pressure data extended from classical thin boundary layer regime to near-free-molecule flow in study of low density effects in hypersonic wedge flows 11 p1633 A66-22928

Flow over sharp and blunt flat plates zero angle of attack in hypersonic shock tunnel, measuring surface skin friction, heat transfer, static pressure and shock layer pitot pressure 11 p1633 A66-22925

Pressure distribution and low density effects on sharp flat plates and sharp blunt cones measured in hypersonic wind tunnel 11 p1634 A66-22928

Flat plate in hypersonic flow analysis shock tunnel, obtaining surface pressure using electron beam densitometer 11 p1634 A66-22928

Hypersonic rarefied gas flow in shock ducts, measuring wall static pressure and stream total pressure distributions 11 p1634 A66-22928

Modified Newtonian-Prandtl Meyer approximation technique to determine pressure distribution over blunt body 12 p1796 A66-23606

Inviscid hypersonic flow over compressed side of delta wing of moderate aspect ratio 12 p1796 A66-23606

Steady state expansion of gas into vacuum considering continuum inviscid analysis collision-free analysis, supersonic flow at hypersonic limits, etc, for spherical and cylindrical symmetry 12 p1860 A66-23606

Simplified Navier-Stokes equations for steady hypersonic viscous flow past slender shapes with sharp leading edges 12 p1796 A66-23606

Langmuir probe measurements in hypersonic plasma flow, evaluating properties of plasma jet wind tunnel electron temperature and plasma density 12 p1920 A66-23806

Hypersonic flow of equilibrium dissociated air around sphere numerically analyzed Lunev method 12 p1796 A66-23806

Radiative heat transfer near stagnation point of blunt body in hypersonic flow noting effect on convective heat transfer 12 p1978 A66-24206

Boundary value problems in plane axisymmetric hypersonic flow of viscous ideal gas past blunt body 12 p1797 A66-24306

Hypersonic flow of inviscid gas past cone obtaining solution for entire flow including turbulent boundary layer and velocity field using zero approximation method 12 p1798 A66-24406

Aerodynamic characteristics of rectangular plates in hypersonic flow of rarefied gas differing in aspect ratio, thickness and angles of attack, determining maximum lift drag ratio 12 p1798 A66-24406

Hypersonic or supersonic flow of gas past yawing delta wing with stall fence 12 p1799 A66-24406

Properties of compressible boundary layer with heat transfer and arbitrary pressure gradients calculated, using integral equation and correlation concept for application to hypersonic flows 12 p1865 A66-24506

Laminar hypersonic flow past sphere based on constant-density approximation, solving Navier-Stokes equations and comparing with values of shock Reynolds number 12 p1800 A66-24906

Fundamental phenomena in hypersonic flow - Conference, Buffalo, June 1966 13 p2060 A66-25106

Asymptotic behavior of two-dimensional inviscid flow at infinite Mach number past power-law body, considering flow over flat plate and blunt body followed by cylindrical afterbody 13 p2060 A66-25106

Chemical reactions in gas flows including relation between dissociation and recombination kinetics, thermal decomposition of hydrazine, kinetics of high temperature air, etc, analyzed, using shock tube 13 p2016 A66-25106

Langmuir probe to measure stagnation region shock layer ionization distribution under nonequilibrium hypersonic flow conditions [AIAA PAPER 66-167] 13 p2138 A66-25106

Hypersonic flow field about slender cone derived from heat-pressure-wake survey 13 p1990 A66-25106

Distribution, as function of azimuth, static pressure and mass and heat transfer coefficients for case of interaction between detached shock wave on cylinder nose and hypersonic flow and turbulent boundary



- layer along wall 13 p1991 A66-25464  
 Inviscid hypersonic flow of nonuniform  
 incident stream over wedge, noting vorticity  
 effects, perturbation equations and boundary  
 conditions 13 p1992 A66-26665  
 Rotational flow properties in ideal inviscid  
 near layer about arbitrarily shaped blunt-  
 based body in hypersonic  
 flow 13 p1993 A66-26727  
 First-collision process at sharp leading  
 edge of flat plate aligned with hypersonic  
 free stream 13 p1993 A66-26728  
 Shock bounded self-similar flows over  
 slender bodies with volumetric mass,  
 momentum and energy 13 p2071 A66-26731  
 Addition 13 p2071 A66-26731  
 Laminar separated hypersonic flow over  
 spiked bodies in gun tunnel for analyzing  
 parameters influencing heat transfer rates  
 in reattachment region 14 p2218 A66-27403  
 Mach number, Reynolds number and  
 boundary layer trip devices effect on base  
 pressure 14 p2219 A66-27443  
 Streamline flow of ideal stable gas with  
 constant ratio of specific heats around  
 conical body with arbitrary taper,  
 determining flow velocity  
 components 14 p2220 A66-27679  
 Plane or axisymmetric hypersonic ideal gas  
 flow in divergent nozzle with parabolic wall  
 shape 14 p2221 A66-28056  
 MHD equations applied to hypersonic flow  
 of solar plasma around magnetosphere and  
 approximation with simpler equations of gas  
 dynamics 15 p2483 A66-28815  
 Variation problem solution in hypersonic  
 gas dynamics, noting intake portion  
 construction for body with minimum  
 resistance for limited length and flat  
 end 15 p2477 A66-28956  
 Conditions at head shock wave in viscous  
 hypersonic flow past blunt body for study  
 of boundary layer 15 p2423 A66-28960  
 Separation 15 p2423 A66-28960  
 Flow pattern and heat transfer distribution  
 in regions of adverse pressure gradient and  
 separated flow over two-dimensional models  
 at Mach 10 airflow 15 p2424 A66-29271  
 Unsteady flow during starting process in  
 hypersonic nozzle, discussing initial pressure  
 effect and behavior of secondary shock  
 wave 15 p2425 A66-29684  
 Boltzmann equation for Pitot tube  
 problem, using distribution function,  
 deriving equations for rarefied gas flow in  
 impact tube under hypersonic and adiabatic  
 conditions 15 p2481 A66-29739  
 Book on dynamics and thermodynamics of  
 gases, emphasizing modern theory of gas  
 behavior at hypersonic velocities and  
 extremely high altitudes 15 p2482 A66-29914  
 Terrestrial origin of tektites, noting  
 possible connection with cometary collision  
 and evidence of lunar origin for  
 some 16 p2802 A66-30926  
 Stagnation region of solid body of  
 revolution in low density hypersonic flow  
 with low Reynolds 16 p2629 A66-31033  
 Stagnation region for body of revolution in  
 analyzing temperature, velocity and atom  
 hypersonic flow with low Reynolds number,  
 concentration under aerodynamic  
 heating 16 p2686 A66-31037  
 Skin friction methods compared for  
 problem of turbulent compressible boundary  
 layer on flat plate at hypersonic Mach  
 numbers 16 p2686 A66-31118  
 Approximation of Chaplygin plane motion  
 equations of gas flow at high supersonic  
 velocities 16 p2688 A66-31304  
 Hypersonic flow past blunt body near  
 stagnation point examined, noting surface  
 layer, characterized by increased density  
 and decreased entropy of 16 p2630 A66-31305  
 Hypersonic laminar boundary layer flow of  
 equilibrium dissociating 16 p2630 A66-31306  
 Three-dimensional boundary layer flow  
 over windward side of flat delta wing in  
 hypersonic flow at moderate angle of attack,  
 examining viscous-inviscid interaction  
 [AIAA PAPER 66-492] 16 p2631 A66-31477  
 Hypersonic source flow effect on shock  
 shape and surface pressure of sharp-nosed  
 slender bodies 16 p2632 A66-31592  
 Hypersonic strong-interaction similarity  
 solutions for viscous compressible flow past  
 plate analyzed using Navier-Stokes  
 equations 16 p2632 A66-31655  
 Inviscid hypersonic flow past circular cone  
 at finite angle of attack with attached shock  
 wave in presence of dissociation air behind  
 shock wave 17 p2837 A66-32033  
 Pressure distribution, skin friction and  
 heat transfer for sharp- and blunt-nosed  
 slender bodies in hypersonic air  
 flow 17 p2837 A66-32070  
 Source type hypersonic free stream effects  
 on flow field about axisymmetric cone,  
 obtaining properties in shock layer,  
 boundary layer, pressure gradient,  
 etc 17 p2837 A66-32080  
 Base, recompression and laminar near wake  
 regions of cones in hypersonic  
 flow 17 p2838 A66-32438  
 Static and dynamic stability derivatives of  
 sharp wedges in viscous laminar hypersonic  
 flow determined, using approximate  
 pressure relations 17 p2839 A66-32444  
 Hypersonic self-similarity of barrel shock  
 in source-type free jets at high pressure  
 ratio 17 p2839 A66-32468  
 Gap size effect on pressure and  
 aerodynamic heating over flap of blunt delta  
 wing in hypersonic flow  
 [AIAA PAPER 66-408] 17 p2840 A66-32747  
 Laminar separation in supersonic and  
 hypersonic flow analyzed in gun tunnel,  
 noting concept of incipient separation and  
 free interaction principle  
 [AIAA PAPER 66-455] 17 p2910 A66-32761  
 Head wave of frictionless flow of real gas  
 past positioned circular cone for small or  
 zero angles of attack 17 p2842 A66-33169  
 Implicit finite difference method applied  
 to plane hypersonic flow over blunt circular  
 cylinder 17 p2842 A66-33170  
 Extremization of products of powers of  
 functionals as applied to flat top wings for  
 maximizing lift drag ratio in hypersonic  
 flow 17 p2842 A66-33242  
 Hypersonic argon beam flow past  
 cylindrical thermal nozzle 17 p2974 A66-33287  
 Hypersonic low-density free-stream viscous-  
 inviscid interaction along intersection of two  
 planes 17 p2916 A66-33480  
 Inviscid hypersonic flow of perfect gas  
 past symmetric two-dimensional and  
 axisymmetric blunt bodies at angle of attack  
 [AIAA PAPER 66-411] 18 p3045 A66-33636  
 Nose bluntness and angle of attack effects  
 on hypersonic flow, noting shock wave  
 deflection decrease of minimum possible  
 shock angle, varying specific heat ratio,  
 convective heating, boundary layer  
 transition, etc 18 p3046 A66-33639  
 [AIAA PAPER 66-414] 18 p3046 A66-33639  
 Lift, drag and static pitching  
 measurements on lifting bodies at simulated  
 hypersonic cold-wall conditions  
 [AIAA PAPER 66-467] 18 p3046 A66-33651  
 Laminar, transitional and turbulent  
 boundary layer flows with adverse pressure  
 gradient on axisymmetric blunted conical  
 flared body at Mach 10  
 [AIAA PAPER 66-493] 18 p3047 A66-33658  
 Average pressure and skin friction on  
 slender two-dimensional wings in hypersonic  
 flow, taking into account displacement  
 effects of boundary layer 18 p3048 A66-33823  
 Approximation method for compressible  
 laminar heat transfer to blunt axisymmetric  
 bodies in high speed flow 18 p3048 A66-33824  
 Shock wave boundary layer interactions  
 and shear flow regimes in hypersonic inlet  
 flows 18 p3049 A66-34447  
 [AIAA PAPER 66-606] 18 p3049 A66-34447  
 Diffusion of chemically frozen partially  
 dissociated gas over surfaces with  
 discontinuous catalytic 18 p3266 A66-34928  
 Binary flutter of wedges in hypersonic  
 flow according to piston theory and  
 McIntosh derivatives 19 p3473 A66-35625  
 Hall effect influence on steady hypersonic  
 flow of inviscid compressible gas past  
 wedge 19 p3275 A66-35736  
 Optimum form for hypersonic profile with  
 minimum drag for given bending strength  
 solved by variational 20 p3491 A66-36922  
 Hypersonic plasma generator for reentry  
 vehicles with arc tunnel experimental data  
 and analysis of nonequilibrium chemical  
 reaction between cesium atoms and ionized  
 air species 20 p3497 A66-37158  
 Book on transonic and hypersonic flow  
 theory covering motion and shock equations,  
 application of Newtonian theory,  
 temperature effect, behavior of minimum  
 drag bodies, etc 20 p3492 A66-37495  
 Localized convection coefficient for  
 hypersonic separation line along delta wing  
 leading edge calculated, using Mangler and  
 Stewartson transformation 20 p3492 A66-37818  
 Inviscid hypersonic nonequilibrium flow of  
 three-component gas past circular cone,  
 using exact reaction-rate equations to  
 correct solution first obtained from  
 approximate equations 21 p3693 A66-38711  
 Stability derivatives of sharp cones  
 performing pitching oscillations in viscous  
 hypersonic flow 21 p3693 A66-38723  
 Conical MHD shock wave in  
 axisymmetric hypersonic viscous-layer  
 flow 21 p3727 A66-39185  
 Dissociation of hypersonic airflow past  
 circular cylinder at zero angle of  
 incidence 21 p3695 A66-39230  
 Oblique shock wave formal determination  
 of aerodynamic forces and pressure  
 distribution on delta wings in supersonic or  
 moderately hypersonic  
 flow 21 p3695 A66-39602  
 Hypersonic flow, discussing heat effect on  
 flow parameters, shock and motion  
 equations, drag increase,  
 etc 22 p3897 A66-39699  
 Hypersonic gas flow past blunt body  
 problem solved by integral correlation  
 method, taking into account radiation  
 effects and gas dynamic parameter  
 distribution in shock wave  
 layer 22 p3897 A66-39902  
 Model of laminar hypersonic base flow  
 region of slender bodies, introducing base  
 height and Reynolds number variation of  
 base pressure ratio 22 p3843 A66-40345  
 Flow field study of shock wave and  
 boundary layer development at leading edge  
 of sharp flat plate in rarefied hypersonic  
 flow 22 p3844 A66-40349  
 [AIAA PAPER 66-31] 22 p3844 A66-40349  
 Probe design for mass flux, stagnation  
 point heat transfer and total enthalpy  
 measurements of high temperature  
 hypersonic gas flows  
 [AIAA PAPER 66-750] 22 p3919 A66-40635  
 Shock impingement on blunt body in  
 hypersonic flow, noting alteration of flow  
 and local heat transfer rate near  
 impingement point 22 p3846 A66-40641  
 [AIAA PAPER 66-756] 22 p3846 A66-40641  
 Reentry simulation systems using MHD  
 accelerators, technical difficulties,  
 performance and efficiency  
 [ICAS PAPER 66-39] 22 p3896 A66-40661  
 Aerodynamic analysis of complex shapes in  
 hypersonic flow, using digital computer  
 [ICAS PAPER 66-25] 22 p3847 A66-40665  
 Surface catalytic and Reynolds number  
 effects on nonequilibrium hypersonic  
 stagnation flow of air or diatomic gas on  
 highly cooled blunt body 22 p3847 A66-40919  
 Moment method in hypersonic flow of  
 rarefied gas around bodies of arbitrary  
 shape 23 p4054 A66-41357  
 Similarity laws in hypersonic flow of real  
 gas around thin blunted bodies, particularly  
 bodies with rough lateral  
 surface 23 p4009 A66-41720  
 Heat transfer to blunt bodies with catalytic  
 and noncatalytic surfaces in nonequilibrium  
 dissociated hypersonic flow  
 [AIAA PAPER 66-3] 23 p4150 A66-41878  
 Perturbation analysis of radiative cooling  
 in shock layers and radiative heat transfer  
 effects on hypersonic flow over wedge and  
 circular cone 23 p4011 A66-41882  
 Shock wave transport effects on  
 hypersonic leading edge flow past sharp  
 plate, discussing Rankine-Hugoniot  
 relations 23 p4058 A66-41910  
 Flow visualization via afterglow produced  
 in pure low temperature nitrogen and air by  
 electron beam projection 23 p4058 A66-41911  
 Optimization of lift-drag ratio of power law  
 half-bodies in hypersonic viscous flows,  
 considering interrelation between body  
 shape and skin friction 23 p4012 A66-41915  
 Diameter and location of wake neck and  
 trailing wake shock for pointed and blunt



slender hypersonic cones 23 p4012 A66-41919  
 Hypersonic small disturbance theory of unsteady inviscid flow past thin wedge oscillating in pitch motion and effects of wave reflections 23 p4012 A66-41925  
 Inviscid flow near stagnation point of blunt body in hypersonic stream, using thin shock layer theory with very small density ratio 23 p4013 A66-42013  
 Inviscid hypersonic flow past flat wings at large angle of attack analyzed, using homogeneous layer concept of shock layer theory 23 p4013 A66-42014  
 Series truncation applied to hypersonic flow problems by treating elliptic partial differential equation as parabolic or hyperbolic 23 p4014 A66-42060  
 Functional interdependence of four distinctly different parameters represented by gamma in study of thermodynamical relations for shock waves 24 p4193 A66-42270  
 Analytical method for studying pattern of flow from nozzle into vacuum used to calculate plume shape for rocket exhausting into hypersonic stream 24 p4158 A66-42790  
 Reentry and recovery of space vehicles in reliable shock free landings, using modified helicopter rotor for hypersonic flow and thermal problems 24 p4284 A66-43073

**HYPERSONIC GLIDER**  
 Hypersonic wind tunnel measurements to Mach 17 of aerodynamic characteristics of family of hypersonic gliders [ONERA TP 331] 11 p1635 A66-23199

**HYPERSONIC HEAT TRANSFER**  
 Spectral and total radiation studies of bodies traveling at hypersonic speed in simulated Martian and Venusian atmospheres [AIAA PAPER 65-116] 03 p0315 A66-12783  
 Aerodynamic heating of vehicles entering Earth atmosphere at hypersonic speed, noting blunt body concept, radiative and convective heating, heat shield weights, etc 13 p1989 A66-25153  
 Estimates of expected relative magnitudes of convective and radiative heat transfer at stagnation point of blunt body for superorbital speeds and attitudes with continuum flow 13 p1989 A66-25154  
 Foreign planetary atmospheric effect on hypersonic laminar stagnation region heat transfer and skin friction studied for various dissociating gases 13 p1993 A66-26729  
 Design, fabrication and test of sandwich construction box beam made of D-43 columbium and Haynes 25 superalloy for use as hot redundant structure for hypersonic vehicles 16 p2816 A66-30894  
 Hypersonic tunnel measurements of turbulent heat transfer for thin walled slender cone 17 p3039 A66-33474  
 Effect of mass injection into cavity on hypersonic boundary layer transition and on heating downstream 21 p3835 A66-38734

**HYPERSONIC INLET**  
 Diffusion in supersonic duct flow composed of boundary layers, with application to hypersonic inlet with internal compression [AIAA PAPER 64-245] 05 p0606 A66-15071  
 Busemann inlet flow field calculation for hypersonic speeds, considering internal-compression inlet geometry and performance 20 p3493 A66-38178

**HYPERSONIC NOZZLE**  
**SA SPRAY NOZZLE**  
 Displacement and heat transfer effects of laminar and turbulent boundary layers far downstream in slowly expanding hypersonic nozzle, determining inviscid core flow 15 p2424 A66-29273  
 Reduction of thick boundary layers in low density wind tunnel by applying suction to nozzle, using high-speed cryopump 16 p2673 A66-30381  
 Vibrational and rotational nonequilibrium flow effects in hypersonic conical nozzle expansion of nitrogen flows and airflows 17 p2842 A66-33478

**HYPERSONIC REENTRY**  
 Optical radiation transfer equations applied to imaging instruments used in radiometry of hypersonic reentry bodies 08 p1222 A66-18709  
 Electromagnetic wave propagation near missiles during hypersonic atmospheric reentry and computer program for determination of dissociated and ionized particle density in nonequilibrium nitrogen-

plasma flow 13 p2150 A66-26374  
 Graphite composites suitability for use on hypersonic entry vehicle components 14 p2319 A66-28014  
 High temperature refractory alloy fabrication for microwave antennas in hypersonic glide reentry vehicles 19 p3370 A66-36158  
 Flexible uniform-stress truncated disk spinning about central hub for aerodynamic braking useful as reentry decelerator, noting low decelerator weight fractions for wide range of mission parameters 22 p3845 A66-40599  
 Plasma-electromagnetic wave interactions during hypersonic reentry of space vehicle into lower layers of atmosphere [ICAS PAPER 66-37] 22 p3957 A66-40666  
 Hypersonic entry vehicle measurement of Mars atmospheric density, pressure, composition, temperature and detection spectrometry of chemical species in shock layer 24 p4277 A66-42680

**HYPERSONIC SHOCK**  
 Hypersonic shock tunnel study, examining effects of roughness, bluntness and angle of attack on boundary layer transition 08 p1166 A66-19813  
 Instability of hypersonic shock layer flow over blunt bodies with surface cavities coupled to dynamic stability of body 10 p1619 A66-21156  
 Viscous hypersonic blunt body problem examined, using Newtonian thin-shock-layer theory, slip effect, Navier-Stokes shock structure, etc 13 p1990 A66-25157  
 Scattered light spectrum of thermal sound waves used to provide velocity and absorption data about hypersonic waves in several liquids 16 p2745 A66-30300  
 Unification of various small-epsilon theories of real gas flows based on assumption of specific-heat ratio near unity 23 p4151 A66-42050  
 Microwave experimental technique for continuous velocity measurement of shock and contact discontinuities bounding air plasma generated in cylindrical hypersonic shock tube 24 p4190 A66-42173  
 Network for compensating electrical output of thin film resistance thermometers for deviations due to large heat-transfer rates 24 p4207 A66-42176

**HYPERSONIC SPEED**  
 Law of plane cross section applicability to hypersonic motion of deformable bodies in inhomogeneous nonstationary media with time dependent parameters 01 p0006 A66-10460  
 Forced Mandelstam-Brillouin scattering in gases, determining hypersonic velocity for three gases 09 p1408 A66-20770  
 Non slender bodies of revolution with minimum pressure drag, noting derivation of minimizing curves for Newtonian flow 11 p1631 A66-22514  
 Transversal contour of minimum total drag of body in Newtonian flow 11 p1631 A66-22518  
 Inviscid unsteady flow field disturbances caused by blast-generated normal shock wave sweeping past slender wedge moving at hypersonic speed 12 p1795 A66-23577  
 Equations for translatory motion of lifting body moving at hypersonic speed, considering Earth sphericity, noting effect of centrifugal forces 13 p2193 A66-26448  
 Forced Mandelstam-Brillouin scattering in gases, determining hypersonic velocity for three gases 14 p2341 A66-27305  
 PDE of terminal shape of ablating body as function of time derived, noting mass and energy flow, boundary layer thickness, etc 16 p2628 A66-30219  
 Lift-to-drag ratio attainable by slender, homothetic body at hypersonic speeds, assuming Newtonian pressure distribution and constant skin-friction coefficient 17 p2838 A66-32348  
 Oscillatory motion of angle of attack for space vehicles entering Earth atmosphere at hypersonic speeds from satellite orbits 17 p3016 A66-32893  
 Similarity laws for bodies maximizing lift-to-drag ratio at hypersonic speeds, considering longitudinal and transversal contours 19 p3276 A66-36245  
 Newtonian variational problem for pressure

on surface of nonshallow body moving hypersonic velocity 19 p3276 A66-364  
 Wind tunnel testing of delta-like lift bodies at low, supersonic and hypersonic speeds, noting lift to drag ratios and of design performance of caret wave-rid wings [ICAS PAPER 66-24] 23 p4007 A66-410

**HYPERSONIC TEST APPARATUS**  
 Hypersonic shock tunnel study, examining effects of roughness, bluntness and angle of attack on boundary layer transition 08 p1166 A66-19813  
 Laminar separation in supersonic air hypersonic flow analyzed in gun tunnel noting concept of incipient separation as free interaction principle [AIAA PAPER 66-455] 17 p2910 A66-327  
 High Mach and Reynolds number hypersonic facility, noting available stagnation pressure, running time and a storage system [AIAA PAPER 66-758] 22 p3894 A66-406  
 Short-duration aerodynamic testing techniques and new usage of hypersonic shock tunnels [AIAA PAPER 66-762] 23 p4052 A66-413

**HYPERSONIC VEHICLE**  
 Preliminary design for optimum combination of insulating and structural materials for hypersonic cruise vehicles 03 p0436 A66-127  
 Plasma sheaths on radiation patterns antennas on hypersonic vehicles, noting permittivity and transmission loss 04 p0474 A66-134  
 Sounding rocket instability, covering exact and approximate solution and Magnus moment coefficient for hypersonic roll vehicle /Sandia Nitehawk rocket system [AIAA PAPER 66-62] 06 p0958 A66-162  
 X-20 program for maneuverable hypersonic reentry vehicle, noting boost-glide dynamics soaring 08 p1300 A66-185  
 NASA mission, discussing V/STOL transports, SST and hypersonic cruise vehicles [SAE PAPER 660169] 14 p2416 A66-272  
 Hypersonic cruise vehicles for military and civil requirements, considering air breathing propulsion and structural weight 24 p4296 A66-422  
 Structural design problems of hypersonic air vehicles with air breathing propulsion discussing relation to future hypersonic commercial air transport [ICAS PAPER 66-31] 24 p4281 A66-424

**HYPERSONIC WAKE**  
 Hypersonic laminar near wake of blunt bodies considered in terms of dual region model [AIAA PAPER 65-52] 03 p0315 A66-127  
 Hypersonic wake transition map noting free wake, near wake and interpolation phenomena 03 p0356 A66-128  
 Hypersonic wakes, effects of turbulent fluctuations on air ionization reaction rate measured by averaging and regrouping perturbed source terms of chemical rate equations [AIAA PAPER 65-819] 03 p0359 A66-132  
 Mach-Zehnder interferometer study of fluctuations in turbulent wakes of slender cones and spheres in ballistic flight [AIAA PAPER 65-809] 04 p0455 A66-136  
 Hypersonic wake ionization dependence of ablation products, investigating laminar and turbulent flow regions [AIAA PAPER 65-54] 05 p0793 A66-157  
 Spatial distributions of free electrons in near wakes of spheres in hypersonic flight [AIAA PAPER 66-55] 07 p0983 A66-184  
 Aerodynamic characteristics of wake behind hypervelocity bodies [AIAA PAPER 66-53] 08 p1162 A66-189  
 Conservation laws involving mass, momentum and energy applied to asymptotic properties of hypersonic flow 09 p1327 A66-202  
 Stability of laminar boundary layers and wakes at hypersonic speeds, noting existence conditions for subsonic disturbances and effect of hot wake core 13 p2061 A66-251  
 Schlieren photographs of turbulent hypersonic wakes behind cones and spheres at various Mach numbers and pressure analyzing laminar wake core, wake diameter



- and distance to transition 13 p1992 A66-26664
- Hypersonic wake studies in ballistic missile research program, discussing reentry of hypervelocity vehicles, laminar flow, atmospheric turbulence, 14 p2218 A66-27402
- Enthalpy and density fluctuations in high speed wakes, noting typical reentry and ballistic range cases 14 p2219 A66-27431
- Static enthalpy and velocity profile within viscous wake of circular cylinder at Mach 0 18 p3049 A66-34582
- Distance of transition to turbulence of wake measured behind spherical and blunt-cone models at hypersonic speeds in ballistic range 23 p4011 A66-41883
- Transient ionization levels of hypersonic velocity projectile wakes measured by open microwave resonators phase shift observation 24 p4209 A66-42194
- Transmission resonant cavity measurements of electron line densities and collision frequencies in ionized wakes of hypervelocity projectiles 24 p4191 A66-42195
- Coherent CW superheterodyne radar system for studying backscattering from hypersonic velocity projectile wakes 24 p4191 A66-42196
- Supersonic and hypersonic wake flow dependence on near wake pressure, using momentum integral 24 p4158 A66-42775
- HYPERSONIC WIND TUNNEL**
- Pressure and temperature distribution measurements in test chamber of hypersonic blow-down wind tunnel located at University of Tokyo 01 p0053 A66-10632
- Air condensation in hypersonic wind tunnel strongly related to flow expansion rate 01 p0059 A66-10808
- Textbook on design, calibration and operation of near-sonic, transonic, supersonic and hypersonic wind tunnels 03 p0351 A66-12284
- Aerodynamic blast simulation in hypersonic tunnels, noting unsteady tunnel flow behind blast wave 03 p0316 A66-12794
- Design and fabrication of air receiver of hypersonic wind tunnel at University of Tokyo 03 p0438 A66-13084
- Hypersonic pilot wind tunnel using compression heater gives Mach-14 flows 03 p0353 A66-13223
- Scramjet design and combustion testing in hypersonic wind tunnels with arc-heating and MHD accelerators 06 p0805 A66-16320
- Rarified gas dynamics in space flight and hypersonic low density wind tunnel of Goettingen Aerodynamics Research Facility 07 p1017 A66-17479
- NAE helium hypersonic wind tunnel for hypersonic flight simulation and boundary layer studies 07 p1018 A66-18050
- Heat-sensitive paint in measuring kinetic heating in hypersonic wind tunnel 08 p1316 A66-18720
- Heat transfer in 20-inch hypersonic wind tunnel to two-dimensional inlet ramp at various angles of attack 08 p1318 A66-19147
- Magnetic suspension for aerodynamic wind tunnel models in Mach 8 airstream controlled in five degrees of freedom 09 p1364 A66-20664
- Pressure and heat transfer measurement by FM telemetry for models flying freely in hypersonic wind tunnel streams 10 p1538 A66-22041
- Microwave transmission tests in pure air plasma using hypersonic shock tunnel, obtaining electron density and collision frequency profiles, predicting propagation path signal loss and antenna radiation pattern distortion [AIAA PAPER 66-173] 11 p1742 A66-22211
- Refinements of hypersonic testing techniques in 100-inch tunnel F of von Karman gas dynamics facility 11 p1686 A66-22842
- Supersonic jet interaction for hypersonic flow of Mach 7.1 and for variable Mach number, noting jet instability, stagnation pressure, drag variation, wind tunnel, etc 14 p2220 A66-27467
- ONERA research on use of magnetic suspension systems in hypersonic wind tunnels and measurement of base pressure and heat transfer rates 16 p2683 A66-31699
- Hypersonic wind-tunnel test program giving data on turbulent boundary layer with mass addition including Mach number effect on heat transfer and skin friction reduction and massive blowing 17 p2839 A66-32477
- Hypersonic wind tunnel, noting hot gas generation by piston drive in gun barrel, stagnation temperatures and other operating parameters 17 p2904 A66-32895
- Piezoelectric balance for aerodynamic force measurements in hypersonic shock tunnel, discussing design, calibration and performance characteristics 24 p4190 A66-42174
- Stagnation pressure, temperature and static pressure measurement in shock driven facilities, using equipment with piezoelectric crystal and fast response thermocouple 24 p4207 A66-42175
- Pyroelectric heat-transfer sensor performance compared with thin skin thermocouple heat sensors, noting discrepancy in measurement results in severe environment 24 p4207 A66-42177
- HYPERSONICS**
- Brillouin scattering in liquids examining velocity, frequency and lifetime of thermally excited hypersonic sound waves, using laser light sources 03 p0376 A66-12422
- HYPERTENSION**
- S BLOOD PRESSURE**
- HYPERVELOCITY**
- S HYPERSONIC SPEED**
- HYPERVELOCITY ACCELERATOR**
- Glass tube containing pressurized helium progressively imploded by coaxial explosive charge, considering application to hypervelocity guns 11 p1686 A66-22840
- Explosive gas guns for hypervelocity acceleration 11 p1686 A66-22841
- Macroscopic particle acceleration to meteoritic velocities by trapping and accelerating superconducting solenoid in front of magnetic traveling wave 24 p4237 A66-42401
- HYPERVELOCITY CRATERING**
- Hypervelocity impact force per crater surface area correlated to stress-to-fracture of target, experimenting with aluminum and copper as targets and projectiles 01 p0154 A66-10496
- Hypervelocity crater depth and target strength 03 p0437 A66-12802
- Cavity depth for waterdrop impacts against water, discussing apparatus, equation for cavity depth, effect of gravitational potential energy, liquid surface behavior, etc 15 p2477 A66-28716
- Metal behavior during hypervelocity cratering, noting momentum and energy equations for impulsive loading, including anisotropic stress and strain rate tensors, etc 17 p3022 A66-32013
- Hypervelocity projectile impact cratering from Ranger photographs of lunar surface 19 p3457 A66-35443
- Micrometeoroid environment effect on metal surface thermal properties, using simulated space vehicle placed in solar space environment chamber [AIAA PAPER 65-138] 23 p4140 A66-41894
- High velocity impact range diagnostic instrumentation including timing and triggering devices, laser and spark photography, radiation monitors, ballistic pendulum, etc 24 p4191 A66-42187
- HYPERVELOCITY FLOW**
- Electron density decay in wakes of hypervelocity aluminum and copper spheres in air and nitrogen as function of time, using transmission resonant cavity 02 p0267 A66-11529
- Simultaneous streak and frame interferometry for short duration hypervelocity facilities 03 p0370 A66-12962
- Aerodynamic characteristics of wakes behind hypervelocity bodies [AIAA PAPER 66-53] 08 p1162 A66-18952
- Hypervelocity techniques - Symposium, Tullahoma, Tennessee, November 1965 11 p1683 A66-22826
- Flow velocity, static pressure and test-section pitot pressure of expansion tube, using unheated /room temperature/ hydrogen driver 11 p1683 A66-22827
- Modified Expansion Tube /MET/ and high density shock tube operated in expansion tube mode for use in hypervelocity flow research 11 p1684 A66-22829
- Nonsteady isentropic compression wave to generate high-velocity air flows with very low ambient dissociation levels 11 p1684 A66-22831
- Momentum and energy accommodation for hypervelocity gas particles on crystal surface, using Lennard Jones potential and approximating lattice by system of independent forced harmonic oscillators 16 p2752 A66-30388
- Spark discharge generated blast wave application to shock on shock simulation, free-stream sound speed determination and hypervelocity flow measurements [AIAA PAPER 66-763] 22 p3894 A66-40645
- Windowless total radiation gauge for shock tube measurements of high temperature gas radiance 24 p4208 A66-42183
- Closed form relationship for estimation of flat plate turbulent heating rates at hypervelocities 24 p4158 A66-42788
- HYPERVELOCITY GUN**
- Wall friction, heat transfer and real-gas propellant effects in two-stage light gas guns 11 p1685 A66-22837
- Packaging techniques for telemetry components and systems to withstand gun-launch accelerations up to 250,000 g 16 p2651 A66-30561
- HYPERVELOCITY IMPACT**
- Linear accelerator for micrometeoroids operated in radially stable mode and variable frequency for hypervelocity impact studies 01 p0053 A66-10852
- Localized bonding or spot welding of aluminum plates by high velocity impact with microparticles 02 p0242 A66-11562
- Hypervelocity impact cratering materials and impact conditions 02 p0300 A66-11855
- Micrometeoroid impact effect on candidate skin materials, determining change in optical properties 03 p0382 A66-12793
- Hypervelocity impacts into space radiator materials, discussing material evaluation for waste heat shield 05 p0701 A66-14931
- Meteoroid protection weight requirements effects on space exploration costs, examining environment and hypervelocity impact penetration [SAE PAPER 650786] 05 p0774 A66-15011
- Ratio of maximum wall thickness to crater depth as function of impact velocity of meteoric particles 06 p0961 A66-17173
- Plates spot welded by hypervelocity impact of microparticle 07 p1037 A66-17468
- IR sensor detection of hypervelocity meteoroid puncture radiation emission 08 p1225 A66-19520
- Hypervelocity particle penetration of manned space station structure, discussing hole formation and repair 10 p1612 A66-21931
- Hypervelocity impact data applied to synthesis of meteoroid barriers in spacecraft design 10 p1612 A66-21954
- Helium gas gun for studying penetration and shock reflection from hypervelocity impact 11 p1687 A66-23263
- Depth of penetration of projectiles impacting at hypervelocities predicted, using dynamic yield strength of material with phenomenological model 12 p1957 A66-23592
- Strong plane shock produced in Al by hypervelocity impact and late stage equivalence examined, using analytical and graphical solution of method of characteristics and realistic state equation 13 p2194 A66-25061
- Meteoroid hazard to space power plant, reevaluating particle mass, flux, density and impact [AIAA PAPER 64-759] 13 p2194 A66-26622
- Material and geometry aspects of meteoroid armor protection for space radiator tubes, discussing bumper-fin concept 14 p2407 A66-28029
- Cratering in materials analysis, considering transient, primary, secondary and recovery phases, using rod projectiles at high velocity impact 15 p2607 A66-28702
- Terrestrial origin of tektites, noting possible connection with cometary collision and evidence of lunar origin for some 16 p2802 A66-30926
- Mathematical model for predicting strength and density of material from deceleration-time history of instrumented impact probe 18 p3253 A66-33805



Peculiarities of dispersion of matter resulting from meteorite impact on lunar surface as explanation of concentric nature of structure of crater 19 p3455 A66-35284

Radiation flux from meteoritic collision with obstacle 19 p3341 A66-35744

Photographic measurement on optical radiation associated with hypervelocity impact of projectile on target 23 p4091 A66-41909

Strength factor expressed as empirical penetration equation for impact target, combining effects of resistance to penetration and strain hardening 23 p4140 A66-41918

### HYPERVELOCITY LAUNCHER

Launching of beryllium, aluminum and steel projectiles up to 54,100 ft/sec 11 p1685 A66-22838

### HYPERVELOCITY PROJECTILE

Head-on interaction of plane shock wave and supersonic cone-cylinder projectile 03 p0316 A66-12813

Autocorrelation functions and gas density spectra from microdensitometer tracings of schlieren photographs of turbulent wakes behind hypervelocity spheres 03 p0317 A66-12947

Laser technique to photograph hypervelocity projectiles in free-flight range 03 p0379 A66-13248

Elastic impact and perforation of aluminum plates at minimal velocities by projectiles 05 p0775 A66-15299

High precision transient measurement of submicrosecond response of shock-loaded materials by instrumentation techniques and target alignment 08 p1226 A66-19694

Equilibrium air total radiation mechanism, vacuum UV radiation and relation to hypervelocity entry studied, using shock tube blunt model test flow [AIAA PAPER 66-103] 09 p1469 A66-20087

Projectile detection in hyperballistics range by using electro-optics and triggering of instrumented stations with luminous and nonluminous projectiles 10 p1538 A66-22042

Orthogonal x radiographs determination of hypervelocity fragment characteristics from shaped charge for potential terminal ballistics application 11 p1685 A66-22839

Behavior of projectiles in hyperballistic tunnel analyzed by photographs of their shock waves, using array of spark gaps flashes correlated with cameras 16 p2673 A66-30313

Moving source scanning spectrometer for ballistic range radiometry noting spectral resolution, operation and performance characteristics 24 p4208 A66-42180

Radiometer system with photomultiplier tube for measuring absolute radiation from hypervelocity projectile flow fields 24 p4208 A66-42181

Vacuum UV radiation measurement from high temperature nitrogen, detecting radiation from shock layer of ballistic model 24 p4208 A66-42182

Projectile-borne and gaseous impurity effects on spectroscopic turbulence and velocity measurements at reentry simulating range 24 p4190 A66-42184

Microwave reflectometer instrumentation for Ames light-gas guns, measuring time-distance values of projectiles during acceleration 24 p4209 A66-42185

Mass of shaped charge accelerator generated fragments determined via high speed flash X-ray photography of projectiles in flight 24 p4209 A66-42186

Transient ionization levels of hypersonic velocity projectile wakes measured by open microwave resonators phase shift observation 24 p4209 A66-42194

Transmission resonant cavity measurements of electron line densities and collision frequencies in ionized wakes of hypervelocity projectiles 24 p4191 A66-42195

Coherent CW superheterodyne radar system for studying backscattering from hypersonic velocity projectile wakes 24 p4191 A66-42196

Double Langmuir probe measurement of turbulent structure and ionization intensity of hypervelocity projectile and spectral characteristics of probe signal fluctuation 24 p4192 A66-42198

## HYPERVELOCITY WIND TUNNEL

Variable-volume arc chamber in Ling-Temco-Vought hypervelocity wind tunnel, examining design, performance and calibration technique 11 p1686 A66-22843

Source type hypersonic free stream effects on flow field about axisymmetric cone, obtaining properties in shock layer, boundary layer, pressure gradient, etc 17 p2837 A66-32080

Free flight model technique in hypervelocity shock tunnel for aerodynamic force and moment measurement by optical instrumentation [AIAA PAPER 66-771] 22 p3847 A66-40652

### HYPERVENTILATION

Shape changes in human chest wall during static respiration at end of spontaneous expiration, maximum expiration and maximum inspiration 15 p2441 A66-29649

### HYPOELASTICITY

Thermodynamics utilized to show that there is no difference between bodies defined as hypoelastic, elastic and hyperelastic 12 p1980 A66-23957

### HYPOTENSION

### S BLOOD PRESSURE

### HYPOTHALAMUS

Blood pressure and heart rate during hypothalamic self-stimulation in dogs, discussing experimental methods and results, physiological response, etc 16 p2640 A66-31154

Medial forebrain bundle, lateral hypothalamic area and reinforcing brain stimulation, discussing self-stimulation 17 p2859 A66-32552

Induction and suppression of hypothalamic self-stimulation behavior by microinjection of endogenous substances at self-stimulation site 20 p3506 A66-37603

### HYPOTHERMIA

Effects of cold and abnormal atmosphere discussing tolerance limits to hypercapnia, anoxia induced hypothermia and hypoxia 04 p0464 A66-14067

Semiconductor cooler creating hypothermia in small animals, operating on Peltier effect and employing quaternary metal alloy 15 p2444 A66-29497

Automatic device for reversible hypothermia in living organism, considering parameters of physiological functions, included in logic circuits 15 p2444 A66-29498

Hematocrit index and arterial-blood gas composition in white rats during artificial hypothermia 15 p2440 A66-29511

### HYPOTHESIS

### S BOWEN HYPOTHESIS

### S INTERMITTENCY HYPOTHESIS

### S NULL HYPOTHESIS

### S SIMILARITY HYPOTHESIS

### HYPOXIA

### SA ANOXIA

Hypoxia protection on taking of second graft of homologous bone marrow in previously irradiated and grafted mice 01 p0020 A66-10609

Effects of cold and abnormal atmosphere discussing tolerance limits to hypercapnia, anoxia induced hypothermia and hypoxia 04 p0464 A66-14067

Thermal homeostasis under hypoxia in man, discussing thermal stress adaptation and physiological responses in oxygen-deficient environment 04 p0465 A66-14068

Gastric secretion after simultaneous action of radiation and hypoxia 06 p0810 A66-16058

Protective effect of adrenaline, subgaleally injected, on survival time of rats subjected to acute hypoxia 06 p0811 A66-16064

Computational analysis employing digital computers to evaluate hypoxic stress reactions in man 07 p0998 A66-17659

Carbon dioxide induced mild hypoxia, correction of alterations on performance of psychologic and psychomotor systems 07 p0998 A66-17661

Cytoplasmic alterations and fat vacuole formation in pneumocytes of guinea pigs exposed to severe hypoxia in low pressure chamber 08 p1175 A66-18769

Effect of oxygen deficiency on acoustic organ of cats, determining content of potassium and sodium ions in perilymph, cerebrospinal fluid and blood serum 13 p2011 A66-26251

Chronic hypoxia effects on thyroid

function of rats, discussing radiolod trapping and acinar cell length 14 p2227 A66-261

Resistance to hypoxia by individuals height of 1650 m trained for high altitude climbing, noting equipment 15 p2435 A66-29

Rats resistance to oxygen deficiency while suffering effects of 750 roentgen dose X-ray exposure 15 p2438 A66-29

Hypoxia in cats and rats due to gradual and abrupt drops in oxygen content of air 15 p2439 A66-29

Superacute hypoxia in cats exposed to pure nitrogen followed by artificial respiration 15 p2439 A66-29

Hypoxic hypoxia attenuation mechanism carbon dioxide enrichment of alveolar intake 16 p2638 A66-30

Hypoxia and lower body negative pressure effects on blood volume, and orthostatic physical tolerance after four weeks hypoxic bed rest 16 p2640 A66-31

Human reaction to pure oxygen inhalation interrupting previous hypoxia 17 p2849 A66-31

Accelerographic and ballistocardiographic evidence of increased stroke volume secondary to acute high altitude hypoxia 17 p2855 A66-32

Retinal adjustment to light at different levels of hypoxia 17 p2859 A66-32

Lifetime high altitude environment effect on man, noting Peruvian natives adapted to constant hypoxia 22 p3854 A66-40

Hypoxia of simulated high altitude exposure prolongs synaptic delay conduction time in brain system of rats 22 p3855 A66-40

Levy hypoxia test and associated arterial oxygen desaturation and increased cardiac output 24 p4163 A66-42

Effects of meprobamate and hypoxia on psychomotor performance during bidimensional tracking, coded problem solving and response to auditory signals 24 p4164 A66-42

### HYSTERESIS

### SA ANTIFERROMAGNETISM

### SA DAMPING

Forced vibration of system with polygenic hysteresis loops in presence of constant force 01 p0159 A66-11

Russian monograph on turbulent plasma theory covering turbulence formation, hysteresis, plasma oscillations, self-consistent wave interactions, etc 03 p0406 A66-13

Electrostatic hysteresis synchronous motion discussing development, operation characteristics, test results, advantages and limitations 04 p0459 A66-13

Polarization and domain structure barium titanate single crystals with double hysteresis loop 06 p0926 A66-16

Capacitance-voltage curves in MOS devices indicating difference in relaxation time of surface states 06 p0940 A66-17

Brushless induction hysteresis motor extreme environments 07 p0991 A66-17

Hysteresis effect in long term variation of cosmic radiation, investigating whether its effect appears during short term Forbush decreases 07 p1125 A66-18

Empirical and experimental modulation functions for cosmic ray intensity variation showing rigidity dependence of intensity changes 07 p1128 A66-18

Digital simulation of magnetic hysteresis using analytic approximation of magnetic curves by seventh degree polynomials 08 p1187 A66-19

Effect of thermal and thermomagnetic treatment of nickel-cobalt ferrite single crystal on rotational magnetic hysteresis losses 09 p1412 A66-19

Hysteresis nature of current-voltage characteristics observed in p-n junctions obtained by bombarding germanium crystal with fast electrons 09 p1413 A66-20

Hysteresis properties of thin ferromagnetic films of nickel-iron and of nickel-iron molybdenum compositions, noting anisotropic dispersion effect 09 p1431 A66-20

Magnetic hysteresis and associated current-carrying capacity of type II superconductor on pinning of flux threads by inter-



- effects 10 p1573 A66-21246
- Stability of steady state response of one degree of freedom double bilinear hysteretic model ASME PAPER 65-WA/APM-4]
- Magnetoresistance effect applied to Rotatable Initial Susceptibility II films, explaining resulting hysteresis loops and torque curves 13 p2161 A66-25183
- Layered film of Cr and NiFe exhibit biased hysteresis loop in easy axis direction and asymmetric hysteresis loops in hard axis direction 14 p2353 A66-26901
- Magnetic torque and hysteresis loop measurements, examining exchange anisotropy in sulfided Fe films 14 p2354 A66-26907
- Magnetic hysteresis and switching property of manganese-bismuth thin magnetic films epitaxially grown by vapor deposition technique 14 p2355 A66-26913
- Dual input describing function (DIDF) of two-state relay with hysteresis 14 p2265 A66-27481
- Hysteresis effects in one-dimensional conducting gas flow through rectangular MHD converter channel with constant magnetic gap and variable electron spacing 15 p2428 A66-29219
- Hysteresis phenomena in He-Ne gas laser in axial magnetic field and polarization of oscillating mode within certain tuning region 15 p2516 A66-29385
- Tuning of ammonia beam maser resonator based on frequency shift method, noting hysteresis appearance and elimination 16 p2720 A66-31696
- Critical current enhancement and degradation due to hysteresis in nonideal type II superconductors in axial magnetic fields 18 p3153 A66-33612
- First-order modulation effects of galactic cosmic radiation, considering hysteresis effect and variation of energy spectrum in 11-yr modulation 18 p3186 A66-34811
- Micromagnetic theory of ferromagnetics, discussing magnetization curve, saturation and hysteresis effects 19 p3439 A66-35714
- Magnetization curve and magnetic hysteresis of ferromagnetic single crystals 19 p3439 A66-35715
- Hysteresis effect in ionospheric propagation indices studied by separating data concerning solar cycle portion with increasing solar activity from decreasing solar activity data 20 p3551 A66-37570
- Magnetization curves for two specimens of semiconducting strontium titanate of given electron density, noting magnetic hysteresis and heat capacity 21 p3796 A66-38553
- Control of magnetic hysteresis mechanism, increasing damping torque for use in gravity-oriented satellite stabilization 21 p3820 A66-38862
- Quenching and hysteresis effects between Zeeman oscillations on single axial mode observed in near-zero magnetic fields for short planar laser 21 p3747 A66-39116
- Esaki diode oscillator, investigating oscillation waveform, conductance characteristics, constants, hysteresis and parasitic oscillation 21 p3712 A66-39221
- Competition, hysteresis and reactive Q-switching in carbon dioxide lasers at 10.6 microns, using moving mirror technique 23 p4079 A66-41631
- Optimizing procedures using Fortran II FAP programming on IBM 709/7090 computers, comparing eight known techniques 19 p3308 A66-35868
- Saturn computer design and fault simulation on IBM 7090 computer 22 p3871 A66-40744
- ICBM
- S INTERCONTINENTAL BALLISTIC MISSILE /ICBM/
- ICE
- Equations describing crystallization process in low level clouds as function of ice crystal penetration from upper clouds or from artificial seeding 02 p0254 A66-12023
- Detection of 3.1 micron mu cepheid absorption band due to interstellar ice particles 05 p0768 A66-15770
- Growth and destruction of ice mantles on interstellar graphite grains by sputtering, thermal evaporation and cloud collisions 05 p0765 A66-15845
- Flows and fractures as types of deformation occurring on Earth under huge loads of ice suggested by isostatic compensation of Antarctica, Arctic basin and glaciated region in North America 12 p1875 A66-24894
- Ice crystal size during expansion of humid air in supersonic nozzle 17 p2948 A66-32417
- ICE FORMATION
- SA DEICING SYSTEM
- Growth of ice crystals freely falling in atmosphere and form when produced by cloud element coagulation analyzed, using low pressure chamber 01 p0097 A66-11105
- Nucleation of ice formation in supercooled clouds as result of lightning-initiated sound waves 04 p0542 A66-13674
- Ice and snow fields in polar regions as observed by high resolution camera on Nimbus satellite 11 p1729 A66-22327
- Urea effective ice nucleant in supercooled clouds due to endothermic heat of solution and high solubility 13 p2122 A66-26125
- Rime effect on reflection efficiency of microwave reflectors, noting surface roughness irregularity and relation between icing and meteorological topographical conditions 20 p3516 A66-37726
- ICE NUCLEUS
- Carbon dioxide effect on shattering of freezing water drops, using methanol-cooled chamber with variable temperature control 10 p1552 A66-21290
- Ice crystallization on solid-insoluble nuclei in high humidity air, noting two measuring methods for nuclei concentration 14 p2327 A66-28134
- Cometary nuclei discussing brightness, models, evidence from photometry, spectrography, dynamic properties of nuclei, and meteors 17 p3009 A66-33368
- Radioactive heating effect on icy conglomerate cometary nucleus and splitting from solar heat shock 17 p3009 A66-33370
- ICE SURVEILLANCE
- Water, ice and slush effects on traction characteristics of runway pavement, noting aquaplaning and aircraft braking criteria 02 p0216 A66-12223
- Airborne albedo measurements of ice in Ross Sea, Antarctica, for various solar elevations and altitudes 05 p0669 A66-14937
- ICING
- S DEICING SYSTEM
- IDEAL FLUID
- Masses attached to body of revolution estimated by Vandrey method of calculating disturbed velocity potential of flow of ideal fluid 01 p0058 A66-10462
- Ordinary differential equations theory yielding hydrodynamics conditions of stability with respect to finite perturbations for plane stationary curvilinear flow of ideal fluid 02 p0219 A66-12104
- Solid bodies in plane parallel flow of ideal fluid, discussing one-parameter family of ablation bodies with steady shape 04 p0596 A66-13554
- Longitudinal motion effect on lateral vibrations of prolate body of revolution in ideal fluid 05 p0775 A66-15315
- Behavior of fluids under weightlessness and in weak gravitational fields, formulating small linear oscillations of ideal fluid under surface tension 06 p0873 A66-18708
- Flow parameters of incompressible ideal fluid in axisymmetric curvilinear channel, obtaining and solving nonlinear differential equation 12 p1863 A66-24243
- Oscillations of cylindrical orthotropic three-layer shell having ideal fluid flow at variable rate, establishing parametric resonance and determining limits of shell motion instability regions 13 p2206 A66-26461
- Laminar fluid flow of two-phase ideally viscous medium between two parallel surfaces 13 p2072 A66-26766
- Boundary problem describing plane jet steady state flow of ideal incompressible fluid, reducing solution to nonlinear integro-differential equations 14 p2272 A66-26775
- Aerodynamic forces acting on harmonically oscillating thin profile in stalled plane parallel flow of ideal incompressible fluid 14 p2220 A66-27695
- Ideal conducting fluid in electromagnetic and gravitational fields treated by relativistic mechanics, using variational principles 14 p2277 A66-28049
- Natural modes and eigenfunctions of low amplitude oscillation determined by Ritz averaging method for ideal fluid with equilibrium surface in weak force field 16 p2687 A66-31297
- Theory of unsteady one-dimensional motion of ideal incompressible fluid, discussing equation of state 16 p2688 A66-31300
- Book on jet theory in ideal fluids, covering compressible flow, steady jet flow, infinite flow past polygonal obstacle, unsteady flow, etc 16 p2632 A66-31746
- Einstein field equations for perfect fluid, coupled to frozen-in magnetic field, in high-density limit of gravitational collapse 17 p2997 A66-31973
- Variational principle for steady flows of ideal liquid and sufficient conditions for nonlinear stability under finite perturbations 17 p2913 A66-33168
- Hamilton principle extended to compressible MHD flow of perfect conducting fluid 20 p3610 A66-37987
- Coefficients of equations of perturbed motion of body containing ideal incompressible liquid 21 p3770 A66-38973
- Hydrodynamic equations derived for classical multicomponent ideal fluid, using expansions in small parameter mu 21 p3728 A66-39297
- Subsonic jet flow past solids, examining two classes of exact solutions in ideal fluid for plane nonvortical steady state flow 22 p3902 A66-40915
- Stability analysis of discontinuous solution of gas dynamics PDEs for ideal fluid 23 p4055 A66-41559
- Inertial motion equations of rigid body bounded by multiply connected surface in ideal infinite fluid 24 p4237 A66-42846
- Axisymmetric vortex jet behavior of ideal incompressible fluid at large distances from nozzle, noting surface waves 24 p4195 A66-42851
- Two-dimensional bubble contours in steady state turbulence-free flow of ideal incompressible fluid, obtaining solution for all internal pressures 24 p4232 A66-43064
- IDEAL GAS
- SA PERFECT GAS
- Plane adiabatic motion of ideal gas determined by separating variables of motion equations in curvilinear coordinates 01 p0006 A66-10471
- Stability of plane stationary detonation wave, using detonation model of ideal perfect gas flowing in pipe at constant supersonic velocity 02 p0217 A66-11391
- Thermodynamic properties of substances in ideal gas state in finite series representation 03 p0443 A66-12512
- Magnetic properties of ideal gas of charged bosons and fermions as affected by dimensionality n of containing space 03 p0409 A66-12630
- Total stopping distance calculated for various experimental conditions for solid piston motion between driver and test gases in closed shock tube 05 p0660 A66-15061
- Power characteristics of linear axisymmetric flow of ideal incompressible conducting gas with Hall effect in two-component magnetic field 08 p1168 A66-18863
- Growth or decay of plane, cylindrical or spherical sonic discontinuity moving in



nonhomogeneous gas in isentropic equilibrium under external forces 08 p1208 A66-19230

Peculiarities of aerodynamic characteristics of flow past plate and pointed and blunt slender cones in viscous hypersonic thermodynamically ideal gas 08 p1165 A66-19571

Thermodynamic property calculations from equations of state and ideal gas properties, using entropy as illustrative example 10 p1619 A66-21077

Scalar formulation of ideal charged adiabatic gas flow in presence of gravitational and electromagnetic fields 10 p1524 A66-21814

Equilibrium flow of ideal gas and condensing vapor mixture from nozzle, using basic equations to describe process 12 p1863 A66-24368

Transition solution of physical state across plane nonrelativistic MHD shock of finite strength in compressible dissipationless perfect gas in uniform magnetic field 12 p1923 A66-24578

Streamline flow of ideal stable gas with constant ratio of specific heats around conical body with arbitrary taper, determining flow velocity components 14 p2220 A66-27679

Book on uniform steady motion of ideal gas and gas dynamics of supersonic wind tunnels 14 p2220 A66-27789

Plane or axisymmetric hypersonic ideal gas flow in divergent nozzle with parabolic wall shape 14 p2221 A66-28056

Ideal gas flow past infinite circular cone at angle of attack, noting finite-difference method for self-similar solution of Prandtl boundary layer equation 14 p2222 A66-28283

Critical flow rate, critical pressure ratio and critical mass flow of dissipative adiabatic nozzle and pipeflow of ideal gas 16 p2690 A66-31635

Physical phenomena occurring within fluid devices, particularly pneumatic devices, considering Maxwellian distribution of velocities, ideal gas law and mean free path 18 p3098 A66-34118

Channel flow general equations including nonviscous uniform flow, steady flow, stagnation state and speed of sound in ideal gas 18 p3098 A66-34121

Friction and heat exchange effects on one-dimensional flow profile of ideal gases 18 p3098 A66-34122

Shock formation in mixture of chemically reacting ideal gases due to piston action 18 p3100 A66-34641

Transformation and solutions of equations of one-dimensional isentropic motion of ideal gas 19 p3342 A66-36467

Correlation formulas improvement for laminar shock tube boundary layer for air and argon 21 p3727 A66-39167

Stability problem of plane steady detonation wave in ideal gas 22 p3898 A66-40156

## IDENTIFICATION

System measurement and identification, considering stochastic transformation between input and output functions, noting connection with radio communication problems 15 p2473 A66-29375

Aircraft accident victim identification techniques 19 p3294 A66-36444

Identifying critical elements /parts and components/ as criteria for system design tradeoff at system and circuit levels 20 p3568 A66-37916

## IE-A

## S EXPLORER XX SATELLITE

## IFR

## S INSTRUMENT FLIGHT RULE /IFR/

## IGNITER

JP-5 fuel-air mixture ignition by platinum catalytic igniters, using ramjet engine baffle combustors 13 p2171 A66-25594

Igniter performance in solid propellant rocket motors, examining mass discharge rate effect on chamber pressure transients [AIAA PAPER 66-680] 18 p3161 A66-34227

Solid propellant motor ignited from aft end, noting igniter 20 p3629 A66-38261

Static firing tests on special small rockets /SSR/ with different igniter cases and combustion instabilities 23 p4119 A66-41436

## IGNITION

## SA COMBUSTION

## SA SOLID PROPELLANT IGNITION

## SA SPARK IGNITION

Tagaform synthetic hypergolic fuel for hybrid rockets, discussing polymerization, ignition delay, etc 11 p1760 A66-22249

Analytical solution to rate equations for branching chain reactions of hydrogen-oxygen reaction under shock tube conditions, for application to ignition problems 13 p2018 A66-26442

Turbulent jet theory, thermal ignition theory and flameout characteristics of bluff body flame stabilizers 14 p2413 A66-27694

Laminar and turbulent diffusion flame combustion mechanisms, stabilization, flame ionization, Bunsen burner, fuel gas jet eddy diffusion, etc 15 p2616 A66-29068

Automatic ignition in methane-chlorine mixture, investigating photochemical and thermal chlorination of methane in gas phase 17 p2989 A66-32824

Ignition model for condensed thermally unstable propellant by exothermal processes taking place in condensed phase 18 p3260 A66-33719

Ignition of powder prepared from nitroglycerin and nitrocellulose by shock wave in sectioned low-high pressure chamber 18 p3260 A66-33721

Bilateral switching thyristor system on common silicon substrate, discussing ignition 19 p3313 A66-35500

Ignition conditions determined based on linearization of initial nonlinear equations 19 p3477 A66-35742

Unstable combustion products of glow discharge, discussing effect of propagation rate of hydrogen-oxygen flame 21 p3834 A66-38473

Laplace transform analysis of solid or hybrid propellant ignition by exothermic heterogeneous reactions in presence of radiant energy flux 21 p3806 A66-38688

Analytic solution for ignition kinetics of dry carbon monoxide-oxygen reaction obtained, assuming initiation reaction followed by chain-branching steps 22 p3998 A66-40115

Detonability of hydrogen-oxygen mixtures in large vessels at low initial pressures, using strong and weak igniters 23 p4120 A66-41890

## IGNITION LIMIT

Measuring apparatus for autoignition times of explosives, propellants and pyrotechnics under various initial vacuum or pressure ranges 01 p0054 A66-10854

Flammability hazards of aircraft hydrocarbon fuels as function of temperature and pressure based on equilibrium conditions [AIAA PAPER 65-801] 03 p0414 A66-12565

Chemical kinetics of nonequilibrium combustion of propane-air and ethane-air mixtures in one-dimensional flow, including ignition delay and reaction time [CI PAPER WSCI-65-19] 05 p0788 A66-15143

Hypergolic ignition of light hydrocarbon fuels with fluorine-oxygen /Flox/ mixtures [CI PAPER WSCI-65-23] 05 p0743 A66-15147

Ignition of hydrogen-oxygen-argon mixtures containing small amounts of hydrocarbons and bromine substituted hydrocarbons in shock tubes 06 p0822 A66-18634

Upper ignition limit for reaction of fluorine with hydrogen 09 p1338 A66-20394

Discontinuity characteristics of trough-shaped flame stabilizers for combustion in wake of poorly streamlined body during period of ignition arrest 20 p3674 A66-36915

Initial air-side boundary layer effect on ignition of slot injected gaseous hydrogen by hot supersonic air stream [AIAA PAPER 66-644] 23 p4149 A66-41513

## IGNITION SYSTEM

## SA CHOKE

## SA IGNITER

Combustion and heat transfer in rocket combustion chamber burning liquid oxygen and gaseous hydrogen 02 p0279 A66-11668

Fuel drop ignition, discussing parametric extension of quasi-flame surface theory to higher reaction orders and arbitrary stoichiometric ratios [AIAA PAPER 66-70] 06 p0970 A66-16415

Ignition mechanisms of solid composite

propellants containing ammonium perchlorate as oxidizer 15 p2569 A66-2930

Thermal explosion equations solved by Dorodnitsyn method of integral equations 17 p3034 A66-3256

Ignition of liquid propellant rocket engines, discussing propellant flow, pressure and mixture ratio 18 p3163 A66-3418

Ignition of solid propellant rocket motor, considering igniter characteristics, components and materials 18 p3160 A66-3418

Error analysis of absorbed energy flux density and ignition exposure time data accuracy, precision and confidence limit estimates for arc image furnace ignition experiments [AIAA PAPER 66-669] 18 p3261 A66-3422

Ignition pressure transient of rocket motor, discussing initial ignition even flame spreading and final chamber filling convective heating effect on burning rate etc [AIAA PAPER 66-666] 18 p3165 A66-3449

Ignition analysis of condensed phase fuel suddenly exposed to stationary hot oxidizing gas, noting strong pressure effect due to feedback mechanism 20 p3626 A66-3738

Electronic devices for ignition of firn mechanisms designed for carrier rocket stage separation 21 p3822 A66-3963

Ignition and controlled burning of liquid oxygen-liquid methane mixture, evaluating use as rocket monopropellants [AICE PREPRINT 28E] 22 p3969 A66-3988

Low pressure low temperature ignition of hypergolic propellants, particularly hydrazine-nitrogen tetroxide systems, in space environment simulator and conclusion on gas phase reactions 22 p3892 A66-4023

Sea level and high altitude ignition of fuel rich gas generator/turbine manifold assembly 24 p4294 A66-4264

## IGNITION TEMPERATURE

## S COMBUSTION TEMPERATURE

## S SPONTANEOUS IGNITION

## TEMPERATURE

## IGY

## S INTERNATIONAL GEOPHYSICAL

## YEAR /IGY/

## IL-62 AIRCRAFT

## S ILYUSHIN IL-62 AIRCRAFT

## ILLUMINANCE

Illuminance of Earth shadow at three wavelengths by numerical integrator accounting for light attenuation, ozone absorption and extinction, Rayleigh scattering and refractive beam divergence 11 p1770 A66-2257

Angular divergence effect of light beam on illuminance of turbid scattering medium 14 p2326 A66-2754

Gated laser night-viewing system, calculating apparent illuminance as function of target distance 20 p3511 A66-3693

## ILLUMINATION

## SA FLARE

Ruby laser with concentric resonator as illumination source of bubble chamber 01 p0084 A66-1118

Ruby laser with concentric resonator as illumination source of bubble chamber 12 p1890 A66-2401

Reflector-light source requirements for homogeneous format illumination in night aerial photography 13 p2081 A66-2600

Dense continuous *Chlorella* culture growth at various illumination levels 15 p2440 A66-2950

Four-horn and five-horn monopulse antenna system properties including illumination tapers, gain factor, temperature, etc 18 p3080 A66-3426

Photoluminescence effect on growth rate of *Chlorella vulgaris*, discussing action spectrum and mechanism of light requirement for heterotrophic growth 20 p3507 A66-3779

## ILLUSION

## S MOON ILLUSION

## S OCULOGRAPHIC ILLUSION

## S OPTICAL ILLUSION

## ILYUSHIN IL-62 AIRCRAFT

Design, performance capabilities and operational characteristics of Russian high speed jet aircraft IL-62 with tail-mounted engine 24 p4160 A66-4307

## IMAGE

## SA AFTERIMAGE



A OPTICAL IMAGE  
 A RETINAL IMAGE  
 Scattering matrix of slot waveguide  
 calculated, using mirror image  
 method 14 p2252 A66-27250  
 IMAGE CONTRAST  
 Structural character of modern black and  
 white aerial photography films and relation  
 to image definition 01 p0068 A66-10694  
 Determination of contrast range of optical  
 images obtained in aerial camera as function  
 of atmospheric and optical  
 factors 03 p0368 A66-12504  
 Photoelectric storage tube capable of long  
 term integration of faint optical images,  
 employing as storage target low density  
 layer of KCl for increased charge  
 multiplication 06 p0893 A66-17017  
 Raster magnification effect of moire  
 images to observe plane deformation in  
 specimens subjected to  
 impact 11 p1782 A66-22857  
 Unsharpness and contrast effect on slit  
 detection studied by  
 radiography 13 p2086 A66-25820  
 Structural character of modern black and  
 white aerial photography films and relation  
 to image definition 15 p2497 A66-28555  
 Influence of object contrast upon partially  
 coherent image formation 15 p2501 A66-28979  
 Image distortion within cinematographic  
 process as related to photography, noting  
 quality estimation, visual perception criteria,  
 etc 16 p2702 A66-30432  
 Image contrast enhancing by matching  
 spectral reflectance or emittance  
 characteristics 17 p2925 A66-32610  
 IMAGE CONVERTER  
 Soviet electronic telescope, indicating  
 possibility of noneclipse observation of  
 coronal lines in IR band 01 p0137 A66-10456  
 Control circuit of image converter  
 tube 01 p0071 A66-11041  
 Temperature in toroidal theta pinch  
 discharge with image converter  
 camera 04 p0553 A66-14284  
 Text on electron optics covering principles  
 and application, electron lenses, cathode ray  
 tubes, mass and beta ray spectrographs,  
 quadrupole systems, image converters,  
 etc 09 p1402 A66-20333  
 Control circuit of image converter  
 tube 11 p1708 A66-23287  
 UV photography and spectroscopy using  
 spectrally selective image converter and  
 photodetection 14 p2293 A66-27330  
 Photographing of satellites, using optical  
 system and image converter for determining  
 coordinates 15 p2453 A66-30002  
 Epitaxial-planar diffusion techniques to  
 fabricate monolithic electro-optical mosaics  
 of 2500 phototransistor element with  
 internal row and surface column  
 interconnections 16 p2665 A66-31431  
 Information content of photoelectric star  
 images determined by background radiation,  
 optical aberrations and photon noise,  
 deriving equations for rms  
 error 16 p2654 A66-31441  
 Power source for image converter tubes  
 /ITC/ with regulated  
 output 20 p3559 A66-37521  
 Proximity focused biplanar image  
 converter diode for high speed photography,  
 discussing basic geometries with respect to  
 quantitative data gathering  
 capabilities 23 p4070 A66-41673  
 Photographic equipment using image  
 converter tube as electronic shutter with  
 exposure times from 0.5 to 5000  
 microseconds 23 p4070 A66-41674  
 Multipurpose ultrahigh speed camera  
 system, noting use as monosecond Kerr cell,  
 image converter and giant laser pulse  
 generator 23 p4071 A66-41675  
 IMAGE CORRELATION  
 Monochromatic atmospheric transluence  
 measured, using logarithmic photometer  
 with diode photomultiplier for remedying  
 image displacement due to atmospheric  
 fluctuations 07 p1034 A66-17925  
 Monochromatic atmospheric transluence  
 measured, using logarithmic photometer  
 with diode photomultiplier for remedying  
 image displacement due to atmospheric  
 fluctuations 12 p1880 A66-23886  
 Conduction mechanism in discontinuous  
 metal films involving image forces, potential

barrier, activation energies, saturation effect  
 in conductivity, etc 16 p2783 A66-31427  
 Radar image edges sharpness relationship  
 to relative humidity near  
 ground 17 p2948 A66-32270  
 Rotating prism design for continuous image  
 compensation cameras, application to UV  
 and IR regions of  
 spectrum 19 p3354 A66-35384  
 IMAGE DISSECTOR TUBE  
 High resolution solid state precision star  
 tracking system using magnetoresistance  
 multiplier and image disector  
 phototube 08 p1250 A66-19349  
 Bore-sighted star tracker using image  
 disector tube as photodetector and  
 incorporating continuous strip electron  
 multiplier 08 p1252 A66-19499  
 Image disector for lunar observation in  
 conjunction with Earth-based telescope,  
 noting efficiency of resolution contrast  
 sensitivity 12 p1883 A66-24678  
 IMAGE FILTER  
 Fresnel diffraction laws for calculation of  
 light amplitude distribution in image spot of  
 point as function of aperture dimensions  
 used on hologram, source function,  
 etc 04 p0532 A66-14173  
 Ten-element band pass filter section and  
 derivatives with classification of image-  
 impedance functions 11 p1669 A66-23113  
 IMAGE FURNACE  
 Error analysis of absorbed energy flux  
 density and ignition exposure time data,  
 accuracy, precision and confidence limit  
 estimates for arc image furnace ignition  
 experiments  
 [AIAA PAPER 66-669] 18 p3261 A66-34224  
 Arc image stagnation-flow reactor for  
 measuring gas-solid reaction rates between  
 2000 and 3000 degrees K 24 p4216 A66-43214  
 IMAGE INTENSIFIER  
 SA LASER  
 Aberration of width of linear image  
 created by skew rays in composite  
 quadrupole lens 02 p0199 A66-11782  
 Electron avalanches in anode and cathode  
 directed streamers detected by high-gain  
 image intensifier and streak  
 shutter 08 p1263 A66-19079  
 Five-stage transmission secondary-emission  
 image intensifier tube as high speed shutter  
 for moment and streak  
 photography 12 p1883 A66-24937  
 X-ray image intensifier in conjunction with  
 motion picture film sequencing of thrust  
 chamber image during hot firing to obtain  
 failure analysis data 13 p2079 A66-25819  
 Aerial image reproduction on Lith type  
 and extreme resolution emulsions, noting  
 experimental results on sharpness, line  
 width changes and methods of testing with  
 photomicrography 19 p3353 A66-35315  
 Image restoration via phase holograms,  
 noting applications to deteriorated  
 photographic negatives and  
 positives 23 p4068 A66-41411  
 Image intensifier application as aid to  
 visual acquisition of weak luminous moving  
 targets against night sky 23 p4071 A66-41676  
 IMAGE ORTHICON TUBE  
 Manned Orbiting Laboratory experiments  
 such as airglow, solar corona, cosmic ray,  
 plasma, far UV image orthicon,  
 etc 04 p0585 A66-13678  
 Image, display and storage tube for scan  
 conversion, digital storage and signal  
 processing 07 p1036 A66-18270  
 Pulsating auroras observed near  
 equatorward boundary of auroral displays  
 during postbreakup phase with image  
 orthicon TV and  
 photometers 18 p3107 A66-34519  
 Image orthicon slit spectrograph for study  
 of aurora and night glow 22 p3921 A66-40898  
 IMAGE TRANSDUCER  
 Film scanning system using GaAs light-  
 emitting diode and phototransistor light  
 detector 11 p1709 A66-23476  
 IMAGE TUBE  
 Remote extraterrestrial surface navigation,  
 discussing image-tube based stellar field  
 acquisition system  
 parameters 04 p0543 A66-13590  
 Luminescent surfaces and structures for  
 information display, discussing cathode ray  
 tube, image intensifier for night vision,  
 spectral emission, etc 19 p3312 A66-35338

Langmuir current-density limit derived for  
 differing axial and radial electron beam  
 temperatures in high-resolution image  
 devices 20 p3524 A66-36899  
 Photographic radar system employing Q-  
 switched ruby laser, Mullard type 6929  
 image tube and conventional  
 camera 21 p3736 A66-38796  
 Signal generating image tubes for photo-  
 optical tracking and surveillance  
 sensors 23 p4070 A66-41669  
 IMAGE VELOCITY SENSOR  
 SA SPATIAL FILTERING  
 Laboratory simulation to test image-  
 velocity measuring device yielding accurate  
 and useful results 02 p0227 A66-11379  
 Signal-generating astronomical sensors,  
 describing Stratoscope II balloon-borne  
 telescope 08 p1222 A66-18732  
 Image movement from aircraft velocity for  
 vertical and oblique panoramic  
 cameras 13 p2078 A66-25605  
 Control signal generator and output  
 characteristics of angular position and  
 velocity sensors used in single-axis Sun-  
 oriented system of Vostok  
 spacecraft 19 p3394 A66-35280  
 Moving image velocity measuring technique  
 using parallel-slit spatial filter is treated as  
 continuous optical correlation  
 processing 20 p3558 A66-37288  
 Signal generating image tubes for photo-  
 optical tracking and surveillance  
 sensors 23 p4070 A66-41669  
 IMAGERY  
 Nimbus I IR scanning radiometry for  
 nocturnal imagery of clouds and other data,  
 IR spectral returns and relation to image  
 gray scale 10 p1531 A66-21519  
 Geoscience information acquisition by  
 radar return studied by means of terrain  
 target scattering coefficients  
 /scatterometry/ 14 p2244 A66-28407  
 Geometric analysis of recordings by IR  
 scanners, emphasizing significance of stereo  
 imagery 24 p4210 A66-42289  
 IMAGING TECHNIQUE  
 Image translation from plate into  
 coordinate system on another plate using  
 homographic coordinates of object applied  
 to astrometry 01 p0135 A66-10276  
 Electron image of CRT cathode formed  
 directly on view screen, eliminating  
 emission patchiness from oxide coated  
 tubes 01 p0036 A66-10395  
 Radiation patterns of transversely polarized  
 corner reflector antenna, using image  
 method 01 p0044 A66-10937  
 Linear filtering concepts in imaging and  
 optical data processing systems, including  
 three-dimensional photography obtained by  
 wave front reconstruction 02 p0240 A66-11453  
 Metal surface structure, semiconductors  
 and dielectric films analyzed, using image  
 orthicon technique for data on work  
 function, electron reflection coefficient and  
 electric resistance 05 p0621 A66-15578  
 Systems design techniques applied to laser  
 rangefinder and imaging devices,  
 emphasizing relation between operational  
 requirements and laser  
 technology 06 p0889 A66-15967  
 Flight simulation developments for  
 V/STOL visual device requirements  
 including mirrors focusing images at  
 infinity, transparency image storage  
 techniques, optical probes,  
 etc 06 p0869 A66-16814  
 Automatic picture transmission of Nimbus  
 I meteorological satellite, considering  
 frequency choice, vehicle position, antenna,  
 image reception, etc 08 p1180 A66-18612  
 Optical radiation transfer equations applied  
 to imaging instruments used in radiometry  
 of hypersonic reentry  
 bodies 08 p1222 A66-18709  
 Solid-state camera system consisting of  
 monolithic phototransistor mosaic sensor and  
 molecular digital readout  
 system 08 p1226 A66-19545  
 Visual display system providing instrument  
 data in one-to-one correspondence with real  
 world, using cathode ray tube images of  
 horizon and runway projected on aircraft  
 windscreen 08 p1203 A66-19784  
 Imaging and altimeter-type radar employed  
 in orbiting spacecraft for high resolution  
 mapping, scattering cross section studies,



climatology, etc 10 p1532 A66-21521  
 Earth atlas based on high altitude photography, Nimbus and IR imagery and high altitude radar 10 p1532 A66-21527  
 imagery  
 Cardinal points and focal lengths of holographic system established by treating holographic imaging as projective transformation between object and image space 11 p1706 A66-22872  
 Ghost imaging of solid objects by holograms formed in near field without using Fourier transforming lenses 11 p1708 A66-23205  
 Microstructure viewed on several different successive parallel planes simultaneously, using multiple positive or negative transparencies, obtaining three-dimensional photomicrograph 12 p1892 A66-23626  
 Observation satellite optics, discussing focal length, resolution, viewing angle, Earth curvature effect, etc 12 p1915 A66-24935  
 Panoramic facsimile camera providing IR and visible spectrum imagery designed for unmanned space operation, noting construction, weight, etc 13 p2077 A66-25236  
 Lens aberration correction using Gabor wavefront reconstruction method to produce hologram of spherically aberrated wavefront emerging from lens 13 p2080 A66-25990  
 Optical system correction through coefficient selection of aspheric surface, computing vector sums of all aberration orders to give spot diagrams and light distribution in image 14 p2334 A66-27317  
 Luna IX imaging system and analysis of pictorial data of lunar surface 15 p2498 A66-28741  
 Subroutines and functions of BE VISION, package of FORTRAN programs for drawing orthographic views of combinations of plane and quadric surfaces 15 p2510 A66-29770  
 Behavior of projectiles in hyperballistic tunnel analyzed by photographs of their shock waves, using array of spark gaps flashes correlated with cameras 16 p2673 A66-30313  
 Writing rate of rotating-mirror streak camera determined, using Q-switched laser technique 16 p2702 A66-30419  
 Partial coherence theory, discussing mutual coherence function, coherent fields, imaging theory, etc 16 p2748 A66-31241  
 Image related scanning systems for visual simulation display for space rendezvous and docking [AIAA PAPER 65-263] 18 p3093 A66-33788  
 Life detection on Mars by visual techniques, discussing imaging devices, filters, shutters and microcopy 18 p3063 A66-34371  
 Pinhole array camera for multiple image production for integrated circuits 19 p3354 A66-35385  
 Geologic evaluation of simultaneously produced like-and cross-polarized radar imagery 19 p3351 A66-36390  
 Holography principles, discussing basic equation, Fourier transform holograms and hologram interferometry 20 p3556 A66-36929  
 Holography theory and construction methods including experiments with thick or three-dimensional recording media, considering applications to microscopy, X-ray holography and TV 20 p3560 A66-37620  
 Imaging techniques to obtain temperature and emissivity measurements and phase diagrams of high melting point ceramic oxides with aid of solar furnace 21 p3738 A66-39102  
 Modulation transfer function shown to reduce harmonic distortion by forming positive images, provided exposure and development conditions are met 21 p3738 A66-39127  
 Holography, discussing potential uses, frozen wave fields, holograms at X-ray wavelength and stress 21 p3739 A66-39199  
 Finite grain size of photographic film effect on holography for cylindrical wavefronts 21 p3740 A66-39393  
 Imaging performance of error-free optical system limited by deviations in optical imaging surfaces, discussing aperture efficiency 21 p3773 A66-39395  
 Holographic processes, uses and limitations, discussing coherent imaging, holographic

information storage and information display 22 p3918 A66-40292  
 Dependence of complex optical transfer function of image forming system on horizontal range through turbulent atmosphere 22 p3949 A66-40890  
 Computer ray tracing study of image-forming in eyes as affected by pupil size, refractive indices and curvatures of cornea and lens 23 p4025 A66-41149  
 Electronic imaging techniques for engineering, laboratory, astronomical and other scientific measurements - Seminar, Los Angeles, April 1965 23 p4069 A66-41664  
 Radiometric capability of S-10 image orthicon system evaluated for quantitative radiation measurements against reentry vehicles 23 p4070 A66-41668  
 Advanced imaging techniques for Metro camera for space applications 23 p4070 A66-41670  
 Millimeter wave resonant interferometer capable of measuring spatial distribution of electrons in low density transient plasma column subject to perturbation 24 p4209 A66-42191  
 Wide field active imaging, image processing in which pictorial information is placed within laser cavity 24 p4222 A66-42559  
 Correlation of like and cross polarized side-looking radar images with geologic features for terrain discrimination 24 p4173 A66-42634  
 Noise limitations in obtaining three-dimensional images by holographic techniques, considering graininess of photographic emulsion 24 p4212 A66-42752  
**IMBEDDING**  
 SA INVARIANT IMBEDDING  
 Broadband X to K band varactor frequency doubler, noting efficiency increase by replacing variable resistance element with varactor 12 p1832 A66-23908  
**IMIDE**  
 S PYRIMIDINE  
**IMMERSION**  
 Effects of water immersion, recumbency and activity without negative breathing pressures, measuring heart rate and blood pressure with and without tilting 11 p1642 A66-22573  
 Bed rest and water immersion effects on plasma volume and catecholamine response to tilting, noting urinary excretion of norepinephrine and epinephrine 15 p2430 A66-28661  
 Comparative insulative properties of wet and dry type immersion protection flight clothing 16 p2643 A66-31127  
 Buoyancy and magnetohydrostatic stability of magnetic body immersed in magnetizable fluid 16 p2749 A66-31757  
 Characteristic equation for linear flutter problem of elastic cylindrical shell immersed in gas flow, discussing energy radiation, traveling wave propagation and discontinuity problem 22 p3995 A66-40510  
**IMMUNOLOGY**  
 Comparison methods for relationship among enzymes that are same but belong to different organisms 04 p0460 A66-13367  
 Antibody globulin coupled to diazotized aminoaryl derivative of carboxymethyl-cellulose to form immunoadsorbent for extracting antigens 12 p1805 A66-23568  
 Immunochemical studies on interspecies molecular hybrids of hemoglobin 13 p2010 A66-25898  
 Immunological reactions of Russian spacemen before and after space flight 15 p2436 A66-29468  
**IMP**  
 Observations of interplanetary magnetic field by Mariner and Imp spacecraft confirm predictions based on behavior of cosmic rays 03 p0429 A66-13263  
 Solar wind observations with Explorer XII and IMP, noting periodic fluctuations in solar proton flux and detection of 3 mev electrons of interplanetary origin 18 p3167 A66-34335  
 Solar wind in framework of Parker theory, summarizing data obtained from IMP and energetic-particle experiments 18 p3167 A66-34338  
 IMP satellite data on lunar magnetospheric MHD wake and interaction with solar wind 18 p3231 A66-34358  
 Energetic electron spikes in and beyond transition region of Earth radiation zone from IMP observations 18 p3196 A66-3487

**IMP-A**  
 S EXPLORER XVIII SATELLITE  
**IMP-D**  
 S EXPLORER XXXIII SATELLITE  
**IMP-E**  
 Comparison of interplanetary magnetic field measurements obtained by Pioneer V space probe and IMP-III satellite 18 p3233 A66-3454  
**IMPACT**  
 SA ELECTRON IMPACT  
 SA HYPERVELOCITY IMPACT  
 SA ION IMPACT  
 SA PROTON IMPACT  
 Computational method for determination of corridors of launch vehicle trajectory and impact dispersions [AIAA PAPER 66-483] 18 p3226 A66-3362  
**IMPACT ACCELERATION**  
 Cratering in materials analysis, considering transient, primary, secondary and recovery phases, using rod projectiles at high velocity impact 15 p2607 A66-2870  
 Physiological and biomechanical reactions of humans exposed to action of g forces examining effects of impact acceleration 24 p4166 A66-4312  
**IMPACT DAMAGE**  
 SA METEOR HAZARD  
 SA RAIN IMPACT DAMAGE  
 Micrometeoroid impact effect on candidate skin materials, determining change in optical properties 03 p0382 A66-1277  
 Hypervelocity crater depth and target strength 03 p0437 A66-1280  
 Dynamic flexural buckling of rods with axial plastic compression wave, noting strain-hardening law [ASME PAPER 65-APMW-32] 04 p0593 A66-1422  
 Elastic impact and perforation of aluminum plates at minimal velocities by projectiles 05 p0775 A66-1529  
 Ratio of maximum wall thickness to crater depth as function of impact velocity of meteoric particles 06 p0961 A66-1717  
 Hypervelocity particle penetration of manned space station structure, discussing hole formation and repair 10 p1612 A66-2193  
 Meteoroid environment, meteoroid impact hazard on spacecraft structure and meteoroid shields 13 p2193 A66-2584  
 Dynamic flexural buckling of rods with axial plastic compression wave, noting strain-hardening law [ASME PAPER 65-APMW-32] 18 p3247 A66-3356  
 High strain rate deformation of solids under liquid impact examined via photographic methods 20 p3588 A66-3780  
 Germanium damage due to low energy He, Ne, Ar and Kr ion bombardment 20 p3623 A66-3839  
 Criticism of article on microparticle impact effect on metal optical properties 21 p3818 A66-3879  
 Photomicrographs of pressure crack figures on silicon single crystals at room temperature 21 p3803 A66-3929  
**IMPACT DECELERATION**  
 Mathematical model for predicting strength and density of material from deceleration time history of instrumented impact probe 18 p3253 A66-3380  
 Thromboelastographic investigation of short duration high-intensity chest-to-back impact deceleration in rats 22 p3856 A66-4050  
 Periodic symmetric two-impacts-per-cycle motion of impact damper solved, determining asymptotically stable regions 24 p4216 A66-4214  
**IMPACT LOAD**  
 Central maximum loading by transverse impact on beams independent of boundary conditions calculated by simplified integrals and verified by measurements 03 p0433 A66-1231  
 Dynamic stability of elastic and rigid rod under longitudinal impact 03 p0441 A66-1329  
 Stress wave propagation theory for long bars and stepped shafts under impact loads 04 p0525 A66-1340  
 Breaking strength of plastic metals under impulse loading by measuring axial tensile



resses 05 p0699 A66-14685  
Estimation of die loads in impact forging  
axially symmetric disks and flat slabs  
ASME PAPER 65-WA/PROD-1]

Measurements of dynamic behavior of  
tors supported by externally pressurized  
as bearings subjected to impact  
ASLE PREPRINT 65AM 3A4]

Results of aircraft accidents in terms of  
injury and death in-flight, on impact, after  
impact and during escape 10 p1495 A66-22141  
Critical impact load under which  
axisymmetric deformation of perfect elastic  
isotropic cylindrical shell becomes unstable  
determined, using deflection  
theory 12 p1959 A66-23746  
Nonsymmetric strain response of simply-  
supported cylindrical shells to localized  
impact loads expressed as step, ramp and  
sawtooth functions and rectangular  
impulse 12 p1972 A66-25007  
Photoelastic intensity variations in glass  
beam following impact of steel ball,  
registering values 13 p2198 A66-26300  
Response of vibrating body with two  
degrees of freedom when colliding with stiff  
body, useful for communication relays and  
terminal analysis 14 p2407 A66-28040  
Unstabilized rod buckling from impact load  
with longitudinal compression wave  
deflection 15 p2607 A66-28736  
Dynamic elastic response of inner and  
outer edges of ring to distributed impact  
loads 18 p3247 A66-33570  
Physical and mechanical properties of  
cermets obtained by sintering powdered  
iron at high temperatures under dynamic  
impact compression 20 p3583 A66-37413  
Stress wave, deformation and fracture  
caused by liquid impact, noting analogy with  
solid and explosive impact and loading  
fracture formation, propagation,  
etc 20 p3588 A66-37803  
Initial stages of deformation in metals  
subjected to repeated liquid impact  
compared to loading from shock waves in  
liquid 20 p3586 A66-37808

IMPACT PREDICTION  
Calibrating geodetic and geophysical errors  
effect on Minuteman trajectory, noting  
instrument errors 14 p2390 A66-28449  
High-speed photographic techniques,  
recording impact and postimpact  
phenomena, used in prediction of flow  
resulting from hypervelocity impact of  
pellet with thin plate 20 p3560 A66-37740

IMPACT PRESSURE  
Increasing plastic buckling resistance of  
thin cylindrical /Mg and Al/ shell by means  
of elastic core /polyurethane foam/  
[ASME PAPER 65-APMW-18]  
04 p0592 A66-14219  
Interaction of light pulse from ruby laser  
with mercury surface, observing mechanical  
impact believed to be rapid vaporization  
process 04 p0533 A66-14373  
Impact of rigid or flexible body on surface  
of compressible fluid, noting impact of rigid  
wedge and linear supersonic airfoil theory  
[ASME PAPER 65-WA/UNT-3]  
05 p0663 A66-15600  
Excitation of phosphorus suspension in  
electroluminescent panel by steel ball  
impact 06 p0928 A66-16887  
Increasing plastic buckling resistance of  
thin cylindrical /Mg and Al/ shell by means  
of elastic core /polyurethane foam/  
[ASME PAPER 65-APMW-18]  
10 p1615 A66-21475  
Impact tube pressure probe response to  
free molecular rarefied gas flow for  
arbitrary angle of attack 11 p1692 A66-22939  
Longitudinal impact between cylindrical  
rods, considering local deformations and  
wave propagation in rods, showing solution  
through dimensionless equation of Sears  
theory 12 p1968 A66-24242  
Boltzmann equation for Pitot tube  
problem, using distribution function,  
deriving equations for rarefied gas flow in  
impact tube under hypersonic and adiabatic  
conditions 15 p2481 A66-29739  
Structure and properties of free supersonic  
jets including impact pressure and velocity  
distribution measurements, condensation,

etc 16 p2628 A66-30376  
Response of impact and static pressure  
probes in rarefied high speed gas  
flow 16 p2628 A66-30378  
Static pitching moment coefficient  
determination from location of center of  
pressure in right circular cone, using  
Newtonian impact  
mechanics 17 p2840 A66-32494  
Munroe jet formation when small cavity or  
bubble in liquid is subjected to impact or  
shock 20 p3546 A66-37804  
Impact of elastic conical shell of revolution  
moving with constant axial velocity toward  
rigid obstacle 21 p3827 A66-38692  
Impact of rigid or flexible body on surface  
of compressible fluid, noting impact of rigid  
wedge and linear supersonic airfoil theory  
[ASME PAPER 65-WA-UNT-3]  
21 p3731 A66-39531  
Vertical impact of spherical solid half-  
submerged in fluid of finite depth,  
examining effect of bottom on occurring  
phenomena 23 p4056 A66-41728

IMPACT SENSITIVITY  
Input initiation energy and potential  
impact energies available under processing  
conditions, interpreting test  
data 05 p0787 A66-15138  
Liquid nitrogen dilution effect on LOX  
impact sensitivity of selected  
materials 10 p1590 A66-21951  
Nonmonotonicity in sensitivity test data,  
noting results of liquid oxygen impact tests  
on Mylar-aluminum-Mylar laminate bonded  
to polyester foam 12 p1958 A66-23648  
Explosive sensitivity of dust or sprays  
ignited behind reflected shock simulated by  
shock tube, measuring ignition delay  
dependence on shock  
temperature 20 p3680 A66-38039  
Drop-weight tester/photographic apparatus  
for studying impact initiation-explosion  
process in nitroglycerin 23 p4119 A66-41243

IMPACT TEST  
Mechanical properties of commercial heats  
of Al and vacuum melted steel, deriving  
data from impact and tensile tests, noting  
ways of increasing  
toughness 01 p0086 A66-10413  
Impact process beyond limits of Hertz  
theory 01 p0154 A66-10478  
Hypervelocity impact force per crater  
surface area correlated to stress-to-fracture  
of target, experimenting with aluminum and  
copper as targets and  
projectiles 01 p0154 A66-10496  
Wide wedge penetration into thick  
aluminum target, noting adiabatic heating  
and softening 02 p0300 A66-11854  
Charpy test modification using ram to  
deform sample, obtaining data on elastic  
limit corresponding to high stress  
rates 02 p0246 A66-12005  
Fracture toughness of X7000-series  
aluminum alloy plate  
weldments 05 p0686 A66-14695  
Stroboscopic arrangement for photoelastic  
investigation on longitudinal stressed  
beams 05 p0773 A66-14990  
Drop-weight impact sensitivity testing of  
explosives  
[CI PAPER WSCI-65-27] 05 p0788 A66-15140  
Slow-bend impact testing of embrittlement  
of zirconium by hydrogen 06 p0895 A66-16356  
Yield stress dependence on strain rates in  
annealed steel and aluminum subjected to  
ball-indentation tests 08 p1315 A66-19803  
Photoelastic measurement of dynamic  
stresses and loading of structures,  
examining impact stress phenomena, stress  
waves, vibrations, stress distribution,  
etc 08 p1316 A66-19805  
Acoustic detection of micrometeoroids  
from rockets, discussing experimental setup,  
calibration methods and analysis of  
results 09 p1381 A66-20367  
High-chromium ferrite steel Kh25T  
brittleness at 475 degrees C investigated,  
using neutron structural  
analysis 09 p1391 A66-20872  
Impact properties of six materials  
compared on two falling-weight tensile  
impact testers, pendulum tester and high  
speed universal tensile tester, giving stress-  
strain curves 13 p2197 A66-26110  
Reactivity of titanium alloy oxidizer tank  
with nitrogen tetroxide oxidizer under

vibration analyzed for LEM when subjected  
to impact 13 p2111 A66-26222  
Model tests for determination of structural  
response of Apollo command module to  
water impact 14 p2393 A66-28020  
Material and geometry aspects of  
meteoroid armor protection for space  
radiator tubes, discussing bumper-fin  
concept 14 p2407 A66-28029  
Human response to predicted Apollo  
landing impacts in selected body  
orientations 15 p2430 A66-28663  
Cavity depth for waterdrop impacts against  
water, discussing apparatus, equation for  
cavity depth, effect of gravitational  
potential energy, liquid surface behavior,  
etc 15 p2477 A66-28716  
Microscopic strain rate equation  
interpreting macroscopic creep, stress-strain  
and impact test results 24 p4288 A66-42274  
Impact of compact mass of tungsten  
particles on obstacles of polystyrene and  
steel, as meteoritic impact  
model 24 p4292 A66-42886

IMPACT TESTING MACHINE  
Performance of impact machines for  
testing explosive sensitivity to impact  
[CI PAPER WSCI-65-33] 05 p0787 A66-15137  
Drop-weight sensitivity of explosive liquids  
tested with impact apparatus, showing  
increase with temperature  
[CI PAPER WSCI-65-28] 05 p0788 A66-15139  
Docking of logistics vehicle to space  
station investigated, using airbearing  
postimpact dynamic docking  
simulator 08 p1303 A66-18808  
Closed loop hydraulic high-speed universal  
testing machine and simulation of high  
strain rate conditions 13 p2197 A66-26108  
Impulse-impact shock simulation system  
with initial peak sawtooth  
capability 16 p2680 A66-30484  
Notched bar impact testing machine with  
solid slab pendulum and no material  
protruding beyond striking  
edge 22 p3988 A66-39670  
High velocity impact range diagnostic  
instrumentation including timing and  
triggering devices, laser and spark  
photography, radiation monitors, ballistic  
pendulum, etc 24 p4191 A66-42187

IMPACT TOLERANCE  
Human tolerance limits in water impact,  
identifying environmental and trauma  
characteristics 03 p0327 A66-12356  
Structural design of transport aircraft to  
reduce fatalities, analyzing protective shell  
to withstand ground impact load and fuel  
containment  
[AIAA PAPER 65-773] 03 p0434 A66-12592  
Impact strength of austenitic stainless  
steel welds discussing effects of heat  
treatment, carbon and ferrite content  
[ASME PAPER 65-WA/MET-1]  
05 p0704 A66-15692  
Balsa-wood impact limiter for hard landing  
on Mars surface, noting testing,  
performance, parameters and  
manufacture 13 p2191 A66-25264  
Impact dynamics of landing systems using  
material crushing to absorb kinetic energy  
of body impacting at very high  
velocities 14 p2402 A66-27895  
Human reaction to simulated landing  
impact overload, including analysis of EKG,  
kinetocardiogram, blood pressure and  
respiration data 15 p2443 A66-29445  
Skirt Jet peripheral retrorocket for  
lightweight terminal impact attenuation  
system using multiple nozzle rocket motors  
assembled to form annulus around outer  
periphery of vehicle 22 p3986 A66-40598

IMPEDANCE  
SA ACOUSTIC IMPEDANCE  
SA ELECTRIC IMPEDANCE  
SA MECHANICAL IMPEDANCE  
SA RESPIRATORY IMPEDANCE  
Electric field and wave impedance in spin  
wave propagation in ferrimagnetic  
materials 06 p0847 A66-16101  
Slot admittance for two-layer compressible  
plasma sheath-ion sheath in plasma half-  
space 14 p2235 A66-27128  
Receiver noise-temperature measurement  
uncertainty and dependence on source  
impedance 14 p2238 A66-27584  
Two-dimensional excitation problem of  
circular cylinder with surface impedance



varying over cylinder circumference 17 p2874 A66-32247

Electromagnetic field penetration into magnetoactive plasma with calculation of total surface impedance of plasma 20 p3512 A66-37135

Traveling wave phototube /TWP/ theory in terms of modified TWT coupled mode theory, noting equivalent impedance concept and noise output calculation 24 p4184 A66-42746

**IMPEDANCE MATCHING**

**SA ANTENNA COUPLER**

Integral restrictions on time delay of linear phase low pass matching networks with prescribed parasitic loads 02 p0208 A66-11909

Impedance of growing wave in interaction region used to calculate minimum value of traveling wave tube noise coefficient 06 p0837 A66-17190

Strip transmission line for microwave circuit design such as varactor multiplier frequency sources, filters, multiple pole diode switches, etc 09 p1356 A66-20672

Wide-angle impedance matching /WAIM/ method reducing variation of reflection coefficient with scan angle and polarization by dielectric sheet located in front of array antenna face 11 p1656 A66-22547

Equation governing properties encountered in Gaussian beam propagation represented graphically on impedance chart, showing relation between Gaussian mode and geometrical optics 11 p1656 A66-23089

Complex normalization of scattering matrices, noting application to impedance transformation 11 p1678 A66-23239

Coupling impedance selection for Perceptron-like adaptive pattern recognition system 13 p2045 A66-25338

High gain low-noise electronic amplifier with field effect transistor at UHF range, noting design parameters and performance 13 p2040 A66-25832

Optimum shape of multimode rectangular waveguide transition by comparing smoothed with stepwise transition 14 p2251 A66-27239

Cumulative coupling and impedance mismatch and radiation pattern problems in large uniformly spaced flat phased array 15 p2456 A66-28585

Wide angle impedance matching /WAIM/ of planar array antenna by dielectric sheet for reduction of reflection coefficient variation with scan angle and polarization 15 p2456 A66-28587

General broadband matching for passive and active 1-port load impedance and application to tunnel diode amplifier 15 p2464 A66-29321

Bit error rate improvement without source coding, using matched filters 16 p2659 A66-30548

Impedance of growing wave in interaction region used to calculate minimum value of traveling wave tube noise coefficient 19 p3297 A66-35548

Wall interaction digital stream amplifier with increased flow gain, impedance matching, outputs decoupled and noise reduction 19 p3283 A66-36812

Transfer functions, optimum impedance matching conditions, input and output admittances and voltage spectra of transistorized frequency converters 20 p3525 A66-37125

**IMPEDANCE MEASUREMENT**

Field analysis of plasma filled disk-loaded waveguide, obtaining TWT interaction impedance 03 p0339 A66-12436

Mode of use and effect of precision coaxial connectors on precise methods of impedance measurement 03 p0344 A66-13017

Plasma impedance measurement including block diagram of electronic system 03 p0371 A66-13254

Impedance of dielectric oxide with uniformly distributed monoenergetic traps 04 p0501 A66-14253

Distributed stepped impedance low-pass prototype filter, giving impedance values for filters with Chebyshev equal-ripple characteristics 06 p0844 A66-16082

Interdigital band pass filters and related coupled structures, deriving exact equivalent circuits from impedance matrices 06 p0845 A66-16085

Quarter-wavelength inhomogeneous impedance transformers, discussing design parameter calculation for nearly equal-ripple performance 06 p0845 A66-16090

Impedance variation in scanning arrays approximated without beam forming and steering system 06 p0850 A66-16398

Equivalent h parameters for n transistors connected in cascade, establishing effect of circuit impedances 06 p0854 A66-16687

Effect of various geometries on performance and characteristics of helical antennas, considering input impedance and radiation pattern 07 p1006 A66-17474

Plasma sheath effects on antenna impedance probe and retarding potential probe installed on two Aerobee 150 rockets 08 p1181 A66-18746

Saturation of microwave impedance and occurrence of microwave emission in indium antimonide for strong longitudinal or transverse magnetic fields 08 p1270 A66-19059

Evaluation and comparison of methods of calculating antenna impedance in ionized medium 09 p1349 A66-19844

Radiative and capacitive terms of impedance of finite cylindrical antenna calculated in magnetoplasma with losses by using Kogelnik theory 09 p1349 A66-19845

LF admittance measurements on orthogonal dipoles in ionosphere 09 p1341 A66-19855

Photoimpedance measurement as function of AC field of CdS crystals coated with SiO films or situated between polystyrene foils 09 p1425 A66-20189

Antenna impedance behavior in plasma related to radio astronomy, emphasizing electrically small antennas used in space vehicles 10 p1507 A66-21118

Ionospheric aerial impedance measurements of wire dipole at frequency of 60 kc and plasma electron and collision frequency estimations 10 p1526 A66-21119

Plasma electron density and temperature from measurement of LF impedance of Langmuir probe, noting ionospheric probing 10 p1536 A66-21549

Impedances of offset parallel-coupled strip transmission lines analyzed by conformal mapping techniques 10 p1514 A66-21906

Input impedance of spherical emitter in infinite homogeneous isotropic conducting medium 11 p1656 A66-23031

Distributed RC network synthesis, determining necessary and sufficient conditions for driving point impedance frequency response of transfer functions and Foster type realizations 11 p1678 A66-23240

Relative impedance and transmission techniques for measuring small-signal parameters of varactor diodes at UHF and X-band 12 p1831 A66-23787

Fluid flow impedance parameters and properties, discussing nonlinear orifice resistors in fluidic circuitry, tube resistance and fluid capacity 12 p1803 A66-24384

Measurement of three-terminal immittance at VHF and UHF frequencies 13 p2026 A66-26101

Complex transfer admittance in quadriple transistors from Schottky measuring principle for transconductance of electron tubes 14 p2246 A66-26797

Analysis of antenna parameters for determining equivalent radius of noncircular antennas 14 p2253 A66-27531

Mutual and self-impedance of linear antennas in interface between dielectric layers computed, noting cases of symmetric and antisymmetric excitations 14 p2256 A66-27914

Theoretical calculation of effective load impedance of tunnel diode mounted in microwave structure 15 p2462 A66-29016

Impedance measurement of 39.5 meter tip-to-tip dipole antenna made during ionospheric rocket flight 15 p2469 A66-30046

Electrophysiological patterns and cerebral impedance characteristics in orienting and discriminative behavior 17 p2860 A66-32832

Microwave power generation and amplification via transistors, noting optimum source and load impedance for microwave transistors under large signal conditions 19 p3319 A66-36166

Computer analysis of interference in complex network resulting from common impedance coupling of signals 20 p3538 A66-37119

Resistive and reactive components of impedance of short dipole in lower ionosphere 20 p3525 A66-37300

Constant impedance antennas, noting applicability for high gain broadband performance 20 p3530 A66-37770

Antenna measurement for input impedance, gain and directivity characteristics 20 p3531 A66-37772

Iterated theoretical admittance of cylindrical antenna, determining effective length and approximating ideal independence 20 p3534 A66-38360

Conductance and capacitance of metal-insulator-semiconductor diodes or any two terminal complex admittance plotted automatically as function of applied bias 22 p3882 A66-40819

Bolometer mount efficiency measurement technique by impedance method 24 p4205 A66-42100

**IMPEDANCE PROBE**

**SA RADIO FREQUENCY IMPEDANCE PROBE**

Circuits for variable impedance control at centimeter-wave frequencies, using varactor semiconductors and dephasing ferrites in waveguide 07 p1002 A66-17820

Fredholm integral equation system for magnetic currents induced on wedge under impedance boundary condition 09 p1344 A66-20444

RC network and ideal current negative immittance converter with unity gain used in obtaining RLC voltage transfer functions 15 p2471 A66-29322

Ionospheric thin-layer stratifications and valley region analyzed by integrational propagation method and by impedance probe 15 p2494 A66-30044

Impedance plethysmographic system for monitoring right ventricular output to obtain cardiac output 17 p2924 A66-32144

Scaling procedure for deriving approximate closed-form expression for impedance of spherical probe immersed in cold magnetoplasma 18 p3109 A66-33544

Resistance and frequency response range of sheath surrounding electrostatic probe floating in tenuous plasma 19 p3357 A66-35800

Ionospheric electron density measured by rocket carrying new gyro-plasma impedance probe 24 p4199 A66-42460

**IMPELLER**

**SA PUMP IMPELLER**

**SA ROTOR BLADE**

**SA STATOR**

**SA TURBINE WHEEL**

Boundary layer influence on performance of centrifugal-compressor impellers, measuring discharge velocity profile [ASME PAPER 65-WA/FE-7] 05 p0609 A66-15720

Boundary layer influence on performance of centrifugal-compressor impellers, measuring discharge velocity profile [ASME PAPER 65-WA/FE-7] 12 p1799 A66-24538

Three-dimensional flow visualization approach to complex flow characteristics in centrifugal impeller [ASME PAPER 66-GT-83] 14 p2274 A66-26980

Degree of partiality effect on centrifugal turbine operation 23 p4122 A66-41799

**IMPELLER BLADE**

Laminar boundary layer behavior of centrifugal impeller blades, discussing exact solution via perturbation technique [ASME PAPER 65-WA/FE-15] 05 p0608 A66-15612

Stresses calculated in centrifugal impeller with cover disk by two-dimensional stress analysis and digital computer program [ASME PAPER 65-WA/FE-17] 05 p0780 A66-15701

Gas temperature effect on thermal condition of vanes during acceleration of gas turbine engine 08 p1281 A66-18866

Laminar boundary layer behavior of centrifugal impeller blades, discussing exact solution via perturbation technique [ASME PAPER 65-WA/FE-15] 12 p1799 A66-24543



Geometrically different volutes effect on  
impeller of centrifugal pump performance,  
discussing radial thrust, head and runout  
capacity  
[ASME PAPER 66-FE-14] 17 p2932 A66-33268  
Optimal centripetal turbine impellers with  
radial blade inlet and semiaxial  
discharge 21 p3807 A66-38931  
Inhomogeneity of axial velocity component  
in or near blades forming impeller intake of  
radial compressor attributed to flow  
deflection 24 p4158 A66-43067  
**IMPINGEMENT**  
**JET IMPINGEMENT**  
**IMPLOSION**  
Spherical and cylindrical implosive waves  
and system of generating detonation wave  
that converges to given  
focus 03 p0445 A66-13131  
Imploding cylindrical shock wave  
production through imploding detonation  
waves in oxygen-acetylene mixtures, using  
Chapman-Jouguet theory 08 p1204 A66-18523  
Experiments on jets formed from  
imploding bubbles, indicating that Munro  
jets are formed when hemispherical cavities  
on liquid surface collapse by shock wave  
travelling from below 10 p1607 A66-21292  
Hydromagnetic disturbances during radial  
implosion phase of preionized theta pinch  
Cariddi/ 19 p3414 A66-36510  
Implosion of fast nonpreionized theta pinch  
studied, using first and second harmonic of  
ruby laser light 20 p3609 A66-37638  
Hydrodynamic implosion mechanism and  
impact of liquid jets formed by collapsing  
cavitation bubbles, examining damage to  
solid boundaries 20 p3547 A66-37811  
Neutron star rotational flattening after  
formation in supernova  
implosion 21 p3810 A66-38467  
Implosion experiment, discussing methods  
for detonation and shock wave propagation  
phase calculation 21 p3837 A66-39503  
**IMPREGNATED MATERIAL**  
Ablation mechanism for impregnated  
tungsten materials 02 p0303 A66-11552  
Capillary impregnation for preparing  
corrosionless materials from titanium carbide and  
nichrome 08 p1238 A66-18896  
Refractory properties and resistance to  
thermal shock of sintered tantalum carbide  
impregnated with copper or silver at high  
temperature  
[CONERA TP 323] 11 p1718 A66-23201  
Operating lifetime of porous bearings,  
discussing dependence on quality of  
impregnating lubricant 17 p2930 A66-33143  
**IMPREGNATION**  
**IS DOPING**  
**IS FINISH**  
**IMPULSE**  
**IS ELECTRIC IMPULSE**  
**IS SPECIFIC IMPULSE**  
**IMPULSE GENERATOR**  
Pulse repetition rate of magnetic pulse  
generators increased by transforming  
generator power supply frequency, using  
static frequency  
multipliers 09 p1352 A66-20301  
Sinusoidal voltage converted to rectangular  
voltage, using charge storage  
diodes 11 p1668 A66-23064  
Pulse generator consisting of active  
unidirectional nonlinear quadrupole having  
feedback circuit with linear quadrupole  
containing reactive  
elements 14 p2251 A66-27233  
Differential minority carrier storage circuit  
with avalanche pulse energization and fast  
rise/fall adjustable length pulse  
output 22 p3872 A66-39717  
Construction method for pulse generator in  
digital magnetic devices and current  
generators in magnetic deflecting  
system 23 p4046 A66-41521  
**IMPULSE NOISE**  
Signal to noise ratio characteristics  
measured for square-law detector, extracting  
signals from non-Gaussian  
noise 06 p0831 A66-16341  
Degradation of matched filter receiver  
operating in non-Gaussian noise, considering  
performance in presence of ideal impulse  
noise 06 p0856 A66-16864  
Hearing impairment from overexposure to  
impulsive noise, noting relationship between  
temporary threshold shift and peak level

and duration of impulsive  
noise 17 p2862 A66-31948  
Combined use of time-domain waveforms,  
detection probability and false alarm  
probability for selection of optimum sample  
period and quantization interval for  
detection of impulse  
waveforms 19 p3299 A66-35663  
Speech communications effects and  
temporary threshold shift reduction  
characteristics of British-made earplugs  
under quiet and high intensity impulsive  
noise backgrounds 24 p4168 A66-42857  
**IMPULSE ORBITAL TRANSFER**  
Optimal free-space fixed thrust trajectories  
using impulsive trajectories as starting  
iteratives  
[AIAA PAPER 66-96] 06 p0956 A66-17094  
Minimum fuel transfer solution of Lawden  
problem involving finite number of impulse  
thrusts separated by coasting arcs  
[AIAA PAPER 66-7] 07 p1136 A66-17881  
First-order perturbation solution to  
problem of minimum-fuel orbit transfer in  
form of equal slope guidance constraint  
[AIAA PAPER 66-11] 07 p1137 A66-17883  
Two-body problem applied to elliptic orbit,  
comparing three-impulse with single-impulse  
plane change applied at  
node 08 p1289 A66-18837  
Optimum impulsive transfer between  
elliptic and noncoplanar circular orbits,  
noting paths with up to three apsidal  
impulses 09 p1459 A66-20884  
Two-body problem of two-impulse transfer  
to or from given circular orbit and given  
nonplanar hyperbolic  
asymptote 10 p1608 A66-21788  
Optimum orbital transfer from circular to  
nonintersecting elliptical orbit with use of  
two impulses of unequal specific  
impulses 14 p2387 A66-28181  
Canonical transformation in optimal  
steering and cut-off-relight programs for  
orbital transfer about central  
field 14 p2387 A66-28182  
Analytical dynamics and optimal transfers  
between orbits 15 p2596 A66-29154  
Impulse functions associated with two-  
impulse transfer between nearly tangent  
noncoplanar coplanar elliptical  
orbits 16 p2805 A66-31539  
Optimum three-impulse rotation of plane  
of circular orbit 16 p2806 A66-31627  
Optimal free-space fixed thrust trajectories  
using impulsive trajectories as starting  
iteratives  
[AIAA PAPER 66-96] 17 p3001 A66-32457  
Minimum impulse orbital transfer between  
coplanar elliptical orbits with aligned axes,  
noting advantage of three- and two-impulse  
transfers 18 p3227 A66-33760  
Single-impulse transition in Newtonian  
central force field from hyperbolic to  
elliptical orbit in case of radial  
impulse 19 p3455 A66-35276  
Infinitesimal economic pulse transfers  
between quasi-circular noncoplanar  
orbits 19 p3459 A66-35583  
Coplanar orbit transfers by tangential  
impulses at apse point in graphical  
presentation of solutions 20 p3657 A66-38176  
Optimum impulsive transfers between  
noncoplanar elliptic orbits having collinear  
major axes and common center of  
attraction, noting overlap configuration of  
initial and final elliptic  
orbits 23 p4129 A66-41686  
**IMPURITY**  
**SA ATMOSPHERIC IMPURITY**  
Incremental-elasticity vs charge  
relationship used for impurity profile of p-n  
junction measurement 01 p0119 A66-10398  
Optimum conditions for improving  
sensitivity of spectral analysis and plotting  
calibration curves for determining impurity  
elements in silicon  
carbide 02 p0188 A66-11995  
Spectral determination of impurities in  
silicon carbide based on evaporation in  
argon atmosphere from cavity cut into  
graphite electrode 02 p0188 A66-11996  
Impurity bandwidth and separation from  
conduction band in n-type GaAs determined  
from electroconductivity and Hall effect  
data 02 p0278 A66-12077  
Impurity concentration dependence of  
difference between heat capacities at

constant pressure and at constant volume in  
Ge 02 p0277 A66-12093  
Anderson model to obtain transition metal  
impurities effect on superconductors due to  
resonance scattering 03 p0407 A66-12331  
Impurity concentration fluctuations in  
silicon crystals, discussing striation  
visualization technique and Czochralski  
method 05 p0729 A66-14512  
Gallium arsenide recombination-radiation  
spectrum discussing effects of impurities on  
short wave radiation band  
energy 05 p0731 A66-14657  
Thermal diffusion of impurity atoms  
suggested as possible cause of GaAs Esaki  
diode deterioration by Weisberg and  
Gold 05 p0733 A66-14672  
Qualitative interpretation of negative  
resistance by impact ionization of deep level  
impurities noting temperature, impurity  
concentration and energy  
level 05 p0735 A66-14964  
Vacuum technique for obtaining thin layers  
of semiconductor material with varying  
impurity distribution across depth of  
layer 06 p0924 A66-16545  
Anomalous diffusion of some group III and  
group V impurities in  
silicon 08 p1268 A66-18657  
Built-in electric field effect on  
simultaneous diffusion of oppositely charged  
impurities in  
semiconductors 08 p1268 A66-18659  
Nonharmonicity effect on dispersion of  
light by impurity centers of solid  
body 08 p1273 A66-19256  
Pressure effect and superconducting  
transition temperature effect on thallium  
and mercury-impure  
thallium 09 p1411 A66-19957  
Dependence of expansion ratio on impurity  
concentration for silicon samples differing  
in impurity and dislocation  
content 09 p1412 A66-19991  
Electronic thermal conductivity,  
longitudinal sound wave decay and nuclear-  
spin temperature in superconductors with  
paramagnetic impurities 09 p1421 A66-20054  
Diamagnetic impurity effect on  
temperature of superconducting transition  
for Fermi surface topology sensitive to  
impurity additions 09 p1428 A66-20594  
Electron paramagnetic resonance, electrical  
conductivity and impurity diffusion in doped  
boron 10 p1580 A66-21724  
Impurity atom diffusion through narrow  
diffusion mask opening determined by  
relaxation method 10 p1512 A66-21762  
IR absorption spectrum of local H-ion  
oscillations in KCl crystals doped with Na,  
Rb, Cs, I, Br and F 10 p1588 A66-22158  
Range of importance of molecular  
impurities on nitrogen vibrational relaxation  
determined, using spectroscopic sodium line  
reversal techniques 11 p1741 A66-23218  
Green function random phase decoupling  
scheme investigation of magnetic impurities  
effect on thermal properties of cubic spin-  
1/2 Heisenberg  
ferromagnet 11 p1758 A66-23394  
Quantum mechanical formula for low-field  
Hall effect in density matrix approach,  
treating this effect in disordered  
systems 12 p1927 A66-23723  
Superconductivity variation in tantalum  
noting dependence of critical current,  
transition temperature and magnetic field  
on impurity concentration 12 p1927 A66-23856  
Antimony ionization in p-germanium single  
crystals, based on diffusion of Sb into  
Ge 12 p1930 A66-24460  
Gold or copper diffusion effect on  
breakdown and multiplication characteristics  
of high voltage silicon p-n junctions, noting  
presence and formation of  
microplasma 13 p2161 A66-25194  
Gallium arsenide recombination-radiation  
spectrum, discussing effects of impurities on  
short wave radiation band  
energy 13 p2167 A66-25932  
Optical linewidth study of energy transfer  
between impurity ions and homogeneous  
broadening and lineshape changes in optical  
transitions 13 p2098 A66-26176  
Avalanche breakdown voltages of abrupt  
and linearly graded p-n junction in Ge, Si,  
GaAs and GaP 14 p2356 A66-27027  
Propagation distribution of impurity atoms



- in heavily doped semiconductors 14 p2356 A66-27068
- Band shift in strongly doped semiconductor under influence of impurity atom electrostatic field 14 p2356 A66-27069
- Hot electron recombination at repulse impurity centers in germanium containing copper 14 p2357 A66-27074
- Optical absorption in semiconductors with impurity center participation in external magnetic field 14 p2358 A66-27082
- Thermoconductivity of germanium alloyed with arsenic and gallium depends on impurity type starting from certain impurity concentration 14 p2359 A66-27178
- Critical temperature of two-band superconductor model with paramagnetic impurity 14 p2360 A66-27194
- Quantitative determination of impurities in organic compounds using flame ionization detector 14 p2232 A66-27610
- Impurity scattering in theory of interband magneto-optical effects, noting inadequacy of first-order perturbation treatment and low and high impurity-atom concentration with weak interaction 15 p2558 A66-28610
- Effect of impurity atoms or neutron irradiation on X-ray diffraction intensities of silicon and germanium crystals 15 p2559 A66-28625
- Light dispersion and absorption by impurity centers in solids calculated via two-particle Green function method, assuming weak electron-phonon interaction 15 p2559 A66-28632
- Impurity photovoltaic effect in cadmium sulfide, noting radiative enhancement of spectral response upon illumination with green light 15 p2561 A66-28709
- In, Ga and Cu impurity effects on absorption spectrum of zinc telluride 15 p2565 A66-29199
- Bulk oscillations in n-type Si compensated with either Au or Co deep level impurities 16 p2778 A66-31078
- Electrical conductivity of metals, explaining electron scattering amplitude changes, phonon spectrum distortion and temperature effects caused by impurity concentration in conductor 16 p2780 A66-31180
- Impurity energy levels in semiconductors described by equivalent Schrodinger equation containing short-range as well as conventional terms for long-range Coulomb potential 16 p2784 A66-31446
- Laser mode operation in pressure of radiation absorbing impurity analyzed by extended Thomson type system 16 p2720 A66-31558
- Epitaxial growth techniques for silicon and germanium, discussing hydrogen reduction methods, doping and impurity control, etc 17 p2976 A66-32259
- Electrostatic field gradient effect in semiconductors with diffused impurities investigated, using basic diffusion theory 17 p2980 A66-32645
- Single donor-type randomly distributed impurity and effect on electron energy spectrum of semiconductor 17 p2982 A66-32969
- In, Ga and Cu impurity effects on absorption spectrum of zinc telluride 17 p2982 A66-33048
- Negative photoconductivity in germanium at temperature and doping levels important with impurity conduction 17 p2985 A66-33293
- Impurity concentration and electric field distribution determined in drift region of silicon p-i-n detectors from capacity as function of reverse voltage 17 p2986 A66-33303
- Tunnel diode capacitance relation to displacement interpreted in terms of impurity drift in nonuniform field of p-n junction in highly doped germanium diodes 19 p3433 A66-35302
- Diffusion and melting techniques used to determine effect of Ni, W, Ti and Ta impurities on lifetime of minority carriers in n-base of silicon p-n junctions 19 p3433 A66-35310
- Impurity conduction for arsenic diffused into p-type germanium and boron into n-type silicon 19 p3433 A66-35342
- Controlled doping of germanium layers during evaporation, noting behavior differences for p- and n-type impurities and concentration dependence 19 p3434 A66-35344
- Chemical sectioning of p-type surface layers on silicon, presenting electrical and X-ray measurements of boron-induced defect distribution 19 p3436 A66-35424
- IR absorption spectrum of local H-ion oscillations in KCl crystals doped with Na, Rb, Cs, I, Br and F 19 p3440 A66-35772
- Trace impurity determination in semiconductors by spectral analysis, using plasma generator 19 p3442 A66-35944
- Diffusion parameters of impurities from polycrystalline Si in hydrogen flux, noting formula for boundary conditions 19 p3321 A66-36457
- Neutral-impurity scattering and scaled electron-hydrogen-atom collision problem for hydrogenic-type impurities in semiconductor studied by method using highly spin-polarized carriers 19 p3448 A66-36763
- Neutral-impurity scattering experiments in silicon with highly spin-polarized electrons 19 p3448 A66-36764
- Recombination radiation from Ga-Sb p-n junctions, noting spectral composition as function of current density and impurity concentration 20 p3618 A66-37563
- Antimony ionization in p-germanium single crystals, based on diffusion of Sb into Ge 20 p3620 A66-37692
- Electrical and photoelectrical properties of silicon photocells with different impurities, examining load characteristics, V-I forward and reverse branches plotted for silicon cells 20 p3502 A66-37734
- Impurity concentration effect on maximum continuous wave power from gallium arsenide lasers at 77 degrees K 20 p3580 A66-37782
- Diamagnetic impurity effect on temperature of superconducting transition for Fermi surface topology sensitive to impurity additions 20 p3622 A66-38128
- Stimulated emission of radiation in semiconductors, calculating dependence on temperature and impurity concentration, using Kane model with Gaussian band tail for density of states and optical model 21 p3795 A66-38547
- Effects of nonmagnetic impurities upon anisotropy of superconducting energy gap 21 p3797 A66-38559
- Impurity atom behavior in diatomic InSb and GaSb crystal lattices analyzed, using nuclear gamma resonance, measuring absolute values of f, chemical displacements and line widths 21 p3799 A66-38922
- Relation between electrical properties and structural features of gold- and antimony-doped germanium single crystals, noting abrupt decrease in mobility 21 p3799 A66-38928
- Electrical properties of indium antimonide single crystals with noncompensated impurity concentration, determining position of deep-seated levels in forbidden band 21 p3799 A66-38929
- Steady state donor-acceptor recombination rate and effects on diode current and injection electroluminescence, using Shockley-Read-Hall semiconductor phenomenological model 21 p3800 A66-38993
- Impurity conduction effect on electron donor recombination cross section in n-type germanium and silicon at liquid helium temperatures 21 p3801 A66-39001
- Anomalous behavior of superconducting transition temperature for certain magnetic ordering of paramagnetic impurities 21 p3803 A66-39264
- Linear flow equation motion of fluid with suspended impurities, noting that under certain assumptions velocity fields can be described by family of potential functions 21 p3729 A66-39448
- Gold doping effects on recovery time of phosphorus, boron and arsenic impurity gaseous-diffused junction diodes and estimated gold recombination center densities 22 p3873 A66-39749
- Energy and wave functions of singly charged donor impurity centers in silicon and germanium 22 p3959 A66-39772
- Jahn-Teller shift reorientation in Ni impurity centers of diamond and rise of C-N pair EPR spectrum with temperature 22 p3964 A66-40307
- Ionization relaxation in impure shock heated argon studied by magnetic mass spectrometer 22 p3899 A66-4038
- Propagation distribution of impurity atom in heavily doped semiconductors 22 p3966 A66-4082
- Band shift in strongly doped semiconductor under influence of impurity atom electrostatic field 22 p3966 A66-4082
- Hot electron recombination at repulse impurity centers in germanium containing copper 22 p3966 A66-4083
- Optical absorption in semiconductors with impurity center participation in external magnetic field 22 p3967 A66-4083
- Metallic impurities effect on tensile strength of binary nickel alloys under tension 22 p3937 A66-4092
- Magnetostriction constants measured at room temperature for YIG single crystals after replacing fraction of iron ions by silicon 23 p4114 A66-4162
- Thermoelectric power and electric resistivity of copper-gold alloy doped with 3d transition metals as function of temperature and atomic number of impurity 23 p4114 A66-4171
- IR active localized vibrational modes absorption in lithium and copper compensated silicon doped gallium arsenide 24 p4251 A66-4224
- Generation-recombination noise and lifetime measured using photoconductivity decay in n- and p-type Ge samples doped with shallow impurities 24 p4253 A66-4235
- Energy levels and wave function of hole in field of two acceptor ions and nearest ion donor for p-type Ge and Si 24 p4255 A66-4245
- Matrix elements of Coulomb potential between Schechter functions and overlaid integrals necessary in determining two-center acceptor states in p-type Ge and Si 24 p4255 A66-4245
- Energy levels and wave function of hole in field of two acceptor ions and nearest ion donor for p-type Ge and Si, noting numerical results 24 p4255 A66-4245
- Impurity photoconductivity spectra of p-type germanium at low temperatures, noting parameters of relative depth of equidistant minima oscillations 24 p4256 A66-4251
- Static Jahn-Teller effect on impurity centers in semiconductors, discussing nature and magnitude of splitting of ground state 24 p4256 A66-4252
- Solid state maser oscillator operating in zero field configuration, using ferric ion substituted as impurity in aluminum nitrate host crystal 24 p4221 A66-4255
- Crystalline solid lasers, considering rare Earth and transition metal impurities and host materials, noting CW laser characteristics 24 p4224 A66-4278
- Critical temperature of two-band superconductor model with paramagnetic impurity 24 p4259 A66-4309
- ### IN-FLIGHT MONITORING
- Parameter dependent approach mechanization for in-flight testing of aircraft system, considering electronic subsystems 01 p0010 A66-1009
- In-flight entertainment system discussing video, audio and motion picture systems 02 p0231 A66-1201
- Maintenance recordings of aircraft parameters, discussing signal conditioning economics and application [ISA PREPRINT 1.3-1-65] 05 p0794 A66-1549
- Spacecraft crew monitoring system for evaluating performance capabilities an physiological state 06 p0818 A66-1624
- In-flight pilot responses to new nongyroscopic blind flight Kenyon instrument 15 p2442 A66-2866
- Airborne performance analysis by multiparameter sampling applied to aircraft maintenance and benefits including prediction of impending malfunctions 17 p2842 A66-3195
- Optimal trajectory problem solution using in-flight guidance computers for control rockets and aircraft under influence of random disturbances 17 p2956 A66-3323
- Real time cardiorespiratory rate monitor for data converter on Gemini space program 19 p3288 A66-3570
- Automatic self-monitor techniques for



- altitude and heading reference  
systems 20 p3596 A66-37188
- Automatic built-in test of advanced  
ionics systems, noting advantages of  
airborne computer in sequencing, conducting  
and evaluating in-flight  
performance 20 p3522 A66-37245
- Parotid fluid collection technic for  
determining in-flight biochemical responses  
or 17-OHCS levels 22 p3854 A66-39791
- Aircraft in-flight vs ground testing, noting  
better SNR, freedom of jamming and  
decreased parameter requirements for  
vibration and transient  
monitoring 22 p3917 A66-39995
- Medico-biological methods based on data  
recording on board rockets and spacecraft  
and telemetering information to  
earth 24 p4169 A66-43141
- INCIDENCE  
FILAMENT  
INCIDENCE  
WAVE INCIDENCE CONTROL  
INCIDENT RAY  
Resolving power and microphotometric  
granularity of IR films measured with  
resolvometer, noting dependence on  
frequency of incident  
light 10 p1534 A66-21332
- Estimation of incidence angles for which  
resolution limit of real Fabry-Perot etalon  
approaches value of ideal  
etalon 10 p1537 A66-22030
- Estimation of incidence angles for which  
resolution limit of real Fabry-Perot etalon  
approaches value of ideal  
etalon 16 p2706 A66-30850
- Absorbance and emittance of metal  
surfaces, determined via cyclic incident  
radiation, noting error computation and  
method accuracy parameters  
[AIAA PAPER 66-416] 18 p2829 A66-31487
- Microwave beam incident on linearly  
graded plasma for electron density profile  
determination, using ray  
theory 22 p3861 A66-39723
- GENERATOR  
BURNER  
FURNACE  
COHERENT SCATTERING  
A NEUTRON SCATTERING  
Holograms of object illuminated with  
spatially incoherent light from low pressure  
mercury lamp, using afocal lens in  
interferometer for wavefront  
splitting 15 p2497 A66-28694
- Incoherent scattering of microwaves by HF  
oscillations resulting from beam-plasma  
instability 18 p3066 A66-33669
- Topside ionosphere, emphasizing  
experiments with incoherent scatter radars  
and topside sounder  
satellites 22 p3908 A66-39970
- Electron density, electron and ion  
temperature and ionic composition  
measurements in Peru, using incoherent  
scattering technique 22 p3910 A66-39977
- INCOMPRESSIBLE FLOW  
High efficiency radial ventilator design and  
frictionless incompressible flow treated by  
conformal mapping 01 p0005 A66-10199
- Axisymmetric steady flow of  
incompressible viscous fluid in circular tube  
of constant porosity treated by small  
parameter method 01 p0059 A66-11003
- Transfer of heat or nonstationary mass in  
circular cylindrical laminar flow  
tube 01 p0166 A66-11086
- Incompressible laminar axisymmetric near  
wake behind very slender cylinder in axial  
flow 02 p0175 A66-11527
- Three-dimensional theory of incompressible  
and inviscid flow through mixed flow  
turbomachines  
[ASME PAPER 64-WA/GTP-1] 02 p0176 A66-11765
- Wind tunnel contraction study of inviscid  
incompressible flow using rheoelectrical  
analogy, discussing experimental techniques,  
contour velocity distribution, optimum  
smoke injector and adverse pressure  
gradient estimation 03 p0352 A66-12719
- Flow resistance of partially permeable  
wedge to incompressible fluid incident on  
base or vertex 03 p0359 A66-13185
- Effect of incompressible fluid flow  
boundaries on unsteady aerodynamic  
properties of thin curved profile undergoing  
small amplitude  
oscillations 04 p0454 A66-13574
- Incompressible laminar boundary layer for  
plate with slot suction at high Reynolds  
number 04 p0509 A66-13654
- Variational principle generalization for  
elimination of simplifying assumptions in  
convective heat transfer model in forced  
incompressible flows 07 p1155 A66-18127
- Pressure distribution on oscillating two-  
dimensional symmetric airfoil in  
incompressible flow, examining trailing edge  
angle influence 07 p0982 A66-18133
- Two-dimensional viscous incompressible  
wedge flow treated by Navier-Stokes  
equation with Prandtl boundary layer  
approximation 07 p0982 A66-18138
- Power characteristics of linear  
axisymmetric flow of ideal incompressible  
conducting gas with Hall effect in two-  
component magnetic field 08 p1168 A66-18863
- Oscillations of oval pipes in  
incompressible-liquid flow treated by  
method based on Mathieu  
functions 08 p1313 A66-19440
- Laminar boundary layer problems for  
compressible and incompressible  
fluids 09 p1368 A66-20751
- Approximate analysis of onset of  
undamped oscillations in plate on which  
impinges ideal compressible fluid  
flow 11 p1779 A66-22234
- Flow regime data for wide range of conical  
diffuser geometries determined from clear  
plastic diffuser  
experiments 11 p1687 A66-22331
- First-order boundary proximity effect on  
Stokes resistance of body, using integral  
equation approach 11 p1693 A66-23008
- Heat transfer in turbulent flow of  
incompressible fluid in plane curved  
channel 11 p1694 A66-23317
- Stability of vortex-free incompressible  
fluid flow 11 p1694 A66-23331
- Transverse flow velocity effect on laminar  
flow shape stability 12 p1863 A66-24428
- Approximate solution of Navier-Stokes  
equations applicable to viscous and  
incompressible fluids 13 p2062 A66-25429
- Velocity defect law for turbulent  
incompressible boundary layer with wall  
injection or suction 13 p2063 A66-25430
- Self-similar solutions for Mises equation of  
boundary value problem in incompressible  
gas flow 13 p2065 A66-26486
- Forced turbulent convective incompressible  
flow along rough plates, measuring velocity  
and temperature profiles 14 p2410 A66-26934
- Variational principle extended to problems  
of nonself-adjoint differential equations,  
with application to slow viscous  
incompressible Poiseuille  
flow 14 p2273 A66-26935
- Boundary layer generation for viscous  
incompressible fluid flow past rigid wall or  
obstacle to which fluid  
adheres 14 p2274 A66-26940
- Variational problem solved, giving lower  
stability bounds for finite disturbances of  
viscous incompressible  
flow 15 p2478 A66-29245
- Three-dimensional viscous free mixing,  
describing numerical and experimental  
solutions for wake and jet flows  
[AIAA PAPER 65-49] 15 p2424 A66-29272
- Mellor solutions for linearized wakes and  
jets in laminar and turbulent flow for class  
of pressure gradients 15 p2424 A66-29293
- Airfoil theory in incompressible flow for  
boundary layer suction or Helmholtz type  
wake 16 p2629 A66-31039
- Aerodynamic lift and moment during  
unsteady flow of ideal incompressible fluid  
around lattice of thin bent  
profile 16 p2690 A66-31620
- Derivation of constitutive equations for  
incompressible mixtures of Newtonian fluids  
using entropy production  
inequality 17 p2905 A66-31926
- Two-dimensional wake in incompressible  
unsteady vortex flow downstream of  
cylindrical body 17 p2907 A66-32279
- Book on theory of steady viscometric flows  
of non-Newtonian fluids, discussing design  
and interpretation of  
experiments 17 p2912 A66-32992
- Hot wire measurements in radial turbulent  
incompressible air jet 18 p3045 A66-33593
- Turbulent boundary layers in compressible  
and incompressible flow, examining pressure  
gradients, temperature distribution and heat  
transfer effects 18 p3097 A66-33595
- Laminar steady incompressible nonuniform  
flow in rectangular duct, stream tube and  
pipe 18 p3099 A66-34124
- Incompressible turbulent two-dimensional  
wall jet flow, discussing viscous interactions  
with surrounding fluid attachment  
streamline, momentum-flux equations,  
etc 18 p3099 A66-34125
- Boundary layer equations for nonstationary  
plane flow of viscous incompressible  
fluid 18 p3100 A66-34545
- Internal waves of finite amplitude and  
permanent form propagating on horizontal  
stream of incompressible  
fluid 18 p3101 A66-34664
- Velocity profile downstream from stepped  
wall having incompressible turbulent fluid  
flows 19 p3340 A66-35580
- Laminar boundary layer stability of  
incompressible fluid at elastic  
surface 19 p3342 A66-36463
- Navier-Stokes equations for plane interface  
with stagnation point formed by expelling  
different gas from leading edge of airfoil  
opposite to main flow 19 p3277 A66-36635
- Oscillating airfoils in incompressible flow  
in Possio equation, with solutions obtained  
in closed form 21 p3832 A66-39378
- Vector equations of steady incompressible  
viscous flow in absence of extraneous  
forces, discussing Beltrami flow, doubly  
laminar flow and plane  
flow 21 p3728 A66-39435
- Extension of extremum principles  
concerned with velocity fields for boundary  
value problems of incompressible rigid  
viscoplastic /Bingham/  
solid 21 p3832 A66-39440
- Laminar incompressible axisymmetric free  
jet with swirl, examining perturbation  
scheme for stream function and asymptotic  
series 21 p3729 A66-39453
- Nonlinear computational instability and  
long-term numerical integration of two-  
dimensional incompressible flow  
equation 21 p3730 A66-39473
- Mean viscous dissipation and bulk  
temperature variation in incompressible  
fully developed duct heat transfer, using  
Green theorem 22 p3998 A66-40033
- Performance of two-dimensional curvilinear  
jets of air cushion vehicles based on  
incompressible flow theory, noting stability  
criteria 22 p3844 A66-40499
- Book on MHD covering fundamental  
equations, boundary conditions,  
incompressible flow, steady flow MHD  
simple and shock waves,  
etc 22 p3957 A66-40619
- Approximate solution of second-order  
incompressible boundary layer equations,  
using mathematical model reformulated for  
application in vicinity of separation  
point 23 p4058 A66-41924
- Hydrodynamic phenomena in rotating fluid  
systems, characterizing flow of fluid whose  
viscosities, thermal conductivity and specific  
heats are constant 23 p4058 A66-41940
- Boundary layer solutions to two-  
dimensional stationary viscous  
incompressible flow past finite object under  
vanishing skin friction 23 p4060 A66-42009
- Experimental verification of stability  
criteria for incompressible inviscid flow  
with helical streamlines, using rotating  
cylinders 23 p4062 A66-42046
- Incompressible flow in two-dimensional  
bends treated by Rayleigh-Ritz method in  
Kamlyama modification of conformal  
mapping 24 p4157 A66-42264
- Incompressible viscous flow around right  
angle corner, noting effect of geometry on  
boundary layer and cross  
flow 24 p4194 A66-42410
- Regular solutions of laminar boundary  
layer equations near point of vanishing skin  
friction, calculating pressure  
gradient 24 p4194 A66-42413
- Velocity profile in isobaric zone  
downstream from step-shaped wall in case  
of incompressible fluid 24 p4197 A66-43002
- Compressible and incompressible flows  
made visible by optical method sensitive to  
density variations, shadowgraph, schlieren



system, Mach-Zehnder interferometer and holographic interferometry with lasers 24 p4192 A66-43196

## INCOMPRESSIBLE FLUID

Coupling method for determining natural oscillations of ideal incompressible liquid in vessel consisting of two regions 01 p0059 A66-11017

Stability analysis of adiabatic flow of incompressible fluid without equation linearization and by constructing functional from hydrodynamic fields 02 p0220 A66-12170

Transient heat transfer between thin circular tube and incompressible fluid, considering radial conduction and heat loss [ASME PAPER 65-HT-2] 04 p0595 A66-13393

Transverse current MHD conduction generators for AC power 04 p0459 A66-13467

Boundary layer control by blowing, analyzing turbulent boundary layer for flow about flat plate of incompressible fluid with intense cross flows 04 p0509 A66-13573

Injection on surface friction and on parameters of turbulent boundary layer, noting semiempirical Prandtl theory 04 p0509 A66-13655

Book on motions of viscous incompressible fluids, covering laminar and turbulent jets and solutions, based on exact Navier-Stokes equations 06 p0872 A66-16562

Shape and gravitational field of Earth calculated by using  $N$  homogeneous incompressible fluid shells to represent distribution of terrestrial mass 07 p1028 A66-17422

Kelvin-Helmholtz instability in fully ionized plasma in magnetic field, assuming variable streaming velocity 07 p1089 A66-17961

Shock wave propagation in electrically conducting incompressible fluid imbedded in magnetic field 07 p1089 A66-17975

Uniform motion of vortex system in inviscid fluid, examining effect of compressibility on motion of vortex singularities 08 p1204 A66-18528

Acceleration potentials applied to motion, at arbitrary Froude numbers, of high-aspect-ratio wing immersed in incompressible ideal fluid 08 p1205 A66-18601

Thermal laminar boundary layer formation on semiinfinite isothermal plate during uniform motion in viscous incompressible fluid over Prandtl number ranges 08 p1206 A66-18874

Velocity profile of main section of axisymmetric turbulent jet of incompressible fluid flowing into homogeneous companion flow of same fluid 08 p1206 A66-18876

Charge density distribution, electric field strength and flow rate of turbulent flow of incompressible fluid in flat nonconducting channel 08 p1263 A66-19172

Motion of three-dimensional diffusing vortex tube in incompressible viscous fluid 08 p1210 A66-19634

Stationary flow of viscous incompressible anisotropically conducting fluid in coaxial channel 11 p1743 A66-22235

Effect of incompressibility of substance on gravitational instability, deriving dispersion equation and comparing results with problem of incompressible fluids 11 p1735 A66-22410

Marginal convection in self-gravitating sphere of uniform incompressible fluid with uniform heat sources distribution 11 p1785 A66-22437

Small oscillations of pendulum with spherical cavity filled with viscous incompressible liquid 12 p1882 A66-24357

Propagation modes of small disturbances in homogeneous incompressible magnetoelastic medium at Alfvén velocities 12 p1929 A66-24379

Numerical method of calculating unsteady flow past arbitrary thin wing moving in ideal incompressible fluid 12 p1797 A66-24430

Flow graph in model of jet curtain in ideal incompressible weightless fluid with isolated vortex 12 p1798 A66-24433

Linearization of Rayleigh problem for viscous compressible conducting fluid, considering compressibility effects by evaluating solution of pressure equation 12 p1924 A66-24580

MHD gyroscope with axial magnetic field, plotting design parameters, estimating performance, etc 13 p2078 A66-25513

Vortex flow of ideal incompressible fluid past plate or slender wing near solid wall 13 p2067 A66-26532

Incompressible fluid static thrust augmentation devices for aircraft propulsion for cases of presence and absence of heat and work exchange [ASME PAPER 66-GT-116] 14 p2373 A66-27008

Solution of boundary layer equation for two-dimensional laminar steady motion of viscous incompressible fluid in convergent channel with suction at wall 14 p2276 A66-27728

Spin angular velocity stability of gyroscope with incompressible fluid-filled cavity as function of three degrees of freedom 14 p2277 A66-28051

Universal laminar boundary layer equations for incompressible fluid and homogeneous and dissociated gases derived, using parametric approximations 14 p2278 A66-28054

Laminar flow of incompressible fluid in rectangular channel, determining temperature distribution over channel cross section and thermal flux through wall for case of energy dissipation 14 p2415 A66-28317

Potential complex and forces in perfect incompressible fluid at rest at infinity with free vortices determined by pointless profiles excited by arbitrary motion 15 p2479 A66-29637

MHD drag of dielectric oscillating sphere in incompressible conducting fluid with uniform magnetic field aligned along axis of oscillation 15 p2553 A66-29689

Plane rotational motion of incompressible fluids in presence of homogeneous porous circular cylinder 15 p2481 A66-29856

Isotropic turbulence theory for incompressible fluid 16 p2683 A66-30165

Complex flow-perturbing potential for Joukowski profile in incompressible fluid with parabolic velocity distribution, using Jacob first order approximation to solve Dirichlet problem 16 p2627 A66-30211

Pressures in incompressible fluid around obstacle for parabolic velocity distribution at infinite distance upstream 16 p2627 A66-30212

Flow in viscous incompressible conducting fluid subjected to magnetic field in concentric cylinders rotating at different angular velocities, assuming planar motion, using differential equations 16 p2757 A66-30214

Motion equations for incompressible viscous fluid with constant vortex derived, using complex variable 16 p2683 A66-30216

Flow of turbulent incompressible fluid downstream from step-shaped wall, determining velocity fields in isobaric region, considering existence of boundary layer thickness at separation point 16 p2687 A66-31205

Linearized unsteady nonequilibrium flows produced by unsteady motion of thin foil or circular cylindrical shell in incompressible gas 16 p2687 A66-31288

Motion of viscous incompressible fluid in interspace between rotating and parallel fixed permeable plane through which supplementary fluid is injected, solved by Navier-Stokes equations 16 p2687 A66-31293

Steady motion of viscous incompressible fluid between concentric spheres, injecting and ejecting fluid through inlet and outlet holes, describing boundary conditions by series expansion 16 p2687 A66-31294

Navier-Stokes equations for rotational motion of incompressible viscous fluid at small Reynolds numbers between rotational surfaces 16 p2688 A66-31298

Theory of unsteady one-dimensional motion of ideal incompressible fluid, discussing equation of state 16 p2688 A66-31300

Stationary viscous incompressible fluid flow past rough surface, noting solution stability and friction stress determination for given pressure gradient 16 p2688 A66-31301

Flow instability of incompressible nonconducting fluid in thin cylindrical conducting elastic pipe in constant uniform magnetic field 16 p2764 A66-31310

MHD boundary layer flow of incompressible conducting rotational fluid over infinite dielectric disk 16 p2765 A66-31414

Velocity and temperature profiles, hydrodynamic elements, heat transfer and friction coefficients of turbulent incompressible flow through circular arc flat tube 17 p2909 A66-32515

Stationary boundary value problem Navier-Stokes equation for incompressible viscous fluids 17 p2911 A66-32818

Self-similar solutions of two-dimensional laminar flow of incompressible electroconductive fluid in channel in cross electric and magnetic fields, using Jacobi elliptic integrals 17 p2971 A66-32818

Performance of hydrodynamic, hydrostatic or hybrid bearings determined by numeric solution of Reynolds lubrication equation for incompressible fluid films [ASME PAPER 66-LUBS-4] 17 p2932 A66-33117

Profile of supercavitating lattice traced for certain parameter values, using perturbative theory of perfectly irrotational incompressible fluid 17 p2914 A66-33218

Vekua method to solve Oseen form Navier-Stokes equation for incompressible viscous fluid flow 18 p3097 A66-33717

Motion of three-dimensional diffusible vortex tube in incompressible viscous fluid 18 p3099 A66-34117

Two-dimensional solution of Laplace equation for vortex formations in incompressible fluid 18 p3100 A66-34618

Hartree solution of MHD laminar boundary layer incompressible conducting fluid, specifically considering flow at inlet semiinfinite flat channel 18 p3147 A66-34618

Flow of incompressible viscous fluid subject to conditions governed by Navier-Stokes equation, examining fluid velocity time tends to infinity 18 p3101 A66-34618

Instability of free laminar boundary layer between parallel streams analyzed for incompressible fluid, noting values Reynolds number 18 p3102 A66-34918

Stress effects on plane creeping Newtonian flows of incompressible second-order fluids 18 p3103 A66-34918

Navier-Stokes equations solutions for incompressible fluid representing boundary layer flows with suction along corners of cylindrical bodies 19 p3341 A66-35819

Steady state heat convection in viscous incompressible fluid sandwiched between two surfaces perpendicular to direction of force of gravity 19 p3342 A66-36419

Behavior of solution of system of equations for unsteady boundary layer of two-dimensional liquid as time approaches infinity 19 p3343 A66-36819

Electromagnetic field effect on heat transfer during laminar flow of electrically conducting incompressible fluid in flat channel 20 p3607 A66-36919

Viscosity effect on small periodic oscillatory disturbance of rigidly rotating incompressible fluid 20 p3545 A66-37419

Plane nonlinear creep of free boundary in incompressible isotropic viscous fluid body 20 p3669 A66-37519

Radial flow of incompressible viscous fluid between two parallel disks 20 p3548 A66-37919

Navier-Stokes equation series form radial flow of incompressible fluid between two rotating parallel disks 20 p3548 A66-37919

Integral-diffusion analysis of turbulent flow of incompressible liquid 20 p3548 A66-38119

Apparent additive mass coefficient for three-dimensional hydrodynamic impact problem of floating sphere in incompressible fluid 20 p3548 A66-38119

Free laminar boundary layer flow between parallel streams of different magnetic field and temperatures for incompressible viscous fluid 21 p3776 A66-38619

Coefficients of equations of perturbed motion of body containing ideal incompressible liquid 21 p3770 A66-38919

Sufficient conditions for instability against small oscillations of symmetric laminar flow of inviscid incompressible perfect magnetofluid 21 p3791 A66-39119



Alfven wave propagation in incompressible fluid stratified by inhomogeneous fluid density or magnetic field strength 21 p3791 A66-39170

Unsteady convective heat transfer of incompressible fluid between two solid channel walls 21 p3728 A66-39340

Velocity distribution of fluctuating axisymmetric flow of incompressible second-order fluid near stagnation point 21 p3728 A66-39346

Two-dimensional unsteady flow of second-order incompressible fluids, noting analogies to Newtonian case 21 p3728 A66-39437

Steady laminar flow of viscous incompressible fluid through two-dimensional channel with fluid sucked or injected with different velocities through uniformly porous parallel walls 21 p3730 A66-39461

Small parameter method to study steady state flow of viscous incompressible fluid in journal bearing 22 p3928 A66-40688

Alfven shocks for flow of highly conducting incompressible fluid over blunt body where magnetic and flow vectors are not aligned 22 p3957 A66-40705

Laminar heat transfer in plane channel with nonuniform temperature field at inlet 22 p4000 A66-40812

Pressure induced flow of elasticoviscous electrically conducting incompressible fluid between relatively moving porous walls in presence of transverse magnetic field 23 p4053 A66-41121

Slow steady flow of viscous incompressible fluid between two coaxial circular cylinders with axial roughness 23 p4054 A66-41122

Existence theorem for stationary flow in magnetic field of incompressible viscous fluid electrically conductive around solid electrically conducting obstacle 23 p4100 A66-41173

Earth shape, moment of inertia and gravitational field determined from two nonlinear integral equations for potential of rotating incompressible fluid 23 p4063 A66-41202

Heat transfer in entrance section in rectangular duct for incompressible fluid in laminar pulsating flow with periodic pressure gradient 23 p4148 A66-41216

Constitutive and balance equations derived in tensorial form for incompressible fluid with nonlinear viscous characteristics 23 p4055 A66-41382

Incompressible fluid motion inside cylinder rotating at constant angular velocity with generatrix forming curve 23 p4055 A66-41560

Unsteady state lift and moment action on lattice of profiles moving in incompressible fluid, determining suction originating at leading edges of profiles 23 p4009 A66-41723

Laminar boundary layer in incompressible fluid, noting effect of variation of kinematic viscosity and density on stability 23 p4056 A66-41725

Volterra equation and Green function to solve MHD problem of unsteady flow of viscous incompressible conducting fluid with time dependency 23 p4106 A66-41837

Boundary value problem of steady two-dimensional MHD flow of viscous incompressible fluid past rigid plate 23 p4106 A66-41875

Steady three-dimensional rotational vortex flow of incompressible fluid, considering viscosity effects 23 p4058 A66-41929

Parametric method in laminar boundary layer theory, noting reduction of equations for incompressible fluid 23 p4059 A66-42008

Hydrodynamic stability of incompressible fluid based on Navier-Stokes equations including numerical calculations of boundary layer disturbances and temperature-independent material constants 23 p4060 A66-42021

Heat transfer in incompressible viscous fluid between two nearly parallel walls with harmonically varying distance, determining velocity field and temperature distribution 23 p4150 A66-42029

Plane laminar jet of incompressible conducting fluid propagating homogeneous magnetic field at magnetic Reynolds number 24 p4196 A66-42872

Laminar flow of fluid with varying viscosity in tube with walls at constant

temperature, analyzing equations of motion and equations for conservation of energy 24 p4197 A66-42991

Two-dimensional bubble contours in steady state turbulence-free flow of ideal incompressible fluid, obtaining solution for all internal pressures 24 p4232 A66-43064

# INCONEL

Nickel-based superalloy Inconel 713C easily forged when made by powder metallurgy methods but not when prepared by casting 11 p1715 A66-22536

Lightweight titanium and Inconel pressure vessel for Apollo cryogenic hydrogen and oxygen storage systems 20 p3541 A66-37092

# INDENTATION

Dynamic indentation of metals with conical projectiles and dynamic tip flattening of projectiles, noting inertia and strain rate effect 02 p0243 A66-11691

Variation of mean applied pressure with deformation size when prismatic body slowly indents semilinear block 08 p1311 A66-19294

Deformation and strength properties of refractory solids at temperatures up to 2000 degrees C, using indentation hardness measurements for stress-strain measurements in strength properties 18 p3254 A66-33967

Indentation damage and subsequent annealing effect on etch-polished Ge surfaces at room temperature examined with optical microscope, using interference contrast techniques 19 p3434 A66-35401

Wiener-Hopf and series solutions to BVP of indentation stresses and displacements in infinite hollow elastic cylinder for axisymmetric punch of finite length and arbitrary profile 22 p3990 A66-40139

# INDEPENDENT VARIABLE

Transformation of unknown functions and independent variables entering into differential equations for motion of nonviscous nonheat-conducting gas 02 p0220 A66-12178

Monograph on Levy method for deflection of loaded simply-supported infinite plate strip, introducing class of real functions 04 p0589 A66-14011

Transition variable as function of superconductor reduced temperature, showing temperature dependency of penetration depth, acoustical attenuation and thermoconductivity 16 p2777 A66-30937

Summability of independent random variables, discussing convergence properties of sequence 19 p3389 A66-35982

Asymptotic behavior of transition probability matrices, analyzing limit theorems involving capacities in Markov chains 19 p3389 A66-35984

Character of continuity of solutions to second-order linear elliptic equations with many independent variables 20 p3592 A66-38421

Synthesis of optimal Liapunov-Bellman function, noting sequential solution method for independent variables and method using first-order partial differential equation 21 p3758 A66-39281

Geometrical properties of partial differential equations with independent variables, using Cartan method 23 p4084 A66-41061

# INDEX

S ABSORPTIVE INDEX  
S MORPHOLOGICAL INDEX  
S REFRACTIVE INDEX

# INDIA

India space research program 01 p0170 A66-10437

Indian National Aeronautics Laboratory annual report 1964-1965 14 p2269 A66-26872

Aerospace research programs in India 1965-1966, emphasizing equatorial aeronomy including meteorology up to 170 km 18 p3238 A66-35234

Ionospheric electron content over Ahmedabad and Bombay from differential Faraday rotations of plane polarized radio waves from Beacon satellite 21 p3734 A66-39229

# INDICATOR

SA ATTITUDE INDICATOR  
SA DETECTOR  
SA ENGINE FAILURE INDICATOR  
SA FLOW DIRECTION INDICATOR  
SA FORCE DISPLACEMENT INDICATOR

SA POSITION INDICATOR  
SA RANGE INDICATOR  
SA TEMPERATURE INDICATOR  
SA VOLTAGE VARIATION INDICATOR

Blood flow measurement by indicators by taking samples in situ-dyes, thermomodulation, krypton 85 14 p2230 A66-27552

# INDIUM

Radiation damage to germanium, silicon, indium and gallium antimonides and arsenides 01 p0119 A66-10373

Neutron flux in atmosphere measured by method of indium activation 02 p0284 A66-12130

Electron energy diffusion in superconducting thin Sn and In films bombarded by alpha particles observed in terms of IR drop 06 p0927 A66-16755

Critical magnetic field and temperature in superconducting metal 08 p1278 A66-19637

Ultrasound absorption by superconducting indium single crystals, noting nonlinear dependence on sonic field amplitude 09 p1428 A66-20592

Distribution coefficient and electrical behavior of indium in cadmium telluride crystals, using In 114 /half-life 49 days/ as tracer 10 p1574 A66-21352

Behavior of trace elements in gallium arsenide and materials and methods used for ohmic contacts to n-and p-type specimens, stressing importance of indium 11 p1757 A66-23283

Diffusion of indium along sessile dislocation in silicon 14 p2356 A66-27070

Neutron irradiation effect on superconductive properties of tin and indium foils at low temperatures, noting decrease of critical temperature and field 14 p2364 A66-27641

Neutron flux in atmosphere measured by method of indium activation 14 p2377 A66-28087

Geometrical resonance and boundary effects in tunneling from superconducting indium 16 p2767 A66-30126

Energy spacing of geometrical resonance structure in very thick indium films, noting interference between electron-like states which propagate with different velocities 16 p2769 A66-30159

Anisotropy of electrical resistance of indium in magnetic field shown to be nearly absent, confirming absence of open Fermi surface 17 p2977 A66-32315

Fermi surface of indium investigated by means of RF size effect at 3 Mc 17 p2977 A66-32316

Critical magnetic field and temperature in superconducting metal 18 p3155 A66-34180

Resonant frequency of helicon waves in indium, deriving high field Hall coefficient 19 p3445 A66-36331

Ultrasound absorption by superconducting indium single crystals, noting nonlinear dependence on sonic field amplitude 20 p3622 A66-38125

Critical magnetic field and transition temperature measurements of superconducting indium in porous glass, using LF mutual inductance technique 21 p3796 A66-38549

Cyclotron resonance observation of electron scattering by Ga and In atoms in Ge 21 p3797 A66-38754

Indium and thallium first spectra sp2 atom configurations and configuration mixing 22 p3960 A66-39801

Photoionization cross section of negatively charged In atoms in n-type silicon from comparison of intrinsic photoconductivity with impurity photoconductivity 22 p3964 A66-40309

Angular variation of position of energy loss maxima in indium 23 p4110 A66-41180

# INDIUM ALLOY

Thermal and electric properties of indium antimonide/indium telluride alloys as function of composition and annealing temperature 01 p0116 A66-10188

Impurity-recombination emission in diodes of n-type Si single crystals alloyed with In 02 p0206 A66-12092

Magnetic and resistive superconducting transitions on bulk samples of indium-lead alloys in alpha-phase region, considering results relative to Glag



theory 09 p1423 A66-20067  
 Indium-cadmium alloy superconducting transition temperatures for varying compositions, noting electronic structure 13 p2169 A66-26278  
 Semiconducting properties of several gallium and indium antimony tellurides systems and their metallurgical aspects 17 p2986 A66-33296  
 Temperature dependence of mixed-state thermoconductivity of type II superconducting In-Pb alloys in magnetic field 21 p3797 A66-38751  
 New phase in mercury-indium alloy system established by resistance, superconductivity transition temperature and X-ray diffraction measurements 24 p4255 A66-42486

**INDIUM ANTIMONIDE**  
 Microwave radiation and surface patterns formed during application of high currents and magnetic fields to n-InSb 01 p0117 A66-10244  
 Theories of damped oscillations and microwave radiation from InSb in breakdown state 01 p0112 A66-10512  
 Negative resistance and oscillation generation in current voltage characteristics of indium antimonide point contacts connected with oxide layers on crystal surface 01 p0043 A66-10764  
 Variation in thermoelectromotive force and magnetoresistance in quantizing magnetic field in indium antimonide semiconductor, considering electron spin and conduction band nonparabolicity 01 p0124 A66-10770  
 Electrical properties of copper diffused p-type indium antimonide crystals 01 p0127 A66-11030  
 Crystal Hall detectors prepared by gluing thin indium antimonide wafer on rectangular parallelepiped ferrite base 01 p0045 A66-11031  
 Quantum oscillation associated with quantization of electron energy spectrum of n-type indium antimonide 02 p0274 A66-11735  
 Helicon effect in semiconductors, using indium antimonide in resonant cavities 02 p0276 A66-12004  
 Electron energy and momentum dissipation in n-type InSb at low temperatures, discussing collision effects on hot electron escape 02 p0276 A66-12079  
 Propagation of LF helicon waves in strongly doped cadmium arsenide and indium antimonide 03 p0410 A66-12944  
 Capacitance-voltage characteristics of anodized InSb surface measured, using metal oxide semiconductor method 03 p0411 A66-13005  
 High electric fields effect on propagation of 24-GHz microwaves along surface on n-type indium antimonide 04 p0562 A66-13749  
 Temperature dependence of electric conductivity in indium antimonide and gallium arsenide measured by noncontact method in terms of Q-factor change 04 p0563 A66-13892  
 Magnetic resonance applied to semiconductors, determining electron density at nucleus sites and kinetic energy temperature of hot electrons in indium antimonide 04 p0563 A66-14030  
 Microwave emission at O-band from n-and p-type indium antimonide subjected to applied electric and magnetic fields 04 p0564 A66-14103  
 Parameters associated with inelastic polar electron scattering in indium antimonide 04 p0565 A66-14267  
 Temperature dependence of effective electron mass of indium antimonide 04 p0565 A66-14275  
 Noise and lifetime of nonequilibrium current carriers in p-indium antimonide 04 p0566 A66-14276  
 Transport coefficients of intrinsically conducting InSb above room temperature in magnetic field of medium strength 04 p0566 A66-14288  
 Influence of microinhomogeneities under magnetic field on Nernst effect in InSb 04 p0568 A66-14345  
 High pressure high current argon discharge covering statistical variations of nonblack body, photon and IR radiation and measurement with InSb photodiode 05 p0720 A66-14507  
 Optical properties of polycrystalline InSb

films noting index of refraction, absorption coefficient and transmission 05 p0741 A66-15852  
 Lattice thermal conductivity of GaAs and InSb calculated for 2 to 300 degrees K, considering separate contributions of longitudinal and transverse phonons 05 p0742 A66-15872  
 Electron drift velocity and mobility of indium antimonide obtained from pulsed measurements of conductivity and Hall effect at various temperatures 06 p0922 A66-16173  
 Direct measurement of energy relaxation time between hot electrons and lattice in n-type indium antimonide in hydrogen temperature range 06 p0929 A66-17036  
 X-ray diffraction method for measuring thermal expansion coefficient of germanium, silicon, indium antimonide and gallium arsenide 06 p0930 A66-17047  
 In-pile neutron and gamma-ray irradiation of n-type indium antimonide, isochronous annealing indicating existence of five recovery stages 06 p0936 A66-17134  
 Magnetic field effects on spectrum and intensity of spontaneous emission in InSb luminescent diode 07 p1094 A66-17316  
 Carrier temperature injected into InSb effect on shape of direct intrinsic line 07 p1095 A66-17317  
 Laser action achieved in n-type indium antimonide excited by 15-kv electron beam at 20 and 4 degrees K 07 p1043 A66-17341  
 Wave propagation in Q band of n-type indium antimonide at low temperature as function of longitudinal magnetic field, noting helicon waves 07 p1101 A66-18200  
 Nonlinearities in helicon wave propagation through InSb cooled by liquid nitrogen 07 p1102 A66-18202  
 Hall current and Hall drift velocity in single crystal indium antimonide under electric and magnetic field 07 p1103 A66-18214  
 Helical oscillations of plasma immersed in time-varying static magnetic field, measuring frequency, amplitude and transition modes 07 p1103 A66-18216  
 Microwave emission from InSb, measuring energy generated at low temperatures and intense electric and magnetic fields 07 p1103 A66-18218  
 Microwave emission from InSb in magnetic fields, explaining experimental results via modified traveling wave helicon model 07 p1104 A66-18219  
 Electron gas energy scattering in n-type indium antimonide at helium temperatures under action of DC field 07 p1104 A66-18259  
 Thermal ionization of small traps in cubic piezoelectric 07 p1105 A66-18377  
 Electron spin effect on quantum oscillations of magnetoresistance and Hall effect in n-InSb single crystal 08 p1269 A66-18971  
 Saturation of microwave impedance and occurrence of microwave emission in indium antimonide for strong longitudinal or transverse magnetic fields 08 p1270 A66-19059  
 Recombination of nonequilibrium charge carriers in p-type indium antimonide, using steady state photomagnetolectric effect 08 p1272 A66-19246  
 Irradiation of indium antimonide with slow neutron 08 p1276 A66-19614  
 Electric properties of single crystal p-type InSb, obtaining samples by zone melting, thermal processing, etc, noting hole concentration plotting 08 p1278 A66-19625  
 Mobility of hot electrons in runaway regime of n-type InSb and GaAs at low temperatures 09 p1412 A66-19987  
 Capacitance of alloyed p-n junctions in p-type InSb is inversely proportional to square root of bias voltage 09 p1429 A66-20814  
 Electron gas energy scattering in n-type indium antimonide at helium temperatures under action of DC field 09 p1431 A66-20903  
 Effective mass in InAs and InSb from Landau shift of peak emission in laser diodes 10 p1543 A66-21579  
 Current-controlled negative-resistance effect between nonsymmetrical ohmic contacts on opposite side of p-type indium antimonide 10 p1585 A66-22081

Current oscillations and microwave emission in indium antimonide subjected high applied parallel electric and magnetic fields at 77 degrees K 10 p1585 A66-22081  
 Indium antimonide optical absorption shift forbidden band narrowing and tin alloy induced by neutron bombardment 10 p1587 A66-22111  
 Temperature and alloying effect on indium antimonide reflection spectrum 10 p1588 A66-22111  
 Hall effect in alloyed crystals of n-type indium antimonide 10 p1589 A66-22111  
 Negative resistance and oscillation generation in current voltage characteristics of indium antimonide point contacts connected with oxide layers on crystal surface 11 p1661 A66-22211  
 Variation in thermoelectromotive force at magnetoresistance in quantizing magnetic field in indium antimonide semiconductor, considering electron spin and conduction band nonparabolicity 11 p1749 A66-22211  
 Neutron irradiation of InSb single crystals noting conductivity type change in p-type and conductivity magnitude in n-type crystals 11 p1749 A66-22211  
 Effect of plastic bending on indium antimonide electrical properties, measuring crystal dislocations, Hall coefficient etc 11 p1751 A66-22211  
 Indium antimonide diodes of various thickness for high injection levels, results in graphical form applied to magnetic diode production 11 p1666 A66-22211  
 Indium antimonide thin film preparation via vacuum deposition, noting evaporation rate effects on electrical properties of film 11 p1756 A66-23011  
 New semiconductor materials produced oriented inclusion of very highly conductive phases in semiconductor, noting In properties and application 13 p2161 A66-25111  
 Semiconductor bulk injection laser compared to junction lasers, noting In npp structures 13 p2091 A66-25511  
 Stimulated emission from electron beam excitation of tellurium and pure and n-type doped indium antimonide in semiconductor lasers 13 p2099 A66-26111  
 Photoluminescence and stimulated emission of gallium arsenide and indium antimonide obtained by optical pumping, noting effect of applied magnetic field on laser and diode emissions 13 p2099 A66-26111  
 Propagation of circularly polarized electromagnetic waves in circular semiconductor cylinder surrounded by metal tube and immersed in DC magnetic field 13 p2169 A66-26211  
 Dislocation structure in single crystal indium antimonide and gallium arsenide studied by X-ray diffraction 14 p2357 A66-27011  
 Spin-lattice relaxation of conduction electrons in semiconductors of n-InSb type with scattering at acoustical and optical phonons 14 p2358 A66-27011  
 Microwave radiation from inductive post of indium antimonide in broadband spectrum occurring when placed in a magnetic field and pulsed to average electric field, results suggest solid state plasma instabilities 14 p2363 A66-27511  
 Nonlinear galvanomagnetic effects in type InSb in quantum limit, using uncompensated and compensated samples 14 p2366 A66-27711  
 Anomalous diffusion of zinc in indium antimonide, noting two diffusion currents 14 p2367 A66-28211  
 Influence of microinhomogeneities under magnetic field on Nernst effect in InSb 14 p2367 A66-28211  
 Sectorial structure effect on current carrier concentration of germanium doped indium antimonide single crystals 15 p2558 A66-28511  
 Electron gas electroconductivity relaxation time and energy loss in n-type InSb cryogenic temperatures 15 p2558 A66-28611  
 Hall coefficient increase with temperature and electron transition to second conduction band in InSb 15 p2558 A66-28611  
 Helicon wave propagation in InSb and In at room temperature 15 p2559 A66-28611  
 Heterodyne detection at millimeter



- wavelengths shown in distributed structure of bulk indium antimonide, noting conversion loss and noise properties 15 p2462 A66-29017
- New type of oscillation when n-type indium antimonide is placed in steady magnetic field at 78 degrees K and pulsed with electric field 15 p2566 A66-29392
- Transport properties in indium antimonide under magnetic field at microwave frequency, showing effect of angular frequency times relaxation time /of electrons and holes/ 15 p2566 A66-29393
- Temperature dependence of electric conductivity in indium antimonide and gallium arsenide measured by noncontact method in terms of Q-factor change 15 p2568 A66-29705
- Spectral distribution of recombination radiation caused by electroluminescence /EML/ in indium antimonide 15 p2568 A66-29726
- Resistance anomaly in n-type InSb at very low temperatures, noting experimental results 16 p2768 A66-30140
- Hydrostatic pressure effect on energy gap, carrier concentration and electron and hole mobilities of indium antimonide 16 p2784 A66-31447
- Generation-recombination and modulation noise power spectrum of high purity p-type InSb at 77 degrees K 16 p2784 A66-31449
- High-mobility InSb thin film preparation by flash evaporation of elemental In and Sb in vacuum and oxidation of film surface prior to recrystallization in inert atmosphere 16 p2785 A66-31575
- Indium arsenic antimonide single crystals in p-n junction laser 16 p2721 A66-31767
- Spontaneous and induced coherent radiation from indium antimonide electron-hole plasma 16 p2721 A66-31768
- Photo-Hall effect and photoconductivity on compensated p-InSb at low temperatures, examining temperature dependence of carrier mobility 16 p2788 A66-31773
- Optical reflection, transparency and Faraday effect for indium antimonide, calculating effective electron mass, relation between energy and wave number, etc 16 p2788 A66-31777
- Electron mobility in p-type indium antimonide, noting entrainment of minority carriers by majority 16 p2789 A66-31784
- Harmonic generation in microwave emission from InSb, attributing resonance type radiation to stimulated cyclotron radiation and plasma wave excitation 17 p2978 A66-32410
- Quantum theory of electric conductivity of semiconductors with nonstandard band, discussing influence of spin splitting of Landau levels on oscillations of transverse magnetoresistance in n-InSb 17 p2978 A66-32508
- Irradiation of indium antimonide with slow neutron 17 p2983 A66-33128
- Electric properties of single crystal p-type InSb, obtaining samples by zone melting, thermal processing, etc., noting hole concentration plotting 17 p2984 A66-33139
- Thermal conversion mechanism in heat treatment of InSb indicates hydrogen dissolved plays role of donor while behavior of oxygen is not yet known 19 p3433 A66-35331
- Indium antimonide optical absorption shift, forbidden band narrowing and tin alloying induced by neutron bombardment 19 p3440 A66-35764
- Temperature and alloying effect on indium antimonide reflection spectrum 19 p3440 A66-35773
- Hall effect in alloyed crystals of n-type indium antimonide 19 p3441 A66-35779
- Attenuation, guide wavelength and characteristic impedance of rectangular waveguides with indium antimonide side wall derived for propagating modes 20 p3524 A66-37113
- Pinch effect in InSb degenerate plasma, discussing electric conductivity and recombination emission spectra 20 p3615 A66-37371
- Dependence of Hall effect and conductivity of irradiated samples on reciprocal temperature in nuclear transmutations produced in InSb by bombardment with slow neutrons 20 p3617 A66-37485
- Gamma irradiation from Co 60 effect on indium antimonide, determining defect formation on dose and limiting position of Fermi level for n-and p-type material 20 p3617 A66-37552
- Quantum oscillation of transverse and longitudinal magnetothermal emf in n-type indium antimonide compared with oscillations of transverse and longitudinal magnetoresistance and Hall coefficient 20 p3618 A66-37557
- Electron tunneling from metal to doped indium antimonide through oxide layer measured, obtaining characteristics of conductance vs applied voltage for n-and p-type crystals 20 p3620 A66-37769
- Receiver with n-type indium antimonide detector for investigating absorption spectra in submillimeter wave range 20 p3561 A66-37999
- Vacuum thermal decomposition of InSb and GaSb surfaces, noting evaporation rates 20 p3624 A66-38411
- Effective electron mass dependence on pressure in InSb determined by measuring electron concentration and thermal emf 20 p3624 A66-38427
- Impurity atom behavior in diatomic InSb and GaSb crystal lattices analyzed, using nuclear gamma resonance, measuring absolute values of f, chemical displacements and line widths 21 p3799 A66-38922
- Quantum oscillations of Hall effect and longitudinal and transverse reluctance in n-indium antimonide, noting spin splitting and temperature and electron concentration effect on oscillation maximum 21 p3799 A66-38924
- Electrical properties of indium antimonide single crystals with noncompensated impurity concentration, determining position of deep-seated levels in forbidden band 21 p3799 A66-38929
- Effective electron mass dependence on pressure in InSb determined by measuring electron concentration and thermal emf 21 p3800 A66-38960
- Isochronal and isothermal stage II recovery in high energy electron irradiated n-type InSb semiconductor, based on Hall coefficient and electroconductivity 21 p3800 A66-38994
- Cryogenic optically excited recombination emission in single crystal InSb semiconductor and transitions involving phonon creation, acceptor impurities and band-to-band emissions 21 p3800 A66-38996
- Current density, electron mobility, magnetoresistance, negative resistance and impact-ionization-produced solid state magnetoplasma oscillations in InSb single crystal semiconductor at high electric and magnetic fields 21 p3805 A66-39568
- Thermal emf of semiconductors in strong magnetic field, examining formation of spherically symmetric zone subject to arbitrary conduction-electron energy dispersion law 22 p3960 A66-39824
- Nonequilibrium charge carrier lifetime in indium antimonide single crystals with Ge and Au impurities 22 p3965 A66-40315
- Coherent radiation generation in electron-hole indium antimonide plasma, discussing emission spectrum 22 p3965 A66-40319
- Dislocation structure in single crystal indium antimonide and gallium arsenide studied by X-ray diffraction 22 p3966 A66-40829
- Spin-lattice relaxation of conduction electrons in semiconductors of n-InSb type with scattering at acoustical and optical phonons 22 p3967 A66-40839
- Large-signal AC field effect experiments with A and B real surfaces of indium antimonide exposed to various chemical reactions and high electric field described by tunnel equation 23 p4111 A66-41185
- Sectorial structure effect on current carrier concentration of germanium doped indium antimonide single crystals 23 p4112 A66-41286
- Indium antimonide diodes of various base thickness for high injection levels results in graphical form applied to magnetic diode production 23 p4045 A66-41478
- Nonequilibrium plasmas produced in InSb by both impact ionization and injection, examining instabilities due to HF oscillations and negative resistance 23 p4114 A66-41582
- Magnetic pinch formation in indium antimonide and possibility of population inversion in pinch, using strong current supported by electron-hole plasma 24 p4249 A66-42224
- Thermal conductivity change in single crystal InSb irradiated with electrons, noting additive thermal resistivity increases 24 p4249 A66-42228
- Anisotropic electron distribution in pure semiconductors near avalanche, considering indium antimonide 24 p4252 A66-42355
- ### INDIUM ARSENIDE
- Semiconductor maser design and principles tabulating indium phosphide, gallium and indium arsenide types 04 p0532 A66-14183
- Recombination of nonequilibrium charge carriers in indium arsenide, noting radiative and impact recombination 04 p0569 A66-14357
- Transport coefficients of n-indium arsenide to calculate electron concentration, mobility and three-band scattering mechanism 04 p0570 A66-14481
- Stimulated emission in indium arsenide shows excitation threshold low and light emission highly directional 06 p0893 A66-17026
- Injection luminescence in InAs diodes 07 p1094 A66-17315
- Hall effect measured by splitting alternating voltage produced in Hall circuit into two components, one with phase coinciding with Hall emf and other with phase departing by 90 degrees 08 p1273 A66-19289
- Specific conductivity, Hall, Nernst, Ettingshausen and other transfer effects in InAs-CdTe and InAs-ZnTe alloys 09 p1428 A66-20539
- Thermal emf quantum oscillation and quantization of electron energy spectrum of n-InAs 09 p1429 A66-20768
- Microwave emission from bulk n-type indium arsenide in presence of applied electric and magnetic fields at liquid nitrogen temperatures 10 p1572 A66-21069
- Effective mass in InAs and InSb from Landau shift of peak emission in laser diodes 10 p1543 A66-21579
- Indium arsenide diodes for thermophotovoltaic conversion at 1000 K 11 p1639 A66-22248
- Carbon and ethylene tetrachloride ultrasonic modulators applied to IR laser heterodyne experiments on InAs photodiode 11 p1714 A66-23353
- Hall generator constructed by vapor deposition of thin films of indium arsenide from 4 to 500 degrees K 12 p1838 A66-24407
- Ettingshausen-Nernst effects in InAs-InP solid solutions, discussing differential thermal emf, scattering at acoustical and thermal oscillations of lattice, ionic impurities, etc 12 p1930 A66-24685
- InAs laser emission, discussing radiative transitions, coherent emission from InAs diodes, recombination mechanisms in IR radiation spectra, etc 13 p2089 A66-25065
- Optical excitation in indium arsenide and gallium antimonide yielding laser radiation 13 p2090 A66-25438
- Thermal emf quantum oscillation and quantization of electron energy spectrum of n-InAs 14 p2361 A66-27303
- V-I characteristics of alloyed p-n junctions in InAs in temperature range from 78 to 296 degrees K 14 p2364 A66-27745
- Recombination of nonequilibrium charge carriers in indium arsenide, noting radiative and impact recombination 14 p2368 A66-28255
- Helicon wave propagation in InSb and InAs at room temperature 15 p2559 A66-28630
- Traveling solvent technique for p-n-p or n-p-n semiconductor structures with highly doped middle layer demonstrated on indium arsenide 16 p2779 A66-31088
- Structure and electron mobility of thin indium arsenide films prepared by co-evaporation technique 16 p2780 A66-31094
- Coherent emission of indium arsenide phosphide p-n junction 16 p2721 A66-31788
- Chemical etchants for In As noting functions, rate dependence on bromine in methanol, p-n junction delineation,



etc 19 p3434 A66-35349  
 Thermal and electric properties of InAs-GaAs alloy as function of composition, impurity additions and temperature 19 p3436 A66-35427  
 Quantum oscillations in magnetoresistance, Hall coefficient and thermoelectric power in strong transverse and longitudinal magnetic fields for n-InAs polycrystals at liquid helium temperature 19 p3438 A66-35479  
 Indium arsenide lasers and HgTe-CdTe photodetectors with very fast time constants for IR spectral band 19 p3376 A66-36268  
 Effective electron mass in n-type indium arsenide at high temperatures and high carrier density, noting temperature dependence of effective electron mass 20 p3616 A66-37444  
 Gunn oscillations in indium arsenide, measuring electrical properties of diodes, noting current voltage characteristics as function of applied stress 20 p3620 A66-37773  
 Scattering mechanism in space charge region as possible explanation of temperature fluctuations of carrier mobility in n-and p-type indium arsenide 23 p4115 A66-41829

## INDIUM COMPOUND

Transverse Dember effect in anisotropy of electrical and photoelectrical characteristics of indium selenide 04 p0565 A66-14259  
 Hall coefficient, electric resistance and thermoelectric power in indium-rich solid solutions measured at various pressures and at 110 degrees C 06 p0922 A66-16172  
 Semiconductor radiation damage in III-V compounds indium antimonide, gallium arsenide and indium arsenide, including values of threshold displacement energies, post-irradiation recovery, etc 06 p0935 A66-17129  
 Optical properties of indium oxide, noting direct and indirect transitions in thin films and crystal plates, absorption coefficient as function of photon energy, etc 10 p1577 A66-21560  
 Photoconductivity and optical transmission of cadmium-indium-telluride, noting temperature dependence 13 p2165 A66-25685  
 Cadmium and indium thio germanates, properties and synthesis 14 p2361 A66-27339  
 Fermi surface of metals and semimetals and quantum oscillations in ultrasonic attenuation and magnetic susceptibility of InBi 14 p2366 A66-27763  
 Optical and electrical characteristics of n-type indium oxide films prepared by spraying, noting relation between carrier mobility and particular impurity used 15 p2559 A66-28623

## INDIUM PHOSPHIDE

Temperature dependence of heat conductivity and thermal emf in n-type InP 02 p0277 A66-12094  
 Semiconductor maser design and principles tabulating indium phosphide, gallium and indium arsenide types 04 p0532 A66-14183  
 Intrinsic optical absorption in indium phosphide single crystals mechanically polished and plotted vs photon energy 07 p1095 A66-17318  
 Instabilities of current and potential distribution in n-type GaAs and InP in electric field of several thousand v/cm 07 p1104 A66-18221  
 Mossbauer effect in polycrystalline indium phosphide and gallium arsenide 08 p1277 A66-19618  
 Temperature dependence of integral light flux of recombination radiation in indium phosphide n-p junction 09 p1431 A66-20935  
 Elastic constants obtained from longitudinal and transverse acoustic waves propagated in single-crystal indium phosphide 10 p1578 A66-21585  
 Ettingshausen-Nernst effects in InAs-InP solid solutions, discussing differential thermal emf, scattering at acoustical and thermal oscillations of lattice, ionic impurities, etc 12 p1930 A66-24685  
 Intervally scattering in III-V semiconductors, noting relation to Gunn effect, scattering in GaAs by longitudinal optic phonons, in InP by longitudinal acoustic phonons 16 p2776 A66-30733  
 InP spontaneous and simulated emission spectra, noting separation of lines by longitudinal optical phonon energy,

threshold current magnitude, etc 17 p2886 A66-32407  
 Mossbauer effect in polycrystalline indium phosphide and gallium arsenide 17 p2983 A66-33132  
 Volt-ampere characteristics and photomicrographs of p-n junctions produced by diffusion of Zn and Cd into InP 21 p3798 A66-38918  
 Thermal conductivity of InP-GaAs solid solutions in vacuum 22 p3962 A66-40051  
 Stable space-charge layers in two-valley semiconductors 22 p3963 A66-40101

## INDIUM TELLURIDE

Deviations from stoichiometry in indium telluride, finding that no impurity conduction occurs in this semiconductor 07 p1099 A66-17916  
 Deviations from stoichiometry in indium telluride, finding that no impurity conduction occurs in this semiconductor 18 p3155 A66-34182

## INDOLE

New synthesis of o-nigrophenylacetaldehyde 16 p2646 A66-30621

## INDUCED FLUID FLOW

EHD traveling potential wave interaction inducing electroconvection in slightly conducting current without electrical contact with flow 23 p4104 A66-41496

## INDUCER

SA HELICAL INDUCER  
 Analog computer solution to nonlinear dynamic system model of oscillations associated with cavitating inducers and sequence of trend-and-effect of constituent influences [ASME PAPER 65-FE-14] 06 p0870 A66-16210  
 Hubless inducer with shroud eliminates vane clearance cavitation, noting test data, suction speed, interrelation of boundary layer transition and cavitation, etc [ASME PAPER 66-FE-8] 17 p2932 A66-33262

## INDUCTANCE

Topological analysis for networks containing nonreciprocal components and mutual inductance 02 p0208 A66-11907  
 Inductance of superconducting solenoid calculated from AC resistance and discharge oscillograms 05 p0737 A66-15336  
 Active filters and oscillators using simulated inductance 11 p1661 A66-22387  
 Switch and load inductances and relation to performance reduction in superconductor energy storage systems 12 p1928 A66-24303  
 Inductance of superconducting solenoid calculated from AC resistance and discharge oscillograms 15 p2569 A66-29983  
 Nonlinear inductance effect on leading edge of high voltage nanosecond pulses during passage through ferrite magnetic field 21 p3801 A66-39156

## INDUCTION

SA MAGNETIC INDUCTION  
 SA RLC CIRCUIT  
 Dielectric diode induction effect demonstrated through equivalent circuit 14 p2252 A66-27491

## INDUCTION HEATING

Self-induction of ellipsoidal plasmoid, deriving relevant equations 21 p3787 A66-39051  
 Compressible fuel mixture deflagration perturbation stability in induction regime characteristic of heat-stressed combustion chambers of rocket engines 23 p4122 A66-41790

## INDUCTION SYSTEM

Discharge chamber with water-cooled metallic walls and HF induction 09 p1407 A66-20144  
 Plasma cluster and shock wave acceleration using plasma induction accelerator with radial magnetic field 09 p1333 A66-20984  
 Behavior of current carrying superconducting coil with heat generation in windings, noting voltage-current characteristics 10 p1509 A66-21562  
 Conical induction plasma gun construction in strongly preionized regime and results of electrostatic probe measurements made with discharge camera 17 p2969 A66-32547  
 Discharge chamber with water-cooled metallic walls and HF induction 21 p3793 A66-39415  
 Faraday unipolar induction in solid cylinder of nonideal type II superconductor, noting contributions to observed

emf 23 p4114 A66-41622  
 Rapid transfer of magnetic energy via exploding foils, noting inductive storage 24 p4239 A66-43211

## INDUCTOR

## SA MAGNETIC COIL

Thin film inductors design limitations due to low inductance values, low Q and undesirable coupling 17 p2882 A66-32111  
 Optimal lumped constant dispersive network design with inductors and capacitors functioning independently 23 p4034 A66-41011

## INDUSTRIAL SAFETY

Computer-directed malfunction checkout of rockets, boosters and modern military aircraft 04 p0526 A66-14021  
 Task Committee on Factors of Safety structural reliability and safety evaluation 15 p2614 A66-29611

## INDUSTRY

## SA AIR FREIGHT INDUSTRY

## SA AIRCRAFT INDUSTRY

SA DEFENSE INDUSTRY  
 Book on titanium covering extraction processes, commercial manufacture and fabrication, cost estimates, marketing, etc 15 p2521 A66-28869

Industry approach to determining weapon system concepts in terms of desired system functions and attainable subsystem performance capabilities 19 p3480 A66-35553

LEM program at RCA, discussing history, management, lunar landing, rendezvous, tracking antenna, radar, etc 21 p3714 A66-39511

LEM program history and management at RCA, discussing Apollo mission studies and initial assignments 21 p3822 A66-39511

## INELASTIC BODY

Stress analysis in inelastic range at elevated temperature covering stress-strain law, point/axially symmetric deformations of thick-walled sphere and cylinder with numerical values 03 p0436 A66-12711

## INELASTIC COLLISION

Quantitative comparison of systematic approaches to generation of inelastic impact cross section with aid of simple universal excitation cross section function [AIAA PAPER 66-150] 06 p0913 A66-17059

Cosmic ray particle interaction at hundred bev range, discussing parameters of inelasticity for collision with nucleus 07 p1113 A66-17531

Nucleon-nucleon collisions at high energies describing statistically independent successive interactions of incident particles with target nucleus 07 p1113 A66-17541

Coefficients of inelasticity of interaction between cosmic ray particles with iron and carbon nuclei 07 p1114 A66-17541

Two-fluid shock wave model involving Boltzmann equation and inelastic collision theory for rarefied gas 08 p1204 A66-18521

High energy cosmic ray jet showers noting energy, angular momentum, collisions, inelasticity, secondary meson distribution, etc 11 p1763 A66-22701

Nonequilibrium internal distributions effect on rates of chemical gas-phase exchange reactions 11 p1650 A66-23211

Spectral line broadening due to collision in stimulated Raman effect 14 p2309 A66-27941

Molecular inelastic collision cross section from radiometer force curve 15 p2543 A66-28781

Quantitative comparison of systematic approaches to generation of inelastic impact cross section with aid of simple universal excitation cross section function [AIAA PAPER 65-150] 15 p2545 A66-29261

Meson emission asymmetry, inelastic particle collisions and multiplicity in ultrahigh energy interactions in nuclear emulsion 15 p2545 A66-29541

Collision cross sections of high energy nucleon-nucleon interactions in nuclear emulsion 15 p2583 A66-29541

Experimental data analysis of cosmic ray showers, secondary particle production by nucleon-nucleon collision at high energy, momentum distribution in pions and primary energy-inelasticity relation 15 p2583 A66-29541

U.S.S.R. accelerator experiments in high



- energy nuclear interaction cross section and elasticity, primary and secondary cosmic ray particle energies, charged nuclear-active particle energy spectra, momenta measurements, etc 15 p2545 A66-29549
- Peripheral inelastic encounters, complex orbital momenta and cosmic ray analyses of interactions, noting hydrodynamical model and Regge pole method 15 p2585 A66-29562
- Muon charge ratio derived from inelastic collision model of pion production, considering just average multiplicities 15 p2588 A66-29575
- Line width and shifts in molecular spectra of gases, giving general formulas for pressure broadening, phase shift of rotation, amplitude modulation of radiation and statistically inelastic collisions 16 p2750 A66-30118
- Balance equations derived from kinetic equations for nonequilibrium plasma, considering radiative processes and inelastic collisions between electrons and ions 16 p2766 A66-31603
- Sufficient conditions for absolute stability servosystem with backlash, taking into account plant inertia and hypothesis of absolutely inelastic collisions 17 p2901 A66-32258
- Primary cosmic ray energy spectrum measurements via Proton I satellite, noting inelastic interaction cross sections, chemical composition, etc 18 p3175 A66-34746
- Inelastic neutron cross section for interaction with Pb and C nuclei near 100 ev 18 p3216 A66-35165
- Inelastic n-p cross section at 60 gev determined from attenuation of penetrating power-producing cosmic ray neutrons in paraffin and graphite 18 p3216 A66-35167
- Energy transfer in low velocity inelastic atomic collisions 19 p3401 A66-35464
- Electron velocity distribution function in nonequilibrium plasma having spatial distribution governed by electron-electron and inelastic collisions 20 p3606 A66-36974
- Radiation peak formation in inhomogeneous gas behind shock wave due to radiating atom distribution and heating of electron gas by inelastic molecular collisions 21 p3728 A66-39334
- Radiation peak formation in inhomogeneous gas behind shock wave due to radiating atom distribution and heating of electron gas by inelastic molecular collisions 22 p3897 A66-39704
- Time resolved emission measurements for Ar-Ar mixtures in three spectral regions and ionization occurrence in excited state elastic collisions 23 p4033 A66-42083
- Phenomenological picture of production of secondary particles in nucleon interactions of energies of hundreds and thousands of ev 24 p4267 A66-42902
- Elementary particles interaction with atomic nuclei with energies from tens to thousands of bev 24 p4267 A66-42903
- High energy inelastic interactions, discussing necessity of statistical methods, secondary particle composition and angular distribution, etc 24 p4267 A66-42904
- Inelastic interactions at ultrahigh energies, discussing secondary particle jets production moving in same direction as colliding particles 24 p4268 A66-42912
- ELASTIC SCATTERING**
- ELASTIC SCATTERING**
- NEUTRON SCATTERING**
- Phonon spectra in aluminum single crystals investigated by means of inelastic scattering of slow neutrons 02 p0277 A66-12083
- Parameters associated with inelastic polar electron scattering in indium antimonide 04 p0565 A66-14267
- Anomalies in low temperature properties of noble metal alloys such as thermoelectric power and nonmonotonic behavior of resistivity with temperature 08 p1274 A66-19362
- Compton process argument for quasar relative nearness to our Galaxy and contrast between Compton and synchrotron radiation scattering effects 12 p1950 A66-24389
- Angular distributions of elastic and inelastic alpha-particle scattering in even tin isotopes, using 40 mev alpha beam 18 p3138 A66-34166
- Absorption spectrum of sulfur hexafluoride in far UV due to electron impact and inelastic scattering and oscillator strengths for three absorption bands 21 p3774 A66-38524
- Sudden approximation applied to rotational transition probabilities and inelastic total cross sections for scattering of homonuclear diatomic molecules by atoms 21 p3774 A66-38526
- INELASTICITY**
- Anelasticity and relaxation time in metals and nonmetals, particularly as manifested by internal friction peak as function of frequency or temperature in study of crystalline material defects 05 p0772 A66-14548
- Design analysis related to structures using materials exhibiting inelastic responses, noting deformation analysis for operational loads and instability analysis for structural failure 06 p0963 A66-16473
- Shear stress, shear rate, inelastic thixotropic properties and speed-torque curves for time-independent non-Newtonian fluids 10 p1618 A66-21885
- Displacement bound theorems for work hardening continua subjected to impulsive loading in inelastic continua 11 p1781 A66-22610
- Young air electron-photon showers at 3200 m altitude, noting average nucleon energy and inelasticity coefficient 15 p2583 A66-29552
- High energy muon energy spectrum, energy loss rate, primary nucleon energy spectrum and inelasticity fluctuations 15 p2587 A66-29571
- Inelastic buckling of rib-cored orthotropic sandwich cylinders under external hydrostatic pressure evaluated by deformation theory of plasticity 24 p4285 A66-42147
- Inelasticity in carbon particle nuclei interactions evaluated by variation with depth of energy of electron photon shower in thick absorber 24 p4268 A66-42910
- INEQUALITY /MATH/**
- Starlike solutions of optimum transversal contour problem treated by Young inequality 11 p1631 A66-22519
- Controllability of general class of nonlinear systems describable by nth order ODE with bounded state and control spaces 13 p2052 A66-26079
- Inequality constraints in open-loop minimum time control problem 13 p2053 A66-26080
- Error bounds based on a priori inequalities for solutions of boundary value problems for linear elliptic partial differential equations 16 p2731 A66-30236
- Matrix algebra, discussing factorization, determinants, eigenvalues, polynomials, inequalities, etc 17 p2945 A66-31869
- Garding inequality and Green transformation applied to elliptic operators in eigenvalue problems 21 p3755 A66-38465
- INERT GAS**
- S RARE GAS**
- INERTIA**
- Motion equations for deep spherical shells including effects of transverse shear deformations and rotatory inertia 05 p0781 A66-15740
- Book on time and space, weight and inertia in terms of relativity theory, including accelerations and rotations, dynamical tensor of matter, ideal clock, rigid body, etc 14 p2330 A66-26808
- Longitudinal and circumferential inertial effects on dynamic response of cylindrical shell to time-varying loads 17 p3025 A66-32470
- Inertia and pressure effects on energy potential of homogeneous and isotropic turbulence in weakly compressible medium 18 p3100 A66-34608
- Motion of solid body with rotating flywheels rotating at constant velocities relative to inertial space and body 22 p3948 A66-40682
- INERTIA MOMENT**
- SA ANGULAR MOMENTUM**
- Mechanical model for representing moment of inertia and fuel sloshing in baffled cylindrical missile tanks 08 p1205 A66-18834
- Moon shape related to distribution of continents and maria and relationship between shape and inertia moments 10 p1605 A66-21203
- Kinetic moment variation theorem for deformable system of material points of variable composition 11 p1735 A66-22239
- Motion of gyroscope with variable moments of inertia on movable base, deriving motion equations 14 p2291 A66-27165
- Servomechanism design, noting optimum response parameters, physical characteristics as functions of inertia, external force, energy dissipation, kinetic energy for operation, etc 16 p2671 A66-31062
- Gyroscopic rotor vibrations excited by effect of lubrication layer in sliding bearings and stabilized with intervening elastodamping supports, taking into account moment of inertia of rotor 17 p3027 A66-32605
- Natural oscillation frequency of gyro mounted in torsional suspension, taking into account moments of inertia of sensitive element 17 p2926 A66-32799
- Section moments of inertia by approximation method 17 p3030 A66-32967
- Design of integrating and position servomechanisms having tachometer-generator feedback, noting role of inertial moments effect 20 p3540 A66-38444
- Elastic stability of cylindrical shells reinforced by one or two frames and subjected to external radial pressure, noting inertia moment about skin line and frame bending stiffness 21 p3828 A66-38703
- Optimization DODGE satellite will be capable of two- and three-axis gravity-gradient stabilization at near synchronous altitude, using moment-of-inertia distributions and libration damping 21 p3820 A66-38860
- Gyrorotor shape with minimum aerodynamic resistance, discussing cases with constant and varying moment of inertia 21 p3739 A66-39327
- Gyro in Cardan suspension, discussing stability criteria for rotations about largest or smallest moment of inertia 22 p3947 A66-39695
- Theorem concerning use of instantaneous axis of rotation for simplification of small oscillation equation of angular momentum 22 p3992 A66-40300
- Static stability of rolling motion of aircraft for given aileron angle when inertia cross-coupling is present, with numerical solution of nonlinear equations 22 p3848 A66-40493
- INERTIA PRINCIPLE**
- SA MACH INERTIA PRINCIPLE**
- Energy function and conservation of inertial mass and three-momentum from relativity principle and conservation of energy in particle collisions 05 p0719 A66-15530
- INERTIAL ACCELEROMETER**
- Inertial gyroscope and accelerometer design and components 13 p2076 A66-25127
- INERTIAL COORDINATE SYSTEM**
- Inertial system using gyros and accelerometers, determining autonomously plant curvilinear coordinates and plant space orientation parameter 02 p0260 A66-12168
- Joint motion of two solids and motion of rotating body relative to other due to external forces 12 p1914 A66-24359
- INERTIAL FORCE**
- SA FROUDE NUMBER**
- High speed compression of viscoplastic thin disk between smooth dies considering inertia effects 02 p0299 A66-11690
- Internal or external pressure effect on natural frequencies of conical shell, noting role of inertia forces, using linear shell theory 11 p1780 A66-22330
- Transient response of value-controlled actuator with inertial loading to step input excitation, considering fluid compressibility 11 p1640 A66-22622
- Friction and inertia fields induced by electromagnetic effects arising in motion of hard magnetic moment in thin circular film 11 p1753 A66-22808
- Gravitation theory and new principle of equivalence of inertial and gravitational energies 12 p1913 A66-23770
- Theoretical behavior and frequency response of electrohydraulic valve-controlled cylindrical vibrator capable of high thrust over wide frequency



- range 12 p1803 A66-23798
- Mathematical model of human body predicting inertial properties in any fixed body position, including location of mass center 12 p1810 A66-24719
- [AIAA PAPER 65-498] 12 p1810 A66-24719
- Axisymmetric form of stability loss of cylindrical shell under effect of load suddenly applied along generatrix, considering inertia forces and obtaining differential equations 13 p2206 A66-28456
- Lift, drag and inertial forces due to uniform unsteady flow with constant acceleration past fixed circular cylinder, determining vorticity flux 13 p1993 A66-26705
- Lumped inertia force method for obtaining mode shape and corresponding natural frequencies 17 p3023 A66-32078
- Oscillations and stability of cylindrical shell in gas flow, taking into account inertia forces 17 p3029 A66-32804
- Rotating masses effect on inertial frames, analyzing stress energy tensor and Schwarzschild geometry 22 p3979 A66-40113
- Stability conditions for system with two degrees of freedom, considering effect of inertial and resistance forces on inertialess body 23 p4137 A66-41001
- Dynamic aeroelastic motion resulting from inertial and aerodynamic effects, coupled through elastic deformation, applied to jet aircraft, considering flutter, buffet, wakes and turbulence 23 p4015 A66-41035
- Inertia product terms effect on satellite gravitational torques 24 p4283 A66-42781
- ### INERTIAL GUIDANCE
- #### SA STELLAR INERTIAL GUIDANCE
- Low cost inertial guidance system commands missile attitude so that modified ballistic trajectory is followed along direct line of sight to target 01 p0098 A66-10003
- Unconventional attitude sensors required to make strapped-down gimballess inertial guidance system practical 01 p0139 A66-10004
- Locating low cost aircraft inertial navigation system being designed for compatibility with high performance tactical aircraft 01 p0099 A66-10010
- Microelectronic integrated circuits and thin films applied to inertial navigation systems to achieve cost reduction 01 p0034 A66-10011
- Design philosophy for low cost inertial navigation system including subsystem characteristics 01 p0099 A66-10012
- SGN-10 Inertial Navigator, pure inertial system with no damping or other external input designed for commercial aircraft 01 p0099 A66-10013
- Operation theory and functional elements of low cost Honeywell SIGN I Strapdown Inertial Guidance and Navigation System 01 p0099 A66-10015
- Inertially augmented radio altimeter guidance system for space booster missions with over-horizon orbital injection requirements 01 p0100 A66-10023
- Review of current knowledge and techniques for stabilizing test pads for high precision inertial guidance and control components 01 p0051 A66-10028
- Accelerometers and gyroscopes tested underground, discussing ground motion attenuation with depth investigated in Deep-Hole program 01 p0051 A66-10038
- Isolation of test pads for inertial guidance systems, investigating soil dynamics for proper selection of sites 01 p0052 A66-10039
- Site selection, construction features and acceleration criteria for inertial test facility 01 p0052 A66-10040
- Terminal prediction guidance for rocket vehicles in terms of strapped-down and gimbaled platform concepts 01 p0101 A66-10042
- Navigation, guidance and control systems to meet basic trajectory and crew safety requirements of LEM 01 p0102 A66-10043
- Central Inertial Guidance Test Facility /CIGTF/ at Holloman AFB, outlining tradeoff between operational and analytical considerations 01 p0102 A66-10047
- Inertial-grade gyroscope theory and application, noting two-degree and single degree of freedom gyros, reference frames and gyrocompasses 01 p0067 A66-10488
- Basic navigation concepts and techniques used by MIT Instrumentation Laboratory to design Apollo guidance and navigation system 02 p0254 A66-11316
- Flight testing of Litton LN-12 inertial navigation system consisting of four-gimbal two-gyro platform and analog computer 02 p0259 A66-12049
- Phase II inertial navigation system design and testing 02 p0259 A66-12050
- USAF Central Inertial Guidance Test Facility for testing aircraft navigation systems 02 p0259 A66-12051
- Inertial navigation and accelerometers deriving law of gyroscopics, noting design of gyroscopes like ball and gas bearings, gimbal suspension, electrostatic, laser, etc 04 p0543 A66-13362
- Portable inertial navigator consisting of platform assembly, computer, power supply and mounting base that eliminates warm-up delays 04 p0544 A66-13925
- Evaluation of methods for estimating circular error probable /CEP/ or system accuracy of ballistic missiles employing inertial navigation systems 04 p0544 A66-14444
- Shipboard inertial navigation system recalibration, using periodic position information from communications satellite 05 p0712 A66-14604
- Effectiveness of split cross-flow heat exchangers, emphasizing uniform exit temperature distribution for unmixed fluids [ASME PAPER 65-HT-24] 05 p0783 A66-14745
- Voltage stabilization using cold cathode trigger tubes 05 p0647 A66-14769
- Slide wire accelerometer, considering factors responsible for sensitivity loss and gain 07 p1031 A66-17410
- Design of low-cost inertial navigation system 07 p1063 A66-17445
- Inertial navigation and guidance systems applied to civil air transport from systems engineering viewpoint 07 p1067 A66-17695
- Route structure and navigation system error over North Atlantic and advantages of SST inertial navigation system 07 p1068 A66-17701
- Flight testing of Phillips vertical reference inertial navigator on DC-8 aircraft 07 p1069 A66-17708
- Differences between inertial equipment and that in current use, emphasizing economic aspects 07 p1069 A66-17710
- Inertial navigation systems for automatic landing, using category I instrument landing system 07 p1069 A66-17714
- Up-dating of self-contained navigational aids such as Doppler, inertial and Doppler/inertial systems 07 p1070 A66-17717
- Doppler-inertial system combination applied to avoid deterioration of navigational accuracy with time 07 p1070 A66-17719
- Schuler tuned inertial system as flight sensor and control of VTOL aircraft translational velocity during hover phase and landing 07 p1070 A66-17724
- Design of Elliott E.5, low cost inertial navigation system for civil aircraft 07 p1071 A66-17727
- International Air Transport Association, Technical Conference, Miami, April 1965, Volume 2 07 p1071 A66-17757
- Automatic airborne navigation facilities in civil aircraft 07 p1073 A66-17767
- Flight evaluation of long range inertial navigation and steering in autopilot and manual operation 07 p1076 A66-17791
- Accurate light-weight self-contained low-cost inertial autonavigational system including gyroscopes, accelerometer and DYDAN computer 07 p1076 A66-17793
- Inertial navigation on north transatlantic route, examining inertial equipment, flight planning and preflight cockpit checks 07 p1076 A66-17798
- Military inertial navigation equipment applied to civil aircraft, evaluating accuracy, reliability and cost 07 p1077 A66-17799
- Modern inertial navigation system development, describing accuracy, reliability and operational use of SGN-10 system 07 p1077 A66-17804
- Development of inertial navigation system based on Electrically Suspended Gyroscope /ESG/, with comparison to conventional inertial and hybrid systems 07 p1078 A66-17807
- Motion of orthogonal trihedron, determining accurately angular position translational motion relative to coordinate system 08 p1249 A66-18181
- Gyroscopes, accelerometers and error sources in inertial navigation systems 08 p1249 A66-19194
- Vehicle angular velocity determined, using configurations with only linear accelerometers and no gyroscopes inertial navigation systems 08 p1224 A66-19194
- Error damping procedures for gimbal inertial navigational systems 08 p1253 A66-19194
- Digital computers for aerospace guidance and control, including Gemini inertial guidance and B-70 aircraft navigation systems 08 p1187 A66-19194
- Low cost inertial guidance for tactical missiles 09 p1400 A66-20194
- Inertial techniques extended to heli measurement in supersonic aircraft simple computing addition to main navigation platform 09 p1400 A66-20194
- Navigational inertial system dynamic property analysis at high flight speed using hodographic characteristic equation for longitudinal and lateral aircraft motion error determination 09 p1401 A66-20194
- Stereographic mapping of plane Cartesian coordinate grid onto sphere for position navigation use 09 p1401 A66-20194
- Electro-optic system superiority over radio and inertial techniques for space navigation determined by simulation studies 10 p1554 A66-21194
- Radio augmented and calibrated inertial navigation equipment and operation 10 p1554 A66-21194
- Operation and structural components inertial navigation system, noting accelerometers, gyroscopic platform stabilizers, error effect, etc 13 p2123 A66-25194
- ESG strapdown inertial navigation system based on double integration of acceleration and analysis of electronic gimbal-induced errors 13 p2124 A66-25194
- Digital airborne computer for navigation problem solutions including inertial navigation, flight path, time-to-go and arrival time, etc 13 p2124 A66-25194
- Inertial navigation and guidance systems applied to civil air transport from systems engineering viewpoint 13 p2125 A66-25194
- Inertial guidance systems using three gimbal, four-gimbal and ball-type platform operative control of aircraft, ships, ballistic missiles 13 p2125 A66-26194
- Orion Inertial Navigation System, detail accelerometers, gyroscopes, computer components, maintenance, operation, etc 13 p2125 A66-26194
- Effect of faulty compensation accelerating force of Earth gravity accuracy in determination by inertial navigation system of coordinate of object flight 14 p2328 A66-27194
- Statistical optimization of rate-compos inertial navigation system based on Phil theory of servo systems 14 p2328 A66-27194
- Flight control systems, automatic land devices and inertial navigation with gyroscopes 15 p2534 A66-29194
- Inertial navigation - Colloquium, Dusseldorf, January 1965 15 p2535 A66-29194
- Inertial navigation systems, examining basic principles of operation and possible time-dependent errors 15 p2535 A66-29194
- Inertial navigation application to aeronautics, requiring accelerometers and inertial platform with turning motion sensors 15 p2536 A66-29194
- Inertial navigation for commercial aviation economically justified by fuel economy and to reduced flight time 15 p2536 A66-29194
- Inertial navigation application to space navigation and guidance systems, considering optimum design requirements 15 p2536 A66-29194
- Pyrotechnic shock testing of Titan airborne inertial guidance equipment not requirements, techniques, etc 16 p2678 A66-30194
- Inertial components and systems evaluated with figures of merit for requirements noting accelerometer errors, limit response, etc 16 p2707 A66-31194



Integrating error equations of inertial navigation system for objects in Keplerian motion 16 p2744 A66-31507  
 Inertial navigation system theory that uses increased numbers of newtonometers /force measuring devices/ in place of gyroscopic sensitive elements 17 p2926 A66-32800  
 Inertial navigation system performance and self-test capability, noting errors from gyro drift 17 p2954 A66-33217  
 Low cost self-monitored inertial navigation system for civil aviation 17 p2955 A66-33218  
 Inertial navigation system reliability and effects of computer and chart display noise 17 p2955 A66-33222  
 Inertial system testing and errors resulting from platform misalignments 17 p2928 A66-33460  
 Thermal noise in internal measuring instruments affecting limitations on spacecraft open-loop inertial autonomous control system precision 18 p3132 A66-33872  
 Inertial navigation technique based on least squares criteria of optimality with error providing estimates of system errors 19 p3396 A66-35517  
 Analytic thermal compensation technique eliminating thermal stabilization time, applied to inertial navigation systems operating in military environment 19 p3397 A66-35518  
 Error equations of inertial navigation with special application to elliptical orbital determination and guidance [AIAA PAPER 65-691] 19 p3397 A66-35898  
 Linear filtering technique for estimation of azimuth alignment of inertial guidance system in presence of disturbances with no measurement noise 19 p3398 A66-36689  
 Passive stabilization of space vehicles with symmetric mass distribution, using coupled system with optimum 20 p3659 A66-36869  
 Optimum control theory applied to shipboard inertial navigation systems with position and azimuth errors because of gyroscope drift-rate 20 p3595 A66-36873  
 Radar-updated inertial navigation of continuously-powered space vehicle during boost phase of flight prior to lunar landing 20 p3596 A66-37221  
 Continuous time multivariate optimal filter for feedback realization applied to augmentation and rapid alignment of inertial systems 20 p3596 A66-37231  
 Reliability program, determining assurance and stabilization trend by analysis of lots applied to testing high reliability parts for return V inertial guidance 20 p3570 A66-37934  
 Central Telecommunications Laboratory 882 arithmetical airborne computer 20 p3523 A66-38013  
 Steering philosophy for rocket booster, using position and/or velocity profiles until desired injection speed is attained [AIAA PAPER 64-639] 20 p3597 A66-38157  
 Inertial navigation in relation to animal navigation, considering three principal characteristics and biological analogs 21 p3760 A66-38450  
 Error sources in strapdown inertial attitude reference system consisting of three pulse torqued gyros and digital differential analyzer 21 p3763 A66-38840  
 Computational errors and requirements evaluated for free and restrained strapdown sensor mechanization, based on analytic models 21 p3763 A66-38841  
 Strapdown inertial sensor configuration based on time modulated torquing approach of gyro and accelerometer readout 21 p3764 A66-38849  
 Strapdown inertial sensor loops design criterion for desired total system performance, noting loop dynamic error 21 p3764 A66-38850  
 Vibration measurement results on air supported isolation platforms, noting effects of heavy vehicle passing sound pressure 21 p3722 A66-38874  
 Apollo inertial navigation system estimation, using statistical filtering to reduce computation 21 p3767 A66-38886  
 Master reference system for reducing sea alignment time of aircraft inertial navigation

systems 21 p3767 A66-38890  
 Integrated navigation system /INS/ using stellar inertial subsystem with optimum data processing 21 p3767 A66-38891  
 Iterative guidance mode with application to three-dimensional upper stage vacuum flight 21 p3768 A66-38897  
 Book on spacecraft navigation systems covering sensors operation and construction, with emphasis on astronomical, inertial and complex navigation systems 21 p3768 A66-39289  
 Inertial and electromagnetic guidance and navigation systems for vehicular and global application 22 p3944 A66-40124  
 Bottom-moored sonar beacons surveyed in absolute position coordinates, noting transmitter-receiver and celestially augmented inertial navigator and error minimization techniques 22 p3945 A66-40323  
 Inertial navigation for civil airline operations, noting azimuth alignment made by automatic gyrocompassing [ICAS PAPER 66-6] 22 p3946 A66-40677  
 Inertially augmented radio altimeter guidance system for space booster missions with over-horizon orbital injection requirements 23 p4088 A66-41099  
 Error sources in strapdown inertial attitude reference system consisting of three pulse torqued gyros and digital differential analyzer 23 p4088 A66-41101  
 Analytic axes alignment for strapdown inertial system, describing computational procedures for ground-based and in-flight correction of attitude parameters 23 p4088 A66-41115  
 Stability analysis of inertial guidance platform control system with saturation and Coulomb friction nonlinearities, using Liapunov method 23 p4089 A66-41319  
 Stability, control, navigation, guidance and air traffic control of hypersonic vehicles noting inertial technology, flight planning and optimal control 24 p4235 A66-42239  
 Space vehicle guidance and navigation, noting instrument techniques, gyroscopic units for reference coordinate realization, inertial navigation systems, etc [AGARDOGRAPH 105] 24 p4235 A66-43123  
**INERTIAL MEASURING UNIT**  
 Internal measurement of latitude, radius vectors and other geophysical properties from center of mass of astronomical system to space vehicle 16 p2698 A66-31386  
 Inertial sensor performance degradation in strapped-down environment, noting gyro drift error and accelerometer bias 21 p3763 A66-38839  
 Six-component balance equipped with semiconductor strain gauges and inertial compensated for hotshot wind tunnels 24 p4206 A66-42167  
 IMU /inertial measurement unit/ gyroscope as attitude reference in space 24 p4214 A66-42955  
 Book on space navigation guidance and control covering manned lunar landing guidance, pulse torquing and inertial measurement units, computer utilization, control systems, etc [AGARDOGRAPH 105] 24 p4235 A66-43122  
 Inertial measurement unit and pulse torquing of Apollo spacecraft, noting components and operation [AGARDOGRAPH 105] 24 p4215 A66-43126  
**INERTIAL NAVIGATION**  
**S SCHULER TUNING**  
**INERTIAL PLATFORM**  
**SA NAVIGATION INSTRUMENT**  
 Floated inertial platform, gimballless all-attitude device utilizing floated sphere to isolate inertial components from acceleration and vibration environments 01 p0099 A66-10014  
 Slab motions affecting test mounts for gyroscopes and accelerometers investigated at underground and surface test locations 01 p0051 A66-10029  
 Control problems associated with stable platforms using single-axis integrating gyroscopes including axes design, drift due to vibration and compensation 03 p0390 A66-12533  
 Response of inertial platform in orbital gyrocompass mode studied for satellite vehicle [AIAA PAPER 64-238] 03 p0369 A66-12736

Specific initial alignment problems and techniques of analytic inertial platform systems 04 p0543 A66-13617  
 Doppler-inertial system combination applied to avoid deterioration of navigational accuracy with time 07 p1070 A66-17719  
 Effect of environmental extremes on Miniature Inertial Navigation System, showing vibration and centrifuge testing data 08 p1251 A66-19491  
 Processing signal information from digital rate gyros and accelerometers in analytic, gimballless inertial platform 08 p1253 A66-19530  
 Inertial techniques extended to height measurement in supersonic aircraft by simple computing addition to main navigation platform 09 p1400 A66-20427  
 Elimination of coupling error between gyroscope and platform, considering rate-integrating gyros with inertial platform 09 p1382 A66-20563  
 Concorde navigation system noting inertial platform, digital computer using integrated circuits and microminiaturization 09 p1401 A66-20685  
 Staff flight test design velocity comparison technique for estimating in-flight inertial platform attitude 18 p3132 A66-34044  
 Slew plane technique for locating two gyro input axes without removing platform from test vehicle and with limited optical access 18 p3133 A66-34048  
 Mechanization of vectorial equations by means of four-gimbal platform and speed sensor for automatic setting of hybrid inertial systems 20 p3597 A66-37395  
 Inertial platform test station for shipboard maintenance and calibration of platform used in A6A and E2A aircraft, examining accelerometer bias and gyro drift tests 21 p3723 A66-38889  
 First-order Markovian gyro drift numerically evaluated and square root plotted vs interval and gyro correlation time 23 p4068 A66-41318  
**INERTIAL REFERENCE SYSTEM**  
**SA GIMBALLLESS INERTIAL REFERENCE SYSTEM**  
 Conditions satisfied by transformation equations connecting inertial and relativistic accelerated systems are deduced for rectilinear motion 03 p0392 A66-12609  
 Lunar orbiter objectives, mission and spacecraft configuration, detailing inertial reference unit 04 p0543 A66-13581  
 Method for initial azimuth alignment of inertial heading reference proven to accuracy of 0.1 percent 07 p1078 A66-17809  
 Inertial reference unit to provide attitude and thrust maneuver measurements for Lunar Orbiter spacecraft 08 p1253 A66-19529  
 Relativistic rocket mechanics, considering coordinate transformation, velocity and dependence of mass on inertial reference system 11 p1775 A66-23118  
 Attitude detectors, characteristics and performance 12 p1879 A66-23745  
 Integration of equations determining location coordinates of moving object on terrestrial sphere 12 p1909 A66-24358  
 Goedel universe analyzed, noting generalized Poisson equation, angular velocity in perturbed metric, equations of motion in inertial frame of reference, etc 13 p2183 A66-25609  
 Variational problem of transition of aircraft with inertial system without stabilizers solved by reduction to Lagrange problem 15 p2534 A66-29336  
 Versatile air-bearing table with three-axis attitude control system for variety of nonspinning zero-g space stations 15 p2534 A66-29362  
 Third-order orbital gyrocompass horizontal and vertical damping techniques to eliminate gyro and bias errors in horizon sensor 18 p3110 A66-33828  
 Time-mass dependent events during motion of material particle, using Hamilton-Jacobi equation of relativistic mechanics in Minkowski continuum 21 p3772 A66-39276  
 Optimizer for shaping control signal of hunting-type system with plant in form of nonlinear inertialess element, examining inadequacy for system operation 22 p3883 A66-39659



## INFINITE SOLID

Equations relating maximum temperature stresses in infinite plate and dimensionless numbers, determining heating rate 09 p1468 A66-20832

## INFLATABLE SPACECRAFT

Parametric requirements for eliminating coupling between bending, sloshing and control in large liquid-propelled elastic space vehicles 10 p1612 A66-21941  
Prestressed circular membrane shell subjected to uniform radial line load, determining stresses and displacements from material properties, internal pressure and original size 24 p4288 A66-42272

## INFLATABLE STRUCTURE

## SA BALLOON

Full scale ground inflation tests to evaluate structural and RF backscatter characteristics of Echo II prototype spheres as function of their internal pressures 01 p0055 A66-11123  
Inflatable plastic structures for space application in U.S. and Germany 06 p0960 A66-17077

## INFLATION

Filling or inflation process of flat circular solid-cloth type parachute canopy operating under finite mass conditions 04 p0457 A66-13530

## INFLUENCE COEFFICIENT

## SA STRUCTURAL INFLUENCE

COEFFICIENT /SIC/  
Influence coefficients for computation of atmospheric components of reentry vehicle circular error probable /CEP/, using Bliss adjoint method, noting effects of certain inadequacies on system performance [AIAA PAPER 66-358] 12 p1908 A66-24517  
Bending behavior of spherical shells through second-order differential equation with complex coefficients, noting effect of load 18 p3253 A66-33765  
Bending characteristics of tapered cylindrical shells, discussing edge and internal influence coefficients 18 p3253 A66-33806  
Block sensitivity coefficient analysis in application of method of transformed circuits to closed-loop control systems, noting dynamic accuracy problem 19 p3327 A66-36014  
Influence coefficients for externally pressurized spherical shells 21 p3828 A66-38724  
Influence coefficients for semifinite and infinite circular cylindrical elastic shell subject to self-equilibrating edge loads 22 p3995 A66-40451

## INFORMATION

Effectetics, informetics, control and stability in modern flight vehicle systems [AIAA PAPER 66-131] 08 p1254 A66-19565  
Effectetics, informetics, control and stability in modern flight vehicle systems [AIAA PAPER 66-131] 18 p3267 A66-33786

## INFORMATION PROCESSING

Energy patterns from space accessible to human senses through data sensors and information acquisition 04 p0472 A66-14093  
Optimum signal shape for transmission of discrete information, discussing signal-noise characteristics 04 p0488 A66-14414  
TV camera, visual display and video-signal information storage tubes, noting secondary electron conduction camera tube 05 p0642 A66-14561  
Error effect in a priori information on sequential estimate variance of linear system states, noting optimal filter synthesis 05 p0653 A66-14601  
Psychological research relevant to human factors engineering of man-machine systems, discussing information processing 05 p0626 A66-14616  
Optical and electro-optical information processing technology - Symposium, Boston, November 1964 05 p0636 A66-14818  
Semiconductor injection laser for use in electro-optical and optical information processing 05 p0692 A66-14823  
Data systems requirement for geographic research, noting use of orbiting sensors to obtain information on terrain, vegetation, human and animal activities, etc 10 p1532 A66-21522  
American Federation of Information Processing Societies, Joint Computer

Conference, Las Vegas, November 1965 12 p1825 A66-23824

Satellite Educational and Informational Television, noting management, market and development problems in terms of profit, demand and growth potential [AIAA PAPER 66-274] 12 p1981 A66-24747

Periodically alternating noise as design problem in theory of information transmission 12 p1824 A66-24854  
Limitations and reliability of human operator of control systems to process information, noting importance of endurance and sensory perception 12 p1807 A66-25012  
Information display techniques for man-machine system 14 p2229 A66-26916  
Collection of information and announcements pertaining to rocket and satellite launchings including objectives, stations, data exchange, etc 15 p2600 A66-29902  
AFIPS Joint Computer Conference, Boston, April 1966 16 p2656 A66-31239

Low-cost computer design using electro-optics for information processing 16 p2657 A66-31240  
Coherent optical transducer for optical information processing 16 p2657 A66-31244  
Information content of photoelectric star images determined by background radiation, optical aberrations and photon noise, deriving equations for rms error 16 p2654 A66-31441

Optimum discrete information system and relations between measurement quality, decisions and system performance 19 p3310 A66-36681  
Information center concept for accurate acquisition and processing of parts, materials and components reliability and maintainability information for task performance 20 p3572 A66-37947  
Vertical sinusoidal vibration as psychological stress in considering capacity for handling information 22 p3854 A66-40007  
Information display - National Symposium, New York, September 1965 22 p3927 A66-40286

Frog retina layered model, stereoscopic system and decision/control system in connection with robot data reduction in Voyager missions 24 p4168 A66-43081

## INFORMATION RETRIEVAL

## SA DATA RETRIEVAL

ESRO/ELDO Space Documentation Service, describing system characteristics, NASA agreement, indexing and search strategy 09 p1473 A66-20658  
Traceability and configuration data system /TAC/ used to determine location of individual parts and assemblies 15 p2506 A66-28791  
R and D problem solving and information gathering in engineering design, reviewing M.I.T. research program on management of science and technology 18 p3268 A66-34064  
Probe and edge theorems for nonlinear optimization algorithms using stored-program computers 19 p3309 A66-35873  
Optimal computer search and application to engineering design 19 p3309 A66-35875  
Maintenance on long-duration manned space flight facilitated by maintenance job aid information stored in high density retrieval and display system 19 p3309 A66-35950  
Satellite instrumentation, discussing data handling systems, cosmic ray detection, signal and information processing, etc 20 p3556 A66-36963  
Delay-line content-addressed memory with information retrieval by word association 24 p4177 A66-43185

## INFORMATION THEORY

## SA COMMUNICATION THEORY

Electronic systems in marine, air and space transportation noting radar, ultrasonic devices, computer techniques, etc 02 p0206 A66-12033  
Information theory applications to angle and line measuring devices with description of use in geodetic instruments 03 p0368 A66-12506  
Textbook on communication engineering emphasizing random processes, information and detection theory, statistical communication theory, applications, etc 03 p0335 A66-12992  
Value of information concept relating

Shannon information theory to theory of optimal solutions 03 p0336 A66-13013  
Existence of statistical relationships between features of different classes of objects determines amount of information obtainable by 03 p0338 A66-13014  
Identification 03 p0338 A66-13014  
Relationship between distribution entropy and variation in distribution of almost periodic channels 05 p0638 A66-15015  
Limitations of communication systems transmitting data from analog sources obtained, using theorem in Shannon paper on information theory 06 p0828 A66-16016  
Scanning slit across point or line space function in determination of radiation irradiance distribution 07 p1081 A66-18018  
Information matrices for estimating parameters of moving targets obtained by combining a priori information with reflected radar signals with additive white Gaussian noise 08 p1180 A66-18018  
Optimum /in Shannon sense/ truncation probability of signal for case of constant power and other conditions 08 p1182 A66-18018  
Spaceflight data handling with emphasis on data compaction techniques based on weighted-information theory, Karhunen-Loeve theory, area recording and transmission procedure 08 p1187 A66-18019  
Upper and lower estimates derived from Shannon reliability of information transmission in channel that is symmetrical with respect to input 09 p1397 A66-20019  
Radio waves and circuits - U.S. Conference, Tokyo, September 1963 11 p1653 A66-22015  
Information recovery from noisy measurements, employing steady quantum measurements, known waveform detection and transfer function evaluation 11 p1656 A66-22015  
Error propagation at above information limits postulated by Shannon sampling theorem and Gabor expansion theorem 11 p1657 A66-23015  
Information theory techniques for sea and analysis of radio signals from extraterrestrial civilizations 12 p1814 A66-23015  
Optimization of high resolution radar based on mathematical results regarding linear transformation of signals and ambiguity functions 12 p1819 A66-24015  
Likelihood detection with multiple Markov process, by expressing statistics distribution function terms 13 p2019 A66-25015  
Man-machine systems for interplanetary exploration, using functional analysis techniques for system design 13 p2013 A66-25015  
Antenna array response to pulsed compression signals, showing dependence of array response on compressed pulse shape 13 p2023 A66-25015  
Radar range measurement accuracy shown to depend on receiver filter 13 p2023 A66-25015  
Quantum information generalizes classical Shannon concept 13 p2025 A66-26015  
Quantum communication channel entropy and information analysis using noncommutative output and input variables including waveguide carrying capacity thermal noise calculations 13 p2025 A66-26015  
Information theory, role in communication systems, detailing coding systems 14 p2239 A66-27015  
Information theory for describing electric and magnetic fields of one-dimensional collisionless plasma 14 p2346 A66-28015  
PCM picture transmission, pseudorandom scanning, noise, bandwidth compression, digital simulation 15 p2450 A66-28015  
Entropy concept of information theory applied to space flight physiological control analysis 15 p2444 A66-28015  
Riemannian signal mapping theory used to clarify stochastic structure of modulation and demodulation in information system 15 p2453 A66-29015  
Coherent optical systems in signal processing techniques, information theory and antenna pattern simulation 16 p2657 A66-31015  
Synthesis of phase synchronization systems



providing maximum-level filtering of internal fluctuation noise, using generalized integral criterion 17 p2898 A66-31853

Easily mechanized method of using stored samples to approximate set of distributions for adaptive pattern recognizer 18 p3073 A66-34073

Value of information concept relating Shannon information theory to theory of optimal solutions 18 p3072 A66-34997

Existence of statistical relationship between features of different classes of objects determines amount of information obtainable by 18 p3074 A66-35002

Information theory criterion applied to nonlinear processing antenna systems yielding optimum system, considering SNR 19 p3318 A66-35885

Learning control system design, discussing hill-climbing and pattern recognition schemes in framework of statistical decision, automata and information 19 p3333 A66-36662

Information theory - IEEE International Symposium, University of California, Los Angeles, January-February 21 p3703 A66-39134

Systematic method of obtaining complex formulations of problems involving white noise, considering deterministic narrow-band signal detection of random phase 21 p3721 A66-39642

**INFRARED ASTRONOMY**

Thermal anomalies found in IR lunar observations attributed to lunar roughness in centimeter scale 01 p1038 A66-10884

Sky survey in two IR spectral ranges, obtaining unbiased census of objects emitting in atmospheric window 04 p0575 A66-13399

Thermal maps of Murray about Venus atmosphere statistically analyzed into solar effects, latitude variations and limb darkening 04 p0579 A66-14450

Visible and IR radiation observations made above atmosphere 10 p1603 A66-21107

Venus IR limb darkening observations by Mariner II 10 p1603 A66-21110

IR emission lines possibly originating from galactic, interstellar and stellar hydrogen regions 10 p1599 A66-21113

12.8-micron IR emission lines observed by glow from planetary nebula IC 17 p3003 A66-32656

IR astronomical measurements for computation of bolometric corrections and effective temperatures of stars of various spectral types 21 p3815 A66-39486

IR observation of Mercury as evidence of nonsynchronous rotation, considering energy radiation as function of position 22 p3979 A66-40305

**INFRARED DETECTOR**

Resistance microwelding process evaluated by IR energy measurements to determine mechanical strength of joint 02 p0234 A66-11328

Hertzian and IR radiometry applied to temperature determination for use in aerial navigation 02 p0257 A66-12032

High detectivity gallium doped germanium detector for far IR 02 p0231 A66-12062

Single crystal semiconductor thermal detector with constant bias current and self-cooling, taking into account end cooling 02 p0232 A66-12063

Graphical method to determine detection range for narrow IR windows in dependence of atmospheric absorption and emission 02 p0223 A66-12064

Varying deposition and firing conditions effect on range of detection of chemically deposited lead sulfide IR detector cells 03 p0407 A66-12332

Design, performance and operation of high-resolution IR radiometer mounted on Nimbus satellite 04 p0518 A66-13468

IR detector types and component structure noting bolometer, thermistor, thermocouple and semiconductor photoelectric type 05 p0676 A66-14679

Cavity type radiometer for absolute total intensity measurement of visible and IR radiation [ISA PREPRINT 1.11-3-65] 05 p0683 A66-15505

IR detectors based on photon-electronic interaction and sensor thermal changes 06 p0880 A66-16559

HF response of copper doped p-type germanium IR detectors 06 p0882 A66-16764

Thermoelectric cooling of IR detectors, examining thermistor bolometers and photoconductive detectors 08 p1221 A66-18683

IR sensor detection of hypervelocity meteoroid puncture radiation emission 08 p1225 A66-19520

Near IR detection system using phototube with type S1 phosphor photocathode, noting tunnel diode discriminator S/N ratio 08 p1227 A66-19696

Sensitivity measure for optical and IR detectors clarified by analysis of noise equivalent power for photodiode 09 p1351 A66-19940

Seasonal variation of atmospheric ozone, determining via IR method total amount and vertical distribution 10 p1526 A66-21124

Terrestrial test sites and aircraft flights used in preparing for remote sensing from Earth orbital spacecraft 10 p1532 A66-21525

Sensitivity and operation of IR detector using avalanche multiplication in microplasmas in silicon junctions, noting SNR at room temperature 13 p2164 A66-25490

Low noise preamplifier with field effect transistors for use with IR detectors 14 p2249 A66-27116

Clear air turbulence detection by measuring associated air temperature gradient by airborne IR radiometer 15 p2500 A66-28927

Indium arsenide lasers and HgTe-CdTe photodetectors with very fast time constants for IR spectral band 19 p3376 A66-36268

Solid cryogenics as heat sinks for cooling electronic components, particularly IR detectors in aircraft and spacecraft 20 p3676 A66-37073

TACITE rocket sounding of characteristics of IR contrast between Earth and space 20 p3663 A66-38033

Gas laser alignment, obtaining oscillation on three lines of He-Ne laser 22 p3930 A66-39718

Double cloud vortex near Antarctica detected by Nimbus I high resolution IR 22 p3942 A66-40053

Low level amplifier for IR receiver for Earth-space IR contrast study 24 p4180 A66-42341

IR sensor classification and selection for specific application 24 p4192 A66-42342

**INFRARED FILTER**

Dimensional filtering in IR technology for background noise elimination, discussing Fourier analysis treatment of system 21 p3768 A66-39646

**INFRARED HORIZON SCANNER**

Automatic control in space reviewing tracking techniques, IR horizon sensors, Apollo spacecraft guidance computer and control systems and terminal guidance system of Surveyor spacecraft 03 p0351 A66-13258

IR planet horizon sensor design, noting filter for uniform radiance, wide angle lens and special detector 11 p1706 A66-22891

IR horizon sensor for determining orbiting satellite attitude with respect to Earth 18 p3110 A66-33873

**INFRARED INSPECTION**

IR nondestructive testing system for usability analysis in production line inspection of Polaris A-3 motors 03 p0373 A66-12996

Thermal IR inspection for bond integrity in solid propellant rocket motors 21 p3808 A66-39154

Magneto-optical phenomena studied by extension of wavelength range of electroradiance measurements in solids using electrolyte into near IR 23 p4111 A66-41263

**INFRARED INSTRUMENT**

Nondispersive IR equipment and techniques for chopping and scanning incident radiation 06 p0880 A66-16560

IR polariscopy method applied to study of photo- and electromechanical effects of n-type silicon films 07 p1034 A66-17875

IR AM TV transmitter and receiver using

GaAs diode and telescope with photomultiplier 08 p1184 A66-19348

Fabry-Perot interferometer with mirrors in form of metallic strips to facilitate use in far IR and microwave spectral regions 11 p1704 A66-22347

Image converter tube for middle IR, noting sensitivity dependence on photoconductor properties 14 p2331 A66-27100

Selection and processing of IR materials and optical glass, discussing similarities and differences between specification and fabrication techniques 15 p2524 A66-28829

Replacing heated tungsten filament and IR filter by GaAs electroluminescent diode without filter for IR illumination 19 p3320 A66-36266

IR spectrometers, radiometers, horizon sensors, rotating-prism planet-seekers and detector cooling using solid cryogenics, for use in high altitude rockets and Earth satellites 24 p4211 A66-42679

**INFRARED MASER**

Quantum-electronic cross-modulation effect noted while monitoring IR laser interferometric fringes 02 p0240 A66-11449

CW IR laser oscillation in HBr and HI gas discharge 06 p0892 A66-16756

Carbon and ethylene tetrachloride ultrasonic modulators applied to IR laser heterodyne experiments on InAs photodiode 11 p1714 A66-23353

Nonequilibrium population buildup and detection for IR solid state lasers and IR-optical double resonance in lanthanum chloride crystal 13 p2098 A66-26177

Far-IR laser molecular spectroscopy including IR laser oscillators, photon noise, detectors and nuclear optics 13 p2100 A66-26195

Optical-and IR-maser spectroscopy of inhomogeneously broadened resonances, using gas lasers 13 p2100 A66-26196

IR maser action on vibrational transitions of thermally pumped polyatomic molecules 13 p2101 A66-26203

IR and visible helium-neon laser modulation using Faraday rotation in YIG 14 p2305 A66-26881

Isotope shifts and Fermi resonance role in carbon dioxide IR laser 16 p2716 A66-30176

Gallium arsenide diode laser as pulsed IR source for experiment and design considerations for radar indication of cloud height and visibility 18 p3066 A66-33616

GaAs crystal as electro-optic modulator at 10.6 microns due to small carrier absorption, freedom from interband transitions and high resistivity 24 p4222 A66-42553

IR GaAs laser amplifier with gains as high as 2000, output powers of 150 mw and saturation occurring with current increase at low light levels 24 p4223 A66-42562

**INFRARED PHOTOGRAPHY**

Design, performance and operation of high-resolution IR radiometer mounted on Nimbus satellite 04 p0518 A66-13468

Resolving power and microphotometric granularity of IR films measured with resolvometer, noting dependence on frequency of incident light 10 p1534 A66-21332

Lunar mapping in far IR, including hot spots during total eclipse of December 19, 1964 16 p2698 A66-31225

IR pyrometry of lunar surface 19 p3457 A66-35447

Quantitative IR radiometric skin temperature measurements, using simple radiometer and method for measuring surface temperature of forearm and hand 20 p3507 A66-38418

Antarctic pack ice boundaries established from TV and IR pictures taken by Nimbus I meteorological satellite 21 p3735 A66-39491

IR photometric measurement of Comet 1965f, noting absolute intensity dependence on distance from Sun, tail intensities and nature of particle emissions 21 p3816 A66-39557

**INFRARED RADIATION**

Visible and IR radiation attenuation by artificial fogs found to depend on droplet size and distribution 01 p0097 A66-10860

IR radiation of refractory solids with radiation properties of flame-sprayed ceramic coatings, determining normal spectral emittance, integrated normal total



emittance and IR intensity curves at 1300 K 03 p0386 A66-13100  
P-n junction of semiconductor CdHgTe behaved as detectors and emitters of IR radiation, showing possibility of laser effect in such alloys 04 p0559 A66-13480  
Two ohmic electrodes or one ohmic and one barrier electrode for current-voltage stable-negative characteristic of cadmium sulfide, noting IR radiation effects 04 p0568 A66-14351  
High pressure high current argon discharge, calculating statistical variations of photon radiation, electron and ion densities 05 p0720 A66-14504  
High pressure high current argon discharge covering statistical variations of nonblack body, photon and IR radiation and measurement with InSb photodiode 05 p0720 A66-14507  
Minority carrier lifetime in silicon measured by contactless method, using laser induced modulation of IR transmission in silicon /LIMIRIS/ effect 05 p0729 A66-14563  
IR emission observation used to deduce composition, temperature and energy budget of stratosphere and mesosphere 05 p0672 A66-15024  
Nitrogen and nitrogen-foreign gas mixtures, determining absorption profile shapes, binary and ternary absorption coefficients and molecular quadrupole moment 06 p0908 A66-16281  
Vacuum fusion and IR absorption determination of bulk oxygen content of germanium crystals 07 p1098 A66-17743  
Time dependent fluctuations in photoconductivity of Cu doped low ohmic n-type gallium arsenide exposed to IR radiation 07 p1099 A66-17876  
Flame as source of emission of visible UV and IR radiation and ionization source for certain combinations of fuels and oxidants 08 p1317 A66-18856  
IR fluctuations radiated by fluid mechanical turbulence of hot shear layers analyzed, assuming gas mixture is black body [AIAA PAPER 66-107] 08 p1206 A66-18955  
Radiometersonde observations of atmospheric IR irradiance, noting measurement results with improved equipment 09 p1369 A66-19869  
Relation between ascending fluxes of Earth and troposphere long-wave IR radiation and temperature of mean energy level 09 p1398 A66-19889  
Handbook of geophysics and space environments, 1965 09 p1370 A66-20267  
IR radiation source, characteristics, transmission and detection, noting atmospheric absorption and emission, IR celestial backgrounds, etc 09 p1371 A66-20277  
Monograph on microwave and IR techniques to investigate plasmas 09 p1402 A66-20328  
Spectroradiometric pyrometry of shock heated gases by IR emission and absorption measurements 09 p1382 A66-20508  
Stationary IR quenching of photocurrent in CdS, discussing recombination channels 09 p1428 A66-20538  
IR and sub-mm wave modulation using free carrier absorption in p-n junction, examining reverse and forward-biased configurations 09 p1432 A66-20972  
Angular distribution of IR radiation of Earth and atmosphere from rocket and balloon sounding 09 p1376 A66-20997  
Angular and spectral distribution of IR radiation emitted by Earth 09 p1376 A66-20998  
IR radiation in upper atm layers investigated by rocket and balloon, noting solar radiation effect 09 p1377 A66-21000  
Interpretation of outgoing IR radiation data from meteorological satellites, including cloud cover identification and Earth surface temperature 10 p1525 A66-21046  
Variation of IR emission from Mars surface with Mars local time in terms of diurnal temperature variations, including atmosphere effect, results suggest low thermoconductivity 10 p1604 A66-21201  
Bipolar excitation of photoconductivity in silicon due to structural disarrangement caused by IR radiation 10 p1583 A66-22019  
IR cooling rate in planetary atmospheres,

noting Curtis-Godson approximation, Doppler line shape, water vapor rotation band, etc 11 p1695 A66-22264  
He-Ne laser IR radiation emission attenuated by atmospheric methane 11 p1657 A66-23090  
Text on engineering radiation heat transfer emphasizing IR energy 12 p1977 A66-23655  
IR radiation effect on photovoltaic effect in cadmium sulfide excited by visible light 12 p1927 A66-23772  
IR applications to reliability assessment, stress analysis, testing, etc, of electrically energized components, thermally or by power dissipation 12 p1842 A66-24671  
Field emission of germanium alloyed with silver and irradiated with IR 13 p2160 A66-25108  
IR emission and electrical resistivity measurements of TA 2000 plasma by interference spectrometer 13 p2138 A66-25124  
Microwave absorption in compressed carbon dioxide between 150 and 300 gc measured, detecting no losses at 150 gc 13 p2021 A66-25383  
IR laser radiation with power of 5.7 watts in vicinity of 10.69  $\mu$ m in sealed tube containing pure carbon dioxide excited by AC or DC current 13 p2131 A66-25410  
IR radiation measurement from Earth-space transition region /project TACITE/ 13 p2192 A66-25498  
IR radiation deficiency of Sun determined by interferometric measurement of solar spectrum 13 p2182 A66-25572  
Atmospheric absorption in IR region, noting effects of water vapor, ozone, carbon dioxide and collision-induced dipole moments 13 p2075 A66-26603  
Simultaneous IR emission and auroral X-ray observations from high altitude balloon flights 14 p2376 A66-27399  
Concepts, symbols, units and nomenclature for transmission of radiant flux through Earth /variable density/ atmosphere 14 p2335 A66-27776  
IR radiation from interstellar grains, measuring intensity as wavelength function and radiation polarization for information on grain temperature and composition and galactic magnetic fields 14 p2377 A66-28122  
Two ohmic electrodes or one ohmic and one barrier electrode for current-voltage stable-negative characteristic of cadmium sulfide, noting IR radiation effects 14 p2368 A66-28249  
IR radiation from gallium arsenide prepared with ohmic contacts and excited by various nanosecond pulses, noting radiation above Gunn effect instability region 15 p2561 A66-28688  
Vacuum spectrometer measurement of absorption band of atmospheric water vapor 15 p2542 A66-29346  
IR transition zone between Earth and space studied by gyro-stabilized satellite 15 p2494 A66-30048  
Possible use of IR radiation to improve visibility through fog, including atmospheric attenuation effects and radiant energy source 16 p2740 A66-30088  
Fundamental vibration spectrum of HD in liquid argon, noting rotation-translation coupling, quantized translational energy levels and perturbation treatment of interaction 16 p2645 A66-30120  
Field emission of germanium alloyed with silver and irradiated with IR 16 p2771 A66-30287  
Radiative flux divergence for lower few centimeters of atmosphere, accounting for combined effects of water vapor, particle absorption and scattering 16 p2699 A66-31640  
Integrating sphere for IR noting efficiency parameters construction, application, etc 17 p2958 A66-32626  
Perturbation approach to IR absorption in p-type semiconductor with zincblende or zinc telluride structure 17 p2982 A66-32971  
Far IR radiation detected at visible frequency, using nonlinear optical mixing with lasers 17 p2959 A66-33322  
IR emitting flares, examining major parameters governing methods of analysis and performance 18 p3135 A66-34192  
IR measurements on eclipsed Moon,

discovering hot spots on lunar surface 19 p3457 A66-354  
Tiros IV atmospheric IR radiati measurements and application to weather analysis, using quasi-global synoptic maps troposphere relative 19 p3393 A66-356  
humidity 19 p3393 A66-356  
Intensity and center-to-limb variation continuous solar spectrum for several models of chromosphere 20 p3650 A66-373  
Vacuum spectrometer measurement absorption band of atmospheric water vapor 20 p3602 A66-373  
IR radiation absorption in imperfect ion crystals 21 p3802 A66-393  
IR and microwave radiations associated with current controlled instability /negative resistance/ in GaAs, noting Gunn threshold and V-I characteristics 21 p3802 A66-393  
IR absorption, reflectivity and transmission in n-type gallium arsenide single crystals at room temperature due to impurities at high carrier concentration 21 p3805 A66-393  
Spontaneous-emission probability and absolute intensity for IR absorption band of nitrous oxide 22 p3947 A66-393  
IR fluctuations radiated by fluid mechanical turbulence of hot shear layers analyzed, assuming gas mixture is black body [AIAA PAPER 66-107] 22 p3899 A66-402  
Statistical correlation of IR cooling measurements by Tiros II /Channel 2 and Channel 4/ and radiometersonde measurements of radiation divergence within atmospheric layers 22 p3944 A66-402  
Radiant energy transfer below cloud cover in Venus atmosphere, noting greenhouse effect caused by atmosphere containing components capable of IR absorption 22 p3980 A66-402  
Monograph on absorption, scattering and attenuation of light and IR radiation in atmosphere 23 p4087 A66-412  
**INFRARED REFLECTION**  
Dispersion theory and multilayer structure approximation of IR reflectivity semiconductor with n on n plus stratified structure 05 p0736 A66-142  
IR spectral reflectance of some common minerals and use in identifying extraterrestrial surfaces 09 p1402 A66-20972  
Heavily doped semiconductor parameters determined from spectral behavior coefficient of reflection and transmission 14 p2357 A66-270  
Heat treatment effect on IR reflectivity of heavily doped n-type silicon 17 p2988 A66-333  
Radio measurements of Moon, particularly IR, showing brightness-temperature maps new, half-and full Moon 19 p3458 A66-356  
Heavily doped semiconductor parameters determined from spectral behavior coefficient of reflection and transmission 22 p3966 A66-402  
**INFRARED SCANNER**  
Nonuniform cooling of lunar surface detected by IR scanning during totality eclipse 02 p0285 A66-113  
Multilayer circuit board defect detection and repairing using computer-controlled radiometer 04 p0498 A66-142  
Continuous moving-scene display system for output of airborne mapping sensors such as radars, microwave radiometers and scanners 06 p0878 A66-159  
Fast scanning IR microscope for semiconductor evaluation used for engineering design analysis, reliability improvement, failure analysis, etc 12 p1843 A66-246  
High resolution IR scanning system a vidicon automatic picture transmission Nimbus II and ground station print instrumentation 21 p3821 A66-393  
Geometric analysis of recordings by scanners, emphasizing significance of stereo imagery 24 p4210 A66-422  
**INFRARED SPECTROMETER**  
Superhigh speed IR spectrometers used for detection and study of free radicals in photochemical reaction, pulse discharges gases, etc 05 p0685 A66-158  
Littrow-type IR spectrometer with diffraction grating 14 p2292 A66-273  
Contaminating effect of water vapor



Optical path of spectrometer on measurements of stratospheric water vapor absorption 15 p2530 A66-28601  
 Transmits 1 to 5 chemical composition and far transmittance measured by vacuum radiating spectrometer 15 p2524 A66-28847  
 Atmospheric temperature profile determination by satellite-borne IR spectrometer, noting instrument design 18 p3113 A66-34556  
 Airborne IR system to detect temperature discontinuities characterizes some forms of near air turbulence /CAT/ (AIAA PAPER 65-459) 19 p3360 A66-36482  
 Near IR two-beam interferometer built for astronomical observations by Fourier transform spectroscopy, noting resolution of spectra of Venus and Mars 20 p3556 A66-36939  
 Optical determination of hole concentration dependence in p-type silicon semiconductors measuring absorption coefficients 21 p3798 A66-38765  
**INFRARED SPECTROPHOTOMETER**  
 IR spectrophotometry of Moon and Jovian satellites of Jupiter, noting surface properties, thermal radiation and albedo increase with wavelength 08 p1298 A66-19458  
 Laboratory method for determining spectral emittance of partially transparent materials in IR 09 p1380 A66-20362  
 Terrestrial thermal radiation field from IR diffraction scanning spectrophotometer aboard Cosmos XLV 09 p1376 A66-20995  
 Optimum wavelength intervals for surface temperature radiometry from total reflectance measurement of common surface minerals 15 p2498 A66-28833  
 Rapid remote sensing method using IR spectrum matching for determining material composition from both terrestrial and extraterrestrial sources 18 p3111 A66-34013  
 Polarization and visible and IR reflectivity studies of Mars indicate that hematite is stable form on Martian surface 18 p3228 A66-34016  
 IR spectrophotometry of Moon and Jovian satellites of Jupiter, noting surface properties, thermal radiation and albedo increase with wavelength 18 p3232 A66-34487  
 Laboratory method for determining spectral emittance of partially transparent materials in IR 19 p3353 A66-35320  
 Chlorine trifluoride analysis using combination of gas chromatography and IR spectrophotometry, noting column containing dichloroethylene 23 p4032 A66-41239  
 Nondestructive detection technique of phosphosilicate layer on semiconductor wafers, using IR spectrophotometer 24 p4181 A66-42390  
**INFRARED SPECTROSCOPY**  
**A RAMAN SPECTROSCOPY**  
 Survey of IR measurement techniques and computational methods in radiant heat transfer (AIAA PAPER 65-657) 01 p0162 A66-10598  
 Mechanical and electro-optical parameters for some acetylene derivatives evaluated from IR spectra 01 p0109 A66-11004  
 IR spectroscopic instrument modifications and innovations, noting filter grating permitting measurement in far IR 02 p0230 A66-11794  
 Electrical, IR property measurements and annealing experiments on electron-irradiated oxygen doped germanium 04 p0562 A66-13747  
 Far IR observation of plasma emitted radiation and observation of plasma effect in propagation of externally generated radiation 04 p0522 A66-14196  
 IR spectroscopy to determine constant of self-combination of donor acceptors of protons in dilute solution 08 p1257 A66-18645  
 Mechanical and electro-optical parameters for some acetylene derivatives evaluated from IR spectra 09 p1404 A66-19942  
 Line-of-sight IR spectral temperature profile measurements in inhomogeneous hot gases 09 p382 A66-20505  
 Transmission of IR radiation from flames through various carbon dioxide wavelengths 09 p1471 A66-20509  
 IR spectroscopic observations with balloon-borne telescope, Stratoscope 10 p1603 A66-21108

IR absorption spectrum of local H-ion oscillations in KCl crystals doped with Na, Rb, Cs, I, Br and F 10 p1588 A66-22158  
 Vanadium oxide bands in near-IR spectra of three Mira stars 13 p2182 A66-25578  
 Humidity attenuation in 8 to 13 micron IR window used in radiance measurement from orbiting satellite 15 p2531 A66-28848  
 Efficiency of radiation sources in IR gas analyzer 16 p2706 A66-30849  
 Liquid oxygen purity control for onboard breathing equipment by IR absorption spectrophotometry and gas chromatography 17 p2866 A66-32233  
 Chemical bonds between rare earth metals and nitrate radicals in lanthanum, gadolinium and yttrium nitrates studied from IR absorption spectra 18 p3063 A66-33842  
 Survey of IR measurement techniques and computational methods in radiant heat transfer (AIAA PAPER 65-657) 19 p3477 A66-35595  
 IR absorption spectrum of local H-ion oscillations in KCl crystals doped with Na, Rb, Cs, I, Br and F 19 p3440 A66-35772  
 Electrolysis of wet hydrogen fluoride, noting analysis of anode products by gas chromatography and water content measurement by IR spectroscopy 23 p4118 A66-41236  
 Spectroscopy of IR emission and laser oscillation resulting from transient population inversions on electronic transitions in molecular nitrogen 24 p4221 A66-42550  
**INFRARED SPECTRUM**  
**SA NEAR INFRARED**  
 Soviet electronic telescope, indicating possibility of noneclipse observation of coronal lines in IR band 01 p0137 A66-10456  
 Oxygen impurity atom interaction with radiation-induced defects in germanium over wide temperature range, producing optically active oxygen defect complexes 02 p0272 A66-11486  
 IR-active lattice vibrational spectra of alpha-aluminum oxide and chromium oxide analyzed by reflection and transmission measurements 03 p0380 A66-12341  
 IR absorption spectra of aluminum and boron doped semiconducting synthetic diamonds 03 p0411 A66-13145  
 IR and UV absorption spectra of free radical NCN observed following photolysis of matrix isolated cyanogen nitride 04 p0473 A66-13644  
 Impurity concentration on semiconductor surface observing photoconductivity of silicon in IR region of spectrum 04 p0569 A66-14356  
 Tellurium alloyed impurity on IR absorption spectrum in n-type gallium arsenide 04 p0569 A66-14360  
 Absorption spectrum sidebands for quasi-local oscillation in KCl-H crystals 05 p0730 A66-14648  
 Unified refractive index and dispersion equations for IR materials in high speed computer calculations 05 p0715 A66-14922  
 IR spectral reflectance of terrestrial atmosphere including ground cover effect, noting data from airborne equipment and instrumented rocket 05 p0669 A66-14947  
 Stain film of chemical species formed by gas phase reaction on silicon 05 p0736 A66-14978  
 IR spectrum of clavacin structure 05 p0629 A66-15107  
 Measurement of surface emittance of surface coatings for selected metals, providing low-thermal emittance characteristics in IR spectrum for thermal and corrosion control (AIAA PAPER 66-18) 05 p0705 A66-15849  
 Fine structure exhibited by near IR absorption and emission spectra of copper ions in ZnS and CdS crystals recorded at low temperatures 05 p0742 A66-15874  
 Internal and vibrational partition functions of carbon dioxide and rotational line intensities arising from transitions from ground and first excited states 06 p0907 A66-15945  
 Kinetics of HF decomposition in HF mixtures behind incident shock waves over various temperature ranges, using IR emission 06 p0941 A66-16127

Free radical CCO spectroscopy when produced by vacuum UV photolysis of matrix isolated carbon suboxide 06 p0821 A66-16128  
 Silicon recombination radiation, describing long wave IR radiation effect and photon energy gain via conversion into short wave radiation 06 p0924 A66-16515  
 Changes in ordinary refractive index and birefringence of gallium sulfide and gallium selenide as function of wavelength for visible and near IR at low temperatures 06 p0929 A66-16940  
 Theoretical model of isolated Lorentz line of IR absorption by gases applied to atmospheric optics and spectroscopy problems 08 p1248 A66-19307  
 Beer and square root law compared in relation to use for atmospheric extinction correction in IR spectrum 09 p1372 A66-20292  
 Silicon recombination radiation, describing long wave IR radiation effect and photon energy gain via conversion into short wave radiation 09 p1431 A66-20896  
 Raman scattering and IR absorption spectra of gaseous, liquid and crystalline benzoyl benzoic acid and O-and M-toluic acids 09 p1339 A66-20941  
 Vertical water vapor distribution to determine absorption function from high altitude measurements of solar IR radiation spectrum 09 p1375 A66-20942  
 Nimbus I IR scanning radiometry for nocturnal imagery of clouds and other data, IR spectral returns and relation to image gray scale 10 p1531 A66-21519  
 IR absorption spectra of oxygen-defect complexes in irradiated silicon 10 p1581 A66-21737  
 Vanadium pentoxide-boron oxide-lead oxide system IR absorption spectra and electroconductivity 10 p1582 A66-21917  
 Broadening of IR absorption lines by HF local oscillations attributed to either modulation effects or decay processes 10 p1588 A66-22162  
 IR spectral study of water deficiency in S stars and water abundance variation with Mira phase 11 p1771 A66-22771  
 Spectral emissivity measurements of carbon dioxide at high temperatures 11 p1738 A66-22870  
 Conductivity effective-mass of holes of gallium arsenide crystals with various hole concentrations determined from frequency dependence of spectral reflectivity in IR 12 p1928 A66-23942  
 Spectral and vertical distribution of atmospheric IR radiation flux divergence for five model atmospheres, noting dependence on sighting angle 12 p1874 A66-24868  
 InAs laser emission, discussing radiative transitions, coherent emission from InAs diodes, recombination mechanisms in IR radiation spectra, etc 13 p2089 A66-25065  
 Panoramic facsimile camera providing IR and visible spectrum imagery designed for unmanned space operation, noting construction, weight, etc 13 p2077 A66-25236  
 IR reflection spectrum of Jupiter from second flight of Stratoscope II, discussing deep absorption features 13 p2184 A66-25619  
 Normal emittance, reflectance and transmittance spectra of roughened rock and mineral surfaces from 8 to 25 micron wavelengths 13 p2017 A66-25873  
 Absorption spectrum sidebands for quasi-local oscillation in KCl-H crystals 13 p2167 A66-25923  
 Solar near-IR scattering by sunlit terrestrial clouds as affected by cloud type, altitude and scattering angle 13 p2073 A66-25989  
 Effect of longitudinal magnetic field on output power of gas laser operating in IR spectrum, noting gas-mixture pressure in discharge tube role 14 p2307 A66-27156  
 Transmission and reflection coefficients of semiconductors and insulators for use in visible and IR spectral regions 14 p2334 A66-27334  
 Laser oscillator study of coherent stimulated emission of IR transitions in rare gases 14 p2308 A66-27336  
 Effect of radiative sound absorption in atmosphere, calculating absorption due to radiation by water vapor in far-IR rotation



spectrum 14 p2334 A66-27659  
Faraday effect in rare earth garnet ferrites and metallic ion  $g$  values in IR spectrum 14 p2364 A66-27703  
Characteristic spectral information obtained from surface of fine particles if spectrum is observed at high SNR or particles are compacted 14 p2335 A66-27809  
Reflection spectra of rock powders compared with Stratoscope II spectrum of Mare Tranquillitatis 14 p2386 A66-28126  
Impurity concentration on semiconductor surface, observing photoconductivity of silicon in IR region of spectrum 14 p2368 A66-28254  
Tellurium alloyed impurity on IR absorption spectrum in  $n$ -type gallium arsenide 14 p2369 A66-28258  
Vertical water vapor distribution to determine absorption function from high altitude measurements of solar IR radiation spectrum 15 p2483 A66-28530  
Outgoing Earth and atmospheric radiation observed in IR spectrum at various altitudes by geophysical balloons and rockets 15 p2483 A66-28739  
Optical properties and thermal behavior of new absorption bands in oxygen doped silicon irradiated at low temperatures 15 p2564 A66-28874  
Cloud top heights and areal coverage obtained from satellite IR measurements, noting error estimation and effect of cloud size on accuracy 15 p2485 A66-28938  
IR spectral reflectance of water frost and solid carbon dioxide 15 p2501 A66-28977  
IR absorption of arsenic monoselenide 15 p2565 A66-29198  
IR absorption spectrum of neutron bombarded silicon 15 p2565 A66-29202  
Optical harmonic generation in IR in zinc blende, hexagonal and trigonal crystals, using unfocused carbon dioxide laser in CW and Q-switched operation 16 p2716 A66-30182  
Surface IR photoconductivity spectra of chemically etched  $p$  and  $n$  silicon, noting energy distribution, activation energies of centers, etc 16 p2788 A66-31774  
Low noise photodiodes with avalanche multiplication for high sensitivity, noting capability for low intensity wideband signal detection, performance in IR region, etc 17 p2880 A66-31934  
Phosphorus I lines identified in lambda greater than 2935 region of solar spectrum with aid of tables of Fraunhofer lines 17 p2999 A66-32267  
IR absorption of arsenic monoselenide 17 p2982 A66-33047  
IR absorption spectrum of neutron bombarded silicon 17 p2982 A66-33051  
Profile and center-to-limb variation of IR helium I triplet at 10,830 angstrom photoelectrically observed in spectrum of undisturbed solar disk 18 p3237 A66-35045  
Broadening of IR absorption lines by HF local oscillations attributed to either modulation effects or decay processes 19 p3441 A66-35776  
Silicon IR absorption spectra at various wavelengths before and after irradiation with neutron fluxes 19 p3442 A66-35821  
Theoretical model of isolated Lorentz line of IR absorption by gases applied to atmospheric optics and spectroscopy problems 19 p3400 A66-36043  
Vibrational spectrum of liquid, solid and gaseous tetradeuterated hydrazine and Raman study of hydrogen bonding in hydrazine 19 p3295 A66-36801  
Detectability of coronal IR lines due to Mg, Al and Si ions with practicable IR spectrometers and photoconductive detectors, considering atmospheric attenuation 20 p3649 A66-37333  
Coherent radiation generation in IR region by nonlinear optics 20 p3582 A66-38429  
Coherent radiation generation in IR region by nonlinear optics 21 p3746 A66-38962  
Birefringence of certain crystals sufficiently large to allow collinear backward wave interaction of three electromagnetic waves with signal frequency tunable over large portion of IR spectrum 21 p3771 A66-39113  
Temperature dependence of integral

absorption and band half-width in IR spectra of methyl and ethyl siloxanes 21 p3802 A66-39160  
High frequency-stability EM wave source, applying thermal excitation methods to pencil quantum generator in IR region 21 p3749 A66-39336  
High frequency-stability EM wave source, applying thermal excitation methods to pencil quantum generator in IR region 22 p3929 A66-39706  
IR I and visual V magnitudes of comet Ikeya-Seki determined, using photoelectric measurements 22 p3977 A66-39863  
Helium atoms in 2P level contribute to formation of excited helium molecules in positive column of DC discharge, noting IR portion of pumping radiation is responsible for enhancement of molecular population 22 p3950 A66-39918  
IR absorption band growth and decay in spectra of oxygen-doped Si irradiated with fast neutron 22 p3962 A66-40085  
Spectral and vertical distribution of atmospheric IR radiation flux divergence for five model atmospheres, noting dependence on sighting angle 22 p3912 A66-40329  
New absorption bands in near IR spectrum of Mars found by Fourier spectroscopy via carbon dioxide absorption measurements 22 p3981 A66-40486  
IR active localized vibrational modes absorption in lithium and copper compensated silicon doped gallium arsenide 24 p4251 A66-42298  
Brightness variation from center to limb for Sun in submillimeter and IR range calculated from some available models of solar atmosphere 24 p4278 A66-42708  
Photodetectors capable of microwave modulation frequency response operating in visible or near IR portion of optical spectrum 24 p4212 A66-42808  
Effect of longitudinal magnetic field on output power of gas laser operating in IR spectrum, noting gas-mixture pressure in discharge tube 24 p4225 A66-42977  
Light emission in near IR by semiconducting GaAs under current oscillations caused by electron-phonon coupling 24 p4258 A66-43000

## INFRARED TRACKING

Packaging design of electronics portion of missiles IR tracker 13 p2040 A66-25841  
IR trackers, discussing method of operation, performance characteristics and application 13 p2025 A66-25983  
Propellant rocket exhaust plume effect on error calculation for radiation balance IR tracker 18 p3240 A66-33798

## INFRASONIC FREQUENCY

LF and infrasonic noise effects on mans cardiac rhythm, hearing, vision, motor control, spatial orientation, speech and subjective tolerance 07 p0999 A66-17656  
Propagation modes of infrasonic waves in isothermal atmosphere with constant horizontal winds and under effect of gravity 17 p2959 A66-33032  
Infrasonic frequency spectrum transformation using magnetic signal recording and reproduction 21 p3713 A66-39322

## INHOMOGENEITY

High field magnetoresistance and random inhomogeneities in arsenic- or antimony-doped  $n$ -type germanium 12 p1931 A66-24805  
Random phase approximation of electron conductivity of turbulent plasma and effects of random static inhomogeneities 13 p2149 A66-26245  
Galerkin vector for elastodynamic problem of isotropic inhomogeneous body 16 p2823 A66-31707  
Overall elastic moduli of inhomogeneous system composed of various solid phases firmly bonded together at arbitrary concentration 17 p3029 A66-32791  
Resistivity of semiconductors with periodic inhomogeneity, noting cases of surface perpendicular and surface parallel stratifications 18 p3155 A66-34229

## INITIAL VALUE PROBLEM

Buckling mechanism for uniform external pressured spherical shell, evaluating transcendental functions via solution of initial value problem 03 p0435 A66-12616

Spectral dynamics of laminar convection, discussing transformation of Benard convection problem into spectral domain 04 p0599 A66-144  
Unique solvability of certain initial boundary problems with equations of mixed type 05 p0727 A66-153  
Initial value problem for Boltzmann-Vlasov and Poisson equation for one-dimensional plasmas 06 p0915 A66-161  
Optimal estimation of initial conditions for numerical prediction 07 p1055 A66-173  
Slow decay of solution of initial boundary value problem for wave equation unbounded region 07 p1059 A66-179  
Landau solution of plasma oscillation problem, discussing dielectric function Lorentzian distribution and cut-off distribution 08 p1260 A66-185  
Nonlinear weather prediction by optimum method of control theory for combining past forecasts with current observations 08 p1248 A66-193  
Geometric program for processing penetrating cosmic ray shower data, consisting of individual track processing at initial point location 09 p1441 A66-202  
Convergence of numerical solutions of OI initial value problems 09 p1394 A66-208  
Initial value problem of converging shock wave propagation in quiescent gas variable density 10 p1521 A66-212  
Stability of baroclinic circular vortex incompressible inviscid fluid for axisymmetric disturbances 10 p1530 A66-212  
Approximate solution of initial boundary value problems involving heat conduction inhomogeneous and anisotropic media 10 p1620 A66-213  
Dependence of hyperbolic equations apex of characteristic cone on initial functions 10 p1551 A66-219  
Initial conditions determination in aircraft takeoff from mobile platform required for solution of differential equations of motion of gravity center 11 p1734 A66-233  
General solution for class of initial value problems for systems of aerodynamic equations, constructing reference solution Cauchy problem involving shock wave expansion waves 11 p1694 A66-233  
Northward momentum transfer across asymmetric jet in three-dimensional atmosphere analyzed, using initial value problem, noting energy transfer across transformation 13 p2064 A66-261  
Cauchy problem of first-order nonlinear partial differential equations 13 p2121 A66-265  
Initial value problem for Navier-Stokes equation 14 p2273 A66-269  
Decay of solutions of initial boundary value problem for hyperbolic equations unbounded regions 14 p2322 A66-276  
Linear initial value problems involving first order differential equations transformed into higher order systems and treated boundary value problems, using numerical techniques 15 p2529 A66-297  
Multidimensional generalized transport equations solutions and calculation difference methods 16 p2732 A66-302  
Gurtin variational principles characterizing linear elastodynamics initial value problem extended to dynamic viscoelasticity theory 16 p2813 A66-302  
Short-range forecasting of stratified cloudiness, noting linear dependence between variations in dew point and air temperature near Earth surface for aperiodic processes 16 p2742 A66-307  
Cause and effect interdependence in line system, noting distribution theory ar double Laplace transform 16 p2670 A66-310  
Nonlinear system position in phase space determined from approximate solution integral equations yielding initial values 16 p2748 A66-315  
Initial value problem for small amplitude wave perturbations solved on zon atmospheric flow with constant vertical shear and vanishing temperature lapse rate 16 p2699 A66-316  
Textbook on numerical solution of initial value problems and approximate numerical integration 17 p2948 A66-334  
Initial boundary value problems involving Maxwell equations in isotropic media solved



merically 18 p3065 A66-33533  
 Partial differential equation describing  
 transient conduction in multidimensional  
 homogeneous media solved by method  
 based on use of known boundary  
 conditions 18 p3262 A66-34380  
 Dependence of hyperbolic equations in  
 hex of characteristic cone on initial  
 functions 19 p3389 A66-36184  
 Wellerstrass necessary condition and basic  
 equations for optimal control of initial or  
 boundary states of continuum mechanical  
 HD and hypersonic partial differential  
 systems 20 p3535 A66-36853  
 Asymptotic behavior of solutions to  
 boundary value and initial problems for ODE  
 with small parameter, using functions of  
 lower law boundary layer 20 p3590 A66-37109  
 Convergence of difference approximations  
 rectangular grids for general first-order  
 quasi-linear hyperbolic initial value problems  
 two independent variables 20 p3590 A66-37526  
 Comparison variables transformation of  
 linearized perturbation initial value  
 problems for nonlinear ordinary first-order  
 differential equation 21 p3756 A66-38817  
 Asymptotic time behavior of longitudinal  
 waves in one-dimensional plasma of  
 relativistic electrons and stationary ions  
 studied, using collisionless Boltzmann  
 equation 21 p3775 A66-39189  
 Initial value problem solution variation  
 linearized by simple transformation 21 p3758 A66-39273  
 Dynamic behavior of soap film stretched  
 between two coaxial rings, assuming  
 potential energy of this surface to be  
 proportional to surface area 21 p3772 A66-39353  
 Implosion experiment, discussing methods  
 for detonation and shock wave propagation  
 phase calculation 21 p3837 A66-39503  
 Cauchy problem of first-order nonlinear  
 partial differential equations 22 p3939 A66-40439  
 Book on numerical processes in differential  
 equations including initial value and  
 boundary value problems 22 p3941 A66-40620  
 Difference assessment between secular and  
 long period perturbations generated by  
 similar initial conditions for celestial  
 mechanics problems 22 p3985 A66-40959  
 Parameters of dynamic systems described  
 by PDEs determined by replacing PDE with  
 integral equation and eliminating via  
 recursion process terms resulting from  
 initial and boundary conditions 23 p4084 A66-41396  
 Radiation and propagation of  
 electromagnetic waves, noting solution to  
 initial value problem for moving point  
 source in infinite homogeneous  
 medium 23 p4040 A66-41635  
 Existence of new isolating integral in  
 restricted three-body problem, computing  
 orbits for various parameter values and  
 initial conditions 24 p4272 A66-42202  
 Vibrations of systems governed by  
 nonlinear partial differential equations  
 analyzed by perturbation method 24 p4236 A66-42267  
 Weak and strict solution existence theorem  
 for initial-boundary value problem for  
 nonlinear hyperbolic equation in relativistic  
 quantum mechanics 24 p4237 A66-42829  
 INITIATION  
 6 GENERATION  
 6 INDUCTION  
 6 STARTING  
 INJECTION  
 6A BLOWING  
 6A CARRIER INJECTION  
 6A FLUID INJECTION  
 6A FUEL INJECTION  
 6A GAS INJECTION  
 6A ION INJECTION  
 6A LIQUID INJECTION  
 6A SECONDARY INJECTION  
 Energetic neutral hydrogen atom injection  
 into ECP in magnetic mirror and plasma  
 shielding against trapped thermal neutral  
 gas 19 p3422 A66-36547  
 Injection electroluminescence in AlAs-GaAs  
 p-n junction diodes of graded energy  
 gap 24 p4251 A66-42300  
 INJECTION LASER  
 6 CHEMICAL LASER

INJECTOR  
 SA PUMP  
 Two propellant injector designs for plasma  
 accelerators that minimize or avoid bearing  
 seal difficulty, using piezoelectric element  
 and pulsed vaporization of filament of liquid  
 conductor [AIAA PAPER 66-241] 12 p1936 A66-24519  
 INJUN I SATELLITE  
 Injun I and III particle observations  
 discussing methods and results on fast  
 electrons, particle counters, energy  
 separation, spectra, flux variation, angular  
 distributions, etc 03 p0363 A66-12647  
 Particle precipitation measurements with  
 Injun satellites, discussing space and time  
 variations of electron precipitation, trapped  
 Van Allen particles and auroral light  
 emission latitude distribution 03 p0363 A66-12648  
 Temporal stability of inner zone protons  
 determined by Injun I satellite  
 measurements in vicinity of South Atlantic  
 magnetic anomaly 20 p3638 A66-38311  
 INJUN III SATELLITE  
 Motions of geomagnetically trapped  
 particles and asymmetric configuration of  
 magnetospheric trapping region caused by  
 solar wind 01 p0060 A66-10159  
 Injun I and III particle observations  
 discussing methods and results on fast  
 electrons, particle counters, energy  
 separation, spectra, flux variation, angular  
 distributions, etc 03 p0363 A66-12647  
 Particle precipitation measurements with  
 Injun satellites, discussing space and time  
 variations of electron precipitation, trapped  
 Van Allen particles and auroral light  
 emission latitude distribution 03 p0363 A66-12648  
 Proton whistler observations from Injun III  
 VLF data, including spectrograms, time-  
 latitude-altitude graphs and  
 theory 08 p1217 A66-19392  
 Fractional concentration of hydrogen ions  
 in ionosphere from VLF proton whistler  
 measurement 08 p1218 A66-19393  
 Auroral zone electron flux and relation to  
 broadbeam radiowave  
 absorption 11 p1703 A66-23495  
 INJURY  
 SA BACK INJURY  
 SA CRASH INJURY  
 SA EJECTION INJURY  
 SA HEAT STROKE  
 SA NOISE INJURY  
 Choriorretinal lesion produced by pulsed  
 ruby laser beam and complex changes in  
 retinal excitability in cats 16 p2641 A66-31761  
 INLET  
 S AIR INLET  
 S CONICAL INLET  
 S HYPERSONIC INLET  
 S SUPERSONIC INLET  
 INLET FLOW  
 Behavior of unassisted annular cowed  
 compressor intakes under cross-flow  
 conditions [AIAA PAPER 65-707] 01 p0130 A66-10945  
 Axial compressors with nonuniform inlet  
 flow, investigating size of gap between  
 blade rows and rotating stall 01 p0008 A66-10953  
 Inlet region of laminar meridional flow in  
 arbitrarily shaped narrow gap between two  
 axisymmetrically formed walls 02 p0217 A66-11585  
 Entrance region Newtonian flow analysis in  
 tube of circular cross section for possible  
 use in viscometry and flow stability studies  
 [AICE PREPRINT 19D] 04 p0511 A66-13935  
 Characteristics of jet ejector with faired  
 inlets as augmenters treated by continuity  
 and momentum equation 04 p0456 A66-14388  
 Unsteady state heat transfer with flowing  
 fluid through porous solids [ASME PAPER 65-HT-10] 05 p0782 A66-14736  
 Diffusion in supersonic duct flow composed  
 of boundary layers, with application to  
 hypersonic inlet with internal compression  
 [AIAA PAPER 64-245] 05 p0606 A66-15071  
 Pressure drop in entrance region of abrupt  
 inlet circular tube for continuum laminar  
 flow conditions [ASME PAPER 65-WA/APM-5] 05 p0663 A66-15428  
 Laminar heat transfer in inlet tube,  
 determining velocity and temperature

distribution [ASME PAPER 65-WA/HT-36] 05 p0792 A66-15671  
 Influence of inlet flow profile  
 characteristics on diffuser static pressure  
 efficiency, achieving pressure increase if  
 flow has high decay rate 06 p0801 A66-16002  
 Inlet of XB-70 consisting of two separate  
 parts located under wing, each part  
 supplying air to three of six J-93  
 engines 07 p0987 A66-17278  
 Motion of particles of dispersed phase at  
 inlet to sampling probe analyzed for  
 application to two-phase medium  
 flow 07 p1031 A66-17417  
 Heat transfer in 20-inch hypersonic wind  
 tunnel to two-dimensional inlet ramp at  
 various angles of attack 08 p1318 A66-19147  
 Pressure drop in entrance region of abrupt  
 inlet circular tube for continuum laminar  
 flow conditions [ASME PAPER 65-WA/APM-5] 10 p1523 A66-21471  
 Losses in vaneless diffusers of centrifugal  
 compressors and pumps due to wall friction  
 and sudden expansion mixing at entrance  
 [ASME PAPER 65-FE-1] 10 p1540 A66-21504  
 Behavior of unassisted annular cowed  
 compressor intakes under cross-flow  
 conditions [AIAA PAPER 65-707] 10 p1594 A66-21890  
 Initial flow in entrance of straight circular  
 pipe computed as refinement of Atkinson  
 and Goldstein solution 12 p1867 A66-24980  
 Rarefied gas flow in hydrodynamic  
 entrance region of circular tube, noting  
 variation with density level, velocity profile  
 and pressure drop for developing  
 flow 13 p2070 A66-26713  
 Secondary flow in entrance section of  
 straight rectangular duct, measuring primary  
 and secondary velocities, turbulence, axial  
 component, Reynolds stress gradients,  
 etc 13 p2070 A66-26714  
 Long-life base load service at 1600 F  
 turbine inlet temperature, noting fuel-air  
 and temperature controls [ASME PAPER 66-GT-98] 14 p2372 A66-27000  
 Heat transfer rate in thermal inlet of  
 circular tube, describing experimental  
 apparatus and observational  
 results 14 p2411 A66-27313  
 Pressure drop for non-Newtonian flow in  
 inlet length of straight  
 channel 14 p2279 A66-28464  
 Two-dimensional flow of incompressible  
 conducting viscous liquid in inlet region of  
 straight channel under magnetic field,  
 obtaining flow characteristics 15 p2553 A66-29742  
 Velocity profile of incompressible and  
 electrically conducting flow in entrance  
 region of constant area MHD  
 channel 16 p2763 A66-31255  
 Turbine blades suitable for supersonic  
 relative inlet velocities and performance in  
 cascade 17 p2841 A66-32889  
 Flow characteristics, design and  
 performance data for subsonic two-  
 dimensional straight centerline diffusers  
 [ASME PAPER 66-FE-10] 17 p2915 A66-33264  
 Inlet/door performance characteristics of  
 VTOL lift-engines studied in full-scale wind  
 tunnel tests [AIAA PAPER 66-655] 18 p3048 A66-34222  
 Shock wave boundary layer interactions  
 and shear flow regimes in hypersonic inlet  
 flows [AIAA PAPER 66-606] 18 p3049 A66-34447  
 MHD flow with parabolic velocity at  
 entrance region of flat  
 channel 18 p3149 A66-34915  
 Supersonic compressor flow induction  
 process as affected by Mach number, cone  
 angle, rotational speed and blade angle  
 [AIAA PAPER 66-615] 19 p3275 A66-35943  
 Busemann inlet flow field calculation for  
 hypersonic speeds, considering internal-  
 compression inlet geometry and  
 performance 20 p3493 A66-38178  
 Bell-shape diffuser for rotationally  
 symmetrical flow 21 p3694 A66-38815  
 Slip flow in hydrodynamic entrance region  
 of tube and parallel plate channel  
 determined by solving linearized momentum  
 equation 21 p3730 A66-39459  
 Velocity distribution for inlet flow in finite  
 radial diffuser 21 p3731 A66-39591



Jet V/STOL aircraft inlet temperature rise caused by recirculation of hot exhaust gases in ground proximity [AIAA PAPER 66-740] 22 p3851 A66-40629

Dynamic test method for characteristics and interactions of supersonic aircraft propulsion systems, particularly inlet/engine performance and control compatibility aspects [AIAA PAPER 66-741] 22 p3893 A66-40630

Bluntness and boundary layer displacement effects on air breathing engine hypersonic inlet flow fields [AIAA PAPER 65-617] 23 p4007 A66-41109

Model determination of effects of injecting and mixing fuel in inlet diffuser of two-shock inlet hypersonic ramjet or scramjet [AIAA PAPER 66-648] 24 p4261 A66-42641

Pressure effects of flexible walls on boundary layer transition in turbulent pipe inlet flow 24 p4195 A66-42859

**INNER RADIATION BELT**

SA ARTIFICIAL RADIATION BELT

SA OUTER RADIATION BELT

SA VAN ALLEN BELT

Directional intensity of electron distribution of energies larger than 40 kev with respect to pitch angles in inner belt from Cosmos V data 06 p0951 A66-17172

Relay I satellite mapping of energy spectrum and spatial distribution of protons in inner radiation belt 08 p1283 A66-19396

Particle transfer across drift shells as basic mechanism of acceleration of protons and electrons in outer radiation belt and formation of inner radiation belt 09 p1444 A66-21023

Terrestrial radiation belt during solar minimum, noting results from measurement with Elektron satellite series 18 p3175 A66-34745

German-French high-altitude rocket measurement of inner radiation belt and artificial ion clouds at altitude of 2000 km 19 p3348 A66-36286

Latitude and longitude variation of count rate and intensity-time dependence of proton flux in inner radiation belt measured by Anton 302 G-M counter in Ariel I satellite 20 p3638 A66-38306

Acceleration of electrons in inner radiation belt by magnetic field variations over slope of geomagnetic anomaly in resonance with longitudinal drift frequencies of electrons 20 p3638 A66-38308

Energy spectrum of inner zone protons with conclusions drawn about source and loss mechanisms for protons in inner radiation zone 20 p3638 A66-38309

Temporal stability of inner zone protons determined by Injun I satellite measurements in vicinity of South Atlantic magnetic anomaly 20 p3638 A66-38311

Injection of protons into inner radiation belt caused by decay of fast cosmic ray albedo neutrons and superimposition of low-energy protons of unknown origin 20 p3639 A66-38318

**INORGANIC COMPOUND**

Radiation induced chemical decomposition in inorganic solids such as alkali metals and metallic sulfates 23 p4111 A66-41212

Radiolysis applied to effects of ionizing radiation on volatile inorganic compounds of fluorine, oxygen and nitrogen, noting mass spectrometric peaks 23 p4032 A66-41235

Wolf Trap Mars microorganism detection, assuming photosynthetic and respiration cycles in inorganic biochemical compounds 24 p4168 A66-42676

**INPUT**

Manual methods of entering navigational data on cards for input into computer 17 p2956 A66-33447

**INSECT**

S DROSOPHILA

**INSERT**

S NOZZLE INSERT

**INSERTION**

Radio interference control component RF characteristics and insertion loss measuring techniques 11 p1665 A66-22681

Synthesizing group of parallel-input filters while minimizing insertion loss and reflection coefficient 11 p1656 A66-23065

**INSULATION**

Utilization tests of nonradiating Francia cellular structures placed on spiral insulator

and heated to low and medium temperatures 22 p3852 A66-40247

**INSPECTION**

SA DETECTION

SA INFRARED INSPECTION

SA QUALITY CONTROL

SA X-RAY INSPECTION

NASA Quality Program for Space System Contractors /NPC 200-2/ serves as standard for quality control

Inspectors 03 p0373 A66-12628

Endoscopes in aviation noting role in inspection of wing interiors, power plants, etc 07 p1040 A66-18330

General family of two-stage chain sampling inspection plans 15 p2506 A66-28789

Numerical control for inspection of machine tools and parts 15 p2506 A66-28790

Inspection techniques for NASA, discussing control of supplier plants, Quality Requirements for Hand Soldering of Electrical Connections and personnel accountability 15 p2506 A66-28792

Maintenance and inspection of air transport vehicle structures 19 p3278 A66-35399

Planned inspection of hardware based on warning analysis, relation to improved cost effectiveness 20 p3569 A66-37921

**INSTABILITY**

SA COMBUSTION INSTABILITY

SA MAGNETOSPHERIC INSTABILITY

SA PLASMA INSTABILITY

SA SPUTTERING

SA TAYLOR INSTABILITY

SA THERMAL INSTABILITY

SA WHIRL INSTABILITY

Boltzmann equation for Gunn effect in GaAs, discussing scattering processes, unjustifiability of use of drifted Maxwell distribution, etc 10 p1583 A66-22067

Curve analysis of current instabilities including Gunn effect in n-type gallium arsenide 22 p3961 A66-40045

**INSTRUMENT**

SA TEACHING MACHINE

Instructional System model for meeting USAF maintenance technical training requirements for complying with weapon system requirements 23 p4030 A66-41578

**INSTRUMENT**

SA APPROACH AND LANDING

INSTRUMENT

SA ELECTROMAGNETIC INSTRUMENT

SA ELECTROSTATIC INSTRUMENT

SA FLIGHT INSTRUMENT

SA INFRARED INSTRUMENT

SA MAGNETIC INSTRUMENT

SA OPTICAL INSTRUMENT

SA RECORDING INSTRUMENT

SA SOLAR INSTRUMENT

Instruments and measurements, automatic control - International Conference, Stockholm, September 1964 16 p2706 A66-30879

**INSTRUMENT APPROACH**

Helicopter landing in zero-zero weather, describing experiment in England involving landing in dense fog 17 p2844 A66-32728

**INSTRUMENT ERROR**

Slab motions affecting test mounts for gyroscopes and accelerometers investigated at underground and surface test locations 01 p0051 A66-10029

Test pad stability measurement using two accelerometers and recording autocollimator 01 p0065 A66-10031

Technique for controlling logarithmic amplitude response /LAR/ and regulating logarithmic amplifiers under industrial conditions 01 p0035 A66-10219

Cryogenic problems in temperature and level sensing discussing thermocouples, resistance sensors, vapor and gas bulb thermometers and level gauges and probes 01 p0070 A66-10955

Calibration procedures and statistical analysis for error reduction in ballistic camera lead-screw type comparator 02 p0228 A66-11380

Reseau techniques application to cartographic photography to improve analytical procedures, reduce mensuration errors and aid in automating systematic corrections 02 p0228 A66-11382

Photographic pyrometer using variable-density filter noting temperature master curve, attenuation, calibration and error

sources 02 p0229 A66-115

Doppler radar performance in al navigation noting calibration error, dispersion, hole-altitude phenomena, etc 02 p0256 A66-118

Altimetry methods reviewed for altitudinal in 40,000 to 80,000 ft range, noting calibration and instrument accuracy 02 p0231 A66-119

Errors in Doppler system determination ground speed and improvement trends wider application 02 p0258 A66-120

Angular velocity and linear acceleration measurement by three mutually orthogonal rotating disks 03 p0369 A66-126

Nonlinear analog-to-digital converter for more constant accuracy 03 p0338 A66-129

Assured performance calibration discussion statistical quality control, instrument variability, vacuum tube and digit voltmeter histories, calibration costs etc 04 p0520 A66-139

Bead leakage affect on voltmeter discussing quality control measurement at thermal effects on electric equipment 04 p0521 A66-139

Use of two reference noise sources for measurement of effective noise temperature of conventional receiver system leads serious errors 04 p0484 A66-140

Heat conductivity measurement of solids determine exact values of experiment error 04 p0521 A66-141

Meridian astronomy methods including determination of instrumental error derivation of systems of right ascension and declinations and determining systematic errors 05 p0761 A66-150

Deformation calculation of RM-700 telescope mounting 05 p0680 A66-152

Geocentric pendular control for detection of direction of terrestrial field 05 p0713 A66-154

Effect of lateral refraction and therm conditions near Pavlov passage instrument on azimuthal position values and time measurement results 05 p0766 A66-154

Instrument errors in neutron monitor affected by contact oxide film 06 p0881 A66-166

Instrumental effects distorting data telescopically observed meteors analyzed simultaneously observation with various binocular telescopes and naked eye 07 p1135 A66-176

Checking and calibration of aircraft compasses, discussing compass base Dublin Airport and effect of lightning strikes 07 p1032 A66-176

Controlled direct current applied to flapper valve to stimulate rotation of aircraft compass swing 07 p1033 A66-177

Error of airborne Doppler navigational system 07 p1073 A66-177

Feedback transfer function analyzer for error reduction in performance measurement for servocontrol systems 07 p1016 A66-178

Indicator design for semiconductor strain gauges, discussing basic circuitry, calibration and stability 08 p1226 A66-195

Digital cross multiplication used in cross coupling and off-leveling errors in gravimetric measurements at sea 09 p1369 A66-198

Height measurement from Doppler navigation, examining accuracy of pressure altimeter 09 p1381 A66-204

Measurement error for pulmonary ventilation during sinusoidal vibration and correcting device consisting of time delay and summing circuit 09 p1335 A66-205

Microwave phase measurement technique using slotted-line interferometer for optimum accuracy 10 p1537 A66-2187

Manual control sextant sighting performance for space navigation, using simulated and real celestial targets 10 p1554 A66-2188

Errors of charged-particle analyzer, resulting from expansion of plasma beam within and without 11 p1744 A66-2245

Measurements of decay curves of stored Aitken nuclei with photoelectric nucleus counter show small nonrandom divergence from theoretical curves 11 p1707 A66-2309

Solar-diurnal cosmic-ray variations



- alyzed, showing that averaging  
observational data over worldwide network  
stations leads to large  
errors 12 p1943 A66-24183
- High altitude mesospheric temperature  
measurements, discussing air-to-sensor heat  
transfer mechanism, bead thermistor and  
ascend rate 13 p2124 A66-25256
- [IAA PAPER 66-388] 12 p1908 A66-24510
- Interplanetary trajectory adaptive  
gyrocompass system, discussing orbital  
angular velocity, angular acceleration, error  
sensitivity coefficients, error sources,  
etc 13 p2124 A66-25256
- Controlled direct current applied to flux  
drive to stimulate rotation of aircraft in  
compass swing 13 p2079 A66-25866
- Surface temperature measurement using  
thermocouples, noting error  
sources 13 p2081 A66-26221
- Accuracy of test device determining  
conductivity of semiconductor materials  
increased by using error calculation and  
design systematology 13 p2085 A66-26761
- Compensation for error resulting from  
inclination of frame of gyrocompass with  
elastic recovery moment, based on shifting  
gravity center along major  
axis 14 p2294 A66-27363
- Utilization of confidence interval concept  
for instrument calibration 14 p2296 A66-27818
- Reduction of measurement error in devices  
for testing semiconductors, employing  
mechanical techniques 14 p2297 A66-28132
- Gravimeter error in recording of Earth  
tides, examining levelling and calibration  
problems 14 p2298 A66-28400
- Time jitter due to inherent noise when  
sampling intervals in Fourier transform  
spectroscopy by interferometer, examining  
effects and elimination  
methods 15 p2499 A66-28849
- Errors in wind speed measurements under  
conditions of turbulence, noting quantitative  
aspects of lateral, vertical and data  
processing errors 15 p2533 A66-28940
- Random error estimation for Mach-Zehnder  
interferometer interference fringe  
measurements 15 p2502 A66-29383
- Potentiometric type pressure transducer  
optimization for low static error  
band 16 p2704 A66-30538
- Calibration and testing of temperature  
measuring devices in -200 to 3000 degrees  
16 p2704 A66-30632
- Symmetry measurements in  
communications device and systems, noting  
error 16 p2707 A66-31030
- Error determination in autonomous  
determination of coordinates, obtaining  
solution for kinematic equations of  
navigation in near-polar  
region 16 p2744 A66-31146
- Inertial components and systems evaluation  
with figures of merit for requirements,  
noting accelerometer errors, limiting  
response, etc 16 p2707 A66-31148
- Wire-to-surface heat transfer and error in  
hot-wire anemometer  
measurements 16 p2708 A66-31256
- Nonstationary aerodynamic load for  
harmonically oscillating body in fluid flow  
with constant mean velocity measured,  
determining errors as functions of system  
parameters 16 p2630 A66-31302
- Angular transducer using Hall effect,  
noting errors due to distortions in magnetic  
circuit and temperature  
effects 16 p2709 A66-31577
- Static errors in Hall effect multiplying  
devices 16 p2667 A66-31580
- Maximum absolute error of temperature  
measurements by means of standard  
platinum resistance  
thermometer 16 p2709 A66-31610
- Technique for controlling logarithmic  
amplitude response /LAR/ and regulating  
logarithmic amplifiers under industrial  
conditions 17 p2880 A66-31902
- Russian monograph on gyroscopic stabilizer  
theory and error  
assessment 17 p2925 A66-32567
- Inertial system testing and errors resulting  
from platform  
misalignments 17 p2928 A66-33460
- Propellant rocket exhaust plume effect on  
error calculation for radiation balance IR  
tracker 18 p3240 A66-33798
- Test pad stability measurement using two  
accelerometers and recording  
autocollimator 18 p3110 A66-33815
- Third-order orbital gyrocompass horizontal  
and vertical damping techniques to  
eliminate gyro and bias errors in horizon  
sensor 18 p3110 A66-33828
- Random and systematic errors in satellite  
trajectory computations 18 p3227 A66-33870
- Upper wind theodolite measurement error  
caused by ambiguous utilization of rate of  
climb of balloon 18 p3128 A66-33962
- Optical system for measurement of aerial  
profile accuracy of large parabolic reflector  
noting design principles, instrument  
composition and experimental  
results 18 p3113 A66-34276
- Energy measurement errors effect on  
characteristics of elementary  
interactions 18 p3140 A66-35168
- Constant current sources consisting of  
sealed ionization chambers for calibrating  
electrometers 19 p3357 A66-35809
- Signal processor recovery time effects on  
photon counting accuracy, observed counts  
and true events in some derived  
curves 19 p3359 A66-35919
- Strain gauge strip chart error  
determination, elimination and effects on  
accuracy of electric  
calibration 19 p3360 A66-36307
- Ephemeral geopotential variations from  
deviations in quartz oscillator clocks of  
Paris and Greenwich  
observatories 19 p3351 A66-36370
- Fourier transform used in correction of  
instrument contour error when observing  
solar spectral line profile 20 p3647 A66-37042
- Symbolic programming digital computer  
techniques, hardware interfacing and system  
errors in simulation of lunar midcourse  
guidance and navigation  
systems 20 p3543 A66-37250
- Fuel and propellant gauging, using method  
of capacitance change induced by liquid  
dielectrics 20 p3664 A66-38251
- Ellipsoid mirror reflectometer using  
radiant flux from IR  
monochromator 20 p3561 A66-38297
- Transistorized portable UV dosimeter for  
use in medicine, climatology, physiotherapy,  
meteorology and stimulated plant growth  
study 20 p3562 A66-38436
- Spectral line profiles corrected for  
influence of apparatus 21 p3736 A66-38636
- Radial velocity measurements with  
objective prisms, discussing error sources,  
luminosity, etc 21 p3737 A66-38821
- Error sources in strapdown inertial  
attitude reference system consisting of  
three pulse torqued gyros and digital  
differential analyzer 21 p3763 A66-38840
- Gyro and accelerometer errors in ternary  
torqued inertial components mounted on  
surface to surface missile, noting angular  
vibration environment 21 p3764 A66-38848
- Gemini VII star sightings analyzed, using  
handheld space sextant in Gemini VI,  
discussing effect of bias, timing, angle  
measurement and trajectory  
errors 21 p3767 A66-38893
- Elimination of rate gyro angular  
acceleration error and scale factor  
sensitivity to wheel speed by integration of  
output signal 21 p3767 A66-38895
- Flow velocity effect on thermometer  
reading and consequences for measuring  
thermodynamic efficiency of hydraulic  
machines 21 p3737 A66-38935
- Legibility analysis to investigate effects of  
scale factors, graduation marks, etc, on  
speed and accuracy of reading moving tape  
instruments 21 p3701 A66-39422
- Noise-signal receiver amplitude-limitation  
effect on noise measurement in presence of  
pulsed interference 22 p3861 A66-39655
- Bottom-moored sonar beacons surveyed in  
absolute position coordinates, noting  
transmitter-receiver and celestially  
augmented inertial navigator and error  
minimization techniques 22 p3945 A66-40323
- Narrow laser beam pointing technique in  
deep space-to-earth data transmission for  
reduction in error  
sources 22 p3867 A66-40496
- Observed Faraday polarization variation of  
satellite transmission radio signals due to  
ionospheric irregularities, latitudinal  
electron density variations and antenna  
geometry readout error 22 p3867 A66-40556
- Distortions in aerial photographs due to  
errors in cameras, noting determination  
methods in various  
countries 22 p3919 A66-40622
- Monograph on theory of gyroscopic  
instruments and devices 23 p4066 A66-41052
- Error sources in strapdown inertial  
attitude reference system consisting of  
three pulse torqued gyros and digital  
differential analyzer 23 p4088 A66-41101
- Fluid stratification in floated gyroscope,  
estimating drift rate as function of time,  
geometry and flotation  
mixture 23 p4066 A66-41102
- Error of measurement of mean square  
value of fluctuation signals due to voltmeter  
calibration 23 p4038 A66-41523
- Elastic microstrain of polycrystalline  
titanium measuring device, discussing  
measurement error 24 p4227 A66-42222
- Error of two-rotor gyrohorizon compass  
caused by hydraulic damper during stop or  
steady motion 24 p4210 A66-42447
- Potential sensitivity of energy radiation  
detectors, examining measurement error  
causes for radiation power of natural and  
artificial sources 24 p4172 A66-42523
- Plane gridded retarding potential analyzer  
for measuring dominant constituent ion  
concentrations, temperature and instrument  
potential in planetary  
ionospheres 24 p4201 A66-42605
- Meteorological measurement systems in  
relation to aerospace problems, using flight  
history of rocket vehicle and root mean  
square accuracy 24 p4214 A66-43043
- Sporadic E layer reflection used to  
determine instrument constant in measuring  
radio wave absorption in  
ionosphere 24 p4205 A66-43156
- INSTRUMENT FLIGHT RULE /IFR/**  
Mixed translation and attitude control  
system using single cockpit stick for low-  
speed flight control of VTOL  
aircraft 05 p0610 A66-15078
- EEG experiments on men exposed to  
intermittent photic stimulation under  
simulated IFR conditions produced  
drowsiness as primary  
response 17 p2864 A66-32165
- Cruising level systems and semicircular  
rule 17 p2950 A66-32354
- INSTRUMENT LANDING SYSTEM**  
Adaptive coupler providing extended  
automatic glide slope beam following by  
compensating for beam  
convergence 01 p0101 A66-10036
- Flight control by ground-based radio  
system discussing aerial navigation safety,  
operating principles, equipment for VOR  
and ILS and importance of  
calibration 03 p0390 A66-13011
- Flight testing of distance measuring  
equipment for instrument landing system  
with results shown in  
histograms 07 p1067 A66-17691
- Inertial navigation systems for automatic  
landing, using category I instrument landing  
system 07 p1069 A66-17714
- Onboard equipment designed for transport  
aircraft landings with visibilities less than  
200 ft and runways less than 2600 ft, having  
all devices duplicated 10 p1554 A66-21368
- TALAR, tactical aircraft landing aid-radio  
uses ground-based Cassegrain antenna,  
magnetron transmitter and 4-lb receiver in  
aircraft while providing ILS  
functions 20 p3596 A66-37232
- Integral monitor development for ILS  
localizer, predicting changes in track  
position and width, noting principles of  
operation and  
performance 23 p4044 A66-41322
- INSTRUMENT ORIENTATION**  
Orientation detector mechanism for high  
altitude cosmic ray research utilizing  
directional East-West symmetry in  
geomagnetic rigidity  
cut-off 07 p1034 A66-17980
- Optical rangefinder design using movable  
plane mirrors as optical compensators and  
focusing systems with fixed basis at  
instrument 09 p1380 A66-20312
- INSTRUMENTATION**  
**SA ADVANCED RANGE**  
**INSTRUMENTATION SHIP /ARIS/**



- SA AIRCRAFT INSTRUMENTATION  
SA BIOINSTRUMENTATION  
SA MICROINSTRUMENTATION  
SA RADAR INSTRUMENTATION  
SA ROCKET INSTRUMENTATION  
SA SATELLITE INSTRUMENTATION  
SA SPACECRAFT INSTRUMENTATION  
Book on navigation principles including instrumentation, control, speed, radio, radar, sonar, position finding, route, etc 14 p2328 A66-26874  
Diodes, transistors, rectifiers and inverters application to control and instrumentation systems, providing phase changing, frequency stabilization, source voltage, etc 14 p2249 A66-27118  
Range instrumentation systems calibration and evaluation at Air Force Eastern Test Range 14 p2272 A66-28447  
Calibration ensuring optimal instrument performance, using statistical quality control, noting background of Assured Performance Calibration program 15 p2508 A66-28810  
Instrument methods determining function and density of length distribution of random radio emissions 15 p2451 A66-29123  
Performance of SNAP-10A instrumentation during component qualification, ground system and flight system tests, noting environmental conditions 16 p2744 A66-30439  
Apparatus for analysis and preparation of magnetic properties of thin ferromagnetic films in vacuo, noting hysteresis loop, thermal evaporation, etc 16 p2661 A66-30697  
Sonic boom - Symposium, Saint Louis, November 1965 17 p2846 A66-33020  
Sonic boom measurement instrumentation noting use of frequency response, vibration isolation, wind screening, etc 17 p2926 A66-33025  
Instrumentation of ESRO telemetry receiving stations noting receiver, recording, monitoring and demodulation equipment 21 p3702 A66-38604  
Instrumentation in aerospace simulation facilities - International Conference, Stanford, August 1966 24 p4205 A66-42166  
Field effect transistors in shock tunnel instrumentation circuitry associated with piezoelectric transducers operating in environment of widely ranging pressures, temperatures and testing times 24 p4207 A66-42170  
Mechanical electrical transducers for aerospace instrumentation and control, noting strain gauge, inductive and potentiometric types 24 p4215 A66-43082
- INSTRUMENTATION PROGRAM**  
SNAP-8 instrumentation, emphasizing selection and installation of aerospace type transducers for liquid metal service [ISA PREPRINT 1.11-4-65] 05 p0683 A66-15510  
Radio astronomy instrumentation, describing antenna parameters, design characteristics, instrumentation needs, etc 20 p3524 A66-36962  
Space vehicle guidance and navigation, noting instrument techniques, gyroscopic units for reference coordinate realization, inertial navigation systems, etc [AGARDOGRAPH 105] 24 p4235 A66-43123
- INSULATED STRUCTURE**  
Preliminary design for optimum combination of insulating and structural materials for hypersonic cruise vehicles 03 p0436 A66-12752  
Thermionic converters, discussing resistant metal-bond use for collector-emitter insulation 05 p0622 A66-15590  
Hall effect in two-dimensional flow of conducting gas interacting with external inhomogeneous magnetic field along insulating plane 08 p1205 A66-18533  
Ferrite component for radio relay equipment such as antenna insulator, waveguide and coaxial equipment insulator and circulator 11 p1664 A66-22658  
Ferrites for resonance-directional insulators and circulators, noting properties at microwave frequencies and applicability 11 p1664 A66-22659  
RF sputtering of insulators, noting effects of auxiliary magnetic field, electrode size, oxygen concentration, substrate temperature and target material on thin dielectric film formation 13 p2157 A66-25039  
Current voltage characteristics of dielectric films 13 p2157 A66-25040  
Lightweight insulations for space vehicle cryogenic storage tanks based on design principles of multilayer radiation shields 19 p3473 A66-35598  
Transient gas-flow process in multilayer insulation systems during evacuation predicted by equations in conjunction with measured permeabilities and diffusion coefficients 20 p3675 A66-37065  
Convection effect in helium charged insulation with partially foam-filled honeycomb core 20 p3675 A66-37066  
Gas flow equations for multilayer insulation systems for both continuum and free molecular flow regimes of interest in cryogenic space vehicle design [AICE PREPRINT 22A] 22 p3897 A66-39888
- INSULATION**  
SA ELECTRIC INSULATION  
SA TEMPERATURE CONTROL  
SA THERMAL INSULATION  
SA WATERPROOFING  
Insulation materials and processes for aerospace and hydrospace applications - SAMPE Symposium, San Francisco, May 1965 06 p0898 A66-16284  
Properties of nonirradiated heat-shrinkable silicone and fluorosilicone rubbers for insulating and encapsulating electrical and electronic apparatus, including resistance to aging, fuels, ozone, etc 06 p0900 A66-16298
- INSULATOR**  
SA EXCITON  
Transient effect of ionizing radiation on semiconductor and insulating materials 05 p0739 A66-15488  
Insulators from high purity oxides used in nuclear thermionic power converters, tabulating refractory materials compatibility and noting thermal expansion, electrical conductivity, etc 05 p0714 A66-15592  
Polyimide resins for extreme environments, discussing chemical structure, application, electrical, thermal and mechanical properties, radiation resistance, etc 06 p0899 A66-16292  
Cellular room-temperature-vulcanizing silicone-rubber, describing compound properties, application and possible structural modifications 06 p0900 A66-16295  
New thermal insulations and product design 09 p1393 A66-20937  
Static characteristics of insulated gate field effect transistor with gate electrodes at both sides of semiconducting channel, including space charge limited currents analysis 09 p1359 A66-20974  
Contact barriers on insulating semiconductor cadmium sulfide measurements, based on pulsed light and bridge 10 p1573 A66-21245  
Numerical method of Schrodinger equation and WKB approximation compared in determination of transmission coefficients for thin insulating films 10 p1577 A66-21558  
Segmented electrode MHD generator performance for various electrode-insulator length ratios 13 p2000 A66-25714  
Compressible metal for turbine seal, discussing Nicroseal coating used in sealing clearance between rotor and adjacent stationary parts 13 p2109 A66-25777  
Electric breakdown and insulation properties of vacuum and design of vacuum devices 14 p2249 A66-27105  
Transmission and reflection coefficients of semiconductors and insulators for use in visible and IR spectral regions 14 p2334 A66-27334  
Thermal model for performance of cork insulation on Minuteman missile in launch environment [AIAA PAPER 65-117] 16 p2827 A66-30893  
Behavior of ceramic insulating materials under nonisothermal conditions at high temperatures 16 p2731 A66-31605  
Experimental assembly for measuring true heat capacity of heat resistant insulating materials during natural cooling at temperatures from 1200 to 2400 degrees K 20 p3556 A66-36989  
Lightweight superinsulation testing for cryogenic tank application 20 p3675 A66-37063  
Thermal conductivity of gas-charged cryogenic powder
- Insulation 20 p3675 A66-37063  
Saturn S-IV and S-IVB liquid hydrogen tank internal insulation, using polyurethane foam reinforced with fiberglass threads 20 p3675 A66-37063  
Reinforced plastic materials evaluated a potential low temperature structural insulators 20 p3676 A66-37081  
Sheet cork as thermal protection during vehicle launch and ascent flight [AIAA PAPER 65-356] 22 p3999 A66-40351  
Effectiveness parameters of spherical shield electrode surrounding negative dielectric junction of insulator in high vacuum 23 p4042 A66-41041
- INSULIN**  
Performance and physiological effects of adrenalin or insulin in human subjects 06 p0813 A66-16822
- INTAKE**  
S FOOD INTAKE  
S WATER INTAKE
- INTEGER**  
Gomory all-integer linear programming algorithm based on lexicographical ordering principle and relation to cost function 19 p3309 A66-35871  
Fortran program for finding minimum value of monotonic function defined on ordered sets of positive integers 19 p3309 A66-36049
- INTEGRAL**  
SA CAUCHY INTEGRAL  
SA ELLIPTIC INTEGRAL  
SA FRESNEL INTEGRAL  
SA JACOBI INTEGRAL  
SA PHASE-SPACE INTEGRAL  
SA RIEMANN INTEGRAL  
SA TRANSFORM INTEGRAL  
Approximation formulas for certain collision integrals of gas transport 03 p0395 A66-12834  
Dual-operator Stieltjes integrals 08 p1245 A66-19636  
Integral curves of particular ordinary differential equation containing singularity 11 p1721 A66-22641  
Integrals of equations of small axisymmetrical oscillations of thin elastic shell of revolution 12 p1966 A66-24068  
Integrals of system of equations describing natural oscillations of dome shaped shell 12 p1966 A66-24068  
General vector notation for multiple integrals 12 p1903 A66-24099  
Adiabatic invariants and third integrals of motion in periodic potentials in periodically time-dependent Hamiltonian systems of degrees of freedom 17 p2945 A66-32293  
Approximation formulas for certain collision integrals of gas transport 19 p3404 A66-36777
- INTEGRAL EQUATION**  
SA FREDHOLM INTEGRAL EQUATION  
SA SINGULAR INTEGRAL EQUATION  
SA TRANSPORT THEORY  
SA VOLTERRA EQUATION  
Radiative transfer equation for isothermal model of solar corona, noting radiation flux and electron density variation 01 p0131 A66-10261  
Approximate calculation of Wiener integration 01 p0092 A66-10311  
Charge trapped in electron or ion beams at pressures below breakdown determined from general integro-differential equation using approximation method 01 p0111 A66-10373  
Solving integrals with Bessel functions as integrand 01 p0095 A66-11002  
Plate theory for case of thin elastic deformable circular plate under rotationally symmetrical stress 02 p0296 A66-11242  
Laplace transform technique to develop asymptotic solutions to integral equations describing influence of scattering law or radiation damage displacement cascade 02 p0245 A66-11944  
Necessary and sufficient criteria for absolute minimum of multidimensional integrals, depending on arbitrary number of real functions of real variables and partial derivatives of arbitrary maximum order 03 p0387 A66-12686  
Laminar stability of incompressible and stationary flows with curved streamlines applying integral method and noting time dependence of flow 03 p0357 A66-13081



Number theoretic method to approximate solution of linear integral equations 04 p0539 A66-13488

Reduction of Rabotnov approximate equation describing steady creep in circular cylindrical shells, under axisymmetric loading, to system of integral equations 04 p0588 A66-13567

Forced torsional motion of semiinfinite isotropic elastic cylinder with vibrations excited by harmonically oscillating rigid disk, using integral equation 04 p0589 A66-13829

Nonlinear eigenvalue problem for equilibrium state of rotating rod solved by perturbation procedures and Leray-Schauder degree theory 04 p0589 A66-13948

Rotating polytrope structure analyzed, using approximation technique of integrating outwards from center and inward from surface 04 p0578 A66-14018

Solving integral in propeller design and second-order effects in subsonic airfoil theory 05 p0606 A66-15082

Solutions for integral equation associated with equation of radiative transfer for isotropic scattering and complete redistribution in frequency cases 05 p0762 A66-15276

Recomputation of values of numerical approximation of integral in gain limitations of large antennas, considering sidelobe level 06 p0844 A66-16044

Averaging systems of integrodifferential equations for small parameter and real  $n$  vector functions 06 p0902 A66-16535

Modified Karman-Pohlhausen pulse integral equation for calculating boundary layers is more accurate when seeking flow separation point 07 p1019 A66-17391

Radiant transport with isotropic scattering, evaluating approximate solutions for reflection and transmission of parallel plane radiation 07 p1152 A66-17589

Heat exchange through absorbing media, determining combined modes of radiation and conduction via exchange factor approximation 07 p1152 A66-17590

Solvability of general mixed boundary value problems for multidimensional hyperbolic integro-differential equation of arbitrary order with analytic coefficients 07 p1056 A66-17608

Boundary problems concerning linear integro-differential equations with calorific operator and delayed arguments 07 p1057 A66-17842

Effectiveness of stagnant layer of radiating gas in shielding surface from radiation flux formulated as integral equation, with heat transfer results presented graphically 07 p1155 A66-18346

Continuation of certain classes of differentiable functions beyond limits of region 07 p1060 A66-18465

Compressible turbulent boundary layer as momentum integral and moment-of-momentum integral equations for arbitrary pressure gradient, noting surface heat-transfer effects 08 p1207 A66-19126

Heat capacity expression due to chemical reaction, relating composition variations and binary diffusion coefficient with Lewis number, presenting integral equation for system enthalpy 08 p1318 A66-19164

Idealized cylindrical shell buckling under axial compression derived from generalized integral expression 08 p1310 A66-19166

Stress-strain state of infinite plate with two holes of different diameter solved, using integral equation derived for two-dimensional problem in elasticity theory for anisotropic medium 08 p1314 A66-19578

Stress-strain state of shell having one end clamped and other under concentrated bending moments and concentrated force acting along generatrix solved by integral equation 08 p1314 A66-19579

Method of induced emf and integral antenna equation 08 p1197 A66-19605

Kilatskin objections and improvements concerning integral equation describing current distribution in rectilinear antenna 08 p1197 A66-19607

Boundary problems for differential and integro-differential equations 08 p1245 A66-19631

Conservation laws involving mass,

momentum and energy applied to asymptotic properties of hypersonic flow 09 p1327 A66-20266

Proof, by degenerate kernel method of existence and uniqueness of solution for one class of nonlinear integral equations 09 p1394 A66-20455

Approximate solution of nonlinear heat conduction problems for boundary conditions of first and third kind, using Leibenson integral relations 09 p1471 A66-20750

Ablation of blunt metallic body near stagnation point solution using integral equations, noting pressure effect 09 p1472 A66-20833

Eigenvalues of integral equations in laser resonant cavities 10 p1542 A66-21343

Integral equation formulation of Oseen flow past obstacles and approximate solution of integral equations for low Reynolds numbers 10 p1525 A66-21848

Integration of equations, approximating Maxwell equations, in curvilinear coordinates separating scalar Laplace equation, with vectors representing electric and magnetic fields 10 p1556 A66-21994

Current distribution and input resistance of T-type, corner and bent tape vibrators powered by lumped electromotive force, using method of integro-differential equations 11 p1666 A66-22719

Atomic integral obtained with magnetic dipole-dipole operator in form of finite sum of integrals over hypergeometric functions 11 p1739 A66-22887

Internal flow problems in free, nearly free molecular regimes and higher transition flows, using Boltzmann equation and series expansion to solve integral equation for surface collision density 11 p1693 A66-22940

First-order boundary proximity effect on Stokes resistance of body, using integral equation approach 11 p1693 A66-23008

Spherical summability of Fourier series of function integrable on unitary group 11 p1723 A66-23360

Cauchy type integral on hypersphere, defining Cauchy principal values, noting role in theory of functions of complex variables 11 p1724 A66-23366

Quasi-linear boundary value problems solved with Galerkin convergence method 12 p1902 A66-23863

Approximate solution of equation with normally distributed operators 12 p1902 A66-23899

Stress-strain state of shells of revolution of variable thickness and elastic parameters under effect of external loads and secondary strains obtaining strain, equilibrium and elasticity equations 12 p1963 A66-24043

Forced oscillations of coaxial multidisk rotors, allowing for gyroscopic effect and rotating at different angular velocities determined by replacing differential equations with integral equations 12 p1964 A66-24050

Evaluation of total square integrals arising in minimization problems of discrete data systems not requiring expansion of determinant for solution 12 p1850 A66-24265

Solution of dual integral equations containing Legendre conic functions and trigonometric functions 12 p1905 A66-24344

Kinetic theory of dense gases generalized for all orders, deriving integral equations for transport coefficients and showing temperature dependence of bulk viscosity 12 p1979 A66-24565

Properties of compressible boundary layers with heat transfer and arbitrary pressure gradients calculated, using integral equation and correlation concept for application in hypersonic flows 12 p1865 A66-24581

Two-dimensional Stokes flows for functions time-periodic with common frequency, noting analogy to oscillations of long cylinder in viscous fluid 12 p1867 A66-24963

Nonuniqueness of solutions of nonlinear integral equation for Chandrasekhar S-function for homogeneous semiinfinite atmosphere 13 p2127 A66-25612

Equations describing motion of barotropic fluid with free surface solved, using finite difference methods based on two-step Lax-Wendroff scheme 13 p2121 A66-25814

Asymptotic solution of Cauchy problem for integro-differential equation with small parameter associated with derivative 13 p2119 A66-25908

Functional integration analysis of exponential behavior of nonlinear feedback control systems 13 p2052 A66-26076

Integral equation for slender wing oscillating in subsonic flow near solid wall 13 p2067 A66-26538

Circulation distribution over rectangular wings, based on Chushkin algorithm and lifting surface equation calculated by digital computer 13 p2068 A66-26540

Properties of laminar boundary layer undergoing surface catalysis with two reactants and two products obeying Langmuir-Hinshelwood mechanism, solving concentration field by integral equation 13 p2019 A66-26663

Heat transfer in Couette flow of radiating fluid with viscous dissipation, noting conduction coupling, effects of temperature level, profile, wall emission, fluid optical thickness, etc 13 p2210 A66-26718

Ionospheric electron density profile and Schlomilch integral equation for oblique incidence 13 p2075 A66-26740

Integral equations for radial distribution functions in classical fluid 14 p2273 A66-26828

Electromagnetic scattering by circular wire loops loaded with lumped impedances, obtaining solution to integral equation by Fourier series 14 p2247 A66-26863

Radiation pattern of dielectric antenna using integral equations, noting differences between real antenna and idealized linear traveling wave antenna 14 p2250 A66-27140

Solution of set of  $n$  dual integral equations with Hankel kernel 14 p2321 A66-27377

Newton-Kantorovich method solution of Hammerstein type nonlinear integral equation, with application to elasticity theory of buckling of thin spherical shell 14 p2322 A66-27628

Integral equations derived from correlation functions, determining transport coefficients in classical fluid, formally valid to general order in density 14 p2276 A66-27635

Chemical potential and integral equation for correlation functions of classical fluids, using Percus method when functions exhibit cluster properties 14 p2276 A66-27637

Integral equations defining transport coefficients of moderately dense gas obtained from Boltzmann equation shown to be identical to first order in density, with results obtained by autocorrelation function method 14 p2276 A66-27639

Resonators with confocal mirrors with variable reflection coefficients calculated, using integral equations for field distributions 14 p2254 A66-27746

Radiation from vertical dipole in warm plasma determined by asymptotic series expansion of integral solutions, noting surface wave propagation, transformation from acoustic to electromagnetic mode on boundary, etc 14 p2240 A66-27917

Newtonian approximation for irregularities in statistically homogeneous and isotropic dust-filled universe 14 p2386 A66-28119

Stationary phase technique synthesis of continuous linear antenna and integral equation for determining radiation pattern 14 p2259 A66-28158

Soviet book on geodetic gravimetry including disturbing potential calculation methods based on Molodenskii integral equation 14 p2288 A66-28209

Effect of slope and curvature of Earth surface on disturbing potential, using Molodenskii integral equation, obtaining deflection of vertical, disturbing potential and Stokes constant 14 p2288 A66-28210

Numerical integration principle in calculation of disturbing potential verified, using conical Earth model 14 p2288 A66-28211

Dual trigonometric integral equations solved, then applied to determining stress field due to crack 14 p2325 A66-28391

Numerical solution of integral equation for diffraction by soft strip applied in wave scattering by obstacles with dimensions comparable to wavelength 14 p2325 A66-28399

Numerical solution of nonlinear integro-differential boundary value problems with



parabolic operators and retarded argument 15 p2525 A66-28519

Resonant modes in ring shaped resonators formed by reflector strip bent into circle, noting eigenfunctions and eigenvalues of integral equation 15 p2457 A66-28786

Input and output coupling constants of spin-2 mesons with two pseudo-scalar mesons obtained by producing resonances at experimentally observed positions 15 p2544 A66-28947

Expansion of arbitrary function of Mehler-Fok integral form in terms of spherical functions 15 p2526 A66-28952

Dual integral equation and dual series analysis and application to mixed boundary value problems in elasticity, hydrodynamics and electrostatics 15 p2526 A66-28953

Dual integral equations in elasticity theory, noting Mehler-Fok transformation of spherical functions, Fredholm equation and application to mixed boundary value problems 15 p2526 A66-28954

Boundary between applicability ranges of network and steepest descent methods in equation integration of Timoshenko theory in analysis of plate deformation 15 p2608 A66-28962

Integral equations in determining periodic regimes for nonlinear dynamic systems and for linear systems with periodically varying parameters 15 p2541 A66-29167

Approximate method, using power polynomials, for calculating distance between detached shock wave and profile 15 p2425 A66-29721

Green-Hadamard functions of Tricomi singular problems for generalized wave equation, expressing equation integrals as hypergeometric Humbert and Horn series 15 p2530 A66-29855

Multidimensional generalized transport equations solutions and calculation by difference methods 16 p2732 A66-30240

Noether theorems applied to degenerate cases of improper integral equations with Cauchy kernels 16 p2733 A66-30745

General theory of linear integral equations with power kernel 16 p2734 A66-30746

Solution of boundary value problems describing two-dimensional flow in plastic regions 16 p2815 A66-30789

Averaging systems of integro-differential equations for small parameter and real n vector functions 16 p2736 A66-30973

Boundary problems for differential and integro-differential equations 16 p2736 A66-30980

Volterra series analysis of aperiodic solutions to certain second order integrodifferential equations with nonlinear damping and nonlinear restoring force 16 p2737 A66-31334

Integrating error equations of inertial navigation system for objects in Keplerian motion 16 p2744 A66-31507

Integral equivalence of two given systems of square integral matrices, reducing problem to determination of principal ideal Z ring 16 p2738 A66-31563

Exact determination of electron density distribution in finite anisotropic plasma by integral equation relating tangential electric field and HF plasma current 16 p2767 A66-31691

Asymptotic behavior of nonlinear integral equations with certain conditions on kernel and nonlinearities 16 p2738 A66-31705

Iteration methods for solution of integro-differential equations 17 p2945 A66-31807

Sound power from nonuniform flow determined by summing surface and volume integral over sound sources 17 p2905 A66-31949

Local emissivity of vertex point of diffuse conical or V-groove cavity, noting dependence on wall material, angle factor and agreement with theoretical solution 17 p3035 A66-32613

Arc operation under nonsteady electrical inputs, noting initial conditions, energy equation solution, temperature profiles, application of Green function for moving boundary problem, etc [AIAA PAPER 66-480] 17 p2970 A66-32769

Control forces in nonlinear integral equations solved by iteration method 17 p2902 A66-32816

Loading of thin ring airfoil in unbounded spherical source flow field, calculating vortex distribution, strength, etc [ASME PAPER 66-FE-3] 17 p2914 A66-33259

First transcendent integrals of motion equations of heavy solid about fixed point 18 p3135 A66-34546

Numerical solution of integral form of radiative transfer equation from measurements in finite set of spectral intervals for deducing atmospheric temperature profiles, using satellites 18 p3129 A66-34554

Solution for inhomogeneous differential linear equation in integral form obtained from Wronskian 18 p3128 A66-34701

Poiseuille flow of rarefied gas in annular tube analyzed numerically for inverse Knudsen number, using Bhatnagar-Gross-Krook model and transport integro-differential equation 18 p3102 A66-34920

Klitskin objections and improvements concerning integral equation describing current distribution in rectilinear antenna 18 p3087 A66-34963

Integration of equations, approximating Maxwell equations, in curvilinear coordinates separating scalar Laplace equation, with vectors representing electric and magnetic fields 18 p3136 A66-34971

Relations between primary spectrum, pion multiplicity and sea level muon spectra, using integral equations 18 p3219 A66-35190

Quadratic integral equation solution for bandlimited signal design for binary communication, using memoryless correlation detection 19 p3296 A66-35339

Numerical integration based on definition of Riemann integral, describing application to nonlinear integral equations of isotropic scattering of radiation in plane parallel atmosphere 19 p3388 A66-35830

Dynamic system parameters substituting integral equation for differential equation of motion, noting application to nonlinear, differential and PDE systems 19 p3325 A66-35987

Partial step integration equation for use with Adams or Adams-Bashforth method of integration of differential equations 19 p3309 A66-36045

Normalized self and mutual admittances of two identical bare circular loop antennas in air or conducting medium evaluated, obtaining single integral equation for current distribution 19 p3321 A66-36405

Linearized problem of oblique incidence of weightless flow of ideal gas on surface of heavy liquid, using eigenvalues and eigenfunctions of integral equation 19 p3342 A66-36470

Green formula and moment functions, predicting rate of radiative energy loss from boundaries of absorbing-emitting slab or sphere 19 p3479 A66-36597

Complex convolution integral applied to Laplace transform expressions in sampled data theory 19 p3339 A66-36747

Singular integral equations with constant coefficients solved by Jacobi polynomials and applied to problems in fluid dynamics, crack propagation, plane elastic theory, etc 19 p3393 A66-36836

Integration technique for determining unsteady aerodynamic forces at subsonic speeds, noting role of kernel of integral equation 20 p3491 A66-36955

Application of Rayleigh principle to obtain sharp upper bounds for increase of first eigenvalue of membrane submitted to parallel and equidistant rectilinear constraints 20 p3669 A66-37544

Boundary value problem of wave equation with application to antenna theory of singular integral equations 20 p3531 A66-37730

Convolution type integral equation solution via reduction to Riemann problem in class of generalized functions 20 p3591 A66-37755

Incorrect problems of mathematical physics examined and illustrated by classical Cauchy problem for Laplace equation 20 p3591 A66-37756

Solvability and methods of solution of boundary value problems noting uniqueness, potential theory application in solving polyharmonic equations and second-order equation 20 p3591 A66-37757

Reduction of problems of diffraction of scalar and vector waves at open curvilinear screen to integral equations of second kind 20 p3518 A66-37992

Liquid junction cell design, noting equation, integration for ideal diffusion potential and salt effects potential for heterolonic junctions of uniform ionic strength and cation concentration 20 p3502 A66-38184

Numerical extrapolation solution of kernel characterized integral equations for apparent emissivity of conical and cylindrical cavities 20 p3681 A66-38229

Interior regularity theorem for linear elliptic matrix differential operator 21 p3754 A66-38445

Plasma slab resistance between juxtaposed disk electrodes, obtaining exact two-and approximate three-dimensional solution 21 p3776 A66-38544

Self-induction of ellipsoidal plasmoid, deriving relevant equations 21 p3787 A66-39052

Energy levels of rotationally hindered linear molecules calculated, using variational principle based on schrodinger-like integral equation 22 p3949 A66-39662

Plane supersonic flow with Mach reflection, represented by shock wave interaction noting integral equation obtained from linearized shock equations 22 p3897 A66-39692

Laplace transformation simulation by analog computer for real and complex values 22 p3870 A66-39992

Integral equation for heat flux in inverse heat conduction for infinite flat plate as in solid rocket igniters 22 p3998 A66-40032

Conformal mapping technique applied to boundary value problem of plane wave diffraction by perfectly conducting elliptical cylinder, noting integral equation 22 p3866 A66-40182

Integral equation solution through Jacob polynomials employed as eigenfunctions of certain operators 22 p3941 A66-40792

Shell dynamical integral and integro-differential BVPs for linear deformable shells, examining reciprocity theorem and Kirchhoff-Lowe hypothesis 23 p4136 A66-40992

Soviet literature survey of exact and approximate solution of two-and three-dimensional mixed boundary value problems in theory of elasticity 23 p4136 A66-40992

Disperse material heating by simultaneous radiative and convective energy with temperatures expressed as integral equations 23 p4148 A66-41276

Parameters of dynamic systems described by PDEs determined by replacing PDE with integral equation and eliminating via recursion process terms resulting from initial and boundary conditions 23 p4084 A66-41392

Current distribution and input resistance of T type, corner and bent tape vibrators powered by lumped electromotive force, using method of integro-differential equations 23 p4045 A66-41452

Binary communications integral equations in complex variable functions and application of Fourier transform for bandlimited signals 23 p4085 A66-41532

Lienard type of differential equation for oscillatory system representing solution by Krylov-Bogoliubov method, noting inverse problem 23 p4085 A66-41542

Newton iterative procedure extended to solution of nonlinear integral equations 23 p4085 A66-41552

Proof of existence of boundary value solutions for various mixed component equations by reduction to singular integral equation 23 p4085 A66-41562

Correct conductance and susceptance of infinite cylindrical antenna determined via asymptotic evaluation of parametric integrals 23 p4047 A66-41636

Complete Rayleigh scattered field within homogeneous plane parallel atmosphere, noting scalar transfer equation extension 23 p4065 A66-41813

Thermal transport in channel-gas flow, discussing integral equation and power series solution 23 p4150 A66-41862

Boltzmann equation for dilute monatomic gas, discussing asymptotic interpretation of



- Hilbert and Chapman-Enskog 23 p4097 A66-42011
- Theories 23 p4097 A66-42011
- Stress intensity factors for single-edge cracks in rectangular sheets with end moments, reducing stress distribution to Neumann-Hilbert problem 24 p4286 A66-42161
- Screening function of interacting electron as at high and metallic densities by many-body perturbation theory 24 p4236 A66-42294
- Integral equations for weight function of optimum filter and correlation function of random absolute error 24 p4188 A66-42475
- Huygen principle for elastic media, comparing Kupradze formulation with formulations of Knopoff and Volpert 24 p4237 A66-42495
- Hilbert parametrix method of solving linear BVPs for second-order elliptic PDEs, using Green functions 24 p4232 A66-42740
- Integral equation of flat-roof resonator solved by iteration method, deriving mode patterns, phase shifts and power losses 24 p4174 A66-42807
- Flow behind shock wave in long tube analyzed by time effect and integrating equations, using Galerkin method 24 p4197 A66-42997
- Energy dependence of effective interaction in superconductivity, calculating critical field and specific heat 24 p4259 A66-43018
- Unambiguous transition probability densities describing inhomogeneous stochastic continuous-to-right Markov processes with finite number of states 24 p4232 A66-43021
- INTEGRAL FUNCTION**
- Iterative procedure for constructing and evaluation functions consisting of integrals of products of radial atomic wave functions 01 p0108 A66-10385
- Linear differential equation solution nonfluctuation and boundedness estimate in connection with integral inequalities 01 p0094 A66-10650
- Function for which error functional attains its maximum value as sphere constitutes solution of polyharmonic equation 02 p0250 A66-12109
- Book on probability theory covering mathematical models, randomness concepts, switching logic concepts, integration on abstract space, etc 03 p0386 A66-12369
- Commutable matrices, decomposing determinant of general solution of AX equals XB into linear factors 04 p0539 A66-13869
- Multiple Stieltjes integral representation of functions in form of Markov series 04 p0539 A66-13871
- Calculation of integrals of infinitely differentiable functions, showing error estimate by network method for periodic functions 07 p1056 A66-17597
- Representation of arbitrary integral functions by Dirichlet series in entire plane, determining number of rays on which zeros must be located 07 p1058 A66-17912
- Interaction between Kolmogoroff integrals determined with aid of finite partitions and those determined with aid of denumerable partitions 08 p1244 A66-18702
- Energy integral for holonomic system of points of variable mass, transforming Lagrangian form via Hamiltonian function 08 p1256 A66-19583
- Necessary conditions for existence of univalent integrals in equations of motion of heavy gyrost at fixed at one point 08 p1227 A66-19762
- Boundary layer theory applied to solution of problems of combined heat and mass transfer, using approximate single-parameter integral method 09 p1367 A66-20703
- Asymptotic expansions of double and multiple integrals occurring in diffraction theory, using stationary phase method 10 p1550 A66-21850
- Partial differential equation solved by integral transform under prescribed boundary conditions 10 p1550 A66-21914
- Lowering order of transfer function of automatic control system based on use of generalized integral quadratic estimates of transient processes of 11 p1673 A66-22203
- Limit cycles and global structure of integral curves of nonlinear system of differential equations in five-dimensional parameter space 11 p1724 A66-23364
- Linear differential equation solution nonfluctuation and boundedness estimate in connection with integral inequalities 12 p1903 A66-24021
- Commutable matrices, decomposing determinant of general solution of AX equals XB into linear factors 12 p1903 A66-24025
- Multiple Stieltjes integral representation of functions in form of Markov series 12 p1903 A66-24027
- Integral multiplicity and coupling coefficient estimation of muon-meson component of cosmic rays for case of primary particle impinging at arbitrary zenith angle 12 p1943 A66-24182
- Supersonic flow around blunt body calculated via integral relations, using simultaneous approximation function in two directions 12 p1797 A66-24208
- Cesaro summability and Fourier transform for evaluating divergent series and integrals occurring in circuit design and analysis 12 p1856 A66-24730
- Integral relations method to reduce by approximation PDEs to ODEs or to algebraic or transcendental equations 13 p2119 A66-25854
- Interaction between atoms of solid surface and gas phase, obtaining closed-form solution of motion equations 16 p2753 A66-30786
- Representation of arbitrary integral functions by Dirichlet series in entire plane, determining number of rays on which zeros must be located 16 p2736 A66-30975
- Thermal explosion equations solved by Dorodnitsyn method of integral equations 17 p3034 A66-32564
- Supersonic flow around blunt body calculated via integral relations, using simultaneous approximation function in two directions 22 p3844 A66-40572
- Finite integral transform to solve unsteady-state heat conduction problems for hollow cylinders with moving internal boundary 22 p4000 A66-40819
- Feynman integral for classical waves evaluated, using Hamiltonian approach to summation 23 p4086 A66-41867
- Existence of new isolating integral in restricted three-body problem, computing orbits for various parameter values and initial conditions 24 p4272 A66-42202
- INTEGRAL OPERATOR**
- Pseudo-inverse concept extended to Hilbert space unbounded operators with arbitrary range 01 p0092 A66-10179
- Axially symmetric potentials represented as mean values in integral operators given for Stokes-Beltrami equations 01 p0058 A66-10505
- Extreme properties of operator which degenerates to trigonometric polynomials in case of periodic functions 05 p0709 A66-15358
- Algebra of singular integral operators, discussing action on Hilbert space and homomorphism 06 p0901 A66-16008
- Forced oscillations of elastoherededitary systems, using Rabotnov functions as kernels of integral operators, permitting description of creep curves for materials 08 p1307 A66-18884
- Resolvent kernel for class of integral operators with difference kernels on finite interval for transport processes 10 p1549 A66-21301
- Generalized heat equation solution expansion in terms of radial heat polynomials, Appel transforms and Laguerre polynomials 13 p2118 A66-25793
- Complex cycles of differential equations examined, deriving limit cycle of multiplicity, integration by quadrature, etc 13 p2119 A66-25851
- Uniqueness of operator spectral function of self-adjoint boundary value problem involving second-order differential equation with operator coefficients 14 p2320 A66-27158
- Linear integral operators applied to singular differential equations and to computations of compressible fluid flows 16 p2683 A66-30241
- Bergman integral operator to generate families of transonic flow patterns which yield Ringleb pattern as special case 17 p2909 A66-32498
- Powers of integral operator generated by Cauchy problem for second-order hyperbolic equation solved by Riesz method of analytical continuation 21 p3756 A66-38739
- Existence theorems of periodic solutions to integro-differential equation with delayed argument 21 p3756 A66-38742
- Integral operator for solving aerodynamic problems for slightly rarefied viscous gas 23 p4054 A66-41356
- Computer technique for constitutive equations of viscoelastic modulus, using Laplace transform and Volterra integral equation, applied to data on solid propellants 24 p4289 A66-42279
- INTEGRATED CIRCUIT**
- SA PRINTED CIRCUIT**
- Microelectronic integrated circuits and thin films applied to inertial navigation systems to achieve cost reduction 01 p0034 A66-10011
- Stress survival matrix test in evaluating reliability of monolithic silicon integrated circuit, measuring safety margin and performance parameter drift 01 p0035 A66-10082
- Metal oxide semiconductor /MOS/ integrated circuits 01 p0037 A66-10500
- Face-down ultrasonic bonding, assembly technique to bond integrated circuit chips to thin films 01 p0037 A66-10501
- Western Electronic Show and Convention, San Francisco, August 1965, Part 2, Integrated circuits 01 p0046 A66-11135
- Static and dynamic performance of discrete component and integrated micropower transistor digital circuits 01 p0047 A66-11136
- Complementary bipolar transistor NAND gate for reducing power dissipation and increasing switching speed 01 p0047 A66-11137
- Low power consumption, high reliability and fully integrated silicon monolithic complementary flip-flop circuit 01 p0047 A66-11139
- Monolithic silicon class B hearing aid push-pull amplifier with low idling current and low current drain 01 p0047 A66-11140
- Integrated circuits equivalent to discrete component circuits in performance and superior in economy 01 p0048 A66-11141
- Current status of linear integrated circuits 01 p0048 A66-11143
- Integrated sense amplifier usable with most medium to high speed coincident current memory /CCM/ systems with only two power supplies and no external components 01 p0048 A66-11144
- Thin film epitaxial single crystal silicon on insulating substrate sapphire and advantages of these microelectronic devices 01 p0048 A66-11145
- Fabrication of thin single crystal silicon films on sapphire and integrated circuit process technology 01 p0048 A66-11147
- Silicon-on-sapphire integrated microcircuit and micropower concepts 01 p0048 A66-11148
- Metallographic polishing procedures used to reveal failure modes in gold-aluminum thermocompression bonds 01 p0049 A66-11153
- Reliability control in parallel gap welding used to join integrated circuit flat packs to printed circuit assemblies 02 p0234 A66-11324
- Microminiaturization applied to circuit integration techniques, outlining steps to fully integrated device including power supply and controls 02 p0199 A66-11860
- Packaging techniques interrelated with design specification and manufacturing capabilities noting integrated circuit system, circuit reliability and thermal resistance 02 p0200 A66-11891
- Thin film integrated wideband amplifier with details on circuit, construction, performance and outline of design process 02 p0202 A66-11918
- Simple active filters using tantalum thin film technology 02 p0202 A66-11919
- Feasibility of guard channel receiver, transmitter and marker receiver system by thin film circuit techniques, noting reliability with minimum servicing 02 p0203 A66-11920
- Silicon monolithic integrated circuit or solid circuit design, noting electrical and economical features 02 p0209 A66-11923
- Standard amplifier building blocks used in systems design, stressing manufacture by silicon integrated circuit



processes 02 p0203 A66-11924  
 Price determining factors considered in integrated circuit amplifier for AM receiver 02 p0203 A66-11925  
 Microelectronics technology noting integrated circuits, passive and active elements, reliability, etc 02 p0209 A66-11926  
 Hybrid integrated-and-conventional circuit configuration in electronic equipment noting thin film circuits, encapsulation, costs, reliability, etc 02 p0204 A66-11928  
 MOS transistor advantages in various digital integrated circuit applications 02 p0194 A66-11934  
 Integrated current limiter design using transistor circuits, pn-pn switches or field effect transistors 02 p0204 A66-11935  
 Integrated circuit characterization by black-box analysis of interconnection parameters, noting transient response 02 p0204 A66-11937  
 Integrated logic circuits for high speed digital systems, noting transmission line connection between gate and amplifier 02 p0204 A66-11938  
 Integrated logic circuit design through breadboard, model assembly, system development, final layout, construction and testing 02 p0204 A66-11939  
 Packaging method for integrated circuits based on flow soldering components through printed wiring boards to be used in digital computer design 02 p0204 A66-11940  
 High-speed reliable cost-orientated integrated circuits, detailing element design and logic and circuit form 02 p0205 A66-11941  
 Microelectronic integrated system cells /MISC/ considering yield and utility 02 p0194 A66-11942  
 Integrated circuit economics discussing design, construction and running costs 02 p0205 A66-11944  
 Microminiature electronic devices noting thin film, integrated circuits and semiconductor technology 02 p0205 A66-11973  
 Nondestructive X-ray diffraction technique for measuring flexure in single-crystal silicon wafers at different stages of integrated circuit fabrication 02 p0275 A66-11978  
 Glass-jointed silicon mosaic for integrated devices 02 p0206 A66-12163  
 Microminiaturization, three-dimensional stacking, ceramic printed, thin film, hybrid and integrated circuits, discussing reduction in system size, weight and primary power requirement and improved reliability 03 p0343 A66-13001  
 Technical developments in field of semiconductors measured by degree of integration of electrical devices 03 p0345 A66-13236  
 DC testers for integrated circuits evaluated, emphasizing areas of application, testing methods and operating characteristics 03 p0345 A66-13274  
 Thin film hybrid approach to economical and time saving miniaturization of integrated electronic circuits 03 p0346 A66-13328  
 Thin film and monolithic circuits combined to satisfy need to couple integrated circuit designer to fabrication process 03 p0347 A66-13329  
 Linear integrated circuits discussing differential and operational amplifiers, development, use, capabilities, new techniques, special designs and reliability 03 p0347 A66-13340  
 Digital integrated circuits discussing current mode logic, resistor, diode and complementary transistor logic circuits, crossover method, power dissipation, testing, standardization and limiting factors 03 p0347 A66-13341  
 Integrated circuit testing noting dynamic test system capabilities 04 p0491 A66-13385  
 Practical component packaging system for compatible use of integrated and thin film circuits in spaceborne digital command and data handling equipment 04 p0492 A66-13465  
 Integrated circuit for time division multiplexers having flexible integrated gate driver circuit for field effect transistor analog gates 04 p0492 A66-13598  
 Microelectronic PCM multicoader using integrated circuits, noting power dissipation,

circuit design, packaging, etc 04 p0493 A66-13599  
 Microelectronic integrated circuits and functional blocks in future aerospace electronic system 04 p0493 A66-13632  
 Avionics design using integrated electronics or microelectronics, noting reduction of maintenance requirements 04 p0494 A66-13684  
 Logical and computing devices, discussing construction of homogeneous functional structure using integral circuits 04 p0494 A66-13704  
 Inductance into integrated circuit, noting techniques involving RC networks 04 p0503 A66-13765  
 Numerical characteristics of signal-noise mixture at output of autocorrelation device for sinusoidal signal and Gaussian noise 04 p0501 A66-14407  
 Monolithic silicon integrated circuit technology noting thin film, insulating and conducting layers, microelectronics, MOS systems, etc 05 p0642 A66-14559  
 High performance operational amplifier design, discussing monolithic circuit construction and performance parameters 05 p0642 A66-14567  
 Metal oxide semiconductor structures in integrated circuits as high and low resistances, inverters and AC amplifiers 05 p0643 A66-14569  
 Integrated circuit current switching logic element fabrication, using transistors and standard isolation techniques 05 p0643 A66-14570  
 Diffusion and film techniques combined in design and fabrication of complex integrated computer logic circuits on small die 05 p0643 A66-14571  
 Integrated monolithic circuits for compact intermediate frequency amplifier 05 p0644 A66-14579  
 Problem of DC coupling between integrated circuit devices and silicon substrates 05 p0646 A66-14637  
 Integrated DC differential instrumentation amplifier discussing drift, gain and common-mode rejection 05 p0646 A66-14641  
 Monolithic integrated circuits regenerative interaction between substrate parasitics and intended semiconductor circuit elements exposed to ionizing radiation 05 p0734 A66-14852  
 Modular synthesis of sequential machines, discussing external variable dependent single memory element devices 05 p0637 A66-14927  
 Reliability of integrated circuits noting stress test schedules, failure rates and sources 05 p0650 A66-15369  
 Yields, costs and reliability of monolithic integrated circuits 05 p0650 A66-15496  
 Thermal-electrical systems for showing effect of variations in integrated circuit geometry and packaging on thermal response characteristics of simple structure 06 p0841 A66-15972  
 Stable tunable RC filters with fixed capacitors, variable resistances and positive feedback 06 p0853 A66-16653  
 Radiation damage to integrated silicon circuit and individual transistors when exposed to neutron flux 06 p0853 A66-16665  
 Reliability of integrated circuits 06 p0856 A66-16925  
 Design of digital monolithic integrated circuit 06 p0856 A66-16926  
 Resistor values in semiconductors calculated from diffusion parameters and vice versa 06 p0857 A66-16928  
 Quadrature modulation single-sideband circuit as frequency translating two-port, comparing performance with conventional modulator-with-SSB filter circuit 07 p1015 A66-17746  
 Microminiature element packaging and multilayer circuits, discussing design and production 07 p1010 A66-18247  
 Crystal oscillator described, using quartz as series resonant element with integrated solid state circuit 07 p1010 A66-18250  
 MOS transistor and application to integrated circuits 07 p1012 A66-18274  
 Semiconductor integrated circuits, discussing diffusion preparation techniques, components used, manufacturing,

interconnecting and packaging and combining with evaporated circuitry 08 p1200 A66-18996  
 Gain in signal to noise ratio obtained with integrated circuit connected behind detector and gain determination 08 p1183 A66-19100  
 Microminiaturization in control equipment and computers 08 p1194 A66-19300  
 Pulse-radar altimeter for Saturn launch vehicle incorporating molecular and monolithic integrated circuits 08 p1225 A66-19520  
 Low-cost fast development capability of master-dice technique for custom line integrated circuits 08 p1196 A66-19525  
 Transit time creates current lag transistor, making it inductive for developing integrated frequency selective circuits 08 p1197 A66-19560  
 Probability of signal acquisition by phase locked oscillator system operating frequency search mode, determining maximum admissible search rate without noise 09 p1345 A66-20440  
 Integrated circuit reliability control at determination 09 p1354 A66-20560  
 Digital systems research model design containing logic gates in integrated circuit packages 09 p1356 A66-20670  
 Design of circuits around off-shelf line microcircuits including sine wave oscillator, voltage-to-frequency converter, logarithmic amplifier, etc 09 p1359 A66-20900  
 Microelectronic devices and circuit including integrated, monolithic, diffuse and deposited, noting reliability and costs 10 p1507 A66-21200  
 Design problems involved in transition from discrete-component circuits to integrated microelectronic circuits, noting conversion of analog and digital circuits to system packaging 10 p1512 A66-21700  
 Hybrid circuit rejects avoided by using ceramic channels and ultrasonic bonding during assembly of active semiconductor devices and integrated circuits to thin film network 10 p1512 A66-21700  
 Package densities and power dissipation requirements in hybrid integrated circuit solved by modular arrays 10 p1512 A66-21700  
 Microwave circuit design for HF amplifiers and radar systems using either hybrid approach with germanium transistors or monolithic one with silicon transistors 10 p1512 A66-21700  
 Microminiature Loran-C Receiver/Indicator for analog-to-digital conversion, using integrated circuit technology 10 p1555 A66-22000  
 Parallel-gap soldering technique for interconnecting integrated circuit flat pack and etched circuit board, noting test procedures 11 p1665 A66-22600  
 Variable threshold logic, integrated logic circuits which eliminate noise effects in digital equipment 11 p1676 A66-22600  
 DC-9 flight simulator using monolithic integrated-circuit GP-4 computer 11 p1683 A66-22600  
 Monolithic circuit with chip of semiconductor material having diffuse active and passive elements 11 p1668 A66-23000  
 Batch-fabrication of beam-lead transistor integrated circuits and other components with leads serving as structural, protective and electrical functions 11 p1669 A66-23000  
 Reliability and failure mechanisms in integrated circuits 11 p1669 A66-23100  
 Transistor-tunnel diode flip-flop with built in gating 11 p1669 A66-23100  
 Integrated circuit gate ring counter noting flip-flop variety comparison 11 p1677 A66-23100  
 Monostable and bistable counting circuit synthesis and analysis of volt-ampere characteristics 11 p1678 A66-23200  
 Circuit design techniques for line integrated circuits, noting manufacturing methods, achievement of monolithic construction, etc 11 p1670 A66-23200  
 Integrated modular digital computer system for ICETAN /ICES-FORTRAN programming of engineering problems 12 p1827 A66-23800  
 Silicon monolithic Semiconductor Memory Integrated Device /SMID/ memory system and memory storage



- ement 12 p1827 A66-23834
- Component reliability, especially in 12 p1827 A66-23834
- transistors, noting techniques, design, tests and mounting as monolithic 12 p1833 A66-24082
- circuits 12 p1833 A66-24082
- Integrated circuits containing transistor, diode and resistor with unilateral and bilateral switches, noting 12 p1834 A66-24087
- application 12 p1834 A66-24087
- Multipurpose chips for reduction of analog computer integrated circuit 12 p1834 A66-24101
- ost 12 p1834 A66-24101
- Integrated stability augmentation circuits 12 p1837 A66-24381
- AN/ASW-16 automatic flight control system 12 p1837 A66-24381
- Integrated circuit processing, particularly array technology, noting key problems 12 p1840 A66-24619
- Microwave integrated circuits in radar systems, detailing airborne forward-looking radar, using phased arrays and pulse compression 12 p1840 A66-24620
- Integrated mixers in S-band construction, using bilithic Schottky barrier diode chip and evaporated microstrip circuitry on alumina dielectric 12 p1840 A66-24621
- Solid state UHF telemetry converter using microwave interdigital multiplexing filter containing integrated semiconductor elements 12 p1840 A66-24622
- Tunnel diode amplifier for broadband radio communication using integrated circuits, noting noise figure, stability and saturation effect 12 p1840 A66-24623
- Monolithic silicon-transistorized integrated amplifier for use as stabilized gain block element in linear circuit 12 p1842 A66-24656
- realizations 12 p1842 A66-24656
- Matrix methods for design of HF integrated circuit 12 p1844 A66-24729
- amplifier 12 p1844 A66-24729
- Polysilicon insulated gate field effect transistor having active element fabricated in epitaxially deposited film on oxidized single crystal silicon 12 p1845 A66-24831
- substrate 12 p1845 A66-24831
- MOS FETs in microelectronics, including digital arrays and logic 12 p1845 A66-24847
- gates 12 p1845 A66-24847
- Metal oxide silicon integrated circuits subsystem size, weight, power and cost compared with double diffused counterpart 12 p1845 A66-24848
- Silicon monolithic circuit development, discussing cost reduction and performance improvement in 12 p1845 A66-24850
- microcircuits 12 p1845 A66-24850
- Properly controlled high-stress life testing used to evaluate failure rate of high reliability solid state components of integrated circuits 12 p1846 A66-24913
- Integrated circuit selective amplifier for intermediate frequency application, using RC active networks 12 p1846 A66-24915
- Thermocompression bonding applied to integrated circuits of semiconductor and thin film type, noting resistance, ultrasonic and electron beam 12 p1846 A66-24916
- welding 12 p1846 A66-24916
- Semiconductor technology applied to design of electronic microsystems 13 p2029 A66-25118
- Optically coupled linear circuit techniques, discussing GaAs p-n junction diode, noncoherent light emitters and silicon p-n junction photosensors 13 p2036 A66-25521
- Design and integrated circuit fabrication of negative impedance converter, using two transistors and two resistors 13 p2036 A66-25523
- Integrated circuits with propagation delays in nanosecond range, noting emitter coupled logic circuit 13 p2036 A66-25534
- Passive thin-film component materials, vacuum evaporation and sputtering processes 13 p2039 A66-25645
- Direct-coupled multistage integrated amplifier design for optimum performance under arbitrary cascade configuration, noting power gain and frequency range 13 p2040 A66-25831
- Band pass characteristics realized by four-layer distributed RC network without series resistance and amplifier scheme used as model for integrated circuits, noting frequency characteristics 13 p2051 A66-26069
- variation 13 p2051 A66-26069
- Reliability assessment techniques for microelectronics, considering integrated circuits, testing procedures, etc 13 p2043 A66-26226
- Electronically tunable circuits for integrated circuits 14 p2263 A66-27047
- Integrated circuit as exclusive-OR gate or as linear amplifier, using transistor or tunnel diode shunted by resistor 14 p2263 A66-27051
- Ministick packaging system for integrated circuits 14 p2249 A66-27109
- Capacitors for monolithic integrated circuits 14 p2252 A66-27306
- Integrated circuit binary counters using majority logic current mode gate element 14 p2255 A66-27803
- Microelectronic PCM multicode using integrated circuits, noting power dissipation, circuit design, packaging, etc 14 p2243 A66-28349
- Logical and computing devices, discussing construction of homogeneous functional structures using integral circuits 15 p2454 A66-28545
- Integrated circuit fabrication noting diffusion steps, temperature and time dependency, doping solid solubility, impurity distribution, etc 15 p2465 A66-29602
- Nondestructive attachment of small electronic components and integrated circuits for simulated mounting in vibration and shock testing 16 p2680 A66-30481
- FM/FM and PAM/PM integrated telemetry systems with MDI for missile evaluation system 16 p2651 A66-30562
- MOS circuit design noting economics, chip area, integrated arrays, etc 16 p2660 A66-30577
- MOS arrays and IC techniques including boxing out, eliminating columns and rows with bad circuits, Fairchild approach, etc 16 p2660 A66-30578
- Transformerless chopper built with integrated circuits, noting low power consumption, offset voltages and HF operation 16 p2661 A66-30660
- Materials science and technology in integrated electronics - Conference, San Francisco, September 1965 16 p2781 A66-31414
- Integrated circuit technology, noting array trend 16 p2664 A66-31415
- Thin film transistors and use in integrated circuits 16 p2664 A66-31416
- Cryoelectronic integrated circuits utilizing superconducting storage and switching devices 16 p2665 A66-31417
- Selective epitaxial deposition of semiconducting GaAs for p-n junction and integrated circuit application 16 p2665 A66-31418
- Fabrication of linear integrated amplifier circuits 16 p2665 A66-31430
- Fabrication of interconnections for integrated circuits operating at microwave frequencies 16 p2665 A66-31433
- Discoloration in contamination area of aluminum bonds in integrated circuits, noting cause and effect on interconnection bond integrity 16 p2665 A66-31434
- Hall voltages in silicon obtained by combining MOS transistor structure with Hall effect of material, noting experimental results, design criteria, etc 16 p2667 A66-31581
- Compatible thin film resistor-capacitor process using nichrome and alumina-silica glass for silicon integrated circuits 16 p2667 A66-31595
- Characteristic parameter selection and transient performance capabilities of integrated logic microcircuit 17 p2880 A66-32057
- Integrated and transistor circuit design, discussing parasitic effects, diode structures, volt-ampere characteristics, capacitors and resistors, temperature and doping effect, etc 17 p2881 A66-32104
- Thin film passive devices combined with monolithic silicon techniques to produce circuits superior in electrical and environmental performance to conventional integrated circuit 17 p2882 A66-32106
- Metal oxide semiconductor transistors use in integrated circuits, discussing field effect devices, analog circuits configurations and applications 17 p2882 A66-32108
- MOS transistors in integrated switching circuits to obtain desirable characteristics of pentode vacuum tubes and bipolar transistors 17 p2882 A66-32109
- Basic guidelines, including estimate of difficulty in incorporating various components into integrated circuits design 17 p2882 A66-32110
- Integrated circuit design, examining layout, tolerances and component interactions 17 p2882 A66-32111
- Step-stress technique to induce failures in integrated circuits to pinpoint source of reliability problems 17 p2882 A66-32114
- Turtle, microcircuit logic or transistor resistor transistor logic /TRTL/ for integrated circuits 17 p2883 A66-32117
- Pulse duration modulator /PDM/ conversion into integrated silicon functional electronic block 17 p2883 A66-32119
- Integrated high speed diode-transistor-logic gate /DTL/ design, discussing, stray capacitance, resistors, diode combination and switching transistors 17 p2883 A66-32121
- Integrated circuit design optimization, using modified direct coupled transistor logic NOR gate 17 p2883 A66-32122
- MOS arrays in improving system size, reliability and power consumption 17 p2883 A66-32126
- Breadboard approach for integrated circuits with reduction of lost and development time, tabulating resistor and transistor parameters 17 p2884 A66-32128
- Integrated circuit breadboarding time saving procedures 17 p2884 A66-32129
- Black-box specifications for best compromise of linear integrated circuit design 17 p2884 A66-32130
- Integrated circuit testing by sequential, go-no-go and programming methods 17 p2884 A66-32131
- Papers on RCA computer progress 17 p2877 A66-32510
- Monolithic silicon integrated circuit application in design of two third-generation computers 17 p2877 A66-32511
- Monolithic silicon integrated circuit used for current-mode logic of RCA Spectra 70/45 and 70/55 computers 17 p2886 A66-32512
- MOS transistor suitability to integrated logic networks, using arrays of many identical elements with superimposed connections 17 p2901 A66-32514
- Batch fabrication of large-capacity memory stacks, using integration of monolithic-ferrite stack with integrated MOS circuitry 17 p2886 A66-32515
- Developmental memory using monolithic-ferrite integrated arrays of magnetic storage elements provides cost and power savings 17 p2886 A66-32516
- Technique for formation of thin tantalum film resistors on silicon integrated circuits 17 p2887 A66-32699
- Microcircuit design, manufacture and application, noting use of silicon monolithic integrated circuits, performance characteristics, reliability, etc 17 p2894 A66-33101
- Program-controlled module design using strips of nickel foil for welding of flatpack assemblies 17 p2930 A66-33121
- Thick film hybrid integrated circuits 17 p2897 A66-33366
- Thermoconductivity, mechanical stress, processing characteristics, etc, of various adhesives used in integrated circuits, noting neoprene cement 18 p3077 A66-34051
- Integrated circuit connecting and packing, discussing cost flexibility and performance characteristics 18 p3086 A66-34399
- Monolithic, thin-film and hybrid integrated circuits technology 18 p3087 A66-34703
- Quartz crystal active filters noting design and operation of multiresonator filters 19 p3312 A66-35337
- Pinhole array camera for multiple image production for integrated circuits 19 p3354 A66-35385
- Automatic failure detection, location and correction system for failures in unmanned spacecraft using frequency-shift-keyed subcarrier 19 p3316 A66-35679
- Catastrophic failures in glass diode packages and integrated circuit chips exposed to high-intensity electron pulse 19 p3318 A66-35920
- Solid structure tunnel diode, discussing



design and manufacture, noting use of thin film photolithographic process for improved reliability 19 p3319 A66-36164

Circuit functions, electrical parameters and fabrication of integrated analog switch in monolithic silicon block 19 p3320 A66-36322

Integrated circuits, examining thin film evolution, noting advantages of size reduction, reliability and functional value 19 p3322 A66-36817

Applicability of microelectronic technique to construction of integrated wideband amplifier consisting of symmetrical differential circuit and common-emitter circuit 19 p3323 A66-36818

Optimum fabrication of microelectronic devices by interconnection of integrated circuits on ceramic 19 p3323 A66-36820

Homogeneous microelectronic structures using integrated circuit technology for fabrication of logical and sequential facilities 19 p3323 A66-36821

Physical limits of miniaturization, noting element size, packing density, heat dissipation, etc, in connection with integrated circuits 19 p3323 A66-36825

Miniature shaft-angle encoder with integrated-circuit encoding matrix and built-in memory potential using single static commutation ring 20 p3558 A66-37217

Transient radiation response and permanent radiation damage in monolithic silicon-junction-transistorized integrated circuit 20 p3526 A66-37318

Direct-coupled gyrator suitable for integrated circuits and time variation 20 p3527 A66-37447

Acceptance checkout system for checkout assistance to Apollo CSM and LEM facilities during countdown, discussing system configuration variability, composition and operation 20 p3543 A66-37579

Gold-plated nickel used for printed wiring in parallel-gap welding of integrated circuits to provide visual criteria for acceptable welds 20 p3562 A66-37621

Integrated circuits economics, discussing design, construction and running costs 20 p3531 A66-37830

Multilayer board and chip production techniques 20 p3535 A66-38414

Substrate properties effect on processing and reliability of tantalum thin film circuits [ACS PAPER 2-S5-65] 21 p3710 A66-38678

Integrated electronic arrays, examining fabrication, logical design, application and packaging 21 p3710 A66-38828

Microcircuits in ground radar, emphasizing phased array techniques and digitalization of beam steering functions 21 p3710 A66-38829

Assembly and packaging of microelectronic systems by integrated circuits, considering spatial configuration, maintainability, interconnection, thermal transfer and environmental resistance 21 p3710 A66-38830

Component characteristics in integrated circuits 21 p3716 A66-39621

Electronic component, ferrite memory cores, filters and inductances adapted to integrated circuit 21 p3716 A66-39622

utilization 21 p3716 A66-39622

Selective amplification of signal voltages in analog computers with integrated circuitry 21 p3716 A66-39623

Miniaturization of logic components for modular and monolithic integrated circuits in computer design 21 p3708 A66-39624

Boolean algebraic analysis of AND, OR, NAND and NOR functions in electronic integrated circuits 21 p3720 A66-39625

Frequency meter for measuring center frequency of random pulses distributed according to Poisson law, consisting of integrating circuit with high time constant 22 p3918 A66-40404

Nondigital applications and interconnection aspects of integrated electronics - WESCON, Los Angeles, August 1966 22 p3878 A66-40713

Packaging monolithic integrated circuits in UNIVAC 1824 Aerospace Computer Central Processor 22 p3878 A66-40714

Power and control integrated circuits - WESCON, Los Angeles, August 1966 22 p3880 A66-40739

Inverter with integrated components and direct coupled inverter circuit not needing transformers for space

applications 22 p3880 A66-40740

Integrated circuit arrays for solid state inverters, noting Johnson counter and packaging 22 p3881 A66-40742

Microbonding - Colloquium, Sunbury-on-Thames, Middlesex, England, January 1966 23 p4043 A66-41188

Microbonding techniques such as thermocompression bonding, soldering, electrical resistance and ultrasonic welding, noting applicability in transistor manufacture 23 p4043 A66-41190

Integrated circuit welding into electronic equipment via parallel gap method, noting military applications in forward area communications 23 p4044 A66-41198

Active and passive multiplication of RC time constants for subaudio frequency integrated filters 23 p4046 A66-41581

Thin films and semiconductors for integrated circuits in microelectronics, for application to aeronautics and astronautics 23 p4048 A66-41657

Reliability prediction, failure rates, fail-safe design and packaging of integrated circuit and MOS-FET microminiaturized electronic equipment 24 p4179 A66-42098

Optimum use of microelectronic reliability data in system development, discussing relation to sources 24 p4179 A66-42099

Performance modeling procedure to determine characteristics of integrated logic devices 24 p4177 A66-42100

Silicon integrated circuits in rocket telemetry transmitter phase-lock frequency stabilization unit 24 p4180 A66-42262

Contour epitaxial deposition for semiconductor devices and integrated circuits, producing regions with well defined doping and geometry in crystal with flat surface 24 p4181 A66-42386

Systems design and packaging with integrated circuits, discussing proper circuit selection guidelines and parameters 24 p4182 A66-42499

Amplifiers using field effect device in first stage and bipolar transistor in second with limited drain-source voltage 24 p4185 A66-43031

Flat-pack case for thermal resistance of integrated circuit to space environment 24 p4186 A66-43059

Transistor parameters in integrated circuits including saturation resistance, voltage breakdown and frequency response and optimization of operation dependence on impurity concentration, geometry, etc 24 p4186 A66-43079

INTEGRATION

SA BINARY INTEGRATION

SA FUNCTIONAL INTEGRATION

SA NUMERICAL INTEGRATION

SA RUNGE-KUTTA INTEGRATION

Conditions of integrability for certain normal systems of equations with partial derivatives 04 p0538 A66-13469

Statistical approach to derivation of quadrature formulas 07 p1061 A66-18510

Integration of Laplace transformed elastokinetic equations, examining stress function, displacement vector field and boundary and initial value problems 10 p1555 A66-21226

Asymptotic integration of elasticity theory equations and analysis of stressed state of anisotropic shell 15 p2609 A66-28963

Curve fitting technique for integration of hydrostatic equilibrium equations of planetary constitution simplified by introduction of homology-invariant variables 16 p2799 A66-30619

Integration of near equilibrium flows in propulsive nozzles, estimating length of transition region from equilibrium condition to kinetic solution [AICE PREPRINT 28C] 22 p3971 A66-39884

INTEGRATOR

SA DIGITAL INTEGRATOR

Surveying transistorized differentiators and integrators, giving fundamental RC and equivalent circuits 01 p0045 A66-11022

Circuitry of diode pump integrator used for generating mean voltage which is function of repetition rate of applied pulse train 03 p0345 A66-13241

Correlation relations of output voltage of switched RC integrator 06 p0823 A66-15888

Properties of second-gate electrode of

MOS-FET and application as voltage controlled integrator 14 p2248 A66-2705

Integrator, whose transfer function has simple pole in z plane, modified to make possible greater stability with no loss increase or improved signal to noise ratio 15 p2449 A66-2864

LF drift reduction for integrators of repetitive signals 15 p2475 A66-2986

Ideal integrator compared with low pass filters 18 p3076 A66-3383

Noise characteristics at integrator input 1 nonstationary regime 19 p3311 A66-3529

High-quality transistorized gyrator for integration 20 p3528 A66-3744

Rheoelectric integrator simulation method for charge carrier lifetime determination 1 transistor 21 p3713 A66-3932

INTELLIGENCE

S ARTIFICIAL INTELLIGENCE

INTELSAT SATELLITE

International Telecommunications Satellite /INTELSAT/ Consortium and COMSAT participation in program [AIAA PAPER 66-332] 12 p1982 A66-2479

INTENSIFIER TUBE

S IMAGE INTENSIFIER

INTENSITY

S ELECTRON INTENSITY

S LIGHT INTENSITY

S LUMINESCENT INTENSITY

S LUMINOUS INTENSITY

S MAGNETIC FIELD INTENSITY

S NOISE INTENSITY

S PARTICLE INTENSITY

S RADIATION INTENSITY

INTERACTION

S ELECTROMAGNETIC INTERACTION

S ELECTRON INTERACTION

S ELECTRON-PHONON INTERACTION

S FLAME INTERACTION

S GAS-GAS INTERACTION

S GAS-ION INTERACTION

S GAS-LIQUID INTERACTION

S GAS-METAL INTERACTION

S GYROINTERACTION

S HIGH ENERGY INTERACTION

S ION-ATOM INTERACTION

S MOLECULAR INTERACTION

S NUCLEAR INTERACTION

S SPIN-ORBIT INTERACTION

S SURFACE INTERACTION

S WAVE INTERACTION

INTERCEPTION

Probability of overlapping intercept by system of random intercepts and application to detection of flying objects in cloud, skies 24 p4231 A66-4247

INTERCEPTION + RENDEZVOUS

Selection of comet intercept mission, based on predictability of future returns obtainability of spectroscopic data from Earth during intercept and launch energy limitations 17 p3011 A66-3336

INTERCEPTOR

SA SATELLITE INTERCEPTOR

U.S. tactical defense systems noting SAM types, interceptors, technical problems, data handling, radar, etc 24 p4297 A66-4295

INTERCONTINENTAL BALLISTIC MISSILE /ICBM/

SA MINUTEMAN ICBM

SA TITAN II ICBM

Recent developments in Minuteman ICBM system and projected improvements such as increased mobility, better site hardening, and defense systems 13 p2192 A66-2568

Problems when using RF diagnostic systems in flight test evaluation of ICBM systems, specifically when using EM system during reentry [AIAA PAPER 66-406] 18 p3239 A66-3363

INTERFACE

SA GAS-SOLID INTERFACE

SA LIQUID-LIQUID INTERFACE

SA LIQUID-SOLID INTERFACE

SA LIQUID-VAPOR INTERFACE

Interface between aerospace systems with man, spacecraft and supporting ground stations 20 p3662 A66-3718

Symbolic programming digital computer techniques, hardware interfacing and system errors in simulation of lunar midcourse guidance and navigation systems 20 p3543 A66-3725

Method for calculating distribution of electric potential above conducting media with parallel interfaces for general case of



layers and arbitrary resistivities of base 20 p3551 A66-37512

Subsystem interfacing in Titan III space launching system, discussing contractual requirements, interface program timing, interface documentation and coordination, review and approval procedures 20 p3687 A66-38186

Two-dimensional time-space analysis of Doppler-effect-like phenomena in refraction and reflection of waves propagating through moving boundary between two media 21 p3706 A66-39574

**INTERFACE STABILITY**

Physical mechanisms of instabilities altering two-phase flow pattern of liquid film 01 p0165 A66-10907

Surface coating of lyophobic films in affecting surface interactions at phase interfaces of heterogeneous systems during transfer process 01 p0166 A66-10997

Stabilizing effect of surface active agents on wave formation in contaminated falling liquid film 07 p1023 A66-18125

Schottky barrier from silicon surfaces with controlled exposure to oxygen and water vapor, noting work function, semiconductor surface state and thickness of interface layer 07 p1107 A66-18406

Metal-ceramic boundary structures and reactions, considering metal-oxide and metal-glass interfaces, ionic and covalent bonds, oxidation, reduction, solution and precipitation 13 p2108 A66-25767

Taylor-Helmholtz instability between liquid of constant shear and vacuum 13 p2068 A66-26682

Inversion layer drift, surface charge, minority carrier recombination rates and lateral current flow effects on silicon-silicon dioxide interface, using MOS capacitance-voltage curve technique 17 p2884 A66-32197

Longitudinal magnetic field reduction of growth rate of gravitational type acceleration instability of liquid metal by vapor 17 p2967 A66-32452

**INTERFACIAL ENERGY**

**IS SURFACE ENERGY**

**INTERFACIAL STRAIN**

Rhenium effect on interface energies of Cr, Mo and W, noting liquid surface tension, solid surface energy and grain-boundary grooving 18 p3121 A66-33726

Constitutive equations for nonlinear elastic solid-linear viscous fluid mixture and for mixture of two nonlinear elastic solids 22 p3898 A66-40140

Heat flux dependence and directional effect of thermal contact resistance for interface between dissimilar metals 22 p4000 A66-40921

**INTERFERENCE**

**SA ELECTROMAGNETIC COMPATIBILITY**

**SA RADIO INTERFERENCE**

**SA WAVE DIFFRACTION**

Interference effects at thin transparent cylindrical glass fibers exposed to coherent light from He-Ne laser 01 p0081 A66-10368

Statistical properties of output of double-sideband receiver when nonlinear mechanisms at input admit unwanted double-sideband signals with Gaussian modulation 05 p0630 A66-14593

Fraunhofer pattern of laser light transmitted through optical fiber, noting spatial frequency of interference fringes between light waves 05 p0696 A66-14972

Maximum likelihood detection of band limited binary signals perturbed by Gaussian noise and intersymbol interference 06 p0829 A66-16193

Learning-type signal processing receivers for binary communication channels with intersymbol interference 06 p0830 A66-16196

Interference phenomenon of serrated system of rings surrounding central beam of gas laser analyzed, using helium neon tube placed between two exterior mirrors 06 p0893 A66-17064

Hologram-generated ghost image experiments to verify fragment displacement theory and diffuse light waveforms 10 p1534 A66-21249

Verification of Klesig equation for interference fringes formed by X-rays scattered from thin films 12 p1926 A66-23712

Moire fringes formed by two zonal gratings

of equal or slightly different pitches 12 p1960 A66-23951

Electron density at large distances from Sun determined by photoelectric measurements during total solar eclipse of July 20, 1963 13 p2187 A66-26134

Anomalous phase variations of GBR transmissions as received in New Zealand correlated with solar season and probably due to long path

Interference 14 p2237 A66-27401

Pressure distribution along wing and body of wing-body combination 14 p2221 A66-28185

Coherence in radiation peaks of ruby laser studied through interference field 17 p2938 A66-33510

Electromagnetic interference from pulse circuits, switches and relays produced by photo-optical control systems 21 p3709 A66-38608

Microwave interference measurement of shock velocity in shock tube, noting standing wave pattern 21 p3738 A66-38798

Plane surface deviation from ideal plane measured by interference method, applied to testing of interferometer plates 21 p3738 A66-39131

Inverse transfer function of pulse-forming network for binary code transmission with small intersymbol interference in time domain and narrow bandwidth in frequency domain 22 p3866 A66-40182

Angle of arrival in amplitude-comparison monopulse antenna arrangement including thermal noise as interference and pulsed radar with ideal radar target 23 p4044 A66-41314

Coherence in radiation peaks of ruby laser studied through interference field 24 p4218 A66-42124

Diffraction gratings by recording laser-generated interference pattern on high resolution film as two-beam hologram 24 p4210 A66-42259

High energy muon flux in interference radiation incident to fast charged particle constant-speed trajectories through periodic laminar medium 24 p4271 A66-42939

**INTERFERENCE DRAG**

Configuration synthesis and optimal utilization of supersonic favorable interference to obtain high lift-drag ratios [AIAA PAPER 65-752] 03 p0315 A66-12732

Interference effect for biconvex aerofoil in wind tunnel with slotted liners 13 p1992 A66-26698

**INTERFERENCE FACTOR TABLE**

Interference ratios in space telecasting, considering methods of control for cochannel broadcasting [AIAA PAPER 66-283] 12 p1821 A66-24754

Basic performance thresholds for 23 desired and undesired modulation types, noting application to interference prediction 23 p4040 A66-41598

**INTERFERENCE GRATING**

Random error estimation for Mach-Zehnder interferometer interference fringe measurements 15 p2502 A66-29383

Transmission characteristics of Fabry-Perot aluminum-magnesium fluoride-aluminum interference filters in far UV region, noting preparation methods, optical properties, etc 17 p2958 A66-32617

Grille spectrometer, noting greater signal to noise ratio than that of scanning Fabry-Perot spectrometer for airglow observations 19 p3353 A66-35378

Interference filter of Fabry-Perot interferometer-type for studying millimeter and submillimeter plasma radiation 22 p3958 A66-40936

Edser-Butler band amplitude dependence on modulating effect of interference grating 24 p4212 A66-42819

**INTERFERENCE LIFT**

Airflow interference theory applied to streamlined wings and bodies undergoing simple harmonic oscillations 07 p0981 A66-18102

**INTERFERENCE MONOCHROMATIZATION**

Wave front shearing interferometer applied to chromatic and monochromatic aberration testing 06 p0878 A66-16117

Coherence properties of optical fields, examining interference effects, intensity fluctuations, photoelectric effects and pulsations 16 p2749 A66-31584

**INTERFEROMETER**

**SA FABRY-PEROT INTERFEROMETER**

**SA MACH-ZEHNDER INTERFEROMETER**

**SA MICHELSON INTERFEROMETER**

**SA MICROWAVE INTERFEROMETER**

**SA RADIO INTERFEROMETER**

Laser interferometer to measure time and spatial variation in repetitively pulsed plasma 01 p0079 A66-10243

Aerodynamic and heat transfer measurements using interferometer with continuous wave laser as source 01 p0069 A66-10849

Spectral measurement of solar simulator sources using polarization interferometer spectrometer 02 p0226 A66-11219

Correlation of phase fluctuations of optical field by photoelectric predetection interferometer 03 p0367 A66-12304

HF direction finder consisting of two orthogonal interferometers built and tested by 16,000 direction-of-arrival measurements 03 p0344 A66-13019

He-Ne laser incorporated into arm of interferometer used to measure fringe shift in small transient plasma 04 p0529 A66-13743

Measurement of electron density of gas discharge plasma by laser interferometer 06 p0916 A66-16379

Interferometer for measurement of ratio of small changes in wavelength of spectral line to linewidth, as basis for measuring plasma electron temperature 06 p0883 A66-16943

Advantages of gas lasers as light sources in aerodynamic research interferometers 06 p0893 A66-16944

Two-element interferometer to investigate Jupiter decimeter circularly polarized radiation 08 p1288 A66-18789

Interferometer for interference perturbation of electromagnetic three-cm waves 08 p1224 A66-19320

Diane ground station interferometry antenna, examining choice of polarization and use of slots for precise measurements 10 p1511 A66-21708

Interferometric determination of radio source positions and use of Royal Radar Establishment Interferometer 11 p1657 A66-23191

Interferometric measurement of ultrasonic velocity in gases at frequencies around 100 kc/s to determine vibrational relaxation 12 p1913 A66-23821

Dependence of Zeeman beat frequency on interferometer tuning in single-mode He-Ne laser with various gas pressures and magnetic field strengths 13 p2101 A66-26201

Multiple element swept-lobe interferometer for study of solar radio bursts 13 p2084 A66-26569

Wavefront shearing prism interferometer applied to testing of chromatic aberration of simple and compound lenses and waveforms characterizing monochromatic aberrations 14 p2291 A66-27319

Lateral shearing interferometer with gas-laser light source for testing large optical systems 14 p2307 A66-27320

Mock interferometer theory with calculation of luminosity and resolving power 14 p2294 A66-27496

Three-meter Ebert grating spectrometer with mock interferometer attachment 14 p2294 A66-27497

Electrostatic probe measurements of velocity displacement and electron density of plasma using laser compared with measurements using microwave interferometer 14 p2346 A66-28269

Optical beam deflection technique using interferometer cavity illuminated by gas laser beam 15 p2512 A66-28689

Holograms of object illuminated with spatially incoherent light from low pressure mercury lamp, using afocal lens in interferometer for wavefront splitting 15 p2497 A66-28694

Gas laser output wavelength stabilization by use of external passive optical interferometer 15 p2513 A66-28835

Fourier transform spectroscopy, history and current status 15 p2498 A66-28838

Collected reports on new development of telescopic, photometric, spectrometric, meteorological, interferometric and detection equipment at various solar and stellar observatories 17 p2923 A66-32020



Plasma density using laser based interferometer, interpreting phase shift of laser signal as time dependent laser frequency variation 19 p3374 A66-35817

Near IR two-beam interferometer built for astronomical observations by Fourier transform spectroscopy, noting resolution of spectra of Venus and Mars 20 p3556 A66-36939

Radio-source fringe visibility survey with NRAO interferometer of 21,500-wavelength base line 20 p3649 A66-37323

Multiple-pass laser interferometer used to confirm electron density inferred from Stark broadening of hydrogen beta line 23 p4101 A66-41260

Optical interferometers for low electron density measurements of transient plasmas 23 p4068 A66-41289

Electron and neutral atom densities in helium and argon afterglow plasma obtained by two helium-neon laser interferometers, noting temporal dependence of electron decay 23 p4101 A66-41364

Low accuracy of interferometric measurement of coefficient of ultrasound absorption in gas 23 p4068 A66-41414

Millimeter wave resonant interferometer capable of measuring spatial distribution of electrons in low density transient plasma column subject to perturbation 24 p4209 A66-42191

**INTERFEROMETER SYSTEM**

Adjustable compensator for Mach-Zehnder interferometer which is suited for large-aperture systems 02 p0233 A66-12216

Laser oscillations and self Q-switching, discussing pulsed flash-lamp excitation experiments with triply activated confocal barium crown glass etalon 04 p0531 A66-13980

Mach-Zehnder interferometer for electromagnetically accelerated shock waves in hydrogen 04 p0554 A66-14285

Two lenses with focal ratios of  $f/4$  and  $f/2.65$  used to collimate light from helium-neon laser 05 p0695 A66-14921

Observation location and instrument vagaries cause discrepancy between photographic and photoelectric interferometric measurements of dayglow at 6300 angstroms 05 p0671 A66-14958

Wave front shearing interferometer applied to chromatic and monochromatic aberration testing 06 p0878 A66-16117

Interferometric examination of Jupiter decimeter radio emission, noting equipment, polarization characteristics and distribution of nonthermal emission 09 p1450 A66-20106

Interferometric measurement of large indices of refraction, noting applicability and accuracy 09 p1403 A66-20516

Gemini rendezvous radar using interferometric angle measuring system, digital range data readout, analog range display and target vehicle command link 09 p1346 A66-20583

RADINT rocket tracking station combines Doppler and interferometer techniques, eliminating need for three or four separate ground stations 09 p1355 A66-20588

Ground station characteristics and requirements in fields of tracking, telemetry and remote control 10 p1520 A66-21706

Long-baseline radio interferometer for radio astronomy, combining wideband signal and one-dimensional linear array to restrict spatial response in two dimensions 11 p1704 A66-22562

Laser application and techniques noting amplification, modulation, interferometry, scattering, plasma diagnostics, nonlinear optics, etc 12 p1889 A66-23931

Power response of two-element interference frequency correlation interferometer to point source of broadband random noise 12 p1840 A66-24626

Holographic interferometry, advantages and operation 13 p2076 A66-25048

Gemini noncoherent pulse radar system using interferometer methods for angle information, noting failures of diode capacitor combination and methods of reliability improvement 13 p2035 A66-25508

Radiotelescope of 40-sec-of-arc resolving power, composed of compound interferometers with small antennas 13 p2058 A66-25569

Radio astronomy antenna theory, discussing antenna resolution, brightness distribution of celestial bodies, interferometer patterns, actual antennas, etc 20 p3530 A66-37721

Intracavity interferometer laser measurements of power gain and output in single-frequency Ar laser and 6328-angstrom Ne isotope shift 22 p3932 A66-40110

Soret Zone Plate simulation by longitudinally distributed coaxial aperture system, noting system activation and operation 23 p4068 A66-41622

Laser induced plasma density measurement using multiple beam interferometry 23 p4105 A66-41630

Zeeman laser interferometer, using axial magnetic field to obtain simultaneous left- and right-hand circularly polarized oscillation modes at upper and lower cavity resonances 24 p4219 A66-42248

**INTERFEROMETRY**

**SA DIFFERENTIAL INTERFEROMETRY**

Interferometric system of Diane satellite tracking stations permits high altitude tracking and measurements with larger solid angle 01 p0030 A66-10788

Ruby crystal optical properties investigated by interference rings from reflecting He-Ne laser beam from crystal face 01 p0083 A66-11045

Polar interferometric method for measuring north-south component of ultrashort wave refraction in ionosphere and optical thickness gradient 02 p0190 A66-11415

Quantum-electronic cross-modulation effect noted while monitoring IR laser interferometric fringes 02 p0240 A66-11449

Laser application problems in interferometry, radar and holography including mechanical stability, noise suppression, dirty laser beam restoration, etc 02 p0240 A66-11454

Schlieren interferometer operating with one prism and single passage 02 p0229 A66-11566

Diane, European interferometric tracking station noting antenna system, calibration operations, angular measurement, etc 03 p0333 A66-12478

Plasma electron density measurements, interferometric and spectroscopic techniques compared with Stark H-beta line and absolute continuum intensity method 03 p0405 A66-13136

Interferometry with holographically reconstructed comparison beam discussing principles, techniques and error sources 04 p0521 A66-13985

Optical interferometry theory, application and verification in plasma study 04 p0522 A66-14197

Heat and mass transfer from vertical plates boundary layer in convection at low Reynolds number by interferometry [ASME PAPER 65-WA/HT-39] 05 p0664 A66-15669

Lens primary aberration evaluation using Twyman interferometer, developing exact equations for high-order lens defects 06 p0879 A66-16118

Book on Fourier transform spectrometry detailing interferometers and programming procedures 06 p0908 A66-16225

Length of compact function estimated from noisy measurement of modulus of Fourier transform 06 p0867 A66-16977

Conventional flow visualization using laser light source [AIAA PAPER 66-127] 06 p0870 A66-17104

Interferometric hologram evaluation and real time vibration analysis of diffuse objects 07 p1144 A66-18040

Interferometric techniques in visual and radio regions for astrophysics 07 p1035 A66-18151

Optical thickness measurement of transparent films on silicon, using spectrophotometric interference technique 07 p1036 A66-18404

Laser application in photography, noting interferometric and holographic techniques 10 p1535 A66-21333

Wave front reconstruction /holography/, hologram production, interferometry, schlieren photography and shadowgrams applied to fluid mechanics 10 p1536 A66-21750

Low-pressure mercury vapor lamp for

interferometric and spectrometric work, noting electrodes, main discharge tube, electrical circuit, etc 10 p1538 A66-22059

Expansion tube for interferometric observation of hypersonic flow fields 11 p1684 A66-22830

Resolution and noise in Fourier transform spectrometer, considering mechanical limitations and diffraction effects 11 p1705 A66-22869

Two-beam interferometry by wavefront reconstruction from hologram recorded with coherent background successively interfered in same latent image 11 p1708 A66-23204

Ruby crystal optical properties investigated by interference rings from reflecting He-Ne laser beam from crystal face 11 p1714 A66-23292

Dissociation rate of nitrogen behind strong shock waves in nitrogen-argon mixtures determined, using time-resolved interferometric measurements of gas density 12 p1861 A66-23616

Polish-made He-Ne red gas lasers, describing power outputs, gas pressure, He/Ne ratio, mirror transmission coefficient and interferometric application 12 p1889 A66-23946

Dual and multiple-beam interferometry by wave front reconstruction from surfaces of standard engineering components, applicable to structural dilatation problems 12 p1884 A66-24967

Interferometric determination of temperature field compared with exact analytical solutions for laminar boundary layer in case of free convection 13 p2208 A66-25314

Interferogram interpretation to determine carbon dioxide concentration in air mixture 13 p2208 A66-25315

Interferometry methods using scatter plate and plane mirror to test long focus optical systems 13 p2080 A66-25992

Lateral, radial and rotational shearing interferometry 13 p2080 A66-25993

Optical length variations in laser amplifiers determined during pumping and amplification, using interferometry 13 p2092 A66-25999

Optical system for schlieren recording/deflection mapping, shadowgraphy and interferometry achieved for laser light, used in recording of refractive index fields 13 p2082 A66-26307

Hyperfrequency interferometer measurement of plasma profile and electron density 14 p2290 A66-26821

Laser beam techniques for study of plasmas with high electron densities 14 p2305 A66-26822

Two-beam interferometry in coherence theory 14 p2330 A66-26965

Theoretical and experimental study of accuracy of Diane interferometric tracking network 14 p2238 A66-27545

Interferometric method for determining stress distributions in semiinfinite plate due to loaded pin 14 p2401 A66-27771

Electron density in laser-induced spark in air determined, measuring simultaneously fundamental laser wavelength and second harmonic 15 p2512 A66-26865

Temperature shift of ruby laser emission measured interferometrically for temperatures between 66 and 210 degrees K 15 p2512 A66-28701

Time jitter due to inherent noise when sampling intervals in Fourier transform spectroscopy by interferometer, examining effects and elimination methods 15 p2499 A66-28849

Shock transition in multihead spin structure of self-sustaining gaseous detonations in oxyacetylene mixtures, including interferometric and schlieren photographic density, temperature and pressure measurements 15 p2618 A66-29607

Gas lasers for interferometric measurements of lengths, noting methods that stabilize wavelengths of lasers 16 p2720 A66-31697

Optical coherence functions and properties from statistical viewpoint for application to spectroscopy and stellar interferometry 17 p2957 A66-31987

Qualitative results on transport mechanisms around dropping mercury



electrode, using long path laser  
interferometry 18 p3110 A66-33924  
Shadowgrams, schlieren photographs and  
interferograms produced from reconstructed  
wavefront 19 p3354 A66-35386  
Preionization and shock wave ionization in  
cylindrical crossed-field plasma source, using  
microwave diagnostic methods including  
interferometry 19 p3408 A66-36277  
Interferometric techniques in visual and  
radio regions for  
astrophysics 21 p3735 A66-38508  
Interferometric measurement of density  
distributions in shock layer of  
nonequilibrium flow field around  
cone 21 p3694 A66-39168  
Interferometric observation of cosmic  
emission at OH frequency, noting emission  
source dimensions 21 p3814 A66-39268  
Line width of well-stabilized laser  
operating far above threshold determined by  
phase random fluctuation, using  
interferometer 21 p3749 A66-39394  
Hologram recording system as  
interferometer 22 p3920 A66-40887  
**INTERGALACTIC MEDIUM**  
Propagation of light in universe with  
inhomogeneously distributed matter,  
considering presence of component  
uniformly spread in space /intergalactic  
gas/ 01 p0135 A66-10281  
Radio galaxies contribution to kinetic  
temperature of intergalactic gas on basis of  
cosmological model 03 p0426 A66-12909  
Density of neutral hydrogen in  
intergalactic space, using spectroscopic  
examination of quasi-stellar source 3C  
9 08 p1288 A66-18782  
Interaction of radiation from distant  
sources with intervening  
medium 08 p1288 A66-18785  
Interstellar and intergalactic plasma  
instability effects on energy distribution  
functions, cosmic ray diffusion and direction  
and interspace field  
interaction 08 p1285 A66-19448  
Radio galaxies contribution to kinetic  
temperature of intergalactic gas on basis of  
cosmological model 14 p2380 A66-27257  
Intergalactic matter temperature  
parameters such as heating by cosmic ray  
ionization, dissipation of hydrodynamic  
turbulence, inelastic electron collision with  
H, He and He-ions 17 p2996 A66-31912  
Interstellar and intergalactic plasma  
instability effects on energy distribution  
functions, cosmic ray diffusion and direction  
and interspace field  
interaction 18 p3169 A66-34477  
Relativistic gas expansion into intergalactic  
space noting energy content, modes of  
expansion and radio source  
distribution 18 p3236 A66-34761  
Intergalactic photon density estimated  
based on luminosity function of  
galaxies 18 p3186 A66-34812  
Principle source of radiative energy loss in  
intergalactic medium in spectral region from  
2 to 18 angstroms is line emission from ions  
of elements oxygen, carbon, neon,  
magnesium and silicon 18 p3237 A66-35046  
Primary gamma ray production, arrival  
directions, particle collisions and  
distribution of EAS penetrating particles in  
intergalactic space 18 p3209 A66-35120  
Expanding universe theory of hot ionized  
intergalactic gas and blackbody radiation  
and X-ray emission energy  
spectra 21 p3817 A66-39561  
Kaufman assumption regarding universe  
expansion considered untenable because it  
requires intergalactic hydrogen temperature  
to remain constant while hydrogen has  
expanded in volume 22 p3978 A66-40008  
**INTERIOR BALLISTICS**  
Development of 23KS20000 motor for Black  
Brant IIB vehicle with emphasis on internal  
ballistics 06 p0942 A66-16702  
Book on quasi-stationary conditions in open  
systems with short reaction times in solid  
propellant rocket engines 09 p1432 A66-20487  
Geometrical quality of elements of exterior  
orientation after double and single point  
resection in space, noting position  
determining characteristics of linear and  
angular parameters 16 p2704 A66-30515  
**INTERMEDIATE FREQUENCY AMPLIFIER**  
Digital IF amplifier for thin film radar

receiver 02 p0202 A66-11917  
Integrated monolithic circuits for compact  
intermediate frequency  
amplifier 05 p0644 A66-14579  
Wideband solid state intermediate  
frequency repeater for communications  
satellites, using waveguide-cavity diode  
down converter transistor amplifier and  
varactor up converter  
[AIAA PAPER 66-300] 12 p1823 A66-24767  
Integrated circuit selective amplifier for  
intermediate frequency application, using  
RC active networks 12 p1846 A66-24915  
Functional approach to electronic  
packaging of 60-mc intermediate frequency  
amplifier using thin film  
circuits 12 p1847 A66-24952  
Signal handling curves in receiver design  
including vacuum-tube capability,  
demodulator circuit, etc 16 p2660 A66-30579  
Receiver consisting of integrated  
millimeter wave mixer and solid state IF  
amplifier chain for operation at 94  
gc 17 p2895 A66-33118  
Black-box approach applied to design of 60-  
megacycle IF amplifier, considering  
application of AGC to circuit and design of  
phase modulator and balanced  
mixer 19 p3321 A66-36423  
Solid state millimeter wave receivers for  
space vehicle environments, discussing  
integral mixer IF amplifiers, oscillators and  
varactor multipliers 22 p3879 A66-40733  
**INTERMETALLICS**  
SA ALLOY  
SA SEMICONDUCTOR  
Joining and metal deposition portion of  
time-temperature effects on gold-aluminum  
thermo-compression bonds 01 p0049 A66-11154  
Electrolytic isolation and precise  
composition of intermetallic phase of  
titanium silicide formed in alloys of system  
Ti-Al-Fe-Si-B-Cr 02 p0245 A66-11994  
Knight shift for nuclear resonance lines of  
intermetallic Nb-Sn phase varies with  
transition temperature 04 p0566 A66-14289  
Physical factors determining hardening of  
nimonic type alloy with high niobium  
content, discussing formation of  
intermetallic phase 05 p0704 A66-15820  
Synthesis and fabrication methods for  
intermetallic carbides, borides, beryllides,  
nitrides and silicides, decreasing  
susceptibility to brittle  
fracture 07 p1051 A66-18298  
Electrochemical and corrosion behavior of  
Al-based Fe, Ni, Ti, Cu and Sb alloys and  
intermetallic compounds 09 p1390 A66-20840  
K absorption spectra of germanium and  
selenium in germanium selenide based on  
band theory of solids by assuming electrons  
transfer, using X-ray  
spectroscopy 11 p1758 A66-23368  
Magnetic and electrical properties of  
intermetallic compound FeRh, discussing  
preparation of thin films 14 p2355 A66-26911  
Heat magnetization in simple model  
applied to thulium intermetallic  
compounds 16 p2745 A66-30177  
Rolling friction studies of intermetallic and  
zirconium oxide for control surface bearings  
for space reentry vehicle  
[ASLE PAPER 66AM 5D4] 16 p2712 A66-30413  
Cold working effect on room temperature  
tensile properties of TiNi intermetallic  
compound 18 p3123 A66-33756  
Aluminide-ductile binder composite alloys  
containing high volume of nickel-aluminum  
compounds and CoAl prepared by powder  
blending and hot  
extrusion 20 p3585 A66-37783  
NaK-77 suitability for 1000-F liquid-metal  
hydraulic flight control  
systems 22 p3852 A66-40498  
Physical factors determining hardening of  
nimonic type alloy with high niobium  
content, discussing formation of  
intermetallic phase 23 p4080 A66-41385  
Magnesium antimonide and magnesium  
bismuthide as materials for power  
generating thermocouples 24 p4227 A66-42111  
Equatorial rare earth germanide magnetic  
structural characteristics 24 p4252 A66-42353  
**INTERMITTENCY HYPOTHESIS**  
Improvement on Montgomery prediction of  
error probability in intermittent system  
operating during short intervals when SNR

is above certain threshold  
level 12 p1816 A66-24138  
Effect of single or periodic disturbances  
on intermittency in pipe flow at various  
Reynolds numbers, noting relation of  
disturbance input frequency to output  
frequency of turbulent  
slugs 16 p2688 A66-31394  
**INTERMODULATION**  
Distortion measurement by total harmonic  
distortion analysis and intermodulation  
distortion analysis 01 p0037 A66-10499  
Intermodulation effects and rule of thumb  
for spurious free dynamic range in  
wideband high sensitivity  
amplifiers 01 p0044 A66-10929  
Nonlinear distortions of HF transistors  
with variable amplification, discussing cross  
and intermodulation  
behavior 04 p0501 A66-14132  
Balanced mixer array with two nonlinear  
elements, one excited in phase and other  
out of phase, has no intermodulation  
outputs, including even-order harmonics of  
out of phase signal 06 p0853 A66-16673  
Cross modulation in varactor-tuned  
limiters 08 p1191 A66-18944  
Fourier analysis of modulation products in  
nonlinear device output and optimum  
frequency conversion for n-frequency  
input 09 p1396 A66-20639  
Nonlinear transfer characteristics derived  
from measured harmonic levels in output  
when input is sinusoidal  
wave 11 p1661 A66-22393  
Intermodulation effect on measurement of  
small Hall coefficients with double AC  
method 16 p2702 A66-30424  
Intermodulation elimination in transistors,  
determining figure of merit and sensitivity  
as function of operating  
current 17 p2895 A66-33115  
First- and second-order sidebands due to  
strong CW signal intermodulation effect in  
3.39 mu He-Ne laser 18 p3117 A66-33615  
**INTERNAL COMBUSTION ENGINE**  
SA PISTON ENGINE  
3-kw internal combustion engine using  
hydrogen and oxygen, discussing design and  
testing for use as space power generator  
[AIAA PAPER 64-756] 13 p2008 A66-26657  
Book on fuel behavior in piston-engine, jet  
and rocket 21 p3306 A66-38950  
**INTERNAL ENERGY**  
Free energy of pure fluids as function of  
thermodynamic temperature determined  
from measurements of internal energy,  
noting case of carbon  
dioxide 12 p1981 A66-24997  
Base drive and internal structural  
irregularities of transistor effect on internal  
current distribution and second breakdown  
characteristics of device 19 p3312 A66-35343  
**INTERNAL FRICTION**  
Mechanical energy dispersion by internal  
friction mechanism of ferromagnetic metals  
in alternating magnetic  
field 01 p0116 A66-10193  
Dislocation relaxation of silver and copper  
and asymmetry of Bordoni internal friction  
peak of metals 01 p0087 A66-10603  
Internal friction and elastic modulus of  
compressor and turbine blade  
materials 03 p0372 A66-12399  
Internal friction, damping and cyclic  
plasticity - ASTM Symposium, Chicago, June  
1964 05 p0771 A66-14546  
Anelasticity and relaxation time in metals  
and nonmetals, particularly as manifested  
by internal friction peak as function of  
frequency or temperature in study of  
crystalline material 05 p0772 A66-14548  
Internal friction measurements for  
studying mechanical properties due to  
crystal dislocations 05 p0698 A66-14550  
Boron addition induced nickel heat  
resistance measured by internal friction as  
function of elastic  
oscillations 05 p0699 A66-14690  
Lithium transformation by plastic  
deformation from bcc to fcc lattice analyzed  
by measuring damping of free torsional  
oscillations of samples, noting role of  
internal friction 05 p0740 A66-15822  
Isothermal annealing effect on internal  
friction and Young modulus of cold-rolled  
aluminum with different



purities 08 p1240 A66-19088  
 Interrelation between relaxation center in tungsten and molybdenum and high temperature internal friction background of spectrum 11 p1719 A66-23386  
 Granato-Luecke frequency dependent internal friction calculated for pinning point distributions after vibration at dislocation temperature 12 p1971 A66-24922  
 Defects in gallium arsenide crystals studied by internal friction with measurements showing damping peak at 140 degrees C 13 p2157 A66-25045  
 Recording assembly for measurement of flexural and torsional moduli and internal friction at various frequencies and temperatures of small samples, using constant amplitude undamped oscillations 13 p2077 A66-25324  
 Low-temperature internal friction peaks in germanium and oxygen-doped and pure silicon crystals 13 p2170 A66-26586  
 LF internal friction of beryllium, noting strain amplitude dependency variation with temperature and purity, obtaining activation energies 16 p2724 A66-31265  
 Mechanical properties of semiconductors, such as elastic modulus and internal friction determined, noting vacuum and temperature conditions 16 p2785 A66-31669  
 Plastic expansion in metals due to alternating torsional and static tensile loading 17 p3029 A66-32808  
 O-O and O-N clusters in niobium detected via internal friction and elastic aftereffect measurements, noting equilibrium, kinetic properties, binding enthalpy, etc 18 p3121 A66-33728  
 Internal friction as function of temperature in cold worked tantalum and niobium containing oxygen and nitrogen 19 p3387 A66-36729  
 Dislocation-induced relaxation in silicon single crystals by measuring internal friction and Young's modulus at temperatures from 77 to 300 degrees K 20 p3618 A66-37561  
 Lithium transformation by plastic deformation from bcc to fcc lattice analyzed by measuring damping of free torsional oscillations of samples, noting role of internal friction 23 p4113 A66-41387  
 Damping mechanisms and phenomenology in materials 23 p4145 A66-41985

**INTERNAL PRESSURE**  
 Full scale ground inflation tests to evaluate structural and RF backscatter characteristics of Echo II prototype spheres as function of their internal pressures 01 p0055 A66-11123  
 Radio beacon telemetry system for measuring orbital performance of Echo II satellite, including internal pressure and skin temperature 01 p0032 A66-11125  
 Stress distribution in vicinity of infinite row of collinear Griffith cracks in elastic body calculated for internal pressure distribution 02 p0298 A66-11577  
 Cylinders subjected to internal and external pressure and axial stress with equations for radial and tangential direction 02 p0299 A66-11706  
 Shells and tubes subjected to internal and external pressures including analysis of transition theory for sheet-bending, considering creep rupture and relaxation 03 p0436 A66-12696  
 Symmetric deformation of viscoelastic-plastic hollow circular cylinder under internal pressure [ASME PAPER 65-APMW-24] 04 p0592 A66-14225  
 Circumferential creep strain of cylinders subjected to internal pressure 12 p1959 A66-23797  
 Time to viscous failure of tubes subjected to internal pressure and axial load 12 p1967 A66-24066  
 Heated cylindrical shell with braces subjected to given compression and internal pressure, having elastic beams along edges, analyzing local deformations effect on shell strength and stability 14 p2400 A66-27684  
 Supersonic flutter of circular cylindrical shells subjected to internal pressure and axial compression [AIAA PAPER 65-407] 15 p2610 A66-29281  
 Bending stresses in cylindrical shell with rigid circular inclusion examined under axial

tension and internal pressure [AIAA PAPER 66-525] 16 p2813 A66-30526  
 Symmetric deformation of viscoelastic-plastic hollow circular cylinder under internal pressure [ASME PAPER 65-APMW-24] 18 p3248 A66-33579  
 Isotherms and isobars for polymer liquids using corresponding states principle to establish function describing dependence of internal pressure on volume or temperature 18 p3124 A66-33692  
 Solutions for large plastic deformations of cylindrical membrane shells under internal pressure 18 p3252 A66-33764  
 In-plane stiffness matrices for composite cylinders of filament winding determined by internal pressure, axial tension and torsion tests 20 p3666 A66-37440  
 Nonsteady state zero-moment creep in shells of revolution with clamped edges under internal pressure, finding change range in stresses in time 21 p3826 A66-38612  
 Strength test results on special small rocket covering bending, stiffness and internal pressure strength of various components 23 p4133 A66-41423  
 Photoelastic analysis of stress and strain distributions of case-bonded propellant grains, calculating internal pressure and dependence on mechanical properties of grain material 23 p4120 A66-41440  
 Two-dimensional bubble contours in steady state turbulence-free flow of ideal incompressible fluid, obtaining solution for all internal pressures 24 p4232 A66-43064

**INTERNAL STRESS**  
 Mechanisms and relative magnitudes of internal damping in structural metals subjected to multiaxial state of stress 01 p0150 A66-10153  
 Temperature cycling effect on welds of known strength which are encapsulated with several types of resins to determine internal stress in electronic modules 02 p0234 A66-11326  
 Tangential force and bending moment effect on behavior of internal stresses and moments near application point in spherical shell analysis 04 p0588 A66-13565  
 Dynamic transient response of cylindrical shell to internal pressure pulse generated by blast wave 12 p1959 A66-23799  
 Extensive creep deformation of thin zero-moment shell of revolution under action of internal and axial load 12 p1966 A66-24059  
 Shells produced by rotation of second-order curves about axis of symmetry evaluated for symmetric and antisymmetric loads 13 p2202 A66-26418  
 Variational solution of simultaneous stability equations boundary value problem for transverse displacements and stress state 16 p2819 A66-31137  
 Internal fracture of spheruloids caused by focusing explosive waves 17 p3027 A66-32636  
 Bending characteristics of tapered cylindrical shells, discussing edge and internal influence 18 p3253 A66-33806  
 Characteristic microstresses in plastically deformed iron and aluminum alloy under tensile testing studied by X-ray techniques 19 p3376 A66-35400  
 High speed ferrimagnetic microtransducer capable of embedding in wide variety of materials and sensors to explore stress characteristics and pressure profiles 20 p3555 A66-36851  
 Embedded foil strain gauges for three-dimensional stress measurements 20 p3668 A66-37499  
 Shallow conical shell stability under pneumatic and hydraulic internal loading 20 p3670 A66-37673

**INTERNATIONAL COOPERATION**  
 European Space Research Organization /ESRO/ objectives and program including sounding rockets, satellite payloads and astronomical satellite 01 p0170 A66-10248  
 Methodology for numerically defining international magnitude of space rescue requirements 01 p0143 A66-10792  
 San Marco project, joint effort of NASA and Italian Space Commission to launch satellite for atmospheric and ionospheric measurements 01 p0143 A66-10809  
 Suggestions concerning cooperation of U.S.

and European industry in space projects 02 p0305 A66-11250  
 Advantages and disadvantages between U.S. and Europe in space projects 02 p0305 A66-11250  
 International TV communications using satellite relaying systems noting Telstar Relay and Syncom satellites and frequency sharing, video bandwidth, etc 02 p0190 A66-11511  
 Objectives, nature, origin and organization of Eurospace, noting communications satellite and space transport committees 02 p0306 A66-11674  
 NASA international program including satellite experiments, sounding rocket investigations, etc 02 p0306 A66-12237  
 Station network designed for CNES using Doppler frequency tracking, coherent systems of demodulation, polarization etc 03 p0351 A66-12477  
 Devices on ESRO satellite to be launched in 1967 by NASA rocket, noting photometer for auroral measurements, plasma probe for electron density, scintillation counter etc 03 p0430 A66-12484  
 Historical development of rules governing international cooperation on aircraft accident investigations [AIAA PAPER 65-768] 03 p0446 A66-12597  
 Worldwide F-104 program, discussing licensing agreements and weapons system management [AIAA PAPER 65-776] 03 p0447 A66-13068  
 NASARR international program concerning F-15 fire-control systems for F-104 Starfighter [AIAA PAPER 65-777] 03 p0447 A66-13068  
 Forensic medicine in space environment with reference to international responsibility, noting risks, medicolegal implications, cybernetics, contamination, pollution, etc 03 p0447 A66-13070  
 Space law basis with practical application noting sources, future legal systems, cooperation, etc 03 p0448 A66-13080  
 Astronomical constants system approved by International Astronomical Union at Hamburg in August 1964 05 p0759 A66-14888  
 West Germany and international cooperation in aerospace engine development, noting VTOL aircraft and supersonic and hypersonic spacecraft 06 p0943 A66-16797  
 Radio communication between U.S.S.R. and Great Britain via passive Earth satellite Echo II and Moon signal reflection 07 p1001 A66-17349  
 International coordination and standardization of HF quantity measurements, considering economic, psychologic and accuracy benefits 07 p1002 A66-18224  
 Worldwide civilian communications, satellite system concept, discussing agreements between U.S. and foreign governments or corporation establishment 08 p1179 A66-18566  
 Defense Communication Satellite Program for reliable worldwide military communications 08 p1179 A66-18566  
 International Geophysical Calendar for 1966 prepared by International Ursigram and World Days Service with advice of IQSY reporters 08 p1219 A66-19410  
 Italian participation in COMSAT 09 p1473 A66-20548  
 European and U.S. space transport models characteristics, noting possible cooperation because of costs 09 p1473 A66-20552  
 International cooperation in space law in connection with future space laboratories and lunar and Martian landings 09 p1473 A66-20558  
 Difficulties encountered in applying system of overall project management to ELDO initial program, noting PERT use, costs plans, etc 09 p1473 A66-20657  
 ESRO/ELDO Space Documentation Service, describing system characteristics, NASA agreement, indexing and search strategy 09 p1473 A66-20658  
 Brazilian space research program including geomagnetic field, radio propagation and development of sounding rocket station near magnetic equator 09 p1458 A66-20709  
 Space research activity in Denmark, discussing international cooperation and ionospheric sounding 09 p1458 A66-20712



Scientific experiments for manned orbital flight - Goddard Memorial Symposium, Washington, D.C., March 1965 10 p1607 A66-21517

NASA program, national and international participation, scientific missions, launching of manned and unmanned satellites, etc 10 p1623 A66-21518

Text on international cooperation in space, institutions involved and technical and political constraints 10 p1623 A66-21765

International sanitary regulations and air traffic, noting uniform code for quarantine practices 11 p1647 A66-22479

European space organizations, particularly ESRO and ELDO 11 p1788 A66-23117

Joint experiment of U.S. Naval Observatory and Japan Radio Research Laboratories for synchronizing standard time pulses, using Relay II satellite 12 p1818 A66-24473

Power, industrial and general applications - IEEE International Convention, New York, March 1966 12 p1803 A66-24658

Communications satellites for small nations, describing requirements of worldwide multiple access system [AIAA PAPER 66-281] 12 p1821 A66-24753

International Telecommunications Satellite (INTELSAT) Consortium and COMSAT participation in program [AIAA PAPER 66-332] 12 p1982 A66-24799

Role of International Telecommunication Union in satellite communication development, noting history, organization, operation [AIAA PAPER 66-443] 12 p1983 A66-24800

Report of Panel on International Meteorological Cooperation to Committee on Atmospheric Sciences, NAS/NRC, on global scientific observation 14 p2326 A66-27843

International RF space allocation for astronomical purposes 15 p2449 A66-28743

International coordination of satellite communications by nongovernmental agencies [AIAA PAPER 66-333] 15 p2621 A66-29866

Space research activities in Rumania 15 p2599 A66-29896

Space research in Hungary in 1965 including satellite tracking, ionospheric sounding, solar activity, etc, noting international data 15 p2600 A66-29907

Pakistan space program including rocket soundings, satellite tracking, meteorological research, etc 15 p2601 A66-29913

Polish space program noting international cooperation, satellite observation, radio astronomy, rocket sounding, etc 15 p2601 A66-29932

Space research programs in Italy since May 1965 and cooperation with NASA 15 p2602 A66-29940

Global TV communications systems utilizing Telstar and Early Bird 17 p2875 A66-32900

CNES network of stations for FR-1 and D-1A, discussing checks of proper functioning, orbital corrections, telemetry, ground control, etc 18 p3094 A66-33978

European Space Research Organization (ESRO) history, objectives, organization and activities 18 p3269 A66-34732

Legal question of Moon ownership, discussing international implications of manned landing 19 p3480 A66-35733

Law of outer space - Colloquium, Athens, September 1965 19 p3480 A66-36201

Space vehicle and astronaut assistance and liability for damage 19 p3481 A66-36202

Proposals for international convention on liability for damage caused by spacecraft, noting principles, preparatory work done and future measures 19 p3481 A66-36203

Noncoercive and coercive processes of international law for space use, discussing factors, functions, and applications 19 p3481 A66-36204

Commercial space communication and growth of regional-national organizations 19 p3481 A66-36205

Space legal liability and damage in UN resolution 19 p3482 A66-36206

Global space communications and international cooperation 19 p3482 A66-36209

Space law in planetary explorations 19 p3482 A66-36211

Influence of outer space activities on

development and evolution of international law 19 p3483 A66-36216

Space law education 19 p3483 A66-36217

International agreements as sources of law of outer space including atomic weapons testing, Comsat agreement, etc 19 p3483 A66-36218

UN General Assembly resolutions on outer space as sources of space law 19 p3484 A66-36222

Proposal that International Civil Aviation Organization (ICAO) might serve as specialized agency for administering outer space 19 p3484 A66-36226

Subjective approach to work of UN Committee on Peaceful Uses of Outer Space 19 p3485 A66-36227

Legal problems concerning name, definition and classification of space objects, noting special problems space stations will entail 19 p3485 A66-36228

Processing of satellite observations obtained within INTEROBS program dealing with atmospheric density determination and calculation of satellite orbital elements 20 p3518 A66-37847

Mediterranean cooperation for solar energy - Meeting, Marseille, May 1966 22 p3851 A66-40242

British-French cooperation in aeronautics, discussing Concorde SST, variable geometry aircraft, Olympus 593 turbojet, etc 23 p4016 A66-42069

Breguet 1150 high seas reconnaissance aircraft, noting design features and technological problems 24 p4159 A66-42489

**INTERNATIONAL GEOPHYSICAL YEAR (IGY)**

Geomagnetic pulsation pc-5 in and near auroral zones based on data collected during IGY period, noting local time dependence 01 p0062 A66-10889

Progressive change in worldwide current systems and auroral zone electrojets with geomagnetic bays examined with magnetic data during IGY 01 p0063 A66-10890

Quiet solar diurnal variations of geomagnetic field at middle and low latitudes during IGY to determine coordinate system and equatorial electrojet 02 p0224 A66-12118

Behavior patterns exhibited by polar ionospheric phenomena indicated by statistical analysis of IGY data 03 p0364 A66-12664

Thermal balance of Earth in light of IGY data 05 p0674 A66-15223

IGY geomagnetic observations, notably magnetic storms in Soviet Union and Antarctic 05 p0674 A66-15224

Cosmic radiation studies in U.S.S.R. during IGY noting 11-year variations, Forbush effect, solar particle propagation, etc 05 p0749 A66-15232

Space-time distribution of perturbed solar diurnal variation at high latitudes during IGY 08 p1214 A66-19033

Geomagnetic and ionospheric observations of 1964 expedition of Zaria 08 p1214 A66-19041

Graph for system of currents of solar diurnal variation during IGY winter season, considering night and evening vorticity individually and using coordinate system 08 p1221 A66-19797

Noncyclic variation during magnetically quiet days, examining seasonal changes in geomagnetic field value at night during IGY 11 p1696 A66-22420

Total counting rate and detected multiplicity spectrum of standard IGY neutron monitor analyzed on basis of neutron production and cosmic radiation components 11 p1765 A66-23144

Cosmic rays, collected papers on international geophysical projects 12 p1939 A66-24159

Cosmic ray variations analysis based on IGY and IGC data, discussing diurnal variations, cosmic ray burst, Forbush effect and existence of interplanetary magnetic field and of solar magnetic traps 12 p1940 A66-24161

Magnetospheric and upper atmospheric meteorological effects on cosmic ray intensity variation and solar corpuscular streams 12 p1940 A66-24163

Cosmic ray variations and solar corpuscular

stream in interplanetary space during March 1958 magnetic storm 12 p1940 A66-24164

Forbush, geomagnetic interaction, cosmic ray variation and solar corpuscular flux effects during magnetic storms in period of maximum solar activity 12 p1940 A66-24165

Variations in cosmic ray neutron component intensity and solar corpuscular flux with H-component of geomagnetic field during magnetic storm 12 p1941 A66-24166

Magnetic storms during IGY, assuming effect on cosmic ray intensity is associated with influence on galactic cosmic rays of magnetic fields of solar and corpuscular fluxes 12 p1941 A66-24169

Calculations of effects of solar cosmic ray flares on instruments and distribution of stations, considering index of differential spectrum of additional flux pulses 12 p1942 A66-24180

IGY and IGC data on atmospheric washout of radioactive fission products by precipitation 14 p2376 A66-27540

Quiet solar diurnal variations of geomagnetic field at middle and low latitudes during IGY to determine coordinate system and equatorial electrojet 14 p2286 A66-28077

IGY data on solar flares emitting energetic protons in sunspot groups with delta configuration, noting occurrence where magnetic fields have steep gradients 20 p3630 A66-37330

Graph for system of currents of solar diurnal variation during IGY winter season, considering night and evening vorticity individually, using coordinate system 21 p3733 A66-38793

Magnetic field of ring current on Earth surface according to observations during IGY 22 p3914 A66-40768

**INTERNATIONAL LAW**

Comments on various aspects of air and space penal law noting principles, penalties, frontiers, etc 02 p0306 A66-11747

Responsibilities of transport aircraft constructor and subcontractor noting damage risk of third party and purchaser, guarantees, etc 02 p0306 A66-11748

Development, organization and legal bases of satellite communication system developed by U.S., noting details on COMSAT 02 p0306 A66-11888

Law of Outer Space Colloquium, Warsaw, September 1964 03 p0447 A66-13074

Sovereignty with respect to outer space especially celestial bodies and space stations, noting international law for free exploration, navigation, etc 03 p0447 A66-13075

Legal problems in organization and establishment of manned Lunar International Laboratory noting exploitation of lunar lands, sovereignty, communications, etc 03 p0447 A66-13077

Codification to determine international law of celestial bodies resulted in formulation of general principles 03 p0448 A66-13079

Air and space flight legal problems concerning property, noise, liability, aircraft mortgaging and seizure and penal laws 04 p0599 A66-13506

Rule of exhaustion of local remedies and liability for space vehicle accidents 06 p0973 A66-16403

Possible infringement liability regarding unlicensed transmission of copyrighted works via communications satellites 07 p1155 A66-17227

Text on international law of territorial air space, discussing civil aviation, trespassing and crime aboard aircraft 08 p1322 A66-19237

Text on space law including historical, scientific and political background of activities in space 09 p1472 A66-19952

Commercial communications satellite system, impact and problems [AIAA PAPER 66-273] 12 p1981 A66-24746

Communications satellites, legal analysis and prognosis [AIAA PAPER 66-277] 12 p1982 A66-24749

Social and legal questions posed by development of large-scale information grids [AIAA PAPER 66-318] 12 p1982 A66-24789

Legal question in air traffic control concerning recommendation for proof of fault system without limitation on liability 14 p2416 A66-27840



Overcapacity in U.S. international air transport industry due to transition to jet between 1954 and 1963 14 p2417 A66-27841

## INTERNATIONAL QUIET SUN YEAR

## /IQSY/

Aerospace techniques used for research during International Quiet Sun Years /IQSY/ 08 p1286 A66-18570

Cerenkov counter measurement of nuclear component of cosmic rays onboard Elektron II satellite as function of solar activity during IQSY 10 p1595 A66-21043

Comet observations in IQSY 11 p1771 A66-22768

Vertical measurement of ionospheric absorption at continuously varying frequency, showing diurnal variation of absorption 12 p1870 A66-24289

Polar-based riometric observations of solar cosmic ray events during IQSY 15 p2592 A66-30034

Non-Stoermer cut-off variation with geomagnetic latitude of PCA during quiet Sun period 20 p3635 A66-38225

Spatial distribution of auroral radio signal reflection centers based on radar observations 22 p3915 A66-40777

## INTERNATIONAL SATELLITE FOR

## IONOSPHERIC STUDY

## S ISIS SATELLITE

## INTERPLANETARY COMMUNICATION

Interplanetary spacecraft telecommunications system design including block diagrams 14 p2239 A66-27822

Attenuation of radio waves from Taurus A in interplanetary space and in space about Sun 14 p2242 A66-28152

Communication and data transmission techniques via unmanned interplanetary satellites, examining video and telemetry systems 21 p3703 A66-38750

Spacecraft and Earth-terminal antennas for interplanetary communication via high power information transmission 22 p3881 A66-40748

## INTERPLANETARY DUST

## SA ZODIACAL DUST CLOUD

Mariner IV Cosmic Dust Detector measurement of momentum, mass distribution, flux densities and time histories of dust particles near Earth and in space 01 p0073 A66-11113

Data on origin and effects of dust particles in interplanetary space obtained from solar corona, zodiacal light and meteor observation 03 p0425 A66-12850

Mass accretion and variation in shape and dimensions of comet orbits 05 p0761 A66-15130

Velocities of dust particles in cislunar space 05 p0762 A66-15266

Interplanetary dust particles, size distribution, mass density, structure and shape 05 p0767 A66-15752

Chemical nature and origin of solid particles formed in primordial solar nebula, examining growth mechanism based on screw dislocations present in preplanetary nebula 05 p0767 A66-15753

Interplanetary dust dynamics, discussing comet tails, electric charge carrying properties, etc 08 p1287 A66-18635

Particle distribution and motion in field of force, discussing density profile, energy dissipation, Coulomb charge shielding for local thermodynamic equilibrium and free orbital motion 08 p1261 A66-18743

Deposition of black magnetic spherules from atmosphere at two stations in New Mexico believed to be of extraterrestrial origin 09 p1370 A66-19879

Interplanetary dust measurements by satellites indicate meteoric fluxes and dust clouds hazardous to manned spaceflight 10 p1600 A66-21048

Dynamical and light scattering properties of small dust grains orbiting Earth 10 p1529 A66-21154

Cosmic dust particles of interplanetary space hypothesized to carry electrical charges, based on irregularities in zodiacal light, night airglow and noctilucent clouds 12 p1945 A66-23510

Al-26 and Be-10 radioactivities in cores of Pacific sediments and implications regarding low-energy proton flux in interplanetary space over last 100,000 years 12 p1943 A66-24236

Newtonian approximation for irregularities in statistically homogeneous and isotropic dust-filled universe 14 p2386 A66-28119

Dynamics of type II comet trails, noting physical analogy in head and trail with rarified partially ionized gas 17 p3012 A66-33392

Cometary trail classification using Bredikhin method, noting spectrophotometric data on meteoritic microstructure 17 p3012 A66-33393

Comet Moorhouse III photographic analysis, noting tail motion, composition, angular motion of rays, etc 17 p3012 A66-33395

Force action on charged spherical dust particles in cometary atmospheres, noting interaction with ions 17 p3012 A66-33399

Relation between optical and electrical properties of interplanetary dust in upper atmosphere and comparison with twilight-optical and ionospheric parameters 18 p3105 A66-33961

Cosmic radiation age spectrum of chondrites by calculation based on interplanetary erosion rate, discussing asteroidal origin for meteorites 18 p3232 A66-34528

Cosmic dust particles of interplanetary space hypothesized to carry electrical charges, based on irregularities in zodiacal light, night airglow and noctilucent clouds 20 p3646 A66-37023

Comet disintegration as basic source of interplanetary dust based on zodiacal isophots 20 p3549 A66-37037

Flare ion fluxes in space by mass-spectrometric measurements of solar flare rare-gas ions stopped in extraterrestrial material 22 p3973 A66-40016

Zodiacal light, airglow and falling atmospheric dust measurements and observations in terms of solar orbiting small diameter particle clouds 24 p4276 A66-42663

## INTERPLANETARY EXPLORER

## S EXPLORER XVIII SATELLITE

## S EXPLORER XXXIII SATELLITE

## S IMPE

## INTERPLANETARY FLIGHT

Data automation system /DAS/ on Mariner IV Mars probe involving real and nonreal time for experiments during cruise and encounter flights 01 p0034 A66-11119

Interplanetary flight reliability problem treated by availability concept in terms of function, duty cycle and subsequent reliability 02 p0235 A66-11619

Manned Venus and Mars flybys and Mars landings using only Saturn-Apollo hardware 02 p0290 A66-12067

Corpuscular radiation effect on electronic components during interplanetary flight, assigning safety margins to each component 04 p0493 A66-13606

Optimal interplanetary guidance, discussing optimization of variable observation rate and correction schedule to achieve desired terminal accuracy 04 p0544 A66-13992

Clinical aspects of interplanetary flights noting models of future cosmic diseases, automation of diagnostics, medical aid aboard spacecraft, etc 06 p0815 A66-16052

Developing trends in space flight, considering eventual exploration and conquest of entire solar system 07 p1156 A66-17832

Civilian and Military Uses of Aerospace-Conference, New York, January 1965 08 p1299 A66-18547

Stochastic optimal control problem solution by dynamic programming and relation to interplanetary guidance 09 p1360 A66-19908

Radiation hazards to astronauts in interplanetary flight from primary cosmic rays, Van Allen belts and chromospheric bursts 10 p1595 A66-21047

NERVA electric manned Mars vehicle design, performance and operation for interplanetary missions 13 p2190 A66-25263

Integrated space suit, suit loop and backpack system for intravehicular operation on interplanetary missions 13 p2013 A66-25277

Man-machine systems for interplanetary exploration, using functional analysis techniques for system design 13 p2013 A66-25281

Trajectory energy requirements for low-thrust flights throughout solar system using

nuclear-electric propulsion [AIAA PAPER 66-497] 16 p2805 A66-31495

Interplanetary mission planning including energy requirements, payload definition, spacecraft design, launching, cost data, etc 19 p3470 A66-36314

Using Mars and Phobos to advanced interplanetary flight 19 p3464 A66-36315

Trajectory corrections of space vehicle launched toward planet, noting fuel consumption 20 p3595 A66-36872

## INTERPLANETARY GAS

Interplanetary medium observation from zodiacal light and radio wave scattering during radio source occultation and influence on galactic and solar cosmic rays 03 p0425 A66-12852

Galactic cosmic ray intensity modulation by interplanetary plasma turbulence, noting cosmic ray and geomagnetic storm 07 p1122 A66-17987

Galactic cosmic ray modulation by interplanetary plasma, deriving by method of best fit, direction and energy spectrum of anisotropy outside of geomagnetic field 07 p1128 A66-18020

Mariner II solar wind measurements including data on Venus electromagnetic radiation, space magnetic fields and charged particles, energy spectra, solar plasma, etc 07 p1130 A66-18077

Penetration of interplanetary plasma into magnetosphere, connected to aurorae and magnetic storms, noting that plasma need not behave like magnetofluid 07 p1138 A66-18081

Current sheet formation on plasma magnetospheric boundary at hyperbolic null point, noting possible connection with solar flare mechanism 07 p1138 A66-18082

Interplanetary medium properties considered in scaling of observed effects of interaction of solar wind with Earth dipolar magnetic field 08 p1292 A66-19123

Exospheric model of solar wind for ionized atmosphere with velocity-dependent collision cross section 10 p1605 A66-21206

Objections to idea of solar ejection of neutral hydrogen and responsibility for geomagnetic storm 11 p1776 A66-23496

Electron irregularity size and motion in interplanetary medium determined from radio source scintillation phenomena 13 p2182 A66-25571

Interplanetary plasma stream analysis using bistatic radar transmissions, considering wave propagation in presence of uniform magnetic field, stream velocity, Faraday rotation, etc 16 p2801 A66-30716

Quasar 3C-48 radio wave scattering by interplanetary plasma inhomogeneities 17 p3003 A66-32666

Type I comet trail relation to interaction of solar wind with geomagnetic field, noting tail ray formation mechanism, interplanetary plasma measurements, etc 17 p3012 A66-33396

Comet gas trail connection with interplanetary plasma and solar activity, noting agreement of results with Mariner II measurements 17 p3012 A66-33397

Compositional, anisotropic and nonradial flow characteristics of solar wind as observed by ARC high-resolution Pioneer VI plasma probe 18 p3170 A66-34542

Cosmic ray origin, discussing role of plasma effects in galaxies, radiogalaxies, metagalactic space, etc 18 p3175 A66-34747

Dynamical behavior of cosmic ray gases, noting modes of hydromagnetic wave propagation and static equilibrium configurations for thermal interstellar gas and field 18 p3178 A66-34759

Long-term modulation of cosmic ray intensity in interplanetary medium 18 p3180 A66-34774

Hydromagnetic wave induced variations in plasma velocity and magnetic field in interplanetary space measured by Mariner II 19 p3466 A66-36766

Interplanetary plasma stream velocities measured by bistatic radar transmissions from Earth to spacecraft, considering presence of uniform interplanetary magnetic field 20 p3648 A66-37214

Correlation between lunar eclipse brightness and interplanetary plasma flux, examining lunar



- luminescence 23 p4131 A66-41862
- Anisotropy of cosmic rays in N-S direction determined by comparison of intensity variations observed in Arctic and Antarctic regions 24 p4263 A66-42464
- Interplanetary exploration space mission objectives, discussing magnetic fields, energetic particles, cosmic radiation, etc 24 p4264 A66-42660
- INTERPLANETARY MAGNETIC FIELD**
- Interplanetary magnetic field model developed by Elliot from data of intensity variation of low energy cosmic rays 02 p0281 A66-11332
- Interplanetary magnetic effects of solar flares recorded by Explorer XVIII and Pioneer V 03 p0419 A66-12681
- Explorer XVIII continuous monitoring of vector field data deemed plausible correlation with noncontinuous data coverage of Pioneer V 03 p0419 A66-12682
- Diffusion of solar particles by interplanetary magnetic field 03 p0422 A66-12872
- Observations of interplanetary magnetic field by Mariner and Imp spacecraft confirm predictions based on behavior of cosmic rays 03 p0429 A66-13263
- Quasi-stationary corotating structure in interplanetary magnetic field observed with Imp I satellite during three solar rotations, noting data on solar wind 05 p0746 A66-14783
- Cosmic rays from solar flare and interplanetary space properties, covering particle scattering and magnetic field induced one-dimensional particle diffusion 05 p0751 A66-15377
- Interplanetary medium phenomena, MHD theory of solar wind and solar rotation as cause of Archimedean spiral twisting of interplanetary magnetic lines 05 p0767 A66-15749
- Cosmic ray diffusion, discussing existence and influence of radial magnetic field 06 p0947 A66-16574
- Frequency distribution of time and energy characteristics of cosmic ray bursts used to construct model of interplanetary magnetic field 06 p0948 A66-16580
- Survey in satellite era of energetic particle radiations, plasmas and magnetic fields in space, including solar wind, solar cosmic rays, etc 06 p0951 A66-16612
- Extraordinarily enhanced radio emission when radio source Taurus A was occulted by supercorona, concluding that supercorona shape is affected by intensity and direction of inclined interplanetary magnetic field 07 p1136 A66-17643
- Cosmic ray variations as affected by space electromagnetic conditions 07 p1121 A66-17986
- Scale and lifetime of magnetic transition region between interplanetary and interstellar space deduced from primary cosmic ray spectrum 07 p1122 A66-17989
- Contribution of spallation and ionization loss to operator that modulates cosmic ray nuclei with Z greater than or equal to 2 during propagation 07 p1124 A66-17998
- Cosmic ray modulation by interplanetary magnetic field indicated by dependence of secular, 27-day and diurnal variations on solar activity 07 p1124 A66-17999
- Active regions on Sun responsible for modulation process evidenced by correlation of cosmic radiation intensity variation with solar activity features 07 p1125 A66-18002
- Forbush effect and region of decreased cosmic ray intensity extending from Earth to Sun 07 p1129 A66-18024
- Asymmetry of cosmic ray variations and structure of interplanetary magnetic field, based on data recorded at Yakutsk and Tiksi 07 p1130 A66-18026
- Motion state of interplanetary plasma and properties of interplanetary magnetic fields, including relation to those of Sun 07 p1138 A66-18078
- Sudden commencement of magnetic storms in outer space caused by oblique MHD shock wave from corpuscular stream 08 p1290 A66-19032
- Spectra of solar, diurnal and secular variations, relation to modulation of cosmic rays by interplanetary magnetic field 09 p1438 A66-20216
- Solar cosmic rays and interplanetary magnetic field, showing polar cap absorption 09 p1439 A66-20218
- Energy dependence of transparency of walls of transition region shell obtained from Forbush effects, in connection with cosmic ray intensity 09 p1439 A66-20221
- Interplanetary space and solar atmospheric particles and fields in various models 09 p1454 A66-20285
- Comparison of interplanetary magnetic field measurements made by Imp-I satellite and those obtained with solar magnetograph at Mount Wilson 09 p1455 A66-20402
- Anisotropic diffusion of solar cosmic rays due to interplanetary magnetic field 09 p1443 A66-20890
- Upper bounds on steady state and pulse outflow of neutrons from Sun determined by assuming neutron-decay protons diffuse in interplanetary magnetic field 11 p1764 A66-23131
- Cosmic ray variations analysis based on IGY and IGC data, discussing diurnal variations, cosmic ray burst, Forbush effect and existence of interplanetary magnetic field and of solar magnetic traps 12 p1940 A66-24161
- 27-day cosmic ray variations from July 1957 to December 1960 and general characteristic of electromagnetic conditions in interplanetary space 12 p1942 A66-24177
- Space probe observations of solar wind, solar magnetic field and interplanetary magnetic field 13 p2187 A66-26286
- Data from satellite 1963 38C, showing existence of 27-day periodicity in intensities of trapped electrons undergoing two increases and linked to interplanetary magnetic field 13 p2175 A66-26353
- Outer solar corona during declining portion of solar activity cycle, noting discrepancy between radio and optical values of electron density 15 p2593 A66-28816
- High energy solar proton propagation in interplanetary magnetic field by Fokker-Planck equation 15 p2575 A66-29081
- Comparison of magnetic and cosmic ray data of Pioneer VI with particle guidance properties of interplanetary magnetic field 15 p2591 A66-30023
- Solar wind interaction with solar dipole magnetic field in coupled hydrodynamic and hydromagnetic equations [AIAA PAPER 66-509] 16 p2793 A66-30608
- Measurements of geomagnetic field at various distances using IMP-I satellite, noting magnetically neutral sheet in tail and observation of five magnetic storms 16 p2695 A66-30715
- Argument in support of Dessler long-tail model of magnetosphere in answer to Van Allen questions 16 p2795 A66-30725
- Type I comet tail origin due to energetic electrons in shock structure, noting inertial slowing down of interplanetary field lines trapped in solar wind 16 p2801 A66-30919
- Origin and propagation of cosmic radiation, discussing interplanetary magnetic fields, plasmas, Faraday rotation of polarized radiation, Zeeman splitting of hydrogen line, etc 17 p2964 A66-32029
- Variations in polarity distribution of interplanetary magnetic field from observations by Mariner II and IV and IMP I 17 p3002 A66-32531
- Cometary tail phenomena interpreted, using plasma dynamics theory coupled with observed solar wind activity 17 p3011 A66-33390
- Correction of magnetic measurements made by Mariner II, noting use of second-order approximation for interplanetary magnetic field 18 p3106 A66-34333
- Interplanetary magnetic-field measurements taken by Interplanetary Monitoring Platform /IMP-I/ 18 p3231 A66-34336
- Solar wind models analyzed, taking into account solar ejected high-velocity gas jets and southward component of interplanetary magnetic field 18 p3167 A66-34339
- Astronomical model study of physics of penetration of interstellar cosmic rays into solar system 18 p3168 A66-34342
- Solar wind origin, examining steady state energy and momentum balance, coronal heating, viscosity effects, velocity distributions and field effects 18 p3168 A66-34343
- Reconnection mechanism for geomagnetic and interplanetary field lines, estimating field-cutting efficiency at magnetopause 18 p3231 A66-34348
- Magnetosphere topology changes due to solar wind interactions, geomagnetic storms and interactions with interplanetary magnetic field outside magnetosphere 18 p3106 A66-34349
- Solar wind interaction with type I comet tails in interplanetary magnetic field 18 p3231 A66-34356
- Anisotropic cosmic radiation with flare effects flowing out of Sun and along filamentary magnetic structures imbedded in solar wind 18 p3170 A66-34537
- Interplanetary magnetic field measurements using flux gate magnetometer sensor mounted on Pioneer VI space probe, noting various graphs 18 p3108 A66-34538
- Collimation of cosmic rays by interplanetary magnetic field based on Pioneer VI measurements during flare event 18 p3170 A66-34539
- Comparison of interplanetary magnetic field measurements obtained by Pioneer VI space probe and IMP-III satellite 18 p3233 A66-34540
- Cosmic radiation, interplanetary magnetic field, solar proton propagation long-term /solar cycle/ modulation of intensity, Forbush effect and daily intensity variation 18 p3175 A66-34741
- Satellite and space probe measurements indicate continual confinement of geomagnetic field by solar wind forming magnetosphere and Earth magnetic tail 18 p3235 A66-34742
- Explorer XVIII satellite measurements of proton energy spectra in region corotating with Sun, noting modulation of galactic cosmic radiation and source of continuous particle accelerations 18 p3177 A66-34754
- Sidereal time variation of cosmic rays explained by diffusion in galactic arm for colinear magnetic field and proximity of solar system 18 p3178 A66-34762
- Anisotropy of cosmic ray with gradient and curvature drifts in spiral interplanetary magnetic field 18 p3181 A66-34780
- Semidiurnal anisotropy of cosmic radiation observed from neutron monitor data treated by numerical filter techniques 18 p3182 A66-34783
- Twenty Forbush decreases with amplitude greater than 4 percent in neutron intensity 18 p3184 A66-34796
- Flux gate magnetometer for interplanetary magnetic field measurements 19 p3356 A66-35674
- Low energy cosmic ray modulation relationship to observed interplanetary magnetic field irregularities in terms of diffusion, using space probes 19 p3454 A66-36765
- Hydromagnetic wave induced variations in plasma velocity and magnetic field in interplanetary space measured by Mariner II 19 p3466 A66-36766
- Diurnal cosmic-ray anisotropy in studying temporal independence of small scale irregularities in interplanetary magnetic field 20 p3630 A66-37302
- Astronomical model for diffusion of galactic cosmic rays in solar system, based on zonal character of solar activity 20 p3630 A66-37329
- Final estimate of interplanetary magnetic field at 1 AU provided by Pioneer V uniaxial induction-coil magnetometer 20 p3649 A66-37336
- Magnetic intensity distribution, polarity and macrostructure of solar and interplanetary magnetic fields 20 p3635 A66-38218
- Ground magnetogram-IMP I data comparison and geomagnetic field effects on interplanetary magnetic field sector structure 20 p3657 A66-38219
- Phase anomaly detected by chemical test D during decreasing phase of last solar cycle 21 p3732 A66-38629
- Acceleration of high energy electrons by means of Parker-Wentzel version of Fernald mechanism due to geometry and distorted structure of interplanetary magnetic field near magnetopause in transition region 22 p3972 A66-40003



Dense particle population of Van Allen belts formed by interaction of high energy corpuscular radiation with interplanetary magnetic field and geomagnetic field 23 p4123 A66-41186

Interplanetary exploration space mission objectives, discussing magnetic fields, energetic particles, cosmic radiation, etc 24 p4264 A66-42660

Anisotropy of Forbush effect in ascertaining structure and intensity of interplanetary magnetic field 24 p4272 A66-43159

# INTERPLANETARY MONITORING PLATFORM /IMP/ S IMP

## INTERPLANETARY NAVIGATION

Manned interplanetary flight, emphasizing nonstop flybys past Mars and Venus, reviewing launch and departure modes, energy requirements, environmental control, navigation spacecraft power source, etc 08 p1286 A66-18561

Navigation, guidance and control of spacecraft in interplanetary space, considering free-fall flight and thrust-vector stabilization during accelerated flight 08 p1248 A66-18586

Electro-optical attitude and velocity sensors for interplanetary navigation and stellar aberration and Doppler shift measurements 08 p1252 A66-19502

Six midcourse guidance techniques, noting Earth-Mars and Earth-Venus trajectory with small and large injection error 13 p2123 A66-25252

Interplanetary midcourse navigation by measuring differential stellar aberration, using Space Velocity Meter /SVM/ 13 p2123 A66-25255

Navigation for spin stabilized deep space interplanetary spacecraft such as Pioneer VI, for missions to Venus, Mars and Jupiter 14 p2329 A66-28456

Optimization of midcourse velocity corrections, applying for variable-time-of-arrival guidance and determining optimum correction time as function of miss parameter 18 p3131 A66-33850

Optimized spacecraft control process eliminates gravitational field-caused nonlinearities by taking as control parameters osculating characteristics of planetocentric motion 18 p3242 A66-33851

Guidance and control systems of Mariner planetary spacecraft, noting requirements, flight performance, systems configuration, etc 18 p3242 A66-33852

Handbook on theory of space flight and navigation of spaceships in interplanetary space, emphasizing characteristics of space trajectories, rocket engines and space vehicles 21 p3812 A66-38947

## INTERPLANETARY PROPULSION CONFIGURATION

Optimization of guidance laws to achieve orbital rendezvous with propulsion system of only moderate throttling capability 01 p0100 A66-10027

Nuclear electric propulsion applied to manned Mars missions, presenting analytical tool to simultaneously optimize interplanetary vehicle design and trajectory [AIAA PAPER 65-414] 23 p4120 A66-41110

Optimization of guidance laws to achieve orbital rendezvous with propulsion system of only moderate throttling capability 24 p4235 A66-42766

## INTERPLANETARY SPACE

Scale of distances and masses in solar system, IR characteristics of Venus and interplanetary space fields and particles revealed by Mariner II 03 p0425 A66-12867

Staudte-Hoffmeister integral for abundance of sporadic meteoric bodies 03 p0427 A66-12921

Interplanetary plasma origin, behavior and effects on space flight studied by space probe 04 p0576 A66-13501

Diffusion coefficient of solar protons in steady state electromagnetic medium of interplanetary space increases with increase in proton momentum 04 p0574 A66-13839

Solar particles zones of incidence during maximum and minimum solar activity 05 p0751 A66-15376

Soviet and other literature on diurnal

variations of cosmic ray intensity used for analysis of electromagnetic conditions in outer space 06 p0949 A66-16587

Total radiation intensity in interplanetary space before and after solar events of March 29 and April 9, 1960 07 p1120 A66-17978

Solar corpuscular radiation behavior, including dynamics of origin at Sun 07 p1130 A66-18079

Energy sources of lunar luminescence noting effects of solar wind, corpuscular radiation, electromagnetic radiation and radioactivity 07 p1139 A66-18090

Propagation mechanisms of solar cosmic radiation in interplanetary space other than classical diffusion 09 p1438 A66-20212

Solar cosmic ray generation, interplanetary proton diffusion and stratospheric showers 10 p1595 A66-21045

Parameters of dynamic modulation determined from measurements of proton and alpha particle spectra, used in cosmic-ray modulation in interplanetary space 11 p1762 A66-22411

Cosmic ray variations and solar corpuscular stream in interplanetary space during March 1958 magnetic storm 12 p1940 A66-24164

Small cosmic ray bursts effect on geomagnetic activity and nature of high-energy solar cosmic ray propagation in interplanetary space 12 p1942 A66-24179

Staudte-Hoffmeister integral for abundance of sporadic meteoric bodies 14 p2380 A66-27270

Interplanetary-space temperature profile appropriate to uniformly expanding corona model 15 p2597 A66-29256

Mariner IV observation of 500-kev protons in interplanetary space 16 p2792 A66-30164

Celestial mechanics covering two-body problem, planetary and asteroid theory, interplanetary trajectories, lunar probe, spherical harmonics, etc 17 p2997 A66-32019

Solar corona and interplanetary plasma noting solar wind effect on comet tails and shock wave caused by interaction of geomagnetic field and plasma 17 p3000 A66-32272

Detection and measurement techniques for collisionless MHD shock wave propagation in interplanetary space, using bistatic-radar Earth-to-spacecraft transmissions 17 p3002 A66-32522

Solar flare electron propagation observations in interplanetary space 18 p3166 A66-34239

Solar wind - Conference, California Institute of Technology, Pasadena, April 1964 18 p3166 A66-34330

Mariner II data analysis on effect of magnetic field on radiation and high energy particles in interplanetary space and solar plasma 18 p3167 A66-34334

Solar wind observations with Explorer XII and IMP, noting periodic fluctuations in solar proton flux and detection of 3 mev electrons of interplanetary origin 18 p3167 A66-34335

Radio astronomy observations applied to solar wind problem, results include radial variation of electron density, size of coronal irregularities and coronal magnetic field direction 18 p3231 A66-34337

Collision-free hydromagnetic shock observed simultaneously in interplanetary space on October 7, 1962 by Mariner II and Explorer XIV 18 p3168 A66-34340

Isotopic changes in materials caused by high energy nuclear active particles and solar wind in interplanetary space and on Earth 18 p3176 A66-34750

Energy characteristics of 11-year cosmic ray variations, evaluating electromagnetic conditions in interplanetary space for proton, alpha particle and electron variations in energy 18 p3176 A66-34752

Relativistic gas expansion into intergalactic space noting energy content, modes of expansion and radio source distribution 18 p3236 A66-34761

Modulation effects in galactic and solar cosmic rays in interplanetary space 18 p3185 A66-34806

Gas tails of brighter comets that may reach 150,000,000 km in length reveal direction and velocity of solar

wind 19 p3452 A66-35797

Interplanetary medium and S-band telecommunications obtained from tracking data from Mariner II and Mariner IV spacecraft 20 p3520 A66-38187

Pioneer VI MIT experimental results on interplanetary plasma 20 p3657 A66-38210

Soviet papers on solar corona and corpuscular radiation in interplanetary space 21 p3812 A66-39119

Interplanetary space environment effect on surface thermal radiative properties, noting results of exposure to simulated solar plasma, solar UV, solar wind, etc 22 p3889 A66-40218

Antenna in interplanetary plasma, noting fluctuation noise in exosphere and radiation impedance when exposed to solar wind 22 p3877 A66-40466

Celestial bodies nature and structure effect on space flights, detailing interplanetary space properties and orbital motion 24 p4280 A66-43131

Interplanetary space and celestial observations from ground stations, satellites and space rockets 24 p4280 A66-43133

INTERPLANETARY SPACECRAFT

Optimum guidance in two dimensions of constant acceleration low-thrust vehicle spiraling away from and in toward planet 01 p0100 A66-10026

Spacecraft design for manned planetary missions, emphasizing early Mars landings 01 p0143 A66-10802

Cosmic ray telescope /CRT/ carried on Mariner IV Mars probe to measure flux and energy of protons and alpha particles in interplanetary space and near Mars 01 p0072 A66-11112

History of Mariner space program and discussion of future unmanned vehicles for exploration of interplanetary space 02 p0296 A66-11677

Rocket engine generated voltage as source of electromagnetic interference and electronic component damage on interplanetary vehicles 04 p0480 A66-13628

Requirements and performance expectations of chemical and nuclear propulsion systems for manned Mars and Venus missions 06 p0942 A66-16499

Study of protection requirements for resistance of meteorite penetration damage for various interplanetary spacecraft systems [AIAA PAPER 65-693] 08 p1303 A66-18807

Feasibility design study of solar powered ion propulsion system for interplanetary spacecraft [AIAA PAPER 66-214] 12 p1936 A66-24524

Optimum guidance in two dimensions of constant acceleration low-thrust vehicle spiraling away from and in toward planet 14 p2328 A66-27419

Recovery of interplanetary vehicles by low thrust braking outside atmosphere 14 p2391 A66-27472

Motion equations and simulation of spin-stabilized interplanetary spacecraft closed-loop pitch control system, using low-thrust gas jet torquers with rate gyro sensors 14 p2392 A66-27881

Spacecraft orientation during interplanetary flights, using system employing two rigidly connected telescopes, one aimed at Sun and other aimed at stars 15 p2447 A66-28506

Mariner program results of Venus and Mars exploration, discussing atmospheres, surfaces, exospheres, etc 16 p2798 A66-30359

Future spacecraft projects, emphasizing roles of space scientist and industrial manager as illustrated by using Jupiter flyby mission spacecraft design 16 p2808 A66-30364

Reliability, maintainability, and spacecraft safety in hypothetical manned Mars mission 17 p2930 A66-33174

Interplanetary manned spacecraft maneuvers including perihelion brake, off-perihelion acceleration and retromaneuvers and heliocentric planet-approach maneuvers [AIAA PAPER 65-695] 19 p3462 A66-35902

Maintenance on long-duration manned space flight facilitated by maintenance job aid information stored in high density retrieval and display system 19 p3309 A66-35950

## INTERPLANETARY TRAJECTORY

Spacecraft-comet rendezvous trajectory



analyzed in terms of comet properties and spacecraft capabilities to determine feasibility of interception mission  
[AIAA PAPER 63-413] 03 p0424 A66-12739  
Solution to boundary value problems associated with artificial satellite, lunar impact trajectory and interplanetary trajectory 04 p0579 A66-14445  
Mars capture probe planned for 1971 using willight orbit with optimization of payload, propulsion and trajectory 08 p1303 A66-18830  
Gravity assisted trajectories to solar system targets analyzed by two-dimensional solar system model  
[AIAA PAPER 66-10] 08 p1289 A66-18984  
Venus swingby used to decelerate manned spacecraft returning from Mars 10 p1609 A66-21928  
Earth departure plane change, interplanetary mission launches and launch windows 10 p1609 A66-21929  
Interplanetary trajectory adaptive gyrocompass system, discussing orbital angular velocity, angular acceleration, error sensitivity coefficients, error sources, etc 13 p2124 A66-25256  
Matching planetocentric and heliocentric low-acceleration trajectories in analysis of propulsion system performance 15 p2598 A66-29297  
Swing-by and capture-orbit trajectories for Mars or Venus exploration described by numerical methods 16 p2798 A66-30358  
NASA Voyager project, discussing planetary orbit design and selection and Mars orbiter trajectory 16 p2808 A66-30365  
Unmanned spacecraft trajectory and guidance considerations for close flyby of planet Mercury 16 p2801 A66-30885  
Matched asymptotic expansions and patched conics used to simplify flyby interplanetary trajectories  
[AIAA PAPER 65-689] 19 p3462 A66-35895  
Gravity assisted trajectories to solar system targets analyzed by two-dimensional solar system model  
[AIAA PAPER 66-10] 23 p4127 A66-41103  
Graphical construction and geometrical interpretation of particular analytical solution for determining ionic orbits subject to certain boundary conditions 24 p4277 A66-42685  
Trajectory characteristics for unmanned interplanetary missions, propulsion requirements for Earth departure and effect capture at target planets 24 p4277 A66-42686  
Interplanetary trajectories, considering gravity effect, free flight trajectory and forces acting on space vehicle 24 p4280 A66-43132  
INTERPLANETARY TRANSFER  
Fehlberg integration method used to calculate optimum interplanetary transfer orbits at low thrust 04 p0576 A66-13527  
Low energy transfer from Earth to Mars via Venus, considering launch window and planet orientation  
[AIAA PAPER 64-647] 18 p3227 A66-33812  
Steepest descent method of trajectory optimization for computing lunar and interplanetary transfer missions, noting terminal constraints 20 p3651 A66-37391  
Transfer paths to Mars via Venus compared with direct flight, discussing direct free fall transfer, flyby and free fall transfer 20 p3651 A66-37392  
INTERPOLATION  
SA COMPUTATION  
Zeros of general orthogonal polynomials as interpolation modes and relation to Jacksonian properties 07 p1058 A66-17865  
Stability of complex moment problems determined by constructing sequence of interpolation polynomials which converge uniformly to solution in bounded region 07 p1060 A66-18099  
Interpolation function of real variable, investigating process constructed for given system of points 09 p1394 A66-20456  
Deriving interpolatory type quadrature formula by inverting linear systems of differentiation formulas 09 p1395 A66-20622  
Carpet plotting technique for increased interpolation accuracy 13 p2031 A66-25363  
Minimal element determination for certain set related to interpolation of second-order

linear ordinary differential equations 18 p3126 A66-33954  
Erdos and Turan theory of fine and rough convergence of interpolation and quadrature processes 18 p3127 A66-34543  
Lacunary interpolatory polynomials, and Mth derivatives prescribed in roots of unity, examining Dini-Lipschitz condition for convergence 18 p3127 A66-34638  
Auxiliary polynomials for direct determination of Chebyshev interpolation polynomial 19 p3389 A66-35936  
INTERPRETATION  
SA PHOTOGRAPH INTERPRETATION  
Image interpretation in manned space surveillance systems 18 p3060 A66-33742  
INTERSTELLAR COMMUNICATION  
Search via laser receivers for interstellar communications 06 p0892 A66-16669  
Search for intelligent signals from space 12 p1880 A66-23894  
Propagation of radio waves in interstellar medium and Earth atmosphere and effect on visible angular dimensions 12 p1814 A66-23897  
INTERSTELLAR GAS  
General dynamical effects of suprathermal gas particles on hydromagnetic wave propagation in interstellar space 05 p0749 A66-15275  
Origin of solar system, discussing monistic and dualistic theory, interstellar gas characteristics, star formation and planetary development 05 p0767 A66-15756  
Solar magnetic field may have originated during process of Sun formation from galactic magnetic field which pervaded interstellar gas from which Sun condensed 08 p1292 A66-19261  
Discrepancy between theoretical calculation and measurement of far UV radiation from hot stars 10 p1598 A66-21094  
IR emission lines possibly originating from galactic, interstellar and stellar hydrogen regions 10 p1599 A66-21113  
Data on large-scale distribution of interstellar hydrogen important for studies of spiral arms and galactic disk 11 p1766 A66-22257  
Interstellar molecular hydrogen abundance and possible source from giant stars 13 p2182 A66-25579  
Book on interstellar gas dynamics 14 p2378 A66-26807  
Formulae relating 21-cm emission intensity to density of interstellar hydrogen gas 14 p2383 A66-27799  
Astronomical satellite application to sky mapping, stellar photometry, interstellar grains and gas study and statistical stellar sampling 15 p2594 A66-28987  
Irregularity of galactic magnetic field structure in vicinity of Sun indicated by starlight polarization, interstellar cloud motion and Milky Way photography 15 p2595 A66-29130  
Energy dissipation channels of nuclear and electron components of cosmic rays in Galaxy and Metagalaxy 15 p2576 A66-29131  
Solar wind computations beyond one angstrom, noting shock wave formation indicating hot tenuous gas region surrounding solar system 15 p2576 A66-29229  
Interstellar medium survey including cloud structure and velocity field of interstellar gas, galactic magnetic field, etc 16 p2799 A66-30575  
Interstellar plasma wave damping by relativistic suprathermal particles, noting magnetosonic and Alfvén waves 17 p2996 A66-31915  
Presence and detectability of hydrogen in molecular form in galaxy 17 p3001 A66-32365  
Control of abundance of neutral hydroxyl radical in unionized interstellar gas 17 p3003 A66-32658  
Virial theorem study of magnetic field effect on gravitational instability of primeval gas cloud, noting possibility of collapse upon change in magnetic flux 17 p3005 A66-33002  
Proton energy density, pressure and compressibility of galactic cosmic ray gas 18 p3165 A66-34140  
Low rigidity end of differential power spectra of proton and helium components of primary cosmic radiation, considering ionization loss and interaction with

interstellar hydrogen 18 p3189 A66-34830  
Principle source of radiative energy loss in intergalactic medium in spectral region from 2 to 18 angstroms is line emission from ions of elements oxygen, carbon, neon, magnesium and silicon 18 p3237 A66-35046  
Delta electrons formed in interstellar hydrogen-galactic ray collision 19 p3452 A66-35283  
Galactic magnetic fields, considering magnetic flux, frequency of fields in radio galaxy, disk, interstellar gas dynamics and spiral structure 20 p3645 A66-36958  
Nonrelativistic equations of bulk motion of relativistic /cosmic ray/ gas derived by taking moments of collisionless Boltzmann equation 20 p3649 A66-37327  
Molecular hydrogen structure, considering planetary and stellar atmospheres and interstellar space 21 p3815 A66-39487  
Thermal instabilities role in star formation, discussing intercloud medium, magnetic pressure and gravitational collapse 23 p4125 A66-41062  
INTERSTELLAR MAGNETIC FIELD  
Interstellar and intergalactic plasma instability effects on energy distribution functions, cosmic ray diffusion and direction and interspace field interaction 08 p1285 A66-19448  
Virial theorem study of magnetic field effect on gravitational instability of primeval gas cloud, noting possibility of collapse upon change in magnetic flux 17 p3005 A66-33002  
Interstellar and intergalactic plasma instability effects on energy distribution functions, cosmic ray diffusion and direction and interspace field interaction 18 p3169 A66-34477  
Dynamical requirements for existence of interstellar magnetic field in solar neighborhood 23 p4124 A66-41812  
INTERSTELLAR MATERIAL  
SA COSMIC DUST  
SA INTERPLANETARY DUST  
Interstellar and intergalactic gas, dust and magnetic fields 05 p0765 A66-15381  
Detection of 3.1 micron  $\mu$  cepheid absorption band due to interstellar ice particles 05 p0768 A66-15770  
Growth and destruction of ice mantles on interstellar graphite grains by sputtering, thermal evaporation and cloud collisions 05 p0765 A66-15845  
Mie scattering calculation to support theory that interstellar extinction is caused by graphite particles 08 p1288 A66-18786  
Elongation of characteristic curve of polarization for interstellar particles due to surface molecular scattering 11 p1769 A66-22535  
IR radiation from interstellar grains, measuring intensity as wavelength function and radiation polarization for information on grain temperature and composition and galactic magnetic fields 14 p2377 A66-28122  
Hyperbolic comets and Oort hypothesis of cometary cloud, discussing probability distribution and existence of interstellar source 17 p3013 A66-33406  
Solar wind proton, solar flare proton and galactic ray effect on interstellar solids /comet/ 17 p3013 A66-33409  
Dynamical aspects of Oort hypothesis on cometary origin 17 p3014 A66-33413  
Interstellar molecules relation to corresponding cometary phenomena 17 p3014 A66-33415  
Plane interstellar polarization dependence on wavelength observed in 18 stars with UV and IR filter 18 p3235 A66-34657  
Total cross sections for arbitrarily oriented dielectric circular cylinders used in obtaining extinction and polarization by realistically oriented interstellar particles, noting refractive index 20 p3649 A66-37325  
Corpuscular radiation from UV Ceti stars assumed to be mainly protons, noting role of interstellar matter 20 p3652 A66-37611  
Spiral patterns of disk-like galaxies explained in terms of density waves that are collective modes of stellar system analogous to plasma waves 24 p4273 A66-42266  
Source spectra and composition of galactic cosmic rays implied by analysis of interstellar and interplanetary travel, noting



solar modulation 24 p4265 A66-42716

**INTERSTELLAR MICROWAVE SPECTRUM**

Galactic center dynamics revealed by hydroxyl radicals present in interstellar medium, noting detection of radio emissions caused by star-excited atoms and molecules 09 p1453 A66-20239

Observational needs for galactic research, discussing stellar luminosity, interstellar absorption, etc 15 p2594 A66-28986

Maser amplifier based on UV continuum pumping from nearby stars, explaining 18-cm OH emission from anomalous H-2 regions 24 p4280 A66-43042

**INTERSTELLAR RADIATION**

Observation of plane interstellar polarization of 22 stars indicates wavelength dependence of position angles and polarization 02 p0292 A66-12188

Secondary protons from interstellar cosmic-ray collisions, noting solar modulation effects on detection 05 p0747 A66-14796

RF spectrum of OH radiation in interstellar space, including emission intensity and linear polarization 11 p1774 A66-22963

Astronomical model study of physics of penetration of interstellar cosmic rays into solar system 18 p3168 A66-34342

Balloon-borne nuclear emulsion detection of finite fluxes of low energy cosmic ray heavy nuclei and interstellar cosmic radiation propagation 18 p3191 A66-34838

Differential spectra of charge components of primary cosmic ray heavy nuclei at different solar modulation levels and effects of interstellar propagation 18 p3191 A66-34839

Stimulated emission processes interpreting OH microwave emission from points in sky, using anisotropic UV radiation which leads to molecule alignment and population inversion 20 p3650 A66-37343

Interstellar X-ray absorption edges due to K-shell photoionization of oxygen and neon, using element abundances and atomic photoelectric cross section data 21 p3809 A66-38658

Diameters and positions of three sources of 18-cm OH emission determined, using 90-ft steerable paraboloids 21 p3814 A66-39269

Cosmic ray modulations in solar system and in interstellar space, presenting graphs of rigidity spectra of protons and helium 22 p3973 A66-40524

**INTERSTELLAR SPACE**

Goals of future space exploration including atmospheric studies, solar activity effects, planetary characteristics and interstellar space interaction effects 02 p0291 A66-12071

Interstellar extinction in UV by measurement of stellar energy distributions between 3000 and 1200 angstroms 08 p1288 A66-18787

Galactic center dynamics revealed by hydroxyl radicals present in interstellar medium, noting detection of radio emissions caused by star-excited atoms and molecules 09 p1453 A66-20239

Spectra of generically related cosmic ray species 09 p1443 A66-20688

Propagation and attenuation of radio waves in interstellar and near solar space 09 p1348 A66-21014

Interstellar polarization measurement for eight stars 13 p2185 A66-25811

Interstellar space navigation, considering problem of observables, navigation schemes and instrumentation 21 p3767 A66-38894

**INTERSTELLAR TRAVEL**

Interstellar travel using ramjet technique and interstellar gas in conjunction with nuclear fusion 06 p0953 A66-16073

Interstellar vehicle propelled by terrestrial laser beam 19 p3449 A66-35488

Book on possibility of extrasolar intelligence covering origin of planetary systems, development of life and terrestrial biological evolution 20 p3506 A66-37305

**INTERSTITIAL ATOM**

Tungsten single crystal structure and mechanical properties as affected by saturation of carbon, oxygen and nitrogen 01 p0089 A66-10998

Tungsten single crystal study by electron microdiffraction for distribution and effects of interstitial phases 03 p0385 A66-13194

Lattice vacancies and interstitials in II-VI

compounds of cadmium sulfide and zinc selenide caused by electron bombardment often determine advantages or limits of material 06 p0935 A66-17130

Electronic states of single defects in diamond calculated by comparing electronic states of single vacancies and single interstitial carbon atoms 06 p0938 A66-17148

Heat transfer between two metallic cylinders in close contact, examining effect of interstitial gas on thermal contact resistances 07 p1149 A66-17452

Concentration dependence of thermodynamical functions of interstitial solid solutions, calculating energy of formation 08 p1258 A66-18897

Equation for entropy of formation of interstitial solid solution with two interstitial sublattices, using phase diagram for constants in free energy and activity equations 08 p1258 A66-18903

Anisotropy of Snoek relaxation measured for oxygen and nitrogen in niobium 10 p1576 A66-21554

Interference maxima changes in X-ray photographs of neutron irradiated metals attributed to interstitial atoms in lattice 13 p2106 A66-25332

Lattice defect distribution effect on degradation of solid solution of interstitial impurities in cast molybdenum 16 p2727 A66-31530

O-O and O-N clusters in niobium detected via internal friction and elastic aftereffect measurements, noting equilibrium, kinetic properties, binding enthalpy, etc 18 p3121 A66-33728

Elastic relaxation effect due to diffusion of interstitial hydrogen in tantalum and niobium 18 p3123 A66-34058

Thermal conductivity of finely divided and granular materials through solid phase and interstitial gas or by radiation between granules 21 p3835 A66-38768

**INTESTINE**

**SA DIGESTIVE SYSTEM**

**SA GASTROINTESTINAL SYSTEM**

Stress and dietary influence on direct oxidative pathway of carbohydrate metabolism in jejunal mucosa of rats 16 p2641 A66-31383

**INTRUDER AIRCRAFT**

**S A-6 AIRCRAFT**

**INVARIANCE**

**SA GAUGE INVARIANCE**

Conditions that principal invariants of tensor must satisfy to be symmetric or orthogonal 12 p1902 A66-23948

Invariant hyperplanes for linear dynamical systems, discussing geometric properties and relation to controllability and observability 12 p1849 A66-24256

UHF transistor design and performance, noting power gain, stability, low noise figure and correlation between circuit invariants and transistor parameters 13 p2038 A66-25560

Invariance principle applied to motions of material particle that do not depend on particle mass 13 p2127 A66-25625

Synthesis of correcting units for automatic control systems, using quasi-invariance condition 15 p2476 A66-29995

Invariance effect for finite number of coordinates in infinite dimensional automatic control system 19 p3325 A66-35986

Synthesis of control systems invariant to parameter changes, examining sensitivity and advantages over self-adjusting systems 19 p3328 A66-36023

Stability, reproducibility and sensitivity of combined systems of automatic control with variable structure determined by presence of sliding mode region 19 p3329 A66-36025

Coordinate control theory of self-adapting systems, considering problems of sensitivity, optimization and invariance 20 p3535 A66-36852

Group theory of invariance of finite linear state-variable transformations generating new linear dynamic system and application to electric network 20 p3539 A66-38147

Theoretical interpretation of expansions in nonzero determinants formed from vertex and circuit matrices 20 p3539 A66-38283

**INVARIANT IMBEDDING**

Second-order linear partial differential equation transformed to normal form, obtaining invariant representation without

Ricci calculus 07 p1055 A66-1730

Existence and uniqueness theorems for invariant-imbedding nonlinear ODE system for absorption loss rate satisfying Lipschitz condition 07 p1059 A66-1797

Fluctuation problem in electromagnetism cascade theory analyzed, using invariant imbedding method 07 p1083 A66-1797

Invariant imbedding in transport processes and theorems of uniqueness and existence for derived hyperbolic equation 09 p1393 A66-1990

Internal diffuse radiation field computed in finite homogeneous isotropically scattering slab illuminated by parallel rays 10 p1556 A66-219

Nonlinear circuit theory, discussing invariant imbedding, dynamic programming and quasi-linearization 11 p1675 A66-2262

Mathematical programming methods for solving nonlinear state-constrained discrete optimal control problems 13 p2047 A66-2538

Invariant imbedding as basis for integration theory for canonical equations of motion with parallels to Jacobi's theory 17 p2947 A66-3250

Intensity of emergent radiation in finite homogeneous slab absorbing and scattering it isotropically, viewed as boundary value problem determined by imbedding techniques 17 p3037 A66-3300

Sensitivity analysis and Liapunov stability discussing correctly set problem and parametric imbedding within theory of partial differential equations 19 p3326 A66-3600

Sensitivity analysis and invariant imbedding, discussing application to adaptive control theory and reduction of boundary value problems to initial value problems 19 p3326 A66-3600

Nonlinear filtering theory based on invariant imbedding for orbit determination and adaptive control problems 19 p3303 A66-3624

Laplace integral application to inversion of three solar limb-darkening curves obtained in UV 19 p3464 A66-3628

First- and second-order constitutive equations of viscoelasticity based on mechanical and invariant theory, discussing relaxation under finite twist of incompressible isotropic bar 19 p3475 A66-3662

Acquisition phase of attitude control function of space vehicle, using noise measurements on one state 20 p3658 A66-3686

Invariant imbedding and scattering of light in one-dimensional medium with moving boundary, noting relaxation of photoemission and Doppler frequency shift 23 p4087 A66-4154

**INVENTORY CONTROL**

Air cargo transport development, and freight classification and inventory balancing 15 p2620 A66-2979

**INVERSION**

**SA POPULATION INVERSION**

Capacitance-voltage characteristics of anodized InSb surface measured, using metal oxide semiconductor method 03 p0411 A66-1300

Inversion of Hilbert type matrix for finite and infinite cases 10 p1550 A66-2134

Matrix inversion algorithm from Cayley-Hamilton 11 p1724 A66-2340

Radius of convergence of power series obtained by inversion of universal Kepler equation 17 p3001 A66-3234

Charge distribution in thermally grown silicon dioxide and silicon n-type inversion layer 22 p3962 A66-4008

**INVERTER**

**SA STATIC INVERTER**

Worst case design of diode transistor logic inverters, considering resistor end-of-life tolerance, supply voltage variations and minimum beta of switching transistor 10 p1508 A66-2128

Operational characteristics of LC tuned solid state static inverter used as power supply in autopilot gyros of Titan rocket, noting power oscillator circuit 12 p1804 A66-2466

Three-phase half-wave inverter circuit consisting of ring of three SCRs and converting DC into AC power supplied into



azag motor load 12 p1804 A66-24662  
 Transistor inverter with 80 percent efficiency for 400 mv source voltage, noting simplicity of design 17 p2848 A66-31810  
 Inverter with integrated components and direct coupled inverter circuit not needing transformers for space  
 Applications 22 p3880 A66-40740  
 Dual-element power devices for solid state inverters, evaluating potential hazards of reverse second  
 Breakdown 22 p3881 A66-40741  
 Integrated circuit arrays for solid state inverters, noting Johnson counter and packaging 22 p3881 A66-40742  
 Analytic model for describing operation of Parzolf tunnel diode  
 Inverter 24 p4187 A66-43181  
**INVESTMENT CASTING**  
 Investment castings in advanced high strength steels and titanium alloys, noting reliability and quality control  
 [SAE PAPER 650770] 05 p0688 A66-15009  
 Capability of investment casting process in production of integrally cast turbine wheels and nozzles for high temperature gas turbine application  
 [SAE PAPER 650706] 07 p1037 A66-17249  
 Investment cast 17-4PH incorporated into actuating and supporting mechanism double loop leading edge of wing of F-8E/FN/French Crusader 17 p2929 A66-32693  
**INVISCID FLOW**  
**A VISCOUS FLOW**  
 Chemical reaction occurring between low temperature plasma jet and nearly inviscid fluid /water/ 02 p0264 A66-11388  
 Introductory book on hypersonic aerodynamics covering continuum flow of inviscid nonequilibrium perfect gas and real gas, viscous and low density effects in hypersonic flow 02 p0176 A66-11875  
 Stabilization of inviscid pure-vortex flow with finite conductivity, using axially applied magnetic field  
 [AIAA PAPER 64-435] 03 p0399 A66-12787  
 Dissociation or ionization effects of air on inviscid hypersonic flow past circular cone with attached shock wave 03 p0316 A66-12928  
 Numerical solutions for inviscid nitrogen gas flows over circular cylinder where nonequilibrium prevails through nose region 03 p0317 A66-13211  
 Hydrodynamic instability of shear layers, using inviscid linearized stability theory of partially growing  
 Disturbances 04 p0513 A66-14474  
 Flow function equations for transonic flow past closed profile  
 Contours 07 p0982 A66-18121  
 Asymmetric hypersonic blunt body problem of determining two-dimensional steady rotational flow field between profile and detached shock 07 p0982 A66-18132  
 Surface pressure, heat transfer coefficient, wave structure and shock disturbances of inviscid supersonic flow field along corner of intersecting wedges  
 [AIAA PAPER 66-128] 07 p0984 A66-18462  
 Stability of frictionally heated Couette and Poiseuille flows, specifically Couette flow in inviscid limit 08 p1204 A66-18527  
 Clear air turbulence, considering energy source by transfer from large to small flow in gravity wave spectra, noting shear role and motion equations 10 p1552 A66-21289  
 Hypersonic flow of air past circular cylinder with nonequilibrium oxygen dissociation, including dissociation of free stream 10 p1479 A66-21375  
 Numerical method for calculating flow, including gas reactions and nonequilibrium, behind given axisymmetric detached shock wave 10 p1481 A66-21892  
 Inviscid flow of compressible conducting gas with aligned magnetic field through axially symmetric Laval nozzle in various transition regions 11 p1636 A66-23256  
 Shock layer approximation used in inverse hypersonic blunt body  
 Problem 12 p1795 A66-23574  
 Inviscid hypersonic flow over compression side of delta wing of moderate aspect ratio 12 p1796 A66-23605  
 Steady state expansion of gas into vacuum, considering continuum inviscid analysis, collision-free analysis, supersonic flow and hypersonic limits, etc, for spherical and

cylindrical symmetry 12 p1860 A66-23607  
 Analytic design of turbine blades based on inviscid isentropic supersonic vortex flow theory and performance in  
 cascades 12 p1796 A66-23800  
 Stability of plane inviscid jet and wake studied for possible growth in downstream spatial direction 12 p1865 A66-24582  
 Long finite amplitude wave motions and interactions in inviscid fluid  
 flows 15 p2478 A66-29242  
 Direct numerical method for calculation of supersonic inviscid flow about axisymmetric blunt body at large angle of attack [AIAA PAPER 65-24] 15 p2423 A66-29269  
 Displacement and heat transfer effects of laminar and turbulent boundary layers far downstream in slowly expanding hypersonic nozzle, determining inviscid core  
 flow 15 p2424 A66-29273  
 Inviscid and viscous flow in central core of supersonic free jet in wind tunnel, noting shock wave location at high Reynolds number 16 p2628 A66-30375  
 Behavior of inviscid supersonic conical flow fields near crossflow stagnation points studied by constructing coordinate expansions of exact conical flow equations [AIAA PAPER 66-491] 16 p2631 A66-31494  
 Self-similarity criteria in radiative flow for unsteady one-dimensional inviscid flow of perfect gas 17 p3034 A66-32471  
 Head wave of frictionless flow of real gas past positioned circular cone for small or zero angles of attack 17 p2842 A66-33169  
 Method of characteristics computer code applied to partial differential equations of inviscid fluid, calculating flow fields [AIAA PAPER 66-412] 18 p3097 A66-33637  
 Partial differential equations for three-dimensional inviscid flow solved for flow field over blunt body shapes at various angles of attack, for application to Apollo spacecraft  
 [AIAA PAPER 66-413] 18 p3045 A66-33638  
 Channel flow general equations including nonviscous uniform flow, steady flow, stagnation state and speed of sound in ideal gas 18 p3098 A66-34121  
 Boundary layer of steady incompressible plane crossed fields MHD flow at large Reynolds number 18 p3147 A66-34663  
 Newton law for simple inviscid fluid using Hamilton principle, emphasizing physical interpretation of  $\Gamma$   
 constraint 18 p3102 A66-34922  
 Hamilton principle applied to force equation for nonrelativistic and relativistic flow of compressible inviscid fluid with polarization and magnetization in connection with electromagnetic  
 momentum 18 p3102 A66-34923  
 MHD flow past semi-infinite plate under conditions where viscosity is  
 destroyed 20 p3609 A66-37537  
 Flutter of infinitely long panel of finite width with upper surface exposed to inviscid flow, noting critical wavelength and flutter velocity 21 p3827 A66-38691  
 Inviscid hypersonic nonequilibrium flow of three-component gas past circular cone, using exact reaction-rate equations to correct solution first obtained from approximate equations 21 p3693 A66-38711  
 Sufficient conditions for instability against small oscillations of symmetric laminar flow of inviscid incompressible perfect magnetofluid 21 p3791 A66-39169  
 Pseudoviscosity method using finite difference equations for calculating two-dimensional flow fields for supersonic motion of inviscid gas 22 p3901 A66-40494  
 Surface mass transfer effect for supersonic flow over cone, examining solution of equations of motion for inviscid compressible gas with velocity field normal to surface of inner cone 23 p4011 A66-41898  
 Inviscid flow model for stagnation region behind strong shock, examining inviscid energy for radiating gas including self-absorption effects 23 p4150 A66-41906  
 Inviscid flow near stagnation point of blunt body in hypersonic stream, using thin shock layer theory with very small density ratio 23 p4013 A66-42013  
 Three-dimensional oscillatory vortex instability in uniform inviscid rotating fluid 23 p4061 A66-42043

Experimental verification of stability criteria for incompressible inviscid flow with helical streamlines, using rotating cylinders 23 p4062 A66-42046  
**IODATE**  
 Gas laser output and threshold in population inversion from photodissociation of methyl iodide and fluoro iodo methylidyne 06 p0892 A66-16771  
 Gas laser output and threshold in population inversion from photodissociation of methyl iodide and fluoriodo methylidyne 19 p3372 A66-35368  
**IODIDE**  
 SA SILVER IODIDE  
 SA SODIUM IODIDE  
 Oxygen inhibition of grain boundary movement and stabilization of optical transmission in cuprous iodide thin film 23 p4110 A66-41152  
 Thermally initiated reaction between tert-butyl iodide and tetrafluorohydrazine provides synthetic route to tert-butyl difluoramine 23 p4118 A66-41234  
**IODINE**  
 Kinetics of reactions in iodide method of growing epitaxial germanium layers 08 p1268 A66-18797  
 Iodine evaluated as working fluid in supersonic wind tunnel through study of iodine dissociation process 11 p1683 A66-22594  
 Solar nucleosynthesis of extinct isotopic iodine, noting incorporation of Nakhilic meteorite material and subsequent decay into fissionogenic xenon 18 p3225 A66-33623  
 Hall effect in poly-n-vinylcarbazole-iodine charge-transfer complex, noting sign discrepancy of majority carrier 22 p3963 A66-40109  
 Transitions of first two band systems of iodine excited in argon suitable for laser action 23 p4079 A66-42085  
**ION**  
 S CESIUM ION  
 S FERRIC ION  
 S FREE RADICAL  
 S HEAVY ION  
 S HYDROGEN ION  
 S METAL ION  
 S NITROGEN ION  
**ION-ATOM INTERACTION**  
 Oxygen impurity atom interaction with radiation-induced defects in germanium over wide temperature range, producing optically active oxygen defect complexes 02 p0272 A66-11486  
 Wave function, polarization and decay of negative ion atoms in electric field 03 p0395 A66-12833  
 Interaction mean free path of nuclear-active particles in iron determined by measuring number of interactions in each iron layer in ionization calorimeter 07 p1115 A66-17550  
 Electromagnetic isotope separators used in nuclear physics for analysis of ion-matter interaction 08 p1257 A66-18694  
 Electron loss rate dependence on internal excitation and deactivation processes in F region ion-molecule reactions 08 p1218 A66-19405  
 Specific reaction rates measured as function of ion energy for low energy ion-molecule reaction 08 p1259 A66-19698  
 Intensity variation of 6300 angstrom night airglow and rate coefficient of ion-atom interchange reaction 09 p1372 A66-20381  
 Reaction rate of atomic oxygen with nitrous oxide in shock tube at high temperatures 11 p1649 A66-22881  
 Perturbation effects in differential elastic ion-atom scattering generated by crossing of molecular states from even potentials 11 p1740 A66-22972  
 Ion beam elastic scattering cross section for proton-helium systems 14 p2337 A66-27978  
 Intensity of oxygen red line in night airglow analyzed, obtaining temperature dependence of rate coefficients of ion atom interchange reaction and collisional deactivation, noting red line intensity dependence on solar activity 15 p2484 A66-28905  
 Mass spectrometric investigations of interaction of atmospheric ions with molecules of rocket gas



- release 15 p2495 A66-30061  
Fast ion molecule reaction in carbon dioxide analyzed, using mass spectrometer 16 p2645 A66-30116  
Electron secondary emission from interaction of ion, atom and molecular energetic beams with solids, especially when kinetic energy is significant 16 p2776 A66-30796  
Collision integrals calculated for interactions Li-H, Li-Li, H-H and H-H plus in LiH system 16 p2766 A66-31612  
Composition of cosmic rays of supernova origin, noting limited mixing and enrichment of elements of outer layer with thermonuclearly synthesized core substances due to shock acceleration 18 p3177 A66-34755  
MHD power generator in which ionization of alkali atoms occurs by collision with excited noble gas atoms, calculating velocity-dependent cross section 19 p3406 A66-35436  
Wave function, polarization and decay of negative ion atoms in electric field 19 p3404 A66-36775  
Instrumentation for plasma diagnostics noting electron density profile, temperature, ion-atom and electron-atom interaction, etc 20 p3556 A66-36964  
Ionospheric ion-molecular reaction rates, discussing various measurement results 21 p3734 A66-39319  
Reaction rates for charge transfer reactions of carbon monoxide with oxygen and carbon dioxide measured at 300 degrees K in pulse-discharge flowing afterglow system 22 p3859 A66-39907
- ION BEAM**  
Noble gas ion beams produced by duoplasmatron magnetically analyzed while varying gas pressure in source 01 p0114 A66-10850  
Duoplasmatron with electrostatic lens decreasing ion energy while focusing ions for maximum density parallel beam 01 p0114 A66-10851  
Charge distribution in ion beams after passage through nitrogen and inert gases 02 p0267 A66-11724  
Nonlinear theory LF oscillation excited in magnetoplasma by ion beam 02 p0268 A66-11779  
Interaction mechanisms of neutralized beam of ions and two symmetric neutralized ion beams flowing parallel to magnetic field 03 p0404 A66-12979  
Neutralizer configurations, immersed and withdrawn filaments, for given ion gun based on two-dimensional computer simulation of ion-beam neutralization [AIAA PAPER 65-380] 05 p0723 A66-15168  
Stability of monoenergetic ion beam injected across magnetic field into plasma-filled magnetic trap, noting oscillation excitation 06 p0914 A66-16142  
Plasma emission properties of vacuum spark when producing high current H and D ion beams 06 p0919 A66-16884  
Turbulent condition in plasma beam with virtual cathode characterized by electric field oscillation spectrum, off-center plasma torch spinning into ion side and ion acceleration 08 p1264 A66-19270  
Electron bombardment ion thrusters with two accelerator-grid systems for producing ion beams in directions 180 or 90 degrees apart [AIAA PAPER 66-248] 10 p1593 A66-21457  
Microthruster ion engine system with thrust vector control, using ion beam deflection [AIAA PAPER 66-204] 12 p1937 A66-24526  
Synthesis of plasma by ion beam bombardment, discussing electrostatic instabilities and collisional and noncollisional damping 14 p2339 A66-26816  
Neutralizer configurations, immersed and withdrawn filaments, for given ion gun based on two-dimensional computer simulation of ion-beam neutralization [AIAA PAPER 65-380] 14 p2342 A66-27411  
External injection of ions into cyclotron, examining case of injection of beam in median plane of magnet 14 p2347 A66-28310  
High intensity sharply-focused ion beam from plasma expansion ion source 15 p2552 A66-29405  
Stability of monoenergetic ion beam injected across magnetic field into plasma-filled magnetic trap, noting oscillation excitation 15 p2556 A66-29872  
Ion beam velocity measurement, using radial electric and tangential magnetic field 16 p2701 A66-30347  
Multistage ion gun using separate acceleration and deceleration stages and eucriptite or spodumene emitters 16 p2760 A66-30428  
Quasi-linear theory of plasma cyclotron instability for one-dimensional oscillation spectrum, noting energy of interaction with electromagnetic field, ion velocities, etc 16 p2762 A66-31172  
Positive ion beam polishing of optical surfaces 17 p2958 A66-32625  
Two-stream instability for longitudinal waves in plasma traversed by ion beam 18 p3148 A66-34909  
Hydrogen density in coaxial plasma injector prior to application of high voltage to electrodes, noting experimental setup and results 18 p3151 A66-35072  
Instrument for continuous variation of angle of incidence between ion beam and axis of RF quadrupole mass spectrometer from zero to 90 degrees 20 p3561 A66-38174  
Ion beam interaction with electron plasma and resultant parameter changes and cyclotron instability 21 p3783 A66-39026  
Operation and design principles of mass spectrometer using system of diaphragms and modulators to extract well-constrained ion bunch from plasma beam 21 p3784 A66-39031
- ION BOMBARDMENT**  
Range formula calculation of neodymium ion concentration in two samples of CdS crystals after bombardment at 200 kev Nd ion energies 01 p0126 A66-10970  
Construction problems of continuous-duty DC excited ion lasers 04 p0530 A66-13956  
Temperature, annealing time and radiation dosage effect on electroconductivity of inversion layers generated in n-type silicon during bombardment with boron ions 05 p0730 A66-14646  
Neutron activation and cesium-aluminum sputtering in oxygenated gas atmosphere [AIAA PAPER 66-77] 06 p0913 A66-17103  
Ion damage and successive annealing of germanium observed by electron microscope 07 p1097 A66-17528  
Induced electric conductivity in germanium bombarded by potassium ion in different crystallographic directions 07 p1104 A66-18363  
Formation of photoelectric converters of solar energy by penetration of high-energy phosphorus ions into p-type silicon 07 p1105 A66-18367  
Contact-making process in cadmium sulfide crystals, examining influence on plasma electron efficiency in glow discharge effect 08 p1272 A66-19243  
Electron excitation in germanium by alkali metal ions, noting effect on electrical conductivity 10 p1587 A66-22154  
Temperature, annealing time and radiation dosage effect on electroconductivity of inversion layers generated in n-type silicon during bombardment with boron ions 13 p2167 A66-25921  
Surface blistering of metals due to low energy hydrogen ion bombardment, determining solar absorptance change in gold-plated specimens 14 p2316 A66-28007  
Secondary emission of excited cesium atoms during bombardment of molybdenum and tantalum by fast cesium ions 14 p2338 A66-28248  
Damaged depth in germanium thin films induced by bombardment with low energy argon ions measured, using differences in sputtering yield for given energy 15 p2561 A66-28705  
Radioactive tracer technique to measure yield and angular distribution of copper sputtered from monocrystalline target subject to cesium ion bombardment [AIAA PAPER 65-379] 15 p2566 A66-29290  
Ion bombardment damage of molybdenum sulfide lattice studied by transmission electron microscopy, noting broadening of extinction contours and dislocation lines 15 p2567 A66-29404  
Fast emitted and reflected particles during ionic bombardment of metallic surfaces, considering two-atom collision rules, light emission, ion scattering, etc 16 p2753 A66-30798  
Change in resistance of titanium film deposited in high vacuum from argon ion bombardment, noting dependence on energy value 16 p2789 A66-3178  
Exchange reactions of charges appearing when beam of fast ions passes into thin gas target, examining characteristics of source of high energy neutral particles 17 p2961 A66-3294  
Radiation-induced electroconductivity and secondary emission in alkalal halide single crystals under positive ion bombardment 17 p2988 A66-3341  
Energy distribution of electrons emitted from alkali halide films on Mo substrate during positive helium and argon ion bombardment 17 p2988 A66-3345  
Sputtering yields of various semiconducting single crystals under argon ion bombardment 19 p3436 A66-3542  
Temperature dependence of sputtering yields of germanium under low energy ion bombardment, observing atom ejection patterns above annealing temperatures 19 p3436 A66-3542  
Electron excitation in germanium by alkali metal ions, noting effect on electrical conductivity 19 p3440 A66-3576  
Anisotropy of secondary electron emission in ion bombarded Si single crystals, using electron microscope 19 p3445 A66-3634  
Dislocation dipoles produced by ion bombardment of thin gold films, noting that during annealing dipoles can condense to form only one dipole 19 p3447 A66-3672  
Germanium damage due to low energy He, Ne, Ar and Kr ion bombardment 20 p3623 A66-3838  
Atom ejection patterns for sputtering of semiconductor single crystals 22 p3963 A66-4008  
Reverse breakdown voltage increase resulting from ion drift in silicon p-junctions formed by sodium ion bombardment 24 p4257 A66-4262
- ION CHAMBER**  
Small lightweight ion chamber dosimeter for monitoring radiation exposure to spacecraft crew members 05 p0676 A66-1465  
Rigidity response of ionization chambers in high atmosphere and deep space for study of rigidity dependence of solar cycle modulation of primary cosmic ray 18 p3179 A66-3476  
Cosmic ray ionization intensity measurement using special ion chamber 24 p4264 A66-4260
- ION CHARGE**  
Rate coefficients of ion charge exchange reaction between atomic oxygen ions and oxygen-nitrogen molecules measured at thermal energies by afterglow method 02 p0263 A66-1150
- ION CURRENT**  
Ionization currents in diamond exposed to pulsed excitation and to applied pulse electric field 10 p1586 A66-2215  
Quasi-stationary distributions of potential in one-dimensional ion-electron current near emitting surface, noting unstable regimes regarding slow variations in boundary conditions 14 p2338 A66-2877  
Electron-ion current partitioning effect efficiency of pulsed plasma accelerators due to viscous drag caused by ions carrying current to cathode [AIAA PAPER 65-335] 18 p3147 A66-3458  
Ionization currents in diamond exposed to pulsed excitation and to applied pulse electric field 19 p3440 A66-3575  
Current jet and plasma produced by coaxial plasma gun which is source of abundant slow deuterium plasma and fast plasma, examining acceleration mechanism 19 p3425 A66-3656  
Charged particle diffusion in plasma discharge in chamber with nonconducting walls, noting relations of various parameters 21 p3784 A66-3903
- ION CYCLOTRON**  
Experiments on ion cyclotron heating of plasma generated by Joule heating in Heliotron-B 12 p1919 A66-2385  
Ion cyclotron instabilities in bounded column-plasma system, noting growth rate parameters, instability conditions,



Langmuir probe measurement of electromagnetic field present in cyclotron oscillations 13 p2140 A66-25426  
Landau damping of transverse oscillations in collisionless plasma at ion cyclotron resonance and collisional damping in zero-temperature plasma 13 p2142 A66-25706  
Ion heating by ion cyclotron wave generation in dense plasma created by HF generator in metal discharge chamber, determining ion temperature 14 p2341 A66-27150  
LF wave in cylindrical plasma in magnetic field where ion beam is flowing and modes are nonaxisymmetric 15 p2553 A66-29629  
Nonresonant coupling of, RF power to plasma during ion cyclotron resonance heating in Model C stellarator 17 p2962 A66-31822  
Plasma formation by fast atom injection into mirror magnetic field and well, showing effect of geometric transition on hydromagnetic drift and ion-cyclotron instability 19 p3421 A66-36541  
Ion cyclotron resonance heating and trapping and adiabatic compression of plasma in QP machine 19 p3431 A66-36590  
HF heating of plasma in metallic vacuum chamber, noting generation and absorption of ion cyclotron waves, estimating plasma density 19 p3431 A66-36593  
Ion cyclotron resonance heating applied to stellarator plasma formed by ohmic heating, noting Alfvén wave generation by stix coil 19 p3432 A66-36594  
Higher harmonics generation of ion cyclotron frequency in longitudinally magnetized plasmas, noting experimental setup and pressure effects 21 p3777 A66-38766  
Boundary behavior of plasma heated by ion cyclotron waves 21 p3780 A66-39003  
Electromagnetic wave propagation in plasma along weakening magnetic field, considering spatial dispersion associated with ion thermal motion 21 p3781 A66-39010  
Solid state plasma microwave oscillations and dispersion conditions for ion-cyclotron instability excitation in semiconductor 21 p3804 A66-39335  
Solid state plasma microwave oscillations and dispersion conditions for ion-cyclotron instability excitation in semiconductor 22 p3959 A66-39705  
Ion heating by ion cyclotron wave generation in dense plasma created by HF generator in metal discharge chamber, determining ion temperature 24 p4244 A66-42970  
ION DENSITY  
IONOSPHERIC ION DENSITY  
MAGNETOSPHERIC ION DENSITY  
Charge trapped in electron or ion beams at pressures below breakdown determined from general integro-differential equation, using approximation method 01 p0111 A66-10375  
Data from ion energy spectrometer mounted on Ariel I satellite indicating increased concentration of oxygen ions during afternoon at high altitudes 01 p0061 A66-10498  
Pressure volume recombination coefficient in oxygen, using capacitor to determine average ion density 04 p0549 A66-14286  
Frequency dependence of resistivity, absorption and emission processes in fully ionized plasma 05 p0726 A66-15245  
Electron temperature and ion density profiles across interelectrode gap of thermionic diode operating in ignited mode 05 p0621 A66-15573  
Radar echo effects of satellite disturbance in plasma medium, noting electron and positive ion density distribution 08 p1302 A66-18755  
Thermal conductivity of NaCl crystals and dependence on Ag, Br, Li, K, I and Rb ion concentration 08 p1278 A66-19627  
Composition of outer ionosphere measured, using RF mass spectrometers mounted on board Elektron I and II satellites 09 p1378 A66-21008  
Local magnetic field, ion density flow and electric field in plasma measured downstream of theta-pinch accelerator in presence of uniform guide field

[AIAA PAPER 66-155] 10 p1565 A66-21684  
Ion density profiles in boundary layers associated with supersonic flow of shock heated air over flat plate measured by cylindrical and flush-mounted electrostatic probes  
[AIAA PAPER 66-159] 10 p1565 A66-21686  
Coefficients of space charge effects for growing oxide films, derived from perturbation treatment, evaluated in terms of boundary concentrations of diffusing species 12 p1811 A66-23624  
Correlation between plasma and ion density fluctuations as detected by magnetic probe, spectral emission techniques and Langmuir probe 13 p2142 A66-25703  
Stratospheric small-ion density measurement from high-altitude jet aircraft, noting dust effect 14 p2297 A66-28334  
Perturbations caused by cylindrical body in plasma, obtaining electric field and electron and ion concentration dependences on distance 15 p2595 A66-29086  
Color centers in alkali metal azides, noting change of ion from linear to bent configuration 16 p2777 A66-31023  
Critical electric field for charged droplets atomizing, noting spark discharge and ion concentration in clouds 16 p2742 A66-31109  
Thermal conductivity of NaCl crystals and dependence on Ag, Br, Li, K, I and Rb ion concentration 17 p2984 A66-33141  
Hollow electric collector probe for measuring ion density in rapidly flowing slightly ionized gas 18 p3112 A66-34244  
Mass and energy spectra of ions in Bostik-type plasma source studied by time-of-flight mass spectrometer 21 p3784 A66-39033  
Visibility and small ion density correlated by comparing light scattering with ion attachment processes on airborne scatters 23 p4065 A66-41842  
ION DISTRIBUTION  
Ion direct heating in nonlinear absorption of transverse waves during scattering on plasma ions, noting equation for ion distribution function 03 p0396 A66-12283  
Cyclotron instability dependence on nonmonotonic ion distribution function of plasma with cyclotron resonance 03 p0396 A66-12289  
Structure of disturbed plasma in thermodynamic equilibrium situated near charged solid surface ideally reflecting incident particles 03 p0397 A66-12381  
D-region atmospheric processes such as electron attachment, photo and other detachment processes, recombination and neutralization as studied in laboratory 03 p0362 A66-12640  
Ogo-A first results on mass spectrometry measurements of thermal positive ion composition at high altitudes 05 p0746 A66-14781  
Ion direct heating in nonlinear absorption of transverse waves during scattering on plasma ions, noting equation for ion distribution function 05 p0727 A66-15455  
Ion composition model representing conditions at low temperatures, assuming that solar cycle variation ions are distributed according to diffusive equilibrium theory 06 p0876 A66-18611  
Kelvin-Helmholtz instability in fully ionized plasma in magnetic field, assuming variable streaming velocity 07 p1089 A66-17961  
Flute modes at ion gyrofrequency propagating perpendicular to magnetic field 08 p1260 A66-18535  
Ion distribution in plasma of vacuum spark 10 p1569 A66-21886  
Physical state of water in living cell and model systems such as collagen and wool 11 p1645 A66-22989  
Chemical and photochemical reactions controlling ion composition of atmosphere between 150 and 300 km 11 p1699 A66-23041  
Relative drift between ions in adjacent layers exciting Kelvin-Helmholtz instability analyzed in thermally ionized cesium plasma, noting range of frequency oscillations 12 p1923 A66-24577  
Structure of disturbed plasma in thermodynamic equilibrium situated near charged solid surface ideally reflecting incident particles 13 p2139 A66-25386  
Ionospheric flight simulation in which ion distribution of neutral gas expanding into

rarefied ionized gas under magnetic field is measured 16 p2759 A66-30374  
Instability of nonlinear stationary oscillations of potential in electron-ion flows useful in distribution functions of ions and electrons 16 p2754 A66-31174  
Hydrogen and helium ions formation and destruction, charge transfer, diffusion, role during solar activity, using mass spectrometry, ground radar, etc 19 p3350 A66-36356  
Excitation of collective motions in collisionless plasma in magnetic field for case of large temperature anisotropy 21 p3783 A66-39024  
Lithium ion drift and density distribution in electric field of Si p-n junction 24 p4253 A66-42359  
Average properties of positive-ion component of solar wind observed by Mariner II 24 p4263 A66-42586  
ION EMISSION  
Energy and intensity of ions emitted by metal target as function of characteristics of laser and nature of metal 05 p0697 A66-15109  
Time resolution of electron and ion emission produced by Q-switched ruby laser pulse focused on metal surface 07 p1045 A66-18358  
Surface physics of ion and electron emission during cesium adsorption on polycrystalline wire surfaces [AIAA PAPER 66-222] 10 p1575 A66-21450  
Electron and ion emission from pulsed ruby laser illuminated metallic surface into vacuum, determining application to pulsed ion thruster [AIAA PAPER 66-230] 10 p1542 A66-21453  
Cesium ion emission patterns obtained from rear-fed porous refractory metals, using thermal emission microscope [AIAA PAPER 66-220] 11 p1746 A66-23086  
Energy spectra of ions emitted by beryllium, carbon and molybdenum heated by laser 13 p2131 A66-25479  
Surface temperature determination procedure for laser heated metals based on heat conduction equations and ion emission from surface 15 p2514 A66-29035  
Actual line shape expected from accelerating radiating ion, errors due to Lorentzian approximation and results for ion laser transition in rare gas lasers 16 p2716 A66-30181  
Collisional Stark broadening in RF discharges, noting large ion and electron broadening contribution 17 p2960 A66-31921  
Electron-ion emission pattern distribution obtained by pulsed laser focusing on solid target 17 p2937 A66-33256  
Large amplitude oscillations with frequencies corresponding to ion transit times in thermal cesium plasma diodes with parallel plane construction 19 p3313 A66-35425  
Secondary ions energy spectra dependent on incidence angle of primary ions for varying escape angles, using molybdenum targets 19 p3403 A66-36454  
Electron and ion emission from polycrystalline surface of Be, Ti, Cr, Ni, Cu, Pt and type-304 stainless steel in cesium vapor 20 p3623 A66-38400  
Energies of ions generated from metal surface irradiated by single giant pulse laser 20 p3582 A66-38412  
Beam foil excitation technique application in measuring mean lives of 2p and 3p levels of hydrogen 21 p3774 A66-38543  
Flare ion fluxes in space by mass-spectrometric measurements of solar flare rare-gas ions stopped in extraterrestrial material 22 p3973 A66-40016  
ION ENGINE  
SA PLASMA ENGINE  
Focusing and accelerating electrode materials for cesium contact ion engines, noting advantages of copper, beryllium and molybdenum [AIAA PAPER 64-684] 02 p0278 A66-11537  
Optimum sastrugi ion optical engine design for uniform emission, considering perveance and electrode clearance [AIAA PAPER 65-69] 03 p0416 A66-12765  
Drain currents from iron and copper ion accelerator electrodes of ion engine as functions of cesium flux, temperature, voltage difference and oxygen pressure



[AIAA PAPER 64-686] 03 p0416 A66-12782  
Electrostatic engine with HF ion source  
uses mercury as fuel 04 p0573 A66-13542  
Radiation tolerant electric propulsion  
system to operate on SNAPSHOT satellite,  
permitting orbital test of ion engine and ion  
propulsion with nuclear power supply  
/SNAP-10A/ 04 p0544 A66-13630  
Electrostatic hysteresis synchronous motor  
discussing development, operation  
characteristics, test results, advantages and  
limitations 04 p0459 A66-13681  
Electric rocket propulsion system  
requirements for space propulsion,  
comparing capabilities with chemical and  
electrical rockets 08 p1280 A66-18575  
Electrostatic ion propulsion and  
electromagnetic engine experiments in  
Germany for application to space travel,  
noting nuclear energy power source 08 p1281 A66-18614  
Electric propulsion systems development,  
discussing ion beam neutralization, nuclear  
power sources, contact ionization engine,  
etc 09 p1434 A66-20248  
Sputtering yields of aluminum, copper and  
titanium measured as function of cesium ion  
energies for use as electrodes on cesium ion  
engines  
[AIAA PAPER 66-203] 10 p1575 A66-21445  
Ion engine arcing frequency from  
micrometeoroid impact  
[AIAA PAPER 66-205] 10 p1592 A66-21446  
Electron-ion emitting characteristics of  
various electrode materials with cesiated  
surfaces for cesium contact ion thrusters  
[AIAA PAPER 66-208] 10 p1592 A66-21447  
Comparison of various electrostatic  
thrusters and proposed low pressure  
colloidal power converter for high payload  
lunar and planetary missions  
[AIAA PAPER 66-211] 10 p1592 A66-21448  
Plasma measurements in cesium electron  
bombardment ion engine indicate that  
reversed cathode-anode configuration  
improves radial ion distribution  
[AIAA PAPER 66-246] 10 p1593 A66-21455  
Ion thruster, including mercury feed  
system and shielded neutralizer, designed  
and tested for spacecraft station keeping  
and attitude control  
[AIAA PAPER 66-247] 10 p1593 A66-21456  
Electron bombardment ion thrusters with  
two accelerator-grid systems for producing  
ion beams in directions 180 or 90 degrees  
apart  
[AIAA PAPER 66-248] 10 p1593 A66-21457  
Ion propulsion by electrostatic acceleration  
of cesium ions subjected to transverse  
magnetic field, using negative space charge  
sheath  
[AIAA PAPER 66-256] 10 p1563 A66-21461  
Life testing of electron-bombardment  
cesium ion engine designed for power-to-  
thrust ratio of 160 kw/lb  
[AIAA PAPER 66-233] 10 p1594 A66-21701  
Discharge and exhaust beam of small low-  
power DC magnetic expansion thruster  
[AIAA PAPER 66-195] 11 p1743 A66-22216  
Durability test of mercury electron-  
bombardment ion thrusters, measuring  
lifetime, output, power efficiency, etc  
[AIAA PAPER 66-231] 11 p1760 A66-22218  
Surface ionization engine development,  
considering life testing of sastrugi thrusters  
[AIAA PAPER 66-236] 11 p1760 A66-22219  
Zero-g vapor feed system with no moving  
parts, noting ion engine testing, propellant  
use efficiency and surface tension storage  
[AIAA PAPER 66-249] 11 p1761 A66-23083  
Feasibility design study of solar powered  
ion propulsion system for interplanetary  
spacecraft  
[AIAA PAPER 66-214] 12 p1936 A66-24524  
Porous structures for ion engine  
application, discussing ionizer materials  
preparation, based on powder metallurgy  
and two-phase tungsten base alloy  
[AIAA PAPER 66-221] 12 p1896 A66-24528  
Power conditioning system for ion engine  
used in Sert-I flight test  
[AIAA PAPER 64-681] 12 p1937 A66-24691  
Glessen ion engine utilizing HF mercury  
ion source 12 p1938 A66-24905  
Lightweight flight prototype mercury ion  
engine system development and testing  
[AIAA PAPER 66-216] 13 p2172 A66-25170  
Electron bombardment thrusters using

liquid mercury cathodes, noting lifetime,  
propellant and power efficiency, feed  
system, temperature limits, etc  
[AIAA PAPER 66-232] 13 p2172 A66-25172  
Multistrip cesium contact thrusters,  
integral focus life test engine and various  
integral focus ionizers  
[AIAA PAPER 66-235] 13 p2172 A66-25174  
Zero-gravity mercury feed system for  
mercury-electron bombardment spacecraft  
engines  
[AIAA PAPER 66-250] 13 p2172 A66-25176  
Weight criteria for integration of nuclear-  
electric power supply with electric thruster  
system as primary spacecraft propulsion  
[AIAA PAPER 64-765] 13 p2173 A66-26611  
Power conditioner, source and heat  
removal equipment considered for ion  
engines  
[AIAA PAPER 64-764] 13 p2174 A66-26659  
Power conditioning and ion thruster  
module size and number effect in terms of  
reliability  
[AIAA PAPER 65-68] 14 p2375 A66-27883  
Power conditioning and advanced  
propulsion system of ionic engine, noting  
high voltage inverter design and vaporizer  
heater circuit 14 p2375 A66-28416  
Cesium contact ion engine construction and  
performance and engine neutralizer  
[AIAA PAPER 65-375] 16 p2791 A66-30906  
Axially symmetric or two-dimensional  
electrode system with emitting surface,  
discussing convergence and accuracy criteria  
of iteration methods 17 p2887 A66-32700  
Electrostatic ion drive measuring methods,  
noting Faraday collector for ion current  
density 17 p2991 A66-33197  
Electrostatic ion drives technology  
problems, considering conversion efficiency,  
thrust, reliability, high voltage, mass per  
unit thrust, etc 17 p2991 A66-33231  
Electron bombardment ion thrusters and  
electrostatic accelerators, discussing  
electrode geometry and composition and  
electrode erosion 17 p2991 A66-33233  
Electrostatic ion drives technology  
problems, discussing gaseous discharge ion  
sources, duoplasmatron and electron  
bombardment ion generator 17 p2991 A66-33234  
Surface tension propellant storage and  
feed systems for zero-g ion  
engines 19 p3450 A66-35615  
Ion engine satellite control system noting  
design and laboratory tests  
[AIAA PAPER 65-417] 19 p3450 A66-35616  
Comparison of electromagnet and  
permanent magnet versions of electron  
bombardment cesium ion engine  
[AIAA PAPER 65-373] 19 p3450 A66-35617  
Thruster device using self-induced  
magnetic Lorentz forces to attain velocities  
up to 50,000 m/sec for plasma jet ejected by  
electric arc engines 19 p3451 A66-36637  
Low thrust divergent flow cesium-on-  
tungsten contact ionization electrostatic  
thruster for satellite attitude control and  
stationkeeping missions  
[AIAA PAPER 66-569] 20 p3628 A66-37051  
Lightweight power-conditioning system for  
ion engines using energy-storage  
transformers for conversion, nondissipative  
regulation and protection 20 p3628 A66-37172  
Ion propulsion engine with replenishable  
liquid-film-protected tungsten electrode,  
discussing construction and mass loss rate  
vs temperature  
[AIAA PAPER 65-378] 20 p3629 A66-38167  
Digital computer program for solution of  
space-charge-flow problem applied to design  
of thrusters with variable thrust vector,  
analyzing two ion-thruster configurations  
with aid of computer 20 p3629 A66-38179  
Automatic double probe to determine  
electron temperatures in ion engine  
exhaust 24 p4215 A66-43208

**ION EXCHANGE**  
Classification of ions capable of replacing  
Ti in barium titanate 06 p0927 A66-16719  
Ion exchange in phospholipid  
monomolecular films 12 p1805 A66-23917  
Computer program for current profile and  
trajectory analysis for cesium contact  
thruster leading to integral focus  
configuration of multistrip contact engines  
for long space missions  
[AIAA PAPER 66-206] 16 p2792 A66-31690

**ION EXCHANGE MEMBRANE**

Gas permeation measurements on ion  
exchange fuel cell membranes using  
chromatography 05 p0611 A66-1453  
Heat and mass transfer in ion exchange  
membrane fuel cells 07 p0995 A66-1832  
Hydrogen-oxygen fuel cells, using ion  
exchange electrolytes 07 p0996 A66-1847

**ION EXTRACTION**

Plasma Separator Thruster, advanced ion  
thruster design based on independent  
operation and optimization of plasma source  
and plasma extraction system  
[AIAA PAPER 66-598] 18 p3163 A66-3421  
Plasma potential and ion energy  
determination via ion extraction and energy  
analysis 24 p4247 A66-4320

**ION GAUGE**

Gauges and systems applicable to  
measurement of extremely high vacuum  
considering ion gauges with modulators  
suppressor gauges, extractor gauges and  
cold cathode type gauges 24 p4215 A66-4306

**ION IMPACT**

Optical excitation due to impact of ver-  
slow helium ions on Ar and Kr attributed to  
transfer of kinetic energy into internal  
electron energy 11 p1740 A66-2297  
Phase difference due to elastic wave  
produced by cyclic heating of targets by  
impacting ions from pulsed  
beam 13 p2159 A66-2507  
Long-lived impact excitation states of  
particles measured from cross section of  
nonelastic collision with second  
particle 18 p3137 A66-3402  
Intensity distribution in rotational  
structure of molecular spectra bands upon  
excitation by ion impacts 20 p3604 A66-3736  
Nonequilibrium plasmas produced in InS  
by both impact ionization and injector  
examining instabilities due to HF  
oscillations and negative  
resistance 23 p4114 A66-4158  
Decaying free carrier concentration  
increase in GaAs when subjected to  
increased level of drive during first  
cycle 24 p4253 A66-4237

**ION INJECTION**

Proton injection into radiation belts by  
large B-L space regions by cosmic ray and  
solar proton albedo neutron decay  
injection 11 p1764 A66-2313  
External injection of ions into cyclotron  
examining case of injection of beam in  
median plane of magnet 14 p2347 A66-2831  
Plasma formation by high energy molecular  
hydrogen ion injection followed by  
dissociation and accumulation in static  
magnetic mirror  
configuration 19 p3422 A66-3654  
Aspa device designed for study of  
composition, energy and density  
distributions produced when plasma blob is  
injected into mirror trap with adiabatic  
plasma compression 19 p3423 A66-3655  
Increasing plasma density in Ogr  
1 20 p3610 A66-3805  
Plasma blob capture when injected  
perpendicular to magnetic force line  
attributed to electrostatic repulsion of  
polarization space charge formed by  
interaction 20 p3610 A66-3805  
Deflection of plasma jet generated by  
coaxial gun and injected along axis of  
quadrupole magnetic field eliminates neutral  
gas, producing complete  
ionization 20 p3610 A66-3805  
Plasma injection from coaxial plasma gun  
into magnetic trap with opposite  
fields 21 p3788 A66-3905  
Deep 1/10 micron/ penetration of ion  
implanted donors in silicon, measuring  
density profiles via C-V method and  
parameter of penetrating tail  
section 24 p4250 A66-4225

**ION MICROSCOPE**

Cesium ion emission patterns obtained  
from rear-fed porous refractory metal  
using thermal emission microscope  
[AIAA PAPER 66-220] 11 p1746 A66-2308  
Scanning microscope for studying Si p-  
junctions by electron or ion  
bombardment 17 p2927 A66-3345

**ION MOBILITY**

Tropospheric ion mobility distribution  
conductivity and densities above exchange  
layer 02 p0222 A66-1182



- Effects of variable ionic mobility on current collection by cylindrical body and of ring electric field on sheath size, noting role of diffusion 05 p0722 A66-14724
- Phenomenon 05 p0722 A66-14724
- Pressurizing thrust bearings through use of ions and high electric fields ASME PAPER 65-WA/LUB-1]
- 05 p0689 A66-15525
- Time dependence of electron density during afterglow of plasma in helium-hydrogen, neon-hydrogen and argon-hydrogen mixtures measured by microwave cavity 07 p1091 A66-18398
- Effect of ion drift from discharge on ionization state of helium-plasma model 08 p1265 A66-19374
- Conductivity measurements on silver bromide and silver 09 p1426 A66-20194
- Pressurizing thrust bearings through use of ions and high electric fields ASME PAPER 65-WA/LUB-1]
- 12 p1888 A66-24546
- Mobility of various ions in nitrogen and argon and mobility and diffusion of ions in hydrogen 14 p2345 A66-28138
- Motion of slow positive potassium and nitrogen ions in nitrogen, measuring mobility and diffusion coefficients with apparatus whose characteristics are given 14 p2345 A66-28139
- Motion of potassium ions in argon, using apparatus for simultaneous measurement of mobility and diffusion coefficients 14 p2345 A66-28140
- Ionic drift velocity peak function for two interconverting nitrogen ion species drifting in gas in electric field 15 p2550 A66-28756
- Effect of ion drift from discharge on ionization state of helium-plasma model 18 p3146 A66-34176
- Gerdien type chamber for measurements of ion mobility spectrum in terrestrial mesosphere and Mars atmosphere 18 p3114 A66-34712
- ION MOTION
- SA PENNING DISCHARGE
- Oscillations of electron-ion plasma in external electric field assuming uniformly accelerated motion of plasma components 02 p0268 A66-11784
- Electron beam-hot plasma interaction at low frequencies, explaining cesium discharges and gas noise 03 p0398 A66-12539
- Frequency oscillation role as drift waves excited during interaction of electron beams with plasma, made impossible by ion transverse motion 05 p0722 A66-14723
- Ion motions in theta pinch discharge studies from time-resolved profile measurements of impurity lines 06 p0921 A66-17050
- Kelvin-Helmholtz instability in fully ionized plasma in magnetic field, assuming variable streaming velocity 07 p1089 A66-17961
- Particle localization in spark chamber and ion drift in Wilson cloud chamber, noting experimental result of simultaneous observation of identical particles 09 p1379 A66-20233
- Plasma density drops developing when injecting plasma into trap with combined field, noting rise of HF field and acceleration of fraction of plasma ions with each drop 13 p2137 A66-25104
- Depopulation of ground state chromium ions in ruby under optical pumping explained via rate equations 13 p2089 A66-25188
- Steady state motion of Couette plasma flow in electric field, assuming transfer of collective motion is effected by ions and heat transfer by 14 p2339 A66-26774
- Electrons 14 p2339 A66-26774
- Drift and diffusion of slow positive ions in hydrogen, using redesigned apparatus 14 p2345 A66-28141
- Unified field theory applied to relaxation of ion velocity distribution in plasma 15 p2552 A66-29396
- Wind shear theory of formation of temperate zone blanketing sporadic E layers, noting motion equation for ions in ionospheric E region 15 p2490 A66-29948
- Plasma density drops developing when injecting plasma into trap with combined field, noting rise of HF field and acceleration of fraction of plasma ions with each drop 16 p2758 A66-30283
- Ion motion effects on ionospheric radio wave propagation 17 p2917 A66-32306
- X-ray irradiated MOS structure behavior, noting ionic charge motion in oxidized silicon that depends on electric field 18 p3155 A66-34083
- Fluid equations used in describing electron and ion motion perpendicular to field lines in slab of plasma supported against gravitational field by sheared magnetic field 19 p3417 A66-36527
- MOS capacitance of p-type silicon in inversion layer and ion drift in fringing field 22 p3872 A66-39744
- Electron-ion motion effect on electromagnetic wave reflection from plasma 22 p3955 A66-39997
- Lithium ion drift and density distribution in electric field of Si p-n junction 24 p4253 A66-42359
- Reverse breakdown voltage increase resulting from ion drift in silicon p-n junctions formed by sodium ion bombardment 24 p4257 A66-42621
- Three-dimensional voltage traps for charged particles, using equilibrium equations with or without thermal agitation 24 p4245 A66-42996
- Effect of ion motion along magnetic field on plasma stability 24 p4245 A66-43052
- ION OSCILLATION
- Plasma ion and electron oscillation 05 p0725 A66-15235
- Secondary emission ratio and multiplication constant of electron-ion oscillatory discharge 06 p0919 A66-16872
- Simultaneous electron and ion oscillations on discharge gap of four-electrode chamber 06 p0919 A66-16881
- IR absorption spectrum of local H-ion oscillations in KCl crystals doped with Na, Rb, Cs, I, Br and F 10 p1588 A66-22158
- Decaying plasma density determined from high-mode oscillations produced in magnetic trap with metallic chamber at 2000 to 6000 oe 16 p2756 A66-30099
- Plasma-ion oscillations in drifted plasma effected in diode-type discharge tube by varying longitudinal magnetic field or cathode temperature 17 p2972 A66-32974
- IR absorption spectrum of local H-ion oscillations in KCl crystals doped with Na, Rb, Cs, I, Br and F 19 p3440 A66-35772
- Ion oscillations in high temperature electron-ion plasma with HF fluctuations 23 p4102 A66-41485
- Flute type oscillations of hot ion plasma in homogeneous magnetic field with wave-plasma resonances 23 p4105 A66-41705
- ION PROBE
- Probes in atmospheric pressure argon plasma where ion diffusion is function of temperature 03 p0406 A66-13280
- In situ probe measuring nonthermal components of electron energy distribution in ionosphere, small-scale ionization inhomogeneities and negative ion concentrations in lower ionosphere 08 p1223 A66-18745
- Potential profile around negatively biased spherical and cylindrical ion probes in collisionless plasma computed numerically 13 p2142 A66-25707
- Polarized pyrometric probe for direct measurement of ion and electron energy in hot dense plasma 14 p2290 A66-26825
- Hollow electric collector probe for measuring ion density in rapidly flowing slightly ionized gas 18 p3112 A66-34244
- Vacuum system of ion microprobe mass spectrometer noting design criteria, operation and results 24 p4215 A66-43162
- ION PRODUCTION
- Discrepancy between observed ion production rate in cesium thermionic converter and Saha-Langmuir equation prediction suggests locality of ion formation 05 p0612 A66-14984
- Ion-electron interaction in plasma 05 p0725 A66-15243
- Photolionization upstream of strong shock wave determined by ion continuity and radiative transfer 07 p1022 A66-18107
- Optimum ionizer structure, examining cesium transport through tungsten capillaries
- [AIAA PAPER 66-207] 12 p1922 A66-24529
- Estimation of ion formation rate at various altitudes in ionosphere and zenith angles during low and high solar activity periods 15 p2487 A66-29105
- H, C, N, O, Cl, Ca and Al negative ion formation in plasma, noting role of continuous radiation, formation temperature and metastable and stable states 18 p3144 A66-34041
- Ionization due to alpha, beta and gamma radiation from ground and atmosphere in ground proximity, noting ion pair production rate and energy spectra 20 p3552 A66-37759
- ION PUMP
- Cathode sputtering theory, explaining sputtering dependence on ion angle of incidence, with application in electromagnetic isotope separators, etc 08 p1257 A66-18695
- Molybdenum and titanium cathodes applied in getter ion pump, noting improvement of initial and average performance 13 p2078 A66-25649
- Vacuum equipment selection for thin film processing line, comparing diffusion and ion-pumped evaporation systems 13 p2040 A66-25843
- Space simulation facility, based on ion-getter pump system, using ion and titanium sublimation pumps and stainless steel shrouds for thermal conditioning 16 p2677 A66-30453
- Optimizing performance of ultra high thermal vacuum system 16 p2681 A66-30499
- Diffusion, getter-ion and cryogenic high vacuum pumping methods, showing relationship of pressure vs gas load, operating efficiency and cost as function of system size 17 p2930 A66-32945
- ION RECOMBINATION
- SA ELECTRON-ION RECOMBINATION
- Ion recombination effects on inhomogeneous cylinder deceleration in rarefied plasma 04 p0551 A66-13858
- Helium-plasma decay in spherical balloon and volume removal by electron-ion recombination 06 p0914 A66-16146
- Departures from local thermal equilibrium in helium plasma produced by magnetically-driven shock wave in T-tube 10 p1566 A66-21811
- Helium afterglow in HF pulse-discharge plasma at 77 K from dissociative recombination of molecular helium ion with thermal electron 10 p1572 A66-22022
- Mixtures of ions in wind-shear theory of sporadic E layer, noting ion recombination 14 p2281 A66-26845
- Recombination coefficient and high electron temperature in midlatitude sporadic E layer with ions of oxygen and nitrogen oxide 14 p2281 A66-26849
- Helium-plasma decay in spherical balloon and volume removal by electron-ion recombination 15 p2556 A66-29876
- Rate constant of ion molecular processes in ionosphere, tabulating results of laboratory analyses 15 p2495 A66-30054
- Helium afterglow in HF pulse-discharge plasma at 77 degrees K from dissociative recombination of molecular helium ion with thermal electron 16 p2760 A66-30841
- Plasma model representing phenomena occurring in cesium thermionic converters operating in collisional ignited mode 19 p3406 A66-35429
- Temperature dependence of dissociative recombination coefficients in argon according to hypotheses of Bates and Palgarno 19 p3404 A66-36758
- Altitude profiles for dayglow emissions excited by molecular ion dissociative recombination, solar radiation fluorescence, oxygen photodissociation, electron collisions and chemical reactions 23 p4064 A66-41680
- ION SCATTERING
- Anomalous scatter and energy loss of ions penetrating crystalline semiconductors 05 p0737 A66-15303
- Measurement of equilibrium fractions of helium ions present in helium beams scattered at zero degrees through carbon foils 06 p0912 A66-17038
- Plasma compression effect of space vehicle in magnetolonic medium, discussing injection and removal of quasi-trapped



ions 08 p1302 A66-18756  
Freezing potential for ammonia and sodium chloride solution at constant freezing rates, noting stationary nature of potential under stationary conditions 13 p2121 A66-26124  
Book on electronics and electron physics advances including fast ion scattering, kinetic ejection of electrons, plasma application in microwaves, etc 16 p2747 A66-30794  
Fast emitted and reflected particles during ionic bombardment of metallic surfaces, considering two-atom collision rules, light emission, ion scattering, etc 16 p2753 A66-30795

## ION SHEATH

Thin electrostatic sheath near body immersed in weakly ionized flowing gas in mean free path regime for relatively small Debye length [AIAA PAPER 66-6] 06 p0921 A66-17102  
Satellite charge and sheath formation resulting from photoelectric and secondary emission 08 p1302 A66-18748  
Electromagnetic wave scattering by satellite caused by ionized coating, noting effect on echo 08 p1182 A66-18754  
Plasma and electron gyroresonance effects on admittance of RF plasma probe surrounded by ion sheath 09 p1381 A66-20373  
Drift instabilities in thermionic plasmas, noting excitation of LF oscillations with finite perturbation amplitude around cathode ion sheath 13 p2145 A66-25729  
RF impedance of absorptive surface plasma probe for case of collapsed ion sheath 13 p2136 A66-26294  
Slot admittance for two-layer compressible plasma sheath-ion sheath in plasma half-space 14 p2235 A66-27128  
Normally incident plane electromagnetic wave scattering by circular cylinder coated with radially stratified sheath 14 p2238 A66-27587

## ION SOURCE

Mass spectrometry of positive ion beam produced by nonmagnetic emitter, using electron beam passing through electrostatic field for rare isotope analysis 03 p0397 A66-12391  
Electrostatic engine with HF ion source uses mercury as fuel 04 p0573 A66-13542  
Power transistors used for stabilization of emission current of electron bombardment ion source for mass spectrograph 04 p0498 A66-14037  
Ionization characteristics of various porous metal ionizers and suitability for use in cesium contact thrusters [AIAA PAPER 66-218] 11 p1756 A66-23094  
Mass spectrometry of positive ion beam produced by nonmagnetic emitter, using electron beam passing through electrostatic field for rare isotope analysis 13 p2139 A66-25397  
Polarized ion source yielding current of 0.1 microamperes, with background of unpolarized deuterons of 1-2 percent and of protons 10-15 percent 13 p2134 A66-26244  
Diagnostic work on ion sources in Germany, including electrostatic drive research, duoplasmatron and porosity of tungsten emitter [DGR PAPER 66-005] 13 p2059 A66-26492  
Thin Permalloy film deposition by controlled high-vacuum ion source, noting design of apparatus 16 p2661 A66-30691  
Electrostatic ion sources, noting simulation chamber for tests and measurement results on emissive power of porous tungsten 16 p2791 A66-31191  
Electrostatic ion sources, assessing thrust output and lifetime for various space missions and satellite attitude control 16 p2791 A66-31192  
Mass spectra of isotopically labeled tetraboranes obtained under zero ion source contact conditions, observing parent peak and metastable transition 16 p2647 A66-31379  
Electrostatic ion drives technology problems, discussing gaseous discharge ion sources, duoplasmatron and electron bombardment ion generator 17 p2991 A66-33234  
Quadrupole mass filter coupled to shock tube for analysis of reaction kinetics noting ion source, time constant, smoothness of leak, etc 17 p2904 A66-33464

Laser vaporization and ionization of solid materials to obtain ions for time-of-flight mass spectrometer 21 p3749 A66-39385

## ION TEMPERATURE

Microwave scattering from nonequilibrium plasmas where electrons have large steady drift velocity with respect to ions 02 p0266 A66-11479  
Electron and ion temperatures determination for helium plasma produced by theta-pinch with azimuthal magnetic field, using Doppler broadening and X-ray absorption 03 p0396 A66-12292  
Ratio of ionospheric electron to ion temperature determined independently of spectral measurements, using electron density data obtained with topside sounder 04 p0517 A66-14374  
Ionospheric diffusion probe determining ion and electron temperatures 05 p0674 A66-15112  
Electron and ion temperatures in ionosphere show no temperature equilibrium in F region 06 p0877 A66-17171  
Ion temperature measurement of streaming helium plasma by Langmuir double probe method, discussing effect of stream velocity 10 p1558 A66-21071  
Plasma electron density as function of radius compared with ion cyclotron heating theory and stability criteria [AIAA PAPER 66-158] 10 p1560 A66-21423  
Conductance and susceptance of neon plasma measured by Q-meter method in frequency range from 0.5 to 25 mc 11 p1745 A66-22587  
Electron density distributions in daytime F-2 layer and dependence on neutral gas, ion and electron temperatures 11 p1699 A66-23135  
Ionospheric processes and measurement of variations in ion temperature and concentration using satellites, noting connection with magnetosphere 12 p1871 A66-24400  
Ion heating by ion cyclotron wave generation in dense plasma created by HF generator in metal discharge chamber, determining ion temperature 14 p2341 A66-27150  
Plasma ion and electron temperature measurement via forward scattering spectrum of deuterium plasma 18 p3146 A66-34235  
Nonuniform plasma stability in magnetic field gradient 19 p3417 A66-36530  
Ionospheric ion temperature from cyclotron damping of proton whistler 20 p3554 A66-38195  
Emission spectrum of plasma consisting of colliding blobs, noting photographic and photoelectric recording and ion temperature measurement 21 p3790 A66-39070  
Electron density and electron and ion temperatures in F region studied by ground-based radar observations at Millstone Hill 22 p3909 A66-39976  
Electron density, electron and ion temperature and ionic composition measurements in Peru, using incoherent scattering technique 22 p3910 A66-39977  
Incoherent scattering of radio waves by plasma extended to include effects of unequal ion and electron temperatures and magnetic field 22 p3867 A66-40550  
Ion temperature measurements around 1000 km altitude, using ion energy analyzer and mass spectrometer mounted on rocket 22 p3913 A66-40551  
Ion energy balance equation for ionosphere including effects of O, He, and H ions, thermoconductivity and cooling by atomic hydrogen and helium 24 p4198 A66-42431  
Ruby laser light scattering measurements of electron and ion temperatures of hydrogen and deuterium plasmas produced in theta pinch devices 24 p4222 A66-42558  
Plane gridded retarding potential analyzer for measuring dominant constituent ion concentrations, temperature and instrument potential in planetary ionospheres 24 p4201 A66-42605  
Ion heating by ion cyclotron wave generation in dense plasma created by HF generator in metal discharge chamber, determining ion temperature 24 p4244 A66-42970

## ION TRAP

Ion escape from magnetic mirror trap due to nonlinear stage of plasma instability related to loss cone 01 p0109 A66-10261  
Asymmetric instability and charge motion in metal-silicon oxide-silicon structures 12 p1932 A66-24823  
Ion escape from magnetic mirror trap due to nonlinear stage of plasma instability related to loss cone 13 p2148 A66-25979  
Plane gridded retarding potential analyzer for measuring dominant constituent ion concentrations, temperature and instrument potential in planetary ionospheres 24 p4201 A66-42605

**IONIC COLLISION**  
Cylindrical plasma rotational velocity formulas derived by calculating Boltzmann collision integral in stationary momentum equation 04 p0556 A66-14333  
Charge transfer between helium ions and molecules of nitrogen and oxygen in crossed-beam experiment within energy range 3 to 600 ev 05 p0671 A66-14959  
Elastic differential scattering in low energy helium ion collisions, discussing quantal and secondary interference and two-state theory 05 p0719 A66-15768  
Shock wave frontal ionization effect on electromagnetic transmission and reception from telemetering equipment on ELDIC satellite launching vehicle 09 p1406 A66-19851  
Charge transfer and charge rearrangement in atmospheric ion-neutral particle collisions 10 p1557 A66-21143  
Plasma density instability induced by electron-hole generation in impact ionization as affected by electric field 10 p1575 A66-21536  
Weak collisions effect on ion waves instability in cesium plasma solved via linearized Fokker-Planck equation 10 p1568 A66-21823  
Quasi-linear current instability in two-temperature plasma for Coulomb collision and free electron acceleration 10 p1569 A66-21972  
Born approximation of cross sections for electron and proton impact ionization of Na and Mg 11 p1737 A66-22496  
Cross sections of inelastic collisions of hydrogen and nitrogen molecular ions with hydrogen molecules 11 p1738 A66-22879  
Kinetic oscillation of nonhomogeneous collision plasma, discussing drift instability, ionization, longitudinal current effect, etc 12 p1921 A66-24204  
Ionospheric radio wave propagation and ionization inhomogeneity drift measured, using doubly reflected signals 12 p1873 A66-24687  
Threshold data for ruby and neodymium laser pulse-induced breakdown in Xe, Ar, Kr, Ne, He, oxygen, nitrogen, air and carbon dioxide 13 p2100 A66-26191  
Ion beam elastic scattering cross section for proton-helium systems 14 p2337 A66-27978  
Seaton formulas used to determine when gas is collision-dominated 14 p2337 A66-28115  
Ionic drift velocity peak function for two-interconverting nitrogen ion species drifting in gas in electric field 15 p2550 A66-28756  
Collision cross sections of ions in isoelectronic sequence of lithium, noting dipolar transitions of type 2s to np 16 p2754 A66-31261  
VLF dipole antenna impedance values, magnetotelluric and collision effects in ionospheric magnetoplasma 17 p2874 A66-32386  
Effective ionization and charge exchange areas of certain gases undergoing collisional ionization by accelerated ions 17 p2961 A66-32954  
Spectrographic investigation of luminescence of carbon monoxide and dioxide excited by collisions with accelerated ions 17 p2961 A66-33403  
Discrepancies in electron-impact broadening of isolated ion lines due to neglect of collision-induced transitions between upper and lower levels of line and Coulomb interactions with perturbed ions 22 p3951 A66-40419

## IONIC CONDUCTION

Electrical damage to cathode ray tube safety glass attributed to current passing



through cathode ray tube face and safety  
 class as result of ionic  
 conduction 10 p1504 A66-21659  
 Anodic oxide film growth on sputtered  
 tantalum films in dilute sulfuric acid, noting  
 ionic conductivity, dielectric constant and  
 optical properties 15 p2562 A66-28718  
 Atmospheric electric field change  
 compensation during measuring air-Earth  
 ionic conduction and electron precipitation  
 current densities 22 p3920 A66-40804  
 Propagation of nervous impulse down  
 unmodulated and unmodulated fibers,  
 obtaining expression involving ionic  
 conductances 23 p4025 A66-41045  
**IONIC CRYSTAL**  
 Physics of luminescent ionic crystal -  
 Conference, Lvov, Ukrainian SSR, January-  
 February 1964 15 p2568 A66-29728  
 Optical properties of complex compounds  
 of divalent platinum, noting absorption  
 spectra, forbidden transitions,  
 etc 15 p2569 A66-29730  
 IR radiation absorption in imperfect ionic  
 crystals 21 p3802 A66-39158  
**IONIC DIFFUSION**  
 Measuring drift velocities of mixed  
 nitrogen ion population in nitrogen gas,  
 noting need of ionization condition control  
 and ion mass analysis 04 p0547 A66-13714  
 Vortical electric field effect on  
 inhomogeneities spreading in weakly ionized  
 plasma /ionosphere/ in magnetic  
 field 04 p0577 A66-13842  
 Diffusion of Li and Cu in GaAs crystals  
 indicates reaction involving divacancies in  
 donor-doped and undoped  
 crystals 06 p0935 A66-17132  
 Diffusion and lifetime of plasma charged  
 particles in magnetic field covering  
 instability, contraction, decay,  
 recombination, etc 13 p2138 A66-25222  
 Precipitation effects in phosphorus-diffused  
 silicon after gold diffusion, using  
 transmission X-ray diffraction  
 microscopy 15 p2561 A66-28700  
 Nonlinear instability theory of weakly  
 inhomogeneous hot-ion plasma when loss cone  
 exists in ion velocity  
 Distribution 17 p2964 A66-31890  
 Ion drift and diffusion of magnetically  
 confined plasma due to inclination of  
 conducting end-plate having electron sheath  
 which reflects ions 18 p3149 A66-34912  
 Instabilities in plasma produced by  
 magnetron source diffusing along static  
 magnetic field, examining effect on particle  
 diffusion perpendicular to magnetic  
 field 19 p3416 A66-36521  
 Volt-ampere characteristics and  
 photomicrographs of p-n junctions produced  
 by diffusion of Zn and Cd into  
 InP 21 p3798 A66-38918  
 Internal electric field effect on singly  
 ionized acceptor or donor impurity diffusion  
 in uniformly doped n-or p-type  
 semiconductors 21 p3804 A66-39468  
**IONIC PROPULSION**  
 Space travel projects noting ion propulsion,  
 electromagnetic drive and tests of flight  
 simulation 03 p0415 A66-12483  
 Propulsion efficiency of magnetic annular  
 arc /MAARC/  
 [AIAA PAPER 66-115] 06 p0808 A66-16251  
 Kaufman-type mercury ion accelerator and  
 efficiency as affected by operating  
 parameters 08 p1281 A66-18722  
 SERT capsule tested two ion engines in  
 space 08 p1281 A66-18735  
 Negatively charged colloid generation by  
 electrostatic spraying, with capillaries  
 arrayed alternately positive and negative  
 [AIAA PAPER 66-251] 10 p1594 A66-21702  
 Cesium-vapor ion electrostatic drives for  
 long-term space flight 11 p1761 A66-23129  
 Colloid particle electrostatic thrusters for  
 lunar ferry missions in specific impulse  
 range 1000-3000 sec 12 p1937 A66-24903  
 Electrical propulsion of space vehicles  
 using solar energy, electrostatic drive,  
 drifting field plasma accelerator, etc  
 [ONERA TP 328] 12 p1937 A66-24904  
 Electrostatic ion sources, noting simulation  
 chamber for tests and measurement results  
 on emissive power of porous  
 tungsten 16 p2791 A66-31191  
 Electrostatic ion sources, assessing thrust  
 output and lifetime for various space

missions and satellite attitude  
 control 16 p2791 A66-31192  
 Melting of solid bodies in chondrule size,  
 discussing accumulation mechanisms  
 involving electrostatic acceleration and gas  
 motions 18 p3225 A66-33622  
 Plasma Separator Thruster, advanced ion  
 thruster design based on independent  
 operation and optimization of plasma source  
 and plasma extraction system  
 [AIAA PAPER 66-598] 18 p3163 A66-34217  
 Propulsion efficiency of magnetic annular  
 arc /MAARC/  
 [AIAA PAPER 65-115] 23 p4107 A66-41901  
 Electrical propulsion devices for space  
 vehicles related to plasma physics, ion-beam  
 generation and particle  
 dynamics 24 p4262 A66-43120  
**IONIC REACTION**  
 Helium afterglow discussing stability of  
 collisional-radiative recombination of ions  
 with electrons and neutral  
 particles 04 p0547 A66-13652  
 Linear free energy relationship between  
 benzoyl and acetyl ion intensities in mass  
 spectra of benzo- and acetophenones  
 explained by kinetic  
 argument 10 p1495 A66-21165  
 Ion-molecule reaction rates and  
 recombination coefficients from mass  
 spectrometric ionospheric  
 data 11 p1702 A66-23492  
 Metal-ceramic boundary structures and  
 reactions, considering metal-oxide and  
 metal-glass interfaces, ionic and covalent  
 bonds, oxidation, reduction, solution and  
 precipitation 13 p2108 A66-25767  
 Proton transfer between hydrogen and  
 methane, ethane, propane and butanes, using  
 high-pressure mass spectrometry, employing  
 ion source with beta rays as ionizing  
 medium 13 p2018 A66-26443  
 IR quantum counter based on energy  
 transfer between two rare-earth ions in  
 tungstate mixture 15 p2568 A66-29642  
 Rate constant for atomic oxygen ion  
 destruction by carbon dioxide measured in  
 pulsed flowing afterglow  
 system 16 p2645 A66-30115  
 Ion-molecular reactions of hydrogen with  
 inert gases caused by low energy electrons  
 in low temperature plasmas, considering  
 energy level populations, reaction cross  
 sections, etc 18 p3064 A66-34026  
 Chemical kinetics of electron plasma  
 reactions, discussing energy states, ion-  
 molecule reactions, charge transfer,  
 transport properties, phase interactions,  
 etc 21 p3702 A66-38448  
 Ionospheric ion-molecular reaction rates,  
 discussing various measurement  
 results 21 p3734 A66-39319  
 Negative ion associative detachment  
 reaction with atomic oxygen in  
 determination of nighttime D region  
 electron density profiles at high  
 latitudes 22 p3905 A66-39945  
 Attachment coefficient and temperature  
 dependence of ionic reactions in F layer for  
 various activation  
 energies 22 p3908 A66-39968  
 Rate constants for atomic and molecular  
 hydrogen ion transfer from tri- and tetra-  
 atomic carbon paraffins to propylene and  
 cyclopropane molecular  
 ions 22 p3861 A66-40905  
 Ionic reaction in nitrogen-oxygen system,  
 discussing reactions of He and N  
 ions 23 p4063 A66-41039  
 Heat of formation of perfluoroammonium  
 ion estimated from thermochemical  
 correlations and compared with estimates by  
 means of Kapustinskii approximation for  
 lattice energies 23 p4031 A66-41222  
 Charge exchange cross sections for argon  
 ions incident on hydrogen and deuterium  
 measured over energy range of 30 to 1000  
 ev, taking into account ion-molecule  
 reactions 23 p4098 A66-41267  
 Cross sections for charge transfer reactions  
 of nitric oxide with atomic and molecular  
 ions of oxygen and  
 nitrogen 24 p4200 A66-42590  
 Ionic reactions of gaseous methane using  
 tandem mass spectrometer, noting  
 translational energy  
 effects 24 p4170 A66-43035

**IONIC WAVE**  
**SA IONOSPHERIC CONDUCTIVITY**  
 Ionic waves amplified by collective  
 behavior in alkali plasma obtained by  
 contact ionization of cesium or potassium  
 vapors on surface of two coaxial tantalum  
 cylinders 01 p0110 A66-10331  
 Saturation and short-time behavior of  
 unstable ion waves in collisionless alkali  
 plasmas in thermal  
 equilibrium 01 p0110 A66-10339  
 Node in radial velocity as boundary  
 condition for ion waves in low pressure  
 plasma and dispersion relations for space  
 charge sheath 01 p0113 A66-10622  
 Collisionless plasma flow over cone when  
 flow velocity is greater than ion wave speed  
 [AIAA PAPER 65-125] 02 p0287 A66-11534  
 Plasma kinetic theory effect of magnetic  
 field on dispersion relation for ionic sound  
 wave 02 p0269 A66-11836  
 Ionization excitation of ionic sound in  
 nonequilibrium discharge plasma and  
 resultant instabilities 03 p0400 A66-12835  
 Steady state jump equations for normal  
 ionizing shock wave propagating into  
 nonconducting gas in electromagnetic  
 field 07 p1087 A66-17939  
 Collision effect on coupling of ion-acoustic  
 waves to neutral acoustic waves at diffuse  
 boundary consisting of partially ionized  
 gas 07 p1088 A66-17955  
 Plasma permittivity modulation by ion  
 waves for thermally ionized alkali plasma in  
 microwave resonator 08 p1266 A66-19811  
 Stagnation layer of rigid plate resulting  
 from cool energetic plasma stream  
 interaction 10 p1567 A66-21820  
 Weak collisions effect on ion waves  
 instability in cesium plasma solved via  
 linearized Fokker-Planck  
 equation 10 p1568 A66-21823  
 Resonant excitation by external forces,  
 propagation and reflection of ion acoustic  
 standing waves between electrodes in  
 mercury vapor discharge 10 p1568 A66-21831  
 Excitation of LF ionic plasma oscillations  
 by HF electronic Langmuir  
 waves 12 p1921 A66-24205  
 Charge sheath role at discharge wall in  
 determining boundary conditions for LF  
 wave in low pressure discharge, using  
 hydrodynamical model 12 p1923 A66-24571  
 Ion acoustic waves propagating along  
 cylindrical plasma column analyzed, deriving  
 boundary condition at plasma  
 surface 12 p1923 A66-24572  
 Excitation of ion-acoustic waves in  
 potassium-cesium plasma when passing  
 current through it, finding natural  
 frequencies of system when plasma is  
 drifting along axis 15 p2550 A66-29214  
 HF heating of dense plasma by resonance  
 excitation of cyclotron-type ion waves and  
 fast magnetoacoustic  
 waves 16 p2756 A66-30095  
 Transverse electromagnetic wave  
 transformation into ion-acoustic plasma  
 oscillations with formation of intermediate  
 Langmuir electron wave 17 p2969 A66-32542  
 Nonlinear ion-acoustic wave propagation  
 in collisionless hot electron plasma with at  
 least one cold ion stream 17 p2973 A66-32976  
 Standing ion acoustic waves in mercury  
 vapor discharges 17 p2973 A66-32983  
 Dispersion of ion waves in mercury vapor  
 discharges, carrying out spectral analysis of  
 acoustic and plasma  
 oscillations 18 p3146 A66-34234  
 Transverse boundary effects on ionic-  
 acoustic wave propagation in  
 magnetoplasma 18 p3150 A66-34938  
 Ionization excitation of ionic sound in  
 nonequilibrium discharge plasma and  
 resultant instabilities 19 p3433 A66-36777  
 Generation of ion plasma waves in weakly  
 ionized gases with measurement of phase  
 velocity and damping 20 p3609 A66-37597  
 Standing ion acoustic waves between  
 cathode and electrically floating auxiliary  
 metal electrode, noting discharges in  
 mercury vapor between plane oxide-coated  
 cathode and nickel anode 22 p3954 A66-39817  
 Excitation of LF ionic plasma oscillations  
 by HF electronic Langmuir  
 waves 22 p3956 A66-40569  
 Ion-acoustic wave propagation and damping  
 in plasma with negative



ions 23 p4104 A66-41505

**IONIZATION**

SA ATMOSPHERIC IONIZATION

SA AURORAL IONIZATION

SA ELECTRON IONIZATION

SA EXCITATION

SA FLAME IONIZATION

SA GASEOUS IONIZATION

SA METEORITIC IONIZATION

SA NONEQUILIBRIUM IONIZATION

SA PHOTODISSOCIATION

SA PHOTOIONIZATION

SA SURFACE IONIZATION

Chromospheric emission lines of magnesium iodine analyzed, calculating hydrogen concentration and ionization degree at 1000 km 01 p0134 A66-10269

Hypersonic wakes, effects of turbulent fluctuations on air ionization reaction rates measured by averaging and regrouping perturbed source terms of chemical rate equations 03 p0359 A66-13230

[AIAA PAPER 65-819] 03 p0359 A66-13230

Resonances below inelastic threshold of electron hydrogen scattering using Feshbach projection-operator technique, converting to eigenvalue problem for projected Hamiltonian 04 p0547 A66-13711

Qualitative interpretation of negative resistance by impact ionization of deep level impurities noting temperature, impurity concentration and energy level 05 p0735 A66-14964

Microwave switching and pulse modulation by impact ionization, using DC electric field to break down n-type germanium 06 p0851 A66-16454

Equilibrium constant of thermal and photolionization of conducting particles present as impurities in partially ionized gas 06 p0918 A66-16838

Low temperature and ionization effects on stability of close-pair defects in semiconductors and behavior at higher temperatures 06 p0932 A66-17113

Satellite ionization effects, CW-reflection and pulse radar techniques in 10 to 20 mc frequency range 08 p1181 A66-18749

Discharge in germanium thin films at liquid helium temperatures, noting electrostatic ionization of impurities and shock-ionization region expansion 09 p1412 A66-19990

Ionization effect on plasma thermoconductivity, noting expressions for conductivity due to energy transfer or dissociation 09 p1407 A66-20136

Average electrical conductivity and state of ionization in RF plasma flow device [AIAA PAPER 66-165] 11 p1742 A66-22209

Radio wave propagation in artificial ionized cloud in upper atmosphere determined, using geometrical optics 12 p1817 A66-24274

Antimony ionization in p-germanium single crystals, based on diffusion of Sb into Ge 12 p1930 A66-24460

Gabor type auxiliary discharge thermionic converter producing ions for space charge neutralization by impact, noting critical converter equation 13 p1998 A66-25530

Ionization calorimeter for measuring primary cosmic ray components, discussing nuclear interactions, energy spectra, EM cascades, etc 13 p2175 A66-26011

Ionization process in comets does not depend on solar electromagnetic or corpuscular radiation, considering it as intrinsic property of cometary atmospheres 15 p2598 A66-29267

Electric current density in ionizing discharge layer determined, using multifluid equations of conservation of momentum and gas mass 17 p2967 A66-32435

Electron scattering interpretation of ionization, emission and absorption line spectra of quasi-stellar object 17 p3004 A66-32928

Effective ionization and charge exchange areas of certain gases undergoing collisional ionization by accelerated ions 17 p2961 A66-32954

Microwave limiter device, based on impact ionization of deep levels in silicon 17 p2897 A66-33461

Ionization probability of bound state of atoms in variable electric field 18 p3140 A66-34690

Book on glow discharge and plasma physics

including collisional processes, ionization, vacuum systems, application in electronics, etc 18 p3150 A66-34946

Range fluctuation of high energy mesons including effect of logarithmic increase of ionization loss derived, using analytical solution, considering effects of bremsstrahlung, pair, etc 18 p3222 A66-35209

Prelonization and shock wave ionization in cylindrical crossed-field plasma source, using microwave diagnostic methods including interferometry 19 p3408 A66-36277

Antimony ionization in p-germanium single crystals, based on diffusion of Sb into Ge 20 p3620 A66-37692

Intense beams of fast neutral hydrogen atoms injected into magnetic trap by ionization in strong magnetic field 21 p3789 A66-39060

Ionization and secondary effects during reflection of shock waves in argon 21 p3726 A66-39086

Ionization effect on plasma thermoconductivity, noting expressions for conductivity due to energy transfer or dissociation 21 p3793 A66-39408

Quasi-linear current instability in two-temperature plasma for Coulomb collision and free electron acceleration 21 p3794 A66-39551

Flare stars as sources of cosmic X-rays, spectra contain 4686-angstrom line of doubly ionized helium indicating that atmospheres contain either ionizing radiation or electrons 22 p3972 A66-39707

Nonequilibrium plasmas produced in InSb by both impact ionization and injection, examining instabilities due to HF oscillations and negative resistance 23 p4114 A66-41582

Photographic measurement on optical radiation associated with hypervelocity impact of projectile on target 23 p4091 A66-41909

Approximate differential operator replacing integral operator, taking ionization losses into account in electromagnetic cascade theory 24 p4269 A66-42923

**IONIZATION CHAMBER**

Ionization chamber for measuring interplanetary space radiation, using Geiger-Mueller counter as secondary detector 01 p0073 A66-11115

Four-year cosmic ray ionization bursts, using ASK-2-34 ionization chamber 06 p0949 A66-16589

Laboratory simulation, in continuum and rarefied flow regimes, of perturbations of ionosphere by satellite and rocket exhaust 06 p0869 A66-16908

Nuclear active particles analysis by observing integral spectrum of ionization bursts under thick layer of dense material at low altitudes 07 p1115 A66-17554

Ionization bursts in shielded spherical chambers with burst data transformed to give integral energy distribution of muon intensity at sea level 07 p1116 A66-17563

Muon detection and energy determination in multilayer system of ionization chambers and probability of finding muon in n-electron shower at depth 07 p1117 A66-17569

Extensive air shower high energy gamma rays in upper third of atmosphere 07 p1118 A66-17573

Cosmic ray intensity measured during geomagnetically quiet and active days from 1959 to 1963 by using balloon flights, noting role of ionization, Forbush effect, etc 07 p1124 A66-18000

Extensive air showers at various atmospheric depths analyzed, using hodoscope counters and ionization chambers, noting differential spectra of densities 15 p2580 A66-29528

Delta-electron generation by muons and fluctuations in soft cosmic ray component, assuming thick absorption layer 15 p2547 A66-29598

Photoelectric yields of alkali halides measured, using rare gas ion chamber to determine flux distribution of helium continuum and obtain absorption coefficients 16 p2754 A66-30855

Tien-Shan high altitude installation for studying strong interactions at 100-1000 gev of cosmic ray nucleons and

ions 18 p3214 A66-3515

Nuclear cascade particles ionization at various depths in iron compared with experimental data in ionization calorimeter 18 p3214 A66-3515

Nuclear active component of cosmic ray studied with arrangement consisting of ionization calorimeter, Geiger counter, hodoscope and two large spark chambers 18 p3215 A66-3515

Ionization chamber to investigate distribution of energy portion transferred to photons by nuclear active particles colliding with atomic nuclei of C, Fe and Pb 18 p3215 A66-3515

Absorption path of high-energy protons in atmosphere measured by ionization calorimeter 18 p3216 A66-3516

Tskhra-Tskaro installation for study of high-energy cosmic particle interaction with matter 18 p3218 A66-3518

Relationship of neutral and charged particles generating electron-nuclear showers studied by ionization calorimeter 18 p3218 A66-3518

Constant current sources consisting of sealed ionization chambers for calibrating electrometers 19 p3357 A66-3580

Pressurized Ar-filled ionization chamber response to charged particles in cosmic radiation determined as function of atmospheric depth 24 p4284 A66-4260

Interaction of 1000 bev particles in ionization calorimeter technique suggests free path of nuclear active particles in atmosphere decreases as particle energy increases 24 p4287 A66-4290

**IONIZATION COEFFICIENT**

Photolionization and absorption coefficient of carbon oxide measured below 100 angstroms, using Seya-Namioka scanning vacuum UV monochromator with helium continuum as background 02 p0263 A66-1183

Electron-ion recombination rate and effective ionization calculated for cesium plasma by Bates method 03 p0398 A66-1251

Comparison of diurnal variations of ionization level in F region at geographically and geomagnetically conjugate stations in Arctic and Antarctic 04 p0516 A66-1385

Two-fluid approximation of one-dimensional steady state flow of inviscid plasma with thermal gradients, considering ionization and recombination processes 08 p1265 A66-1946

Electric discharges in gases analyzed in terms of ion and electron drift velocity and ionization coefficient 10 p1558 A66-2205

Meteor luminosity/ionization ratio dependence on air density found through analysis of ablation rate of meteor 14 p2387 A66-2817

Ionization and diffusion cross sections of Ca, Fe, Si and Mg atoms of disintegrated meteors 19 p3455 A66-3527

Electron drift velocity, ionization attachment coefficients in water vapor and dry air measured by recording short photoelectron pulses 20 p3605 A66-3809

Magnetic field-aligned ionization detected during minimum sunspot activity, using radio telescopes of radio interferometer 22 p3908 A66-3996

**IONIZATION COUNTER**

Measurement and evaluation of radiation exposure in space flight, noting tissue equivalent system for ionization recording 02 p0182 A66-1164

Pulse ionization manometer based on open 6Zn2P pentode with oxide cathode for measuring fluctuating inactive-gas pressure 04 p0520 A66-1389

Pulse ionization manometer based on open 6Zn2P pentode with oxide cathode for measuring fluctuating inactive-gas pressure 15 p2503 A66-2970

Electron-photon and nuclear active components energy of young air shower measured by ionization calorimeter, determining inelasticity coefficient 18 p3206 A66-3510

Ionization calorimetry of energy spectrum of leading particles in cores of EAS compared with data from model 18 p3206 A66-3510

Measurement and evaluation of radiation exposure in space flight, noting tissue equivalent system for ionization recording 20 p3509 A66-3816



- ionization calorimeter measurement of number of particles in electron photon cascade with energy transferred from ionization calorimeter 24 p4269 A66-42924
- IONIZATION CROSS SECTION**
- Charge exchange and ionization cross sections for hydrogen ions passing through ordinary and heavy hydrogen 01 p0107 A66-10194
- Average energy loss per ion pair of low energy nitrogen and oxygen ions in nitrogen, argon and helium 01 p0107 A66-11096
- Dielectronic recombination for low density plasma, estimating coefficient and ionization balance for iron and calcium ions in corona 02 p0286 A66-11357
- Electron collision cross sections of atoms and molecules of argon, helium, nitrogen and dissociation products of carbon dioxide by dual beam radiosonde methods to study low temperature plasma behind shock front 02 p0268 A66-11780
- Modifications of impulse approximation allowing for motion of bound electrons, providing simple analytic expressions for atomic ionization and detachment cross sections 03 p0394 A66-12328
- Impact ionization coefficient for electrons and holes in silicon determined from distribution function of hot carriers and shown to be weakly dependent on ionization cross section 04 p0565 A66-14262
- Ionization cross section of ground state helium cation by electron impact in Born exchange approximation 04 p0549 A66-14312
- Elastic differential scattering of helium ions discussing energy analysis, geometry and target particle motion effects, and interference phenomena 05 p0719 A66-15767
- Ionization of inert-gas atoms and of hydrogen and nitrogen molecules by alkali metal ions of energies greater than 1 to 30 ev 06 p0915 A66-16151
- Hydrogen molecule multiphoton ionization, determining probability of absorption, affected by ruby laser emission 06 p0891 A66-16517
- Bethe approximation of ionization cross sections of excited states of atomic hydrogen by high energy electrons 06 p0912 A66-17037
- Neutral atomic beam used to measure total ionization cross section of argon atoms incident on low density argon 07 p1083 A66-18421
- Absolute cross section for single ionization of lithium ions by electron impact over 75.6 to 800 ev electron energy 07 p1084 A66-18425
- Nonequilibrium radiative and collision ionization, photoionization and shock wave structure in high temperature hypervelocity low density gas 08 p1204 A66-18521
- Radar echo effects of satellite disturbance in plasma medium, noting electron and positive ion density distribution 08 p1302 A66-18755
- Appleton anomaly of F-2 layer examined, assuming ionization induced horizontal motion of neutral air 08 p1215 A66-19207
- Hydrogen molecule multiphoton ionization, determining probability of absorption, affected by ruby laser emission 09 p1387 A66-20898
- Effective excitation cross sections of alkali metal atoms during collision with slow electrons 09 p1406 A66-20940
- Absolute cross section for ionization of atoms and diatomic molecules by electron impact 09 p1410 A66-20958
- Dielectronic recombination for low density plasma, estimating coefficient and ionization balance for iron and calcium ions in corona 10 p1602 A66-21088
- Exospheric model of solar wind for ionized atmosphere with velocity-dependent collision cross section 10 p1605 A66-21206
- Ionosphere formation theory, reviewing solar radiation, absorption, ionization cross section rate, electron renewal in F and upper E layer, etc 10 p1533 A66-21851
- Multiphoton ionization of xenon atom in powerful electric field by ruby laser radiation 10 p1543 A66-21966
- Born approximation of cross sections for electron and proton impact ionization of Na and Mg 11 p1737 A66-22496
- Born-exchange and Ochkur approximations used to calculate electron impact ionization cross sections for He, Li, Be, Na and Mg atoms in ground states 11 p1737 A66-22497
- Ionization charge stage for spectral lines determined by sending particle beam through field which separates components of different net charge 11 p1739 A66-22949
- Langmuir probe to measure stagnation region shock layer ionization distribution under nonequilibrium hypersonic flow conditions [AIAA PAPER 66-167] 13 p2138 A66-25168
- Ionizing collisions between alkali metal atoms and gas molecules, with measured cross sections applied to physics of atomic collisions 13 p2131 A66-25966
- Ionization cross section for rare gases and hydrogen atoms calculated from perturbation theory, noting ruby laser photon absorption 13 p2133 A66-26188
- Atomic ionization by intense optical field, noting ruby laser-pulse effect on inert gas between electrodes 13 p2134 A66-26189
- Ionization enhancement from Van Allen electrons in South Atlantic magnetic anomaly, noting longitudinal variation of trapped electrons, electron-ion recombination, etc 13 p2176 A66-26362
- Bethe-Born approximation and partial ionization cross sections of singly and doubly charged helium and neon ions 14 p2336 A66-26830
- Bethe-Born approximation and partial ionization cross sections of argon, krypton and xenon ions 14 p2336 A66-26831
- Ionization cross sections for low energy collisions of neutral nitrogen molecules or neutral argon atoms, using asymmetric charge transfer 14 p2337 A66-27980
- Effective excitation cross sections of alkali metal atoms during collision with slow electrons 15 p2543 A66-28529
- Energy spectrum of primary photoelectron, using data from atmospheric density distribution, fluxes of solar XUV radiations and absorption and ionization cross sections 15 p2574 A66-28906
- Asymptotic form of wave function and threshold behavior of cross section for ionization of atomic hydrogen by electron impact 15 p2544 A66-29116
- Photoionization of atoms in coherent states 15 p2515 A66-29205
- Variation of most probable muon energy loss with momentum, noting density effect and decrease in ionization loss 15 p2589 A66-29586
- Cesium ionization cross section measurement from threshold to 50 ev, noting apparatus used and results obtained 15 p2548 A66-29814
- Ionization of inert-gas atoms and of hydrogen and nitrogen molecules by alkali metal ions of energies greater than 1 to 30 kev 15 p2548 A66-29881
- Photoionization of atoms in coherent states 17 p2936 A66-33054
- Ionization of low temperature supersonic plasma jets, noting kinetics of elementary processes, gas dynamic parameters and effects of combustion and alkali metal admixtures 18 p3143 A66-34030
- Retarding potential measurement of kinetic energy of electrons released in Penning ionization by excited helium atoms in metastable electron states 18 p3139 A66-34505
- MHD power generator in which ionization of alkali atoms occurs by collision with excited noble gas atoms, calculating velocity-dependent cross section 19 p3406 A66-35436
- Ionization of hydrogen and hydrogenic positive ions by electron impact 19 p3409 A66-36324
- Second Born and Born-exchange approximations used in calculation of ionization cross sections for Fe XV and Fe XVI 19 p3403 A66-36325
- Excitation of lithium-like ions by electron impacts, with computation of cross sections for resonance and nonresonance transitions 19 p3409 A66-36326
- Photoionization cross sections calculated for carbon, nitrogen and oxygen ions, using Hartree-Fock approximation for final transition stages 19 p3405 A66-36805
- Ionization due to alpha, beta and gamma radiation from ground and atmosphere in ground proximity, noting ion pair production rate and energy spectra 20 p3552 A66-37759
- Ionization of oxygen examined, using charge exchange in double mass spectrometer, noting break in electron impact ionization efficiency curve and constructing breakdown graph 20 p3605 A66-38097
- Multiphoton ionization of xenon atom in powerful electric field by ruby laser radiation 21 p3749 A66-39545
- Replacement of Poisson by Polya distribution in calculating laser intensity threshold necessary to induce ionization breakdown in gases 22 p3929 A66-39715
- Photoionization cross section of negatively charged In atoms in n-type silicon from comparison of intrinsic photoconductivity with impurity photoconductivity 22 p3964 A66-40309
- Ionization cross sections and efficiencies by electron impact and photoionization for molecular ionization at low energies 23 p4098 A66-41268
- Small neutral hydrogen flux in total solar wind flux and electron impact and photoionization mechanisms 23 p4123 A66-41689
- Initial phase of shock produced ionization in argon, krypton and xenon to elucidate atom-atom ionization reaction to determine cross section 23 p4098 A66-42079
- Shock tube monitoring of electron-generation rate in argon-xenon ionization cross section implies that atom-atom processes in noble gases ionization cross section is independent of electronic structure 23 p4099 A66-42080
- IONIZATION FREQUENCY**
- Ionization bursts observed in chambers used for continuous registration of intensity variations in hard component of cosmic radiation, correlating variation frequency with solar cycle 06 p0950 A66-16591
- Diffusion technique preparation of GaP p-n junctions and relation of p-i-n junction electric field calculation to Baraff carrier ionization rate theory 07 p1108 A66-18415
- Dependence of variations in critical F-2 ionization on solar activity 08 p1220 A66-19791
- Loss rates of charged particles from ohmically-heated discharges in C-Stellarator, showing confinement time parameters 10 p1568 A66-21825
- Ion-molecule reaction rates and recombination coefficients from mass spectrometric ionospheric data 11 p1702 A66-23492
- Computer method for determination of distribution of low lying ionization, using ordinary and extraordinary wave traces in ionograms 12 p1873 A66-24838
- Critical ionization frequencies in F-2 layer in near-polar region observed at Northern Hemisphere high latitude stations 15 p2487 A66-29107
- Perturbation theory approach to calculation of autoionization rates 15 p2548 A66-29807
- Dependence of variations in critical F-2 ionization on solar activity 21 p3733 A66-38787
- Time resolved emission measurements for Cr-Ar mixtures in three spectral regions and ionization occurrence in excited state inelastic collisions 23 p4033 A66-42083
- IONIZATION GAUGE**
- Nuclear interaction at high energies, discussing active component structure ionization calorimeter application, energy spectrum of particles, etc 07 p1113 A66-17536
- Modulation method applied to Bayard-Alpert and suppressor ionization gauges for reducing lower pressure limits 07 p1033 A66-17742
- Electrode geometry, optimum configuration of hot-filament vacuum ionization gauges, and ion-collector burying technique 17 p2923 A66-31981
- Hydrogen, nitrogen, oxygen and helium gas pumping by ionization pressure gauges in space simulators 22 p3891 A66-40233
- Ionization gauge for transient gas pressure measurement 24 p4215 A66-43210
- IONIZATION POTENTIAL**
- Alkali-ion desorption energies measured on



polycrystalline refractory metals at low surface coverage by electron work function 02 p0263 A66-11483

Ionization potential of thulium obtained from hfs of thulium I, using discharge tube and Fabry-Perot etalon 03 p0393 A66-12322

Relative density and shock front velocity for strong shock waves in hydrogen, helium and argon, using ionization-potential drop deducible from Debye-Huckel theory 04 p0556 A66-14338

Ionization under laser action extended to metals and dielectrics, noting influence on thresholds 06 p0893 A66-17065

Partition function of hydrogen plasma derived classically and by quantum mechanics, obtaining Saha equation containing effective lowering of ionization potential 07 p1090 A66-18155

Mass spectrometric electron impact ionization potentials rapidly obtained by electronic control and automatic data processing systems 07 p1091 A66-18489

Potential and charge density distributions derived for stationary charged sphere and charged body moving through plasma 08 p1261 A66-18744

Potential striae determined in hollow cathode plasma 08 p1264 A66-19183

Ionization energy in silicon carbide and germanium irradiated by electrons 08 p1278 A66-19628

Solar radiation effect on Langmuir frequency, noting ionization of cesium vapor at low potential differences 09 p1409 A66-20925

Ionization threshold observation in Si Zener diodes and multiplication factor 10 p1509 A66-21586

Ionization phenomena in argon due to laser radiation by measuring electron density and energy as time function after laser pulse initiation at different gas pressures and preionized conditions [AIAA PAPER 66-176] 10 p1565 A66-21690

Electron impact ionization cross section of H<sup>+</sup>/2s/ and H<sup>+</sup>/2p/ in Born A, Born B, Born-Ochkur and classical approximations 11 p1738 A66-22498

Ionization charge stage for spectral lines determined by sending particle beam through field which separates components of different net charge 11 p1739 A66-22949

Hydrogen plasma ionization density calculation by three methods 11 p1747 A66-23265

Diurnal and seasonal altitude variations of E and F layers analyzed for geomagnetic activity from rocket measurement of electron concentration 12 p1869 A66-24269

Electrical characteristics of linear, segmented electrode, Hall and Faraday MHD generators operating in equilibrium and nonequilibrium ionization modes, obtaining data on loss mechanisms 13 p2001 A66-26256

Band shift in strongly doped semiconductor under influence of impurity atom electrostatic field 14 p2356 A66-27069

Franck-Condon factors for ionization of hydrogen and deuterium, noting vibrational eigenenergies of D sub 2 14 p2387 A66-27972

Temperature dependence of mean ionization energy changes in germanium and silicon samples exposed to X-rays caused by changes in forbidden bandwidth 16 p2788 A66-31782

Molecular orbital method for boron hydrides from self-consistent field, analyzing dipole moments, ionization potentials, molecular charge distributions, wave functions, etc 17 p2870 A66-32851

Lanthanum oxide as crystal growth modifier, noting habit modifications, optical quality, etc 17 p2982 A66-33060

Ionization energy in silicon carbide and germanium irradiated by electrons 17 p2984 A66-33142

Laboratory work on comets, discussing spectroscopic data, incompleteness of knowledge of dissociation energies and ionization potentials, etc 17 p3012 A66-33400

Ionization potential, dissociation energy and electron affinity for molecular oxygen 18 p3137 A66-33989

Electrostatic potential near nucleus immersed in plasma evaluated, using finite-temperature Thomas-Fermi model 18 p3230 A66-34152

Multiphoton ionization of krypton and argon by ruby laser radiation may occur by absorption 19 p3403 A66-36721

Barium ion concentration computed from Ba II 4554 angstrom line and Lyman alpha radiation intensity in lower chromosphere 20 p3646 A66-37013

Saha equation correction based on consideration of ionization energy reduction from particle interaction in thermal plasma 21 p3793 A66-39371

Dissociation energies of GaF, InF and TiF measured by high temperature mass-spectrometric techniques, noting possibility of potential maxima in excited states 22 p3859 A66-39917

Band shift in strongly doped semiconductor under influence of impurity atom electrostatic field 22 p3966 A66-40828

Mercury, cesium and rubidium vapors ionization in intense radiation flux by Q-switched ruby laser 23 p4076 A66-41156

Qualitative detection of alkyl-free radicals generated by pyrolyzing certain organic compounds, using modified commercial mass spectrometer 23 p4067 A66-41246

Cosmic ray ionization intensity measurement using special ion chamber 24 p4264 A66-42603

Plane gridded retarding potential analyzer for measuring dominant constituent ion concentrations, temperature and instrument potential in planetary ionospheres 24 p4201 A66-42605

**IONIZED GAS**

**SA PLASMA**

Electric conductivity of N-component gas mixture containing one partially ionized component 02 p0265 A66-11389

Positive gas discharge column equilibrium and instability factors, noting increase in ionization and plasma conductivity from decreased electron heating 03 p0398 A66-12509

Quasi-one-dimensional ionized gas motion through channels of arbitrary cross section in crossed electrical and magnetic field 03 p0398 A66-12516

Quantum statistical theory of multicomponent systems applied to fully ionized gas in thermal equilibrium 03 p0398 A66-12605

Macroscopic theory for fully ionized plasma waves 03 p0399 A66-12785

Ring of ionized hydrogen in region 3.5 to 4.5 kpc from galactic center 03 p0426 A66-12908

Total thermoconductivity of ionized gas calculated with no simplification of components 03 p0401 A66-12964

Physics of ionized media - French Society of Physics, National Colloquium, Toulouse, France, May 1965 03 p0401 A66-12965

Ohm law for partially ionized gases and plasmas 03 p0403 A66-12974

Structure of steady plane shock in partially ionized gas, using three-fluid Navier-Stokes model, obtaining velocities, temperatures, electric field and potential distributions through shock 03 p0357 A66-12976

Travelling fields in interaction of ionized gases with electromagnetic field currents checking Lorentz force and magnetic induction 03 p0404 A66-12980

Dispersion relation for plane longitudinal waves within macroscopic theory, considering collisions and viscosity of neutral particles, noting acoustical and ionic modes 03 p0404 A66-12983

Relativistic theory for plane shock wave in ionized hydrogen 03 p0358 A66-13140

Space shift between electron density and luminous intensity of plasma in stationary striation by microwave resonator 03 p0372 A66-13282

Radiation resistance of antennas in gyroelectric media 04 p0492 A66-13424

Ray dispersion of electromagnetic waves by free electrons produced in cone-shaped ionized wake 04 p0481 A66-13843

Electromagnetically driven ionizing shock waves propagating in hydrogen at speeds to relativistic conditions 04 p0511 A66-14010

Spectral line intensities of hydrogen and helium plasma in P.I.G. discharge 04 p0553 A66-14283

Small amplitude wave propagation in hot ionized gases, noting magnetic field

presence 05 p0721 A66-147

Computation of shock wave parameter partially ionized hydrogen 05 p0662 A66-148

Speed of sound in ionized argon, noting electronic excitation influence 05 p0723 A66-151

Estimation in equilibrium state surface potential and distributions of electric potential field and electron density vicinity of object moving in ionized medium 05 p0685 A66-157

Nonequilibrium ionization of K-seeded Na-seeded argon for MHD generators, noting current density-electric field characteristics 05 p0625 A66-158

Plasma generation of ionized gases electromagnetic field and properties 05 p0729 A66-158

Plasma velocity in weakly ionized gas with strong magnetic field and neutral component velocity determined independently [AIAA PAPER 66-4] 06 p0916 A66-162

Equilibrium constant of thermal arc photoionization of conducting particles present as impurities in partially ionized gas 06 p0918 A66-168

Physics of spark discharges igniting gaseous mixtures, noting increase in thermal power of discharge by gas preionization resulting from energy redistribution 06 p0919 A66-168

Radial distribution of electrical conductivity in ionized gas jet based on value measured by induction method at known temperature distribution 06 p0919 A66-168

Photon momentum distribution in fully ionized gas 07 p1082 A66-174

Steady state jump equations for nonionizing shock wave propagating in nonconducting gas in electromagnetic field 07 p1087 A66-178

Current density and heat flux expression in terms of transport coefficients partially ionized gas, noting thermoconductivities 07 p1088 A66-179

Detection of ionized gas front passage at differentiating it from current sheet magnetically driven shock tube 07 p1020 A66-179

Isotope shift, linewidth and predicted wavelength of laser emission in ionized Hg 07 p1044 A66-180

Steady state exothermal hydromagnetic discontinuity in perfectly conducting gas in arbitrarily oriented magnetic field 08 p1267 A66-198

Electron and ion recombination coefficient in weakly ionized gas of homopolar molecules 09 p1407 A66-199

Nonequilibrium transport properties of electron relaxation at cooled surface partially ionized argon 10 p1559 A66-212

Boltzmann transport equation solution for electrons in ionized gas with nonuniform electron concentration gradient 12 p1916 A66-237

Transference numbers in ionized gas contrasting current flow in electrolytes with steady state current flow in weakly ionized gases 12 p1920 A66-240

Electrical precursors in immediate vicinity of ionizing shock waves in argon analyzed using model describing electron diffusion through shock 12 p1923 A66-245

Nonequilibrium effect in two-dimensional steady flow of ionizing gas past magnetized wall, calculating velocity distribution along wall 12 p1924 A66-248

Measurement of effective cross sections of double charge of hydrogen, lithium, sodium and potassium ions in gases, considering error due to unequal scattering of primary and secondary particles 12 p1918 A66-248

Metal wall ionized argon lasers, discussing use of water-cooled quartz discharge channels, CW lasers, development of satisfactory metal, etc 13 p2091 A66-255

Electrical and gas dynamical parameter effect on length of linear constant Mach number MHD duct, assuming gas is ionized by neutron irradiation in expansion nozzle preceding duct and electron recombination takes place in duct 13 p2000 A66-257

Partially ionized plasma drift across toroidal magnetic field arises from collision with neutral gas 13 p2146 A66-257



- Transition probabilities and lifetimes in ionized argon gas lasers 13 p2102 A66-26207
- Differential scattering of ionized helium on neon and argon and ionized argon on argon measured at various relative energies and scattering angles 13 p2135 A66-26269
- Current density in slightly ionized gas for arbitrary collision cross section 13 p2150 A66-26274
- Numerical solution of steady state jump equations for normal ionizing shock waves in hydrogen, assuming upstream and downstream states at chemical equilibrium 13 p2154 A66-26661
- Shock and ionization fronts propagation in gas-dust medium 14 p2380 A66-27255
- Ring of ionized hydrogen in region 3.5 to 4.5 kpc from galactic center 14 p2380 A66-27256
- Mobility of various ions in nitrogen and argon and mobility and diffusion of ions in hydrogen 14 p2345 A66-28138
- Propagation of ionizing fronts across magnetic field, examining flow behind and ahead of front 14 p2347 A66-28305
- Electrical discharge in air, mercury vapor and nitrogen, using RF signal probe, determining electron density and temperature and random velocity in plasma 15 p2548 A66-29715
- Ambipolar diffusion of plasma cloud imbedded in ionized gas with homogeneous magnetic field, assuming electric current is not vanishing 15 p2494 A66-30045
- Spectrum of plasma fluctuations in ionized turbulent gas explained by statistical turbulence theory, noting that electron temperature is larger than gas temperature 16 p2757 A66-30173
- Steady flow of highly rarefied ionized gas through channel with magnetic field solved by Monte Carlo method obtaining density, energies, wall shear stress, etc 16 p2759 A66-30371
- Transistor surface properties degradation by simulated space radiation environment 16 p2662 A66-30998
- Ionized gas flow rate behind detonation wave used with Chapman-Jouguet condition to determine speed of sound in reaction products 16 p2687 A66-31160
- Spectroscopy of plasmajets and electric arcs, noting spectral intensity, line width, etc 16 p2707 A66-31188
- Mean probability of coupling between electrons of flame on electronegative gas and radioactive bromine tracer injected into flame, calculating electrons coupling cross section on bromine 16 p2763 A66-31208
- Ionization equation for optically thin plasma, considering collisional ionization and recombination 16 p2763 A66-31350
- Effect of degree of expansion of ionized gas in nozzle on specific power of MHD generator 16 p2637 A66-31377
- Electron motion examined as major contributor to conductivity of thermally ionized gas in electrical field 17 p2964 A66-31892
- Origin and propagation of cosmic radiation, discussing interplanetary magnetic fields, plasmas, Faraday rotation of polarized radiation, Zeeman splitting of hydrogen line, etc 17 p2964 A66-32029
- Electron velocity distribution in ionized gas under alternating electric field as function of density, temperature, etc, including effects of recombination, ionization, etc 17 p2960 A66-32426
- Electric conductivity of multicomponent partially ionized gas calculated by simplified Chapman-Enskog method 17 p2967 A66-32446
- Steady-state axially-symmetric channel flow of ionized gas in external electromagnetic field in one-dimensional approximation 17 p2971 A66-32867
- Longitudinal Faraday emf, thermoelectric and Hall effects on channel flow of ionized gas 17 p2972 A66-32868
- Measurable range of ionizational relaxation behind shock front in argon extended to equilibrium region by mm-wave technique 17 p2912 A66-32982
- Spectroscopy of highly ionized atoms in problems which arose from solar spectrum study 17 p3006 A66-33074
- Ion lasers involving electron transitions in atoms or molecules with lost electrons 17 p2937 A66-33249
- Dynamics of type II comet trails, noting physical analogy in head and trail with rarified partially ionized gas 17 p3012 A66-33392
- Laminar boundary layer heat transfer measurements by thick-film calorimeter gauges on flat plate in dissociated and partially ionized air 17 p3039 A66-33483
- Theta pinch discharge study of four times ionized nitrogen /N V/ spectrum 18 p3136 A66-33628
- Radiation-induced gas ionization effects on surface properties of shielded transistors 18 p3076 A66-33984
- Magneto-Fanno flow shock tube experiments to determine one-dimensional MGD interactions between partially ionized gas flow and external magnetic field 18 p3145 A66-34111
- Hot flame gases ionization by electron reactions at atmospheric pressure 18 p3137 A66-34116
- Hollow electric collector probe for measuring ion density in rapidly flowing slightly ionized gas 18 p3112 A66-34244
- Transport properties of ionized monatomic gases, using Chapman-Enskog-Burnett approximation method for determination of thermal conductivity, diffusion coefficients and viscosity 18 p3149 A66-34927
- Boundary layer behavior in fully ionized two-temperature plasma 19 p3433 A66-36827
- Interaction between weakly ionized plasma cylinder and electromagnetic fields, plotting dependences between resonance current vs frequency for different gases 20 p3612 A66-38446
- Emission spectra of ionized argon and H in electromagnetic shock tube, giving frame scans of spectra 21 p3726 A66-39081
- Electron, charged particle density spectrum and temperature measurements in arc jet of partially ionized argon 21 p3790 A66-39082
- Velocity dependent collision frequency effect on harmonic generation in ionized gas through which electromagnetic wave passes 21 p3792 A66-39180
- Saha equation correction based on consideration of ionization energy reduction from particle interaction in thermal plasma 21 p3793 A66-39371
- Plasma waveguide parameter changes due to additional gas ionization from microwave field 22 p3952 A66-39651
- Ionization relaxation in impure shock-heated argon studied by magnetic mass spectrometer 22 p3899 A66-40380
- RF induced gas plasma at 250-300 kc/s 22 p3956 A66-40401
- Gas ionization by fast electron beam directed along waveguide leading to longitudinal distribution of secondary electron concentration 22 p3958 A66-40938
- Measurement of effective cross sections of double charge of hydrogen, lithium, sodium and potassium ions in gases, considering error due to unequal scattering of primary and secondary particles 23 p4097 A66-41083
- Mercury, cesium and rubidium vapors ionization in intense radiation flux by Q-switched ruby laser 23 p4076 A66-41156
- Boundary conditions for unique solution to linearized warm plasma equations 23 p4105 A66-41640
- Hall effect in MHD generator using partially ionized gas 23 p4108 A66-42031
- MHD stability of toroidal gas discharge for perfectly ionized gas 23 p4108 A66-42041
- High density highly ionized nitrogen flow in plasma wind tunnel 24 p4191 A66-42192
- Transmission resonant cavity measurements of electron line densities and collision frequencies in ionized wakes of hypervelocity projectiles 24 p4191 A66-42195
- Theta pinch discharge as spectroscopic light source in highly ionized gas spectroscopy 24 p4241 A66-42393
- Nonsymmetric inflation of dipole magnetic field by ionized gas, noting nonsymmetric gas dissipation 24 p4199 A66-42587
- Numerical solution of Boltzmann kinetic equation for weakly ionized plasma in thermoelectronic converter 24 p4239 A66-42871
- Spectrum of three-times ionized nitrogen analyzed in wavelength region 300-8000 angstroms, using theta pinch discharge, connecting singlets and triplets 24 p4240 A66-43104
- Laboratory methods of producing ionized gases, examining properties of real plasmas 24 p4247 A66-43118
- ### IONIZING RADIATION
- #### SA PENNING DISCHARGE
- Ionizing radiation dosimetry for space pilots on short-and long-term space flights 01 p0021 A66-10803
- Radiobiological effects caused by ionizing radiation in mice pre-exposed to effect of acceleration 02 p0182 A66-11664
- Self-acceleration of ionizing particles in electric field of polarized ionization trail 02 p0270 A66-12279
- Particle bombardment produces ionized layers in high latitude ionosphere similar to sporadic E layers of lower latitudes 03 p0363 A66-12657
- Adsorption at semiconductor and gel surfaces discussing chemisorption theory, ionizing radiation effect and structural parameters 04 p0563 A66-13768
- Linvill lumped model in analysis of semiconductor devices in pulsed ionizing radiation environment 05 p0734 A66-14849
- Mid-day dayglow intensities arising from solar ionizing radiation fluorescence 05 p0748 A66-14942
- Self-acceleration of ionizing particles in electric field of polarized ionization trail 05 p0727 A66-15458
- Average energy expended per ionized electron-hole pair in silicon and germanium as function of temperature 05 p0742 A66-15871
- Energy dependence of threshold curve in separating collision from ionization effects and in interpreting anisotropies of electron threshold energies 06 p0938 A66-17150
- Electron mobility changes in GaAs single crystals due to electron irradiation interpreted in terms of ionized-scattering theory 06 p0939 A66-17151
- Ionizing irradiation effects on oxide covered silicon surface properties, measuring changes in inversion layer conductance 06 p0940 A66-17164
- Degradation of silicon dioxide coated silicon planar transistors after exposure to space-type ionizing radiation, using MOS structure 07 p1010 A66-18148
- Ionizing radiation effects in mice protected with hypoxia or with chemicals 08 p1175 A66-19086
- Radiation measurement equipment on Cosmos 41 satellite including scintillation counter, gas discharge counter, etc 08 p1228 A66-19798
- Upper atmospheric parameters that control daytime electron density distributions in F-1 region determined with use of N/h profiles 09 p1372 A66-20369
- Ionizing role of photon radiation in gas thermionic converter, noting experimental results and application to solar energy converters, tubular emitter converters, etc 09 p1405 A66-20923
- Soft electron fluxes in upper atmosphere measured, using open type secondary electron multiplier ejected in container from rocket 09 p1443 A66-21012
- Radiation hazards to astronauts in interplanetary flight from primary cosmic rays, Van Allen belts and chromospheric bursts 10 p1595 A66-21047
- Diode and transistor response to ionizing radiation, describing generation of transients qualitatively and quantitatively 12 p1843 A66-24681
- Frequency deviations in carrier frequencies of ionospherically propagated HF radio waves produced by fluctuations in solar ionizing radiation 14 p2286 A66-27903
- Electron spin resonance of gamma irradiated single crystal of barbituric acid dihydrate, noting formation and Hamiltonian parameters of free radicals 14 p2367 A66-27979
- Particle size and heat treatment effects on stability and reflectance of thermal control glass pigment coatings under UV radiation [AIAA PAPER 65-136] 15 p2616 A66-29288
- Postirradiation restitutive capacity of yeast cell suspensions in wort-agar and water after exposure to 1300 rad/min ionizing



radiation 15 p2438 A66-29485  
 Physiologically active compounds and cultured antibiotic fluids used to eliminate effects of ionizing beta radiation on plant seeds 15 p2438 A66-29487  
 Atmospheric neutral and ion composition and ionization radiation rates from rocket data compared with electron densities around 200 km 15 p2496 A66-30081  
 Physical process effect on structure of H II regions, noting ionization, Lyman continuum spectral distribution and radiative transfer frequency dependence on absorptive processes 17 p3003 A66-32655  
 Ionizing radiation effect on FET with silicon nitride as insulating layer, noting reduction of shift in gate turn-on voltage 17 p2983 A66-33105  
 Geomagnetically trapped proton and electron fluxes in immediate vicinity of Earth 18 p3186 A66-34809  
 Increases of ionizing radiation in stratosphere correlated with recurrent magnetic storms, ionospheric perturbations in auroral zone, etc, possibly due to electrons from outer radiation belt 18 p3197 A66-34874  
 Pulse shape discrimination technique using scintillation counter, distinguishing events of nuclear disintegration from those due to minimum ionizing particles 18 p3115 A66-35229  
 Ionizing particle trajectory analysis via vidicon TV techniques, noting methods of increasing system sensitivity 18 p3115 A66-35230  
 Fast overlap of microwave radiation by ionization aureole of spark in laser beam 19 p3376 A66-36719  
 Instability effect in n-channel silicon MOS transistors bombarded with ionizing radiation 20 p3526 A66-37317  
 Ionizing radiation effects on silicon planar bipolar transistors to determine degradation mechanisms 20 p3526 A66-37319  
 Time variation in solar X-ray ionizing radiation intensity in short wave fadeout SIDs 20 p3635 A66-38217  
 Upper atmospheric parameters that control daytime electron density distributions in F-1 region determined with use of N/h profiles 20 p3636 A66-38235  
 Radiation measurement equipment on Cosmos XLI satellite including scintillation counter, gas discharge counter, etc 21 p3736 A66-38794  
 Seed water content influence on oxygen effect as detected in gamma irradiated barley seeds and prolonged post-storage period in terms of biological effect and paramagnetic resonance signal 22 p3855 A66-40378  
 Radiolysis applied to effects of ionizing radiation on volatile inorganic compounds of fluorine, oxygen and nitrogen, noting mass spectrometric peaks 23 p4032 A66-41235  
 Peculiarities in effects of ionizing radiation on space vehicle crew and on functioning of central nervous system 23 p4026 A66-41335  
 Sporadic E layer formation at night, noting ionization sources and intensity 23 p4064 A66-41645

**IONOSONDE**  
 Auroral disturbances resulting in multipath distortion in propagation by ionospheric reflection and description of chirp ionosonde and antenna systems 23 p4036 A66-41143

**IONOSPHERE**  
 SA D LAYER  
 SA E LAYER  
 SA F LAYER  
 SA ISIS SATELLITE  
 SA LOWER IONOSPHERE  
 SA NIGHT IONOSPHERE  
 SA UPPER ATMOSPHERE  
 SA UPPER IONOSPHERE  
 Sporadic E layer characteristics compared to regular ionospheric layers and formation at various latitudes 01 p0063 A66-11032  
 Monographs on auroras, geomagnetic disturbances and ionosphere at high latitudes 01 p0064 A66-11160  
 Ionospheric effect on spectrum of general background galactic radio emission below 10 mc/s 02 p0284 A66-12192  
 Controlling instabilities in numerical representation of diurnal and geographic

variation of ionospheric data 03 p0361 A66-12501  
 Ionic reactions and photolization processes in D, E and F regions of ionosphere 03 p0365 A66-12874  
 Quiet diurnal solar variations and relation to ionospheric parameters 04 p0516 A66-13852  
 Ionospheric ionization physics 09 p1371 A66-20279  
 Cosmic space physics - All-Union Conference, Moscow, June 1965 09 p1460 A66-20986  
 Amplification coefficient for weak electric field arising on surface of large body in ionosphere in absence of magnetic effect, photoeffect and secondary emission 09 p1465 A66-21019  
 Two Project High Water experiments producing optical, ELF, RF, and radar data on ionospheric absorpt. of large water quantities and expansion process 14 p2289 A66-28417  
 Rate constant of ion molecular processes in ionosphere, tabulating results of laboratory analyses 15 p2495 A66-30054  
 Disturbances about solid body in flowing low density plasma applied to satellite-ionosphere interactions and Langmuir probe data analysis 16 p2759 A66-30373  
 Ionospheric flight simulation in which ion distribution of neutral gas expanding into rarefied ionized gas under magnetic field is measured 16 p2759 A66-30374  
 Ionospheric research in Japan with brief outline of work in various areas of study 17 p2917 A66-32507  
 Solar flare effects and relaxation time of ionosphere 17 p2993 A66-32532  
 Ionospheric effects over Delhf of Russian high altitude nuclear explosions in Central Asia and of U.S.A. explosions at Johnston Island, autumn 1962 17 p2918 A66-32695  
 Kinetic theory of ionospheric satellite trail, discussing neutral and charged components from BGK model equation [AIAA PAPER 66-477] 18 p3226 A66-33654  
 Ionosphere as anisotropic dissipative medium where charged particles random thermal motion acts as thermal radiation source, noting relation between driven AC conduction current density and applied AC electric field intensity 19 p3352 A66-36630  
 Ionospheric ion temperature from cyclotron damping of proton whistler 20 p3554 A66-38195  
 Tropospheric and ionospheric refraction, aspect sensitivity and height of radio aurora, backscatter radar aurora observation and geomagnetic field anomalies 20 p3520 A66-38199  
 Magnetospheric and ionospheric plasma wave model based on theory for MHD waves in slightly ionized gas 22 p3912 A66-40426  
 Mariner IV models of three Mars atmospheric layers analogous to terrestrial E, F-1 and F-2 layers, considering relative mass densities, temperatures, carbon dioxide photodissociation and ionization profile 23 p4129 A66-41779

**IONOSPHERE EXPLORER-A**  
**S EXPLORER XX SATELLITE**  
**IONOSPHERIC ABSORPTION**  
 Nondeviated absorption of radio waves in intermediate region between E and F layers 01 p0031 A66-11051  
 Electromagnetic wave absorption and cosmic noise absorption measurements useful in radio communication 01 p0072 A66-11101  
 MHD absorption of internal gravitational waves in ionospheric F layer in terms of traveling disturbances 02 p0283 A66-12116  
 Auroral type of riometer absorption and magnetic disturbances for stations situated at different longitudes in auroral zone 03 p0364 A66-12660  
 Multiple antenna based on corner reflector used in absorption measurements in magnetically conjugate regions 03 p0334 A66-12661  
 Auroral absorption height obtained from statistical satellite data on average precipitation rate of electrons in auroral zone as function of energy 03 p0364 A66-12663  
 Excessive cosmic radiation absorption in lower nocturnal ionosphere at middle geomagnetic latitudes during Forbush

effects 04 p0514 A66-13443  
 Frequency dependence of cosmic noise levels during anomalous type II absorption, noting shielding sporadic E layer 04 p0574 A66-13859  
 Seasonal variation in short-wave signal absorption at different latitudes reflected in seasonal variation of gas density and ionospheric absorption at D region and lower E region 05 p0672 A66-15025  
 Coronal and prominence phenomena accompanying solar flares noting shock wave, radio burst, ionospheric fadeouts and absorptions, coronal density and temperature increases, etc 07 p1130 A66-18071  
 Spatial and time variations in ionospheric absorption at long wavelengths for small elevations of Sun and at nighttime 08 p1220 A66-19778  
 Annual variations of ionospheric absorption at medium and long wavelengths measured by A3 method at midlatitudes 08 p1220 A66-19779  
 Energy spectrum for auroral zone X-rays, measuring simultaneously bremsstrahlung X-rays and ionospheric absorption 10 p1599 A66-21146  
 Anomalous ionization of lower ionosphere at medium latitudes during worldwide geomagnetic storm result in increased radio wave absorption in ionosphere 11 p1696 A66-22416  
 Radio wave absorption at high latitudes dependent on frequency, noting AZA and PCA are inversely proportional to powers of frequency 12 p1817 A66-24276  
 Vertical measurement of ionospheric absorption at continuously varying frequency, showing diurnal variation of absorption 12 p1870 A66-24289  
 Cosmic radio emission attenuation in ionosphere measurements including characteristic period and seasonal absorption measurements 13 p2186 A66-26050  
 Anomalous ionospheric radio wave absorption during winter in 40 degree northern latitude 13 p2026 A66-26741  
 MHD absorption of internal gravitational waves in ionospheric F layer in terms of traveling disturbances 14 p2286 A66-28075  
 Anomalous polar type radio emission absorption in ionosphere on April 4, 1965 measured, using radio astronomy 14 p2377 A66-28476  
 Proton flux measured by satellite at high latitude compared to ionospheric absorption, measured with riometers, noting absorption variation with latitude across polar caps 15 p2576 A66-29228  
 Winter anomaly of nondeviative ionospheric absorption of radio waves and relation to diurnal, seasonal, local and solar cycle variations 15 p2490 A66-29948  
 Vertical drift of charged particles effect on electron density profile as cause of seasonal variations in ionospheric absorption 15 p2490 A66-29944  
 Ionospheric absorption effects in D and E layers, noting refraction role and effective collision frequency 15 p2493 A66-30036  
 Early morning ionospheric characteristics measured by geophysical rocket, noting electron concentration, solar UV emission, intensity changes, electron temperature, absorption profile, etc 15 p2494 A66-30052  
 Electron precipitation in auroral zone, using observations from riometer, balloon rocket and satellite experiments 17 p2917 A66-32363  
 Riometer recordings at high geomagnetic latitude of intense and sporadic absorptions events correlated with occurrence of auroral and geomagnetic disturbances 18 p3108 A66-34532  
 Stability of Earth radiation belts, considering wave absorption in ionosphere noting role of proton fluxes, Alfvén wave generation, etc 18 p3197 A66-34877  
 Auroral absorption of cosmic radio noise 18 p3238 A66-35086  
 Ionospheric radio wave absorption, noting inverse correlation between solar activity with stability of reflections from sporadic E layer 19 p3344 A66-35262  
 Position of anomalous radio absorption in ionosphere during various phases of solar activity cycle 19 p3345 A66-35269



- Latitudinal effect on behavior of  
ionospheric absorption determined by  
absorption measurements at four  
stations 19 p3350 A66-36358
- Ionospheric absorption measurement by A3  
method in which field strength of distant  
CW transmitter is continuously  
recorded 19 p3351 A66-36359
- Low and medium frequency absorption  
measurements at steep ionospheric  
incidence for demonstrating diurnal, annual  
and sunspot cycle changes in lower  
ionosphere 19 p3351 A66-36360
- Cosmic radio noise used to measure  
ionospheric absorption, comparing  
extraordinary and ordinary wave flux effect  
in overcoming measurement  
problems 19 p3351 A66-36361
- Ionospheric absorption relation to solar  
activity, considering sudden ionospheric  
disturbances, polar cap absorption and  
sudden storm  
commencement 19 p3453 A66-36362
- Separation of D-E and F-layer contribution  
to integral absorption of cosmic noise by  
means of combined pulse reflection and  
cosmic noise  
measurements 19 p3351 A66-36363
- Spatial and time variations in ionospheric  
absorption at long wavelengths for small  
elevations of Sun and at  
nighttime 21 p3732 A66-38774
- Annual variations of ionospheric absorption  
at medium and long wavelengths measured  
by A3 method at  
midlatitudes 21 p3732 A66-38775
- Computer calculations from Sen-Wyller  
expression for specific absorption of radio  
wave in lower ionosphere 22 p3906 A66-39954
- Riometric data on ionospheric absorption  
applied to determination of dissociative  
recombination coefficient, noting  
ionospheric ionization by fragment gamma-  
radiation 22 p3973 A66-40468
- Ionization level of D region at middle  
geomagnetic latitudes as affected by fast  
proton flux 24 p4265 A66-42757
- Nondeviative radiowave absorption in plane  
and parabolic ionospheric layers, noting  
change with time 24 p4174 A66-42760
- Sudden cosmic radio noise absorption,  
polar cap absorption and auroral  
absorption 24 p4202 A66-42832
- Sporadic E layer reflection used to  
determine instrument constant in measuring  
radio wave absorption in  
ionosphere 24 p4205 A66-43156
- Differential absorption and Faraday  
rotation in D region, using closed loop  
feedback system and two signals of  
different frequencies 24 p4205 A66-43218
- IONOSPHERIC COMPOSITION**
- Space studies of Cosmos and Elektron  
satellites including space radiation hazards,  
particle observation, ionosphere chemical  
composition, onboard equipment,  
etc 01 p0136 A66-10415
- RF mass spectrometer measuring ionic and  
neutral particle composition of outer  
ionosphere, mounted on Elektron  
satellites 02 p0229 A66-11662
- Ariel I measurement of ionospheric  
electron density, temperature and ion  
composition 03 p0366 A66-12877
- Communications system of Explorer XX  
ionospheric satellite 04 p0481 A66-13801
- Space exploration discussing terrestrial  
effects of electromagnetic and corpuscular  
solar radiation 04 p0574 A66-13805
- Rocketborne resonance probe experiments  
for measurement of electron temperature,  
density and collision  
frequency 05 p0669 A66-14944
- Atmospheric ionization, discussing  
formation of different ionospheric  
regions 05 p0675 A66-15744
- Ion composition model representing  
conditions at low temperatures, assuming  
that solar cycle variation ions are  
distributed according to diffusive  
equilibrium theory 06 p0876 A66-16611
- Ionospheric research from space vehicles,  
comparing experimental data with  
theoretical models of D, E and F  
regions 07 p1029 A66-18089
- In situ probe measuring nonthermal  
components of electron energy distribution  
in ionosphere, small-scale ionization  
inhomogeneities and negative ion  
concentrations in lower  
ionosphere 08 p1223 A66-18745
- Limit on stably trapped particle fluxes  
determined theoretically and compared with  
data from Explorer  
satellites 08 p1184 A66-19391
- Ionospheric composition and density from  
90 to 1200 km determined from  
measurements made during solar minimum  
period 08 p1284 A66-19413
- Composition of outer ionosphere measured,  
using RF mass spectrometers mounted on  
board Elektron I and II  
satellites 09 p1378 A66-21008
- Role of coupling phenomena in  
recombination processes of complex  
ionosphere composed of two types of  
positive ions examined via wind-shear  
theory 10 p1526 A66-21123
- Ionosphere formation theory, reviewing  
solar radiation, absorption, ionization cross  
section rate, electron renewal in F and  
upper E layer, etc 10 p1533 A66-21851
- Space exploration, discussing terrestrial  
effects of electromagnetic and corpuscular  
solar radiation 12 p1938 A66-23638
- Upper atmospheric model of variations for  
solar minimum conditions based on satellite  
drag and rocket sounding 13 p2073 A66-26130
- Laboratory instrumentation for testing and  
calibration of in situ probes for lower  
ionosphere, mesosphere and  
stratosphere 13 p2059 A66-26549
- Aerobee-borne magnetic mass  
spectrometric measurements of neutral  
composition of lower  
thermosphere 15 p2490 A66-29946
- Electron-ion recombination coefficients for  
atmospheric ions determined in laboratory  
and compared with ionospheric  
analysis 15 p2548 A66-29947
- Role of corpuscular radiation in lower  
ionosphere formation, noting charged  
particle flux, energy spectra,  
etc 15 p2591 A66-30024
- Subsonic parachute-borne blunt probes for  
charged particle measurement in  
ionosphere 15 p2493 A66-30039
- Neutral particle densities of nitrogen,  
molecular and atomic oxygen and argon in  
upper atmosphere, noting density profile  
irregularities, diffusive separation altitude,  
etc 15 p2497 A66-30086
- Lyman alpha ionization of nitric oxide and  
ion molecule reactions accounting for ionic  
nitric oxide content of D and E  
regions 16 p2694 A66-30705
- Alouette satellite observation of  
ionospheric cyclotron resonance, obtaining  
plasma frequency at particular  
height 17 p2920 A66-33085
- Soft electrons and ions study by traps on  
Cosmos V satellite 19 p3451 A66-35248
- Electron and ion concentrations as function  
of solar radiation intensity and variation of  
ionospheric conditions, noting nitrous oxide/  
oxygen ion ratio 19 p3345 A66-35287
- Resistive and reactive components of  
impedance of short dipole in lower  
ionosphere 20 p3525 A66-37300
- Chemical equilibrium in nighttime  
ionosphere, estimating diffusion coefficients,  
noting role of transport  
processes 20 p3554 A66-38207
- Ionospheric ion-molecular reaction rates,  
discussing various measurement  
results 21 p3734 A66-39319
- Topside ionosphere constitution, examining  
electron and ion distribution, charged  
particle scale height, ion composition,  
electron and ion temperatures and  
magnetosphere 22 p3909 A66-39971
- VLF resonances in conjunction with  
topside sounder provide information about  
composition and temperature of terrestrial  
ionosphere 22 p3909 A66-39975
- Electron density, electron and ion  
temperature and ionic composition  
measurements in Peru, using incoherent  
scattering technique 22 p3910 A66-39977
- Ionospheric ionic composition and  
temperatures as function of altitude in  
radar spectrographic  
estimates 22 p3910 A66-39981
- Role of positive ion composition in wind  
shear theory of sporadic E layers, examining  
cases for meteoritic, No and oxygen  
ions 23 p4063 A66-41644
- IONOSPHERIC CONDUCTIVITY**
- SA IONIC WAVE
- Electric current system arising from  
sudden enhancement of ionospheric  
conductivity in auroral  
zone 04 p0516 A66-13853
- Exchange of energy between ionosphere  
and protonosphere, noting nonlocal heating  
by photoelectrons, thermal conductivity and  
heat input by downward  
flux 08 p1215 A66-19204
- Admittance measurements for antenna in  
ionosphere, effect of local magnetic field  
variations, plasma frequency and  
gyrofrequency 09 p1341 A66-19854
- LF admittance measurements on  
orthogonal dipoles in  
ionosphere 09 p1341 A66-19855
- Nocturnal electrical conductivity of  
equatorial ionosphere 09 p1373 A66-20384
- Ionospheric electrodynamics, discussing  
conductivity, wind and dynamo theory, drift  
effect on ionospheric formation and wind-  
electromagnetic field  
interaction 10 p1533 A66-21852
- Correction of Fatkullin expressions for LF  
conductivities of homogeneous plasma in  
presence of electron-ion collisions in  
ionosphere 15 p2488 A66-29109
- LF ionospheric measurement of  
admittances of three orthogonal short  
dipoles, noting impedance variation with  
respect to frequency attitude and  
voltage 15 p2493 A66-30038
- IONOSPHERIC CROSS MODULATION**
- Solar wind modulation of far daytime field  
of extra-long radio waves in ionospheric C  
layer 19 p3345 A66-35268
- Ionospheric cross modulation analysis by  
computer-oriented simulation process, noting  
D region electron density and collision  
frequency profiles 23 p4041 A66-41641
- IONOSPHERIC CURRENT**
- Progressive change in worldwide current  
systems and auroral zone electrojets of  
geomagnetic bays examined with magnetic  
data during IGY 01 p0063 A66-10890
- Diurnal velocity variations of ionospheric  
wind in auroral zones and disturbance daily  
solar variation 01 p0064 A66-11161
- Homogeneous auroral arcs orientation and  
relation to magnetic disturbance  
currents 01 p0064 A66-11164
- Book on lower ionosphere physics noting  
radio wave propagation, ionospheric  
currents, solar radiation and flares, ion  
kinetics, electron collision frequencies,  
etc 04 p0515 A66-13835
- Current system of solar disturbed diurnal  
variations of magnetic field at high latitudes  
in terms of dynamo theory, taking into  
account forward and Hall  
conductivities 04 p0516 A66-13854
- Midlatitude ionospheric currents detected  
by rocketborne rubidium vapor  
magnetometers in Nike-Apache  
rockets 05 p0667 A66-14791
- Electric currents in ionosphere measured  
by sounding rockets equipped with nuclear  
free precession magnetometers and  
Langmuir probes launched near  
Peru 05 p0668 A66-14800
- Lower ionospheric wind effect on  
geomagnetic field variation 05 p0668 A66-14935
- Cosmic ray intensity and geomagnetic field  
changes induced by electric current systems  
excited in ionosphere, noting seasonal  
changes in diurnal  
variations 06 p0950 A66-16596
- Sporadic E layer at middle and low  
latitudes and relation to solar quiet daily  
variations in ionosphere 08 p1213 A66-19027
- Aurora relations with ionospheric currents  
responsible for magnetic disturbance, noting  
sign of bay 08 p1215 A66-19054
- Ionospheric dynamo  
theory with  
consideration for magnetospheric current  
along geomagnetic force lines, noting Sq  
variation in solstices 09 p1372 A66-20374
- Magnetospheric electric fields, noting  
implications of magnetic storm  
theories 10 p1528 A66-21149
- Changes in current kinetic theory of No-O  
reaction, based on observation of release of  
nitric oxide in E region 11 p1703 A66-23494
- Magnetic disturbances at midlatitudes,



noting origin from locally generated currents 12 p1871 A66-24292

Equatorial electrojet cross section profile, describing longitudinal variations, current density, magnetic field produced and electron drift velocity 13 p2074 A66-26357

Sporadic E and ionospheric current correlation in summary of E layer, wind-shear theory and wind 14 p2281 A66-26846

Overhead ionospheric current function corresponding to  $S_q$  field, examining assumption of rotation of quiet day horizontal component 15 p2488 A66-29231

Three-dimensional polarizations of high-latitude micropulsations derived for conjugate point observatories from hydromagnetic wave-ionospheric current model 18 p3107 A66-34527

Ionospheric electric current effects on upper atmospheric electromagnetic wave transmission and propagation, discussing magnetospheric effects, solar wind, geomagnetic field, etc 20 p3550 A66-37434

Successive hourly variations of equivalent current systems of magnetic bay disturbance patterns and F layer minimum frequency increases 20 p3658 A66-38232

Geomagnetic field model based on definition of core field, crustal field, ionospheric currents and plasma pressures, examining trapped particle behavior 20 p3555 A66-38302

Acceleration of electrons in inner radiation belt by magnetic field variations over slope of geomagnetic anomaly in resonance with longitudinal drift frequencies of electrons 20 p3638 A66-38308

Generalization of differential equation of dynamo theory of geomagnetic variations to include unsteady dynamo effect in ionosphere 22 p3914 A66-40759

Rocket observation of upper atmospheric wind around ionospheric E layer by sodium release method, noting cloud drift 24 p4199 A66-42466

Ionospheric winds measurement by luminous trimethyl aluminum trails produced by gun-launched projectiles 24 p4200 A66-42592

Power spectrum analysis of mean daily values of magnetic data for 27 observatories 24 p4201 A66-42597

**IONOSPHERIC DRIFT**

Ionospheric irregularities and drift parameters deduced from fading records of second-order echoes of radiowave reflected vertically from ionosphere 01 p0022 A66-10160

Nocturnal auroral drift in meridional direction 01 p0064 A66-11163

Magnetic activity effect on F-2 region drifts and variation with time at low latitude station 03 p0361 A66-12633

Soviet report on ionospheric structure variations, drift magnitude, velocity and direction 05 p0874 A66-15226

Photographic and radar observations of meteors, discussing pulse coherent techniques for studying ionospheric drifts and winds 05 p0761 A66-15227

Ionospheric drift in F region compared with overall circulation in troposphere and stratosphere 08 p1214 A66-19048

Appleton anomaly of F-2 layer examined, assuming ionization induced horizontal motion of neutral air 08 p1215 A66-19207

Equilibrium electron density distribution in F-2 region of equatorial ionosphere, noting effects of photoionization, loss, diffusion along geomagnetic field lines and electromagnetic drift 08 p1216 A66-19210

Equilibrium theory of ionization transport in ionosphere predicts tendency for thin layers of overdense ionization to form in E region 10 p1531 A66-21279

CW bistatic radar design with arrival direction, distance and Doppler measurements obtained from phase comparisons and used in ionospheric wind determination from meteor trails 10 p1501 A66-21626

Measurement of horizontal ionospheric drifts in E and F regions over magnetic equator 11 p1696 A66-22381

Inhomogeneities shape effect on drift rate in ionosphere under wind and electric field effect 11 p1696 A66-22413

Upper atmospheric diurnal tide determined via sodium vapor trail measurements 11 p1701 A66-23146

Winds in upper atmosphere as revealed by sodium vapor trails explained on basis of prevailing and tidal components critically analyzed 11 p1701 A66-23147

Ionospheric radio wave propagation and ionization inhomogeneity drift measured, using doubly reflected signals 12 p1873 A66-24687

Ionospheric wind patterns studied by distortion of chemiluminous vapor trails from rockets 14 p2280 A66-26838

Ionospheric winds characteristics from observation of motions and growth of sunlit trails of alkali vapor compared to rocket probing of electron concentration 14 p2280 A66-26839

Ionospheric winds from midlatitude winds delineated by luminous trails in five reports at Estes Park seminar 14 p2282 A66-26852

Atmospheric motions from sodium cloud firings in 80 to 200 km height region, noting internal gravity waves, atmospheric tides and drift 15 p2489 A66-29661

Equatorial ionospheric drifts observed at Ibadan, Nigeria, during solar activity minimum, and relation to diurnal variation of sunspot cycle and drift velocity variations in E and F region 16 p2700 A66-31759

Magnitude of vertical drifts in F-region during high and low sunspot years, considering effect of ambipolar diffusion along geomagnetic lines of force 19 p3347 A66-35923

Coupling phenomena in recombination processes of complex ionosphere composed of positive ions under vertical field of ionization drift applied to wind shear theory of sporadic E layers 22 p3907 A66-39962

Ionospheric drift and radio wave dispersion determined from selective fading records and symmetry of cross correlation functions, using Fourier transforms 22 p3916 A66-40807

Geomagnetic disturbances due to dynamo effect of ionospheric winds in lower layers of ionosphere 24 p4204 A66-43150

**IONOSPHERIC ELECTRON DENSITY**

Radio propagation experiment using transmitted VHF waves from OGO-A to deduce electron density in ionosphere and magnetosphere 01 p0063 A66-10892

Book on satellite-caused ionospheric disturbances, particularly in particle density and electric and magnetic fields in vicinity of artificial body 01 p0138 A66-10975

Electron concentration-distribution data for ten quiet days during spring 1958 in F-2 layer 01 p0063 A66-11027

Minimum ionospheric electron density needed for radio reflection in F-2 layer 01 p0031 A66-11037

Mean electron density and collision frequency determined from radio noise absorption, average electron drift velocity and magnetic disturbance intensity observations 01 p0065 A66-11167

Variation of total ionospheric electron content up to 1000 km between sunspot maximum and minimum measured by Faraday fading of Sputnik III signals 02 p0279 A66-11262

Ionosphere electron content near auroral zone obtained from differential Faraday observations of multifrequency beacon satellite Explorer XXII, noting corpuscular radiation role 02 p0223 A66-12017

Electron density and collision frequency observation during auroral absorption event, discussing rocket experiment techniques and results of analysis 03 p0363 A66-12645

Electron-density variation at 1000 km observed by Alouette 03 p0419 A66-12674

Equatorial F-region electron density distribution is natural steady state distribution for charged fluids as shown by momentum transport equation for charged gaseous fluids 03 p0364 A66-12678

Photoelectron energy distribution in F region 03 p0364 A66-12684

Ionospheric interference with cosmic radio waves, analyzing scintillation, noting diffraction of wavefront passing through ionospheric electron density layer 03 p0335 A66-12855

Ariel I measurement of ionospheric electron density, temperature and ion

composition 03 p0366 A66-12877

Ionospheric electron density measured by rocketborne RF spectrometer, dispersive Doppler measurements and variable-frequency impedance probe 03 p0366 A66-12878

Electron density and collision frequency in lower D region measured by rocket sounding 03 p0366 A66-12879

Recombination coefficient and electron production rate in lower D region during solar flare 04 p0574 A66-13444

Accuracy estimation in determination of maximum values of electron production 04 p0514 A66-13444

Spatial distribution of electron density along given path inferred from oblique incidence soundings taken at terminal of path 04 p0515 A66-13679

Difference in Doppler shifts of radio waves emitted at various frequencies by satellite, Elektron I radio station, plotting electron concentration dependence on altitude 04 p0515 A66-13837

Effective ion mass in upper ionosphere from electron-density profiles obtained from Alouette satellite, compared with theory 04 p0517 A66-14177

Electrostatic probe, discussing Explorer XXII measurements of electron concentration and temperature at 1000 km altitude 05 p0746 A66-14782

Ion distribution and temperature in topside ionosphere from plasma scale height profiles from Alouette electron density data 05 p0687 A66-14788

Electric currents in ionosphere measured by sounding rockets equipped with nuclear free precession magnetometers and Langmuir probes launched near Peru 05 p0688 A66-14800

Electron distribution in quiet D region derived from rocket measurements of wavefield generated by LF ground transmitter 05 p0670 A66-14948

Ionospheric F region electron density and electron and ion temperatures measured by ground-based radar backscatter 05 p0670 A66-14950

Electron energy loss rate for D region determined by Maxwellian velocity distribution of thermal component brought about by collisions with molecular nitrogen involving rotational transition 05 p0672 A66-15021

Vertical electron transport velocity in ionosphere 06 p0877 A66-16895

F-layer structure at subauroral and auroral latitudes measured by multifrequency beacon satellite Explorer XXII 08 p1212 A66-18610

Faraday rotation analysis of single frequency radio transmission from satellites to determine local electron density 08 p1181 A66-18752

Inhomogeneities of ionospheric electron concentration in Pacific Ocean region obtained with aid of signals from Explorer VII satellite 08 p1213 A66-19025

Electron concentration profiles above maximum of F layer calculated from measurements made on Earth surface 08 p1213 A66-19026

Geomagnetic sudden-commencement storms effect on electron concentration in F-2 layer above Europe 08 p1215 A66-19082

Ionospheric plasma diffusion, noting electric field effect in derived equation of continuity for F region 08 p1215 A66-19206

Equilibrium electron density distribution in F-2 region of equatorial ionosphere, noting effects of photoionization, loss, diffusion along geomagnetic field lines and electromagnetic drift 08 p1216 A66-19210

Power series solution of F-2 layer diffusor equation, calculating equilibrium electron density from equatorial profile 08 p1216 A66-19211

Ionospheric F-2 region equatorial anomaly may not be caused by geomagnetic field 08 p1217 A66-19211

Improved HF prediction using ray tracing techniques to determine F-2 layer scale heights and scale height  $h'$  for alpha Chapman electron density distribution 08 p1217 A66-19211

Thermospheric heating effect on F-region ionization and electron density in daily back-



- Faraday polarization rotation of linearly polarized lunar-reflected radio waves used to measure ionospheric electron content during July 20, 1963 solar eclipse 08 p1284 A66-19412
- Electron concentration data obtained by rocket probes in quiet ionosphere with solar and geomagnetic activity, as function of time of day, season and altitude 08 p1285 A66-19776
- VLF sudden phase anomaly data for 1963 compared with solar X-ray emission measurements made by Vela satellites 09 p1435 A66-19972
- Upper atmospheric parameters that control daytime electron density distributions in F-1 region determined with use of N/h profiles 09 p1372 A66-20369
- Binary transport of electrons and ions in equatorial ionosphere and effect on brightness of 6300 angstrom airglow at Huancayo 09 p1372 A66-20376
- Source energy spectrum of solar XUV produced photoelectrons in ionosphere 09 p1372 A66-20382
- Latitudinal dependence of sunrise effect in F region determined from Schermerling data for four ground stations 09 p1373 A66-20383
- Structure, ionization-neutralization balance and dynamics of stratified formation in ionosphere 09 p1373 A66-20483
- Electron production, density and absorption in D region as effected by X-radiation 09 p1373 A66-20484
- Relation between height-time distribution of electron concentration and inhomogeneous formations of outer ionosphere 09 p1377 A66-21001
- Radiophysical investigations of outer ionosphere with aid of Cosmos II and Elektron I satellites and certain geophysical rockets 09 p1377 A66-21002
- Physical experimental data collected by Cosmos II satellite dealing with ionospheric structure 09 p1377 A66-21004
- Electron and ion concentration measurements in ionosphere at altitudes of up to 200 km, using rockets and satellites from 1960-64 09 p1377 A66-21005
- Variation and behavior of ionospheric electron concentration at altitudes of 100 to 200 km as measured by rocket probes 09 p1378 A66-21007
- Vertical electron density profiles determined at 725 and 1525 kc, using Elektron II satellite /1964 10 p1600 A66-21050
- Ionospheric aerial impedance measurements of wire dipole at frequency of 60 kc and plasma electron and collision frequency estimations 10 p1526 A66-21119
- Lower ionosphere measurements at solar minimum, discussing positive ion density, electron density, solar radiation optical depth, etc 10 p1527 A66-21139
- Integrated electron content of ionosphere determined from measurements of polarization angle received from Syncom III transmissions, presenting mean diurnal variation 10 p1528 A66-21148
- Simultaneous comparison of RF standing wave impedance probe, plasma frequency probe and resonance rectification probe techniques in determining ionospheric electron density 10 p1529 A66-21155
- Diurnal changes in total ionospheric electron content measured, using Randle Cliff antenna 10 p1530 A66-21162
- Plasma electron density and temperature from measurement of LF impedance of Langmuir probe, noting ionospheric probing 10 p1536 A66-21549
- Ground station installations for observation in ionosphere of noncoherent diffusion of plasma by electrons 10 p1532 A66-21711
- VHF ionospheric radio signal cross correlation coefficients determined, using pulse counting techniques 10 p1505 A66-21731
- Ionospheric electrodynamics, discussing conductivity, wind and dynamo theory, drift effect on ionospheric formation and wind-electromagnetic field interaction 10 p1533 A66-21852
- Spiralling electrons in geomagnetic field and superimposed electric field aligned with magnetic field lines 11 p1695 A66-22371
- Central Italy ionospheric electron density, examining Faraday rotation of 54 mc signals from Transit IVA satellite 11 p1695 A66-22377
- Curves of difference in Doppler shift in observations of transmitter of Elektron I satellite, noting fluctuations in electron concentration 11 p1762 A66-22409
- Focusing inhomogeneities in ionospheric electron density investigated by radio astronomical techniques at frequencies from 13 to 54 megacycles 11 p1696 A66-22415
- Critique of local ionospheric electron concentration determined by dispersion method with aid of satellite and new ionization maximum 11 p1697 A66-22429
- Substantiating possibility of determining local electron concentration by dispersion method with aid of satellites and new ionization maximum 11 p1697 A66-22429
- Effective electron collision frequency from electron temperature profile for ionospheric heating in F region 11 p1697 A66-22499
- Electron density distributions in daytime F-2 layer and dependence on neutral gas, ion and electron temperatures 11 p1699 A66-23135
- Satellite observational data indicates that nighttime electron temperatures in upper F region are larger than neutral gas temperature 12 p1868 A66-23559
- Spectrometer for measuring electron flux and energy at Gemini orbital altitudes 12 p1876 A66-23682
- Diurnal and seasonal altitude variations of E and F layers analyzed for geomagnetic activity from rocket measurement of electron concentration 12 p1869 A66-24269
- Electron distribution from 400 to 1200 km measured, using Ariel I satellite, noting latitudinal and longitudinal anomalies associated with geomagnetic field [AIAA PAPER 66-395] 12 p1872 A66-24511
- Effects of solar flare radiation on electron density of F-2 layer at maximum level in zone 12 p1944 A66-24834
- Explorer XX satellite observations of plasma resonances at fixed frequencies in topside ionosphere, noting patterns, effect of geomagnetic field, electron concentration, etc 13 p2074 A66-26352
- Sporadic E layer electron density detected from VHF ionospheric propagation and reflection 14 p2234 A66-26836
- Ionospheric winds characteristics from observation of motions and growth of sunlit trails of alkali vapor compared to rocket probing of electron concentration 14 p2280 A66-26839
- Rocket probing of winds and charge particle density and temperature in sporadic E layer 14 p2280 A66-26841
- Sporadic E layer electron density from rocket probing 14 p2280 A66-26842
- Sporadic E layer structure from very low electron density probing by radio during sunrise period on July 15, 1964 14 p2280 A66-26843
- Wind-shear theory of sporadic E layer at temperate zone with single ion and many ions, noting electron density 14 p2281 A66-26844
- Mixtures of ions in wind-shear theory of sporadic E layer, noting ion recombination 14 p2281 A66-26845
- Midlatitude sporadic E layer formation from vertical gradients of charge density, electric and geomagnetic fields 14 p2281 A66-26847
- Rocket measuring techniques for E layer charge particles and magnetic field discontinuities 14 p2282 A66-26851
- Unique ionospheric electron density distribution from ionograms from valley between E and F region 14 p2283 A66-27126
- Solution of continuity equation for electrons leads to high loss rate in prenoon maximum of electron density in F-2 layer 14 p2283 A66-27397
- Helium whistler detection by VLF receiver aboard Canadian satellite Alouette II, noting application to composition and electron density measurement of ionosphere 14 p2285 A66-27847
- Ionospheric electron density distribution investigated by ground reception of satellite signals from Elektron I 15 p2482 A66-28495
- Cyclic variations in maximum electron concentration of F-2 layer with solar activity explained by upper atmosphere temperature variations 15 p2486 A66-29093
- Dependence of electron concentration in F-1 layer on zenith angle of Sun 15 p2486 A66-29095
- Electron-concentration distribution in ionospheric F-2 layer with vertical distribution of electron-ion gas 15 p2486 A66-29096
- Relation between solar radiation and electron concentration up to F layer analyzed in winter and summer 15 p2487 A66-29106
- Formation mechanism of ionospheric narrow sporadic E layers by high energy electron fluxes captured by geomagnetic field 15 p2488 A66-29110
- Ionospheric D-region electron distributions in middle latitudes deduced from reflection of long radio waves 15 p2489 A66-29631
- Total electron content from S-66 satellite received at nine stations, using differential Faraday technique 15 p2491 A66-30017
- Upper ionospheric electron density measurement by signals propagated between two parts of high altitude rocket 15 p2493 A66-30037
- Ionospheric thin-layer stratifications and valley region analyzed by integrating propagation method and by impedance probe 15 p2494 A66-30042
- Ionospheric electron density measurement by gyroplasma probe, using sweep frequency impedance technique 15 p2604 A66-30047
- Total ionospheric electron content measurements at Delhi using Faraday fading of satellite beacon transmissions during solar minimum 15 p2495 A66-30067
- Electron content for ionospheric station located 47 degrees N determined from observation of Faraday polarization rotation 15 p2496 A66-30073
- Atmospheric neutral and ion composition and ionization radiation rates from rocket data compared with electron densities around 200 km 15 p2496 A66-30081
- Electron density in E-and D-regions above Kjeller, Norway, from rocket measurements of absorption and height of reflection of radio waves 16 p2692 A66-30332
- Total electron content of ionosphere in middle latitudes, noting results of satellite Doppler measurements, effect of solar radio noise flux, etc 16 p2694 A66-30706
- F-layer nightglow 6300 angstrom emission intensity and electron density data, noting variations in emissions 16 p2694 A66-30708
- Altitude-time distribution of electron concentration, noting satellite measurements of ionospheric inhomogeneities and difference in Doppler shifts of coherent radio waves emitted by Elektron I satellite 16 p2696 A66-30920
- Ionospheric electron density measurement by radio-frequency probes, noting error correction 16 p2697 A66-30994
- Field potential, electron and ion concentration contours in wake of orbiting body 16 p2631 A66-31540
- Variational method calculation of refraction angle in inhomogeneous laminar medium, using approximate integration of series of exponential functional of electron concentration 17 p2873 A66-32241
- Variations in electron density with reflection of long waves in D region 17 p2918 A66-32878
- Altitude variations of frequencies and electron density with reflection in D region 17 p2919 A66-32879
- Dependence of electron density in E layer on Sun zenith distance, based on new ionospheric data and ionization neutralization phenomena 17 p2919 A66-32880
- Anomalous behavior in correlating maximum electron density dependence on solar zenith distance and asymmetry in critical frequency for E layer 17 p2919 A66-32881
- Ionospheric electron generation formula derived, based on analysis of interaction of cosmic radiation on ionosphere 17 p2994 A66-32882
- Ionospheric electron content determined from satellite measurements, noting seasonal and diurnal variation of content and utilization of Faraday fading for



measurements 17 p2920 A66-33069  
 Topside ionograms electron density data both at and below orbit of Alouette I satellite 17 p2920 A66-33092  
 Height distribution of electron density accounting for behavior of LF and VLF radio wave propagation during sudden ionospheric disturbance 17 p2922 A66-33349 /SID/  
 Lunar semidiurnal tides in ionosphere over Puerto Rico determined from electron density profiles for heights between 150 and 300 km 17 p2923 A66-33362  
 Ionospheric electron content determined by closely spaced frequency and rotation rate methods, using satellite transmission 18 p3104 A66-33547  
 Three rocket tests described for measurement of ionospheric electron density 18 p3105 A66-33983  
 Faraday rotation from 24-hr satellite at high frequencies provides means of studying electron content of ionosphere and fluctuations 18 p3106 A66-34200  
 Correlation of geomagnetic index and plasma scale height in topside ionosphere observed from Alouette topside sounder and planetary geomagnetic data 18 p3169 A66-34517  
 Temporal variations in temperature and drift velocity in ionosphere determined from nighttime variations of F-region electron density profiles at Puerto Rico 18 p3107 A66-34522  
 Ionospheric Faraday effect and determination of total electron content in ionosphere 18 p3109 A66-35042  
 Local electron concentration determination by dispersion method and satellite proved unreliable because of horizontal ionization gradient and ionospheric instability 19 p3344 A66-35259  
 Total electron component of ionosphere column between satellite and Earth calculated, using differential Doppler effect 19 p3361 A66-36654  
 Occurrence frequency patterns of topside spread-F on Alouette satellite ionograms, discussing radio propagation, magnetic irregularities, electron density-induced refraction, etc 20 p3554 A66-38196  
 Very steep latitudinal electron density gradients in topside F layer at high altitudes 20 p3554 A66-38197  
 Ionospheric electron content variation with solar radio flux from Faraday rotation data at magnetic equator 20 p3633 A66-38198  
 Modification to theory of differential absorption experiment involving Fresnel reflection coefficient of ionospheric irregularities 20 p3555 A66-38209  
 Upper atmospheric parameters that control daytime electron density distributions in F-1 region determined with use of N/h profiles 20 p3636 A66-38235  
 Alouette satellite, topside sounder measurement of ionosphere electron density from above 20 p3639 A66-38313  
 Relativistic electron production by cosmic radiation in lower ionosphere 20 p3645 A66-38437  
 E-layer critical frequency variations conditioned by solar zenith angle, taking account of transport, gradient and time variations of height scale 21 p3732 A66-38664  
 Electron concentration data obtained by rocket probes in quiet ionosphere with solar and geomagnetic activity, as function of time of day, season and altitude 21 p3809 A66-38772  
 Ionospheric electron content over Ahmedabad and Bombay from differential Faraday rotations of plane polarized radio waves from Beacon 21 p3734 A66-39229  
 Electron density profiles in ionosphere and exosphere - NATO Advanced Study Institute, Flinse, Norway, April 1965 22 p3903 A66-39943  
 Negative ion associative detachment reaction with atomic oxygen in determination of nighttime D region electron density profiles at high latitudes 22 p3905 A66-39945  
 Faraday rotation experiment for determination of electron density and collision frequency observations in arctic D region 22 p3905 A66-39946

Collision frequency in E and D regions of ionosphere for electrons and neutral molecules 22 p3906 A66-39948  
 Partial reflections utilizing different amplitudes of ordinary and extraordinary backscattered waves for electron number densities and collision frequency measurement in lowest ionosphere 22 p3906 A66-39949  
 Electron density and collision frequency profiles for D region obtained through simultaneous measurement of radio wave phase and amplitude 22 p3906 A66-39953  
 Electron density measurements in D layer obtained, using LF radio wave propagating into ionosphere and rocketborne receivers 22 p3906 A66-39955  
 Electron density profiles in D layer measured through Doppler shift on VLF signal propagating from ground up and received by rocket 22 p3907 A66-39957  
 Number densities of ions and electrons in D region measured, using Arcas rocket 22 p3907 A66-39958  
 Mean variation of electron density profile of ionosphere above Lindau/Harz, noting semiannual variation of F-2 layer peak height related to solar activity 22 p3908 A66-39965  
 Lunar tidal effects on noon real-height F-2 electron density profile data from two-year interval 22 p3908 A66-39967  
 True height in-line computation of electron density profile from ionograms, using analog computer in real time 22 p3908 A66-39969  
 Seasonal, diurnal and latitudinal variations of electron density distributions in topside of ionosphere as revealed by Alouette I satellite 22 p3909 A66-39974  
 Electron density and electron and ion temperatures in F region studied by ground-based radar observations at Millstone Hill 22 p3909 A66-39976  
 Electron density, electron and ion temperature and ionic composition measurements in Peru, using incoherent scattering technique 22 p3910 A66-39977  
 F layer electron temperature fluctuations and resultant electron density changes in daytime 22 p3910 A66-39980  
 Nighttime F layer recombination and diffusion coefficients estimated from incoherent scatter measurements of electron densities and electron and ion temperatures 22 p3910 A66-39983  
 Midlatitude ionospheric electron content variation with season and solar cycle 22 p3911 A66-39984  
 Latitudinal and diurnal variations of ionospheric electron content near auroral zone in winter from Faraday rotation data 22 p3911 A66-39985  
 Ionospheric electron content variation at low latitude, noting correlation with solar and geophysical phenomena 22 p3911 A66-39986  
 Faraday rotation measurements of decimeter wavelength radiation from Jupiter, calculating ionospheric electron content 22 p3977 A66-39987  
 Upper ionospheric electron density, electron gyrofrequency, ion density and ion gyrofrequency deduced from whistler-mode waves group index, energy distribution and dispersion curves 22 p3911 A66-39989  
 Observed Faraday polarization variation of satellite transmission radio signals due to ionospheric irregularities, latitudinal electron density variations and antenna geometry readout error 22 p3867 A66-40556  
 Doppler frequency shift for radio waves radiating coherently from satellite in ionosphere, considering electron concentration and angles of refraction 22 p3869 A66-40779  
 Guiding of whistlers due to exospheric anisotropy, electron density and geomagnetic field effects 22 p3915 A66-40803  
 Cosmic radio wave, whistler and transmitted radio wave interactions with ionospheric magnetoplasma in collision-dominated, photoequilibrium and photoionization-dominated regions 22 p3916 A66-40873  
 Rocketborne RF electron density probe for ionospheric profile determination 23 p4064 A66-41683

Anomalous enhancement of ionospheric F-2 region electron density at post-sunset time in low and equatorial latitudes 24 p4198 A66-42462  
 Ionospheric electron density measured by rocket carrying new gyro-plasma impedance probe 24 p4199 A66-42465  
 Ionospheric electron content at temperature latitudes during declining phase of sunspot cycle determined by observation of Faraday effect 24 p4200 A66-42595  
 Decrease in electron density of ionospheric F region following passage of powered rocket 24 p4201 A66-42609  
 F-1 layer formation as affected by solar activity, seasons and time of day 24 p4202 A66-42766  
 Ionospheric constituent parameters at altitude between 78 and 100 km by local measurements of VLF field radiated from ground transmitter 24 p4203 A66-43074  
**IONOSPHERIC F-SCATTER**  
 Dense sporadic E cloud effects on high latitude HF backscatter observation 05 p0667 A66-14792  
 Times of peak cosmic radio noise concentration and usefulness to forward propagation ionospheric scatter reception on DEW-Line as performance monitor, etc 06 p0825 A66-15985  
 Received field strength dependence on maximum and minimum usable carrier frequency range for ionospheric scattering 06 p0836 A66-17034  
 Ambipolar diffusion parameter calculation by Quinn and Nisbet found erroneous for night F layer 08 p1219 A66-19420  
 Short wave radio transmission and reception, examining masking by E region, focusing and attenuation due to scattering at ionospheric and other nonuniformities 08 p1186 A66-19780  
 Ionosphere formation theory, reviewing solar radiation, absorption, ionization cross section rate, electron removal in F and upper E layer, etc 10 p1533 A66-21851  
 Fluctuations in diurnal variations of ionization of F-2 layer interfering with radio wave propagation determined by series expansion 12 p1869 A66-24270  
 Geophysical rocket determination of aerosol scattering coefficient variation from brightness values at 70-450 km heights 15 p2495 A66-30057  
 Contribution to dependence of variation of unperturbed ionospheric F-2 critical frequencies on season and solar activity 18 p3105 A66-34097  
 Phase fluctuations of ground-backscattered signals recorded, noting phase stability of sporadic E-layer-supported and F-2-layer-supported ground backscatter 18 p3071 A66-34534  
 Short wave radio transmission and reception, examining masking by E region focusing and attenuation due to scattering at ionospheric and other nonuniformities 21 p3703 A66-38776  
 Electron density and electron and ion temperatures in F region studied by ground-based radar observations at Millstone Hill 22 p3909 A66-39976  
 Diurnal behavior of topside and bottomside spread F at equatorial latitudes and association with geomagnetic activity 24 p4200 A66-42595  
**IONOSPHERIC HEATING**  
 Heat transfer and mass flux expressions for recombination interactions at solid-gas interface due to transport of atomic and ionized particles to spacecraft in ionosphere 08 p1161 A66-18747  
 Ionospheric heating by magnetic conjugate point photoelectrons, showing variation of electron temperature with time 08 p1218 A66-19402  
 Effect of heating of ionosphere by photoelectrons coming from magnetically conjugate point, using electron temperature measurements 16 p2698 A66-31214  
 Ionospheric heating by photoelectrons streaming from sunlit magnetic conjugate point established from incoherent backscatter spectra data 22 p3910 A66-39977  
**IONOSPHERIC ION DENSITY**  
 Time dependency effect on effective recombination coefficient in lower ionosphere 02 p0223 A66-12111



Current theories for auroral excitation, general excitation and ionization by fast particles in air and relation between luminosity and ionization in aurora 03 p0418 A66-12656

Ion distribution and temperature in topside ionosphere from plasma scale height profiles from Alouette electron density data 05 p0667 A66-14788

Correction to paper on rocket studies of sporadic-E ionization and ionospheric winds 05 p0671 A66-14957

Ionosphere and plasma in near space, discussing Soviet rocket observations on ionospheric structure, expansion and space ionization 05 p0749 A66-15231

Fractional concentration of hydrogen ions in ionosphere from VLF proton whistler measurement 08 p1218 A66-19393

Electron and ion concentration measurements in ionosphere at altitudes of up to 200 km, using rockets and satellites from 1960-64 09 p1377 A66-21005

Lower ionosphere measurements at solar minimum, discussing positive ion density, electron density, solar radiation optical depth, etc 10 p1527 A66-21139

Midlatitude trough in F-region ionization of night ionosphere revealed by ion trap on solar-orbiting satellite 11 p1699 A66-23134

Ion-molecule reaction rates and recombination coefficients from mass spectrometric ionospheric data 11 p1702 A66-23492

Inhomogeneity, transparency and ionospheric ion density parameters for screening and semitransparent sporadic E layers 12 p1873 A66-24686

Rocket probing of winds and charge particle density and temperature in sporadic E layer 14 p2280 A66-26841

Midlatitude sporadic E layer formation from vertical gradients of charge density, electric and geomagnetic fields 14 p2281 A66-26847

Smith subprotonospheric whistlers and digital computation of ion effects on whistler-mode ray tracing 14 p2282 A66-26858

Time dependency effect on effective recombination coefficient in lower ionosphere 14 p2286 A66-28074

High incidence and erraticism of sporadic E occurrence in temperate zones where horizontal component of geomagnetic field is greatest, attributed to horizontal wind shear 15 p2490 A66-29949

Atomic ions of meteoric origin indicated as source of midlatitude E region in IQSY rocket measurement 15 p2492 A66-30033

Nike-Cajun rocket investigation of equatorial D and E region parameters and effect on electrojet 15 p2493 A66-30035

Ionospheric plasma movement, neutral-neutral and charged-neutral particle collisional interactions, electron-ion collision frequencies, mobility and LF Hall conductivity, irregularities, etc 15 p2495 A66-30053

Ion composition and effective recombination coefficient variation of ionosphere in study of X and UV radiation ionization of E layer 15 p2495 A66-30059

Macroscopic equations describing effect of negative ions on diffusion of electrons and positive ions in lower ionosphere 17 p2917 A66-32255

Nitric oxide distribution in lower ionosphere calculated from reaction coefficients and mass spectrometric measurements of density 17 p2922 A66-33354

Meteoric atomic ions in lower ionosphere 17 p2922 A66-33355

First-order correction to Hault theory for measuring ion density in D region, especially those involving heat transfer and compressibility 18 p3107 A66-34523

Electron and ion concentrations as function of solar radiation intensity and variation of ionospheric conditions, noting nitrous oxide/oxygen ion ratio 19 p3345 A66-35287

Positive ion composition in lower ionosphere, particularly D region, considering sources for water ions, stratification of metallic ions, etc 19 p3350 A66-36354

Negative ion density and composition in lower ionosphere 19 p3350 A66-36355

Chemical composition of ionized

components of outer ionosphere above main ionization maximum region measured by satellites 19 p3350 A66-36357

Ionospheric ionization produced by precipitation of particles from Van Allen belts, examining influence of magnetic anomalies, longitudinal drift and local effects during magnetically quiet periods 20 p3641 A66-38325

Gerdien-condenser rocketborne probe used to measure ion densities in D region of atmosphere 22 p3905 A66-39947

Ion mass spectrometry of D layer, using magnetic fields and cyclotron resonance principle 22 p3907 A66-39956

Number densities of ions and electrons in D region measured, using Arcas rocket 22 p3907 A66-39958

Ionospheric ionic composition and temperatures as function of altitude in radar spectrographic estimates 22 p3910 A66-39981

Upper ionospheric electron density, electron gyrofrequency, ion density and ion gyrofrequency deduced from whistler-mode waves group index, energy distribution and dispersion curves 22 p3911 A66-39989

Minimum effective heights of ionospheric layers in continuous recording for study of ionization and disturbance 22 p3920 A66-40773

Role of positive ion composition in wind shear theory of sporadic E layers, examining cases for meteoritic, No and oxygen ions 23 p4063 A66-41644

Plane gridded retarding potential analyzer for measuring dominant constituent ion concentrations, temperature and instrument potential in planetary ionospheres 24 p4201 A66-42605

Measurement technique for variations in optical path of gyroelectric echoes generated by long wave transmitter and propagating in whistler mode 24 p4176 A66-42995

## IONOSPHERIC IRREGULARITY

### SA SUDDEN IONOSPHERIC DISTURBANCE /SID/

Ionospheric irregularities and drift parameters deduced from fading records of second-order echoes of radiowave reflected vertically from ionosphere 01 p0022 A66-10160

Satellite probe measurements of irregularities of electron density distribution above F-2 layer in polar region 03 p0363 A66-12642

Radar echoes explained in terms of backscatter from field-aligned irregularities in F region 03 p0334 A66-12679

Discrete radio source scintillation, considering irregular diffraction pattern caused by ionospheric irregularities 04 p0575 A66-13380

Ionospheric disturbances traveling at subauroral latitudes compared at different altitudes 04 p0514 A66-13481

Vortical electric field effect on inhomogeneities spreading in weakly ionized plasma /ionosphere/ in magnetic field 04 p0577 A66-13842

Small amplitude LF waves in ionosphere covering momentum and energy dissipation, zero temperature plasma and waves in nonuniform plane-stratified medium 04 p0516 A66-13961

F-layer behavior over Genoa-Monte Capellino noting diurnal and seasonal variation, solar activity, nighttime concentration, spread-F, ionospheric and geomagnetic perturbations 05 p0671 A66-14982

Laboratory simulation, in continuum and rarefied flow regimes, of perturbations of ionosphere by satellite and rocket exhaust 06 p0869 A66-16908

Characteristic distortion of Doppler curves and radio signals of artificial satellite from behind horizon 07 p1000 A66-17209

Satellite charge and sheath formation resulting from photoelectric and secondary emission 08 p1302 A66-18748

Satellite ionization effects, CW-reflection and pulse radar techniques in 10 to 20 mc frequency range 08 p1181 A66-18749

Space-time distribution of perturbed solar diurnal variation at high latitudes during IGY 08 p1214 A66-19033

Planet-wide characteristics of ionospheric perturbation as indication of solar radiation 08 p1214 A66-19047

Ionospheric E region inhomogeneity investigated by photographic recordings of reflected signal fading 08 p1214 A66-19049

Ionospheric inhomogeneity movements in E and F-2 regions and height variation of drift velocity 08 p1215 A66-19052

Comparison of signals received on two VHF scatter circuits of different geometry but viewing common scattering region 08 p1184 A66-19211

Ionograms showing satellite traces interpreted as inverted trough disturbance traveling in F region 08 p1216 A66-19212

True height variations of F-2 layer for bay disturbances of geomagnetic field obtained from ionograms, assuming they are caused by horizontal electric field 08 p1216 A66-19213

Satellite emission of variable frequency signal guided by ionization irregularity existing along force line of geomagnetic field 09 p1374 A66-20886

Seasonal variation of F-region parameters at sunspot minimum, noting effects of ionospheric disturbances 11 p1695 A66-22368

Inhomogeneities shape effect on drift rate in ionosphere under wind and electric field effect 11 p1696 A66-22413

Internal gravity wave propagation in thermally stratified atmosphere 11 p1697 A66-22567

Relation between magnetic activity and ionospheric disturbances in F-2 layer studied on basis of 30-year data 12 p1870 A66-24285

Statistical distribution of monthly median noon critical frequency of F-2 layer from ionospheric stations at mid-latitudes, auroral regions and at polar cap 12 p1870 A66-24286

Ionospheric radio wave propagation and ionization inhomogeneity drift measured, using doubly reflected signals 12 p1873 A66-24687

Ionograms made at Australian ionosonde stations during magnetically quiet world day interval, obtaining information on F region ionization, noting existence of universal time control of ionization 12 p1873 A66-24835

Signal amplitude of Transit IVA satellite recorded at two stations, using time difference between observing similar fluctuations in fading period to determine height of ionospheric irregularities 12 p1874 A66-24843

D-region electron distribution, collision frequency and amplitudes of partially reflected waves 13 p2075 A66-26739

Cause and structure of temperature latitude sporadic E - Seminar, Swiss Village, Colorado, June 1965 14 p2279 A66-26834

Sporadic E layer from causal standpoint 14 p2280 A66-26835

Cross correlation of satellite signals through slab containing small anisotropic irregularities 14 p2237 A66-27398

Frequency deviations in carrier frequencies of ionospherically propagated HF radio waves produced by fluctuations in solar ionizing radiation 14 p2286 A66-27903

Scintillations of Jupiter decametric radio wave emission explained in terms of diffraction and refraction by single ionospheric irregularities 15 p2593 A66-28903

Electron concentration inhomogeneities during traveling gravity wave propagation through F layer 15 p2485 A66-29084

Ionospheric plasma movement, neutral-neutral and charged-neutral particle collisional interactions, electron-ion collision frequencies, mobility and LF Hall conductivity, irregularities, etc 15 p2495 A66-30053

Latitudinal variations of ionospheric irregularities studied via synchronous and 1000 km satellites, noting Early Bird data, scintillation index graphs, radio star signals, etc 15 p2496 A66-30071

Scintillation height measurement, noting irregularity distribution during various ionospheric conditions 16 p2691 A66-30230

Spectrum analysis of critical frequency of F-2 layer 16 p2692 A66-30330

Day-to-day variations in F-2 critical frequency 16 p2693 A66-30339

Maximum ionization in ionospheric F region around geomagnetic equator, noting



instruments and observed variations 16 p2697 A66-30995

Solar class 2 flares, noting activity on September 16, 1963, associated ionospheric disturbances, etc 16 p2795 A66-31149

Frequency of strong ionospheric disturbances, noting effect of high and low solar activity, deviations from monthly median, use of statistical analysis, etc 16 p2699 A66-31387

Spread F and ionospheric F region irregularities relation to magnetic field alignment, discussing radio star scintillations 17 p2923 A66-33433

Correlation of peak occurrence of HF radar echoes and high-latitude spread-F measurements near time of local sunset 18 p3107 A66-34525

Horizontal dimensions of ionospheric irregularities determined from differences in angular diameter observed in discrete radio sources 18 p3108 A66-34533

Nature of middle-latitude ionospheric perturbations 19 p3344 A66-35262

Solar activity dependence of sporadic E layer, noting cyclic variation in characteristics from 1957 to 1964 19 p3344 A66-35264

Two-year variation in troposphere, ionosphere and stratosphere regions, noting sporadic E layer in Far East 20 p3552 A66-37571

Anomalous enhancement of F-2 ionization in high latitude around geomagnetic noon due to formation of irregularity or new layer around locality 20 p3658 A66-38234

LF incompressible waves and gradient instabilities in ionosphere 21 p3733 A66-39183

Explorer XX topside sounder observations of ionospheric irregularities in electron density and plasma wave electrostatic resonances 22 p3909 A66-39972

Ionospheric electron content variation at low latitude, noting correlation with solar and geophysical phenomena 22 p3911 A66-39986

Ionization irregularities in bottomside and topside ionosphere, noting circulation effect 22 p3911 A66-39988

Data processing of signal reception from Soviet satellites indicates radio signals scintillation caused by diffraction of waves from ionospheric nonuniformities 22 p3866 A66-40467

Observed Faraday polarization variation of satellite transmission radio signals due to ionospheric irregularities, latitudinal electron density variations and antenna geometry readout error 22 p3867 A66-40556

Automatic, multichannel system for data recording and processing obtained in studies of ionospheric structural inhomogeneities, containing magnetic-tape memory and device for digital tape memory and device for digital computer input 22 p3920 A66-40772

16-megacycle backscatter echoes from sporadic E region recorded near Brisbane, Australia, examining dimensions of horizontally moving irregularities 23 p4064 A66-41685

Nonsymmetric inflation of dipole magnetic field by ionized gas, noting nonsymmetric gas dissipation 24 p4199 A66-42587

Traveling disturbance in ionosphere due to nuclear detonation detected as acoustic-gravity wave modes, noting range-time diagrams 24 p4200 A66-42594

Diurnal variation of ionospheric irregularities, using differential Doppler method for analysis of data transmitted by Beacon satellite 24 p4200 A66-42596

Irregular diffraction analysis with ultrasonic waves, measuring air stream temperature fluctuations and velocity 24 p4176 A66-43020

# IONOSPHERIC NOISE

Broadband VLF emissions observed to determine whether whistler mode signals appearing below ionosphere travel toward polar regions and at low latitude from auroral zone 01 p0012 A66-10893

Theory of thermal noise in ionosphere developed from Nyquist theorem expressing thermal fluctuations of current in localized resistance 09 p1340 A66-19846

Polar cap absorption effect on polar VLF emissions used for analysis of solar proton events 09 p1374 A66-20880

UK-2 satellite measurement of ionospheric noise bands and propagation of waves in Z mode, including orientation determination methods 10 p1604 A66-21117

Effect of Soviet atmospheric nuclear explosions on D and F-2 ionospheric layers, particularly observing enhancement of atmospheric noise 10 p1600 A66-22058

SEA effect at VLF 11 p1651 A66-22373

VHF hiss zone morphology and correlation with particle precipitation events, from Alouette I satellite observations 11 p1700 A66-23136

Simultaneous appearance of in-phase ULF geomagnetic pulses at two conjugate points 13 p2076 A66-26759

Radioelectric emission of VLF at two conjugate points 16 p2693 A66-30590

Frequency-time spectrograms supporting discovery of two whistlers in VLF radio noise data from Injun III satellite 17 p2919 A66-32930

Ionospheric thermal radiation, discussing noise power per unit volume, spectral distribution, frequency, etc 19 p3352 A66-36631

# IONOSPHERIC PROPAGATION

SA RADIO PROPAGATION

SA WAVE PROPAGATION

Pisa University research program since 1958 on AM waves which have undergone linear distortions in ionospheric propagation 01 p0022 A66-10332

Coherent nonlinear interaction of two electromagnetic waves in plasma, noting F layer radio communication 01 p0029 A66-10594

Polar interferometric method for measuring north-south component of ultrashort wave refraction in ionosphere and optical thickness gradient 02 p0190 A66-11415

Time measurement as applied to aerial navigation noting atomic clocks, time transmission by ionospheric propagation of electromagnetic radiation, etc 02 p0257 A66-12031

Damping of longitudinal plasma waves emitted by artificial Earth satellite moving in ionosphere 02 p0269 A66-12132

Radio emission in ionosphere during high solar activity explained as electron emission produced by particles moving as corpuscular fluxes 02 p0284 A66-12133

LF propagation and probe experiment yielding profile of ionospheric D region, discussing experimental techniques, computations, RF impedance probes and formulas for ionospheric data derivation 03 p0334 A66-12643

Schumann resonances of Earth ionosphere cavity and excitation by lightning flashes 04 p0474 A66-13427

VLF radio wave propagation in Earth ionosphere waveguide assuming finite ground conductivity 04 p0475 A66-13429

Sporadic E layer characteristics according to data on ionospheric propagation at ultrashort wavelengths 04 p0514 A66-13445

Refractive index obtained from equation describing electromagnetic wave propagation in ionosphere 04 p0481 A66-13826

Magnetotonic splitting of radio signal in E and F layers, comparing calculated and theoretical gyrofrequency values 04 p0482 A66-13861

French FR-1 satellite for observation of ionized layers of atmosphere by propagation of VLF waves in ionosphere 04 p0586 A66-14385

Phase steps and amplitude fading of VLF signals at dawn and dusk, supposing two waveguide modes exist in dark part of path and one in daylight 05 p0632 A66-14838

Electromagnetic wave propagation in multimode Earth waveguides of variable height 05 p0632 A66-14839

Comments on Volland paper about analytical model of Earth-ionosphere waveguide supposedly agreeing with Austin radio transmission formula 05 p0632 A66-14840

Azimuthal propagation in nonuniform concentric cylindrical waveguide with application to Earth-ionosphere waveguide 06 p0835 A66-16978

Planar gap in plasma medium as idealized model for studying electromagnetic and plasma waves in plasma sheaths and

ionospheric layers 06 p0920 A66-17015

Linear demodulation of AM electromagnetic wave propagating through dispersive medium 06 p0836 A66-17033

/ionosphere/ Improved F-1 layer prediction system that can be used to predict maximum usable frequency /MUF/ for northern latitudes 07 p1000 A66-17213

Frequency-dependent ionospheric refraction effects on Doppler shift of satellite signals 08 p1181 A66-18714

Limiting frequencies of above-ground trajectories for ionospheric radio propagation, estimating attenuation and coverage of satellite radiation 08 p1186 A66-19789

Cylindrical and truncated cone-type metallic dipole antennas for reception of VLF, examining theory of behavior in ionosphere 09 p1340 A66-19847

Lower ionospheric characteristics determined by VLF radio waves propagated over long distances by multiple reflections between Earth and D region 09 p1370 A66-19979

Sporadic E signal strength calculator useful for estimating interference in UHF or HF communications 09 p1344 A66-20380

Ionospheric parameter measurements based on ground reception of radio signals broadcast from Elektron I satellite 09 p1377 A66-21003

Ionospheric focusing of extraterrestrial radio waves received by satellite antenna 10 p1496 A66-21120

Field produced at 100 km altitude by ground located VLF transmitter examined noting absorption, power propagation and propagation variation 10 p1526 A66-21127

High RF magnetotonic propagation effects on polarization scattering matrix 10 p1501 A66-21628

Diurnal phase variation of VLF signals propagated through Arctic polar cap as affected by solar plasma and associated ionospheric activity 11 p1657 A66-23107

Auroral zone, ionospheric scattering and nongreat-circle HF propagation statistically analyzed 11 p1700 A66-23140

Amplitude and phase velocity of electromagnetic waves in 1-30 kc range near Earth surface for plane and spherical Earth-ionosphere waveguide 12 p1817 A66-24278

Ionospheric effect of sudden magnetic storm eruption, noting propagation of disturbance above terrestrial surface 12 p1870 A66-24288

Long distance propagation of ultrashort radio waves by ionospheric scattering in subpolar region, noting graphs of signal level changes 12 p1817 A66-24290

Lower ionosphere guidance of HF and VHF waves for global communications, outlining computer simulation of phenomenon of whispering galleries 13 p2023 A66-25780

Scientific satellite FR-1 and VLF radio transmission 13 p2193 A66-26232

Skip distance and horizontal range of microwave propagation, assuming spherical Earth and ionosphere 13 p2028 A66-26235

Lower hybrid resonance in VLF range in satellites, noting noise emission due to trapping of electromagnetic wave propagation in transverse magnetic field 13 p2074 A66-26364

Sporadic E layer propagation and reflection of VHF signals 14 p2234 A66-26837

Sporadic E layer support of radio transmission by specular reflection and scattering 14 p2281 A66-26850

Doppler frequency changes in vertically incident and reflecting sounding wave associated with geomagnetic disturbances yields information on ionospheric electric field 14 p2234 A66-26856

Spatial selective fading as random process, discussing spatial coherence, wave number, dispersion profile, time delay profile, etc, in ionospheric propagation 14 p2234 A66-26858

VLF electromagnetic propagation parameter determination by field strength measurements over medium distances in ionosphere 14 p2235 A66-27130

Anomalous phase variations of GBR transmissions as received in New Zealand correlated with solar season and probably due to long path



- interference 14 p2237 A66-27401
- Field separation of ground transmitter into ordinary and extraordinary modes when traversing lower boundary of anisotropic ionosphere, noting effect of incidence angle, magnetic azimuth, etc, on energy dissipation of VLF ground wave 14 p2238 A66-27613
- Frequency deviations in carrier frequencies of ionospherically propagated HF radio waves produced by fluctuations in solar ionizing radiation 14 p2286 A66-27903
- Damping of longitudinal plasma waves emitted by artificial Earth satellite moving in ionosphere 14 p2345 A66-28089
- Radio emission in ionosphere during high solar activity explained as electron emission produced by particles moving as corpuscular fluxes 14 p2241 A66-28090
- Satellite emitted radio wave propagation mechanism based on radio wave paths in horizontally inhomogeneous spherically stratified ionosphere with variable electron density 15 p2447 A66-28492
- Radiation of prescribed polarization from cross-dipole antenna on aircraft carrier 15 p2447 A66-28570
- Low power long-range digital communications system based on narrow bandwidth portable transmitter and fixed station receiver 15 p2450 A66-28972
- Electron concentration inhomogeneities during traveling gravity wave propagation through F layer 15 p2485 A66-29084
- Frequency correlation of ionospheric radio waves in inhomogeneous thin layer medium and effect of irregular horizontal ionization gradients 15 p2451 A66-29111
- Delayed cyclotron pulse generation in topside ionosphere deduced from Alouette I data 15 p2452 A66-29678
- Naturally occurring electromagnetic radiation in audiofrequency range studied at Kiruna Geophysical Observatory 16 p2691 A66-30232
- Transmission loss in whistler mode of propagation of VLF radio waves for path propagation underneath ionosphere, using geometrical optics 16 p2652 A66-30709
- Propagation characteristics of whistler mode radio signal over one-hop path from transmitter magnetic conjugate point to far-away receiver, noting transmission loss 16 p2652 A66-30710
- Communication effectiveness over VLF paths impaired by variability of VLF field strength due to modal interference effects 16 p2653 A66-30723
- Phase variation of vlf radio waves received from NPG/NLK 16 p2653 A66-30799
- Occurrence percentage of spread F in world-wide maps drawn from ionosonde data during years of high and low sunspot numbers 16 p2696 A66-30818
- Alouette I satellite data on extraordinary wave resonance trace propagation along ionospheric magnetic field-aligned waveguide 16 p2697 A66-31001
- Ion motion effects on ionospheric radio wave propagation 17 p2917 A66-32306
- Frequency variation of ionospherically propagated radio waves by spectrum analysis of received signal 17 p2874 A66-32384
- Sonic diffraction mechanism used in tropospheric transhorizon propagation 17 p2876 A66-33361
- Coupled electromagnetic and electroacoustic wave propagation in inhomogeneous compressible plasma 18 p3069 A66-34089
- Equatorial transmission of geomagnetic micropulsations through ionosphere and lower exosphere below 2000 km altitude 18 p3107 A66-34526
- Flat Earth approximation of LF propagation theory 18 p3072 A66-34711
- Longitudinal propagation of superlow frequency electromagnetic waves through plane-laminar magnetoactive ionospheric plasma 19 p3296 A66-35298
- Radio wave guiding in horizontally stratified magnetoionic medium in which electron density varies monotonically with height 19 p3305 A66-36629
- Theoretical calculation of propagation path geometry of VHF aurora backscatter communications compared with experimental observations 19 p3306 A66-36653
- Hysteresis effect in ionospheric propagation indices studied by separating data concerning solar cycle portion with increasing solar activity from decreasing solar activity data 20 p3551 A66-37570
- Latitudinal variation of Pc-1 micropulsation propagation, examining attenuation by ionospheric F region duct that acts as waveguide for hydromagnetic waves 20 p3554 A66-38203
- Phase angle irregularities in scattering of ionospheric radio waves 20 p3521 A66-38357
- Limiting frequencies of above-ground trajectories for ionospheric radio propagation, estimating attenuation and coverage of satellite radiation 21 p3703 A66-38777
- Nonlinear modulation distortions of high power radio waves propagating in ionosphere, noting electron temperature increase from radio wave 22 p3861 A66-39647
- Whistler mode excitation in ionosphere by leakage from VLF guide-wave modes, noting nonreciprocal attenuation over north-south propagation path 22 p3863 A66-39932
- HF and VHF guided propagation in ionospheric whispering gallery treated by geometrical optics, emphasizing long-range paths between two terminals in ionosphere 22 p3863 A66-39933
- VLF radio wave propagation in model Earth-ionosphere waveguide of arbitrary height and finite surface impedance boundary 22 p3863 A66-39936
- Electron density measurements in D layer obtained, using LF radio wave propagating into ionosphere and rocketborne receivers 22 p3906 A66-39955
- Polarization characteristic variations of HF signal received over short-range ionospheric path, noting phase measurement of elliptically polarized wave components, using receiving dipoles 22 p3864 A66-40065
- Polar auroral radar system using ionospheric propagation effects for aspect sensitive backscatter 22 p3916 A66-40811
- Sunrise effect on amplitude of very-long-wave signal level 23 p4036 A66-41201
- Group velocity of wave packet propagating radially across plasma immersed in static axial magnetic field, examining ringing phenomena due to pulsed transmission 23 p4101 A66-41261
- Daily and seasonal variation of long distance propagation related to horizontal ionospheric gradients, particularly height of layer on wave path 24 p4174 A66-42739
- Electromagnetic structure of radioelectric whistlers, considering wavefront curvature in D layer, noting signal reception at two distant ground stations 24 p4176 A66-43001
- ### IONOSPHERIC REFLECTION
- Ionospheric irregularities and drift parameters deduced from fading records of second-order echoes of radiowave reflected vertically from ionosphere 01 p0022 A66-10160
- Minimum ionospheric electron density needed for radio reflection in D layer 01 p0031 A66-11037
- Polar aurorae as radar targets and calculation of ionospheric-tropospheric conditions for interpretation of radio observation results 02 p0189 A66-11343
- Relative backscatter coefficients for 16-mc backscatter from land and sea 02 p0190 A66-11472
- Focusing effects estimated for radio propagation along ricochet trajectory, considering ionospheric refraction 04 p0482 A66-13860
- Dense sporadic E cloud effects on high latitude HF backscatter observation 05 p0667 A66-14792
- Wave propagation for LF radio waves analogous to geometrical optics with path integral describing effects of Earth conductivity, curvature and reflection height 05 p0632 A66-14841
- Propagation between Earth and ionosphere up to 100 km of VLF radio waves sent by ground transmitter, calculating field pattern 05 p0672 A66-15041
- Time-dependent changes caused by fluctuations in tracking parameters in radio signals reflected from ionosphere or Moon and dispersed by troposphere 06 p0832 A66-16514
- HF radar search for effects of Earth satellites upon ionosphere, discussing reflection, perturbation and anomalies within F layer 08 p1213 A66-18751
- Ionospherically reflected backscattered radar pulse structure analyzed, using simplified geometry 09 p1341 A66-19867
- Motion of D region under daytime conditions 09 p1374 A66-20485
- Reception of LF signals by radio astronomy satellites, utilizing mathematical techniques for ray tracing in spherical ionosphere 11 p1651 A66-22367
- Excitation, internal reflection and limiting polarization of whistler waves in lower ionosphere, establishing reciprocity relation between incident waves from above and below 11 p1651 A66-22369
- Ground diffraction pattern caused by radio wave reflection from F region, using array of three aerials 11 p1651 A66-22374
- Antenna orientation effect on polarization components of radio waves reflected from ionosphere, noting occurrence and properties of magnetoionic component of polarization 12 p1869 A66-24273
- Ionospheric-plasma density determined by phase difference of incident waves on and reflected from plasma 12 p1870 A66-24284
- Parametric analysis of stability of reflection from sporadic E layer during 11-year solar cycle 12 p1870 A66-24287
- Polarization of atmospheric pulses due to successive reflections at ionosphere in echo type atmospherics 12 p1873 A66-24839
- Height of peaks of ionospheric layers using five-point Kelso analysis and single polynomial analysis 12 p1874 A66-24846
- Oscillations of vertical component of ionospheric refraction measured, using cliff radio interferometer and signals from satellites 13 p2020 A66-25223
- Continuous measurement of ionospheric winds based on observation of meteor trails 13 p2072 A66-25449
- Results of daily recordings of characteristics of some sporadic E layers, noting occurrence of layers as discontinuous succession of two types of structures 13 p2072 A66-25466
- Time-dependent changes caused by fluctuations in tracking parameters in radio signals reflected from ionosphere or Moon and dispersed by troposphere 13 p2024 A66-25954
- D-region electron distribution, collision frequency and amplitudes of partially reflected waves 13 p2075 A66-26739
- Ionospheric electron density profile and Schlomilch integral equation for oblique incidence 13 p2075 A66-26740
- Satellite-emitted short radio wave field intensity and ionospheric parameters 15 p2447 A66-28493
- VLF radio wave propagation in model Earth ionosphere waveguide with finite surface impedance and arbitrary height 15 p2449 A66-28598
- Fast phase fluctuations of signal reflected from F-2 layer 15 p2451 A66-29094
- Ionospheric D-region electron distributions in middle latitudes deduced from reflection of long radio waves 15 p2489 A66-29631
- Effect of meteor activity on fading of radiowave reflected from E region 16 p2692 A66-30331
- Complex refractive index of Earth surface and ionospheric Faraday effect measurements 17 p2873 A66-32200
- Phase observations of 20- and 60-khz signals received at different locations 17 p2875 A66-32535
- Variations in electron density with reflection of long waves in D region 17 p2918 A66-32878
- Altitude variations of frequencies and electron density with reflection in D region 17 p2919 A66-32879
- Backscatter returns from ionospheric sporadic E on sea and land 17 p2923 A66-33357
- Angular scattering of reflected radio waves from ionosphere, giving results of 300 cases 19 p3344 A66-35266
- Modification to theory of differential absorption experiment involving Fresnel reflection coefficient of ionospheric irregularities 20 p3555 A66-38209
- Collision effects on full-wave and ray-



optics virtual height computations for LF radio waves reflected from stratified ionosphere 20 p3521 A66-38360

Partial reflections utilizing different amplitudes of ordinary and extraordinary backscattered waves for electron number densities and collision frequency measurement in lowest ionosphere 22 p3906 A66-39949

Winter variability of electron number density and collision frequency in lower ionosphere measured, using partial reflection method 22 p3906 A66-39950

Electron density profile measurements in auroral zone D layer during quiet ionospheric conditions, using partial reflection method 22 p3906 A66-39951

Collision frequency gradient effect on weak partial reflections from ionosphere 22 p3906 A66-39952

Plasma lines caused by radar incoherent scattering from longitudinal electrostatic plasma oscillations in ionosphere 22 p3910 A66-39982

Statistical properties of phase and amplitude fluctuations during total reflection of waves from ionospheric layer 22 p3869 A66-40762

Reception of signals reflected from ionosphere in vertical radar probing, examining frequency-difference combinations 22 p3869 A66-40780

Auroral disturbances resulting in multipath distortion in propagation by ionospheric reflection and description of chirp ionosonde and antenna systems 23 p4036 A66-41143

Transmission curves for retrodiffusion echoes, identifying propagation modes and synthesizing equivalent vertical ionograms 23 p4063 A66-41182

Seasonal and diurnal fluctuation of radio wave in ionosphere in connection with fading process of reflected signal 24 p4204 A66-43155

Sporadic E layer reflection used to determine instrument constant in measuring radio wave absorption in ionosphere 24 p4205 A66-43156

Optimum communications working frequencies for F-2 layer reflection selected with aid of communications reliability function 24 p4176 A66-43160

**IONOSPHERIC SOUNDING**

**SA DORNIER PARAGLIDER ROCKET**

Oblique incidence sounding of ionosphere based on short wave scattering by Earth surface at Murmansk 01 p0065 A66-11168

Ionospheric, auroral and geomagnetic observation at Syowa Base, Antarctic 02 p0222 A66-11684

Computer processing of data obtained from panoramic vertical sounding of ionosphere to separate reliable portions of height-frequency characteristic from total 02 p0224 A66-12122

Positive system of recording ionospheric characteristics on ionosonde of automatic ionospheric station 02 p0232 A66-12144

Ionosphere and high latitude particles - COSPAR Symposium, Alpbach, Tirol, Austria, March 1964 03 p0361 A66-12639

Probe techniques in polar ionosphere covering cylindrical Langmuir, RF and mobility probes, Gerden condensers, error sources, techniques, etc 03 p0362 A66-12641

Ionospheric plasma density measurement utilizing variable frequency impedance probe, dispersive Doppler measurements and RF spectrometer field strength detection theory 03 p0398 A66-12644

Injun I and III particle observations discussing methods and results on fast electrons, particle counters, energy separation, spectra, flux variation, angular distributions, etc 03 p0363 A66-12647

Rocket and satellite methods for studying ionosphere 03 p0370 A66-12862

Electron energy spectrum during auroral absorption measured by Nike-Cajun analyzer 03 p0366 A66-12880

X-ray photograph confirmation in 1964 of solar brightness distribution derived from ionospheric observations during solar minimum in 1954 04 p0579 A66-14179

Ratio of ionospheric electron to ion temperature determined independently of spectral measurements, using electron

density data obtained with topside sounder 04 p0517 A66-14374

Ionospheric magnetic dipole transition, noting radiative transfer equation for atomic oxygen and nitric oxide 05 p0667 A66-14793

Admittance of short dipole antenna in ionosphere measured during rocket flights, deducing values of plasma frequency 05 p0669 A66-14945

Ionospheric diffusion probe determining ion and electron temperatures 05 p0674 A66-15112

Airborne ionospheric probes on both sides of magnetic equator at low African latitudes during equinoctial and solstice periods, obtaining daily behavior of F layer 05 p0674 A66-15113

Evaluation of sounding rockets for meteorology for 30 to 200-km altitude range, noting role in X and gamma ray detection, sporadic E layer, etc 07 p1140 A66-17610

Resonant effects theory observed by sounding equipment on ionospheric satellite Alouette 08 p1212 A66-18620

Geomagnetic and ionospheric observations of 1964 expedition of Zaria 08 p1214 A66-19041

Ionospheric triplet observation at low latitude by vertical sounding 08 p1214 A66-19051

Upper atmosphere sounding rocket program in increased space research activities in Australia 09 p1458 A66-20707

Space research activity in Denmark, discussing international cooperation and ionospheric sounding 09 p1458 A66-20712

Space and atmospheric research programs in Pakistan 09 p1459 A66-20720

Space research in Sweden including cosmic rays, aurora, radio astronomy, rocket sounding, etc 09 p1459 A66-20724

Correlation characteristics of signal reflection and magnetoionic components obtained in phase fluctuation measurements 11 p1696 A66-22414

Data on satellite orbits used for Earth figure, upper atmosphere density, solar radiation, etc 12 p1868 A66-23637

Enhanced ionization along midnight auroral zone during elementary geomagnetic disturbances 12 p1872 A66-24472

FR-1 French satellite, functions, structure and performance 13 p2192 A66-25493

Ionospheric station simultaneous observations of sporadic E layer critical frequency variations 13 p2073 A66-26236

Cross sections of geomagnetic field intensity and ionospheric characteristics obtained by airborne equipment crossings of geomagnetic dip equator 13 p2074 A66-26358

Oblique ionospheric sounding at medium-sweep frequencies, noting performance of chirp techniques 14 p2233 A66-26771

Plasma oscillation resonance phenomena of ionospheric antenna excitation near lower hybrid resonant frequency 14 p2340 A66-27127

Ringling phenomena in ionospheric magnetoplasma as evidenced by spikes on ionograms from Alouette satellite 14 p2283 A66-27513

Computer processing of data obtained from panoramic vertical sounding of ionosphere to separate reliable portions of height-frequency characteristic from total 14 p2287 A66-28081

Positive system of recording ionospheric characteristics on ionosonde of automatic ionospheric station 14 p2297 A66-28100

Soviet space research in 1965 including Moon and planets, magnetosphere, radiation belt, upper atmosphere, space vehicle dynamics, etc 15 p2599 A66-29897

Danish space program, emphasizing polar ionosphere and high energy primary cosmic radiation studies 15 p2601 A66-29936

Polar cap absorption observational results from ionospheric soundings, proton flares before 1956 and prediction for 1966-68 15 p2591 A66-30019

Impedance measurement of 39.5 meter tip-to-tip dipole antenna made during ionospheric rocket flight 15 p2469 A66-30046

Early results from topside sounder experiments in Alouette II satellite, presenting ionograms, plasma spike, electron number density and scale 15 p2496 A66-30075

Rocket borne ionospheric direct sounding instruments to measure ion and electron density, electron temperature, thermal electron energy distribution and space electric potential versus rocket potential 16 p2705 A66-30819

Ionospheric sounding using random diffusion of electromagnetic wave by ionospheric plasma with continuous wave through two separate antennas 16 p2653 A66-30953

Klystron transmitter for ionospheric diffusion soundings, noting method to obtain high stability in output power 16 p2661 A66-30954

Transmitting antenna of Cassegrain type, noting conical horn, primary and secondary mirror, etc 16 p2661 A66-30955

Geometrical characteristics of framework and reflecting surface of ionospheric diffusion probe antenna, noting specifications on design, manufacture, erection, alignment and adjustment 16 p2662 A66-30956

Receiver of ionospheric diffusion probe, noting radio telescope, low noise parametric amplifier, filters, signal detection, etc 16 p2662 A66-30957

Satellite signals wave polarization by ionosphere above 18 p3106 A66-34366

Antarctic Diffusion spectrum modifications due to positive ions collision with neutral particles, observed through ionospheric probe in E layer 19 p3346 A66-35590

Nitrogen temperature and density in thermosphere region from thermosphere probe data, examining inconsistency with satellite drag estimates 19 p3349 A66-36347

Ion temperature measurements around 1000 km altitude, using ion energy analyzer and mass spectrometer mounted on rocket 22 p3913 A66-40551

Relation between diurnal, seasonal and cyclic variations of stratifications in E layer and fine structure of sporadic E layer and E-2 layer 22 p3914 A66-40761

**IONOSPHERIC STORM**

**SA SUDDEN IONOSPHERIC DISTURBANCE /SID/**

MHD absorption of internal gravitational waves in ionospheric F layer in terms of traveling disturbances 02 p0283 A66-12116

Energy characteristics of ionospheric disturbances and nature of geomagnetic and ionospheric disturbances 02 p0284 A66-12117

Anomalous polar cap absorption during chromospheric flare of July 7, 1958 02 p0285 A66-12247

Ionospheric and polar-geomagnetic disturbance and PCA event on February 11, 1958 caused by solar flare 03 p0360 A66-12345

Effects connected with auroras and magnetic storms in lower ionosphere considering radio wave attenuation, cosmic ray absorption, etc 03 p0365 A66-12854

E-layer disturbances caused by particles, impinging upon atmosphere during auroras, noting ionization, X-rays and electrical conductivities 03 p0365 A66-12858

Continuous recording of CW transmission frequency M.S.F. Rugby permits study of effects of traveling ionospheric disturbances, on phase height of reflection levels of both magnetoionic components 04 p0488 A66-14379

Ionospheric magnetic perturbations at high latitudes of northern hemisphere during years of maximum solar activity 08 p1213 A66-19028

Ionospheric disturbances following geomagnetic sudden commencements propagating from two isolated locations in high latitudes which are conjugate points 08 p1216 A66-19214

Long-period acoustic-gravity waves launched into F region by Alaskan earthquake of March 28, 1964 08 p1219 A66-19418

Lower ionosphere ionization for quiet and disturbed Sun calculated for comparison of experimental and theoretical values for electron concentration and effective recombination 11 p1696 A66-22417

MHD absorption of internal gravitational waves in ionospheric F layer in terms of traveling disturbances 14 p2286 A66-28075

Energy characteristics of ionospheric disturbances and nature of geomagnetic and



- ionospheric disturbances 14 p2377 A66-28076  
Microbarographic analysis of troposphere-ionospheric storm relationship, ground level pressure fluctuations and polar region traveling pressure waves 17 p2920 A66-33088  
Initial disturbances in F-2 layer at middle altitudes during magnetic storms which begin with sudden commencement and relation to magnetic field 17 p2922 A66-33353  
Cosmic ray meson component distribution with time plots of particle flux revealed characteristic disturbances accompanying sudden commencements of geomagnetic storms associated with Forbush decreases 20 p3632 A66-38074  
Simultaneous long term ionospheric variation in midday averages of critical frequency E and F-2 at Washington, D.C. before and after increased geomagnetic activity 22 p3914 A66-40560  
Dependence of seasonal occurrence probability of F-zero layer on level of geomagnetic activity and ionospheric activity observed above 22 p3914 A66-40760  
Soviet book on high latitude research in field of geomagnetism and aeronomy including ionospheric storm, atmospheric absorption, etc 24 p4203 A66-43149  
Classification system of ionospheric storms by degree of anomalous absorption, average duration, gradual or sudden commencement, etc 24 p4204 A66-43154
- IONOSPHERIC TEMPERATURE**  
Ion distribution and temperature in topside ionosphere from plasma scale height profiles from Alouette electron density data 05 p0687 A66-14788  
Resonance radiation emitted by alkali cloud for ionospheric temperature measurement, considering multiple scattering and radiative transfer inside cloud 05 p0672 A66-15040  
Electron and ion temperatures in ionosphere show no temperature equilibrium in F region 06 p0877 A66-17171  
Ionospheric processes and measurement of variations in ion temperature and concentration using satellites, noting connection with magnetosphere 12 p1871 A66-24400  
Sounding rocket measurement of ionospheric electron temperature 15 p2494 A66-30043  
Neutral atmosphere reduces electron gas thermal conductivity below 200 km during both day and night 20 p3552 A66-37590  
E layer properties noting role of pressure, temperature, composition and recombination coefficient when varying with height and time 22 p3907 A66-39960  
Topside ionosphere constitution, examining electron and ion distribution, charged particle scale height, ion composition, electron and ion temperatures and magnetosphere 22 p3909 A66-39971  
VLF resonances in conjunction with topside sounder provide information about composition and temperature of terrestrial ionosphere 22 p3909 A66-39975  
Time dependent thermal behavior of ionospheric electron gas 22 p3913 A66-40552  
Nighttime electron temperatures in upper F region suggest corpuscular energy input 23 p4064 A66-41682  
Ion energy balance equation for ionosphere including effects of O, He, and H ions, thermoconductivity and cooling by atomic hydrogen and helium 24 p4198 A66-42431
- ISY**  
**S INTERNATIONAL QUIET SUN YEAR**  
/ISY/  
**IRAN**  
Space research activities in Iran 15 p2600 A66-29905
- IRIDIUM**  
Iridium coating for graphite oxidation protection at temperatures over 2000 degrees C 23 p4083 A66-41891
- IRON**  
Silicon and iron effects on embrittlement of cobalt-base alloy 01 p0085 A66-10357  
Asymmetric line near  $\lambda$  equals 2.00 of paramagnetic resonance spectrum of MgO powder as polycrystalline spectrum of ferric ions in cubic field 01 p0123 A66-10602  
Chemical reaction between iron and extreme pressure agents like chlorine and sulfur for corrosion mechanism analysis [ASLE PREPRINT 65-LC-11] 02 p0237 A66-12254  
Transition temperature dependence on thickness of superimposed films of iron and tin 03 p0407 A66-12323  
Heat conductivity measurement of solids at 200 to 1000 degrees C from radial thermal flux, specifically Armco iron and stainless steel 03 p0443 A66-12513  
Nature of interaction between titanium nitride and metals of iron, molybdenum and tungsten groups 04 p0535 A66-13436  
Fe and Mn variation in tektites, significance in identification of parent material 04 p0575 A66-13454  
Oxidation kinetics of tantalum-iron and tantalum-cobalt alloys and iron and cobalt at 500-900 degrees C 04 p0535 A66-13696  
Dissolution kinetics of iron filamentary single crystals in dilute acidic environments shown to obey Frank topographical theorems describing etch-rate anisotropy 07 p1107 A66-18412  
Calculation of intensity and polarization of forbidden lines of Fe XIII ion in solar corona in presence of nonradial magnetic field 08 p1287 A66-18640  
Specific heat of iron, cobalt and nickel in high temperature range measured, using quasi-adiabatic operating calorimeter 08 p1240 A66-19255  
Fe, Ni and Co in gallium arsenide determined by tunnel spectroscopy 08 p1278 A66-19624  
Compositional variations in thin evaporated nickel-iron films 10 p1577 A66-21555  
High energy subdivided walls origin in silicon-iron suggested by reverse domain nucleation 10 p1582 A66-21887  
Coercive force of single crystal iron films with two-axial magnetic anisotropy 11 p1754 A66-22817  
Linear heat conduction in metals with temperature-dependent physical properties and constant illumination 11 p1787 A66-23264  
Initial yielding characteristics of vacuum-melted iron as function of thermal history after slow cooling or quenching, noting interstitial segregation into grain boundaries 11 p1719 A66-23398  
Solubility of niobium carbide in gamma iron from carbon content of series of iron-niobium alloys equilibrated with hydrogen-methane mixtures 11 p1719 A66-23401  
Classification of iron VIII to XII and XIV lines in solar extreme UV spectrum and isoelectronic sequences from Ar to Ni 12 p1947 A66-23730  
Chemical reaction between iron and extreme pressure agents like chlorine and sulfur for corrosion mechanism analysis [ASLE PREPRINT 65-LC-11] 12 p1889 A66-24993  
Condensed nickel and iron films measured for tensile strength and microhardness 13 p2106 A66-25333  
Temperature dependence on Hall effect of thin iron layers 13 p2162 A66-25412  
Relation between angular dispersion and grain size in evaporated permalloy films 14 p2352 A66-26892  
Magnetostatic model for perpendicular anisotropy in polycrystalline nickel-iron thin films 14 p2352 A66-26893  
Anisotropic resistance in permalloy films based on imperfection orientation model 14 p2352 A66-26895  
Magnetostatic interaction effect on real and imaginary parts of transverse biased permeability in thin Ni-Fe films 14 p2352 A66-26896  
Lever mechanism for magnetization creep in nickel-iron thin films in longitudinal DC and transverse AC field 14 p2353 A66-26898  
Layered film of Cr and NiFe exhibit biased hysteresis loop in easy axis direction and asymmetric hysteresis loops in hard axis direction 14 p2353 A66-26901  
Anisotropy spectrum in nonmagnetostrictive permalloy films 14 p2353 A66-26902  
Uniaxial anisotropy field measurement for magnetic annealing of permalloy films 14 p2353 A66-26903  
Composition dependence of irradiation-induced uniaxial magnetic anisotropy energy of permalloy films 14 p2354 A66-26904  
Torsional strain sensitivity and absolute compositional analysis of permalloy films 14 p2354 A66-26905  
Magnetic torque and hysteresis loop measurements, examining exchange anisotropy in sulfided Fe films 14 p2354 A66-26907  
Magnetic properties of vacuum deposited iron nickel films 14 p2354 A66-26908  
Bias-sputtering of nickel-iron thin films for memory elements 14 p2354 A66-26909  
Positive and negative NiFe magnetostriction film exhibits striped domain when evaporated at oblique incidence 14 p2355 A66-26912  
Temperature dependence of Hall emf and electrical resistance of Sendust type Fe-Si-Al alloys 15 p2560 A66-28678  
Zero magnetic field millimeter maser using trivalent iron ion in host crystalline structure of rutile /titanium dioxide/ as active material 15 p2514 A66-29018  
Temperature dependences of coercive force, hysteresis loops and domain structure of thin iron-gadolinium alloy films 16 p2774 A66-30698  
Domain structure and hysteresis loops of thin iron-gadolinium films of different thicknesses 16 p2775 A66-30699  
Mechanical behavior of polycrystalline iron and single crystal molybdenum in compression over various strain rate ranges, noting temperature role 16 p2724 A66-31264  
Copper and Armco iron structural defects during cyclic deformation studied by electron-microscope and optical-microscope techniques 16 p2727 A66-31528  
Paramagnetic iron and chromium ion impurities effect on absorption spectrum and microhardness of rutile single crystals 16 p2786 A66-31733  
Compactibility of iron, stainless steel and titanium powder of various dispersity and bulk density 17 p2940 A66-32847  
Fe, Ni and Co in gallium arsenide determined by tunnel spectroscopy 17 p2984 A66-33138  
Energy gaps of Ag-Sn, Fe-Sn and Sn film studied by electron tunneling method for various temperatures 18 p3156 A66-34474  
Silicon, iron and nickel in solar corona determined by method of Pottasch 18 p3233 A66-34575  
Spectral analysis methods used to calculate iron abundance in solar corona 18 p3233 A66-34577  
Iron and nickel lines in solar UV spectrum, abundance of various metallic elements in solar atmosphere, electron collision cross sections and oscillator f-values of electron transitions 18 p3237 A66-35050  
Powder iron compact properties evaluated by sonic tests, noting elastic modulus dependence on porosity 19 p3376 A66-35328  
Second Born and Born-exchange approximations used in calculation of ionization cross sections for Fe XV and Fe XVI 19 p3403 A66-36325  
Nature of interaction between titanium nitride and metals of iron, molybdenum and tungsten groups 20 p3586 A66-38138  
Oblique detonation impacts in pentolite on iron treated by methods of plane steady compressible flow, discussing regular and shock Mach reflection and expansion 21 p3727 A66-39172  
Electric resistance of amorphous iron films, noting film structure dependence on evaporation parameters 23 p4110 A66-41138  
Temperature homogenization effect on structure of industrial aluminum, determining mechanical properties dependency on Fe/Si ratio 23 p4081 A66-41403
- IRON ALLOY**  
**SA PERMALLOY**  
**SA STEEL**  
Graphite content effect on antifriction properties of graphitized nickel-based copper and iron alloys 01 p0087 A66-10745  
Polycrystalline niobium elastic properties and effects of alloying with chromium and iron 03 p0383 A66-13128  
Decay of K-state in Ni-Cr, Ni-Cr-Mo and Fe-Ni-Cr-Mo alloys studied in terms of electric conductivity during plastic



deformation 06 p0896 A66-16606  
 Phase work hardening of austenitic Fe-Ni alloys in phase transformation 06 p0896 A66-16607  
 process 06 p0896 A66-16607  
 Martensitic transformation kinetics and maraging mechanisms in Fe-Mn-Ni-Ti alloy observed by electron and X-ray diffraction 08 p1236 A66-18762  
 Iron and nickel concentrations effect on composition, quality and current yield of electrodeposition of titanium from aqueous solutions 08 p1229 A66-18794  
 Perpendicular anisotropy of Ni and Fe films and saturation magnetization under various pressures 08 p1270 A66-19011  
 Structural change effects on plasticity and fracture characteristics on iron alloys with annealing 11 p1716 A66-22745  
 Crystalline structure and magnetic properties of single-crystal films of iron-nickel alloys, for application as memory elements of computers 11 p1753 A66-22807  
 Induced anisotropy of ferromagnetic atom pairs and magnetostriction stresses in Fe-Ni thin films subject to annealing 11 p1755 A66-22818  
 Creep behavior in Ni-Fe alloys at high temperatures, using one composition inside ordered regions and another 11 p1717 A66-22993  
 Age hardening response correlated with structural observations of iron-nickel-cobalt alloys 12 p1895 A66-24374  
 Effect of preparation conditions on formation of carbide phases in iron-carbon thin films, using vacuum condensation 12 p1933 A66-25025  
 Magnetoresistance effect applied to Rotatable Initial Susceptibility II films, explaining resulting hysteresis loops and torque curves 13 p2161 A66-25183  
 Age-hardening of Fe-Ni-Ti alloy martensite associated with formation of ordered Ni-Ti phase 13 p2106 A66-25331  
 Martensitic transformation of Ni-Fe alloy from fcc to bcc lattice, noting stress produced by chemical free energy difference between austenite and martensite structure 15 p2520 A66-28649  
 Trace element effect on lifetime of iron-chromium-aluminum heat-resisting alloy 16 p2723 A66-30311  
 Grain growth from solution precipitation and grain coalescence in liquid phase sintering of W-Ni-Fe and W-Ni-Cu alloys 17 p2939 A66-32393  
 Element distribution in cermet alloys of W-Ni-Fe system determined by X-ray spectral analysis 17 p2940 A66-32848  
 Structural transformations in alnico alloy with titanium studied by X-ray 18 p3123 A66-34401  
 Graphite content effect on antifriction properties of graphitized nickel-based copper and iron alloys 18 p3117 A66-34981  
 Characteristic microstresses in plastically deformed iron and aluminum alloy under tensile testing studied by X-ray techniques 19 p3376 A66-35400  
 Plessite composition and texture, discussing possible origin in terms of meteorite thermal history 19 p3460 A66-35732  
 Phase separation from tempering of martensite in iron-nickel alloys with aluminum additions 19 p3386 A66-36426  
 Phase and chemical compositions of structural components forming in iron-nickel-chromium alloys with aluminum and titanium content 22 p3936 A66-40787  
 Magnetic transformation and effect of plastic strain on shear modulus of Fe-Cr-Ni alloys 24 p4227 A66-42310  
 Alpha and gamma solubility limits in Fe-Ni phase diagram at temperatures above 500 degrees C, using quench-and-anneal and diffusion-couple techniques and electron probe microanalyzer 24 p4227 A66-42365  
**IRON COMPOUND**  
**SA FERRITE**  
 Mariner IV observations of Mars surface, showing no detectable magnetic field or radiation belts, suggest iron on surface oxidized from photodissociation of water vapor 10 p1606 A66-21211  
 Sublimation rate of iron fluoride and identification of vapor species by Knudsen technique, using mass spectrometer 11 p1651 A66-23413

Iron selenides of nickel arsenide structure analyzed, noting dependence of semiconductor characteristics on iron gap arrangements 13 p2164 A66-25471  
 Paleogenetic study of ferredoxin structure, reconstructing evolution from amino acid sequence 14 p2228 A66-27810  
 Niobium dissolution kinetics in iron carbide 19 p3386 A66-36447  
 Microwave energy attenuation by dissipative material consisting of epoxy resin loaded with fine powder of iron carbonyl 20 p3587 A66-37585  
 Properties of ferrous ion in iron germanium oxide studied in terms of Mossbauer effect and susceptibility measurements 20 p3621 A66-37823  
 Kinetic energy causing anomalous increase in thermoelectric power in semiconducting p-type iron-chromium sulfide near Curie temperature 21 p3803 A66-39261

**IRON METEORITE**

Gallium concentrations in iron phases of several chondritic meteorites 02 p0290 A66-11962  
 Cl 36 in stony meteorites produced by spallation reactions and neutron capture 04 p0579 A66-14318  
 Rare gas measurements in iron meteorites and troilite and schreibersite inclusions, using mass spectrometer 04 p0580 A66-14484  
 Cosmic ray induced lithium and calcium in iron meteorites by improved technique of potassium isotope 04 p0580 A66-14487  
 Isostructural and jadeite mineral called ureyite found as rare emerald-green grains in iron meteorites Coahuila, Toluca and Hex River Mountains 05 p0674 A66-15197  
 Mineral content and structure of graphite and sulfide inclusions in iron meteorites measured by reflected light and microprobe 06 p0952 A66-15940  
 Concentration gradients in meteoritic kamacite predicted from Fe-Ni phase diagram and diffusion 06 p0955 A66-16787  
 Strontium-rubidium age of iron meteorite 07 p1132 A66-17234  
 Discovery of new fragments of typical iron meteorite near Wolf Creek, Australia 07 p1133 A66-17457  
 Low-background gamma-ray spectrometry of induced radioactivity resulting from Bogou meteorite cosmic radiation 08 p1291 A66-19094  
 Polyminal contents of globular and elongated nodules in Odessa iron meteorite 08 p1292 A66-19259  
 Radionuclide production in iron targets bombarded with 400-mev protons investigated by Monte Carlo method for cosmic ray effects on meteorites 11 p1775 A66-23145  
 Iron meteorites with low cosmic ray exposure ages examined via analysis of product of argon 39 and 38 13 p2177 A66-25135  
 Aerodynamic heating of ferrous Santa Catharina meteorite 14 p2381 A66-27350  
 Iron and stony meteorite evolution, cosmic radiation ages and space erosion model 14 p2390 A66-28409  
 Fe-Ni-P system and structure of iron meteorites 15 p2603 A66-29967  
 X-ray diffraction study of minerals from shocked iron meteorites 16 p2803 A66-31014  
 Ferrous /manganous/ orthophosphates, sarcoside and grafitonite found in four iron and pallasite meteorites 16 p2803 A66-31221  
 Isotopic abundance and content used to trace history of 20 iron and stony meteorites 16 p2803 A66-31223  
 Mass spectrometric measurement of distribution of spallation produced chromium nuclides between alloys in iron meteorite 17 p3007 A66-33282  
 Isotopic composition of silver in Canyon Diablo iron meteorite 18 p3228 A66-34017  
 Cosmic ray produced lithium and calcium in iron meteorites 18 p3236 A66-34890  
 Radiation age of 74 iron meteorites estimated from content of cosmogenic isotopes Ga and Ge 19 p3456 A66-35361  
 Determination of constancy of cosmic radiation and of terrestrial and cosmic ages of ferrous meteorites by radioactivity of Al 26 and Be 10 20 p3651 A66-37411

Widmanstätten patterns for electrolytic dissolution of iron meteorites and separation of nonmetallic portions, particularly kamacite 21 p3816 A66-39493  
 Butler iron meteorite composition, noting unusually high cobalt and germanium content and low cooling rate 22 p3978 A66-40013  
 Butler iron meteorite composition, noting very high concentration of germanium, gallium and nickel exhibiting Widmanstätten pattern 22 p3978 A66-40014  
 Revision of Levin average value of accommodation coefficient K for iron meteoric bodies 22 p3984 A66-40783  
 Shield of volatile matter acting as cosmic radiation barrier as possible explanation of contraction between radiation ages of stony and iron meteorites 23 p4065 A66-41832

**IRON OXIDE**

Electrical properties of alpha ferric oxide containing magnesium, noting temperature effect, carrier concentration, conductivity variations, etc 08 p1271 A66-19221  
 Structure and properties of intermediate components of iron-oxide-germanium-oxide system analyzed, using heat treatment 13 p2162 A66-25355  
 Combustion behavior of aluminum-ferric oxide thermite with aluminum oxide additions used as combustion model for involatile condensed systems 18 p3259 A66-33718  
 Mossbauer, X-ray and magnetic measurements of wustite structural and magnetic decomposition properties 20 p3623 A66-38391

**IRRADIATION****SA PROTON IRRADIATION****SA X-RAY IRRADIATION**

Free radical reactions in irradiation of model systems and role of radicals in radiation damage 13 p2010 A66-26227  
 Conversion of 2-formyl dienone III into dienone IV upon irradiation in acetic acid followed by base-catalyzed deformation of crude photoproduct 15 p2446 A66-28873  
 Generation recombination noise in Ge single crystals under fast neutron irradiation, using reversible technique to vary noise parameters 16 p2778 A66-31072  
 Irradiation system for experiments with Plum Brook Reactor in nuclear rocket program, noting cryogenic system, dynamic testing, etc 17 p2956 A66-32045  
 Thermal neutron irradiation effect on superconducting properties of niobium aluminum and vanadium silicide doped with fissionable impurities 17 p2979 A66-32630  
 Oxygen defect complexes in neutron irradiated germanium 17 p2980 A66-32647  
 Silicon IR absorption spectra at various wavelengths before and after irradiation with neutron fluxes 19 p3442 A66-35821  
 Q-switch pulsed ruby laser irradiation-induced chemical dissociation and ionization in residual gases 23 p4079 A66-42076  
 2-carboxy-3-keto-9-methyl hexahydronaphthalene converted in high yield into 5/7 fused products on irradiation in aqueous and nonaqueous media 24 p4171 A66-43101

**IRREVERSIBLE PROCESS**

Text on theory of heat and mass transfer from viewpoint of thermodynamics of irreversible processes 01 p0161 A66-10237  
 Irreversible tempering brittleness of spring steel with Mn, Cr, Si and C 01 p0086 A66-10452  
 Heat and mass transfer treated by thermodynamics of irreversible processes 01 p0162 A66-10623  
 Parameters of internal heat and mass transfer determined from temperature and moisture content measurements and using characteristic function of irreversible thermodynamics 01 p0162 A66-10624  
 Molecular transfer equations derived on basis of irreversible thermodynamics and law of conservation of matter 01 p0163 A66-10625  
 Heat and mass transfer in nonuniform gas-suspension flow treated by irreversible thermodynamics 01 p0163 A66-10628  
 Nonequilibrium thermodynamics applied to problem of solid carrying electric and heat currents in presence of external magnetic field



ASME PAPER 65-HT-1] 05 p0782 A66-14732  
Kinetic equations of complex reactions  
derived, using conical graphs, reducing  
reversible reaction problems to problems of  
irreversible kinetics 06 p0822 A66-16544  
Nonequilibrium thermodynamics applied to  
problem of solid carrying electric and heat  
currents in presence of external magnetic  
field  
ASME PAPER 65-HT-1] 11 p1785 A66-22186  
Generalized form of variational principle  
for minimum dissipation of energy applied  
to anisotropic thermal conductivity  
formulation 11 p1788 A66-23448  
Thermodynamics of irreversible processes  
applied to continuum mechanics, deriving  
classical rheological  
equations 12 p1976 A66-23546  
Two branches of fluctuation theory,  
conventional thermostatics or equilibrium  
statistical mechanics and time-dependent  
correlation functions 12 p1976 A66-23553  
Variational calculus methods for convective  
heat transfer to nonhomogeneous fluids and  
fluids with thermal  
expansion 12 p1979 A66-24817  
Heat and mass transfer phenomena  
analyzed, using thermodynamics of  
irreversible processes and incorporating  
certain particular data of kinetic and  
statistical theories 12 p1980 A66-24910  
Irreversible form of chemisorption by  
semiconductor as affected by volume  
impurity and reaction with  
chemisorbate 13 p2017 A66-25696  
Relativistic hydrothermodynamics in  
covariant form for simple viscous fluid,  
omitting infinite heat conduction velocity  
and instantaneous diffusion flux theory from  
treatment of Eckart 13 p2210 A66-26333  
Heat and mass transfer treated by  
thermodynamics of irreversible  
processes 14 p2416 A66-28486  
Second law of thermodynamics, discussing  
Clausius and Boltzmann mathematical  
expressions of entropy, role of  
irreversibility and relationship between  
increase of entropy and increase of  
disorder 15 p2616 A66-29062  
Planck entropy equation and irreversibility  
of radiation matter interaction for stationary  
isothermal gas emitting resonance lines of  
two-level atoms 17 p2957 A66-32044  
Nonisothermal deformation of viscoelastic  
medium analyzed on basis of  
thermodynamically irreversible  
processes 20 p3671 A66-38112  
Thermodynamics of irreversible processes  
methods applied to stress-strain relations of  
single-phase nonelastic continuous  
medium 21 p3830 A66-38986  
Solution to chain of kinetic gas equations,  
showing effect of fast reversible and slow  
irreversible processes on particle  
distribution function 21 p3771 A66-39248  
Irreversible thermodynamics of large  
viscoelastic deformations, showing hidden  
coordinates as scalar functionals and  
applicability to quasi-equilibrium  
states 22 p3999 A66-40456  
Generalized strain and transition concepts  
for elastic-plastic deformation creep and  
relaxation 23 p4144 A66-41973  
Inequality, derived from entropy law, for  
irreversible processes of nonequilibrium  
thermodynamics, with attention to  
viscoelastic materials 24 p4293 A66-42136  
Stress-strain temperature equations and  
energy equation with heat conduction for  
isotropic nonlinear viscoelastic materials,  
using irreversible  
thermodynamics 24 p4289 A66-42280  
ROTATIONAL FLOW  
Maximum friction along jet path in mixing  
zone at constant pressure applied in finding  
irrotational wall velocity 13 p2063 A66-25468  
Potential complex and forces in perfect  
incompressible fluid at rest at infinity with  
free vortices determined by pointless  
profiles excited by arbitrary  
motion 15 p2479 A66-29637  
SCHEMIA  
Effect of head-to-foot accelerations of up  
to 10 g on rabbits, noting changes in ECG,  
EEG, brain histology, etc, leading to  
ischemic conditions 18 p3060 A66-34408  
ENTROPIC PROCESS  
Isentropic expansion of argon plasma in

Laval nozzle, discussing parallel flow  
parameters, frozen flow, thermodynamic  
equilibrium, energy balance,  
etc 05 p0720 A66-14509  
Self-similarity of solutions to motion  
equations for relativistic gas possessing  
point symmetry and nonexistence of  
isentropic flow 06 p0954 A66-16538  
Approximate methods for integration of  
equations of plane isentropic motion of gas  
at supersonic velocities 08 p1165 A66-19572  
Polytropic technique for gas turbine  
performance, prediction and evaluation,  
noting use of sophistication factor  
[SAE PAPER 660161] 09 p1434 A66-20161  
Inviscid flow of compressible conducting  
gas with aligned magnetic field through  
axially symmetric Laval nozzle in various  
transition regions 11 p1636 A66-23256  
Analytic design of turbine blades based on  
inviscid isentropic supersonic vortex flow  
theory and performance in  
cascades 12 p1796 A66-23800  
Nonrelativistic force in simple  
magnetizable fluid derived from  
thermodynamic information about energy  
and power 12 p1915 A66-24651  
Incompressible fluid static thrust  
augmentation devices for aircraft propulsion  
for cases of presence and absence of heat  
and work exchange  
[ASME PAPER 66-GT-116] 14 p2373 A66-27008  
Circumventing turbine inlet temperature  
limitation of gas turbines by direct fluid-to-  
fluid energy exchanger, using isentropic  
compression waves to avoid shock losses  
[ASME PAPER 66-GT-117] 14 p2373 A66-27009  
Self-similarity of solutions to motion  
equations for relativistic gas possessing  
point symmetry and nonexistence of  
isentropic flow 15 p2603 A66-29978  
Supersonic diffuser for eliminating  
separation of boundary layer in isentropic  
compression 19 p3276 A66-36084  
Isentropic two-dimensional nonstationary  
flow of polytropic gas adjoining region with  
quiescent gas, constructing approximate  
picture of motion near arbitrary  
discontinuities 24 p4195 A66-42723  
Argon entropy diagram calculation from  
sound velocity data and P-V-T  
relation 24 p4238 A66-42887  
ISIS SATELLITE  
Canadian ISIS program for launching of  
satellites containing enough instrumentation  
to measure all ionospheric parameters  
simultaneously 24 p4283 A66-42696  
ISLAND  
Optical absorption of island films of gold  
as function of island density obtained from  
electron micrographs and film  
thickness 19 p3435 A66-35416  
ISOBAR  
Isotherms and isobars for polymer liquids  
using corresponding states principle to  
establish function describing dependence of  
internal pressure on volume or  
temperature 18 p3124 A66-33692  
ISOBUTYLENE  
SA POLYISOBUTYLENE  
Pressure drop as function of flow rate for  
helical flow of non-Newtonian  
polyisobutylene solution 15 p2477 A66-28615  
ISOCYANATE  
Phosgenation procedure for synthesis of  
carbon-14 labeled isocyanates, noting isotope  
distribution in  
compounds 14 p2231 A66-26871  
ISOLATION  
SA SOCIAL ISOLATION  
Disorientation, time perception and  
isolation 11 p1642 A66-22487  
Matrix equations of rigid-body motion for  
general vibration isolation system, analyzing  
conditions for decoupling translational and  
rotational motions 21 p3770 A66-38650  
Transmissibility, isolator mass effects,  
vibration source and receiver characteristics  
for HF vibration isolation  
problem 24 p4291 A66-42860  
ISOLATOR  
Spacecraft sterilization problem using  
gnotobiotic techniques and isolators, noting  
peracetic acid role and hot wire techniques  
for insertions 13 p2014 A66-25289  
Damping constant of electromagnetic wave

in plane parallel waveguide with ferrite  
resonant isolator, using perturbation theory,  
considering dielectric and magnetic  
losses 14 p2250 A66-27143  
Ferromagnetic microwave resonance  
isolators for use in  
waveguides 15 p2459 A66-28936  
Change in ferrite transverse dimensions,  
examining effect on variable-field isolator  
performance in X-band 15 p2565 A66-29059  
ISOMER  
SA TAUTOMER  
High sensitivity optical resolution of amine  
diastereoisomers by gas liquid  
chromatography 17 p2869 A66-31873  
GLC-mass spectrometric stereoisomer  
discrimination as means of detecting  
biological processes 18 p3059 A66-34372  
Gas liquid chromatography resolution of  
racemic hydroxy and beta-mercapto-amino  
acids involving suitable derivation of  
functional group 20 p3510 A66-37606  
Optical resolution and absolute  
configuration of trans-beta-phenylglycidic  
acid 21 p3702 A66-38449  
ISOMERIZATION  
Rates and activation parameters  
determined from nuclear magnetic  
resonance spectra for degenerate  
isomerizations of disubstituted benzofuran  
oxides 05 p0629 A66-15155  
Master equation for intramolecular  
relaxation processes, with application to  
internal vibrational relaxation and  
isomerization reactions 06 p0911 A66-16170  
Conversion of 2-carboxy-3-keto-9-methyl-  
unsubstituted hexahydronaphtalene into 5/7-  
fused products on irradiation in aqueous and  
nonaqueous media, observing photochemical  
rearrangements 24 p4170 A66-42314  
ISOPHOTE  
Mapping 6300 angstrom airglow isophotes  
from observations of scanning photometer at  
Haleakala, Hawaii 17 p2918 A66-32534  
Profiles of isophotes and relative  
intensities for Aristarchus region of Moon  
taken during total eclipse on December 19,  
1964 18 p3237 A66-35048  
Comet disintegration as basic source of  
interplanetary dust based on zodiacal  
isophotes 20 p3549 A66-37037  
ISOPROTENOL  
S ADRENERGICS  
ISOSTATIC PRESSURE  
Statics and kinematics of rigid bodies in  
structural mechanics, establishing isostatic  
support conditions 03 p0436 A66-12733  
ISOTHERM  
Isotherms and isobars for polymer liquids  
using corresponding states principle to  
establish function describing dependence of  
internal pressure on volume or  
temperature 18 p3124 A66-33692  
ISOTHERMAL FLOW  
Interaction or coupling of radiation with  
conduction and convection mechanisms in  
nonisothermal nongray gas flowing in  
entrance region of tube with isothermal  
black walls  
[AIAA PAPER 66-136] 06 p0875 A66-17090  
Superfluid critical velocity in He 2  
isothermal gravitational flow in narrow  
channels 09 p1366 A66-20018  
Critical velocities and supercritical velocity  
dissipation effects in isothermal flow of  
liquid He 2 in narrow  
channels 09 p1366 A66-20019  
Exact solutions for triple wave type  
hydrodynamic equations for confined  
isothermic gas flow and polytropic gas  
efflux into vacuum 12 p1863 A66-24360  
ISOTHERMAL LAYER  
Turbulent velocity fluctuation field in  
isothermal boundary layer with  
homogeneous injection and combustion  
[AIAA PAPER 65-820] 04 p0510 A66-13689  
First-order perturbation analysis of free  
convection of liquid metal from isothermal  
vertical finite plate extended to uniform  
heat flux 10 p1619 A66-21054  
Surface boundary layer charge of  
isothermal atmosphere of fully ionized  
equilibrium plasma in gravitational  
field 10 p1609 A66-21813  
Justification for multiple isothermal layer  
approximation to real atmospheric acoustic-  
gravity wave propagation 14 p2234 A66-26857  
Internal atmospheric gravity waves in



isothermal medium, solving hydrodynamic equations, determining wave propagation in realistic atmosphere for range of wave parameters, wind amplitude, reflected energy, etc 20 p3554 A66-38202

## ISOTHERMAL PROCESS

Statistical behavior of reacting mixture in incompressible isotropic turbulence when reaction rate is quadratic function of local concentration of reactant, using Kraichnan direct interaction hypothesis [ATAA PAPER 65-812] 03 p0358 A66-13180

Practical Philips cycle for low temperature refrigeration, noting equal coefficient of performance to that of ideal Carnot cycle under isothermal 09 p1472 A66-20879

Decaying second-order isothermal reaction in limit of homogeneous turbulence in final period of decay 10 p1496 A66-21828

Compact Ackeret-Keller closed cycle thermodynamic nuclear turbine power plant [ASME PAPER 66-GT/CLC-6] 14 p2329 A66-26980

Mutual reactions occurring between various allotropic forms of TA6A during isothermal treatments of austenitized beta alloy 17 p2939 A66-32327

Steady isothermal motion of viscous gas between outer fixed sphere and eccentrically located rotating inner sphere 19 p3371 A66-36481

Boundary value problem for isothermal unidirectional deformation of hyperelastic material applied to inflation of thick walled sphere 22 p3988 A66-39673

## ISOTOPE

SA BERYLLIUM 10

SA DEUTERIUM

SA NUCLEAR ISOTOPE

MONOPROPELLANT

SA RADIOACTIVE ISOTOPE

SA TRITIUM

Mass spectrometry of positive ion beam produced by nonmagnetic emitter, using electron beam passing through electrostatic field for rare isotope analysis 03 p0397 A66-12391

Holbrook meteorite discussing abundance of lithium isotopes, measurement techniques, apparatus, and concentration pattern over surface 03 p0429 A66-13268

Cohen theory of square cascades and countercurrent separation processes for thermal diffusion columns 04 p0598 A66-14317

Performance of thermal diffusion columns studied for limits of validity of theory of isotopic mixtures in case of mixtures of gases 04 p0598 A66-14325

Isotopic ratios and location of light primordial rare gases in stony meteorites and correlation with diffusion coefficients 04 p0580 A66-14482

Rare gas measurements in iron meteorites and troilite and schreibersite inclusions, using mass spectrometer 04 p0580 A66-14484

Potassium content and K-A ages of 18 amphoterite chondrites determined from isotope dilution technique 04 p0580 A66-14486

Cosmic ray induced lithium and calcium in iron meteorites by improved technique of potassium isotope detection 04 p0580 A66-14487

Separation of gases from isotopes in compression shock produced in expanding gas flow past obstruction, dependent on gas density and hydrokinetic properties of components 06 p0875 A66-17052

Isotope shift, linewidth and precise wavelength of laser emission in ionized Hg 07 p1044 A66-18035

Critical magnetic field curves of superconducting Ru isotopes and dependence of superconducting transition temperature on isotopic mass 07 p1109 A66-18443

Electromagnetic isotope separators used in nuclear physics for analysis of ion-matter interaction 08 p1257 A66-18694

Low temperature chromatographic separation of hydrogen isotopes based on interaction with alumina surface electric fields 11 p1650 A66-23209

Mass spectrometry of positive ion beam produced by nonmagnetic emitter, using electron beam passing through electrostatic

field for rare isotope

analysis 13 p2139 A66-25397

Rare gas concentrations and isotopic compositions in Khor Temiki meteorite 13 p2186 A66-25877

Capillary viscosity meter measurements of hydrogen-deuterium solutions 13 p2114 A66-25970

Telescopic measurements of primary energy spectra and abundances of He 3 and He 4 in galactic cosmic radiation 16 p2793 A66-30198

Isotopic abundance and content used to trace history of 20 iron and stony meteorites 16 p2803 A66-31223

Angular distributions of elastic and inelastic alpha-particle scattering in even tin isotopes, using 40 mev alpha beam 18 p3138 A66-34166

Isotopic changes in materials caused by high energy nuclear active particles and solar wind in interplanetary space and on Earth 18 p3176 A66-34750

Abundance of isotopic helium 3 nuclei in primary cosmic radiation, using nuclear emulsion stack 18 p3189 A66-34828

Tracks of nuclei of primary cosmic rays that ended within nuclear emulsions and possibility of separating isotopes 18 p3192 A66-34842

Relative abundance of carbon isotopes in primary cosmic radiation estimated by separation of isotopes method in nuclear emulsion 18 p3192 A66-34843

Balloon-borne scintillation counter measurements of isotopic composition, energy/nucleon and rigidity spectra of primary cosmic helium nuclei 18 p3193 A66-34848

Isotopic composition of xenon extracted from Ca-poor achondrites, noting relation between enstatite achondrites and enstatite chondrites 22 p3983 A66-40558

Isotopic composition of Xe indicates that two Ca-rich achondrites comprise group of diopside-olivine achondritic meteorites containing fission-produced Xe 24 p4264 A66-42606

## ISOTOPE SHIFT

Isotopic volume shift in X-ray molybdenum K alpha 1 line 01 p0084 A66-10255

Isotopic shift in components of five even ytterbium isotopes measured on ten spectral lines of neutral and ionized atom 09 p1431 A66-20938

Isotope shift measurement for 6328 angstroms helium-neon laser transition 10 p1540 A66-21070

Isotopic volume shift in X-ray molybdenum K alpha 1 line 13 p2110 A66-25972

Isotopic shift in components of five even ytterbium isotopes measured on ten spectral lines of neutral and ionized atom 15 p2557 A66-28527

Spectroscopic analysis of isotope shift between tetraborane /10/ and pentaborane /11/ 15 p2446 A66-29236

Isotope shifts and Fermi resonance role in carbon dioxide IR laser 16 p2716 A66-30176

Solar nucleosynthesis of extinct isotopic iodine, noting incorporation of Nakhilite meteorite material and subsequent decay into fissionogenic xenon 18 p3225 A66-33623

Isotope shifts for zero-phonon absorption lines associated with radiation induced color centers in lithium fluoride single crystals 18 p3154 A66-33921

Generically related cosmic ray spectrum explaining variations in abundance ratios of helium isotopes and light to medium elements in terms of solar and geomagnetic modulation 18 p3178 A66-34758

He-3-He-4 isotopic composition of primary cosmic ray helium flux in terms of energy, rigidity and solar modulation 18 p3192 A66-34841

Intracavity interferometer laser measurements of power gain and output in single-frequency Ar laser and 6328-angstrom Ne isotope shift 22 p3932 A66-40110

Homogeneous isotopic exchange reaction between hydrogen and deuterium in single-pulse shock tube with excess argon 22 p3860 A66-40902

## ISOTROPIC MEDIUM

Longitudinal elastic wave of finite amplitude propagation in isotropic solid 01 p0057 A66-10421

Electromagnetic wave propagation through multilayer isotropic and anisotropic structure 01 p0025 A66-10525

Approximate solution of principal boundary value problem of electrostatics 02 p0262 A66-12246

Shock waves in elasticity discussing upstream, downstream and Lagrange coordinate-related configurations, propagation conditions in isotropic medium and developing equations for arbitrary shock amplitudes 03 p0392 A66-12535

Vacuum and low temperature X-ray camera for structural analysis of oxidized materials 04 p0518 A66-13499

Background radiation density in isotropic homogeneous universe, discussing Olbers paradox 04 p0574 A66-14017

Linearized version for isotropic elastic plates and shells by series expansion method obtained as Euler equations 04 p0591 A66-14201

Static deformation of model of three-constant isotropic elastic material exhibiting phenomenon of couple stresses [ASME PAPER 65-WA/APM-3] 05 p0776 A66-15427

Stress relaxation of wound reel of magnetic tape, assuming homogeneous and isotropic material, exhibits instantaneous and delayed elasticity, creep under shear and elastic behavior under hydrostatic stress [ASME PAPER 65-WA/APM-8] 05 p0689 A66-15430

Three-dimensional linear elasticity problems in homogeneous transversely isotropic elastic materials like infinite circular cylinder, using potential function method [ASME PAPER 65-WA/APM-26] 05 p0778 A66-15447

Maxwell equations for isotropic medium bounded by conductors in three-space dimensions solved by applying Laplace equations described in Minkowski space 06 p0851 A66-16450

Radiant transport with isotropic scattering, evaluating approximate solutions for reflection and transmission of parallel plane radiation 07 p1152 A66-17589

Elastic interaction energy of two infinitesimal dislocation loops in a transversely isotropic medium estimated from fundamental elasticity tensor 07 p1144 A66-18044

Stressed state of unbounded nonlinear isotropic plate with square hole during triaxial uniform tension 08 p1307 A66-18880

Dynamic problems of transversely isotropic half-space and elastic layer, solving contact and boundary value problems 08 p1315 A66-19708

Approximate solution for elasticity problems, noting mathematical determination of stress distribution in any homogeneous isotropic body 09 p1468 A66-20642

Static deformation of model of three-constant isotropic elastic material exhibiting phenomenon of couple stresses [ASME PAPER 65-WA/APM-3] 10 p1615 A66-21480

Stress relaxation of wound reel of magnetic tape, assuming homogeneous and isotropic material, exhibits instantaneous and delayed elasticity, creep under shear and elastic behavior under hydrostatic stress [ASME PAPER 65-WA/APM-8] 10 p1539 A66-21481

Longitudinal elastic wave of finite amplitude propagation in isotropic solid 11 p1738 A66-22606

Polarization and birefringence of photoelastic plastic medium 11 p1781 A66-22613

Input impedance of spherical emitter in infinite homogeneous isotropic conducting medium 11 p1656 A66-23031

Propagation of MHD emissions in Alfvén mode along high latitude geomagnetic field lines, auroral zone signal energy penetration and isotropic wave mode transformation 11 p1701 A66-23151

Potential representation of solution of equations for homogeneous and isotropic medium in presence of magnetic and temperature fields 13 p2195 A66-25401

Buckling of unstable perfectly elastic isotropic rectangular 13 p2195 A66-25401



- plate 14 p2396 A66-27312
- Stresses and displacements in circular cylinder of transversely isotropic material for mixed boundary conditions, obtaining solution by using partial differential equation 14 p2397 A66-27388
- Stresses in composite spheroids of two different isotropic elastic materials under compressive forces acting along common axis of revolution 14 p2397 A66-27391
- Dislocation problems of circular ring with simple type nonhomogeneity and of isotropic circular ring with thickness varying inversely with square of radial distance 14 p2397 A66-27392
- Fundamental equations for birefringence of isotropic elastic solids and isotropic viscous fluid derived from Toupin theory of photoelasticity and stress 14 p2408 A66-28388
- Optics 14 p2408 A66-28388
- Huygen principle for electromagnetic field in moving, isotropic, homogeneous and linear medium, using Maxwell-Minkowski equations and Green function for field equation 15 p2537 A66-28783
- Theory of transversely isotropic fluids for fluid having rigid microstructure 15 p2480 A66-29692
- Galerkin vector for elastodynamic problem of isotropic inhomogeneous body 16 p2823 A66-31707
- Finite rotational and inflational deformation of incompressible homogeneous isotropic torus 17 p3018 A66-31928
- Variational and reciprocity theorems on thermoelastic distortions in homogeneous isotropic body 17 p3032 A66-33331
- Three-dimensional linear elasticity problems in homogeneous transversely isotropic elastic materials like infinite circular cylinder, using potential function method [ASME PAPER 65-WA/APM-26] 18 p3248 A66-33582
- Elastic equilibrium of infinite isotropic homogeneous plate with soldered circular isotropic ring 18 p3251 A66-33703
- Second-order volumetric change in isotropic elastic materials without external loads 18 p3258 A66-34639
- Transfer efficiency of laser pumping cavities with diffusely reflecting wall determined, based on approximately isotropic nature of light inside cavity 19 p3372 A66-35379
- Numerical integration based on definition of Riemann integral, describing application to nonlinear integral equations of isotropic scattering of radiation in plane parallel atmosphere 19 p3388 A66-35830
- Photoelastic Wertheim law in general tensor coordinate system derived for linearly anisotropic or isotropic homogeneous matter 19 p3474 A66-36320
- First- and second-order constitutive equations of viscoelasticity based on mechanical and invariant theory, discussing relaxation under finite twist of incompressible isotropic bar 19 p3475 A66-36639
- Linear model for macroscopically uniform elastic medium, deriving expression for Green tensor in weakly and highly dispersed isotropic media 19 p3476 A66-36834
- Elastic deformation of unbounded transversely isotropic body with internal plane-circular slot under slot surface load 19 p3476 A66-36839
- Bending problems of transversely isotropic circular plates based on Ambartsumian theory of anisotropic plates 21 p3830 A66-38980
- Heat transfer in conducting, absorbing, emitting, scattering and heat generating medium 21 p3836 A66-39438
- Input resistance of short filamental antenna in warm isotropic plasma from kinetic /Vlasov equation/ rather than hydrodynamic approach 22 p3874 A66-39939
- HF conductivity of quasi-equilibrium isotropic fully ionized two-temperature plasma 23 p4102 A66-41367
- Electromagnetic wave transmission through and reflection from homogeneous nonlinear anisotropic slab between two linear isotropic media 24 p4173 A66-42706
- Numerical integration of equations of Love first approximation for thin isotropic shells, presenting results for torus and flask having variable wall thickness 24 p4292 A66-42964
- ISOTROPIC TURBULENCE**
- Weak turbulence in media with decay spectrum, analyzing second component of collision term with isotropic model 02 p0264 A66-11385
- Dynamic equations for two-point double correlations of fluid pulsation velocities and particles suspended in it, noting isotropic turbulence degeneration 02 p0217 A66-11393
- Statistics of locally-isotropic turbulent field for gas with density sensitive heating mechanism [AIAA PAPER 65-38] 02 p0302 A66-11532
- Damping of longitudinal plasma waves emitted by artificial Earth satellite moving in ionosphere 02 p0269 A66-12132
- Statistical behavior of reacting mixture in incompressible isotropic turbulence when reaction rate is quadratic function of local concentration of reactant, using Kraichnan direct interaction hypothesis [AIAA PAPER 65-812] 03 p0358 A66-13180
- Presence of suspended particles leads to more rapid attenuation of pulsations in final stage of degeneration of isotropic turbulence 04 p0512 A66-14436
- Turbulence in hydrodynamics and plasma physics 05 p0727 A66-15260
- Anisotropic grid-generated turbulence passed through axisymmetric nozzle of small contraction ratio followed by straight section 12 p1866 A66-24947
- Damping of longitudinal plasma waves emitted by artificial Earth satellite moving in ionosphere 14 p2345 A66-28089
- Inertia and pressure effects on energy potential of homogeneous and isotropic turbulence in weakly compressible medium 18 p3100 A66-34608
- Cosmic ray isotropy mechanism, examining plasma beam instability and cosmic ray scattering at plasma turbulent pulsations 20 p3629 A66-37032
- Contraction to improve isotropy of grid-generated turbulence 22 p3899 A66-40381
- Four-plasmon hydrodynamic equations describing weak turbulence spectrum in universal equilibrium region of plasma without magnetic field 24 p4243 A66-42532
- Channel flow deriving equation for /proper/ turbulence spectrum and expression for spectrum of dynamic and turbulent quantities 24 p4197 A66-43061
- ISOTROPISM**
- SA ANISOTROPY**
- Near-isotropic circularly polarized antenna 13 p2035 A66-25503
- ISRAEL**
- Aerospace and related research conducted at various universities, institutes and agencies in Israel during 1964 and 1965 09 p1458 A66-20716
- ITALIAN SATELLITE**
- S SAN MARCO SATELLITE**
- ITALY**
- Milan airport system noting air traffic 05 p0661 A66-15846
- European Miniature Electronic Components and Assemblies Data 1965-1966, Part I, Germany and Italy 06 p0858 A66-17158
- Italian participation in COMSAT 09 p1473 A66-20548
- Aerospace research in Italy including San Marco project, ionospheric measurements, cooperation with NASA, rocket experiments, etc 09 p1458 A66-20717
- Space research programs in Italy since May 1965 and cooperation with NASA 15 p2602 A66-29940
- ITERATION**
- Convergence, oscillation, functional stability and reliability of m-by-1 homogeneous polyfunctional nets under iteration 10 p1517 A66-21691
- Axially symmetric or two-dimensional electrode system with emitting surface, discussing convergence and accuracy criteria of iteration methods 17 p2887 A66-32700
- Programming tasks optimization through infinite iteration procedure 22 p3941 A66-40542
- ITERATIVE NETWORK**
- New block diagram compiler for sampled data system simulation 12 p1828 A66-23827
- Iterated theoretical admittance of cylindrical antenna, determining effective length and approximating ideal independent susceptance 20 p3534 A66-38365
- ITERATIVE SOLUTION**
- Solution to linear programming problems, using iterative method 01 p0050 A66-10170
- State assignment effect on sequential circuit reliability represented by Markov chain, using iterative assignment method with dynamic programming 02 p0207 A66-11521
- Theorems for determining common point of convex sets by method of successive projection 02 p0250 A66-12097
- Isotropic scattering of radiation from point source in finite atmosphere bounded by totally absorbing spherical shell, deriving iterative series solution 04 p0548 A66-13828
- MHD equations linearized by Newton iteration method, describing weak perturbation propagation 04 p0574 A66-13841
- Iterative process to refine solution to system of linear equations 04 p0540 A66-14392
- Iterative procedure for analyzing linear electrical networks by digital computer 05 p0638 A66-15127
- Computer analysis of axisymmetric free vibrations of orthotropic shells of revolution and elastic rings [AIAA PAPER 65-109] 05 p0781 A66-15790
- Circuit network in designing low pass filters with minimum attenuation requirements in stopbands and optimum transient behavior, using Schussler technique and iterative process 07 p1008 A66-17751
- Iterative procedure for determining linear separability of Boolean function and threshold functions for logical switching circuit design 07 p1059 A66-17971
- Computational reduction of high speed memory requirements in solving optimization problems by dynamic programming and supersonic transport trajectory application 07 p1004 A66-17976
- Iteration technique used to study minimum climb time of rockets 07 p1141 A66-18232
- Rapidly convergent iterative unique determination of linear steering function for desired orbit conditions 08 p1289 A66-18826
- Iterative guidance law for Saturn launch vehicle for lunar landing, examining trajectory optimization 08 p1253 A66-19539
- Formulation and iterative solution of small strain plasticity problems, using Hencky-Nadai hardening law as mathematical model for material behavior 09 p1466 A66-20263
- Globally convergent iteration function for solution of polynomial equations according to certain algorithms 09 p1395 A66-20624
- Tensor product analysis of alternating direction implicit iteration techniques for approximate solution of elliptic partial differential equations 09 p1396 A66-20637
- Dynamic stability of circular elastic rods, noting iteration method analysis of nonlinear coupling effect between axial force and curvature in forced in-plane vibrations 09 p1467 A66-20638
- Iterative method for computing optimum values of parameters for best agreement in least squares sense between given values and corresponding calculated values 10 p1507 A66-21213
- Iterative technique for determination of prime implicants of switching functions specified in maxterm form 10 p1517 A66-21695
- Chaplygin asymptotic series solution method for differential equation systems 10 p1551 A66-21915
- Numerical solution to first geodetic problem of ellipsoid of rotation, using iterative application of Runge-Kutta method to differential equations of geodetic line 11 p1698 A66-22767
- Numerical convergence of iterative solution to complete Bhattacharya-Gross-Krook equation for strong shock waves 11 p1690 A66-22909
- Iterative solution to shock wave structure in highly rarefied flows through kinetic theory and full Boltzmann equation 11 p1690 A66-22910
- Successive approximation methods of solving optimal control problems, based on variational calculus and Euler-Lagrange equation 11 p1679 A66-23273
- Newton-Raphson method iterative solution



of two-point boundary value problem and application to trajectory optimization and tubular reactor design 11 p1680 A66-23276

Successive approximations to determine vector in theory of optimal control 13 p2045 A66-25294

Mathematical programming methods for solving nonlinear state-constrained discrete optimal control problems 13 p2047 A66-25352

Iterative method solution of kinetic equation with functional derivatives for ionized plasma 13 p2141 A66-25476

Combined optimization problem, equivalent to dual control problem, considering determination of optimal control policies for plant under random disturbances, using iterative equations 13 p2051 A66-26065

Method for automatically adjusting networks for best approximation to desired responses, using iterative gradient techniques, constraint equations and Carroll programming technique 13 p2051 A66-26070

Iterative approximation of rational transfer function in Laplace transform variable  $s$ , optimal with respect to given input and output time functions, and deviation from desired output-input-time functional relation 13 p2054 A66-26087

Reflection coefficient for arbitrary lossy waveguide with large number of identical periodically positioned inhomogeneities determined by iteration 14 p2250 A66-27145

Boundary value problem of elastic/viscoplastic beams solved, using iteration method, noting wave propagation and effect of shear and inertia of axial motion of beam in motion equation 14 p2397 A66-27386

Approximate iterative calculation of non-Newtonian supersonic gas flow past highly blunt bodies 15 p2423 A66-28959

Iterative derivation of approximation of real function by exponential series 15 p2527 A66-29056

Tesseral harmonics of coordinates using Baker-Nunn data and geopotential and dynamical procedures, noting iterative cycle for correction 15 p2491 A66-29999

A posteriori error bounds in iterative matrix inversion 16 p2732 A66-30238

Iteration method of general linear programming on digital computer, using penalty functions, compared to equilibrium problem of mechanical system 16 p2669 A66-30759

Function approximation from finite number of arbitrary points, using iteration methods 16 p2734 A66-30760

Stresses and displacements in linearly elastic and toroidal shells of circular cross section determined by nonlinear numerical method [AIAA PAPER 65-144] 16 p2816 A66-30905

Iterative solution to Krook-Boltzmann kinetic equation noting Navier-Stokes numerical solution, computation and analysis of distribution function within shock wave 16 p2685 A66-30945

Molecular-kinetics experiments /trajectory calculation of particle interaction/ using digital computer iterative method for theoretical comparison 16 p2656 A66-30947

Iteration methods for solution of integro-differential equations 17 p2945 A66-31807

Rayleigh scattering scalar source functions and source matrix computed by iteration of auxiliary equation 17 p2917 A66-31922

Control forces in nonlinear integral equations solved by iteration 17 p2902 A66-32816

Iteration scheme based on Newton approximation method applied to two-dimensional and rotationally symmetric flows past obstacles 17 p2913 A66-33066

Iterative gradient method application to trajectory optimization problems, noting feasibility to systems with continuous bang-bang controls 17 p2903 A66-33254

Iterative solution of large signal abrupt junction varactor doubler as input frequency is varied, given power of source and load impedance 17 p2895 A66-33276

Simplification of steepest-ascent method for determining optimal control program by introducing penalty method to eliminate

adjoint variables 18 p3089 A66-33603

Digitally computed tables of Chebyshev approximations of Laplace shift operator transfer function enabling analog simulation of time delay systems 18 p3090 A66-34069

Iterative determination of space flight trajectory and velocity represented as sum of Kepler motions about celestial bodies 18 p3234 A66-34635

Computer iteration scheme for calculating arbitrary hyperbolic transfer orbit in field of attracting center, based on Gauss equations 19 p3455 A66-35278

Space mission trajectory optimization by iterative minimizing of residual vector, using linear correction [AIAA PAPER 65-697] 19 p3462 A66-35903

Iterative solutions to high-speed actions, noting reduction to successive problems of maximization of linear form from finite state 19 p3325 A66-35931

Numerical integration of primitive equations by simulated backward difference method, using two-step iteration for divergent barotropic model of atmosphere 19 p3393 A66-36057

Class  $K$  matrices, discussing new methods and application to convergence rate of iteration procedures 19 p3391 A66-36335

Iterative approximation method for solution of proper elements /eigenvalue/ of Sturm-Liouville equation 19 p3392 A66-36783

Fourth-order multipoint iterative methods for solving equations which cost one function and two derivative evaluations per iteration, for use in root finding 19 p3392 A66-36786

Iterative solution of time optimal control boundary value problem resulting from application of Pontryagin maximum principle 20 p3535 A66-36850

Iterative computational procedures applicable to optimal control problems including treatment of minimum-error regulator, minimum-error rendezvous and minimum-fuel terminal control 20 p3536 A66-36855

Unimodal function minimum located by successive approximations to interval of uncertainty 20 p3589 A66-36903

Acoustic oscillations in solid propellant rocket chambers, discussing cases of small amplitude perturbations and solving wave equations 20 p3628 A66-37387

Iterative method for extracting annual and Chandlerian terms of variation of Earth rotation from experimental data of universal time 20 p3550 A66-37410

Iterative guidance mode with application to three-dimensional upper stage vacuum flight 21 p3768 A66-38897

Communication possibility over memoryless channel with computational iterative decoding scheme that is asymptotically complex 21 p3704 A66-39141

Iterative solution of equations for diffuse reflection and transmission in finite plane-parallel atmosphere with arbitrary stratification 21 p3734 A66-39220

Simultaneous nonlinear estimation of parameter vector via iterative procedure for known and unknown covariance matrix 22 p3939 A66-40000

Newton iterative procedure extended to solution of nonlinear integral equations 23 p4085 A66-41556

Singular solutions for Chaplygin equations using generalized wave functions, noting iteration method for finding wave equation corresponding to first terms of expansion series 23 p4085 A66-41561

Energy dependence of effective interaction in superconductivity, calculating critical field and specific heat 24 p4259 A66-43018

Iterative design procedure for optimum placement of vapor deposited Nb-Sn ribbon superconductors in high field large bore modular magnets 24 p4186 A66-43175

Boundary layer equation transformation, using special curvilinear coordinates 08 p1206 A66-18872

Two-dimensional isothermal liquid flow electrically conducting in channel under electromagnetic fields, finding self-modeling solutions, using Jacobi functions 15 p2551 A66-29221

Invariant imbedding as basis for integration theory for canonical equations of motion with parallels to Jacobi theory 17 p2947 A66-32500

Self-similar solutions of two-dimensional laminar flow of incompressible electroconductive fluid in channel in crossed electric and magnetic fields, using Jacobi elliptic integrals 17 p2971 A66-32866

Existence of new isolating integral in restricted three-body problem, computing orbits for various parameter values and initial conditions 24 p4272 A66-42202

**JACOBI POLYNOMIAL**

Multistage rocket trajectory optimization, extending maximum principle to include Weierstrass and Jacobi conditions 11 p1733 A66-23337

Bilinear expansions treating Euler transform of special integrand, reviewing properties of Jacobi function for application in quantum mechanics or plasma physics 12 p1905 A66-24566

Locating zeros of complex functions by computing topological index 13 p2121 A66-26326

Contact problem of half-plane inelasticity theory using Jacobi polynomials and taking into account thermal stresses and presence of adhesion and friction in contact area 19 p3476 A66-36835

Singular integral equations with constant coefficients solved by Jacobi polynomials and applied to problems in fluid dynamics, crack propagation, plane elastic theory, etc 19 p3393 A66-36836

Integral equation solution through Jacobi polynomials employed as eigenfunctions of certain operators 22 p3941 A66-40798

**JAHN-TELLER EFFECT**

Jahn-Teller effect in excited 4-T-2 state of trivalent Cr ions in ruby, discussing unilateral elastic strain effect splitting of pure electronic line 597 nm in U band 03 p0410 A66-12941

Dynamic Jahn-Teller effect in excited state vanadium doped aluminum oxide 17 p2981 A66-32717

Three-dimensional X-ray diffraction data to determine structure of crystal of potassium barium hexanitrocobaltate, discussing Jahn-Teller effect 17 p2871 A66-33486

Jahn-Teller shift reorientation in Ni impurity centers of diamond and rise of C-N pair EPR spectrum with temperature 22 p3964 A66-40307

Static Jahn-Teller effect on impurity centers in semiconductors, discussing nature and magnitude of splitting of ground state 24 p4256 A66-42527

**JAMMING**

Selection of optimum ranging signal for jam resistant satellite communications system [AIAA PAPER 66-292] 12 p1822 A66-24762

**JAPAN**

F-104J production program from Japanese standpoint [AIAA PAPER 65-804] 03 p0446 A66-12600

Japanese space research during 1964, particularly meteorological rocket observation, satellite tracking and space experimental techniques and data 09 p1458 A66-20718

Heat transfer bibliography of 32 Japanese works including heat transfer application, phase change, separated flow, radiation, transpiration and mass transfer 14 p2410 A66-26937

Space research in Japan in 1965 15 p2602 A66-29941

Height distributions of atmospheric refractive index variations over Japan 16 p2653 A66-30796

Japanese air traffic control using real time computer data processing 22 p3945 A66-40617

**JEANS THEORY**

First order /Jeans/ stability analysis of infinite uniform medium pervaded by magnetic field 13 p2187 A66-26138

## JACOBI INTEGRAL

First order nonlinear partial differential equation discussing global locally-Lipschitzian solutions via Jacoby theorem extension 06 p0901 A66-16006



- Homogeneous rotating low density plasma permeated by magnetic field with anisotropic velocity distribution may exhibit homogeneous instability as well as gravitational instability 21 p3794 A66-39562
- ET**
- SA AIR JET
- SA ANNULAR JET
- SA ARC JET
- SA EXHAUST JET
- SA FLUID JET
- SA FREE JET
- SA GAS JET
- SA LAMINAR JET
- SA PERIPHERAL JET
- SA PLASMA JET
- SA REACTION JET
- SA SUPERSONIC JET
- SA TURBULENT JET
- SA TWIN JET
- SA TWO-DIMENSIONAL JET
- SA VAPOR JET
- SA WALL JET
- Accelerator for jets formed by shaped charges, using principles of detonation waves 14 p2329 A66-27475
- Particle energy measurements in high energy jets with large stacks of nuclear emulsion 15 p2584 A66-29557
- High energy jets produced by heavy primary nuclei of cosmic origin and fragmentation products 18 p3215 A66-35160
- High energy cosmic ray jets studied in large nuclear emulsion stacks at Krakow 18 p3215 A66-35161
- ET AIRCRAFT**
- Development of air transport in East Germany after World War II including route charts of Lufthansa 01 p0170 A66-11071
- Breguet 941 STOL aircraft advantages over conventional commercial jet aircraft to solve requirements imposed on airport facilities 02 p0177 A66-11749
- Cost effectiveness of VTOL short range jet airlines, discussing significance of block time
- [AIAA PAPER 65-797] 03 p0320 A66-12598
- Design and market research aspects of Hamburger HFB 320 jet executive aircraft 10 p1482 A66-21360
- Stick pushers in new medium range jet transports, noting aerodynamics of aircraft stall 11 p1637 A66-23072
- Supersonic business aircraft design problems related to payload and range 12 p1800 A66-23643
- Design of V/STOL aircraft including propulsion systems, control and lift configurations 14 p2222 A66-26924
- Design and mission requirements and weight penalties claimed for jet VTOL tactical aircraft 16 p2633 A66-30597
- Statistical analysis of vertebral fracture in U.S. Navy during 1959-1963 period 16 p2644 A66-31132
- Function, method of operation, complexity and effect on weight and cost for BITE /built-in test equipment/ as applied to electric power systems for jet aircraft 20 p3499 A66-37189
- Flight recorder utilization in British civilian jet and turboprop aircraft 21 p3696 A66-38603
- Vehicle Millemile concept in ascertaining composite mix of load and revenue needed to meet cost of operating large jet aircraft 21 p3838 A66-39244
- Dynamic aeroelastic motion resulting from inertial and aerodynamic effects, coupled through elastic deformation, applied to jet aircraft, considering flutter, buffet, wakes and turbulence 23 p4015 A66-41035
- Design, performance capabilities and operational characteristics of Russian high speed jet aircraft IL-62 with tail-mounted engine 24 p4160 A66-43075
- ET AIRSTREAM**
- Position of tropopause in middle latitude jet flow 18 p3108 A66-34607
- ET AMPLIFIER**
- Flueric control devices physical mechanisms, including jet-on-jet and turbulence amplifiers, vortex and boundary layer control devices [ASME PAPER 65-WA/AUT-21] 05 p0624 A66-15615
- Fluid amplifier analysis predictions for prime-element conceptual models and jet amplifier dynamic effects 09 p1333 A66-20327
- Stream-interaction amplifiers and uses in fluidic circuits, discussing momentum exchange, pressure differential and Coanda effect 18 p3053 A66-33898
- Fluidic electro-fluid converter development from study of jet separation from curved surface as affected by geometry, Reynolds number and wall temperature 19 p3282 A66-36673
- Static characteristics of symmetrical wall reattachment jet amplifier over range of Reynolds number 20 p3501 A66-37646
- JET BLAST EFFECT**
- Experiments on jets formed from imploding bubbles, indicating that Munro jets are formed when hemispherical cavities on liquid surface collapse by shock wave traveling from below 10 p1607 A66-21293
- JET BOUNDARY**
- Jet boundary determination of underexpanded two-phase carbon dioxide supersonic nozzle flow 14 p2219 A66-27445
- Hydrodynamic implosion mechanism and impact of liquid jets formed by collapsing cavitation bubbles, examining damage to solid boundaries 20 p3547 A66-37811
- Performance of two-dimensional curtain jets of air cushion vehicles based on incompressible flow theory, noting stability criteria 22 p3844 A66-40499
- JET DRAGON AIRCRAFT**
- S DE HAVILLAND DH-125 AIRCRAFT
- JET ENGINE**
- SA PULSE JET ENGINE
- SA RESISTOJET ENGINE
- SA T56 JET ENGINE
- Laboratory, component and engine tests for lubricant properties of J-79 jet engine including elastomer volume swell, oxidation-corrosion, lubricity, etc [SAE PAPER 650816] 01 p0078 A66-10821
- Dynamic pressure and temperature measurements of forward gas expulsion during high speed stall of jet engines [SAE PAPER 650840] 01 p0130 A66-10832
- Correction factors derived for avoiding formation of stagnation cores near hub of axial compressors 01 p0008 A66-11094
- JR 100 lightweight lift jet engine outline for National Aerospace Laboratory 02 p0278 A66-11306
- New titanium alloy for 900 degrees F surface in jet engines 02 p0242 A66-11513
- Combustion phenomena in model combustion chamber of lift jet engine in terms of efficiency, pressure loss and extinction limit 03 p0443 A66-12400
- Photoelastic analysis and theoretical considerations to minimize stress concentration of blade joints of compressor and turbine of jet engine 03 p0373 A66-12402
- Erosion, oxidation, loss of strength and reduction of ductility resulting from long-time elevated temperature stressed exposure of nickel alloy used in jet engine design [AIAA PAPER 65-744] 03 p0381 A66-12583
- Engine thrust and heat mass in air breathing jet engine for space flight 04 p0572 A66-13441
- Olympus 593 jet engine for Concorde SST, development, performance and reliability 05 p0744 A66-14768
- ONERA experimental wind tunnel research with jet engine intakes and exits [ONERA TP 292] 05 p0606 A66-15159
- Rolls-Royce RB 108 lift-jet engine design, characteristics and V/STOL research 05 p0745 A66-15298
- Jet engine models applicable to analog and Dynasir simulation for transient performance analysis [ASME PAPER 65-WA/MD-16] 05 p0745 A66-15521
- Heat-and fatigue-resistant metal alloys for construction of jet aircraft combustion chambers, including 18 NiCoMo alloy suitable for temperatures up to 650 degrees C 05 p0704 A66-15806
- M.A.N. RB 153 jet engine development, characteristics and capabilities 06 p0943 A66-17019
- Rolls-Royce RB 108 jet engine, discussing project history, test results and current application 06 p0943 A66-17021
- Inlet of XB-70 consisting of two separate parts located under wing, each part supplying air to three of six J-93 engines 07 p0987 A66-17278
- Metallurgical factors for materials in jet engines, considering ductility, strength loss, strain-cycling criteria, etc [SAE PAPER 660057] 09 p1388 A66-20155
- Gimballed jet engine development, noting application to V/STOL aircraft and design of plenum chamber burning engine 10 p1591 A66-21366
- Effect of bleeding air behind compressor for VTOL stabilization on dynamic behavior of jet engine 10 p1591 A66-21405
- High activity of alkali metal salts of carboxylic acids and substituted phenols as synergists for arylamine antioxidants in ester-type synthetic lubricating oils 11 p1711 A66-23123
- Design of system analyzing operating conditions of jet engine up to overhaul, recording regime of engine revolutions, exhaust gas temperatures, accelerations, etc 13 p2076 A66-25078
- Noise suppression for jet engine 14 p2269 A66-26770
- Supersonic transport engine requirements in light of past jet transport operation [SAE PAPER 660296] 14 p2373 A66-27291
- Plasma sprayed and detonation-flame-plated protective wear-resistant coatings to extend life of aircraft jet engine parts [SAE PAPER 660310] 14 p2301 A66-27292
- Liquid cooled high specific impulse arc jet engine has measured engine thrust not completely aerodynamic in nature [AIAA PAPER 64-669] 14 p2374 A66-27470
- Random balance statistical method of identifying major causes of performance variations in jet engine fuel control units 15 p2572 A66-28863
- Dual-flow and single-flow jet engines 15 p2572 A66-29364
- Creep fatigue, thermal cycling, vibration control, transient thermal response control, structural loads and hot part reliability relating to long-life jet engine failure [SAE PAPER 660311] 15 p2572 A66-29836
- Jet engine reliability at various stages /planning, production, in-service, etc/ noting its economic aspects and global methods analyzed 16 p2790 A66-30316
- Jet engine transient thrust response for V/STOL aircraft 16 p2791 A66-30598
- Jet engine technology, including spinoff from lift jet, propulsion systems, cost estimates, etc 16 p2791 A66-31280
- Operating stability of turbojet engines improved by use of double-rotor compressor 17 p2992 A66-33487
- Cracking of jet engine components made of titanium alloys results from silver chloride stress corrosion 19 p3473 A66-35655
- Variable geometry jet engine control using advanced hydromechanical, microelectronic and fluidic techniques 19 p3450 A66-36364
- Decision table for determining base depot maintenance policy for aircraft engines 20 p3566 A66-37888
- Combustion efficiency measurement of jet-engine systems, noting role of static pressure in outflow nozzle 20 p3681 A66-38443
- Additives effect on antioxidant stability and antilabration characteristics of lubricating oils used in jet and turboprop engines 20 p3575 A66-38445
- Turbine engine self-excited vibrations from thermal deformation of engine components during transient operating conditions, noting vibration elimination and preventive measures 21 p3807 A66-38622
- JET EXHAUST**
- Scaling of near field pressure correlation patterns around jet exhaust 01 p0010 A66-10123
- Flow field about subsonic jet exhausting into quiescent and low velocity air stream [AIAA PAPER 65-704] 01 p0008 A66-10942
- Nonreturn circuit V/STOL wind tunnel to reduce external wind effects 02 p0216 A66-11964
- Form rolling used to form L-shaped strips from L605 alloy for economical fabrication of supports for jet engine exhaust nozzles 10 p1545 A66-21220
- Effect of supersonic aircraft on cirrus formation and climate, noting influence of combustion products on stratosphere



[AIAA PAPER 66-369] 12 p1907 A66-24497  
Steady nonisentropic jet expansion in vacuum with pressure tensor approximated by second-order moment technique and BGK model 16 p2684 A66-30605

**JET FLAME**  
Laminar diffusion flame occurring in mixing zone between undiluted fuel and undiluted oxidizer by process of molecular diffusion 03 p0443 A66-12489

**JET FLAP**  
Ground effect on pressure distribution and lift coefficient of jet-flap wing tested in wind tunnel 07 p0981 A66-18095  
Jet drag solutions for symmetrical struts of various shapes, thickness ratios and slot widths in quiescent and uniform streaming flow 12 p1800 A66-25005  
Jet-flap controlled lifting propeller, examining power and efficiency 21 p3731 A66-39592

**JET FLIGHT**  
Flight data used to determine relationship between atmospheric temperature changes and clear air turbulence occurrence at jet altitudes [AIAA PAPER 66-365] 12 p1906 A66-24477

**JET FLOW**  
Velocity distribution in laminar viscous liquid-into-liquid jet 01 p0057 A66-10407  
Condensation in underexpanded jet issuing from sonic orifice into quiescent atmosphere 01 p0007 A66-10617  
Expansion of plane nonisothermal jet of liquid dropping into space filled with same liquid at different temperature 01 p0059 A66-11019  
Attraction switching through use of parallel secondary injection in Coanda-effect nozzle 03 p0355 A66-12775  
Iterative solution of Navier-Stokes equations for class of flows generated within rectangular cavity by surface passing over open end 03 p0356 A66-12888  
Turbulence in free shear layer in mixing region of circular jet, comparing statistical characteristics of mathematical and physical models [AIAA PAPER 65-805] 03 p0357 A66-13081  
Turbulent mixing of axisymmetric jet of partially dissociated nitrogen with ambient air, establishing mixing and decay characteristics [AIAA PAPER 65-823] 03 p0359 A66-13231  
Jet deflection by curvilinear walls in VTOL takeoff, examining parameters affecting flow separation 04 p0572 A66-13512  
Turbulent jet axis under crossflow of different density assuming static pressure, excess heat content and projection of mean jet velocity 04 p0509 A66-13656  
Characteristics of jet ejector with faired inlets as augmenters treated by continuity and momentum equation 04 p0456 A66-14388  
Comparison of Landau and Schlichting solution for Laminar submerged jet discharging from infinitely thin pipe 04 p0512 A66-14439  
Liquid-phase viscosity effect on disruption of hydrodynamic stability of bubble boiling in large liquid volume 04 p0599 A66-14441  
Mixed flow of five plane turbulent air jets discharged into atmosphere through slotted nozzles 06 p0872 A66-16470  
Mean flow pattern of round air jet in ambient airstream parallel to jet axis 06 p0802 A66-16504  
Steady flow interactions of supersonic airstream and jet blown from hemispherical and flat body noses 07 p0982 A66-18137  
Flow of thin jets in vicinity of solid walls with diverging profiles 07 p1026 A66-18230  
Papers on fluidics, analyzing digital and fluid amplifier design 09 p1331 A66-20316  
Flow induction by rotary jets, involving isentropic flow deflection followed by constant-area mixing 09 p1327 A66-20737  
Initial velocity and density conditions for three-dimensional boundary layer equations, noting wakes and jets 10 p1522 A66-21303  
Corresponding compressible and incompressible jets and wakes in boundary layer equations of turbulent and laminar cases 10 p1480 A66-21411  
Hot-wire measurements in plane turbulent jet of air 10 p1480 A66-21466  
Spectroscopic and optical studies of high pressure underexpanded jet produced by

expanding DC arc plasma generator through sonic orifice [AIAA PAPER 66-164] 10 p1565 A66-21688  
Plasma burner in which heating of gas is effected in jet discharge stabilized by vortex or flow methods 11 p1748 A66-23417  
Hydrodynamics of free steady state jet subject to axial tension, numerical computation of perturbation corrections for Newtonian jets 12 p1797 A66-24031  
Flow graph in model of jet curtain in ideal incompressible weightless fluid with isolated vortex 12 p1798 A66-24433  
Crosswind effect on turbulent jet parameters for submerged jet propagation at angle to unrestricted flow 12 p1864 A66-24445  
Stability of plane inviscid jet and wake studied for possible growth in downstream spatial direction 12 p1865 A66-24582  
Condensation in underexpanded jet issuing from sonic orifice into quiescent atmosphere 13 p1990 A66-25178  
Heat exchange between axisymmetric jet flow and plate situated normal to flow 13 p2208 A66-25313  
Shape of plane and circular jet deformed by gas flow impinging at angle of incidence determined from head drag of jet relative to flow 13 p2062 A66-25320  
Fluid devices as affected by delay for signal transmission in lines, jet behavior and Coanda effect 13 p2062 A66-25366  
Velocity variation along two types of confined jets, with and without lateral flow, in presence of transverse magnetic field 13 p2140 A66-25444  
Boundary problem describing plane jet steady state flow of ideal incompressible fluid, reducing solution to nonlinear integro-differential equations 14 p2272 A66-26775  
Three-dimensional periodic oscillations in jet at high Reynolds number 14 p2273 A66-26929  
Heat transfer equation to find temperature distribution in two-dimensional and circular jets 14 p2274 A66-27378  
Supersonic jet interaction for hypersonic flow of Mach 7.1 and for variable Mach number, noting jet instability, stagnation pressure, drag variation, wind tunnel, etc 14 p2220 A66-27467  
Trails arising in wake of fan-type jets in transverse gas flow during uniform fuel-air mixture combustion 14 p2413 A66-27693  
Three-dimensional MHD flow with jet and vortex nature in viscous incompressible conducting fluid 14 p2348 A66-28393  
Mellor solutions for linearized wakes and jets in laminar and turbulent flow for class of pressure gradients 15 p2424 A66-29293  
Empirical relationships between momentum, kinetic energy and displacement thicknesses for uniform-density turbulent boundary layer and wall jet flows 15 p2479 A66-29301  
Monte Carlo technique to examine four-momentum transfer in jets 15 p2586 A66-29566  
Exact solution derived for gas jet flow with three characteristic high subsonic velocities, using Falkovich extension of Chaplygin hodographic method 15 p2425 A66-29850  
Continuum source molecular beam facility, examining effect of source-skimmer distance variation on flux and spatial distribution of beam in collimation chamber downstream 16 p2746 A66-30386  
Jet oil lubrication and scavenging technique for 20 mm high speed ball bearing [ASLE PAPER 66AM 1B4] 16 p2710 A66-30402  
Mixing of free jet boundary which includes laminar and turbulent flow region in tandem 16 p2685 A66-30805  
Stream function for plane free sonic gas jet flowing past profile 16 p2630 A66-31290  
Two-dimensional MHD jet flow of conducting fluid in coplanar magnetic field and nonstationary flow past body with magnetic field perpendicular to surface 16 p2765 A66-31402  
Low-speed capillary jets of Newtonian liquids discharging into air in perturbation analysis and boundary layer analysis 16 p2691 A66-31662

Book on jet theory in ideal fluids, covering compressible flow, steady jet flow, infinite flow past polygonal obstacle, unsteady flow, etc 16 p2632 A66-31746  
Jet flow effect on electrical discharge in conducting viscous fluid based on magnetic boundary layer theory 17 p2964 A66-31895  
Hall current effect on capillary instability of finitely conducting liquid jet carrying axial volume current 17 p2908 A66-32432  
Jet disintegration into large drops in Vivdenko and Shabalin paper 17 p2909 A66-32566  
Flow characteristics, design and performance data for subsonic two-dimensional straight centerline diffusers [ASME PAPER 66-FE-10] 17 p2915 A66-33264  
Flow in two-dimensional plane wall jet in still air with various initial gaps between nozzle exit and leading edge of wall 18 p3097 A66-33951  
Navier-Stokes equations, differences for laminar jets and turbulent jets, submerged jets and transition layer stability 18 p3099 A66-34123  
Overall structure of combustion process in jet flow of hydrocarbon-air mixtures stressing conditions for ramjet engines, noting flame propagation angles, flow computation, etc [AIAA PAPER 66-573] 18 p3264 A66-34444  
Liquid high-velocity jets dispersion from variable-rugosity injector nozzles, considering effect of roughness of nozzle walls near orifice 19 p3340 A66-35579  
Critical jets of symmetrical perfect-gas flow determined by analogy between impedance network node equation and velocity potential and stream function in Tricomi plane 19 p3341 A66-36250  
Rotary jet flow induction studied with analytical flow model, noting mutual deflection of primary and secondary flow and jet dissipation 19 p3277 A66-36488  
Simultaneous passage of two unmixed gas flows through joint two-circuit turbojet nozzle into ambient medium 20 p3627 A66-36917  
Jet deflection in drifting subsonic flow 20 p3491 A66-36919  
Flow model analysis of shape of curved two-dimensional jet reattaching to offset inclined wall with ventilated cavity beneath jet 20 p3501 A66-37647  
Munroe jet formation when small cavity or bubble in liquid is subjected to impact or shock 20 p3546 A66-37804  
Penetration distance for secondary liquid injection into supersonic airstream, emphasizing jet flow far from injection orifice 20 p3548 A66-38151  
Jet flow turbulence characteristics, calculating vertical wind velocity pulsation component, determining thermodynamic characteristics of atmosphere 20 p3595 A66-38381  
Self-preserving flow in outer part of two-dimensional curved turbulent wall jet for constant ratio of jet thickness to wall radius of curvature 22 p3844 A66-40489  
Jet oil lubrication and scavenging technique for 20 mm high speed ball bearing [ASLE PAPER 66AM 1B4] 22 p3928 A66-40657  
Solution of motion and energy equations in boundary layer of main portion of vortex jet 22 p3902 A66-40817  
Subsonic jet flow past solids, examining two classes of exact solutions in ideal fluid for plane nonvortical steady state flow 22 p3902 A66-40915  
Liquid drop flow in twisted fan-shaped nonisothermic jet allowing change in viscosity coefficient in flow field, using boundary layer equations 23 p4055 A66-41567  
Microstructure of turbulent jet in concurrent flow, analyzing wake parameter and measuring profiles of pulsation velocity components and Reynolds shear stresses 23 p4056 A66-41726  
Similar solution of laminar mixing of curved half-jet and curvature effect of boundary layer flow along curved surface 23 p4059 A66-42003  
Axisymmetric vortex jet behavior of ideal incompressible fluid at large distances from nozzle, noting surface



- waves 24 p4195 A66-42851
- Fragmentation of liquid jet in gaseous medium at high velocities 24 p4196 A66-42868
- FUEL**
- SA JP-4 JET FUEL
- SA JP-5 JET FUEL
- Heat transfer unit, operational method and data relating heat exchanger performance to deposit forming tendencies of jet fuel for supersonic aircraft
- [SAE PAPER 650803] 01 p0128 A66-10845
- Current status of technology of using liquid hydrogen in manned aircraft systems [AIAA PAPER 66-671] 18 p3162 A66-34443
- IMPINGEMENT**
- Flow rate distribution and mixing ratio of two impinging jets in simulation of bipropellant liquid rocket system, using hypergolic propellants 02 p0278 A66-11590
- Variation of local heat-transfer coefficients produced by impinging jets reexamined in light of velocity and turbulence distributions effects 02 p0304 A66-12197
- Thermal and pressure effects of rocket exhaust impinging on flat plate surface at high vacuum
- [AIAA PAPER 66-46] 07 p1154 A66-17895
- Expansion parameters of liquids expelled into vacuum as related to orbital perturbations arising from liquid venting and impingement on adjacent hardware 10 p1481 A66-21947
- Approximate analysis of onset of undamped oscillations in plate on which impinges ideal compressible fluid flow 11 p1779 A66-22234
- Model study of thrust loss due to recirculation of gases from jets of V/STOL aircraft to engine intakes 18 p3162 A66-33683
- Flow field of highly underexpanded axisymmetric jet impinging on flat convex or concave surface calculated by modified inverse method 18 p3100 A66-34600
- Shock impingement on blunt body in hypersonic flow, noting alteration of flow and local heat transfer rate near impingement point
- [AIAA PAPER 66-756] 22 p3846 A66-40641
- Round turbulent low speed airjet impingement on flat surface and application to theoretical analysis of inviscid rotational flow 23 p4012 A66-42002
- LIFT**
- DO-31 VTOL transport design, specifications and testing, using direct jet lift for takeoff and transition to conventional flight 07 p0986 A66-17270
- Conically spiraling ascent or descent trajectory of spacecraft in application of jet lift, noting characteristic mission parameters 09 p1457 A66-20557
- Inlet/door performance characteristics of VTOL lift-engines studied in full-scale wind tunnel tests
- [AIAA PAPER 66-655] 18 p3048 A66-34222
- MIXING**
- Wake pressure of blunt body moving at supersonic speed calculated by analysis of curved half-jet mixing 01 p0007 A66-10630
- Performance of supersonic bypass nozzle with small and large secondary flow evaluated theoretically and experimentally [ONERA TP 287] 03 p0316 A66-12897
- Warren momentum integral method for predicting compressible free mixing of two dissimilar gases
- [AIAA PAPER 65-822] 03 p0357 A66-13083
- Two sets of Tollmein and Goertler equations derived for two-dimensional compressible free jet mixing layer, using similarity assumption
- [AIAA PAPER 65-821] 04 p0510 A66-13692
- Qualitative and quantitative solution of linearized approximations to boundary layer equations, noting free jet and wall-slot injection into moving stream
- [ASME PAPER 65-APMW-6] 04 p0512 A66-14212
- Axial deviation of gas flow resulting from mixing turbulent gas jets 07 p1019 A66-17395
- Qualitative and quantitative solution of linearized approximations to boundary layer equations, noting free jet and wall-slot injection into moving stream
- [ASME PAPER 65-APMW-6] 10 p1523 A66-21470
- Two-dimensional isoenergetic compressible mixing of jet with fluid at rest for laminar and turbulent mixing 12 p1795 A66-23572
- Mixing of laminar viscous incompressible jets expelled from equally spaced holes in vertical wall, obtaining solution by using Navier-Stokes equation 12 p1864 A66-24444
- Maximum friction along jet path in mixing zone at constant pressure applied in finding irrotational wall velocity 13 p2063 A66-25468
- Horizontal slot jet mixing effect on sedimentation removal, neglecting boundary shear 13 p2071 A66-26732
- Turbulent mixing of rotationally symmetric jet in flow of equal velocity and equal density, including similarity models 15 p2423 A66-28522
- Three-dimensional viscous free mixing, describing numerical and experimental solutions for wake and jet flows [AIAA PAPER 65-49] 15 p2424 A66-29272
- Flow diagram for dimensioning of jet compressors to plot irreversible mixing, noting shape of mixing channel, design guidelines, etc 16 p2632 A66-31645
- Laminar argon arcjet mixing with coaxial flow of cool helium, considering turbulent characteristics and heat transfer [AIAA PAPER 65-587] 17 p3033 A66-32442
- Subsonic-supersonic speed jet turbulent mixing 17 p2840 A66-32489
- Turbulent gas jet mixing in chamber with four inlet nozzles 20 p3627 A66-36925
- Aerodynamic effect of free transverse gas flow on propagation of turbulent gas jet, analyzing jet mixing process and jet axis curvature 21 p3727 A66-39255
- Equivalent problem method of heat conduction theory applied to mixed flow produced by convergence of two jets ejected from two plane-parallel nozzles with parallel axes 21 p3728 A66-39256
- Laminar gas jet mixing as affected by periodic vorticity produced by mechanical vibration of orifice 23 p4055 A66-41497
- Time of establishment of steady state mixing in plane and axially symmetrical jets determined, using self-similar motions in unsteady state boundary layer and free turbulence 23 p4010 A66-41734
- NOISE**
- Stress response and fatigue life of acoustically excited brazed steel honeycomb panels for variations in thickness 01 p0147 A66-10133
- Analog computer application to prediction of nonlinear response of panel structure to random forcing function 01 p0148 A66-10134
- Aeroacoustic excitation of aerospace structures for design purposes, sources being jets of gas turbines and rockets and turbulent boundary layers
- [SAE PAPER 650823] 01 p0156 A66-10824
- Effect of exit velocity profile /shear/ on jet noise analyzed, considering structure of turbulence in mixing region of jets 02 p0176 A66-11587
- Effect of nozzle geometry and jet interference on noise generation and mechanism of noise reduction of noise suppressors 02 p0177 A66-11588
- Sound pressure and acoustic spectrum associated with it calculated for predetermination of ground noise during takeoff period of future aircraft [ONERA TP 250] 02 p0177 A66-11679
- Refraction of injected point source of sound by cold nitrogen jet, noting effects of temperature and velocity fields 07 p1080 A66-17500
- Horizontal propagation of sound from jet engine at ground proximity, discussing effects of vector wind, ground absorption and temperature gradient 07 p1080 A66-17730
- Noise generation mechanisms, discussing pressure-time histories, frequency spectra, sound pressure levels, directionality, etc 09 p1402 A66-20240
- Word-intelligibility tests in presence of recorded noise from jet and propeller aircraft 09 p1338 A66-20957
- FAA study of jet takeoff and landing noise effect on population around airport, establishing numerical value of noisiness 10 p1482 A66-21373
- Optimum magnitude of jet-noise reduction in cylindrical muffler 13 p2056 A66-25090
- Acoustic power emitted by coaxial subsonic jets in relation to aerodynamic parameter 13 p2063 A66-25432
- Sequential Noise Output Recording Equipment /SNORE/, aircraft engine noise test facility, for jet noise and compressor noise and acoustic absorption materials test facility [ASME PAPER 66-GT/N-41] 14 p2269 A66-26986
- Optimum magnitude of jet-noise reduction in cylindrical muffler 21 p3721 A66-38515
- Interactions among technical, economic and political aspects of aircraft noise problem, examining relation between thrust and jet engine noise
- [ICAS PAPER 66-5] 23 p4152 A66-42068
- Mean flow refraction of self noise and generation of shear noise in jets 24 p4194 A66-42414
- NOZZLE**
- Jet tab system influence on pressure distribution within rocket nozzle for missile control 03 p0431 A66-12749
- Thrust measurement for calibrating nozzle flow coefficients by direct primary method [ASME PAPER 64-WA/FM-3] 06 p0871 A66-16220
- Chemical reaction kinetics and gas dynamics combined to analyze processes occurring in combustion chambers and nozzles of jet and rocket engines 10 p1620 A66-21367
- Axisymmetric shock wave formation at nozzle exit when jet pressure is less than ambient pressure 12 p1799 A66-24447
- Acoustic output, turbulence in jets and noise sources in fluid amplifiers noting design, noise reduction by jet edge, input nozzle design, forced secondary flow, etc 18 p3054 A66-34132
- Binary adder and other pneumatic logic elements producing any two-valued function of three two-valued input parameter by proper arrangement of input jet nozzles 20 p4946 A66-36862
- PILOT**
- Medical aspects of commercial jet pilot fatigue, examining effects of socio-economic and off-duty activities 15 p2442 A66-28665
- PLUME**
- Highly underexpanded sonic jet in wind-tunnel study of stagnation temperature-pressure and shock profiles 08 p1164 A66-19134
- Propellant rocket exhaust plume effect on error calculation for radiation balance IR tracker 18 p3240 A66-33798
- Multiple rocket engine exhaust plumes calculated by method of characteristics and finite difference and compared with schlieren data
- [AIAA PAPER 66-651] 18 p3264 A66-34448
- Wind tunnel test program for simulation of gas-particle rocket exhaust plume, separated flow around nozzle and base recirculation [AIAA PAPER 66-767] 22 p3895 A66-40648
- Wind tunnel tests determining plume induced flow separation pattern on missile configurations as ratio of nozzle to ambient pressure 23 p4012 A66-41914
- Laminar shock layer structure in which streamlines retain appropriate momentum, calculating exhaust plume structure for rocket nozzle 23 p4012 A66-41921
- Absorption cross section, scattering cross section and angular scattering distribution of solid alumina particles emitted in homogeneous solid propellant rocket plume 24 p4294 A66-42778
- PROPULSION**
- Production and recent developments in gas turbines and propulsive engines in West Germany 06 p0942 A66-16795
- High by-pass turbofan for business aircraft, comparing jet propulsion system efficiency with fan engines, cost factors and market potentials [SAE PAPER 660221] 13 p2173 A66-26400
- Dynamic test method for characteristics and interactions of supersonic aircraft propulsion systems, particularly inlet/engine performance and control compatibility aspects [AIAA PAPER 66-741] 22 p3893 A66-40630
- PUMP**
- Design charts for determining ejector characteristics for optimum performance of jet pump systems [ASME PAPER 65-WA/FE-32] 05 p0691 A66-15709



Optimum design parameters for water ejectors  
[ASME PAPER 65-WA/FE-31] 05 p0691 A66-15710

Jet inducer with multiple nozzles calibrated in liquid mercury and water to minimize feed pump performance degradation due to off-design operation and cavitation 07 p1025 A66-18170

Jet pump cavitation correlation by similarity parameter 07 p1025 A66-18171

Jet pump development and testing on Lear Jet Model 24 and Model 40, noting fuel pump system performance, requirements and configuration  
[SAE PAPER 660223] 13 p2002 A66-26398

High-lift jet-pump boundary layer control system for STOL short haul S-1600 transport 16 p2633 A66-31282

Variable fluid-transformer control of fluid flow in increasing efficiency of hydraulic control systems 19 p3281 A66-36671

**JET STREAM**

Quasi-Lagrangian study of inviscid barotropic fluid for analysis of certain ageostrophic jet flows 02 p0222 A66-11825

Vertical velocity fluctuations in nocturnal low level jet examined by sonic anemometers 04 p0541 A66-13666

Energy distribution near jet stream and associated wave amplitude relations 05 p0711 A66-14544

Annual variation of wind direction and jet stream across Greenwich meridian 07 p1063 A66-18337

Winter jet stream structure and turbulence over Australia 10 p1552 A66-21317

Observational study of cloud forms in vicinity of jet streams as viewed from ground and Tiros meteorological satellite 11 p1727 A66-22316

Reliability of locating jet streams by means of cloud patterns in Tiros pictures, determining most definitive characteristics of those patterns 13 p2121 A66-25813

Wind tunnel experiments on thin two-dimensional airfoil with sharp leading edge and with jet blowing through mid-chord slot on upper surface in order to control boundary layer and circulation around it 18 p3048 A66-33950

One-dimensional analysis used by Hope and Segars invalid for ejector with supersonic primary stream 18 p3100 A66-34604

Wall interaction digital stream amplifier with increased flow gain, impedance matching, outputs decoupled and noise reduction 19 p3283 A66-36812

Jet impact on plane surface at oblique angle, noting transformation from jet to thin sheet and role of stagnation pressure 20 p3546 A66-37805

Supersonic gas flow states in transition regime, discussing change from dynamical to molecular flow, velocity and pressure distribution and conditions for freezing of translational degrees of freedom 20 p3548 A66-38084

Clear air turbulence near jet stream, discussing velocity profiles and various meteorological parameters 22 p3902 A66-39677

High altitude turbulence in presence of strong jet stream or under influence of orographic systems 22 p3942 A66-39730

Stress, eddy viscosity and viscous dissipation estimations in jet stream obtained during Project TOPCAT in Australia, using aircraft soundings 24 p4234 A66-42984

**JET TRANSPORT**

SA BOEING 737 AIRCRAFT

Fail-operative stability augmentation system for C-141 jet transport aircraft yaw control axis, using triple redundant sensors and signaling 01 p0011 A66-10662

Slender wing research and short-range transport operation are among studies at Royal Aircraft Establishment 03 p0321 A66-12885

Takeoff and overshoot director system for jet transport aircraft 05 p0712 A66-14701

Short-range jet transport operating cost reduction through technical innovation, labor cost and research 06 p0804 A66-15992

Possible cost reduction with all-wing short-range aircraft, noting ogee design 06 p0804 A66-15993

Design trends in landing gear for medium- and short-range jet transports 07 p0987 A66-17286

VC10 C Mk I jet transport for troop transport, freighting, casualty evacuation and refueling 07 p0989 A66-18163

Passenger injuries due to decompression, impact and explosion from dynamite in rear lavatory of Boeing 707 at high altitude 09 p1336 A66-20522

V/STOL transport aircraft design and application, noting performance with varying number of propulsion units 10 p1482 A66-21369

Wind tunnel, simulator and flight test results to evaluate cockpit accelerations, handling qualities and stability and control of jet transports in severe turbulence  
[AIAA PAPER 65-330] 16 p2634 A66-31317

Operational cargo handling requirements to make economically feasible supersonic transport and giant subsonic jet 22 p3848 A66-40021

New jet transports, discussing subsonic, SST and stretched versions of subsonic transports 23 p4016 A66-41302

Promotion of aviation safety, discussing adoption of new accident statistics, elimination of catastrophes and STOL design extension to medium and long-range aircraft 23 p4152 A66-41305

**JET VANE**

S GUIDE VANE

**JETSTREAM AIRCRAFT**

S HANDLEY PAGE HP-137 AIRCRAFT

**JETTISON SYSTEM**

Frequency, dynamic response and jettison analyses for payload shrouds, with application to OAO 16 p2808 A66-30468

Environment simulation for space vehicle explosive separation system testing, noting equipment, performance, etc 16 p2679 A66-30470

**JOINT**

SA BONDING

SA FASTENER

SA LAP JOINT

SA METAL JOINT

SA RIVETED JOINT

SA SOLDERED JOINT

SA WELDED JOINT

Strength of adhesive joints showing ratio of normal and shear stress as important parameter, using crack propagation theory 01 p0152 A66-10380

Attachment and joining aspects in space age structures noting selection of materials  
[SAE PAPER 650788] 01 p0156 A66-10842

Double universal joints for transmission of mechanical power 04 p0526 A66-13800

Qualities required of materials for joint sealing, particularly elastomers, noting properties and possibilities 12 p1899 A66-23818

Approximation method for checking stability of compression members in rigid-joint space truss or stability against out-of-plane buckling of compression members in rigid-joint plane truss 19 p3475 A66-36489

Energy dissipation effect on panel vibration damping due to structural joints 21 p3827 A66-38693

Spacecraft joint design for fabric-type flexible structures with nonflexible structural components 22 p3926 A66-40281

Joint designs for reinforced plastic structures, emphasizing unidirectional mechanical properties 22 p3927 A66-40282

Joint strength analysis for brittle materials 22 p3927 A66-40283

Optimum seal and sealants for joints and connections in spacecraft 22 p3927 A66-40285

**JOINT /BIOL/**

S BONE

**JORDAN FORM**

Completely plastic torsion of cylindrical bar with simply connected cross sections examined, using ridge of Jordan domain analogy 09 p1466 A66-20130

Structure and representations of noncommutative Jordan algebras, using proof of analog of Jacobson coordinatization theorem 18 p3127 A66-34456

Construction of Cayley-Dickson type and involution type bimodules for composition algebras 22 p3939 A66-40002

**JOSEPHSON CURRENT**

Quantitative electrodynamic experiment on

Josephson oxide tunneling junction, verifying time dependence of Josephson equation 07 p1108 A66-18438

Tunnel junction RF modes driven by AC Josephson current 09 p1417 A66-20030

Persistent currents and flux quantization in superconducting rings interrupted by Josephson junction 09 p1417 A66-20031

Flux quantization, Josephson tunneling and persistent currents in superconductor studied by model of charged Bose gas at zero K 09 p1417 A66-20034

Dependence of step-like structure of volt-ampere characteristics of superconducting Sn-I-Sn tunnel junction as function of temperature, magnetic field and junction dimensions 09 p1428 A66-20593

Josephson effect in superconductors with paramagnetic impurities in absence of potential difference between superconductors 14 p2361 A66-27197

Josephson effect in superconducting bodies 14 p2370 A66-28355

Josephson type superconducting tunnel junction for generation of microwaves and submillimeter waves 15 p2461 A66-29012

Dependence of step-like structure of volt-ampere characteristics of superconducting Sn-I-Sn tunnel junction as function of temperature, magnetic field and junction dimensions 20 p3622 A66-38128

Spectral response curves of superconducting point contacts, noting existence of frequency dependent Josephson current amplitudes peaking in vicinity of energy gap 21 p3803 A66-39282

Kinetic tunneling theory in superconductors, clarifying conditions for onset of Josephson current 21 p3803 A66-39309

Tunnel current dependence on magnetic field for two superconductors with thin dielectric interface 21 p3804 A66-39314

Josephson effect in superconductors with paramagnetic impurities in absence of potential difference between superconductors 24 p4259 A66-43095

**JOULE HEATING**

Hydrodynamic acceleration of plasma in discharge tube into which energy is released in form of Joule heat 04 p0552 A66-14154

Heating of completely ionized quasi-neutral gas by Joule energy dissipation 04 p0556 A66-14420

Ionizing role of photon radiation in gas thermionic converter, noting experimental results and application to solar energy converters, tubular emitter converters, etc 09 p1405 A66-20923

Experiments on ion cyclotron heating of plasma generated by Joule heating in Heliotron-B 12 p1919 A66-23851

High magnetic field limit of shock wave in steady state model plasma moving along x axis studied transverse to magnetic field 18 p3148 A66-34905

Integral method derivation of thermoconductivity coefficient of cylindrical semiconductor immersed in liquid He and superheated by Joule heating 24 p4255 A66-42494

**JOURNAL BEARING**

Vibrational and stability behavior of unbalanced shaft running in cylindrical journal bearing, noting oil film elastic effects 01 p0151 A66-10285

Stability of symmetrical elastic rotor in journal bearings with flexible damped supports  
[ASME PAPER 65-APMW-8] 04 p0528 A66-14214

Exact thermoelastic solutions for clearance variation in short cylindrical dry journal bearings with unsymmetrical frictional heating  
[ASME PAPER 65-LUB-3] 04 p0527 A66-14239

Whirl instability and pneumatic hammer for rigid rotor in pressurized gas journal bearings  
[ASME PAPER 65-LUB-12] 04 p0527 A66-14245

Cylindrical squeeze-film gas journal bearing, noting load deflection experiments  
[ASME PAPER 65-LUB-13] 04 p0527 A66-14246

Reynolds equation for compressible and incompressible lubrication for load



- coefficients and attitude angles of axial groove cylindrical bearings  
[ASME PAPER 65-LUB-16] 04 p0528 A66-14248
- Prandtl mixing-length theory used to predict performance of journal bearings operating in turbulent regime  
[ASME PAPER 65-LUB-17] 04 p0528 A66-14249
- Self-excited torsional vibrations of power transmission drives under boundary lubrication, developing rotating shaft/bearing relations 05 p0772 A66-14643
- Load capacity and attitude angle of gas lubricated short journal bearing 06 p0885 A66-16224
- Dynamic stability conditions of self-acting gas lubricated journal bearings 07 p1039 A66-18231
- Continuous fluid film self-acting cylindrical journal bearing theory and design data, introducing isothermal bulk modulus into lubrication equations  
[ASME PREPRINT 65AM 3A2] 07 p1039 A66-18285
- Externally pressurized nonrotating porous wall air lubricated journal bearing properties, taking into account surface roughness effects  
[ASME PREPRINT 65AM 3A5] 07 p1039 A66-18286
- Mercury lubricated hybrid bearings for lubrication requirements of mercury Rankine Silent Compact Auxiliary Power (SCAP) system  
[ASME PREPRINT 65AM 3A3] 07 p1039 A66-18288
- Stability of symmetrical elastic rotor in journal bearings with flexible damped supports  
[ASME PAPER 65-APMW-8] 10 p1539 A66-21488
- Cylindrical squeeze-film gas journal bearing, noting load deflection experiments  
[ASME PAPER 65-LUB-13] 12 p1888 A66-24551
- Load capacity of condensing vapor-lubricated long self-acting journal bearing, examining two-phase and single-phase regions  
[ASME PAPER 65-LUBS-5] 12 p1888 A66-24554
- Test rig for gas-lubricated journal bearings measuring frictional torque, gas film pressure distribution, static and dynamic eccentricity changes, etc 12 p1859 A66-24929
- Designing hydrostatic journal-and thrust-gas bearings 13 p2085 A66-25365
- Externally pressurized gas journal bearings, evaluating various design parameters for operating at high temperatures and high speeds  
[ASME PAPER 66AM 4B2] 16 p2711 A66-30410
- Rotor-tilting pad gas lubricated journal bearing system performance determined by solving dynamic equations together with time-transient Reynolds equation  
[ASME PAPER 66-LUBS-3] 17 p2931 A66-33177
- Turbulent hydrodynamic lubrication theories and solution of Constantinescu equation for finite-length journal bearing  
[ASME PAPER 66-LUBS-11] 17 p2931 A66-33184
- Eigenvalues and eigenvectors obtained by numerical solution of special Hill equation in lubrication theory  
[ASME PAPER 66-LUBS-13] 17 p2932 A66-33185
- Prediction of hydrostatic gas journal bearing performance by solving simultaneous flow equations with Fortran II computer program  
[ASME PAPER 66-LUBS-16] 17 p2932 A66-33187
- Small parameter method to study steady state flow of viscous incompressible fluid in journal bearing 22 p3928 A66-40688
- P-4 JET FUEL
- Measurement of friction of materials sliding in JP-4 fluid to predict performance of hydraulic pump 06 p0884 A66-16136
- P-5 JET FUEL
- JP-5 fuel-air mixture ignition by platinum catalytic igniters, using ramjet engine baffle combustors 13 p2171 A66-25594
- JUMP
- Jump conditions at point of contact for corresponding cases of sliding and rolling contact in plane motion 21 p3769 A66-38476
- JUNCTION
- SA BARRIER LAYER
- SA N-P JUNCTION
- SA N-P-N JUNCTION
- SA NIP JUNCTION
- SA P-N JUNCTION
- SA P-N-P JUNCTION
- SA SILICON JUNCTION
- Wideband junction circulator design with maximum product of isolation and frequency bandwidth but maintaining minimum temperature and DC magnetic field variation 01 p0040 A66-10548
- Electron distribution disruption by electric current across n-n heterojunction resulting in heating and cooling of respective electron gases in each of semiconductors, noting electron scattering 07 p1104 A66-18362
- Quantitative electrodynamic experiment on Josephson oxide tunneling junction, verifying time dependence of Josephson equation 07 p1108 A66-18438
- Transport equation for germanium-gallium arsenide-iodine system and epitaxial vapor growth preparation of GaAs-Ge heterojunction by closed tube process 13 p2161 A66-25185
- Injection and extraction of hot electrons in n-n heterojunctions with rapid Maxwellization of electron gas, negative resistance and semiconductor characteristics 13 p2166 A66-25920
- Design of lossless junction, given one row in scattering matrix 14 p2268 A66-27965
- Flow graph analysis of lossless nonideal 3- and 4-port junction circulators for visualizing scattering matrices and calculating coefficients of combined networks 17 p2896 A66-33277
- Perturbation theorems for waveguide junctions expressing changes in impedance or admittance matrix elements 18 p3077 A66-34057
- Numerical solution of problems on discontinuity at junction between homogeneous and inhomogeneous waveguides 18 p3078 A66-34094
- Hybrid junction diplexer connecting transmitter and receiver to common antenna 22 p3873 A66-39784
- Effectiveness parameters of spherical shield electrode surrounding negative dielectric junction of insulator in high vacuum 23 p4042 A66-41040
- Alloyed semiconductor heterojunction metallurgy and physics, noting processes of interface alloying, solution growth and vapor transport-interface alloy 24 p4252 A66-42348
- JUNCTION DIODE
- P-n transitions in gallium arsenide investigated as factor in performance of such diodes as converters of ultrasonic into electrical oscillations 01 p0036 A66-10422
- Increased efficiency and power-handling capability of high order idlerless frequency multipliers by using hyperabrupt varactors 02 p0195 A66-11363
- Large signal transient response simulation of p-n junction diode using RC analog network 02 p0200 A66-11882
- Microwave power measuring device using p-n junction diodes and operating at 8, 4 and 2 mm 02 p0200 A66-11885
- Impurity-recombination emission in diodes of n-type Si single crystals alloyed with In 02 p0206 A66-12092
- Semiconductor diodes discussing germanium and silicon diode structures, ultrasonic chip bonding and epitaxial material effects on structures 03 p0348 A66-13344
- Temperature sensitivity of p-n junction volt-ampere characteristic may make such devices suitable for meteorological sensors 04 p0519 A66-13675
- Aircraft and commercial application of three-phase direct current resistance welding, using silicon diodes 05 p0685 A66-14518
- Rise of junction temperature during continuous operation of GaAs injection laser 05 p0692 A66-14771
- Operating principles of pulse and frequency modulation, using step-recovery diodes as circuit elements 05 p0651 A66-15835
- Transient process during instantaneous switching of semiconductor junction diode from forward to neutral direction 06 p0852 A66-16546
- Characteristics of spontaneous IR source for which external quantum efficiency of forward-biased GaAs p-n junction measures 40 percent at 20 degrees K 06 p0855 A66-16766
- Emitter degeneration effects in design of transistor amplifiers when it is desirable to predict and control amount of distortion produced by nonlinearity of transistor input characteristic 06 p0857 A66-16974
- Switching transients of semiconductor junction diodes with arbitrarily thick base 06 p0859 A66-17189
- Injection luminescence in InAs diodes 07 p1094 A66-17315
- Energy spectrum of recombination radiation from forward-biased heavily doped GaAs diodes at 4.2, 77 and 290 degrees K as function of current density 07 p1096 A66-17326
- Temperature dependence of loss and gain factor of GaAs diode and threshold current density of GaAs laser and junction luminescence of GaAs 07 p1042 A66-17332
- Uniaxial strain effects in /100/ junction orientation GaAs laser diodes, discussing photon polarization 07 p1042 A66-17335
- Stimulated emission in GaSb diodes made from crystals prepared by Czochralski method 07 p1096 A66-17336
- Amplification factors and optimum matching conditions calculated for complex capacitive diode frequency converters 07 p1005 A66-17347
- Effect of irradiation of silicon by fast neutrons on switching time of alloy diode synthesized on silicon base 07 p1099 A66-17929
- Current-voltage relationship of Au on GaAs Schottky barrier, examining introduction of single temperature independent parameter 07 p1106 A66-18399
- Neutron and electron irradiation damage in uniform silicon avalanche junction diode and effect on avalanche pulse rate 07 p1012 A66-18410
- Formed point contact gallium arsenide backward diodes compared with conventional millimeter-wave diodes show advantage as low level baseband current detectors 08 p1189 A66-18658
- Rectifying and ohmic contacts used in manufacture of gallium phosphide diodes that emit light when current is reversed 08 p1273 A66-19291
- Room temperature capacitance voltage characteristics and built-in diffusion voltages in n Ge-n Si double saturation heterojunction 09 p1411 A66-19912
- Gallium arsenide phosphide heterojunction diode used to triple from X band to Ka band 09 p1350 A66-19924
- Electrical contact for very small planar junctions and embodiment in millimeter-wave mixer diode 09 p1350 A66-19926
- Effect of thickness nonuniformity on capacitance of Al-Al<sub>2</sub>O<sub>3</sub>-Al tunnel junction structure compared with device with uniform thickness 09 p1426 A66-20198
- Dependence of step-like structure of volt-ampere characteristics of superconducting Sn-I-Sn tunnel junction as function of temperature, magnetic field and junction dimensions 09 p1428 A66-20593
- IR and sub-mm wave modulation using free carrier absorption in p-n junction, examining reverse and forward-biased configurations 09 p1432 A66-20972
- Directional radiation from incoherent electroluminescent diodes, noting increase in refractive index for dielectric slab model 10 p1509 A66-21581
- P-i-n diode modulators for K and Q frequency bands, extending operation from 18 to 40 gc 10 p1513 A66-21856
- Time dependence of multiplication and refinement in silicon technology needed to establish uniform multiplication for Read diode prototype 10 p1515 A66-22089
- Silicon diode microwave oscillators and amplifiers, noting application of avalanche transit time for increased efficiency of p-n



junctions 10 p1515 A66-22090  
 Indium arsenide diodes for thermophotovoltaic conversion at 1000 K 11 p1639 A66-22248  
 Schottky diode and metal-base transistor design and operation with metal-semiconductor contact 11 p1660 A66-22271  
 P-n transitions in gallium arsenide investigated as factor in performance of such diodes as converters of ultrasonic to electrical oscillations 11 p1664 A66-22608  
 Cadmium sulfide space charge limited diodes, noting current voltage characteristics and field and electron density distributions 11 p1668 A66-23026  
 Scanning electron microscope observation of electrical leakage paths due to crystal defects in silicon diodes 11 p1668 A66-23028  
 Sinusoidal voltage converted to rectangular voltage, using charge storage diodes 11 p1668 A66-23064  
 Semiconductor diode mixer relatively free of modulation distortion and cross modulation 11 p1669 A66-23066  
 Volt-ampere characteristics of short semiconductor diode at high injection levels 11 p1757 A66-23229  
 Parameter dependence of intermediate frequency voltage indicated during establishment of optimum conditions for optical receivers and merit of subcarrier mixing 12 p1832 A66-23960  
 Radiative recombination in gallium arsenide p-n junctions for weak currents, obtaining relation between emission spectra and current-voltage characteristics of diodes 12 p1929 A66-24456  
 Reverse current across collector-base junction in transistor 12 p1844 A66-24822  
 Quantitative observation of light modulation by electro-optic effect in reverse-biased GaAs p-n junctions at wavelength of 1.15 microns 13 p2159 A66-25067  
 Hot-carrier diode characteristics and application to HF and microwave devices such as mixers and detectors 13 p2031 A66-25359  
 Optically coupled linear circuit techniques, discussing GaAs p-n junction diode, noncoherent light emitters and silicon p-n junction photosensors 13 p2036 A66-25521  
 Voltage buildup on p-n junction and base of semiconductor diode during jump in forward current 13 p2041 A66-25943  
 Voltage dependence of barrier height in Al-AlN-Mg tunnel junction 13 p2170 A66-26596  
 Radiation effects on silicon p-n junction diode solar cell and use of transparent radiation shield 14 p2225 A66-27107  
 Green emission lines from solution-grown p-n junctions in GaP diodes doped with shallow donors and acceptors 14 p2251 A66-27231  
 Formula derivation for dynistor delay time and switching-on time on basis of system of charge equations 14 p2254 A66-27741  
 Long diode theory not limited by conditions of quasi-neutrality, noting V-I characteristics 14 p2254 A66-27744  
 Exact circuit analysis of abrupt-junction varactor diode frequency doubler 14 p2268 A66-27957  
 Conventional point-contact diodes and junction diodes with point-contact geometry, examining fabrication techniques and millimeter wave application 15 p2461 A66-29013  
 Bandwidth of nonoverdriven abrupt-junction varactor-frequency doubler, deriving upper bounds for minimum constant T for lossless case 15 p2465 A66-29323  
 Stable microwave oscillations in single crystal Ge alloy p-n junction diodes 15 p2567 A66-29402  
 Reverse recovery phenomena in silicon alloyed p-n junction 15 p2467 A66-29710  
 Minimum spectral line width, threshold current density, radiation-peak displacement and possible recombination mechanism for GaSb laser diode p-n junctions in coherent radiation 16 p2721 A66-31764  
 Origin of polarization of radiation from GaAs diodes, noting intensity dependence on current density and effect of anisotropic electron velocity

distribution 16 p2667 A66-31770  
 Varactor frequency doubler response to amplitude and phase modulated signals 17 p2878 A66-31811  
 Silicon microwave p-n diode design and use as variable resistance 17 p2891 A66-32909  
 Signal analysis of abrupt and graded junction varactor harmonic generators with idlers, showing how load and source resistances may be optimized 17 p2893 A66-32922  
 Iterative solution of large signal abrupt junction varactor doubler as input frequency is varied, given power of source and load impedance 17 p2895 A66-33276  
 Strong injection in nondegenerated p-n junction producing electron-hole plasma in n region near junction 17 p2986 A66-33307  
 Photocurrent and leakage current in zinc diffused GaAs junction diodes in terms of channel effect 17 p2987 A66-33319  
 Microplasma internal parameter measurement including switch-on voltage, switch-off voltage, plasma resistance, parallel capacity and internal series resistance 17 p2896 A66-33320  
 One-dimensional diode model with high resistivity n region and built-in electrical field 18 p3088 A66-35038  
 Energy band structure, carrier behavior and characteristic curve of p-n junction diode at high-current level, solving transport and Poisson equations 19 p3312 A66-35346  
 Switching transients of semiconductor junction diodes with arbitrarily thick base 19 p3314 A66-35547  
 Gallium arsenide lasers operating at room temperature investigated, based on diffusion p-n junctions, discussing emission spectrum 19 p3375 A66-36070  
 Low-distortion modulation of IR and submillimeter waves, using free-carrier absorption in pair of crossed reverse-biased junction diodes 20 p3528 A66-37452  
 Avalanche transistor generation of jitter-free nanosecond current pulses for driving GaAs laser diodes at low temperatures 20 p3528 A66-37453  
 Radiative recombination in gallium arsenide p-n junctions for weak currents, obtaining relation between emission spectra and current-voltage characteristics of diodes 20 p3619 A66-37688  
 Signal analysis of abrupt and graded junction varactor harmonic generators with idlers, showing how load and source resistances may be optimized 20 p3531 A66-37831  
 Dependence of step-like structure of volt-ampere characteristics of superconducting Sn-I-Sn tunnel junction as function of temperature, magnetic field and junction dimensions 20 p3622 A66-38126  
 RC network model applied to study of transient response of semiconductor diode, obtaining accuracy estimates for finite-difference representation of one-dimensional diffusion equation 21 p3713 A66-39298  
 Avalanche breakdown voltage of quasi-planar /circular cylindrical/ silicon junction and relation to increased electric field intensity in curved portion 22 p3959 A66-39741  
 Far-field light emission mode pattern of GaAs diode injection lasers, dielectric gradient in inversion layer and refractive index in junction 22 p3930 A66-39743  
 Gold doping effects on recovery time of phosphorus, boron and arsenic impurity gaseous-diffused junction diodes and estimated gold recombination center densities 22 p3873 A66-39749  
 Four-layer p-n-p-n diodes having two separate capacitance modes enables use as controlled element in frequency keying circuits 22 p3875 A66-40074  
 Injection luminescence in forward-biased CdTe p-n junction diode 23 p4112 A66-41298  
 Capture effect on I-V characteristics of junction diodes and injection coefficients in forbidden transition zone 23 p4045 A66-41444  
 I-V characteristics of junction diode with antibarrier layer and oxide film pressed on rear contact 23 p4045 A66-41445  
 Unidirectional semiconductor-diode parametric amplifier and mixer, emphasizing power transfer and low noise characteristics 23 p4048 A66-41856

Avalanche radiation from bulk of long thin forward-biased p-n-p silicon diodes 24 p4180 A66-42258  
 Injection electroluminescence in AlAs-GaAs as p-n junction diodes of graded energy gap 24 p4251 A66-42300  
 Multiple energy bands effects on stress dependence of breakdown and order of magnitude in breakdown voltage of Ge and Si junction diodes 24 p4251 A66-42306  
 Transistor theory approximation of DC and small signal I-V characteristics of p-n-p-n junction diodes and triodes 24 p4184 A66-42744

**JUNCTION TRANSISTOR**  
 General progress of semiconductor junction and ruby lasers, especially in experimental field 02 p0238 A66-11370  
 Collector-to-base junction breakdown occurring in planar transistors over whole surface due to emitter presence 02 p0205 A66-12002  
 Synthesis of equivalent circuits consisting of lumped elements for active region of distributed model of junction transistor 03 p0346 A66-13321  
 Increase in collector voltage at constant power dissipation will increase junction temperature and give apparent effect of higher thermal resistance 04 p0500 A66-14102  
 Electrical and radiation storage time in transistors with respect to majority carrier storage in base, calculating photocurrent 05 p0735 A66-14855  
 Punch-through avalanche phenomena, describing fast rise pulse production in junction transistors of variable base width 05 p0651 A66-15840  
 Characteristics of electrochemical cells in which concentration of ionic species in chamber can be varied via applied electrical signal as analog of junction transistor 06 p0852 A66-16637  
 Distributed model of junction transistor and application in prediction of emitter-base diode characteristic, base impedance and pulse response of device 06 p0855 A66-16785  
 Current amplification factors of micropower silicon planar transistors in low current common-base and common-emitter circuits 06 p0860 A66-17196  
 Current voltage characteristics of four-layer structures with common diffusion p-n junction and two emitters 06 p0860 A66-17197  
 Heterojunction preparation by vacuum evaporation, describing epitaxial deposition of germanium on gallium arsenide substrate 08 p1270 A66-19058  
 Unifron, junction-type unipolar field transistor, design, operation, parameter, production technology and uses in electronic circuitry 08 p1193 A66-19277  
 Small signal properties of field effect devices, junction and MOS 08 p1195 A66-19356  
 Switching waveform prediction of simple transistor inverter circuit from charge control equations 08 p1195 A66-19358  
 Light activated low level switch consisting of electroluminescent GaAs p-n diode and double emitter silicon transistor 08 p1195 A66-19359  
 Analog multiplier-divider based on properties of saturated transistors 08 p1198 A66-19735  
 Tunnel junction RF modes driven by AC Josephson current 09 p1417 A66-20030  
 Electrical properties, solubility and diffusion characteristics of gold in silicon, noting discrepancy between theoretical calculations and experimental measurements 09 p1432 A66-20975  
 Nonresonant solid state magnetic, semiconductor and dielectric devices, noting operation characteristics, control parameters, etc 10 p1509 A66-21418  
 Field effect transistor input capacitance in pinch-off region derived by using two parallel coupled condensers as equivalent 10 p1510 A66-21657  
 Impurity atom diffusion through narrow diffusion mask opening determined by relaxation method 10 p1512 A66-21762  
 Dynamic transient thermal response and voltage feedback in junction transistors 10 p1512 A66-21764  
 Polarity and harmonics of nonlinear



distortion sources in common emitter transistor amplifiers operated in normal domain 11 p1661 A66-22391

Dependence of recombination-generation current and injection coefficient of p-n junction on forward bias 11 p1666 A66-22730

Minority carrier flow in base region of Graded Band Gap Base /GBGB/ transistor, determining effect of injected current level upon carrier transit time 11 p1668 A66-23024

Mathematical approximation for alpha of drift transistors derived in terms of equivalent dominant pole and excess phase 11 p1671 A66-23245

Component reliability, especially in transistors, noting techniques, design, tests and mounting as monolithic circuits 12 p1833 A66-24082

Existence of limitation on properties and diffusion mode in junction and insulated gate field effect transistors 12 p1837 A66-24306

Noise figure of microwave transistors, noting effect of parasitics associated with wafer and package 13 p2038 A66-25562

Normalized low-level characteristics of saturated transistor 14 p2247 A66-27043

Junction field effect transistor used for switching 14 p2252 A66-27459

Synthesis of equivalent circuits consisting of lumped elements for active region of distributed model of junction transistor 14 p2260 A66-28295

Thermal noise of input conductance and gate-drain conductance in junction-gate FET 15 p2458 A66-28892

Unijunction transistor parameter and design charts 17 p2888 A66-32780

Secondary breakdown in transistors, noting effect of irregularities in collector base junction and tunneling sites 17 p2894 A66-33108

Direct current volt-ampere characteristics of junction gate germanium alloy FET, including field-dependent mobility effect and channel-height distribution 17 p2897 A66-33463

DC theory of unijunction transistor, calculating idealized one-dimensional model, neglecting diffusion currents but taking into account bulk recombination effects 18 p3076 A66-33934

Current amplification factors of micropower silicon planar transistors in low current common-base and common-emitter circuits 19 p3315 A66-35554

Current voltage characteristics of four-layer structures with common diffusion p-n junction and two emitters 19 p3315 A66-35555

Differential low level junction field effect transistor commutators performance and characteristics for design considerations 19 p3317 A66-35702

Varactor characteristics, applications, equivalent circuits, measurement problems, etc 19 p3319 A66-36165

Frequency variations of pi-equivalent circuit parameters of junction transistor, noting expansion of hyperbolic function into Taylor series 22 p3873 A66-39815

Monograph on electronic theory of heavily doped semiconductors covering energy spectrum, perturbation theory, absorption of electromagnetic waves, density states, etc 23 p4109 A66-41119

Heterojunction formation between substrate and compound semiconductor synthesized by substitution reaction during alloying process 23 p4113 A66-41300

Dependence of recombination-generation current and injection coefficient of p-n junction on forward bias 23 p4045 A66-41468

HF transistor stability in common emitter configuration, examining performance of input admittance in circuit design and analysis 24 p4181 A66-42377

Charge transport through hemispherical metal contacts on semiconductors, calculating V-I characteristics and injection ratios 24 p4254 A66-42388

Small signal forward and reverse transfer parameters derived for metal oxide semiconductor and junction-gate field effect transistors from simple unified charge-control analysis 24 p4185 A66-43030

JUPITER /PLANET/

Jupiter radio emission, with plasma waves in planet ionosphere as source of radiation 01 p0131 A66-10273

Spectral index of radiation from Jupiter between 178 and 810 02 p0282 A66-11502

Visual data of sudden changes in motion of Jupiter Great Red Spot during 1962 02 p0292 A66-12191

Spectral data of Galilean satellites of Jupiter 03 p0427 A66-12919

Simultaneous passage of shadows of two Jupiter satellites across planet disk, including tabulation of dates and times of phenomenon 05 p0758 A66-14731

Concepts concerning Jupiter surface revised following transformations observed since 1962 and estimation of ash particles in planet atmosphere 05 p0759 A66-14880

Jupiter emission data re-analyzed, supporting Bigg finding of control by satellite X 05 p0760 A66-14946

Decameter emission from Jupiter, discussing polarization characteristics such as direction, magnitude, measurement techniques and data 05 p0762 A66-15280

Geometrical UV reflectivity of Jupiter in terms of Rayleigh scattering determined from objective-grating rocket spectrometer 05 p0762 A66-15281

Radiation from Jupiter magnetospheric tail contributes to decametric noise 07 p1133 A66-17467

Effects of commensurability with mean motion of Jupiter upon distribution of mean motions of short-periodic comets 07 p1135 A66-17640

Two-element interferometer to investigate Jupiter declimeter circularly polarized radiation 08 p1288 A66-18789

Jovian phase variations and limb-darkening of surface detail examined by scanning isodensitometer 08 p1293 A66-19266

IR spectrophotometry of Moon and Galilean satellites of Jupiter, noting surface properties, thermal radiation and albedo increase with wavelength variation 08 p1298 A66-19458

Decametric radiation of Jupiter, discussing environment of planet and properties of magnetosphere 09 p1449 A66-20102

Decametric radiation of Jupiter, discussing effect of Io satellite and asymmetrical stop zones 09 p1449 A66-20103

Frequency and polarization structure of Jupiter decametric emission on 10-msec scale 09 p1450 A66-20104

Jupiter microwave emission, noting brightness distribution, Van Allen belt flux density and polarization 09 p1450 A66-20105

Interferometric examination of Jupiter declimeter radio emission, noting equipment, polarization characteristics and distribution of nonthermal emission 09 p1450 A66-20106

Relation of Jupiter declimeter radiation intensity and polarization to distribution of synchrotron radiating electrons in Van Allen belt 09 p1450 A66-20107

Simultaneous observations of Jupiter on three frequencies, noting phase consistency of flux variations, Faraday rotation and flux density 09 p1450 A66-20108

High-resolution spectra of decametric radio bursts from Jupiter 09 p1457 A66-20470

Jupiter in 1964/65 photographic observation 11 p1771 A66-22648

Postdetector correlation interferometry of size of noise burst at decameter wavelengths from Jupiter 13 p2182 A66-25552

IR reflection spectrum of Jupiter from second flight of Stratoscope II, discussing deep absorption features 13 p2184 A66-25619

Short-period Trojan orbits in restricted three-body problem numerically determined, using Jupiter and Sun as principal masses 13 p2185 A66-25807

Spectral data of Galilean satellites of Jupiter 14 p2380 A66-27268

Conceptual unmanned spacecraft designs for Jupiter exploration including flyby and orbiter missions 14 p2394 A66-28176

[AIAA PAPER 65-388] 14 p2394 A66-28176

Relation between RF of Jovian decametric emission bursts and modulation by Io searching for modulation by three outer Galilean satellites 15 p2597 A66-29232

Measurements of location of centroid of

Jovian radio emission relative to nearby radio source 15 p2597 A66-29259

Jupiter decametric radio emission spectrum noting power at various frequencies, mean flux density, magnetic pole locations, etc 16 p2801 A66-30922

Jupiter planetary surface observations show slow evolution of atmospheric phenomena 16 p2804 A66-31310

Jupiter Red Spot coordinate measurement from recent plates 17 p3006 A66-33011

Radio noise bursts from Jupiter at decameter wavelengths noting Cerenkov emission, Doppler-shifter cyclotron emission and escaped-whistler models 18 p3225 A66-33550

Nonsolar absorption lines in spectra of inner three Galilean satellites of Jupiter 18 p3230 A66-34155

Thermal contrast of satellite eclipse shadows and band structure during 1965 apparition of Jupiter 18 p3230 A66-34156

IR spectrophotometry of Moon and Galilean satellites of Jupiter, noting surface properties, thermal radiation and albedo increase with wavelength variation 18 p3232 A66-34487

Angular sizes of sources of Jovian radio bursts measured by using interferometers suggest they are produced by diffraction or focusing process in interplanetary space 18 p3237 A66-35083

Growth rate of forward-subliminuous-mode electromagnetic wave excited in helical stream-plasma used to calculate Jupiter decametric emission 19 p3463 A66-35924

Magnetic fields and trapped radiation intensities of other planets in solar system, particularly Jupiter 20 p3639 A66-38316

Faraday rotation measurements of decameter wavelength radiation from Jupiter, calculating ionospheric electron content 22 p3977 A66-39987

Millisecond radio pulses from Jupiter 22 p3980 A66-40400

Jovian radio bursts containing millisecond pulses, noting effect of Io position on probability of decametric emission 22 p3982 A66-40521

Polarization, periodicity and angular diameter of radiation from Jupiter at 610 mc/s 23 p4125 A66-41064

Hot shadows cast on Jupiter by satellites explained in terms of freezing of supercooled ammonia 23 p4128 A66-41308

Periodicities in Jupiter decametric radiation and methods of assessing statistical and physical significances, noting natural satellites effects 23 p4129 A66-41684

Jupiter radiation recorded almost every night with antenna arrays shows emission dependency on Jupiter longitude and Io position 23 p4131 A66-41817

Radio emission from Venus, Jupiter, Pluto and other planets at 1.9 cm analyzed, using radio telescope, noting effective temperatures 23 p4131 A66-41818

Asteroid belt flyby spacecraft concepts based on Atlas family with potential growth for Jupiter flyby 24 p4278 A66-42691

**JUPITER ATMOSPHERE**

Jupiter photoelectric spectral scan in UV reproduced as geometric reflectivity vs wavelength, using Aerobee rocket 02 p0286 A66-11359

Discrepancy between derived temperature for cloud tops of Jupiter and Saturn and expected value for model in simple equilibrium with solar radiation attributed to presence of ammonia 04 p0579 A66-14180

Optical thickness of Jupiter isothermal atmosphere assuming it consists of hydrogen, methane and ammonia 05 p0759 A66-14879

Separation between fluid phases in multicomponent atmosphere as possible explanation of Jupiter great red spot 08 p1298 A66-19592

Jupiter photoelectric spectral scan in UV reproduced as geometric reflectivity vs wavelength, using Aerobee rocket 10 p1603 A66-21099

Image converter tube spectrophotometry of zonal variation of methane absorption bands on Jovian disk in near IR region 12 p1944 A66-23504

Jovian rotational effects on magnetospheric



- model and conditions of fluting and two-stream instability 15 p2602 A66-29952  
 Rapid drift in longitude of small dark spot on south edge of Jupiter North Temperate Belt, noting sinusoidal displacement characteristics and measurement with blue and UV photography 17 p3005 A66-33009  
 Experimental analysis of Taylor columns likely to bear on processes occurring in Jupiter atmosphere 17 p3006 A66-33013  
 Image converter tube spectrophotometry of zonal variation of methane absorption bands on Jovian disk in near IR region 20 p3646 A66-37017  
 Spectral study of Jupiter, Saturn and rings of Saturn, determining methane concentration in cloud layers 20 p3647 A66-37035  
 Planetary scale atmospheric circulations of Jupiter and Saturn using fluid dynamics, noting rotation effects 23 p4129 A66-41679
- JUPITER PROJECT**  
 Reliability design requirements for Data Transmission System for Jupiter Precursor Spacecraft 20 p3513 A66-37208

## K

## K-BAND

- K absorption spectra of germanium and selenium in germanium selenide based on band theory of solids by assuming electrons transfer, using X-ray spectroscopy 11 p1758 A66-23368  
 K emission band of graphite examined, using grazing incidence spectrometer and Gaussian window function 12 p1931 A66-24802  
 K beta 5 emission band and fundamental K-edge absorption of vanadium analyzed and results compared with vanadium spectra from other series 12 p1898 A66-25024  
 Emission and absorption bands in K spectral region of titanium, using single setup 14 p2314 A66-27371  
 K-band Fabry-Perot resonator using plane and concave mirrors, determining overvoltage factors in interferometer, noting diffraction losses 16 p2707 A66-31207

## K-MESON

## S KAON

## KALMAN-SCHMIDT FILTER

- Self-contained orbital navigation system using Earth-horizon measurements in 14-16  $\mu$  carbon dioxide absorption band, using Kalman linear filter theory 01 p0100 A66-10024  
 Kalman filter divergence control, noting analytical and empirical modification methods 21 p3766 A66-38883  
 Apollo inertial navigation system estimation, using statistical filtering to reduce computation 21 p3767 A66-38886  
 Integrated navigation system /INS/ using stellar inertial subsystem with optimum data processing 21 p3767 A66-38891

## KAMACITE

- Concentration gradients in meteoritic kamacite predicted from Fe-Ni phase diagram and diffusion 06 p0955 A66-16787  
 Widmanstätten patterns for electrolytic dissolution of iron meteorites and separation of nonmetallic portions, particularly kamacite 21 p3816 A66-39493

## KAMAN MILITARY HELICOPTER

## S UH-2 HELICOPTER

## KAON

- Normal scalar nonet, K1 meson-2 pion decay, K1-K2 mass difference and S-wave pion scattering 15 p2544 A66-28946  
 Cosmic ray measurements, muon production from decay of charged pions and kaons, muon polarization, momentum spectra, atmospheric gamma cascades and derivation of kaon/pion ratio 15 p2587 A66-29573

## KAON PRODUCTION

- Kaon decay contribution to sea level muon flux at large zenith angles, using Ashton and Wolfendale procedure 15 p2588 A66-29579

## KARHUNEN-LOEVE EXPANSION

- Spaceflight data handling with emphasis on data compaction techniques based on weighted-information theory, Karhunen-Loeve theory, area recording and

- transmission procedure 08 p1187 A66-19536
- KARMAN-BODEWADT FLOW**  
 Coupled flow problem, comparing flow induced by steady rotation of permeable and impermeable disks 06 p0871 A66-16353
- KARMAN VORTEX STREET**  
 Karman vortex street pattern of mesoscale eddies in wake of islands [AIAA PAPER 65-16] 02 p0221 A66-11548  
 Turbulence wake suppression in Karman vortex street of circular cylinders by controlling transverse oscillations of vortex generating cylinder in transition range 04 p0453 A66-13514  
 Mesoscale eddies in wake of islands describing properties, characteristic parameters via Karman vortex street pattern, drag theory and empirical observation 07 p1061 A66-17365
- KAWASAKI KH-4 HELICOPTER**  
 Flight test determination of parasite drag area and required power of Kawasaki Bell KH-4 single-rotor helicopter 07 p0988 A66-17525
- KEPLER LAW**  
 Orbits of artificial satellites for suitable variables, noting oblate shape of Earth and air resistance 02 p0285 A66-11256  
 Kepler method in determining length of satellite radius vector independent of linear measurements from Earth, discussing accuracy in geodetic measurement 03 p0366 A66-13197  
 Optimum transfer between Kepler ellipses, noting Hohmann orbital transfer method and geodesics and metric tensors in phase space 04 p0579 A66-14459  
 Approximate value of mass of Moon calculated, using noncalculus derivation of Newton modification of Kepler third law 08 p1296 A66-19380  
 Solution of Kepler equation by stepwise approximation, discussing elliptical orbit, parabolic ellipse and hyperbolic orbit 12 p1950 A66-24398  
 Book on satellite orbital flight trajectory theory and celestial mechanics 15 p2595 A66-29128  
 Simplified method for derivation of universal gravitation law from Kepler law of planetary orbits 16 p2747 A66-30870  
 Integrating error equations of inertial navigation system for objects in Keplerian motion 16 p2744 A66-31507  
 Radius of convergence of power series obtained by inversion of universal Kepler equation 17 p3001 A66-32347  
 Iterative determination of space flight trajectory and velocity represented as sum of Kepler motions about celestial bodies 18 p3234 A66-34635  
 Elliptic restricted problem of three bodies, discussing analytical determination of characteristic exponent to equilibrium solutions [AIAA PAPER 65-685] 19 p3461 A66-35892
- KERNEL FUNCTION**  
 Nonlinear viscoelastic incompressible materials under small finite deformation for short time ranges, noting kernel functions for tensor tests [ASME PAPER 65-APMW-31] 04 p0593 A66-14231  
 Poisson pseudokernel and pseudodifferential operators on manifold with boundary 05 p0708 A66-15093  
 Classes of uniqueness for solutions of Cauchy problem and representation of positively defined kernels 07 p1056 A66-17598  
 Improved numerical procedure for harmonically deforming lifting surfaces from supersonic kernel function method [AIAA PAPER 66-78] 08 p1163 A66-18995  
 Kernel function procedure for solving oscillatory lifting surface problem at subsonic speeds, using least squares method 08 p1165 A66-19149  
 Proof, by degenerate kernel method of existence and uniqueness of solution for one class of nonlinear integral equations 09 p1394 A66-20455  
 Nonlinear system analysis by Volterra-Wiener functionals, considering convergence and kernels 09 p1363 A66-20797  
 Resolvent kernel for class of integral operators with difference kernels on finite interval for transport processes 10 p1549 A66-21301

- Nonlinear filters, including system analysis optimization, realization via Volterra functionals, etc 11 p1675 A66-22630  
 Construction of rational second order kernels with aid of rational functions of order  $n$ , applying result to theory of approximation of functions 12 p1902 A66-23765  
 Plane stationary problem of heat conduction for mixed boundary conditions solved, using Fredholm integral equation with symmetrical kernel 12 p1979 A66-24372  
 Dynamic optimization and minimizing kernel function for dual control problem 13 p2117 A66-25348  
 Generalized heat equation solution expansion in terms of radial heat polynomials, Appel transforms and Laguerre polynomials 13 p2118 A66-25793  
 Circular kernels and circular transformations in analysis of infinite sequences 14 p2322 A66-27627  
 Noether theorems applied to degenerate cases of improper integral equations with Cauchy kernels 16 p2733 A66-30745  
 General theory of linear integral equations with power kernel 16 p2734 A66-30746  
 Asymptotic behavior of nonlinear integral equations with certain conditions on kernel and nonlinearities 16 p2738 A66-31705  
 Two Fredholm integral equations encountered in elasticity theory solved by Wiener-Hopf method 17 p2947 A66-32783  
 Nonlinear viscoelastic incompressible materials under small finite deformation for short time ranges, noting kernel functions for tensor tests [ASME PAPER 65-APMW-31] 18 p3248 A66-33577  
 Estimation of Poisson kernels of elliptic operator with variable coefficients by using maximum principle and Fatou theorem 19 p3390 A66-36248  
 Integration technique for determining unsteady aerodynamic forces at subsonic speeds, noting role of kernel of integral equation 20 p3491 A66-36955  
 Numerical extrapolation solution of kernel-characterized integral equations for apparent emissivity of conical and cylindrical cavities 20 p3681 A66-38298  
 Subsonic aerodynamic loading on harmonically oscillating nonplanar lifting surfaces in kernel-function formulation 21 p3694 A66-38733  
 Spline theory methods of interpolating linear functional containing Peano kernel 21 p3757 A66-39257
- KEROSENE**  
 Thermal stability aspects of commercial kerosene for supersonic transport [AIAA PAPER 66-670] 18 p3162 A66-34442
- KERR CELL**  
 Optically biased pulsed transmission mode operation of Q-switched laser, in connection with Kerr cells inhibiting lasing action 09 p1386 A66-19937  
 Kerr cell as shutters and laser modulators in high speed photography 10 p1537 A66-21869  
 Segmented-rod ruby laser structure operated as giant pulse laser, using Kerr cell to provide Q-switching, noting number of oscillating modes 13 p2088 A66-25038  
 High speed stroboscopic photography using Kerr cell modulated laser source 16 p2705 A66-30828  
 High power nonspiking operation of ruby laser for continuous output on microscopic and macroscopic scale 20 p3581 A66-38242  
 Multipurpose ultrahigh speed camera system, noting use as monosecond Kerr cell, image converter and giant laser pulse generator 23 p4071 A66-41675  
 Carbon disulfide traveling wave Kerr cells with identical microwave and dielectric constants, noting light modulator construction at microwave frequencies 24 p4185 A66-42814
- KERR EFFECT**  
 Free-carrier magneto-Kerr effect analysis considering amplitude ratio of two polarized components of reflected wave and phase difference between these two components 03 p0412 A66-13151  
 Kerr effect measurement of coercive force, nucleation field and saturation field for thin films 11 p1754 A66-22814



- Magneto-optical study of critical curves of thin films by observing domain structures during magnetization process 11 p1755 A66-22820
- Self-focusing of light from Kerr effect and changes in density of matter 13 p2127 A66-25109
- Domain wall mobility effect on multilayer magnetic thin films consisting of permalloy layers separated by silicon oxide 14 p2351 A66-26888
- Magneto-Kerr effect at surface of laboratory plasma 15 p2556 A66-29811
- Self-focusing of light from Kerr effect and changes in density of matter 16 p2745 A66-30288
- Pulse switching of permalloy films by use of interrupted pulses and Kerr magneto-optical effect 16 p2773 A66-30683
- Amplitude and phase of complex Kerr magneto-optic coefficients measured, describing technique and results 17 p2958 A66-32623
- Linear instability of laser propagation in fluid with coupling between light and medium 18 p3120 A66-35034
- Laser light modulation by Pockels or Kerr effect for application to telecommunications system, examining electrical birefringence modulation 19 p3304 A66-36262
- Fermi surface interpretation of band structure, electron energy levels, optical properties and ferromagnetic structure of transition and noble metals 20 p3613 A66-37274
- Spin wave excitation by ferromagnetic resonance, measuring coercive field as function of temperature by Kerr effect method and determining magnetic properties of thin films 20 p3621 A66-38085
- Optical deflection of light beams via Kerr effect, ultrasonic waves, piezoelectric crystals and mirror galvanometer 22 p3877 A66-40293
- Electro-optic light modulation using Pockel and Kerr effects in crystals for communications applications, using lasers 24 p4225 A66-42811
- ESTREL AIRCRAFT**
- S HAWKER P 1127 AIRCRAFT**
- ETONE**
- Thermal decomposition of tert.-butyl hydroperoxide with oxygen and acetone addition studied by isotopic tracer 13 p2017 A66-26305
- Sensitization of polyvinyl cinnamate, using Michler ketone 14 p2290 A66-27016
- Tandem column gas-liquid chromatography labeling technique for mass spectrometry, noting ketones exchange and data on deuterium and oxygen compounds 15 p2446 A66-28872
- KEYING**
- S FREQUENCY-SHIFT KEYING**
- S PHASE-SHIFT KEYING**
- KH-4 HELICOPTER**
- S KAWASAKI KH-4 HELICOPTER**
- KIDNEY**
- S RENAL FUNCTION**
- S URINE**
- KINEMATIC EQUATION**
- Kinematic and physical relations for small motion superposed on initial motion defined in fixed reference frame 01 p0106 A66-10735
- Force and moment response of pneumatic tires undergoing nonstationary lateral motions, using motion equations [ASME PAPER 65-AV-2] 11 p1636 A66-22471
- Error determination in autonomous determination of coordinates, obtaining solution for kinematic equations of navigation in near-polar region 16 p2744 A66-31146
- Laminar boundary layer in incompressible liquid, noting effect of variation of kinematic viscosity and density on stability 23 p4056 A66-41725
- KINEMATICS**
- SA BODY KINEMATICS**
- SA MICROWAVE REFLECTOMETRY**
- Kinematic systems and reduction gears used in turboprop engines, outlining design features 01 p0079 A66-11060
- Statics and kinematics of rigid bodies in structural mechanics, establishing isostatic support conditions 03 p0436 A66-12733
- Book on MHD including kinematic aspect, magnetic force effects, boundary conditions, MGD, etc 04 p0556 A66-14384
- Kinematic computer calculations of energy distribution among products of repulsive, mixed and attractive energy release exothermic reactions 11 p1787 A66-23213
- Small motion superposed on stationary slow deformation process of viscoelastic material with fading memory, based on Rivlin and Ericksen differential equation 14 p2397 A66-27384
- Similarity method for accelerations and velocities 17 p2960 A66-33424
- Mayor-Mises method for solution of kinematic and kinetostatic problems of three-dimensional mechanisms [ASME PAPER 66-MD-2] 21 p3741 A66-38475
- Continuous media model theory and comparison with theory of many-dimensional non-Euclidean manifolds, noting kinematic characteristics of particle deformation, variational principles, thermodynamic equation, etc 21 p3756 A66-38627
- Graph theory and enumeration of basic kinematic chains and mechanisms 23 p4097 A66-41978
- KINETIC ENERGY**
- SA FROUDE NUMBER**
- Tapered circuit TW amplifier experiments considering circuit phase velocity tapering effects on small signal gain, bandwidth, dynamic power limiting, etc 01 p0036 A66-10394
- Stationary and kinetic methods determining parameters of sensitizing recombination r-center in high resistivity monolayer photoconductors 02 p0273 A66-11718
- Steady flow possessing extremal kinetic energy compared to equivortex flow for stability analysis 02 p0219 A66-12169
- Modifications of impulse approximation allowing for motion of bound electrons, providing simple analytic expressions for atomic ionization and detachment cross sections 03 p0394 A66-12328
- Kinetic energy in unstable and weakly stable plasma noting optical and acoustical modes in electron-ion system, Vlasov term in quasi-linear theory and two-particle correlation term 04 p0550 A66-13406
- Energy conversion from available potential to kinetic broken into spectral components permitting analysis in vicinity of extratropical cyclone 04 p0541 A66-13665
- Magnetic resonance applied to semiconductors, determining electron density at nucleus sites and kinetic energy temperature of hot electrons in indium antimonide 04 p0563 A66-14030
- Input initiation energy and potential impact energies available under processing conditions, interpreting test data 05 p0787 A66-15138
- Atmospheric energetics during January-February 1963 stratospheric warming investigated, using spectral energy equations for zonal and eddy kinetic and potential energies 07 p1027 A66-17360
- Identification of charged fast particles in nuclear emulsions, measuring multiple scattering of protons and mesons along track with various kinetic energies 07 p1114 A66-17543
- Kinetic energy variations in different parts of baric centers during atmospheric motion 08 p1217 A66-19301
- Unbounded isothermal atmosphere response to time harmonic point disturbances, exact solutions obtained for frequency ranges of acoustic waves, trapped oscillations and gravity 13 p2183 A66-25613
- Amplification of interaction of atoms and of pulsed or periodic cooling of transparent media produced by laser beam, noting changes in kinetic energy of atoms 13 p2093 A66-26021
- Limiting cases of screened Coulomb T matrix in complex energy plane 15 p2547 A66-29618
- Electron secondary emission from interaction of ion, atom and molecular energetic beams with solids, especially when kinetic energy is significant 16 p2776 A66-30796
- Epitaxial growth of low pressure sputtered-silver films, noting dependence of growth on kinetic energy distribution of sputtered atoms 16 p2784 A66-31532
- Retarding potential measurement of kinetic energy of electrons released in Penning ionization by excited helium atoms in metastable electron states 18 p3139 A66-34505
- Kinetic energy variations in different parts of baric centers during atmospheric motion 19 p3348 A66-36038
- Temperature potentials in cylinder of known radius, investigating optimal heating regime and thermal kinetic factor effect on maximum potential magnitude 20 p3665 A66-36912
- Collision integrals, effective cross sections and deflection angles for Morse potential calculated, using dimensionless relative kinetic energy of pair of atoms 21 p3775 A66-39073
- Kinetic energy causing anomalous increase in thermoelectric power in semiconducting p-type iron-chromium sulfide near Curie temperature 21 p3803 A66-39261
- Frequency dependence of electrostatic energy density in undamped longitudinal plasma oscillation, noting contribution of kinetic and thermal energy 23 p4104 A66-41507
- Rotating body in vacuum, examining motion dependency on body configuration and kinetic energy distribution, noting effect of change in energy on motion 24 p4281 A66-42337
- Plasma temperature increase by randomization of kinetic plasma energy through acceleration stages, obtaining higher plasma velocities 24 p4244 A66-42888
- KINETIC EQUATION**
- Self-field electron kinetic reaction to electromagnetic propagation in three-fluid Brownian plasma 01 p0110 A66-10335
- Singularities of kinetic /plasma/ dispersion equation 01 p0113 A66-10637
- Kinetic equation of laser optimum emission, determining pumping efficiency, value of losses in special modes, etc 01 p0084 A66-11058
- Equilibrium configuration of plasma confined by magnetic field on kinetic equations of particle drift without considering collisions 02 p0268 A66-11781
- Static force factor introduced into kinetic longitudinal plasma oscillation equation, noting Landau damping factor 03 p0397 A66-12382
- Kinetic equation with relativistic interaction correlation for homogeneous plasma 03 p0405 A66-13139
- Hydrodynamic systems expressed by kinetic equations, deriving equations of aerodynamics without knowledge of interaction of gas molecules 04 p0510 A66-13879
- Electrical conductivity of polar semiconductors in electric fields, calculating lattice and Coulomb electron scattering mechanism by kinetic equation method 04 p0568 A66-14350
- Structure of solutions of chain of equations for deriving Boltzmann kinetic equation of gases 05 p0663 A66-15344
- Kinetic equations of complex reactions derived, using conical graphs, reducing reversible reaction problems to problems of irreversible kinetics 06 p0822 A66-16544
- Lagrangian formulation of wave kinetics in weakly turbulent plasma, taking into account interaction of plasma oscillations 07 p1085 A66-17647
- Thermal conditions in boiling liquids including container wall damage-flux density relationship, stable and unstable boiling in bubble evaporation region and film vaporization 07 p1154 A66-18066
- Kinetic equations, considering free and bound charges in weakly ionized hydrogen plasma, noting self-consistent approximation for second distribution function 08 p1265 A66-19375
- Kinetic equation for plasma in strong static magnetic field derived, using Bogoliubov method 09 p1408 A66-20371
- Balescu-Lenard kinetic equation derived for fully ionized zero-external-field homogeneous unbounded plasma, with relativistic corrections for thermal motion 10 p1567 A66-21816
- Kinetic equation for density matrix of discrete system undergoing relaxation in



presence of instantaneous collisions 10 p1622 A66-21983

Second harmonic generation by laser beams of finite spectral width, using quantum transitions and kinetic equations, noting shape of pumping line at fundamental frequency 10 p1544 A66-22026

Coulomb collisions and equilibrium states in fully ionized plasma, deriving kinetic equation in pairwise collision approximation 10 p1572 A66-22037

Kinetic moment variation theorem for deformable system of material points of variable composition 11 p1735 A66-22239

Kinetics and gas dynamics equations derived to determine state of gas behind strong shock waves, accounting for all excited states of neutral atoms 11 p1688 A66-22586

Properties of moving dislocations in unstabilized creep at various temperatures analyzed by kinetic equations in Akulov theory 11 p1784 A66-23323

Hydrodynamic approximation of interaction between charged particle beam and plasma confined by ideally conducting sheath 13 p2139 A66-25389

Nonlinear kinetic equation for waves and particles in nonisotropic plasma where anisotropy is due to magnetic field, noting probability of wave absorption-emission by particles 13 p2140 A66-25409

Iterative method solution of kinetic equation with functional derivatives for ionized plasma 13 p2141 A66-25476

Second optical harmonic generation equations for steady state laser derived from density matrix 13 p2092 A66-25682

Phase stability of system of particles in cyclic accelerator with automatic frequency correction of accelerating field, noting kinetic equation method 13 p2147 A66-25748

Solution of reactor kinetics equation numerically unconditionally stable for all values of reactivity or integration step size 13 p2126 A66-25791

Transport equation for classical unstable electron plasma extended to quantum mechanical multicomponent case, rewriting kinetic equation 13 p2155 A66-26674

Hydrodynamic systems expressed by kinetic equations, deriving equations of aerodynamics without knowledge of interaction of gas molecules 14 p2275 A66-27569

Electrical conductivity of polar semiconductors in electric fields, calculating lattice and Coulomb electron scattering mechanism by kinetic equation method 14 p2368 A66-28247

Difference equations arising when one-velocity kinetic equation is solved by characteristics method, estimating error 14 p2338 A66-28280

Structure of solutions of chain of equations for deriving Boltzmann kinetic equation of gases 15 p2482 A66-29972

Second harmonic generation by laser beams of finite spectral width, using quantum transitions and kinetic equations, noting shape of pumping line at fundamental frequency 16 p2718 A66-30845

Parametric resonance in plasma situated in magnetic field, noting oscillation, frequency stability, kinetic equations, electric field effect, etc 16 p2762 A66-31170

Balance equations derived from kinetic equations for nonequilibrium plasma, considering radiative processes and inelastic collisions between electrons and atoms 16 p2766 A66-31603

Book on laser theory based on kinetic equations with emphasis on emission from luminescent center transitions, semiconductor junctions and Raman scattering 17 p2934 A66-32558

Successive approximation solution to integral kinetic equation and corrections to moments of distribution function for viscous and rarefied gases 17 p2909 A66-32585

Electron capture detector parameters in pulse sampling mode analyzed, noting kinetic processes, temperature effect, etc 17 p2961 A66-32660

Radiation control of ruby laser by diffraction modulator with traveling ultrasonic wave, noting computer solution of kinetic equations of population balance,

radiation density, characteristic damping, etc 17 p2938 A66-33515

Kinetic equations, considering free and bound charges in weakly ionized hydrogen plasma, noting self-consistent approximation for second distribution function 18 p3146 A66-34177

Light absorption by free current carriers role in kinetic equations of semiconductor laser/radiation system 18 p3119 A66-34691

Longitude dependence of distribution function of electrons for fixed value of McIlwain parameter, using kinetic equation 18 p3197 A66-34873

Quantum theory of laser model, deriving kinetic equations for radiation and single-particle density matrices, using Bogoliubov expansion procedure 19 p3374 A66-36008

Nonlinear plasma wave interaction, discussing Langmuir wave scattering on particles and energy transformation 19 p3418 A66-36532

Quadrupole relaxation in multilevel systems by method of kinetic equations 20 p3512 A66-37140

Digital computer analysis of kinetic equations for CO burning in presence of hydrogen 20 p3679 A66-37702

Improvement of gyroscopic accuracy by increased kinetic moment, noting use of gyromotor with rotors placed inside each other 21 p3739 A66-39326

Flow of strongly rarefied ionized plasma past electrically charged body solved by kinetic and Poisson equations in absence of magnetic field 21 p3795 A66-39604

Integration of near equilibrium flows in propulsive nozzles, estimating length of transition region from equilibrium condition to kinetic solution [AICE PREPRINT 28C] 22 p3971 A66-39884

Kinetic equations in hydrodynamic approximation for weakly reacting and excited Bose systems, finding asymptotic expressions for Green function 23 p4055 A66-41412

Radiation control of ruby laser by diffraction modulator with traveling ultrasonic wave, noting computer solution of kinetic equations of population balance, radiation density, characteristic damping, etc 24 p4219 A66-42128

Nonlinear integral equations formulated that are equivalent to Krook kinetic equation for steady problems in two and three space dimensions 24 p4193 A66-42407

Statistical mechanics methods applied to plasma, deducing kinetic equation 24 p4246 A66-43111

## KINETIC FRICTION

Turbine rotor subject to thermal stresses due to friction of accidental contact with stator 23 p4075 A66-41995

## KINETIC HEATING

Radio galaxies contribution to kinetic temperature of intergalactic gas on basis of cosmological model 03 p0426 A66-12909

Reversed heat conduction in natural convection at thermal leading edge on vertical wall [ASME PAPER 65-WA/HT-34] 05 p0792 A66-15672

Heat-sensitive paint in measuring kinetic heating in hypersonic wind tunnel 08 p1316 A66-18720

Structural design of Concorde supersonic airliner, noting airframe strength parameters 10 p1483 A66-21717

Radio galaxies contribution to kinetic temperature of intergalactic gas on basis of cosmological model 14 p2380 A66-27257

Homogeneous nucleation of liquid drops in supersaturated vapors, noting kinetic treatment for heating of growing clusters and irreversible thermodynamics of nonisothermal nucleation 19 p3477 A66-35566

Equilibrium deviation occurring in plasma with variable kinetic temperature due to radiation transport within plasma volume and outflow beyond limits of volume 20 p3606 A66-36973

Kinetics of heating and evaporation of exploding copper and brass wires in air and polyethylene tubes studied by X-ray techniques 24 p4238 A66-42976

## KINETIC THEORY

SA BOKINETIC THEORY  
SA DIFFUSION

Kinetic theory of Lorentz plasma in rotating magnetic fields and electromagnetic fields based on Boltzmann equation 01 p0113 A66-10640

Electromagnetic H-wave propagation of given frequency along plasma sheet surrounded by vacuum 01 p0030 A66-10897

Cauchy problem for linearized Boltzmann equation in kinetic theory of gases 01 p0107 A66-11011

Plasma kinetic theory effect of magnetic field on dispersion relation for ionic sound wave 02 p0269 A66-11836

Dissociation of oxygen molecules by vibrational excitation 03 p0396 A66-13211

Kinetic theory of unstable plasma covering growth and stabilization of spatially homogeneous electron plasma in uniform neutralizing positive charge field, Pines-Schrieffer and formally equivalent kinetic equations and Balescu theory 03 p0406 A66-13359

Kinetic processes in simple plasma, using linear Liouville equation for N-body particle distribution and expanding solution as power series 05 p0727 A66-15259

Book on physical gas dynamics including transport theory, kinetic theory, thermodynamics, equilibrium, fluid flow, radiative transfer, etc 05 p0666 A66-15848

Kinetic theory approach to plasma fluctuations taking particle pair collisions into account 06 p0918 A66-16778

Class of exact solutions for one-dimensional single-relaxation equation with arbitrary collision frequency 08 p1316 A66-18532

Acoustic and optical phonon drag of pure ionic n-type semiconductors having NaCl structure, calculating kinetic coefficients 08 p1273 A66-19252

Book on dynamics of rarefied gas discussing kinetic theory, shock wave structure, Couette flow, gas flow between coaxial cylinders and plasma dynamics 08 p1208 A66-19321

Book on kinetic theory of simple liquids including equilibrium properties, time-dependent system, Markov processes, Brownian motion, transport coefficients, etc 08 p1209 A66-19463

Initial stage of motion in Rayleigh problem, calculating time variable velocity of tangential stress on and velocity of gas near plate 08 p1209 A66-19477

Kinetic model construction of maximum number of Boltzmann collision integral properties 08 p1259 A66-19577

Kinetic instability of terrestrial outer radiation belts calculated, using magnetospheric electron flux data 08 p1286 A66-19789

Superfluid basic theory noting Josephson tunneling, liquid helium kinetic theory, quantized vortex lines, etc 09 p1415 A66-20005

Kinetic approximation of passage of electromagnetic wave through plasma layer, noting angle of incidence of wave on layer 10 p1506 A66-21993

Kinetic theory of passage of electromagnetic waves through plasma layer 10 p1506 A66-22004

Kinetic approximation of electromagnetic surface wave propagation in infinite plasma sheath solved by Fourier method, noting resulting dispersion equation 11 p1743 A66-22441

Rarefied gas dynamics - International Symposium, Institute for Aerospace Studies, University of Toronto, July 1964, Volume 1 11 p1688 A66-22901

Sound wave propagation in rarefied gas dynamics, using kinetic theory 11 p1736 A66-22903

Accuracy of kinetic theory approximations assessed by comparison of approximate and exact solutions of Krook kinetic equation for Couette flow and shock wave structure 11 p1690 A66-22906

Iterative solution to shock wave structure in highly rarefied flows through kinetic theory and full Boltzmann equation 11 p1690 A66-22910

Shock structure calculations from kinetic theory, using ellipsoidal distribution function 11 p1690 A66-22912

Rayleigh problem at low Mach numbers



and arbitrary Knudsen number investigated in rarefied gas dynamics according to kinetic theory 11 p1692 A66-22922

Kinetic theory of leading edge of plate interacting with streaming gas evaluated by Bhatnagar-Gross-Krook equation of statistical mechanics 11 p1633 A66-22924

Transport properties, thermoconductivity, molecular collision and viscosity of polyatomic gas of circular cylindrical molecules with hemispherical caps 11 p1741 A66-23215

Electromagnetic H-wave propagation of given frequency along plasma sheet surrounded by vacuum 11 p1658 A66-23299

Kinetic oscillation of nonhomogeneous collision plasma, discussing drift instability, ionization, longitudinal current effect, etc 12 p1921 A66-24204

Kinetic theory of passage of s-and p-polarized electromagnetic waves through thin inhomogeneous plasma layer 12 p1816 A66-24225

Kinetic theory of dense gases generalized for all orders, deriving integral equations for transport coefficients and showing temperature dependence of bulk viscosity 12 p1979 A66-24565

Brillouin scattering by gases as experimental test of kinetic theory away from hydrodynamic regime 12 p1917 A66-24585

Milne-Eddington model in heat and mass transfer, showing analogy between radiation and particle transfer and correspondence to simplified Boltzmann equation 13 p2208 A66-25162

Two-time probability distribution function, autocorrelation function, Liouville equation and fluctuation theory of plasma kinetics 13 p2156 A66-26685

Rarefied gas flow in hydrodynamic entrance region of circular tube, noting variation with density level, velocity profile and pressure drop for developing flow 13 p2070 A66-26713

Text on vacuum science and technology including kinetic theory of gases, gas flow, pumps, vacuum measurements and equipment, etc 14 p2335 A66-27721

Solution to dispersion equation of linearized Boltzmann equation in kinetic theory of rarefied gases, noting root behavior and distribution function structure 14 p2278 A66-28285

Kinetic theory of two-photon absorption from single mode of radiation field, noting dependence on coherence properties of field 15 p2544 A66-28943

Classical analytical mechanics applied to mechanics of continua, noting relation between kinetic-stress functions and Ostrogradskii-Hamilton principle and stress tensor and finite deformation tensor 15 p2539 A66-29148

Surface protrusions and holes, Maxwell kinetic gas theory and surface interaction of current of free molecules and rigid body 16 p2686 A66-31042

Textbook on molecular thermodynamics, statistical mechanics and kinetic theory of gases, with applications to ideal gas, crystal, radiation field, etc 16 p2829 A66-31312

Kinetic theory of electromagnetic propagation in confined magnetoactive plasma 17 p2968 A66-32539

Pulsating plasma column acceleration in high current pulsed accelerator 17 p2972 A66-32870

Linearized model of Boltzmann equation to examine problems of kinetic theory of nonuniform gases 17 p2911 A66-32961

Kinetic theory of liquid viscosity made tractable by using approximation of perturbation of radial distribution function of monatomic liquid by nonuniform flow field 17 p2940 A66-33335

Kinetic theory of ionospheric satellite trail, discussing neutral and charged components from BGK model equation [ATAA PAPER 66-477] 18 p3226 A66-33654

Computer programs for combustion rates of hydrogen-air mixture 18 p3063 A66-33830

Physical phenomena occurring within fluid devices, particularly pneumatic devices, considering Maxwellian distribution of velocities, ideal gas law and mean free path 18 p3098 A66-34118

Boltzmann equation, interpreted in terms of certain correlation functions known as product densities, applied to fluctuation theorem and gases and liquids not in equilibrium 18 p3136 A66-34706

Variational principle applied to boundary value problems in kinetic theory, specifically examining Kramer problem, plane Couette flow and plane Poiseuille flow 18 p3102 A66-34919

Kinetic approximation of passage of electromagnetic wave through plasma layer, noting angle of incidence of wave on layer 18 p3072 A66-34970

Kinetic theory approach to plasma fluctuations taking particle pair collisions into account 19 p3405 A66-35375

Wall term in Boltzmann H relationship leads to increase in entropy for solutions to Boltzmann equations 19 p3401 A66-35584

Kinetic theory of passage of electromagnetic waves through plasma layer 19 p3303 A66-36088

Relation of kinetic theory to unstable plasmas /weak turbulence/, noting expansion parameters and extension to include discrete particle effects 19 p3418 A66-36536

Rarefied gas motion instability, constructing general solution for effect of various force fields 19 p3343 A66-36846

Necessary and sufficient conditions of kinetic processes involving two systems of point masses 20 p3598 A66-36910

Electrodynamic properties of homogeneous magnetoactive plasmas including wave propagation, excitation, scattering, etc 20 p3608 A66-37488

Metastable dislocation crack transformation into polygonal walls of edge dislocations caused by diffusion over crack surface 20 p3669 A66-37551

Rotary inertia and shear deformation as finite approach of kinetic beam and plate problems 21 p3826 A66-38585

Kinetic instability of terrestrial outer radiation belts calculated, using magnetospheric electron flux data 21 p3809 A66-38785

Solution to chain of kinetic gas equations, showing effect of fast reversible and slow irreversible processes on particle distribution function 21 p3771 A66-39248

Kinetic oscillation of nonhomogeneous collision plasma, discussing drift instability, ionization longitudinal current effect, etc 22 p3956 A66-40568

Kinetic theory of passage of s-and p-polarized electromagnetic waves through thin inhomogeneous plasma layer 22 p3867 A66-40587

Orientation relaxation in symmetrical-top gases and binary gas mixtures, noting prediction of cross sections from kinetic theory data for molecules 22 p3860 A66-40901

Monograph on kinetic theory of plasmas, deriving state equation, Maxwell equation for plasma-magnetic field interaction and boundary layer heat transfer expressions 23 p4102 A66-41400

Boltzmann equation for dilute monatomic gas, discussing asymptotic interpretation of Hilbert and Chapman-Enskog theories 23 p4097 A66-42011

Static elastic and thermoelastic stability, discussing kinetic theory and physical interpretation of energy methods 24 p4287 A66-42271

Monte Carlo analysis of plasma of heavy ions, obtaining thermodynamic properties, potential energy and pair distribution 24 p4245 A66-43036

# KINETICS

SA CHEMICAL KINETICS  
SA ELECTROKINETICS  
SA HYDROKINETICS

Soviet and foreign papers on physics of boiling including heat transfer, heat release, bubbling processes, kinetics and sonic aspects of boiling and bibliography 09 p1469 A66-20100

Kinetics of CN radicals association generated by shocking cyanogen-argon mixtures at high temperatures in reflected shock region of expansion 12 p1811 A66-23615

Soviet and foreign papers on physics of boiling covering heat transfer, heat release, bubbling processes, kinetics and sonic

aspects of boiling, including bibliography 21 p3834 A66-38509

Kinetics of nonuniform generation of longitudinal plasma waves by transverse wave beam with narrow spectrum, noting effect of magnetic field 22 p3958 A66-40931

Turbulence in conducting medium treated by fluid mechanical approach and kinetic theory, noting energy transfers between eddies 23 p4108 A66-42033

# KIRCHHOFF LAW

Finite linear time-invariant passive reciprocal electrical networks including Kirchhoff generalized constraints 07 p1014 A66-17745

Validity of Kirchhoff law for apparent local spectral emittance and absorbance and total flux calculations for spacetrack cavities [ATAA PAPER 65-135] 08 p1316 A66-18793

Notions of one-and two-dimensional topology in network theory as applied to Kirchhoff laws and network duality 13 p2050 A66-26058

Combined frequency and space correlation of wave fields scattered by rough surfaces where conditions of applicability of Kirchhoff approximation hold true 14 p2236 A66-27144

Differential equations of linear theory of elastic shells derived under Kirchhoff-Love hypothesis with aid of static-geometric analog 23 p4142 A66-41956

# KIWI ROCKET REACTOR

Behavior of Kiwi-and Nerva-type nuclear rocket reactors under induced failure conditions to determine validity of theoretical prediction of total energy released 09 p1401 A66-20585

# KLEIN-GORDON EQUATION

Stochastic processes in microscale relativistic fluid mechanics, discussing Dirac fluid, Klein-Gordon equation, diffusion, quantum potential, spin fluids, etc 12 p1914 A66-24093

Irreducible unitary representations of restricted Lorentz group on manifolds of time-, light-and spacelike 4-vectors, obtaining plane-wave solutions of Klein-Gordon equation 15 p2528 A66-29622

# KLYSTRON

Periodic electrostatic focusing scheme for ungridded multicavity klystron amplifier 01 p0044 A66-10932

Synchronization of reflex klystron loaded with resonator with nonlinear capacitance from p-n junction of semiconductor diode at third harmonic of external signal 03 p0342 A66-12626

Two-cavity klystron frequency multiplier for generating waves less than 1 mm 03 p0342 A66-12881

CW klystron frequency multiplier for generating submillimeter waves 04 p0492 A66-13422

Microwave amplifier, electrostatically focused klystron, for spaceborne equipment used in telecommunications of deep space 04 p0493 A66-13603

Microwave tube technology noting klystrons, crossed field devices, traveling wave tubes, etc 05 p0642 A66-14560

Experimental verification of spectrum asymmetry at output of pulsed RF klystron amplifier transmitter leads to modulation technique called Control of Unwanted Radiated Energy /CURE/ 06 p0841 A66-15956

Ballistic klystron theory approximation for bunching enhancement of three-cavity klystron whose center cavity is detuned to HF side for maximum efficiency 06 p0852 A66-16643

Reflex klystron as subcarrier detector for microwave signals modulated by RF carriers in 100 to 500 kc range 06 p0853 A66-16651

Coupled monotron analysis of band-edge oscillations in high power traveling wave tubes, discussing electron beam interaction with coupled-cavity structure 06 p0855 A66-16768

Predicting and measuring FM of reflex klystron noise performance when subjected to random acoustical and mechanical vibration 07 p1008 A66-17512

Difference frequency between harmonics of millimeter wave oscillators at submillimeter wavelength, using crossed waveguide harmonic generator as harmonic mixer 07 p1008 A66-17514



Klystrons, cross field devices and traveling-wave tubes, including design and application 07 p1011 A66-18269

Frequency stabilization method for reflex klystrons and other self-excited microwave oscillators 09 p1357 A66-20780

Spectra of amplitude and phase fluctuations in drift klystron under initial energy spectra of randomly correlated fluctuations of current and velocity 09 p1358 A66-20810

Microwave regenerative amplifier using reflex klystron, considering beam current, supply voltages, mismatch, input and output amplitudes, phase lead, etc 11 p1655 A66-22725

Reflex klystrons as microwave FM detector and theoretical circuit predictions 11 p1670 A66-23160

FM and AM noise spectra of low-noise microwave tubes, solid state klystrons and solid state chains 12 p1835 A66-24135

Klystron and TWT, generating high powers at millimeter wavelengths, combined in single amplifier for radar systems 12 p1839 A66-24614

Noise and amplification characteristics of millimeter-wave reflex klystron amplifiers 13 p2037 A66-25549

High power generators for studying interaction of oscillating fields with plasmas 14 p2246 A66-26818

Short circuited crossguide coupling used to stop oscillation of reflex klystrons and convert them into stable millimeter wave amplifiers 14 p2248 A66-27058

Extension of nonlinear TWT equations to floating drift relativistic klystron, noting formulas for first harmonic of current in two- and three-cavity klystron 14 p2250 A66-27139

Spurious X-band output signals observed during interaction of dual reflex klystron cavities and klystron beams 14 p2258 A66-27956

Submillimeter wave mixing of output of carinotron and output of klystron in crossed-waveguide harmonic generator 15 p2463 A66-29025

Klystron transmitter for ionospheric diffusion soundings, noting method to obtain high stability in output power 16 p2661 A66-30954

Three-cavity extended-interaction klystron with cavities consisting of resonated sections of bar structure tested in pulsed operation, noting relation between cavity length and efficiency 16 p2663 A66-31020

Frequency stabilization method for reflex klystrons and other self-excited microwave oscillators 22 p3874 A66-39839

Traveling wave tubes and klystrons, discussing microwave power generation efficiency, application for satellite communications, etc 22 p3878 A66-40701

Microwave regenerative amplifier using reflex klystron, considering beam current, supply voltages, mismatch, input and output amplitudes, phase lead, etc 23 p4045 A66-41463

**KNUDSEN CELL**

High temperature equilibria among vapor species produced by fluorination of beryllium in Knudsen effusion cell, using mass spectrometer, deriving dissociation energy 12 p1811 A66-23621

Knudsen gauge designed by university sophomores, measuring molecular collision cross sections 15 p2498 A66-28787

**KNUDSEN FLOW**

Adherence of gas to wall, investigating Boltzmann equations for perfect fluid, Prandtl-type flow and state of rest fluid 05 p0661 A66-14535

Tube gas flow theory applicable to laminar flow, slip flow, transition region of flow and free molecular flow 07 p1023 A66-18131

Rarefied gas dynamics - International Symposium, Institute for Aerospace Studies, University of Toronto, July 1964, Volume 1 11 p1688 A66-22901

Mass flow of nitrogen gas through circular orifice at five Knudsen number values from 0.13 to 1.78 and range of upstream to downstream pressure 11 p1692 A66-22936

Internal flow problems in free, nearly free molecular regimes and higher transition

flows, using Boltzmann equation and series expansion to solve integral equation for surface collision density 11 p1693 A66-22940

Boltzmann-Krook equation in Knudsen layers for Rayleigh shear flow and related flow of rarefied gas 21 p3731 A66-39578

**KNUDSEN NUMBER**

Transition flow of nitrogen through short circular tubes with length-to-diameter ratios from 0.005 to 1 and pressure ratios from 1 to 20 05 p0605 A66-14704

Aerodynamic properties of simple bodies in hypersonic transition regime 08 p1164 A66-19132

Cylindrical Poiseuille flow of rarefied gas for inverse Knudsen number from zero to 10 10 p1524 A66-21806

Boltzmann equation behavior, at large Knudsen numbers, for free molecular interactions with infinite collision cross section 11 p1691 A66-22918

Rayleigh problem at low Mach numbers and arbitrary Knudsen number investigated in rarefied gas dynamics according to kinetic theory 11 p1692 A66-22922

Aerodynamic drag torque on rotating sphere in transition regime, noting dependence of gas inertia on Reynolds number 11 p1635 A66-22935

Poiseuille flow of rarefied gas in annular tube analyzed numerically for inverse Knudsen number, using Bhatnagar-Gross-Krook model and transport - integro-differential equation 18 p3102 A66-34920

**KOLMOGOROFF THEORY**

Contraction to improve isotropy of grid-generated turbulence 22 p3899 A66-40381

Grid turbulence for large Reynolds numbers, noting consistency of power spectra values with Kolmogoroff scaling, decay law and Reynolds number effect on turbulence 24 p4194 A66-42408

Extension of formalism of theory of branching random processes applied to fluctuations in development of extensive air shower cascade by Kolmogoroff method 24 p4269 A66-42920

**KONIG THEOREM**

Critical analysis of certain conformal mappings of ellipsoid of revolution onto plane 18 p3109 A66-34739

**KROOK EQUATION**

Class of exact solutions for one-dimensional single-relaxation equation with arbitrary collision frequency 08 p1316 A66-18532

Cylindrical Poiseuille flow of rarefied gas for inverse Knudsen number from zero to 10 10 p1524 A66-21806

Linearized one-dimensional Krook equation solved for half-space of gas bounded by oscillating wall 11 p1736 A66-22902

Accuracy of kinetic theory approximations assessed by comparison of approximate and exact solutions of Krook kinetic equation for Couette flow and shock wave structure 11 p1690 A66-22906

Numerical calculations of axially symmetric two-dimensional steady expansions of monatomic gas, using approximate Boltzmann equation with Krook collision term 11 p1690 A66-22908

Numerical convergence of iterative solution to complete Bhatnagar-Gross-Krook equation for strong shock waves 11 p1690 A66-22909

Internal flow problems in free, nearly free molecular regimes and higher transition flows, using Boltzmann equation and series expansion to solve integral equation for surface collision density 11 p1693 A66-22940

Iterative solution to Krook-Boltzmann kinetic equation noting Navier-Stokes numerical solution, computation and analysis of distribution function within shock wave 16 p2685 A66-30945

Kinetic theory of ionospheric satellite trail, discussing neutral and charged components from BGK model equation [AIAA PAPER 66-477] 18 p3226 A66-33654

Numerical solutions of Krook kinetic equation for Couette flow and plane shock wave 18 p3101 A66-34665

Boltzmann-Krook equation in Knudsen layers for Rayleigh shear flow and related flow of rarefied gas 21 p3731 A66-39578

Nearly free molecular flow in rarefied gas dynamics in comparison of theoretical and experimental results with reference to

drag 23 p4060 A66-42025

Numerical solution of Bhatnagar-Gross-Krook model for shock wave structure problem, noting Chapman-Enskog approximation 23 p4061 A66-42037

Nonlinear integral equations formulated that are equivalent to Krook kinetic equation for steady problems in two and three space dimensions 24 p4193 A66-42407

**KRYPTON**

Radioactive krypton-85 diffusion technique for temperature mapping of turbine blade surfaces [SAE PAPER 650704] 06 p0944 A66-17078

Xenon, radiogenic Xe 129R and krypton contents and xenon and krypton isotopic composition of Bruderheim meteorite 08 p1297 A66-19409

Sensitivity and safety of Kr-85 /radiokrypton/ for leak detection 22 p3928 A66-40497

X-rays and Auger electron emission by krypton 81 measured, using proportional counter 24 p4262 A66-42430

**KU-BAND**

Solid-dielectrically loaded strip transmission line techniques extended to Ku-band region 08 p1192 A66-18946

**L-BAND**

Sinusoidal step response of L-band waveguide to step-modulated RF excitation 03 p0332 A66-12432

Experimental L-band traveling wave maser developed with exceptionally wide tuning range 06 p0889 A66-15958

Parametric generation and amplification of magnetoelastic waves in single-crystal yttrium iron garnet cylinder at L-band at room temperature 06 p0851 A66-16457

Ground clutter shields for L-band radar using 60-ft parabolic reflector with Cassegrain geometry 15 p2457 A66-28596

Nuclear radiation hardened telemetry transmitter in L-band, noting tests and radiation effect problems 16 p2650 A66-30554

L-band traveling wave maser using chromium doped rutile, discussing inverted susceptibility as figure of merit 20 p3580 A66-38239

**L-2000 AIRCRAFT**

**S LOCKHEED L-2000 AIRCRAFT**

**LABORATORY**

SA ASTRONOMICAL OBSERVATORY

SA ENGINE TESTING LABORATORY

SA ENVIRONMENTAL LABORATORY

SA LUNAR MOBILE LABORATORY /MOLAB/

SA MANNED ORBITAL LABORATORY /MOL/

SA MANNED ORBITAL RESEARCH LABORATORY /MORL/

SA MISSILE TESTING LABORATORY

SA SPACE LABORATORY

SA TEST FACILITY

Air Force Avionics Laboratory and problem of transition from exploratory development to operational hardware 15 p2618 A66-28746

**LABORATORY APPARATUS**

Laboratory simulation to test image-velocity measuring device yielding accurate and useful results 02 p0227 A66-11379

Cesium diode thermionic converter, noting design, operation, application 10 p1485 A66-21515

Lunar dust depth in Mare Cognitum determined by comparing Ranger VII photographs with laboratory crater photographs 11 p1770 A66-22571

Laboratory duplication of processes exciting airglow, noting green line of oxygen atoms 11 p1699 A66-23116

Laboratory instrumentation for testing and calibration of in situ probes for lower ionosphere, mesosphere and stratosphere 13 p2059 A66-26549

Automated Biological Laboratory for Mars mission exobiological experiments controlled by computer routines 18 p3062 A66-34369

Laser application survey 19 p3374 A66-35798

Laboratory simulation of thermal shock failure in tungsten under missile firing conditions 19 p3385 A66-36154



Laboratory equipment protection from vibration environment, noting instrumentation and results 21 p3722 A66-38873

**ABYRINTH**  
Measurement of oculogravic illusion in subjects with or without labyrinthine defects, showing validity as specific response to stimulation of otolith organs 06 p0813 A66-16828  
Vestibular function in conditions of subgravity 11 p1641 A66-22481  
Labyrinthine nystagmus and sensation of turning evoked by impulsive stimuli in yaw, pitch and roll compared for subjects in plane of rotation and in tilted position 24 p4163 A66-42448

**ACTIC ACID**  
Crystalline lactic dehydrogenases in reaction with p-hydroxymercuribenzoate in urea 13 p2009 A66-25796

**LAGRANGE COORDINATE**  
Lagrange theorem extended for solution of three-body problem to regular configurations of more than three particles 16 p2804 A66-31393  
Motion equations of rigid body, discussing transformation from Lagrange equation to Euler equation 19 p3400 A66-35831  
Three-body model including low thrust forces used to generate artificial libration points or assure stability of five Lagrangian libration points in Earth-Moon space [AIAA PAPER 65-682] 19 p3461 A66-35889  
Lagrange libration points in plane of two mutually gravitating heavy masses applied to theory of SYNCOM lunar satellites 22 p3979 A66-40176

**LAGRANGE EQUATION**  
Global maximum for particle idealization of rocket propelled vehicle moving in calculus of variations, noting Lagrange equation 04 p0538 A66-13462  
Correlation matrix of natural thermal noise put forward for arbitrary passive linear system described by Lagrange equations and thermal equilibrium 07 p1013 A66-17431  
Partial-fraction expansion of transfer matrix, using Lagrange interpolation formula 08 p1246 A66-19738  
Non-Einsteinian gravitation, noting that expression for invariant density of free Lagrange gravitational field holds only for slowly varying weak fields 09 p1403 A66-20769  
Strict complementary energy theorem for finite deformation of elastic continuum established, using Lagrange strain and stress tensors as conjugate deformation and stress tensors characterizing deformation 10 p1615 A66-21478  
Variational principle application to heat conduction in solids, noting temperature dependence, physical meaning of Lagrangian heat flow between parallel plates, etc 12 p1975 A66-23542  
Lagrangian for particular collisional models in fluid dynamics, considering fluctuation theory relations and stability in presence of external field 12 p1918 A66-23552  
Lagrange equations of motion for solid body with liquid-filled cavities derived, using Hamilton-Ostrogradskii principle of least action 13 p2127 A66-25628  
Lunar origin hypothesis suggesting capture in gravitational field of Earth following storage in solar system 13 p2188 A66-26366  
Lagrange equation approach to linear aeroelasticity in modern aircraft from structural and aerodynamic data 13 p1997 A66-26696  
Non-Einsteinian gravitation, noting that expression for invariant density of free Lagrange gravitational field holds only for slowly varying weak fields 14 p2334 A66-27304  
Active-control and similar-control stabilization of Lagrange solutions of restricted three-body linear perturbation problem 14 p2382 A66-27559  
New method of introducing nonholonomic constraints into Lagrangian formulation of mechanics 16 p2749 A66-31724  
Lagrange equation for symmetric, nonhomotropic, spherical, cylindrical and one-dimensional unsteady flow of perfectly conducting gas behind normal shock wave of variable strength 18 p3102 A66-34728

Generalizations of functional Lagrange expansion to multivariable nonlinear systems such as state space and functional equations in s domain for control problems application 19 p3391 A66-36704  
Generalized Lagrange equations for rheonomic-holonomic mechanical system 20 p3602 A66-37542  
Inadequacy of Corson variational principle as foundation of classical and quantum dynamics 24 p4237 A66-42406  
Correction of motion of two degree of freedom system with one cyclic coordinate 24 p4189 A66-42837

**LAGRANGE MULTIPLIER**  
Rayleigh-Ritz method, stationary complementary and potential energy principles and Lagrange undetermined multipliers applied to free vibration of elastic body 11 p1781 A66-22611  
Lagrange and Mayer problems of optimal control of cost 11 p1680 A66-23277  
Existence theorems for optimal control solutions of Pontryagin and Lagrange problems 11 p1725 A66-23458  
Dual quadratic programming of dynamic response of frictionless mechanical system with one-sided constraints 13 p2117 A66-25347  
Variational problem of Lagrange with inequality, analyzing splitting of extremals, dead-end, entry and exit from boundary, etc 13 p2120 A66-26139  
Lagrangian multiplier representation for coast periods of optimum trajectories 14 p2381 A66-27433  
Variational problem of transition of aircraft with inertial system without stabilizers solved by reduction to Lagrange problem 15 p2534 A66-29336  
Lagrangian multiplier method applied to mixed boundary value problems such as stresses due to temperature changes in semiinfinite slab 15 p2615 A66-29733  
Natural frequencies of all-clamped rectangular sandwich panel vibrations, using Lagrange multipliers 24 p4286 A66-42160

**LAGRANGE SIMILARITY HYPOTHESIS**  
Quasi-Lagrangian study of inviscid barotropic fluid for analysis of certain ageostrophic jet flows 02 p0222 A66-11825  
Single fluid heat exchanger, using Lagrange method and thin walled stainless steel tube for theoretical and experimental dynamic response analysis [ASME PAPER 65-WA/HT-9] 05 p0791 A66-15653  
Lagrangian similarity hypothesis to determine structure of turbulence that arises during fluid flow over rough rigid wall 07 p1022 A66-18103  
Single fluid heat exchanger, using Lagrange method and thin walled stainless steel tube for theoretical and experimental dynamic response analysis [ASME PAPER 65-WA/HT-9] 11 p1785 A66-22193

**LAGUERRE FUNCTION**  
Linear system impulse response approximation, determining time-scaling factor via orthonormal Laguerre functions 06 p0866 A66-16748  
Second derivatives of Legendre and Laguerre polynomials based on Markov inequalities 08 p1244 A66-18792  
Inverse Laplace transformations in terms of Laguerre functions 12 p1905 A66-24654  
Generalized heat equation solution expansion in terms of radial heat polynomials, Appel transforms and Laguerre polynomials 13 p2118 A66-25793  
Functional integration analysis of exponential behavior of nonlinear feedback control systems 13 p2052 A66-26076  
Signal analysis with aid of Laguerre polynomials 16 p2655 A66-31688

**LALLEMAND CAMERA**  
Vectorial photoelectric effect and quantum efficiency measurement in thin gold films for two light polarizations, using Lallemant electronic camera 20 p3614 A66-37279

**LAMB WAVE**  
Lamb shift in lithium isotope measured by determining lifetime from photon emission and employing analog formula of Bethe and Salpeter 11 p1739 A66-22948

**LAME WAVE EQUATION**  
Stress-strain distribution of sharp corners

effect on surface of elastic body, examining mathematical difficulties in application of Lame equation and boundary data smoothing 23 p4135 A66-40991

**LAMINA**  
**S LAMINAR BOUNDARY LAYER SEPARATION**  
**S MONOMOLECULAR LAYER**  
**LAMINAR BOUNDARY LAYER**  
Three-dimensional laminar boundary layer on body of revolution at small incidence at its stability 01 p0055 A66-10203  
Two-phase flow over flat plate analyzing velocity profile, shear coefficient and heat transfer of laminar boundary layer formed over plate 01 p0006 A66-10423  
Laminar boundary layer of nitrogen flow over helium cooled sphere with porous wall 01 p0162 A66-10463  
Heat transfer data obtained in combined convection regime for rotating isothermal cone, noting influence of cone vertex angle 01 p0164 A66-10902  
Surface modifications of recovered small-scale plastic models after high speed flight used to estimate extent of laminar and turbulent flow over surface related to ablation studies 02 p0303 A66-11560  
Three-dimensional laminar boundary layer flow on rotating helical blade 02 p0176 A66-11952  
Multiphase flow system with regard to chemical and nuclear processes, rocketry and air pollution control noting adiabatic potential, laminar and electrodynamic flow 03 p0354 A66-12312  
Laminar boundary layer transition on highly cooled 10 degree cone in hypersonic flow, using heat gauges to study turbulent burst propagation 03 p0315 A66-12788  
Laminar boundary layer control wind tunnel results, using perforated plastic reinforced by glass fiber 04 p0453 A66-13513  
Incompressible laminar boundary layer for plate with slot suction at high Reynolds number 04 p0509 A66-13654  
Porous blowing and suction for laminar boundary layer during free convection at vertical surface 04 p0597 A66-13820  
Laminar boundary layer on impulsively started rotating sphere, discussing viscous incompressible axially symmetric flow in terms of nonsteady partially linearized Navier-Stokes equations 04 p0513 A66-14477  
Interaction of radiation and convection in laminar boundary layer of perfect gas on flat black plate [ASME PAPER 65-HT-54] 05 p0785 A66-14760  
Integral method based on method of moments to investigate compressible laminar boundary layers 05 p0607 A66-15466  
Cylinders in reciprocating harmonic rotation, calculating momentum, heat and mass transfer in forced convective field via perturbation technique [ASME PAPER 65-WA/HT-6] 05 p0791 A66-15654  
Quasi-linearization solution of two-component laminar compressible boundary layer with heat transfer on ablating wall [ASME PAPER 65-WA/HT-41] 05 p0792 A66-15667  
Viscous fluid flow, examining effect of time dependent suction applied at wall of infinite extent 06 p0871 A66-16351  
Temperature distribution of fluid in laminar boundary layer of flat plate and heat flow from fluid to plate 06 p0872 A66-16467  
Aerodynamic calculations for diffusion combustion in laminar boundary layer between two plane parallel conducting gas flows in transverse magnetic field 06 p0918 A66-16844  
Linear stability of laminar boundary layers for asymptotic suction profile, obtaining solution of inviscid equation in terms of hypergeometric function 06 p0874 A66-16998  
Pressure gradient effect on stability of laminar boundary layer when skin friction at wall vanishes, noting Reynolds number of flow 06 p0874 A66-16999  
Controlled three-dimensional roughness effect on hypersonic laminar boundary layer transition [AIAA PAPER 66-26] 06 p0804 A66-17092  
Wake from bluff bodies interaction with initially laminar boundary layer



[AIAA PAPER 66-126] 06 p0875 A66-17096  
Concentration profile in laminar boundary layer frozen to wall by catalytic chemical reaction 07 p1019 A66-17245  
Combined free and forced convection flows with heat and mass transfer in laminar boundary layers on vertical surfaces 07 p1150 A66-17579  
Incompressible laminar boundary layer equations for flow due to jet against body of revolution extending to infinity in absence of pressure gradient but with axially symmetrical swirl 07 p0981 A66-18045  
Similar solutions to laminar boundary layer equations affected by Prandtl number, viscosity-temperature variation, mass transfer and hypersonic parameter 07 p1023 A66-18136  
Laminar boundary layer on cone with uniform mass transfer, discussing velocity and energy fields 08 p1161 A66-18530  
Pressure distribution and heat transfer for laminar boundary layer flow over highly swept blunt delta wings in hypersonic free stream  
[AIAA PAPER 66-130] 08 p1162 A66-18953  
Axisymmetric stagnation-point boundary layer with constant shear inner layer solution 08 p1207 A66-19150  
Laminar boundary layer in gas flow with arbitrary external velocity and temperature gradient solved by single-parameter approximation 08 p1319 A66-19424  
Hypersonic shock tunnel study, examining effects of roughness, bluntness and angle of attack on boundary layer transition 08 p1166 A66-19813  
Distribution of specific thermal flux on body surface heated by plasma jet 09 p1407 A66-20139  
Heat exchange, friction and mass exchange in laminar multicomponent boundary layer during injection of extraneous gases 09 p1368 A66-20705  
Laminar boundary layer problems for compressible and incompressible fluids 09 p1368 A66-20751  
Onset of turbulence in detached laminar shear layer 09 p1368 A66-20803  
Numerical solution of laminar boundary layer momentum, energy and diffusion differential equations for heat and mass transfer on moving continuous flat surface with injection or suction 10 p1619 A66-21053  
Heat transfer and distribution of velocity, temperature and concentration in laminar supersonic boundary layers with blowing of light gas with desired pressure and heat distribution 10 p1620 A66-21394  
Transition region and amplification factor of unstable disturbances in laminar boundary layers with distributed suction 10 p1522 A66-21408  
Dissociated laminar boundary layer with heterogeneous recombination 10 p1524 A66-21805  
Thickness of laminar liquid film draining from vertical surface analytically determined by assuming evaporation rate is known constant  
[ASME PAPER 65-HT-39] 11 p1785 A66-22189  
Laminar MGD boundary layer on conducting surface in crossed electric and magnetic fields for flow core of constant temperature 11 p1745 A66-22590  
Heat exchange, friction and mass exchange in laminar multicomponent boundary layer during injection of extraneous gases 11 p1688 A66-22591  
Thick laminar boundary layer influence at supersonic speeds and low Reynolds numbers 11 p1634 A66-22933  
Asymptotic expansions to heat-transfer rate for laminar boundary layer flow at small or large Prandtl number 11 p1786 A66-23012  
Book on basic developments in fluid dynamics including numerical solution of problems in gas dynamics, stability of parallel flows, blast wave theory, etc 12 p1861 A66-23806  
Analytical solution for surfaces with longitudinal curvature of larger magnitude than that considered in early forms of boundary layer theory, noting condition for self-similar solutions, main flow, boundary layer equations, etc 12 p1861 A66-23811  
Similar solution of differential equations

for compressible laminar boundary layers in case of insulated walls 12 p1862 A66-23861  
Equation for laminar boundary layer on flat plate in viscous compressible gas flow under chemical relaxation, solved by approximate method in series 12 p1863 A66-24244  
Parametric method of solving equations of laminar boundary layer with longitudinal pressure gradient during equilibrium gas dissociation 12 p1863 A66-24367  
Heat transfer and mass transfer near stagnation point during injection and suction of various gases through blunt body surface 12 p1979 A66-24427  
Transverse flow velocity effect on laminar flow shape stability 12 p1863 A66-24428  
Properties of compressible boundary layers with heat transfer and arbitrary pressure gradients calculated, using integral equation and correlation concept for application in hypersonic flows 12 p1865 A66-24581  
Stability of laminar boundary layers and wakes at hypersonic speeds, noting existence conditions for subsonic disturbances and effect of hot wake core 13 p2061 A66-25165  
Interferometric determination of temperature field compared with exact analytical solutions for laminar boundary layer in case of free convection 13 p2208 A66-25314  
Porous blowing and suction for laminar boundary layer during free convection at vertical surface 13 p2209 A66-25319  
Compressible laminar boundary layer equations solved, noting wall flow and suction problem 13 p2063 A66-25467  
Laminar boundary layer characteristics determined by Howarth and Kochin-Loitianskii methods, using simple quadratures 13 p2066 A66-26487  
Surface roughness effect on laminar-turbulent transition, noting plane flow past isolated cylindrical element in laminar boundary layer 13 p2068 A66-26542  
Properties of laminar boundary layer undergoing surface catalysis with two reactants and two products obeying Langmuir-Hinshelwood mechanism, solving concentration field by integral equation 13 p2019 A66-26663  
Approximate methods of computing heat transfer through laminar boundary layer, considering boundary layer along flat plate and second order effects 13 p1993 A66-26712  
Thermal insulation of surfaces by cold gas injection into laminar compressible boundary layer of air in chemical equilibrium 13 p1993 A66-26730  
Nonequilibrium laminar boundary layer of binary dissociating gas determined by solving nonlinear partial differential equations governing system  
[AIAA PAPER 65-129] 14 p2274 A66-27406  
Finite-difference method for computing transient velocity profiles in laminar boundary layer around two-dimensional cylinder, noting Blasius flow oscillations 14 p2274 A66-27434  
Solution of boundary layer equation for two-dimensional laminar steady motion of viscous incompressible fluid in convergent channel with suction at wall 14 p2276 A66-27728  
Universal laminar boundary layer equations for incompressible fluid and homogeneous and dissociated gases derived, using parametric approximations 14 p2278 A66-28054  
Laminar air flow past porous plate through which fuel and oxidizer mixture is injected, deriving diffusion combustion processes that develop in laminar boundary layer 14 p2371 A66-28318  
Integration of third-order differential equation of laminar boundary layer on porous surface 15 p2477 A66-28777  
Series expansion solutions for shock tube laminar wall boundary layer, taking into account mutual interaction between boundary layer and free stream 15 p2479 A66-29270  
Displacement and heat transfer effects of laminar and turbulent boundary layers far downstream in slowly expanding hypersonic nozzle, determining inviscid core

flow 15 p2424 A66-29273  
Double unsteady laminar boundary layers on solid bodies in presence of oscillating external flow of small amplitude 15 p2480 A66-29686  
Laminar boundary layer of low temperature plasma on isolator walls in channel of MHD generator in presence of transverse magnetic field 16 p2758 A66-30327  
Asymptotic behavior of solutions to equations for laminar boundary layer far from wall 16 p2684 A66-30582  
Laminar boundary layer separation in supersonic flow on body with symmetry of revolution 16 p2629 A66-30583  
Stability of idealized laminar boundary flow, determining phase velocity, amplification rate and wave number of all disturbances 16 p2686 A66-30948  
Interaction of radiation and convection in laminar boundary layer of perfect gas on flat black plate  
[ASME PAPER 65-HT-54] 16 p2828 A66-30988  
Laminar boundary layer in oscillatory flow along infinite flat plate with variable suction 16 p2686 A66-31107  
Hypersonic laminar boundary layer flow of equilibrium dissociating gas 16 p2630 A66-31306  
Laminar boundary theory perturbation solutions modified by formulating perturbation about Blasius solution 16 p2691 A66-31663  
Source type hypersonic free stream effects on flow field about axisymmetric cone, obtaining properties in shock layer, boundary layer, pressure gradient, etc 17 p2837 A66-32080  
Momentum-integration method for laminar boundary layer interactions in rotating flow 17 p2907 A66-32278  
Response of two-dimensional laminar boundary layer to fluctuating free stream or surface oscillation 17 p2908 A66-32443  
Laminar boundary layer on cylinder with symmetric cross section bounded by two equal circular arcs treated by Pohlhausen method 17 p2911 A66-32836  
Laminar boundary layer on cylinder with symmetric cross section bounded by two equal circular arcs 17 p2911 A66-32837  
Electric and magnetic fields effect on three-dimensional laminar boundary layer of conducting fluid near line of intersection of two surfaces 17 p2971 A66-32865  
Mangler rectilinearization of axisymmetric laminar boundary layer flows and Prandtl boundary layer hypotheses, applicability to non-Newtonian fluids 17 p2912 A66-33045  
Laminar boundary layer heat transfer measurements by thick-film calorimeter gauges on flat plate in dissociated and partially ionized air 17 p3039 A66-33483  
Laminar, transitional and turbulent boundary layer flows with adverse pressure gradient on axisymmetric blunted conical flared body at Mach 10  
[AIAA PAPER 66-493] 18 p3047 A66-33658  
Boundary layer problem concerned with effects of radiation absorption and emission for flow of high speed gas over flat plate  
[AIAA PAPER 66-521] 18 p3047 A66-33662  
Step function distribution of heat transfer for laminar supersonic boundary layer described as function of decay factor 18 p3261 A66-34363  
Hartree solution of MHD laminar boundary layer incompressible conducting fluids, specifically considering flow at inlet to semiminfinite flat channel 18 p3147 A66-34636  
Instability of free laminar boundary layer between parallel streams analyzed for incompressible fluid, noting values of Reynolds number 18 p3102 A66-34921  
Hydrogen combustion in air above solid noncatalytic wall heated to 800 degrees C, examining diffusion equation for slow combustion and laminar boundary layer flow over noncatalytic wall 19 p3479 A66-36249  
Laminar boundary layer stability of incompressible fluid at elastic surface 19 p3342 A66-36463  
Finite difference method approach to discontinuity in parabolic equations for shear laminar boundary layer flow of injected gas past wall 19 p3342 A66-36477  
Separation of laminar boundary layer of gas flow from cone as function of angle of



- attack, Mach number, etc 19 p3277 A66-36478
- Flow coefficient of nozzle calculated by thickness of quantity of motion of laminar boundary layer at nozzle 20 p3545 A66-37412
- exit 20 p3545 A66-37412
- General theorems for dissociated and chemically reacting compressible laminar unsteady two-component boundary layers derived, based on Nirenberg maximum principle 20 p3510 A66-37524
- Approximate method of integrating linearized equation for laminar boundary layer to establish relations of velocity distribution with friction 20 p3546 A66-37679
- stress 20 p3546 A66-37679
- Free laminar boundary layer flow between parallel streams of different magnetic fields and temperatures for incompressible viscous fluid 21 p3776 A66-38682
- Free convection boundary layer along isothermal plate, using equation of laminar compressible flow and heat transfer, noting profile dependency upon wall coordinate 21 p3835 A66-38945
- Correlation formulas improvement for laminar shock tube boundary layer for air and argon 21 p3727 A66-39167
- Distribution of specific thermal flux on body surface heated by plasma jet 21 p3793 A66-39411
- Von Karman integral concept for incompressible laminar boundary layers extended to second-order for two-dimensional or axisymmetric flow by generalizing definition of displacement and momentum thickness 22 p3898 A66-40137
- Strouhal number effect on sound-excited laminar-turbulent transition in separated boundary layers formed by round or plane nozzle 22 p3899 A66-40382
- Short duration technique providing simulation of thermodynamic properties and composition of exhaust products of liquid and solid propellant rocket engines [AIAA PAPER 66-760] 22 p3894 A66-40643
- Laminar boundary layer equations solved in presence of nonuniform velocity and enthalpy profiles in initial cross section or on bodies extending to infinity upstream and downstream 22 p3901 A66-40685
- Heat transfer in nonisothermal plate with laminar boundary layer 22 p4000 A66-40822
- Pressure gradient calculation in three-dimensional laminar boundary layer, using method of local similarity 23 p4009 A66-41724
- Laminar boundary layer in incompressible liquid, noting effect of variation of kinematic viscosity and density on stability 23 p4056 A66-41725
- Approximation of self-similar plane and axisymmetric problems for high temperature laminar boundary layer, based on equations for boundary layer of finite thickness for high temperature gas 23 p4149 A66-41783
- Nongray radiation effects on laminar boundary layer of absorbing gas over flat plate, using absorption coefficient with stepwise frequency dependence 23 p4012 A66-41903
- Plaint coatings applied to streamlined bodies to reduce hydrodynamic drag by stabilizing laminar boundary layer against transition to turbulence 23 p4059 A66-41943
- Similar solutions for laminar boundary layer under forced convection of mixture of fluids with constant mass density and temperature and composition dependent parameters for flat plate analysis 23 p4059 A66-42007
- Parametric method in laminar boundary layer theory, noting reduction of equations for incompressible fluid 23 p4059 A66-42008
- Separation point of laminar boundary layer before dihedron, determining conservation of momentum and mass 23 p4013 A66-42010
- Shear flow transition to turbulence and instability phenomena, discussing parallel and laminar flows 23 p4060 A66-42019
- Stability of laminar boundary layers at concave wall with vortex type disturbance introduced by interference baffles 23 p4060 A66-42022
- Flow coefficient of elliptical cylindrical pipe, analyzing boundary layer at exit for various Reynolds numbers, noting velocity profile 23 p4014 A66-42057
- Flat plate laminar boundary layer in supersonic wind tunnel, measuring pressure distribution and profiles and heat transfer rates, noting dissociation fraction effects 24 p4194 A66-42411
- Laminar boundary layer characteristics on continuous moving surface, noting high critical Reynolds number, disturbance amplitude function and energy criterion for stability 24 p4194 A66-42412
- Regular solutions of laminar boundary layer equations near point of vanishing skin friction, calculating pressure gradient 24 p4194 A66-42413
- LAMINAR BOUNDARY LAYER SEPARATION**
- Pohlhausen method applied to shock wave/boundary layer interaction, calculating flow characteristics of laminar separation region 04 p0455 A66-14138
- Solving supersonic laminar boundary layer separation by velocity profile and energy momentum concept, noting application to wedges and curved surfaces [ASME PAPER 65-APMW-19] 04 p0512 A66-14220
- Laminar boundary layer behavior of centrifugal impeller blades, discussing exact solution via perturbation technique [ASME PAPER 65-WA/FE-15] 05 p0608 A66-15612
- Separation point position determined for laminar layer on cylindrical surface at various Reynolds numbers 09 p1368 A66-20835
- Solving supersonic laminar boundary layer separation by velocity profile and energy momentum concept, noting application to wedges and curved surfaces [ASME PAPER 65-APMW-19] 10 p1523 A66-21469
- Laminar boundary layer behavior of centrifugal impeller blades, discussing exact solution via perturbation technique [ASME PAPER 65-WA/FE-15] 12 p1799 A66-24543
- Laminar boundary layer separated flow of particulate suspension, including Brownian diffusion, jet flow, etc 14 p2275 A66-27561
- LAMINAR FLAME**
- Laminar diffusion flame occurring in mixing zone between undiluted fuel and undiluted oxidizer by process of molecular diffusion 03 p0443 A66-12489
- Laminar flame speeds predicted by Spalding formulation in stoichiometric mixtures with nonnormal diffusion 03 p0443 A66-12490
- Burning modes in initially unmixed reactants, describing stagnation region formation by interaction of opposed flows of fuel and oxidant [AIAA PAPER 66-71] 06 p0969 A66-16258
- Time dependent stability of one-dimensional laminar flames with distributed heat losses 10 p1621 A66-21809
- Effect contributing to laminar flame stability with surface variations 14 p2410 A66-26780
- Laminar and turbulent diffusion flame combustion mechanisms, stabilization, flame ionization, Bunsen burner, fuel gas jet eddy diffusion, etc 15 p2616 A66-29068
- Plasma behavior in laminar and turbulent hydrocarbon-air flames, discussing flame ionization, electron concentration and recombination, detonation wave ionization data, ignition, etc 18 p3143 A66-34027
- LF self-vibrations of laminar diffusion flames in axial mode at frequencies corresponding to fuel system natural frequencies [WSCF 66-30] 18 p3263 A66-34414
- Stability analysis of one-dimensional steady laminar flame propagation with conductive heat loss 20 p3680 A66-38045
- LAMINAR FLOW**
- Laminar flow through parallel and uniformly porous walls of different permeability 01 p0057 A66-10425
- Interaction of two identical spheres falling freely in viscous fluid under laminar flow conditions 01 p0058 A66-10487
- Transfer of heat or nonstationary mass in circular cylindrical laminar flow tube 01 p0166 A66-11086
- Inlet region of laminar meridional flow in arbitrarily shaped narrow gap between two axisymmetrically formed walls 02 p0217 A66-11585
- Heat transfer and friction for laminar flow of gas in circular tube at high heating rate, using finite difference method 02 p0304 A66-12198
- Nonisothermal wall problem for vertical right circular cone in laminar free convection for fluids with low Prandtl numbers 02 p0305 A66-12200
- Rheology of liquids discussing viscometers, models for prediction and industrial and biological application 03 p0355 A66-12601
- Hypersonic laminar near wake of blunt bodies considered in terms of dual region model [AIAA PAPER 65-52] 03 p0315 A66-12789
- Combustion and sublimation in aerothermochemical interaction between dissociated air stream and graphite surface in hypersonic laminar viscous flow [AIAA PAPER 65-42] 03 p0444 A66-12797
- Stabilization of laminar conducting fluid flowing down inclined plane in transverse magnetic field 03 p0356 A66-12946
- Laminar stability of incompressible and stationary flows with curved streamlines, applying integral method and noting time dependence of flow 03 p0357 A66-13089
- Viscous dissipation effect on temperature profile in thermal entrance region between parallel plates, considering flow laminar and velocity profile developed 03 p0358 A66-13092
- Extremal concentrations in laminar flow of incompressible viscous liquid along tube of constant cross section, noting recombination reactions 04 p0597 A66-13695
- Laminar and turbulent flow in eccentric annular ducts compared 04 p0511 A66-13938
- Laminar flow development of incompressible Newtonian fluid in hydrodynamic entrance region of flat duct 04 p0511 A66-13939
- Hydrodynamic behavior of mercury in laminar and turbulent flow in tube, discussing effect of vacuum and protective gas 04 p0511 A66-14185
- Convective mass exchange in heterogeneous chemical reactions in laminar flow along wall 04 p0597 A66-14186
- Laminar flow stability of layer of viscoelastic fluid flowing down infinite inclined plane under action of gravity 04 p0512 A66-14428
- Laminar flow in two-dimensional channel with uniformly porous walls through which fluid is uniformly injected 05 p0662 A66-15057
- Pressure drop in entrance region of abrupt inlet circular tube for continuum laminar flow conditions [ASME PAPER 65-WA/APM-5] 05 p0663 A66-15428
- Heat pipes as heat removal systems in space thermionic power supplies, discussing laminar, turbulent flow and heat transfer efficiency 05 p0789 A66-15542
- Heat transfer and velocity characteristics of thermal and hydrodynamic laminar flow in ducts of arbitrary cross section, considering boundary conditions at wall [ASME PAPER 65-WA/HT-13] 05 p0790 A66-15650
- Nonsimilar boundary layer flow and heat transfer of cone rotating in forced flow [ASME PAPER 65-WA/HT-31] 05 p0608 A66-15674
- Local heat transfer coefficients in nozzle under conditions of cold-wall low density high speed laminar flow 05 p0609 A66-15774
- MHD boundary layer equations with explicit solutions for longitudinal field in plane stationary incompressible laminar flow 06 p0920 A66-17007
- Convective heat transfer in thin rectangular channels commonly found in nuclear reactor fuel assemblies 07 p1148 A66-17299
- Laminar and turbulent boundary layer flow in ablating cones in hypervelocity flight [AIAA PAPER 66-27] 07 p1020 A66-17889
- Mass transfer method for measuring skin friction from isothermal adiabatic leading-edge flat plate in compressible laminar airflow with negligible pressure gradient 07 p0980 A66-17943
- Electron diffusion in mutually perpendicular static electric and magnetic fields based on stability of laminar flow 07 p1081 A66-17953



Wall jet on rotating disk totally immersed in fluid, with derivation of laminar flow velocity profiles 07 p0981 A66-18047

Heat transfer and stability of laminar hypersonic separated flow around annular cavity conical model 07 p0981 A66-18117

Tube gas flow theory applicable to laminar flow, slip flow, transition region of flow and free molecular flow 07 p1023 A66-18131

Performance of air Tesla turbine for various flows investigated by differential equation of motion 08 p1161 A66-18824

Electron conservation equation and effects of laminar or turbulent flow on breakdown in gases 08 p1206 A66-18933

Book on two-dimensional laminar boundary layers with and without suction noting velocity profile role, wind tunnel models, transition measurements, etc 08 p1208 A66-19355

Adiabatic laminar flow in concentric sleeve seal where rotating shaft changes fluid temperature and viscosity [ASLE PREPRINT 65AM 4C3] 08 p1232 A66-19382

Laminar circulation and thermal equilibrium in stars generated by nonspherical perturbations 09 p1448 A66-20096

Forced convection problem for steady fully-developed laminar flow in straight channel when fluid properties are functions of temperature 09 p1366 A66-20175

Heat transfer in laminar flow between parallel porous walls with discontinuous change in wall temperature 09 p1470 A66-20176

Laminar fully-developed flow of water between parallel flat plates examined, using motion equation with experimental values for viscosity, conductivity, specific heat and density 09 p1470 A66-20179

Interaction of two identical spheres falling freely in viscous fluid under laminar flow conditions 09 p1367 A66-20701

Parameter estimation for laminar conical flow of viscous inelastic non-Newtonian fluids 10 p1521 A66-21056

Mathematical model of flame propagation in laminar and turbulent flow 10 p1619 A66-21072

Pressure drop and heat transfer to Newtonian fluids in cooled pipes for laminar flow, establishing empirical correlation 10 p1620 A66-21272

Electrical conduction behavior of laminar arc-heated flow in contact with cooled anode, noting anode current parameters [AIAA PAPER 66-188] 10 p1561 A66-21435

Friction factors and mean electrical conductivity for argon arc plasma flow, examining laminar-turbulent flow modes [AIAA PAPER 66-189] 10 p1561 A66-21436

Pressure drop in entrance region of abrupt inlet circular tube for continuum laminar flow conditions [ASME PAPER 65-WA/APM-5] 10 p1523 A66-21471

Velocity overshoot within boundary layer in alternating laminar air flow near mouth of square channel 10 p1524 A66-21827

Combined free and forced laminar convection heat transfer inside inclined circular tubes of varying position [ASME PAPER 65-WA/HT-3] 11 p1785 A66-22191

Mean and dynamic skin friction, separation and transition in low-speed laminar and turbulent flow measured by thin-film heated element 11 p1693 A66-23013

Mechanical flow processes and variational methods based on fluctuation theory, noting relations on minimum entropy production, two-dimensional laminar flow of incompressible fluid, etc 12 p1975 A66-23543

Elgensolutions for laminar flow in porous two-dimensional channel subject to certain boundary conditions 12 p1862 A66-23994

Asymptotic series solution to problem of laminar film condensation on nonisothermal vertical plate, considering inertia and convection effects 12 p1978 A66-23996

Liquid film flow stability, considering two-dimensional perturbations, hydrodynamic friction with allowance for finite curvature radius of bounding surface 12 p1864 A66-24435

Mixing of laminar viscous incompressible

jets expelled from equally spaced holes in vertical wall, obtaining solution by using Navier-Stokes equation 12 p1864 A66-24444

Laminar hypersonic flow past sphere based on constant-density approximation, solving Navier-Stokes equations and comparing with values of shock Reynolds number 12 p1800 A66-24943

Transition from laminar to turbulent flow, establishing critical Reynolds number of 2223 for steady pipeflow 13 p2069 A66-26702

Laminar fluid flow of two-phase ideally viscous medium between two parallel surfaces 13 p2072 A66-26766

Hypersonic wake studies in ballistic missile research program, discussing reentry of hypervelocity vehicles, laminar flow, atmospheric turbulence, etc 14 p2218 A66-27402

Laminar ducted flow of viscous electrically conducting fluid under uniform arbitrarily oriented magnetic field for rectangular duct with nonconducting walls 14 p2342 A66-27407

Effect of instantaneous change in viscosity on laminar vortex of flow through suddenly widening pipe 14 p2277 A66-27933

Oscillating laminar separated flow formed ahead of forward facing step oscillating transversely to hypersonic free stream, noting phase differences between separation point movement and that of step 14 p2221 A66-28110

Laminar fluid flow in channel generated by arbitrary generatrix, allowing for interaction between boundary layer and flow core, calculating boundary layer 14 p2278 A66-28316

Laminar flow of incompressible fluid in rectangular channel, determining temperature distribution over channel cross section and thermal flux through wall for case of energy dissipation 14 p2415 A66-28317

Two-dimensional laminar MHD flow in convergence channel with uniform input, finding effect of flow convergence on boundary development for arbitrary magnetic field induction 15 p2549 A66-28638

Three-dimensional viscous free mixing, describing numerical and experimental solutions for wake and jet flows [AIAA PAPER 65-49] 15 p2424 A66-29272

Mixing of free jet boundary which includes laminar and turbulent flow region in tandem 16 p2685 A66-30805

Laminar steady motion transition to turbulent flow in systems described by hydrodynamic equations, including small amplitude steady periodic motion analysis 16 p2689 A66-31512

Laminar electrohydrodynamic flow in plane diffusor, taking into account molecular diffusion of space charge 17 p2969 A66-32544

MHD approximation of laminar duct and channel flow of electroconductive viscous Newtonian fluid 17 p2971 A66-32861

Self-similar solutions of two-dimensional laminar flow of incompressible electroconductive fluid in channel in crossed electric and magnetic fields, using Jacobi elliptic integrals 17 p2971 A66-32866

Gravitational stability of laminar liquid layer flowing down inclined plane and heated from below 17 p2914 A66-33172

Laminar flow velocity field and pressure distribution in inlet region of rectangular ducts [ASME PAPER 66-FE-7] 17 p2914 A66-33261

Approximate solution of boundary layer problems by variational techniques, using multiparameter approach 18 p3096 A66-33594

Fully developed laminar incompressible flow in stepped rectangular channel, with velocity profiles obtained by variational method 18 p3097 A66-33596

Laminar steady incompressible nonuniform flow in rectangular duct, stream tube and pipe 18 p3099 A66-34124

Critical parameters and flow characteristics of swept wings with full-chord laminar flow, noting boundary layer disturbance effects 18 p3050 A66-34950

Interface propagation in mixed laminar-turbulent flow between counter-rotating concentric cylinders, noting spiral turbulence as dominant feature of Couette flow transition 20 p3547 A66-37979

Distortion of laminar circular Couette flow measured by end effects, noting two-

dimensional tangential motion near axial plane of symmetry 20 p3547 A66-37980

Laminar and turbulent boundary layer flow in ablating cones in hypervelocity flight [AIAA PAPER 66-27] 21 p3723 A66-38686

Quantities and relations for describing two-phase flows, kinematics and kinetics of both phases of laminar pipeflow 21 p3724 A66-38933

Sufficient conditions for instability against small oscillations of symmetric laminar flow of inviscid incompressible perfect magnetofluid 21 p3791 A66-39169

Vector equations of steady incompressible viscous flow in absence of extraneous forces, discussing Beltrami flow, doubly laminar flow and plane flow 21 p3728 A66-39435

Pressure distribution in laminar flow between parallel disks, noting inertia effects 21 p3729 A66-39439

Heat transfer in laminar flow of Bingham material through circular pipe, taking into account dissipation effect 21 p3836 A66-39441

Steady laminar flow of viscous incompressible fluid through two-dimensional channel with fluid sucked or injected with different velocities through uniformly porous parallel walls 21 p3730 A66-39461

Laminar forced-convective heat transfer for dissipative fluid in tube bounded by concentric circles 21 p3837 A66-39610

Pitot tube technique for measuring velocity profiles, using Bernoulli equation in stress measurement in laminar viscoelastic flow 22 p3898 A66-40010

Model of laminar hypersonic base flow region of slender bodies, introducing base height and Reynolds number variation of base pressure ratio 22 p3843 A66-40345

Gaseous dispersion in laminar flow through circular tube with mass transfer to retentive layer 22 p3900 A66-40411

Heat transfer in entrance section in rectangular duct for incompressible fluid in laminar pulsating flow with periodic pressure gradient 23 p4148 A66-41216

Laminar shock layer structure in which streamlines retain appropriate momentum calculating exhaust plume structure for rocket nozzle 23 p4012 A66-41921

Temperature distribution of laminar channel flow with tangential stress and wall temperature 24 p4294 A66-42720

Secondary steady or periodic flow generation from stability loss by laminar flow of viscous incompressible fluid, noting nonuniqueness of solution 24 p4195 A66-42840

Laminar flow of fluid with varying viscosity in tube with walls at constant temperature, analyzing equations of motion and equations for conservation of energy 24 p4197 A66-42991

Generalization of experimental data on hydraulic resistance in tubes with ribbon turbulizers for laminar flow with macrovortices and turbulent flow 24 p4198 A66-43223

**LAMINAR FLOW AIRFOIL**

Drag reduction for sailplanes, investigating adoption of laminar foil section 01 p0008 A66-11097

Preventing turbulent contamination of laminar flow on highly swept wings by attaching bump on leading edge 06 p0801 A66-15998

Laminar profile characteristics affected by wind tunnel flow turbulence 07 p1018 A66-17857

**LAMINAR FLOW CONTROL**

Laminar flow control /LFC/, aircraft performance benefits include increased endurance, loiter time and cruise altitude 18 p3050 A66-34948

Flight testing of laminar flow control on X-21 aircraft, noting degradation of laminar performance in proximity of clouds or atmospheric turbulence, feasibility, handling, etc 18 p3050 A66-34949

Aerodynamic design criteria for maintaining laminar flow control including instability limit, surface roughness, acoustical environment, etc 18 p3050 A66-34951

Optimum high payload laminar flow control aircraft offer 20 to 25 percent range improvement, indicated by design studies of



- large logistics aircraft 18 p3053 A66-34952  
Flight testing of laminar flow control on full-scale swept wings, examining total pressure probes, wing wake drag and boundary layer stability utilizing pressure transducer [AIAA PAPER 66-734] 22 p3846 A66-40625
- LAMINAR HEAT TRANSFER**  
Transfer of heat or nonstationary mass in circular cylindrical laminar flow tube 01 p0166 A66-11086  
Heat transfer by laminar forced convection for dissipative fluid in annulus calculated, using complex variable method 04 p0598 A66-14211  
Limiting relative laws of friction and heat transfer applicable to nonisothermal gas flow with finite Reynolds numbers 04 p0598 A66-14440  
Spectral dynamics of laminar convection, discussing transformation of Benard convection problem into spectral domain 04 p0599 A66-14472  
Free convection on laminar forced flow heat transfer in horizontal circular tube [ASME PAPER 65-HT-23] 05 p0783 A66-14744  
Laminar flow heat transfer in polygonal ducts, covering analog solution by Moire and point matching method [ASME PAPER 65-HT-27] 05 p0784 A66-14746  
Laminar boundary-layer heat transfer and shear stress predictions from similarity solutions, emphasizing large free-stream velocity gradients and highly cooled walls [ASME PAPER 65-HT-62] 05 p0786 A66-14763  
Quasi-linearization solution of two-component laminar compressible boundary layer with heat transfer on ablating wall [ASME PAPER 65-WA/HT-41] 05 p0792 A66-15667  
Laminar heat transfer and pressure distribution in open cavity supersonic flow, noting heat-transfer coefficient [ASME PAPER 65-WA/HT-37] 05 p0808 A66-15670  
Laminar heat transfer in inlet tube, determining velocity and temperature distribution [ASME PAPER 65-WA/HT-36] 05 p0792 A66-15671  
Nonsimilar boundary layer flow and heat transfer of cone rotating in forced flow [ASME PAPER 65-WA/HT-31] 05 p0608 A66-15674  
Stagnation point heat transfer for binary pair diffusion model including dissociation and ionization 05 p0665 A66-15775  
Reference-point results applied to variations in laminar heat transfer to total vehicle over range of vehicle attitudes and associated trajectories [AIAA PAPER 66-28] 07 p0980 A66-17890  
Thermal laminar boundary layer formation on semilinear isothermal plate during uniform motion in viscous incompressible fluid over Prandtl number ranges 08 p1206 A66-18874  
Heat exchange, friction and mass exchange in laminar multicomponent boundary layer during injection of extraneous gases 09 p1368 A66-20705  
Local boundary layer approximations of first order for steady laminar convection flow produced by nonuniform axisymmetric heating or cooling of infinite horizontal surface 10 p1620 A66-21276  
Heat exchange, friction and mass exchange in laminar multicomponent boundary layer during injection of extraneous gases 11 p1688 A66-22591  
Laminar free convection flow and velocity and temperature distributions in air above thin horizontal electrically heated wire 12 p1980 A66-24906  
Mars atmospheric composition and laminar convective heating and ablation studied to predict performance of heat protection systems during entry 13 p2208 A66-25274  
Unsteady laminar forced and free convection in coaxial sector tubes in presence of constant axial temperature gradient, accounting for oscillation and resonance 13 p2210 A66-26719  
Heat and mass transfer process in reacting boundary layer of compressible gas in laminar flow along semilinear porous plate 14 p2416 A66-28484  
Free convection on laminar forced flow heat transfer in horizontal circular tube [ASME PAPER 65-HT-23] 16 p2828 A66-30983  
Laminar flow heat transfer in polygonal ducts, covering analog solution by Moire and point matching method [ASME PAPER 65-HT-27] 16 p2828 A66-30985  
Text on convective heat and mass transfer for first-year graduate students in mechanical, nuclear and aeronautical engineering 16 p2829 A66-31315  
Heat transfer of forced laminar convection in multiply connected regions 16 p2830 A66-31708  
Approximation method for compressible laminar heat transfer to blunt axisymmetric bodies in high speed flow 18 p3048 A66-33824  
Electromagnetic field effect on heat transfer during laminar flow of electrically conducting incompressible fluid in flat channel 20 p3607 A66-36980  
Integral solution of laminar film condensation with combined gravitational-type body force and forced convection concurrent and parallel to surface 20 p3678 A66-37118  
Laminar forced convection heat transfer to gas from circular tube, achieving boundary condition of uniform heat flux 20 p3679 A66-37508  
Calculation of heat transfer in laminar flows of structurally viscous fluids in tubes with constant thermoconductivity, heat capacity and density 20 p3681 A66-38122  
Regression rate for gas-solid hybrid motor described by convective heat transfer feedback mechanism through laminar sublayer [AICE PREPRINT 34B] 22 p3970 A66-39876  
Laminar boundary-layer heat transfer and shear stress predictions from similarity solutions, emphasizing large free-stream velocity gradients and highly cooled walls [ASME PAPER 65-HT-62] 22 p3997 A66-40024  
Laminar heat transfer in plane channel with nonuniform temperature field at inlet 22 p4000 A66-40812
- LAMINAR JET**  
Velocity distribution in laminar viscous liquid-into-liquid jet 01 p0057 A66-10407  
Comparison of Landau and Schlichting solution for laminar submerged jet discharging from infinitely thin pipe 04 p0512 A66-14439  
Laminar and turbulent MHD free jet, using Peskin analysis 05 p0721 A66-14719  
Book on motions of viscous incompressible fluids, covering laminar and turbulent jets and solutions, based on exact Navier-Stokes equations 06 p0872 A66-16562  
Asymptotic derivation for viscous decay of wake behind plane plate in fluid with power law 07 p1019 A66-17841  
Magnetic forces effect on laminar wall jet of electrically conducting incompressible fluid of constant properties 12 p1796 A66-23594  
Laminar jets in nitrogen from DC plasma torch analyzed, using schlieren and spectroscopic techniques, noting jet form dependency on Reynolds number 14 p2344 A66-27849  
Diffusion combustion in laminar boundary layer between two plane-parallel co-current streams 14 p2416 A66-28485  
Laminar to turbulent transition in free jets 15 p2424 A66-29303  
Laminar argon arcjet mixing with coaxial flow of cool helium, considering turbulent characteristics and heat transfer [AIAA PAPER 65-587] 17 p3033 A66-32442  
Velocity distribution in laminar plasma jet determined from energy equation and spectroscopic measurement of temperature distribution 17 p2967 A66-32459  
Navier-Stokes equations, differences for laminar jets and turbulent jets, submerged jets and transition layer 18 p3099 A66-34123  
Similarity solutions of heated two-dimensional laminar free jets with arbitrary Prandtl number and nonlinear viscosity-temperature energy dissipation relationships 18 p3103 A66-34932  
Acoustic sensitivity and logic circuitry of fluidic turbulence amplifiers for application to laminar jet streams 18 p3056 A66-35012  
Turbulence amplifier developed as pure fluid amplifier and logic element in which laminar jet is directed at mouth of collector tube and pressure at any input causes turbulence, reducing output to zero 20 p3501 A66-37653  
Laminar incompressible axisymmetric free jet with swirl, examining perturbation scheme for stream function and asymptotic series 21 p3729 A66-39453  
Plane laminar jet of incompressible conducting fluid propagating homogeneous magnetic field at magnetic Reynolds number 24 p4196 A66-42872
- LAMINAR MIXING**  
Inviscid stability of laminar mixing of two parallel streams of compressible fluid with respect to three-dimensional wavy disturbances 02 p0218 A66-11955  
Two-dimensional isoenergetic compressible mixing of jet with fluid at rest for laminar and turbulent mixing 12 p1795 A66-23572  
Laminar mixing of two parallel streams of compressible fluid stability with respect to supersonic disturbances 22 p3900 A66-40385  
Laminar gas jet mixing as affected by periodic vorticity produced by mechanical vibration of orifice 23 p4055 A66-41497  
Similar solution of laminar mixing of curved half-jet and curvature effect of boundary layer flow along curved surface 23 p4059 A66-42003
- LAMINAR WAKE**  
Incompressible laminar axisymmetric near wake behind very slender cylinder in axial flow 02 p0175 A66-11527  
Relationship of laminar wake width to wake transition distance for cones 02 p0175 A66-11561  
Stagnation temperature measurement in laminar wakes behind wedge and cone in hypersonic shock tunnel, noting effect of Reynolds number variation [AIAA PAPER 65-53] 03 p0315 A66-12790  
Wake from bluff bodies interaction with initially laminar boundary layer [AIAA PAPER 66-126] 06 p0875 A66-17096  
Aerodynamic characteristics of wakes behind hypervelocity bodies [AIAA PAPER 66-53] 08 p1162 A66-18952  
Stability of plane inviscid jet and wake studied for possible growth in downstream spatial direction 12 p1865 A66-24582  
Laminar viscous wake interaction with supersonic external inviscid flow downstream treated by implicit finite difference method [AIAA PAPER 66-454] 16 p2689 A66-31468  
Base, recompression and laminar near wake regions of cones in hypersonic flow 17 p2838 A66-32438  
Static enthalpy and velocity profile within viscous wake of circular cylinder at Mach 20 18 p3049 A66-34582  
Interaction between hypersonic wake flow and aerodynamic deployable decelerator, predicting pressure and heat transfer of decelerator 22 p3846 A66-40605  
Diameter and location of wake neck and trailing wake shock for pointed and blunt slender hypersonic cones 23 p4012 A66-41919
- LAMINATE**  
**SA MULTILAYER STRUCTURE**  
Printed circuit laminate measilng, definition, origin, effects and control 11 p1664 A66-22673  
Multilayer circuit laminate fabrication and comparison of glass-base laminates with phenolic-paper-base and epoxy-paper-base grades 11 p1664 A66-22675  
Prestressing effect on fiber alignment and strength of glass fiber laminates 24 p4289 A66-42338
- LAMINATED MATERIAL**  
Modification of Ritz equations for natural frequencies of homogeneous isotropic plates to apply to natural frequencies of laminated panels 01 p0149 A66-10150  
Physical properties of 181 glass cloth laminates of diallyl orthophthalate and isophthalate in high temperature range 02 p0248 A66-11689  
Thin copper clad laminates and problems arising in application to multilayer printed circuit boards 03 p0347 A66-13330  
Curves relating loss factor, characteristic mode value and frequency parameter for designing damped sheet laminates 05 p0687 A66-14992  
Vibrational characteristics, natural



frequencies and associated composite loss factor of finite-length laminated beam with alternate elastic and viscoelastic layers [ASME PAPER 65-WA/APM-1] 05 p0776 A66-15425

Vibrational characteristics, natural frequencies and associated composite loss factor of finite-length laminated beam with alternate elastic and viscoelastic layers [ASME PAPER 65-WA/APM-1] 10 p1616 A66-21483

Strength of structural composites of orthotropic materials with arbitrary thickness and orientation including lamination and anisotropy effects [AIAA PAPER 65-75] 10 p1617 A66-21781

Nonmonotonicity in sensitivity test data, noting results of liquid oxygen impact tests on Mylar-aluminum-Mylar laminate bonded to polyester foam 12 p1958 A66-23648

Strain gauge load measuring transducer operating in bending mode and based on elastic properties of epoxide glass fabric laminate 12 p1884 A66-24985

Impact fracture toughness of brazed laminates of maraging steels and titanium alloys found to be 2 to 7.8 times greater than homogeneous specimens of like size [AIAA PAPER 65-566] 19 p3377 A66-35620

Plastic laminates use for ablation shields, noting importance of heat flow and comparison of thermal screens 22 p3938 A66-40417

High temperature structural properties of glass fabric-reinforced polybenzimidazole, polyimide and phenolic laminates for aerospace application 23 p4083 A66-41389

Laminated reinforced plastics used in construction of jettisonable fuel tank, aircraft equipment components, radomes, missiles and satellite parts 23 p4074 A66-41654

Laminated structure with dominant displacement from reference point for solid medium working beyond elastic limit 23 p4144 A66-41969

**LAMP**

SA ARC LAMP

SA ELECTROLUMINESCENT LAMP

Demountable high-power xenon arc lamp with replaceable silica discharge tube 08 p1168 A66-19296

Low-pressure mercury vapor lamp for interferometric and spectrometric work, noting electrodes, main discharge tube, electrical circuit, etc 10 p1538 A66-22059

**LAND**

S EARTH

**LANDAU DAMPING**

Static force factor introduced into kinetic longitudinal plasma oscillation equation, noting Landau damping factor 03 p0397 A66-12382

Resonance and response characteristics of unbounded one-dimensional plasma immersed in nonuniform static field 03 p0400 A66-12951

Plasma waves propagating transverse to uniform external magnetic field discussing electron motion, wavelength magnitude, frequencies and application of results 03 p0406 A66-13358

Plasma resonance of cylindrical plasma in absence of magnetic field noting conductivity kernel, scattering of radiation, nonuniformity of plasma sheath and Landau damping 04 p0474 A66-13425

Laminar Landau collisionless damping of finite amplitude disturbances in collision-free plasmas 05 p0727 A66-15257

Landau solution of plasma oscillation problem, discussing dielectric function, Lorentzian distribution and cut-off distribution 08 p1280 A66-18536

Equivalence of oscillating electric field on plasma boundary, with specularly reflecting bounding wall, to unbounded plasma with planar oscillating grid at wall position 08 p1261 A66-18546

Quantum statistical electromagnetic wave propagation and relativistic damping effects in uniformly magnetized electron-positron gas 08 p1187 A66-19809

Landau damping and velocity Fourier transform of initial perturbation in longitudinal plasma oscillations 10 p1567 A66-21817

Hydrodynamic approximation of interaction

between charged particle beam and plasma confined by ideally conducting sheath 13 p2139 A66-25389

Landau damping of transverse oscillations in collisionless plasma at ion cyclotron resonance and collisional damping in zero-temperature plasma 13 p2142 A66-25706

Cross section for inelastic scattering of electromagnetic radiation by electron density fluctuations in anisotropic solids, using laser sources, investigating Landau and collision damping of plasmons 13 p2132 A66-26153

Transverse reluctance of bismuth telluride in pulsed magnetic fields revealing fine structure of Shubnikov-De Haas oscillations interpreted as spin-splitting of Landau levels 16 p2786 A66-31695

Gravitational instability of magnetoplasma in radial electric field, noting resistive drift modes, stabilization criterion effect of Coriolis force, Landau damping, etc 17 p2966 A66-32425

Landau damping in inhomogeneous plasmas indicated by solution of Vlasov equation 18 p3150 A66-34936

Verification of Landau theory that longitudinal electron waves in plasma of finite temperature are damped even in absence of collisions 19 p3416 A66-36522

Drift-wave instability in weakly inhomogeneous fully ionized plasma confined in strong magnetic field in Q machine 19 p3416 A66-36523

Electrostatic-wave propagation in collisionless plasma, noting Landau damping 19 p3432 A66-36760

Electrostatic wave dispersion characteristics in one-dimensional plasma exhibiting Landau damping 19 p3432 A66-36761

Reversible property of Vlasov equation describing thermalization of electron beam in plasma and Landau damping, noting entropy is constant in nonlinear approximation 20 p3608 A66-37460

Asymptotic time behavior of longitudinal waves in one-dimensional plasma of relativistic electrons and stationary ions studied, using collisionless Boltzmann equation 21 p3775 A66-39189

Landau damping of longitudinal electron plasma waves in finite-diameter uniform-density cylindrical plasma, assuming Maxwellian velocity distribution 22 p3955 A66-40104

**LANDING**

S AIRCRAFT LANDING

S APPROACH AND LANDING

S GLIDE LANDING

S LUNAR LANDING

S PLANETARY LANDING

S SOFT LANDING

S TAKEOFF

S TAKEOFF AND LANDING

S WATER LANDING

**LANDING AID**

SA AIR TRAFFIC CONTROL

SA AIRPORT

SA APPROACH AND LANDING

INSTRUMENT

SA RUNWAY

Landing task and pilot acceptance of displays for landing in reduced weather minimums [AIAA PAPER 65-722] 03 p0328 A66-12579

Airborne navigation and flight-control equipment for reducing weather minimums to lowest possible level 06 p0907 A66-16427

Direct lift control as landing approach aid by providing more rapid means of changing and controlling flight path than conventional methods [AIAA PAPER 66-14] 08 p1167 A66-18985

Optimum antenna requirements for radio-slope guidance system and vertical control in blind landing procedures 08 p1254 A66-19833

Radio augmented and calibrated inertial navigation equipment and operation 10 p1554 A66-21898

Head-up display system as aid in bad-weather landing 17 p2951 A66-33199

Bendix microvision head-up display system all-weather landing aid 17 p2952 A66-33201

Head-up display systems, discussing state of the art and arguments in favor of their use 17 p2952 A66-33202

Blind landing equipment, discussing type 191 collimator unit tested on Caravelle aircraft 17 p2952 A66-33203

Pilot performance and problems arising during transition from instrument to visual flight in landing approach with low visibility 17 p2952 A66-33204

TALAR, tactical aircraft landing aid-radio, uses ground-based Cassegrain antenna, magnetron transmitter and 4-lb receiver in aircraft while providing ILS functions 20 p3596 A66-37232

**LANDING DEVICE**

Rotor recovery system for spacecraft landing 08 p1303 A66-1882

Onboard equipment designed for transport aircraft landings with visibilities less than 200 ft and runways less than 2600 ft, having all devices duplicated 10 p1554 A66-21368

Unmanned planetary probe and lander capsule design, emphasizing Mars lander capsules 16 p2808 A66-30366

**LANDING GEAR**

SA AIRCRAFT TIRE

SA AIRFRAME

SA FAIRING

Cause and elimination of vertical oscillations of aircraft landing gear system in motion of aircraft over unpaved airfield 01 p0011 A66-10470

Landing gear with one to eight wheels, weight, wheel well volume and allowable traffic on heavy airplanes, noting flexible pavement design and tire pressure [SAE PAPER 650799] 01 p0053 A66-10815

Soft and rough airfield landing gears, discussing ground flotation and shock absorbers for aircraft of several sizes [SAE PAPER 650844] 01 p0011 A66-10834

Analytical landing simulation to analyze dynamic loads and aircraft response, particularly high sink speed landing gear [SAE PAPER 650845] 01 p0011 A66-10835

Landing gear design challenges for V/STOL service XC-142A and relative success or failure [SAE PAPER 650843] 01 p0012 A66-10848

Statistical analysis of dynamic system response used to design aircraft undercarriage systems [AIAA PAPER 65-710] 01 p0013 A66-10947

C-5A aircraft design load criteria for landing gear of large aircraft that must operate from semi-improved airfields [AIAA PAPER 65-711] 01 p0013 A66-10948

Airport pavement roughness data and aircraft response data evaluated to determine pavement design and construction criteria [AIAA PAPER 65-712] 01 p0055 A66-10949

British Lockheed undercarriage and hydraulic system for German HFB 320 Hansa aircraft 04 p0458 A66-13932

Aircraft landing gear designs in past 12 years 05 p0611 A66-15134

XB-70 landing gear inspection, describing hydraulic jack used 06 p0869 A66-16793

Design of landing gear for military cargo aircraft and supersonic transports 07 p0985 A66-17255

Two-stage /descent and ascent/ Lunar Excursion Module control system for landing gear, ascent stage, liftoff from lunar surface, etc 07 p1140 A66-17280

Design trends in landing gear for medium- and short-range jet transports 07 p0987 A66-17286

Aircraft landing gear design, evaluating undercarriage of research aircraft and weapons systems 07 p0987 A66-17359

British and French VTOL landing gear design, describing unique SConc fixed-wing VTOL aircraft 08 p1167 A66-18627

Aircraft landing gear design and maintenance, noting elimination of sharp corners and radii, weldability criterion, joints, part identification, bushings, etc 10 p1482 A66-21135

Modern landing gear design as function of aircraft type and size 13 p1997 A66-25499

Concorde aircraft front and rear auxiliary landing gear noting geometry, steering and anti-shimmy control, etc 16 p2633 A66-30317

Airport pavement roughness data and aircraft response data evaluated to determine pavement design and construction criteria [AIAA PAPER 65-712] 16 p2683 A66-31590



- Landing gears and operation illustrated in modern aircraft 16 p2635 A66-31681
- Main landing gear design for Concorde SST 17 p2846 A66-32950
- Air cushion landing gear for aircraft, noting rubber tubing under fuselage forming pneumatic bumper blown up by turbine engine 17 p2848 A66-33082
- P-3 tricycle landing gear assembly, examining mechanical and hydraulic mechanisms for brakes and steering, using graphic charts 19 p3279 A66-36059
- Maraging steels for landing gear forgings, noting fabrication, distortion and fatigue tests 21 p3751 A66-39237
- Airframe and landing gear of Beagle B.206 series II low-wing monoplane of all-metal stressed skin construction 22 p3848 A66-39687
- LANDING MODULE**
- SA LUNAR LANDING MODULE
- SA MARS EXCURSION MODULE /MEM/
- Model tests for determination of structural response of Apollo command module to water impact 14 p2393 A66-28020
- Next-generation lunar transports for multimanned crew landing [SAE PAPER 660443] 17 p3017 A66-33158
- Electric power generator selection for Mars probe/lander 23 p4020 A66-41748
- LANDING SIMULATION**
- Analytical landing simulation to analyze dynamic loads and aircraft response, particularly high sink speed landing gear [SAE PAPER 650845] 01 p0011 A66-10835
- Lunar landing research vehicle used for simulated lunar landings on Earth 04 p0585 A66-13636
- Man, system and vehicle simulation program for landing and docking phases of Apollo lunar landing mission 08 p1202 A66-18577
- Full-scale and model test for dynamic effects of LEM landing 14 p2393 A66-28019
- Human reaction to simulated landing impact overload, including analysis of EKG, kinetocardiogram, blood pressure and respiration data 15 p2443 A66-29445
- Dynamic and steady state flow disturbances encountered by aircraft during carrier landing approach in water tunnel simulation study [AIAA PAPER 65-332] 16 p2634 A66-31319
- Landing run and taxiing problems in very low visibility 17 p2952 A66-33206
- Pilot dynamic response in bank angle control maneuver simulation of sidewind landing of aircraft [ICAS PAPER 66-14] 22 p3945 A66-40672
- Full-scale and model test for dynamic effects of LEM landing 24 p4283 A66-42771
- LANDING SITE**
- SA LUNAR LANDING SITE
- Military STOL and conventional civil aircraft behavior on rudimentary airstrips 18 p3051 A66-33686
- Technological approaches to use of aircraft on undeveloped or semideveloped field from standpoint of load and terrain roughness 18 p3051 A66-33937
- Engineering constraints involved in selection of Martian landing site for lander vehicles 18 p3232 A66-34367
- LANDING SPEED**
- Discrete control signal effect on lateral motion of aircraft landing in presence of correction, considering slideslip equation 23 p4089 A66-41355
- LANDING SYSTEM**
- SA AUTOMATIC LANDING SYSTEM
- SA INSTRUMENT LANDING SYSTEM
- Advanced integrated landing system /AILS/ consisting of azimuth and elevation ground station, ground display site and airborne unit, emphasizing scanning-beam technique 01 p0101 A66-10034
- Lateral maneuver capability of high lift-drag ratio used to extend period of daylight landings from orbit 03 p0390 A66-12774
- Spacecraft landing systems, examining laboratory and full-size studies with steerable parachutes 04 p0584 A66-13529
- Aircraft braking system, determining energy absorbed during landing or interrupted takeoff 06 p0807 A66-16970
- Flight deck display for future aircraft projects, emphasizing vertical scale director instruments for cockpit display 11 p1649 A66-23250
- Fog chamber tests and runway lighting requirements, considering landing, cockpit vision and photometry [AIAA PAPER 65-333] 12 p1857 A66-23801
- Impact dynamics of landing systems using material crushing to absorb kinetic energy of body impacting at very high velocities 14 p2402 A66-27895
- Flight simulator techniques applied to all-weather landing problems 17 p2899 A66-33205
- Landing approach navigational problems, discussing transition to visual flight at low altitude of 100 ft 17 p2898 A66-33209
- Pilot acceptance factors in development of all-weather landing and SST navigation systems 17 p2955 A66-33219
- All-weather landing system for Caravelle aircraft in joint Sud Aviation-Lear program 18 p3133 A66-34680
- Parachute and cushion landing system for specific payload geometry for touchdown with gliding descent, considering minimum weight design 19 p3278 A66-35626
- Radiation attenuation effect of atmospheric aerosols on all-weather aircraft landing guidance systems using lasers 19 p3397 A66-36051
- Aerodynamic deceleration systems - AIAA Conference, Houston, September 1966 22 p3848 A66-40589
- Base-mounted landing rocket system for Apollo-type vehicle evaluated for heat-shield water pressure, ground effect, vehicle dynamics, etc 22 p3987 A66-40612
- Land landing system for Apollo spacecraft with roll control, steerable parachutes and landing rocket 22 p3987 A66-40613
- All-weather landing systems in U.K., examining safety and reliability criteria in connection with trident airborne equipment [ICAS PAPER 66-8] 22 p3946 A66-40676
- LANGMUIR PROBE**
- Effect produced by nonhomogeneous HF field on distributed plasma parameters 01 p0115 A66-11050
- Nonlinear scattering effect of Langmuir oscillations on electrons of plasma located in strong magnetic field 01 p0115 A66-11055
- Beam width of two antenna systems measured and compared for accuracy in determining plasma density 02 p0269 A66-11969
- Probe techniques in polar ionosphere covering cylindrical Langmuir, RF and mobility probes, Gerding condensers, error sources, techniques, etc 03 p0362 A66-12641
- Langmuir probes in spacecraft, considering plasma effects 03 p0370 A66-12876
- Plasma instabilities in dipole magnetic field 03 p0400 A66-12893
- Comparing data of two Langmuir probes placed in cesium plasma 04 p0550 A66-13476
- Inhomogeneous plasma from hot-cathode arc discharge at various pressures using various gases, recording oscillations from plasma instability with Langmuir probes 04 p0552 A66-13868
- One-dimensional self-consistent problems involving interaction between Langmuir and ionic-acoustic plasma oscillations caused by induced combination scattering of former on latter 04 p0556 A66-14418
- Inhomogeneous plasma from hot-cathode arc discharge at various pressures using various gases, recording oscillations from plasma instability with Langmuir probes 05 p0727 A66-15459
- Cesium plasma created in thermionic converter investigated by Langmuir probe to determine potential, gain, velocity and oscillations 05 p0620 A66-15571
- Behavior of small cylindrical Langmuir probe in steady low density flow of argon plasma [AIAA PAPER 66-5] 07 p1034 A66-17880
- In situ probe measuring nonthermal components of electron energy distribution in ionosphere, small-scale ionization inhomogeneities and negative ion concentrations in lower ionosphere 08 p1223 A66-18745
- Stable plasma belt trapped in permanent dipolar magnetic field, measuring floating potential, electric and magnetic drifts, etc 08 p1265 A66-19408
- Computation and measurement of Hall potentials and flow field perturbations in MGD flow of axisymmetric free jet 08 p1266 A66-19815
- Solar radiation effect on Langmuir frequency, noting ionization of cesium vapor at low potential differences 09 p1409 A66-20925
- Ion temperature measurement of streaming helium plasma by Langmuir double probe method, discussing effect of stream velocity 10 p1558 A66-21071
- Langmuir probe velocity and acceleration measurements for coaxial Hall accelerators [AIAA PAPER 66-196] 10 p1562 A66-21441
- Single and double Langmuir probe for low density plasma, noting measurement of electron temperature and density 10 p1535 A66-21514
- Plasma electron density and temperature from measurement of LF impedance of Langmuir probe, noting ionospheric probing 10 p1536 A66-21549
- Electron density and temperature measured in exhaust of magnetoplasma dynamic (MPD) source, using Langmuir probe and spectrometry [AIAA PAPER 65-298] 10 p1594 A66-21780
- Feasibility of using Langmuir probe for measuring statistical properties of unsteady or turbulent electron-rich plasmas [AIAA PAPER 65-544] 12 p1919 A66-23580
- Langmuir probe measurements in hypersonic plasma flow, evaluating properties of plasma jet wind tunnel, electron temperature and plasma density 12 p1920 A66-23853
- Low pressure plasma electron temperature inferred from Langmuir probe measurements differs from plasma mean electron energy 12 p1920 A66-23959
- Approximate equality of drift and random currents at boundary between Faraday dark space and head of striated positive column in discharges through neon 12 p1920 A66-23961
- Hot-wire anemometer determination of electron and ion temperature, neutral particle temperature, concentration and velocity and potential of partially ionized helium plasma 12 p1882 A66-24223
- Plasma edge phenomena in unified Langmuir treatment for probe in collisionless plasma 12 p1925 A66-24816
- Disturbance of thermal equilibrium of weakly ionized cesium contact plasma due to wall losses measured by Langmuir probe 13 p2137 A66-25117
- Langmuir probe to measure stagnation region shock layer ionization distribution under nonequilibrium hypersonic flow conditions [AIAA PAPER 66-167] 13 p2138 A66-25168
- Langmuir probe measurement of electromagnetic field present in cyclotron ion oscillations 13 p2140 A66-25426
- Correlation between plasma and ion density fluctuations as detected by magnetic probe, spectral emission techniques and Langmuir probe 13 p2142 A66-25703
- Time resolved Langmuir probe measurements of plasma density in electromagnetic shock tubes 13 p2149 A66-26243
- Resonance probe with variable HF voltage superimposed on DC voltage applied to conventional Langmuir plasma probe 14 p2289 A66-26820
- Plasma potential and sheath radius of positive cylindrical and spherical Langmuir probes 14 p2339 A66-26829
- Response of Langmuir probes in rocket exhaust jets, noting sensitivity to chamber temperature and pressure and alkali metal concentration 14 p2294 A66-27421
- Comparison between microwave and Langmuir probe plasma diagnostic techniques 14 p2343 A66-27506
- Electroconductivity of combustion products of propane-air mixture determined by double Langmuir probes 15 p2617 A66-29312
- Electron temperature correlation with excitation in temperature in argon plasma established, using spectral analysis and Langmuir probe 15 p2555 A66-29762
- Electric potential and space charge density near Langmuir probe in hot rarefied plasma at rest, calculating current collected from plasma 16 p2759 A66-30372



Disturbances about solid body in flowing low density plasma applied to satellite-ionosphere interactions and Langmuir probe data analysis 16 p2759 A66-30373

Scattering of electromagnetic waves in plasma, noting effect of eddy current fluctuations 16 p2654 A66-31179

Ultrahigh frequency plasma oscillations, noting Maxwellian equilibrium between plasma electrons and primary, monoenergetic electrons 16 p2766 A66-31651

Sublimation of rhenium and Langmuir method vapor pressure measurements using vacuum microbalance 17 p2938 A66-31882

Langmuir probe curves for pulsed plasma obtained by time-sampling probe technique and compared with BBM analysis for ion saturation current 19 p3405 A66-35411

Instrumentation for plasma diagnostics noting electron density profile, temperature, ion-atom and electron-atom interaction, etc 20 p3556 A66-36964

Plasma decay technique to measure density in discharge tubes compared to value obtained by Langmuir 21 p3792 A66-39182

Behavior of small cylindrical Langmuir probe in steady low density flow of argon plasma [AIAA PAPER 66-5] 22 p3918 A66-40350

Langmuir type probe in argon arc jet, discussing surface contamination problems, causes of high electron temperature and development of automatic cleaning technique 22 p3899 A66-40368

Hot-wire anemometer determination of electron and ion temperature, neutral particle temperature, concentration and velocity and potential of partially ionized helium plasma 22 p3919 A66-40585

Electron number densities measured behind shock wave in pressure driven shock tube by microwave resonant cavity technique and by electrostatic quasi-Langmuir probe 24 p4191 A66-42197

Double Langmuir probe measurement of turbulent structure and ionization intensity of hypervelocity projectile and spectral characteristics of probe signal fluctuation 24 p4192 A66-42198

**LANGUAGE**

**SA MACHINE LANGUAGE**

**SA SPEECH**

Dictionary of mathematical terms in English, French, Russian, German and Armenian, with English terms in alphabetical order 04 p0540 A66-14003

Space technology jargon, noting language used, origin and formation of words, acronyms, etc 16 p2831 A66-31151

Facilitating effect of repetition on recall of word from list of unconnected words 23 p4025 A66-41044

**LANGUAGE PROGRAMMING**

**SA BLOCK DIAGRAM COMPILER /BLODIB/**

Universal programming languages and processors, survey and new concepts 12 p1826 A66-23825

Digital simulation languages, discussing history, input format, effectiveness, programming error diagnostics, etc 12 p1826 A66-23826

New block diagram compiler for sampled data system simulation 12 p1826 A66-23827

User-oriented computer programming system using Flexowriter modified to construct new two-dimensional programming language 12 p1826 A66-23828

Integrated modular digital computer system for ICETAN /ICES-FORTRAN/ programming of engineering problems 12 p1827 A66-23833

Symbolic programming digital computer techniques, hardware interfacing and system errors in simulation of lunar midcourse guidance and navigation 20 p3543 A66-37250

Abstract machine design with recursive function programming language, showing simulator construction in Fortran 20 p3523 A66-38018

Aitol computer programming language for spacecraft checkout systems and automatic support operations in Saturn launch vehicle 20 p3544 A66-38257

Optimization of two-way space frame with single column supports for minimum weight

of steel by digital language programming techniques 21 p3833 A66-39539

**LANSRAUX SERIES**

**S BESSEL FUNCTION**

**S HANKEL FUNCTION**

**LANTHANIDE**

Solid state reduction of lanthanide ions in laser hosts, effect of presence of recombination hole-centers in photoreduced samples and elimination during electrochemical process 14 p2362 A66-27464

**LANTHANUM**

Energy gap and thermoconductivity of normal and superconducting fcc lanthanum 03 p0407 A66-12320

Staining properties of trivalent lanthanum cation on cell membranes 06 p0812 A66-16565

Ultrasonic absorption in superconducting lanthanum explained by two models for loss of energy from low-energy phonon field in London superconductor 09 p1415 A66-20021

Magnetic state of gadolinium impurities in superconducting lanthanum 16 p2768 A66-30134

Thermal conductivity of lanthanum and monochalcogenides, noting role and temperature dependence of crystal-lattice conductivity 20 p3617 A66-37556

**LANTHANUM ALLOY**

High temperature oxidation of liquid yttrium and liquid lanthanides and their alloys with gold, obtaining parabolic diffusion-controlled rate constants 08 p1235 A66-18622

Molybdenum recrystallization as affected by La and Y additions under various types of heat treatment 15 p2520 A66-28670

**LANTHANUM CHLORIDE**

Nonequilibrium population buildup and detection for IR solid state lasers and IR-optical double resonance in lanthanum chloride crystal 13 p2098 A66-26177

**LANTHANUM COMPOUND**

Crystalline structure of simplest lanthanum and samarium silicates 05 p0702 A66-15337

Surface ionization of Cs atoms on lanthanum hexaboride cathode with intrinsic thermionic emission of cathode observed from mass-spectrometric measurement of ion current 06 p0912 A66-16885

Thermionic emission properties of rhenium tape coated with lanthanum hexaboride, examining usefulness as low temperature emitter 06 p0883 A66-17029

Superconducting transition temperature of stoichiometric lanthanum sulfide 07 p1108 A66-18437

Specific heat evidence for gapless superconductivity, examining experimental results on lanthanum doped with magnetic impurity gadolinium 09 p1420 A66-20053

Conductivity of working fluid of MHD generator, using thermionic emission from suspended lanthanum hexaboride powder 15 p2552 A66-29408

Lanthanum hexaboride evaporation from Knudsen cell studied by mass spectrography for composition, sublimation heat and ion current 17 p2981 A66-32849

X-ray and metallographic examination of tungsten alloys, noting decrease of work function during thermal emission upon addition of lanthanum hexaboride 20 p3584 A66-37414

Lanthanum germanide synthesis using arc furnace, noting chemical properties 20 p3584 A66-37416

**LANTHANUM OXIDE**

Lanthanum oxide as crystal growth modifier, noting habit modifications, optical quality, etc 17 p2982 A66-33060

**LANTHANUM TELLURIDE**

Superconductivity of chalcogenide lanthanum telluride, noting temperature variations relationship to stoichiometric composition of samples 16 p2772 A66-30290

**LAP JOINT**

Load partition in double-lap butt joints for bearing type connections including expressions for stress-strain relationship and bolt shear deformation 02 p0302 A66-12242

Strength of adhesive-bonded lap joints as affected by changes in temperature and fatigue 14 p2401 A66-27772

**LAPLACE EQUATION**

**SA STOKES-BELTRAMI EQUATION**

Approximation of spherical functions by analogs of Fejer and Vallée-Poussin

sums 04 p0539 A66-13488

Numerical solution to Laplace equation in two dimensions, subject to boundary conditions imposed by conducting surfaces and dielectrics, applied to transmission line problems 06 p0846 A66-16097

Maxwell equations for isotropic medium bounded by conductors in three-space dimensions solved by applying Laplace equations described in Minkowski space 06 p0851 A66-16450

Integration of equations, approximating Maxwell equations, in curvilinear coordinates separating scalar Laplace equation, with vectors representing electric and magnetic fields 10 p1556 A66-21994

Cauchy problem for two-dimensional Laplace equation in infinite strip 11 p1722 A66-22646

Approximate continuation of harmonic and parabolic functions as solutions of Laplace and heat equations 16 p2732 A66-30242

Noniterative finite-difference method for solution of Poisson and Laplace equations for linear boundary conditions, discussing slow viscous flow results [ASME PAPER 66-FE-1] 17 p2914 A66-33258

Two-dimensional solution of Laplace equation for vortex formations in incompressible fluid 18 p3100 A66-34634

Integration of equations, approximating Maxwell equations, in curvilinear coordinates separating scalar Laplace equation, with vectors representing electric and magnetic fields 18 p3136 A66-34971

Laplace integral application to inversion of three solar limb-darkening curves obtained in UV 19 p3464 A66-36258

Incorrect problems of mathematical physics examined and illustrated by classical Cauchy problem for Laplace equation 20 p3591 A66-37758

Stress separation in photoelasticity, using series solution of Laplace equation and least squares method 24 p4292 A66-42862

**LAPLACE OPERATOR**

Digitally computed tables of Chebyshev approximations of Laplace shift operator transfer function enabling analog simulation of time delay systems 18 p3090 A66-34069

Elliptic BVP in equilibrium theory of thin plates employing iterated Laplace operator 21 p3822 A66-38464

Eigenvalue problem for Laplace operator for two-dimensional region with boundary composed of piecewise-analytical simple closed curves solved by finite difference method 22 p3938 A66-39901

**LAPLACE TRANSFORM**

**SA MELLIN TRANSFORM**

Stability analysis of multiloop multirate sampled systems using identities expressing Laplace transforms of sampled signals in terms of shifted transforms of same signals sampled with smaller periods 01 p0100 A66-10018

Lubich generalization of Laplace transform as related to Cauchy problem 01 p0094 A66-10651

Laplace transform technique to develop asymptotic solutions to integral equations describing influence of scattering law on radiation damage displacement cascade 02 p0245 A66-11946

Fodor terminal-state problem solved on basis of distribution theory without using heuristic operators 03 p0388 A66-12703

Distribution theory used to remove apparent contradictions observed when applying Laplace transform to discontinuous functions 03 p0388 A66-12704

Transistor equivalent circuit parameters by inverse Laplace transform of time behavior 04 p0497 A66-13966

Donnell-type nonlinear theory for instability of cylindrical shell subjected to axisymmetric moving loads with constant velocity [ASME PAPER 65-APMW-35] 04 p0594 A66-14235

Transient response of narrow-band networks to narrow-band signals, using Laplace transforms with positive frequencies 05 p0652 A66-14595

Asymptotic expressions for axial stress in thin viscoelastic shells due to longitudinal impact obtained, using Laplace transform, determining viscosity effect on propagating



wave shape  
[ASME PAPER 65-WA/APM-10]  
05 p0776 A66-15432  
Random vibrational system, solving first passage time via conversion to first order Markov process  
[ASME PAPER 65-WA/APM-18]  
05 p0777 A66-15440  
Necessary and sufficient condition for matrix distribution to have positive-real Laplace transform  
09 p1396 A66-20641  
Laplace transform and analog computation applied to simulation of heat transfer between wall separated fluids, determining transfer functions and frequency responses  
09 p1472 A66-20908  
Integration of Laplace transformed elastokinetic equations, examining stress function, displacement vector field and boundary and initial value problems  
10 p1555 A66-21226  
Asymptotic expressions for axial stress in thin viscoelastic shells due to longitudinal impact obtained, using Laplace transform, determining viscosity effect on propagating wave shape  
[ASME PAPER 65-WA/APM-10]  
10 p1615 A66-21476  
Laplace transform solution for small time used as complement to problem of one-dimensional propagation of stress pulse in bar with continuously nonhomogeneous elastic modulus  
10 p1617 A66-21498  
Space and time dependent randomly distributed stress and temperature fields in cylinder with deformable surface calculated, using approximation  
12 p1959 A66-23864  
Random vibrational system, solving first passage time via conversion to first order Markov process  
[ASME PAPER 65-WA/APM-18]  
12 p1961 A66-23990  
Liubich generalization of Laplace transform as related to Cauchy problem  
12 p1903 A66-24022  
N-dimensional two-sided Laplace transformation and n-dimensional Mellin transformation of  
12 p1904 A66-24194  
Inverse Laplace transformations in terms of Laguerre functions  
12 p1905 A66-24654  
Exact solution, using Laplace transform, for problem of transient characteristic of semiconductor diode, challenging Nosov view  
13 p2031 A66-25229  
Iterative approximation of rational transfer function in Laplace transform variable s, optimal with respect to given input and output time functions, and deviation from desired output-input-time functional relation  
13 p2054 A66-26087  
Nonhomogeneous solid sphere radiative cooling asymptotic representation based on heat conduction theory by Laplace transforms  
14 p2414 A66-28144  
Evaluation of solution moduli of nonlinear contour problems pertaining to polyvibrant systems with delayed remainders and arguments  
15 p2529 A66-29653  
Interaction between atoms of solid surface and gas phase, obtaining closed-form solution of motion  
16 p2753 A66-30786  
Cause and effect interdependence in linear system, noting distribution theory and double Laplace transform  
16 p2670 A66-31024  
Generalization of Barbier-Eddington approximation, for inversion of darkening law  
16 p2803 A66-31258  
Green functions for heat source and concentrated force acting in unbounded thermoelastic space, applying perturbation method and Laplace transforms  
17 p3018 A66-31836  
Symmetrical stress wave propagation in thin plate with small, circular hole at center, noting boundary conditions and solutions via Laplace transforms and by method of characteristics  
17 p3022 A66-32012  
Donnell-type nonlinear theory for instability of cylindrical shell subjected to axisymmetric moving loads with constant velocity  
[ASME PAPER 65-APMW-35]  
18 p3248 A66-33574  
Numerical inversion of Laplace transform  
18 p3127 A66-34082

Pressure distribution, surface roughness, dry friction and elastic coupling effects on wave propagation and reflection in elastic rod, using modified-Laplace transformations  
18 p3259 A66-34940  
Functional polynomial fitting of continuous functional, using Laplace transforms to reduce number of measured records for identifying kernels of second-degree approximation  
19 p3391 A66-36703  
Complex convolution integral applied to Laplace transform expressions in sampled data theory  
19 p3339 A66-36747  
Series expansion of inversion of n-dimensional Laplace transforms in terms of ultraspherical polynomials having coefficient computed recursively  
19 p3392 A66-36784  
Transient processes in linear automatic control systems dependent on parameters which appear when differential equations of analyzing system are transformed by Laplace-Karson method  
20 p3537 A66-36892  
Unified approach to synthesis of orthonormal exponential functions with elements whose asymptotic order may be chosen arbitrarily and poles that may be real, complex or both  
20 p3522 A66-37665  
Laplace transform applied to small pressure variations effect on gunpowder burning stability  
20 p3681 A66-38121  
Laplace transform analysis of solid or hybrid propellant ignition by exothermic heterogeneous reactions in presence of radiant energy flux  
21 p3806 A66-38688  
Laser amplifier theory using Fabry-Perot interferometer and Laplace transform for obtaining transient solutions in addition to steady state solutions  
21 p3748 A66-39224  
Minimum mean-square-error design of distributed-parameter control systems characterized by Laplace transform transfer functions  
21 p3720 A66-39430  
Laplace transformation simulation by analog computer for real and complex values  
22 p3870 A66-39996  
Transient response of narrow band networks to narrow band signals, using Laplace transforms with positive frequencies  
22 p3864 A66-40063  
Criterion for spatial-amplification or nontransmittance using double Laplace transforms in light of complex values of wave vector  
22 p3869 A66-40928  
Fresnel formulas for transformation of transverse electromagnetic wave into longitudinal plasma wave at dielectric-plasma interface, using Laplace transforms  
22 p3869 A66-40929  
Linear viscoelastic bending analysis of anisotropic plates  
23 p4145 A66-41975  
Power spectrum analysis of short-time transient response of one degree of freedom system to random excitation, evaluating error generated, using Laplace method  
24 p4286 A66-42164  
Computer technique for constitutive equations of viscoelastic modulus, using Laplace transform and Volterra integral equation, applied to data on solid propellants  
24 p4289 A66-42279  
Combination of probability density functions for system error analysis, using convolution or transformation methods  
24 p4189 A66-42827  
Laplace transform analysis of transistor switching circuit controlled by RC time constant, using PWM circuit as example  
24 p4185 A66-42946  
**LARMOR ORBIT**  
Reflection and transmission of charged particles incident on plane moving plasma shock with small thickness compared to Larmor radius of  
04 p0552 A66-14019  
Plasma conductivity as function of Larmor electron frequency and mean electron-atom collision interval in transverse magnetic field of argon and mercury plasma  
06 p0918 A66-16835  
Flute instability of plasma of finite pressure and zero pressure, examining stabilizing effect of finite larmor radius  
07 p1086 A66-17651  
First mode of flute disturbances in axisymmetric plasma will be unstable for very large Larmor ion  
07 p1086 A66-17653  
Larmor precession of charged particles

effect on nonstationary temperature field in plane channel  
12 p1922 A66-24361  
Growth rate of sheet pinch instability calculated in small Larmor radius limit, using integration along unperturbed orbits, finding instability driven by resonant electrons  
12 p1951 A66-24573  
MHD instability in plasmas during pinch discharge, noting wave velocity dependence on Larmor radius, Hall effect, electron temperature fluctuations, etc  
13 p2142 A66-25704  
Charged particles in nonadiabatic magnetic traps, noting behavior in mirror machine with spatially modulated central field, using model with square wave modulation  
13 p2145 A66-25727  
Finite Larmor radius equations for plasma, noting pressure tensor modification and approximate moment equations  
15 p2555 A66-29757  
MHD theory of stability reduced to fourth-order differential equation with arbitrary parameter for highest order derivative  
17 p2964 A66-31893  
Set of fluid equations in finite Larmor radius obtained by systematic asymptotic expansion, using gyration period and radius as small space and time parameters  
18 p3150 A66-34965  
Drift-wave instability in weakly inhomogeneous fully ionized plasma confined in strong magnetic field in Q machine  
19 p3416 A66-36523  
Drift instabilities calculated in beta limit, examining influence on electron cyclotron harmonic waves, Larmor radius flute, structure of infinite plasma in magnetic field, etc  
19 p3418 A66-36535  
Macroscopic hydromagnetic equations with magnetic viscosity for collisionless plasma, determining Larmor radius ratio to characteristic length, using Vlasov equation in drift frame  
20 p3610 A66-38054  
Short-circuit effects by metal walls and influence on plasma boundary stability  
21 p3791 A66-39177

# LASER

SA CHEMICAL LASER  
SA FABRY-PEROT LASER  
SA GAS LASER  
SA LIQUID LASER  
SA MASER  
SA ORGANIC LASER  
SA PULSED LASER  
SA RUBY LASER  
SA SEMICONDUCTOR LASER  
SA SOLID STATE LASER  
SA TRANSIENT OSCILLATION  
Optical phase modulator using ferroelectric barium titanate crystal  
01 p0117 A66-10240  
Laser characteristics of and coherent oscillations from trivalent Tm, Ho, Yb and Er ions in yttrium aluminum garnet  
01 p0079 A66-10241  
Laser interferometer to measure time and spatial variation in repetitively pulsed plasma  
01 p0079 A66-10243  
Economical feasibility requirements for optical maser communications systems  
02 p0189 A66-11301  
Laser bibliography covering devices and related systems for period January-June 1965  
02 p0239 A66-11372  
Reflection coefficient of mirrors measured on operating wavelength of laser in which they are used  
02 p0239 A66-11420  
Laser beam modulation methods assessed for making use of capability of laser for carrying multitude of signals simultaneously  
02 p0191 A66-11692  
Multiphonon absorption in laser GaAs and ruby crystal of optical generator  
02 p0241 A66-11727  
Laser mirrors consisting of alternating lead-oxide and cryolite films  
02 p0241 A66-11820  
Superconducting states in impurity-free semiconductors created by laser illumination  
02 p0242 A66-12091  
Fabry-Perot interferometric modulator for laser beam, noting error of precise alignment of reflecting surfaces and Gaussian type of imperfections  
02 p0232 A66-12202  
Angular scanning of laser beam forming multiple beam phased array, making use of



- time coherence 03 p0377 A66-12445  
 Light emission in forward biased semiconductor p-n junction 03 p0409 A66-12577  
 Possible materials for second harmonic generation and laser action discussing centrosymmetric and piezoelectric crystals and single crystal plate with alternate layers of noncentrosymmetric composition 03 p0378 A66-12940  
 Biological effects of laser radiation with reference to intact animals, primate eyes and skin and malignant tumors of animal and human origin 03 p0325 A66-12994  
 Optical data processing techniques considering storage, manipulation, holography and pattern recognition using matched filters 03 p0378 A66-12997  
 Physical fundamentals of lasers such as population inversion, induced emission and principal optical apparatus explained for communications engineers 03 p0379 A66-13233  
 Laser technique to photograph hypervelocity projectiles in free-flight range 03 p0379 A66-13248  
 Magnitude of anisotropic line broadening in ruby 03 p0413 A66-13278  
 Preparation of single crystals of double molybdates of Na and La /or other rare earth elements/ doped with Nd, Tb or Pr for laser application 04 p0529 A66-13478  
 Hazards, effect, safety and precaution for prevention of physical injuries from laser radiation 04 p0529 A66-13694  
 He-Ne laser incorporated into arm of interferometer used to measure fringe shift in small transient plasma 04 p0529 A66-13743  
 Optical resonator using cylindrical mirror with variable radius of curvature 04 p0530 A66-13890  
 Semiconductor laser radiation by direct zone-to-zone transitions 04 p0532 A66-14273  
 Angular width and intensity of light from two lasers that cause plasma to oscillate and in turn are scattered by induced fluctuations 04 p0533 A66-14328  
 Local electron temperature and electron density in theta pinch measured by means of scattering of laser beam 04 p0555 A66-14334  
 Optically connected laser constructed on gallium arsenide p-n junction, noting coherent radiation 04 p0533 A66-14363  
 Production laser welding of intricate and critical subassemblies incorporated into space vehicles and components 05 p0691 A66-14514  
 Laser beam welding electronic-component leads 05 p0685 A66-14517  
 Trimming microcircuit elements like evaporated thin-film and silk-screened cermet-film resistors attempted with CW and pulsed lasers 05 p0692 A66-14562  
 Laser welding evaluated with regard to performance and production application 05 p0686 A66-14692  
 Laser digital devices, examining quenching of gain and optical absorption 05 p0693 A66-14826  
 Waveguide coupling between adjacent parallel fibers as means of transferring radiation from one element to another 05 p0693 A66-14827  
 Some laser properties from viewpoint of second law of thermodynamics of irreversible processes 05 p0694 A66-14899  
 Automatic frequency control of laser local oscillator for heterodyne detection of laser signal and use of 2.5 gc frequency offset to permit retrieval of microwave data 05 p0633 A66-14908  
 Radiation damage and annealing of gallium arsenide laser diode 05 p0696 A66-14979  
 History and development of molecular amplification by stimulated emission of radiation, noting various laser types 05 p0696 A66-15034  
 Molecular anisotropy of propagation of intense light beam, noting Raman and Brillouin effects 05 p0696 A66-15106  
 Energy and intensity of ions emitted by metal target as function of characteristics of laser and nature of metal 05 p0697 A66-15109  
 Heating process in laser welding of metal sheets, taking into account energy distribution, heat transfer and flux densities 05 p0688 A66-15347  
 Transmission through tapered quartz tube in laser near field 05 p0697 A66-15481  
 Interaction mechanism between laser beam and surface in ultrahigh vacuum 05 p0697 A66-15484  
 Instrumentation techniques for new type of gas density measuring system using light scattered from laser beam as measured quantity 05 p0698 A66-15794  
 Second harmonic light generated on reflection of giant-pulse laser beam from surface of silver mirror 06 p0921 A66-16072  
 Local laser heating of cathode for electron extraction from plasmoid 06 p0889 A66-16149  
 Continuous optical second-harmonic generation using ND/YAG laser and crystal of single-domain lithium niobate 06 p0889 A66-16378  
 Measurement of electron density of gas discharge plasma by laser interferometer 06 p0916 A66-16379  
 Frequency-selective transmission etalon replaces end mirror of FM laser so that total power is obtained as single optical frequency 06 p0890 A66-16381  
 Gain measurements of Raman amplifier pumped by diffuse ruby radiation 06 p0891 A66-16388  
 Photon trapped wave effect for developing optical waveguides in which optical beam creates waveguide as it propagates 06 p0892 A66-16662  
 Line narrowing of neodymium glass laser with reflection 07 p1041 A66-17291  
 Atmospheric turbulence, power fluctuation and radar detection in laser systems design 07 p1041 A66-17294  
 Lock-on band of continuously operating laser oscillator determined for traveling wave circuit 07 p1043 A66-17623  
 Estimation of energy parameters of laser light beam used to weld metals 07 p1037 A66-17626  
 Brillouin scattering of light by phonons and phonon maser in derivation of conservation theorems from basic equations 07 p1045 A66-18397  
 Coherence and stimulation threshold of Stokes line 08 p1232 A66-18648  
 New optics techniques including interference filters, lasers and optical fibers 08 p1255 A66-19118  
 Onset of retonation, laser technology and high repetition-high resolution schlieren stroboscopic wave phenomena records 08 p1318 A66-19200  
 Optical laser pumps, high power CW laser operation by cathodoluminescence and suitable selection of phosphors 08 p1234 A66-19546  
 First-order relativity test using phase change of two coherent beams 09 p1385 A66-19935  
 Continuous optical quantum generator operating at room temperature on calcium tungstate doped with neodymium ions 09 p1386 A66-19956  
 Earth-Moon distance measurement using laser technique 09 p1453 A66-20129  
 Electronics methods used in laser technology and vice versa, emphasizing microwave photoelectronic devices, self-consistent gas discharges at optical frequencies, etc 09 p1386 A66-20434  
 Quantum theory of interaction of electromagnetic waves in plasma considered in terms of light-light scattering and plasma-laser beam interaction 10 p1558 A66-21173  
 Laser application in photography, noting interferometric and holographic techniques 10 p1535 A66-21333  
 Eigenvalues of integral equations in laser resonant cavities 10 p1542 A66-21343  
 Spontaneous emission noise effects on coherence properties of laser 10 p1542 A66-21550  
 Diffusion of light by plasma electrons produced in laboratory for very small effective diffusion area 10 p1566 A66-21712  
 Coherent laser light for conventional and unconventional photographic situations 11 p1705 A66-22670  
 Bibliography of open literature on lasers, Part V 11 p1712 A66-22876  
 Quantum optics theorem on classical source for which effect of detector and dissipation mechanism is negligible 11 p1713 A66-22967  
 Laser scattering by bound charged particles 11 p1713 A66-23080  
 Irregular bends and lens displacements effect on wavelength and modes in laser waveguide 11 p1713 A66-23103  
 Dismountable flash lamp for laser, including cross sectional scale drawing and wiring diagram 11 p1714 A66-23296  
 Raman laser materials selection, emphasizing frequency shifts and excitation power threshold 11 p1721 A66-23477  
 Clear air turbulence detection with laser Doppler optical radar [AIAA PAPER 66-374] 12 p1818 A66-24498  
 Consistent theory of nonlinear optical effects in bounded light beams by extending parabolic equations to nonlinear problems 12 p1891 A66-24888  
 Stimulated Raman effect and tunability of Raman laser 13 p2089 A66-25062  
 Optical communication for Mars exploration with outline of laser modulators and antennas 13 p2021 A66-25251  
 Electron-beam-controlled CRT scanlaser 13 p2091 A66-25557  
 Quantum theory for noise in steady state of laser oscillator above threshold, comparing semiclassical and quantized linear theories 13 p2091 A66-25650  
 Optical instrumentation radar for real-time positional data on high-speed cooperative targets 13 p2023 A66-25654  
 Thermally-induced optical path distortions in laser rods measured by obtaining time resolved interferograms, using Mach-Zehnder interferometer and Q-switched laser 13 p2092 A66-25994  
 Thermal optical behavior of glasses and other potential laser materials and thermal distortion in air, water, benzene, ethanol and toluene 13 p2092 A66-25996  
 FM laser and optical heterodynes in optical communication systems 13 p2093 A66-26004  
 Laser welding of aerospace structural alloys and resultant joint properties 13 p2087 A66-26019  
 Monte Carlo technique to determine total energy and energy distribution in laser crystal due to optical pumping 13 p2093 A66-26028  
 Neodymium-doped yttrium-aluminum garnet crystal laser oscillator as regenerative amplifier of noise 13 p2103 A66-26212  
 Nonlinear quantum mechanical analysis of laser steady motion, stability under deviations and noise effect on line width and intensity fluctuations 13 p2103 A66-26213  
 Quantum theory of lasers presented in terms of correlation functions of second-quantized electromagnetic and matter fields 13 p2103 A66-26214  
 Thermalization of plasma by creating imploding shock wave driven by laser energy release 13 p2106 A66-26683  
 Production of neutral or ionized gas plasmoids by focusing beam of coherent light emitted by ruby laser on target of pure metal or metal containing gas 14 p2339 A66-26819  
 Laser beam techniques for study of plasmas with high electron densities 14 p2305 A66-26822  
 Laser frequency tuning by dielectric material interaction to produce nonlinear effects 14 p2305 A66-26887  
 Optical communication using laser techniques 14 p2234 A66-26918  
 Monograph on lasers including gas lasers, ruby lasers, giant-pulse techniques, oscillation modes, etc 14 p2305 A66-26961  
 Nonlinear optics, considering Maxwell equation and nonlinear material response 14 p2330 A66-26964  
 Solid state reduction of lanthanide ions in laser hosts, effect of presence of recombination hole-centers in photoreduced samples and elimination during electrochemical process 14 p2362 A66-27464  
 Laser radiation to determine electron density in dense high temperature plasma 14 p2374 A66-27507  
 Protection and hazard to eyes of uninformed operators and bystanders from laser light 14 p2309 A66-27668  
 Ultrasonic modulation of laser oscillation from neodymium glass rod 14 p2309 A66-28044  
 Optically connected laser constructed on gallium arsenide p-n junction, noting



- coherent radiation 14 p2310 A66-28262
- Parametric amplifiers and 14 p2310 A66-28358
- lasers 14 p2310 A66-28358
- Perspective rendering of field intensity 14 p2310 A66-28358
- diffracted at circular aperture with reference to laser-scanning technique 15 p2499 A66-28843
- Quantum theory of laser having only single-mode oscillation and ignoring atomic motion and spatial variations in cavity mode 15 p2515 A66-29117
- Open laser resonator composed of two ideally spherical mirrors with rectangular aperture 15 p2515 A66-29200
- Relation between nonlinear luminescence quenching and concentration of luminescence centers in laser crystal 15 p2515 A66-29204
- Thermal effects in various media due to laser beam 15 p2515 A66-29209
- Shape and dimension of spark arising during focusing of laser emission 15 p2516 A66-29210
- Two-quanta absorption and scattering loss in powerful laser 15 p2516 A66-29350
- Regenerative helium-neon laser with amplification coefficient of 1000 15 p2516 A66-29352
- Optical resonator using cylindrical mirror with variable radius of curvature 15 p2518 A66-29703
- Local laser heating of cathode for electron extraction from plasmoid 15 p2519 A66-29879
- Heating process in laser welding of metal sheets, taking into account energy distribution, heat transfer and flux densities 15 p2511 A66-29989
- Satellite range measurements using laser in conjunction with photoelectric receiver and Baker-Nunn camera 15 p2453 A66-29998
- Single-mode laser field model consisting of amplitude stabilized sine wave with slowly varying random phase plus stationary noise field 16 p2716 A66-30127
- Laser communication by optical beam waveguide 16 p2717 A66-30594
- Paramagnetic resonance spectra shift due to temperature change in cross-relaxation rutile maser 16 p2718 A66-30820
- Growth of single crystals of rare-earth fluorides for laser application, using hydrogen fluoride atmosphere, noting ion exchange purification 16 p2779 A66-31082
- Laser welding for advanced electronic packaging 16 p2715 A66-31593
- Polarizing properties of laser reflector consisting of two identical rectangular prisms 16 p2721 A66-31803
- Laser for photoelasticity including scattered-light method, conventional transmission polariscope with static loads and dynamic photoelasticity 17 p3022 A66-32072
- Book on laser theory based on kinetic equations with emphasis on emission from luminescent center transitions, semiconductor junctions and Raman scattering 17 p2934 A66-32558
- Parametric oscillator threshold with single mode optical masers and observation of amplification in lithium niobate 17 p2935 A66-32716
- Retardation-type laser modulators, examining driving power, transmission and dynamic range 17 p2935 A66-32820
- Open laser resonator composed of two ideally spherical mirrors with rectangular aperture 17 p2935 A66-33049
- Relation between nonlinear luminescence quenching and concentration of luminescence centers in laser crystal 17 p2936 A66-33053
- Thermal effects in various media due to laser beam 17 p2936 A66-33058
- Shape and dimension of spark arising during focusing of laser emission 17 p2936 A66-33059
- Physical mechanism of molecular lasers and vibrational rotation relation 17 p2936 A66-33246
- Fluorescent-solid lasers design and performance noting materials 17 p2937 A66-33250
- Readout technique for laser fog disdrometer 17 p2927 A66-33346
- Space communication requirements using lasers and microwaves in manned Mars flights
- [AIAA PAPER 65-324] 18 p3067 A66-33794
- Electron temperature and concentration in DC plasma arc determined from Thomson scattering of laser radiation 18 p3118 A66-33840
- Laser system for measuring surface contours in large steerable antennas 18 p3119 A66-34296
- Yttrium vanadate crystals grown and processed for optical purposes 19 p3373 A66-35434
- Interstellar vehicle propelled by terrestrial laser beam 19 p3449 A66-35488
- Cooperative scattering of laser light by thetatron plasma 19 p3373 A66-35489
- Quantum theory of laser model, deriving kinetic equations for radiation and single-particle density matrices, using Bogolubov expansion procedure 19 p3374 A66-36008
- Radiation attenuation effect of atmospheric aerosols on all-weather aircraft landing guidance systems using lasers 19 p3397 A66-36051
- Transmission of luminous flux due to ionization of gases by high power laser, measuring energy absorption in ionized zone 19 p3403 A66-36255
- Two-laser cavity in tandem to resolve components with homogeneously broadened /Doppler/ line 19 p3376 A66-36720
- Book on lasers including pulsed and organic, Q modulation and modes in optical resonators 20 p3575 A66-36967
- Q modulation of laser theory and application, presenting giant pulse production, phenomenological theory, output response to step function change, electro-optic and mechanical modulators 20 p3576 A66-36971
- Two-quanta absorption and scattering loss in powerful laser 20 p3576 A66-37355
- Regenerative helium-neon laser with amplification coefficient of 1000 20 p3576 A66-37357
- Laser theory and application 20 p3577 A66-37420
- Laser application as measuring equipment in metal working, discussing surface-grazing interferometer, feedback laser device and length measuring laser [ASME PAPER 66-MD-43] 21 p3742 A66-38491
- Polarizing properties of laser reflector consisting of two identical rectangular prisms 21 p3747 A66-39105
- Laser bibliography July-December 1965, including references to holograms 21 p3749 A66-39541
- Powerful laser employing induced two-quanta luminescence 22 p3930 A66-39771
- Temperature distribution in two-layer plate during welding by laser light flux 22 p3923 A66-40194
- Consistent theory of nonlinear optical effects in bounded light beams by extending parabolic equations to nonlinear problems 23 p4076 A66-41095
- Time dependent Schroedinger equation for Bloch electron in presence of laser field, using WKB approximation method, compared with perturbation theory 23 p4077 A66-41266
- Laser technique acquisition of data on exploding-wire phenomena in explosion model, supersonic model and ablation model 23 p4091 A66-41701
- Superconductor solenoid application to laser devices and development of magnetic plasma traps for research in controlled thermonuclear reactions 23 p4115 A66-41743
- Wide field active imaging, image processing in which pictorial information is placed within laser cavity 24 p4222 A66-42559
- Signal excitation in negatively charged antenna rod in effect of unfocused laser beam 24 p4224 A66-42753
- Magnetic dipole moment in spark produced by focusing laser radiation 24 p4226 A66-43055
- Compressible and incompressible flows made visible by optical method sensitive to density variations, shadowgraph, schlieren system, Mach-Zehnder interferometer and holographic interferometry with lasers 24 p4192 A66-43196
- experiments 07 p1001 A66-17217
- Oscillation, modulation and transmission problems regarding long distance electric signal communication possibilities of lasers 07 p1045 A66-18359
- Data pulsed transmission over electron-injection laser communication system, using continuous waves 09 p1385 A66-19934
- Microwave communications, discussing radio relay techniques, carrier telephony, satellite microwave communications, television, laser light wave communication, etc 11 p1655 A66-22696
- Optical communication for Mars exploration with outline of laser modulators and antennas 13 p2021 A66-25251
- Solar noise in optical communications, background radiation dependence on detector aperture, noise power and application to GaAs diodes and gas lasers 13 p2024 A66-25833
- FM laser and optical heterodynes in optical communication systems 13 p2093 A66-26004
- Optical communication using laser techniques 14 p2234 A66-26918
- Atmospheric turbulence effects on laser beam propagation, noting beam cross section, phase variation, AM and FM, etc 14 p2235 A66-27035
- Coherent transmission of optical radar from laser source and use of RF subcarriers placed on optical beams for wideband communications purposes 14 p2244 A66-28404
- Multiple scattering effects on propagation of coherent optical signals studied for laser communications application 15 p2448 A66-28580
- Laser communication by optical beam waveguide 16 p2717 A66-30594
- P-n junction lasers for short range communications, examining design, technological problems and performance 17 p2933 A66-31956
- Space communication requirements using lasers and microwaves in manned Mars flights
- [AIAA PAPER 65-324] 18 p3067 A66-33794
- Acquisition and reacquisition in spacecraft-spacecraft and spacecraft-to-Earth communications using laser systems 18 p3067 A66-33795
- Ultrasonic cell which modulates intensity of He-Ne laser beam for communication of intelligence 18 p3118 A66-34059
- System design analysis of laser methods of deep space communication, examining local heterodyne system /LHS/, direct detection system /DDS/ and transmitted reference system 19 p3300 A66-35666
- Book on laser receivers covering noise performance, atmospheric effects, detection techniques, hardware and systems available, optical communication in visible and IR spectrum, etc 19 p3375 A66-36060
- Laser light modulation by Pockels or Kerr effect for application to telecommunications system, examining electrical birefringence modulation 19 p3304 A66-36262
- Coherent laser light use in atmospheric communications system, discussing effect of atmospheric turbulence and small vibrations on coherent detection efficiency and SNR 20 p3511 A66-36930
- Laser communications system design, describing range equation, modulation and detection techniques, atmospheric effects, etc 20 p3515 A66-37257
- Narrow laser beam pointing technique in deep space-to-earth data transmission for reduction in error sources 22 p3867 A66-40496
- Atmospheric turbulence effect on laser beam intensity distribution 23 p4035 A66-41030
- Atmospheric turbulence effect on frequency spectra of light intensity fluctuations examined, using He-Ne laser 23 p4035 A66-41031
- Tropospheric propagation using laser as transmitter, analyzing effects of Benard cells, turbulence, wind shear, etc 24 p4171 A66-42367
- Optical communication systems, discussing available equipment, transmission characteristic, lack of long distance operation reliability, etc 24 p4174 A66-42805
- Electro-optic light modulation using Pockel and Kerr effects in crystals for



- communications applications, using  
lasers 24 p4225 A66-42811  
Book on laser applications in radio  
communication systems 24 p4226 A66-43226
- LASER MODE**  
Self-locked gas laser mode dependence on  
cavity length and position of laser medium  
in cavity 01 p0081 A66-10347  
Phase relations of longitudinal modes in  
gas laser with annular  
resonator 01 p0082 A66-10726  
Induced emission modes of traveling wave  
laser 01 p0082 A66-10778  
Gas laser interferometers for plasma low  
electron density  
measurement 01 p0069 A66-10856  
Two-and three-step laser cascades detected  
experimentally in helium-neon mixtures,  
analyzing two-step cascade starting with  
density matrix  
formulation 02 p0241 A66-11477  
Laser model possessing two modes of  
different vibrational  
frequency 02 p0241 A66-11728  
Optical whispering mode of polished  
cylinders and implication in laser  
technology, noting trapped fluorescent  
light 02 p0262 A66-12203  
Mode-controlled giant pulse laser used to  
produce two-beam hologram in short  
exposure time of 30 nsec 02 p0233 A66-12215  
Synchronized mode of excitation for  
diffraction-coupled laser 03 p0375 A66-12293  
Laser excitation in quartz of elastic modes  
of thick plate, suggesting energy coupling  
mechanisms 03 p0376 A66-12423  
Pressure dependence of dominant emission  
modes from PbSe diode  
laser 03 p0378 A66-13003  
Multireflector Fabry-Perot laser resonators,  
discussing suppression effect against  
unwanted modes 03 p0380 A66-13325  
Time characteristics in generation of giant  
laser pulse studied by circuit with prismatic  
shutters 04 p0530 A66-13889  
Mode guiding and gain in junction laser  
due to dielectric sandwich confining wave  
propagation 04 p0530 A66-13952  
FM laser oscillation theory discussing  
effect of arbitrary atomic line shape,  
saturation, mode pulling, power output,  
sideband amplitude, distortion,  
etc 04 p0530 A66-13954  
Modes of emission-vs-time spectrum,  
optical emission spectrum and superposition  
spectrum of short confocal ruby laser in  
near field 04 p0532 A66-14290  
Spatial distribution of hollow-cone shaped  
emission of modes which are totally  
reflected in neodymium-glass  
lasers 04 p0532 A66-14291  
Mode selective characteristics of plane-  
parallel dielectric plate as reflector for  
ruby laser resonator 04 p0533 A66-14330  
Mode of operation of various ruby lasers  
with plane-parallel mirrors at room  
temperature 04 p0534 A66-14500  
Laser deflection and scanning by means of  
multimode cavities with dynamic spatial  
filters 05 p0693 A66-14829  
Laser light redistribution in illuminating  
optical signal processing systems noting  
apodization, spatial modes and aspheric  
elements 05 p0693 A66-14830  
Microwave beats identified between modes  
in bromine-argon mixture 05 p0695 A66-14923  
Peripheral modes in chelate laser, noting  
luminescence emitted by axis of cylindrical  
cell and lateral face 05 p0697 A66-15171  
Mode competition and coupling in Q-  
switched ruby laser 06 p0890 A66-16383  
CW laser oscillation between 11.48 and  
11.55 microns from nitrogen-carbon disulfide  
system 06 p0890 A66-16384  
Time dependence of laser operation modes,  
using laser model with two oscillation  
types 06 p0891 A66-16626  
Multiple internal-reflection folded-path  
rectangular laser configuration for obtaining  
length of active media between Fabry-Perot  
reflectors 06 p0891 A66-16652  
CW IR laser oscillation in HBr and HI gas  
discharge 06 p0892 A66-16756  
Derivation of two  
electromagnetic field and population  
inversion in solid state  
laser 06 p0893 A66-16773  
Self-modulation of laser with two-mode  
resonator 06 p0893 A66-16775  
Oscillation mode control in p-n junction  
lasers for current density reduction for  
stimulated emission 07 p1041 A66-17329  
Intensity distribution of fringe systems  
used to verify phase inversion between two  
lobes of laser in TEM-10  
mode 07 p1043 A66-17453  
Solid state laser system, describing  
quantum mechanical treatment of self-  
sustained oscillation for one  
mode 07 p1044 A66-17817  
Generation of induced laser radiation in  
prestationary regime 07 p1044 A66-17877  
Quasi-Fermi level, frequency, threshold  
pumping value and particular mode in  
radiative intraband  
transition 07 p1045 A66-18361  
Phase-locking effect and phase sum of LF  
and HF oscillating modes in  
laser 07 p1046 A66-18413  
Laser emission in pure cadmium sulfide  
crystals bombarded by electron  
beams 08 p1233 A66-18650  
HF modulation of radiation spikes due to  
beats between oscillation modes in optical  
ruby laser 09 p1386 A66-19955  
Time dependent emission behavior of  
single axial mode of diffraction limited ruby  
laser at room  
temperature 09 p1386 A66-20420  
Neodymium doped glass laser found to  
oscillate in conventional random pulsating  
manner under mode-locked  
conditions 10 p1541 A66-21251  
Single filament junction laser emitting  
coherent light of simpler modes, showing  
that laser has two portions, each with  
selective diffused region 10 p1542 A66-21357  
Induced emission modes of traveling wave  
laser 11 p1711 A66-22290  
Quantum mechanical nonlinear theory of  
intensity and phase fluctuations of  
homogeneously broadened laser  
noise 11 p1711 A66-22466  
Parasitic internal oscillations in laser  
crystal with dielectric rod caused by total  
reflection from generatrix of cylindrical  
sample 11 p1712 A66-22739  
Standing waves in laser resonators verified  
by placing thin metallic films between  
external mirrors of pulsed neodymium  
laser 11 p1713 A66-22893  
Mode suppression techniques for gas laser  
single axial mode operation for large mirror  
separations 11 p1713 A66-23093  
Excitation of axial oscillation modes in  
semiconductor lasers analyzed, based on rate  
equations for chemical potentials of carriers  
and number of photons 12 p1890 A66-24455  
Equations of motion governing interaction  
of optical modes in presence of time-varying  
parameters 12 p1890 A66-24559  
Two-level atom interaction with multimode  
gas laser cavity, obtaining stationary state  
and solving unique eigenvalue in special  
cases 12 p1891 A66-24568  
Dependence of beat frequency of  
neodymium laser axial modes on distance  
between mirrors and neodymium rod  
position within resonator 12 p1891 A66-24881  
Segmented-rod ruby laser structure  
operated as giant pulse laser, using Kerr  
cell to provide Q-switching, noting number  
of oscillating modes 13 p2088 A66-25038  
Multimode ruby resonator output as  
affected by mode number and mode  
degeneracy 13 p2088 A66-25043  
Second harmonic generated by transmitting  
laser radiation through tellurium  
monocrystal, while filtering out fundamental  
frequency 13 p2090 A66-25437  
Digital-mode FM CW laser ranging and  
tracking system using compound axis  
servomechanism 13 p2024 A66-25982  
Natural modes of plane and cylindrical  
dielectric resonators in optical  
band 13 p2093 A66-26042  
Laser oscillation and energy losses in  
medium containing active  
molecules 13 p2093 A66-26043  
Atmospheric observation with advanced  
light radar, noting equipment characteristics,  
molecular scattering mechanism,  
etc 13 p2122 A66-26133  
Parametric oscillator theory applied to  
tunable coherent optical parametric  
oscillation in lithium  
niobate 13 p2096 A66-26145  
Raman light forward emission in liquids  
when illuminated by laser, obtaining  
stimulated Raman action without feedback,  
which suggests existence of mechanism  
contributing to modulation of medium  
polarizability 13 p2097 A66-26160  
Laser action in gallium antimonide diodes,  
examining emitted light spectrum vs  
injected current, temperature effect,  
radiative efficiency, etc 13 p2100 A66-26184  
Spontaneous and coherent emission from  
lead sulfide, telluride and selenide diode  
lasers in oriented magnetic field,  
determining band edge parameters from  
spin-split zero order Landau level  
transitions 13 p2100 A66-26185  
Multiple quantum equations for mode  
amplitude and frequency determination for  
magnetic field-tuned gas optical  
maser 13 p2101 A66-26200  
Dependence of Zeeman beat frequency on  
interferometer tuning in single-mode He-Ne  
laser with various gas pressures and  
magnetic field strengths 13 p2101 A66-26201  
High resolution piezoelectrically scanned  
Fabry-Perot interferometer used to study  
gain profiles, mode structures and emission  
line widths of CW Ar, Kr and Xe ion lasers  
and Hg-He pulsed laser 13 p2102 A66-26208  
Correlations and intensity fluctuations in  
light from individual lasing and nonlasing  
modes of CW GaAs laser and threshold  
noise change in laser  
emission 13 p2102 A66-26210  
Periodic undamped oscillations in power  
intensity of two-mode optical  
maser 13 p2103 A66-26217  
Absolute flux measurement for pulsed and  
triggered lasers requiring only quantum  
receivers 13 p2104 A66-26375  
Phase locking of one laser to another by  
direct injection of first laser beam into  
second laser cavity 13 p2105 A66-26593  
Relaxation oscillation in single-mode  
operation of room-temperature CW ruby  
laser 14 p2306 A66-27028  
Steady state regime of electromagnetic  
oscillation in laser 14 p2306 A66-27065  
Axial and transverse mode selection,  
emission spectrum and transient emission  
behavior of confocal ruby laser operated in  
ellipsoidal pumping  
system 14 p2308 A66-27606  
Experimental observation of regular  
spiking in neodymium doped glass laser rod  
attributed to simultaneous oscillation of  
many transverse and longitudinal  
modes 15 p2513 A66-28727  
Solar pumping and modulation of various  
laser materials for deep space  
communication, noting TV picture  
transmission 15 p2513 A66-28971  
Hysteresis phenomena in He-Ne gas laser  
in axial magnetic field and polarization of  
oscillating mode within certain tuning  
region 15 p2516 A66-29385  
Reversible bleachable dye-solutions for  
expander elements in  
laser 15 p2517 A66-29388  
Ultrashort optical pulses generated by  
mode locking continuous neodymium doped  
yttrium-aluminum garnet  
laser 15 p2517 A66-29391  
Time characteristics in generation of giant  
laser pulse studied by circuit with prismatic  
shutters 15 p2518 A66-29702  
Crystal motion effect on time behavior of  
laser generation mode, using high speed  
photography and  
oscillograms 15 p2518 A66-29725  
Length dependent threshold data for  
stimulated Raman emission in liquids, noting  
correlation between laser beam self-focusing  
and onset of Raman  
emission 16 p2716 A66-30157  
Nonuniform pumping effects on near-axial  
low-order transverse mode structure in solid  
state laser cavity 16 p2719 A66-31087  
Mode locking in gaseous laser whose cavity  
is length modulated at mode separation  
frequency 16 p2719 A66-31095  
Modes of tilt-mirror optical resonator,  
using spillover radiation to extract coherent  
far IR 16 p2747 A66-31134  
Ionization of air with laser radiation in  
spike mode 16 p2762 A66-31150  
Linear absorption effect on threshold for



self-focusing of laser beam in cadmium sulfide, noting variation of absorption coefficient 16 p2720 A66-31537

Laser mode operation in pressure of radiation absorbing impurity analyzed by extended Thomson type system 16 p2720 A66-31558

Low noise photodiodes with avalanche multiplication for high sensitivity, noting capability for low intensity wideband signal detection, performance in IR region, etc 17 p2880 A66-31934

Second-harmonic enhancement in nonlinear crystal by loss modulator coupling of pulsed ruby laser modes 17 p2933 A66-31939

Steady state oscillations of molecular beam laser with inhomogeneous sinusoidal field in resonator 17 p2885 A66-32243

Laser operated with saturable filter for Q-switching, noting two modes of excitation soft and hard regime/ 17 p2934 A66-32314

Effect of anomalous dispersion on stimulated emission spectrum of doped cadmium fluoride crystals 17 p2977 A66-32317

Selective diffused junction laser, discussing GaAs laser used for quenching experiment 17 p2934 A66-32408

Fabry-Perot etalon use for interferometry and laser control, noting low angle scattering, laser oscillation, thermal tuning sensitivity, etc 17 p2925 A66-32619

Oscillation conditions for feedback lasers, superradiant directionally coherent emission lasers and coherence brightened emission lasers 17 p2934 A66-32628

Michelson interferometer used to study modes of red He-Ne laser 17 p2937 A66-33316

Laser radar ranging system using pseudorandom code modulation, considering application to pulse and digital circuitry, statistical communication theory and electro-optical engineering 18 p3117 A66-33557

Mode characteristics of solid state lasers from analytical solution of conservative equation 18 p3118 A66-33839

Optical frequency breakdown threshold of inert gas mixtures, using focused beam radiation from Q-spoiled neodymium laser 18 p3138 A66-34236

Derivation of two equations for electromagnetic field and population inversion in solid state laser 19 p3372 A66-35370

Self-modulation of laser with two-mode resonator 19 p3372 A66-35372

Transfer efficiency of laser pumping cavities with diffusely reflecting wall determined, based on approximately isotropic nature of light inside cavity 19 p3372 A66-35379

Doppler shift and high velocity mirror translation effects on mutual optical coherence function of gas laser Michelson interferometers 19 p3354 A66-35387

Laser mirror transducer decoupling from mechanical resonances of laser cavity 19 p3374 A66-35813

Mode theory of spherical mirror resonators, discussing diffraction losses, resonant conditions, mode patterns, internal focusing elements, mode selection, etc 20 p3599 A66-36972

Second harmonic frequency generation obtained in process of optical mixing of collinear neodymium laser beams in potassium dihydrogen phosphate 20 p3578 A66-37550

Phase relations of longitudinal modes in gas laser with annular resonator 20 p3579 A66-37663

Excitation of axial oscillation modes in semiconductor lasers analyzed, based on rate equations for chemical potentials of carriers and number of photons 20 p3579 A66-37687

Electron beam scanlaser based on laser cavity directly and/or transversely degenerate having Q-spoiled for all modes but one 20 p3581 A66-38244

Pulsed-mode gain characteristics in neodymium-doped silicate glass laser experimentally related to giant-pulse laser energy output 20 p3582 A66-38396

Coupling of adjacent axial modes in external Raman resonator observed as first Stokes frequency with benzene as Raman medium and Q-switched ruby laser as pump source 21 p3747 A66-39109

Quenching and hysteresis effects between

Zeeman oscillations on single axial mode observed in near-zero magnetic fields for short planar laser 21 p3747 A66-39116

Laser mode-locking during resonator Q-factor modulation 21 p3748 A66-39303

Stable limiting cycles of laser resulting from mutual synchronization of phase-shifted oscillation modes 22 p3929 A66-39653

Frequency doubling of laser light with variable Q-switched resonator 22 p3929 A66-39654

Intensity and frequency equations for interband optical transitions and multimode properties in semiconductor lasers 22 p3929 A66-39666

Atomic degeneracy influence on mode interactions in gas laser 22 p3931 A66-39930

CW ruby laser of 10-mm length in ellipsoidal pumping system under water cooling, noting various modes 22 p3931 A66-40100

Electron thermalization effect on semiconductor laser behavior, noting optical transition between impurity level and band, taking into account diffusion process 22 p3933 A66-40790

Steady state regime of electromagnetic oscillation in laser 22 p3933 A66-40824

Dependence of beat frequency of neodymium laser axial modes on distance between mirrors and neodymium rod position within resonator 23 p4076 A66-41088

Theory of steady multimode oscillation of solid state laser extended to cavities with inefficient end mirrors or losses dependent on frequency 23 p4077 A66-41274

Frequency tuning of coherent emission over vibronic continuum of phonon-terminated optical masers by thermal tuning and wavelength-selective feedback 23 p4077 A66-41369

Quantum theory of Q-spoiled laser, noting statistics of number of photons in mode bear qualitative resemblance to Poisson statistics 23 p4077 A66-41373

Parasitic internal oscillations in laser crystal with dielectric rod caused by total reflection from generatrix of cylindrical sample 23 p4078 A66-41477

Ruby laser giant pulse off-axial modes detected with high resolution spherical Fabry-Perot interferometer 23 p4079 A66-41627

Spectral width of peak type and monopulse type radiation of solid-body laser in nonstationary regime 24 p4219 A66-42133

Photoelectron emission statistics determining probability distribution of photoelectron counts in photomultiplier illuminated by laser below and above threshold of oscillation 24 p4220 A66-42543

Mode selection, relaxation oscillations, mode interaction and thermal effects in room temperature CW lasers in ellipsoidal pumping systems 24 p4221 A66-42546

Spectroscopy of IR emission and laser oscillation resulting from transient population inversions on electronic transitions in molecular nitrogen 24 p4221 A66-42550

Current measuring device for EHV transmission line, obtaining instantaneous magnetic field by gauging Faraday rotation angle of laser beam in flint glass rod 24 p4222 A66-42556

Single transverse and longitudinal modes observed in output of passive Q-switched ruby laser when two spherical mirrors are used for resonator 24 p4223 A66-42563

Mode coupling in ruby laser with reactance placed within cavity resonator with modulation frequency close to separation of axial modes, examining electric field envelope 24 p4223 A66-42565

Scattering matrix analysis of single frequency Michelson type He-Ne gas laser, including frequency and amplitude stability analysis of oscillation spectrum 24 p4223 A66-42566

Laser beams and resonators, discussing beam propagation in free space, geometrical optics application and resonator modes in view of aperture diffraction effects 24 p4225 A66-42806

Laser mode control and stabilization using internal time-varying perturbation 24 p4174 A66-42813

# LASER OUTPUT

Pentacarbocyanine compound used to reduce monopulse duration in neodymium laser 01 p0080 A66-10262

Fast photoionization aureole detection and cloud of concentrated long-lived ionization from spark shock wave in laser beam 01 p0080 A66-10263

Ruby laser output exhibiting regular spikes 01 p0080 A66-10324

Focused laser as accelerating cavity for cyclic particle accelerator 01 p0080 A66-10328

Peak power transients of near confocal helium-neon laser working at 6328 angstroms on pulsed discharge basis 01 p0080 A66-10329

Self-locked gas laser mode dependence on cavity length and position of laser medium in cavity 01 p0081 A66-10347

Laser transition identification in electron beam pumped gallium arsenide, primarily on concentration of shallow donors and acceptors 01 p0081 A66-10348

Electron beam pumping of noble gas ion laser 01 p0081 A66-10350

Laser oscillation increase in efficiency in neodymium doped glass produced through energy transfer 01 p0081 A66-10352

Gallium arsenide injection laser for prolonged operation at liquid nitrogen temperatures 01 p0081 A66-10369

Atomic beam lasers, particularly for population inversion in levels of optical transition 01 p0082 A66-10448

Laser with diffraction limited radiation pattern 01 p0082 A66-10450

Breakdown of gases under influence of laser spark phenomena with subsequent absorption of laser radiation and gas heating 01 p0082 A66-10646

Current and voltage distribution over length of HF discharge in helium-neon laser 01 p0082 A66-10704

Nonlinear interaction of oscillations of two types in laser does not affect stationary operation when oscillations are sufficiently apart in band 01 p0082 A66-10724

Aerodynamic and heat transfer measurements using interferometer with continuous wave laser as source 01 p0069 A66-10849

Thermal limitations on capabilities of gallium arsenide p-n junction lasers 01 p0082 A66-10895

Two-dimensional laser deflection using Fourier optics 01 p0083 A66-10897

Carrier frequency stabilization of FM laser with respect to center of atomic gain profile, using small distortion present in laser oscillation 01 p0083 A66-10966

Laser-action threshold in electron-beam excited gallium arsenide and effect of temperature and doping 01 p0083 A66-10971

UV and visible laser oscillations in fluorine, phosphorus and chlorine atoms in pulsed chlorine, phosphorus fluoride and sulfur fluoride gas 01 p0083 A66-10972

Discharges sharply directional coherent radiation generation by synchronized lasers or multimirrored resonator of single laser 01 p0083 A66-11007

Kinetic equation of laser optimum emission, determining pumping efficiency, value of losses in special modes, etc 01 p0084 A66-11058

Cadmium telluride laser with electron excitation 01 p0084 A66-11188

Metallic plasma tube for ion lasers allows them to run at higher current densities than with ceramic tubes 02 p0239 A66-11373

Pressure dependence of output of helium-neon gaseous laser in high pressure range 02 p0239 A66-11375

Second harmonic light generation, stressing saturation effects occurring at high laser power levels, solving nonlinear coupled Maxwell equations 02 p0239 A66-11443

Quantum-electronic cross-modulation effect noted while monitoring IR laser interferometric fringes 02 p0240 A66-11449

Laser transition in vibrational state of ground electronic state of CN from rotational level 8 to 7 with population inversion as result 02 p0240 A66-11451

Laser application problems in interferometry, radar and holography including mechanical stability, noise suppression, dirty laser beam restoration,



etc 02 p0240 A66-11454  
 Development in U.S. of laser application with table including government supported programs in photography, data processing, radar, etc 02 p0240 A66-11455  
 Linear coefficient of amplification of carbon dioxide subjected to HF excitation field for laser emission 02 p0241 A66-12003  
 Current status of theoretical and experimental studies of variant of Raman effect encountered in scattering of laser light 02 p0241 A66-12065  
 Quantum yield coefficient of stimulated emission and angular distribution of laser diode emission 02 p0242 A66-12086  
 Lossless conversion of plane laser wave to plane wave of uniform irradiance, noting planoaspheric lenses method and aberrated lens system 02 p0242 A66-12204  
 Gain and bandwidth narrowing in regenerative helium-xenon laser amplifier 03 p0376 A66-12308  
 Brillouin scattering in liquids examining velocity, frequency and lifetime of thermally excited hypersonic sound waves, using laser light sources 03 p0376 A66-12422  
 GaAs optically coupled transistor structure with lasing emitter 03 p0377 A66-12442  
 Cut-off of ruby laser emission by pulsed electron and bremsstrahlung radiation, using adiabatic temperature 03 p0377 A66-12447  
 Output power and pulse duration of ruby laser 03 p0378 A66-12602  
 Pulsed laser-created plasmas by light absorption by skin effect 03 p0403 A66-12975  
 Intense laser beam focusing effect in gas to study light-induced discharges by time-resolved spectroscopy and photography 03 p0378 A66-12978  
 Internal bubble formation and cracking in rods of Q-switched ruby and Nd-glass lasers caused by laser light, and in case of Nd-glass rods, by platinum inclusions in glass 03 p0378 A66-13002  
 Pressure dependence of dominant emission modes from PbSe diode laser 03 p0378 A66-13003  
 Polarization of light from glass laser doped with two percent positive trivalent neodymium measured with time resolution of less than microsecond 03 p0378 A66-13006  
 Intensity distribution in Fabry-Perot interferometer producing resonant waves for large Fresnel number applied in model for filament-form laser mechanism 03 p0379 A66-13097  
 Model for behavior of optical maser in static magnetic field of arbitrary strength in Z direction and in electromagnetic field composed of traveling waves 03 p0379 A66-13135  
 Pulse energy and power of lasers under continuous operating conditions measured, using calorimeters, photoelectric effect of radiation, etc 03 p0379 A66-13205  
 Lasers as triggering mechanism for spark gaps, noting delay time between pulse arrival and current flow 03 p0379 A66-13247  
 Quantum statistics for analyzing radiation fields interacting with other systems applied to model laser operating as linear amplifier 03 p0379 A66-13260  
 Pentacarbocyanine compound used to reduce monopulse duration in neodymium laser 03 p0379 A66-13307  
 Fast photoionization aureole detection and cloud of concentrated long-lived ionization from spark shock wave in laser beam 03 p0379 A66-13308  
 Atomic beam lasers, particularly for population inversion in levels of optical transition 03 p0380 A66-13311  
 Laser with diffraction limited radiation pattern 03 p0380 A66-13313  
 Measuring device for pulsed laser output power using bolometer, amplifier and oscilloscope 04 p0520 A66-13888  
 Experiments on helium-neon FM lasers covering phase-locked and FM region power output, modulation index and distortion experiments 04 p0530 A66-13955  
 Construction problems of continuous-duty DC excited ion lasers 04 p0530 A66-13956  
 Laser oscillations and self Q-switching, discussing pulsed flash-lamp excitation experiments with triply activated confocal barium crown glass etalon 04 p0531 A66-13980

High power Brewster window laser with gas fills, discussing power output and efficiency parameters 04 p0531 A66-13983  
 Static characteristics of gas laser internal modulation circuit, using electro-optical crystal inserted into gas laser resonator 04 p0531 A66-14059  
 Fractures in neodymium-doped alkaline silicates and borosilicates produced by laser beam 04 p0532 A66-14174  
 Conical emission in ruby lasers with exterior mirrors 04 p0532 A66-14278  
 Spikefree emission from laser using long ruby crystal doped heavily with chromium and suitable symmetry for pump radiation 04 p0533 A66-14331  
 Rise time and output power of single pulse in He-Ne laser measured by method of changing Q-factor by plate located in resonant cavity 04 p0533 A66-14332  
 Interaction of light pulse from ruby laser with mercury surface, observing mechanical impact believed to be rapid vaporization process 04 p0533 A66-14373  
 Laser beam use in biology and medicine, noting interaction of electromagnetic radiation with biological systems, hazards, diagnostics, therapeutics, etc 04 p0534 A66-14455  
 Plasma generation by focusing laser beam in air at atmospheric pressure and room temperature indicate connection with luminous energy absorption during breakdown 05 p0692 A66-14538  
 Minority carrier lifetime in silicon measured by contactless method, using laser induced modulation of IR transmission in silicon /LIMIRIS/ effect 05 p0729 A66-14563  
 Gallium arsenide p-n junction laser diode covering injection current distribution, density and emission spectra variation 05 p0692 A66-14659  
 Thomson scattering measurements of magnetic annular shock tube plasmas using Q-switched ruby laser light beam 05 p0680 A66-14707  
 Rise of junction temperature during continuous operation of GaAs injection laser 05 p0692 A66-14771  
 Atmospheric breakdown limitations to optical maser propagation 05 p0632 A66-14837  
 Helium-neon laser output characteristics as function of laser parameters 05 p0694 A66-14897  
 Laser oscillation in calcium tungstate crystals activated with trivalent praseodymium 05 p0694 A66-14898  
 Stimulated Raman and Brillouin scattering for Stokes radiation parallel to laser beam in rectangular waveguide 05 p0694 A66-14901  
 Output spectra of argon ion laser in ring resonator and two mirror resonators 05 p0694 A66-14904  
 Ruby lasers discussing output characteristics, beam divergence, beat modes and respective experimental techniques 05 p0695 A66-14919  
 Photographic film used for quantitative measurements of intensity distribution in Q-switched laser beam 05 p0695 A66-14920  
 Electrodeless excitation of discharge in helium-neon gas laser tube applied to voice transmission 05 p0696 A66-14924  
 Fraunhofer pattern of laser light transmitted through optical fiber, noting spatial frequency of interference fringes between light waves 05 p0696 A66-14972  
 Laser oscillations of silicon tetrachloride, silicon tetrafluoride and ethyl silicate in gaseous discharge 05 p0696 A66-14973  
 Time dependent emission behavior of ruby laser discussing rate equations, Q-value, output power, steady state values, etc 05 p0696 A66-14981  
 Evolution of luminous zone of plasma generated by focusing laser beam in air 05 p0723 A66-15097  
 Airborne laser-radar light detection and ranging /LIDAR/ systems applied to detection of clear air turbulence /CAT/ 05 p0697 A66-15297  
 Propagation rate of high power laser light pulse in inversely populated medium 05 p0717 A66-15333  
 Optical range parametric amplification, describing power output experiment with glass-laser-excited potassium dihydrogen phosphate crystal 05 p0697 A66-15352

Modulation of laser light with composite Fabry-Perot resonator, using more than three multiple reflecting plates 05 p0698 A66-15836  
 Intensity distribution of radiation immediately after leaving laser and after focusing within lens, noting optimum focusing conditions 05 p0698 A66-15853  
 Optical-misalignment effect on threshold power of solid state laser and compensation via lens in resonator 05 p0698 A66-15854  
 Energy losses in ruby laser due to heat evolution during optical pumping, noting relation between energy absorption and population inversion 05 p0698 A66-15858  
 Powerful pulse of ruby laser emission generated by ultrasonic traveling wave diffraction modulator 05 p0698 A66-15861  
 Variation of scattering cross section with beam intensity for ruby laser light on atomic hydrogen 05 p0698 A66-15864  
 Dispersion resonator performance in ruby laser, showing generation of R sub 1 and R sub 2 lines 06 p0889 A66-16346  
 CW laser action in carbon dioxide-helium mixtures 06 p0890 A66-16385  
 Ruby laser noise radiation consisting of increased luminescence and laterally dispersed generation determined from energy level populations 06 p0891 A66-16628  
 Optical design of elliptical cavities and comparison of energy transfers from light source to ruby laser with cylindrical cavities 06 p0891 A66-16647  
 Laser communications link security against interception, examining frequency bandwidth for minimum SNR 06 p0891 A66-16650  
 Helium-neon gas lasers, discussing amplitude variation suppression technique 06 p0892 A66-16670  
 Regular periodic spiking in output of pulsed neodymium doped borate glass laser at pumping levels slightly above threshold 06 p0892 A66-16672  
 Life performance characteristics of uncoated ruby laser Q-switched by rotating prism forming end reflector of laser resonator 06 p0892 A66-16675  
 Ground state ESR saturation effect on ruby laser output frequency at cryogenic temperature 06 p0892 A66-16753  
 CW high-power carbon dioxide-nitrogen-helium laser operation, noting helium addition 06 p0892 A66-16754  
 Stimulated emission in indium arsenide shows excitation threshold low and light emission highly directional 06 p0893 A66-17026  
 Gas breakdown by laser can be accounted for by both microwave breakdown theory and inverse bremsstrahlung 06 p0893 A66-17040  
 Ionization under laser action extended to metals and dielectrics, noting influence on thresholds 06 p0893 A66-17065  
 Conventional flow visualization using laser light source [ATAA PAPER 66-127] 06 p0870 A66-17104  
 Light output from helium-neon gas maser photographed with and without intracavity modulation at locking frequency, using high speed rotating mirror 07 p1040 A66-17205  
 Fused silica output coupling component for laser system, using frustrated total internal reflection configuration 07 p1040 A66-17287  
 Recording sampling system for measuring energy incident on biological system exposed to laser beam 07 p1030 A66-17293  
 Laser radiation absorbed along slant paths, spectral line overlapping and center line shift with pressure variation 07 p1041 A66-17295  
 Temperature dependence of emission spectrum and threshold current in GaAs lasers 07 p1042 A66-17333  
 Excitation of semiconductor lasers by beam of fast electrons, discussing work of Shockley, Popov, Keldysh and Krokhin 07 p1043 A66-17337  
 Laser-beam scattering by individually introduced charged polystyrene spherical particles and droplets of naphthalene and water in combination 07 p1043 A66-17473  
 Oscillation spikes in quasi-continuous operation of ruby laser at room temperature, noting threshold pumping energy 07 p1043 A66-17532



- Compton scattering of laser photons, noting transformation into gamma radiation photons upon collision with high energy electrons 07 p1044 A66-17816
- Isotope shift, linewidth and precise wavelength of laser emission in ionized g 07 p1044 A66-18035
- Pulsed laser welding, wire-to-wire, sheet-to-sheet, circuit board, vacuum tube, etc 07 p1038 A66-18153
- Diffraction velocimeter detecting and measuring transverse movement of surface by sensing light backscattered by it when laser illuminated 07 p1044 A66-18333
- Electron energy spectra in neon, xenon and helium-neon laser discharges, calculating production and destruction rate parameters 07 p1045 A66-18354
- Stable single-frequency output from laser cavity obtained by filter method and resonance suppression 07 p1045 A66-18356
- Frequency stabilization of gas lasers, using atomic resonance and interferometers 07 p1045 A66-18357
- Time resolution of electron and ion emission produced by Q-switched ruby laser pulse focused on metal surface 07 p1045 A66-18358
- Replica techniques and electron and optical microscopy to study laser irradiated metal surfaces 07 p1052 A66-18393
- Organic cations effect on laser threshold of solutions of tetrakis form of europium benzoyltrifluoroacetate 07 p1046 A66-18418
- Laser action on rotational transitions of  $10_0-9_8$ ,  $8-7$ ,  $7-6$  and  $6-5$  vibrational bands of ground electronic state 07 p1046 A66-18424
- Intensity fluctuations in output of four-level CW laser oscillators by linearized rate equations 07 p1047 A66-18434
- Peak irradiance of optical pump and total pump-energy incident upon laser crystal determined, accounting for temperature variation effects 07 p1047 A66-18487
- Helium-neon gas discharge intensification for 6328A laser wavelength, discussing measurement techniques, gain parameters and results 08 p1232 A66-18632
- Statistical model of random quasi-sinusoidal function of constant amplitude represented by emission of laser or radio transmitter 08 p1244 A66-18637
- Laser development, discussing basic theory, pumping methods and laser types 08 p1233 A66-18700
- Cross section measurement for electromagnetic backscattering of laser beams from rough aluminum and magnesium oxide surfaces 08 p1182 A66-18930
- Laser with neodymium-glass Q-factor modulation 08 p1233 A66-18970
- Heating by laser beam with application to lithium, noting use for high temperature plasma production 08 p1233 A66-18972
- Higher order calculation of laser output, noting approximation method for linewidth parameter and Lamb dip shape 08 p1233 A66-19063
- Correlation factor for induced radiation frequency shifts and crystal temperature variations in ruby laser 08 p1233 A66-19269
- Gas laser emission solution by determining emission field density dependence on resonator parameters, relaxation characteristics and atom excitation in gas discharge plasma 08 p1234 A66-19271
- Laser regime with giant pulses generated in dysprosium doped cadmium fluoride under continuous pumping by xenon lamps, obtaining Q factor modulation by rotating prism 08 p1234 A66-19376
- Threshold parameters and spectral composition of radiation of neodymium-glass laser in dispersion 08 p1234 A66-19669
- Micromachining with pulsed helium-neon gas laser, noting experimental techniques, operation and application 08 p1232 A66-19734
- Decay time of regular spiking in ruby laser in nearly concentric cavity and photomixing of light output 08 p1235 A66-19812
- Wavelength change of spontaneous and stimulated emission with uniaxial pressure under CW operation of GaAs diode laser at 4 degrees K 09 p1385 A66-19922
- Optically biased pulsed transmission mode operation of Q-switched laser, in connection with Kerr cells inhibiting lasing action 09 p1386 A66-19937
- Sharply directional coherent radiation generation by synchronized lasers or multimirrored resonator of single laser 09 p1386 A66-19945
- Spark discharge in air induced by focusing laser radiation, determining temperature of plasma produced near focus 09 p1386 A66-19959
- Induced radiation at high photon densities, noting applicability of perturbation theory to multiphoton resonance radiation of lasers 09 p1386 A66-20344
- Output power of CW laser measured by wire bolometer in form of plane single-layer spiral as sensitive element 09 p1381 A66-20364
- Effect of load mismatch on laser output, determining nonlinear dependence of equivalent negative conductance as function of oscillation amplitude in laser resonator cavity 09 p1386 A66-20435
- Intense UV pumping effect on ruby laser output 09 p1387 A66-20519
- Solid state laser output exhibiting regular and irregular spikes analyzed through relaxation oscillations and classical physics 09 p1387 A66-20568
- Superconductors applied to magnets, lasers and MHD power generation 09 p1429 A66-20674
- Optical range parametric amplification, describing power output experiment with glass-laser-excited potassium dihydrogen phosphate crystal 09 p1387 A66-20893
- Laser radar as instrument to obtain operational meteorological information 10 p1540 A66-21067
- Isotope shift measurement for 6328 angstroms helium-neon laser transition 10 p1540 A66-21070
- Laser configuration generating single frequency radiation in single spatial mode with high output achieved by suppressing all resonances but one 10 p1541 A66-21250
- Dielectric cavity maser composed of ruby rod separating metal plates, noting strength saturation behavior, power output, etc 10 p1541 A66-21308
- Pump power dependence of ruby laser starting and stopping time predicted via rate equation analysis 10 p1541 A66-21309
- Spiking behavior of multimode ruby laser in spherical resonator, interpreting near-field patterns, frequency spectrum, etc 10 p1542 A66-21311
- Laser induced gas breakdown at high pressures, noting effect of plasma density on index of refraction via optical frequency resonance measurement 10 p1542 A66-21564
- CW laser action on triple state phosphorus-sulfur transition, using hydrogen sulfide-noble gas mixtures 10 p1543 A66-21577
- Effective mass in InAs and InSb from Landau shift of peak emission in laser diodes 10 p1543 A66-21579
- Carnahan proposed first order ether drift experiment using two lasers shown to be of second order nature, noting role of phase shifts 10 p1543 A66-21656
- Ionization phenomena in argon due to laser radiation by measuring electron density and energy as time function after laser pulse initiation at different gas pressures and preionized conditions 10 p1565 A66-21690
- [AIAA PAPER 66-176] 10 p1565 A66-21690
- Threshold parameters and spectral composition of radiation of neodymium-glass laser in dispersion 10 p1543 A66-21836
- Silicon and selenium doping effects on gallium arsenide laser characteristics 10 p1543 A66-21879
- Soviet and foreign papers on plasma diagnostics by scattering of laser beams at plasma electrons 10 p1569 A66-21990
- Second harmonic generation by laser beams of finite spectral width, using quantum transitions and kinetic equations, noting shape of pumping line at fundamental frequency 10 p1544 A66-22026
- Degree of excitation of metastable state determined, using luminescence saturation phenomenon, calculating population of working level of laser substance 10 p1544 A66-22027
- Measurement of radiation pattern of ruby laser emission for various resonators and operating regimes, noting laser effect on angular half-width values 10 p1544 A66-22028
- High sensitivity fast-response laser detection system, describing microwave response photoelectric detector with amplification and mixing functions 10 p1544 A66-22046
- Gallium arsenide laser excitation by fast electrons 10 p1544 A66-22146
- Plasma production by optical irradiation of gases and by solids, considering interaction of laser radiation with surfaces and irradiation of particles of solid material in vacuum [AIAA PAPER 66-174] 11 p1742 A66-22212
- Dispersion resonator performance in ruby laser, showing generation of R sub 1 and R sub 2 lines 11 p1711 A66-22345
- Equations obtained from Hamiltonian for coupling, first Stokes line, first anti-Stokes line and coherent field for Raman laser 11 p1711 A66-22490
- Wavelength measurement of helium-neon laser emission by double-channel recording interferometer, using krypton-86 primary standard 11 p1712 A66-22874
- Optical diffraction velocimeter, using backscattered laser light to measure relative velocity between light source and surface 11 p1706 A66-22958
- Moon shape determined by measuring distance from lunar surface points to lunar center of mass, using optical laser radar 11 p1774 A66-22964
- Design and operation of helium-neon laser noting radiation, frequency structure, power density, external magnetic field effect, application, etc 11 p1713 A66-22980
- He-Ne laser IR radiation emission attenuated by atmospheric methane 11 p1657 A66-23090
- Current and voltage distribution over length of HF discharge in helium-neon laser 11 p1714 A66-23309
- Mach-Zehnder laser interferometer as diagnostic tool in shock tube experiments 11 p1714 A66-23352
- Carbon and ethylene tetrachloride ultrasonic modulators applied to IR laser heterodyne experiments on InAs photodiode 11 p1714 A66-23353
- Laser action on rotational line in carbon dioxide and nitrous oxide vibrational spectra in both P and R branches up to J values of over 50 11 p1714 A66-23357
- Efficient conversion of electrical energy into laser radiation, using coaxial optical pump 11 p1715 A66-23479
- Single pulse operation of lasers, noting energy storage and amplification effect for four- and three-level active medium 12 p1889 A66-23667
- Laser ranging via digital counter coupled photomultiplier tube, noting spectral response, gain transit time dependence, output coupling and effective cathode diameter 12 p1830 A66-23759
- Spatial amplitude of field of ideally parallel laser beam focused by optical systems with spherical aberration 12 p1889 A66-23778
- Laser application and techniques noting amplification, modulation, interferometry, scattering, plasma diagnostics, nonlinear optics, etc 12 p1889 A66-23931
- Polish-made He-Ne red gas lasers, describing power outputs, gas pressure, He/Ne ratio, mirror transmission coefficient and interferometric application 12 p1889 A66-23946
- Cadmium telluride laser with electron excitation 12 p1890 A66-24009
- Optically pumped rubidium 87 maser oscillator 12 p1890 A66-24124
- Focused energy techniques for joining, including laser welding [ASTME PREPRINT AD66-718] 12 p1886 A66-24413
- Laser welding for production microwelding, noting design, construction and application [ASTME PREPRINT MM66-707] 12 p1886 A66-24415
- Spatially independent laser rate equation generalized for multimode effects, noting steady state oscillation threshold singularities, spiking parameters,



etc 12 p1891 A66-24560  
 Steady state value of inverted population, power output, threshold behavior and spiking characteristics for single-mode laser when radiation intensity has spatial dependence 12 p1891 A66-24562  
 Pulsed induced emission in hydrogen beam laser for case of two relaxation times, determining polarization only by number of active particles in resonator 12 p1891 A66-24884  
 Dependence of emission intensity of gas laser on longitudinal and transverse magnetic fields, using simplified model 12 p1891 A66-24885  
 Treatment of steel with laser beam, obtaining precision holes without affecting microhardness of metal 12 p1888 A66-24898  
 Correlation functions of amplitude and intensity fluctuation for laser model near threshold obtained by using distribution functions evaluated by Fokker-Planck equation, treating amplitude as random variable 12 p1892 A66-25018  
 Segmented-rod ruby laser structure operated as giant pulse laser, using Kerr cell to provide Q-switching, noting number of oscillating modes 13 p2088 A66-25038  
 Ruby laser amplifier dynamics, noting amplification in energy gain regimes and correlation to theoretical equations 13 p2089 A66-25049  
 Formation of ultrasonically gated giant laser pulses by Q-spilling, noting photographs of ruby and role of cavitation in gating mechanism 13 p2089 A66-25057  
 Traveling wave beats created by ring laser on rotating platform, noting frequency division rotating rate and capture band parameters 13 p2089 A66-25102  
 Frequency shift in resonance transition induced in potassium vapor by ruby laser pulse 13 p2089 A66-25103  
 Holograms and wavefront reconstruction techniques involving prismatic refraction of monochromatic and coherent laser light causing interference pattern on photographic emulsion 13 p2076 A66-25144  
 Cavity loss and optimum reflectivity of output mirror in ruby laser with external mirror 13 p2089 A66-25187  
 Angular distribution of stimulated Raman radiation, discussing axial and off-axial Stokes and surface radiation mechanism 13 p2090 A66-25189  
 Optical resonator diffraction loss, noting laser oscillations in high loss arrangements, output beam power, field patterns, etc 13 p2090 A66-25195  
 Laser producing two or three light pulses in sequence with interval between pulses mechanically controlled by optical wedge inserted into resonator 13 p2090 A66-25322  
 Adjustment procedure for laser with polygonal resonator, noting spatial mirror adjustment in addition to angular adjustment 13 p2090 A66-25323  
 Effective diffusion cross section of ultrasonic and laser beam while acting on turbulent flow 13 p2062 A66-25404  
 IR laser radiation with power of 5.7 watts in vicinity of 10.69  $\mu$ m in sealed tube containing pure carbon dioxide excited by AC or DC current 13 p2131 A66-25410  
 Second harmonic generated by transmitting laser radiation through tellurium monocrystal, while filtering out fundamental frequency 13 p2090 A66-25437  
 Optical excitation in indium arsenide and gallium antimonide yielding laser radiation 13 p2090 A66-25438  
 Energy spectra of ions emitted by beryllium, carbon and molybdenum heated by laser 13 p2131 A66-25479  
 Neodymium doped YAG crystal and lithium meta niobate as CW laser materials and potassium tantalum niobate as optical modulator material 13 p2164 A66-25518  
 Optical ray tracing to predict focusing characteristics of laser light in refractive targets, calculating heating effects in target, noting target geometry, refractive index, thickness of skin layers, etc 13 p2090 A66-25531  
 Coherent light recording/reproducing techniques based on Debye theory of coherent light source focusing 13 p2091 A66-25541

Output power of 6328 angstrom He-Ne gas laser as function of laser gain, cavity loss and output coupling 13 p2091 A66-25651  
 Alignment of laser mirrors using gas laser with highly collimated beam of small diameter 13 p2092 A66-25824  
 Gallium arsenide p-n junction laser diode, injection current distribution, density and emission spectra variation 13 p2092 A66-25934  
 Sensitivity and tracking capabilities of precision laser automatic tracking system 13 p2025 A66-25984  
 Laser pumping by intense noble gas discharge in zeta-pinch geometry 13 p2092 A66-25995  
 Spectroscopy of lithium fluoride crystals activated with uranium trioxide for laser action, showing anomalous fluorescent decay under high intensity pumping 13 p2092 A66-25997  
 Elliptic cavity design for solid state lasers, discussing multiple reflections, absorption coefficient, refraction losses, etc 13 p2092 A66-25998  
 Optical length variations in laser amplifiers determined during pumping and amplification, using interferometry 13 p2092 A66-25999  
 Photographic copies of holograms taken with laser light noting film, light source, directional effect, processing, etc 13 p2081 A66-26000  
 Microwave models of optical resonators, discussing correction of discrepancies resulting from approximations in measurements 13 p2093 A66-26006  
 Amplification of interaction of atoms and of pulsed or periodic cooling of transparent media produced by laser beam, noting changes in kinetic energy of atoms 13 p2093 A66-26021  
 Automodulation of emission from solid state laser 13 p2093 A66-26041  
 Helium-neon laser multibeam generation in gas discharge tube, using spherical mirrors and tapered plates 13 p2093 A66-26053  
 Magnetization induced by circularly polarized laser light incident on nonabsorbing material, in absence of external magnetic field, in doped calcium fluoride proportional to light intensity and Verdet constant 13 p2131 A66-26142  
 Second harmonic generation of light analyzed, stressing saturation effects occurring at high laser power, solving nonlinear Maxwell equations 13 p2096 A66-26144  
 Light frequency multipliers for nonlinear optical effects at various wavelengths, considering focusing, laser beam finite divergence, air breakdown, stimulated Raman emission, etc 13 p2096 A66-26146  
 Nonlinear light scattering in pressurized methane, noting displacement of spectral line from laser frequency 13 p2132 A66-26148  
 Nonlinear susceptibility describing second harmonic generation of light measured in semiconductors with zinc-blende symmetry, using quantum mechanics and laser wavelength 13 p2168 A66-26149  
 Cross section for inelastic scattering of electromagnetic radiation by electron density fluctuations in anisotropic solids, using laser sources, investigating Landau and collision damping of plasmons 13 p2132 A66-26153  
 Scattering of electron beam by standing waves of photons inside laser cavity corresponds to stimulated Compton effect 13 p2096 A66-26155  
 Effect of fluctuating laser pump on stimulated Raman scattering, noting growth of coupled Stokes-anti-Stokes waves in presence of two-mode pump 13 p2096 A66-26158  
 Absorption spectra in optical region when laser radiation and continuous radiation are simultaneously incident on molecular medium 13 p2133 A66-26161  
 Interaction between stimulated Brillouin and Raman scattering in carbon sulfide, using optical resonator and laser beam 13 p2097 A66-26162  
 Velocity and lifetime of microwave thermal phonons in liquids and solids determined by spectrum of light scattering from laser illuminated sample 13 p2133 A66-26166  
 Excitation radiation transfer from trivalent

chromium to neodymium examined via fluorescence spectroscopy, noting energy transfer parameters and effect on laser output 13 p2098 A66-26175  
 Photoluminescence and stimulated emission of gallium arsenide and indium antimonide obtained by optical pumping, noting effect of applied magnetic field on laser and diode emissions 13 p2099 A66-26182  
 Steady state variation of light intensity with distance for monochromatic light, noting dependence of absorption coefficient on degree of excitation of electronic system 13 p2099 A66-26183  
 Electrical breakdown of gases by optical frequency radiation, noting laser beam attenuation and subsequent energy absorption by plasma 13 p2134 A66-26190  
 Growth rate of ionization by electron impact in presence of laser beam, elastic and inelastic scattering cross sections, free-free absorption, excitation and ionization coefficients, breakdown times and thresholds 13 p2134 A66-26193  
 Pressure effects in Fabry-Perot lossy-cavity gas laser output 13 p2101 A66-26199  
 Threshold studies of ion laser oscillations in sulfur and saturation and quenching of laser intensity 13 p2102 A66-26209  
 Optical system for schlieren recording, deflection mapping, shadowgraphy and interferometry achieved for laser light, used in recording of refractive index fields 13 p2082 A66-26307  
 Magnitude and phase of complex spatial coherence of He-Ne laser beam 13 p2104 A66-26334  
 Helium-neon laser emission on 6401 angstrom line, noting intensity vs mirror shift and optical cavity 13 p2104 A66-26336  
 Self-pumping chemical laser theory and operation, noting chemical pumping 13 p2104 A66-26382  
 Cooler for semiconductor lasers and photodetectors using low temperature gas 13 p2104 A66-26559  
 Alignment of angular positions of spherical mirror and grating of Fastie-Ebert spectrometer, using bright collimated monochromatic beam of He-Ne laser 13 p2084 A66-26564  
 Maximum output power approximated for 6328 angstrom He-Ne gas laser, noting optimum mirror transmission and laser geometry 13 p2105 A66-26571  
 Mathematical model of GaAs injection laser applied in determining maximum obtainable power output, using rate equations of electron and photon densities and thermal resistance for optimum value 13 p2105 A66-26572  
 Cataphoresis, moving striations and associated noise in He-Ne laser 13 p2105 A66-26591  
 IR and visible helium-neon laser modulation using Faraday rotation in YIG 14 p2305 A66-26881  
 Laser oscillations in CdSe and CdS bombarded by fast electron beam 14 p2306 A66-27031  
 Laser Doppler velocimeter for measuring localized flow velocities in liquids 14 p2306 A66-27053  
 Ruby laser energy reflected off Explorer XXII satellite 14 p2306 A66-27054  
 Laser radiation coherence property deterioration and molecular scattering during propagation through turbulent atmosphere 14 p2236 A66-27131  
 Effect of longitudinal magnetic field on output power of gas laser operating in IR spectrum, noting gas-mixture pressure in discharge tube role 14 p2307 A66-27156  
 Semiconductor GaAs quantum generator with two-photon absorption of neodymium laser emission 14 p2307 A66-27187  
 Pumping neodymium lasers through use of coherent emission of ruby lasers, finding threshold energy 14 p2308 A66-27605  
 Energy-rich plasmas produced by light pulses from Q-switched laser, noting energy transfer from electrons to ions during expansion process 14 p2308 A66-27607  
 Time parameters of powerful laser measured with GaAs photodiode, noting time constant and time resolution of photodiode 14 p2309 A66-27750



Laser safety standards, discussing nature of photobiological mechanisms responsible for tissue damage upon exposure to laser radiation 14 p2309 A66-27775

Fluorescent lifetimes of neodymium, ytterbium and samarium incorporated in ordered perovskite-type compounds determined, noting crystal structure potential for laser emission 14 p2367 A66-27976

Performance of two-photon laser operating in continuous wave mode, deriving formula for pulse frequency 14 p2310 A66-28166

Electrostatic probe measurements of velocity displacement and electron density of plasma using laser compared with measurements using microwave interferometer 14 p2346 A66-28269

Measurements of maser beam propagated through atmosphere, emphasizing beam broadening and signal fluctuation due to clear air turbulence 15 p2448 A66-28581

Atmospheric exploration with lidar, noting high resolution and sensitivity 15 p2530 A66-28600

Light transmission through optical diffraction lattice consisting of medium in EM field of laser beam 15 p2511 A66-28626

Electron density in laser-induced spark in air determined, measuring simultaneously fundamental laser wavelength and second harmonic 15 p2512 A66-28685

Coherent emission from trivalent holmium ions in rare earth substituted yttrium aluminum garnet, noting three energy transfer combinations in YAG 15 p2512 A66-28690

Measurement of single line in P branch of carbon dioxide vibro-rotational absorption band using tuned optical maser spectroscopy, noting presence of shifted frequencies 15 p2512 A66-28691

Radiative cascade patterns in helium-neon gas system using idealized model, computing spontaneous decays which are compared with laser experiments 15 p2512 A66-28699

Temperature shift of ruby laser emission measured interferometrically for temperatures between 66 and 210 degrees K 15 p2512 A66-28701

Damage thresholds for various glasses exposed to laser pulses, emphasizing internal damage 15 p2524 A66-28732

Intensity distribution at focus of high power laser, noting measuring method 15 p2513 A66-28834

Gas laser output wavelength stabilization by use of external passive optical interferometer 15 p2513 A66-28835

Pulsed toroidal excitation of gas ion lasers extended to drive high power CW laser transitions in Ar, Kr, Cl and Br, noting operating parameters and power output 15 p2513 A66-28877

CW IR laser oscillation in atomic Cl in HCl and HI gas discharges, noting use of two power supplies and energy level diagram 15 p2513 A66-28880

Stimulated Raman effect in acetone and acetone-carbon disulfide mixtures, noting similarity of Stokes radiation pattern to Raman effect 15 p2513 A66-28881

Dependence of magnitude of Herschel bleaching in photographic emulsion on delay between forward and bleaching exposure, using laser radiation 15 p2513 A66-28884

118-micron wavelength water vapor gas laser with 4-inch diameter two-meter focal length mirror resonator system 15 p2514 A66-29010

Surface temperature determination procedure for laser heated metals based on heat conduction equations and ion emission from surface 15 p2514 A66-29035

Resonator geometry and mirror positions and effect on radiation output in helium-neon laser 15 p2515 A66-29201

Spectral composition of laser light within framework of theory of nonlinear optical effects 15 p2542 A66-29356

Relation between laser parameters and cathode diameter in excitation of He-Ne mixture by discharge of hollow cylinder 15 p2516 A66-29357

Hole burning in bleachable absorbers used as laser Q-spoller 15 p2517 A66-29387

Laser oscillation with totally reflecting roof prism as cavity, noting output vs

mirror alignment for two rotation axes 15 p2517 A66-29414

Pulsed laser operation in wedge-shaped ruby rod at room temperature 15 p2517 A66-29415

Neon level broadening under effect of laser radiation studied by observing Hanle effect on fluorescent light 15 p2517 A66-29640

Detection of very low levels of modulation on laser beam to determine performance of microwave light modulators 15 p2518 A66-29682

Measuring device for pulsed laser output power using bolometer, amplifier and oscilloscope 15 p2503 A66-29701

Dynamics of field and generation frequencies in giant pulse of ruby laser with passive shutter, using solution of cryptocyanine in ethanol, noting mirror reflection coefficient 15 p2518 A66-29727

Output power frequency response of single mode helium neon laser, determining effects of atomic collisions on frequency response of individual atoms 15 p2518 A66-29812

Statistical analysis of light fields created by superposition of laser light and chaotic light 15 p2519 A66-29815

Second harmonic generation /SHG/ by focused laser beams in nonlinear crystals 15 p2519 A66-29816

Coupling and synchronization of lasers, noting field amplitudes, delayed interaction and dielectric constant dispersion 15 p2519 A66-29885

Propagation rate of high power laser light pulse in inversely populated medium 15 p2543 A66-29980

Cooperative interactions between ions and electrons in forward scattering of ruby laser beam from plasma 16 p2716 A66-30153

Unmodulated laser output at controlled frequency, using correcting beats from reference laser 16 p2717 A66-30205

Traveling wave beats created by ring laser on rotating platform, noting frequency division rotating rate and capture band parameters 16 p2717 A66-30281

Frequency shift in resonance transition induced in potassium vapor by ruby laser pulse 16 p2717 A66-30282

Laser action with nonresonant feedback using high gain ruby crystals 16 p2717 A66-30297

Writing rate of rotating-mirror streak camera determined, using Q-switched laser technique 16 p2702 A66-30419

Topocentric distance of geodetic satellite GEOS-A measured by laser telemetry from station 16 p2652 A66-30586

Demodulation method in which phase modulation of laser beam is converted to amplitude modulation by autocorrelation 16 p2717 A66-30616

Radiative corrections to Thomson scattering in laser beams arising from damping of electron motion and photon density, using quantum mechanics 16 p2717 A66-30628

High speed stroboscopic photography using Kerr cell modulated laser source 16 p2705 A66-30828

Second harmonic generation by laser beams of finite spectral width, using quantum transitions and kinetic equations, noting shape of pumping line at fundamental frequency 16 p2718 A66-30845

Degree of excitation of metastable state determined, using luminescence saturation phenomenon, calculating population of working level of laser substance 16 p2718 A66-30846

Measurement of radiation pattern of ruby laser emission for various resonators and operating regimes, noting laser effect on angular half-width values 16 p2718 A66-30847

Breakdown by neodymium glass laser radiation in atomic and molecular gases, determining power densities, noting relation of pressure to breakdown power 16 p2718 A66-30938

Dislocations and precipitates in GaAs injection lasers revealed by new A-B etchant 16 p2718 A66-31071

Collision broadened linewidth and saturation parameters for 6328 angstrom transition of Ne in He-Ne laser 16 p2718 A66-31084

Time resolution of laser-induced electron emission from cesium diode at high laser power 16 p2719 A66-31135

Statistical effects during generation of second harmonic in optically transparent crystals, noting coefficient of correlation between harmonic and fundamental radiation power of solid state laser 16 p2747 A66-31167

Recording of light-induced light scattering using laser beam, calculating cross section of photon-photon scattering 16 p2748 A66-31175

Giant coherent light pulse generation by Q-factor-modulated laser 16 p2719 A66-31183

Initial pulse in luminous emission of discharge laser, using photomultiplier preceded by mobile iris, determining geometrical distribution of discharge brightness 16 p2719 A66-31209

Laser beam energy profile determined by multiple-layer aluminum foil technique 16 p2719 A66-31217

Effects and parameters influencing optical path length within pumping process in ruby and doped glass laser rods 16 p2719 A66-31443

High voltage pulsed electrodeless discharge in rare gas as light source for ruby and Nd glass laser excitation and observation of output characteristics 16 p2720 A66-31448

Laser cavity output optimization for maximum external quantum efficiency showing dependence on length and reflectivity for given current density 16 p2720 A66-31535

Laser induced spontaneous electron emission from rear side of metal foils, noting electron energy vs laser energy pulse magnitude, etc 16 p2784 A66-31536

Granularity characteristics of scattered light from helium-neon laser directed onto moving surface 16 p2720 A66-31725

Near-field diffraction of helium-neon laser at circular apertures 16 p2720 A66-31727

Laser beam effect on hardening of steel 16 p2721 A66-31802

Breakdown of gases under influence of laser spark phenomena with subsequent absorption of laser radiation and gas heating 17 p2933 A66-32061

Static characteristics of gas laser internal modulation circuit, using electro-optical crystal inserted into gas laser resonator 17 p2933 A66-32225

Laser and maser development, discussing design improvements and application for television, space communications, etc 17 p2934 A66-32353

Nonlinear scattering of ruby laser beam by plasma at second and third harmonic 17 p2967 A66-32433

Sun pumped continuous wave one-watt YAG crystal laser, noting equipment setup and output duration 17 p2934 A66-32620

Internal phase modulation in He-Ne laser using electro-optic effect in crystal quartz, observing spectrum and RF mode beats 17 p2934 A66-32621

Frequency shift relative to spectral width for single pulses of triggered laser determined by measuring variations of emitted wavelength as function of time 17 p2934 A66-32622

Stimulated Brillouin scattering from nitrogen and methane using giant pulse laser, noting convergence angle of backscattered beam sound, velocity measurement, etc 17 p2961 A66-32627

Heat transfer and stress wave evolution prior to ablation and thermal equilibrium in exposure of solid and liquid materials to laser sources 17 p2979 A66-32638

Intensity noise in multimode GaAs laser emission 17 p2935 A66-32689

Power enhancement in pulsed He-Ne lasers, noting overshooting for RF discharge modulation with square wave 17 p2935 A66-32963

Resonator geometry and mirror positions and effect on radiation output in helium-neon laser 17 p2935 A66-33050

Strong axial magnetic field effect on constant current discharge in continuous-duty ion laser, noting plasma diffusion, charged particle density and laser output decrease 17 p2936 A66-33117

Ion lasers involving electron transitions in atoms or molecules with lost



electrons 17 p2937 A66-33249  
Far IR radiation detected at visible frequency, using nonlinear optical mixing with lasers 17 p2959 A66-33322  
Low threshold neodymium glass laser oscillator with high repetition 17 p2937 A66-33325  
High power continuous wave four-level solid neodymium glass laser showing length and host loss as dominant factors in limiting output power 17 p2937 A66-33334  
Experimental study of emission control in ruby laser using diffraction modulator with modulated traveling ultrasonic wave 17 p2938 A66-33516  
Optical modulation in bulk gallium arsenide, using Gunn effect 18 p3152 A66-33606  
Ionized noble gas lasers, considering problems at higher powers, especially those of inversion mechanism and magnetic field effects 18 p3118 A66-33767  
Communication systems at microwave and optical frequencies for future Mars missions 18 p3067 A66-33793  
Qualitative results on transport mechanisms around dropping mercury electrode, using long path laser interferometry 18 p3110 A66-33924  
Photoconductivity induced in uncolored sodium chloride and aluminum oxide single crystals by radiation from ruby laser 18 p3154 A66-33939  
Ruby photoconductivity when exposed to laser irradiation, noting oscillograms 18 p3154 A66-33941  
Laser action on several hyperfine transitions in Mn I 18 p3118 A66-34000  
Coherent and spontaneous emission from lead-tin telluride alloys upon excitation by GaAs diode laser, noting band structure of alloy system 18 p3119 A66-34159  
Laser regime with giant pulses generated in dysprosium doped cadmium fluoride under continuous pumping by xenon lamps, obtaining Q factor modulation by rotating prism 18 p3119 A66-34178  
Ne-He laser output dependence on pressure and nonexcited atom concentration 18 p3119 A66-34696  
Energy and power of Q-switched neodymium glass laser measured, using calorimetric devices, vacuum photodiodes, etc 18 p3120 A66-34904  
Soviet and foreign papers on plasma diagnostics by scattering of laser beams at plasma electrons 18 p3150 A66-34967  
Holography principles and development, considering wave front reconstruction, Lippmann photography, laser light, application to TV, etc 18 p3115 A66-35244  
Output power of CW laser measured by wire bolometer in form of plane single-layer spiral as sensitive element 19 p3353 A66-35321  
Helium-neon laser assessment as source in high precision range measurements 19 p3372 A66-35362  
Light energy measurements made with argon bomb used as chemically powered laser pump 19 p3373 A66-35388  
CW He-Ne laser measurement of light scattering in crystals noting laser output, performance and crystal imperfections 19 p3373 A66-35402  
Orientation effect in GaAs injection lasers, noting emission characteristics and structural spectra 19 p3373 A66-35404  
Laser action in closed molecular system with mixture of carbon dioxide, nitrogen and water vapor, noting coupling-out plate reflectivity and population inversion 19 p3373 A66-35433  
Laser illuminated electro-optical imaging noting energy variation parameters, equipment used and results obtained in TV reception 19 p3355 A66-35531  
Multicolor laser display, discussing components and future application 19 p3355 A66-35532  
Ring laser sensor parameters and characteristics, noting application to measurement of angular rate, mass flow, navigation and guidance 19 p3356 A66-35533  
Spatial coherence measurement of He-Ne laser output 19 p3373 A66-35592  
Laser application for vibration measurement utilizing Doppler shift

produced on wave reflected from surface vibrating normal to beam 19 p3356 A66-35673  
path 19 p3356 A66-35673  
Gallium arsenide laser excitation by fast electrons 19 p3374 A66-35760  
Laser application survey 19 p3374 A66-35798  
Plasma density using laser based interferometer, interpreting phase shift of laser signal as time dependent laser frequency variation 19 p3374 A66-35817  
Laser output energy controller having eight-to-one improvement in pulse repeatability in solid state lasers 19 p3374 A66-36034  
Valence band spin-orbit splitting in highly degenerate semiconductors determined from splitting of peak laser diode emission in high magnetic fields 19 p3374 A66-36036  
Resonant birefringence in potassium vapor under influence of electric field of ruby laser emission 19 p3375 A66-36066  
Gallium arsenide lasers operating at room temperature investigated, based on diffusion p-n junctions, discussing emission spectrum 19 p3375 A66-36070  
Pulsed discharges of OCS molecular laser 19 p3375 A66-36080  
Measurements on physical and laser properties of vapor-grown ruby single crystals prepared by epitaxial growth 19 p3375 A66-36081  
Coherent laser-type light generators with capability of adjusting frequency over visible spectrum 19 p3375 A66-36265  
Plasma production by firing giant pulse laser at solid deuterium pellet /ice/, noting strong anisotropy in plasma outburst 19 p3432 A66-36595  
High temperature high-density plasma from single solid particle of lithium hydride suspended in vacuum, using ruby laser irradiation 19 p3432 A66-36596  
Fast overlap of microwave radiation by ionization aureole of spark in laser beam 19 p3376 A66-36719  
Multiphoton ionization of krypton and argon by ruby laser radiation may occur by absorption 19 p3403 A66-36721  
Gated laser night-viewing system, calculating apparent illuminance as function of target distance 20 p3511 A66-36938  
Pulsed ruby lasers, considering pumping and threshold, output, quantum mechanics and variation on basic device 20 p3575 A66-36968  
Frequency spectrum of laser impulse in Q-switching regime wider than that of single impulse radiated by laser in ordinary regime 20 p3576 A66-37141  
Solid laser radiation operating in Q-switched resonator regime noting effect of finite rate of switching, finiteness of relaxation time, transmission coefficient factor, etc 20 p3576 A66-37142  
Two-photon laser excitation conditions deteriorated by presence of resonator tuned on transition frequency between operating levels of matter 20 p3576 A66-37143  
Frequency doubling in resonance laser, obtaining second harmonic field for laser radiation by giant pulses 20 p3576 A66-37144  
High time resolution polarimeter for laser analysis, beam intensity after passing through analyzers measured by photomultipliers 20 p3558 A66-37285  
Q-switched ruby laser output increased by use of saturable dye solution in laser cavity 20 p3576 A66-37290  
Spectral composition of laser light within framework of theory of nonlinear optical effects 20 p3602 A66-37360  
Relation between laser parameters and cathode diameter in excitation of He-Ne mixture by discharge of hollow cylinder 20 p3576 A66-37361  
Giant pulse formation theory, measuring shape and duration of neodymium glass laser pulses for various values of inverse population 20 p3577 A66-37367  
Crystal growth, diffusion and fabrication of gallium arsenide-phosphide junction lasers with low threshold current densities 20 p3577 A66-37401  
Nonreciprocal effects associated with excitation current observed in DC-excited He-Ne ring laser, noting coupling phenomena between right and left waves 20 p3577 A66-37408

Magnitude of Hanle effect of neon atoms emitted by laser dependence on excitation, discharge intensity explained by multiple coherent diffusion at metastable level 20 p3577 A66-3740  
Optical techniques in laser detection systems 20 p3516 A66-3743  
Laser emission interferograms obtained with Fabry-Perot cross-grating interferometer in submillimeter wavelength range 20 p3559 A66-3754  
Submillimeter laser emission from ICH noting interferograms 20 p3578 A66-3754  
Single cavity microwave laser amplifier analysis, determining gain, bandwidth, noise cavity Q-factor effect and width of magnetic resonance line 20 p3578 A66-3758  
Identification of number of lines at 1 microns emitted from pulsed carbon dioxide laser as P branch of carbon dioxide vibrational transition 20 p3579 A66-3762  
Nonlinear interaction of oscillations of two types in laser does not effect stationary operation when oscillations are sufficiently apart in band 20 p3579 A66-3766  
Laser TV system operation, performance characteristics and application 20 p3517 A66-3774  
Pulsed operation of electron-beam pumped zinc oxide laser emitting radiation in UV at very low temperatures, noting importance of use of cavity 20 p3579 A66-3776  
Continuous wave UV ionized gas laser, emission over four transitions in neon krypton and argon 20 p3579 A66-3777  
Upper laser states deriving population through cascade transitions from higher layer states of argon ion noting consistency of laser output current dependence with current dependence of cascade rate 20 p3579 A66-3777  
Degradation of continuous argon laser performance when positioned in axial magnetic field, noting role of quenching radiation trapping and excitation mechanisms 20 p3579 A66-3777  
Photodissociation laser system, discussing output energy dependence on pressure, temperature and number of successive optical pumping flashes 20 p3579 A66-3778  
Submillimeter wavelength electronic devices, examining development of lasers, and reflected wave tubes with overlapping effective wave range 20 p3580 A66-38004  
Stimulated emission spectrum in axial-mode model of plane resonator in stationary generation regime 20 p3580 A66-38127  
Trajectories of light rays through medium subjected to acoustic waves examined, knowing that acoustic waves in laser medium function as optical waveguide 20 p3580 A66-38238  
Discharge current and laser light noise measurements effect in gas discharge helium-neon laser, using equivalent circuit 20 p3580 A66-38240  
Frequency stabilization of gas laser to lock output to center of atomic resonance, using error signal 20 p3580 A66-38242  
High power nonspiking operation of ruby laser for continuous output on microscopic and macroscopic scale 20 p3581 A66-38242  
Confocal resonator theory instead of diffraction as explanation of 90 degree rotation between near and far fields of ruby lasers 20 p3581 A66-38243  
Spontaneous emission noise power added to amplified signal in laser amplifier in He-Xe gas discharge and saturation relation to population inversion 20 p3581 A66-38387  
Laser machining, discussing hole drilling, microwelding metal removal and application to hard brittle materials [ASME PAPER 66-MD-28] 21 p3742 A66-38484  
Unfocused ruby laser radiation field-biphenyl compound interaction, resulting luminescence and apparent multiphoton absorption 21 p3745 A66-38528  
Second-harmonic generation by focused laser beams based on experiments using He-Ne gas laser, noting SHG should be strongly peaked when focus is at either of crystal surfaces 21 p3746 A66-38554  
Fokker-Planck equation applied to laser under influence of quantum fluctuations connected with dissipation, pumping and cavity thermal noise, noting distribution and



correlation function 21 p3746 A66-38930  
 Performance of GaAs semiconductor laser with resonator, noting dependence of forbidden zone width and absorption coefficient on free carrier concentration and incident photon energy 21 p3746 A66-38955  
 Interchannel generation transfer and multichannel generation in laser with four splits levels, noting radiation density, temperature effect and variations in coefficients of losses 21 p3746 A66-38956  
 Modulation by ultrasonic diffraction of 10.6 micron laser radiation in photoelastic CdS, GaAs and Si crystals 21 p3747 A66-39112  
 Optical spectra of ultrashort optical pulses generated by mode-locked glass-doped neodymium lasers, considering saturable absorber cell placed parallel to Fabry-Perot reflector 21 p3747 A66-39115  
 Neodymium laser oscillator using time-variable reflector, noting loading and pumping of optical cavity with nearly maximum amount of energy 21 p3747 A66-39118  
 Photoconductive and luminescent behavior of undoped cadmium sulfide single crystals at room temperature under laser excitation 21 p3748 A66-39165  
 Molecular laser action by vibrational excitation of nitric oxide during flash photolysis of nitrosyl chloride 21 p3748 A66-39166  
 Laser amplifier theory using Fabry-Perot interferometer and Laplace transform for obtaining transient solutions in addition to steady state solutions 21 p3748 A66-39224  
 Gas laser frequency and emitted power dependence on resonator tuning 21 p3748 A66-39308  
 High frequency-stability EM wave source, applying thermal excitation methods to pencil quantum generator in IR region 21 p3749 A66-39336  
 Line width of well-stabilized laser operating far above threshold determined by phase random fluctuation, using interferometer 21 p3749 A66-39394  
 High frequency-stability EM wave source, applying thermal excitation methods to pencil quantum generator in IR region 22 p3929 A66-39706  
 Single pulse operation of lasers, noting energy storage and amplification effect for four- and three-level active medium 22 p3929 A66-39711  
 Replacement of Poisson by Polya distribution in calculating laser intensity threshold necessary to induce ionization breakdown in gases 22 p3929 A66-39715  
 Far-field light emission mode pattern of GaAs diode injection lasers, dielectric gradient in inversion layer and refractive index in junction 22 p3930 A66-39743  
 Laser radiation effect on metals, noting disintegration mechanism, indentation formation and vapor formation 22 p3930 A66-39763  
 Ruby laser pumping threshold energy, divergence angle and output power as affected by resonator length 22 p3930 A66-39769  
 Effective brightening of laser radiation propagating in strongly absorbing medium 22 p3930 A66-39770  
 Thermoelastic wave equations in continuum mechanics model of laser-induced fracture in transparent media in terms of laser beam energy absorption 22 p3931 A66-40089  
 Spectral hole burning and cross relaxation effects on steady state gain saturation of laser amplifier with inhomogeneously broadened linewidth 22 p3931 A66-40098  
 Intracavity interferometer laser measurements of power gain and output in single-frequency Ar laser and 6328-angstrom Ne isotope shift 22 p3932 A66-40110  
 Reflecting mirrors in laser oscillators treated as reflecting elements and transducers for coupling power from oscillator to external space 22 p3932 A66-40184  
 Temperature measurements of laser sparks from relative intensity of X-ray flux transmitted through beryllium foils of different thickness 22 p3933 A66-40421  
 Dynamic laser wavelength selection by insertion of dispersive tunable electro-optic Q-spoller within laser

cavity 22 p3933 A66-40866  
 Paschen series laser lines in atomic and molecular hydrogen 22 p3933 A66-40892  
 Spectral analysis of laser discharge in pure and impure He, obtaining spectra of spark at various pressures, determining electron concentration at various stages 22 p3934 A66-40946  
 Quantitative photographic determinations of laser beam power density distributions and Q-switched ruby oscillator-amplifier system divergence characteristics 23 p4075 A66-41032  
 Neodymium doped glass laser using saturable liquid Q-switch 23 p4075 A66-41033  
 Transients and stability of idealized two-level laser system, obtaining rate equation solution, noting characterization by relaxation times 23 p4076 A66-41034  
 Pulsed induced emission in hydrogen beam laser for case of two relaxation times, determining polarization only by number of active particles in resonator 23 p4076 A66-41091  
 Dependence of emission intensity of gas laser on longitudinal and transverse magnetic fields, using simplified model 23 p4076 A66-41092  
 Mercury, cesium and rubidium vapors ionization in intense radiation flux by Q-switched ruby laser 23 p4076 A66-41156  
 Internal self-damage in 25 mw ruby laser oscillator rod 23 p4076 A66-41160  
 Crystal defects and performance in ruby laser, measuring coherence function of light and output energy and crystal homogeneity 23 p4077 A66-41291  
 Master equation solved to obtain diagonal elements of density matrix for laser light, taking into account pumping scheme characterizing three-level laser 23 p4077 A66-41374  
 Laser beam effect on hydrodynamic bearings, discussing microcracks and critical energy, explaining breakdowns 23 p4078 A66-41409  
 Estimated greatest permissible mirror misalignment, active medium inhomogeneity and extra-axial beam losses for artificial realization of very narrow radiation pattern in real laser 23 p4078 A66-41449  
 Radiative power amplification of He-Ne laser with nearly confocal resonators 23 p4078 A66-41453  
 Linearly and circularly polarized fields in laser amplifier interaction with axial magnetic field, emphasizing combination tone production 23 p4079 A66-41624  
 Laser induced plasma density measurement using multiple beam interferometry 23 p4105 A66-41630  
 Multipurpose ultrahigh speed camera system, noting use as monosecond Kerr cell, image converter and giant laser pulse generator 23 p4071 A66-41675  
 Resonator misalignment effect on output of neon-helium laser with spherical mirrors 23 p4079 A66-41830  
 Transitions of first two band systems of iodine excited in argon suitable for laser action 23 p4079 A66-42085  
 Experimental study of emission control in ruby laser using diffraction modulator with modulated traveling ultrasonic wave 24 p4219 A66-42129  
 Conductivity modulation by heavy-to-light hole transitions in p-type germanium noting carrier lifetime and ringing of laser pulse 24 p4219 A66-42249  
 Time dependency of phase difference of two weakly coupled nonlinear optical oscillators, considering coupling of two traveling waves in laser 24 p4220 A66-42257  
 Q-switching laser system to obtain simultaneous giant pulses from five ruby laser oscillators 24 p4220 A66-42302  
 Giant pulse generation range in transverse direction after Q-switching in ruby laser, examining resonator properties 24 p4220 A66-42516  
 Multiple cyclotron resonance absorption lines in degenerate valence bands of Ge semiconductor studied with far IR laser submillimeter spectrometer 24 p4257 A66-42545  
 Linearized population rate equations and quantum noise sources used to calculate spectra of intrinsic second moment intensity

fluctuations in 3- and 4-level CW laser oscillators 24 p4221 A66-42548  
 Radiation interaction between laser oscillators with different active materials and frequencies 24 p4221 A66-42549  
 Self-trapping of laser beam due to diffraction from dielectric waveguide arising from permittivity increase of birefringent beam 24 p4222 A66-42554  
 Ring laser rotation rate sensor noting relation to electromagnetic radiation 24 p4223 A66-42564  
 Gas pumping effect on output of repetitively pulsed ion lasers 24 p4223 A66-42569  
 Narrow spectral outputs from actively Q-switched lasers, deriving fractional energy expression for injected mode group 24 p4223 A66-42570  
 Configurations for realization of multiple laser light scattering using microwave acoustic waves and two Porro prisms 24 p4224 A66-42636  
 Radiation of giant pulses of superluminescence by highly excited active medium of Nd glass with rapid cut-in of amplification 24 p4224 A66-42755  
 Glass lasers, comparing glass with crystals as hosts for laser ions, considering neodymium laser properties 24 p4224 A66-42800  
 Lasers applied to logic, memory, input-output and data transmission-linkages parts of computers 24 p4225 A66-42804  
 Nonlinear optics emphasizing parametric oscillation, self-focusing and trapping of laser beams and stimulated Raman, Rayleigh and Brillouin scattering, using Maxwell equations and electric dipole approximation 24 p4225 A66-42810  
 Laser beam deflection and scanning techniques 24 p4175 A66-42817  
 Current transducer for measuring current pulses in kiloampere range and suitable for laser research applications 24 p4213 A66-42820  
 Effect of longitudinal magnetic field on output power of gas laser operating in IR spectrum, noting gas-mixture pressure in discharge tube 24 p4225 A66-42977  
 Optical transmission of plasma column generated by ionized gas explosion determined, using laser beam 24 p4245 A66-42998  
 Perturbation of ruby laser by vibrating one of mirrors constituting resonant cavity 24 p4225 A66-42999  
 Spectroscopic, chemical and laser properties of piperidinium salt of europium tetrakis 24 p4226 A66-43034  
 Laser system for meteorological data using oscilloscope to display return signal, translated as concentrations of matter or aerosols 24 p4226 A66-43044  
 Semiconductor GaAs quantum generator with two-photon absorption of neodymium laser emission 24 p4226 A66-43085  
**LASER RADAR**  
**S LIDAR**  
**LATERAL OSCILLATION**  
 Rotating orbiting cables, determining lateral vibration in orbital plane via mathematical model analysis [AIAA PAPER 66-98] 06 p0962 A66-16264  
 Force and moment response of pneumatic tires undergoing nonstationary lateral motions, using motion equations [ASME PAPER 65-AV-2] 11 p1636 A66-22471  
 Lateral vibration of rotating bar with circular cross section under simultaneous axial force and torque, noting eigenvalue equations and damping effects 21 p3833 A66-39598  
**LATERAL STABILITY**  
 Lateral buckling of I-beam, examining stress and strain induced change in elasticity moduli and rigidity 06 p0964 A66-16479  
 Variational analysis of stability of infinitely long cylindrical panel under constant evenly distributed lateral loading 08 p1308 A66-18890  
 Stability of bending-torsional equilibrium of cantilevered bar subjected at end to follower force, as in case of wing under jet, determining critical thrust 19 p3475 A66-36432  
 Three-dimensional parachute dynamic stability theory 22 p3845 A66-40593



## LATERAL STABILITY AND CONTROL

Lateral-directional handling qualities of large transport, examining factors involved in pilot maneuvers 01 p0101 A66-10037

Lateral-directional handling qualities of large transport, examining factors involved in pilot maneuvers 16 p2634 A66-31318

## LATEX

## S RUBBER

## LATITUDE

## SA GEOMAGNETIC LATITUDE

Existence of significant latitudinal variation in density from 200 to 800 km 12 p1868 A66-23556

Seasonal-latitudinal variations in lower thermospheric density, temperature and composition 15 p2490 A66-29820

Atmosphere models for seasonal and latitudinal variation in thermosphere as function of solar flux and geomagnetic index 15 p2492 A66-30031

Latitudinal variations of ionospheric irregularities studied via synchronous and 1000 km satellites, noting Early Bird data, scintillation index graphs, radio star signals, etc 15 p2496 A66-30071

Latitudinal effect on behavior of ionospheric absorption determined by absorption measurements at four stations 19 p3350 A66-36358

## LATITUDE SENSING

Azimuth and latitude determination without time recording based on observation of stars at same horizontal elevation 02 p0255 A66-11694

Azimuth and latitude determination without time recording based on observation of stars at same horizontal elevation 02 p0255 A66-11702

Internal measurement of latitude, radius vectors and other geophysical properties from center of mass of astronomical system to space vehicle 16 p2698 A66-31386

## LATTICE

## SA CRYSTAL LATTICE

## SA MOLECULAR CHAIN

## SA SPIN-LATTICE RELAXATION

Phase transition in two-dimensional lattice gas of hard-square molecules 17 p2978 A66-32505

Profile of supercavitating lattice traced for certain parameter values, using perturbation theory of perfectly irrotational incompressible fluid 17 p2914 A66-33253

## LATTICE IMPERFECTION

## SA INTERSTITIAL ATOM

Determination methods for various types of dislocation in germanium lattice and influence on physical properties of germanium 02 p0276 A66-12066

Symmetry of ground states of P, As and Sb donors in silicon determined optically 03 p0411 A66-13144

Individual and group defect contribution to variation in carrier concentration and mobility in n-type germanium irradiated with fast neutrons 05 p0730 A66-14644

Lattice vacancies and interstitials in II-VI compounds of cadmium sulfide and zinc selenide caused by electron bombardment often determine advantages or limits of material 06 p0935 A66-17130

Implementation of Kossel line technique of crystallographic analysis and lattice parameter measurement in study of lattice defects in semiconductor crystals 06 p0935 A66-17133

Diffuse X-ray scattering in crystal structure of Ni-Be and Cu-Be alloys during first stage of aging due to anisotropic monoclinic lattice distortions 08 p1235 A66-18589

Interrelation between relaxation center in tungsten and molybdenum and high temperature internal friction background of spectrum 11 p1719 A66-23386

Zeta phase in tantalum-carbon system, noting diffusionless transformation of carbon-deficient lattice under compressive stress 12 p1892 A66-23566

Individual and group defect contribution to variation in carrier concentration and mobility in n-type germanium irradiated with fast neutrons 13 p2166 A66-25917

Propagation distribution of impurity atoms in heavily doped semiconductors 14 p2356 A66-27068

Cuprous oxide conductivity caused by

ionization of thermal lattice defects 14 p2358 A66-27091

Lattice distortions and field gradients in alkali halide solutions, noting discrepancy in calculation of electric field gradients 16 p2775 A66-30731

Lattice defect distribution effect on degradation of solid solution of interstitial impurities in cast

molybdenum 16 p2727 A66-31530

Phonon-drag thermopower variation in dilute copper alloys assuming Rayleigh law for phonon scattering 17 p2884 A66-33152

Crystal lattice defects in metals caused by neutron irradiation 18 p3120 A66-33621

Radiation damage in solids including crystal lattice defects, thermal migration, channeling and focusing effects, etc 18 p3155 A66-34136

Magnetic properties of lattice imperfections in lithium fluoride, potassium chloride and sodium chloride single crystals 18 p3157 A66-34499

Lattice defects and tensile strength 20 p3584 A66-37694

Structure and properties of thin films in terms of deposition conditions, noting conditions for continuity, surface roughness, grain size, lattice defect density, crystalline orientation, purity, etc 20 p3621 A66-38087

Interband microwave scattering of holes by cyclotron resonance in Ge 21 p3797 A66-38753

Propagation distribution of impurity atoms in heavily doped semiconductors 22 p3966 A66-40827

Cuprous oxide conductivity caused by ionization of thermal lattice defects 22 p3967 A66-40847

LATTICE POINT

Location and nature of singularity of Ising square lattice susceptibility, using Padé approximation based on Clapp spin-spin correlation function 02 p0263 A66-11887

Detailed account of dislocation loops according to continuum theory 04 p0590 A66-14164

LATTICE VIBRATION

Space and time dependence of increased phonon population /amplitude of lattice vibration/ in amplifying cadmium sulfide crystal 01 p0122 A66-10575

IR-active lattice vibrational spectra of alpha-aluminum oxide and chromium oxide analyzed by reflection and transmission measurements 03 p0380 A66-12341

Interaction of conduction electrons with lattice vibrations in semiconductor produces additional transmission bands or disappearance of resonance absorption region 04 p0564 A66-14251

Group II-VI semiconductors, examining theory of bound exciton complexes, lattice vibrations, phonon-assisted edge emission and higher energy bands 08 p1271 A66-19239

Neutron diffraction in ordered nickel-manganese alloys with near equilibrium distribution of atoms over lattice points 09 p1389 A66-20612

Interaction potential of inert gases defined in terms of transport properties, noting contribution of nonadditivity to static lattice energy 12 p1917 A66-23936

Electron and lattice heat conductivity of mercury selenide crystals 14 p2356 A66-27066

Temperature dependent soft-mode lattice vibration in perovskite-type ferroelectric crystal single-oscillator 15 p2567 A66-29394

Lattice vibrational properties of hexagonal CdSe 16 p2778 A66-31075

Electron vibration spectra of light absorption in molecular crystals, taking oscillation frequency changes as principal mechanism of exciton-phonon interaction 16 p2780 A66-31178

Current-carrier scattering in germanium telluride 16 p2788 A66-31780

Vibration spectrum of lattice of rectilinear vortices in charged and neutral superfluid systems studied in terms of Landau superfluid hydrodynamics 19 p3400 A66-35997

X-radiation alignment of quartz crystals for generation and detection of reverberating acoustic echoes at liquid-helium temperatures 20 p3624 A66-38409

Ruby laser-induced effect of pulsed pressure on KDP crystal surface and thermal bulk effect on excitation of

ultrasonic oscillation in crystal 22 p3932 A66-40318

Electron and lattice heat conductivity of mercury selenide crystals 22 p3966 A66-40825

Nitrate heat of formation value revised by re-evaluating lattice energy of cesium nitrate, considering charge distribution in anion 23 p4031 A66-41221

## LAUE DIFFRACTION

Pendellosing fringes in elastically deformed silicon, observing X-ray wavefield beam interference upon superimposition on crystal exit surface 07 p1098 A66-17815

Preparation, X-ray measurements and photovoltaic properties of Ge-epitaxial-Pb heterojunctions 15 p2562 A66-28711

Von Laue and Cowley diffraction theories of coherent diffuse X-ray scattering from random alloys, predicting diffuse intensity singularities at reciprocal lattice points 22 p3948 A66-40084

Laue reflection method of X-ray diffraction, determining single crystal orientation 24 p4255 A66-42506

## LAUNCH

## S LUNAR LAUNCH

## S ORBITAL LAUNCH

## S PRELAUNCH TESTING

## S SEA LAUNCH

## LAUNCH COMPLEX

Moon launch pads at Cape Kennedy noting structural and functional groups, crawlerway, propellant facilities, etc 01 p0054 A66-10862

Ground support equipment and launch installations for Apollo launch operation and testing 02 p0215 A66-11614

Orbital Launch Facility for performing launch operations of advanced planetary missions 02 p0293 A66-11620

Gemini spacecraft and launch vehicle interface design, development and configuration control 02 p0294 A66-11636

Hammaguir firing range facilities and planned launch of D-1A geodesic satellite 11 p1687 A66-23378

Launch operations and safety analysis of first test flight of SNAP-10A in SNAPSHOT satellite 12 p1953 A66-23678

## LAUNCH SITE

Siting of manned lunar launch facilities 09 p1365 A66-20699

Wind and turbulence distribution caused by barriers and complex surfaces adjacent to missile launching sites [AIAA PAPER 66-335] 12 p1906 A66-24483

Launching range facilities of Diamant rocket including equipment, radars, interferometers, telemetry, data processing, etc 16 p2682 A66-31233

## LAUNCH TIME

Plane trajectory with multistage rocket in minimum climb-time 02 p0296 A66-11703

Linear interpolation method for analyzing wind conditions at Wallops Island for launch operational problem [AIAA PAPER 66-340] 12 p1906 A66-24486

Gemini rendezvous launch operations planning for simultaneous launch countdown 14 p2394 A66-28438

## LAUNCH VEHICLE

SA ATLAS AGENA LAUNCH VEHICLE

SA ATLAS CENTAUR LAUNCH VEHICLE

SA ATLAS LAUNCH VEHICLE

SA BOOSTER

SA CENTAUR LAUNCH VEHICLE

SA DIAMANT LAUNCH VEHICLE

SA ELDO LAUNCH VEHICLE

SA LITTLE JOE II LAUNCH VEHICLE

SA MISSILE LAUNCHER

SA RECOVERY LAUNCH VEHICLE

SA SATURN I LAUNCH VEHICLE

SA SATURN IB LAUNCH VEHICLE

SA SATURN V LAUNCH VEHICLE

SA SATURN LAUNCH VEHICLE

SA THOR LAUNCH VEHICLE

SA TITAN III LAUNCH VEHICLE

SA TITAN LAUNCH VEHICLE

Major phases in total testing program to validate booster in man-rated launch vehicle 01 p0141 A66-10107

Electromagnetic waves and effect of plasma from vehicle exhaust on microwave communication link between in-flight launch vehicle and ground station 01 p0027 A66-10549

Difficulties in control system synthesis for



- launch vehicles exhibiting severe mode interaction 01 p0104 A66-10673
- Design of reusable space launch vehicle systems considering propulsion, structural weights, heat protection and cost [SAE PAPER 650801] 01 p0144 A66-10816
- Structural, propulsion, guidance and flight control systems of Saturn IB and V Apollo launch vehicles 02 p0294 A66-11629
- Launch vehicle guidance, premidcourse orbit determination and midcourse maneuver of Ranger IX spacecraft lunar mission and merger 02 p0260 A66-12056
- Turboramjet-powered hypersonic aircraft evaluated for cruise and boost mission for orbital launching [AIAA PAPER 65-759] 03 p0318 A66-12553
- Turborocket application to air breathing satellite launcher program describing engine design, performance and weight characteristics 04 p0572 A66-13539
- Design and comparison of apogee impulse systems developed for booster rocket thrust augmentation 04 p0573 A66-13541
- Structural dynamic load and instability problems in launch vehicles and spacecraft in lunar exploration emphasizing reliability, crew safety and mission success 04 p0585 A66-13549
- Gemini System Interference Monitor /SIM/ for simultaneous monitoring and remote control of many widely separated test points from central location 05 p0645 A66-14592
- Design and manufacture of Blue Streak satellite launcher structure, noting propellant tank 06 p0888 A66-17070
- Solid propellants for future large launch vehicles noting motor configurations, costs, thrust, size, etc 07 p1110 A66-17613
- Support Evaluation Technique for computer simulation, evaluation and control of complex logistic problems 08 p1203 A66-19527
- Booster rocket survey of U.S. and Western Europe 10 p1612 A66-21958
- Satellite and launch vehicles since Sputnik 13 p2189 A66-25129
- Orbital satellite launching systems, problem of increasing percentage orbital payload at minimum cost and advantages of air breathing engines 14 p2391 A66-27010
- Survival probability of launch vehicle rising through random wind field determined from component responses 14 p2391 A66-27870
- Flight Load Survey program, written in Fortran IV, for accurate and rapid sounding of wind-induced loads on aerospace launch vehicle [AIAA PAPER 66-470] 16 p2811 A66-31473
- Propulsion systems for European launch vehicles for scientific satellites, interplanetary probes and orbiting astronomical observatories 17 p2990 A66-32370
- Launch vehicle development, discussing requirements to support program, economic and operational development and reusability [SAE PAPER 660452] 17 p3017 A66-33161
- Computational method for determination corridors of launch vehicle trajectory and impact dispersions [AIAA PAPER 66-483] 18 p3226 A66-33656
- Structural dynamics research on launch vehicles at Langley Research Center, examining analytical method limitations and need for improved mathematical models for vibrational characteristics 18 p3240 A66-33818
- Gain specification of linear controller for large launch booster, using new application of linear control theory 19 p3471 A66-36687
- Computerized cost-effectiveness model for large payload test vehicle system of 50-150 launch program 20 p3684 A66-37901
- Aircraft, missile and space launch systems, considering in-flight transportation and separate and multiple orbital missions [AIAA PAPER 65-344] 20 p3664 A66-38150
- Titan III launch vehicle development in engine, material and flight control for various orbits and trajectories [AIAA PAPER 65-309] 20 p3664 A66-38152
- Adaptive control system requirements for launch vehicles includes insensitivity to parameter variations and adjustability as function of measured flight conditions 20 p3664 A66-38182
- Turboramjet powered hypersonic aircraft evaluated for cruise and boost mission for orbital launching [AIAA PAPER 65-759] 23 p4015 A66-40974
- Payload capabilities of launch vehicles, particularly for missions with high velocity requirements, analyzing various propulsion systems 23 p4121 A66-41315
- Launch vehicle and spacecraft cost trends including larger vehicles, post Saturn phase, performance improvement by throttling, etc [SAE PAPER 660463] 24 p4281 A66-42394
- Titan III standard space-launch system configuration, describing booster-spacecraft and physical-electrical interfaces 24 p4282 A66-42693
- LAUNCH VEHICLE CONFIGURATION**
- Estimation technique for combined effect of all variables acting simultaneously on mission of large launch vehicles 03 p0416 A66-12768
- Design criteria for launch-vehicle high-energy stage, emphasizing operational reliability, mission range and low development effort 06 p0959 A66-16494
- Launch vehicle parameter design for optimal support of communications satellites [AIAA PAPER 66-285] 12 p1955 A66-24756
- LAUNCH WINDOW**
- Missile and spacecraft countdown and meeting prespecified launch window probabilities by Markov chain techniques 01 p0140 A66-10087
- Earth departure plane change, interplanetary mission launches and launch windows 10 p1609 A66-21929
- Low energy transfer from Earth to Mars via Venus, considering launch window and planet orientation [AIAA PAPER 64-647] 18 p3227 A66-33812
- Guidance, navigation and two phases of targeting of Saturn V lunar landing mission, analyzing launch, boost to orbit and iterative guidance 21 p3768 A66-38898
- Optimum launch and transfer conditions for two concentrations of orbits within meteor stream associated with Kreutz group of sun-grazing comets in space mission 22 p3976 A66-39859
- LAUNCHING**
- SA INFRARED TRACKING**
- SA SATELLITE LAUNCHING**
- Responsibility for damage caused by space launchings 03 p0447 A66-13076
- Probability distribution of number of system failures and generating function for compound probability distribution of required launches 09 p1463 A66-19911
- Trajectory corrections of space vehicle launched toward planet, noting fuel consumption 20 p3595 A66-36872
- Launch and recovery system for large instrumented free flight models in high speed wind tunnel, using miniaturized telemetry and recording equipment [AIAA PAPER 66-776] 22 p3896 A66-40656
- LAUNCHING DEVICE**
- SA GUN LAUNCHING DEVICE**
- SA HYPERVELOCITY LAUNCHER**
- SA MISSILE LAUNCHER**
- SA ROCKET LAUNCHING DEVICE**
- Optimum design in fabricating rocket launcher rail, considering use of beryllium and boron carbide materials for weight reduction 17 p3030 A66-32883
- Launching device for free flying models in conventional wind tunnels consisting of split hollow shell enclosing model [AIAA PAPER 66-773] 23 p4052 A66-41332
- LAUNCHING FACILITY**
- Cost factors in launch operations controlled by management techniques and tools used in other facets of research and development 01 p0141 A66-10105
- Launching facilities for space rockets including buildings, assembly and test program and platforms for Saturn V Moon shot 01 p0054 A66-10873
- Dragon rocket probe, launch history and flight modifications 10 p1611 A66-21397
- Space station design trends, noting functional requirements, payload capability, logistics and launch requirements 13 p2193 A66-25759
- LAVA**
- S MAGMA**
- LAVAL NUMBER**
- Laval points in ideal gas expansion with energy losses in nozzle or turbine-blade cascade 19 p3276 A66-36305
- LAW**
- S CAUCHY LAW**
- S CHILD LAW**
- S CLOSURE LAW**
- S CONSERVATION LAW**
- S FOURIER LAW**
- S HOOKE LAW**
- S INTERNATIONAL LAW**
- S KEPLER LAW**
- S KIRCHHOFF LAW**
- S NEWTON-BUSEMANN LAW**
- S NEWTON PRESSURE LAW**
- S OHM LAW**
- S RADIATION LAW**
- S REGULATION**
- S SCALING LAW**
- S SIMILITUDE LAW**
- S SNELL LAW**
- S SPACE LAW**
- S STEFAN-BOLTZMANN LAW**
- S STOKES LAW**
- S STRESS-OPTIC LAW**
- LAYER**
- S BARRIER LAYER**
- S BOUNDARY LAYER**
- S D LAYER**
- S E LAYER**
- S EKMAN LAYER**
- S F LAYER**
- S FLAT LAYER**
- S ISOTHERMAL LAYER**
- S MONOMOLECULAR LAYER**
- S PLASMA LAYER**
- S SHEAR LAYER**
- S SHOCK LAYER**
- S STRATIFIED LAYER**
- S SUBSTRATE**
- S SURFACE LAYER**
- S TRANSITION LAYER**
- LC CIRCUIT**
- Possibility of circuit designs without inductors in future multiplex technique systems 02 p0194 A66-11246
- Form, period and spectrum of free oscillations in LC circuits with nonlinear capacitive p-n alloy junctions 02 p0198 A66-11704
- Combination of approximations method for natural oscillations in circuit containing p-n junction capacitance and nonlinear inductance 02 p0199 A66-11846
- Operational characteristics of LC tuned solid state static inverter used as power supply in autopilot gyros of Titan rockets, noting power oscillator circuit 12 p1804 A66-24661
- Synchronous-phase LC oscillator 14 p2259 A66-28184
- LCRE**
- S LITHIUM COOLED REACTOR**
- EXPERIMENT /LCRE/**
- LEAD**
- SA ELECTRIC LEAD**
- Interaction mean free path of nuclear-active particles in iron determined by measuring number of interactions in each iron layer in ionization calorimeter 07 p1115 A66-17550
- Angular correlation of photons measured for positrons annihilating in normal and superconducting lead without observing any effect on Fermi surface 07 p1109 A66-18440
- Tunneling characteristics of superconducting energy gap of lead above critical magnetic field 09 p1416 A66-20027
- Temperature range of transition from superconducting to normal state in very pure lead determined from variation of specific heat and magnetic susceptibility 09 p1419 A66-20044
- Batch-fabrication of beam-lead transistors, integrated circuits and other components with leads serving as structural, protective and electrical functions 11 p1669 A66-23087
- Absorption bands in thin lead films, vacuum prepared, considering general analysis of elements in group IVA of periodic table 14 p2369 A66-28271
- Subharmonic structure in superconductive Pb-Pb tunneling junctions, noting energy gap values and background current temperature dependence 16 p2769 A66-30160
- Oscillating tunneling characteristics from electron interference in normal metal induced by superconducting contacts between silver and lead 16 p2769 A66-30168
- Ultrasonic attenuation dependence on



frequency in Pb crystals at low temperatures 16 p2770 A66-30179

Parallel and perpendicular magnetic transitions of superconducting lead films and foils determined from transverse magnetization and AC susceptibility measurements 16 p2770 A66-30190

Attenuation of longitudinal sound in pure crystals of superconducting lead 17 p2978 A66-32506

Negative temperature coefficient of electrical resistance, anomalous Hall constant and magnetoresistance constant for thin films of Be and Pb 18 p3157 A66-34627

Grain boundary migration in pure aluminum and lead under reversed torsional and bending stresses at elevated temperatures 19 p3386 A66-36365

High temperature fatigue in pure lead and aluminum observed continuously by microscopic cinecamera combined with fatigue machine 19 p3386 A66-36366

Troilite-graphite phase from Toluca meteorite analyzed to determine concentration and isotopic composition of lead using mass spectrometer, noting radiogenic problem 22 p3976 A66-39684

## LEAD ALLOY

Klim-Anderson model of flux pinning to compute magnetization of cylindrical hard superconductor, e.g. lead alloy 03 p0413 A66-13277

Magnetic and resistive superconducting transitions on bulk samples of indium-lead alloys in alpha-phase region, considering results relative to Glag theory 09 p1423 A66-20067

Phonon spectrum of lead indium alloys noting distinctness of impurity band as inferred from electron tunneling measurements 16 p2768 A66-30130

Au-Sn-Pb section of Au-Pb-Sn phase diagram, examining solderability of gold coatings of electronic components 16 p2722 A66-30223

Temperature dependence of mixed-state thermoconductivity of type II superconducting In-Pb alloys in magnetic field 21 p3797 A66-38751

## LEAD COMPOUND

Ferroelectric properties and morphotropic phase boundary in phase diagram of ternary system of compounds of lead, titanium and nickel 06 p0927 A66-16720

Synthesis, X-ray studies and dielectric measurements of lead containing perovskites 07 p1092 A66-17220

Temperature dependence of optical birefringence on single crystals of lead zirconate-titanate solid solution measured, noting they are optically negative 08 p1269 A66-19006

Lead stearate effect on thermodynamic properties of propellant, using heat-of-explosion test 16 p2790 A66-31685

Synthesis, X-ray studies and dielectric measurements of lead containing perovskites 17 p2976 A66-31991

Temperature and magnetic field effect on flux pinning by superconducting Sn precipitates in lead-indium matrix, noting occurrence of magnetic hysteresis 19 p3444 A66-38077

Lead stearate effect on heat of explosion in nitro-cellulose propellant combustion at various pressure levels 20 p3626 A66-38041

## LEAD OXIDE

Lead oxides formed from tetraethyl lead /TEL/ in combustion zone identified in analysis of antiknock properties 03 p0413 A66-12486

Vanadium pentoxide-boron oxide-lead oxide system IR absorption spectra and electroconductivity 10 p1582 A66-21917

Properties of hydrothermally grown single crystals of tetragonal lead monoxide, with contacts applied by metal evaporation 14 p2359 A66-27099

## LEAD SELENIDE

Pressure dependence of dominant emission modes from PbSe diode laser 03 p0378 A66-13003

Photo-induced recombination radiation from single crystals of PbSe and PbTe as function of carrier concentration and temperature 07 p1094 A66-17312

Spontaneous emission band analyzed to invoke principle of detailed

balance 07 p1094 A66-17313

Spontaneous and coherent emission from lead sulfide, telluride and selenide diode lasers in oriented magnetic field, determining band edge parameters from spin-split zero order Landau level transitions 13 p2100 A66-26185

Preparation temperature and condensation rate effect on current carrier mobility in lead selenide and telluride films 16 p2787 A66-31769

## LEAD SULFIDE

Silicon and lead sulfide electron paramagnetic resonance spectra, showing gas action and temperature effect on EPR signal amplitude and absorption 01 p0124 A66-10765

Varying deposition and firing conditions effect on range of detection of chemically deposited lead sulfide IR detector cells 03 p0407 A66-12332

Reflectivity of n-type lead sulfide measured as function of wavelength, temperature and carrier density 03 p0412 A66-13147

Radiative recombination emission and photoconduction in lead sulphide, emphasizing chemical deposition or vacuum evaporated layers 07 p1094 A66-17311

Numbers theory for lead sulfide photoconducting films, noting balancing of n and p-type impurities, various activation energies, etc 10 p1578 A66-21574

Photoconduction model for illuminated lead sulfide films with shunt path increase during barrier modulation 10 p1578 A66-21575

Silicon and lead sulfide electron paramagnetic resonance spectra, showing gas action and temperature effect on EPR signal amplitude and absorption 11 p1748 A66-22276

Spontaneous and coherent emission from lead sulfide, telluride and selenide diode lasers in oriented magnetic field, determining band edge parameters from spin-split zero order Landau level transitions 13 p2100 A66-26185

Preparation, X-ray measurements and photovoltaic properties of Ge-epitaxial-PbS heterojunctions 15 p2562 A66-28710

## LEAD TELLURIDE

Thermal and magnetic properties of GeTe and PbTe semiconductors containing transition elements in solution 01 p0127 A66-11079

NaCl substrate surface temperature and structure effect on orientation, structure and characteristics of vacuum-deposited PbTe film 04 p0564 A66-14255

Lead telluride single crystal grown on cleaved rock-salt substrates for thin-film field effect transistors 06 p0854 A66-16679

Photo-induced recombination radiation from single crystals of PbSe and PbTe as function of carrier concentration and temperature 07 p1094 A66-17312

Spontaneous emission band analyzed to invoke principle of detailed balance 07 p1094 A66-17313

Effect of sample geometry on frequency of helicon waves in lead telluride at low temperature 07 p1101 A66-18201

Cyclotron resonance in Azbel-Kaner geometry in n- and p-type lead telluride, examining anisotropy of absorption under anomalous skin effect conditions 07 p1102 A66-18205

Magneto-optical reflection measurements at liquid-helium temperature for p-type PbTe samples in Faraday and Voigt configuration 07 p1102 A66-18206

Pressure induced change in energy gap and forbidden bandwidth of lead telluride 10 p1587 A66-22152

Hall mobility and Hall constant variation for lead telluride-tin telluride polycrystals at high temperatures 13 p2163 A66-25419

Spontaneous and coherent emission from lead sulfide, telluride and selenide diode lasers in oriented magnetic field, determining band edge parameters from spin-split zero order Landau level transitions 13 p2100 A66-26185

Microscopic and electron diffraction structural analysis of epitaxial growth of PbTe by sublimation on split surface of NaCl at 150 degrees C in vacuum 13 p2170 A66-26757

Hall coefficient and thermal emf of electron gas of PbTe in strong magnetic field 14 p2358 A66-27088

Temperature dependence of Hall effect and conductivity of lead telluride single crystals containing bismuth 14 p2364 A66-27645

Entropy and heat of formation of lead telluride determined by emf temperature coefficient measurement 14 p2369 A66-28330

Preparation temperature and condensation rate effect on current carrier mobility in lead selenide and telluride films 16 p2787 A66-31769

Multiphoton plasma production and stimulated recombination radiation in lead telluride, considering electron-hole pair production rate 17 p2975 A66-31884

Coherent and spontaneous emission from lead-tin telluride alloys upon excitation by GaAs diode laser, noting band structure of alloy system 18 p3119 A66-34159

Pressure induced change in energy gap and forbidden bandwidth of lead telluride 19 p3440 A66-35766

Sublimation rates of pressed-and-sintered lead telluride and lead stannous telluride thermoelements 19 p3281 A66-36294

Predicted plasma mode in microwave frequency range for magnetoplasma excitations in germanium, applying theory to n-type and p-type lead telluride 22 p3960 A66-39805

Vibration modes frequencies of lead telluride propagating in certain symmetric direction determined by inelastic neutron scattering 22 p3966 A66-40405

Hall coefficient and thermal emf of electron gas of PbTe in strong magnetic field 22 p3967 A66-40844

Bond degradation and diffusion of braze and shoe constituents in lead telluride thermoelectric elements 24 p4247 A66-42107

Evaporation rates of lead telluride and lead tin telluride in pressed and sintered thermoelement form 24 p4247 A66-42108

Neutron activation analysis of sodium dopant concentrations and distributions in lead telluride thermoelectric materials during couple operation in vacuum and argon atmosphere 24 p4247 A66-42109

Thermoelectric material testing and selection for high-performance generator, noting lead telluride 24 p4160 A66-42112

Silicon-germanium lead-telluride segmenting for improved thermoelectric efficiency, noting sequential fabrication process difficulties 24 p4248 A66-42115

W-diffusion bonding in preparing segmented silicon-germanium-lead telluride thermoelements, noting properties 24 p4248 A66-42116

W-diffusion bonding of lead telluride base thermoelements with nonmagnetic electrodes 24 p4216 A66-42117

## LEAD TITANATE

Design and fabrication techniques for high voltage impulse generation by conversion of mechanical to electrical energy, using piezoelectric ceramics 01 p0016 A66-10916

Temperature and bias characteristics of ceramics of Pb/Zr-Ti/O-3 and its families, using schematic model on reorientations of 180 and 90 degree domains 08 p1243 A66-19061

## LEADING EDGE

## SA LEADING-EDGE SWEEP

## SA SHARP LEADING EDGE

Simplified leading-edge flow boundary value problem of Bhatnagar-Gross-Krook equation solved by finite difference method 01 p0058 A66-10633

Gas dynamics equation for wing of zero-thickness with two subsonic leading edges in supersonic flow reduced to wave equation 06 p0803 A66-17006

Leading edge pressure distributions measured on circular cylinders in normal cross flow, obtaining data from tests in arc heated perfect gas and variable atmosphere wind tunnels 11 p1686 A66-22845

Kinetic theory of leading edge of plate interacting with streaming gas evaluated by Bhatnagar-Gross-Krook equation of statistical mechanics 11 p1633 A66-22924

Flow field near leading edge of heated flat plate in Mach 0.5 airflow 11 p1634 A66-22934

Effect of variation in thermal expansion



- coefficient upon thermal stress in thin leading edge to set upper and lower limits 12 p1957 A66-23597
- First-collision process at sharp leading edge of flat plate aligned with hypersonic free stream 13 p1993 A66-26728
- Subsonic wing design, classical linearization technique used to describe leading edge boundary 15 p2425 A66-29638
- Shape of head wave in linearized supersonic flow past finite span wing, considering waves with convex and concave leading edge 16 p2632 A66-31792
- Nonlinear theory for flow past slender wings with leading edge vortices in sudden plunging motion 17 p2837 A66-32082
- Turbulent heat transfer measurements on transpiring flat plate in Mach 8 tunnel using nitrogen, helium and argon as injection gases 17 p2838 A66-32439
- Separated unsteady flow about flat plate rotating impulsively from rest to uniform angular velocity about axis along leading edge, noting torsional oscillations [AIAA PAPER 66-427] 17 p2910 A66-32753
- Wind tunnel experiments on thin two-dimensional airfoil with sharp leading edge and with jet blowing through mid-chord slot on upper surface in order to control boundary layer and circulation around it 18 p3048 A66-33950
- Flow in two-dimensional plane wall jet in still air with various initial gaps between nozzle exit and leading edge of wall 18 p3097 A66-33951
- Linearized calculation of subsonic wings with rounded leading edge 20 p3491 A66-36949
- Localized convection coefficient for hypersonic separation line along delta wing leading edge calculated, using Mangler and Stewartson transformation 20 p3492 A66-37818
- Nonlinear inductance effect on leading edge of high voltage nanosecond pulses during passage through ferrite magnetic field 21 p3801 A66-39156
- Welded titanium wing leading edge design and manufacture for increased range and load carrying capacity 22 p3924 A66-40256
- Lifting wings in supersonic regime, analyzing flow separation at leading edges [ICAS PAPER 66-20] 22 p3847 A66-40670
- Theory of wings with curved leading edges in supersonic flow, including delta wings with straight leading edges in case where motion is conical 23 p4008 A66-41379
- Supersonic unsteady gas flow around bodies at low Strouhal numbers, noting angle of attack amplitude and leading edge shock wave 23 p4009 A66-41719
- Unsteady state lift and moment action on lattice of profiles moving in incompressible fluid, determining suction originating at leading edges of profiles 23 p4009 A66-41723
- Shock wave transport effects on hypersonic leading edge flow past sharp plate, discussing Rankine-Hugoniot relations 23 p4058 A66-41910
- LEADING-EDGE SWEEP**
- Angle of attack, leading edge sweep and thickness effects on hypersonic flow field of slender delta wing 08 p1164 A66-19135
- Boundary layer transition measurements on swept wings with supersonic leading edges 14 p2219 A66-27439
- LEAKAGE**
- Leak detection methods and equipment for testing propellant actuated cartridges, missile fuses and timers 11 p1708 A66-23257
- Multiple quick-disconnect valve used in auxiliary power unit /APU/ of aircraft and serving several systems at once while preventing fluid leakage from one system to another 14 p2226 A66-28032
- Leak-rate transducers capable of aerospace flight detection of small gas flow rates in critical joints of Saturn engine systems 20 p3557 A66-37215
- Electronic hydrogen leak and fire detector systems installed on Saturn S-IVB static test firing stands, discussing installation and operational problems 20 p3557 A66-37216
- Sensitivity and safety of Kr-85 /radiokrypton/ for leak detection 22 p3928 A66-40497
- Control valve seat leakage as function of fluid viscosity, density, pressure drop and cube function of gap between two surfaces 23 p4017 A66-41145
- Leak specifications for gas-filled electronic enclosures, discussing molecular, slow viscous, capillary and ordinary leak patterns 24 p4182 A66-42574
- LEARNING**
- SA CONDITIONED RESPONSE
- SA MACHINE LEARNING
- SA MEMORY
- SA TRAINING
- Macromolecular parameters of memory and learning and information processing in molecular genetics, molecular immunology and molecular neurology 24 p4182 A66-42313
- LEARNING SYSTEM**
- Automatic evaluation of echo signals from circular-scan radar using learning system 04 p0543 A66-13497
- Training and instruction by means of teaching machines in field of aviation 04 p0469 A66-13508
- Learning matrices based on redundancy principle as nonadaptive self-correcting adjustment switches and error detectors in electronic systems 04 p0489 A66-13510
- Error correcting learning machines application to unknown linear dynamic systems 05 p0653 A66-14602
- Heuristic approach to reinforcement learning control systems, describing operation and simulation on IBM 1710-GEDA hybrid computer 06 p0864 A66-16734
- Adaptation theory concepts, examining threshold learning process, Markov chain, learning wave, feedback adaptivity, etc 11 p1647 A66-22299
- Man-machine systems involved in on-line man/ computer interaction, manned space systems, satellite communication and display systems 14 p2230 A66-27820
- Self-learning control system theory, discussing power yield, adaptive and extremum systems, nondeterministic systems, combined deterministic/ self-organizing systems, etc 19 p3330 A66-36433
- On-line and off-line self-organizing control systems for space vehicle application 19 p3333 A66-36661
- Learning control system design, discussing hill-climbing and pattern recognition schemes in framework of statistical decision, automata and information theory 19 p3333 A66-36662
- Markov chain hill-climbing scheme for probable fast-time learning absorbing model 19 p3333 A66-36663
- Estimation method of learning time of time-varying threshold learning processes /TLP/ 19 p3333 A66-36664
- Algorithm for learning without external supervision and application to learning control systems 19 p3333 A66-36666
- Pattern recognition techniques applied to process identification, examining capability of mode learning machines for on-line identification of both linear and nonlinear processes 19 p3310 A66-36712
- Learning curve theory used to explain tendency toward decreasing downtime observed in maintenance of many systems 20 p3569 A66-37924
- On-line-learning and off-line-learning self-organizing control systems 21 p3720 A66-39431
- LEAST SQUARES METHOD**
- Order in equiatomic germanium silicon solid solution, using diffusion scattering of X-rays calculated by least squares method 01 p0124 A66-10768
- Geomagnetic field represented as dipoles located by least squares gradient method 01 p0063 A66-11052
- Second derivatives of gravity calculated from interdependences between coefficients of formulas, using least squares method, weight coefficients being variable 01 p0063 A66-11098
- Linear smoothing method minimizing mean-square error in time series where signal statistics are unknown and noise is additive, deriving filter 05 p0653 A66-14600
- Error correcting learning machines application to unknown linear dynamic systems 05 p0653 A66-14602
- Computer algorithm determination of nonlinear system dynamics, using least squares method 05 p0636 A66-14605
- Recursive procedure based on orthonormalization for discrete sample least mean square error estimation of non-Markovian random process 05 p0706 A66-14614
- Smoothing, filtering and prediction problems of filtering theory correspond in field of orbit determination to ephemeris reconstruction, navigation and orbital prediction 05 p0631 A66-14630
- Filtering techniques for estimating nonlinear discrete-time processes, including Bayesian estimation and weighted least squares approach 05 p0656 A66-14631
- Nonlinear inverse heat conduction problem solved by finite difference method, using least squares and future temperatures [ASME PAPER 65-HT-40] 05 p0784 A66-14753
- Least squares method to determine diurnal lunar tide fluctuations from observations of Pulkovo, Greenwich and Tokyo Time Services 06 p0954 A66-16426
- Least squares recursive differential-correction estimation in nonlinear problems, examining equations and stochastic interpretation 06 p0903 A66-16735
- Least squares technique for identification of linear time-invariant plant in sampled data system corrupted by additive noise 06 p0866 A66-16750
- Kernel function procedure for solving oscillatory lifting surface problem at subsonic speeds, using least squares method 08 p1165 A66-19149
- Iterative method for computing optimum values of parameters for best agreement in least squares sense between given values and corresponding calculated values 10 p1507 A66-21213
- Random errors of derivatives obtained from least squares approximations to empirical functions 10 p1550 A66-21341
- Order in equiatomic germanium silicon solid solution, using diffusion scattering of X-rays calculated by least squares method 11 p1748 A66-22279
- Least squares estimator computed by method which reduces problem subject to constraints to no constraints 11 p1725 A66-23452
- Quasi-optimal minimum-time controllers for high-order dynamic systems obtained by least-squares fitting points on optimal switching surface 12 p1849 A66-24253
- Convergence rate of method of least squares and some approximate Galerkin type methods in eigenvalue problems 15 p2526 A66-28696
- Best straight line calculated by least squares method 16 p2736 A66-31007
- Partial totals method of estimation for one parameter exponential model, comparing procedure with maximum likelihood, least squares and weighted least squares estimators 16 p2737 A66-31384
- Robbins-Monro stochastic approximation method extended and results applied to least squares method 17 p2946 A66-32296
- Least squares method to solve linear integral and differential equations 17 p2947 A66-32608
- Inertial navigation technique based on least squares criteria of optimality with filter providing estimates of system errors 19 p3396 A66-35517
- Linear least-squares filtering problem in geometrical interpretation 19 p3318 A66-35731
- Reduction of variance by least squares polynomial approximations, noting exact functional dependence of variance on degree of polynomial 19 p3388 A66-35832
- Limitations of method of least squares in terms of quality of estimates it provides in geodetic measurements 20 p3590 A66-37471
- Least squares iterative procedure for resolving individual particle distributions comprising model atmosphere density profile above 110 km 20 p3551 A66-37516
- Span loading on wing of complete aircraft configuration determined, using segmented wing in wind tunnel test technique and least squares method [AIAA PAPER 66-768] 22 p3895 A66-40649
- First-order Markovian gyro drift numerically evaluated and square root plotted vs interval and gyro correlation time 23 p4068 A66-41318



Approximate solution to digital sequential least squares estimation of eigenstates of nonlinear processes 23 p4050 A66-41614

Real time computer technique for least squares estimates of current system state for noisy nonlinear system, using Pontryagin maximum principle 23 p4050 A66-41615

Least squares estimates and random sampling theory, examining outliers in samples of size three 23 p4086 A66-41930

Stress separation in photoelasticity, using series solution of Laplace equation and least squares method 24 p4292 A66-42862

**LEE WAVE**

Mountain lee waves at White Sands Missile Range investigated by balloon soundings 02 p0253 A66-11970

**LEGAL LIABILITY**

Law of outer space - Colloquium, Athens, September 1965 19 p3480 A66-36201

Space vehicle and astronaut assistance and liability for damage 19 p3481 A66-36202

Proposals for international convention on liability for damage caused by spacecraft, noting principles, preparatory work done and future measures 19 p3481 A66-36203

Space legal liability and damage in UN resolution 19 p3482 A66-36206

Liability resulting from space activities 19 p3482 A66-36208

Legal problems and general principles of space law 19 p3484 A66-36224

**LEGENDRE FUNCTION SERIES**

Solution of dual integral equations containing Legendre conic functions and trigonometric functions 12 p1905 A66-24344

Maximum error curves for Lanczos selected point method of polynomial solution to ordinary differential equations, using Chebyshev and Legendre functions 17 p2947 A66-32858

Fourier series of Gegenbauer function, examining convergence characteristics 18 p3126 A66-33696

Transformation of infinite Legendre sums into finite series of Legendre polynomials by transforming sum into integral leading to difference equations 22 p3995 A66-40458

**LEGENDRE POLYNOMIAL**

Second derivatives of Legendre and Laguerre polynomials based on Markov inequalities 08 p1244 A66-18792

Approximate theory of shells of revolution of average thickness, using seminverse method and expansion into series in Legendre polynomials 11 p1779 A66-22229

**LEGENDRE TRANSFORM**

Thermodynamic formalism based on fundamental relation and Legendre transformation, with macroscopic and statistical application 08 p1319 A66-19292

Decomposition technique by which convex control programming problem, having coupled subsystem constraints, can be decomposed into smaller subproblems 13 p2117 A66-25349

Legendre transformation and characteristics of MGD potential equation 13 p2142 A66-25708

**LEGIBILITY**

Effect of color and brightness contrast, direction of contrast and contrast values on legibility of circular dial 21 p3701 A66-39420

Legibility analysis to investigate effects of scale factors, graduation marks, etc, on speed and accuracy of reading moving tape instruments 21 p3701 A66-39422

**LEM**

**S LUNAR EXCURSION MODULE /LEM/ LENS**

**SA LUNEBERG LENS**

**SA QUADRUPOLE LENS**

**SA VISUAL ACCOMMODATION**

**SA WIDE ANGLE LENS**

Statistics of beam waveguide light-ray propagation extended to include correlations between displacements of different lenses 05 p0634 A66-15179

Design of intentional bends of beam waveguide, giving relations between waveguide parameters and radius of curvature of guide axis 06 p0846 A66-16093

Transverse beam width and phase constant of nonsquare law media for light propagation in imperfect lenslike media requiring repeater 13 p2127 A66-25539

Lens aberration correction using Gabor

wavefront reconstruction method to produce hologram of spherically aberrated wavefront emerging from lens 13 p2080 A66-25990

Fast lens component for SFR high speed photographic recorder with asymmetric objectives 17 p2927 A66-33439

**LENS ANTENNA**

Beam waveguides for long distance electromagnetic wave transmission at optical wavelengths described by theory of focusing antennas 11 p1656 A66-22737

Thinned lens approach in optimizing cost and performance of phased array antenna 15 p2455 A66-28568

Beam waveguides for long distance electromagnetic wave transmission at optical wavelengths described by theory of focusing antennas 23 p4037 A66-41475

**LENS DESIGN**

**SA OPTICAL CORRECTION PROCEDURE**

Duoplasmatron with electrostatic lens decreasing ion energy while focusing ions for maximum density parallel beam 01 p0114 A66-10851

Constructing and evaluating electrostatic filter lenses with wide image angles for low voltage electron microscope 02 p0228 A66-11498

Electron microscope filter lenses with unconventionally shaped electrodes and large image angles 02 p0228 A66-11499

Lossless conversion of plane laser wave to plane wave of uniform irradiance, noting planoaspheric lenses method and aberrated lens system 02 p0242 A66-12204

Two lenses with focal ratios of f/4 and f/2.65 used to collimate light from helium-neon laser 05 p0695 A66-14921

Light waveguide for general lens-like media, ideal lenses and continuous media with square-law index variation 05 p0634 A66-15178

Periodic gas lenses, discussing structure ray optics properties of alternating gradient focusing systems 05 p0717 A66-15180

Cardinal points of optical glass lenses and technique for converting thick single lenses into equivalent lenses of zero thickness 07 p1030 A66-17202

Lens centering errors effect on optical image quality and wave front aberration 08 p1255 A66-19220

Best-fit sphere approximation to general aspheric lens surface, discussing computer program 09 p1402 A66-20514

Irregular bends and lens displacements effect on wavelength and modes in laser waveguide 11 p1713 A66-23103

Two wide-angle camera lenses, one adapted by NASA for Tiros satellite, noting freedom from astigmatism and distortion correction by choosing refractive index 14 p2291 A66-27318

Wavefront shearing prism interferometer applied to testing of chromatic aberration of simple and compound lenses and waveforms characterizing monochromatic aberrations 14 p2291 A66-27319

Lens decentering distortion using thin prism and Conrady models, noting application of precise calibration to photogrammetry 16 p2746 A66-30514

LASL lens design program for Doublet Achromat, from existing Fraunhofer design, used in solar corona monochromatic photography 19 p3354 A66-35383

Lens design by computer methods known as Flair and Triplet 19 p3399 A66-35824

Flexible lens design program system for determining optimum solution to set of requirements 19 p3399 A66-35825

Structural design relationship to optical design with reference to tolerance in range tracking instruments 19 p3358 A66-35826

Two-dimensional microwave lenses with large angular field for radar antenna, noting residual aberrations 20 p3527 A66-37427

**LENTICULAR BODY**

Feasibility study indicates that cap-type microwave reflectors can be used as communication satellites 04 p0586 A66-13927

Martian clouds analysis and topographical relationships, discussing white and yellow classification and frequency of occurrences 15 p2602 A66-29951

**LEONID METEOR**

Luster micrometeoroid sampling payload

launched during Leonid meteor shower November 16, 1965 at White Sands Missile Range 15 p2604 A66-30066

Aerobee rocket measurement in sampling of micrometeoroid debris during peak of Leonid meteor shower 15 p2605 A66-30068

**LEPTON**

Effects of derivative terms in leptonic current of photon interaction yielding neutrino and antineutrino 07 p1083 A66-18239

Static properties and interactions of neutrinos noting mass, spin, helicity, charge, lepton number, etc 15 p2546 A66-29582

Statistical equilibrium of fundamental particles at elevated temperatures, determining degeneration parameters 15 p2618 A66-29645

**LES**

**S LINCOLN EXPERIMENTAL SATELLITE /LES/**

**LESA**

**S LUNAR EXPLORATION SYSTEM FOR APOLLO /LESA/**

**LEWIS NUMBER**

Convective heat transfer measurements for partially dissociated carbon monoxide and hydrogen with high Lewis number [ASME PAPER 65-WA/HT-27] 05 p0793 A66-15676

Heat capacity expression due to chemical reaction, relating composition variations and binary diffusion coefficient with Lewis number, presenting integral equation for system enthalpy 08 p1318 A66-19164

**LIAPUNOV FUNCTION**

Collected works of Liapunov on equilibrium configurations of fluids 01 p0056 A66-10304

Liapunov work on equilibrium configuration of inhomogeneous rotating fluid 01 p0056 A66-10305

Series of equilibrium configurations for homogeneous rotating fluid in monograph of Liapunov 01 p0056 A66-10306

Liapunov monograph on equations for surfaces of equilibrium configurations of rotating fluid deriving from ellipsoids 01 p0056 A66-10307

Stability equilibrium criteria for orthotropic rectangular plates discussing Liapunov and other theories 01 p0154 A66-10476

Liapunov function determining sufficient conditions for stability of autonomous functional differential equations with finite time lag 02 p0249 A66-11900

Stability of solution to autonomous Liénard equation, using second Liapunov method 03 p0392 A66-12688

Current trends in nonlinear control theory 03 p0349 A66-12701

Stability of automatic control system with nonlinear elements, obtaining quadratic equations by using Liapunov method 03 p0349 A66-12707

Axiomatic approach to control system theory as generalization of dynamic systems, noting weak and strong stability and Liapunov function 03 p0351 A66-13255

Book on motion stability using Liapunov method noting motion equations, perturbing forces effect on equilibrium, instability, Lagrange theorem, etc 03 p0393 A66-13286

Liapunov stability equilibrium for systems with infinite number of degrees of freedom, discussing stability criteria 04 p0545 A66-13558

Quadratic form as Liapunov function for linear homogeneous vector differential equation with constant coefficient matrix 04 p0539 A66-13825

Book on state variables for control theory noting transfer functions, time domain, nonlinear system stability using Liapunov method, optimization, etc 04 p0504 A66-13836

Global asymptotic stability problem for complex high order system solved by transformation into interconnected set of lower subsystems 05 p0654 A66-14608

Optimization theory and converse of circle criterion for simple time-varying feedback system 05 p0655 A66-14620

Solution method for Poincaré problem concerning periodic solutions of nonautonomous systems with analytical right-hand side 05 p0708 A66-15338

Equilibrium solution stability of discrete systems represented by origin in state space



- studied by Liapunov functions and quadratic moments  
ASME PAPER 65-WA/AUT-17] 05 p0710 A66-15619
- Describing-function method for approximate representation of stability boundaries for typical nonlinear systems  
ASME PAPER 65-WA/AUT-3] 05 p0711 A66-15704
- Controller analytical design for nonautonomous systems, deriving necessary and sufficient conditions for existence of optimum control 06 p0862 A66-16522
- Convex programming problems, developing parametric gradient method for approximate solution 06 p0838 A66-16526
- Optimum transfer function determination, using Liapunov method and superposition theorem 06 p0864 A66-16683
- Upper bound on dynamic/transient and steady state/quantization error in digital control systems, using direct method of Liapunov 06 p0865 A66-16741
- Nonlinear differential equation stability, describing technique for Liapunov function construction 06 p0865 A66-16743
- Liapunov function construction, using stochastic analog of deterministic method of partial integration 06 p0865 A66-16745
- Nonlinear differential equation analysis of motion stability of plant with automatic control device 07 p1080 A66-17858
- Permanent axes of rotation for gyrostabilizer under influence of forces depending only on position of gyrostabilizer 07 p1035 A66-18191
- Stability of bodies with holonomically constrained moving parts, using method of Liapunov to demonstrate dependence of motion stability on potential function of generalized coordinates  
AIAA PAPER 66-101] 07 p1082 A66-18457
- Techniques for synthesis of control systems, based on Liapunov second method 08 p1200 A66-19016
- Liapunov stability criterion for panel flutter in supersonic flow derived from second method of Liapunov 08 p1310 A66-19160
- Discontinuous Liapunov functions applied to stability analysis of position-controlled system with symmetrically-controlled asynchronous motor 08 p1201 A66-19685
- Generalization of some theorems concerned with Liapunov direct method in connection with equations of perturbed motion 09 p1394 A66-20162
- Generation of Liapunov functions for second method solution of stability problems in automatic control 09 p1362 A66-20650
- Direct method of Liapunov used to study stability of ordinary differential equation by obtaining linear bounds on vector components 09 p1363 A66-20654
- Stability in elastic and aeroelastic systems analyzed by Liapunov direct method 09 p1468 A66-20800
- Oscillation stability criteria for simple surge tank obtained from second method of Liapunov 10 p1523 A66-21497
- Theorems and corollaries describing bounds for quadratic Liapunov functions 10 p1551 A66-21918
- Unilateral estimates under conditions of asymptotic stability of solutions to differential equations with unbounded operators 10 p1552 A66-21985
- Liapunov first method and applicability to asymptotic stability of stationary points of nonlinear differential systems 11 p1721 A66-22641
- Sufficient conditions for asymptotic dynamic stability of linear differential system with random retardation, using Liapunov function method 11 p1736 A66-22643
- Liapunov function for case of stability with constantly acting disturbances in nonlinear spaces 11 p1723 A66-23316
- Stability and boundedness for solutions of class of complex differential systems obtained in terms of Liapunov-like functions 11 p1725 A66-23426
- Existence of Liapunov functions for problem of Lure with removal of complete controllability and observability 11 p1681 A66-23451
- Liapunov second method applied to interconnected differential systems 11 p1682 A66-23456
- Overall stability of equilibrium position in critical Liapunov case, using extension of Malkin method 12 p1848 A66-24030
- Liapunov second method applied to stability of general second order bang-bang control systems 12 p1850 A66-24259
- Two theorems on Liapunov second method, discussing related automatic control system techniques and asymptotic system stability 12 p1850 A66-24264
- Stability and quality evaluation of nonlinear sampled data control systems using Popov criteria for continuous nonlinear systems 12 p1852 A66-24325
- Dynamic system stability, developments, application and literature 12 p1854 A66-24636
- Stability of pulse frequency modulated closed-loop control systems determined, using state variables which define system output and error 12 p1855 A66-24640
- Man-machine systems for interplanetary exploration, using functional analysis techniques for system design 13 p2013 A66-25281
- Stability criteria of trivial solution of rheolinear differential equation verified by calculating Liapunov function for nonlinear equations 13 p2117 A66-25399
- Plasma stability problem, discussing macroscopic and microscopic approaches and application of Liapunov method 13 p2141 A66-25583
- Averaging method for differential equations with retarded arguments 13 p2118 A66-25827
- Countable systems of differential equations, considering differential operator theory and infinite systems 13 p2119 A66-25850
- Equations for two coupled van der Pol oscillators, Liapunov function used to find four-dimensional phase space nonperiodicity cylinder and subspace of exiting trajectories 13 p2042 A66-26088
- Liapunov stability and instability in critical case of determining equation with even number of zero roots 14 p2336 A66-28065
- Domains of attraction in large of periodic solutions of weakly nonlinear systems, using Liapunov function and differential equations 15 p2525 A66-28509
- Existence, boundedness, decay and exponential decay of solutions of classes of nonlinear systems of differential equations, using suitable Liapunov functions 15 p2525 A66-28510
- Sufficient conditions for recurrence and positivity of diffusion process defined by stochastic differential equation, using Liapunov function 15 p2525 A66-28512
- Singular characteristics of dynamic systems with steady state motion, noting effect of constantly acting small perturbations 15 p2537 A66-28950
- Liapunov stability of motion of heavy rigid body with fixed point moving along spherical surface 15 p2537 A66-28966
- Liapunov method and dynamic programming of stability of motion of variable mass point in Oxyz coordinate reference system, allowing for Earth rotation effects 15 p2538 A66-29046
- Existence and stability theorems for almost periodic solutions of nearly Liapunov systems 15 p2527 A66-29050
- Control system stability under external forces discussing Liapunov function construction, transfer functions and matrix analysis, frequency conditions of absolute stability, etc 15 p2470 A66-29147
- Dynamic system stability, control and observation, noting optimal system synthesis, application of functional analysis, Liapunov function and dynamic programming 15 p2470 A66-29149
- Liapunov function method used simultaneously as criterion of motion stability of several Liapunov functions and of derivatives of higher order than first 15 p2539 A66-29151
- Liapunov methods of studying motion stability of solid bodies with liquid-filled cavities 15 p2539 A66-29155
- Differential equations for motion stability of systems with time delay solved, using Liapunov function methods 15 p2540 A66-29156
- Stability of gyroscopes, gyrostabilizers and gyroscopic systems treated by methods of Liapunov and Chetaev 15 p2542 A66-29173
- Stochastic extensions of techniques for using Liapunov second method in design and analysis of feedback controls, using differential equations 15 p2473 A66-29376
- Normal solvability of Dirichlet problem for Bitsadze elliptic system, noting conditions under which homogeneous problem has nonzero regular solutions 16 p2734 A66-30784
- Controller analytical design for nonautonomous systems, deriving necessary and sufficient conditions for existence of optimum control 16 p2670 A66-30832
- Convex programming problems, developing parametric gradient method for approximate solution 16 p2656 A66-30836
- Solution method for Poincare problem concerning periodic solutions of nonautonomous systems with analytical right-hand side 16 p2735 A66-30968
- Stability analysis for steady disk movement over rough horizontal plane, using Liapunov function method 16 p2715 A66-31616
- Book on stability, oscillation and time lags in differential and differential-difference equations, discussing Liapunov stability theorem 16 p2739 A66-31754
- Stability of constant solutions for second-order nonlinear differential equation which uses Hahn notations and definitions 17 p2945 A66-31837
- Basic theorems of Liapunov direct method with theory of first approximation/linearization/ and stability criteria for linear motions 17 p2946 A66-32325
- Topological classification of higher dimensional systems of ordinary differential equations by Liapunov functions 18 p3127 A66-33976
- Discontinuous Liapunov functions applied to stability analysis of position-controlled system with symmetrically-controlled asynchronous motor 18 p3091 A66-34671
- Poincare-Liapunov systems of ordinary differential equations, qualitatively investigating plane and rough systems, singular points, periodic solutions, etc 18 p3128 A66-34966
- Absolute stability criteria of control system with one nonlinear element, using Liapunov functions 18 p3092 A66-35016
- Sensitivity analysis and Liapunov stability, discussing correctly set problem and parametric imbedding within theory of partial differential equations 19 p3326 A66-36010
- Unilateral estimates under conditions of asymptotic stability of solutions to differential equations with unbounded operators 19 p3390 A66-36190
- Liapunov second method and stability theory of autonomous and certain nonautonomous systems 19 p3391 A66-36438
- Electromagnetic instabilities in collisionless plasma obtained, using Liapunov function 19 p3423 A66-36554
- Liapunov method synthesis of time variable nonlinear multivariable systems, deriving simplified control law for tracking of linear noninteracting model 19 p3335 A66-36697
- Model reference adaptive control system synthesis based on Liapunov direct method 19 p3335 A66-36698
- Interpretation of results obtained by Liapunov method, using parallelepiped imbedded in region of asymptotic stability 19 p3337 A66-36717
- Liapunov functions for finite time stochastic stability and analysis of tracking system 19 p3338 A66-36738
- Transformation matrix converting phase variable form into Schwartz form for application to Liapunov function and Hurwitz criterion 19 p3392 A66-36742
- Motion of arbitrary gyrostabilizer in central Newtonian force field, applying Liapunov stability conditions for regular precession 19 p3362 A66-36841
- Conditional stability and boundedness of conditionally invariant sets derived from vector Liapunov function 21 p3755 A66-38538
- Stability of bodies with holonomically constrained moving parts, using method of Liapunov to demonstrate dependence of



motion stability on potential function of generalized coordinates

[AIAA PAPER 66-101] 21 p3827 A66-38695  
Dynamical system stability examined using direct method of Liapunov, noting application to periodic solutions 21 p3718 A66-39104

Existence of q-ary uniform convolutional codes where q is any prime-power, noting error-correcting ability comparable to familiar maximal-length block codes 21 p3704 A66-39138

Synthesis of optimal Liapunov-Bellman function, noting sequential solution method for independent variables and method using first-order partial differential equation 21 p3758 A66-39281

Normal solvability of Dirichlet problem for Bitsadze elliptic system, noting conditions under which homogeneous problem has nonzero regular solutions 22 p3940 A66-40446  
Liapunov function and Meyer-Kalman-Yakubovich lemma used to obtain frequency domain stability criteria for linear plant with both monotone increasing and odd monotone increasing nonlinear feedback functions 22 p3940 A66-40529

Stability analysis of inertial guidance platform control system with saturation and Coulomb friction nonlinearities, using Liapunov method 23 p4089 A66-41319

Existence and uniqueness theorems in Poincare-Liapunov theory for multipoint control boundary value problems 23 p4085 A66-41539

Perron theorem, Liapunov functions and stability analysis of certain perturbed systems 23 p4085 A66-41552

Nonlinear methods to describe stability motion of solids with liquid-filled cavities 23 p4059 A66-41982

Equations describing stability in Liapunov sense with respect to permanently existing perturbation 24 p4230 A66-42217

Asymptotic stability of linear systems, using matrix analysis 24 p4187 A66-42375

Book on dynamic stability theory using Liapunov second method 24 p4237 A66-42612

Quadratic Liapunov functional derivation for time-delay system 24 p4232 A66-42845

#### LIBRATION

Space probe at Trojan libration point of Earth-Sun system 14 p2384 A66-27890

Stability of spacecraft motion in Earth-Moon system near equilateral libration point 16 p2810 A66-31252

Spacecraft mission to libration centers of Earth-Moon system for collecting meteoroids and photographic program carried out for establishing presence of material at centers 18 p3236 A66-34955

#### LIBRATIONAL MOTION

Routh criterion concerning existence of periodic solutions around triangular libration centers is shown to be valid only at first order [AIAA PAPER 65-681] 01 p0134 A66-10235

Nonlinear resonance effect on attitude librations of undamped rigid gravity gradient stabilized satellite in circular Earth orbit 01 p0143 A66-10811

Material elasticity effects on planar librational motion of rigid satellite under action of gravity 01 p0144 A66-10812

Solar influence on libration point satellite motion for 2500 days in vicinity of Earth-Moon system [AIAA PAPER 65-88] 02 p0288 A66-11556

Lunar physical libration constants determination based on position of crater Mesting A with respect to lunar limb 02 p0293 A66-12265

Lunar topographical asphericity, lunar coordinates, absolute and relative, harmonic analytical interpolation, formations, stratigraphy and optical librations 07 p1139 A66-18265

Limiting periodic solutions around triangular libration centers and Routh criterion 13 p2184 A66-25806

Space probes and Earth-Moon libration points 13 p2186 A66-26012

Cislunar libration point as place of departure, rendezvous and parking for lunar operation 14 p2390 A66-28450

Uniqueness of equilibrium attitudes for Earth-pointing satellites 16 p2806 A66-31541

Gravity gradient stabilization of near-Earth satellite with extensible boom and libration damping with combined lossy spring and magnetic hysteresis rods 18 p3244 A66-33862

Tesseral perturbations of repeating ground track synchronous satellite orbits in gravitational potential 18 p3233 A66-34595

Lagrange-Laplace theory of lunar physical librations extended to include reduced estimate of mechanical ellipticity of lunar equator 19 p3460 A66-35791

Book on methods in astrodynamics and celestial mechanics including libration points, satellite motion, orbit determination, optimization, optimal control, etc 19 p3460 A66-35887

Theory and application of motion associated with equilibrium configurations of dynamical systems applied to astronomy and space dynamics 19 p3461 A66-35888

Three-body model including low thrust forces used to generate artificial libration points or assure stability of five Lagrangian libration points in Earth-Moon space [AIAA PAPER 65-682] 19 p3461 A66-35889

Effect of Sun perturbations on motion near Earth-Moon equilateral libration points [AIAA PAPER 65-683] 19 p3461 A66-35890

Satellite motion under influence of longitude-dependent terms of geopotential in reference frame rotating with satellite mean motion, noting tesseral harmonics effect and dynamical and librational resonances 19 p3470 A66-36388

Long-period orbits in vicinity of equilateral equilibria in restricted problem studied by method similar to method explaining frequency pulling in electronics 20 p3654 A66-37799

DODGE satellite will be capable of two- and three-axis gravity-gradient stabilization at near synchronous altitude, using moment-of-inertia distributions and libration damping 21 p3820 A66-38860

Lagrange libration points in plane of two mutually gravitating heavy masses applied to theory of SYNCOM lunar satellites 22 p3979 A66-40176

Dumbbell librations of satellites in elliptic orbits of small eccentricity determined via WKBJ approximation 24 p4272 A66-42158

Normal modes of libration and response to perturbing torques of satellite with attitude stabilized in all libration angles by wire arrangement 24 p4283 A66-42769

#### LIDAR

Airborne laser-radar light detection and ranging /LIDAR/ systems applied to detection of clear air turbulence /CAT/ 05 p0697 A66-15297

Laser radar as instrument to obtain operational meteorological information 10 p1540 A66-21067

Optical instrumentation radar for real-time positional data on high-speed cooperative targets 13 p2023 A66-25654

Atmospheric observation with advanced light radar, noting equipment characteristics, molecular scattering mechanism, etc 13 p2122 A66-26133

High powered Q-switched ruby laser /LIDAR/ for meteorological application, noting system equations, design, operation, etc 13 p2122 A66-26548

Optical communication using laser techniques 14 p2234 A66-26918

Laser Doppler velocimeter for measuring localized flow velocities in liquids 14 p2306 A66-27053

Radio location by coherent light with quantum structure 14 p2242 A66-28157

Coherent transmission of optical radar from laser source and use of RF subcarriers placed on optical beams for wideband communications purposes 14 p2244 A66-28404

Precision automatic tracking using CW He-Ne laser, noting performance and application 14 p2245 A66-28448

Atmospheric exploration with lidar, noting high resolution and sensitivity 15 p2530 A66-28600

Airborne laser radar investigation of clear air turbulence 15 p2533 A66-28928

Optical radar scanning system, using ruby laser source for meteorological studies 15 p2450 A66-28929

Submillimeter and millimeter radar and LIDAR astronomy contribution to solar

system communications, and planetary, and lunar surface studies 15 p2595 A66-29002

Measurement of distance to Moon by optical radar, discussing ruby laser/photomultiplier apparatus and procedure 16 p2647 A66-30291

Cloud height measurement by optical radar systems 17 p2949 A66-32884

Lidar detection of backscatter from upper atmosphere 17 p2875 A66-32929

Gallium arsenide diode laser as pulsed IR source for experiment and design considerations for radar indication of cloud height and visibility 18 p3066 A66-33616

Optical techniques in laser detection systems 20 p3516 A66-37439

Detecting concentration of nitric oxide in metastable state in upper atmosphere, using giant-pulse Raman laser sources 24 p4203 A66-43022

#### LIE GROUP

Group classification of solutions to Hopf equation according to type of viscosity coefficient 08 p1209 A66-19476

Left almost periodic function defined on topological group G is not necessarily right almost periodic even if g is Lie group 18 p3127 A66-34461

Partly invariant solutions of equations admitting Lie group and application to gas dynamics 23 p4086 A66-42024

#### LIFE

S ABIOTIC GENESIS

S BIOGENESIS

S EVOLUTION

S EXTRATERRESTRIAL LIFE

S FATIGUE LIFE

#### LIFE DETECTOR

Martian life-detection instruments and experiments, examining biological criteria and visual, organic, chemical and metabolic tests 02 p0183 A66-11608

Future of environmental biology, discussing space research on living organisms in extraterrestrial environment 04 p0470 A66-14069

Detection of microbial life on near planets by measuring physical parameters 06 p0810 A66-15909

Biosyllektes, device for collecting microorganisms in interplanetary space or upper atmospheric layers 06 p0814 A66-15914

Automated life detection on Martian environment based on metabolism, reproduction and chemistry 06 p0818 A66-16323

Extraterrestrial life detection and life support systems in manned space travel, noting electronic equipment necessary for it 08 p1175 A66-18727

Search for terrestrial life at kilometer resolution, using Tiros and Nimbus meteorological satellite photographs 10 p1605 A66-21209

Spectral reflectance of selected vegetation, animal integuments and minerals for life detection on Mars 10 p1608 A66-21520

Approaches for analyzing possible life forms on other planets, noting detection of microorganisms or enzymes, radio contact and retracing life in laboratory 13 p2009 A66-25798

Pasteur Probe assay of asymmetry of D, L amino acids in detection of Martian life 15 p2447 A66-30025

Book on extraterrestrial biology covering origin processes of life, planets, life detection, etc 16 p2639 A66-30874

Life detection instrument incorporating metabolism and growth experiments including detection of metabolism of radioactive substrates, photosynthesis, etc 18 p3062 A66-34368

Processing of planetary soil samples for detection of extraterrestrial life 18 p3062 A66-34370

Life detection on Mars by visual techniques, discussing imaging devices, filters, shutters and microscopy 18 p3063 A66-34371

Mass spectrometry and gas chromatography in analysis of organic compounds present in extraterrestrial bodies to provide information on existence of life 18 p3059 A66-34373

Mars probe instrument package design for biological exploration 19 p3287 A66-35572

Automated biological laboratory with initial



- missions to Mars, noting functions operation and necessary instrumentation 24 p4167 A66-42671
- Extraterrestrial life detection on Mars and limitations on terrestrial observations and flyby and landing 24 p4167 A66-42673
- missions Wolf Trap Mars microorganism detection, assuming photosynthetic and respiration cycles in inorganic biochemical compounds 24 p4168 A66-42676
- LIFE SCIENCE**
- Possibility of life originating in different forms in various parts of universe as response to changing environmental conditions 01 p0017 A66-10300
- Prevalence and diversity of life in Cosmos, tracing divergent evolution in response to variety of environment 01 p0017 A66-10303
- Papers on experimental and theoretical aspects of exobiology 02 p0181 A66-11601
- Bibliography of current aspects of exobiology dealing with solar system, life detection system, origin of life and life in universe 02 p0182 A66-11612
- Migration of north and south poles by angular displacement of Earth mass, explaining geographical distribution of flora and fauna, past and present 05 p0667 A66-14730
- Chemical evolution studied by finding and reconstructing chemical reactions that might have occurred among primeval molecules on surface of Earth 05 p0629 A66-15017
- Nucleic acid molecule reproduction discussing probability of life development under favorable environmental circumstances 06 p0952 A66-15915
- Text on evolution, interpreting functions of body organs in terms of chemical processes and tracing development of complex organic molecules 10 p1487 A66-22065
- RCA life sciences paper on microscale medical sensors, adaptation theory, logic techniques and human factors engineering 11 p1647 A66-22297
- Mars environmental conditions, life organism detection, evaluation and limiting effects 11 p1771 A66-22715
- Life sciences and space research, Volume 4, International Space Science Symposium, Argentina, May 1965 19 p3283 A66-35567
- Origin of constituents of nucleic acid and protein molecules, noting biological molecules synthesis under conditions similar to those prevailing in prebiotic Earth, following Oparin-Haldane hypothesis 20 p3507 A66-38029
- Book on natural evolution including origins of universe, stellar and planetary evolution, beginnings of life on Earth and development of intelligence and technical civilizations among galactic communities 24 p4163 A66-42347
- NASA Biosatellite Program exploring dynamic space flight effects on terrestrial organisms and Earth diurnal rotation effect on biological rhythm 24 p4168 A66-42675
- LIFE SUPPORT SYSTEM**
- SA CLOSED ECOLOGICAL SYSTEM
- SA PRESSURIZED CABIN
- SA PRESSURIZED SUIT
- Program for engineering development of integrated spacecraft environmental control and life support systems and solution of man-machine integration problems [SAE PAPER 650813] 01 p0021 A66-10820
- Physiological-ecological investigations of *Chlorella* cultures as link in closed ecological system 01 p0018 A66-10981
- Animal and human test of manned spacecraft life support system consisting of closed system with recirculating air loop, examining potassium superoxide-potassium hydroxide chemistry 02 p0183 A66-11492
- Thermal control in advanced integrated life support system design to accommodate four-man crew on one-year Earth orbit mission 02 p0185 A66-11631
- Heat rejection from space radiator of power system used as energy source when integrated with life support system 02 p0186 A66-11642
- Tests of advanced life support and environmental control systems in manned space laboratory 02 p0186 A66-11646
- Apollo space suit design discussing construction, purpose and operating conditions of liquid-cooled life support system 03 p0328 A66-12631
- Electrolysis-Hydrogenomonas bacterial bioregenerative life support system for manned space flight of long duration 06 p0815 A66-15929
- Alkali metal superoxide applied by Soviet as active chemical for space cabin air revitalization 06 p0819 A66-16830
- Life support closed cycles for missions to outer space lasting 12 months or longer, considering recovery and replenishing of water, food and oxygen from wastes 07 p0998 A66-17229
- Zero-gravity effect on opossum fetus observed by TV system in proposed satellite 08 p1176 A66-18726
- Extraterrestrial life detection and life support systems in manned space travel, noting electronic equipment necessary for it 08 p1175 A66-18727
- Drinking water reclamation from urine by thermoelectrics, including operational theory and data for working models 08 p1176 A66-18730
- Oxygen recovery from metabolic carbon dioxide for spacecraft environment 08 p1177 A66-18821
- Recovery of reusable products of human excretory wastes in closed-loop life support systems for long-duration manned spaceflight [AICE PREPRINT 19B] 10 p1491 A66-21185
- Chemical analysis of permanent and trace organic gases in 30-day manned experiment, using gas chromatography 12 p1811 A66-25011
- Integration of life support system and propulsion system for manned interplanetary space missions 13 p2012 A66-25246
- Integrated space suit, suit loop and backpack system for intravehicular operation on interplanetary missions 13 p2013 A66-25277
- Algatron, device for life support systems in space, providing potable water, oxygen supply, stabilizing human wastes by algal photosynthesis 13 p2015 A66-25702
- Thermal integration of electric power for use in life support system to reduce total electrical power requirements [AIAA PAPER 64-722] 13 p2004 A66-26617
- Regenerative life support system for four-man crew on long duration tests, noting biological constraint parameters 17 p2862 A66-32138
- Carbon dioxide control for manned spacecraft, discussing regenerative methods for eliminating system weight dependence on mission duration 17 p2863 A66-32141
- Ideal operation of portable life support system /PLSS/ requires anticipatory response to astronauts changing heat dissipation needs 17 p2863 A66-32152
- Life support subsystem for recovering breathable oxygen by water vapor electrolysis 17 p2866 A66-32194
- Aerospace life support - Conference, American Institute of Chemical Engineers, Houston, February 1965 17 p2866 A66-32667
- Water electrolysis unit designed as flight prototype to support four-man crew for one-year mission with 90-day resupply intervals [AICE PREPRINT 47B] 17 p2867 A66-32671
- Manned spaceflight analytical instrumentation uses design tradeoff of reduction in size with loss of versatility 17 p2867 A66-32677
- Suitability of oxygen-helium atmosphere for manned space missions proven by 56-day human exposure at 258 mm Hg total pressure 18 p3057 A66-33768
- Major and minor constituents of oxygen-helium atmosphere to which humans were exposed for 56 days 18 p3057 A66-33769
- Human renal response to 56-day exposure to oxygen-helium atmosphere at 258 mm Hg total pressure 18 p3057 A66-33770
- Human blood enzyme response to 56-day exposure to oxygen-helium atmosphere at 258 mm Hg total pressure 18 p3057 A66-33771
- Exercise performance and cardiovascular response of man exposed for 56 days to oxygen-helium atmosphere 18 p3057 A66-33772
- Respiratory effects of 56-day human exposure to oxygen-helium atmosphere 18 p3058 A66-33774
- Bite-size foods included in feeding study of man exposed for 56 days to oxygen-helium atmosphere 18 p3061 A66-33775
- Nutritional evaluation of feeding bite-size foods to man exposed for 56 days to oxygen-helium atmosphere 18 p3061 A66-33776
- Lunar Exploration System for Apollo /LESA/, discussing life support, power, fuel, communications systems, mission objectives and base evolution concept phases [SAE PAPER 660449] 18 p3093 A66-33895
- Apollo LEM ECS and main subsystems design emphasizing maintenance of pressure, temperature, relative humidity and oxygen at safe levels 18 p3062 A66-33956
- Life support requirements encountered in manned space flights, considering cycle involving oxygen, food and water in terms of process criteria 19 p3485 A66-36231
- Weight and size optimization of flight type cryogenic storage supply system of oxygen and hydrogen for fuel cell operation and life support in manned spacecraft 19 p3292 A66-36233
- Physical and psychological aspects of man in space, examining oxygen supply, temperature extremes, meteorites, radiation and effects of confinement, isolation and sensory impoverishment 19 p3287 A66-36645
- Two-gas regenerative life support system for pressure, thermal and humidity control, water reclamation, atmospheric circulation, carbon dioxide and trace contaminant removal [AIAA PAPER 65-501] 20 p3510 A66-38172
- Storage, dumping and regeneration techniques in air, water and food needed to keep astronauts alive 22 p3857 A66-40022
- Cleaning techniques for zip gun or hand-held maneuvering unit and environmental life support system or ventilation control module used for astronaut White walk in space 22 p3886 A66-40039
- Life support systems for crew comfort and safety, considering thermal and radiation environmental control, carbon dioxide removal, cryogenic gas storage, etc 22 p3857 A66-40129
- Book on problems of return from space including heat protection, materials, development testing, life support, design, simulation and other related activities 22 p3988 A66-40875
- Tests of advanced life support and environmental control systems in manned space laboratory simulator 24 p4168 A66-42779
- Onboard spacecraft generation system extracts necessary breathing oxygen from ambient air, using electrochemical cell that separates oxygen from inert gases and impurities 24 p4162 A66-42956
- Regenerative air conditioning systems of spacecraft cabins for long missions, analyzing principal parameters of gas mixtures for life requirements 24 p4169 A66-43142
- Physicochemical methods of creating life support systems in spacecraft cabins 24 p4169 A66-43143
- Life support system in spacecraft cabins based on biological circulation of substances 24 p4166 A66-43144
- Safety and survival in manned space flights, discussing space suits, escape, life preservation after soft landing, etc 24 p4169 A66-43145
- LIFETIME**
- SA PLASMA LIFETIME
- SA SATELLITE LIFETIME
- Rotating mirror arrangement with tungsten light source for minority carrier lifetime measurements on semiconductors 03 p0369 A66-12611
- Lifetime of semiconductor devices determined from noise levels 06 p0860 A66-17195
- Transition probabilities and lifetimes in ionized argon gas lasers 13 p2102 A66-26207
- Fluorescence lifetime measuring technique employing pulsed or modulated RF discharges applied to emission of second positive and first negative systems of nitrogen 14 p2337 A66-27974
- Fluorescent lifetimes of neodymium,



ytterbium and samarium incorporated in ordered perovskite-type compounds determined, noting crystal structure potential for laser 14 p2367 A66-27976

Life expectancy of form C dry reed switch as function of operating environment 15 p2460 A66-28992

Lifetime measurement for minority carriers injected into germanium by electron bombardment 15 p2567 A66-29409

Lifetime of semiconductor devices determined from noise levels 19 p3315 A66-35553

Effective charge carrier lifetime in silicon p-i-n junction detectors determined, using transit time for carriers produced by incident radiation 19 p3318 A66-35913

DC-photodecay method for investigating minority-carrier lifetimes in silicon crystals 21 p3736 A66-38747

Coverage dependent evaporative lifetimes of various metals and oxygenated W ribbon filaments at high temperatures 22 p3934 A66-40097

**LIFT**

SA DRAG

SA GROUND EFFECT

SA INTERFERENCE LIFT

SA JET LIFT

Problem of operational flexibility in Mars landing mission, discussing use of lifting vehicles 13 p2191 A66-25273

Aerodynamic lift and moment during unsteady flow of ideal incompressible fluid around lattice of thin bent profile 16 p2690 A66-31620

Prediction of drag due to lift of plane wings at subsonic speeds, based on correlation of wind tunnel measurements in terms of viscosity effect on lift curve slope 16 p2632 A66-31664

Minimum of maximum overload in braking of vehicle in atmosphere, examining aerodynamic lift on basis of Pontryagin maximum principle 22 p3986 A66-40465

**LIFT AUGMENTATION**

SA DOWNWASH

Flight experiments to assess stalling behavior and handling problems arising in design, maintenance and operation of suction wing for high lift [AIAA PAPER 65-750] 03 p0319 A66-12586

Boundary layer control for improvement of lift at lower angles of attack by carrier-based supersonic aircraft [AIAA PAPER 65-751] 03 p0321 A66-13055

Boundary layer control high lift system for high speed aircraft, using ejector for momentum augmentation and air bleed from propulsion system [AIAA PAPER 64-589] 05 p0610 A66-15070

V/STOL aircraft engine technology, discussing engine configuration, lift augmentation, thrust deflection, efficiency parameters, etc 06 p0943 A66-17023

Direct lift control as landing approach aid by providing more rapid means of changing and controlling flight path than conventional methods [AIAA PAPER 66-14] 08 p1167 A66-18985

Jet drag solutions for symmetrical struts of various shapes, thickness ratios and slot widths in quiescent and uniform streaming flow 12 p1800 A66-25005

**LIFT COEFFICIENT**

Theoretical and experimental analysis of structural, functional and design characteristics of air cushion vehicles at zero speed, examining lift coefficient, viscosity effect, static tests, etc 01 p0011 A66-10490

Advances attributable to XB-70 program including aerodynamic concepts, structural material, design, systems and equipment development [SAE PAPER 650798] 01 p0012 A66-10844

Lift coefficient in two-dimensional smoke wind tunnel noting symmetrical, cambered and leading double-edge slot wing section 03 p0317 A66-13216

STOL for high speed aircraft, discussing aerodynamic parameters, lift coefficient, increase methods, etc 09 p1327 A66-20245

Breguet 941 STOL aircraft design and performance, noting maximum lift coefficient and single-shaft power plant 10 p1483 A66-21716

Effects of nonlinearities in lift and pitching moment curves on longitudinal motion of aircraft, comparing approximate analytical method with computer calculations 13 p1995 A66-26285

Short takeoff and landing for high speed aircraft, discussing aerodynamic parameters of lift coefficient of flap system, lift-drag ratio and thrust 18 p3052 A66-33971

STOL flying possibilities and limitations, considering aircraft generating high lift by using fixed wing and airfoil features 23 p4016 A66-41774

Comparison of lifting characteristics of profile with air ejection onto slotted and unslotted flaps, examining dependence on jet impulse coefficient 23 p4010 A66-41795

First-and second-order theory for uniform shear flow past airfoil, obtaining expressions for pressure, lift and moment coefficients 23 p4011 A66-41879

**LIFT DEVICE**

SA HIGH LIFT DEVICE

Rolls-Royce RB 108 lift-jet engine design, characteristics and V/STOL research 05 p0745 A66-15298

Glide slope direct lift control of carrier landings, discussing trim change with actuation and longitudinal stability and control 07 p0986 A66-17272

Jet engine technology, including spinoff from lift jet, propulsion systems, cost estimates, etc 16 p2791 A66-31280

Inlet/door performance characteristics of VTOL lift-engines studied in full-scale wind tunnel tests [AIAA PAPER 66-655] 18 p3048 A66-34222

**LIFT DISTRIBUTION**

Circulation distribution for swept-back wing of finite span and large aspect ratio in subsonic flow by asymptotic method 07 p0981 A66-18033

Idealized ground effect wing, with tips close to ground, assumed to be semicircular lifting line in transverse plane, considering minimum induced drag 12 p1800 A66-25006

Electrical analogy for wing in unsteady supersonic flow, determining distribution of lifting power for various aspect ratios 13 p1990 A66-25405

**LIFT-DRAG RATIO**

Configuration synthesis and optimal utilization of supersonic favorable interference to obtain high lift-drag ratios [AIAA PAPER 65-752] 03 p0315 A66-12732

Lateral maneuver capability of high lift-drag ratio used to extend period of daylight landings from orbit 03 p0390 A66-12774

Maneuvered reentry of vehicle with aerodynamic lift into planet atmosphere, using motion equations and considering reentry trajectories as minor circles 03 p0432 A66-13129

Prediction technique for impulse required to supplement aerodynamic rotation of satellite orbit plane [AIAA PAPER 66-59] 06 p0956 A66-17085

Reference-point results applied to variations in laminar heat transfer to total vehicle over range of vehicle attitudes and associated trajectories [AIAA PAPER 66-28] 07 p0980 A66-17890

STOL for high speed aircraft, discussing aerodynamic parameters, lift coefficient, increase methods, etc 09 p1327 A66-20245

Slender profile of infinitely thin supersonic wing that provides minimum mean heat-transfer coefficient at given lift-drag ratio 09 p1328 A66-20754

Parametric investigations of supersonic long-haul aircraft, discussing operational profile, optimal lift-drag ratio, takeoff weight, civilian and military aircraft 10 p1482 A66-21371

Lift-drag ratio, specific impulse, aspect ratio and weight of payload and power plant considered for STOL aircraft 10 p1483 A66-21398

Boundary layer effect on lift and drag characteristics of hypersonic lifting bodies 10 p1480 A66-21409

Ground proximity effect on maximum lift-drag ratio for wing with uniform spanwise circulation, considering vortex model 11 p1636 A66-23253

Aerodynamic characteristics of rectangular plates in hypersonic flow of rarefied gas

differing in aspect ratio, thickness and angles of attack, determining maximum lift-drag ratio 12 p1798 A66-24442

Maximum lift/drag ratio wing for supersonic environment 13 p1991 A66-25634

Hypersonic lift-drag ratio and landing modes in manned entry vehicle design 15 p2605 A66-28742

L/D ratio for gliding recovery of first stage of launch vehicle, using stage separation conditions as parameters 16 p2807 A66-30348

Lift-to-drag ratio attainable by slender, homothetic body at hypersonic speeds, assuming Newtonian pressure distribution and constant skin-friction coefficient 17 p2838 A66-32348

Extremization of products of powers of functionals as applied to flat top wings for maximizing lift drag ratio in hypersonic flow 17 p2842 A66-33242

Lift, drag and static pitching measurements on lifting bodies at simulated hypersonic cold-wall conditions [AIAA PAPER 66-467] 18 p3046 A66-33651

Elastomeric ablative thermal shield material to meet system requirements for lifting reentry vehicles having lift-drag ratio of 0.5 to 1.5 18 p3240 A66-33801

Atmospheric reentry trajectory of space vehicle at orbital velocities and constant lift-drag ratio 18 p3244 A66-33879

Lift and drag of supercavitating isolated hydrofoil or hydrofoils in cascade, noting characteristics of flat plate and circular arc foils 18 p3100 A66-34642

Wall effect removal on supercavitating flow, estimating effects due to tunnel ducts and boundary layer blocking 18 p3101 A66-34643

Flow analysis of swept back blades in water tunnel, noting flow patterns, surface pressure distribution, lift-drag ratio, etc 18 p3049 A66-34649

Similarity laws for bodies maximizing lift-to-drag ratio at hypersonic speeds, considering longitudinal and transversal contours 19 p3276 A66-36245

Glide range with variable lift drag ratio expressed in power series of speed 20 p3492 A66-37428

Wind tunnel testing of delta-like lifting bodies at low, supersonic and hypersonic speeds, noting lift to drag ratios and off-design performance of caret wave-rider wings [ICAS PAPER 66-24] 23 p4007 A66-41011

Optimal redistribution of lifting surface between wing and stabilizer-elevator unit ensuring minimum reduction of lift-drag ratio 23 p4011 A66-41796

Optimization of lift-drag ratio of power law half-bodies in hypersonic viscous flows, considering interrelation between body shape and skin friction 23 p4012 A66-41915

**LIFT FAN**

Aircraft control power requirements provided by lift fan propulsion system for V/STOL flight, noting gas power transfer [SAE PAPER 650831] 01 p0130 A66-10830

Fan-wing combinations for three-dimensional flow solutions investigated to determine V/STOL aerodynamic characteristics [AIAA PAPER 65-85] 05 p0606 A66-15076

Tip turbine lift-fan system with single rotor for thrust augmentation of gas generator for advanced V/STOL aircraft [AIAA PAPER 65-708] 05 p0611 A66-15163

Lift fans for advanced V/STOL aircraft, describing performance improvement parameters 06 p0807 A66-17020

Fan-wing combinations for three-dimensional flow solutions investigated to determine V/STOL aerodynamic characteristics [AIAA PAPER 65-85] 14 p2274 A66-27415

Lift fan propulsion system using 62.5-inch lift fans flight tested in XV-5A aircraft from hover to subsonic flight regions [AIAA PAPER 66-739] 22 p3972 A66-40628

Balance bridging techniques using air supply lines for powered lift-fan model testing [AIAA PAPER 66-751] 22 p3893 A66-40637

**LIFT FORCE**

Lift force of airfoil section determined for sudden change in angle of attack, analyzing



randtl vortex positions 03 p0314 A66-12526  
 Formula for determining takeoff distance  
 of aircraft, taking into account lifting force,  
 air and motion resistance and transition to  
 larger angle of attack 11 p1637 A66-22849  
 Lifting systems and motion of slender  
 profile at arbitrary distance from liquid or  
 solid boundary, using kernel degeneration  
 method to reduce singular equation to  
 Fredholm equation 13 p2067 A66-26531  
 Stabilizing methods for hypersonic aircraft,  
 noting effect of aircraft characteristic  
 parameters on magnitude of balancing  
 coefficients of lifting 14 p2223 A66-27680  
 Lift engine technology, noting effect on  
 operational transport aircraft design, VTOL  
 capabilities, low speed control, 17 p2844 A66-32732  
 Unsteady state lift and moment action on  
 lattice of profiles moving in incompressible  
 fluid, determining suction originating at  
 leading edges of profiles 23 p4009 A66-41723  
 Single air flow acceleration and deviation  
 for propulsion and lift of high speed  
 aircraft, analyzing long-range flight paths  
 [ICAS PAPER 66-41] 23 p4122 A66-42070  
**LIFTING BODY**  
 Manned lifting body sizing, discussing  
 system requirements, constraints and  
 relationship to parametric vehicle design  
 data [AIAA PAPER 66-47] 06 p0958 A66-16259  
 Use of lifting upper stage to achieve large  
 offsets during ascent to orbit [AIAA PAPER 66-60] 06 p0960 A66-17108  
 Lifting body with controllable radial force,  
 examining acceleration and deceleration,  
 equation of motion, target hitting accuracy  
 improvement via force variation, 11 p1733 A66-23338  
 Optimum autopilot design for  
 maneuverable lifting 11 p1733 A66-23342  
 Dynamic programming method for  
 approximate solution of gliding flight and  
 minimum time to climb problems in  
 boundary value theory 11 p1778 A66-23349  
 Analogy between impulsive flow over  
 circular cylinders and flat plates, and  
 separated flow about lifting bodies moving  
 at high angles of attack in subsonic and  
 supersonic range [AIAA PAPER 65-395] 12 p1795 A66-23575  
 Meteorological environment considerations  
 in terminal flight region relating to all-  
 weather land recovery operations of lifting  
 reentry vehicles [AIAA PAPER 66-360] 12 p1907 A66-24492  
 Vertical profile of wind velocity  
 determined, using lifting sensors for  
 prelaunch rocket operations [AIAA PAPER 65-15] 12 p1883 A66-24698  
 Use of lift to increase payload of  
 unmanned Martian landing capsule,  
 discussing approach corridor and capsule  
 design 13 p2191 A66-25271  
 Equations for translatory motion of lifting  
 body moving at hypersonic speed,  
 considering Earth sphericity, noting effect  
 of centrifugal forces 13 p2193 A66-26448  
 Structural and heat shield designs for  
 lifting entry vehicles for orbital missions  
 analyzed for effects of wall thickness and  
 weight on vehicle size and total  
 weight 14 p2393 A66-28025  
 Oscillatory trajectories in atmospheric  
 entry of lifting vehicles at subcircular  
 speeds and constant angles of attack with  
 initial conditions deviating from equilibrium  
 glide 17 p3016 A66-33065  
 Lift, drag and static pitching  
 measurements on lifting bodies at simulated  
 hypersonic cold-wall conditions  
 [AIAA PAPER 66-467] 18 p3046 A66-33651  
 Similarity laws for bodies maximizing lift-  
 to-drag ratio at hypersonic speeds,  
 considering longitudinal and transversal  
 contours 19 p3276 A66-36245  
 Lifting wings in supersonic regime,  
 analyzing flow separation at leading edges  
 [ICAS PAPER 66-20] 22 p3847 A66-40670  
 Motion of solid body with rotating  
 flywheels rotating at constant velocities  
 relative to inertial space and  
 body 22 p3948 A66-40682  
 Use of lift to increase payload of  
 unmanned Martian landing capsule,

discussing approach corridor and capsule  
 design 23 p4132 A66-41113  
 Use of lifting upper stage to achieve large  
 offsets during ascent to orbit  
 [AIAA PAPER 66-60] 23 p4132 A66-41114  
 Optimization of lift-drag ratio of power law  
 half-bodies in hypersonic viscous flows,  
 considering interrelation between body  
 shape and skin friction 23 p4012 A66-41915  
**LIFTING REENTRY**  
 Controlled ballistic, steady lift and variable  
 lift reentry of winged  
 spacecraft 04 p0584 A66-13526  
 Comparison of adaptive and nonadaptive  
 control systems for lifting entry vehicles  
 [AIAA PAPER 66-48] 06 p0960 A66-17100  
 Rheolectric analogy using apparent mass  
 to obtain static and dynamic stability  
 derivatives for lifting-body reentry vehicles  
 [AIAA PAPER 66-58] 08 p1303 A66-18991  
 Manual guidance system for atmospheric  
 entry of lifting reentry  
 vehicles 10 p1554 A66-21930  
 Reentry scattering due to equilibrium  
 incidence without using Allen  
 hypothesis 16 p2796 A66-30315  
 Motion equations and Pontryagin maximum  
 principle applied to space vehicle reentry  
 trajectory optimization through independent  
 control of lift and drag 16 p2809 A66-30884  
 Viscous aerodynamic contributions to  
 forces and moments on front face of blunt  
 lifting reentry vehicle in producing  
 trajectory error [AIAA PAPER 66-464] 16 p2631 A66-31471  
 Lifting reentry test phases and effect of  
 pilot performance on miss distance in first  
 manned Gemini flight, discussing spacecraft  
 control 17 p3016 A66-32685  
 Trajectory control scheme effect on  
 performance of lifting entry vehicles  
 [AIAA PAPER 66-407] 17 p3016 A66-32746  
 Elastomeric ablative thermal shield  
 material to meet system requirements for  
 lifting reentry vehicles having lift-drag ratio  
 of 0.5 to 1.5 18 p3240 A66-33801  
**LIFTING ROTOR**  
 Stopped and slow rotor aircraft  
 configuration for fundamental limitations on  
 forward flight speed of compound  
 helicopters [SAE PAPER 650806] 01 p0012 A66-10847  
 Annular vortices method applied to  
 determine aerodynamic characteristics of  
 lifting propeller in axial and oblique  
 flows 23 p4010 A66-41785  
**LIFTING SURFACE**  
 Improved numerical procedure for  
 harmonically deforming lifting surfaces from  
 supersonic kernel function method  
 [AIAA PAPER 66-78] 08 p1163 A66-18995  
 Kernel function procedure for solving  
 oscillatory lifting surface problem at  
 subsonic speeds, using least squares  
 method 08 p1165 A66-19149  
 Subsonic aerodynamic loading on  
 harmonically oscillating nonplanar lifting  
 surfaces in kernel-function  
 formulation 21 p3694 A66-38733  
 Supersonic aerodynamic problem of wing-  
 body interaction and solution within lifting-  
 surface theory, using analog method  
 [ICAS PAPER 66-22] 23 p4008 A66-41254  
 Optimal redistribution of lifting surface  
 between wing and stabilizer-elevator unit  
 ensuring minimum reduction of lift-drag  
 ratio 23 p4011 A66-41796  
 Reverse flow and deformation optimization  
 theories applied to subsonic aeroelasticity of  
 lifting surface in harmonic oscillation, using  
 numerical integration and computer  
 programs 24 p4157 A66-42343  
**LIGHT**  
 SA AIRPORT LIGHT  
 SA COHERENT LIGHT  
 SA EXTRAGALACTIC LIGHT  
 SA GLARE  
 SA LAMP  
 SA LUMINESCENCE  
 SA MERCURY LIGHT  
 SA PHOTON  
 SA POLARIZED LIGHT  
 SA QUARTZ LIGHT  
 SA RUNWAY LIGHT  
 SA SUNLIGHT  
 SA ULTRAVIOLET LIGHT  
 SA XENON LIGHT  
 SA ZODIACAL LIGHT

Spatial structure for second harmonic  
 generated in anisotropic medium by finite-  
 aperture light beam 08 p1233 A66-18969  
 Role of light in chemical and biochemical  
 evolution noting photosynthetic reactions  
 depending on chlorophylls, pigment system,  
 etc 17 p2853 A66-32102  
**LIGHT, SPEED OF**  
 Wave attenuation with phase velocity  
 greater than speed of light in infinite  
 plasma layer between ideal metallic  
 plates 02 p0268 A66-11785  
 Second postulate of special theory of  
 relativity proved by existence of short  
 period Cepheids 05 p0759 A66-14888  
 Velocity of light determined from  
 photometric distance comparison, using  
 invar gauges 08 p1256 A66-19344  
 Lorentz-invariant Markov process in  
 relativistic phase space 12 p1914 A66-24406  
 Velocity of light determined from  
 photometric distance comparison, using  
 invar gauges 19 p3400 A66-36052  
 Feasibility of improved accuracy in light  
 velocity measurement in vacuum by using  
 superconducting parallelepiped  
 hyperfrequency cavity 19 p3360 A66-36253  
 Time contraction physically explained for  
 objects moving with velocities significant  
 with respect to velocity of  
 light 21 p3817 A66-39600  
 Augmented special relativity theory to  
 account for Einstein effects, with extension  
 to general scalar field theory and notes on  
 corpuscular light and galactic-centered  
 reference frame 23 p4090 A66-41273  
**LIGHT ABSORPTION**  
 Sedimentation rates of metallic particles in  
 cyclohexane medium measured by light  
 absorption 01 p0069 A66-10750  
 Pulsed laser-created plasmas by light  
 absorption by skin effect 03 p0403 A66-12975  
 Electric field effect on light absorption by  
 silicon throughout region of phonon-assisted  
 indirect transitions 03 p0412 A66-13150  
 Laser digital devices, examining quenching  
 of gain and optical  
 absorption 05 p0693 A66-14826  
 Light scattering in spherical nebula of  
 great optical thickness 05 p0765 A66-15417  
 Wooten method for measurement of true  
 light absorption in aerosols, making it  
 unnecessary to make separate light  
 scattering measurement 06 p0906 A66-17032  
 Comparison of properties of mode and  
 nonmode GaAs diodes, discussing emission  
 spectra oscillations and absorption  
 constant 07 p1042 A66-17334  
 Displacement of absorption band edge into  
 long wave region by phonon-caused  
 damping 07 p1105 A66-18372  
 Mechanism for indirect phototransition in  
 semiconductors near natural absorption edge  
 when interacting with current  
 carriers 07 p1105 A66-18373  
 Particle distribution and motion in field of  
 force, discussing density profile, energy  
 dissipation, Coulomb charge shielding for  
 local thermodynamic equilibrium and free  
 orbital motion 08 p1261 A66-18743  
 Light pulse absorption in gas and  
 measurement of temperatures attained  
 noting hydrodynamic, breakdown and  
 radiative transfer mechanisms and wave  
 velocities 08 p1319 A66-19276  
 Atmosphere of Mars as absorbing, ascribing  
 red color to selective absorption in  
 atmospheric layer 08 p1294 A66-19328  
 Change in photoconductivity and  
 photoelectromagnetic effect of gallium  
 arsenide single crystals caused by constant  
 illumination of spectral  
 compositions 09 p1412 A66-19997  
 Spin-magnetophonon interaction effect on  
 light absorption in  
 semiconductor 09 p1426 A66-20199  
 Accuracy in determination of light  
 absorption coefficient of semiconductors  
 with reflection coefficients of 0.2 to  
 0.5 09 p1431 A66-20943  
 Retention of semiconductor properties by  
 gallium arsenide after irradiation by fast-  
 neutron flux 10 p1589 A66-22167  
 Transmission factor of rectilinearly  
 polarized light as affected by plasma  
 oscillations in granular films of  
 gold 13 p2163 A66-25440  
 Photoabsorption power due to sodium



interband, using orthogonalized plane wave evaluation of matrix elements in oscillator strengths 14 p2365 A66-27753  
 Accuracy in determination of light absorption coefficient of semiconductors with reflection coefficients of 0.2 to 0.5 15 p2557 A66-28531  
 Light dispersion and absorption by impurity centers in solids calculated via two-particle Green function method, assuming weak electron-phonon interaction 15 p2559 A66-28632  
 Resonant absorption of monochromatic light in system with intermediate energy level 15 p2516 A66-29355  
 Electron vibration spectra of light absorption in molecular crystals, taking oscillation frequency changes as principal mechanism of exciton-phonon interaction 16 p2780 A66-31178  
 Light absorption coefficient for indirect photon transitions during Coulomb interaction of electrons at high electron densities 16 p2787 A66-31766  
 Electric field effect for free carrier absorption, determining coefficient for acoustic phonon 17 p2976 A66-32264  
 Diffuse reflection by planetary inhomogeneous atmosphere with albedo for single scattering decreases exponentially with optical depth 18 p3230 A66-34149  
 Light absorption by free current carriers role in kinetic equations of semiconductor laser/radiation system 18 p3119 A66-34691  
 Retention of semiconductor properties by gallium arsenide after irradiation by fast-neutron flux 19 p3441 A66-35781  
 Resonant absorption of monochromatic light in system with intermediate energy level 20 p3604 A66-37359  
 Effective brightening of laser radiation propagating in strongly absorbing medium 22 p3930 A66-39770  
 Light absorption by optically pumped atoms undergoing magnetic resonance, noting modulation amplitudes and modulation frequency limitation for primary interaction 22 p3930 A66-39807  
 Optical pumping on He 4 atom in metastable level, examining modulation of light in absorption in longitudinal and transverse beams and obtaining magnetic resonance curves 22 p3930 A66-39808  
 Magnetic resonance in He 3 ground states examined through interaction with metastable atoms in gas discharge, observing transfer of transverse magnetization by collision 22 p3931 A66-39809  
 Photoabsorption cross section of atomic hydrogen by molecular hydrogen flow through discharge tube 23 p4098 A66-41245  
 Monograph on absorption, scattering and attenuation of light and IR radiation in atmosphere 23 p4087 A66-41272  
 Absorption coefficient of light in semiconductors in crossed electric and magnetic fields, examining conditions for Franz-Keldysh effect occurring in magnetic field 24 p4256 A66-42524

**LIGHT ADAPTATION**

**SA VISUAL ACCOMMODATION**

Human eye adaptation to dark and light, noting threshold dependence on previous history of illumination 04 p0461 A66-13790  
 Light effect on rhythmic excretion of water and electrolytes in humans 09 p1335 A66-20534

**LIGHT AIRCRAFT**

Flight characteristics and test program of CL-84 light tilt-wing V/STOL Army support vehicle 07 p0986 A66-17271  
 Supercharging turbojet engine for light aircraft compared to piston and turbojet engines 10 p1591 A66-21393  
 Lift-drag ratio, specific impulse, aspect ratio and weight of payload and power plant considered for STOL aircraft 10 p1483 A66-21398  
 Light aircraft lateral stability augmentation system for wing leveling, noting operation and pilot performance [SAE PAPER 660220] 13 p1996 A66-26397  
 Aeroelastic stability of light aircraft, examining appearance of structural nonlinearities in global vibration test for determining critical flutter speed 17 p3023 A66-32331

British Executive and General Aviation /BEAGLE/ and development of Beagle B.206 S twin-engine executive aircraft 22 p3847 A66-39686

**LIGHT AMPLIFIER**

**SA LASER**

High speed streak camera using electronic control circuits, light amplifier and time calibrator 02 p0230 A66-11816  
 Cathode ray tube measurements indicate that noise in cathodoluminescence is mainly caused by shot noise of primary beam 02 p0206 A66-12161  
 Light flow amplification in inhomogeneous layer taking nonlinearity into account 05 p0692 A66-14725  
 Waveguide coupling between adjacent parallel fibers as means of transferring radiation from one element to another 05 p0693 A66-14827  
 Spontaneous emission noise properties of pair of pulsed ruby laser amplifiers 10 p1542 A66-21310  
 Nonlinear amplification of light pulse passing through laser operating at saturation regime 10 p1543 A66-21963  
 Optical length variations in laser amplifiers determined during pumping and interferometry 13 p2092 A66-25999  
 Light frequency multipliers for nonlinear optical effects at various wavelengths, considering focusing, laser beam finite divergence, air breakdown, stimulated Raman emission, etc 13 p2096 A66-26146  
 Light pulse shape variation of laser with modulated Q-factor during nonlinear amplification 14 p2307 A66-27183  
 Coefficient of light amplification in gas discharge 15 p2515 A66-29203  
 Regenerative helium-neon laser with amplification coefficient of 1000 15 p2516 A66-29352  
 Coefficient of light amplification in gas discharge 17 p2935 A66-33052  
 Regenerative helium-neon laser with amplification coefficient of 1000 20 p3576 A66-37357  
 Laser amplifier theory using Fabry-Perot interferometer and Laplace transform for obtaining transient solutions in addition to steady state solutions 21 p3748 A66-39224  
 Nonlinear amplification of light pulse passing through laser operating at saturation regime 21 p3749 A66-39542  
 Spectral hole burning and cross relaxation effects on steady state gain saturation of laser amplifier with inhomogeneously broadened linewidth 22 p3931 A66-40098  
 Radiative power amplification of He-Ne laser with nearly confocal resonators 23 p4078 A66-41453  
 Linearly and circularly polarized fields in laser amplifier interaction with axial magnetic field, emphasizing combination tone production 23 p4079 A66-41624  
 IR GaAs laser amplifier with gains as high as 2000, output powers of 150 mw and saturation occurring with current increase at low light levels 24 p4223 A66-42562  
 Light pulse shape variation of laser with modulated Q-factor during nonlinear amplification 24 p4224 A66-42727

**LIGHT COMMUNICATION DEVICE**  
 Economical feasibility requirements for optical maser communications systems 02 p0189 A66-11301  
 Laser beam modulation methods assessed for making use of capability of laser for carrying multitude of signals simultaneously 02 p0191 A66-11692  
 Electrodeless excitation of discharge in helium-neon gas laser tube applied to voice transmission 05 p0696 A66-14924  
 Transmission of large number of instrumentation channels over parallel pulse-modulated light beams, using electro-optical mosaic sources and detectors 06 p0824 A66-15970  
 Laser communications link security against interception, examining frequency bandwidth for minimum SNR 06 p0891 A66-16650  
 Optimum threshold and associated error probability for detecting binary optical signals 06 p0833 A66-16663  
 Search via laser receivers for interstellar communications 06 p0892 A66-16669

Parameter dependence of intermediate frequency voltage indicated during establishment of optimum conditions for optical receivers and merit of subcarrier mixing 12 p1832 A66-23980  
 Optical communication for Mars exploration with outline of laser modulators and antennas 13 p2021 A66-25251  
 Optical guides stressing lens type beam waveguide 13 p2022 A66-25538  
 Solar noise in optical communications, background radiation dependence on detector aperture, noise power and application to GaAs diodes and gas lasers 13 p2024 A66-25833  
 FM laser and optical heterodynes in optical communication systems 13 p2093 A66-28004  
 Multiple scattering effects on propagation of coherent optical signals studied for laser communications application 15 p2448 A66-28580  
 Communication systems at microwave and optical frequencies for future Mars missions 18 p3067 A66-33793  
 System design analysis of laser methods of deep space communication, examining local heterodyne system /LHS/, direct detection system /DDS/ and transmitted reference system 19 p3300 A66-35666  
 Book on laser receivers covering noise performance, atmospheric effects, detection techniques, hardware and systems available, optical communication in visible and IR spectrum, etc 19 p3375 A66-36060  
 Optical communication systems, discussing available equipment, transmission characteristic, lack of long distance operation reliability, etc 24 p4174 A66-42805

**LIGHT ELEMENT**  
 Collisional excitation in Van de Graaff accelerator of beams of light elements producing light emission in 2700-6600 angstrom range 21 p3776 A66-39396

**LIGHT EMISSION**  
 Second harmonic light generation, stressing saturation effects occurring at high laser power levels, solving nonlinear coupled Maxwell equations 02 p0239 A66-11443  
 Emission factor of radiating inhomogeneous layer determined by Abel integral equation from intensity profile, using analog computer 03 p0398 A66-12524  
 Lasing in p-type GaAs in which population inversion is brought about by avalanche breakdown of high resistivity region in material 03 p0378 A66-13008  
 Beat signal dependence on angular spread of oscillations in light waves heterodyning with incoherent light source 06 p0889 A66-15898  
 Stimulated emission in indium arsenide shows excitation threshold low and light emission highly directional 06 p0893 A66-17026  
 Light emission and photovoltaic effect of GaP diodes near bandgap 07 p1004 A66-17319  
 Anisotropy of balanced photoelectromagnetic emf in p-type germanium sample in which normal to illuminated surface coincides with crystallographic axis 09 p1413 A66-20002  
 Light emission associated with growth defects from reverse biased gallium phosphide p-n junctions 10 p1577 A66-21556  
 Forced emission from electron-excited cadmium selenide 10 p1544 A66-22174  
 Photoelectric observations and orbital solutions of BV 342, obtaining light element and light curve data 11 p1769 A66-22534  
 Laboratory duplication of processes exciting airglow, noting green line of oxygen atoms 11 p1699 A66-23116  
 X-ray produced auroral light emission in air and excitation of second positive and first negative bands in nitrogen 11 p1765 A66-23152  
 Film scanning system using GaAs light-emitting diode and phototransistor light detector 11 p1709 A66-23476  
 InAs laser emission, discussing radiative transitions, coherent emission from InAs diodes, recombination mechanisms in IR radiation spectra, etc 13 p2089 A66-25065  
 Copper diffused gallium arsenide p-n junctions, explaining current-voltage characteristics, light emission and capacitance of diodes at 300 and 77 degrees K 13 p2161 A66-25186



- Laser action in gallium antimonide diodes, examining emitted light spectrum vs injected current, temperature effect, radiative efficiency, etc 13 p2100 A66-26184
- Correlations and intensity fluctuations in light from individual lasing and nonlasing modes of CW GaAs laser and threshold noise change in laser emission 13 p2102 A66-26210
- Absolute flux measurement for pulsed and triggered lasers requiring only quantum receivers 13 p2104 A66-26375
- Gamma photon flux from solar Na 22 disintegration emitted by Sun after chromospheric eruption 13 p2176 A66-26760
- Light output of alpha particles in crystalline and vapor anthracene as function of pressure and temperature 14 p2296 A66-27796
- Short-lived oscillation in light emitted in active aurora 14 p2286 A66-27985
- Coupling efficiency evaluation in light emitting diodes 15 p2514 A66-29032
- Liquid hydrazine decomposition process to determine what chemical or physical changes may be occurring that cause breaks in burning rate/pressure curves, measuring flame temperature and light emission 15 p2570 A66-29610
- Initial pulse in luminous emission of discharge laser, using photomultiplier preceded by mobile iris, determining geometrical distribution of discharge brightness 16 p2719 A66-31209
- Radiation transport in spectral lines as consecutive photon absorptions and emissions, discussing contemporary theories, approximation methods and applications 18 p3120 A66-35076
- Forced emission from electron-excited cadmium selenide 19 p3441 A66-35788
- Semiconductor light emission mechanisms examined including wavelength emitted, width of ray emitted and efficiency of emission 19 p3445 A66-36263
- Replacing heated tungsten filament and IR filter by GaAs electroluminescent diode without filter for IR illumination 19 p3320 A66-36266
- High respiration rate of *Chlorella* maintained by blue-green light 19 p3287 A66-36435
- Optical-electronic components for signal transmission, considering light emission diodes and silicon control switches 19 p3283 A66-36813
- Zodiacal-light photometric measurements, analyzing effect of twilight radiation on observable brightness 20 p3549 A66-37036
- Chemiluminescent NO-O-atom reaction, determining effect of change of emission intensities and third bodies 20 p3604 A66-37309
- Light emission from semiconducting cadmium selenide crystals when not excited with photons, electron beam or tunneling, noting association with acoustoelectric field domain 20 p3620 A66-37767
- Collisional excitation in Van de Graaff accelerator of beams of light elements producing light emission in 2700-6600 angstrom range 21 p3776 A66-39396
- Light emission of electron-excited molecular nitrogen with NO, noting electronic state changes 22 p3949 A66-39910
- Spectral distribution of light from exploding wire sources noting environment, pressure, energy and material effects 22 p3948 A66-40197
- Radiative lifetime and emission intensity measurements, determining oscillator strength and electron transition moment of first positive band system of nitrogen 23 p4033 A66-42082
- Light emission in near IR by semiconducting GaAs under current oscillations caused by electron-phonon coupling 24 p4258 A66-43000
- Electron transitions and sharp emission lines in XUV solar spectral regions with fractionally charged quarks bound to C, N and O nuclei 24 p4280 A66-43189
- from intensity profile, using analog computer 03 p0398 A66-12524
- Measurement of elasto-optic performance of solids in Bragg diffraction devices 04 p0531 A66-13958
- Fresnel diffraction laws for calculation of light amplitude distribution in image spot of point as function of aperture dimensions used on hologram, source function, etc 04 p0532 A66-14173
- Light intensity in homogeneous turbid medium for unresolved absorption bands calculated from distribution of photon optical paths in absence of absorption, considering atmospheric scattering 04 p0542 A66-14302
- Diffuse day skylight intensity rocket measurements, discussing exponential variation of intensity with height in upper atmosphere 05 p0668 A66-14916
- Mixed integration techniques used for signal detection having coherence time less than duration when propagating through time-varying medium 06 p0828 A66-16112
- Intensity of polarized light transmitted through laser amplifier and linear polarizer, as function of axial magnetic field strength 07 p1041 A66-17292
- Photoelectron impact excitation effect on dayglow intensity, calculating energy distribution for various altitudes 07 p1028 A66-17374
- Reduction of diffracted light for astrometry near Sun 07 p1035 A66-18036
- Varying luminance and light-dark ratio effects on brightness enhancement of intermittent light 11 p1736 A66-22873
- Light intensity fluctuations along inclined inhomogeneous path with variable turbulence characteristics in lower atmospheric layer 12 p1913 A66-23776
- Human ability to detect small excursions of apparent movement of point light source, considering visual guidance system application 12 p1808 A66-23923
- Lunar surface luminescence and variations in light flux with solar activity 12 p1948 A66-23943
- Photo emf of gallium arsenide determined as function of temperature, light intensity, external electric field and surface quality 13 p2165 A66-25679
- Steady state variation of light intensity with distance for monochromatic light, noting dependence of absorption coefficient on degree of excitation of electronic system 13 p2099 A66-26183
- Photoluminescence for p-and n-type gallium arsenide as function of exciting light intensity, noting minority carrier recombination mode, electron energy spectrum, etc 13 p2169 A66-26187
- Threshold studies of ion laser oscillations in sulfur and saturation and quenching of laser intensity 13 p2102 A66-26209
- Cosmological theory testing with gravitational lens effect 14 p2383 A66-27710
- Light intensity in homogeneous turbid medium for unresolved absorption bands calculated from distribution of photon optical paths in absence of absorption, considering atmospheric scattering 14 p2327 A66-28216
- Spectral distribution changes occurring in diffuse skylight at zenith in visual region during total solar eclipse, using photoelectric spectrometer 15 p2484 A66-28830
- Resonance signal inversion in Rb optical pumping and relation of mixing of excited state sublevels 15 p2517 A66-29410
- Statistical analysis of light fields created by superposition of laser light and chaotic light 15 p2519 A66-29815
- Daily physiological rhythm changes associated with light intensity and color, noting body temperature oscillations vs light intensity, heart rate changes, etc 15 p2441 A66-29959
- Bibliography of holograms 16 p2702 A66-30433
- Isolation of morphologically intact and photochemically functional chloroplasts from marine chrysomonad *Hymenomonas* sp 16 p2638 A66-30648
- Multiple beam interferometer theory, noting discrepancy between intensity distribution and Airy formula determination of theoretical resolving power 16 p2706 A66-30936
- Coherence properties of optical fields, examining interference effects, intensity fluctuations, photoelectric effects and pulsations 16 p2749 A66-31584
- Photoeffect on barrier capacitance of p-n junction 17 p2988 A66-33326
- Light energy measurements made with argon bomb used as chemically powered laser pump 19 p3373 A66-35388
- Temperature, illumination intensity and degradation factor effects on solar cell output characteristics 20 p3497 A66-37164
- Internal turbulence scale for convection jets determined, using measurements of light intensity fluctuations 21 p3760 A66-39357
- Replacement of Poisson by Polya distribution in calculating laser intensity threshold necessary to induce ionization breakdown in gases 22 p3329 A66-39715
- Photoelectric photometry of Echo II satellite and graphs of light curves giving light intensity logarithm as function of time 22 p3863 A66-39856
- Thresholds, b-wave latencies, stimulus intensity/b wave amplitude relationships and diffuse adaptation effects upon electroretinogram stimulation by light subtending 20 degree visual field 22 p3856 A66-40965
- Photoelectric skylight perimeter for Stokes parameter measurements in plane polarized light 23 p4066 A66-41029
- Atmospheric turbulence effect on laser beam intensity distribution 23 p4035 A66-41030
- Atmospheric turbulence effect on frequency spectra of light intensity fluctuations examined, using He-Ne laser 23 p4035 A66-41031
- Quantitative photographic determinations of laser beam power density distributions and Q-switched ruby oscillator-amplifier system divergence characteristics 23 p4075 A66-41032
- Photoconductivity in homogeneous semiconductors when solution of second-order nonlinear differential equations with indivisible variables is obtained in elementary functions, noting light intensity effect 23 p4113 A66-41564
- Conversion efficiency of GaAs solar cell at various light intensities 24 p4161 A66-42391
- Linearized population rate equations and quantum noise sources used to calculate spectra of intrinsic second moment intensity fluctuations in 3-and 4-level CW laser oscillators 24 p4221 A66-42548
- Photometric device for measuring propagation velocity of light fluctuations in arc-heated plasma jet 24 p4212 A66-42776
- LIGHT MODULATOR**
- SA OPTICAL MASER MODULATOR**
- SA ULTRASONIC LIGHT MODULATOR**
- /ULM/
- Electro-optic diffraction grating for light beam modulation and diffraction 02 p0239 A66-11371
- Magnetostrictive device for light modulator control 03 p0376 A66-12424
- Periodic variation of quality factor of He-Ne gas laser cavity by vibrating quartz-modulation of light beam 04 p0529 A66-13477
- Modulation of laser light with composite Fabry-Perot resonator, using more than three multiple reflecting plates 05 p0698 A66-15836
- Light modulation at microwave frequencies noting single-sideband suppressed-carrier modulation, traveling wave modulation, etc 07 p1003 A66-18328
- Coherent excitation of mercury resonance state by irradiation with light modulated at Larmor frequency 08 p1233 A66-19089
- Gadolinium molybdenate as ferroelectric host in pulsed laser, noting light modulation and crystal domain 11 p1713 A66-23207
- Light beam deflection due to linear temperature gradients across electro-optic modulator crystals 11 p1737 A66-23431
- Balanced mixer for heterodyning light of two different frequencies from independent sources to obtain intermediate frequency in microwave region 12 p1890 A66-24143
- Transverse wave FM phototube system for detection of microwave-frequency modulated



light, noting design, operation and application 12 p1838 A66-24558  
 Neodymium doped YAG crystal and lithium meta niobate as CW laser materials and potassium tantalum niobate as optical modulator material 13 p2164 A66-25518  
 Intensity modulation of light using acoustic standing waves in megacycle range and requiring no high voltages 13 p2091 A66-25540  
 IR and visible helium-neon laser modulation using Faraday rotation in YIG 14 p2305 A66-26881  
 Retardation produced by 45 degree y-cut low voltage light-amplitude modulator and effect of wave-normal ordinary and extraordinary ray directions 14 p2334 A66-27588  
 Optimum processing of photocell output to produce Poisson photoelectron flux 14 p2242 A66-28156  
 Detection of very low levels of modulation on laser beam to determine performance of microwave light modulators 15 p2518 A66-29682  
 Demodulation method in which phase modulation of laser beam is converted to amplitude modulation by autocorrelation 16 p2717 A66-30616  
 Helium-neon laser modulation by positive and negative voltage pulses 16 p2720 A66-31559  
 Retardation-type laser modulators, examining driving power, transmission and dynamic range 17 p2935 A66-32820  
 Laser light modulation by Pockels or Kerr effect for application to telecommunications system, examining electrical birefringence modulation 19 p3304 A66-36262  
 Low-distortion modulation of IR and submillimeter waves, using free-carrier absorption in pair of crossed reverse-biased junction diodes 20 p3528 A66-37452  
 Traveling-wave phase modulation of coherent light propagating in anisotropic medium 22 p3933 A66-40867  
 10.6 micron output of carbon dioxide-He laser modulated, using Bragg diffraction from longitudinal acoustic waves in Te 24 p4219 A66-42251  
 GaAs crystal as electro-optic modulator at 10.6 microns due to small carrier absorption, freedom from interband transitions and high resistivity 24 p4222 A66-42553  
 Electro-optic light modulation using Pockel and Kerr effects in crystals for communications applications, using lasers 24 p4225 A66-42811  
 Carbon disulfide traveling wave Kerr cells with identical microwave and dielectric constants, noting light modulator construction at microwave frequencies 24 p4185 A66-42814  
 Horizontal deflection in TV display produced by Bragg reflection of laser light by ultrasonic waves in water 24 p4212 A66-42816

**LIGHT PRESSURE**

Absolute energy and power measurements from electromagnetic pressure in optical wavelength range 08 p1256 A66-19285  
 Dust particles in laser cavity observed for angular stabilization and constant velocities 13 p2105 A66-26594  
 Momentum transfer caused by focusing laser giant pulse on surface in vacuum investigated for Be, C, Al, Zn, Ag and W 19 p3373 A66-35418

**LIGHT PROBE**

Potential distribution in epitaxial p-n semiconductor measured via moving light spot, determining deposition depth 07 p1106 A66-18382  
 Photoelectric observations and orbital solutions of BV 267, obtaining new light elements, system light change and orbital solutions 11 p1769 A66-22533  
 Amplitude and phase of complex Kerr magneto-optic coefficients measured, describing technique and results 17 p2958 A66-32623  
 Self-focusing and self-trapping of intense light beams in nonlinear medium examined, using approximations of geometrical optics and accounting for diffraction effects 20 p3602 A66-37372

**LIGHT SCATTERING**

**SA ATMOSPHERIC SCATTERING**

Interference effects at thin transparent cylindrical glass fibers exposed to coherent light from He-Ne laser 01 p0081 A66-10368  
 Surface roughness of metallic powder particles determined by light scattering, considering iron particles 01 p0069 A66-10747  
 Effect of incomplete and inaccurate optical information on particle size distribution function, considering transparency and scattering pattern 01 p0097 A66-10758  
 Pore formation in decomposition of solid solutions of bivalent impurities in sodium chloride crystals by studying light scattering in these crystals 01 p0125 A66-10777  
 Two-dimensional laser deflection using Fourier optics 01 p0083 A66-10897  
 Use of Brillouin scattering for optical beam modification, spatial distribution of acoustic energy and coherent sound of great intensity 03 p0376 A66-12421  
 Angular distribution of diffusely reflected light flux as function of scattering indicatrix, survival probability of light quantum and conditions of medium illumination 04 p0541 A66-13415  
 Free photon path distribution during passage through thick plane-parallel light scattering layer 04 p0541 A66-13416  
 Plasma electron concentration, using nonlinear light scattering on geometrical optical path 04 p0554 A66-14295  
 Angular width and intensity of light from two lasers that cause plasma to oscillate and in turn are scattered by induced fluctuations 04 p0533 A66-14328  
 Light scattering theory and generation of second harmonic in plasma in external magnetic field 04 p0555 A66-14333  
 Local electron temperature and electron density in theta pinch measured by means of scattering of laser beam 04 p0555 A66-14334  
 Thomson scattering measurements of magnetic annular shock tube plasmas using Q-switched ruby laser light beam 05 p0680 A66-14707  
 Optical properties of light scattering layer with negative absorption coefficient, discussing layer reflection and transmission 05 p0715 A66-14726  
 Nonlinear Maxwell equation for optics of many-particle system, noting Raman scattering from electron plasma 05 p0695 A66-14905  
 Light beams used as plasma probes, considering scattering effect of refraction 05 p0726 A66-15248  
 Solutions for integral equation associated with equation of radiative transfer for isotropic scattering and complete redistribution in frequency cases 05 p0762 A66-15276  
 Formulas for light passage through planetary atmospheres of finite optical thickness, taking into account polarization 05 p0765 A66-15415  
 Structural changes in radiation field following quantum reemission after photoexcitation of atom when true absorption is low 05 p0765 A66-15416  
 Light scattering in spherical nebula of great optical thickness 05 p0765 A66-15417  
 Photometric measurements of twilight brightness for upper atmospheric temperature determination 05 p0674 A66-15528  
 Variation of scattering cross section with beam intensity for ruby laser light on atomic hydrogen 05 p0698 A66-15864  
 Radiation absorption and scattering by small spherical solid carbon particles in wavelength range 0.2 to 40 mu calculated by classical Mie theory 06 p0911 A66-16261  
 Granularity and radial structure in circular Fraunhofer diffraction fringes produced by lycopodium powder scattering of monochromatic coherent light 06 p0891 A66-16443  
 Laser-beam scattering by individually introduced charged polystyrene spherical particles and droplets of naphthalene and water in combination 07 p1043 A66-17473  
 Diffusive reflection of light from and passage through optically thick atmosphere with nonspherical indicatrix 07 p1080 A66-17921  
 Angular dependence of radiation intensity

scattered from plane diffuse surface illuminated by wideband collimated light 07 p1081 A66-18039  
 Diffraction velocimeter detecting and measuring transverse movement of surface by sensing light backscattered by it when laser illuminated 07 p1044 A66-18333  
 Brillouin scattering of light by phonons and phonon maser in derivation of conservation theorems from basic equations 07 p1045 A66-18397  
 Apparatus for fluoridation of hydroxyl and oxygen contaminated fluoride compounds, obtaining optically clear crystals with no Tyndall scattering for laser application 07 p1047 A66-18488  
 Numerical Neumann solution to scalar equation of transfer in homogeneous layer of optical thickness 08 p1255 A66-18780  
 Nonharmonic effect on dispersion of light by impurity centers of solid body 08 p1273 A66-19256  
 Atmospheric attenuation of light with average turbulence conditions 08 p1248 A66-19319  
 Mars atmospheric optical thickness and scattering from photometric observation 08 p1294 A66-19327  
 Difference between values for atmospheric pressure at Martian surface when obtained by photometry or by spectroscopy, due to nonconsideration of light scattering by aerosol particles 08 p1295 A66-19331  
 Optical turbulence simulation with small transparent solid bodies immersed in index-matching liquids 08 p1186 A66-19702  
 Atmospheric optics noting attenuation, reflectance, flux and optical radiation 09 p1398 A66-20274  
 Lower atmospheric density measurements through light scattering from Q-spoiled ruby laser beam, using optical radar detector 09 p1373 A66-20398  
 H-alpha double limb observed in spectroheliograms is instrumental and not solar phenomenon 09 p1455 A66-20404  
 Mie scattering and absorption cross sections for spherical absorbing particles as function of complex refractive index 09 p1405 A66-20512  
 Spectral distribution of light scattered by density fluctuations in dense monatomic one-component fluid 09 p1404 A66-20960  
 UV color and flux at 2200 and 2600 angstroms measured for A and B stars, using rocketborne photometers 10 p1602 A66-21096  
 Dynamical and light scattering properties of small dust grains orbiting Earth 10 p1529 A66-21154  
 Quantum theory of interaction of electromagnetic waves in plasma considered in terms of light-light scattering and plasma-laser beam interaction 10 p1558 A66-21173  
 Comparison of microwave scaling method and optical simulation technique for obtaining radar cross sections 10 p1502 A66-21630  
 Diffusion of light by plasma electrons produced in laboratory for very small effective diffusion area 10 p1566 A66-21712  
 Internal diffuse radiation field computed in finite homogeneous isotropically scattering slab illuminated by parallel rays of radiation 10 p1556 A66-21923  
 Soviet and foreign papers on plasma diagnostics by scattering of laser beams at plasma electrons 10 p1569 A66-21990  
 Mutual conversion of direct and inverse problems of light scattering by soft-particle system, noting transparency data determining particle spectrum 10 p1553 A66-22029  
 Pore formation in decomposition of solid solutions of bivalent impurities in sodium chloride crystals by studying light scattering in these crystals 11 p1749 A66-22289  
 Elongation of characteristic curve of polarization for interstellar particles due to surface molecular scattering 11 p1769 A66-22535  
 Atmospheric aerosol size distribution from scattered light measurements by rocketborne equipment 11 p1697 A66-22565  
 Illuminance of Earth shadow at three wavelengths by numerical integration, accounting for light attenuation, ozone absorption and extinction, Rayleigh



scattering and refractive beam divergence 11 p1770 A66-22570

Optical diffraction velocimeter, using backscattered laser light to measure relative velocity between light source and surface 11 p1706 A66-22958

Transverse motion modification of longitudinal frequency spectrum resonances of light scattered from plasma 11 p1745 A66-22973

Laser scattering by bound charged particles 11 p1713 A66-23080

Propagation of narrow beam of light in turbid medium with strongly extended scattering 12 p1913 A66-23777

Diffusive reflection of light from and passage through optically thick atmosphere with nonspherical indicatrix 12 p1913 A66-23882

Radiation field in plane-parallel semiinfinite medium illuminated by high-directivity beam bounded from above by mirror surface whose reflection is calculated for various scattering indicatrices 12 p1914 A66-24245

Brillouin scattering by gases as experimental test of kinetic theory away from hydrodynamic regime 12 p1917 A66-24585

Dual-and multiple-beam interferometry by wave front reconstruction from surfaces of standard engineering components, applicable to structural dilatation problems 12 p1884 A66-24967

Light diffusion of Martian atmosphere measured by spectroscopic evaluation of polarization variation from disk center to edge 13 p2181 A66-25461

Physics of quantum electronics - Conference, San Juan, Puerto Rico, June 1965 13 p2093 A66-26141

Nonlinear light scattering in pressurized methane, noting displacement of spectral line from laser frequency 13 p2132 A66-26148

Extension of three-field mixing theory to include effects of convective nonlinearities on excitation in plasma, using correlation function of spectral densities for interpretation of thermally enhanced light-by-light scattering 13 p2132 A66-26151

Nonlinear optical effects in plasma, optical mixing of three light beams and scattering of light-by-light, noting dominant Raman scattering 13 p2132 A66-26152

Cross section for inelastic scattering of electromagnetic radiation by electron density fluctuations in anisotropic solids, using laser sources, investigating Landau and collision damping of plasmons 13 p2132 A66-26153

Light coupling with phonons, magnons and plasmons, deriving wave equations and coupling constants, observing Raman effect in spin systems and in plasmas, noting second harmonic generation 13 p2132 A66-26154

Stimulated Brillouin scattering in quartz analyzed, noting amplification, Stokes wave generation and ruby gain 13 p2097 A66-26165

Velocity and lifetime of microwave thermal phonons in liquids and solids determined by spectrum of light scattering from laser illuminated sample 13 p2133 A66-26166

He-Ne laser homodyne spectrometer observation of broadening of spectral profile of light scattered from carbon dioxide near critical temperature and density due to density fluctuations 13 p2133 A66-26168

Laser radiation coherence property deterioration and molecular scattering during propagation through turbulent atmosphere 14 p2236 A66-27131

Angular divergence effect of light beam on illuminance of turbid scattering medium 14 p2326 A66-27542

Photometric determination of extinction coefficient for optical scattering in turbid medium 14 p2326 A66-27544

Effect of incomplete and inaccurate optical information on particle size distribution function, considering transparency and scattering pattern 14 p2326 A66-27857

Multiple scattering effects on propagation of coherent optical signals studied for laser communications application 15 p2448 A66-28580

Optical beam scattering of gas laser for measurement of photoelastic constants and

application to lithium niobate 15 p2512 A66-28692

CAT detection from Doppler shift in laser light backscattered from atmospheric aerosol 15 p2500 A66-28930

Light diffraction by random fluctuation of refractive index of plasma 15 p2552 A66-29330

Two-quanta absorption and scattering loss in powerful laser 15 p2516 A66-29350

Statistical analysis of light fields created by superposition of laser light and chaotic light 15 p2519 A66-29815

Homogeneous nucleation of water vapor determined by laser beam scattering from cloud 16 p2716 A66-30121

Scattering of light from pulsed ruby laser by plasma jet, noting cross section, electron-phonon interaction, etc 16 p2716 A66-30139

Cooperative interactions between ions and electrons in forward scattering of ruby laser beam from plasma 16 p2716 A66-30153

Scattered light spectrum of thermal sound waves used to provide velocity and absorption data about hypersonic waves in several liquids 16 p2745 A66-30300

Mutual conversion of direct and inverse problems of light scattering by soft-particle system, noting transparency data determining particle spectrum 16 p2747 A66-30848

Recording of light-induced light scattering using laser beam, calculating cross section of photon-photon scattering 16 p2748 A66-31175

Reflection and refraction of light waves at boundary of nonlinear dielectric 16 p2655 A66-31556

Granularity characteristics of scattered light from helium-neon laser directed onto moving surface 16 p2720 A66-31725

Color and light intensity gradient of residual light scattered and refracted into umbra of Earth shadow measured during lunar eclipse 17 p2999 A66-32068

Nonlinear scattering of ruby laser beam by plasma at second and third harmonic 17 p2967 A66-32433

Earth surfaces reflecting and polarizing properties in aerial reconnaissance 17 p2918 A66-32611

Upper atmospheric light scattering of vertically fired ruby-laser pulse 17 p2922 A66-33348

Electron temperature and concentration in DC plasma arc determined from Thomson scattering of laser radiation 18 p3118 A66-33840

Minimization technique for light scatter due to diffuse mirrored birefringent coatings used in performing photoelastic studies by fringe multiplication 18 p3257 A66-34563

Soviet and foreign papers on plasma diagnostics by scattering of laser beams at plasma electrons 18 p3150 A66-34967

CW He-Ne laser measurement of light scattering in crystals noting laser output, performance and crystal imperfections 19 p3373 A66-35402

Plasma diagnostics by Thomson scattering of laser beam, investigating difficulties from particle scattering, absorption, etc 19 p3405 A66-35412

Cooperative scattering of laser light by thiatron plasma 19 p3373 A66-35489

Directional distribution of light reflected from roughened surfaces with measurements made of plane-polarized components of reflected light as well as of mixed radiation 20 p3598 A66-36941

Ultrasonic light diffraction, deriving line intensity in form of quadratures with parametric dependence 20 p3601 A66-37147

Two-quanta absorption and scattering loss in powerful laser 20 p3576 A66-37355

Continuous wave gas laser as light source in scattered light static photoelasticity 20 p3577 A66-37443

Light scattering influence on effective value of extinction coefficient considered as function of optical parameters of medium and of angular characteristics of source and receiver 21 p3760 A66-39361

Particle spectrum determination by inversion of scattering data for high concentrations of sol 21 p3760 A66-39364

Ground state resonance, noting absence of

Doppler broadening of signals in forward scattered light 22 p3931 A66-39810

Light reflection from shock waves clarified through propagation in shock tubes, using gas laser 22 p3898 A66-40012

Screening effect of meteoritic particles, ice grains and ice-coated dust particles entrained in outgoing gases of comets, determining particle size and numbers from momentum/energy balance 22 p3983 A66-40697

Daytime sky brightness relationship to atmospheric anisotropic light scattering 22 p3917 A66-40960

Monograph on absorption, scattering and attenuation of light and IR radiation in atmosphere 23 p4087 A66-41272

Crystal defects and performance in ruby laser, measuring coherence function of light and output energy and crystal homogeneity 23 p4077 A66-41291

Invariant imbedding and scattering of light in one-dimensional medium with moving boundary, noting relaxation of photon emission and Doppler frequency shift 23 p4087 A66-41540

Complete Rayleigh scattered field within homogeneous plane parallel atmosphere, noting scalar transfer equation extension 23 p4065 A66-41813

Visibility and small ion density correlated by comparing light scattering with ion attachment processes on airborne scatters 23 p4065 A66-41842

Ruby laser light scattering measurements of electron and ion temperatures of hydrogen and deuterium plasmas produced in theta pinch devices 24 p4222 A66-42558

Configurations for realization of multiple laser light scattering using microwave acoustic waves and two Porro prisms 24 p4224 A66-42636

Optical heterodyne receiver antenna properties, noting effective aperture of capture cross section vs directional tolerance and detection of doppler shifts in liquid scattered coherent light 24 p4174 A66-42809

Nonlinear optics emphasizing parametric oscillation, self-focusing and trapping of laser beams and stimulated Raman, Rayleigh and Brillouin scattering, using Maxwell equations and electric dipole approximation 24 p4225 A66-42810

Acousto-optical deflection and modulation devices, considering specific geometries and scattering-efficiency-bandwidth products 24 p4174 A66-42812

**LIGHT SOURCE**

Super-radiance source of improved spectral composition with integral radiation directing means especially suitable for use in solar simulators 02 p0214 A66-11234

Photochemical studies of oxygen-ozone and carbon dioxide equilibria with bromine UV lamp 04 p0473 A66-13397

Silicon avalanche light sources for photographic data recording 05 p0677 A66-14831

Triangular resonator for coherent light sources, considering natural oscillations and energy withdrawal 06 p0893 A66-16883

Advantages of gas lasers as light sources in aerodynamic research 06 p0893 A66-16944

Interferometers 06 p0893 A66-16944

Conventional flow visualization using laser light source [AIAA PAPER 66-127] 06 p0870 A66-17104

Electro-optical system measuring spectral response of photosensitive material or device and output under arbitrary light spectrum as in silicon solar cell 07 p0997 A66-18485

Light source having absolute spectral energy distribution for standardizing star tracker calibration 08 p1252 A66-19501

Laser application to streak photography methods of time resolved flow visualization for transient flows 10 p1536 A66-21752

Reflector-light source requirements for homogeneous format illumination in night aerial photography 13 p2081 A66-26005

Photoelectron counts of photomultiplier illuminated by gas laser light source 13 p2102 A66-26211

Phase locking of one laser to another by direct injection of first laser beam into second laser cavity 13 p2105 A66-26593



Monograph on lasers including gas lasers, ruby lasers, giant-pulse techniques, oscillation modes, etc 14 p2305 A66-26961  
 Lateral shearing interferometer with gas-laser light source for testing large optical systems 14 p2307 A66-27320  
 Well shielded ceramic capillary spark source, thermocouple radiation detector and silicon p-n junction diode testing 14 p2293 A66-27329  
 Laboratory simulation of solar radiation under varying atmospheric conditions 14 p2327 A66-28135  
 Hologram reconstruction obtained by illuminating hologram plate with common two-cell flashlight 15 p2502 A66-29033  
 Near-Bose-Einstein probability distribution of photoelectron counts produced by He-Ne gas laser narrow band Gaussian light source operating slightly below oscillation threshold 16 p2717 A66-30645  
 High voltage pulsed electrodeless discharge in rare gas as light source for ruby and Nd glass laser excitation and observation of output characteristics 16 p2720 A66-31448  
 Coherent gas laser light to meet requirements of streak photography for time-resolved flow visualization 17 p2935 A66-32959  
 Small-order vibration displacements measurement by Michelson interferometer, using CW laser source 17 p2926 A66-33037  
 High temperature light source with substantially continuous spectral emission for UV absorption spectroscopy approximating black body in visible and near UV region 19 p3353 A66-35314  
 Partially coherent light, noting distinction between narrow-band coherent and incoherent sources 20 p3575 A66-36935  
 Continuous wave gas laser as light source in scattered light static photoelasticity 20 p3577 A66-37443  
 Spectral distribution of light emission of exploding wire systems measured by high-speed drum camera and rotating shutter 20 p3603 A66-37742  
 Schlieren photographs of plasma discharges in parallel plate rail tube, using pulsed ruby laser as light source 23 p4104 A66-41510  
 Theta pinch discharge as spectroscopic light source in highly ionized gas spectroscopy 24 p4241 A66-42393

**LIGHT TRANSMISSION**

SA DIFFRACTION  
 SA FIBER OPTICS  
 SA ILLUMINATION  
 SA OPTICAL COUPLING  
 SA VISIBILITY

Propagation of light in universe with inhomogeneously distributed matter, considering presence of component uniformly spread in space /Intergalactic gas/ 01 p0135 A66-10281  
 Total reflection technique to achieve effective high absolute photocathode sensitivity 01 p0078 A66-10857  
 Parametric fluctuations of spatially restricted light beam in turbulent atmosphere 02 p0191 A66-11838  
 Optical scintillation frequency noting propagation of electromagnetic and acoustic waves in turbulent atmosphere 02 p0262 A66-12207  
 Multiple light filter narrowing emission bands of ruby laser with multiplex resonator 03 p0378 A66-12627  
 Propagation of optical waves through atmosphere, considering attenuation of optical waves and noise generation 04 p0545 A66-13756  
 Measurement of elasto-optic performance of solids in Bragg diffraction devices 04 p0531 A66-13958  
 Deflection of light rays by gravitational lenses 05 p0757 A66-14526  
 Semiconductor application to coherent optical transducers and spatial filters 05 p0647 A66-14822  
 Molecular anisotropy of propagation of intense light beam, noting Raman and Brillouin effects 05 p0696 A66-15106  
 Light waveguide for general lens-like media, ideal lenses and continuous media with square-law index variation 05 p0634 A66-15178  
 Statistics of beam waveguide light-ray propagation extended to include correlations

between displacements of different lenses 05 p0634 A66-15179  
 Oscillation growth of ray about wavy axis of lens light guide noting spectrum of waves, mechanical stiffness of guide and ray amplitude 05 p0634 A66-15181  
 Transmission through tapered quartz tube in laser near field 05 p0697 A66-15481  
 Second harmonic light generated on reflection of giant-pulse laser beam from surface of silver mirror 06 p0921 A66-16072  
 Design of intentional bends of beam waveguide, giving relations between waveguide parameters and radius of curvature of guide axis 06 p0846 A66-16093  
 Phase perturbation of optical beams due to atmospheric turbulence, using modulated interferometer to produce Doppler beats between two coherent beams 06 p0909 A66-16434  
 Photon trapped wave effect for developing optical waveguides in which optical beam creates waveguide as it propagates 06 p0892 A66-16662  
 Amplitude and phase fluctuations of plane monochromatic light wave propagating in turbulent medium 06 p0910 A66-16777  
 Velocity of light determined from photometric distance comparison, using invar gauges 08 p1256 A66-19344  
 Average transfer function from statistics of wave-front distortions in light propagating through atmosphere 08 p1256 A66-19705  
 Low loss transmission medium for optical frequencies consisting of thin wall dielectric tube separating internal high density gas from external low density gas 08 p1235 A66-19839  
 Optical radiation absorption and attenuation by atmosphere polluted with carbon dust, including transmission coefficient calculation 09 p1402 A66-20313  
 Transmission of IR radiation from flames through various carbon dioxide pathlengths 09 p1471 A66-20509  
 Statistical analysis of light beam propagation in weakly deformed circular mirror tube 09 p1347 A66-20776  
 Mechanical interpretation of problem of passage of light through curved light conductor 09 p1387 A66-20790  
 Irregularities of iris type beam waveguide, noting transmission loss during principal lightwave propagation 11 p1712 A66-22736  
 Cosmological effects in anisotropic inhomogeneous cosmological models including Riemannian geometry, light propagation, gravitational field, etc 11 p1772 A66-22778  
 Weakly focusing transparent media properties and guided transmission of coherent light beams with relatively small loss 11 p1657 A66-23091  
 Irregular bends and lens displacements effect on wavelength and modes in laser waveguide 11 p1713 A66-23103  
 Directional fluctuations in light waves propagating from edge of solar disk caused by atmospheric turbulence 12 p1913 A66-23775  
 Transverse beam width and phase constant of nonsquare law media for light propagation in imperfect lenslike media requiring repeater 13 p2127 A66-25539  
 Random variations in beam waveguide components and effects on light propagation 13 p2024 A66-25939  
 Intense light pulse propagation in optical media, noting polarized nature of transient oscillations, phase and amplitude distortion and two-level composition of medium 13 p2098 A66-26171  
 Light reflection from dielectric films of continuously varying refractive index 14 p2356 A66-26966  
 Atmospheric turbulence effects on laser beam propagation, noting beam cross section, phase variation, AM and FM, etc 14 p2235 A66-27035  
 Transmission spectra, electroluminescence-brightness variations with applied frequency and voltage and physical properties of ZnS thin films 14 p2361 A66-27315  
 Quantitative assessment of deterioration that light beam undergoes on passing through turbulent

atmosphere 15 p2448 A66-28579  
 High amplitude LF current and optical transmission oscillations in CdS single crystals under high electric field and monochromatic illumination near fundamental absorption 15 p2558 A66-28613  
 edge 15 p2558 A66-28613  
 Light transmission through optical diffraction lattice consisting of medium in EM field of laser beam 15 p2511 A66-28626  
 Statistical analysis of ray oscillation suppression in light waveguide, using Liouville theorem 16 p2746 A66-30596  
 Light propagation through Schwarzschild singular sphere, solving problem of visual image of emitting surface of gravitating sphere as seen by observer 16 p2748 A66-31171  
 Misinterpretation of theories of light, noting no clear-cut and simple distinction or opposition between theories of Newton and Huygens 16 p2749 A66-31722  
 Linear instability of laser propagation in fluid with coupling between light and medium 18 p3120 A66-35034  
 Light deflection by solar activity 19 p3455 A66-35249  
 Amplitude and phase fluctuations of plane monochromatic light wave propagating in turbulent medium 19 p3399 A66-35374  
 Design principles of waveguide systems applicable to electromagnetic wave transmission by reflection and refraction 19 p3319 A66-36033  
 Velocity of light determined from photometric distance comparison, using invar gauges 19 p3400 A66-36052  
 Trajectories of light rays through medium subjected to acoustic waves examined knowing that acoustic waves in laser medium function as optical waveguide 20 p3580 A66-38238  
 Normal incidence reflectivity and transmissivity coefficient measurements in Ge thin epitaxial films 20 p3623 A66-38397  
 Self-induced divergence of continuous wave He-Ne laser beams when traversing transparent liquid, noting nonlinear effect in propagation of light 21 p3748 A66-39164  
 Statistical analysis of light beam propagation in weakly deformed circular mirror tube 22 p3947 A66-39835  
 Mechanical interpretation of problem of passage of light through curved light conductor 22 p3931 A66-39849  
 Irregularities of iris type beam waveguide, noting transmission loss during principal lightwave propagation 23 p4078 A66-41474  
 Split angle, total internal reflection and Wollaston prism-digital light deflection techniques 24 p4174 A66-42815  
 Transmittance of gaseous air components for 1850 angstrom radiation 24 p4234 A66-42818  
 Edser-Butler band amplitude dependence on modulating effect of interference grating 24 p4212 A66-42819  
 Optical constants of triple, symmetrical and absorbing thin film used with layer thickness to determine complex transmission factor 24 p4258 A66-42994

**LIGHTHILL METHOD**

LF solutions for dipoles in semiinfinite media found not to be valid for entire range of frequencies 06 p0826 A66-16032  
 Lighthill integral transform methods in hodograph transformation theory of plane compressible transonic shock-free potential flows around airfoil sections in solution space of Chaplygin equation [ICAS PAPER 66-26] 23 p4007 A66-41008

**LIGHTING**

**S AIRCRAFT LIGHTING**

**LIGHTNING**

Lightning discharges investigated by oscillographic method in field laboratory at Pirkuli in 1963 01 p0096 A66-10191  
 Ionizing radiation as potential lightning hazard, noting lightning protection device for medical and industrial buildings 03 p0423 A66-13266  
 Schumann resonances of Earth ionosphere cavity and excitation by lightning flashes 04 p0474 A66-13427  
 Atmospheric radio noise bursts arising from radiation fields of electrical discharge in LF band at Bangalore, India 04 p0475 A66-13428



- Nucleation of ice formation in supercooled clouds as result of lightning-initiated sound waves 04 p0542 A66-13674
- Noise from terrestrial lightning discharges as source of interference to satellite radio reception 05 p0633 A66-14955
- Electrical structure of thunderstorms, particularly weak portion of squall line thunderstorm complex, using aircraft photography, radar data, etc 06 p0905 A66-16270
- Checking and calibration of aircraft compasses, discussing compass base at Dublin Airport and effect of lightning strikes 07 p1032 A66-17675
- Amplitude distributions of radio noise at ELF and VLF related to amplitude distribution of lightning discharges 08 p1184 A66-19403
- Lightning and static electricity discharges effects on helicopter design and performance, noting blade and rotor hub protection, fuel ignition, etc 11 p1638 A66-23259
- Electrical discharge theory of cosmic atmospheric phenomena, relating lightning, novae and quasars 12 p1950 A66-24394
- Lightning discharge radiating sferics near Gulf of Mexico and west coast of U.S. 17 p2923 A66-33358
- Photometric studies of lightning with correlated photographs of discharge channels to determine photoelectric pulse profile characteristics 18 p3129 A66-34018
- Frequency distribution of atmospherics emitted by multiple lightning discharges 20 p3553 A66-38075
- Electric component of radiation field from same flashes recorded with histograms of product of field strength and distance, showing concentration around mean values 20 p3553 A66-38076
- Cathode ray oscillograph-directional antenna recordings of electromagnetic pulses from lightning discharges 20 p3553 A66-38081
- Physical properties of lightning return stroke analyzed by several time-integrated and time-resolved spectroscopy techniques 20 p3555 A66-38384
- Lightning flash mechanisms and electric field strengths in clouds 21 p3759 A66-38533
- Chondrules origin, discussing possible production by lightning in primitive Laplace type nebula 22 p3981 A66-40477
- IMB**
- S LUNAR LIMB**
- LIMESTONE**
- Compressional wave velocity in limestones, marbles and single crystal of calcite under hydrostatic pressure to 20 kbar 19 p3351 A66-36387
- LIMITER**
- SA POWER LIMITER**
- Regenerative frequency converters used as signal limiters, determining characteristics from equivalent circuit of semiconductor diode 02 p0199 A66-11758
- Spectrum of phase-manipulated signal at output of ideal amplitude limiter 04 p0501 A66-14405
- Low level garnet limiter with operating range greater than one octave, using conductivity change due to impact ionization in n-type germanium, noting volt-ampere characteristic 06 p0851 A66-16459
- Phase-advance stabilization of servocontrol systems by use of limiters controlled by error signal 08 p1199 A66-18671
- Two basic semiconductor limiters design and performance as microwave duplexing devices 14 p2253 A66-27529
- Octave band all-pass filter with electronically tunable limiter 15 p2463 A66-29037
- Microwave limiter device, based on impact ionization of deep levels in silicon 17 p2897 A66-33461
- Equilibrium of toroidal magnetically confined plasma, using segmented circular aperture limiter 23 p4102 A66-41484
- LIMITER AMPLIFIER**
- Optimal pulse shape determined for signal which gives maximum response energy in ideal limiter filter system 07 p1001 A66-17354
- P-I-n diode coaxial attenuators and levelers noting design, performance parameters and application 12 p1831 A66-23812
- LINCOLN EXPERIMENTAL SATELLITE**
- /LES/**
- Lincoln experimental satellite program in antenna pointing, solid state repeaters, RF power generation and magnetic torquing of spin axis [AIAA PAPER 66-271] 12 p1821 A66-24744
- LINE**
- S DELAY LINE**
- S FORCE LINE**
- S FRAUNHOFER LINE**
- S H-ALPHA LINE**
- S H-BETA LINE**
- S LOOP**
- S PIPELINE**
- S SIGHT LINE**
- S SPECTRAL LINE**
- S TRANSMISSION LINE**
- LINE CURRENT**
- Magnetohydrostatic cavity formed around system of line currents in infinitely conducting atmosphere 14 p2279 A66-28394
- Boundary of magnetic field of two arbitrary line currents immersed in plasma at uniform pressure 15 p2553 A66-29687
- Field boundary of two line currents immersed in streaming plasma treated by conformal transformation 22 p3956 A66-40386
- Chapman-Ferraro hollows for system of parallel line currents enveloped by stratified corpuscular flux 22 p3975 A66-40806
- LINE SHAPE**
- Resonant frequency equation for line segment with reactive loads at both ends, using Chebyshev principle 02 p0199 A66-11754
- Transition probabilities and line-shape parameters for three argon lines in wall-stabilized Ar arc containing trace of H 08 p1261 A66-18766
- Green function method in theory of dispersion and absorption of electromagnetic radiation in semiconductor, considering resonance line shapes 09 p1411 A66-19961
- Optical linewidth study of energy transfer between impurity ions and homogeneous broadening and lineshape changes in optical transitions 13 p2098 A66-26176
- Actual line shape expected from accelerating radiating ion, errors due to Lorentzian approximation and results for ion laser transition in rare gas 16 p2716 A66-30181
- Catalog of neutral H-line profiles at 21 cm wavelength noting intensity, radial velocity, line widths, etc 19 p3460 A66-35792
- LINE SPECTRUM**
- SA SPECTRAL LINE**
- Line widths of some gallium-substituted polycrystalline garnets prepared at liquid-helium temperature 01 p0121 A66-10561
- Coronal spectrum of eclipse of February 15, 1961 studied at constant height as function of heliographic latitude from circular slit spectrograph 02 p0286 A66-11354
- Quiet chromosphere and corona noting line intensity and coronal electron and kinetic temperature 03 p0420 A66-12841
- Profiles of intense resonance lines and variation from center of limb of solar disk 03 p0427 A66-12917
- Line broadening from Stark effect and Doppler effect for plasma 04 p0553 A66-14193
- Laser radiation absorbed along slant paths, spectral line overlapping and center line shift with pressure 07 p1041 A66-17295
- Line intensities of first negative bands of nitrogen molecular ion measured as function of bombarding electron energy and gas pressure 09 p1404 A66-20377
- Observed line spectra of nine quasi-stellar radio sources representation for single temperature, electron density and ionization level 09 p1456 A66-20416
- Range of importance of molecular impurities on nitrogen vibrational relaxation determined, using spectroscopic sodium line reversal techniques 11 p1741 A66-23218
- Profiles of intense resonance lines and variation from center of limb of solar disk 14 p2380 A66-27266
- Organic flame temperatures and burning velocities at various fuel-air ratios measured, noting band intensity, effect of diluents, etc 14 p2413 A66-27723
- Intensities of optically thick lines emitted by hydrogen-like ions in steady state plasma for various electron temperatures and densities 16 p2758 A66-30276
- Flare observations in H-alpha line, line and continuous spectra of flares, and optical characteristics of proton flares 17 p2993 A66-32364
- Electron scattering interpretation of ionization, emission and absorption line spectra of quasi-stellar object 17 p3004 A66-32928
- Pressure broadening of microwave lines in semiclassical treatment obtained as limit of quantum impact theory and its limitations 20 p3602 A66-37640
- XUV C, Ti, Mn, Fe, Ni, Cu, Zn and Ar line spectra and continuum radiation spectra in plasmas produced by focused ruby laser beam 22 p3954 A66-39812
- LINEAR ACCELERATOR**
- Linear accelerator for micrometeoroids operated in radially stable mode and variable frequency for hypervelocity impact studies 01 p0053 A66-10852
- Vehicle angular velocity determined, using configurations with only linear accelerometers and no gyroscopes for inertial navigation 08 p1224 A66-19488
- RF losses in lead and niobium investigated for possibility of constructing superconducting linear accelerator 09 p1416 A66-20026
- 1 g rotating linear acceleration vector producing compensatory nystagmus, noting effects when rotation axis was vertical and horizontal 11 p1643 A66-22579
- Electrons from linear accelerator directed in collimated beam at normal incidence upon thick targets of various materials, obtaining energy spectra of retrofugal electrons 13 p2136 A66-26280
- Vestibular neuronal response to rotating linear acceleration vectors, noting generation of compensatory ocular nystagmus 17 p2858 A66-32177
- LINEAR ARRAY**
- Linear antennas and characteristics regarding maximum power, directivity, height, sleeve and conical dipoles and current distribution 04 p0491 A66-13402
- Electro-optical signal processors for phased linear array antennas, discussing time and spatial delay multiplexing 05 p0648 A66-14832
- Field of linear array consisting of coaxial spherical antennas, each representing pair of hemispheres separated by narrow clearance with applied voltage 05 p0651 A66-15880
- Multiple-feed system for microwave focusing objective, discussing array factors 06 p0827 A66-16042
- Transient condition effects on radiation resistance and expansion in linear antennas 09 p1352 A66-20348
- Potential analog synthesis of linear arrays and radiation pattern representation as function of single complex variable 09 p1356 A66-20605
- Inaccuracy in normalized space factor of nonuniformly excited and spaced linear antenna array expressed in terms of Poisson sum formulation 11 p1663 A66-22555
- Long-baseline radio interferometer for radio astronomy, combining wideband signal and one-dimensional linear array to restrict spatial response in two dimensions 11 p1704 A66-22562
- Pattern synthesis method for linear array using integral mean of Fourier approximation 12 p1841 A66-24628
- Bilinear transformation reduces linear uniformly spaced array to examination of rational fraction on imaginary axis of complex plane 13 p2029 A66-25202
- Mutual and self-impedance of linear antennas in interface between dielectric layers computed, noting cases of symmetric and antisymmetric excitations 14 p2256 A66-27914
- Eigenvalues design method for nonuniformly spaced arrays that will approximately any required radiation pattern 15 p2463 A66-29026
- Equivalent linear antenna substitution for antenna with plane aperture in statistical



analysis of antennas 17 p2879 A66-31861  
 Haar theorem for synthesis of  
 nonuniformly spaced linear discrete antenna  
 arrays 17 p2886 A66-32389  
 Radiation characteristics of circular  
 aperture and linear antenna with partially  
 coherent illumination 18 p3074 A66-33536  
 Radiation pattern of linear nonequidistant  
 antenna array 19 p3311 A66-35307  
 Broadband signals effect on far-zone field  
 of linear arrays studied in terms of energy  
 radiation pattern 19 p3320 A66-36402  
 Optimal discrete binary system of  
 electrical control of beam position of phased  
 linear antenna array 21 p3712 A66-39251

**LINEAR CIRCUIT**  
 Current status of linear integrated  
 circuits 01 p0048 A66-11143  
 Topological rules for impedance functions  
 of linear reciprocal  
 networks 02 p0208 A66-11906  
 Topological analysis for networks  
 containing nonreciprocal components and  
 mutual inductance 02 p0208 A66-11907  
 Optimal amplitude frequency and transient  
 process characteristics in linear loops of low  
 pass filter type 02 p0209 A66-12268  
 Linear circuit for degenerate parametric  
 amplification, using analog computer  
 elements 03 p0332 A66-12425  
 Invalidity of overall noise bandwidth for  
 receivers using linear or square law  
 envelope detectors for predetection of  
 signal to noise ratio 03 p0332 A66-12430  
 Impedance matrix of single three-pole and  
 two-stage amplifier determined by Kron  
 method 03 p0348 A66-12497  
 General linear time-invariant networks  
 analyzed in time and frequency  
 domain 03 p0349 A66-13022  
 Linear integrated circuits discussing  
 differential and operational amplifiers,  
 development, use, capabilities, new  
 techniques, special designs and  
 reliability 03 p0347 A66-13340  
 Digital computer calculation of linear  
 transistor amplifier performance from two-  
 port y-parameter  
 measurements 05 p0645 A66-14587  
 Iterative procedure for analyzing linear  
 electrical networks by digital  
 computer 05 p0638 A66-15127  
 Gain-bandwidth limitations and optimum  
 design of noninverting frequency converters  
 comprised of parametric conductance in  
 parallel with parametric capacitance pumped  
 in time-quadrature 07 p1017 A66-18348  
 Low-cost fast development capability of  
 master-dice technique for custom linear  
 integrated circuits 08 p1196 A66-19523  
 Circuit design techniques for linear  
 integrated circuits, noting manufacturing  
 methods, achievement of monolithic  
 construction, etc 11 p1670 A66-23243  
 Linear cycle set factorization, showing that  
 uniqueness of canonical procedure is  
 incorrect and introducing new cycle division  
 algorithm 11 p1679 A66-23247  
 Field effect transistor application to linear  
 amplifier and attenuator  
 circuits 11 p1673 A66-23470  
 Insulated gate field effect transistors in  
 HF-UHF linear amplifiers 11 p1673 A66-23471  
 Digital and RF/linear circuits compared  
 noting monolithic, hybrid and thin film  
 circuit limitations, phase locked loop design,  
 etc 12 p1830 A66-23756  
 Optimal amplitude frequency and transient  
 process characteristics in linear loops of low  
 pass filter type 12 p1848 A66-23872  
 Monolithic silicon-transistorized integrated  
 amplifier for use as stabilized gain block  
 element in linear circuit  
 realizations 12 p1842 A66-24656  
 Optically coupled linear circuit techniques,  
 discussing GaAs p-n junction diode,  
 noncoherent light emitters and silicon p-n  
 junction photosensors 13 p2036 A66-25521  
 Distributional study of real frequency  
 behavior of passive  
 systems 13 p2055 A66-26094  
 HF transistor circuit design, noting effect  
 of bias frequency and temperature on y and  
 h parameters 14 p2261 A66-28369  
 Power gain and stability of linear active  
 two-port networks with circuit design  
 equations based on terminal  
 parameters 14 p2268 A66-28371

Multiport linear networks in which pumped  
 variable capacitances shunt and interconnect  
 several ports, exemplifying with varactor  
 parametric amplifier, impedance  
 transformer, coupler, etc 17 p2890 A66-32907  
 Linearizer for constant temperature hot-  
 wire anemometer, detailing linearization  
 circuit 19 p3357 A66-35806  
 Continuous group and infinitesimal  
 transformation in linear dynamic system  
 application, considering linear  
 network 20 p3539 A66-38148  
 Three amplifier and oscillator  
 configurations analyzed for controlling  
 location of dominant poles of feedback  
 circuit within possible realizable  
 region 23 p4050 A66-41612

**LINEAR EQUATION**  
 SA NONLINEAR EQUATION  
 SA REYNOLDS EQUATION  
 SA SIMULTANEOUS LINEAR EQUATION  
 Approximate solution for differential  
 equations, using algorithm applied to  
 boundary value problem involving linear  
 equation 01 p0091 A66-10164  
 Solution to linear difference and  
 differential equation with variable  
 coefficients 01 p0092 A66-10173  
 Error estimates for some finite difference  
 methods of solving ordinary linear  
 differential equations 01 p0092 A66-10315  
 Qualitative-quantitative analysis of  
 solutions of second order ordinary linear  
 homogeneous differential equations and two  
 derivatives 01 p0093 A66-10403  
 Volterra integral equation used in alpha  
 operational method for solution of linear  
 differential equations 01 p0093 A66-10404  
 Linear differential equation solution  
 nonfluctuation and boundedness estimate in  
 connection with integral  
 inequalities 01 p0094 A66-10650  
 Asymptotic behavior of solution to system  
 of differential equations with random  
 limited coefficients 01 p0095 A66-10733  
 Cauchy problem for linearized Boltzmann  
 equation in kinetic theory of  
 gases 01 p0107 A66-11011  
 Nonlinear difference schemes for  
 hyperbolic equation applied to solution of  
 one-and multidimensional transport and  
 quasi-linear equations 01 p0095 A66-11013  
 Existence and formal uniqueness theorem  
 of partial linear differential equations with  
 Cauchy conditions on characteristic multiple  
 hyperplane 01 p0095 A66-11075  
 Wave solutions to linearized quasi-  
 hydrostatic equations for adiabatic  
 nonviscous flow on equatorially oriented  
 beta plane 02 p0254 A66-11982  
 Cauchy problem for infinite order linear  
 differential equation 02 p0250 A66-12019  
 Fragnen-Lindelof type theorems for  
 second-order linear elliptic equation,  
 examining Dirichlet problem solution in  
 infinite region 02 p0250 A66-12100  
 Stability analysis of adiabatic flow of  
 incompressible fluid without equation  
 linearization and by constructing functional  
 from hydrodynamic fields 02 p0220 A66-12170  
 Zeros of solutions of second-order linear  
 differential equation, discussing Sturm  
 comparison theorem 04 p0538 A66-13363  
 Linear theory of optimum variable thrust  
 rendezvous trajectories with power limit  
 propulsion system 04 p0575 A66-13457  
 MHD equations linearized by Newton  
 iteration method, describing weak  
 perturbation propagation 04 p0574 A66-13841  
 Qualitative and quantitative solution of  
 linearized approximations to boundary layer  
 equations, noting free jet and wall-slot  
 injection into moving stream  
 [ASME PAPER 65-APMW-6] 04 p0512 A66-14212  
 Iterative process to refine solution to  
 system of linear  
 equations 04 p0540 A66-14392  
 Transformation and equivalence of higher  
 than second order homogeneous linear  
 differential equations 05 p0708 A66-15153  
 Linearized equation and energy principle  
 for plasma stability  
 problems 05 p0726 A66-15254  
 Stress and strain analysis of sandwich  
 plates, formulating and solving problem of  
 bending for transversally isotropic layers  
 and light core 06 p0964 A66-16477

Correct solvability of Cauchy problem for  
 parabolic systems with coefficients  
 satisfying Dini condition 06 p0902 A66-16534  
 Properties of linearized system of  
 equations of perturbed motion and  
 application to motion of center of mass of  
 space vehicle 06 p0957 A66-17169  
 Second-order linear partial differential  
 equation transformed to normal form,  
 obtaining invariant representation without  
 Ricci calculus 07 p1055 A66-17301  
 Approximate method determining  
 nonstationary thermal fields in solid bodies  
 with thermal capacity and  
 thermoconductivity coefficient depending  
 linearly on temperature 07 p1148 A66-17399  
 Stability in small of two types of extremal  
 systems with modulating action, using linear  
 difference equation with periodic  
 coefficients 07 p1013 A66-17429  
 Perturbation method in theory of dynamic  
 stability of systems with distributed  
 parameters, discussing linear Hamiltonian  
 equation in separable Hilbert  
 space 07 p1056 A66-17606  
 Solution of linear differential equations  
 with quasi-periodic coefficients by method  
 of accelerated  
 convergence 07 p1058 A66-17908  
 Asymptotic behavior of solutions of  
 ordinary linear differential equations  
 involving continuous complex valued  
 functions 07 p1058 A66-17913  
 Improving estimates of solutions of linear  
 perturbed-motion equations of mechanical  
 systems with variable  
 coefficients 07 p1060 A66-18188  
 Evolutionary graphs to solve systems of  
 linear equations 08 p1246 A66-19635  
 One type of infinite-order differential  
 equation with polynomial coefficients of  
 increasing power 08 p1246 A66-19707  
 Second-order linear equations with  
 nonnegative characteristic form in analysis  
 of first boundary value  
 problem 09 p1397 A66-20734  
 Monte Carlo linear extrapolation of  
 multivariable functions, introducing  
 truncation procedure which saves on  
 machine time and serves for variance  
 reduction 10 p1549 A66-21215  
 Hypergeometric solutions of second-order  
 linear ordinary differential equation with n-  
 regular singular points 10 p1550 A66-21305  
 Qualitative and quantitative solution of  
 linearized approximations to boundary layer  
 equations, noting free jet and wall-slot  
 injection into moving stream  
 [ASME PAPER 65-APMW-6] 10 p1523 A66-21470  
 Digital computer solutions to rigorous  
 linear equations system for current density  
 by enforcing boundary conditions at discrete  
 points in scattering body 10 p1497 A66-21589  
 Theorems and corollaries describing  
 bounds for quadratic Liapunov  
 functions 10 p1551 A66-21918  
 Transcendence and algebraic independence  
 of values of E-functions representing  
 solution to third-order linear differential  
 equation 10 p1552 A66-21986  
 Linear ODEs in canonical form with after-  
 effect in functional space of continuous  
 functions 11 p1676 A66-22644  
 Discrete ordinate technique for solution of  
 distribution function of linearized Boltzmann  
 equation, with application to Couette  
 flow 11 p1692 A66-22923  
 Approximation of function of many  
 variables by linear  
 methods 11 p1723 A66-23313  
 Approximate oscillatory solution of second  
 order linear equations, with application to  
 Bessel equation 11 p1724 A66-23425  
 Stress function solution in dynamic linear  
 theory of homogeneous incompressible  
 elastic bodies 12 p1962 A66-23998  
 Linear differential equation solution  
 nonfluctuation and boundedness estimate in  
 connection with integral  
 inequalities 12 p1903 A66-24021  
 Cauchy problem for infinite order linear  
 differential equation 12 p1903 A66-24024  
 Best linear unbiased (BLU)/ estimator for  
 large class of error correlation  
 models 12 p1904 A66-24197  
 Majorants of solutions of first boundary  
 problem for second order linear elliptic



equations 12 p1904 A66-24238  
 Statistical derivation of linear viscoelastic equations, relating stresses to minor deformation 12 p1969 A66-24355  
 Acceleration potential method for solving linear problems of wing hydrodynamics above interface between fluids differing in density, for arbitrary Froude number 13 p2067 A66-26530  
 Linear differential system for rendezvous with target in elliptical orbit 14 p2391 A66-27471  
 Solution of linear system of equations based on determinants 14 p2324 A66-28137  
 Asymptotic estimates of characteristic values of differential equation with periodic coefficients 15 p2524 A66-28507  
 Linear normal form of system of real differential equation, noting disappearance of difference between Hartman and Sternberg hypotheses 15 p2525 A66-28511  
 Multiple characteristics of square systems of linear partial differential equations with constant coefficients, obtaining formal series solutions for systems 15 p2527 A66-29061  
 Linear integral operators applied to singular differential equations and to computations of compressible fluid flows 16 p2683 A66-30241  
 Bending stresses in cylindrical shell with rigid circular inclusion examined under axial tension and internal pressure [AIAA PAPER 66-525] 16 p2813 A66-30526  
 Riemann-Hilbert boundary value problem for elliptic systems of linear partial differential equations of first order 16 p2733 A66-30651  
 Asymptotic behavior of solution to ordinary differential equation, noting transformation to nearly diagonal system of first order 16 p2733 A66-30741  
 General theory of linear integral equations with power kernel 16 p2734 A66-30746  
 Transformation and equivalence of homogeneous linear differential equations of higher than second order, examining equivalence of regular equations with dimension 16 p2734 A66-30778  
 Correct solvability of Cauchy problem for parabolic systems with coefficients satisfying Dini condition 16 p2735 A66-30972  
 Asymptotic behavior of solutions of ordinary linear differential equations involving continuous complex valued functions 16 p2736 A66-30976  
 Quasi-linear equations for inhomogeneous plasma in magnetic field applied to pumping of energy of Langmuir oscillations 16 p2762 A66-31176  
 Extension of problem of singular perturbation for linear scalar constant coefficient differential-difference equation with single retardation to several retardations, noting degenerate equation solution 16 p2737 A66-31230  
 Downrange radar and optical data reduction used for evaluation of ejection velocities of ballistic missile penetration aids at deployment 16 p2804 A66-31464  
 Generalized star-mesh transformation in network theory obtained using fact that Kirchhoff rules, Maxwell rules, Mason rules and Coates formulas can be obtained from each other 17 p2899 A66-32053  
 Generalized solutions to second-order linear or quasi-linear uniform parabolic equation 17 p2947 A66-32664  
 Boundedness of solutions to nearly differential equations with random arguments 17 p2947 A66-32712  
 Textbook on differential equations with deviating arguments, covering existence theorems, linear equations, stability theory, boundary value problems, etc 17 p2947 A66-33188  
 Solution method for use when linear combinations of given approximate solutions are used for representing exact solution of general ordinary linear homogeneous differential equation 18 p3125 A66-33627  
 Sufficient conditions for boundedness of solutions of linear system of differential equations with variable coefficients 18 p3126 A66-33929  
 Minimal element determination for certain set related to interpolation of second-order linear ordinary differential

equations 18 p3126 A66-33954  
 Evolutionary graphs to solve systems of linear equations 18 p3127 A66-34173  
 Solution for inhomogeneous differential linear equation in integral form obtained from Wronskian 18 p3128 A66-34701  
 Graphical analysis of extremal control system stepwise adapted to process with extremal characteristic located between two first-order linear operators 19 p3324 A66-35582  
 Transcendence and algebraic independence of values of E-functions representing solution to third-order linear differential equation 19 p3390 A66-36191  
 Homogeneous linear differential equations, examining stochastic processes for perturbations causing discontinuous solutions and for perturbations acting on entire bounded intervals 19 p3390 A66-36334  
 Contact problem for elastic rectangle solved by reducing problem to solution of quasi-fully regular infinite set of linear algebraic equations with bounded free terms 19 p3476 A66-36837  
 Mean value theorem for curves arising in solution of ordinary differential equation by series method 20 p3590 A66-37525  
 Linear homogeneous third-order differential equations, examining existence, uniqueness and asymptotic behavior of nontrivial nonoscillatory solutions and existence criteria for oscillatory solutions 20 p3591 A66-37608  
 Pulsation properties of stellar models representing RR Lyrae stars obtained, using adiabatic and nonadiabatic linearized pulsation equations 20 p3652 A66-37613  
 Cylindrical shells strengthened by stringers and formers calculated, using double trigonometric series 20 p3670 A66-37672  
 Well-posed BVP for linear partial differential system and relation of weak solution with two Banach spaces 21 p3754 A66-38458  
 Boundary layers with coupled heat and mass transfer for large enthalpy per unit mass of injected material, based on linearity of perturbation equations 21 p3834 A66-38704  
 Approximate method for determining damping factors of mechanical oscillatory systems with many degrees of freedom described by linear differential equations of n-th order with constant coefficients 21 p3770 A66-38971  
 Periodic flows of orientable anisotropic fluids tending to be unoriented at rest considered through linear equations which predict resonance phenomenon 21 p3727 A66-39173  
 Plane supersonic flow with Mach reflection represented by shock wave interaction, noting integral equation obtained from linearized shock equations 22 p3897 A66-39696  
 Reinforced cylindrical shell stability under axial compressive force, using linear and quasi-linear formulation 22 p3990 A66-40146  
 Linear theory of micropolar elasticity, noting all components of asymmetric stress tensor are determined and motion of media is fully described when deformation and microrotation vectors are known 22 p3995 A66-40566  
 Book on numerical processes in differential equations including initial value and boundary value problems 22 p3941 A66-40620  
 Impulse response of second-order time varying systems of differential equation obtained without knowledge of independent solutions of associated homogeneous equation 23 p4086 A66-41694  
 Linear perturbation theory of flow due to convection of entropy and vorticity in nonuniform flow field, noting sound generation 23 p4062 A66-42051  
 Generalized solution to linear second-order parabolic equation showing that first boundary value problem has unique solution, obtaining estimates of Holder norms of solutions 24 p4231 A66-42233  
 Book on asymptotic methods of integrating linear differential equations with varying coefficients, emphasizing equations for oscillatory processes 24 p4231 A66-42613  
 Hilbert parametrix method of solving linear BVPs for second-order elliptic PDEs, using Green functions 24 p4232 A66-42740

Asymptotic behavior of solution to system of differential equations with random limited coefficients 24 p4232 A66-42749  
 Single second-order oblique derivative problem with elliptic operator 24 p4232 A66-42830  
 Linear second-order partial differential equations of elliptic type analyzed, using maximum principle and barrier functions 24 p4233 A66-43065  
 Numerical solution of linear boundary value problems 24 p4233 A66-43201  
**LINEAR FILTER**  
**SA WIENER FILTER**  
 Self-contained orbital navigation system using Earth-horizon measurements in 14-16  $\mu$  carbon dioxide absorption band, using Kalman linear filter theory 01 p0100 A66-10024  
 Recursive space navigation applied to navigating in near orbit of planet by measuring directions to known landmarks 01 p0100 A66-10025  
 Linear filtering concepts in imaging and optical data processing systems, including three-dimensional photography obtained by wave front reconstruction 02 p0240 A66-11453  
 Stochastic differential equations specifying dynamical structure of filters generating posterior probability distribution when inputs are time functions 03 p0351 A66-13259  
 Nonsteady optimum-filtering problems where useful and noise signals are related to white noise by different equations 04 p0505 A66-13979  
 Linear smoothing method minimizing mean-square error in time series where signal statistics are unknown and noise is additive, deriving filter 05 p0653 A66-14600  
 Power spectral density analysis, reviewing signal wave, time, rate and system parameters [ISA PREPRINT 1.5-3-65] 05 p0683 A66-15508  
 Communications and control systems that require faithful transmission of amplitude-modulated signals through linear filters 06 p0823 A66-15964  
 Finite wide-sense stationary sequence followed by another sequence corresponding to linear filtering without delay, minimizing mean square error 06 p0828 A66-16116  
 Recovery of continuous signal from samples taken at periodically varying rate, determining optimum mean-squared realizable filter and error 06 p0829 A66-16195  
 Optimum linear separation of random message from additive white noise of given spectral height realized as unity feedback system 06 p0832 A66-16449  
 Nonlinear optimal filtration problem solved, using quasi-orthogonal representations of random functions 07 p0104 A66-17432  
 Optimal filter in solution of linear mean square estimation problem when process statistics are undefined 12 p1848 A66-24249  
 Algebraic conditions of controllability and observability and relation between two Riccati-type matrix equations, deriving one from optimal regulation and second from optimal linear filtering 12 p1854 A66-24339  
 Optimum linear filtering of integrated signal in white noise, deriving expression for minimum mean square error 13 p2023 A66-25664  
 Lumped-constant filters whose bandpass depends only on one parameter of transmission coefficient, having lower bandpass for given transient process delay time 15 p2464 A66-29120  
 Linear stochastic filtering theory assessing Kalman-Bucy filter and equivalence with Kolmogorov-Wiener problem 15 p2473 A66-29377  
 Feedback realization of continuous-time optimal filter, with application in redundant signal mixing 15 p2474 A66-29382  
 Synthesis of linear digital recursive filters, noting application to arbitrary amplitude frequency transfer function synthesis 15 p2475 A66-29772  
 Effect of modifying digital filter weights derived on least squares error basis through multiplication by certain weighting functions 16 p2859 A66-30535  
 Nonstationary problem of linear filtering in presence of additive noise solved by computer simulation 16 p2869 A66-30762



Optimum estimate of nonlinear process in presence of non-Gaussian noise and disturbances, deriving algorithm for correcting approximation 19 p3323 A66-35340

Linear least-squares filtering problem in geometrical interpretation 19 p3318 A66-35731

Linear filtering technique for estimation of azimuth alignment of inertial guidance system in presence of disturbances with no measurement noise 19 p3398 A66-36689

Automatic tracking radar control via nonstationary filter, noting design principle and operation 20 p3536 A66-36866

Graphic solution for factoring higher-order polynomials of response function resulting from analysis of linear filter networks 21 p3756 A66-38672

Horizon sensor data processing with compensation for statistical properties of errors, noting application of optimal filtering theory 21 p3766 A66-38882

Kalman filter divergence control, noting analytical and empirical modification methods 21 p3766 A66-38883

Simulation experiments to describe effects of measurement function nonlinearity and ambiguities when linear filters are applied in distant planet satellite orbit parameter estimation 21 p3766 A66-38885

Apollo inertial navigation system estimation, using statistical filtering to reduce computation 21 p3767 A66-38886

Optimum realizable linear filter role in some communication problems, considering detection and continuous estimation 22 p3879 A66-40716

Maximum a posteriori /MAP/ interval estimation for state vector of random process, solving fixed delay filtering and deriving error matrix 22 p3868 A66-40718

Reentry filtering prediction and smoothing in application of satellite and spacecraft trajectory estimation techniques [AIAA PAPER 65-319] 23 p4132 A66-41098

## LINEAR PREDICTION

Linear estimation for log Weibull distribution from random sample of ordered failure time 01 p0091 A66-10120

Recursive procedure based on orthonormalization for discrete sample least mean square error estimation of non-Markovian random process 05 p0706 A66-14614

Parameter evaluation of delta modulation encoding techniques for image communication applications by computer simulation 20 p3513 A66-37201

Linear prediction theory for maximum load tolerance of oscillator and lossless embedding required to induce oscillation 20 p3540 A66-38288

## LINEAR PROGRAMMING

### SA DUAL CONTROL PROBLEM

### SA NONLINEAR PROGRAMMING

Solution to linear programming problems, using iterative method 01 p0050 A66-10170

Selection of maximum number of constraints for which solution can be obtained for problems of linear or nonlinear programming and approximation of functions 01 p0051 A66-10707

Nonlinear optimal design problem reduced to linear programming problem for worst-case circuit design 05 p0656 A66-14626

Research and Development Effectiveness /RDE/ computerized planning program, utilizing analytical techniques in management of research and development resources 08 p1322 A66-19461

Gradient systems of differential equations for solution of linear and quadratic programming problems on analog computer 08 p1188 A66-19687

Stochastic linear programming as activity analysis model for determination of maximal profit operations for companies 09 p1349 A66-20635

Integer linear programming to design combinatorial network of threshold gates capable of evaluating partially specified Boolean function 10 p1517 A66-21698

Selection of maximum number of constraints for which solution can be obtained for problems of linear or nonlinear programming and approximation of functions 11 p1675 A66-22619

Linear graphs theory as part of topology

solving problems in circuitry, psychology, linear programming, matrices, network theory, etc 11 p1675 A66-22627

Alternative method of determining incentive fee schedule for government contracts, based on linear programming and system reliability 12 p1888 A66-24669

New algorithm for quadratic programming problems with application to control, determining input requiring minimum time from initial state to target 13 p2046 A66-25341

Gomory method of linear programming [PST PAPER NT-148] 14 p2324 A66-27836

Iteration method of general linear programming on digital computer, using penalty functions, compared to equilibrium problem of mechanical system 16 p2669 A66-30759

Tucker linear programming concept of combinatorial equivalent matrices extended to network synthesis 16 p2739 A66-31721

Optimal solution method for linear program in which second member and several constraint matrices depend linearly on one parameter 18 p3127 A66-34389

Gradient systems of differential equations for solution of linear and quadratic programming problems on analog computer 18 p3073 A66-34673

Gomory all-integer linear programming algorithm based on lexicographical ordering principle and relation to cost function 19 p3309 A66-35876

Reliability-maintainability cost tradeoff via dynamic and linear programming, discussing states, alternatives within states, transition rates and expected costs 20 p3568 A66-37911

Product form of inverses of sparse matrices, discussing geometrical interpretation and Gauss-Jordan method 24 p4233 A66-43203

## LINEAR RECEIVER

Minimum noise of linear receiver in formulas of Heffner and Nyquist 08 p1183 A66-19112

## LINEAR SYSTEM

### SA NONLINEAR SYSTEM

Best stabilizing control for linear system under given class of perturbations 01 p0050 A66-10354

Existence of explicit stable difference scheme in correct Cauchy problem for linear systems of partial differential equations with constant coefficients 01 p0094 A66-10654

Gradient method of solving terminal control problems in linear automatic control system 01 p0051 A66-11012

Statistical probability problems of optimal control for linear systems 01 p0051 A66-11183

Existence and uniqueness of solution for second boundary value Neumann problem in linear flow theory 02 p0296 A66-11242

Disturbance signals used to synthesize optimal structure of rapid action automatic systems 02 p0206 A66-11311

Linear quartz crystal temperature sensing element for digital data presentation 02 p0228 A66-11516

System coefficient matrices and finite number of derivatives are sufficient conditions for controllability of linear time-variable systems 02 p0208 A66-11901

Stability of single-frequency solutions to quasi-linear autonomous systems with two degrees of freedom 02 p0262 A66-12175

Quartz thermometer measuring temperatures automatically and directly on digital display, using quartz wafer with linear coefficient cut 03 p0367 A66-12373

Monograph on boundary problems for linear parabolic systems with complex coefficients 03 p0386 A66-12456

Three independent systems of matrix equations for solving transfer function of multiparameter linear system handling by human operator 03 p0328 A66-12699

Plotting of radius of controllability sphere for linear dynamic systems bounded with respect to control actions and having fixed time of motion 03 p0350 A66-13042

Plotting in phase space controllability region for unstable linear system of differential equations 03 p0350 A66-13043

Textbook employing signal analysis theory in treating linear systems and communication theory including Fourier series, Fourier and Laplace transforms,

convolution integral, etc 03 p0336 A66-13073

Motion stability of linear continuous systems noting influence of various forces 03 p0438 A66-13094

Optimization of linear servosystem comprising ideal proportional, integral and differential control regulator and order system 03 p0350 A66-13095

Optimal fixed time constant-energy regulator for linear plants with perturbations operating within bounding hypersurface 03 p0350 A66-13176

Linear system using differential circuits for indirect measurement of perturbations 04 p0503 A66-13771

Analytical design of controller for stabilization of linear system with random delay in form of intermittent Markov process 04 p0504 A66-13973

Pontryagin maximum principle to solve zeroing problem for nonsteady linear systems optimum in integral sense 04 p0504 A66-13978

Time domain and frequency domain analysis of linear time invariant systems applied to radar return signal analysis 04 p0506 A66-14108

Response of linear and nonlinear devices to noise calculated by constant time-varying parameters, covariance, integral transform and characteristic function methods 04 p0485 A66-14110

Steady states of mechanical system using perturbation method, assuming primary and secondary oscillators are tuned to single pulse, each involving Duffing type nonlinearity 04 p0545 A66-14169

Viscoelastic contact problem for linear materials and quadratic surfaces of bodies [ASME PAPER 65-APMW-36] 04 p0594 A66-14236

Generalized convolution theorems of periodic functions based on Fourier series formalism used to study processes in linear systems 04 p0506 A66-14402

Error effect in a priori information on sequential estimate variance of linear system states, noting optimal filter synthesis 05 p0653 A66-14601

Time-varying linear differential systems, discussing minimum time identification via scalar valued transform of Zadeh 05 p0654 A66-14607

Synthesis method for linear time-varying systems, discussing integral formulation and approximation functions 05 p0654 A66-14609

Controllability and observability matrices in time-variable linear systems 05 p0655 A66-14618

Composite state vector method for linear time-varying system 05 p0655 A66-14619

Relative stability of linear feedback systems noting Hurwitz, Nyquist and Mikhailov stability criteria 05 p0707 A66-14623

Approximation formulas for minimum and maximum roots of nth order polynomials 05 p0707 A66-14624

Absolute stability of multiply connected pulse systems containing linear continuous portion, pulse elements in phase and nonlinear elements with time dependent characteristics 05 p0658 A66-15331

Stability of linear stochastic distributed parameter dynamical systems by differential integral equations [ASME PAPER 65-WA/APM-12] 05 p0717 A66-15434

Sufficient condition for existence of admissible control for optimization systems [ASME PAPER 65-WA/AUT-12] 05 p0710 A66-15607

Transfer function identification of linear time-varying system with input and output signals available in sampled data form [ASME PAPER 65-WA/AUT-16] 05 p0659 A66-15620

Output moments of linear system determined in terms of corresponding moments of input and input-output relationship of average correlations and spectra, defining nonstationary processes 06 p0902 A66-16188

Maximization of output voltage of linear time-invariant system noting effect of input admittance, assuming input pulse is equal to zero 06 p0860 A66-16190

Vector equation  $F/X/$  equals zero solved



by transforming nonlinear algebraic equation into nonlinear differential equation 06 p0865 A66-16746

Linear system impulse response approximation, determining time-scaling factor via orthonormal Laguerre functions 06 p0866 A66-16748

Least squares technique for identification of linear time-invariant plant in sampled data system corrupted by additive noise 06 p0866 A66-16750

Optimal control of distributed parameter systems governed by systems of linear partial differential equations 06 p0866 A66-16964

Linear time-invariant systems, noting relation between transient response duration and differential equation coefficients 06 p0867 A66-16990

Criterion of nonrigorous hyperbolicity for equation system with nondiagonal quasi-linear partial derivatives after putting system in diagonal quasi-linear form for relativistic MHD 06 p0921 A66-17058

Complete resolution of concentrated load of limiting contour, determining spectrum of functional linear operator attached to interior region 06 p0967 A66-17061

Optimum transient response of linear systems with rational transfer functions 07 p1013 A66-17402

Optimal program control for minimization of finite state vector norm of linear system with two types of sets of permissible controls 07 p1013 A66-17425

Correlation matrix of natural thermal noise put forward for arbitrary passive linear system described by Lagrange equations and thermal equilibrium 07 p1013 A66-17431

Amplitude modulated carrier frequency signal circuit analyzed, showing open loop linear pulse system 07 p1014 A66-17439

Linear vibratory system response to random impulses, describing nonstationary white noise and mean square resonance 07 p1143 A66-17731

Resolving matrix of normal system of ordinary linear differential equations in complex independent variable for multiply connected fields 07 p1057 A66-17835

Stationary queue length Poisson distribution in single channel service system, considering reliability of device 07 p1003 A66-17862

Existence of logarithm for nonsingular square matrix, uniqueness for linear ordinary differential equation systems, logarithms of operators and spectral mapping 07 p1058 A66-17966

Characteristics of pulsed wave at output of linear system with pulsed rectangular wave input 07 p1016 A66-18071

Existence and uniqueness of piecewise-continuous solution to two-dimensional linear first order hyperbolic system with discontinuous coefficients 07 p1060 A66-18100

Asymptotic stability of periodic solutions of nonautonomous quasi-linear systems with two degrees of freedom 07 p1016 A66-18187

General performance indices for time and frequency response for free motion of linear discrete control systems 07 p1016 A66-18280

Distortions of linear system reactions with change in amplitude-frequency and phase-frequency characteristics 08 p1183 A66-19102

Root hodograph method for determining amplitude and phase frequency characteristics of dynamic linear systems 08 p1202 A66-19692

Partial-fraction expansion of transfer matrix, using Lagrange interpolation formula 08 p1246 A66-19738

Dynamic programming in linear vector system and application in switching system 09 p1393 A66-19909

Linear system induced amplitude-frequency and phase-frequency distortions 09 p1361 A66-20296

Weighting function and frequency response determination of linear system with N degrees of freedom, using convergent series solution 09 p1396 A66-20636

Necessary and sufficient condition for matrix distribution to have positive-real Laplace transform 09 p1396 A66-20641

Stability of characteristic indices of limiting solutions of linear

systems 10 p1549 A66-21236

Nonresonant solid state magnetic, semiconductor and dielectric devices, noting operation characteristics, control parameters, etc 10 p1509 A66-21418

Equations of linear automatic control systems decomposed asymptotically 10 p1518 A66-21979

Dynamic characteristics of linear plant determined under noise conditions, allowing for error in input-signal measurement 11 p1673 A66-22202

Stability of linear time-lag systems with stochastic parameters examined, deriving sufficient condition for asymptotic stability 11 p1674 A66-22224

Optimum control in nonlinear automatic control systems and linear systems with distributed parameters 11 p1674 A66-22352

Synthesis of time-optimal control for third-order linear discrete objects 11 p1676 A66-22754

Accuracy and optimality of estimates of discrete pulse transfer function of linear unsteady plant 11 p1677 A66-22758

Model of spectrotron with external feedback in dynamic behavior analysis, considering control pulse and transient process 11 p1677 A66-22761

Amplitude calculation of forced mass vibrations in damped linear mechanical system from column matrices of oscillation modes of eigenfrequencies 11 p1783 A66-23018

Linear quadrupoles, wave and operating parameters, transfer loss and phase coefficient for mismatched network 11 p1677 A66-23063

Linear system dynamics, discussing time function vector space, spectral coefficients, orthonormal and transfer functions, parameter variation, Fourier approximation, etc 11 p1679 A66-23269

Automata theory and control theory analytically compared for general and linear systems and tolerance 11 p1680 A66-23275

Existence and uniqueness of minimum effort control for wide class of effort functions, using generalization of Neustadt problem 11 p1681 A66-23424

Complete controllability of particular plant 11 p1682 A66-23455

Circuit theory reciprocity theorem for dynamic linear systems with gyroscopic coupling for steady state response 12 p1912 A66-23611

Response of logarithmic frequency characteristics of dynamic linear systems to small parameter variations 12 p1848 A66-23780

Stability of linear stochastic distributed parameter dynamical systems by differential integral equations [ASME PAPER 65-WA/APM-12] 12 p1914 A66-23989

Statistical probability problems of optimal control of linear systems 12 p1848 A66-24016

Existence of explicit stable difference scheme in correct Cauchy problem for linear systems of partial differential equations with constant coefficients 12 p1903 A66-24023

Properties helping design of linear sampled data systems containing periodically time-varying components like parametric amplifiers 12 p1848 A66-24139

Linear distributed parameter systems with bounded input in minimization of difference between desired response and obtainable response 12 p1849 A66-24251

Invariant hyperplanes for linear dynamical systems, discussing geometric properties and relation to controllability and observability 12 p1849 A66-24256

Optimal control and stability for stochastic systems, viewing linear diffusion models based upon Gaussian-Markov process as finite dimensional linear system driven by white noise 12 p1854 A66-24637

Absolute and relative stability of linear control systems containing transport or distributed lag 12 p1855 A66-24643

Response to multiple random excitation of system with multiple degrees of freedom, connecting spectral density matrix of generalized coordinates with corresponding generalized forces 12 p1972 A66-25004

Noise factor of linear receiving systems in

quantum and classical regions, noting role of dual push-pull amplifier and frequency converter 13 p2020 A66-25226

Matrix solution of limit problems of linear system of ordinary differential equations 13 p2117 A66-25414

Functional analysis demonstrating existence and uniqueness of displacement field, providing solution for linear viscoelasticity problem for medium having behavior satisfying coercivity condition 13 p2195 A66-25463

Linear power amplification with switching techniques, using pulse width modulation 13 p2036 A66-25522

Mathematical methods for examining stability of linear and nonlinear systems, with survey of stability criteria 13 p2118 A66-25581

Asymptotically stable linear system controlled by scalar random input 13 p2048 A66-25849

Dynamic programming for stochastic systems applied in designing controller for transferring linear system from initial to final position in specified time interval 13 p2048 A66-25852

Control system design, analyzing sensitivity of system performance to parameter variations by obtaining time domain measure of sensitivity 13 p2050 A66-26062

Optimum control of linear systems in presence of random disturbances, noting choice between cost design and cost variance methods 13 p2051 A66-26066

Components of gradient of performance criterion in adaptive control systems, employing correlation technique by use of time delay 13 p2051 A66-26067

Multiparameter sensitivity matrix analysis of linear feedback multiloop systems 13 p2053 A66-26082

State-variable feedback decoupling of multivariable linear plants with cross coupling between various input-output pairs 13 p2053 A66-26083

Markov parametric algorithm for effective construction of minimal realizations of linear state-variable finite-dimensional dynamical systems from input-output data 13 p2053 A66-26084

Satisfaction approach to synthesis and control of linear systems 13 p2055 A66-26097

Stability limits of linear system of k-th-order with periodic coefficients 13 p2055 A66-26340

Approximating probability characteristics of mismatch for steady mode of operation of astatic servosystem with modulation 13 p2056 A66-26480

Lagrange equation approach to linear aeroelasticity in modern aircraft from structural and aerodynamic data 13 p1997 A66-26696

Effect of relay response time on dynamic properties of automatic system incorporating linear group and relay element with pure delay 14 p2264 A66-27358

Restrictions placed on transfer function of linear system with input and output coordinates in presence of given plant in control loop 14 p2265 A66-27522

Stability of nonlinear control systems, noting Hermitian matrix for linear system of ordinary differential equations and analogous problem for difference equations 15 p2525 A66-28513

Mean square asymptotic stability of linear system described by nth order equation with random coefficients 15 p2537 A66-28964

Letov problem and analytical construction of optimal controller from motion equations of linear servosystem 15 p2469 A66-29045

Stability of variable-structure control systems, noting two-stage motion in linear system stabilization and image point impingement on switching surface 15 p2471 A66-29161

Destabilization of linear system with N degrees of freedom without damping subjected to nonconservative forces 15 p2609 A66-29251

State variable determination for linear time invariant plants with known parameters, noting noise suppressing characteristics of technique 15 p2471 A66-29329

Absolute stability of multiply connected



pulse systems containing linear continuous portion, pulse elements in phase and nonlinear elements with time-dependent characteristics 15 p2475 A66-29976

Optimization of linear control systems when placing step limitations on control, using functional analysis 16 p2668 A66-30751

Synthesis problem of optimum dynamic characteristics of multivariate linear control systems with random input signals 16 p2668 A66-30752

Cause and effect interdependence in linear system, noting distribution theory and double Laplace transform 16 p2670 A66-31024

Analytical design method for synthesis of feedback controller for multivariable linear control systems, considering transfer function 16 p2671 A66-31111

Pole-zero method to determine frequency response of second-order linear control systems with phase-advance signal shaping 16 p2671 A66-31157

Tabulated data method for synthesizing third order linear transfer functions, using chain of inverted L-sections of passive resistor-capacitor elements in conjunction with single operational amplifier 16 p2671 A66-31203

Simulation of fourth order type I linear system, using one-operational amplifier and two-terminal network consisting of four resistors and four capacitors 16 p2672 A66-31385

Linear system damping while using minimum control intensity treated as functional analysis problem 16 p2672 A66-31504

Periodic and quasi-periodic solutions to differential equations describing pulsed systems 16 p2738 A66-31709

Maximum increase in system error due to computer round-off errors for closed loop linear sampled data system 17 p2900 A66-32075

Variation of mean square error of linear system with time, applying parameter perturbation process to random or deterministic input 17 p2901 A66-32289

Dynamic programming applied to synthesis of linear optimal or suboptimal multivariable control systems in which control-signal vector depends only on certain prescribed state variables 17 p2901 A66-32291

Sequential linear estimation when measurement function is nonlinear, not considering system dynamics, applied to space trajectories 17 p2946 A66-32456

Stability analysis of linear dynamic system in form of rigid straight shaft having several stable mathematical pendulums 17 p2958 A66-32607

Viscoelastic contact problem for linear materials and quadratic surfaces of bodies [ASME PAPER 65-APMW-36] 18 p3249 A66-33589

Necessary and sufficient conditions for existence of classical normal and quasi-normal modes in damped linear dynamic systems [ASME PAPER 65-WA/APM-25] 18 p3134 A66-33592

Reduction of Gilchrist two-equation set for free oscillations in conservative quasi-linear systems with two degrees of freedom 18 p3134 A66-33602

Sensitivity of eigenvalue to changes in matrix, noting development of computational formula 18 p3127 A66-34077

Exact evaluation of responses of feedback control system with time delay to deterministic input 18 p3090 A66-34081

Piecewise linear system modeling via topological techniques, using flowgraph method for network synthesis 18 p3090 A66-34247

Linear system induced amplitude-frequency and phase-frequency distortions 18 p3091 A66-34959

Equivalent systems with identical accuracy at fixed moment of time through transfer function of steady state correcting device 18 p3091 A66-34988

Plotting of radius of controllability sphere for linear dynamic systems bounded with respect to control actions and having fixed time of motion 18 p3092 A66-35005

Plotting in phase space controllability region for unstable linear system of

differential equations 18 p3092 A66-35006

Transient and steady state responses of linear systems under oscillation and PAM 19 p3303 A66-35834

Equations of linear automatic control systems decomposed asymptotically 19 p3324 A66-35857

Optimal control of time-varying linear systems subject to additive noises and load disturbances, based on exact plant equations 19 p3325 A66-35877

Iterative solutions to high-speed actions, noting reduction to successive problems of maximization of linear form from finite state 19 p3325 A66-35931

Monotonic stability of motion for neutral linear solution 19 p3400 A66-35932

Sensitivity points method for linear systems based on structural interpretation of logarithmic sensitivity functions, introducing sensitivity dipole 19 p3327 A66-36015

Synthesis of automatic control systems for linear plants with variable parameters satisfying specified performance criteria 19 p3328 A66-36024

Stability of characteristic indices of limiting solutions of linear systems 19 p3389 A66-36183

Stability and sensitivity of terminal linear feedback control systems 19 p3334 A66-36668

Gain specification of linear controller for large launch booster, using new application of linear control theory 19 p3471 A66-36687

Rigid body rotational attitude control in three dimensions with linear transformation as output variable, noting advantages, applications and results 19 p3471 A66-36693

Linear optimal control in systems with uncertain parameters, noting application to design of compensating network for flexible booster for uncertain value of first bending mode 19 p3471 A66-36696

Rapid parameter identification system for linear time-invariant plant with only input and output measurable 19 p3336 A66-36709

Design synthesis of adaptive control system for linear discrete plants with time varying parameters, noisy measurements and statistical and deterministic disturbances 19 p3337 A66-36711

Optimization criterion capable of simultaneously considering different performance aspects applied to linear second-order control system with acceleration, velocity and displacement feedback loops 19 p3337 A66-36714

Sequential estimation on states of linear systems disturbed by white noise, determining relations between covariance matrices 19 p3338 A66-36736

Horowitz root-locus compensation method extended to analysis and design of high-gain linear control systems with variable coefficients 19 p3338 A66-36741

Forced modes of automatic continuous system with linear controlled plant with variable dynamic properties and learning model self-adjusted by search modulation 20 p3536 A66-36878

Linear system with given structure identified from measured input and output time histories of frequency responses including curve-fitting, equation of motion and set of equations of motion methods 20 p3537 A66-36885

Optimum transformation of linear system with minimal rms error from given point to fixed delta-environment of another given point 20 p3537 A66-36890

Equivalent transfer function of linear two-channel system of automatic control, discussing system stability dependence on cross links 20 p3537 A66-36891

Transient processes in linear automatic control systems dependent on parameters which appear when differential equations of analyzing system are transformed by Laplace-Karson method 20 p3537 A66-36892

Optimal control analysis of system behavior described by linear stochastic differential equations 20 p3537 A66-36893

Indirect testing of dynamic systems involving maximum measure of parameter values from minimum test points, noting dependency of error propagation on system structure 20 p3521 A66-37210

Linear system providing maximum signal

to noise ratio for given parameters of correlation function of incoming quasi-harmonic signal mixed with white noise 20 p3515 A66-37379

Plane linearly polarized electromagnetic wave diffraction on several spheres forming linear system, showing solution of boundary value problems 20 p3603 A66-37754

Group theory of invariance of finite linear state-variable transformations generating new linear dynamic system and application to electric network 20 p3539 A66-38147

Linear elliptic partial differential systems, eigenvalue and boundary value problems - Johns Hopkins University, Lectures, March-May 1965 21 p3754 A66-38457

Interior regularity theorem for linear elliptic matrix differential operator 21 p3754 A66-38459

Optimal control problem for linear systems with phase constraints 21 p3717 A66-38540

Equations of transient motion of linear systems solving methods including analytical, progressive and shock-spectra for application to aircraft, packaging, etc 21 p3824 A66-38572

Dynamic instability in linear vibrating system when linked to unlimited energy reservoir 21 p3825 A66-38577

Free vibration of composite system analyzed, using Rayleigh-Ritz method 21 p3825 A66-38583

Feedback control system behavior, examining influence of values of structural parameters and variations in domain of complex variable 21 p3718 A66-38806

Eigenvalue problems with monotonic operators and error estimation for operator equations with continuous homogeneous operators in semiordeered normalized vector space 21 p3757 A66-38942

Movchan theorem for stability of continuous systems, considering example of vibrating string and derivation of stability criterion for nonlinear elasticity 22 p3990 A66-40134

Decomposition of system of linear differential equations, using asymptotic techniques of Krylov and Bogolubov 22 p3940 A66-40459

Development of family of standard polynomials with adjustable damping, noting first- and second-degree numerators 22 p3884 A66-40514

Reduction principle applied to nominal stability, determining perturbation function for case where equations of perturbed motion are autonomous and characteristic equation of linear system has double zero root 22 p3941 A66-40796

Stability of trivial solution to system of linear differential equation with distributed delay, determining majorant of solutions to Cauchy problems 22 p3941 A66-40797

Analytical design of controllers for linear autonomous systems of arbitrary order 23 p4048 A66-40969

Sufficient conditions for linear time optimal control system on compact real intervals in Euclidean n space 23 p4049 A66-41536

Bang-bang principle in problem of epsilon-stabilization of linear control systems extended to systems of arbitrary dimension 23 p4051 A66-41874

Inequality, derived from entropy law, for irreversible processes of nonequilibrium thermodynamics, with attention to viscoelastic materials 24 p4293 A66-42136

Rotor instability factors, noting difficulty of applying linear theory to actual damping forces in rotor 24 p4287 A66-42269

Asymptotic stability of linear systems, using matrix analysis 24 p4187 A66-42375

Analytical method based on Taylor series to substitute linear control system for nonlinear control system 24 p4188 A66-42482

Optimal control problem formulated for linear constant-coefficient system subjected to class of amplitude bounded load disturbances 24 p4189 A66-43205

## LINEAR TRANSFORMATION

Transformation of equivalent nth order linear differential equations 03 p0388 A66-13154

Controller analytical design for nonautonomous systems, deriving necessary and sufficient conditions for existence of optimum control 06 p0862 A66-16522



Pulse compression by dispersive gratings on crystal quartz, describing ultrasonic method and wave transformation of frequency-swept radar 06 p0857 A66-16958

Linear and antilinear transformations for real and complex Hilbert space 07 p1058 A66-17963

Rapidly convergent iterative unique determination of linear steering function for desired orbit conditions 08 p1289 A66-18826

Linear perturbation theory computation of target errors in lunar impact trajectories due to random injection 08 p1289 A66-18828

Optimization of high resolution radar based on mathematical results regarding linear transformation of signals and ambiguity functions 12 p1819 A66-24601

EPr and normal EPr matrices, noting linear transformation on vector space 14 p2320 A66-27113

Minimum effort control problem in rotund reflexive Banach space and extension to Hilbert space under bounded linear transformation 14 p2266 A66-27631

Controller analytical design for nonautonomous systems, deriving necessary and sufficient conditions for existence of optimum control 16 p2670 A66-30832

Group theory of invariance of finite linear state-variable transformations generating new linear dynamic system and application to electric network 20 p3539 A66-38147

Matrix displacement method applied to anisotropic plate and shell theory, including parallelogram and triangular configurations under bending, membrane forces and shear strains 21 p3831 A66-39352

Piecewise linear transformations to simplify multiple threshold rules in statistical decision theory of pattern recognition systems 23 p4040 A66-41595

**LINEAR VIBRATION**

Progress in mechanics of linear vibrations - Symposium, Paris, April 1965 21 p3823 A66-38560

Recent progress of mechanics of linear vibrations - Symposium, Paris, April 1965 21 p3824 A66-38571

Mechanics of linear vibrations - Symposium, Paris, April 1965 21 p3824 A66-38576

Dynamic instability in linear vibrating system when linked to unlimited energy reservoir 21 p3825 A66-38577

Shell immersion in moving fluid under vibrations which can be damped or amplified, analyzing instability due to fluid constituting energy reservoir 21 p3825 A66-38578

Haag general synchronization theory for oscillating systems with one degree of freedom applied to boundary value problems for multivibrating systems 21 p3774 A66-39607

**LINEARITY**

SA NONLINEARITY

Linearity, stress, strain, time and birefringence relations in plastic model materials, using Hooke law 20 p3668 A66-37498

**LINEARIZATION**

SA BERNOULLI EQUATION

Quasi-linearization used to determine orbits from observational data such as angular data, range and range rate 02 p0288 A66-11547

Quantum theory for noise in steady state of laser oscillator above threshold, comparing semiclassical and quantized linear theories 13 p2091 A66-25650

Differential approximation linearization technique compared with Galerkin method 16 p2732 A66-30265

Distribution function, harmonic and statistical linearization methods applied to study forced oscillations in nonlinear oscillatory system 17 p2959 A66-32801

Motion equations for large-amplitude transverse vibrations of tensioned string and necessary conditions for linearization 17 p2959 A66-33033

Ignition conditions determined based on linearization of initial nonlinear equations 19 p3477 A66-35742

Suboptimal adjoint-vector control theory for linearization of feedback control systems

independent of nominal trajectory 20 p3535 A66-36849

Approximate method of integrating linearized equation for laminar boundary layer to establish relations of velocity distribution with friction stress 20 p3546 A66-37679

Comparison variables transformation of linearized perturbation initial value problems for nonlinear ordinary first-order differential equation 21 p3756 A66-38817

**LING-TEMCO-VOUGHT MILITARY AIRCRAFT**

S A-7 AIRCRAFT

S F-8 AIRCRAFT

**LINK**

SA CROSS LINKING

SA DATA LINK

Jump conditions at point of contact for corresponding cases of sliding and rolling contact in plane motion 21 p3769 A66-38476

Graph theory and enumeration of basic kinematic chains and mechanisms 23 p4097 A66-41978

**LIOUVILLE EQUATION**

Structural classification of global master equation by means of projector operator formalism 01 p0105 A66-10320

Kinetic processes in simple plasma, using linear Liouville equation for N-body particle distribution and expanding solution as power series 05 p0727 A66-15259

Equations of motion of turbulent gas and formulation of simple model of turbulence from classical Liouville equation and aerodynamics of rarefied gas 06 p0802 A66-16537

Solution to Liouville equation, obtaining expression for singlet distribution function for system under arbitrary perturbation from equilibrium, leading to solution of linear Boltzmann equation 06 p0912 A66-16633

Couette flow, Neumann-Liouville series expansion convergence for various flow regimes and related Fredholm integral equation solutions 07 p1020 A66-17964

Two-time probability distribution function, autocorrelation function, Liouville equation and fluctuation theory of plasma kinetics 13 p2156 A66-26885

Equations of motion of turbulent gas and formulation of simple model of turbulence from classical Liouville equation and aerodynamics of rarefied gas 15 p2482 A66-29973

**LIOUVILLE THEOREM**

Transformation of error ellipsoid in motion of material point, with selection of invariant parameters 06 p0954 A66-16423

Statistical analysis of ray oscillation suppression in light waveguide, using Liouville theorem 16 p2746 A66-30596

**LIPID**

SA FATTY ACID

Ion exchange in phospholipid monomolecular films 12 p1805 A66-23917

Sulfur compounds analysis in lipid extracts from Orgueil meteorite support concept of low temperature environment on parent body and differ from petroleum 20 p3648 A66-37304

**LIPID METABOLISM**

Mechanism of in vivo rbc damage by oxygen, noting effect on canine erythrocytes 03 p0326 A66-13348

Nature of particles involved in lipid synthesis in yeast 06 p0822 A66-16566

Cytoplasmic alterations and fat vacuole formation in pneumocytes of guinea pigs exposed to severe hypoxia in low pressure chamber 08 p1175 A66-18769

Effects of alpha glycerophosphate and of palmitoyl-coenzyme A on lipid synthesis in yeast extracts 15 p2429 A66-28616

High oxygen at reduced pressure effect on metabolism of radioactive acetate in rats 15 p2430 A66-28658

Acceleration stress-induced changes in fat metabolism, level of circulating glucose and corticosterone level in rats 15 p2431 A66-28868

Lysosomal enzymes in rats exposed to 100 percent oxygen to determine possibility of accelerated in vivo lipid peroxidation 17 p2857 A66-32169

**LIPSCHITZ CONDITION**

First order nonlinear partial differential

equation discussing global locally-Lipschitzian solutions via Jacoby theorem extension 06 p0901 A66-16006

Uniform structure for Lipschitz condition on functions between sets, extensions to nonmetric spaces and fixed point theorem for uniform spaces 07 p1059 A66-17969

Existence and uniqueness theorems for invariant-imbedding nonlinear ODE systems for absorption loss rate satisfying Lipschitz condition 07 p1059 A66-17972

General convergence theorem for gradient method of minimizing functions with Lipschitz continuous first partial derivatives, noting role of steepest descent algorithms 11 p1724 A66-23402

Sufficient conditions for optimal stochastic control of diffusion processes governed by vector equations satisfying local Lipschitz conditions 11 p1682 A66-23459

Quasi-linear boundary value problems solved with Galerkin convergence method 12 p1902 A66-23863

Optimal control for stochastic differential equation system, noting existence and uniqueness of solution for coefficients satisfying Lipschitz condition 19 p3325 A66-35983

**LIQUID**

SA ORGANIC LIQUID

Liquids used in manometers for pressure and pressure difference measurement in rarefied gases, considering cadmium boron tungstate, polymethylsiloxanes, etc, noting lack of toxicity, low viscosity, etc 03 p0371 A66-13204

Itinerant oscillator model of liquids covering classical velocity autocorrelation function of atom and neutron scattering experiments 04 p0547 A66-13809

Book on kinetic theory of simple liquids including equilibrium properties, time-dependent system, Markov processes, Brownian motion, transport coefficients, etc 08 p1209 A66-19463

Specific heat of liquids with constant volume determined, using pycnometer cell, obtaining formula for specific heat in terms of measurable thermal parameters 13 p2077 A66-25354

Nonlinear optical polarization of gases and liquids, stressing second degree contribution in macroscopic electric field 13 p2132 A66-26147

Angular emission properties of stimulated Raman radiation from liquids, noting two classes of radiation 13 p2097 A66-26159

Multiple stimulated Brillouin emission exhibited by liquids exposed to pulsed ruby laser, noting scattering events, Stokes orders identification and iteration mechanism 13 p2097 A66-26164

Complex dielectric constants of lossy liquids measured by transmission measurements in X-band waveguide 13 p2082 A66-26342

Liquid phase compression in closed cycle gas turbine by using particular working fluids for application to nuclear power stations [ASME PAPER 66-GT-111] 14 p2411 A66-27005

Variational principle for steady flows of ideal liquid and sufficient conditions for nonlinear stability under finite perturbations 17 p2913 A66-33168

**LIQUID AMMONIA**

Organic and liquid ammonia electrolyte systems in combination with active anode materials to achieve high energy output battery system [AIAA PAPER 64-750] 13 p2007 A66-26651

**LIQUID ATOMIZATION**

Mathematical models to explain parametric dependence of specific charge of liquid droplets produced by electrical spraying through metallic capillary at high potential [AIAA PAPER 66-252] 10 p1522 A66-21458

Vaporization and atomization theoretically calculated to be controlling parts of combustion process in determining rocket combustion instability [AICE PREPRINT 28D] 22 p3971 A66-39879

Combustion of atomized liquid fuels, noting optimum value of atomization fineness affecting completeness of combustion 24 p4293 A66-42208



## LIQUID BREATHING

Liquid breathing effects on dogs in hyperbaric chamber 21 p3699 A66-38447

## LIQUID COOLING

Liquid cooling of thin film resistors including use of nucleate boiling 02 p2023 A66-11921

Liquid cooling on semiconductor devices noting natural convection, nucleated boiling, forced convection and forced convection with boiling 02 p2023 A66-11922

Apollo space suit design discussing construction, purpose and operating conditions of liquid-cooled life support system 03 p0328 A66-12631

Heat pipe performance, emphasizing heat carrying and waste heat dissipation functions, construction and materials testing 05 p0616 A66-15543

Heat pipe characteristics covering performance analysis and experimental results such as heat transfer rate, life tests, working liquid selection, etc 05 p0616 A66-15544

Direct-immersion liquid cooling of modularized microelectronic systems on system-wide basis 06 p0841 A66-15973

High power phase shifter for phased array systems, using temperature compensated garnet along with dielectric liquid cooling technique 07 p1007 A66-17507

Saturated vapor spherical bubble collapse in uniformly subcooled liquids 08 p1320 A66-19559

Design and application of dry, dielectric and water-cooled dummy loads 12 p1829 A66-23537

High field liquid-neon-cooled superconducting electromagnet for cryogenic solid state research 20 p3601 A66-37106

Water-circulation-cooled space suit, discussing heat dissipation mechanism, body temperature maintenance, metabolic rates, astronaut comfort, etc 20 p3509 A66-38164

One-dimensional heat flow equation for liquid nitrogen end-cooled ruby laser rod 20 p3581 A66-38386

## LIQUID DROP

Thermal radiation absorption by droplet or spray during ignition and combustion of atomized liquid fuels 01 p0164 A66-10899

Electrohydrostatic boundary equations solving two- and three-dimensional axisymmetric situation and sessile drop problem 04 p0545 A66-13808

Fuel drop ignition, discussing parametric extension of quasi-flame surface theory to higher reaction orders and arbitrary stoichiometric ratios [AIAA PAPER 66-70] 06 p0970 A66-16415

Mass and momentum transfer between droplets and turbulent medium in which they move 06 p0972 A66-16896

Flow separation, wake configuration and droplet motion in purified systems shadowgraphically analyzed 10 p1524 A66-21808

Quasi-steady spherically symmetric burning of monopropellant liquid droplet in stagnant atmosphere 14 p2412 A66-27560

Cavity depth for waterdrop impacts against water, discussing apparatus, equation for cavity depth, effect of gravitational potential energy, liquid surface behavior, etc 15 p2477 A66-28716

Convective diffusion of material from single drop moving in liquid medium at low Reynolds numbers, using quasi-stationary approximation 16 p2689 A66-31516

Liquid water and nitrogen drops vibrating in natural frequencies above hot plate on vapor cushion analyzed by photographic techniques and used to simulate atomic nuclei fission 18 p3262 A66-34377

Homogeneous nucleation of liquid drops in supersaturated vapors, noting kinetic treatment for heating of growing clusters and irreversible thermodynamics of nonisothermal nucleation 19 p3477 A66-35566

Freezing of supercooled water drops to determine dependence of heterogeneous nucleation on temperature and on duration of supercooling 19 p3394 A66-36384

Chemical etch pitting techniques, determining dislocations in crystal structure caused by liquid droplet impacts, calculating stress distribution due to collision 20 p3547 A66-37806

Solids erosion by repeated liquid impact at relatively low velocities to determine impact pressure and load 20 p3586 A66-37807

distribution Reaction rates of decomposition burning of small spheres of liquid 20 p3626 A66-38043

hydrazine Distance/time records, drag coefficients and Reynolds numbers of single freely-falling drops of pentane, heptane and benzene burning in cold atmosphere 20 p3626 A66-38044

Cloud and fog droplet spectra rearrangement due to external conditions calculated from distribution function of water content 20 p3594 A66-38374

Charge transfer between water drops relevance to radiation problem and efficiency of conversion of electrostatic to electromagnetic energy 22 p3942 A66-39679

Aerodynamic breakup of liquid drops in flow behind plane shock wave analyzed via high speed photography, noting experimental setup, parameter variation, etc 22 p3899 A66-40198

Liquid drop flow in twisted fan-shaped nonisothermic jet allowing change in viscosity coefficient in flow field, using boundary layer equations 23 p4055 A66-41567

Drop bursting by surface forces such as electric fields and fluid environments with larger viscosity 23 p4060 A66-42018

Atomization of water drops by high speed airstreams, noting dependency on time 23 p4016 A66-42053

## LIQUID-FILLED SHELL

Unsteady motion of rotating fluid in cavity neglecting viscous dissipation 01 p0058 A66-10485

Temperature distribution and thermal stresses in liquid-filled cylindrical shell 07 p1143 A66-17397

Pressure wave propagation velocity in horizontal liquid-filled flexible tubes 07 p1146 A66-18277

Approximation method of calculating axisymmetric oscillations of shells of revolution filled with liquid 08 p1308 A66-18891

Small axisymmetric oscillations of fluid inside elastic cylindrical shell with elastic bottom determined by reducing problem to internal Neumann problem for circular cylinder 09 p1368 A66-20756

Oscillations of cylindrical shell filled with incompressible fluid of variable depth 10 p1614 A66-21328

Asymptotic solution to motion of solid containing cylindrical or spherical cavities filled with viscous liquid 12 p1863 A66-24356

Small oscillations of pendulum with spherical cavity filled with viscous incompressible liquid 12 p1882 A66-24357

Lagrange equations of motion for solid body with liquid-filled cavities derived, using Hamilton-Ostrogradskii principle of least action 13 p2127 A66-25628

Axially symmetric oscillations of elastic spherical shell partially filled with liquid, considering shell as joined hemispheres with or without same thickness 14 p2400 A66-27682

Spin angular velocity stability of gyroscope with incompressible fluid-filled cavity as function of three degrees of freedom 14 p2277 A66-28051

Parametric oscillations of cylindrical shell filled with liquid of variable depth 15 p2607 A66-28768

Steady and unsteady perturbed motion effect on solid body containing cavity filled with liquid in analyzing dynamic stability of mechanical systems 15 p2539 A66-29152

Liapunov methods of studying motion stability of solid bodies with liquid-filled cavities 15 p2539 A66-29155

Theoretical and experimental analysis of Korotkoff sounds at diastole which are interpreted as dynamic instability induced by application of pressure cuff 19 p3286 A66-36431

Liquid instability of vibrating partially filled elastic tank, emphasizing resonant breathing mode and frequency response 20 p3672 A66-38153

Monograph on dynamics of body with liquid-filled cavities associated with practical problems of rocket technology such as

seismic stability of liquid propellant tank 21 p3831 A66-39287

Nonlinear methods to describe stability motion of solids with liquid-filled cavities 23 p4059 A66-41982

## LIQUID FLOW

### SA WATER FLOW

Rheology of liquids discussing viscometers, models for prediction and industrial and biological application 03 p0355 A66-12601

Flow of non-Newtonian liquids in cylindrical pipes containing cylindrical parallel cores moving longitudinally at constant speed 03 p0358 A66-13099

Wave flow of thinly layered fluid on vertical plane, noting fluid-gas interface stress 04 p0510 A66-13821

Liquid-phase viscosity effect on disruption of hydrodynamic stability of bubble boiling in large liquid volume 04 p0599 A66-14441

Approximation method of calculating axisymmetric oscillations of shells of revolution filled with liquid 08 p1308 A66-18891

Hydrodynamic problem of nonviscous liquid flow past two spheres solved, using new method of solution 10 p1525 A66-21919

Expansion parameters of liquids expelled into vacuum as related to orbital perturbations arising from liquid venting and impingement on adjacent hardware 10 p1481 A66-21947

Visualization technique for solving three-dimensional liquid flow problems, using small particles suspended in and moving with liquid 11 p1682 A66-22206

Coaxial capacitor for measuring density of fluids in both liquid and gaseous phase over wide range of temperatures and pressures 11 p1707 A66-22961

Stability of vertical water jet examined by imposing audiofrequency disturbances 13 p2060 A66-25133

Taylor-Helmholtz instability between liquid of constant shear and vacuum 13 p2068 A66-26682

Mechanics of contained fluids in subgravity 14 p2275 A66-27558

Pressure in sealing groove and increase time due to pumping action of moving wall applied to force cylinder of translational motion, considering liquid in groove laminar 14 p2225 A66-27688

Liquid flow with viscosity changing under effect of nonisothermicity 15 p2478 A66-29222

Motion of non-Newtonian liquid through two coaxial curved pipes, noting relation between pressure gradient and outflow rate, curvature effect and secondary flow 15 p2479 A66-29397

Fringing effect on sensitivity of magnetic flow meter 17 p2926 A66-32874

Gravitational stability of laminar liquid layer flowing down inclined plane and heated from below 17 p2914 A66-33172

Differential equation system describing nonsteady state motion of liquid in open channel 18 p3097 A66-33932

Book on mechanics of liquids and gases 18 p3102 A66-34731

Velocity profile measurements in turbulent liquid jets via photography, noting calculation of flow turbulence characteristics 18 p3114 A66-34894

High strain rate deformation of solids under liquid impact examined via photographic methods 20 p3588 A66-37802

Outflow of liquid from cylindrical tank through central outlet for cases where effect of gravity is small, noting distortion of liquid surface [AICE PREPRINT 17D] 22 p3897 A66-39885

Marangoni flow, motion of liquid surfaces under influence of surface tension gradients, explaining high fluxes obtained in boiling heat transfer 22 p3999 A66-40303

Steady liquid flow between rotating coaxial cylinders with arbitrary dependence of viscosity on temperature 22 p3902 A66-40814

Viscoelastic properties of liquids under steady flow determined experimentally in frequency range 5-75 mc/s, using internal reflection of pulse of shear wave at surface of fused quartz bar 23 p4066 A66-41159

Approximation method for wall effect in cavitation flow around bodies in water tunnel, examining effect of solid boundary



- on resistance factor 23 p4056 A66-41727
- Instantaneous shear stress at liquid flow boundary, measuring turbulence and velocity fluctuation in close proximity of pipe wall 24 p4194 A66-42415
- Fragmentation of liquid jet in gaseous medium at high velocities 24 p4196 A66-42868
- LIQUID GAS**
- Low temperature physics - International Conference, Columbus, Ohio, August-September 1964 09 p1413 A66-20004
- Viscosity of liquid nitrogen and oxygen measured as function of temperature and pressure 14 p2276 A66-27642
- Sound velocity measurements in liquid argon, liquid oxygen and liquid nitrogen 14 p2336 A66-28276
- Density, viscosity, surface tension, vapor pressure and vapor liquid equilibria data of liquid ozone-fluorine mixtures considered as Newtonian fluids 23 p4119 A66-41244
- LIQUID-GAS MIXTURE**
- Cold neutron scattering by hydrogen in liquid argon, calculating scattering cross section and length for monatomic liquid 04 p0548 A66-13810
- Violent bubble behavior in liquids contained in vertically vibrated tanks caused by water hammer type of resonance [AIAA PAPER 66-86] 06 p0875 A66-17099
- Bubble coalescence in longitudinally vibrated liquid column 07 p1025 A66-18173
- Shock phenomena with mixtures of water and nitrogen in two-phase supersonic tunnel [AIAA PAPER 66-87] 07 p0984 A66-18453
- Liquid-gas coexistence curve shape near critical point, allowing for volume and temperature deviations and for mathematical singularities 08 p1316 A66-18796
- Atomization of liquid-spray particles in Venturi scrubber, investigating acceleration by high-speed photography 08 p1208 A66-19422
- Relationship between shock wave phenomena during collapse of cavitation bubbles in water and temperature and gas content of water 13 p2060 A66-25091
- Violent bubble behavior in liquids contained in vertically vibrated tanks caused by water hammer type of resonance [AIAA PAPER 66-86] 16 p2685 A66-30913
- Relationship between shock wave phenomena during collapse of cavitation bubbles in water and temperature and gas content of water 21 p3723 A66-38516
- LIQUID HELIUM**
- Ultrahigh vacuum chamber with liquid-helium-cooled liner for space environment simulation 08 p1202 A66-18926
- Superfluid basic theory noting Josephson tunneling, liquid helium kinetic theory, quantized vortex lines, etc 09 p1415 A66-20005
- Superfluid hydrodynamics and kinetic theory of superfluids, noting relation of macroscopic concepts of Bardeen-Cooper-Schrieffer theory to microscopic characteristics 09 p1415 A66-20006
- Strong coupling cell theory of liquid helium, noting heat capacity 09 p1391 A66-20011
- Acoustic impedance of liquid He 3 under vapor pressure 09 p1391 A66-20012
- Acoustic impedance of liquid He 3 under pressure of up to 12.5 atm 09 p1391 A66-20013
- Heat capacity measurements of liquid He 3 to improve precision in determination of effective mass ratio 09 p1392 A66-20014
- Turbulent vortices in quantum and classical fluid and time dependent meniscus depth of water, He I and He II 10 p1525 A66-21965
- Interaction between vortices and solid surface manifested as pulling away of freely suspended disk in rotating liquid helium 2 from suspension head, performing additional rotational motion, determining vortex slip coefficient 12 p1865 A66-24879
- Acoustically induced cavitation in liquid helium analogous to unfiltered air-saturated water 14 p2334 A66-27663
- Effect of temperature changes on flux-jumping behavior of niobium stannide superconducting solenoids in superfluid helium 15 p2560 A66-28686
- Logarithmic decrements of quartz crystal driven in torsional vibration mode at resonant frequency determined as function of temperature in liquid helium 15 p2537 A66-28869
- Text on experimental low temperature physics covering experimental techniques, liquid helium, superconductivity and electronic properties in metals 15 p2566 A66-29320
- Liquid filled electrostatic generation, noting charge transporting and insulating function of liquid helium 17 p2848 A66-31814
- Electrically cryopumped system for liquid helium transfer continuously at low flow rates 20 p3542 A66-37105
- Impurity conduction effect on electron donor recombination cross section in n-type germanium and silicon at liquid helium temperatures 21 p3801 A66-39001
- Characteristics of efficient semiconductor lasers in UV portion of spectrum obtained at both liquid helium and nitrogen temperatures, using pulsed electron beam excitation on ZnS crystals 21 p3747 A66-39114
- Turbulent vortices in quantum and classical fluid and time dependent meniscus depth of water, He I and He II 21 p3731 A66-39544
- Interaction between vortices and solid surface manifested as pulling away of freely suspended disk in rotating liquid helium 2 from suspension head, performing additional rotational motion, determining vortex slip coefficient 23 p4053 A66-41086
- Integral method derivation of thermoconductivity coefficient of cylindrical semiconductor immersed in liquid He and superheated by Joule heating 24 p4255 A66-42494
- LIQUID HELIUM 2**
- Turbulent effects in liquid He 2 stationary flow 09 p1365 A66-20015
- Damping of small amplitude vibrations of fine wire as probe of onset and development of critical flow phenomena in He 2 at moderate Reynolds numbers 09 p1365 A66-20016
- Vorticity growth when steady heat current is applied to liquid He 2 in narrow tube 09 p1366 A66-20017
- Superfluid critical velocity in He 2 isothermal gravitational flow in narrow channels 09 p1366 A66-20018
- Critical velocities and supercritical velocity dissipation effects in isothermal flow of liquid He 2 in narrow channels 09 p1366 A66-20019
- LIQUID HYDROGEN**
- Materials for use as rolling-contact bearing lubricants in liquid hydrogen environment [ASLE PREPRINT 65-LC-9] 02 p0238 A66-12255
- Liquid hydrogen flow system startup of full scale simulated nuclear rocket engine 03 p0391 A66-12350
- Saturn Launch Vehicle Program technical equipment and engineering techniques for solving structural, propulsion, launch and control problems 06 p0959 A66-16496
- Model simulating energy distribution process /thermal stratification/ within liquid hydrogen stored aboard moving rocket to avoid pump cavitation [AIAA PAPER 64-426] 08 p1279 A66-18809
- Platinum resistance thermometers with interchangeable characteristics for liquid hydrogen measurements, discussing standardization and calibration 08 p1226 A66-19598
- Ultrasonic velocity of compressed fluid hydrogen between 15 and 100 degrees K and in normal and parahydrogen of saturated liquid between 14.5 and 32.2 degrees K 09 p1392 A66-20081
- Liquid hydrogen tank level in space measured by applying known impulse and determining resulting acceleration of container 11 p1706 A66-22957
- Liquid hydrogen flow system performance during startup transient of nuclear rocket measured in full-scale simulated engine system, approximating in-flight exhaust conditions 12 p1911 A66-23699
- Tank design, optimization program and testing for effect on storage penalties associated with liquid hydrogen for hypersonic aircraft 14 p2394 A66-28026
- Impact of propellant heating on nuclear spacecraft insulation and pressurization systems design 18 p3240 A66-33816
- Current status of technology of using liquid hydrogen in manned aircraft systems [AIAA PAPER 66-671] 18 p3162 A66-34443
- Hydrogen pumping by means of phenomenon of hydrogen absorption by solid layer of carbon dioxide condensed at temperature of 20.4-14 degrees K 19 p3400 A66-36099
- Fluid hydrogen slush, discussing advantage of reduced evaporation loss during storage and handling, refrigeration and density 20 p3625 A66-37074
- Heat of fusion and density of solid and slush hydrogen at pressures to about 400 atm 20 p3625 A66-37081
- Nuclear radiation and liquid hydrogen effect on environmental mechanical properties of phenolic asbestos, glass and linen resins 20 p3587 A66-37097
- Childdown rate and equilibrium heat-leak storage loss measurements in liquid hydrogen storage dewars 20 p3541 A66-37101
- Heat exchangers for liquid hydrogen conversion to ambient temperature hydrogen gas, using water heat source 20 p3677 A66-37102
- Heat transfer coefficients over range of Reynolds numbers for solid-vapor mixture of parahydrogen discharge below triple point pressure 20 p3679 A66-37511
- RL10 pump-fed rocket engine modified for fluorine-hydrogen application [ASME PAPER 66-MD-74] 21 p3806 A66-38501
- Heating environment for space vehicle, examining wind and incident radiation effects on heat transfer to liquid hydrogen, insulation surface thermal properties and optimization of insulation system 22 p3986 A66-39777
- Testing for mechanical properties of materials at liquid hydrogen temperatures, noting liquid transfer system and safety regulations [AICE PREPRINT 22B] 22 p3886 A66-39890
- Liquid hydrogen tank insulation constructed of honeycomb core containing polyurethane foam for S-II booster 22 p3997 A66-39892
- Thermal conductivity of formed-plastic composite insulation systems for liquid hydrogen storage tank [AICE PREPRINT 22D] 22 p3997 A66-39893
- LIQUID INJECTION**
- SA FUEL INJECTION**
- Liquid injection thrust vector control noting general requirements, injectant metering point, stream solidity collimators, secondary flow, metering configuration and nozzle back pressure 02 p0180 A66-11972
- Thermodynamic analysis of MHD generator with vapor liquid injector 03 p0323 A66-12831
- Increased heat of ablation and performance of injection cooling by addition of surface active agent [ASME PAPER 65-WA/HT-49] 05 p0792 A66-15660
- Solid propellant rocket engine omniaxis liquid injection thrust vector control system, using function generator in signal-summing feedback loop to control flow in servovalves and increase motor reliability 14 p2226 A66-27700
- Liquid film cooling of small diameter throat tubes 18 p3263 A66-34385
- Vaporization of liquid fuel injected in heated horizontal circular pipe for straight and swirl air flow, noting increased rate of vaporization in swirl airflow for increased heat supply 18 p3265 A66-34490
- Thermodynamic analysis of MHD generator with vapor liquid injector 19 p3282 A66-36773
- Penetration distance for secondary liquid injection into supersonic airstream, emphasizing jet flow far from injection orifice 20 p3548 A66-38151
- Mass transfer and hydrodynamics of gas jet injection into liquid surface, deriving empirical equations for hollow truncated point formed around injection point 21 p3836 A66-38958
- LIQUID LASER**
- Theoretical optical resonator for laser with rare earth liquid solutions as active components 10 p1543 A66-21970



Coupled wave formalism, giving unified description of parametric down conversion of light, stimulated Brillouin and Raman effects, etc, stressing exponential character of gain 13 p2132 A66-26156

Recirculation of liquid through cell and external heat exchanger to solve problem of repeated flashing in europium chelate lasers 21 p3747 A66-39108

Trivalent neodymium in selenium oxychloride, inorganic liquid laser without limitations of europium chelates and matching in threshold and output neodymium-doped crystals 21 p3747 A66-39110

Performance characteristics of room temperature liquid laser, using trivalent ion neodymium-doped selenium oxychloride 21 p3747 A66-39111

Theoretical optical resonator for laser with rare earth liquid solutions as active components 21 p3749 A66-39549

### LIQUID LEVEL

Four major methods of liquid level control in tanks 01 p0069 A66-10866

Cryogenic problems in temperature and level sensing discussing thermocouples, resistance sensors, vapor and gas bulb thermometers and level gauges and probes 01 p0070 A66-10955

Bubble level for sensing local vertical of attitude stabilized satellite 08 p1223 A66-18816

Ultrasonic echo method of level measuring and monitoring in which acoustic pulse is emitted by vertical transducer and reflected from surface of liquid or gas 10 p1535 A66-21337

Oscillation stability criteria for simple surge tank obtained from second method of Liapunov 10 p1523 A66-21497

Liquid hydrogen tank level in space measured by applying known impulse and determining resulting acceleration of container 11 p1706 A66-22957

Method for measuring amount of liquid remaining in tank under near-zero-g conditions based on relation between gas ullage, volume and pressure 13 p2000 A66-25693

Fluid content measurement in storage tanks under zero-g conditions discussing gas law system, trace material, capacitive panel and RF methods 19 p3340 A66-35611

Fluid amplifier application to process control including turbulence amplifiers, logic function performance, etc [ASME PAPER 66-MD-8] 21 p3697 A66-38477

VECO 32A11 thermistor element for temperature and liquid level sensing in hazardous gases such as Freon 12 21 p3740 A66-39388

### LIQUID-LIQUID INTERFACE

#### SA SURFACE TENSION

Velocity distribution in laminar viscous liquid-into-liquid jet 01 p0057 A66-10407

Expansion of plane nonisothermal jet of liquid dropping into space filled with same liquid at different temperature 01 p0059 A66-11019

Surface instabilities discussing stability of movement of nonrigorous planar surface of liquid layer when subjected to motion in direction perpendicular to its face 03 p0354 A66-12537

Acceleration potential method for solving linear problems of wing hydrodynamics above interface between fluids differing in density, for arbitrary Froude number 13 p2067 A66-26530

### LIQUID MERCURY

#### S MERCURY /METAL/

#### LIQUID METAL

#### SA MERCURY /METAL/

Liquid metal embrittlement noting stress and intergranular corrosion, hydrogen embrittlement and behavior of silver chloride crystal 02 p0243 A66-11698

Shaft seals to contain liquid metals in mechanisms exposed to space environment 03 p0374 A66-13108

Electrophoretic motion of dielectric particle determined from flow rate of liquid metals and semiconductors near infinite plane 05 p0733 A66-14688

Transient quenching method of determining critical heat flux and transfer

coefficients in film and nucleate boiling liquid metals, specifically magnesium [ASME PAPER 65-HT-49] 05 p0785 A66-14757

High temperature electromagnetic transducers applied as sensors for physical variables, including mechanical displacement and liquid metal flow and level 05 p0676 A66-14775

Liquid-metal heat transport fluid circulation, discussing molten lithium pump development and testing for high performance mobile nuclear plants [ASME PAPER 65-WA/FE-18] 05 p0689 A66-15611

Minimum heat transfer levels and vapor formation in boiling liquid metals 06 p0972 A66-16843

Experimental assembly using liquid gallium cycle for testing electromagnetic pumps and flow meters 06 p0918 A66-16847

Heat transfer coefficients in liquid metal concurrent flow double pipe heat exchangers 07 p1150 A66-17582

Surface heat flux removal by lithium-sodium-mercury spray cooling, noting vaporization mechanism 07 p1151 A66-17586

Liquid metal condensation, noting two-phase turbulent condensation mechanism and determining heat transfer coefficients 07 p1152 A66-17592

Cavitation damage in high-temperature liquid metal pumps for Rankine cycle space power plants studied in water model 07 p1038 A66-18175

Boiling heat transfer in liquid metals including boiling instability, superheats, two-phase flow, forced convection, heat flux, etc 08 p1316 A66-18684

Hydrogen solubility in liquid niobium at high temperatures and partial pressures 08 p1241 A66-19377

Russian monograph on MHD of liquid metals, discussing application for transport and technological treatment of metals, molten salts and slags 08 p1266 A66-19566

Cavitation damage in alkali liquid metals predicted from properties of water, aviation gasoline and sodium-potassium eutectic 08 p1211 A66-19721

First-order perturbation analysis of free convection of liquid metal from isothermal vertical finite plate extended to uniform heat flux 10 p1619 A66-21054

Liquid-metal heat transport fluid circulation, discussing molten lithium pump development and testing for high performance mobile nuclear plants [ASME PAPER 65-WA/FE-18] 10 p1539 A66-21502

Thermionic energy-conversion diode using liquid metal as electron oscillator 11 p1640 A66-23404

Chemical behavior of metallic elements predicted by periodic table, noting formation of liquid and solid metallic solutions, binary and complex metallides and nature of chemical bond 12 p1896 A66-24897

Electron bombardment thrusters using liquid mercury cathodes, noting lifetime, propellant and power efficiency, feed system, temperature limits, etc [AIAA PAPER 66-232] 13 p2172 A66-25172

Nonrotating MHD liquid-metal power system, noting nozzle and separator configuration 13 p1998 A66-25527

Space power systems using liquid metal /LM/ working fluids in boiling-condensing cycle, specifically condensing-ejector LMMHD power system 13 p1998 A66-25528

Electrical analogy for turbulent liquid metal heat transfer in noncircular duct entrance region, solving Fourier equation, determining fluid boundary conditions, temperature distribution, etc 13 p2210 A66-26717

Two-phase flow and material attrition problems for Rankine cycle liquid metal power plants [ASME PAPER 66-GT/CLC-4] 14 p2224 A66-26979

DC liquid-metal MHD generator tested with cold NaK to determine power efficiency 14 p2225 A66-27408

Forced convection heat transfer in symmetrical ducts when fluid is liquid metal, examining new prediction methods for engineering analysis and design 16 p2824 A66-30304

Large quantities of high-purity carbides and carbide solid solutions produced by auxiliary metal bath in carbon tube furnace 16 p2723 A66-30638

Thermal emf of metallic liquid couples measured as function of thermal difference between junctions and alloys composition, noting correlation between thermodynamic and thermoelectric properties of alloys 16 p2781 A66-31410

Longitudinal magnetic field reduction of growth rate of gravitational type acceleration instability of liquid metal by vapor 17 p2967 A66-32452

Effect of temperature, pressure and initial wall treatment on thermal resistance at stainless steel-liquid metal interface 17 p3036 A66-32845

Centrifugal pump for liquid metal power-transmission in flight control systems [ASME PAPER 66-FE-20] 17 p2932 A66-33273

Kinetic theory of liquid viscosity made tractable by using approximation of perturbation of radial distribution function of monatomic liquid by nonuniform flow field 17 p2940 A66-33335

Forced convection heat transfer for liquid metal flow in rectangular channels with prescribed wall heat fluxes and heat sources in fluid stream 17 p3038 A66-33468

Critical heat flux for boiling water, sodium and rubidium, correlating burnout data for liquid metals only and as relation for metallic and nonmetallic fluids 18 p3262 A66-34376

Accelerated cavitation damage in liquid sodium and mercury of stainless steels and superalloys under consideration for use in liquid metal power conversion systems 19 p3380 A66-35804

Drag coefficient of turbulent flow of electrically conducting liquid metal in MHD channels of round cross section 19 p3407 A66-36098

Oxygen role in oxidation/reduction reaction and polyoxide formation mechanisms associated with refractory metal corrosion by liquid alkali metals 19 p3383 A66-36135

Welding and annealing procedures for fabrication of Nb alloy liquid metal loop and operation in boiling alkali metals 19 p3370 A66-36139

Thermodynamics of MHD converter cycles with previously mixed liquid metal used as working body, discussing thermal, electrical and energetic efficiency 20 p3496 A66-36986

Simultaneous measurement of heat conductivity, heat capacity and thermal diffusivity of solid and liquid metals at high temperature 20 p3678 A66-37120

Resistance and heat transfer coefficient relation theoretically determined for flow of electrically conducting liquid in magnetic field 20 p3679 A66-37614

NaK-77 suitability for 1000-F liquid-metal hydraulic flight control systems 22 p3852 A66-40498

Steady state flow of liquid metal in MGD channel of rectangular section, noting magnetic field effect on resistance factor 23 p4106 A66-41729

Nozzle design using liquid metal vapor condensation Mach number as design parameter 24 p4294 A66-42786

### LIQUID METAL COOLED REACTOR /LMCR/

Liquid metals as coolants or working fluids in nuclear auxiliary power systems for extended space missions 11 p1735 A66-23267

Performance efficiency and weight considerations for liquid MHD power conversion [AIAA PAPER 64-760] 13 p2008 A66-26660

Applicability of refractory metals to solid propellant rockets, lifting and guidance structure for glide reentry vehicles and liquid metal containment for nuclear space power systems 19 p3382 A66-36105

### LIQUID NITROGEN

Two-phase flow and heat transfer for boiling liquid nitrogen in horizontal tubes 01 p0165 A66-10909

Dynamic measurements of speed of pumping by activated charcoal cooled to liquid nitrogen temperatures to evaluate cryosorption 02 p0261 A66-11591

Cold wall space simulating installation and technique for cooling wall with liquid



- nitrogen 02 p0216 A66-11895  
 Film boiling of saturated nitrogen flowing upward in vertical heated tube, noting annular-flow regime change to vapor matrix [ASME PAPER 65-WA/HT-26]  
 Multistage cryogenic trapping system 05 p0793 A66-15677  
 Cooling design, operation and application 07 p1032 A66-17665  
 Shock wave attenuation experiment by liquid nitrogen injection 08 p1210 A66-19594  
 Liquid nitrogen dilution effect on LOX impact sensitivity of selected materials 10 p1590 A66-21951  
 Superhigh vacuum creation in OGRA-1 facility, using titanium sputtered liquid nitrogen-cooled copper surfaces 12 p1922 A66-24218  
 Axisymmetric liquid nitrogen turbulent jet propagating under supercritical pressure in gaseous nitrogen medium 12 p1864 A66-24446  
 Liquid nitrogen-cooled shield against oil vapor contamination of proton accelerator in vacuum chamber 19 p3381 A66-35814  
 Dimensional and experimental analyses of helium bubble motion in liquid nitrogen 20 p3545 A66-37104  
 Fine structure in direct absorption edge of cleaved type IIA diamond determined from reflectance data obtained from 5.5 to 11.5 eV at room and liquid-nitrogen temperatures 20 p3622 A66-38248  
 One-dimensional heat flow equation for liquid nitrogen end-cooled ruby laser rod 20 p3581 A66-38386  
 Man rating requirements of space environment simulation laboratory, consisting of two large chambers with floors which can be cooled by liquid nitrogen down to 92 degrees K 22 p3892 A66-40239  
 Superhigh vacuum creation in OGRA-1 facility, using titanium sputtered liquid nitrogen-cooled copper surfaces 22 p3957 A66-40582
- LIQUID OXIDIZER**  
 Hypergolic ignition of composite solid propellants, examining oxidizer concentration, heat flux and exothermic reactions 22 p3969 A66-39871  
 Ablation velocity, rocket motor working conditions and combustion instabilities for hybrid rockets, using solid fuel and liquid or gaseous oxidizer 24 p4261 A66-42695
- LIQUID OXYGEN /LOX/**  
**SA FLUORINE-LIQUID OXYGEN /FLOX/**  
**SA LOX-HYDROGEN ENGINE**  
 Liquid oxygen density as function of temperature and pressure 08 p1280 A66-19428  
 Contamination control in missile systems, considering rocket engine cleanliness as equality control parameter 09 p1432 A66-19954  
 Liquid nitrogen dilution effect on LOX impact sensitivity of selected materials 10 p1590 A66-21951  
 Nonmonotonicity in sensitivity test data, noting results of liquid oxygen impact tests on Mylar-aluminum-Mylar laminate bonded to polyester foam 12 p1958 A66-23648  
 Gaseous hydrogen and liquid oxygen combustion and heat transfer in small rocket chamber 14 p2375 A66-28104  
 LOX-compatible packaging films for maintaining cleanliness of supercleaned components 17 p2943 A66-32203  
 Liquid oxygen purity control for onboard breathing equipment by IR absorption spectrophotometry and gas chromatography 17 p2866 A66-32233  
 Axial pressure gradient change with geometry in combustion chambers formed by cylindrical and conical sections, using rocket motors burning LOX and JP-5A 19 p3450 A66-35624  
 Ignition and controlled burning of liquid oxygen-liquid methane mixture, evaluating use as rocket monopropellants [AICE PREPRINT 28E] 22 p3969 A66-39880  
 LOX characteristics for on board breathing equipment including contaminants noxious to people, clogging of equipment, explosiveness and possible use of contaminated LOX 22 p3858 A66-40504
- LIQUID PHASE**  
 Hydrogen bonding kinetics in free radical liquid-phase reactions 21 p3702 A66-38520  
 Triplet states of liquid benzene and toluene studied, using biacetyl phosphorescence
- sensitization 23 p4032 A66-42077
- LIQUID POTASSIUM**  
 Potassium condensing tests of horizontal multitube convective and radiative condensers operating at vapor temperatures from 1250 to 1500 degrees 05 p0786 A66-14932
- LIQUID PROPELLANT**  
**SA AEROZINE**  
 Machine computation of thermodynamic properties of hydrazine from 32 degrees F to 1.02 times critical density 03 p0414 A66-12760  
 Drop-weight sensitivity of explosive liquids tested with impact apparatus, showing increase with temperature [CI PAPER WSCI-65-28] 05 p0788 A66-15139  
 Immiscibility and rapid interface reaction rate as cause of disruption in nitrogen tetroxide-hydrazine impinging jets [CI PAPER WSCI-65-20] 05 p0743 A66-15145  
 Droplet combustion fronts in hydrazine-nitrogen tetroxide system determined from kinetics of vapor decomposition, noting two-flame front model [CI PAPER WSCI-65-21] 05 p0743 A66-15146  
 Hypergolic ignition of light hydrocarbon fuels with fluorine-oxygen /flox/ mixtures [CI PAPER WSCI-65-23] 05 p0743 A66-15147  
 Specific impulse of solid and liquid propellants to increase performance 09 p1433 A66-20801  
 Overpressure of liquid propellant explosion in vacuum and atmosphere 14 p2370 A66-27451  
 Probability model for defining explosive yield and spill of liquid propellant 14 p2371 A66-28442  
 Yield and combustion physics of liquid propellant explosions determined from analytic charts 14 p2371 A66-28443  
 Ignition and combustion mechanism of liquid propellant consisting of aliphatic alcohols and mixed acid, using calcium and potassium permanganates as catalysts 17 p2989 A66-32458  
 Flox-light hydrocarbon combinations desirable as liquid rocket propellants due to high specific impulse, hypergolicity and cooling properties [AIAA PAPER 66-581] 18 p3159 A66-33809  
 Test for space storability of liquid propellants by suitably coating storage tanks [AIAA PAPER 65-534] 19 p3448 A66-35613  
 Thermodynamic properties and solubilities of He molecular nitrogen, molecular oxygen, Ar and nitrogen trioxide in liquid nitrogen tetroxide 19 p3449 A66-36368  
 Liquid methane fueled propulsion system for SST application, noting increased payload capacity, propellant characteristics and design criteria for storage within aircraft [AIAA PAPER 66-685] 20 p3625 A66-37259  
 Monograph on dynamics of body with liquid-filled cavities associated with practical problems of rocket technology such as seismic stability of liquid propellant tank 21 p3831 A66-39287  
 Small liquid propulsion systems testing in space environment simulator with high vacuum and low pumping capacity 22 p3890 A66-40226  
 Liquid methane as fuel for SST propulsion in terms of cost, combustion heat and cooling capacity 24 p4261 A66-42240
- LIQUID PROPELLANT ROCKET ENGINE**  
**SA HYDROX ENGINE**  
 Reliability prediction for rocket engines based on initial-failure-symptom and failure-cause estimates and uses experienced development efficiencies and effort 01 p0129 A66-10083  
 Convective heat transfer behavior of 90 percent hydrogen peroxide studied with reference to possible use as rocket propellant 01 p0164 A66-10903  
 Parameter relationship governing construction of models for combustion of liquid fuels in rocket engines 02 p0279 A66-11707  
 Unsteady boundary layer flow of multicomponent gas mixtures, investigating combustion instability in liquid and hybrid rocket motors [AIAA PAPER 65-41] 03 p0444 A66-12796  
 Oscillations in liquid fuel rocket combustion chambers covering LF and HF theory, stability requirements and optimal performance criteria 04 p0594 A66-14463  
 Flight tests and observations with S-IV stage of Saturn I carrier rocket, discussing design, reliability, developmental problems and difficulties 05 p0770 A66-14674  
 Short-circuiting gas metal-arc welding of high nickel alloys for manufacture of liquid rocket engine components with aerospace quality 05 p0686 A66-14691  
 Combustion instability in liquid propellant rocket motors causing pressure fluctuations [CI PAPER WSCI-65-22] 05 p0788 A66-15144  
 Test method evaluating explosive sensitivity, due to shock, of materials immersed in oxygen difluoride for application to rocket propulsion systems [CI PAPER WSCI-65-34] 05 p0743 A66-15150  
 Quasi-linear partial differential equations of transients in liquid rocket engine propellant feed system solved, determining transient pressure ratio [ASME PAPER 65-FE-23] 06 p0942 A66-16217  
 Heterogeneous detonations, discussing polydisperse and monodisperse spray detonations and liquid fuel film shock-induced combustion [AIAA PAPER 66-109] 06 p0969 A66-16256  
 Liquid chemical propulsion rocket engines development problems, specifically propulsion system for Titan rocket 08 p1280 A66-18572  
 Coupling of conversion process and internal field related to effect of injector design on unstable burning of liquid propellant rocket motors 08 p1282 A66-19136  
 Design and development of first liquid-fueled stage of Diamant launch vehicle 10 p1611 A66-21256  
 Propellant injection distribution effect on transverse modes of liquid rocket engine instability [AIAA PAPER 65-613] 12 p1977 A66-23587  
 Metals for liquid propellant rocket systems in terms of environments in which performance is required 13 p2109 A66-25778  
 Relation between pressure-type fuel supply system and pressure variation in combustion chamber of rocket engine 14 p2373 A66-27382  
 Longitudinal wave histories in liquid rocket motor 14 p2374 A66-27450  
 Dynamic differential equation relating perturbations in feeding system with transient states in combustion chamber of liquid fuel rocket engine 17 p2989 A66-31388  
 Longitudinal instability in liquid rockets analyzed by digital computer assembling of coupled structural and fluid systems [AIAA PAPER 66-472] 17 p3016 A66-32765  
 Heterogeneous detonations, discussing polydisperse and monodisperse spray detonations and liquid fuel film shock-induced combustion [AIAA PAPER 66-109] 17 p3037 A66-33237  
 Ignition of liquid propellant rocket engines, discussing propellant flow, pressure and mixture ratio 18 p3163 A66-34186  
 Computer-simulated mathematical model of thermal environmental effects on expulsion system design parameters for liquid-propellant gas-generator rocket engine [AIAA PAPER 66-686] 18 p3163 A66-34228  
 Combustion instability in MMH-NTO liquid rocket engine as affected by propellant mixture ratio, injection velocity, droplet size and distribution and chamber pressure [AIAA PAPER 66-603] 18 p3164 A66-34432  
 Combustion stability development with storable propellants for liquid rocket engines, showing coupling between technology and engine system [AIAA PAPER 65-614] 19 p3448 A66-35609  
 Axial pressure gradient change with geometry in combustion chambers formed by cylindrical and conical sections, using rocket motors burning LOX and JP-5A 19 p3450 A66-35624  
 Calibration device for flow and volume meters for liquid rocket engine propellant 20 p3561 A66-38066  
 Liquid rocket POGO oscillations caused by closed-loop interaction between longitudinal structural mode of vibration and propulsion system 20 p3629 A66-38154  
 Project Scorpio USAF Cellular Combustion Chamber Program for cost reduction and injection pattern simplification in liquid propellant rocket engines 20 p3629 A66-38256



Storable metallized liquid propellants for rocket engine systems, noting gains in specific impulse and/or propellant density 20 p3626 A66-38258

RL10 pump-fed rocket engine modified for fluorine-hydrogen application [ASME PAPER 66-MD-74] 21 p3806 A66-38501

Liquid-propellant rocket engine design and propellant types 22 p3971 A66-40121

Liquid rocket propulsion system weldment design and quality requirements, noting efficiency parameters 22 p3924 A66-40257

**LIQUID SLOSHING**

Experimental study of damping of planar wave motion in vicinity of resonance 01 p0059 A66-10644

Coupling method for determining natural oscillations of ideal incompressible liquid in vessel consisting of two regions 01 p0059 A66-11017

Violent bubble behavior in liquids contained in vertically vibrated tanks caused by water hammer type of resonance [AIAA PAPER 66-86] 06 p0875 A66-17099

Mechanical model for representing moment of inertia and fuel sloshing in baffled cylindrical missile tanks 08 p1205 A66-18834

Damping of liquid oscillations in cylindrical tanks, determining rigid and flexible baffle loss coefficients, baffle efficiency and maximum bending stress [AIAA PAPER 66-97] 08 p1207 A66-19000

Piezoelectric acceleration sensors and fluid interaction with spherical shell container undergoing translational oscillatory motion 08 p1228 A66-19769

Parametric requirements for eliminating coupling between bending, sloshing and control in large liquid-propelled elastic space vehicles 10 p1612 A66-21941

Nondimensional theoretical and experimental pressures and forces acting on flat ring baffle under sloshing conditions 10 p1525 A66-21952

Composite motion stability for partially filled cylinder rotating at constant velocity and resting on elastic supports 11 p1779 A66-22233

Sloshing motion control of liquid-vapor interface in spacecraft fuel tanks, using dielectrophoresis 16 p2684 A66-30466

Violent bubble behavior in liquids contained in vertically vibrated tanks caused by water hammer type of resonance [AIAA PAPER 66-86] 16 p2685 A66-30913

Flexible baffle effect on nature and magnitude of damping and sloshing motions of liquid propellants over wide range of conditions 16 p2685 A66-30915

Liquid sloshing effect on axisymmetric vibrations of liquid-filled cylindrical shell 16 p2819 A66-31139

Fluid hydrogen slush, discussing advantage of reduced evaporation loss during storage and handling, refrigeration and density 20 p3625 A66-37074

Particle size distribution, aging effects, terminal velocity measurements and production techniques of slush hydrogen investigated as potential upgraded spacecraft fuel 20 p3676 A66-37075

Three superconducting niobium stannide liquid level sensors tested in triple point slush or liquid hydrogen for capability of detecting liquid-vapor interface 20 p3557 A66-37076

Propellant sloshing in tanks of guided missile, giving mathematical description and numerical and experimental results in Coralie stage 21 p3818 A66-38642

Stability problems of solid body with liquid filler, noting small partial damping of liquid 21 p3770 A66-38972

Coefficients of equations of perturbed motion of body containing ideal incompressible liquid 21 p3770 A66-38973

Coupling between spin-stabilized rocket motion and propellant sloshing tested in zero gravity environment [AICE PREPRINT 17C] 22 p3897 A66-39887

Planar and rotary sloshing motion of liquid, using analytic mechanical model that consists of mass point constraint to parabolic surface 22 p3993 A66-40361

**LIQUID SODIUM**

Heat transfer to in-line turbulent flow of NaK through unbaffled bundle of circular

rods 05 p0783 A66-14737

Transient heat transfer from liquid sodium spray impinging on vertical plate 07 p1151 A66-17587

**LIQUID-SOLID INTERFACE**

Energy distribution in cavitation bubble collapsing at interface between liquid and solid approximated by localized explosion in ideal gas 06 p0870 A66-16200

Transient heat transfer from liquid sodium spray impinging on vertical plate 07 p1151 A66-17587

Stabilizing effect of surface active agents on wave formation in contaminated falling liquid film 07 p1023 A66-18125

Liquid titanium reaction with nonmetallic refractory ceramics, Ti melting behavior and electron-probe microstructural analysis 08 p1236 A66-18759

Surface phenomena on interface between liquid metals and various refractory compounds, determining surface energy and angle of contact 08 p1238 A66-18898

Internal wave ripples from fluid impacts on base of stably stratified fluid region, calculating particular case of single ripple in viscous fluid 11 p1693 A66-23009

Energy distribution in cavitation bubble collapsing at interface between liquid and solid approximated by localized explosion in ideal gas 13 p2064 A66-25916

Mathematical analysis of thermal wave technique for linear kinetics from viewpoint of solid-liquid interface motion 18 p3265 A66-34508

Ion propulsion engine with replenishable liquid-film-protected tungsten electrode, discussing construction and mass loss rate vs temperature [AIAA PAPER 65-378] 20 p3629 A66-38167

**LIQUID SURFACE**

Liquid surface instability caused by sliding detonation and shock waves of gas mixture 01 p0060 A66-11192

Dynamics of axisymmetric liquid free surface following stepwise acceleration change 16 p2684 A66-30502

Linearized problem of oblique incidence of weightless flow of ideal gas on surface of heavy liquid, using eigenvalues and eigenfunctions of integral equation 19 p3342 A66-36470

Outflow of liquid from cylindrical tank through central outlet for cases where effect of gravity is small, noting distortion of liquid surface [AICE PREPRINT 17D] 22 p3897 A66-39885

**LIQUID-VAPOR EQUILIBRIUM**

Thermal events in diurnal breathing cycle and vapor loss reduction in volatile liquid storage [AICE PREPRINT 11C] 10 p1521 A66-21181

Liquid-vapor phase equilibria of neon-normal hydrogen system 20 p3676 A66-37087

Low temperature liquid-vapor equilibrium in neon-oxygen system at pressures up to 5000 psi from 63 to 152 degrees K 20 p3601 A66-37088

Hydrodynamic equations for liquid with intrinsic rotation applicable to suspensions and liquid/vapor systems 21 p3728 A66-39312

**LIQUID-VAPOR INTERFACE**

Physical mechanisms of instabilities altering two-phase flow pattern of liquid film 01 p0165 A66-10907

Localization caused by capillary effects in gas-liquid interface such as epidermis and wicks depends upon gas phase unsaturated with liquid vapor 03 p0355 A66-12779

Wave flow of thinly layered fluid on vertical plane, noting fluid-gas interface stress 04 p0510 A66-13821

Phase change across interface of suddenly pressurized binary liquid-vapor system [ASME PAPER 64-WA-AV-1] 04 p0597 A66-14026

Heat transfer during film condensation of liquid metal vapor, discussing thermal resistance effect of condensation coefficient [ASME PAPER 65-HT-29] 05 p0784 A66-14748

Ultrasonic wave effect on mass transfer rate of selected fluid liquid phase in capillary 08 p1210 A66-19680

Heat transfer during film condensation of liquid metal vapor, discussing thermal resistance effect of condensation coefficient [ASME PAPER 65-HT-29] 11 p1784 A66-22182

Thickness of laminar liquid film draining

from vertical surface analytically determined by assuming evaporation rate is known constant [ASME PAPER 65-HT-39] 11 p1785 A66-22189

Load capacity of condensing vapor-lubricated long self-acting journal bearing, examining two-phase and single-phase regions [ASME PAPER 65-LUBS-5] 12 p1888 A66-24554

Sloshing motion control of liquid-vapor interface in spacecraft fuel tanks, using dielectrophoresis 16 p2684 A66-30466

Localization of gas-liquid interface by capillary effects, noting error in adverse acceleration equation 16 p2685 A66-30917

Shape and stability of liquid-gas interface in annular tank in force field determined by numerical integration of boundary value problem and eigenvalue [AIAA PAPER 66-425] 16 p2689 A66-31488

Longitudinal magnetic field reduction of growth rate of gravitational type acceleration instability of liquid metal by vapor 17 p2967 A66-32452

Nozzle cooling and infiltrant loss from infiltrated refractory metal composites at high gas propellant temperature 19 p3385 A66-36157

Three superconducting niobium stannide liquid level sensors tested in triple point slush or liquid hydrogen for capability of detecting liquid-vapor interface 20 p3557 A66-37076

Entry problem of thin symmetric wedge impinging normally on free surface of compressible inviscid liquid, neglecting gravitational effects 20 p3547 A66-37981

Static and dynamic behavior of liquid-vapor interface during weightlessness [AICE PREPRINT 17A] 22 p3897 A66-39886

**LITHERGOLIC PROPELLANT**

Calculation of performance data of seven lithergic propellant combinations with determination of principal thermodynamic coefficients 20 p3626 A66-38015

**LITHIUM**

Level-crossing spectroscopy with electric field, Stark shift of 3P term of lithium subject to electric and magnetic field 03 p0395 A66-13133

Ion-pairing process in nickel and lithium doped germanium 04 p0565 A66-14270

Reflex arc in lithium vapor analyzed, using spectrographic, mass spectrometric and probe measuring techniques 04 p0554 A66-14293

Pseudopotential method for determining temperature-dependent electric resistance of lithium, neglecting free electron approximation and examining electron-phonon interaction 04 p0566 A66-14316

Heat pipe characteristics covering performance analysis and experimental results such as heat transfer rate, life tests, working liquid selection, etc 05 p0616 A66-15544

Lithium transformation by plastic deformation from bcc to fcc lattice analyzed by measuring damping of free torsional oscillations of samples, noting role of internal friction 05 p0740 A66-15822

Absolute cross section for single ionization of lithium ions by electron impact over 75.6 to 800 ev electron energy range 07 p1084 A66-18425

Schottky and Langmuir laws verification by thermionic emission of lithium aluminosilicate with respect to current limitation caused by space charge 13 p2163 A66-25436

Lithium/calcium ratio of five F giant and six G giant stars 13 p2183 A66-25611

Lithium-hydrogen bipropellant arc jet 14 p2374 A66-27426

Regression rates of metallized hybrid fuel systems applied to lithium hydride butyl rubber-fluorine-oxygen system, oxidizer flow, etc 15 p2569 A66-29289

Atmospheric decay of rocket-released Li due to diffusion, wind and chemical reaction 16 p2697 A66-31008

Cosmic ray produced lithium and calcium in iron meteorites 18 p3236 A66-34890

Drift rate and precipitation of lithium ion in germanium as affected by resistivity, acceptors, carrier lifetime and copper diffusion 19 p3442 A66-35914

Lithium-drifted germanium detector



resolution and efficiency as function of temperature for gamma rays 19 p3359 A66-35915

Fine and hyperfine structure of term in 3p level of lithium studied by level-crossing spectroscopy technique, determining fine structure separation 19 p3443 A66-35989

Corrosion tests on eight refractory metals and alloys in liquid lithium and cesium vapors 19 p3383 A66-36136

Ephemeral-corrosion tests of refractory metals in molten lithium between 2000 and 3000 degrees F 19 p3383 A66-36138

Excitation of lithium-like ions by electron impacts, with computation of cross sections for resonance and nonresonance transitions 19 p3409 A66-36326

Adsorption of lithium on /110/, /111/ and /112/ planes of single-crystal tungsten in field-emission projector, measuring work function dependence on concentration 20 p3618 A66-37558

Lithium use in silicon solar cell for radiation resistance improvement, noting preservation of minority carrier lifetime 20 p3502 A66-37775

Fabrication methods for lithium drifted surface barrier silicon detectors, discussing lithium diffusion, stain etching, preparation for and final etch 20 p3535 A66-38417

Nonisotropic nonequilibrium lithium plasma flow through nozzle with allowance for friction and heat transfer 21 p3694 A66-39088

Lithium transformation by plastic deformation from bcc to fcc lattice analyzed by measuring damping of free torsional oscillations of samples, noting role of internal friction 23 p4113 A66-41387

Nonaqueous lithium-nickel halide batteries capabilities and limitations, explaining methods of selection and evaluation of solvent, solutes and combinations for electrolytes 23 p4021 A66-41752

Lithium ion drift and density distribution in electric field of Si p-n junction 24 p4253 A66-42359

Lithium cleavage of unsaturated vicinal di-tert-phosphines producing lithium diphenylphosphide 24 p4170 A66-42889

**LITHIUM ALLOY**

Continuous optical second-harmonic generation using ND/YAG laser and crystal of single-domain lithium niobate 06 p0889 A66-16378

Electronic packaging weight reduction by using magnesium-lithium alloy 19 p3376 A66-35327

**LITHIUM ALUMINUM HYDRIDE**

Synthesis of complex lithium aluminum hydride, lithium hexahydroalenate, having hydrogen to aluminum ratio greater than four 11 p1649 A66-22400

Combustion and performance characteristics of lithium aluminum hydride/hydrogen peroxide hybrid rocket [AICE PREPRINT 34D] 22 p3969 A66-39878

**LITHIUM CHLORIDE**

Lithium chloride power plant theory and technology, noting application to critical weapons systems 23 p4021 A66-41758

**LITHIUM COMPOUND**

Complex permittivity and permeability of lithium aluminum ferrite in cavity resonator determined, using perturbation theory 01 p0123 A66-10590

Phase transitions in lithium niobate and tantalate, discussing ferroelectricity 07 p1092 A66-17221

Sunspot spectra, determining lithium abundance and ratio of Li 6/Li 7 isotopes 07 p1136 A66-17736

Sequence of crystallization during heat treatment of ternary system of lithium aluminosilicate glasses 12 p1900 A66-24860

Mechanical properties of lithium silicate glasses at different stages of crystallization and relation to microstructure 12 p1900 A66-24862

Density, microhardness, elastic constants and surface strength relation to microstructure of lithium aluminosilicate glass crystallized under various conditions of heat treatment 12 p1901 A66-24863

Parametric oscillator theory applied to tunable coherent optical parametric oscillation in lithium

niobate 13 p2096 A66-26145

Electro-optic effect and elastic wave propagation in single-domain ferroelectric lithium tantalate 13 p2170 A66-26589

Cis- and trans-beta-bromostyrene reaction with lithium diphenylphosphide in tetrahydrofuran producing cis- and trans-beta-styryldiphenylphosphine, discussing proton magnetic resonance and configuration retention 14 p2232 A66-27498

Optical beam scattering of gas laser for measurement of photoelastic constants and application to lithium niobate 15 p2512 A66-28692

Phase transitions in lithium niobate and tantalate, discussing ferroelectricity 17 p2976 A66-31992

Parametric oscillator threshold with single mode optical masers and observation of amplification in lithium niobate 17 p2935 A66-32716

Thermodynamics of molten lithium nitrite galvanic cell, noting emf temperature dependence 20 p3503 A66-38189

**LITHIUM COOLED REACTOR EXPERIMENT /LCRE/**

Liquid-metal heat transport fluid circulation, discussing molten lithium pump development and testing for high performance mobile nuclear plants [ASME PAPER 65-WA/FE-18] 05 p0689 A66-15611

Liquid-metal heat transport fluid circulation, discussing molten lithium pump development and testing for high performance mobile nuclear plants [ASME PAPER 65-WA/FE-18] 10 p1539 A66-21502

**LITHIUM FLUORIDE**

Spectroscopy of lithium fluoride crystals activated with uranium trioxide for laser action, showing anomalous fluorescent decay under high intensity pumping 13 p2092 A66-25997

Thermal energy storage using solar Brayton cycle cavity receiver with lithium fluoride heat storage [AIAA PAPER 64-727] 13 p2006 A66-26636

Ionized electron centers in irradiated lithium fluoride crystals investigated by observing emission and absorption spectra 15 p2568 A66-29641

Impurity absorption of LiF crystals in vacuum UV 15 p2568 A66-29729

Ultrasonic attenuation changes due to dislocation formation during yielding of magnesium, molybdenum and LiF 16 p2726 A66-31458

Isotope shifts for zero-phonon absorption lines associated with radiation induced color centers in lithium fluoride single crystals 18 p3154 A66-33921

UV transmittance of LiF and BaF under various storage conditions 18 p3134 A66-34001

Ultrasonic attenuation in lithium fluoride from liquid helium to room temperature, finding anharmonic attenuation of slow transverse mode to vary with frequency 19 p3447 A66-36398

**LITHIUM HYDRIDE**

Constrained variation method in molecular quantum mechanics, presenting wave function, degree of constraint and energy loss values for lithium hydride molecule 13 p2130 A66-25372

Collision integrals calculated for interactions Li-H, Li-Li, H-H and H-H plus in LiH system 16 p2766 A66-31612

High temperature high-density plasma from single solid particle of lithium hydride suspended in vacuum, using ruby laser irradiation 19 p3432 A66-36596

Perturbation theory of constraints applied to variational calculation on ground state of lithium hydride molecule, using 28-term wave function 22 p3947 A66-39925

**LITHOLOGY**

Epitaxial, diffusion and photolithographic processes in manufacture of semiconductor component 10 p1514 A66-22056

**LITHOSPHERE**

**S EARTH SURFACE**

**LITTLE JOE II LAUNCH VEHICLE**

Nitrogen powered hydraulic attitude control system of Little Joe II solid propellant launch vehicle for flight testing escape mechanism used on Apollo 20 p3499 A66-37314

**LIVER**

Protein synthesis in liver of adrenalectomized and hypophysectomized rats exposed to centrifugation stress 13 p2010 A66-25899

Age effect on liver glycogenesis in rats exposed to acceleration stress 17 p2860 A66-32555

**LMCR**

**S LIQUID METAL COOLED REACTOR /LMCR/**

**LOAD DISTRIBUTION**

Strains and internal force in bending of two coupled orthotropic plate strips of different rigidity under effect of uniformly distributed loads 01 p0152 A66-10406

Fabrication, testing and experimental results for rigid-vinyl plastic monocoque domes subjected to external pressure loads 01 p0156 A66-10918

Beam forced vibration with harmonically time-variant motion produced by uniformly distributed load, assuming one boundary condition is nonlinear 01 p0157 A66-10926

Equations for rotational motion of satellite and rods with end loads as stabilizer, considering rods elastic deformation caused by load bending oscillations 02 p0295 A66-11651

Resonant frequency equation for line segment with reactive loads at both ends, using Chebyshev principle 02 p0199 A66-11754

Rationalized method for beam deflection under concentrated loading 02 p0299 A66-11796

Nonlinear boundary value problem solution as applied to effect of uniformly distributed pressure and concentrated load on spherical dome 02 p0301 A66-12174

Stress repetitions as design parameter for pavements, considering traffic load on roads 02 p0216 A66-12220

Load partition in double-lap butt joints for bearing type connections including expressions for stress-strain relationship and bolt shear deformation 02 p0302 A66-12242

Optimizing fatigue life of flexibly mounted rolling bearings, discussing shaft and housing structure 03 p0373 A66-12929

Elasticity determined for axial fir-tree-type connections of turbine blade roots 03 p0440 A66-13201

Lambda method for numerical solution of rectangular plate problem under wide range of loadings and boundary conditions 03 p0440 A66-13270

Quadrature solution to one-dimensional problem for helicoidal shell with given load and desired force distributions, moments and displacements 04 p0588 A66-13564

Stress concentration of various intensities in quasi-half-plane and other semilinear regions 04 p0589 A66-14144

Donnell-type nonlinear theory for instability of cylindrical shell subjected to axisymmetric moving loads with constant velocity [ASME PAPER 65-APMW-35] 04 p0594 A66-14235

Steady state and transient response of arbitrary tapered distributed RC networks with lumped load terminations 05 p0651 A66-14574

Book on minimum structure weight and effect on design, with application to planar and three-dimensional structures 05 p0774 A66-15064

Telescope components and subassemblies, covering structural element analysis techniques on experimental basis 05 p0680 A66-15208

Astronomical telescope, discussing support mechanism design for constant mirror shape 05 p0680 A66-15209

Torsional instability of cantilevered bars, describing effects of distributed nonconservative compressive load at free end [ASME PAPER 65-WA/APM-19] 05 p0777 A66-15441

Exact solution for Green function of open spherical shell subjected to harmonically oscillating concentrated load and any consistent boundary conditions [ASME PAPER 65-WA/APM-24] 05 p0778 A66-15446

Lubricant effect on fatigue life of



stationary ball on flat contact subjected to oscillatory normal load  
[ASME PAPER 65-WA/CF-3]

05 p0690 A66-15622

Optimal design for lightweight structures, considering material properties, shape and interaction forces

06 p0963 A66-16474

Crack propagation in quasi-brittle solid deformed by external load, using thermodynamic laws

06 p0965 A66-16491

Complete resolution of concentrated load of limiting contour, determining spectrum of functional linear operator attached to interior region

06 p0967 A66-17061

Infinitely-long thin elastic circular cylindrical shells loaded along segment of generatrix by arbitrarily distributed loads

07 p1143 A66-17627

Plane disk design calculations for uniform strength under asymmetric and axisymmetric load

07 p1038 A66-18096

Asymptotic solution to elasticity theory problem for hollow isotropic cylinder of finite dimensions and small thickness under axisymmetric load distributed over entire surface

07 p1144 A66-18183

Fatigue testing machine with two shaft-rotation speeds for HF and LF testing

07 p1147 A66-18388

Two-dimensional problem of disturbance propagation in elastic plate under concentrated load moving along boundaries at constant speed, pressure and stress-strain pattern

08 p1305 A66-18598

Error estimates in application of linear plate theory to deflection and stress determination as function of boundary conditions, correlation between geometric plate parameters and load

08 p1305 A66-18599

Nonuniform load distribution among transistors of multitransistor circuit in parallel connection

08 p1190 A66-18772

Minimum rigidity of ribs ensuring cylindrical shell stability under external load determined, using matrix

08 p1308 A66-18887

Series solution for deflection of rectangular plate subjected to concentrated load at arbitrary location, using Green function

08 p1310 A66-19161

Stress-strain state of shell having one end clamped and other under concentrated bending moments and concentrated force acting along generatrix solved by integral equation

08 p1314 A66-19579

Antisymmetric disk loading effect on distribution of induced rotor

09 p1327 A66-20252

Deflection of thin circular plate under eccentric loading using complex variables, obtaining expressions in series

09 p1467 A66-20581

Electromagnetic scattering from conducting object controlled by loading portions of surface with impedances, distributed or lumped

10 p1499 A66-21610

Stressed state of spherical shell weakened by square aperture with rounded corners, under uniform internal

11 p1779 A66-22238

Takeoff load distribution predetermination for commercial transport craft based on appropriate weight ratios

12 p1800 A66-23784

Torsional instability of cantilevered bars, describing effects of distributed nonconservative compressive load at free end

[ASME PAPER 65-WA/APM-19]

12 p1961 A66-23979

Bending of cylindrical shell clamped at one end and reinforced by elastic ring at free end, with vertical forces uniformly distributed acting over

12 p1964 A66-24044

Effect on long shell of circumferential and uniformly distributed load /due to explosion/ at constant rate along shell

12 p1964 A66-24048

Effect of external or internal static pressure on natural frequencies of unstiffened, cross-stiffened and sandwich cylindrical shells

13 p2194 A66-25142

Stressed state of isotropic elastic medium with two circular holes solved, using approximation method for concentrated loads

13 p2202 A66-26417

Shells produced by rotation of second-order curves about axis of symmetry evaluated for symmetric and antisymmetric loads

13 p2202 A66-26418

Shell with positive curvature and zero moment state examined, determining sufficient condition for secondary potential load

13 p2203 A66-26420

Elimination of stress concentrations at holes in plates, noting selection of compensating reinforcement

13 p2204 A66-26434

Differential equilibrium equations for shallow shells of constant curvature under effect of concentrated load, using Fourier transform

13 p2205 A66-26440

Effect of stress concentrations on load carrying capacity of brittle materials of nonuniform microstructure, considering iron plates with holes

13 p2205 A66-26441

Approximate solution for stress-strain concentration in plate with central circular orifice during uniaxial tension by distributed load calculated, using Timoshenko method

13 p2207 A66-26495

Stresses in concentric and eccentric compound rings

13 p2207 A66-26499

Stress and deformation in cross section of beam during complex loading, using steepest-descent method

14 p2400 A66-27685

Axially loaded cylindrical structures analyzed for optimum weight construction consistent with cost constraint, emphasizing beryllium-aluminum alloys

14 p2406 A66-28023

Tension shell theory applied to Voyager mission, noting equations for lateral loading for entry at zero angle of attack, shear and bending of wall role, etc

14 p2407 A66-28027

Problem of rectangular plate clamped all round transformed into generalized plane stress problem for

14 p2409 A66-28396

Central deflection of simply supported centrally loaded rhombic plate with formula depending on first coefficient obtained in mapping of rhombus

14 p2409 A66-28397

Mass forces for infinite elastic space expressed by generalized functions

15 p2615 A66-29852

Maximum load of thin walled I-beam producing beam surface buckling calculated and total stresses defined

16 p2815 A66-30675

Transverse cut-out effect on fatigue strength of rotating shaft under constant bending load, noting fatigue stress concentration factor

16 p2815 A66-30679

Energy feedback adaptive control system for elimination of effects of load inertia variations in servomechanisms

16 p2670 A66-30812

Hollow metallic O rings used for sealing as thin shells under axisymmetric loading

17 p3020 A66-32002

Radial loading effect on vibration frequencies of thin spherical shells

17 p3024 A66-32362

Large deflections of symmetrically loaded shallow membrane shells of revolution, considering existence of boundary layer near edges and using asymptotic analysis

17 p3025 A66-32480

Plane elasticity theory problem for curve with mixed boundary conditions having radial load distribution

17 p3028 A66-32784

Donnell-type nonlinear theory for instability of cylindrical shell subjected to axisymmetric moving loads with constant velocity

[ASME PAPER 65-APMW-35]

18 p3248 A66-33574

Exact solution for Green function of open spherical shell subjected to harmonically oscillating concentrated load and any consistent boundary conditions

[ASME PAPER 65-WA/APM-24/]

18 p3248 A66-33576

Stress analysis of junction of thin elastic shells of revolution, considering axisymmetric wind and sinusoidal load distributions

18 p3253 A66-33804

Snapping of shallow simply supported sinusoidal arch under sinusoid step pressure load, using motion equations and infinitesimal stability analysis

18 p3257 A66-34591

Complex loading problems in plastic flow theory solved by analogy with elastic solutions in elastoplastic

19 p3473 A66-35755

theory

External and internal loads and environment effects on space vehicle, especially motor case, noting stresses, structural design, fatigue behavior, safety, etc

19 p3474 A66-36313

Elastic deformation of unbounded transversely isotropic body with internal plane-circular slot under slot surface load

19 p3476 A66-36839

Solids erosion by repeated liquid impact at relatively low velocities to determine impact pressure and load

20 p3586 A66-37807

Steel testing at 580 degrees C during stress relaxation with repeated load increases

21 p3827 A66-38616

Complex load effect on shell buckling, determining compliance tensor components during stability loss

22 p3989 A66-39820

Residual stresses and strains for cases with/ without secondary plastic deformations during unloading under nonuniform heating

22 p3990 A66-40144

Stressed state near round opening in orthotropic cylindrical shell solved for various loading and boundary conditions by Bubnov-Galerkin variational method

22 p3990 A66-40145

Deformation of aluminum single crystals during constant load tensile test

22 p3935 A66-40201

Centricity effect on magnitude of discontinuity stresses in unsymmetrically loaded shells of revolution, discussing results of numerical calculations

22 p3993 A66-40366

Buckling of stiffened cylindrical shells under various loads and load combinations, noting optimization procedure for elastic stability

22 p3996 A66-40673

[ICAS PAPER 66-13] Membrane of constant strength subjected to load uniformly distributed in horizontal plane, using yield condition of maximum principal normal stress

22 p3996 A66-40708

Creep analysis of stress-strain-time relation in metal with complex loading

23 p4136 A66-40998

Longitudinal and tangential local and strip loads effect on magnitude of forces, moments and displacements in circular cylindrical shell

23 p4139 A66-41788

Stresses in shells under arbitrarily concentrated loads calculated numerically

23 p4142 A66-41958

Power series solutions to homogeneous shallow shell equations for point load concentrated on vertex of shell

24 p4285 A66-42145

Plastic theory of structures for collapse under highly localized loading

24 p4286 A66-42152

Certain tensorial character of concentrated loads

24 p4289 A66-42288

Torsion of elastic rectangular bar with similarly distributed external tangential loads applied at both ends

24 p4289 A66-42436

LOAD FACTOR

SA SHOCK LOAD

SA TRANSIENT LOAD

Weight and load factor modification of V/STOL aircraft design when aircraft is used as weapon system

01 p0011 A66-10186

Crack initiation and propagation in aluminum sheets, noting ductile fracture and load limit for design purposes

01 p0156 A66-10920

C-5A aircraft design load criteria for landing gear of large aircraft that must operate from semi-improved airfields

[AIAA PAPER 65-711]

01 p0013 A66-10948

Thin homogeneous shell stability loss under arbitrary loading, noting equations for stress and deflection functions

02 p0297 A66-11395

Minimum weight circular plate under two independent systems of loading, noting Tresca yield condition

04 p0587 A66-13487

Linear isotropic strain-hardening applied to load-deformation characteristics of cylindrical shells under internal pressure, obtaining Tresca yield criterion and stress profiles

07 p1147 A66-18349

Fuel cell considered from viewpoint of fuel costs, noting hydrocarbon fuel for application with low load factor and instant



starting 07 p0997 A66-18478  
 Effect of load mismatch on laser output, determining nonlinear dependence of equivalent negative conductance as function of oscillation amplitude in laser resonator cavity 09 p1386 A66-20435  
 Load factor estimation for flights in turbulent conditions by replacing exact transfer function with equivalent statistical model 10 p1482 A66-21385  
 Effect of conventional ammunition on aluminum honeycomb paneling, noting reduction of load-bearing and peel-strength properties 13 p2196 A66-25599  
 Bending moment of thin nonlinearly elastic plates, noting dependence of coefficient of moment concentration on external load and material properties 13 p2203 A66-26429  
 Lubrication parameters with respect to experimental values and reproducibility 14 p2305 A66-28465  
 Plastic strain effect on fatigue strength of aircraft skin sheets with hole subjected to constant loading, noting stress concentration at hole 16 p2815 A66-30678  
 Optimum parameters of three-layer plates and shallow shells filled with reinforced and nonreinforced foam plastic under compression 16 p2817 A66-31048  
 Transport aircraft economics of load factor and wasted seat problem 17 p2846 A66-32795  
 Shaft-rotor system with bearing configuration such that load-deflection relation at rotor is nonlinear and radially symmetric, noting harmonic whirl and free undamped vibrations 17 p2930 A66-32892  
 Aircraft taxi loads, discussing runway transfer function, random profiles, analog mathematical model, analog taxi simulation program and peak count [AIAA PAPER 66-469] 18 p3050 A66-33652  
 Bending behavior under lateral loads and stretching effects due to in-plane forces described by two uncoupled differential equations governing circular plates 18 p3253 A66-33803  
 Technological approaches to use of aircraft on undeveloped or semideveloped field from standpoint of load and terrain roughness 18 p3051 A66-33937  
 Load characteristics and characteristic curves for proportional and bistable fluid amplifier noting output, input and dynamic effects 18 p3054 A66-34133  
 Load level as stability loss condition for bulging of elastoplastic rod in presence of creep 19 p3473 A66-365753  
 Transonic buffeting effects on hammerhead shaped payloads analyzed, using power spectral techniques and wind tunnel tests 20 p3672 A66-38170  
 Safety-factor problem in glider design, discussing limiting load concept in form of extreme load in exceptional cases of operation 21 p3696 A66-38620  
 Load carrying capacities of rotationally symmetric plates and shells for limited anisotropic behavior and different yield stresses in tension and compression 21 p3831 A66-39375  
 Carrying capacity and moment of friction calculated for cylindrical MHD bearing for small magnitude of radial clearance 23 p4074 A66-41736  
 Concentrated forces on shells, discussing load distributions and pressure variations 23 p4142 A66-41957  
 Nonlinear programming problem of yield point load of perfectly plastic structure, using limit analysis theorems, with application to curved beam 23 p4146 A66-41992  
 Reinforced semiinfinite under concentrated loads, noting flange stress magnitude and distribution 24 p4285 A66-42144

**LOAD TEST**

Photoelastic investigation of stresses in cemented joints, particularly scarf and butt bonding 02 p0298 A66-11582  
 Comparative design study of low-disk-loading VTOL concepts including stopped-rotor, tilt-propotor, tilt-wing, transport effectiveness, etc [AIAA PAPER 65-756] 03 p0318 A66-12551  
 Cylindrical squeeze-film gas journal bearing, noting load deflection experiments [ASME PAPER 65-LUB-13] 04 p0527 A66-14246

Breaking strength of plastic metals under impulse loading by measuring axial tensile stresses 05 p0699 A66-14685  
 Design for structural reliability discussing safety factors, probable variations in applied loads, temperatures, materials, geometry and strength 05 p0775 A66-15074  
 Pressure peaks in hydraulic actuator inertia load aggravated in presence of valve overlap, noting cavitation damage [ASME PAPER 65-FE-4] 06 p0808 A66-16213  
 Notched structure load analysis, discussing planar stress distribution in flat bar for various points of application of force 06 p0964 A66-16478  
 Four-point loading bend test on specimen of full plate thickness with sharp notch to 20 percent depth, with ductility criterion as fully plastic angle of bend before fracture 06 p0965 A66-16492  
 Polymeric material deformation under harmonically varying load action, noting steady state regime temperature distribution effects 08 p1243 A66-18879  
 Cylindrical squeeze-film gas journal bearing, noting load deflection experiments [ASME PAPER 65-LUB-13] 12 p1888 A66-24551  
 High temperature structural properties of polybenzimidazole, polyimide and phenolic laminates under different loading conditions 13 p2113 A66-25311  
 High speed tensile testing of materials under destructive loads at high strain rates 13 p2197 A66-26107  
 Static and high strain rate tensile behavior of epoxy, polyester and urethane resins reinforced with 181-S, 184-E and woven roving glass materials and nylon 13 p2114 A66-26111  
 Approximation method for determining limit and breaking load for infinite brittle body weakened by plane crack, noting crack propagation 13 p2203 A66-26423  
 Limit load of flat notched bars subject to tension, discussing rupture force magnitude, plastic strain occurrence, rupture stress and yield limit curves, etc 14 p2398 A66-27394  
 Mechanical strength of plastic buckling of sheet metals under lateral hydraulic loads 15 p2510 A66-29778  
 Structural mounting of large diameter cylindrical missile section in centrifuge for high acceleration environmental testing 16 p2677 A66-30458  
 Loading of thin ring airfoil in unbounded spherical source flow field, calculating vortex distribution, strength, etc [ASME PAPER 66-FE-3] 17 p2914 A66-33259  
 Complex load action on elastic-plastic structures in light of limit analysis, discussing safety criterion 21 p3826 A66-38591  
 SH-3A airframe fatigue test facility for automatic simulation of helicopter flight and landing loads 22 p3992 A66-40251  
 Automated minimum weight structural design for various load conditions, integrating matrix displacement analysis and operations research 22 p3995 A66-40490

**LOAD TESTING MACHINE**

Calibration problem of load-measuring instruments solved, using automatic digital voltmeter [ASTME PREPRINT IQ66-705] 12 p1882 A66-24412  
 Strain gauge load measuring transducer operating in bending mode and based on elastic properties of epoxide glass fabric laminate 12 p1884 A66-24985  
 Calibration method for tensile testing apparatus for testing elongated high modulus fibers and graphing of typical load elongation curves 17 p2943 A66-32400

**LOADING**

SA AERODYNAMIC LOAD  
 SA AXIAL LOAD  
 SA BLAST LOADING  
 SA COMPRESSION LOADING  
 SA CRITICAL LOADING  
 SA CYCLIC LOAD  
 SA DUMMY LOAD  
 SA DYNAMIC LOAD  
 SA EDGE LOADING  
 SA GUST LOAD  
 SA HUGONIOT EQUATION OF STATE  
 SA IMPACT LOAD  
 SA RANDOM LOAD

SA STATIC LOADING  
 SA STRESS AND LOAD  
 SA TRANSIENT LOAD  
 SA VIBRATORY LOADING  
 SA WING LOADING

Surface roughness and loading effect on actual contact surface of metals 01 p0079 A66-11062  
 Minimization of radar cross section of thin cylinder by central loading, calculating backscatter field 05 p0632 A66-14842  
 Machine part design by limit loads and Mohr circles, using trial and error dimension minimization 14 p2397 A66-27389  
 Equilibrium equations for closed circular cylindrical rib-reinforced shells under arbitrary loading 16 p2819 A66-31138  
 Loading considerations in design of large helicopters for transport of externally suspended cargo 17 p2845 A66-32741  
 Flying qualities and aircraft control during tandem rotor helicopter external sling load operations 17 p2846 A66-32742  
 Load carrying capacity of circular plates under antisymmetric load 17 p3029 A66-32806

**LOADING APPARATUS**

Helicopter airframe fatigue testing noting fail-safe design, crack detection, loads applied, test facilities and techniques, etc 17 p3027 A66-32737  
 Heavy equipment short-range transportation with crane-type helicopters, noting correlation between lift capacity and aircraft weight 17 p2845 A66-32739  
 Static perturbation technique used in analysis of stability relationship to shape of equilibrium surface for finite-dimensional problems 22 p3992 A66-40202

**LOADING MOMENT**

Approximation method for momentary peak shaft loads, computing starting and stalling torques of power transmission system 02 p0238 A66-12266  
 Optimum speed control of automatic system, noting nonlinear mechanical characteristics of slave motor and speed dependence of load moment 06 p0863 A66-16531  
 Symmetric bending of circular orthotropic plate of systematically variable thickness for different types of loading 15 p2613 A66-29435  
 Rigorous solutions for loadings applied at apex of spherical shell, noting cases of concentrated radial and tangential force, concentrated moment about polar and planar axis, etc 20 p3670 A66-37761  
 Side forces and moments on Tomahawk sounding rocket with and without spin at high Reynolds number and Mach 5 [AIAA PAPER 66-754] 23 p4008 A66-41329

**LOADING RATE**

Rockwell hardness test discussing standardization by cycle control and equipment modification 03 p0439 A66-13158  
 Two-parametric classification of load cycles on construction elements connected with fatigue limit tests and service life 06 p0964 A66-16483  
 Instantaneous strength, rigidity and strain characteristics of reinforced plastics surface-heated on one side 12 p1899 A66-24041  
 Metal behavior during hypervelocity cratering, noting momentum and energy equations for impulsive loading, including anisotropic stress and strain rate tensors, etc 17 p3022 A66-32013  
 Longitudinal and circumferential inertial effects on dynamic response of cylindrical shell to time-varying loads 17 p3025 A66-32470  
 Fatigue damage accumulation in materials at high temperatures under variable loads, noting calculation of fatigue life 18 p3254 A66-34230  
 Fatigue curve for one type of loading determined from stress variation during cyclic deformation and fatigue curve from other type of load application 18 p3254 A66-34231  
 Load-supporting capacity of vertical plasma cylinder contained by axial pinch effect analyzed for applications to bearings with electrically conducting lubricants 23 p4101 A66-41293  
 Elastodynamic buckling of circular cylindrical shells, unstiffened and longitudinal stringers-stiffened 23 p4147 A66-42000



## LOADING WAVE

Shock wave, plane loading and unloading wave propagation in prismatic rod with variable cross section and curvilinear stress-strain relation 17 p3031 A66-33329

## LOCALIZATION

## SA SOUND LOCALIZATION

Effects of physical location of visual stimuli on intentional response time /IRT/ 02 p0183 A66-12075  
Total complexions for isolated assembly of N quasi-independent localized systems with equally spaced energy levels 03 p0444 A66-12610

Localized diffusion of phosphorus in silicon used to produce deep p-n junctions with Gaussian P distribution 08 p1268 A66-18678

## LOCKHEED XV-4A AIRCRAFT

## S AIRCRAFT

## LOCKHEED L-2000 AIRCRAFT

Thermal management of Lockheed L-2000 supersonic transport heat sources and sinks, considering flight profile, aircraft configuration and heat transfer modes [ASME PAPER 65-AV-40] 09 p1329 A66-20298  
Operation and maintenance of Lockheed L-2000 double delta SST aircraft with high thrust engine and large delta wings, designed to meet civil aviation requirements [SAE PAPER 660295] 15 p2427 A66-29832

## LOCKHEED MILITARY AIRCRAFT

## S C-5 AIRCRAFT

## S C-141 AIRCRAFT

## S F-104 AIRCRAFT

## S P-3 AIRCRAFT

## LOCOMOTION

## SA ASTRONAUT LOCOMOTION

Simulated fish propulsion analysis of boundary layer transition and vortex chain shedding 13 p2071 A66-26725  
Dolphin body design for integrating resistance and propulsion mechanisms 19 p3279 A66-36050

## LOG PERIODIC ANTENNA

Log-periodic dipole antenna array and conical logarithmic spiral antenna design and performance 04 p0491 A66-13404

Sampling of independent orthogonally polarized antenna output to increase signal levels at least 10 decibels over one-antenna systems 04 p0481 A66-13729

Wideband annular-zone directional antenna, with individual radiators arranged in log-periodic concentrated groups on ring fed by conical line 08 p1190 A66-18682

Log periodic Yagi-Uda dipole antenna array and extension of frequency bandwidth 14 p2256 A66-27920

One-port log-periodic circuits, determining conditions for which phase of input reflection coefficient varies linearly with logarithm of frequency 19 p3324 A66-35717

## LOG SPIRAL ANTENNA

Log-periodic dipole antenna array and conical logarithmic spiral antenna design and performance 04 p0491 A66-13404

Vector potential representation of planar logarithmic spiral antenna field 14 p2259 A66-28159

## LOGARITHM

Existence of logarithm for nonsingular square matrix, uniqueness for linear ordinary differential equation systems, logarithms of operators and spectral mapping 07 p1058 A66-17966

Logarithmic pulse storage device, basic characteristics and choice of parameters as function of pulse length and measurable frequency range 09 p1356 A66-20773

Range fluctuation of high energy mesons including effect of logarithmic increase of ionization loss derived, using analytical solution, considering effects of bremsstrahlung, pair, etc 18 p3222 A66-35209

Logarithmic pulse storage device, basic characteristics and choice of parameters as function of pulse length and measurable frequency range 22 p3873 A66-39832

## LOGARITHMIC RECEIVER

Technique for controlling logarithmic amplitude response /LAR/ and regulating logarithmic amplifiers under industrial conditions 01 p0035 A66-10219

Logarithmic region of planar triode with Maxwellian distribution of initial velocities of electrons 02 p0205 A66-11974

Automatic gain control of emitter current to increase dynamic range and calculate

amplitude characteristics of transistorized resonance amplifier 04 p0496 A66-13914

Logarithmic amplifier with pulse-length discrimination followed by high-pass filter for reducing adverse effects of distributed clutter in radar receivers 08 p1180 A66-18712

Transistorized logarithmic amplitude converter for recording pulses of radiation detector, automatic switching of conversion scale permits amplitude measurements 13 p2077 A66-25321

Technique for controlling logarithmic amplitude response /LAR/ and regulating logarithmic amplifiers under industrial conditions 17 p2880 A66-31902

Automatic gain control of emitter current to increase dynamic range and calculate amplitude characteristics of transistorized resonance amplifier 20 p3532 A66-37872

amplitude characteristics of transistorized resonance amplifier 20 p3532 A66-37872

## LOGIC

## SA BOOLEAN ALGEBRA

## SA FLUID LOGIC

## SA THRESHOLD LOGIC

## SA TRANSISTOR LOGIC

Convergence, oscillation, functional stability and reliability of m-by-1 homogeneous polyfunctional nets under iteration 10 p1517 A66-21691

RCA life sciences paper on microscale medical sensors, adaptation theory, logic techniques and human factors engineering 11 p1647 A66-22297

Neural, threshold, majority and Boolean logic techniques compared for reliability and efficiency in adaptive machines and data handling systems 11 p1659 A66-22300

Digital simulation languages, discussing history, input format, effectiveness, programming error diagnostics, etc 12 p1826 A66-23826

Exactness of majorants of Dirichlet problem solution and uniqueness conditions for linear elliptic equations 17 p2947 A66-32581

Probabilistic logical analysis of neurons and neurophysiological functional organization of core of reticular formation 18 p3056 A66-33761

Theoretical static I-V characteristics of surface gate dielectric triode and geometric factors influence on amplification factor at cut-off 22 p3872 A66-39746

Exactness of majorants of Dirichlet problem solution and uniqueness conditions for linear elliptic equations 17 p2947 A66-32581

Probabilistic logical analysis of neurons and neurophysiological functional organization of core of reticular formation 18 p3056 A66-33761

Theoretical static I-V characteristics of surface gate dielectric triode and geometric factors influence on amplification factor at cut-off 22 p3872 A66-39746

Exactness of majorants of Dirichlet problem solution and uniqueness conditions for linear elliptic equations 17 p2947 A66-32581

Probabilistic logical analysis of neurons and neurophysiological functional organization of core of reticular formation 18 p3056 A66-33761

Theoretical static I-V characteristics of surface gate dielectric triode and geometric factors influence on amplification factor at cut-off 22 p3872 A66-39746

Exactness of majorants of Dirichlet problem solution and uniqueness conditions for linear elliptic equations 17 p2947 A66-32581

Probabilistic logical analysis of neurons and neurophysiological functional organization of core of reticular formation 18 p3056 A66-33761

Theoretical static I-V characteristics of surface gate dielectric triode and geometric factors influence on amplification factor at cut-off 22 p3872 A66-39746

Exactness of majorants of Dirichlet problem solution and uniqueness conditions for linear elliptic equations 17 p2947 A66-32581

Probabilistic logical analysis of neurons and neurophysiological functional organization of core of reticular formation 18 p3056 A66-33761

Theoretical static I-V characteristics of surface gate dielectric triode and geometric factors influence on amplification factor at cut-off 22 p3872 A66-39746

Exactness of majorants of Dirichlet problem solution and uniqueness conditions for linear elliptic equations 17 p2947 A66-32581

Probabilistic logical analysis of neurons and neurophysiological functional organization of core of reticular formation 18 p3056 A66-33761

Theoretical static I-V characteristics of surface gate dielectric triode and geometric factors influence on amplification factor at cut-off 22 p3872 A66-39746

Exactness of majorants of Dirichlet problem solution and uniqueness conditions for linear elliptic equations 17 p2947 A66-32581

and logic and circuit

form 02 p0205 A66-11941  
Turbulence amplifier system noting principles and application 02 p0180 A66-11963

Computer logical gates for characteristics of large systems as local guidance control and regulation systems of plants 03 p0348 A66-12603

Digital integrated circuits discussing current mode logic, resistor, diode and complementary transistor logic circuits, crossover method, power dissipation, testing, standardization and limiting factors 03 p0347 A66-13341

Oscillograms and circuit diagrams of counter in which storage of preceding state is performed by trigger with direct coupling by means of unित्रons 04 p0490 A66-13917

Diffusion and film techniques combined in design and fabrication of complex integrated computer logic circuits on small die 05 p0643 A66-14571

Adaptive logic network structure matched to relationships in input environment, defining task network has to learn, using switching functions 05 p0653 A66-14599

Transistor astable multivibrators for solid state logic elements for use in digital control and indication 05 p0647 A66-14770

Reliability and fault-masking in n-variable two-input and multiple input NOR trees discussing system, function and signal-state reliability measures 05 p0648 A66-14928

Active two-input pure fluid OR-NOR gate fabrication by logic binary-to-decimal converter [ASME PAPER 65-WA/AUT-13] 05 p0624 A66-15606

Fluidic devices, discussing design, equivalence to logic circuits, fluid amplifier application to build flip-flops, etc 06 p0809 A66-16794

Reliability of logical elements and systems with given probabilities of individual elements 07 p1013 A66-17387

Alloying technique through doped diffused layer for production of high speed silicon tunnel diodes for logic circuits and memory functions 08 p1188 A66-18653

System designing with all-magnetic logic circuits based on resistance shift register circuit 08 p1187 A66-19101

Ternary-pentary majority algebra, Boolean-to-majority function conversion, and derivative identities 08 p1188 A66-19672

Digital fluid amplifiers and application, noting breadboard miniaturization 09 p1332 A66-20321

Integrated circuit for switching-type high-efficiency power supply with feedback regulation 09 p1354 A66-20566

Coincidence detector circuit provides complement of exclusive OR, restores signal level and has high fan-out 09 p1359 A66-20920

Integrated circuit gate ring counters, noting flip-flop variety comparison 11 p1677 A66-23178

Silicon monolithic Semiconductor Memory Integrated Device /SMID/ memory system and memory storage element 12 p1827 A66-23834

Redundancy method based on circuit failure asymmetries for reliability improvement in digital circuits 12 p1842 A66-24668

Reliability improvement through redundancy at various system levels in analog systems 12 p1844 A66-24733

MOS FETs in microelectronics, including digital arrays and logic gates 12 p1845 A66-24847

Periodically operating gate circuit with negative feedback for sampling in micro- and millisecond range 12 p1847 A66-24938

Harmonic linearization of logic law control systems, deriving complex equivalent transmission coefficient for nonlinear part of circuit with variable structural elements 13 p2045 A66-25299

Various methods of implementing minimized logic circuits entirely with NAND gates 13 p2047 A66-25361

Integrated circuits with propagation delays in nanosecond range, noting emitter coupled logic circuit 13 p2036 A66-25534

Gating circuit concept, using carrier frequency approach, applied to inverter,



- converter and cycloconverter  
circuits 13 p2043 A66-26296
- Approaches to microelectronics, application of microelectronics to telecommunication equipment, noting logic circuits, radio relay, etc 13 p2043 A66-26316
- Optimum design of emitter follower transistor logic /ETL/ circuits and comparison with various other logic circuits 14 p2263 A66-27023
- Integrated circuit as exclusive-OR gate or as linear amplifier, using transistor or tunnel diode shunted by resistor 14 p2263 A66-27051
- Diode gate design, using bridge circuit to eliminate spurious gating signals 14 p2267 A66-27802
- Automatic speech analyzer capable of detecting frequencies of three primary voice formants 14 p2296 A66-27864
- Adaptive method for synthesis of circuit of majority decision elements which realizes given logical function 14 p2268 A66-28043
- Dynamic logic chassis analyzer /DLCA/, diagnostic tool for isolating faults to circuit board or component level in programmer test station /PTS/ and component test station /CTS/ ground support equipment 14 p2260 A66-28266
- Thin film hybrid packaging method for series of computer logic circuits designed to operate at 100-mc clock rate 14 p2260 A66-28267
- Dielectric-tape TV camera for panoramic scanning application in meteorological satellite, discussing subject logic and control system design 14 p2262 A66-28418
- Optimal scientific satellite PFM encoding system circuit design and digital data processing 14 p2244 A66-28429
- Automatic systems for diagnostic medical tests onboard spacecraft, using algorithms given in matrix form 15 p2444 A66-29462
- Automatic device for reversible hypothermia in living organism, considering parameters of physiological functions, included in logic circuits 15 p2444 A66-29498
- Diode transistor logic /DTL/ circuit stage delay and transistor speed parameters 16 p2668 A66-30125
- Characteristic parameter selection and transient performance capabilities of integrated logic microcircuit 17 p2880 A66-32057
- MOS transistors in integrated switching circuits to obtain desirable characteristics of pentode vacuum tubes and bipolar transistors 17 p2882 A66-32109
- Integrated high speed diode-transistor-logic gate /DTL/ design, discussing stray capacitance, resistors, diode combination and switching transistors 17 p2883 A66-32121
- Integrated circuit design optimization, using modified direct coupled transistor logic NOR gate 17 p2883 A66-32122
- Computer assemblies packaging analysis for optimum logic gates and inputs as function of leads 17 p2883 A66-32124
- Current-mode logic gates in building differential amplifier for memory-core readout 17 p2884 A66-32127
- Monolithic silicon integrated circuit used for current-mode logic of RCA Spectra 70/45 and 70/55 computers 17 p2886 A66-32512
- Developmental memory using monolithic-ferrite integrated arrays of magnetic storage elements provides cost and power savings 17 p2886 A66-32516
- Logic circuit construction problems in multicore magnetic elements with magnetic flow switching 17 p2878 A66-33495
- Analog computer and logic circuitry combination for variable frequency signal production, noting application to adaptive control systems 18 p3089 A66-33561
- Carrier travel time in transistor region where changeover from neutral region to depletion layer takes place 18 p3076 A66-33936
- Fluid interaction devices, noting induction and turbulence amplifiers, impact modulators, logic gates, inverters, etc 18 p3054 A66-34131
- Acoustic sensitivity and logic circuitry of fluidic turbulence amplifiers for application to laminar jet streams 18 p3056 A66-35012
- Tuning of power amplifiers without standard servoloop and electromechanical variable RF element, for application to transceiver 19 p3324 A66-35515
- Silicon-on-sapphire batch-fabrication of computer logic and memories, describing SOS diode matrix 19 p3314 A66-35526
- Changing of PCM telemetry, from individual, integrated bipolar and/or MOS logic elements to complex MOS subsystems 19 p3317 A66-35700
- Trainable nonlinear function generator using threshold logic elements for pattern classifiers 19 p3338 A66-36737
- Pneumatic control system based upon dual membrane relay permitting all fundamental logic operations 19 p3282 A66-36808
- Realization of arbitrary storage structures using newly developed pneumatic logic system as elements 19 p3310 A66-36809
- Homogeneous microelectronic structures using integrated circuit technology for fabrication of logical and sequential facilities 19 p3323 A66-36821
- Space control system using digital SUBORDINATE OR logic blocks to add optimum response capability to maneuver commands 20 p3662 A66-37229
- Ternary-pentary majority algebra, Boolean-to-majority function conversion and derivative identities 20 p3522 A66-37264
- Fluid logic and amplification - International Conference, England, September 1965 20 p3500 A66-37642
- Operation principles of turbulence amplifiers, considering application to low cost automation, using conventional pneumatic valves and cylinders 20 p3502 A66-37655
- Oscillograms and circuit diagrams of counter in which storage of preceding state is performed by trigger with direct coupling by means of unitrons 20 p3522 A66-37875
- Integrated electronic arrays, examining fabrication, logical design, application and packaging 21 p3710 A66-38828
- Miniaturization of logic components for modular and monolithic integrated circuits in computer design 21 p3708 A66-39624
- Boolean algebraic analysis of AND, OR, NAND and NOR functions in electronic integrated circuits 21 p3720 A66-39625
- Design formulae and comparative tables of three n-input universal logic circuits 22 p3883 A66-39727
- Design principles and block diagrams of self-adaptive universal logic circuit with trainable elements 22 p3883 A66-39728
- Digital computer program for static worst case design of diode transistor logic 22 p3870 A66-40396
- Complementary symmetry flip-flop and similar transistor micropower digital logic circuit design 23 p4048 A66-41144
- Structural diagram for loading of potential element transistors operating in complex logic circuit 23 p4041 A66-41397
- Performance modeling procedure to determine characteristics of integrated logic devices 24 p4177 A66-42100
- Lasers applied to logic, memory, input-output and data transmission-linkages parts of computers 24 p4225 A66-42804
- Controllable threshold circuit using interconnection simple toroids for all-magnetic logic to select signal paths 24 p4189 A66-43178
- Tabular minimization procedure for ternary switching functions in obtaining minimal irredundant function form, using limited set of reduction rules 24 p4177 A66-43186
- Multifunction monolithic thin film compatible diode-transistor logic circuits for data processing 24 p4178 A66-43187
- LOGIC NETWORK**
- Logical and computing devices, discussing construction of homogeneous functional structure using integral circuits 04 p0494 A66-13704
- Pneumatic logic elements for sequential control of machines and individual processes 07 p0991 A66-17416
- System reliability by analyzing reliability of components in connection with operation of logic structures 08 p1187 A66-19447
- Modular system of logic for nuclear detectors onboard Vela satellite 09 p1463 A66-19969
- Fluid mechanics, fluidic devices and systems, noting design, manufacturing techniques and application 09 p1332 A66-20317
- Digital and RF/linear circuits compared noting monolithic, hybrid and thin film circuit limitations, phase locked loop design, etc 12 p1830 A66-23756
- Associative parallel processor using word and bit logic and sequential-state-transformation mode, with application to picture processing and pattern recognition 12 p1827 A66-23830
- Near minimal set of tests detecting all single faults in combinational logic net, using shortcut methods 13 p2040 A66-25804
- Integrated circuit binary counters using majority logic current mode gate element 14 p2255 A66-27803
- Logical and computing devices, discussing construction of homogeneous functional structures using integral circuits 15 p2454 A66-28545
- Realization of numerical counters with micrological elements, discussing flip-flop and memory elements 16 p2656 A66-30964
- Papers on RCA computer progress 17 p2877 A66-32510
- MOS transistor suitability to integrated logic networks, using arrays of many identical elements with superimposed connections 17 p2901 A66-32514
- Nonlinear operational amplifier with high power switching devices, noting volt-ampere characteristics 18 p3086 A66-34494
- Intermittent connection testing for digital logic module 20 p3523 A66-37949
- Fluid amplifier application to process control including turbulence amplifiers, logic function performance, etc [ASME PAPER 66-MD-8] 21 p3697 A66-38477
- SESIAC, electronic machine for statistical simulation consisting of stochastic generator, containing no equations or tabulated functions, only random pulse sources and logic networks 23 p4053 A66-41604
- LOGICAL DESIGN**
- Integrated circuit current switching logic element fabrication, using transistors and standard isolation techniques 05 p0643 A66-14570
- Switching circuit theory and logical design - IEEE Annual Symposium, University of Michigan, Ann Arbor, October 1965 05 p0637 A66-14926
- Book on unified treatment of switching theory, emphasizing synthesis and analysis aspects of switching circuits 06 p0861 A66-16198
- Area boundaries and design implications of mutually stable logical element characteristics 07 p1014 A66-17435
- Iterative procedure for determining linear separability of Boolean function and threshold functions for logical switching circuit design 07 p1059 A66-17971
- Russian monograph on algorithm of machine search for logical natural derivation of investigated formulas from initial formulas via propositional calculus 07 p1004 A66-18464
- Redundant microelectronic system and reliability 11 p1661 A66-22272
- Infinite automata theory and structural logical design of digital machines 11 p1659 A66-22707
- Flow of data and control information from apparatus to computer and use of microprogrammed controller 12 p1827 A66-23829
- Self-diagnosable DX-1 computer design to achieve maximum operational availability 12 p1828 A66-23843
- PERT statistical design of logic systems, discussing expected delays, critical timing paths, timing slack between various inputs and probability of achieving specific output by given time 14 p2284 A66-27232
- Computer design of programmable decommutator for multiformat PCM telemetry data 14 p2246 A66-28432
- Book on automatic communication switching systems, logic, logical switching components, storage elements, relay centers, etc 15 p2465 A66-29644
- Program for calculating and designing diode switching circuits consisting of AND and OR gates, where interrelationship of input variable is determined by single switching function 15 p2453 A66-29867



Optimum dimensioning of diode transistor logic /DTL/ circuit equipped with silicon epitaxial planar transistor BSX20 operating in saturated mode 16 p2668 A66-30124

Turtle, microcircuit logic or transistor resistor transistor logic /TRTL/ for integrated circuits 17 p2883 A66-32117

Characteristics of pneumatic logical elements including membrane-type elements, noting design and construction in Eastern Europe 19 p3280 A66-35723

Binary adder and other pneumatic logic elements producing any two-valued function of three two-valued input parameter by proper arrangement of input jet nozzles 20 p3496 A66-36862

Cascade free jet logical element interactions and application to multiple-parameter logical function 20 p3496 A66-36863

Logical element geometry effect on fluid flow in turbulent reattachment device 20 p3501 A66-37645

Digital computer program for static worst case design of diode transistor logic 22 p3870 A66-40396

Minimization of logical functions in normal disjunctive form, using Gavrillova method and ALGOL 60 algorithm 22 p3941 A66-40541

Logical processing units and interconnection networks design noting reliability, fault diagnosis, computer coordination of data and control processes, etc 22 p3871 A66-40728

Saturn computer design and fault simulation on IBM 7090 22 p3871 A66-40744

**LOGISTICS**

SA MAINTENANCE

SA SPACE LOGISTICS

SA TRANSPORTATION

Digital simulation of scheduling logistic support by helicopter, using Backtrack techniques 12 p1858 A66-24683

Mathematical models for logistics planning providing complete analysis of requirements through computer simulation 14 p2245 A66-27122

Titan II operational base management, organization and responsibilities, noting logistic requirements, concurrency problems, etc 14 p2416 A66-27123

Military air cargo transport technology and logistic systems 15 p2620 A66-29793

Mathematical model used by Army Missile Command for establishing priorities for reliability and logistics improvement 20 p3684 A66-37886

VTOL operational availability computer simulation model, studying initial and tradeoff design, maintenance, logistics, manpower and flight operational requirements 20 p3543 A66-37909

Locating general drop zone and desired impact point, identifying receiving unit and dropping supplies for aerial delivery systems 22 p3850 A66-40615

**LOMMEL FUNCTION**

Fresnel gain of aperture antenna, developing rigorous analytical formula for circular aperture antennas with parabolic tapered illumination 05 p0651 A66-15837

**LONG PERIOD EFFECT**

Climatic conditions at Earth surface, relation to long-term planetary trends in atmospheric circulation 05 p0712 A66-15221

Cell voltages and Coulomb efficiency in oxygen electrodes and hydrogen and hydrazine fuel cells for long duration discharges 08 p1172 A66-19652

Long duration flight physiological data on ducks and chickens in closed ecological systems, including oxygen and food requirements and carbon dioxide output 15 p2435 A66-29452

**LONG RANGE NAVIGATION**

SA LORAN

SA LORAN C

Automatic star trackers for long range aircraft navigation, discussing instrumentation methods and use of pulse code modulation for sensor design 02 p0257 A66-12029

Ground-based radio aids and self-contained aids for long range navigation 02 p0258 A66-12040

VLF radio propagation conditions and phase delays in design of long range

navigation aids 02 p0259 A66-12053

Future trends in long range aircraft navigation 02 p0260 A66-12058

Long distance air navigation across North Atlantic 07 p1063 A66-17444

Evaluation of four different types of Doppler radar as long range self-contained navigation aid 07 p1065 A66-17689

Long range navigation in jet operations, discussing problems and limitations 07 p1065 A66-17670

Universal long range radio navigational system, discussing purpose and function of ground-based system 07 p1065 A66-17671

DECTRA long range navigational aid, DECTRA airborne receiver and Omnitrac computer 07 p1068 A66-17702

Up-dating of self-contained navigational aids such as Doppler, inertial and Doppler/inertial systems 07 p1070 A66-17717

MOA/BOAC Doppler/Loran A trials 1963-64, discussing navigational accuracy during transatlantic flights 07 p1072 A66-17759

Accuracy of navigation techniques for North Atlantic flights evaluated, based on Loran A and Doppler/GM compass automatic dead reckoning system 07 p1072 A66-17760

Safety and economic factors which determine navigational requirements in long range traffic area 07 p0988 A66-17764

Automatic Astro Tracker as part of long-range aircraft navigation complex heading reference system 07 p1075 A66-17786

Flight evaluation of long range inertial navigation and steering in autopilot and manual operation 07 p1076 A66-17791

Astronavigation applied to piston aircraft and supersonic jets, advantages and shortcomings 07 p1076 A66-17797

Air collision risk and traffic control in long-range air traffic systems as basis for safe procedural separation standards 09 p1401 A66-20431

All-weather operations, head-up displays, long range navigational aids - Symposium, International Federation of Air Line Pilots Associations, Rotterdam, October 1965 17 p2951 A66-33198

Separation standards and navigation in long-range air traffic control region 17 p2954 A66-33213

Worldwide civilian-aircraft navigation system based on VLF radio using ground stations or satellites 17 p2954 A66-33214

Doppler navigation system accuracy improvement and evaluation of inertial navigator with steering 17 p2954 A66-33215

Deetra long-range navigational system giving area coverage position fixing for multiplicity of North Atlantic transocean routes 17 p2954 A66-33216

Efficient and accurate orbit prediction for very long periods of time using analytic perturbation technique in conjunction with multistep methods 19 p3462 A66-35899

[AIAA PAPER 65-692]

Safe separation standards estimation for analyzing long-range air traffic systems, emphasizing flying errors observation in operational conditions 21 p3760 A66-38452

Costing of parallel route systems for supersonic traffic, examining diurnal traffic patterns, sensitivities to fuel requirements, sonic bang avoidance and layout of track systems 21 p3761 A66-38453

**LONG WAVE RADIATION**

Equations for reflecting effect of underlying surfaces on long wave radiation fluxes in free atmosphere 01 p0062 A66-10761

Solar radiation measurements made in four stations from 1957 to 1963 show dependence of atmospheric long-wave radiation on water-vapor pressure and cloudiness 04 p0542 A66-13818

Long-wave recombination radiation of germanium associated with optical transitions involving photon emission and current carrier heating 04 p0568 A66-14348

Silicon recombination radiation, describing long wave IR radiation effect and photon energy gain via conversion into short wave radiation 06 p0924 A66-16515

Ascending and descending fluxes of long wave radiation in free winter atmosphere as affected by temperature stratification, water-vapor distribution and clouds 07 p1029 A66-17923

Radiometersonde observations of atmospheric IR irradiance, noting measurement results with improved equipment 09 p1369 A66-19869

Silicon recombination radiation, describing long wave IR radiation effect and photon energy gain via conversion into short wave radiation 09 p1431 A66-20896

Effects of long-wave radiation exchange near Earth surface, extrapolating air temperature measurements to ground to estimate surface temperature, obtaining equivalent black body temperature of ground 11 p1702 A66-23155

Ascending and descending fluxes of long wave radiation in free winter atmosphere as affected by temperature stratification, water-vapor distribution and clouds 12 p1869 A66-23884

Long wave radiation and total radiation balance at Earth surface in Arctic region, based on Stefan-Boltzmann formula 12 p1869 A66-24202

Normally incident plane electromagnetic wave scattering by circular cylinder coated with radially stratified sheath 14 p2238 A66-27587

Equations for reflecting effect of underlying surfaces on long wave radiation fluxes in free atmosphere 14 p2285 A66-27860

Long-wave recombination radiation of germanium associated with optical transitions involving photon emission and current carrier heating 14 p2368 A66-28245

Observational data obtained in determinations of photographic positions of satellites, noting long wave vibrations of images role in position error 20 p3517 A66-37835

Long-wave radiative heat transfer between clouds and free atmosphere as basic factor in weather forecasting 20 p3594 A66-38371

**LONGITUDE**

SA PLANETARY LONGITUDE

SA SOLAR LONGITUDE

Method for calculating longitude dependence of geomagnetically trapped electrons at low altitude, based of scattering and energy loss due to atmospheric interactions 20 p3640 A66-38324

**LONGITUDINAL CONTROL**

Flight evaluation of various longitudinal handling qualities involving parameters and region of pilot acceptance [AIAA PAPER 65-780] 03 p0322 A66-13067

Automatic system ensuring landing in absence of visibility and atmospheric turbulence by controlling motion of aircraft leveling out, consisting of time-dependent input signal shaping device and amplifiers 12 p1909 A66-24321

Flight control system design for high performance aircraft, particularly longitudinal transient response handling qualities 19 p3278 A66-35509

Short period longitudinal aerodynamics of reentry vehicle flight control system, using sensitivity techniques 19 p3396 A66-35510

**LONGITUDINAL STABILITY**

Wind tunnel research of deep stall aerodynamic characteristics of T tail analyzed as preliminary design guide [AIAA PAPER 65-737] 03 p0317 A66-12547

Reduced stiffness responses of airplane to longitudinal control, noting elevator flutter and stick-fixed dynamic longitudinal stability [AIAA PAPER 65-784] 03 p0320 A66-12594

Experimental fixed and moving-base flight simulator investigation of generalized aircraft longitudinal pilot induced oscillations [AIAA PAPER 65-793] 03 p0352 A66-12596

Effect of canard foreplane on longitudinal long-period perturbed motion of aircraft depends on change in hinge moments with Mach number change 04 p0458 A66-14152

Parametric response of elastic columns discussing longitudinal inertia effects, analytic stability criteria and results [ASME PAPER 65-WA/APM-13] 05 p0777 A66-15435

Quasi-linear partial differential equations of transients in liquid rocket engine propellant feed system solved, determining transient pressure ratio [ASME PAPER 65-FE-23] 06 p0942 A66-16217

Parametric response of elastic columns, discussing longitudinal inertia effects,



analytic stability criteria and results  
[ASME PAPER 65-WA/APM-13] 12 p1961 A66-23985

Text on longitudinal static stability of low-speed aircraft including effect on pilot, flight test, pitch maneuverability, etc 14 p2222 A66-26792

Longitudinal instability in liquid rockets analyzed by digital computer assembling of coupled structural and fluid systems [AIAA PAPER 66-472] 17 p3016 A66-32765

Oscillatory motion of angle of attack for space vehicles entering Earth atmosphere at hypersonic speeds from satellite orbits 17 p3016 A66-32893

Longitudinal motion of piloted aircraft during rapid dropping of concentrated loads in comparison of numerical solution with flight data 17 p2848 A66-33076

Exact analytic solution, in confluent hypergeometric functions, to problem of stability of conical shell under uniformly distributed longitudinal compressive forces 18 p3252 A66-33709

Reduced stiffness responses of airplane to longitudinal control, noting elevator flutter and stick-fixed dynamic longitudinal stability [AIAA PAPER 65-784] 19 p3279 A66-36485

Wind tunnel research of deep stall aerodynamic characteristics of T tail analyzed as preliminary design guide [AIAA PAPER 65-737] 19 p3280 A66-36491

Linearized motion equations for low-altitude flight pitching stability of aircraft with control surface 21 p3696 A66-38937

Three-dimensional parachute dynamic stability theory 22 p3845 A66-40593

**LONGITUDINAL STABILITY AND CONTROL**

Aerothermoelasticity effect on longitudinal stability and control of winged aerospace vehicles [AIAA PAPER 64-489] 05 p0775 A66-15075

Glide slope direct lift control of carrier landings, discussing trim change with actuation and longitudinal stability and control 07 p0986 A66-17272

Response of hypersonic aircraft to abrupt control displacements, determining vehicle characteristics, design and operational parameters 09 p1330 A66-20739

Spacecraft longitudinal and lateral stability along reentry trajectory during deceleration period determined, using equations of motion 17 p2846 A66-32897

**LONGITUDINAL WAVE**

Longitudinal wave decay in inhomogeneous plasma may vary with distance 01 p0109 A66-10257

Longitudinal elastic wave of finite amplitude propagation in isotropic solid 01 p0057 A66-10421

Four-plasmon decay effects for longitudinal waves show broadening of noise spectrum 09 p1407 A66-19964

Longitudinal elastic wave of finite amplitude propagation in isotropic solid 11 p1736 A66-22606

Wave propagation during gyroresonance interaction, noting nonlongitudinal characteristics of waves generated in magnetosphere between beams of charged particles 13 p2072 A66-25462

Longitudinal wave decay in inhomogeneous plasma may vary with distance 13 p2148 A66-25974

Stability criteria of system with negative differential conductivity showing generation of longitudinal waves, noting amplitude buildup increment 14 p2358 A66-27085

Longitudinal and transverse waves transformation in nonuniform plasma 17 p2969 A66-32543

Quasi-linear hyperbolic equations governing one-dimensional longitudinal wave propagation in viscoelastic material 17 p3032 A66-33502

Longitudinal wave propagation in plasma waveguide, observing lower and higher modes 18 p3072 A66-34567

Two-stream instability for longitudinal waves in plasma traversed by ion beam 18 p3148 A66-34909

Longitudinal sound waves attenuation in superconductor with spatially dependent energy gap by Green function method applied to ultrasonic attenuation in type II superconductor 21 p3795 A66-38548

Microwave plasma diagnostics using

longitudinal radio wave propagation 21 p3790 A66-39068

Longitudinal wave in cylinder of viscoelastic material for case of small frequencies, obtaining propagation equations by using stress-strain relations, compatibility conditions and motion 22 p3996 A66-40703

Stability criteria of system with negative differential conductivity showing generation of longitudinal waves, noting amplitude buildup increment 22 p3967 A66-40841

Monochromatic longitudinal wave amplification by charged particle beam in nonlinear plasma, noting amplitude dependence on coordinate 24 p4243 A66-42520

**LOOP**

SA CIRCUIT

SA CLOSED LOOP SYSTEM

SA RING

SA SERVO LOOP

Acquisition behavior of phase-locked loops analyzed by treating loop as first-order loop with slowly varying dependent bias 12 p1856 A66-24648

Divergent vertical helicopter oscillations due to pilot presence in collective control loop and physiological response of pilot to oscillations 17 p2843 A66-32719

**LOOP ANTENNA**

Radiation from dielectric coated cylindrical core loop antenna surrounded by lossy plasma sheath 01 p0040 A66-10552

Circular filament of electric current in unbounded magnetotonic medium, measuring radiation resistance for constant current distribution 05 p0633 A66-15122

Current distribution on L-band loop antenna composed of four quarter-circular sections 06 p0850 A66-16446

Russian text on diffraction and radiation of waves 08 p1257 A66-19755

Transient processes in thin open-loop and closed-loop antennas studied by method that takes transmission line processes into account 08 p1199 A66-19759

Current distribution along circular loop antenna, obtaining backscattering patterns as function of rotation angle 10 p1510 A66-21592

Matrix analysis of scattering from conjugate-matched antenna 11 p1662 A66-22541

Electromagnetic scattering by circular wire loops loaded with lumped impedances, obtaining solution to integral equation by Fourier series 14 p2247 A66-26863

Impedance integral evaluation for antenna loop immersed in conducting medium 14 p2256 A66-27923

Radiation pattern of dielectric coated cylindrical core loop antenna in lossy plasma sheath 15 p2452 A66-29712

Normalized self-and mutual admittances of two identical bare circular loop antennas in air or conducting medium evaluated, obtaining single integral equation for current distribution 19 p3321 A66-36405

Broadening frequency bandwidth of full-wave directive loop antennas employing reflectors and directors 20 p3531 A66-37727

Cardioid whip-loop receiving antenna system using only passive circuitry to bring normal and abnormal components of VLF sky waves into phase with each other 22 p3872 A66-39732

Propagation and radiation of radio waves from dielectric coated prolate spheroidal core loop antenna surrounded by plasma sheath 24 p4184 A66-42745

**LOLAN**

Signal simulator for testing Loran A and Loran C airborne receivers in laboratory, using digital simulator circuits to test dynamic response of tracking circuits 23 p4088 A66-41253

**LOLAN C**

Loran C system and technique of ground stations for giving ships fixes 02 p0257 A66-12037

Loran C navigational system considering sky waves and future of Loran D system 02 p0258 A66-12043

Loran C navigation system using pulsed hyperbolic radio signals, noting factors influencing range and accuracy 02 p0258 A66-12045

Airborne hyperbolic coordinate converter for Loran C signals, noting flight testing 02 p0258 A66-12047

Flight testing of FAA-Lear Siegler receiver/converter airborne system with Loran-C hyperbolic navigation system 07 p1069 A66-17706

Microminiature Loran-C Receiver/Indicator for analog-to-digital conversion, using integrated circuit technology 10 p1555 A66-22047

Direct frequency comparison of atomic hydrogen masers in different places and conditions by simultaneous monitoring of Loran C signals 12 p1890 A66-21445

Loran C receiving equipment using microcircuits, noting error 17 p2955 A66-33220

Central Telecommunications Laboratory 882 P arithmetical airborne computer 20 p3523 A66-38013

Photographic integration process using Loran-C pulses for precise synchronization of timing signals at any point in continental U.S. 22 p3862 A66-39733

**LORENTZ**

Actual line shape expected from accelerating radiating ion, errors due to Lorentzian approximation and results for ion laser transition in rare gas lasers 16 p2716 A66-30181

**LORENTZ FORCE**

Traveling fields in interaction of ionized gases with electromagnetic field currents checking Lorentz force and magnetic induction 03 p0404 A66-12980

Lorentz force maximization in continuous-flow Hall current plasma accelerators, using either axial electric field and radial magnetic field or radial electric field and slanted magnetic field 08 p1263 A66-19154

Nonrelativistic force in simple magnetizable fluid derived from thermodynamic information about energy and power 12 p1915 A66-24651

Voltage drop in direction of current flow produced in superconducting alloys by current perpendicular to magnetic field explained by assuming Abrikosov filaments move under influence of Lorentz force 13 p2168 A66-26022

Temperatures, Lorentzian widths and drift velocities of excited neutral and ionic species in argon-ion laser, noting thermal equilibrium achievement 15 p2512 A66-28695

Nonlinear terms of electromagnetic field in ionized gas reduced to linear system and single nonlinear equation 15 p2547 A66-29648

Nonlinear flux flow in type II superconductor, noting resistance characteristics 16 p2768 A66-30135

Mean Lorentz force field of electrically conducting medium in turbulent motion affected by Coriolis force 16 p2763 A66-31349

Spatial charge region, excess electron concentration, capacitance and conductivity in semiconductor layer with Lorentz forces acting on carrier determined as functions of surface potential and applied electromagnetic field 19 p3442 A66-35819

Microinstability-driven losses in energetic proton plasma formed by single transit of 600-keV hydrogen ion beam through magnetic mirror field 19 p3421 A66-36543

**LORENTZ GAS**

Kinetic theory of Lorentz plasma in rotating magnetic fields and electromagnetic fields based on Boltzmann equation 01 p0113 A66-10640

Electron distribution function of homogeneous Lorentzian plasma calculated by successive approximation method 01 p0115 A66-11077

Self-modulation and Luxembourg effect in electromagnetic wave propagation in isotropic and homogeneous Lorentz plasma 01 p0031 A66-11083

Theoretical model of isolated Lorentz line of IR absorption by gases applied to atmospheric optics and spectroscopy problems 08 p1248 A66-19307

Microinstability limitations of DCX-1 energetic plasma from gas dissociation and Lorentz force dissociation 10 p1568 A66-21826

Relaxation of isotropic distribution of test particles in homogeneous background gas, including nonzero temperature effects 11 p1741 A66-23390

Minimum internal energy calculation of



anisotropic oxygen polarizability and Lorentz correction in barium titanate crystal 11 p1758 A66-23408

HF and LF alternating electric fields effect on weakly ionized argon, temperature modulation and production of harmonics 13 p2141 A66-25447

Nonlinear interaction between two modulated electromagnetic waves propagating in homogeneous anisotropic Lorentz plasma 14 p2344 A66-27941

Approximation method for thermal diffusion factor of almost Lorentzian gas mixture with better convergence properties than Chapman-Enskog approximation 16 p2824 A66-30119

Nonlinear effects in homogeneous Lorentz plasma, calculating anisotropies of electron distribution function 17 p2963 A66-31842

Experimental study of isotropic term of acoustic radiation intensity in gas 18 p3136 A66-34724

Theoretical model of isolated Lorentz line of IR absorption by gases applied to atmospheric optics and spectroscopy problems 19 p3400 A66-36043

**LORENTZ TRANSFORMATION**

Uniqueness of gravitation theory developed by method of classical Lorentz covariant field theory 01 p0107 A66-11095

New tests for invariance of vacuum state under Lorentz group 04 p0546 A66-13456

Lorentz-invariant theories of gravitation analyzed, using astronomical tests for comparing results predicted by theories with general relativity formulas 05 p0716 A66-15088

Lorentz-invariant Markov process in relativistic phase space 12 p1914 A66-24406

Traveling wave interaction in nonlinear medium Lorentz transformation 13 p2163 A66-25434

Potential equations in homogeneous isotropic moving media derived, using Minkowski theory 14 p2340 A66-27040

Basic premises of tetrad formulation of general relativity theory and relationship to generalized Lorentz transforms 14 p2332 A66-27212

Lorentz-equivalence generalization in substratum theory 15 p2593 A66-28652

Lorentz-covariant theory of gravitation constructed with linear field equations 15 p2542 A66-29332

Irreducible unitary representations of restricted Lorentz group on manifolds of time-, light- and spacelike 4-vectors, obtaining plane-wave solutions of Klein-Gordon equation 15 p2528 A66-29622

Lorentz invariant space-time gravitational field theory, Maxwellian gravitokinetic field of potential and kinetic components and precession of orbit of Mercury analyzed by Einstein restricted theory of relativity 16 p2802 A66-31011

Energy pulse tensor formulation of law of conservation of energy in interacting electromagnetic field, using complete inhomogeneous Lorentz group 18 p3135 A66-34579

Lorentz transformation of thermodynamic quantities, noting application of formalism of statistical mechanics, validity of Planck-Einstein equations for total energy and momentum 22 p3997 A66-39806

Radiation in relativistically moving anisotropic plasma medium, noting Lorentz type transformation of plasma electron volume density 23 p4105 A66-41638

**LOSS**

S ENERGY LOSS

S HEARING LOSS

S LEAKAGE

S OHMIC LOSS

S PLASMA LOSS

S TRANSMISSION LOSS

**LOUDSPEAKER**

Design technique for large capacity acoustic instrument 14 p2296 A66-28036

**LOW ALTITUDE**

Decreased flying ability of pilots in simulated low altitude high speed flight from 0.4 to 0.9 Mach 12 p1809 A66-23928

Linearized motion equations for low-altitude flight pitching stability of aircraft with control surface 21 p3696 A66-38937

**LOW ASPECT RATIO WING**

Flow past slender bodies of revolution or

low aspect ratio wings with finite span or cross-sectional area 04 p0454 A66-13517

Subsonic flow near trailing edge of low aspect ratio delta wing 04 p0454 A66-13518

Matrix scheme using two-way spline curves for interpolating low aspect ratio lifting surface mode deflections for use in aeroelastic calculations 05 p0774 A66-15058

Aircraft with wings of low aspect ratio 09 p1329 A66-20556

Low aspect ratio wing moving above interface of two fluids of different density, replacing value of velocity potential by value obtained at large distance downstream from wing 13 p2068 A66-26539

Theoretical nonlinear method for calculating aerodynamic forces on low-aspect-ratio wings at high angles of attack and wide range of Mach numbers 20 p3491 A66-36907

Downwash angles behind rectangular wings of small aspect ratio calculated at subsonic velocities according to nonlinear theory 23 p4010 A66-41781

**LOW DENSITY GAS**

Introductory book on hypersonic aerodynamics covering continuum flow of inviscid nonheat-conducting perfect gas and real gas, viscous and low density effects in hypersonic flow 02 p0176 A66-11875

Neutral atomic beam used to measure total ionization cross section of argon atoms incident on low density argon gas 07 p1083 A66-18421

Single and double Langmuir probe for low density plasma, noting measurement of electron temperature and density 10 p1535 A66-21514

Interferometer apparatus used in combination with Fabry-Perot etalon to study properties of low density air streams 11 p1709 A66-23298

Tenuous hydrogen plasma injection into axial magnetic cusp field at entrance of long solenoid 13 p2147 A66-25749

Spectral energy distribution and Doppler broadening of Rayleigh light scattered from hydrogen and argon gas at low density, using Fabry-Perot interferometer 13 p2133 A66-26169

Argon flow through long tube compared with Weber theoretical model, applying classical continuum equations 14 p2274 A66-27444

Plasma stability analysis, discussing low density fluid equations, variational principle and sufficiency condition at moderate densities, electric field effect, etc 15 p2554 A66-29746

Supersonic section of nondissipative sectional low density plasma accelerator, calculating two-dimensional cold plasma flow 17 p2964 A66-31894

Anomalous electron diffusion and ion acceleration measured in steady state low-density weakly-turbulent plasma subjected to crossed E and B fields 18 p3149 A66-34913

**LOW DENSITY WIND TUNNEL**

Rarified gas dynamics in space flight and hypersonic low density wind tunnel of Goettingen Aerodynamics Research Facility 07 p1017 A66-17479

Low density plasma jet wind tunnel for investigation of low density high-enthalpy high-speed flow 09 p1364 A66-20253

Pressure distribution and low density effects on sharp flat plates and sharp and blunt cones measured in hypersonic wind tunnel 11 p1634 A66-22930

**LOW FREQUENCY**

Filtering properties of frequency-stability transport circuits of molecular beam generator, noting design considerations for high efficiency 09 p1353 A66-20442

Lumped-circuit LF general three-resonator filter in rectangular wave guide using inductive susceptances as coupling elements 10 p1514 A66-21911

Charge sheath role at discharge wall in determining boundary conditions for LF wave in low pressure discharge, using hydrodynamical model 12 p1923 A66-24571

5 kw LF power amplifier with improved frequency response, noting design and operation 12 p1843 A66-24682

Drift instabilities in thermionic plasmas, noting excitation of LF oscillations with finite perturbation amplitude around

cathode ion sheath 13 p2145 A66-25729

LF spectrum measurements of radio source 3C84, including plot of flux density vs frequency 14 p2384 A66-27846

Shear relaxation time of monatomic fluids for liquid and dense gas phases calculated, using LF viscosity data and estimates of HF elastic moduli 14 p2277 A66-27977

LF wave in cylindrical plasma in magnetic field where ion beam is flowing and modes are nonaxisymmetric 15 p2553 A66-29629

LF resonances in mixed state of pure niobium, noting line shape and damping decrease 16 p2770 A66-30186

Chain code method of eliminating LF drift disturbance error in calculation of impulse-response function of time-invariant system 24 p4187 A66-42368

**LOW LEVEL TURBULENCE**

Vertical velocity fluctuations in nocturnal low level jet examined by sonic anemometers 04 p0541 A66-13666

Low altitude turbulence model for aircraft gust load estimation related to meteorological parameters, terrain conditions and height [AIAA PAPER 65-14] 09 p1400 A66-20741

Severely turbulent airflow at low levels over United Kingdom 11 p1730 A66-23015

Low level wind jets at White Sands Missile Range 17 p2949 A66-33339

**LOW PASS FILTER**

Integral restrictions on time delay of linear phase low pass matching networks with prescribed parasitic loads 02 p0208 A66-11909

Optimal amplitude frequency and transient process characteristics in linear loops of low pass filter type 02 p0209 A66-12268

Filter techniques for high-speed diode switches designed to suppress troublesome switching transients 06 p0842 A66-15974

Distributed stepped impedance low-pass prototype filter, giving impedance values for filters with Chebyshev equal-ripple characteristics 06 p0844 A66-16082

Band stop filters, discussing insertion loss vs frequency characteristics for large and small dissipation and arbitrary number of resonators 06 p0845 A66-16088

New low-pass filter with attenuation by dissipation, noting reflection and attenuation vs frequency 06 p0846 A66-16098

L-band waffle-iron filter fabrication and modifications for high power characteristics 06 p0847 A66-16100

Circuit network in designing low pass filters with minimum attenuation requirements in stopbands and optimum transient behavior, using Schussler technique and iterative process 07 p1008 A66-17751

Schussler-elliptic low pass filters, discussing solution of approximation problem for low pass filters with good transient response 08 p1198 A66-19748

Seven-stage RL feedback amplifier with 500-mc low-pass bandwidth and 52 db gain, employing frequency compensation technique 11 p1671 A66-23244

Optimal amplitude frequency and transient process characteristics in linear loops of low pass filter type 12 p1848 A66-23872

Dielectric layers of alternating low and high dielectric constant used as filters in millimeter wave, IR and optical regions 12 p1831 A66-23906

Optimum realizable transmitter waveforms for high-speed data transmission, noting application to low pass filter channel 13 p2019 A66-25146

Asymmetrical property of binary pseudorandom noise generators, noting Gaussian probability density function in output of low pass filter 17 p2894 A66-33110

Ideal integrator compared with low pass filters 18 p3076 A66-33835

Pulse-shaping networks with frequency-band limitation, noting approximation of idealized networks with echo equalizers 19 p3306 A66-36656

Low-pass filter characteristics, particularly phase and group delay and magnitude characteristics, considering various network types 21 p3709 A66-38671

Steady state and transient response characteristics of class of low pass filters noting transmission properties, frequency



and time domain considerations, etc 21 p3713 A66-39271  
 Surface effects at interface between linear and nonlinear media representing transmission lines of low pass filter type 22 p3861 A66-39656  
 Low pass elliptic function filter fabricated from RC network and low gain voltage amplifier 23 p4050 A66-41611

## LOW PRESSURE CHAMBER

Growth of ice crystals freely falling in atmosphere and form when produced by cloud element coagulation analyzed, using low pressure chamber 01 p0097 A66-11105  
 Solar simulator with pumping setup to obtain low pressure atmosphere for simulated space environment, noting construction, operation and results 13 p2057 A66-25495  
 Aerospace medical advances in Polish military aviation and pilot testing procedures and equipment, particularly low pressure chamber and centrifuge 14 p2271 A66-28365  
 Low atmospheric pressure and oxygen-rich environment effect on characteristics of uninterrupted long-term exposure to toxic gases of space cabin atmospheres, noting animal testing 16 p2642 A66-30623  
 Man-rating of low-pressure chambers at Crew Systems Division and Structures and Mechanics Division of NASA Manned Spacecraft Center /MSC/ at Houston 19 p3289 A66-35842

## LOW SPEED HANDLING

Aerodynamic characteristics of fixed-geometry double delta wing SST, noting low speed handling improvement due to vortex flow [AIAA PAPER 64-591] 05 p0610 A66-15069  
 F5D-1 aircraft delta wing modification, describing wind tunnel and flight test results with ogive wing 06 p0802 A66-16805  
 VTOL control power requirements under low speed flight conditions for randomly disturbed mechanical system 09 p1330 A66-20736  
 Double-delta supersonic air transport low-speed operational characteristics, noting wind tunnel tests and design parameters 13 p1991 A66-25760  
 Low speed handling with special reference to super stall, emphasizing rate of change of angle of attack and flight trials of BAC 111 and VC10 aircraft 19 p3280 A66-36748

## LOW SPEED STABILITY

Stability and control characteristics of STOL aircraft in low speed landing approach portion of flight regime [AIAA PAPER 65-715] 01 p0013 A66-10952  
 Boundary layer control high lift system for high speed aircraft, using ejector for momentum augmentation and air bleed from propulsion system [AIAA PAPER 64-589] 05 p0610 A66-15070  
 Text on longitudinal static stability of low-speed aircraft including effect on pilot, flight test, pitch maneuverability, etc 14 p2222 A66-26792  
 Stability and control characteristics of STOL aircraft in low speed landing approach portion of flight regime [AIAA PAPER 65-715] 16 p2635 A66-31591

## LOW SPEED WIND TUNNEL

Low speed wind tunnel design and testing including V/STOL aircraft, helicopters, reentry vehicles, etc 20 p3540 A66-37009

## LOW TEMPERATURE ENVIRONMENT

Fluids and elastomers for low temperature heat transfer and hydraulic systems [ASLE PREPRINT 65-LC-7] 02 p0249 A66-12256  
 Microwave emission from InSb, measuring energy generated at low temperatures and intense electric and magnetic fields 07 p1103 A66-18218  
 Commercial fuel cells, noting biochemical, regenerative and low temperature carbon monoxide fuel cell 07 p0996 A66-18476  
 Occurrence of supernumerary fogbows at subfreezing temperatures, noting interval of appearance and possible formation mechanism 09 p1400 A66-20733  
 Low temperature resistivity of yttrium-based alloys containing small amounts of rare earth metals, deriving exchange integrals from resistivity data 09 p1430 A66-20846

Practical Philips cycle for low temperature refrigeration, noting equal coefficient of performance to that of ideal Carnot cycle under isothermal conditions 09 p1472 A66-20879

Combined cryostat/oven and specimen transfer device for tensile testing, noting design, operation and results 11 p1683 A66-22699

Plastic deformation of Charpy specimens under plane stress-strain conditions, noting low temperature brittle fracture behavior, effects of notch geometry and loading, etc 12 p1969 A66-24532

Test program evaluating protective clothing and safety equipment for personnel working in Saturn booster at minus 100 F in oxygen-rich or deficient environment, noting problems with communications, visibility, breathing, etc 12 p1810 A66-24958  
 Fluids and elastomers for low temperature heat transfer and hydraulic systems [ASLE PREPRINT 65-LC-7] 12 p1901 A66-24992

Low temperature transport properties of hydrogen, deuterium and HD, noting quantum phase shift, intermolecular potentials, etc 14 p2414 A66-27973

Resistance anomaly in n-type InSb at very low temperatures, noting experimental results 16 p2768 A66-30140

Laminar boundary layer of low temperature plasma on isolator walls in channel of MHD generator in presence of transverse magnetic field 16 p2758 A66-30327  
 Refrigerated mass spectrometer inlet serving also as low temperature reactor and rough separative device for compounds stable only at very low temperatures 16 p2645 A66-30420

Optical phonon production, showing existence of electric field strength range at low temperature scattering in which phonon emission results in electron stoppage 20 p3577 A66-37376  
 Minimum changes in viscosity of liquid lubricants with temperature, discussing low temperature lubricating oils [ASME PAPER 66-MD-68] 21 p3743 A66-38497

Cryogenic, flame and nuclear radiation temperature effects on pressure transducers, noting zero and sensitivity shifts and thermal gradients 21 p3740 A66-39427

Man rating requirements of space environment simulation laboratory, consisting of two large chambers with floors which can be cooled by liquid nitrogen down to 92 degrees K 22 p3892 A66-40239

High energy density Zn/O battery system, noting good low oxygen pressure and low temperature performance characteristics 23 p4022 A66-41759

Gas chromatography analysis of ambient gas and vapor effects on semiconductor and solid state devices at low temperatures 24 p4179 A66-42095

## LOW TEMPERATURE PHYSICS

### SA CRYOGENICS

Phase diagram from thermodynamic data of complex solution of nitric acid and nitrogen tetraoxide at low temperature 01 p0163 A66-10626

Superconducting critical field curves for tin, indium and mercury below one degree K, with entropy difference linear in temperature for free electron gas 02 p0271 A66-11480

Silver bonded diode for parametric amplifiers improves performance when cooled at liquid nitrogen temperature 02 p0198 A66-11520

Temperature dependent component in low temperature thermoelectric power of doped n-germanium observed in liquid helium region, noting negative magnetoresistance 04 p0570 A66-14369

One- and two-dimensional superconductivity, discussing effect of thermodynamic fluctuations on off-diagonal long-range order 05 p0718 A66-15865

Low temperature alpha radiation and subsequent isothermal recovery effects on electron structure of gold, relating resulting failures to Frenkel defects 07 p1048 A66-17303

Single injection measurements in n-type

silicon at liquid-helium temperatures under transient conditions, using pulse measurements 07 p1107 A66-18414

Anomalies in low temperature properties of noble metal alloys such as thermoelectric power and nonmonotonic behavior of resistivity with temperature 08 p1274 A66-19362

Book on theory and measuring techniques for electrical resistance of metals at low temperatures and cryogenics 09 p1388 A66-19976

Low temperature physics - International Conference, Columbus, Ohio, August-September 1964 09 p1413 A66-20004

Effect of static magnetic field on millimeter wave absorption in superconducting aluminum at reduced temperature 09 p1416 A66-20025

Low temperature physics LT9 - International Conference, Columbus, Ohio, August 1964 09 p1424 A66-20075

Thermoelectric power of actual ferromagnetic metals over wide temperature range, examining effect of alloying and solute magnetic ions 09 p1425 A66-20080

Low temperature chromatographic separation of hydrogen isotopes based on interaction with alumina surface electric fields 11 p1650 A66-23209

Low temperature techniques in satellite communications systems, noting maser, cooled parametric amplifier and trend toward closed-cycle refrigerators 13 p2042 A66-26104

Effect of temperature on cyclic minimum creep rate and other phenomena associated with cycle dependent deformation from 77.4 to 295 degrees K [ASME PAPER 66-MET-7] 14 p2395 A66-26975

Text on experimental low temperature physics covering experimental techniques, liquid helium, superconductivity and electronic properties in metals 15 p2566 A66-29320

Heat capacity of high purity beryllium measured at temperatures below 30 degrees K 16 p2775 A66-30727

Thermal ionization for low temperature plasma confined in magnetic field, examining magnetic field effect on ionization 16 p2762 A66-31166

Textbook on specific heats at low temperatures, including electronic, magnetic and lattice contributions of solids, gases and liquids, calorimetry, refrigeration, internal energy, etc 16 p2748 A66-31313

Thermal expansion and electrical resistivity measurements below 400 degrees K on niobium and two niobium alloys containing tungsten 16 p2725 A66-31454

Inverse Compton X-ray and gamma ray flux due to high energy electron interaction with cosmic blackbody radiation at 3.5 degrees K 17 p2992 A66-31914

Elementary processes in low-temperature plasma 18 p3143 A66-34029

Quantum corrections to second virial coefficient for low-temperature gas 21 p3836 A66-39175

Book on low temperature techniques and common cryogenic systems 24 p4238 A66-43161

## LOW THRUST PROPULSION

Optimum guidance in two dimensions of constant acceleration low-thrust vehicle spiraling away from and in toward planet 01 p0100 A66-10026

Perturbation solutions of differential equations of motion for low-thrust rocket trajectories 02 p0288 A66-11546

Low thrust spiral trajectory of satellite of variable mass 02 p0288 A66-11551

Linear theory of optimum variable thrust rendezvous trajectories with power limit propulsion system 04 p0575 A66-13457

Fehlberg integration method used to calculate optimum interplanetary transfer orbits at low thrust acceleration 04 p0576 A66-13527

Optimum guidance in two dimensions of constant acceleration low-thrust vehicle spiraling away from and in toward planet 14 p2328 A66-27419

Recovery of interplanetary vehicles by low thrust braking outside atmosphere 14 p2391 A66-27472



Low-thrust engine spacecraft control during boost phase, independent of velocity vector determination, by stabilizing osculating orbit plane relative to planetocentric coordinate system 15 p2534 A66-28490

Low thrust space flight mechanics and optimal control of low thrust engine spacecraft 15 p2596 A66-29157

Matching planetocentric and heliocentric low-acceleration trajectories in analysis of propulsion system 15 p2598 A66-29297

Trajectory energy requirements for low-thrust flights throughout solar system using nuclear-electric propulsion [AIAA PAPER 66-497] 16 p2805 A66-31495

Bibliography of programmed low-thrust trajectories and optimal low-thrust trajectories 17 p3001 A66-32350

Low-power electric propulsion systems characteristics and design [AIAA PAPER 66-578] 18 p3165 A66-34445

Microrocket technology utilizing solid, liquid and gaseous propellants for spacecraft control, including performance measurement techniques [AIAA PAPER 65-620] 20 p3629 A66-38149

Asymptotic solution for optimum power-limited orbit transfer 21 p3811 A66-38736

Low-thrust rockets for spacecraft attitude control, noting subliming solid rockets 21 p3807 A66-38800

Optimum parameters for low-thrust propulsion system with energy storage for specific maneuver 21 p3808 A66-38974

**LOWER ATMOSPHERE**

Simultaneous lower atmosphere observations with radar and aerological measurements by airborne meteorograph and electrometeorograph 02 p0253 A66-11273

Vertical profile of refractive index in lower atmospheric layer measured by modified A-22-IV radio probe on captive balloon 02 p0253 A66-11274

Vertical and horizontal turbulent diffusion in lower atmospheric layer as two-layer problem 04 p0513 A66-13442

Electrical effect of large meteorite moving in lower atmosphere 04 p0577 A66-13846

Spectra of vertical turbulent thermal fluxes and momenta in lower atmospheric layer, including review of relevant literature sources 09 p1398 A66-19893

Lower atmospheric density measurements through light scattering from Q-spoiled ruby laser beam, using optical radar detector 09 p1373 A66-20398

IGY and IGC data on atmospheric washout of radioactive fission products by precipitation 14 p2376 A66-27540

Air-temperature and wind profiles in atmospheric boundary layer and dependence upon stability criteria of ground layer 16 p2741 A66-30772

Wind velocity spectra and correlation functions statistically analyzed in ULF range for lowest levels of atmosphere 16 p2742 A66-30773

Lower atmospheric diurnal variations in air temperature, directional wind velocity and gradients during clear anticyclonic weather 16 p2742 A66-30774

Cosmic ray neutron flux as function of altitude measured near Earth surface, using boron trifluoride detectors 17 p2992 A66-31974

Solar radiation control for changing meteorological conditions in lower atmospheric layer 20 p3594 A66-38373

**LOWER IONOSPHERE**

Time dependency effect on effective recombination coefficient in lower ionosphere 02 p0223 A66-12115

Book on lower ionosphere physics noting radio wave propagation, ionospheric currents, solar radiation and flares, ion kinetics, electron collision frequencies, etc 04 p0515 A66-13835

Lower ionospheric wind effect on geomagnetic field variation 05 p0668 A66-14935

Lower ionospheric characteristics determined by VLF radio waves propagated over long distances by multiple reflections between Earth and D region 09 p1370 A66-19973

Excitation, internal reflection and limiting

polarization of whistler waves in lower ionosphere, establishing reciprocity relation between incident waves from above and below 11 p1651 A66-22369

Anomalous ionization of lower ionosphere at medium latitudes during worldwide geomagnetic storm result in increased radio wave absorption in ionosphere 11 p1696 A66-22416

Lower ionosphere ionization for quiet and disturbed Sun calculated for comparison of experimental and theoretical values for electron concentration and effective recombination 11 p1696 A66-22417

Time dependency effect on effective recombination coefficient in lower ionosphere 14 p2286 A66-28074

Vertical drift of charged particles effect on electron density profile as cause of seasonal variations in ionospheric absorption 15 p2490 A66-29944

Macroscopic equations describing effect of negative ions on diffusion of electrons and positive ions in lower ionosphere 17 p2917 A66-32255

Nitric oxide distribution in lower ionosphere calculated from reaction coefficients and mass spectrometric measurements of density 17 p2922 A66-33354

Meteorite atomic ions in lower ionosphere 17 p2922 A66-33355

Partial reflections utilizing different amplitudes of ordinary and extraordinary backscattered waves for electron number densities and collision frequency measurement in lowest ionosphere 22 p3906 A66-39949

Computer calculations from Sen-Wyller expression for specific absorption of radio wave in lower ionosphere 22 p3906 A66-39954

Long VLF path propagation measurements, determining characteristics of lower ionosphere, noting role of phase and amplitude variations during solar flares 22 p3907 A66-39959

Effective recombination coefficient in lower ionosphere, deriving expression for dependence of dissociative recombination on temperature and solar distance 24 p4201 A66-42758

**LOX**

**S LIQUID OXYGEN /LOX/**

**LOX-HYDROGEN ENGINE**

Reliability design concepts in cryogenic fluid systems in Saturn S-IV stage propulsion system, noting hydrogen and LOX tank pressurization systems 01 p0129 A66-10079

Applicability of liquid hydrogen-oxygen technology to development of European launch vehicles 02 p0295 A66-11671

Base thermal environment measured on flight tests of eight-engine LOX/RP-1 propelled Saturn I booster [AIAA PAPER 65-212] 14 p2391 A66-27873

**LRV**

**S LUNAR ROVING VEHICLE /LRV/**

**LUBRICANT**

SA GAS LUBRICANT

SA GRAPHITE

SA GREASE

SA HIGH TEMPERATURE LUBRICANT

SA OIL

SA SOLID LUBRICANT

Sliding friction tests at ultrahigh load of eight greases and 18 dry lubricants and various base materials [ASLE PREPRINT 65-LC-23] 02 p0237 A66-12249

Materials for use as rolling-contact bearing lubricants in liquid hydrogen environment [ASLE PREPRINT 65-LC-9] 02 p0238 A66-12255

Physical properties of new class of lubricants, methyl alkyl silicones, illustrating exceptional lubricating ability [ASLE PREPRINT 65-LC-4] 02 p0238 A66-12261

Fuels and lubricants with thermally stable molecular structure and antioxidants to meet requirements of supersonic transport 03 p0414 A66-13221

Density and viscosity changes of lubricants in contact due to pressure changes in concentrated-contact lubrication [ASME PAPER 65-LUB-4] 04 p0527 A66-14240

Partial porous metal bearings performance

during steady state operation with full film of lubricant, determining pressure distribution [ASME PAPER 65-WA/LUB-3] 05 p0689 A66-15526

Lubricant effect on fatigue life of stationary ball on flat contact subjected to oscillatory normal load [ASME PAPER 65-WA/CF-3] 05 p0690 A66-15622

Gold thin films of 1800 angstroms to be used as lubricants were vapor-deposited on Ni, Ni-Cr and Ni-Re substrates in vacuum 06 p0884 A66-15937

Aircraft turbine lubricant technology for high Mach number engines especially SST, noting stability, autoignition, coking, toxicity, etc [SAE PAPER 660071] 09 p1434 A66-20156

Means of assessing aviation turbine lubricant quality, considering specification, maintenance, operational factor and equipment strip approach [SAE PAPER 660074] 09 p1434 A66-20159

Solid and dry-film lubricants, tabulating kinetic coefficients of friction, noting particle size, viscosity, costs, wear life, application, etc 12 p1885 A66-24099

Physical properties of new class of lubricants, methyl alkyl silicones, illustrating exceptional lubricating ability [ASLE PREPRINT 65-LC-4] 12 p1889 A66-24989

Structural changes in metal surface layers under boundary friction conditions in presence of surface active lubricant additives 13 p2086 A66-25884

Nonstructural materials for space utilization including lubricants, sliding electrical contacts and dielectrics 14 p2319 A66-28006

Metal flow, friction and lubricant performance during stamping of thin titanium alloy blanks 14 p2304 A66-28202

Thermal stability, adhesion prevention, stress and die wear reduction and air pollution of industrial lubricants 14 p2304 A66-28207

Grease lubricants for aerospace application, determining physical properties and testing them at 400 degrees F and under high vacuum [ASLE PAPER 66AM 3C2] 16 p2711 A66-30409

Lubricant selection for lunar missions and manned spacecraft based on compatibility with oxygen-rich environment, propellant, anodic coatings and sliding friction behavior in vacuum [ASLE PAPER 66AM 7A2] 16 p2712 A66-30415

Sliding friction tests at ultrahigh load of eight greases and 18 dry lubricants and various base materials [ASLE PREPRINT 65-LC-23] 16 p2713 A66-30571

Differential thermal analysis for study of thermal decomposition of organic lubricant system 17 p2928 A66-31899

Vapor deposited gold thin films to obtain adhesion and durability between film and substrate essential as lubricants in high vacuum 17 p2929 A66-31979

Operating lifetime of porous bearings, discussing dependence on quality of impregnating lubricant 17 p2930 A66-33143

**LUBRICATING OIL**

Laboratory, component and engine tests for lubricant properties of J-79 jet engine including elastomer volume swell, oxidation-corrosion, lubricity, etc [SAE PAPER 650816] 01 p0078 A66-10821

Disengaging gear lubrication through heat dissipation as factor in Ryder rating of rocket lubricant [ASLE PREPRINT 65-LC-16] 02 p0237 A66-12253

Polyolefin fluids with wide viscosity range compared with petroleum oils and existing synthetic lubricants for extreme temperature application [ASLE PREPRINT 65-LC-1] 02 p0238 A66-12259

Lubricant film thickness in elastohydrodynamic range measured as function of speed in rolling configuration for mineral oils and esters 07 p1040 A66-18292



High activity of alkali metal salts of carboxylic acids and substituted phenols as synergists for arylamine antioxidants in ester-type synthetic lubricating oils 11 p1711 A66-23123

Simulation of lubricating oil circulation in aviation turbine engines by constructed model, noting change of viscosity, acid number and electrical conductivity at high temperatures 12 p1803 A66-23751

Constant oil monitoring system using electric conductivity tester for extending oil life in gas turbine engines [SAE PAPER 650814] 12 p1935 A66-23844

Vacuum effects on lubricants and bearing materials due to reduced ambient pressure and low concentration of oxidizing gases 12 p1885 A66-24383

Polyolefin fluids with wide viscosity range compared with petroleum oils and existing synthetic lubricants for extreme temperature application [ASLE PREPRINT 65-LC-1] 12 p1888 A66-24986

Oil cushion resilience in hydrodynamic bearings, examining effect on dynamic behavior of unsymmetrical shaft with one disk 12 p1889 A66-24999

Friction and lubrication of polymers 13 p2087 A66-26304

Lubrication parameters with respect to experimental values and reproducibility 14 p2305 A66-28465

Jet oil lubrication and scavenging technique for 20 mm high speed ball bearing [ASLE PAPER 66AM 1B4] 16 p2710 A66-30402

Ball bearing life operating in vacuum with molybdenum disulfide and oils as lubricant [ASLE PAPER 66AM 7A3] 16 p2712 A66-30416

Disengaging gear lubrication through heat dissipation as factor in Ryder rating of rocket lubricant [ASLE PREPRINT 65-LC-16] 16 p2713 A66-30574

Detection and causes of fretting corrosion, discussing prevention via lubrication, effects of load, surface finish, material hardness, friction coefficient, vibration, etc 18 p3117 A66-34400

Spectrometric oil analysis for assessing failure probability of turbojet-engine oil-wetted parts 19 p3355 A66-35524

Additives effect on antioxidant stability and antiabrasion characteristics of lubricating oils used in jet and turboprop engines 20 p3575 A66-38445

Minimum changes in viscosity of liquid lubricants with temperature, discussing low temperature lubricating oils [ASME PAPER 66-MD-68] 21 p3743 A66-38497

Jet oil lubrication and scavenging technique for 20 mm high speed ball bearing [ASLE PAPER 66AM 1B4] 22 p3928 A66-40657

**LUBRICATION**

SA BOUNDARY LUBRICATION

SA SELF-LUBRICATING MATERIAL

SA SPACE ENVIRONMENTAL LUBRICATION

SA SPACECRAFT MECHANISM LUBRICATION

Gas-lubricated bearing equations derived that are valid for wide range of temperature and Mach numbers 04 p0526 A66-14156

Microirregularity lubrication to improve reliability of liquid lubricated rotary shaft face seal [ASME PAPER 65-LUB-11] 04 p0527 A66-14244

Prandtl mixing-length theory used to predict performance of journal bearings operating in turbulent regime [ASME PAPER 65-LUB-17] 04 p0528 A66-14249

Aircraft turbine engine oil drain practices, discussing engine design and materials and minimum and maximum drain time [SAE PAPER 660073] 09 p1434 A66-20158

Pressure distribution of viscous electrically conducting fluid in lubricating layer of cylindrical bearing 12 p1887 A66-24425

Microirregularity lubrication to improve reliability of liquid lubricated rotary shaft

face seal [ASME PAPER 65-LUB-11] 12 p1888 A66-24550

Liquid solid film lubrication of hydrodynamic bearings, including effects of solid particles in liquid base lubricant [ASLE PAPER 66AM 5DE] 16 p2711 A66-30412

Gyroscopic rotor vibrations excited by effect of lubrication layer in sliding bearings and stabilized with intervening elastodamping supports, taking into account moment of inertia of rotor 17 p3027 A66-32605

Steady-state and dynamic characteristics of full circular bearing and centrally loaded arc bearing presented in design charts for turbulent lubrication analysis [ASME PAPER 66-LUBS-4] 17 p2931 A66-33178

MHD lubrication flow in thrust bearing, noting fluid inertia effect on load capacity and flow rate [ASME PAPER 66-LUBS-8] 17 p2931 A66-33181

Surface roughness effects in hydromagnetically lubricated externally pressurized bearings and hydromagnetic squeeze film between two circular plates [ASME PAPER 66-LUBS-9] 17 p2931 A66-33182

Split-inner-race ball bearings design for use as thrust bearings on aircraft gas turbines [ASME PAPER 66-LUBS-10] 17 p2931 A66-33183

Turbulent hydrodynamic lubrication theories and solution of Constantinescu equation for finite-length journal bearing [ASME PAPER 66-LUBS-11] 17 p2931 A66-33184

Eigenvalues and eigenvectors obtained by numerical solution of special Hill equation in lubrication theory [ASME PAPER 66-LUBS-13] 17 p2932 A66-33185

Performance of hydrodynamic, hydrostatic or hybrid bearings determined by numerical solution of Reynolds lubrication equation for incompressible fluid films [ASME PAPER 66-LUBS-4] 17 p2932 A66-33186

Aircraft turbine engine oil drain practices, discussing engine design and materials and minimum and maximum drain time [SAE PAPER 660073] 20 p3628 A66-37255

Lubrication review, 1964 24 p4217 A66-42579

**LUBRICATION SYSTEM**

Process fluid lubrication of system bearings 01 p0079 A66-10867

Mercury lubricated hybrid bearings for lubrication requirements of mercury Rankine Silent Compact Auxiliary Power /SCAP/ system [ASLE PREPRINT 65AM 3A3] 07 p1039 A66-18288

Friction stresses in turbulent lubrication film and dependence on Reynolds number and pressure distribution studied, using mixing-length hypothesis [ASLE PREPRINT 65AM 3A1] 07 p1039 A66-18289

Pressure distribution, surface temperature and deformation profile in conjunctive region of lubricated cylindrical disks rolling or sliding on their peripheral surfaces [ASLE PREPRINT 65AM 4A3] 07 p1039 A66-18290

Thermal elastohydrodynamic lubrication of rolling and sliding cylinders, noting correlation with film thickness and friction experimental data [ASLE PREPRINT 65AM 4A2] 07 p1040 A66-18291

High temperature bearing lubricant requirements for jet engine lubrication systems [SAE PAPER 660072] 09 p1383 A66-20157

Cermet face seals for inert gas environment sealing shaft of liquid-metal pumps employing conventional lubrication system [ASLE PREPRINT 65AM 4C4] 10 p1540 A66-22039

Operation, maintenance and installation of friction and nonfriction bearings, noting characteristics, problems, etc 11 p1711 A66-22951

Experimental friction and lubrication system parameters including load coefficient, oil volume, friction coefficient and bearing temperature characteristics, in mathematical terms 15 p2505 A66-28523

Wear and grease lubrication effects in matched aircraft spline specimens subjected to oscillatory motion 16 p2713 A66-30572

Spherical squeeze-film hybrid bearing with small steady-state radial displacement treated by perturbation method [ASME PAPER 66-LUBS-5] 17 p2931 A66-33179

**LUBRICATION TESTING MACHINE**

Lubricant testing for supersonic aircraft, examining temperature requirements, viscosity, evaporation characteristics, etc 10 p1539 A66-21399

Four-ball wear tester to evaluate solid lubricant dispersions including molybdenum disulfide 14 p2302 A66-27774

Lubricant testing system optimizing with respect to machine ability and cost [ASLE PAPER 66AM 5D2] 16 p2711 A66-30411

Measuring wear life and friction coefficient of dry film and solid film lubricants and plastic materials in ultrahigh vacuum 22 p3923 A66-40216

**LUCITE**

Gauge, using spherical Lucite shell as active element for measuring peak pressures in strong shock waves, designed for underground nuclear explosion 13 p2083 A66-26557

**LUMINESCENCE**

SA CHEMILUMINESCENCE

SA ELECTROLUMINESCENCE

SA FLUORESCENCE

SA LIGHT

SA LUNAR LUMINESCENCE

SA PHOSPHORESCENCE

SA PHOTOLUMINESCENCE

SA THERMOLUMINESCENCE

Cathode ray tube measurements indicate that noise in cathodoluminescence is mainly caused by shot noise of primary beam 02 p0206 A66-12161

Rare earth chelates preparation, luminescence behavior and laser action 05 p0741 A66-15833

Injection luminescence in InAs diodes 07 p1094 A66-17315

Phonon series in cadmium sulfide single crystal emissions at low temperature range 10 p1583 A66-22025

Sensitized and unsensitized phosphorescence and energy transfer properties of series of aliphatic alpha diketones in fluid solution 12 p1916 A66-23620

Laser-generation-type luminescence CdS-CdSe crystals exposed to double photon excitation from ruby laser 14 p2308 A66-27647

Meteor luminescence during atmospheric motion, obtaining radiation coefficient as function of cross sections of particle excitation and pulse transfer processes 15 p2596 A66-29143

Relation between nonlinear luminescence quenching and concentration of luminescence centers in laser crystal 15 p2515 A66-29204

Absorption, excitation, and emission spectra of TI-activated NaI single crystals at liquid helium temperatures 15 p2566 A66-29347

Physics of luminescent ionic crystal - Conference, Lvov, Ukrainian SSR, January-February 1964 15 p2568 A66-29728

Phonon series in cadmium sulfide single crystal emissions at low temperature range 16 p2776 A66-30844

Red and blue flashes in silicate luminescence excited by low-energy proton and lunar reddening by solar-ion excitation 16 p2802 A66-30930

Relation between nonlinear luminescence quenching and concentration of luminescence centers in laser crystal 17 p2936 A66-33053

Spectral distribution of ruby luminescence yield, noting absorption coefficient and excitation band 17 p2938 A66-33509

Quantitative analysis of transient luminous phenomena on lunar surface and relation to solar electromagnetic or corpuscular



excitations 19 p3457 A66-35446  
 Terrestrial aureole structure in daylight, twilight and night and explanation for luminous particles observed in wake of Voskhod spacecraft 19 p3347 A66-35646  
 Organic laser systems including luminescence for achieving laser action, fluorescent and phosphorescent systems and chemistry and spectroscopic properties of rare earth chelates 20 p3576 A66-36970  
 Absorption, excitation, and emission spectra of TI-activated NaI single crystals at liquid helium temperatures 20 p3615 A66-37352  
 Photoconductive and luminescent behavior of undoped cadmium sulfide single crystals at room temperature under laser excitation 21 p3748 A66-39165  
 MHD analysis of luminescence and widening of tail of Finsler 1937 V Comet passing through solar corpuscular stream containing frozen-in magnetic field 21 p3814 A66-39277  
 Stimulated emission, absorption spectra and luminescence of neodymium-activated YAG crystals in pulsed laser 21 p3748 A66-39306  
 Silicon dioxide complexes and deposition of excess oxygen at dislocations and structural defects, examining creation of microplasma breakdown of silicon p-n junctions 22 p3965 A66-40320  
 Spectral distribution of ruby luminescence yield, noting absorption coefficient and excitation band 24 p4249 A66-42123  
 Luminescence spectra of meteorites of different classes using proton excitation, giving estimates of radiation conversion efficiency 24 p4273 A66-42363  
 Radiation of giant pulses of superluminescence by highly excited active medium of Nd glass with rapid cut-in of amplification 24 p4224 A66-42755

**LUMINESCENT INTENSITY**  
**SA LIGHT INTENSITY**  
 Short period fluctuations in intensity of auroral luminescence and relation to geomagnetic fluctuations 01 p0065 A66-11166  
 Sudden decrease in brightness of Encke comet in 1964 07 p1134 A66-17520  
 Anodic luminescence in electrochemical oxidation of silicon crystal 09 p1410 A66-19897  
 Possible luminescence effects on Mercury 12 p1945 A66-23558  
 Space correlation of main emission lines for night sky emission spectra and altitude distribution of sodium luminescence 15 p2495 A66-30060  
 Spectrographic investigation of luminescence of carbon monoxide and dioxide excited by collisions with accelerated ions 17 p2961 A66-33403  
 Rapid secular decrease in absolute brightness and commensurability effects with mean motion of Jupiter studied in evolution of short periodic comets 17 p3013 A66-33407  
 Secular brightness changes in periodic comets and relation to solar activity 17 p3013 A66-33408  
 Luminescent surfaces and structures for information display, discussing cathode ray tube, image intensifier for night vision, spectral emission, etc 19 p3312 A66-35338  
 Minerals responsible for thermoluminescence of meteorites identified and radiation age derived 19 p3465 A66-36386  
 Intensity measurements on molecular oxygen Herzberg I system emitting in afterglow of microwave discharge, noting dependence of transition moment on internuclear distance 20 p3555 A66-38208  
 Scattering and transformation of electromagnetic waves during critical fluctuations in nonequilibrium plasma 21 p3789 A66-39065  
 Air flow luminescence front propagation in electromagnetic shock tube measured, using phase synchronized high-speed photography 21 p3790 A66-39080  
 Single crystal wurtzite CdS luminescence as function of exciting intensity, noting shift of overlapping band structure of green-edge emission indicative of electron-hole recombination 24 p4219 A66-42250

**LUMINOSITY**  
**SA STELLAR LUMINOSITY**

Luminosity distribution of radio galaxies in terms of flux density 02 p0292 A66-12189  
 Aircraft illumination utilizing electroluminescent panels 11 p1640 A66-22666  
 Fast auroral waves differ from flaming aurora in which waves of luminosity appear to converge toward magnetic zenith 15 p2484 A66-28820  
 Intergalactic photon density estimated based on luminosity function of galaxies 18 p3186 A66-34812  
 Observed regularities of contrast characteristics of human visual system in photopic luminance region examined by psychophysics of response/stimulus peak-to-peak measurements of spatial sine wave patterns 21 p3700 A66-39129

**LUMINOUS INTENSITY**  
 Space shift between electron density and luminous intensity of plasma in stationary striation by microwave resonator 03 p0372 A66-13282  
 Visibility conditions for fibrous structure of auroral arcs and bands 04 p0516 A66-13863  
 Appearance frequency and brightness distribution of band and other auroral forms 04 p0516 A66-13864  
 Sky scanner to record luminance distribution over entire sky vault 06 p0883 A66-16948  
 Mount Bezovec meteor expedition /1961/ observations on luminosity function of visual Persels and sporadic meteors 07 p1135 A66-17634  
 Isophotometric representation of solar corona, using photographs of equal density 07 p1136 A66-17735  
 Validity of Kirchhoff law for apparent local spectral emittance and absorbance and total flux calculations for spacecraft cavities [AIAA PAPER 65-135] 08 p1316 A66-18793  
 Radial inhomogeneity, temperature dependence and ion and atom concentration of growing luminous cloud from arc discharge 08 p1266 A66-19771  
 Faraday effect method for measuring magnetic fields of extremely short duration and device for observing slightly luminous phenomena 14 p2290 A66-26824  
 Sky luminance distribution for upper and lower sky at various levels 15 p2484 A66-28831  
 Solar eclipse coronal isotopes, noting spectrum in region of maximum visual sensitivity, ellipticity figures, Ludendorff coefficient, luminosity gradients, etc 15 p2593 A66-28867  
 Nonlinear diffusion equations in electron beam excited plasma noting two- and three-body recombination, radial distribution of electron density, light intensity, etc 15 p2555 A66-29761  
 Spectroscopic data from argon and nitrogen supersonic plasma jets, noting line width, intensity, temperature, etc 16 p2763 A66-31189  
 Velocity dependence of meteor luminous efficiency evaluated, using statistical analysis [AIAA PAPER 66-515] 16 p2805 A66-31482  
 Galactic evolution examined, using luminosity and volume emissivity diagrams 18 p3178 A66-34760  
 Solar altitude relationship to scene luminance for aerial photographs determined by photographic photometry 19 p3358 A66-35816  
 Pinhole photometric observation of umbra intensity profiles of large sunspot 21 p3808 A66-38469  
 Electric field domain motion in Ge samples with Au and Sb impurities, noting temperature and illumination effect on V-I characteristics 22 p3964 A66-40312  
 Image intensifier application as aid to visual acquisition of weak luminous moving targets against night sky 23 p4071 A66-41676  
 Height-luminosity distribution of auroral hydrogen beta emission measured with rocket mounted photometer 23 p4065 A66-41690

**LUNAR ATMOSPHERE**  
 Lunar atmosphere and hydrosphere, predicting dimensional correlation for craters and maria of primordial lunar life, noting dark and smooth appearance 02 p0181 A66-11606  
 Shear strength of idealized granular media

in vacuum, in conditions simulating environmental pressure of lunar surface layer 14 p2288 A66-28180  
 Lunar magnetosphere, Moon-solar wind interaction, X-ray flux measurement and possible hazards to astronauts 18 p3231 A66-34357  
 IMP satellite data on lunar magnetospheric MHD wake and interaction with solar wind 18 p3231 A66-34358  
 Solar wind disturbance detected by ground facility and Explorer XVIII while behind Moon 22 p3983 A66-40562

**LUNAR BASE**  
 Manufacture of propellants by aerogel carbothermal process involving reduction of silicates with methane and/or carbon [SAE PAPER 650835] 01 p0053 A66-10831  
 Nuclear lunar base power plant based on SNAP-8 components 13 p2004 A66-26606  
 Lunar base nuclear power plant and communications and command requirements, noting alternative power source 16 p2649 A66-30537  
 Lunar Exploration System for Apollo /LESA/, discussing life support, power, fuel, communications systems, mission objectives and base evolution concept phases [SAE PAPER 660449] 18 p3093 A66-33895  
 Meteorological observations of Earth from lunar surface 19 p3455 A66-35286

**LUNAR CINEMATOGRAPHY**  
 Lunar facsimile camera, noting large angular field coverage and electromechanical scanning system with optically narrow instantaneous field 19 p3356 A66-35675

**LUNAR COMMUNICATION**  
 Spacecraft and ground equipment design of lunar orbiter telecommunications system 04 p0477 A66-13580  
 S-band tracking and communication system to connect 15 ground stations with large parabolic antennas and Apollo command module and lunar excursion module 07 p1018 A66-18391  
 Lunar communication satellites, discussing satellite relay, librational, random, and synchronous satellite design, lunar orbits, etc [AIAA PAPER 66-315] 12 p1823 A66-24781  
 Design of Apollo project lunar-based telemetry system for transmitting experiment data to Earth for one year 19 p3300 A66-35671

**LUNAR COMPOSITION**  
 Role of solar furnaces in production of water on Moon [ASME PAPER 65-WA/SOL-2] 05 p0661 A66-15633  
 Surface of Moon composed of solid material with different physical properties from terrestrial rock 09 p1453 A66-20173  
 Bronzite and hypersthene chondrites, evaluating lunar or asteroidal origin 12 p1948 A66-23903  
 Tekites, approximate age and probable lunar origin 14 p2383 A66-27823  
 Rapid remote sensing method using IR spectrum matching for determining material composition from both terrestrial and extraterrestrial sources 18 p3111 A66-34013  
 Chemical reactor on-site manufacture of propellant oxygen from metallic silicates found on Moon [AICE PREPRINT 46C] 22 p3977 A66-39895

**LUNAR CRATER**  
 Age of craters and relative rate of formation on Mars and Moon 01 p0136 A66-10438  
 Catalog of all craters in third lunar quadrant recognizable on photographs and having diameter greater than 3.5 km 02 p0286 A66-11465  
 Volcanic sublimates and secondary impact craters of Llamana Volcano, Hawaii, with reference to lunar craters 02 p0288 A66-11500  
 Lunar crater-diameter-depth relationship from Ranger VII photographs in excellent accord with terrestrial impact crater parameters 02 p0291 A66-12186  
 Inapplicability of Baldwin relation for determining causes of lunar crater formation 05 p0764 A66-15332  
 Origin and nature of three structures in 235-mi diameter lunar crater photographed by Ranger VII 07 p1133 A66-17456



Structural analysis of lunar crater  
Alphonsus, using Ranger IX  
photographs 09 p1455 A66-20397  
Lunar dust depth in Mare Cognitum  
determined by comparing Ranger VII  
photographs with laboratory crater  
photographs 11 p1770 A66-22571  
Origin of lunar craters from statistical  
analysis of distribution over lunar surface,  
reviewing Fleder theory 12 p1949 A66-24033  
Comparison of cratering on Earth and  
Moon, resulting from high velocity impact of  
solid objects upon planetary  
masses 12 p1949 A66-24199  
Baldwin formula for diameter and depth of  
lunar ring mountains and craters in sea of  
clouds, noting Ranger VII  
photos 14 p2379 A66-27182  
Circularity index of lunar craters indicate  
two populations as shown by frequency  
distribution curve 15 p2597 A66-29257  
Number density of all observable lunar  
craters as function of diameter and of time,  
examining meteoroidal impact  
hypothesis 15 p2598 A66-29262  
Lunar crater filling by dust or lava in  
stochastic model based on impact  
formation 15 p2598 A66-29263  
Statistical test of randomness applied to  
lunar crater data, noting distribution and  
density 15 p2598 A66-29264  
Frequency distribution of secondary lunar  
craters determined from Ranger VII  
photographs, hypothesizing that part of  
these depressions are subsidence  
formations 15 p2598 A66-29265  
Inapplicability of Baldwin relation for  
determining causes of lunar crater  
formation 15 p2603 A66-29974  
Volcanic origin of lunar and Martian  
craters, noting distribution, diameters,  
etc 18 p3225 A66-33625  
Similarity in frequency distribution of  
Martian and lunar craters with terrestrial  
volcanic craters 18 p3226 A66-33626  
Randomness tests of lunar crater  
distribution based on data from relatively  
small regions or most recent craters, results  
indicate internal origin 18 p3233 A66-34573  
Geographic and topography features of  
lunar crater Caramuel based on 1965  
photographs 18 p3239 A66-35245  
Peculiarities of dispersion of matter  
resulting from meteorite impact on lunar  
surface as explanation of concentric nature  
of structure of crater 19 p3455 A66-35284  
Ranger VII, VIII and IX lunar probes  
scientific results on texture of maria, crater  
rays, crater classification, mare ridges, rilles,  
lineaments and bearing strength of mare  
floor 19 p3457 A66-35441  
Terrestrial calderas, defined as basins of  
subsidence larger than volcanic craters,  
associated pyroclastic deposits and possible  
lunar application 19 p3458 A66-35450  
Softened appearance of certain large lunar  
craters explained by ash flow  
theory 19 p3458 A66-35451  
Early lunar cratering, circumterrestrial  
swarm as hypothetical origin of  
planetesimals 20 p3655 A66-38026  
Volcanic vs meteoritic origin of lunar  
craters, discussing survival advantages in  
lunar landing 22 p3980 A66-40398  
Baldwin formula for diameter and depth of  
lunar ring mountains and craters in sea of  
clouds, noting Ranger VII  
photos 24 p4279 A66-42722  
Impact theory of crater formation on  
surfaces of Moon and Mars not as consistent  
with evidence as endogenous cratering  
theory 24 p4280 A66-43028  
**LUNAR CRUST**  
Moon shape related to distribution of  
continents and maria and relationship  
between shape and inertia  
moments 10 p1605 A66-21203  
Note on paper discussing lunar shape and  
internal structure in connection with  
inhomogeneity of density distribution,  
showing incompatibility of hypothesis with  
measurements 10 p1605 A66-21210  
Thermal conductivity equation solved for  
four combinations of concentration of  
radioactive elements in lunar crust, using  
result for crust thickness  
estimate 20 p3648 A66-37151

**LUNAR DISK**  
Lunar profiles determined from  
photographs of annular solar eclipses of 1962  
and 1963 20 p3655 A66-38021  
**LUNAR DUST**  
Lunar dust layer with protons in solar  
wind displacing atoms in grains, thus  
sintering dust through diffusion into porous  
structure 03 p0429 A66-13338  
Depth of lunar dust estimated by  
comparison with laboratory craters overlain  
by various thicknesses of sand, including  
Ranger VII photographs 06 p0955 A66-16783  
Strength of overlay of granular material on  
Moon estimated from Ranger VII  
photographs, showing fairly steep slopes  
covered with dust 06 p0955 A66-16784  
Lunar dust depth in Mare Cognitum  
determined by comparing Ranger VII  
photographs with laboratory crater  
photographs 11 p1770 A66-22571  
Structure and coherency of lunar dust  
layer, considering corpuscular radiation such  
as solar wind and meteorite  
bombardment 12 p1952 A66-24892  
Dust layers on lunar  
maria 23 p4128 A66-41309  
**LUNAR ECHO**  
Radio communication between U.S.S.R. and  
Great Britain via passive Earth satellite  
Echo II and Moon signal  
reflection 07 p1001 A66-17345  
Combined Faraday polarization and Doppler  
frequency measurements of lunar radar  
echoes of Earth magnetospheric  
wake 08 p1296 A66-19401  
Multifrequency radar as remote sensor for  
exploration of Earth and Moon surfaces,  
examining variation of backscattering with  
change in wavelength 09 p1341 A66-19868  
Relationship between geometric optic and  
autocorrelation approach to lunar and  
planetary radar echoes for Gaussian  
autocorrelation function 09 p1341 A66-19870  
Lunar radar scattering behavior indicates  
wide range of structure sizes on  
Moon 09 p1452 A66-20124  
Total radar cross section of Moon has  
much larger value in decimeter region than  
at shorter wavelengths 09 p1452 A66-20125  
Radar scattering maps of Moon created by  
delay-frequency analysis of lunar radar  
echo 09 p1452 A66-20126  
Angular dependence of mean power  
backscattered from Moon and Venus  
indicates greater smoothness of Venus  
surface 09 p1452 A66-20127  
Radio reflectivity measurements have  
provided more data on lunar surface than  
radar observation 09 p1452 A66-20128  
Radar cross polarization measurements for  
target surface property determination,  
noting application to lunar  
studies 12 p1819 A66-24603  
Vector scatter theory for backscatter of  
circularly polarized waves from Moon and  
Venus 22 p3866 A66-40174  
**LUNAR ECLIPSE**  
Radio emission of Moon during lunar  
eclipse 08 p1298 A66-19459  
Partial and total lunar eclipses from 1964  
to 2163 10 p1606 A66-21265  
Electrical and mechanical features of  
millimeter-wave antenna facility, including  
measurement of lunar surface during eclipse  
of December 1963 11 p1770 A66-22551  
Illuminance of Earth shadow at three  
wavelengths by numerical integration,  
accounting for light attenuation, ozone  
absorption and extinction, Rayleigh  
scattering and refractive beam  
divergence 11 p1770 A66-22570  
Radio emission intensity measurements of  
Moon at 1.8 cm during lunar eclipse of June  
25, 1964 12 p1945 A66-23507  
Three-color photometric study of  
atmospheric extinction by dust particles  
from lunar eclipse photoelectric  
measurements of Mare Crisium  
region 13 p2185 A66-25810  
Luminescence in December 1964 lunar  
eclipse, noting brightness measurement  
results in Mare Nubium  
region 16 p2800 A66-30644  
Observations of lunar radio eclipses at mm  
wavelengths 16 p2806 A66-31542  
Color and light intensity gradient of  
residual light scattered and refracted into

umbra of Earth shadow measured during  
lunar eclipse 17 p2999 A66-32068  
Earth shadow enlargement during lunar  
eclipse, noting contacts of lunar formations  
with shadow 17 p3000 A66-32341  
Solar eclipse observations by orbiting  
spacecraft will provide data on solar  
atmosphere, Earth upper atmosphere and  
role of multiple  
scattering 17 p3001 A66-32349  
Radio emission of Moon during lunar  
eclipse 18 p3232 A66-34488  
IR measurements on eclipsed Moon,  
discovering hot spots on lunar  
surface 19 p3457 A66-35448  
Radio emission intensity measurements of  
Moon at 1.8 cm during lunar eclipse of June  
25, 1964 20 p3646 A66-37020  
Terrestrial penumbra density variation  
with solar activity during lunar eclipses in  
11-year cycle 22 p3976 A66-39857  
Photoelectric observation of Moon during  
total lunar eclipse of June 24-25, 1964,  
noting bluing of color B-V before Mare  
Imbrium enters umbra 22 p3976 A66-39858  
Correlation between lunar eclipse  
brightness and interplanetary plasma flux,  
examining lunar  
luminescence 23 p4131 A66-41862  
**LUNAR EFFECT**  
Lunar-diurnal variation of cosmic ray  
intensity based on observations of neutron  
and meson component 02 p0281 A66-11336  
Lunar inequality on time of perihelion  
passages of Earth 04 p0576 A66-13481  
Effect of Moon phase and celestial latitude  
on lunar modulation of geomagnetic  
activity 10 p1529 A66-21157  
Lunar influence in terrestrial meteor rates  
investigated for unusual periodicities by  
spectral analysis of meteor rate  
data 11 p1775 A66-23140  
Variations of zodiacal light and airglow,  
suggesting correlation with solar and lunar  
cycle 14 p2283 A66-27096  
Lunar modulation of geomagnetic activity  
from 1884 to 1959 analyzed using magnetic  
character figure, noting relation to solar  
activity 24 p4201 A66-42598  
**LUNAR ENVIRONMENT**  
Lunar atmosphere, terrain and  
temperature 09 p1454 A66-20286  
Space suit for thermal, radiation and  
exposure protection for man on  
Moon 14 p2231 A66-28413  
Lunar environmental effects and logistics  
problems in industrial chemical processing  
of lunar resources  
[AICE PREPRINT 46A] 22 p3977 A66-39894  
Design and operational performance  
criteria for adequate simulation of thermal  
environment of spacecraft at lunar  
surface 22 p3888 A66-40209  
**LUNAR EVOLUTION**  
Equilibrium shape of Moon, assuming  
homogeneity computing mean rotation  
configuration and pertinent single parameter  
equilibrium shapes 07 p1133 A66-17304  
Thermal history of Moon and development  
of surface, discussing nearly simultaneous  
formation of maria 19 p3458 A66-35452  
Hypothesis concerning evolution of lunar  
surface, discussing infall of surface dust and  
bombardment by  
planetesimals 19 p3460 A66-35793  
Lunar origin, tidal evolution of Earth-Moon  
system, thermal background of lunar  
interior, figure and composition of Moon  
and radial density profile 20 p3647 A66-37038  
Statistical petrographic analysis of  
meteorite and carbonaceous chondrite  
evolution on Moon and Mars from rocket  
photographs 23 p4132 A66-42075  
**LUNAR EXCURSION MODULE /LEM/**  
Navigation, guidance and control systems  
to meet basic trajectory and crew safety  
requirements of LEM 01 p0102 A66-10043  
Measurement schedules effect on work  
load of astronaut performing navigation  
function, stressing tradeoff between number  
of measurements and accuracy  
level 01 p0102 A66-10044  
Design requirements for LEM, describing  
stabilization and control elements of abort  
system 01 p0140 A66-10046  
Apollo extension systems, developing  
technology for long-term manned space  
mission 02 p0293 A66-11509



LEM integrated guidance and control system consisting of digital computer, inertial measuring unit and various navigational sensors 02 p0255 A66-11628

Lunar landing research vehicle used for simulated lunar landings on Earth 04 p0585 A66-13636

LEM mission and pilot role in spacecraft control including guidance and control systems, retromaneuvering, landing-site inspection, etc 05 p0713 A66-15166

Two-stage /descent and ascent/ Lunar Excursion Module control system for landing gear, ascent stage, liftoff from lunar surface, etc 07 p1140 A66-17280

Apollo and LEM mission simulators, noting computer complex providing real time simulation, mathematical models, telemetry, display equipment, aural effects, etc 07 p1018 A66-18331

Apollo lunar landing spacecraft design noting command, service, lunar excursion module, etc 08 p1300 A66-18553

Design and program for Apollo Lunar Excursion Module, noting propulsion, guidance, control, ground support, etc 08 p1300 A66-18554

Man, system and vehicle simulation program for landing and docking phases of Apollo lunar landing mission 08 p1202 A66-18577

High efficiency lightweight DC-DC power converter with step-width modulating preregulator for use in Apollo Lunar Excursion Module 08 p1169 A66-19496

Functional electronic block used to breadboard molecular circuits of prototype lunar TV camera for Apollo Lunar Excursion Module /LEM/ 08 p1196 A66-19524

System and mission requirements of Lunar Mobile Laboratory, noting design and operation characteristics 09 p1364 A66-20160

Measurement schedules effect on work load of astronaut performing navigation function, stressing tradeoff between number of measurements and accuracy 10 p1554 A66-21953

Hybrid computer simulation of lunar excursion module and maneuvers with orbiting command service 12 p1828 A66-23839

Design of electronics packaging for LEM, considering reliability, low-weight, integration, control, etc 12 p1847 A66-24956

Reactivity of titanium alloy oxidizer tank with nitrogen tetroxide oxidizer under vibration analyzed for LEM when subjected to impact 13 p2111 A66-26222

Full-scale and model test for dynamic effects of LEM landing 14 p2393 A66-28019

Integrated checkout of Apollo payloads, command module, lunar excursion module and service module 14 p2271 A66-28423

Apollo Manned Space Flight Network /MSFN/ tracking and communications systems for tracking lunar spacecraft 15 p2450 A66-28748

Guidance and navigational system hardware for Apollo Command Module and LEM 18 p3132 A66-33877

Apollo LEM ECS and main subsystems design emphasizing maintenance of pressure, temperature, relative humidity and oxygen at safe levels 18 p3062 A66-33956

LEM Data Reduction System that performs concurrent data processing and telemetry conversion on computer time-shared arrangement 19 p3299 A66-35662

VHF communications system for S-band transmission link 20 p3515 A66-37228

Acceptance checkout system for checkout assistance to Apollo CSM and LEM facilities during countdown, discussing system configuration variability, composition and operation 20 p3543 A66-37579

Maintainability program for lunar excursion module considering prelaunch, inflight and lunar launch operations 20 p3574 A66-37962

Trajectories for manned lunar landing, discussing various mission alternatives in planning and realized stages and Apollo project characteristics 20 p3656 A66-38032

Manual steering, hybrid guidance system, in-flight computations and trajectory for automatic descent and landing system for LEM 21 p3768 A66-38899

LEM program at RCA, discussing history, management, lunar landing, rendezvous,

tracking antenna, radar, etc 21 p3714 A66-39515

LEM program history and management in RCA, discussing Apollo mission studies and initial assignments 21 p3822 A66-39516

Attitude, translation and descent engine control for attitude and position control of LEM 21 p3808 A66-39518

Mechanical and thermal requirements of attitude, translation and descent engine controls of Lunar Excursion Module /LEM/ 21 p3808 A66-39519

Lunar Excursion Module /LEM/ reliability program, discussing engineering, manufacturing and techniques of design and qualification testing of electronic components 21 p3714 A66-39520

Communications subsystem providing S-band link between LEM and Earth and VHF link between LEM and Command Module 21 p3714 A66-39521

Erectable antenna for S-band communication between LEM and Earth 21 p3714 A66-39522

LEM rendezvous radar for tracking transponder on lunar surface or on Command Module 21 p3714 A66-39523

Cassegrain monopulse tracking antenna for LEM and Command Module rendezvous guidance 21 p3714 A66-39524

Solid state frequency multipliers for LEM landing and rendezvous 21 p3715 A66-39525

Lunar Excursion Module rendezvous radar and transponder receivers 21 p3715 A66-39526

Full-scale and model test for dynamic effects of LEM landing 24 p4283 A66-42771

Onboard calculation for navigation and guidance of Apollo mission vehicle [AGARDOGRAPH 105] 24 p4236 A66-43125

**LUNAR EXPLORATION**

Legal problems in organization and establishment of manned Lunar International Laboratory noting exploitation of lunar lands, sovereignty, communications, etc 03 p0447 A66-13077

Structural dynamic load and instability problems in launch vehicles and spacecraft in lunar exploration emphasizing reliability, crew safety and mission success 04 p0585 A66-13549

Apollo unified S-band system covering station locations, uplink and downlink spectrums, spacecraft gross parameters, theory of operation, etc 04 p0478 A66-13589

Space flight posture of U.S. at completion of AES program and alternate approaches for further lunar exploration and exploitation [SAE PAPER 650833] 05 p0760 A66-15015

Extravehicular mobility unit /EMU/ to be worn by astronauts on Apollo lunar landing mission 08 p1176 A66-18584

Lunar crater distribution measurement from Ranger VII photographic data analysis, deriving approximate expression for secondary distribution 08 p1297 A66-19417

Layman book on lunar exploration including topographical data, lunar water, food, shelter and travel, space suits, working conditions, etc 10 p1609 A66-21900

Fuel cells compared with other power systems for space application [AIAA PAPER 64-723] 13 p2005 A66-28618

Cislunar libration point as place of departure, rendezvous and parking for lunar operation 14 p2390 A66-28450

Titan III guidance and navigation system modification for lunar mission application 14 p2329 A66-28451

Soviet space research in 1965 including Moon and planets, magnetosphere, radiation belt, upper atmosphere, space vehicle dynamics, etc 15 p2599 A66-29897

U.S. space research in 1965 including lunar missions, Venus and Mars projects, manned space flights, meteorological satellites, etc 15 p2599 A66-29899

Projected rotary-percussive drilling system for obtaining lunar surface samples within specified payload and size requirements, considering drive systems 18 p3094 A66-34139

Steepest descent method of trajectory optimization for computing lunar and interplanetary transfer missions, noting terminal constraints 20 p3651 A66-37391

Luna X measurement of fields, radiation and micrometeorites near

Moon 22 p3980 A66-40377

**LUNAR EXPLORATION SYSTEM FOR APOLLO /LESA/**

Lunar Exploration System for Apollo /LESA/, discussing life support, power, fuel, communications systems, mission objectives and base evolution concept phases [SAE PAPER 660449] 18 p3093 A66-33895

**LUNAR FAR SIDE**

Photographic data relative to hidden face of Moon from Russian probe Zond III on July 20, 1965 10 p1608 A66-21755

Lunar basins and lunar lineaments on far side of Moon from analysis of Zond III photographs 22 p3982 A66-40544

**LUNAR FLIGHT**

Three-body problem of cislunar space flight, noting effect of solar gravitational field on spacecraft trajectory 16 p2804 A66-31332

Simultaneous observation of two trial distances of stars, stellar occultation, etc, for determining position of space vehicle during mission from Earth to Moon 20 p3597 A66-38014

**LUNAR GEOLOGY**

**SA SELENOGRAPHY**

Lunar rock petrography by X-ray diffraction system in soft-landed unmanned spacecraft 01 p0067 A66-10312

Moon structure, origin, morphology and surface properties of polarization, radio and radar wavelength-emission, etc 05 p0767 A66-15758

Propellant extraction from lunar material, giving cost analysis of manufacture and use in Earth-Moon space flight with expendable and reusable tankers 10 p1610 A66-21943

Text on lunar geology /selenology/, discussing photographic methods, lunar craters, ring-structures, soil, faulting, tectonic synthesis, maria origin, etc 14 p2381 A66-27490

Lunar and asteroidal meteorites 14 p2382 A66-27603

Results and goals of lunar geological studies from Ranger and Luna satellite observations of surface 16 p2806 A66-31701

Thermal history, chemical composition and interior of Moon evaluated from Ranger VII, VIII and IX and terrestrial photographs 19 p3456 A66-35438

Mechanism for selenological processes assuming lunar surface is anorogenically molded and crater pattern stems from reactivation of anorogenic zones 19 p3464 A66-36312

**LUNAR GRAVITATION**

Clairaut theorem of normal gravity at surface and configuration of Moon 03 p0427 A66-12918

Approximate value of mass of Moon calculated, using noncalculus derivation of Newton modification of Kepler third law 08 p1296 A66-19380

Clairaut theorem of normal gravity at surface and configuration of Moon 14 p2380 A66-27287

Lunar models of figure, density distribution and gravity field from Earth telescope data 21 p3812 A66-38822

Tracking data for Lunar Orbiter I producing first estimate of overall gravitational field of Moon, noting spacecraft will not impact on Moon before completing photographic mission 22 p3979 A66-40302

**LUNAR GRAVITATIONAL EFFECT**

Tracking geometry and dynamics of lunar satellite, estimating orbital elements and lunar gravitational field parameters through Earth-based range and range rate observations [AIAA PAPER 66-39] 07 p1139 A66-18448

Testing lunar surface vehicles under simulated lunar gravity conditions, discussing mobility test article configurations and gravity simulator designs [SAE PAPER 660144] 12 p1858 A66-24534

Lunar origin hypothesis suggesting capture in gravitational field of Earth following storage in solar system 13 p2188 A66-26366

Langley Lunar Landing Research Facility for flight tests of landing vehicle and simulation of lunar gravity field 21 p3821 A66-38900

**LUNAR LANDING**

**SA SOFT LANDING**



- Lunar landing research vehicle used for simulated lunar landings on Earth 04 p0585 A66-13636
- Simulation study of human performance in manual control tasks in orbital rendezvous and lunar landing 06 p0818 A66-16245
- Soviet space program, development of proton booster and proton and electron satellites and likelihood of Russia winning Moon race 06 p0955 A66-16802
- Man in Project Apollo including module to module docking, lunar landing, maneuvering, eentry, etc 07 p1140 A66-17279
- Man, system and vehicle simulation program for landing and docking phases of Apollo lunar landing mission 08 p1202 A66-18577
- Extravehicular mobility unit (EMU) to be worn by astronauts on Apollo lunar landing mission 08 p1176 A66-18584
- Iterative guidance law for Saturn launch vehicle for lunar landing, examining trajectory optimization 08 p1253 A66-19539
- International cooperation in space law in connection with future space laboratories and lunar and Martian landings 09 p1473 A66-20558
- Jodrell Bank observations of landing phase and TV signals of Luna 9 soft landing 12 p1948 A66-23915
- Lunar landing spacecraft analysis and Surveyor reliability data acquisition 13 p2192 A66-25506
- Informed guesses as to mode of landing of Luna IX, based on data available through news media 14 p2392 A66-27896
- Simulated lunar landing maneuver of Apollo spacecraft, determining pilot control problems and handling qualities 16 p2743 A66-30886
- Guidance control technique for soft automatic lunar landing 16 p2743 A66-30887
- Legal question of Moon ownership, discussing international implications of manned landing 19 p3480 A66-35733
- Radar-updated inertial navigation of continuously-powered space vehicle during deboost phase of flight prior to lunar landing 20 p3596 A66-37221
- Surveyor vernier propulsion system, discussing design of thrust chamber, propellant tank assemblies, functions of VPS, etc [AIAA PAPER 66-593] 20 p3629 A66-37632
- Trajectories for manned lunar landing, discussing various mission alternatives in planning and realized stages and Apollo project characteristics 20 p3656 A66-38032
- Performance capabilities of Surveyor spacecraft lunar landing TV system operating in mode that reduces RF power requirements for lunar distances 20 p3562 A66-38383
- Guidance, navigation and two phases of targeting of Saturn V lunar landing mission, analyzing launch, boost to orbit and iterative guidance 21 p3768 A66-38898
- Apollo mission evolution, with particular reference to lunar descent, landing, takeoff and rendezvous performed by LEM 21 p3822 A66-39517
- Landing dynamics analysis of ability of Moon surface to support Luna IX landing capsule 22 p3981 A66-40518
- Book on space navigation guidance and control covering manned lunar landing guidance, pulse torquing and inertial measurement units, computer utilization, control systems, etc [AGARDOGRAPH 105] 24 p4235 A66-43122
- Navigation, guidance and control system instrumentation for Apollo manned lunar landing mission [AGARDOGRAPH 105] 24 p4236 A66-43124
- LUNAR LANDING MODULE**
- Surveyor midcourse guidance treated by minima and maxima theory, noting terminal phase 19 p3397 A66-35600
- Langley Lunar Landing Research Facility for flight tests of landing vehicle and simulation of lunar gravity field 21 p3821 A66-38900
- LUNAR LANDING SITE**
- Lunar landing site selection by Earth-based manual control, using televised landing area picture 01 p0104 A66-10682
- Accuracy of spacecraft landing location on lunar surface determined from postarrival tracking, considering effect of various mission-dependent parameters [AIAA PAPER 65-694] 19 p3462 A66-35901
- LUNAR LAUNCH**
- Moon launch pads at Cape Kennedy noting structural and functional groups, crawlerway, propellant facilities, etc 01 p0054 A66-10862
- Siting of manned lunar launch facilities 09 p1365 A66-20699
- LUNAR LIMB**
- Preliminary drawings of lunar limb areas from 30 degrees north latitude to north pole 02 p0287 A66-11496
- Preliminary drawings of lunar limb areas from 30 degrees south latitude to south pole 02 p0288 A66-11497
- LUNAR LUMINESCENCE**
- Energy sources of lunar luminescence noting effects of solar wind, corpuscular radiation, electromagnetic radiation and radioactivity 07 p1139 A66-18090
- Determination of lunar luminance to set video gain of Ranger TV cameras 08 p1222 A66-18733
- Estimation of ozone concentration at altitudes of 44 to 102 km from nighttime geophysical rocket measurements of atmospheric brightness 08 p1221 A66-19796
- Statistical correlation between transient lunar luminescence and sunspot number distribution 11 p1775 A66-23193
- Lunar surface luminescence and variations in light flux with solar activity 12 p1948 A66-23943
- Model explaining negative polarization of moonlight at small lunar phase angles 12 p1949 A66-24235
- Visibility of lunar luminescence, noting favorable possibilities at new Moon, dark eclipses and far side and energy sources for luminescence 13 p2188 A66-26350
- Luminescence in December 1964 lunar eclipse, noting brightness measurement results in Mare Nubium region 16 p2800 A66-30644
- Lunar luminescence and photographic observation techniques, noting solar activity effect 17 p3006 A66-33010
- Profiles of isophotes and relative intensities for Aristarchus region of Moon taken during total eclipse on December 19, 1964 18 p3237 A66-35048
- Estimation of ozone concentration at altitudes of 44 to 102 km from nighttime geophysical rocket measurements of atmospheric brightness 21 p3733 A66-38792
- Terrestrial penumbra density variation with solar activity during lunar eclipses in 11-year cycle 22 p3976 A66-39857
- Correlation between lunar eclipse brightness and interplanetary plasma flux, examining lunar luminescence 23 p4131 A66-41862
- LUNAR MAGNETIC FIELD**
- Imp-I observation of magnetic wake of Moon or Earth 11 p1697 A66-22424
- Statistical-probability determination of lunar-solar daily and seasonal magnetic variations and geomagnetic effects 12 p1951 A66-24463
- Lunar magnetosphere, Moon-solar wind interaction, X-ray flux measurement and possible hazards to astronauts 18 p3231 A66-34357
- IMP satellite data on lunar magnetospheric MHD wake and interaction with solar wind 18 p3231 A66-34358
- LUNAR MAP**
- SA SELENOGRAPHY**
- Horizontal and vertical control system for determining three-dimensional coordinates in lunar charting by aeronautical chart and information center 08 p1293 A66-19263
- Statistical comparison of lunar maps of U.S. Army with Baldwin maps, determining true precision of individual values on both maps 13 p2177 A66-25119
- Reduction of measures for position on single lunar photograph to determine refraction-free photographic coordinates 15 p2603 A66-29969
- Selenographic measures on Yerkes Lunar Photograph No. 1170, noting refraction-free coordinate 15 p2603 A66-29970
- Solid selenographic coordinates computation, using librations for lunar photographs 15 p2603 A66-29971
- Lunar charting for project Apollo 16 p2743 A66-30669
- Lunar mapping in far IR, including hot spots during total eclipse of December 19, 1964 16 p2698 A66-31225
- Radio measurements of Moon, particularly IR, showing brightness-temperature maps of new, half-and full Moon 19 p3458 A66-35453
- LUNAR MARE**
- Lunar maria surface features and formation from Ranger VII photographs 03 p0424 A66-12455
- Moon shape related to distribution of continents and maria and relationship between shape and inertia moments 10 p1605 A66-21203
- Possible origin of lunar maria, suggesting they may be scars of mechanical damage wrought on lunar hemisphere by disruptive tides of Earth 14 p2384 A66-27900
- Lunar surface roughness in Mare Cognitum analyzed spectrally and compared with two terrestrial areas 14 p2387 A66-28336
- Indigenous organic matter on Moon by comparing Gilvarry and Sagan theories 17 p3005 A66-33006
- Model formulation of fine structure of lunar topography in Mare Cognitum based on Ranger VII satellite photographs 19 p3456 A66-35439
- Ranger VII, VIII and IX lunar probes scientific results on texture of maria, crater rays, crater classification, mare ridges, rilles, lineaments and bearing strength of mare floor 19 p3457 A66-35441
- Thermal history of Moon and development of surface, discussing nearly simultaneous formation of maria 19 p3458 A66-35452
- LUNAR MOBILE LABORATORY /MOLAB/**
- Apollo extension systems for lunar and planetary mission 02 p0288 A66-11510
- Data handling and telemetry requirements for manned scientific traverse, discussing MOL instrumentation and data parameters 04 p0478 A66-13591
- Space flight posture of U.S. at completion of AES program and alternate approaches for further lunar exploration and exploitation [SAE PAPER 650833] 05 p0760 A66-15015
- System and mission requirements of Lunar Mobile Laboratory, noting design and operation characteristics 09 p1364 A66-20160
- Testing lunar surface vehicles under simulated lunar gravity conditions, discussing mobility test article configurations and gravity simulator designs [SAE PAPER 660144] 12 p1858 A66-24534
- Human physiological and psychological characteristics effects on design of mobile lunar laboratory 17 p2904 A66-32944
- /MOLAB/ Digital computer optimization program, determining minimum weight fuel cell primary power system for MOLAB 20 p3496 A66-37156
- LUNAR OBSERVATORY**
- Communications of Arizona Lunar and Planetary Laboratory, Volume 3 09 p1455 A66-20291
- Lunar astronomical research, establishment of lunar observatory and mathematical model for analysis of logistics implications 14 p2390 A66-28410
- Lunar motion and shape, reviewing observational and theoretical work of various observatories and laboratories 17 p2998 A66-32024
- LUNAR OCCULTATION**
- X-ray source identified from Aerobee rocketborne Geiger counters, noting lunar occultation of Crab Nebula 02 p0282 A66-11360
- Metropolitan area man-made VHF/UHF noise in 200 to 500-mc frequency range 03 p0333 A66-12568
- Spectra of lunar occultations of emission source 3C 273 08 p1297 A66-19449
- X-ray source identified from Aerobee rocketborne Geiger counters, noting lunar occultation of Crab Nebula 10 p1598 A66-21101
- Radio sources observation during immersion phase of lunar occultation 13 p2183 A66-25608
- Radio source location by observing occultation of source by Moon 16 p2806 A66-31582



Lunar occultation and identification of MSH 19-27 radio source, noting computer analysis of brightness distribution 18 p3225 A66-33549

Spectra of lunar occultations of emission source 3C 273 18 p3232 A66-34478

Brightness distribution of 3C444 radio source obtained from lunar occultation 18 p3235 A66-34658

**LUNAR ORBIT**

Computation of approximate coordinates of Moon with estimation of accuracy over time interval of 50 years 02 p0292 A66-12235

Tidal de-spin of Mercury and Moon noting solar torque on planets 03 p0426 A66-12892

Variation of Earth-Moon distance and inclination angle of orbital planes during period of tidal evolution 03 p0427 A66-12920

Onboard lunar orbital navigation system simulation, using minimum variance estimation 08 p1249 A66-18818

Motions of perigee and node and distribution of mass in Moon determined by treating Sun, Earth and Moon as point masses 08 p1296 A66-19352

Inertial reference unit to provide attitude and thrust maneuver measurements for Lunar Orbiter spacecraft 08 p1253 A66-19529

Space probes and Earth-Moon libration points 13 p2186 A66-26012

Variation of Earth-Moon distance and inclination angle of orbital planes during period of tidal evolution 14 p2380 A66-27269

Variation in Earth-Moon distance as result of meteoritic impact 15 p2597 A66-29261

Semianalytical solution of motion of satellite in lunar orbit, considering perturbations due to lunar and Earth gravity and solar attraction 15 p2604 A66-30016

Secular variations of lunar orbit due to tidal friction 17 p3005 A66-33005

AIMP-D spacecraft mission analysis, determining launch conditions and trajectory shaping for attaining lunar orbit, noting errors, flight path angle, etc [AIAA PAPER 66-535] 18 p3226 A66-33665

Dynamical system of two degrees of freedom, with application to restricted problem and lunar theory 18 p3234 A66-34654

Brown lunar theory interpretation of observed lunar motion and associated rectangular-to-polar lunar coordinate transformations 18 p3234 A66-34655

Lagrange-Laplace theory of lunar physical librations extended to include reduced estimate of mechanical ellipticity of lunar equator 19 p3460 A66-35791

Lunar orbit evolution caused by tidal friction in Earth and Moon interiors 22 p3985 A66-40956

**LUNAR ORBITER**

Systems design analysis of lunar survey viewfinder /LSV/ consisting of pointing and tracking telescope for high-resolution lunar surface survey 20 p3558 A66-37225

U.S. Lunar Orbiter program 20 p3663 A66-38063

Trajectory optimization as part of real time flight operations in Lunar Orbiter program 21 p3765 A66-38866

Tracking data for Lunar Orbiter I producing first estimate of overall gravitational field of Moon, noting spacecraft will not impact on Moon before completing photographic mission 22 p3979 A66-40302

**LUNAR PERTURBATION**

Lunar physical libration constants determination based on position of crater Mestling A with respect to lunar limb 02 p0293 A66-12265

Lunar-solar perturbation effect on satellites with eccentric orbits, noting lifetimes on perigee heights 16 p2802 A66-30923

Brown lunar theory interpretation of observed lunar motion and associated rectangular-to-polar lunar coordinate transformations 18 p3234 A66-34655

**LUNAR PHASE**

Model explaining negative polarization of moonlight at small lunar phase angles 12 p1949 A66-24235

Interrelation between lunar phase and occurrence of precipitation larger than 10.0 mm per day in northern Germany 16 p2742 A66-31113

Variation of geomagnetic activity with

phase of Moon tested for statistical significance, noting fluctuations at lunar period 22 p3982 A66-40555

**LUNAR PHOTOGRAPH**

Ranger television system designed to transmit close-up pictures of lunar surface to Earth 02 p0189 A66-11364

Zond III photographs of lunar far side taken July 20, 1965 noting Oceanus Procellarum, Mare Orientale and thalassoids 04 p0578 A66-14023

Ranger lunar probe photograph analysis, crater size and shape measurements and dominant topographic features, including camera and command systems 07 p1132 A66-17208

Origin and nature of three structures in 235-mi diameter lunar crater photographed by Ranger VII 07 p1183 A66-17456

Structural analysis of lunar crater Alphonsus, using Ranger IX photographs 09 p1455 A66-20397

Ephemeris time determined by photographic observation of Moon 10 p1606 A66-21261

Data processing procedures used on flights of Rangers VII, VIII and IX, evaluating lunar photographs 11 p1775 A66-23079

Reduction of measures for position on single lunar photograph to determine refraction-free photographic coordinates 15 p2603 A66-29969

Selenodetic measures on Yerkes Lunar Photograph No. 1170, noting refraction-free coordinate 15 p2603 A66-29970

Solid selenodetic coordinates computation, using librations for lunar photographs 15 p2603 A66-29971

**LUNAR PHOTOGRAPHY**

Photographic determination of dependence of topocentric coordinates of Moon on geocentric coordinates 03 p0366 A66-13031

Long-focus horizontal telescope with coelostat for photographing position of Moon 05 p0681 A66-15217

Ranger Block III television system for lunar surface photography 06 p0958 A66-15934

History, background and purpose of Ranger missions to Moon, including spacecraft, television subsystem, testing and calibration 07 p1139 A66-18360

Lunar surface shape and altitude determination via stereophotogrammetric processing of telescopic Moon photographs 07 p1036 A66-18482

Stereoscopic camera system design for use on lunar orbiting vehicle including illumination, lunar albedo, resolution and signal to noise ratio 08 p1222 A66-18734

Zond III photographic survey of far side of Moon 09 p1463 A66-19904

Light-colored rays radiating from some lunar craters, hypotheses advanced and Ranger VII photographs 11 p1771 A66-22770

Design parameters of astronomical camera for lunar charting 12 p1876 A66-23644

Image dissector for lunar observation in conjunction with Earth-based telescope, noting efficiency of resolution contrast sensitivity 12 p1883 A66-24678

Lunar photographs received from Luna IX 13 p2177 A66-25137

Large-scale photography and mapping problems in lunar photogrammetry 13 p2182 A66-25601

Photometric method for deriving lunar surface elevation information from single picture 13 p2183 A66-25603

NASA Lunar Orbiter program to place unmanned spacecraft into orbit around Moon 13 p2078 A66-25604

Frequency distribution of secondary lunar craters determined from Ranger VII photographs, hypothesizing that part of these depressions are subsidence formations 15 p2598 A66-29265

Surveyor I data analyzed, noting lunar photographs, topography and instrumentation 15 p2599 A66-29657

Monographs from Lunar and Planetary Laboratory of University of Arizona, 1965 15 p2603 A66-29968

High resolution lunar satellite photography capable of 1-ft ground resolution [SMPT PREPRINT 98-63] 16 p2707 A66-31152

Lunar photographs of Ranger VII analyzed,

noting lunar surface 16 p2806 A66-31700

Photographic atlas of Moon, particularly Ranger VII transmissions and Pic-du-Midi ground observation, with discussion of lunar physical and dynamic properties 16 p2807 A66-31747

Lunar photography with 74-inch reflector of Helwan Observatory, detailing original negatives 17 p3006 A66-33018

Lunar photometric brightness variational function based on JPL study of Moon topology 18 p3235 A66-34656

Luna IX photographs indicate lunar surface composition of weakly cohesive poorly sorted fragmental material of unknown source 22 p3978 A66-40017

Cathode ray tube device for digital video processing of Ranger pictures 23 p4071 A66-41677

**LUNAR PROBE**

SA EXPLORER XXXIII SATELLITE

SA LUNIK IX LUNAR PROBE

SA PIONEER SPACE PROBE

SA RANGER VII LUNAR PROBE

SA RANGER VIII LUNAR PROBE

Lunar photographs received from Luna IX 13 p2177 A66-25137

Informed guesses as to mode of landing of Luna IX, based on data available through news media 14 p2392 A66-27896

Hypothesis that Luna IX rocket exhaust during soft landing caused formation of shallow crater visible in Ranger VII lunar probe photographs 15 p2593 A66-28681

Luna IX imaging system and analysis of pictorial data of lunar surface 15 p2498 A66-28741

Celestial mechanics covering two-body problem, planetary and asteroid theory, interplanetary trajectories, lunar probe, spherical harmonics, etc 17 p2997 A66-32019

First Soviet automatic station Luna IX to land on Moon, discussing flight stages and reproductions of lunar surface images transmitted to Earth 17 p3004 A66-32958

Lunar figure and orbit parameters measured by optical location method 19 p3455 A66-35285

Ranger VII, VIII and IX lunar probes scientific results on texture of maria, crater rays, crater classification, mare ridges, rilles, lineaments and bearing strength of mare floor 19 p3457 A66-35441

Auxiliary autonomous piggyback detector and recorder system for spacecraft failure detection following touchdown 19 p3315 A66-35676

Luna X measurement of fields, radiation and micrometeorites near Moon 22 p3980 A66-40377

**LUNAR PROGRAM**

Scientific and industrial reasons for manned lunar missions 04 p0576 A66-13576

Equipment design and weight estimates for lunar production of oxygen and water 22 p3977 A66-39896

**LUNAR RADIATION**

Heat flux from lunar emission incident on surface in circular orbit as function of orbital parameters [AIAA PAPER 64-336] 03 p0425 A66-12756

Intensity estimation for lunar X-rays excited by high energy terrestrial electrons from solar stream induced geomagnetic cavity 09 p1442 A66-20388

Lunar X-ray detectability, noting generation by solar wind electron bombardment and flux intensity 09 p1459 A66-20885

Ozone number densities in 30 to 75 km altitude determined at night by rocket measurements of lunar UV radiation absorption in various bands 15 p2492 A66-30030

Red and blue flashes in silicate luminescence excited by low-energy proton and lunar reddening by solar-ion excitation 16 p2802 A66-30930

**LUNAR RAY**

Ranger VII and VIII photography shows nature of lesser lunar ray systems, including images of crater Delambre and Bonpland J 08 p1293 A66-19265

Light-colored rays radiating from some lunar craters, hypotheses advanced and Ranger VII photographs 11 p1771 A66-22770

**LUNAR ROVING VEHICLE /LRV/**

Lunar-surface fixed shelter and roving



- vehicle designed for lunar exploration 02 p0289 A66-11618
- Preliminary mobility tests of scale model lunar roving vehicle [SAE PAPER 660147] 07 p1017 A66-17250
- One-man lunar Rover craft design and performance, considering bipropellant rocket powered platform kinesthetically controlled by astronaut 08 p1303 A66-18822
- Apollo extension system /AES/ for lunar surface exploration [SAE PAPER 660145] 08 p1296 A66-19390
- System design technique for extraterrestrial vehicles which maximizes effectiveness of complex system operating in partially defined environment 13 p2057 A66-25247
- Unmanned lunar roving vehicle power requirements, comparing radioisotope thermoelectric generator and solar cell/battery systems 23 p4017 A66-41104
- Isotope power systems for lunar roving vehicles noting fuel, radiation shielding, performance, weight, etc 23 p4024 A66-41770
- LUNAR SATELLITE**
- Tracking geometry and dynamics of lunar satellite, estimating orbital elements and lunar gravitational field parameters through Earth-based range and range rate observations [AIAA PAPER 66-39] 07 p1139 A66-18448
- Lunar communication satellites, discussing satellite relay, librational, random, and synchronous satellite design, lunar orbits, etc [AIAA PAPER 66-315] 12 p1823 A66-24781
- High resolution lunar satellite photography capable of 1-ft ground resolution [SMPT PREPRINT 98-63] 16 p2707 A66-31152
- Lagrange libration points in plane of two mutually gravitating heavy masses applied to theory of SYNCOM lunar satellites 22 p3979 A66-40176
- LUNAR SCATTERING**
- Dependence of mean scattered power on scattering geometry and wavelength in terms of scale roughness and rms slope of components for bistatic scattering 10 p1499 A66-21612
- Specular returns and diffuse scattering from Moon and ocean bottom 16 p2653 A66-30932
- Lunar line waveguide parameters calculated for inner conductor displacement and ratio of radii 19 p3311 A66-35301
- LUNAR SEISMOGRAPH**
- Velocity distribution of P and S waves in lunar interior, based on elastic wave propagation in rocks and P and S wave distribution in upper Earth layer 10 p1607 A66-21287
- Interior structure of Moon and planets studied by geophysical seismic methods 20 p3647 A66-37039
- LUNAR SHADOW**
- Photoelectric observation of Moon during total lunar eclipse of June 24-25, 1964, noting bluing of color B-V before Mare Imbrium enters umbra 22 p3976 A66-39858
- LUNAR SHELTER**
- Lunar-surface fixed shelter and roving vehicle designed for lunar exploration 02 p0289 A66-11618
- Lunar shelter design and support system imposed by lunar environment [SAE PAPER 650834] 05 p0660 A66-15016
- LUNAR SOIL**
- Environmental test criteria for lunar and planetary soils, discussing particle size, clay, hydrothermal alteration, cohesion, adhesion, vacuum and temperature effects, etc 14 p2387 A66-28179
- Shear strength of idealized granular media in vacuum, in conditions simulating environmental pressure of lunar surface layer 14 p2288 A66-28180
- Mechanical properties of lunar dust, consolidated lunar conglomerates and lunar rocks described by macrorheological constants 16 p2805 A66-31483
- Solar energy vs electrical or nuclear power for recovery of water, oxygen and various chemicals from lunar soil [AICE PREPRINT 46B] 22 p3977 A66-39897
- LUNAR SPACECRAFT**
- SA APOLLO SPACECRAFT
- Apollo manned space flight program including mission profile, spacecraft and constituent systems 01 p0143 A66-10799
- Lunar orbiter objectives, mission and spacecraft configuration, detailing inertial reference unit 04 p0543 A66-13581
- Classical spectroscopic binary star orbit determination techniques to provide orbital elements for lunar satellite tracked by Earth-based Doppler radar [AIAA PAPER 66-40] 08 p1298 A66-19727
- Electronic predictor instruments for dynamic control and simulation and possible application to lunar spaceship 13 p2048 A66-25896
- Series power switch for orientation and position computer of small lunar-orbit spacecraft designed to reduce weight and cost 17 p2878 A66-33122
- Next-generation lunar transports for multiman crew landing [SAE PAPER 660443] 17 p3017 A66-33158
- Terminal guidance system instrumentation for Surveyor project lunar soft-landing spacecraft 18 p3132 A66-33881
- Classical spectroscopic binary star orbit determination techniques to provide orbital elements for lunar satellite tracked by Earth-based Doppler radar 18 p3234 A66-34596
- Symbolic programming digital computer techniques, hardware interfacing and system errors in simulation of lunar midcourse guidance and navigation systems 20 p3543 A66-37250
- Microbiological decontamination of lunar spacecraft during mechanical integration and assembly 22 p3857 A66-40044
- LUNAR SURFACE**
- SA SELENOGRAPHY**
- Lunite model based on astronomical and radar data of radio wave reflectance from lunar surface, showing dependence of reflection coefficient on wavelength 01 p0135 A66-10274
- Martian surface age calculated from rate of meteorite infall in analogy to lunar case 01 p0136 A66-10440
- Apollo extension systems for lunar and planetary mission 02 p0288 A66-11510
- Radar backscattering for tenuous surface layer on Moon 04 p0577 A66-13895
- Bearing strength of lunar surface, optical properties suggest rock particles which maintain high porosity by interparticle adhesion 06 p0955 A66-16788
- Directional radiative characteristics of conical cavities and relation to reflective characteristics of Moon 07 p1136 A66-17729
- Lunar surface ideal for thermal neutron, molecular and atomic beam measurements 08 p1287 A66-18768
- Coefficients of expansion into spherical harmonics of Moon surface as presented by selenodetic control system of USAF 08 p1217 A66-19264
- Lunar crater distribution measurement from Ranger VII photographic data analysis, deriving approximate expression for secondary distribution 08 p1297 A66-19417
- IR spectrophotometry of Moon and Galilean satellites of Jupiter, noting surface properties, thermal radiation and albedo increase with wavelength 08 p1298 A66-19458
- Lunar and planetary surfaces investigated from thermal radiation standpoint 09 p1451 A66-20114
- Surface of Moon composed of solid material with different physical properties from terrestrial rock 09 p1453 A66-20173
- Lunar atmosphere, terrain and temperature 09 p1454 A66-20286
- Lunar X-ray detectability, noting generation by solar wind electron bombardment and flux 09 p1459 A66-20885
- Intensity Remote measurement of trace amounts of vapors in lunar and planetary atmospheres as indicator of biologic and geologic surface conditions 10 p1608 A66-21532
- Lunar and planetary terrain roughness in terms of curvature statistics, based on Ranger VII and Bonita Lava Flow contour map analysis [AIAA PAPER 65-389] 10 p1610 A66-21955
- Lunar spectral reflectivity distribution determined by comparison of lunar spectra with solar spectrum and spectra of early star classes 12 p1945 A66-23506
- Nondispersive X-ray spectrometer for remote geochemical analysis of lunar or planetary surfaces 12 p1878 A66-23694
- Luna 9 TV photographs of Moon 12 p1948 A66-23916
- Radar maps of Moon and planets using bistatic continuous wave mode of radar operation between orbiting spacecraft and ground station 12 p1825 A66-24891
- Neutron analysis techniques for determining hydrogen presence on lunar or planetary surfaces, based on measurement of gamma radiation 14 p2233 A66-28105
- Reflection spectra of rock powders compared with Stratoscope II spectrum of Mare Tranquillitatis 14 p2386 A66-28128
- Radar cross section of Earth surfaces as affected by wavelength, with reference to probing lunar surfaces 15 p2448 A66-28572
- Hypothesis that Luna IX rocket exhaust during soft landing caused formation of shallow crater visible in Ranger VII lunar probe photographs 15 p2593 A66-28681
- Objections to Gehrels model explaining observations on wavelength dependence of optical properties of lunar surface 15 p2597 A66-29260
- Surveyor I data analyzed, noting lunar photographs, topography and instrumentation 15 p2599 A66-29657
- Diffusely reflecting surfaces for simulating brightness of lunar surfaces, noting pronounced rise of reflectivity at small phase angles 16 p2802 A66-30929
- Lunar photographs of Ranger VII analyzed, noting lunar surface 16 p2806 A66-31700
- Characteristics of lunar radio emission considered, taking into account averaging effect of antenna radiation pattern 17 p2999 A66-32237
- Lunar surface layer radioactivity from diffusion of radon and thoron 17 p3004 A66-32942
- First Soviet automatic station Luna IX to land on Moon, discussing flight stages and reproductions of lunar surface images transmitted to Earth 17 p3004 A66-32958
- Lunar structural lineaments as boundary conditions for convection theory 17 p3007 A66-33235
- Thermal energy calculations from circular and elliptical spots in area of crater Aristarchus to support volcanic origin 18 p3228 A66-34099
- IR spectrophotometry of Moon and Galilean satellites of Jupiter, noting surface properties, thermal radiation and albedo increase with wavelength 18 p3232 A66-34487
- Nature of lunar surface - IAU/NASA Symposium, Goddard Space Flight Center, Greenbelt, Maryland, April 1965 19 p3456 A66-35437
- Lunar and Planetary Laboratory of University of Arizona, summarizing conclusions concerning lunar surface 19 p3457 A66-35440
- Ranger VII, VIII and IX lunar probes scientific results on texture of maria, crater rays, crater classification, mare ridges, rilles, lineaments and bearing strength of mare floor 19 p3457 A66-35441
- Lunar surface, discussing radar scattering, optical scattering, thermal and photographic data, etc 19 p3457 A66-35442
- Hypervelocity projectile impact cratering from Ranger photographs of lunar surface 19 p3457 A66-35443
- Optical photometric properties of lunar surface, discussing brightness effects, solar wind, albedo, reflectivity, backscatter, chemical composition, ion bombardment effects, etc 19 p3457 A66-35444
- Polarized light study of lunar surface dust composition 19 p3457 A66-35445
- Quantitative analysis of transient luminous phenomena on lunar surface and relation to solar electromagnetic or corpuscular excitations 19 p3457 A66-35446
- IR measurements on eclipsed Moon, discovering hot spots on lunar surface 19 p3457 A66-35448
- Lunar surface radar observation techniques and results on dielectric constant of surface material, surface undulations, reflectivity, roughness, etc 19 p3458 A66-35449
- Thermal history of Moon and development



- of surface, discussing nearly simultaneous formation of maria 19 p3458 A66-35452
- Hypothesis concerning evolution of lunar surface, discussing infall of surface dust and bombardment by planetesimals 19 p3460 A66-35793
- Mechanism for selenological processes assuming lunar surface is anorogenically molded and crater pattern stems from reactivation of anorogenic zones 19 p3464 A66-36312
- Lunar spectral reflectivity distribution determined by comparison of lunar spectra with solar spectrum and spectra of early star classes 20 p3646 A66-37019
- Role of radiative transfer in mechanism of heat flow in lunar surface, noting magnitude of contribution to transfer 20 p3648 A66-37260
- Vacuum upwellings of simulated basalt and granite magma, showing correlation with lunar surface by photometry 20 p3655 A66-38025
- Viscosity distribution within Moon analyzed, using Navier-Stokes and continuity equations, abnormal inertia moment explained, maria and continent distribution examined for understanding internal state of Moon 20 p3656 A66-38030
- Energy reflected from subsolar point on Moon determined, noting energy balance and radiated energy 20 p3656 A66-38052
- Origin of tektites with Moon considered most likely extraterrestrial source 22 p3656 A66-38059
- Behavior of postulated lunar surface materials due to environmental high vacuum, examining micrometeoroid impact and solar radiation effect 21 p3810 A66-38506
- Statistical method for determining preferential directions shown by lunar surface formations known as lunar grid system 21 p3811 A66-38637
- Luna IX photographs indicate lunar surface composition of weakly cohesive poorly sorted fragmental material of unknown source 22 p3978 A66-40017
- Conceptual analytical method for simulating lunar surface environment, using computer program for parametric curves 22 p3888 A66-40210
- Volcanic vs meteoritic origin of lunar craters, discussing survival advantages in lunar landing 22 p3980 A66-40398
- Landing dynamics analysis of ability of Moon surface to support Luna IX landing capsule 22 p3981 A66-40518
- Photographic evidence from Luna IX indicating Moon may have surface made up largely of fine rock particles 22 p3982 A66-40522
- Translunar communication using pumice-like outer layer as propagation medium 23 p4036 A66-41151
- Lunar domes defined, observed and listed 23 p4128 A66-41209
- Dust layers on lunar maria 23 p4128 A66-41309
- Penetrating radiation measurement on Moon surface obtained by Luna IX spacecraft 23 p4128 A66-41410
- Magnetic spherules in silurian and permian salt samples suggest constant meteoric influx useful in determination of lunar surface age 24 p4198 A66-42435
- LUNAR SURFACE VEHICLE**
- Standard vehicular systems for operation on lunar surface with model of lunar exploration program [SAE PAPER 650838] 02 p0216 A66-12224
- Remote extraterrestrial surface navigation, discussing image-tube based stellar field acquisition system parameters 04 p0543 A66-13590
- Scale model testing of lunar surface vehicles in simulated low gravity field [SAE PAPER 660148] 07 p1017 A66-17251
- Lunar and terrestrial vehicle wheels, frame, steering, suspension, electrochemical energy converters, electric traction power systems and vehicular propulsion [SAE PAPER 660150] 07 p1018 A66-17867
- Locomotion energy requirements for lunar surface vehicles, noting parameters affecting requirements, resistance factors, etc [SAE PAPER 660149] 12 p1858 A66-24530
- Testing lunar surface vehicles under simulated lunar gravity conditions, discussing mobility test article configurations and gravity simulator designs [SAE PAPER 660144] 12 p1858 A66-24534
- Dynamic analysis of lunar surface vehicle including power spectral density terrain definition, vehicle velocity limiting criteria and nonlinear analysis of vehicle freedom to pitch, bounce and roll 14 p2393 A66-28022
- Human and man/system requirements to provide criteria for choosing alternative mission and lunar surface roving vehicles design concepts 17 p2903 A66-32170
- Mobility aids for wheeled surface vehicles and flyers for Apollo lunar surface exploration 19 p3340 A66-35963
- Movable platform and differential throttle control configurations for lunar manned flying vehicle 24 p4284 A66-42954
- LUNAR TEMPERATURE**
- Thermal anomalies found in IR lunar observations attributed to lunar roughness on centimeter scale 01 p0138 A66-10884
- Nonuniform cooling of lunar surface detected by IR scanning during total eclipse 02 p0285 A66-11302
- Heat flux from lunar emission incident on surface in circular orbit as function of orbital parameters [AIAA PAPER 64-336] 03 p0425 A66-12756
- Central lunar temperature measured at 1 mm wavelength as time and phase function during total eclipse 05 p0763 A66-15290
- Radio emission of Moon during lunar eclipse 08 p1298 A66-19459
- Radiometric mapping and determination of lunar brightness temperature at 3 mm wavelength 09 p1455 A66-20389
- Electrical and mechanical features of millimeter-wave antenna facility, including measurement of lunar surface during eclipse of December 1963 11 p1770 A66-22551
- Observations of lunar radio eclipses at mm wavelengths 16 p2806 A66-31542
- Radio emission of Moon during lunar eclipse 18 p3232 A66-34488
- IR pyrometry of lunar surface 19 p3457 A66-35447
- Thermal conductivity equation solved for four combinations of concentration of radioactive elements in lunar crust, using result for crust thickness estimate 20 p3648 A66-37151
- LUNAR TIDE**
- Lunar tidal effect on oxygen green line in night airglow at Honolulu from 1961 to 1963 05 p0668 A66-14801
- Least squares method to determine diurnal lunar tide fluctuations from observations of Pulkovo, Greenwich and Tokyo Time Services 06 p0954 A66-16426
- Lunar tide calculated by analysis of perturbations in inclinations of two nearly polar satellites 06 p0877 A66-16781
- Possible effects of oceans on atmospheric lunar tide 07 p1061 A66-17363
- Phillips frequency-dependence rule for sporadic E extended for better statistical coincidence with lower frequency data 11 p1695 A66-22372
- Lunar tidal effect on daily and monthly variation of polarized sky light 12 p1874 A66-24844
- Lunar tidal variations in monthly median noon critical frequency in American zone during low solar activity 14 p2285 A66-27727
- Classical theory of tidal oscillations of plumb line acting under solar and lunar tidal forces 15 p2596 A66-29142
- Annual variations in atmospheric lunar tides attributed primarily to vertical shear of zonal wind systems 16 p2698 A66-31112
- Lunar semidiurnal tides in ionosphere over Puerto Rico determined from electron density profiles for heights between 150 and 300 km 17 p2923 A66-33362
- Lunar tidal effects on noon real-height F2 electron density profile data from two-year interval 22 p3908 A66-39967
- Lunar tidal variations, geopotential velocity and calculation of Love number 24 p4198 A66-42246
- LUNAR TOPOGRAPHY**
- SA SELENOGRAPHY**
- Lunar topographical asphericity, lunar coordinates, absolute and relative, harmonic analytical interpolation, formations, stratigraphy and optical librations 07 p1139 A66-18265
- Moon shape related to distribution of continents and maria and relationship between shape and inertia moments 10 p1605 A66-21203
- Note on paper discussing lunar shape and internal structure in connection with inhomogeneity of density distribution, showing incompatibility of hypothesis with measurements 10 p1605 A66-21210
- Layman book on lunar exploration including topographical data, lunar water, food, shelter and travel, space suits, working conditions, etc 10 p1609 A66-21900
- Moon shape determined by measuring distance from lunar surface points to lunar center of mass, using optical laser radar 11 p1774 A66-22964
- Photometric method for deriving lunar surface elevation information from single picture 13 p2183 A66-25603
- Lunar topography and cartography, noting application to lunar atlas preparation, absence of magnetic field, etc 17 p2999 A66-32132
- Harmonics of absolute lunar elevations, discussing stability criteria and spherical harmonic analysis of geometric figure of Moon 17 p3006 A66-33019
- Lunar photometric brightness variational function based on JPL study of Moon topology 18 p3235 A66-34656
- Model formulation of fine structure of lunar topography in Mare Cognitum based on Ranger VII satellite photographs 19 p3456 A66-35439
- Lunar models of figure, density distribution and gravity field from Earth telescope data 21 p3812 A66-38822
- Lunar basins and lunar lineaments on far side of Moon from analysis of Zond III photographs 22 p3982 A66-40544
- LUNAR TRACKING**
- Systems design analysis of lunar survey viewfinder /LSV/ consisting of pointing and tracking telescope for high-resolution lunar surface survey 20 p3558 A66-37225
- Optimal correlation of tracking data determining Surveyor I location 23 p4129 A66-41780
- LUNAR TRAJECTORY**
- SA EARTH-MOON TRAJECTORY**
- Solution to boundary value problems associated with artificial satellite, lunar impact trajectory and interplanetary trajectory 04 p0579 A66-14445
- Russian book on three-dimensional problem of reaching Moon, covering power optimized trajectories, initial velocity minimum, lunar orbit, perturbation factors, etc 06 p0954 A66-16563
- Linear perturbation theory computation of target errors in lunar impact trajectories due to random injection errors 08 p1289 A66-18828
- Sensor requirements for midcourse guidance phase of spacecraft on lunar trajectories, with attention to optical measurements and statistical combining for trajectory estimates [AIAA PAPER 64-234] 12 p1910 A66-24692
- LUNEBERG LENS**
- Spherical radar reflectors with high-gain omnidirectional response, noting structure, efficiency and achievement of isotropic response 10 p1503 A66-21642
- LUNG**
- S PULMONARY CIRCULATION**
- S PULMONARY FUNCTION**
- LUNIX IX LUNAR PROBE**
- Jodrell Bank observations of landing phase and TV signals of Luna 9 soft landing 12 p1948 A66-23915
- Luna 9 TV photographs of Moon 12 p1948 A66-23916
- Lunar photographs received from Luna IX 13 p2177 A66-25137
- Luna IX imaging system and analysis of pictorial data of lunar surface 15 p2498 A66-28741
- Luna IX photographs indicate lunar surface composition of weakly cohesive poorly sorted fragmental material of unknown source 22 p3978 A66-40017
- Landing dynamics analysis of ability of Moon surface to support Luna IX landing capsule 22 p3981 A66-40518
- Photographic evidence from Luna IX indicating Moon may have surface made up



largely of fine rock  
 particles 22 p3982 A66-40522  
**TUTETIUM COMPOUND**  
 Electric resistivity of solid phase of  
 lutetium hydrogen system noting action of  
 hydrogen atom 01 p0127 A66-11090  
**LUXEMBOURG EXPERIMENT**  
**S LANGMUIR PROBE**  
**LYMAN ALPHA RADIATION**  
 Extreme UV solar spectrum analysis  
 between Lyman alpha lines of H-I and C-VI,  
 using rocket  
 spectrography 02 p0286 A66-11356  
 Scattered Lyman alpha radiation  
 measurements near Earth and in  
 interplanetary space by Zond I, using NO-  
 filled photon counters with LiF  
 windows 10 p1596 A66-21049  
 Extreme UV solar spectrum analysis  
 between Lyman alpha lines of H-I and C-VI,  
 using rocket  
 spectrography 10 p1597 A66-21079  
 UV radiation from galaxies, radio sources,  
 quasi-stellar objects and Seyfert galaxies,  
 examining Lyman alpha

fluxes 10 p1598 A66-21098  
 Lyman alpha ionization of nitric oxide and  
 ion molecule reactions accounting for ionic  
 nitric oxide content of D and E  
 regions 16 p2694 A66-30705  
 Altitude distribution of atmospheric  
 molecular and atomic hydrogen, showing  
 results of Lyman alpha absorption  
 measurements 17 p2919 A66-32995  
 Lyman alpha airglow observations indicate  
 diurnal variation of atomic hydrogen in  
 thermosphere and exosphere with  
 abundance change with solar  
 activity 19 p3349 A66-36349  
 Barium ion concentration computed from  
 Ba II 4554 angstrom line and Lyman alpha  
 radiation intensity in lower  
 chromosphere 20 p3646 A66-37013  
 Magnetospheric phenomena related to  
 geomagnetic tail noting F region, polar  
 auroras and solar Lyman alpha radiation  
 scattering in night sky 24 p4203 A66-43029  
**LYMAN BETA RADIATION**  
 Ratio of average transmission coefficients

of L-beta and H-alpha and reabsorption in  
 hydrogen pulsed  
 discharge 01 p0111 A66-10390  
**LYMAN SPECTRUM**  
 Wing broadening in plasma of hydrogen  
 Lyman-alpha line by local electron and  
 quasi-static ion fields calculated, considering  
 impact theory of electron collisions,  
 quadrupole and dipole interactions and  
 existent asymmetries 03 p0405 A66-13138  
 X-ray photographs of Sun using Fresnel  
 zone plate camera mounted on Skylark  
 rocket, noting Lyman C-VI emission line in  
 solar spectrum 10 p1607 A66-21291  
 Physical process effect on structure of H  
 II regions, noting ionization, Lyman  
 continuum spectral distribution and  
 radiative transfer frequency dependence on  
 absorptive processes 17 p3003 A66-32655  
 Quasi-stellar radio sources correlated for  
 prediction of Lyman lines relative strengths  
 and optical depth of nebulas beyond Lyman  
 continuum, using simple  
 models 23 p4130 A66-41807

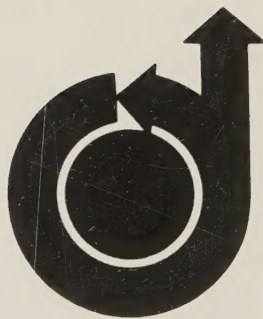












**AIAA TECHNICAL INFORMATION SERVICE**

750 THIRD AVENUE

NEW YORK, N. Y. 10017